PHYTOSOCIOLOGY OF WEED COMMUNITY IN CULTURE OF COWPEA (*VIGNA UNGUICULATA* L. WALP) AND CONTROLLING POSSIBILITIES WITH PRE-EMERGENT HERBICIDES

GONZAGA, G. DA S.[1] – SOUZA CRUZ , A. B. DE[1] – ALBUQUERQUE, J. A. A.[1] – SANTOS, G. X. L. DOS[2] – SOARES, M. B. B.[2*] – RIBEIRO ROCHA, P. R.[1] – ALVES, J. M. A.[1] – CASTRO, T. S. DE[1] – SANTOS, T. S. DOS[1] – SOUZA CRUZ, D. L. DE[3]

[1]*Federal University of Roraima (UFRR), BR 174, Km 12, S/N, Campus do Cauamé, Bairro Monte Cristo, Boa Vista, RR, CEP 69310-250, Brazil (phone: +55-95-3627-2573)*

[2]*Agribusiness Technology Agency of São Paulo (APTA) PO Box 24, Pindorama-SP, CEP 15830-000, Brazil (phone: +55-17-3572-2008; fax: +55-17-3572-1592)*

[3]*Federal Institute of Education, Science and Technology of Amazonas BR 307, São Gabriel da Cachoeira, AM, 69750-000, Brazil (phone: +55-97-3471-1470)*

**Corresponding author*
e-mail: beatriz@apta.sp.gov.br

(Received 23rd Oct 2017; accepted 20th Jun 2018)

Abstract. This study has aimed to diagnose and compare the predominant weed species in cowpea crop in the Amazon region and to evaluate the effectiveness of herbicides applied in pre-emergence. The weed sampling was obtained before planting, the cowpea cultivar was BRS Aracê, by collecting all the plants present within a 0.25 m² hollow frame, randomly thrown 40 times in experimental area to calculate the phytosociological indices. The herbicide efficiency experiment was conducted in a randomized block design with four replications, in time subdivided plot model. Treatments were applied one day after crop planting, their doses (g/ha ai) were: metribuzin (360), sulfentrazone (600), S-metolachlor (1200), pendimethalin (750), oxadiazon (1000), alachlor (2400), metribuzin + pendimethalin (360 + 750), metribuzin + alachlor (360 + 2400), manual weeding and weedy check. The evaluations of weed control were done at 21, 28 and 35 DAP. The most important weed in phytosociology was *Tridax procumbens*. Cultivation of the crop with weeds caused a reduction of more than 66% in crop productivity. The application of the metribuzin herbicide prevented the emergence of all cowpea seedlings while oxadiazon satisfactorily controlled the weeds without affecting the crop yield.
Keywords: *importance value index, chemical control, selectivity, tolerance*

Introduction

Cowpea (*Vigna unguiculata* (L.) Walp) is an annual grain legume (Fabaceae) native to west Africa, and possibly originated in Nigeria (Rachie and Roberts, 1974).

Cowpea is a widely adapted, stress tolerant grain, vegetable, and fodder crop grown on about 7 million ha in warm to hot regions of Africa, Asia, and the Americas (Yadav et al., 2017). Historically, cowpea production is made by small producers using a low technology level (Costa et al., 2017), from the North and Northeast regions of Brazil. The Brazilian average productivity of cowpea is between 300 and 400 kg/ha, considered low when compared to its productive potential (1000 kg/ha) (Mancuso et al., 2016).

http://www.aloki.hu ● ISSN 1589 1623 (Print) ● ISSN 1785 0037 (Online)
DOI: http://dx.doi.org/10.15666/aeer/1605_53115322
© 2018, ALÖKI Kft., Budapest, Hungary

The factors contributing to the low productivity of cowpea in Brazil are mainly related to the absence of mechanization and the low investment in the control of weeds and pests (Filgueiras et al., 2009).

Therefore, one of the major problems encountered by producers in the northern region of Brazil is the interference of weeds in the crop, since sowing is done in wide spacing and the initial growth of cowpea is slow (Costa et al., 2017). The problem of weed has been reported more severe during rainy season, as weeds come in 2-3 flushes and growth is very fast, therefore, they compete for light, nutrient and space and are responsible for reduction in crop yield and productivity by up to 70% (Moody,1973).

Type of weeds, weed density, their persistence and crop management practices determine the magnitude of yield loss (Omisore et al., 2016). The identification of weeds at the level of genus and species is a basic task, constituting a fundamental instrument of phytosociological surveys that will be the basis for the knowledge of the main weeds present in a given area. The progress of phytosociological evaluations has been slow and non-isochronous in the different research groups in the country.

The critical period of crop weed competition in cowpea has been identified as 20-30 days after sowing and presence of weeds beyond this period causes severe reduction in yields (Gupta et al., 2016). Hence, weed control needs to be undertaken during initial period of crop growth.

The occurrence of weed flora under any crop production system greatly influenced by range of factors such as history of the planting area, soil seed bank, tillage operations, selection of crops, application of chemical fertilizer, irrigation and agronomic practices etc (Saved et al., 1990). Beside these, the weed control measures (Hass and Streibig, 1982) and environment factors (Schemer and Chilcote, 1969) also significantly influenced the distribution of weed flora. Therefore, it is fundamental to know the phytosociology of weeds that compete with a crop, understanding the plant communities from a floristic and structural point of view and knowing the species present in a specific area (Braun-Blanquet, 1979).

Still widely used by smallholders, manual weeding although proven effective, it is not economically viable on a large scale because of the high labor cost, so integrated weed management is the best approach to minimize weed interference and productivity losses (Kumar and Singh, 2017). The suggestion that integrated weed management can be useful to provide better weed control measures should further be assessed. Omisore et al. (2016) compared different weed control methods in cowpea production and pre-emergence herbicide + hoe weeding at 6 weeks after planting was more effective in controlling weeds and increase grain yield.

Chemical weed control, i.e. use of herbicide proved the most practical, effective and economical means of controlling even unapproachable or in accessible weed or noxious weed (Yadav et al., 2017).

There are no registered herbicides for cowpea in Brazil, which prevents recommendations, however for crops belonging to the same botanical family (Fabaceae) as common bean (*Phaseolus vulgaris* L.) and soybean (*Glycine max* L.) are registered 27 and 55 herbicides, respectively.

Another aspect to be considered in the application of herbicides in this crop is the lack of knowledge about the tolerance of the many varieties to the herbicides (Harrison and Fery, 1993). There is great variability in the tolerance of cowpea genotypes to herbicides such as bentazon, in which more susceptible genotypes were killed, or very affected, with applications of 2000 g ai ha^{-1}, while the most tolerant ones resisted at the dose of 16.000 g ai ha^{-1} (Harrison and Fery, 1993).

http://www.aloki.hu ● ISSN 1589 1623 (Print) ● ISSN 1785 0037 (Online)
DOI: http://dx.doi.org/10.15666/aeer/1605_53115322
© 2018, ALÖKI Kft., Budapest, Hungary

Study the selectivity of herbicides to this culture is promising because the chemical control ensure less dependence on labour, efficiency even during the rainy season, effectiveness in controlling weeds in the planting furrow and not affecting the root system of the crops and being efficient in controlling vegetative propagation in the weeds (Costa et al., 2017). Herbicides already available in the Brazilian market, especially those used in common bean and soybean crops, can be effective for the control of weeds in cowpea, without causing injury or yield losses,.

The aim of this study was to get to know the characteristics of the characteristics of weed community of cowpea crop in the Amazon region of northern Brazil and to evaluate the selectivity and efficiency of herbicides applied in pre-emergence in cowpea crop.

Materials and methods

The experiment was conducted in the Agricultural Sciences Center of Federal University of Roraima, Cauamé Campus, municipality of Boa Vista in the State of Roraima, latitude 2°52'15.49" N, longitude 60°42'39.89" W and 85 m of altitude, with annual average precipitation of 1.678 mm (Araújo et al., 2001).

The soil of the experimental area was classified as Yellow Udox Soil and based on interpretation of chemical analysis, the soil was fixed using 1.500 kg/ha of limestone, 50 kg/ha of FTE BR 12, 90 kg/ha of P_2O_5 in the form of simple superphosphate and 60 kg/ha of K_2O in the form of potassium chloride.

Weed collection was performed immediately before planting, by the square inventory standard method. A 0.25 m^2 square was used, which was randomly launched for 40 times in the usable area. All weeds that were contained in the square were collected with root system and aerial part.

The collected species were identified and quantified according to family, genus and species by analysis of the external morphological characteristics of the vegetative and reproductive plant parts, according to literature, by comparison with other species identified and also by consulting experts.

The floristic list with families and species was organized according to the classification system established in the Angiosperm Phylogeny Group III guidelines (APG III, 2009). All scientific names and their authors were confirmed after verification in the International Plant Names Index (IPNI, 2013).

Phytosociological structure was assessed based on parameters such as the relative values of frequency, density and abundance and the importance value for each species according the methodology proposed by Braun-Blanquet (1979) (*Table 1*).

Table 1. *Description of the evaluated characteristics, formulas and evaluation method for the phytosociological survey based on the methodology proposed by Braun-Blanquet (1979)*

Characteristics	Method
Frequency (F)	Number of releases that contain the species/Total number of releases
Density (D)	Total number of individuals per species/Total area collected
Abundance (A)	Total number of individuals per species/Nº of releases that contain the species
Relative frequency (RF)	(Species frequency x 100)/Total frequency of all species
Relative density (RD)	(Species density x 100)/Total density of all species
Relative abundance (RA)	(Species abundance x 100)/Total abundance of all species
Importance value (IV)	RF + RD + RA

http://www.aloki.hu ● ISSN 1589 1623 (Print) ● ISSN 1785 0037 (Online)
DOI: http://dx.doi.org/10.15666/aeer/1605_53115322
© 2018, ALÖKI Kft., Budapest, Hungary

The seeds of the BRS Aracê cowpea variety, used in this study, were inoculated with the *Bradyrhizobium* BR 3262 strain recommended for the state of Roraima. The soil management system of the area was no-tillage, with sowing done with a mechanized planter at a spacing of 0.5 m between rows and planting density of 10 seeds per linear meter.

The experiment was designed in randomized blocks with 4 replicates in the time subdivided plot model. The plots consisted of herbicides applied in pre-emergence (*Table 2*) and the subplots consisted of 3 evaluation periods with a 7-day interval between them (21, 28 and 35 days after emergence). Pre-emergent herbicides, registered for the cultivation of soybeans and common bean, were used, in addition to some mixtures, except oxadiazon (registered for some horticultural crops, rice and sugar cane). These herbicides, although presenting different mechanisms of action, presented some degree of selectivity to other varieties of cowpea or to soy or bean crops.

Table 2. *Herbicides used in pre-emergence as a strategy to control weeds in cowpea, their modes of action, crops for which they are registered in Brazil, Boa Vista-RR, 2016*

	Pre-emergent herbicides	**Mode of action**	**Crop (Fabaceae)**	**Dose (g ha^{-1} a.i.)**
T1	Metribuzin	Selective, systemic with contact and residual activity. Inhibits photosynthesis (photosystem II)	Soybeans	360
T2	Sulfentrazone	Cell membrane disruption - PPO inhibitor	Soybeans	600
T3	S-metolachlor	Selective, absorbed through roots and shoots. Inhibition of VLCFA (inhibition of cell division)	Soybeans; Common bean	1200
T4	Pendimethalin	Selective, absorbed by roots and leaves. Inhibition of mitosis and cell division. Microtubule assembly inhibition	Soybeans	750
T5	Oxadiazon	Selective with contact action. Inhibits protoporphyrinogen oxidase, leading to irreversible cell membrane damage	-	1000
T6	Alachlor	Selective, systemic action absorbed by germinating shoots. Inhibition of VLCFA (inhibition of cell division)	Soybeans, Peanuts	2400
T7	Metribuzin +Pendimethalin	Inhibits PSII+ Microtubule assembly	Soybeans	360+750
T8	Metribuzin+ Alachlor	Inhibits PSII+Inhibition of VLCFA	Soybeans	360+2400
T9	Weed-free (manual weeding)	-	-	-
T10	Weedy check	-	-	-

The experimental plot consisted of six rows with 5 m of length, however, it was considered useful area of the plot the two central rows. The two lateral rows in addition to 0.5 of the frontal ends of the plot were considered border. The total area of the experiment was 600 m^2 and the total useful area was 200 m^2.

The herbicides were applied one day after planting and a costal spray, equipped with two TT 110.02 nozzles, spaced 0.5 m, maintained at a pressure of 2 bar, and a syringe volume of 170 L/ha was used.

http://www.aloki.hu ● ISSN 1589 1623 (Print) ● ISSN 1785 0037 (Online)
DOI: http://dx.doi.org/10.15666/aeer/1605_53115322
© 2018, ALÖKI Kft., Budapest, Hungary

The evaluation of control efficiency at 21, 28 and 35 days after planting (DAP) was based on a visual scale recommended by the Brazilian Society of Weeds. Percentage notes were assigned from 0 to 100%, where 0 (zero) indicates the absence of control and 100 the total control of weeds.

The results were submitted to the normality test of Shapiro-Wilk, visual control rating data were arc-sine square root transformed prior to analysis. Back-transformed are presented with mean separation based on transformed values. Data were subjected to ANOVA, when the variances were significant, the means were compared by the Tukey test at $p \leq 0.05$, using the software R™ version 2.12.2 and the package ExpDes english (R Core Team, 2017).

Results

This weed community was represented by 29 weed species from 10 different botanical families, 34.5% were monocots and 65.5% were dicots. *Table 3* shows the weed species found in the area and their respective common names and EPPO codes subdivided into botanical families.

Table 3. *Weed species found in the area with their common names and EPPO codes, distributed by botanical families*

Botanic family	Scientific name	Common name	EPPO code[1]
Asteraceae	*Acanthospermum australe* (Loefl.) Kuntze	Paraguayan starbur	ACNAU
	Emilia coccinea (Sims) G. Don	Scarlet tasselflower	EMICO
	Emilia sonchifolia (L.) DC. ex Wight	Lilac tasselflower	EMISO
	Praxelis clematidea (Griseb.) R.M.King and H.Rob.	Praxelis	PRACL
	Tridax procumbens L.	Coat buttons	TRQPR
Fabaceae	*Chamaecrista conferta* (Benth.) H. S. Irwin and Barneby	Pig's senna	CASAB
	Desmodium tortuosum (Sw.) DC.	Florida beggar weed	DEDTO
	Indigofera hisurta L.	Hairy indigo	INDHI
	Mimosa candolei R. Grether	Sensitive plant	SCNLE
	Zornia latifólia Sm.	Zornia	ZORLF
	Chamaecrista hispidula (Vahl) H.S.Irwin and Barneby	Cassia	CASHP
	Calopogonium mucunoides Desv.	Wild ground nut	CLOMU
Poaceae	*Cenchrus echinatus*L.	Southern sandbur	CCHEC
	Digitaria horizontalis Willd.	Jamaican crabgrass	DIGHO
	Digitaria insularis (L.) Fedde	Sourgrass	TRCIN
	Digitaria sanguinalis (L.) Scop.	Common crabgrass	DIGSA
	Paspalum dilatatum Poir.	Dallisgrass	PASDI
	Brachiaria decumbens Stapf. Prain.	Signal grass	BRADC
Cyperaceae	*Cyperus ferax* L.	Flatsedge	CYPFE
	Cyperus flavus (Vahl) Nees	Inflatedscale flatsedge	CYPFW
	Cyperus rotundus L.	Nutgrass	CYPRO
Malvaceae	*Waltheria indica* L.	Indian waltheria	WALAM
Convolvulaceae	*Ipomoea nil* (L.) Roth	Japanese morning glory	IPONI
Commelinaceae	*Commelina benghalensis* L.	Bengal day flower	COMBE
Amarantaceae	*Amaranthus viridis* L.	Slender amaranth	AMAVI
	Alternanthera tenella Colla	Perrotleaf	ALRFI
Nictaginaceae	*Boerhavia diffusa* L.	Red spiderling	BOEDI
Euphorbiaceae	*Chamaesyce hirta* (L.) Mills.	Hairy spurge	EPHHI
	Chamaesyce hyssopifolia (L.) Small	Hyssop spurge	EPHHS

[1]EPPO code: also known as Bayer code, is an encoding system used by the European and Mediterranean Plant Protection Organization (EPPO) to designate plants, pests and pathogens that are important for agriculture, 2014

http://www.aloki.hu ● ISSN 1589 1623 (Print) ● ISSN 1785 0037 (Online)
DOI: http://dx.doi.org/10.15666/aeer/1605_53115322
© 2018, ALÖKI Kft., Budapest, Hungary

The botanical families with the highest number of species were Fabaceae, Poaceae and Asteraceae with 7, 6 and 5 species, respectively, representing 62% of the weed species found in the studied area. There is a high number of weed species in the area belonging to the same botanical family of cowpea (Fabaceae).

Table 4 shows the phytosociological parameters (RF, RD, RA and IV) of weed species found in the experimental area. For the values of relative density, there are 5 prominent species: *Tridax procumbens* (21.21%), *Praxelis pauciflora* (13.26%), *Digitaria insularis* and *Digitaria sanguinalis*, (10.23% both) and *Chamaesyce hirta* (9.47%). The other species showed relative density (RD) lower than 5%.

Table 4. *Phytosociological parameters (RF, RD, RA and IV) of weed species found in the experimental area*

Species	RD	RF	RA	IV
Acanthospermum australe	1.89	9.71	2.32	13.92
Alternanthera tenella	4.17	2.18	6.8	13.15
Amaranthus viridis	1.52	2.18	2.47	6.17
Boerhavia diffusa	0.38	0.73	1.86	2.96
Brachiaria decumbens	1.52	2.18	2.47	6.17
Calopogonium mucunoides	0.38	0.73	1.86	2.96
Cenchrus echinatus	2.65	3.64	2.6	8.89
Chamaecrista conferta	0.38	0.73	1.86	2.96
Chamaecrista hispidula	0.38	0.73	1.86	2.96
Chamaesyce hirta	9.47	8.01	4.22	21.7
Chamaesyce hyssopifolia	1.52	1.46	3.71	6.68
Commelina benghalensis	3.03	2.91	3.71	9.65
Cyperus ferax	0.76	1.46	1.86	4.07
Cyperus flavus	0.38	0.73	1.86	2.96
Cyperus rotundus	1.52	0.73	7.42	9.66
Desmodium tortuosum	2.65	4.37	2.16	9.19
Digitaria horizontalis	1.89	2.18	3.09	7.17
Digitaria insularis	10.23	12.38	2.95	25.55
Digitaria sanguinalis	1.14	1.46	2.78	5.38
Emilia coccinea	10.23	6.55	5.57	22.35
Emilia sonchifolia	1.89	1.46	4.64	7.99
Indigofera hisurta	0.38	0.73	1.86	2.96
Ipomoea nil	0.38	0.73	1.86	2.96
Mimosa candolei	0.38	0.73	1.86	2.96
Paspalum dilatatum	2.27	0.73	11.13	14.13
Praxelis clematidea	13.26	12.38	3.82	29.46
Tridax procumbens	21.21	12.38	6.11	39.7
Waltheria indica	2.27	3.64	2.23	8.14
Zornia latifólia	1.89	2.18	3.09	7.17

The species *T. procumbens, P. pauciflora* and *D. insularis* stand out for their high frequency in the study area, as well as *Acanthospermum australe* and *C. hirta*.

http://www.aloki.hu ● ISSN 1589 1623 (Print) ● ISSN 1785 0037 (Online)
DOI: http://dx.doi.org/10.15666/aeer/1605_53115322
© 2018, ALÖKI Kft., Budapest, Hungary

Paspalum dilatatum showed the highest value of relative abundance (11.13%) followed by *Cyperus rotundus* (7.42%) and *Alternanthera tenella* (6.80%).

From the values of relative density, frequency and abundance the importance value index (IV) was calculated and it is possible to observe in the results the prominence of 5 species, *Tridax procumbens*, *Praxelis pauciflora*, *Digitaria insularis*, *Emilia coccinea* and Chamaesyce hirta, considering the most important with IV of the order of 39.7%, 29.46%, 25.55% 22.35% and 21.70%, respectively. The other species belong to groups that present important value indices ranging from intermediate to low.

Although studies suggest that the best strategy for weed management is the application of pre-emergence herbicides and manual weeding 40 days after planting (Yadav et al., 2015), it was decided to only apply pre-emergence herbicides with the intention of reducing manual labor costs.

Table 5 shows the efficiency of the pre-emergence herbicides applied to control the weed community of cowpea in the Amazon region. There was a significant interaction between the herbicide used and the weed control efficiency at different evaluation times after application

Table 5. *Herbicides efficiency (%) in weed control at 21, 28 and 35 days after planting of cowpea and grain yield (kg/ha)*

Herbicides (H)	**Days after planting (DAP)**			**Yield (kg/ha)[2]**
	21	**28**	**35**	
	Weed control efficiency (%)[1, 2]			
Metribuzin	92.5 Aa	88.7 ABa	91.2 ABa	0.00 D
Sulfentrazone	81.2 ABa	75.0 BCa	80.0 ABCa	617.53 C
S-metolachlor	68.7 BCa	45.0 DEb	52.5 DEb	1315.52 B
Pendimethalin	45.0 DEab	40.0 DEb	52.5 DEa	1436.92 B
Oxadiazon	77.5ABa	57.5 CDb	77.5 ABCa	1668.93 A
Alachlor	52.5 CDEa	50.0 DEa	60.0 CDa	1377.16 B
Metribuzin +Pendimethalin	67.5 BCDa	55.0 CDEb	42.5 DEc	395.79 C
Metribuzin+ Alachlor	86.2 ABa	86.2 ABa	76.2 BCa	559.89 C
Weed-free (manual weeding)	100.0 Aa	100.0 Aa	100.0 Aa	1681.62 A
Weedy check	35.0 Ea	32.5 Ea	30.0 Ea	565.90 C
CV%	21.93%			8.21%
F(H)	25.85**			13.27**
F(DAP)	14.12**			-
F(HxDAP)	4.41**			-

[1]Data were arc-sine transformed before analysis; however, back-transformed actual mean values are presented based on the interpretation from the transformed data

[2]Means followed by the same letters, lowercase in the rows and uppercase in columns, do not differ significantly by Tukey's test ($p < 0.05$); **Significant at $p \leq 0.01$ by the F-test

Cowpea grain yield was significantly reduced by weed interference (565.90 kg/ha), evidencing the low competitive capacity of the crop. the treatment without weed control when compared to the treatment maintained under manual weeding, which obtained the highest recorded productivity (1668.93 kg/ha), was responsible for a loss equivalent to 66.09%.

http://www.aloki.hu ● ISSN 1589 1623 (Print) ● ISSN 1785 0037 (Online)
DOI: http://dx.doi.org/10.15666/aeer/1605_53115322
© 2018, ALÖKI Kft., Budapest, Hungary

The herbicides Metribuzin, Sulfendrazone, Oxadiazon and the mixture of Metribuzin with Alachlor showed, until 35 days after sowing the cowpea, weed control efficiency means higher than 75%.

The application of the metribuzin herbicide prevented the emergence of all cowpea seedlings resulting in no grain yield and the mixture of metribuzin with Alachlor or Pendimethalin caused enough crop injury to reduce yields by 66.45% and 76.28%, respectively. These crop yield reductions are superior to the loss caused by weed competition in the treatment without control of the infestation (66.09%). Sulfentrazone reported control results of weed plants (80% at 35 DAP) similar to the herbicide metribuzin, causing severe injury and loss of cowpea productivity compared to weed-free treatment (62.99%).

The herbicide oxadiazon presented a good result in relation to weed control (77.5%), without affecting crop yield.

The herbicides S-metolachlor and Pendimethalin showed good crop yields (1315.52 kg/ha and 1436.92 kg/ha), although not very good weed control efficiency (52.5% for both). The other herbicides tested were statistically placed in intermediate groups regarding weed control efficiency and weedy check plots presented the worst results, being used as a parameter to evaluate herbicides with less efficiency of weed control (Alachlor and the Metribuzin + Pendimethalin mixture) (*Table 5*).

Discussion

The greater infestation of dicots in cowpea compared to monocots was also observed by Batista et al. (2017) and the fact that these weeds belong to the same class of cowpea makes their control, especially the chemical, difficult.

Several authors have highlighted the predominance of Fabaceae, Poaceae and Asteracerae families in the Amazon region, especially in agricultural areas. Marques et al. (2010), while evaluating the floristic composition of weeds in the cowpea culture in the mulch system, verified that the Cyperaceae, Fabaceae, Poaceae, Malvaceae, Asteraceae and Rubiaceae families were the ones presenting the highest number of species and greatest importance. Leal et al. (2006) studying the seed bank in systems of production of agriculture with burning and without burning in the State of Pará, also cited these families as predominant in the area and highlighting their aggressive potential in the Amazon region.

There is a high number of weed species in the area belonging to the same botanical family of cowpea (Fabaceae). Although the relationship between competition between plants and phylogenetic proximity is unimportant in comparison to competitive capacity and functional characteristics of plants, such as height, for example (Cahill et al., 2008), weed species belonging to the same family have botanical characteristics and nutritional requirements similar to those of the crop, which can make them aggressive competitors in the agricultural environment

Tridax procumbens, Praxelis pauciflora, Digitaria insularis, Digitaria sanguinalis and *Chamaesyce hirta* were the species that had higher relative density (RD). According to Swanton et al. (2015), the time of weed emergence relative to the crop is the most important factor in the crop-weed competition, with the density of weed seedlings being the second major variable. There is a relationship between weed density and duration of interference. The length of a critical period for weed control varies with density just as density thresholds vary with time of weed emergence relative to the crop (Dunan et al., 1995).

http://www.aloki.hu ● ISSN 1589 1623 (Print) ● ISSN 1785 0037 (Online)
DOI: http://dx.doi.org/10.15666/aeer/1605_53115322
© 2018, ALÖKI Kft., Budapest, Hungary

Frequency (F) is the proportion of sampling units (e.g., quadrat; field) that contains the species. *Tridax procumbens, Praxelis pauciflora, Digitaria insularis, Acanthospermum australe* and *Chamaesyce hirta* stand out for their high relative frequency (RF) in the study area. Recording frequency is fast and nondestructive is less prone to incorrect estimates than density. In situations where appropriate sampling techniques are employed and sampling points are uniformly distributed across the sampled area, frequency can be a good indicator of the spatial distribution of a species within the sampled area (Nkoa et al., 2015)

The species with the greatest abundance (RA) were *Paspalum dilatatum, Cyperus rotundus* and *Alternanthera tenella.* Abundance measures the quantitative significance of a species in its habitat. It describes the species' success in terms of numbers. High relative abundance is related to the appearance of weeds in reeds, and it is fundamental to indicate local actions to control weeds not only in cowpea but also in crops in general (Dias et al., 2007).

The importance value index (IV) was calculated from the values of relative density, frequency and abundance. The IV groups the parameters mentioned above and classifies each species in the weed community according to its ability to cause damage and reduce the productivity of cowpea. The IV groups the parameters mentioned above and classifies each species in the weed community according to its ability to cause damage and reduce the productivity of cowpea (Concenço et al., 2013). *Tridax procumbens, Praxelis pauciflora, Digitaria insularis, Emilia coccinea* and *Chamaesyce hirta* were considered the 5 most important species of the studied area.

In their studies, Kissmann and Groth (1999) also emphasized the importance of the species *T. procumbens*, which, in addition to high relative density and relative frequency, also shows concentration of individuals in specific areas, as shown by the high relative abundance. The IV of this species reveals its competitive potential in relation to the crops. *T. procumbens* is an annual herbaceous species propagated by seeds and should be controlled in the early stages of development or by the use of pre-emergent herbicides. *P. pauciflora* presented the second highest IV, it is an annual herbaceous species and often forms dense populations due to the ease of germination and high potential for spread of seeds which are easily transported by wind.

D. insularis is an annual species and reproduces by seeds and rhizomes. Jakelaitis et al. (2003) emphasize its importance, mainly due to its habit of overgrown growth, which besides competing for area, water and nutrients, can exceed the plants of cowpea in height, harming its development. It is also worth mentioning that its habit of growth facilitates the development of pests and diseases in cowpea. The species *E. coccinea* and *C. hirta* are annual herbaceous plants propagated by seeds and should also be considered important when thinking about weed control to maintain good productivity levels of cowpea.

Due to the short cycle, cowpea becomes extremely susceptible to competition with weeds, especially at the beginning of their development (Lamego et al., 2011). The phytosociological study was done before planting the cowpea to know the local weed community and then defining a weed control strategy.

Although studies suggest that the best strategy for weed management is the application of pre-emergence herbicides and manual weeding 40 days after planting (Yadav et al., 2015), it was decided to only apply pre-emergence herbicides with the intention of reducing manual labor costs.

http://www.aloki.hu ● ISSN 1589 1623 (Print) ● ISSN 1785 0037 (Online)
DOI: http://dx.doi.org/10.15666/aeer/1605_53115322
© 2018, ALÖKI Kft., Budapest, Hungary

Cowpea grain yield was significantly reduced by weed interference. In other field experiments, yield reductions reach 90% (Freitas et al., 2009) in the absence of weed control. Untreated weed treatment presented average productivity comparable to treatments that used nonselective herbicides, so interference from competition for essential factors equates to damage caused by the phytotoxicity of the applied products. Pre-emergent herbicides with prolonged residual effect have been used as an effective strategy to control weeds during the critical period of competition with the crop (Monquero et al., 2008).

The herbicide metribuzin is not selective for cowpea and in field experiments the cowpea presented marginal tolerance to the herbicide presenting severe injuries and drastic yield reduction. (Costa et al., 2017). Although promising results for selectivity of cowpea to sulfentrazone (Costa et al., 2017), the use of this herbicide drastically decreased the productivity of the crop in this study, this behavior may be due to the dosage of the sulfentrazone applied or the variety of cowpeas used, since it is known that sulfentrazone can cause phytotoxicity to cowpea in high doses as there is a difference in the effect of the herbicide between the cultivars (Azevedo et al., 2016). For varieties with lower tolerance to sulfentrazone, growers need to ensure the quality of application in relation to soil type and pH, otherwise the herbicide may present phytoxicity.

The herbicide oxadiazon presented a good result in relation to weed control without affecting crop yield. Fontes et al. (2010) obtained similar weed control (82%) in the Amazon region without affecting the BRS Guariba variety using the 600 g ia. ha^{-1} dose. Oxadiazon has as its mechanism of action the inhibition of the enzyme protoporphyrinogen oxidase (PPO) e and when applied in pre-emergence of weeds, phytotoxic actions occur during emergence of seedlings, close to the soil surface in a 0-5 cm depth range. Fontes et al. (2010) obtained similar weed control (82%) in the Amazon region without affecting the BRS Guariba variety using the 600 g ia. ha^{-1} dose. Oxadiazon has as its mechanism of action the inhibition of the enzyme protoporphyrinogen oxidase (PPO) e and when applied in pre-emergence of weeds, phytotoxic actions occur during emergence of seedlings, close to the soil surface in a 0-5 cm depth range (Silva et al., 1999).

Conclusion

Tridax procumbens, *Praxelis pauciflora*, *Digitaria insularis*, *Emilia coccinea* and *Chamaesyce hirta* were the species with the highest index of importance (IV) in the Amazonian cowpea area, difficult to control plants with high reproductive rates, these weeds play aggressive competition with cowpea plants for environmental resources and need to be controlled in the early stages of their development, so the use of pre-emergent herbicides are recommended as a control strategy.

Weed competition severely reduces cowpea productivity. The herbicides metribuzin, sulfentrazone and oxadiazon were satisfactory levels of weed control; however, the use of metribuzin resulted in no yield of the culture, preventing its germination. The sulfentrazon, which is considered selective for cowpea beans, significantly reduced the yield of the crop under the tested conditions and variety. The use of oxadiazon in pre-emergence was an effective strategy for weed control up to 35 DAP without reducing crop yield.

http://www.aloki.hu ● ISSN 1589 1623 (Print) ● ISSN 1785 0037 (Online)
DOI: http://dx.doi.org/10.15666/aeer/1605_53115322
© 2018, ALÖKI Kft., Budapest, Hungary

REFERENCES

[1] Angiosperm Phylogeny Group (2009): APG III. – Botanical Journal of the Linnean Society 161(2): 105-121.
[2] Azevedo, R., Ikeda, F., Olibone, A., Da Costa, W. B., Poltronieri, F., Olibone, D., Cavalieri, S. (2016): Seletividade de doses de sulfentrazone em cultivares de feijão-caupi. – Congresso Brasileiro Da Ciência Das Plantas Daninhas, 30, Curitiba.
[3] Batista, P. S. C., Oliveira, V. S., Souza, V. B., Carvalho, A. J., Aspiazu, I. (2017): Phytosociological survey of weeds in erect prostrate cowpea cultivars. – Planta Daninha 35: e017160273.
[4] Braun-Blanquet, J. (1979): Fitosociologia: bases para el estudio de las comunidades vegetales. – H. Blume, Madrid.
[5] Cahill, J. F., Kembel, S. W., Lamb, E. G., Keddy, P. (2008): Does phylogenetic relatedness influence the strength of competition among vascular plants? – Perspect. Plant Ecol. Evol. Syst. 10: 41-50.
[6] Concenço, G., Ceccon, G., Correia, I. V. T., Leite, L. F., Alves, V. B. (2013): Occurrence of weed species under crop succession. – Planta Daninha 31(2): 359-368.
[7] Costa, A. F. da, do Vale, L. S., de Oliveira, A. B., de Brito Neto, J. F., Cardoso, G. D. (2017): Selectivity of pre-and post-emergent herbicides for cowpea (*Vigna unguiculata*). – African Journal of Agricultural Research 12(11): 881-887.
[8] Dias, A. C. R., Carvalho, S. J. P., Nicolai, M., Christoffoleti, P. J. (2007): Understanding the occurrence of different species of crabgrass (Digitaria spp.) in sugar cane crop. – Planta Daninha 25(2): 489-499.
[9] Dunan, C. M., Westra, P., Schweizer, E. E., Lybecker, D. W., Moore, F. D. (1995): The concept and application of early economic period threshold: the case of DCPA in onions (Allium cepa). – Weed Sci. 43: 634-639.
[10] Filgueiras, G. C., Santos, M. A. S., Homma, A. K. O., Rebello, F. K. Cravo, M. S. (2009): Aspectos socioeconômicos. – In: Zilli, J. E., Vilarinho, A. A., Alves, J. M. A. (eds.). A cultura do feijão-caupi na Amazônia brasileira. Embrapa Roraima, Boa Vista, pp. 23-58.
[11] Fontes, J. R. A, Gonçalves, J. R. P, Morais, R. de (2010): Tolerância do feijão-caupi ao herbicida oxadiazon. – Pesquisa Agropecuária Tropical 40(1): 110-115.
[12] Freitas, F. C. L., Medeiros, V. F. L. P., Grangeiro, L. C., Silva, M. G. O., Nascimento, P. G. M. L., Nunes, G. H. (2009): Weed Interference in Cowpea. – Planta Daninha 27(2): 241-247.
[13] Gupta, K. C., Gupta, A. K., Saxena, R. (2016): Weed management in cowpea [*Vigna unguiculata* (L.) Wasp.] under rainfed conditions. – Int. J. Agri. Sci. 12(2): 238-240.
[14] Harrison, H. F., Fery, R. L. (1993): Differential bentazon response in cowpea (*Vigna unguiculata*). – Weed Technology 7(3): 756-758.
[15] Hass, H., Streibig, J. C. (1982): Changing Pattern of Weed Distribution as a Result of Herbicides Use and Other Agronomic Factor. – In: Le Baron, H. M., Gressel, J. (eds.) Herbicides Resistance in Plants. Wiley, New York, pp. 57-59.
[16] International Plant Names Index (2013): Disponível em. – http://www.ipni.org. Accessed on 10 Jan 2018.
[17] Jakelaitis, A., Ferreira, L. R., Silva, A. A. D., Agnes, E. L., Miranda, G. V., and Machado, A. F. L. (2003): Weed population dynamics under different corn and bean production systems. – Planta Daninha 21(1): 71-79.
[18] Kissmann, K. G., Groth, D. (1999): Plantas infestantes e nocivas. Tomo III. 2. ed. – BASF, São Paulo.
[19] Kumar, P., Singh, R. (2017): Integrated weed management in cowpea (*Vigna unguiculata* (L.) Wasp.) under rainfed conditions. – Int. J. Curr. Microbiol. App. Sci 6(3): 97-101.

http://www.aloki.hu ● ISSN 1589 1623 (Print) ● ISSN 1785 0037 (Online)
DOI: http://dx.doi.org/10.15666/aeer/1605_53115322
© 2018, ALÖKI Kft., Budapest, Hungary

[20] Lamego, F. P., Basso, C. J., Vidal, R. A., Trezzi, M. M., Santi, A. L., Ruchel, Q., Kaspary, T. E., Gallon, M. (2011): Selectivity of metolachlor and alachlor for the "Carioca" bean. – Planta Daninha Viçosa-MG 29(4): 877-8837.
[21] Leal, E. C., Vieira, I. C. G., Kato, M. D. S. A. (2006): Banco de sementes em sistemas de produção de agricultura com queima e sem queima no município de Marapanim, Pará. – Boletim do Museu Paraense Emílio Goeldi Ciências Naturais 1(1): 19-29.
[22] Mancuso, M. A. C., Aires, B. C., Negrisoli, E., Corrêa, M. R., Soratto, R. P. (2010): Seletividade e eficiência de herbicidas no controle de plantas daninhas na cultura do feijão-caupi. – Revista Ceres 63(1): 025-032.
[23] Marques, L. J. P., Silva, M. R. M., Araújo, M. S. D., Lopes, G. D. S., Corrêa, M. J. P., Freitas, A. C. R. D., Muniz, F. H. (2010): Floristic composition of weeds in the cowpea (*Vigna unguiculata*) culture under the chopped secondary forest system. – Planta Daninha 28(5): 953-961.
[24] Monquero, P. A., Binha, D. P., Silva, A. C., Silva, P. V., Amaral, L. R. (2008): Efficiency of pre-emergence herbicides after different periods of drought. – Planta Daninha 26(1): 185-193.
[25] Moody, K. (1973): Weed control in cowpeas. – Proc. Weed Sci. Soc. Nigeria 3: 14-22.
[26] Nkoa, R., Owen, M. D., Swanton, C. J. (2015): Weed abundance, distribution, diversity, and community analyses. – Weed Science 63(sp1): 64-90.
[27] Omisore, J. K., Aboyeji, C. M., Daramola, O. F. (2016): Comparative evaluation of weed control methods on cowpea (*Vigna unguiculata* (L.) Walp) production in the savanna agro-ecological zone of Nigeria. – Scientia Agriculturae 14(3): 279-283.
[28] Rachie, K. O., Roberts, L. M. (1974): Grain legumes of the lowland tropics. – Adv. Agron. 26(1): 132.334.
[29] R Core Team (2017): R: A language and environment for statistical computing. – Vienna, Austria: R Foundation for Statistical Computing; 2016
[30] Saved, K., Torres, L. G., Bermejo, E. H. and Hildago, B. (1990): Influence of environmental factor on the weed flora in crops in Guadalquivir Valley. – Weed Res. 30:363-374
[31] Schemer, D. E., Chilcote, D. O. (1969): Factors influencing persistence and depletion in buried seed population. A model for analysis of parameter of buried seed persistence and depletion. – Crop Sci. 9: 417-19.
[32] Silva, J. B. F., Pitombeira, J. B., Nunes, R. P., Pinho, J. L. N., Cavalcante Júnior, A. T. (2003): Weed control in cowpea under no-nill system. – Planta Daninha 21(1): 151-157.
[33] Swanton, C. J., Nkoa, R., Blackshaw, R. E. (2015): Experimental methods for crop–weed competition studies. – Weed Science 63(sp1): 2-11.
[34] Yadav, T., Chopra, N. K., Chopra, N. K. (2015): Efficacy of pre-and post-emergence herbicides with and without weeding in forage cowpea (*Vigna unguiculata*). – Indian Journal of Agronomy 60(4): 622-625.
[35] Yadav, T., Nisha, K. C., Chopra, N. K., Yadav, M. R., Kumar, R., Rathore, D. K., ... Ram, H. (2017): Weed management in cowpea. A review. – Int. J. Curr. Microbiol. App. Sci. 6(2): 1373-1385.

http://www.aloki.hu ● ISSN 1589 1623 (Print) ● ISSN 1785 0037 (Online)
DOI: http://dx.doi.org/10.15666/aeer/1605_53115322
© 2018, ALÖKI Kft., Budapest, Hungary

COMMUNITY ANALYSIS AND CHARACTERIZATION OF FUNGI FROM BATURA GLACIER, KARAKORAM MOUNTAIN RANGE, PAKISTAN

HASSAN, N.[1,2] – HASAN, F.[1] – NADEEM, S.[1] – HAYAT, M.[1] – ALI, P.[1] – KHAN, M.[1] – SAJJAD, W.[1] – ZADA, S.[1] – RAFIQ, M.[1,2,*]

[1]*Applied, Environmental and Geomicrobiology Laboratory, Department of Microbiology, Faculty of Biological Sciences, Quaid-i-Azam University, Islamabad-45320, Pakistan*

[2]*Bristol Glaciology Centre, School of Geographical Sciences, Faculty of Science, University of Bristol, Bristol BS8 1SS, United Kingdom*

**Corresponding author*
e-mail: m.rafiq@bristol.ac.uk; muhammadrafiq61@yahoo.com
(phone: +44-745-980-4496)

(Received 15th May 2018; accepted 27th Jun 2018)

Abstract. Karakoram mountain range contains the tallest mountain peaks of the world with thousands of glaciers which are microbiologically untapped. This is a pioneer approach of isolation and characterization of fungi from Batura glacier, Karakoram, Pakistan. Total number (CFU/mL or g) was determined at 4 °C and 15 °C to isolate psychrophilic and psychrotrophic fungi, respectively. About 33 different fungi were isolated from sediment (29), ice (2) and water (2) and were identified morphologically and by sequencing of specific internal transcribed spacer region of the species through internal transcribed spacer 1 (ITS1) and internal transcribed spacer 2 (ITS2) primers. Mostly, the fungal isolates belonged to genus *Penicillium*, followed by *Cladosporium*, *Geomyces*, *Cordyceps*, *Mrakia*, *Cadophora*, *Tetracladium*, *Eupenicillium, Trametes*, *Mortierella*, *Scopulariopsis*, *Beauveria, Candida* and *Pseudogymnoascus*. They showed growth at wide temperature range from 4–37 °C, few at 45 °C as well. Most of the isolates were able to grow at pH 1–13. Fungal isolates were able to grow in 2–26% NaCl, with the highest tolerance (26%) by *Mrakia robertii.* All study isolates showed inhibitory activity against *Staphylococcus* sp., and four industrially important enzymes (cellulase, DNase, lipase and phosphatase) were produced by *Mrakia robertii.* The fungal isolates of such cold habitats are potential sources of various industrial and environmental application.
Keywords: *non-polar glaciers, diversity, psychrotrophs, antimicrobial activity, industrial applied enzymes*

Introduction

Psychrophiles are known as cryophile or 'cold-loving' organisms (Margesin et al., 2007) having ability to grow and survive in cold environment. According to Morita (Morita, 1975), psychrophiles grow and survive below 20 °C providing 15 °C as optimum growth temperature. However, the psychrophiles in cold environment are also accompanied by psychrotrophs. The psychrotrophs possess ability to grow below and above 20 °C but their growth optimum has been observed beyond 20 °C (Baross and Morita, 1978; Cavicchioli et al., 2002; Gounot, 1986). Psychrotrophic community have been described as "the survivor's community" by Friedmann (1994) because of their survival strategies and their normal physiological state under low temperature (Morita, 2000).

Psychrophilic and psychrotrophic fungi have widely been studied for their presence in several cold environments as reviewed by Hassan et al. (2016) such as Arctic and Antarctic region (Azmi and Seppelt, 1997; Babjeva and Reshetova, 1998; Selbmann et al., 2005; Vishniac, 2006). Furthermore, different cold environments including permafrost (Broady et al., 1998), cold water (Botha and Wolfaardt, 2000; Dmitriev et al., 1997), ice

http://www.aloki.hu ● ISSN 1589 1623 (Print) ● ISSN 1785 0037 (Online)
DOI: http://dx.doi.org/10.15666/aeer/1605_53235341
© 2018, ALÖKI Kft., Budapest, Hungary

in glacial habitats (Ma et al., 1999), snow and below snow-covered tundra (Schadt, 2000), polar water present in off shore area (Broady et al., 1998) and massive glacial sheets of ice and ice shelves freshwater (Bridge, 2010; Tojo and Newsham, 2012) have been investigated for cold adapted fungi. Limited research data is available on the fungal diversity and characterization in non-polar regions such as Hindukush, Karakoram, and Himalayas (HKKH). A proper investigation was needed for existence of cold adapted and psychrophilic life (microorganisms) in the HKKH glaciers.

The rate of discovery of new antibiotics is very slow as compared to emerging of antibiotic resistant pathogens in the current era. Treatment of several pathogens are now difficult due to dearth of operative antibiotics, e.g. Enterobacteriaceae bacteria producing extended spectrum beta-lactamase (ESBL), *Enterococci* sp. with vancomycin resistant abilities and *Staphylococcus aureus* with methicillin-resistant capabilities. It is important to explore extreme habitats for new antibiotics having diverse and unique characteristics. There is many diverse type of extreme environments however cold habitats could be among important sources for the discovery of novel antibiotics. Therefore, we need to investigate novel antibiotics from extreme and unexplored sites against both multi-drug resistant bacteria and fungi.

Pakistan has one of the world's largest glacier reserves in the Karakoram–Hindu Kush–Himalaya ranges. According to Rahman et al. (2008), the junction of the Karakoram Western Himalayan and Hindu Kush mountain ranges are accompanied by the Northern Areas of Pakistan. Batura glacier considered as the largest glaciers located exterior the polar region. It is present in the north of Passu 7,500 m above sea level. Batura glacier has not been explored yet for the presence of psychrophilic and psychrotrophic fungi. Isolation and characterization of the psychrophilic and psychrotrophic fungal community from samples of glacier (ice sediments and water) taken from Batura glacier was the ambition of the current research.

Materials and methods

Sampling

The length of Batura glacier is 57 km with a termination point of ~3000 m altitude in the valley of Hunza, Pakistan, given in *Figure 1*. Several highlighted peaks of Karakoram (>7000 m in south and >5500 m in the north) surrounded the Batura glacier. Ice, water and sediments samples were taken from Batura glacier (36°30.302N to 074°51.138E) following standard microbiological procedures. Approximately 200–300 g sediments were taken using sterilized gloves and scoops to avoid sample contamination. Nasco Whirl–Pak™ bags (Fisher Scientific) were used to place individual sample (for sediments) and sterilized polyethylene bottles (for ice and water samples). The pH of all samples were 7.0 whereas temperature of glacial sediments and water were 1 °C while glacial ice had –2 °C. All the collected samples were kept at 4 °C until transported to Department of Microbiology Quaid-i-Azam University Islamabad and stored at –20 °C.

Isolation of fungi

For isolation of fungi Sabouraud Dextrose Agar (Sigma – Aldrich) (g/L; 10% mycological peptone 40% dextrose 15% Agar) Potato Dextrose Agar (Sigma – Aldrich) (g/L; 4% potato extract 20% dextrose 15% agar) and Malt Extract Agar (Sigma – Aldrich) (g/L; 30% malt extract 10% mycological peptone 15% Agar) were used as

http://www.aloki.hu ● ISSN 1589 1623 (Print) ● ISSN 1785 0037 (Online)
DOI: http://dx.doi.org/10.15666/aeer/1605_53235341
© 2018, ALÖKI Kft., Budapest, Hungary

growth medium. Incubation temperatures were set at 4 °C and 15 °C. Total viable counts were determined in terms of fungal colony forming units (CFUs/mL or /g) and morphologically distinct colonies were further subcultured to get the pure cultures. Potato Dextrose Agar (PDA) slants were used for preservation of fungal isolates at 4°C and also under mineral oil till further use.

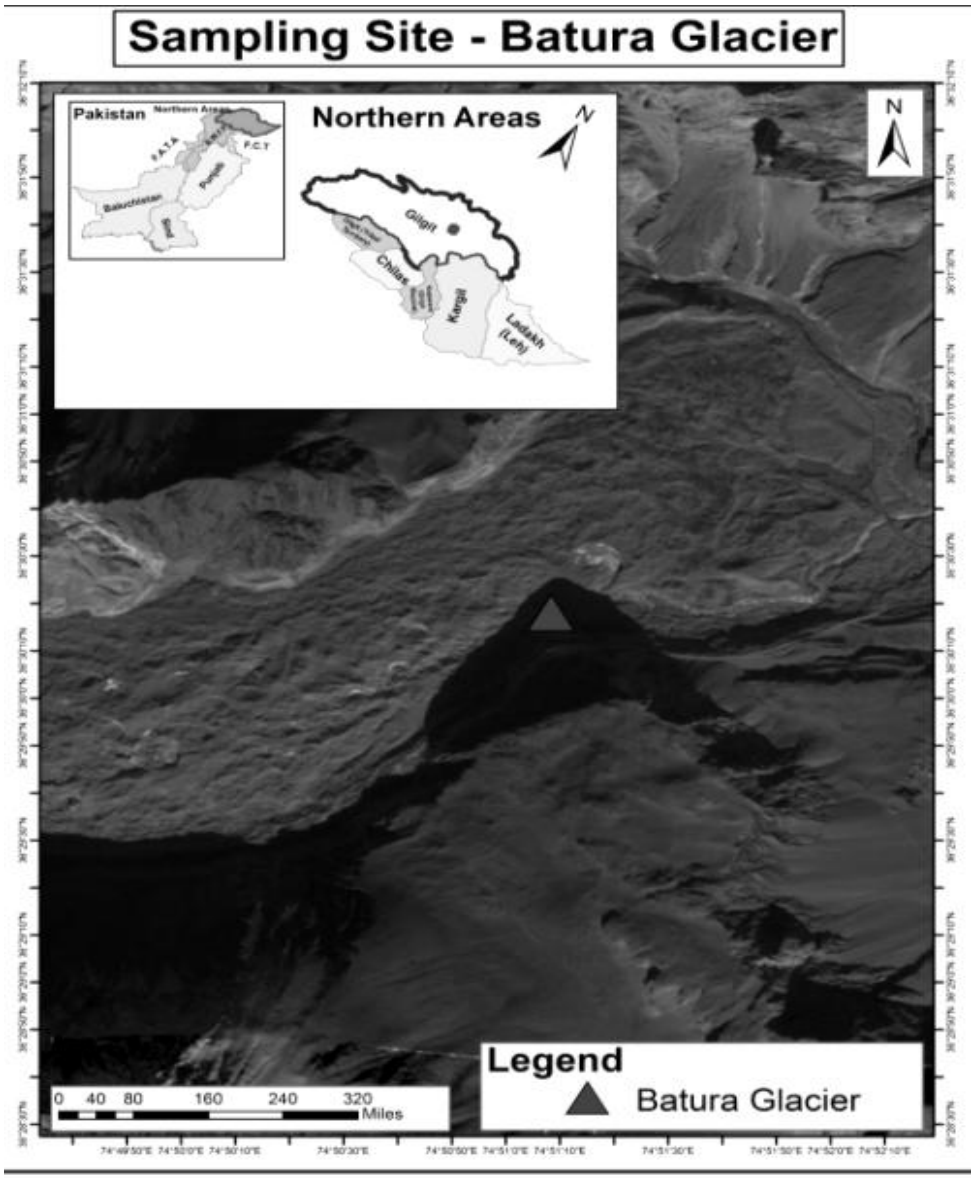

Figure 1. *Location of Batura glacier*

Morphological characterization

Different media such as PDA, Tryptic Soy Agar (Sigma – Aldrich) (g/L; 15% casein peptone 5% soya peptone 5% sodium chloride 15% agar) Sabouraud Dextrose Agar (SDA) and Malt Extract Agar (MEA) was used as growth media for fungal isolates. Color, texture and size (both front and reverse sides) were observed and recorded at 4 C and 15 C. Microscopic examination of fungal isolates was carried out following the protocol of Hassan et al. (2017).

http://www.aloki.hu ● ISSN 1589 1623 (Print) ● ISSN 1785 0037 (Online)
DOI: http://dx.doi.org/10.15666/aeer/1605_53235341
© 2018, ALÖKI Kft., Budapest, Hungary

Physiological characterization

All the physiological parameters were measured using SDA, MEA and PDA. Cultures were grown for 10 days. Diverse temperatures from 4 to 50 C (4, 15, 37, 45, and 50 C) were used to determine temperature optima of the fungal isolates. pH tolerance of the fungal isolates was determined by inoculating them separately in a medium adjusted to varying pH values (1, 3, 5, 7, 9, 11 and 13). For determination of halophilic nature of the fungal isolates, SDA complemented with NaCl up to 26% was used. All physiological examinations were carried out at 4 °C and 15°C.

DNA extraction and amplification

Rosa et al. (2009) DNA extraction protocol was used to extract the DNA of all the fungal isolates. The extracted DNA was amplified using internal transcribed spacer 1 (ITS1) – 5.8S – internal transcribed spacer 2 ITS2 region prior to sequencing following the protocol described by Hassan et al. (2016). T100™ Thermal Cycler (Bio Rad) was used for PCR amplification. Agarose gel electrophoresis was used to confirm PCR products *using standard DNA ladder.*

Phylogenetic analysis

Sequencing was done commercially by Macrogen (Macrogen Inc. Seoul Korea) and the sequences obtained were analysed by Chromas Lite, while further evaluation was done using National Center for Biotechnology Information (NCBI) database by comparing with available nucleotide sequences (Thompson et al., 1997). The GenBank sequence database was used to compare the obtained FASTA sequences to data using BLASTn (Altschul et al., 1990; Zhang et al., 2000). Accession no. of all fungal isolates were obtained by depositing sequences to National Centre for Biotechnological Information (NCBI). Tamura–Nei model of Maximum Likelihood method used to infer evolutionary history of fungal isolates (Tamura and Nie, 1993). MEGA6 software following maximum likelihood method has been used to construct phylogenetic tree (Tamura et al., 2013) at the bootstrap value of 1,000.

Evaluation of antimicrobial activity

Antimicrobial activity of isolated fungal isolates was checked against *Staphylococcus aureus* (Multi-drug resistant), *E. coli* (MDR), *Staphylococcus* sp., *Klebsiella pneumoniae* (MDR), vancomycin resistant *Enterococcus* species and fungal isolates *Candida albicans* and *Aspergillus niger* following the protocol described by Hassan et al. (2017).

Screening for extracellular enzyme activity

Extracellular enzyme activity of all fungal isolates was determined on solid media. Ten days old fungal cultures were used as inoculum. Hankin and Anagnostakis (1975) protocol was used to determine amylase, deoxyribonuclease, lipase and protease activities. The phosphatase activity was determined on Pikovskaya's medium (Pikovskaya, 1948). Carboxymethylcellulose (CMC) was used as a substrate for screening cellulolytic activity of all fungal isolates. 0.5% Congo red solution and 1 M NaCl were used to visualize zones of inhibition around fungal colonies formed due to cellulolytic activity. 15 °C were used for all assays of qualitative extracellular enzyme activities.

http://www.aloki.hu ● ISSN 1589 1623 (Print) ● ISSN 1785 0037 (Online)
DOI: http://dx.doi.org/10.15666/aeer/1605_53235341
© 2018, ALÖKI Kft., Budapest, Hungary

Results

33 fungal isolates were isolated in this study. The highest CFU/g/mL was observed in sediments ($1.11 \times 10^3$and 7.75×10^2 at 4 and 15 °C, respectively) and given in *Table 1*.

Table 1. *Total viable count (CFU/mL/gm) of fungal isolates at 15 °C and 4 °C*

Temperature (°C)	Samples	No. of colonies/200 µL	CFU/mL/gm
4	Glacier ice	2	1.0×10^1
	Glacier water	3	1.5×10^1
	Glacier sediment	2.2×10^2	1.11×10^3
15	Glacier ice	7	3.5×10^1
	Glacier water	4	2.0×10^1
	Glacier sediment	1.55×10^1	7.75×10^2

Morphology

Colony morphology of all the fungal isolates were different, mostly they were of cottony to powdery textures irregular shapes and sizes and of blue to green in color. The macroscopic and microscopic features of the isolated fungal strains are specified in *Table A1* in the *Appendix*. The hyphae were septate colorless and spores were mostly cylindrical to ovoid in shape.

Molecular characterization

On the basis of DNA sequence of internal transcribed spacer region by (ITS1 – ITS2), all isolated fungal isolates have shown diverse groups of taxonomy. The evolutionary relationships, respective homology and resemblance directory of the isolated fungal strains with narrowly correlated species of fungi as well as their accession no. is summarized in *Table 2* and *Figure 2*.

Physiological characterization

Temperature tolerance of the fungal isolates showed variable results. All were capable to grow between 4 and 37 °C. Two isolates, HB_3 and LB_{13} were capable to grow above 37°C (*Table 3*). However, 4 and 15 °C temperatures were found to be optimum growth temperature values, except for HB_2, HB_7 and HB_{14} in the case of which the optimum growth temperature was 37 °C. The growth pattern of the fungal isolates at varying pH (1, 3, 5, 7, 9, 11 and 13) was very broad. The optimum pH for growth was found to be between 4 and 9. Most of the isolates (79%) grew in acidic range, 7 could not grow at pH 1 while all other isolates showed growth at the lowest pH. All fungal isolates have survived at extreme alkaline pH up to 13. The fungal isolates have tolerated salt concentration between 2 and 26% (33 between 2 and 14% 32 at 16% 24 at 18% 17 at 20% 11 at 22 and 24% and 1 showed growth at 26% salt concentration), given in *Table 3*. Based on such results, the fungal isolates could be categorized as polyextremophiles.

http://www.aloki.hu ● ISSN 1589 1623 (Print) ● ISSN 1785 0037 (Online)
DOI: http://dx.doi.org/10.15666/aeer/1605_53235341
© 2018, ALÖKI Kft., Budapest, Hungary

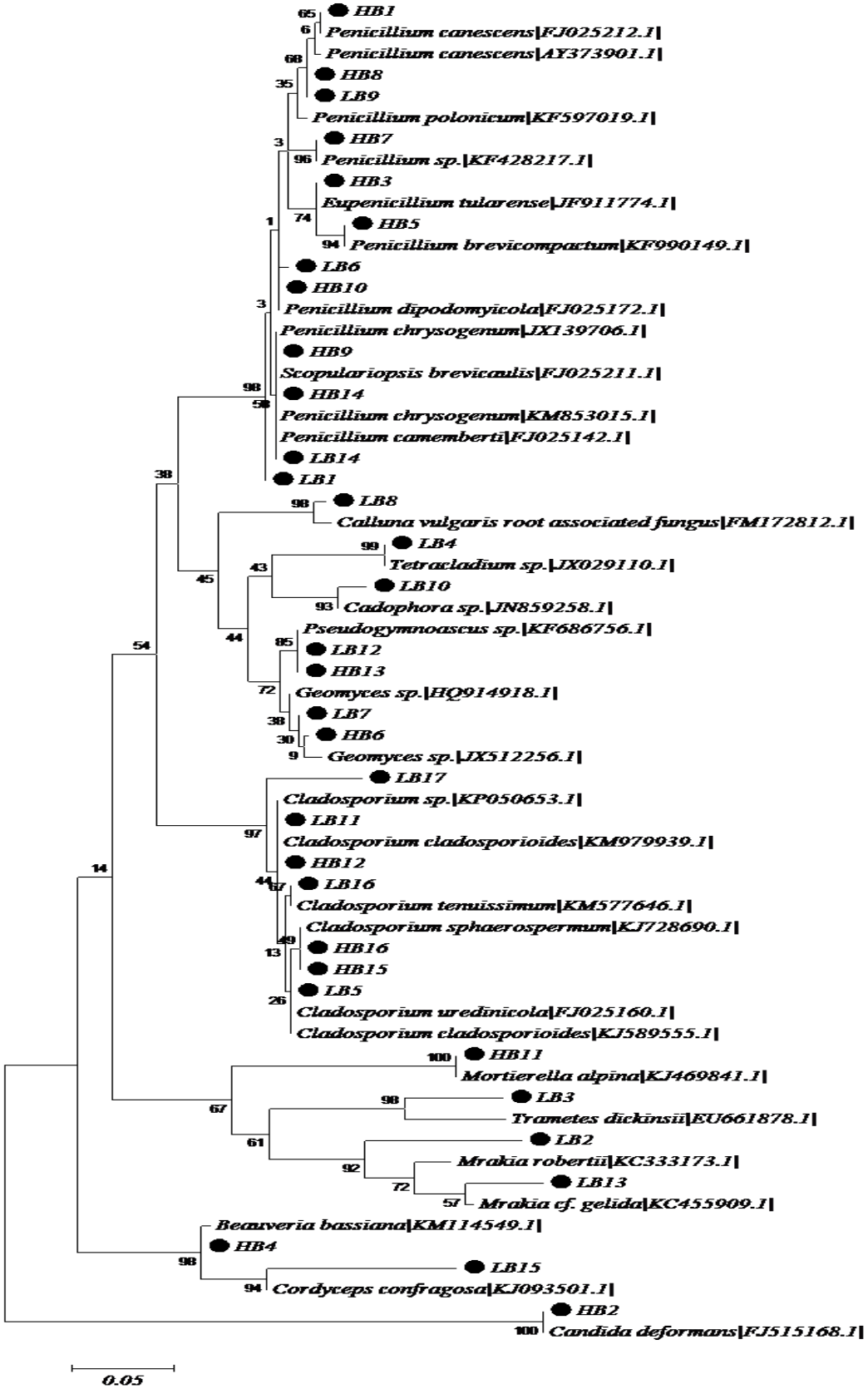

Figure 2. *Phylogenetic tree by Maximum likelihood method of the study isolates and homologous ITS data set from NCBI*

http://www.aloki.hu ● ISSN 1589 1623 (Print) ● ISSN 1785 0037 (Online)
DOI: http://dx.doi.org/10.15666/aeer/1605_53235341
© 2018, ALÖKI Kft., Budapest, Hungary

Table 2. *The resemblance directory of the fungal isolates with respect to homologous strains*

Isolates	Accession no.	Homologous strains with accession no.	Identity (%)
LB_1	KR0(19737	*Penicillium camemberti* (FJ025142.1)	99
LB_2	KR0(19738	*Mrakia robertii* (KC333173.1)	84
LB_3	KR0(19739	*Trametes dickinsii* (EU661878.1)	87
LB_4	KR0(19740	*Tetracladium* sp. (JX029110.1)	100
LB_5	KR0(19741	*Cladosporium uredinicola* (FJ025160.1)	99
LB_6	KR0(19742	*Penicillium polonicum* (KF5970(19.1)	97
LB_7	KR0(19743	*Geomyces* sp. (HQ914918.1)	99
LB_8	KR0(19744	Calluna vulgaris root associated fungus (FM172812.1)	99
LB_9	KR0(19745	*Penicillium canescens* (AY373901.1)	100
LB_{10}	KR0(19746	*Cadophora* sp. (JN859258.1)	99
LB_{11}	KR0(19747	*Cladosporium cladosporioides* (KM979939.1)	100
LB_{12}	KR0(19748	*Geomyces* sp. (JX512256.1)	99
LB_{13}	KR0(19749	*Mrakia cf. gelida* (KC455909.1)	99
LB_{14}	KR0(19750	*Penicillium chrysogenum* (JX139706.1)	99
LB_{15}	KR0(19751	*Cordyceps confragosa* (KJ093501.1)	91
LB_{16}	KR0(19752	*Cladosporium tenuissimum* (KM577646.1)	100
LB_{17}	KR0(19753	*Cladosporium cladosporioides* (KJ589555.1)	95
HB_1	KR0(19754	*Penicillium canescens* (FJ025212.1)	99
HB_2	KR0(19755	*Candida deformans* (FJ515168.1)	100
HB_3	KR0(19756	*Eupenicillium tularense* (EU142874.1)	99
HB_4	KR0(19757	*Beauveria bassiana* (KM114549.1)	100
HB_5	KR0(19758	*Penicillium brevicompactum* (KF990149.1)	99
HB_6	KR0(19759	*Geomyces* sp. (HQ914918.1)	99
HB_7	KR0(19760	*Penicillium* sp. (KF428217.1)	100
HB_8	KR0(19761	*Penicillium canescens* (AY373901.1)	100
HB_9	KR0(19762	*Scopulariopsis brevicaulis* (FJ025211.1)	100
HB_{10}	KR0(19763	*Penicillium dipodomyicola* (FJ025211.1)	100
HB_{11}	KR0(19764	*Mortierella alpine* (KJ469841.1)	100
HB_{12}	KR0(19765	*Cladosporium* sp. (KP050653.1)	100
HB_{13}	KR0(19766	*Pseudogymnoascus* sp. (KF686756.1)	100
HB_{14}	KR0(19767	*Penicillium chrysogenum* (KM853015.1)	100
HB_{15}	KR0(19768	*Cladosporium sphaerospermum* (KJ728690.1)	99
HB_{16}	KR0(19769	*Cladosporium sphaerospermum* (KJ728690.1)	99

LB: Low (Temperature, 4 °C) Batura Isolates, HB: High (Temperature, 15 °C) Batura Isolates

http://www.aloki.hu ● ISSN 1589 1623 (Print) ● ISSN 1785 0037 (Online)
DOI: http://dx.doi.org/10.15666/aeer/1605_53235341
© 2018, ALÖKI Kft., Budapest, Hungary

Table 3. *Temperature, pH and salt tolerance range of the fungal isolates. (Numbers between brackets are the optimal growth values)*

Isolates	Temperature (°C) range	pH range	Salt range (%)
LB_1	4−37, opt. 4	1−13, opt. 5–8	2−24, opt. 2–8
LB_2	4−37, opt. 4	1−13, opt. 5–7	2−26, opt. 2–10
LB_3	4−37, opt. 4	1−13, opt. 5–7	2−16, opt. 2–6
LB_4	4−37, opt. 4	1−13, opt. 5–8	2−18, opt. 2–6
LB_5	4−37, opt. 4	1−13, opt. 5–8	2−16, opt. 2–6
LB_6	4−37, opt. 4	1−13, opt. 5–7	2−24, opt. 2–8
LB_7	4−37, opt. 4	2−13, opt. 5–7	2−16, opt. 2–6
LB_8	4−37, opt. 4	1−13, opt. 5–8	2−16, opt. 2–6
LB_9	4−37, opt. 4	1−13, opt. 5–8	2−18, opt. 2–6
LB_{10}	4−37, opt. 4	1−13, opt. 5–8	2−16, opt. 2–6
LB_{11}	4−37, opt. 4	1−13, opt. 5–7	2−18, opt. 2–6
LB_{12}	4−37, opt. 4	1−13, opt. 5–7	2−16, opt. 2–6
LB_{13}	4−45, opt. 4	1−13, opt. 5–7	2−18, opt. 2–6
LB_{14}	4−37, opt. 4	1−13, opt. 5–7	2−18, opt. 2–6
LB_{15}	4−37, opt. 4	1−13, opt. 5–8	2−16, opt. 2–6
LB_{16}	4−37, opt. 4	1−13, opt. 5–8	2−16, opt. 2–6
LB_{17}	4−37, opt. 4	1−13, opt. 5–8	2−20, opt. 2–6
HB_1	4−37, opt. 15	2−13, opt. 5–7	2−24, opt. 2–10
HB_2	4−37, opt. 15	1−13, opt. 5–8	2−20, opt. 2–8
HB_3	4−37, opt. 15	2−13, opt. 5–7	2−24, opt. 2–10
HB_4	4−37, opt. 15	1−13, opt. 5–8	2−20, opt. 2–8
HB_5	4−37, opt. 15	2−13, opt. 5–7	2−24, opt. 2–10
HB_6	4−37, opt. 15	1−13, opt. 5–8	2−14, opt. 2–6
HB_7	4−37, opt. 15	1−13, opt. 5–8	2−24, opt. 2–10
HB_8	4−37, opt. 15	2−13, opt. 5–7	2−18, opt. 2–8
HB_9	4−37, opt. 15	1−13, opt. 5–8	2−20, opt. 2–8
HB_{10}	4−37, opt. 15	1−13, opt. 5–8	2−24, opt. 2–8
HB_{11}	4−37, opt. 15	2−13, opt. 5–7	2−18, opt. 2–8
HB_{12}	4−37, opt. 15	2−13, opt. 5–7	2−24, opt. 2–8
HB_{13}	4−37, opt. 15	2−13, opt. 5–7	2−24, opt. 2–10
HB_{14}	4−37, opt. 15	2−13, opt. 5–7	2−20, opt. 2–8
HB_{15}	4−37, opt. 15	1−13, opt. 5–7	2−20, opt. 2–8
HB_{16}	4−37, opt. 15	1−13, opt. 5–8	2−20, opt. 2–8

http://www.aloki.hu ● ISSN 1589 1623 (Print) ● ISSN 1785 0037 (Online)
DOI: http://dx.doi.org/10.15666/aeer/1605_53235341
© 2018, ALÖKI Kft., Budapest, Hungary

Evaluation of antimicrobial activity

Screening of the fungal isolates for antimicrobial activity showed greater antibacterial than antifungal activities and summarised in *Table 4*. Five fungal isolates exhibited inhibitory activity against *Staphylococcus aureus*, 21 showed such activity against *Staphylococcus* sp., 3 against *Enterococcus* sp., 2 against *E. coli* but none showed antimicrobial activity against *Klebsiella pneumoniae*. The number of fungal isolates that displayed inhibitory activity against *Candida albicans* and *Aspergillus niger* were 10 and 4, respectively.

Table 4. *Production of various extracellular enzymes by the fungal isolates*

Isolates	Enzymes					
	Amylase	**Cellulase**	**DNase**	**Lipase**	**Phosphatase**	**Protease**
LB_1	−	−	−	−	+	−
LB_2	−	+	+	+	+	−
LB_3	−	−	−	−	−	−
LB_4	−	−	−	+	−	−
LB_5	−	−	−	−	−	−
LB_6	++	+	−	−	+	−
LB_7	++	++	−	++	−	−
LB_8	−	−	−	−	−	−
LB_9	−	−	−	−	+	−
LB_{10}	++	−	−	−	−	−
LB_{11}	−	−	−	−	−	−
LB_{12}	−	−	−	++	−	−
LB_{13}	+	−	−	−	−	−
LB_{14}	−	+	−	−	+	−
LB_{15}	−	−	−	−	+	−
LB_{16}	++	−	−	−	−	++
LB_{17}	−	−	−	−	−	−
HB_1	−	−	−	−	+	−
HB_2	−	−	−	−	−	−
HB_3	−	−	−	++	+	−
HB_4	−	−	−	−	++	−
HB_5	+	−	−	−	+	−
HB_6	−	−	−	++	−	−
HB_7	−	−	−	++	+	−
HB_8	−	++	−	+++	−	−
HB_9	−	+++	−	−	+	−
HB_{10}	−	++	−	−	+	−
HB_{11}	−	−	−	−	−	−
HB_{12}	−	−	−	−	−	−
HB_{13}	−	−	−	−	−	−
HB_{14}	−	−	−	−	−	−
HB_{15}	−	−	−	−	−	−
HB_{16}	−	−	−	−	−	−

(–) No Zone, (+) Zone up to 6 mm, (++) Zone up to 12 mm, (+++) Zone above 12 mm

http://www.aloki.hu ● ISSN 1589 1623 (Print) ● ISSN 1785 0037 (Online)
DOI: http://dx.doi.org/10.15666/aeer/1605_53235341
© 2018, ALÖKI Kft., Budapest, Hungary

Screening for extracellular enzyme activity

In this study, maximum number of fungal isolates were found to produce phosphate (13 fungal isolates) followed by lipases (10), cellulases (7), amylases (6), DNases (1) and proteases (1) and summarized in *Table 5*. They were good in lipase production but were very poor in the production of DNase and protease. This research openly revealed that fungal isolates could be a good source of industrially important biocatalysts.

Table 5. *Screening for antimicrobial compounds against different bacteria and fungi*

Isolates	Bacteria					Fungi	
	E. coli	*Klebsiella pneumonie*	*Staph. Aureus*	*Staph.* sp.	*Enterococcus* sp.	*Aspergillus niger*	*Canda albicans*
LB_1	–	–	–	++	–	–	+
LB_2	–	–	–	–	++	–	–
LB_3	–	–	–	+++	–	–	++
LB_4	+	–	–	+++	–	–	+
LB_5	–	–	–	+++	–	–	–
LB_6	–	–	–	–	–	–	–
LB_7	–	–	–	+++	–	–	–
LB_8	–	–	–	+++	++	–	+
LB_9	–	–	+	+	–	++	++
LB_{10}	–	–	–	+++	–	–	–
LB_{11}	–	–	–	+++	–	–	+
LB_{12}	–	–	–	++	–	–	–
LB_{13}	–	–	–	+++	–	–	–
LB_{14}	–	–	–	+++	–	–	++
LB_{15}	–	–	++	++	–	–	+
LB_{16}	–	–	–	++	–	–	–
LB_{17}	–	–	–	–	–	–	–
HB_1	–	–	–	–	–	++	–
HB_2	–	–	–	+++	–	–	–
HB_3	–	–	–	–	–	–	–
HB_4	–	–	++	+	–	–	–
HB_5	–	–	+++	–	++	+	–
HB_6	–	–	–	–	++	–	–
HB_7	–	–	–	+	–	–	–
HB_8	–	–	++	–	–	++	+
HB_9	–	–	–	–	–	–	–
HB_{10}	–	–	–	++	–	–	–
HB_{11}	–	–	–	+++	–	–	–
HB_{12}	++	–	–	+++	–	–	–
HB_{13}	–	–	–	+++	–	–	–
HB_{14}	–	–	–	–	–	–	–
HB_{15}	–	–	–	–	–	–	–
HB_{16}	–	–	–	–	–	–	–

(–) No Zone, (+) Zone up to 8 mm, (++) Zone up to 16 mm, (+++) Zone above 16 mm

http://www.aloki.hu ● ISSN 1589 1623 (Print) ● ISSN 1785 0037 (Online)
DOI: http://dx.doi.org/10.15666/aeer/1605_53235341
© 2018, ALÖKI Kft., Budapest, Hungary

Discussion

The main objective of this research was to isolate and characterize the psychrotrophs and in the current study, a combination of morphological analysis and molecular methods were carried out for the identification of the fungal isolates. Out of 33 fungal isolates, four isolates LB_2 LB_3 LB_{15} and LB_{17} showed a similarity index up to 84, 87, 91 and 95% respectively and their sequences are deposited in database and to determine their taxonomic affiliation further investigations are needed. The fungal isolates were found to belong to mostly genus *Penicillium* (10) followed by *Cladosporium* (7) *Geomyces* (3) *Cordyceps* (1) *Mrakia* (2) *Cadophora* (1) *Tetracladium* (1) *Trametes* (1) *Mortierella* (1) *Scopulariopsis* (1) *Beauveria* (1) *Candida* (1) *Eupenicillium* (1) and *Pseudogymnoascus* (1).

The members of the genus *Geomyces,* are keratinophilic, psychrophilic and psychrotolerant in nature as have been reported by Blehert et al. (2009) and Arenz et al. (2011) from Antarctica and Arctic habitats as well as characterized as halotolerant and moderately cellulolytic. Fell and Stalzell-Tallman (1998) and Margesin et al. (2005) have earlier been documented *Mrakia* species with obligate psychrophilic nature from Antarctica, Alpine and Arctic habitats. Fungal species isolated in the present study that related to *Penicillium*, Candida, *Cladosporium*, *Pseudogymnoascus* and *Cadophora* have previously been reported in Antarctica and Alpine habitats (Burgaud et al., 2010; Dhakar et al., 2014; Duncan et al., 2006; Goncalves et al., 2012; Wang et al., 2015).

Tetracladium species have been found in alpine glaciers and snow-covered soil therefore considered to be cold-adapted (Kuhnert et al., 2012; Robinson et al., 2000). *Mortierella* species have been reported from Antarctic soil and mosses (Bridge and Newsham, 2009). The fungal species *Eupenicillium tularense Beauveria bassiana* and *Scopulariopsis brevicaulis* have not been reported from the low temperature habitats previously these species have been isolated for the first time from non-polar glacier in this study. Although *Trametes* sp. and *Cordyceps* sp. have been found for the first time in non-polar glaciers in this study but as the isolates showed low similarity (87% and 91% respectively) which most probably belong to genera other than *Trametes* and *Cordyceps* because they have homology less than 97% (Goncalves et al., 2012).

Batura glacier is one of the coldest non-polar glacier having very low temperature often below freezing point (–2 °C). In this study fungal isolation from such low temperature habitat indicate the possible role of the spores in their survival. Spores facilitate the existence of both bacteria and fungi in extreme environments as they protect them from UV-radiation and DNA damages (Ma et al., 2000). According to Robinson (2001), fungal persistence may possible due to cold circumvention rather than cold tolerance in Arctic and Antarctic habitats. Vishniac (1996) believed that spores helped more fungi to endure freezing than vulnerable hyphomycete hyphae. Catranis and Starmer (1991) and Ma et al. (2000) have isolated several of fungal isolates up to 140,000 years old from ice cores of Greenland. These studies show that fungal spores are central to survival of fungi in cold environments.

In the current study, the fungal isolates survived and grown at various extreme physiological parameters including temperature, NaCl and pH. Based on such results, fungal isolates grouped as psychrotolerants, halotolerants and thermotolerants as they tolerated broad range of temperature i.e. low and high temperature (from 4 to 45 °C) and the highest NaCl concentration (up to 26%). The isolates are highly diverse in terms of temperature requirement. They showed growth at lower temperature range (4–15 °C) which is a key property of psychrophilic organisms but they also showed growth at

http://www.aloki.hu ● ISSN 1589 1623 (Print) ● ISSN 1785 0037 (Online)
DOI: http://dx.doi.org/10.15666/aeer/1605_53235341
© 2018, ALÖKI Kft., Budapest, Hungary

higher temperatures. The ability of fungal isolates to grow at low and high temperature and high concentrations of salt possibly indicated mechanisms involved in the protection against such stressful conditions. Production of polyols, lipid/fatty acids and antifreeze proteins, etc. by cold adapted microbes are central mechanisms to overcome stressful conditions (Robinson et al., 2001). In this study the isolate *Mrakia cf. gelida* was capable of surviving at 45 °C and this was the first report of *Mrakia cf. gelida* from the glacier habitat that shown such a thermophilic nature because members of genus *Mrakia* have been reported as of psychrophilic nature (Xin and Zhou, 2007). Maheshwari[46] defined thermophilic fungi as they are able to grow between 20 and 55 °C. Our results are supported by Zucconi et al. (1996), who isolated thermotolerant-mesophilic fungi from Victoria Land Antarctica that was able to grow at 45 °C.

Fungal isolates showed growth on wide range of pH (1–13) which is a remarkable discovery of current research. Generally, acidic environment favors growth of fungi. On the other hand, the isolated fungal strains tolerated diverse salt concentrations (2–26%). Several fungal isolates showed growth at 24% (NaCl), whereas 1 of the fungal isolates could grew at 26% salt concentration as well. According to existing literature, many of the fungal isolates representing different genera isolated from the low temperature environments (*Cladosporium Cordyceps Mrakia Cadophora Tetracladium Trametes, Mortierella, Scopulariopsis, Beauveria, Candida, Eupenicillium* and *Pseudogymnoascus*) were characterized for the first time at such an extreme pH and salt conditions in the present study. However, species of the genera *Penicillium, Geomyces* and a few others (isolated from cold and other habitats) have been observed to grow at both high and low pH as well as the highest salts concentrations (Dhakar et al., 2014; Eliades et al., 2006; Grum-Grzhimaylo et al., 2013; Kochkina et al., 2007).

Secondary metabolites production by fungal isolates most importantly represented by antimicrobial activity have also been investigated in this study. Previously many fungal isolates have been found to produce secondary metabolites with bactericidal and fungicidal activity. In our study, fungal isolates exhibited decent antimicrobial activities against genus *Staphylococcus* as compared to other bacterial fungal genera. Screening of fungi from cold habitats against clinical bacterial isolates and fungal strains has not yet been reported. However, Brunati et al. (2009) screened more than 150 fungi and 165 yeasts (benthic mats of Antarctic lakes) against bacterial and fungal human pathogens from Merck Culture Collection (MB MY) and American Type Culture Collection (ATCC) including *Staphylococcus aureus, Enterococcus faecium, Escherichia coli, Moraxella catarrhalis, Pseudomonas aeruginosa, Candida albicans, Aspergillus fumigatus* and *Cryptococcus neoformans* but they were not found to be multi-drug resistant. A total of 47 (29%) filamentous fungi repressed growth of *Escherichia coli* (10%), *Staphylococcus aureus* (14%) and *Cryptococcus neoformans* (8%) *Candida albicans* (11%).

Based on the previous studies Arctic and Antarctic fungal isolates have been very poorly studied for the enzyme production. Currently, applications of cold adaptive fungi in biotechnological industries are becoming of great interest. Due to the cold adapted nature of various enzymes produced by psychrophilic fungi such as amylases, lipases, cellulases and proteases, their applications are increasing in various industrial fields (Feller and Gerday, 2003; Leary, 2008). In our study fungal isolates showed a broad range of extracellular enzyme production. Generally fungal isolates were reported as good producers of lipases phosphatases and cellulases. In various research studies many of the fungi from cold regions have been found good producers of different extracellular

http://www.aloki.hu ● ISSN 1589 1623 (Print) ● ISSN 1785 0037 (Online)
DOI: http://dx.doi.org/10.15666/aeer/1605_53235341
© 2018, ALÖKI Kft., Budapest, Hungary

enzymes cluding amylase, lipase, cellulose, chitinase, polygalacturonase and phosphatase (Fenice et al., 1997; Inglis et al., 2000; Singh et al., 2012, 2014).

Conclusions

Diversity evaluation of psychrotrophic and psychrophilic fungi in Batura glacier was conducted for the first time. Most of the fungal isolates belonging to Ascomycetes followed by Basidiomycetes and Zygomycetes were identified in this study. They were very versatile, capable to survive and grow at different extreme salt concentrations, temperature and pH and were also capable of producing antibiotics and enzymes of industrial importance at low temperatures. In the future, the isolated fungi of this study would be a great source of novel antibiotics and cold active enzymes that need to be properly characterized via both genetic and analytical tools. But utilizing cloning and other genetic manipulation approaches, the polyextremophilic nature of fungal isolates could be a good source of acid, salinity and alkalinity stable enzymes that would contribute greatly to the food, feed, paper and pulp industries, known for their extreme and environmental friendly processes.

Acknowledgments. Higher Education Commission of Pakistan for providing research funds for this project.

Conflict of interest. The authors declare that the research was conducted in the absence of any commercial or financial relationships that could be construed as a potential conflict of interest.

Author contributions. All authors have made contributions to the work and writing of this manuscript.

REFERENCES

[1] Altschul, S. F., Gish, W., Miller, W., Myers, E. W., Lipman, D. J. (1990): Basic local alignment search tool. – Journal of Molecular Biology 215(3): 403–410.
[2] Arenz, B. E., Held, B. W., Jurgens, J. A., Blanchette, R. A. (2011): Fungal colonization of exotic substrates in Antarctica. – Fungal Diversity 49(1): 13–22.
[3] Azmi, O. R., Seppelt, R. D. (1997): Fungi of the Windmill Islands, continental Antarctica. Effect of temperature, pH and culture media on the growth of selected microfungi. – Polar Biology 18(2): 128–134.
[4] Babjeva, I., Reshetova, I. (1998): Yeast resources in natural habitats at polar circle latitude. – Food Technol. Biotechnol. 36: 1–5.
[5] Baross, J. A., Morita, R. Y. (1978): Microbial Life at Low Temperatures: Ecological Aspects. – In: Kushner, D. J. (ed.) Microbial Life in Extreme Environments. Academic Press, London, pp. 9–71.
[6] Blehert, D. S., Hicks, A. C., Behr, M., Meteyer, C. U., Berlowski–Zier, B. M., Buckles, E. L., Coleman, J. T., Darling, S. R., Gargas, A., Niver, R., Okoniewski, J. C. (2009): Bat white-nose syndrome: an emerging fungal pathogen? – Science 323(5911): 227–227.
[7] Bridge, P. D., Newsham, K. K. (2009): Soil fungal community composition at Mars Oasis, a southern maritime Antarctic site, assessed by PCR amplification and cloning. – Fungal Ecology 2(2): 66–74.
[8] Bridge, P. D., Spooner, B. M., Roberts, P. J. (2008): Non–lichenized fungi from the Antarctic region. – Mycotaxon 106: 485–490.
[9] Broady, P. A., Weinstein, R. N. (1998): Algae, lichens and fungi in la Gorce Mountains, Antarctica. – Antarctic Science 10(4): 376–385.

http://www.aloki.hu ● ISSN 1589 1623 (Print) ● ISSN 1785 0037 (Online)
DOI: http://dx.doi.org/10.15666/aeer/1605_53235341
© 2018, ALÖKI Kft., Budapest, Hungary

[10] Brunati, M., Rojas, J. L., Sponga, F., Ciciliato, I., Losi, D., Göttlich, E., de Hoog, S., Genilloud, O., Marinelli, F. (2009): Diversity and pharmaceutical screening of fungi from benthic mats of Antarctic lakes. – Marine Genomics 2(1): 43–50.
[11] Burgaud, G., Arzur, D., Durand, L., Cambon–Bonavita, M. A., Barbier, G. (2010): Marine culturable yeasts in deep–sea hydrothermal vents: species richness and association with fauna. – FEMS Microbiology Ecology 73(1): 121–133.
[12] Catranis, C., Starmer, W. T. (1991): Microorganisms entrapped in glacial ice. – Antarctic Journal of the United States 26(5): 234–236.
[13] Cavicchioli, R., Siddiqui, K. S., Andrews, D., Sowers, K. R. (2002): Low–temperature extremophiles and their applications. – Current Opinion in Biotechnology 13(3): 253–261.
[14] Dhakar, K., Sharma, A., Pandey, A. (2014): Cold, pH and salt-tolerant Penicillium spp. inhabit the high-altitude soils in Himalaya, India. – World Journal of Microbiology and Biotechnology 30(4): 1315–1324.
[15] Dmitriev, V. V., Gilichinski, D. A., Faizutdinova, R. N., Shershunov, I. N., Golubev, W. I., Duda, V. I. (1997): Occurrence of viable yeasts in 3–million–year–old permafrost in Siberia. – Mikrobiologiya 66: 655–660.
[16] Duncan, S. M., Farrell, R. L., Thwaites, J. M., Held, B. W., Arenz, B. E., Jurgens, J. A., Blanchette, R. A. (2006): Endoglucanase-producing fungi isolated from Cape Evans historic expedition hut on Ross Island, Antarctica. – Environmental Microbiology 8(7): 1212–1219.
[17] Elíades, L. A., Cabello, M. N., Voget, C. E. (2006): Contribution to the study of alkalophilic and alkali–tolerant Ascomycota from Argentina. – Darwiniana 44(1): 64–73.
[18] Fell, J. W., Statzell–Tallman, A. (1998): Methods for the Isolation, Maintenance and Identification of Yeasts. – In: Kurtzman, C. P., Fell, J. W. (eds.) The Yeasts. A Taxonomic Study. Elsevier, Amsterdam.
[19] Feller, G., Gerday, C. (2003): Psychrophilic enzymes: hot topics in cold adaptation. – Nature Reviews Microbiology 1(3): 200.
[20] Fenice, M., Selbmann, L., Zucconi, L., Onofri, S. (1997): Production of extracellular enzymes by Antarctic fungal strains. – Polar Biology 17(3): 275–280.
[21] Friedmann, E. I., Druk, A. Y., McKay, C. P. (1994): Limits of life and microbial extinction in the Antarctic desert. – Antarctic Journal of the United States 29: 176–180.
[22] Gonçalves, V. N., Vaz, A. B., Rosa, C. A., Rosa, L. H. (2012): Diversity and distribution of fungal communities in lakes of Antarctica. – FEMS Microbiology Ecology 82(2): 459–471.
[23] Gounot, A. M. (1986): Psychrophilic and psychrotrophic microorganisms. – Experientia 42: (192–197).
[24] Grum–Grzhimaylo, A. A., Debets, A. J. M., van Diepeningen, A. D., Georgieva, M. L., Bilanenko, E. N. (2013): *Sodiomyces alkalinus*, a new holomorphic alkaliphilic ascomycete within the Plectosphaerellaceae. – Persoonia: Molecular Phylogeny and Evolution of Fungi 31: 147.
[25] Hankin, L., Anagnostakis, S. L. (1975): The use of solid media for detection of enzyme production by fungi. – Mycologia 1: 597–607.
[26] Hassan, N., Rafiq, M., Hayat, M., Shah, A. A., Hasan, F. (2016): Psychrophilic and psychrotrophic fungi: a comprehensive review. – Reviews in Environmental Science and Bio/Technology 15(2): 147–172.
[27] Hassan, N., Rafiq, M., Hayat, M., Nadeem, S., Shah, A. A., Hasan, F. (2017): Potential of psychrotrophic fungi isolated from Siachen glacier, Pakistan, to produce antimicrobial metabolites. – Applied Ecology and Environmental Research 15(3): 1157–1171.
[28] Inglis, G. D., Popp, A. P., Selinger, L. B., Kawchuk, L. M., Gaudet, D. A., McAllister, T. A. (2000): Production of cellulases and xylanases by low–temperature basidiomycetes. – Canadian Journal of Microbiology 46(9): 860–865.

http://www.aloki.hu ● ISSN 1589 1623 (Print) ● ISSN 1785 0037 (Online)
DOI: http://dx.doi.org/10.15666/aeer/1605_53235341
© 2018, ALÖKI Kft., Budapest, Hungary

[29] Kochkina, G. A., Ivanushkina, N. E., Akimov, V. N., Gilichinskii, D. A., Ozerskaya, S. M. (2007): Halo–and psychrotolerant *Geomyces* fungi from Arctic cryopegs and marine deposits. – Microbiology 76(1): 31–38.
[30] Kuhnert, R., Oberkofler, I., Peintner, U. (2012): Fungal growth and biomass development is boosted by plants in snow–covered soil. – Microbial Ecology 64(1): 79–90.
[31] Leary, D. K. (2008): Bioprospecting in the Arctic. – UNU–IAS Report, United Nations University, Institute of Advanced Studies, Yokohama, Japan.
[32] Ma, L., Catranis, C. M., Starmer, W. T., Rogers, S. O. (1999): Revival and characterization of fungi from ancient polar ice. – Mycologist 13(2): 70–73.
[33] Ma, L. J., Rogers, S. O., Catranis, C. M., Starmer, W. T. (2000): Detection and characterization of ancient fungi entrapped in glacial ice. – Mycologia 286–295.
[34] Maheshwari, R., Bharadwaj, G., Bhat, M. K. (2000): Thermophilic fungi: their physiology and enzymes. – Microbiology and Molecular Biology Reviews 64(3): 461–488.
[35] Margesin, R., Fauster, V., Fonteyne, P. A. (2005): Characterization of cold-active pectate lyases from psychrophilic *Mrakia frigida*. – Letters in Applied Microbiology 40(6): 453–459.
[36] Margesin, R., Fonteyne, P. A., Schinner, F., Sampaio, J. P. (2007): Novel psychrophilic basidiomycetous yeasts from Alpine environments: *Rhodotorula psychrophila* sp. nov., *Rhodotorula psychrophenolica* sp. nov. and *Rhodotorula glacialis* sp. nov. – Int J Syst Evol Microbiol 57: 2179–2184.
[37] Morita, R. (2000): Low–Temperature Environments. – In: Lederberg J. (ed.) Encyclopedia of Microbiology, Vol. 3 L–P. Academic Press, New York.
[38] Morita, R. Y. (1975): Psychrophilic bacteria. – Bacteriological Reviews 39(2): 144.
[39] Otha, A., Wolfaardt, G. M. (2000): Yeast Biofilms: An Unexplored Natural Phenomenon. – In: Van Dijken, J. P., Scheffers, W. A. (eds.) The Rising Power of Yeasts in Science and Industry, Papendal, Arnhem, The Netherlands, Symposium Book. – Delft University Press, Delft.
[40] Pikovskaya, R. I. (1948): Mobilization of phosphorus in soil in connection with vital activity of some microbial species. – Mikrobiologiya 17: 362–370.
[41] Rahman, A., Duncan, A. J., Miller, D. W., Clemens, J., Frutos, P., Gordon, I. J., Rehman, A. U., Baig, A., Ali, F., Wright, I. A. (2008): Livestock feed resources, production and management in the agro–pastoral system of the Hindu Kush–Karakoram–Himalayan region of Pakistan: The effect of accessibility. – Agricultural Systems 96(1–3): 26–36.
[42] Robinson, C. H. (2001): Cold adaptation in Arctic and Antarctic fungi. – New Phytologist 151(2): 341–353.
[43] Robinson, C. T., Gessner, M. O., Callies, K. A., Jolidon, C., Ward, J. V. (2000): Larch needle breakdown in contrasting streams of an alpine glacial floodplain. – Journal of the North American Benthological Society (19(2): 250–262.
[44] Rosa, L. H., Vaz, A. B., Caligiorne, R. B., Campolina, S., Rosa, C. A. (2009): Endophytic fungi associated with the Antarctic grass *Deschampsia antarctica* Desv. (Poaceae). – Polar Biology 32(2): 161–167.
[45] Schadt, C. W., Martin, A. P., Lipson, D. A., Schmidt, S. K. (2003): Seasonal dynamics of previously unknown fungal lineages in tundra soils. – Science 301(5638): 1359–1361.
[46] Singh, S. M., Singh, S. K., Yadav, L. S., Singh, P. N., Ravindra, R. (2012): Filamentous soil fungi from Ny–Ålesund, Spitsbergen, and screening for extracellular enzymes. – Arctic 45–55.
[47] Singh, S. M., Singh, P. N., Singh, S. K., Sharma, P. K. (2014): Pigment, fatty acid and extracellular enzyme analysis of a fungal strain *Thelebolus microsporus* from Larsemann Hills, Antarctica. – Polar Record 50(1): 31–36.
[48] Tamura, K., Nei, M. (1993): Estimation of the number of nucleotide substitutions in the control region of mitochondrial DNA in humans and chimpanzees. – Molecular Biology and Evolution 10(3): 512–526.

http://www.aloki.hu ● ISSN 1589 1623 (Print) ● ISSN 1785 0037 (Online)
DOI: http://dx.doi.org/10.15666/aeer/1605_53235341
© 2018, ALÖKI Kft., Budapest, Hungary

[49] Tamura, K., Stecher, G., Peterson, D., Filipski, A., Kumar, S. (2013): MEGA6: molecular evolutionary genetics analysis version 6.0. – Molecular Biology and Evolution 30(12): 2725–2729.
[50] Thompson, J. D., Gibson, T. J., Plewniak, F., Jeanmougin, F., Higgins, D. G. (1997): The CLUSTAL_X windows interface: flexible strategies for multiple sequence alignment aided by quality analysis tools. – Nucleic Acids Research 25(24): 4876–4882.
[51] Tojo, M., Newsham, K. K. (2012): Snow moulds in polar environments. – Fungal Ecology 5(4): 395–402.
[52] Vishniac, H. S. (1996): Biodiversity of yeasts and filamentous microfungi in terrestrial Antarctic ecosystems. – Biodiversity and Conservation 5(11): 1365–1378.
[53] Vishniac, H. S. (2006): Yeast Biodiversity in the Antarctic. – In: Rosa, C. A., Péter, G. (eds.) Biodiversity and Ecophysiology of Yeasts. Springer, Berlin, Heidelberg.
[54] Wang, M., Jiang, X., Wu, W., Hao, Y., Su, Y., Cai, L., Xiang, M., Liu, X. (2015): Psychrophilic fungi from the world's roof. – Persoonia: Molecular Phylogeny and Evolution of Fungi 34: 100.
[55] Xin, M. X., Zhou, P. J. (2007): *Mrakia psychrophila* sp. nov., a new species isolated from Antarctic soil. – Journal of Zhejiang University Science B 8(4): 260–265.
[56] Zhang, Z., Schwartz, S., Wagner, L., Miller, W. (2000): A greedy algorithm for aligning DNA sequences. – Journal of Computational Biology 7: 203–214.
[57] Zucconi, L., Pagano, S., Fenice, M., Selbmann, L., Tosi, S., Onofri, S. (1996): Growth temperature preferences of fungal strains from Victoria Land, Antarctica. – Polar Biology 16(1): 53–61.

APPENDIX

Table A1. *Colony morphology and microscopic characteristics of fungal isolates on SDA*

Isolate	Sample form	Temperature (°C)	Colony morphology		Microscopic characteristics
			Front	Reverse	
LB_1	Sediment	4	Powdery, initially cottony, white with white margins then turned to dim gray	Golden to brown center with dim gray margins	Branched and septate hyphae, smooth-walled to broadly ellipsoidal and scattered conidia, cylindrical phialides and metulae
LB_2	Sediment	4	Mucoid, light goldenrod center with off-white edges	Lemmon chiffon center with off-white margins	Cylindrical to ovoid shaped and scattered spores, no pseudo- hyphae observed
LB_3	Sediment	4	Cottony, initially salmon to white with salmon edges then turned to slate gray to white	Saddle brown center with golden edges	Hyaline, thin-walled and branched hyphae with frequent clamp connections, chlamydospores hyaline, pear to oval shaped.
LB_4	Sediment	4	Velvety, initially dry mucoid to yellow then turned to dark orange with goldenrod margins	Saddle brown center with golden edges	Hyphae septate, branched, Conidiophores simple or sparsely branched and scattered conidiophores

http://www.aloki.hu ● ISSN 1589 1623 (Print) ● ISSN 1785 0037 (Online)
DOI: http://dx.doi.org/10.15666/aeer/1605_53235341
© 2018, ALÖKI Kft., Budapest, Hungary

LB_5	Sediment	4	Velvety, initially dark olive green with light yellow edges then turned to black to dark green with white surface	Black center with off-white edges	Branched, pale olivaceous brown hyphae, conidia ellipsoidal to limoni-form, smooth-walled or slightly verrucose, olivaceous brown	
LB_6	Sediment	4	Cottony, initially white velvety with off-white margins then turned to dim gray	Golden to brown center with dim gray margins.	Terverticillate to quaterverticillate conidiophores, smooth-walled, globose to suglobose conidia and cylindrical metulae and phialides	
LB_7	Sediment	4	Cottony, initially yellow to green then turned to sea green with dim gray edges	Dark brown center with saddle brown edges	Hyphae hyaline to pale yellow and septate, scattered and erect conidiophores, and branched conidia	
LB_8	Sediment	4	Velvety, initially cottony white then turned to gray with slate gray margins	Dark brown center with light goldenrod margins	Septate and branched hyphae, globose to subglobose shaped conidia, scattered conidiophores	
LB_9	Sediment	4	Cottony, initially velvety with blue to green center, white margin then turned to light gray to dark sea green	Dark orange to brown center with off-white margins	Branched and septate hyphae, conidiophores biverticillate, grey to green and echinulate to globose shaped conidia	
LB_{10}	Sediment	4	Velvety, initially gray to black center with off-white edges then turned to light slate gray	Gray to black center and light yellow edges	Hyaline, smooth and thin-walled conidia, ovoidal to ellipsoidal shaped spores	
LB_{11}	Sediment	4	Cottony, initially slate gray center with white margins then turned to dim gray	Brown center and yellow to off-white margins	Conspicuously roughened and branched conidiophores, septate hyphae, scattered conidia	
LB_{12}	Sediment	4	Velvety, initially white center with off-white margins then turned into light gray	Black to brown center with brown margins	Scattered and branched hyphae, curved, branched and pale greenish conidia	
LB_{13}	Sediment	4	Dry mucoid, initially white center with off-white margins then turned to light goldenrod	Golden center and light goldenrod margins	Spores are globose to ovoid shape, no pseudohyphae was observed	
LB_{14}	Sediment	4	Powdery, initially cottony, white with white margins then turned to dim gray	Golden to brown center with dim gray margins	Cylindrical metulae and phialides, scattered and branched hyphae, scattered conidiophores	

http://www.aloki.hu ● ISSN 1589 1623 (Print) ● ISSN 1785 0037 (Online)
DOI: http://dx.doi.org/10.15666/aeer/1605_53235341
© 2018, ALÖKI Kft., Budapest, Hungary

LB_{15}	Sediment	4	Velvety, initially white with white edges then turned to light cyan	Saddle brown center with light goldenrod yellow edges	Septate to multiseptate and branched hyphae, colorless and cylindrical to ovoid shape spores	
LB_{16}	Ice	4	Velvety, initially dark olive green gray center with off-white edges then turned to dark green to black	Black center with off-white edges	Septate and branched hyphae, elliptical to cylindrical in shape, pale to dark brown in color	
LB_{17}	Water	4	Velvety, dark olive green with light yellow edges	Black center with light goldenrod yellow edges	Branched hyphae, conidia ellipsoidal to limoni-form, smooth-walled or slightly verrucose, olivaceous brown	
HB_1	Sediment	15	Cottony, initially green to blue then turned to dim gray with white margins	Brown center with golden-rod margins	Septate, branched hyphae, longer and visibly roughened conidiophores producing smooth to finely roughened conidia	
HB_2	Sediment	15	Cottony, initially white to light yellow then converted to gray with whit to off-white edges	Khaki center with pale goldenrod edges	Pseudomycelium and septate hyphae, cylindrical to ovoid shaped and scattered conidia	
HB_3	Sediment	15	Powdery, initially dark sea green then turned to black with pale green edges	Black center with dark orange to golden edges	Branched, septate hyphae, numerous, large and densely packed phialides conidiophore	
HB_4	Sediment	15	Cottony, light yellow to light golden-rod yellow center with white margins	Golden center with light goldenrod margins	Septate and hyaline hyphae, short and globose to ovoid conidiophore, scattered conidia	
HB_5	Sediment	15	Cottony, initially white to gray then turned to brown-black with off-white edges	Off-white to yellow center and light yellow edges	Round to ovoid in shape conidia, septate and branched hyphae, and scattered conidiophores	
HB_6	Sediment	15	Cottony, white to light goldenrod yellow center with white margins	Dark orange to brown center with goldenrod margins	Short distinct branched conidiophores, conidia are 1-celled and either white or yellow	
HB_7	Sediment	15	Cottony, initially green center with white margins then turned to light gray to white	Off-white to yellow center and light yellow edges	Conspicuously roughened and branched conidiophores, septate hyphae, scattered conidia	
HB_8	Sediment	15	Cottony, initially velvety with blue to green center, white margin then turned to light gray to dark sea green	Dark orange to brown center with off-white margins	Conidiophores biverticillate, grey to green and echinulate to globose shaped conidia	

http://www.aloki.hu ● ISSN 1589 1623 (Print) ● ISSN 1785 0037 (Online)
DOI: http://dx.doi.org/10.15666/aeer/1605_53235341
© 2018, ALÖKI Kft., Budapest, Hungary

HB_9	Sediment	15	Powdery, initially cottony with dark green center and white edges then turned to dim gray	Off-white to yellow center and light yellow edges	Hyphae are septate and hyaline, kidney-shaped to brush-shaped conidiophores on conidia
HB_{10}	Sediment	15	Cottony, initially gray center with white edges then turned to light gray	Off-white to yellow center and light yellow edges	Divergent biverticillate to terverticillate conidiophores, smooth-walled and scattered conidia
HB_{11}	Sediment	15	Cottony, white center with white margins	Golden to yellow center and off-white margins	Sporangiophores subulate, hyaline, smooth, unbranched. Sporangia mainly globose
HB_{12}	Sediment	15	Powdery, initially white center with dark sea green margins then turned into black to brown	Black center with dark olive green margins	Septate and brown hyphae erected and pigmented conidiophores with conidia
HB_{13}	Sediment	15	Cottony, white center with dark salmon margins	Golden to brown center and yellow margins	Short chains or branched conidiophores, obovoidal and scattered conidia
HB_{14}	Sediment	15	Powdery, initially velvety with blue to green center, white margin then turned to gray to green	Light golden-rod center with light golden-rod yellow margin	Septate and branched hyphae, chains of spores (or conidia) from brush-shaped conidiophores
HB_{15}	Ice	15	Velvety, initially dark olive green with light yellow edges then turned to black to green	Black center with light goldenrod yellow edges	Septate, light colored hyphae, erect, pigmented, scattered conidiophores, and conidia
HB_{16}	Water	15	Velvety, dark olive green with light yellow edges	Black center with light golden red yellow edges	Septate and branched hyphae, elliptical to cylindrical in shape conidia, scattered conidiophores

LB: Low (Temperature, 4 °C) Batura Isolates, HB: High (Temperature, 15 °C) Batura Isolates

http://www.aloki.hu ● ISSN 1589 1623 (Print) ● ISSN 1785 0037 (Online)
DOI: http://dx.doi.org/10.15666/aeer/1605_53235341
© 2018, ALÖKI Kft., Budapest, Hungary

DIVERSITY ASSESSMENT OF GRAPEFRUIT (*CITRUS × PARADISI*) AND TANGELO (*CITRUS × TANGELO)* UNDER INDIAN CONDITIONS USING PHYSICO-CHEMICAL PARAMETERS AND SSR MARKERS

AHMED, S.* – RATTANPAL, H. S. – SINGH, G.

Department of Fruit Science, PAU, Ludhiana, Punjab, 141004 India

**Corresponding author*
e-mail: shahnawazpomol@gmail.com

(Received 24th Apr 2018; accepted 5th Jul 2018)

Abstract. In a previous report, grapefruit (*Citrus × paradisi* Macfad.) and tangelo (*Citrus × tangelo* J.W. Ingram & H.E. Moore, 1975) landraces from diversity rich Indo-Gangetic Plain and arid regions of India were characterised using specific SSR markers. Eight grapefruit and two tangelo varieties were compared with germplasm of diverse origin comprising of cultivars, landraces and wild types. Significant differences were observed for different morphological characters studied. The highest phenotypic co-efficient of variance (PCV) and genotypic co-efficient of variance (GCV) were determined for seed weight (104.4 and 103.7, respectively), number of seeds per fruit (102.3 and 101.9, respectively), number of fruits per tree (60.0 and 60.0, respectively) and acidity (40.4 and 38.8, respectively). These mentioned characters were more influenced by environment than other characters. A total of 75 alleles were amplified by 26 polymorphic simple sequence repeat (SSR) loci and the number of alleles ranged from 1 to 4 with an average of 2.88 alleles per locus. The highest number of alleles per locus was four as amplified by CAT01, CS05, CCSM204, CCSM70, CIBE5156, ATC09 and CMS26 followed by three alleles per locus each by CCSM77, CCSM156, CL11, OP29, CMS46, CMS09, CIBE4728, CMS3O and AG14 and the remaining markers amplified two alleles. The highest number of alleles among grapefruit varieties was found in Ray Ruby (75) while the lowest number of alleles was found in Flame (61) while among tangelo varities the highest number of alleles was found in Pearl (64). Average polymorphism (%) of all the polymorphic primer pairs across all the varieties of grapefruit was 69.55 and the highest polymorphism among grapefruit varieties was found in Marsh (82.09) while among tangelo varieties the highest polymorphism was found in Pearl (81.25). The measure of allelic diversity that is PIC value ranged from 0.17 (CS06) to 0.75 (CAT01) with an average value of 0.53.
Keywords: *citrus, germplasm, morphological characterization, molecular markers, polymorphism*

Introduction

Citrus is a sub-tropical fruit that belongs to the family of *Rutaceae.* It is grown commercially throughout India and is known worldwide of its characteristic flavour, attractive evergreen foliage and flower as well as the extraordinary fragrance, which are added aesthetic values (Rabha et al., 2013). In India, it is grown in acreage of 935 thousand hectares with the production of 11515 thousand MT and productivity of 12181 MT/ha respectively (NHB, 2016).

The grapefruit (*Citrus × paradisi* Macfad.) originated from Barbados in the Caribbean islands, is a natural hybrid between pummelo (*Citrus maxima* (Burm.) Merr.) and sweet orange (*C. sinensis* L. Osb). It was first named as *Citrus paradise* Macfad. by James Macfadyen in 1837 (Scora et al., 1982 and Scora, 1988). The tangelo (*Citrus × tangelo* J.W. Ingram & H.E. Moore, 1975) probably originated in southeastern Asia over 3,500 years ago. Tangelo is most likely a result of insect cross pollination of the mandarin orange and the pummelo (pummelo is the ancestor of the grapefruit).

http://www.aloki.hu ● ISSN 1589 1623 (Print) ● ISSN 1785 0037 (Online)
DOI: http://dx.doi.org/10.15666/aeer/1605_53435358
© 2018, ALÖKI Kft., Budapest, Hungary

Grapefruit is the fourth most important citrus fruit economically in the world. It is rich in various nutrients, phytochemicals, vitamin C and fiberpectin with pink and red hues that contain the beneficial antioxidants lycopene (Silver et al., 2011). There are many benefits of this fruit worth mentioning: (i) peel and seed extract of grapefruit have antifungal properties (Okunowo et al., 2013), (ii) it helps in lowering cholesterol (Platt, 2000) and also (iii) in animals cell studies, grapefruit powder, limonin and naringenin decrease growth and increase self-destruction of colon, mouth, skin, lung, breast and stomach cancer (Chidambara et al., 2011). Citrus varieties show more diversity in their morphological traits such as size and shape of canopy, color, type, number of seeds, fruit weight, fruit diameter, flower diameter, TSS, acidity etc. Generally in plants, the diversity at the phenotypic level is much larger than at genetic level, as selectively neutral molecular markers are used to evaluate the extent of genetic variation.

For future variety management and conservation purposes this adaptive genetic diversity represents important potential. Recently researchers (Amara et al., 2011; Ahmed et al., 2012; Jianfeng et al., 2012; Uzun and Yesiloglu, 2012), have observed the significant diversity among cultivated genotypes of Citrus genus in respect of physiological, morphological and agronomic traits but very little DNA variation has been detected using DNA-markers. Likewise, in other cases markers were used to determine genetic diversity, characterization and phylogenetic relationships among the Citrus and related genera (Gulsen and Roose, 2001; Shahsavar et al., 2007; Uzun et al., 2009; Marak and Laskar, 2010; Golein et al., 2011). Grapefruits are highly polyembryonic and have low genetic variation due to nucellar and mutation origin (Fang and Roose 1997 and Corazza-Nunes et al., 2002). Substantial genetic variation among citrus species and cultivars is due to frequent bud mutation, interspecific and intergeneric hybridization, apomixes and long history of cultivation. There is an urgent need for diversification of scion citrus cultivars for Punjab citriculture for reducing the high risks associated with the outbreaks of new and more severe diseases and pests. Secondly, there is more variation in characters in citrus than in other fruit crops (Reuther et al., 1967) and citrus is phenotypically the most heterogeneous group (Moore, 2001). In the present study ten varieties of grapefruit and tangelo were studied with the aim (a) to correlate the physico-chemical variation with the genetic diversity (b) to estimate genetic polymorphism and relationships among grapefruit and tangelo varieties based on SSR markers.

Materials and methods

Plant material

In this study we investigate eight grapefruit and two tangelo cultivars (*Table 1*) from the College Orchard, Department of Fruit Science, Punjab Agricultural University, Ludhiana, India in the year 2015-16. Observations were recorded for different morphological characters at different growth and development stages. All the trees received recommended doses of fertilizers and other cultural practices during the course of these investigations.

Morphological evaluation

Morphological evaluation was carried out for two years, i.e. from 2015 to 2016. Fruits were harvested at full maturity, yield and quality parameters data were recorded.

http://www.aloki.hu ● ISSN 1589 1623 (Print) ● ISSN 1785 0037 (Online)
DOI: http://dx.doi.org/10.15666/aeer/1605_53435358
© 2018, ALÖKI Kft., Budapest, Hungary

Characterization of grapefruit and tangelo cultivars was conducted on ten genotypes on the basis of IPGRI (International Plant Genetic Resources Institute) citrus descriptors (Anonymous, 1999). Twenty fruits were sampled from each cultivar for quality analysis, and characteristics evaluated including number of seed per fruit, peel thickness, fruit weight, fruit size, juice content, peel content and rag content. Juice was filtered through filter paper, thereafter, juice samples were examined to determine the following parameters; pH, total soluble solids (TSS), titratable acidity (% of citric acid) using N/10 NaOH and phenolphthalein as indicator, using digital refractometer, and ascorbic acid (mg/100 ml of juice) using a dye (2, 6-dichlorophenol indophenol) according to the standard method (Rangana, 1986). Design of experiment was in randomized block with five replications. Data were subject for analysis of variation to one way ANOVA. Statistical analysis was performed using analysis of variance. P values ≤ 0.05 were considered as significant. A cluster analysis was performed using the unwieghted pair group method with arithmetic average (UPGMA) based on simple matching coefficient in NTSYS software. The phenotypic and genotypic coefficients of variation were calculated as per formula described by Burton (1952) and Burton and de Vane (1953). Heritability, in broad sense, was calculated as suggested by Allard (1960) and genetic advance percent of mean was calculated following the method suggested by Johnson et al. (1955).

Table 1. *Citrus paradisi Macf. cultivars and variants used in the study of germplasm characterization*

S. no.	Varieties	Origin
Grapefruit		
1	Flame	Originated in Florida – budwood registration program, winter haven in 1988
2	Foster	Originated as a branch sport of a selection called 'Walters' in Florida, USA in 1907
3	Marsh	Originated as seedling trees on the property of a Mrs. Rushin near Lakeland, Florida, USA (1862)
4	Ray Ruby	Originated in Texas in 1985
5	Red Blush	Originated as sports–lower branches–growing out of 'Thompson' trees in USA in 1929
6	Rio Red	Originated in Texas in 1985
7	Ruby Red	Originated in Texas in 1988
8	Star Ruby	Originated as a lower branch mutation bearing red-blushed fruits, noticed on a 'Foster' tree at San Benito, Texas, USA in 1930
Tangelo		
9	Minneola	Produced at John Carpenter, USDCS, Indio CA in 1961
10	Pearl	Hybrid produced at UCR in 1945

Isolation and purification of genomic DNA

Genomic DNA was extracted from 5 g of well ground tissue using the protocol described by Gusmini et al. (2004). DNA was extracted from young leaves of five randomly selected plants for each variety and then subsequent molecular analysis. Air dried DNA pellets were dissolved in 50 l of 1X TE buffer (Tris-EDTA buffer- 10 mM Tris-HCl, I mM EDTA, pH 8.0. Quantity and quality of DNA was determined by

http://www.aloki.hu ● ISSN 1589 1623 (Print) ● ISSN 1785 0037 (Online)
DOI: http://dx.doi.org/10.15666/aeer/1605_53435358
© 2018, ALÖKI Kft., Budapest, Hungary

Nanodrop 1000 instrument (Thermo Scientific, USA) using 2 l of genomic DNA. Absorbance was recorded at 260/280 nm and readings were taken for both the quantity (ng µ/l) and quality (Absorbance). Only the samples having absorbance value from 1.90-2.00 were taken for DNA analysis. And the samples with absorbent values less are repeated till the desired amount of DNA is achieved.

Selection of primers

The DNA was amplified through polymerase chain reaction (PCR) using 60 SSR primer pairs (synthesized by Integrated DNA Technologies) previously described and used (Ahmad et al., 2003; Barkley et al., 2006; Ollitrault et al., 2010; Soriano et al., 2012; Yaly et al., 2011; Meral et al., 2011) for citrus germplasm characterization. PCR amplification of 20 µl total volume was performed in 2.0 µl of 10X PCR buffer, 2.5 µl of 1 mM dNTPs, 1.25 µl of each of forward and reverse primer (5 µM), 0.25 µl of Taq polymerase (5 units/µl of Promega, USA), 4.0 µl of DNA (15 ng) and distilled de-ionized water using an Eppendorf thermal cycler. The PCR profile consisted of initial denaturation at 94 °C for 3 min and subsequent 35 cycles each with denaturation at 94 °C for 30 s, primer annealing at 48-57 °C for 1 min and primer extension at 72 °C for 1 min. Final extension step was performed at 72 °C for 7 min. Annealing temperature was modified to optimize the reaction conditions for individual primers. PCR products were stored at 4 °C before analysis. PCR-amplified DNA fragments were separated on a 1.5% agarose gel containing 1X TBE (45 mM Tris-borate1 mM EDTA) and 0.5 µg/ml aqueous solution of ethidium bromide. The agarose gel was run at a constant voltage of 100 V for 2–3 h in 0.5 × TBE buffer. Gels were visualized under UV light and photographed using photo documentation system (Alphaimager system). The repeatability of the markers was verified in the whole collection and all null alleles were confirmed by a second amplification.

Data collection and analysis

SSR alleles were scored for the presence (1) and absence (0) of the SSR bands. Polymorphism information content (PIC) for each SSR marker was determined as per the procedure outlined by Senior et al. (1998).

$$PIC = 1 - \Sigma\,(Pij)^2$$

$$i = 1$$

where *Pij* is the frequency of *j*th allele in *i*th primer and summation extends over 'n' patterns.

Genetic similarity coefficients between various genotypes (in pair-wise comparisons) were calculated from the SSR data matrix using dice coefficient and the resulting genetic similarity matrix was analyzed using NTSYS-PC version 2.02 to produce an agglomerative hierarchical classification (Rohlf, 1989) by employing Unweighted Pair Group Method using Arithmetic Averages (UPGMA). For estimating the similarity matrix, null alleles (no SSR allele in a given *citrus* genotype) were treated as missing data to reduce the biased genetic or similarity measures (Warburton and Crossa, 2000).

Genetic diversity (GD) was calculated according to the following formula of Nei (1987):

http://www.aloki.hu ● ISSN 1589 1623 (Print) ● ISSN 1785 0037 (Online)
DOI: http://dx.doi.org/10.15666/aeer/1605_53435358
© 2018, ALÖKI Kft., Budapest, Hungary

$$GD = n\,(1 - p^2)/(n - 1)$$

where (n) is the number of samples and (p) is the frequency of one allele.

Results and discussion

Clustering studies based on morphological diversity

Grapefruit and tangelo varieties consist of four clusters (*Fig. 1*), cluster I consists of only one variety Flame with an average distance of 0.37 cm (*Table 2*) from other varieties. Cluster II consists of two varieties namely Marsh and Red Blush, which are more associated with each other with an average distance of 0.10 cm. While in cluster III there were four varieties namely Foster, Ray Ruby, Star Ruby and Rio Red. Foster have an average distance of 0.13 cm as compared to Rio Red which has 0.24 cm distance from the other varieties. In cluster IV there were three verities Ruby Red, Minneola and Pearl. Minneola and Pearl were closely associated with each other with an average distance of 0.25 cm while Ruby Red have less association with other varieties with an average distance of 1.37 cm from other varieties. Further, the study on inheritance of agronomic traits of citrus reports them to be controlled by multiple genes which can be assessed only through morphological assessment (Liu and Deng, 2007).

Table 2. *Root mean-square distance between grapefruit and tangelo varieties within clusters based on morphological characteristics.*

Number of clusters	Clusters joined		Freq	Norm RMS distance (cm)
9	Ray Ruby	Star Ruby	2	0.0136
8	Marsh	Red Blush	2	0.1072
7	Foster	CL9	3	0.1349
6	CL7	Rio Red	4	0.2447
5	Minneola	Pearl	2	0.2573
4	Flame	CL8	3	0.3715
3	CL4	CL6	7	0.5285
2	Ruby Red	CL5	3	0.7395
1	CL3	CL2	10	1.3799

However, Dorji and Yapwattanaphun (2011) concluded that the groups diverged having similarity coefficient of 0.79 in contrast to 0.41. There is not much variation with respect to qualitative characters of the groups. Golein et al. (2005) reported that the analyzed accessions having high average similarity coefficient (0.91) indicated that all mandarins represented variations of single clones. Likewise, analysis of 43 morphological characters in the 22 cultivars of *C. sinensis* revealed that maximum similarity (0.64) occurred between the cultivars Campbell Valencia and Vanale, both of which are exotic in origin and are most similar in terms of qualitative fruit, leaf and seed characters (Malik et al., 2012). Minimum similarity (0.18) was observed between the

http://www.aloki.hu ● ISSN 1589 1623 (Print) ● ISSN 1785 0037 (Online)
DOI: http://dx.doi.org/10.15666/aeer/1605_53435358
© 2018, ALÖKI Kft., Budapest, Hungary

cultivars Washington navel and Mosambi, which may be attributed to their different centres of origin where they have developed their distinct characters.

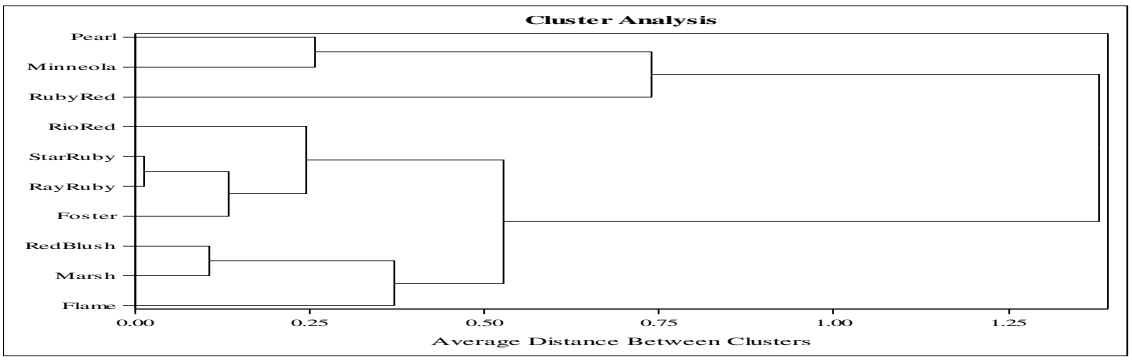

Figure 1. *Dendrogram of grapefruit and tangelo varieties based on morphological characteristics using the UPGMA method*

Variability, heritability and genetic advance in grapefruit and tangelo varieties based on morphological characteristics.

Estimation of genotype for phenotypic variance (PV) and genotypic variance (GV) indicated that variance was recorded maximum for number of fruits per tree, fruit weight, and fruit diameter, number of seeds per fruit and seed weight (*Table 3*). The variation present in population is due to genotypic and environmental effects. It includes both genotypic and environmental condition. The highest phenotypic co-efficient variance (PCV) and genotypic co-efficient variance (GCV) were recorded for seed weight (104.4 and 103.7, respectively), number of seeds per fruit (102.3 and 101.9, respectively), number of fruits per tree (60.0 and 60.0, respectively) and acidity (40.4 and 38.8, respectively). These mentioned characters were much more influenced by the environment than other characters.

In the present investigation of genetic advance coupled with high heritability was observed for seed weight, number of seeds per fruit, number of fruits per tree and acidity. Thus the results indicated that selection would be highly effective for above mentioned characters. Similar finding was made by Baswal et al. (2016), who concluded that the co-efficient of variation (both genotypic and phenotypic) was higher for the characters like density of oil glands/cm^2 (35.1 and 34.8, respectively) followed by albedo thickness (19.5 and 19.4, respectively). GCV associated with high heritability (80% or more) indicated that selection would be effective for the improvement of these characters. Also Roy et al. (2014) concluded that in pummelo germplasm while studying variability, a wide range of variability was observed for almost all variables or characters. The co-efficient of variation was higher (>20) for characters like yield per plant, fruit rind thickness, seed weight and number of fruits per plant.

Burton (1952) observed that if GCV associated with high heritability (80% or more) indicated that selection would be effective for the improvement of these characters but if a character with low heritability (40% or less) selection may be comparatively difficult or virtually impractical due to masking effect of the environment on the genotypic effects. This indicated that selection for density of oil glands, albedo thickness, fruit weight and fruit diameter would be effective. In a similar study, Panse

http://www.aloki.hu ● ISSN 1589 1623 (Print) ● ISSN 1785 0037 (Online)
DOI: http://dx.doi.org/10.15666/aeer/1605_53435358
© 2018, ALÖKI Kft., Budapest, Hungary

(1957) suggested that a high genetic advance coupled with high heritability may be expected if heritability is mainly due to additive genetic effects.

Table 3. *Variability, heritability and genetic advance in grapefruit and tangelo varieties based on morphological characteristics*

Characters (Grapefruit)	PV	GV	PCV	GCV	h^2 (%)	GA (%) of mean
Leaf lamina length (mm)	79.5	63.4	8.4	7.5	79.7	13.9
Leaf lamina width (mm)	42.4	28.1	9.6	7.8	66.3	13.2
Rootstock bud circumference (cm)	148.3	145.4	12.5	12.3	97.9	25.2
Leaf area	16.1	14.3	14.8	13.9	88.5	27.1
Scion truck circumference	216.9	212.5	16.5	16.4	97.9	33.4
Average number of seeds per fruit	193.9	192.1	102.3	101.9	99.0	209.0
Seed weight per fruit (g)	190.7	189.4	104.1	103.7	99.3	213.0
Seed length (mm)	7.8	6.8	18.2	16.9	86.8	32.5
Seed width (mm)	1.5	1.4	17.9	17.2	92.3	34.1
Flower diameter (mm)	5.5	4.0	7.0	6.0	73.3	10.6
Staminate (%)	3.0	2.9	26.4	25.7	94.7	51.6
Perfect (%)	4.4	2.3	2.2	1.6	52.9	2.4
Pollen viability (%)	150.2	145.6	20.2	19.8	96.9	40.3
Pollen germination	47.9	45.8	17.5	17.1	95.5	34.5
Fruit diameter (mm)	246.6	235.7	16.2	15.9	95.5	32.0
Fruit length (mm)	110.8	102.3	12.0	11.5	92.3	22.9
Fruit rind thickness (mm)	3.6	3.2	24.3	22.7	87.1	43.7
Number of segments per fruit	13.0	8.9	23.7	19.5	68.1	33.2
Diameter of fruit axis (mm)	13.8	11.8	27.9	25.8	85.3	49.2
Total soluble solids (%)	0.4	0.3	8.4	6.9	67.1	11.7
Acidity (%)	0.1	0.1	40.4	38.8	92.1	76.7
Ph	0.1	0.0	8.8	5.4	37.1	6.7
VIT C	59.1	50.4	17.5	16.2	85.2	30.8
JUICE %	66.2	56.2	15.9	14.7	84.8	27.9
PEEL %	18.2	9.0	13.7	9.6	49.2	13.9
RAG %	42.4	19.0	36.4	24.4	44.8	33.6
Number fruits per tree	22200.2	22161.3	60.0	60.0	99.8	123.5
Fruit weight (g)	12060.5	11900.6	30.8	30.6	98.6	62.7

PV = phenotypic variance, GV = genotypic variance, PCV = phenotypic coefficient of variance, GCV = genotypic coefficient of variance, h^2 = heritability in broad sense and GA = genetic advances

Allele amplification in grapefruit and tangelo varieties

Allele frequency or the frequency at which alleles are found at any locus of interest is used to estimate the frequency of given genetic profile. In grapefruit and tangelo varieties a total of 75 alleles were amplified by 26 polymorphic SSR loci and the number of alleles ranged from 1 to 4 with an average of 2.88 alleles per locus. The highest number of alleles per locus was four as amplified by CAT01, CS05, CCSM204,

http://www.aloki.hu ● ISSN 1589 1623 (Print) ● ISSN 1785 0037 (Online)
DOI: http://dx.doi.org/10.15666/aeer/1605_53435358
© 2018, ALÖKI Kft., Budapest, Hungary

CCSM70, CIBE5156, ATC09 and CMS26 followed by three alleles per locus each by CCSM77, CCSM156, CL11, OP29, CMS46, CMS09, CIBE4728, CMS3O and AG14 and the remaining markers amplified two alleles (*Table 4*).

Table 4. *Number of alleles amplified, polymorphism (%), polymorphic information content (PIC) value and genetic diversity of SSR markers in grapefruit and tangelo varieties*

S. no.	SSR marker	Monomorphic allele	Polymorphic allele	Total no. of alleles	Polymorphism (%)	PIC	Genetic diversity
1	CS05	1	3	4	75.00	0.69	0.76
2	CCSME15	0	2	2	100.00	0.30	0.33
3	OP571	1	1	2	50.00	0.49	0.55
4	CAT01	1	3	4	75.00	0.75	0.83
5	CCSM77	0	3	3	100.00	0.59	0.65
6	CCSM156	1	2	3	66.67	0.61	0.67
7	CCSM170	1	1	2	50.00	0.50	0.55
8	CCSM201	1	1	2	50.00	0.28	0.31
9	CCSM204	1	3	4	75.00	0.64	0.71
10	CCSM68	0	2	2	100.00	0.43	0.47
11	CCSM70	1	3	4	75.00	0.74	0.82
12	CCSME15	0	2	2	100.00	0.18	0.20
13	CIBE5156	1	3	4	75.00	0.74	0.83
14	CL11	1	2	3	66.67	0.51	0.56
15	CS06	1	1	2	50.00	0.17	0.18
16	CS09	1	1	2	50.00	0.41	0.45
17	CIBE5720	1	1	2	50.00	0.49	0.55
18	GT03	1	1	2	50.00	0.49	0.55
19	ATC09	1	3	4	75.00	0.68	0.75
20	0P29	1	2	3	66.67	0.38	0.42
21	CMS46	1	2	3	66.67	0.61	0.67
22	CMS09	2	1	3	33.33	0.60	0.67
23	CIBE4728	2	1	3	33.33	0.66	0.73
24	CMS26	1	3	4	75.00	0.68	0.75
25	CMS30	0	3	3	100.00	0.55	0.61
26	AG14	0	3	3	100.00	0.55	0.61
	Total	**22**	**53**	**75**	**1808.34**	**13.72**	**15.18**
	Mean	**0.85**	**2.04**	**2.88**	**69.55**	**0.53**	**0.58**

Polymorphic information content and percentage of polymorphism among grapefruit and tangelo varieties based on SSR markers

In Grapefruit and tangelo varieties the percentage of polymorphism of the 26 polymorphic markers ranged from 50 to 100 (*Table 4*). Among these, 6 exhibited 100 percent polymorphism; seven were having 75 %, four having 66.66 % and remaining had 50 %. Average polymorphism (%) of all the polymorphic primer pairs across all the varieties of grapefruit was 69.55. The PIC value which is a measure of allelic diversity

http://www.aloki.hu ● ISSN 1589 1623 (Print) ● ISSN 1785 0037 (Online)
DOI: http://dx.doi.org/10.15666/aeer/1605_53435358
© 2018, ALÖKI Kft., Budapest, Hungary

at a locus ranged from 0.17 (CS06) to 0.75 (CAT01) with an average value of 0.53. Fourteen SSR markers revealed PIC value more than 0.53. Primer CAT01 amplified 4 alleles and had the highest PIC value of 0.75 followed by CSM70 and CIBE5156 in which 3 alleles were amplified and had PIC value of 0.74 (*Table 4*). All the alleles amplified by CAT01 primer pairs on all the varieties of grapefruit were all distinguishable. It has been observed that marker OP29 amplified 3 alleles and had PIC value of 0.38 while GT03 amplified 2 alleles and had PIC value of 0.49. Therefore, there seemed to be no strong correlation between the PIC value and the number of alleles amplified. Across all varieties, a total of 663 alleles (*Table 5*) were amplified by 58 SSR primers with an average of 63.30 alleles for each variety. The average amplified fragments for polymorphic marker was 51.90 whereas for monomorphic, it was 14.40. The maximum number of alleles (75) was detected in Ray Ruby whereas Minneola showed the least number of alleles (52). However, the percent of polymorphic markers was maximum (82.09) in Marsh followed by 81.25 % in Pearl.

Table 5. *Total number of alleles amplified in grapefruit and tangelo varieties using SSR markers*

S. no.	Genotypes	Number of amplified alleles		Total	Polymorphism (%)
		Monomorphic markers	Polymorphic markers		
Grapefruit					
1	Foster	12	48	60	80.00
2	Flame	13	48	61	78.69
3	Marsh	12	55	67	82.09
4	Ray Ruby	15	60	75	80.00
5	Red Blush	20	52	72	72.22
6	Rio Red	16	56	72	77.78
7	Ruby Red	14	60	74	81.08
8	Star Ruby	15	51	66	77.27
Tangelo					
9	Pearl	12	52	64	81.25
10	Minneola	15	37	52	71.15
	Total	**144**	**519**	**663**	**781.53**
	Mean	**14.40**	**51.90**	**66.30**	**78.15**

Likewise, Meral et al. (2011) reported narrow genetic diversity in Satsuma mandarins clones suggesting that the observed morphological polymorphism within the group must be associated with somatic mutations which were not detected by SSR molecular markers. Similarly, Singh et al. (2016) concluded that among 19 different mandarin genotypes that 57 SSR markers amplified, a total of 96 alleles were detected by 39 polymorphic SSR loci and maximum 5 alleles were amplified with an average of 2.46 alleles per primer pair. The CAT01 was the highly informative marker as it revealed maximum number of alleles (5), PIC value (0.75) and genetic diversity (0.79). Across the genotypes, maximum number of alleles (83) was detected in Daisy hybrid and the percentage of polymorphic marker was maximum (80.32) in Nova hybrid. The markers with low number of alleles were able to differentiate the varieties with specific alleles.

http://www.aloki.hu ● ISSN 1589 1623 (Print) ● ISSN 1785 0037 (Online)
DOI: http://dx.doi.org/10.15666/aeer/1605_53435358
© 2018, ALÖKI Kft., Budapest, Hungary

Simple Sequence Repeats (SSRs) have proven to be efficient genetic markers for comparative genetic mapping between Citrus species (Luro et al., 2008). Although some SSRs were identified based on EST database in previous studies (Chen et al., 2006) no system analysis of SSRs in citrus has been reported because of incomplete citrus genome. Recently, the Clementine mandarin genome has been sequenced (Gmitter et al., 2012) and the completion of these genome sequences provided an opportunity for us to scan the entire genome for SSR discovery in citrus. In this study, we present our results on the SSR survey for the development of citrus SSR markers.

Genetic diversity

Genetic diversity among grapefruit and tangelo varieties ranged from 0.18 (CS06) to 0.83 (CAT01 and CIBE5156). The average value of genetic diversity across all the primers was 0.58 (*Table 4*). The dendrogram (*Fig. 2*) depicting the genetic relationship classified the genotypes into 3 major clusters (I, II and III). The cluster I contains single variety (Minneola) but cluster II was further sub divided into two sub clusters IIA and IIB with three (Rio Red, Star Ruby and Pearl) and two (Flame and Foster) varieties respectively. While four (Ray Ruby, Marsh, Ruby Red and Red Blush) varieties were clustered in cluster III. The similarity coefficient based on DNA amplification of grapefruit and tangelo varieties using SSR primer was estimated by dice similarity coefficient (*Table 6*). The varieties Ruby Flame and Foster, Ruby Red and Red Blush showed the highest genetic similarity having coefficient of 0.90 and were closely related. However, Rio Red and Pearl showed lowest (0.68) genetic similarity coefficient and these were genetically distinct from each other. Similarly, 19 different mandarin genotypes (Singh et al., 2016) were classified in three clusters, i.e. cluster I, cluster II and cluster III. All the indigenous genotypes (selections) were grouped in cluster -I and it had maximum genetic similarity coefficient. However, the exotic genotypes (hybrids) were grouped in cluster II and cluster III. Clustering was according to the breeding history of genotypes but independent of their geographic origin.

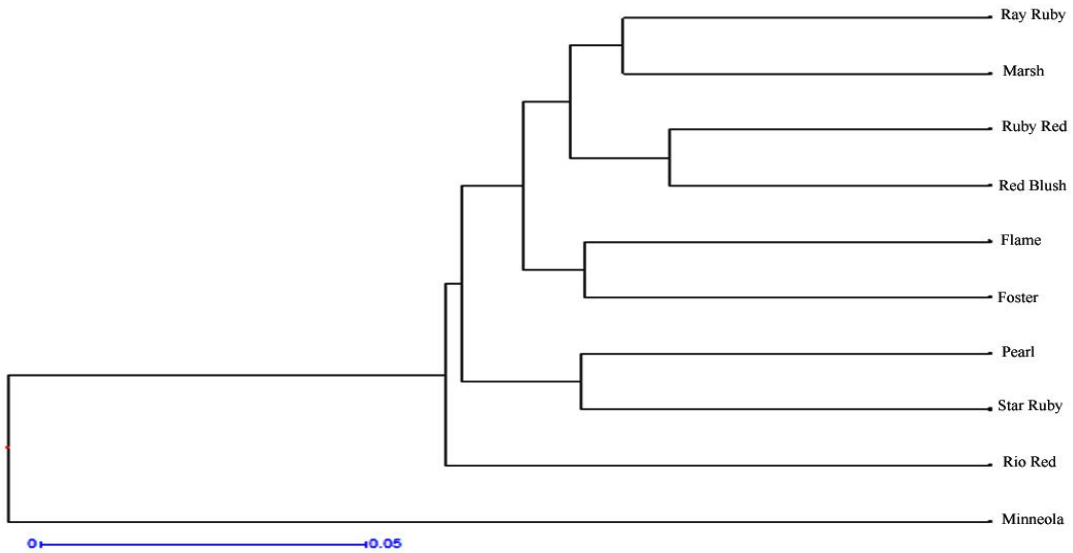

Figure 2. *Dendrogram illustrating genetic relationship among grapefruit and tangelo varieties based on the SSR markers generated by UPGMA tree analysis*

http://www.aloki.hu ● ISSN 1589 1623 (Print) ● ISSN 1785 0037 (Online)
DOI: http://dx.doi.org/10.15666/aeer/1605_53435358
© 2018, ALÖKI Kft., Budapest, Hungary

Table 6. *Similarity coefficient based on DNA amplification of grapefruit and tangelo varieties estimated by dice similarity coefficient*

Varieties	1	2	3	4	5	6	7	8	9
2	0.76								
3	0.88	0.71							
4	0.85	0.73	0.87						
5	0.87	0.69	0.85	0.89					
6	0.83	0.76	0.83	0.83	0.86				
7	0.82	0.68	0.82	0.82	0.85	0.83			
8	0.87	0.73	0.87	0.89	0.90	0.90	0.87		
9	0.85	0.71	0.81	0.81	0.83	0.84	0.83	0.88	
10	0.86	0.68	0.82	0.82	0.84	0.83	0.84	0.86	0.87

Legend: Marsh, Ray Ruby, Rio Red, Star Ruby, Flame, Red Blush, Ruby Red, Foster, Minneola, and Pearl

The results revealed that the difference in the dendrogram of morphological and molecular data could be due to action of diverse evolutionary forces and environmental attributes. This hypothesis was supported by the findings of Paudyal and Haq (2008) who reported that environmental factors affected up to 40% in pummelo accessions in an un-controlled field survey. The morphological difference in individual accession was supported by the observation of Dorji and Yapwattanaphun (2011a) who reported that phenotypic variation could be attributed to mutations, cross pollination and environmental interactions (*Figs. 3, 4* and *5; Table 7*).

Table 7. *Physico-chemical parameters of grapefruit and tangelo varieties*

Varieties	Average number of seeds per fruit	Seed weight per fruit (g)	Rootstock diameter (mm)	Scion diameter (mm)	Spine length (mm)	Leaf lamina length (mm)	Leaf lamina width (mm)	Leaf area (cm^2)	Petiole wing width (mm)	Flower diameter (mm)	Pollen viability (%)	Pollen germination (%)
Grapefruit												
Flame	3.3	2.3	94.3	90.1	5.6	117.6	76.9	32.7	12.9	32.8	51.4	32.9
Foster	34.5	30.2	83.2	80.3	5.7	105.9	66.1	27.7	16.3	35.0	54.9	38.2
Marsh Seedless	3.2	2.9	104.6	100.6	4.8	110.1	68.5	29.8	18.8	31.3	50.2	29.9
Ray Ruby	4.5	3.6	110.5	105.1	4.3	114.2	74.1	31.6	22.0	37.1	55.9	39.7
Red Blush	3.8	3.1	115.1	112.2	6.3	104.2	64.7	25.3	15.6	33.1	57.6	40.4
Rio Red	1.8	1.1	108.0	96.1	5.1	99.1	65.2	23.9	17.8	31.6	53.2	36.6
Ruby Red	3.5	3.3	87.3	74.1	5.5	97.0	73.3	23.1	14.5	35.6	53.5	34.7
Star Ruby	35.8	33.1	79.5	65.6	4.3	110.9	63.3	30.4	19.8	34.0	66.7	42.4
Tangelo												
Minneola	21.5	24.7	92.0	80.1	3.4	101.7	61.1	24.5	23.3	30.4	77.7	46.9
Pearl	24.0	28.3	98.7	84.5	3.6	90.7	60.0	21.7	20.7	32.2	85.7	53.0
SEm±	2.3	1.9	1.0	1.2	0.6	6.9	6.5	2.4	0.9	2.1	3.7	2.5
LSD (p=0.05)	0.8	0.7	3.0	3.6	0.2	2.3	2.2	0.8	0.3	0.7	1.2	0.8

http://www.aloki.hu ● ISSN 1589 1623 (Print) ● ISSN 1785 0037 (Online)
DOI: http://dx.doi.org/10.15666/aeer/1605_53435358
© 2018, ALÖKI Kft., Budapest, Hungary

Varieties	Fruit diameter (mm)	Fruit length (mm)	Fruit rind thickness (mm)	Number of segments per fruit	Total soluble solids (Brix)	Acidity (%)	pH	Ascorbic acid (mg/100g)	Juice content (%)	Peel content (%)	Rag content (%)	Fruit weight (g)
Grapefruit												
Flame	93.0	83.7	7.2	12.8	7.3	1.13	4.1	52.9	52.3	34.9	12.8	258.9
Foster	99.1	91.3	8.5	15.4	8.7	0.90	4.2	40.9	45.6	33.4	21.2	431.9
Marsh Seedless	103.1	93.9	8.5	12.6	7.5	1.45	4.5	54.7	46.8	32.8	20.5	337.1
Ray Ruby	111.6	96.9	7.7	14.4	7.9	1.80	5.0	50.9	48.4	31.3	20.2	384.0
Red Blush	84.9	75.9	10.4	13.7	8.2	0.62	4.8	35.8	51.9	31.5	16.6	313.7
Rio Red	114.4	98.8	9.7	15.4	8.2	1.16	4.4	41.5	44.0	32.1	23.9	456.5
Ruby Red	109.1	97.5	9.3	13.0	8.5	1.03	4.8	43.9	40.4	34.4	25.2	561.8
Star Ruby	104.9	87.0	7.5	13.5	8.0	0.78	4.3	46.6	53.7	30.7	15.6	359.4
Tangelo												
Minneola	70.5	68.0	4.4	19.5	9.4	0.54	4.7	36.9	64.3	26.7	9.0	203.6
Pearl	74.0	81.1	5.6	22.3	8.4	0.64	4.8	34.0	62.5	23.7	13.8	236.2
SEm±	5.7	5.0	1.2	3.5	0.7	0.19	0.6	5.1	5.5	5.3	8.4	21.9
LSD (p=0.05)	1.9	1.7	0.4	1.2	0.2	0.07	0.2	1.7	1.8	1.8	2.8	7.3

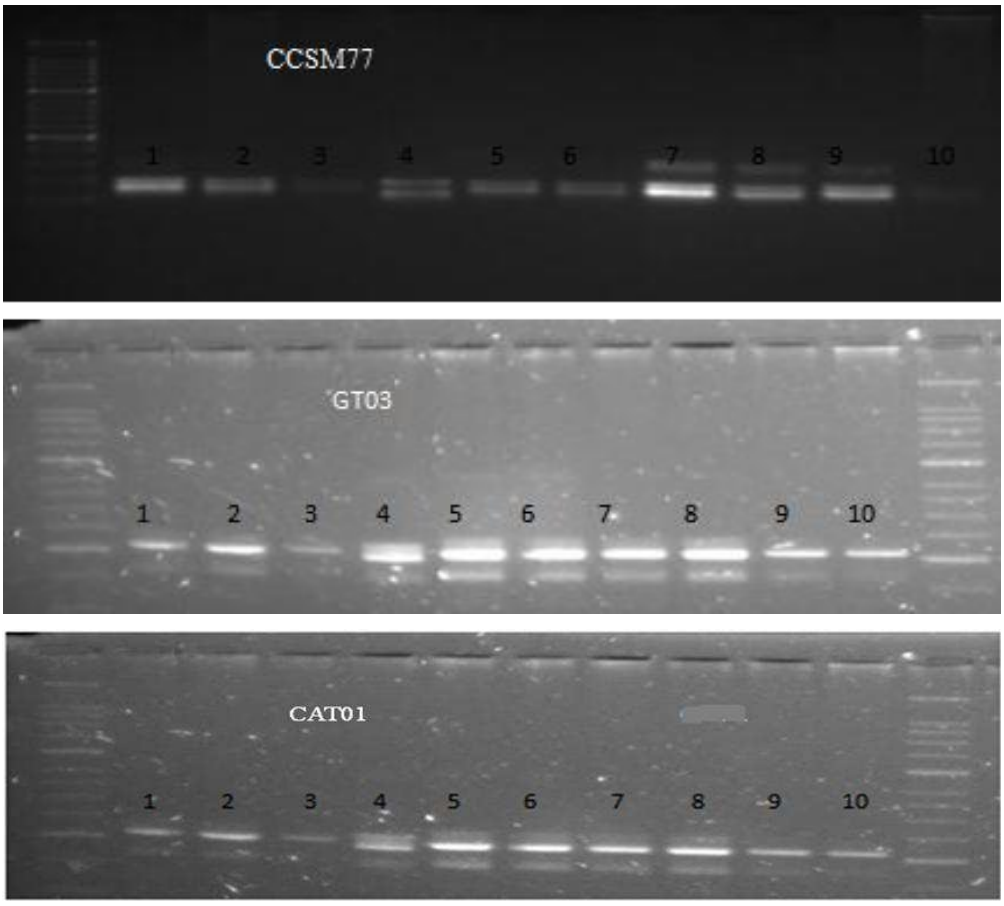

Figure 3. *Agarose gel showing SSR amplification profile by different primer in different grapefruit and tangelo varieties Flame, Foster, Marsh, Ray Ruby, Red Blush, Rio Red, Ruby Red, Star Ruby, Minneola and Pear*

http://www.aloki.hu ● ISSN 1589 1623 (Print) ● ISSN 1785 0037 (Online)
DOI: http://dx.doi.org/10.15666/aeer/1605_53435358
© 2018, ALÖKI Kft., Budapest, Hungary

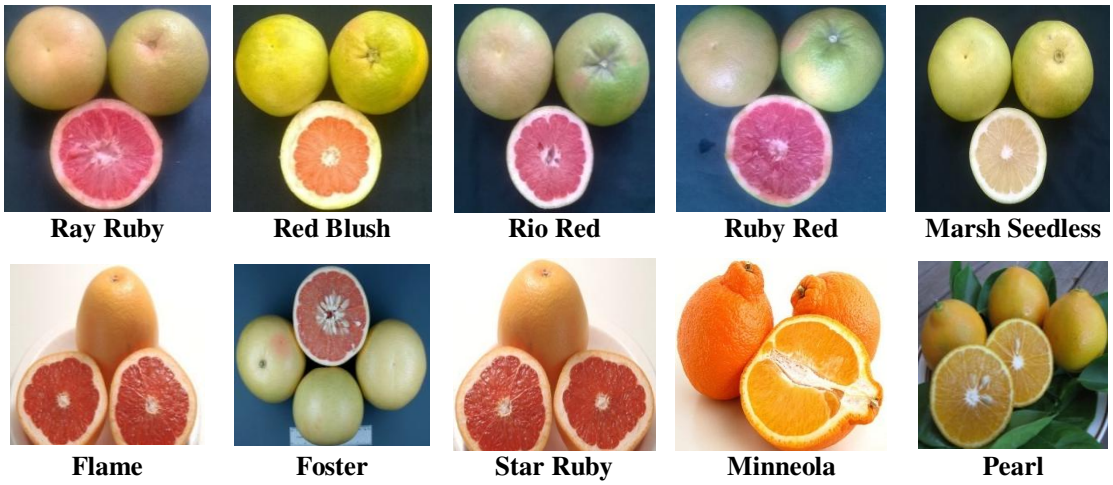

Figure 4. *Diversity in fruit size and shape of different grapefruit and tangelo varieties*

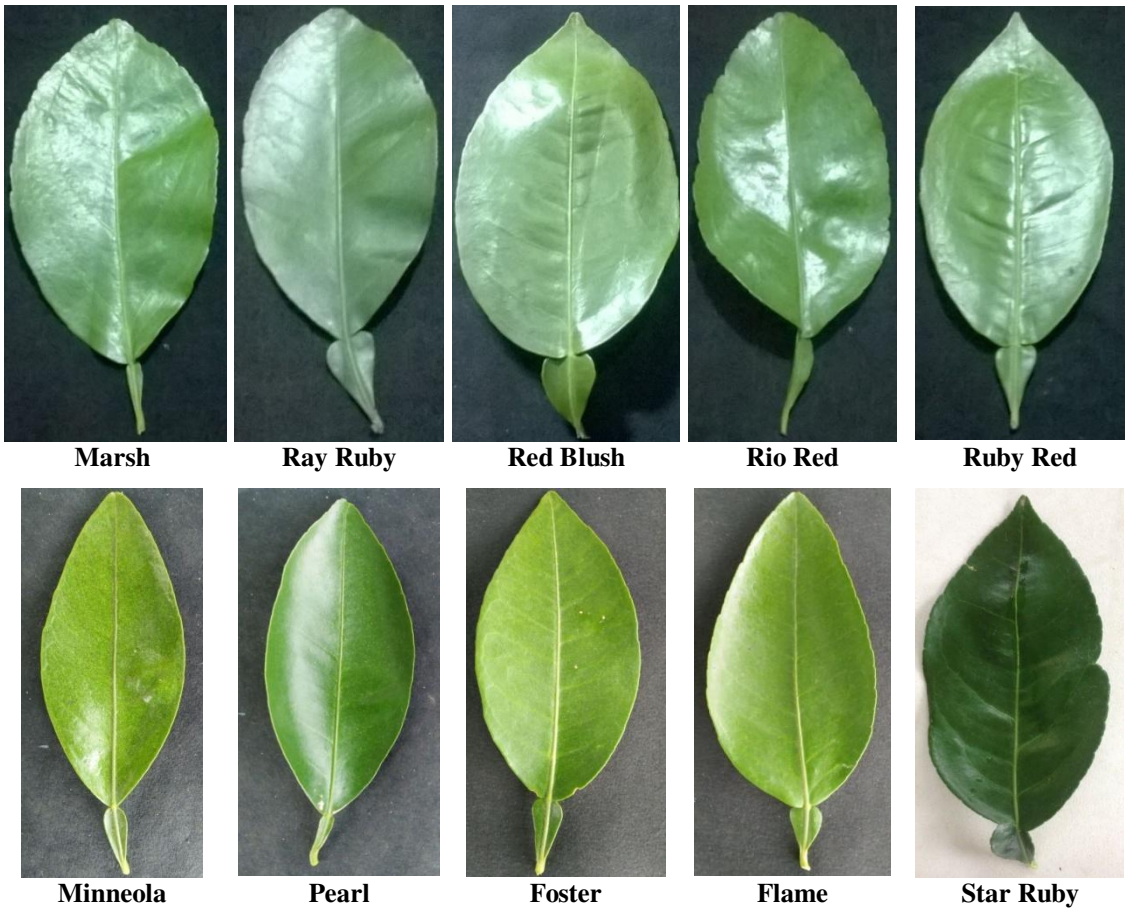

Figure 5. *Diversity in leaf size and shape of different grapefruit and tangelo varieties*

Conclusions

Present study indicated that genetic diversity in grapefruit and tangelo varieties was found to be very low, despite having high morphological variability, which could be elucidated by the fact that much of the phenotypic variation witnessed may be due to

http://www.aloki.hu ● ISSN 1589 1623 (Print) ● ISSN 1785 0037 (Online)
DOI: http://dx.doi.org/10.15666/aeer/1605_53435358
© 2018, ALÖKI Kft., Budapest, Hungary

somatic mutations. Genetic diversity among grapefruit and tangelo varieties ranged from 0.18 (CS06) to 0.83 (CAT01 and CIBE5156). Furthermore, based on molecular analysis, varieties Ruby Flame and Foster, Ruby Red and Red Blush showed the highest genetic similarity having coefficient of 0.90 and were closely related. However, Rio Red and Pearl showed the lowest (0.68) genetic similarity coefficient and these were genetically distinct from each other.

Acknowledgements. The first author is thankful to the Department of Science and Technology, New Delhi, India for providing INSPIRE fellowship during this study.

REFERENCES

[1] Ahmad, M., Javaid, A., Rahman, H., Hussain, S. I., Ramzan, A., Ghafoor, A. (2012): Identification of mandarin x orange hybrids using simple sequence repeat markers. – J Agric Res. 50: 225-232.
[2] Ahmad, R., Struss, D., Southwick, S. M. (2003): Development and characterization of micro satellite markers in citrus. – J Amer Soc Hort Sci 128: 584-90.
[3] Allard, R. W. (1960): Principles of Plant Breeding. – John Wiley and Sons Inc., New York, United States of America, pp. 83-108.
[4] Amara, M. H., Biswasa, M. K., Zhangc, Z., Guoa, W. W. (2011): Exploitation of SSR, SRAP and CAPS-SNP markers for genetic diversity of citrus germplasm collection. – Sci Horti 128: 220-227.
[5] Anonoymus (1999): IPGRI. Descriptors of Citrus. – International Plant Genetic Resource Institute. Rome. Italy. http:/www.cgiar.org/ipgri/.
[6] Barkley, N. A., Roose, M. L., Krueger, R. R., Federici, C. T. (2006): Assessing genetic diversity and population structure in a citrus germplasm collection utilizing simple sequence repeat markers (SSRs). – Theor Appl Genet 112: 1519-31.
[7] Baswal, A. K., Rattanpal, H. S., Sidhu, G. S. (2016): Varietal assessment and variability studies in grapefruit (citrus paradisi aradisi aradisi mac fadyen) genotypes in subtropical zones of Punjab al zones of Punjab, India. – The Bioscan 11(2): 1369-71.
[8] Burton, G. W. (1952): Quantitaive inhereitance in grasses. – Proc. 6th Intercropping. Grassland Cong., Pp. 277-283.
[9] Burton, G. W., Vane, E. W. (1953): Estimating herita-bility in tall fescue (*Festuca arundinacea*) from replicated clone material. – Agron J 45: 475-81.
[10] Chen, C., Zhou, P., Choi, Y. A., Huang, S., Gmitter, Jr. F. G. (2006): Mining and characterizing microsatellites from citrus ESTs. – Theoretical and Applied Genetics 112: 1248-1257.
[11] Chidambara, Murthy, K. N., Jayaprakasha, G. K., Kumar, V., Rathore, K. S., Patil, B. S. (2011): Citrus limonin and its glucoside inhibit colon adenocarcinoma cell proliferation through apoptosis. – J Agri Food Chem 59: 2314-2323.
[12] Chowdhury, N. H. (1991): Studies on Quality of Rice in Bangladesh. – In: Proceeding of the Workshop on Chemical Aspects of Rice Grain Quality, IRRI, Philippines, pp. 23-127.
[13] Corazza-Nunes, M. J., Machado, M. A., Nunes, W. M. C., Cristofani, M., Targon, M. L. P. N. (2002): Assessment of genetic variability in grapefruits (*Citrus paradisi* Macf.) and pummelos (*C. maxima* Burm. Merr.) using RAPD and SSR markers. – Euphytica 126: 169-76.
[14] Dorji, K., Yapwattanaphun, C. (2011): Morphological identification of mandarin (*Citrus reticulata* Blanco) in Bhutan. – Kasetsart J Nat Sci 45: 793-802.
[15] Fang, D. Q., Roose, M. L. (1997): Identification of closely related Citrus cultivars with inter simple sequence repeat markers. – Theor Appl Genet 95: 408-17.

http://www.aloki.hu ● ISSN 1589 1623 (Print) ● ISSN 1785 0037 (Online)
DOI: http://dx.doi.org/10.15666/aeer/1605_53435358
© 2018, ALÖKI Kft., Budapest, Hungary

[16] Gmitter, Jr. F. G., Chen, C., Machado, M. A., Souza, A. A., Ollitrault, P. (2012): Citrus genomics. – Tree Genetics & Genomes 8: 611-626.
[17] Golein, B., Talaie, A., Zamani, Z., Eabadi, A., Behjatnia, A. (2005): Assessment of Genetic Variability in Some Iranian Sweet Oranges (Citrus sinensis [L.] Osbeck) and Mandarins (Citrus reticulata Blanco) Using SSR Markers. – International Journal of Agriculture & Biology 7(2): 167-170.
[18] Golein, B., Fifaei, R., Ghasemi, M. (2011): Identification of zygotic and nucellar seedlings in citrus interspecific crosses by inter simple sequence repeats (ISSR) markers. – Afr J Biotechnol 10: 18965-18970.
[19] Gulsen, O., Roose, M. L. (2001): Lemons: diversity and relationships with selected Citrus genotypes as measured with nuclear genome markers. – J Amer Soc Hort Sci. 126: 309-327.
[20] Gusmini, G., Wehner, T., Jarret, R. (2004): Inheritance of egusi seed type in watermelon. – J. Hered. 95: 268-270.
[21] Jianfeng, H., Yonghua, Q., Hongxia, M., Chunyan, Z., Zixing, Ye., Guibing, Hu. (2012): Molecular marker analysis of 'Shatangju' and 'Wuzishatangju' mandarin (Citrus reticulata Blanco). – Afr J Biotechnol 11: 15501-15509.
[22] Johnson, H. W., Robinson, H. F., Comstock, R. E. (1955): Estimates of genetics and environmental variability in soyabean. – Agron J 47: 314-18.
[23] Liu, Y. Z., Dang, X. X. (2007): Citrus breeding and genetics in China. – The Asian Australian J Plant Sci Biotechnol pp. 23-28.
[24] Luro, F., G. Costantino, J., Terol, X., Argout, T., Allario, P., Wincker, M., Talon, P., Ollitrault, R. Morillon. (2008): Transferability of the EST-SSRs developed on Nules clementine (Citrus clementina Hort ex Tan) to other citrus species and their effectiveness for genetic mapping. – BMC Genomics 9: 287.
[25] Malik, S. K., Rohini, M. R., Kumar, S., Choudhary, R., Pal, D., Chaudhury, R. (2012): Assessment of genetic diversity in sweet orange [*Citrus sinensis* (L.) Osbeck] cultivars of India using morphological and RAPD markers. – Agric Res 1: 317-24.
[26] Marak, C. K., Laskar, M. A. (2010): Analysis of phonetic relationship between Citrus indica Tanaka and a few commercially important citrus species by ISSR markers. – Sci Hortic124: 345-348.
[27] Meral, N., Tuzcu, O., Yeilolu, T., Kacar, Y. A., Yildirim, B., Boncuk, M., Cimen, B. (2011): Molecular diversification and preliminary evaluations of some Satsuma selections performance under Mediterranean conditions. – Afri J Biotech 10: 4347-57.
[28] Moore, G. A. (2001): Oranges and lemons: clues to the taxonomy of Citrus from molecular markers. – Trends Genet 17(9): 536-40.
[29] Nei, M. (1987): Molecular Evolutionary Genetics. – Columbia University Press, New York.
[30] NHB (2016): Fruit Production Database. – National Horticulture Board, New Delhi, India. www.nhb.in.
[31] Okunowo, W., Oyedeji, O., Afolabi, L., Matanmi, E. (2013): Essential oil of grapefruit (Citrus paradisi) peels and its antimicrobial activities. – Amr J Plant Sci 4: 1-9.
[32] Ollitrault, F., Terol, J., Pina, J., Navarro, A., Talon, L., Ollitrault, P. (2010): Development of SSR markers from *Citrus clementina* (Rutacea) BAC end sequences and interspecific transferability in citrus. – Amer J Bot 124e-29 e.
[33] Panse, V. G. (1957): Genetics of quantitative characters in selections to plant breeding. – Ind Jour Genet 17: 318-28.
[34] Paudyal, K., Haq, N. (2008): Variation of pomelo [Citrus grandis (L.) Osbeck] in Nepal and participatory selection of strains for further improvement. – Agroforestry Systems 72: 195-204.
[35] Platt, R. (2000): Current concepts in optimum nutrition for cardio vascular disease. – Prev Cardiol 3: 83-87.

http://www.aloki.hu ● ISSN 1589 1623 (Print) ● ISSN 1785 0037 (Online)
DOI: http://dx.doi.org/10.15666/aeer/1605_53435358
© 2018, ALÖKI Kft., Budapest, Hungary

[36] Rabha, A., Wangchu, L., and Singh, B. (2013): Studies on genetic diversity of citrus in east Siang district of Arunachal Pradesh. – Int J Agric Environ Biotech 6: 131-37.
[37] Rangana, S. (1986): Hand Book of Analysis and Quality Control for the Fruit and Vegetable Products. – Tata McGraw Hills, New Delhi.
[38] Reuther, E., Batcheler, L. D., Webber, H. J. (1967): The Citrus Industry. Vol. 1. – Agr. Sci. University of California, Berkeley.
[39] Rohlf, F. J. (1989): NTSYS-pc Numerical Taxonomy and Multivariate Analysis System, version 2.02. – Exeter Publication, Sarauket, NY.
[40] Roy, D., Kundu, S., Ghosh, B., Dutta, P., Pal, R. (2014): Performance of pummelo germplasm in new alluvial zone of West Bengal. – J Crop Weed 10: 179-82.
[41] Scora, R. W. (1988): Biochemistry, Taxonomy and Evolution of Modern Cultivated Citrus. Proc Int Soc Citricult VI. Congr. vol. 1. – Margraf Publishers, Weikersheim, Germany, pp. 277-289.
[42] Scora, R. W., Kumamoto, J., Soost, R. K., and Nauer, E. M. (1982): Contribution to the origin of the Grapefruit, *Citrus paradisi* (Rutaceae). – Syst Bot 7: 170-77.
[43] Senior, M. L., Murphy, J. P., Goodman, M. M., Stuber, C. W. (1998): Utility of SSRs for determination genetic similarities and relationship in maize using an agarose gel system. – Crop Sci 38: 1088-98.
[44] Shahsavar, A. R., Izadpanah, K., Tafazoli, E., Tabatabaei, B. E. S. (2007): Characterization of Citrus germplasm including unknown variants by inter-simple sequence repeat (ISSR) markers. – Sci Hortic 112: 310-314.
[45] Silver, H. J., Dietrich, M. S., Niswender, K. D. (2011): Effects of grapefruit, grapefruit juice and water preloads on energy balance, weight loss, body composition, and cardio metabolic risk in free-living obese adults. – Nutri Metabol 8: 8.
[46] Singh, P., Singh, A., Navraj K, S., Sidhu G, S., Rattanpal, H. S. (2016a): Genetic diversity and DNA fingerprinting of indigenous and exotic mandarin genotypes in India using SSR markers. – Aus J Crop Sci 10(1): 24-31.
[47] Singh, P., Singh, A., Rattanpal, H. S. (2016b): Genetic divergence of indigenous and exotic mandarin (*Citrus reticulata* Blanco) accessions based on fruit morphological and physiological traits. – Res Crops 17(3): 538-44.
[48] Soriano, J., Zuriage, E., Rubio, P., Llacer, G., Infante, R., Badenes, M. (2012): Development and characterization of microsatellite markers in pomegranate (*punica granatum* L). – Mol Breed 27: 119-28.
[49] Uzun, A., Yesiloglu, T. (2012): Genetic Diversity in Citrus. – In: Caliskan, M. (ed.) Genetic Diversity in Plants. InTech, London. http://www.intechopen.com/books/geneticdiversity-inplants/genetic-diversity-in-citrus.
[50] Uzun, A., Gulsen, O., Kafa, G., Seday, U., Tuzcu, O., Yesiloglu, T. (2009): Characterization for yield, fruit quality, and molecular profiles of lemon genotypes tolerant to 'mal secco' disease. – Sci Hortic.122: 556-561.
[51] Warburton, M., Crossa, J. (2000): Data Analysis in the CIMMYT Applied Biotechnology Centre for Fingerprinting and Genetic Diversity Analysis. – CIMMYT, Texcoco, Mexico.
[52] Yaly, M. C., Novelli, V. M., Bastianel, M., Machado, M. A. (2011): Transferability and level of heterozygosity of microsatellite markers in citrus species. – Plant Mol Biol Rep 29: 418-23.

http://www.aloki.hu ● ISSN 1589 1623 (Print) ● ISSN 1785 0037 (Online)
DOI: http://dx.doi.org/10.15666/aeer/1605_53435358
© 2018, ALÖKI Kft., Budapest, Hungary

INTERPOLATION METHODS FOR GROUNDWATER QUALITY ASSESSMENT IN TANK CASCADE LANDSCAPE: A STUDY OF ULAGALLA CASCADE, SRI LANKA

KUMARI, M. K. N.[1,2*] – SAKAI, K.[3*] – KIMURA, S.[3] – NAKAMURA, S.[3] – YUGE, K.[4] – GUNARATHNA, M. H. J. P.[1,2] – RANAGALAGE, M.[5] – DUMINDA, D. M. S.[2]

[1]*United Graduate School of Agricultural Sciences, Kagoshima University, 1-21-24 Korimoto, Kagoshima-shi, Kagoshima 890-0065, Japan*

[2]*Faculty of Agriculture, Rajarata University of Sri Lanka, Puliyankulama, Anuradhapura 50000, Sri Lanka*

[3]*Faculty of Agriculture, University of the Ryukyus, 1 Senbaru, Nishihara-cho, Okinawa 903-0213, Japan*

[4]*Faculty of Agriculture, Saga University, 1 Honjo-machi, Saga 840-8502, Japan*

[5]*Faculty of Social Science and Humanities, Rajarata University of Sri Lanka, Mihintale, Anuradhapura 50000, Sri Lanka*

**Corresponding authors*
e-mail/phone/fax: nadeeta@gmail.com, +81-80-1787-5910 (M. K. N. Kumari); ksakai@agr.u-ryukyu.ac.jp, +81-89-895-8783, +81-89-895-8734 (K. Sakai)

(Received 22nd May 2018; accepted 11th Jul 2018)

Abstract. Interpolation methods are extensively used to map the spatial distribution of water quality parameters. However, the selection of the most appropriate method is a critical issue in environmental studies. The relative performances of deterministic and geostatistical methods in explaining the spatiotemporal variation of water quality parameters/indices in a tank cascade landscape were assessed. Inverse distance weighted (IDW), global polynomial interpolation (GPI), local polynomial interpolation (LPI), radial basis function (RBF), kriging (KR), and empirical Bayesian kriging (EBK) methods were evaluated using root mean square error (RMSE) in a leave-one-out cross-validation. Coefficient of variance, normality, level of autocorrelation, and extreme values near boundaries of the dataset showed a clear relationship with the relative performances of the different interpolation methods. Therefore, a clear understanding of the quality of the dataset is required in order to select the appropriate method to interpolate water quality parameters. EBK performed well for most parameters throughout the study period and is recommended as the best method to interpolate water quality parameters/indices in the Ulagalla cascade and other tank cascade landscapes in Sri Lanka and similar environments.
Keywords: *deterministic interpolation, empirical Bayesian kriging (EBK), geostatistical methods, root mean square error (RMSE), spatial variability*

Introduction

The tank cascade system (TCS) is a unique water storage and supply system used in the intermediate and dry zones of Sri Lanka. The system has been in use since the third century BCE (Madduma Bandara, 1985), mainly for irrigation and domestic water use. The main principle behind the TCS is re-use and recycling of water through a connected series of tanks. Hence, the TCS is defined as a connected series of tanks arranged within a micro- (or meso-) catchment of the dry zone landscape for storing, conveying and utilizing of water from an ephemeral rivulet (Madduma Bandara, 1985). As can be seen

http://www.aloki.hu ● ISSN 1589 1623 (Print) ● ISSN 1785 0037 (Online)
DOI: http://dx.doi.org/10.15666/aeer/1605_53595380
© 2018, ALÖKI Kft., Budapest, Hungary

in *Figure 1,* the major elements of TCS are categorized as meso-catchment, micro-catchment (catchment area of the individual tanks within the cascade), the main valley, side valleys and irrigated paddy lands. It has been recognized as globally important agricultural heritage site by Food and Agriculture Organization of the United Nations (FAO).

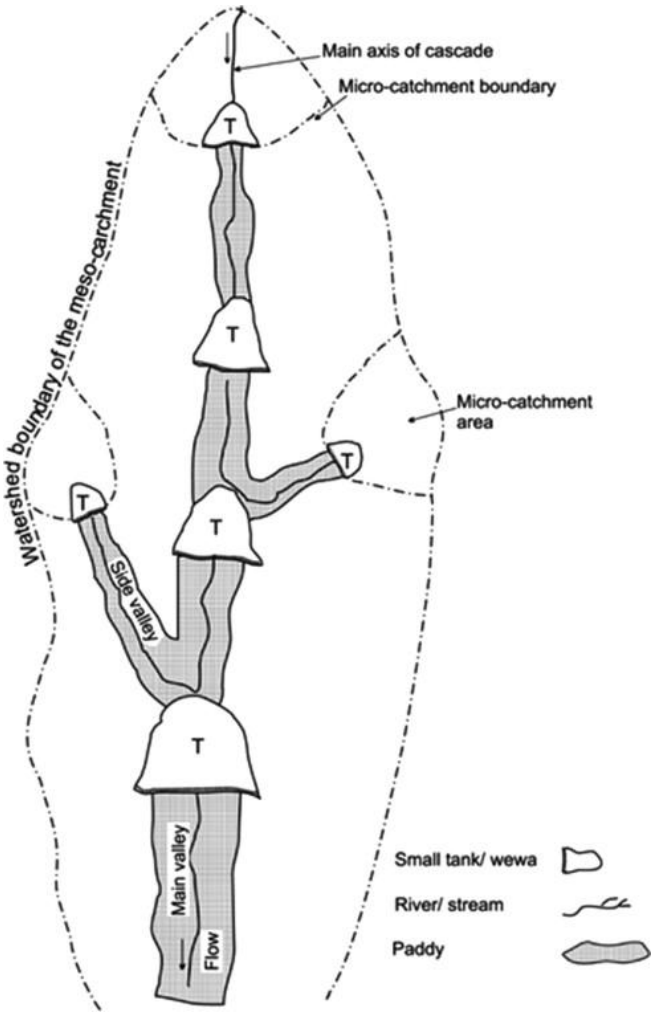

Figure 1. *Schematic representation of tank cascade system in dry zone of Sri Lanka (adapted from Panabokke et al., 2002)*

The dry zone of Sri Lanka receives an annual rainfall less than 1750 mm whereas, annual evaporation ranges from 1700-1900 mm, which implies the water stress condition during dry periods (Panabokke et al., 2002). This area is characterized with short rainy period (from September to January) which receives 80% of the total rainfall and long dry period (from February to October). As this area is dominated with reddish brown earth with low water retention capacity, the water scarcity problem is intensified in this area (Panabokke et al., 2002). This spatial and temporal variation of rainfall has led the ancient farming communities to invent TCS which can act as a sustainable water management system. TCS provides cooler micro-climate which enhances the plant and animal biodiversity while providing habitat for endangered elephants, resident and migrant water birds. Though it is not totally similar to Sri Lankan tank cascade systems,

http://www.aloki.hu ● ISSN 1589 1623 (Print) ● ISSN 1785 0037 (Online)
DOI: http://dx.doi.org/10.15666/aeer/1605_53595380
© 2018, ALÖKI Kft., Budapest, Hungary

comparable environments are in use for paddy irrigation in India (Bitterman et al., 2016; Van Meter et al., 2016; Bebermeier et al., 2017).

As a convenient substitute for insufficient surface water resources in the dry zone of Sri Lanka, groundwater use has dramatically increased during the last three decades, coinciding with changes in agriculture and livelihoods (Jayakody, 2006; Kumari et al., 2013). Moreover, a close relationship between the groundwater and surface water has been identified in tank cascade landscape (Bebermeier et al., 2017). Hence, the sustainability of the tank cascade landscape is endangered along with the overexploitation and quality deterioration of groundwater. Thus, an increasing amount of attention has been given to sustainably managing water resources in tank cascade landscapes, and several monitoring studies of groundwater in this landscape have been conducted (Wijesundara et al., 2012; Gunarathna et al., 2016a, b; Kumari et al., 2016). However, no appropriate continuous monitoring system has been put in place, because continuous monitoring of groundwater over a large area for an extended duration is expensive and labor intensive. Therefore, a suitable method for estimating groundwater availability and quality is needed that requires a minimum number of sampling sites in order to better manage the water resources in tank cascade landscapes.

Spatial interpolation, including deterministic and geostatistical interpolation techniques in ArcGIS, has been used to understand the spatial and temporal variation of natural resources, including groundwater, and related environmental concerns (Chai et al., 2011; Gunaalan et al., 2018). Deterministic interpolation techniques include inverse distance weighted (IDW), radial basis functions (RBFs), global polynomial interpolation (GPI), and local polynomial interpolation (LPI) methods; geostatistical interpolation techniques include kriging/co-kriging (ordinary kriging [OK], simple kriging [SK], universal kriging [UK], etc.), areal interpolation, and empirical Bayesian kriging (EBK). The ArcGIS Geostatistical Analyst extension can fill the gap between geostatistics and GIS analysis and has been used to characterize the spatial variability of variables in detail (Kumar et al., 2007; Uyan and Cay, 2013; Bao et al., 2014).

Interpolation accuracy is sensitive to the precise demarcation of boundaries and areas (Mirzaei and Sakizadeh, 2016; Gunaalan et al., 2018), the effectiveness of predicting parameters of unknown locations using known values, sample size (Stahl et al., 2006), spatial distribution of sampling sites (Güler, 2014), normality of the dataset (Wu et al., 2016), grid size or resolution (Hengl, 2007), and interpolation method (Luo et al., 2008; Xie et al., 2011). Moreover, if the distribution of sampling locations or wells does not appropriately represent the spatial variation of water quality parameters, any biases will be intensified (Heistermann and Kneis, 2011; Wagner et al., 2012). However, different interpolation methods tend to provide similar predictions at low (Mirzaei and Sakizadeh, 2016) and very high sampling densities (Gunnink and Burrough, 1996). In most cases, interpolation methods have been used without proper assessment of their accuracy. Only a few assessments of accuracy have been conducted. Mirzaei and Sakizadeh (2016) evaluated three interpolation methods to estimate a water quality index and found EBK to be the best method. Xie et al. (2011) stated that the best interpolation method to explain the spatial variation of heavy metals in soil varied with the size of the polluted area. Seyedmohammadi et al. (2016) compared five interpolation methods to estimate the spatial variation of electrical conductivity (EC) in groundwater and reported that OK was superior to the others. Based on the relative performance of four interpolation methods to interpolate EC, total dissolved solids (TDS), and pH, EBK was found as the best method (Gunarathna et al., 2016a, b).

http://www.aloki.hu ● ISSN 1589 1623 (Print) ● ISSN 1785 0037 (Online)
DOI: http://dx.doi.org/10.15666/aeer/1605_53595380
© 2018, ALÖKI Kft., Budapest, Hungary

To date, no study has evaluated these interpolation methods with an extensive number of parameters covering all contaminant groups (anions, cations, nutrients) and water quality indices along with temporal effects. Because the assessment of spatial and temporal variation of groundwater is essential in sustainable management of water resources, the objective of this study was to describe and predict the relative performance of deterministic (IDW, LPI, GPI, and RBFs) and geostatistical (UK, OK, and EBK) interpolation methods and to select the best interpolation method to explain the spatial and temporal variation of groundwater quality in the Ulagalla cascade, Sri Lanka. Many physicochemical parameters were studied, including anions, cations, nutrients, and other water quality indices, as well as temporal effects. The relationships between characteristics of datasets and those of different interpolation methods were also examined.

Materials and methods

Study area

Ulagalla cascade covers approximately 51 km^2 in the Anuradhapura district of Sri Lanka (8°5'–8°14'N; 80°31'–80°34'E). The economy of this area is based on agriculture, which comprises tank-based paddy cultivation and rainfed or irrigated upland crop cultivation using groundwater. Mean annual rainfall in Anuradhapura is 1255 mm, and there is a distinct dry period from May to September. The monthly average maximum and minimum temperatures in the dry zone range from 25.0 to 37.7 °C and 17.4 to 26.8 °C, respectively. (Gunarathna and Kumari, 2013; Abeysekara and Punyawardena, 2016). A shallow regolith aquifer of the hard rock region is the main aquifer type in the study area. Groundwater potential is comparatively limited because of the low groundwater storage capacity and transmissivity of the underlying crystalline basement (Sirimanne, 1952).

Data collection and data preparation

The total cascade area was divided into 1-km^2 cells, and one agro-well was purposely selected to represent each cell so as to evaluate the quality of groundwater in the study area. Within the existence of agro-wells and the availability of water in the agro-wells throughout the study period, a total of 29 wells were selected (*Fig. 2)*. Three replicates from aforesaid 29 wells were collected monthly from April 2016 to March 2017 to measure the water quality parameters using standard procedures (APHA, 2005). All the chemical analyses were carried out at the laboratory of soil and water sciences, Department of Agricultural Engineering and Soil Science, Faculty of Agriculture, Rajarata University of Sri Lanka. Sodium adsorption ratio (SAR) (Wilcox, 1955) and total hardness (TH) (Todd and Mays, 2005) were calculated from measured data. The following 12 water quality parameters or indices were used: electrical conductivity (EC); pH; concentrations of sodium (Na^+), potassium (K^+), calcium (Ca^{2+}), magnesium (Mg^{2+}), chloride (Cl^-), nitrate (NO_3^--N), phosphate (PO_4^{3-}), and bicarbonate (HCO_3^-); sodium adsorption ratio (SAR); and total hardness (TH).

Attribute data containing information about the physicochemical parameters/indices were joined with geographic coordinates obtained with a handheld global positioning system (GPS) receiver (eXplorist 510, Magellan, USA) of each sampling point (*Table A1* in the *Appendix*). ArcGIS 10.2 (ESRI, California, USA) and R statistical

http://www.aloki.hu ● ISSN 1589 1623 (Print) ● ISSN 1785 0037 (Online)
DOI: http://dx.doi.org/10.15666/aeer/1605_53595380
© 2018, ALÖKI Kft., Budapest, Hungary

software (R Foundation for Statistical Computing, Vienna, Austria) (Team R, 2016) were used for the interpolation analysis and statistical analysis, respectively.

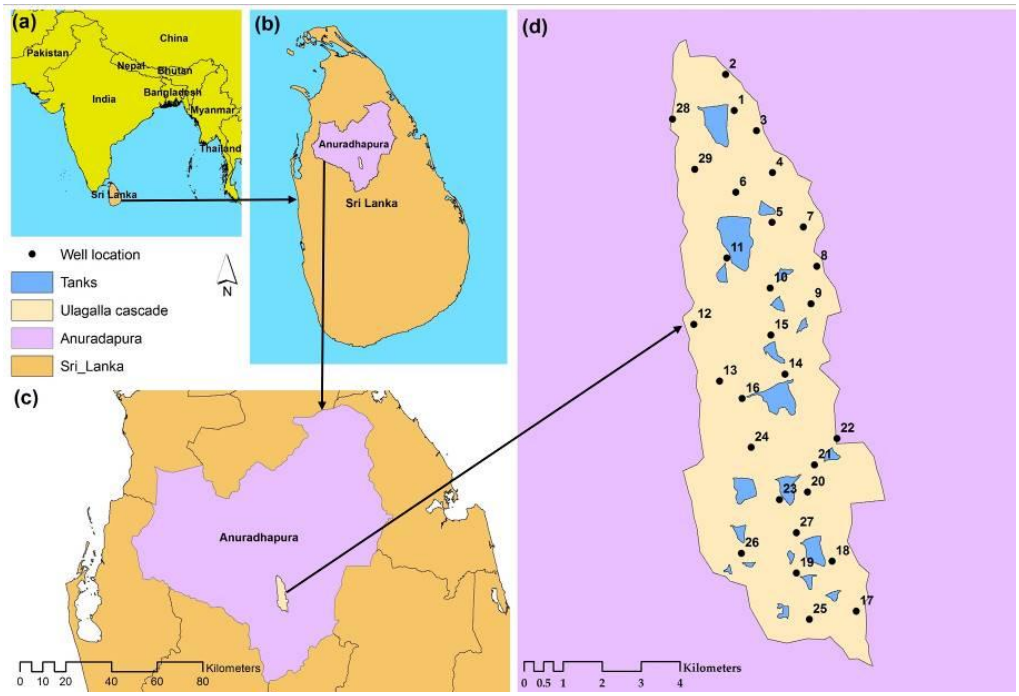

Figure 2. *Location of the study areas: (a) South Asia; (b) Sri Lanka; (c) Anuradhapura district; (d) groundwater sampling locations in Ulagalla cascade*

Interpolation methods

Inverse distance weighted (IDW)

In IDW, the interpolation weights are calculated as a function of the observed sampling point and the prediction point (Gunnink and Burrough, 1996). The accuracy of IDW depends on the number of closest neighboring sampling points (Yao et al., 2013). The values for unknown points are estimated with *Equation 1:*

$$Z(x_0) = \frac{\sum_{i=1}^{n} \frac{x_i}{h_{ij}^{\beta}}}{\sum_{i=1}^{n} \frac{1}{h_{ij}^{\beta}}} \qquad \text{(Eq.1)}$$

where $Z(x_0)$ is the interpolated value, x_i is the i^{th} data value, β is the user-defined exponent for weighting, n is the total number of sampling data values and h_{ij} is the distance between the known point and the unknown point (Seyedmohammadi et al., 2016).

Global polynomial interpolation (GPI)

The GPI method positions a plane between sample points by fitting a polynomial formula to the points. Using a value on the plane that relates to the prediction location,

http://www.aloki.hu ● ISSN 1589 1623 (Print) ● ISSN 1785 0037 (Online)
DOI: http://dx.doi.org/10.15666/aeer/1605_53595380
© 2018, ALÖKI Kft., Budapest, Hungary

the unknown point is determined by minimizing the errors (Webster and Oliver, 2008) With the use of low order polynomials GPI creates slowly while describing the physical processes. However, with complex polynomials, it is difficult to ascribe physical meaning to GPI (Johnston et al., 2003).

Local polynomial interpolation (LPI)

Whereas GPI fits one polynomial to the entire surface, LPI fits many polynomials, each within specified overlapping local neighborhoods. Although this method produces smooth surfaces, it is best suited for use only with data that have a narrow range of variation. LPI creates a surface from many different polynomial formulas, each of which is optimized for a specified neighborhood, neighborhood shape, and maximum and minimum number of points. LPI is sensitive to the neighborhood distance, and the sample points in a neighborhood can be weighted by their distance from the prediction location. Because LPI is sensitive to neighborhood distance and a small search neighborhood may create empty areas in the prediction surface, the method shows better results with grid-based sampling data than with random point sampling (Johnston et al., 2003; Hani et al., 2011).

Radial basis functions (RBFs)

RBFs are a form of artificial neural networks with a series of exact interpolation techniques. They use an equation derived from the distance between an interpolated point and the sampling points (Lin and Chen, 2004; Aguilar et al., 2005). The method consists of five deterministic interpolation techniques: thin plate spline, spline with tension, completely regularized spline, multi-quadratic function, and inverse multi-quadratic function. The RBF method is used mainly to create smooth surfaces from a large number of data points. Although RBFs give good results for areas with gently varying surfaces, the method will not provide accurate results if there are any large variations in the surface within a short horizontal distance (Johnston et al., 2003). The most commonly used RBF technique, completely regularized spline was used for this analysis.

Kriging

Kriging is a linear interpolation method that assumes that the parameter to be interpolated can be modeled by random processes with spatial autocorrelation. Hence, kriging techniques are widely used to describe and model spatial patterns and predict values at unmeasured locations. Three types of kriging were evaluated in this study: ordinary kriging, universal kriging and empirical Bayesian kriging.

Ordinary kriging (OK)

OK is the most widely used kriging method. It uses an average of a subset of neighboring points to produce a particular interpolation point. OK can use either semivariograms or covariances to explain the autocorrelation and can use transformations to avoid trends (Johnston et al., 2003), but the semivariance function plays a major role in deriving weights of OK (Johnston et al., 2003). The empirical semivariance function can be used to estimate the parameters of the semivariogram function and the nugget effect as expressed in *Equation 2:*

http://www.aloki.hu ● ISSN 1589 1623 (Print) ● ISSN 1785 0037 (Online)
DOI: http://dx.doi.org/10.15666/aeer/1605_53595380
© 2018, ALÖKI Kft., Budapest, Hungary

$$\gamma(h) = \frac{1}{2N(h)} \sum_{i=1}^{N(h)} [Z(x_i) - Z(x_i + h)]^2 \quad \text{(Eq.2)}$$

where γ is the semivariance, $N(h)$ is the number of data pairs within a given class of distance and direction, h is the lag distance, and $Z(x_i)$ and $Z(x_i + h)$ are the sample values at two points separated by the distance interval h (Xie et al., 2011).

Universal kriging (UK)

UK can be used to produce prediction, quantile, probability, or standard error maps. The method is used to estimate the spatial means when the data have a strong trend, and the trend is modeled using simple functions. The use of UK is limited to large surfaces, such as a large country, because it is difficult to follow a trend along the direction of spreading (Kis, 2016).

Empirical bayesian kriging (EBK)

EBK is different from other classical kriging methods because the parameters are automatically optimized using a number of semivariogram models instead of a single semivariogram. The following steps are used in EBK: (1) A semivariogram model is estimated using available data. (2) A new value is simulated for each input data location using the semivariogram model. (3) Based on the simulated data, a new semivariogram model is estimated. Bayes's rule is then used to calculate the weight of the new semivariogram model. By repeating the steps 2 and 3, the semivariogram estimated in step 1 is used to simulate a new set of values at the input locations (Krivoruchko, 2012).

Data preprocessing

Because the Kriging methods require the sample distribution to be normal, Shapiro Wilk test was performed for all 144 datasets (12 water quality parameters/indices × 12 months) to check the goodness-of-fit of the data ($P < 0.05$). The results showed that K^+, Mg^{2+}, NO_3^--N, Cl^- and EC were not normally distributed at any time, and the other parameters and indices were normally distributed only during several months. Hence, datasets that were not normally distributed were log-transformed and thereafter except very few, all the other data sets were normally distributed.

Validation and model evaluation

Cross-validation and validation with an independent dataset are the most common methods used to compare different interpolation methods, whereby the data are divided into a training set and a validation set. The validation set is used to test the model acquired from the training set. Those allowed us to assess the goodness-of-fit of interpolation methods and the appropriateness of the neighborhood (Dashtpagerdi et al., 2013; Gunarathna et al., 2016a, b). Because the number of sampling points was limited, we used leave-one-out cross-validation (Gunarathna et al., 2016a, b) to estimate the spatial variation of water quality parameters/indices in the study area, removing one data point from the known dataset and estimating its value from the other known values. If a model has a standardized mean error close to 0, the RMSE and average standard error are as small as possible as compared with other models, which means the model

http://www.aloki.hu ● ISSN 1589 1623 (Print) ● ISSN 1785 0037 (Online)
DOI: http://dx.doi.org/10.15666/aeer/1605_53595380
© 2018, ALÖKI Kft., Budapest, Hungary

provides the most accurate predictions. Hence, we used RMSE (*Eq. 3*) to compare the models:

$$RMSE = \sqrt{\frac{1}{n}\left(Z_i - \hat{Z}_i\right)^2} \quad \text{(Eq.3)}$$

where $\hat{Z}_i$ is the estimated value, Z_i is the measured value at sampling point i (i = 1,.., n), and n is the total number of observations.

The coefficient of variance (CV), which is the ratio of standard deviation to the mean of each parameter/index, was used to study the relative variability of the dataset. We used the local Moran's Index (MI), one of the most commonly used criteria for spatial autocorrelation of quantitative data (Moran, 1950), to estimate the level of spatial autocorrelation of water quality parameters/indices in the Ulagalla cascade.

Results and discussion

Relative performance of deterministic and geostatistical interpolation methods

The RMSE values of cross-validation for the 12 water quality parameters/indices during 12 consecutive months are summarized in *Tables A2–A13* in the *Appendix*. Note that the RMSE values of the OK and UK interpolation methods were similar to each other for all the parameters/indices, and are considered together as kriging (KR). EBK was superior to all other interpolation methods in estimating spatial variation of K^+, Mg^{2+}, NO_3^--N, and EC in all 12 months (*Tables 1, A4, A6, A7* and *A11*); of Na^+, HCO_3^-, Cl^-, and TH in 11 months (*Tables 1, A3, A9, A10* and *A13*); of SAR in 10 months and of pH and PO_4^{3-} in 7 months (*Tables 1, A2, A12, A8*). EBK was outperformed in only 6 months in the interpolation of Ca^{2+} (*Tables 1* and *A5*). Overall, EBK was the best method for interpolating groundwater quality parameters/indices in 121 out of the 144 incidences.

Table 1. *Summary of selected best interpolation methods for different parameters/indices during the study period*

	pH	Na^+	K^+	Ca^{2+}	Mg^{2+}	NO_3^--N	PO_4^{3-}	HCO_3^-	Cl^-	EC	SAR	TH
Apr	EBK	EBK	EBK	GPI	EBK	EBK	EBK	EBK	KR	EBK	RBF	EBK
May	EBK	EBK	EBK	EBK	EBK	EBK	KR	EBK	EBK	EBK	KR	EBK
Jun	EBK	EBK	EBK	EBK	EBK	EBK	EBK	EBK	EBK	EBK	EBK	EBK
Jul	IDW	EBK	EBK	EBK	EBK	EBK	RBF	EBK	EBK	EBK	EBK	EBK
Aug	GPI	EBK	EBK	EBK	EBK	EBK	RBF	EBK	EBK	EBK	EBK	EBK
Sep	EBK	EBK	EBK	GPI	EBK	EBK	KR	EBK	EBK	EBK	EBK	EBK
Oct	EBK	EBK	EBK	LPI	EBK	EBK	EBK	EBK	EBK	EBK	EBK	LPI
Nov	EBK	IDW	EBK	GPI	EBK	EBK	RBF	EBK	EBK	EBK	EBK	EBK
Dec	GPI	EBK	EBK	EBK	EBK	EBK	RBF	KR	EBK	EBK	EBK	EBK
Jan	LPI	EBK	EBK	GPI	EBK	EBK	EBK	EBK	EBK	EBK	GPI	EBK
Feb	LPI	EBK	EBK	LPI	EBK	EBK	EBK	EBK	EBK	EBK	RBF	EBK
Mar	EBK	EBK	EBK	EBK	EBK	EBK	RBF	EBK	EBK	EBK	RBF	EBK

http://www.aloki.hu ● ISSN 1589 1623 (Print) ● ISSN 1785 0037 (Online)
DOI: http://dx.doi.org/10.15666/aeer/1605_53595380
© 2018, ALÖKI Kft., Budapest, Hungary

Based on the number of success incidences obtained from the cross-validation results, the interpolation methods can be sorted, as EBK > LPI > GPI > IDW > KR > RBF (*Table 1*). This ranking supports the findings of Gunarathna et al. (2016a, b) and Mirzaei and Sakizadeh (2016), who also found EBK to be superior to other interpolation methods with the use of a limited number of variables. Even though EBK recorded the lowest RMSE value for most of the parameters/indices that was not the case with Ca^{2+} and PO_4^{3-}, for which several methods had the lowest RMSE during different months (*Table 1*). Hence, we selected Ca^{2+} (*Table 2*) and PO_4^{3-} (*Table 3*) to elucidate differences in the methods.

As inexact interpolators among the selected methods, GPI and LPI showed quite similar results compared to other methods used in the present study and this was supported by Wang et al. (2014). Xiao et al. (2016) also confirmed that GPI is suitable only when the variability of the dataset is relatively small. Although GPI can be used to analyze the surface trend of regionalized variables, it is not accurate when extreme values are present (Mutuna and Kurima, 2012; Wang et al., 2014). LPI is also capable of simulating a narrow range of variability with high accuracy (Xiao et al., 2016). GPI was ranked in the top three methods during 10 months of the study period, and the CV was relatively small in 6 of those 10 months (*Table 2*). Moreover, no extreme values were recorded near the boundaries in those 6 months. In the other 4 months, the variation of the dataset was moderate, and no extreme values were recorded near the boundaries (*Table 2*). According to the summary statistics of phosphate concentration (*Table 3*), the conditions of low variation and no extreme values near boundaries were met in only 3 months, and GPI was ranked among the top three only once.

Table 2. *Summary statistics of calcium concentration in Ulagalla cascade*

	Apr	**May**	**Jun**	**Jul**	**Aug**	**Sep**	**Oct**	**Nov**	**Dec**	**Jan**	**Feb**	**Mar**
Mean	*182.9*	*38.2*	*63.6*	*70.4*	*35.3*	*49.7*	*30.1*	*35.0*	*92.2*	*86.4*	*84.5*	*37.3*
Standard deviation	*89.7*	*28.4*	*30.3*	*47.2*	*19.5*	*25.1*	*20.6*	*17.5*	*44.0*	*36.5*	*53.8*	*23.1*
CV	49	74	48	67	55	50	69	50	48	42	64	62
Moran's Index (MI)	−0.19	−0.12	−0.39	0.04	−0.18	−0.30	0.13	−0.26	−0.26	−0.22	−0.03	−0.07
P-value of MI	0.31	0.57	0.02	0.60	0.32	0.08	0.22	0.13	0.12	0.22	0.96	0.79
Skewness (original data)	*0.40*	*1.28*	*0.62*	*0.91*	*1.45*	*0.84*	*1.99*	*0.81*	*1.22*	*0.22*	*1.62*	*1.66*
Skewness (after log transformation)	0.4	0.07	0.62	−0.18	0.33	0.84	−0.19	0.81	−1.04	0.22	−0.43	−0.07
Range	*350*	*114*	*117*	*161*	*85*	*106*	*100*	*80*	*226*	*129*	*264*	*100*
Lowest RMSE	**GPI**	**EBK**	**EBK**	**EBK**	**EBK**	**GPI**	**LPI**	**GPI**	**EBK**	**GPI**	**LPI**	**EBK**
2nd lowest RMSE	**LPI**	**KR**	**KR**	**GPI**	**KR**	**EBK**	**EBK**	**LPI**	**GPI**	**EBK**	**EBK**	**KR**
3rd lowest RMSE	**KR**	**LPI**	**GPI**	**LPI**	**GPI**	**KR**	**RBF**	**EBK**	**LPI**	**LPI**	**GPI**	**GPI**
4th lowest RMSE	EBK	GPI	LPI	KR	LPI	LPI	IDW	KR	KR	KR	KR	LPI
5th lowest RMSE	IDW	RBF	IDW	IDW	RBF	IDW	KR	IDW	IDW	IDW	IDW	RBF
6th lowest RMSE	RBF	IDW	RBF	RBF	IDW	RBF	GPI	RBF	RBF	RBF	RBF	IDW
Well numbers with extreme values		1		10, 14	1	10	27, 28	10	10		10	1, 10

http://www.aloki.hu ● ISSN 1589 1623 (Print) ● ISSN 1785 0037 (Online)
DOI: http://dx.doi.org/10.15666/aeer/1605_53595380
© 2018, ALÖKI Kft., Budapest, Hungary

Table 3. *Summary statistics of phosphate concentration in Ulagalla cascade*

	Apr	**May**	**Jun**	**Jul**	**Aug**	**Sep**	**Oct**	**Nov**	**Dec**	**Jan**	**Feb**	**Mar**
Mean	0.04	0.05	0.06	0.57	0.58	0.06	0.11	0.16	0.09	0.04	0.32	0.70
Standard deviation	0.04	0.06	0.05	0.24	0.27	0.08	0.16	0.15	0.12	0.05	0.06	0.78
CV	97	119	87	42	47	135	139	91	134	106	20	111
Moran's Index (MI)	0.33	0.26	0.37	0.43	0.36	0.25	0.17	0.26	0.25	0.23	0.03	0.20
P-value of MI	0.00	0.02	0.00	0.00	0.00	0.03	0.14	0.04	0.04	0.06	0.61	0.09
Skewness (original data)	*2.24*	*2.88*	*2.42*	*1.93*	*1.89*	*2.42*	*2.20*	*2.01*	*2.05*	*2.01*	*−2.06*	*2.72*
Skewness (after log transformation)	0.80	0.78	0.23	0.97	0.49	0.80	0.53	1.24	0.49	0.67	−2.55	1.00
Range	0.15	0.26	0.26	0.99	1.30	0.34	0.63	0.57	0.44	0.17	0.26	3.69
Lowest RMSE	**IDW**	**RBF**	**RBF**	**EBK**	**RBF**	**RBF**	**EBK**	**EBK**	**EBK**	**EBK**	**EBK**	**EBK**
2nd lowest RMSE	**EBK**	**KR**	**EBK**	**KR**	**EBK**	**KR**	**RBF**	**GPI**	**RBF**	**RBF**	**LPI**	**LPI**
3rd lowest RMSE	**RBF**	**LPI**	**IDW**	**RBF**	**KR**	**LPI**	**IDW**	**KR**	**KR**	**KR**	**GPI**	**GPI**
4th lowest RMSE	LPI	EBK	KR	IDW	IDW	EBK	LPI	LPI	IDW	IDW	IDW	KR
5th lowest RMSE	GPI	IDW	GPI	LPI	LPI	IDW	GPI	RBF	LPI	GPI	RBF	RBF
6th lowest RMSE	KR	GPI	LPI	GPI	GPI	GPI	KR	IDW	GPI	LPI	KR	IDW
Well numbers with extreme values	14, 16, 12	14, 16	2, 14	14, 16	1, 2, 14, 15, 16	1, 2, 11, 14, 15, 16	14, 16, 11	11, 14, 16, 25	14, 16, 11	14, 11	14, 16, 11	16, 15, 11

IDW is widely used in the field of environmental sciences, but it is rarely recommended as the best interpolation method in comparison studies (Li and Heap, 2011). In their review, Li and Heap (2011) reported that IDW is highly sensitive to sample density and data variation (CV). The poor performance of IDW in our study could be attributed to the high spatial data variation and relatively low sample size. In the classification using Ca^{2+} and PO_4^{3-}, IDW was never the best-fit model when the CV was high. Therefore, we do not recommend the use of IDW to interpolate spatial variation of groundwater quality parameters/indices in tank cascade landscapes unless the data show low spatial variation and have a higher sample density with an evenly distributed sampling pattern.

Kriging (KR) is one of the most widely used interpolation methods in the field of environmental sciences, and it has been recommended in comparison studies (Li and Heap, 2011). Basic assumptions of KR are spatially autocorrelated observations (a function of distance between observations) and normally distributed data (Zimmerman et al., 1999). Therefore, KR has a strong ability to predict the overall trend of groundwater contamination when a dataset is autocorrelated (Ahmed, 2002; Nas, 2009; Xie et al., 2011; Mutuna and Kurima, 2012; Zehtabian et al., 2013). As shown in *Table 3,* KR was ranked on first three during 6 months when the data was significantly autocorrelated in 8 months and was in the top three in 5 of those 8 months. This characteristic was also observed in the Ca^{2+} dataset where KR performed well in June when the data were autocorrelated.

http://www.aloki.hu ● ISSN 1589 1623 (Print) ● ISSN 1785 0037 (Online)
DOI: http://dx.doi.org/10.15666/aeer/1605_53595380
© 2018, ALÖKI Kft., Budapest, Hungary

Because EBK divides the dataset into subsets and simulates a semivariogram for each subset to reduce the uncertainty relative to that in KR, it provides relatively better interpolation accuracy on small datasets and non-stationary datasets than KR (ESRI, 2015). In *Tables 2* and *3,* EBK was listed in the top three in 21 of 24 incidences. This shows that EBK performs well irrespective of CV, MI, extreme values near boundaries (EVnB), and skewness (SK). However, when the dataset was less variable, showed autocorrelation, and had no EVnB, other interpolation methods performed better than EBK. Hence, we recommend using EBK when data show high variability and no autocorrelation, and extreme values near boundaries and are not normally distributed.

As the quality of the dataset determines the accuracy of different interpolation methods, we assessed the importance of CV, MI, SK, and EVnB (characteristics that show the quality of a dataset) to the success of each method using an attribute evaluation option available in the CORElearn package (Robnik-Sikonja and Savicky, 2017) of R software (*Table 4*). The relative importance of the characteristics can be sorted as EVnB > CV > SK > MI for GPI and EVnB > SK > CV > MI for LPI. These results confirm the sensitivity of GPI and LPI to CV and EVnB. The relative importance for RBF was CV > EVnB > SK > MI, demonstrating that RBF is sensitive to the variability of the dataset and EVnB. The relative failure of RBF in this study can be explained by the high spatial variation of the water quality parameters/indices. The relative importance for IDW was EVnB > CV > MI > SK, confirming its sensitivity to dataset variability and extreme values. The relative importance for KR was EVnB > MI > CV > SK, confirming that KR can be successfully used when the dataset is autocorrelated with low variability while lacking extreme values near boundaries.

Table 4. *Relative importance of attributes on different interpolation methods*

	Relative importance					
Attributes	**GPI**	**LPI**	**RBF**	**IDW**	**KR**	**EBK**
CV	0.013	0.036	0.181	0.274	0.013	0.025
MI	−0.031	0.010	0.010	0.243	0.052	0.009
SK	−0.02	0.081	0.050	0.730	0.001	−0.013
EVnB	0.262	0.093	0.077	0.422	0.218	0.154

CV – coefficient of variance, MI – Moran's Index, SK – Skeweness, EVnB – extreme values near boundary

Distribution pattern of observed and simulated data using EBK method

Figure 3 shows boxplot diagrams of the observed and EBK-predicted values of the 12 parameters/indices. The measured and predicted values of almost all the parameters/indices were right skewed except pH, showing that the majority of the values are clustered below the median and the means are greater than the median (*Table A14*). Further, it can be noted that EBK was unable to properly predict extreme values, but there were no significant differences between observed and predicted values. The final spatial distribution maps of water quality parameters/indices prepared using the EBK interpolation method for the mean values of the 12 parameters/indices are shown in *Figure 4*. It was observed that the concentration of most parameters/indices were comparatively low at the upper part of the cascade and it has increased at the lower part of the cascade due to the accumulation effect.

http://www.aloki.hu ● ISSN 1589 1623 (Print) ● ISSN 1785 0037 (Online)
DOI: http://dx.doi.org/10.15666/aeer/1605_53595380
© 2018, ALÖKI Kft., Budapest, Hungary

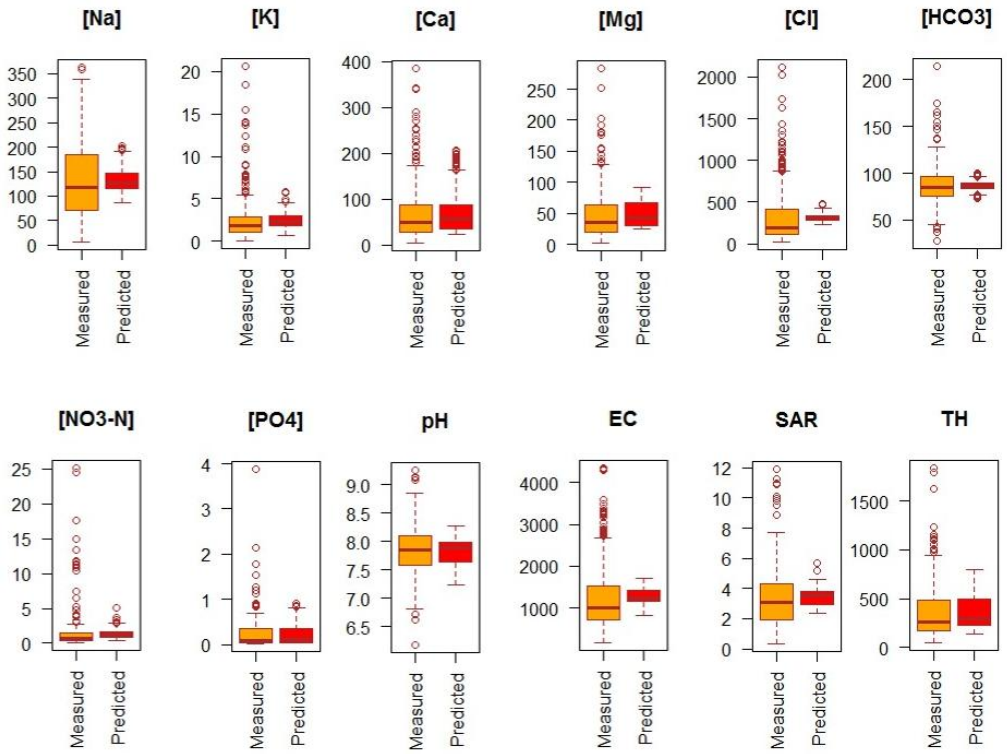

Figure 3. *Boxplot diagrams of observed and EBK-predicted values of (a) Na^+ (mg/l) (b) K^+ mg/l), (c) Ca^{2+}(mg/l), (d) Mg^{2+} (mg/l), (e) Cl^- (mg/l), (f)HCO_3^- (mg/l), (g) NO_3^--N (mg/l), (h) PO_4^{3-} (mg/l), (i) pH, (j) EC (µS/cm), (k) SAR and (l) TH (mg/l) in Ulagalla cascade*

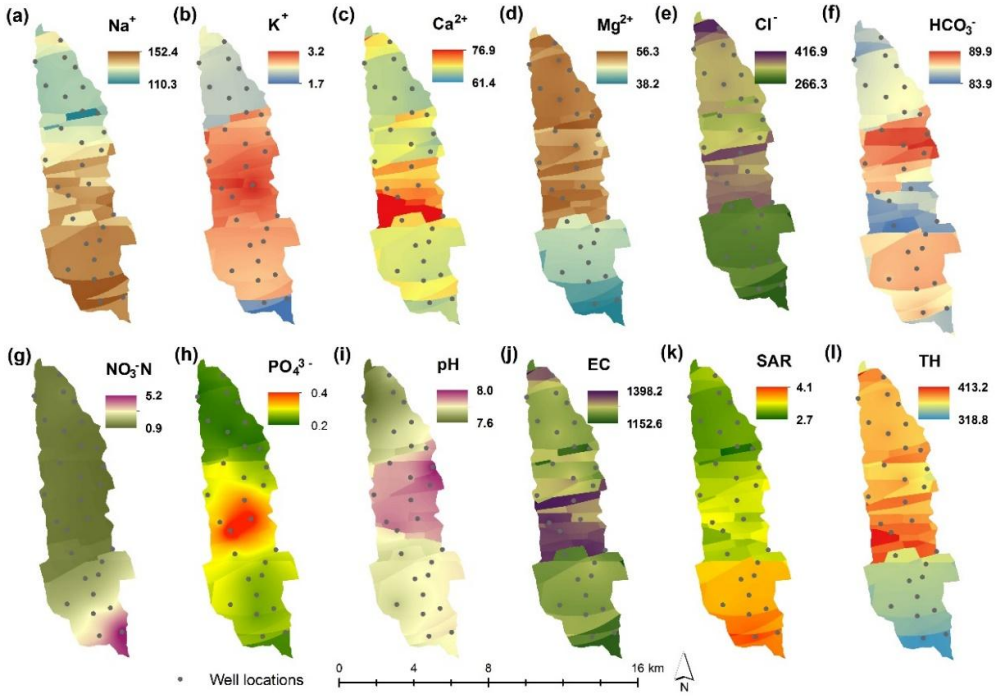

Figure 4. *Spatial distribution of (a) Na^+ (mg/l), (b) K^+ (mg/l), (c) Ca^{2+}(mg/l), (d) Mg^{2+} (mg/l), (e) Cl^- (mg/l), (f)HCO_3^- (mg/l), (g) NO_3^--N (mg/l), (h) PO_4^{3-} (mg/l), (i) pH, (j) EC (µS/cm), (k) SAR, and (l) TH (mg/l) in Ulagalla cascade*

http://www.aloki.hu ● ISSN 1589 1623 (Print) ● ISSN 1785 0037 (Online)
DOI: http://dx.doi.org/10.15666/aeer/1605_53595380
© 2018, ALÖKI Kft., Budapest, Hungary

Conclusions

A clear understanding of spatial and temporal variation in water quality parameters/indices is a key issue in agriculture as well as in environmental studies. At present, many algorithms are used with the aim of selecting the best interpolation method for delineation of the spatial distribution of water quality parameters/indices. We investigated the interpolation accuracy of a variety of methods in a tank cascade landscape.

The EBK method proved superior to deterministic and other geostatistical methods in interpolating groundwater quality parameters (anions, cations, and nutrients) and indices associated with tank cascade landscapes. Kriging interpolation was successful when the dataset was autocorrelated with low variability. IDW had the worst results in estimating the spatial distribution of water quality parameters/indices. Better performance was obtained with the GPI and LPI methods when the dataset was less variable and had no extreme values near boundaries.

Because groundwater monitoring is labor intensive and expensive, it is important to use optimum sampling density and to choose the design in a methodical way. Furthermore, it is advisable to decide on the interpolation method before sampling and then schedule sample density and design accordingly. This study can be used as a guide for such decision making for groundwater monitoring in a tank cascade landscape.

In general, the preparation of composite water quality zonation map for the Ulagalla cascade with the integration of EBK method and water quality indices/parameters can be carried out. Future research can be conducted to find out the optimum number of sampling points to obtain precise estimation of water quality in tank cascade landscape.

Acknowledgements. This work was financially supported by Research, Publication and Higher Degrees Committee, Rajarata University of Sri Lanka, Mihintale, Sri Lanka, under the grant number RJT/RP&HDC/2016/Agri/R/3.

REFERENCES

[1] Abeysekara, A. B., Punyawardena, B. V. R. (2016): Potential and Constraints of Climate for Groundwater Management in the Dry Zone of Sri Lanka. – In: Pathmarajah, S. (ed.) Groundwater Availability and Use in the dry Zone of Sri Lanka. Cap-Net Lanaka, Postgraduate Institute of Agriculture, University of Peradeniya, Sri Lanka, pp.1–32.

[2] Aguilar, F. J., Aguera, F., Aguilar, M. A., Carvajal, F. (2005): Effects of terrain morphology, sampling density, and interpolation methods on grid DEM accuracy. – Photogrammetric Engineering & Remote Sensing 71: 805–816. doi: 10.14358/PERS.71.7.805.

[3] Ahmed, S. (2002): Groundwater Monitoring Network Design: Application of Geostatistics with a Few Case Studies from a Granitic Aquifer in a Semiarid Region. – In: Sherif, M. M., Singh, V. P., Al-Rashed, M. (ed.) Groundwater Hydrology, vol. 2, pp. 37–57. Balkema, Rotterdam.

[4] APHA (2005): Standard Methods for the Examination of Water and Wastewater, Standard Methods. – American Public Health Association/American Water Works Association/Water Environment Federation, Washington D. C.

[5] Bao, Z., Wu, W., Liu, H., Chen, H., Yin, S. (2014): Impact of long-term irrigation with sewage on heavy metals in soils, crops and groundwater. A case study in Beijing. – Polish Journal of Environmental Studies 23(2): 309–318.

http://www.aloki.hu ● ISSN 1589 1623 (Print) ● ISSN 1785 0037 (Online)
DOI: http://dx.doi.org/10.15666/aeer/1605_53595380
© 2018, ALÖKI Kft., Budapest, Hungary

[6] Bebermeier, W., Meister, J., Withanachchi, C. R., Middelhaufe, I., Middlehaufe, B. (2017): Tank cascade systems as a sustainable measure of watershed management in South Asia. – Water (Switzerland) 9(3): 1–16. DOI: 10.3390/w9030231.
[7] Bitterman, P., Tate, E., Van Meter, K. J., Basu, M. B. (2016): Water security and rainwater harvesting: A conceptual framework and candidate indicators – Applied Geology 76: 75–84. DOI: 10.1016/j.apgeog.2016.09.013.
[8] Chai, H., Cheng, W., Zhou, C., Chen, X., Ma, X., Zhao, S. (2011): Analysis and comparison of spatial interpolation methods for temperature data in Xinjiang Uygur Autonomous Region, China. – Natural Science 3(12): 999–1010. doi: 10.4236/ns.2011.312125.
[9] Dashtpagerdi, M. M., Vagharfard, H., Honarbakhsh, A. (2013): Application of cross-validation technique for zoning of groundwater levels in Shahrekord plain. – Agricultural Sciences 4(7): 329–333.
[10] ESRI (2015): What is empirical bayesian kriging. – http://desktop.arcgis.com/en/arcmap/10.3/guide-books/extensions/geostatistical-analyst/what-is-empirical-bayesian-kriging-.htm. Accessed on 12.12.2017.
[11] Güler, M. (2014): Comparison of different interpolation techniques for modelling temperatures in Middle Black Sea region. – Journal of Agricultural Faculty of Gaziosmanpasa University 31(2): 61–71. DOI: 10.13002/jafag714.
[12] Gunaalan, K., Ranagalage, M., Gunarathna, M. H. J. P., Kumari, M. K. N., Vithanage, M., Saravanan, S., Warnasuriya, T. W. S. (2018): Application of geospatial techniques for groundwater quality and availability assessment : A case study in Jaffna Peninsula, Sri Lanka. – International Journal of Geo-Information 7: 20. DOI: 10.3390/ijgi7010020.
[13] Gunarathna, M. H. J. P., Kumari, M. K. N. (2013): Rainfall trends in Anuradhapura : Rainfall analysis for agricultural planning. – Rajarata University Journal 1: 38–44.
[14] Gunarathna, M. H. J. P., Kumari, M. K. N., Nirmanee, K. G. S. (2016a): Evaluation of interpolation methods for mapping pH of groundwater. – International Journal of Latest Technology in Engineering, Management and Applied Science 5(3): 1–5.
[15] Gunarathna, M. H. J. P., Nirmanee, K. G. S., Kumari, M. K. N. (2016b): Are geostatistical interpolation methods better than deterministic interpolation methods in mapping salinity of groundwater? – International Journal of Research and Innovations in Earth Sciences 3(3): 59–64.
[16] Gunnink, J. L., Burrough, P. A. (1996): Interactive Spatial Analysis of Soil Attribute Patterns Using Exploratory Data Analysis (EDA) and GIS. – In: Masser, I., Salge, F. (ed.) Spatial Analytical Perspectives on GIS. Taylor & Francis, New York.
[17] Hani, A., Ali, S., Abari, H. (2011): Determination of Cd, Zn, K, pH, TNV, organic material and electrical conductivity (EC) distribution in agricultural soils using geostatistics and GIS (Case Study : South- Western of Natanz-Iran). – World Academy of Science, Engineering and Technology 5(12): 852–855.
[18] Heistermann, M., Kneis, D. (2011): Benchmarking quantitative precipitation estimation by conceptual rainfall-runoff modeling. – Water Resources Research 47(6): 1–23. DOI: 10.1029/2010WR009153.
[19] Hengl, T. (2007): A Practical Guide to Geostatistical Mapping of Environmental Variables. – Office for Official Publication of the European Communities, Luxembourg.
[20] Jayakody, A. N. (2006): Large diameter shallow agro-wells. A national asset or a burden for the nation? – The Journal of Agricultural Science 2(1): 1–10.
[21] Johnston, K., Ver Hoef, J., Krivoruchko, K., Lucas, N. (2003): Using ArcGIS Geostatistical Analyst. – ESRI press, Redlands, California.
[22] Kis, I. M. (2016): Comparison of ordinary and universal kriging interpolation techniques on a depth variable (a case study of the Šandrovac Field). – The Mining-Geology-Petroleum Engineering Bulletin: 41–58. DOI: 10.17794/rgn.2016.2.4.
[23] Krivoruchko, K. (2012): Empirical Bayesian Kriging - Implemented in ArcGIS Geostatistical Analyst. – ESRI Press, Redlands, CA.

http://www.aloki.hu ● ISSN 1589 1623 (Print) ● ISSN 1785 0037 (Online)
DOI: http://dx.doi.org/10.15666/aeer/1605_53595380
© 2018, ALÖKI Kft., Budapest, Hungary

[24] Kumar, A., Maroju, S., Bhat, A. (2007): Application of ArcGIS geostatistical analyst for interpolating environmental data from observations. – Environmental Progress 26(3): 220–225. DOI: 10.1002/ep. 10223.
[25] Kumari, M. K. N., Pathmarajah, S., Dayawansa, N. D. K. (2013): Characterization of agro-well water in Malwathu Oya cascade-I in Anuradhapura district of Sri Lanka. – Tropical Agricultural Research 25(1): 46–55.
[26] Kumari, M. K. N., Pathmarajah, S., Dayawansa, N. D. K., Nirmanee, K. G. S. (2016): Evaluation of groundwater quality for irrigation in Malwathu Oya cascade-I in Anuradhapura district of Sri Lanka. – Tropical Agricultural Research 27(4): 310–324.
[27] Li, J., Heap, A. D. (2011): A review of comparative studies of spatial interpolation methods in environmental sciences: Performance and impact factors. – Ecological Informatics 6: 228–241. DOI: 10.1016/j.ecoinf.2010.12.003.
[28] Lin, G., Chen, L. (2004): A spatial interpolation method based on radial basis function networks incorporating a semivariogram model. – Journal of Hydrology 288: 288–298. DOI: 10.1016/j.jhydrol.2003.10.008.
[29] Luo, W., Taylor, M., Paker, S. (2008): A comparison of spatial interpolation methods to estimate continous wind speed surfaces using irregularly distributed data from England and Wales. – International Journal of Climatology 28: 947–956. DOI: 10.1002/joc.1583.
[30] Madduma Bandara, C. M. (1985): Catchment Ecosystem and Village Tank Cascade in the Dry Zone of Sri Lanka: A time-Tested System of Land and Water Resources Management. – In: Lundqvist, J., Lohm, U., Falkenmark, M (ed.) Strategies for River Basin Management. Linkoping, Sweden.
[31] Mirzaei, R., Sakizadeh, M. (2016): Comparison of interpolation methods for the estimation of groundwater contamination in Andimeshk-Shush Plain, Southwest of Iran. – Environmental Science and Pollution Research 23(3): 2758–2769. DOI: 10.1007/s11356-015-5507-2.
[32] Moran, P. A. P. (1950): Notes on Continuous Stochastic Phenomena. – Biometrika 37: 17–23. DOI: 10.2307/2332142.
[33] Mutuna, F., Kurima, D. (2012): A comparison of spatial rainfall estimation techniques: A case study of Nyando river basin Kenya. – Journal of Agriculture, Science and Technology 14(2): 149–165.
[34] Nas, B. (2009): Geostatistical approach to assessment of spatial distribution of groundwater quality. – Polish J. of Environ. Stud. 18(6): 1073–1082.
[35] Panabokke, C. R., Sakthivadivel, R., Weerasinghe, A. D. (2002): Small Tanks in Sri Lanka: Evolution, Present Status and Issues. – International Water Management Institute, Colombo, Sri Lanka.
[36] Robnik-Sikonja, M., Savicky, P. (2017): CORElearn: Classification, Regression and Feature Evaluation. R package version 1.50.3. – https://cran.r-project.org/package=CORElearn.
[37] Seyedmohammadi, J., Esmaeelnejad, L., Shabanpour, M. (2016): Spatial variation modeling of groundwater electrical conductivity using geostatistics and GIS. – Modeling Earth Systems and Environment 2(169): 1–10. DOI: 10.1007/s40808-016-0226-3.
[38] Sirimanne, C. H. L. (1952): Geology for water supply Ceylon. – As. Advmt. Sci. 8th Annual Session, pp. 87–118.
[39] Stahl, K., Moore, R. D., Floyer, J. A., Asplin, M. G., Mckendry, I. G. (2006): Comparison of approaches for spatial interpolation of daily air temperature in a large region with complex topography and highly variable station density. – Agricultural and Forest Meteorology 139: 224–236. DOI: 10.1016/j.agrformet.2006.07.004.
[40] Team R, R. C. (2016): A language and environment for statistical computing. R foundation for statistical computing: Vienna, Austria. – http://www.r-project.org/.
[41] Todd, D. K., Mays, L. (2005): Groundwater Hydrology. – John Wiley & Sons, USA, New York.

http://www.aloki.hu ● ISSN 1589 1623 (Print) ● ISSN 1785 0037 (Online)
DOI: http://dx.doi.org/10.15666/aeer/1605_53595380
© 2018, ALÖKI Kft., Budapest, Hungary

[42] Uyan, M., Cay, T. (2013): Spatial analyses of groundwater level differences using geostatistical modeling. – Environmental and Ecological Statistics 20: 633–646. DOI: 10.1007/s10651-013-0238-3.
[43] Van Meter, K. J., Steiff, M., McLaughlin, D. L., Basu, N. B. (2016): The socioecohydrology of rainwater harvesting in India: Understanding water storage and release dynamics across spatial scales. – Hydrology and Earth Sciences 20(7): 2629–2647. DOI: 10.5194/hess-20-2629-2016.
[44] Wagner, P. D., Fiener, P., Wilken, F., Kumar, S., Schneider, K. (2012): Comparison and evaluation of spatial interpolation schemes for daily rainfall in data scarce regions. – Journal of Hydrology 464–465: 388–400. DOI: 10.1016/j.jhydrol.2012.07.026.
[45] Wang, S., Huang, G. H., Lin, Q. G., Li, Z., Zhang, H., Fan, Y. R. (2014): Comparison of interpolation methods for estimating spatial distribution of precipitation in Ontario, Canada. – International Journal of Climatology 34: 3745–3751. DOI: 10.1002/joc.3941.
[46] Webster, R., Oliver, M. (2008): Geostatistics for Environmental Scientists. – John Wiley & Sons, Ltd, New York.
[47] Wijesundara, W. M. G. D., Nandasena, K. A., Jayakody, A. N. (2012): Spatial and temporal changes in nitrogen, phosphorus and potassium concentration in water in the Thirappane tank cascade in dry zone of Sri Lanka. – Journal of Environmental Professionals Sri Lanka 1(1): 70–81.
[48] Wilcox, L. V. (1955): Classification and Use of Irrigation Waters. – SDA Circular No. 969, United States Department of Agriculture. Washington, D. C.
[49] Wu, W., Tang, X., Ma, X., Liu, H. A. (2016): A comparison of spatial interpolation methods for soil temperature over a complex topographical region. – Theoretical and Applied Climatology 125(3–4): 657–667.
[50] Xiao, Y., Gu, X., Yin, S., Shao, J., Cui, Y., Zhang, Q., Niu, Y. (2016): Geostatistical interpolation model selection based on ArcGIS and spatio-temporal variability analysis of groundwater level in piedmont plains, northwest China. – SpringerPlus 5: 425. DOI: 10.1186/s40064-016-2073-0.
[51] Xie, Y., Chen, T. B., Lei, M., Yang, J., Guo, Q. J., Song, B., Zhou, X. Y. (2011): Spatial distribution of soil heavy metal pollution estimated by different interpolation methods: Accuracy and uncertainty analysis. – Chemosphere 82: 468–476. DOI: 10.1016/j.chemosphere.2010.09.053.
[52] Yao, X., Fu, B., Lu, Y., Sun, F., Wang, S., Liu, M. (2013): Comparison of four spatial interpolation methods for estimating soil moisture in a complex terrain catchment. – PLoS ONE 8(1): 1–13. DOI: 10.1371/journal.pone.0054660.
[53] Zehtabian, G., Asgari, H., Tahmouresc, M. (2013): Assessment of spatial structure of groundwater quality variables based on the geostatistical simulation. – Desert 17: 215–224.
[54] Zimmerman, D., Pavlik, C., Ruggles, A. (1999): An experimental comparison of ordinary and universal kriging and distance weighting. – Mathematical Geology 31(4): 375–390.

http://www.aloki.hu ● ISSN 1589 1623 (Print) ● ISSN 1785 0037 (Online)
DOI: http://dx.doi.org/10.15666/aeer/1605_53595380
© 2018, ALÖKI Kft., Budapest, Hungary

APPENDIX

Table A1. *Longitude and latitude of the sampling locations*

Well no.	Longitude	Latitude	Well no.	Longitude	Latitude
1	80° 32' 28" E	8° 13' 35" N	16	80° 32' 35" E	8° 9' 34" N
2	80° 32' 21" E	8° 14' 5" N	17	80° 34' 11" E	8° 6' 36" N
3	80° 32' 47" E	8° 13' 18" N	18	80° 33' 51" E	8° 7' 18" N
4	80° 33' 1" E	8° 12' 43" N	19	80° 33' 21" E	8° 7' 8' N
5	80° 33' 0" E	8° 12' 1" N	20	80° 33' 30" E	8° 8' 16" N
6	80° 32' 30" E	8° 12' 27" N	21	80° 33' 36" E	8° 8' 38" N
7	80° 33' 27" E	8° 11' 58" N	22	80° 33' 55" E	8° 9' 0" N
8	80° 33' 38' E	8° 11' 25" N	23	80° 33' 7" E	8° 8' 9" N
9	80° 33' 33" E	8° 10' 53" N	24	80° 32' 43" E	8° 8' 53" N
10	80° 32' 59" E	8° 11' 6" N	25	80° 33' 32" E	8° 6' 29" N
11	80° 32' 23" E	8° 11' 32" N	26	80° 32' 35" E	8° 7' 24" N
12	80° 31' 55" E	8° 10' 36" N	27	80° 33' 21" E	8° 7' 42" N
13	80° 32' 16" E	8° 9' 49" N	28	80° 31' 37" E	8° 13' 28" N
14	80° 33' 11" E	8° 9' 54" N	29	80° 31' 56" E	8° 12' 46" N
15	80° 32' 60" E	8° 10' 27" N			

Table A2. *Accuracy of different methods at predicting pH*

	RMSE						
	IDW	**GPI**	**RBF**	**LPI**	**OK**	**UK**	**EBK**
April	0.422	0.421	0.442	0.440	0.482	0.482	*0.393*
May	0.294	0.269	0.294	0.276	0.270	0.270	*0.266*
June	0.406	0.430	0.425	0.438	0.409	0.409	*0.402*
July	*0.303*	0.314	0.319	0.310	0.313	0.313	0.306
August	0.401	*0.392*	0.412	0.400	0.413	0.413	0.404
September	0.468	0.456	0.486	0.469	0.499	0.499	*0.451*
October	0.417	0.395	0.426	0.406	0.440	0.440	*0.391*
November	0.397	0.398	0.408	0.405	0.398	0.398	*0.370*
December	0.394	*0.356*	0.397	0.357	0.395	0.395	0.377
January	0.373	0.358	0.375	*0.352*	0.367	0.367	0.359
February	0.355	0.373	0.359	*0.344*	0.351	0.351	0.347
March	0.257	0.249	0.252	0.246	0.243	0.243	*0.236*

Table A3. *Accuracy of different methods at predicting sodium concentration*

	RMSE						
	IDW	**GPI**	**RBF**	**LPI**	**OK**	**UK**	**EBK**
April	92.45	92.48	95.10	94.76	96.52	96.52	*90.46*
May	78.64	79.38	79.95	81.00	81.91	81.91	*77.20*
June	72.20	64.76	74.33	67.48	63.97	63.97	*63.13*
July	69.93	64.29	70.40	67.04	64.68	64.68	*62.25*

http://www.aloki.hu ● ISSN 1589 1623 (Print) ● ISSN 1785 0037 (Online)
DOI: http://dx.doi.org/10.15666/aeer/1605_53595380
© 2018, ALÖKI Kft., Budapest, Hungary

August	76.94	71.68	80.03	74.68	77.974	77.974	*70.36*
September	78.63	76.92	78.91	79.49	82.32	82.32	*70.71*
October	59.37	57.47	60.22	59.78	62.48	62.48	*52.50*
November	*59.40*	61.57	60.22	59.60	60.392	60.392	60.15
December	101.53	101.44	103.13	104.55	104.267	104.267	*98.98*
January	66.72	66.66	65.96	68.75	67.62	67.62	*63.51*
February	91.87	94.39	93.75	97.04	94.024	94.024	*91.52*
March	77.68	77.91	79.63	78.36	82.09	82.09	*71.69*

Table A4. *Accuracy of different methods at predicting potassium concentration*

	RMSE						
	IDW	**GPI**	**RBF**	**LPI**	**OK**	**UK**	**EBK**
April	2.497	2.512	2.509	2.461	2.435	2.435	*2.413*
May	2.094	2.149	2.099	2.131	2.095	2.095	*2.040*
June	3.008	2.922	2.954	2.847	2.886	2.886	*2.841*
July	2.853	2.805	2.872	2.783	2.818	2.818	*2.693*
August	2.272	2.311	2.297	2.256	2.187	2.187	*2.190*
September	1.873	1.907	1.881	1.842	1.810	1.810	*1.795*
October	1.509	1.566	1.528	1.553	1.486	1.486	*1.453*
November	1.710	1.712	1.707	1.703	1.707	1.707	*1.652*
December	3.669	3.686	3.694	3.674	3.659	3.659	*3.500*
January	2.753	2.719	2.777	2.710	2.661	2.661	*2.558*
February	3.300	3.482	3.324	3.307	3.249	3.249	*3.198*
March	1.043	1.041	1.040	1.016	1.075	1.075	*1.011*

Table A5. *Accuracy of different methods at predicting calcium concentration*

	RMSE						
	IDW	**GPI**	**RBF**	**LPI**	**OK**	**UK**	**EBK**
April	99.562	*90.209*	100.446	91.437	93.295	93.295	94.296
May	32.981	30.199	32.803	30.184	29.581	29.581	*28.213*
June	36.401	32.650	37.321	33.056	32.387	32.387	*31.622*
July	49.471	47.518	50.900	47.606	49.863	49.863	*45.759*
August	23.423	20.558	23.355	20.890	20.212	20.212	*19.383*
September	29.037	*26.220*	29.319	26.744	26.700	26.700	26.594
October	20.529	21.708	20.212	*17.601*	20.772	20.772	20.183
November	19.873	*17.981*	20.212	18.285	18.807	18.807	18.682
December	49.393	45.419	49.848	45.836	46.767	46.767	*43.777*
January	41.396	*38.672*	42.099	38.988	39.115	39.115	38.914
February	55.709	53.134	56.238	*51.639*	54.282	54.282	52.781
March	25.096	23.094	25.008	23.289	22.864	22.864	*22.832*

http://www.aloki.hu ● ISSN 1589 1623 (Print) ● ISSN 1785 0037 (Online)
DOI: http://dx.doi.org/10.15666/aeer/1605_53595380
© 2018, ALÖKI Kft., Budapest, Hungary

Table A6. *Accuracy of different methods at predicting magnesium concentration*

	RMSE						
	IDW	**GPI**	**RBF**	**LPI**	**OK**	**UK**	**EBK**
April	52.09	48.59	51.09	49.33	51.61	51.61	*46.22*
May	38.74	35.86	38.09	36.70	36.62	36.62	*33.58*
June	33.33	30.96	33.06	31.05	30.94	30.94	*29.02*
July	48.02	48.26	46.85	46.06	45.52	45.52	*43.98*
August	21.45	19.44	21.72	19.79	22.28	22.28	*18.13*
September	20.26	18.93	19.76	19.02	19.11	19.11	*17.84*
October	19.94	19.19	19.09	18.96	19.80	19.80	*18.59*
November	24.27	23.11	23.92	23.12	23.69	23.69	*21.57*
December	59.82	57.08	58.69	57.28	59.94	59.94	*53.49*
January	37.24	37.04	35.26	36.30	36.45	36.45	*34.28*
February	55.12	56.53	53.29	53.73	54.51	54.51	*52.07*
March	25.35	23.85	25.07	24.16	24.28	24.28	*23.55*

Table A7. *Accuracy of different methods at predicting nitrate nitrogen concentration*

	RMSE						
	IDW	**GPI**	**RBF**	**LPI**	**OK**	**UK**	**EBK**
April	3.449	3.572	3.563	3.526	3.349	3.349	*3.192*
May	3.035	2.890	3.188	2.884	2.794	2.794	*2.735*
June	2.519	2.349	2.527	2.449	2.256	2.256	*2.170*
July	2.684	2.685	2.829	2.670	2.529	2.529	*2.490*
August	0.801	0.840	0.773	0.805	0.778	0.778	*0.750*
September	2.334	2.395	2.416	2.382	2.247	2.247	*2.119*
October	4.982	5.147	5.200	5.209	4.904	4.904	*4.718*
November	4.537	4.770	4.691	4.694	4.344	4.344	*4.299*
December	2.162	2.195	2.265	2.157	2.039	2.039	*1.969*
January	2.181	2.246	2.260	2.217	2.067	2.067	*2.027*
February	2.166	2.190	2.267	2.148	2.049	2.049	*1.985*
March	3.316	3.147	3.507	3.164	3.052	3.052	*2.906*

Table A8. *Accuracy of different methods at predicting phosphate concentration*

	RMSE						
	IDW	**GPI**	**RBF**	**LPI**	**OK**	**UK**	**EBK**
April	*0.0383*	0.0411	0.0393	0.0400	0.0419	0.0419	0.0387
May	0.0550	0.0579	*0.0429*	0.0539	0.0522	0.0522	0.0544
June	0.0521	0.0554	*0.0510*	0.0561	0.0547	0.0547	0.0519
July	0.2372	0.2508	0.2351	0.2505	0.2299	0.2299	*0.2289*
August	0.2376	0.2847	*0.2137*	0.2559	0.2203	0.2203	0.2185
September	0.0791	0.0845	*0.0665*	0.0772	0.0761	0.0761	0.0784
October	0.1630	0.1643	0.1583	0.1641	0.1666	0.1666	*0.1543*
November	0.1601	0.1547	0.1578	0.1577	0.1561	0.1561	*0.1456*

http://www.aloki.hu ● ISSN 1589 1623 (Print) ● ISSN 1785 0037 (Online)
DOI: http://dx.doi.org/10.15666/aeer/1605_53595380
© 2018, ALÖKI Kft., Budapest, Hungary

December	0.1233	0.1252	0.1184	0.1251	0.1214	0.1214	*0.1165*
January	0.0511	0.0513	0.0494	0.0514	0.0505	0.0505	*0.0478*
February	0.0644	0.0642	0.0660	0.0638	0.0678	0.0678	*0.0609*
March	0.8531	0.8177	0.8526	0.8143	0.8521	0.8521	*0.7667*

Table A9. *Accuracy of different methods at predicting bicarbonate concentration*

	RMSE						
	IDW	**GPI**	**RBF**	**LPI**	**OK**	**UK**	**EBK**
April	7.635	8.537	7.152	7.084	7.484	7.484	*7.791*
May	10.472	12.321	10.672	10.795	10.583	10.583	*10.177*
June	25.261	25.468	25.984	26.111	25.386	25.386	*23.049*
July	26.454	28.259	27.438	28.560	27.723	27.723	*25.567*
August	26.394	25.871	27.128	26.459	25.518	25.518	*23.879*
September	21.248	21.488	21.703	21.815	21.398	21.398	*20.118*
October	24.846	24.494	24.940	24.767	26.945	26.945	*22.679*
November	37.413	36.044	36.765	36.308	36.299	36.299	*33.808*
December	23.242	22.315	23.540	22.811	*21.880*	*21.880*	22.271
January	23.791	22.593	24.270	23.372	22.774	22.774	*21.953*
February	13.513	13.121	13.770	13.571	13.889	13.889	*13.124*
March	16.755	16.211	16.609	16.734	16.073	16.073	*15.043*

Table A10. *Accuracy of different methods at predicting chloride concentration*

	RMSE						
	IDW	**GPI**	**RBF**	**LPI**	**OK**	**UK**	**EBK**
April	523.00	472.00	514.00	479.00	*473.57*	*473.57*	474.63
May	437.00	399.00	432.00	405.00	397.85	397.85	*377.13*
June	299.00	260.00	303.00	266.00	256.10	256.10	*243.52*
July	339.00	295.00	340.00	303.00	292.21	292.21	*275.89*
August	340.00	310.00	340.00	316.00	301.81	301.81	*290.23*
September	380.00	352.00	380.00	358.00	349.04	349.04	*331.90*
October	349.00	320.00	349.00	324.00	317.13	317.13	*301.21*
November	348.00	323.00	350.00	327.00	319.33	319.33	*302.74*
December	467.00	426.00	473.00	433.00	423.95	423.95	*401.40*
January	347.00	321.00	351.00	327.00	322.52	322.52	*304.87*
February	366.00	341.00	368.00	347.00	341.23	341.23	*325.94*
March	332.00	301.00	336.00	308.00	301.53	301.53	*288.31*

Table A11. *Accuracy of different methods at predicting electrical conductivity*

	RMSE						
	IDW	**GPI**	**RBF**	**LPI**	**OK**	**UK**	**EBK**
April	556.00	522.00	562.00	533.00	511.68	511.68	*485.51*
May	1014.00	972.00	1020.00	991.00	954.44	954.44	*900.32*

http://www.aloki.hu ● ISSN 1589 1623 (Print) ● ISSN 1785 0037 (Online)
DOI: http://dx.doi.org/10.15666/aeer/1605_53595380
© 2018, ALÖKI Kft., Budapest, Hungary

June	901.00	789.00	915.00	809.00	781.29	781.29	*733.61*
July	889.00	775.00	894.00	796.00	760.98	760.98	*717.11*
August	966.00	861.00	974.00	883.00	846.27	846.27	*800.76*
September	20.00	24.00	19.00	19.00	19.22	19.22	*18.55*
October	1048.00	980.00	1049.00	999.00	961.50	961.50	*907.20*
November	1052.00	985.00	1057.00	1002.00	961.89	961.89	*914.46*
December	771.00	719.00	775.00	732.00	703.45	703.45	*669.21*
January	843.00	797.00	849.00	812.00	779.35	779.35	*739.80*
February	598.00	560.00	602.00	571.00	549.77	549.77	*522.34*
March	824.00	764.00	817.00	780.00	762.11	762.11	*719.89*

Table A12. *Accuracy of different methods at predicting sodium adsorption ratio*

	RMSE						
	IDW	**GPI**	**RBF**	**LPI**	**OK**	**UK**	**EBK**
April	1.571	1.667	*1.446*	1.546	1.459	1.459	1.639
May	2.298	2.442	2.197	2.306	*2.110*	2.110	2.231
June	1.394	1.367	1.435	1.421	1.449	1.449	*1.311*
July	2.046	1.950	2.118	2.040	2.057	2.057	*1.886*
August	2.458	2.420	2.526	2.475	2.779	2.779	*2.269*
September	2.568	2.591	2.601	2.673	2.564	2.564	*2.372*
October	2.177	2.187	2.217	2.261	2.253	2.253	*2.012*
November	2.027	2.122	2.047	2.086	2.225	2.225	*1.949*
December	2.150	2.186	2.160	2.196	2.142	2.142	*2.100*
January	1.788	*1.749*	1.843	1.817	1.829	1.829	2.148
February	1.921	2.008	*1.622*	1.872	1.781	1.781	1.694
March	2.168	2.319	*2.097*	2.157	2.104	2.104	2.159

Table A13. *Accuracy of different methods at predicting total hardness*

	RMSE						
	IDW	**GPI**	**RBF**	**LPI**	**OK**	**UK**	**EBK**
April	364.00	338.00	363.00	339.00	357.00	357.00	*349.00*
May	228.00	207.00	225.00	210.00	208.57	208.57	*195.55*
June	202.00	185.00	204.00	186.00	183.93	183.93	*170.94*
July	290.00	295.00	288.00	283.00	275.66	275.66	*267.19*
August	134.00	120.00	135.00	122.00	117.87	117.87	*113.19*
September	143.00	131.00	141.00	132.00	132.02	132.02	*123.10*
October	117.00	117.00	111.00	*103.00*	114.81	114.81	110.32
November	139.00	130.00	138.00	131.00	137.79	137.79	*122.21*
December	344.00	325.00	340.00	325.00	336.25	336.25	*307.04*
January	227.00	223.00	220.00	220.00	228.00	228.00	*222.00*
February	338.00	339.00	331.00	324.00	332.00	332.00	*318.69*
March	158.00	146.00	156.00	148.00	146.53	146.53	*144.43*

http://www.aloki.hu ● ISSN 1589 1623 (Print) ● ISSN 1785 0037 (Online)
DOI: http://dx.doi.org/10.15666/aeer/1605_53595380
© 2018, ALÖKI Kft., Budapest, Hungary

Table A14. *Summary of Whisker boxplot diagram*

Parameter	Measured					Predicted				
	Median	**Mean**	**Q1**	**Q3**	**Asym.**	**Median**	**Mean**	**Q1**	**Q3**	**Asym.**
Na	118.4	133.0	71.94	183.8	RS	126.5	132.9	114.8	145.7	RS
K	1.845	2.48	1.04	2.88	RS	2.30	2.44	1.81	2.96	RS
Ca	48.8	67.15	27.77	88.15	RS	55.85	67.77	36	87.4	RS
Mg	34.88	47.29	19.67	63.07	RS	41.88	48.26	29.35	66.51	RS
Cl	190.0	325.5	118.8	420.0	RS	320.4	356.5	285.4	339.6	RS
HCO3	85.5	86.7	75	96.7	RS	86.0	87.0	86.0	89.0	RS
NO3-N	0.72	1.54	0.41	1.44	RS	1.14	1.36	0.85	1.64	RS
PO4	0.085	0.234	0.03	0.35	RS	0.106	0.23	0.05	0.346	RS
pH	7.86	7.83	7.58	8.1	LS	7.89	7.83	7.65	7.8	RS
EC	1016	1259	1719	1350	RS	1239	1261	1165	1403	RS
SAR	3.12	3.42	1.96	4.31	RS	3.49	3.41	2.97	3.83	LS
TH	261.4	361.0	168.1	485.7	RS	294.3	364.9	222.7	497.8	RS

RS - right skewed; LS - left skewed; Q1 - 1st quartile; Q3 - 3rd quartile; Asym. - asymmetry

http://www.aloki.hu ● ISSN 1589 1623 (Print) ● ISSN 1785 0037 (Online)
DOI: http://dx.doi.org/10.15666/aeer/1605_53595380
© 2018, ALÖKI Kft., Budapest, Hungary

ESTIMATING THE COUNTRY-LEVEL WATER CONSUMPTION FOOTPRINT OF SELECTED CROP PRODUCTION

HARUN, S. N. – HANAFIAH, M. M.*

School of Environmental and Natural Resource Sciences, Faculty of Science and Technology, Universiti Kebangsaan Malaysia, 43600 Bangi, Selangor, Malaysia

**Corresponding author*
e-mail: mhmarlia@ukm.edu.my

(Received 28th May 2018; accepted 31st Jul 2018)

Abstract. Agriculture has become a major user of global freshwater resources. This study measured the consumptive water use of 15 selected crops (cash crops, vegetables, and fruits) in Malaysia. The results indicated that the green water consumption footprint (129.8 m^3/ton -1586.0 m^3/ton) was higher compared to the blue water consumption footprint (21.0 m^3/ton - 931.0 m^3/ton) for all 15 crops in Malaysia. Paddy crop had the highest total water consumption footprint for both off and main seasons with 2265 m^3/ton and 2255 m^3/ton, respectively, due to the cultivation practices under flood conditions. The water consumption footprint depends on the crop yield, implying that the higher the crop yield, the lower the value is. This paper provides a comprehensive review of the assessment of the water consumption footprint of crop production in Southeast Asia from 2007 to 2017 (10 years). The paper also highlights and discusses a feasibility study for the water consumption footprint of crops and future outlooks in Southeast Asia following an LCA-based approach.
Keywords: *water footprint, water scarcity, agriculture water management, sustainability, Malaysia*

Introduction

In line with the increasing world population, increased water use and management issues have become a major global sustainability debate in recent years. A large amount of water is required to satisfy the needs of various sectors. A better understanding of water use and management is necessary to improve water resource stewardship and management at the local, regional, and global levels. The agriculture sector has become a major global freshwater consumer due to the irrigation sector, which consumes about 70% of freshwater around the world (Scanlon et al., 2007; Gordon et al., 2010; WWAP, 2012). Some regions, such as Southeast Asia, have a tropical climate and receive a sufficient amount of rainfall throughout the year, which allows for growing a variety of crops and has made the region a major global agriculture producer. The agriculture sector also makes a significant contribution to economic growth, as there is a high exportation of agricultural products, such as palm oil and rice; however, intensive anthropogenic activities and unforeseen natural events have affected the availability of surface and groundwater. The water footprint (WF) is a sustainability indicator that has been introduced to assess water consumption and the availability for different sectors (e.g., industrial, agricultural, domestic, etc.) and levels (global, national, regional, watershed, etc.). The WF was introduced to assess and quantify the water required for the production of a product and to assess the potential environmental impacts related to water use (Hoekstra, 2017, 2003; Babel et al., 2011; Chapagain and Hoekstra, 2004). WF is categorized into three components (green, blue, and grey)

http://www.aloki.hu ● ISSN 1589 1623 (Print) ● ISSN 1785 0037 (Online)
DOI: http://dx.doi.org/10.15666/aeer/1605_53815403
© 2018, ALÖKI Kft., Budapest, Hungary

based on a spatial and temporal water consumption evaluation of the source (Hoekstra et al., 2011; Aldaya et al., 2010).

Development of the water footprint concept

The concept of virtual water and the WF indicator were developed over the last decade. The virtual water concept was first introduced by Allan (1998), who defined it as the volume of freshwater used to produce a product. In other words, virtual water is the volume of water required to produce a product at the consumption level. WF is defined as the volume of water used in the production of a product or service consumed by an individual or group (Hoekstra, 2017). Hoekstra (2003) introduced the concept of WF by developing a framework to analyse the ratio of spatially and temporally explicit water consumption per water availability. The focus of the WF in early studies was quantifying the WF of processes, products, companies, and consumer groups. The WF consists of three components, which are specified geographically and temporally: green, blue, and grey water. The green WF refers to the total rainwater evapotranspiration and water incorporated into harvested crops used in the production of goods or services. The blue WF is defined as the volume of surface and groundwater consumed during the production of a product. The grey WF refers to the volume of freshwater required to dilute pollutants so that the quality of the polluted water complies with ambient water quality standards.

In the 2000s, Hoekstra and Hung (2002), Chapagain and Hoekstra (2003), Hoekstra (2003), Oki et al. (2003), Zimmer and Renault (2003), and De Fraiture et al. (2004) conducted studies to assess virtual water at a global scale. Hoekstra and Hung (2002) and Chapagain and Hoekstra (2004) provided global WF statistics of the agricultural, domestic, and industrial sectors and virtual water flows between nations due to international trade. Early studies of the WF focused on blue and green water consumption, and later, the grey WF was included to assess how much water is needed to dilute the pollutants in a body of water (Chapagain and Hoekstra, 2008). The WF has been further improved in terms of its definition and methodology for the agriculture, industry, and domestic sectors at a global scale by applying high spatial and resolution aspects (Mekonnnen and Hoekstra, 2011). Hoekstra et al. (2011) also developed the Global WF Standard to ensure that a reliable method is applied and a fair comparison can be formed between various WF studies.

ISO 14046 is the standard guideline for reporting WF, and it was launched by the International Standard Organization (ISO) in 2014. The factors that must be considered when applying ISO 14046 include societal, environmental, legal, cultural, and organizational diversity as well as differences in economic conditions (ISO, 2014). The framework consists of four phases: goal and scope definition, WF inventory, analysis, and water impact assessment. WF assessments can be performed either individually or as part of the Life Cycle Assessment (LCA) to identify the hot spots of the process throughout its supply chain; thus, significant environmental impacts from water consumption can be reduced (Sabli et al., 2017). *Figure 1* provides a brief description of the development of the WF assessment concept.

Although several WF studies have been conducted in many developed countries, this approach is still nascent in Southeast Asian countries, especially Malaysia. For the WF of agriculture, few studies have been conducted in Malaysia for cash crops (Harun and Hanafiah, 2017) and palm oil (Aminordin et al., 2014; Vijaya et al.,

http://www.aloki.hu ● ISSN 1589 1623 (Print) ● ISSN 1785 0037 (Online)
DOI: http://dx.doi.org/10.15666/aeer/1605_53815403
© 2018, ALÖKI Kft., Budapest, Hungary

2014; Zulkifli et al., 2014; Muhammad et al., 2012). Therefore, the present study aimed to assess the water consumption footprint of selected crops in Malaysia and to provide a comprehensive review of the current state of the water consumption footprint of crops in Southeast Asia from 2007 to 2017 (10 years). Recommendations and potential approaches to the sustainability of water resources in Malaysia are discussed as well.

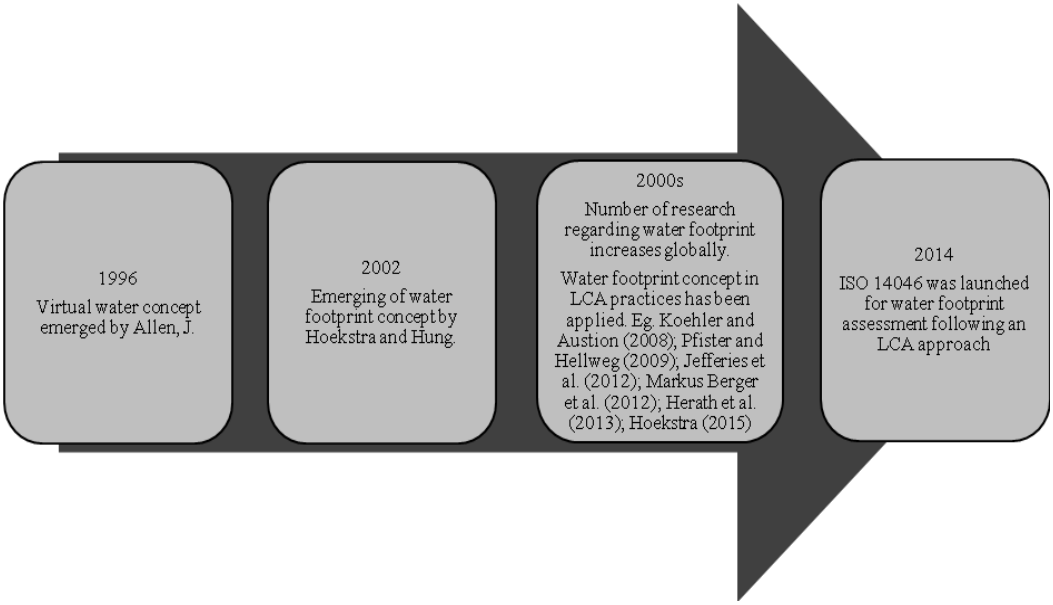

Figure 1. *Development of WF assessment concept*

Assessment of the water consumption footprint of selected crops in Malaysia

Malaysia receives a high amount of rainfall, with an average of 3,000 mm per year, implying a high dependence on rainfall for its water resources (GWP, 2017; WHO, 2011). The area of Malaysia's water supply is around 566 km^2 and includes catchment areas, rivers, lakes, and reservoirs. In Malaysia, the agriculture sector recorded an annual growth rate of 5.6% in 2015 compared to 2010 with a contribution of 8.9% to the Gross Domestic Product (GDP). Palm oil was a major contributor to the GDP of the agriculture sector, followed by other agriculture, livestock, fishery, rubber, and forestry and logging sectors, as shown in *Figure 2*.

According to the World Wildlife Fund (WWF), inefficient agricultural water use is a major issue that must be addressed to ensure the sustainability of water resources, as agriculture consumes about 68% of total water use in Malaysia. The agriculture sector plays an important role in national economic development by securing national food security and also contributes to public incomes, especially for people living in rural areas. Therefore, farmers in Malaysia as well as across the world have taken a step further to strengthen food security, and the government has also allocated billions of Ringgit Malaysia (RM) to maximise Malaysian agriculture production over the past 50 years (Zaim et al., 2013).

http://www.aloki.hu ● ISSN 1589 1623 (Print) ● ISSN 1785 0037 (Online)
DOI: http://dx.doi.org/10.15666/aeer/1605_53815403
© 2018, ALÖKI Kft., Budapest, Hungary

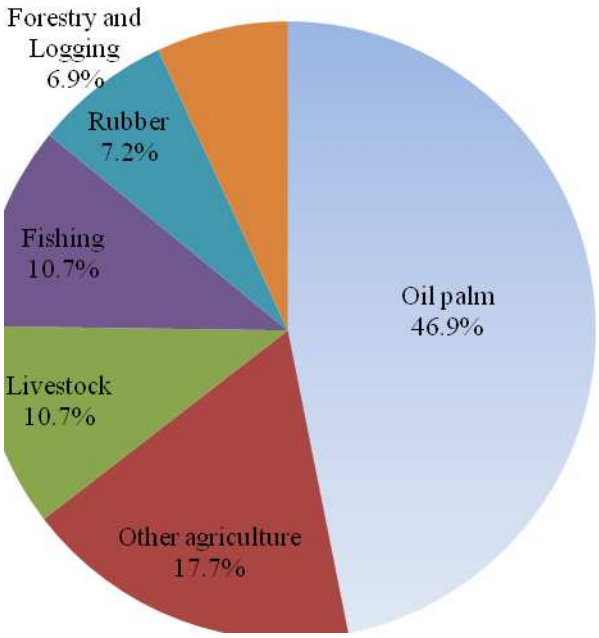

Figure 2. *Malaysia Gross Domestic Products (GDP) 2015 (Department of Statistics Malaysia, 2016)*

Methodological framework

In an agricultural context, the water consumption footprint (WCF) is used to quantify how much water has been consumed to grow a crop, and it is applicable to both annual and perennial crops (Hoekstra, 2011). In the present study, the WCF of three crop categories (cash crops, vegetables, and fruits) in Malaysia was assessed. Fifteen crops from the three crop categories grown in Peninsular Malaysia were selected: cassava, maize, sugarcane, sweet potato, pomelo, mandarin, banana, mango, pineapple, watermelon, cucumber, eggplant, green bean, lettuce, and rice. These 15 crops were chosen based on the high demand and their major contributions to the Malaysian economic sector. The total WCF of the crop cultivation process (WCF_{crop}) was adapted from the general formula of Hoekstra et al. (2011), as shown in *Equation 1.*

$$WCF_{crop} = WCF_{green,crop} + WCF_{blue,crop}\ m^3/ton \quad \text{(Eq.1)}$$

where,

WCF_{crop} = total water consumption footprint
$WCF_{green,crop}$ = green water consumption footprint
$WCF_{blue,crop}$ = blue water consumption footprint

The green water used in the process of the WCF of a crop ($WCF_{green,crop,}$ m^3/ton) was calculated by dividing the green component in the water use of a crop with the crop yield (Y, ton/ha) as shown in *Equation 2*. The blue component ($WCF_{blue,crop}$) was calculated similarly to the green WF and is expressed in m^3/ton.

$$WCF_{crop} = \frac{CWU_{green,crop}}{Y_{crop}} + \frac{CWU_{blue,crop}}{Y_{crop}} \left(\frac{m^3/ha}{ton/ha}\right) \quad \text{(Eq.2)}$$

http://www.aloki.hu ● ISSN 1589 1623 (Print) ● ISSN 1785 0037 (Online)
DOI: http://dx.doi.org/10.15666/aeer/1605_53815403
© 2018, ALÖKI Kft., Budapest, Hungary

where,

$CWU_{green,crop}$ = crop water use (green component)
$CWU_{blue,crop}$ = crop water use (blue component)
Y = crop yield

The crop evapotranspiration (ET), which is the combination of the two processes whereby water is lost from the soil surface and from crops by transpiration, was calculated using the following formulae (*Eqs. 3* and *4*) to determine the WCF_{green} and WCF_{blue}:

$$CWU_{green} = 10 \times \sum_{d=1}^{lgp} ET_{green} \ (m^3/ha) \quad \text{(Eq.3)}$$

$$CWU_{blue} = 10 \times \sum_{d=1}^{lgp} ET_{blue} \ (m^3/ha) \quad \text{(Eq.4)}$$

where,

ET_{green} = green water evapotranspiration
ET_{blue} = blue water evapotranspiration

A factor 10 was applied to convert water depths in millimeters into water volumes per land surface in m^3/ha, and lgp is the length of the growing period in days. The Penman-Monteith method by Allen et al. (1998) was used to calculate the evapotranspiration of crops (*Eqs. 5* and *6*). Crops coefficient used in this study was based on the length of crop development stages according to Food Agriculture Organization (FAO).

$$ET_{crop} = K_c \times ET_0 \ (mm/day) \quad \text{(Eq.5)}$$

where,

ET_{crop} = crop evapotranspiration (mm/day)
K_c = crop coefficient
ET_0 = Penman-Monteith crop evapotranspiration (mm/day)

$$ET_o = \frac{0.408\Delta(R_n - G) + \gamma \frac{900}{T+273} u_2 (e_s - e_a)}{\Delta + \gamma(1 + 0.34u_2)} \quad \text{(Eq.6)}$$

where,

ET_o = reference evapotranspiration (mm day^{-1})
Rn = net radiation at the crop surface (MJ m-2 day^{-1})
G = soil heat flux density (MJ m-2 day^{-1})
T = air temperature at 2 m height (°C)
u2 = wind speed at 2 m height (m s^{-1})
es = saturation vapour pressure (kPa)
ea = actual vapour pressure (kPa)
es – ea = saturation vapour pressure deficit (kPa)
D = slope vapour pressure curve (kPa $°C^{-1}$)
G = psychrometric constant (kPa $°C^{-1}$)

http://www.aloki.hu ● ISSN 1589 1623 (Print) ● ISSN 1785 0037 (Online)
DOI: http://dx.doi.org/10.15666/aeer/1605_53815403
© 2018, ALÖKI Kft., Budapest, Hungary

A statistical analysis was also used to estimate the rainfall deficit for irrigation water requirements based on long-term rainfall records. This analysis was determined as part of the rainfall, which effectively contributes to cover crop water requirements (CWR). Information from the inventory database was compiled, and all data were used to model the WCF of the selected crop cultivation in Malaysia. Finally, a set of recommendations and suggestions was developed. The conceptual framework of the present study is shown in *Figure 3*.

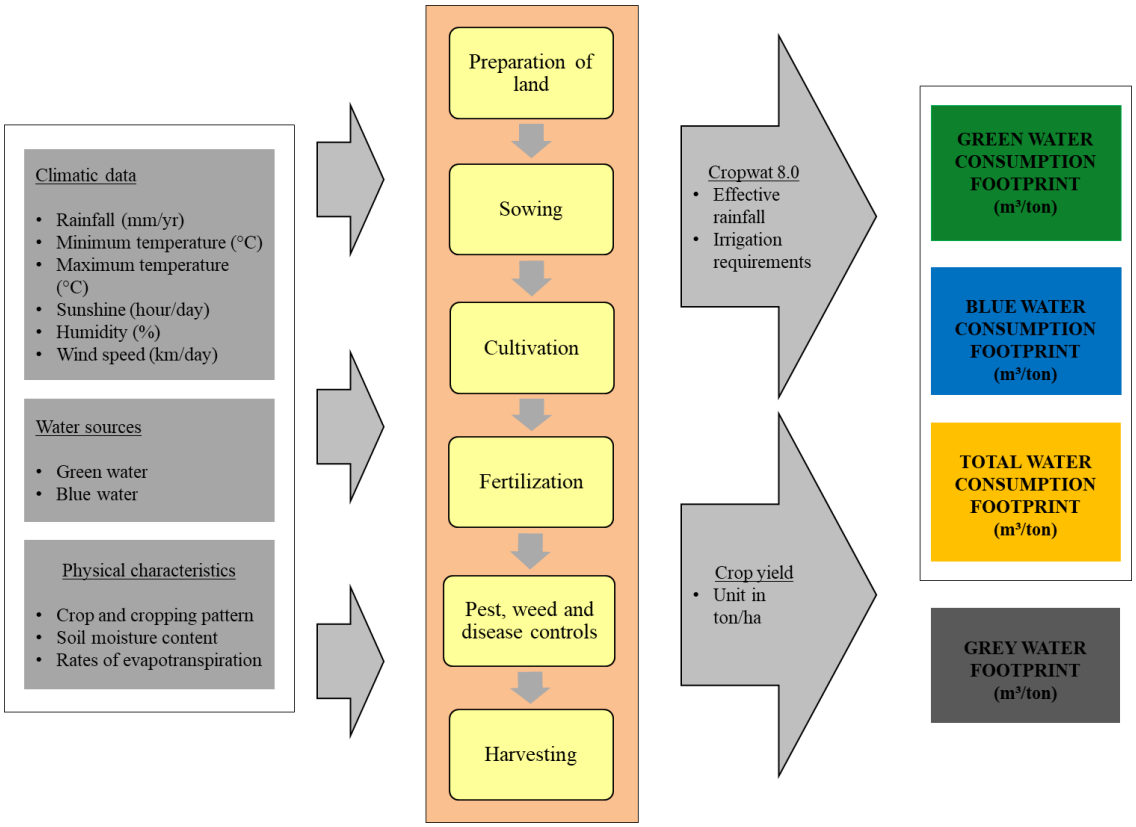

Figure 3. *Conceptual frameworks for WCF study of crop cultivation in Malaysia*

For this research study, data were compiled from various secondary data sources, such as books, publications, reports, government agencies related to the field of studies, including the Department of Irrigation and Drainage (DID), Malaysian Meteorological Department (MMD), Department of Agriculture for Peninsular Malaysia (DOA), Department of Statistics, Malaysian Agricultural Research and Development Institute (MARDI), and National Water Services Commission (SPAN), Malaysian rice cultivation, and Malaysian hydrological information. Foreground data were obtained through a series of site visits by communicating with data providers and administering questionnaires.

Result and discussion

Climatic data

For the WCF analysis, the climatic data provided by Malaysian Meteorological Department (MMD) consisted of minimum and maximum temperature, humidity,

http://www.aloki.hu ● ISSN 1589 1623 (Print) ● ISSN 1785 0037 (Online)
DOI: http://dx.doi.org/10.15666/aeer/1605_53815403
© 2018, ALÖKI Kft., Budapest, Hungary

sunshine, rainfall rate, and wind speed for nine years (2005 to 2013), which were used to estimate the water use for crops. Crop water requirements and irrigation requirements were calculated using the CROPWAT 8.0 Model, which is a decision support tool developed by the Land and Water Development Division of FAO. In addition to climatic data, other parameters, such as crop data and soil conditions, were included in the CROPWAT 8.0 model to estimate crop performance under both rain-fed and irrigated conditions.

Peninsular Malaysia experienced a uniform temperature throughout the year and ranged from 24 to 34 °C, while the average temperature over a period of nine years (2005 to 2013) recorded in this study was 28.7 °C. Due to the high evaporation rate, Malaysia's humidity ranged between 80% to 86%, with an average humidity of 82%, which can be considered high with an average of six hours of sunshine per day. In this study, the highest humidity rate was found in November at 85.8%, while the lowest humidity at 78.9% was observed in February. On the other hand, the highest wind speed rates were recorded in January and February at 155.5 and 146.9 km/day, respectively. The lowest wind speed rate of 121.0 km/day was recorded from April to July and September to November. *Figure 4* shows the average temperature, relative humidity, wind speed, and monthly sunshine for Malaysia over the nine-year period.

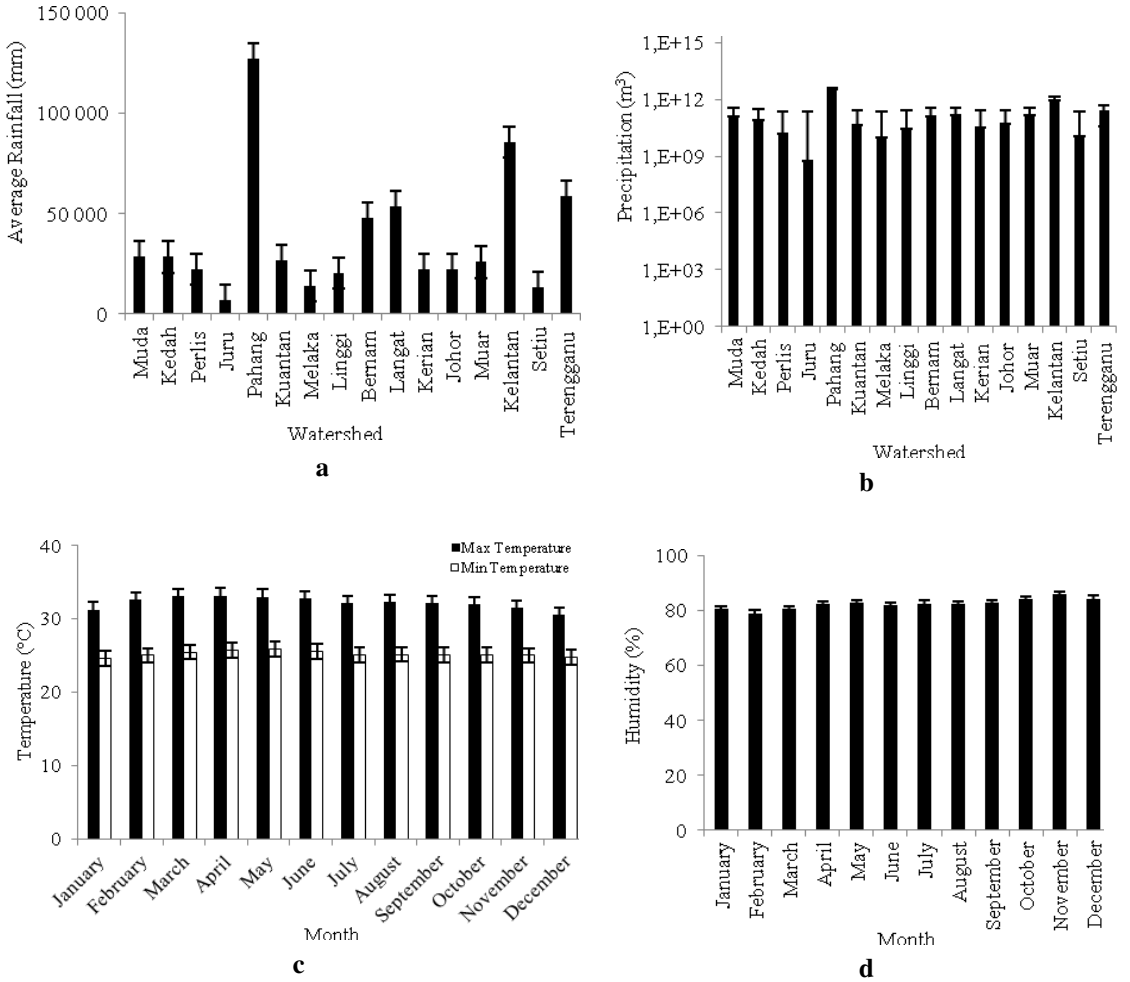

http://www.aloki.hu ● ISSN 1589 1623 (Print) ● ISSN 1785 0037 (Online)
DOI: http://dx.doi.org/10.15666/aeer/1605_53815403
© 2018, ALÖKI Kft., Budapest, Hungary

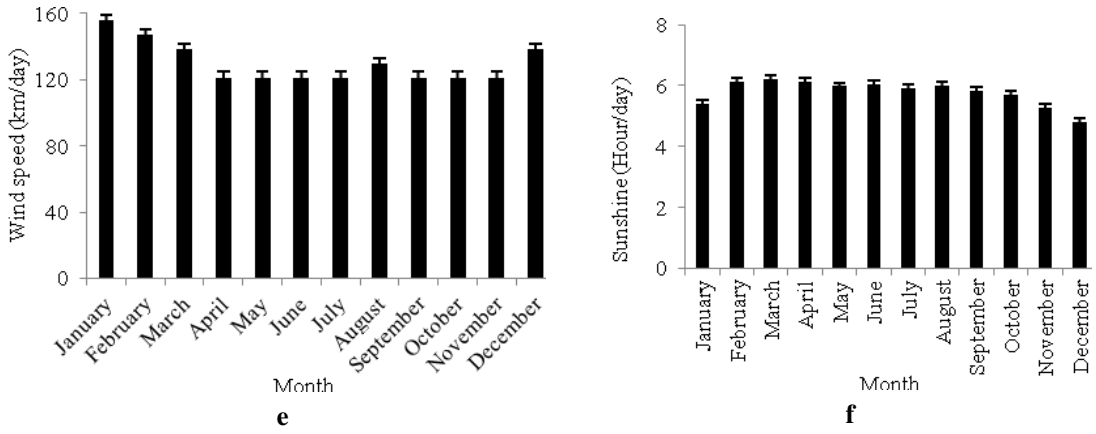

Figure 4. *Average a) rainfall, b) precipitation, c) temperature, d) humidity, e) wind speed, and f) monthly sunshine hours in Peninsular Malaysia over nine years (2005–2013)*

Water consumption footprint of selected crops

The green, blue, and total WCF for each crop along with the average yield from the year 2005 to 2013 are shown in *Figure 5*. The results indicated that perennial trees (banana, mango, and pineapple) require the highest amount of water per ton of crop production because perennial trees require water year-round, unlike annual trees. Variations in the blue and green WCF of crop production were related to the volume of water use, consumption patterns, climate factors, and agricultural management practices (Le Roux et al., 2017; Mekonnen et al., 2011). The evapotranspiration rate, which is mostly determined by climate conditions, is another factor that affects the WCF of crops.

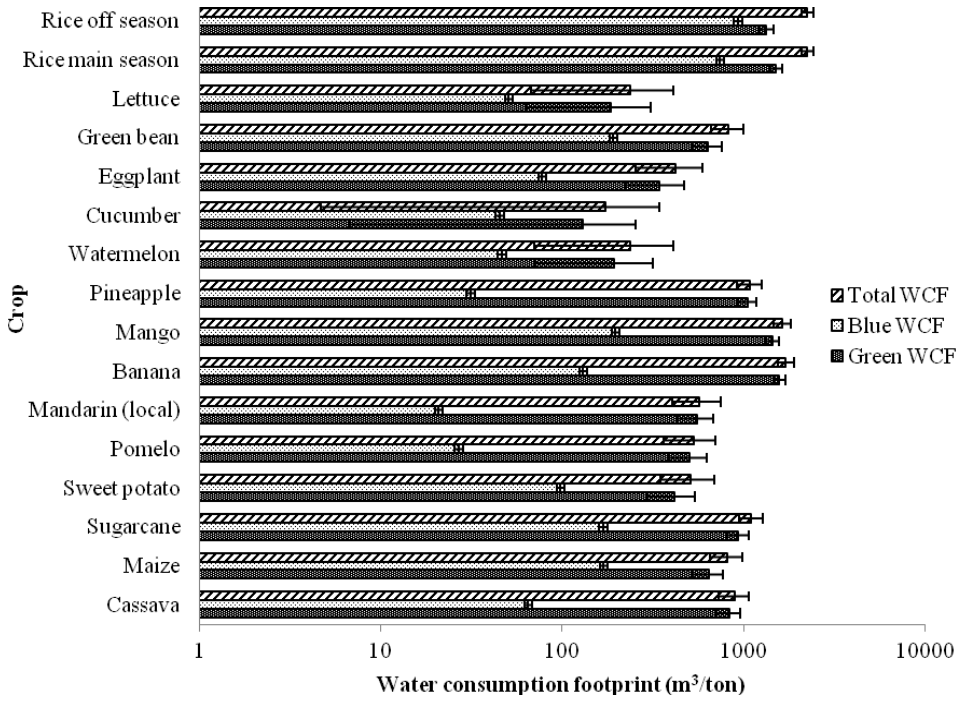

Figure 5. *Average blue, green, and total WCF of 15 crops for nine states in Peninsular Malaysia*

http://www.aloki.hu ● ISSN 1589 1623 (Print) ● ISSN 1785 0037 (Online)
DOI: http://dx.doi.org/10.15666/aeer/1605_53815403
© 2018, ALÖKI Kft., Budapest, Hungary

Green WCF had the highest value compared to blue WCF for all 15 crops in Peninsular Malaysia over the nine-year period. In Malaysia, 80% of irrigation water originates from green water, contributing to a higher green WCF compared to the blue WCF of crop production. In the agricultural sector, the blue water used depends on the crop, crop tolerance to water deficits, irrigation efficiency and green water availability (Lovarelli et al., 2016). If the evapotranspiration rate is higher than the rainfall rate, WCF_{blue} is potentially equal to the difference between evapotranspiration and rainfall (Bochiolla et al., 2013). Crop irrigation systems in Malaysia highly depend on rainwater, especially during the wet season (November to March), and there is a uniform temperature and high humidity throughout the year. It has been shown that the average of the green WCF was higher compared to the blue WCF for nine cultivated crops in Malaysia Ghazali and Hanafiah, 2016). Malaysia usually uses rainfall to meet crop water requirements, and the irrigation supply is only needed when rainfall is not sufficient (Abdul Samad et al., 2017; Ghazali and Hanafiah, 2016). Green water consumption causes less damage to the environment compared to blue water consumption (Falkenmark and Rockström, 2004) because high blue water usage will eventually lead to water scarcity (Gheewala et al., 2014). Terengganu has the highest average of green and total WCF among nine states in Peninsular Malaysia, and the lowest WCF was found for Selangor (*Figure 6*). This is because Terengganu has the lowest yield value compared to all crops included.

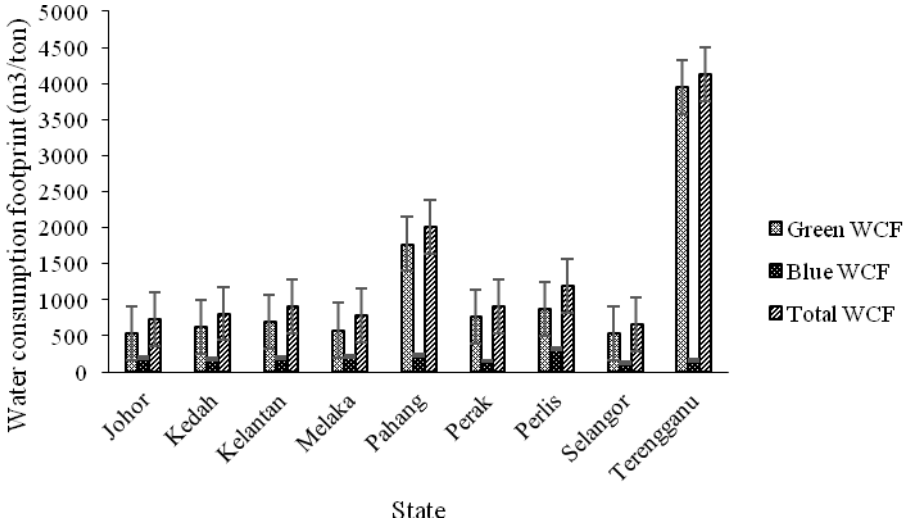

Figure 6. *Average of WCF (nine years) of 15 crops for nine states in Peninsular Malaysia*

The results for total WCF indicate that the cultivation of rice requires the highest amount of irrigation in both seasons compared to other crops, i.e., 2265 m^3/ton and 2255 m^3/ton in the off-seasons and main seasons, respectively, followed by mangoes and green beans. Based on this study, in the off-season, rice has the highest WCF values and contributes 15% of the total WCF of 15 crops in Peninsular Malaysia (*Fig. 7*). Rice requires two or three times more water than any other crop because paddy fields are cultivated under flood conditions (Gheewala et al., 2014; Maclean et al., 2013). Chapagain and Hoekstra (2011) reported that rice is one of the largest water consumers in the world, and large areas are required to irrigate paddy fields. Compared to other

http://www.aloki.hu ● ISSN 1589 1623 (Print) ● ISSN 1785 0037 (Online)
DOI: http://dx.doi.org/10.15666/aeer/1605_53815403
© 2018, ALÖKI Kft., Budapest, Hungary

selected Southeast Asian countries, Malaysia was ranked 8th for the highest paddy production at 2674.4 tons after Indonesia (recorded the highest paddy production), Vietnam, Thailand, Myanmar, Philippines, Cambodia, and Laos in 2015 (Economic Planning Unit, 2016).

Cucumbers had the lowest WCF (175.07 m^3/ton) compared to other crops due to the higher production yield (19.66 ton/ha). WCF is based on several factors; however, the most important factor is related to crop yield (Gheewala et al., 2014; Bulsink et al., 2010). A higher crop yield results in a lower WCF of crops (Gheewala et al., 2014; Bulsink et al., 2010; Chu et al., 2017). To reduce the WCF, the productivity of the crop per hectare of area must be improved. For instance, improving agriculture practices, such as by using organic fertilizer and regular weed control, can be applied. The results of the total WCF of the present study are similar to the previous study presented by Mekonnen et al. (2014), which reported the average of WCF for crops at the global scale; however, there are some crops that have different WCF values due to regional and climate factors, including climate variability, productivity, and agriculture practices (Gheewala et al., 2014; Mekonnen and Hoekstra, 2014; Bulsink et al., 2010; Hoekstra and Chapagain, 2006).

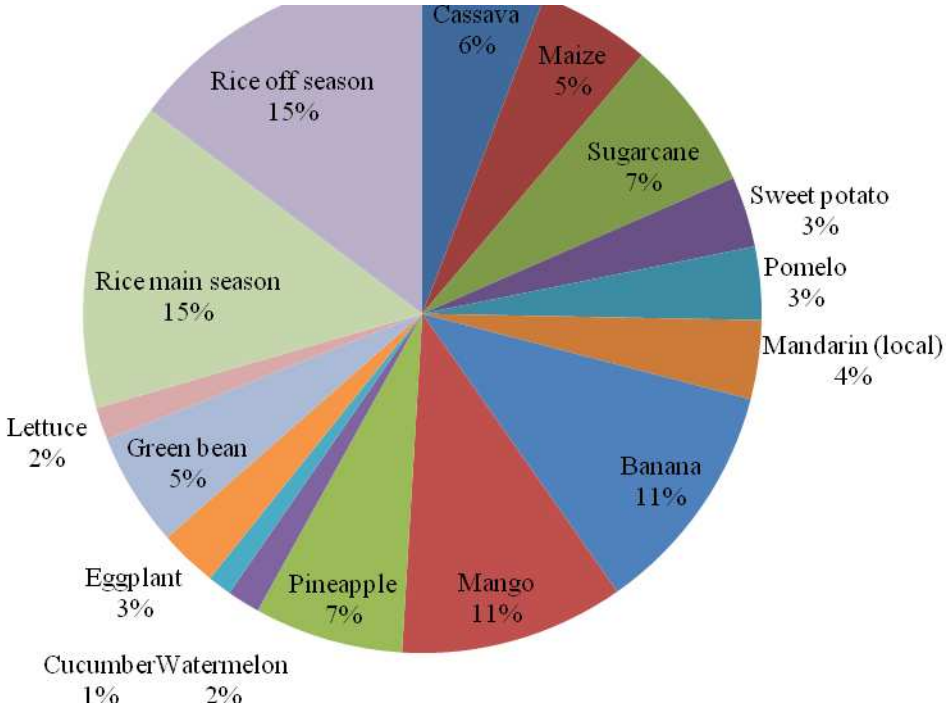

Figure 7. *Percentages of total WCF of 15 crops in Malaysia*

Previous studies of the WCF of crops in Southeast Asia

The next sections of this paper discuss previous studies of the WF of crops conducted in the Southeast Asian region that were published from 2007 to 2017 (10 years). The keywords used to search for published studies included water footprint, blue water, green water, water consumption, water use, water scarcity, agriculture, crop production, and Southeast Asia. Literature from several established databases, such as Scopus and Science Direct, were included. Southeast Asia has a tropical humid climate

http://www.aloki.hu ● ISSN 1589 1623 (Print) ● ISSN 1785 0037 (Online)
DOI: http://dx.doi.org/10.15666/aeer/1605_53815403
© 2018, ALÖKI Kft., Budapest, Hungary

and consists of 11 countries: Brunei, Cambodia, East Timor, Indonesia, Laos, Malaysia, Myanmar, Philippines, Singapore, Thailand, and Vietnam. Agriculture is the primary economic activity in Southeast Asia, and approximately 16% of the land area is planted with crops. Many Southeast Asian countries heavily depend on the export of plantation crops, such as coconut, sugar, rubber, tea, bananas, and abaca, to maintain the balance of trade. Southeast Asian countries are among the largest exporters of commodity crops, such as palm oil and rice. Furthermore, rice is one of the staple foods of Malaysia, Thailand, and Indonesia.

Aim and scope

WF is a new approach used to assess water use in the agricultural sector of Southeast Asia, and few studies have been conducted in this region. *Table 1* provides an overview of studies on the WCF of crops that have been conducted in Southeast Asia. To satisfy the growing demand for food, feed, and biofuel production in the future, information related to water resource availability and crop water requirements is needed for water resource sustainability planning (Gheewala et al., 2014).

Table 1. *Previous study on WCF of crops in Southeast Asia from 2010-2017*

Authors	Location	Phases assessed	Functional unit	WCF (m^3/ton)			
				Blue	Green	Grey	Total
SUGARCANE							
Babel et al. (2011)	KhlongPhlo sub-basin, Rayong province, Thailand	Production	m^3/GJ	81	147	n.a	228
Kongboon and Sampattagul (2012)	Northern provinces, Thailand	Cultivation	m^3/ton	31	146	49	226
Sangchan (2015)	Eastern Thailand	Cultivation	m^3/ton	Rain-fed 0.0 Irrigated 10.21	153.31 136.18	18.17 15.90	171.48 162.29
Gheewala et al. (2014)	Thailand	Cultivation	m^3/ton	2442	7920	n.a	10362
Kongboon and Sampattagul (2012)	Thailand	Cultivation, production	m^3/ton	31	146	49	226
Present study	Malaysia	Cultivation	m^3/ton	168.40	941.60	n.a	1109.50
OIL PALM							
Silalertruksa et al. (2017)	Thailand	Cultivation	m^3/ton	773.2	1145.8	n.a	1919
Suttayakul et al. (2016)	Thailand	Cultivation, Mill	m^3/ton	191.34	722.84	148.82	1063
Babel et al. (2011)	KhlongPhlo sub-basin, Rayong province, Thailand	Production	m^3/GJ	421	756	62	1239
Seewiseng et al. (2012)	Chaipattana-Mae FahLuang Reforestation Project, Phetchaburi province, Thailand	Oil palm production	m^3/ton	1829	524	1636	3989

http://www.aloki.hu ● ISSN 1589 1623 (Print) ● ISSN 1785 0037 (Online)
DOI: http://dx.doi.org/10.15666/aeer/1605_53815403
© 2018, ALÖKI Kft., Budapest, Hungary

Mungkalasiri et al. (2015)	Thailand Pathumthani and Chonburi	Cultivation	m^3/ton	Pathumthani 92.22 Chonburi 302.70	Pathumthani 423.77 Chonburi 635.65	Pathumthani 92.22 Chonburi 131.96	Pathumthani 678.84 Chonburi 1070.65
Bulsink et al. (2010)	Indonesia	Cultivation Trading	m^3/ton	0	802	51	853
Seewiseng et al. (2012)	Thailand (Phetchaburi province)	Production (land preparation, cultivation, harvesting and transportation steps)	m^3/ton	4657	1333	4160	10150
Gheewala et al. (2014)	Thailand	Cultivation	m^3/ton	5405	8323	n.a	13728
Muhammad et al. (2012)	Malaysia	Nursery (seedling)	m^3/ton	0.157	0.310	0.002	0.469
Vijaya et al. (2014)	Malaysia	Cradle-to-gate (from nursery and ends in the palm oil mill.	m^3/ton	21.48	5275.00	535.30	5831.78
Zulkifli et al. (2014)	Malaysia	Fresh fruit bunch	m^3/ton	17.00	5273.45	535	5825.45
PADDY							
Shrestha et al. (2017)	Thailand	Cultivation	m^3/ton	600	1678	585	3209
Bulsink et al. (2010)	Indonesia	Cultivation Trading	m^3/ton	735	2527	212	3473
Gheewala et al. (2014)	Thailand	Cultivation	m^3/ton	Major rice 1275 Second rice 3948	Major rice 4079 Second rice 1179	n.a	Major rice 5354 Second rice 5127
Chatpanyacharoen et al. (2015)	Thailand (Nan Province)	Cultivation 4 stages of rice development namely, land preparation and vegetative growth, reproductive growth, grain development and harvest	m^3/ton	0	1470.33	788.49	2258.82
Present study	Malaysia	Cultivation	m^3/ton	Main Season: 747.33 Off season: 931.82	Main Season: 1508.40 Off season: 1333.20	n.a	Main Season: 2255.8 Off season: 2265.10
CORN							
Cheroennet and Suwanmanee (2017)	Thailand	Cultivation, Ethanol production	m^3/ton	0	0.77	0.63	1.4
Present study	Malaysia	Cultivation	m^3/ton	170.6	649.3	n.a	819.9
COCOA							
Bulsink et al. (2010)	Indonesia	Cultivation Trading	m^3/ton	0	8895	519	9414
PINEAPPLE							
Gheewala et al. (2014)	Thailand	Cultivation	m^3/ton	5402	8323	n.a	13725
Present study	Malaysia	Cultivation	m^3/ton	31.34	1060.20	n.a	1091.60
CASSAVA							
Bulsink et al. (2010)	Indonesia	Cultivation Trading	m^3/ton	8	487	19	514

http://www.aloki.hu ● ISSN 1589 1623 (Print) ● ISSN 1785 0037 (Online)
DOI: http://dx.doi.org/10.15666/aeer/1605_53815403
© 2018, ALÖKI Kft., Budapest, Hungary

Tiewtoy et al. (2013)	Eastern Thailand	Cultivation	m^3/ton	Rain-fed 0.0 Irrigated 23.8	Rain-fed 335.8 Irrigated 393.9	Rain-fed 58.5 Irrigated 58.9	Rain-fed 386.8 Irrigated 413.2
Babel et al. (2011)	Thailand	Production	m^3/GJ	n.a	n.a	n.a	103
Gheewala et al. (2014)	Thailand	Cultivation	m^3/ton	1297	6529	n.a	7827
Namchancharoen et al. (2015)	Thailand	Cultivation and harvesting of feedstock, feedstock transport, feedstock processing, ethanol conversion, by products processing and on-site waste management.	m^3/ton	0	178.08	78.58	256.96
Present study	Malaysia	Cultivation	m^3/ton	65.42	853.56	n.a	900.98

n.a = not available

Functional unit

The WCF is expressed in terms of water volume per unit of product or as water volume per unit of time (Hoekstra et al., 2011). In an agricultural context, the functional unit frequently used is the volume of water per ton of crop product (m^3/ton); however, m^3/GJ is sometimes used as a functional unit when an analysis of energy crops is conducted. For example, Babel et al. (2011) examined the WCF of the biofuel energy production of palm oil, cassava, and sugarcane.

Component

The WCF considers both the direct and indirect water use of a process or product, which includes water consumption and water pollution throughout the full production cycle. The green, blue, and grey WCF were calculated separately, as they measure different types of water appropriation. The green and blue WCF are quantified to assess water quantity, while the grey WCF focuses on water quality.

Type of crops

Figure 8 shows the type of crops analyzed by the reviewed papers. CROPWAT 8.0 was applied to calculate the water used to cultivate crops. Most reviewed WCF studies assessed the WF of palm oil, followed by sugarcane and cassava, due to the promotion of biofuel in many countries, such as the US, Brazil, China, India, Thailand, and Malaysia. Biofuel use is promoted to reduce fossil fuel consumption, oil imports, and greenhouse gas emissions as well as to decrease the poverty rate of rural communities (Dufey, 2006; De Fraiture et al., 2008).

http://www.aloki.hu ● ISSN 1589 1623 (Print) ● ISSN 1785 0037 (Online)
DOI: http://dx.doi.org/10.15666/aeer/1605_53815403
© 2018, ALÖKI Kft., Budapest, Hungary

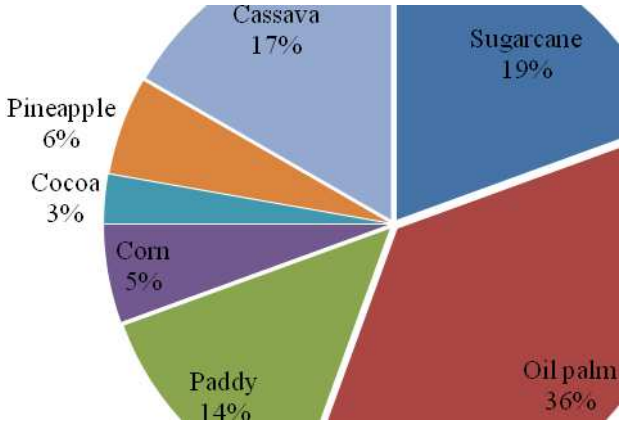

Figure 8. *Type of crops analysed in the reviewed papers*

The government of Thailand has planned to increase the share of renewable energy in the total energy consumption from 0.5% in 2002 to 20.3% by 2022 (Preechajarn and Prasertsri, 2010), many studies on biofuel crops have been carried out in Thailand (e.g., Silalertruksa et al., 2017; Suttayakul et al., 2016; Mungkalasiri et al., 2015; Pongpinyopap et al., 2014; Tiewtoy et al., 2013; Babel et al., 2011; Seewiseng et al., 2012; Gheewala et al., 2014; Namchancharoen et al., 2015; Kongboon and Sampattagul, 2012). In Thailand, biofuel is projected to replace 4928 million liters of fossil fuel annually by the year 2022 (Preechajarn and Prasertsri, 2010). The increase in biofuel crops will lead to land use changes and the replacement of native rainforests and wetlands due to shortages of land for agricultural purposes (Muller et al., 2007). Land use changes affect water resources and the aquatic environment. In addition, the changes can influence evapotranspiration and interception, thus reducing effective rainfall sources and affecting surface runoff and groundwater recharge (Stephan et al., 2001). As biofuel crops are crucial to supporting renewable and sustainable energy, it is necessary to determine which crop is produced in the most water-efficient manner (Babel et al., 2011). Several researchers, such as Gerbens-Leenes et al. (2009), Yang et al. (2009), and Mekonnen and Hoekstra (2011), conducted WCF studies on biofuel production. For instance, Yang et al. (2009) investigated the water requirements of biofuel in China based on the government's biofuel development plans.

Agriculture is a major source of livelihood in Southeast Asia. The Asian Development Bank (ADB) (1999) reported that there are approximately 115 million ha of land that are devoted to the production of rice, maize, palm oil, and natural rubber. Rice is a staple food for about 557 million people in Southeast Asia (Manzanilla et al., 2011); hence, this region is one of the largest producers and exporters of rice at a global scale. An assessment of the WCF of rice was carried out by Chatpanyacharoen et al. (2015) to evaluate water requirements for rice cultivation in the Wang Pha district, Nan Province, Thailand. The WCF of rice in the Nan province was 2258.82 m^3/ton. The green WCF accounted for 1470.33 m^3/ton, and the grey WCF was 788.49 m^3/ton. The results indicated that the value of WCF was within the range of the WCF of rice found by Mekonnen and Hoekstra (2014) (range from 638-2874 m^3/ton). The blue WCF was not assessed because cultivation occurs under rain-fed conditions. The results of the WCF were affected by the maximum evapotranspiration (ET_o) and rice maximum coefficient (K_c). Only two components of WCF (green and grey WCF) were used for

http://www.aloki.hu ● ISSN 1589 1623 (Print) ● ISSN 1785 0037 (Online)
DOI: http://dx.doi.org/10.15666/aeer/1605_53815403
© 2018, ALÖKI Kft., Budapest, Hungary

the study because the green WCF was related to rainfall data, and for grey WCF, the phosphate was selected as the other pollutant (nitrate, ammonia) reduction parallel to the reduction of phosphate concentrations during the cultivation process. Numerous studies have been conducted on the WCF of rice across the globe, including studies by Chapagain and Hoekstra (2011), Bulsink et al. (2010), Aldaya et al. (2010), Yoo et al. (2013), Shresta et al. (2013), Gheewala et al. (2014), Marano and Filippi (2015), and Su et al. (2015). Shresta et al. (2013) estimated the WCF of rice and other crops in different districts, development regions, and physiographic divisions of Nepal. Marano and Filippi (2015) determined the WCF for rice production in two areas in Argentina located in the central-east Entre Rios and Santa Fe regions.

The volumetric WCF indicator does not provide the actual impact of water use directly (Wichelns, 2010); thus, it underestimates the water scarcity or water stress of a specific area. Water scarcity generally varies based on geographical, climate condition, environmental, social, economic, and political factors. The water stress index (WSI) developed by Pfister (2009) is a commonly applied method used to measure water scarcity. The WSI can serve as a characterization factor for freshwater deprivation. The evaluation of the impacts of crop water use in different regions or watersheds using the water stress index and the indication of water deprivation potential was studied by Gheewala et al. (2014) for 10 crops, including rice, maize, soybeans, mung beans, peanuts, cassava, sugarcane, pineapple, and palm oil. The highest amount of water use in irrigation was rice farming, which amounted to 10,489 million m^3/year volume of water used, followed by maize, sugarcane, palm oil, and cassava. In addition, major rice cultivation contributes to the highest water deprivation rate, which is around 1862 million m^3H_2Oeq/year, followed by sugarcane, second rice, and cassava. Crops such as rice, maize, cassava, soybeans, groundnuts, coconut, palm oil, bananas, coffee, and cocoa, which were analyzed by Bulsink et al. (2010), accounted for 86% of total Indonesian water use.

The factors that generally determine the WCF are volume of consumption, consumption patterns, climate, and agricultural practices (Hoekstra and Chapagain, 2008). Several studies have compared the WCF value of crops among provinces. Mungkalasiri et al. (2015) conducted a study to evaluate the WCF of palm oil and fresh fruit bunches (FFB) in two provinces in Thailand (Pathumthani and Chonburi). The results showed that the WCF of palm oil in Chonburi province (1070.65 m^3/ton of FFB) was higher than Pathumthani (678.84 m^3/ton of FFB) due to the lower yield and annual precipitation. The green and blue water WCF mainly depend on climate conditions. Areas with higher precipitation and yield rates have lower WCF values compared to areas with lower precipitation and yield rates (Mungkalasiri et al., 2015). Agricultural practices vary depending on farmers and the technology used and thus influence the yield and WCF values of the crops studied. Bulsink et al. (2010) found that the WCF of the population of Java was low due to high yields, the average consumption rate was just below average, and the evapotranspiration rate was lower compared to other regions.

Water management in Southeast Asia: future outlook following an LCA-based approach

Urbanization and industrialization have grown rapidly in Southeast Asia, thus affecting water resources. Other factors, such as water-related disasters, climate change,

http://www.aloki.hu ● ISSN 1589 1623 (Print) ● ISSN 1785 0037 (Online)
DOI: http://dx.doi.org/10.15666/aeer/1605_53815403
© 2018, ALÖKI Kft., Budapest, Hungary

and poor governance, have worsened the water sustainability issue. In acknowledgement of the importance of managing water resources for sustainability, Global Water Partnership (GWP) Southeast Asia was established to develop and influence sustainable water management policies at the national and regional levels (Lautze et al., 2011). The GWP drafted the water vision and framework, which is comprised of at least five countries (Cambodia, Indonesia, Philippines, Thailand, and Vietnam), and has incorporated Integrated Water Resources Management (IWRM). At the regional level, GWP Southeast Asia is working with ASEAN and has contributed to adding water sustainability to the ASEAN agenda through the creation of the ASEAN Working Group on Water Resources Management (AWGWR) (Global Water Partnership, 2017).

Agriculture is a primary sector that contributes to economic growth in Southeast Asian countries; however, it has a significant impact on water consumption. This could lead to water deprivation and scarcity if water resources are not managed properly. As mentioned, considerable efforts have been devoted to improving water management as well as to promoting green and sustainable development. As part of the initiative to sustain water resources, the WCF approach has been adopted in Southeast Asia. As shown by previous studies, Southeast Asian countries have begun to implement WCF in water resource management.

For Malaysia, the country has sufficient water to supply the needs of the agriculture, domestic, industrial, energy production, and environmental sectors; however, water resources must be managed properly to ensure that the resource is sustainable for future generations. The government of Malaysia has put forth various efforts to manage water resources. In the 11th Malaysia Plan (2016-2020), water resources and the agriculture sector were two primary focuses due to the awareness of global climate change (Economic Planning Unit, 2015). The National Water Resources Policy was launched by the Malaysian government in 2012, which provides holistic strategies for water resource management in Malaysia. The policy includes governance collaboration to ensure water security and continued sustainability. In addition, the federal government prioritized the restoration program for water resources by enhancing the IWRM program. Improvements in water quality in some rivers in Malaysia and the water shortage issue in Klang Valley were addressed through this program.

Moreover, a water demand management master plan was established by the Ministry of Energy, Green Technology, and Water (KeTTHA), which provides Malaysia with a better approach to water demand management and a tool to forecast water demands. For the river basin, agencies at the state level (i.e., Lembaga Urus Air Selangor [LUAS], Syarikat Air Kelantan [SAK], Syarikat Air Negeri Sembilan [SAINS], Pengurusan Air Pahang Berhad [PAIP], etc.) that have been established are responsible for effectively managing the river basins due to various legislations related to water management. In addition, communication, public awareness, and education programs for all ages were increased to promote a more efficient and prudent use of water. Awareness campaigns and activities with the cooperation of the relevant non-governmental organizations (NGOs) have also been implemented to promote the efficient use of water and river conservation for local commodities.

The WCF assessment is a nascent approach in Malaysia, especially in the agriculture sector. The actual impact of water use cannot be provided directly through a volumetric WCF indicator because water scarcity issues vary based on geographical, climate condition, environmental, social, economic, and political factors (Gheewala et al.,

http://www.aloki.hu ● ISSN 1589 1623 (Print) ● ISSN 1785 0037 (Online)
DOI: http://dx.doi.org/10.15666/aeer/1605_53815403
© 2018, ALÖKI Kft., Budapest, Hungary

2014). Hence, the assessment of WCF is useful to determine the impact of water consumption regarding water deprivation potential. Water deprivation can be calculated by multiplying the blue WCF of crops by the water stress index. Furthermore, the WCF approach following an LCA approach could improve the understanding of water consumption scenarios in crop production. Several WCF studies have been conducted in Southeast Asia following the LCA approach, such as Cheroennet and Suwanmanee (2017), Gheewala et al. (2014) and Silalertruksa et al. (2017). Silalertruksa et al. (2017) determined the impact of greenhouse gases and water use on palm oil cultivation in Thailand. The study combined two methods, including the life cycle greenhouse gas emissions assessment and the water scarcity footprint assessment.

The ISO WF (ISO, 14046) was launched in 2014, and it focuses on water availability and degradation. The LCA and ISO address all input and output in the WF inventory analysis; hence, all environmental effects of water use are also included in the assessment (Pfister et al., 2015; Quinteiro et al., 2015; Núnez et al., 2013; Ridoutt et al., 2010, 2012; Canals et al., 2009). By adopting the WF assessment, relevant input can be applied for the formulation of various types of government policies, such as national or state water policies, river basin policies, local water policies, trade policies, foreign policies, and development cooperation policies (Hoekstra, 2011). ISO 14046 (2014) lists the benefits of WF assessments:

- WF can help in assessing the magnitude of potential environmental impacts related to water.
- Identifying ways to reduce potential water-related impacts of products at various life cycle stages, and of processes and organizations.
- Facilitating water efficiency and optimization of water management at product, process and organizational levels.
- Provide scientifically consistent and reliable information for reporting WF results.

Limitations and uncertainties

During the assessment of the WF, uncertainty is an important factor that must be taken into account, as several variables must be characterized. In most studies, the WF assessment was conducted based on several assumptions and limitations in the data section due to the difficulty in obtaining data from data providers. In addition, it is sometimes impossible to obtain actual data, such as data on water availability, crop water requirements, and crop water use. Another issue is that different irrigation methods, such as surface, sprinkler, and drip irrigation, might contribute to different irrigation efficiencies. Therefore, to limit the uncertainty level of a crop system assessment, the cultivation technique and geographical data should be carefully determined. In the present study, the grey WCF was excluded because the assessment aims to quantify the water quantity instead of the water quality; however, it is important to consider water quality, as shown by several studies conducted in Southeast Asia, because the assessment of green and blue water consumption is more related to water balance than the WF (Loverelli et al., 2016).

In Southeast Asia countries, technology constraints could lead to high water consumption even if water use efficiency and water management are applied. According to Mekonnen and Hoekstra (2015) and Pfister and Bayer (2014), considerations of the available technology and practices (i.e., crop residue management, optimized nutrient

http://www.aloki.hu ● ISSN 1589 1623 (Print) ● ISSN 1785 0037 (Online)
DOI: http://dx.doi.org/10.15666/aeer/1605_53815403
© 2018, ALÖKI Kft., Budapest, Hungary

management, and effective rainfall enhancement) could be useful in WF evaluations. Nevertheless, these aspects do not represent actual farming contexts. Regional conditions and technologies in different countries have significant effects on water management in the agricultural sector. Policies on more sustainable agricultural techniques must be endorsed to help reduce stress on the water use system. In addition, a more environmentally friendly system must be introduced to farmers to improve environmental quality (i.e., reducing fossil fuel dependence, mitigating soil erosion, improving soil quality, optimizing water use), economy (i.e., reducing operating costs) and public health safety (i.e., avoiding hazardous pesticides and fertilizers, producing more nutritious crops, producing food that safe for communities).

Conclusion

Based on this study's results, the green WCF had the highest value compared to the blue WCF for all 15 crops in Peninsular Malaysia for an average of nine years. The results for total WCF indicated that the cultivation of rice requires the highest amount of irrigation in both seasons compared to other crops, i.e., 2265 m^3/ton in the off-season and 2255 m^3/ton in the main season, followed by mangoes and green beans. Cucumbers had the lowest WCF compared to other (175.07 m^3/ton) crops due to higher production (19.66 ton/ha). The value of the WCF depends on the crop yield, and a higher crop yield results in a lower WCF of crops (Gheewala et al., 2014; Bulsink et al., 2010; Chu et al., 2017).

In conclusion, some improvements can still be achieved in WCF calculations and are required to make this indicator more valid in a crop production context. The WCF can be used to compare the water use efficiency of each product, particularly during a water shortage period, so that policies can be developed to determine which plant to promote in consideration of the net profit of a product, market requirements, labour requirements, etc. The findings of this study could be used as a guideline and can provide useful information for both stakeholders and policymakers for better water management practices, particularly in Malaysia.

Acknowledgements. Marlia M. Hanafiah was funded by the research grant (DIP-2017-006).

REFERENCES

[1] Abdul Samad, M. N. S., Hanafiah, M. M., Abdul Hasan, M. J., Ghazalli, N. F., Harun, S. N. (2017): Ratio of water withdrawal to availability in Kelantan watersheds, Malaysia. – Journal Clean WAS 1(1): 39-42.

[2] Aldaya, M. M., Hoekstra, A. Y. (2010): The water needed for Italians to eat pasta and pizza. – Agricultural System 103(6): 351-360.

[3] Allan, J. A. (1998): Virtual water: a strategic resource, global solutions to regional deficits. – Groundwater 36: 545-546.

[4] Allen, R. G., Pereira, L. S., Raes, D., Smith, M. (1998): Crop Evapotranspiration – Guidelines for Computing Crop Water Requirements. – FAO Irrigation and Drainage Paper 56. FAO, Rome.

[5] Aminordin, M. M., Hanafiah, M. M. (2014): Water footprint assessment of oil palm in Malaysia: a preliminary study. – AIP Conference Proceedings 1614(1): 803-807.

http://www.aloki.hu ● ISSN 1589 1623 (Print) ● ISSN 1785 0037 (Online)
DOI: http://dx.doi.org/10.15666/aeer/1605_53815403
© 2018, ALÖKI Kft., Budapest, Hungary

[6] Asian Development Bank (1999): Water in the 21st Century. – Asian Development Bank Annual Report 1999. Asian Development Bank, Manila, Philippines.
[7] Babel, M. S., Shrestha, B., Perret, S. (2011): Hydrological impact of biofuel production: A case study of the Khlong Phlo Watershed in Thailand. – Agricultural Water Management 101(1): 8-26.
[8] Bocchiola, D., Nana, E., Soncini, A. (2013): Impact of climate change scenarios on crop yield and water footprint of maize in the Po valley of Italy. – Agriculture Water Management 116: 50-61.
[9] Bulsink, F., Hoekstra, A. Y., Booij, M. J. (2010): The water footprint of Indonesian provinces related to the consumption of crop products. – Hydrology and Earth System Science 14: 119-128.
[10] Canals, L. M., Chenoweth, J., Chapagain, A., Orr, S., Anton, A., Clift, R. (2009): Assessing freshwater use impacts in LCA. Part 1. Inventory modelling and characterisation factors for the main impact pathways. – The International Journal of Life Cycle Assessment 14(1): 28-42.
[11] Chapagain, A. K., Hoekstra, A. Y. (2003): Virtual water trade. Virtual water flows between nations in relation to trade in livestock and livestock products. – International Expert Meeting on Virtual Water Trade 13(11): 1-202.
[12] Chapagain, A. K., Hoekstra, A. Y. (2004): Water footprint of Nations; Value of Water Research Report Series No. 16; The United Nations Educational, Scientific and Cultural Organization – International Institute for Hydraulic and Environmental Engineering (UNESCO-IHE), Delft, the Netherlands.
[13] Chapagain, A. K., Hoekstra, A. Y. (2008): The global component of freshwater demand and supply: an assessment of virtual water flows between nations as a result of trade in agricultural and industrial products. – Water International 33(1): 19-32.
[14] Chapagain, A. K., Hoekstra, A. Y. (2011): The blue, green and grey water footprint of rice from both a production and consumption perspective. – Ecological Economics 70: 749-758.
[15] Chatpanyacharoen, W., Hungspreug, N., Anurugsa, B., Taweesuk, S. (2015): Water footprint evaluation of oryza sativa in Tha Wang Pha district, Nan Province. – Thammasat International Journal of Science and Technology 20(4): 21-28.
[16] Cheroennet, N., Suwanmanee, U. (2017): Net energy gain and water footprint of corn ethanol production in Thailand. – Energy Procedia 118: 15-20.
[17] Chu, Y., Shen, Y., Yuan, Z. (2017): Water footprint of crop production for different crop structures in the Hebei Southern Plain, North China. – Hydrology and Earth System Sciences 21(6): 30.
[18] De Fraiture, C. (2004): Does International Cereal Trade Save Water? The Impact of Virtual Water Trade on Global Water Use. Comprehensive Assessment Research Report, Vol. 4. – International Water Management Institute, Sri Lanka.
[19] De Fraiture, C., Giordano, M., Liao, Y. (2008): Biofuels and implications for agricultural water use: blue impacts of green energy. – Water Policy 10(S1): 67-81.
[20] Dufey, A. (2006): Biofuels Production, Trade and Sustainable Development: Emerging Issues. Environmental Economics Programme, Sustainable Markets Discussion Paper No. 2. – International Institute for Environment and Development (IIED), London, UK.
[21] Economic Planning Unit (2010): The Malaysian Economy in Figures. – Prime Minister's Department, Kuala Lumpur, Malaysia.
[22] Economic Planning Unit (2015): Eleventh Malaysia Plan, 2016-2020: Anchoring Growth on People. – Prime Minister's Department, Kuala Lumpur, Malaysia.
[23] Economic Planning Unit (2016): The Malaysian Economy in Figures. – Prime Minister's Department, Kuala Lumpur, Malaysia.
[24] Falkenmark, M., Rockström, J. (2004): Balancing Water for Humans and NATURE: THE NEW APPROACH in Ecohydrology. – Earthscan, London.

http://www.aloki.hu ● ISSN 1589 1623 (Print) ● ISSN 1785 0037 (Online)
DOI: http://dx.doi.org/10.15666/aeer/1605_53815403
© 2018, ALÖKI Kft., Budapest, Hungary

[25] Gerbens-Leenes, P. W., Hoekstra, A. Y., van der Meer, Th. (2009): The water footprint of bioenergy. – Proceedings of the National Academy of Sciences of the United States of America 106: 10219-10223.
[26] Ghazali, N. F., Hanafiah, M. M. (2016): Malaysian water footprint accounts: Blue and green water footprint of rice cultivation and the impact of water consumption in Malaysia. – AIP Conference Proceedings 1784(1).
[27] Gheewala, S. H., Silalertruksa, T., Nilsalab, P., Mungkung, R., Perret, S. R., Chaiyawannakarn, N. (2014): Water footprint and impact of water consumption for food, feed, fuel crops production in Thailand. – Water 6(6): 1698-1718.
[28] Global Water Partnership (GWP) (2017): GWP Gender Strategy. – GWP, Stockholm, Sweden.
[29] Gordon, L. J., Max Finlayson, C., Falkenmark, M. (2010): Managing water in agriculture for food production and other ecosystem services. – Agriculture Water Management 97: 512-519.
[30] Harun, S. N., Hanafiah., M. M. (2017): Consumptive use of water by selected cash crops in Malaysia. – Malaysian Journal of Sustainable Agriculture 1(2): 06-08.
[31] Hoekstra, A. Y. (2003): Virtual water trade. – Proceedings of the International Expert Meeting on Virtual Water Trade, Value of Water Research Report Series No. 12, The United Nations Educational, Scientific and Cultural Organization-International Institute for Hydraulic and Environmental Engineering (UNESCO-IHE), Delft, the Netherlands.
[32] Hoekstra, A. Y. (2011): The global dimension of water governance: Why the river basin approach is no longer sufficient and why cooperative action at global level is needed. – Water 3(1): 21-46.
[33] Hoekstra, A. Y. (2017): Water footprint assessment: evolvement of a new research field. – Water Resources Management 31(10): 3061-3081.
[34] Hoekstra, A. Y., Chapagain, A. K. (2006): The water footprints of Morocco and the Netherlands. – Water Research Report Series No. 21. UNESCO-IHE, Delft, The Netherlands.
[35] Hoekstra, A. Y., Chapagain, A. K. (2008): Globalization of Water. Sharing the Planet's Freshwater Resources. – Blackwell Publishing, Oxford.
[36] Hoekstra, A. Y., Hung, P. Q. (2002): Virtual Water Trade: A Quantification of Virtual Water Flows between Nations in Relation to International Crop Trade. Value of Water. – Research Report Series No. 11. UNESCO-IHE, Delft, The Netherlands.
[37] Hoekstra, A. Y., Chapagain, A. K., Aldaya, M. M., Mekonnen, M. M. (2011): The Water Footprint Assessment Manual: Setting the Global Standard. – Earthscan, London, Washington.
[38] ISO 14046 (2014): Environmental Management, Water Footprint Principles, Requirements and Guidelines. – International Standards Organizations (ISO), Geneva.
[39] Kongboon, R., Sampattagul, S. (2012): Water footprint of bioethanol production from sugarcane in Thailand. – Journal of Environment and Earth Science 2(11): 61-67.
[40] Lautze, J., De Silva, S., Giordano, M., Sanford, L. (2011): Putting the cart before the horse: Water governance and IWRM. – Natural Resources Forum 35(1): 1-8.
[41] Le Roux, B., Van Der Laan, M., Vahrmeijer, T., Bristow, K. L., Annandale, J. G. (2017): Establishing and testing a catchment water footprint framework to inform sustainable irrigation water use for an aquifer under stress. – Science of the Total Environment 599: 1119-1129.
[42] Lovarelli, D., Bacenetti, J., Fiala, M. (2016): Water footprint of crop productions: a review. – Science of the Total Environment 548: 236-251.
[43] Maclean, J., Hardy, B., Hettel, G. (2013): Rice Almanac: Source Book for One of the Most Important Economic Activities on Earth. – IRRI, Los Baños, Philippines.
[44] Manzanilla, D. O., Paris, T. R., Vergara, G. V., Ismail, A. M., Pandey, S., Labios, R. V., Tatlonghari, G. T., Acda, R. D., Chi, T. T. N., Duoangsila, K., Siliphouthone, I., Manikmas, M. O. A., Mackill, D. J. (2011): Submergence risks and farmers preferences:

http://www.aloki.hu ● ISSN 1589 1623 (Print) ● ISSN 1785 0037 (Online)
DOI: http://dx.doi.org/10.15666/aeer/1605_53815403
© 2018, ALÖKI Kft., Budapest, Hungary

Implications for breeding Sub1 rice in Southeast Asia. – Agricultural Systems 104: 335-347.

[45] Marano, R. P., Filippi, R. A. (2015): Water footprint in paddy rice systems. Its determination in the provinces of Santa Fe and Entre Ríos, Argentina. – Ecological Indicators 56: 229-236.

[46] Mekonnen, M. M., Hoekstra, A. Y. (2011): The green, blue and grey water footprint of crops and derived crop products. – Hydrology and Earth System Sciences 8(47): 763-809.

[47] Mekonnen, M. M., Hoekstra, A. Y. (2014): Water footprint benchmarks for crop production: a first global assessment. – Ecological Indicator 46: 214-223.

[48] Mekonnen, M. M., Hoekstra, A. Y. (2015): Global grey water footprint and water pollution levels related to anthropogenic nitrogen loads to fresh water. – Environment Science and Technology 49(21): 12860-12868.

[49] Muhammad, H., Sahid, I. B., Surif, S., Ai, T. Y., May, C. Y. (2012): A gate-to-gate case study of the life cycle assessment of an oil palm seedling. – Tropical Life Sciences Research 23(1): 15.

[50] Muller, A., Schmidhuber, J., Hoogeveen, J., Steduto, P. (2007): Some insights in the effect of growing bio-energy demand on global food security and natural resources. – Proceedings of International Conference on Linkages between Energy and Water Management for Agriculture in Developing Countries, Hyderabad, India.

[51] Mungkalasiri, J., Wisansuwannakorn, R., Paengjuntuek, W. (2015): Water footprint evaluation of oil palm fresh fruit bunches in Pathumthani and Chonburi (Thailand). – International Journal of Environmental Science and Development 6(6): 445.

[52] Namchancharoen, T., Papong, S., Malakul, P., Mungcharoen, T. (2015): The carbon and water wootprint assessment of cassava-based bioethanol production in Thailand. – Proceeding International Conference on Biological, Environment and Food Engineering, (BEFE 2015) May 15-16, 2015, Singapore.

[53] Núnez, M., Pfister, S., Roux, P., Antón, A. (2013): Estimating water consumption of potential natural vegetation on global dry lands: Building an LCA framework for green water flows. – Environmental Science and Technology 47(21): 1225-1226.

[54] Oki, T., Sato, M., Kawamura, A. (2003): Virtual water trade to Japan and in the world. – Virtual Water Trade 1-13.

[55] Pfister, S., Bayer, P. (2014): Monthly water stress: spatially and temporally explicit consumptivewater footprint of global crop production. – Journal of Cleaner Production 73: 52-62.

[56] Pfister, S., Koehler, A., Hellweg, S. (2009): Assessing the environmental impacts of freshwater consumption in LCA. – Environmental Science and Technology 43: 4098-4104.

[57] Pfister, S., Vionnet, S., Levova, T., Humbert, S. (2015): Ecoinvent 3: Assessing water use in LCA and facilitating water footprinting. – International Journal of Life Cycle Assessment 21(9): 1349-1360.

[58] Pongpinyopap, S., Saibuatrong, W., Mungkalasiria, J., Wisansuwannakorn, R., Mungcharoen, T., Srinophkun, T. R. (2014): water footprint assessment of palm oil biodiesel production in southern part of Thailand. – Environment and Natural Resources Journal 12(2): 42-46.

[59] Preechajarn, S., Prasertsri, P. (2010): Thailand Biofuels Annual 2010. Gain Report Number Th0079. – USDA Foreign Agricultural Service, Global Agricultural Information Network, Washington.

[60] Quinteiro, P., Dias, A. C., Silva, M., Ridoutt, B. G., Arroja, L. (2015): A contribution to the environmental impact assessment of green water flows. – Journal of Cleaner Production 93: 318-329.

[61] Ridoutt, B. G., Juliano, P., Sanguansri, P., Sellahewa, J. (2010): The water footprint of food waste: case study of fresh mango in Australia. – Journal of Cleaner Production 18: 1714-1721.

http://www.aloki.hu ● ISSN 1589 1623 (Print) ● ISSN 1785 0037 (Online)
DOI: http://dx.doi.org/10.15666/aeer/1605_53815403
© 2018, ALÖKI Kft., Budapest, Hungary

[62] Ridoutt, B. G., Sanguansri, P., Freer, M., Harper, G. S. (2012): Water footprint of livestock: comparison of six geographically defined beef production systems. – International Journal of Life Cycle Assessment 17: 165-17.
[63] Sabli, N. S. M., Noor, Z. Z., Kanniah, K., Kamaruddin, S. N., Rusli, N. M. (2017): Developing a methodology for water footprint of palm oil based on a methodology review. – Journal of Cleaner Production 146: 173-180.
[64] Sangchan, S. (2015): Impact of biofuel production on hydrology: a case study of Klong Phlo watershed, Eastern Thailand. – Journal of Agricultural Technology 11(8): 1743-1754.
[65] Scanlon, T. M., Caylor, K. K., Levin, S. A., Rodriguez-Iturbe, I. (2007): Positive feedbacks promote power-law clustering of Kalahari vegetation. – Nature 449(7159): 209-212.
[66] Seewiseng, L., Bhaktikul, K., Aroonlertaree, C., Suaedee, W. (2012): The water footprint of oil palm crop in Phetchaburi province. – International Journal of Renewable Energy 7(2): 49-54.
[67] Shrestha, S., Pandey, V. P., Chanamai, C., Ghosh, D. K. (2013): Green, blue and grey water footprints of primary crops production in Nepal. – Water Resources Management 27(15): 5223-5243.
[68] Shrestha, S., Chapagain, R., Babel, M. S. (2017): Quantifying the impact of climate change on crop yield and water footprint of rice in the Nam Oon irrigation project, Thailand. – Science of the Total Environment 599-600(Supplement C): 689-699.
[69] Silalertruksa, T., Gheewala, S. H., Pongpat, P., Kaenchan, P., Permpool, N., Lecksiwilai, N., Mungkung, R. (2017): Environmental sustainability of oil palm cultivation in different regions of Thailand: greenhouse gases and water use impact. – Journal of Cleaner Production 167(Supplement C): 1009-1019.
[70] Stephens, W., Hess, T., Knox, J. (2001): Review of the Effects of Energy Crops on Hydrology. – Institute of Water and Environment. Cranfield University, UK.
[71] Su, M. H., Huang, C. H., Li, W. Y., Tso, C. T., Lur, H. S. (2015): Water footprint analysis of bioethanol energy crops in Taiwan. – Journal of Cleaner Production 88: 132-138.
[72] Suttayakul, P., H-Kittikun, A., Suksaroj, C., Mungkalasiri, J., Wisansuwannakorn, R., Musikavong, C. (2016): Water footprints of products of oil palm plantations and palm oil mills in Thailand. – Science of the Total Environment 542(Part A): 521-529.
[73] Tiewtoy, S., Somjai, T., Suwan, C. (2013): Water footprint of energy crops under rain-fed and irrigated cultivation in Eastern Thailand. – International Journal of Environmental and Rural Development 4(2): 138-142.
[74] Vijaya, S., Ngan, M., May, C., Nik, M. (2008): Environmental performance of the milling process of Malaysian palm oil using the life cycle assessment approach. – American Journal of Environmental Sciences 4(4): 310-315.
[75] Wichelns, D. (2010): Virtual water and water footprints offer limited insight regarding important policy questions. – International Journal of Water Resources Development 26(4): 639-651.
[76] World Health Organisation (WHO) (2011): World Water Day 2006. – Resource Sheet Number 2.
[77] World Water Assessment Programme (WWAP) (2012): The United Nations World Water Development Report 4. – Managing Water under Uncertainty and Risk, Paris, UNESCO.
[78] Yang, H., Zhou, Y., Liu, J. (2009): Land and water requirements of biofuel and implications for food supply and the environment in China. – Energy Policy 37: 1876-1885.
[79] Yoo, S. H., Choi, J. Y., Lee, S. H., Kim, T. (2013): Estimating water footprint of paddy rice in Korea. – Paddy and Water Environment 12(1): 43-54.

http://www.aloki.hu ● ISSN 1589 1623 (Print) ● ISSN 1785 0037 (Online)
DOI: http://dx.doi.org/10.15666/aeer/1605_53815403
© 2018, ALÖKI Kft., Budapest, Hungary

[80] Zaim, F., Bahaman, A. S., Haslinda, A. (2013): Paddy industry and paddy farmers well-being: A success recipe for agriculture industry in Malaysia. – Asian Social Science 9: 177-181.
[81] Zimmer, D., Renault, D. (2003): Virtual water in food production and global trade: Review of methodological issues and preliminary results. – Virtual Water Trade: Proceedings of the International Expert Meeting on Virtual Water Trade, Value of Water Research Report Series 12(1): 1-19.
[82] Zulkifli, H., Halimah, M., Vijaya, S., Choo, Y. M. (2014): Water footprint: Part 2 – FFB production for oil palm planted in Malaysia. – Journal of Oil Palm Research 26(4): 282-291.

http://www.aloki.hu ● ISSN 1589 1623 (Print) ● ISSN 1785 0037 (Online)
DOI: http://dx.doi.org/10.15666/aeer/1605_53815403
© 2018, ALÖKI Kft., Budapest, Hungary

ALLELOPATHIC ACTIVITY OF SOLVENT EXTRACTS OF *RHAZYA STRICTA* DECNE. AGAINST SELECTED WEEDS OF WHEAT CROP

ANWAR, T.[1] – ILYAS, N.[1] – QURESHI, R.[1*] – MUNAZIR, M.[2] – KHAN, A. M.[1] – ANSARI, L.[3] – RAHIM, B. Z.[4] – ANSARI, K. A.[5] – PANNI, M. K.[6]

[1]*Department of Botany, Pir Mehr Ali Shah Arid Agriculture University Murree Road, Shamsabad, Rawalpindi, 46300, Punjab, Pakistan*

[2]*Department of Botany, Government College Women University, 51040, Sialkot, Punjab, Pakistan*

[3]*Department of Forestry and Range Management, Pir Mehr Ali Shah Arid Agriculture University Murree Road, Shamsabad, Rawalpindi, 46300, Punjab, Pakistan*

[4]*Department of Botany, Baluchistan University, Quetta, 87500, Baluchistan, Pakistan*

[5]*Department of Botany, Shah Abdul Latif University, Khairpur, 66020, Sindh, Pakistan*

[6] *Bioactive Natural Products and Phytoceuticals Laboratory, Department of Horticulture, Plant and Soil Building, Michigan State University, East Lansing, Michigan, 48823, U.S.A.*

**Corresponding author*
e-mail: rahmatullahq@yahoo.com

(Received 31st May 2018; accepted 31st Jul 2018)

Abstract. The experiment was designed to study allelopathic effect of *Rhazya stricta* Decne. against selected weeds of wheat crop by using aqueous, hexane and methanolic extracts on filter paper and soil. The germination percentage, radicle length and plumule length were observed. The results revealed that *R. stricta* methanolic extract showed the highest degree of seed germination percentage inhibition of *C. album*, *P. minor* and *R. dentatus* with 47%, 43% and 42%, respectively in soil, and minimum germination for *C. album* (53%). The same extract caused significant radical length reduction of *R. dentatus* and *A. fatua* measuring 51% and 50%, respectively. The highest degree of inhibition in plumule length was measured for *A. fatua* and *R. dentatus* with 55% and 34%, respectively by *R. stricta* methanolic extract. Based on the results, it can be concluded that *R. stricta* showed good allelopathic activity that may be used in future herbicide screening program to launch in the market.
Keywords: *allelopathic effect, seed germination, radicle length, plumule length, Phalaris minor, Avena fatua, Chenopodium album, Euphorbia helioscopia, Triticum aestivum*

Introduction

Weeds are regarded as a major problem in agricultural productivity of various crops globally. For controlling weeds, synthetic chemicals (weedicides) are used which possess negative effect on human health and cause environmental pollution (Dallali et al., 2017) that augments to develop alternate weed management strategies (Thi et al., 2008). Allelopathy offers an important strategy for biological weed management (Arora et al., 2015) by production and release of chemical substances from leaves, flowers, seeds, stems or roots of plants which ultimately affect growth and development of other plants (Delcour et al., 2015). The most auspicious scheme to replace synthetic herbicides is to use environmental friendly natural chemical plant products. The synthesis of biochemical based on natural plant products and management of the allelopathy towards improvement

http://www.aloki.hu ● ISSN 1589 1623 (Print) ● ISSN 1785 0037 (Online)
DOI: http://dx.doi.org/10.15666/aeer/1605_54055421
© 2018, ALÖKI Kft., Budapest, Hungary

of crop productivity are the major areas that has gained attention of allelopathy research (Chon et al., 2005). The phytotoxic potential of these biologically active substances is widely searched by using highly advanced procedures for chemical identification (Dayan et al., 2000).

Rhazya stricta Decne., is an evergreen medicinal shrub of the family Apocynaceae distributed abundantly across Western and South Asia (Sabir et al., 2016). In Pakistan, it is commonly reported from Salt Range as well as periphery of District Khushab, Punjab, Pakistan (Qureshi et al., 2011). This plant has various ethno-medicinal values which may be attributed due to the presence of various phytochemicals in the plant. *R. stricta* invades and has deteriorated rangelands and have harmful effects on the growth and development of various plants by causing reduced seed germination (Ebid, 2016). Several alkaloids, glycosides, triterpenes, tannins and volatile compounds are present in the leaves of *R. stricta* (Khan et al., 2011). It has been reported to develop an ecological hazard such as autotoxicity to other plants due to presence of allelopathic potential (Alqarawi et al., 2018). So, it was assumed that due to presence of some chemicals *R. stricta* could be employed in biological weed management strategies. The aim of the present study was to explore the possible allelopathic potential of different leaf extracts of *R. stricta* on seed germination and seedling growth of selected weed species.

Materials and methods

Collection and processing of R. stricta

This research was carried out at Plant Physiology Laboratory, Department of Botany, Pir Mehr Ali Shah Arid Agriculture University, Rawalpindi (PMAS-AAUR), Pakistan. The mature leaves of *R. stricta* were collected from district Bahawalpur (73°15′12″ E longitude and 29°59′55″ N latitude, 159 m above sea level), Punjab, Pakistan and washed for several times under running tap water to remove dust following the methodology of Manimegalai et al. (2012) and Omar and Almaghrabi (2008). The same were dried in blotting paper for 4 weeks under shade at room temperature (20-25 °C). These were crushed using heavy duty blender (waring Lab.) to make fine powder (500 g), passed through mesh of 2 mm size and kept in air tight plastic zip lock bags separately at 4 °C (Anwar et al., 2013).

Procurement and surface sterilization of test species seeds

Seeds of monocotyledonous (*Phalaris minor, Avena fatua*) and dicotyledonous weeds (*Chenopodium album, Euphorbia helioscopia* and *Rumex dentatus*) were collected since all these are sensitive to herbicide (Shahid et al., 2006). These weeds are reported to be the most densely populated weeds of wheat crop (Qureshi et al., 2009). Wheat seeds were procured from the Barani Agricultural Research Institute (BARI), Chakwal (72.7211° E longitude and 32.9309° N latitude). Seeds were surface sterilized with 2% (w/v) solution of Sodium hypochlorite (NaOCl) for 5-8 min. After disinfection, these seeds were washed several times with distilled water (Biljana and Kragujevac, 2015; Anwar et al., 2016).

Studied parameters

Three growth parameters were used for screening allelopathic potential (Anwar et al., 2017 a, b) as follows:

(a) Germination percentage

http://www.aloki.hu ● ISSN 1589 1623 (Print) ● ISSN 1785 0037 (Online)
DOI: http://dx.doi.org/10.15666/aeer/1605_54055421
© 2018, ALÖKI Kft., Budapest, Hungary

(b) Radical length (cm)
(c) Plumule length (cm)

Aqueous extract preparation

An aliquot (10 g) of dried leaf powder of *R. stricta* was soaked in 100 ml distilled water in a flask and agitated at room temperature (20-25 °C) for 24 h on an orbital shaker (160 rpm). The extract was strained through muslin cloth and finally filtered through Whatman filter paper No. 1. Aqueous extract was obtained as filtrate of the mixture and final volume was attuned to 100 ml giving 10% water extract. This stock solution was then diluted with distilled water to prepare the different concentration of the extract i.e. T_1 (100%), T_2 (75%), T_3 (50%) after Sahu and Devkota (2013). Distilled water (0%) was used as control and indicated as T_4. The extract was stored at 4 °C in pre-disinfected flasks. To evade adulteration and forthcoming chemical modifications, the extracts were ensured to be used within 3-4 days (Anwar et al., 2017 a, b).

Hexane extract preparation

An aliquot (300 g) of dried leaf powder of *R. stricta* was mixed with hexane (2 L) repeated three times for 6 h on shaker. This extract was filtered, concentrated and dried over a rotary evaporator in pre-weighed flask. The obtained residue was 6.14 g. The stock solution was then diluted with hexane to prepare three concentrations i.e. T_1 (100%), T_2 (75%), T_3 (50%) and T_4 (0% control). These stored at 4 °C in pre-sterilized flasks (Sahu and Devkota, 2013).

Methanolic extract preparation

The defatted marc (after hexane extraction), was again placed on shaker with methanol (2 L) repeated three time for 6 h on shaker. This extract was filtered, concentrated, and dried over a rotary evaporator in pre-weighed flask. The obtained residue was 25.29 g. The stock solution was than diluted with methanol to prepare three concentrations i.e. T_1 (100%), T_2 (75%), T_3 (50%) and T_4 (0% control). These stored at 4 °C in pre-sterilized flasks (Sahu and Devkota, 2013).

Bioassay techniques

An aliquot (15 ml) of *R. stricta* extract was added to 25 g soil per Petri dish and 5 ml extract was added to filter paper in per Petri dish; while distilled water, hexane and methanol used as control in aqueous, hexane and methanolic extracts, respectively. Ten seeds of selected test species were sown in per Petri dish. Each treatment was replicated for five times. The Petri dishes were wrapped with squash tape, enclosed with Aluminium foil and incubated in the growth chamber (NTS Model MI-25S) at room temperature (20-25 °C) for 15 days. The data on germination percentage, radical length (cm) and plumule length (cm) were recorded and calculated of each test species by comparing with control (Khan et al., 2008).

Statistical analysis

A completely randomized design (CRD) was used for the experiment. The statistical analysis was done by using STATISTIX 9 and means were separated by using Fisher's protected LSD test (Nekonam et al., 2014).

http://www.aloki.hu ● ISSN 1589 1623 (Print) ● ISSN 1785 0037 (Online)
DOI: http://dx.doi.org/10.15666/aeer/1605_54055421
© 2018, ALÖKI Kft., Budapest, Hungary

Results

Allelopathic potential of R. Stricta aqueous extract

Germination percentage

The results revealed that *R. stricta* aqueous extract significantly inhibited germination of *C. album* (35%), followed by *R. dentatus* (32%) and *P. minor* (31%) on filter paper (*Table 1*); whereas, no significant effect on germination percentage was recorded for *T. aestivum*, *A. fatua* and *E. helioscopia*. On the soil, *R. stricta* aqueous extract also significantly inhibited seed germination of *R. dentatus* (50%), followed by *C. album* (45%) and *P. minor* (47%) compared to control (*Tables 1* and *2*). In the case of filter paper and soil, minimum germination percentage was noted for *R. dentatus* (50%) and *C. album* (55%), respectively. It has been noted that maximum germination percentage reduction of the *C. album*, *R. dentatus* and *P. minor* was accomplished at 100% concentration revealing concentration dependent (*Fig. 1a*).

Table 1. *Allelopathic effect of R. stricta leaf aqueous extract (AE) on germination percentage (%) of test species on filter paper*

Treatments	Test species					
	T. aestivum	*A. fatua*	*R. dentatus*	*P. minor*	*E. helioscopia*	*C. album*
$T_{1\ AE}$	86^{a}	81^{a}	55^{c}	59^{c}	88^{a}	58^{c}
$T_{2\ AE}$	88^{a}	80^{a}	59^{c}	61^{c}	90^{a}	67^{c}
$T_{3\ AE}$	89^{a}	82^{a}	70^{b}	74^{b}	91^{a}	78^{b}
$T_{4\ AE}$	90^{a}	83^{a}	81^{a}	85^{a}	92^{a}	89^{a}
LSD	14.722	18.56	16.974	17.874	17.529	17.504
F-value	27.64*	25.08*	13.29*	14.98*	21.73*	14.97*

Means followed by different letters within one column differ significantly at ($P < 5\%$)
*Significant at ($P < 1\%$)

Table 2. *Allelopathic effect of R. stricta leaf aqueous extract (AE) on germination percentage (%) of test species on soil*

Treatments	Test species					
	T. aestivum	*A. fatua*	*R. dentatus*	*P. minor*	*E. helioscopia*	*C. album*
$T_{1\ AE}$	87^{a}	80^{a}	50^{c}	53^{b}	89^{a}	55^{c}
$T_{2\ AE}$	89^{a}	82^{a}	56^{c}	58^{b}	91^{a}	64^{c}
$T_{3\ AE}$	90^{a}	83^{a}	67^{b}	71^{b}	92^{a}	75^{b}
$T_{4\ AE}$	91^{a}	84^{a}	82^{a}	86^{a}	93^{a}	90^{a}
LSD	15.722	19.46	15.774	14.474	16.529	17.967
F-value	26.64*	24.07*	12.39*	15.68*	22.73*	31.90*

Means followed by different letters within one column differ significantly at ($P < 5\%$)
*Significant at ($P < 1\%$)

Radical length

The data revealed that the highest radical length inhibition activity was exhibited by *R. dentatus* (44%) and *A. fatua* (40%) in *R. stricta* aqueous extract on filter paper.

http://www.aloki.hu ● ISSN 1589 1623 (Print) ● ISSN 1785 0037 (Online)
DOI: http://dx.doi.org/10.15666/aeer/1605_54055421
© 2018, ALÖKI Kft., Budapest, Hungary

Likewise, extract on soil caused significant radical length reduction of *R. dentatus* (48%) followed by *A. fatua (*45%) as compared to control. The data suggested that radical length of *C. album*, *P. minor, E. helioscopia* and *T. aestivum* remained unaffected. The results also illustrated that minimum radical length was noted for *A. fatua* (56%) and *R. dentatus* (52%) on filter paper and soil, respectively. The final data concluded that maximum radical length (97%) was noted for *C. album*, *P. minor, E. helioscopia* and *T. aestivum* (*Tables 3* and *4*). The results revealed that allelopathic inhibitory effect was concentration dependent for *R. dentatus* and *A. fatua* (*Fig. 1b*).

Table 3. *Allelopathic effect of R. stricta aqueous extract (AE) on radical length (cm) of test species on filter paper*

Treatments	Test species					
	T. aestivum	*A. fatua*	*R. dentatus*	*P. minor*	*E. helioscopia*	*C. album*
$T_{1\ AE}$	9.03^{a}	4.99^{c}	5.08^{d}	8.11^{a}	9.13^{a}	8.12^{a}
$T_{2\ AE}$	9.06^{a}	5.87^{c}	6.82^{c}	8.14^{a}	9.22^{a}	8.19^{a}
$T_{3\ AE}$	9.08^{a}	7.13^{b}	8.04^{b}	8.18^{a}	9.37^{a}	8.21^{a}
$T_{4\ AE}$	9.14^{a}	8.35^{a}	9.14^{a}	8.20^{a}	9.41^{a}	8.24^{a}
LSD	4.2679	0.9692	0.7136	2.4388	1.403	0.9741
F-value	20.22*	486.76*	278.70*	58.00*	55.71*	161.39*

Means followed by different letters within one column differ significantly at ($P < 5\%$)
*Significant at ($P < 1\%$)

Table 4. *Allelopathic effect of R. stricta aqueous extract (AE) on radical length (cm) of test species on soil*

Treatments	Test species					
	T. aestivum	*A. fatua*	*R. dentatus*	*P. minor*	*E. helioscopia*	*C. album*
$T_{1\ A}$ a	9.12^{a}	4.75^{c}	4.82^{c}	8.18^{a}	9.22^{a}	8.27^{a}
$T_{2\ A}$	9.26^{a}	5.02^{c}	6.55^{b}	8.23^{a}	9.41^{a}	8.31^{a}
$T_{3\ AE}$	9.32^{a}	6.99^{b}	7.09^{b}	8.40^{a}	9.55^{a}	8.46^{a}
$T_{4\ AE}$	9.38^{a}	8.65^{a}	9.35^{a}	8.49^{a}	9.67^{a}	8.59^{a}
LSD	1.1360	1.540	0.999	1.1125	1.0662	1.320
F-value	127.48*	45.47*	66.33*	111.84*	95.32*	56.72*

Means followed by different letters within one column differ significantly at ($P < 5\%$)
*Significant at ($P < 1\%$)

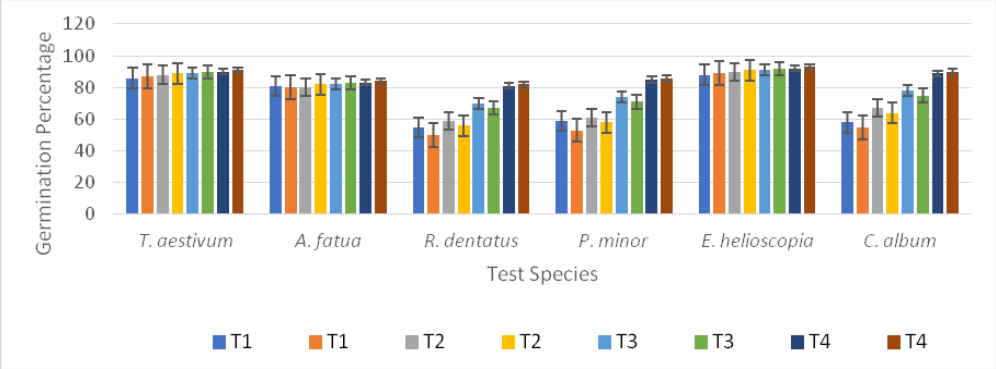

http://www.aloki.hu ● ISSN 1589 1623 (Print) ● ISSN 1785 0037 (Online)
DOI: http://dx.doi.org/10.15666/aeer/1605_54055421
© 2018, ALÖKI Kft., Budapest, Hungary

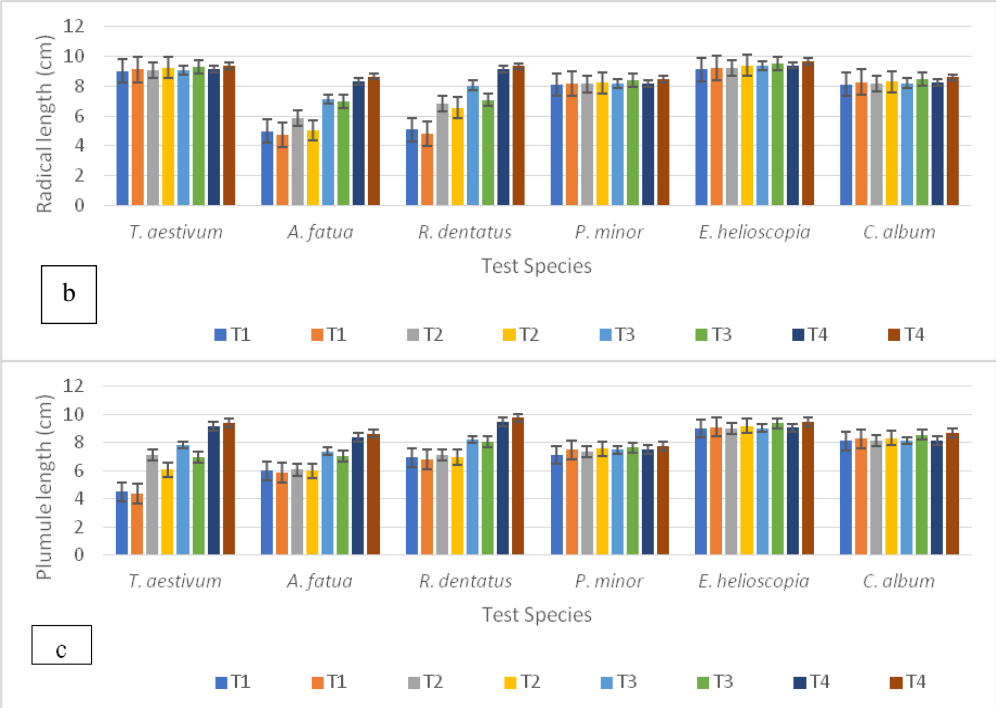

Figure 1. *Allelopathic potential of R. stricta aqueous extract against test species on filter paper (FP) and soil (S) on: (a) germination percentage (b) radical length (c) plumule length*

Plumule length

The experimental results of the current study indicated that aqueous extract of *R. stricta* significantly inhibited the plumule length of *T. aestivum* (51%), *A. fatua* (28%) and *R. dentatus* (27%) as compared to control, on filter paper. Interestingly, there was no significant effect on plumule elongation of *P. minor*, *E. helioscopia* and *C. album*. The statistical study recommended that *R. stricta* aqueous extract significantly inhibited plumule length of *T. aestivum* (53%), *A. fatua* (32%) and *R. dentatus* (30%) in soil. The statistical data concluded that minimum plumule length was noted for *T. aestivum* i.e. 49% and 47% on filter paper and soil, respectively (*Tables 5* and *6*). The statistical figures also proposed that maximum plumule length (96%) was noted for *P. minor*, *E. helioscopia* and *C. album* (*Fig. 1c*).

Table 5. *Allelopathic effect of R. stricta aqueous extract (AE) on plumule length (cm) of test species on filter paper*

Treatments	Test species					
	T. aestivum	*A. fatua*	*R. dentatus*	*P. minor*	*E. helioscopia*	*C. album*
$T_{1\ AE}$	4.49^{c}	5.99^{c}	6.93^{c}	7.12^{a}	9.01^{a}	8.11^{a}
$T_{2\ AE}$	7.12^{b}	6.06^{c}	7.13^{c}	7.36^{a}	9.02^{a}	8.12^{a}
$T_{3\ AE}$	7.81^{b}	7.39^{b}	8.24^{b}	7.48^{a}	9.04^{a}	8.13^{a}
$T_{4\ AE}$	9.14^{a}	8.39^{a}	9.46^{a}	7.52^{a}	9.06^{a}	8.14^{a}
LSD	3.7846	1.2971	0.9640	0.8718	0.0182	0.6156
F-value	8.44**	46.74*	57.31*	55.81*	14.11*	111.35*

Means followed by different letters within one column differ significantly at ($P < 5\%$)
*Significant at ($P < 1\%$)

http://www.aloki.hu ● ISSN 1589 1623 (Print) ● ISSN 1785 0037 (Online)
DOI: http://dx.doi.org/10.15666/aeer/1605_54055421
© 2018, ALÖKI Kft., Budapest, Hungary

Table 6. *Allelopathic effect of R. stricta aqueous extract (AE) on plumule length (cm) of test species on soil*

Treatments	Test species					
	T. aestivum	*A. fatua*	*R. dentatus*	*P. minor*	*E. helioscopia*	*C. album*
$T_{1\ AE}$	4.36[c]	5.86[c]	6.82[c]	7.48[a]	9.12[a]	8.26[a]
$T_{2\ AE}$	6.08[b]	5.99[c]	6.96[c]	7.56[a]	9.20[a]	8.32[a]
$T_{3\ AE}$	6.95[b]	7.06[b]	8.07[b]	7.63[a]	9.37[a]	8.57[a]
$T_{4\ AE}$	9.38[a]	8.65[a]	9.76[a]	7.72[a]	9.46[a]	8.69[a]
LSD	2.7846	1.3971	0.9140	0.8618	0.1182	0.4294
F-value	6.44**	45.74*	56.31*	55.91*	14.21*	196.36*

Means followed by different letters within one column differ significantly at ($P < 5\%$)
*Significant at ($P < 1\%$)

Allelopathic potential of R. stricta hexane extract

Germination percentage

There was significant reduction of germination of *C. album* (42%), *R. dentatus* (45%) and *P. minor* (41%) as compared to control on filter paper, whereas, no significant effect was observed on the germination of *T. aestivum*, *A. fatua* and *E. helioscopia* showing resistance to the allelopathic effect. Similarly, the highest seed germination inhibition was noted for *C. album* (51%), *P. minor* (50%) and *R. dentatus* (51%) by incorporation of *R. stricta* hexane extract into soil. It was experiential that the maximum (97%) germination noted for *T. aestivum*, *A. fatua* and *E. helioscopia*. In the present study, minimum germination was noted for *R. dentatus* (65%) and *C. album* (49%) on filter paper and soil, respectively (*Tables 7* and *8*). The statistics also recommended that allelopathic inhibitory effect was concentration dependent for *C. album*, *P. minor* and *R. dentatus* with concentration increase, suppression potential was gradually enhanced (*Fig. 2a*).

Table 7. *Allelopathic effect of R. stricta leaf hexane extract (HE) on germination percentage (%) of test species on filter paper*

Treatments	Test species					
	T. aestivum	*A. fatua*	*R. dentatus*	*P. minor*	*E. helioscopia*	*C. album*
$T_{1\ HE}$	86[a]	81[a]	55[c]	59[c]	88[a]	58[c]
$T_{2\ HE}$	88[a]	80[a]	59[c]	61[c]	90[a]	67[c]
$T_{3\ HE}$	89[a]	82[a]	70[b]	74[b]	91[a]	78[b]
$T_{4\ HE}$	90[a]	83[a]	81[a]	85[a]	92[a]	89[a]
LSD	14.722	18.56	16.974	17.874	17.529	17.504
F-value	27.64*	25.08*	13.29*	14.98*	21.73*	14.97*

Means followed by different letters within one column differ significantly at ($P < 5\%$)
*Significant at ($P < 1\%$)

http://www.aloki.hu ● ISSN 1589 1623 (Print) ● ISSN 1785 0037 (Online)
DOI: http://dx.doi.org/10.15666/aeer/1605_54055421
© 2018, ALÖKI Kft., Budapest, Hungary

Table 8. *Allelopathic effect of R. stricta leaf hexane extract (HE) on germination percentage (%) of test species on soil*

Treatments	Test species					
	T. aestivum	*A. fatua*	*R. dentatus*	*P. minor*	*E. helioscopia*	*C. album*
$T_{1\ HE}$	89^{a}	82^{a}	49^{c}	50^{d}	91^{a}	49^{d}
$T_{2\ HE}$	91^{a}	84^{a}	56^{c}	61^{c}	93^{a}	64^{c}
$T_{3\ HE}$	92^{a}	85^{a}	68^{b}	71^{b}	94^{a}	75^{b}
$T_{4\ HE}$	93^{a}	86^{a}	84^{a}	88^{a}	95^{a}	92^{a}
LSD	13.588	17.910	15.07	13.844	15.480	15.874
F-value	13.93*	22.96*	37.71*	22.94*	54.38*	12.98*

Means followed by different letters within one column differ significantly at ($P < 5\%$)
*Significant at ($P < 1\%$)

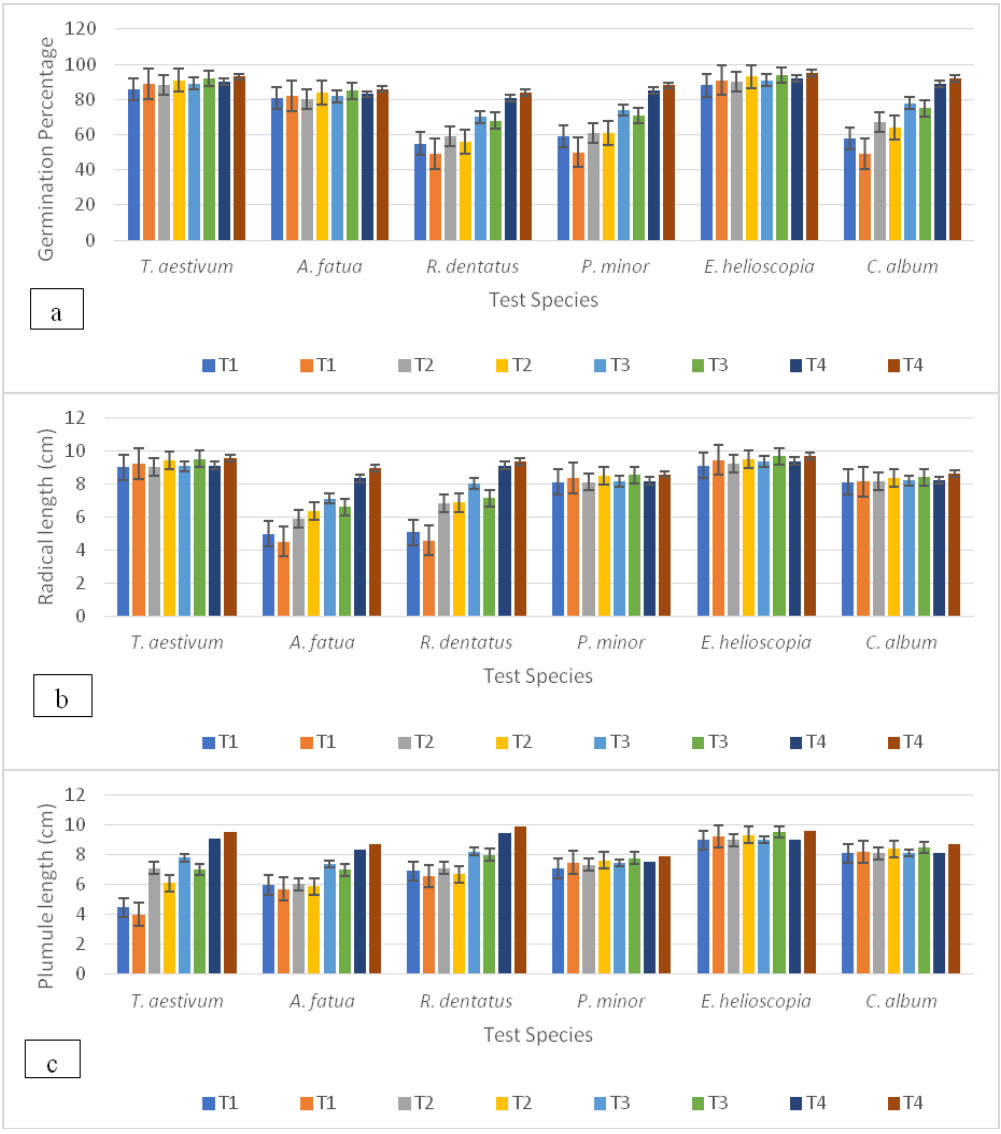

Figure 2. *Allelopathic potential of R. stricta hexane extract against test species on filter paper (FP) and soil (S) on: (a) germination percentage (b) radical length (c) plumule length*

http://www.aloki.hu ● ISSN 1589 1623 (Print) ● ISSN 1785 0037 (Online)
DOI: http://dx.doi.org/10.15666/aeer/1605_54055421
© 2018, ALÖKI Kft., Budapest, Hungary

Radical length

The statistical data concluded that the highest radical length inhibition activity was exhibited by *R. dentatus* (44%) and *A. fatua* (40%) in *R. stricta* hexane extract on filter paper. Similarly, hexane extract on soil caused significant reduction in radical length of *R. dentatus* (51%) and *A. fatua* (50%) compared to control, while *T. aestivum*, *P. minor, E. helioscopia* and *C. album* remained unaffected. The results also illustrated minimum radical length for *R. dentatus* i.e. 46% and 49% on filter paper and soil, respectively (*Tables 9* and *10*). The maximum radical length (96%) was noted for *T. aestivum*, *P. minor, E. helioscopia* and *C. album* (*Fig. 2b*).

Table 9. *Allelopathic effect of R. stricta leaf hexane extract (HE) on radical length (cm) of test species on filter paper*

Treatments	Test species					
	T. aestivum	*A. fatua*	*R. dentatus*	*P. minor*	*E. helioscopia*	*C. album*
$T_{1\ HE}$	9.03[a]	4.99[c]	5.08[d]	8.11[a]	9.13[a]	8.12[a]
$T_{2\ HE}$	9.06[a]	5.87[c]	6.82[c]	8.14[a]	9.22[a]	8.19[a]
$T_{3\ HE}$	9.08[a]	7.13[b]	8.04[b]	8.18[a]	9.37[a]	8.21[a]
$T_{4\ HE}$	9.14[a]	8.35[a]	9.14[a]	8.20[a]	9.41[a]	8.24[a]
LSD	4.2679	0.9692	0.7136	2.4388	1.403	0.9741
F-value	20.22*	486.76*	278.70*	58.00*	55.71*	161.39*

Means followed by different letters within one column differ significantly at ($P < 5\%$)
*Significant at ($P < 1\%$)

Table 10. *Allelopathic effect of R. stricta leaf hexane extract (HE) on radical length (cm) of test species on soil*

Treatments	Test species					
	T. aestivum	*A. fatua*	*R. dentatus*	*P. minor*	*E. helioscopia*	*C. album*
$T_{1\ HE}$	9.26[a]	4.52[c]	4.58[c]	8.39[a]	9.48[a]	8.15[a]
$T_{2\ HE}$	9.46[a]	6.34[b]	6.87[b]	8.48[a]	9.52[a]	8.35[a]
$T_{3\ HE}$	9.52[a]	6.61[b]	7.16[b]	8.56[a]	9.69[a]	8.43[a]
$T_{4\ HE}$	9.58[a]	8.99[a]	9.40[a]	8.61[a]	9.70[a]	8.66[a]
LSD	1.8406	1.3918	1.9912	1.5634	0.3063	1.4662
F-value	51.46*	97.97*	84.01*	76.89*	125.70*	93.12*

Means followed by different letters within one column differ significantly at ($P < 5\%$)
*Significant at ($P < 1\%$)

Plumule length

The *R. stricta* hexane extract significantly inhibited the plumule length of *T. aestivum* (51%), *A. fatua* (29%) and *R. dentatus* (27%) on filter paper. Interestingly, there was no significant effect on plumule elongation of *P. minor, E. helioscopia* and *C. album*. Likewise, *R. stricta* hexane extract significantly inhibited plumule length of *T. aestivum* (58%), *A. fatua* (34%) and *R. dentatus* (34%) in soil. The statistical data concluded that minimum plumule length was noted for *T. aestivum* i.e. 49% and 42% on filter paper and soil, respectively (*Tables 11* and *12*). The statistical analysis revealed

http://www.aloki.hu ● ISSN 1589 1623 (Print) ● ISSN 1785 0037 (Online)
DOI: http://dx.doi.org/10.15666/aeer/1605_54055421
© 2018, ALÖKI Kft., Budapest, Hungary

that maximum plumule length (95%) was noted for *P. minor, E. helioscopia* and *C. album* (*Fig. 2c*).

Table 11. *Allelopathic effect of R. stricta leaf hexane extract (HE) on plumule length (cm) of test species on filter paper*

Treatments	Test species					
	T. aestivum	*A. fatua*	*R. dentatus*	*P. minor*	*E. helioscopia*	*C. album*
$T_{1\ HE}$	4.49^{c}	5.99^{c}	6.93^{c}	7.12^{a}	9.01^{a}	8.11^{a}
$T_{2\ HE}$	7.12^{b}	6.06^{c}	7.13^{c}	7.36^{a}	9.02^{a}	8.12^{a}
$T_{3\ HE}$	7.81^{b}	7.39^{b}	8.24^{b}	7.48^{a}	9.04^{a}	8.13^{a}
$T_{4\ HE}$	9.14^{a}	8.39^{a}	9.46^{a}	7.52^{a}	9.06^{a}	8.14^{a}
LSD	3.7846	1.2971	0.9640	0.8718	0.0182	0.6156
F-value	8.44**	46.74*	57.31*	55.81*	14.11*	111.35*

Means followed by different letters within one column differ significantly at ($P < 5\%$)
*Significant at ($P < 1\%$)

Table 12. *Allelopathic effect of R. stricta leaf hexane extract (HE) on plumule length (cm) of test species on soil*

Treatments	Test species					
	T. aestivum	*A. fatua*	*R. dentatus*	*P. minor*	*E. helioscopia*	*C. album*
$T_{1\ HE}$	4.01^{c}	5.72^{c}	6.59^{c}	7.51^{a}	9.24^{a}	8.21^{a}
$T_{2\ HE}$	6.13^{b}	5.90^{c}	6.72^{c}	7.65^{a}	9.33^{a}	8.42^{a}
$T_{3\ HE}$	7.04^{b}	7.01^{b}	8.01^{b}	7.79^{a}	9.56^{a}	8.51^{a}
$T_{4\ HE}$	9.58^{a}	8.77^{a}	9.94^{a}	7.89^{a}	9.61^{a}	8.71_{a}
LSD	3.7946	2.2971	1.9640	2.8718	4.0182	0.9841
F-value	9.34**	41.64*	53.41*	58.71*	16.31*	246.78*

Means followed by different letters within one column differ significantly at ($P < 5\%$)
*Significant at ($P < 1\%$)

Allelopathic potential of R. stricta methanolic extract

Germination percentage

The methanolic extract of *R. stricta* significantly inhibited germination of *P. minor* (49%), *R. dentatus* (48%) and *C. album* (47%) on filter paper, whereas, no significant effect was noted on the germination of *T. aestivum*, *A. fatua* and *E. helioscopia* showing resistance against extract. Similarly, the same extract significantly suppressed seed germination of *C. album* and *R. dentatus* (51% each), followed by *P. minor* (50%) on soil. It was noted that maximum (95%) germination was observed for *T. aestivum*, *A. fatua* and *E. helioscopia*. Besides, minimum germination was noted for *P. minor* i.e. 51% and *R. dentatus* (49%) on filter paper and soil, respectively (*Tables 13* and *14*). The results revealed that germination reduction of the *C. album*, *P. minor* and *R. dentatus* was concentration dependent (*Fig. 3a*).

http://www.aloki.hu ● ISSN 1589 1623 (Print) ● ISSN 1785 0037 (Online)
DOI: http://dx.doi.org/10.15666/aeer/1605_54055421
© 2018, ALÖKI Kft., Budapest, Hungary

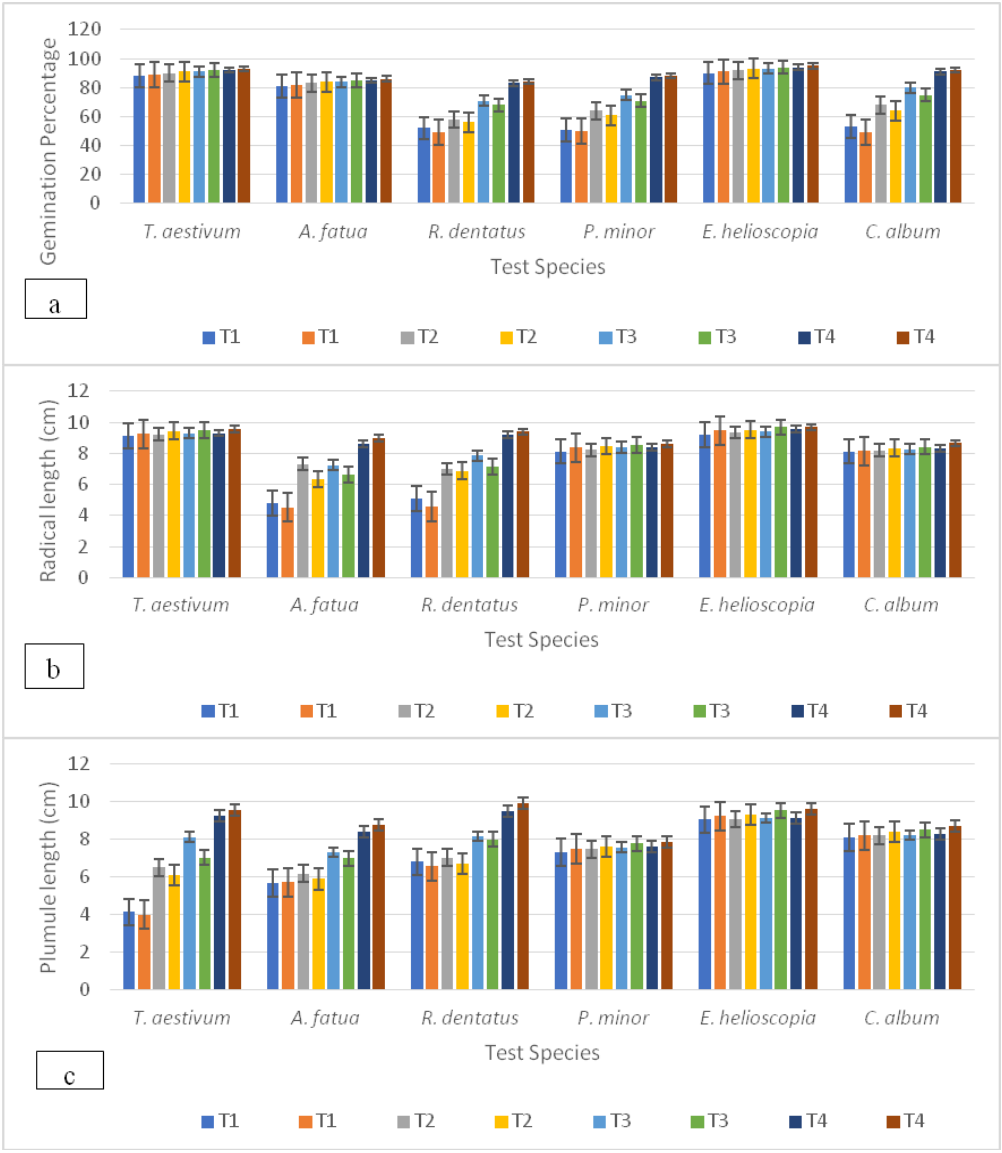

Figure 3. *Allelopathic potential of R. stricta methanolic extract against test species on filter paper (FP) and soil (S) on: (a) germination percentage (b) radical length (c) plumule length*

Table 13. *Allelopathic effect of R. stricta leaf methanolic extract (ME) on germination percentage (%) of test species on filter paper*

Treatments	Test species					
	T. aestivum	*A. fatua*	*R. dentatus*	*P. minor*	*E. helioscopia*	*C. album*
$T_{1\ ME}$	88^{a}	81^{a}	52^{c}	51^{d}	90^{a}	53^{d}
$T_{2\ ME}$	90^{a}	83^{a}	58^{c}	64^{c}	92^{a}	68^{c}
$T_{3\ ME}$	91^{a}	84^{a}	71^{b}	75^{b}	93^{a}	80^{b}
$T_{4\ ME}$	92^{a}	85^{a}	83^{a}	87^{a}	94^{a}	91^{a}
LSD	16.722	16.62	12.74	14.174	15.529	18.34
F-value	28.64*	21.18*	11.39*	12.67*	23.73*	14.75*

Means followed by different letters within one column differ significantly at ($P < 5\%$)
*Significant at ($P < 1\%$)

http://www.aloki.hu ● ISSN 1589 1623 (Print) ● ISSN 1785 0037 (Online)
DOI: http://dx.doi.org/10.15666/aeer/1605_54055421
© 2018, ALÖKI Kft., Budapest, Hungary

Table 14. *Allelopathic effect of R. stricta leaf methanolic extract (ME) on germination percentage (%) of test species on soil*

Treatments	Test species					
	T. aestivum	*A. fatua*	*R. dentatus*	*P. minor*	*E. helioscopia*	*C. album*
$T_{1\ ME}$	89^{a}	82^{a}	49^{c}	50^{d}	91^{a}	49^{d}
$T_{2\ ME}$	91^{a}	84^{a}	56^{c}	61^{c}	93^{a}	64^{c}
$T_{3\ ME}$	92^{a}	85^{a}	68^{b}	71^{b}	94^{a}	75^{b}
$T_{4\ ME}$	93^{a}	86^{a}	84^{a}	88^{a}	95^{a}	92^{a}
LSD	13.588	17.910	15.07	13.844	15.480	15.874
F-value	13.93*	22.96*	37.71*	22.94*	54.38*	12.98*

Means followed by different letters within one column differ significantly at ($P < 5\%$)
*Significant at ($P < 1\%$)

Radical length

The methanolic extract significantly inhibited radical length for *R. dentatus* (45%) and *A. fatua* (44%) on filter paper, whereas, no significant effect was noted for *T. aestivum P. minor, E. helioscopia* and *C. album* showing resistance against extract. Similarly, the applications of extract into soil significantly suppressed radical length of *R. dentatus* (51%) and *A. fatua* (50%) as compared to control. The maximum (96%) radical length was observed for *T. aestivum P. minor, E. helioscopia* and *C. album* (*Tables 15* and *16*). The final data concluded that minimum radical length was noted for *R. dentatus* i.e. 55% and 49% on filter paper and soil, respectively (*Fig. 3b*).

Table 15. *Allelopathic effect of R. stricta methanolic extract (ME) on radical length (cm) of test species on filter paper*

Treatments	Test species					
	T. aestivum	*A. fatua*	*R. dentatus*	*P. minor*	*E. helioscopia*	*C. album*
$T_{1\ ME}$	9.16^{a}	4.81^{c}	5.11^{c}	8.14^{a}	9.19^{a}	8.14^{a}
$T_{2\ ME}$	9.22^{a}	7.31^{b}	7.01^{b}	8.22^{a}	9.36^{a}	8.21^{a}
$T_{3\ ME}$	9.29^{a}	7.25^{b}	7.85^{b}	8.39^{a}	9.40^{a}	8.27^{a}
$T_{4\ ME}$	9.31^{a}	8.64^{a}	9.21^{a}	8.41^{a}	9.56^{a}	8.32^{a}
LSD	3.1490	0.8763	1.7841	1.2929	0.8953	1.340
F-value	22.59*	129.81*	34.17*	66.06*	50.17*	42.47*

Means followed by different letters within one column differ significantly at ($P < 5\%$)
*Significant at ($P < 1\%$)

Table 16. *Allelopathic effect of R. stricta methanolic extract (ME) on radical length (cm) of test species on soil*

Treatments	Test species					
	T. aestivum	*A. fatua*	*R. dentatus*	*P. minor*	*E. helioscopia*	*C. album*
$T_{1\ ME}$	9.26^{a}	4.52^{c}	4.58^{c}	8.39^{a}	9.48^{a}	8.15^{a}
$T_{2\ ME}$	9.46^{a}	6.34^{b}	6.87^{b}	8.48^{a}	9.52^{a}	8.35^{a}
$T_{3\ ME}$	9.52^{a}	6.61^{b}	7.16^{b}	8.56^{a}	9.69^{a}	8.43^{a}
$T_{4\ ME}$	9.58^{a}	8.99^{a}	9.40^{a}	8.61^{a}	9.70^{a}	8.66^{a}
LSD	1.8406	1.3918	1.9912	1.5634	0.3063	1.4662
F-value	51.46*	97.97*	84.01*	76.89*	125.70*	93.12*

Means followed by different letters within one column differ significantly at ($P < 5\%$)
*Significant at ($P < 1\%$)

http://www.aloki.hu ● ISSN 1589 1623 (Print) ● ISSN 1785 0037 (Online)
DOI: http://dx.doi.org/10.15666/aeer/1605_54055421
© 2018, ALÖKI Kft., Budapest, Hungary

Plumule length

Analysis of the data revealed that *R. stricta* methanolic extract significantly suppressed the plumule length of *T. aestivum* (55%), *A. fatua* (33%) and *R. dentatus* (28%) as compared control on filter paper. Interestingly, there was no significant effect on plumule elongation of *P. minor, E. helioscopia* and *C. album*. Likewise, *R. stricta* methanolic extract significantly inhibited plumule length of *T. aestivum* (58%), *A. fatua* (35%) and *R. dentatus* (34%) in soil. The statistical data concluded that minimum plumule length was noted for *T. aestivum* i.e. 45% and 42% on filter paper and soil, respectively (*Tables 17* and *18*). The statistical figures also proposed that maximum plumule length (96%) was noted for *P. minor, E. helioscopia* and *C. album* (*Fig. 3c*).

Table 17. *Allelopathic effect of R. stricta methanolic extract (ME) on plumule length (cm) of test species on filter paper*

Treatments	Test species					
	T. aestivum	*A. fatua*	*R. dentatus*	*P. minor*	*E. helioscopia*	*C. album*
$T_{1\ ME}$	4.15^{d}	5.68^{c}	6.81^{c}	7.32^{a}	9.06^{a}	8.12^{a}
$T_{2\ ME}$	6.52^{c}	6.20^{c}	7.05^{c}	7.48^{a}	9.09^{a}	8.21^{a}
$T_{3\ ME}$	8.14^{b}	7.31^{b}	8.16^{b}	7.59^{a}	9.13^{a}	8.23^{a}
$T_{4\ ME}$	9.28^{a}	8.42^{a}	9.52^{a}	7.62^{a}	9.16^{a}	8.29^{a}
LSD	6.4846	1.4971	0.9240	0.8728	0.2182	1.4428
F-value	5.43**	44.74*	55.31*	55.01*	14.13*	28.95*

Means followed by different letters within one column differ significantly at ($P < 5\%$)
*Significant at ($P < 1\%$)

Table 18. *Allelopathic effect of R. stricta methanolic extract (ME) on plumule length (cm) of test species on soil*

Treatments	Test species					
	T. aestivum	*A. fatua*	*R. dentatus*	*P. minor*	*E. helioscopia*	*C. album*
$T_{1\ ME}$	4.01^{c}	5.72^{c}	6.59^{c}	7.51^{a}	9.24^{a}	8.21^{a}
$T_{2\ ME}$	6.13^{b}	5.90^{c}	6.72^{c}	7.65^{a}	9.33^{a}	8.42^{a}
$T_{3\ ME}$	7.04^{b}	7.01^{b}	8.01^{b}	7.79^{a}	9.56^{a}	8.51^{a}
$T_{4\ ME}$	9.58^{a}	8.77^{a}	9.94^{a}	7.89^{a}	9.61^{a}	8.71^{a}
LSD	3.7946	2.2971	1.9640	2.8718	4.0182	0.9841
F-value	9.34**	41.64*	53.41*	58.71*	16.31*	246.78*

Means followed by different letters within one column differ significantly at ($P < 5\%$)
*Significant at ($P < 1\%$)

Discussion

This study was aimed at investigating allelopathic potential of *R. stricta* by using various solvent (i.e. aqueous, methanolic, hexane) leaf extracts against selected noxious weeds of wheat crop. The germination percentage, radicle length and plumule length were observed. The results revealed that all plant extracts showed significant allelopathic activity, however, the same was varied from species to species as well as solvents. Overall, methanolic extract showed the highest degree of seed germination

http://www.aloki.hu ● ISSN 1589 1623 (Print) ● ISSN 1785 0037 (Online)
DOI: http://dx.doi.org/10.15666/aeer/1605_54055421
© 2018, ALÖKI Kft., Budapest, Hungary

percentage inhibition, radical and plumule length for *C. album*, *P. minor* and *R. dentatus*.

The results revealed that *R. stricta* aqueous extract significantly inhibited germination percentage of *C. album, R. dentatus* and *P. minor* (*Tables 1* and *2*). The results revealed that germination percentage reduction of the *C. album*, *R. dentatus* and *P. minor* was concentration dependent (*Fig. 1a*). As far as radical length is concerned, the aqueous extract had significantly affected radical length for *R. dentatus* and *A. fatua* (*Tables 3* and *4*). The results revealed that allelopathic inhibitory effect was concentration dependent for *R. dentatus* and *A. fatua* (*Fig. 1b*). The current study indicated that aqueous extract of *R. stricta* significantly inhibited the plumule length of *A. fatua* and *R. dentatus* as compared to control, on filter paper as well as on soil (*Tables 5* and *6*). The results agree with that of Khan et al. (2011) who reported germination inhibition of *Zea mays* by stem aqueous extracts of *R. stricta*, while plumule and radical growth was significantly decreased by aqueous leave extract. Like the present investigation, the later study also revealed that the inhibitory effects were directly proportional to the extract concentration. In another study, leaf extracts of *R. stricta* significantly inhibited germination percentage and decreased plumule and radical length of seedlings of *Vicia faba, Hordeum vulgare* and *Triticum aestivum* (Ebid, 2016). Aqueous extracts from the leaves of *R. stricta* significantly reduced germination and growth of *Salsola villosa* by hampering functioning of the membrane and photosynthetic capacity due to reduced synthesis of chlorophyll pigments (Alqarawi et al., 2018).

R. stricta leaf aqueous extract owed to some toxic factors of the extract. Noteworthy, there was variation among the test treatments of different concentrations of *R. stricta* extract and control. There was significant morphological variation in the radical and plumule elongation of the tested weeds that may be attributed due to the presence of various allelochemicals in plant extract. Allelopathic interaction more effectively inhibited growth on soil in contrast to filter paper (Hegazy and Fadl-Allah, 1995; El-Khatib, 2000). These findings agreed with those of Migahid and El-khazan (2002), who studied the allelopathic effect of *Zygophyllum* aqueous extract on sesame and corn.

This study exhibited the allelopathic activity of various solvents on the germination and growth parameters of selected weeds. Overall, the activity of *R. stricta* extracts was found concentration dependent. Wardle et al. (1992) reported a concentration dependent inhibition of radical, plumule growth and seed germination for some weeds by *R. stricta* extract. Besides, Alam (1990) and Bora et al. (1999) also observed concentration dependent inhibition of plumule length by *R. stricta* extract. Another study revealed that there was significant reduction in germination, radical and plumule length of *Z. mays* by *R. stricta* extract (Zackrisson and Nilsson, 1992). El-khawas and Shehata (2005) stated that the inhibitory effect of allelochemicals on seed growth due to changes in enzyme activities that affect the transport of storage substances.

Our results revealed that *R. stricta* methanolic leaf extract imposed significant inhibitory effects on the germination and growth parameters of all the tests weeds. The findings of current study confirmed the earlier findings on cowpea and rice plumule, radicle length and germination that were significantly checked with increasing concentration of *R. stricta* methanolic leaf extract (Jadhar and Gayanar, 1992). Moreover, seed germination and seedling growth of different crops and weed had been significantly checked by inhibitory potential of *R. stricta* extracts (Lisanework and Michelson, 1993; Khan et al., 2008).

http://www.aloki.hu ● ISSN 1589 1623 (Print) ● ISSN 1785 0037 (Online)
DOI: http://dx.doi.org/10.15666/aeer/1605_54055421
© 2018, ALÖKI Kft., Budapest, Hungary

Suppressive effect on plumule length and seed germination was also described by Tefera (2002) and Siddiqui et al. (2009). These findings were in accordance to previous studies who stated that *R. stricta* leaf extract reduced growth of weeds species (Maciel et al., 2003; Kaul and Bansal, 2002). Germination response of various field crops varies in the presence of *R. stricta* leaf extract that confirms our observation of the differences in germination response of tested species. Several studies demonstrated the allelopathic potential of *Parthenium hysterophorus* (Tawaha and Turk, 2003), *Brassica nigra* (Singh et al., 2003) and *Raphanus raphanistrum* (Batish et al., 2002).

The leaf extracts were more toxic and more allelopathic in nature owing to relatively higher inhibitory potential in contrast to other plant parts (Hussain and Gadoon, 1981; Norsworthy, 2003). Similar allelopathic effects were reported from other plants (Inderjit and Duke, 2003; Hussain et al., 2011).

Conclusion

This study was aimed at evaluation of allelopathic potential of *R. stricta* against some noxious weeds of wheat crop by using aqueous, hexane and methanolic extracts on filter paper and soil. The results revealed that methanolic extract highly reduced seed germination percentage of *C. album*, *P. minor* and *R. dentatus*. The same extract caused significant radical and plumule length reduction of *R. dentatus* and *A. fatua*. Based on the results, it can be concluded that *R. stricta* showed good allelopathic activity that may be used in future herbicide screening program prior to launch in the market.

Acknowledgements. This paper is extracted from the PhD thesis of the first author.

REFERENCES

[1] Alam, S. M. (1990): Effect of wheat straw extract on germination and seedling growth of wheat (cv. Pavon). – Wheat Informative Service 71: 16-18.

[2] Alqarawi, A. A., Hashem, A., Kumar, A., Al-Arjani, A. B. F., Abd-Allah, E. F., Dar, B. A., Egamberdieva, D. (2018): Allelopathic effects of the aqueous extract of Rhazya stricta on growth and metabolism of *Salsola villosa*. – Plant Biosystematics DOI: 10.1080/11263504.2018.1439117.

[3] Anwar, T., Khalid, S., Arafat, Y., Sadia, S., Riaz, S. (2013): Allelopathic suppression of *Avena fatua* and *Rumex dentatus* in associated crops. – Pakistan Journal of Weed Science Research 19: 31-43.

[4] Anwar, T., Khalid, S., Saeed, M., Mazhar, R.., Qureshi, H., Rashid, M. (2016): Allelopathic interference of leaf powder and aqueous extracts of hostile weed: *Parthenium hysterophorus* (Asteraceae). – Science International 4: 86-93.

[5] Anwar, T., Khalid, S., Mazhar, R., Qureshi, H., Rashid, M. (2017a): Herbicidal potential of selected species to overcome weed infestation in *Triticum aestivum*, *Zea mays* and *Helianthus annuus*. – Pakistan Journal of Weed Science Research 23: 49-63.

[6] Anwar, T., Khalid, S., Panni, M. K., Qureshi, H., Rashid, M. (2017b): Allelopathic effect of *Euphorbia helioscopia* on *Avena fatua*, *Rumex dentatus*, *Helianthus annuus*, *Zea mays* and *Triticum aestivum*. – Pakistan Journal of Weed Science Research 23: 165-177.

[7] Arora, K., Batish, D. R., Singh, H. P., Kohli, R. K. (2015): Allelopathic potential of the essential oil of wild marigold (Tagetes minuta L.) against some invasive weeds. – Journal of Environmental & Agricultural Sciences 3: 56-60.

http://www.aloki.hu ● ISSN 1589 1623 (Print) ● ISSN 1785 0037 (Online)
DOI: http://dx.doi.org/10.15666/aeer/1605_54055421
© 2018, ALÖKI Kft., Budapest, Hungary

[8] Batish, D. R., Singh, H. P., Kohli, R. K., Saxena, D. B., Kaur, S. (2002): Allelopathic effect of *Parthenium* against two weedy species, *Avena fatua* and *Bidens pilosa*. – Environmental Experimental Botany 47: 149-155.
[9] Biljana, M. B., Kragujevac, D. Z. J. (2015): Allelopathic relations of selected cereal and vegetable species during seed germination and seedling growth. – Journal of Science 37: 135-142.
[10] Bora, I. P., Singh, J., Borthakur, R., Bora, E. (1999): Allelopathic effect of leaf extracts of *Acacia auriculiformis* on seed germination of some agricultural crops. – Annals Forestry 7: 143-146.
[11] Chon, S. U., Jang, H. G., Kim, D. K., Kim, Y. M., Boo, H. O., Kim, Y. J. (2005): Allelopathic potential in lettuce (Lactuca sativa L.) plants. – Scientia Horticulture 106(3): 309-317.
[12] Dallali, S., Rouz, S., Aichi, H., Hassine, H. B. (2017): Phenolic content and allelopathic potential of leaves and rhizosphere soil aqueous extracts of white horehound (*Maribum vulgare* L.). – Journal of New Sciences 39: 342-353.
[13] Dayan, F. E., Romagni, J. G., Duke, S. O. (2000): Investigating the mode of action of natural phytotoxins. – Journal of Chemical Ecology 20: 2079-2093.
[14] Delcour, I., Spanoghe, P., Uyttendaele, M. (2015): Literature Review: Impact of climate change on pesticide use. – Food Research International 68: 7-15.
[15] Ebid, A. I. (2016): Allelopathic effect of three wild species on seed germination and seedling growth of *Vicia faba*, *Hordeum vulgare* and *Triticum aestivum*. – Journal Agricultural Ecology Research International 6(1): 1-7.
[16] El-Khatib, A. A. (2000): The ecological significance of allelopathy in the community organization of allhagrae-corum. – Biology Plantarum 43: 42-431.
[17] El-Khawas, S. A., Shehata, M. M. (2005): The allelopathic potentialities of *Acacia nilotica* and *Eucalyptus rostrata* on monocot (*Zea mays* L.) and dicot (*Phaseolus vulgaris* L). – Plant Biotechnology 4: 23-34.
[18] Hegazy, A. K., Fadl-Allah, E. M. (1995): Inhibition of seed germination and seedling growth by *Cleome droserifolia* and allelopathic effect on fungi. – Egypt Journal Arid Environment 29: 3-13.
[19] Hussain, F., Gadoon, M. A. (1981): Allelopathic effects of *Sorghum vulgare* Pers. – Oecologia 51: 284-288.
[20] Hussain, M. I., Gonzalez, L., Reigosa, M. J. (2011): Allelopathic potential of *Acacia melanoxylon* on the germination and root growth of native species. – Weed Biology Management 11: 18-28.
[21] Inderjit, Duke, S. O. (2003): Eco-physiological aspects of allelopathy. – Planta 217: 529-539.
[22] Jadhar, B. B., Gayanar, D. G. (1992): Allelopathic effect of *Acacia auriculiformis* on germination of rice and cowpea. – Indian Journal Plant Physiology 1: 86-89.
[23] Kaul, S., Bansal, G. L. (2002): Allelopathic effect of *Ageratina adenophora* on growth and development of *Lantana camara.* – Indian Journal of Plant Physiology 7: 195-197.
[24] Khan, M., Hussain, F., Musharaf, S. (2011): Allelopathic effects of *Rhazya stricta* decne on seed germination and seedling growth of maize. – African Journal Agricultural Research 6(30): 6391-6396.
[25] Khan, M. A., Hussain. I., Ahmad, E. (2008): Allelopathic effect of *Eucalyptus* (*Eucalyptus camaldulensis* L.) on germination and seedling growth of (*Triticum aestivum* L.). – Pakistan Journal of Weed Science Research 14: 9-18.
[26] Lisanework, N., Michelen, A. (1993): Allelopathy in agro forestry systems. The effects of leaf extracts of *Eucalyptus* species on three crops. – Agro-forestry Systematics 21: 63-74.
[27] Maciel, C. D. G., Correa, M. R., Alves, E., Negrisoli, E., Velini, E. D., Rodrigues, J. D., Ono, E. O., Boaro, C. S. F. (2003): Influence of *Brachiaria decumbens* straw management on the initial development of *Glycine max* and *Euphorbia heterophylla*. – Plant Weed 213: 635-637.

http://www.aloki.hu ● ISSN 1589 1623 (Print) ● ISSN 1785 0037 (Online)
DOI: http://dx.doi.org/10.15666/aeer/1605_54055421
© 2018, ALÖKI Kft., Budapest, Hungary

[28] Manimegalai, A., Manikandan, T., Sheela, R., Geetha, S. (2012): Allelopathic influence of *Tectona grandis* leaves on the germination of black gram (*Vigna mungo* L.) and green gram (*Vigna radiate* L.). – International Journal of Current Science 12: 241-244.
[29] Migahid, M. M., El-khazan, M. M. (2002): Allelopathic potential in *Zygophyllum album* and its effect on growth and metabolism of some crop plants. – International Conference on Biological Sciences Tanta Uni. 2: 46-63.
[30] Nekonam, M. S., Kraimmojeni, H., Sharifnabi, B., Razmjoo, J., Amini, H., Bahrami, F. (2014): Assessment of some medicinal plants for their allelopathic potential against redroot pigweed (*Amaranthus retroflexus*). – Journal of Plant Protection and Research 54: 90-95.
[31] Norsworthy, J. K. (2003): Allelopathic potential of wild radish (*Raphanus raphanistrum*). – Weed Technology 17: 307-313.
[32] Omar, A., Almaghrabi. (2008): Allelopathic effect of *Rhazya stricta* leaves leachate on germination and seedlings of some plants. – Egypt Journal of Experimental Biology 4: 99-103.
[33] Qureshi, R., Waheed, A., Arshad, M. (2009): Weed communities of wheat crop in district Toba Tek Singh, Pakistan. – Pakistan Journal of Botany 41: 239-245.
[34] Sabir, S. H., Khan, E. A., Shah, H., Ahmed, N., Khan, J., Sadozai, G. U. (2016): Allelopathic sorghum water extract helps to improve yield of sunflower (*Helianthus annuus* L.). – Pakistan Journal of Botany 48: 1197-1202.
[35] Sahu, A., Devkota, A. (2013): Allelopathic effects of aqueous extract of leaves of *Mikania micrantha* H. B. K. on seed germination and seedling growth of *Oryza sativa* L. and *Raphanus sativus* L. – Science World Journal 11: 90-93.
[36] Shahid, M., Ahmad, B., Khattak, R. A., Hassan, G. Khan, H. (2006): Response of wheat and its weeds to different allelopathic plant water extracts. – Pakistan Journal of Weed Science Research 12: 61-68.
[37] Siddiqui, S., Meghvansi, M. K., Yadav, K., Yadav, R., Wani, F. A., Ahmad, A. (2009): Efficacy of aqueous extracts of five arable trees on the seed germination of *Pisum sativum* L. var. VRP-6 and KPM-522. – Botany Research International 2: 30-35.
[38] Singh, H. P., Batish, D. R., Pandher, J. K., Kohli, R. K. (2003): Assessment of allelopathic properties of *Parthenium hysterophorus* residues. – Agricultural Ecosystem and Environment 95: 537-541.
[39] Tawaha, A. M., Turk, M. A. (2003): Allelopathic effects of black mustard (*Brassica nigra*) on germination and growth of wild barley (*Hordeum spontaneum*). – Journal Agronomy and Crop Sciences 189: 298-303.
[40] Tefera, T. (2002): Allelopathic effects of *Parthenium hysterophorus* extracts on seed germination and seedling growth of *Eragrostis tef* (Zucc.) Trotter. – Journal Agronomy and Crop Sciences 188: 306-310.
[41] Thi, H. L., Lan, P. T. P., Chin, D. V., Kato-Noguchi, H. I. S. A. S. H. I. (2008): Allelopathic potential of cucumber (Cucumis sativus) on barnyard grass (Echinochloa crus-galli). – Weed Biology Management 8(2): 129-132.
[42] Wardle, D. A., Nicholson, K. S., Ahmed, M. (1992): Comparison of osmotic and allelopathic effects of grass leaf extracts on grass seed germination and radicle elongation. – Plant and Soil 140: 315-319.
[43] Zackrisson, O., Nilsson, M. C. (1992): Allelopathic effects by *Empetrum hermaphroditum* on seed germination of two boreal tree species. – Canadian Journal of Forest Research 22: 1310-131.

http://www.aloki.hu ● ISSN 1589 1623 (Print) ● ISSN 1785 0037 (Online)
DOI: http://dx.doi.org/10.15666/aeer/1605_54055421
© 2018, ALÖKI Kft., Budapest, Hungary

SPATIAL DISTRIBUTION OF THERMAL STRESSES IN IRAN BASED ON PET AND UTCI INDICES

MOHAMMADI, B.[1*] – GHOLIZADEH, M. H.[1] – ALIJANI, B.[2]

[1]*Department of Climatology, Faculty of Natural Resources, University of Kurdistan Sanandaj, Iran*

[2]*Center of Excellence for Spatial Analysis of Environmental Hazard, Kharazmi University Tehran, Iran*

**Corresponding author*
e-mail: b.mohammadi@uok.ac.ir; phone: 98-918-877-5160

(Received 9th Jun 2018; accepted 1st Aug 2018)

Abstract. Cognition of the bioclimatic conditions in any place can be the first step in conducting many environmental studies. This study was performed with the aim of determining the thermal stress of Iran. For this purpose, the daily data of the climatic variables in 288 synoptic stations were prepared from the Iran Meteorological Organization during the period 1981-2010. First, the bioclimatic conditions in each of the stations were calculated based on UTCI (Universal Thermal Climate Index) and PET (Physiologically Equivalent Temperature) indices. Then, using the thermal stress of 288 synoptic stations, the bioclimatic conditions throughout Iran were interpolated using a Simple Kriging method. The results of this study showed that the bioclimatic conditions are immensely varied spatially and temporally, such that in specific times all bioclimatic conditions can be seen in Iran. Also, during the year, each place can experience different bioclimatic conditions. Based on UTCI, extreme cold and extreme heat stress are the only bioclimatic conditions that do not exist during the year. However, based on PET, all bioclimatic conditions exist during the year. Also July and January, respectively, are the hottest and coldest months of the year. Based on UTCI in April, October and November, more than 70% of Iran has comfortable conditions, whereas PET showed that in March and October 24.6 and 23.7% experienced comfortable conditions respectively. It seems that the obtained results of PET index have high efficiency in relationship with UTCI index to show Iran's bioclimatic conditions.
Keywords: *applied climatology, bioclimatic conditions, climatic comfort, human heat balance, extreme climatic conditions*

Introduction

Climate and weather conditions are the most important components of the environment. Atmospheric conditions can have an effect on some activities and even create restrictions in our lives. Identification and understanding the weather conditions in any place is inevitable and necessary. It is clear that there is no place in the world experiencing favourable conditions and thermal comfort throughout the year. Nowadays, there has been much interest in the study of differentiation of bioclimatic conditions in outdoor spaces (Nikolopoulou, 2004; Geletič et al., 2018). Most of the research performed in different countries has been focusing on aspects such as the relations between thermal comfort, microclimate, behavior and use of place and spatial variation (Nikolopoulou and Lykoudis, 2006 and 2007; Thorsson et al., 2007; Kántor et al., 2012a, b). Such research is often carried out because of climate change and increased occurrence of heat stress in the earth's surface (Frich et al., 2002; Givoni et al., 2003; Matzarakis et al., 2013). An important use of bioclimatic studies is energy management and architecture. In many parts of Iran, architecture is designed to harmonize with the climate (Pourvahidi and Ozdeniz, 2013). In general, for

http://www.aloki.hu ● ISSN 1589 1623 (Print) ● ISSN 1785 0037 (Online)
DOI: http://dx.doi.org/10.15666/aeer/1605_54235445
© 2018, ALÖKI Kft., Budapest, Hungary

comprehensive and sustainable development, environmental studies, especially bioclimatic studies are very important. In the past years, many indices on different aims and goals were developed to assess the suitability of climate for tourism activities and thermal stress issues including adaptation factors (Morgan et al., 2000; Maddison, 2001; Lise and Tol, 2002; Potchter et al., 2018). The recognition of human bioclimatic comfort in geographical areas is important for the planning of tourism (Matzarakis, 2006; Kovács et al., 2017). It could also help in the planning of building and housing, architectural patterns and the use of natural attractions of ecotourism in environmental planning (Ramazani Gourbi, 2010; Milošević et al., 2016).

The evaluation of bioclimatic conditions and atmospheric variables in each place can be used to choose the best time and place to travel, requirements that are important for tourism purposes (Caliskan et al., 2012). For example, research by Shakoor (2011) showed that in the Yazd province, the best season for tourists activities is autumn and the most ideal bioclimatic conditions with the emphasis on tourists health is seen in the Anar region (south west of Yazd province). Evaluation of the role of climate on tourism in the northwest of Iran, using the PET (Physiologically Equivalent Temperature) index showed that the months of June, July and August are in the comfortable category representing the most suitable months for tourism and tourist activities (Farajzadeh and Matzarakis, 2009). In another study using the Predicted Mean Vote (PMV) index the highest level of climatic comfort for Tabriz is in August, July and September, while the lowest value of climatic comfort is in November, December, January, February and March (Ghavidel Rahimi and Ahmadi, 2013). In another study, Eslami and Tirandaz (2011) showed up in their study that there are suitable conditions during the days, from May to November and during the night, from June to September in the Gilan province. There are several indicators to check the bioclimatic conditions. According to research by Cendrowska (2013) UTCI (Universal Thermal Climate Index) compared to the PET index is more efficient in assessing the bioclimatic conditions of urban areas for tourism and recreational purposes. In addition, climatic conditions can affect the health and welfare of humans. For example cold or very hot weather types, especially in young people and children can aggravate respiratory diseases (Lecha Estela, 1998). Several studies on bioclimatic conditions in different regions have been carried out.

Most studies that have been done in this field in Europe and the United States have been centered on human health (Scott et al., 2004; Ruuhela et al., 2017; Basarin et al., 2018). For example, the role of the climate on mortality rates in US cities was studied by Kalkstein (2008). The Dadbakhsh et al. (2017) study was conducted to evaluate the relation between respiratory-related mortality and temperature in Shiraz, Iran. Heat stress in Greece stuadied by Matzarakis and Mayer (1997). In Austria, has been studied heat-related mortality in Vienna (Matzarakis et al., 2011). A similar study was conducted by Nastos and Matzarakis (2008) on Athens. Such studies in Japan, to assess the environmental effects and in particular the effect of weather conditions on human activities and behaviors have also been done (Ichinose et al., 2008; Matzarakis, 2008). Studies in this discipline have progressed in China, similarly to popular studies in Europe, although the climatological background and acclimation potential of the peoples of China are partially similar to those of Japan.

Temperature and humidity are the important determinants of the bioclimatic conditions in any place. In addition to these two variables, wind speed, cloudiness and vapor pressure have an important role in our sense of climatic conditions. Though, each person is affected by a series of climatic variables simultaneously, their perception,

http://www.aloki.hu ● ISSN 1589 1623 (Print) ● ISSN 1785 0037 (Online)
DOI: http://dx.doi.org/10.15666/aeer/1605_54235445
© 2018, ALÖKI Kft., Budapest, Hungary

feeling and response to these factors, however, due to physiological characteristics and coverage, are different (Lin et al., 2011). The review of a number of recent studies has shown that identification of bioclimatic regions has become an attractive issue worthy of investigation. These studies were focusing on tourism activities, diseases and health (Matzarakis, 2006). In this study, bioclimatic zones of Iran were identified by UTCI and PET indices. These indices are the best indicators used to assess the bioclimatic conditions in all climatic regions (Richards and Havenith, 2007; Bröde et al., 2009; Matzarakis et al., 1999).

The main purpose of current research is study of the bioclimatic conditions of Iran using PET and UTCI indexes. In fact, the obtained results of research can be the foundation of other research including planning of building and housing, architectural patterns, ecotourism, health, and so on. It is pinpointed that the two mentioned indexes rarely have been performed to show the bioclimatic conditions of Iran based on monthly scale in previously. Therefore, the characteristics and scope of each area based on bioclimatic regions were evaluated and final results of both indices were compared.

Materials and methods

In this study, the bioclimatic conditions in 288 synoptic stations of Iran based on the PET and UTCI indices were evaluated. However, these stations studied, did not have the statistical period equal. For example, Tehran, Isfahan, Tabriz, Mashhad and some old stations had a statistical period of more than 30 years, while in some other stations; the length of the survey period was less than 10 years.

Therefore, due to the inequality of the length of the study period, their long-term average daily was used. If the station has daily 10-year data, the long- term daily average of that station is calculated based on 10 years. For stations with more or less data, the same calculations have been done. In fact, in this study have been used long-term average daily data and maps provide with this data.

Atmospheric variables including average temperature, wind speed, relative humidity, cloudiness, and water vapor pressure were used. A database of meteorological variables mentioned was created for each station on a daily basis. After calculating the bioclimatic conditions of each station on daily, the long-term average daily thermal stress was calculated. Then, using interpolation techniques, bioclimatic conditions in Iran was estimated. The PET and UTCI indices were calculated by RayMan and BioKlima software respectively. Both indices can be calculated by several meteorological variables manually. But manual calculations are often difficult and very complex. Therefore, in most bioclimatic indices related software are often used in these cases (Mohammadi and Karimi, 2017). In this research, the homogeneity of the data was done using a Kolmogorov-Smirnov test .The data used were normal distribution, so their homogeneity was confirmed. The data used was obtained from the Meteorological Organization of Iran (*Fig. 1*).

Usually studies carried out in the field of bioclimatic conditions are in two different groups; bioclimatic conditions in outdoor and indoor spaces. Theoretically, the same indicators that the study of thermal stress indoors (climate discussion of architecture) are used, can also be used in open spaces of thermal stress. But the indices used for any geographic environment should be precisely identified. In fact, in evaluating thermal stress in outdoor spaces, many climate variables are not in the control of the researcher. So to solve this problem, the UTCI and PET, with the aim of a better assessment of

http://www.aloki.hu ● ISSN 1589 1623 (Print) ● ISSN 1785 0037 (Online)
DOI: http://dx.doi.org/10.15666/aeer/1605_54235445
© 2018, ALÖKI Kft., Budapest, Hungary

thermal stress for the outdoors, were presented. In this study, to investigate thermal conditions of Iran, two indices (UTCI and PET) as the biometeorological indices based on the human heat budget are applied (Cendrowska, 2013). In fact, UTCI offers a better portrayal of biothermal conditions for human beings compared to other indices Temperature Effective (TE), Wet Bulb Globe Temperature (WBGT), Heat Stress Index (HIS), Wind Chill Temperature (WCT), Physiological Subjective Temperature (PST) and Physiological Strain (PhS) (Blażejczyk et al., 2012). Many variables are used to calculate and estimate this index. In addition to climatic variables, some personal variables such as metabolic rate and thermal resistance of clothes, was chosen. Another benefit of using PET and UTCI indices is their calculating units (°C). Calculation in degrees Celsius creates a better understanding of these indices by experts in the fields of energy management, health and environmental planing (Lin and Matzarakis, 2008). To calculate the UTCI index, variables of air temperature (°C), relative humidity (%), vapor pressure (hPa), wind speed (m/s) and the sun altitude (degree), during the period 1981-2010, were used. Therefore, a database of these variables for each of the stations was prepared to a dimension of 365 * 5. In this database, 5 is the number of variables and 365 is also the number of days of the year. For each station, bioclimatic conditions of Iran were calculated individually. Although UTCI index can be calculated by complex equations, in this study Bioklima 2.6 software was used to assess of thermal stresses. Different values of the UTCI have been classified according to thermal stress (*Table 1*). All steps for calculating the UTCI index were also performed for the PET index. The PET Index is one of the best indicators that based on the human energy balance equation (Matzarakis et al., 1999; Gulyas and Matzarakis, 2007; Charalampopoulos et al., 2013). The results of this index can be displayed as bioclimatic maps. The PET index is appropriate to evaluate the bioclimatic conditions in different geographical regions (Gulyas, 2005; Matzarakis et al., 2013). In this research, air temperature (°C), relative humidity (%), average wind speed (m/s), and cloudiness (Octas) were used to calculate PET values for Iran.

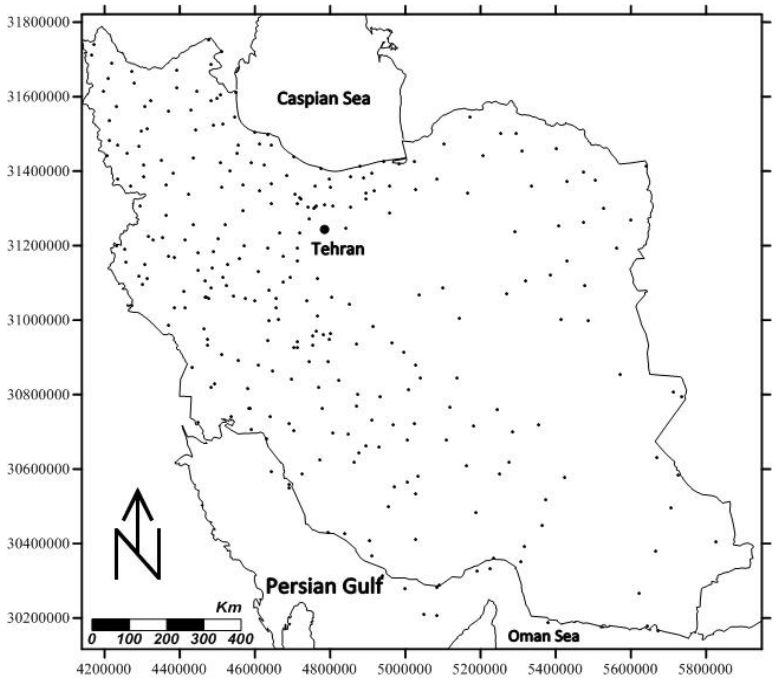

Figure 1. *The geographic distribution of 288 synoptic stations in Iran*

http://www.aloki.hu ● ISSN 1589 1623 (Print) ● ISSN 1785 0037 (Online)
DOI: http://dx.doi.org/10.15666/aeer/1605_54235445
© 2018, ALÖKI Kft., Budapest, Hungary

Table 1. *Ranges UTCI and of PET indices for different grades of thermal stress and thermal perception by human beings (Ketterer and Matzarakis, 2012)*

Thermal stress based on UTCI index (°C)		**Thermal perception based on PET index (°C)**	
Extreme heat stress	above +46	Very hot	below 4
Very strong heat stress	+38 to +46	Hot	4 to 8
Strong heat stress	+32 to +38	Warm	8 to 13
Moderate heat stress	+26 to +32	Slightly warm	13 to 18
No thermal stress	+9 to +26	Comfortable	18 to 23
Slight cold stress	+9 to 0	Slightly cool	23 to 29
Moderate cold stress	0 to -13	Cool	29 to 35
Strong cold stress	-13 to -27	Cold	35 to 41
Very strong cold stress	-27 to -40	Very cold	above 41
Extreme cold stress	below -40	-	-

Due to the complexity of the calculations, in this study, PET and UTCI indices were calculated using RayMan 1.2 and BioKlima 2.6 software respectively.

The PET index is calculated as follows in several stages:

- In the first step body temperature must be calculated with MEMI (Munich Energy balance Model for Individuals) model based on meteorological parameters.
- In the second step the calculated values of mean skin temperature and core temperature imported into the MEMI model and energy balance equation for air temperature based on T_a (with v = 0.1 m/s, VP = 12 hPa and $T_{mrt} = T_a$) dissolved. Eventually air temperature obtained is equivalent to the PET.

The UTCI is defined as the air temperature (t) of the reference condition causing the same physiological response as the actual condition. Thus, UTCI is the air temperature which would produce under reference conditions the same thermal strain as in the actual thermal environment. Therefore, with the help of the mathematical relation, the UTCI can be calculated:

$$UTCI = CalcUTCI\ (temp, wind, mrt, hum)$$

Where temp: air temperature (°C); wind: wind speed (m/s); mrt: mean radiant temperature (°C); hum: humidity ratio (%).

By calculating the bioclimatic conditions of all stations, two databases from output UTCI and PET indices with dimensions of 288 * 365 were prepared. In this database, 365 and 288, respectively, are the numbers of days of the year and stations. One purpose of this research was the mapping of Iran's bioclimatic conditions. To draw these maps from the estimated heat stress, data of 288 of Iran's synoptic stations based on PET and UTCI were used. In fact, using thermal stress to calculate these stations, interpolation was performed. In the atmospheric and geographical field of numerical analysis, interpolation is a method of constructing new data points within the range of a discrete set of known data points. In some cases it may be the average value of a parameter to be estimated over an area. This average, by the Simple Kriging method

http://www.aloki.hu ● ISSN 1589 1623 (Print) ● ISSN 1785 0037 (Online)
DOI: http://dx.doi.org/10.15666/aeer/1605_54235445
© 2018, ALÖKI Kft., Budapest, Hungary

will be calculated on different parts of that region and from their average the results will be achieved. Therefore, in this study, the Simple Kriging method was used to estimate Iran's bioclimatic conditions. In Simple Kriging, all input points are used to calculate each output pixel value. The output of a Simple Kriging method is a raster map. For each pixel in the output map, a value is calculated by an interpolation on input point values. Finally, based on this database, bioclimatic conditions in Iran were estimated. Thus, for each day throughout the country, a bioclimatic map was prepared. In addition to using monthly averages of bioclimatic conditions, bioclimatic maps were drawn.

Results

Annual and seasonal differentiation of bioclimatic conditions

Based on the UTCI index, Iran's bioclimatic conditions during the year showed, on average, a comfort bioclimatic condition prevailing in 45% of Iran. In total, 31.7% of Iran has gone towards a warming condition over the year (the moderate heat stress, strong and very strong heat stress). On the other hand, cold bioclimatic conditions (slight cold stress, moderate cold stress, strong cold stress and very strong cold stress) in 21.3% of Iran have been seen. It should be noted, according to UTCI, strong and very strong heat stress condition, did not prevail in any part of Iran over the year. Each of the bioclimatic conditions during different months of the year, have shown a different situation. So, strong cold stress and strong heat stress conditions have not been seen, at any time, in Iran. Other bioclimatic conditions, such as very strong cold stress, has been record in Iran, for both January (0.9%) and February (0.2%). Also a very strong heat stress condition has been determined in Iran, for June (6.5%), July (10.7%) and August (6.8%). PET analysis on Iran's bioclimatic conditions during the year showed that, on average, a comfort bioclimatic condition has been experienced in 11.9% of Iran. In total, 55.6% of Iran has experienced warming conditions over the year (slightly warm, warm, hot and very hot). On the other hand, 32.5% of Iran has experienced cold conditions (low cold stress, cold stress, strong and very strong cold stress). It should be noted, according to this index, very cold and hot bioclimatic conditions, 3.5 and 15.1%, respectively, are in the lowest and highest parts of Iran. In general, according to *Table 2,* we can say that each of the bioclimatic conditions during the year have shown a different situation. For example, comfortable and slightly warm conditions were seen throughout the year in Iran. Other bioclimatic conditions, like very cold, have been reported in Iran, during winter and autumn. Also a very hot condition has been experienced in Iran during spring and summer. Other conditions and affected zones in different seasons can be seen in *Table 2* and *Figure 2*.

In general, in the annual assessment of PET and UTCI indices from Iran, significant differences were observed in thermal stress. Comparing Iran's annual differentiation of bioclimatic conditions based on mentioned indices, suggests that the PET index has a more reasonable estimate of Iran's thermal comfort compared to the UTCI index. Because Iran was located in the world's desert belt and also identified as an arid and semi-arid region, the thermal comfort does not dominate climatic conditions. Hence PET's assessment of Iran's thermal comfort is closer to the climatic reality. The difference in the quality of assessment of these indices can also be seen clearly in monthly maps.

http://www.aloki.hu ● ISSN 1589 1623 (Print) ● ISSN 1785 0037 (Online)
DOI: http://dx.doi.org/10.15666/aeer/1605_54235445
© 2018, ALÖKI Kft., Budapest, Hungary

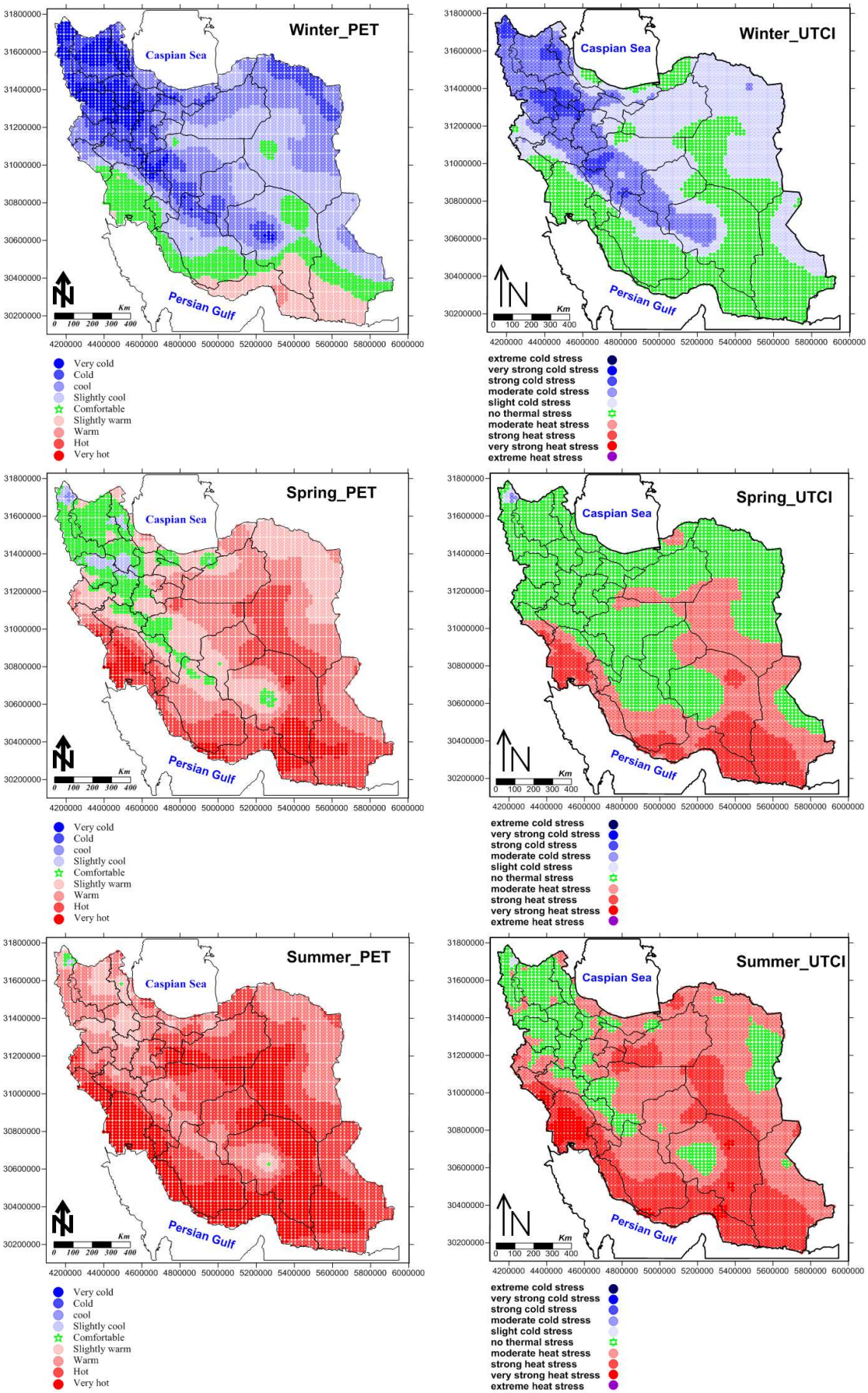

http://www.aloki.hu ● ISSN 1589 1623 (Print) ● ISSN 1785 0037 (Online)
DOI: http://dx.doi.org/10.15666/aeer/1605_54235445
© 2018, ALÖKI Kft., Budapest, Hungary

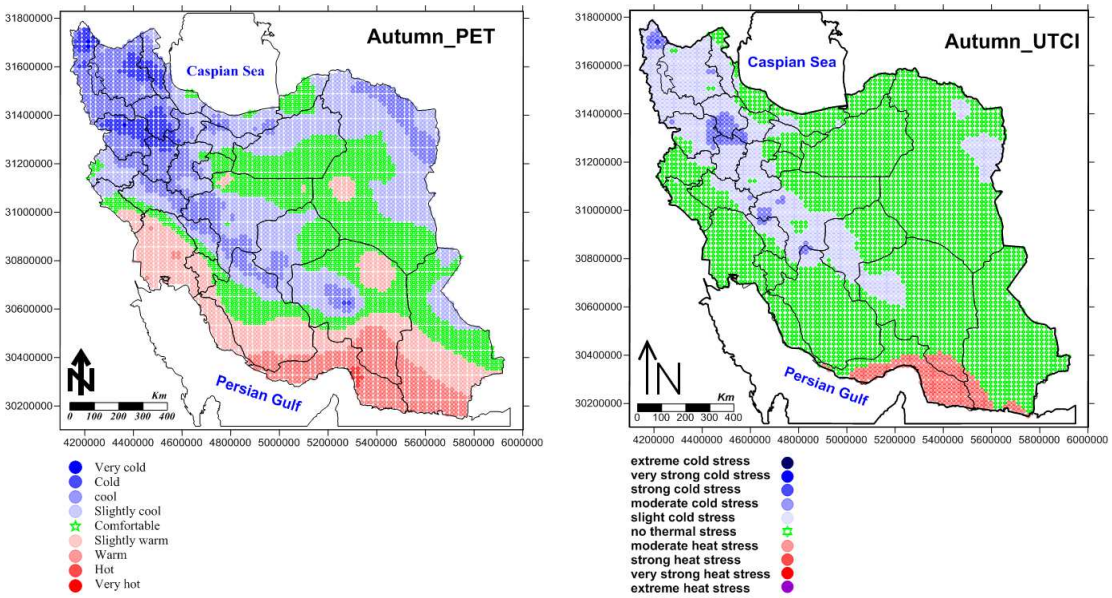

Figure 2. *Iran's bioclimatic conditions in winter, spring, summer and autumn*

Table 2. *The spatial extent (percent of the territory of Iran) of various categories of thermal stress and thermal perception in Iran, mean seasonal values for the period 1981-2010*

UTCI	Winter	Spring	Summer	Autumn
Extreme cold stress	0.0	0.0	0.0	0.0
Very strong cold stress	0.4	0.0	0.0	0.0
Strong cold stress	4.9	0.0	0.0	0.4
Moderate cold stress	19.3	0.1	0.0	6.9
Slight cold stress	32.9	2.7	0.1	21.7
No thermal stress	42.3	52.0	22.5	63.1
Moderate heat stress	0.3	28.3	40.3	7.1
Strong heat stress	0.0	14.7	31.3	0.7
Very strong heat stress	0.0	2.2	5.8	0.0
Extreme heat stress	0.0	0.0	0.0	0.0
PET	**Winter**	**Spring**	**Summer**	**Autumn**
Very cold	10.5	0.0	0.0	3.5
Cold	14.4	0.1	0.0	7.5
Cool	26.9	4.0	0.0	17.5
Slightly cool	22.1	18.8	0.1	20.1
Comfortable	15.7	36.0	0.7	19.3
Slightly warm	8.9	61.8	7.7	17.1
Warm	1.5	74.9	23.5	9.9
Hot	0.0	60.8	35.1	4.8
Very hot	0.0	43.8	32.8	0.1

http://www.aloki.hu ● ISSN 1589 1623 (Print) ● ISSN 1785 0037 (Online)
DOI: http://dx.doi.org/10.15666/aeer/1605_54235445
© 2018, ALÖKI Kft., Budapest, Hungary

Monthly differentiation of bioclimatic conditions

January

Studying the bioclimatic conditions of Iran by UTCI showed that extreme heat stress, strong and very strong heat stress, moderate heat stress and strong cold stress conditions in January, have not been experienced in Iran. In 27.4% of Iran's territory, any thermal stress has not been seen. In this month, southern and southwestern regions of Iran, as well as scattered parts of the Caspian Sea coasts do not have heat stress. In January, slight cold stress in large parts of Iran (37.8% of Iran) was dominant. In addition, moderate cold stress, strong cold stress and very strong cold stress, with 25.6, 8.3 and 0.9%, respectively, covered a considerable part of Iran in northern latitudes and higher elevations. In January, by reducing the height and latitude, Iran's bioclimatic conditions have changed to climatic comfort. Based on the PET index, Iran does not have warm, hot and very hot bioclimatic conditions in January. In this month, cold conditions are dominant from the south to the northwest and northeast of Iran. However, the northwest of Iran, Kurdistan and Hamadan provinces are coldest places in Iran. Of course, on along the northwest to the southeast of Iran to the center of Kerman province, also Alborz Mountains and some parts of northeast and north of Iran, cold conditions has been experienced. On the other hand, slight warmth is experienced only in some parts of Hormozgan, Sistan and Baluchistan provinces. Generally, in this month, cool, cold and very cold conditions, 32.3, 20.3 and 18.2%, respectively, covered most parts of the country. Also, 10% of Iran was located in differentiation of bioclimatic conditions (*Fig. 3*).

February

Bioclimatic conditions of Iran in February revealed a very similar thermal stress to that of January. In this month, extreme heat stress, very strong heat stress, strong heat stress and moderate heat stress was not observed in Iran. In addition, extreme cold stress in any part of Iran cannot be seen. In this month, bioclimatic conditions with no thermal stress, compared to January, have shown a significant increase. The scope of areas without any thermal stress has increases from 27.4% in January to 33.2% in February. Slight cold stress in large parts of Iran (37.7%) has not been experienced. In this month, the extent of areas under moderate cold stress, strong cold stress and very strong cold stress has been reduced. In February, very hot and hot conditions cannot be seen in Iran. Compared to January, the extent of the areas that had experienced cold conditions has reduced. As well as the extent of areas with differentiation of bioclimatic conditions, slightly warm and warm conditions increased. From the southwest to the southeast of Iran, thermal comfort and slightly warm conditions are prevalent. In this month, in the highlands, as well as high latitude, there are cold conditions. In February such as in January, the northwest experienced colder conditions than other regions of Iran. Cool, cold and slightly cool conditions were experienced in 27.5, 24.4 and 16.5% of Iran, respectively (*Fig. 3*).

March

In March, extreme cold stress and very strong cold stress in the territory of Iran had not been seen. Compared to the months of January and February, cold stress in March is dominant in smaller parts of Iran. Therefore, it can be said that in March the beginning

http://www.aloki.hu ● ISSN 1589 1623 (Print) ● ISSN 1785 0037 (Online)
DOI: http://dx.doi.org/10.15666/aeer/1605_54235445
© 2018, ALÖKI Kft., Budapest, Hungary

of heat stress become evident in Iran, meaning that in March, the comfort conditions, compared to January and February, have been experienced in more parts of Iran. In fact, thermal comfort in March is the most abundant bioclimatic conditions of Iran. These conditions prevailed in 66.2% of the territory of Iran. By reducing the height and latitude, cold stress conditions in Iran has declined. Also start of heat stress can be seen in the Persian Gulf and Southeast of Iran. There is an obvious difference among Iran's bioclimatic conditions in March compared to January and February. In March, the heat stress conditions in large parts of this country have developed. In other words, in this month, Iran was beginning to get out of the cold climatic conditions (slightly cool to very cold). There are cold and very cold conditions in less than 8% of Iran. In contrast, slightly cool, comfortable and cool conditions, have been experienced, in 25.5, 24.6 and 20.8% respectively, of Iran. In this month, more than 20% of Iran's climatic conditions tend to be warm. For example, areas that are in high latitudes and with greater height have experienced relatively colder bioclimatic conditions (*Fig. 3*).

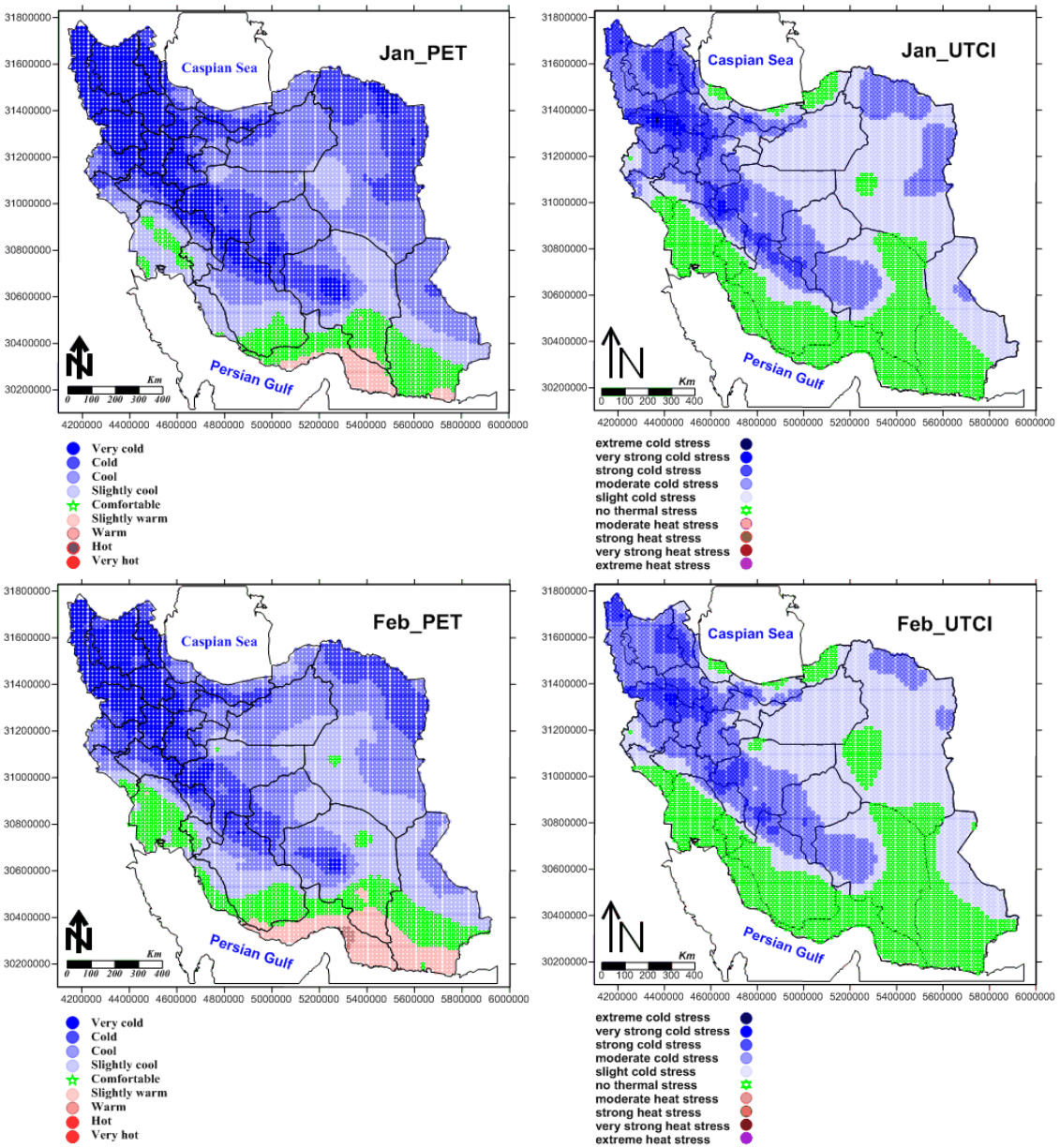

http://www.aloki.hu ● ISSN 1589 1623 (Print) ● ISSN 1785 0037 (Online)
DOI: http://dx.doi.org/10.15666/aeer/1605_54235445
© 2018, ALÖKI Kft., Budapest, Hungary

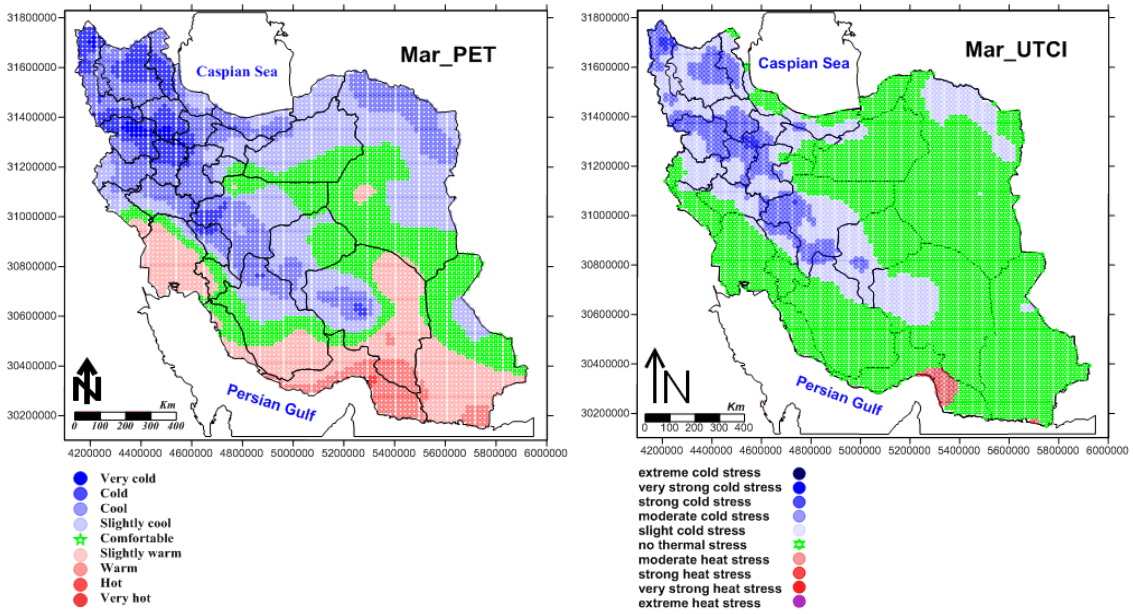

Figure 3. *Iran's bioclimatic conditions in January, February and March*

April

In April, bioclimatic conditions of extreme cold stress, very strong cold stress, strong cold stress, extreme heat stress, very strong heat stress and strong heat stress has not been seen in Iran. No thermal stress conditions in April, compared to the previous months (winter), in the wider parts have expanded. In this month, more than 76% of Iran has experienced no thermal stress conditions. The important point in this month is an increase in the range of moderate heat stress conditions that Iran has experienced. Within 15.5% of Iran, there was moderate heat stress. The belt of the south, southeast, parts of the southwest of Iran as well as parts of Kerman province are in the territories of moderate heat stress. In this month, scattered parts of the Kurdistan province and also along the Zagros Mountains have cold stress. In April, Iran's bioclimatic conditions have changed compared to winter, especially in the months of January and February. In this month, severe bioclimatic conditions (very cold and very hot) are not experienced in Iran. In general, slightly cool, cool, cold conditions ruled about 20% of Iran's territory. Unlike March, in this month, the extent of the regions with climatic comfort is reduced. Warm conditions also extended in large areas of Iran. In this month slightly warm, warm and comfort to the respectively 28.8, 23.1 and 21% in the major part of Iran have been seen. Southern of Iran being the warmest in this month and the northwest of Iran to the Alborz and Zagros Mountains being the coolest parts of the country (*Fig. 4*).

May

Bioclimatic conditions prevailing in May show a significant increase in heat stress. In this month, only a small part in the northwest of Azerbaijan is experiencing slight cold stress. From the beginning of the year (from January to May) cold stress with different intensities is seen in a small region of Iran. The important point in this month is the reduction in areas affected by thermal comfort. From January to April, the extent

http://www.aloki.hu ● ISSN 1589 1623 (Print) ● ISSN 1785 0037 (Online)
DOI: http://dx.doi.org/10.15666/aeer/1605_54235445
© 2018, ALÖKI Kft., Budapest, Hungary

of comfort conditions showed an increasing trend. This condition in Iran has shown a significant reduction (dropping from 76.6% in April to 54.6% in May). By contrast, moderate heat stress and strong heat stress were observed in 29.7 and 15.3% of Iran's territory. Therefore the warming trend of Iran in this month suddenly increased. In this month, in reduced elevation and latitude, heat stress has increased. In fact, large parts of central Iran and also Iran's southern tapes have experienced this situation. Iran's bioclimatic conditions in May, is very similar to April. In May, bioclimatic conditions of very cold, cold and cool have almost left Iran. Moreover, only 2.4% has experienced slightly cool conditions. Comfort condition in less than 15% (highlands and higher latitudes) has prevailed. Also for the first time, about 10% of Iran is in hot conditions. Hot, warm, and slightly warm conditions have covered Iran, 28.3, 23.4 and 22.1%, respectively. In this month, only scattered parts of the northwest of Iran have slightly cool conditions (*Fig. 4*).

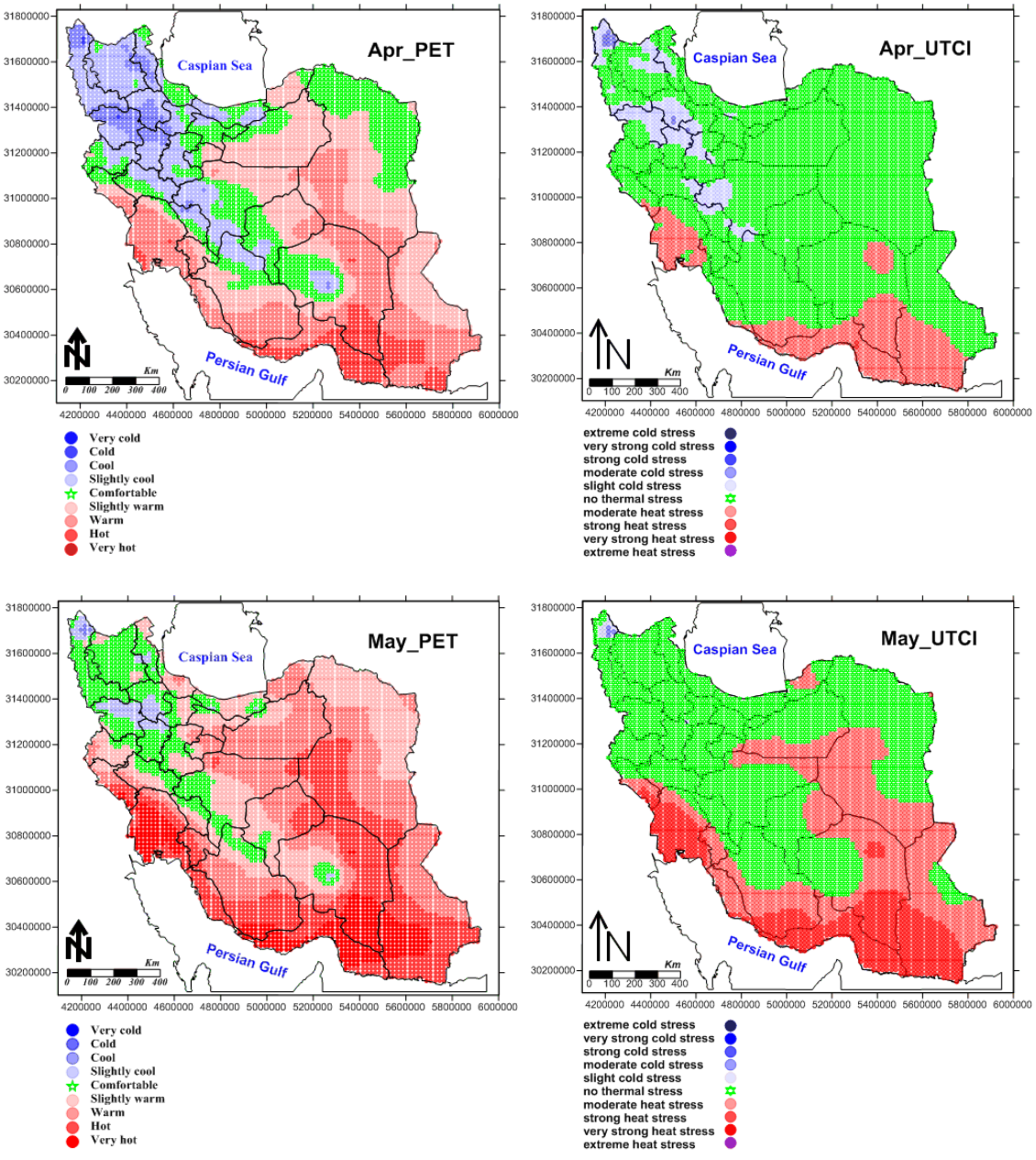

http://www.aloki.hu ● ISSN 1589 1623 (Print) ● ISSN 1785 0037 (Online)
DOI: http://dx.doi.org/10.15666/aeer/1605_54235445
© 2018, ALÖKI Kft., Budapest, Hungary

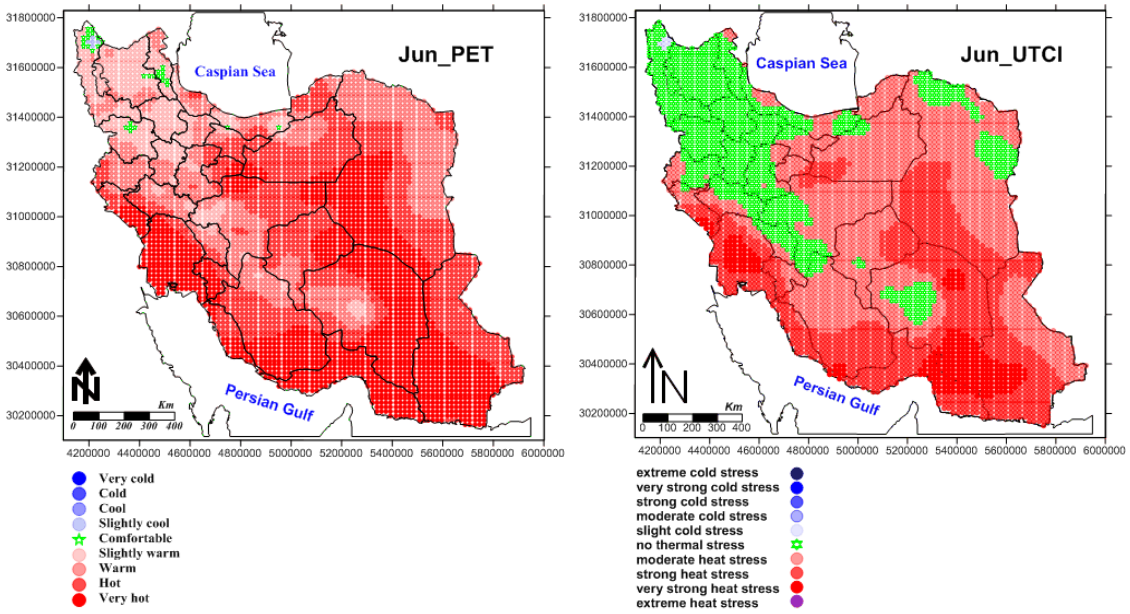

Figure 4. *Iran's bioclimatic conditions in April, May and June*

June

In June, almost all cold stress bioclimatic conditions in Iran have vanished based on the UTCI index. In only 0.1% of Iran slightly cold stress conditions prevailed. From the northwest of Iran to the south of Isfahan province, scattered areas in the northeast of Iran and the middle of Kerman province comfort conditions prevail. These areas include about 24.9% of Iran. Other parts of Iran are under the influence of moderate heat stress (39.8%); strong heat stress (28.7%) and very strong heat stress (6.5%), respectively. Generally, in June, the severe heat stress can be seen. Heat stress in the lower latitude and longitude, as well as Iran's low-lying areas, is more than other regions. Based on the PET, very cold, cold, cool conditions have not been seen in Iran. However, there is a slightly cool condition in about 0.1% and thermal comfort in about 0.6% of a small part of the northwest of Iran. Thus, in more than 99% of Iran, warm conditions with different intensities have been reported. It should be noted that in the highlands and of course the higher latitude there is less intense heat. In this month, very hot, hot, and warm conditions are seen in 34.4, 30.6 and 23.5%, respectively, of Iran (*Fig. 4*).

July

Iran's bioclimatic condition in July is similar to June. In July, almost no cold stress is seen in Iran. Less than 0.1% of the Iranian region has experienced slight cold stress conditions. However, there is a significant difference in July compared to June. Thermal stress in this month has declined to 7.8%. Only in small parts of Iran, no thermal stress can be seen. In this month, more elevated areas and areas with higher latitude have experienced thermal comfort conditions. Reduced thermal stress and the lack of cold stress condition in this month, expanding heat stress condition with varying severity, have been confirmed. Overall, more than 90% of the region has experienced heat stress conditions with different intensities. The current bioclimatic conditions of this month, is a strong heat stress condition (42.2% of Iran). Bioclimatic conditions of moderate heat

http://www.aloki.hu ● ISSN 1589 1623 (Print) ● ISSN 1785 0037 (Online)
DOI: http://dx.doi.org/10.15666/aeer/1605_54235445
© 2018, ALÖKI Kft., Budapest, Hungary

stress with 38.3% and very strong heat stress with 10.7% prevailed in large parts of the country. The PET index showed that in July, no part of Iran experienced slightly cool, cool, cold and very cold conditions. In this month, the thermal comfort condition was experienced in only in 0.2% of Iran (a small part of the northwest of the country). Therefore, 99.8% of Iran's territory experienced warm conditions. Large parts of the country (45.1, 33.3 and 18.9%) were in very hot, hot, and warm conditions, respectively. Heat intensity in the higher places (Alborz and Zagros mountains) and the northwest is less than other parts of Iran (*Fig. 5*).

August

No significant changes can be seen in the bioclimatic conditions of Iran in August compared to July and June. In August, only 0.1% is under the influence of slight cold stress. Cold stress with more intensity like Jun and July cannot be seen in any part of Iran. In August, comfort conditions, compared to previous months, increased slightly. In this month, 13% of Iran, including parts of the northwest and northeast of the country, west of Isfahan province and central Kerman, experienced no thermal stress conditions. Increasing climatic comfort conditions (no thermal stress condition), on the one hand, and a reduction in the range of areas that have experienced very strong heat stress and strong heat stress on the other hand, indicates the relative cool air in Iran. In this month, very strong heat stress conditions are limited to 6.8%. Also the strong heat stress conditions decreased to 35.1%. In this month, the thermal stress condition reduction in the highlands and northern latitudes is remarkable. Based on the PET index, Iran's bioclimatic conditions in August are very similar to July. In this month 99.8% of Iran is experiencing hot conditions (with different intensities). In total, only 0.2% of Iran is in thermal stress and slightly cool conditions. In this month, cool, cold and very cold conditions in the scope of Iran cannot be seen. However, a significant difference is in the extent of very hot bioclimatic conditions between July and August. The extent of the hot condition in August (39.3%) is lower than in July (45.1%) in Iran. However, hot and warm conditions in August compared to July have increased significantly (*Fig. 5*).

September

Bioclimatic conditions in September showed that in many parts of Iran, the severity of heat stress is reduced. Contrary to June, July and August, very strong heat stress conditions in the territory of Iran have been eliminated. In addition, strong heat stress and moderate heat stress in comparison with the months before 16.5 and 37.6%, respectively, has decreased. Among the bioclimatic conditions, no thermal stress conditions were experienced in 45.8% of the territory of Iran. An increase in the range of areas that have no thermal stress conditions on the one hand, and a reduction in the severity of heat stress on the other hand, represent a new stage entering Iran's bioclimatic conditions. In this month highlands (including the Zagros mountain range, Alborz and northeast of Iran) and also northern latitudes of Iran have bioclimatic comfort conditions (no thermal stress). In the lowlands and lower latitude, strong heat stress can be seen. Based on the PET index, the intensity of heat over Iran has reduced in September. In addition, comfort condition has expanded to 1.8%. Along the Zagros and Alborz mountains, and generally highlands, heat with intensity is further reduced (*Fig. 5*).

http://www.aloki.hu ● ISSN 1589 1623 (Print) ● ISSN 1785 0037 (Online)
DOI: http://dx.doi.org/10.15666/aeer/1605_54235445
© 2018, ALÖKI Kft., Budapest, Hungary

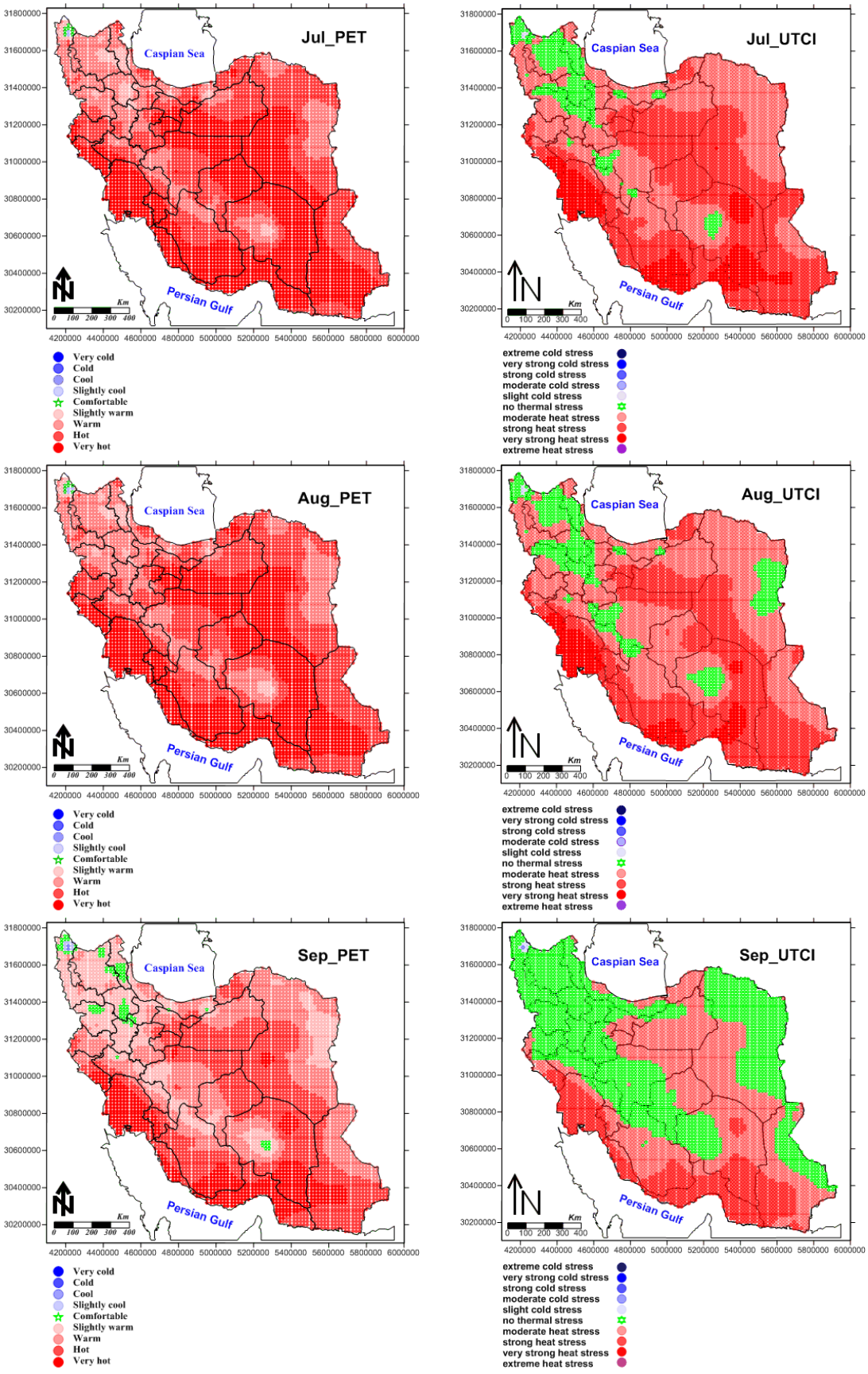

Figure 5. *Iran's bioclimatic conditions in July, August and September*

APPLIED ECOLOGY AND ENVIRONMENTAL RESEARCH 16(5):5423-5445.
http://www.aloki.hu ● ISSN 1589 1623 (Print) ● ISSN 1785 0037 (Online)
DOI: http://dx.doi.org/10.15666/aeer/1605_54235445
© 2018, ALÖKI Kft., Budapest, Hungary

October

With the onset of autumn in October, significant changes in Iran's bioclimatic conditions have occurred. In this month, limited parts of Iran are under slight cold stress (0.7%) and moderate cold stress (less than 0.1%). The province of west Azarbaijan and Kurdistan, Zanjan and Hamedan experienced such conditions. The most important bioclimatic characteristics of this month, is the lack of heat stress conditions in 79.1% of the country. Most parts of Iran compared to other months are in the range of climatic comfort. Cold stress conditions in the narrow strip of the southwest to the southeast can be seen. Moderate heat stress and strong heat stress was reported only in 18 and 2.1% of Iran. The increasing extent of no thermal stress on the one hand and reduced thermal stress on the other hand, are indicative of the start of the cold period. Based on PET, slightly cool and cold conditions can be seen in less than 0.10 of Iran. However, in October, cold and very cold conditions have not yet begun. Heat conditions in this month to the lower latitude and low-lying areas have receded. In fact, the highlands with high-latitude have moved towards cold conditions. In this month, slightly warm, comfortable and warm conditions were seen in 30.6, 23.7 and 22.3% of Iran, respectively. Very hot conditions are in less than 5.0% of Iran. Therefore, October, can be called a transitional month moving towards cold conditions (*Fig. 6*).

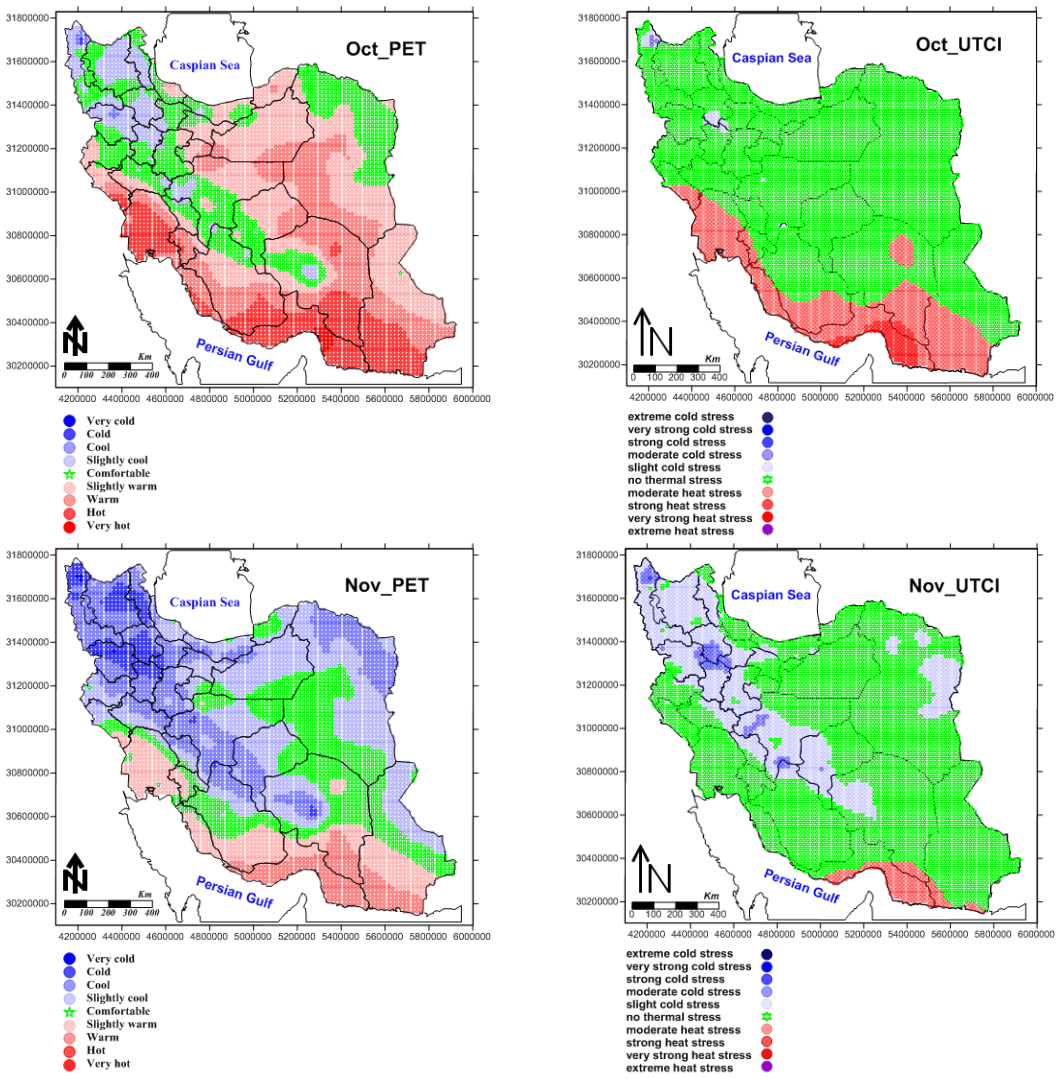

APPLIED ECOLOGY AND ENVIRONMENTAL RESEARCH 16(5):5423-5445.
http://www.aloki.hu ● ISSN 1589 1623 (Print) ● ISSN 1785 0037 (Online)
DOI: http://dx.doi.org/10.15666/aeer/1605_54235445
© 2018, ALÖKI Kft., Budapest, Hungary

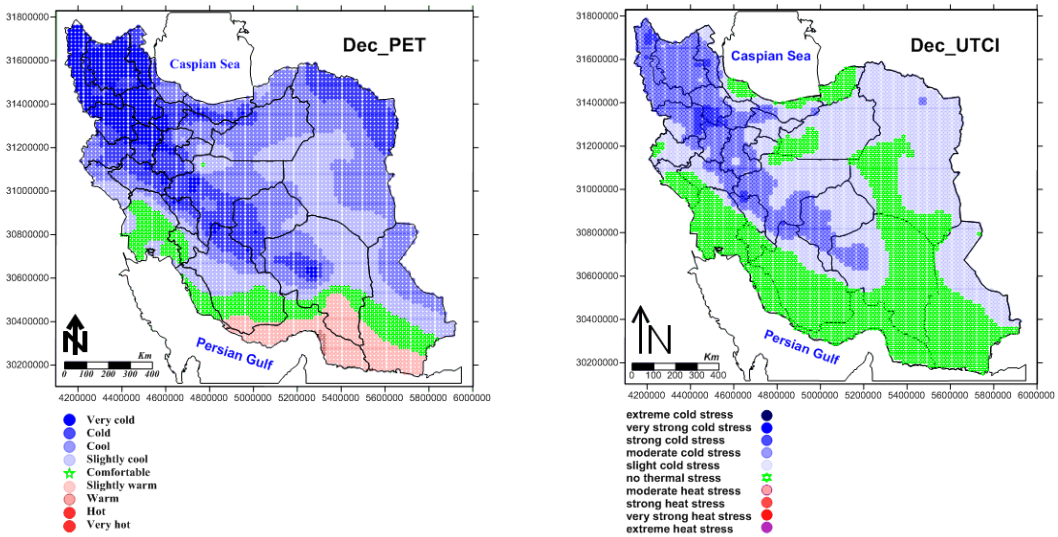

Figure 6. *Iran's bioclimatic conditions in October, November and December*

November

In November, only 3.3% of the territory of Iran (including southern Iran) has reported heat stress conditions. In fact, with the exception of the southern coast, heat stress conditions with different intensities are not seen in Iran. In parts of the Khorasan province and from the northwest of Iran to Kerman province, slight cold stress and moderate cold stress dominates the region. What is obvious is that compared to October, conditions of heat stress and no thermal stress conditions have shown a significant decrease. Moreover, significant increase, especially in slight cold stress condition (23.5%) and moderate cold stress (1.9%) can be observed. Based on the PET index, the bioclimatic condition in November shows a major difference with October. In this month, very hot and hot conditions have left Iran and on the other hand very cold and cold conditions are reported only in about 5% of the region. Overall, in about 20% of Iran, slightly warm and warm conditions can be seen. Compared to October, in November, there is a slight increase in the expansion of thermal comfort (24%). In this month 29, 24 and 22% of Iran respectively, is surrounded by slightly cool, comfort and cool conditions. Also thermal stress to the low latitudes and low-lying areas has been displaced (*Fig. 6*).

December

The Cooling trend in Iran that began in September has become more intense in December. In December, in no part of this country have heat stresses been experienced. In addition, thermal stress conditions of 71.3% in November decreased to 39% in December. In this month, no thermal stress conditions are experienced in low-lying areas and low latitudes especially in coastal areas as well as parts of the Caspian Sea. Overall, more than 60% of Iran has experienced cold stress with different intensities. Highlands and higher latitudes have more severe cold stress conditions. Temperature reduction in December continues based on the PET index. In this month, only 0.2% is in hot conditions and 7.9% of Iran was in slightly warm conditions. Therefore, any effect of hot and very hot conditions cannot be seen in Iran. On the other hand, very cold and

http://www.aloki.hu ● ISSN 1589 1623 (Print) ● ISSN 1785 0037 (Online)
DOI: http://dx.doi.org/10.15666/aeer/1605_54235445
© 2018, ALÖKI Kft., Budapest, Hungary

cold conditions have shown a significant increase in December compared to April to November. In fact December, after the months of January and February, is the coldest month in Iran. In addition, significant reductions in thermal stress can be seen in this month. In this month, thermal stress can be seen in about 10% of Iran. Cold severity to the northwest of Iran and highlands is more. However, in some parts of the south coast, slightly warm conditions can still be experienced (*Fig. 6*).

Discussion

Iran is one of the largest countries that located in Middle East. Iran has an area of 1,648,195 square kilometres. It lies between latitudes 24° to 40° N, and longitudes 44° to 64° E. Iran consists of the Iranian Plateau and it is one of the world's most mountainous countries, its landscape dominated also by rugged mountain ranges. Therefore, Iran's climate is very diverse ranging from arid and semi-arid, to subtropical along the Caspian coast and the northern forests. This study was performed with the aim of determining the thermal stress and bioclimatic conditions of Iran. Most of the researches in terms of bioclimatic conditions in Iran have been done within the cities and/or provinces. However, in the estimation of bioclimatic conditions of Iran, the different indices are used. Comparison of this research to other researches that have been conducted in different parts of the country shows there are slight differences in the estimation of bioclimatic conditions. Without a doubt, such differences may be caused by the type and volume of data and the different methods used. However, analysis of bioclimatic conditions in Iran is the most important feature of this research. The impact of bioclimatic conditions on thermal comfort in different areas of the world has been carried out recently, indicating the impact of urban bioclimatic on human morbidity (Schwartz et al., 2004; Nastos and Matzarakis, 2006), tourism potential and decision making (Didaskalou and Nastos, 2003; Hamilton and Lau, 2003), urban planning (Nikolopoulou and Lykoudis, 2006; Thorsson et al., 2007), and mortality (Analitis et al., 2008; Almeida et al., 2010). In general, the result of this research is almost in alignment with the work of Ramazani Gourbi (2010). Looking at the map of bioclimatic Iran, it can be said that in the eastern and western parts of the Gilan province, comfort conditions can be seen throughout the year. However, the eastern parts of this province have more thermal comfort. The results of this study have some differences to the research that Shakoor (2011) conducted on on Yazd. Shakoor believes that in the months of October, November and January, favourable climatic conditions exist in Yazd. The findings of this study are no in alignment with the findings of Ghavidel Rahimi and Ahmadi (2013). The results of this study are however in line with the studies of Tavoosi and Sabzi (2013) and Mohammadi (2014). However, there are the slight differences between findings of this study and other researches, a part or parts of Iran have studied. In these regions, temperatures rarely fall below freezing and the area remains humid for the rest of the year. To the west, settlements in the Zagros basin experience lower temperatures, severe winters with below zero average daily temperatures and heavy snowfall. The eastern and central parts of Iran are arid, with less than 250 mm of precipitation, and have occasional deserts. Average summer temperatures rarely exceed 38 °C. The coastal plains of southern Iran have mild winters, and very humid, sultry and hot summers with annual precipitation of less than 350 mm. Generally the results of this study showed that Iran's bioclimatic conditions are very diverse during the year.

http://www.aloki.hu ● ISSN 1589 1623 (Print) ● ISSN 1785 0037 (Online)
DOI: http://dx.doi.org/10.15666/aeer/1605_54235445
© 2018, ALÖKI Kft., Budapest, Hungary

According to UTCI, all bioclimatic conditions (except extreme cold and extreme heat stress conditions) in a limited time and a small territory of Iran were at least experienced. In contrast to some areas experiencing cold condition in winter (with different intensities), some areas of Iran show a thermal comfort conditions which highlights the climatic diversity of the country as well as high tourism potential throughout the year. These regions are mostly located in south latitudes and Iran's lowland areas which display the lowest thermal stress conditions. In spring, cold stress and comfort conditions is reduced. However in this season, especially, thermal stress condition is prevalent in considerable parts of Iran, but heat stress conditions with different intensities is expanding. At the beginning of the summer the regions that have experienced thermal stress conditions have decreased. The results of this research reveal that heat stress with different intensities has been experienced in more than half of Iran. In late summer, heat stress in Iran will gradually decline. In the autumn, with the increasing cold stress and reducing heat stress, we can see the cooling process in Iran. The other results of this study showed that moderate cold stress and thermal stress conditions can be seen all year round. In fact, the existence and expansion of thermal comfort and generally bioclimatic conditions with different intensities at any time of year (in large or small parts of Iran), shows Iran's bioclimatic ability. The occurrence of simultaneous bioclimatic conditions also reflects the fact that Iran is a country of four seasons. This means, when many parts of Iran (northwest, west and northeast) are experiencing strong cold stress conditions in December, January and February, other parts of the country are experiencing comfort and moderate heat stress conditions. Such a contradiction in the bioclimatic conditions event is even in some provinces of the country. For example, very diverse bioclimatic conditions have been experienced in the months of June and July in the Isfahan province. Kerman province has this climate variety in August, September and December. Comparisons of the results of PET and UTCI indices showed that in some months of the year (such as January and February) there is very little difference between the estimated bioclimatic conditions in Iran. However, in March, April, May, September, October and November, there are considerable differences in bioclimatic conditions estimated by these indices.

Compared with previous studies of thermal stresses in other parts of Iran, the advantage of the method employed in this research is that the PET index is more understandable for people who (tourists) can assess the outdoor thermal condition based on their experience in an indoor environment (Farajzadeh et al., 2015; Roshan et al., 2018). About half the country is covered with mountains and moreover due to the vastness of Iran, it has various and different climates. Iran's climatic diversity in terms of spatial and temporal scale is visible. According to studies that published in Farsi, Iran is divided into several climatic regions. The south of Iran has very humid hot weather. Winters are very pleasant. Iranians travel to the south of Iran in winters; especially Kish and Gheshm islands have the best weather in winters. Therefore, the temperature difference in different parts of Iran can reach up 40 to 50 degrees in winter. Considering such explanations, we can say it seems that the PET index compared to the UTCI index showed a great ability in estimating Iran's bioclimatic conditions. In fact, the PET Index shows Iran's climatic diversity better than the UTCI index. Bioclimatic maps that are presented in this study can provide a good platform for doing a lot of planning, energy management, human activities such as tourism and even other environmental studies. Furthermore, the results of this study are important for government agencies to offer detailed tourism climate information to improve the success of the tourism industry.

http://www.aloki.hu ● ISSN 1589 1623 (Print) ● ISSN 1785 0037 (Online)
DOI: http://dx.doi.org/10.15666/aeer/1605_54235445
© 2018, ALÖKI Kft., Budapest, Hungary

Conclusion

The evaluation of the bioclimatic conditions for Iran was carried out based on the analysis of the UTCI and PET indices. The results of this study showed that at the spatial and temporal scales Iran has different bioclimatic conditions. The results of this research have several applications in the fields of tourism, agriculture, medical, and architecture, etc. In general, bioclimatic maps in this research have a useful uses for decision makers on various levels, including health, tourism and regional planning. The results of this study suggest that the bioclimatic conditions of Iran during the year are very diversity. However, warm and very warm bioclimatic conditions in most cases have been experienced in the southern parts of Iran and areas with lower altitude. These regions are affected by heat stress in spring and summer seasons. Analysis of the bioclimatic conditions is subject of applied investigation among various scientists such as urban planners, climatologists, architects, and biologists. According to the studies mentioned in discussion section can be said that there are several research recommendations in the field of bioclimatic conditions in Iran. To better understand the bioclimatic conditions of Iran, the trend analysis of the Iran's bioclimatic conditions has been suggested. Also, the relationship between bioclimatic conditions and the rate of hospital admissions for cardiovascular disease in Iran can be the other topic for future research.

REFERENCES

[1] Almeida, S. P., Casimiro, E., Calheiros, J. (2010): Effects of apparent temperature on daily mortality in Lisbon and Oporto, Portugal. – Environmental Health 9(1): Article 12.

[2] Analitis, A., Katsouyanni, K., Biggeri, A. et al. (2008): Effects of cold weather on mortality: results from 15 European cities within the PHEWE project. – American Journal of Epidemiology 168: 1397-1408.

[3] Basarin, B., Lukic, T., Mesaros, M., Pavic, D., Dordevic, J., Matzarakis, A. (2018): Spatial and temporal analysis of extreme bioclimate conditions in Vojvodina, Northern Serbia. – Int. J. Climatol 38: 142-157.

[4] Blażejczyk, K., Epstein, Y., Jendritzky, G., Staiger, H., Tinz, B. (2012): Comparison of UTCI to selected thermal indices. – International Journal of Biometeorology 56: 515-535.

[5] Bröde, P., Fiala, D., Blazejczyk, K., Epstein, Y., Holmér, I., Jendritzky, G., Kampmann, B., Richards, M., Rintamäki, H., Shitzer, A., Havenith, G. (2009): Calculating UTCI Equivalent Temperature. – In: Castellani, J. W., Endrusick, T. L. (eds.): Environmental Ergonomics XIII. University of Wollongong, Wollongong, pp. 49-53.

[6] Caliskan, O., Cicek, I., Matzarakis, A. (2012): The climate and bioclimate of Bursa (Turkey) from the perspective of tourism. – Theor Appl Climatol 108: 417-425.

[7] Cendrowska, K. L. (2013): Assessment of bioclimatic conditions in cities for tourism and recreational purposes (A Warsaw case study). – Geographia Polonica 86: 55-66.

[8] Charalampopoulos, I., Tsiros, I., Chronopoulou-Sereli, A., Matzarakis, A. (2013): Analysis of thermal bioclimate in various urban configurations in Athens, Greece. – Urban Ecosyst 16: 217-233.

[9] Dadbakhsh, M., Khanjani, N., Bahrampour, A., Haghighi, P. S. (2017): Death from respiratory diseases and temperature in Shiraz, Iran (2006-2011). – Int J Biometeorol 61: 239-246.

[10] Didaskalou, E. A., Nastos, P. T. (2003): The role of climatic and bioclimatic conditions in the development of health tourism product. – Anatolia 14(2): 107-126.

http://www.aloki.hu ● ISSN 1589 1623 (Print) ● ISSN 1785 0037 (Online)
DOI: http://dx.doi.org/10.15666/aeer/1605_54235445
© 2018, ALÖKI Kft., Budapest, Hungary

[11] Eslami, A. R., Tirandaz, M. (2011): The use of GIS on bioclimatic zoning for tourism settlement (case study: Polroud basin, Guilan province). – Annals of Biological Research 2: 44-51.
[12] Farajzadeh, H., Matzarakis, A. (2009): Quantification of climate for tourism in the northwest of Iran. – Meteorol Appl 16: 545-555.
[13] Farajzadeh, H., Saligheh, M., Alijani, B., Matzarakis, A. (2015): Comparison of selected thermal indices in the northwest of Iran. – Natural Environment Change 1: 61-80.
[14] Frich, P., Alexander, L. V, Della-Marta, P., Gleason, B., Haylock, M., Klein Tank, A. M. G., Peterson, T. (2002): Observed coherent changes in climatic extremes during the second half of the twentieth century. – Clim. Res. 19: 193-212.
[15] Geletič, J., Lehnert, M., Savić, S., Milošević, D. (2018): Modelled spatiotemporal variability of outdoor thermal comfort in local climate zones of the city of Brno, Czech Republic. – Science of the Total Environment 624: 385-395.
[16] Ghavidel Rahimi, Y., Ahmadi, M. (2013): Estimation of climatic comfort in Tabriz. – Geography and Development 33: 182-173.
[17] Givoni, B., Noghuchi, M., Saaroni, H., Pochter, O., Yaacov, Y., Feller, N., Becker, S. (2003): Outdoor comfort research issues. – Energy and Building 35: 77-86.
[18] Gulyas, A. (2005): Differences in human comfort conditions within a complex urban environment: a case study. – Acta Climatologica et Chorologica 38-39: 71-84.
[19] Gulyas, A., Matzarakis, A. (2007): Selected examples of bioclimatic analysis applying the physiologically equivalent temperature in Hungary. – Acta Climatologica et Chorologica 40-41: 37-46.
[20] Hamilton, J. M., Lau, M. A. (2005): The role of climate information in tourist destination choice decision-making. –Proceedings of the 17th International Congress of Biometeorology, Garmisch-Partenkirchen (Germany), 5-9 Sep 2005, pp. 608-611.
[21] Ichinose, T., Matuschek, O., Jing, Y. (2008): Biometeorology for tourism/recreation in Japan: a review. – Global Environmental Research 12: 123-128.
[22] Kalkstein, A. (2008): Geographical variations in seasonal mortality across the United States: a bio climatological approach. – A dissertation presented in partial fulfillment of the requirements for the degree doctor of philosophy, Arizona State University, UMI Number: 3319075.
[23] Kántor, N., Égerházi, L., Unger, J. (2012a): Subjective estimation of thermal environment in recreational urban spaces—Part 1: Investigations in Szeged, Hungary. – International Journal of Biometeorology 56(6): 1075-1088.
[24] Kántor, N., Unger, J., Gulyás, Á. (2012b): Subjective estimations of thermal environment in recreational urban spaces—Part 2: International comparison. – International Journal of Biometeorology 56: 1089-1101.
[25] Ketterer, C., Matzarakis, A. (2012): Development and application of assessment methods for thermal bioclimate conditions in Stuttgart. – ICUC8, 8th International Conference on Urban Climates, 6th-10th August, UCD, Dublin Ireland.
[26] Kovács, A., Németh, A., Unger, J., Kántor, N. (2017): Tourism climatic conditions of Hungary–present situation and assessment of future changes. – Journal of the Hungarian Meteorological Service 121: 79-99.
[27] Lecha Estela, L. B. (2008): Biometeorological classification of daily weather types for the humid tropics. – Int J Biometeorol 42: 77-83.
[28] Lin, T. P., Matzarakis, A. (2008): Tourism climate and thermal comfort in Sun Moon Lake, Taiwan. – International Journal of Biometeorology 52: 281-290.
[29] Lin, T. P., De Dear, R., Hwang, R. L. (2011): Effect of thermal adaptation on seasonal outdoor thermal comfort. – International Journal of Climatology 31: 302-312.
[30] Lise, W., Tol, R. S. J. (2002): Impact of climate on tourism demand. – Clim Change 55: 429-449.
[31] Maddison, D. (2001). In search of warmer climate? The impact of climate change on flows of British tourists. – Clim Change 49: 193-208.

http://www.aloki.hu ● ISSN 1589 1623 (Print) ● ISSN 1785 0037 (Online)
DOI: http://dx.doi.org/10.15666/aeer/1605_54235445
© 2018, ALÖKI Kft., Budapest, Hungary

[32] Matzarakis, A. (2006): Weather- and climate-related information for tourism. – Tourism and Hospitality Planning and Development 3: 99-115.
[33] Matzarakis, A. (2008): Relevance of thermal bioclimate for tourism in Japan. – Global Environmental Research 12: 129-136.
[34] Matzarakis, A., Mayer, H. (1997): Heat stress in Greece. – Int J Biometeorol 41: 34. https://doi.org/10.1007/s004840050051.
[35] Matzarakis, A., Mayer, H., Iziomon, M. (1999): Applications of a universal thermal index: physiological equivalent temperature. – Int. J. Biometeor 43: 76-84.
[36] Matzarakis, A., Muthers, S., Koch, E. (2011): Human biometeorological evaluation of heat-related mortality in Vienna. – Theor Appl Climatol 105: 1. https://doi.org/10.1007/s00704-010-0372-x.
[37] Matzarakis. A; Rammelberg. J., Junk. J. (2013): Assessment of thermal bioclimate and tourism climate potential for central Europe, the example of Luxembourg. – Theor Appl Climatol 114: 193-202.
[38] Milošević, D., Bajšanski, I., Savić, S., Žiberna, I. (2016): Benefits of the environmental simulations for the urban planning process. – 4th eCAADe International Regional Workshop, Faculty of Technical Sciences, University of Novi Sad, May 19-20, 2016.
[39] Mohammadi, B. (2014): An estimation and spatio-temporal analysis of climatic comfort conditions in Kurdistan province. – Geographical Research Quarterly 113: 159-176.
[40] Mohammadi, B., Karimi, S. (2017): The relationship between thermal sensation and the rate of hospital admissions for cardiovascular disease in Kermanshah, Iran. – Theoretical and Applied Climatology. https://doi.org/10.1007/s00704-017-2332-1.
[41] Morgan, R., Gatell, E., Junyent, R., Micallef, A., Ozhan, E., Williams, A. (2000): An improved user- based beach climate index. – J Coast Conserv 6: 41-50.
[42] Nastos, P. T., Matzarakis, A. (2006): Weather impacts on respiratory infections in Athens, Greece. – International Journal of Biometeorology 50: 358-369.
[43] Nastos, P., Matzarakis, A. (2008): The effect of air temperature and the thermal index PET on mortality in Athens, Greece. – Proceedings 18th International Congress on Biometeorology, Tokio, 22-26 September 2008, pp. 1-4.
[44] Nikolopoulou, M. (2004): Outdoor Comfort. – In: Steemers, K., Steane, M. A. (eds.) Architecture and Variety: Environmental Perspectives. Spon Press, London.
[45] Nikolopoulou, M., Lykoudis, S. (2006): Thermal comfort in outdoor urban spaces: Analysis across different European countries. – Building and Environment 41: 1455-1470.
[46] Nikolopoulou, M.-H., Lykoudis, S. (2007): Use of outdoor spaces and microclimate in a Mediterranean urban area. – Building and Environment 42: 3691-3707.
[47] Potchter, O., Cohen, P., Lin, T. P., Matzarakis, A. (2018): Outdoor human thermal perception in various climates: A comprehensive review of approaches, methods and quantification. – Science of the Total Environment 631: 390-406.
[48] Pourvahidi, P., Ozdeniz, M. B. (2013): Bioclimatic analysis of Iranian climate for energy conservation in architecture. – Scientific Research and Essays 8: 6-16.
[49] Ramazani Gourbi, B. (2010): The zoning of human bioclimatic comfort for ecotourism planning in Gilan, Iran South Western of Caspian Sea. – Australian Journal of Basic and Applied Sciences 4(8): 3690-3694.
[50] Richards, M., Havenith, G. (2007): Progress towards the Final UTCI Model. – In: Mekjavic, I. B., Kounalakis, S. N., Taylor, N. A. S. (eds.) Environmental Ergonomics XII. Biomed, Ljubljana, pp. 521-524.
[51] Roshan, G., Yousefi, R., Kovács, A., Matzarakis, A. (2018): A comprehensive analysis of physiologically equivalent temperature changes of Iranian selected stations for the last half century. – Theoretical and Applied Climatology 131: 19-41.
[52] Ruuhela, R., Jylhä, K., Lanki, T., Tiittanen, P., Matzarakis, A. (2017): Biometeorological Assessment of Mortality Related to Extreme Temperatures in Helsinki Region, Finland,

http://www.aloki.hu ● ISSN 1589 1623 (Print) ● ISSN 1785 0037 (Online)
DOI: http://dx.doi.org/10.15666/aeer/1605_54235445
© 2018, ALÖKI Kft., Budapest, Hungary

in 1972-2014. – International Journal of Environmental Research and Public Health 944: 1-19.

[53] Schwartz, J., Samet, J. M., Patz, J. A. (2004): Hospital admissions for heart disease: the effects of temperature and humidity. – Epidemiology 15: 755-761.

[54] Scott, D., Jones, B., McBoyle, G. (2004): Climate, Tourism and Recreation: A Bibliography. – University of Waterloo, Waterloo.

[55] Shakoor, A. (2011): Investigating biophysics and bioclimate effect on the health of tourists in Yazd Province using tourism climate index (TCI). – International Journal of the Physical Science 6: 6607-6622.

[56] Tavoosi, T., Sabzi, B. (2013): Assess the extent of climatic comfort zone Ilam province Evans index. – Geography and Urban Regional Planning 7: 21-34.

[57] Thorsson, S., Honjo, T., Lindberg, F., Eliasson, I., Lim, E. M. (2007): Thermal comfort and outdoor activity in Japanese urban public places. – Environment and Behavior 39: 660-684.

http://www.aloki.hu ● ISSN 1589 1623 (Print) ● ISSN 1785 0037 (Online)
DOI: http://dx.doi.org/10.15666/aeer/1605_54235445
© 2018, ALÖKI Kft., Budapest, Hungary

LAND SURFACE ENERGY BALANCE OF OASIS-DESERT ECOTONE AND ITS RELATIONSHIP WITH SURFACE TEMPERATURE DURING THE SUMMER

LI, L.[1,2] – YAN, R.[1*] – XIONG, H.[3]

[1]*State Key Laboratory of Lake Science and Environment, Nanjing Institute of Geography and Limnology, Chinese Academy of Sciences, 210008 Nanjing, China*

[2]*University of Chinese Academy of Sciences, 100049 Beijing, China*

[3]*College of Arts and Sciences of Beijing Union University, 100083 Beijing, China*

**Corresponding author*
e-mail: rhyan@niglas.ac.cn

(Received 16th Jun 2018; accepted 10th Aug 2018)

Abstract. In this study, land surface energy balance in the oasis-desert ecotone of the northern piedmont of the East Tianshan Mountains, Xinjiang, China was calculated using meteorological data from a Bowen ratio system, in conjunction with modified Bowen ratio method. The daily variation in land surface energy balance was then investigated, along with energy partitioning under different weather conditions. The four weather conditions including sunny day, overcast day, rainy day and average condition. Finally, based on the analysis of relationship between land surface energy and land surface temperature, prediction models for land surface temperature were constructed and validated. The results show that the *splendens* grassland soil has a cache energy function. Latent heat (*LE*) plays a dominant role in the energy budget of the oasis-desert zone for all weather conditions, which is inconsistent with some previous studies on other arid areas. The average value of *LE/Rn* (59%) of this zone is between those of the desert and of the oasis due to the transitional thermal-hydrologic property of the land surfaces and the local circulation. The variations of energy partitioning during the daytime are the same among the different weather conditions, while these curves fluctuate continuously at night, especially before sunrise and after sunset. Except for *H*, the correlations between each energy component and the surface temperature for different conditions are ordered as follows: clear days > average values> overcast days > rainy days. The same rule is also found in the response intensities (regression coefficients) of the land surface temperature to energy change. The established and validated models for land surface temperature suggest that the soil surface layer temperature is mainly influenced by dry heat energy factors (*Rn*, *G*, and *H*) because of not in the summer monsoon zone and coarser soil particle, rather than the hygrothermal energy factor (*LE*).
Keywords: *Bowen ratio, latent heat, sensible heat, energy budget, temperature, Xinjiang*

Introduction

Land surface processes describe the exchange of matter and energy between the earth surface and the atmosphere, which closely connect the atmosphere, hydrosphere, biosphere, and pedosphere (Mathew et al., 2018; Pal and Ziaul, 2017; Xystrakis et al., 2017; Yaşar Korkanç, 2018). The atmosphere-land energy exchange dominated by land surface energy balance significantly impacts the formation and evolution of regional environments and global climate change. Thus, land surface energy balance is the main topic of research on land surface processes. This energy balance directly influences the changes in land surface (soil) temperature. On the other hand, land surface temperature also exert significant effect on energy exchange at the land-atmosphere interface (Burakowski et al., 2018; Wang et al., 2018). Hence, several

http://www.aloki.hu ● ISSN 1589 1623 (Print) ● ISSN 1785 0037 (Online)
DOI: http://dx.doi.org/10.15666/aeer/1605_54475465
© 2018, ALÖKI Kft., Budapest, Hungary

large-scale field experiments on land surface processes consider land surface energy and temperature to be major observational items, such as EFEDA (Osann Jochum et al., 2006), NOPEX (Halldin et al., 1998), BOREAS (Sellers et al., 1995), and EBEX-2000 (Oncley et al., 2007). Significant progress has been made in understanding the land surface energy balance and temperature for different land surfaces/ecosystems, including studies on plateaus (Luo et al., 2018; Zhang et al., 2014), mountains (Gualtieri, 2018; Wagner et al., 2014), deserts (Urqueta et al., 2018), and forests (Gage and Cooper, 2017). Moreover, many studies have found a problem with the unclosure of the energy balance, i.e., the available energy is found to be larger than the sum of the turbulent fluxes of sensible and latent heat measured in these land surfaces (Foken, 2008). This energy unclosure is mainly attributed to the energy storage in the upper soil layer and the heterogeneity of the land surface (Foken et al., 2006). Thus, these two reasons must be considered and corrected through studying the land surface processes, especially in the ecotone where vertical sensible heat advection may generate due to the heterogeneous land surface (Zhang et al., 2012a).

The oasis-desert ecotone that lies between the oases and deserts is an ecologically fragile zone (Tiyip et al., 2005), where characteristics of land surface energy balance strongly affect regional atmospheric circulation and surface temperature. In addition, there are some significant differences in the response of land surface energy balance with surface temperatures to different weather conditions. However, very few studies have focused on these aspects concerning oasis-desert ecotones thus far. Hence, investigating the land surface energy balance and its relationship with land surface temperature in this area can contribute to the research on regional surface energy balance and improve the regional weather and global climate model. It will also provide references for the optimal regulation of water resources in this region. The objectives of this study are: (1) to compare the characteristics of surface energy balance under different weather conditions; (2) to compare the patterns of surface energy partitioning with those of other nine land surfaces in the arid zone of Northwest China; and (3) to quantify the relationship between land surface temperature and energy component.

Materials and methods

Study area

The trial was conducted on the *Achnatherum splendens* grassland near the Wanmuchun forest-farm, Qitai County, Xinjiang Province, China. The area is 2 km southeast of the Gurbantunggut Desert in the northern piedmont of the East Tianshan Mountains. It represents a typical oasis-desert ecotone in northwest China (*Fig. 1*). The geographic location of the study site is 44°11′19″ N, 89°25′32″ E, and the altitude is 693 m above sea level. The climate of the region is temperate continental and arid climate with an annual mean precipitation of only 150 mm, whereas annual potential evaporation reaches above 2100 mm. The average annual temperature is approximately 5 °C, with 2933.6 annual sunshine hours.

The area of experimental zone is approximately 2100 ha (3000 m × 7000 m). It is mainly covered with *A. splendens*, a perennial, densely tufted Gramineae, accompanied by sparse *Sophora alopecuroides* and *Salsola collina Pall*. The total coverage is roughly 30%. The soil is sandy loam, and the groundwater depth range from 3 to 5 m.

http://www.aloki.hu ● ISSN 1589 1623 (Print) ● ISSN 1785 0037 (Online)
DOI: http://dx.doi.org/10.15666/aeer/1605_54475465
© 2018, ALÖKI Kft., Budapest, Hungary

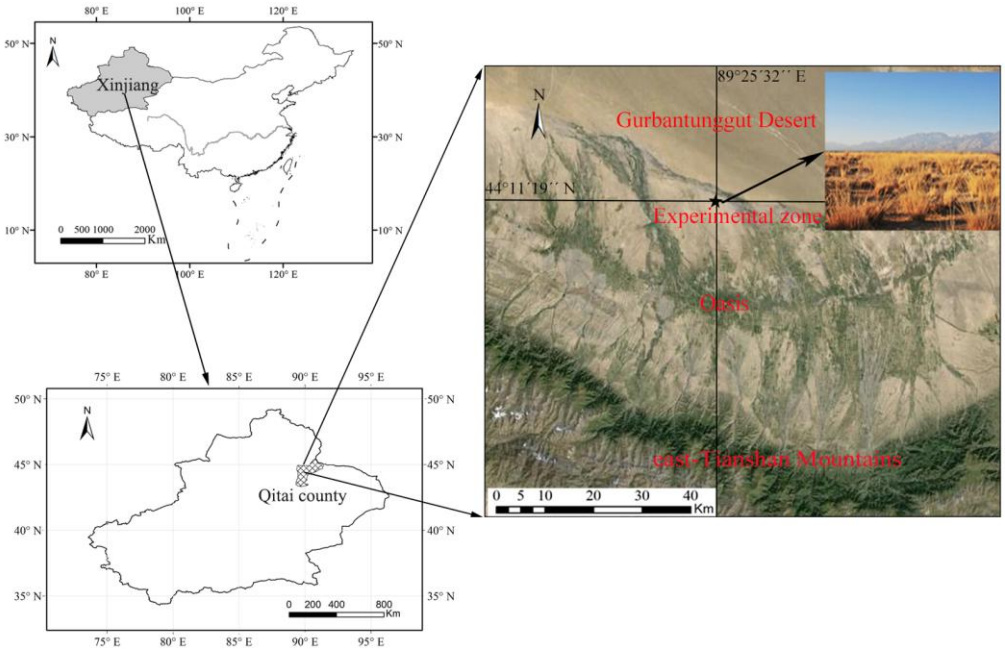

Figure 1. *Location of the study area*

Bowen ratio/energy balance method and its modification

The Bowen ratio/energy balance (BREB) method (Bowen, 1926) has been widely used to measure land surface energy. This method can provide accurate, continuous measurement of micrometeorological elements and energy balance components over an extensive surface area (Dugas and Mayeux Jr, 1991). The core concept of BREB method is to divide the available energy into turbulent sensible heat and latent heat fluxes by using the Bowen ratio (Uddin et al., 2013).

The energy balance of land surface, neglecting small amount of photosynthetic energy storage, can be expressed as:

$$Rn = LE + H + G \quad \text{(Eq.1)}$$

where Rn is the net radiation (W/m^2), LE the latent heat of evapotranspiration (W/m^2), H the sensible heat flux (W/m^2), and G the soil heat flux (W/m^2). Rn and G are obtained from the observation. Except in extremely unstable or stable atmospheric situation, The Bowen ration (β) is defined as the ratio of sensible heat flux to the latent heat (H/LE) (Bowen, 1926). Therefore, *Equation 1* can be rewritten as (*Eq. 2*):

$$LE = (Rn - G) / (1 + \beta) \quad \text{(Eq.2)}$$

The Bowen ratio (β) can be calculated as

$$\beta = H / LE = \rho c_p K_H \Delta t / \rho c_p K_V \Delta e = \gamma (\Delta t / \Delta e) \quad \text{(Eq.3)}$$

where ρ is air density, c_p the specific heat of air at a constant pressure (cal·g^{-1}·K^{-1}). K_H and K_V are the turbulent transfer coefficients for heat and vapour, respectively. γ is

http://www.aloki.hu ● ISSN 1589 1623 (Print) ● ISSN 1785 0037 (Online)
DOI: http://dx.doi.org/10.15666/aeer/1605_54475465
© 2018, ALÖKI Kft., Budapest, Hungary

psychrometric constant, Δt and Δe the differences in the air temperature (°C) and water vapor pressure (hPa) between the two heights, respectively. In *Equation 3,* K_H is assumed to be equal to K_V for neutral to moderately unstable atmospheric condition over smooth terrain (Spittlehouse and Black, 1980). And this assumption is usually valid except in extremely unstable or stable atmospheric condition (Dugas and Mayeux Jr, 1991). For instance, K_H is greater than K_V for stable conditions.

Many previous studies assumed the G to be the direct measured value of soil heat flux transducer at 0.05 m below the soil surface, but in reality G also includes the heat stored in the 0 to 0.05 m layer computed from measurement of the change in temperature of the layer with time and the heat capacity of the layer. Thus its computation should be modified as (*Eq. 4*):

$$G = G_{0.05} + C_S \frac{\partial T}{\partial t} \Delta Z \quad \text{(Eq.4)}$$

where $G_{0.05}$ denotes heat flux obtained from heat flux transducer at 0.05 m below the soil surface (W/m^2), C_S the specific heat of dry soil (J·kg^{-1}·°C^{-1}), $\frac{\partial T}{\partial t}$ is the rate of change in soil temperature over time, and ΔZ the depth of the soil layer measured, i.e., 0.05 m.

Additionally, with respect to the flat and homogeneous surface, vertical sensible heat advection can be not taken into account due to its almost no occurrence. However, since there are some differences in surface thermodynamic properties between the oasis and the desert surface, sensible heat can be advected vertically to some extent in the inhomogeneous surfaces of ecotones, thereby generating vertical sensible heat advection (H_{vad}) (Zhang et al., 2012a, b). Thus, here the sensible heat (H) comprises not only the turbulent sensible heat (H_0) but also comprises the vertical sensible heat advection (H_{vad}) (*Eq. 5*):

$$H = H_0 + H_{vad} \quad \text{(Eq.5)}$$

where H_0 and H_{vad} can be calculated as follows (*Eqs. 6* and *7*):

$$H_0 = \beta LE \quad \text{(Eq.6)}$$

$$H_{vad} = -\rho c_p z_r w_r \frac{\Delta T}{\Delta Z} \quad \text{(Eq.7)}$$

where ρ is air density; c_p is the specific heat capacity of air at a constant pressure (cal·g^{-1}·K^{-1}); w_r is the vertical wind speed of height Z_r; and $\Delta T / \Delta Z$ is the vertical gradient of temperature.

Experimental design

The Bowen ration system (Delta-T Devices Ltd., UK), similar to that used in (Peacock and Hess, 2004; Todd et al., 2000), was set up on the center of the experimental zone. Its main observed elements included net radiation, air temperature, air humidity, wind speed, soil temperature, soil moisture, the soil heat flux, and precipitation. Net radiation was measured at 0.5 m above the maximum height of the

http://www.aloki.hu ● ISSN 1589 1623 (Print) ● ISSN 1785 0037 (Online)
DOI: http://dx.doi.org/10.15666/aeer/1605_54475465
© 2018, ALÖKI Kft., Budapest, Hungary

splendens canopy by a net radiometer. Sensors of air temperature and air humidity were installed in two layers, that is, 0.5 m and 2.5 m above the height of the canopy. Sensors of soil temperature and moisture were arranged in eight layers, that is, 0.05, 0.1, 0.15, 0.2, 0.4, 0.6, 0.8, and 1 m underground. The soil heat flux was measured with soil heat flux plate at 0.05 m below the soil surface. More details on each sensor are listed in *Table 1,* including sensitivity and estimation of errors. The diagrams of measurement configurations Bowen ratio system is seen in *Figure 2*. All observed data were automatically recorded at 30-min intervals by a data collector and then exported by a computer. Measurements were taken from 22 July to 3 September 2010. The distance between the site of instrument setup and the boundary of the experimental zone varied from 1510 m to 3534 m, which meets the fetch requirement that the ratio of fetch (upwind distance of uniform conditions) to the height of the instrument above the surface needs to be greater 100 (Wiernga, 1993).

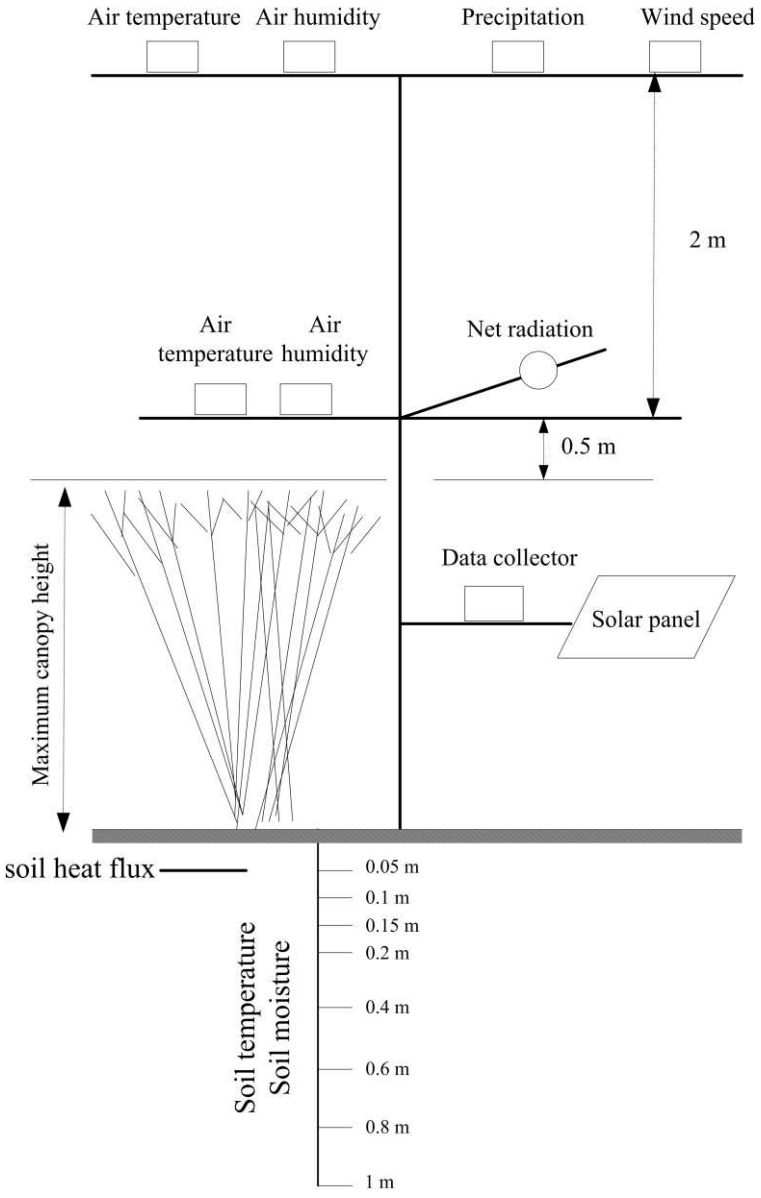

Figure 2. *The scheme of Bowen ratio system*

http://www.aloki.hu ● ISSN 1589 1623 (Print) ● ISSN 1785 0037 (Online)
DOI: http://dx.doi.org/10.15666/aeer/1605_54475465
© 2018, ALÖKI Kft., Budapest, Hungary

Table 1. *Details on each sensors of Bowen ratio system*

Sensor type	Observed item	Measurement range	Sensitivity	Accuracy
NR2	Net radiation	-500~2000W/m^2	0.09049-0.11210mV/W/m^2	±5%(20°C)
RHT2	Air humidity	0–100%	10mV/%RH	±2% (5%<RH<95%); ±2.5%(RH<5%, RH>95%)
AT2	Air temperature	-20–80°C	10mV/°C	±0.5% (0.5°C)
AN3	Wind speed	0.15–75m/s	0.8Hz/m.s^{-1}	±0.1m/s
TRIME-PICO-32	Soil temperature	-15–50°C	–	±0.2°C
TRIME-PICO-64	Soil moisture	0–100%	–	±1% (0<RH<40%); ±2% (40%<RH<70%)
HFP01	Soil heat flux	-2000–2000W/m^2	63.6μV/W/m^2	±5%
RE1	Precipitation	0–500mm/h	–	±0.2mm/h

In addition, in order to analyze the effect of different land surfaces types on energy partitioning, we collected observation data of nine other stations with different surfaces types in the same arid zone of Northwest China, which were mainly obtained from previous published papers (*Fig. 3*). These stations are classified into three groups, namely, Desert/Gobi, Oasis-desert ecotone, and Oasis. *Table 2* lists their geographic information, land surfaces types, and climatic backgrounds.

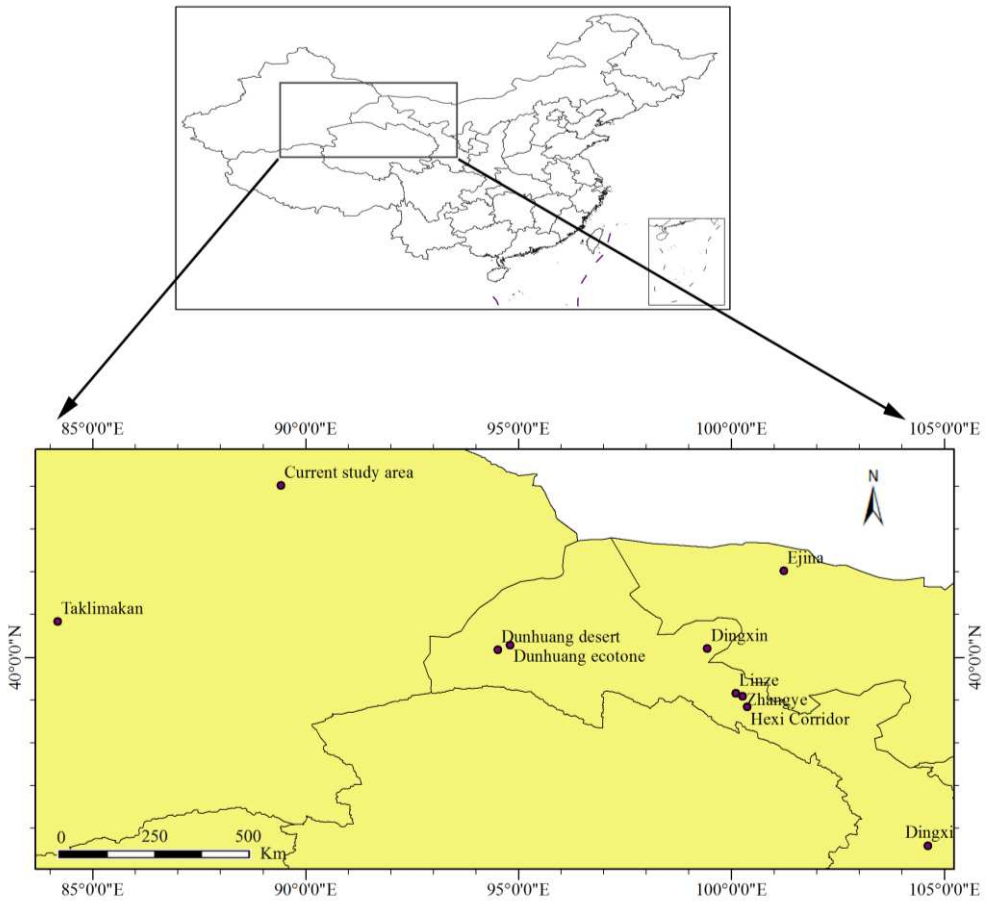

Figure 3. *Location of ten selective observation stations in the arid zone of Northwest China*

http://www.aloki.hu ● ISSN 1589 1623 (Print) ● ISSN 1785 0037 (Online)
DOI: http://dx.doi.org/10.15666/aeer/1605_54475465
© 2018, ALÖKI Kft., Budapest, Hungary

Table 2. *Stations' geographic information and climatic backgrounds in Northwest China*

Land surfaces	Station	Latitude/ Longitude	Altitude (m)	Land cover	Precipitation (mm/yr)	Annual average temperature (°C)	Clear day	Overcast day	Rainy day	Average
Desert/Gobi	Dunhuang[a]	40°10′ N/ 94°31′ E	1150	Desert	39	9.4	√	√	√	√
	Taklimakan[b]	40°48′ N/ 84°18′ E	912	Desert	100	11.5	√	√		√
	Dingxin[c]	40°12′ N/ 99°26′ E	1192	Bare land	65	8.6	√	√	√	√
	Linze[d]	39°09′ N/ 100°06′ E	1480	Desert	95	7.6				√
Oasis–desert ecotone/ Oasis–gobi ecotone	Zhangye[e]	39°05′ N/ 100°16′ E	1480	Sparse grassland	107	7.8	√			
	Ejina[f]	42°01′ N/ 101°14′ E	927	*Phragmites* grassland	38	8.2				√
	Dunhuang[g]	40°30′ N/ 94°75′ E	1090	Sparse *sparsifolia* grassland/Bare land	40	8.9	√			
	Current study area	**44°01′ N/ 89°25′ E**	**693**	***Splendens* grassland**	**150**	**5.5**	√	√	√	√
Oasis	Dingxi[h]	35°35′ N/ 104°37′ E	1897	Non-irrigated farmland	386	6.7	√	√		√
	Hexi Corridor[i]	38°50′ N/ 100°22′ E	1565	Irrigated farmland	100	7.6				√

[a]Zhang and Cao (2003); [b]Wang et al. (2014); [c]Wang et al. (2008); [d]Zheng et al. (2000); [e]Zhang et al. (2007); [f]Si et al. (2010); [g]Wang et al. (2005); [h]Yang et al. (2004); [i]Zheng et al. (2000)
√ in the body of table indicates that the observation data is available

Examining relationship between land surface energy and temperatures

In order to investigate the relationship between soil temperature and surface energy accurately, a Pearson correlation coefficient (Pearson, 1895) and linear regression (Weisberg, 1985) method were used to quantify the relationship between land surface energy and temperatures. More detailed information about the methods can be found in Pearson (1895) and Weisberg (1985)

Results and discussion

Daily variation in land surface energy

In order to analyze the effects of different weather conditions on the land surface energy, 14 typical clear days (total cloud cover < 1 okta), 5 overcast days (total cloud cover > 7 okta), and 2 rainy days (1.2 mm/h, 3–7 okta) are derived from the observation period as sample data. Then, the daily variation in land surface energy at half-hour scales for different weather conditions are shown in *Figures 2–5*. These curves are generated according to the average of the sample data with similar weather conditions.

Clear days

On clear days, all of the surface energy components (*Rn*, *LE*, *H*, and *G*) display a single peak with a clear day-night difference (*Figure 4*). Although the general pattern of *LE* change is the same as that of *Rn* change, its daily maximum is half an hour later than that of *Rn*. *LE* become negative after sunset because of the water vapor exchange

http://www.aloki.hu ● ISSN 1589 1623 (Print) ● ISSN 1785 0037 (Online)
DOI: http://dx.doi.org/10.15666/aeer/1605_54475465
© 2018, ALÖKI Kft., Budapest, Hungary

between soil and atmosphere over a desert surface near an oasis in the summer. After midnight, it shifted to a low positive, thus implying that slight evapotranspiration still occur. *H* is positive in the daytime and negative at night, which suggests that the *H* flux moves from the land surface to the atmosphere in the daytime, while it moves from atmosphere to land surface at night. The range of the daily variation in *G* is only approximately 80 W/m^2, and its daily maximum is more than two hours later than that of *Rn*. When the value of *G* is greater than 0 in the daytime, the soil absorbed heat as a heat sink. By contrast, the soil releases heat as a heat source when the value of *G* is less than 0 at night.

The total daily values on clear day of *Rn*, *LE*, *H*, and *G* are 13.53×10^6, 9.41×10^6, 3.91×10^6, and 0.27×10^6 J/m^2, respectively. This finding indicates that *LE*, rather than *H*, is dominant in terms of surface energy budget (accounting for 70% of *Rn*) on clear days. This is significantly different from the other arid regions in northwest China under the same weather condition. For instances, the value of *LE* is lower than that of *H* in Zhangye oasis-desert ecotone (Zhang et al., 2007) and Dunhuang oasis-gobi ecotone (Wang et al., 2005) over the same period (*Table 3*). This result can be attributed to the fact that the vegetation coverage index of the Zhangye oasis-desert ecotone is only 37% of that of the current study area. Furthermore, the Dunhuang oasis-gobi ecotone is mainly covered with *Alhagi sparsifolia*, where PAI (plant area index, which is the sum of the leaf area index and the woody area index) and annual precipitation is low. Thus, *LE* induced by plant transpiration is lower in the Zhangye and Dunhuang ecotone than that in the current study area. Likewise, *H* is dominant in the Dunhuang Desert (Zhang and Cao, 2003), Taklimakan Desert (Wang et al., 2014), and Dingxin Gobi (Wang et al., 2008) because of sparse vegetation and bare soil (*Table 2*). Although *LE* is dominant in the non-irrigated farmland of Dingxi Oasis (Yang et al., 2004), its proportion is smaller than that of the current study area. This is because farmland is converted into bare land, after reaping wheat in mid-August. These comparisons showed that different vegetation cover conditions significantly affect the surface energy partitioning.

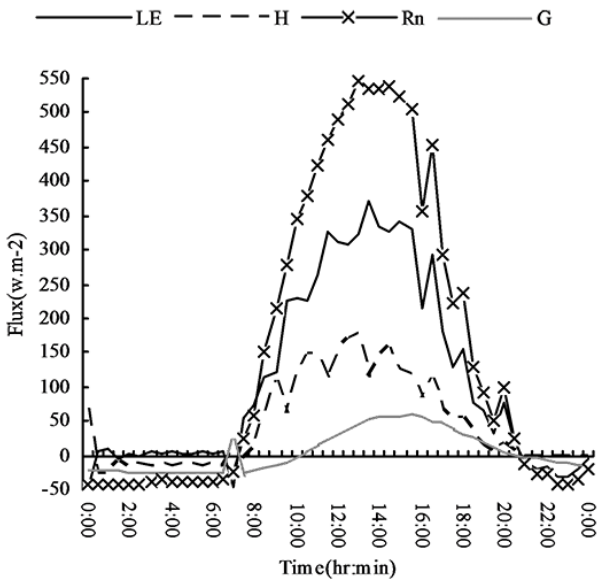

Figure 4. *Daily variations in surface energy balance on clear days in splendens grassland. LE is the latent heat of evapotranspiration, H the sensible heat flux, Rn the net radiation, and G the soil heat flux*

http://www.aloki.hu ● ISSN 1589 1623 (Print) ● ISSN 1785 0037 (Online)
DOI: http://dx.doi.org/10.15666/aeer/1605_54475465
© 2018, ALÖKI Kft., Budapest, Hungary

Table 3. *LE/Rn and H/Rn of different land surfaces on clear and overcast summer days*

Types of underlying surfaces	Clear day		Overcast day	
	LE/Rn	***H/Rn***	***LE/Rn***	***H/Rn***
Current study area	*69.58%*	*28.94%*	*130.80%*	*21.37%*
Dunhuang Desert[a]	1.64%[a]	83.60%[a]	2.73%[a]	155.60%[a]
Taklimakan Desert[b]	21.62%[b]	72.97%[b]	12.83%[b]	92.10%[b]
Dingxin Gobi[c]	8.10%[c]	86.80%[c]	−6.30%[c]	102.20%[c]
Dunhuang oasis–gobi ecotone[d]	18.69%[d]	76.87%[d]	--	--
Zhangye oasis–desert ecotone[e]	9.84%[e]	66.57%[e]	--	--
Dingxi Oasis[f]	54.97%[f]	29.13%[f]	57.65%[f]	27.16%[f]

[a]Zhang and Cao (2003); [b]Wang et al. (2014); [c]Wang et al. (2008); [d]Wang et al. (2005); [e]Zhang et al. (2007); [f]Yang et al. (2004)
-- in the body of table indicates that the observation data is not available

Overcast days

On overcast days, energy curves affected by fluctuating cloudiness are divided into multiple peaks and troughs (*Figure 5*). The highest peaks of *Rn*, *LE*, and *H* are lowered to 46%, 40%, and 45% of the corresponding values on sunny days, respectively. With the exception of the period from 12:00 to 13:30, the value of *G* is less than 0 throughout the day, thus indicating that soil mainly releases heat into the atmosphere as a heat source to compensate for the insufficient *Rn* on overcast days.

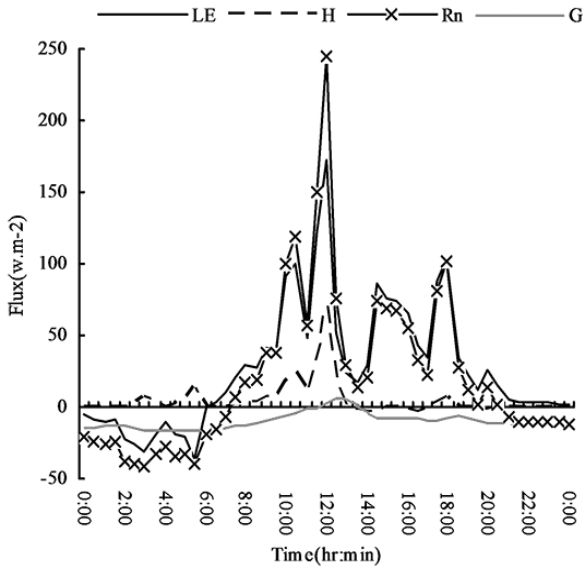

Figure 5. *Daily variations in surface energy balance on overcast days in splendens grassland. LE is the latent heat of evapotranspiration, H the sensible heat flux, Rn the net radiation, and G the soil heat flux*

The total daily values on overcast day of *LE*, *H*, and *G* are 2.32×10^6, 0.38×10^6, and -0.92×10^6 J/m^2. These values account for 130.80%, 21.37%, and −52.16% of *Rn*, respectively. The reason why *LE*/*Rn* > 1 and *G*/*Rn* < 0 is that the soil continually releases heat to the atmosphere to replenish the inadequate energy for evaporation.

http://www.aloki.hu ● ISSN 1589 1623 (Print) ● ISSN 1785 0037 (Online)
DOI: http://dx.doi.org/10.15666/aeer/1605_54475465
© 2018, ALÖKI Kft., Budapest, Hungary

Therefore, the value of *LE* which also includes the additional heat derived from soil, is higher than *Rn*. This phenomenon is specific for the *splendens* grassland and not the Dunhuang Desert, Taklimakan Desert, Dingxin Gobi, and Dingxi Oasis (*Table 3*). That may be explained by the differences in the soil property and vegetation cover among them. Although the value of *Rn* decreased, the large heat storage capacity of *splendens* grassland soil can provide sufficient energy for evapotranspiration on overcast days. As a result, $LE > Rn$ and $G < 0$. This finding demonstrates that *splendens* grassland soil stores heat on clear days, and then releases it on overcast days, that is, it has a cache energy function.

Rainy days

On rainy days, moderate amounts of rain fell early in the morning and stopped at noon. The weather then turned fine. As a result of precipitation, the time-point of each energy balance component begins to increase rapidly is more than four hours later than that on sunny days (*Figure 6*). This lag contributes to the "lagged peak" of each energy curve. The maxima of *Rn* and *H* are 117% and 214% of those generated during sunny days, respectively. This result shows that the few clouds and low air turbidity might enhance the energy exchange between atmosphere and land when the sun shines again once the rain ceases. The peak value of *LE* is similar to that on sunny days. This finding implies that grassland evapotranspiration rate remains high due to the increased available water and increased *Rn* on rainy days. *G* remains negative during rainfall, that is, the soil releases heat to the atmosphere. Once the rain stopped, *G* reaches the minimum value, i.e., the soil releases more energy to the atmosphere and promotes the appearance of the *LE* peak.

The total daily values of *LE*, *H*, and *G* on rainy day are 6.35×10^6, 3.49×10^6, and -6.35×10^5 J/m^2, respectively. These values are responsible for 68.96%, 37.94%, and −6.90% of *Rn*, respectively. This finding indicates that *LE* is dominant in rainy days. That is consistent with the results of Dingxin Gobi and Dunhuang Desert, where *LE* is also dominant because of rainfall.

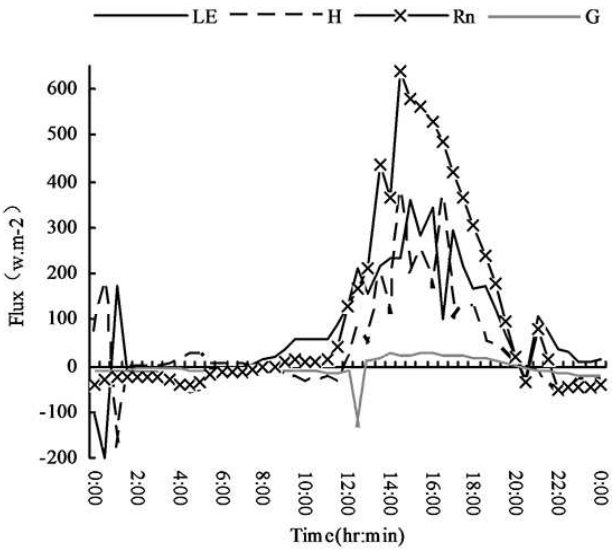

Figure 6. *Daily variations in surface energy balance on rainy days in splendens grassland. LE is the latent heat of evapotranspiration, H the sensible heat flux, Rn the net radiation, and G the soil heat flux*

http://www.aloki.hu ● ISSN 1589 1623 (Print) ● ISSN 1785 0037 (Online)
DOI: http://dx.doi.org/10.15666/aeer/1605_54475465
© 2018, ALÖKI Kft., Budapest, Hungary

Average

The average values of each energy components (calculated from the average of all observed data during the observation period) decrease compared to those of clear days. Nonetheless, the general trends of the daily variation curves are consistent with those observed on clear days (*Figure 7*). The average value of *LE/Rn* (59%) is significantly higher than that observed in the Linze Desert (Zheng et al., 2000), Dunhuang Desert, Taklimakan Desert, and Dingxin Gobi over the same period. However, this value is lower than that obtained in the irrigated farmland of the Hexi Corridor Oasis (Zheng et al., 2000; *Table 4*). As a result of the dry climate and sparse vegetation, the reduced capability of holding and retaining water leads to the severe scarcity of water for evapotranspiration in the first four ecosystems. Nevertheless, in the irrigated farmland of the Hexi Corridor Oasis, the high water content of the soil and vegetation due to the high vegetation coverage and artificial irrigation induces vigorous evapotranspiration. Therefore, *LE* plays a predominant role in the energy exchange, whose proportion is 9.2% larger than that observed in the current study area. The current study area's transition property in the energy partitioning might be attributed to the thermal-hydrologic property between deserts and oases and the local circulation. The differences in the thermal property between the oasis and the desert cause the local circulation. Then the horizontal advection caused by local circulation transfers the hot and dry air from the desert to the oasis-desert ecotone. Consequently, the temperature gradient decreases and the humidity gradient increases that leads to a reduction in *H* and increase in *LE* so that *LE* become predominant in the surface energy budget of ecotone. Moreover, the value of *LE*/*Rn* is slightly higher than that of the Ejina oasis-desert ecotone (Si et al., 2010) because the annual precipitation in the Ejina oasis-desert is only one quarter of that in the current study area. This suggests that surface energy balance is not entirely controlled by vegetation cover, and climatic conditions may be also important.

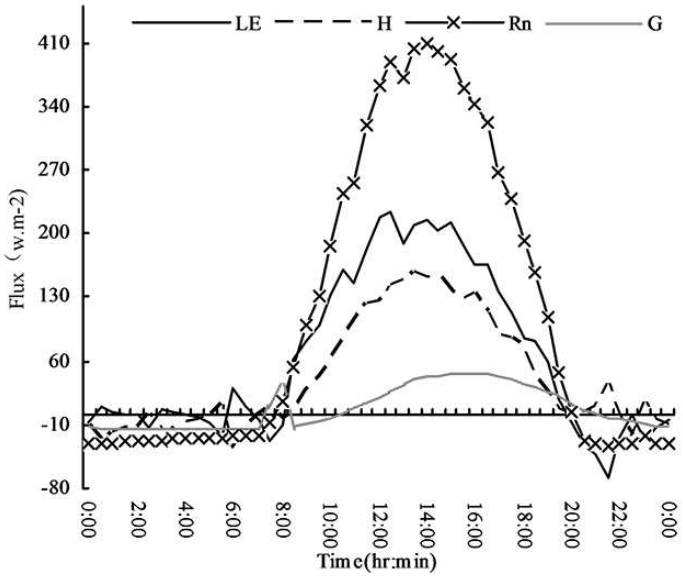

Figure 7. *Daily variations in surface energy balance under the average condition in the splendens grassland. LE is the latent heat of evapotranspiration, H the sensible heat flux, Rn the net radiation, and G the soil heat flux*

http://www.aloki.hu ● ISSN 1589 1623 (Print) ● ISSN 1785 0037 (Online)
DOI: http://dx.doi.org/10.15666/aeer/1605_54475465
© 2018, ALÖKI Kft., Budapest, Hungary

Table 4. *LE/Rn and H/Rn values of different land surfaces under the average condition in summer*

Types of underlying surfaces	*LE/Rn*	*H/Rn*
Current study area	*58.8%*	*37.1%*
Dunhuang Desert [a]	3.80% [a]	86% [a]
Linze Desert[b]	6.70%[b]	88%[b]
Taklimakan Desert[c]	4.5%[c]	52.5%[c]
Dingxin Gobi[d]	5.2%[d]	87%[d]
Ejina oasis–desert ecotone[e]	49.6%[e]	46.2%[e]
Dingxi Oasis[f]	55.5[f]	42.9[f]
Hexi Corridor Oasis[g]	60%–79%[g]	7%–20%[g]

[a]Zhang and Cao (2003); [b]Wang et al. (2005); [c]Wang et al. (2014); [d]Wang et al. (2008); [e]Si et al. (2010); [f]Yang et al. (2004); [g]Zheng et al. (2000)

Daily variation in energy partitioning

Figure 8 shows the daily variations in energy partitioning for different weather conditions. The general pattern in the daytime variation of energy partitioning is similar among the four different weather conditions. The available surface energy is primarily transformed into *LE*, as indicated in the order *LE/Rn* > *H/Rn* > *G/Rn*. However, before midnight (20:30–24:00), *LE/Rn* > *G/Rn* > *H/Rn* is observed for clear days and the average condition, thus suggesting that a certain amount of evapotranspiration still occur (*Fig. 8a* and *d*). By contrast, *H/Rn* is highest on overcast and rainy days at the same time (*Fig. 8b* and *c*). After midnight (24:00–8:00 the next day), *G* is dominant in the energy balance for all different weather conditions except rainy days. It implies that the soil becomes the main heat source of the soil–plant–atmosphere continuum (SPAC) system in the grassland after midnight.

In the daytime, the curves of *G/Rn*, *H/Rn*, and *LE/Rn* have not significant change for each weather condition (*Fig. 8*). However, at night, these curves fluctuated continuously. At sunrise and sunset, with the conversion of the heat source between the atmosphere and the soil (from soil to atmosphere or from atmosphere to soil), the changes in the direction of energy transport and energy intensity trigger the severe oscillation of curves, thus resulting in large peaks or troughs. The range of fluctuation in *LE/Rn* is the widest among all of the curves at sunrise. The result might be because following night condensation, much dew available for evapotranspiration is generated on the soil surface and the vegetation surface at sunrise. Although the value of *Rn* changes from negative to a relatively low positive, this value is far lower than that of *G* (whose direction is negative). Thus, at this point, the value of *LE* is almost equal to the sum of *Rn* and *G.* As a result, *LE/Rn* is greater than 1 (on rainy days, this value is close to 10), thereby mutating *LE/Rn* significantly. It also explains why the trend of change in the curve of *LE/Rn* is opposite to that of *G/Rn* in the peak. The time-points at which all of the curves change substantially in the mornings and evenings of overcast days are half an hour later and half an hour earlier, respectively, than those under the average condition because of the decreased solar radiation and reduced sunshine hours. On sunny days, the time-points are half an hour earlier and four hours later than those under the average condition because of the strong radiation and long sunshine hours. On rainy

http://www.aloki.hu ● ISSN 1589 1623 (Print) ● ISSN 1785 0037 (Online)
DOI: http://dx.doi.org/10.15666/aeer/1605_54475465
© 2018, ALÖKI Kft., Budapest, Hungary

days, the time-points at which all energy curves deviate to the right are one and a half hours later than that under the average condition.

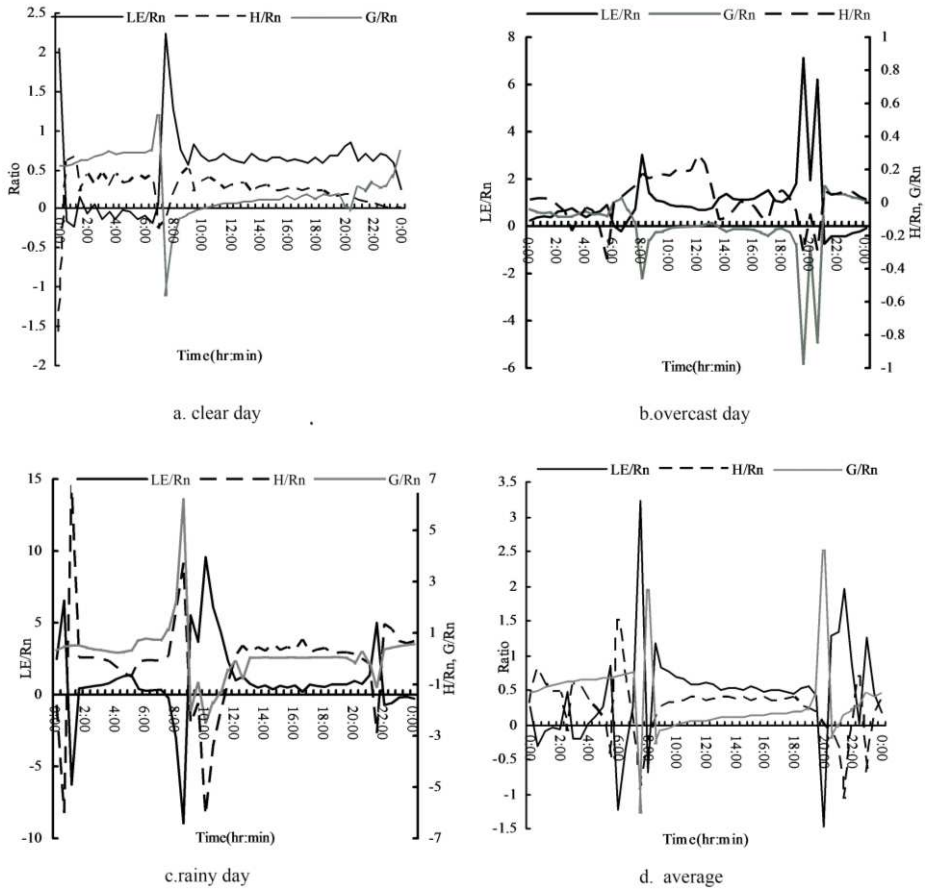

Figure 8. *Daily variations in energy partitioning under different weather conditions. LE is the latent heat of evapotranspiration, H the sensible heat flux, Rn the net radiation, and G the soil heat flux*

Relationship between land surface energy and surface temperature

Correlations between land surface energy and soil temperature at different depths

In order to investigate the relationship between soil temperature and surface energy accurately, this study stratified soil into four layers measuring, namely, 5, 10, 15, and 20 cm. Since surface energy exchange mainly occurs during the daytime, only the results during daytime (8:00–18:00) over the observation period are analyzed here (*Table 5*). Moreover, their significance level is also tested.

The correlation between each energy component and soil temperature decreases gradually and is increasingly negatively correlated, with increasing soil depth (*Table 5*). This finding is due to the gradual delay in the peak time of soil temperature with the increase in depth, which enhanced the non-synchronism between the soil temperature and land surface energy. At 20 cm, the trend of soil temperature is opposite to that of land surface energy; therefore, the correlation between both is predominantly negative. Among the layers, the soil temperature at 5 cm displays the best correlation with energy components. For instance, the coefficient between the soil temperature at 5 cm and *G* is

http://www.aloki.hu ● ISSN 1589 1623 (Print) ● ISSN 1785 0037 (Online)
DOI: http://dx.doi.org/10.15666/aeer/1605_54475465
© 2018, ALÖKI Kft., Budapest, Hungary

0.61, 5.81, 1.72, and 0.54 times larger than those at 10, 15, and 20 cm on average, respectively. This result is ascribed to the fact that the energy exchange firstly begins in the topsoil which is the critical plane of the SPAC system. Therefore, only the relationship between the soil temperature at 5 cm and energy components is analyzed as presented in the following section.

Table 5. *Correlation coefficients between the energy components and soil temperature. ** represents $p < 0.01$, denoting the correlation between the two corresponding variables is statistically highly significant*

	Rn	***G***	***LE***	***H***
$T_{soil\text{-}5cm}$	0.4234**	0.8754**	0.2328**	0.2804**
$T_{soil\text{-}10cm}$	0.0556**	0.5426**	−0.0145	−0.0337
$T_{soil\text{-}15cm}$	−0.2289**	0.1286**	−0.1733**	−0.2675**
$T_{soil\text{-}20cm}$	−0.3653**	−0.3215**	−0.1955**	−0.3667**
$T_{soil\text{-}average}$	0.1410**	0.5695**	0.0707**	0.0241**

The correlations between each energy component (*Rn*, *LE*, *H*, and *G*) and soil temperature are all significant; however, that of *G* and soil temperature is the best. The correlations of *Rn* and *H* with soil temperature are intermediate, while the correlation of *LE* with soil temperature is the least significant (*Table 5*). This finding is mainly resulted from the fact that *G* has the most direct effect on the change in soil temperature compared to other energy components, because it represents the amount of heat passing in and out of the soil. For instance, when the value of *G* is positive and high, the heat flow transferred continuously from the land surface to soil layers, thus accumulating soil energy and increasing soil temperature. However, *Rn*, *LE*, and *H* exerted their indirect effects on the soil temperature by means of *G*. These results demonstrate that soil temperature is more sensitive to *G* than to other energy components.

Relationship between land surface energy and soil temperature under different weather conditions

G is most closely related to soil temperature under sunny conditions, followed by its correlations under overcast and rainy conditions (*Table 6*). On overcast days, the negative correlation between the amount of clouds and soil temperature on overcast days weakens the relationship between *G* and soil temperature. In addition, *Rn* and air temperature decrease on overcast days because of clouds. Thus, *G* lessens and soil temperature changes very slowly. Finally, the correlation coefficient (R^2) between *G* and soil temperature is only 81% of what it is on sunny days (*Table 6b*). On rainy days, a significant cooling effect of precipitation on soil temperature contributes to a negative correlation between precipitation and soil temperature. It interferes with the synchronism of *G* and soil temperature. Thus, the coefficient on rainy days is equivalent to only 50% of that on sunny days (*Table 6c*). Since there are less overcast and rainy days during the observation period, the value of the coefficient under the average condition is similar to that on sunny days (approximately 0.61) (*Table 6d*). The response sensitivity (linear regression coefficient) of soil temperature to change in *G* indicates that the values observed during sunny days are equivalent to those generated under the

http://www.aloki.hu ● ISSN 1589 1623 (Print) ● ISSN 1785 0037 (Online)
DOI: http://dx.doi.org/10.15666/aeer/1605_54475465
© 2018, ALÖKI Kft., Budapest, Hungary

average condition, followed by those observed on overcast days. Those observed on rainy days are the lowest.

Similar to *G*, the linear correlations between *Rn*, *LE*, and soil temperature among different conditions are ordered as follows: sunny days > average condition > overcast days > rainy days. On sunny days, the soil temperature change substantially because of the increased *Rn* and *LE*. Therefore, soil temperature is mostly close to *Rn* and *LE on sunny day* compared to that under other weather condition. On overcast and rainy days, the correlations observed are weakened because of the the interference of clouds and precipitation on these energy components.

The linear correlations between *H* and soil temperature under different conditions are arranged as follows: average condition > rainy days > sunny days > overcast days. The response sensitivity (linear regression coefficients) of soil temperature to change in *H* demonstrates that average condition > sunny days > rainy days > overcast days.

Table 6. *Relationship between land surface energy and soil temperature ($T_{soil\text{-}5cm}$) under different weather conditions*

a.

Items		Regression equation	R^2	P
Sunny day	*G*	$T_{soil\text{-}5cm} = 0.1397\ G + 31.835$	0.6196	0.0000
	Rn	$T_{soil\text{-}5cm} = 0.0102\ Rn + 30.572$	0.1749	0.0034
	LE	$T_{soil\text{-}5cm} = 0.0145\ LE + 30.582$	0.1312	0.0123
	H	$T_{soil\text{-}5cm} = 0.0258\ H + 30.976$	0.0932	0.0369

b.

Items		Regression equation	R^2	P
Overcast day	*G*	$T_{soil\text{-}5cm} = 0.1120G + 27.299$	0.5202	0.0001
	Rn	$T_{soil\text{-}5cm} = 0.0049Rn + 26.967$	0.0942	0.0331
	LE	$T_{soil\text{-}5cm} = 0.0058LE + 27.012$	0.0388	0.1748
	H	$T_{soil\text{-}5cm} = 0.0087H + 27.046$	0.0152	0.3987
	Amount of clouds	$T_{soil\text{-}5cm} = -0.6095AC + 21.527$	0.2812	0.0008

c.

Items		Regression equation	R^2	P
Rainy day	*G*	$T_{soil\text{-}5cm} = 0.0596G + 27.334$	0.3027	0.0003
	Rn	$T_{soil\text{-}5cm} = 0.0036Rn + 26.470$	0.0924	0.0337
	LE	$T_{soil\text{-}5cm} = 0.0009LE + 26.823$	0.0023	0.7450
	H	$T_{soil\text{-}5cm} = 0.0101\ H + 26.488$	0.1837	0.0021
	Precipitation	$T_{soil\text{-}5cm} = -1.3911RF + 27.261$	0.1117	0.0189

d.

Items		Regression equation	R^2	P
Average value	*G*	$T_{soil\text{-}5cm} = 0.1523G + 27.968$	0.6152	0.0000
	Rn	$T_{soil\text{-}5cm} = 0.0107Rn + 27.513$	0.1571	0.0048
	LE	$T_{soil\text{-}5cm} = 0.0126LE + 27.880$	0.0609	0.0874
	H	$T_{soil\text{-}5cm} = 0.0309H + 27.437$	0.1791	0.0025

Surface temperature model

As overcast and rainy days are rare in the observation period, the observed half-hour scale data of thirteen sunny days, four overcast days, and two rainy days derived from

http://www.aloki.hu ● ISSN 1589 1623 (Print) ● ISSN 1785 0037 (Online)
DOI: http://dx.doi.org/10.15666/aeer/1605_54475465
© 2018, ALÖKI Kft., Budapest, Hungary

sample data are used to establish the land surface temperature model using the stepwise multiple linear regression (*Table 7*). In these empirical statistical models, soil temperature is chosen as a dependent variable, where each energy components as independent variables (the amount of clouds and rainfall may be included in overcast and rainy days, respectively). Then, the remaining sample data for different weather conditions are applied to validate the models.

Table 7. *Soil temperature models for different weather conditions*

	Equation for multiple linear stepwise regression	**R^2**	**p**	**F**
Sunny days	$T_{soil\text{-}5cm} = 3.085 \times 10^{-1}G - 2.547 \times 10^{-2}Rn + 2.004 \times 10^{-3}H + 30.427$	0.8093	0.0000	895.19
Overcast days	$T_{soil\text{-}5cm} = 2.469 \times 10^{-1}G - 1.662 \times 10^{-2}Rn + 28.726$	0.6623	0.0000	141.23
Rainy days	$T_{soil\text{-}5cm} = 3.576 \times 10^{-2}G - 3.794 \times 10^{-3}Rn + 1.034 \times 10^{-2}H + 28.203$	0.2112	0.0002	8.39
Average	$T_{soil\text{-}5cm} = 3.444 \times 10^{-1}G - 3.755 \times 10^{2}Rn + 1.8470 \times 10^{-2}H + 30.455$	0.9471	0.0000	268.77

The established models for different weather conditions are all highly significant ($p < 0.01$). However, the models for sunny days ($R^2 = 0.8093$) and for the average condition ($R^2 = 0.9471$) performed best, followed by those for overcast ($R^2 = 0.6623$) and rainy days ($R^2 = 0.2112$) (*Table 7*). For validation, all simulation results agree with the measured values ($p < 0.01$, slope ≈1, the mean bias error MBE is little) (*Fig. 9*). Nonetheless, the sunny model displays a superior R^2 value and slope, followed by the overcast and rainy models. These results might be because the sample size for constructing models is different among different weather conditions.

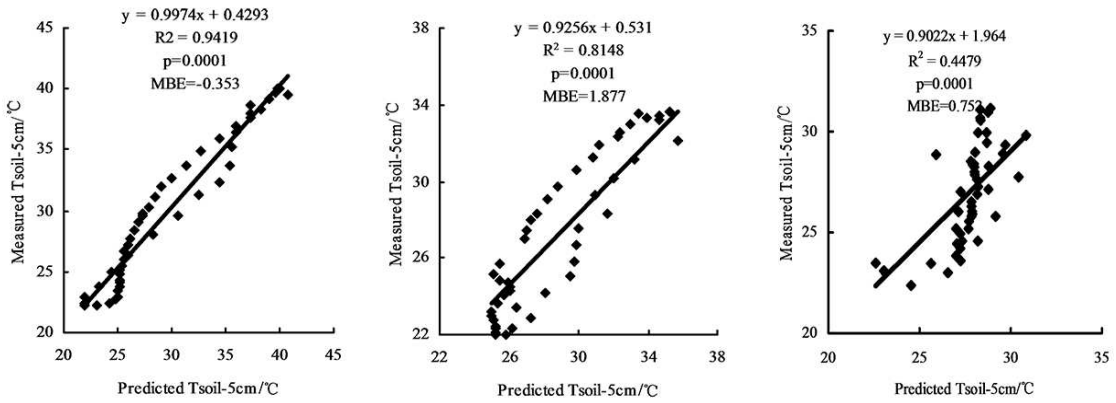

a. sunny day b. overcast day c. rainy day

Figure 9. *Comparisons of simulated versus observed (half-hour) land surface temperatures for model validation*

LE is excluded in the established models using stepwise multiple linear regression method. This result shows that surface layer soil temperature is mainly affected by dry heat energy factors (*Rn*, *G*, and *H*) than to *LE* under various weather conditions (*Table 7*). It might be attributed to the fact that the oasis-desert ecotone in Northwest China is outside the East Asian summer monsoon zone. Thus, there is only minimal

http://www.aloki.hu ● ISSN 1589 1623 (Print) ● ISSN 1785 0037 (Online)
DOI: http://dx.doi.org/10.15666/aeer/1605_54475465
© 2018, ALÖKI Kft., Budapest, Hungary

amount of water available for evapotranspiration in the surface layer soil. Furthermore, the precipitation primarily infiltrates into the deeper soil because of coarser soil particle (sandy loam). Consequently, the strong evapotranspiration power does not directly impact the surface layer temperature, but can affect deeper layer temperature. The result is in contrast to that observed in Northeast China and Loess Plateau (Zhang et al., 2012b), where the soil temperature is sensitive to both dry heat energy factors (*Rn*, *G*, and *H*) and *LE* due to monsoon precipitation and loamy or clay soil.

Conclusions

Unlike the *LE* reported in most previous studies in the Desert/Gobi, the *LE* in the current study area is dominant in the energy exchange for all weather conditions. The average value of *LE*/*Rn* (59%) over the observation period is between that of desert and oasis. These results might be explained by the transitional thermal-hydrologic property and the local circulation. The comparisons of energy partitioning among the ten selected station in the Northwest China, show that the general pattern in energy partitioning is significantly affected by the vegetation coverage, as well as climatic condition.

At sunrise and sunset, the conversion of the heat source between the atmosphere and the soil contributes to large peaks or troughs in the energy fluxes curves. At sunrise, the fluctuation amplitude of *LE/Rn* is the greatest among all of the curves. As a result of different radiation intensities and sunshine hours, there is a difference in the time-point at which energy fluxes begins to change violently in mornings and evenings among the four different weather conditions.

The correlations between each energy component and soil temperature imply that they are all highly significant for all weather conditions. However, they are ordered as follows: $G > Rn > H > LE$. The correlations of *G*, *Rn*, *LE*, and soil temperature under different weather conditions can be ranked as follows: sunny days > average value > overcast days > rainy days. Moreover, the response sensitivity (regression coefficients) of soil temperature to change in each energy component indicates that the average and sunny conditions are equal, followed by the overcast and rainy conditions.

The prediction models for land surface temperature without *LE* under different weather conditions imply that soil surface layer temperature is mainly affected by dry heat energy factors (*Rn*, *G*, and *H*) and less sensitive to the hygrothermal energy factor (*LE*) in the oasis-desert ecotone. It is difficult for us to make an in-depth, detailed analysis on the mechanism of land surface process in the oasis-desert ecotone due to the limited temporal coverage. Thus, it's necessary to accumulate longer time series of observational data for refining our findings.

Acknowledgements. This study is supported by Major Science and Technology Program for Water Pollution Control and Treatment (2017ZX07203002-02), National Natural Science Foundation of China (41701031), Water Resources Science and Technology Program of Jiangsu Water Resources Department (2017002ZB), and Talents-Import Program in Nanjing Institute of Geography and Limnology (NIGLAS2017QD06).

REFERENCES

[1] Bowen, I. S. (1926): The ratio of heat losses by conduction and by evaporation from any water surface. – Physical Review 27: 779.

http://www.aloki.hu ● ISSN 1589 1623 (Print) ● ISSN 1785 0037 (Online)
DOI: http://dx.doi.org/10.15666/aeer/1605_54475465
© 2018, ALÖKI Kft., Budapest, Hungary

[2] Burakowski, E., Tawfik, A., Ouimette, A., Lepine, L., Novick, K., Ollinger, S., Zarzycki, C., Bonan, G. (2018): The role of surface roughness, albedo, and Bowen ratio on ecosystem energy balance in the Eastern United States. – Agricultural and Forest Meteorology 249: 367-376.
[3] Dugas, W. A., Mayeux Jr, H. S. (1991): Evaporation from rangeland with and without honey mesquite. – Journal of Range Management 161-170.
[4] Foken, T. (2008): The energy balance closure problem: an overview. – Ecological Applications 18: 1351-1367.
[5] Foken, T., Wimmer, F., Mauder, M., Thomas, C., Liebethal, C. (2006): Some aspects of the energy balance closure problem. – Atmospheric Chemistry and Physics 6: 4395-4402.
[6] Gage, E. A., Cooper, D. J. (2017): Urban forest structure and land cover composition effects on land surface temperature in a semi-arid suburban area. – Urban Forestry & Urban Greening 28: 28-35.
[7] Gualtieri, G. (2018): Surface turbulence intensity as a predictor of extrapolated wind resource to the turbine hub height: method's test at a mountain site. – Renewable Energy 120: 457-467.
[8] Halldin, S., Gottschalk, L., van de Griend, A. A., Gryning, S.-E., Heikinheimo, M., Högström, U., Jochum, A., Lundin, L.-C. (1998): NOPEX—a northern hemisphere climate processes land surface experiment. – Journal of Hydrology 212: 172-187.
[9] Luo, D., Jin, H., Marchenko, S. S., Romanovsky, V. E. (2018): Difference between near-surface air, land surface and ground surface temperatures and their influences on the frozen ground on the Qinghai-Tibet Plateau. – Geoderma 312: 74-85.
[10] Mathew, A., Khandelwal, S., Kaul, N., Chauhan, S. (2018): Analyzing the diurnal variations of land surface temperatures for surface urban heat island studies: Is time of observation of remote sensing data important? – Sustainable Cities and Society 40: 194-213.
[11] Oncley, S. P., Foken, T., Vogt, R., Kohsiek, W., DeBruin, H., Bernhofer, C., Christen, A., Van Gorsel, E., Grantz, D., Feigenwinter, C. (2007): The energy balance experiment EBEX-2000. Part I: overview and energy balance. – Boundary-Layer Meteorology 123: 1-28.
[12] Osann Jochum, M. A., de Bruin, H. A. R., Holtslag, A. A. M., Belmonte, A. C. (2006): Area-averaged surface fluxes in a semiarid region with partly irrigated land: Lessons learned from EFEDA. – Journal of Applied Meteorology and Climatology 45: 856-874.
[13] Pal, S., Ziaul, S. (2017): Detection of land use and land cover change and land surface temperature in English Bazar urban centre. – The Egyptian Journal of Remote Sensing and Space Science 20: 125-145.
[14] Peacock, C., Hess, T. (2004): Estimating evapotranspiration from a reed bed using the Bowen ratio energy balance method. – Hydrological Processes 18: 247-260.
[15] Pearson, K. (1895): Note on regression and inheritance in the case of two parents. – Proceedings of the Royal Society of London 58: 240-242.
[16] Sellers, P., Hall, F., Ranson, K. J., Margolis, H., Kelly, B., Baldocchi, D., den Hartog, G., Cihlar, J., Ryan, M. G., Goodison, B. (1995): The boreal ecosystem-atmosphere study (BOREAS): an overview and early results from the 1994 field year. – Bulletin of the American Meteorological Society 76: 1549-1577.
[17] Si, J., Feng, Q., Zhang, Y., Chang, Z., Zhang, K. (2010): Research on evapotranspiration and energy budget of phragmites australis stand in Oasis. – Arid Zone Research 27: 160-168.
[18] Spittlehouse, D., Black, T. (1980): Evaluation of the Bowen ratio/energy balance method for determining forest evapotranspiration. – Atmosphere-Ocean 18: 98-116.
[19] Tiyip, T., CUI, J.-y., DING, J.-l. (2005): Study on the means of groundwater distribution beneath the oasis-desert ecotone in an arid area by using thermal infrared data. – Arid Land Geography 2: 025.
[20] Todd, R. W., Evett, S. R., Howell, T. A. (2000): The Bowen ratio-energy balance method for estimating latent heat flux of irrigated alfalfa evaluated in a semi-arid, advective environment. – Agricultural and Forest Meteorology 103: 335-348.

http://www.aloki.hu ● ISSN 1589 1623 (Print) ● ISSN 1785 0037 (Online)
DOI: http://dx.doi.org/10.15666/aeer/1605_54475465
© 2018, ALÖKI Kft., Budapest, Hungary

[21] Uddin, J., Hancock, N. H., Smith, R. J., Foley, J. P. (2013): Measurement of evapotranspiration during sprinkler irrigation using a precision energy budget (Bowen ratio, eddy covariance) methodology. – Agricultural Water Management 116: 89-100.
[22] Urqueta, H., Jódar, J., Herrera, C., Wilke, H.-G., Medina, A., Urrutia, J., Custodio, E., Rodríguez, J. (2018): Land surface temperature as an indicator of the unsaturated zone thickness: A remote sensing approach in the Atacama Desert. – Science of the Total Environment 612: 1234-1248.
[23] Wagner, M. J., Bladon, K. D., Silins, U., Williams, C. H., Martens, A. M., Boon, S., MacDonald, R. J., Stone, M., Emelko, M. B., Anderson, A. (2014): Catchment-scale stream temperature response to land disturbance by wildfire governed by surface-subsurface energy exchange and atmospheric controls. – Journal of Hydrology 517: 328-338.
[24] Wang, H., HU, Z., Ma, W., LI, D. (2008): The seasonal variation of microclimate characteristics and energy transfer in the surf ace layer over Dingxin Gobi. – Chinese Journal of Atmospheric Sciences 32: 1458-1470.
[25] Wang, S., Zhang, Q., Wei, G. (2005): Analyses on characters of surface radiation and energy at oasis-desert transition zone in Dunhuang. – Plateau Meteorology 24: 556-562.
[26] Wang, S., Ma, Q., Ding, H., Liang, H. (2018): Detection of urban expansion and land surface temperature change using multi-temporal landsat images. – Resources, Conservation and Recycling 128: 526-534.
[27] Wang, Y., Ali, M., He, Q., Yang, X., Huo, W., Zhang, J. (2014): Research on surface energy budget in the north margin of Taklimakan Desert. – Desert and Oasis Meterorology 8: 34-41.
[28] Weisberg, S. (1985): Applied Linear Regression. – Wiley, New York, pp. 371-372.
[29] Wiernga, J. (1993): Representative roughness parameters for homogeneous terrain. – Boundary-Layer Meteorology 63: 323-363.
[30] Xystrakis, F., Psarras, T., Koutsias, N. (2017): A process-based land use/land cover change assessment on a mountainous area of Greece during 1945–2009: Signs of socio-economic drivers. – Science of the Total Environment 587-588: 360-370.
[31] Yang, X., Zhang, Q., Wang, R., Ma, P., Yang, Q., Liu, H. (2004): Experimental study on surface energy balance over Loess Plateau of middle part Gansu in summer. – Plateau Meteorology 23: 828-834.
[32] Yaşar Korkanç, S. (2018): Effects of the land use/cover on the surface runoff and soil loss in the Niğde-Akkaya Dam Watershed, Turkey. – Catena 163: 233-243.
[33] Zhang, K., Wang, R., Zhang, Q., Si, J., Yang, Q., Liu, H., Wang, H. (2007): Characteristics of surface radiation and energy balance as well microclimate within oasis-desert ecotone of Zhangye on typical clear days in summer. – Journal of Desert Research 27: 1055-1061.
[34] Zhang, Q., Cao, X. (2003): The influence of synoptic conditions on the averaged surface heat and radiation budget energy over desert or Gobi. – Chinese Journal of Atmospheric Sciences 27: 245-254.
[35] Zhang, Q., Li, H., Zhao, J. (2012a): Modification of the land surface energy balance relationship by introducing vertical sensible heat advection and soil heat storage over the Loess Plateau. – Science China Earth Sciences 55: 580-589.
[36] Zhang, Q., Zeng, J., Zhang, L. (2012b): Characteristics of land surface thermal-hydrologic processes for different regions over North China during prevailing summer monsoon period. – Science China Earth Sciences 55: 1872-1880.
[37] Zhang, Q., Zhang, L., Huang, J., Zhang, L. Y., Wang, W. Y., Sha, S. (2014): Spatial distribution of surface energy fluxes over the Loess Plateau in China and its relationship with climate and the environment. – Sci. China-Earth Sci. 57: 2135-2147.
[38] Zheng, H., Wang, J., Maitani, T., Ohtaki, E., Huang, Z., Zhao, S. (2000): Some characteristics of energy exchange at the underlying surface of desert and oasis in Hexi Corridor. – Acta Ecologica Sinica 20: 88-92.

http://www.aloki.hu ● ISSN 1589 1623 (Print) ● ISSN 1785 0037 (Online)
DOI: http://dx.doi.org/10.15666/aeer/1605_54475465
© 2018, ALÖKI Kft., Budapest, Hungary

GENOME-WIDE CHARACTERIZATION AND ANALYSIS OF SBP TRANSCRIPTION FACTOR FAMILY IN COMMON BEAN (*PHASEOLUS VULGARIS* L.)

ILHAN, E.

Department of Molecular Biology and Genetics, Erzurum Technical University
Erzurum, Turkey
(e-mail: emre.ilhan@erzurum.edu.tr; phone:+90-444-5388-2387)

(Received 6th Jul 2018; accepted 14th Aug 2018)

Abstract. SQUAMOSA promoter binding proteins (SBPs) are considered as being a major family of plant-specific transcription factors which plays an important role in flower improvement process. To discover SBP genes in common bean [*Phaseolus vulgaris* (L.)] genome, in silico analysis methods were carried out in this study. Twenty-three members of Pvul-SBP gene family were identified from common bean genome. A phylogenetic tree drawn using SPB proteins of *Phaseolus vulgaris*, *Arabidopsis thaliana* and *Glycine max* was separated into three main groups (A, B, and C). The C group was clustered into nine subclades. The chromosome locations of *Pvul-SBP* genes showed that *Pvul-SBP-1*/*Pvul-SBP-6*, *Pvul-SBP-2*/*Pvul-SBP-16*, *Pvul-SBP-5*/*Pvul-SBP-14* and *Pvul-SBP-9*/*Pvul-SBP-15* gene couples were segmentally-duplicated. Also, orthologue genes were defined using SBP proteins of *Arabidopsis thaliana* and *Glycine max*. The expression levels of *Pvul-SBP* genes in different plant tissues such as roots, leaf and floral organs showed some of *Pvul-SBP* genes were up or down regulated in certain tissue types. The results of this research would provide the estimation of the evolutionary relationships between *SBP* genes in various plants such as *P. vulgaris*, *G. max* and *A. thaliana*.
Keywords: *gene expression, orthologue relationship, phylogeny, synteny*

Introduction

Identification and characterization of transcription factor (TF) families in plants has been turned into one of the most important topics for plant scientists in recent years due to their importance in regulation networks of plant growing processes (Buyuk et al., 2016; Inal et al., 2017; Ilhan et al., 2018). There have been many well-conducted studies for characterization of several plant-specific TFs in many plant species. However, there is no information about some of them including SBP (SQUAMOSA promoter binding protein family) in certain plant species (Wang et al., 2015).

SBPs are considered as being a major family of plant-specific transcription factors which plays an important role in flower improvement processes (Pan et al., 2017). SBP domain, a highly-conserved DNA-binding domain, has specific properties for each member of this TF family. Even though this domain is known to be a zinc-binding domain, structures within this domain are not similar to those ones in other zinc-binding domains and thus has been declared as representing a novel type of zinc binding motif (Wang et al., 2015).

Recent studies which were aimed at defining the roles of SBP family of transcription factors showed divergent roles of them in plant developmental processes (Zhang et al., 2016).

Among sixteen identified *SBP* genes in *Arabidopsis* genome, many of them have been revealed to play role in embryogenesis (Unte et al., 2003), development of shoots and leaves (Schwarz et al., 2008), flowering process (Gandikota et al., 2007), transition

http://www.aloki.hu ● ISSN 1589 1623 (Print) ● ISSN 1785 0037 (Online)
DOI: http://dx.doi.org/10.15666/aeer/1605_54675480
© 2018, ALÖKI Kft., Budapest, Hungary

between vegetative and generative phases (Jung et al., 2012) and plant hormone signaling (Zhang et al., 2007)

Genome-wide characterization and expression studies of SBP genes have been conducted in a number of plant species including *Betula pendula*, *Chlamydomonas*, *Oryza sativa*, *Zea mays*, *Populus trichocarpa*, *L. esculentum*, *Malus* × *domestica* Borkh., *Salvia miltiorrhiza*, *Gossypium hirsutum*, *Arachis hypogaea* L., petunia, *Capsicum annuum* L., *Chrysanthemum morifolium*, *Phyllostachys edulis*, *Solanum tuberosum*, *Ziziphus jujuba* and (Lannenpaa et al., 2004; Kropat et al., 2005; Xie et al., 2006; Chuck et al., 2010; Lu et al., 2011; Salinas et al., 2012; Li et al., 2013; Zhang et al., 2014, 2015, 2016; Li et al., 2016; Preston et al., 2016; Song et al., 2016; Pan et al., 2017; Kavas et al., 2017; Shao et al., 2017).

The common bean [Phaseolus vulgaris (L.)] is a self-pollinated legume species. It has a small genome size of 588 Mbp and a diploid genome ($2n = 2x = 22$) (Arumuganthan and Earle, 1991). It is one of the earliest plant species cultivated. As a result of its nitrogen fixation ability, it enriches the nitrogen content of soil. It has an important role in human nutrition, especially in developing countries, due to its high protein content (Broughton et al., 2003). It has been possible to analyze and characterize the SBP gene family with the publication of the whole genome sequence of common bean by Schmutz in 2014 (Schmutz et al., 2014). However, the SPB proteins in *Phaseolus vulgaris* L. have not been identified and characterized yet. To fill this gap in the literature and due to importance of this gene family in plant developmental processes, this study aimed at describing and characterizing SBP proteins in *Phaseolus vulgaris* L. Accordingly, 23 Phvul-SBP members were identified and comprehensive analysis of the sequence phylogeny, genomic organization, exon-intron architecture variation, conserved protein motifs, gene duplication events, and expression analysis were performed.

Materials and methods

Identification of SBP genes in P. vulgaris genome

Phaseolus vulgaris of SBP protein sequences were retrieved from Phytozome database v12.1 (www.phytozome.net) using keyword searching with Pfam Accession Number (PF03110) obtained from Pfam Database (http://pfam.xfam.org). BLASTP and BLASTX searches (National Center for Biotechnology Information [NCBI]: http://www.ncbi.nlm.nih.gov) was used to confirm Pvul-SBP proteins. Non-redundant sequences were obtained using decrease redundancy tool (http://web.expasy.org/decrease_redundancy/). SBP domains in non-redundant sequences were checked by HMMER (http://www.ebi.ac.uk). The solid and chemical traits of SBP proteins in *Phaseolus vulgaris*, such as the theoretical isoelectric point (pI), the number of amino acids, and the molecular weight (Da), were identified using the ProtParam tool (http://web.expasy.org/protparam/).

Phylogenetic analysis, physical location, conserved motifs of phvul-SBP genes, gene structure and gene duplication events

Chromosomal locations and CDS sizes (bp) were identified by using Phytozome database v12.1. The *Pvul-SBP* genes were mapped with MapChart (Voorrips, 2002).

http://www.aloki.hu ● ISSN 1589 1623 (Print) ● ISSN 1785 0037 (Online)
DOI: http://dx.doi.org/10.15666/aeer/1605_54675480
© 2018, ALÖKI Kft., Budapest, Hungary

Multiple sequence alignment of Pvul-SBP proteins was conducted with ClustalW. Phylogenetic analysis was performed using MEGA v7 (Tamura et al., 2013) and Neighbor-joining (NJ) algorithm with 1000 replicated-bootstrap value.

The conserved motifs in Pvul-SBP protein sequences were identified using the MEME (Multiple Expectation Maximization for Motif Elucidation) online tool (Bailey et al., 2006). The limits for maximum number of motifs and minimum/maximum width were adjusted as 20 and 2, 50, respectively. Motif sites were among 2 and 300. Site distribution was set as any number of repetitions. The described conserved motifs were examined in InterProscan with default adjusting (Quevillon et al., 2005).

Online Gene Structure Display Server program tool (GSDS) was used (Guo et al., 2007) to predict the exon/intron organization of the *Pvul-SBP* genes. Genomic DNA sequences and coding sequences of Pvul-SBP genes were utilized.

Segmental duplicate gene pairs were examined on the Plant Genome Duplication Database server (PGDD) (Lee et al., 2013), with a display range of 100 kb. The nonsynonymous rates (Ka), synonymous rates (Ks) and developmental constraints (Ka/Ks) with the duplicated pairs of Pvul-SPLs were evaluated using the CODEML program in PAML (Yang, 2007). The roughly date of the duplication events was determined using $T = Ks / 2\lambda \times 10^{-6}$ Mya (million years ago), in terms of the synonymous substitution rates (λ) in common bean of 8.46×10^{-9} (Schmutz et al., 2014).

Synteny analysis

P. vulgaris and *A. thaliana*, *P. vulgaris* and *G. max* of orthologue *SBP* genes were identified with PGDD (Lee et al., 2013). Then, the protein sequences of orthologue genes were retrieved from Phytozome v12.1. The retreived synteny map was created using iTAK - Plant Transcription factor & Protein Kinase Identifier and Classifier (Zheng et al., 2016).

Gene expression analysis in silico

The expression levels of Pvul-SBP genes examined in special tissue libraries of plants at different stages of growth, including root_10 (10 days after planting), nodules, root_19 (19 days after planting), young pods, stem_10 (10 days after planting), stem_19 (19 days after planting), green mature buds, leaves, young triloliates, flower buds and flowers were retrieved from Phytozome Database v12.1 (http://phytozome.jgi.doe.gov/pz/portal.html#!info?alias=Org_Pvulgaris). FPKM (expected number of fragments per kilobase of transcript sequence per millions base pairs sequenced) units were used for the expression levels *in silico*. FPKM values were log2 transformed and the heatmap was produced with the algorithm CIMMiner (http://discover.nci.nih.gov/cimminer).

Results and discussion

Identification of SBP gene family in common bean

Sequences of SBP proteins in the *P. vulgaris* genome were downloaded from Phytozome database v12.1 (www.phytozome.net) using keyword searching with Pfam Accession Number (PF03110) retrieved from Pfam Database. Subsequently, SBP domains were analyzed by searching HMMER and Pfam databases in candidate Phvul-

http://www.aloki.hu ● ISSN 1589 1623 (Print) ● ISSN 1785 0037 (Online)
DOI: http://dx.doi.org/10.15666/aeer/1605_54675480
© 2018, ALÖKI Kft., Budapest, Hungary

SBP proteins and the redundant sequences were discarded after the confirmation. A total of 23 candidate *Phvul-SBP* genes in *Phaseolus vulgaris* genome was discovered and some descriptive information was given in *Table 1* which involves the information about chromosomal location, the coding sequences (CDS, lengths), amino acid (length), molecular weight and number of isoelectric point (pI). As shown in *Table 1* and *Figure 1,* all of the non-redundant *Phvul-SBP* genes were distributed on 10 chromosomes of P. vulgaris. While the lowest number of *Phvul-SBP* genes was obtained on chromosome 11 (one *Phvul-SBP* gene), the highest number of Phvul-SBPs was found on chromosome 3 (4 *Phvul-SBP* genes) (*Fig. 1*). The CDS of the *Phvul-SBP* genes extended from 378 (*Phvul-SBP-4*) to 3210 (*Phvul-SBP-9*). The length of Phvul-SBP proteins extended from 125 (Phvul-SBP-4) to 1039 (Phvul-SBP-9) amino acids (aa). pIs of Phvul-SBP proteins were among 5.8 (Phvul-SBP-15) and 9.46 (Phvul-SBP-12) ranging from acidic to alkaline, and the molecular weight of Phvul-SBPs were between 14756.09 Da (Phvul-SBP-14) and 114838.01 Da (Phvul-SBP-9) (*Table 1*). *SBP* gene family which is essential to plants was detected and classified in various species such as *Arabidopsis* (Rhoades et al., 2002), rice (Xie et al., 2006), tomato (Salinas et al., 2012), *Citrus* (Shalom et al., 2015), *Gossypium raimondii* (Ali et al., 2017), wheat (Wang et al., 2015), maize (Mao et al., 2016) and grape (Hou et al., 2013).

Table 1. *The information of 23 Phvul-SBP proteins*

Gene ID	Phytozome ID	Chromosomal location	CDS length	aa length	Molecular weight (kDa)	pI
Phvul-SBP-1	Phvul.001G091400	Chr01:15552500..15556152	1095	364	40.66	7.16
Phvul-SBP-2	Phvul.001G141000	Chr01:38299114..38303396	1074	357	38.20	8.97
Phvul-SBP-3	Phvul.001G262600	Chr01:50971750..50975439	1362	453	49.63	7.58
Phvul-SBP-4	Phvul.002G114500	Chr02:24504136..24505511	378	125	13.99	9.19
Phvul-SBP-5	Phvul.002G230300	Chr02:40279842..40282041	510	169	19.49	5.47
Phvul-SBP-6	Phvul.002G286000	Chr02:45529658..45533339	1152	383	41.91	8.82
Phvul-SBP-7	Phvul.003G008800	Chr03:989197..995182	3030	1009	111.88	8.45
Phvul-SBP-8	Phvul.003G039600	Chr03:4337189..4341787	1443	480	53.96	6.4
Phvul-SBP-9	Phvul.003G120700	Chr03:30548630..30555522	3120	1039	114.84	7.35
Phvul-SBP-10	Phvul.003G182900	Chr03:40612076..40617217	1650	549	60.30	6.49
Phvul-SBP-11	Phvul.005G074000	Chr05:13162582..13164100	576	191	21.61	8.86
Phvul-SBP-12	Phvul.005G101900	Chr05:31789454..31791276	510	169	19.30	9.46
Phvul-SBP-13	Phvul.006G159700	Chr06:26373187..26387876	2289	762	85.64	6.85
Phvul-SBP-14	Phvul.006G183900	Chr06:28501741..28503445	384	127	14.76	6.45
Phvul-SBP-15	Phvul.007G210600	Chr07:33265157..33272512	3045	1014	112.51	5.8
Phvul-SBP-16	Phvul.007G258400	Chr07:37986117..37990987	1107	368	39.58	8.76
Phvul-SBP-17	Phvul.008G157100	Chr08:28607666..28613632	1035	344	37.55	9.15
Phvul-SBP-18	Phvul.008G157200	Chr08:28427029..28429343	951	316	34.55	8.82
Phvul-SBP-19	Phvul.009G165100	Chr09:24615068..24618431	1194	397	43.71	7.67
Phvul-SBP-20	Phvul.009G219200	Chr09:33103356..33114413	3096	1031	113.97	6.59
Phvul-SBP-21	Phvul.010G056000	Chr10:10002440..10005618	993	330	36.35	8.85
Phvul-SBP-22	Phvul.010G056200	Chr10:10088279..10091188	1119	372	41.02	6.9
Phvul-SBP-23	Phvul.011G164800	Chr11:46749842..46751202	561	186	20.80	8.97

pI: Theoretical isoelectric point, kDa: kiloDalton

http://www.aloki.hu ● ISSN 1589 1623 (Print) ● ISSN 1785 0037 (Online)
DOI: http://dx.doi.org/10.15666/aeer/1605_54675480
© 2018, ALÖKI Kft., Budapest, Hungary

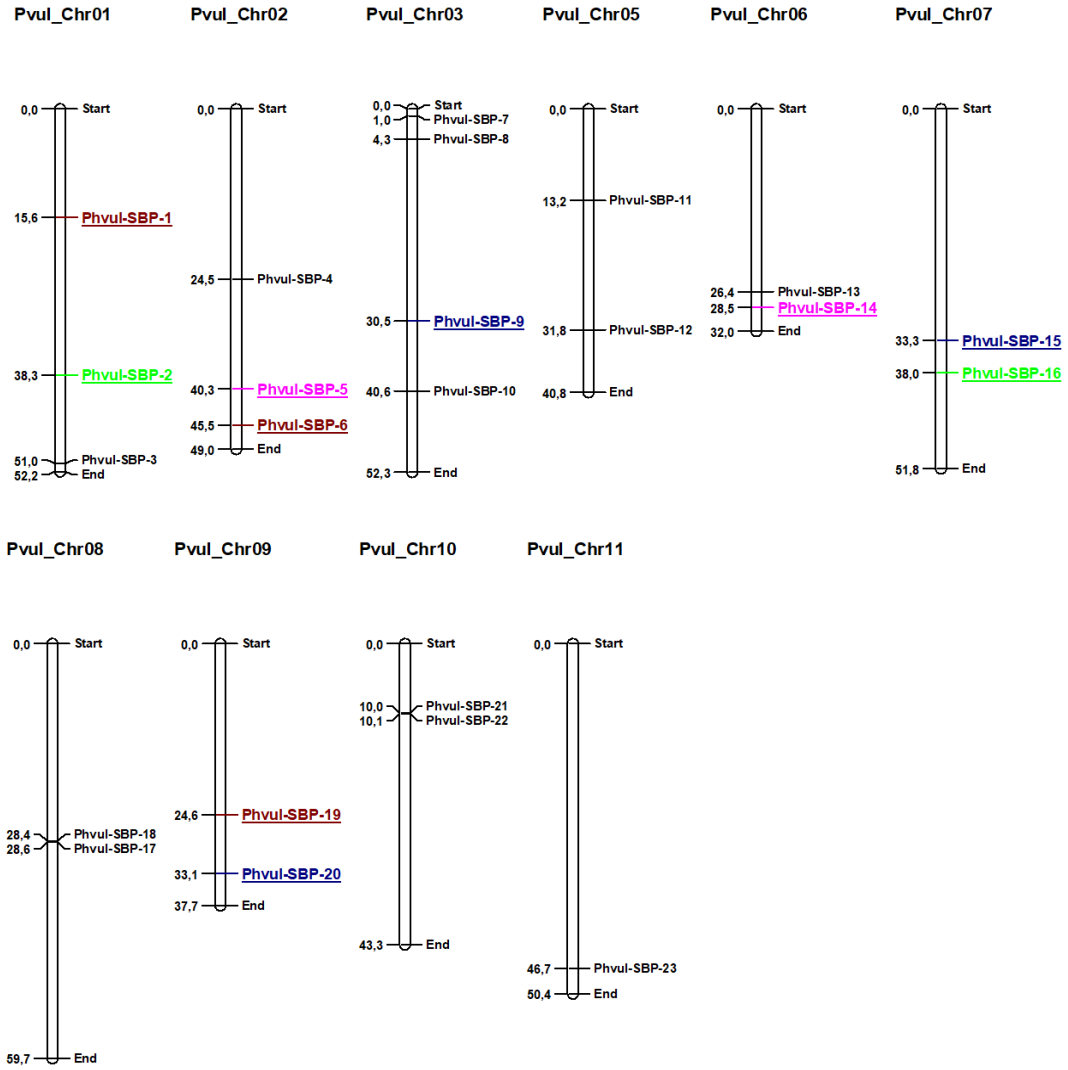

Figure 1. *Distribution of Phvul-SBP genes on common bean chromosomes. Similar colors present segmentally – duplicated genes*

Several paralogous gene pairs are originated from gene duplication events (Cannon et al., 2004). Furthermore, organisms adapt to different environments via gene duplication events throughout processes of development and growth (Bowers et al., 2003; Gu et al., 2003). Plant genomic structure, which can occur by independent events involving in segmental or tandem duplications, is one of most important characteristics of gene duplication (Flagel and Wendel, 2009). Based on significance of gene duplications on evolution of gene families in plants, the gene duplication events of putative *Phvul-SBP* genes in common bean genome have been examined. After the duplication analysis, six segmentally-duplicated gene couples (*Phvul-SBP-1*/*Phvul-SBP-19*, *Phvul-SBP-2*/*Phvul-SBP-16*, *Phvul-SBP-5*/*Phvul-SBP-14*, *Phvul-SBP-6*/*Phvul-SBP-19*, *Phvul-SBP-9*/*Phvul-SBP-15* and *Phvul-SBP-9*/*Phvul-SBP-20*) among the identified 23 *Phvul-SBP* genes in common bean (*Table 2*) were detected. According to the gene duplication analysis, none of the gene couples have been found to include tandem repeats.

http://www.aloki.hu ● ISSN 1589 1623 (Print) ● ISSN 1785 0037 (Online)
DOI: http://dx.doi.org/10.15666/aeer/1605_54675480
© 2018, ALÖKI Kft., Budapest, Hungary

The Ka/Ks ratio has been become a popular parameter for genome-wide identification researches of gene families in recent years. This ratio gives a worthwhile information about the selective evolutionary pressures that are acting on that gene (Yang and Swanson, 2002; Kryazhimskiy and Plotkin, 2008). According to Juretic et al. (2005), a Ka/Ks larger than 1 reflects the positive selection during the evolution of the gene sequence. Additionally, a Ka/Ks lower than 1 indicates duplications have undergone purifying selection and a Ka/Ks = 1 means neutral selection in duplication events. As displayed in *Table 2,* the divergence time of segmentally duplicated Phvul-SBP gene pairs extended from 32.77 to 101.61 million years (MYA). Except for one, all of the duplicated Phvul-SBP gene pairs showed Ka/Ks ratio lower than 1 which reflects the occurrence of purifying selection after the duplication events. The Ka/Ks ratio (=1) of Phvul-SBP-1/Phvul-SBP-19 indicated the predominance of neutral selection during duplication events of this gene pair (*Table 2*).

Table 2. *The Ka/Ks ratios and identified divergence times for the segmentally duplicated Phvul-SBP proteins*

Paralogous gene pairs		Ka	Ks	Ka/Ks	Duplication date (MYA)
Phvul-SBP-1	Phvul-SBP-19	0	0	1	-
Phvul-SBP-2	Phvul-SBP-16	0.1922	0.8346	0.2075	49.33
Phvul-SBP-5	Phvul-SBP-14	0.3358	1.0685	0.0917	63.15
Phvul-SBP-6	Phvul-SBP-19	0.2174	0.7511	0.2834	44.39
Phvul-SBP-9	Phvul-SBP-15	0.3989	1.7193	0.1484	101.61
	Phvul-SBP-20	0.1836	0.5544	0.2868	32.77

Phylogenetic analysis, gene structure and conserved motifs of Phvul-SBPs

To discover the relationships between Phvul-SBP proteins, a phylogenetic tree of SBP domain proteins in *Phaseolus vulgaris*, *Arabidopsis* and *Glycine max* was structured using amino acid sequences with contributed bootstrap values (1000 replicates; *Fig. 2*) via neighbour joining method. Phvul-SBP proteins were clustered into twelve groups, A - C9 (*Fig. 2*). Similar coding and exon-intron sequences were observed in most of the Phvul-SBP genes which were found in the same subgroup in phylogenetic tree.

To investigate conserved motifs in Phvul-SBP proteins, MEME (v5.0.1) was used. MEME software finds the most statistically significant (low E-value) motifs based on its log likelihood ratio, its width and number of occurrences, the background letter frequencies and the size of the training set. Motifs with E-values larger than 0.01 (1e-2) are possibly just statistical artifacts, and not real motifs (Bailey et al., 2009).

A total of 20 conserved motifs were described (*Fig. 3* and *Table 3*). The lengths of identified motifs were between 8 and 50 amino acids. A total of Phvul-SBP proteins consist of Motif 1 which is one of the two motifs which have SBP domain among all motifs. A similar result was found in Ali et al. (2017).

Twenty-three common bean SBP gene structures were investigated and the estimated number of exons among the 23 *Phvul-SBP* genes extended from two to 10 (*Fig. 4*). As seen in *Figure 4,* these genes were also clustered into twelve groups in terms of the gene structure analysis in line with the phylogenetic tree of Phvul-SBP proteins shown in *Figure 2*. Deep examinations of the segmentally duplicated gene pairs, which have

http://www.aloki.hu ● ISSN 1589 1623 (Print) ● ISSN 1785 0037 (Online)
DOI: http://dx.doi.org/10.15666/aeer/1605_54675480
© 2018, ALÖKI Kft., Budapest, Hungary

same exon–intron structures and similar motifs, would contribute to a comprehension of the different roles they play in development and growth. In a recent research, it has been reported that the gene pairs, which have similar motif sequences and orders could show similar functions in moso bamboo (Pan et al., 2017). These gene pairs could be originated from an ancestor in evolutionary process.

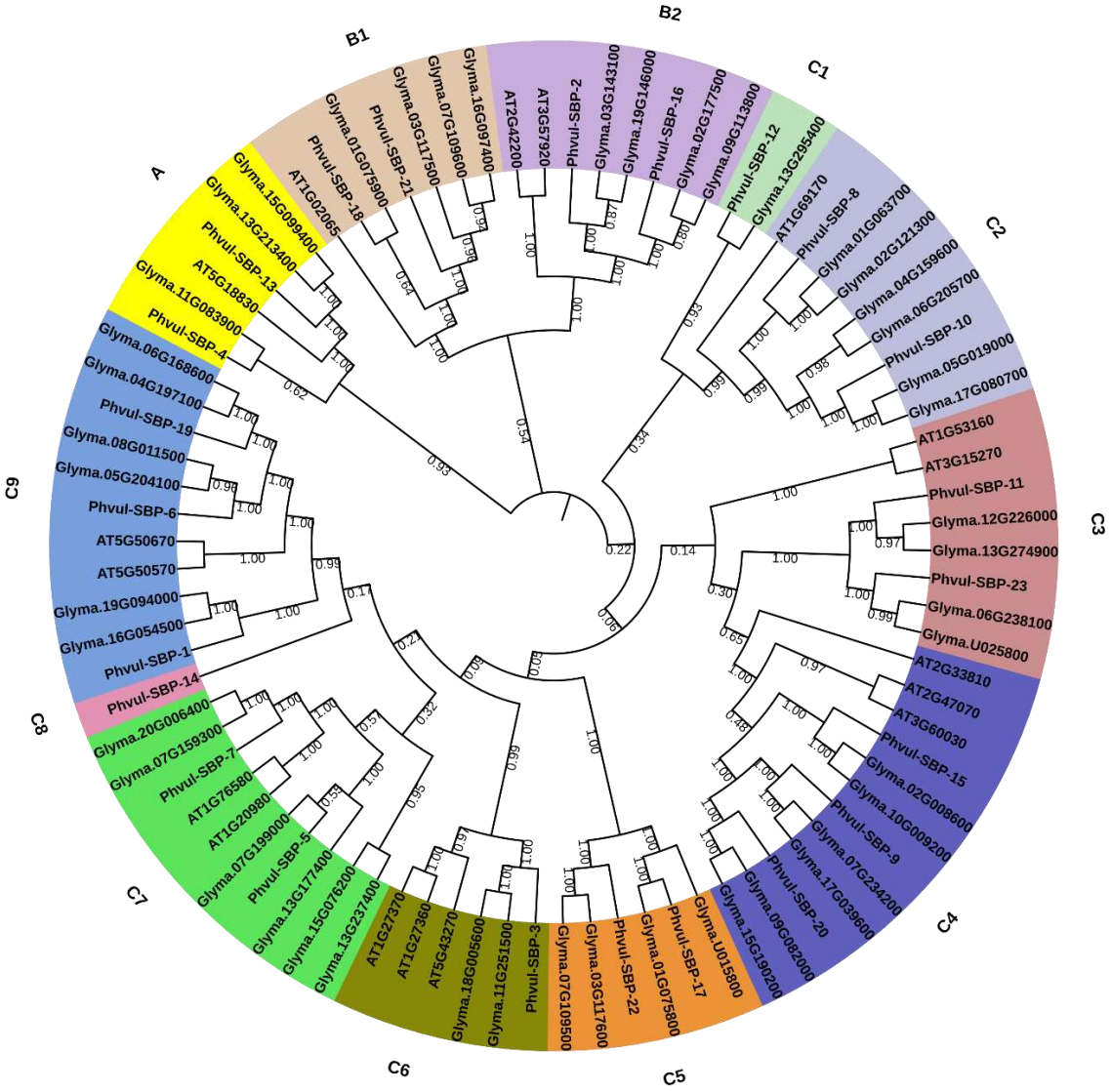

Figure 2. *A phylogenetic tree of SBP proteins of common bean, soybean and Arabidopsis thaliana. The tree was generated with MEGA v7 and Neighbor-joining (NJ) algorithm with 1000 replicated-bootstrap values*

Table 3. *The MEME motif sequences and length of Pvul-SBP proteins*

Motif ID	Conserved sequence	E-value*	Sites	Width	Domain
1	RCQVEGCNADLSNAKDYHRRHKVCEMHSKAP KVJVAGLEQRFCQQCSRFH	2.3E-730	23	50	SBP
2	VLSEFDEGKRSCRRRLAGHNERRRKPQPE	5.5E-351	22	29	SBP
3	RTDRIVFKLFGKDPNDFPLVLRAQILNWLSHSP TEIESYIRPGCIILTIY	5E-92	5	50	Unknown

http://www.aloki.hu ● ISSN 1589 1623 (Print) ● ISSN 1785 0037 (Online)
DOI: http://dx.doi.org/10.15666/aeer/1605_54675480
© 2018, ALÖKI Kft., Budapest, Hungary

4	PAGLTPLHVAASISGSDNVLDALTDDPGMVGIE AWKSARDSTGLTPHDYA	8E-48	4	50	Unknown
5	TAMVYRPAMLSMVAIAAVCVCVALLFKSSPKV YYVFRPF	7E-41	4	39	Unknown
6	FIQEMGWLLHRSRLKVRLGPVAPIQDJFQFNRF KWLVDFSMDHDWCAVMK	3E-34	3	50	Unknown
7	GKRSLEWDLNDWKWDGDLFTASRLNSVPSDC	1E-24	3	31	Unknown
8	PKILCVKPLAVPASKRAQFIVKGVNLLQPATRL LCALEGKYLVCE	1E-24	5	45	Unknown
9	FWRTGWVYVRVQHQLAFLYNGQVVIDVPL	1E-21	4	29	unknown
10	DSSCALSLLSSQSW	2E-16	10	14	Unknown
11	SLIGLKLGKRIYFED	5E-15	9	15	Unknown
12	ALLEMGLLHKAVKRNSRPMVELLLRYVP	1E-13	4	28	Unknown
13	PVIVAEEEICSEICTLENVJE	2E-11	5	21	Unknown
14	YLLMSLLRILSNMHSNGSDHTTBQDILSHLLRN LASLAGPNNG	2E-13	3	43	Unknown
15	HJKFSCTIPNVVGRGFIEVED	2E-10	5	21	Unknown
16	WEELDYGT	6E-09	10	8	n/a
17	LRGHYSYIQLVQKKINKKGGAAHVVDIP	1E-08	3	28	Unknown
18	WVQCDSLKSSPPQTSRNSDSTSTQ	9E-09	3	24	Unknown
19	MDWNLKAPSWDLVEVDKANJPNIESMEEHNRF GMFRMEGEFSVDLKLGQV	2E-07	2	50	Unknown
20	CRQADERGRIQMNJPRNSGYKSFHIR	5E-06	3	26	Unknown

*The expected value of each motif prediction was given in the MEME program

Figure 3. *Shematic representation of the 20 conserved motifs in Pvul-SBP proteins. The 20 conserved motifs were classified using MEME Suite v5.0.1. Each motifs were shown by different colored boxes. The numbers in the boxes represent motif 1 – motif 20, respectively*

http://www.aloki.hu ● ISSN 1589 1623 (Print) ● ISSN 1785 0037 (Online)
DOI: http://dx.doi.org/10.15666/aeer/1605_54675480
© 2018, ALÖKI Kft., Budapest, Hungary

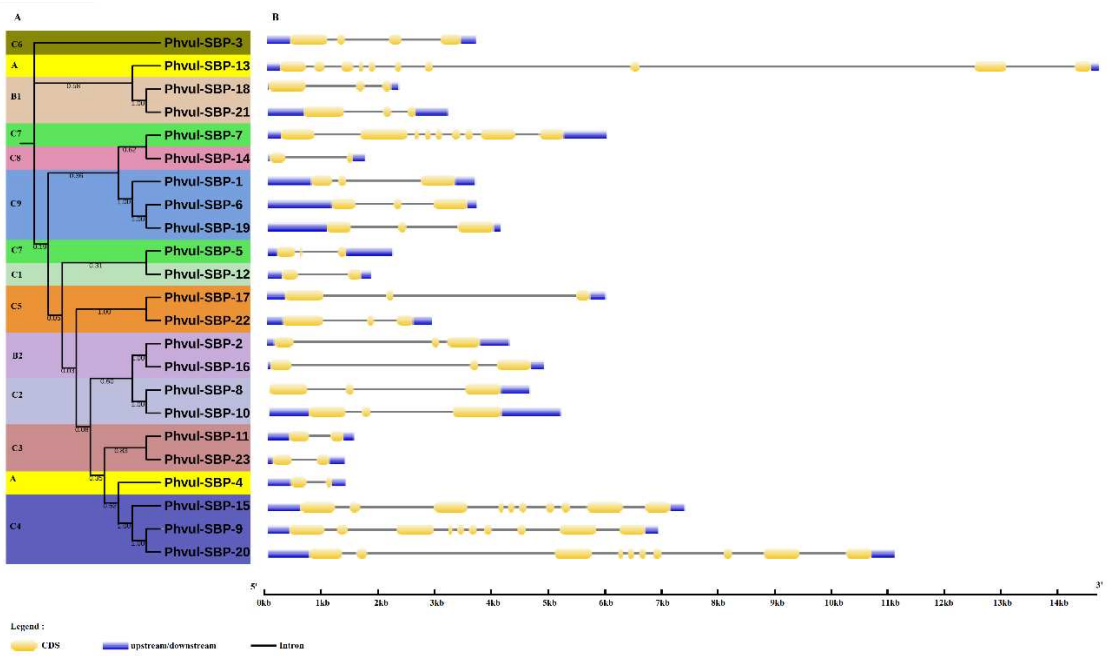

Figure 4. *Gene structure of Phvul-SBP genes.* ***A.*** *The number of below branches of the phylogenetic tree display bootstrap values. The tree was structured with MEGA v7 by the Neighbor-Joining (NJ) method with 1000 bootstrap replicates. The A – C9 numerals on the tree correspond to 12 Pvul-SBP groups shown in Figure 2.* ***B.*** *Yellow colors represent exons, grey lines represent introns and blue colors represent untranslated regions (UTRs)*

Comparative and synteny events among SBP genes of P. vulgaris, Arabidopsis thaliana and Glycine max

To calculate evolutionary relationship of the *SBP* gene family in *P. vulgaris*, *Arabidopsis* and *Glycine max*, the synteny events among SBP protein sequences of these plants are shown in *Figure 5*.

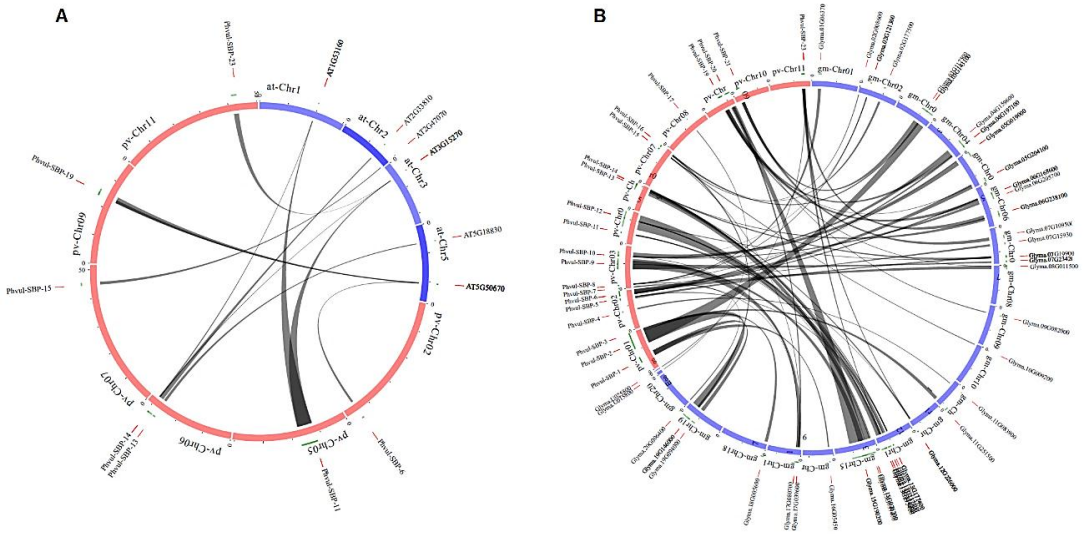

Figure 5. *Genome wide synteny analysis of SBP genes.* ***A.*** *Comparative map between P. vulgaris and A. thaliana.* ***B.*** *Comparative map between P. vulgaris and G. max*

http://www.aloki.hu ● ISSN 1589 1623 (Print) ● ISSN 1785 0037 (Online)
DOI: http://dx.doi.org/10.15666/aeer/1605_54675480
© 2018, ALÖKI Kft., Budapest, Hungary

This synteny analysis was established on SBP proteins of 6 *Arabidopsis* and 40 *Glycine max*. Since *P. vulgaris* and *G. max* were closely related genomes (Schmutz et al., 2014), *SPB* genes of these plants showed high similarity. However, 22 *Pvul-SBP* genes were matched to 40 *G. max SBP* genes distributed on all chromosomes of *G. max*. In a recent study, it was reported that some *Arabidopsis SBP* genes were syntenic to those of diploid cotton genes and these genes showed an evolutionary relationship (Ali et al., 2017). In another study, the synteny analysis between apple and *Arabidopsis* demonstrated that 11 apple and *Arabidopsis* genes were located in the duplicated genomic regions. In the same study, it was notified that duplications such as segmental, tandem and genomic duplications have important roles in evolutionary processes (Li et al., 2013).

Expression profiles of Phvul-SBPs in different tissues

In this research, a common mRNA analysis of *Phvul-SBP* genes were performed via publicly available expression data in Phytozome v12.1 online plant genomics resource (https://phytozome.jgi.doe.gov). The heatmap shows the expression variance between identified 21 *Phvul-SBP* genes in different plant tissues (*Fig. 6*).

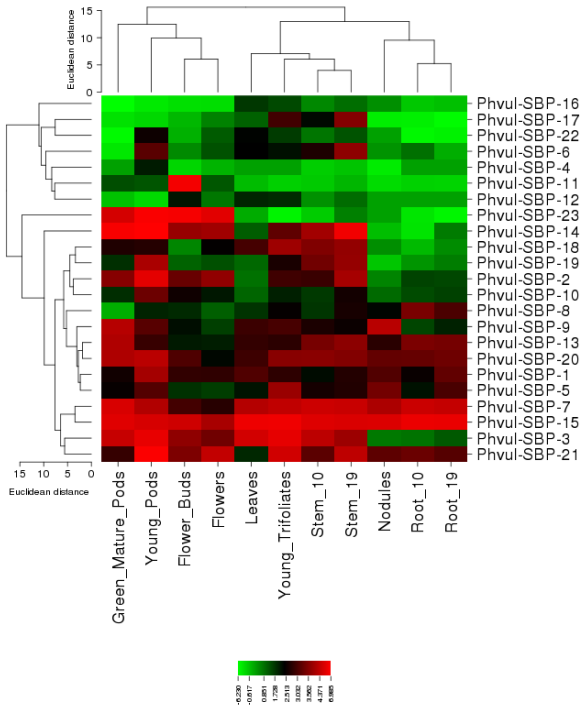

Figure 6. *Hierarchical clustering of expression profiles of Phvul-SBP genes in 11 different tissues of common bean. Heat map was drawn with CIMminer online tool*

As seen in the *Figure 6,* the *Phvul-SBP-16*, *-17*, *-22*, *-6*, *-4*, *-11* and *-12* genes revealed relatively low expression levels in almost all tissues including green mature pods, young pods, flower buds, flowers, leaves, young trifoliates, stem_10, stem_19, nodules, root_10 and root_19. The rest of the *Phvul-SBP* genes exhibited relatively high mRNA levels in most of the developmental stages of common bean. *Phvul-SBP-14*, *-15* and *-23* were the genes which exhibited the highest expression levels at least in one of the

http://www.aloki.hu ● ISSN 1589 1623 (Print) ● ISSN 1785 0037 (Online)
DOI: http://dx.doi.org/10.15666/aeer/1605_54675480
© 2018, ALÖKI Kft., Budapest, Hungary

certain tissue types among all genes. Additionally, some of the genes were only up- or down-regulated in certain tissue types. For instance, *Phvul-SBP-1*, *-3*, *-5*, *-7*, *-8*, *-9*, *-13*, *-15*, *-20* and *-21* were highly expressed in root tissues. *Phvul-SBP-1*, *-2*, *-3*, *-5*, *-7*, *-8*, *-9*, *-10*, *-13*, *-14*, *-15*, *-18*, *-19*, *-20* and *-21* were highly expressed in stem tissues. *Phvul-SBP-1*, *-2*, *-3*, *-5*, *-7*, *-8*, *-9*, *-10*, *-13*, *-14*, *-15*, *-18*, *-19*, *-20*, *-21* and *-23* were highly expressed in floral organs. The other *Pvul-SBP* genes were low expressed in these tissues of *P. vulgaris*. Similar results were obtained in grapevine genome (Wang et al., 2010). *SBP* genes in this genome were up or down regulated in various tissues such as root, leaf, flower and fruit. *SBP* genes in *P. vulgaris* were suggested to express in different tissues.

Conclusion

In this study, genome sequences, identification, conserved motifs of 23 *Pvul-SBP* genes were identified in *P. vulgaris* genome. The Pvul-SBPs were divided into twelve classes and 23 *Pvul-SBP* genes were distributed across 10 chromosomes with different densities. Also, expression levels of 23 *Pvul-SBP* genes in different plant tissues such as roots, leaf and floral organs were determined using *in silico* analysis. To the best of our knowledge, this is the first report of a genome wide analysis of the common bean SBP gene family. This study would provide beneficial information for understanding the classification and functions of the *SBP* genes in common bean.

REFERENCES

[1] Ali, M. A., Alia, K. B., Atif, R. M., Rasul, I., Nadeem, H. U., Shahid, A., Azeem, F. (2017): Genome-wide identification and comparative analysis of squamosa-promoter binding proteins (Sbp) transcription factor family in *Gossypium raimondii* and *Arabidopsis thaliana*. – Pakistan Journal of Botany 49: 1113-1126.

[2] Arumuganthan, K., Earle, E. (1991): Nuclear DNA content of some important plant species. – Plant Molecular Biology Reports 9: 208-218.

[3] Bailey, T. L., Boden, M., Buske, F. A., Frith, M., Grant, C. E., Clementi, L., Ren, J., Li, W. W., Noble, W. S. (2009): MEME SUITE: tools for motif discovery and searching. – Nucleic Acids Research 37(suppl_2): W202-W208.

[4] Bailey, T. L., Williams, N., Misleh, C., Li, W. W. (2006): MEME: discovering and analyzing DNA and protein sequence motifs. – Nucleic Acids Research 34: W369-W373.

[5] Bowers, J. E., Chapman, B. A., Rong, J., Paterson, A. H. (2003): Unravelling angiosperm genome evolution by phylogenetic analysis of chromosomal duplication events – Nature 422(6930): 433-8.

[6] Broughton, W. J., Hernandez, G., Blair, M., Beebe, S., Gepts, P., Vanderleyden, J. (2003): Beans (*Phaseolus* spp.) – model food legumes. – Plant and Soil 252(1): 55-128.

[7] Buyuk, I., Inal, B., Ilhan, E., Tanriseven, M., Aras, S., Erayman, M. (2016): Genome-wide identification of salinity responsive HSP70s in common bean. – Molecular Biology Reports 43: 1251-1266.

[8] Cannon, S. B., Mitra, A., Baumgarten, A., Young, N. D., May, G. (2004): The roles of segmental and tandem gene duplication in the evolution of large gene families in *Arabidopsis thaliana*. – BMC Plant Boilogy 4(1): 10.

[9] Chuck, G., Whipple, C., Jackson, D., Hake, S. (2010): The maize SBP-box transcription factor encoded by tasselsheath4 regulates bract development and the establishment of meristem boundaries. – Development 137: 1585-1585.

http://www.aloki.hu ● ISSN 1589 1623 (Print) ● ISSN 1785 0037 (Online)
DOI: http://dx.doi.org/10.15666/aeer/1605_54675480
© 2018, ALÖKI Kft., Budapest, Hungary

[10] Flagel, L. E., Wendel, J. F. (2009): Gene duplication and evolutionary novelty in plants. – New Phytologist 183: 557-564.
[11] Gandikota, M., Birkenbihl, R. P., Hohmann, S., Cardon, G. H., Saedler, H., Huijser, P. (2007): The miRNA156/157 recognition element in the 3' UTR of the *Arabidopsis* SBP box gene SPL3 prevents early flowering by translational inhibition in seedlings. – Plant Journal 49: 683-693.
[12] Gu, Z. L., Steinmetz, L. M., Gu, X., Li, W. H. (2003): Role of duplicate genes in genetic robustness against null mutations. – Nature 421: 63-6.
[13] Guo, A., Zhu, Q., Chen, X., Luo, J. (2007): GSDS: a gene structure display server. Yi chuan. – Hereditas 29: 1023-1026.
[14] Hou, H. M., Li, J., Gao, M., Singer, S. D., Wang, H., Mao, L. Y., Fei, Z. J., Wang, X. P. (2013): Genomic organization, phylogenetic comparison and differential expression of the SBP-box family genes in grape. – Plos One 8.
[15] Ilhan, E., Buyuk, I., Inal, B. (2018): Transcriptome - Scale characterization of salt responsive bean TCP transcription factors. – Gene 642: 64-73.
[16] Inal, B., Buyuk, I., Ilhan, E. and Aras, S. (2017): Genome-wide analysis of *Phaseolus vulgaris* C2C2-YABBY transcription factors under salt stress conditions. – 3Biotech 7(5): 302.
[17] Jung, J. H., Ju, Y., Seo, P. J., Lee, J. H., Park, C. M. (2012): The SOC1-SPL module integrates photoperiod and gibberellic acid signals to control flowering time in *Arabidopsis.* – Plant Journal 69: 577-588.
[18] Juretic, N., Hoen, D. R., Huynh, M. L., Harrison, P. M., Bureau, T. E. (2005): The evolutionary fate of MULE-mediated duplications of host gene fragments in rice. – Genome Research 15: 1292-1297.
[19] Kavas, M., Kızıldoğan, A. K., Abanoz, B. (2017): Comparative genome-wide phylogenetic and expression analysis of SBP genes from potato (*Solanum tuberosum*). – Computational Biology and Chemistry 67: 131-140.
[20] Kropat, J., Tottey, S., Birkenbihl, R. P., Depege, N., Huijser, P., Merchant, S. (2005): A regulator of nutritional copper signaling in Chlamydomonas is an SBP domain protein that recognizes the GTAC core of copper response element. – Proceedings of the National Academy of Sciences of the United States of America 102: 18730-18735.
[21] Kryazhimskiy, S., Plotkin, J. B. (2008): The population genetics of dN/dS. – Plos Genetics 4.
[22] Lannenpaa, M., Janonen, I., Holtta-Vuori, M., Gardemeister, M., Porali, I. and Sopanen, T. (2004): A new SBP-box gene BpSPL1 in silver birch (*Betula pendula*). – Physiologia Plantarum 120: 491-500.
[23] Lee, T. H., Tang, H. B., Wang, X. Y., Paterson, A. H. (2013): PGDD: a database of gene and genome duplication in plants. – Nucleic Acids Research 41: D1152-D1158.
[24] Li, J., Hou, H. M., Li, X. Q., Xiang, J., Yin, X. J., Gao, H., Zheng, Y., Bassett, C. L., Wang, X. P. (2013): Genome-wide identification and analysis of the SBP-box family genes in apple (*Malus* × *domestica* Borkh.). – Plant Physiology and Biochemistry 70: 100-114.
[25] Li, M., Zhao, S. Z., Zhao, C. Z., Zhang, Y., Xia, H., Lopez-Baltazar, J., Wan, S. B., Wang, X. J. (2016): Cloning and characterization of SPL-family genes in the peanut (*Arachis hypogaea* L.). – Genetics and Molecular Research 15.
[26] Lu, S. F., Yang, C. M., Chiang, V. L. (2011): Conservation and diversity of MicroRNA-associated copper-regulatory networks in *Populus trichocarpa.* – Journal of Integrative Plant Biology 53: 879-891.
[27] Mao, H. D., Yu, L. J., Li, Z. J., Yan, Y., Han, R., Liu, H., Ma, M. (2016): Genome-wide analysis of the SPL family transcription factors and their responses to abiotic stresses in maize. – Plant Gene 6: 1-12.

http://www.aloki.hu ● ISSN 1589 1623 (Print) ● ISSN 1785 0037 (Online)
DOI: http://dx.doi.org/10.15666/aeer/1605_54675480
© 2018, ALÖKI Kft., Budapest, Hungary

[28] Pan, F., Wang, Y., Liu, H. L., Wu, M., Chu, W. Y., Chen, D. M., Xiang, Y. (2017): Genome-wide identification and expression analysis of SBP-like transcription factor genes in Moso Bamboo (*Phyllostachys edulis*). – BMC Genomics 18: 486.
[29] Preston, J. C., Jorgensen, S. A., Orozco, R., Hileman, L. C. (2016): Paralogous SQUAMOSA PROMOTER BINDING PROTEIN-LIKE (SPL) genes differentially regulate leaf initiation and reproductive phase change in petunia. – Planta 243: 429-440.
[30] Quevillon, E., Silventoinen, V., Pillai, S., Harte, N., Mulder, N., Apweiler, R., Lopez, R. (2005): InterProScan: protein domains identifier. – Nucleic Acids Research 33: W116-W120.
[31] Rhoades, M. W., Reinhart, B. J., Lim, L. P., Burge, C. B., Bartel, B., Bartel, D. P. (2002): Prediction of plant microRNA targets. – Cell 110: 513-520.
[32] Salinas, M., Xing, S. P., Hohmann, S., Berndtgen, R., Huijser, P. (2012): Genomic organization, phylogenetic comparison and differential expression of the SBP-box family of transcription factors in tomato. – Planta 235: 1171-1184.
[33] Schmutz, J., McClean, P. E., Mamidi, S., Wu, G. A., Cannon, S. B., Grimwood, J., Jenkins, J., Shu, S. Q., Song, Q. J., Chavarro, C., Torres-Torres, M., Geffroy, V., Moghaddam, S. M., Gao, D. Y., Abernathy, B., Barry, K., Blair, M., Brick, M. A., Chovatia, M., Gepts, P., Goodstein, D. M., Gonzales, M., Hellsten, U., Hyten, D. L., Jia, G. F., Kelly, J. D., Kudrna, D., Lee, R., Richard, M. M. S., Miklas, P. N., Osorno, J. M., Rodrigues, J., Thareau, V., Urrea, C. A., Wang, M., Yu, Y., Zhang, M., Wing, R. A., Cregan, P. B., Rokhsar, D. S., Jackson, S. A. (2014): A reference genome for common bean and genome-wide analysis of dual domestications. – Nature Genetics 46: 707-713.
[34] Schwarz, S., Grande, A. V., Bujdoso, N., Saedler, H., Huijser, P. (2008): The microRNA regulated SBP-box genes *SPL*9 and *SPL*15 control shoot maturation in *Arabidopsis*. – Plant Molecular Biology 67: 183-195.
[35] Shalom, L., Shlizerman, L., Zur, N., Doron-Faigenboim, A., Blumwald, E., Sadka, A. (2015): Molecular characterization of SQUAMOSA PROMOTER BINDING PROTEIN-LIKE (SPL) gene family from *Citrus* and the effect of fruit load on their expression. – Frontiers in Plant Science 6: 389.
[36] Song, A., Gao, T., Wu, D., Xin, J., Chen, S., Guan, Z., Wang, H., Jin, L., Chen, F. (2016): Transcriptome-wide identification and expression analysis of chrysanthemum SBP-like transcription factors. – Plant Physiology and Biochemistry 102: 10-16.
[37] Tamura, K., Stecher, G., Peterson, D., Filipski, A., Kumar, S. (2013): MEGA6: Molecular Evolutionary Genetics Analysis Version 6.0. – Molecular Biology and Evolution 30: 2725-2729.
[38] Unte, U. S., Sorensen, A. M., Pesaresi, P., Gandikota, M., Leister, D., Saedler, H., Huijser, P. (2003): SPL8, an SBP-Box gene that affects pollen sac development in *Arabidopsis*. – Plant Cell 15: 1009-1019.
[39] Voorrips, R. E. (2002): MapChart: Software for the graphical presentation of linkage maps and QTLs. – Journal of Heredity 93: 77-78.
[40] Wang, B. N., Geng, S. F., Wang, D., Feng, N., Zhang, D. D., Wu, L., Hao, C. Y., Zhang, X. Y., Li, A. L., Mao, L. (2015): Characterization of SQUAMOSA promoter binding protein-like genes in wheat. – Journal of Plant Biology 58: 220-229.
[41] Wang, Y., Hu, Z., Yang, Y., Chen, X., Chen, G. (2010): Genome-wide identification, phylogeny, and expression analysis of the SBP-box gene family in grapevine. – Russian Journal of Plant Physiology 57: 273-282.
[42] Xie, K. B., Wu, C. Q., Xiong, L. Z. (2006): Genomic organization, differential expression, and interaction of SQUAMOSA promoter-binding-like transcription factors and microRNA156 in rice. – Plant Physiology 142: 280-293.
[43] Yang, Z. H. (2007): PAML 4: Phylogenetic analysis by maximum likelihood. – Molecular Biology and Evolution 24: 1586-1591.

http://www.aloki.hu ● ISSN 1589 1623 (Print) ● ISSN 1785 0037 (Online)
DOI: http://dx.doi.org/10.15666/aeer/1605_54675480
© 2018, ALÖKI Kft., Budapest, Hungary

[44] Yang, Z. H., Swanson, W. J. (2002): Codon-substitution models to detect adaptive evolution that account for heterogeneous selective pressures among site classes. – Molecular Biology and Evolution 19: 49-57.
[45] Zhang, H. X., Jin, J. H., He, Y. M., Lu, B. Y., Li, D. W., Chai, W. G., Khan, A., Gong, Z. H. (2016): Genome-wide identification and analysis of the SBP-box family genes under Phytophthora capsici stress in pepper (*Capsicum annuum* L.). – Frontiers in Plant Science 7: 504.
[46] Zhang, L. S., Wu, B., Zhao, D. G., Li, C. L., Shao, F. J., Lu, S. F. (2014): Genome-wide analysis and molecular dissection of the SPL gene family in *Salvia miltiorrhiza*. – Journal of Integrative Plant Biology 56: 38-50.
[47] Zhang, X. H., Dou, L. L., Pang, C. Y., Song, M. Z., Wei, H. L., Fan, S. L., Wang, C. S., Yu, S. X. (2015): Genomic organization, differential expression, and functional analysis of the SPL gene family in *Gossypium hirsutum*. – Molecular Genetics and Genomics 290: 115-126.
[48] Zhang, Y., Schwarz, S., Saedler, H., Huijser, P. (2007): SPL8, a local regulator in a subset of gibberellin-mediated developmental processes in *Arabidopsis*. – Plant Molecular Biology 63: 429-439.
[49] Zheng, Y., Jiao, C., Sun, H. H., Rosli, H. G., Pombo, M. A., Zhang, P. F., Banf, M., Dai, X. B., Martin, G. B., Giovannoni, J. J., Zhao, P. X., Rhee, S. Y., Fei, Z. J. (2016): iTAK: A program for genome-wide prediction and classification of plant transcription factors, transcriptional regulators, and protein kinases. – Molecular Plant 9: 1667-1670.

http://www.aloki.hu ● ISSN 1589 1623 (Print) ● ISSN 1785 0037 (Online)
DOI: http://dx.doi.org/10.15666/aeer/1605_54675480
© 2018, ALÖKI Kft., Budapest, Hungary

APPLICATION OF SWAT MODEL IN ASSESSING THE IMPACT OF LAND USE CHANGE IN RUNOFF OF MAROON RIVER IN IRAN

SHAFIEI MOTLAGH, K.[1] – PORHEMMAT, J.[2*] – SEDGHI, H.[1] – HOSSENI, M.[2]

[1]*Department of Water Resource Engineering, Science and Research Branch, Islamic Azad University, Tehran, Iran*

[2]*Hydrology and Water Resources of Soil Conservation and Watershed Management Research Institute (SCWMRI), Tehran, Iran*

**Corresponding author*
e-mail: porhemmat@scwmri.ac.ir

(Received 21st Feb 2018; accepted 17th Jul 2018)

Abstract. Proper management of watersheds is one of the most important methods for using water and soil resources. In the last few decades, accurate and timely estimates of the quantitative and qualitative runoff status are one of the major concerns of large-scale management. The aims of this research are a simulation of monthly runoff, sensitivity analysis, optimization of sensitive parameters, investigation of the effect of land use change over the last four decades on the quantity and quality of the Maroon River (southwest of Iran) at the exit point of the Maroon Watershed (Idnak) in Iran using the SWAT model. For this purpose, the semi-distributed SWAT model and the SUFI2 program were used in the SWAT CUP software package for sensitivity analysis, calibration, validation and uncertainty analysis. In this research, the map of land use change and soil mapping and vegetation cover in the Maroon watershed were first identified over the course of the four decades between 1970 and 2010, using TM and ETM satellite measurements in Landsat. Observations of the Idnak Hydrometer Station were used as the base station during 1970 to 2010 over a period of four decades. Comparison of the effects of land use management options on various components of the hydrological cycle as well as different runoff rates show that if the pessimistic scenario occurs, and with the continuation of the destructive trend in land use to the retreat, values of runoff will increase and there will be more permeability and the drainage will go down to deeper aquifers.
Keywords: *watershed, SUFI 2, management, Iran*

Introduction

The proper management of watersheds is one of the most important methods for optimal use of water and soil resources. For this purpose, comprehensive information of different methods of management and executive is needed. In our country, more catchments, especially mountainous watersheds lack sufficient numbers of measurement stations which will cause any development planning and management schemes to fail. To tackle this issue, practitioners and researchers in water and irrigation management have offered solutions such as empirical formulae and mathematical models. So far, no optimal solutions have been provided. It is believed that simulation of hydrological phenomena of basins could be the optimal solution (Rostamian et al., 2010). During the past few decades, correct and timely estimates of the quantity and quality of runoff are one of the concerns of senior management. Watershed management, water resources management, especially management of reservoir exploitation and water supply network are faced with challenges. Generally, to understand and predict the processes of generation and transmission to the output stream basin is one of the most fundamental discussions in

http://www.aloki.hu ● ISSN 1589 1623 (Print) ● ISSN 1785 0037 (Online)
DOI: http://dx.doi.org/10.15666/aeer/1605_54815502
© 2018, ALÖKI Kft., Budapest, Hungary

hydrology (Salmani, 2011). Rainfall-runoff simulations are one of the key issues considered in hydrologic sciences and environmental management. In recent years, the need for water is growing rapidly. There is an increasing demand for water resources to integrate, sustain and manage basins as well as the proper understanding of water balance in basins (Anwar, 2010). Therefore, hydrologic models have been developed to simulate rainfall-runoff, river flow analysis and to better understand the factors affecting the hydrological cycle in watersheds (Alavinia et al., 2010). These basin hydrological models are vital tools to better understand different hydrological processes, to optimize management strategies and evaluate the impact of land use changes in different time periods (Spruill et al., 2000). In these models, studying the processes of rainfall - runoff is difficult and there are uncertainties due to the influence of various parameters. These models are accurate in predicting the hydrological response of basins and can be improved with localization of optimal parameter values (Karlinger et al., 1988). The purpose of the model is to find, and as a representational image, to simply represent the facts and phenomena. The mathematical model describes the behavior of a system mathematically. These models have many applications, especially in the natural sciences and engineering systems (Mirabzadeh et al., 2005). Due to the temporal and spatial variations in the water cycle factors affecting natural watershed, identifying all components through analysis or theory of the water cycle is often impossible and time consuming. Hydrological models have been developed to overcome this problem and have been used in watersheds around the world. Since the results of some of these models matched the actual values, there has been an increase in using these models in watershed studies. With access to distributed spatial information, distributive hydraulic models are increasingly used to simulate the various hydrological processes in order to identify and manage natural and human activities that affect the watershed systems (Zhang et al., 2008). SWAT is a model in catchment basin scale that is provided by Jeff Arnold. The SWAT model is a multi-purpose simulation model for watershed management. This model is developed using several other models to estimate and predict the impact of different land management practices on water levels, sediment and chemical-agricultural watersheds within complex and large data without soil, land use and conditions management in the long run. This model has been used successfully to simulate the runoff, sediment and nutrient loads to many basins throughout North America, Asia and Europe (Duan, 2009). The review of the Omani studies showed that to predict the effects of changes in land use and conservation activities on the amount of suspended sediment Gharehsou basin with an area of 5739 km^2 using SWAT2000, this model can be used as an effective tool to review basin hydrological components used in response to corresponding changes in land use (Omani et al., 2007). In basins of West Africa using SWAT model caused changes of conditions in changing areas of forest, grassland and shrub land in relation to agricultural land or natural hydrology in urban areas resulting in areas becoming watershed transformations and resulting in an increase in the volume of surface runoff, groundwater resources and water-based power reduction as well as changes in the amount and intensity of river erosion and sedimentation (Liu, 2009). Wang et al. showed by modeling the effect of different land use options in a basin in China that it is evident that land use has different effects on the amount of runoff and underground water basin and converts forest land to pasture land within the basin leading to an increase in annual runoff and reduction in permeability of the soil and groundwater due to reduced transpiration reduction in basin (Willems, 2009). Palamuleni (2011) examined time changes in land cover and land use and its effects on river flow regime Prshayr during the

http://www.aloki.hu ● ISSN 1589 1623 (Print) ● ISSN 1785 0037 (Online)
DOI: http://dx.doi.org/10.15666/aeer/1605_54815502
© 2018, ALÖKI Kft., Budapest, Hungary

two time periods (1989 and 2002). The SWAT model (Phomcha et al., 2011) showed that the result of converting forest land to pasture, farmland and residential areas are effective on the rate of runoff and concentration time (t_c). Salmani (2011) simulated the effects of changes in land use on runoff in the Qazzaqli catchment in Golestan province using the SWAT model and showed that this model can be used as an effective tool in the study of the hydrological basin Qazzaqli catchment in components used in response to changes in land use (Salmani, 2011). Land use changes in a basin could significantly impact the hydrological cycle and water resources in the basin, therefore effects of land use changes on watershed hydrology are a guideline to determine appropriate strategies for sustainable development of water resources within a watershed. Natural earth ecosystem exploitation along with changes in land cover and land use especially in ecosystem environmental conditions affect hydrological responses to such as floods, erosion and sedimentation. Land use and land cover is one of the main factors in water resources management, erosion, and sedimentation basin. This complexity is not easy to study and analyze. Considering the importance of the subject and to aid in improved management of water resources, this study will utilize the Maroon Basin model and will be provided with SWAT as semi-distributed hydrological model. Accordingly, weather, soil, topography, observational discharge outlet of the basin, changes in land use and types of vegetation factors affecting the quantity and quality of water resources at the basin scale will also be investigated.

The studied area

Maroon basin is located in the southern and south-western domains of Central Zagros 50° 05' East longitude and North latitude are 30° 39' and 31° 21', respectively. The study area is supervised by the Regional Water Company in Kohgiloyeh and Boerahmad Province. The area of this range is 3801 km^2. The maximum height of this area is 3403.4 m and the minimum is 397 m. The highlands area is 3703.8 km^2 and the plain area is 196.9 km^2. The average height in highlands is 1689.22 m and in plains it is 984.32 m (Water Resources Management Co of Iran, 2009). The climate of the affected area is of low latitude with elevation changes, and is adjacent to the Persian Gulf in the southern areas. The geology of Maroon basin consists of outcrops of sandstone, conglomerate and alternation of colored marl and silty limestone. The type of precipitation at higher elevations is in the form of rain and in the form of snow at lower altitudes. Average annual precipitation in this basin is 150 mm in the coastal plains, and 900 mm in elevations. *Figure 1* shows the location of the studied area that is characterized by 7 sub-basins with numbers 1-7.

Materials and methods

The SWAT model is a continuous and semi-distributed physical model that is used to simulate complex hydrological processes in watersheds with respect to changes in soil, land use and weather conditions for long periods of time. This model requires comprehensive information, including topographic maps, digital elevation model (DEM), land use, utilized soil properties, management information, meteorological data and other watershed characteristics to simulate watershed hydrological process. The topography defined by a digital elevation model (DEM) represents the height of each point in each region with specific spatial resolution that is displayed by a cellular network. DEM map of the area with 1: 50000 scale is provided by the Forest

http://www.aloki.hu ● ISSN 1589 1623 (Print) ● ISSN 1785 0037 (Online)
DOI: http://dx.doi.org/10.15666/aeer/1605_54815502
© 2018, ALÖKI Kft., Budapest, Hungary

Rangelands and Watershed Organization. Geographical coordinates were then entered into the model. In this study, the DEM map is used to specify the basin and sub-basins surface drainage pattern analysis. Sub-basin parameters such as length and width of the channel slope are extracted from the DEM map. Maroon watershed DEM map is shown in *Figure 2*.

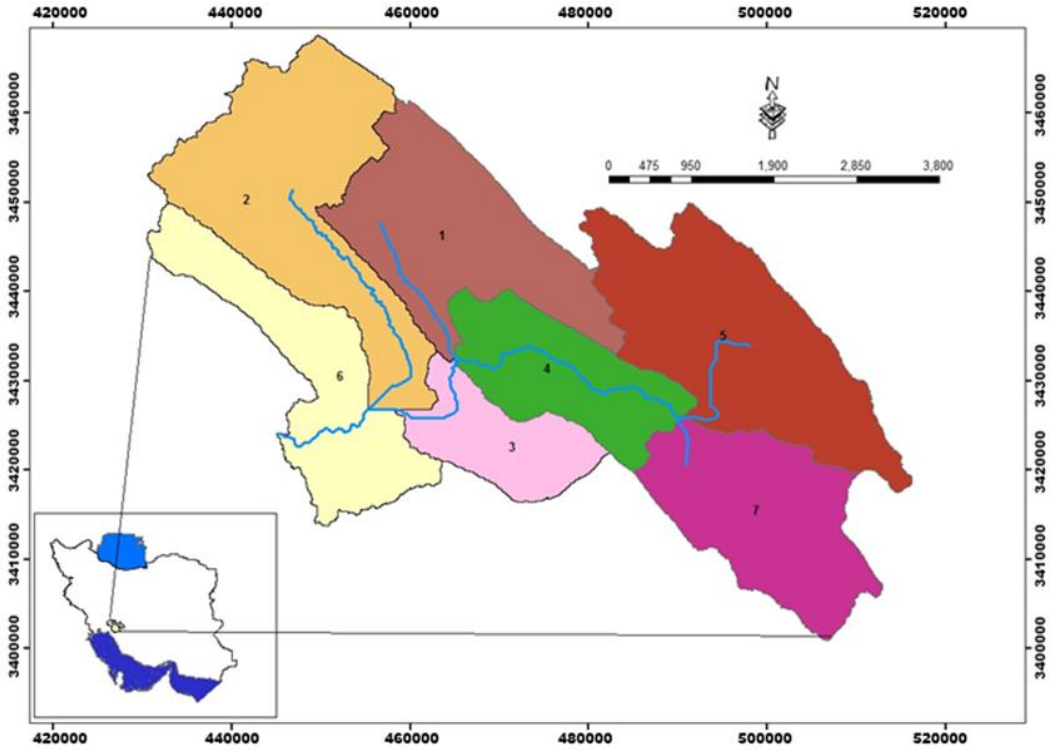

Figure 1. *Location of the studied area in the southwest of Iran*

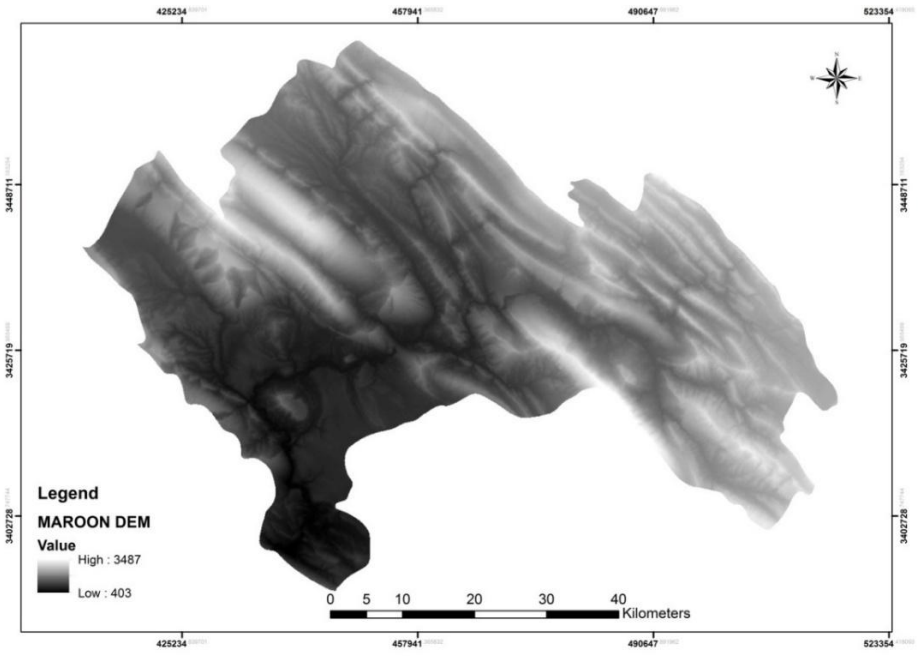

Figure 2. *DEM map of the catchment area of Maroon*

http://www.aloki.hu ● ISSN 1589 1623 (Print) ● ISSN 1785 0037 (Online)
DOI: http://dx.doi.org/10.15666/aeer/1605_54815502
© 2018, ALÖKI Kft., Budapest, Hungary

Digital River network with SHAPE file format was introduced to the model as shown in *Figure 3*. The database of drainage network is added to the DEM map to determine the state of the river network. Map drainage network is used to draw more precise drainage pattern details in the event that the DEM basin used is not able to specify this pattern.

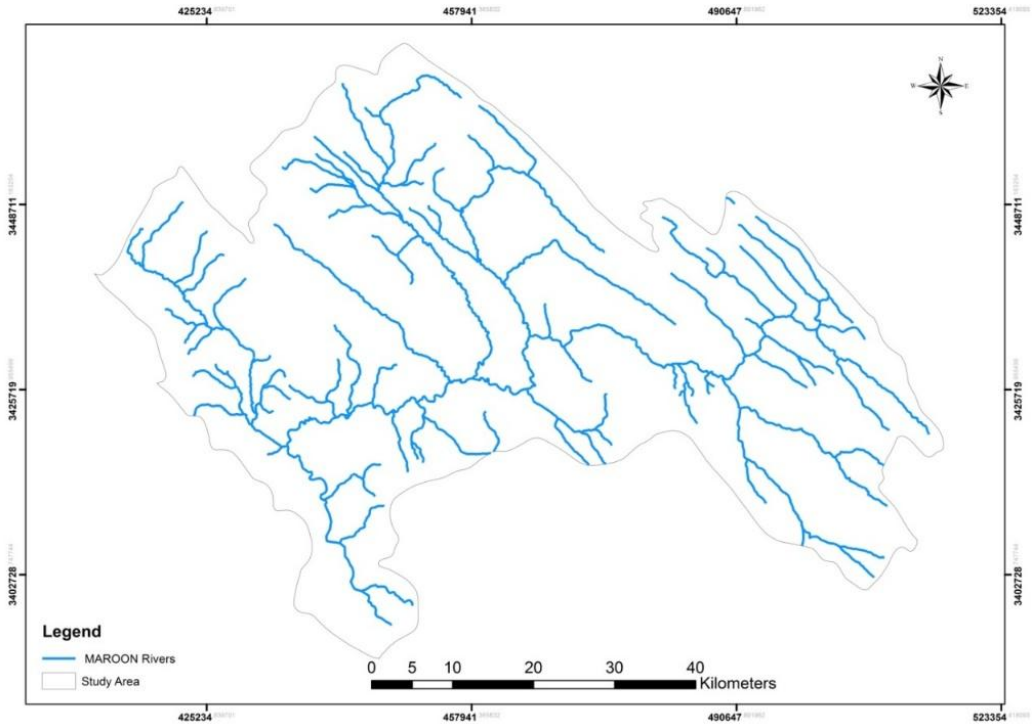

Figure 3. *Network River Maroon Basin*

One of the requirements for each hydrological basin simulation is the map of land use and vegetation. In the simulations with the SWAT model, the land use map is one of the essential items. Land use is one of the most important factors that affect the amount of runoff, evapotranspiration and surface erosion in the basin. Land cover information is important for many activities including land use planning and land management. Nowadays, satellite images and remote sensing techniques have been widely used in land use mapping to provide updated data, high capability analysis, variety of forms, digitization and processing in all sectors, including agriculture, natural resources and land use mapping as base maps. In the current study aimed at extracting Maroon watershed land use, initially, the images of land sat satellite for 1980-1990 and 2000-2010 were prepared. Then, topographic map digitization and mosaic, slope maps, aspect and elevation from sea map were prepared to identify the area in GIS software. Subsequently, correcting and processing operations on satellite images using 30 ground control points were done using Geomatica software. Furthermore, the supervised classification map of the area was produced by combining bands 3, 4, 5, and the final map was obtained after applying the filter operation. Type of land use with a four-digit code can be identified by the model. Land use map of the study area was classified again by the SWAT model as shown in *Figures 4, 5, 6* and 7. Land use changes per hectare during four decades clearly shown in *Table 1*.

http://www.aloki.hu ● ISSN 1589 1623 (Print) ● ISSN 1785 0037 (Online)
DOI: http://dx.doi.org/10.15666/aeer/1605_54815502
© 2018, ALÖKI Kft., Budapest, Hungary

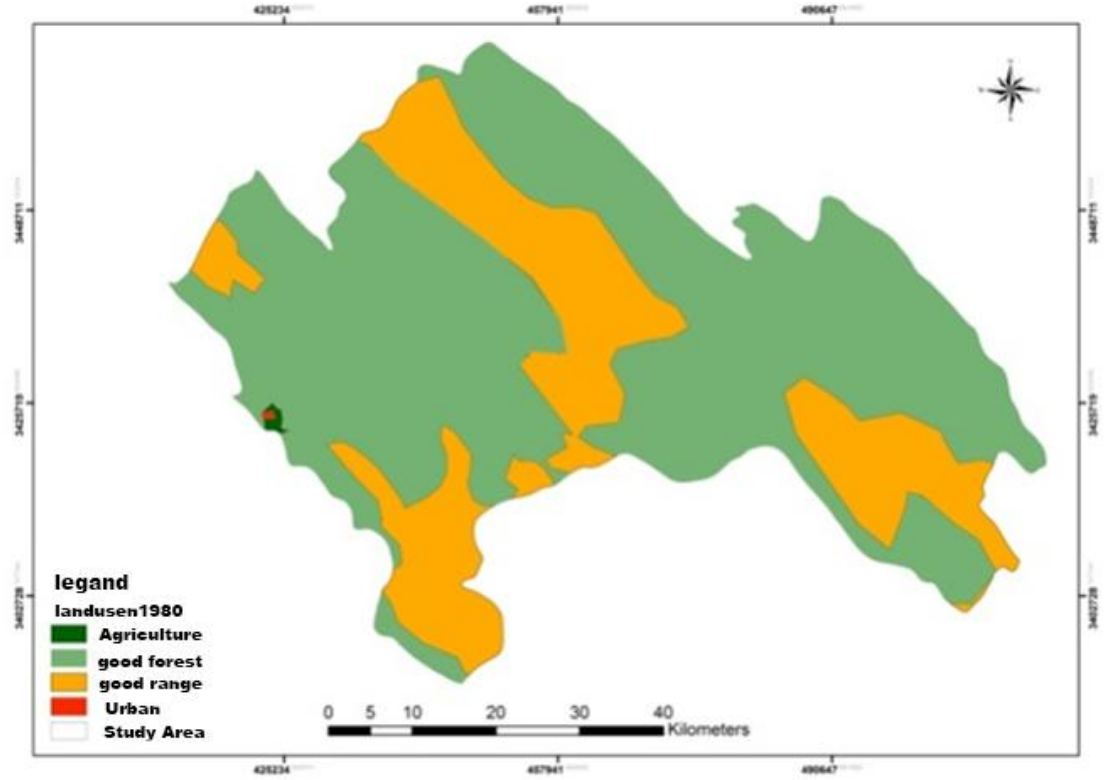

Figure 4. *Land use map (1980)*

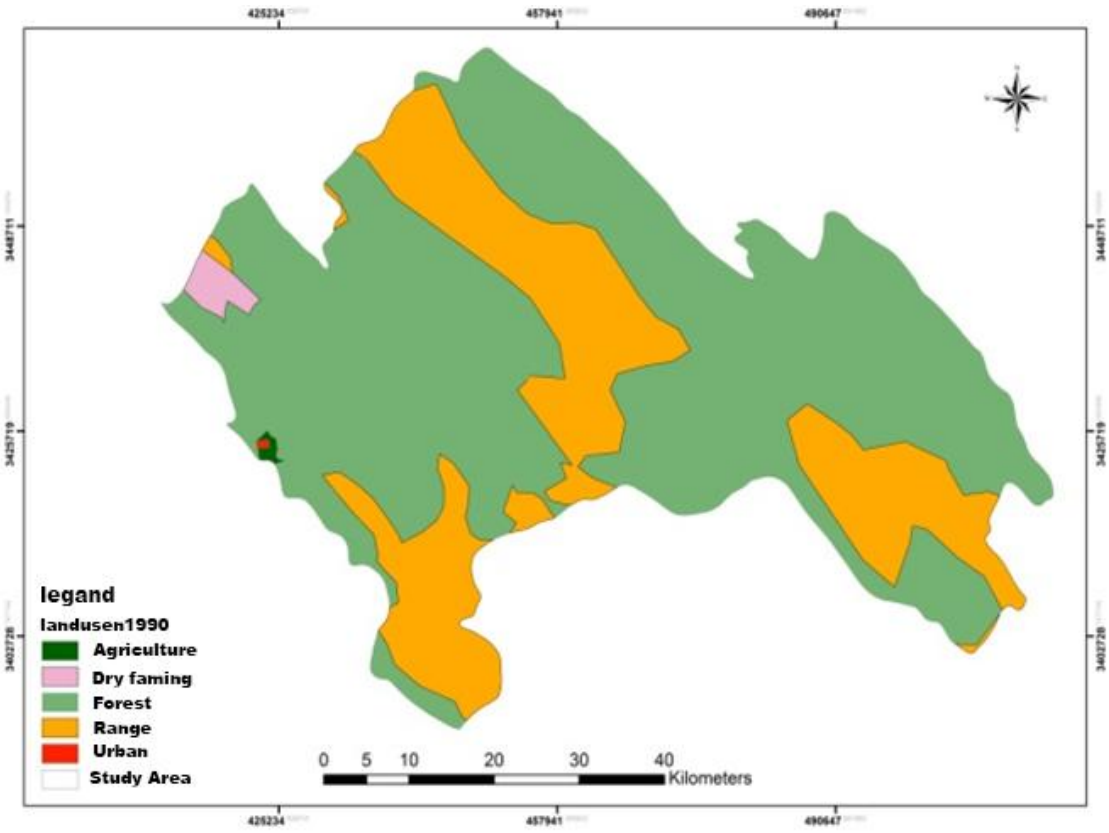

Figure 5. *Land use map (1990)*

http://www.aloki.hu ● ISSN 1589 1623 (Print) ● ISSN 1785 0037 (Online)
DOI: http://dx.doi.org/10.15666/aeer/1605_54815502
© 2018, ALÖKI Kft., Budapest, Hungary

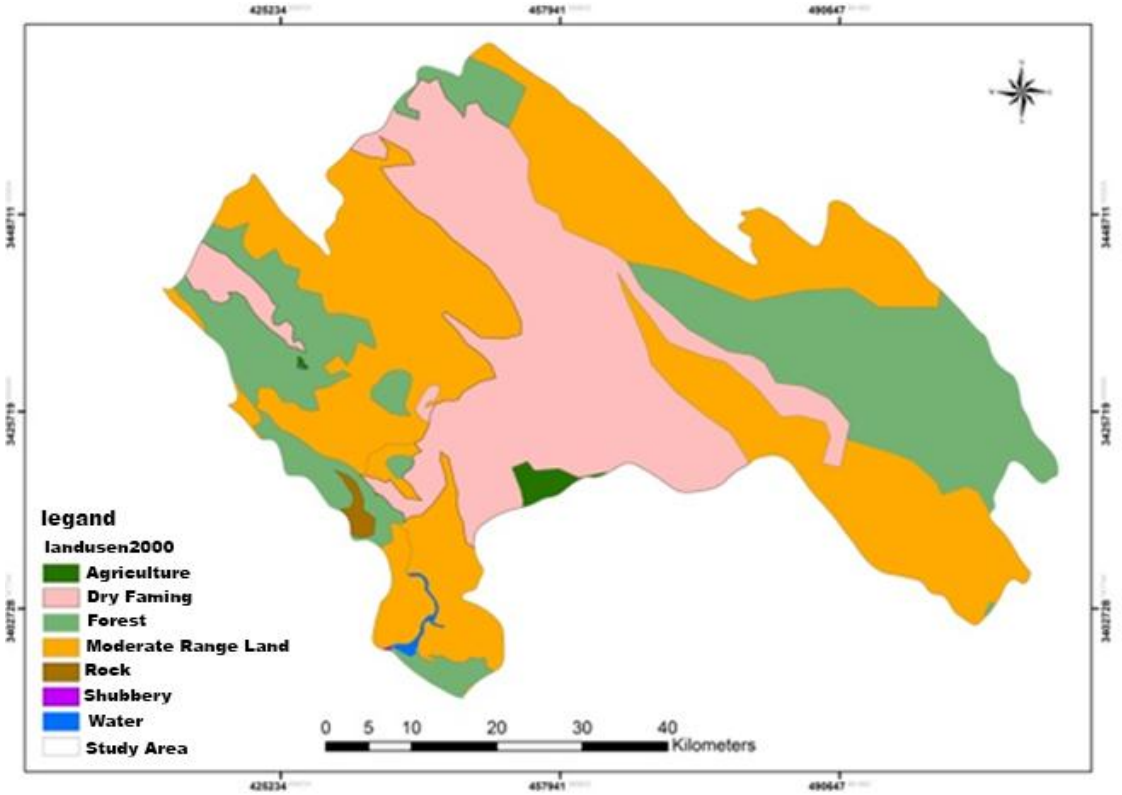

Figure 6. *Land use map (2000)*

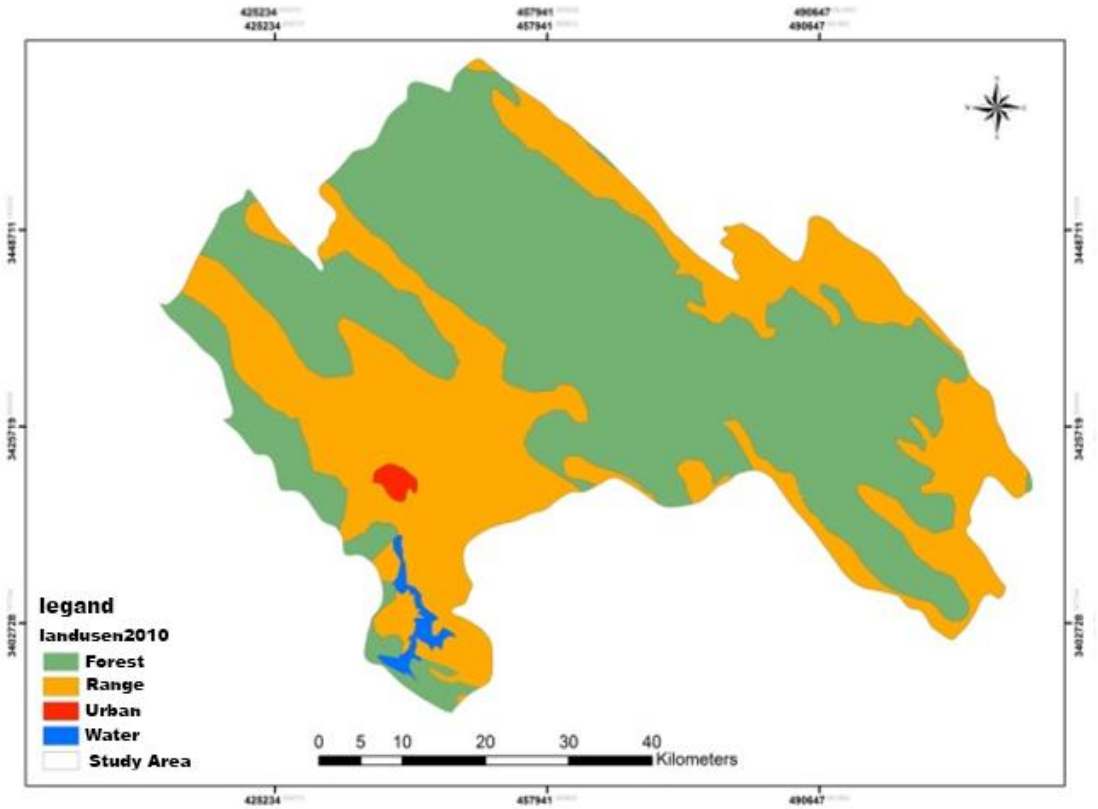

Figure 7. *Land use map (2010)*

http://www.aloki.hu ● ISSN 1589 1623 (Print) ● ISSN 1785 0037 (Online)
DOI: http://dx.doi.org/10.15666/aeer/1605_54815502
© 2018, ALÖKI Kft., Budapest, Hungary

Table 1. *Land use area changes in Maroon during four recent decades/ha*

Use type	1980 **Use**	1990 **Use**	2000 **Use**	2010 **Use**
Agriculture	535	612	916	1344
Forest	272258	264458	256186	224458
Pasture	108375	116097	123415	154063
Urban area	126	127	752	1409
Water	0	0	25	20

Soil texture map of the study area

Soil data is the most basic information required for this model. The SWAT requires various physico-chemical properties of the soil, such as soil texture, available moisture content in the soil, hydraulic conductivity, bulk density, organic carbon content and model of different soil layers to simulate the characteristics of the basin. The map of the re-categorized soil map of the Maroon watershed land use and the map of vegetation during four decades from 1980 to 2010 were prepared using satellite images shown in *Figure 8*. Considering that 100 years of time is required to change the texture of the soil and the timeframe for this research is 40 years the soil texture map is identical in four decades and the model of 2010 is used in the model.

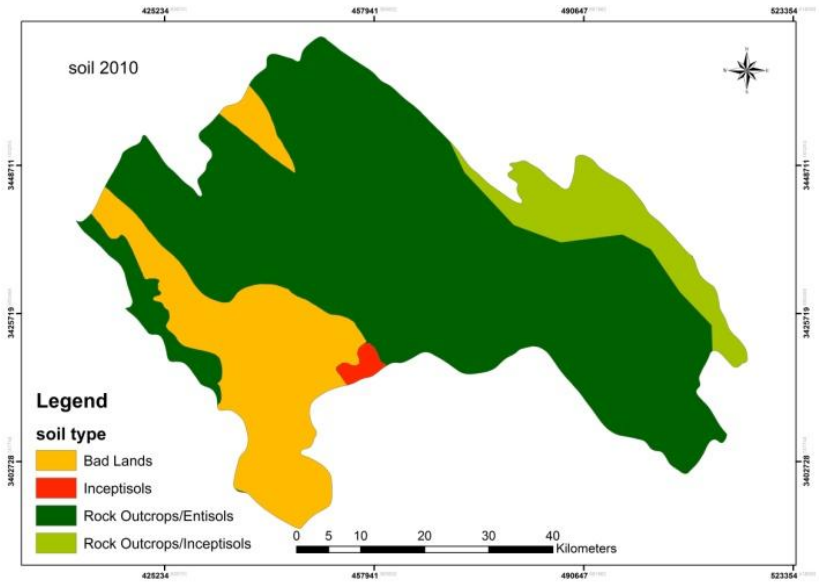

Figure 8. *The soil maps of the study area during 2010*

Meteorological and hydrological data

Climate as the source of input energy, determines the humidity of basins and controls water balance as well as determines the relative importance of different components of the hydrological cycle. The SWAT model requires information on basic daily climate variable rainfall, maximum and minimum temperature, solar radiation, relative humidity and wind speed for simulating the conditions of the basin. This information may be read as an input file, observational values or be created by the SWAT model by using monthly average values summarized in the weather generator input file (userwgn.dbf).

http://www.aloki.hu ● ISSN 1589 1623 (Print) ● ISSN 1785 0037 (Online)
DOI: http://dx.doi.org/10.15666/aeer/1605_54815502
© 2018, ALÖKI Kft., Budapest, Hungary

Hydrological data are required for sensitivity analysis, calibration, and validation analysis of hydrological models uncertainty. Hydrological data used in this study consist of monthly and daily discharge values at Idnak stations located at the basin output. This data was collected from Khuzestan Province Regional Water Organization. Idnak gauging stations are used as base stations for the runoff changes. This data is converted into the format required for the model. The simulation is done automatically. Then, upon parameter optimization, the simulated value is closer into the observed data. *Figure 9* shows the position and number of meteorological and hydrometric stations in the studied area.

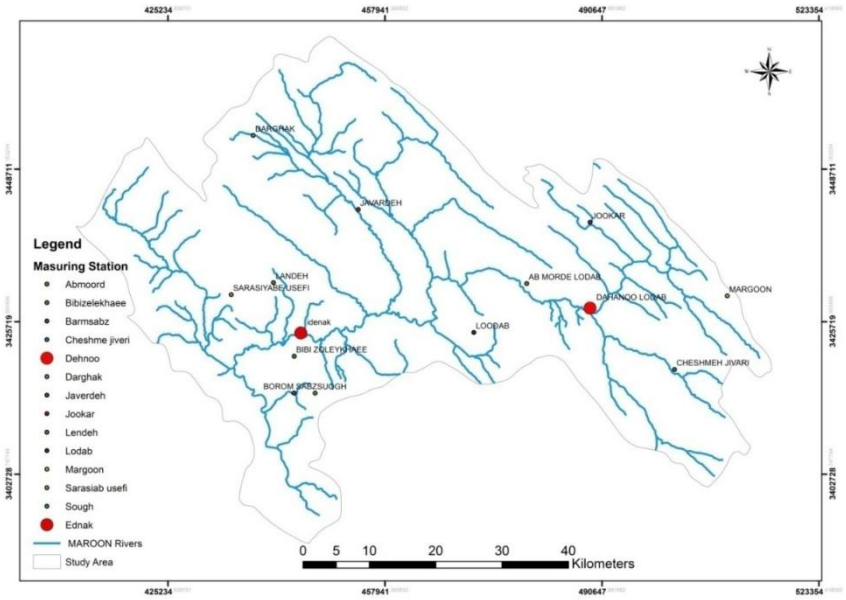

Figure 9. *Position of meteorological stations in the studied area*

Running the SWAT 2012 model

In this study, a semi-distributed SWAT model 2012 with a GIS extension was used for analysis and simulation. Basically, the SWAT model database is designed for the conditions of the United States of America. So to use this model in other areas the input information should be modified including data related to soil (usersoil.dbf), land (landuse.dbf), weather generator stations (userwgn.dbf) as well as management information. Data related to GIS development of the SWAT model is identified with unique functions to determine the Basin Hydrological Response Unit (HRU). The model used the data digital elevation model data to automatically divide each area based on current conditions and then accumulated the data into several sub-basins. In general, there are 25 sub-basins in the Maroon watershed with 21 sub-basin located at the outlet. Also the number 5 sub-basin with an area of 27.5 km^2 is the smallest sub-basin. The sub-basin number 2 with an area of 278.36 km^2 is the largest sub-basin. The hydrological response units are integrated lands that are located within the sub-basin and in the areas where land use, soil, slope and management is homogeneous and monolithic. To determine the HRU map, the gradient map was used. Different tilt classes were obtained based on the characteristics of the study area and aimed at the DEM map. According to a wide range of sub-basins in the studied area, using several

http://www.aloki.hu ● ISSN 1589 1623 (Print) ● ISSN 1785 0037 (Online)
DOI: http://dx.doi.org/10.15666/aeer/1605_54815502
© 2018, ALÖKI Kft., Budapest, Hungary

slopes to a common dip for all sub-basins is a priority. The slope classes are different in each area depending on the characteristics of the topography of the area. In various studies done in this area, there is no single classification for slope classes. Thus, the user selects the slope classes based on topography. Generally, in the study area 4 gradient classes (0-2, 2-10, 10-20, and > 20%) were introduced to the model.

The sensitivity analysis of the model

Sensitivity analysis is the study of quantitative and qualitative changes based on input variables for Output Models. In other words, in this analysis, the effective variables ordered in the model is based on their role in the amount of general error. Maroon watershed, in terms of hydrological basin is very complex. Also sensitivity analysis was performed using the indicators t-stat and p-value SUF12 program in the bundle SWA CUP. Generally, higher absolute value of t-stat represents the most sensitive parameter. The closer the p-value is to zero, the more sensitive the parameter is. It should be mentioned that in this study, the parameter range has been set at default values for the Maroon watershed model.

The calibration model

After identifying the most critical parameters affecting the flow rate, calibration was performed to describe the optimal values. Calibration is the modification of input parameters, so that it is the best fit for the observed data. Inverse modeling in recent years is used as a suitable method in many branches of Earth Sciences and environmental studies. Maybe it is because direct measurement is time-consuming, expensive and often faced with limitations while measuring a few output parameters makes it easier for some of the input parameters (Rostamian, 2009). The calibration process may be performed in the form of trial and error methods (manually) and automatic (using computer programs). Automatic calibration is more optimal compared to manual methods and its implementation is easier (Liu, 2009). In this study, automatic calibration methods were used to identify the optimal values of model parameters. This process was done by changing the parameters specified in the input file and by using the qualitative evaluation model (Himesh, 2000). The calibration process was conducted both on a monthly and daily basis and based on the Maroon basin flow. At first, the model was simulated for a suitable period (the period of warming-up) and based on the initial values obtained for a given period which was implemented in the model. In total, 27 parameters were selected based on various studies conducted in this area that upon sensitivity analysis and identification decreased to 13 parameters, which were the most effective parameters. Reducing the number of parameters during sensitivity analysis caused reductions in the implementation time and increased accuracy by reducing the uncertainty of the model. So, after knowing the most sensitive parameter, the model was run using critical parameters affecting the discharge.

Validation of the model

When calibration is performed to check the accuracy of the calibrated model for use in estimation and subsequent management activities, the independent model using observed data was implemented (1970 and 1971 in the first decade, 1980 and 1981 in the second decade, 1990 and 1991 in the third decade, 2000 and 2001 in the fourth decade) without changing the parameters of the calibration. The model validation will

http://www.aloki.hu ● ISSN 1589 1623 (Print) ● ISSN 1785 0037 (Online)
DOI: http://dx.doi.org/10.15666/aeer/1605_54815502
© 2018, ALÖKI Kft., Budapest, Hungary

be done to ensure that the calibration model on the output of all variables and conditions that affect calibration, correctly evaluates models of the relevant periods. Here, the same validation method and calibration process was done using the software package SWAT CUP and SUFI2program.

Model performance evaluation

To evaluate the performance of the model to simulate hydrological processes, it can be compared and simulated using different statistical models with observational data (Green, 2006). It is very difficult to only investigate one statistical method for the model's performance, therefore to evaluate the efficiency of the model; several statistical methods were used simultaneously. Williams used the correlation coefficient (R2) plus the efficiency factor Nash - Sutcliffe (ENS) proposed as a way to assess and analyze the data simulated (Willems et al., 2009). In this study, the SWAT model is used for evaluating performance.

Results and discussion

The first model was run by using input data and relevant default data. *Figures 10-17* show the output in the initial run based on monthly time period. As shown in these figures, the simulated basin in the initial run is very weak. In order to check the quality of simulation in the initial run, the Nash-Sutcliffe (E_{NS}) coefficients of correlation between observed and simulated values were used.

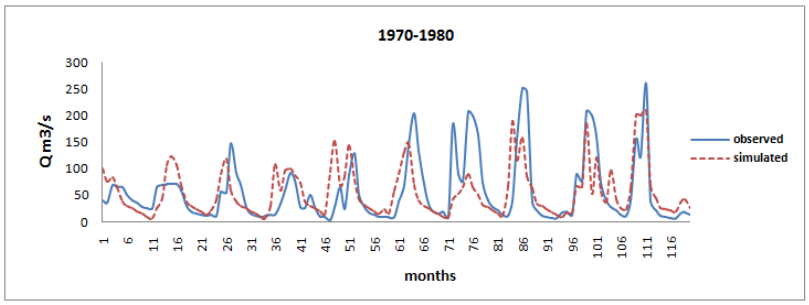

Figure 10. *Values of runoff simulated and observed in the first decade of the initial run of Maroon area on a monthly basis*

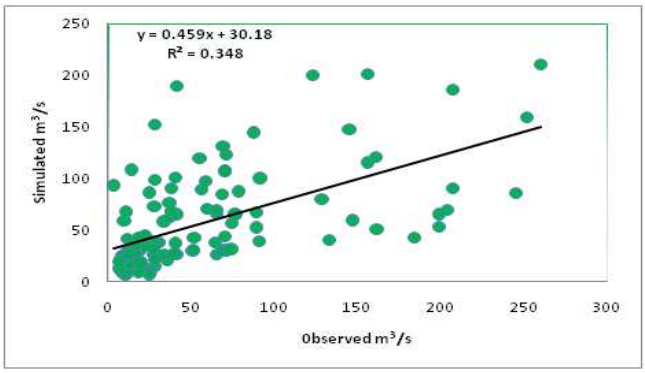

Figure 11. *Correlation between observed runoff and simulated runoff in the first decade of the initial run on a monthly basis*

http://www.aloki.hu ● ISSN 1589 1623 (Print) ● ISSN 1785 0037 (Online)
DOI: http://dx.doi.org/10.15666/aeer/1605_54815502
© 2018, ALÖKI Kft., Budapest, Hungary

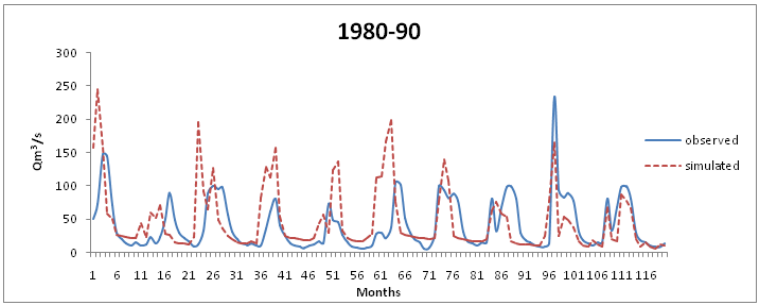

Figure 12. *Values of runoff simulated and observed of Maroon area in the second decade of the initial run on a monthly basis*

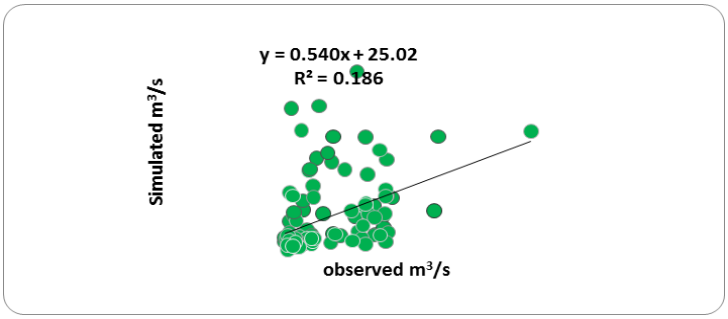

Figure 13. *The correlation between observed runoff and simulated runoff in the second decade of run of the model on a monthly basis*

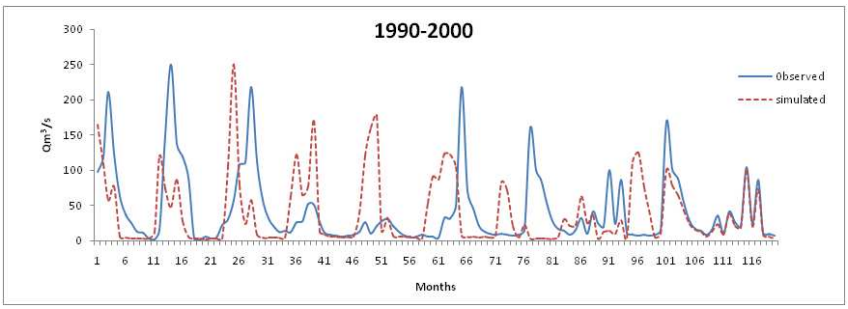

Figure 14. *Values observed and simulated runoff in Maroon watershed in the third decade in the initial run the model on a monthly basis*

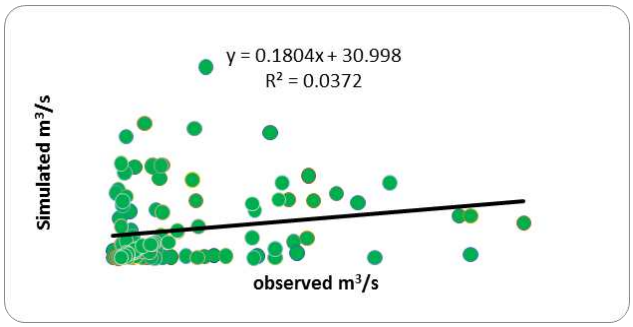

Figure 15. *The correlation between observed and simulated runoff in the third decade in the initial run model on a monthly basis*

http://www.aloki.hu ● ISSN 1589 1623 (Print) ● ISSN 1785 0037 (Online)
DOI: http://dx.doi.org/10.15666/aeer/1605_54815502
© 2018, ALÖKI Kft., Budapest, Hungary

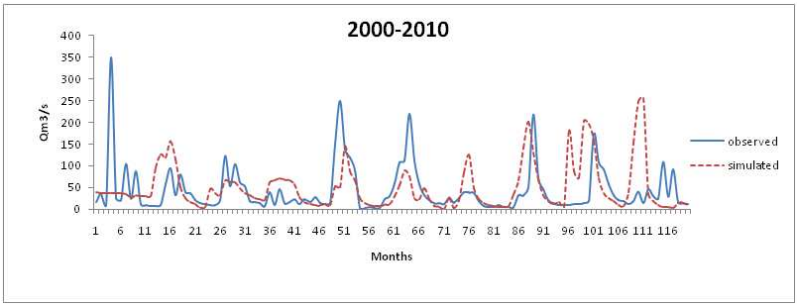

Figure 16. *Values of observed and simulated runoff in Maroon watershed in the fourth decade in the initial run model on a monthly basis*

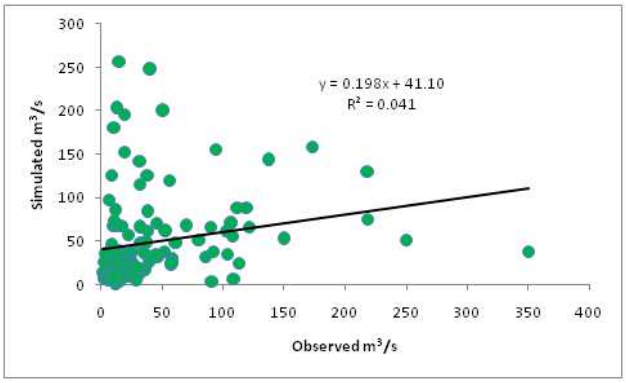

Figure 17. *The correlation between observed and simulated runoff in the fourth decade of the first run model based on a monthly basis*

Sensitivity analysis

After the initial run off, sensitivity analysis was carried out on the output model of the basin. In sensitivity analysis, the effect of various parameters on model output based on objective function (in this study, Nash was considered as the objective function) were clearly identified. For the sensitivity analysis and to determine the relative importance of each model parameter, the SWAT, SWAT CUP and LH-OAT methods were used in addition to the SUF12 program during calibration. Sensitivity analysis in the LH-OAT method presented is based on 27 selected parameters. Also, the identification of sensitive parameters on a monthly basis was conducted using SUF12 programs on 27 parameters as shown in *Table 2*.

Table 2. *Priority of critical parameters based on t-stat and p-value values using the SUF12 program after calibration on a monthly basis average of the four periods*

Range	Parameters
20-90	r_ CN2
0-2000	r_SOL_K()
0-150	v _CH_ K2
0-1	v _CH_ N2
0-1	v_ ALPHA _BNK
10-150	r _SLSUBBSN

http://www.aloki.hu ● ISSN 1589 1623 (Print) ● ISSN 1785 0037 (Online)
DOI: http://dx.doi.org/10.15666/aeer/1605_54815502
© 2018, ALÖKI Kft., Budapest, Hungary

0-5000	v_GWQMN
0-50	v _TLAPS
0-10	v _SMFMX
0-0.25	r_SOL_ALB()
0-500	v_ GW_ DELAY
0-1	r_SOL_AWC()
0.01-0.1	r_ EPCO
0-1.5	v_ GW REVAP
0-1	v_ ALPHA_ BF
-5-+5	v_ SFTMP
0-180	r_ LAT TTIME
0-10	v _SMFMN
0-1	r _ESCO
0-2.5	r_SOL_BD()
0-25	v_ SMTMP
0-100	v _CANMX
0-0.6	r_SLOPE()
1-24	v_ SURLAG
0-1	v_RCHRG_DP
0-1	v_ TIMP
0-500	v_ REVAPMN
0-25	r _SOL _Z
0-1	v _BLAI
0-1	v_ BIOMIX
0-10	v_ SHALLIST _N

The results of the sensitivity analysis carried out using the LH-OAT method on the 27 parameters indicated that GWQMN, RCHRG-DP, CN2 SMFMN ESCO flow are the most sensitive parameters on a monthly basis. The most sensitive parameters affecting the discharge area of Maroon on a monthly basis using the SUF12 program software are SWAT CUP SOL-K, CN2 ESCO, SMFMN, RCHRG-DP, REVAPMN, GWQMN, SLSUBBSN ALPHA-BNK, excluding the most critical parameters affecting the discharge of Maroon River. In general, due to the different regional and climatic conditions, sensitive and effective parameters are different for the studied region on a daily and monthly basis (Sangjun, 2007). As seen in all methods and based on the daily and monthly activities, CN2 is the most sensitive parameter. The CN2 Parameter (number of CSC curve for the average moisture conditions (II) and the slope 5%) is a function of the soil permeability, land use and former humidity conditions. The value of this parameter is different for the various soil types, land use and for each sub-basin. Generally, increasing the amount of CN2 increases runoff volume. The high sensitivity of this parameter indicates the important role of land use in the amount of runoff from the basin. Also, most of the region is mountainous, which increases the amount of runoff by reducing the amount of permeability. In this case, In this case more runoff is outside of catchment area. CH-N2 (Manning roughness coefficient of Main River) is an effective parameter on the routing of stream flow and is used to calculate the concentration of the watershed. High sensitivity of CH-K2 (effective hydraulic conductivity river bed) in this region indicates the presence of lateral branches in the area to form intermittent or seasonal activities that impact the flow of the main river

http://www.aloki.hu ● ISSN 1589 1623 (Print) ● ISSN 1785 0037 (Online)
DOI: http://dx.doi.org/10.15666/aeer/1605_54815502
© 2018, ALÖKI Kft., Budapest, Hungary

(Beven, 2001). This basin has rigid seasonal streams and numerous rivers, especially in semi-arid areas that in the case of rain and flooding, has considerable impact on the outflow at Idnak gauging stations. SOLK (saturated hydraulic conductivity of soil layers) is scaled to facilitate movement of water in soil layers that represent a balance between water flow and hydraulic gradient. Other important parameters on the HRU level include SUBBAN (average length of the slope of the land in each HRU) that may have the same value for each HRU as well as the ESCO parameter (evaporation from soil coefficient offsetting) which is an important parameter influencing the hydrological cycle surface. Generally, decline in this parameter increases surface runoff base flow and vice versa. ESCO reduction causes the transmission of more water from the lower layers to the upper layers of the soil and consequently the amount of surface runoff and base flow will increase. Effective parameters on groundwater are effective on surface water. These parameters show that the river flow is mainly controlled by groundwater flow. GWQMN (minimum shallow water table depth required for the reverse flow) is relevant to current production base. Considering the depth of the water in the aquifer level, groundwater flow occurs when the water level in the aquifer level is equal to or greater than GWQMN. This parameter has an impact on base flows and affects the flow of the river (Reungsang et al., 2005). RCHRG-DP (recharge percentage deep aquifer from shallow or confine aquifer) represents the percentage drop of water from the root zone that feeds the deep aquifers. The high sensitivity of this parameter in the studied area entails the probability of water transfer from the shallow aquifer to the deep aquifer and may create problems in water balance and consequently for the region (Sanjay, 2010). REVAPMN (minimum depth of water table levels in shallow aquifers to climb through the capillary or recharge deep aquifer) is representative of the water movement to the unsaturated zone and deep aquifers. ALPHA-BMK (alpha factor for storing base flow the sidebar) represents the side which is affected on the main channel or sub-basin within the range.

Model calibration

After the initial run the SWAT CUP software package and SUF12 programs were implemented for calibration and uncertainty analysis to determine variable Maroon River discharge areas in the basin outlet. According to various studies conducted in this field, about 27 parameters are effective and important for calibration. Varying ranges of parameters were set according to their default model and based on hydrometric station of Idnak. Each parameter was entered in the model within the limits of permitted changes, and implemented in order to optimize the output of the simulation model. Then, sensitivity analysis reduced the number of parameters. A total of 13 known parameters from the 27 selected primary parameters were more effective and were entered in the final stage of the model. Calibration was performed on a monthly basis during various stages for various parameters. Finally, the optimal values of parameters were determined to simulate the monthly watershed runoff. *Table 3* shows optimal values of parameters that affect the rainfall-runoff (amount or percentage changes) upon simulation and calibration of the parameters after the 2000 runoff model. Also *Figures 18-25* show calibration results based on a monthly time period using the SUF12 program and also the correlation coefficient between observed and simulated runoff model.

http://www.aloki.hu ● ISSN 1589 1623 (Print) ● ISSN 1785 0037 (Online)
DOI: http://dx.doi.org/10.15666/aeer/1605_54815502
© 2018, ALÖKI Kft., Budapest, Hungary

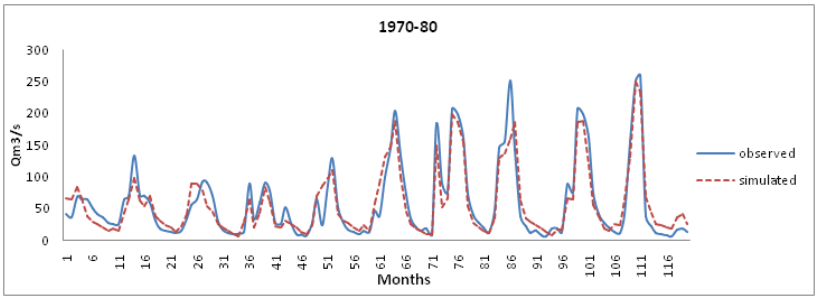

Figure 18. *Values of runoff Maroon areas simulated and observed using the sufi2 program in calibration stage on a monthly basis in the first decade*

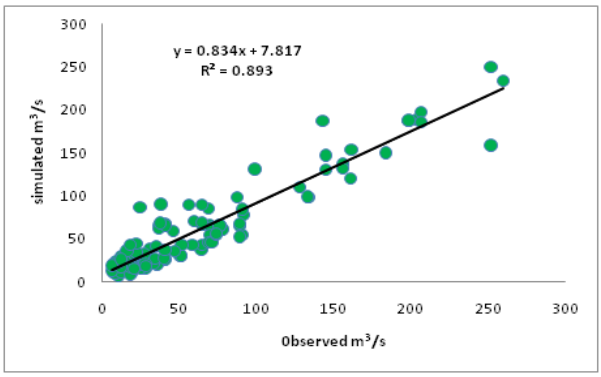

Figure 19. *The correlation between simulated and observed runoff model calibration using the sufi2 program stage on monthly basis - the first decade period*

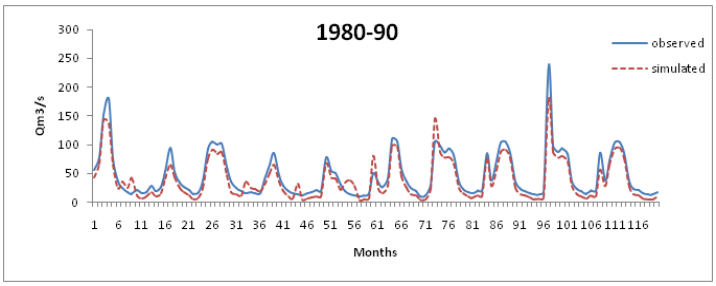

Figure 20. *Values of simulated and observed runoff areas at the base of Maroon using the sufi2 program model calibration phase on a monthly basis - second decade period*

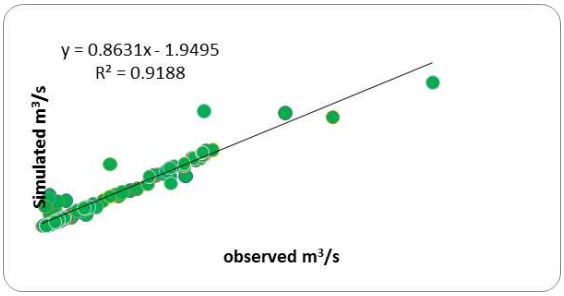

Figure 21. *The correlation between simulated and observed runoff model calibration using the sufi2 program stage at the base monthly time period - second decade*

http://www.aloki.hu ● ISSN 1589 1623 (Print) ● ISSN 1785 0037 (Online)
DOI: http://dx.doi.org/10.15666/aeer/1605_54815502
© 2018, ALÖKI Kft., Budapest, Hungary

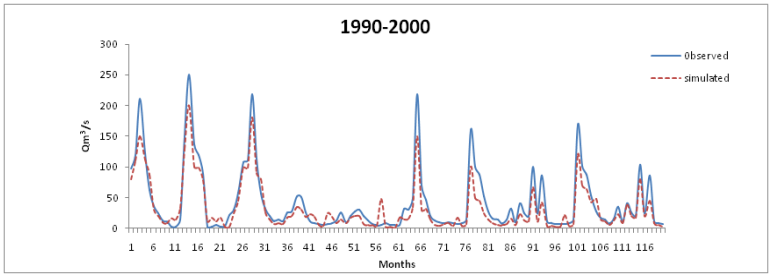

Figure 22. *Observed and simulated runoff values of the Maroon basin by using the sufi2 program calibration model on a monthly basis - the third decade*

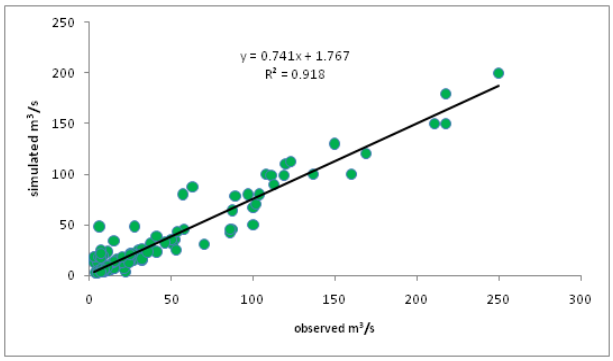

Figure 23. *The correlation between simulated and observed runoff model calibration by using the sufi2 program stage on a monthly basis - third decade*

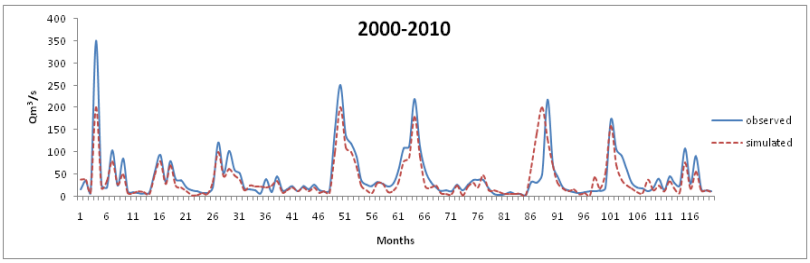

Figure 24. *The values of simulated and observed runoff of the Maroon basin by using the sufi2 program model calibration on a monthly basis - fourth decade*

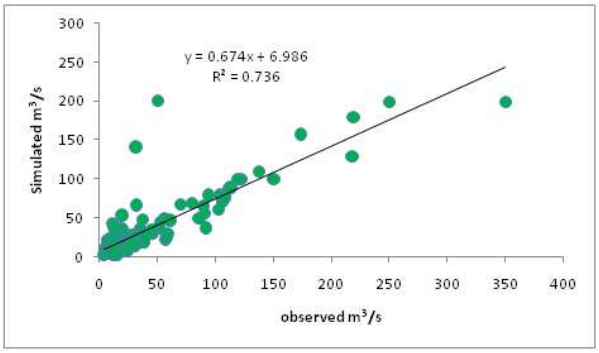

Figure 25. *The correlation between simulated and observed runoff model calibration by using the sufi2 program stage on a monthly basis - fourth decade*

http://www.aloki.hu ● ISSN 1589 1623 (Print) ● ISSN 1785 0037 (Online)
DOI: http://dx.doi.org/10.15666/aeer/1605_54815502
© 2018, ALÖKI Kft., Budapest, Hungary

Table 3. *The final value parameters (amount or percentage changes) by using SUF12 program on a monthly basis*

Range	Parameter description	Parameter name
60-70	The primary SCS Curve Number for average moisture conditions (II)	CN2
15-30	Saturated hydraulic conductivity of the soil layer (mm/hr)	SOL_K
0.01-0.1	Constant depletion of ground water days	ALPHA _BF
10-150	The average length of the slope of the land in each HRU (m)	SLSUBBSN
0-1	The minimum rate of snow melt during the year (mmH2O/0C-day)	SMFMN
0.1-0.25	The maximum rate of snowmelt during the year (mmH2O/0C-day)	SMFMX
0.1-0.2	Factor soil evaporation	ESCO
0.2-0.4	Shallow or deep aquifer fed percent of non-enclosed table	RCHRG_DP
2-3	Snow or rain turned to snow average air temperature	SFTMP
80-95	Water kept up by vegetation (mmH2O)	CANMX
0-0.5	The base temperature of melting snow	SMTMP
0-150	The main river bed effective hydraulic conductivity (mm / hr)	CH-K2

Validation of the model

In this research, Idnak hydrometric station was an aid and supplement for computational parameters required for the SWAT model during calibration and validation. In accordance to studies conducted by Omani et al., two-thirds of the available data for calibration and one-third was used for validation. Statistical and graphical simulation results indicate acceptable water flow for the period of calibration results at this stage. For validation of the model, optimized parameters were used in the calibration stage from the SWAT CUP software package and the SUFi2 program.

Model evaluation

To evaluate the performance of the SWAT model in the simulation of monthly discharge at Idnak hydrometric station, indicators were presented during calibration and validation based on the criteria for evaluating the accuracy of the simulation. Numerous researchers have recommended using several methods for parameter optimization and uncertainty analysis instead of one particular method (Abbaspour et al., 2004), (Abbaspour et al., 2007). This is the reason that for this study, the SUFi2 program was used in the form of an extension in the SWAT model bundle within the SWAT CUP software package. The usefulness of model was examined by coefficients such as p-factor, r-factor, R2, ENS, bR2, MSE and RMSE in the watershed outlet (*Table 4)*. In this study, the Nash-Sutcliffe efficiency was used as an objective function for the model calibration and verification. P-factor index in watershed Maroon is from 0.72 to 0.92 for the monthly period variable. The greater the index, the more effective the simulation is. The value of this parameter in these areas is low which indicates great uncertainty in forecasts. One of the reasons for low p-factor is that the current value is greater than the values predicted by the model base. The results for the observed data are located outside the 95% prediction uncertainty ranges. Lack of information about the uptake and upstream water use is a reason for the incompetency of the base flow prediction model. Therefore, in order to reduce uncertainty in models, there is a need to use comprehensive data on water management in the studied area. R-factor is the average

http://www.aloki.hu ● ISSN 1589 1623 (Print) ● ISSN 1785 0037 (Online)
DOI: http://dx.doi.org/10.15666/aeer/1605_54815502
© 2018, ALÖKI Kft., Budapest, Hungary

thickness of the band 95 PPU which is divided by the standard deviation measured data. The less the value of this index, the less the simulation is done with greater precision so that the optimal value is zero. This index regarding Maroon basin is a variable for monthly periods showed values of 0.93 to 90.2 during the calibration. Relatively small values of p-factor and r-factor in this basin on a monthly basis indicate good calibration and runoff in the basin and there is lower prediction uncertainty. The value of R2 (R2 coefficient multiplied by the coefficient of linear regression) using the SUFI2 program for calibration for the monthly period is 0.75. The value of this coefficient for the validation period is 0.82 on a monthly basis. The Mean Square Error (MSE) is scaled to consider the random mean difference between simulation and observations. MSE and RMSE Square represent the value of these parameters which can be varied from zero to infinity and the optimal value is zero. In addition, these factors along with E_{NS} and R_2 coefficients were used to determine suitability. The optimal value of R_2 is one. Although, there is no specific rule as reported by (Santi et al., 2001) that 0.5 is not acceptable for hydrological models. According to *Table 5,* the index in the SUFI2 program at calibration period is 0.84 and for validation period 0.82 on a monthly basis. In general, according to the simulation results, the accuracy of the model for the basin hydrological process simulation was relatively good. Finally, this model can be used for future analyses of basins and sub-basins and to check the different components of the hydrological cycle.

Table 4. *The statistical coefficients evaluation of the accuracy of the model to simulate the monthly runoff during calibration and validation*

SUF12		The statistical indices
Validation	**Calibration**	
0.92	0.79	P_factor
2.91	1.51	R_factor
0.86	0.85	R^2
0.82	0.86	E_{NS}
0.829	0.654	bR^2
82.07	58.88	MSE
9.05	7.6	RMSE

Conclusion

One of the specific applications to examine different components of the hydrological cycle is to utilize the SWAT model based on different scenarios. The results of this study states that SUF12 program and the basic monthly runoff curve number are the most sensitive parameters. On the other hand, there is a direct relationship between this parameter and land use. Parameter CN2 (primary SCS Curve Number for average moisture conditions (II) and the slope 5%) is a function of the soil permeability, land use and previous humidity conditions. The value of this parameter for different soil types and land use is different for each sub-basin. In general, increasing the amount of CN2 increases the volume of runoff water and reduces power losses, waterborne rivers and underground water resources, soil erosion and sediment changes (Setegn et al., 2010). The high sensitivity of this parameter indicates the important role of land use in these areas in the amount of runoff from the basin. A comparison of the effect of land

http://www.aloki.hu ● ISSN 1589 1623 (Print) ● ISSN 1785 0037 (Online)
DOI: http://dx.doi.org/10.15666/aeer/1605_54815502
© 2018, ALÖKI Kft., Budapest, Hungary

use management options on different hydrological cycle components show different amounts of runoff over the past four decades. A pessimistic scenario occurs with the continuing damage to the state in land use regression and various increases of runoff amounts which decrease permeability and gullies to the shallow and deep aquifers, stream sub cortical and results in actual evapotranspiration. *Figure 26* shows a comparison of the flow surface runoff, base flow and susceptibility of model to CN.

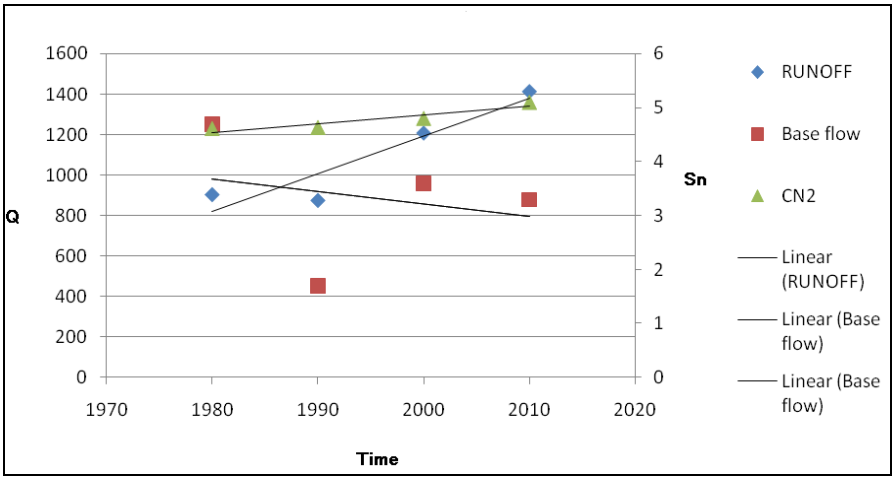

***Figure 26**. Comparison of the flow surface runoff, base flow and susceptibility of model to CN*

As evident in each scenario, by changing land use, changes in runoff peak values should entail a positive trend for reducing the negative trend for an increase in peak flow and peak values. This is due to change in the type of vegetation, and the result is a change in the runoff curve number. In this case, by reducing the permeability, greater quantities of rainfall run off the surface. Thus, the hydrological response basin in a state of regression and degradation is more severe than in the user regenerative mode; Hence, the need to maintain the current state of the basin and improving land use is one of the basic strategies for managing surface runoff.

REFERENCES

[1] Abbaspour, K. C., Johnson, C. A., Vangenuchten, T. M. (2004): Estimating uncertain flow and transport parameters using a sequential uncertainty fitting procedure. – Vadose Zone Journal 3: 1340-1352.

[2] Abbaspour, K. C., Yang, J., Maximov, I., Siber, R., Bogner ,K., Mieleitner, J., Zobrist, J., Sirinsivasan, R. (2007): Modeling Hydrology and water quality in the per-alpine Thure watershed using SWAT. – Journal of Hydrology 333:413-430.

[3] Alavinia, M., Nasiri, F. (2010): Compare the HSPF model and SWAT model simulation of sediment (case study catchment area of the Abroo). – The fifth National Congress of Civil Engineering, Ferdowsi University of Mashhad.

[4] Anwar, N. S. (2010): Simulated Impact of land use dynamics on Hydrology during a 20-ear-period of Deles Basin in Ethiopia. – TRITA-LWR Master Thesis, Department of Land and Water Resources Engineering, Royal Institute of Technology (KTH), Stockholm, Sweden, pp. 1-33.

[5] Beven, K. J. (2001): Rainfall-Runoff Modeling: the Primer. – Wiley, Chichester, UK.

http://www.aloki.hu ● ISSN 1589 1623 (Print) ● ISSN 1785 0037 (Online)
DOI: http://dx.doi.org/10.15666/aeer/1605_54815502
© 2018, ALÖKI Kft., Budapest, Hungary

[6] Duan, Z., Song, X., Liu, J. (2009): Application of SWAT for sediment yield estimation in a mountainous agricultural basin. – Graduate University of Chinese Academy of Sciences (GUCAS), Conservation Sedny. 76: 501-521.
[7] Green, C. H., Tomer, M. D., DiLuzio, M., Arnold, J. G., James, D. (2006): Hydrologic calibration of the soil and water assessment tool for a large tile-drained watershed in Iowa. – Transactions of the American Society of Agricultural and Biological Engineers (ASABE). 2(49): 411-413.
[8] Himesh, S., Rao, C., Mahajan, A. (2000): Calibration and Validation of Water Quality Model. – CSIR Centre for Mathematical Modelling and Computer Simulation, Technical Report CM 0002, Bangalore, India.
[9] Karlinger, M. R., Guertin, D. P., Troutman, B. M. (1998): Regression estimates for topological—hydrograph input. – J. Water Resour. 114: 446-456.
[10] Liu, Y. (2009): Automatic calibration of a rainfall–runoff model using a fast and elitist multi objective particle swarm algorithm. – Expert Systems with Applications 36: 9533-9538.
[11] Mirabzadeh, M., Globoidnia, M. (2005): The structure of mathematical modelsand theirapplication in groundwater systems. – Modeling Workshop onIrrigation andDrainage, The National Committee on Irrigation and Drainage. 18-20 November 2005, Tehran, Iran.
[12] Omani, N., Tajrishy, M., Abrishamchi, A. (2007): Modeling of a river basin using SWAT model and GIS. – International Conference on Managing Rivers in the 21 century, Reversid Kuching, Saravak, Malaysia, pp. 510-517.
[13] Palamuleni, L.G. (2011): Evaluating land cover change and its impact on hydrological regime in Upper Shire river catchment, Malawi. – Reg Environ Change 113:145-155.
[14] Phomcha, P., Wirojanagud, P., Vangpaisal, T., …, Thaveevouthti, T. (2011): Predicting sediment discharge in an agricultural watershed: A case study of the Lam Sonthi watershed Thailand. – J of Science Asia 37: 43-50.
[15] Reungsang, P., Kanwar, R. S., Jha, M., Gassman, P. W., Ahmad, K., …, Saleh, A. (2005): Calibration and Validation of SWAT for the Upper Maquoketa River Watershed. – Working Paper 05-WP 396, Center for Agricultural and Rural Development (CARD) at Iowa State University, pp. 1-19.
[16] Rostamian, R. (2006): Estimating runoff and sediment in Beheshtabad in North Karun Using SWAT2000. – Master of Science, Water Engineering, College of Agriculture, Isfahan University of Technology, pp. 43-48.
[17] Rostamian, R., Jaleha, A., Afyunia, M., Mousavian, S. F., Heidarpour, M., Jalalian, A., Abbaspour, K. C. (2010): Application of a SWAT model for estimating runoff and sediment in two mountainous basins in central Iran. – Hydrological Sciences Journal 53: 977-988.
[18] Salmani, H. (2011): Optimization parameters of rainfall - runoff in the semi-distributed model SWAT Ghazaghli basin in Golestan Province. – M.Sc. Thesis, Department of Rehabilitation Desert, Department of Natural Resources, Tehran University, pp. 234-236.
[19] Sangjun, I., Brannan, K. M., Mostaghimi, S., , Sang, M. K. (2007): Comparison of HSPF and SWAT models performance for runoff and sediment yield prediction. – Journal of Environmental Science and Health 11: 1561-1570.
[20] Sanjay, J. (2010): Simulation of runoff and sediment yield for a Himalayan watershed using SWAT model. – Journal of Water Resource and Protection 2: 267-281.
[21] Setegn, S. G., Dargahi, B., Srinivasan, R., …, Melesse, A. M. (2010): Modeling of sediment yield from Anjeni-Gauged watershed, Ethiopia using SWAT model. – Journal of the American Water Resources Association (JAWRA) 46(3): 514-526.
[22] Spruill, C. A., Workman, S. R., …, Taraba, J. L. (2000): Simulation of daily and monthly stream discharge from small watershed using the SWAT model. – Soil and Water Division of ASAE, pp. 1431-1440.

http://www.aloki.hu ● ISSN 1589 1623 (Print) ● ISSN 1785 0037 (Online)
DOI: http://dx.doi.org/10.15666/aeer/1605_54815502
© 2018, ALÖKI Kft., Budapest, Hungary

[23] Water Resources Management Company of Iran (2009): Report on Updating Integration of Studies on Water Resources in Maroon Watershed, 3rd ed. – Khuzestan Province Water and Electricity Organization (Public Joint Stock). Base Studies on Water Resources Assistance, pp. 177-189.
[24] Willems, P. (2009): A time series tool to support the multi-criteria performance evaluation of rainfall-runoff models. – Environmental Modelling & Software 24: 311-321.
[25] Zhang, X., Srinivasan, R., Van Liew, M. (2008): Multi-site calibration of the SWAT model for Hydrologic modeling. – Soil & Water Division of ASABE, American Society of Agricultural and Biological Engineers 51(6): 2039-2049.

http://www.aloki.hu ● ISSN 1589 1623 (Print) ● ISSN 1785 0037 (Online)
DOI: http://dx.doi.org/10.15666/aeer/1605_54815502
© 2018, ALÖKI Kft., Budapest, Hungary

EFFECT OF HYDROPHILIC POLYMER IN THREE GREEN ROOF SUBSTRATES ON GROWTH, FLOWER DEVELOPMENT, AND OVERWINTERING OF *AGASTACHE RUGOSA* (KOREAN MINT) WITHOUT IRRIGATION

XU, H.[1] – YEUM, K.-J.[2] – YOON, Y.-H.[1] – JU, J.-H.[3*]

[1]*College of Landscape Architecture, Central South University of Forestry and Technology No. 498 Shaoshan South Road, 410004 Changsha, China*

[2]*Division of Food Bioscience, KonKuk University, 268 Chungwondaero, 27478 Chungju-si, Chungcheongbuk-do, South Korea*

[3]*Department of Green Convergence Technology, KonKuk University, 268 Chungwondaero, 27478 Chungju-si, Chungcheongbuk-do, South Korea*

**Corresponding author*
e-mail: jjhkkc@kku.ac.kr; phone: +82-43-840-3541; fax: +82-43-851-4169

(Received 27th Apr 2018; accepted 11th Jul 2018)

Abstract. Some herb plants can be adapted to green roof systems when provided with better growing conditions such as irrigation. The aim of this study was to determine the effects of different amounts of water retentive, hydrophilic polymers used in green roof substrate mixtures, on the growth of *Agastache rugosa*. Coir dust and perlite were mixed at a ratio of 80 to 20% (coir dust to perlite, v/v) (termed C_4P_1), 50 to 50% (C_1P_1) or 20 to 80% (C_1P_4) at a substrate depth of 20 cm. Hydrophilic polymer was added to the substrate mixtures at 0 (polymer: medium (w/v), dry weight basis) (control), 0.25, 0.5, 1.0 or 2.0 $kg \cdot m^{-3}$. Our study indicated that *Agastache rugosa* can withstand extended dry conditions experienced in green roofs. Substrates C_4P_1 and C_1P_1 with high coir dust matter are not suitable for *Agastache rugosa* because of the low growth and poor ornamental quality observed in these plants, especially during the summer rainy season. For the determination of difference in growth, flower development and overwintering of *Agastache rugosa* among the different substrate conditions, Duncan's multiple range test was conducted. It was found that the addition of 1.0 $kg \cdot m^{-3}$ hydrophilic polymer to C_1P_4 significantly increased the number of inflorescences and resulted in good growth and ornamental quality during both drought and rainy seasons. Moreover, higher overwintering rate was associated with lower coir dust and hydrophilic polymer content. These results indicated that addition of 1.0 $kg \cdot m^{-3}$ hydrophilic polymer to C_1P_4 was optimal for the growth of *Agastache rugosa* in green roofs under dry and rainy seasons.
Keywords: *rooftop, hydrogel, native herb, water content, urban agriculture*

Introduction

Green roof is an environmentally friendly way to reduce urban heat island, noise and air pollution. At the same time, it can improve storm water management with delayed runoff, water quality, building's microclimate as well as aesthetic value and habitats for wildlife (Santamouris, 2014). Because of their numerous environment benefits, and more green, and open-air amenities without additional land acquisition cost, green roofs has become popular in many cities around the world. However, environmental conditions on the rooftops are often extreme compared to those on the ground, such as high temperature, strong wind, and long-term drought. Extensive green roof with light and thin layer of substrate demonstrate water deficit conditions (Dunnett and Nolan, 2004). The composition and characteristics of green roofs depend on many factors.

http://www.aloki.hu ● ISSN 1589 1623 (Print) ● ISSN 1785 0037 (Online)
DOI: http://dx.doi.org/10.15666/aeer/1605_55035516
© 2018, ALÖKI Kft., Budapest, Hungary

With the tremendous upsurge of interest in increasing the diversity of plant species in green roof systems, the edible plants were used extensively in recent year (Butler et al., 2012). It is also important to choose an appropriate substrate in which plants demonstrate drought-tolerant growth and can withstand the harsh rooftop environment.

Agastache rugosa is a perennial herb native to Korea, China and Japan that can grow to a height of 100-150 cm with quadrangular stems, displaying mauve or purple - blue flowers between June and September (Schafer, 2011). *Agastache rugose* thrives in warm and humid weather. It does grow best in full sun and well-drained sandy loam rich in organic matter, but also tolerate under somewhat poor soil and dry conditions. It can survive winter temperatures of at least -10 °C without protection. It can propagate by seeds in the spring and autumn, as well as with rooted cutting (Yamani et al., 2014). The flowers attract various species of butterflies and are also known as a valuable source of nectar for honeybees and native bees. It is also used in traditional Chinese medicine to treat cholera, vomiting, fever, headaches, colds, vomiting, nausea, and stomach problems, as well as in other eastern Asia countries (Choi and Seo, 2007).

Hydrophilic polymers (hydrogel), able to hold water several hundred times their weight, are widely used to improve the moisture of soil in the field of agriculture, horticulture and forestry (Baran et al., 2015). Since the 2000's, studies have been conducted on the application of hydrophilic polymers in green roofs, along with the development of high interest in green roofs. Hydrophilic polymers are used in green roof substrates to enhance the water holding capacity and improve the growth of plants. Young et al. (2017) revealed that coarser particle size substrates amended with 1% (v/v) dry hydrophilic polymer can significantly improve the drought tolerance of green roof plants， such as *Festuca ovina* and *Linaria vulgaris*. The growth of *Salvia officinalis* in 8 cm deep substrate mixed with hydrophilic polymer at a rate of 0.6% was the best under drought stress (Savi et al., 2014). Farrell et al. (2013) examined the impact of hydrophilic polymer addition to two green roof substrates, scoria-based and crushed terracotta roof-tile based, on the growth of winter wheat (*Triticum aestivum* L.) and white lupin (*Lupinus albus* L.). The results suggest that hydrogel addition can improve the plant available water, but had no effect on increasing wilting time. Olszewski et al. (2010) reported that the use of hydrophilic polymers increased the total porosity and container capacity of the substrate. The study also showed that hydrophilic polymer addition improved the initial plant growth of *Sedum floriferum* and *Sedum spurium*. Oschmann et al. (2007) conducted a three-year experiment with extensive green roof systems using crushed expanded slate substrates with 12 species of wild plants. The results revealed that use of hydrophilic polymers can enhance the water holding capacity and plant available water of substrates. In addition, the plants in substrates showed the best growth, especially at a concentration of 3 $g \cdot L^{-1}$, which resulted in the best coverage and regeneration. Meanwhile, our previous study found that the use of hydrophilic polymers in peat moss-based substrates significantly increased the substrate water content, but adversely affected plant growth, flowering and the visual quality of the drought-tolerant plant *Aster koraiensis* under no irrigation conditions (Xu et al., 2014). The response to hydrophilic polymers will thus depend upon the specific plant species and environmental conditions in the area. The objectives of this study were to determine the effect of different levels of water-retentive, hydrophilic polymer in three types of substrates on the growth, flower development and overwintering of *Agastache rugosa* in green roofs during the dry as well as rainy season.

http://www.aloki.hu ● ISSN 1589 1623 (Print) ● ISSN 1785 0037 (Online)
DOI: http://dx.doi.org/10.15666/aeer/1605_55035516
© 2018, ALÖKI Kft., Budapest, Hungary

Material and methods

Substrate preparation

A total of 45 square containers ((50 cm (L) × 50 cm (W) × 25 cm (H)) were installed on the flat rooftop of the Complex Practice Building in Konkuk University, Chungju, Chungcheongbuk-do, South Korea located at latitude 35°49' N and longitude 127°08' E (*Fig. 1*). Monthly precipitation was about 88.2, 110.6, 277.7, 122.7, and 153.8 mm in June, July, August, September, and October, respectively, with very little precipitation in May and November. Diurnal maximum air temperature was 35.3 °C, 31.7 °C, 34.4 °C, 34.4 °C, 31.0 °C, 27.2 °C, and 17.5 °C in May, June, July, August, September, October, and November, respectively. Minimum air temperature was 4.6 °C, 15.1 °C, 17.0 °C, 17.4 °C, 9.5 °C, 1.6 °C, and -4.5 °C, respectively.

Figure 1. *Experimental blocks on flat rooftop of the Complex Practice Building in Konkuk University, Chungju, Chungcheongbuk-do, South Korea*

From top to bottom, each container was filled with the following four layers: vegetation, growing medium, geotextile filter, and plastic drainage. A geotextile filter with good air permeability and water permeability was used to filter the substrate and separate it from the drainage layer. Plastic drainage was used to support the three layers above, to cut off roots, increase insulation, and retain excess water (Papafotiou et al., 2013). Based on the growth habits of *Agastache rugosa* and previous studies on green roof substrates, experimental substrates were formulated consisting of 80, 20, or 50% (by volume) coir and 20, 80, or 50% (by volume) perlite. Hydrophilic polymer (K-SAM, Kolon Chemical Co., Ltd., Korea) was incorporated into the substrates at concentrations of 0 (referred as control), 0.25, 0.5, 1.0, or 2.0 $kg \cdot m^{-3}$ (polymer: medium (w/v), dry weight basis) with three replicates per treatment. Organic fertilizers were

http://www.aloki.hu ● ISSN 1589 1623 (Print) ● ISSN 1785 0037 (Online)
DOI: http://dx.doi.org/10.15666/aeer/1605_55035516
© 2018, ALÖKI Kft., Budapest, Hungary

added to the substrates at 5% total volume to ensure that the same quantity was applied in each substrate which depth was 20 cm.

Plant material

Seedlings of *Agastache rugosa* were obtained from a commercial nursery, grown on 10 cm-diameter pots. Three seedlings of *Agastache rugosa* with consistent heights of 20 cm were transplanted into green roof containers on the 14th of May 2014. The initial height of the transplants differed by <1 cm. All plants were watered every 2 days in the first week followed by no watering when they were considered well established.

Measurement of volumetric water content of the substrate and plant growth

The volumetric water content in the top 10 cm of the substrates were monitored using a portable soil humidity tester (DM-5, Takemura®, Japan), respectively, at four locations selected randomly. Three replications were performed at 5 p.m. every week during the experimental period. Meteorological data were recorded every 30 min using an automatic weather station (Sensus, Casella Group Ltd., UK).

The growth parameters observed were plant height, leaf number of all the plants (n = 9) in June (dry season) and August (rainy season), respectively. Plant height (H) above the stem base, widest width at the widest vegetative point of the plant passing through the center (W1), and widest width perpendicular to W1 (W2) were measured. The data for the height and width were used to calculate the growth index (GI) ([W1 + W2]/2 + H)/2, commonly used as an indicator of plant size (Hammond et al., 2007). The relative appearance of the plant was evaluated based on its visual quality. The visual quality evaluations were divided into five grades, with grade 1 standing for severely stressed and completely dried out, grade 2 for stressed with less than 50% of the leaves retaining green pigmentation, grade 3 for mildly stressed with 50% of the leaves retaining green pigmentation, grade 4 for minor stress with over 50% of the leaves appearing to be healthy, and grade 5 for unstressed with all leaves appearing healthy (Nagase and Dunnett, 2010).

Leaf color was measured using a Chroma meter (CR-400, Konica Minolta Group, Japan) with L*, a*, and b* mode. The L* values ranged from black (L* = 0) to white (L* = 100). The a* values ranged from red (a* = 100) to green (a* = -100). The b* values ranged from yellow (b* = 100) to blue (b* = -100). Chroma C* was calculated as $(a^*2 + b^*2)^{1/2}$ measures for color saturation or intensity. Hue angle h was calculated as $\tan^{-1}$ (b* / a*). When a* was less than 0 and b* was greater than 0, h was 180 + $\tan^{-1}$ (b* / a*). The value of h is a 360° color wheel, with 0°, 90°, 180°, and 270° representing red-purple, yellow, bluish-green, and blue, respectively (Wang and Camp, 2000). The leaves measured were the third from the top to the bottom of the plant. The Leaf color, chlorophyll contents of leaves and number of inflorescences were measured in August when plants were at peak flower time.

The chlorophyll meter (SPAD-502) is a simple tool used to measure the relative chlorophyll content or greenness, thus is an efficient indicator of stress in plants (Netto et al., 2005). The chlorophyll contents were measured for 9 leaves per container using a SPAD-502 meter (Minolta Camera Co., LTd, Osaka, Japan).

All the herb plants in green roofs overwinter with no protection. Overwintering survival rates and self-sown seeding number for all plants were recorded in May and

http://www.aloki.hu ● ISSN 1589 1623 (Print) ● ISSN 1785 0037 (Online)
DOI: http://dx.doi.org/10.15666/aeer/1605_55035516
© 2018, ALÖKI Kft., Budapest, Hungary

June 2015 by measuring the number of sprouts aboveground from the roots and growing seedlings from seeds, respectively.

Experiment design and statistical analysis

This experiment was a completely randomized design with two factor, substrate design and hydrophilic polymer rate. There were three replicates for each treatment and each replicate consisted of three plants. Data were subjected to analysis of variance (ANOVA) with SAS 9.1 software package (SAS version 9.1, SAS Institute, Cary, NC). Significant mean separation was indicated by Duncan's multiple range test. Statistical significance was considered when the p value was less than 0.05.

Results

Volumetric water content of substrate

Under C_4P_1 treatment, the average volumetric water content was 52.7, 60.3, 61.3, 66.5, or 85.3% with 0 (control), 0.25, 0.5, 1.0, or 2.0 $kg \cdot m^{-3}$ of hydrophilic polymer, respectively. Under C_1P_4 treatment, it was 14.0, 14.1, 14.4, 17.8, or 25.3%, respectively, and 48.9, 50.4, 53.4, 58.5, or 82.6% under C_1P_1 treatment (*Fig. 2*). The moisture contents of substrate C_4P_1 and C_1P_1 under the control treatment were almost 3.8- and 3.5- fold higher than that of substrate C_1P_4, respectively. There was a significant ($p < 0.001$) interactive effect of the substrate and the hydrophilic polymer content on the volumetric water content. The temperatures of the substrates were significantly affected by treatment with hydrophilic polymer during the study (data not shown). The temperature of the substrate dropped significantly ($p < 0.001$) as the hydrophilic polymer content in the substrate was increased.

Plant growth

As shown in *Table 1,* the growth index of *Agastache rugosa* was not significantly different among the three substrates when measured in June. However, the leaf number ($p = 0.009$) and visual rating ($p = 0.028$) were significantly greater in substrate C_1P_4 than in substrate C_4P_1 in August. In addition, the growth index ($p < 0.001$), leaf number ($p < 0.001$) and visual rating ($p < 0.001$) of *Agastache rugosa* were significantly greater in substrate C_1P_4 than those in other two substrates when they were measured.

Flower development

The purple-blue flowers of *Agastache rugosa* started to bloom from mid-July to mid-October, with a flowering period extending more than 90 days. The peak blooming period was from mid-August to early September. The total number of inflorescences per *Agastache rugosa* plant was significantly ($p = 0.002$) higher in C_1P_4 than in the other substrates (*Fig. 3*). Incorporation of 1.0 $kg \cdot m^{-3}$ hydrophilic polymer significantly increased the total number of inflorescences per *Agastache rugosa* plant in C_1P_4, which was more than 2- fold higher than those in either the control or other hydrophilic polymer treatments. However, there was no significant difference in the total number of inflorescences per plant between the control and hydrophilic polymer treatment in C_4P_1 and C_1P_1.

http://www.aloki.hu ● ISSN 1589 1623 (Print) ● ISSN 1785 0037 (Online)
DOI: http://dx.doi.org/10.15666/aeer/1605_55035516
© 2018, ALÖKI Kft., Budapest, Hungary

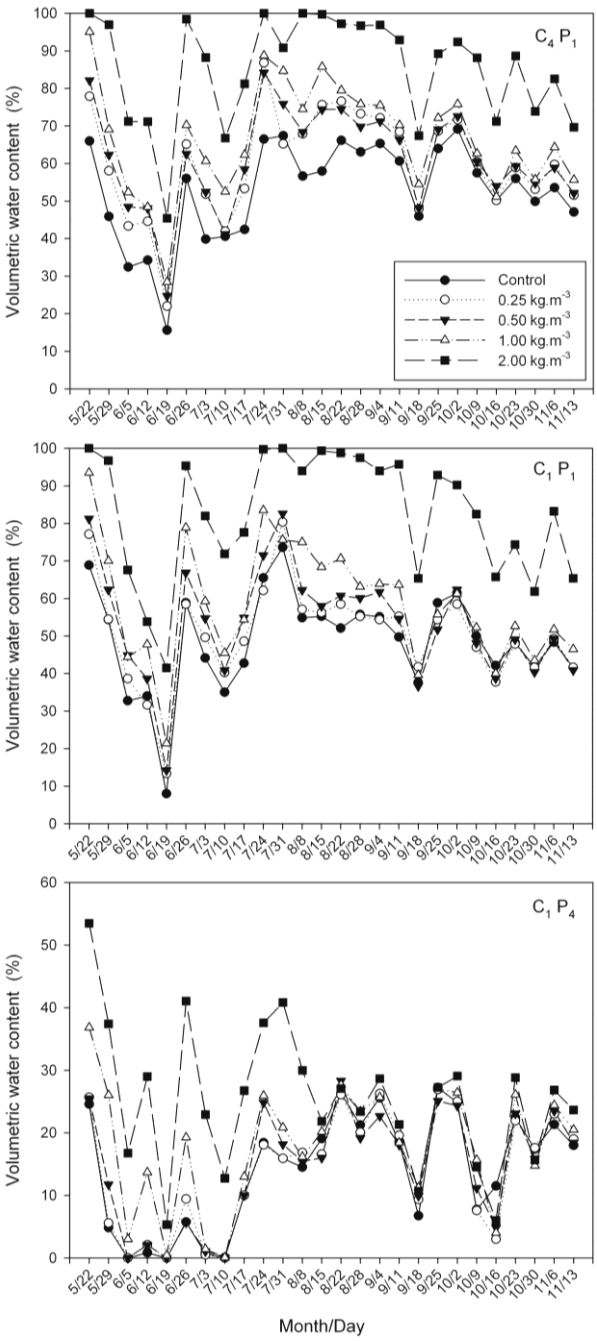

Figure 2. *Volumetric water content of three different green roof substrates (C_4P_1: coir 80%, perlite 20%; C_1P_1: coir50%, perlite 50%; C_1P_4: coir 20%, perlite 80% (% by vol.)) containing different amounts of hydrophilic polymer: 0 (Control), 0.25, 0.5, 1.0, and 2.0 kg·m^{-3} (polymer: medium (w/v), dry weight basis)*

http://www.aloki.hu ● ISSN 1589 1623 (Print) ● ISSN 1785 0037 (Online)
DOI: http://dx.doi.org/10.15666/aeer/1605_55035516
© 2018, ALÖKI Kft., Budapest, Hungary

Table 1. *Growth index, leaf number and visual rating of Agastache rugosa grown in different green roof substrates during the dry season (June) and the rainy season (August)*

Substrate	Polymer rate ($kg \cdot m^{-3}$)	June (dry season)			August (rainy season)		
		Growth index	Leaf number (per plant)	Visual rating	Growth index	Leaf number (per plant)	Visual rating
C_4P_1[y]	Control[x]	17.50ab[z]	13.1b	3.8b	20.09bc	12.0c	2.2cd
	0.25	16.60b	14.6ab	3.9ab	20.43bc	14.4bc	2.3c
	0.5	16.90ab	16.6ab	4.3ab	19.65c	8.7c	2.3c
	1.0	17.39ab	16.8ab	4.1ab	22.99a-c	12.3c	2.4c
	2.0	17.82ab	11.1b	3.9ab	21.09bc	10.3c	1.6d
C_1P_1	Control	19.44a	22.1a	3.9ab	24.75a-c	13.3bc	2.6bc
	0.25	17.56ab	15.4ab	4.2ab	19.53c	10.7c	2.8bc
	0.5	17.68ab	17.3ab	4.1ab	22.29a-c	14.4bc	2.8bc
	1.0	17.60ab	19.6ab	4.1ab	24.77a-c	14.4bc	2.9b
	2.0	17.31ab	17.4ab	3.9ab	20.09bc	9.7c	2.3c
C_1P_4	Control	19.31ab	18.8ab	4.1ab	28.43a	22.9a	4.0ab
	0.25	17.10ab	16.3ab	4.2ab	25.12a-c	25.7a	4.1ab
	0.5	18.53ab	22.4a	4.3ab	28.16a	26.4a	4.2ab
	1.0	18.10ab	19.6ab	4.4a	27.86a	20.7ab	4.4a
	2.0	17.46ab	17.1ab	4.4a	26.39ab	20.3ab	3.8b
Significance	Substrate	NS	**	*	***	***	***
	Polymer rate	NS	NS	NS	NS	NS	*
	Interaction	NS	NS	NS	NS	NS	NS

***, **, *: $p < 0.001$, $p < 0.01$, $p < 0.05$, respectively. NS: not significant

[x]Hydrophilic polymer rate: 0 (referred as control), 0.25, 0.5, 1.0, and 2.0 $kg \cdot m^{-3}$ [polymer: medium (w/v), dry weight basis]

[y]Substrate: C_4P_1: coir 80%, perlite 20%; C_1P_1: coir 50%, perlite 50%; C_1P_4: coir 20%, perlite 80% (% by volume)

[z]Means within columns by substrate were determined by Duncan's multiple rang test at $p \leq 0.05$ level

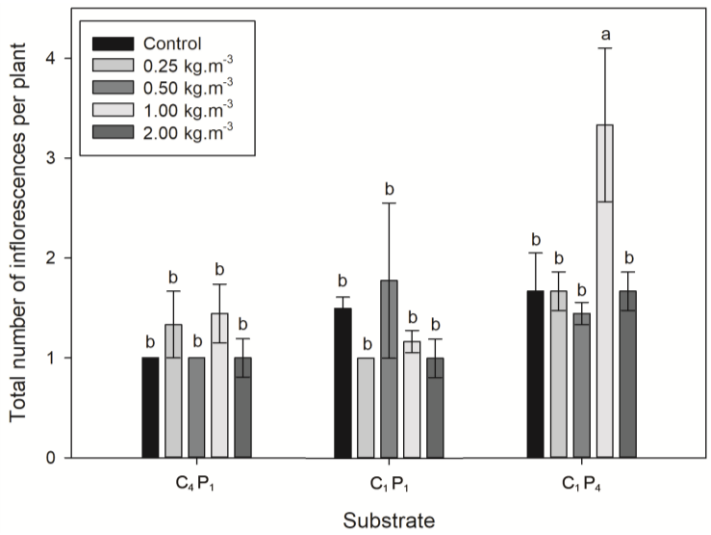

Figure 3. *Effect of total number of inflorescences per plant for Agastache rugosa in the three different green roof substrates (C_4P_1: coir 80%, perlite 20%; C_1P_1: coir50%, perlite 50%; C_1P_4: coir 20%, perlite 80% (% by vol.)) containing different amounts of hydrophilic polymer: 0 (Control), 0.25, 0.5, 1.0, and 2.0 $kg \cdot m^{-3}$ (polymer: medium (w/v), dry weight basis)*

http://www.aloki.hu ● ISSN 1589 1623 (Print) ● ISSN 1785 0037 (Online)
DOI: http://dx.doi.org/10.15666/aeer/1605_55035516
© 2018, ALÖKI Kft., Budapest, Hungary

As shown in *Table 2,* there was an interactive effect between the substrate and the hydrophilic polymer on lightness (L*) (interaction $p = 0.010$), values of a* (interaction $p = 0.003$), b* (interaction $p = 0.009$), Chroma (C*) (interaction $p = 0.007$) and hue angle (h) (interaction $p = 0.040$) in August when plants were at the peak flowering stage. Lower values of L* and a* as well as higher hue angles were recorded in the leaves of plants in C_1P_4, confirming the darker green color of the foliage compared to C_4P_1 and C_1P_1. The leaves in C_4P_1 had a less vivid green color than those in C_1P_4 and C_1P_1. Treatment with 1.0 $kg \cdot m^{-3}$ hydrophilic polymer greatly increased the value of L* (brighter), b* (more yellow) and Chroma (more vivid), but decreased the value of a* (more green) in substrate C_4P_1. In C_1P_1, hydrophilic polymer amendment increased the value of L* (brighter), b* (more yellow), and C* (more vivid), but decreased a* values (more green) and h values (greener). The SPAD value for all treatments in C_1P_4 was better than for other substrates. Moreover, the leaf performances were the highest under C_1P_4 treatment when measured in August, with large leaf sizes and green healthy leaves (*Fig. 4*).

Table 2. *Color measurements and SPAD values of Agastache rugosa grown in three different green roof substrates in August at the peak flowing time*

Substrate	Polymer rate ($kg \cdot m^{-3}$)	L*	a*	b*	C*	h	SPAD value
C_4P_1[y]	Control[x]	40.10c-f[z]	-2.51a-c	23.85c-f	24.59b-c	91.56ab	17.13d
	0.25	35.22d-f	-2.65a-c	19.10d-f	19.91cd	91.98ab	20.76cd
	0.5	52.52a	-17.79e	42.07a	45.68a	112.92a	20.06cd
	1.0	36.90c-f	-6.59b-d	20.19c-f	21.24cd	108.08a	23.11bc
	2.0	32.79f	2.50ab	13.46f	16.22d	65.74b	19.48cd
C_1P_1	Control	34.59ef	6.28a	14.45ef	16.80d	62.19b	19.77cd
	0.25	44.84a-d	-11.42c-e	29.59a-d	31.91a-c	108.84a	24.16bc
	0.5	50.42a	-18.38e	38.60ab	42.75a	115.46a	23.80bc
	1.0	51.34ab	-18.87e	40.38ab	44.57a	115.07a	26.14b
	2.0	46.48a-c	-12.72de	34.15a-c	36.44ab	110.43a	20.53cd
C_1P_4	Control	41.47b-f	-16.73e	27.67b-e	32.34a-c	121.20a	30.71a
	0.25	43.55a-e	-17.34e	31.12a-d	35.63ab	119.24a	30.99a
	0.5	44.47a-d	-16.78e	32.14a-d	36.26ab	117.68a	34.94a
	1.0	41.18b-f	-16.45e	27.95a-e	32.46a-c	120.52a	35.06a
	2.0	44.34a-d	-17.23e	32.61a-d	36.90ab	117.78a	31.20a
Significance	Substrate	NS	***	*	**	**	***
	Polymer rate	**	**	**	**	NS	***
	Interaction	**	**	**	**	*	NS

***, **, *: $p < 0.001$, $p < 0.01$, $p < 0.05$, respectively. NS: not significant

[x]Hydrophilic polymer rate: 0 (referred as control), 0.25, 0.5, 1.0, and 2.0 $kg \cdot m^{-3}$ [polymer: medium (w/v), dry weight basis]

[y]Substrate: C_4P_1: coir 80%, perlite 20%; C_1P_1: coir 50%, perlite 50%; C_1P_4: coir 20%, perlite 80% (% by volume)

[z]Means within columns by substrate were determined by Duncan's multiple rang test at $p < 0.05$ level

Overwintering

There was an interactive effect between substrate and hydrophilic polymer rate on overwintering rate (interaction $p = 0.041$) and self-sown seedling number (interaction $p < 0.001$) of *Agastache rugosa*, with significantly higher overwintering rate and self-sown seedling number in substrate C_1P_4 than that in C_4P_1 and C_1P_1 (*Table 3*). In

http://www.aloki.hu ● ISSN 1589 1623 (Print) ● ISSN 1785 0037 (Online)
DOI: http://dx.doi.org/10.15666/aeer/1605_55035516
© 2018, ALÖKI Kft., Budapest, Hungary

substrate C_1P_4, the addition of hydrophilic polymer decreased the overwintering rate, especially at rate of 2.0 kg·m^{-3}. However, hydrophilic polymer increased self-sown seedling number of *Agastache rugosa* in substrate C_1P_4, especially at the rate of 1.0 and 2.0 kg·m^{-3} compared to other hydrophilic polymer treatments or control. While in substrate C_4P_1 and C_1P_1, self-sown seedling number decreased by hydrophilic polymer treatment.

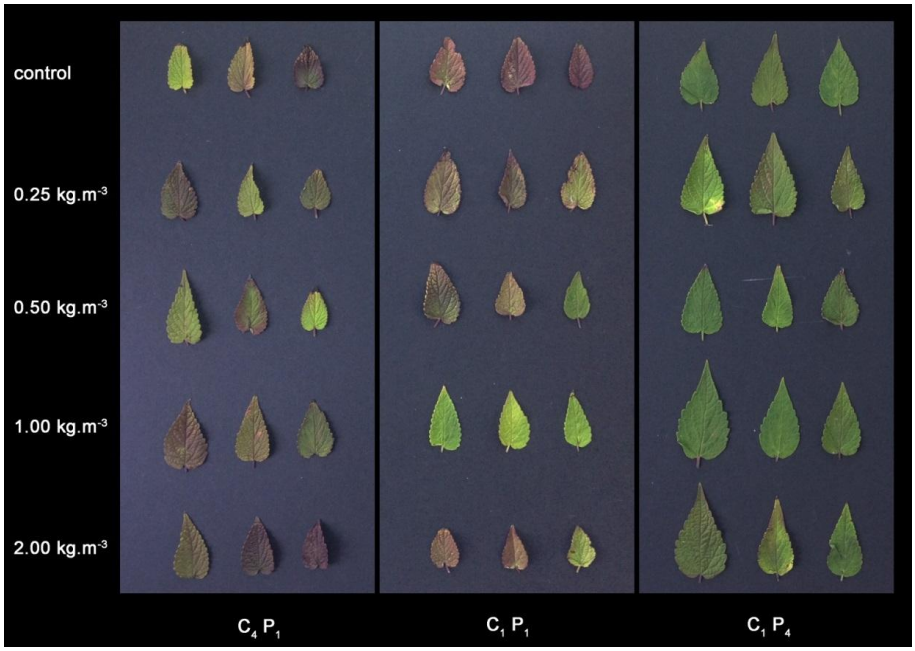

Figure 4. *Leaf performance for Agastache rugosa in the three different green roof substrates (C_4P_1: coir 80%, perlite 20%; C_1P_1: coir50%, perlite 50%; C_1P_4: coir 20%, perlite 80% (% by vol.)) containing different amounts of hydrophilic polymer: 0 (Control), 0.25, 0.5, 1.0, and 2.0 kg·m^{-3} (polymer: medium (w/v), dry weight basis) in August at peak blooming time*

Table 3. *Overwintering rate and self-sown seeding number of Agastache rugosa grown in three different green roof substrates*

Polymer rate (kg·m^{-3})	Overwintering rate (%)			Self-sown seedling number		
	C_4P_1[y]	C_1P_1	C_1P_4	C_4P_1	C_1P_1	C_1P_4
Control[x]	33.3d[z]	33.3d	100.0a	22.3de	30d	49.0c
0.25	55.6cd	50.0cd	77.8a-c	20.3d-f	22.0de	57.3bc
0.5	33.3d	66.7b-d	88.9ab	12.0e-g	15.0d-g	65.0b
1.0	44.4d	50.0cd	77.8a-c	13.5e-g	13.5e-g	90.5a
2.0	33.3d	33.3d	55.6cd	4.0g	6.0gf	80.5a
Significant						
Substrate	***			***		
Polymer rate	NS			NS		
Interaction	*			***		

***, **, *: $p < 0.001$, $p < 0.01$, $p < 0.05$, respectively. NS: not significant

[x]Hydrophilic polymer rate: 0 (referred as control), 0.25, 0.5, 1.0, and 2.0 kg·m^{-3} [polymer: medium (w/v), dry weight basis]

[y]Substrate: C_4P_1: coir 80%, perlite 20%; C_1P_1: coir 50%, perlite 50%; C_1P_4: coir 20%, perlite 80% (% by volume)

[z]Means within columns by substrate were determined by Duncan's multiple rang test at $p < 0.05$ level

http://www.aloki.hu ● ISSN 1589 1623 (Print) ● ISSN 1785 0037 (Online)
DOI: http://dx.doi.org/10.15666/aeer/1605_55035516
© 2018, ALÖKI Kft., Budapest, Hungary

Discussion

Our results revealed that more water was retained in the substrates when hydrophilic polymers were added compared to the control substrate. However, the amounts of additional volumetric water content in the three substrates depended on the compositions of the substrate. Hydrophilic polymer at 2.0 $kg \cdot m^{-3}$ significantly increased the average volumetric water content to values 1.62-, 1.81-, and 1.69- fold greater than that with no hydrophilic polymer in substrates C_4P_1, C_1P_4, and C_1P_1, respectively. In agreement with our study results, many studies have demonstrated that water retention in soil was increased with the addition of hydrophilic polymers, particularly in coarse-textured sandy soil (Dorraji et al., 2010). As the hydrophilic polymer content in the substrate increased, the substrate water content also increased, resulting in decreased temperature in the substrate (Nardini et al., 2012). The difference in volumetric water content between substrates with and without hydrophilic polymers decreased over time, especially in the coarse-textured substrate C_1P_4 starting from August. The difference also decreased with hydrophilic polymer concentrations less than 2.0 $kg \cdot m^{-3}$ in other substrate treatments. This reduction might be due to the loss of hydrophilic polymer effectiveness with time (Geesing and Schmidhalter, 2004). According to Han et al. (2013), the capacity of absorbing and desorbing water decreased with time and outside water condition. However, Jobin et al. (2004) found that there was no difference in available water and air-filled porosity in three substrates containing hydrophilic polymer after 9 weeks. Bai et al. (2010) studied the soil moisture of sandy soils mixed with four types of super-absorbent polymers under alternating dry and wet conditions. They found that the water retention capacity of the polymer decreased sharply when soil moisture was lower than a critical threshold. In addition, the water holding capacity of hydrophilic polymers could be affected by the extreme environmental conditions on the rooftop such as intensive solar radiation, high temperature, water deficits, freeze-thaw cycles caused by season change, and wetting-drying cycle due to weather change (Andry et al., 2009). In the present study, high temperature and frequent rainfall during the summer rainy season in August might have resulted in frequent wetting and drying of the substrates, leading to the loss of hydrophilic polymer effectiveness. This was associated with coarse-textured substrates, such as C_1P_4, that have a lower holding capacity, even with 2.0 $kg \cdot m^{-3}$ hydrophilic polymer.

Our study revealed that the C_4P_1 and C_1P_1 substrates, which have high coir dust content, are not ideal for *Agastache rugosa* in green roofs, either under drought stress or frequent rainfall. In our study, the moisture contents of substrate C_4P_1 and C_1P_1 under the control treatment were almost 3.8- and 3.5- fold higher than that of substrate C_1P_4, respectively. Although high coir dust content can increase the water content of substrates remarkably, it had no significant effect on plant growth for *Agastache rugosa* in June with little rainfall. Conversely, decreased leaf number and visual rate were observed in C_4P_1 with high coir dust content. In this study, the high coir dust content significantly decreased the number of inflorescences and ornamental quality in the peak flower period. Because of the high water-holding capacity, high organic content substrates are commonly used as container media, but are not recommended in green roofs in many studies (Cho et al., 2006). Beattie and Berghage (2004) suggested that substrates composed of 80-100% mineral matter and 0-20% organic matter suited for green roofs. Dunnett and Kingsburry (2004) also stated that low proportions of organic matter should be used, at between 10% and 20% of the total volume. The result is also consistent with the study findings that the substrate containing 10% organic matter was

http://www.aloki.hu ● ISSN 1589 1623 (Print) ● ISSN 1785 0037 (Online)
DOI: http://dx.doi.org/10.15666/aeer/1605_55035516
© 2018, ALÖKI Kft., Budapest, Hungary

optimal for *Allium schoenoprasum*, *Limonium latifolium*, *Melica ciliate* and *Nepeta* × *faassenii* because of stable growth under dry and wet conditions in green roofs (Nagase and Dunnett, 2011). Bates et al. (2015) conducted a six-year experiment which showed that the substrate with low organic matter content was suitable for brown (biodiversity) roofs. In our study, the peak flower time for *Agastache rugosa* was the summer rainy season with high temperatures and frequent rainfall, which might have resulted in frequent wetting and drying of the substrates in the green roof. Increased coir dust content could result in lush growth that may suffer damage under drought stress or frequent rainfall, resulting in frequent drying and wetting. Rowe et al. (2006) found that high organic matter in substrates may result in shrinkage because of decomposition. They may also increase poor growth of *Agastache rugosa* in the substrates C_4P_1 and C_1P_1, with worse flowering and reddish purple leaves in August. In our study, the results showed that hydrophilic polymer addition had no significant effect on the growth of *Agastache rugosa* in June, during which plants were exposed to less rainfall, though the hydrophilic polymer significantly increased the water content of the substrates. The results indicated that *Agastache rugosa* has high drought tolerance that can withstand extended dry conditions on green roofs. Although mineral-based substrates are recommended in green roofs, water scarcity is typically the main problem because of extreme environmental conditions, even in the rainy season. The flowering is the most sensitive phase to water stress (Álvarez et al., 2013) and the effect of water deficits on flowering has been suggested in many studies. Koshita and Takahara (2004) found that water stress reduced the number of flowers produced by *Citrus unshiu* during flower-bud induction periods. Caser et al. (2017) showed that severe water stress significantly decreased flower number and delayed the flowering period of *Primula vulgaris* 'Heidy'. The importance of water stress was also examined by Razmjoo et al. (2008), who found that the number of flowers produced by *Matricaria chamomile* decreased with long interval irrigation. Similar effects of water stress on flower production have also been observed in crops. Passioura (2006) observed that water deficit greatly affected crop productivity, especially when it occurred at the flowering stage. The number of flowers and yield of *Solanum melongena* L. was markedly decreased when water regimes were adopted (Lovelli et al., 2007). In our study, hydrophilic polymer addition at a concentration of 1.0 $kg \cdot m^{-3}$ increased the water content in substrate C_1P_4, thereby improving the substrate condition and significantly increasing the number of flowers produced by *Agastache rugosa*.

The *Agastache rugosa* in substrate C_1P_4 had high rate of overwintering success with over 70%, except in 2.0 $kg \cdot m^{-3}$ hydrophilic polymer treatment. Higher overwintering rate was associated with lower coir dust and hydrophilic polymer content. The low temperature injures the growth of plant roots, and cold weather freezes the surface soil sometimes, inflicting damage on shallow roots such as those planted in green roofs. Another type of winter root injury is caused by frost heaving, which is the result of the formation of ice lenses in the soil caused by a segregation of the soil water. Ice lenses are growing from below and pushed upward, which cause the plants to move upwards in the soil, sometimes pushing them out of the soil altogether. This can break many of the fine roots (Cleavitt et al., 2008). Injury or death usually follows if roots are broken or the shoots and exposed roots become dried out. Frost heaving is most likely to occur in fine-textured soils with high water content (Tarnocai and Bockheim, 2017). The higher coir dust and hydrophilic polymer content resulted in higher water content in substrates, thus leading to the low rate of overwintering.

http://www.aloki.hu ● ISSN 1589 1623 (Print) ● ISSN 1785 0037 (Online)
DOI: http://dx.doi.org/10.15666/aeer/1605_55035516
© 2018, ALÖKI Kft., Budapest, Hungary

The result also confirmed that the self-sown seedling number was affected by the composition of substrate, hydrophilic polymer rate. The germination of seed associated with moisture content, suitable temperature, and adequate supply of oxygen (Finch-Savage and Leubner-Metzger, 2006). However, long-term high moisture maintenance may result in seeds of some species rotting. As to *Agastache rugosa,* there was more number of seed starting seedlings under the C_1P_4 treatment by the perlite based (perlite) substrate, compared to coir dust based substrate.

Conclusions

Our results indicated that higher moisture was retained in substrates with hydrophilic polymers compared to that in the control substrate. We found that *Agastache rugosa* had a high drought tolerance capable of withstanding extended dry conditions in green roofs. The C_4P_1 substrate, which has high coir dust content, is not recommended for *Agastache rugosa* because of its low growth and poor ornamental quality, especially in the rainy season. Addition of 1.0 $kg \cdot m^{-3}$ hydrophilic polymer to substrate C_1P_4 increased the inflorescences number and resulted in good growth and ornamental quality both under drought and rainy seasons. Higher overwintering rate was associated with lower coir dust and hydrophilic polymer content. A greater number of seeds started seedling in substrate C_1P_4, especially at rates of 1.0 and 2.0 $kg \cdot m^{-3}$. These results indicated that the addition of 1.0 $kg \cdot m^{-3}$ hydrophilic polymer to substrate C_1P_4 is optimal for *Agastache rugosa* in green roofs. Further research studies are needed to determine the physical and chemical properties of substrates with different amounts of hydrophilic polymers. In addition, a follow up study on the effects of hydrophilic polymers on overwintering and the growth of *Agastache rugosa* in the second year would be useful.

Acknowledgements. This research was supported by Basic Science Research Program through the National Research Foundation of Korea (NRF) funded by the Ministry of Science, ICT & Future Planning (2015RIC1A2A01052633).

REFERENCES

[1] Álvarez, S., Bañón, S., Sánchez-Blanco, M. J. (2013): Regulated deficit irrigation in different phenological stages of potted geranium plants: water consumption, water relations and ornamental quality. – Acta Physiologiae Plantarum 35: 1257-1267.

[2] Andry, H., Yamamoto, T., Irie, T., Moritani, S., Inoue, M., Fujiyama, H. (2009): Water retention, hydraulic conductivity of hydrophilic polymers in sandy soil as affected by temperature and water quality. – Journal of Hydrology 373: 177-183.

[3] Bai, W., Zhang, H., Liu, B., Wu, Y., Song, J. (2010): Effects of super-absorbent polymers on the physical and chemical properties of soil following different wetting and drying cycles. – Soil Use and Management 26: 253-260.

[4] Baran, A., Zaleski, T., Kulikowski, E., Wieczorek, J. (2015): Hydrophysical and biological properties of sandy substrata enriched with hydrogel. – Polish Journal of Environmental Studies 24: 2355-2362.

[5] Bates, A. J., Sadler, J. P., Greswell, R. B., Mackay, R. (2015): Effects of recycled aggregate growth substrate on green roof vegetation development: A six year experiment. – Landscape and Urban Planning 135: 22-31.

http://www.aloki.hu ● ISSN 1589 1623 (Print) ● ISSN 1785 0037 (Online)
DOI: http://dx.doi.org/10.15666/aeer/1605_55035516
© 2018, ALÖKI Kft., Budapest, Hungary

[6] Beattie, D. J., Berghage, R. (2004): Green roof media characteristics: the basics. – Proc. of 2nd North American Green Roof Conference: Greening Rooftops for Sustainable Communities, Portland, Oregon, pp. 411-416.
[7] Butler, C., Butler, E., Orians, M. (2012): Native plant enthusiasm reaches new heights: Perceptions, evidence, and the future of green roofs. – Urban Forestry & Urban Greening 11: 1-1.
[8] Caser, M., Lovisolo, C., Scariot, V. (2017): The influence of water stress on growth, ecophysiology and ornamental quality of potted *Primula vulgaris* 'Heidy' plants. New insights to increase water use efficiency in plant production. – Plant Growth Regulation 83: 361-373.
[9] Cho, M. S., Park, Y. Y., Jun, H. J., Chung, J. B. (2006): Growth of Gerbera in mixtures of coir dust and perlite. – Horticulture Environment and Biotechnology 47: 211-216.
[10] Choi, S., Seo, Y. (2007): Effect of sta-green and activated carbon on growth of *Agastache rugosa* in green house. – Korean Journal of Plant Resources 20: 255-257.
[11] Cleavitt, N. L., Fahey, T. J., Groffman, P. M., Hardy, J. P., Henry, K. S., Driscoll, C. T. (2008): Effects of soil freezing on fine roots in a northern hardwood forest. – Canadian Journal of Forest Research 38: 82-91.
[12] Dorraji, S. S., Golchin, A., Ahmadi, S. (2010): The effects of hydrophilic polymer and soil salinity on corn growth in sandy and loamy soils. – Clean-Soil, Air, Water 38: 584-591.
[13] Dunnett, N., Kingsbury, N. (2004): Planting Green Roofs and Living Walls. – Timber Press, Portland, Oregon.
[14] Dunnett, N., Nolan, A. (2004): Effect of substrate depth and supplementary watering on the growth of nine herbaceous perennials in a semi-extensive green roof. – Acta Horticulturae 643: 305-309.
[15] Farrell, C., Ang, X. Q., Rayner, J. P. (2013): Water-retention additives increase plant available water in green roof substrates. – Ecological Engineering 52: 112-118.
[16] Finch Savage, W. E., Leubner Metzger, G. (2006): Seed dormancy and the control of germination. – New Phytologist 171: 501-523.
[17] Geesing, D., Schmidhalter, U. (2004): Influence of sodium polyacrylate on the water-holding capacity of three different soils and effects on growth of wheat. – Soil Use and Management 20: 207-209.
[18] Hammond, H. E., Norcini, J. G., Wilson, S. B., Schoellhorn, R. K., Miller, D. L. (2007): Growth, flowering, and survival of firewheel *Gaillardia pulchella* Foug. based on seed source and growing location. – Native Plants Journal 8: 25-39.
[19] Han, Y., Yu, X., Yang, P., Li, B., Xu, L., Wang, C. (2013): Dynamic study on water diffusivity of soil with super-absorbent polymer application. – Environmental Earth Sciences 69: 289-296.
[20] Jobin, P., Carno, J., Bernier, P. Y., Dansereau, B. (2004): Impact of two hydrophilic acrylic-based polymers on the physical properties of three substrates and the growth of Petunia xhybrida 'Brilliant Pink'. – Journal of the American Society for Horticultural Science 129: 449-457.
[21] Koshita, Y., Takahara. T. (2004): Effect of water stress on flower-bud formation and plant hormone content of satsuma mandarin (*Citrus unshiu* Marc.). – Scientia Horticulturae 99: 301-307.
[22] Lovelli, S., Perniola, M., Ferrara, A., Di Tommaso, T. (2007): Yield response factor to water (Ky) and water use efficiency of *Carthamus tinctorius* L. and *Solanum melongena* L. – Agricultural Water Management 92: 73-80.
[23] Nagase, A., Dunnett, N. (2010): Drought tolerance in different vegetation types for extensive green roofs: effects of watering and diversity. – Landscape and Urban Planning 97: 318-327.

http://www.aloki.hu ● ISSN 1589 1623 (Print) ● ISSN 1785 0037 (Online)
DOI: http://dx.doi.org/10.15666/aeer/1605_55035516
© 2018, ALÖKI Kft., Budapest, Hungary

[24] Nagase, A., Dunnett, N. (2011): The relationship between percentage of organic matter in substrate and plant growth in extensive green roofs. – Landscape and Urban Planning 103: 230-236.
[25] Nardini, A., Andri, S., Crasso, M. (2012): Influence of substrate depth and vegetation type on temperature and water runoff mitigation by extensive green roofs: shrubs versus herbaceous plants. – Urban Ecosystems 15: 697-708.
[26] Netto, A. T., Campostrini, E., de Oliveira, J. G., Bressan-Smith, R. E. (2005): Photosynthetic pigments, nitrogen, chlorophyll a fluorescence and SPAD-502 readings in coffee leaves. – Scientia Horticulturae 104: 199-209.
[27] Olszewski, M. W., Holmes, M. H., Young, C. A. (2010): Assessment of physical properties and stonecrop growth in green roof substrates amended with compost and hydrogel. – HortTechnology 20: 438-444.
[28] Oschmann, C., Kobayashi, N., Perkuhn, C., Grüneberg, H., Wissemeier, A. H. (2007): Study to expand the range of wild plants for extensive roof greening systems using superabsorbent polymers (SAP). – Acta Horticulturae 813: 421-426.
[29] Papafotiou, M., Pergialioti, N., Tassoula, L., Massas, I., Kargas, G. (2013): Growth of native aromatic xerophytes in an extensive Mediterranean green roof as affected by substrate type and depth and irrigation frequency. – HortScience 48: 1327-1333.
[30] Passioura, J. (2006): Increasing crop productivity when water is scarce-from breeding to field management. – Agricultural Water Management 80: 176-196.
[31] Razmjoo, K., Heydarizadeh, P., Sabzalian, M. R. (2008): Effect of salinity and drought stresses on growth parameters and essential oil content of *Matricaria chamomile*. – International Journal of Agriculture and Biology 10: 451-454.
[32] Rowe, D. B., Monterusso, M. A., Rugh, C. L. (2006): Assessment of heat-expanded slate and fertility requirements in green roof substrates. – HortTechnology 16: 471-477.
[33] Santamouris, M. (2014): Cooling the cities–a review of reflective and green roof mitigation technologies to fight heat island and improve comfort in urban environments. – Solar Energy 103: 682-703.
[34] Savi, T., Marin, M., Boldrin, D., Incerti, G., Andri, S., Nardini, A. (2014): Green roofs for a drier world: Effects of hydrogel amendment on substrate and plant water status. – Science of the Total Environment 490: 467-476.
[35] Schafer, P. (2011): The Chinese Medicinal Herb Farm: A Cultivator's Guide to Small-Scale Organic Herb Production. – Chelsea Green Publishing, White River Junction, Vermont.
[36] Tarnocai, C., Bockheim, J. G. (2017): Soils of Cold and Permafrost Affected Landscapes. – In: Richardson, D. et al. (eds.) The International Encyclopedia of Geography. Wiley, New York.
[37] Wang, S. Y., Camp, M. J. (2000): Temperatures after bloom affect plant growth and fruit quality of strawberry. – Scientia Horticulturae 85: 183-199.
[38] Xu, H., Yoon, Y. H., Choi, E. Y., Kang, H. K., Ju, J. H. (2014): Combination effects of the use of hydrophilic polymer for green roof substrate and rainy season condition on growth and biomass partitioning of *Aster koraiensis*. – Journal of Food Agriculture and Environment 12: 1177-1181.
[39] Yamani, H., Mantri, N., Morrison, P. D., Pang, E. (2014): Analysis of the volatile organic compounds from leaves, flower spikes, and nectar of Australian grown *Agastache rugosa*. – BMC complementary and Alternative Medicine 14: 495.
[40] Young, T. M., Cameron, D. D., Phoenix, G. K. (2017): Increasing green roof plant drought tolerance through substrate modification and the use of water retention gels. – Urban Water Journal 14: 551-560.

http://www.aloki.hu ● ISSN 1589 1623 (Print) ● ISSN 1785 0037 (Online)
DOI: http://dx.doi.org/10.15666/aeer/1605_55035516
© 2018, ALÖKI Kft., Budapest, Hungary

EFFECTS OF LONG-TERM CONSERVATION TILLAGE ON SOIL NITROGEN CONTENT AND ORGANIC NITROGEN COMPONENTS IN A CHINESE MOLLISOL

HUANG, D. D.[1,2#] – CHEN, X. W.[2,3#] – CAO, G. J.[1*] – LIANG, A. Z.[2,3] – JIA, S. X.[2,3] – LIU, S. X.[1]

[1]*College of Resource and Environment, Jilin Agricultural University 130118 Changchun, China*

[2]*Key Laboratory of Mollisols Agroecology, Northeast Institute of Geography and Agroecology, Chinese Academy of Sciences, 130102 Changchun, China*

[3]*University of Chinese Academy of Sciences, 100049 Bejing, China*

[#]*These authors contributed equally*

**Corresponding author*
e-mail: cgj72@126.com

(Received 31st May 2018; accepted 1st Aug 2018)

Abstract. The effect of different long-term (2001-2016) tillage practices on soil nitrogen forms in different soil layers were studied to provide a scientific basis for evaluating soil fertility and establishing rational fertilization measures. Soil contents of total nitrogen (TN), particulate organic nitrogen (PON), microbial biomass nitrogen (MBN), water soluble organic nitrogen (WSON), NO3-N content, NH4-N content ammonium nitrogen and organic acid nitrogen component contents were measured under no-tillage (NT) and mould plow (MP) treatments based on a long-term (16 year) conservation tillage experiment in Northeast China. The results showed that no-tillage increased soil total nitrogen, active nitrogen, inorganic nitrogen and organic nitrogen content, which varied with soil depth. Compared with MP, NT significantly ($p < 0.05$) increased total nitrogen and active nitrogen content in the surface soil (0-30 cm); TN, PON, MBN and WSON increased significantly ($p < 0.05$) by 28.32%, 23.07%, 15.13% and 25.21% in 0-5 cm and by 10.17%, 19.4%, 15.97%, and 31.33% in 5-10 cm, respectively. For soil inorganic nitrogen, the content of ammonium nitrate at 0-5 cm and at 5-10 cm under NT was significantly ($p < 0.05$) higher than that of MP by 28.1% and 32.13%, respectively, and the content of ammonium nitrogen in soil at 0-5 cm was significantly ($p < 0.05$) higher, by 12.86%, than that of MP. No-tillage significantly increased the content of total hydrolysable nitrogen, hydrolysable ammonia nitrogen, hydrolysable amino acid nitrogen and hydrolysable unidentified nitrogen in the 0-10 cm soil layer, but no significant effect was found on the content of hydrolysable amino sugar nitrogen. Soil nitrogen content was closely related to tillage practices. These results suggest that no-tillage was beneficial in augmenting soil nitrogen supply capacity by increasing soil total nitrogen, active nitrogen, inorganic nitrogen and organic nitrogen content.

Keywords: *no-tillage, mould plow, soil nitrogen forms, straw returning, Northeast China*

Introduction

Soil nitrogen (N) is one of the necessary nutrients for plant growth and development, as well as a major nutrient limiting factor for crop yield (Gao et al., 2008; Karra et al., 2018; Lenssen et al., 2007; Sainju et al., 2009). Soil organic and inorganicnitrogen are the main forms of the nitrogen pool. Soil organic nitrogen content of approximately 70%-90% in surface soil could not only maintain soil nitrogen fertility (Xu et al., 2003), but also has an important function for soil nitrogen supply capacity (Ju et al., 2004). Soil inorganic nitrogen pools with ammonium and nitrate, is the most effective nitrogen pool type for crop absorption (Mkhabela et al., 2008). Approximately 50% of the

http://www.aloki.hu ● ISSN 1589 1623 (Print) ● ISSN 1785 0037 (Online)
DOI: http://dx.doi.org/10.15666/aeer/1605_55175528
© 2018, ALÖKI Kft., Budapest, Hungary

accumulated nitrogen in crops comes from soil, especially for the black soil of Northeast China where more than 70% of the plant's accumulated nitrogen comes from the soil (Fuzzi, 1996; Ballb et al., 1999). Therefore, soil N mineralization from organic to inorganic N is the key process for crop absorbing and utilizing N.

Tillage practices have a great impact on soil N availability and nitrogen reserves. Intensive agricultural systems may deplete soil N pools by removal of the above ground portion of the plants, which may result in negative nutrient balance depleting soil fertility. Conservation tillage with returned straw could improve the soil aggregate structure, maintain soil moisture, reduce water runoff and evaporation, increase water infiltration, stabilize soil temperature changes, promote the reproduction of beneficial microorganisms and regulate nutrient metabolism, thus affecting the mineralization and transportation of soil N and plant absorption and utilization (Patra et al., 1993; Ram et al., 2003; Barajas-Guzmán et al., 2006). Therefore, it is critical to understand the dynamic and cycling of the soil N pools and their fractions under different agriculture management styles. Previous studies have shown that compared with traditional tillage, conservation tillage changed the soil microenvironment, thus affecting the mineralization and content of soil N, such as no-tillage significantly increasing the total N content in the 0-5 cm soil layer (Lou et al., 2012; Varvel et al., 2011; Sainju et al., 2009; Dikgwatlhe et al., 2014). However, the soil total N pool changes slowly responding to the management practice changes because of its large size, inherent spatial variability, and small fraction available to plants. Therefore, more attempts have been made to labile fractions as plant-available N (Wander, 2004; Haynes, 2005), which is the most active component of soil organic N. Particulate organic nitrogen (PON), microbial nitrogen (MBN) and water-soluble organic nitrogen (WEON) are the important active N pools, which play an essential role in the process of soil N cycle (Jones et al., 2004). No-tillage (NT) may temporarily increase N immobilization leading to reduced plant-available N, while long-term NT can also increase soil labile N pool to improve the availability of N to crops in the upper soil layers (Sun et al., 2015; Sainju et al., 2013).

The mollisol area in Northeast China is the main grain-producing area in the country. With the increment of reclamation years and predatory production, fertility degradation of the mollisol has become more and more prominent. It is now considered urgent to change the traditional farming methods and carry out conservation tillage as an effective means of preservation. Several previous studies have focused mainly on soil total nitrogen content change under conservation tillage, but focused less on soil active nitrogen, inorganic nitrogen and organic nitrogen components. Thus, in the current study, soil organic nitrogen contents between conservation tillage and conventional tillage were analyzed based on a long-term conservation experiment started in 2001. This involved analysis of soil nitrogen and organic nitrogen components under protective tillage and conventional tillage conditions, with a view to evaluating soil fertility, formulating reasonable fertilization measures and providing a scientific basis for sustainable development of agriculture.

Material and methods

Study site

The study was conducted on Dehui Experimental Station (44°12'N, 125°33'E) of the Northeast Institute of Geography and Agroecology, Chinese Academy of Sciences, in

http://www.aloki.hu ● ISSN 1589 1623 (Print) ● ISSN 1785 0037 (Online)
DOI: http://dx.doi.org/10.15666/aeer/1605_55175528
© 2018, ALÖKI Kft., Budapest, Hungary

Dehui County, Jilin Province, China. The climate is described as a temperate continental monsoon; based on data from the past 30 years, the annual mean air temperature is 4.4 °C, and the annual mean precipitation is 520.3 mm, with more than 70% of the rain occurring in June, July, and August. The winter (November–April) is long and cold. The soil is a clay loam (Typic Hapludoll) unusually covered with snow in winter. More details about the soil can be found in *Table 1* (Chen et al., 2018). Conventional management practices were used on the land to grow a monoculture of maize for more than 20 years before the establishment of this tillage experiment.

Experimental design

The present study was conducted using monoculture maize in a long-term (2001-2016) tillage field experiment. The tillage and rotation treatment are as follows. The tillage treatments consisted of no-tillage (NT), mould plow (MP) tillage and ridge tillage (RT), with two crop rotations (continuous maize (*Zea mays L.*), and maize-soybean (*Glycine max L.*). All the treatments were arranged in a randomized complete block design with four replicates at the whole plot level, and each plot was 5.2 m × 20 m. The NT treatment had no soil disturbance except for planting, usually in early May. The RT treatment included ridging in June and less than one-third row width smashing of maize stalks/roots in fall. The MP treatment included one approximately 15 cm in depth moldboard plowing after maize harvest, generally in early October, and one 7.5 to 10 cm in depth disking during the spring, as well as field cultivation (ridging in June). Herbicides were applied before and after seeding for all the tillage treatments to control weeds. Starter fertilizer (100 kg·ha^{-1} N, 45.5 kg·ha^{-1} P and 78 kg·ha^{-1} K) and an additional 50 kg·ha^{-1} N at the V-6 stage were applied for maize. Starter fertilizers (40 kg·ha^{-1} N, 60 kg·ha^{-1} P and 80 kg·ha^{-1} K) were applied concurrently at the time of planting for soybean. The crop residues were returned onto the soil surface after harvest under NT and RT treatments with the exception of the plots under MP.

Table 1. *Selected soil physical and chemical properties in 2001 prior to the tillage experiment (Chen et al., 2018)*

Depth (cm)	pH	Clay (%) (<2 µm)	Silt (%) (2-20 µm)	Sand (%) (20-200 µm)	Bulk density (g/cm^3)	Soil organic carbon (g/kg)	Total soil nitrogen (g/kg)
0-5	6.48	36.03	24.00	39.97	1.24	16.48	1.42
5-10	6.45	35.83	23.78	40.39	1.38	16.29	1.39
10-20	6.51	35.68	24.35	39.98	1.36	16.08	1.37
20-30	7.03	36.56	25.00	38.72	1.38	14.22	1.16

Soil sampling and measurements

Soil samples (7 replicates per plot) were collected at depths of 0-5 cm, 5-10 cm, 10-20 cm and 20-30 cm with S-type sampling on 23 April, 2017. The collected samples were divided into two parts, one was stored at 4 °C as a fresh sample for determination of microbial biomass nitrogen (MBN) and water-soluble organic nitrogen (WSON), and the other was air-dried for soil total nitrogen (TN), organic nitrogen components, etc. Soil total nitrogen was determined by an elemental analyzer (Flash EA1112, Thermo Finnigan, Italy). Particle organic nitrogen (PON) was extracted first and then analyzed

http://www.aloki.hu ● ISSN 1589 1623 (Print) ● ISSN 1785 0037 (Online)
DOI: http://dx.doi.org/10.15666/aeer/1605_55175528
© 2018, ALÖKI Kft., Budapest, Hungary

by elemental analysis (Cambardella et al., 1992). Soil water-soluble organic nitrogen was determined by the TOC-VCPH automatic analyzer (Model TOC-VCPH, Shimadzu, Tokyo, Japan) (Gigliotti et al., 2002). Soil microbial nitrogen (MBN) was determined by a modified CHCL3 fumigation-extraction method (Vance et al., 1987), and the extractions were analyzed by the automatic TOC-VCPH analyzer. Soil organic nitrogen components were determined according to Bremner's method (Bremner, 1965). Soil inorganic nitrogen was determined by a fully automatic continuous flow analyzer (SKALAR SAN + +, The Netherlands).

Data analysis

Statistical analyses were carried out using SPSS (Version 11.5, SPSS Inc., Chicago, IL, USA). Treatment means were compared using the least significant difference (LSD) and a significance level of $P < 0.05$.

Results

Total nitrogen content

Compared with MP, NT significantly ($p < 0.05$) increased the total nitrogen content by 28.32% and 10.17%, in the 0-5 cm and 5-10 cm soil depth intervals, respectively (*Fig. 1*). While the total nitrogen content of the 10-20 cm and 20-30 cm layers under NT treatment was slightly lower than that of MP, the difference was not significant. Under both NT and MP, soil total N decreased with increased soil depth.

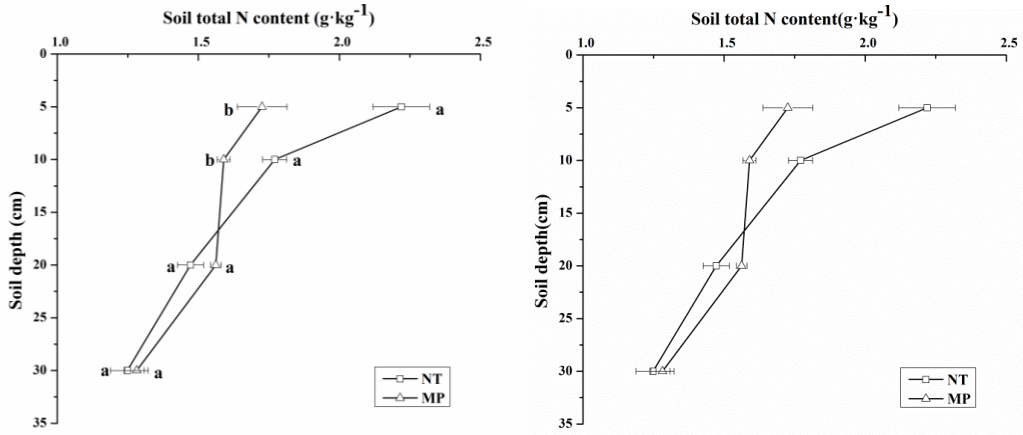

Figure 1. *Soil total nitrogen at different soil depths under different tillage practices ($P < 0.05$). (NT: no tillage; MP: mould plow. Different letter indicates significant difference of soil total N content between different tillage practices at the same depth)*

Active nitrogen

NT significantly ($p < 0.05$) increased soil active nitrogen in the 0-5 cm and 5-10 cm soil layers more than MP (*Fig. 2*). Particulate organic nitrogen increased by 23.07% and 19.4%, microbial biomass N increased by 15.13% and 15.97%, and soil soluble organic nitrogen increased by 25.21% and 31.33% in the 0-5 cm and 5-10 cm soil layers, respectively (*Fig. 2*). No significant differences were found between NT and MP for

http://www.aloki.hu ● ISSN 1589 1623 (Print) ● ISSN 1785 0037 (Online)
DOI: http://dx.doi.org/10.15666/aeer/1605_55175528
© 2018, ALÖKI Kft., Budapest, Hungary

PON, MBN, and WSON in the 10-30 cm soil layer. With the increment of soil depth, PON, MBN, and WSON showed a decreasing trend.

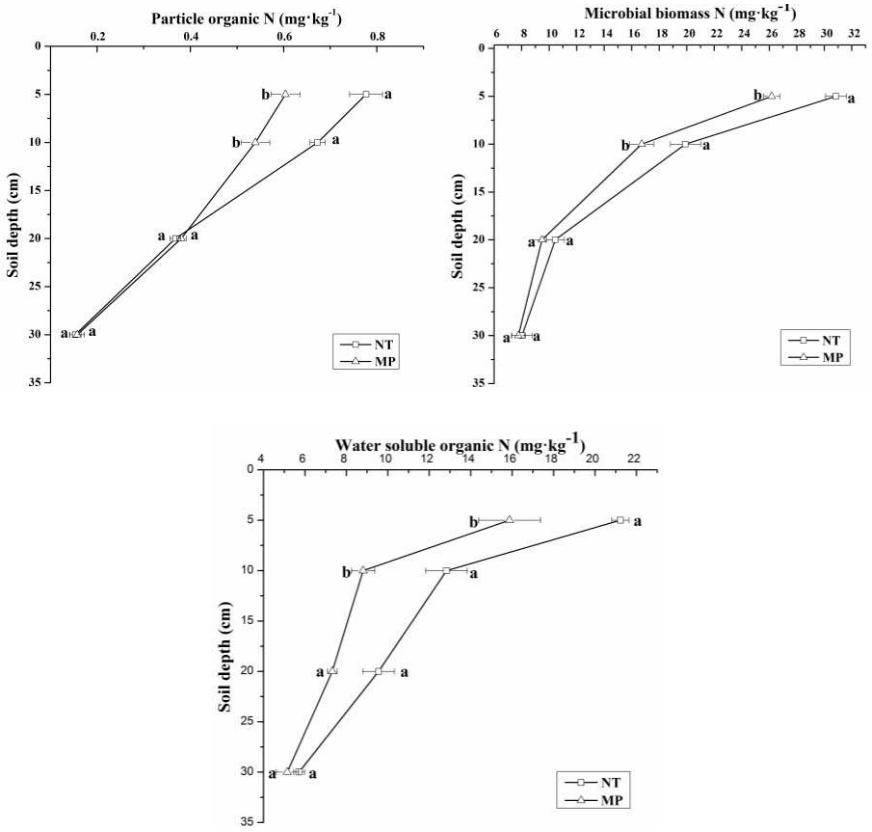

Figure 2. *Depth distributions of particulate organic N, microbial biomass N and water soluble organic N under different tillage practices ($P < 0.05$). (NT: no tillage; MP: mould plow. Different letter indicates significant difference of particulate organic N, microbial biomass N and soluble water soluble organic N between different tillage practices at the same depth)*

Soil inorganic nitrogen

The NO_3^-N content in the 0-5 cm and 5-10 cm soil layers under NT were 28.10% and 32.13%, significantly ($p < 0.05$) higher than that of MP, respectively (*Fig. 3*).

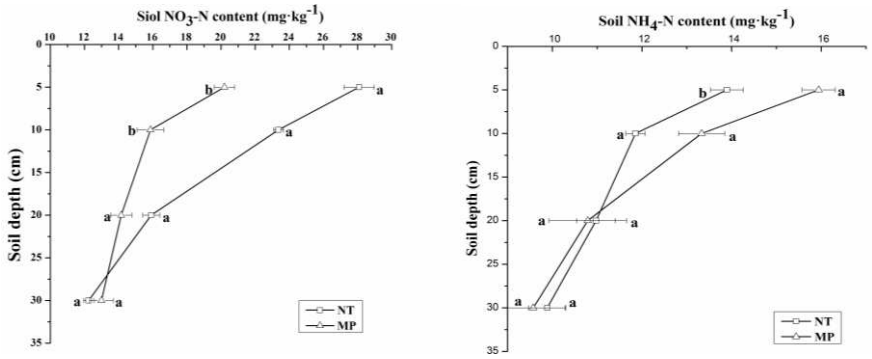

Figure 3. *Depth distributions of soil NO_3^-N and NH_4^-N under different tillage practices ($P < 0.05$). (NT: no tillage; MP: mould plow. Different letter indicates significant difference of soil NO_3-N and NH_4-N between different tillage practices at the same depth)*

http://www.aloki.hu ● ISSN 1589 1623 (Print) ● ISSN 1785 0037 (Online)
DOI: http://dx.doi.org/10.15666/aeer/1605_55175528
© 2018, ALÖKI Kft., Budapest, Hungary

The NH_4^-N content in the 0-5 cm soil layer under MP was 12.86% significantly ($p < 0.05$) higher than that of NT, the NH_4^-N content under MP in the 5-10 cm soil layer was also higher than NT although the difference was not significant. There was no significant difference between NT and MP for NO_3-N and NH4-N in the 10-30 cm soil layer. With the increment of soil depth, the content of nitrate nitrogen and ammonium nitrogen decreased.

Soil organic nitrogen components

NT significantly ($p < 0.05$) increased total hydrolysable nitrogen content, hydrolysable ammonia nitrogen content, and hydrolysable amino acid nitrogen in topsoil (0-5 and 5-10 cm) more than MP (*Table 2*). Compared with MP, total hydrolysable nitrogen content increased by 22.03%, and 9.67%, hydrolysable ammonia nitrogen increased by 22.24% and 19.67%, and hydrolysable amino acid nitrogen increased by 21.48% and 22.95% in the 0-5 cm and 5-10 cm soil layers, respectively (*Table 2*). No significant difference was observed in the 10-30 cm soil layers for the hydrolysable nitrogen. Tillage practices had no significant effect on the content of hydrolysable amino sugar nitrogen. The content of hydrolysable amino sugar nitrogen in the 10-30 cm soil layer was slightly lower than MP, but the difference was not significant. The hydrolysable unidentified nitrogen content in the 0-5 cm soil layer of the NT treatment was 30.87% significantly ($p < 0.05$) higher than that in MP, while the differences between the two nitrogen types for NT and MP in the 5-30 cm depth interval were not significant. The differences of all types of nitrogen between NT and MP in the 10-30 cm soil layer were not significant.

Table 2. *Soil organic nitrogen components under different tillage practices*

Soil depth (cm)		0-5	5-10	10-20	20-30
Total hydrolysable nitrogen	NT	1438.76a	1249.49a	957.18a	812.79a
	MP	1121.87b	1038.37b	1015.78a	839.70a
Hydrolysable ammonia nitrogen	NT	587.23a	510.45a	412.49a	348.84a
	MP	484.31b	410.01b	437.46a	357.63a
Hydrolysable amino sugar nitrogen	NT	44.21a	35.54a	29.82a	24.29a
	MP	34.13a	31.72a	31.68a	24.87a
Hydrolysable amino acid nitrogen	NT	482.82a	450.74a	294.44a	250.21a
	MP	379.11b	347.28b	344.20a	281.50a
Hydrolysable unidentified nitrogen	NT	324.51a	252.76a	220.42a	189.46a
	MP	224.32b	249.36a	202.44a	175.70a

Same letter means no significant difference under different layers and tillage practices for a single soil nitrogen property. NT: no tillage; MP: mould plow

Discussion

Effect of tillage on soil total nitrogen content

After 16 years of conversion from traditional farming to conservation tillage, the TN content in the 0-10 cm surface layer increased under no-till practices. Our results were consistent with other research, such as that no-tillage had shown that total nitrogen at 0-5 cm and 0-30 cm layers was higher than that for other tillage (Power et al., 1998;

http://www.aloki.hu ● ISSN 1589 1623 (Print) ● ISSN 1785 0037 (Online)
DOI: http://dx.doi.org/10.15666/aeer/1605_55175528
© 2018, ALÖKI Kft., Budapest, Hungary

Purakayastha et al., 2009). As a result of the NT straw surface coverage, soil disturbance decreased, leading to a reduction of total nitrogen mineralization and eventually an increase in total nitrogen (Franzluebbers et al., 1999). No-tillage straw also increased the soil C/N ratio by adding organic matter to the soil, thus enhancing the solid holding capacity of nitrogen (Kushwaha et al. al., 2000; Hemwong et al., 2008; Zavalloni et al., 2011). The total nitrogen content both in NT and MP decreased with increases in soil depth. This was due to the accumulation of organic matter in the surface NT soil. In the 10-30 cm soil layer, total nitrogen content under MP treatment was higher than NT (*Fig. 1*). For this phenomenon, underground biomass may play an important role. In traditional farming, the stubble was turned into the deeper layer of soil. However, in NT, the root system showed a high density in the soil surface and a low density in the deep soil (Qin et al., 2006). Therefore, different subsurface biomass in NT and MP may cause the difference of total nitrogen in various soil layers between treatments. The results of the present study are consistent with other findings; no-tillage straw returning to the soil led to accumulation of soil nitrogen on the soil surface (Torbert et al., 1995; Thomas et al., 2005).

Effect of tillage on soil active nitrogen

Soil particulate organic nitrogen (PON) was considered as a stable part of soil organic nitrogen, as it could be converted into inorganic nitrogen, which could then be used to supply nitrogen sources for plant growth and crop yield, and maintain soil nitrogen balance (Rosell et al., 2000). PON was sensitive to farmland management practices such as soil disturbance and crop straw inputs; therefore, it responded quickly to management practice changes (Cambardella et al., 1992). These results showed that conservation tillage mainly increased the PON content in the 0-5 cm and 5-10 cm soil layers, which is consistent with other related studies (Fabrizzi et al., 2003; Bessam et al., 2003; Malhi et al., 2006; Sainju et al., 2012). There are three reasons for this. First, no-till straw returning could provide a good environment for soil aggregate formation, and a large amount of PON could be physically protected in soil aggregates. Second, cultivation such as autumn plowing could disturb the soil and destroy soil aggregates, thus accelerating PON mineralization (Wander, 2004). Third, the location of crop straw returning may affect the distribution of PON. In the NT treatment, the straw covered the soil surface. However, in the MP treatment, straws were buried in the soil stubble in more close contact with the soil. The variable distribution of straw returning to the field could explain that the PON content in NT treatment was significantly higher than MP in the 0-10 cm soil layer. To summarize, the results showed that no-tillage straw returned to the soil helps increase soil PON content.

Soil microbial biomass nitrogen was the source and reservoir of nitrogen nutrients and an important biological indicator of soil quality (Shukla et al., 2017). In the present study, conservation tillage significantly increases soil microbial biomass nitrogen. This may be due to the higher total nitrogen content in conservation tillage soils, which provided a higher material basis for MBN formation. The positive impact of NT on soil microbial communities could also be attributed to the reduction of soil disturbance, which led to the reduction of fungal mycelium damage, the conservation of microbial habitat, the improvement of soil moisture conditions and the reduction of extreme temperature conditions (Rhoton, 2000). In short, NT increased soil microbial and physic-chemical conditions, improved microbial habitat, disturbed soil less, and

http://www.aloki.hu ● ISSN 1589 1623 (Print) ● ISSN 1785 0037 (Online)
DOI: http://dx.doi.org/10.15666/aeer/1605_55175528
© 2018, ALÖKI Kft., Budapest, Hungary

provided relatively high levels of organic nitrogen, ultimately resulting in an increase in surface microbial biomass nitrogen.

Soil soluble organic nitrogen played an important role in the farmland nitrogen circulation system (Kranabetter et al., 2007). In this study, no-tillage straw surface coverage resulted in an increase in soil soluble organic nitrogen in the 0-10 cm soil layer. The disturbance of mould plow tillage soils improved the aeration of the soil and destroyed the soil aggregates, thus accelerating the mineralization of PON. Therefore, the soil soluble organic nitrogen tended to decrease, resulting in the decrease in the surface layer content. Meanwhile, no-tillage straw covering the surface could improve soil moisture and boost nitrogen fixation.

Effect of tillage on soil inorganic nitrogen

Soil inorganic nitrogen played an important role in the forms of nitrate nitrogen and ammonium nitrogen in the soil nitrogen cycle, and was the main form of crop absorption and utilization, although only a minor portion of the total nitrogen (Nguyen et al., 2017). Halvorson found that the NO_3-N content in mould plow tillage in the northern plains of the United States was higher than that of no-tillage systems (Halvorson et al., 2000). In this study NO_3-N content in 0-10 cm soil under NT layer was significantly higher than that of MP, which is not consistent with this finding. which may be related to different crop types, tillage years, soil types and planting systems. Our results showed that no-tillage with straw returned to the soil would increase the number and continuity of macropores in the topsoil and may cause a large amount of NO_3-N to be stored in the surface soil (Li et al., 2007). At the same time, no-tillage could effectively store soil moisture and reduce NO_3-N leaching to the lower soil. In addition, the straw covered the surface of no-tillage soil, which increased soil nitrogen fixation, thereby reducing the loss of NO_3-N. In contrast, conventional farming led to large disturbances of surface soil with high porosity with NO_3-N tending to move downwards. Sainju et al. (2013) found that the NH_4-N content in MP was higher than in NT, which is consistent with our findings. Under dry land conditions, Li et al. (2007) found that no-tillage increased the quantity of earthworms in farmland and the number and continuity of macropores in the soil, thus improving soil aeration. In well-aerated soil, NH_4-N was more easily transferred into NO_3-N, resulting in soil NH_4-N content decreasing under no-tillage.

Effect of tillage on soil organic activated nitrogen components

Soil organic nitrogen is the source of mineral nitrogen for crops, and as the main form of soil nitrogen, it plays a key role in the stability of farmland ecosystems (Schulten et al., 1997). In this study, no-tillage significantly affected the total hydrolysable nitrogen, hydrolysable ammonia nitrogen and hydrolysable amino acid nitrogen in the 0-10 cm soil layer, and hydrolysable unidentified nitrogen in the 0-5 cm soil layer. The reason may be that no-tillage increased the total nitrogen content of soil, and the increase in total nitrogen would inevitably lead to the increase in soil hydrolysable ammonia nitrogen (Follett et al., 1989). Hydrolysable ammonia nitrogen was composed of inorganic exchangeable ammonium and part of the fixed ammonium composition, the mineralization of two ammonium after soil disturbance accelerated under conventional farming, and the absorption and utilization of crops to ammonia, led to the average content of hydrolysable ammonia nitrogen decreasing obviously; hence,

http://www.aloki.hu ● ISSN 1589 1623 (Print) ● ISSN 1785 0037 (Online)
DOI: http://dx.doi.org/10.15666/aeer/1605_55175528
© 2018, ALÖKI Kft., Budapest, Hungary

hydrolysable ammonia nitrogen in the 0-10 cm layer of mould plow tillage was significantly lower than no-tillage (Jiang, 2005). The addition of organic material under no-tillage increased the soil organic matter content, which was continuously converted into humus under the action of microorganisms. Soil amino acids nitrogen and other compounds of N were fixed into humic acid during the humification (Porter et al., 1964). Under acidic conditions, the amino acid nitrogen released, which made the higher hydrolysable amino acid nitrogen content of the 0-10 cm soil layer than that of conventional tillage. Hydrolysable unidentified nitrogen is a difficult component to mineralization in soil organic nitrogen pools of acidolysis, and the mineralization rate of unknown nitrogen of acidolysis is very small, so it is easy to accumulate in soil (Stevenson, 1982). The increase in total nitrogen in the surface layer under no-tillage also leads to the increase in hydrolysable unidentified nitrogen. Tillage practices have no significant effect on hydrolysable amino sugar nitrogen. Since hydrolysable amino sugar nitrogen is mainly derived from residues of microbial cell walls, and hydrolysable amino sugar nitrogen reflects the accumulation of dead microorganisms rather than live microorganisms. Therefore, hydrolysable amino sugar nitrogen is a very small percentage of soil total nitrogen, and it is less affected by tillage practices (Stevenson, 1982). Liu's preliminary studies conducted in the same site reported that the soil organic nitrogen mineralization plays an important role in the nitrogen nutrition of crops. The total soil nitrogen mineralization rate in no-tillage has a significant stratification phenomenon. The contribution of no-till active organic nitrogen to total mineralization rate (75-89%) was significantly greater than that of conventional tillage (31-45%), indicating that tillage practices will affect the source of soil organic nitrogen mineralization. The degree of humification, humic acid content, and aromaticity of organic matter in long-term no-tillage mollisol were significantly lower than that of mould plow tillage, so the mineralization of active organic nitrogen pool contributed more to the total primary mineralization rate. This means that much more organic nitrogen in no-till agecan be converted into inorganic nitrogen and absorbed by plants (Liu et al., 2017).

Conclusion

The results of this study showed that the effects of conservation tillage on the soil nitrogen pool occurred in the surface layer by significantly increasing the contents of total nitrogen, particulate nitrogen, microbial biomass nitrogen, water-soluble organic nitrogen, nitrate nitrogen and acidolysis of organic nitrogen components. In sum, no-tillage was suitable to increase the accumulation of nitrogen in dry farming areas, which would provide a theoretical basis for optimizing mollisol management and sustainable development of agriculture with rational fertilizing in Northeast China.

Acknowledgements. This research was supported by the National Natural Science Foundation of China (41430857), Key Research Program of Frontier Sciences, Chinese Academy of Sciences (Grant No. QYZDB-SSW-DQC035), Youth Innovation Promotion Association, Chinese Academy of Sciences (2015183), National Key R&D Program of China (2017YFC0504200), "135" project planning of Northeast Institute of Geography and Agroecology, Chinese Academy of Sciences (Y6H2042001), Open Research Funds from the Key Laboratory of Mollisols Agroecology, Chinese Academy of Sciences (2016ZKHT-02).

http://www.aloki.hu ● ISSN 1589 1623 (Print) ● ISSN 1785 0037 (Online)
DOI: http://dx.doi.org/10.15666/aeer/1605_55175528
© 2018, ALÖKI Kft., Budapest, Hungary

REFERENCES

[1] Ballb, C., Scott, A., Parker, J. P. (1999): Field N_2O, CO_2 and CH_4 fluxes in relation to tillage compaction and soil quality in Scotland. – Soil & Tillage Research 53: 29-39.
[2] Barajas-Guzmán, M. G., Campo, J., Barradas, V. L. (2006): Soil water, nutrient availability and sapling survival under organic and polyethylene mulch in a seasonally dry tropical forest. – Plant and Soil 287(1-2): 347-357.
[3] Bessam, F., Mrabet, R. (2003): Long-term effect of tillage and cropping systems on particulate organic matter of a Calcixeroll soil of semi-arid Morocco. – Proceedings 16th Triennial Conference of International Soil Tillage Research Organization, Brisbane, Australia, 13–18 July, pp. 144-149.
[4] Bremner, J. M., Edwards, A. P. (1965): Determination and isotope-ratio analysis of different forms of nitrogen in soils: I. Apparatus and procedure for distillation and determination of ammonium. – Soil Science Society of America Journal 29(5): 504-507.
[5] Cambardella, C. A., Elliott, E. T. (1992): Particulate soil organic-matter changes across a grassland cultivation sequence. – Soil Science Society of America Journal 56(3): 777-783.
[6] Chen, X. W., Chang, L., Liang, A. Z., Wu, D. H., Zhang, X. P. Yang, J. M. (2018): Effects of long term conservation tillage on soil nitrogen content and organic nitrogen components in a Chinese Mollisol. – Applied Ecology and Environmental Research 16(1): 663-675.
[7] Dikgwatlhe, S. B., Chen, Z. D., Lal, R. (2014): Changes in soil organic carbon and nitrogen as affected by tillage and residue management under wheat-maize cropping system in the North China Plain. – Soil and Tillage Research 144: 110-118.
[8] Fabrizzi, K. P., Moron, A., García, F. O. (2003): Soil carbon and nitrogen organic fractions in degraded vs. non-degraded Mollisols in Argentina. – Soil Science Society of America Journal 67(6): 1831-1841.
[9] Follett, R., Schimel, D. S. (1989): Effect of tillage practices on microbial dynamics. – Soil Soc Am J 53: 1091-1096.
[10] Franzluebbers, A. J., Langdale, G. W., Schomberg, H. H. (1999): Soil carbon, nitrogen, and aggregation in response to type and frequency of tillage. – Soil Science Society of America Journal 63(2): 349-355.
[11] Fuzzi, S. (1996): Overview of the biogenic sources of atmospheric trace compounds due to agricultural activities. – Aerobiologia 12: 129-132.
[12] Gao, Y. H., Luo, P., Wu, N. (2008): Impacts of grazing intensity on nitrogen pools and nitrogen cycle in an alpine meadow on the eastern Tibetan plateau. – Applied Ecology and Environmental Research 3(6): 69-79.
[13] Gigliotti, G., Kaiser, K., Guggenberger, G. (2002): Differences in the chemical composition of dissolved organic matter from waste material of different sources. – Biology and Fertility of Soils 36(5): 321-329.
[14] Halvorson, A. D., Black, A. L., Krupinsky, J. M., Merrill, S. D., Wienhold, B. J., Tanaka, D. L.(2000): Spring wheat response to tillage and nitrogen fertilization in rotation with sunflower and winter wheat. – Agronomy Journal 92(1): 136-144.
[15] Haynes, R. J. (2005): Labile organic matter fractions as central components of the quality of agricultural soils: an overview. – Advances in Agronomy 85(4): 221-268.
[16] Hemwong, S., Cadisch, G., Toomsan, B. (2008): Dynamics of residue decomposition and N_2 fixation of grain legumes upon sugarcane residue retention as an alternative to burning. – Soil and Tillage Research 99(1): 84-97.
[17] Jiang, X. D., Li, Z. J., Hou, L. T. (2005): Impacts of minimum tillage and no-tillage systems on soil NO_3-N content and water use efficiency of winter wheat summer corn cultivation. – Transactions of the CSAE 21(7): 20-24.
[18] Jiang, X. F. (2005): The effect on soil organic nitrogen under the different tillage in dryland. – Doctoral dissertation, Gansu Agricultural University.

http://www.aloki.hu ● ISSN 1589 1623 (Print) ● ISSN 1785 0037 (Online)
DOI: http://dx.doi.org/10.15666/aeer/1605_55175528
© 2018, ALÖKI Kft., Budapest, Hungary

[19] Jones, D. L., Shannon, D., Murphy, D. V., Farrar, J. (2004): Role of dissolved organic nitrogen (DON) in soil N cycling in grassland soils. – Soil Biology & Biochemistry 36: 749-756.
[20] Ju, X. T., Liu, X. J., Zhang, F. S. (2004): Effects of long-term fertilization on soil organic nitrogen fractions. – Scientia Agricultura Sinica 37(1): 87-91.
[21] Karra, R., Maslouhi, A., Bamba, Y. O. (2018): Modeling of nitrogen transport in variably saturated soils. – Applied Ecology and Environmental Research 2(6): 1427-1444.
[22] Kranabetter, J. M., Dawson, C. R., Dunn, D. E. (2007): Indices of dissolved organic nitrogen, ammonium and nitrate across productivity gradient of boreal forests. – Soil Biology Biochemistry 39(12): 3147-3158.
[23] Kushwaha, C. P., Tripathi, S. K., Singh, K. P. (2000): Variations in soil microbial biomass and N availability due to residue and tillage management in a dryland rice agroecosystem. – Soil and Tillage Research 56(3): 153-166.
[24] Lenssen, A. W., Waddell, J. T., Johnson, G. D. (2007): Diversified cropping systems in semiarid Montana: Nitrogen use during drought. – Soil and Tillage Research 94(2): 362-375.
[25] Li, H., Gao, H., Wu, H., Li, W. Y., W, X. Y., H, J. (2007): Effects of 15 years of conservation tillage on soil structure and productivity of wheat cultivation in northern China. – Soil Research 45(5): 344-350.
[26] Liu, S. Y., Zhang, X. P., Zhao, J. (2017): Effects of long-term no tillage treatment on gross soil N transformations in black soil in Northeast China. – Geoderma 301: 42-46.
[27] Lou, Y., Xu, M., Chen, X. (2012): Stratification of soil organic C, N and C: N ratio as affected by conservation tillage in two maize fields of China. – Catena 95: 124-130.
[28] Malhi, S. S., Lemke, R., Wang, Z. H. (2006): Tillage, nitrogen and crop residue effects on crop yield, nutrient uptake, soil quality, and greenhouse gas emissions. – Soil and Tillage Research 90(1): 171-183.
[29] Matthews, A. M., Armstrong, A. C. (2000): Development and testing of a model for predicting tillage effects on nitrate leaching from cracked clay soils. – Soil and Tillage Research 53(3): 245-254.
[30] Mkhabela, M. S., Madani, A. Gordon, R. (2008): Gaseous and leaching nitrogen losses from no-tillage and conventional tillage systems following surface application of cattle manure. – Soil and Tillage Research 98(2): 187-199.
[31] Nguyen, T. T. N., Xu, C. Y., Tahmasbian, I., Che, R. W., Xu, Z. H., Zhou, X. H., Wallacea, H. M., Bai, S. H. (2017): Effects of biochar on soil available inorganic nitrogen: A review and meta-analysis. – Geoderma 288: 79-96.
[32] Patra, D. D., Ram, M., Singh, D. V. (1993): Influence of straw mulching on fertilizer nitrogen use efficiency, moisture conservation and herb and essential oil yield in Japanese mint (*Mentha arvensis L.*). – Fertilizer Research 34(2): 135-139.
[33] Porter, L. K., Stewart, B., A., Haas, H., J. (1964): Effect of long-term cropping on hydrolysable organic nitrogen fraction in some Great Plant soils. – Soil Sci. Soc. Am. Proc 28: 368-370.
[34] Power, J. F., Peterson, G. A. (1998): Nitrogen transformations, utilization, and conservation as affected by fallow tillage method. – Soil and Tillage Research 49(1): 37-47.
[35] Purakayastha, T. J., Smith, J. L., Huggins, D. R. (2009): Microbial biomass and N cycling under native prairie, conservation reserve and no-tillage in Palouse soils. – Geoderma 152(3): 283-289.
[36] Qin, R., Stamp, P., Richner, W. (2006): Impact of tillage on maize rooting in a Cambisol and Luvisol in Switzerland. – Soil and Tillage Research 85(1): 50-61.
[37] Ram, M., Ram, D. Roy, S. K. (2003): Influence of anorganic mulching on fertilizer nitrogen use efficiency and herb and essential oil yields in geranium Pelargonium graveolens. – Bioresource Technology 87(3): 273-278.

http://www.aloki.hu ● ISSN 1589 1623 (Print) ● ISSN 1785 0037 (Online)
DOI: http://dx.doi.org/10.15666/aeer/1605_55175528
© 2018, ALÖKI Kft., Budapest, Hungary

[38] Rhoton, F. E. (2000): Influence of time on soil response to no-till practices. – Soil Science Society of America Journal 64(2): 700-709.
[39] Rosell, R. A., Galantini, J. A., Suner, L. G. (2000): Long-term crop rotation effect on organic carbon, nitrogen, and phosphoru: Haplustoll soil fraction. – Arid Soil Research and Rehabilitation 14(14): 309-315.
[40] Sainju, U. M., Caesar-Tonthat, T., Lenssen, A. W., Evans, R. G., Kolberg, R. (2009): Tillage and cropping sequence impacts on nitrogen cycling in dryland farming in eastern Montana, USA. – Soil and Tillage Research 103(2): 332-341.
[41] Sainju, U. M., Lenssen, A. W., Caesartonthat, T. (2012): Dryland soil nitrogen cycling influenced by tillage, crop rotation, and cultural practice. – Nutrient Cycling in Agroecosystems 93(3): 309-322.
[42] Sainju, U. M., Stevens, W. B., Evans, R. G., Iversen, W. M. (2013): Irrigation system and tillage effects on soil carbon and nitrogen fractions. – Soil Science Society of America Journal 77: 1225-1234.
[43] Schulten, H. R., Schnitzer, M. (1997): The chemistry of soil organic nitrogen: a review. – Biology & Fertility of Soils 26(1): 1-15.
[44] Shukla, S. K., Yadav, R. L., Awasthi, S. K., Gaur, A. (2016): Soil Microbial Biomass Nitrogen, In Situ Respiration and Crop Yield Influenced by Deep Tillage, Moisture Regimes and N Nutrition in Sugarcane-Based System in Subtropical India. – Sugar Tech 19(2): 1-11.
[45] Stevenson, F. J. (1982): Organic forms of soil nitrogen. – Nitrogen in Agricultural Soils: 67-122.
[46] Sun, L., Chang, S. X., Feng, Y. S., Dyck, M. F., Puurveen, D. (2015) : Nitrogen fertilization and tillage reversal affected water-extractable organic carbon and nitrogen differentially in a Black Chernozem and a Gray Luvisol. – Soil Tillage Res 146: 253-260.
[47] Thomas, G. A., Dalal, R. C., Standley, J. (2007): No-till effects on organic matter, p H, cation exchange capacity and nutrient distribution in a Luvisol in the semi-arid subtropics. – Soil and Tillage Research 94: 295-304.
[48] Torbert, H. A., Reeves, D, W. (1995): Interactions of traffic and tillage applied to cotton on N movement below the root zone of a subsequent wheat crop. – Soil and Tillage Research 33: 3-16.
[49] Vance, E. D., Brookes, P. C., Jenkinson, D. S. (1987): An extraction method for measuring soil microbial biomass C. – Soil biology and Biochemistry 19(6): 703-707.
[50] Varvel, G. E., Wilhelm, W. W. (2011): No-tillage increases soil profile carbon and nitrogen under long-term rainfed cropping systems. – Soil and Tillage Research 114(1): 28-36.
[51] Wander, M., Magdoff, F., Ray, R. W. (2004): Soil Organic Matter Fractions and Their Relevance to Soil Function. – In: Magdoff, F., and Weil, R. R. (eds.) Soil Organic Matter in Sustainable Agriculture. CRC Press, Boca Raton, FL.
[52] Xu, Y. C., Shen, Q. R. Ran, W. (2003): Content and distribution of forms of organic N in soil and particle size fractions after long-term fertilization. – Chemosphere 50(6): 739-745.
[53] Zavalloni, C., Alberti, G., Biasiol, S. (2011): Microbial mineralization of biochar and wheat straw mixture in soil: A short-term study. – Applied Soil Ecology 50: 45-51.

http://www.aloki.hu ● ISSN 1589 1623 (Print) ● ISSN 1785 0037 (Online)
DOI: http://dx.doi.org/10.15666/aeer/1605_55175528
© 2018, ALÖKI Kft., Budapest, Hungary

GAMMA-AMINO BUTYRIC ACID METABOLISM UNDER HIGH TEMPERATURE STRESS IN TWO LICHEN SPECIES

CEKIC, F. O.[1] – GOREN-SAGLAM, N. [2*] – TORUN, H.[3] – YIGIT, E.[4] – UNAL, D.[5,6]

[1]*Department of Biology, Faculty of Science and Letters, Aksaray University, Aksaray, Turkey*

[2]*Department of Biology, Faculty of Science, Istanbul University, Istanbul, Turkey*

[3]*Department of Biosystem Engineering, Faculty of Agriculture and Natural Science, University of Düzce, Düzce, Turkey*

[4]*Department of Biology, Faculty of Science and Letter, University of İnönü, Malatya, Turkey*

[5]*Department of Molecular Biology and Genetic, Faculty of Science and Letter, University of Bilecik S. E., Bilecik, Turkey*

[6]*Biotechnology Application and Research Center, University of Bilecik S. E., Bilecik, Turkey*

**Corresponding author*
e-mail: gorenn@istanbul.edu.tr; phone: +90-212-455-5700; fax: +90-212-522-6562

(Received 6th Jun 2018; accepted 14th Aug 2018)

Abstract. High temperature stress is a major environmental stress factor for all photosynthetic organisms. Some lichen species could have the ability of tolerance against global warming. In the present study, we investigated the effects of high temperature on GABA metabolism in two different lichen species *Evernia prunastri* and *Usnea* sp.. *Evernia* and *Usnea* sp. were collected from unpolluted locations in Bilecik, TURKEY. *Evernia* and *Usnea* sp. were kept at 45 °C for 0, 24 and 48 h. We analyzed GABA content, glutamate dehydrogenase (GDH) and glutamate decarboxylase (GAD) activities and also chlorophyll and MDA contents in the thalli of the lichens. The chlorophyll degradation and lipid peroxidation data indicated that *E. prunastri* thalli showed tolerance to high temperature while *Usnea* sp. thalli were found to be sensitive under these conditions. GABA content was enhanced by high temperature stress in *E. prutastri* thalli, while GAD and GDH activities were decreased. According to our results, we can suggest that GABA accumulation in lichen thalli could occur via different metabolic pathways.
Keywords: *Evernia, GABA, glutamate decarboxylase, glutamate dehydogenase, high temperature, Usnea*

Abbreviations: GABA: gamma-amino butyric acid; GAD: glutamate decarboxylase; GDH: glutamate dehydrogenase; MDA: malondialdehyde

Introduction

Global warming is one of the most serious problems for all organisms, populations, and ecological communities (Walther et al., 2002; Liu et al., 2003; Pisani et al., 2007). Climatic changes can negatively influence photosynthetic organisms; disrupt cellular homeostasis, and alter their morphology, biochemical structure, and physiology (Karl et al., 2007; Bita and Greats, 2013). High temperature stress can cause membrane damages, inhibit protein and carbohydrate metabolisms via inactivation of the enzymes in mitochondria and chloroplasts (Bita and Greats, 2013).

Gamma-amino butyric acid (GABA) plays different roles in plant metabolism including carbon–nitrogen metabolism, energy balance, signaling and development. It is found in a wide range of organisms including plants, algae and lichens (Bouché and Fromm, 2004;

http://www.aloki.hu ● ISSN 1589 1623 (Print) ● ISSN 1785 0037 (Online)
DOI: http://dx.doi.org/10.15666/aeer/1605_55295538
© 2018, ALÖKI Kft., Budapest, Hungary

Yolcu et al., 2013). GABA probably plays a dual role as both a signaling molecule and a metabolite (Fait et al., 2008). GABA is mainly synthesized in metabolic pathway known as GABA shunt. It plays a major role in primary C/N metabolism. GABA shunt includes three main enzymes; cytosolic enzyme glutamate decarboxylase (GAD; EC 4.1.1.15), the mitochondrial enzymes GABA transaminase (GABA-T; EC 2.6.1.19), and succinic semialdehyde dehydrogenase (SSADH; EC 1.2.1.16). Enhancement in GABA content under various stress conditions such as drought, chilling, salt, heavy metal stresses was reported by several researchers (Bor et al., 2009; Al-Quraan et al., 2013; Wang et al., 2016). Previous studies demonstrated that GABA shunt pathway plays an important role in the alleviation of oxidative stress caused by high temperature stress (Cao et al., 2013; Nayyar et al., 2014).

Lichens are poikilohydric organisms and highly adapted to osmotic dehydration (Hájek et al., 2006). Most of the species have ability of tolerance against global warming and can live in the range of 35-46 °C and survive even at 70 °C (Pisani et al., 2007; Dyakov et al., 2015), although some air-dried lichen species are being sensitive to high temperature stress (Van Herk et al., 2002). Similarly, in higher plants, high temperature could have an effect on the growth and physiological process of the lichens (Pissani et al., 2007). Previously studies demonstrated that increasing temperature caused to a reduction in chlorophyll content and directly or indirectly altered the synthesis of lichen substances (Bjerke et al., 2003). In the literature, there are very limited studies on the heat tolerance or stress, and physiological mechanisms of high temperature tolerance are not fully known in lichens. Moreover, the role of GABA metabolic pathway under high temperature conditions is not clearly elucidated yet. In the present study, our aim was to determine the role of GABA shunt under high temperature conditions. To find out the answers of these questions, we showed that the alteration of GABA accumulation, and activities of GAD and GDH enzymes in different lichen species; *E. prunastri* and *Usnea* sp. under high temperature.

Materials and methods

Materials

The lichen species, *E. prunastri* and *Usnea* sp. were collected from unpolluted locations from Bilecik Center Forest, Turkey (N 40° 11.526', E 029° 57.962') at February 2017. 90 individual samples were transferred to the laboratory in the plastic bags, cleaned from impurities, and washed three times for 5 s with distilled water to remove dust from the surface. All lichen species were transferred to petri dishes and incubated in a growth chamber under 100 µmol m^{-2} s^{-1} light intensity and 16:8 light/dark cycle at 23 ± 2 °C and humidity was %38 for 48 h (Hall et al., 2002). Lichens were sprayed with distilled water once a day according to Calatayud et al. (1997). After laboratory adaptation, experimental conditions were designed. Lichen thalli was used as a control after the incubation for 48 h in normal growth conditions (as seen in *Table 1;* 0 h data).

For temperature experiments, 30 individual thalli of *E. prunastri* and *Usnea* sp. in petri dishes were kept for 0, 24 and 48 h in an incubator 100 µmol m^{-2} s^{-1} light intensity and 16:8 light/dark cycle at 45 ± 2 °C and likewise watered once a day. Heat stress temperature was chosen according to Pissani et al (2007) studies. The data presented in this study are the averages of three independent experiments.

http://www.aloki.hu ● ISSN 1589 1623 (Print) ● ISSN 1785 0037 (Online)
DOI: http://dx.doi.org/10.15666/aeer/1605_55295538
© 2018, ALÖKI Kft., Budapest, Hungary

Table 1. *Chlorophyll a, and b content and Chlorophyll a/b ratio in thalli of E. prunastri and Usnea sp. under heat stress for 0 (as a control), 24 and 48 h*

Groups	n	*E. prunastri*			*Usnea* sp.		
		Chl*a* **(µg/mg fw)**	**Chl*b*** **(µg/mg fw)**	**Chl*a/b*** **(µg/mg fw)**	**Chl*a*** **(µg/mg fw)**	**Chl*b*** **(µg/mg fw)**	**Chl*a/b*** **(µg/mg fw)**
0 h	3	1.385±0.11	0.444±0.09	3.12±0.03	1.456±0.33	0.455±0.13	3.20±0.03
24 h	3	1.132±0.16	0.481±0.04	2.39±0.01	0.884±0.76	0.424±0.40	2.09±0.02
48 h	3	0.867±0.20	0.308±0.03	2.87±0.13	1.089±0.19	0.713±0.06	1.49±0.01
p-value		<0.0001	<0.0001	0.0005	0.0003	0.0002	<0.0001
F probability		802.63	291085.45	92.12	115.73	133.25	6600.25

Chlorophyll content analysis

Chlorophyll analysis was determined using the method described by Wellburn (1994). Approximately 20 mg of thalli were extracted in the dark for 1 h at 65 °C in 3.0 mL of dimethyl sulfoxide (DMSO) in the presence of polyvinylpolyrrolidone to minimise chlorophyll degradation. The absorbances of the extracts were measured using a UV-visible spectrophotometer (Perkin Elmer). For the chlorophyll analysis, measurements were taken at the wavelengths 665.1 and 649.1 nm.

Lipid peroxidation

Formation of malondialdehyde (MDA) was evaluated as an indicator of lipid peroxidation. The determination of MDA was performed by the thiobarbituric acid reactive substances method (Heath and Packer, 1968). The absorbance differences between 532 and 600 nm was used to calculate MDA formation as a by-product of lipid peroxidation.

GABA analysis

GABA content was detected by HPLC (Agilent 1200) according to Bor et al. (2009). 0.1 g of lichen samples (*E. prunastri* and *Usnea* sp. were homogenized in 5 mL solution of water:chloroform:methanol (3:5:12 v/v/v), and centrifuged at 4 °C for 10 min. The supernatant was dried. The dried samples were dissolved in water, Borax buffer (pH 8.0) and 2-hydroxynaphthaldehyde (0.3% in methanol) and heated at 80 °C for 30 min. The samples were separated by reversed-phase column Supelco LC18 (250 × 4.6 mm^2, 5 µm) at 330 nm with a mobile phase of methanol:water (62:38 v/v). The injection volume was 5 µL. GABA content was calculated according to the peak areas of GABA standarts.

GAD and GDH enzyme analysis

GDH activity was measured according to Akihiro et al. (2008) and Yolcu et al. (2013). The extracts were mixed with the assay mixture containing 50 mM $(NH_4)_2SO_4$, 13 mM α-ketoglutarate, 0.25 mM NADPH and 1 mM $CaCl_2$ in 100 mM Tris-HCl buffer (pH 8.0). GDH activity was measured according to the absorbance differences at 340 nm and expressed as micromoles per minute per gram fresh weight (FW).

http://www.aloki.hu ● ISSN 1589 1623 (Print) ● ISSN 1785 0037 (Online)
DOI: http://dx.doi.org/10.15666/aeer/1605_55295538
© 2018, ALÖKI Kft., Budapest, Hungary

GAD activity was assayed according to Bartyzel et al. (2003) and Yolcu et al. (2013). 100 µL of sample was mixed with reaction mixture containing 3 mM L-glutamate, 20 µM pyridoxal phosphate and 50 mM potassium phosphate (pH 5.8) and incubated at 30 °C for 1 h for the decarboxylation process. HCl (0.5 M) was added to the mixture to stop the reaction. The samples were derivatized with 0.35% (w/v) ninhydrin solution. GAD activity was determined spectrophotometrically by comparing with the standard GABA values, and calculated as micromoles per minute per gram.

Statistics

Statistical analysis was performed with one-way analysis of variance (ANOVA) and Student's t-test followed by *posthoc* Tukey test as appropriate (SPSS for Windows version 11.0). The critical values for statistical significance was $p < 0.05$ and 0.01.

Results

Malondialdehyde (MDA) is often used as an indicator of oxidative damage at the cellular level. *Figure 1* shows the MDA content of thalli after exposure to high temperature for 0, 24 and 48 h. In *E. prunastri* thallus, MDA content was not significantly changed at 24 h, but the MDA content significantly increased ($p < 0.001$) at 48 h under high temperature (*Fig. 1*). In *Usnea* sp. thallus, the MDA content significantly increased at 24 h and 48 h.

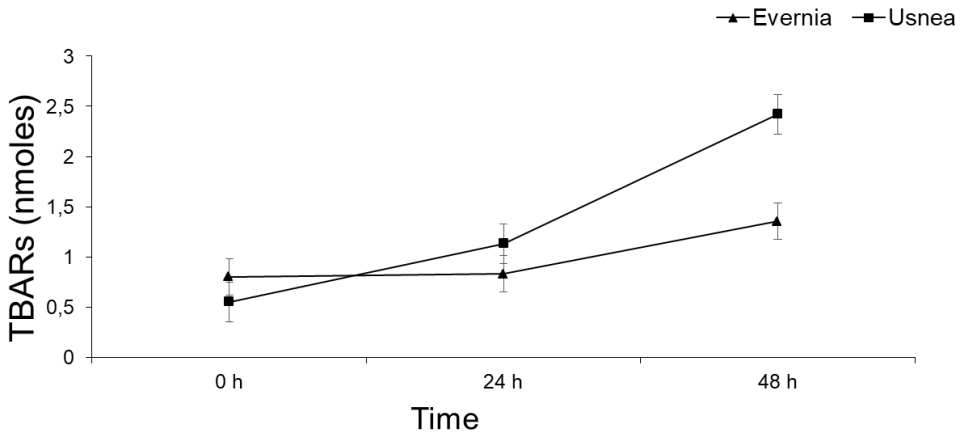

Figure 1. *Lipid peroxidation of different two lichen species under heat stress (45 °C) for 0 h, 24 h and 48 h*

The results of this study showed that the chlorophyll *a* content was significantly ($p < 0.001$) altered by high temperature treatment at 24 h and 48 h between lichen species. In *E. prunastri* thalli, however the chlorophyll *a* content gradually decreased at 24 and 48 h, chlorophyll *b* content was not significantly changed at 24 h (*Table 1*). The chlorophyll *a/b* ratio in the thallus of *E. prunastri* showed differences under 24 and 48 h exposures. In *Usnea* sp. The chlorophyll a content was significantly decreased at 24 and 48 h when compared to the control groups ($p < 0.001$) (0 h, as seen in *Table 1*). The content of chlorophyll *b* increased significantly under 48 h high temperature exposure. The chlorophyll *a/b* ratio decreased significantly after 24 h and 48 h exposures in *Usnea* sp. (*Table 1*).

http://www.aloki.hu ● ISSN 1589 1623 (Print) ● ISSN 1785 0037 (Online)
DOI: http://dx.doi.org/10.15666/aeer/1605_55295538
© 2018, ALÖKI Kft., Budapest, Hungary

As shown in *Figure 2,* GABA was enhanced under heat especially by time exposures. The highest increase was determined in *E. prunastri* under 48 h heat treatment. The lowest increase was detected in *Usnea* sp. However, we did not find any significant increase in the GABA content under 24 h treatment in *Usnea* sp.

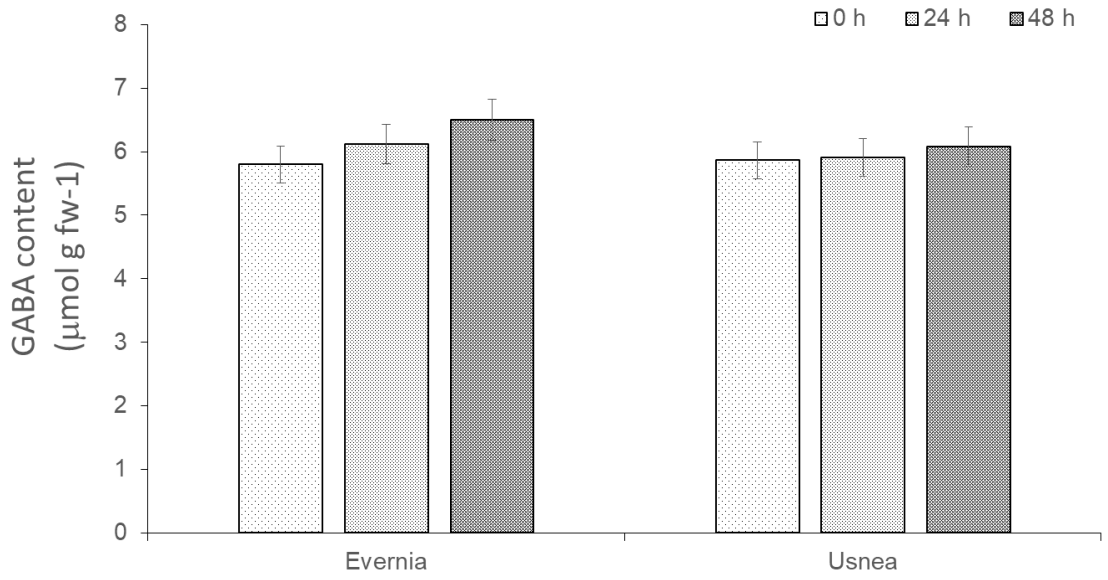

Figure 2. *GABA content of different two lichen species under heat stress (45 °C) for 0 h, 24 h and 48 h*

GAD activity was significantly decreased by heat treatments in *E. prunastri* when compared to the control group (*Fig. 3*). However, it was significantly increased by 24 h heat treatment in *Usnea* sp. as compared to the control group ($p < 0.05$). 48 h heat treatment did cause a decline in GAD activity in all of the species.

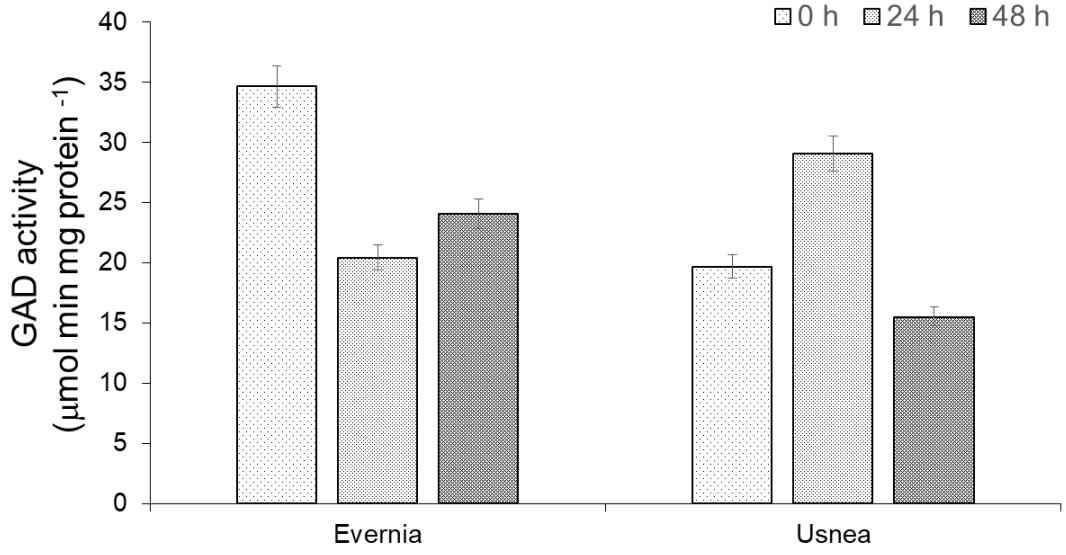

Figure 3. *GAD enzyme activities of different two lichen species under heat stress (45 °C) for 0 h, 24 h and 48 h*

http://www.aloki.hu ● ISSN 1589 1623 (Print) ● ISSN 1785 0037 (Online)
DOI: http://dx.doi.org/10.15666/aeer/1605_55295538
© 2018, ALÖKI Kft., Budapest, Hungary

GDH activity was not significantly changed in both lichen species as compared to their control groups. However, GDH activity was increased under 24 h heat treatment in *E. prunastri* when compared to the control group (*Fig. 4*). In addition, GDH activity was significantly increased when compared to 48 h heat teratment in the thalli of *Usnea* sp ($p < 0.05$).

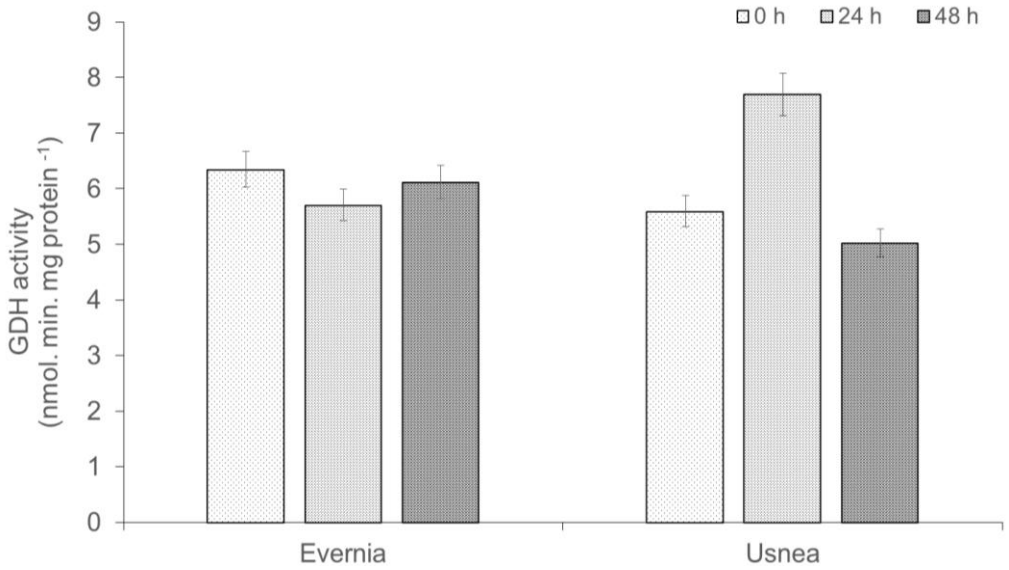

Figure 4. *GDH enzyme activities of different two lichen species under heat stress (45 °C) for 0 h, 24 h and 48 h*

Discussion

High temperature can induce oxidative stress via ROS production and lead can cause loss of cellular homeostasis in the photosynthetic organisms (Liu et al., 2003; Almeselmani et al., 2006). Oxidative stress also causes destruction of cell membranes via lipid peroxidation (Almeselmani et al., 2006). Malondialdehyde, MDA, is produced naturally as a result of lipid peroxidation and is often used as an indicator of oxidative damage at the cellular level (Mittler, 2002). Previous studies reported that high membrane damage occurs at higher temperatures and this could cause to the loss of structural organization of the membranes (Liu et al., 2003; Almeselmani et al., 2009; Hafmann, 2012). In our study, lipid peroxidation rate increased in *Usnea* sp., while MDA content did not significantly change in *E. prunastri* thalli at 24 h (*Fig. 1*). Our results indicate that thallus of *E. prunastri* could be more tolerant to heat stress.

Chlorophyll content is an important indicator for the photosynthetic process. It is also very sensitive to stress-initiated oxidative stress such as photo-oxidation (Chettri et al., 1998). Chlorophyll *b* is formed from chlorophyll *a* by the oxidation of the methyl group on the ring II to the aldehyde group (Chettri et al., 1998), and the ratio of chlorophyll *a/b* is more sensitive to the modification than chlorophyll *a+b*. In green plants, the antenna size is determined by the amount of light-harvesting chlorophyll *a/b* protein complex that is associated with the PSII (Takana and Takana, 2006). Conversion of chlorophyll *b* to chlorophyll *a* is the first step in chlorophyll degradation, as well as influencing chlorophyll a / b ratio (Chettri et al., 1998; Takana and Takana, 2006). Therefore, chlorophyll degradation is frequently used to identify the physiological

http://www.aloki.hu ● ISSN 1589 1623 (Print) ● ISSN 1785 0037 (Online)
DOI: http://dx.doi.org/10.15666/aeer/1605_55295538
© 2018, ALÖKI Kft., Budapest, Hungary

conditions of the lichens (Chettri et al., 1998; Bačkor and Zetiková, 2003). Many lichen species could have tolerance to climate change and high temperature (Pisani et al., 2007). Pisani et al. (2007) showed that the content of photosynthetic pigments was not significantly changed at 40 °C for 24 h in *E. prunastri*. Similarly, in our study, chlorophyll degradation was not decreased in the range of 4-2 in *E. prunastri* thalli under high temperature stress (*Table 1*). However, the chl *a/b* ratio significantly decreased in the thalli of *Usnea sp.* during 24 and 48 h. Exposure of *Usnea* sp. to the temperature of 45 °C had significantly negative effect on the content of photosynthetic pigments (*Table 1*). Our results indicated that *E. prunastri* has more tolerance capacity than *Usnea* sp. under high temperature stress.

GABA biosynthesis is enhanced via various stress conditions (Bor et al., 2009; Al-Quraan et al., 2011; Paradisone et al., 2015), and GABA pathway could regulate the adaptation mechanisms (Al-Quraan and Al-Share, 2016). GABA is synthesized from glutamate by the activity of cytosolic GAD (Bouche et al., 2003). In higher plants, many researchers have suggested that GAD activity played a dominant role in the accumulation of GABA (Cao et al., 2012). Yolcu et al. (2013) also reported that GAD activity is highly correlated with high GABA levels. GDH is an enzyme found in the mitochondria that catalyzes the deamination of glutamate which is then converted to GABA by the action of GAD (Andersson and Rager, 2003; Forde and Lea, 2007). In higher plants, GABA accumulation can have a role in the tolerance under many environmental stress conditions (Nayyar et al., 2014). Previous studies also demonstrated that rapid accumulation of GABA in response to heat-stress (Bouche et al., 2004; Nayyar et al., 2014). In the present study, high GABA accumulation could decrease lipid peroxidation at 48 h with increasing lipid peroxidation rate at 48 h exposure in *E. prunastri* thalli (*Figs. 1* and *2*). Therefore, we can suggest that GABA could be a signal for high temperature tolerance.

Among lichens, Jager and Weigel (1978) reported that GABA is one of the predominant amino acids in the lichen *P. furfuracea*. Yolcu et al. (2013) also found that lowest GDH activity showed in *P. furfuracea* thalli as compared to higher plant species. In *Usnea* sp. under 24 h heat treatment, we can suggest that GABA could be synthesized by the activity of GAD via GABA pathway. However; under 48 h heat treatment GAD activity did not increase when compared to control group while GABA contents were enhanced under the same conditions (*Fig. 3*). In *E. prunastri* thalli, GDH and GAD enzymes activities did not show any relation with GABA accumulation under high temperature stress (*Figs. 3* and *4*). Numerous publications in higher plants link GABA metabolism with polyamine biosynthesis pathways, however there is not any information in lichens. GABA can also be synthesized via polyamine pathway by polyamine degradation or reduction (Moschou et al., 2008; Yolcu et al., 2013). Moreover, Wang et al. (2016) showed that the elevated chilling tolerance in NO-treated banana fruit may be attributed to enhanced accumulation of polyamines and GABA.

Conclusion

According to our results, we can suggest that GABA could be mainly synthesized via GAD activity during normal conditions in *Evernia* and *Usnea*, but in stress conditions, GABA can be synthesized via polyamine accumulation. However, further studies should be done to identify the effects of polyamine pathway on GABA metabolism in lichens both under normal and stress conditions.

http://www.aloki.hu ● ISSN 1589 1623 (Print) ● ISSN 1785 0037 (Online)
DOI: http://dx.doi.org/10.15666/aeer/1605_55295538
© 2018, ALÖKI Kft., Budapest, Hungary

Author contributions. All authors conceived research. Dr. Dilek Unal designed the experimental framework and chlorophyll and lipid peroxidation analysis. Dr. Fazilet Ozlem Cekic performed GABA and enzyme analyses. Dr. Nihal Goren-Saglam, Dr. Emel Yigit and Dr. Hulya Torun participated the experimental analysis. Dr. Dilek Unal and Dr. Nihal Goren-Saglam drafted the manuscript. All authors have read and approved the manuscript.

REFERENCES

[1] Akihiro, T., Koike, S., Tani, R., Tominaga, T., Watanabe, S., Iijima, Y., Aoki, K., Shibata, D., Ashihara, H., Matsukura, C., Akama, K., Fujimura, T., Ezura, H. (2008): Biochemical mechanism on GABA accumulation during fruit development in tomato. – Plant and Cell Physiology 49: 1378-1389.

[2] Al-Quraan, N. A., Locy, R. D., Singh, N. K. (2011): Implications of paraquat and hydrogen peroxide-induced oxidative stress treatments on the GABA shunt pathway in *Arabidopsis thaliana* calmodulin mutants. – Plant Biotechnology Reports 5: 225-234.

[3] Al-Quraan, N. A., Sartawe, F. A., Qaryouti, M. M. (2013): Characterization of ɤ-aminobutyric acid metabolism and oxidative damage in wheat (*Triticum aestivum L.*) seedlings under salt and osmotic stress. – Journal of Plant Physiology 170: 1003-1009.

[4] Al-Quraan, N. A., Al-Share, A. T. (2016): Characterization of the γ-aminobutyric acid shunt pathway and oxidative damage in Arabidopsis thaliana pop 2 mutants under various abiotic stresses. – Biologia Plantarum 60: 132-138.

[5] Almeselmani, M., Deshmukh, P. S., Sairam, R. K., Kushwaha, S. R., Singh, T. P. (2006): Protective role of antioxidant enzymes under high temperature stress. – Plant Science 171: 382-388.

[6] Andersson, J. O., Roger, A. J. (2003): Evolution of GDH genes: evidence for lateral gene transfer within and between prokaryotes and eukaryotes. – BMC Evolutionary Biology 3: 14.

[7] Bačkor, M., Zetiková, J. (2003): Effects of copper, cobalt and mercury on the chlorophyll content of lichens *Centraria islandica* and *Flavocetraria cucullata*. – Journal of the Hattori Botanical Laboratory 93: 175-187.

[8] Bartyzel, I., Pelczar, K., Paszkowski, A. (2003): Functioning of the gamma-aminobutyrate pathway in wheat seedlings affected by osmotis stress. – Biologia Plantarum 47: 221-225.

[9] Bita, C. E., Gerats, T. (2013): Plant tolerance to high temperature in a changing environment: scientific fundamentals and production of heat stress-tolerant crops. – Frontiers in Plant Science 4: 273. DOI: 10.3389/fpls.2013.00273.

[10] Bjerke, J. A., Zielke, M., Solheim, B. (2003): Long-term impacts of simulated climatic change on secondary metabolism, thallus structure and nitrogen fixation activity in two cyanolichens from the Arctic. – New Phytologist 159: 361-367.

[11] Bor, M., Seckin, B., Ozgur, R., Yılmaz, O., Ozdemir, F., Turkan, I. (2009): Comparative effects of drought, salt, heavy metal and heat stresses on gamma-aminobutryric acid levels of sesame. – Acta Physiologia Plantarum 31: 655-659.

[12] Bouche, N., Fait, A., Bouchez, D., Moller, S. G., Fromm, H. (2003): Mitochondrial succinic-semialdehyde dehydrogenase of the gamma-aminobutyrate shunt is required to restrict levels of reactive oxygen intermediates in plants. – Proceedings of the National Academy of Sciences 100: 6843-6848.

[13] Bouche, N., Fromm, H. (2004): GABA in plants : just a metabolite ? – Trends in Plant Science 9: 110-115.

[14] Calatayud, A., Deltoro, V. I., Barreno, E., de Valle-Tascon S (1997): Changes in in vivo chlorophyll fluorescence quenching in lichen thalli as a function of water content and suggestion of zeaxanthin-associated photoprotection. – Physiologia Plantarum 101: 93-102.

http://www.aloki.hu ● ISSN 1589 1623 (Print) ● ISSN 1785 0037 (Online)
DOI: http://dx.doi.org/10.15666/aeer/1605_55295538
© 2018, ALÖKI Kft., Budapest, Hungary

[15] Cao, J., Barbosa, J. M., Singh, N., Locy, R. D. (2013): GABA shunt mediates thermotolerance in Saccharomyces ceresiae by reducing reactive oxygen production. – Yeast 30: 129-144.
[16] Chettri, M. K., Cook, C. M., Vardaka, E., Sawidis, T., Lanaras T (1998): The effect of Cu, Zn, and Pb on the chlorophyll content of lichens *Cladonia convolute* and *Cladonia rangiformis*. – Environmental and Experimental Botany 39: 1-10.
[17] Dyakov, M. Y., Insarova, I. D., Kharabadze, D. E., Ptushenko, V. V., Shtaer, O. V. (2015): Influence of extreme ambient temperatures and anaerobic conditions on Peltigera aphthosa (L.) Wild. viability. – Life Sciences in Space Research 7: 66-72.
[18] Fait, A., Fromm, H., Walter, D., Galili, G., Fernie, A. R. (2008): Highway or byway: the metabolic role of the GABA shunt in plants. – Trends in Plant Science 13: 14-9.
[19] Forde, B. G., Lea, P. J. (2007): Glutamate in plants: metabolism, regulation and signalling. – Journal of Experimental Botany 58: 2339-2358.
[20] Hall, R. S. B., Bornman, J. F., Björn, L. O. (2002): UV-induced changes in pigment content and light penetration in the fruticose lichen Cladonia arbuscular ssp. mitis. – Journal of Photochemistry and Photobiology: Biology 66: 13-20.
[21] Hájek, J., Barták, M., Dubová, J. (2006): Inhibition of photosynthetic processes in foilose lichens induced by temperature and osmotic stress. – Biologia Plantarum 50: 624-634.
[22] Heath, R. L., Packer, L. (1968): Photoperoxidation in isolated chloroplast: 1. Kinetics and stoichiometry of fatty acid peroxidation. – Archives of Biochemistry and Biophysics 125: 189-198.
[23] Jager, H. J., Weigel, H. J. (1978): Amino acid metabolism in lichens. – Bryologist 81: 107-113.
[24] Karl, T. R., Kukla, G., Razuvayev, V. N., Changery, M. J., Quayle, R. G., Heim, R. R., Easterling, D. R., Kotak, S., Larkindale, J., Lee, U., von Koskull-Döring, P., Vierling, E., Scharf, K. D. (2007): Complexity of the heat stress response in plants. – Current Opinion Plant Biology 10: 310-316.
[25] Liu, Y., Cao, T, Glime, J. M. (2003): The Changes of membrane permeability of mosses under high temperature stress. – Bryologist 106: 53-60.
[26] Mittler, R. (2002): Oxidative stress, antioxidants and stress tolerance. – Trends in Plant Science 7: 405-410.
[27] Moschou, P. N., Paschalidis, K. A., Roubelakis-Angelakis, K. A. (2008): Plant polyamine catabolism: the start of the art. – Plant Signal Behaviour 3: 1061-1066.
[28] Nayyar, H., Kaur, R., Kaur, S, Singh R (2014): γ-aminobutyric acid (GABA) imparts partial protection from heat stress injury to rice seedlings by improving leaf turgor and upregulating osmoprotectants and antioxidants. – Journal of Plant Growth Regulation 33: 408-419.
[29] Paradisone, V., Barrameda-Medina, Y., Montesinos-Pereira, D., Romero, L., Esposito, S., Ruiz, J. M. (2015): Roles of some nitrogenous compounds protectors in the resistance to zinc toxicity in Lactuca sativa cv. Phillipus and Brassica oleracea cv. Bronco. – Acta Physiologia Plantarum 37: 1-8.
[30] Pisani, T., Paoli, L., Gaggi, C., Pirintsos, S. A., Loppi, S. (2007): Effects of high temperature on epiphytic lichens: Issues for consideration in a changing climate scenario. – Plant Biosystem 141: 164-169.
[31] Tanaka, A., Tanaka, R. (2006): Chlorophyll metabolism; a review. – Current Opinion Plant Biology 9: 248-255.
[32] Van Herk, C. M., Aptroot, A., van Dobben, H. F. (2002): Long-term monitoring in the Netherlands suggests that lichens respond to global warming. – Lichenologist 34: 141-154.
[33] Walther, G. R., Post, E., Convey, P., Menzel, A., Parmesan, C., Beebee, T. J. C., Fromentin, J. M., Hoegh-Guldberg, O., Bairlein, F. (2002): Ecological responses to recent climate change. – Nature 416: 389-395.

http://www.aloki.hu ● ISSN 1589 1623 (Print) ● ISSN 1785 0037 (Online)
DOI: http://dx.doi.org/10.15666/aeer/1605_55295538
© 2018, ALÖKI Kft., Budapest, Hungary

[34] Wang, Y., Luo, Z., Mao, L., Ying, T. (2016): Contribution of polyamines metabolism and GABA shunt to chilling tolerance induced by nitric axide in cold-stored banana fruit. – Food Chemistry 197: 333-339.
[35] Wellburn, A. R. (1994): The spectral determination of chlorophylls a and b, as well as total carotenoids, using various solvents with spectrophotometers of different resolution. – Journal of Plant Physiology 144: 307-313.
[36] Yolcu, S., Ozdemir, F., Bor, M. (2013): Gamma-amino butyric acid, glutamate dehydrogenase and glutamate decarboxylase levels in phylogenetically divergent plants. – Plant Systematics and Evolution 299: 403-412.

http://www.aloki.hu ● ISSN 1589 1623 (Print) ● ISSN 1785 0037 (Online)
DOI: http://dx.doi.org/10.15666/aeer/1605_55295538
© 2018, ALÖKI Kft., Budapest, Hungary

SPATIAL DISTRIBUTION PATTERN AND ECOLOGICAL NICHE CHARACTERISTICS OF *P. SYLUESTRIFORMIS* POPULATION IN CHANGBAI MOUNTAIN AREA, CHINA

JIN, H.* – ZHAO, Y. – YIN, H. – HUANG, L. – LIU, L. – CHEN, Q. – DAI, Y. – QIN, L.

Jilin Provincial Joint Key Laboratory of Changbai Mountain Biocoenosie an Biodiversity, Changbaishan Academy of Science, CN-133613 Yanbian, P. R. China

**Corresponding author*
e-mail: fivecl10jinhui@163.com

(Received 13th Jun 2018; accepted 1st Aug 2018)

Abstract. *P. syluestriformis* is an endemic plant in Changbai Mountain area of China. Some sample plots were set up in natural distribution communities of *P. syluestriformis*. Based on the survey data of the plots, the spatial distribution pattern of *P. syluestriformis* population was studied by the aggregation index. The niche breadth of Levins, Hurlbert and the Pianka niche overlap methods were used to analyze the niche characteristics of *P. syluestriformis* population in different communities. The results showed that in the pure forest of *P. syluestriformis* at about 700 m above sea level, *P. syluestriformis* population was in an aggregate distribution state, and in the scattered community of *P. syluestriformis*, *P. syluestriformis* population was randomly distributed in different forest stands under natural conditions, *P. syluestriformis* population had obvious advantages in each resource location. The maximum niche breadth of Levins was 5.3094. In the aspect of niche overlap index, there was a large niche overlap between the population of *P. syluestriformis* and *U. japonica*, which had obvious sharing advantages. Followed by *L. olgensis*, *A. tegmentosum*, *Q. mongolica*, *A. nephrolepis*. *P. syluestriformis* population and the above-mentioned associated species had the same or similar requirements for the same resource, and competition would occur when the resources were insufficient. The succession dynamics of *P. syluestriformis* populations were mainly characterized by narrow geographical distribution and narrow habitat, few populations, no individual seedlings and saplings, and lack of self-renewal ability, so they belonged to the recession-type populations.
Keywords: *P. syluestriformis, aggregation degree, niche overlap, niche breadth*

Introduction

The niche is the smallest unit of species distribution. Since Grinnell J proposed niche conception in 1917. The study of niche theory has been one of the research hotspots in the field of world ecology (Grinnell, 1917). Niche theory is widely used in species relations, biodiversity, community structure and function, community succession dynamics, intraspecific and interspecific competition studies.

To analyze the status and relationship of target species in communities, Chinese and foreign scholars used multiple niche breadth and niche overlap formulas to measure the niche characteristics of main populations of different communities. Seen from the existing results, the plant communities that developed on different types of landforms in different regions have different manifestations of their population niche characteristics (Chang et al., 2015; Chen et al., 2010). Among them, Chinese scholars have made relatively successful attempts to study the niche of plant populations in Changbai Mountain, China (Chen et al., 2009; Ye et al., 2011). The research on the population niche characteristics of rare and endangered plants is of great significance for further exploring the utilization of space resources and the interrelationships between other

http://www.aloki.hu ● ISSN 1589 1623 (Print) ● ISSN 1785 0037 (Online)
DOI: http://dx.doi.org/10.15666/aeer/1605_55395549
© 2018, ALÖKI Kft., Budapest, Hungary

endangered plants and other populations, and revealing the mechanism of endangered plants.

P. syluestriformis, is an evergreen tree of *Pinus* L. and a rare and endangered tree species in Changbai Mountain area of China. The natural population is relatively narrow and is located at N 42°06' - 42°32', E 128°07' - 128°21', scattered on the northern slope of Changbai Mountain, China (Jin et al., 2015).

Due to population increase, economic development and environmental destruction, the distribution area of natural population of *P. syluestriformis* have gradually narrowed and it has reached the edge of extinction. At present, the number of existing plants of *P. syluestriformis* is less than 110000 (Wang, 2007).

Since the 1980s, some Chinese scholars began to pay attention to the special species of *P. syluestriformis*. Aiming at the ecological characteristics, the growth pattern, the introduction and afforestation techniques, the biomass, diversity of interspecific seed traits in population, and so on (Lu et al., 2004; Cheng et al., 2013; Zou et al., 1995), and research cases on the niche characteristics of the rare population of *P. syluestriformis* have not been reported so far. Therefore, in this paper, the field survey data of community of *P. syluestriformis* population distribution as the data source were used to quantitatively measure the niche characteristics of the dominants to reveal the function and status of *P. syluestriformis* population in the community and analyze the interrelation between various groups. It will provide scientific support for judging the stability of *P. syluestriformis* population and theoretical basis for revealing its endangered mechanism.

Material and methods

Regional survey of research

The research area is located in the Changbai Mountain Nature Reserve in Jilin, China. The zonal climate belongs to the continental mountain climate with monsoon influence. Winter is cold and dry; summer is warm and humid. The precipitation is mostly concentrated in July-August, with an average annual temperature of 4.4 °C, extreme minimum temperature of -40 °C, the extreme maximum temperature of 37.5 °C, annual precipitation of 600-1340 mm, relative humidity of more than 70%, and the frost-free period of 90-100 days. The soil in the distribution area of *P. syluestriformis* is mostly formed dark brown soil on volcanic ash. The soil layer is thin, the pH is 4.2-4.9, the content of humus is low, and the water holding capacity is poor.

The plant in the area belongs to floristic plant of Changbai Mountain. The upper part of the natural distribution area of *P. syluestriformis* is mixed with coniferous forest, and the lower part is interlaced with coniferous and broad-leaved mixed forest belt, forming a unique mixed forest and a small piece of pure forest of *P. syluestriformis*.

Sampling method

In 2015, one sample plots of 30m × 30m were set up in the pure forest of *P. syluestriformis*, two sample plots of 30m × 30m were set up in the scattered forest of *P. syluestriformis* in Changbai Mountain Nature Reserve. The species, crown width, coverage and diameter at breast height (DBH) of woody plants with DBH ≥ 1.3 cm were investigated and recorded in detail. The sample area was summarized in *Table 1*. The distribution map of *P. syluestriformis* is shown in *Figure 1*.

http://www.aloki.hu ● ISSN 1589 1623 (Print) ● ISSN 1785 0037 (Online)
DOI: http://dx.doi.org/10.15666/aeer/1605_55395549
© 2018, ALÖKI Kft., Budapest, Hungary

Table 1. *Community habitat and vegetation status in the survey area*

Sample number	Forest type	Altitude/m	Falling gradient	Aspect	Crown density	Geographic coordinates	Dominant species of Arbor layer
P1	The pure forest of *P. syluestriformis*	700-740	<1	Northeast, near the plains	70	N 42°25' E128°07'	*P.syluestriformis, Q.mongolica, A.mono, U.japonica, A.pseudosieboldianum, F.mandshurica, T.mandschurica*
P2	The scattered forest of *P. syluestriformis*	890-984	3	Southeast	75	N 42°18' E128°06'	*P.syluestriformis, Q.mongolica, A.nephrolepis, L.olgensis, A.mono, T.amurensis, P.koraiensis, A. kalkora, P jezoensis*
P3	The scattered forest of *P. syluestriformis*	1100-1180	<3	North	80	N42°10' E128°08'	*P.syluestriformis, T.amurensis, A.nephrolepis, L.olgensis, A. mono, B.platyphylla, P.davidiana, T.amurensis, P.jezoensis, A.tegmentosum*

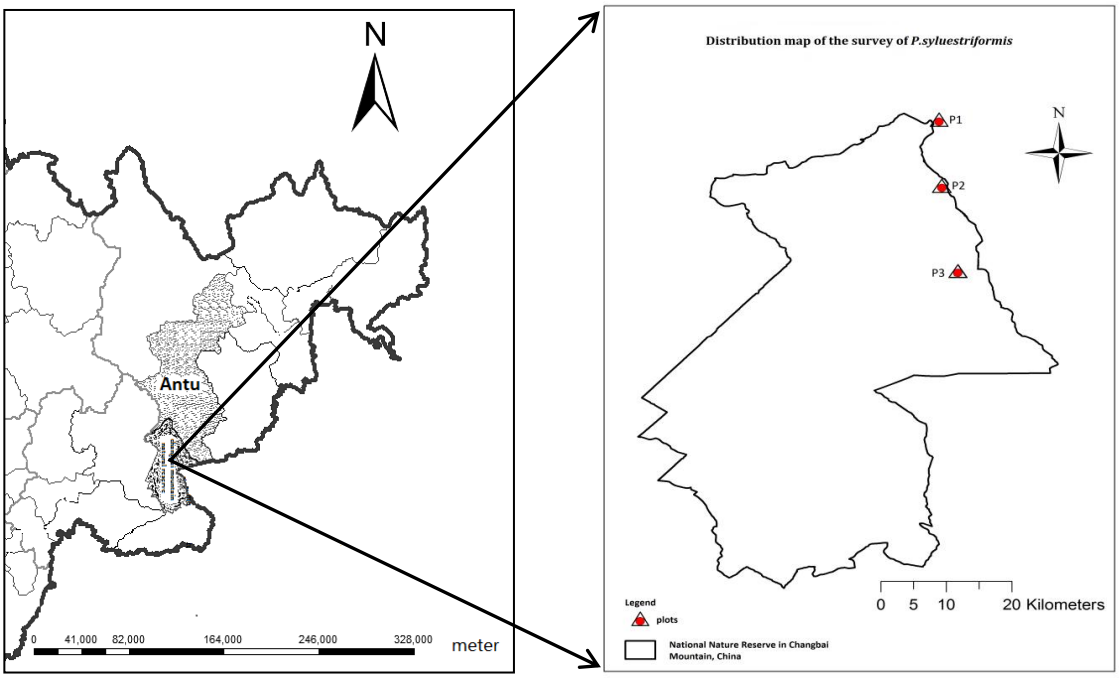

Figure 1. *Distribution map of the survey of P. syluestriformis*

http://www.aloki.hu ● ISSN 1589 1623 (Print) ● ISSN 1785 0037 (Online)
DOI: http://dx.doi.org/10.15666/aeer/1605_55395549
© 2018, ALÖKI Kft., Budapest, Hungary

Data processing

Population distribution pattern measurement method

There are many mathematical models for determining the types of distribution patterns of biological populations. In practical applications, each model has its adaptive application effect and the method is simple and effective. This paper combines with five kinds of aggregation index, such as the diffusion coefficient (C), aggregation index (I), average congestion (M^*), convergence index (M^*/x) and M index (C_A). The distribution pattern is determined by means of t test of mean variance and F test of deviation degree of random distribution, and the population aggregation is determined by negative binomial parameters (K) (Wang, 2012; Guo, 2004).

Niche breadth (Hurlbert, 1978; Li et al., 2003)

$$Bi = \frac{1}{r\sum_{j=1}^{r} P_{ij}^2} \quad \text{(Eq.1)}$$

Equation 1 of Levins (1968) is quantitatively calculated, γ is the number of resource bits, P_{ij} is the proportion of the species is using the j-th resource for all resources and is the population number; the niche breadth range is [1/γ, 1].

$$B_a = \frac{1}{\sum_{j=1}^{n} \frac{p_j^2}{a_j}} \quad \text{(Eq.2)}$$

Equation 2 stands for Hurlbert niche breadth index. P_j is the proportion of the species i that uses the j-th resource to the total resource bit used by the species, a_j is the number of items available in resources j($\Sigma a_j = 1.0$), B_a is the standardized Hurlbert niche breadth index.

Niche overlap (Hurlbert, 1978)

$$O_{ik} = \sum_{j=1}^{r} P_{ij}P_{kj} \Big/ \sqrt{\left(\sum_{j=1}^{r} P_{ij}\right)^2 \left(\sum_{j=1}^{r} P_{kj}\right)^2} \quad \text{(Eq.3)}$$

Pianka (1973) overlap index was used for analysis. In *Equation 3,* O_{ik} value is between 0 and 1.

Age class division of P. syluestriformis

For the classification of age class of *P. syluestriformis*, this paper takes 30 years as an age class, altogether divides into 8 age classes, which are I grade, II grade, III grade, IV grade, V grade, VI grade, VII grade, VIII grade. Those over 240 years old are classified as VIII grade.

http://www.aloki.hu ● ISSN 1589 1623 (Print) ● ISSN 1785 0037 (Online)
DOI: http://dx.doi.org/10.15666/aeer/1605_55395549
© 2018, ALÖKI Kft., Budapest, Hungary

Data statistical analysis

The original data is input into Excel table, and the data format can be read by R software according to the need of analysis. The spatial distribution pattern is analyzed, using the Riplely correlation function in the Spatstat library of R software.

Results

Spatial distribution pattern of P. syluestriformis population

According to the survey sample data, the indexes mentioned above of aggregation were measured by distribution (*Table 2*). It could be seen from the results in the table that the maximum diffusion coefficient of P2 sample plot was 2.243, which was greater than 1, and the diffusion coefficient of other sample plots was less than 1. After comparing t and $t0.05(36\text{-}1)$, both reached significant level of difference. According to the analysis of sample plots, the pure forest community of *P. syluestriformis* presented a clustered distribution. While in the scattered forests, the distribution state showed random and scattered in various forest communities. The M^*/x index was greater than 1 in P2 sample plots, the indexes in the other samples were all less than 1. To more accurately reflect the spatial pattern of a natural population of *P. syluestriformis* in different habitats, the regression analysis of 6 plots M^*/x of scattered forests was carried out. The regression equation was as follows: $M^* = -0.05161 + 0.43806x$ $R = 0.6927$. In the regression relationship, the α value was -0.05161, which was approximately 0, indicating that the basic component of the distribution was a single individual. The space β used to explain the basic component, the β value was 0.43806, and the value β was < 1, which was a uniform distribution. Using the statistical method of Taylor's power law, the regression equation was: $lgS^2 = -0.16858 + 0.88407lgx$ $R = 0.9959$, further confirmed that the populations of *P. syluestriformis* were scattered in the communities in the scattered state.

Table 2. *Spatial distribution and aggregation index of P. syluestriformis population*

Sample number	$\bar{x}$	S^2	Diffusion coefficient C	I index	Average congestion M^*	M^*/x index	C_A index	Distribution pattern
P1	1.750	2.243	2.4933**	1.4933	2.0317	1.1610	0.1610	*C*
P2	0.278	0.201	0.7221**	-0.2779	-0.0001	-0.0004	-1.0004	*R*
P3	0.056	0.052	0.9437**	-0.0563	-0.0007	-0.0128	-1.0128	*R*

C: cluster distribution, *R:* random

The spatial distribution pattern of a natural population of *P. syluestriformis* was analyzed by using C, M^*, C_A index. The results showed in *Table 3* that in pure forest there was no individual of *P. syluestriformis* in addition to VIII age-class, and there were distributions at all other levels, of which III and IV age-classes were clustered, and other age-classes were random. It also showed that the population had a certain diffusivity from young to mature individuals, and C, C_A had the same result of judgment. In pure forest community, the spatial distribution pattern of *P. syluestriformis* population changed from young to mature, which was a general trend from random type to clustered type and then to random type.

http://www.aloki.hu ● ISSN 1589 1623 (Print) ● ISSN 1785 0037 (Online)
DOI: http://dx.doi.org/10.15666/aeer/1605_55395549
© 2018, ALÖKI Kft., Budapest, Hungary

Table 3. *Aggregation degree of distribution pattern of different age classes of P. syluestriformis population*

Sample number	Age-class	Diffusion coefficient *C*	Average congestion *M**	*M*/x* index	C_A index	Distribution pattern
P1	I	0.9306	0.0000	0.0001	-0.9999	*R*
	II	0.8472	0.2222	0.5926	-0.4074	*R*
	III	1.0708	0.9180	1.0836	0.0836	*C*
	IV	1.0853	0.5714	1.1755	0.1755	*C*
	V	0.9722	-0.0000	-0.0005	-1.0005	*R*
	VI	0.9583	0.0000	0.0001	-0.9999	*R*
	VII	0.9722	-0.0000	-0.0005	-1.0005	*R*
	VIII	-	-	-	-	*N*
P2	I	1.0000	0.0069	1.0000	0.0000	*R*
	II~III	-	-	-	-	*N*
	IV	0.9930	0.0069	0.4972	-0.5028	*R*
	V	0.9650	0.0067	0.1608	-0.8392	*R*
	VI	0.9720	0.0068	0.1946	-0.8054	*R*
	VII	0.9720	0.0068	0.1946	-0.8054	*R*
	VIII	0.9510	0.0066	0.1187	-0.8813	*R*
P3	I~V	-	-	-	-	*N*
	VI	0.9444	-0.0000	-0.0002	-1.0002	*R*
	VII	0.9167	0.0000	0.0001	-0.9999	*R*
	VIII	0.9861	-0.0000	-0.0005	-1.0005	*R*

C: cluster distribution, *R:* random, *N:* lack of this type

However, aggregation index of *P. syluestriformis* population of the scattered community below 1000 m above sea level showed that only one individual of I age-class was present in the investigated community, the individuals of II-III age-classes were missing, and the individuals of IV-VIII age-classes were randomly distributed.

Aggregation index of *P. syluestriformis* population of the scattered community above 1000 m above sea level showed that there were no individuals of I-V age-classes in the community, and only individuals of VI-VIII age-classes had the spatial distribution pattern of random distribution.

Analysis of niche breadth measurement results

Niche breadth is an indirect measurement of the scale and population dynamics of the population's ability to use environmental resources. The niche breadth depends on the quantitative expression of species' position and role in the community, which can better explain the environmental adaptability and resource utilization ability of the population during the succession process. The greater the niche breadth of the population, the stronger its ability to adapt to the environment, the fuller the utilization of various resources, and the more dominant position it often plays in the community. To overcome the impossibility of comparing the niche of different communities and within the same community, levins index and Hurlbert index were used to study the niche breadths of major populations. Comprehensive analysis of survey plots, niche

http://www.aloki.hu ● ISSN 1589 1623 (Print) ● ISSN 1785 0037 (Online)
DOI: http://dx.doi.org/10.15666/aeer/1605_55395549
© 2018, ALÖKI Kft., Budapest, Hungary

breadths were calculated of 12 species with relatively high important value and wide distribution range by using *Equations 1* and *2*.

It could be seen in *Table 4* that the order of the levins niche breadth index was P. syluestriformis > A. nephrolepis>L. olgensis>B. platyphylla>T. amurensis>U. japonica >A. tegmentosum>Q. mongolica>P. jezoensis> A. mono>S. pohuashanensis>P. koraiensis. The maximum of Levins niche breadth of P. syluestriformis population was 5.3094, indicating that P. syluestriformis had obvious superiority in each resource location. As one of the community species, it was distributed in 8 resource locations. The second was A. nephrolepis, and the Levins niche breadth was 4.1782, and it also occupied a wide range of niches. It was distributed in all six resource locations except for pure forests. B. platyphylla and T. amurensis had wide niche amplitude and wide distribution, the Levins niche breadth was 3.3196 and 3.1864, respectively. L. olgensis and P. koraiensis were the main associated tree species in the arbor layer of scattered communities, and the Levins niche breadth was 3.4050 and 2.3611, respectively.

Table 4. *Niche breadth of main species in arbor layer of P. syluestriformis community*

Species number	*Pi*1	*Pi*2	*Pi*3	*Pi*4	*Pi*5	*Pi*6	*Pi*7	*Pi*8	*Bi*	*Ba*
P. syluestriformis	0.265	0.273	0.083	0.083	0.040	0.130	0.021	0.106	5.3094	0.6637
Q. mongolica	0.034	0.009	0.134	0.505	0.000	0.000	0.000	0.318	2.6626	0.5325
T. amurensis	0.048	0.018	0.000	0.462	0.242	0.000	0.197	0.034	3.1864	0.5311
U. japonica	0.314	0.228	0.456	0.000	0.000	0.000	0.000	0.000	2.7771	0.9257
P. jezoensis	0.000	0.016	0.000	0.299	0.000	0.011	0.534	0.139	2.5296	0.5059
L. olgensis	0.000	0.000	0.339	0.290	0.000	0.299	0.072	0.000	3.4050	0.8513
B. platyphylla	0.049	0.004	0.383	0.054	0.000	0.035	0.370	0.104	3.3196	0.4742
A. mono	0.001	0.000	0.208	0.000	0.000	0.103	0.580	0.108	2.4885	0.4977
P. koraiensis	0.000	0.000	0.011	0.034	0.572	0.021	0.302	0.059	2.3611	0.3935
A. nephrolepis	0.000	0.000	0.001	0.355	0.090	0.141	0.205	0.209	4.1782	0.6964
S. pohuashanensis	0.000	0.000	0.026	0.061	0.000	0.061	0.270	0.583	2.3638	0.4728
A. tegmentosum	0.029	0.000	0.107	0.126	0.000	0.555	0.184	0.000	2.7089	0.5418

Taking full account of the fact that the resource status was highly variable under actual circumstances, the Hurlbert niche breadth value was calculated. The index took into account the magnitude of each resource's state. The analysis data showed that the Hurlbert niche breadth was the largest due to *U. japonica,* it had a larger important value in the *P. syluestriformis* pure forest, its utilization of resources and space in forest was similar to that of *P. syluestriformis*. The Hurlbert niche breadth of other species were basically the same as the Levins niche breadth, which reflected the status and the distribution range of major arbor populations determined the niche breadth.

Analysis of niche overlap measurement results

Niche overlap is the similarity between two species in relation to ecological factors. Niche overlap occurs when two species use the same resource or share one resource (food, nutrients, space, etc.). Niche overlaps make connections between species, and the niche overlap value can explain the competition or coexistence between species.

http://www.aloki.hu ● ISSN 1589 1623 (Print) ● ISSN 1785 0037 (Online)
DOI: http://dx.doi.org/10.15666/aeer/1605_55395549
© 2018, ALÖKI Kft., Budapest, Hungary

Calculation of niche overlap index by *Equation 3,* as shown in *Table 5,* the maximum niche overlap occurred between *A. mono* and *B. platyphyll*, followed by *A. Nephrolepis* and *T. amurensis*, indicating that there may be higher niche overlap among species with narrow niche breadth. There was a large niche overlap between *P. syluestriformis* and *U. japonica* population, with an overlap index of 0.704, followed by *L. olgensis*, *A. tegmentosum*, *Q. mongolica*, *L. olgensis* and *A. nephrolepis*, with niche overlap indices of 0.395, 0.392, 0.369, 0.368 and 0.367, respectively.

In the communities of natural *P. syluestriformis* population, the degree of niche overlap of various populations was great, the relationship between species was complex, the trend of resource sharing was obvious, and the utilization of resources by species was similar. The niche overlap of populations with large importance value and wide niche breadth was greater than that of other populations. On the contrary, the niche overlap of populations with small importance value and narrow niche breadth was smaller than that of other populations.

Table 5. *Niche overlaps of main species in arbor layer of P. syluestriformis community*

Species	*P. syluestriformis*	*Q. mongolica*	*T. amurensi*	*U. japonica*	*P. jezoensis*	*L. olgensis*	*B. platyphylla*	*A. mono*	*P. koraiensi*	*A. nephrolepis*	*S. pohuashanensis*	*A. tegmentosum*
P. syluestriformis	1	0.368	0.302	0.704	0.206	0.395	0.310	0.198	0.148	0.367	0.291	0.392
Q. mongolica		1	0.716	0.201	0.507	0.578	0.337	0.161	0.094	0.820	0.550	0.212
T. amurensis			1	0.058	0.703	0.488	0.337	0.331	0.590	0.849	0.276	0.280
U. japonica				1	0.007	0.477	0.583	0.251	0.013	0.002	0.029	0.160
P. jezoensis					1	0.377	0.664	0.820	0.440	0.801	0.602	0.371
L. olgensis						1	0.614	0.416	0.118	0.604	0.178	0.765
B. platyphylla							1	0.888	0.349	0.454	0.493	0.409
A. mono								1	0.450	0.504	0.563	0.482
P. koraiensis									1	0.442	0.284	0.183
A. nephrolepis										1	0.651	0.539
S. pohuashanensis											1	0.235
A. tegmentosum												1

Discussion

The niche breadth of the populations in each community depends on the adaptability of the species to the environment, the intensity of interspecific competition, and the distribution of environmental factors (Chen et al., 2014).

This research found that the niche breadth of *P. syluestriformis* was large in the community, indicating that the species had strong adaptability to the environment. Wei Zhiqin and others thought that rare and endangered plants were mostly inhibited in the community, and the niche was very narrow (Wei et al., 2004). The conclusion of this study is contrary to it. The reason may be that, on the one hand, it is possible that the purpose of the study is to use *P. syluestriformis* as the target tree. When selecting the

http://www.aloki.hu ● ISSN 1589 1623 (Print) ● ISSN 1785 0037 (Online)
DOI: http://dx.doi.org/10.15666/aeer/1605_55395549
© 2018, ALÖKI Kft., Budapest, Hungary

plots, the gathering community of *P. syluestriformis* was artificially selected as the survey site, but this did not affect the community structure and its status in the community. On the one hand, it may be because *P. syluestriformis* itself had a special habitat requirement, and the population had a widening niche breadth to obtain sufficient resources (Zhang, 2011).

This research reflects that the view is consistent with Liu Wei's research on the niche of main plant species of the Spruce-fir forests in Changbai Mountain, that is, the greater niche breadth, the greater overlap (Liu and Cao, 2011). However, due to the individual niche breadth, the species' biological and ecological characteristics are unnecessarily the same, and the niche overlap between them is unnecessarily high. It is considered that the decrease in the degree of overlap reflects the differentiation of inter-species resource utilization (Du et al., 2015). Therefore, for species pairs with large niche overlap in the community, it is considered that there are two possibilities: one is that there is a competitive relationship while sharing resources among the species, and the other is that the resources are similarly used while promoting the relationship between the species (Xu et al., 2014). Vannette proposed the niche construction hypothesis, which held the view that if the niche of species was divided into three parts: niche overlap between species, the environmental impact niche and the requirement niche of environmental resources, the prediction of community construction based on niche would be more accurate (Vannette and Fukami, 2014).

Field investigations showed that there were fewer young seedlings of *P. syluestriformis* under the forest, indicating that the habitat of *P. syluestriformis* was higher than the interaction between the species. This paper only explored the resource utilization status between *P. syluestriformis* and the current community dominant species from the perspective of community science. The resource utilization ability of *P. syluestriformis* under different growth conditions was not compared, and further research would be needed. Besides, the distribution of two communities of *P. syluestriformis* could be regarded as the key protection habitat, and the difference of population dynamics caused by the difference of their habitats needed to be further explored.

Conclusions

The research showed that populations with similar habitat requirements could form a good symbiotic relationship under the condition of sufficient resources, which supported the theory that niche overlap and competition were not related. There were relatively few individuals in each resource location of *P. syluestriformis*, and most of them were older, occupying the absolute superiority in the height niche of the arbor layer, and occupying the upper layer of the forest canopy and occupying the absolute dominant position in the community.Therefore, this advantage of *P. syluestriformis* was temporary, and the succession dynamics of *P. syluestriformis* populations were mainly characterized by narrow geographical distribution and narrow habitat, few populations, no individual seedlings and saplings, and lack of self-renewal ability, so they belonged to the recession-type populations. After a certain period of succession, it would probably be replaced by other arbor species, which had many saplings, and had relatively large niche overlap with its *P. syluestriformis,* such as *P. koraiensis, A. nephrolepis,* and so on.

http://www.aloki.hu ● ISSN 1589 1623 (Print) ● ISSN 1785 0037 (Online)
DOI: http://dx.doi.org/10.15666/aeer/1605_55395549
© 2018, ALÖKI Kft., Budapest, Hungary

The reason for the rarity of *P. syluestriformis* was mainly caused by the combination of internal and external factors. The internal factors were the defects of ecological and biological characteristics of *P. syluestriformis*. The ecological adaptability of *P. syluestriformis* was relatively narrow and the distribution area was limited; the seed regeneration was difficult, and the ability of self-regeneration was extremely lacking; the resources for the growth of seedlings and saplings were limited. External factors included historical overuse and habitat destruction, and natural communities were largely absent. Therefore, the community resources of Changbai Mountain area were very rare. The protection of wild populations and their habitats of *P. syluestriformis* was the most effective protection measure. With establishment of a different forest for further implementation of *P. syluestriformis* by local conservation and artificial cultivation, the artificial cultivated individuals were transplanted into their original habitats. In this way, they could be naturalized into the natural environment, could develop normally and produce future generations, and consequently expand the size of natural populations.

Acknowledgements. This research was financially supported by the 12th Five-Year Plan National Science and Technology support Project of China (Grant No. 2012BAD22B040102), and the Scientific and Technological Development Project of Jilin Province, China (Grant No. 20180101017JC).

REFERENCES

[1] Chang, C., Wang, X., Yang, R. et al. (2015): A quantitative characterization method for alpine vegetation zone based on DEM and NDVI. – Geographical Research 34(11): 2113-2123.

[2] Chen, J., Liu, X. L., He, F. et al. (2010): Niche characteristics of dominant woody populations in *Quercus Aquifo Liodes* shrub community in Balangshan Mountain in Wolong Nature Reserve. – Scientia Silvae Sinicae 46(3): 23-28.

[3] Chen, X., Bu, Z. J., Wang, S. Z. et al. (2009): Niches of seven bryophyte species in Hani peat land of Changbai Mountains. – Yingyong Shengtai Xuebao 20(3): 574-578.

[4] Chen, Y. K., Yang, Q., Mo, Y. N. et al. (2014): A study on the niches of the state's key protected plants in Bawangling, Hainan Island. – Chinese Journal of Plant Ecology 38(6): 576-584.

[5] Cheng, J. Y., Cao, W. J., Yang, L. (2013): Research on wild interindividual seed trait diversity of *P. syluestriformis*. – Journal of Jilin Forestry Science and Technology 42(1): 1-5.

[6] Du, D. L., Su, J., Liu, Y. C. et al. (2015): Study on the niche of *Gordonia acuminata* population in Jinyun mountain. – Guihaia 19(4): 315-322.

[7] Grinnell, J. (1917): The niche-relations of the California Thrasher. – Auk 34: 427-433.

[8] Guo, H. (2004): Studies on Spatial Pattern of *Larix chinensis* Populations in Qinling Mountain. – Shanxi Normal University, Xi'an, China.

[9] Hurlbert, S. H. (1978): The measurement of niche overlap and some relatives. – Ecology 59: 67-77.

[10] Jin, H., Zhao, Y., Zhao, W. et al.(2015): Natural population status and endangered mechanism of *Pinus sylvestriformis* in Changbai Mountain. – Journal of Beihua University (Natural Science) 16(5): 661-665.

[11] Levins, R. (1968): Evolution in Changing Environments: Some Theoretical Explorations. – Princeton University Press, USA.

[12] Li, J., Zhu, J. Z., Zhu, Q. K.(2003): A review on niche theory and niche metrics. – Journal of Beijing Forestry University 25(1): 100-107.

http://www.aloki.hu ● ISSN 1589 1623 (Print) ● ISSN 1785 0037 (Online)
DOI: http://dx.doi.org/10.15666/aeer/1605_55395549
© 2018, ALÖKI Kft., Budapest, Hungary

[13] Liu, W., Cao, W. (2011): Niche characteristics of main plant species in spruce-fir forests in Changbai Mountains. – Chinese Journal of Ecology 30(8): 1766-1774.
[14] Lu, Z., Ni, B. C., Fan, R. H. et al. (2004): Introduction research on *P. sylvestriformis*. – Forestry Survey and Design 141(1): 32-34.
[15] Pianka, E. R. (1973): The structure of lizard communities. – Annual Review of Ecology and Systematics 4: 53-74.
[16] Vannette, R. L., Fukami, T. (2014): Historical contingency in species interactions: towards niche-based predictions. – Ecology Letters 17(1): 115-124.
[17] Wang, S. X. (2007): Biological Resources of Changbai Mountain Protection and Development Zone. – Liaoning Science and Technology Press, Shenyang, China.
[18] Wang, W. (2012): Characteristics of Reproduction and Spread for *Aconitum leucostomum* Worosch Population in Nalati Mountain Meadow. – Xinjiang Agricultural University, Urumchi, China.
[19] Wei, Z. Q., Li, X. G., He, Y. Q. et al. (2004): Study of niche characteristics of the main tree populations of a rare and endangered plant community. – Journal of Southwest Agricultural University (Natural Science) 26(1): 1-4.
[20] Xu, D. J., Wang, P. P., He, Y. J. et al. (2014): Niche characteristics of dominant plant populations of *Alsophila spinulosa* community of Danxia landform in North Guizhou. – Bulletin of Botanical Research 34(5): 612-618.
[21] Ye, J., Hao, Z. Q., Xie, P. et al. (2011): Habitat associations of saplings and adults in an old-growth temperate forest in the Changbai Mountains, northeastern China. – Forestry Studies in China 13(1): 13-22.
[22] Zhang, J. T. (2011): Mathematical Biology. – Science Press, Beijing, China.
[23] Zou, C. J., Bu, J., Xu, W. D. (1995): Biomass and productivity of *P. sylvestriformis* plantation. – Chinese Journal of Applied Ecology 6(2): 123-127.

http://www.aloki.hu ● ISSN 1589 1623 (Print) ● ISSN 1785 0037 (Online)
DOI: http://dx.doi.org/10.15666/aeer/1605_55395549
© 2018, ALÖKI Kft., Budapest, Hungary

THE IMPORTANT ROLE OF AMINOETHOXYVINYLGLYCINE (AVG) PRE-HARVEST APPLICATION IN FRUIT HARVEST TIME, FRUIT QUALITY AND MINERAL ELEMENT CONTENTS OF 'AKÇA' (*PYRUS COMMUNIS* L.)

ÇETINBAŞ, M.

Fruit Research Institute, Egirdir, Isparta, Turkey
(e-mail: melikecetinbas@gmail.com; phone:+90-246-313-2420; fax:+90-246-313-2425)

(Received 19th Jun 2018; accepted 7th Aug 2018)

Abstract. 'Akça' pear is one of the most grown early varieties in Turkey. Although it is of high quality, it forms smaller fruits than other early varieties. In order to investigate the role of aminoethoxyvinylglycine (AVG) application in the harvest time, fruit yield and quality of 'Akça' pears, this study was carried out for 2 years in 2012 and 2013 in an orchard located in Isparta-Egirdir (Turkey) Fruit Research Institute. ReTain plant growth regulator was used for AVG. ReTain containing 15% AVG was applied to the 'Akça' pear fruits and leaves. Four concentrations of AVG (0, 100, 125, 150 ppm) and three application times [30, 21, 7 days before commercial harvest (DBH)] were evaluated using the field system. Harvest time, fruit yield, fruit size, fruit weight, fruit flesh firmness, titratable acidity (TA), soluble solid contents (SSC), fruit color, ethylene production and respiration rate, and nutritional status of fruits were determined at the harvest time. In addition, the effect of AVG applications on some leaf properties (macro-micro element content, leaf area and chlorophyll) was determined. As a result, 30 and 21 DBH AVG applications delayed the harvest time for 3 days. AVG applications reduced both ethylene production and respiration rate. All AVG applications dramatically increased fruit size (2-16%) and fruit weight (7-57%) as well as fruit flesh firmness (1-55%) of the 'Akça' pear. Given all these results, it is considered that 21 DBH AVG applications at 100 ppm will be suitable for the 'Akça' pear in terms of harvest time and fruit and leaf quality parameters.
Keywords: *ethylene inhibitor, pear, leave properties, plant growth regulator, nutritional status*

Introduction

The amount of pears produced in the world is 25.798.644 tons and, with a production amount of 462.336 tons, pear takes the 5th place in Turkey (FAOSTAT, 2018). However, it falls behind other European countries in terms of both yield per decare and exportation. One of the biggest reasons for this is that products with sufficient quality cannot be obtained due to problems related to cultivation techniques. There are many studies conducted in the world for the purpose of increasing fruit quality, and most of them are on plant growth regulators. The most frequently used natural plant growth regulator in the world is the ethylene group (23%), followed by the auxin group and gibberellins (17%), respectively. Cytokinin and Dormin are not yet widely used in the world (Barut, 1995). In recent years, AVG (aminoethoxyvinylglycine), an ethylene blocker, has been used to increase pre-harvest fruit fall and fruit quality. AVG is commercially sold worldwide as ReTain® plant growth regulator. ReTain contains 15% AVG and is a human and environmentally friendly, organic commercial product (Rath and Prentice, 2004) registered in 2001 for use in apples, peaches and nectarine fruits in Australia. Preharvest application of AVG 1–4 weeks prior to harvest inhibits biosynthesis of ethylene and influences abscission, ripening and senescence and reduces quality loss after harvest in many crops (Martinez-Romero et al., 2007; Lurie, 2008; Pech et al., 2012; Kuçuker et al., 2015b; Pasa, et al., 2017). Jobling et al. (2003) found

http://www.aloki.hu ● ISSN 1589 1623 (Print) ● ISSN 1785 0037 (Online)
DOI: http://dx.doi.org/10.15666/aeer/1605_55515569
© 2018, ALÖKI Kft., Budapest, Hungary

that AVG treated plums allowed a delay in harvested timing, and resulted in retaining higher firmness and SSC in comparison with untreated fruit, suggesting that accumulation of soluble solids can take place when fruits are on trees for longer. Dussi et al. (2002) applied 14 DBH 125 and 180 ppm AVG to 'Williams' pears. In this study, AVG had no effect on pre-harvest fall, but both fruit size and fruit hardness increased. It was reported that 21, 14 and 7 DBH 125 ppm AVG applied to 'Abbe Fetel' pear delayed the harvest for 5 to 15 days (Andreotti et al., 2004). The pear variety 'Akça' is desired by producers and consumers for being an early comer and its quality characteristics. The fruit size of this variety is slightly smaller than other early comers, meaning a decrease in its market price and a disadvantage for producers. The purpose of this study is to determine the appropriate dose and application time of AVG as well as the effectiveness of AVG applications to improve the fruit quality of the 'Akça' pear.

Material and methods

Plant-chemical materials and experiment design

The plant material of the study was the 12-year-old Akça/Quince A trees in the pear orchard of Egirdir Fruit Research Institute Directorate Isparta, Turkey) Cultural practices such as irrigation, fertilization, plant protection and pruning were carried out regularly during the trial. Thinning was not performed for the fruits. In our study, ReTain (15% AVG) plant growth regulator (Valent BioScience Corporation) was used as the chemical material, and AVG doses were calculated based on the active substance. Four doses of AVG – namely, 0 (control), 100, 125 and 150 ppm – were used. These doses were applied to all fruits and leaves of the 'Akça' pear 30, 21, 7 days before harvest (DHB) for two years. All spray solutions contained 0.2% 'Tween 20' as surfactant. Control trees were sprayed with water + surfactant. A knapsack sprayer was used to apply AVG onto fruits and leaves at the rate of 8 L per tree (*Fig. 1*). The experiment was set up according to the design pattern of 4 repetitive random blocks, and each repetition consisted of 1 tree.

Figure 1. *'Akça' pear and application*

Determination of the effect of applications on harvest time

Determination of harvest time; observation of the fruit size, greenish-yellow coloration of the fruit ground color, hardness of the fruit flesh, and formation of the fruit top color. Harvest was carried out according to these harvest criteria and harvest time

http://www.aloki.hu ● ISSN 1589 1623 (Print) ● ISSN 1785 0037 (Online)
DOI: http://dx.doi.org/10.15666/aeer/1605_55515569
© 2018, ALÖKI Kft., Budapest, Hungary

scales (Ozelkok and Kaynaş, 1995), and the effect of AVG applications on harvest time was determined.

The effect of applications on yield and some fruit quality properties

Of the trees from each application, yield (kg tree^{-1}) per tree and yield (kg cm^{-2}) per trunk section area were determined. Average values were calculated by measuring the width (mm) and length (mm) of the fruit with the help of a calliper. The average fruit weight (g) of the fruit was calculated by weighing. Flesh firmness measurements were determined as Newton (N) with Lloyd Instruments LF Plus (Ametek, U.K.) texturing equipment. Using a CR-300 Minolta (Japan) color meter and taking measurements from both cheek areas of the fruits, fruit color was determined by CIE L*, a*, b*, C* and Hu°. SSC (with digital refractometer, %) and TA (titration method, %) were determined.

The effect of applications on ethylene production and respiratory rate in fruits

As reported by Dilmaçunal (2009), pears weighing approximately 1 kg were put into jars and kept at 20 ± 1 °C for 24 h to determine ethylene production (μL kg^{-1} h) and respiratory rate (μL kg^{-1} h). Ethylene production and respiratory rate were determined by using gas chromatography.

The effect of applications on fruit and leaf mineral element contents

N (nitrogen) analysis in fruit and leaf

In the plant sample burned with a salicylic-sulfuric acid mixture of 2.5%, ammonia formation was obtained in the base environment of the kjeldahl distillation unit. The ammonia formed was then kept in boric acid and titrated with 0.1 N sulfuric acid. It was calculated as shown in the formula below (Ryan et al., 2001) (*Eq. 1*).

$$N\% = \frac{(T-B) \times N \times 1.4}{S} \quad \text{(Eq.1)}$$

T: Amount of sulfuric acid consumed for plant sample titration
B: Amount of sulfuric acid consumed for stratum corneum (witness) titration
N: Normality of sulfuric acid
S: Amount of plant sample used in the analysis
1.4: Coefficient

P (phosphorus), K (potassium), Ca (calcium), Mg (magnesium), Cu (copper), Fe (iron), Mn (manganese), Zn (zinc), B (boron) analysis in fruit and leaf

Since a considerable amount of boron is lost during wet combustion, dry combustion was performed. Reading was made by ICP (Inductively Coupled Plasma Atomic Emission Spectophometer) (Ryan et al., 2001). The following steps were taken as part of dry combustion: 0.5 g ground plant material was put into porcelain crucibles, which were then placed into the muffle furnace. Furnace temperature was gradually increased to 550 °C. After reaching 550 °C, combustion continued for 6 h. Following combustion, 5 ml 2 N HCl was added into the cooled porcelain crucibles and the samples were dissolved and stirred with a plastic stick. After 15-20 min, pure water was added until

http://www.aloki.hu ● ISSN 1589 1623 (Print) ● ISSN 1785 0037 (Online)
DOI: http://dx.doi.org/10.15666/aeer/1605_55515569
© 2018, ALÖKI Kft., Budapest, Hungary

reaching 50 ml and thoroughly stirred. 30 min later, it was filtered using a filter paper, and the extract obtained was read by ICP.

The effect of application on leaf area (LA) and total chlorophyll (spad value)

Total chlorophyll was measured using a portable chlorophyll meter on July 15 (first year) – July 10 (second year) (Minolta SPAD-502, Osaka, Japan). Designed and manufactured based on the principles of Inada (1963), this chlorophyll meter measures the amount of chlorophyll in leaves indirectly. It measures the red and infrared regions in the leaf structure (at 659 nm and 940 nm wavelengths, respectively) to determine the relative chlorophyll density. 15 leaf samples were taken in total from four sides of the trees in all applications, and the surface area of one side of each leaf was calculated as a cm^2 by a digital planimeter (Koizumi KP-90 N) (Kucukyumuk et al., 2015).

Statistical analysis of results

Variance analysis was performed with the obtained data, and differences between the treatments were tested by Duncan's multiple range test at $P < 0.05$ using SSPS (V. 18; Statiscal software, SPSS. Inc., USA) software program. The experiment was based as a completely randomized blocking pattern as four replications and was assigned as one tree for each replication, and was assigned to one tree at each replication with each plot having 20 pear fruits.

Results

Fruit harvest time and yield

The harvest was made 2 times a year for both years, and it was seen that the applications affected harvest dates. In the 1st and 2nd years, the control group and the fruits with 7 DBH AVG ripened at the same time, while the fruits with 30 and 21 DBH AVG ripened later. After reaching maturity for the first harvest, the control and the fruits with 7 DBH AVG were harvested on July 14 in the first year and on July 6 in the second year. On the other hand, other fruits with 30 and 21 DBH AVG were harvested on July 18 in the first year and on July 9 in the second year. It was determined that AVG applications (except for 7 DBH) delayed the harvest maturity of Akça pear for up to 3-4 days. AVG applications did not have any statistically significant effect on yield per tree or yield per trunk section in both years (*Table 1*).

Table 1. *The effect of AVG treatments on yield in the 'Akça' pear, 2012 and 2013*

Application time[1]	AVG doses (ppm)	Yield (kg $tree^{-1}$)		Yield (kg cm^{-2})	
		I. Year	II. Year	I. Year	II. Year
30 d	0	8.52	12.78	0.02	0.29
	100	8.93	13.40	0.02	0.28
	125	9.27	13.90	0.02	0.28
	150	9.60	14.40	0.03	0.32
21 d	0	8.68	12.78	0.03	0.29
	100	10.33	15.50	0.03	0.33
	125	10.73	16.10	0.03	0.36
	150	10.33	15.50	0.03	0.40

http://www.aloki.hu ● ISSN 1589 1623 (Print) ● ISSN 1785 0037 (Online)
DOI: http://dx.doi.org/10.15666/aeer/1605_55515569
© 2018, ALÖKI Kft., Budapest, Hungary

7 d	0	8.22	12.78	0.02	0.29
	100	13.20	19.80	0.04	0.48
	125	10.70	16.05	0.03	0.37
	150	9.80	14.70	0.03	0.36
Time means					
30		9.08	13.62	0.02	0.29
21		10.02	14.97	0.03	0.34
7		10.48	15.83	0.03	0.37
	Dose means				
	0	8.47	12.78	0.02	0.29
	100	10.82	16.23	0.03	0.36
	125	10.23	15.35	0.03	0.34
	150	9.91	14.87	0.03	0.36
P values					
Time (T)		0.275	0.251	0.267	0.096
AVG dose (D)		0.702	0.748	0.956	0.864
T x D		0.283	0.326	0.730	0.231

[1]Days before harvest (DBH)

Fruit quality

As a result of the variance analysis performed in both application years, the time x dose interactions were found statistically significant ($p < 0.05$) in terms of fruit width (*Table 2*). In both years, the AVG applications increased fruit width. The applications with the highest fruit width in the first and second years were 21 DBH 100 ppm AVG (48.32 mm) and 30 DBH 100 ppm AVG (49.54 mm), respectively (*Table* 2). The effect of AVG applications on fruit length was statistically significant ($p < 0.05$) only in the first year as time x dose interaction (*Table* 2). Just like in fruit width, the applications with the highest fruit length were 21 DBH 100 ppm AVG (1st year). On the other hand, the lowest fruit length was observed in the control fruits with 7 DBH AVG application (1st year) (*Table 2*). Fruit weight increased with the applications in both years, and the time x dose interaction was found to be statistically significant in the analysis of variance ($p < 0.05$). The heaviest fruits were obtained from 30 and 21 DBH 100 ppm AVG applications. The least heavy fruits were again obtained from the controls (*Table 2*).

Table 2. *The effect of AVG treatments on fruit width, length and weight in the 'Akça' pear, 2012 and 2013*

Application time[1]	**AVG doses (ppm)**	**Fruit width (mm)**		**Fruit length (mm)**		**Fruit weight (g)**	
		I. Year	**II. Year**	**I. Year**	**II. Year**	**I. Year**	**II. Year**
30 d	0	45.02c-e*	42.53b*	56.79e-g*	79.55	53.17de*	47.86c*
	100	47.81ab	49.54a	63.32bc	69.64	68.07a	71.28a
	125	47.54ab	48.75a	64.72b	68.89	64.39ab	70.42a
	150	47.07a-d	48.01a	62.81b-d	68.08	60.27bc	67.00a

http://www.aloki.hu ● ISSN 1589 1623 (Print) ● ISSN 1785 0037 (Online)
DOI: http://dx.doi.org/10.15666/aeer/1605_55515569
© 2018, ALÖKI Kft., Budapest, Hungary

21 d	0	45.74b-e	42.30b	55.97fg	60.81	53.71c-e	46.50c
	100	48.32a	49.23a	68.61a	70.64	67.10a	73.26a
	125	47.62ab	48.44a	65.68ab	66.09	64.06ab	67.41a
	150	46.31a-d	48.76a	62.16b-d	69.99	57.17cd	71.77a
7 d	0	44.05e	42.79b	53.78g	63.30	49.01e	49.17c
	100	45.89b-e	48.38a	60.09c-e	65.58	55.84cd	67.43a
	125	44.97de	48.99a	59.50d-f	65.14	52.62de	68.20a
	150	47.12a-c	44.10b	60.97cd	56.09	60.14bc	61.12b
Time means							
30		46.86	47.21	61.91	71.54	61.48	64.14
21		47.00	47.18	63.11	66.88	60.51	64.74
7		45.51	46.07	58.59	62.53	54.40	61.48
	Doses means						
	0	44.94	42.54	55.52	67.89	51.97	47.84
	100	47.34	49.05	64.01	68.62	63.67	70.66
	125	46.71	48.73	63.30	66.71	60.36	68.68
	150	46.83	46.96	61.98	64.72	59.19	66.63
P values							
Time (T)		0.037	0.629	0.032	0.083	0.015	0.710
AVG Doses (D)		0.649	0.499	0.459	0.177	0.283	0.807
T x D		0.002	0.000	0.000	0.465	0.000	0.000

[1]Days before harvest (DBH)
*Each column, values followed by the same letter are not significantly different at $p < 0.05$ level according to Duncan's multiple range test

The time x dose interaction of AVG applications was statistically significant ($p < 0.05$) in terms of fruit flesh firmness in both years. In both years, fruit flesh firmness increased with the applications, and the fruit flesh firmness of the applications of 21 DBH was higher than others. 21 DBH 100 ppm AVG in the first year and 30 DBH 150 ppm AVG in the second year gave the hardest fruits (*Table 3*).

Table 3. *The effect of AVG treatments on fruit flesh firmness, SSC and TA in the 'Akça' pear, 2012 and 2013*

Application time[1]	**AVG doses (ppm)**	**Firmness (N)**		**SSC (%)**		**TA (%)**	
		I. Year	**II. Year**	**I. Year**	**II. Year**	**I. Year**	**II. Year**
30 d	0	88.99c*	82.22b*	12.73b*	12.13	0.17a-d*	0.17b-d*
	100	89.77bc	94.14ab	11.23d	12.83	0.17a-d	0.17b-d
	125	92.33b	97.00ab	11.33d	12.27	0.15d	0.16d
	150	90.93b	104.13a	11.87cd	12.33	0.17a-d	0.17b-d
21 d	0	86.30c	83.33b	12.80ab	12.27	0.17a-d	0.16d
	100	95.15a	93.83ab	11.90cd	12.00	0.19a	0.19a
	125	93.00a	96.95ab	12.53bc	12.07	0.17a-d	0.16d
	150	95.02a	100.08ab	12.60b	12.23	0.16b-d	0.17b-d

http://www.aloki.hu ● ISSN 1589 1623 (Print) ● ISSN 1785 0037 (Online)
DOI: http://dx.doi.org/10.15666/aeer/1605_55515569
© 2018, ALÖKI Kft., Budapest, Hungary

7 d	0	89.83bc	63.97c	12.90ab	12.33	0.17a-d	0.18ab
	100	91.35b	89.60ab	12.83ab	12.37	0.16cd	0.17b-d
	125	91.98b	87.21ab	13.47a	11.80	0.17a-c	0.18ab
	150	87.39c	99.37ab	12.87ab	12.67	0.18ab	0.18ab
Time means							
30		90.51	94.37	11.79	12.39	0.17	0.01
21		92.37	93.55	12.46	12.14	0.17	0.01
7		90.14	85.04	13.02	12.29	0.18	0.02
	Dose means						
	0	88.37	76.51	12.81	12.24	0.17	0.01
	100	92.09	92.52	11.99	12.40	0.17	0.01
	125	92.44	93.72	12.44	12.04	0.17	0.01
	150	91.11	101.19	12.44	12.41	0.17	0.01
P values							
Time (T)		0.406	0.176	0.000	0.371	0.375	0.001
AVG Dose (D)		0.954	0.943	0.370	0.219	0.375	0.896
T x D		0.044	0.006	0.000	0.237	0.051	0.004

[1]Days before harvest (DBH)
*Each column, values followed by the same letter are not significantly different at $p < 0.05$ level according to Duncan's multiple range test

In the first year, the applications increased the amount of SSC, and the time x dose interaction was found to be significant ($p < 0.05$) as a result of the variance analysis. In the second year, however, the applications were statistically insignificant. In the first year, the highest SSC (13.47%) was found in 7 DBH 125 ppm AVG *(Table 3*). The time x dose interaction was statistically significant ($p < 0.05$) in terms of TA in both years, and the highest TA was obtained from 21 DBH 100 ppm AVG (*Table 3*).

In the first year, the effect of AVG applications on fruit color values (L*, a*, b*, C*, h°) was statistically significant ($p < 0.05$) in time x dose interactions (*Table 4*).

Table 4. *The effect of AVG treatments on fruit color (L*, a*, b*, C*, h°) in the 'Akça' pear, 2012*

Application time[1]	**AVG doses (ppm)**	**L***	**a***	**b***	**C***	**h°**
30 d	0	72.79a*	-19.11a*	48.47ab*	52.16bc*	111.54f*
	100	70.43de	-21.19cd	48.01bc	52.52bc	113.82b-d
	125	69.19f	-21.84de	47.32d	52.13bc	114.79ab
	150	69.92d-f	-21.59c-e	47.37d	52.07c	114.51a-c
21 d	0	72.53ab	-19.18a	48.60ab	52.32bc	111.55f
	100	67.96g	-22.21e	47.16d	52.14bc	115.23a
	125	69.54ef	-21.82de	47.58cd	52.35bc	114.64a-c
	150	70.48de	-21.30c-e	48.23a-c	52.74ab	113.84b-d
7 d	0	71.62bc	-20.15b	48.18bc	52.26bc	112.72e
	100	70.65c-e	-21.07b-d	48.85a	53.24a	113.35de
	125	70.52de	-20.82bc	48.43ab	52.76ab	113.27de
	150	70.71cd	-20.98b-d	48.00bc	52.41bc	113.63c-e

http://www.aloki.hu ● ISSN 1589 1623 (Print) ● ISSN 1785 0037 (Online)
DOI: http://dx.doi.org/10.15666/aeer/1605_55515569
© 2018, ALÖKI Kft., Budapest, Hungary

Time means						
30		70.58	-20.93	47.79	52.22	113.66
21		70.13	-21.13	47.89	52.39	113.82
7		70.87	-20.75	48.37	52.67	113.24
	Dose means					
	0	72.31	-19.48	48.42	52.24	111.94
	100	69.68	-21.49	48.01	52.63	114.13
	125	69.75	-21.49	47.78	52.41	114.23
	150	70.37	-21.29	47.87	52.41	113.99
P values						
Time (T)		0.431	0.706	0.041	0.032	0.517
AVG Dose (D)		0.902	0.965	0.758	0.670	0.218
T x D		0.000	0.000	0.000	0.006	0.000

[1]Days before harvest (DBH)
*Each column, values followed by the same letter are not significantly different at $p < 0.05$ level according to Duncan's multiple range test

The values of L*, which indicates brightness, decreased with the AVG applications. The lowest L* was obtained from 21 DBH 100 ppm AVG (67.96). The values of a*, which indicates redness, also decreased with the applications, and the lowest value was obtained from 21 DBH 100 ppm AVG, which also gave the value of b* indicating yellowness. On the other hand, the highest value of b* was obtained from 7 DBH 100 ppm AVG. As in b* values, the highest C* value was produced by 7 DBH 100 ppm AVG. The hue values of AVG-applied fruits were higher than those of the control fruits, and the highest h° value was produced by 21 DBH 100 ppm AVG (*Table 4*). In the second year of the project, the time x dose interactions of L*, a*, h° values were found to be statistically significant ($p < 0.05$). L* and a* values decreased with the AVG applications, and the lowest L* (67.78) and a* (22.58) values were observed in 21 DBH 150 ppm AVG. It was found that the h° values of the AVG applications were higher than the control fruits, and the highest h° value was obtained from 21 DBH 125 ppm AVG (*Table 5*).

Table 5. *The effect of AVG treatments on fruit color (L*, a*, b*, C*, h°) in the 'Akça' pear, 2013*

Application time[1]	**AVG doses (ppm)**	**L***	**a***	**b***	**C***	**h°**
30 d	0	73.90a*	-19.66ab*	48.36	52.32	112.12b-d*
	100	69.17b	-22.32c	47.46	52.46	115.19a
	125	70.08b	-22.00c	47.53	52.38	114.85a
	150	69.96b	-22.49c	47.19	52.28	115.49a
21 d	0	73.46a	-19.35ab	48.60	52.48	111.69cd
	100	68.95b	-22.21c	47.93	52.83	114.87a
	125	69.96b	-22.01c	47.69	52.54	114.78a
	150	67.78b	-22.58c	47.10	52.24	115.62a

http://www.aloki.hu ● ISSN 1589 1623 (Print) ● ISSN 1785 0037 (Online)
DOI: http://dx.doi.org/10.15666/aeer/1605_55515569
© 2018, ALÖKI Kft., Budapest, Hungary

7 d	0	74.50a	-18.68a	48.74	52.30	110.94d
	100	69.68b	-21.82c	48.42	53.13	114.29ab
	125	70.73b	-21.07bc	48.19	52.66	113.63a-c
	150	69.93b	-21.30bc	47.72	52.29	114.07a-c
Time means						
30		70.78	-21.62	47.63	52.36	114.41
21		70.04	-21.54	47.83	52.52	114.24
7		71.21	-20.72	48.27	52.60	113.23
	Dose means					
	0	73.95	-19.23	48.56	52.37	111.58
	100	69.27	-22.12	47.93	52.81	114.78
	125	70.25	-21.69	47.80	52.53	114.42
	150	69.22	-22.12	47.34	52.27	115.06
P values						
Time (T)		0.499	0.328	0.115	0.505	0.266
AVG Dose (D)		0.804	0.843	0.471	0.122	0.883
T x D		0.000	0.003	0.066	0.601	0.003

[1]Days before harvest (DBH)
*Each column, values followed by the same letter are not significantly different at $p < 0.05$ level according to Duncan's multiple range test

Ethylene production and respiration rate

In the first year, ethylene production could not be determined. In terms of respiration rate, the time x dose interaction was found statistically significant ($p < 0.05$). In the second year, however, the effect of the applications on both ethylene production and respiration rate was found to be statistically significant ($p < 0.05$) in terms of time x dose interaction (*Table 6*). All AVG applications slowed both ethylene production (μL kg^{-1} h) and respiratory rate (μL kg^{-1} h) in the fruit. The lowest ethylene production was 0.15 μL kg^{-1} h and the lowest respiration rate was 12.32 μL kg^{-1} h obtained from 21 DBH 150 ppm AVG (*Table 6*).

Table 6. *The effect of AVG treatments on ethylene production and respiration rate in the 'Akça' pear, 2012 and 2013*

Application time[1]	**AVG doses (ppm)**	**Ethylene production (μL kg^{-1} h)**		**Respiration rate (μL kg^{-1} h)**	
		I. Year	**II. Year**	**I. Year**	**II. Year**
30 d	0	-	3.54a*	15.41a-c*	28.16a*
	100	-	0.86d-f	15.13bc	18.22b-d
	125	-	1.12c-f	15.87a-c	15.06cd
	150	-	0.28ef	15.96a-c	13.80cd
21 d	0	-	2.98ab	16.72ab	27.38a
	100	-	0.56d-f	16.06a-c	16.55b-d
	125	-	0.82d-f	14.61c	19.08b-d
	150	-	0.15f	15.66a-c	12.32d

http://www.aloki.hu ● ISSN 1589 1623 (Print) ● ISSN 1785 0037 (Online)
DOI: http://dx.doi.org/10.15666/aeer/1605_55515569
© 2018, ALÖKI Kft., Budapest, Hungary

7 d	0	-	2.09bc	17.07a	23.51ab
	100	-	2.02bc	15.06bc	21.41a-c
	125	-	1.56cd	16.54ab	18.14b-d
	150	-	1.23c-e	15.96a-c	17.17b-d
Time means		-			
30		-	1.45	15.59	18.81
21		-	1.13	15.76	18.84
7		-	1.72	16.16	20.06
	Dose means	-			
	0	-	2.87	16.40	26.35
	100	-	1.15	15.41	18.73
	125	-	1.17	15.68	17.43
	150	-	0.55	15.86	14.43
P values		-			
Time (T)		-	0.441	0.427	0.851
AVG Dose (D)		-	0.166	0.218	0.181
T x D		-	0.000	0.049	0.001

[1]Days before harvest (DBH)
*Each column, values followed by the same letter are not significantly different at $p < 0.05$ level according to Duncan's multiple range test

Fruit and leave mineral element contents determination

The effect of AVG applications on the nitrogen contents of fruits was found to be statistically significant ($p < 0.05$) in both years as time x dose interaction. In both years, nitrogen contents increased with 30 and 21 DBH AVG applications but decreased with 7 DBH AVG applications. The highest and lowest nitrogen contents were obtained from 30 DBH 150 ppm AVG and from 7 DBH 125 ppm AVG, respectively (*Table 7*).

Table 7. *The effect of AVG treatments on nitrogen, calcium, magnesium in the 'Akça' pear fruit, 2012 and 2013*

Application time[1]	**AVG doses (ppm)**	**Nitrogen (%)**		**Calcium (ppm)**		**Magnesium (ppm)**	
		I. Year	**II. Year**	**I. Year**	**II. Year**	**I. Year**	**II. Year**
30 d	0	0.50bc*	0.52a*	0.08	0.07a-c*	0.06	0.06
	100	0.56b	0.57ab	0.09	0.09ab	0.07	0.07
	125	0.54bc	0.55ab	0.08	0.07a-c	0.06	0.06
	150	0.72a	0.72a	0.09	0.09a	0.07	0.07
21 d	0	0.39c	0.50b	0.07	0.06c	0.06	0.06
	100	0.55b	0.56ab	0.10	0.09a	0.06	0.06
	125	0.51bc	0.50b	0.05	0.07bc	0.05	0.05
	150	0.55bc	0.55ab	0.09	0.09a	0.07	0.07
7 d	0	0.50bc	0.48b	0.07	0.06c	0.05	0.07
	100	0.42bc	0.42b	0.08	0.08abc	0.05	0.05
	125	0.41bc	0.41b	0.08	0.08abc	0.06	0.06
	150	0.46bc	0.46b	0.08	0.08abc	0.06	0.06

http://www.aloki.hu ● ISSN 1589 1623 (Print) ● ISSN 1785 0037 (Online)
DOI: http://dx.doi.org/10.15666/aeer/1605_55515569
© 2018, ALÖKI Kft., Budapest, Hungary

Time means							
30		0.58	0.59	0.08	0.08	0.06	0.07
21		0.50	0.53	0.08	0.08	0.06	0.06
7		0.45	0.44	0.08	0.08	0.06	0.06
	Dose means						
	0	0.46	0.50	0.07bc	0.07	0.06	0.06
	100	0.51	0.52	0.09ab	0.09	0.06	0.06
	125	0.49	0.49	0.07c	0.07	0.06	0.06
	150	0.57	0.58	0.09a	0.09	0.07	0.07
P values							
Time (T)		0.008	0.002	0.732	0.683	0.155	0.237
AVG Dose (D)		0.154	0.347	0.025	0.000	0.175	0.144
T x D		0.004	0.041	0.195	0.030	0.239	0.187

[1]Days before harvest (DBH)
*Each column, values followed by the same letter are not significantly different at $p < 0.05$ level according to Duncan's multiple range test

In the variance analysis made for calcium content, only the time x dose interaction of the applications in the second year was found statistically significant ($p < 0.05$). In general, calcium content increased with the applications. In terms of magnesium content, however, no statistically significant difference was observed in both years (*Table 7*). In terms of phosphorus and potassium, there was no statistically significant difference in phosphorus content in both years, while the difference between dose averages was statistically significant ($p < 0.05$) in potassium content and the dose of 150 ppm had the highest amount of potassium (*Table 8*).

Table 8. *The effect of AVG treatments on phosphorus, potassium, copper, zinc in the 'Akça' pear fruit, 2012 and 2013*

Application time[1]	**AVG doses (ppm)**	**Phosphorus (ppm)**		**Potassium (ppm)**		**Copper (ppm)**		**Zinc (ppm)**	
		I. Year	**II. Year**	**I. Year**	**II. Year**	**I. Year**	**II. Year**	**I. Year**	**II. Year**
30 d	0	0.12	0.12	1.18	1.18	1.82	1.83	9.17b*	9.41
	100	0.13	0.14	1.21	1.22	3.65	3.76	12.64a	12.80
	125	0.11	0.11	1.04	1.04	2.28	2.15	11.28ab	12.29
	150	0.14	0.14	1.28	1.29	2.68	3.10	13.92a	14.08
21 d	0	0.12	0.12	1.16	1.12	1.74	2.44	9.09b	9.42
	100	0.12	0.12	1.14	1.14	2.30	2.30	11.25ab	11.81
	125	0.08	0.08	0.79	0.79	3.08	2.98	10.90ab	11.20
	150	0.13	0.13	1.21	1.22	3.31	3.21	10.95ab	10.97
7 d	0	0.12	0.12	1.16	1.12	1.67	2.63	9.14b	9.21
	100	0.11	0.11	1.01	1.01	2.44	2.61	8.25b	8.17
	125	0.11	0.12	1.03	1.04	2.56	2.66	8.85b	9.26
	150	0.12	0.12	1.07	1.12	2.93	3.10	10.85ab	10.98

http://www.aloki.hu ● ISSN 1589 1623 (Print) ● ISSN 1785 0037 (Online)
DOI: http://dx.doi.org/10.15666/aeer/1605_55515569
© 2018, ALÖKI Kft., Budapest, Hungary

Time means									
30		0.13	0.13	1.18	1.18	2.61	2.71	11.75	12.15a*
21		0.11	0.11	1.08	1.07	2.61	2.73	10.55	10.85ab
7		0.11	0.12	1.07	1.07	2.40	2.75	9.27	9.40b
	Dose means								
	0	0.12	0.12	1.17a*	1.14a*	1.74	2.30	9.13	9.34
	100	0.12	0.12	1.12a	1.12a	2.79	2.89	10.72	10.93
	125	0.10	0.10	0.95b	0.96b	2.64	2.60	10.34	10.92
	150	0.13	0.13	1.18a	1.21a	2.97	3.14	11.91	12.01
P values									
Time (T)		0.331	0.335	0.260	0.219	0.882	0.995	0.016	0.016
AVG Dose (D)		0.107	0.110	0.017	0.019	0.101	0.300	0.051	0.130
T x D		0.272	0.276	0.059	0.078	0.596	0.608	0.015	0.055

[1]Days before harvest (DBH)
*Each column, values followed by the same letter are not significantly different at $p < 0.05$ level according to Duncan's multiple range test

In both years, the effect of AVG applications on iron content was statistically significant ($p < 0.05$) as time x dose interaction. However, manganese and boron contents were not found to be statistically significant (*Table 9*). The effect of AVG applications on copper and zinc contents is given in *Table 8*. In zinc content, the time x dose interaction was statistically significant ($p < 0.05$) only in the first year of AVG applications. The application with the highest iron content was 30 DBH 150 ppm AVG in both years. On the other hand, the lowest iron content was observed in the control fruits with 7 DBH AVG (*Table 9*).

Table 9. *The effect of AVG treatments on iron, manganese, boron in the 'Akça' pear fruit, 2012 and 2013*

Application time[1]	**AVG doses (ppm)**	**Iron (ppm)**		**Manganese (ppm)**		**Boron (ppm)**	
		I. Year	**II. Year**	**I. Year**	**II. Year**	**I. Year**	**II. Year**
30 d	0	13.90e*	14.45cd*	5.27	5.61	12.00	11.48
	100	19.27ab	18.91ab	7.23	7.73	17.73	17.99
	125	17.33b-d	17.37b-d	6.14	6.41	11.97	12.03
	150	21.21a	21.22a	7.07	7.20	14.71	15.36
21 d	0	13.87e	13.82d	4.84	5.32	12.14	12.71
	100	17.04b-e	17.09b-d	6.60	6.78	12.41	12.28
	125	17.78bc	17.75bc	6.24	6.57	13.02	12.60
	150	17.01b-e	16.86b-d	6.11	6.55	13.39	13.46
7 d	0	14.03e	14.09cd	4.75	5.26	12.60	11.19
	100	14.45de	14.91cd	5.40	5.74	15.21	15.51
	125	14.98c-e	14.96cd	5.87	6.09	14.90	15.18
	150	16.37b-e	16.21b-d	5.67	6.00	11.82	13.40
Time means							
30		17.93	17.99	6.43	6.74	14.10	14.21
21		16.43	16.38	5.95	6.30	12.74	12.76
7		14.96	15.04	5.42	5.77	13.63	13.82

http://www.aloki.hu ● ISSN 1589 1623 (Print) ● ISSN 1785 0037 (Online)
DOI: http://dx.doi.org/10.15666/aeer/1605_55515569
© 2018, ALÖKI Kft., Budapest, Hungary

	Dose means						
	0	13.93	14.12	4.95	5.40	12.25	11.79
	100	16.92	16.97	6.41	6.75	15.12	15.26
	125	16.70	16.69	6.08	6.36	13.30	13.27
	150	18.20	18.10	6.28	6.58	13.31	14.07
P values							
Time (T)		0.019	0.019	0.159	0.107	0.625	0.582
AVG Dose (D)		0.003	0.007	0.055	0.042	0.361	0.191
T x D		0.000	0.002	0.310	0.171	0.659	0.453

[1]Days before harvest (DBH)
*Each column, values followed by the same letter are not significantly different at $p < 0.05$ level according to Duncan's multiple range test

The effect of AVG applications was found to be statistically insignificant on the nitrogen content of leaves but statistically significant ($p < 0.05$) on the magnesium content as time x dose interaction only in the second year and again statistically significant ($p < 0.05$) on the calcium content as time x dose interaction in both years of the project (*Table 10*).

Table 10. *The effect of AVG treatments on nitrogen, calcium, magnesium in the 'Akça' pear leave, 2012 and 2013*

Application time[1]	**AVG doses (ppm)**	**Nitrogen (%)**		**Calcium (ppm)**		**Magnesium (ppm)**	
		I. Year	**II. Year**	**I. Year**	**II. Year**	**I. Year**	**II. Year**
30 d	0	1.98	1.92	1.98b*	1.80b*	0.43	0.47ab*
	100	1.95	1.82	1.78bc	1.55cd	0.40	0.39c
	125	2.07	1.99	2.03ab	2.06a	0.44	0.48a
	150	2.05	1.85	1.95bc	1.64b-d	0.40	0.39c
21 d	0	1.93	1.79	1.79bc	1.82b	0.42	0.48a
	100	1.97	1.89	2.42a	1.76bc	0.42	0.43a-c
	125	1.95	1.91	2.03ab	1.81b	0.43	0.46ab
	150	2.02	1.89	1.76bc	1.72b-d	0.41	0.45ab
7 d	0	2.00	1.76	1.50c	1.78bc	0.25	0.45ab
	100	2.03	1.95	1.89bc	1.51d	0.42	0.43a-c
	125	2.04	1.83	1.97bc	1.60b-d	0.40	0.42bc
	150	1.96	1.90	1.92bc	1.83b	0.43	0.46ab
Time means							
30		2.01	1.89	1.94	1.76	0.42	0.43
21		1.97	1.87	2.00	1.78	0.42	0.46
7		2.01	1.86	1.82	1.68	0.38	0.44
	Dose means						
	0	1.97	1.83	1.75	1.80	0.37	0.47
	100	1.98	1.89	2.03	1.61	0.41	0.42
	125	2.02	1.91	2.01	1.82	0.43	0.45
	150	2.01	1.88	1.88	1.73	0.41	0.44
P values							
Time (T)		0.262	0.818	0.322	0.352	0.296	0.299
AVG Dose (D)		0.498	0.549	0.152	0.037	0.404	0.033
T x D		0.349	0.609	0.034	0.001	0.161	0.009

[1]Days before harvest (DBH)
*Each column, values followed by the same letter are not significantly different at $p < 0.05$ level according to Duncan's multiple range test

http://www.aloki.hu ● ISSN 1589 1623 (Print) ● ISSN 1785 0037 (Online)
DOI: http://dx.doi.org/10.15666/aeer/1605_55515569
© 2018, ALÖKI Kft., Budapest, Hungary

The leaves with the highest calcium content (2.42 ppm) were obtained from 21 DBH 100 ppm AVG in the first year and from 30 DBH 125 ppm AVG in the second year (*Table 10*). In terms of magnesium contents, the amount of magnesium decreased with the applications in the second year in general; it increased only in 30 DBH 125 ppm AVG (*Table 10*). With respect to the effect of AVG applications on phosphorus and potassium contents, the time x dose interaction for phosphorus and the difference between doses for potassium were found statistically significant ($p < 0.05$) (*Table 11*). *Table 11* shows the effect of AVG applications on the copper and zinc contents of the Akça leaves. It was seen that the applications increased the copper content. The effect of AVG applications was statistically significant on the iron and boron contents of leaves as well. As time x dose interaction, iron content in both years and boron content only in the second year were found statistically significant ($p < 0.05$) (*Table 12*). Iron content had the highest value in 30 DBH 125 ppm AVG in the first year and in 7 DBH 100 ppm AVG in the second year. For boron, however, it was 7 DBH 100 ppm AVG with a value of 36.72 ppm (*Table 12*).

Table 11. *The effect of AVG treatments on phosphorus, potassium, copper, zinc in the 'Akça' pear leave, 2012 and 2013*

Application time[1]	AVG doses (ppm)	Phosphorus (ppm)		Potassium (ppm)		Copper (ppm)		Zinc (ppm)	
		I. Year	II. Year	I. Year	II. Year	I. Year	II. Year	I. Year	II. Year
30 d	0	0.19a-d*	0.16	1.04	1.32	10.25d*	9.61	34.91	36.74
	100	0.17b-d	0.17	1.18	1.37	14.25ab	12.86	40.40	35.99
	125	0.18b-d	0.16	1.32	1.30	12.89a-d	13.55	38.71	33.40
	150	0.16c	0.16	1.34	1.28	12.83a-d	10.26	31.70	29.81
21 d	0	0.22a	0.16	1.04	1.21	10.49cd	9.37	35.80	34.58
	100	0.21a-c	0.15	1.36	1.25	14.76ab	9.76	36.06	28.35
	125	0.17b-d	0.16	1.23	1.26	13.64ab	12.13	39.73	30.51
	150	0.16c	0.15	1.09	1.33	15.33a	9.65	34.82	31.23
7 d	0	0.21ab	0.15	0.97	1.24	10.13d	9.65	36.60	35.22
	100	0.16c	0.15	1.16	1.31	13.30a-c	15.04	33.82	31.84
	125	0.16c	0.15	1.15	1.45	11.98b-d	11.34	37.22	31.19
	150	0.18b-d	0.16	1.04	1.41	12.58a-d	12.55	37.79	34.03
Time means									
30		0.17	0.16	1.22	1.32	12.56	11.57	36.43	33.99
21		0.19	0.15	1.18	1.26	13.56	10.23	36.60	31.17
7		0.18	0.16	1.08	1.35	12.00	12.15	36.36	33.07
	Dose means								
	0	0.21	0.16	1.02b*	1.26	10.29	9.54	35.77	35.52
	100	0.18	0.16	1.23a	1.31	14.11	12.55	36.76	32.06
	125	0.17	0.16	1.24a	1.34	12.84	12.34	38.56	31.70
	150	0.17	0.16	1.15ab	1.34	13.58	10.82	34.77	31.69
P values									
Time (T)		0.281	0.085	0.149	0.220	0.182	0.246	0.987	0.159
AVG Dose (D)		0.006	0.919	0.025	0.465	0.000	0.080	0.155	0.067
T x D		0.015	0.232	0.053	0.534	0.002	0.187	0.134	0.065

[1]Days before harvest (DBH)

*each column, values followed by the same letter are not significantly different at $p < 0.05$ level according to Duncan's multiple range test

http://www.aloki.hu ● ISSN 1589 1623 (Print) ● ISSN 1785 0037 (Online)
DOI: http://dx.doi.org/10.15666/aeer/1605_55515569
© 2018, ALÖKI Kft., Budapest, Hungary

Table 12. *The effect of AVG treatments on iron, manganese, boron in the 'Akça' pear leave, 2012 and 2013*

Application time[1]	AVG doses (ppm)	Iron (ppm)		Manganese (ppm)		Boron (ppm)	
		I. Year	II. Year	I. Year	II. Year	I. Year	II. Year
30 d	0	62.37ab*	59.36ab*	57.25	176.43	32.03	32.84bc*
	100	67.46a	51.82c-e	69.46	147.17	34.71	33.90bc
	125	71.00a	58.83a-c	65.42	166.37	36.88	33.29bc
	150	69.33a	51.09de	53.55	144.13	33.71	32.08cd
21 d	0	54.19b	59.24a-c	56.79	158.95	31.70	32.75bc
	100	67.19a	52.48b-e	51.36	151.43	36.63	29.95de
	125	64.96a	49.36e	61.15	146.80	34.05	29.19e
	150	70.40a	56.95a-d	65.22	148.10	37.70	35.41ab
7 d	0	62.17ab	59.84ab	59.66	139.71	31.12	32.86bc
	100	69.39a	61.71a	72.77	175.83	35.55	36.72a
	125	69.07a	57.34a-d	66.52	154.23	32.12	31.66c-e
	150	64.49a	56.62a-d	60.85	158.60	31.66	32.97bc
Time means							
30		67.54	55.27	61.42	158.53	34.33	33.03
21		64.19	54.51	58.63	151.32	35.02	31.83
7		66.28	58.88	64.95	157.09	32.62	33.55
	Dose means						
	0	59.58	59.48	57.90	158.36	31.62	32.82
	100	68.01	55.33	64.53	158.14	35.63	33.52
	125	68.34	55.17	64.37	155.80	34.35	31.38
	150	68.07	54.89	59.87	150.28	34.36	33.49
P values							
Time (T)		0.406	0.074	0.414	0.736	0.199	0.186
AVG Dose (D)		0.001	0.170	0.543	0.883	0.069	0.180
T x D		0.011	0.008	0.546	0.700	0.124	0.000

[1]Days before harvest (DBH)
*Each column, values followed by the same letter are not significantly different at $p < 0.05$ level according to Duncan's multiple range test

The effect of applications on leaf area (cm^2) and chlorophyll value (spad value) in the leaves of 'Akça' variety

The effect of AVG applications on the leaf area of 'Akça' variety was statistically significant ($p < 0.05$) as time x dose interaction only in the first year. Leaf area expanded with the applications, and the largest leaf area was observed in 21 DBH 125 ppm AVG (*Table 13*). Their effect on the chlorophyll value of the leaves of 'Akça' variety was found statistically significant ($p < 0.05$) as time x dose interaction in both years. The amount of chlorophyll increased in general with the applications. The highest spad value was obtained from 30 DBH 125 ppm AVG and 21 and 7 DBH 100 ppm AVG (*Table 13*).

http://www.aloki.hu ● ISSN 1589 1623 (Print) ● ISSN 1785 0037 (Online)
DOI: http://dx.doi.org/10.15666/aeer/1605_55515569
© 2018, ALÖKI Kft., Budapest, Hungary

Table 13. *The effect of AVG treatments on Leaf area and total chlorophyll in the 'Akça' pear leave, 2012 and 2013*

Application time[1]	AVG doses (ppm)	Leaf area (cm^2)		Total chlorophyll (spad value)	
		I. Year	II. Year	I. Year	II. Year
30 d	0	33.01cd*	34.65	44.12b-d*	45.74cd*
	100	33.48cd	30.95	45.47a-c	46.78bc
	125	36.32b-d	36.73	46.07ab	49.86a
	150	36.04b-d	39.45	44.07b-d	47.74a-c
21 d	0	32.33d	33.62	41.74d	44.11d
	100	36.70bc	36.23	48.16a	49.60a
	125	41.01a	38.41	44.87a-d	48.78ab
	150	36.17b-d	38.27	45.14a-d	47.92a-c
7 d	0	33.11cd	32.21	42.95b-d	43.99d
	100	34.50cd	34.57	46.13ab	48.99ab
	125	38.96ab	38.35	42.24cd	48.40ab
	150	39.56ab	38.49	42.63b-d	48.30ab
Time means					
30		34.71	35.45	44.93	47.53
21		36.55	36.63	44.98	47.60
7		36.53	35.90	43.49	47.42
	Dose means				
	0	32.82	33.49	42.93	44.61
	100	34.89	33.92	46.59	48.46
	125	38.76	37.83	44.40	49.01
	150	37.26	38.74	43.95	47.99
P values					
Time (T)		0.283	0.816	0.221	0.981
AVG Dose (D)		0.106	0.201	0.022	0.598
T x D		0.000	0.322	0.000	0.000

[1]Days before harvest (DBH)
*Each column, values followed by the same letter are not significantly different at $p < 0.05$ level according to Duncan's multiple range test

Discussion

It was determined that 30 DBH and 21 DBH AVG applications (all doses) delayed the harvest maturity of Akça pear for up to 3-4 days. It was well documented that AVG inhibits ethylene biosynthesis, thus retards fruit ripening (Amarante et al., 2002; Schupp and Greene, 2004; Petri et al., 2006; Kang et al., 2007). Similar results were also observed in this study. Clayton et al. (2000) reported that ReTain applied 14 and 7 days before harvest delayed the harvest for up to 4-10 days in the Bartlett pear. The increase in fruit weight with the AVG applications also led to an increase in fruit yield. As reported by Romani et al. (1983), since AVG allows for late ripening, fruit continues to grow, leading to an increase in size and yield. Delayed harvest provides flexibility in fruit processing-packing, storage and marketing planning. Pasa et al. (2017) stated that fruit set, number of fruit per tree and yield were significantly improved by AVG sprayed one week after full bloom with doses ranging from 40 to 100 mg L^{-1} for 'Santa

http://www.aloki.hu ● ISSN 1589 1623 (Print) ● ISSN 1785 0037 (Online)
DOI: http://dx.doi.org/10.15666/aeer/1605_55515569
© 2018, ALÖKI Kft., Budapest, Hungary

Maria', while for 'Abate Fetel' the most responsive dose was 100 mg L^{-1}. Fruit quality attributes and fruit size were not affected by treatments. Dussi et al. (2002) applied 14 DBH 125 and 180 ppm AVG to Williams pears**.** In this study, AVG did not have any effect on pre-harvest fall, but an increase in size and hardness was detected. Pre-harvest AVG applications to Williams pear caused a delay in fruit ripening and increased fruit size (Romani et al., 1983). In our study, compared to the control fruits, the AVG applications increased fruit width by about 2-16% and fruit weight by 7-57%.

In the study performed by Clayton et al. (2000) on Bartlett pear, it is reported that AVG increased fruit firmness compared to the control group and maintained both their shelf life and storage as well as their firmness more than controls. The 'Akça' pear is in demand in both domestic and international markets because it is an early comer summer variety. Therefore, shelf life shortens during transport. Higher fruit firmness means a longer shelf life. For this reason, in line with the data obtained by this study, an increase in fruit firmness is considered to reduce quality losses during transport. According to our findings, L* values expressing brightness decreased with the AVG applications. a* values indicating redness were lower in the AVG applications, which is parallel with AVG's retardant effect on ripening and thus coloring.

All AVG applications slowed both ethylene production (μL kg^{-1} h) and respiratory rate (μL kg^{-1} h) in the fruit. Similar to our findings, Clayton et al. (2000) and Butar and Çetinbaş (2017) reported that AVG reduced both ethylene amount and respiration rate and that the application doses had the same effect in Williams pear. In the AVG studies conducted on other varieties, it was reported that ethylene production and respiration rate slowed down (Amarante et al., 2002; Schuup and Greene, 2004; Petri et al., 2006; Kang et al., 2007; Ozturk et al., 2012; Yıldız et al., 2012).

When applied externally, plant growth regulators, which are synthesized naturally in the plant, may have different physiological effects depending on application period and concentration (Salisbury and Ross, 1985). In our study, different application periods and doses of AVG plant growth regulator affected fruits' mineral element contents differently even in different years. Butar and Çetinbaş (2017) stated that a change in AVG application time and dose led to different mineral element contents in 'Williams' pear fruits. In a study conducted on the 'Akça' pear, the contents of N, P, K, Ca, Mg, Zn, Fe, Mn and Cu in the fruit were found to be 3.37, 0.73, 8.25, 0.65, 8.25, 6.63, 4.08, 3.01 mg kg^{-1}, respectively (Kuçuker et al., 2015a). Partly similar results were obtained in our study. AVG applications affect mineral element contents in different ways in leaves as in fruits. It is reported that pear contains 1.134-1.682% nitrogen, 0.46-1.08% potassium, 1.81-3.1% calcium, 0.28-0.55% magnesium, 0.078-0.22% phosphorus, 51.5-197.5 mg kg^{-1} iron, 4.85-8.0 mg kg^{-1} copper, 16-57.5 mg kg^{-1} zinc, and 20-99.5 mg kg^{-1} manganese (Gunen et al., 2003). In our study, these elements were found to exist in the above-given ranges. AVG plant growth regulator is thought to have both increasing and decreasing effects on the mineral element contents in the fruits and leaves of 'Akça' pear. However, decreases did not negatively affect fruit or leaf quality in our study.

Since ethylene hormone causes chlorophyll decomposition in plants (Taiz and Zieger, 2008; Karaçalı, 2009), in an environment where ethylene hormone is suppressed, chlorophyll decomposition is either delayed or slowed down. Accordingly, in our opinion, the AVG applications in our study led to an increase in both leaf area and chlorophyll amount because delayed ethylene production enabled the leaves to nourish and photosynthesize more and have a larger area, and delayed chlorophyll decomposition gave rise to a higher chlorophyll amount.

http://www.aloki.hu ● ISSN 1589 1623 (Print) ● ISSN 1785 0037 (Online)
DOI: http://dx.doi.org/10.15666/aeer/1605_55515569
© 2018, ALÖKI Kft., Budapest, Hungary

Conclusion

Taking all results into account, it was concluded in present study that AVG was definitely effective in increasing the quality of 'Akça' pears. The treatments applied in a dose of 100 ppm 21 days before the anticipated harvest time had more effective results in 'Akça' pear in terms of harvest time and fruit quality. Furthermore, since plant nutrients (macro and micro) and plant growth regulator are in interaction with each other, more detailed studies are necessary on this subject.

Acknowledgements. The author is thankful to Mr. Sinan Butar in the Fruit Research Institute, for help field management and chemical analysis.

REFERENCES

[1] Amarante, C. V. T., Anderson, S., Megguer, C. A., Blum, L. E. B. (2002): Effect of minoethoxyviınilglycine (AVG) on preharvest fruit drop and maturity of apples. – Revista Brasileira de Fruticultura 24: 661-664.
[2] Andreotti, C., Bregoli, A. M., Costa, G. (2004): Pre- and post-harvest aminoethoxyvinylglycine (AVG) application affects maturity and storage of pear fruit. – European Journal of Horticultural Science 69(4): 147-152.
[3] Barut, E. (1995): The use of plant growth regulator on horticulturae in future. – Derim 11: 141-144.
[4] Butar, S., Çetinbaş, M. (2017): Pre-Harvest application of Retain [aminoethoxyvinylglycine (AVG)] influences pre-harvest drop and fruit quality of 'Williams' pears. – Journal of Agricultural Sciences 23: 353-365.
[5] Clayton, M., Biasi, W. V., Southwick, S. M., Mitcham, E. J. (2000): ReTain affects maturity and ripening of 'Bartlett' pear. – HortScience 35(7): 1294-1299.
[6] Dilmaçunal, T. (2009): Normal and controlled atmosphere storage of some apple cultivars grown in organic and conventional farming conditions. – PhD Thesis, SDU Institute of Natural and Applied Sciences, Horticulture, Isparta, Turkey.
[7] Dussi, M. C., Sosa, D., Calvo, G. S. (2002): Effects of ReTain™ on fruit maturity and fruit set of pear cultivars Williams and Packham S Triumph. – Acta Horticulturae 596: 767-771.
[8] FAOSTAT (2018): http://www.faostat.fao.org. – Accessed in May 2018.
[9] Gunen, Y., Yagmur, B., Mısırlı, A., Gulcan, R. (2003): Determination of mineral nutrients in some pear cultivars resistant and susceptible to fire blight. – Ege Journal of Agricultural Research 40(3): 65-72.
[10] Inada, K. (1963): Studies on a method for determining the deepness of green color and chlorophyll content of intact crop leaves and its practical applications principles for estimating the deepness of green color and chlorophyll content of whole leaves. – Japanese Journal of Crop Science 32: 157-162.
[11] Jobling, J., Pradhan, R., Morris, S., Mitchell, L., Rath, A. (2003): The effect of ReTain™ plant growth regulator [aminoethoxyvinylglycine (AVG)] on the postharvest storage life of 'Tegan Blue' plums. – Australian Journal of Experimental Agriculture 43: 515-518.
[12] Kang, I. K., Byun, J. K., Kweon, H. J., Kim, M. J., Kwon, S., Park, M. Y., Lee, D. H., Choi, C., Choi, D. G. (2007): Effects of aminoethoxyvinylglycine on preharvest drop, fruit color, and quality of Tsugaru apples. – Horticulture, Environment, and Biotechnology 48(3): 159-164.
[13] Karaçalı, I. (2009): Conservation and Marketing of Horticultural Products (in Turkish). – Ege University Agricultural Faculty, Bornova, Izmir, Turkey.

http://www.aloki.hu ● ISSN 1589 1623 (Print) ● ISSN 1785 0037 (Online)
DOI: http://dx.doi.org/10.15666/aeer/1605_55515569
© 2018, ALÖKI Kft., Budapest, Hungary

[14] Kuçuker, E., Ozturk, B., Ozkan, Y., Yıldız, K. (2015a): The effect of foliar urea treatment on yield, fruit quality and bioactive compounds of different pear varieties (*Pyrus communis* L.). – Ömer Halisdemir University Engineering Sciences Journal 4(2): 78-86.
[15] Kuçuker, E., Ozturk, B., Aksit, H., Genç, N. (2015b): Effect of pre-harvest aminoethoxyvinylglycine (avg) application on bioactive compounds and fruit quality of plum (*Prunus salicina* lindell cv. black beauty) at the time of harvest and during cold storage. – The Journal of Animal & Plant Sciences 25(3): 763-770.
[16] Kucukyumuk, C., Sarısu, H. C., Yıldız, H., Kaçal, E., Koçal, H. (2015): Farklı anaçlar üzerine aşılı 0900 Ziraat Kiraz çeşidinde su stresinin bazı vejetatif gelişim parametrelerine etkisi. – Yüzüncü Yıl University Journal Agriculture Science 25(2): 180-192.
[17] Lurie, S. (2008): Regulation of ethylene biosynthesis in fruits by aminoethoxyvinylglycine and 1-methylcyclopropene. – Acta Horticulturae 796: 31-41.
[18] Martinez-Romero, D., Bailen, G., Serrano, M., Guillén, F., Valverde, J. M., Zapata, P., Castillo, S., Valero, D. (2007): Tools to maintain postharvest fruit and vegetable quality through the inhibition of ethylene action: a review. – Critical Reviews in Food Science and Nutrition 47: 543-560.
[19] Ozelkok, S., Kaynaş, K., Buyukyılmaz, M. (1995): Investigate the physiology of the possible types of important arms foreseen in production. – Scientific Research and Review 48.
[20] Ozturk, B., Kuçuker, E., Karaman, S., Ozkan, Y. (2012): The effects of cold storage and aminoethoxyvinylgcine (AVG) on bioactive compounds of plum fruit (*Prunus salicina* Lindell cv. 'Black Amber'). – Postharvest Biology and Technology 72: 35-41.
[21] Pasa, M. S., Silva, C. P., Carra, B., Brighenti, A. F., Souza, A. L. K., Schmitz, J. D., Katsurayama, J. M., Ciotta, M. N. (2017): Fruit set and yield of 'Santa Maria' and 'Abate Fetel' pears are increased by early spring application of aminoethoxyvinilglycine (AVG). – Revista de Ciências Agroveterinárias, Lages 16(4): 487-491.
[22] Pech, J. C., Purgatto, E., Bouzayen, M., Latche, A. (2012): Ethylene and fruit ripening. – Annual Plant Reviews 44: 275-304.
[23] Petri, J. L., Leite, G. B., Argenta, L. C., Basso, C. (2006): Ripening delay and fruit drop control in 'Imperial Gala' and 'Suprema' ('Fuji' sport) apples by applying AVG (aminoethoxyvinylglycine). – Acta Horticulturae 727: 519-524.
[24] Rath, A. C., Prentice, A. J. (2004): Yield increase and higher flesh firmness of 'Arctic Snow' nectaries both at harvest in Australia and after export to Taiwan following pre-harvest application of retain plant growth regulator (aminoethoxyvinylglycine, AVG). – Australian Journal of Experimental Agriculture 44: 343-351.
[25] Romani, R., Labavitch, J., Yamashita, T., Hess, B., Rae, H. (1983): Preharvest AVG treatment of 'Bartlett' pear fruits: Effects on ripening, color change, and 104 volatiles. – Journal of the American Society for Horticultural Science 108(6): 1046-1049.
[26] Ryan, J., Estafan, G., Rashid, A. (2001): Soil and Plant Analysis Laboratory Manual. 2nd ed. – ICARDA and NARS, Aleppo, Syria, pp. 135-140.
[27] Salisbury, F. B., Ross, C. W. (1985): Plant Physiology. 3rd ed. – Wadsworth, Belmont, California.
[28] Schupp, J. R., Greene, D. W. (2004): Effect of aminoethoxyvinylglycine (AVG) on preharvest drop, fruit quality, and maturation of 'McIntosh' apples. I. Concentration and timing of dilute applications of AVG. – HortScience 39: 1030-1035.
[29] Taiz, L., Zieger, E. (2008): Plant Physiology (in Turkish translation, editor: İsmail Turkan). – Palme Publishing, Ankara, Turkey.
[30] Yıldız, K., Ozturk, B., Ozkan, Y. (2012): Effects aminoethoxyvinylglycine (AVG) on preharvest fruit drop, fruit maturity, and quality of 'Red Chief' apple. – Scientia Horticulturae 144: 121-124.

http://www.aloki.hu ● ISSN 1589 1623 (Print) ● ISSN 1785 0037 (Online)
DOI: http://dx.doi.org/10.15666/aeer/1605_55515569
© 2018, ALÖKI Kft., Budapest, Hungary

ASSESSMENT OF THE EFFECT OF VARIOUS BIOSTIMULANTS ON *MEDICAGO X VARIA* T. MARTYN YIELDING AND CONTENT OF SELECTED ORGANIC COMPONENTS

GODLEWSKA, A.* – CIEPIELA, G. A.

Institute of Health Sciences, Faculty of Natural Science, Siedlce University of Natural Sciences and Humanities, B. Prusa st. 14, 08-110 Siedlce, Poland

**Corresponding author*
e-mail: agnieszka.godlewska@uph.edu.pl

(Received 25th Jun 2018; accepted 7th Aug 2018)

Abstract. The objective of the present work was to determine the effect of various biostimulants on sand lucerne yielding and content of chlorophyll, proteins, and simple sugars against the background of nitrogen fertilisation regime. A field experiment was arranged as a randomized subblock design (split-plot) with three replicates at the Siedlce Experimental Unit of the University of Natural Sciences and Humanities in Poland in the second decade of August 2013). The following factors were examined: type of biostimulant: Algex, Tytanit, Asahi SL and a control (no biostimulant addition); nitrogen application rate: 0 (control) and 30 kg ha^{-1}. Statistical analysis demonstrated that the biostimulants applied significantly increased plant biomass yields but the effect was more beneficial in plots to where no nitrogen had been applied. Chlorophyll content in lucerne leaves and monosaccharide content were significantly higher following an application of all the biostimulants. Their effect on the sand lucerne content of protein compounds varied. An application of Tytanit and Algex contributed to an increase in protein compounds in test plants but, for Algex, the differences were statistically insignificant. By contrast, an application of Asahi SL was followed by a significant decline in the concentration of protein compounds in lucerne plants. Significantly higher average dry matter yields, a higher average chlorophyll content and a higher average concentration of protein compounds were noted in plots fertilised with nitrogen compared with non-fertilised units. However, nitrogen fertilisation regime significantly reduced the sand lucerne content of simple sugars.
Keywords: *chlorophyll, protein compounds, monosaccharides, Algex, Tytanit, Asahi SL*

Introduction

At present, a challenge for scientists is to look for new technological solutions which would beneficially affect the growth, development, yielding and chemical composition of plants, coupled with limiting e.g. natural environment pollution, and production of healthy food. Recently, products which stimulate metabolic processes in plants, even if they are grown under unfavourable conditions, have been appearing, including biostimulants or growth stimulants (Kocira et al., 2016) of mineral or organic origin (alga and seaweed extracts, phytohormones, micro- and macroelements such as titanium). Biostimulants are products which contain biologically active substances which, by influencing metabolism, contribute to an increase in yields. As it is frequently accompanied by an improvement in yield quality (Kocira et al., 2015; Godlewska and Ciepiela, 2017), the products supplement an application of plant protection preparations and mineral fertilisation. When rationally used, they may be one of the main factors which positively affect the environment and soil productivity (Murawska et al., 2017). According to many authors, an application of biostimulants significantly contributes to an increase in yield, nutrient content, e.g. protein (Szabo et al., 2011), sugars (Godlewska and Ciepiela, 2016), and chlorophyll. It is well known that the effect of

http://www.aloki.hu ● ISSN 1589 1623 (Print) ● ISSN 1785 0037 (Online)
DOI: http://dx.doi.org/10.15666/aeer/1605_55715581
© 2018, ALÖKI Kft., Budapest, Hungary

biostimulants depends on many factors, including crop plant species (Sultana et al., 2005). There are few reports in scientific literature on the effect of biostimulants in herbage legume cultivation, which prompted the authors to undertake research in this field.

The objective of the present work was to determine the effect of various biostimulants on sand lucerne yielding and content of chlorophyll, proteins, and simple sugars against the background of nitrogen fertilisation regime. Protein compounds and monosaccharides are basic components in an assessment of nutritional value of roughages. Chlorophyll content in lucerne leaves is indicative of photosynthesis which has a direct influence on plant growth and development.

Materials and methods

A field experiment was arranged as a randomised sub-block design (split-plot) with three replicates at the Siedlce Experimental Unit of the University of Natural Sciences and Humanities in Poland (52.169° N, 22.280° E) in mid-August 2013. The plot area was 10 m^2 (2.5 m × 4.0 m). According to the Polish soil classification system (Systematics of Polish Soils, 2011), the soil used in the experiment was Hortic Anthrosol (WRB), developed from loamy sand. Based on the analysis performed at the Regional Chemical Station in Wesoła, it was found that the soil was of neutral reaction (pH in 1n KCL = 6.8), with a high humus content (3.78%), available phosphorus content ($H_2PO_4^-$ − 170 mg·kg^{-1}) and magnesium content (Mg^{2+} − 84 mg·kg^{-1}), and average total nitrogen (N – 1.3 g·kg^{-1}) and available potassium (K^+ − 114 mg·kg^{-1}) contents. The following factors were examined:

- Type of biostimulant: Algex, Tytanit, Asahi SL and a control (no biostimulant addition)
- Nitrogen application rate: 0 (control) and 30 kg·ha^{-1}

Algex is an extract of the sea alga *Ascophyllum nodosum* which contains vitamins, amino acids, phytohormones (auxins, cytokinins, gibberellins), polysaccharides, betaine as well as macro- and microelements such as N − 8%, P − 3.6%, K − 7%, B − 0.036%, Zn − 0.025%, Cu − 0.009%, Fe − 0.016%, Mn − 0.036% and Mo − 0.0036%. Algex is manufactured by Rosier, Moustier, Belgium.

Tytanit is produced by INTERMAG Ltd., Olkusz, Poland. Tytanit contains 8.5 g Ti per 1 dm^3 (0.8% m/m) in the form of Ti-ascorbate.

Asahi SL is produced by Arysta Life Science Ltd., Warsaw, Poland. The product contains the following phenolic compounds: sodium p-nitrophenolate − 0.3%, sodium o-nitrophenolate − 0.2% and sodium 5-nitroguaiacolate − 0.1%.

The sowing rate of *Medicago x varia* T. Martyn cv. Marshal was calculated based on the standards drawn up by IMUZ (the Institute for Land Reclamation and Grassland Farming) (Jankowski et al., 2005). Standard cultivation methods were applied in the experiment and, additionally, plants were fertilised with different biostimulants.

The lucerne sowing rate was 23 kg·ha^{-1}. In 2013, when seeds were sown, neither biostimulants or nitrogen fertiliser was applied. In October 2013 only one cut was performed at the plant height of 10 cm. Over the study period (2014-2016), the cutting regime consisted of three harvests per year. Ammonium nitrate was applied three times per year. The total nitrogen amount was split into three equal rates which were applied before each cutting. P and K fertilisation was applied to all the plots. Phosphorus was

http://www.aloki.hu ● ISSN 1589 1623 (Print) ● ISSN 1785 0037 (Online)
DOI: http://dx.doi.org/10.15666/aeer/1605_55715581
© 2018, ALÖKI Kft., Budapest, Hungary

applied once as triple superphosphate at the rate of 40 kg·ha^{-1} P_2O_5 in the spring. The amount of potassium (160 kg·ha^{-1} K_2O) was split into three equal rates and applied prior to each cutting as 60% potash salt. The biostimulants was sprayed as an aqueous solution. The spraying was performed before each cutting: the first application was three weeks before the first cutting, the second one two weeks after the first harvest and the last one three weeks after the second harvest. Biostimulant rates following each cut were applied as recommended by the manufacturer, that is thinned with water to obtain the volume of 400 dm^3: Algex − 6 dm^3·ha^{-1}, Tytanit − 0.4 dm^3·ha^{-1}, Asahi SL − 0.6 dm^3·ha^{-1}.

Leaf chlorophyll was determined using a Minolta Chlorophyll Meter SPAD-502. It measures the light absorption by leaves at the wavelength of 650 and 940 nm. The quotients of light absorption at the two wavelengths are unitless and are called SPAD values. They reflect the leaf greenness index which corresponds to the total chlorophyll content (Machul, 2005; Pacewicz and Gregorczyk, 2009). Measurements were taken in each plot on 10 randomly selected sand lucerne leaves (top leaves) the day before harvest.

During harvest of each cut, green matter from each plot (whole area, that is 10 m^2) was weighed to determine the yield, and 0.5 kg green matter samples of lucerne were taken to determine the drying-up coefficient, and to carry out chemical analyses. The samples were left to dry in a ventilated room. Airy dry matter was weighed (to determine dry matter yield per plot) and was then shredded and ground. The obtained material was subjected to chemical analysis to determine dry matter (by determining moisture content), protein compounds, and monosaccharides. The method of determination was near-infrared spectroscopy (NIRS) using a NIRFlex N-500 spectrometer and ready-to-use INGOT calibration applications.

Statistical analysis was conducted by means of the program STATISTICA StatSoft, Inc. (2011). STATISTICA (data analysis software system), version 10 (www.statsoft.com) was used. Significance of differences between means was checked using the Tukey test at the significance level of $\alpha \leq 0.05$.

Meteorological conditions during the study period were changeable and precipitation was very unevenly distributed (*Table 1*). The mean air temperature in the 2015 growing season was by 2 degrees lower than the mean across 2006-2016 whereas precipitation sum in 2016 was by 24 mm higher than the value for the preceding decade. July 2016 was of particular interest as the precipitation sum was twice as high as the mean across 2006-2016 and amounted to 25.6% of the precipitation sum for the whole growing season. By contract, unusual precipitation shortages occurred in September 2014, April and July 2015, and May and September 2016.

Table 1. *Meteorological condition in years 2014-2016 by Meteorological station in Siedlce*

Years	Means monthly air temperatures (°C)						Means in growing season (IV-IX) (°C)
	Month						
	IV	V	VI	VII	VIII	IX	
2014	9.7	13.7	15.1	20.4	17.8	13.7	15.1
2015	8.1	12.3	16.5	14.3	21.1	8.8	13.5
2016	8.8	14.6	18.1	19.0	17.9	14.4	15.5
Mean of 2006-2016	9.6	14	17.2	19.9	18.4	13.6	15.5

http://www.aloki.hu ● ISSN 1589 1623 (Print) ● ISSN 1785 0037 (Online)
DOI: http://dx.doi.org/10.15666/aeer/1605_55715581
© 2018, ALÖKI Kft., Budapest, Hungary

Years	Monthly precipitation (mm)						Sum in season (IV-IX) (mm)
	Month						
	IV	V	VI	VII	VIII	IX	
2014	39.5	79.3	50.3	62.5	66.3	26.7	324.6
2015	29.7	100.6	41.1	68.3	12	77.5	329.2
2016	55.1	36.8	56.9	112.5	73.3	15.2	349.8
Mean of 2006-2016	26.9	68.9	64.6	55.8	65.3	44.3	325.8

Results and discussion

An analysis of average results for three study years demonstrated significant variation in sand lucerne yields regardless of the experimental factors (*Table 2*).

Table 2. *Dry matter yield of Medicago x varia T. Martyn (t ha^{-1}) (sum of three cuts)*

Year	Dose of N kg ha^{-1}	Biostimulant				Mean
		Without biostimulant (control)	Algex	Tytanit	Asahi SL	
2014	0	9.6 a	14.7 b	13.1 bc	12.7 c	12.5 A
	30	15.3 a	15.7 a	16.1 a	20.3 b	16.9 B
2015	0	18.2 a	20.5 b	20.1 b	18.7 ab	19.4 A
	30	21.7 a	23.1 a	23.3 a	22.9 a	22.8 B
2016	0	12.7 a	18.8 b	16.8 c	14.3 a	15.7 A
	30	19.5 a	20.6 ab	21.5 b	24.0 c	21.4 B
2014	Mean	12.5 a	15.2 bc	14.6 b	16.5 c	14.7 A
2015		20.0 a	21.8 a	21.7 a	20.8 a	21.1 B
2016		16.1 a	19.7 b	19.2 b	19.1 b	18.5 C
Mean	0	14.0 a	18.7 b	17.3 b	15.5 a	16.4 A
	30	19.5 a	20.6 a	21.2 ab	23.0 b	21.1 B
Mean		16.8 a	19.7 b	19.3 b	19.3 b	18.9

Different lower-case letters within the same line indicate significant differences. Different uppercase letters indicate that the values in the column for individual factors (Dose N and Years) and their interaction differ significantly

Significantly the lowest biomass yields were obtained in the first study year, them being the highest in the second year. Precipitation amount is an important factor which determines yield levels. Thus, it can be inferred that such low yields in the first study year may have been due to relatively the lowest precipitation amounts (*Table 1*). An application of biostimulants, regardless of the study years and nitrogen fertilisation regime, increased plant yields (by 15.6%, on average). The effect of biostimulants in the individual study years and in combination with nitrogen rates was equivocal. In non-fertilised plots, the biostimulants Algex and Tytanit contributed to a significant increase in lucerne yields in each study year compared with yields harvested from plots not treated with the biostimulants. Such an effect for Asahi SL was observed in the first study year only. A significant rise in yields obtained from plots fertilised with nitrogen

http://www.aloki.hu ● ISSN 1589 1623 (Print) ● ISSN 1785 0037 (Online)
DOI: http://dx.doi.org/10.15666/aeer/1605_55715581
© 2018, ALÖKI Kft., Budapest, Hungary

was observed following an application of Asahi SL (in the first and third study year) and Tytanit (in the third year). Also Tan et al. (2011), Kováčik et al. (2018) and Whitted-Haag et al. (2014) obtained significant plant yield increases following an application of Tytanit. In each study year, the biostimulant Algex increased lucerne yields in plots fertilised with nitrogen but the differences were insignificant, which is in disagreement with results obtained by other researchers. Many authors have reported a significant effect of an application of sea alga extract on plant yields (Kumar and Sahoo, 2011; Sabir et al., 2014; Nerrisa et al., 2016). However, one should bear in mind that the effect of natural biostimulants is to a great extent determined by crop plant species and cultivar (Sultana et al., 2005; Godlewska and Ciepiela, 2016). Regardless of the remaining factors, nitrogen fertilisation regime significantly influenced yields produced by the test plant.

Dry matter yield (t ha^{-1}) harvested with individual cuts as affected by nitrogen fertilisation regime and type of biostimulant is presented in *Table 3*.

Table 3. *Dry matter yield of Medicago x varia T. Martyn (t ha^{-1}) (average of three years)*

Cut	Dose of N kg ha^{-1}	Biostimulant				Mean
		Without biostimulant (control)	Algex	Tytanit	Asahi SL	
1	0	3.3 a	5.0 b	4.1 c	3.4 a	4.0 A
	30	5.1 a	5.5 a	5.6 a	5.4 a	5.4 B
2	0	6.5 a	8.6 b	8.4 b	7.6 c	7.8 A
	30	9.1 a	9.3 a	9.7 a	11.5 b	9.9 B
3	0	4.3 a	5.1 b	4.7 ab	4.5 ab	4.7 A
	30	5.3 a	5.8 ab	5.9 ab	6.1 b	5.8 B
1	Mean	4.2 a	5.2 b	4.9 bc	4.4 ac	4.7 A
2		7.8 a	9.0 b	9.1 b	9.5 b	8.8 B
3		4.8 a	5.4 a	5.3 a	5.3 a	5.2 A
Mean	0	4.7 a	6.2 b	5.8 bc	5.2 ac	5.5 A
	30	6.5 a	6.9 a	7.1 ab	7.7 b	7.0 B
Mean		5.6 a	6.6 b	6.4 b	6.4 b	6.3

Different lower-case letters within the same line indicate significant differences. Different uppercase letters indicate that the values in the column for individual factors (Dose N and Cut) and their interaction differ significantly

Regardless of the experimental factors, the lowest lucerne yields were harvested in the first cut, them being the highest for the second cut (mean across years), which should be linked with the meteorological conditions (*Table 1*). Irrespective of the biostimulants, nitrogen regime increased yields harvested in each cut. The effect of the biostimulants on lucerne yields was favourable but the differences were not always significant. Regardless of the N fertiliser factor, in the first and second cut, the biomass of plants in plots treated with biostimulants was significantly higher compared with control yields. In individual cuts, the effect of biostimulants as influenced by nitrogen regime was equivocal. In units without nitrogen application, a significant increase in yield was observed for the first cut following an application of Algex and Tytanit, for the second

http://www.aloki.hu ● ISSN 1589 1623 (Print) ● ISSN 1785 0037 (Online)
DOI: http://dx.doi.org/10.15666/aeer/1605_55715581
© 2018, ALÖKI Kft., Budapest, Hungary

cut following spraying with all the biostimulants, and for the third cut after Asahi SL had been applied. Significantly higher yields harvested in plots fertilised with nitrogen were recorded for the second and third cut only after spraying with Asahi SL compared with control yields.

The nitrogen status of plants, important in terms of the effectiveness of crop plant production and yield quality, can be determined by means of an application of a test which measures the chlorophyll content in leaves (Rostami et al., 2008). Chlorophyll content in the leaves of sand lucerne harvested in individual cuts and study years as affected by nitrogen fertilisation and biostimulant application is presented in *Table 4*. Data analysis revealed that nitrogen regime increased SPAD in lucerne leaves by 7.66%, the differences being significant. In their study, Szulc et al. (2012) found similar relationships. The effect of biostimulants examined in the experiment reported here was unidirectional. Regardless of the nitrogen regime, cuts and study years, each biostimulant significantly increased chlorophyll content in test plants (by 6.70%, on average). The obtained results correspond to data presented by other authors. Murawska et al. (2017) applied Asahi SL, a sea alga extract and Tytanit, and observed a clear increase in chlorophyll content in winter wheat leaves. Also, El-Miniawy et al. (2014) demonstrated in their work a banaficial effect of a sea alga extract on SPAD in strawberry leaves. Research by other workers revealed that an application of Tytanit increased chlorophyll content in the leaves of timothy (Radkowski, 2013), winter wheat and winter oilseed rape (Kováčik etal., 2014).

Table 4. *The effect of the biostimulants on content of chlorophyll in leaves of Medicago x varia T. Martyn (value of SPAD) by nitrogen fertilization, cut and study year*

Tested trait		Biostimulant				Mean
		Without biostimulant (control)	Algex	Tytanit	Asahi SL	
Dose of N kg ha^{-1}	0	51.7 a	56.3 b	55.4 b	55.8 b	54.8 A
	30	56.7 a	58.7 b	59.7 bc	61.0 c	59.0 B
Cut	1	53.7 a	56.3 b	56.3 b	57.6 c	56.0 A
	2	57.5 a	59.8 b	60.6 b	59.9 b	59.4 B
	3	51.5 a	56.5 b	55.8 b	57.9 c	55.4 A
Year	2014	54.3 a	55.8 b	56.8 b	56.8 b	55.9 A
	2015	54.9 a	57.9 b	57.7 b	57.8 b	57.1 B
	2016	53.7 a	57.9 b	57.8 b	59.4 c	57.2 B
Mean		54.2 a	57.4 b	57.6 b	58.5 b	56.9

Different letters within the same line indicate significant differences. Values in column for individual factors indicated with different, capital letters differ significantly

Chlorophyll content in the plants of individual cuts (mean across years) changed during the growing period, it being significantly the highest in the second cut lucerne. Also, analysis of the obtained results demonstrated that, in each cut, an application of biostimulants significantly increased chlorophyll content in lucerne compared with control plants which had not been treated with biostimulants. The biostimulant Asahi SL significantly increased chlorophyll content in the first and third cut lucerne leaves compared with all the remaining treatments. Moreover, the chlorophyll content in

http://www.aloki.hu ● ISSN 1589 1623 (Print) ● ISSN 1785 0037 (Online)
DOI: http://dx.doi.org/10.15666/aeer/1605_55715581
© 2018, ALÖKI Kft., Budapest, Hungary

lucerne leaves was observed to increase in individual study years. Similar relationships were reported in the works by Olszewska (2008) and Ciepiela et al. (2013). Soil moisture may be one of the factors affecting chlorophyll content in plants. Thus, the highest chlorophyll content in the second cut plants may have been due to a large amount of precipitation accompanied by high 24-hour air temperatures during the period of growth of these plants.

The sand lucerne content of protein compounds in dry matter averaged 176.3 g·kg^{-1} DM (*Table 5*) and was affected by all the experimental factors. Regardless of biostimulant application and nitrogen regime, significantly the lowest level of protein compounds was recorded for the second cut lucerne, it being the highest for the third cut plants. When study years are taken into consideration, the lowest concentration of protein compounds was determined in the second cut plants, it being the highest in the third cut.

Table 5. *The effect of the biostimulants on content of protein compounds in Medicago x varia T. Martyn by nitrogen fertilization, cut and study year (g kg^{-1} DM)*

Tested trait		Biostimulant				Mean
		Without biostimulant (control)	Algex	Tytanit	Asahi SL	
Dose of N kg ha^{-1}	0	165.7 a	172.3 ab	177.2 b	154.8 c	167.5 A
	30	185.4 a	191.9 ab	196.8 b	181.9 ac	189.0 B
Cut	1	174.2 a	180.3 abc	186.7 b	171.6 ac	178.2 A
	2	156.1 a	163.3 ab	168.3 b	150.8 ac	159.6 B
	3	196.3 a	202.6 ab	206.1 b	182.6 c	196.9 C
Year	2014	165.2 a	169.9 ab	176.2 b	155.6 ac	166.7 A
	2015	152.2 a	159.3 ab	164.7 b	143.9 ac	155.0 B
	2016	194.5 a	201.3 ab	205.5 b	188.8 ac	197.5 C
Mean		175.5 a	182.1 ab	187.0 b	168.3 c	176.3

Different letters within the same line indicate significant differences. Values in column for individual factors indicated with different, capital letters differ significantly

The effect of biostimulants varied considerably. The most beneficial effect of Titanit was observed on protein compound content in sand lucerne. The biostimulant significantly increased (by 6.55%, on average) this content compared with control plants. The results correspond to findings reported by Murawska et al. (2017) who observed an increase in the winter wheat grain content of protein after spraying with Tytanit. An application of Algex contributed to an increase in protein compounds compared with their concentration in control plants (by 3.76%, on average) but the differences were statistically insignificant. However, a significant effect of sea alga extracts has been reported in many works (Matysiak et al., 2012; Ciepiela and Godlewska, 2014). It may follow from the fact that components in sea alga extracts (auxins, cytokinins, gibberellic acid and amino acids) increase plant physiological activity including protein synthesis (Szabo et al., 2011).

The biostimulant Asahi SL applied in the experiment contributed to a decline in protein compound content (by 4.28%, on average) in sand lucerne plants harvested in each cut (mean across years) compared with control plants. Significant differences

http://www.aloki.hu ● ISSN 1589 1623 (Print) ● ISSN 1785 0037 (Online)
DOI: http://dx.doi.org/10.15666/aeer/1605_55715581
© 2018, ALÖKI Kft., Budapest, Hungary

between values reflecting the decline in the content of this component were recorded for plants harvested in the third cut only.

Regardless of biostimulant application, cuts and study years, nitrogen fertilisation regime significantly increased the concentration of protein compounds in lucerne (by 12.8%, on average) compared with the content in lucerne harvested in plots where no nitrogen had been applied.

Monosaccharide content (*Table 6*) was significantly the highest in the dry matter of the first cut sand lucerne (mean across years) compared with plants in the second and third cut. This was due to the fact that these compounds were used in large amounts during increased plant respiration under the conditions characterised by high temperatures (the second and third cut) when sugars are utilised. The findings correspond to results of the study reported by Ciepiela and Godlewska (2014). Moreover, statistical analysis confirmed significantly the highest concentration of simple sugars in plants harvested in the third study year compared with the first and second study year.

Table 6. *The effect of the biostimulants on content of monosaccharides in Medicago x varia T. Martyn by nitrogen fertilization, cut and study year (g kg^{-1} DM)*

Tested trait		Biostimulant				Mean
		Without biostimulant (control)	Algex	Tytanit	Asahi SL	
Dose of N kg ha^{-1}	0	51.9 a	58.3 b	62.4 bc	55.0 ab	56.9 A
	30	38.8 a	45.8 b	49.5 bc	43.6 ab	44.4 B
Cut	1	62.5 a	70.2 b	74.7 bc	67.3 ab	68.7 A
	2	34.3 a	39.8 b	42.7 bc	36.7 ab	38.4 B
	3	39.3 a	46.3 b	50.4 bc	44.0 ab	45.0 C
Year	2014	39.5 a	47.0 ab	54.7 b	45.1 ab	46.5 A
	2015	42.6 a	49.4 ab	53.7 b	47.1 ab	48.2 A
	2016	49.2 a	55.6 b	57.9 b	52.2 ab	53.7 B
Mean		45.4 a	52.1 b	56.0 b	49.3 c	50.2

Different letters within the same line indicate significant differences. Values in column for individual factors indicated with different, capital letters differ significantly

Biostimulants tested in this study significantly increased monosaccharide content in lucerne compared with control plants (by 10.6%, on average), regardless of nitrogen application regime, cuts and study years. An application of Algex and Tytanit to plots which were and were not fertilised with nitrogen contributed to a significant increase in the lucerne content of monosaccharides. A beneficial effect of sea alga extracts on the concentration of simple sugars in plants has been confirmed in research by other authors (Roussos et al., 2009; Pacholczak et al., 2012; Godlewska and Ciepiela, 2013; El-Miniawy et al., 2014). However, there is no data available for sand lucerne. The biostimulant Asahi SL increased monosaccharide content in plants, too, but the differences were insignificant. Contrasting findings were reported by Cwalina-Ambroziak and Amarowicz (2012) who applied Asahi SL and found a decline in sugar content in tomato and red pepper fruit.

http://www.aloki.hu ● ISSN 1589 1623 (Print) ● ISSN 1785 0037 (Online)
DOI: http://dx.doi.org/10.15666/aeer/1605_55715581
© 2018, ALÖKI Kft., Budapest, Hungary

Regardless of biostimulants, nitrogen fertilisation regime significantly reduced monosaccharide content in lucerne dry matter, which corresponds to research results reported by Godlewska and Ciepiela (2013).

Conclusions

Statistical analysis demonstrated that the biostimulants applied significantly increased plant biomass yields but the effect was more beneficial in plots to where no nitrogen had been applied. Chlorophyll content in lucerne leaves and monosaccharide content were significantly higher following an application of all the biostimulants. Their effect on the sand lucerne content of protein compounds varied. An application of Tytanit and Algex contributed to an increase in protein compounds in test plants but, for Algex, the differences were statistically insignificant. By contrast, an application of Asahi SL was followed by a significant decline in the concentration of protein compounds in lucerne plants. Significantly higher average dry matter yields, a higher average chlorophyll content and a higher average concentration of protein compounds were noted in plots fertilised with nitrogen compared with non-fertilised units. However, nitrogen fertilisation regime significantly reduced the sand lucerne content of simple sugars.

Acknowledgements. The results of the research carried out under the research theme No. 340/S/13 were financed from the science grant granted by the Ministry of Science and Higher Education.

REFERENCES

[1] Ciepiela, G. A., Godlewska, A. (2014): Changes in protein compounds and momosaccharidesin selected grass species following an application of seaweed extract. – Polish Journal of Environmental Studies 23(1): 29-35.
[2] Ciepiela, G. A., Godlewska, A., Jankowska, J. (2013): The effect of biostimulant on yields of mixed grass/red clover stands and chlorophyll content in crop plant leaves under different nitrogen fertilisation regimes. – Fresenius Environmental Bulletin 22(12b): 3700-3708.
[3] Cwalina-Ambroziak, B., Amarowicz, R. (2012): Effects of Biological and Fungicidal Environmental protection on chemical composition of tomato and red pepper fruits. – Polish Journal of Environmental Study 21(4): 831-836.
[4] El-Miniawy, S. M., Ragab, M. E., Youssef, S. M., Metwally, A. A. (2014): Influence of foliar spraying of seaweed extract on growth, yield and quality of strawberry plants. – Journal of Applied Sciences Research 10(2): 88-94.
[5] Godlewska, A., Ciepiela, G. A. (2013): The effect of natural growth regulators obtained from Ecklonia maxima and mineral nitrogen on true protein and simple sugar contents of Dactylis glomerata L. and Festulolium braunii (K. Richt) A. Camus. – Turkish Journal of Fild Crops 18(2): 247-253.
[6] Godlewska, A., Ciepiela, G. A. (2016): The effect of growth regulator on dry matter yield and some chemical components in selected grass species and cultivars. – Soil Science and Plant Nutrition 62(3): 297-302. DOI: 10.1080/00380768.2016.1185741.
[7] Godlewska, A., Ciepiela, G. A. (2017): Effectiveness of fertilization of Dactylis glomerata and Festulolium braunii with nitrogen and the biostimulant Kelpak SL . – Romanian Agricultural Research 34: 197-206.

http://www.aloki.hu ● ISSN 1589 1623 (Print) ● ISSN 1785 0037 (Online)
DOI: http://dx.doi.org/10.15666/aeer/1605_55715581
© 2018, ALÖKI Kft., Budapest, Hungary

[8] Jankowski, K., Ciepiel, A. G. A., Jodełka, J., Kolczarek, R. (2005): Grassland. – University of Podlasie Press, Siedlce, pp. 119-122 (in Polish).
[9] Kocira, A., Kocira, S., Stryjecka, M. (2015): Effect of Asahi SL application on comman bean yield. – Agriculture and Agricultural Science Procedia 7: 103-107.
[10] Kocira, A., Świeca, M., Kocira, S., Złotek, U., Jakubczyk, A. (2016): Enhancement of yield, nutritional and nutraceutical properties of two common bean cultivars following the application of seaweed extract (*Ecklonia maxima*). – Saudi Journal of Biological Sciences 25: 563-571.
[11] Kováčik, P., Baran, A., Filová, A., Vician, M., Hudec, J. (2014): Content changes of assimilative pigments in leaves aftere fertilizer Mg-Titanit application. – Acta Fytotechnica et Zootechnika 17(2): 58-64. DOI: 10.15414/ afz.2014.17.02.58-64.
[12] Kováčik, P., Wiśniowska-Kielian, B., Smoleń, S. (2018): Effect of application of mg-tytanit stimulator on winter wheat yielding andquantitative parameters of wheat straw and grain. – Journal of Elementology 23(2): 697-708. DOI: 10.5601/jelem.2017.22.2.1461.
[13] Kumar, G., Sahoo, D. (2011): Effect of seaweed liquid extract on growth and field of *Triticum aestivum* var. Pusa Gold. – Journal of Applied Phycology 23: 251-255.
[14] Machul, M. (2005): Use of the SPAD test to determine a supplementary nitrogen rate for maize. – Pulawskie Memoirs 40: 160-172 (in Polish).
[15] Matysiak, K., Kaczmarek, S., Leszczyńska, D. (2012): Influence of liquid seaweed extract of *ecklonia maxima* on Winter wheat cv Tonacja. – Journal of Research and Applications in Agricultural Engineering 57(4): 44-47.
[16] Murawska, B., Gabrowska, M., Spychaj-Fabisiak, E., Wszelaczynska, E., Chmielewski, J. (2017): Production and environmental aspects of the application of biostymulators Asahi SL, Kelpak SL and stymulator Tytanit with limited doses of nitrogen. – Environmental Protection and Natural Resources 28(4-74): 10-15. DOI: 10.1515/OSZN-2017-0024.
[17] Nerissa, A., Farrell, A., Ramsubhag, A., Jayaraman, J. (2016): The effect of *Ascophyllum nodosum* extract on the growth, yield and fruit quality of tomato grown under tropical conditions. – Journal Applied Phycology 28: 1353-1362. DOI: 10.1007/s10811-015-0608-3.
[18] Olszewska, M. (2008): Productivity of *Festulolium braunii (K. Richt)* A. Camus and *Festuca pratensis* L. Grown in mixtures with *lotus corniculatus* L. depending on multiple nitrogen rates. – Acta Scientiarum Polonorum, Agricultura 7(2): 101-104 (in Polish).
[19] Pacewicz, K., Gregorczyk, A. (2009): Comparision values of chlorophyll content by chlorophyll meter SPAD-502 and N-tester. – Folia Pomeranae Universitatis Technologiae Stetinensis, Agricultura, Alimentaria, Piscaria et Zootechnica 269(9): 41-46 (in Polish).
[20] Pacholczak, A., Szydło, W., Jacygard, E., Federowicz, M. (2012): Effect of auxins and the biostimulator algaminoplant on rhizogenesis in stem cuttings of two dogwood cultivars (*Cornus alba* 'Aurea' and 'Elegantissima'). – Acta Scientiarum Polonorum, Hortorum Cultus 11(2): 93-103.
[21] Radkowski, A. (2013): Leaf greenness (SPAD) index in timothy-grass seed plantation at different doses of titanium foliar fertilization. – Ecological Chemistry and Engineering A 20(2): 167-174.
[22] Rostami, M., Koocheki, A., Mahallati, M. N., Kafi, M. (2008): Evaluation of chlorophyll meter (SPAD) data for prediction of nitrogen status in corn (Zea mays L.). – American-Eurasian Journal of Agricultural and Environmental Sciences 3: 79-85.
[23] Roussos, P. A., Denaxa, N. K., Damvakaris, T. (2009): Strawberry fruit quality attributes after application of plant growth stimulating compounds. – Scientia Horticulturae 119: 138-146. DOI: 10.1016/j.scienta.20008.07.021.
[24] Sabir, A., Yazar, K., Sabir, F., Kara, Z., Yazici, M., Goksu, N. (2014): Vine growth, yield, berry quality attributes and leaf nutrient content of grapevines as influenced by seaweed extract (Ascophyllum nodosum) and nanosize fertilizer pulverizations. – Scientia Horticulturae 175: 1-8.

http://www.aloki.hu ● ISSN 1589 1623 (Print) ● ISSN 1785 0037 (Online)
DOI: http://dx.doi.org/10.15666/aeer/1605_55715581
© 2018, ALÖKI Kft., Budapest, Hungary

[25] Sultana, V., Ehteshamul-Haque, S., Ara, J., Athar, M. (2005): Comparative efficacy of brown, green and red seaweeds in the control of root infesting fungi and okra. – International Journal of Environment Science and Technology 21(1): 75-81.
[26] Szabo, V., Sarvari, A., Hrotko, K. (2011): Treatment of Stockplants with biostimulators and their effects on cutting propagation of prunus Marianna GF8-1. – Acta Horticulturae 923: 277-282. DOI: 10.17660/ActaHortic.2011.923.41.
[27] Szulc, P., Bocianowski, J., Rybus-Zając, M. (2012): The effect of soil supplementation with nitrogen and elementar sulphur on chlorophyll kontent and grain field of maize (Zea mays L.). – Zemdirbystre-Agriculture 99(3): 247-254.
[28] Tan, Z., Wang, Z. (2011): Demonstration for application of "Fengtaibao", a new water soluble titanium-containing foliar fertilizer, in potato. – Chinese Potato Journal 4: 234-237.
[29] Whitted-Haag, B., Kopsell, D. E., Kopsell, D. A., Rhykerd, R. L. (2014): Foliar silicon and titanium application influence growth and quality characteristics of annual bedding plants. – Open Horticulture Journal 7: 6-15. DOI: 10.2174/1874840601407010006.

http://www.aloki.hu ● ISSN 1589 1623 (Print) ● ISSN 1785 0037 (Online)
DOI: http://dx.doi.org/10.15666/aeer/1605_55715581
© 2018, ALÖKI Kft., Budapest, Hungary

ASSOCIATION OF DIESEL EXHAUST PARTICLE EXPOSURE WITH ERYTHROCYTES DEFORMATION OF MALE MICE

WARDOYO, A. Y. P.* – JUSWONO, U. P. – NOOR, J. A. E.

Laboratory of Air Quality and Astro Imaging, Department of Physics, Brawijaya University
Jl. Veteran 65145, Malang, East Java, Indonesia
(phone: +62-341-575-833; fax: +62-341-585-834)

**Corresponding author*
e-mail: a.wardoyo@ub.ac.id

(Received 26th Jun 2018; accepted 14th Aug 2018)

Abstract. Many epidemiological studies, whether in vivo or in vitro in human or mammals indicate that particulate matters emitted by diesel vehicles have impacts on health. While the effects of daily particulate matter exposure have been well reviewed, the physiological evidence of mice blood alteration associated with the exposure to the diesel exhaust particles has not been investigated well. In this study, we examined the association between the exposure to ultrafine particles contained in the diesel exhaust emission and mice erythrocyte deformation. Ultrafine particles (diameter: 0.02 μm to 0.10 μm) were filtered from three different diesel engine cars. There were 50 male mice used as the experimental animals. The mice were exposed to the ultrafine particles in the different concentration for eight consecutive days. The total concentration of ultrafine particles was measured using a P-Trak Ultrafine Particle Counter (TSI, Model 8525). The mice were sacrificed after the eight-day exposures. The blood samples were observed using a Binocular BX-51 Computer Microscope to examine the level of erythrocyte deformation. The results showed that the increasing amount of the ultrafine particle concentrations caused the increasing extent of the erythrocytes deformation level significantly.
Keywords: *particulate matter, ultrafine particle, diesel vehicle, mice erythrocyte, deformation level*

Introduction

Diesel engines are widely used as a rapid mass transportation mode. The increasing amount of diesel engines is correlated with the exhaust emission. One of the problems with the diesel engine use is the exhaust particles. Diesel exhaust particles are the particles that generated from a diesel engine and become the major constituents of the ambient air pollutant. They consist of ultrafine particles or $PM_{0.1}$ (particulate matter with an aerodynamic diameter ≤ 0.1 μm) (Waly et al., 2013), PM_1 (particulate matter with an aerodynamic diameter ≤ 1 μm) (Xu et al., 2013, Wierzbicka et al., 2014), and $PM_{2.5}$ (particulate matter with an aerodynamic diameter < 2.5 μm) (Hemmingsen et al., 2009). Considering toxicity level, ultrafine particles, as the smallest particulate matter has become a prevalent problem in the whole world regarding both quality and quantity.

There is a well-established correlation between exposure to ultrafine particles emission and health and environment. Inhalation of ultrafine particles increases the risk of adverse health effects associated with the endothelial progenitor cells (Jantzen et al., 2016), abnormal sedimentation, hemagglutination, dose-dependent hemolysis in erythrocytes (Li et al., 2008), increasing of oxidative stress in human embryonic kidney cells (Wang et al., 2009), and a potential risk for atherosclerotic vascular disease (Stewart et al., 2010). Especially the impacts of ultrafine particles in the blood, the erythrocyte deformation or the morphological changes may relate to the abnormal function of blood. Any alteration due to erythrocytes deformation become a marker of iron deficiency anemia and thalassemia (Zhang et al., 2012). Similarly, a previous study

http://www.aloki.hu ● ISSN 1589 1623 (Print) ● ISSN 1785 0037 (Online)
DOI: http://dx.doi.org/10.15666/aeer/1605_55835593
© 2018, ALÖKI Kft., Budapest, Hungary

showed that the erythrocyte deformation was related to the sickle cell disease (Charrin et al., 2016). Our previous studies confirmed the correlation between the exposure to particulate matters from motorcycle exhaust emission and the cell deformations in mice model, in red blood cells (Wardoyo et al., 2017) and kidney cells (Wardoyo et al., 2018). However, there are no published novel data reporting the trends of ultrafine particles concentration from diesel exhaust emission and erythrocyte cell alteration, which are determined useful for investigating a deeper impact of particulate matters emission in the road traffic. Furthermore, the degree to which ultrafine particles from heavy vehicles mean a risk in the organ is a scientific scope that has not previously been tested by direct exposure in human and experimental animals. Although there have been numerous researchers that investigated this case, the sharp mechanisms and effects of the ultrafine particles in the erythrocytes are poorly understood. In this study, exposure to the ultrafine particles focused on the diesel exhaust emission (as a heavy-duty motor vehicle) was chosen due to the negative impact possibilities in health, i.e., in mice erythrocytes. This study is also needed to develop a biomarker for assessing a better understanding of the effect of the ultrafine particles for an acute exposure in the blood.

Materials and Methods

Ultrafine Particles

Three diesel engine cars (D1, D2, and D3) were preferred as the motor samples chosen based on the availability around the University of Brawijaya Malang, Indonesia. The diesel exhaust emission was filtered using a particulate filtering system that consists of an N95 particulate respirator (3M, Model 8210) and a sucking pump (constant debit: 33.05 cm^3/s; flow rate: 2.03 m/s) as described in our previous study (Wardoyo et al., 2018). The filtered ultrafine particles (diameter: 0.02 μm to 0.10 μm) were injected into the exposure chambers in three different injection times (20 - 60 seconds) in order to generate the varied ultrafine particle concentrations of C1 (20 seconds), C2 (40 seconds), and C3 (60 seconds). The concentrations of the ultrafine particles were measured using a P-Trak Ultrafine Particle Counter (TSI, model 8525) (*Fig. 1*) (Wardoyo et al., 2007). The different injection times were used to generate different concentrations of ultrafine particles.

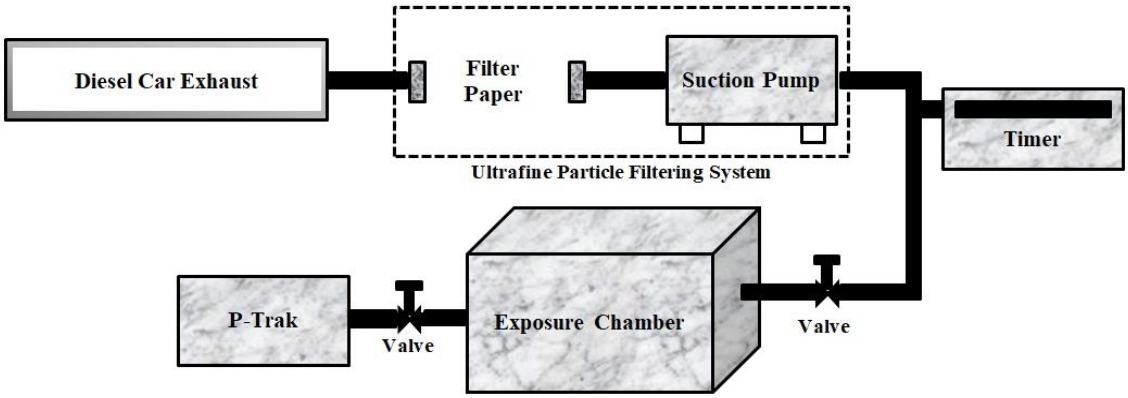

Figure 1. *The schematic of the ultrafine particle concentration measurements*

http://www.aloki.hu ● ISSN 1589 1623 (Print) ● ISSN 1785 0037 (Online)
DOI: http://dx.doi.org/10.15666/aeer/1605_55835593
© 2018, ALÖKI Kft., Budapest, Hungary

Experimental Animals and Treatments

The study included 50 male Wistar mice (12 weeks old, body weight: 21 - 23 g). All mice were treated humanely, provided with water and foods *ad libitum*, and kept under controlled light (12:12 dark-light cycle) and room temperature (27.4 - 28.1^{o}C). An acclimatization period of three days was allowed for the mice before any exposure treatment. All animal treatment procedures were approved by the Animal Care and Use Committee of Brawijaya University Malang, Indonesia (Ethical Clearance number: 541-KEP-UB).

After the acclimation, the mice were randomly divided into a control group (C0) - the group of unexposed mice (n = 5) - and the exposure groups (C1, C2, and C3, n = 5 per car sample per group). The mice from C1 groups were exposed to the ultrafine particles with the car sample D1, D2, and D3 with the injection time of 20 seconds. The mice from C2 and C3 groups were exposed to the ultrafine particles with the car sample D1, D2, and D3 with the injection times of 40 and 60 seconds, respectively. The exposures were conducted for 100 seconds on eight consecutive days (100 seconds per day). Our previous research gave us information that the mice collapsed more than eight days after the exposure. After the last day of the exposure, all mice were sacrificed using a cervical vertebra dislocation method in order to take the blood drop samples. The blood was collected in tubes, and the smears were made on object glasses and fixed with methanol solutions (70%). When they came dried (±5 minutes), they were colored using Giemsa-buffer pro-Giemsa solution (1:3) as long as 15 minutes. The samples were washed in running tap water. Any section showing abnormal morphology caused by the drying procedure was discarded.

Deformation Calculation

Digital images of the blood samples were taken with a 400x magnification of areas can reliably be judged from an overall evaluation of the slide. Five different investigators scored random fields of view using a Binocular BX-51 Computer Microscope (Wang et al., 2017, Cannizzaro et al., 2009). The deformation level (DL) of the mice erythrocytes was calculated using equation (1) (Wardoyo et al., 2017). The total of deformed and normal erythrocytes were averaged from those ten fields of view for each animal and then averaged from 5 animals.

$$DL = \frac{\sum deformed\ erythrocytes}{\sum erythrocytes} x\ 100\% \qquad \text{(Eq.1)}$$

Statistical Analysis

Values are expressed as the means ± SD (standard deviation). The differences between two groups (C0 and an exposure group) were evaluated using a Student's *t*-test. We compared the results obtained in the control group and the D1 group, the control group and the D2 group, and the control group and the D3 group. The association between the exposure to the ultrafine particles and the erythrocyte deformation level was interpreted by a linear regression analysis using Microsoft Excel 2016. $R^2 > 0.85$ was considered as significantly correlated, and $p < 0.05$ was considered to show statistical significance (Eeftens et al., 2015).

http://www.aloki.hu ● ISSN 1589 1623 (Print) ● ISSN 1785 0037 (Online)
DOI: http://dx.doi.org/10.15666/aeer/1605_55835593
© 2018, ALÖKI Kft., Budapest, Hungary

Results

Ultrafine Particles Concentration

The concentrations of ultrafine particles mice were exposed to for eight consecutive days are presented in *Table 1*. Based on the measurement results, a longer time needed to inject the exhaust emission to the exposure chamber generates a higher ultrafine particle concentration. Compared to C1, the concentrations of C2 and C3 are higher, in which the highest concentration is found in C3. On the other hand, the lowest ultrafine particle concentration is found in C1.

Table 1. *Ultrafine particles concentration mice were exposed to(mean ± SD)*

Ultrafine Particle Concentrations	Ultrafine Particles Concentration (x10^7 particles/ cm^3)		
	D1	D2	D3
C1	3.65 ± 0.04	2.26 ± 0.02	1.03 ± 0.10
C2	4.87 ± 0.26	2.87 ± 0.16	1.10 ± 0.07
C3	5.46 ± 0.35	3.28 ± 0.08	1.22 ± 0.01

Deformation Level

The digital images used to observe histological changes (deformation) in the mice erythrocytes are shown in *Fig. 2*. The erythrocytes in those examples are obtained from the control and the exposure groups. The control group is used to observe the native deformation of the healthy mice (normal mice, without exposure). According to *Fig. 2*, there are significant differences in the deformation level between the control mice and the exposed mice. The normal erythrocytes are interpreted as the red circles, and the abnormal ones are shown by the black circles. A normal erythrocyte has a biconcave shape. The abnormal erythrocytes are obtained as (1) teardrop-shaped, (2) helmet-shaped cells, (3) sickle-shaped cells, (4) ovalocytes, (5) saddle-shaped, and (6) stomatocytes (Zhang et al., 2009). *Table 2* below interprets the calculated deformation levels of the mice erythrocytes.

Table 2. *Deformation levels from the control and exposure groups ($p < 0.05$ between two groups: the control group and an exposure group)*

Ultrafine Particle Concentration	Deformation Levels (%)		
	D1	D2	D3
Control	12 ± 1	12 ± 1	12 ± 1
C1	32 ± 1	31 ± 1	25 ± 2
C2	33 ± 3	32 ± 1	26 ± 1
C3	35 ± 2	33 ± 3	29 ± 1

Figure 2 shows that the exposure of ultrafine particles with the concentration of C1 induces a significant increase in the deformed erythrocytes compared to the control group. It has been observed that the exposure to ultrafine particles with the

http://www.aloki.hu ● ISSN 1589 1623 (Print) ● ISSN 1785 0037 (Online)
DOI: http://dx.doi.org/10.15666/aeer/1605_55835593
© 2018, ALÖKI Kft., Budapest, Hungary

concentration of C1 induced 110 ± 5, 119 ± 3, and 93 ± 9 deformed erythrocytes in D1, D2, and D3 car samples, respectively. In the group of C2, the exposed ultrafine particles significantly decrease the number of normal erythrocytes compared to the control group (245 ± 7 cells). The deformed erythrocytes in the group of C2 for the car sample D1, D2, and D3 are 103 ± 11 cells, 111 ± 6 cells, and 99 ± 5 cells, respectively. Similarly, a significant difference is also found in the other exposure group among the C3 and the control groups. The erythrocyte deformation in the group of C3 for the car sample D1, D2, and D3 involved 107 ± 5 cells, 135 ± 16 cells, and 81 ± 5 cells, respectively.

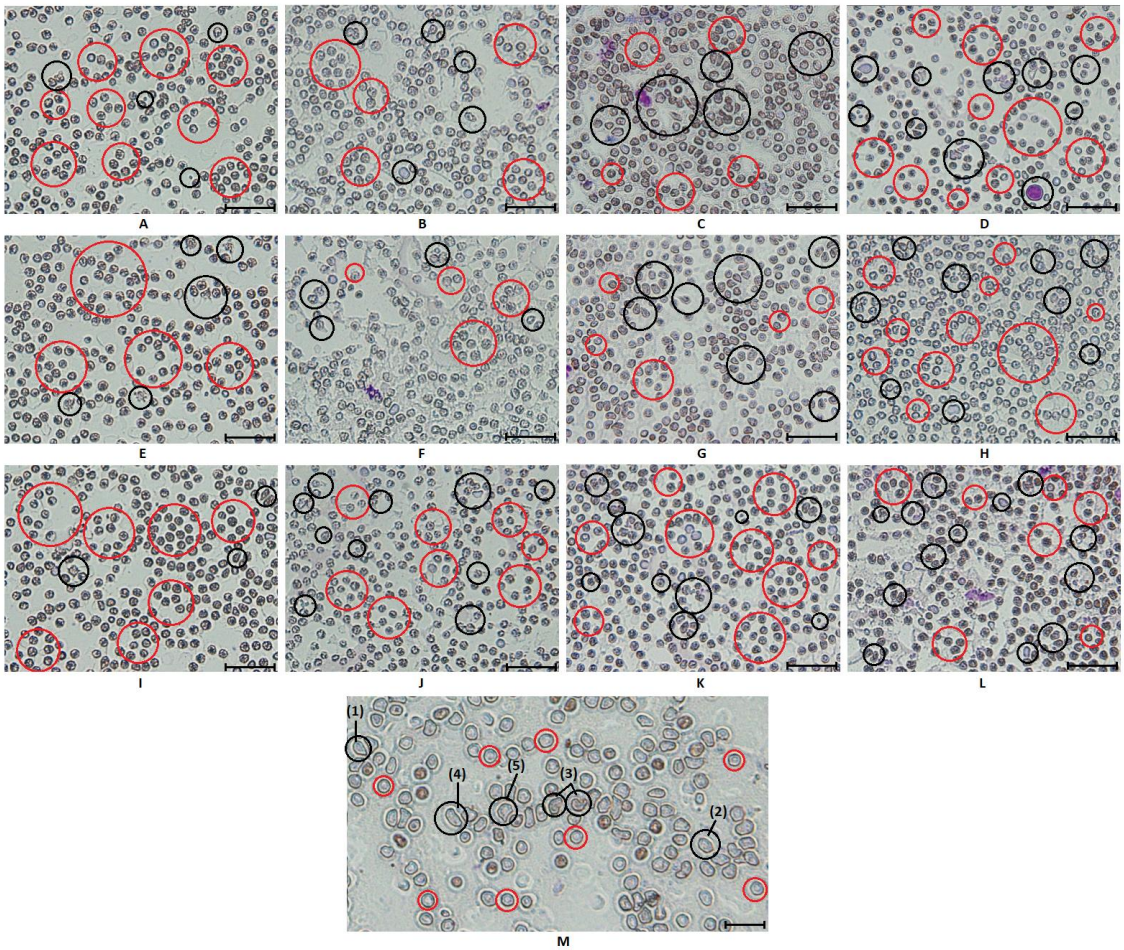

Figure 2. *Digital images from the control group (A; E; and I) and the treatment groups, with 400x of magnification (scale bar: 30 µm): B-D = C1 groups; F-H = C2 groups; and J-L = C3 groups. The normal and deformed erythrocytes (M), scale bar: 20 µm*

Ultrafine Particle Concentration vs Deformation Level

For a better understanding, *Fig. 3* depicts the correlation between the exposure to the ultrafine particles and the deformation levels of the mice erythrocytes (D1-D3). In order to investigate the influence of the exposure to ultrafine particles, the deformation levels of the mice erythrocytes were alleviated by the deformation level obtained in the control group. The correlation between the ultrafine particle concentration and the erythrocyte deformation was interpreted in a linear regression. In the car sample of D1, the

http://www.aloki.hu ● ISSN 1589 1623 (Print) ● ISSN 1785 0037 (Online)
DOI: http://dx.doi.org/10.15666/aeer/1605_55835593
© 2018, ALÖKI Kft., Budapest, Hungary

increasing amount of the ultrafine particle concentrations increase the level of erythrocytes deformation (R^2 = 0.86). Interestingly, the similar trend is found in the different car samples D2 (R^2 = 0.99) and D3 (R^2 = 0.98). The increased concentrations of ultrafine particles in the diesel exhaust emission cause more deformation on the erythrocytes. Based on *Fig. 3*, it is confirmed that a higher dose of ultrafine particles enhanced the deformation levels compared to the control group (see *Table 2*). The figure above shows that the concentration of the ultrafine particles contained in the car exhaust emission had direct influences on the mice erythrocytes deformability (R^2 > 0.85). All graphs indicate a high correlation, since the values of each R^2 approach 1.

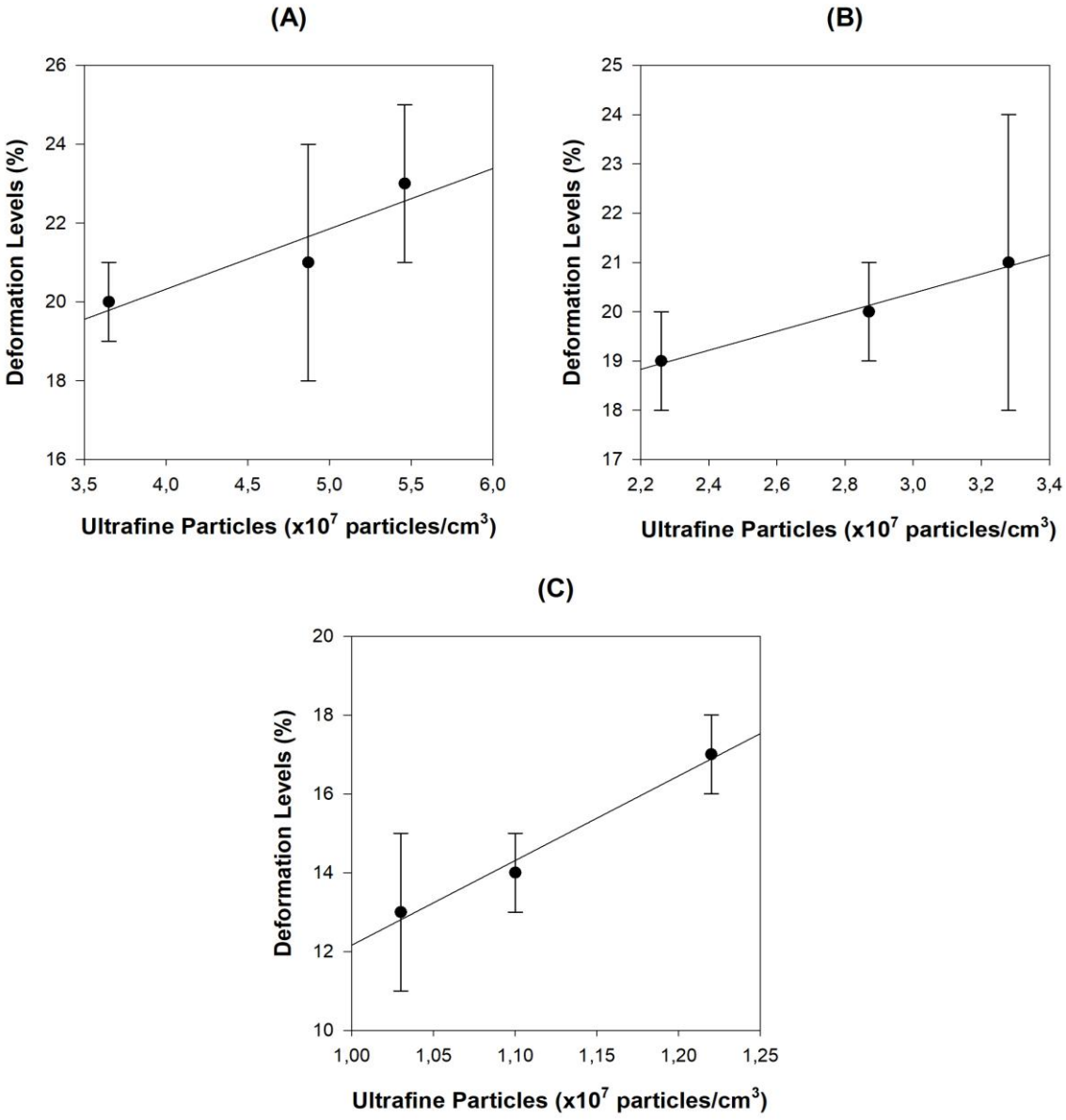

Figure 3. *The correlations between the concentration of ultrafine particles in the car exhaust smoke and the mice erythrocytes deformation: A). D1; B). D2; and C). D3*

http://www.aloki.hu ● ISSN 1589 1623 (Print) ● ISSN 1785 0037 (Online)
DOI: http://dx.doi.org/10.15666/aeer/1605_55835593
© 2018, ALÖKI Kft., Budapest, Hungary

Discussion

The present study of the erythrocyte deformability is of great importance in hemorheology. This study reveals a novel association between exposure to ultrafine particles contained in the exhaust emission emitted by diesel engine cars and mice erythrocytes deformation. The deformation was indicated by the alteration in the erythrocyte shape that might be related to the erythrocyte function in the body system. As we know, a normal erythrocyte needs flexibility in transporting gases in the body. A biconcave shape of a normal erythrocyte is related to its work in squeezing through capillaries. It is necessary to investigate the erythrocytes morphological changes (deformation). The existence of erythrocyte deformation or the morphological changes may relate to the abnormal function of blood. For example, a previous study showed that the erythrocyte deformation was related to the sickle cell disease (Charrin et al., 2016). Similarly, any alteration due to erythrocytes deformation becomes a marker of iron deficiency anemia and thalassemia (Zhang et al., 2012), as well as the sickle cell disease (Charrin et al., 2016).

Our findings suggest that the cell alteration by exposure to ultrafine particles is confined to the erythrocyte deformation. In this study, unexposed mice (control group) had healthier erythrocytes with normal biconcave cells, and on the contrary, the exposed mice showed a positive correlation with the abnormal erythrocytes ($p < 0.05$) (*Fig. 3*). In addition to the cell alteration, the deformation of the mice erythrocytes can be linked to the cell physical alteration (Yoon and You, 2016) and the existence of eryptosis, suicidal death erythrocytes (Mischitelli et al., 2016). Consistent with this assessment, we found that deformation level, as well as the deformed erythrocytes, were significantly increased in the mice exposed to the ultrafine particles. The deformation effects of the exposure to ultrafine particles are in accordance with a previous study (Wardoyo et al., 2017), confirming that exposure to ultrafine particles contained in the motorcycle exhaust emission induces erythrocytes deformation, such as sickle-shaped cells, teardrop-shaped cells, and helmet-shaped cells, which then increase the level of erythrocyte deformation.

This study corroborates previous findings obtained from mice exposed to acute ultrafine particles contained in the motorcycle exhaust emission (ten consecutive days), implicating the deformation effects in the mice tubular epithelial cells (Wardoyo et al., 2018) and erythrocytes (Wardoyo et al., 2017). Consistent with this result, erythrocytes are highly deformable and may also exhibit reduced deformability and stronger aggregation in many pathological situations, such as sickle cell anemia (Popel and Johnson, 2005). Eryptosis itself can be triggered by any kind of erythrocyte injury, including oxidative stress due to reactive oxygen species (Mischitelli et al., 2016). This deformation effect is likely to be due to the continuous exposure of diesel exhaust particles which alter the lipid bilayer. This suggests that an important role may exist between exposure to diesel exhaust particles and erythrocyte deformation, oxidative stress, and chronic inflammation. Interestingly, there is a significant correlation between erythrocyte deformability and oxidative stress and chronic inflammation markers (Gyawali et al., 2015). This probably may develop due to the erythrocyte responses in countering the effects of oxidative stress and chronic inflammation. Oxidation of membrane lipids and proteins may alter the erythrocytes (Richards et al., 1998).

The oxidative stress and chronic inflammation can be related to the production of reactive oxygen species (Jantzen et al., 2016). The generation of reactive oxygen species due to the exposure to ultrafine particles might be related to the cytotoxic effect

http://www.aloki.hu ● ISSN 1589 1623 (Print) ● ISSN 1785 0037 (Online)
DOI: http://dx.doi.org/10.15666/aeer/1605_55835593
© 2018, ALÖKI Kft., Budapest, Hungary

on endothelial cells (Mo et al., 2012). Reactive oxygen species can be related to the translocation of particles. When particles transport through the bloodstream or lymphatic system to vital organs, they can cross the lung-blood barrier and translocate into the blood circulation, unite to erythrocytes, and disturb the cation transport on the membrane causing erythrocytes deformation (Li et al., 2008, Delfino et al., 2005). This deformation can be linked to the decreasing amount of mice antioxidant (becoming the free radicals generators) (Kampa and Castanas, 2008). However, the effect of deposited particulate matters in altering the mice erythrocytes was found in some abnormal forms of erythrocytes. Diesel exhaust particles exposures indeed had a significant role in generating the inflammatory and genotoxic effects (Hougaard et al., 2008). The form of a normal erythrocyte in the two-dimensional model is a biconcave capsule, and its radius is ± 3.91 μm (Zhang et al., 2009). However, this form may change due to the existence of particles, as explained above. In addition, the most erythrocytes found in our research are in a normal form. This state becomes the evidence that not all erythrocytes can be influenced by the particles. We consider that the membrane rigidity prevents large deformation and large cell contact area, resulting in a less dense erythrocytes cores (Zhang et al., 2009). Moreover, the deformations were influenced by some factors, such as neo-Hookean elastic (Bagchi et al., 2005) and the local tangential and the normal directions of the membrane (Zhang et al., 2009). The above analysis conveyed that the possible interactions occurred between exposure to diesel exhaust particles and erythrocyte deformability.

Motor vehicle emission may consist of polycyclic aromatic hydrocarbons (Lai et al., 2013) and volatile organic compounds (Ge et al., 2018). Similarly, previous studies measured the substances of particulate matters emitted by motor vehicles, including polycyclic aromatic hydrocarbons and volatile organic compounds (Pham et al., 2013, Yan et al., 2015, Wierzbicka et al., 2014). Epidemiologic studies have investigated the toxic impacts related to the exposure to polycyclic aromatic hydrocarbons and volatile organic compounds. Polycyclic aromatic hydrocarbon substances, such as anthracene, phenanthrene, fluoranthene, benzo(a)pyrene, pyrene, and naphthalene, and many other forms are well-known to be the carcinogens for human health (Tongo et al., 2017, Sarigiannis et al., 2015, Bortey-Sam et al., 2017, Louis et al., 2016, Pham et al., 2013). On the other hand, volatile organic compounds also become hazardous chemicals and toxic to human health due to the carcinogenic and mutagenic characteristics (Kumar et al., 2018).

Conclusion

In conclusion, diesel exhaust ultrafine particles significantly affect the mice erythrocyte deformation. The dose concentration of diesel exhaust ultrafine particles have an influence on the erythrocyte deformation level. The more diesel ultrafine particles mice were exposed to the more damage to the erythrocytes was observed. The correlation between the ultrafine particle exposure and the erythrocyte deformation was obtained proportionally with the $R^2 > 0.85$.

Acknowledgements. All the authors are grateful to Directorate General of Higher Education, for providing funding for conducting this research project. The kind hands of Arif Budianto, Mia Anggun P., Eko T.P.A., Arsyal K.R., Renado Anggara, and M. Nurhuda Arifandi involving in this study are gratefully acknowledged.

http://www.aloki.hu ● ISSN 1589 1623 (Print) ● ISSN 1785 0037 (Online)
DOI: http://dx.doi.org/10.15666/aeer/1605_55835593
© 2018, ALÖKI Kft., Budapest, Hungary

REFERENCES

[1] Bagchi, P., Johnson, P.C., Popel, A.S. (2005): Computational fluid dynamic simulation of aggregation of deformable cells in a shear flow. – Journal of Biomechanical Engineering 127(7): 1070–1080.

[2] Bortey-Sam, N., Ikenaka, Y., Akoto, O., Nakayama, S.M.M., Asante, K.A., Baidoo, E., Obirikorang, C., Saengtienchai, A., Isoda, N., Nimako, C., Mizukawa, H., Ishizuka, M. (2017): Oxidative stress and respiratory symptoms due to human exposure to polycyclic aromatic hydrocarbons (PAHs) in Kumasi, Ghana. – Environmental Pollution 228: 311–320.

[3] Cannizzaro, V., Berry, L.J., Nicholls, P.K., Zosky, G.R., Turner, D.J., Hantos, Z., Sly, P.D. (2009): Lung volume recruitment maneuvers and respiratory system mechanics in mechanically ventilated mice. – Respiratory Physiology and Neurobiology 169(3): 243–251.

[4] Charrin, E., Ofori-Acquah, S.F., Nader, E., Skinner, S., Connes, P., Pialoux, V., Joly, P., Martin, C. (2016): Inflammatory and oxidative stress phenotypes in transgenic sickle cell mice. – Blood Cells, Molecules, and Diseases 62: 13–21.

[5] Delfino, R.J., Sioutas, C., Malik, S. (2005): Review potential role of ultrafine particles in associations between airborne particle mass and cardiovascular health. – Environmental Health Perspectives 113(8): 934–947.

[6] Eeftens, M., Phuleria, H.C., Meier, R., Aguilera, I., Corradi, E., Davey, M., Ducret-Stich, R., Fierz, M., Gehrig, R., Ineichen, A., Keidel, D., Probst-Hensch, N., Ragettli, M.S., Schindler, C., Künzli, N., Tsai, M.-Y. (2015): Spatial and temporal variability of ultrafine particles, NO2, PM2.5, PM2.5 absorbance, PM10 and PMcoarse in Swiss study areas. – Atmospheric Environment 111(2): 60–70.

[7] Ge, J.C., Kim, H.Y., Yoon, S.K., Choi, N.J. (2018): Reducing volatile organic compound emissions from diesel engines using canola oil biodiesel fuel and blends. – Fuel 218(January): 266–274.

[8] Gyawali, P., Richards, R.S., Bwititi, P.T., Nwose, E.U. (2015): Association of abnormal erythrocyte morphology with oxidative stress and inflammation in metabolic syndrome. – Blood Cells, Molecules, and Diseases 54(4): 360–363.

[9] Hemmingsen, J.G., Hougaard, K.S., Talsness, C., Wellejus, A., Loft, S., Wallin, H., Møller, P. (2009): Prenatal exposure to diesel exhaust particles and effect on the male reproductive system in mice. – Toxicology 264: 61–68.

[10] Hougaard, K.S., Jensen, K.A., Nordly, P., Taxvig, C., Vogel, U., Saber, A.T., Wallin, H. (2008): Effects of prenatal exposure to diesel exhaust particles on postnatal development, behavior, genotoxicity and inflammation in mice. – Particle and Fibre Toxicology 5(3).

[11] Jantzen, K., Møller, P., Karottki, D.G., Olsen, Y., Bekö, G., Clausen, G., Hersoug, L.G., Loft, S. (2016): Exposure to ultrafine particles, intracellular production of reactive oxygen species in leukocytes and altered levels of endothelial progenitor cells. – Toxicology 359–360: 11–18.

[12] Kampa, M., Castanas, E. (2008): Human health effects of air pollution. – Environmental pollution (Barking, Essex : 1987) 151(2): 362–367.

[13] Kumar, A., Singh, D., Kumar, K., Singh, B.B., Jain, V.K. (2018): Distribution of VOCs in urban and rural atmospheres of subtropical India: Temporal variation, source attribution, ratios, OFP and risk assessment. – Science of the Total Environment 613–614: 492–501.

[14] Lai, C.-H., Chuang, K.-Y., Chang, J.-W. (2013): Characteristics of nano-/ultrafine particle-bound PAHs in ambient air at an international airport. – Environmental science and pollution research international 20(3): 1772–80.

[15] Li, S.-Q., Zhu, R.-R., Zhu, H., Xue, M., Sun, X.-Y., Yao, S.-D., Wang, S.-L. (2008): Nanotoxicity of TiO2 nanoparticles to erythrocyte in vitro. – Food and Chemical Toxicology 46(12): 3626–3631.

http://www.aloki.hu ● ISSN 1589 1623 (Print) ● ISSN 1785 0037 (Online)
DOI: http://dx.doi.org/10.15666/aeer/1605_55835593
© 2018, ALÖKI Kft., Budapest, Hungary

[16] Louis, C., Liu, Y., Tassel, P., Perret, P., Chaumond, A., Andre, M. (2016): PAH, BTEX, carbonyl compound, black-carbon, NO2 and ultrafine particle dynamometer bench emissions for Euro 4 and Euro 5 diesel and gasoline passenger cars. – Atmospheric Environment 141(2): 80–95.
[17] Mischitelli, M., Jemaa, M., Almasry, M., Faggio, C., Lang, F. (2016): Triggering of suicidal erythrocyte death by fascaplysin. – Cellular Physiology and Biochemistry 39(September): 1638–1647.
[18] Mo, Y., Wan, R., Feng, L., Chien, S., Tollerud, D.J., Zhang, Q. (2012): Combination effects of cigarette smoke extract and ambient ultrafine particles on endothelial cells. – Toxicology in vitro : an international journal published in association with BIBRA 26(2): 295–303.
[19] Pham, C.T., Kameda, T., Toriba, A., Hayakawa, K. (2013): Polycyclic aromatic hydrocarbons and nitropolycyclic aromatic hydrocarbons in particulates emitted by motorcycles. – Environmental Pollution 183: 175–183.
[20] Popel, A.S., Johnson, P.C. (2005): Microcirculation and hemorheology. – Annual Review of Fluid Mechanics 37(1): 43–69.
[21] Richards, R.S., Roberts, T.K., McGregor, N.R., Dunstan, R.H., Butt, H.L. (1998): The role of erythrocytes in the inactivation of free radicals. – Medical Hypotheses 50(5): 363–367.
[22] Sarigiannis, D.A., Karakitsios, S.P., Zikopoulos, D., Nikolaki, S., Kermenidou, M. (2015): Lung cancer risk from PAHs emitted from biomass combustion. – Environmental Research 137: 147–156.
[23] Stewart, J.C., Chalupa, D.C., Devlin, R.B., Frasier, L.M., Huang, L., Little, E.L., Lee, S.M., Richard, P., Anthony, P., Taubman, M.B., Utell, M.J., Frampton, M.W. (2010): Vascular effects of ultrafine particles in persons with type 2 diabetes. – Environmental Health Perspectives 118(12): 1692–1699.
[24] Tongo, I., Ogbeide, O., Ezemonye, L. (2017): Human health risk assessment of polycyclic aromatic hydrocarbons (PAHs) in smoked fish species from markets in Southern Nigeria. – Toxicology Reports 4: 55–61.
[25] Waly, M.I., Ali, B.H., Nemmar, A. (2013): Acute effects of diesel exhaust particles and cisplatin on oxidative stress in cultured human kidney (HEK 293) cells, and the influence of curcumin thereon. – Toxicology in Vitro 27(8): 2299–2304.
[26] Wang, F., Gao, F., Lan, M., Yuan, H., Huang, Y., Liu, J. (2009): Oxidative stress contributes to silica nanoparticle-induced cytotoxicity in human embryonic kidney cells. – Toxicology in Vitro 23(5): 808–815.
[27] Wang, T., Miao, M., Bai, M., Li, Y., Li, M., Li, C., Xu, Y. (2017): Effect of sophora japonica total flavonoids on pancreas, kidney tissue morphology of streptozotocin-induced diabetic mice model. – Saudi Journal of Biological Sciences 24(3): 741–747.
[28] Wardoyo, A.Y.P., Juswono, U.P., Noor, J.A.E. (2017): A study of the correlation between ultrafine particle emissions in motorcycle smoke and mice erythrocyte damages. – Experimental and Toxicologic Pathology 69(8): 649–655.
[29] Wardoyo, A.Y.P., Juswono, U.P., Noor, J.A.E. (2018): Varied dose exposures to ultrafine particles in the motorcycle smoke cause kidney cell damages in male mice. – Toxicology Reports 5: 383–389.
[30] Wardoyo, A.Y.P., Morawska, L., Ristovski, Z.D., Jamriska, M., Carr, S., Johnson, G. (2007): Size distribution of particles emitted from grass fires in the Northern Territory, Australia. – Atmospheric Environment 41(38): 8609–8619.
[31] Wierzbicka, A., Nilsson, P.T., Rissler, J., Sallsten, G., Xu, Y., Pagels, J.H., Albin, M., Österberg, K., Strandberg, B., Eriksson, A., Bohgard, M., Bergemalm-rynell, K., Gudmundsson, A. (2014): Detailed diesel exhaust characteristics including particle surface area and lung deposited dose for better understanding of health effects in human chamber exposure studies. – Atmospheric Environment 86: 212–219.

http://www.aloki.hu ● ISSN 1589 1623 (Print) ● ISSN 1785 0037 (Online)
DOI: http://dx.doi.org/10.15666/aeer/1605_55835593
© 2018, ALÖKI Kft., Budapest, Hungary

[32] Xu, Y., Barregard, L., Nielsen, J., Gudmundsson, A., Wierzbicka, A., Axmon, A., Jönsson, B.A.G., Kåredal, M., Albin, M. (2013): Effects of diesel exposure on lung function and inflammation biomarkers from airway and peripheral blood of healthy volunteers in a chamber study. – Particle and Fibre Toxicology 10(60): 1–9.
[33] Yan, C., Zheng, M., Yang, Q., Zhang, Q., Qiu, X., Zhang, Y., Fu, H., Li, X., Zhu, T., Zhu, Y. (2015): Commuter exposure to particulate matter and particle-bound PAHs in three transportation modes in Beijing, China. – Environmental Pollution 204: 199–206.
[34] Yoon, D., You, D. (2016): Continuum modeling of deformation and aggregation of red blood cells. – Journal of Biomechanics 49(11): 2267–2279.
[35] Zhang, J., Johnson, P.C., Popel, A.S. (2009): Effects of erythrocyte deformability and aggregation on the cell free layer and apparent viscosity of microscopic blood flows. – Microvascular Research 77(3): 265–272.
[36] Zhang, Y., Zhang, W., Wang, S., Wang, C., Xie, J., Chen, X., Xu, Y. Mao, P. (2012): Detection of human erythrocytes influenced by iron deficiency anemia and thalassemia using atomic force microscopy. – Micron 43(12): 1287–1292.

http://www.aloki.hu ● ISSN 1589 1623 (Print) ● ISSN 1785 0037 (Online)
DOI: http://dx.doi.org/10.15666/aeer/1605_55835593
© 2018, ALÖKI Kft., Budapest, Hungary

ANALYSIS OF FLOWER BUD DIFFERENTIATION OF *JATROPHA NIGROVIENSRUGOSUS* AT DIFFERENT DEVELOPMENTAL STAGES

XIAO, F.[1,2] – WANG, X. R.[1*] – ZHAO, Y.[1,2] – HE, H.[1]

[1]*Foresty College of Guizhou University, 550225 Guiyang, China*

[2]*Institute for Forest Resources & Environment of Guizhou, 550225 Guiyang, China*

**Corresponding author*
e-mail: wxr7211@126.com

(Received 27th Jun 2018; accepted 2nd Aug 2018)

Abstract. The female to male flower ratio of *Jatropha nigroviensrugosus*, a new cultivar, is higher than that of the common *J. curcas*. However, the sex determination mechanism of *J. curcas* remains elusive. In the present study, gene expression analysis of inflorescence buds, female and male flowers, and new leaf buds of *J. nigroviensrugosus* was performed, using second-generation sequencing. The results demonstrated that high expression of genes related to sucrose phosphate synthase, soluble starch synthase (EC:2.4.1.21) and granule-bound starch synthase promoted the formation and development of male flowers, and the genes CUP-SHAPED COTYLEDON 2 (*CUC2)* and *CUC3*, played pivotal roles in regulating the formation and development of female flowers. The initial development of female flower primordia required cytokinins (CTK) induction, while late developmental stages only required a low concentration of CTK. The characteristic genes for floral organ development were conservatively expressed in the four tested parts. In this investigation, we not only provide genetic information regarding the differential developmental processes between female and male flowers, but also deepen our understanding of *J. nigroviensrugosus*.
Keywords: *Jatropha, new cultivar, differential expressed gene, transcription factor*

Introduction

Jatropha curcas L., a plant of the *Jatropha* genus in the *Euphorbiaceae* family, is an important energy-bearing tree which is extensively distributed worldwide. *J. curcas* has a high, untapped potential to contribute towards sustainable production of food and bioenergy, rehabilitation of degraded land, and reduction of atmospheric carbon dioxide, its potential oil productivity is 1.9 t/ha, beginning the fourth year after planting (Montes et al., 2016; Dias et al., 2012). However, the low seed yield of has been a stumbling block in realizing its full potential as an ideal bioenergy crop, the small number of female flowers and a low female to male flower ratio (ranges from1:20 to 1:108) are the main factors limiting its seed yield (Gangwar et al., 2018; Ashoke et al., 2005). Breeders are mainly concerned with shortening the young growth cycle of *J. curcas*; increasing the ratio of female to male flowers; increasing oil content, seed weight, seed volume and other traits. Seed weight had positive correlation with seed length, breadth, thickness and oil content (Kaushik et al., 2007). The shortening of the breeding cycle and the increasing the number of female flowers contribute to the number of seeds, and the traits such as seed size, density and volume are important indicators affecting yield. Changing the offspring traits through interspecific hybridization in *J. curcas*, or through the method of discovery, identification, promotion and application of high-yield new varieties is a necessary way to genetic improvement.

http://www.aloki.hu ● ISSN 1589 1623 (Print) ● ISSN 1785 0037 (Online)
DOI: http://dx.doi.org/10.15666/aeer/1605_55955610
© 2018, ALÖKI Kft., Budapest, Hungary

J. nigroviensrugosus CV Yang, a new variant of *J. curcas* discovered in 2005, its main features are the downward cotyledons and true leaves, bulged leaf tissues (wrinkled leaves). It has a larger number of female flowers and a higher female to male flower ratio, which means a higher seed yield, the experimental plots for many years of afforestation showed that the dry seed yield per hectare of five-year-old stands in *J. nigroviensrugosus* reached 3196.8 kg/ha, which was 6 times higher than *J. curcas* (349.5~559.5 kg/ha); the oil content of the seeds in *J. nigroviensrugosus* was 40~42%, which was higher than *J. curcas* (30 ～ 40%) (Yang et al., 2012, 2013, 2015). Comparison of the $\delta^{13}C$ values and various photosynthetic indices between *J. nigroviensrugosus* and *J. curcas*, with respect to different flowering stages, demonstrated that during the leaf bud stage, *J. nigroviensrugosus* transported a large amount of nutrients to the leaf buds for their differentiation to flower buds. Therefore, flower differentiation is likely determined during the transformation from leaf to flower buds, and the flowering numbers may be determined during the inflorescence stage (He et al., 2016).

Flower formation has continuously been a focus in Plant developmental biology. Studies regarding sex expression and floral morphology are essential for deep understanding of breeding and for the determination of the reproductive potential of plant genotypes (De Lourdes Adriano-Anaya et al., 2016). The transcriptome describes all RNA transcribed by a certain tissue or cell at a certain developmental stage or in a specific physiological state, reflecting the overall expression pattern and regulation of genes. The female or male favorable analysis of floral development in both monoecious and dioecious plants by transcriptome profiling or microarray analysis may help to better understand flower development and the gender regulatory network (Mao et al., 2017; Gao et al., 2013; Rocheta et al., 2014). Hence, we performed high-throughput RNA sequencing (RNA-Seq) and differential analysis on the inflorescence buds, leaf buds, and male and female flowers of *J. nigroviensrugosus*. The present study shed light on the molecular basis of sex determination of *J. nigroviensrugosus* and elucidated the expression patterns of flowering-related genes prior to and following inflorescence and leaf bud differentiation, providing directions for the study of the flowering mechanism of *J. nigroviensrugosus*.

Materials and methods

Materials

The tested plants were collected from Qiaoma Experimental Foreast, Ceheng County, Guizhou Province, China. The place is a typical dry-hot valley climate which is situated 830 m above sea level, with an annual average temperature 19.2 °C, rainfall 1340.7 mm, sunshine duration 1514 h and annual frost-free period is 305 days. It is known as the “natural greenhouse”. The soil is yellow sandy loam developed from sand shales, slightly acidic.. Three 8-year-old *J. nigroviensrugosu* (JCw) plants were selected for the present investigation. The following four tissues were collected from each of the three plants: inflorescence buds at the terminal vegetative shoots (JCw_p) (early-forming adaxial bulges with a diameter <0.3 cm); slightly red new leaf buds at the branch tips (JCw_l); female flowers not yet open (JCw_f) (slightly visible white ovules showing after vertical cut); and male flowers not yet open (JCw_m) (slightly visible yellow anthers showing after vertical cut). Immediately after sample collection, wrap it

http://www.aloki.hu ● ISSN 1589 1623 (Print) ● ISSN 1785 0037 (Online)
DOI: http://dx.doi.org/10.15666/aeer/1605_55955610
© 2018, ALÖKI Kft., Budapest, Hungary

in foil paper and put it into liquid nitrogen. Bring it back to the laboratory and transpose it in a -80 °C ultra-low temperature freezer.

RNA extraction and transcriptome sequencing

Total RNA was extracted from the above-mentioned tissue samples, using TRIzol (Invitrogen, USA). After passing the quality examination, the RNA samples were sent to Shanghai Meiji Biological Cooperation for sequencing from both ends with an Illumina Hiseq sequencing platform.

Sequencing

Following completion of the sequencing, the raw data were quality controlled and compared with the genome of *J. curcas* (https://www.ncbi.nlm.nih.gov/genome/915). The read counts were transformed into FPKM (expected number of fragments per kilobase of transcript sequence per million base pairs sequenced) values for gene expression analysis. The thresholds of $|\log_2 (\text{fold change})| \geq 1$ and q-value < 0.05 were used to determine the differential expressed genes (DEGs) in the resulting reads. The related DEGs were subjected to Gene Ontology (GO, http://www.geneontology.org/) functional enrichment and Kyoto Encyclopedia of Genes and Genomes (KEGG, http://www.genome.jp/kegg/) pathway enrichment.

Results

Transcriptome sequencing and alignment

FastQC (https://www.bioinformatics.babraham.ac.uk/projects/fastqc/) was used to perform quality control on the raw data, demonstrating a Q20 above 97%, a Q30 above 93%, and an average QC content of 43.5%. HISAT2 (https://ccb.jhu.edu/software/hisat2/index.shtml) was used to align the sequenced transcriptome data of *J. nigroviensrugosus* with the genome of *J. curcas* (https://www.ncbi.nlm.nih.gov/genome/915), demonstrating alignment rates higher than 96% (*Table 1*).

Table 1. *Transcriptome sequence number of J. nigroviensrugosus and alignment rate against J. curcas genome*

Sample	Total_seq_num	Aligned_seq_num	Alignment_rate	Uniq_aligned_num	Uniq_rate	Multi_aligned_num	Multi_rate
JCw_p1	61561080	59770212	97.09%	47954394	77.90%	11815818	19.19%
JCw_p2	68567902	66625809	97.17%	53415546	77.90%	13210263	19.27%
JCw_p3	59863830	58056039	96.98%	46249509	77.26%	11806530	19.72%
JCw_l1	65790812	63842133	97.04%	50803720	77.22%	13038413	19.82%
JCw_l2	57042156	55510903	97.32%	44681167	78.33%	10829736	18.99%
JCw_l3	54306178	52727027	97.09%	42234790	77.77%	10492237	19.32%
JCw_f1	63398574	61833649	97.53%	49485973	78.06%	12347676	19.48%
JCw_f2	51699528	50312809	97.32%	40301836	77.95%	10010973	19.36%
JCw_f3	65665646	63948655	97.39%	51294438	78.11%	12654217	19.27%
JCw_m1	61817828	60212667	97.40%	47821892	77.36%	12390775	20.04%
JCw_m2	55453444	54036050	97.44%	42977841	77.50%	11058209	19.94%
JCw_m3	59762748	58184393	97.36%	46342932	77.54%	11841461	19.81%

http://www.aloki.hu ● ISSN 1589 1623 (Print) ● ISSN 1785 0037 (Online)
DOI: http://dx.doi.org/10.15666/aeer/1605_55955610
© 2018, ALÖKI Kft., Budapest, Hungary

Form 40.30 to 53.41 million sequences were aligned to unique positions in the genome, the alignment rates is ranging from 77.22 to 78.33%, form 18.99 to 20.04% sequences is aligning to multiple positions in the genome. These indicating overall matched *J. nigroviensrugosus* sequences with the *J. curcas* genome. Consequently, the sequences may be analyzed as reference-based transcriptome. The small differences between the sequences indicate that the data were highly qualified to reveal differences in inflorescences prior to and subsequent to leaf bud differentiation.

PCA and gene expression analyses

The gene expression of four samples of *J. nigroviensrugosus*, based on the quantitative results of FPKM, was subjected to principal component analysis (PCA), using R (https://www.r-project.org/) which is an open source software. The results denote that the tip inflorescence buds (JCw_p) were closely related to the new leaf buds (JCw_l), with a PC1 value on the X axis of 44.4% and a PC2 value on the Y axis of 31.5%. Three-dimensional (3D) visualization shows significantly clustered samples with no outliers, suggesting good biological repeatability (*Fig. 1a*). According to the DEG screening thresholds, statistical analysis of all pairs of *J. nigroviensrugosus* samples, there were 2995 DEGs between JCw_m and JCw_f, with 1733 upregulated and 862 downregulated genes in JCw_m; 4238 DEGs between JCw_p and JCw_f, with 2138 upregulated and 2100 downregulated genes in JCw_p; 6153 DEGs between in JCw_p and JCw_m, with 3226 upregulated and 2927 downregulated genes in JCw_p. There were 74 genes specifically expressed in JCw_f or JCw_m (*Fig. 1b*).

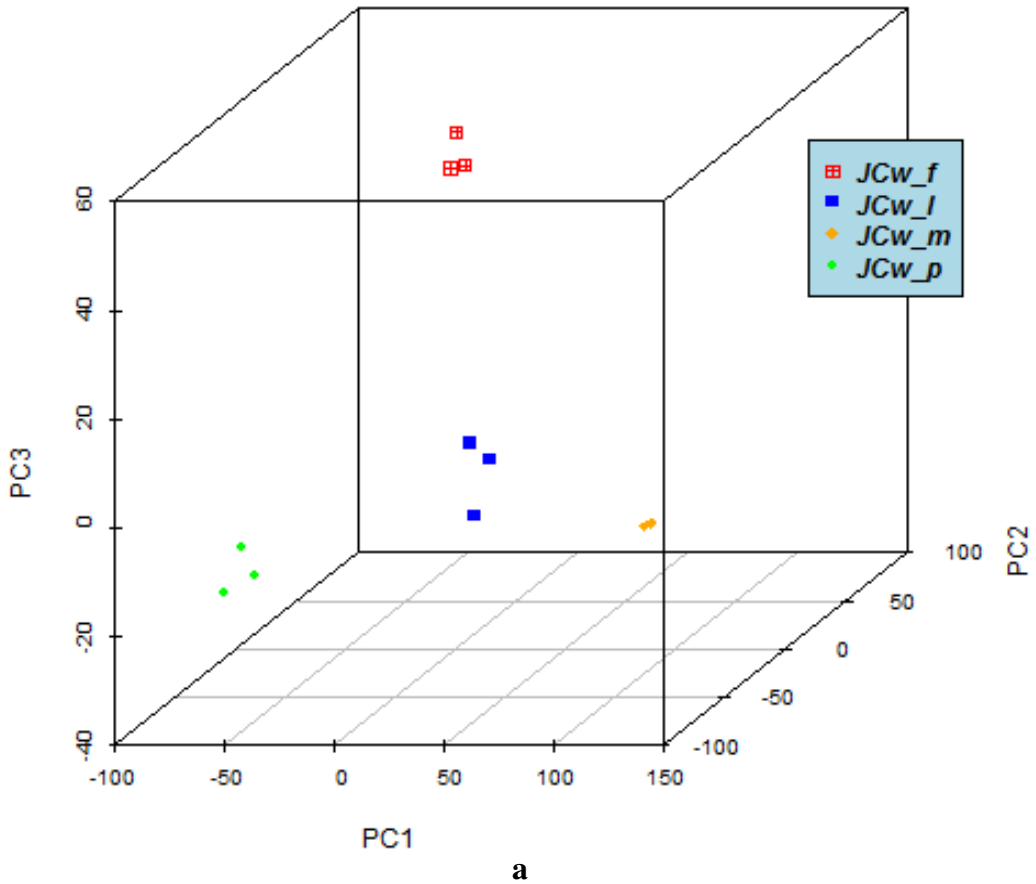

a

http://www.aloki.hu ● ISSN 1589 1623 (Print) ● ISSN 1785 0037 (Online)
DOI: http://dx.doi.org/10.15666/aeer/1605_55955610
© 2018, ALÖKI Kft., Budapest, Hungary

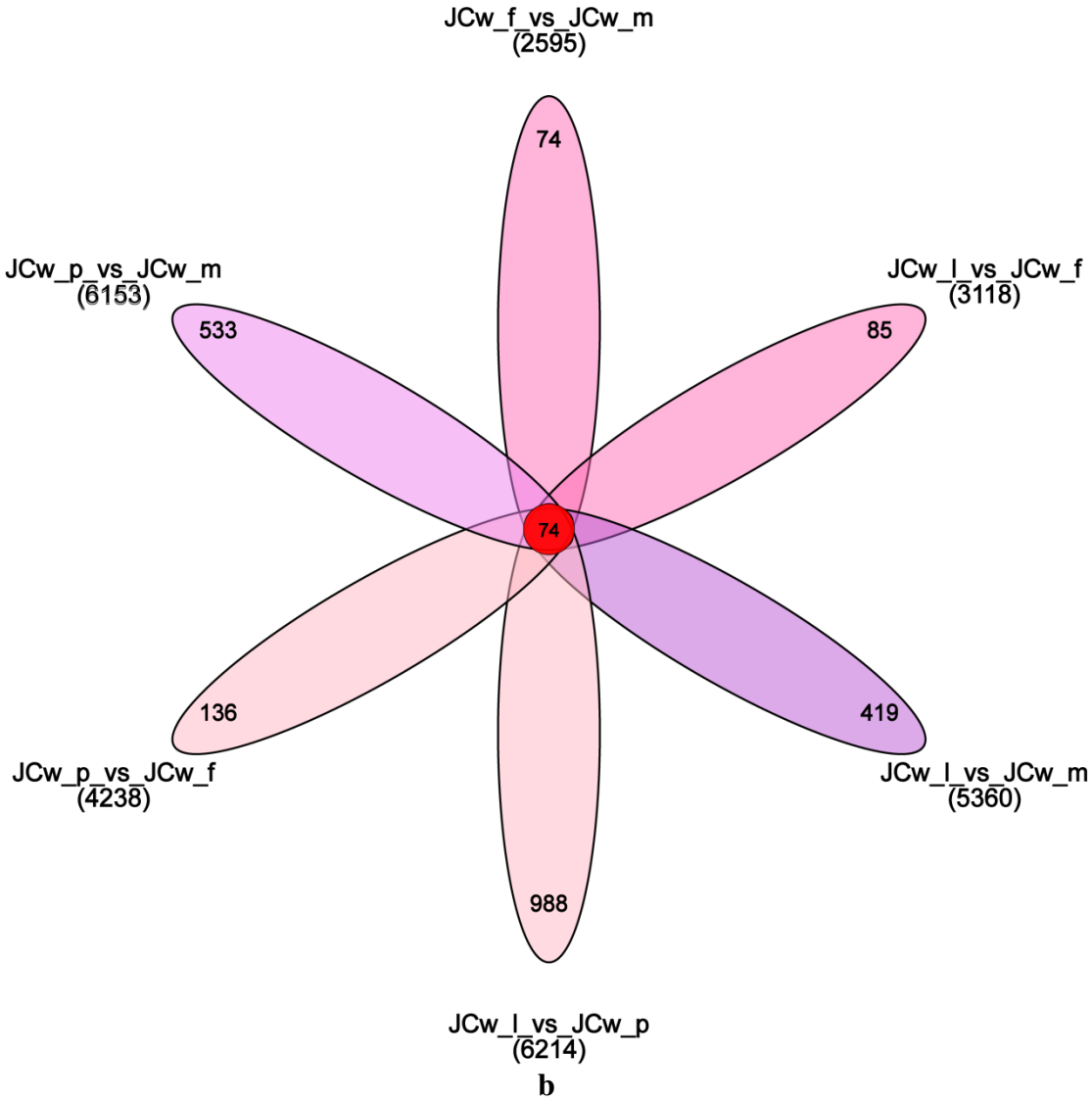

Figure 1. a. *PCA of the different tissues of J. nigroviensrugosus with 3D visualization.* ***b.*** *Venn diagram of DEGs between pairs of J. nigroviensrugosus samples*

Functional enrichment of female and male flowers of J. nigroviensrugosus

GO functional enrichment analysis was conducted on the DEGs between male and female flowers. With respect to the biological process, genes related to carbohydrate metabolism, including glucose, sucrose, polysaccharides and starch, were significantly enriched. With respect to the cell components, genes associated with inner and outer membranes, extracellular regions, transcription factor complexes and the cell skeleton were significantly enriched. In molecular function, genes coupled to glucosidase, hydrolase and oxidoreductase were significantly enriched. Pathway enrichment analysis of DEGs between male and female flowers (*Fig. 2a*) displays significantly enriched metabolic pathways such as starch and sucrose (ko00500), and pentose and glucuronic acid interconversion (ko00040). Moreover, there were significant differences in the plant hormone signal transduction pathway (ko04075), with a total of 16 hormone synthesis-related genes upregulated in female flowers and 18 upregulated in male

http://www.aloki.hu ● ISSN 1589 1623 (Print) ● ISSN 1785 0037 (Online)
DOI: http://dx.doi.org/10.15666/aeer/1605_55955610
© 2018, ALÖKI Kft., Budapest, Hungary

flowers. The abscisic acid (ABR) synthesis-related genes SnRK2 (gene 20150) and ABF (gene 13255 and gene 14512) were significantly upregulated in male flowers. The cytokinin (CTK) synthesis-related gene A-ARR (gene 13354) was significantly upregulated in female flowers, and B-ARR (gene 20147) was significantly upregulated in male flowers.

DEGs analysis between inflorescence and leaf buds, and female and male flowers

Between inflorescence buds and male flowers, the starch and sucrose metabolic pathway (ko00500) was significantly enriched (*Fig. 2b*). In male flowers, the expression of 84 genes related to fructokinase (EC: 2.7.1.4) (gene 5753, gene 8905, and gene 17326), starch synthase (EC: 2.4.1.21) (gene 4801), granule-bound starch synthase (EC: 2.4.1.242) (gene 13471) and sucrose-phosphate synthase (EC: 2.4.1.14) (gene 7836, gene 12091, and gene 14471) were significantly upregulated, and 21 were downregulated. However, there was no significant enrichment of the starch and sucrose metabolic pathway between inflorescence buds and female flowers. The pathway enrichment of the DEGs between inflorescence buds and female flowers reveals enriched metabolic processes such as ribosomes, plant hormone signaling and DNA replication (*Fig. 2c*). With respect to the phytohormone signaling pathway, the ethylene synthesis-related gene ERF1/2 (gene 18694) was upregulated in female flowers. The pathway enrichment of the DEGs between inflorescence and leaf buds displayed enriched metabolic processes such as ribosomes, photosynthesis, photosynthesis-antenna proteins, and plant hormone signaling (*Fig. 2d*). With respect to the photosynthetic pathway, with the exception of gamma (gene 7618) being upregulated in inflorescence buds, the remaining 48 DEGs involved in photosynthesis and 15 DEGs associated with photosynthesis-antenna proteins were all upregulated in leaf buds.

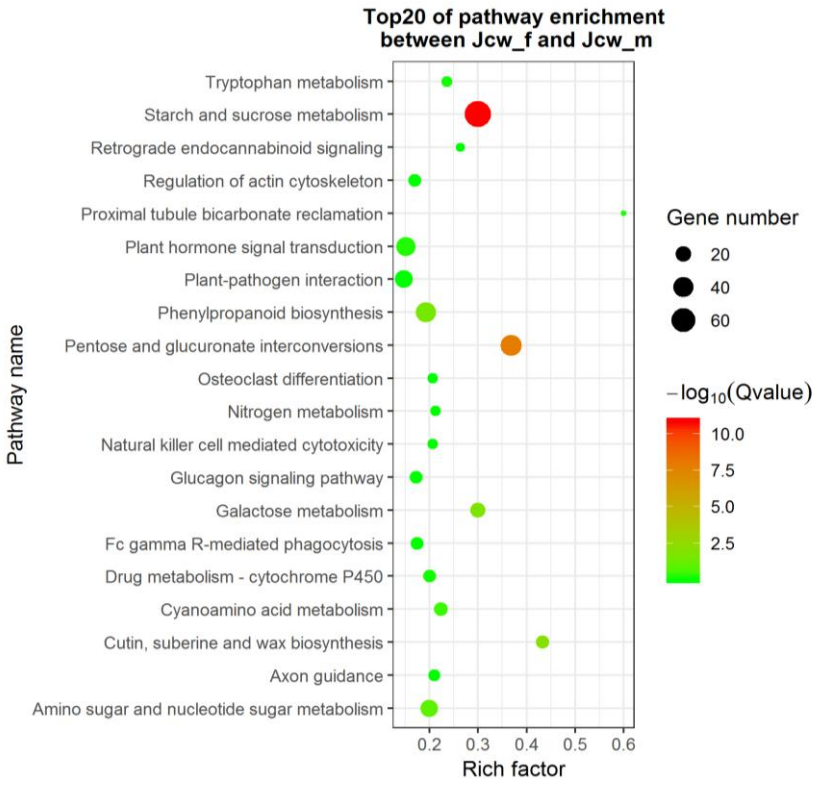

a

http://www.aloki.hu ● ISSN 1589 1623 (Print) ● ISSN 1785 0037 (Online)
DOI: http://dx.doi.org/10.15666/aeer/1605_55955610
© 2018, ALÖKI Kft., Budapest, Hungary

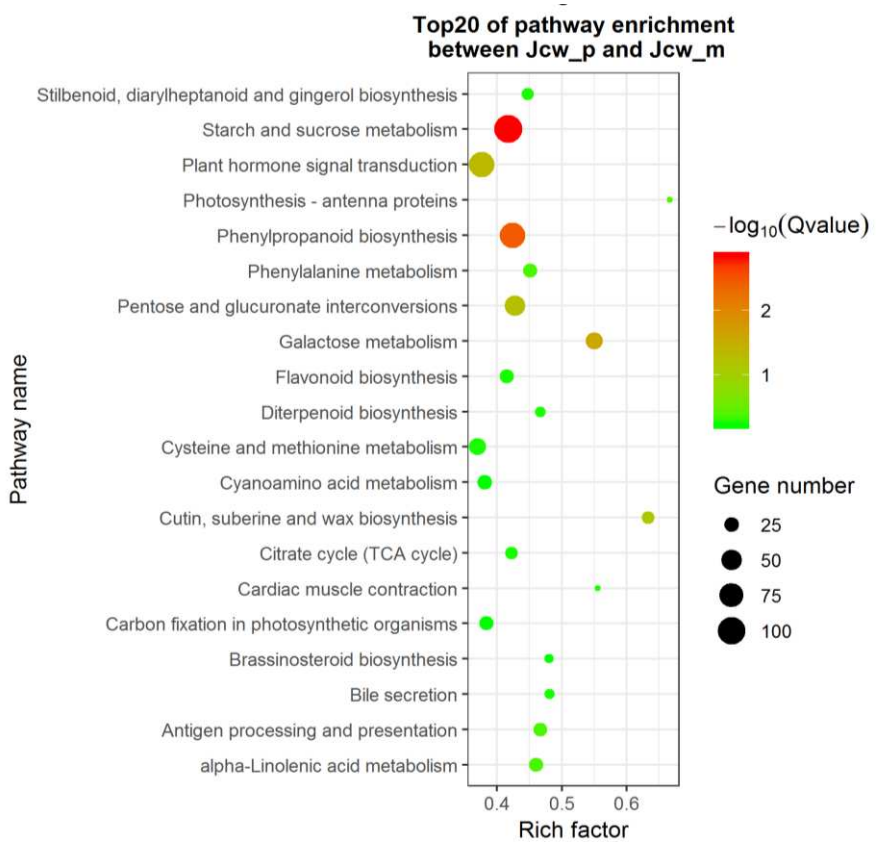

b

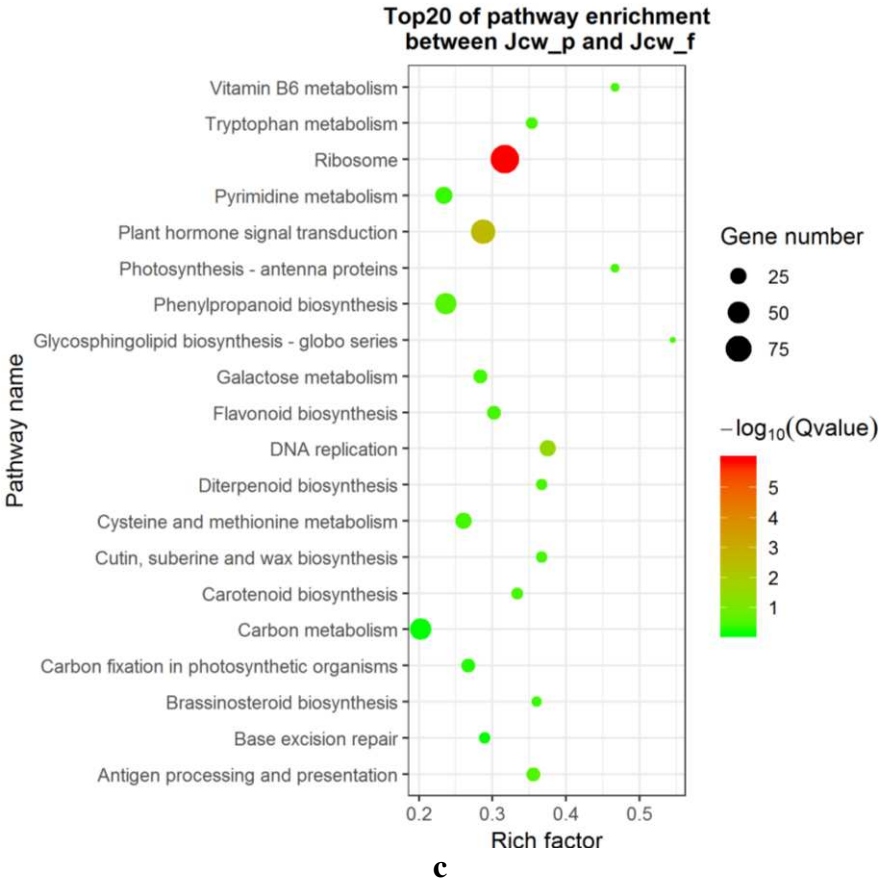

c

http://www.aloki.hu ● ISSN 1589 1623 (Print) ● ISSN 1785 0037 (Online)
DOI: http://dx.doi.org/10.15666/aeer/1605_55955610
© 2018, ALÖKI Kft., Budapest, Hungary

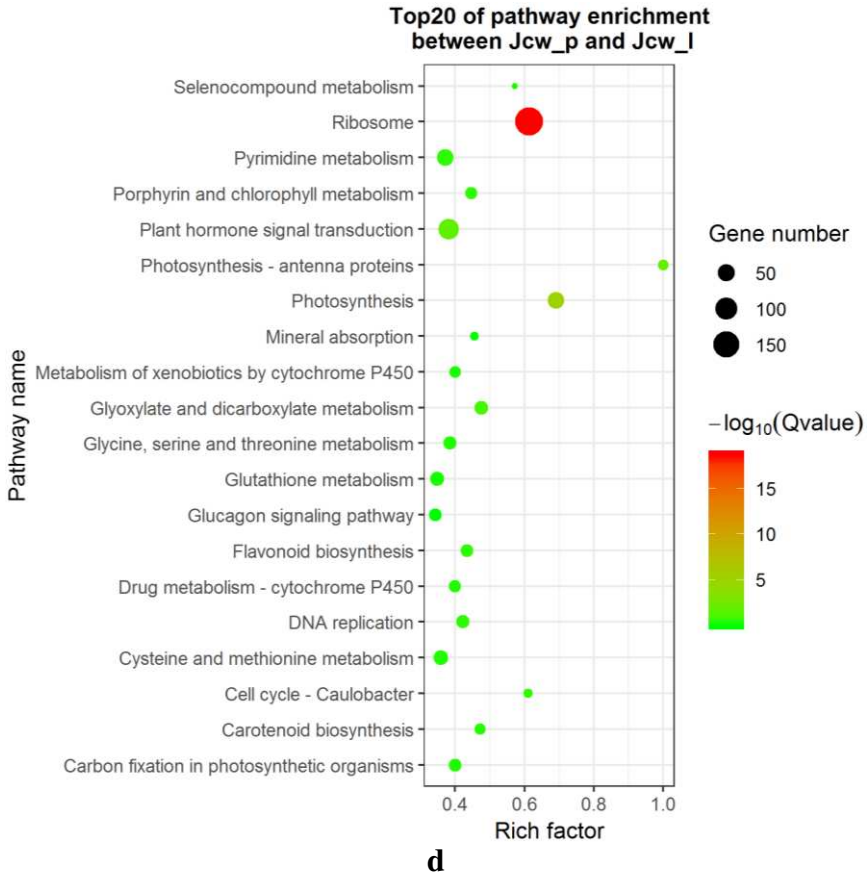

Figure 2. a. *Bubble map for the top 20 enriched pathways in female and male flowers.* ***b.*** *Bubble map for the top 20 enriched pathways in inflorescence buds and male flowers.* ***c.*** *Bubble map for the top 20 enriched pathways in inflorescence buds and female flowers.* ***d.*** *Bubble map for the top 20 enriched pathways in inflorescence and leaf buds*

Changes in MADS-box gene expression

Download the *J. curcas* proteinome data (http://www.ncbi.nlm.nih.gov/genome/915) (Sato et al., 2010) and the MADS-box Hidden Markov Model (HMM) model file (PF00319, http://pfam.sanger), using the HMM file as a seed, run HMM search in the *J. curcas* proteinome database (e-value < 1e-20). Construct a *J. curcas*-specific HMM model based on the screening results, then perform HMM search again (e-value < 0.01), non-repetitive MADS-box related protein ID are extracted and the corresponding gene ID sequence and length information are extracted according to genomic annotation file. Search through the Pfam database, NCBI conserved domain database (https://www.ncbi.nlm.nih.gov/Structure/cdd/wrpsb.cgi) and SMART (http://smart.embl-heidelberg.de/) to confirm that all predicted genes contain the MADS-box domain. The MADS-box gene family is divided into two main lineages, type-I and type-II, that origi- nated from a duplication of ancestor genes during the divergence of plants and animals, the major difference between type-I and type-II genes is that type-II genes possess the K-box domain (Alvarez-Buylla et al., 2000; Theißen et al., 1996). Contained the K-box domain was identified as the type-II MADS-box gene, the otherwise is identified as the type-I MADS-box gene. Heatmap clustering and multiple annotations are performed using the circlize package (Gu et al., 2014). Two

http://www.aloki.hu ● ISSN 1589 1623 (Print) ● ISSN 1785 0037 (Online)
DOI: http://dx.doi.org/10.15666/aeer/1605_55955610
© 2018, ALÖKI Kft., Budapest, Hungary

types of MADS-box-related genes were subjected to hierarchical cluster analysis and visualized as four clusters according to the number of tissue samples (*Fig. 3*). The results show that for *J. nigroviensrugosus*, the MADS-box-related genes could be divided into two expression patterns (clustered by sample), one expressed in female and male flowers, and the other in inflorescence and leaf buds. In addition, the gene highly expressed in all samples is the type-II MADS-box gene.

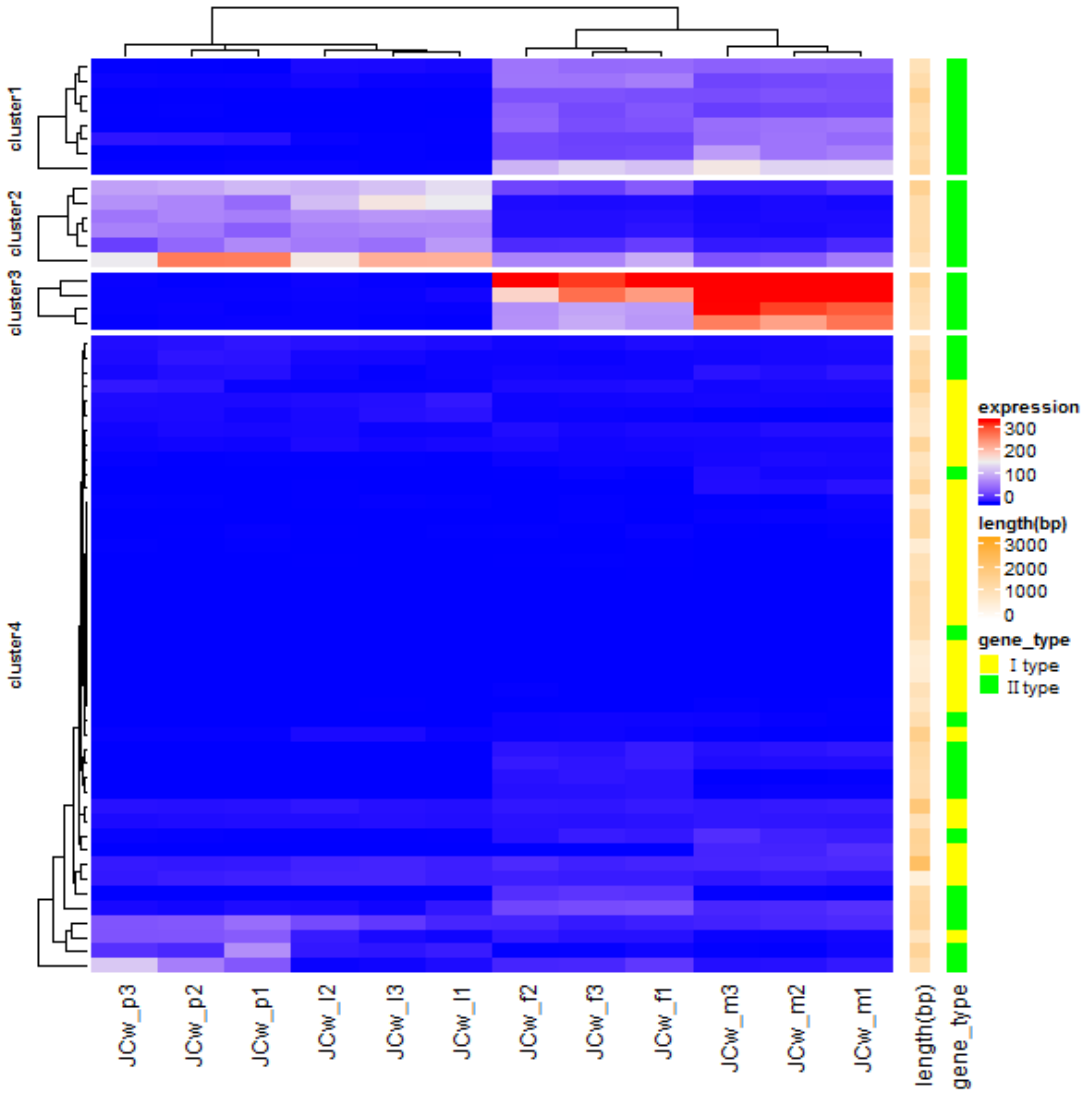

Figure 3. *MADS-box gene expression profile of the four parts of J. nigroviensrugosus*

Discussion

The low yield and low oil content of *J. curcas* seeds are the biggest problems encountered in the current planting of *J. curcas* trees; therefore, the identification of the most favorable genotypes is extremely important (Junqueira et al., 2016). As a new species, *J. nigroviensrugosus* has a higher female to male ratio and a higher seed yield than common *J. curcas.* Several papers have investigated flower induction of *J. curcas* in China and abroad, for instance, histological analysis of the differentiation of male and female flowers at different developmental stages (Xu et al., 2016), transcriptome

http://www.aloki.hu ● ISSN 1589 1623 (Print) ● ISSN 1785 0037 (Online)
DOI: http://dx.doi.org/10.15666/aeer/1605_55955610
© 2018, ALÖKI Kft., Budapest, Hungary

differences between pure female and bisexual inflorescences (Chen et al., 2017), and gene responses subsequent to hormone induction (Ghosh et al., 2010; Pan et al., 2016). However, there is a lack of information regarding the flowering mechanism of *J. nigroviensrugosus*, and whether the relevant measures applied to the common *J. curcas* can be applied to *J. nigroviensrugosus*. Studies of *J. nigroviensrugosus* prior to and subsequent to inflorescence differentiation are beneficial for expanding knowledge of the sex determination mechanism of this energy-rich plant.

A plant undergoes a major physiological change during the transition from vegetative growth to reproductive development, and this transition is a result of responses to various endogenous and exogenous signals (Srikanth and Schmid, 2011). The expression of a specific gene, including the tissue specificity and the difference in transcriptional level, may influence the sex determination of a flower (Ramos et al., 2017). The differentially-expressed genes in the comparison group of female and male flowers may be involved in the regulation of gender differentiation. During this period, carbohydrates may act as mobile signals to regulate flower morphogenesis (Turnbull, 2011; Corbesier et al., 2006). Sugar catabolism enzymes may increase the assimilation ability of the shoots, thereby accelerating shoot growth and increasing primordium numbers (Ito et al., 2002). Low concentrations of sucrose may promote flowering, whereas high concentrations may delay flowering (Ohto et al., 2001). Sucrose-mediated signaling is integrated into the photoperiod pathway, located downstream of the CONSTANS (CO) gene and upstream of the FLOWERING LOCUS T (FT) gene (Seo et al., 2011). Sucrose-phosphate synthase (SPS) (EC: 2.4.1.14) is considered to be a key enzyme in the control of sucrose synthesis (Sawitri et al., 2018). With respect to inflorescence buds and male flowers, the SPS-related genes (gene 7836, gene 12091 and gene 14471) were upregulated in male flowers. In addition, polygalacturonase (PG) was involved in the development of pollen (Ogawa et al., 2009), whichwas significantly upregulated in male flowers. The distribution of sugars and starch is known to be related to flower transformation. Studies conducted on various angiosperm species have shown a correlation between flower abortion and starch content (Reale et al., 2009). Starch is composed of linear and branched glucose (Glc) polymers (Zeeman et al., 2010). The soluble starch synthase (EC: 2.4.1.21) is primarily related to amylopectin catalysis, while granule-bound starch synthase (EC: 2.4.1.242) is primarily associated with the production of amylose, both of which were found to be highly expressed in the male flowers of *J. nigroviensrugosus*. This data indicates that high expression of sucrose and starch synthesis-related genes plays an important role in the development of male flowers in *J. nigroviensrugosus*.

Plant hormones play essential roles in gender determination (Aryal and Ming, 2014). Auxin plays a dominant role in floral organ initiation and organogenesis (Chandler, 2011), and CTK triggers the initiation of female flower primordium (Hui et al., 2017). Application of exogenous cytokinin (6-benzyladenine, BA) on inflorescence buds can significantly increase the number of female flowers, BA treatment may delay floral organ formation by inhibiting the transcription of the A, B and E classes of floral organ-identity genes, which allowing extra time for the plant to produce more primordia in inflorescence meristems (Chen et al., 2014). Type-B Arabidopsis response regulators (ARRs) are positive regulators of the CTX response (Mason et al., 2005), and type-A ARRs are thought to work as negative regulators of CTX to inhibit the activity of type-B ARRs (To and Kieber, 2008; To et al., 2004). B-ARR (gene 8030 and gene 17670) was significantly upregulated in inflorescence buds compared with leaf buds.

http://www.aloki.hu ● ISSN 1589 1623 (Print) ● ISSN 1785 0037 (Online)
DOI: http://dx.doi.org/10.15666/aeer/1605_55955610
© 2018, ALÖKI Kft., Budapest, Hungary

Comparing the male and female flowers, A-ARR (gene 13354) was significantly upregulated in female flowers, whereas B-ARR (gene 20147) was significantly upregulated in male flowers. These data suggest that the initial development of *J. nigroviensrugosus* female flower primordia requires the induction of CTK, but the late developmental stage only needs a low concentration of CTK. As a gaseous plant hormone, ethylene regulates the flowering time of plants through interactions with other plant hormones (Iqbal et al., 2017). In J. *curcas*, treatment with a low concentration of ethephon (25 ppm) is thought to increase the number of female flowers (Makwana and Robin, 2013), and increasing the ethephon concentration has been shown to decrease the number of male and female flowers per inflorescence as well as the total flower number (Costa et al., 2016). Compared with inflorescence buds and male flowers, the expression of ERF1/2 (gene 18694) was significantly increased in female flowers of *J. nigroviensrugosus*, highlighting the importance of ethylene in the regulation of female flower formation and development. In the ABA signaling pathway, the SnRK2 signal plays a crucial role in the sex determination of ferns and regulates the sex ratio of male to hermaphrodite in the reproductive cycle (McAdam et al., 2016). However, there is no related report regarding the impact of SnRK2 on the female to male flower ratio of angiosperms, especially *J. curcas*.

The differential expression of transcription factors (TFs), also known as trans-acting factors, play an essential role in the control of organ development (Latchman, 1997). Six signaling pathways have been identified to regulate the flowering of A. thaliana: photoperiod, vernalization, autonomous, gibberellin (GA), temperature-sensitive, and age-dependent control (Fornara et al., 2010). These signaling pathways are both independent and connected, and converge the flowering signals to several key integrators such as FT, TWIN SISTER OF FT (TSF) and SUPPRESSOR OF OVEREXPRESSION OF CONSTANS 1 (SOC1), activating the expression of meristem-specific genes such as LEAFY (LFY), APETALA1 (AP1) and FRUITFULL (FUL), eventually initiating plant flowering (Cho et al., 2017). Among these, the expression of SOC1 was high in leaf and inflorescence buds, but low in male and female flowers. Conversely, FT was highly expressed in male and female floral organs. The zinc finger transcription factor CONSTANS contains a B-box domain (Gangappa et al., 2014), which plays a central role in photoperiod sensing (Lee et al., 2017). The expression of CONSTANS-LIKE 7 (gene 24482) and CONSTANS-LIKE 3 (gene 12833) were upregulated in both male and female flowers, with respect to inflorescence buds.

NAC genes encode plant-specific transcription factors that are closely related to vegetative reproduction, and embryo and flower development (Olsen et al., 2005). CUP-SHAPED COTYLEDON 1 (CUC1), CUC2 and CUC3 have been shown to regulate organ segregation and meristem formation (Vroemen et al., 2003). In addition to controlling shoot meristem activity, CUC1 and CUC2 also play key roles in female organ development (Kamiuchi et al., 2014). Genetic interaction analyses using single, double and triple mutants of cuc1-1D, cuc2-1D (a CUC2 mutant similar to cuc1-1D), and hws-1, demonstrate that HWS (HAWAIIAN SKIRT), CUC1 and CUC2 act together to control floral organ number (González-Carranza et al., 2017). It is believed that CUC2 is associated with female flower opening of *J. curcas* (Gangwar et al., 2016). Through comparison of female and male flowers of *J. nigroviensrugosus*, we found nine NAC-related genes upregulated in female flowers (including homologous genes of CUC2 and CUC3), and 12 NAC-related genes upregulated in male flowers (including

http://www.aloki.hu ● ISSN 1589 1623 (Print) ● ISSN 1785 0037 (Online)
DOI: http://dx.doi.org/10.15666/aeer/1605_55955610
© 2018, ALÖKI Kft., Budapest, Hungary

NAC2 and NAC29). These data indicate that CUC2 and CUC3 make a contribution in the formation and development of *J. nigroviensrugosus* female flowers.

The MADS-box TFs are the primary components of the current well-known ABCDE model which are closely related to the origin and evolution of plant reproductive organs (Smaczniak et al., 2012; Theissen et al., 2000). The MADS-box TFs play a pivotal role in floristic differentiation (Theissen and Melzer, 2007). Ming et al. (2011) showed that the structural determinants of floral organs are randomly distributed in autosomes, therefore only the spatiotemporal patterns are expressed between sexes, but the expression are not sex-specific. With respect to the DEGs selected in the comparison group of female and male flowers in *J. nigroviensrugosus*, seven genes including ANR1, AGL14 and AGL7 were upregulated in female flowers, while 11 genes including AGL11, AGL62 and AGL20/SOC1 were upregulated in male flowers. The B- and C-class genes, the characteristic genes of flower organ development (Pařenicová et al., 2003), and the dependent SEP1, SEP2 and SEP3 genes, were all similarly expressed in both female and male floral organs of *J. nigroviensrugosus*, and the expression was not sex-specific. The MADS-box-related genes from the four different tissues of *J. nigroviensrugosus* were primarily divided into two expression patterns (*Fig. 3*). Cluster 3-related genes were expressed only in male and female flowers, while cluster 2-related genes were expressed in inflorescences and leaf buds, with a certain degree of conservativity. Two MADS-box-related genes in cluster 3 were only highly expressed in male flowers, spatiotemporally. In addition, the gene highly expressed in all samples belongs to the type-II MADS-box gene. Several cluster 4-related genes, including AGL62 and AGL80, were not expressed in any of the four tissues, suggestive of involvement in early endosperm development (Kang et al., 2008; Portereiko et al., 2006) and regulation of certain physiological activities.

Conclusion

As a new cultivar, transcriptome sequencing of inflorescence and leaf bud differentiation in *J. nigroviensrugosus* was beneficial to analyze the nutrient supply relationship and hormonal regulation of different plant parts. Genes related to sucrose phosphate synthase, soluble starch synthase and granule-bound starch synthase were highly expressed in male flowers of *J. nigroviensrugosus*, suggestive of an important role in the formation and development of male flowers. Initial development of female flower primordia required the induction of CTK, while late stage development only required a low concentration of CTK in coordination with other hormones. CUC2 and CUC3 were very important in the formation and development of female flowers of *J. nigroviensrugosus*. As the most important transcription factors, MADS-box-related genes were conserved throughout different parts of *J. nigroviensrugosus*. Moreover, a number of DEGs were screened during the differentiation of male and female flowers, this study provided an important basis for further research regarding the differentiation of flowers and the molecular mechanism of high-yield *J. nigroviensrugosus* breeding.

Acknowledgements. The work was supported by National Natural Science Foundation of China-Study on flower bud differentiation and flowering mechanism of *Jatropha nigroviensrugosus* CV Yang. (31360165)

http://www.aloki.hu ● ISSN 1589 1623 (Print) ● ISSN 1785 0037 (Online)
DOI: http://dx.doi.org/10.15666/aeer/1605_55955610
© 2018, ALÖKI Kft., Budapest, Hungary

REFERENCES

[1] Alvarez-Buylla, E. R., Pelaz, S., Liljegren, S. J., Gold, S. E., Burgeff, C., Ditta, G. S., de Pouplana, L. R., Martínez-Castilla, L., Yanofsky, M. F. (2000): An ancestral MADS-box gene duplication occurred before the divergence of plants and animals. – Proceedings of the National Academy of Sciences 97(10): 5328-5333.

[2] Aryal, R., Ming, R. (2014): Sex determination in flowering plants: papaya as a model system. – Plant Science 217: 56-62.

[3] Ashoke, B., Kalyani, D., Datta, S. K. (2005): Floral biology, floral resource constraints and pollination limitation in *Jatropha curcas* L. – Pakistan Journal of Biological Sciences 8(3): 456-460.

[4] Chandler, J. W. (2011): The hormonal regulation of flower development. – Journal of Plant Growth Regulation 30(2): 242-254.

[5] Chen, M. S., Pan, B. Z., Wang, G. J., Ni, J., Niu, L., Xu, Z. F. (2014): Analysis of the transcriptional responses in inflorescence buds of *Jatropha curcas* exposed to cytokinin treatment. – BMC Plant Biology 14(1): 318.

[6] Chen, M. S., Pan, B. Z., Fu, Q., Tao, Y. B., Martínez-Herrera, J., Niu, L., Ni, J., Dong, Y. L., Zhao, M. L., Xu, Z. F. (2017): Comparative transcriptome analysis between gynoecious and monoecious plants identifies regulatory networks controlling sex determination in *Jatropha curcas*. – Frontiers in Plant Science 7: 1953.

[7] Cho, L. H., Yoon, J., An, G. (2017): The control of flowering time by environmental factors. – The Plant Journal 90(4): 708-719.

[8] Corbesier, L., Coupland, G. (2006): Coupland. The quest for florigen: a review of recentprogress. – Journal of Experimental Botany 57(13): 3395-3403.

[9] Costa, A. P., Vendrame, W., Nietsche, S., Crane, J., Moore, K., Schaffer, B. (2016): Branching, flowering and fruiting of Jatropha curcas treated with ethephon or benzyladenine and gibberellins. – Anais da Academia Brasileira de Ciências 88(2): 989-998.

[10] De Lourdes Adriano-Anaya, M., Pérez-Castillo, E., Salvador-Figueroa, M., Ruiz-González, S., Vázquez-Ovando, A., Grajales-Conesa, J., Ovando-Medina, I. (2016): Sex expression and floral diversity in *Jatropha curcas*: a population study in its center of origin. – PeerJ 4: e2071.

[11] Dias, L. A. S., Missio, R. F., Dias, D. C. F. S. (2012): Antiquity, botany, origin and domestication of Jatropha curcas (Euphorbiaceae), a plant species with potential for biodiesel production. – Genet. Mol. Res 11(3): 2719-28.

[12] Fornara, F., de Montaigu, A., Coupland, G. (2010): SnapShot: control of flowering in *Arabidopsis*. – Cell 141(3): 550-550.

[13] Gangappa, S. N., Botto, J. F. (2014): The BBX family of plant transcription factors. – Trends in Plant Science 19(7): 460-470.

[14] Gangwar, M., Sood, H., Chauhan, R. S. (2016): Genomics and relative expression analysis identifies key genes associated with high female to male flower ratio in *Jatropha curcas* L. – Molecular Biology Reports 43(4): 305-322.

[15] Gangwar, M., Sood, A., Bansal, A., Chauhan, R. S. (2018): Comparative transcriptomics reveals a reduction in carbon capture and flux between source and sink in cytokinin-treated inflorescences of *Jatropha curcas* L. – Biotech 8(1): 64.

[16] Gao, W. J., Li, S. F., Zhang, G. J., Wang, N. N., Deng, C. L., Lu, L. D. (2013): Comparative analysis of gene expression by microarray analysis of male and female flowers of *Asparagus officinalis*. – Bioscience, Biotechnology, and Biochemistry 77(6): 1193-1199.

[17] Ghosh, A., Chikara, J., Chaudhary, D. R., Prakash, A. R., Boricha, G., Zala, A. (2010): Paclobutrazol arrests vegetative growth and unveils unexpressed yield potential of *Jatropha curcas*. – Journal of Plant Growth Regulation 29(3): 307-315.

http://www.aloki.hu ● ISSN 1589 1623 (Print) ● ISSN 1785 0037 (Online)
DOI: http://dx.doi.org/10.15666/aeer/1605_55955610
© 2018, ALÖKI Kft., Budapest, Hungary

[18] González-Carranza, Z. H., Zhang, X., Peters, J. L., Boltz, V., Szecsi, J., Bendahmane, M., Roberts, J. A. (2017): HAWAIIAN SKIRT controls size and floral organ number by modulating CUC1 and CUC2 expression. – PloS One 12(9): e0185106.
[19] Gu, Z., Gu, L., Eils, R., Schlesner, M., Brors, B. (2014): Circlize implements and enhances circular visualization in R. – Bioinformatics 30(19): 2811-2812.
[20] He, H., Wang, X. R., Hu, Z. (2016): Nutritional transport and photosynthetic characteristics of Guizhou *Jatropha nigroviensrugosus* and ordinary *Jatropha curcas*. – Journal of West China Forestry Science 45(5): 79-83.
[21] Hui, W., Yang, Y., Wu, G., Peng, C., Chen, X., Zayed, M. Z. (2017): Transcriptomeprofile analysis reveals the regulation mechanism of floral sex differentiation in *Jatropha curcas* L. – Scientific Reports 7(1): 16421.
[22] Iqbal, N., Khan, N. A., Ferrante, A., Trivellini, A., Francini, A., Khan, M. I. R. (2017): Ethylene role in plant growth, development and senescence: interaction with other phytohormones. – Frontiers in Plant Science 8: 475.
[23] Ito, A., Hayama, H., Kashimura, Y. (2002): Sugar metabolism in buds during flower bud formation: a comparison of two Japanese pear [*Pyrus pyrifolia* (Burm.) Nak.] cultivars possessing different flowering habits. – Scientia Horticulturae 96(1-4): 163-175.
[24] Junqueira, V. S., de Azevedo Peixoto, L., Laviola, B. G., Bhering, L. L., Mendonça, S., Costa, T. D. S. A., Antoniassi, R. (2016): Bayesian Multi-Trait Analysis Reveals a Useful Tool to Increase Oil Concentration and to Decrease Toxicity in *Jatropha curcas* L. – PloS One 11(6): e0157038.
[25] Kamiuchi, Y., Yamamoto, K., Furutani, M., Tasaka, M., Aida, M. (2014): The CUC1 and CUC2 genes promote carpel margin meristem formation during *Arabidopsis* gynoecium development. – Frontiers in Plant Science 5: 165.
[26] Kang, I. H., Steffen, J. G., Portereiko, M. F., Lloyd, A., Drews, G. N. (2008): The AGL62 MADS domain protein regulates cellularization during endosperm development in *Arabidopsis*. – The Plant Cell 20(3): 635-647.
[27] Kaushik, N., Kumar, K., Kumar, S., Kaushik, N., Roy, S. (2007): Genetic variability and divergence studies in seed traits and oil content of Jatropha (*Jatropha curcas* L.) accessions. – Biomass and Bioenergy 31(7): 497-502.
[28] Latchman, D. S. (1997): Transcription factors: an overview. – The International Journal of Biochemistry & Cell Biology 29(12): 1305-1312.
[29] Lee, B. D., Kim, M. R., Kang, M. Y., Cha, J. Y., Han, S. H., Nawkar, G. M., Kim, W. Y. (2017): The F-box protein FKF1 inhibits dimerization of COP1 in the control of photoperiodic flowering. – Nature Communications 8(1): 2259.
[30] Makwana, V., Robin. P. (2013): Interaction between GA and ethrel in inducing female flowers in *Jatropha curcas*. – Int. J. Biotechnol. Bioeng. Res. 4: 465-472.
[31] Mao, Y., Liu, W., Chen, X., Xu, Y., Lu, W., Hou, J., Wu, L. (2017): Flower development and sex determination between male and female flowers in *Vernicia fordii*. – Frontiers in Plant Science 8: 1291.
[32] Mason, M. G., Mathews, D. E., Argyros, D. A., Maxwell, B. B., Kieber, J. J., Alonso, J. M., Schaller, G. E. (2005): Multiple type-B response regulators mediate cytokinin signal transduction in *Arabidopsis*. – The Plant Cell 17(11): 3007-3018.
[33] McAdam, S. A., Brodribb, T. J., Banks, J. A., Hedrich, R., Atallah, N. M., Cai, C., Geiger, D. (2016): Abscisic acid-controlled sex before transpiration in vascularplants. – Proceedings of the National Academy of Sciences 113(45): 12862-12867.
[34] Ming, R., Bendahmane, A., Renner, S. S. (2011): Sex chromosomes in land plants. – Annual Review of Plant Biology 62: 485-514.
[35] Montes, J. M., Melchinger, A. E. (2016): Domestication and breeding of *Jatropha curcas* L. – Trends Plant Sci 21(12): 1045-1057.
[36] Ogawa, M., Kay, P., Wilson, S., Swain, S. M. (2009): ARABIDOPSISDEHISCENCE ZONE POLYGALACTURONASE1 (ADPG1), ADPG2, and QUARTET2 are

http://www.aloki.hu ● ISSN 1589 1623 (Print) ● ISSN 1785 0037 (Online)
DOI: http://dx.doi.org/10.15666/aeer/1605_55955610
© 2018, ALÖKI Kft., Budapest, Hungary

polygalacturonases required for cell separation during reproductive development in *Arabidopsis*. – The Plant Cell 21(1): 216-233.

[37] Ohto, M. A., Onai, K., Furukawa, Y., Aoki, E., Araki, T., Nakamura, K. (2001): Effects of sugar on vegetative development and floral transition in *Arabidopsis*. – Plant Physiology 127(1): 252-261.

[38] Olsen, A. N., Ernst, H. A., Leggio, L. L., Skriver, K. (2005): NAC transcription factors: structurally distinct, functionally diverse. – Trends in Plant Science 10(2): 79-87.

[39] Pan, B. Z., Luo, Y., Song, L., Chen, M. S., Li, J. L., Xu. Z. F. (2016): Thidiazuron increases fruit number in the biofuel plant *Jatropha curcas* by promoting pistil development. – Industrial Crops and Products 81: 202-210.

[40] Pařenicová, L., de Folter, S., Kieffer, M., Horner, D. S., Favalli, C., Busscher, J., Angenent, G. C. (2003): Molecular and phylogenetic analyses of the complete MADS-box transcription factor family in *Arabidopsis*: new openings to the MADS world. – The Plant Cell 15(7): 1538-1551.

[41] Portereiko, M. F., Lloyd, A., Steffen, J. G., Punwani, J. A., Otsuga, D., Drews, G. N. (2006): AGL80 is required for central cell and endosperm development in *Arabidopsis*. – The Plant Cell 18(8): 1862-1872.

[42] Ramos, M. J. N., Coito, J. L., Fino, J., Cunha, J., Silva, H., de Almeida, P. G., CostaSara, M. M. R., Amâncio, S., Paulo, O. S., Rocheta, M. (2017): Deep analysis of wild *Vitis* flower transcriptome reveals unexplored genome regions associated with sex specification. – Plant Molecular Biology 93(1-2): 151-170.

[43] Reale, L., Sgromo, C., Ederli, L., Pasqualini, S., Orlandi, F., Fornaciari, M., Ferranti, F., Romano, B. (2009): Morphological and cytological development and starch accumulation in hermaphrodite and staminate flowers of olive (*Olea europaea* L.). – Sexual Plant Reproduction 22(3): 109-119.

[44] Rocheta, M., Sobral, R., Magalhães, J., Amorim, M. I., Ribeiro, T., Pinheiro, M., Egas, C., Morais-Cecílio, L., Costa, M. M. (2014): Comparative transcriptomic analysis of male and female flowers of monoecious *Quercus suber*. – Frontiers in Plant Science 5: 599.

[45] Sato, S., Hirakawa, H., Isobe, S., Fukai, E., Watanabe, A., Kato, M., Kawashima, K., Minami, C., Muraki, A., Nakazaki, N., Takahashi, C. (2010): Sequence analysis of the genome of an oil-bearing tree, *Jatropha curcas* L. – DNA Research 18(1): 65-76.

[46] Sawitri, W. D., Afidah, S. N., Nakagawa, A., Hase, T., Sugiharto, B. (2018): Identification of UDP-glucose binding site in glycosyltransferase domain of sucrose phosphate synthase from sugarcane (Saccharum officinarum) by structure-based site-directed mutagenesis. – Biophysical Reviews 10(2): 1-6.

[47] Seo, P. J., Ryu, J., Kang, S. K., Park, C. M. (2011): Modulation of sugar metabolism by an INDETERMINATE DOMAIN transcription factor contributes to photoperiodic flowering in *Arabidopsis*. – The Plant Journal 65(3): 418-429.

[48] Smaczniak, C., Immink, R. G., Angenent, G. C., Kaufmann, K. (2012): Developmental and evolutionary diversity of plant MADS-domain factors: insights from recent studies. – Development 139(17): 3081-3098.

[49] Srikanth, A., Schmid, M. (2011): Regulation of flowering time: all roads lead to Rome. – Cellular and Molecular Life Sciences 68(12): 2013-2037.

[50] Theissen, G., Melzer, R. (2007): Molecular mechanisms underlying origin and diversification of the angiosperm flower. – Annals of Botany 100(3): 603-619.

[51] Theißen, G., Kim, J. T., Saedler, H. (1996): Classification and phylogeny of the MADS-box multigene family suggest defined roles of MADS-box gene subfamilies in the morphological evolution of eukaryotes. – Journal of Molecular Evolution 43(5): 484-516.

[52] Theissen, G., Becker, A., Di Rosa, A., Kanno, A., Kim, J. T., Münster, T., Winter, K., Saedler, H. (2000): A Short History of MADS-Box Genes in Plants. – In: Doyle, J. J., Gaut, B. S. (eds.) Plant Molecular Evolution, pp. 115-149. Springer, Dordrecht.

[53] To, J. P., Kieber, J. J. (2008): Cytokinin signaling: two-components and more. – Trends in Plant Science 13(2): 85-92.

http://www.aloki.hu ● ISSN 1589 1623 (Print) ● ISSN 1785 0037 (Online)
DOI: http://dx.doi.org/10.15666/aeer/1605_55955610
© 2018, ALÖKI Kft., Budapest, Hungary

[54] To, J. P., Haberer, G., Ferreira, F. J., Deruère, J., Mason, M. G., Schaller, G. E., Alonso, J. M., Ecker, J. R., Kieber, J. J. (2004): Type-A Arabidopsis response regulators are partially redundant negative regulators of cytokinin signaling. – The Plant Cell 16(3): 658-671.
[55] Turnbull, C. (2011): Long-distance regulation of flowering time. – Journal of Experimental Botany 62(13): 4399-4413.
[56] Vroemen, C. W., Mordhorst, A. P., Albrecht, C., Kwaaitaal, M. A., de Vries, S. C. (2003): The CUP-SHAPED COTYLEDON3 gene is required for boundary and shoot meristem formation in *Arabidopsis*. – The Plant Cell 15(7): 1563-1577.
[57] Xu, G., Huang, J., Yang, Y., Yao, Y. A. (2016): Transcriptome analysis offlower sex differentiation in *Jatropha curcas* L. using RNA sequencing. – PloS One 11(2): e0145613.
[58] Yang, C. (2013): Phenotypic Characteristics and Genetic Stability of New Varieties of *Jatropha curcas.* – Botany in Ecological Civilization: Present and Future - The Fifteenth Congress of Chinese Society of Botany and the 80th Academic Year Symposium. Session 4 Session: Resource Botany. http://cpfd.cnki.com.cn/Article/CPFDTOTAL-ZGZO201310005036.htm.
[59] Yang, C. Y., Fang, Z., Li, B., Long, Y. F. (2012): Review and prospects of *Jatropha* biodiesel industry in China. – Renewable and Sustainable Energy Reviews 16(4): 2178-2190.
[60] Yang, C. Y., Lu, W., Wu, X., Xu, Z., Long, Y. (2015): Analysis on components of fatty acids from new *Jatropha* cultivars seed oils and their potential of preparing biodiesel. – Botanical Research 4(1): 16-24.
[61] Zeeman, S. C., Kossmann, J., Smith, A. M. (2010): Starch: its metabolism, evolution, and biotechnological modification in plants. – Annual Review of Plant Biology 61: 209-234.

http://www.aloki.hu ● ISSN 1589 1623 (Print) ● ISSN 1785 0037 (Online)
DOI: http://dx.doi.org/10.15666/aeer/1605_55955610
© 2018, ALÖKI Kft., Budapest, Hungary

ECOLOGICAL ASSESSMENT OF PLANT COMMUNITIES ALONG THE EDAPHIC AND TOPOGRAPHIC GRADIENTS OF BIHA VALLEY, DISTRICT SWAT, PAKISTAN

IQBAL, Z.[1] – ZEB, A.[1] – ABD_ALLAH, E. F.[2] – RAHMAN, I. U.[1,3*,†] – KHAN, S. M.[4] – ALI, N.[1] – IJAZ, F.[1] –ANWAR, Y.[5] – MUZAMMIL, S.[5] – ALQARAWI, A. A.[2] – HASHEM, A.[6] – AFZAL, A.[1] – MAJID, A.[1] – KHAN, M. A.[1] – CALIXTO, E. S.[7]

[1]*Department of Botany, Hazara University, Mansehra-21300, KP, Pakistan*

[2]*Department of Plant Production, College of Food & Agricultural Sciences, King Saud University, P.O. Box 2460, Riyadh 11451, Saudi Arabia*

[3]*William L. Brown Center, Missouri Botanical Garden, P.O. Box 299, St. Louis, MO 63166-0299, USA*

[4]*Department of Plant Sciences, Quaid-i-Azam University, Islamabad, Pakistan*

[5]*Department of Biological Sciences, Faculty of Science, King Abdulaziz University, Jeddah 21589, Saudi Arabia*

[6]*Botany and Microbiology Department, College of Science, King Saud University P.O. Box 2460, Riyadh 11451, Saudi Arabia*

[7]*Department of Biology, University of Sao Paolo, SP, Brazil*

**Corresponding author*
e-mail: hajibotanist@outlook.com; irahman@mobot.org
[†]ORCID ID: 0000-0003-3312-7975

(Received 21st Feb 2018; accepted 2nd Aug 2018)

Abstract. A study was conducted to explore the plant biodiversity and vegetation structure of Biha Valley, District Swat, Pakistan. On the basis of the physiognomy of the vegetation the study area was divided into 19 stands. Line transect (50 m) method was used to sample the phytosociological attributes of the study area. PCORD software (version 5) was used to recognize communities by two-way indicator species analysis (TWINSPAN) and CANOCO software (version 5) for ordination analysis was done for detrended correspondence analysis (DCA) and canonical correspondence analysis (CCA) to find variation directories of different plant species. Different life-form classes and leaf size spectra were recorded according to the Raunkiaer classification. The floristic composition of the area consists of 203 plant species belonging to 154 genera and 70 families. The biological spectrum of the area indicated that Therophytes was dominant with 46.60% among the life-classes, followed by Hemicryptophytes having 15.53%. Leaf spectra of study area revealed that Microphylls was dominant (41.26%) followed by Nanophylls (32.04%). Seven plant communities were recognized by TWINSPAN classification, which showed that species diversity decreased with altitude. Moreover, the result indicates the importance of soil organic matter in top soil layers for plant species distribution. The increases in soil nutrients (OM, P, N, and K), improvement in site conditions (community cover, depth of litter, depth of humus, soil water content) and decrease in soil bulk density indicated the natural habitat restoration following abandonment.
Keywords: *multivariate analysis, similarity index, vegetation structure, biological spectrum, Pakistan*

Introduction

Vegetation can be defined as the group of plants growing together in a particular locality. It can also be defined as a unit which retains their structure and physiognomic characteristics to permit their distinction from other units (Khan et al., 2012). Plants are

http://www.aloki.hu ● ISSN 1589 1623 (Print) ● ISSN 1785 0037 (Online)
DOI: http://dx.doi.org/10.15666/aeer/1605_56115631
© 2018, ALÖKI Kft., Budapest, Hungary

common feature of the natural sceneries and grow in all environments. Though, each species being dispersed according to its own unique tolerance of a multitude of factors that consist its environment no species occur all over the world. Species with certain environmental tolerances develop into recognizable plant formations with distinctive floristic and structural characteristics. At a comprehensive scale these signify the major biomes of the world (Archibold, 1995). Vegetation of an area can either be characterized by its component species or by the functional combination and physical qualities that differentiate the physical appearance of vegetation. It is an essential variation that is illustrated by the different methods available for describing vegetation (Goldsmith et al., 1986; Kent and Coker, 1992). Floristic diversity and its biological spectra rely on topography and elevation. Plant-life characters like life form, leaf size spectra, and phenological traits mirror the conditions of the existing ecological and natural surroundings (Rahman et al., 2018).

Phytosociology is the study of the characteristics, classification, relationships and distribution of plant communities and attempts to describe the species diversity in plant communities (Haq et al., 2015a). It displays a high association between vegetation and environmental conditions, enabling us to discover, the complicated relations of ecosystem parts by studying resources and environment (Asri, 1994). Plants of similar nature and ecological needs (niche) are associated with each other, creating plant ecological groups (Braun-Blanquet, 1983). Plant communities include one or more ecological groups (Khademi, 2009). Phytosociology is a branch of plant ecology that explains the association of plant species in communities (Ewald, 2003). Plants type and characteristics of soil are so related that they cannot be isolated from of each other. Phytosociology is the quantitative study of vegetation and its prime purpose is to describe the vegetation its pattern and classify it in a meaningful method. It shows species diversity which determines the dispersal of individuals among the species in a specific habitat (Haq et al., 2015b). A number of quantitative, qualitative and synthetic characteristics of plant communities e.g. density, dominance, richness, floristic composition, structure, physical appearance, development and exchange multilateral relations of plants to one another and to the environmental factors and the classification of communities are examined by phytosociology.

To date, the Biha Valley (Swat) has not been studied using recently developed analytical methods for vegetation characterization. The current study was therefore carried out to document the floristic diversity of the area, to recognize the major plant communities of the site and to identify the key environmental variables influencing vegetation structure, species composition and species diversity in the research area.

Materials and methods

Study area

The study site (Biha Valley) is located in the northwestern part of District Swat in the Hindu Raj series of Hindukush Mountains (*Fig. 1*). The Valley is one of the Union councils of Tehsil Matta that comprises 22991 ha. It is situated in the North West corner of District Swat. It lies between 35° 60 and 35° 20 North latitude and 72° 30 to 72° 40 East longitude (Adnan, 2003). The valley is surrounded by Usherai Dara (Dir) from West, Dir Kohistan on the North, Shawar valley from the South West and Mandal dag, Charma and Sulatan valley from the Eastern North. Pushtoni, Nalkot, Biha, Fazal banda, Chatikal, Dughalgay and Swatai are the important villages situated in this area.

http://www.aloki.hu ● ISSN 1589 1623 (Print) ● ISSN 1785 0037 (Online)
DOI: http://dx.doi.org/10.15666/aeer/1605_56115631
© 2018, ALÖKI Kft., Budapest, Hungary

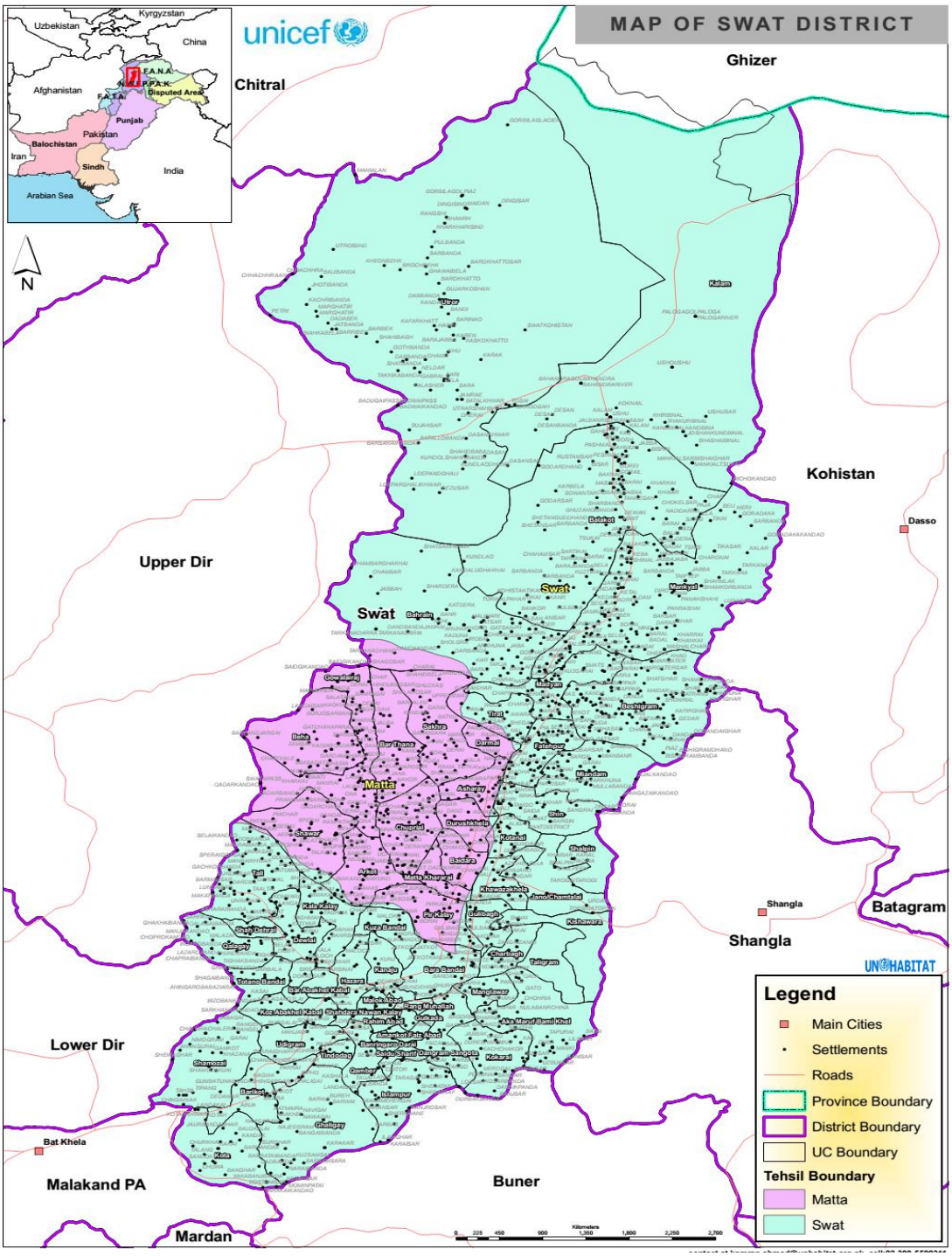

Figure 1. *Map of the study area*

Natural vegetation

The site has diverse vegetation setup and cool climatic condition in summer due to high elevation that varies from 1600 to 4100 m from sea level. Phyto-geographically, the study area lies in Sino-Japanese region (Ahmad and Sirajuddin, 1996). Vegetation of the area consists of moist temperate forests (Champion et al., 1965) extending to sub

http://www.aloki.hu ● ISSN 1589 1623 (Print) ● ISSN 1785 0037 (Online)
DOI: http://dx.doi.org/10.15666/aeer/1605_56115631
© 2018, ALÖKI Kft., Budapest, Hungary

alpine and alpine types. The mountains along the valley are densely forested. The project area has unique flora as it occupies nexus of the three great mountains i.e. Landaysar, Brajosar and Datkor soki. Nature has been very generous to the region in its endowments of very tall invincible peaks, enormous glaciers, majestic streams, and the meadows of high altitude plateaus. Due to its geographical location within the monsoon belt, farmers of the lower parts of the area cultivate orchards, cereals as well as cash crops. In upper parts of the valley forests and alpine pastures prevail widely. Accordingly, the valley gives home to vast diversity of useful plants i.e. edible, medicinal and aromatic plants are common. Various products like honey, morels, and handicrafts are also obtained by the local people from the valley. Doghalgo khvar Chatikal and Swatai are the main streams which meet with each other in Biha Valley.

Regarding the altitude, climate, soil and topography, vegetation of Biha valley can be classified into the following broad categories:

1. *Olive–White Oak Zone:* These forests are located at lower altitudinal ranges from 1400 to 1700 m above sea level.
2. *Blue Pine Zone:* These forests can be observed between 1700 and 2700 m and represent the major part of vegetation in the valley. This type of vegetation is located in Derai sargay, Pakani, Yag bila and Cyakas etc.
3. *Fir Spruce Zone:* Fir spruce forests can be observed above 2700 m upto an elevation of 2900 m at Kotago, Kadyar, Kamali chari, Dolo, Jargogo and Jaby.
4. *Tree Line Iron Oak Forest:* These forests are usually located between 2900 and 3400 m at Goryal, Sangwano kandaow, Mero kandaow and Dat kor. However, in some areas these forests occur from 2750 m where they are usually mixed with fir and spruce at the lower boundary. These forests change to pure iron oak forest as the elevation increases.
5. *Alpine and Sub-Alpine Zone:* This type of vegetation can be observed above 3200 m and is present in Kandaw sar, Mero kandaow, Landay sar, Brajo sar, and Sangwano kandaow.

Climate

Climatically, the area comes under typical sub-tropical dry temperate zone. The sub-tropical, semi-arid climate of Saidu Sharif is comparable to that in the lower parts of the valley while the upper parts of the valley have a climate of temperate type up to 2500 m height and above 2500 m there is subalpine and alpine zone. Winter is hard and summer precipitation remains high at higher altitudes as compared to lower parts of the valley (Weiers, 1995). Monsoon winds (from subtropical regions of the Arabian Sea) bring summer rainfall while westerlies are responsible for winter rain and snowfall in the valley. Due to considerable precipitations in both seasons the upper regions of the Biha valley are comparatively much humid than the lower areas. June and July are the hottest months and December, January and February are the coldest months of the year. Relative humidity is also an important atmospheric factor governing the distribution of plants and vegetation (Hussain and Ilahi, 1991). The value of relative humidity is higher in the months of July, August and September. There are usually two rainy seasons per year: One lasts from January to April (winter rainfall and the other one occurs in July/August (summer rainfall). Snowfall frequently occurs from November to March. Coldest months of the year are December, January and February in which the valley remains permanently under snow cover. The lower snow line in winter in Doghalgay Valley is 1800 to 4000 m. Beside rainfall and snowfall hailing, that damage the crops

http://www.aloki.hu ● ISSN 1589 1623 (Print) ● ISSN 1785 0037 (Online)
DOI: http://dx.doi.org/10.15666/aeer/1605_56115631
© 2018, ALÖKI Kft., Budapest, Hungary

and orchards badly, is also common during May and June (summer) and September and October (autumn) (Khan, 1991). Relative humidity is also an important atmospheric factor governing the distribution of plants and vegetation (Hussain and Ilahi, 1991). The value of relative humidity is higher in the months of July, August and September.

Rock types and soil

The area is characterized by very complicated geological structures and rocks. Quartz and mica, with minor iron garnet or graphite etc are its major components. The rocks are usually dark grey with a micaceous shine on the surface. The main soil materials are silty clay loam and in moderately deep silt loam (Shangla-rockland complex), which is closely related to the parent rock. The area has different parent rocks therefore wide variety of soil types can be found in the area.

Field investigations

The entire study area was surveyed to identify the different stands of vegetation on the basis of the physiognomy of the vegetation. The Geological Positioning System (GPS) coordinates including altitude, longitude and latitude were taken from each stand by using GPS. Line transect method by using 50 m transect was used to sample the phytosociological attributes of the study area (Kent and Coker, 1992). Density, cover, frequency, relative density, relative cover and relative frequency for each species was calculated following Daubenmire (1959) and Hussain (1989). Phenology of the species was documented by visiting the study area in different intervals during 2012-2013. Different life-form classes and leaf size spectra were recorded according to the Raunkiaer classification.

Community homogeneity

Similarity Index determines the interspecific association between the species of plant communities**.** The index of similarity was calculated after Sorenson (1948) by using the following formula (*Eq. 1*):

$$SI = 2C \ / \ A+B \times 100 \qquad \text{(Eq.1)}$$

where, C = the least importance value of common species, A = importance value of community A, B = importance value of community B.

Dissimilarity Index is the reverse sequence of similarity index. It was calculated by using the following formula (*Eq. 2*):

$$ID = 100 - Is \qquad \text{(Eq.2)}$$

where, Is = Index of similarity and S = Sorenson Index.

Soil analyses

For soil analysis, the soil will be dugout, the surface soil up to 10 cm depth was removed and about 500 g of soil from each sample was collected, mixed well individually before the use and analyzed in the soil laboratory at ARI (Agriculture research institute) Mingora, Swat, Pakistan. Then samples were air dried at 20 to 25 °C,

http://www.aloki.hu ● ISSN 1589 1623 (Print) ● ISSN 1785 0037 (Online)
DOI: http://dx.doi.org/10.15666/aeer/1605_56115631
© 2018, ALÖKI Kft., Budapest, Hungary

and passed through a 2 mm sieve and analyzed for different physiochemical characteristics. Soil pH and texture were measured with the help of dynamic digital pH meter and hydrometer respectively (McLean, 1982; Koehler et al., 1984; Rahman et al., 2015, 2017). Nitrogen through Macro-Kjeldahl method (Paul and Berry, 1921), Phosphorus and Potassium were analyzed through ammonium bicarbonate-diethylene triamine penta acetic acid (AB-DTPA) method (Soltanpour and Woekman, 1979). While, soil organic matters were determined by following Nelson et al. (1996).

Data analyses

The data were statistically analyzed to find out the relationship between plant species composition and different physiographic and edaphic attributes. PCORD software (version 5) was used to recognize communities by two-way indicator species analysis (TWINSPAN) and CANOCO software (version 5) for ordination analysis was done for detrended correspondence analysis (DCA) and canonical correspondence analysis (CCA) to find variation directories of different plant species (Ter Braak, 1986, 1994).

Results

Floristic composition

The study area consists of 203 plant species belonging to 70 different families and 154 genera. The biggest family was Asteraceae consisting of 19 species, while the other major families were Rosaceae comprising of 16 species.

Flowering stage

During field observations in the research area two flowering seasons were recorded. The first flowering seasons were observed from May to August, in which total 174 species (85.35%) were observed in flowering and in peak flowering period. The species included herbs (71.41%), shrubs (11.83%), trees (10.65%), ferns (2.37%) with prominent sori (reproductive phase) and climbers were present with 1.78%. While in the second spell (September to October) only 29 plant species with 14.65% were observed in flowering stage in which 62.07% were herbs, 13.79% shrubs, 10.34% trees and 6.90% grasses and ferns each. The flowering stage of the plants starts to decline from 15 October in the Alpine areas and continues from the middle of November in the lower sub-tropical regions. The remaining 80% of the plants were in either fruiting stage or dormant condition and remain dormant till April (*Table 1*). The distribution of flowering species showed significant variations with altitude. Plants living at high elevations especially in alpine and sub-alpine areas were found in blooming condition from July to August while plants at lower altitude were found in blooming condition from May to July.

Table 1. *Flowering seasons of plant species recorded in the Biha Valley*

Season	Herbs		Shrubs		Trees		Grasses		Ferns		Climber		Total	
May-Aug	122	71.4%	20	11.8%	18	10.6%	5	2.3%	6	2.9%	3	1.8%	174	85.3%
Sep-Oct	17	62.1%	4	13.8%	3	10.3%	3	6.9%	2	6.9%	0	0	29	14.6%

http://www.aloki.hu ● ISSN 1589 1623 (Print) ● ISSN 1785 0037 (Online)
DOI: http://dx.doi.org/10.15666/aeer/1605_56115631
© 2018, ALÖKI Kft., Budapest, Hungary

Fruiting stage

The main fruiting period of the study area was recorded from September onward, 185 plant species (91.41%) were observed in fruiting stage while from May to August the poorest fruiting period was recorded during which only 18 plants species (8.59%) were observed (*Table 2*).

Table 2. *Fruiting seasons of plant species recorded in the Biha Valley*

Season	Herbs		Shrubs		Trees		Grasses		Ferns		Climbers		Total	
May-Aug	16	88.2%	1	5.9%	1	5.9%	0		0		0		18	8.6%
Sep onward	123	67.4%	23	12.7%	20	11.1%	8	3.3%	8	3.8%	3	1.7%	185	91.4%

Phytosociology

TWINSPAN classification

The phytosociological data of 19 stands having 203 species were analyzed by TWINSPAN Classification. In this classification a total of seven plant communities were recognized in the study area (*Fig. 2*). These communities are described below.

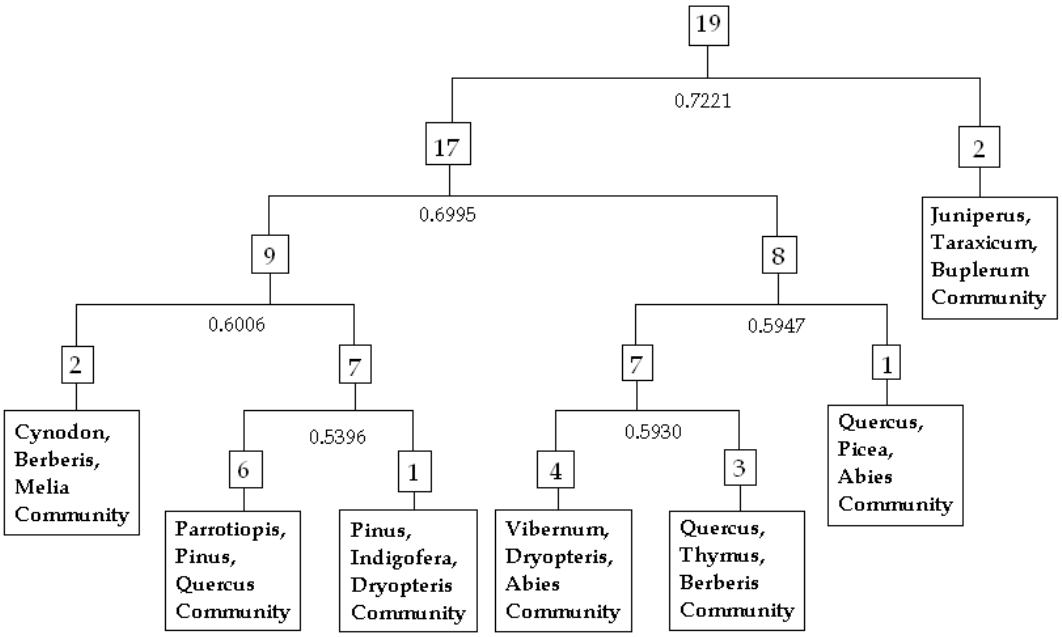

Figure 2. *TWINSPAN classification of plant communities of the Biha Valley*

The Cynodon-Berberis-Melia (CBM) community

This community was recorded at Nalkot sarbira and Nalkot shigartan from longitude (E = 072° 18.127' to 072° 18.127') and latitude (N = 35° 03.516' to35° 04.080') from north-east to south exposure with 15° to 30° slope at 5174-5445 ft elevation. The community consists of 70 plant species including 43 herb species, 12 species of shrubs and trees each, 2 grass species and 1 fern species. The dominant species in this

http://www.aloki.hu ● ISSN 1589 1623 (Print) ● ISSN 1785 0037 (Online)
DOI: http://dx.doi.org/10.15666/aeer/1605_56115631
© 2018, ALÖKI Kft., Budapest, Hungary

community was *Cynodon dactylon* with 32.97 IVI the co-dominant species were *Berberis lyceum* with 13.83 IVI and *Melia azadarach* with 12.92 IVI. In the community, 135.07 IVI contributed by herbs, 68.06 by trees, 61.96 by shrubs, 36.28 by grasses and 0.95 by ferns (*Table 3*). Therophytes was the dominant life form in the community (40%) followed by Nanophanerophytes (17.14%). Microphylls was the dominant leaf spectra in the community (52.86%) followed by Nanophylls (24.29%). This community existed in loamy sand soil with basic nature (pH = 7.2 to 7.6). The organic matter in the soil was 2.90 to 4.28%, nitrogen was 0.14 to 0.21%. Phosphorous was 6.67 to 7.86 mg/kg, potassium was 132 to 138 mg/kg and electric conductivity was 0.03 to 0.09.

Table 3. *Numbers and total importance value contributed by herbs, shrubs and trees in each community of the Biha Valley*

S. no	CBM	PPQ	PID	VDA	QTB	QPA	JTB
Altitude (ft)	5174-5445	5606-7503	7078	7557-8850	9450-10513	10345	11225-11760
Latitude	072°18.127'-072°18.127'	072°17.397'-072°16.852'	072°13.501'	072°13.224'-072°12.207'	072°11.899'-072°11.608'	072°14.678	072°15.842'-072°15.586'
Longitude	35°03.516'-35°04.080'	35°02.675'-35°03.456'	35°05.626'	35°05.776'-35°06.240'	35°06.284'-35°06.567'	35°08.546'	35°08.224'-35°8.292'
Slope angle	15° to 30°	28° to 40°	20°	22° to 33°	24° to 49°	31°	20° to 27°
Slope exposure	North-east to south	S/E, N/W. N/E, E and N	South-west	South-east and North-east	North-east and South-east	South	South-east and North-east
Herbs species	43	58	22	26	31	17	22
Shrubs species	12	19	4	2	6	1	2
Trees species	12	11	2	7	3	3	0
Grass species	2	2	1	0	0	0	3
Fern species	1	5	2	4	1	0	1
Climbers	0	3	0	0	0	0	0
IVI of first 3 dominant species	59.72	50.23	107.73	97.93	80.49	113.15	98.18
By remaining species	212.6	218.32	220.45	204.09	225.65	186.85	201.81
Herbs IVI	135.07	112.58	170.37	126.37	191.2	159.14	212.09
Shrubs IVI	61.96	82.88	52.65	39.86	43.93	18.13	60.12
Trees IVI	68.06	44	42.64	87.92	68.33	113.15	-
Grasses IVI	36.28	3.31	8.41	-	-	-	23.58
Ferns IVI	0.95	22.29	39.90	47.87	2.68	-	4.2
Climbers IVI	-	3.49	-	-	-	-	-

CBM = *Cynodon-Berberis-Melia*, PPQ = *Parrotiopsis-Pinus-Quercus*, PID = *Pinus-Indigofera-Dryopteris*, VDA = *Vibernum-Dryopteris-Abies*, QTB = *Quercus-Thymus-Berberis,* QPA = *Quercus-Pieacea-Abies*, JTB = *Juniperus-Taraxicum-Bupleurum*

The Parrotiopsis-Pinus-Quercus (PPQ) community

From 5606 to 7503 ft altitude, *Parrotiopsis, Pinus and Quercus* community was found in More Khwar, Koza Pakani, Bara Pakani, Sarma Pakanai, Pakani Shaheed and Wale Drab locality. The longitude of the community varies from E = 072° 17.397' to 072° 16.852' and latitude N = 35° 02.675' to 35° 03.456' on S/E, N/W, N/E, E and N exposures with 28° to 40° slope degree. The community comprised of 98 plant species out of which 58 species were herbs, 19 species were shrubs, 11 species were trees, 5 species were ferns, 3 species were climbers and 2 species were grasses. In this

http://www.aloki.hu ● ISSN 1589 1623 (Print) ● ISSN 1785 0037 (Online)
DOI: http://dx.doi.org/10.15666/aeer/1605_56115631
© 2018, ALÖKI Kft., Budapest, Hungary

community *Parrotiopsis jacquemontiana* was the dominant species with 17.33 IVI while the co-dominant species were *Pinus wallichiana* 16.47 and *Quercus incana* with 16.43 IVI. In the community the herbs contributed a total of 112.58 IVI, 82.88 by shrubs, 44 by trees, 22.29 by ferns, 3.49 by climbers and 3.31 by grasses (*Table 3*). The dominant life form class in the community was Therophytes (44.44%) followed by Nanophanerophytes (17.17). The dominant leaf spectrum in the community was Microphylls (45.45%). The loamy sand soil of this community had basic nature (pH = 6.8 to 7.8) in comparison with other communities. The organic matter in the soil was noted 0.69 to 4.14% and nitrogen was 0.03 to 0.21%. The total amount of phosphorous found in the soil was 5.75 to 14.11 mg/kg, potassium was 112 to 162 mg/kg and electric conductivity was 0.02 to 0.08.

The Pinus-Indigofera Dryopteris (PID) community

At 7078 ft elevation, *Pinus-Indigofera-Dryopteris* was observed in Yag bila/Chatikal E = 072° 13.501'. N = 35° 05.626' on the southwest facing with 20° slope. The community consists of 31 plant species out of which 22 species were herbs 4 species were shrubs, 2 species were ferns and trees each, and 1 species was grass. The dominant species in this community was *Pinus wallichiana* with IVI 37.38 while the associated species were *Indigofera heterantha* (36.34) and *Dryopteris blonfordii* with 34.0 IVI. In this community 170.37 IVI contributed by herbs, 52.65 by shrubs, 42.64 by trees, 39.90 by ferns and 8.41 by grasses (*Table 3*). The dominant life form class in this community was Hemicryptophytes (35.71%) followed by Therophytes (32.14%). Based on the leaf spectra the community is categorized in Microphylls (39.29%). The soil chemistry of the community was loamy sand and had a pH of 7. The organic matter in the soil was the lowest as compared to other communities (1.04%) while nitrogen was 0.05%, phosphorous was the highest in the soil (19.57 mg/kg). Potassium was 158 mg/kg and electric conductivity was 0.03 of the soil.

The Vibernum-Dryopteris-Abies (VDA) community

Vibernum grandiflorum, Dryopteris blonfordii and Abies pindrow community was recorded from 7557 to 8850 ft elevation in Jarogo jai, Jarogo khwargai, Jarogo banda and Goryal jai 072° 13.224' to 072° 12.207' E and 35°.05.776' to 35° 06.240' N on the south-east and north-east facing slope with 22° to 33°. The community consists of 39 plant species out of which 26 species were herbs, 7 species were trees, 4 species were ferns and 2 species were shrubs. The highest IVI in community was of *Viburnum grandiflorum* with 39.13 while the associated species were *Dryopteris blonfordii* 29.43 and *Abies pindrow* with 29.38 IVI. In this community a total of 126.37 IVI was contributed by herbs 87.92 by trees 47.87 by ferns and 39.86 by shrubs (*Table 3*). In this community the Therophytes was the dominant life form (41.03%), followed by Hemicryptophytes (25.64%). On the basis of leaf spectra, the community is characterized by Microphylls (30.77%), Nanophylls (25.64%), Mesophylls (20.51%), Leptophylls (15.38%) and Megaphyll (7.69%). The physico-chemical analysis showed that the community was established in pure loamy to loamy sand soil with pH highly acidic slightly neutral 6 to 7.2. Organic contents in the soil were observed (1.73 to 4.83%) the highest in comparison with other communities and nitrogen was 0.09 to 0.17%. Phosphorous was measured 6.14 to 13.12 mg/kg, potassium was 112 to 164 mg/kg and electric conductivity was 0.01 to 0.14.

http://www.aloki.hu ● ISSN 1589 1623 (Print) ● ISSN 1785 0037 (Online)
DOI: http://dx.doi.org/10.15666/aeer/1605_56115631
© 2018, ALÖKI Kft., Budapest, Hungary

The Quercus-Thymus-Berberis (QTB) community

At 9450 to 10513 ft altitude, Goryal 1, Goryal 2 and Kandaow locality 072° 11.899' to 072° 11.608' N and 35° 06.284' to 35° 06.567' E on northeast and southeast exposures with 24° to 49° slopes, the community *Quercus semicarpifolia, Thymus linearis* and *Berberis jaeschkeana* was recorded. The community contains 41 plant species out of which 31 species were herbs, 6 species were shrubs, 3 species were trees and 1 species was fern. In this community *Quercus semicarpifolia* was the dominant species with 41.83 IVI while the co-dominant species were *Thymus linearis* 19.52 and *Berberis jaeschkeana* with 19.14 IVI. In the community the herbs contributed a total of 191.2 IVI, trees 68.33, shrubs 43.93, and ferns 2.68 (*Table 3*). The dominant life form in the community was Therophytes (43.90%) followed by Hemicryptophytes (19.51%). The dominant leaf spectrum in the community was Microphylls (43.90%), Nanophylls (29.27%), Leptophylls (12.20%), Mesophylls (9.76%) and Megaphyll (4.88%). The soil chemistry of the community was loamy sand with highly acidic nature to neutral of 5.8 to 7 pH. The organic content in the soil was observed 2.42 to 4.14%, whereas the nitrogen was 0.12 to 0.21%. The amount of phosphorous was measured high as compared to other communities (6.14 to 19.67 mg/kg), potassium was 138 to 160 mg/kg and electric conductivity was observed 0.02 to 0.12.

The Quercus-Picea-Abies (QPA) community

At an altitude of 10345 ft, *Quercus semicarpifolia*, *Picea smithiana and Abies pindrow community* was recorded in Mero kandaow locality E = 072 ° 14.678', N = 35° 08.546' on south facing slope with 31°. The community comprised of 21 plant species out of which 13 species were herbs, 3 species were trees and 1 species was a shrub. In this community *Quercus semicarpifolia* was the dominant species with 57.97 IVI while the co-dominant species were *Picea smithiana* 28.66 and *Abies pindrow* with 26.52 IVI. In the community the herbs contributed a total of 159.14 IVI, trees 113.15 and shrubs 18.13 (*Table 3*). The dominant life form in the community was Therophytes (47.62%) followed by Hemicryptophytes (19.05%). The dominant leaf spectrum in the community was Microphylls (47.62%). The physiochemical analysis of the soil showed that this community was present in loamy sand soil with a highly basic character (pH = 8) in comparison with other communities. The organic matter in the soil was noted 2.42% and nitrogen was 0.12%. The total amount of phosphorous found in the soil was 7.33 mg/kg, potassium was 156 mg/kg and electric conductivity was 0.01.

The Juniperus-Taraxacum-Bupleurum (JTB)

The community was observed at Landay sar and Sali kandaow of Dughalgo side at longitude E = 072° 15.842' to 072° 15.586' and latitude N = 35° 08.224' to 35° 08.292' of the area on southeast and northeast exposures with 20° to 27° slope at 11225 to 11760 ft elevation. The community comprised of 28 plant species having 22 species of herbs 3 species of grasses 2 species of shrubs and 1 species of ferns. In this community, *Juniperus communis* has the highest importance value index 45.07 followed by the co-dominant species *Taraxacum officinale* and *Bupleurum longicaule* having 34.2 and 18.91 importance value index respectively. A total of 212.09 importance value index was contributed by herbs 60.12 by shrubs, 23.58 by grasses and 4.2 by ferns (*Table 3*). The major life form in the community observed was Therophytes (50%) followed by Chamaephytes (25%). The highest leaf spectra observed in the community was

http://www.aloki.hu ● ISSN 1589 1623 (Print) ● ISSN 1785 0037 (Online)
DOI: http://dx.doi.org/10.15666/aeer/1605_56115631
© 2018, ALÖKI Kft., Budapest, Hungary

Nanophyll (32.14%), followed by Microphyll (28.57%). Physico-chemical analysis showed that the soil of the area was pure loamy to loamy sand with acidic nature of 5.8 to 6 pH. The organic matter noted was 2.76 to 4.83% and nitrogen was 0.14 to 0.24% in the soil of the community while phosphorous was 6.93 to 8.38 mg/kg and potassium was the highest as compared to other communities 144 to 186 mg/kg. The electric conductivity (EC) of the community was also high in comparison with other communities 0.52 to 0.67.

Index of similarity (IS)

The highest index of similarity (50.63%) was recorded between *Vibernum grandiflorum, Dryopteris blonfordii, Abies pindrow,* and Quercus semicarpifolia, *Thymus linearis* and *Berberis jasckeana* communities followed by (48.57%) between *Pinus wallichiana, Indigofera heterantha, Dryopteris blonfordii* and *Vibernum garndiflorum, Dryopteris blonfordii Abies pidrow* communities (36.68%) between *Cynodon dactylon, Berberis lycium, Melia azadarch* and *Parrotiopsis jacquemontiana, Pinus wallichiana, Quercus incana* communities. Intermediate similarity was recorded (27.77%) between *Pinus wallichiana, Indigofera heterentha, Dryopteris blonfordii* and *Quercus semicarpifolia, Thymus linearis* and *Berberis jasckeana* communities (27.53%) between *Parrotiopsis jacquemontiana, Pinus wallichiana, Quercus incana* and *Vibernum garndiflorum, Dryopteris blonfordii Abies pidrow* communities (26.15%), *Parrotiopsis jacquemontiana, Pinus wallichiana, Quercus incana* and *Pinus wallichiana, Indigofera heterantha, Dryopteris blonfordii.* The highest index of similarities ranges from 26.15% to 50.63% between communities due to same conditions of soil such as soil texture, organic matter and pH and physiographic factors such as slope angle, slope exposure and less difference in altitude. The least similarity index (2.02%) was noted between *Cynodon dactylon, Berberis lycium*, *Melia azadarch* and *Juniperus communis, Taraxacum officinale*, *Bupleurm longicaule* communities. Remaining communities also showed less than 20% similarity due to variation in altitude (5350 to 12000 ft), soil condition, organic matter, pH and phosphorus percentage (*Table 4*).

Table 4. *Similarity and dissimilarity index*

Community	CBM	PPQ	PID	VDA	QTB	QPA	JTB
CBM	x	36.68	19.80	14.67	11.88	6.52	2.04
PPQ	63.32	x	26.15	27.53	15.71	9.91	3.14
PID	80.2	73.85	X	48.57	27.77	11.32	3.38
VDA	85.33	72.42	51.43	x	50.63	19.67	2.98
QTB	88.12	84.29	72.23	49.37	x	19.06	11.59
QPA	93.48	90.09	88.68	80.33	80.94	X	4
JTB	97.96	96.86	96.62	97.02	88.41	96	X

CBM = *Cynodon-Berberis-Melia,* PPQ = *Parrotiopsis-Pinus-Quercus,* PID = *Pinus-Indigofera-Dryopteris,* VDA = *Vibernum-Dryopteris-Abies,* QTB = *Quercus-Thymus-Berberis,* QPA = *Quercus-Pieacea-Abies,* JTB = *Juniperus-Taraxicum-Bupleurum*

Index of dissimilarity (ID)

According to Muller-Dumbois and Ellenberg (1974), plant communities having less than 65% similarity were considered as dissimilar. All the plant communities of the

http://www.aloki.hu ● ISSN 1589 1623 (Print) ● ISSN 1785 0037 (Online)
DOI: http://dx.doi.org/10.15666/aeer/1605_56115631
© 2018, ALÖKI Kft., Budapest, Hungary

investigated area showed less than 65% similarity hence considered as different communities. The highest dissimilarity (97.96%) was recorded between *Juniperus communis, Taraxacum officinale*, *Bupleurm longicaule* and *Cynodon dactylon, Berberis lycium, Melia azadarch* communities (97.02%), between *Juniperus communis, Taraxacum officinale*, *Bupleurm longicaule* and *Vibernum garndiflorum, Dryopteris blonfordii Abies pidrow* communities (96.86%), between *Juniperus communis, Taraxacum officnale*, *Bupleurm longicaule* and *Parrotiopsis jacquemontiana, Pinus wallichiana, Quercus incana* communities (96.62%), *Juniperus communis, Taraxacum officnale*, *Bupleurm longicaule* and *Pinus wallichiana, Indigofera heterentha, Dryopteris blonfordii* while the lowest dissimilarity (49.37%) was observed between *Quercus semicarpifolia, Thymus linearis* and *Berberis jasckeana* and *Vibernum grandiflorum, Dryopteris blonfordii, Abies pindrow* communities (51.43%), between *Vibernum garndiflorum*, *Dryopteris blonfordii Abies pidrow* and *Pinus wallichiana, Indigofera heterentha, Dryopteris blonfordii* and *Vibernum garndiflorum.* All the other communities have greater than 60% dissimilarity (*Table 4*).

Ordination

Ordination of species

All species of the 19 stands and 7 communities were analyzed through Detrended Correspondence Analysis DCA which showed that the species of *Cynodon dactylon* and *Melia azadarch, Oenothera rosea* and *Dactylis glumerata, Diospyros lotus* and *Celtis caucasica, Spirea canescens* and *Trifolium repens, Quercus dilatata* and *Berberis lycium, Pinus wallichiana* and *Indigofera heterentha*, *Achyranthes aspera* and *Quercus incana*, *Abies pindrow* and *Rumex dentatus*, *Anemone obtusiloba* and *Viola canescens, Bupleurum longicaule* and *Rumex nephalensis*, *Epilobium hirsutum* and *Juniperus communis* have positive correlation with each other. While the species of *Juglans regia* and *Quercus semicarpifolia, Beberis lycium* and *Juniperus communis, Diospyros lotus* and *Piecea smithiana, Rubus fruticosus* and *Barberis jaeschkena* have negative correlation with each other and *Bistorta amplexicaulis* was found an isolated species as no correlated species was found with it (*Fig. 3*).

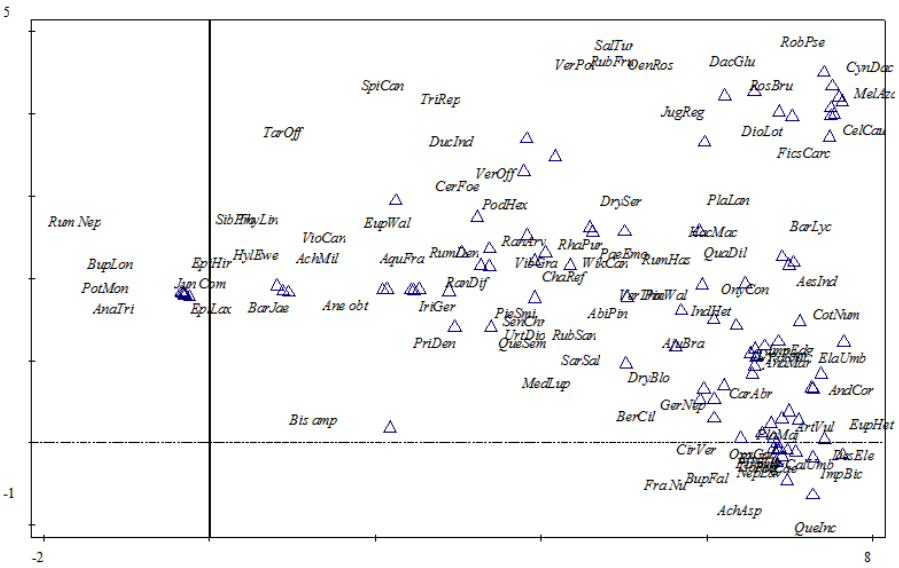

Figure 3. *DCA ordination of species*

http://www.aloki.hu ● ISSN 1589 1623 (Print) ● ISSN 1785 0037 (Online)
DOI: http://dx.doi.org/10.15666/aeer/1605_56115631
© 2018, ALÖKI Kft., Budapest, Hungary

Ordination of stands

The ordination of all stand of the study area given Detrended Correspondence Analysis DCA (*Fig. 4*). The DCA of stand indicated that both stands 1 and 2 correlated with each other, stand 3, 12, 13, 14, 15 and 16 correlated as well, 5, 6, 7 and 8 correlated too, 9, 10 and 11 also correlated, 17 and 19 correlated as well with each other in environmental variables and similar vegetation while stand 4 and stand 18 have no correlation with any stand therefore, these are considered as individual communities.

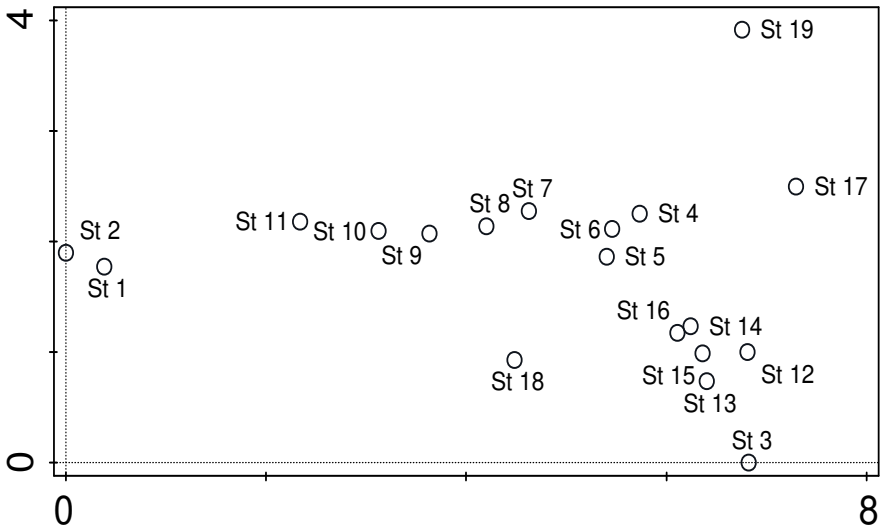

Figure 4. *DCA ordination of stands*

Ordination of species with environmental variables

The correlation between vegetation and environmental variables was indicated in the ordination diagram produced through Canonical Correspondence Analysis (CCA). In which the direction and length of the arrow indicated the environmental variables and the triangle shaped clusters indicated the vegetation while length of the arrow shows the strength of variable between the variable at each axis representing the degree of correlation between them, the variables on the same axis show positive correlation while the variables on the opposite axes indicated negative correlation. As shown in (*Fig. 5*) that *Abies pindrow, Verbena officinalis* and *Rumex dentatus* were highly correlated with slope steepness while these species were less correlated with electric conductivity, silt, soil fertility, pH, latitude and soil classes. *Viburnum grandiflorum, Trifolium repens, Duchesnea indica, Primula denticulate, Sibbaldia procumbens, Viola canescens, Anemone obtusiloba,* were highly correlated with phosphorous and less correlated with silt, latitude, electric conductivity, pH, and classes. *Barberis jaeschkena*, *Taraxacum officinale* and *Hylotelephium ewersii* were highly correlated with potassium and less correlated with classes, pH, latitude, silt, and electric conductivity. Similarly, *Trachydium roylei*, *Bupleurum longicaule*, *Genetiana olivieri*, *Eritrichuim canum, Anaphalis triplenervis, Bergenia stracheyi, Cerastium pusillum, Circea cordata* and *Potentella Monenthes* have close association with electric conductivity and nitrogen and less relationship with slope angle, slope facing, phosphorous and potassium. *Chenopodium album, Calamintha umbrosa, Elscholtzia fruticosa, Baberis lyceum, Andrachne cordifolia* and *Desmodium elegans* were closely associated with latitude and

http://www.aloki.hu ● ISSN 1589 1623 (Print) ● ISSN 1785 0037 (Online)
DOI: http://dx.doi.org/10.15666/aeer/1605_56115631
© 2018, ALÖKI Kft., Budapest, Hungary

less associated with slope steepness, altitude, longitude, slope exposure, clay, soil fertility, potassium and phosphorous. *Carpesium abrotonoide, Artemisia vulgaris* and *Elaeagnus umbellate* were highly associated with pH and less correlated with altitude, longitude clay, slope exposure and slope steepness. No species was found closely associated with altitude and longitude however the density of species decreases with the increase in altitude.

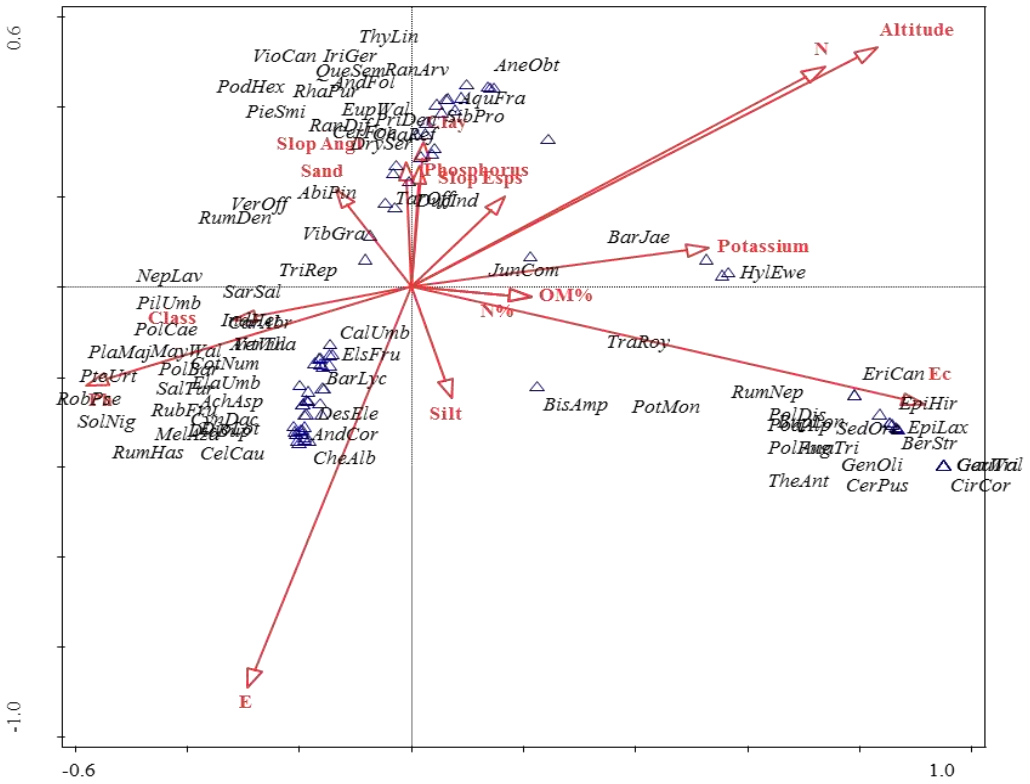

Figure 5. *CCA ordination of species with environmental variables*

Ordination of communities with environmental variables

CCA ordination was used to find the correlation of environmental variables and plant communities of the study area (*Fig. 6*). The maximum strength was recorded for the environmental variables like altitude, electric conductivity and nitrogen. The minimum environmental variable strength was recorded for Organic matter. The stands of *Cyanodon, Berberis, Melia* community and *Parrotiopsis, Pinus, Quercus* community positively correlated with Latitude and pH. *Pinus, Indigofera, Dryopteris* community positively correlated with sand. *Vibernum, Dryopteris, Abies* community positively correlated with sand, slope angle, clay and phosphorous. *Quercus, Thymus, Berberis* community were positively correlated with slope aspect, clay and phosphorous. *Quercus, Picea, Abies* community positively correlated with slope angle and clay. The stands of *Juniperus, Taraxacum, Bupleurum* community positively correlated with electrical conductivity. In constrained CCA ordination the total variation was 5.859, explanatory variables account for 84.5%. The CCA ordinations of different axis are given in *Table 5*.

http://www.aloki.hu ● ISSN 1589 1623 (Print) ● ISSN 1785 0037 (Online)
DOI: http://dx.doi.org/10.15666/aeer/1605_56115631
© 2018, ALÖKI Kft., Budapest, Hungary

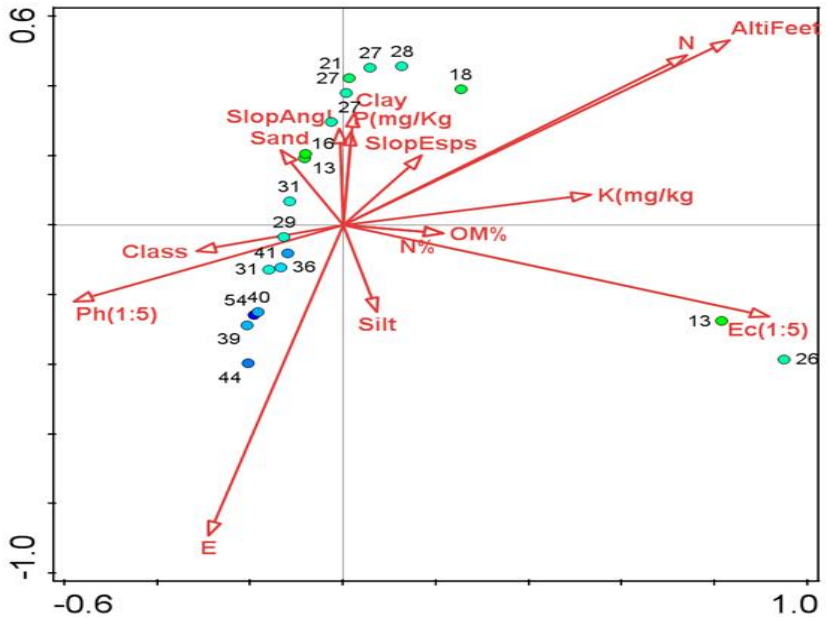

Figure 6. *CCA ordination of stands with environmental variables*

Table 5. *CCA ordination on different axis*

Statistic	Axis 1	Axis 2	Axis 3	Axis 4
Eigenvalues	0.8393	0.7068	0.5418	0.4799
Explained variation	14.32	26.39	35.63	43.82
Pseudo-canonical correlation	0.9982	0.9979	0.9976	0.9561
Explained fitted variation	16.94	31.21	42.15	51.84
Permutation test results: on all axes	Pseudo-F = 1.1, P = 0.256			

Discussion

In the present study a sum of 203 plants species of 70 families were recorded in which the leading families were Asteraceae, Rosaceae and Lamiaceae; therefore, the area was considered rich floristically. Our results are in accordance with previous reports of many researchers of the country. Ijaz (2016) and Khattak et al. (2015) mentioned Asteraceae while Rahman et al. (2016a, b) cited Lamiaceae as the leading families from their study areas. During the present study the ratio of flowering was found different at different time of the year. A very few herbaceous and shrubby plants initiated vegetative growth at the end of April. Early May is the blooming time for few plant species. Plant species such as *Juglans regia*, *Melia azaadarch, Morus alba, Rosa moschata, Rubus fruticosus, Caltha alba* and *Lactuca dissecta* were active during this period. May to August is the favorable season for the flowering for the majority of shrubby, trees and herbaceous species. July and August were the peak flowering months after that flowering stage starts declining. Similarly, Zhanghe et al. (1999) also described that peak of flowering happened during May in various parts of China.

The study of characteristics, classification, relationships and distribution of plant communities is known as phytosociology (Dastagir et al., 1999). From elevation of 5174 ft to 12760 ft 7 different plant communities were established from 19 stands with

http://www.aloki.hu ● ISSN 1589 1623 (Print) ● ISSN 1785 0037 (Online)
DOI: http://dx.doi.org/10.15666/aeer/1605_56115631
© 2018, ALÖKI Kft., Budapest, Hungary

203 plant species in the study area by using TWINSPAN classification. Seasonal fluctuations and sampling time change the structure of the community which is the consequence of the environmental conditions, habitat and existing vegetation types. Champion et al. (1965) and Bano et al. (2018) recognized different communities of plants from various areas and reported that it was due to the degradation of environmental and anthropogenic factors therefore the current investigation also signify that the major vegetation units were degraded by different environmental variables and man-made factors. Kumar (1996) found the relation between species distribution and soil physical factors like soil moisture and texture and El-Ghani (1998) reported a close relationship between soil chemistry (pH), calcium and organic carbon and composition of plant species. Organic matter content as a pivotal soil fertility factor can affect phytodiversity (Zhang et al., 2010). Our results indicate the importance of soil organic matter in top soil layers for plant species distribution. The increases in soil nutrients (OM, P, N, and K), improvement in site conditions (community cover, depth of litter, depth of humus, soil water content) and decrease in soil bulk density indicated the natural habitat restoration following abandonment.

DCA and Cluster analysis are very useful in plant communities and classification of species and other than this to give structure to plant life. Soil pH, texture and density of trees are the major causes of vegetation pattern (Saima et al., 2009).

The ranges of altitude have an important effect on qualitative and quantitative characteristics of trees (Fallah Chay and Marvie, 2005). The mean of temperature, evaporation and transpiration are reducing with increasing altitude range, while the humidity will be increasing. Some species of plants do not prefer the high altitudes because of short growth period and low temperatures. The presence of severe winds in highlands also confines the growth of plant. At lower altitude (5445 ft) of the study area *Cynodon-Berberis-Melia* community exists while the *Parrotiopsis-Pinus-Quercus* was present at 5606 to 7503 ft elevation; similarly, at high elevation of 10000 to 12000 ft the *Quercus-Thymus-Berberis* community and *Juniperus-Taraxacum-Bupleurum* community was recorded. Agreed findings were reported by Bano et al. (2018). They recorded the presence of *Berberis* community at 2485–2937 m. Similarly, *Thymus* and *Artemisia* community is reported by Aleyha and Shokuii (2003) at 2350–2500 m elevation in Semnan. Karimi (1997) documented the *Thymus* and *Agropyron* community in Anzali-Khalkhal area at 1400 to1800 m altitude. The elevation in the area showed positive correlation with the number of species. Our findings are in line with Dasti and Malik (1998) who indicated that altitude is an environmental variable which affects the density and association of plants. Our results reveal that soil characteristics such as electric conductivity, pH, clay and fertility have great effect on community distribution and plants species association.

The results revealed that slope exposure was one of the most important variable influencing the plant distribution. South and north facing slopes have completely unlike vegetation covers. South facing slopes have high temperature and low humidity because of severe solar radiation in comparison with north facing slopes. In contrast, north facing slopes have low temperature and has high humidity because of low radiation. As the community of *Juniperus -Taraxacum* and *Bupleurum* exists on northeast facing slopes and at lesser altitude such a situation is resulted from the deficit of radiation and temperature. *Vibernum-Dryopteris* and *Abies* community was recorded also in north facing slopes. While on south facing slope *Cynodon-Berberis* and *Melia* community was recorded at lower altitude and *Quercus-Picea and Abies*

http://www.aloki.hu ● ISSN 1589 1623 (Print) ● ISSN 1785 0037 (Online)
DOI: http://dx.doi.org/10.15666/aeer/1605_56115631
© 2018, ALÖKI Kft., Budapest, Hungary

community was observed at high elevation. According to Nazarian (2003), the Salix community was present in north-northeast facing slopes, and the thorny assemblages on south, southwest, southeast, north, northwest and northeast facing slopes in Central Alborz. In our investigation direction of east and west slope were only found effective on growth of diameter and north exposure was found effective on species richness, canopy cover and species association (*Fig. 7*). The analysis of site exposure is commonly used for the determination of qualitative and quantitative indices (Corney et al., 2006; Ajbilou et al., 2006).

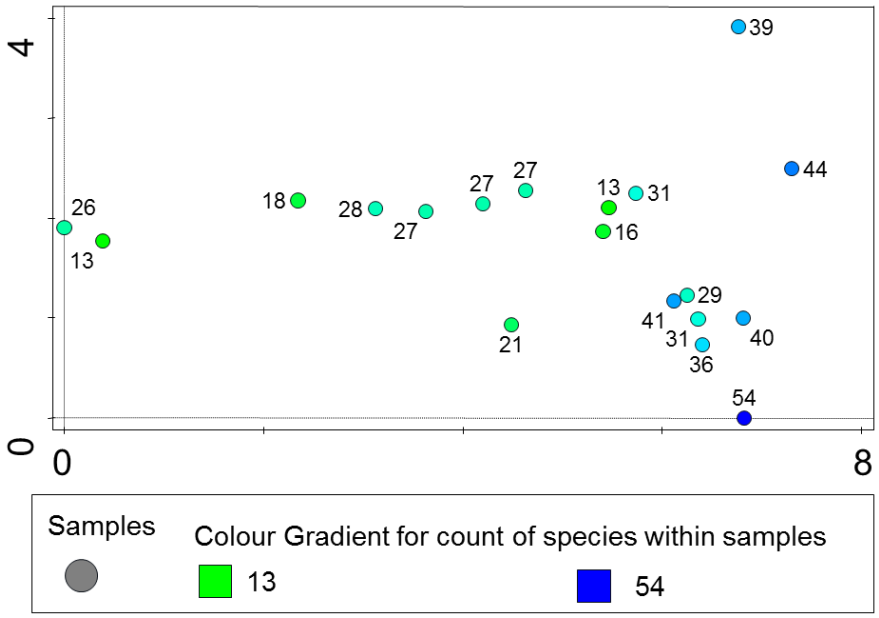

Figure 7. *DCA ordination showing the taxonomic richness of species*

Slope angle or steepness influences the cover of vegetation on different kinds of slopes. In the studied area, *Cyanodon* as a grass, *Pinus* community as a tree and *Juniperus* as a shrub accumulation are present on moderate slopes, but *Parrotiopsis, Vibernum* as a shrub *Quercus* and *Quercus* as tree communities are stretched on sharp slopes. Khageaddin in (2000) described the existence of *Amygdalus haussknechtii* on high slopes of more than 100% in Kolah ghazi National Park.

The distribution and composition of plant communities in the studied area seems to be controlled by different environmental variables together with climate, topography, soil and biotic pressure. These variables go through variations of various points due to relations with each other and may possibly result in micro-gradients (Hanson and Churchill, 1965). The soil characteristics also influence the distribution of plant on smaller scale (Bakkenes et al., 2002). Landscape also plays significant role in physical features of vegetation. It influences the plant life by changing other variables of environment. Diverse aspects, slopes and altitudes support various plant communities in Biha Valley. Similar findings were recorded by Ahmed et al. (2009) during their research work on *Olea ferruginea* forests of lower Dir.

http://www.aloki.hu ● ISSN 1589 1623 (Print) ● ISSN 1785 0037 (Online)
DOI: http://dx.doi.org/10.15666/aeer/1605_56115631
© 2018, ALÖKI Kft., Budapest, Hungary

Conclusion

The present investigated area has rich phytodiversity containing 203 plant species including 137 herbs, 25 shrubs, 21 trees, 8 grasses, 8 ferns and 3 species of climbers. Most of the local inhabitants are depending upon the biodiversity of the area. The local people use plant resources for various purposes including medicinal, for fodder, fruits, vegetables, fuel wood etc. The dominance of Therophytes and Microphylls type of biological spectrum shows that the area has sub-tropical and moist temperate type of climate. The ecological characters of plants such as density, frequency and abundance were completely influenced by the natural as well as biotic pressures mainly at the sites of the investigation area. The highest values of density and frequency were observed in the rainy season and the minimum values in the cold season. Plants have revealed relatively higher frequency and density, consequently higher degree on distribution and numerical strength of species in summer season on account of most sustainable climatic conditions. It seems in such natural communities, that constancy appears to depend on the balance between the stability and variability of the environment. The diversity of plant species decreases with altitude in the site. Soil electric conductivity, pH, slope angle, slope exposure were found to be the highest environmental variables influencing the distribution of species and communities in the area.

It can be concluded that seasons have great effect on characteristics of soil and species diversity. It was observed that species diversity increases during spring and summer season which decreased later as autumn and winter come close which resulted in decline in the diversity due to dry environmental conditions, slow growth rate and other climatic factors. Difference in numerical parameters like, species richness and species diversity is correlated with variations in soil factors, slope aspect elevation, and micro-climatic conditions in different sites of the area.

Further it is concluded that the site faces the pressure from the local inhabitants in the form of overgrazing and deforestation, which have reduced regeneration of woody plants. Overgrazing, human population explosion, uprooting of medicinal plants by the local laypeople and other informal factors are responsible for habitat loss, soil erosion and proper functioning of ecosystems. There is dire need to conserve the biodiversity of the area in order to provide the resources and resource alternatives for the people's survival in the future.

It could be recommended that rare plant species in the specific micro-habitat can further be studied for conservation management purposes and future ethnobotanical projects must be initiated.

Author's Contributions. AZ conducted the fieldwork, collected data, plant species and conducted the herbarium work, SMK helped in the field work. AM identified the plants specimens. IUR drafted the manuscript. ZI and IUR analyzed the data, FI and MAK helped in organizing the data. ZI supervised the work. IUR and NA critically reviewed the manuscript, EFA, AAA, AH and AA helped in discussion. NA and IUR revised the manuscript, MS, YA and ESC helped in the revision. All the authors have read and approved the final manuscript.

Acknowledgements. The authors would like to extend their sincere appreciation to the Deanship of Scientific Research at King Saud University, Saudi Arabia for its funding to the Research Group number (RG-1435-014).

http://www.aloki.hu ● ISSN 1589 1623 (Print) ● ISSN 1785 0037 (Online)
DOI: http://dx.doi.org/10.15666/aeer/1605_56115631
© 2018, ALÖKI Kft., Budapest, Hungary

REFERENCES

[1] Adnan, S. M. (2003): Feasibility of Community Involvement in the Sustainable Use of Medicinal Plants of Roringar Valley, Swat. – Ethnobotany Project WWFP, Peshawar.
[2] Ahmad, M., Sirajuddin (1996): Ethnobotanical Profile of Swat. – Proceedings of the First Training Workshop on Ethnobotany and its Application to Conservation, September 16-24, PARC, WWF, ICIMOD, Islamabad, pp. 202-206.
[3] Ahmed, M., Khan, N., Wahab, M., Hamza, S., Siddiqui, M. F., Nazim, K., Khan, M. U. (2009): Vegetation structure of *Olea ferruginea* Royle Forests of lower Dir district of Pakistan. – Pak. J. Bot. 41(6): 2683-2695.
[4] Ajbilou, R. Maranon, T., Arroyyo, J. (2006): Ecological and biogeographical analyses of Mediterranean forests of northern Morocco. – Acta Ecologica 29: 104-113.
[5] Aleyha, M. Shokuii, M. (2003): Vegetation Types of Semnan Area. – Research Institute of Forests and Rangelands, Tehran, No. 335.
[6] Archibold, O. W. (1995): Ecology of World Vegetation (1st edition). – Chapman & Hall, Great Britain.
[7] Asri, J. (1994): Phytosociology. – Forests and Rangelands Institute, Tehran, pp. 1-134.
[8] Bakkenes, M. Alkemade, J. R. Ihle, F. Leemans, R. Latour, J. B. (2002): Assessing effects of forecasted climate change on the diversity and distribution of European higher plants for 2050. – Glo. Change Bio. 8(4): 390.
[9] Bano, S., Khan, S. M., Alam, J., Alqarawi, A. A., Abd_Allah, E. F., Ahmad, Z., Hashem, A. (2018): Eco-Floristic studies of native plants of the Beer Hills along the Indus River in the districts Haripur and Abbottabad, Pakistan. – Saudi Journal of Biological Sciences 25(4): 801-810.
[10] Braun-Blanquet, J. (1983): Plant Sociology. – Koeltz Scientific Books, Königstein, pp. 35-72.
[11] Champion, H. G., Seth, S. K., Khattak, G. H. (1965): Forest Types of Pakistan. – Pak. Forest Int., Peshawar.
[12] Corney, M. G. Smart, S. M. Kibby, K. J., Buche, R. G. H., Marrs, R. H. (2006): Relationships between the species composition of forest field-layer vegetation and environmental drivers assessed using a national scale survey. – Journal of Ecology 94: 388-401.
[13] Dastagir, G. Haq, I. U., Malik, Z. H. (1999): Phytosociology of Mai Dhani Hill near Muzaffarabad, Azad Kashmir. – Pak. J. Bio. Sci. 2(2): 185-191.
[14] Dasti, A. A., Malik, S. A. A. (1998): A transect of vegetation and soils on the Indus valley scarp slope. – Pakistan. Pak J. Plant Sci. 4(2): 73-84.
[15] Daubenmire, R. (1959): Mountain topography and vegetation pattern. – North West Sci. 54(2): 146-152.
[16] El-Ghani, M. M. (1998): Environmental correlates of species distribution in arid desert ecosystems of eastern Egypt. – J. Arid Environ. 38: 297-313.
[17] Ewald, J. (2003): A critique for phytosociology. – J. Veg. Sci. 14(2): 291-296.
[18] Fallah Chay, M. M., Marvie Mohadjer, M. R. (2005): Ecological role of altitude in diversity of tree species in Siahkal forests, north of Iran. – Iranian J. Nat. Res. 58: 89-100 (in Persian).
[19] Goldsmith, F. B., Harrison, C. M., Morton, A. J. (1986): Description and Analysis of Vegetation. – In: Moore, P. D., Chapman, S. B. (eds.) Methods in Plant Ecology (2nd edition). The Alden Press, Oxford, pp. 437-534.
[20] Hanson, H., Churchill, E. D. (1965): The Plant Community. – Reinhold, New York, pp 219.
[21] Haq, F., Ahmad, H., Iqbal, Z. (2015a): Vegetation description and phytoclimatic gradients of sub-tropical forests of Nandiar Khuwar catchment District Battagram. – Pak. J. Bot. 47(4): 1399-1405.

http://www.aloki.hu ● ISSN 1589 1623 (Print) ● ISSN 1785 0037 (Online)
DOI: http://dx.doi.org/10.15666/aeer/1605_56115631
© 2018, ALÖKI Kft., Budapest, Hungary

[22] Haq, F. Ahmad, H., Iqbal, Z. (2015b): Vegetation composition and ecological gradients of subtropical-moist temperate ecotonal forests of Nandiar Khuwar catchment, Pakistan. – Bangladesh J. Bot. 44(2): 267-276.
[23] Hussain, F. (1989): Field and laboratory manual of plants ecology. – University Grants Commission, Islamabad 3: 27-78.
[24] Karimi, G. H. H. (1997): Vegetation Cover of Anzali-Khalkhal Area. – Research Institute of Forests and Rangelands, Tehran.
[25] Kent, M., Coker, P. (1992): Vegetation Description and Analysis: A practical Approach. – John Wiley and Sons, New York.
[26] Khademi, A., Babaee, S. (2009): Investigation of biomass and its relation with physiographic and soil characteristics in oak forests. – Ir. J. Forest 1: 57-67.
[27] Khageaddin, H. (2000): Phytocociology of Kolahghazi National Park. – The Iranian Journal J. Pajouhesh & Sazandegi 45: 10-16.
[28] Khan, S. M. Page, S., Ahmad, H., Shaheen, H., Harper, D. (2012): Vegetation dynamics in the western Western himalayasHimalayas, diversity indices and climate change. – Sci., Tech. and Dev. 31(3): 232-243.
[29] Khattak, N. S., Nouroz, F., Rahman, I. U., Noreen, S. (2015): Ethnoveterinary uses of medicinal plants of district Karak, Pakistan. – Journal of Ethnopharmacol. 171: 273-279.
[30] Koehler, F. E., Moudre, C. D., McNeal, B. L. (1984): Laboratory Manual for Soil Fertility. – Washington State University, Pulman, USA.
[31] Kumar, S. (1996): Trends in structural compositional attributes of duneinterdune vegetation and their edaphic relations in the Indian desert. Vegetatio 124: 73-93.
[32] Marvie, M. M. R. (1984): The study on Oak forest in Gorgan (case study; Loveh). – Iranian J. Nat. Res. 37: 41-56 (in Persian).
[33] McLean, E. O. (1982): Soil pH and Lime Requirement. – In: Page, A. L., Miller, R. H., Keey, D. R. (eds.) Methods of Soil Analysis Part 2. Amer. Soc. Agron. No. 9, Madison, Wisconsin, USA, pp. 199-209.
[34] Mueller-Dumbois, D., Ellenberg, H. (1974): Aims and Methods of Vegetation Ecology. – John Wiley and Sons, London, pp. 45-58.
[35] Nazarian, H. (2003): Eco-Phytosociological Evaluation of Elika and Dona Watershed of Central Alboorz. – PhD Thesis, Sciences Faculty, Tehran University.
[36] Nelson, D. W., Sommers, L. E., Sparks, D. L., Page, A. L., Helmke, P. A., Loeppert, R. H., Sumner, M. E. (1996): Total Carbon, Organic Carbon, and Organic Matter. – In: Sparks, D. L. (ed.) Methods of Soil Analysis. Part 3. Chemical Methods. American Society of Agronomy-Soil Science Society of America, Madison, WI, pp. 961-1010.
[37] Paul, A. E., Berry, E. H. (1921): The Kjeldahl method and its modifications. – J. Assoc. Agric. Chem. 5: 108-132.
[38] Rahman, I. U., Afzal, A., Iqbal, Z., Ijaz, F., Khan, S. M., Khan, S. A., Shah, A. H., Khan, K., Ali, N. (2015): Influence of foliar nutrients application on growth and yield of onion grown in nutrient deficient soil. – Bangladesh J. Bot. 44: 613-619.
[39] Rahman, I. U., Ijaz, F., Afzal, A., Iqbal, Z., Ali, N., Khan, S. M. (2016a): Contributions to the phytotherapies of digestive disorders. Traditional knowledge and cultural drivers of Manoor Valley, Northern Pakistan. – J. Ethnopharmacol. 192: 30-52.
[40] Rahman, I. U., Ijaz, F., Afzal, A., Iqbal, Z., Ali, N., Afzal, M., Khan, M. A., Muhammad, S., Qadir, G., Asif, M. (2016b): A novel survey of the ethno medicinal knowledge of dental problems in Manoor Valley (Northern Himalaya). – Pakistan. J. Ethnopharmacol. 194: 877-894.
[41] Rahman, I. U., Ijaz, F., Afzal, A. Iqbal, Z. (2017): Effect of foliar application of plant mineral nutrients on the growth and yield attributes of chickpea (*Cicer arietinum* L.) Under nutrient deficient soil conditions. – Bangladesh J. Bot. 46: 111-118.
[42] Rahman, I. U., Afzal, A., Iqbal, Z. et al. (2018): First insights into the floristic diversity, biological spectra and phenology of Manoor Valley, Pakistan. – Pak. J. Bot. 50: 1113-1124.

http://www.aloki.hu ● ISSN 1589 1623 (Print) ● ISSN 1785 0037 (Online)
DOI: http://dx.doi.org/10.15666/aeer/1605_56115631
© 2018, ALÖKI Kft., Budapest, Hungary

[43] Saima, S., Dasti, A. A., Hussain, F., Wazir, S. M., Malik, S. A. (2009): Floristic compositions along an 18 - km long transect in Ayubia National Park district Abbottabad, Pakistan. – Pak. J. Bot. 41(5): 2115-2127.
[44] Shaheen, S., Iqbal, Z., Ijaz, F., Alam, J., Rahman, I. U. (2016): Floristic composition, biological spectrum and phenology of Tehsil Havelian, District Abbottabad, Pakistan. – Pak. J. Bot. 48(5): 1849-1859.
[45] Soltanpour, P. N. (1985): Use of ammonium bicarbonate DTPA soil test to evaluate elemental availability and toxicity. – Commun. Sci. Pl. Anal. 16: 323-338.
[46] Sorenson, T. (1948): A method of establishing groups of equal amplitude in plant sociology based on similarity of species and its application to analyses of the vegetation on Danish commons. – Royal Danish Academy of Sciences and Letters 5(4): 1-34.
[47] Ter Braak, C. J. F. (1986): Canonical correspondence analysis: A new eigenvector technique for multivariate direct gradient analysis. – Ecol. 67: 1167-1179.
[48] Ter Braak, C. J. F. (1994): Canonical community ordination. Part I: Basic theory and linear methods. – Ecoscience 1: 127-140.
[49] Zhang, K., Dang, H., Tan, S., Wang, Z., Zhang, Q. (2010): Vegetation community and soil characteristics of abandoned agricultural land and pine plantation in the Qinling Mountains, China. – Forest Ecol. Manag. 259: 2036-2047.
[50] Zhanghe, C., Jieyuan, C., Yunlong, Z. (1999): Flowering and fruiting phenologies of the woody plants in three floras in China. – J. Trop. Subtrop. Bot. 7: 102-108.

http://www.aloki.hu ● ISSN 1589 1623 (Print) ● ISSN 1785 0037 (Online)
DOI: http://dx.doi.org/10.15666/aeer/1605_56115631
© 2018, ALÖKI Kft., Budapest, Hungary

GENETIC DIVERSITY WITHIN NATURAL POPULATIONS OF THE MEDICINAL PLANT *RHYNCHOSIA MINIMA* (L.) DC.

MUHAMMAD, N.[1] – ALI, N.[1*] – NISAR, M.[2] – ABD_ALLAH, E. F.[3] – HASHEM, A.[4] – ALQARAWI, A.[3] – ALDUBISE, A.[3] – KHAN, U.[1] – RAHMAN, I. U.[1] – AFZA, R.[1] – KHAN, A.[5] – AHMAD, H.[6]

[1]*Department of Botany, Hazara University, Mansehra, Pakistan*

[2]*Department of Botany, University of Malakand, Chakdara, Pakistan*

[3]*Department of Plant Production, College of Food & Agricultural Sciences, King Saud University, P.O. Box 2460, Riyadh 11451, Saudi Arabia*
ORCID ID (E. F. Abd_Allah): 0000-0002-8509-8953

[4]*Department of Botany and Microbiology, College of Science, King Saud University, P.O. Box 2460, Riyadh 11451, Saudi Arabia*

[5]*Department of Microbiology, BUITEMS, Quetta, Pakistan*

[6]*Islamia College University, Peshawar, Pakistan*

**Corresponding author*
e-mail: niazalitk25@gmail.com

(Received 20th May 2018; accepted 31st Jul 2018)

Abstract. Genetic diversity and relationships among 100 genotypes of *Rhynchosia minima* collected from four districts of Malakand Division was assessed using 16 morphological characteristics and total seed protein profile. Based on qualitative characteristics, inter-district trait similarity index among genotypes of Swat-Dir Lower and Swat-Buner was 100%, while for Dir Lower-Buner, Dir Lower-Dir Upper, and Buner-Dir Upper, it was 85.71%, 28.57%, and 42.85%, respectively. Total seed protein profile resulted in 8 reproducible bands/loci, where inter-district locus contribution to the genetic disagreement was 75%. Among the 8 loci, B-6 and B-7 were monomorphic and could be *R. minima* specific, whereas loci B-1, B-4, B-5 and B-8 were observed only in genotypes collected from Buner. All but locus B-1 were present in genotypes of Dir Upper; locus B-8 was missing in genotypes from Dir Lower; loci B-1 and B-4 were absent in genotypes collected from Swat. Two-way cluster analysis resolved genotypes of District Buner and Dir Upper into discrete clusters, highlighting the role of habitat-specific adaptation. Genotypes of Dir Lower and Swat formed mosaic cluster, indicating to the transfer of genes and/or their coevolutionary descent. To the best of our understanding, this is the first ever report addressing genetic variability in *R. minima*.
Keywords: *genetic variability, climate change, SDS-PAGE, two-way cluster analysis, Rynchosia*

Introduction

Grain legumes are important dietary constituents for both humans and livestock and are ranked third in global importance after cereals and oilseeds (Ilyas et al., 2009; Naim-Feil et al., 2017). With the estimated rise in human population, food security is generally uncertain and warrants the need for safeguarding the biodiversity provided by nature and arable land for specific adaptation to stresses as well as ecosystem resilience under changing climatic conditions (Jacobsen et al., 2013; McCouch et al., 2013; Ali et al., 2016). Under these circumstances, demands for grain legume consumption will increase, and biotic and abiotic constraints will push the limits of legume production

http://www.aloki.hu ● ISSN 1589 1623 (Print) ● ISSN 1785 0037 (Online)
DOI: http://dx.doi.org/10.15666/aeer/1605_56335651
© 2018, ALÖKI Kft., Budapest, Hungary

further (Ilyas et al., 2009). Nevertheless, the role of tropical grain legumes is critically important for areas where protein intake from animal sources is low. Population growth and limited land and water resources for agriculture are the major concerns that have gained considerable recent attention (Takeda and Matsuoka, 2008; McCouch et al., 2013). Although there have been consistent increases in crop productivity, these efforts are no longer meet the demands of future populations (Heslop-Harrison and Schwarzacher, 2012). Therefore, exploiting and tapping the wealth of wild and cultivated genetic resources provided by nature and currently warehoused in our seed repositories are vital (Tenskley and McCouch, 1997; Mujeeb-Kazi et al., 2017). However, in spite of all efforts, the world currently faces a greater demand on agricultural output than at any time in history (Tanksley and McCouch, 1997; Naim-Feil et al., 2017).

Indeed, plant breeders have been largely successful in developing high-yielding crop varieties; demands for greater yield potential were previously approached with genetic improvements coupled with increased farming inputs and addition to arable land (Helsop-Harrison and Schwarzacher, 2011). More recently, as the arable land surface has begun to shrink due to population growth, freshwater resources are becoming scarce, and agricultural inputs are associated with increased pollution; thus, major benefits will most likely result from genetic improvement of crops (Lobell et al., 2008; McCouch et al., 2013). However, the last several decades of intense plant breeding and selection are regarded as the most important force that has narrowed the genetic variability of crop species after their domestication some 10,000 years ago (Lu et al., 2009; Schwarzacher et al., 2011; Ali et al., 2012). Today, humanity depends on less than a dozen flowering plant species for 80% of all caloric intake (McCouch et al., 2013). Without sufficient adaptation measures in place, this will not be sufficient to support the feeding demands of 2050 in the face of climate change, habitat fragmentation, and limited water and land resources (Lobell et al., 2008; Mujeeb-Kazi et al., 2017).

Rhynchosia minima (L.) DC., a herbaceous, vining, perennial weed of the family Fabaceae, is found on all five continents (Lopez, 2012). The plant has considerable plasticity and can colonize disturbed areas as well as gaps within natural communities (Shaukat and Burhan, 2000). The plant has tremendous potential to be used in forage, pharmaceutical and other agricultural products, and more importantly, there are no known major threats to this species (Lopez, 2012); however, the plant has negligible uses worldwide, including in Pakistan. Traditionally, *R. minima* is applied to alleviate boils, colds, respiratory infections, diarrhea, dysentery and joint pains, and has been used as an abortifacient and an ecbolic and for general healing. It is also used as a food (in sweets), and its seeds are used as repellents and have antimicrobial potential. Furthermore, a number of important compounds that could fight cancer and may reduce carcinogenesis have been isolated from the seeds (Morris, 2008; Gweru et al., 2009; Jia et al., 2015).

A wide genetic base is critical to adaptation and will determine the future severity of climate change impacts. Genetic bottlenecks jeopardize the potential of crop species for sustainable agriculture and render them vulnerable to stresses (Ali et al., 2012, 2016; McCouch et al., 2013; Mujeeb-Kazi et al., 2017). With the continuous developments in DNA-based technologies and computational tools, more objective measurements of genetic diversity at the genomic level could be made, and important loci could be precisely mapped.

http://www.aloki.hu ● ISSN 1589 1623 (Print) ● ISSN 1785 0037 (Online)
DOI: http://dx.doi.org/10.15666/aeer/1605_56335651
© 2018, ALÖKI Kft., Budapest, Hungary

However, not all of these tools are currently available to plant breeders in developing countries, which house large food-insecure human populations. Plant breeders still rely on traditional approaches to screen entries for a clearly defined character recognizable in the phenotype. Once a line with the desired characteristic is pinpointed, it is crossed with an elite cultivar in order to introduce the genes from the exotic donor into the cultivated type (Tanksley and McCouch, 1997; Mujeeb-Kazi et al., 2017).

Proteins are end products of gene expression, and measuring the diversity of the total seed proteins using the SDS-PAGE method is robust, inexpensive and important in practice to crops such as grain legumes (Nisar et al., 2009, 2016; Zahoor et al., 2015). Furthermore, seed storage protein markers have been successfully used to resolve taxonomic relationships and to identify potential lines in both wild and cultivated crop species (Lioi et al., 1999; Ghafoor et al., 2002; Nisar et al., 2007, 2009; Hameed et al., 2009; Win et al., 20011; Wadood et al., 2016). Overall, a combination of morphology with measurements of SDS-PAGE diversity of the total seed proteins has been largely successful, and the genetic diversity of seed storage proteins has been studied in many plant species of agronomic and commercial importance.

Our understanding of the potential of wild plant species and their objective diversity is still limited and needs enhancement (Payne, 1987; Rogl et al., 1996; Ali et al., 2016; Masood et al., 2017). To date, wild plants have received little attention, and thus, the main objective of the current study was to measure intraspecific genetic variation within the population of *R. minima* naturalized in different geographical regions. The present study was designed to study genetic relationships among natural populations of *R. minima* collected from four districts at random for morphological and seed storage protein evaluation. To the best of our understanding, the present study is the first documented report from Pakistan on the genetic diversity of *R. minima*.

Materials and methods

Climatic conditions of Malakand division

Malakand division in general is a hilly area located within the Northern Pakistan covering an area of nearly 29,872 Km^2 and having a range of climatic conditions (*Fig. 1*). Moving along the foothills of the Hindu Kush, Himalayas and Karakoram ranges, the climate of Malakand division changes from humid subtropical at the foothills to the typical arid climate characteristic of the plains of South Asia (Muhammad et al., 2016). District Swat stretches from 35.2227° North to 72.4258° East longitude and the climatic conditions varies from dry to moist temperate. The climate is influenced by various factors including latitude, altitude, the Indian Ocean Summer, Monsoon and the Western cyclonic currents, coming from the Mediterranean Sea, in the winter. Dir lower is located in the Dry temperate zone (34.9161° N, 71.8097° E; 4411 ft above sea level), Dir upper is a moist temperate region (35.3356° N, 72.0468° E; 3174 ft above sea level) while, District Buner having areas of both Dry and moist temperate regions (34.3943° N, 72.6151° E; 4049 ft above sea level).

Plant materials

Field trips were arranged during 2016–2017, and 100 genotypes of *R. minima* growing in the wild were collected from four districts of Malakand Division, Pakistan (i.e., 25 genotypes from each of District Swat, Dir lower, Buner and Dir upper) and are

http://www.aloki.hu ● ISSN 1589 1623 (Print) ● ISSN 1785 0037 (Online)
DOI: http://dx.doi.org/10.15666/aeer/1605_56335651
© 2018, ALÖKI Kft., Budapest, Hungary

listed in *Table A1* in the *Appendix*. Plants were identified, the genotypes were labeled [first letter(s) corresponding to District, followed by species abbreviated name and accession number], and voucher specimens were submitted to the Herbarium at Hazara University Mansehra, Pakistan. These genotypes were assessed for estimation of inter- and intra-district variation and genetic diversity of morphological traits and total seed storage protein profile.

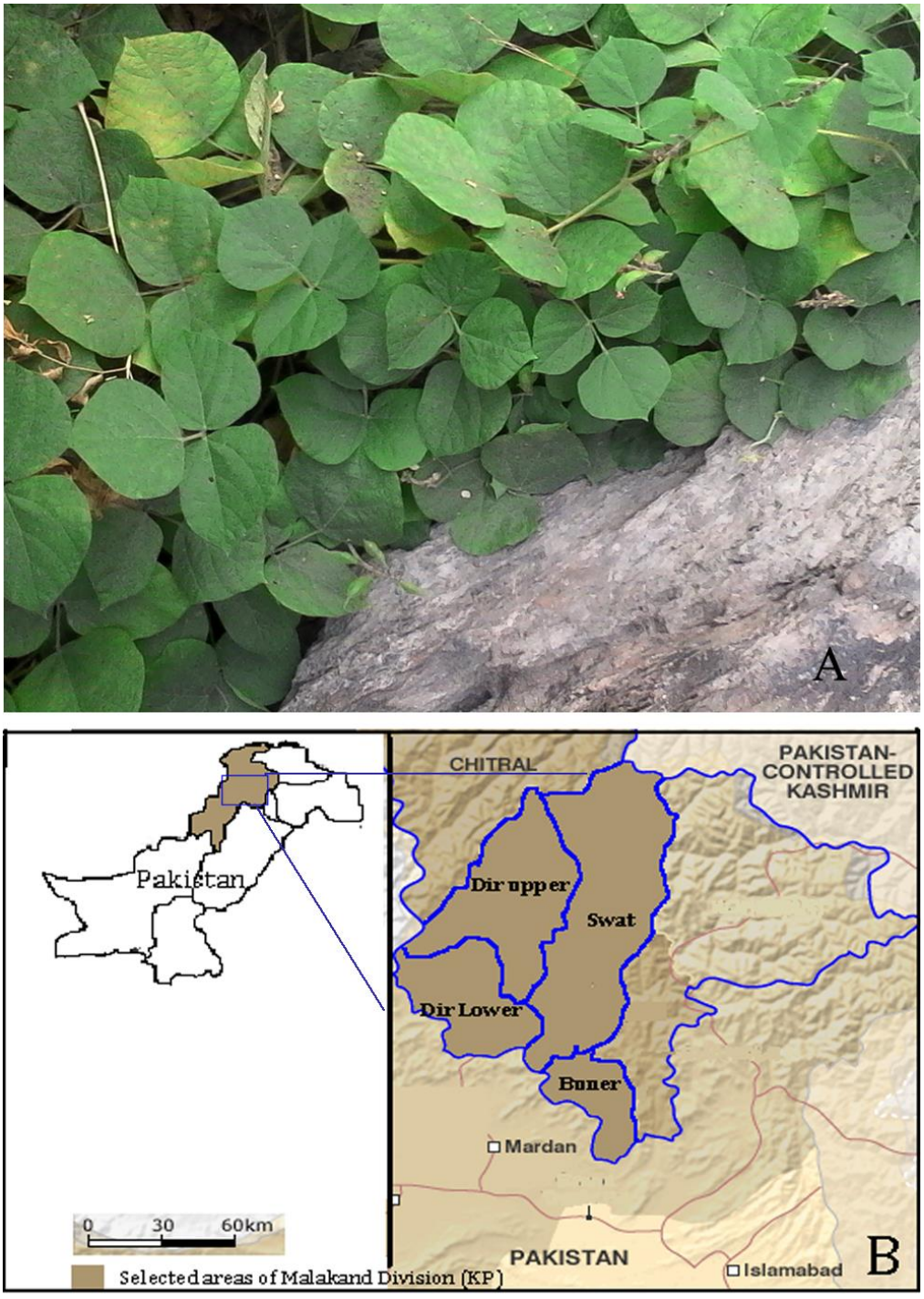

Figure 1. *Rhynchosia minima plants growing on a rocky substrate (A) and map of the study area (B)*

http://www.aloki.hu ● ISSN 1589 1623 (Print) ● ISSN 1785 0037 (Online)
DOI: http://dx.doi.org/10.15666/aeer/1605_56335651
© 2018, ALÖKI Kft., Budapest, Hungary

Morphological characterization

Morphological characterization was registered on site and all randomly selected 25 mature genotypes were accounted (*Fig. 1*). A total of 16 morphological traits, including qualitative and quantitative traits, were scored. Qualitative traits were scored visually and encompassed leaf upper surface color (Luc), leaf lower surface color (Llc), inflorescence color (Ic), seed color (Sc), seed shape (Ss), hilum color (Hc) and testa texture (Tt). Quantitative traits were measured with the help of Vernier calipers or the centimeter scale and encompassed petiole length (PL), leaf length (LL), leaf width (LW), inflorescence length (IL), seed length (SL), seed weight (SW), seed thickness (ST), no. of pods per plant (PP) and 100 seed weight (SWT).

Protein profiling

For a total seed storage protein profile, sodium dodecyl polyacrylamide gel electrophoresis (SDS-PAGE) was performed following the method described by Laemmli (1970) and modified by Zahoor et al. (2015). A single seed of each genotype was crushed into a fine flour, and then 400 µl of protein extraction buffer (0.5 M Tris-HCl, 0.2% SDS, 5 M urea, 1% β-mercaptoethanol pH 8.0) was added to 0.01 g of the fine seed powder in an Eppendorf tube and homogenized with a vortex. The mixture was kept for 20 min at room temperature (RT) for protein extraction. Bromophenol blue (BPB) was added to the sample buffer for observing protein sample movement. Samples were centrifuged at 13,000 rpm for 14 min at RT and the supernatant was transferred to a clean 1.5 ml Eppendorf tube and run on a 12% polyacrylamide gel (composition of resolution gel: 3.0 M Tris-HCl pH 9.0, 0.4% SDS and stacking gel 0.4 M Tris-HCl pH 7.0, 0.4% SDS) at 100 V for 2 hrs. The gel was stained with Coomassie brilliant blue for 20 min and destained (5% methanol, 20% acetic acid) until the background color disappeared.

Data analysis

Morphological and SDS-PAGE data were assembled in an MS Excel sheet. Two-way cluster analysis was based on binary data in PC-ORD software (Lepsˇ and Sˇmilauer, 2003). Genetic similarity estimates (F) were designed following Nei and Li (1979), and CANOCO software was used for specific loci/band enrichment in *R. minima* and to find the influence/relationship of the morphological traits and geographical origin on the total seed protein diversity in *R. minima*.

Results and discussion

Morphological diversity in R. minima genotypes

For morphological diversity, both the qualitative and quantitative characteristics were assessed, revealing substantial variability among genotypes for most traits: plants collected from different districts harbored higher variability than genotypes from within the same district. Descriptive statistics of the morphological parameters are summarized in *Table 1*. The CV% was calculated for petiole length, leaf length, leaf width, stipule length, inflorescence length, seed length, seed width and seed thickness, No. of pods per plant, 100 seed weight.

http://www.aloki.hu ● ISSN 1589 1623 (Print) ● ISSN 1785 0037 (Online)
DOI: http://dx.doi.org/10.15666/aeer/1605_56335651
© 2018, ALÖKI Kft., Budapest, Hungary

Table 1. *Descriptive statistics of the important morphological parameters*

Area/site of collection	Traits	Minimum	Maximum	Mean	Std. Deviation	CV%
District Swat	**PL**	1.3	1.94	1.5749	0.20889	13.2637
	LL	81.98	101.98	94.7232	5.06394	5.3461
	LW	15.33	33.67	22.58	3.74443	16.582
	IL	1.67	4.33	3.2	0.63828	19.943
	SL	5.67	9	7.684	0.87428	11.377
	SW	2.67	5	3.972	0.52323	13.172
	ST	1.6	3.17	2.516	0.38371	15.251
	P/P	12.67	34	22.2667	6.08428	27.324
	SWT	24	33	28.544	2.44916	8.581
District Dir lower	**PL**	2	2.99	2.654	0.28634	10.789
	LL	107.6	137.8	128	7.04929	5.518
	LW	19.67	112	79.072	32.28988	40.836
	IL	3	7.33	5.0493	1.31576	26.0582
	SL	2.96	8	4.3708	1.22465	28.018
	SW	1.83	4.2	2.9333	0.54815	18.687
	ST	1.23	3.27	2.536	0.57702	22.752
	P/P	23	40.33	33.6933	4.02989	11.961
	SWT	9	33	14.0684	7.74323	55.0398
District Buner	**PL**	6	6.99	6.5473	0.33476	5.112
	LL	63.33	89.78	73.6398	6.29928	8.554
	LW	36	122.67	71.5239	27.31532	38.191
	IL	3.33	6	4.1733	0.90329	21.644
	SL	2.65	8.23	4.8076	1.30897	27.227
	SW	1.67	6.8	3.1561	1.04537	33.122
	ST	1.57	3.63	2.6128	0.57634	22.058
	P/P	35.67	78.67	59.9733	17.37813	28.976
	SWT	9.3	15	12.6412	1.7454	13.809
District Dir upper	**PL**	3.99	5.8	4.3719	0.37533	8.585
	LL	23.25	34	29.223	2.53127	8.661
	LW	17	115	46.78	25.44987	54.401
	IL	1.67	7.67	4.7733	1.55075	32.488
	SL	2.67	8.67	6.1688	1.83278	29.711
	SW	1.57	4.67	3.3835	0.85506	25.271
	ST	1.43	3.37	2.3399	0.51268	21.911
	P/P	13	77.33	45.1867	24.76315	54.801
	SWT	12.14	33	20.5656	7.39849	35.975
	CV% = Std. Deviation/Mean * 100					

PL = petiole length, LL = leaf length, LW = leaf width, SL = seed length, SW = seed width, ST = seed thickness, P/P = no. of pods/plant, SWT = 100 seed weight

http://www.aloki.hu ● ISSN 1589 1623 (Print) ● ISSN 1785 0037 (Online)
DOI: http://dx.doi.org/10.15666/aeer/1605_56335651
© 2018, ALÖKI Kft., Budapest, Hungary

Petiole length in genotypes collected from district Swat was 13.2637%, for district Dir lower was 10.789, for district Buner was 5.112 and for district Dir Upper was 8.585. Significant variation was found for the leaf length among the genotypes of four districts; the highest value was observed for genotypes collected from district Buner (8.554) followed by district Dir Upper (8.661%) and Dir lower (5.518%) while, lowest value was recorded for the genotypes collected from Swat (5.3461%). For leaf width in genotypes collected from Swat was (16.582%), Dir lower (40.836%), for district Buner (38.191%) whereas for district Dir Upper was 54.401%. Furthermore highest variation was observed for seed length and seed width. Number of pods/plant varied for genotypes collected from Swat, Dir lower, Buner and Dir Upper was 27.324%, 11.961%, 28.976% and 54.801% respectively (*Table 1*).

Based on qualitative characteristics, the inter-district trait similarity index among genotypes of Swat-Dir Lower and Swat-Buner was 100%, while for Swat- Dir Upper, Dir Lower-Buner, Dir Lower-Dir Upper, and Buner-Dir Upper, it was 28. 571, 85.71%, 28.57%, and 42.85%, respectively (*Table 2*). Similarly, based on quantitative traits inter-district traits similarity index among genotypes of Swat-Dir Lower, Swat-Dir Upper, Swat-Buner, Dir lower-Buner and Dir upper-Swat was 22.2%; while for Dir Lower-Dir upper was 11.1%; Buner-Dir upper was 33.333% and that of Buner-Dir Upper was 42.85%. Furthermore, the Pearson correlation coefficient revealed a significant positive as well as a negative association ($p = 0.05$ and 0.01) among the studied traits of *R. minima* (*Tables 3* and *4*). Several traits revealed strong interrelationships within phenotype categories, particularly leaf traits with yield contributing traits and a few traits correlating with other categories, such as inherently linked growth and phenology-related traits (*Tables 2* and *3*). Furthermore, quantitative data set of 100 genotypes was used for cluster analysis. The dendrogram resolved all the 100 genotypes of *R. minima* into four discrete clusters (groups), each representing the geographical origin of collection and highlighting the determining role of geography rather than variation within the traits themselves (*Fig. 2*).

Table 2. *Region-wise trait similarity index based on qualitative traits*

Traits	S-RM	DL-RM	B-RM	DU-RM	Traits similarity index				
					S-RM & DL-RM	S-RM & B-RM	DL-RM & B-RM	DL-RM & DU-RM	B-RM & DU-RM
Luc	Green	Green	Green	Moss green	Green	Green	NA	NA	NA
Llc	Green	Green	Green	Yellow green	Green	Green	Green	NA	NA
Ic	White yellow	White yellow	White yellow	Yellow green	White yellow	White yellow	white yell	NA	NA
Sc	Brown	Brown	Brown	Dull yellow	Brown	Brown	Brown	NA	NA
Ss	Oblong	Oblong	Oblong	Oblong	Oblong	Oblong	Oblong	Oblong	Oblong
Hc	White	White	White yellow	White yellow	White	White	White yellow	NA	White yellow
Tt	Smooth	Smooth	Smoth	Smoth	Smoth	Smoth	Smoth	Smoth	Smoth
TSI= homologous traits/Total traits*100 =					100	100	85.71	28.57	42.85

Luc = leaf upper surface colour, Llc = leaf lower surface colour, Ic =Inflorescence color, Sc = Seed color, Ss = Seed shape, Hc = Hilum Color, Tt = Testa texture, S = Swat, DL = Dir lower, DU = Dir upper, B = Buner, RM = R. minima

http://www.aloki.hu ● ISSN 1589 1623 (Print) ● ISSN 1785 0037 (Online)
DOI: http://dx.doi.org/10.15666/aeer/1605_56335651
© 2018, ALÖKI Kft., Budapest, Hungary

Table 3. *Correlation coefficient among nine quantitative traits of DL-RM (italic numbers) and S-RM*

Traits	PL	LL	LW	IL	SL	SW	ST	P/P	SWt
PL	1.00	*-0.501**	*0.01*	*0.39*	*0.884***	*-0.580***	*-.910***	*-0.07*	*-0.743***
LL	-0.08	1.00	*-0.03*	*-0.28*	*-0.450**	*0.20*	*.432**	*0.22*	*0.36*
LW	0.12	0.18	1.00	*0.405**	*0.25*	*-0.540***	*0.15*	*-0.08*	*-0.27*
IL	-0.48	0.34	0.21	1.00	*.659***	*-0.30*	*-0.27*	*-0.01*	*-0.08*
SL	0.39	-0.37	0.06	-0.33	1.00	*-0.543***	*-0.765***	*-0.03*	*-0.07*
SW	0.524**	-0.34	-0.06	-0.34	0.828**	1.00	*.417**	*0.17*	*0.622***
ST	0.402*	-0.36	0.11	-0.09	0.611**	0.707**	1.00	*0.641***	*-0.08*
P/P	0.39	-0.17	-0.16	-0.03	-0.14	0.13	0.18	1.00	*0.14*
SWt	-0.13	-0.31	-0.20	-0.25	0.23	0.32	0.07	0.20	1.00

*Correlation is significant at the 0.05 level (2-tailed)
**Correlation is significant at the 0.01 level (2-tailed)
PL = petiole length, LL = leaf length, LW = leaf width, IL = inflorescence, SL = seed length, SW = seed weight, ST = seed thickness, P/P = no. of pod/plant, SWT = seed weight. S = swat, DL = Dir lower, RM = R. minima

Table 4. *Correlation coefficient among nine quantitative traits of DU-RM (italic numbers) and B-RM*

Traits	PL	LL	LW	IL	SL	SW	ST	P/P	SWt
PL	1.00	*-.952***	*0.31*	*0.658***	*0.811***	*-0.841***	*-0.888***	*-0.19*	*-0.34*
LL	-0.415*	1.00	*-0.33*	*-0.662***	*-0.828***	*0.817***	*0.878***	*0.11*	*0.32*
LW	-0.21	0.31	1.00	*0.27*	*-0.05*	*-0.18*	*-0.24*	*0.636***	*0.791***
IL	-0.35	0.657**	0.592**	1.00	*0.04*	*-0.15*	*-0.525***	*-0.565***	*0.911***
SL	0.37	-0.32	-0.12	0.11	1.00	*-0.08*	*-0.11*	*-0.707***	*-0.695***
SW	0.15	0.02	0.30	0.434*	0.806**	1.00	*0.19*	*0.519***	*0.862***
ST	-0.03	0.04	0.28	0.444*	0.448*	0.602**	1.00	*0.18*	*0.33*
P/P	0.35	-0.407*	-0.936**	-0.695**	0.11	-0.34	-0.37	1.00	*-0.18*
SWt	0.24	-0.23	-0.747**	-0.552**	-0.20	-0.528**	-0.530**	.800**	1.00

*Correlation is significant at the 0.05 level (2-tailed)
**Correlation is significant at the 0.01 level (2-tailed)
PL = petiole length, LL = leaf length, LW = leaf width, IL = inflorescence, SL = seed length, SW = seed weight, ST = seed thickness, P/P = no. of pod/ plant, SWT = seed weight. DU = Dir upper, B = buner, RM= R. minima

SDS-PAGE analysis

For exploration of genetic polymorphisms, modern tools can provide better understanding of species relationships and heterogeneity. Furthermore, morphometric, biochemical and molecular marker approaches have been used for examining genetic diversity and for inferring the intra- and interspecies relationships in plants (Tomooka et

http://www.aloki.hu ● ISSN 1589 1623 (Print) ● ISSN 1785 0037 (Online)
DOI: http://dx.doi.org/10.15666/aeer/1605_56335651
© 2018, ALÖKI Kft., Budapest, Hungary

al., 2002). Moreover, isozymes (Jaaska and Jaaska, 1990), low-molecular-weight carbohydrates (Yasui et al., 1985), RFLPs (Fatokun et al., 1993), and nuclear as well as chloroplast DNA, (Vaillancourt and Weeden, 1993), RAPDs (Kaga et al., 1996), SSRs, EST-SSRs (Ali et al., 2016) and AFLPs (Tomooka et al., 2002), among others, have been used to study crop species.

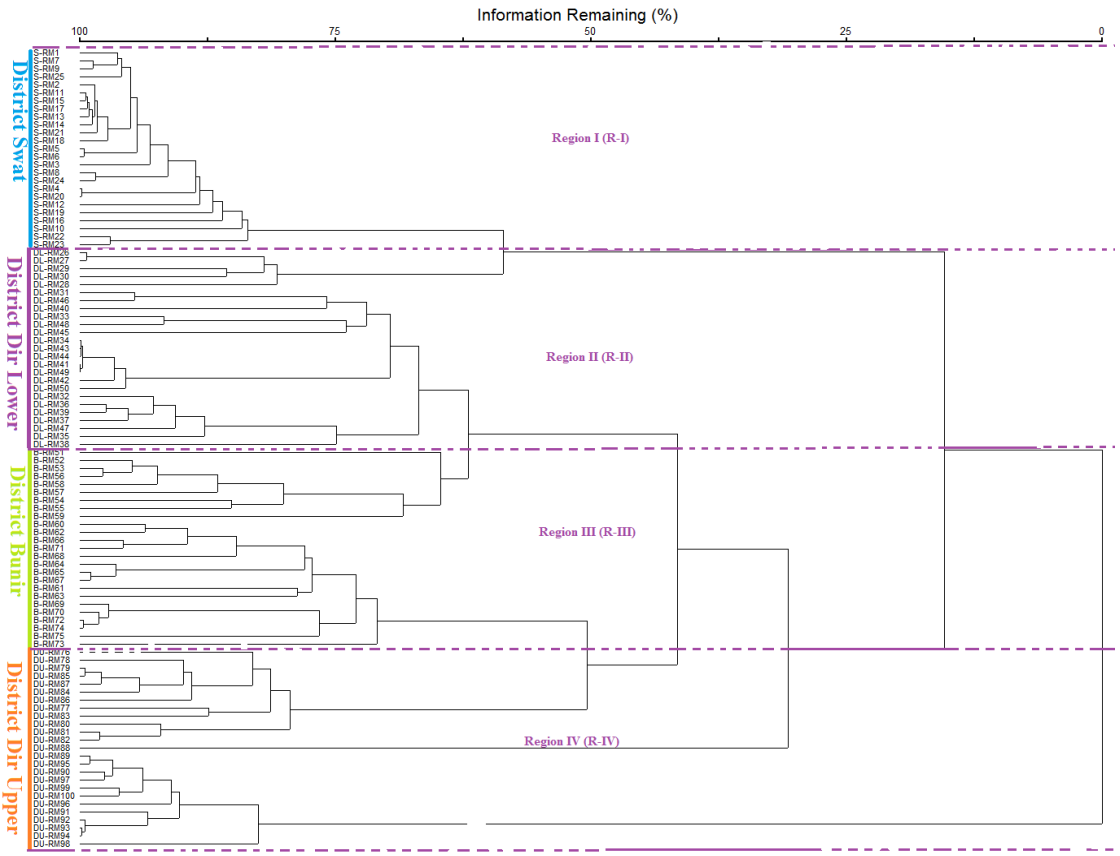

Figure 2. *Intra-species relationship identified through morphological characteristics in different genotypes of R. minima collected from four districts of Malakand Division, Pakistan. RM indicates R. minima, S = Swat, DL = Dir lower, B = Buner and DU = Dir upper*

Eight reproducible bands of ~10–180 kDa were observed in the *R. minima*; a representative PAGE is shown (*Fig. 3*). The binary data of these loci were used to estimate relationships among all genotypes with cluster analysis, and all *R. minima* were divided into six clusters (*Fig. 4*). In cluster-1 (also referred to as Region I, R-I), genotypes collected from District Buner were resolved as having 25% genetic diversity, whereas genotypes of R-II consisted of samples collected from District Dir Upper with 24.07% genetic diversity among genotypes. Genotypes in R-III belonged to District Dir lower with 29.37% genetic variation among genotypes, and R-IV genotypes collected from District Swat had 50% diversity. Similarly, genotypes in R-V and R-VI consisted of genotypes of *R. minima* collected from Dir lower (5 genotypes) and Swat (13 genotypes with 48.07% genetic diversity).

SDS-PAGE has shown promise in understanding the genetic relationships in angiosperms at the generic as well as at the species levels and is reliable for assessing polymorphisms in crops (Payne, 1987; Ghafoor et al., 2002; Nisar et al., 2009; Win et

http://www.aloki.hu ● ISSN 1589 1623 (Print) ● ISSN 1785 0037 (Online)
DOI: http://dx.doi.org/10.15666/aeer/1605_56335651
© 2018, ALÖKI Kft., Budapest, Hungary

al., 2011; Zahoor et al., 2015). The results for the mean square values and response of protein loci/band enrichment within genotypes showed significant variations as indicated (*Fig. 5*). Variability in color and size indicates variation, and the species-specific loci B-6 and B-7 revealed maximum enrichment (present in 100% genotypes), followed by B-8 (72%), B-5 (69%), B-4 (65%), B-3 (63%) and B-2 (50). Furthermore, loci B-2 and B-3 were negatively associated with B-1, B-4 and B-5, while B-8, B-6 and B7 have a neutral association because these bands are evenly distributed among the *R. minima* genotypes collected from these four geographical areas (*Fig. 5*). The overall inter-district locus contribution towards the genetic disagreement was 75%, whereas within the district, it varied from 0.00 to 75%. Among the 8 loci, B-6 and B-7 were monomorphic, present in all genotypes and are likely to be species specific. In contrast, loci B-1, B-4, B-5 and B-8 were observed in genotypes collected from Buner, whereas these genotypes were missing loci B-2 and B-3 and genotypes collected from Dir Upper had all loci except B-1. *R. minima* genotypes collected from Dir Lower and Swat had a mixed protein profile, i.e., showing higher diversity and intermixing within the genotypes. This indicates frequent gene flow within these genotypes and their potential to withstand extreme environmental events (*Fig. 4* and *Table 5*). Details of all of these loci and whether they are monomorphic or polymorphic have been determined and are given in *Table 5*. There was a high inter-district locus contribution towards genetic disagreements among *R. minima* genotypes; SDS-PAGE could be a consistent procedure for documentation of these genotypes, while intra-district locus contributions towards genetic disagreement in genotypes of *R. minima* collected from Swat (S-RM) and Dir lower (DL-RM) were high (100%) compared to those from Buner (B-RM) at 85.71% and from Dir upper (DU-RM) at 28.57% (*Table 2*).

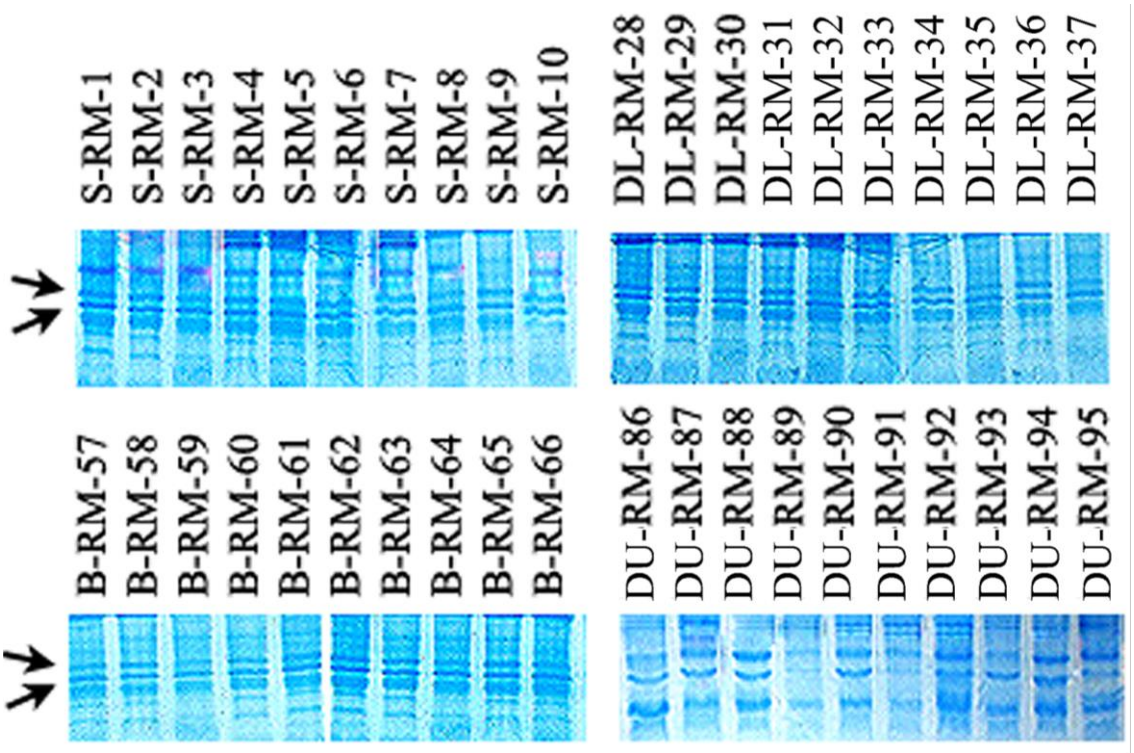

Figure 3. *Representative polyacrylamide gel (12%) electrophoresis showing diversity in total seeds storage proteins among different genotypes of R. minima. Arrow indicates the species-specific loci (B6, B7). S = Swat, DL = Dir lower, B = Buner, DU = Dir upper, RM = R. minima*

http://www.aloki.hu ● ISSN 1589 1623 (Print) ● ISSN 1785 0037 (Online)
DOI: http://dx.doi.org/10.15666/aeer/1605_56335651
© 2018, ALÖKI Kft., Budapest, Hungary

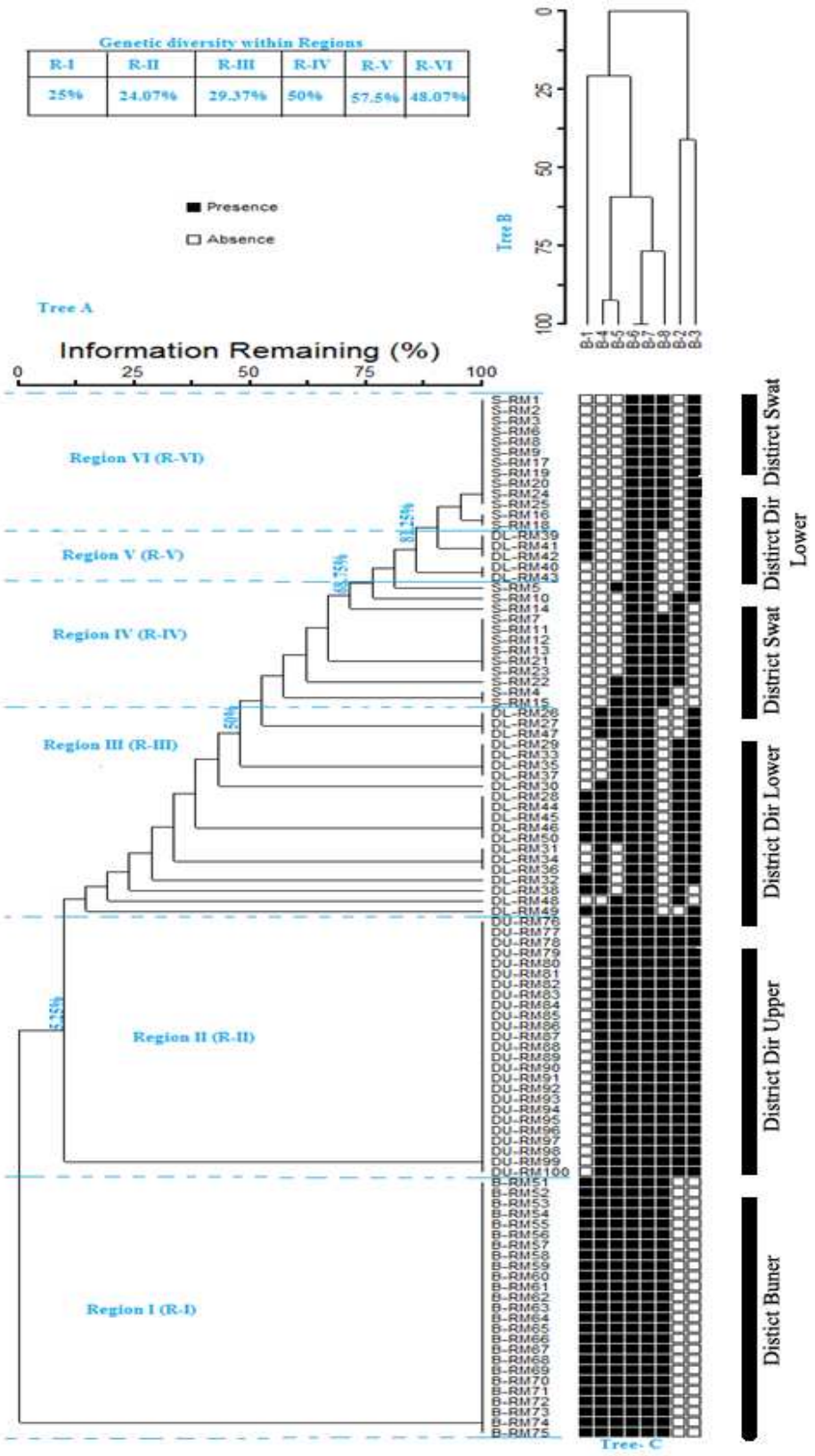

Figure 4. *Two-way cluster dendrogram based on the presence/absence of seed protein bands in different genotypes of R. minima species collected from four districts of Malakand Division, Khyber Pakhtunkhwa, Pakistan. RM indicates genotypes of R. minima, S = Swat, DL = Dir lower, B = Buner and DU = Dir upper*

http://www.aloki.hu ● ISSN 1589 1623 (Print) ● ISSN 1785 0037 (Online)
DOI: http://dx.doi.org/10.15666/aeer/1605_56335651
© 2018, ALÖKI Kft., Budapest, Hungary

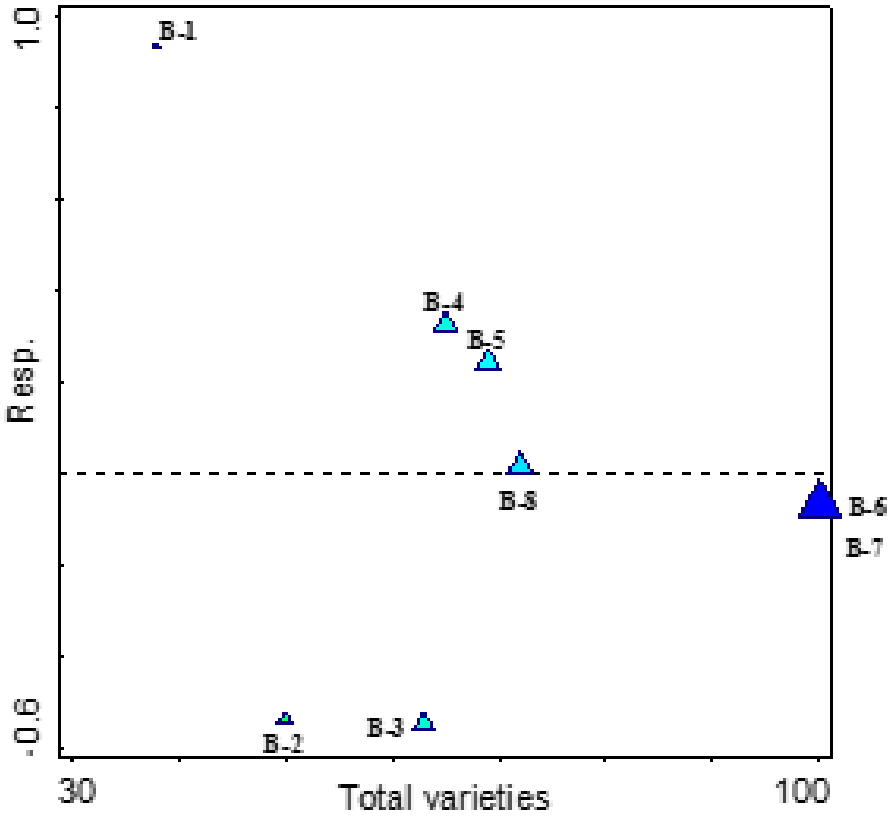

Figure 5. *Different colours showing the R. minima genotype (X-axis) enrichment on the basis of particular loci/band categories*

These four Districts are located adjacent to one another, but altogether, they cover an area of approximately 12,484 km^2, and each District is characterized by distinct environmental conditions and vegetation types. Nonetheless, the wide ecological amplitude and genomic plasticity of *R. minima* allow it to invade new areas and gaps within established plant communities (Shaukat and Burhan, 2000; Jia et al., 2015). This highlights the potential of finding useful genes for adaptation and climatic resilience as well as introgression of genes for improving productivity and resistance in leguminous crops via intergeneric crosses. We have no evidence whether such intergeneric crosses are likely to be successful, but wide crosses (interspecific and intergeneric) have been reported to be tremendously successful in cereals (Ali et al., 2012; Masood et al., 2016; Mujeeb-Kazi et al., 2017). There are numerous reports where not only cultivated plants but also their distant wild relatives have been hybridized successfully, and the size of the alien chromatin associated with linkage drag has then been reduced while still retaining the useful trait (Schwarzacher et al., 2011; Ali et al., 2016; Patokar et al., 2016; Mujeeb-Kazi et al., 2017).

To the best of our knowledge, this is the first study addressing diversity in *R. minima*, although we have no idea whether the seed storage proteins were overlapping as reported in other legumes. Therefore, no attempt was made to assign the recorded polypeptides into respective classes, i.e., legumin and vicilin (Mirali et al., 2007). Instead, for fine resolution, the dendrogram was divided into six regions, and genotypes collected from District Dir lower and Swat segregated with one another, while genotypes from District Dir upper and Buner assorted into discrete clades/groups

http://www.aloki.hu ● ISSN 1589 1623 (Print) ● ISSN 1785 0037 (Online)
DOI: http://dx.doi.org/10.15666/aeer/1605_56335651
© 2018, ALÖKI Kft., Budapest, Hungary

(*Fig. 4*). *R. minima* enrichment on the basis of specific seed protein bands indicated that B-6 and B-7 were species specific and present in all genotypes (*Fig. 5*). The presence of common loci (B-6 and B-7) among these genotypes suggests their close genetic similarity and common ancestry. These loci encoded proteins that have been fixed in different genotypes of *Rhynchosia* over evolutionary time. These findings are in agreement with those of Azeez and Morakinyo (2004), who associated the presence of common protein bands in *Lycopersicum* and *Trichosanthes* species with their common evolutionary origin.

Table 5. *Intra- and inter-district genetic diversity among R. minima genotypes*

Regions	Expressed loci	Status	GD%	Regions	Expressed loci	Status	GD%
S-RM	1	Poly	0.4	B-RM	25	Mono	0.25
	9	Poly	0.36		25	Mono	0.00
	14	Poly	0.56		0.00	Mono	0.00
	0.00	Mono	0.00		0.00	Mono	0.25
	4	Poly	0.16		25	Mono	0.25
	25	Mono	1.00		25	Mono	1.00
	25	Mono	1.00		25	Mono	1.00
	21	Poly	0.84		25	Mono	0.25
GD = poly/Total loci*100 = 62.5				**GD = poly/Total loci*100 = 0.00**			
DL-RM	11	Poly	0.44	DU-RM	0.00	Mono	0.25
	16	**Poly**	0.64		25	Mono	0.00
	23	Poly	0.23		25	Mono	0.00
	15	**Poly**	0.6		25	Mono	0.25
	15	Poly	0.6		25	Mono	0.25
	25	**Mono**	1.00		25	Mono	1.00
	25	Mono	1.00		25	Mono	1.00
	0.00	**Mono**	0.00		25	Mono	0.25
GD = poly/Total loci*100 = 75					**GD = poly/Total loci*100 = 0.00**		

Inter district variation in *R. minima* genotypes

Expressed loci	Status	GD%
37	Poly	0.37
50	Poly	0.5
62	Poly	0.62
65	Poly	0.65
69	Poly	0.16
100	Mono	1.00
100	Mono	1.00
71	Poly	0.71
Intra locus contribution toward GD poly/Total*100 = 75		

S = swat, B = buner DL = Dir lower, DU = Dir upper, RM = Rhynchosia minima, GD = genetic disagreement

Detrended correspondence analysis (DCA) revealed grouping and distribution of *R. minima* genotypes into four patches on the basis of their geographical origin coupled

http://www.aloki.hu ● ISSN 1589 1623 (Print) ● ISSN 1785 0037 (Online)
DOI: http://dx.doi.org/10.15666/aeer/1605_56335651
© 2018, ALÖKI Kft., Budapest, Hungary

with the data of morphological as well as total seed protein diversity. Area of collection (origin) played a marked role in the grouping of *R. minima* genotypes as well as a positive/negative association with a particular set of morphological traits and seed protein profile (*Fig. 6*). Furthermore, comparison of the two cluster dendrograms were in general agreement with one another, indicating the stability of the morphological traits and the potential of *R. minima* to adapt to various climatic and soil conditions (compare *Figs. 2* and *4*). The DCA plot revealed important information regarding the distribution of genotypes with morphological traits and total seed protein profile. Here, the role of geographical origin again was overwhelming and leaf-related traits as well as protein loci B-1 had a strong and positive impact (*Fig. 6*). It will be extremely interesting to study specific genes in *R. minima* that allow adaptation to new habitats and to compare them to those that have previously played an important role in plant domestication under human influence (Baudoin and Marechal, 1985; Chen et al., 2006).

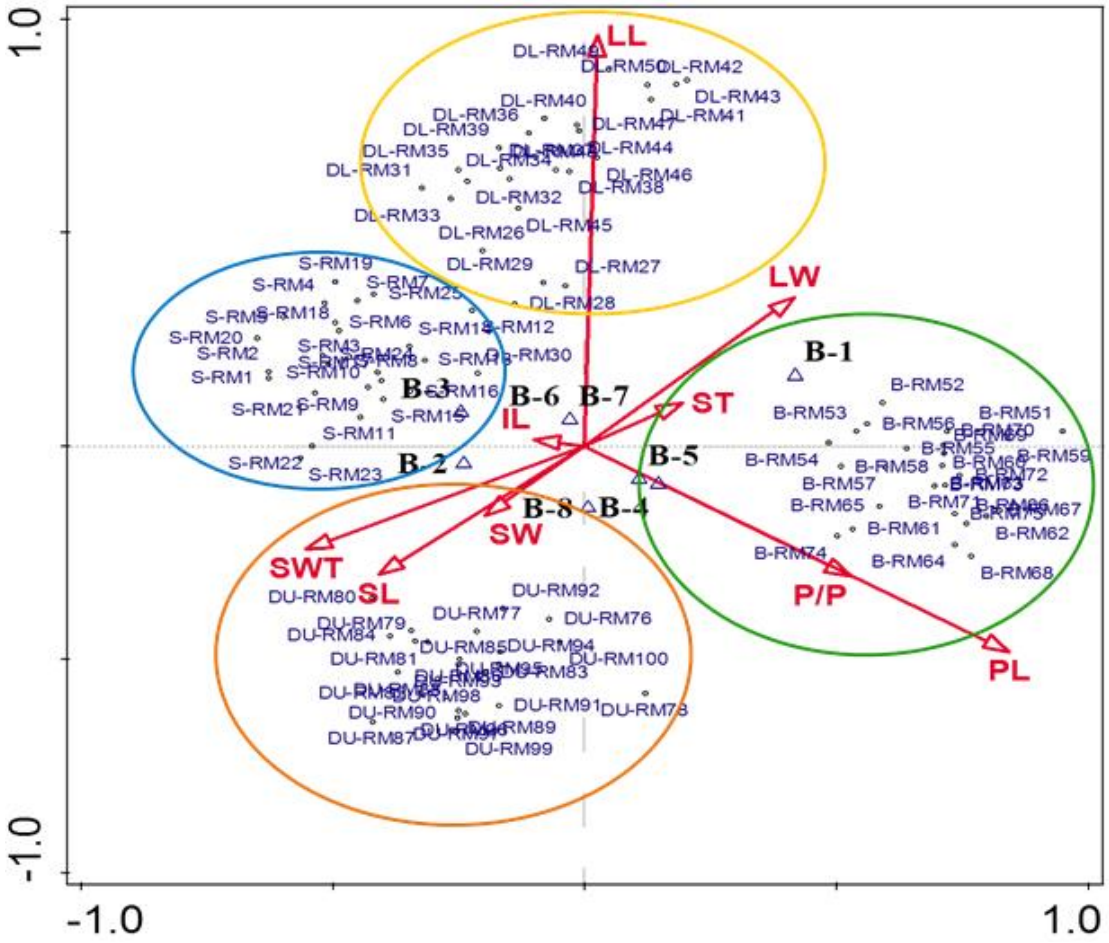

Figure 6. *Detrended correspondence analysis (DCA) diagram showing the distribution of R. minima genotypes and their association/relatedness based on morphological traits and total seed protein profile*

All together, humanity depend on a fraction of the genetic diversity residing in fewer than a dozen of the approximately 300,000 species of angiosperms for 80% of their caloric intake (McCouch et al., 2013). This is not enough to support our food system in

http://www.aloki.hu ● ISSN 1589 1623 (Print) ● ISSN 1785 0037 (Online)
DOI: http://dx.doi.org/10.15666/aeer/1605_56335651
© 2018, ALÖKI Kft., Budapest, Hungary

the future, and unlike conventional breeding that relies on crossing the best with the best, more predictable breeding outcomes are possible with linkages of genes with specific traits. Wild relatives of crops have tremendous genetic potential that can be released by searching for superior genes. In the past, where the increased crop productivity was based on improved agricultural practices and other changes, future gains will rely on improved genetics (Heslop-Harrison and Schwarzacher, 2012).

Conclusion

A total of 16 important morphological traits as well as SDS-PAGE of the total seed protein profile were assessed, and the data revealed the existence of ample diversity. Further, cluster analysis based on seed storage protein analyses demonstrated that the 100 genotypes of *R. minima* collected from four districts had close similarities to each other. The SDS-PAGE electrophoresis results also demonstrated that seed protein profiling provides a powerful tool for genotype discrimination based on geographic differences. Furthermore, the results indicate that high variability exists in *R. minima* and that the differences observed among populations were associated with both genetics and geography. Grain legumes are ranked third after cereals and oilseed crops due to their importance for both humans and livestock (Ilyas et al., 2009; Naim-Feil et al., 2017), and therefore, improvements in leguminous crops are of paramount significance. In the future, where adaptation to stresses is likely to address the severity of climate change impacts as well as worldwide food security concerns (Lobell et al., 2008), minor modifications such as changes in sowing dates are helpful to mitigate negative impacts, but long term benefits will be linked to genetic improvements (Heslop-Harrison and Schwarzacher, 2012). Wild crop relatives offer rich sources of genes for resistance to both biotic and abiotic stresses and therefore could improve agriculture (Vavilov, 1940). Nevertheless, *R. minima*, a distant relatives of crop legumes, has so far undergone only limited utilization in foraging as well as for pharmaceutical purposes (Gundidza et al., 2009; Jia et al., 2015), yet it demands attention for the isolation of important phytochemicals and provides an opportunity for widening the genetic base of important legumes.

Acknowledgements. The authors would like to extend their sincere appreciation to the Deanship of Scientific Research at King Saud University for its funding to the Research Group number (RG-1435-014).

REFERENCES

[1] Ali, N. (2012): Molecular markers, cytogenetics and epigenetics to characterize wheat-*Thinopyrum* hybrid lines conferring wheat streak mosaic virus resistance. – Doctoral dissertation, University of Leicester, UK.

[2] Ali, N., Heslop-Harrison, J. S., Ahmad, H., Graybosch, R. A., Hein, G. L., Schwarzacher, T. (2016): Introgression of chromosome segments from multiple alien species in wheat breeding lines with wheat streak mosaic virus resistance. – Heredity 117: 114-123.

[3] Azeez, M. A., Morkinyo, J. A. (2004): Electrophoretic characterization of crude leaf protein in *Lycopersicum* and *Trichosanthes* cultivars. – African Journal of Biotechnology 3: 585-587.

http://www.aloki.hu ● ISSN 1589 1623 (Print) ● ISSN 1785 0037 (Online)
DOI: http://dx.doi.org/10.15666/aeer/1605_56335651
© 2018, ALÖKI Kft., Budapest, Hungary

[4] Baudoin, J. P., Marechal, R. (1985): Genetic Diversity in *Vigna*. – In: Singh, S. R., Rachie, K. O. (eds.) Cowpea Research, Production and Utilization. John Wiley and Sons Ltd, New York, pp. 3-9.
[5] Chen, C., Pan, L., Hu, Y., Hu, Z., Ding, Y. (2006): Analysis of genetic variation of seed proteins in the genus *Vigna* and among its relatives cultivated in China. – Euphytica 123: 367-378.
[6] Fatokun, C. A., Danesh, D., Young, N. D., Stewart, E. L. (1993): Molecular taxonomic relationships in the genus *Vigna* based on RFLP analysis. – Theoretical and Applied Genetics 86: 97-104.
[7] Ghafoor, A., Ahmad, Z., Qureshi, A. S., Bashir, M. (2002): Genetic relationship in *Vigna mungo* (L.) Hepper and *Vigna radiata* (L.) Wilczek based on morphological traits and SDS- PAGE. – Euphytica 123: 367-378.
[8] Gundidza, M., Gwenu, N., Magwa, M. L., Ramalivhana, N. J., Humphrey, G., Samie, A. (2009): Phytochemical composition and biological activities of *R. minima*. – African Journal of Biotechnology 8: 7221-7229.
[9] Gweru, N., Gundidza, M., Magwa, M. L., Ramalivhana, N. J., Humphrey, G., Samie, A., Mmbengwa, V. (2009): Phytochemical composition and biological activities of essential oil of *Rhynchosia minima* (L., DC. Fabaceae). – African Journal of Biotechnology 8: 721-724.
[10] Hameed, A., Shah, T. M., Atta, B. M., Iqbal, N., Haq, M. A., Ali, H. (2009): Comparative Seed Storage Protein Profiling of Kabuli chickpea genotypes. – Pakistan Journal of Botany 41: 703-710.
[11] Heslop-Harrison, J. P., Schwarzacher, T. (2012): Genetics and Genomics of Crop Domestication. – In: Altman, A., Hasegawa, P. M. (eds.) Plant Biotechnology and Agriculture. Academic Press, Amsterdam, pp. 3-18.
[12] Ilyas, M., Qazi, J., Mansoor, S., Briddon, R. W. (2009): Molecular characterization and infectivity of a Legumovirus (genus *Begomovirus*: family Geminiviridae) infecting the leguminous weed *Rhynchosia minima* in Pakistan. – Virus Research 145: 279-284.
[13] Jaaska, V., Jaaska, V. (1990): Isozyme variation in Asian beans. – Botanica Acta 103: 223-322.
[14] Jacobsen, S. E., Sørensen, M., Pedersen, S. M., Weiner, J. (2013): Feeding the world: genetically modified crops versus agricultural biodiversity. – Agronomy and Sustainable Development 33: 651-662.
[15] Jia, X., Zhang, C., Qiu, J., Wang, L., Bao, J., Wang, K., Zhang, Y., Chen, M., Wan, J., Su, H., Han, J. (2015): Purification, structural characterization and anticancer activity of the novel polysaccharides from Rhynchosia minima root. – Carbohyberate Polymer 132: 67-71.
[16] Kaga, A., Tomooka, N., Egawa, Y., Hosaka, K., Kajima, O. (1996): Species relationships in the subgenus *Ceratotropis* (genus *Vigna*) as revealed by RAPD analysis. – Euphytica 88: 17-24.
[17] Laemmli, U. K. (1970): Cleavage of structural proteins during the assembly of the head of bacteriophage T4. – Nature 227: 680-685.
[18] Lepsˇ, J., Sˇmilauer, P. (2003): Multivariate Analysis of Ecological Data Using CANOCO. – Cambridge University Press, New York.
[19] Lioi, L., Sparvoli, F., Bollini, R. (1999): Variation and genomic polymorphism of lectin-related protein in Lima Bean (*Phaseolus lunatus* L.) seed. – Genetic Research and Crops Evolution 46: 157-182.
[20] Lobell, D. B., Burke, M. B., Tebaldi, C., Mastrandrea, M. D., Falcon, W. P., Naylor, R. L. (2008): Prioritizing climate change adaptation needs for food security in 2030. – Science 319: 607-610.
[21] Lopez, P. L. (2012): *Rhynchosia minima*. – The IUCN Red List of Threatened Species 2012: e.T19379374A20135353.

http://www.aloki.hu ● ISSN 1589 1623 (Print) ● ISSN 1785 0037 (Online)
DOI: http://dx.doi.org/10.15666/aeer/1605_56335651
© 2018, ALÖKI Kft., Budapest, Hungary

[22] Lu, H., Zhang, J., Liu, K. B., Wu, N., Li, Y., Zhou, K., Ye, M., Zhang, T., Zhang, H., Yang, X., Shen, L. (2009): Earliest domestication of common millet (*Panicum miliaceum*) in East Asia extended to 10,000 years ago. – Proceedings of the National Academy of Science 106: 7367-7372.
[23] Masood, R., Ali, N., Jamil, M., Bibi, K., Rudd, J. C., Mujeeb-Kazi, A. (2016): Novel genetic diversity of the alien D-Genome synthetic hexaploid wheat (2n = 6x = 42, AABBDD) germplasm for various phenology traits. – Pakistan Journal of Botany 48(5): 2017-2024.
[24] McCouch, S., Baute, G. J., Bradeen, J., Bramel, P., Bretting, P. K., Buckler, E., Burke, J. M., Charest, D., Cloutier, S., Cole, G., Dempewolf, H. (2013): Agriculture: feeding the future. – Nature 499: 23-25.
[25] Mirali, N., El-Khouri, S., Rizq, F. (2007): Genetic diversity and relationships in some *Vicia* species as determined by SDS-PAGE of seed proteins. – Biosystematics Plant 51: 660-666.
[26] Morris, J. B. (2008): *Rhynchosia minima* (L.) DC. Regeneration, characterization and potential uses for natural products and flavonoids. – Plant Genetic Resources 153: 9-15.
[27] Mujeeb-Kazi, A., Ali, N., Ibrahim, A., Napar, A. A., Jamil, M., Hussain, S., Mahmood, Z., Delgado, R., Rosas, V., Cortes, A., Rajaram, S. (2017): Tissue culture mediated allelic diversification and genomic enrichment of wheat to combat production constraints and address food security. – Plant Tissue Culture and Biotechnology 27: 89-140.
[28] Naim-Feil, E., Toren, M., Aubert, G., Rubinstein, M., Rosen, A., Eshed, R., Sherman, A., Ophir, R., Saranga, Y. and Abbo, S. (2017): Drought response and genetic diversity in Pisum fulvum, a wild relative of domesticated pea. – Crop Science 57(3): 1145-1159.
[29] Nei, M., Li, W. H. (1979): Mathematical model for studying genetic variation in terms of restriction endonucleases. – Proceedings of the National Academy of Sciences 76(10): 5269-5273.
[30] Nisar, M., Ghafoor, A., Khan, M. R., Ahmad, H., Qureshi, A. S., Ali, H. (2007): Genetic diversity and geographic relationship among local and exotic chickpea germplasm. – Pakistan Journal of Botany 39: 1575-1581.
[31] Nisar, M., Ghafoor, A., Asmatullah (2009): First proteomic assay of Pakistani *Pisum sativum,* L. germplasm relation to geographic pattern. – Russian Journal of Genetics 45: 805-810.
[32] Nisar, M., Ghafoor, A., Wadood, S. F., Iqbal, A., Nausheen. (2016): Intra and inter specific profiling of Pakistani *Quercus* Species growing in hilly areas of District Dir Khyber Pukhtunkhwa. – Pakistan Journal of Botany 48: 263-270.
[33] Patokar, C., Sepsi, A., Schwarzacher, T., Kishii, M., Heslop-Harrison, J. S. (2016): Molecular cytogenetic characterization of novel wheat-*Thinopyrum bessarabicum* recombinant lines carrying intercalary translocations. – Chromosoma 125: 163-172.
[34] Payne, P. I. (1987): Genetics of wheat storage proteins and the effect of allelic variation on bread-making quality. – Annual Reviews Plant Physiology 38: 141-153.
[35] Rogle, S., Javornik, B., Sinkovic, T., Batic, F. (1996): Characterization of oak (*Quercus* L.) seed proteins by electrophoresis. – Bioindicator 36: 195-162.
[36] Schwarzacher, T., Ali, N., Chaudhary, H. K., Graybosch, R., Kapalande, H. V., Kinski, E., Heslop-Harrison, J. S. (2011): Fluorescent *in situ* hybridization as a genetic technology to analyzing chromosomal organization of alien wheat recombinant lines. – IAEA-TECDOC-1664: 121-128.
[37] Shaukat, S. S., Burhan, N. (2000): Fecundity, seed characteristics and factors regulating germination of *Rhynchosia minima* (L.) DC. – Pakistan Journal of Botany 32: 211-226.
[38] Takeda, S., Matsuoka, M. (2008): Genetic approaches to crop improvement: responding to environmental and population changes. – Nature Review Genetics 9: 444.
[39] Tanksley, S. D., McCouch, S. R. (1997): Seed banks and molecular maps: unlocking genetic potential from the wild. – Science 277: 1063-1066.

http://www.aloki.hu ● ISSN 1589 1623 (Print) ● ISSN 1785 0037 (Online)
DOI: http://dx.doi.org/10.15666/aeer/1605_56335651
© 2018, ALÖKI Kft., Budapest, Hungary

[40] Tomooka, N., Maxted, N., Thavarasook, C., Jayasuriya, A. H. M. (2002): Two new species, new species combinations and sectional designations in *Vigna* subgenus Ceratotropis (Piper) Verdcourt (*Leguminosae, Phaseoleae*). – Kew Bulletin 57: 613-624.
[41] Vaillancourt, R. E., Weeden, N. F. (1993): Chloroplast DNA phylogeny on old world *Vigna* (*Leguminosae*). – Systematic Botany 18: 642-651.
[42] Vavilov, N. I. (1940): The New Systematics of Cultivated Plants. – Huxley, J. (ed.) New Systematics. Clarendon, Oxford, pp. 549-566.
[43] Wadood, S. F., Hassan, N., Khaliq, A., Nausheen, J. T., Ghafoor, A., Khan, M., Nisar, M. (2016): Genetic polymorphism in *Lens culinaris* collected from Malakand division Khyber Pakhtunkhwa, Pakistan. – Journal of Biology and Environmental Science 8: 53-60.
[44] Win, K. T., Zaw, A., New, K. L., Thein, M. S., Yutaka, H. (2011): Diversity of Myanmar cowpea accessions through seed storage polypeptides and its cross compatibility with the subgenus *Ceratotropis.* – Journal of Plant Breeding and Crop Science 3: 87-95.
[45] Yasui, T., Tateishi, Y., Ohashi, H. (1985): Distribution of low molecular weight carbohydrates in the subgenus *Ceratotropis* of the genus *Vigna* (Leguminosae). – Botanical Magazine Tokyo 98: 75-82.
[46] Zahoor, M., Nisar, M., Islam, N. U. (2015): Genetic variations of *Robinia pseudoacacia* plant using SDS-PAGE. – Pakistan Journal of Botany 47: 2335-2338.

APPENDIX

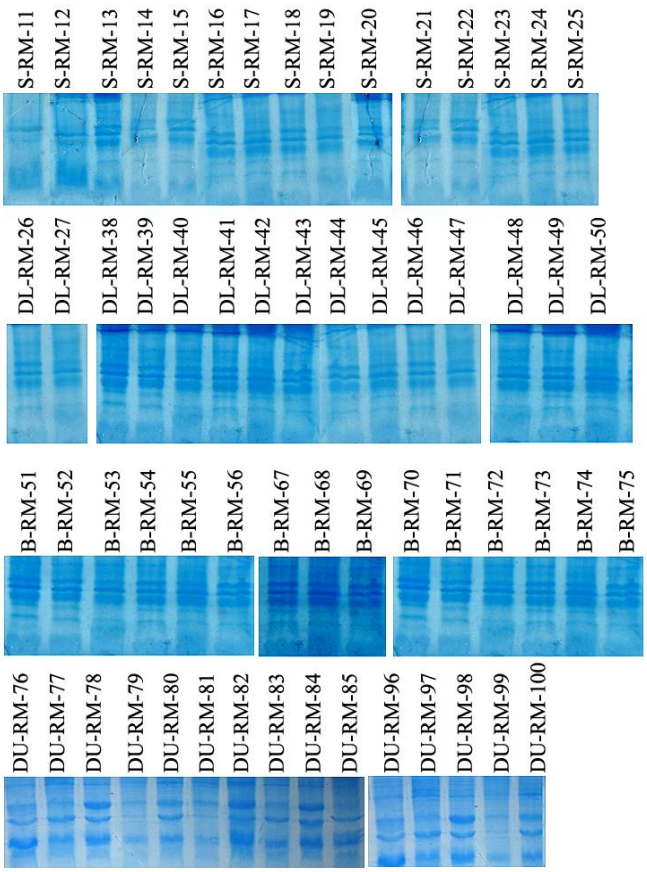

Figure A1. *Polyacrylamide gel (12%) electrophoresis showing diversity in total seed storage protein among different genotypes of R. minima collected from four districts of Malakand Division, Pakistan. S = swat, DL = Dir lower, B = buner, DU = Dir upper, RM = R. minima*

http://www.aloki.hu ● ISSN 1589 1623 (Print) ● ISSN 1785 0037 (Online)
DOI: http://dx.doi.org/10.15666/aeer/1605_56335651
© 2018, ALÖKI Kft., Budapest, Hungary

Table A1. *List of R. minima genotypes collected from four districts of Malakand Division, Pakistan*

S. No.	Species name	District of collection	Specific area of collection	Accession No.	S. No.	District of collection	Specific area of collection	Accession No.
1.	*R. minima*	Swat	Ziarat	S-RM1	51.	Buner	Karakar	B-RM51
2.	*R. minima*	Swat	Swegalai	S-RM2	52.	Buner	Jowar	B-RM52
3.	*R. minima*	Swat	Dadahara	S-RM3	53.	Buner	Toorwarsk	B-RM53
4.	*R. minima*	Swat	Kohay	S-RM4	54.	Buner	Sawarai	B-RM54
5.	*R. minima*	Swat	Gadi	S-RM5	55.	Buner	Chamtalai	B-RM55
6.	*R. minima*	Swat	Sharif Abad	S-RM6	56.	Buner	Matwanai	B-RM56
7.	*R. minima*	Swat	Zarakhela	S-RM7	57.	Buner	Bara	B-RM57
8.	*R. minima*	Swat	Gora Gat	S-RM8	58.	Buner	Nawagai	B-RM58
9.	*R. minima*	Swat	Chongai	S-RM9	59.	Buner	KozaNawagai	B-RM59
10.	*R. minima*	Swat	Qabar Shah	S-RM10	60.	Buner	Narbatawa	B-RM60
11.	*R. minima*	Swat	Landakay	S-RM11	61.	Buner	Naway Kalay	B-RM61
12.	*R. minima*	Swat	Kota	S-RM12	62.	Buner	Anghapur	B-RM62
13.	*R. minima*	Swat	Aboha	S-RM13	63.	Buner	Derai	B-RM63
14.	*R. minima*	Swat	Terang	S-RM14	64.	Buner	Amnawar	B-RM64
15.	*R. minima*	Swat	Dool	S-RM15	65.	Buner	Sangara	B-RM65
16.	*R. minima*	Swat	Chargo Tangay	S-RM16	66.	Buner	Agarai	B-RM66
17.	*R. minima*	Swat	Amlook Garai	S-RM17	67.	Buner	Ashezomaira	B-RM67
18.	*R. minima*	Swat	Shamra	S-RM18	68.	Buner	Bampokha	B-RM68
19.	*R. minima*	Swat	Mula Hassan Baba	S-RM19	69.	Buner	Balo Khan	B-RM69
20.	*R. minima*	Swat	Malak Abad	S-RM20	70.	Buner	Bahi Kaly	B-RM70
21.	*R. minima*	Swat	Soray	S-RM21	71.	Buner	Barjokaney	B-RM71
22.	*R. minima*	Swat	Tangai Chena	S-RM22	72.	Buner	Bar Kaley	B-RM72
23.	*R. minima*	Swat	Qalagay	S-RM23	73.	Buner	Beshonai	B-RM73
24.	*R. minima*	Swat	Sarkhanai	S-RM24	74.	Buner	Bazargey	B-RM74
25.	*R. minima*	Swat	Yakhtangay	S-RM25	75.	Buner	Mula Banda	B-RM75
26.	*R. minima*	Dir lower	Faqir Abad	DL-RM26	76.	Dir upper	Batal	DU-RM76
27.	*R. minima*	Dir lower	Ramora	DL-RM27	77.	Dir upper	Khwage-Oba	DU-RM77
28.	*R. minima*	Dir lower	Gul Abad	DL-RM28	78.	Dir upper	Bekari	DU-RM78
29.	*R. minima*	Dir lower	Shah lam Baba	DL-RM29	79.	Dir upper	Patrok	DU-RM79
30.	*R. minima*	Dir lower	Ouch	DL-RM30	80.	Dir upper	Shoor	DU-RM80
31.	*R. minima*	Dir lower	Asbanr	DL-RM31	81.	Dir upper	Balkot	DU-RM81
32.	*R. minima*	Dir lower	Nawagai	DL-RM32	82.	Dir upper	Jandrai	DU-RM82
33.	*R. minima*	Dir lower	Khwas	DL-RM33	83.	Dir upper	Islam-Gat	DU-RM83
34.	*R. minima*	Dir lower	Totano Bandai	DL-RM34	84.	Dir upper	Jelar	DU-RM84
35.	*R. minima*	Dir lower	Bambolai	DL-RM35	85.	Dir upper	Kakad	DU-RM85
36.	*R. minima*	Dir lower	Kityari	DL-RM36	86.	Dir upper	Haji Shai	DU-RM86
37.	*R. minima*	Dir lower	Shwa	DL-RM37	87.	Dir upper	Kharkani	DU-RM87
38.	*R. minima*	Dir lower	Badwan	DL-RM38	88.	Dir upper	Thal	DU-RM88
39.	*R. minima*	Dir lower	Dalbar	DL-RM39	89.	Dir upper	Kalkot	DU-RM89
40.	*R. minima*	Dir lower	Laaram	DL-RM40	90.	Dir upper	Lamotai	DU-RM90
41.	*R. minima*	Dir lower	Sarkhanai	DL-RM41	91.	Dir upper	Jagram	DU-RM91
42.	*R. minima*	Dir lower	Jawaro	DL-RM42	92.	Dir upper	Bandagai	DU-RM92
43.	*R. minima*	Dir lower	Babar Ghakhey	DL-RM43	93.	Dir upper	Karodara	DU-RM93
44.	*R. minima*	Dir lower	Medan	DL-RM44	94.	Dir upper	Warai	DU-RM94
45.	*R. minima*	Dir lower	Talash	DL-RM45	95.	Dir upper	Laspoor	DU-RM95
46.	*R. minima*	Dir lower	Fingal	DL-RM46	96.	Dir upper	Mastooj	DU-RM96
47.	*R. minima*	Dir lower	Bagh	DL-RM47	97.	Dir upper	Drosh	DU-RM97
48.	*R. minima*	Dir lower	Khaal	DL-RM48	98.	Dir upper	Ashreet	DU-RM98
49.	*R. minima*	Dir lower	Rabaat	DL-RM49	99.	Dir upper	Domail	DU-RM99
50.	*R. minima*	Dir lower	Kotigram	DL-RM50	100.	Dir upper	Qashqar	DU-RM100

http://www.aloki.hu ● ISSN 1589 1623 (Print) ● ISSN 1785 0037 (Online)
DOI: http://dx.doi.org/10.15666/aeer/1605_56335651
© 2018, ALÖKI Kft., Budapest, Hungary

STUDY ON IMMOBILIZED *CHLORELLA SP.* BY NANO MUSSEL-SHELL POWDER AND CHITOSAN

WEI, D. Y.[1] – CAI, L.[2] – JIANG, D. J.[3] – GUO, J.[4] – WANG, Y. N.[5] – JI, L. L.[5*] – SONG, W. D.[6*]

[1]*College of Naval Architecture and Mechanical-electrical Engineering, Zhejiang Ocean University*
Haida South Road No.1, Lincheng Street, Dinghai District, 316022 Zhoushan, China
(phone: +86-580-226-2589; fax: +86-580-226-2063)

[2]*College of Environmental and Science Technology, Donghua University*
201620 Shanghai, China

[3]*College of Marine Science and Technology, Zhejiang Ocean University*
316022 Zhoushan, China

[4]*College of Food and Medical, Zhejiang Ocean University, 316022 Zhoushan, China*

[5]*Institute of Innovation & Application, Zhejiang Ocean University, 316022 Zhoushan, China*

[6]*College of Petrochemical and Energy Engineering, Zhejiang Ocean University*
316022 Zhoushan, China

**Corresponding authors*
L. Ji – e-mail: jll-gb@163.com; W. Song – e-mail: swd60@163.com
phone: +86-580-226-2589; fax: +86-580-226-2063

(Received 25th May 2018; accepted 17th Jul 2018)

Abstract: Shells were used to produce biomass materials through calcining due to their excellent mechanical properties. In this paper, the mussel shells were calcined by the vacuum tube furnace and muffle furnace at 600 °C, 700 °C and 800 °C respectively, and that prepared under optimum conditions was activated by K_2CO_3 in the hydrothermal method. The pore structure and morphology of the sample were characterized by specific surface area analyser (BET) and scanning electron microscopy (SEM). Then the *Chlorella sp.* was immobilized by mussel shell powder and chitosan, which was co-cultured for 60 days. The results showed that calcined shells at 700 °C in a vacuum tube furnace have an optimal specific surface area, up to 4.107 m^2/g. K_2CO_3 hydrothermal modification method could effectively enlarge the pores of shell powder, from 4.107 nm up to 16.557 nm. The shell powder modified by chitosan had positive charges, which could attract the microalgae with negative charges, could live for up to 60 days. This article aims to use waste shells to immobilize microalgae, which is not only of great importance to the protection of the environment but also provides a novel way to immobilize microalgae.
Keywords: *Chlorella sp., immobilization, nanoporous mussel shell materials, microstructural characterization, recovery growth rate*

Introduction

Biomass has been assigned numerous roles to human beings from ancient times because of its massive and recyclable nature, however, with the rapid expansion of man-made materials, like alloy, plastic fibre, and so on, a great number of natural materials have been neglected and abandoned. Most of the non-renewable and non-biodegradable synthetic materials were used and subsequently became wastes, resulting in seriously environmental "white pollution" at present (Wang et al., 2017). Therefore, high-value utilization of biomass resources has been paid more and more attention to researchers

http://www.aloki.hu ● ISSN 1589 1623 (Print) ● ISSN 1785 0037 (Online)
DOI: http://dx.doi.org/10.15666/aeer/1605_56535664
© 2018, ALÖKI Kft., Budapest, Hungary

because of their renewability and biodegradability (Wang et al., 2016). Shells are often used to prepare porous materials by calcination as carrier-loaded functional ions due to its main component is 95% $CaCO_3$ and a small amount of organic matter (Currey et al., 1977; Okumura and Gennes, 2001; Currie et al., 2007). The previous study was performed a shell-based catalyst by the impregnation process using potassium hydroxide to extract economical biodiesel fuel synthesis from castor oil (Nurdin et al., 2015). The current use of seashells is limited to feed additives (J. et al., 2013), adsorbents (Paradelo et al., 2016), cement reinforcing phase (Martinez-Garcia et al., 2016), antimicrobials (Li et al., 2016), and carriers for functional materials (Edralin et al., 2017) at present.

Chlorella sp. is a kind of unicellular green microalgae that around 40% of global photosynthesis is performed by microalgae (Myers, 1980). From the 1960s, Oswald et al. first found the chlorella in the oxidized pond had an excellent removal effect on nitrogen and phosphorus in the water (Oswald et al., 1957). However, due to its small size of single cells, the presence of free-living microalgae in treated effluents remains a problem (Chevalier and Noüe, 1985), so researchers focused on the use of immobilized microalgae (Jiménez-Pérez et al., 2004). Immobilization techniques can be primarily divided into two groups: “passive” and “active” immobilization (Moreno-Garrido, 2008). Because the microalgae tends to adhere and naturally grow on the surface of natural organisms, the “passive” immobilization mostly uses it as a carrier (Robinson et al., 1986), but this process is easily reversed. Therefore, the “active” immobilization method, such as chemical attachment (Moreira et al., 2006), flocculant agents (Seki and Suzuki, 2002), and gel entrapment (Solé and Matamoros, 2016), are most widely used. Alginate gel, a gel entrapment type, has been most widely used because the immobilized cells do not undergo extreme physicochemical changes during the immobilization process (Smidsrød and Skja˚K-Br˛K, 1990).

Most frequent current uses of chlorella sp. are the metabolite production cultured, improvement of culture collections handling, obtaining of energy, nutrients, removement of metal or organic pollutant from aquatic media, measurement of toxicity and co-immobilization system production for different purposes (Abdel-Raouf et al., 2012). The use of immobilized algal cells in water purification processes has been reported previously (Bruun, 2013) as microalgae form part of the organisms fixed in percolating filters of wastewater treatment plants. At present, the immobilization technology of microalgae mostly uses natural polymer materials as carriers, such as agar(Kandilian et al., 2017), alginate (Smidsrød and Skja˚K-Br˛K, 1990) and so on. The advantage of these materials is that they have good biocompatibility, but the immobilization power is not strong, as a result, the microalgae is easy to fall off. In addition, the polymeric polymer material as a carrier to immobilized microalgae has the disadvantages of low biocompatibility and toxicity to microalgae cells (Timofeeva and Kleshcheva, 2011). There are few reports on the use of porous biomass materials as carriers to immobilize microalgae.

In this paper, mussel shell was calcined, activated and modified by chitosan, used to be as a carrier, to immobilize microalgae. Because modified shell has positive charges, it could attract the microalgae with negative charges, and achieve microalgae immobilization with a strong immobilization power. At the same time, Chitosan has the dual functions of electric neutral flocculation and adsorption flocculation, which is not only can provide nutrients for the growth of microalgae, but also non-toxic and harmless. This material will has broad prospects in the field of water quality control.

http://www.aloki.hu ● ISSN 1589 1623 (Print) ● ISSN 1785 0037 (Online)
DOI: http://dx.doi.org/10.15666/aeer/1605_56535664
© 2018, ALÖKI Kft., Budapest, Hungary

Materials and methods

Materials

Mussel shell was provided by a food processing factory (Zhejiang province, China). *Chlorella sorokiniana* was obtained from the laboratory of Marine Biological Chemical Laboratory, Zhejiang Ocean University. BG-11 medium ($NaNO_3$, 1.5 g; K_2HPO_4, 0.04 g; $MgSO_4.7H_2O$, 0.075 g; $CaCl_2.7H_2O$, 0.036 g; Na_2CO_3, 0.02 g; H_3BO_4, 2.86 g; $MnCl_2.4H_2O$, 1.81 g; $ZnSO_4$, 0.222 g; Na_2MoO_4, 0.39 g; $CuSO_4.5H_2O$, 0.079 g; $Co(NO_3)_2.6H_2O$, 49.4 g; Citric acid, 0.006 g; ferric citrate, 0.006 g; ampicillin, 50 μg/mL; distilled water, 1000 mL; agar, 20 g; trace element solution A5, 1 mL). All chemical reagents were analytical grade. All solutions were prepared by using deionized water.

Microalgae cultivation

Chlorella sp. was cultured in the BG-11 medium. The culture broth and the container were sterilized in an autoclave (1.2 kg/cm^2). Under sterile conditions, the algae seeds were evenly inoculated on the medium (300 mL), transferred to a conical flask (500 mL) and placed at 25 (± 1) °C with a sterile breathable film sealing with the bottle mouth; then the whole bottle was illuminated under a LED growth lamp with a red to blue ratio of 5:1 for 24 h, shaken three times a day at regular time.

Shell calcining

The cleaned shells were immersed in 1% HCl for 24 h and calcined at 600 °C, 700 °C and 800 °C for 2 h by using vacuum tube furnace (SKGL-1200-II, SIOMM, Shanghai) and muffle furnace (SX2-5-12, TAISITE, Tianjin), and sieved to < 100 μm (average particle size: 75 μm) mesh particle size by micro-nano-pulverizer (MKCA6-2J, Masuko, Japan; *Table 1*).

Table 1. *Experimental design*

Temperature	Muffle furnace	Vacuum tube furnace	Modified by K_2CO_3
600 °C	MM600 °C	MT600 °C	MMM600 °C
700 °C	MM700 °C	MT700 °C	MTM700 °C
800 °C	MM800 °C	MT800 °C	MTM800 °C

Activation of shell powder

0.5 g shell powder and 30 mL, 1% K_2CO_3 were dissolved to 50 mL tube, sonicated for 30 min by using an ultrasonic cleaning machine (G-040S, Geneng Cleaning Equipment Co., Ltd., Shenzhen, China, 600 w) and the sample was dissolved. The mixture was placed into a Teflon reactor at 160 °C for 24 h. After filtering, precipitation was washed to neutrality and dried at 60 °C for 8 h.

Modification by chitosan

Chitosan, a linear polymer with high specific surface area, has the dual functions of electric neutral flocculation and adsorption flocculation, non-toxic and harmless,

http://www.aloki.hu ● ISSN 1589 1623 (Print) ● ISSN 1785 0037 (Online)
DOI: http://dx.doi.org/10.15666/aeer/1605_56535664
© 2018, ALÖKI Kft., Budapest, Hungary

which is not only can provide nutrients for the growth of microalgae, but also conducive to the immobilization of microalgae.

100 mg chitosan and 10 mL HCl (1%) were dissolved in 100 mL deionized water. The chitosan mixed with activated shell powder with a mass ratio of 1:2, stirring for 1 h and vacuum drying at 80 °C for 24 h. The sample was marked as CS-M (*Fig. 1*).

Preparation of immobilized microalgae

100 mL *Chlorella sp.*, growing in logarithmic phase, 20 mL, 2% tea extract solution, 0.5 g CS-M, stirring for 30 min, standing in layers, removing as much supernatant as possible, adding 0.2 g Sodium alginate, 2 mL, 3% glycerol, stirring for 30 min, standing for 2 h, centrifugal separation, storage of the precipitate in sterile, sealed, dark conditions, storage temperature were 25 °C, 4 °C, -24 °C, respectively. 0.1 g CS-M and 1 mL steamed water, diluted 20 times, injected on slides, covered with coverslips. Optical microscopy (OM) was used to observe the combined situation of microalgae and shell powder under the ratio of 10 ×10 (ECLIPSE Ti, Nikon, Japan).

Determination of chlorophyll-a (chl.a) content in immobilized microalgae

5 mL algae were centrifuged at 5500 r/min for 15 min, collecting the precipitate, adding 5 mL, 80% acetone solution, extracting the chlorophyll-a in darkness at 4 °C for 24 h until the chl.a and acetone were fully mixed, centrifuge at 6000 r/min for 15 min. Finally, measuring the absorbance (OD) of supernatant by using UV-vis (UV-2600, SHIMADZU, Japan) at 663 nm and 645 nm wavelength respectively, with the reference solution of 80% acetone. All tests are repeated three times.

Reference calculation formula of chl.a concentration (Gao and Sun, 2000) is as follows:

$$\text{Concentration of chl. a (mg/L)} = 12.71 \times OD_{663} - 2.59 \times OD_{645}$$

OD_{645}, OD_{663}: OD of the extract at 645 nm and 663 nm wavelengths, respectively.

Test methods of microalgae cell density

Take algae fluid, which cultivated in the BG-11 medium for 24 h, 48 h, 72 h, 96 h, 120 h, and 162 h. The absorbance (OD_{680}) of the algae was measured at a wavelength of 680 nm. After fixing with Rochelle's solution, the *microalgae* was diluted and counted its number using a hemocytometer (Shanghai refinement Biochemical Instrument Co., Ltd., Shanghai, China). Repeat three times and take the average. Establish a standard curve of OD_{680} and the number of *microalgae* cells.

Characterization

The specific surface area and porosity tester (BET) was used to analyze the specific surface area, and pore size distribution of shell powder under 77 k with N_2 is the analysis gas (Quadrasorb SI, Quantachrome, USA). The surface morphology of the sample was observed by using JSM-7800F ultra-high resolution thermal field emission scanning electron microscope (JEOL, Japan).

http://www.aloki.hu ● ISSN 1589 1623 (Print) ● ISSN 1785 0037 (Online)
DOI: http://dx.doi.org/10.15666/aeer/1605_56535664
© 2018, ALÖKI Kft., Budapest, Hungary

Statistical analysis

Statistical analysis was performed using Origin 8.5 (Origin Corp., USA). All the experiments were performed independently at least three times.

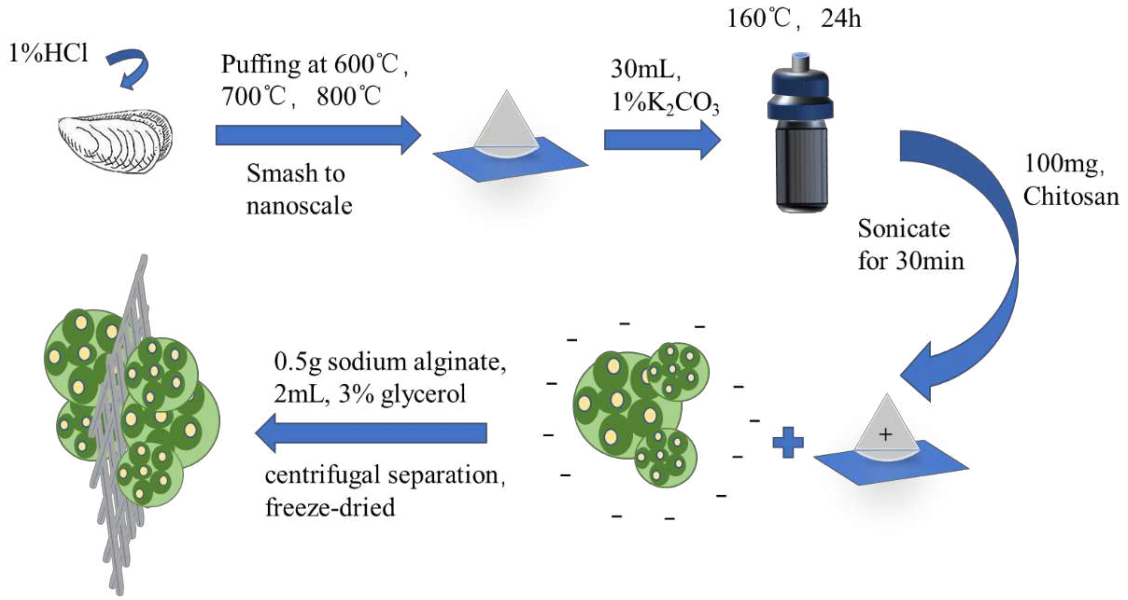

Figure 1. *The schematic illustration of Chlorella sp. immobilized by nano mussel-shell powder and chitosan*

Results and discussion

BET characterization

The curves of adsorption isotherms and pore diameter distribution of MM (mussel powder calcined by muffle furnace) and MT (mussel calcined by tube furnace) under 600 °C (a), 700 °C (b) and800 °C (c) are as shown in *Figure 2*. The isothermal adsorption curves of MM and MT at 600 °C and 700 °C are similar, and all type III (Sing, 1985). The lateral interaction between the adsorbed molecules is greater than the interaction between the adsorbent surface and the adsorbate. Adsorption takes place in multiple layers, and the amount of adsorption increases with enhancement of pressure. While the specific surface area of MM is generally superior to MT under 600 °C, 1.308 m^2/g vs 0.435 m^2/g the average pore diameter of MT is about 5 nm, while that of MM is about 2 nm. The average pore diameters of MM and MT at 800 °C are not significantly different. The reason may be that the organic matter in shell powder has been completely decomposed since 700 °C. Adsorption isotherms of MM at 800 °C has a hysteresis loop, which belongs to type H_1, indicating that the pore distribution of the material is relatively narrow, the particle is spherical and its size is uniform. In general, the organic matter of shell powder will completely break down at 700 °C. According to the average pore size of each material, it can be proved that the shell powder will form a well-distributed, less porous mesoporous material after high-temperature calcination. The puffing effect of the tube furnace is slightly better than that of the muffle furnace (*Tables 2* and *3*).

http://www.aloki.hu ● ISSN 1589 1623 (Print) ● ISSN 1785 0037 (Online)
DOI: http://dx.doi.org/10.15666/aeer/1605_56535664
© 2018, ALÖKI Kft., Budapest, Hungary

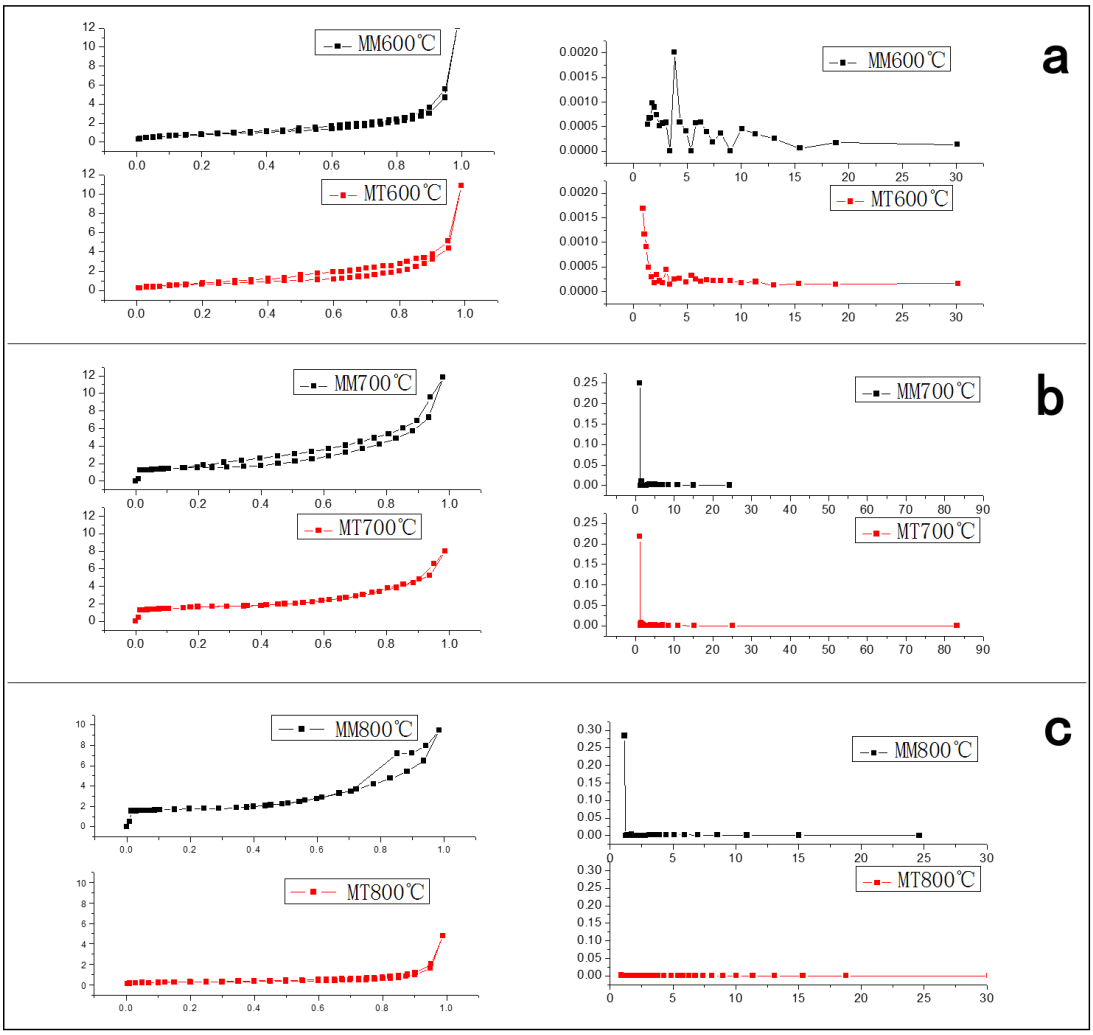

Figure 2. *Adsorption isotherms and pore diameter distribution curves of MM and MT under different expansion temperatures (600 °C, a; 700 °C, b; 800 °C, c)*

Table 2. *The specific surface area and average pore size of MM*

Temperature (°C)	600	700	800
Specific surface area （m^2/g）	1.308	5.538	12.45
Average pore size （nm）	7.627	11.1078	4.9343

Table 3. *The specific surface area and average pore size of MT*

Temperature (°C)	600	700	800
Specific surface area （m^2/g）	0.435	1.2	0.965
Average pore size （nm）	3.406	4.107	3.177

The curves of adsorption isotherms and pore diameter distribution of MMM (MM modified by K_2CO_3) and MTM (MT modified by K_2CO_3) are as shown in *Figure 3,*

http://www.aloki.hu ● ISSN 1589 1623 (Print) ● ISSN 1785 0037 (Online)
DOI: http://dx.doi.org/10.15666/aeer/1605_56535664
© 2018, ALÖKI Kft., Budapest, Hungary

whose calcined condition is 600 °C, 700 °C, 800 °C. All the adsorption isotherms of MTM are type IV (Sing, 1985), similar to type III at first, but at higher pressures, the adsorption increase rapidly with the hole is condensed in capillary. However, the hysteresis loops appeared on the adsorption isotherms of MMM, regardless of temperature, which belongs to type H_1. Comparing the surface area and average pore size of shell powder before and after modifying with K_2CO_3, we found that the average pore diameter of the shell powder, which calcined in the tube furnace, is greatly improved. The average pore size of shell powder increased from 3.406 nm to 15.176 nm at 600 °C, 4.107 nm to 16.557 nm at 700 °C, and 3.177 nm to 7.804 nm at 800 °C. But with the decrease of pore numbers, the specific surface area has reduced. The calcined shell powder in the muffle furnace does not have much difference before and after modification. We chose MTM (700 °C) as the best sample (*Tables 4* and *5*).

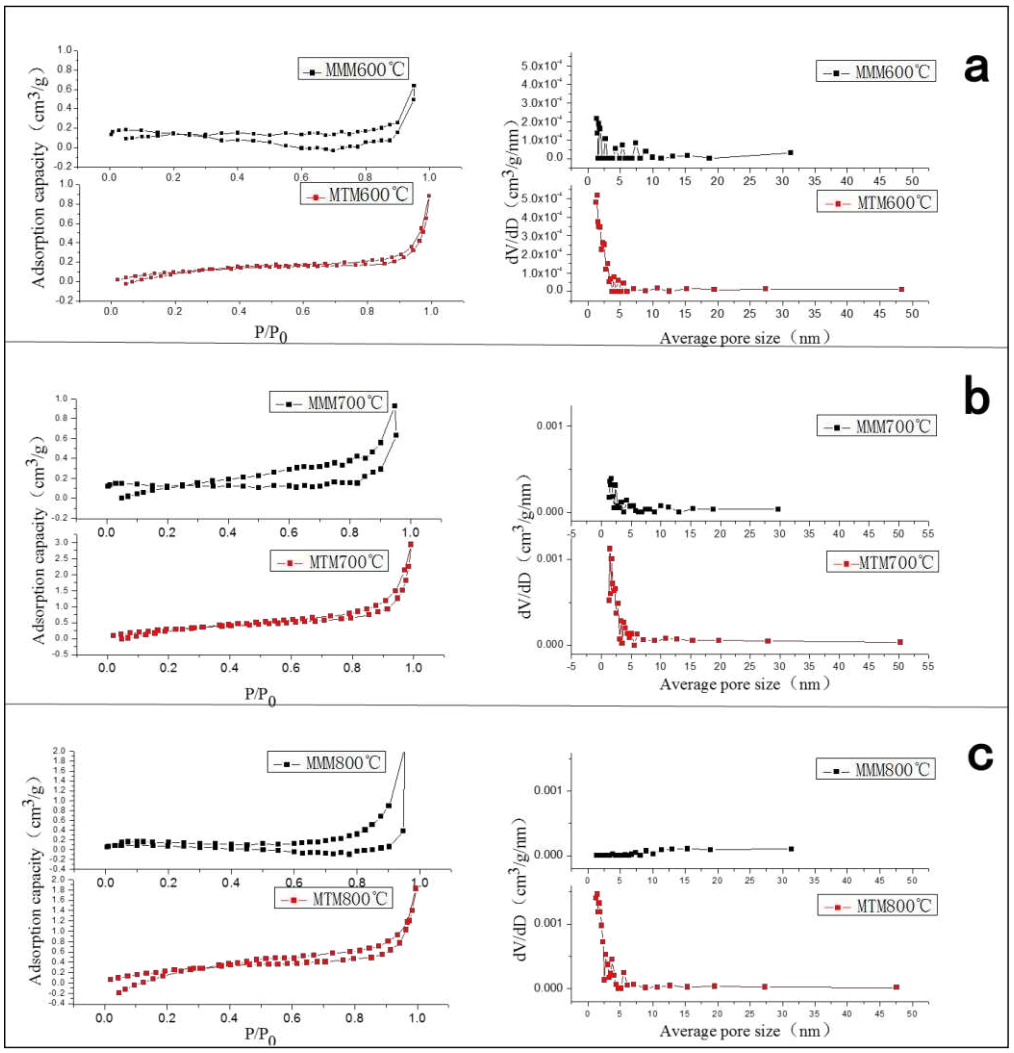

Figure 3. *Adsorption isotherms and pore diameter distribution curves of MMM (MM modified by K_2CO_3) and MTM (MT modified by K_2CO_3) under different expansion temperatures (600 °C, a; 700 °C, b; 800 °C, c)*

There are few reports on the use of biomass materials as carriers to immobilize microalgae. Shell powder, a excellent porous material, immobilizes microalgae by

http://www.aloki.hu ● ISSN 1589 1623 (Print) ● ISSN 1785 0037 (Online)
DOI: http://dx.doi.org/10.15666/aeer/1605_56535664
© 2018, ALÖKI Kft., Budapest, Hungary

means of charge attraction and physical adsorption, has strong immobilization power and can provide certain nutrients to microalgae and prolong its life.

Table 4. *The specific surface area and average pore size of MMM*

Temperature (°C)	600	700	800
Specific surface area（m^2/g）	2.894	5.4272	0.888
Average pore size（nm）	7.086	12.600	9.019

Table 5. *The specific surface area and average pore size of MTM*

Temperature (°C)	600	700	800
Specific surface area（m^2/g）	0.336	0.364	0.123
Average pore size（nm）	15.176	16.557	7.804

SEM characterization

Two SEM photographs of M (Mussel calcined at 700 °C in a vacuum environment), MTM as shown in *Figure 4,* the texture of M is loose, and there are several pores on the surface, with the pore diameter is about 0.5 μm, which determines the excellent adsorption performance of shell powder. The size of pores in MTM is increased, compared with M, which is 1 μm, because 1% potassium carbonate and water vapor have the good pore-forming ability, enhancing adsorption and sustained release capabilities of shell powder.

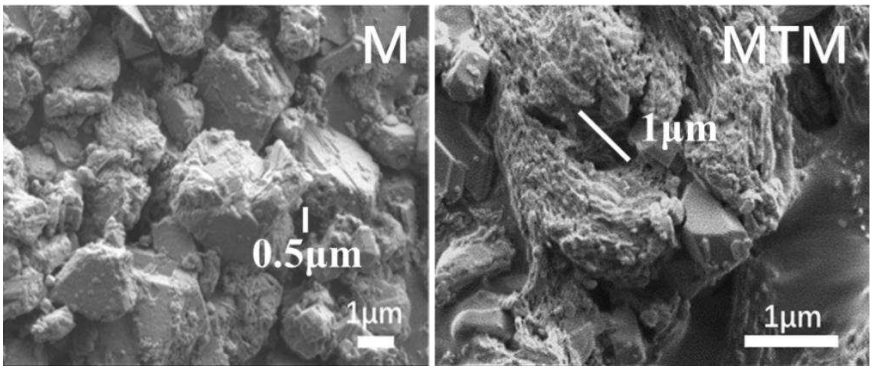

Figure 4. *SEM images of M and MTM*

OM characterization

Photomicrographs of immobilized microalgae under a bio-optical microscope are shown in *Figure 5*. It can be seen that the diameter of shell powder is about 200 μm, and the chlorella sp. cells are about 10 μm with a partial shell powder stacked. A large number of Chlorella sp. cells accumulate around the shell powder, indicating that modification of the shell by CS increased the "fixed" effect of the shell on the microalgae. It is beneficial to the dispersion of microalgae during the use of the immobilized microalgae. Sodium alginate also has a certain reinforcement and moisturizing effect.

http://www.aloki.hu ● ISSN 1589 1623 (Print) ● ISSN 1785 0037 (Online)
DOI: http://dx.doi.org/10.15666/aeer/1605_56535664
© 2018, ALÖKI Kft., Budapest, Hungary

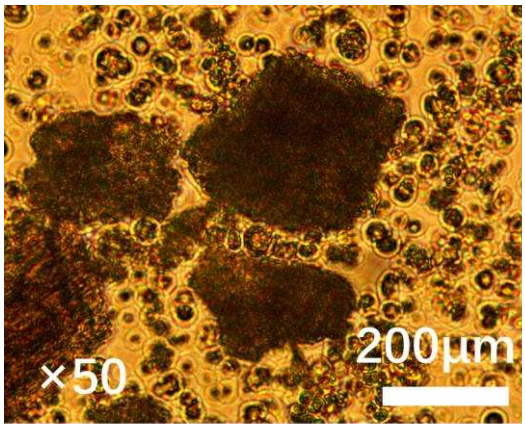

Figure 5. *OM images of immobilized microalgae*

The growth of immobilized microalgae

Growth curve of *microalgae* was determined in *Figure 7a,* during the preservation process, the chl.a content of all samples in the first 20 days changed slowly, however, after 20th day, decreased linearly. Loss rate of chl.a in immobilized microalgae after 60 days are respectively 59.04%, 50.22%, 42.77%, with the content of chl.a are respectively 3.41778 mg/L, 4.72185 mg/L, 5.31715 mg/L, which preserved in 25 °C, 4 °C and -24 °C. The changes of chl.a content in immobilized microalgae at 4 °C and -24 °C are similar. However, it can be observed that there was a greatly decrease from 30th to 40th days at 25 °C, from 6.88823 mg/L to 4.26672 mg/L, which is the best growth temperature of *microalgae*, with a highest activity, but it can only perform respiration and cannot synthesize chl.a due to the dark environment. The nutrients provided by shell powder are limited. Over time, *microalgae* lacks nutrient intake, resulting in the death of a large number of *microalgae* and the loss rate of chl.a increased rapidly. The loss rate of chl.a was the lowest after 60 days, which kept at 24 °C, 42.77%, probably because of the low activity of chlorella sp. at low temperature. In general, microalgae can survive 60 days in immobilized *microalgae,* which is rarely founded in recent research (*Fig. 6* and *Table 6*).

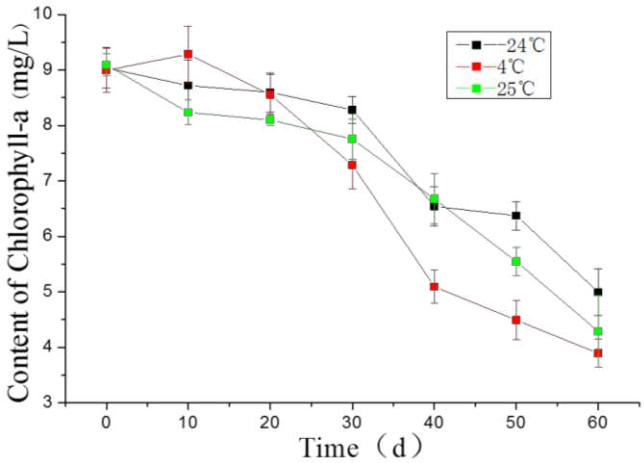

Figure 6. *The curve of microalgae growth within 60 days under different storage conditions (-24 °C, 4 °C, 25 °C)*

http://www.aloki.hu ● ISSN 1589 1623 (Print) ● ISSN 1785 0037 (Online)
DOI: http://dx.doi.org/10.15666/aeer/1605_56535664
© 2018, ALÖKI Kft., Budapest, Hungary

Table 6. *The loss rate of chl.a (%) during 60 days in immobilized microalgae*

Storage conditions (°C)	25	4	-24
Loss rate of chlorophyll-a (%)	59.04	50.22	42.77

Regrowth of immobilized microalgae

Regrowth curve of *microalgae* was determined in *Figure 7b,* the reactivation rate of *microalgae* in the immobilized microalgae at 4 °C is the fastest and the highest, with the cells number is up to 3.41769 × 10^6 cell/mL and the recovery rate is 26% (*Table 7*). The curves of *Chlorella sp.* cells number in immobilized microalgae are similar at 4 °C and -24 °C, which have a rapid recovery period of microalgae from the 15th day to19th day, and reaching the stable at the 9th day. However, the overall growth rate is slow at 25 °C. The reason may be the ultimate mortality of *Chlorella sp.* is high in the preservation process of immobilized microalgae, at 25 °C. Generally, the resuscitation curve of microalgae in immobilized microalgae was consistent with the Logistic growth curve.

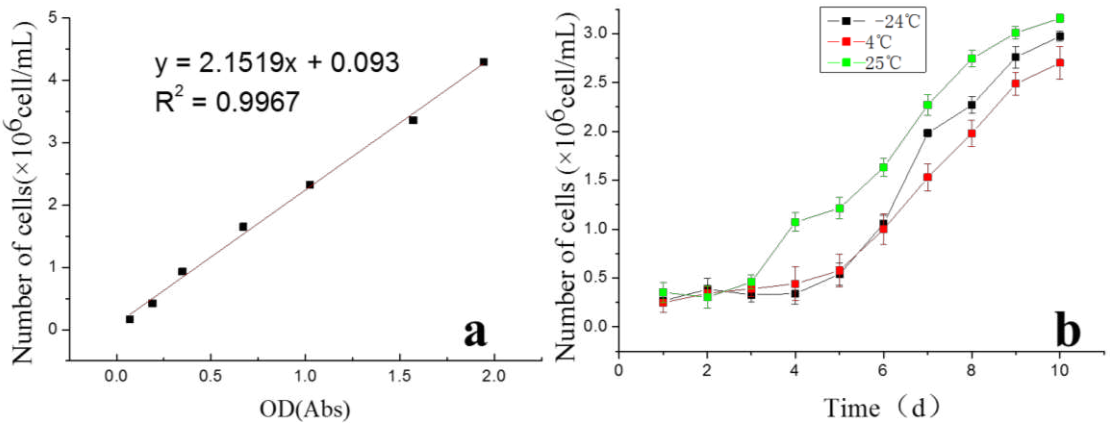

Figure 7. a. *The stand curve of microalgae cells numbers.* ***b.*** *The regrowth curve of microalgae within 10 days under different storage conditions (-24 °C, 4 °C, 25 °C)*

Table 7. *Recovery growth rate of microalgae (%) during 60 days*

Storage conditions (°C)	25	4	-24
Microalgae specific growth rate (%)	23	26	26

Conclusion

In summary, it was found that the shell powder calcined at 700 °C in a vacuum tube furnace and hydrothermal modification with K_2CO_3 has the optimum pore structure with an average pore size of 16.557 nm. The OM picture of CSM clearly shows that the *Chlorella sp.* is fixed with chitosan-modified shell powder, whose surface is positive. This structure can extend the shelf life of *Chlorella sp.* to 60 days and the best sample of the resurrection rate is 26%, the number of cells is 3.41769 × 10^6 cell/mL, reviving at 4 °C. With the rapid development of industrialization, this material has bright prospects. This is a new technology for immobilizing microalgae that can be used in water

http://www.aloki.hu ● ISSN 1589 1623 (Print) ● ISSN 1785 0037 (Online)
DOI: http://dx.doi.org/10.15666/aeer/1605_56535664
© 2018, ALÖKI Kft., Budapest, Hungary

purification, energy harvesting and other fields, not only has the great significance for environmental protection but also for abandoned resources reuse.

Acknowledgements. This study was supported by the Natural Science Foundation of Zhejiang Province of China (No. LQ16D060004), Key Research and Development Projects of Zhejiang Province of China (No. 2018C02043), Demonstration Project of Marine Economic Innovation and Development of Zhoushan City of China, and Demonstration Project of Marine Economic Innovation and Development of Yantai City of China (No. YHCX-SW-L-201705).

REFERENCES

[1] Abdel-Raouf, N., Al-Homaidan, A. A., Ibraheem, I. B. M. (2012): Microalgae and wastewater treatment. – Saudi Journal of Biological Sciences 19(3): 257-275.
[2] Bruun, O. (2013): China's environmental challenges, by Judith Shapiro. – China Journal 70: 215-217.
[3] Chevalier, P., Noüe, J. D. L. (1985): Wastewater nutrient removal with microalgae immobilized in carrageenan. – Enzyme & Microbial Technology 7(12): 621-624.
[4] Currey, J. D. (1977): Mechanical properties of the mother of pearl in tension. – Proceedings of the Royal Society of London 196(1125): 443-463.
[5] Currie, J. A., Harrison, N. R., Wang, L., Jones, M. I., Brooks, M. S. (2007): A preliminary study of processing seafood shells for eutrophication control Asia-Pacific. – Journal of Chemical Engineering 2(5): 460-467.
[6] Edralin, E. J. M., Garcia, J. L., Rosa, F. M. D., Punzalan, E. R. (2017): Sonochemical synthesis, characterization and photocatalytic properties of hydroxyapatite nano-rods derived from mussel shells. – Materials Letters 196: 33-36.
[7] Gao, J. F., Sun, Q. (2000): Botanical Physiology Experiment (Chapter 2). – The World Book Publishing Company, Shanxi.
[8] Jiménez-Pérez, M. V., Sánchez-Castillo, P., Romera, O., Fernández-Moreno, D., Pérez-MartíNez, C. (2004): Growth and nutrient removal in free and immobilized planktonic green algae isolated from pig manure. – Enzyme & Microbial Technology 34(5): 392-398.
[9] Kandilian, R., Jesus, B., Legrand, J., Pilon, L., Pruvost, J. (2017): Radiation transfer in agar immobilized microalgae cell cultures. – Journal of Quantitative Spectroscopy & Radiative Transfer 198: 81-92.
[10] Li, M., Yao, Z. T., Chen, T., Lou, Z. H., Xia, M. (2014): The antibacterial activity and mechanism of mussel shell waste-derived material. – Powder Technology 264(3): 577-582.
[11] Martínez-García, C., González-Fonteboa, B., Martínez-Abella, F., Carro-López, D. (2016): Performance of mussel shell as aggregate in plain concrete. – Construction & Building Materials 139: 570-583.
[12] Moreira, S. M., Moreira-Santos, M., Guilhermino, L., Rui, R. (2006): Immobilization of the marine microalga phaeodactylum tricornutum, in alginate for in situ experiments. Bead stability and suitability. – Enzyme & Microbial Technology 38(1-2): 135-141.
[13] Moreno-Garrido, I. (2008): Microalgae immobilization. Current techniques and uses. – Bioresource Technology 99(10): 3949.
[14] Myers, J. (1980): Primary productivity in the sea. – Bulletin of Marine Science - Miami 32(3): 1-16.
[15] Nurdin, S., Rosnan, N. A., Ghazali, N. S., Gimbun, J., Nour, A. H., Haron, S. F. (2015): Economical biodiesel fuel synthesis from castor oil using mussel shell-base catalyst (ms-bc). – Energy Procedia 79: 576-583.

http://www.aloki.hu ● ISSN 1589 1623 (Print) ● ISSN 1785 0037 (Online)
DOI: http://dx.doi.org/10.15666/aeer/1605_56535664
© 2018, ALÖKI Kft., Budapest, Hungary

[16] Okumura, K., Gennes, P. G. D. (2001): Why is nacre strong? Elastic theory and fracture mechanics for biocomposites with stratified structures. – European Physical Journal E 4(1): 121-127.
[17] Oswald, W. J., Gotaas, H. B., Golueke, C. G., Kellen, W. R., Gloyna, E. F., Hermann, E. R. (1957): Algae in waste treatment [with discussion]. – Sewage and Industrial Wastes 29(4): 437-457.
[18] Paradelo, R., Conde-Cid, M., Cutillas-Barreiro, L., Arias-Estévez, M., Nóvoa-Muñoz, J. C., Álvarez-Rodríguez, E. et al. (2016): Phosphorus removal from wastewater using mussel shell investigation on retention mechanisms. – Ecological Engineering 97: 558-566.
[19] Robinson, P. K., Mak, A. L., Trevan, M. D. (1986): Immobilized algae: a review. – Process Biochemistry 21(4): 122-127.
[20] Seki, H., Suzuki, A. (2002): Adsorption of heavy metal ions to floc-type biosorbents. – Journal of Colloid & Interface Science 249(2): 295-300.
[21] Sing, K. S. W. (1985): Reporting physisorption data for gas/solid systems with special reference to the determination of surface area and porosity (Recommendations 1984). – Pure and Applied Chemistry 57(4): 603-619.
[22] Smidsrød, O., Skja˚K-Br↿K, G. (1990): Alginate as immobilization matrix for cells. – Trends in Biotechnology 8(3): 71-78.
[23] Solé, A., Matamoros, V. (2016): Removal of endocrine disrupting compounds from wastewater by microalgae co-immobilized in alginate beads. – Chemosphere 164: 516-523.
[24] Spångberg, J., Jönsson, H., Tidåker, P. (2013): Bringing nutrients from sea to land – mussels as fertiliser from a life cycle perspective. – Journal of Cleaner Production 51(51): 234-244.
[25] Timofeeva, L., Kleshcheva, N. (2011): Antimicrobial polymers: mechanism of action, factors of activity, and applications. – Applied Microbiology & Biotechnology 89(3): 475-492.
[26] Wang, D., Zhao, T., Yan, L., Mi, Z., Qiang, G., Zhang, Y. (2016): Synthesis, characterization and evaluation of dewatering properties of chitosan-grafting dmdaac flocculants. – International Journal of Biological Macromolecules 92: 761-768.
[27] Wang, J., Qian, W., He, Y., Xiong, Y., Song, P., Wang, R. M. (2017): Reutilization of discarded biomass for preparing functional polymer materials. – Waste Management 65: 11.

http://www.aloki.hu ● ISSN 1589 1623 (Print) ● ISSN 1785 0037 (Online)
DOI: http://dx.doi.org/10.15666/aeer/1605_56535664
© 2018, ALÖKI Kft., Budapest, Hungary

EFFICIENT ELECTROCHEMICAL AMMONIA REMOVAL SYSTEM

WANG, Y.[1] – SONG, W.[2*] – JI, L.[1] – GUO, J.[3] – CAI, L.[1] – ZHANG, Y.[4]

[1]*Institute of Innovation & Application, Zhejiang Ocean University, Zhoushan 316022, China*

[2]*School of Petrochemical & Energy Engineering, Zhejiang Ocean University Zhoushan, 316022 China*

[3]*College of Food and Medical, Zhejiang Ocean University, Zhoushan 316022, China (phone: +86-580-255-0008; fax: +86-580-255-1319)*

[4]*Metalock Engineering Ningbo Co. Ltd., Zhoushan 316022, China (phone: +86-580-801-2252; fax: +86-580-801-2253)*

**Corresponding author e-mail: swd60@163.com; phone: +86-188-580-2759*

(Received 25th May 2018; accepted 31st Jul 2018)

Abstract. Efficient electrochemical ammonia oxidation system was studied with an objective to enhance the selectivity of ammonia to nitrogen gas and to remove the by-products in an undivided electrochemical cell, in which various cathodes (Ti, Cu/Zn, Fe) and Ti/IrO_2-Pt anode were assembled. In the present study, anodic oxidation of ammonia and cathodic reduction of by-products were achieved, especially with Cu/Zn cathode. The ammonia-N decreased from 100.0 mg/L to 0.0 mg/L in the presence of 1.0 g/L NaCl after 120 min electrolysis at the current density of 30.0 mA/cm^2 with Cu/Zn cathode and Ti/IrO_2 anode. No nitrite was detected in the treated solutions. The concentration of chloramine was 0.24 mg/l. About 97.34% of initial TN was transformed into nitrogen gas in Cu/Zn system, indicating that Cu/Zn cathode has better performance than Ti and Fe cathode. The results indicated that Cu/Zn cathode exhibited a little higher reduction ability, possibly attributed by the higher electrocatalytic activity of brass containing Zn (35-41 wt%) which significantly influenced the kinetics of current density. As ammonia could be completely removed by the simultaneous oxidation and reduction in this study, it is suitable for deep treatment of ammonia polluted water.

Keywords: *water pollution, electrocatalysis, ammonia nitrogen, dimensionally stable anode, electrocatalytic activity*

Introduction

Ammonia contamination in water bodies is a widespread environmental problem. Usually, two main categories of treatment processes, physicochemical and biological treatment methods, were employed for ammonia removal from domestic and industrial wastewaters, including ion exchange, air stripping, breakpoint chlorination, and biological process and so on (Rahmani et al., 2004; Du and Liu, 2005; Wang and Liu, 2006). As electrochemical oxidation of ammonia has high treatment efficiency, minimized sludge production, small area occupied and relatively low investment cost, many researchers have focused on it in decades.

The electrochemical method is widely used to remove ammonia from ammonia-containing underground water or industrial wastewater, which contains low concentrations of organic matter and cannot be effectively treated by biological method. In the last decades, researchers have tried to improve electrochemical denitrification by different ways, such as using different electrodes, designing different electrochemical

http://www.aloki.hu ● ISSN 1589 1623 (Print) ● ISSN 1785 0037 (Online)
DOI: http://dx.doi.org/10.15666/aeer/1605_56655680
© 2018, ALÖKI Kft., Budapest, Hungary

cells, addition of different supporting electrolytes and employing different power supply, etc.

In the past years, various electrodes such as Pt, Ru, Ir, Ti, graphite, Ni, Lead dioxide, dimension stable anode (DSA), boron-doped diamond (BDD) and bimetallic or multi-metallic electrodes have been used in electrochemical oxidation (Feng, 2003; Vitse et al., 2005; Chen et al., 2007; De et al., 2009). It was shown that ammonia is effectively removed from solution while active chlorine was electrogenerated on the Ti/PtOx–IrO_2 electrode with nitrogen gaseous being postulated to be the main by-product of ammonia electrolysis (Kapałka et al., 2010a). In general, during the electrochemical process of ammonia, nitrogen gas was the most favorable reduction product. One of the problems is the generation of nitrate, which needs to be further treated.

Although electrochemical method has been investigated and used to deal with ammonia issue, most researchers mainly focused on the anode effect on ammonia removal. However, few of them paid attention to the effect of cathode which may play an important role in the by-products (NO_3^--N, NO_2^--N and chloramines) generated during the process of electrochemical ammonia oxidation. On the other hand, some researchers found that the cathodes such as Cu/Zn and Fe had high efficiency on nitrate and nitrite removal. Therefore, it is possible to decrease the production of side products by employing cathode with high nitrate and nitrite reduction ability.

From previous study, ammonia could be efficient removed by Ti/RuO_2-Pt anode via electrochemical oxidation process (Wang et al., 2012). To compare with previous studies in order to design a better treatment system and study the effects of different anodes on experimental results simultaneously.

In present study, an efficient electrochemical ammonia oxidation system was designed with various cathodes (Ti, Cu/Zn, Fe) and Ti/IrO_2-Pt anode. The effect of different cathodes on the reduction efficiency of ammonia to nitrogen gas and the formation of by-products during the electrochemical process are studied in 2017, at Zhejiang Ocean University labs. The optimum operating conditions are also discussed, to enhance the selectivity of ammonia to nitrogen gas and to remove the by-products simultaneously.

Materials and methods

Electrochemical apparatus

The experiments are carried out in undivided cells using Ti, Fe and Cu/Zn plates as cathodes and Ti/IrO_2–Pt anode, respectively for the treatment of synthetic ammonia solution with anodic ammonia oxidation and cathodic reduction rates being compared. During the experiments, the influence of initial chloride ion concentration, current density, temperature and initial pH are investigated and assessed. The concentrations of ammonia, nitrite, nitrate, chloramine, and dissolved metals are determined with standard methods. The current efficiency (include the average current efficiency (ACE) and the instantaneous current efficiency (ICE), reaction kinetics, oxidation rate and one-way analysis of variance are used to analyze and assess this ammonia removal process.

The average current efficiency (ACE) and the instantaneous current efficiency (ICE) are calculated using *Equations 1* and *2*, respectively (Comninellis and Pulgarin, 1991; Van et al., 2004):

$$ACE = 3FV\left[\left(NH_4^+ - N\right)_0 - \left(NH_4^+ - N\right)_t\right]/14I_t \quad \text{(Eq.1)}$$

http://www.aloki.hu ● ISSN 1589 1623 (Print) ● ISSN 1785 0037 (Online)
DOI: http://dx.doi.org/10.15666/aeer/1605_56655680
© 2018, ALÖKI Kft., Budapest, Hungary

$$ICE = 3FV\left[\left(NH_4^+ - N\right)_t - \left(NH_4^+ - N\right)_{t+\Delta t}\right]/14I_{\Delta t} \quad \text{(Eq.2)}$$

where $(NH_4^+\text{-}N)_0$, $(NH_4^+\text{-}N)_t$ and $(NH_4^+\text{-}N)_{t+\Delta t}$ are the concentration of NH_4^+-N (mg/L) at times zero, t and t + Δt (min), respectively, I is the current density (A), F is the Faraday number (96,485 C/mol), t is the time (min), V is the volume of the electrolyte (L), 3 is the number of exchanged electrons for the electrochemical oxidation of ammonia, and 14 is the molecular mass of ammonia (g/mol).

Batch experiments were conducted in an apparatus at room temperature (about 23.0-26.0 °C). An undivided and unbuffered electrochemical cell was designed in our lab with a networking volume of 400.0 mL. The 400.0 mL electrolysis cell was made of acryl plates with four outer spots for the electrodes assembled. Three metal plates include Cu/Zn (Cu: 62.2 wt.%; Zn: 37.8 wt.%), Ti and Fe plates of 75.0 cm^2 (15.0 cm × 5.0 cm) were used as the cathode respectively with Ti/IrO_2–Pt (TohoTech company, Japan) as the anode at the same area. A distance of 8.0 mm was set between the two electrodes. The immersed areas of the anode and cathode in the treated solution were the same and calculated as 50.0 cm^2. A DC power with a voltage range of 0–50.0 V and current range of 0–5.0 A was employed as a power supply. Test synthetic ammonia solutions were prepared using $(NH_4)_2SO_4$ and distilled water to give a final concentration of 100.0 mg/L with no Cl^- ion. In the solution, free ammonia concentration is only 0.0198 mg/L. The NaCl dosage of 0 g/L, 0.5 g/L, 1.0 g/L, 2.0 g/L (w/v) were added into the synthetic ammonia solutions to investigate the effect of influencing factors (sodium chloride dosage, current density, temperature and initial pH value). The current density was varied from 5.0 mA/cm^2 to 50.0 mA/cm^2, and the initial pH value was adjusted from 3.0 to 11.0 by NaOH (0.1 M) or H_2SO_4 (0.1 M). 0.5 g/L Na_2SO_4 was added in all solution as supporting electrolyte. At different intervals, 1.5 mL of sample was drawn from the electrochemical cell for analysis. The electrolysis was ceased when either 90.0% of initial ammonia was converted or 2 h elapsed.

Analysis

The concentrations of ammonia and nitrate were determined by spectrophotometer (DR/4000U Spectrophotometer, USA) by standard methods (Clesceri and Eaton, 1998). Nitrite was analyzed by ion chromatography (Yokogawa IC7000, AS9-HC column). Total nitrogen (T-N) was determined with a T-N, T-P autoanalyzer (Autoanalyzer 3, Bran+Luebbe). Dissolved copper and zinc contents in the filtered samples were detected using plasma emission spectrophotometer equipment (ICAP-575, Jareruasshu). Surface morphology of electrodes was characterized ex-situ by atomic force microscopy (AFM) (Digital Instruments, DimensionTM3000, USA). Mono-, di- and tri-chloramines were determined by the colorimetric DPD method (Clesceri and Eaton, 1998). All the other analyses were done according to standard methods (Clesceri and Eaton, 1998).

Results and discussion

Influence of NaCl dosages

In the present experiment, as NaCl plays an important role on not only the ammonia oxidation rate but also the formation of the by-product nitrate, the performance of electrochemical ammonia oxidation with different NaCl dosage was investigated.

http://www.aloki.hu ● ISSN 1589 1623 (Print) ● ISSN 1785 0037 (Online)
DOI: http://dx.doi.org/10.15666/aeer/1605_56655680
© 2018, ALÖKI Kft., Budapest, Hungary

Figures 1 and *2* were the concentrations of ammonia-N and nitrate-N concerning time. *Figure 3* was oxidation rate of ammonia with varied chloride concentration.

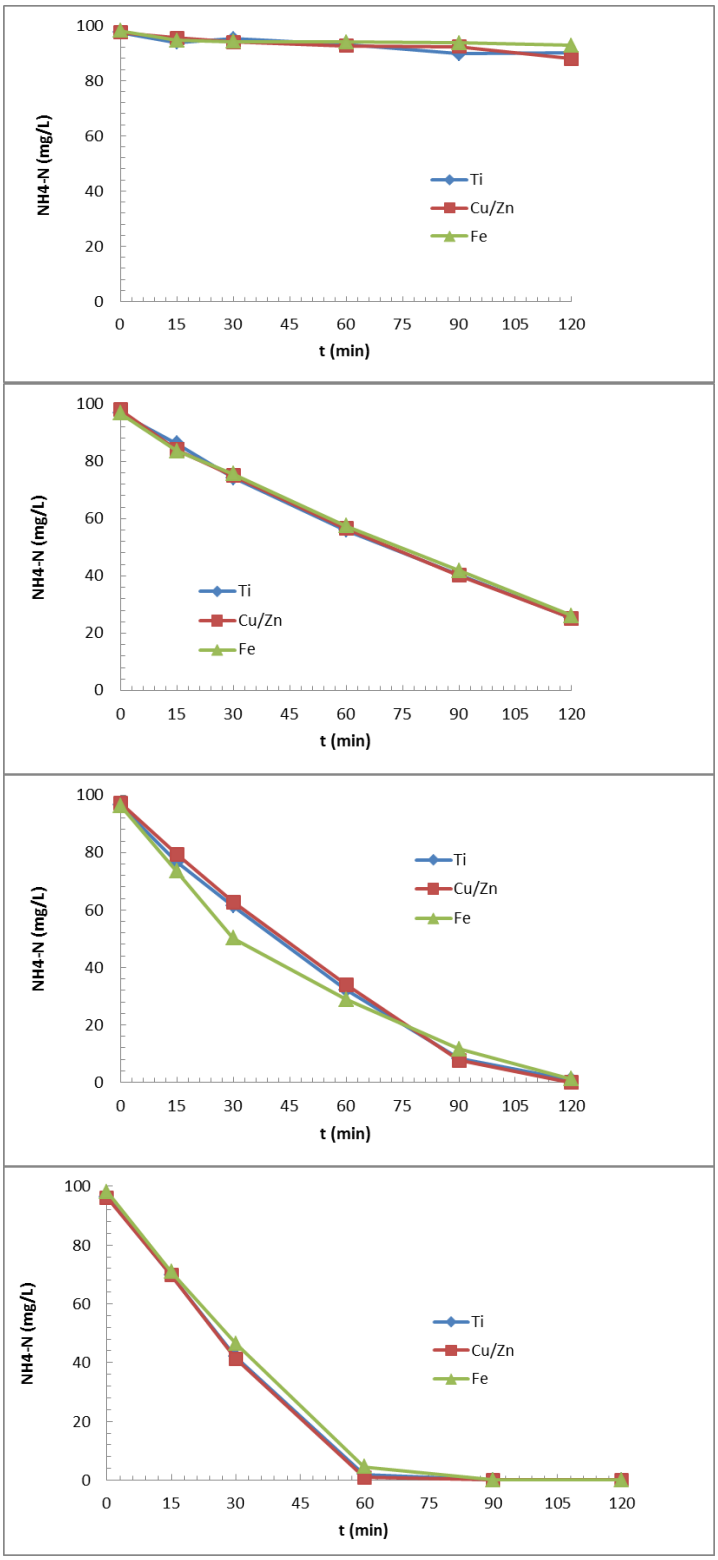

Figure 1. *Concentration of ammonia with respect to reaction time. Anode: Ti/IrO_2-Pt, cathode: Ti, Fe, Cu/Zn, 30.0 mA/cm^2 at 0 (a), 0.5 (b), 1.0 (c), 2.0 (d) g/L of NaCl, respectively*

http://www.aloki.hu ● ISSN 1589 1623 (Print) ● ISSN 1785 0037 (Online)
DOI: http://dx.doi.org/10.15666/aeer/1605_56655680
© 2018, ALÖKI Kft., Budapest, Hungary

a

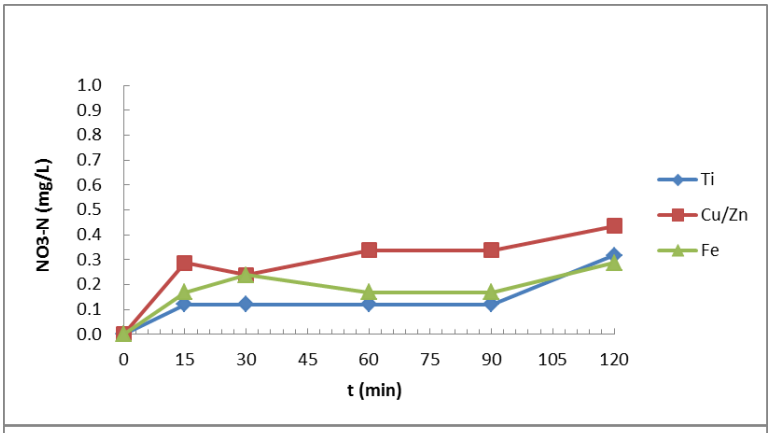

b

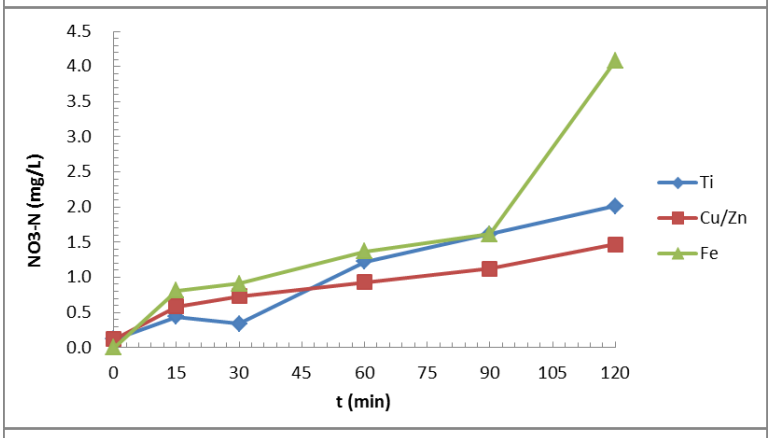

c

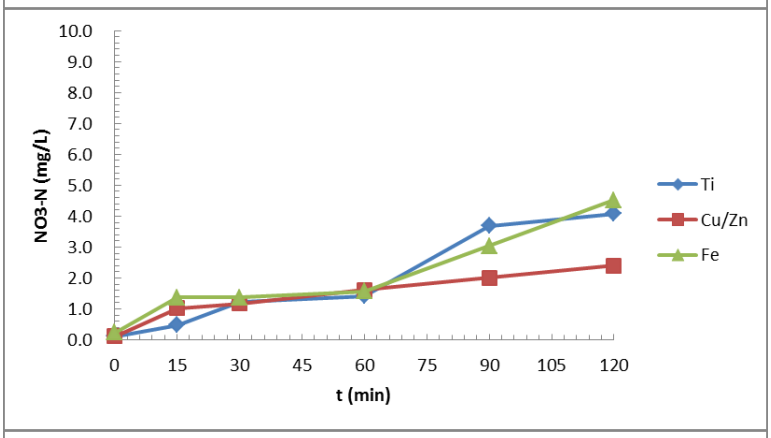

d

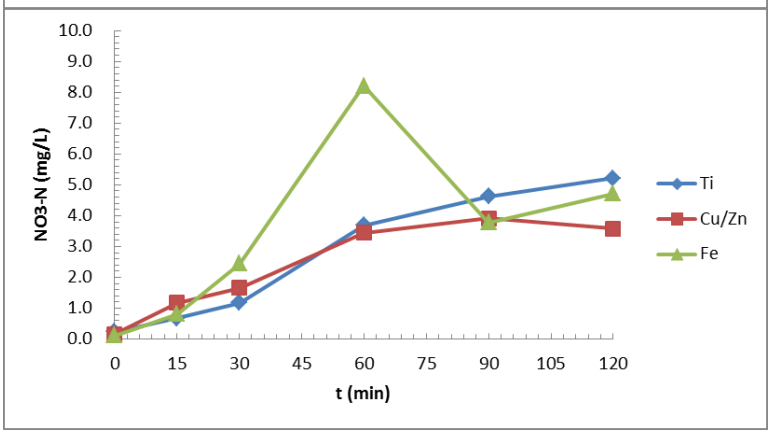

Figure 2. *Concentration of nitrate with respect to reaction time. Anode: Ti/IrO_2-Pt, cathode: Ti, Fe, Cu/Zn, 30.0 mA/cm^2 at 0 (a), 0.5 (b), 1.0 (c), 2.0 (d) g/L of NaCl, respectively*

http://www.aloki.hu ● ISSN 1589 1623 (Print) ● ISSN 1785 0037 (Online)
DOI: http://dx.doi.org/10.15666/aeer/1605_56655680
© 2018, ALÖKI Kft., Budapest, Hungary

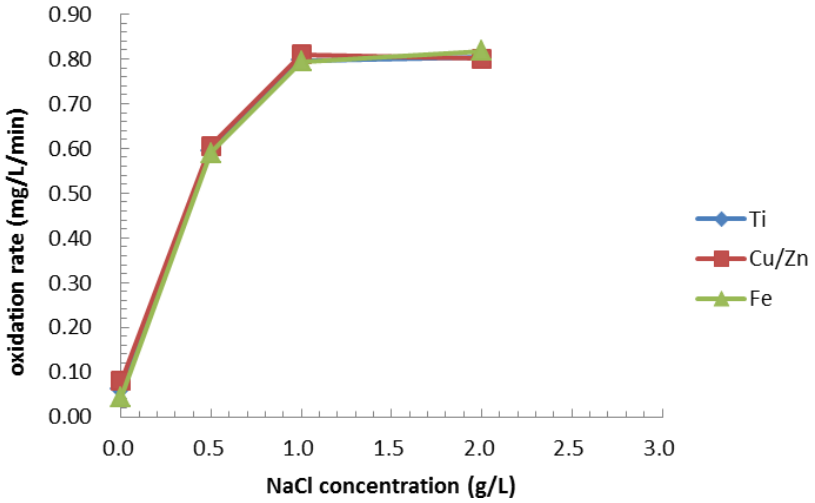

Figure 3. *Influence of NaCl concentrations on the ammonia oxidation rate. Anode: Ti/IrO_2-Pt, cathode: Ti, Fe, Cu/Zn, 30.0 mA/cm^2, respectively*

The results showed that without chloride ion, the ammonia removal efficiencies were 0.08, 0.1 and 0.05 with Ti, Cu/Zn and Fe as cathode employed, respectively. Meanwhile, the different amounts of nitrate formation during the electrochemical oxidation of ammonia can be attributed to the difference of the cathodes in the absence of NaCl, in which Cu/Zn cathode showed the lowest by-product formation. Cupro-zinc materials were well-known for their good corrosion resistance. Moreover, zinc has a good electroactivity while copper displays a good activity of electroreduction. As a result, a synergistic effect of alloying Zn with Cu could be expected. From the observed results, it can be concluded that Cu/Zn cathode is more suitable for ammonia removal than Ti and Fe cathodes in the absence of NaCl because of its high selectivity for ammonia oxidation to nitrogen gas. The effect of varying Cl^- concentration on ammonia-N and nitrate-N removal was also shown. The results indicated that these three cathodes exhibited almost the same performance of ammonia removal after 60 min electrolysis under NaCl addition. In the presence of 0.5 g/L NaCl after 120 min electrolysis, ammonia-N decreased from 100 mg/L to 25.4 mg/L, 25.3 mg/L and 26.1 mg/L respectively with Ti, Cu/Zn and Fe as a cathode. It is clear that the ammonia-N was significantly decreased compared with that in the absence of NaCl, which proved the key role of indirect oxidation during electrochemical oxidation of ammonia (Deng and Englehardt, 2007). Meanwhile, nitrate-N increased from 0 to 2.0 mg/L, 1.5 mg/L and 4.0 mg/L respectively, and no nitrite was detected through the experiments. In the presence of 1.0 g/L and 2.0 g/L NaCl, the ammonia decreased sharply, implying that in the presence of chloride ions, hypochlorite ions may be formed and then oxidize the ammonia and by-product presumably to nitrogen gas (Li et al., 2009) as listed in *Equations 3–7*.

For the indirect oxidation, in the presence of chloride ion, oxidizing hypochlorite ion will be formed during the electrolysis

$$2Cl^- \rightarrow Cl_2 + 2e^- \quad \text{(Eq.3)}$$

$$Cl_2 + H_2O \rightarrow HClO + H^+ + Cl^- \quad \text{(Eq.4)}$$

http://www.aloki.hu ● ISSN 1589 1623 (Print) ● ISSN 1785 0037 (Online)
DOI: http://dx.doi.org/10.15666/aeer/1605_56655680
© 2018, ALÖKI Kft., Budapest, Hungary

$$HClO \rightarrow ClO^- + H^+ \quad \text{(Eq.5)}$$

The hypochlorite acid formed during the electrolysis would efficiently oxidize the ammonia, which is assumed to be oxidized into nitrogen gas and nitrate.

$$2NH_4^+ + 3HClO \rightarrow N_2 + 3H_2O + 5H^+ + 3Cl^- \quad \text{(Eq.6)}$$

$$NH_4^+ + 4HClO \rightarrow NO_3^- + H_2O + 6H^+ + 4Cl^- \quad \text{(Eq.7)}$$

Stated, above 90% of removed ammonia was assumed to transform into N_2 gas with NaCl addition, which was similar to another report (Kim et al., 2005). The production of N_2 could be calculated as equal to the loss of N element according to the N conservation law (Xiao et al., 2009). Simultaneously, intermediate nitrate ions were formed in the water. On the contrary, the by-product formation had different results. The nitrate formation could come from not only the indirect oxidation of ammonia by HClO but also by hydroxyl radicals. The by-product formation generated by Ti and Fe increased during electrolysis while it increased for the first period and then decreased finally under Cu/Zn cathode condition. As Cu/Zn cathode exhibited high reduction ability, the NO_3^- concentration was the lowest. Mácová and Bouzek (2005) found that brass is containing Zn higher than 35 wt. % and lower than 41 wt. % will significantly influence the kinetics of current density, and higher electrocatalytic activity of Cu/Zn than both Cu and Zn was observed.

It can be concluded that ammonia oxidation rate was increased with the increased dosage of NaCl, while nitrate formation was different with various cathodes, which suggested that the cathode and chloride ion concentration can be optimized in the ammonia solution during electrolysis process with effective ammonia removal and relatively low amount of by-products left in the solution. Therefore, the electrochemical process in the presence of chlorides showed a higher capacity and selectivity in ammonia transformation into nitrogen gas (Xiao et al., 2009) In this study, the optimum NaCl concentration was 1.0 g/L and the best cathode was Cu/Zn cathode. As the combination of Ti/IrO_2-Pt anode and Cu/Zn cathode showed a good performance for ammonia oxidation, the influence of several other factors, such as current density initial pH and temperatures were also studied.

Influence of current density

Figure 4 shows that current density had some effect on the removal of ammonia and the nitrate-N production. In this work, current densities ranged from 5.0 mA/cm^2 which is the minimum required to achieve effective oxidation of ammonia (Cossu et al., 1998).

The ammonia concentration decreased from 100.0 mg/L to 80.9 mg/L, 59.3 mg/L, 23.2 mg/L, 0.0 mg/L in 120 min respectively (*Fig. 4a*). This observation is in agreement with the previous report that an increase in current density improves ammonia-N treatment efficiencies under the same charge loading. The possible reason is that the increased current density during electrochemical oxidation could enhance chlorine generation, which was responsible for subsequent removal of pollutions (Deng et al., 2007).

Figure 4b shows the variation of nitrate-N during electrolysis at different current densities. The final concentration of nitrate-N decreased with the increase of current

http://www.aloki.hu ● ISSN 1589 1623 (Print) ● ISSN 1785 0037 (Online)
DOI: http://dx.doi.org/10.15666/aeer/1605_56655680
© 2018, ALÖKI Kft., Budapest, Hungary

density. The nitrate-N increased from 0 to 2.6 mg/L, 2.4 mg/L, 1.3 mg/L, 2.4 mg/L, 3.3 mg/L and 2.8 mg/L in 120 min, respectively. Ammonia oxidation rate has been reported to be linearly by current density (Vanlangendonck et al., 2005), which is in agreement with the present experiments. A similar tendency was obtained in the present experiments. At lower current density, less amount of hypochlorite acid was produced, which was not enough to oxidize all the ammonia present in the solution.

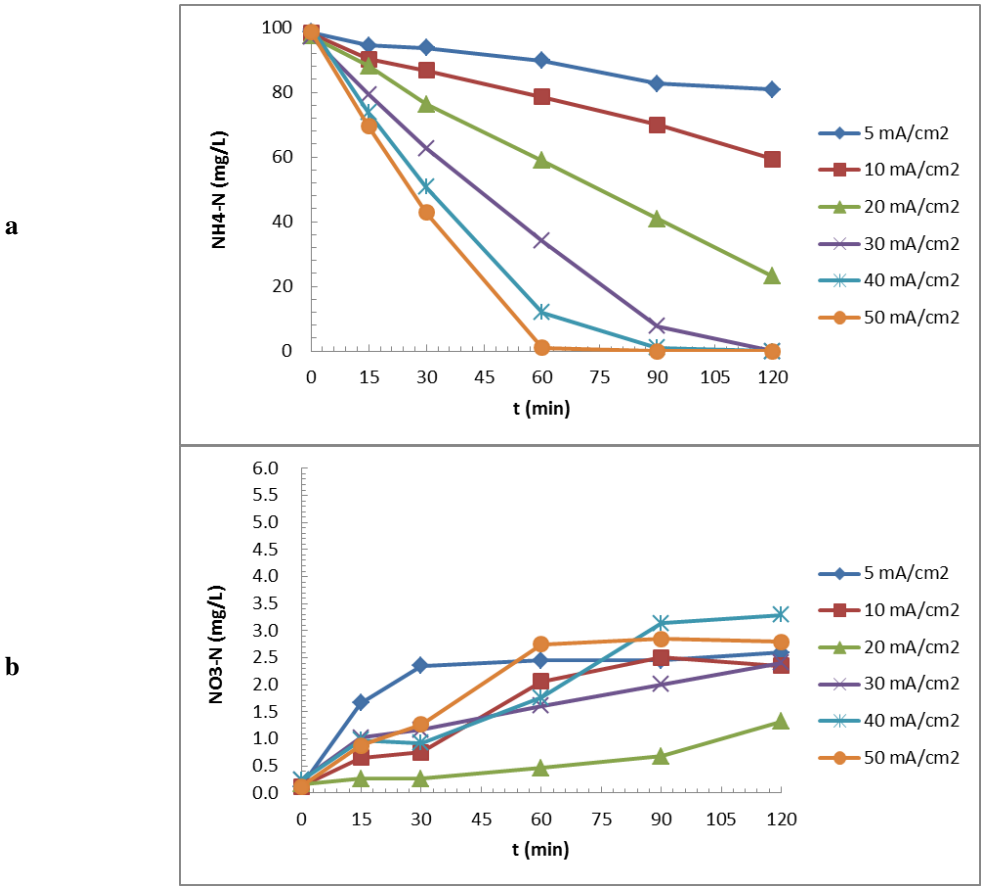

Figure 4. *The concentration of ammonia (a) and nitrate (b) concerning reaction time at different current densities. Anode: Ti/IrO_2-Pt, cathode: Cu/Zn, 1.0 g/L NaCl*

And from *Figure 5,* the ammonia oxidation rate almost increased with current density increased from 5.0 to 50.0 mA/cm^2. This enhancement could be attributed to more chlorine generated responsibly for subsequent removal of pollutions (Deng et al., 2007).

The impact of current density on both ICE and ACE during electrolysis are also investigated (data not shown). At a higher current density, the ICE and ACE decreased rapidly as the duration of electrolysis increased. Initially, the ammonia concentration and chloride ion concentration were high, and the electrical energy was mainly consumed by the ammonia oxidation. With the electrolysis progressed the electrical energy was mainly consumed by oxygen evolution and chlorate formation, thus resulting in a decrease in current efficiency.

http://www.aloki.hu ● ISSN 1589 1623 (Print) ● ISSN 1785 0037 (Online)
DOI: http://dx.doi.org/10.15666/aeer/1605_56655680
© 2018, ALÖKI Kft., Budapest, Hungary

Therefore, in the present experiments, to remove all of the ammonia with the consideration of ACE and ICE, the optimum current density was determined at 30.0 mA/cm^2.

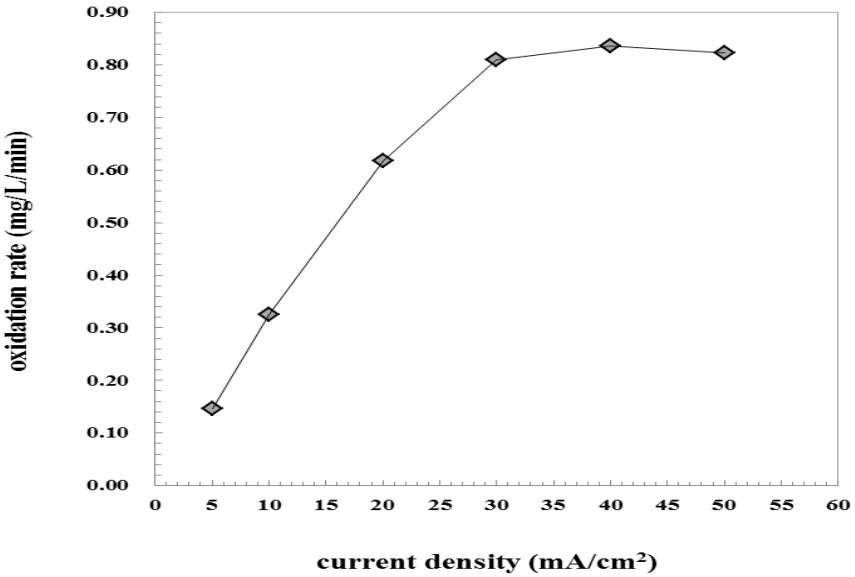

Figure 5. *Effect of current density on ammonia oxidation rate under 1.0 g/L of NaCl condition*

Influence of initial pH

Figures 6 and *7* present the ammonia oxidation rate under different initial pH conditions. Initial pH of 3, 5, 7, 9 and 11 were tested.

The ammonia decreased from 100.0 mg/L to 1.0 mg/L and 0 mg/L in 120 min, respectively under initial pH 3.0, 5.0, 7.0, 9.0 and 11.0 conditions. The oxidation rates were almost 0.8 mg/L/min.

The results of one-way analysis of variance ($p = 0.991$ for NH_4-N and 0.541 for NO_3-N, > 0.05, data not shown) confirmed that electrochemical treatment is independent of initial pH. This result agrees with Lin and Wu (Lin and Wu, 1996), but different from Kapałka et al. (2010b, 2011).

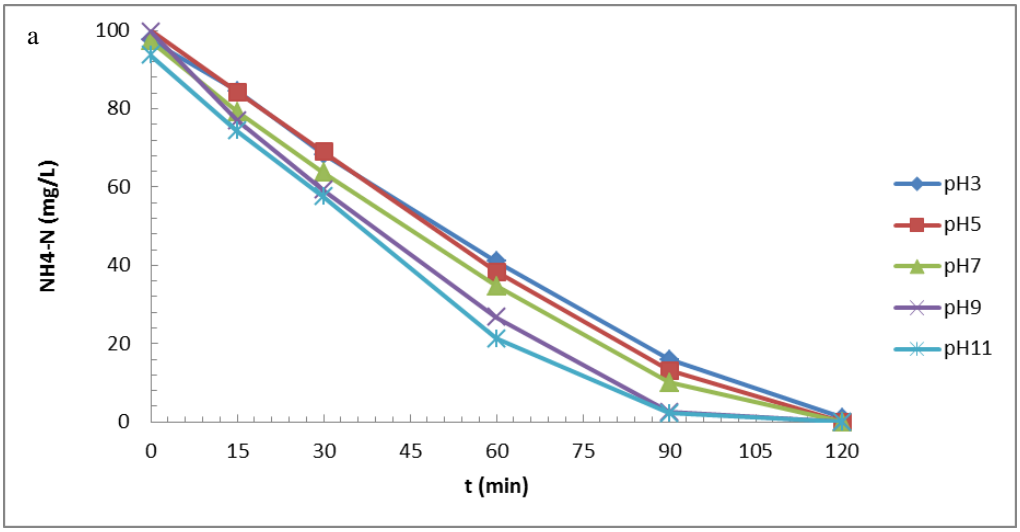

http://www.aloki.hu ● ISSN 1589 1623 (Print) ● ISSN 1785 0037 (Online)
DOI: http://dx.doi.org/10.15666/aeer/1605_56655680
© 2018, ALÖKI Kft., Budapest, Hungary

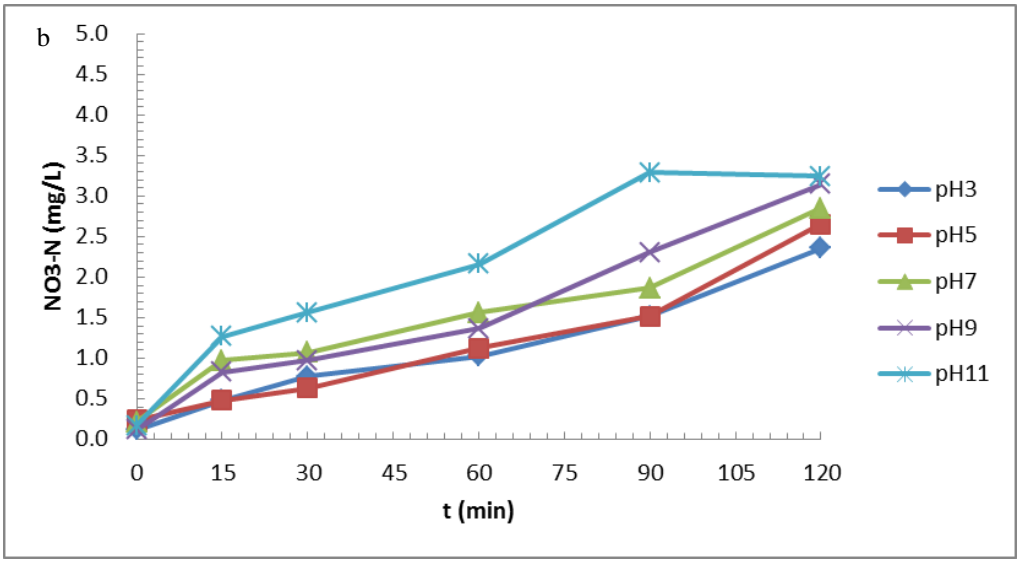

Figure 6. *The concentration of ammonia (a) and nitrate (b) VS time at different initial pH. Anode: Ti/IrO$_2$-Pt, cathode: Cu/Zn, 1.0 g/L NaCl, 30.0 mA/cm^2*

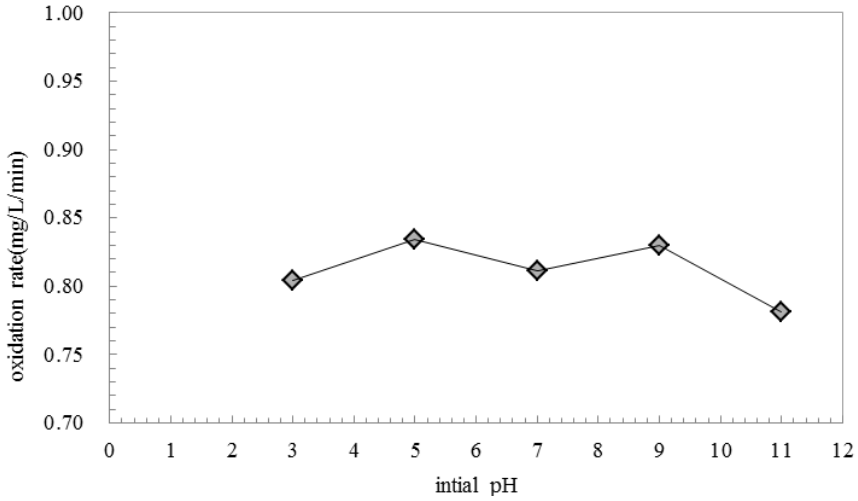

Figure 7. *Electrochemical NH_4^+-N removal as a function of pH under a current density of 30.0 mA/cm^2 and 1.0 g/L of NaCl*

Which can be explained by previously report, in a weak alkaline environment, the circulation of $Cl^- \rightarrow Cl_2 \rightarrow ClO^- \rightarrow Cl^-$ could be formed, making efficient use of chlorine. In a strong alkaline environment, ClO_3^- was present and competes with Cl^- for electrons, decreasing the removal rate (Wang, 2000). The mechanism for the ammonia removal at anode was like the "breaking point reactions" and a stepwise process, and the reaction at cathode was hydrogen evolution reaction.

Influence of temperature

Figure 8 shows the variation of ammonia-N and nitrate-N during electrolysis at different temperature control conditions. As it was difficult to maintain high temperature throughout experiments, the temperature was only set to be at uncontrolled

http://www.aloki.hu ● ISSN 1589 1623 (Print) ● ISSN 1785 0037 (Online)
DOI: http://dx.doi.org/10.15666/aeer/1605_56655680
© 2018, ALÖKI Kft., Budapest, Hungary

and 25.0 °C. Under the uncontrolled temperature condition, the temperature of the treated solution increased from 25.0 to 41.2 °C after 120 min electrolysis with all of the ammonia being destroyed. Under the controlled temperature (25.0 °C) condition, ammonia oxidation was a little slower. This was mainly due to different pH changes in the electrolyte at different temperatures during the electrolysis (data not shown). The pH varied because of the various reactions occurred during ammonia oxidation process. Moreover, increasing temperature could increase the rate of diffusion and the capability of adsorption. Consequently, the ammonia oxidation rate increased when the temperature was increased from 25.0 to 41.2 °C.

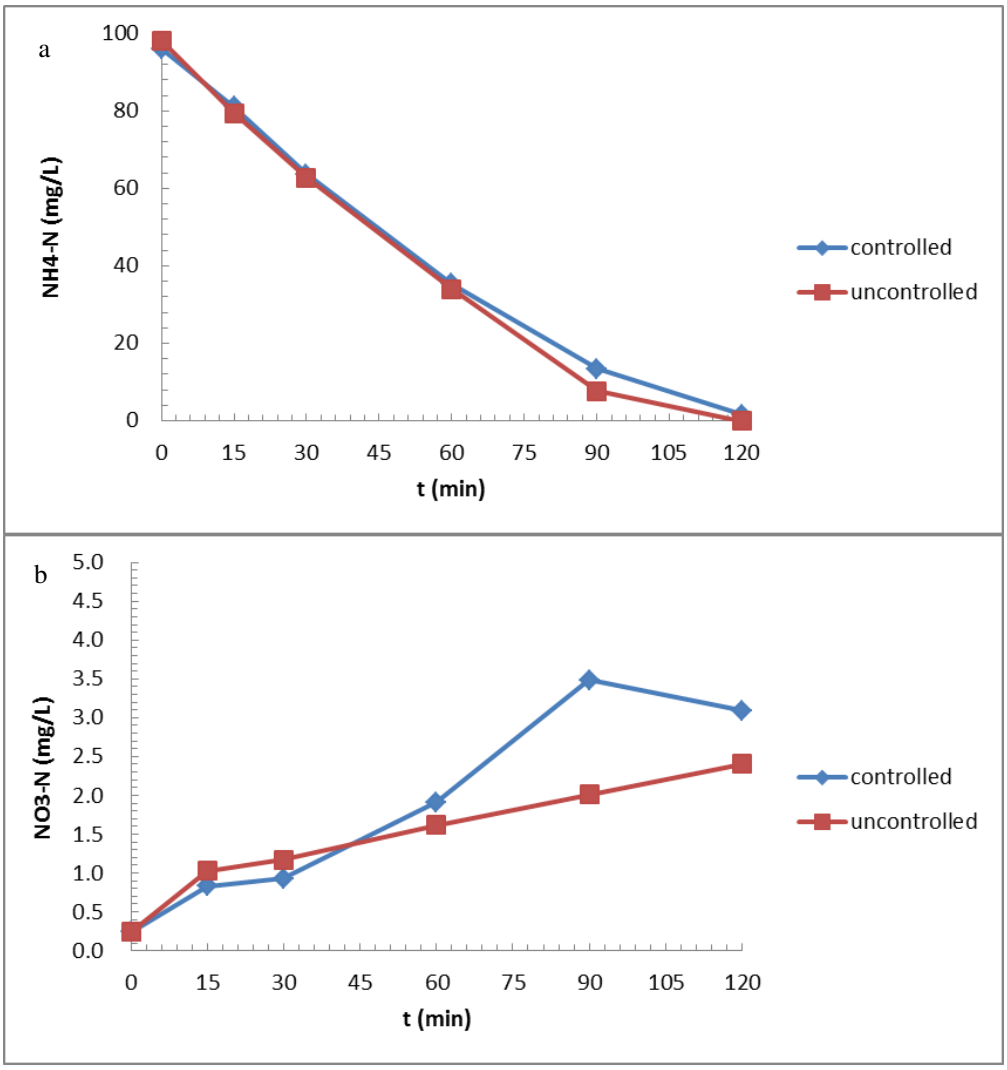

Figure 8. *The concentration of ammonia (a) and nitrate (b) concerning time at temperature control methods. Anode: Ti/IrO_2-Pt, cathode: Cu/Zn, 1.0 g/L NaCl, 30.0 mA/cm^2. The final temperature of the uncontrolled condition is about 41.2 °C*

In addition, ammonia in aqueous solution can exist in two forms: un-ionized form (NH_3) and/or ionized form (NH_4^+) (Körner et al., 2001). Compared these two forms of ammonia, the unionized one is much easier to be oxidized. These two forms of ammonia established an equilibrium following *Equation 8* (Lin and Wu, 1996).

http://www.aloki.hu ● ISSN 1589 1623 (Print) ● ISSN 1785 0037 (Online)
DOI: http://dx.doi.org/10.15666/aeer/1605_56655680
© 2018, ALÖKI Kft., Budapest, Hungary

$$NH_3 + H_2O \leftrightarrow NH_4^+ + OH^- \quad \text{(Eq.8)}$$

Under the uncontrolled condition, with increasing temperature, larger amount of NH_3 formed then subsequently oxidized on the electrode, which also increased ammonia oxidation rate.

The enhancement of ammonia oxidation could also be attributed to either the accelerated diffusion of ammonia from the bulk solution through the diffusive layer to the electrode surface (mass-transfer effect) or the rapid electro-oxidation reactions (activation effect).

In general, increasing temperature could enhance ammonia oxidation rate in several ways; the uncontrolled condition was a little favorable for electrochemical oxidation of ammonia.

Mass balance of nitrogen

Under the optimal condition, the mass balance of nitrogen in each treatment system is shown in *Figures 9* and *10*. The initial mass of ammonia nitrogen in the solution was 100 mg/L. The concentrations of ammonia, nitrite, nitrate and chloramines were determined during the electrolysis as listed in *Table 1*. It can be seen that the ratio of ammonia transferred into nitrogen gas was the highest in Cu/Zn cathode system, 97.34% and the others were 94.91% 94.38% in Ti and Fe cathode systems, respectively. This result indicated that the activity of the Cu/Zn electrode is relatively higher concerning the oxidation of ammonia ions and reduction of nitrate and nitrite.

Table 1. *Final concentrations of N species under different cathode conditions with 30.0 mA/cm^2 and 1.0 g/L NaCl in 120 min*

Cathode	Nitrate-N (mg/L)	Nitrite-N (mg/L)	Chloramine-N (mg/L)	Ammonia-N (mg/L)
Cu/Zn	2.40	0.00	0.24	0.00
Ti	4.08	0	0.24	0.92
Fe	4.52	0	0.00	1.16

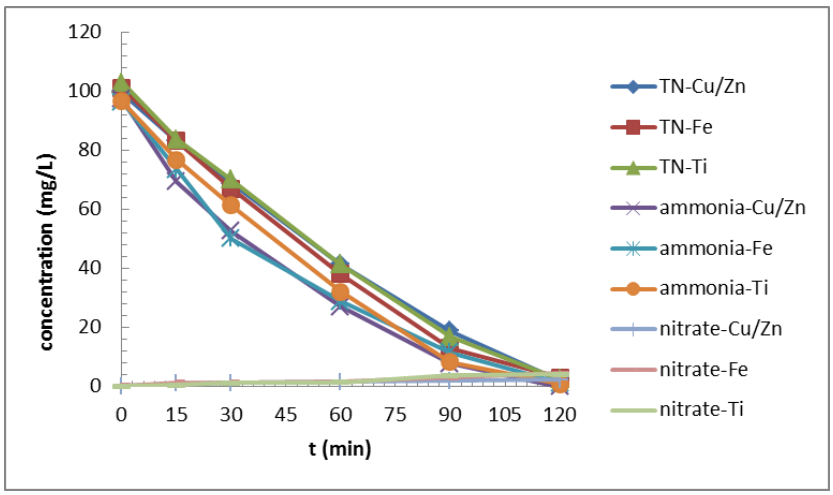

Figure 9. *The concentration of TN, ammonia-N and nitrate-N concerning time. Anode: Ti/IrO$_2$-Pt, cathode: Cu/Zn, Ti and Fe, 1.0 g/L NaCl, 30.0 mA/cm^2*

http://www.aloki.hu ● ISSN 1589 1623 (Print) ● ISSN 1785 0037 (Online)
DOI: http://dx.doi.org/10.15666/aeer/1605_56655680
© 2018, ALÖKI Kft., Budapest, Hungary

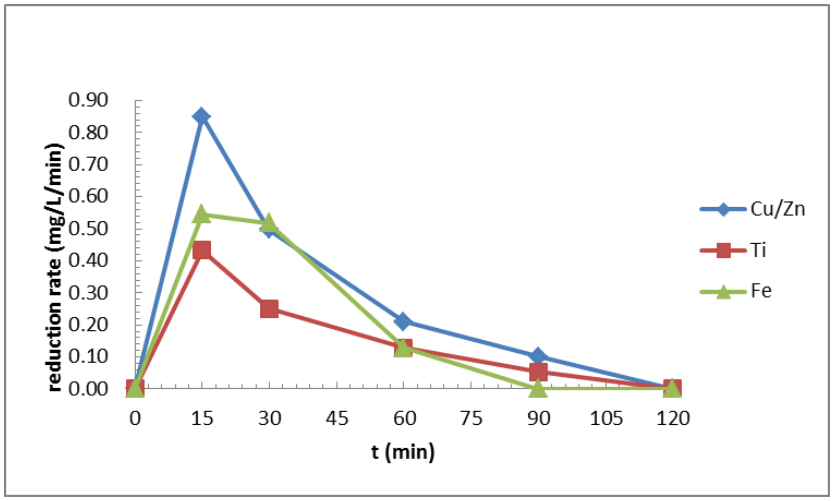

Figure 10. *Reduction rate concerning time. Anode: Ti/IrO_2-Pt, cathode: Cu/Zn, Ti and Fe, 1.0 g/L NaCl, 30.0 mA/cm^2*

Kinetic studies

$$ln\left(\left[NH_4^+ - N\right]_0 / \left[NH_4^+ - N\right]_t\right) = K_t \qquad \text{(Eq.9)}$$

where $[NH_4^+\text{-}N]_0$ and $[NH_4^+\text{-}N]_t$ respectively correspond to the initial ammonia concentration and the concentration after a period of reaction, and K is the reaction rate constant.

Application of *Equation 9* to the experimental data produces straight line plots as shown in *Figure11*. These data can be represented by pseudo first-order kinetics. However, when the NaCl concentration is at low levels (0.0 g/L, 0.5 g/L), the fitness was not good, possibly caused by diffusion and consumption of Cl^- ions during the electrochemical process.

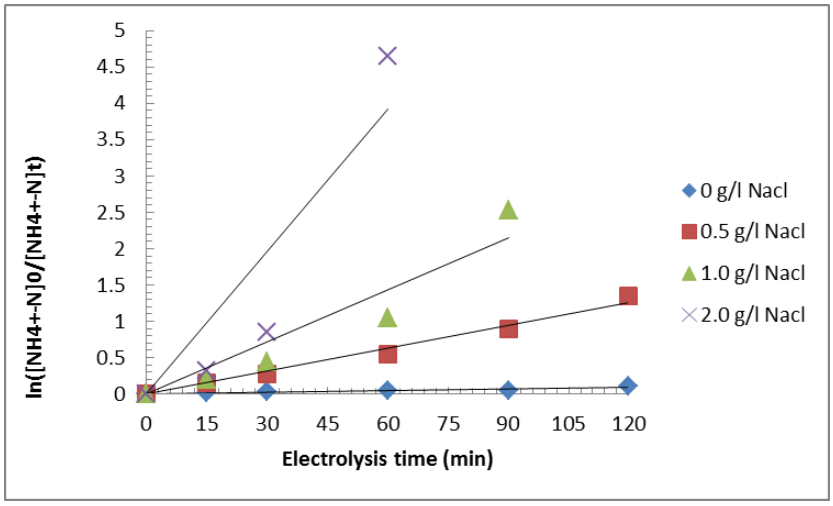

Figure 11. *Pseudo-first-order kinetic model of the electrochemical treatment data, with a current density of 30.0 mA/cm^2*

http://www.aloki.hu ● ISSN 1589 1623 (Print) ● ISSN 1785 0037 (Online)
DOI: http://dx.doi.org/10.15666/aeer/1605_56655680
© 2018, ALÖKI Kft., Budapest, Hungary

The kinetic rate coefficients were determined from the slopes of the straight lines under each set of operating condition (data not shown). The values of the kinetic rate coefficients obtained at different NaCl concentrations ranged between 0.01-0.07 min^{-1}. Higher values of correlation coefficients (R^2 = 0.84-0.98) confirmed the hypothesis of the pseudo first-order reaction of ammonia oxidation. The result also indicated that ammonia could be completely removed if appropriate conditions provided.

Analysis of electrode surfaces and the electrochemical solution

Analysis of the electrolyte after electrolysis for 2 h at the current density of 30.0 mA/cm^2 revealed that the concentrations of copper and zinc in the electrolyte were less than 0.2 and 1.5 mg/L, respectively, which are allowable limits for National Secondary Drinking Water Regulations (EPA 816-F-09-0004, May 2009). The low concentrations of Cu and Zn observed in the solutions may be attributed to limited corrosion of the electrodes under constant potential conditions.

As Ti/IrO_2–Pt anode and Cu/Zn cathode system had the best performance for ammonia oxidation in the presence of NaCl; the AFM investigation was carried out. The surface roughness of the anode had no change after electrolysis, implying that the Ti/IrO_2–Pt anode was stable for ammonia oxidation.

Conclusions

In this work, we have investigated the electrochemical ammonia removal system. To complete electrochemical oxidize of ammonia and reduce the formation of by-products, cathodic reduction of by-products, and anodic oxidation of ammonia was investigated in an undivided cell using Ti/IrO_2-Pt plate as an anode and three plates as a cathode for treatment of the synthetic ammonia solution respectively. It can be concluded:

(1) The ammonia-N decreased from 100.0 mg/L to 0.0 mg/L in the presence of 1.0 g/L NaCl after 120 min electrolysis at the current density of 30.0 mA/cm^2 with Cu/Zn cathode and Ti/IrO_2–Pt anode. No nitrite was detected in the treated solutions. Dissolved copper and zinc were 0.2 mg/l and 1.5 mg/l, respectively. The concentration of chloramine was 0.24 mg/l. About 97.34% of initial TN was transformed into nitrogen gas in Cu/Zn system, indicating that Cu/Zn cathode has good performance on by-production reduction.

(2) Initial pH had no obvious effect on electrochemical ammonia removal.

(3) Cu/Zn cathode possessed the highest ammonia oxidation rate (0.81 mg/L/min) and reduction rate of by-product (0.849 mg/L/min). The ammonia oxidation rates with Cu/Zn cathode was higher than that with Ti and Fe cathode. The nitrate formed during electrolysis with Cu/Zn was the lowest than that with other cathodes. The reason why the nitrate-N concentration was the lowest with Cu/Zn cathode was that because of its high reduction ability

(4) It was a little favorable for electrochemical oxidation of ammonia under uncontrolled temperature condition.

(5) The data obtained from the experiments could be represented by pseudo first-order kinetics.

From above, the mechanism of ammonia electro-oxidation on Cu/Zn cathode and Ti/IrO_2–Pt anode and formation of N_2 as a final product was indicated, that ammonia is

http://www.aloki.hu ● ISSN 1589 1623 (Print) ● ISSN 1785 0037 (Online)
DOI: http://dx.doi.org/10.15666/aeer/1605_56655680
© 2018, ALÖKI Kft., Budapest, Hungary

oxidized through several steps to various nitrogen compounds, which was in accordance with previous reports, as *Equation 10*.

$$\begin{matrix} NH_3 \rightarrow NH_2OH_{ads} \rightarrow NO_x \\ \downarrow \\ N_2 \end{matrix} \quad \text{(Eq.10)}$$

In the present study, the ammonia was completely removed with less amount of by-products using Cu/Zn cathode and Ti/IrO_2-Pt anode electrochemical system.

Present experiments confirmed that the order of oxidation ability of those two anodes was Ti/IrO_2–Pt > Ti/RuO_2–Pt. The possible reasons are listed as follows:

(1) High oxidation ability of the Ti/IrO_2–Pt lead to more amounts of hydroxyl radicals and hypochlorite ion formed than at Ti/RuO_2–Pt anode, and they could lead to the passivation of the cathode, which resulted in the slightly lower ammonia oxidation rate.

(2) As it is likely that, the presence of Cl^- ions affected the performance of each electrode. Experimental data showed that the higher oxidant generation of FAC (Free available chlorine) under Ti/IrO_2-Pt anode condition than the other anode was particularly observed.

(3) On the other hand, previous studies indicated that EAN (anode potential) of Ti/IrO_2–Pt electrode was lower and electrocatalytic activity toward chlorine evolution was higher which was confirmed by Szpyrkowicz et al. (2005).

In general, Ti/IrO_2-Pt anode had highest oxidation ability by various pathways, which combined with Cu/Zn cathode exhibited good performance on ammonia oxidation that could be employed for practical use in the future.

Acknowledgements. This study was supported by the Natural Science Foundation of Zhejiang Province of China (No. LQ16D060004), Key Research and Development Projects of Zhejiang Province of China (No. 2018C02043), Demonstration Project of Marine Economic Innovation and Development of Zhoushan City of China, and Demonstration Project of Marine Economic Innovation and Development of Yantai City of China (No. YHCX-SW-L-201705).

REFERENCES

[1] Chen, J., Shi, H., Lu, J. (2007): Electrochemical treatment of ammonia in wastewater by RuO_2–IrO_2–TiO_2/Ti electrodes. – Journal of Applied Electrochemistry 37(10): 1137-1144.

[2] Clesceri, L. S., Eaton, A. D. (1998): Standard Methods for the Examination of Water and Wastewater. – APHA, AWWA, WEF Publishing, Washington.

[3] Comninellis, C., Pulgarin, C. (1991): Anodic oxidation of phenol for wastewater treatment. – Journal of Applied Electrochemistry 21(8): 703-708.

[4] Cossu, R., Polcaro, A. M., Lavagnolo, M. C., Mascia, M., Palmas, S., Renoldi, F. (1998): Electrochemical treatment of landfill leachate: oxidation at Ti/PbO2 and Ti/SnO2 anodes. – Environmental Science and Technology 32(22): 3570-3573.

[5] De, L. R. M. G., Da, S. W. G. R., Da, C. J. W. S. D., Afonso, J. C. (2009): Removal of ammonium ion from produced waters in petroleum offshore exploitation by a batch single-stage electrolytic process. – Journal of Hazardous Materials 161(2-3): 1560-1564.

http://www.aloki.hu ● ISSN 1589 1623 (Print) ● ISSN 1785 0037 (Online)
DOI: http://dx.doi.org/10.15666/aeer/1605_56655680
© 2018, ALÖKI Kft., Budapest, Hungary

[6] Deng, Y., Englehardt, J. D. (2007): Electrochemical oxidation for landfill leachate treatment. – Waste Management 27(3): 380-388.
[7] Du, Q., Liu, S. (2005): Ammonia removal from aqueous solution using natural Chinese clinoptilolite. – Separation and Purification Technology 44(3): 229-234.
[8] Feng, C. (2003): Development of a high performance electrochemical wastewater treatment system. – Journal of Hazardous Materials 103(1-2): 65-78.
[9] Kapałka, A., Katsaounis, A., Michels, N. L., Leonidova, A., Souentie, S., Comninellis, C., Udert, K. M. (2010a): Ammonia oxidation to nitrogen mediated by electrogenerated active chlorine on Ti/PtOx-IrO2. – Electrochemistry Communications 12(9): 1203-1205.
[10] Kapałka, A., Cally, A., Neodo, S., Comninelli, S. C., Wachter, M., Udert, K. M. (2010b): Electrochemical behavior of ammonia at Ni/Ni(OH)2 electrode. – Electrochemistry Communications 12(1): 18-21.
[11] Kapałka, A., Fierro, S., Frontistis, Z., Katsaounis, A., Neodo, S., Frey, O., De, R. N., Udert, K. M., Comninellis, C. (2011): Electrochemical oxidation of ammonia (NH4+/NH3) on thermally and electrochemically prepared IrO2 electrodes. – Electrochimica Acta 56(3): 1361-1365.
[12] Kim, K. W., Kim, Y. J., Kim, I. T., Park, G. I., Lee, E. H. (2005): The electrolytic decomposition mechanism of ammonia to nitrogen at an IrO2 anode. – Electrochimica Acta 50(22): 4356-4364.
[13] Körner, S., Das, S. K., Veenstra, S., Vermaat, J. E. (2001): The effect of pH variation at the ammonium/ammonia equilibrium in wastewater and its toxicity to Lemna gibba. – Aquatic Botany 71(1): 71-78.
[14] Li, M., Feng, C. P., Zhang, Z. Y., Shen, Z. L., Sugiura, N. (2009): Electrochemical reduction of nitrate using various anodes and a Cu/Zn cathode. – Electrochemistry Communications 11(10): 1853-1856.
[15] Lin, S. H., Wu, C. L. (1996): Electrochemical removal of nitrite and ammonia for aquaculture. – Water Research 30(3): 715-721.
[16] Mácová, Z., Bonzek, K. (2005): Electrocatalytic activity of copper alloys for NO3- reduction in a weakly alkaline solution Part 1: Copper–zinc. – Journal of Applied Electrochemistry 35(12): 1203-1211.
[17] Rahmani, A. R., Mahivi, A. H., Mesdaghinia, A. R., Nasseri, S. (2004): Investigation of ammonia removal from polluted waters by Clinoptilolite zeolite. – International Journal of Environment Science and Technology 1(2): 125-133.
[18] Szpyrkowicz, L., Radaelli, M., Daniele, S. (2005): Electrocatalysis of chlorine evolution on different materials and its influence on the performance of an electrochemical reactor for indirect oxidation of pollutants. – Catalysis Today 100(3-4): 425-429.
[19] Van, H. K., Verhaege, M., Verstraete, W. (2004): Electro-oxidative abatement of low-salinity reverse osmosis membrane concentrates. – Water Research 38(6): 1550-1558.
[20] Vanlangendonck, Y., Corbisier, D., Van, L. A. (2005): Influence of operating conditions on the ammonia electro-oxidation rate in wastewaters from power plants (ELONITA™ technique). – Water Research 39(13): 3028-3034.
[21] Vitse, F., Cooper, M., Botte, G. G. (2005): On the use of ammonia electrolysis for hydrogen production. – Journal of Power Sources 142(1-2): 18-26.
[22] Wang, P., Liu, W., Fang, H. (2000): Electrochemical oxidation of ammonium-N in landfill leachate. – China Environ. Science 1: 289-291.
[23] Wang, Y., Liu, S. (2006): Ammonia removal from leachate solution using natural Chinese clinoptilolite. – Journal of Hazardous Materials 136(3): 735-740.
[24] Wang, Y. N., Guo, X., Li, J. L., Yang, Y. N., Lei, Z. F., Zhang, Z. Y. (2012): Efficient electrochemical removal of ammonia with various cathodes and Ti/RuO_2-Pt anode. – Open Journal of Applied Sciences 2: 241-247.
[25] Xiao, S., Qu, J., Zhao, X., Liu, H., Wan, D. (2009): Electrochemical process combined with UV light irradiation for synergistic degradation of ammonia in chloride-containing solutions. – Water Research 43(5): 1432-1440.

http://www.aloki.hu ● ISSN 1589 1623 (Print) ● ISSN 1785 0037 (Online)
DOI: http://dx.doi.org/10.15666/aeer/1605_56655680
© 2018, ALÖKI Kft., Budapest, Hungary

TRANSCRIPTOME AND PROTEOMICS INTERACTION REVEALS LOW SEED GERMINATION OF *CYCLOBALNOPSIS GILVA* TO SAVE FOREST ECOLOGY

ZAYNAB, M.[1] – FATIMA, M.[2] – ABBAS, S.[3] – SHARIF, Y.[4] – UMAIR, M.[3] – CHEN, S.[5*] – CHEN, W.[1*]

[1]*College of Life Sciences, Fujian Agriculture and Forestry University, 350002 Fuzhou, P. R. China*

[2]*College of Crop Science, Fujian Agriculture and Forestry University, 350002 Fuzhou, P. R. China*

[3]*Department of Biochemistry, Quaid-i-Azam University, Islamabad, Pakistan*

[4]*College of Plant Protection, Fujian Agriculture and Forestry University, 350002 Fuzhou, P. R. China*

[5]*College of Forestry, Fujian Agriculture and Forestry University, 350002 Fuzhou, P. R. China*

**Corresponding authors*
e-mail: weichen@fafu.edu.cn, weichen909@163.com (Wei Chen)
e-mail: fjcsp@126.com; phone: +86-591-8378-9367; fax: +86-591-8378-9352 (Shipin Chen)

(Received 13th Jun 2018; accepted 1st Aug 2018)

Abstract. Tree species display wide range of heterogeneity in their size, type, dormancy and growth of seed. Data about variation in germination under natural conditions and tree growth in connection with mentioned attributes is of immense value to understand tree distribution and forest stand management. Studies dealing with tree seed germination can enable successful nursery operations and healthy seedling production. This may also increase the seedlings' establishment in the forest restoration activities on destructed sites through native plant species. Successful germination is not only critical for plantlet establishment but also necessary for crop yield. As seed detaches from mother plant it desiccates continuously and selects suitable environment for germination activity. To understand the low germination rate in *Cyclobalnopsis gilva* molecular aspects of germination has been elucidated well with the integrated studies of proteomic, transcriptomic molecular biology. In this review, common and different aspects of seed germination including metabolic activation, transcription and translation regulation, have been discussed. This review will help to understand the transcriptomic and proteomic interaction of *C. gilva* which will be helpful to save the forest ecology and solve the problem of woody plants with low germination rate all over the world.
Keywords: *environment, woody plants, forest, metabolic activation, transcription, translation*

Introduction

Seed germination comprises of three interlinked processes, such as (I) rapid water uptake, (II) plateau phase and (III) post-germination. Phase (I) starts with the water absorption which helps in the breakdown of starch, proteins, and lipids along with the continuity of glycolytic and oxidative pentose phosphate pathways (Howell et al., 2007; Macovei et al., 2011). Phase II involves mitochondrial synthesis (Howell et al., 2007) and translation of stored mRNA (Dinkova et al., 2011; *Fig. 1*). Phase III follows the elongation of embryonic axes leading to radicle growth. Previous research studies have explained seed germination with considerable progress from more than two decades. However, there are many small circles of seed germination, which demands more

http://www.aloki.hu ● ISSN 1589 1623 (Print) ● ISSN 1785 0037 (Online)
DOI: http://dx.doi.org/10.15666/aeer/1605_56815692
© 2018, ALÖKI Kft., Budapest, Hungary

exploration for the proper understanding of mutual linkages between various pathways (He and Yang, 2013).

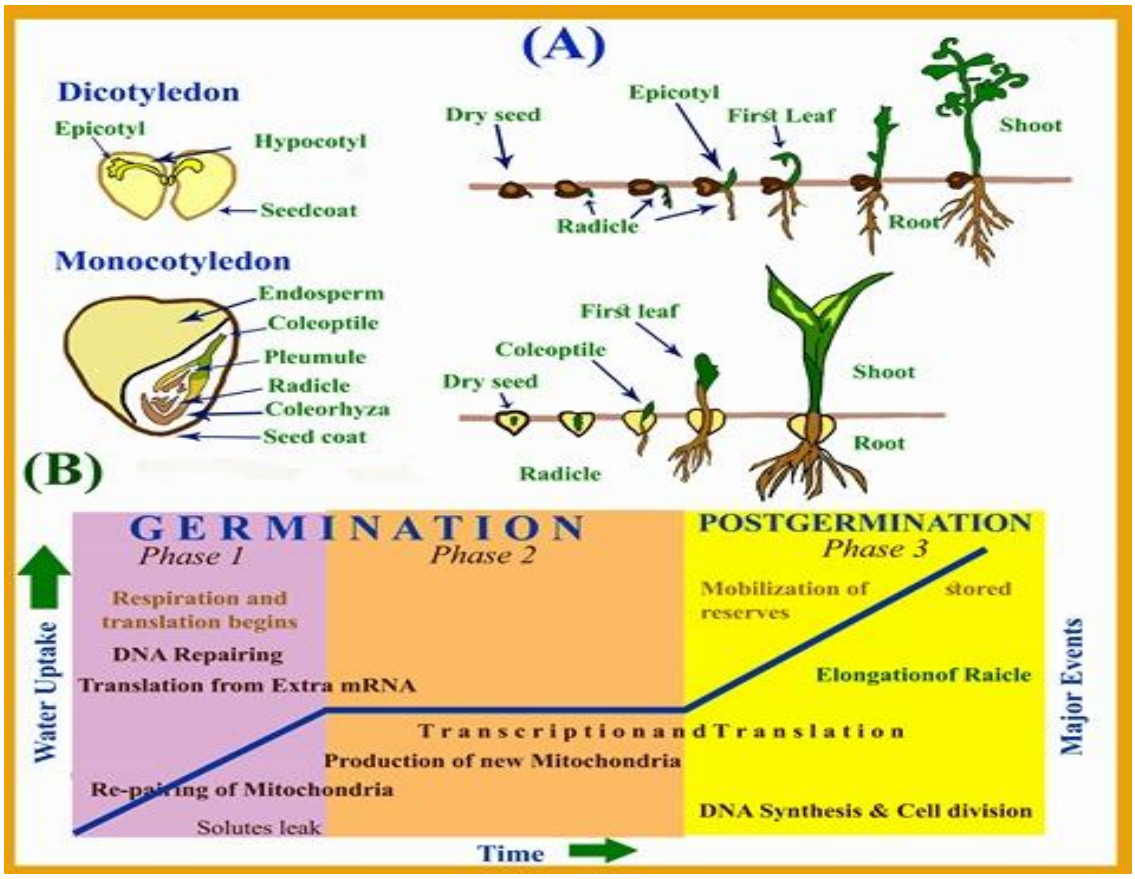

Figure 1. *Following imbibition, seed germination could be divided into three major steps. First of all, rapid uptake of water occurs which results in biosynthesis of mRNA. Second step includes more important activities which involves reactivation of metabolism, mobilization of stored reserves, loosening of cell wall, repair of cell structure and coleoptile enlargement. Again rapid uptake of water occurs during the last step, upon which respiration and TCA recovers, cell multiplication, radical emergence and seedling establishment initiates*

In Arabidopsis, barley and rice more than ten thousand stored mRNA and transcripts have been identified and several studies confirmed that mRNA are stored during seed maturation (Rajjou et al., 2004; Nakabayashi et al., 2005; Kimura and Nambara, 2010; Okamoto et al., 2010; Radchuk et al., 2007). Until now, the confirmed transcriptomes from whole dry seeds have presented the diverse type of transcripts according to their genetic and physiological parts like the embryo and endosperm (Le et al., 2010). Furthermore, the transcriptional theory was genuinely authenticated by Kimura and Nambara (2010). Seed germination depends upon the variation in physio-chemistry of different parts of seeds i.e. embryo, endosperm seed coat and interaction among them (Nonogaki et al., 2000). Embryo is a vital part of the seed, as it contains genetic information required for triggering the seed germination process (Sheoran et al., 2005). There are several enzymes involved in metabolic pathways during seed germination and that stored during seed maturation (www.seed-proteome.com) (Rajjou et al., 2004; Fujino et al., 2008; Gallardo et al., 2001). Okamtao (2010) reported that during

http://www.aloki.hu ● ISSN 1589 1623 (Print) ● ISSN 1785 0037 (Online)
DOI: http://dx.doi.org/10.15666/aeer/1605_56815692
© 2018, ALÖKI Kft., Budapest, Hungary

imbibition transcriptome profile in germinating seed changes and even these changes are tissue specific. During early germination, transcripts are noticed to share similar or common but highly abundant cis-acting elements in their respective gene promotor followed by high expression pattern (Marcus and Feeley, 1964; Dure and Waters, 1965; Comai and Harada, 1990). Degradation of stored mRNA is associated with a change in expression of a gene (Comai and Harada, 1990; Nakabayashi et al., 2005; Howell et al., 2009; Preston and Hileman, 2009). The mechanisms involved in seed germination, numerous broad-spectrum omics studies have been conducted across the globe, involving transcriptomic approaches (Holdsworth et al., 2008; Sghaier-Hammami et al., 2009a, b). Productivity and survival of woody plants is continuously affected by multiple stresses (Pinheiro et al., 2014). Plants growth is negatively affected by surrounding biotic and abiotic stress agents that cause physical and biological dysfunctions and plants differ in their ability to overcome these stresses. Aside from the huge proteomics data available for woody plants, limited information is available on seed germination. Until now, *Fagus sylvatica* is among the limited plants for which attempts has been made to know the proteomic changes associated with seed germination (Pawlowski, 2007), similarly *P. dactylifera* (Sghaier-Hammami et al., 2009a, b), *J. curcas* (Yang et al., 2009) and *P. campanulata* (Lee et al., 2006) are some other examples. Depending upon seed dormancy woody plants have four categories (Gendreau and Corbineau, 2009) that are physical, mechanical, morphological and embryo dormancy. Fukumoto and Kajimura (2001) reported the poor regeneration of Cyclobalnopsis sp is due to insect damage of seeds and deer grazing of regenerating seedlings which are threatening the successful regeneration of Cyclobalnopsis sp. Transcriptome and proteomic interaction of woody plants during the seed germination studies has been ignored till now. *Cyclobalnopsis gilva* a woody plant has low germination rate as compared to other plants (Meiqing et al., 2012). It belongs to *Fagaceae* family and because of its hardness it is used in the furniture industry. (Zaynab et al., 2017). It is native in the southeastern part of China (*Fig. 2*). Among evergreen broad leaves, Cyclobalanopsis is one of an abundantly found woody tree which is a good biological filter that reduces environmental pollution (Deng et al., 2014). Being efficient natural cleaners, trees can help to overcome environmental pollution (Seth et al., 2003). Leaves with hairy, spiny and waxy surface can easily absorb gaseous form of pollutants while particle forms of pollutants can be trapped by twigs, branches and tree stems. Trees reduce carbon oxides, disintegrate waste materials and fix nitrogen in atmosphere. Trees act as pollution sinks and metabolize heavy metals and absorb toxic gases from the surrounding environment (Yang et al., 2017). There are no studies reported transcriptome and proteome changes analysis during seed germination of *C. gilva.* The basic purpose of this study/review is to describe transcript and protein change during the complex mechanisms of seed germination of *C. gilva*.

Transcription and translation activation

Gene expression changes dramatically at proteomic as well as transcriptomics level as seed imbibes water (*Fig. 3*) (Holdsworth, 2008). Weitbrech et al. (2011) reported that these alterations in gene expression are related to germination. It is considered that transcription is not going on in fully ripened seed, but mRNAs which are essential for germination have already been stored (Howell, 2009). Large number of mRNA species are present in fully ripen seed. Over 12000 mRNA have been found in mature seeds of

http://www.aloki.hu ● ISSN 1589 1623 (Print) ● ISSN 1785 0037 (Online)
DOI: http://dx.doi.org/10.15666/aeer/1605_56815692
© 2018, ALÖKI Kft., Budapest, Hungary

Arabidopsis. He et al. (2011) in rice embryo, about 17000 mRNA have been found (Howell, 2009). In rice and Arabidopsis α-amanitin, a transcription inhibitor has found to delay germination but not totally block it (Rajjou, 2004). It looks that transcription inhibitors have greater role to play in seedling establishment than in germination (He et al., 2011). These results suggest that factors assuring the germination speed are synthesized in de novo transcription. High increase in transcription occur in rice embryo after 3 to 12 h of water absorption which results in increased secondary metabolites production that are involved in cell wall, amino acids, carbohydrates metabolism (Howell, 2009). Rice and Arabidopsis germination was diminished in the presence of translation inhibitors which showed that instead of transcription, translation is prerequisite of germination (Rajjou, 2004). New protein synthesis in Arabidopsis starts 8 h after imbibition. That is why it is proposed that stored mRNAs are utilized for this protein synthesis. For metabolites activation and mobilization of reserves translation of stored mRNAs was important in both rice and Arabidopsis seeds (Rajjou, 2012, 2006). In maize seeds in vitro incubation experiments demonstrated that eIF(iso)4E is required for translation of stored mRNAs (Dinkova et al., 2011). Arabidopsis double mutant i4g1/i4g2 knocked out for eIFiso4G1 and eIFiso4G2 (responsible for stored mRNA translation) showed diminished germination rate and long seed viability (Lellis, 2010). Form this experiment it was clear that cereal seeds and Arabidopsis possess similar mode of translation for stored mRNA.

Figure 2. *Presence of C. gilva in the southeastern ecological region of China*

http://www.aloki.hu ● ISSN 1589 1623 (Print) ● ISSN 1785 0037 (Online)
DOI: http://dx.doi.org/10.15666/aeer/1605_56815692
© 2018, ALÖKI Kft., Budapest, Hungary

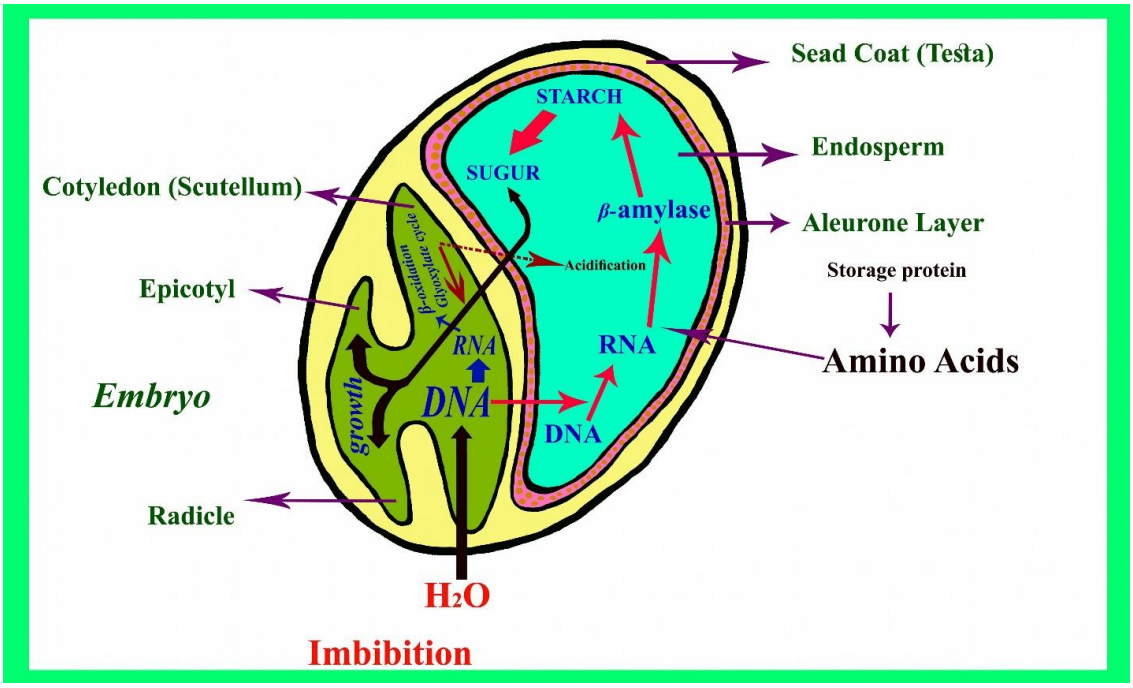

Figure 3. *Molecular processes occurring in embryo and endosperm during C. gilva seed germination*

Role of translation in seed germination

Previous observation inferred that upon imbibition radicle protrude out of seed coat in Arabidopsis seed in the presence a specific, potential inhibitor of DNA-dependent RNA polymerase "α-amanitin", this showed that seed germination is not limited to de novo transcription (Rajjou, 2004). To speed up the germination vigor, de novo synthesis of transcripts encoding proteins and enzymes involved in GAs biosynthesis and involved in germination sensitivity to this hormone is important because germination uniformity and speed is strongly affected under absence of these transcripts. In contrast, under the presence of translation inhibitor "cycloheximide" Arabidopsis germination was totally blocked (Rajjou, 2001). These results highlight the importance of protein synthesis especially from the stored RNA templates in seed for the completion of germination. As seed store RNA and proteins during maturation on source plant, role of these stored elements is clear from these results and for Arabidopsis seed germination potential is planned during seed maturation. For germination, other studies have also identified the core role of translation. During germination of mature seeds high contribution of stored mRNA has been confirmed by transcriptome analysis (Nakabayashi et al., 2005). The study conducted by Nakabayashi et al. (2005) elaborated the importance of protein synthesis during early germination stages, as 2% to 3% genes showed upregulation while evidence was also provided by ribosomal proteins coding genes and translation initiation and elongation factors.

Recent analysis of sugarbeat (*Beta vulgaris* L.) seed proteome identified 758 proteins reconstructing and inferring their detailed metabolic status (Catusse et al., 2008). Seeds are prepared for germination mainly during maturation on plan as indicated by sugar beet seeds, which are prepared to mobilize their reserves including starch, proteins, phytate and triglycerides during germination as occur in Arabidopsis and they also

http://www.aloki.hu ● ISSN 1589 1623 (Print) ● ISSN 1785 0037 (Online)
DOI: http://dx.doi.org/10.15666/aeer/1605_56815692
© 2018, ALÖKI Kft., Budapest, Hungary

identified proteins not mentioned in seeds. Promisingly, data highlight that sugar beet seeds have opportunity to initiate translation either by using cap-independent mechanism or conventional way of cap-dependent mechanism. It is clear that during some events of cell life like during stress conditions or viral infection and mitosis, cell compromises its standard way of translation i.e. 5-end cap-recognition of mRNA while at the same time some mRNA use cap-independent mechanism of initiation as congregation initiation site for initiation factor (Baird et al., 2006). A model is suggested by these findings. In this model germinating seed has two pools of mRNA comprising of de novo synthesized mRNA and stored mRNA and during germination these pools allow their recruitment by either of two initiation pathways (Catusse et al., 2008). In maize seed, during embryonic axis elongation, stored mRNAs were likely to use cap-independent mechanism for translation initiation (Dinkova et al., 2005).

Comparison of the seed transcriptome and proteome

Comparison of several proteome and transcriptome studies carried out in the same environmental conditions and sampling points, showed little correlation between functional gene classes at proteomics and transcriptomics level (Gallardo et al., 2002; Ogawa et al., 2003; Chibani et al., 2006; Carrera et al., 2008). Germination vigor can possibly change the abundance of RNA present in seed for germination completion, some functions associated with establishment of seedling (translation after germination completion), for observation of changes in protein profiles, proteomic approaches are not sensitive enough. Up till now it is also vague that changes in seed dormancy status are controlled by translational or post-translational regulations (Holdsworth et al., 2008). Gene expression study is critically important to understand the molecular network involved in germination regulation as the list of genes regulated in imbibed seeds obtained through either proteomic (Chibani et al., 2006) or transcriptomic (Cadman et al., 2006) approaches showed similarities. Integration of information from proteomic and transcriptomic studies will be the key objective for further post-genomic research. Favorably, some proteomic and transcriptomic based studies under similar time essays and growth conditions are helping to integrate the information from different studies (Cadman et al., 2006; Chibani et al., 2006; Carrera et al., 2008).

Due to less germination rate of woody plants proteomic studies of seed germination are getting more importance (Zaynab et al., 2017; Canovas et al., 2004). It is difficult to examine woody plants due to laborious sample preparation and high concentrations of resins, tannins and phenolic compounds (Sebastiana et al., 2013). In a study, *P. dactylifera* L. (Date palm) proteomic studies for seed development and germination were done by Sghaier-Hammami et al. (2009) and they reported that carbohydrates, the major storage reserves are stored in early seed development which are used during initial stages of seed germination.

Comprehensive information regarding access amount of some functional protein types related to seed ripening, dormancy and germination have been provided by the proteomic analysis of germinating seeds. Many other studies have also shown the proteome changes related to dormancy and germination status (Gallardo et al., 2001, 2002; Job et al., 2005; Chibani et al., 2006; Oracz et al., 2007), regarding this information seed biology is a prominent host of plant proteomics. Proteomics is a strategy for global analysis that provides information on a multitude of processes in complex events, such as germination (Gallardo et al., 2001). Despite the increasing

http://www.aloki.hu ● ISSN 1589 1623 (Print) ● ISSN 1785 0037 (Online)
DOI: http://dx.doi.org/10.15666/aeer/1605_56815692
© 2018, ALÖKI Kft., Budapest, Hungary

interest in plant proteomics, studies on woody plant seed germination are still very limited. To date, the only attempts to understand proteome changes during the germination of woody plants were carried out in *Prunus campanulata* (Lee et al., 2006), *Fagus sylvatica* (Pawlowski, 2007), *Acer platanoides* (Pawlowski, 2009), *Jatropha curcas* (Yang et al., 2009), *Phoenix dactylifera* (Sghaier-Hammami et al., 2010, 2009b) and *Araucaria angustifolia* (Balbuena et al., 2011). Only a limited number of reports about proteomics in woody plant seed germination have been published. Lu et al. (2016) conducted a study to determine the mechanisms involved in seed dormancy breaking of M. sieboldii to better understand the anatomical and translation bases of seed germination in this species and they reported that a small subunit of legumin precursor, ADP-glucose pyrophosphorylase and aspartic proteinase dominate the seed proteome of M. sieboldii. Such studies not only provide information regarding the protein abundance in dry stored seeds and imbibed seeds but also elaborate the post-translational modifications for proteome expression. Gallardo et al. (2001) reported the proteome changes related to imbibition germination while Chilbani et al. (2006) studied the imbibed ripened seeds. Rajjou et al. (2004) noticed that germination in alpha-amanitin treated transparent testa (tt) of mutant seeds was not blocked concluded that transcription was not important for germination. On the other hand, cycloheximide was a potential inhibitor of radicle emergence. If transcription was important for expression of genes involved in synchronization and speed of germination was answered by the α-amanitin treatment. Seeds treated with α-amanitin showed great germination potential, but germination rate was slow and less sensitive to GA application and the level of several key proteins for germination (malate synthase) (Eastmond et al., 2000) were very low in treated seeds. Chibani et al. (2006) reported great difference in protein profiles of after-ripened and imbibed seeds of accession CVI. In dormant seeds lack of germination was not associated with less de novo protein production because 35S methionine incorporation quantification showed the same incorporation level in after-ripened and dormant seeds (Carrera et al., 2008). Exogenous ABA application greatly lowered the germination potential in after-ripened imbibed seeds, but it did not alter dormancy at proteomic level (Chibani et al., 2006). 35S methionine incorporation in ABA treated after-ripened imbibed seeds were greater that non-treated and dormant seeds, this indicated that ABA treatment does not hinder RNA translation protein abundance was also high in treated seeds. Both proteomic and transcriptomic studies showed that instead of seed dormancy ABA treatment use another way of inhibiting germination. This is not surprising because physiologically ABA does not reduce germination potential but only delay it (Muller et al., 2006). It is very likely that ABA application to un-germinated seeds just like drought and salinity causes increased ABA production, these responses have already been observed in germinating seedlings (Lopez-Molina et al., 2002).

Post-translational control of seed germination

A growing number of evidence indicates that large changes in redox state of protein occur as seed germinates. In dry cereal seeds proteins are present in oxidized (S-S) form in embryo and starchy endosperm, upon imbibition these are converted into sulfhydryl (-SH) or reduced form (Buchanan and Balmer (2005)). Thioredoxin (Trx), a regulatory protein seems to play core role in redox conversion. Trx cause reduction enzymatically in the presence of NADPH and facilitates reserves mobilization during germination in

http://www.aloki.hu ● ISSN 1589 1623 (Print) ● ISSN 1785 0037 (Online)
DOI: http://dx.doi.org/10.15666/aeer/1605_56815692
© 2018, ALÖKI Kft., Budapest, Hungary

three ways i.e. enhancing protein susceptibility and sensitivity to proteolysis by reducing them, enhancing breakdown of stored proteins and starch as it inactivates disulfide proteins inhibiting specific proteases and amylases and it activates enzymes functioning in germination (*Fig. 3;* Buchanam and Balmer, 2005). This issue has recently been investigated in barrel clover (*Medicago truncatula*) (Alkhalfoui, 2007). Role of Trx in monocotyledons and dicotyledons seed germination have been proved. It can be summarized that in dry and fully mature seeds oxidized proteome keep seed metabolically dormant, which is activated. It can be summarized that oxidized proteome in metabolically dormant seed is by redox reaction in protein bisulfide bridges in the presence of specific Trx during seed germination. Given the large number of proteins affected (more than 100) Alkhalfioui (2007), post-translational mechanism offers an efficient and simple way of controlling complex pathways critical in seed germination. It follows, that investigation of targets like post-translational modifications becomes an emerging question. As post-translational changes may become key regulators of cell activity upon imbibition, so this question is importance increasingly. Carbonylation of proteins by reactive oxygen species may be another oxidative change. In several model systems carbonylated proteins accumulation is referred to aging, but it is not for Arabidopsis where germination rate is high, and seedlings are vigorous. Results indicates that changes in protein carbonylation patterns may occur to nullify the ROS produced in germinating seeds by recovery of metabolic processes. Job et al. (2005) conducted a study in which it is suggested that carbonylation of proteins stored in seed is to facilitate the protein mobilization at time of seed germination. Jatropha and other woody plants store the metabolic reserves as starch, proteins and lipids in embryo and endosperm (Yang et al., 2009). Triacylglycerol (TAG) the major form of lipids is the storage reserve of oilseed plants. TAG is broken down by lipases to release fatty acids which are further catabolized in glyoxilate cycle and β-oxidation. Seed germination and development mechanism of woody plant *A. angustifolia* was studied by Balbuena et al. (2011). Their study showed the differential expression of proteins in germinated and mature embryos which suggests the activation of robust metabolic pathways, translation initiation and stress regulation, overall indicates active degradation metabolism.

Conclusion and perspectives

Like any other field of plant science seed biology is of importance and attracting attention of plant biologists. Previous studies have suggested complicated signalling network and gene expression regulation are involved in seed germination. Plants may share same molecular mechanisms as transcription and translational activation, phytohormone behavior, radicle protrusion etc. however different plant species possess distinct mechanisms, especially for metabolism activation and reserves mobilization. Furthermore, cross-talk among environmental factor signalling pathways and phytohormones during germination is spurious up till now. With the advent of omics era, molecular pathways underlying the germination are becoming more elaborated. For example, during germination, role of functional proteins and specific signalling components in rice and Arabidopsis have been identified by proteomic and phosphoproteomic studies. However, still much information is required to understand the germination process. Nevertheless, in future integration of newly emerging techniques including ChIP-sequencing, proteomic and transcriptomic techniques and imaging will contribute to understand the process how different signals conciliate seed

http://www.aloki.hu ● ISSN 1589 1623 (Print) ● ISSN 1785 0037 (Online)
DOI: http://dx.doi.org/10.15666/aeer/1605_56815692
© 2018, ALÖKI Kft., Budapest, Hungary

germination. To better understand the underlying mechanisms of desiccation tolerance and intolerance, the physiological responses described require research at the metabolomic and transcriptomic levels in detail.

Acknowledgements. This work was supported by the Industry-University Cooperation Program of Science and Technology Commission Foundation of Fujian Province (Grant No. 2016N5003).

Conflict of interests: The authors declare no conflict of interest.

REFERENCES

[1] Alkhalfioui, F., Renard, M., Vensel, W. H., Wong, J., Tanaka, C. K., Hurkman, W. J., Montrichard, F. (2007): Thioredoxin-linked proteins are reduced during germination of Medicago truncatula seeds. – Plant Physiology 144(3): 1559-1579. http://doi.org/10.1104/pp.107.098103.

[2] Baird, S. D., Turcotte, M., Korneluk, R. G., Holcik, M. (2006): Searching for IRES. – RNA 12(10): 1755-1785.

[3] Buchanan, B. B., Balmer, Y. (2005): Redox regulation: a broadening horizon. – Annu Rev Plant Biol. 56: 187-220.

[4] Cadman, C. S., Toorop, P. E., Hilhorst, H. W., Finch-Savage, W. E. (2006): Gene expression profiles of Arabidopsis Cvi seeds during dormancy cycling indicate a common underlying dormancy control mechanism. – Plant J. 46(5): 805-22.

[5] Carrera, E., Holman, T., Medhurst, A., Dietrich, D., Footitt, S., Theodoulou, F. L., Holdsworth, M. J. (2008): Seed after-ripening is a discrete developmental pathway associated with specific gene networks in Arabidopsis. – The Plant Journal 53(2): 214-224.

[6] Catusse, J., Job, C., Job, D. (2008): Transcriptome- and proteome-wide analyses of seed germination. – C R Biol. 331(10): 815-822.

[7] Chibani, K., Ali-Rachedi, S., Job, C., Job, D., Jullien, M., Grappin, P. (2006): Proteomic Analysis of Seed Dormancy in Arabidopsis. – Plant Physiology 142(4): 1493-1510. http://doi.org/10.1104/pp.106.087452.

[8] Comai, L., Harada, J. J. (1990): Transcriptional activities in dry seed nuclei indicate the timing of the transition from embryogeny to germination. – Proc Natl Acad Sci USA 87: 2671-2674.

[9] Corbineau, F., Xia, Q., Bailly, C., El-Maarouf-Bouteau, H. (2014): Ethylene, a key factor in the regulation of seed dormancy. – Front. Plant Sci 5: 1-13.

[10] Deng, M., Hipp, A., Song, Y. G., Li, Q. S., Coombes, A., Cotto, A. (2014): Leaf epidermal features of Quercus subgenus Cyclobalanopsis (Fagaceae) and their systematic significance. – Bot J Linean Soc. 176(2): 224-259.

[11] Dinkova, T. D., Márquez-Velázquez, N. A., Aguilar, R., Lázaro-Mixteco, P. E. (2011): Tight translational control by the initiation factors eIF4E and eIF(iso)4E is required for maize seed germination. – Seed Sci. Res. 21(2): 85-93.

[12] Dure, L., Waters, L. (1965): Long-lived messenger RNA: evidence from cotton seed germination. – Science 147: 410-412.

[13] Eastmond, P. J., Germain, V., Lange, P. R., Bryce, J. H., Smith, S. M., Graham, I. A. (2000): Postgerminative growth and lipid catabolism in oilseeds lacking the glyoxylate cycle. – Proc. Natl. Acad. Sci. U. S. A. 97: 5669-5674.

[14] Fujino, K., Sekiguchi, H., Matsuda, Y., Sugimoto, K., Ono, K., Yano, M. (2008): Molecular identification of a major quantitative trait locus, qLTG3-1: controlling low-temperature germinability in rice. – Proc Natl Acad Sci USA 105: 12623-12628.

http://www.aloki.hu ● ISSN 1589 1623 (Print) ● ISSN 1785 0037 (Online)
DOI: http://dx.doi.org/10.15666/aeer/1605_56815692
© 2018, ALÖKI Kft., Budapest, Hungary

[15] Fukumoto, H., Kajimura, H. (2001): Guild structures of seed insects in relation to acorn development in two oak species. – Ecological Research 16(1): 145-155.
[16] Gallardo, K., Job, C., Groot, S. P., Puype, M., Demol, H., Vandekerckhove, J., Job, D. (2001): Proteomic analysis of arabidopsis seed germination and priming. – Plant Physiol. 126(2): 835-848.
[17] Gallardo, K., Job, C., Groot, S. P. C., Puype, M., Demol, H., Vandekerckhove, J., Job, D. (2002): Proteomics of Arabidopsis Seed Germination. A Comparative Study of Wild-Type and Gibberellin-Deficient Seeds. – Plant Physiol. 129(2): 823-837.
[18] Gendreau, E., Corbineau, F. (2009): Physiological aspects of seed dormancy in woody ornamental plants. – Propagation of Ornamental Plants. 9(3): 151-158.
[19] Hauvermale, A. L., Ariizumi, T., Steber, C. M. (2012): Gibberellin signaling: a theme and variations on DELLA repression. – Plant Physiol 160: 83-92.
[20] He, D., Yang, P. (2013): Proteomics of rice seed germination. – Front Plant Sci 4: 1-9.
[21] He, D., Han, C., Yao, J., Shen, S., Yang, P. (2011): Constructing the metabolic and regulatory pathways in germinating rice seeds through proteomic approach. – Proteomics 11: 2693-2713.
[22] Holdsworth, M. J., Bentsink, L., Soppe, W. J. (2008): Molecular networks regulating Arabidopsis seed maturation, after-ripening, dormancy, and germination. – New Phytol 179: 33-54.
[23] Howell, K. A., Cheng, K., Murcha, M., Jenkin, L. E., Millar, A. H. Whelan, J. (2007): Oxygen initiation of respiration and mitochondrial biogenesis in rice. – J Biol Chem 282: 15619-15631.
[24] Howell, K. A., Narsai, R., Carroll, A., Ivanova, A., Lohse, M., Usadel, B., Millar, A. H., Whelan, J. (2009): Mapping metabolic and transcript temporal switches during germination in rice highlights specific transcription factors and the role of RNA instability in the germination process. – Plant Physiol 149: 961-980.
[25] Job, C., Rajjou, L., Lovigny, Y., Belghazi, M., Job, D. (2005): Patterns of protein oxidation in Arabidopsis seeds and during germination. Plant Physiol. 138: 790-802.
[26] Kimura, M., Nambara, E. (2010): Stored and neosynthesized mRNA in Arabidopsis seeds: effects of cycloheximide and controlled deterioration treatment on the resumption of transcription during imbibition. – Plant Mol Biol 73: 119-129.
[27] Le, B. H., Cheng, C., Bui, A. Q., Wagmaister, J. A., Henry, K. F., Pelletier, J., Kwong, L., Belmonte, M., Kirkbride, R., Horvath, S. (2010): Global analysis of gene activity during Arabidopsis seed development and identification of seed-specific transcription factors. –Proc Natl Acad Sci USA 107: 8063-8070.
[28] Lee, C. S., Chien, C. T., Lin, C. H., Chiu, Y. Y., Yang, Y. S. (2006): Protein changes between dormant and dormancy-broken seeds of Prunus campanulata – Maxim. Proteomics. 6(14): 4147-4154.
[29] Lellis, A. D., Allen, M. L., Aertker, A. W., Tran, J. K., Hillis, D. M., Harbin, C. R., Browning, K. S. (2010): Deletion of the eIFiso4G subunit of the Arabidopsis eIFiso4F translation initiation complex impairs health and viability. – Plant Molecular Biology 74(3): 249-263.
[30] Lopez-Molina, L., Mongrand, S., McLachlin, D. T., Chait, B. T., Chua, N. H. (2002): ABI5 acts downstream of ABI3 to execute an ABA-dependent growth arrest during germination. – Plant J 2: 317-328.
[31] Macovei, A., Balestrazzi, A., Confalonieri, M., Faé, M., Carbonera, D. (2011): New insights on the barrel medic MtOGG1 and MtFPG functions in relation to oxidative stress response in planta and during seed imbibition. – Plant Physiol Biochem 49: 1040-1050.
[32] Marcus, A., Feeley, J. (1964): Activation of protein synthesis in the imbibition phase of seed germination. – Proc Nat AcadSci USA 51: 1075-1079.
[33] Meiqing, J., Zhihui, L., Mohua, Y., Lijun, W., Qian, S. (2012): The study on seed quality and germination characteristics of cyclobalanopsis gilva (Bl.) Oerst. – Chin Agric Sci Bull. 34: 008-009.

http://www.aloki.hu ● ISSN 1589 1623 (Print) ● ISSN 1785 0037 (Online)
DOI: http://dx.doi.org/10.15666/aeer/1605_56815692
© 2018, ALÖKI Kft., Budapest, Hungary

[34] Müller, K., Tintelnot, S., Leubner-Metzger, G. (2006): Endosperm-limited Brassicaceae seed germination: abscisic acid inhibits embryo-induced endosperm weakening of Lepidium sativum (cress) and endosperm rupture of cress and Arabidopsis thaliana. – Plant Cell Physiol. 47(7): 864-77.
[35] Nakabayashi, K., Okamoto, M., Koshiba, T., Kamiya, Y., Nambara, E. (2005): Genome-wide profiling of stored mRNA in Arabidopsis thaliana seed germination: epigenetic and genetic regulation of transcription in seed. – Plant J 41: 697-709.
[36] Nonogaki, H., Gee, O. H., Bradford, K. J. (2000): A germination-specific endo-β-mannanase gene is expressed in the micropylar endosperm cap of tomato seeds. – Plant Physiol123: 1235-1246.
[37] Ogawa, M., Hanada, A., Yamauchi, Y., Kuwahara, A., Kamiya, Y., Yamaguchi, S. (2003): Gibberellin Biosynthesis and Response during Arabidopsis Seed Germination. – The Plant Cell 15(7): 1591-1604.
[38] Okamoto, M., Tatematsu, K., Matsui, A., Morosawa, T., Ishida, J., Tanaka, M., Endo, T. A., Mochizuki, Y., Toyoda, T., Kamiya, Y. (2010): Genome-wide analysis of endogenous abscisic acid-mediated transcription in dry and imbibed seeds of Arabidopsis using tiling arrays. – Plant J 62: 39-51.
[39] Oracz, K., El-Maarouf Bouteau, H., Farrant, J. M., Cooper, K., Belghazi, M., Job, C., Job, D., Corbineau, F., Bailly, C. (2007): ROS production and protein oxidation as a novel mechanism for seed dormancy alleviation. – Plant J. 50(3): 452-465.
[40] Pawłowski, T. A. (2007): Proteomics of European beech (Fagus sylvatica L.) seed dormancy breaking: influence of abscisic and gibberellic acids. – Proteomics 7(13): 2246-57.
[41] Pawłowski, T. A. (2009): Proteome analysis of Norway maple (Acer platanoides L.) seeds dormancy breaking and germination: influence of abscisic and gibberellic acids. – BMC Plant Biol. 9: 48.
[42] Pinheiro, H. A., DaMatta, F. M., Chaves, A. R. M., Loureiro, M. E., Ducatti, C. (2005): Drought Tolerance is Associated with Rooting Depth and Stomatal Control of Water Use in Clones of Coffea canephora. – Annals of Botany 96(1): 101-108.
[43] Preston, J. C., Hileman, L. C. (2009): Developmental genetics of floral symmetry evolution. – Trends Plant Sci 14: 147-154.
[44] Radchuk, R., Radchuk, V., Götz, K. P., Weichert, H., Richter, A., Emery, R. J., Weschke, W., Weber, H. (2007): Ectopic expression of phosphoenolpyruvate carboxylase in Vicianarbonensisseeds: effects of improved nutrient status on seed maturation and transcriptional regulatory networks. – Plant J 51: 819-839.
[45] Rajjou, L., Gallardo, K., Debeaujon, I., Vandekerckhove, J., Job, C., Job, D. (2004): The effect of α-amanitin on the Arabidopsis seed proteome highlights the distinct roles of stored and neosynthesized mRNAs during germination. – Plant Physiol. 4: 1598-1613.
[46] Rajjou, L. Duval, M. Gallardo, K. Catusse, J., Bally, J., Job, C., Job, D. (2012): Seed Germination and Vigor. – Annu Rev Plant Biol. 63: 507-533.
[47] Sebastiana, M., Figueiredo, A., Monteiro, F., Martins, J., Franco, C., Coelho, A. V., Vaz, F., Simões, T., Penque, D., Pais, M. S., Ferreira, S. (2013): A possible approach for gel-based proteomic studies in recalcitrant woody plants. – Springerplus. 2(1): 210.
[48] Seth, A., Rojas, M., Liebmann, B., Qian, J. H. (2003): Daily rainfall analysis for South America from a regional climate model and station observations. – Geophys Res Lett. 31(7): L07213.
[49] Sghaier-Hammami, B., Valledor, L., Drira, N., Jorrin-Novo, J. V. (2009a): Proteomic analysis of the development and germination of date palm (Phoenix dactylifera L.) zygotic embryos. – Proteomics 9: 2543-2554.
[50] Sghaier-Hammami, B., Drira, N., Jorrín-Novo, J. V. (2009b): Comparative 2-DE proteomic analysis of date palm (Phoenix dactylifera L.) somatic and zygotic embryos. – J Prot 73: 161-177.

http://www.aloki.hu ● ISSN 1589 1623 (Print) ● ISSN 1785 0037 (Online)
DOI: http://dx.doi.org/10.15666/aeer/1605_56815692
© 2018, ALÖKI Kft., Budapest, Hungary

[51] Sheoran, I. S., Olson, D. J., Ross, A. R., Sawhney, V. K. (2005): Proteome analysis of embryo and endosperm from germinating tomato seeds. – Proteomics 5: 3752-3764.
[52] Weitbrecht, K., Müller, K., Leubner-Metzger, G. (2011): First off the mark: early seed germination. – J Exp Bot 62: 3289-3309.
[53] Yang, J., Ji, X., Deane, D. C., Wu, L., Chen, S. (2017): Spatiotemporal Distribution and Driving Factors of Forest Biomass Carbon Storage in China: 1977-2013. – Forest 8: 263.
[54] Yang, M. F., Liu, Y. J., Liu, Y., Chen, H., Chen, F., Shen, S. H. (2009): Proteomic analysis of oil mobilization in seed germination and postgermination development of Jatropha curcas. – J Proteome Res. 8(3): 1441-1451.
[55] Zaynab, M., Kanwal, S., Furqan, M., Islam, W., Noman, A., Ali, G. M., Rehman, N., Zafar, S., Sughra, K. Jahanzeb, M. (2017): Proteomic approach to address low seed germination in Cyclobalnopsis gilva. – Biotechnol Lett 39: 1441.

http://www.aloki.hu ● ISSN 1589 1623 (Print) ● ISSN 1785 0037 (Online)
DOI: http://dx.doi.org/10.15666/aeer/1605_56815692
© 2018, ALÖKI Kft., Budapest, Hungary

ANALYSIS ON LANDSCAPE PATTERN OF LAND USE AND ECO-ENVIRONMENT CHARACTERISTICS OF THREE LAKE BASINS IN YUNNAN PROVINCE, CHINA

FAN, K.[1,2] – PEI, W. J.[1,2] – ZHANG, J. S.[1,2] – YU, J. X.[1,2] – ZENG, W. J.[1,2*]

[1]*College of Water Resources and Hydraulic Engineering, Yunnan Agricultural University Kunming, China*

[2]*Engineering Research Center of Science and Technology of Land and Resources, Yunnan Agricultural University, Kunming, China*
(phone: +86-182-1459-6922)

**Corresponding author*
e-mail: zengweijunde@163.com; phone: +86-136-8871-2698

(Received 13th Jun 2018; accepted 14th Aug 2018)

Abstract. Lake Basin pollution has become an important environmental problem, exploring its landscape pattern of land use and eco-environment characteristics is of great significance for environmental pollution control. Through the analysis of the landscape pattern indices of diversity, evenness, dominance and fragmentation of the three lake basins in Yunnan province of China, and based on the evaluation results of the ecological environment of the lake basins, to explore the relationship and characteristics between the landscape pattern of land use and its ecological environment. Research indicates: (1) According to the analysis of landscape pattern of land use in the basin, the level of landscape diversity and evenness in the Fuxian Lake Basin is the highest, followed by the Erhai Basin. However, the lowest is in the Dianchi Basin; the degree of landscape fragmentation in the Dianchi Basin is the highest, followed by the Fuxian Lake Basin, and the lowest in the Erhai Basin. (2) According to the results of the ecological environmental quality assessment, Dianchi Basin is the worst, while the Erhai Basin and Fuxian Lake Basin are better, and the Fuxian Lake Basin is the best. (3) The landscape pattern of land use in the basin is closely related to the quality of the ecological environment. Basins with good ecological environment quality have a relatively high degree of diversity and evenness, and relatively low fragmentation; in the basins with poor ecological environment, the degree of evenness and diversity of landscape are relatively low, and the degree of landscape fragmentation is relatively high.
Keywords: *plateau lake basin, remote sensing interpretation, land use; landscape pattern index, ecological environment evaluation*

Introduction

Along with the rapid development of social economy and urbanization process accelerated, environmental quality is declining, population is increasing and the environmental problems are increasingly prominent, the land use / cover change and ecological environment research have become a hot topic in the world. The research content mainly includes the land use change rule (Rao, 2015; Yang, 2016; Sharma, 2017; Kumar, 2017), mechanism (Zhang, 2012; Fu, 2012; Martyn et al., 2017), driving force (Li, 2014; Cattarino, 2014; Chai, 2016; Yuan, 2016; Wenban-Smith, 2017), landscape spatial pattern and so on (Xu, 2012; Yu, 2016; Liu, 2015; Lamine, 2018), the research on landscape pattern of land use mainly in provincial (Li, 2005; Zhang, 2009), municipal (country) regions (Ge, 2016; Wang, 2015; Hassan, 2017), a typical river basin (Feng, 2010; Chen, 2009; Mehrian, 2016) as the scale, abundant research results have been achieved. In the above studies, the longitudinal analysis of different phases in the same region is the main research, and the landscape pattern of land use and ecological

http://www.aloki.hu ● ISSN 1589 1623 (Print) ● ISSN 1785 0037 (Online)
DOI: http://dx.doi.org/10.15666/aeer/1605_56935704
© 2018, ALÖKI Kft., Budapest, Hungary

environment were often studied separately, and the research on the relationship and characteristics between landscape pattern of land use and ecological environment in different lake basins was relatively insufficient.

According to "The Environmental Status Bulletin of Yunnan Province in 2015" (Yunnan Environmental Protection Department, 2016), the water quality of Lugu Lake Basin and Fuxian Lake Basin in the nine great plateau lake basins of Yunnan Province in China was excellent, the water quality in the Erhai Basin was good, and the Dianchi Basin was heavily polluted, and land use is closely related to lake pollution. This study selected the Dianchi Basin, Erhai Basin and Fuxian Lake Basin as the research object, the relationship and characteristics between landscape pattern of land use and ecological environment in the three major lake basins were analyzed, which is of great significance for optimizing landscape structure of land use and controlling lake water environment pollution.

Materials and methods

General background of the study area

In order to study the relevance and comparability, this article referred to the two major factors of socio-economic development level and lake pollution degree. The Dianchi Basin (capital of the provincial capital, heavy pollution), the Erhai Basin (prefecture-level city, good water quality) and the Fuxian Lake Basin (County Town, Type I Water Quality) are selected as the research area to explore the characteristics of land use landscape and ecological environment quality in the three major lake basins (*Fig. 1*).

The total area of the Dianchi Basin is 2891.07 km^2. The entire basin's terrain gradually decreased from north to south. With the rapid development of social economy, the rapid expansion of urban built-up areas in Kunming, the landscape pattern of land use in the lake basin has undergone major changes, and the landscape has presented a trend of fragmentation and the development of complex boundaries (Zhang, 2013).

The total area of the Erhai Basin is about 2609.07 km^2, which is second only to Dianchi Basin in the plateau lakes of Yunnan Province. The area along the lake is flat and the periphery is dominated by mountains. The type of land use in the basin is dominated by woodland, grassland and paddy fields. Economic and social development has had a certain impact on the land use structure of the Erhai Basin (Li, 2011).

The total area of the Fuxian Lake Basin is 690.03 km^2. The north of the lake is a basin, with fault cliffs or fault block mountains on the east and west sides, and alluvial plains on the south (Kang, 2011). Since the 1980s, unreasonable development of human activities have caused some damage to the land use structure of the lake basin. However, in recent years, with the emphasis on the ecological environment of the lake basin, the land use structure has gradually been optimized and the lake has always been Class I water quality (Wu, 2002).

Data sources

Part of the research data is from Landsat OLI remote sensing image data from the three major lake basins. The shooting time was March 2015, the line number of Dianchi Basin, Fuxian Lake Basin and Erhai Basin are 43, 43 and 42, respectively, and the band number is 129, 129 and 131, respectively. According to the classification standard of land use status (GB/T 21010-2007), combined with land use status, land use types are

http://www.aloki.hu ● ISSN 1589 1623 (Print) ● ISSN 1785 0037 (Online)
DOI: http://dx.doi.org/10.15666/aeer/1605_56935704
© 2018, ALÖKI Kft., Budapest, Hungary

divided into the dry land, paddy fields, garden lands, forest land, grass land, construction land, water area and unused lands eight types. Used spatial information technology (GIS/RS) and ERDAS software, based on the correction and enhancement processing of remote sensing images in the three lake basins, training samples were selected, supervised classification was conducted, and data such as land use type and area were further extracted. The other part comes from environmental protection agencies and their websites in Yunnan Province, Kunming City, and Dali Prefecture, as well as relevant data released in the "Yunnan Province Environmental Status Bulletin", "Kunming City Environmental Status Bulletin" and "Dali Prefecture Environmental Status Bulletin".

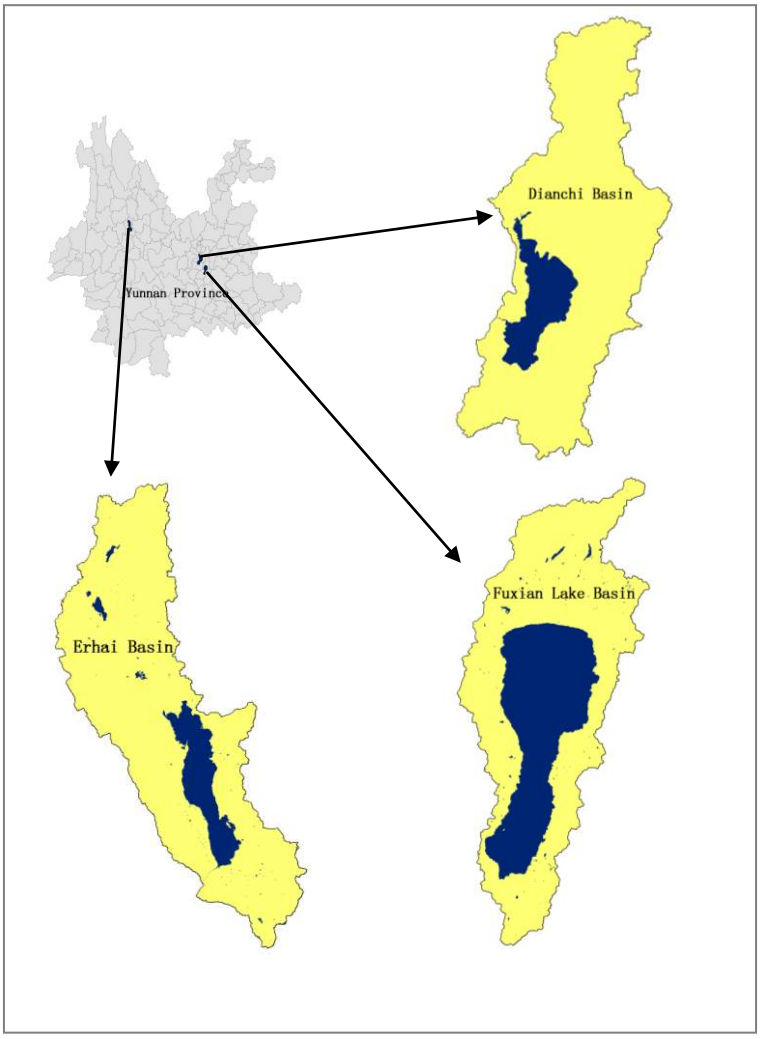

Figure 1. *Study areas*

Research methods

Analysis method of characteristics of land use landscape pattern

Based on the analysis methods of landscape ecology on quantitative structure, the land use diversity, evenness, dominance and fragmentation index of the three lake

http://www.aloki.hu ● ISSN 1589 1623 (Print) ● ISSN 1785 0037 (Online)
DOI: http://dx.doi.org/10.15666/aeer/1605_56935704
© 2018, ALÖKI Kft., Budapest, Hungary

basins were obtained, and the characteristics of land use landscape patterns were analyzed (Liu et al., 2008). The formula is as follows:

- Diversity index (*Eq. 1*)

$$SHDI = -\sum_{i=1}^{m} \left(p_i \ln p_i \right) \quad \text{(Eq.1)}$$

In the formula,, "*SHDI*" is the diversity index, "P_i" is the ratio of landscape plaque type "*i*", and "*m*" is the landscape type.

- Evenness index (*Eq. 2*)

$$SHEI = \frac{H}{H_{\max}} = \frac{-\sum_{k=1}^{n} P_k \ln\left(P_k\right)}{\ln\left(m\right)} \quad \text{(Eq.2)}$$

In the formula,, "*SHEI*" is the evenness index, "*H*" is the measured diversity index, "H_{max}" is the maximum diversity index, and "*m*" is the landscape type.

- Dominance index (*Eq. 3*)

$$LDI = H_{\max} + \sum_{i=1}^{m} P_i \ln\left(P_i\right) \quad \text{(Eq.3)}$$

In the formula,, "*LDI*" is the dominance index, "H_{max}" is the maximum diversity index, "P_i" is the ratio of landscape plaque type "*i*", and "*m*" is the landscape type.

- Fragmentation index (*Eq. 4*)

$$LFI = \sum N_i / \sum A_i \quad \text{(Eq.4)}$$

In the formula,, "*LEI*" is the fragmentation index, "N_i" is the number of plaques in class "*i*", and "A_i" is the total area of class "*i*".

The method of ecological environment evaluation

- Build an evaluation system

Referring to the "Technical Specifications for Eco-environmental Status Assessment" (HJ 192-2015) (Ministry of Ecological and Environment of the People's Republic of China, 2016), published in 2015 by the Ministry of environmental protection, and combined the geographical features of the three lake basins, the evaluation indexes were selected according to the principles of objectivity, comprehensiveness, evaluability, independence and hierarchy. Then the Analytic Hierarchy Process (AHP) was used to determine the degree of association between the adjacent level evaluation indexes in the structural model. For indexes that belong to the same level, the above-mentioned index elements are the criteria. We constructed the pairwise judgment matrix by "1-9 scale method", compared the importance of the evaluation indicators, and calculated the relative weight values until it passed the

http://www.aloki.hu ● ISSN 1589 1623 (Print) ● ISSN 1785 0037 (Online)
DOI: http://dx.doi.org/10.15666/aeer/1605_56935704
© 2018, ALÖKI Kft., Budapest, Hungary

consistency check (CR < 0.1000). Because the selection of each index is extensive and the directions of the indicators are inconsistent, in order to eliminate the influence of the unit of measure, dimension and magnitude differences on the evaluation results, and make the indexes comparable and in the same direction, the linear data is used for non-dimensional treatment of the initial data (*Eqs. 5* and *6*). The evaluation indicator system for the ecological environment of the three lake basins is shown in *Table 1,* and the classification criteria for the evaluation results are shown in *Table 2*.

Index dimensionless processing formula:

$$Y = \frac{X}{X_{\max}} \text{ (Positive indicators)} \quad \text{(Eq.5)}$$

$$Y = \frac{X_{\min}}{X} \text{ (Negative indicators)} \quad \text{(Eq.6)}$$

In the formula, "X" is the original value of a certain evaluation factor, "X_{max} "is the maximum value of a parameter, and "X_{min}" is the minimum value of a parameter.

Table 1. *Evaluation index system of ecological environment in three lake basins*

Target layer	Rule layer	Direction	Weight	Index layer	Weight
Ecological environment quality index (EI)	Biological abundance index (A1)	Positive	0.1589	Arable land ratio (A11)	0.1799
				Forestland area ratio (A12)	0.2965
				Grassland area ratio (A13)	0.2965
				Construction land area ratio (A14)	0.0700
				Wetland area ratio (A15)	0.1112
				Unused area ratio (A16)	0.0460
	Vegetation coverage index (A2)	Positive	0.1589	Forestland area ratio (A21)	0.5695
				Grassland area ratio (A22)	0.3331
				Arable land ratio (A23)	0.0974
	Water network density index (A3)	Positive	0.0967	Water resources/Total area (A31)	0.4934
				Wetland area/ Total area (A32)	0.3108
				The length of the river/Total area (A33)	0.1958
	Soil erosion index (A4)	Negative	0.2409	Severe erosion area ratio (A41)	0.6370
				Moderate erosion area ratio (A42)	0.2583
				Slight erosion area ratio (A43)	0.1047
	Pollution load index (A5)	Negative	0.3447	COD/Total annual precipitation in the region (A51)	0.3000
				NH3—N/Total annual precipitation in the region (A52)	0.3000
				SO2/Total area (A53)	0.3000
				Solid waste emissions/Total area (A54)	0.1000

http://www.aloki.hu ● ISSN 1589 1623 (Print) ● ISSN 1785 0037 (Online)
DOI: http://dx.doi.org/10.15666/aeer/1605_56935704
© 2018, ALÖKI Kft., Budapest, Hungary

Table 2. *Classification criteria for evaluation results of ecological environment*

Level	Index	Status
Excellent	EI ≥ 0.75	Vegetation coverage, biodiversity, and ecological conditions are the best
Good	0.55 ≤ EI < 0.75	Vegetation coverage, biodiversity, and ecological environment are better
General	0.35 ≤ EI < 0.55	Vegetation coverage, biodiversity, and ecological conditions are normal
Poor	0.20 ≤ EI 〈 0.35	The vegetation coverage is poor, with severe drought and less rain, fewer species, and poor ecological environment
Worst	EI < 0.20	Ecological environment and its bad conditions

- Establish a comprehensive evaluation model

Individual indicators include biological abundance index, vegetation coverage index, water network density index, soil erosion index, and pollution load index, which are the composite of different basic indicators of each criterion level. Every single index reflects ecological environmental quality from different aspects, and the calculation of the single index adopted the method of the multi-factor linear weighting function, the calculation formula is as follows (*Eq. 7*):

$$B_i = \sum_{j=1}^{n} Gj * Wj \quad \text{(Eq.7)}$$

In the formula, "B_i" is every single index,, "G_j" is the index score corresponding to each specific evaluation index, and "W_j" is the weight of corresponding evaluation index.

The single-item index evaluated the priority of ecological environment quality in a certain aspect, and a comprehensive evaluation must be conducted to fully reveal. The formula is as follows (*Eq. 8*):

$$B = \sum_{i=1}^{n} Bi * Wi \quad \text{(Eq.8)}$$

In the formula, "B" is the total evaluation score, "B_i" *(i = 1, 2, 3)* is the individual index, "W_i" is the weight corresponding to the basic indicators of each criterion level, the standard value of each indicator is weighted and averaged on a layer-by-layer basis to obtain a composite index.

Results

Through remote sensing image interpretation, land use remote sensing classification maps of three lake basins were obtained (*Fig. 2*), and landscape pattern index is shown in *Table 3*.

Table 3. *Land use landscape pattern index of three lake basins*

Basins	Diversity index	Evenness index	Dominance index	Fragmentation index
Dianchi Basin	1.2966	0.6663	0.6493	0.1780
Erhai Basin	1.3569	0.6973	0.5890	0.0616
Fuxian Lake Basin	1.3852	0.7119	0.5607	0.1167

http://www.aloki.hu ● ISSN 1589 1623 (Print) ● ISSN 1785 0037 (Online)
DOI: http://dx.doi.org/10.15666/aeer/1605_56935704
© 2018, ALÖKI Kft., Budapest, Hungary

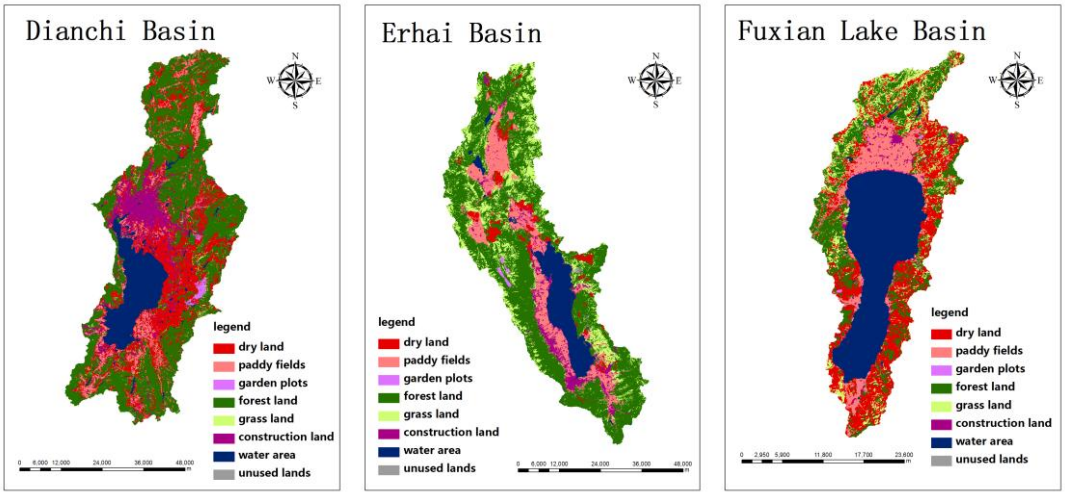

Figure 2. *Classification map of land use in the three major lake basins*

Analysis of landscape pattern characteristics of land use

According to *Table 3,* the landscape pattern of the three lake basins was analyzed horizontally horizontally, that is, the different indexes of the same basin were analyzed, and the results were as follows:

(1) In Dianchi Basin, the diversity index and evenness index were the smallest, while the dominant index and fragmentation index were the largest, indicating that the diversity of landscape structure of land use in Dianchi Basin was the worst, the landscape types were unevenly distributed, and the degree of landscape fragmentation was the most serious;

(2) In addition to the lowest fragmentation index in the Erhai Basin, the diversity, evenness, and fragmentation index are all in the middle level and are closer to the Fuxian Lake Basin. Therefore, overall, the diversity of land use landscape structure in the basin is relatively good. The type distribution is more uniform, and the landscape type is divided into smaller segments with the best connectivity.

(3) The diversity index and evenness index of the Fuxian Lake Basin are the largest, the dominance index is the lowest, and the fragmentation index is at the intermediate level. Based on the comprehensive analysis, the land use landscape structure of the basin is the simplest, and the level of human disturbance is the lowest.

The landscape pattern of the three major lake basins was analyzed longitudinally, that is, the same index of different watersheds is analyzed. The results are as follows:

(1) The order of diversity index which is Fuxian Lake Basin > Erhai Basin > Dianchi Basin, 1.3852, 1.3569, and 1.2966, respectively. The diversity of landscape structure of land use in Dianchi Basin was the lowest, the landscape diversity was poor, and the coordination of various landscape types was low. The diversity of landscape structure of land use in Fuxian Lake Basin was the highest, and the diversity of landscape was well maintained. The degree of coordination is high; the diversity of the Erhai Basin is between the two.

(2) The ranking of evenness index which is Fuxian Lake Basin > Erhai Basin > Dianchi Basin, which is 0.7119, 0.6973, and 0.6663, respectively. The dominance index ranking is Dianchi Basin > Erhai Basin > Fuxian Lake Basin, which are 0.6493, 0.5890,

http://www.aloki.hu ● ISSN 1589 1623 (Print) ● ISSN 1785 0037 (Online)
DOI: http://dx.doi.org/10.15666/aeer/1605_56935704
© 2018, ALÖKI Kft., Budapest, Hungary

and 0.5607, respectively. It showed that the balance of land use landscape structure in Dianchi Basin is poor, and the distribution of land use types is uneven. This is mainly due to the fact that the proportion of forest land and cultivated land in the basin is large, which greatly improves the dominance of the overall landscape. The balance of land use structure in the Fuxian Lake Basin is relatively good, with a balanced distribution across the regions; the landscape evenness in the Erhai Basin is located between the two.

(3) Fragmentation index ranking which is Dianchi Lake Basin > Fuxian Lake Basin > Erhai Lake Basin, which is 0.1780, 0.1167, and 0.0616, respectively. The result showed that the landscape pattern of land use in Dianchi Basin has the highest degree of fragmentation, and the landscape is the most severely fragmented. This is mainly because the Dianchi Basin is located in a karst landscape area and the degree of rocky desertification is relatively deep, resulting in serious landscape fragmentation; The higher degree of fragmentation of land-use landscape structures in the Fuxian Lake Basin is because the basin is located in the central part of the central basin of the central Yunnan basin and the watershed of the Zhujiang River system. The surrounding area is mostly eroded by fault blocks, and the terrain is undulating, scattered and distributed on both sides of the lake. There are 61 sub-watersheds, and special geological conditions have caused great fragmentation of the terrain of the Fuxian Lake Basin. The fragmentation of land use landscape structures in the Erhai Basin is the lowest.

The evaluation results of the ecological environment of the three lake basins

According to *Table 4,* the "*EI*" indexes of the Dianchi Basin, the Erhai Basin, and the Fuxian Lake Basin are 0.5628, 0.7274, and 0.7413, respectively. They are all between 0.55 and 0.75. It showed that the three lake basins have good vegetation coverage, good biodiversity, and good ecological environment.

Table 4. *Evaluation results of ecological environment in the three lake basins*

Evaluation index	Dianchi Basin	Erhai Basin	Fuxian Lake Basin
Biological abundance index (A1)	0.7431	1.0000	0.9624
Vegetation coverage index (A2)	0.6811	1.0000	0.6010
Water network density index (A3)	0.1608	0.1519	1.0000
Soil erosion index (A4)	1.0000	0.9345	0.2135
Pollution load index (A5)	0.2322	0.4926	1.0000
Ecological environment quality index (EI)	0.5628	0.7274	0.7413

Comparative analysis showed that the "*EI*" index is the lowest in the Dianchi Basin, and the ecological environment is the worst in the three lake basins. The "*EI*" index of Erhai Basin is slightly lower than that of Fuxian Lake Basin, which is larger than the Dianchi Basin, and its ecological environment is better than that of the Dianchi Basin, which is slightly inferior to Fuxian Lake Basin. The "*EI*" index is the highest in Fuxian Lake Basin, and the ecological environment is better than the other two lake basins.

Comprehensive analysis of the landscape pattern of land use and eco-environment characteristics

The comprehensive analysis was made on the landscape pattern index of land use and ecological environment index in the three lake basins. The Dianchi Basin landscape

http://www.aloki.hu ● ISSN 1589 1623 (Print) ● ISSN 1785 0037 (Online)
DOI: http://dx.doi.org/10.15666/aeer/1605_56935704
© 2018, ALÖKI Kft., Budapest, Hungary

diversity index and evenness index were the smallest, while the dominance index and fragmentation index were the largest, the ecological environment index was the smallest, and the fragmentation degree of the Erhai Basin was the smallest. In addition to the lowest fragmentation index in the Erhai Basin, the other indices are all in the middle level. The landscape diversity index and evenness index of the Fuxian Lake Basin are the largest, the dominance index is the smallest, the fragmentation index is small, and the ecological environment index is the largest (*Fig. 3*).

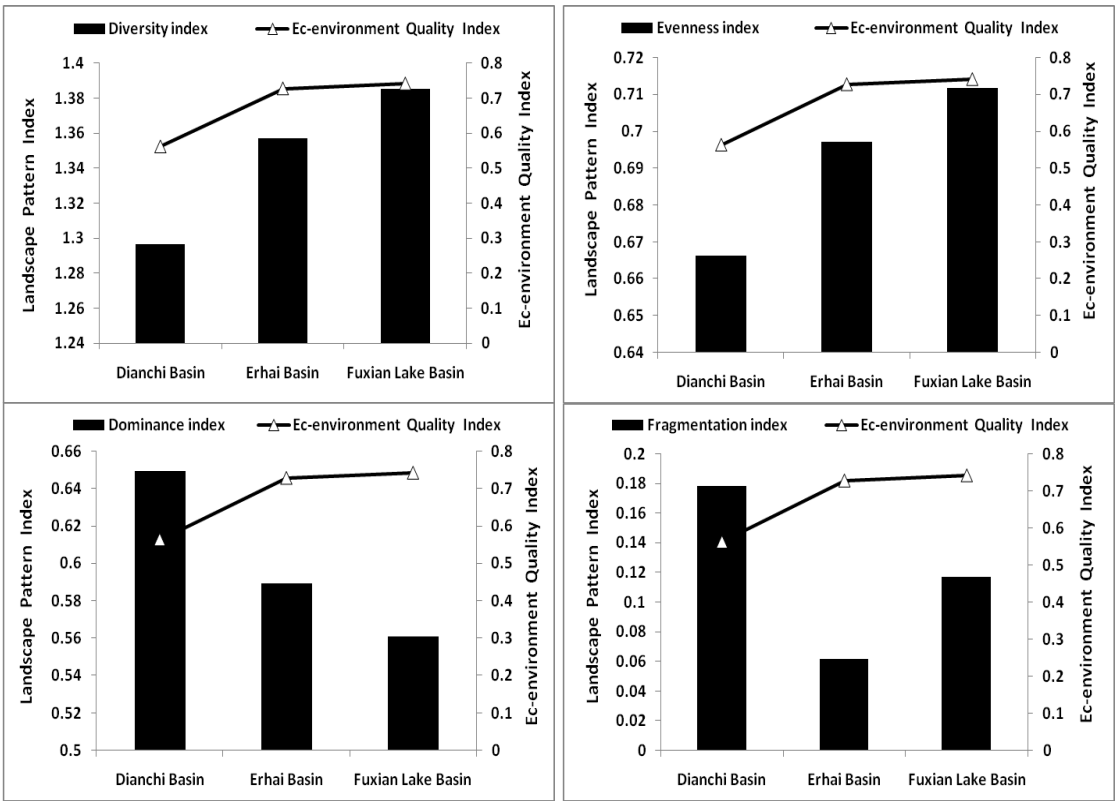

Figure 3. *Landscape pattern index and eco-environment quality index of land use in the three major lake basins*

Through comparison, it is found that the landscape patterns of land use in the three lake basins are closely related to the status of the ecological environment, and the landscape diversity and evenness of the basins with good ecological environment quality are relatively high, and the degree of landscape fragmentation is relatively low. On the contrary, in the basin with poor ecological environment, the degree of diversity and evenness of landscape is relatively low, and the degree of landscape fragmentation is relatively high.

Based on the analysis of the socio-economic development level of the three lake basins, the landscape pattern of land use and eco-environment characteristics of the three lake basins are related to the socio-economic development level of the lake basins. The Dianchi Basin with the highest level of economic development has the lowest landscape diversity. The distribution of landscape types is the lowest, the degree of landscape segmentation is the highest, and the quality of ecological environment is the lowest. The degree of landscape diversity and landscape types in the Erhai Basin and

http://www.aloki.hu ● ISSN 1589 1623 (Print) ● ISSN 1785 0037 (Online)
DOI: http://dx.doi.org/10.15666/aeer/1605_56935704
© 2018, ALÖKI Kft., Budapest, Hungary

Fuxian Lake Basin with a lower level of economic development are relatively evenly distributed. The degree of landscape fragmentation is relatively low, and the quality of ecological environment is the best.

Discussion

At present, there are many researches on the landscape pattern of land use, and the results are relatively fruitful, but mainly based on the study of landscape patterns in different phases of the same study area, and the lateral contrast analysis between different regions of the same time phase is less, most of them take city, county and other areas as the research scale, and few studies take plateau lake basin as the object. This study conducted a comparative analysis on the landscape pattern of land use and eco-environment characteristics among different plateau lake basins in Yunnan Province of China, which can provide scientific basis for optimizing the landscape pattern of land use and protecting the ecological environment. Because the factors affecting regional landscape pattern of land use and ecological environment quality are complex, involving natural conditions such as climate, topography, vegetation, hydrology, and socio-economic factors such as population and economic level, this study is only a brief description from the macro aspect, the next step will focus on the driving factors that affect the landscape pattern and the ecological environment of different basins, so as to make the research more perfect and scientific.

Conclusion

(1) From the analysis of the land use landscape pattern of the lake basins, the degree of landscape diversity and the degree of evenness are the highest in the Fuxian Lake Basin, followed by the Erhai Basin, and the lowest is the Dianchi Basin; the fragmentation of the landscape is highest in the Dianchi Basin and followed by the Fuxian Lake Basin. The lowest is the Erhai Basin.

(2) According to the results of the ecological environmental quality assessment, Dianchi Basin is the worst, while the Erhai Basin and Fuxian Lake Basin are better, and the Fuxian Lake Basin is the best.

(3) The landscape pattern of land use in the basin is closely related to the quality of the ecological environment. Basins with good ecological environment quality have a relatively high degree of diversity and evenness, and relatively low fragmentation; in the basins with poor ecological environment, the degree of landscape evenness and diversity are relatively low, and the degree of landscape fragmentation is relatively high.

The landscape pattern of land use is closely related to the ecological environment, unreasonable land use is one of the important factors of lake pollution, therefore, the relationship between land use and lake water quality should be further explored on the basis of this study, so as to better alleviate the pollution and improve the ecological environment of the lake basins from the perspective of land use.

Acknowledgements. The research was supported by Yunnan Agricultural University Natural Science Foundation for Youths (**NO.2015ZR16**).

http://www.aloki.hu ● ISSN 1589 1623 (Print) ● ISSN 1785 0037 (Online)
DOI: http://dx.doi.org/10.15666/aeer/1605_56935704
© 2018, ALÖKI Kft., Budapest, Hungary

REFERENCES

[1] Cattarino, L., McAlpine, C. A., Rhodes, J. R. (2014): Land-use drivers of forest fragmentation vary with spatial scale. – Global Ecology and Biogeography 23(11): 1215-1224.
[2] Chai, X. K., Jiang, G. T., Gao, P. et al. (2016): Characteristics and driving forces of land use change in Weihe River Basin. – Yellow River 38(8): 77-85.
[3] Chen, Y., Yin, Y. X., Chen, S. (2009): Land use/cover forecasting of catchment and its landscape ecological effects: a case study of XiTiaoXi catchment in the upper reaches of TaiHu basin. – Resources and Environment in the Yangtze Basin 8: 765-770.
[4] Feng, Y. X., Luo, G. P., Zhou, D. C. (2010): Effects of land use change on landscape pattern of a typical arid watershed in the recent 50 years: a case study on Manas River Watershed in Xinjiang. – Acta Ecologica Sinica (16): 4295-4305.
[5] Fu, Q. (2012): Study on land use change of economic zone around capital district based on GIS and logistic regress model. – Territory & Natural Resources Study 1: 34-36.
[6] Ge, J. L., Xie, Q. Y. (2016): Analysis of landscape pattern of land-use and its eco-environmental effect in Dalian. – Territory & Natural Resources Study 3: 53-55.
[7] Hassan, M. M. (2017): Monitoring land use/land cover change, urban growth dynamics and landscape pattern analysis in five fastest urbanized cities in Bangladesh. – Remote Sensing Applications: Society and Environment 7: 69-83.
[8] Kang, J. H. (2011): Talking about the present situation and protection measures of water resources development and utilization in the watershed of Fuxian Lake. – Pearl River 23(1): 75-77.
[9] Kumar, D. (2017): Monitoring and assessment of land use and land cover changes (1977-2010) in Kamrup district of Assam, India using remote sensing and GIS techniques. – Applied Ecology and Environmental Research 15(3): 221-239.
[10] Lamine, S., Petropoulos, G., Singh, P., Kumar, S. et al. (2018): Quantifying land use/land cover spatio-temporal landscape pattern dynamics from Hyperion using SVMs classifier and FRAGSTATS. – Geocarto International 33(8): 862-878.
[11] Li, J. S.(2011): Research on structures and patterns of land Use of Erhai Watershed. – Environmental Science Survey 30(4): 34-39.
[12] Li, P., Yu, S. X. (2014): Analysis of land use driving forces based on canonical correspondence analysis in Dianchi Basin. – China Population, Resources and Environment (S1): 123-126.
[13] Li, Y. C., Gong, P., Chen, J. et al. (2005): Landscape pattern and its dynamical change in north China during 1989-1999. – Journal of Soil Water Conservation 5: 145-148.
[14] Liu, H. Q., Xu, J. W. et al. (2008): Landscape Ecology:265-269.
[15] Liu, Y. B., Dai, L., Dong, Y. Y. (2015): Simulation of landscape pattern change of PoYang Lake area partition. – Resources and Environment in the Yangtza Basin (10): 1762-1770.
[16] Martyn, A., Barvinsky, A., Tykhenko, R. (2017): Problems of conceptual apparatus in environmental economics: relationship between the systems and mechanism of land use. – Zemleustrìj, Kadastr ì Monìtorìng Zemel′ 17(4): 21-28.
[17] Mehrian, M. R., Hernandez, R. P., Yavari, A. R. (2016): Investigating the causality of changes in the landscape pattern of Lake Urmia basin, Iran using remote sensing and time series analysis. – Environmental Monitoring and Assessment 188(8): 1-13.
[18] Ministry of Ecological and Environment of the People's Republic of China (2016): Technical Specifications for Eco-environmental Status Assessment. – HJ 192-2015.
[19] Rao, Y. H., Zhang, J. J., Xu, Q. et al. (2015): A rule of land use change in a mining city based on logistic regression model. – China Mining Magazine 24(3): 70-75.
[20] Sharma, G., Manandhar, R. (2017): Land use change in Banepa Municipality. – Journal of Safety and Crisis Management 7(1): 33-39.

http://www.aloki.hu ● ISSN 1589 1623 (Print) ● ISSN 1785 0037 (Online)
DOI: http://dx.doi.org/10.15666/aeer/1605_56935704
© 2018, ALÖKI Kft., Budapest, Hungary

[21] Wang, P. P. (2015): Study on the county's landscape pattern change characteristics and its driving mechanism in the northeast China. – Northeast Agricultural University, Heilongjiang Sheng.
[22] Wenban-Smith, A. (2017): Land-use drivers of transport emissions revisited. – Transport 170(2): 76-85.
[23] Wu, X. H., Li, Y. X., Hou, C. D. (2002): The current situation analyses of Fuxian Lake. – Journal of Yuxi Teachers College 18(2): 66-68.
[24] Xu, B. S. (2012): Study on Landscape Pattern Evolution of Land Use and Ecological Security Assessment in Jianghan Plain. – Huazhong Normal University, Hubei.
[25] Yang, H. R., Wang, H. Y., Peng, W. F. et al. (2016): Research of spatial and temporal dynamic changes in regional land use/cover. – Chinese Journal of Agricultural Resources and Regional Planning 8: 37-46.
[26] Yu, J., Zhang, L. (2016): The role of village collective in the establishment of large - scale family farm structure. – Chinese Journal of Agricultural Resources and Regional Planning (12): 98-103.
[27] Yuan, L., Yang, K. (2016): An analysis of quantitative impacts of multi-scale factors on driving forces in land use change. – China Land Sciences (12): 63-70.
[28] Yunnan Environmental Protection Department (2016): 2015 Environmental Status Bulletin of Yunnan province. – Yunnan Environmental Protection Department, Yunnan Sheng.
[29] Zhang, B. Y., Shen, H. F., Zheng, J. G. et al. (2009): GIS-based analysis on the landscape spatial patterns of land-use in Henan Province. – Resources Science 2: 317-323.
[30] Zhang, K., Zhao, Y. L., Fu, Y. C. et al. (2013): Fractal dimension dynamics and land use in the Lake Dianchi Watershed from 1974 to 2008. – Resources Science 35(1): 232-239.
[31] Zhang, Y. R., Zhou, Z. F. (2012): MA Shi-bin. Analysis on the mechanism of land use change in industrial resource based city: a case study of downtown zone in Liupanshui in Guizhou Province. – Hubei Agricultural Sciences 51(12): 2461-2465.

http://www.aloki.hu ● ISSN 1589 1623 (Print) ● ISSN 1785 0037 (Online)
DOI: http://dx.doi.org/10.15666/aeer/1605_56935704
© 2018, ALÖKI Kft., Budapest, Hungary

FLAME ATOMIC ABSORPTION SPECTROMETRY DETERMINATION OF SILVER NANOPARTICLES IN ENVIRONMENTAL WATERS USING DISPERSIVE LIQUID-LIQUID MICROEXTRACTION

WU, H. Z.[1,2] – MENG, L. F.[3*]

[1]*Faculty of Land Resources and Engineering, Kunming University of Science and Technology Kunming 650093, China*

[2]*College of Mining Engineering, Guizhou University of Engineering Science Bijie 551700, China*

[3]*College of Chemical Engineering, Guizhou University of Engineering Science Bijie 551700, China*

**Corresponding author*
e-mail: 1025588702@qq.com

(Received 21st Jun 2018; accepted 22nd Aug 2018)

Abstract. A novel, rapid low-density solvent based dispersive liquid-liquid microextraction has been developed for extraction and preconcentration of silver nanoparticles (AgNPs) prior to flame atomic absorption spectrometry analysis. In this study, water samples were first treated with acetonitrile/water (80:20, v/v) which was then utilized as disperser solvent in the dispersive liquid-liquid microextraction process along with using 1-octanol as extractant. An enrichment factor of 57 is obtained, and the recoveries of AgNPs spiked into environmental samples are in the range of 96.7 to 108%. A low limit of detection (LOD) of 6.5 μg/L is achieved using flame atomic absorption spectrometry (FAAS) for quantification. The relative standard deviation (RSD) is 2.1% (n = 9). This proposed method provides an efficient approach for the analysis and tracking of AgNPs in the environmental water samples.
Keywords: *AgNPs, DLLME, extractant, preconcentration, FAAS*

Introduction

Metallic nanoparticles are of high importance in current materials research, with potential applications in biomedicine, energy conversion, imaging, or as pigments (Khaligh et al., 2015; Hartmann et al., 2013). Engineered nanomaterials (NMs) have already yielded a variety of commercially available products including cosmetics, antimicrobials, suntan lotions, paints, stain-resistant clothing and remediation products (Mirzaei et al., 2013). The rapid growth in the commercial use of AgNPs will inevitably increase silver exposure to the general population (Ghaedi et al., 2013). AgNPs may penetrate the skin (Ghaedi et al., 2015) via textile or wound dressing contact, be inhaled from some spray medicine, or ingress into the female genital tract by incorporation into female hygienic products or medical implants (Habila et al., 2015), and it is also toxic to human cells (Altunay et al., 2015; Fan et al., 2012; Choi et al., 2011). Therefore, it is important from an analytical point of view to develop sensitive and economical methods for determination of trace silver nanoparticles.

Because of the complexity of the matrices and trace amounts of metal ions residues in practical samples, sample preparation is necessary and often plays a vital role in the overall analytical scheme (Lambropoulou et al., 2007). In the past few years, a diversity of extraction methods, including liquid-liquid extraction (LLE) (Fernández-Gutiérrez et al., 1998), stir bar

http://www.aloki.hu ● ISSN 1589 1623 (Print) ● ISSN 1785 0037 (Online)
DOI: http://dx.doi.org/10.15666/aeer/1605_57055714
© 2018, ALÖKI Kft., Budapest, Hungary

sorptive extraction (SBSE) (Van et al., 2007), solid-phase micro extraction (SPME) (Beltran et al., 2003) and solid-phase extraction (SPE) (Gil-García et al., 2006), have been developed for sample preparation. A wide range of applications hitherto bears testimony to the fact that they are portable and effective for sample preparation. However, for most of these methods, considerable time and organic solvent are needed for analytes to be extracted into the organic phase or onto the sorbent. In order to increase the throughput for sample pretreatment, the development of time saving and high efficient microextraction techniques has drawn much attention (Ding et al., 2013).

Dispersive liquid-liquid microextraction (DLLME) has been brought up as an exciting microextraction technique in 2006 (Yu et al., 2014; El-Shahawi et al., 2013; Rezaee et al., 2006). In this procedure, a mixture of high density organic solvent (serving as extraction solvent) and water miscible polar dispersive solvent (dispersive solvent) is rapidly injected into an aqueous sample to form an emulsion consisting of fine droplets of the extraction solvent, dispersive solvent, and water. Due to the extraction solvent being highly dispersed in the aqueous phase, the surface area between extraction solvent and sample solution is infinitely large, thus speeding up the extraction. While, the main disadvantage of DLLME is that the extraction solvent is generally limited to solvents with higher density than water in order to be sedimented by centrifugation, typically chlorinated solvents such as chlorobenzene, chloroform, and tetrachloromethane, all of them are potentially toxic to humans and the environment. To date, CPE has already successfully been applied for the quantification of Au-NPs in water samples in combination with electrothermal atomic absorption spectrometry (ET-ASS) (Hartmann et al., 2013). However, ET-AAS measurement, which background absorption signal is large, the relative sensitivity and sample in homogeneity more serious, analytical precision is poor.

In this study, the possibility of AgNPs enrichment by DLLME was considered. A new microextraction method combined with flame atomic absorption spectrometry (FAAS) was developed for separation, enrichment and determination of AgNPs in environmental waters. Factors affecting the extraction efficiency, such as pH, concentration of extractant, extraction time, and nature of the extractant were studied and optimized.

Materials and methods

Materials

All chemicals used were analytical grade or better and all solutions were prepared in deionized water. 1-hexanol, 1-heptanol, 1-octanol, 1-nonanol, 1-decanol and decanoic acid were obtained from the Aladdin Reagent Corporation (Shanghai, China). Tannic acid, sodium carbonate , Ammonium sulfate , hydrochloric acid, silver nitrate, ethanol and sodium thiosulphate, all purchased from (Aladdin, China).

Equipment

A pHSJ-4A pH meter (Shanghai, China), vortex agitator (Shanghai, China) and SK5210LHC ultrasonic instrument (Shanghai, China), centrifuge (Shanghai, China) and flame atomic absorption spectrometer (AA6300, Shimadzu, Japan) were used.

Synthesis of AgNPs nanoparticle

Preparation of $AgNO_3$ solution and tannic acid solution, 0.100 mol/L Na_2CO_3 solution with deionized water; amount of 200 mL tannic acid solution at three mouth bottle

http://www.aloki.hu ● ISSN 1589 1623 (Print) ● ISSN 1785 0037 (Online)
DOI: http://dx.doi.org/10.15666/aeer/1605_57055714
© 2018, ALÖKI Kft., Budapest, Hungary

thermostatic water bath heating, and stirring; adding 5 mL Na_2CO_3 solution to tannin reduction; after 10 min, A certain amount of volume $AgNO_3$ solution, with the constant pressure drop funnel the dropwise added to the above mixture. Three mouth bottle solution color from colorless to light yellow gradually, orange, red, and finally turned a deep red or red brown, continue stirring heating 30 min, obtained the AgNPs. The AgNPs concentration of the solution was determined by FAAS.

Extraction procedure

DLLME of AgNPs step

A 4 mL AgNPs sample solution placed in 10 mL long tapered glass centrifuge tube was adjusted to pH 3.0 with diluted HCl, and then 40 μL of 1 M $Na_2S_2O_3$ and 80 μL of 1-octanol (as extraction solvent of DLLME) were added to the acetonitrile/water (80:20, v/v) extract (used as disperser solvent) and the mixture was diluted to 40 mL by deionized water in a 50 mL vial with conical bottom. Then, the tube was sealed and swirled on a vortex agitator at 2000 rpm for 30 s to accelerate the formation of the fine droplets of the extraction solvent and to enhance the transfer of the analytes. The supernatant aqueous phase can then easily be removed by decanting. The droplet was dissolved in 2 mL of ethanol and transferred to FAAS measurement.

Results and discussion

Optimization of the DLLME conditions

Parameters that commonly affect the DLLME efficiency, such as sample pH, the type and volume of extraction solvent, salt content, equilibration time were investigated.

pH plays an important role on metal chelate formation and subsequent extraction. To optimize the extraction conditions for the nanoparticles pH was varied between 1 and 7 using hydrochloric acid for pH adjustment while the other experimental variables remained constant. The highest extraction efficiency was achieved at pH 3.0 (*Fig. 1*) while the replicate times n = 6. So, pH 3.0 was selected as the optimum for further experiments.

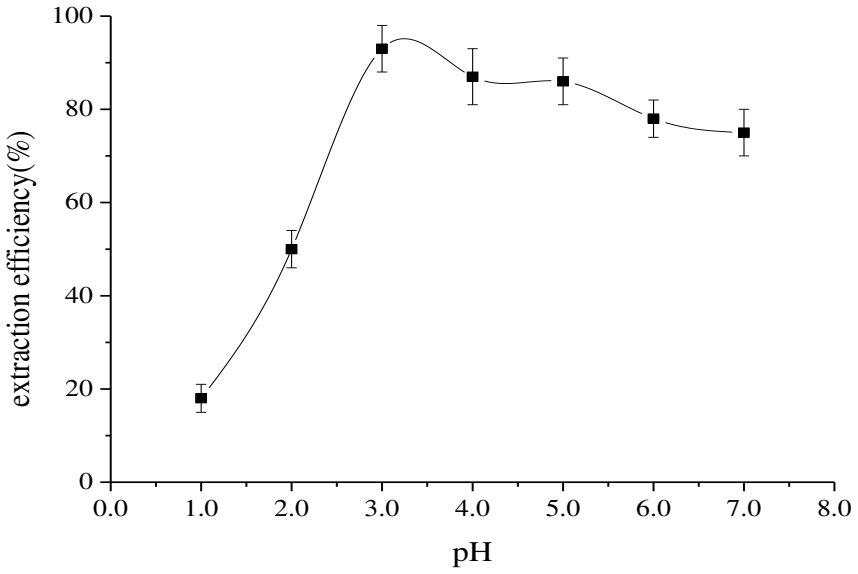

Figure 1. *Effect of pH on DLLME of AgNPs*

http://www.aloki.hu ● ISSN 1589 1623 (Print) ● ISSN 1785 0037 (Online)
DOI: http://dx.doi.org/10.15666/aeer/1605_57055714
© 2018, ALÖKI Kft., Budapest, Hungary

Selection of the disperser solvent

The applicability of several organic solvents including MeOH, MeCN, EtOH, MeOH 80% and MeCN 80% was investigated in the preliminary experiments taking into account that they should be used as primary extracts of the analytes from real water samples must then act as disperser solvent in DLLME process. *Figure 2* shows the recoveries of the whole procedure of all extraction solvents tested. The results revealed that the maximum extraction efficiency was achieved by MeCN/water (80:20 v/v).

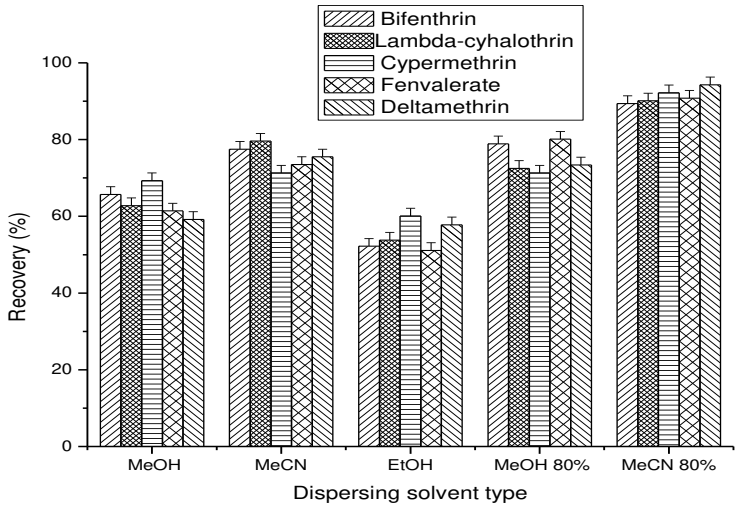

Figure 2. *Effect of dispersing solvent*

To study the volume effect of disperser solvent, it was varied from 4 to 12 mL in the interval of 2 mL while extraction solvent was kept at 80 µL. The obtained results showed that the extraction efficiency increased with increasing the volume of MeCN 80% up to 10 mL and then dropped down slightly above 10 mL due to the increased solubility of AgNPs in the aqueous phase and decreasing the distribution ratio.

Therefore 10 mL MeCN 80% was selected as both the extraction solvent of AgNPs from environmental samples and as disperser solvent in DLLME for subsequent experiments.

In this study $Na_2S_2O_3$ as a masking reagent to cover the interference of Ag^+. When $Na_2S_2O_3$ was added, thiosulfate ions and silver ions generated thiosulfate (*Fig. 3*), which is soluble in water. Therefore, silver ions can be eliminated to the detection of AgNPs.

$$Na_2S_2O_3 + 2Ag^+ = 2Na^+ + Ag_2S_2O_3\downarrow$$

$$Ag_2S_2O_3 + 2Na_2S_2O_3 = Ag_2Na_4(S_2O_3)_3$$

Figure 3. *The reaction of sodium thiosulfate with* Ag^+

Selection of extraction solvent

Selection of appropriate extraction solvent is of great importance in microextraction technique in order to obtain efficient extraction. For the LDS-DLLME, the extraction

http://www.aloki.hu ● ISSN 1589 1623 (Print) ● ISSN 1785 0037 (Online)
DOI: http://dx.doi.org/10.15666/aeer/1605_57055714
© 2018, ALÖKI Kft., Budapest, Hungary

solvent should meet the following requirements: (1) be immiscible with aqueous solution (2) able to extract the analytes, and (3) possess low toxicity. To avoid the use of more highly toxic solvents such as trichloromethane, tetrachloromethane, tetrachloroethylene, chlorobenzene etc., five low density organic alcohol including 1-hexanol (density, d = 0.819 g mL^{-1}), 1-heptanol (d = 0.820 g mL^{-1}), 1-octanol (d = 0.821 g mL^{-1}), 1-nonanol (d = 0.827 g mL^{-1}), and 1-decanol (d = 0.828 g mL^{-1}) were evaluated as extractants. Among them a stable cloudy solution and good extraction recovery were observed with 1-octanol. The fine droplets of 1-octanol afford larger surface area to contact with the water sample and can be completely absorbed by MNPs after magnetic separation, so that higher extraction performance can be attained. As can be seen, 1-octanol has higher extraction recovery than those obtained by other extraction solvents for the AgNPs.

Effect of extraction solvent volume

The volume of extracting solvent is an important parameter which can influence the occurrence of the cloudy state and efficiency of extraction process. To investigate the volume effect of 1-octanol, different quantities of 1-octanol (50-100 μL) were used. Observably, too little 1-octanol may lead to low recoveries and the extraction efficiency was improved with the increase of 1-octanol volume. As shown in *Figure 4,* the recoveries for each of the AgNPs increased from 55-63% to 86.8-109.1% in the range of 50-80 μL of 1-octanol. The highest recovery was obtained when 80 μL of 1-octanol was used for the extraction. Therefore, the volume of 80 μL of 1-octanol was selected as an optimum solvent volume for further studies.

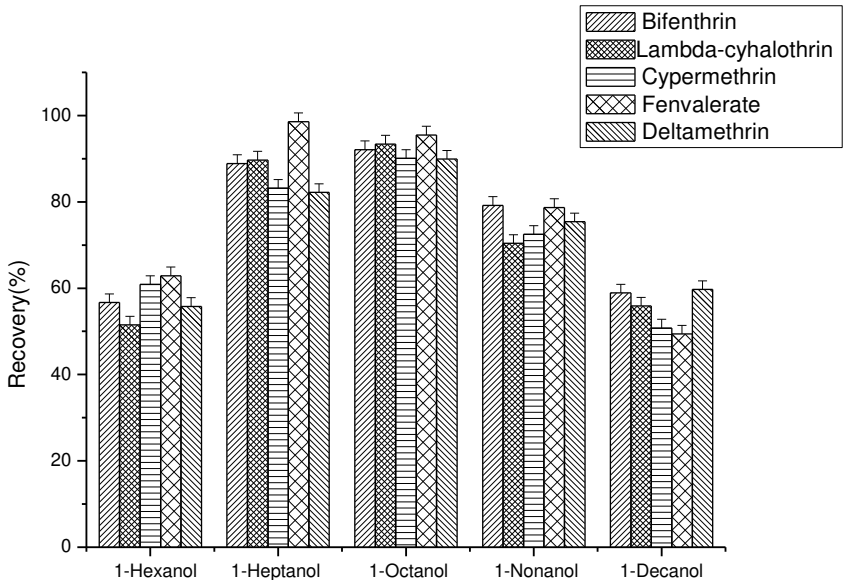

Figure 4. *Selection of extraction solvent*

Effect of equilibration time

In DLLME extraction, equilibration time is defined as an interval time from the occurrence of cloudy solution and before addition of magnetic adsorbents. The effect of extraction time on the adsorption was investigated from 0-120 s. The result showed that

http://www.aloki.hu ● ISSN 1589 1623 (Print) ● ISSN 1785 0037 (Online)
DOI: http://dx.doi.org/10.15666/aeer/1605_57055714
© 2018, ALÖKI Kft., Budapest, Hungary

equilibration time has no influence on extraction efficiency. It is well-known that vortex process is an effective way to enhance mass transfer from aqueous phase to the extraction phase. Consequently, short time was required for extraction. Generally, 30 s of extraction time was enough to achieve high extraction recovery, and prolonged extraction time did not contribute significantly to an increase in extraction recovery. Thereby, vortex time of 30 s was selected.

The high viscosity of the so prepared surfactant rich phase made it necessary to dissolve the sample prior to sample introduction to FAAS. Ethanol appeared to be a feasible solvent since it readily dissolves the surfactant rich phase and it prevents degradation of the enriched nanoparticles.

Evaluation of the preservation of the nanoparticle size distribution

To gain an insight in the size distribution of the nanoparticles in real samples it is necessary to know whether the size distribution of Ag-NPs is changing during the extraction procedure or not. This was studied using TEM for imaging of the particles before and after DLLME. As shown in *Figure 5,* the size of particles that underwent the extraction process is more or less identical to the size before DLLME treatment. Thereby we conclude that the size distribution is not affected by the presented method. This supports the results of Yang et al. (2017) that studied CPE for metal nanoparticles. This finding is especially important because the size determination of nanoparticles is an important issue in current research. DLLME samples of Ag-NPs can therefore be used for size determination after pre-concentration.

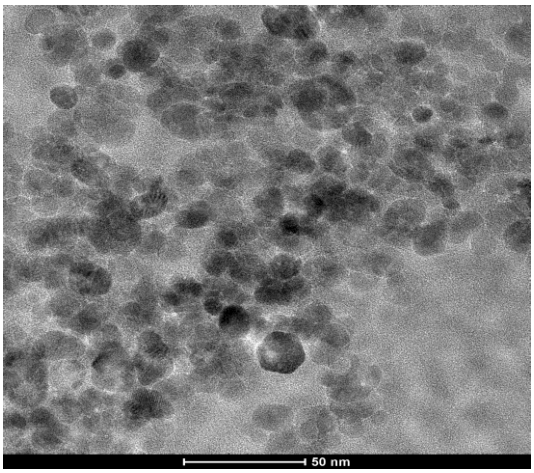

Figure 5. *TEM images of synthesized AgNPs*

Analytical features

The analytical characteristics of the method were evaluated under the optimum experimental conditions (*Table 1*). The enrichment factor (EF), relative standard deviations (RSD) and limits of detection (LOD) are effective factors to evaluate a developed analytical method. With the optimized system, the calibration graph of AgNPs was linear in the range of 10-1000 μg/L. The calibration equation is $A = 7.9 \times 10^{-2}$ C + 0.003 with a correlation coefficient of 0.9999, where A is the absorbance and C is the Ag concentration in μg/L. The detection limits, defined as the

http://www.aloki.hu ● ISSN 1589 1623 (Print) ● ISSN 1785 0037 (Online)
DOI: http://dx.doi.org/10.15666/aeer/1605_57055714
© 2018, ALÖKI Kft., Budapest, Hungary

concentration equivalent to three times the standard deviation of the reagent blank, for AgNPs was 6.5 μg/L. The relative standard deviation for AgNPs was 2.1% (n = 9). The relative recoveries of AgNPs in water samples at the spiking level of 3-20 μg/L ranged from 96.7 to 108%. There are many reasons, such as instrument fluctuations, operating errors, etc., so the calibration curve will appear quantitative. Recovery rates of 80% to 120% are generally considered normal. The enhancement factor, defined as the ratio of slope of preconcentrated samples to that obtained without preconcentration, was 57 for AgNPs.

Table 1. *Analytical characteristics of the method*

Parameter	Analytical feature
Linear range (μg/L)	10-1000
R^2	0.9999
Limit of detection (μg/L)	6.5
RSD (%) (n = 9)	2.1
Enrichment factor	57
Pre-concentration time (min)	<10
Recovery (%)	96.7-108.0

Effect of foreign ions

To regard of the high sensitivity of FAAS, the interference connected with the DLLME procedure was studied. Due to cations may react with AgNPs and lead to the decrease of extraction efficiency.10 mL sample solution containing Ag^+ and other ions were prepared and treated with the developed procedure. The tolerance limit was defined as the foreign ion concentration causing a change in the absorbance of less than ±5%. *Table 2* shows the concentration of the interferential ions, the recovery is tolerable.

Table 2. *Effects of the matrix ions on the recoveries of the examined metal ions*

Ions	Concentration (ug/L)	Recovery (%)	
		Pd	Ag
Na^+	10×10^3	105.0	104.1
K^+	10×10^3	104.2	104.8
Cl^-	10×10^3	103.5	102.2
Ca^{2+}	10	99.1	101.1
Mg^{2+}	0.5	99.2	96.8
Cr^{3+}	0.5	100.7	98.8
Mn^{2+}	0.5	103.4	99.2
Zn^{2+}	0.5	102.2	100.1
Cd^{2+}	0.5	98.7	99.7
Ni^{2+}	0.5	99.6	100.8
Pb^{2+}	0.5	108.7	98.5
Cu^{2+}	0.5	102.6	99.9

http://www.aloki.hu ● ISSN 1589 1623 (Print) ● ISSN 1785 0037 (Online)
DOI: http://dx.doi.org/10.15666/aeer/1605_57055714
© 2018, ALÖKI Kft., Budapest, Hungary

Analysis of real samples

To further evaluate the applicability of the proposed method, real environmental water samples were analyzed and the recoveries were determined by spiking 3-20 μg/L AgNPs. The WWTP water sample was obtained from our laboratory (Bijie, China), the river water sample from LiuCang Qiao River (Bijie, China). As shown in *Table 3,* the obtained recoveries of AgNPs were in the range of 96.7-108%, which was satisfactory with regard to the low spiking level. No significant difference between recoveries for samples with or without filtration was observed, suggesting that the presence of natural particles in the samples had no significant effects on the DLLME of AgNPs at concentrations 20 μg/L. This result indicates that FAAS can be adopted to identify and quantify the AgNPs content in environmental samples.

Table 3. *Determination and identification of AgNPs in environmental waters by the proposed method*

Sample	AgNPs added (μg/L)	AgNPs found (μg/L)	Recovery (%)
River water	0	*ND	–
	5	4.9±0.3	98.0±0.6
	10	10.8±0.5	108.0±5.0
	20	20.5±0.6	102.5±3.0
WWTP	0	*ND	–
	3	2.9±0.5	96.7±16.7
	8	8.1±0.6	101.3±7.5
	15	15.8±0.7	105.3±4.6

Comparison with other measurements

Table 4 compares the characteristic data of the proposed method with other methods for AgNPs reported in literature. As it can be seen, the proposed method has higher RSD and lower detection time.

Table 4. *The comparison of proposed measurement with other measurements*

Measurement	Sample volume (mL)	Detection time (min)	RSD (%) (n = 9)	Injection volume (mL)	LOD (μg/L)	Reference
ICP-MS	9.5	>10	5.6	5	0.006	Hartmann et al. (2013)
ET-AAS	40	5	9.5	0.2	0.005	Hartmann et al. (2013)
FAAS	5	<2	2.1	0.2	6.5	This paper

Conclusion

In the present study, a new microextraction technique, based on dispersive liquid-liquid microextraction (DLLME) was developed for determining AgNPs in environmental water samples. $Na_2S_2O_3$ was added into the extraction system as a masking reagent of Ag^+ to prevent its extraction into the 1-octanol rich phase. The extraction could be achieved within 2 min and good extraction efficiencies were obtained. Such facile separation is essential to improve the operation efficiency which avoiding time-consuming centrifugation or freezing or manual collection of extractant.

http://www.aloki.hu ● ISSN 1589 1623 (Print) ● ISSN 1785 0037 (Online)
DOI: http://dx.doi.org/10.15666/aeer/1605_57055714
© 2018, ALÖKI Kft., Budapest, Hungary

In addition, there are many reasons, such as instrument fluctuations, operating errors, etc., so the calibration curve will appear quantitative. Recovery rates of 80% to 120% are generally considered normal. The type of sample and matrix does not affect the detection of AgNPs. This proposed method provided a simple approach for quantification of AgNPs in environmental water samples.

REFERENCES

[1] Altunay, N., Gürkan, R., Kır, U. (2015): Ultrasound assisted-cloud point extraction combined with flame atomic absorption spectrometry for selective preconcentration and determination of As(V) in selected water and beverage samples. – Analytical Methods 7(16): 6629-6639.

[2] Beltran, J., Peruga, A., Pitarch, E., López, F. J., Hernández, F. (2003): Application of solid-phase microextraction for the determination of pyrethroid residues in vegetable samples by GC-MS. – Anal. Bioanal. Chem. 376(4): 502-11.

[3] Choi, S. Y., Jeong, S., Jang, S. H., Park, J., Park, J. H., Ock, K. S., Lee, S. Y., Joo, S. W. (2012): In vitro toxicity of serum protein-adsorbed citrate-reduced gold nanoparticles in human lung adenocarcinoma cells. – J. Toxicol. In Vitro 26(2): 229-237.

[4] Ding, J., Mao, L. J., Yuan, B. F., Feng, Y. Q. (2013): A selective pretreatment method for determination of endogenous active brassinosteroids in plant tissues: double layered solid phase extraction combined with boronate affinity polymer monolith microextraction. – Plant Methods 9(1): 13.

[5] El-Shahawi, M. S., Al-Saidi, H. M. (2013): Dispersive liquid-liquid microextraction for chemical speciation and determination of ultra-trace concentrations of metal ions. – Trac. Trends Anal. Chem. 44: 12-24.

[6] Fan, J. H., Li, W. T., Hung, W. I., Chen, C. P., Yeh, J. M. (2011): Cytotoxicity and differentiation effects of gold nanoparticles to human bone marrow mesenchymal stem cells. – Biomed. Eng. Appl. Basis Commun. 23(2): 141-152.

[7] Fernández-Gutiérrez, A., Martínez-Vidal, J. L., Arrebola-Liébanas, F. J., Gonzalez-Casado, A., Vílchez, J. L. (1998): Determination of endosulfan and some pyrethroids in waters by micro liquid-liquid extraction and GC-MS. – Fresenius' Journal of Analytical Chemistry 360(5): 568-572.

[8] Ghaedi, M., Niknam, K., Nasiri, K. S., Soylak, K. (2013): Combination of flotation and flame atomic absorption spectrometry for determination, preconcentration and separation of trace amounts of metal ions in biological samples. – Human & Experimental Toxicology 32(5): 504-12.

[9] Ghaedi, M., Karimipour, G., Alambarkat, E., Asfaram, A., Montazerozohori, M. (2015): Solid-phase extraction of Pb^{2+} ion from environmental samples onto L-AC-Ag-NP by flame atomic absorption spectrometry (FAAS). – International Journal of Environmental Analytical Chemistry 95(11): 1030-1041.

[10] Gil-García, M. D., Barranco-Martínez, D., Martínez-Galera, M., Parrilla-Vázquez, P. (2006): Simple, rapid solid-phase extraction procedure for the determination of ultra-trace levels of pyrethroids in ground and sea water by liquid chromatography/electrospray ionization mass spectroscopy Rapid. – Commun. Mass Sp. 20(16): 2395-403.

[11] Habila, M., Unsal, Y. E., Alothman, Z. A., Shabaka, Z. A., Tuzen, M. (2015): Speciation of chromium in natural waters, tea, and soil with membrane filtration flame atomic absorption spectrometry. – Analytical Letters 48(14): 2258-2271.

[12] Hartmann, G., Schuster, M. (2013): Species selective preconcentration and quantification of gold nanoparticles using cloud point extraction and electrothermal atomic absorption spectrometry. – Anal. Chim. Acta. 761: 27-33.

http://www.aloki.hu ● ISSN 1589 1623 (Print) ● ISSN 1785 0037 (Online)
DOI: http://dx.doi.org/10.15666/aeer/1605_57055714
© 2018, ALÖKI Kft., Budapest, Hungary

[13] Khaligh, A. (2015): Graphene oxide-packed micro-column solid-phase extraction combined with flame atomic absorption spectrometry for determination of lead (II) and nickel (II) in water samples. – International Journal of Environmental and Analytical Chemistry 95(1): 16-32.
[14] Lambropoulou, D. A., Albanis, T. A. (2007): Methods of sample preparation for determination of pesticide residues in food matrices by chromatography–mass spectrometry-based techniques: a review. – Anal. Bioanal. Chem. 389(6): 1663-83.
[15] Mirzaei, M., Naeini, A. K. (2013): Determinaton of trace amounts of titanium by flame atomic absorption spectrometry after cloud point extraction. – Journal of Analytical Chemistry 68(7): 595-599.
[16] Rezaee, M., Assadi, Y., Milani Hosseini, M. R., Aghaee, E., Ahmadi, F., Berijani, S. (2006): Determination of organic compounds in water using dispersive liquid-liquid microextraction. – J. Chromatogr. A. 1116(1-2): 1-9.
[17] Van, H. E., David, F., Sandra, P. (2007): Stir bar sorptive extraction for the determination of pyrethroids in water samples: A comparison between thermal desorption in a dedicated thermal desorber, in a split/splitless inlet and by liquid desorption. – J. Chromatogr. A. 1157(1-2): 1-9.
[18] Yang, X., Jia, Z., Yang, X., Li, G., Liao, X. (2017): Cloud point extraction-flame atomic absorption spectrometry for pre-concentration and determination of trace amounts of silver ions in water samples. – Saudi Journal of Biological Sciences 24(3): 589-594.
[19] Yu, C., Zhang, S., Zhang, J., Li, S., Zhou, W., Gao, H., Lu, R. (2014): An in situ ionic liquid dispersive liquid-liquid microextraction method for the detection of pyrethroids by LC-UV in environmental water samples. – J. Brazil. Chem. Soc. 24(6): 1034-104000.

http://www.aloki.hu ● ISSN 1589 1623 (Print) ● ISSN 1785 0037 (Online)
DOI: http://dx.doi.org/10.15666/aeer/1605_57055714
© 2018, ALÖKI Kft., Budapest, Hungary

AGRONOMIC ASPECTS OF SWITCHGRASS CULTIVATION AND USE FOR ENERGY PURPOSES

BRODOWSKA, M. S.[1] – MUSZYŃSKI, P.[2*] – HALINIARZ, M.[3] – BRODOWSKI, R.[4] – KOWALCZYK-JUŚKO, A.[4] – SEKUTOWSKI, T.[5] – KURZYNA-SZKLAREK, M.[1]

[1]Department of Agricultural and Environmental Chemistry, University of Life Sciences in Lublin, Akademicka Street 15, 20-950 Lublin, Poland (phone: +48-81-445-6045)

[2]Department of Chemistry, University of Life Sciences in Lublin Akademicka Street 15, 20-950 Lublin, Poland (phone: +48-81-445-6556)

[3]Department of Herbology and Plant Cultivation Techniques, University of Life Science in Lublin, Akademicka Street 13, 20-950 Lublin, Poland (phone: +48-81-445-6654)

[4]Department of Environmental Engineering and Geodesy, University of Life Sciences in Lublin Leszczyńskiego Street 7, 20-069 Lublin, Poland (phone: +48-81-531-9712)

[5]Department of Weed Science and Tillage Systems, Institute of Soil Science and Plant Cultivation, National Research Institute, Orzechowa Street 61, 50-540 Wrocław, Poland (phone: +48-71-336-2658)

**Corresponding author*
e-mail: pawel.muszynski@up.lublin.pl; phone: +48-81-445-6556

(Received 22nd Jun 2018; accepted 9th Aug 2018)

Abstract. The world's non-renewable energy resources continually decline and therefore there is an urgent need to seek and use any available renewable energy sources. An alternative to conventional fuels can be the usage of plant biomass for energy purposes. This particularly relates to plants with C4 photosynthesis, a large increase in biomass, low habitat requirements, and high resistance to diseases and pests. All these characteristics are met, among others, by switchgrass which in many countries occurs as a common wild plant. In agricultural production, switchgrass does not pose many agronomic problems; moreover, it is a very durable plant that can be used in one stand for even 10 years and can be grown in all soils, even contaminated ones. Effective use of switchgrass for bioethanol, biogas or syngas production provides measurable ecological benefits and in the long term offers a chance to maintain a sustainable national energy balance, given the continuously shrinking non-renewable fuel resources. Due to the multifaceted use of this plant and a number of features important from the point of view of the power generation industry, it is worth having a closer look at the possibility of spreading the cultivation of this species.
Keywords: *Panicum virgatum, cropping, biomass, combustion and co-firing, biofuels*

Introduction

Switchgrass (*Panicum virgatum* L.) belongs to the *Poaceae* family. It is native to North America where it occurs naturally from the Atlantic coast to the Rocky Mountains within the area between 55°N (southern Canada) and 30°N (northern Mexico) (Lewandowski et al., 2003; Wullschleger et al., 2010). This is a perennial grass with erect stems, often with a reddish tinge, and a height from 0.5 to 2.7 m. The

http://www.aloki.hu ● ISSN 1589 1623 (Print) ● ISSN 1785 0037 (Online)
DOI: http://dx.doi.org/10.15666/aeer/1605_57155743
© 2018, ALÖKI Kft., Budapest, Hungary

inflorescence is a branched panicle with a length from 15 to 50 cm. Switchgrass has a very well-developed root system that reaches a depth of even 3 meters (Moser and Vogel, 1995; Christian and Elbersen, 1998; Vogel et al., 2011; Kibet et al., 2016). It is a species with C4 photosynthesis (Hatch-Slack cycle) and due to this it can carry out this process even four times more efficiently compared to C3 type plants (Gołaszewski, 2011; Wang et al., 2012).

Due to the different morphological characteristics and habitat preferences, two ecotypes of this species are distinguished: the lowland ecotype and the upland ecotype (Bals et al., 2010; Casler, 2012; Young et al., 2012). Lowland ecotypes reach a height of more than 3 m, usually grow in clumps in wetland areas, and have thick stiff stems with a large number of branches. Upland ecotypes are shorter, occur in dry areas, have thinner stems with a lower number of branches compared to lowland switchgrass, and form characteristic sods; they are more recommended for growing in a cooler climate (Christensen and Koppenjan, 2010; Casler, 2012).

The first attempts to grow switchgrass began in the 30s and 40s of the 20th century in the USA where many switchgrass cultivars have been bred, including several cultivars also adapted to European climatic conditions: 'Cave-in-Rock', 'Kanlow', and 'Alamo' (McLaughlin and Kszos, 2005). In the United States, this species is recommended for sodding in degraded areas and is grown as an erosion prevention plant. Moreover, switchgrass has the ability to clean soils and waters by removing excess nutrients (N, P) originating, among others, from fertilization. Switchgrass filter strips decrease the amount of reactive phosphorus and reduce the chemical oxygen demand (COD) in surface runoff water, which protects surface waters against eutrophication (Sanderson and Adler, 2008). Switchgrass is used for phytoremediation because it exhibits the capacity to accumulate toxic substances from soils, in particular heavy metals and residues of crop protection chemicals (Chen et al., 2012; Zorer Çelebi and Zorer, 2018). The capacity of switchgrass for significant soil carbon sequestration contributes to a reduction in total environmental CO_2 balance (Liebig et al., 2008; Adkins et al., 2016). This plant is also an excellent growth and living habitat for wildfowl and mammals, in particular in the so-called ecotone zones between forest and crop fields. It is also a very impressive and beautiful ornamental grass sown in gardens and parks (Dudkiewicz and Bolibok, 2011; Elbersen et al., 2013).

At the beginning of the 90s of the last century, an attempt was also made to use switchgrass as an energy crop. The U.S. Department of Energy, among others, conducted research on the use of biomass of this species for energy purposes. Also in Europe, switchgrass arouses an increasingly greater interest as a productive and durable 'energy' species resistant to adverse environmental conditions (Bals et al., 2010; Sanderson and Adler, 2008; Wullschleger et al., 2010). Due to the multifaceted use of this plant and a number of features important from the point of view of the power generation industry, it is worth having a closer look at the possibility of introducing and spreading the cultivation of this species (Bocian et al., 2010; Pszczółkowski et al., 2012).

Plantation establishment and management

Sowing of switchgrass

Switchgrass seeds are very small (depending on the cultivar, 500-1000 seeds·g^{-1}) and characterized by very short viability and low germination capacity. The field emergence

http://www.aloki.hu ● ISSN 1589 1623 (Print) ● ISSN 1785 0037 (Online)
DOI: http://dx.doi.org/10.15666/aeer/1605_57155743
© 2018, ALÖKI Kft., Budapest, Hungary

rate is about 50% (Schmer et al., 2006). To increase their germination capacity, switchgrass seeds should be stratified by subjecting them to low temperatures or NaClO. The recommended seeding depth is from 0.5 to 2.0 cm (Sanderson et al., 2012). In wet areas, it is recommended to grow switchgrass with a row spacing of 60-90 cm, while in dry areas 90-120 cm (Majtkowski, 2006). It has been shown that switchgrass germinates better and besides the growth of seedlings is more intensive after application of selected strains of Cyanobacteria, which have the ability to fix atmospheric nitrogen, as a biofertilizer (Chojnacka et al., 2010). Switchgrass is not resistant to low temperatures and this is why it should be sown in areas with mild winters. Its seeds sprout best in a soil with a pH ranging 6-8 (Hanson and Johnson, 2005).

The field under switchgrass should be very carefully prepared. Switchgrass can be sown in no-till or conventional cultivation practices. No-till allows you to set up switchgrass plantations on fields with a large slope and in areas with low rainfall (Drinnon et al., 2014; Sadeghpour et al., 2014b). Moreover, according to Ashworth et al. (2015) intercropping selected legumes in switchgrass may enhance forage quality and yield, reduce fertilizer costs, and emissions/runoff to air and groundwater.

Plantation evaluation in terms of emergence

The first evaluation of the condition of a plantation is conducted after 6-10 weeks from the date of its establishment. At this time, the number of seedlings per 1 m^2 should be from 100 to 200. The second evaluation of the condition of the plantation is made at the end of the first growing season. To conclude that the plantation has been successfully established, there should be 10-30 plants per m^2 (Douglas et al., 2009). Due to intensive tillering, plants growing at a lower density in the first year will produce a larger number of stems in the next years.

Weed control

One of the major factors that ensure optimal growth and development of switchgrass intended for energy production is to eliminate or at least reduce weed infestation of a plantation, mainly in the first year (Miesel et al., 2012). The slow growth rate of switchgrass (during the first month) and the late time of its sowing (the second decade of April and the beginning of May) promote weed competition. The greatest noxiousness of weeds is observed during the period from emergence to the 8-10-leaf stage of switchgrass (Boydston et al., 2010; Anderson et al., 2014).

Switchgrass badly bears cutting (especially in the first year of cultivation) and damage that can occur during mechanical weed control treatments and therefore mechanical and physical methods are not recommended in switchgrass cultivation. Chemical weed control in switchgrass crops is limited by the small range of agents recommended for use in non-agricultural crops used for energy purposes. The effect of such weed control is partial, since predominantly the annual (mono- and dicotyledonous) species are well destroyed, whereas the perennial deep-rooted species are poorly destroyed and in the next year (during the plant establishment period) they reappear, very frequently with double intensity. Furthermore, inappropriately selected herbicides can produce the following adverse effects: decreased field germination capacity, damage of switchgrass plants, and their reduced biomass (Sekutowski et al., 2009; Boydston et al., 2010; Anderson et al., 2014). A year before the establishment of a switchgrass plantation, it is recommended to use different herbicides that contain in

http://www.aloki.hu ● ISSN 1589 1623 (Print) ● ISSN 1785 0037 (Online)
DOI: http://dx.doi.org/10.15666/aeer/1605_57155743
© 2018, ALÖKI Kft., Budapest, Hungary

their composition mainly glyphosate (following Smeets et al., 2009). According to Bullard and Metcalfe (2001), the optimal rate of glyphosate in switchgrass cultivation is 2.5 $kg \cdot ha^{-1}$. To control dicotyledonous weeds, herbicides with bentazon and 2,4-D can also be used (Samson, 2007; Christensen and Koppenjan, 2010; Scordia et al., 2015). In the professional literature, there is little information and few recommendations concerning weed management in switchgrass plantations using foliar herbicides. The present author's research conducted since 2008 shows that it is possible to use selectively and safely various foliar herbicides recommended for use in cereal, maize or green crops (*Table 1*).

Table 1. *Exemplary active substances of herbicides used in the cultivation of switchgrass. (Own results not published)*

Active substance	Application date	F		Weed management	
		I	II	Monocotyledons	Dicotyledonous
Iodosulfuron-methyl-sodium; Mesosulfuron-methyl	T-3	2-3 (CH)	1-2	+	+
Thifensulfuron methyl; Chlorsulfuron	T-3	2 (CH)	1	+	+
MCPA	T-3	1	1	-	+
2,4-D; Dicamba	T-3	1	1	-	+
Clopyralid; Fluroxypyr; Triclopyr	T-3	1	1	-	+

F – phytotoxicity – sensitivity to the active substance of the herbicide in a 1-9 scale, where: 1 – no effect on switchgrass, 9 – complete destruction of switchgrass; I – 7 days after application of the active substance of the herbicide; II – 28 days after application of the active substance of the herbicide; CH – leaf chlorosis; T-3 – 3-5 switchgrass leaves

Switchgrass insects

Switchgrass is genetically varied and generally resistant to many insects and hence pests usually do not pose a problem in growing switchgrass. Damage caused by insects can be much greater when switchgrass monocultures are grown on large production fields (Sanderson et al., 2012). The most common insects found were Coleoptera, Hemiptera, Diptera and Hymenoptera (Parrish and Fike, 2005; Holguin, 2010).

In the northern states of the USA, Prasifka et al. (2010) recorded the occurrence of *Blastobasis repartella* on a wildly growing switchgrass. Larvae of this moth feed on young tillers of switchgrass. In South Dakota (USA) Boe and Gagne (2011) discovered on switchgrass new species of gall midge. Sometimes plantations of switchgrass can be damaged by grasshoppers and crickets (*Orthoptera*) (Parrish and Fike, 2005; Branson et al., 2006; Holguin, 2010).

Management of pests in grasses involves mainly chemical control. With high pest incidence, insecticides based on malathion and carbaryl, insect growth regulators and pyrethroids are used (Holguin, 2010).

Switchgrass diseases

In wet locations, switchgrass can be infected by fungal diseases, but lowland types are more resistant to rust than upland ones. Especially young plantations can be sometimes attacked by various diseases (Vogel et al., 2011; Uppalapati et al., 2013).

http://www.aloki.hu ● ISSN 1589 1623 (Print) ● ISSN 1785 0037 (Online)
DOI: http://dx.doi.org/10.15666/aeer/1605_57155743
© 2018, ALÖKI Kft., Budapest, Hungary

Rust is the biggest problem in growing switchgrass. Two species of rust fungi, *Uromyces graminicola* and *Puccinia emaculata*, are known to infect switchgrass (Gustafson et al., 2003; Zale et al., 2008; Sanderson et al., 2012; Uppalapati et al., 2013). Rust can be controlled by fungicides, however, some of them negatively affect the quality of the raw material obtained. Hagan and Akridge (2013) achieved the best results by applying azoxystrobin and myclobutanil. A very good way to protect the plantation against rust is also the cultivation of varieties resistant to these pathogens (Gustafson et al., 2003).

Switchgrass may also be attacked by diseases such as: anthracnose (*Colletotricum navitas*), smuts (*Tilletia maclaganii*), Phoma leaf spot (*Phoma spp.*), and *Fursarium* root rot (*Fusarium spp.*), sharp eyespot (*Rhizoctonia cerealis*), leaf spot (*Colletotrichum graminicola*), bunt (*Tilletia pulcherrima*), spot blotch and root rot (*Bipolaris spicifera*) (Vogel, 2004; Carris et al., 2008; Crouch et al., 2010; Vu et al., 2011). In Iowa (USA) Thomsen et al. (2008) estimated yield losses from *Tilletia maclaganii* of 2-40% in switchgrass fields. Leaf spot is caused by fungi from the genus *Bipolaris*. This disease reduces seed germination and yield of switchgrass biomass, particularly if a susceptible cultivar is seeded over a wide area. Control measures against leaf spots include developing resistant cultivars and fungicidal seed treatments (Krupinsky et al., 2004). According to research of Steward et al. (2015) viral diseases raised by Panicum mosaic virus and its satellite virus should be considered important pathogens of switchgrass and serious potential threats to biofuel crop production efficiency.

Fertilization

Switchgrass does not have high soil requirements. Even though it prefers soils with a neutral pH, but it also grows well in slightly acidic and alkaline soils. It can be grown on light or medium cohesive, moderately salinated and agriculturally unsuitable soils (Evanylo et al., 2005; Kabała et al., 2010; Quinn et al., 2015).

Switchgrass is characterized by low nutrient requirement. Bullard and Metcalfe (2001) think that NPK fertilization should be used at the stage of plantation establishment and the fertilizer rates proposed by them are as follows: 80 kg NH_4NO_3 (28 kg $N \cdot ha^{-1}$), 40 kg P_2O_5 (17.5 kg $P \cdot ha^{-1}$), and 60 kg K_2O (49.8 kg $K \cdot ha^{-1}$). Sokhansanj et al. (2009) as well as Christensen and Koppenjan (2010) claim that in the first year of plantation nitrogen fertilizers are not recommended to be applied because weeds characterized by higher biomass increase could suppress the slowly growing young seedlings of switchgrass. Over the plantation lifetime, nitrogen fertilizers are applied to increase biomass yield, but the need to use phosphorus and potassium is determined by the content of these nutrients in the soil (Sanderson et al., 1996; McLaughlin et al., 2002). Nitrogen fertilization also has a beneficial effect on the content of lignin in biomass (Withers, 2010). According to Samson (2007), nitrogen fertilization at a rate of 50-60 kg $N \cdot ha^{-1}$ is appropriate to obtain optimal biomass production in switchgrass, whereas higher rates may reduce its yield. The nitrogen rate that will positively affect switchgrass yield depends on many factors, among others, climatic conditions and the productivity of switchgrass cultivars (An et al., 2018). Thus, in some studies yields have been observed to increase at higher nitrogen rates than those applied by Samson (2007). For example, based on the literature data Gunderson et al. (2008) report that lowland and upland ecotypes reach the maximum yield under nitrogen fertilization at rates of 90 and 100 $kg \cdot ha^{-1}$, respectively. Kering et al. (2012), Giannoulis et al. (2016) and Alexopoulou et al. (2017), on the other hand, observed an

http://www.aloki.hu ● ISSN 1589 1623 (Print) ● ISSN 1785 0037 (Online)
DOI: http://dx.doi.org/10.15666/aeer/1605_57155743
© 2018, ALÖKI Kft., Budapest, Hungary

increase in switchgrass biomass production at a nitrogen doses of 135 kg·ha^{-1} and 80, 160, 240 kg·ha^{-1} and 75, 150 kg·ha^{-1}, respectively. Nitrogen rate should be adjusted depending on the level of this nutrient in the soil (Mitchell et al., 2014). In planning nitrogen fertilization, biomass harvest date should also be taken into account (Miesel et al., 2017). If harvest is to be carried out after the end of the growing season (the first ground frost), the applied nitrogen rate should be lower than in the case of an earlier harvest date (Mitchell et al., 2016). Generally, moderate nitrogen rates under particular soil conditions are entirely sufficient and allow high switchgrass yields to be obtained (Thomason et al., 2004).

Switchgrass is characterized by efficient use of both potassium and phosphorus. Information can be found in the literature which shows that these two elements have effect on biomass yield quantity and quality but also information which proves that they can do not affect the yield of switchgrass. The effect of using K and P fertilizers on the yield of switchgrass depends on the content of these macroelements in the soil. In general, on soils with a deficiency of N and P, switchgrass reacts positively to fertilization of K or P. However, this beneficial effect is not observed on soils that are rich in K and P (Muir et al., 2001; Kering et al., 2012; Shield et al., 2012; Kering et al., 2013). Some studies indicate that the use of multi-ingredient fertilizer increases the yield of switchgrass. Ameen et al. (2018) showed that the fertilizer mixture of N, P, and K (NPK) caused increase in biomass yield of switchgrass compared with the PK, NK, and NP treatments. Mohammed et al. (2015) showed that mixture fertilizer NPK significantly increased biomass yield of switchgrass (by 49%) compared to the control treatment. In turn, calcium fertilizers should only be used when the soil pH is below 5 (Bates et al., 2008).

Good results were obtained using organic cattle manure (CM) and poultry litter (PL) fertilizers on the switchgrass. It was found that these fertilizers increased biomass yield significantly to the extent of 30 and 23% compared with combined chemical fertilizer (12.9 Mg·ha^{-1}) (Mohammed et al., 2015).

Biomass yield and harvest

In the first and second year of cultivation, biomass productivity reaches from 33 to 66% of the maximum production level (McLaughlin and Kszos, 2005). It is only in the 3rd year of plant growth that the biomass production reaches 100% productivity on light soils, whereas on heavy soils this occurs 2-3 years later. Due to this, in the first year switchgrass is usually not harvested, nor is animal grazing recommended, in particular in plantations established in a cooler climate (Christensen and Koppenjan, 2010). From the year in which the optimal productivity is reached, in properly managed switchgrass plantations yields can be maintained at a constant high level for more than 10 next years (Mitchell et al., 2008, 2016; Monti et al., 2009a; Sokhansanj et al., 2009).

The annual switchgrass yield is from several to over a dozen Mg of dry matter (DM) per hectare, though it may exceed 20 Mg DM·ha^{-1} and even more than 30 Mg DM·ha^{-1}, depending on environmental and agronomic factors as well as the cultivar, ecotype and plantation age (Gunderson et al., 2008; Smeets et al., 2009; Hattori and Morita, 2010). Generally, lowland species are characterized by higher yields than upland cultivars. A review of literature data by Heaton et al. (2004) shows that the average annual yield is 10 Mg DM·ha^{-1}. In Poland, the average yield of switchgrass grown on a light soil in the area of Wrocław in the period 2004-2006 was 7.16 Mg DM·ha^{-1} (Dradrach et al., 2007).

http://www.aloki.hu ● ISSN 1589 1623 (Print) ● ISSN 1785 0037 (Online)
DOI: http://dx.doi.org/10.15666/aeer/1605_57155743
© 2018, ALÖKI Kft., Budapest, Hungary

Switchgrass productivity is significantly dependent on the amount of rainfall during the growing season and is higher on well-irrigated soils (Kimura et al., 2015).

Harvest date and frequency depend on climatic and soil conditions, switchgrass ecotype and the future use of biomass harvested (Casler and Boeb, 2003; Jiang et al., 2014). Potentially, switchgrass can be harvested once or several times during the growing season or once after the end of the growing season. In the case of several harvests, a larger amount of nutrients, in particular nitrogen, is removed with the yield (Prieto et al., 2017; Wang et al., 2018). For this reason, plantation operating costs increase due to the need to replenish soil nitrogen at higher nitrogen fertilizer rates. Moreover, each successive harvest requires equipment for biomass cutting and transport, which generates additional economic costs (Christensen and Koppenjan, 2010). A single harvest during the growing season (e.g. in the middle of August or at the turn of summer and autumn) allows a high biomass yield to be obtained (Vogel et al., 2002; Lemus et al., 2008). A late autumn harvest gives a relatively high yield, but the productivity can be lower by 10-20% compared to an earlier harvest (Vogel et al., 2002). But a frequent harvest adversely affects the condition of plants and plantation longevity (Fike et al., 2006; Lee et al., 2014b). It should be stressed that after the end of the growing season nutrients from the aboveground parts of switchgrass plants are transported to the roots (Anderson et al., 2013; Lindsey et al., 2013; Wayman et al., 2014). That is why a single harvest after the end of the growing season is more appropriate in the context of good overwintering of the rhizome (following Mitchell and Schmer, 2012). A spring harvest (before plant growth begins) causes the lowest losses in reserve nutrients (Adler et al., 2006; Samson, 2007; Guretzky et al., 2011; Gamble et al., 2015), but the yield harvested during this period is lower than the yield obtained from an autumn harvest (Adler et al., 2006; Cherney et al., 2018). Yield losses result, among others, from dry and brittle leaves of switchgrass plants being blown away by strong winds. Most frequently, the harvest is carried out once a year, though in the case of upland ecotypes grown in a warmer climate a high yield is also obtained with two biomass harvests per year (Fike et al., 2006).

The harvest is carried out using one-stage technology (simultaneous cutting and grounding) or two-stage technology (first the cutting operation, then grounding). It should be indicated that the grounding operation is important when switchgrass biomass is used for energy purposes. In the case of biomass to be burned or subjected to thermochemical conversion, low moisture, ash, nitrogen, potassium and chlorine contents are also of major importance (Lindsey et al., 2013; Liu et al., 2014; Sadeghpour et al., 2014a; Gorlitsky et al., 2015). It is essential that the values of these parameters are lowest in spring-harvested biomass (*Table 2*) (Adler et al., 2006; Zegada-Lizarazu et al., 2010; Lee et al., 2014b; Cherney et al., 2018). During the summer period, the plant water content is about 70%, at the end of autumn it decreases to about 40% (following Sokhansanj et al., 2009), while in spring-harvested biomass it can be from several to over a dozen percent (Adler et al., 2006; Samson, 2007; Sadeghpour et al., 2014a). It is worth mentioning that a low plant water content facilitates harvest as well as storage and pelletization of the material harvested. But biomass with a water content of > 20% can be stored only for a short time and its drying is costly (Sokhansanj et al., 2009). Harvest at a later time seems to be less favorable when the biomass will be subjected to enzymatic hydrolysis (bioethanol production) because the biomass harvested during this time contains more lignin which hinders this

http://www.aloki.hu ● ISSN 1589 1623 (Print) ● ISSN 1785 0037 (Online)
DOI: http://dx.doi.org/10.15666/aeer/1605_57155743
© 2018, ALÖKI Kft., Budapest, Hungary

process (Lindsey et al., 2013; Aurangzaib et al., 2016; Serapiglia et al., 2017). However, this component increases the energy value of biomass (Williams et al., 2016).

Table 2. *The ash and selected elements content in switchgrass depending on the harvest date. (Adler et al., 2006)*

Harvest date	Ash	N	K	Cl
	% dry matter			
	Experience plots			
Autumn	3.41	0.62	0.33	0.10
Spring	2.47	0.54	0.06	0.03
	Experience canopy			
Autumn	3.46	0.43	0.34	0.06
Spring	2.26	0.40	0.07	0.01

Switchgrass is harvested using conventional farming equipment. It is mowed at a height of 10-15 cm from soil surface and the cut biomass is baled into round or rectangular bales that are stored in a dry place isolated from the ground. To reduce storage losses, biomass with a moisture content > 18% should be field dried before it is baled (Garland, 2008; Monti et al., 2009b; following Mitchell and Schmer, 2012).

The use of biomass for energy purposes

The growing problem of greenhouse emissions and the increasing demand for energy have enhanced the interest in energy sources alternative to fossil fuels. Biomass is an appropriate energy source that can provide in a short time transportation fuels such as biodiesel and bioethanol. Bioethanol is one of the most known biofuels that can be a substitute for petrol (Alvira et al., 2010). The possibility of using first generation bioethanol, produced from maize, wheat, sugar beet, sugar cane, etc., has been studied thus far (Bai et al., 2010). Nevertheless, the production of biofuels from food raw materials arouses a lot of controversy and therefore second-generation biofuels are used, which are produced from lignocellulosic substrates (e.g. switchgrass, straw). Switchgrass biomass can be converted to useful energy by direct combustion or during the production of liquid (bioethanol) and gaseous biofuels (syngas, biogas) (Sanderson et al., 2006; Alvira et al., 2010; Schmer et al., 2014).

Combustion and co-firing of switchgrass

Switchgrass biomass can be used in the burning process as a stand-alone fuel or can be co-fired with coal. However, the use of switchgrass as the only source of fuel or in a mixture with coal in high capacity power plants is not common or economically beneficial. This is due to slagging and contamination of the combustion systems (Karlsson et al., 2015). The reason for this adverse phenomenon is the presence of potassium, calcium, magnesium, chlorine and silicon in biomass in amounts larger than in coal (Qin et al., 2006; Antunes and de Oliveira, 2013). The higher the potassium and sodium content, the lower the biomass ash melting point and as a result of this the greater the slagging and the boiler corrosion. Gaseous chlorine and hydrogen chloride are the main corrosion factors of power boilers, but the action of HCl on boiler metal

http://www.aloki.hu ● ISSN 1589 1623 (Print) ● ISSN 1785 0037 (Online)
DOI: http://dx.doi.org/10.15666/aeer/1605_57155743
© 2018, ALÖKI Kft., Budapest, Hungary

jest less dangerous than that of Cl_2. Chlorides, especially potassium and sodium chlorides, released during biomass burning condense on the surface of the boilers and superheater tubes. Then, in a reaction of the chlorides with iron oxides present in the deposits or SO_2 that occurs in flue gas, chlorine and hydrogen chloride are formed, respectively. The solid products of these reactions, on the other hand, are melted into a glassy viscous layer that captures non-volatile elements (Ca, Si and Mg) from which silicates are formed with lower melting points than in the case of chlorides, which increases the risk of corrosion (Hardy et al., 2009; Kumar et al., 2017).

The effectiveness of switchgrass biomass burning is also dependent on ash and moisture content. The composition and calorific value of switchgrass are shown in *Table 3*. A relatively high ash content in switchgrass is due to the higher proportion of leaves, which can contain 3 times more ash than the stems, in the biomass of this plant (*Table 4*) (Madakadze et al., 1999; Hu et al., 2010; Vamvuka et al., 2010). Ash reduces the calorific value of biomass. A high moisture content of biomass also results in a reduced calorific value and this content should not be more than 23% (Lewandowski and Kicherer, 1997). In the biomass burning process, nitrogen content is also important, since it affects NO_x emissions (Elbersen, 2001). According to Lewandowski and Kicherer (1997), the nitrogen content in dry matter should be < 10 $g \cdot kg^{-1}$ DM (dry matter).

Table 3. *The composition and calorific value of the biomass of switchgrass*

C (% DM)	H (% DM)	N (% DM)	O (% DM)	Ash (% DM)	Moisture (%)	High Heating Value, HHV ($MJ \cdot kg^{-1}$ DM)	Source
44.5	5.8	0.5	45.7	3.7	6.2	19.5	(Pilon and Lavoie, 2011)
46.68	5.82	0.76	37.38	8.98	15.00	18.06	(Tillman, 2000; ECN, 2016)

DM – dry matter

Table 4. *Percentage of internodes, nodes, and leaves of switchgrass in the dry mass. (Hu et al., 2010)*

Variety	Internodes (%)	Nodes (%)	Leaves (%)
Alamo	26.8	3.7	69.5
Kanlow	25.9	3.2	71.0

Research shows that burning switchgrass biomass mixed with coal can bring ecological benefits, such as reduced emissions of some atmospheric pollutants and an increase in biomass heating rate during this process (Kumar et al., 2017). Switchgrass and coal can be co-fired in pulverized coal-fired boilers (which are commonly used in Polish power plants and combined heat and power plants) as well as in fluidized beds. Co-firing in pulverized coal-fired boilers requires the biomass to be converted into a homogeneous material with a grindability similar to that of coal. This is due to the fact that the co-firing process is preceded by biofuel grinding in coal mills, which are structurally unsuitable for co-milling of coal with raw biomass (Zuwała et al., 2014). During the combustion of a coal and biomass mixture in fluidized beds, on the other

http://www.aloki.hu ● ISSN 1589 1623 (Print) ● ISSN 1785 0037 (Online)
DOI: http://dx.doi.org/10.15666/aeer/1605_57155743
© 2018, ALÖKI Kft., Budapest, Hungary

hand, pollutants are deposited on the coils of the secondary superheaters of the boiler which hinder its operation (Hycnar, 2006). It should be added that the risk of chloride corrosion in the co-firing process is not high if the percentage of biomass in the fuel stream does not exceed 10% (Hardy et al., 2009).

Bioethanol production from switchgrass

Switchgrass is considered a good substrate to produce bioethanol because of its biomass yield, high carbohydrate content, good adaptation to various soil and climate conditions, and low agricultural requirements for its production. Preferred ecotypes for bioenergy applications is lowland ecotypes. This is due to the fact that the biomass yield is higher compared to lowland ecotypes (Dien et al., 2013). In studies Dien et al. (2013) the higher content of carbohydrate occurred in upland ecotype and increased with harvest maturity.

The process of bioethanol production is based on the fermentation of monosaccharides (pentoses and hexoses) that are formed as a result of enzymatic hydrolysis of the polysaccharides (cellulose and hemicelluloses) contained in switchgrass biomass. Cellulose and hemicelluloses, together with lignin, are the major components of the lignocellulose polymer which is not very susceptible to enzymatic hydrolysis due to its complex structure (Lee et al., 2014a; Williams et al., 2016; Zabed et al., 2017). In the lignocellulosic complex, lignin is the most difficult to hydrolyze, mainly due to the presence of carbon-carbon bonds and ether-type bonds in its structure, while the hemicelluloses are relatively easiest to hydrolyze. Moreover, the lignin and hemicelluloses surrounding the microfibers of the cellulose effectively impede the degradation of this polysaccharide by the cellulosic enzymes (Waramit et al., 2011; Umezawa, 2018).

Individual varieties of switchgrass differ in the content of carbohydrates and their individual fractions. Studies on biomass composition of five switchgrass genotypes, selected from twenty-two as the best yielding, were carried out by Min et al. (2017). Biomass composition was analyzed for total carbohydrate polymers (glucan + xylan + arabinan), total lignin (acid-soluble lignin + acid-insoluble lignin) and total extractives (water-soluble extractives + ethanol-soluble extractives) contents. The SWG 2007-2 genotype switchgrass had the highest amount of total carbohydrate polymers and the lowest amount of total lignin; therefore, this genotype is the most promising switchgrass line for the bioconversion to produce biofuel through sugar platform route. On the other hand high ratio of [water soluble carbohydrates + starch + cellulose]:hemicellulose showed that biomass of switchgrass stems and whole aboveground part (2.39 and 2.40) could be highly valuable feedstock for liquid biofuel production (Butkutė et al., 2013).

Thus, to reduce the resistance of lignocellulose and its fractions (in particular cellulose and lignin) to enzymatic action, the biomass structure and chemical composition should be changed (Rijal et al., 2012). These effects can be achieved through biomass pretreatment using the following methods: mechanical (grinding, milling), chemical (decomposition using acids (H_2SO_4, HCl) and bases (NaOH, KOH, $Ca(OH)_2$) as well as ammonium and ozone), thermal (in which steam heating, for example, is used), and also biological (the use of microorganisms to degrade or digest the cellulose and lignin) (Xu et al., 2011; Larsen et al., 2012; Karp et al., 2015; Loow et al., 2016; Sharma et al., 2016; Chen et al., 2018; Rajendran et al., 2018). Acid hydrolysis or base hydrolysis is relatively cheap and commonly used methods of

http://www.aloki.hu ● ISSN 1589 1623 (Print) ● ISSN 1785 0037 (Online)
DOI: http://dx.doi.org/10.15666/aeer/1605_57155743
© 2018, ALÖKI Kft., Budapest, Hungary

chemical biomass pretreatment. The study of Rijal et al. (2012) showed the beneficial effect of acid or base pretreatment as well as of grinding and heating in a pellet mill on the efficiency of enzymatic hydrolysis of switchgrass biomass.

The process that follows pretreatment is enzymatic hydrolysis designed to convert the cellulose and hemicelluloses to fermenting sugars, which include glucose and xylose. This method uses the complexes of three enzymes (cellulases and hemicellulases) which are produced by microorganisms and which have a synergistic effect during the hydrolysis of cellulose (endo-β-1,4-glucanases, exo-β-1,4-glucanases, and β-glucosidase) and hemicelluloses (endo-β-1,4-xylanases, exo-β-1,4-xylanases and β-xylosidase). These polysaccharides are hydrolyzed to monosaccharides. The glucose derived from the hydrolysis is usually subjected to fermentation using strains of the yeast *Saccharomyces cerevisiae* and the bacterium *Zymomonas mobilis*. But xylose is converted by other yeasts, such as *Pachysolen tannophilus, Candida shehatae,* and *Pichia stipitis* (following Zabed et al., 2017). However, problems have been noted with the use of xylose-fermenting yeasts due to their low tolerance to ethanol, slow fermentation rate and difficulties with adjusting the reaction conditions (Keshwani and Cheng, 2009). Therefore, strains of bacteria such as *Escherichia coli* and *Zymomonas mobilis* have been modified in recent years using genetic engineering. Nevertheless, the fermentation capacity of these strains is not sufficiently effective. Genetically modified strains of *Sacharomyces cerevisiae* are currently used in the process of biomass conversion to ethanol, which is common for xylose and glucose (Balan et al., 2012).

The results of studies on the efficiency of ethanol from switchgrass biomass, with reference to other biomass resources, using in process *Sachcaromyces cerevisiae* are presented by Guragain et al. (2014) (*Table 5*).

Table 5. *Ethanol production at shake flask level using fermentation of biomass hydrolyzed using S. cerevisiae. (Guragain et al., 2014)*

Type of biomass	Ethanol yield ($g \cdot g^{-1}$ glucose consumed)	Productivity ($g \cdot l^{-1} \cdot h^{-1}$)	Ethanol yield ($g \cdot g^{-1}$ pretreated biomass)	Ethanol yield ($g \cdot g^{-1}$ raw biomass)
Switchgrass	0.492 ± 0.003	2.17 ± 0.039	0.16 ± 0.0029	0.10 ± 0.003
Wheat straw	0.492 ± 0.003	2.87 ± 0.003	0.22 ± 0.0002	0.12 ± 0.003
Miscanthus	0.489 ± 0.007	2.27 ± 0.030	0.17 ± 0.0022	0.10 ± 0.001
Sorghum bagasse	0.494 ± 0.005	2.80 ± 0.081	0.21 ± 0.0061	0.13 ± 0.003

Productivity was measured for 15 h of fermentation at 30 °C and expressed as gram of ethanol produced per liter per hour

The yeast *Saccharomyces cerevisieae* only ferment hexoses and are not able to use pentoses contained in biomass. Therefore, other microorganisms that do not have this negative trait are used for the fermentation of sugars and are competitive to *S. cerevisa* strains in terms of the amount of ethanol produced (Kurylenko et al., 2014). Abdullahi et al. (2017) studied the effect of N fertilization and acidic switchgrass biomass hydrolysis on ethanol yield. Pre-treatment was carried out with HCl (concentrations of 3, 4 and 5%). *Saccharomyces cerevisiae* and Gram-negative *Zymomonas mobilis* were used in the fermentation process. The microorganisms were used singly and in combination. The beneficial effects of nitrogen doses of 50 and 75 kg $N \cdot ha^{-1}$ and treatment with 4% acid on the content of reducing sugars in the hydrolyzate were found.

http://www.aloki.hu ● ISSN 1589 1623 (Print) ● ISSN 1785 0037 (Online)
DOI: http://dx.doi.org/10.15666/aeer/1605_57155743
© 2018, ALÖKI Kft., Budapest, Hungary

The most ethanol was obtained when the hydrolyzate was fermented using the combination of *Saccharomyces cerevisiae* and *Zymomonas mobilis*.

Hydrothermal pretreatment is recommended for grass biomass (Alvira et al., 2010; Kim et al., 2011). As a result of the hydrothermal degradation of lignocellulosic biomass, liquid and solid fractions containing useful bioproducts of the depolymerisation of complex sugars can be obtained. Kim et al. (2011) showed that the content of glucose and xylose in switchgrass biomass processed by hydrothermolysis was higher than after the following pre-treatment methods: AFEX (ammonia fiber exolosion), SAA (soaking aqueous ammonia), lime and dilute sulfuric acid. According to Suryawati et al. (2009) temperature 200 °C and time10 min are the best conditions for the hydrothermolysis of switchgrass. Under these conditions, Suryawati et al. (2008) reported an increase in glucan content from 36.6 to 56.6% (dry basis) and a reduction in the xylan content from 21.0 to 2.4% (dry basis) in the solid fraction of switchgrass.

The most problematic step in the biochemical method of obtaining ethanol is the hydrolysis. It is related to the fact that simple sugars which are the end products of enzymatic hydrolysis inhibit the activity of enzymes: cellulases and hemicellulases. For complete hydrolysis of lignocellulose polysaccharides, the sugars released should be directly (in the same tank) transformed by fermenting organisms into ethanol. It is possible in the process of simultaneous saccharification and fermentation (SSF process) (Kurylenko et al., 2014). Faga et al. (2010) conducted research on fermentation of switchgrass biomass using the SSF process. For the pretreatment of biomass, hydrothermolysis (water in the subcritical state, temperature 200 °C, holding time 10 min, 10% (w/w) solids loading) was applied. The following yeast strains were used for the fermentation: *Kluyveromyces marxianus* IMB 1, IMB 2, IMB 3, IMB 4 and IMB 5 (culture at 45 °C) and *Saccharomyces cerevisiae* D_5A (culture at 37 °C). The fermentation process was carried out for: 72 h (*K. marxianus* IMB 1, IMB 2, IMB 4 and IMB 5), 96 h (*K. marxianus* IMB 3) and 7 days (*S. cerevisiae* D_5A). The effect of buffer pH on bioethanol production by *S. cerevisiae* D_5A was also investigated. It was found that in 96 and 120 h of fermentation, the strains IMB 3 and *S. cerevisiae* D_5A were characterized by a higher yield of ethanol production in relation to other *K. marxianus* strains. In the final fermentation stage, the bioethanol production efficiency for IMB 3, IMB 1, IMB 5 strains was at a similar level, but lower than for IMB 3 and *S. cerevisiae*. With the lowering of the pH from 5.5 to 4.8, reduction of ethanol production by *S. cerevisiae* D_5A was observed. Research Sykes et al. (2016) indicate that ethanol efficiency method is significantly reduced by the use of biomass switchgrass infected with rust.

Bioethanol from switchgrass biomass can also be obtained without pre-treatment, which reduces the costs of the process. Chung et al. (2014) proposed the use of a genetically modified strain of *Caldicellulosiruptor bescii* for fermentation. Genetic modification consisted of among others on the introduction of a gene responsible for coding the enzyme allowing ethanol synthesis. A gene isolated from *Clostridium thermocellum* was used for this purpose. The degree of biomass processing using the *Caldicellulosiruptor bescii* recombinant was about 30% and 1.7 moles of ethanol was obtained from each one mole of glucose. Fu et al. (2011) and Yee et al. (2014) studied the production efficiency of bioethanol from biomass of genetically modified switchgrass. Transgenic switchgrass was characterized by a decreased expression of the COMT (Caffeic acid O-methyltransferase) gene, which is responsible for the coding of one of the key enzymes in the lignin biosynthetic pathway. As a result, with the use of

http://www.aloki.hu ● ISSN 1589 1623 (Print) ● ISSN 1785 0037 (Online)
DOI: http://dx.doi.org/10.15666/aeer/1605_57155743
© 2018, ALÖKI Kft., Budapest, Hungary

Clostridium thermocellum, a greater production of bioethanol from transgenic switchgrass biomass in relation to unmodified biomass was obtained.

Ethanol yield from switchgrass biomass from field-scale production ranged from about 2300 to 3500 $L \cdot ha^{-1}$ in depends on biomass yielding (Schmer et al., 2008). Net Energy Yield (NEY) of this biofuel ranged from 50 to more than 75 $GJ \cdot ha^{-1}$. However the complex technological process of bioethanol production from lignocellulosic feedstocks involves significant costs. Moreover, the technology of producing liquid biofuels from this type of biomass has not been fully identified. In particular, the economic aspect is a barrier to the production of second generation biofuels being quickly spread. Energy inputs on the production and processing of switchgrass under the U.S. conditions are 50% higher than the energy generated from the ethanol produced from this crop (Pimentel and Patzel, 2005).

Conversion of switchgrass biomass to gaseous fuels

In spite of the continuous development of bioethanol production from woody feedstocks, the reaction costs are still high, while the variation in biomass composition requires the selection of appropriate hydrolyzing enzymes. Thus, more practical and less costly possibilities of using biomass are sought. One of them is the production of gaseous fuels (Boateng et al., 2006).

Biomass-derived gaseous fuels can be obtained using various processes, including among others: thermal process (gasification and pyrolysis (*Table 6*)) and biochemical: anaerobic digestion. The former one is high-temperature conversion of biomass to gaseous fuels under the influence of a gasifying agent. On the other hand, pyrolysis is a process that does not require access of external oxidizing and reducing agents and hence can be a stand-alone process or one of the stages of gasification or combustion (Piechocki et al., 2010). The pyrolysis products are: non-condensable gases (CO, CO_2, CH_4, and H_2), bio-oil (liquid) and bio-char (solid). Depending on the time of pyrolysis, the yield of these products varies. As a result of gasification synthesis gas (syngas) is produced, whose main components are as follows: H_2, N_2, H_2O, CH_4, CO and CO_2. The amount and composition of the synthesis gas varies depending on the conditions of the gasification process (Damartzis and Zabaniotou, 2011; Sarkar et al., 2014). Lower heating value (LHV) of gases which produced in gasification and pyrolysis of switchgrass biomass are respectively: 4 $MJ \cdot Nm^{-3}$ and 5.9 $MJ \cdot kg^{-1}$ (Elbersen, 2001).

Table 6. *Thermal conversion products of switchgrass biomass. (Elbersen, 2001)*

Product	Gasification	Pyrolysis
H_2	5%	-
CH_4	3%	5%
CO	11%	32%
Other	tar	Bio-oil, charcoal

Pyrolysis can be carried out in a reactor equipped with a mechanism that provides the flow and simultaneous mixing of the feedstock (e.g. a rotating drum reactor or a screw reactor). The syngas production efficiency is higher and the quality of syngas is better when biomass harvested at later dates is pyrolyzed (Boateng et al., 2006). Subsequently,

http://www.aloki.hu ● ISSN 1589 1623 (Print) ● ISSN 1785 0037 (Online)
DOI: http://dx.doi.org/10.15666/aeer/1605_57155743
© 2018, ALÖKI Kft., Budapest, Hungary

through catalytic conversion bioethanol can be obtained from the synthetic gas derived using this method.

In studies by Boateng et al. (2007) with the use of a fluidized-bed reactor, the bio-oil efficiency was over 60% by mass and the energy conversion efficiency was in the range of 52%-81%. He et al. (2009) studied the effect of feedstock moisture contents and pyrolysis temperature (T) on the yield and physicochemical properties of the obtained bio-oil. It was shown that under conditions: moisture of 10% and T = 450 °C, moisture of 15% and T = 550 °C, the obtained bio-oils were characterized by the best physical properties. In addition, experience has shown that by modifying only two parameters of the pyrolysis process, it is possible to significantly affect the efficiency and properties of the obtained biofuel.

According to Boateng et al. (2007), Bridgeman et al. (2007) and He et al. (2009) the chemical composition of bio-oil made from switchgrass is dominated by oxygen compounds, mainly acids, alcohols, ketones, phenols and furans. The mentioned compounds and the presence of water give the hydrophilic character of bio-oil, which limits its useful properties. It should be noted that the water must be separated if the bio-oil is used to produce fuels (Imam and Capareda, 2012). The aqueous phase contained in bio-oil is attempted to be used for the production of hydrogen by means of microbial electrolysis (Borole and Mielenz, 2011). The presence in char and bio-oil of mainly derivatives of phenols, furans and cyclopentanones was also reported by Pilon and Lavoie (2013), who studied the switchgrass pyrolysis at temperatures 300, 400 and 500 °C and in the atmosphere of two different gases: N_2 and CO_2. The studies also showed the variability of biochar and bio-oil shares as well as their calorific value as a function of temperature and type of inert gas. In the process conducted at 500 °C, less biochar was obtained than at temperatures of 300 and 400 °C in both N_2 and CO_2 environments. At 300 °C and in a CO_2 atmosphere the char content was higher than at this temperature in the N_2 environment. The calorific value of biochar at 300 °C and in the CO_2 atmosphere showed a lower calorific value than at the same temperature under the N_2 atmosphere (22.2 vs. 24.5 $MJ \cdot kg^{-1}$). In turn, the calorific value of bio-oil at the temperature of 300 and 400 °C was similar in both atmospheres (~15 $MJ \cdot kg^{-1}$) and at a temperature of 500 °C it was higher in the atmosphere of CO_2.

Research Mohamed et al. (2016) indicate that the use of catalysts in the pyrolysis process can improve the quality of bio-oil obtained from switchgrass biomass. The catalysts were used individually (K_3PO_4; clinoptilolite; activated carbon) and in a mixture (K_3PO_4 + clinoptilolite; K_3PO_4 + bentonite). It was found that bio-oils obtained in the presence of catalysts (K_3PO_4 (10, 20, 30 wt.%), clinoptilolite (20 wt.%), combinations (10 wt.% K_3PO_4 + 10 wt.% clinoptilolite, 10 wt.% K_3PO_4 + 10 wt.% bentonite, 10 wt.% K_3PO_4 + 10 wt.% bentonite) were characterized by lower water content and viscosity in relation to bio-oil obtained without the use of catalyst. The presence of catalysts also positively influenced the quality parameters of biochar, including composition, surface area and porosity. The variability of bio-oil properties (including viscosity, pH, calorific value) obtained from various tests makes it impossible to determine the appropriate quality standards, which in turn is a barrier to the use of this product on an industrial scale (He et al., 2009).

To gasify switchgrass biomass, fluidized bed boiler technology is most recommended, since fluidized bed boilers can use biofuels with a low volume density and a low ash melting point. In the process of switchgrass gasification using this technology, only light tar fractions are formed and boiler slagging does not occur.

http://www.aloki.hu ● ISSN 1589 1623 (Print) ● ISSN 1785 0037 (Online)
DOI: http://dx.doi.org/10.15666/aeer/1605_57155743
© 2018, ALÖKI Kft., Budapest, Hungary

However, a disadvantage of this gasification method is the high carbon content in ash (Elbersen, 2001).

Methods of pretreatment of biomass, ie torrefaction and densification, may lead to obtaining syngas with better properties. Torrefaction is a high-temperature drying process in which a solid fuel (biocarbon) with improved properties towards the raw biomass is obtained. The basic methods of biomass densification are: briquetting and pelleting. Densification increases the volume density of biomass, which increases its usefulness for energy purposes. Sarkar et al. (2014) studied switchgrass biomass gasification, which was pre-treated with torrefaction (at 230 and 270 °C), densification (pelleting) and combined treatment: torrefaction and densification. Gasification was carried out at 700, 800 and 900 °C. The oxidizing agent was air. An increase in H_2 and CO concentrations in the synthesis gas and its lower heating value (LHV) with increasing temperature was observed. The largest amounts of produced H_2 (0.03 $kg \cdot kg^{-1}$ biomass) and CO (0.72 $kg \cdot kg^{-1}$ biomass) showed synthesis gas (LHV = 5.08 $MJ \cdot m^{-3}$) obtained at 900 °C. This gas came from biomass gasification, which was subjected to a combined treatment.

Research Pasangulapati et al. (2012) indicate that the content of cellulose, hemicellulose and lignin in the switchgrass biomass affects the quality of gas obtained as a result of thermal conversion. According to the authors, higher content of cellulose and hemicellulose in relation to lignins results in a higher proportion of CO and CO_2 than CH_4 in the produced gas. Switchgrass and wheat straw in comparison to other biomass tested (eastern red cedar and dry distilled grains with solubles (DDGS)) were characterized by the highest efficiency of coal conversion: 94 and 95%, respectively. In the studies of Torreiero et al. (2018) biomass gasification process (*Nicotiana glauca, Panicum virgatum, Elytrigia elongata*) was tested. It was shown that the conversion efficiency of carbon from switchgrass biomass was the highest: 80% (oxidizing agent: air) and 91.3% (oxidizing agent: enriched air).

The syngas obtained from switchgrass biomass can be subjected to bacterial fermentation to produce bioethanol. For this purpose is best suited a syngas with a high content of carbon monoxide and hydrogen and small content of tar. Fermentation of syngas occurs with the use of anaerobic microorganisms, including from the genus *Clostridium*. According to Tanner (2008) the fermentation of syngas results in the production of 30% more bioethanol in relation to the biochemical conversion method using the same amount of biomass. Pardo-Planas et al. (2017) conducted simulation studies on the optimization of gasification of biomass with steam to a syngas rich in carbon monoxide and hydrogen. The paper analyzed the values of fuel-air equivalence ratio (ER) and molar ratio of steam to biomass (SBR) and the influence of their value on the quantity and percentage composition (CO and H_2 content) of the produced syngas. It was shown that in simulated conditions the efficiency of synthesis gas conversion to ethanol was 63.5%. According to the authors, the hybrid method, ie the combination of gasification with fermentation, is a promising method for producing bioethanol from switchgrass biomass.

Qian et al. (2013) studied the effect of biomass type (switchgrass, sorghum straw and red cedar) and fuel-air equivalence ratio ER (0.20, 0.25 and 0.28) on the physicochemical properties of char obtained as a result of gasification. It was shown that with the increase of the ER index, the following char parameters increased: Brunauer-Emmett-Teller (BET) surface area and ash content, while the content of moisture and fixed carbon decreased.

http://www.aloki.hu ● ISSN 1589 1623 (Print) ● ISSN 1785 0037 (Online)
DOI: http://dx.doi.org/10.15666/aeer/1605_57155743
© 2018, ALÖKI Kft., Budapest, Hungary

Gaseous fuel from switchgrass biomass can be also obtained in the biochemical conversion process: anaerobic digestion (AD). In this process, microorganisms participate, which under anaerobic conditions convert organic substances of the raw material into biogas. The main components of biogas are: methane and carbon dioxide. The usefulness of switchgrass biomass for biogas production results from its chemical composition. Especially some of switchgrass germplasm could be of interest for biogas producers: biomass of octoploid switchgrass ecotype No. 64 by chemical composition was similar to that of reed canary grass, which is characterized by high energy potential (Butkutė et al., 2013). It should be also noted that the solid fraction of post-fermentation residue can be used for the production of solid biofuels, which increases the energy and economic efficiency of the project (Czekała et al., 2018).

Anaerobic fermentation is a labile process whose normal course depends on many factors, including the content of lignins in the substrate. Lignins are resistant to biodegradation (hardly decomposed by methane bacteria) and therefore cause low methane production and reduce process efficiency. In order to use switchgrass biomass more efficiently for the synthesis of methane, pre-treatment is carried out by various methods: mechanical, chemical, thermal or biological (Rodriguez et al., 2017). These methods are similar to those used at the initial preparation stage for the production of bioethanol. Literature data demonstrate the effect of pre-treatment on the efficiency of methane production from switchgrass biomass (Frigon et al., 2012; Papa et al., 2015; Capecchi et al., 2016). Biological methods of pre-treatment, i.e. ensiling and the use of enzymes, are an alternative to physical and chemical methods due to the less onerousness for the environment. For the production of biogas to be possible throughout the year, the maintenance of switchgrass biomass is necessary. One of the treatments for the preservation of biomass is its ensiling (Bélanger et al., 2012). This process not only allows the biomass to be stored for a long period of time without loss, but also to ensure that physico-chemical composition remains unchanged during storage. The stability of the composition of switchgrass biomass is extremely important when it is used for the production of biogas (Herrmann et al., 2011). This composition, however, is altered due to side reactions, e.g. secondary fermentation, which may occur in the ensiling process. The production of silage is based on the metabolic processes of lactic acid bacteria. Therefore, in order to improve the stability of aerobic silage, it is recommended to use microbiological preparations containing strains of lactic acid bacteria. In view of the further use of ensiled biomass for the production of biogas, absolutely heterofermentative bacterial strains (eg, *Lactobacillus buchneri, Lactobacillus brevis*) are particularly useful (Liu et al., 2016). Under anaerobic conditions, the strains of these bacteria ferment simple sugars, both pentoses and hexoses, among others to lactic acid and acetic acid. Lactic acid is a biomass conservation factor in the ensiling process. Whereas, acetic acid is a component that methane bacteria use in the production of biomethane in methane fermentation. In order to obtain good quality silage, both bacterial and bacterial-enzymatic inoculum are used. Kupryś-Caruk (2017) investigated the effect of the addition of bacterial preparations Lactosil and 11CH4 on the quality of silage and biogas production, among others from switchgrass. Both preparations contained heterofermentative lactic acid bacteria and differed in the absence of homofermentative bacteria (11CH4). It was found that silages made with the addition of both Lactosil and 11CH4 were characterized by a higher content of lactic acid in relation to the control. The content of acetic acid was higher in silage with the addition of Lactosil, and the lower in silage with the preparation 11CH4 compared to silage

http://www.aloki.hu ● ISSN 1589 1623 (Print) ● ISSN 1785 0037 (Online)
DOI: http://dx.doi.org/10.15666/aeer/1605_57155743
© 2018, ALÖKI Kft., Budapest, Hungary

made without the addition of these preparations. Significant more biogas was obtained from silage with the addition of 11CH4, which contained the least hemicelluloses and lignins. The problem of the effect of additives on the quality of silage and biogas yield was also investigated by Zhao et al. (2017). In the conducted experiment, the authors demonstrated a positive effect of the combined addition of the strain of *Lactobacillus brevis* and the xylanase enzyme on the volume of biogas production from switchgrass silage. The xylanase enzyme breaks down the lignocellulose hydrolytically into products that are used by the strain of *Lactobacillus brevis*. The use of this enzyme resulted in lowering the lignin content, which positively affected the quality of the obtained silage. Another way to optimize biogas production is to use mixed fermentation feeds, i.e. prepared on the basis of two types of substrates. One of the most common practices of this type is the mixing of plant biomass with manure. Due to the buffering properties of manure, the risk of lowering the pH in the fermenter and consequently stopping the fermentation process is reduced. Ahn et al. (2010) studied the effect of co-fermentation of manure with switchgrass silage on biogas yield in thermophilic conditions (55 °C). For mixture of switchgrass silage with swine manure, a 53% volatile solids reduction (VS) and a biogas yield of 0.373 L $CH_4 \cdot g^{-1}$VS were noted. However, for the other two mixtures (silage of switchgrass + dairy manure and silage of switchgrass + poultry manure) the reduction rates of VS and biogas yields were clearly lower: 9.3%, 0.028 L $CH_4 \cdot g^{-1}$VS and 20%, 0.002 L $CH_4 \cdot g^{-1}$VS, respectively. It should be noted that the higher share of ensiled biomass in the batch, the more acidification of the digester and the complete refraction of the process may occur. This is due to both the low pH of the silage and the production in the digester with the wrong composition and proportion of the substrate mixture of larger amounts of volatile fatty acids (VFA) (Thamsiriroj et al., 2012). In the studies of Ahn et al. (2010) high concentration of VFA was observed during fermentation of mixtures (silage of switchgrass + dairy manure and silage of switchgrass + poultry manure), which was maintained until the end of the process. The methane bacteria could not digest the accumulated acids, which led to acidification of the fermenter and a decrease in biomethane production capacity from these mixtures. For this reason, it is important to determine the right ratio of substrates used and to select the optimal initial loading of the digester with the charge of organic compounds. In addition, the content of dry matter in the digester, which has a significant influence on the yield of biogas, depends on the proportion of substrates in the mixture. Zheng et al. (2015) investigated the effect of various manure dairy farm to biomass relation to methane production in mesophilic conditions. The substrates were mixed in the following total solid ratios (TS): 4:0, 3:1, 2:2, 1:3 and 0:4. It was found that the co-digestion mixture with the ratio of 2:2 substrates showed the highest efficiency of methane production (158.6 mL $CH_4 \cdot g^{-1}$VS). In comparison to the monofermentation of manure and switchgrass, the increase in methane production was 74.5% and 18.3%, respectively.

Among vegetable raw materials, maize is most commonly used in biogas installations. Research of Barbanti et al. (2014) shows that the production capacity of methane from switchgrass biomass is lower (217 mL $CH_4 \cdot g^{-1}$VS) in relation to maize production (316 mL $CH_4 \cdot g^{-1}$VS). This is due to the higher content of structural carbohydrates and lignins in swtchgrass biomass in relation to maize biomass (Barbanti et al., 2014). The data provided in the literature also indicate differences in the production of biogas from switchgrass resulting from fluctuations in the composition and volume of its biomass yield. These characteristics are influenced by the variety,

http://www.aloki.hu ● ISSN 1589 1623 (Print) ● ISSN 1785 0037 (Online)
DOI: http://dx.doi.org/10.15666/aeer/1605_57155743
© 2018, ALÖKI Kft., Budapest, Hungary

habitat and climate conditions of the crop and the applied agrotechnics. It seems therefore justified that varieties of switchgrass intended for biogas should be selected in terms of the same indicators as in the case of maize. These indicators include the highest possible dry matter content·ha^{-1}, low ash content, and lignin and the ability to ensilage (BiogasMagazine, 2012). Selection of varieties with the use of agrotechnics corresponding to local conditions and optimally selected parameters of methane fermentation should result in intensification of biogas production.

Summary

In the world, switchgrass is a species that is used more and more frequently for energy purposes. This species has many positive traits that make this plant very attractive and worthy of spreading. From the agricultural point of view, an enormous advantage of switchgrass is that it has low soil and fertilization requirements; switchgrass is also characterized by high resistance to diseases and pests and thereby it is relatively easy and cheap to grow. Moreover, it exhibits great durability and high biomass productivity over a long period of time and due to this it can be used in a given field for even 10 years without a significant decrease in yield. When switchgrass is used as an energy crop, it is possible to produce bioethanol, biogas (biomethane) and synthesis gas. Biomass of this species can also be co-fired with coal. The effectiveness of these processes is dependent on the moisture content, the ash content and composition as well as the lignin content in switchgrass biomass.

REFERENCES

[1] Abdullahi, A. A., Aliero, B. L., Aliero, A. A., Zuru, A. A., Rabah, A. B. (2017): Optimization of ethanol production from switchgrass (*Panicum virgatum* L.) grown in Sokoto geoecological zone of Nigeria. – International Journal of Chemistry, Pharmacy & Technology 2(1): 43-56.

[2] Adkins, J., Jastrow, J. D., Morris, G. P., Six, J., de Graaff, M.-A. (2016): Effects of switchgrass cultivars and intraspecific differences in root structure on soil carbon inputs and accumulation. – Geoderma 262: 147-154.

[3] Adler, P. R., Sanderson, M. A., Boateng, A. A., Weimer, P. J., Jung, H. G. (2006): Biomass yield and biofuel quality of switchgrass harvested in fall or spring. – Agronomy Journal 98: 1518-1525.

[4] Ahn, H. K., Smith, M. C., Kondrad, S. L., White, J. W. (2010): Evaluation of biogas production potential by dry anaerobic digestion of switchgrass –animal manure mixtures. – Applied Biochemistry and Biotechnology 160: 965-975. DOI: 10.1007/s12010P009P8624Px.

[5] Alexopoulou, E., Zanettib, F., Papazoglouc, E. G., Christoua, M., Papatheoharic, Y., Tsiotasa, K., Papamichaela, I. (2017): Long-term studies on switchgrass grown on a marginal area in Greece under different varieties and nitrogen fertilization rates. – Industrial Crops and Products 107: 446-452.

[6] Alvira, P., Tomás-Pejó, E., Ballesteros, M., Negro, M. J. (2010): Pretreatment Technologies for an effecient bioethanol production process based on enzymatic hydrolysis: A review. – Bioresource Technology 101: 4851-4861.

[7] Ameen, A., Tang, Ch., Han, L., Xie, G. H. (2018): Short-term response of switchgrass to nitrogen, phosphorus, and potassium on semiarid sandy wasteland managed for biofuel feedstock. – BioEnergy Research 11: 228-238.

http://www.aloki.hu ● ISSN 1589 1623 (Print) ● ISSN 1785 0037 (Online)
DOI: http://dx.doi.org/10.15666/aeer/1605_57155743
© 2018, ALÖKI Kft., Budapest, Hungary

[8] An, Y., Gao, Y., Ma, Y. (2018): Growth performance and weed control effect in response to nitrogen supply for switchgrass after establishment in the semiarid environment. – Field Crops Research 221: 175-181.
[9] Anderson, E. K., Parrish, A. S., Voigt, T. B., Owens, V. N., Hong, C.-H., Lee, D. K. (2013): Nitrogen fertility and harvest management of switchgrass for sustainable bioenergy feedstock production in Illinois. – Industrial Crops and Products 48: 19-27.
[10] Anderson, E. K., Hager, A. G., Voigt, T. B., Lee, D. K. (2014): Switchgrass and prairie cordgrass response to foliar- and soil-applied herbicides. – Weed Technology 28: 633-645.
[11] Antunes, R. A., de Oliveira, M. C. L. (2013): Corrosion in biomass combustion: A materials selection analysis and its interaction with corrosion mechanisms and mitigation strategies. – Corrosion Science 76: 6-26.
[12] Ashworth, A. J., Allen, F. L., Keyser, P. D., Tyler, D. D., Saxton, A. M., Taylor, A. M. (2015): Switchgrass yield and stand dynamics from legume intercropping based on seeding rate and harvest management. – Journal of Soil and Water Conservation 70: 374-384. https://doi: 10.2489/jswc.70.6.374.
[13] Aurangzaib, M., Moore, K. J., Archontoulis, S. V., Heaton, E. A., Lenssen, A. W., Fei, S. (2016): Compositional differences among upland and lowland switchgrass ecotypes grown as a bioenergy feedstock crop. – Biomass and Bioenergy 87: 169-177.
[14] Bai, Y., Luo, L., van der Voet, E. (2010): Life cycle assessment of switchgrass-derived ethanol as transport fuel. – The International Journal of Life Cycle Assessment 15: 468-477.
[15] Balan, V., Kumar, S., Bals, B., Chundawat, S., Jin, M., Dale, B. (2012): Biochemical and Thermochemical Conversion of Switchgrass to Biofuels. – In: Monti, A. (ed.) Switchgrass: A Valuable Biomass Crop for Energy. Springer-Verlag, London.
[16] Bals, B., Rogers, C., Jin, M., Balan, V., Dale, B. (2010): Evaluation of ammonia Fiber Expansion (AFEXTM) pretreatment for enzymatic hydrolysis of switchgrass harvested in different seasons and locations. – Biotechnology for Biofuels 3: 1-11.
[17] Barbanti, L., Di Girolamo, G., Grigatti, M., Bertin, L., Ciavatta, C. (2014): Anaerobic digestion of annual and multi-annual biomass crops. – Industrial Crops and Products 56: 137-144.
[18] Bates, G., Keyser, P., Harper, C., Waller, J. (2008): SP701-B-Using Switchgrass for Forage. The University of Tennessee Agricultural Extension Service, SP701B-5M-3/08(Rep) R12-4110-070-012-08 08-0166, http://trace.tennessee.edu/utk_agexbiof/7 (accessed in May, 2018).
[19] Bélanger, G., Savoie, P., Parent, G., Claessens, A., Bertrand, A., Tremblay, G. F., Massé, D., Gilbert, Y., Babineau, D. (2012): Switchgrass silage for methane production as affected by date of harvest. – Canadian Journal of Plant Science 92: 1187-1197. https://doi.org/10.4141/cjps2011-202.
[20] BiogasMagazine (2012): https://www.deere.pl/pl_PL/docs/product/equipment/self_propelled_forage_harvester/Biogas_Magazine.pdf. – Accessed in July, 2018.
[21] Boateng, A. A., Hicks, K. B., Vogel, K. P. (2006): Pyrolysis of switchgrass (*Panicum virgatum* L.) harvested at several stages of maturity. – Journal of Analytical and Applied Pyrolysis 75: 55-64.
[22] Boateng, A. A., Daugaard, D. E., Goldberg, N. M., Hicks, K. B. (2007): Bench-scale fluidized-bed pyrolysis of switchgrass for bio-oil production. – Industrial & Engineering Chemistry Research 46(7): 1891-1897.
[23] Bocian, P., Golec, T., Rakowski, J. (2010): Modern Technologies of Biomass Production and Use for Energy Purposes. – BiOB, Warsaw (in Polish).
[24] Boe, A., Gagne, R. J. (2011): A new species of gall midge (Diptera: *Cecidomyiidae*) infesting switchgrass in the Northern Great Plains. – BioEnergy Research 4: 77-84. https://doi.org/10.1007/s12155-010-9102-6.

http://www.aloki.hu ● ISSN 1589 1623 (Print) ● ISSN 1785 0037 (Online)
DOI: http://dx.doi.org/10.15666/aeer/1605_57155743
© 2018, ALÖKI Kft., Budapest, Hungary

[25] Borole, A. P., Mielenz, J. (2011): Estimating hydrogen production potential in biorefineries using 534 microbial electrolysis cell technology. – International Journal of Hydrogen Energy 36(22): 14787-14795.
[26] Boydston, R. A., Collins, H. P., Fransen, S. C. (2010): Response of three switchgrass (*Panicum virgatum*) cultivars to mesotrione, quinclorac, and pendimethalin. – Weed Technology 24: 336-341.
[27] Branson, D. H., Joern, A., Sword, G. A. (2006): Sustainable management of insect herbivores in grassland ecosystems: new perspectives in grasshopper control. – Bioscience 56: 743-755. https://doi.org/10.1641/0006-3568(2006)56[743:SMOIHI]2.0.CO;2.
[28] Bridgeman, T. G., Darvell, L. I., Jones, J. M., Williams, P. T., Bridgwater, A. V., Barraclough, T., Shield, I., Yates, N., Thain, S. C., Donnison, I. S. (2007): Influence of particle size on the analytical and chemical properties of two energy crops. – Fuel 86(1-2): 60-72.
[29] Bullard, M., Metcalfe, P. (2001): Estimating the Energy Requirements and CO_2 Emissions from Production of the Perennial Grasses Miscanthus, Switchgrass and Reed Canary Grass. – ETSU B/U1/00645/REP. ADAS Consulting Ltd.
[30] Butkutė, B., Lemežienė, N., Cesevičienė, J., Liatukas, Ž., Dabkevičienė, G. (2013): Carbohydrate and lignin partitioning in switchgrass (*Panicum virgatum* L.) biomass as a bioenergy feedstock. – Zemdirbyste-Agriculture 100(3): 251-260.
[31] Capecchi, L., Galbe, M., Wallberg, O., Mattarelli, P., Barbanti, L. (2016): Combined ethanol and methane production from switchgrass (*Panicum virgatum* L.) impregnated with lime prior to steam explosion. – Biomass and Bioenergy 90: 22-31.
[32] Carris, L. M., Castlebury, L. A., Zale, J. (2008): First report of *Tilletia pulcherrima* bunt on switchgrass (*Panicum virgatum*) in Texas. – Plant Disease 92: 1707. https://doi.org/10.1094/PDIS-92-12-1707C.
[33] Casler, M. D. (2012): Switchgrass Breeding, Genetics, and Genomics. – In: Monti, A. (ed.) Switchgrass: A Valuable Biomass Crop for Energy. Springer-Verlag, London.
[34] Casler, M. D., Boeb, A. R. (2003): Cultivar × environment interactions in switchgrass. – Crop Science 43: 2226-2233. https://doi:10.2135/cropsci2003.2226.
[35] Chen, B-C., Lai, H-Y., Juang, K-W. (2012): Model evaluation of plant metal content and biomass yield for the phytoextraction of heavy metals by switchgrass. – Ecotoxicology and Environmental Safety 80: 393-400.
[36] Chen, J., Adjallé, K., Barnabé, S., Perrier, M., Paris, J. (2018): Mechanical and thermal pretreatment processes for increasing sugar production from woody biomass via enzymatic hydrolysis. – Waste and Biomass Valorization 1-9. https://doi.org/10.1007/s12649-018-0217-x.
[37] Cherney, J. H., Cherney, D. J. R., Paddock, K. M. (2018): Biomass yield and composition of switchgrass bales on marginal land as influenced by harvest management scheme. – BioEnergy Research 11: 33-43.
[38] Chojnacka, A., Romanowska-Duda, Z., Grzesik, M., Pszczółkowski, W., Sakowicz, T. (2010): Cyanobacteria as a Source of Bioactive Compounds for Crop Cultivation. – In: Wołowski, K., Kwandrans, J., Wojtal, A. Z. (eds.) Taxonomy the Queen of Science – The Beauty of Algae. Book of Abstracts of the 29th International Phycological Conference Kraków. Inst. Bot. Polish Acad. Sci., Krakow.
[39] Christian, D. G., Elbersen, H. W. (1998): Switchgrass (*Panicum virgatum* L.). – In: El Bassam, N. (ed.) Energy Plant Species: Their Use and Impact on Environment and Development. James & James (Science Publishers) Ltd., London.
[40] Christensen, C. A., Koppenjan, G. (eds.). (2010): Planting and Managing Switchgrass as a Dedicated Energy Crop, 2nd ed. Blade Energy Crops. – http://switchgrass.okstate.edu/other-information-sources/Blade_Switchgrass_Crop_Guide_2009.pdf (accessed in May, 2018).

http://www.aloki.hu ● ISSN 1589 1623 (Print) ● ISSN 1785 0037 (Online)
DOI: http://dx.doi.org/10.15666/aeer/1605_57155743
© 2018, ALÖKI Kft., Budapest, Hungary

[41] Chung, D., Cha, M., Guss, A. M., Westpheling, J. (2014): Direct conversion of plant biomass to ethanol by engineered *Caldicellulosiruptor bescii*. – Proceedings of the National Academy of Sciences 111(24): 8931. DOI: 10.1073/pnas.1402210111.

[42] Crouch, J. A., Beim, L. A., Cortese, L. M., Bonos, S. A., Clarke, B. B. (2010): Anthracnose disease of switchgrass caused by the novel fungal species *Colletotricum navitas*. – Mycological Research 113: 1411-1421. https://doi.org/10.1016/j.mycres.2009.09.010.

[43] Czekała, W., Bartnikowska, S., Dach, J., Janczak, D., Smurzyńska, A., Kozłowski, K., Bugała, A., Lewicki, A., Cieślik, M., Typańska, D., Mazurkiewicz, J. (2018): The energy value and economic efficiency of solid biofuels produced from digestate and sawdust. – Energy 159: 1118-1122.

[44] Damartzis, T., Zabaniotou, A. (2011): Thermo-chemical conversion of biomass to second generation bio-fuels through integrated process design – a review. – Renewable & Sustainable Energy Reviews 15: 366-378.

[45] Dien, B. S., O'Bryan, P. J., Hector, R. E., Iten, L. B., Mitchell, R. B., Qureshi, N., Sarath, G., Vogel, K. P., Cotta, M. A. (2013): Conversion of switchgrass to ethanol using dilute ammonium hydroxide pretreatment: influence of ecotype and harvest maturity – Environmental Technology 34(13-14): 1837-1848.

[46] Douglas, J., Lemunyon, J., Wynia, T., Salon, P. (2009): Technical Note No. 3. Planting and Managing Switchgrass as a Biomass Energy Crop. – USDA. NRCS. http://www.nrcs.usda.gov/Internet/FSE_DOCUMENTS/stelprdb1042293.pdf (accessed in May, 2018).

[47] Dradrach, A., Gąbka, D., Szlachta, J., Wolski, K. (2007): Energy value of several grass species cultivated on light soil. – Grassland Science in Poland 10: 29-35 (in Polish).

[48] Drinnon, D., McCord, J., Goddard, K., Walton, J., Ownley, B., Jackson, S., Rhodes, G. N., Tyler, D. (2014): Guidebook for the sustainable production practices of switchgrass in the southeastern U.S. – http://nativegrasses.utk.edu/publications/SustainableProductionPracticesSwitchgrass.pdf; http://www.se-ibss.org/publications-and-patents/extension-and-outreach-publications/guidebook-for-the-sustainable-production-practices-of-switchgrass-in-the-southeastern-u.s (accessed in July, 2018).

[49] Dudkiewicz, M., Bolibok, Ł. (2011): Selected energy plants as a landscaping element. – Acta Scientiarum Polonorum, Formatio Circumiectus 10: 13-20 (in Polish).

[50] ECN (Energy Research Centre of the Netherlands). (2016): https://www.ecn.nl/phyllis2/Browse/Standard/ECN-Phyllis#switchgrass. – Accessed in May, 2018.

[51] Elbersen, H. W. (ed.). (2001): Final Report FAIR 5-CT97-3701 "Switchgrass". Switchgrass (*Panicum virgatum* L.) as an alternative energy crop in Europe. Initiation of a productivity network. – https://subsites.wur.nl/en/switchgrass/Publications.htm (accessed in May, 2018).

[52] Elbersen, W., Poppens, R., Bakker, R. (2013): Switchgrass (*Panicum virgatum* L.). A perennial biomass grass for efficient production of feedstock for the biobased economy. – https://subsites.wur.nl/en/switchgrass/Publications.htm (accessed in May, 2018).

[53] Evanylo, G. K., Abaye, A. O., Dundas, C., Zipper, C. E., Lemus, R., Sukkariyah, B., Rockett, J. (2005): Herbaceous vegetation productivity, persistence, and metals uptake on abiosolids-amended mine soil. – Journal of Environmental Quality 34: 1811-1819.

[54] Faga, B. A., Wilkins, M. R., Banat, I. M. (2010): Ethanol production through simultaneous saccharification and fermentation of switchgrass using *Saccharomyces cerevisiae* D_5A and thermotolerant *Kluyveromyces marxianus* IMB strains. – Bioresource Technology 101: 2273-2279.

[55] Fike, J. H., Parrish, D. J., Wolf, D. D., Balasko, J. A., Green, J. T., Rasnake, Jr. M., Reynolds, J. H. (2006): Switchgrass production for the upper southeastern USA:

http://www.aloki.hu ● ISSN 1589 1623 (Print) ● ISSN 1785 0037 (Online)
DOI: http://dx.doi.org/10.15666/aeer/1605_57155743
© 2018, ALÖKI Kft., Budapest, Hungary

Influence of cultivar and cutting frequency on biomass yields. – Biomass and Bioenergy 30: 207-213.

[56] Frigon, J-C., Mehta, P., Guiot, S. R. (2012): Impact of mechanical, chemical and enzymatic pre-treatments on the methane yield from the anaerobic digestion of switchgrass. – Biomass and Bioenergy 36: 1-11.

[57] Fu, C., Mielenz, J. R., Xiao, X., Ge, Y., Hamilton, C. Y., Rodriguez, M., Chen, F., Foston, M., Ragauskas, A., Bouton, J., Dixon, R. A., Wang, Z.-Y. (2011): Genetic manipulation of lignin reduces recalcitrance and improves ethanol production from switchgrass. – Proceedings of the National Academy of Sciences 108(9): 3803-3808. http://www.pnas.org/cgi/doi/10.1073/pnas.1100310108 (accessed in July, 2018).

[58] Gamble, J. D., Jungers, J. M., Wyse, D. L., Johnson, G. A., Lamb, J. A., Sheaffer, C. C. (2015): Harvest date effects on biomass yield, moisture content, mineral concentration, and mineral export in switchgrass and native polycultures managed for bioenergy. – BioEnergy Research 8: 740-749.

[59] Garland, C. D. (2008): Growing and harvesting switchgrass for ethanol production in Tennessee. Ext. Bull. SP701-A. – https://extension.tennessee.edu/publications/Pages/default.aspx (accessed in May, 2018) or http://utextension.tennessee. edu/publications/spfiles/SP701-A.pdf (accessed in May, 2018).

[60] Giannoulis, K. D., Karyotis, T., Sakellariou-Makrantonaki, M., Bastiaans, L., Struik, P. C., Danalatos, N. G. (2016): Switchgrass biomass partitioning and growth characteristics under different management practices. – NJAS - Wageningen Journal of Life Sciences 78: 61-67.

[61] Gołaszewski, J. (2011): The use of agricultural substrats in Polish biogas plants. – Postępy Nauk Rolniczych 2: 64-94 (in Polish).

[62] Gorlitsky, L. E., Sadeghpour, A., Hashemi, M., Etemadi, F., Herbert, S. J. (2015): Biomass vs. quality tradeoffs for switchgrass in response to fall harvesting period. – Industrial Crops and Products 63: 311-315.

[63] Gunderson, C. A., Davis, E. B., Jager, H. I., Perlack, R. D., West, T. O., Brandt, C. C., Wullschleger, S. D., Baskaran, L. M., Wilkerson, E. G., Downing, M. E. (2008): Exploring Potential U.S. Switchgrass Production for Lignocellulosic Ethanol. – ORNL/TM-2007/183 National Laboratory Oak Ridge, Tennessee, USA. http://info.ornl.gov/sites/publications/files/Pub11922.pdf (accessed in May, 2018).

[64] Guragain, Y. N., Ganeshc, K. M., Bansala, S., Sathishc, R. S., Raoc, N., Vadlani, P. V. (2014): Low-lignin mutant biomass resources: Effect of compositional changes on ethanol yield. – Industrial Crops and Products 61: 1-8.

[65] Guretzky, J. A. Biermacher, J. T., Cook, B. J., Kering, M. K., Mosali, J. (2011): Switchgrass for forage and bioenergy: harvest and nitrogen rate effects on biomass yields and nutrient composition. – Plant Soil 339: 69-81.

[66] Gustafson, D. M., Boe, A., Jin, Y. (2003): Genetic variation for *Puccinia emaculata* infection in switchgrass. – Crop Science 43: 755-759. https://doi:10.2135/cropsci2003.7550.

[67] Hagan, A. K., Akridge, J. R. (2013): Efficacy of fungicides for the control of rust on switchgrass. – SNA Research Conference 58, Pathology and Nematology Section: 201-204.

[68] Hanson, J. D., Johnson, H. A. (2005): Germination of switchgrass under various temperature and pH regimes. – Seed Technology 27: 2003-2010.

[69] Hardy, T., Kordylewski, W., Mościcki, K. (2009): Chlorine corrosion hazard due to firing and co-firing of biomass in boilers. – Archiwum Spalania 9: 181-195 (in Polish).

[70] Hattori, T., Morita, S. (2010): Energy crops for sustainable bioethanol production; which, where and how? – Plant Production Science 13: 221-234.

http://www.aloki.hu ● ISSN 1589 1623 (Print) ● ISSN 1785 0037 (Online)
DOI: http://dx.doi.org/10.15666/aeer/1605_57155743
© 2018, ALÖKI Kft., Budapest, Hungary

[71] He, R., Ye, X. Ph., English, B. C., Satrio, J. A. (2009): Influence of pyrolysis condition on switchgrass bio-oil yield and physicochemical properties. – Bioresource Technology 100: 5305-5311.
[72] Heaton, E., Voigt, T., Long, S. P. (2004): A quantitative review comparing the yields of two candidate C4 perennial biomass crops in relation to nitrogen, temperature and water. – Biomass and Bioenergy 27: 21-30.
[73] Herrmann, C., Heiermann, M., Idler, C. (2011): Effects of ensiling, silage additives and storage period on methane formation of biogas crops. – Bioresource Technology 102(8): 5153-5161.
[74] Holguin, C. (2010): Insect diversity and pest status on switchgrass grown for biofuel in South Carolina. – All Theses. https://tigerprints.clemson.edu/all_theses/960 (accessed in July, 2018).
[75] Hu, Z., Sykes, R., Davis, M. F., Brummer, E. Ch., Ragauskas, A. J. (2010): Chemical profiles of switchgrass. – Bioresource Technology 101: 3253-3257.
[76] Hycnar, J. J. (2006): Fluidized beds - an example of rational solution of wastes problems. – Polityka Energetyczna 9: 365-376 (in Polish).
[77] Imam, T., Capareda, S. (2012): Characterization of bio-oil, syn-gas and bio-char from switchgrass pyrolysis at various temperatures. – Journal of Analytical and Applied Pyrolysis 93: 170-177.
[78] Jiang, Q. Z., Webb, S. L., Yesudas, C. R., Bhandari, H. S., Narasimhamoorthy, B., Bouton, J. H., Saha, M. C. (2014): Variance components and heritability of biomass yield in switchgrass (*Panicum virgatum* L.) grown in the Southern Great Plains. – Field Crops Research 168: 148-155. https://doi:10.1016/j.fcr.2014.07.016.
[79] Kabała, C., Karczewska, A., Kozak, M. (2010): Energetic plants in reclamation and management of degraded soils. – Zeszyty Naukowe Uniwersytetu Przyrodniczego we Wrocławiu Rolnictwo T.576(XCVI): 97-118 (in Polish).
[80] Karlsson, S., Âmand, L-E., Lisk, J. (2015): Reducing high-temperature corrosion on high-alloyed stainless steel superheaters by co-combustion of municipal sewage sludge in a fluidised bed boiler. – Fuel 139: 482-493.
[81] Karp, E. M., Resch, M. G., Donohoe, B. S., Ciesielski, P. N., O'Brien, M. H., Nill, J. E., Mittal, A., Biddy, M. J., Beckham, G. T. (2015): Alkaline pretreatment of switchgrass. – ACS Sustainable Chemistry & Engineering 3: 1479-1491.
[82] Kering, M. K., Biermacher, J. T., Butler, T. J., Mosali, J., Guretzky, J. A. (2012): Biomass Yield and Nutrient Responses of Switchgrass to Phosphorus Application. – BioEnergy Research 5: 71-78.
[83] Kering, M. K., Butler, T. J., Biermacher, J. T., Mosali, J., Guretzky, J. A. (2013): Effect of potassium and nitrogen fertilizer on switchgrass productivity and nutrient removal rates under two harvest systems on a low potassium soil. – BioEnergy Research 6: 329-335.
[84] Keshwani, D. R., Cheng, J. J. (2009): Switchgrass for bioethanol and other value-added applications: A review. – Bioresource Technology 100: 1515-1523.
[85] Kibet, L., Blanco-Canqui, H., Mitchell, R. B., Schacht, W. H. (2016): Root biomass and soil carbon response to growing perennial grasses for bioenergy. – Energy, Sustainability and Society 6: 1-8.
[86] Kim, Y., Mosier, N. S., Ladisch, M. R., Pallapolu, V. R., Lee, Y. Y., Garlock, R., Balan, V., Dale, B. E., Donohoe, B. S., Vinzant, T. B., Elander, R. T., Falls, M., Sierra, R., Holtzapple, M. T., Shi, J., Ebrik, M. A., Redmond, T., Yang, B., Wyman, C. E., Warner, R. E. (2011): Comparative study on enzymatic digestibility of switchgrass varieties and harvests processed by leading pretreatment technologies. – Bioresource Technology 102: 11089-11096.
[87] Kimura, E., Collins, H. P., Fransen, S. (2015): Biomass production and nutrient removal by switchgrass (*Panicum virgatum*) under irrigation. – Agronomy Journal 107: 204-210.

http://www.aloki.hu ● ISSN 1589 1623 (Print) ● ISSN 1785 0037 (Online)
DOI: http://dx.doi.org/10.15666/aeer/1605_57155743
© 2018, ALÖKI Kft., Budapest, Hungary

[88] Krupinsky, J. M., Berdahl, J. D., Schoch, C. L., Rossman, A. Y. (2004): Leaf spot on switch grass (*Panicum virgatum*), symptoms of a new disease caused by *Bipolaris oryzae*. – Canadian Journal of Plant Pathology 26: 371-378. https://doi.org/10.1080/07060660409507155.

[89] Kumar, H., Mohapatra, S. K., Singh, R. I. (2017): Review on CFD Modelling of Fluidized Bed Combustion Systems based on Biomass and Co-firing. – Journal of The Institution of Engineers (India): Series C: 1-26. https://doi.org/10.1007/s40032-017-0361-2.

[90] Kupryś-Caruk, M. P. (2017): The effect of microbial silage additives on biogas production from perennial energy grasses. – Journal of Research and Applications in Agricultural Engineering 62: 68-71.

[91] Kurylenko, O. O., Ruchala, J., Hryniv, O. B., Abbas, C. A., Dmytruk, K. V., Sibirny, A. A. (2014): Metabolic engineering and classical selection of the methylotropic thermotolerant yeast *Hansenula polymorpha* for improvement of high-temperature xylose alcoholic fermentation. – Microbial Cell Factories 13: 122-132.

[92] Larsen, S., Bruun, S., Lindedam, J. (2012): Straw yield and saccharification potential for ethanol in cereal species and wheat cultivars. – Biomass and Bioenergy 45: 239-250.

[93] Lee, H. V., Hamid, S. B. A., Zain, S. K. (2014a): Conversion of lignocellulosic biomass to nanocellulose: structure and chemical process. – The Scientific World Journal, Article ID: 631013. DOI: 10.1155/2014/631013.

[94] Lee, D. K., Parrish, A. S., Voigt, T. B. (2014b): Switchgrass and Giant Miscanthus Agronomy. – In: Shastri, Y., Hansen, A., Rodriguez, L., Ting, K. C. (eds.) Engineering and Science of Biomass Feedstock Production and Provision. Springer, New York.

[95] Lemus, R., Brummer, E. C., Burras, C. L., Moore, K. J., Barker, M. F., Molstad, N. E. (2008): Effects of nitrogen fertilization on biomass yield and quality in large fields of established switchgrass in southern Iowa, USA. – Biomass and Bioenergy 32: 1187-1194.

[96] Lewandowski, I., Kicherer, A. (1997): Combustion quality of biomass: Practical relevance and experiments to modify the biomass quality of *Miscanthus x giganteus*. – European Journal of Agronomy 6: 163-177.

[97] Lewandowski, I., Scurlock, J. M. O., Lindvall, E., Christou, M. (2003): The development and current status of perennial rhizomatous grasses as energy crops in the US and Europe. – Biomass and Bioenergy 25: 335-361.

[98] Liebig, M. A., Schmer, M. R., Vogel, K. P., Mitchell, R. B. (2008): Soil carbon storage by switchgrass grown for bioenergy. – BioEnergy Research 1: 215-222.

[99] Lindsey, K., Johnson, A., Kim, P., Jackson, S., Labbe, N. (2013): Monitoring switchgrass composition to optimize harvesting periods for bioenergy and value-added products. – Biomass and Bioenergy 56: 29-37.

[100] Liu, X.-J. A., Fike, J. H., Galbraith, J. M., Fike, W. B. (2014): Switchgrass Response to Cutting Frequency and Biosolids Amendment: Biomass Yield, Feedstock Quality, and Theoretical Ethanol Yield. – BioEnergy Research 7: 1191-1200.

[101] Liu, J., Wang, Y., Wang, X., Cao, Z., Li, S., Cui, Z. (2016): The effect of *Lactobacillus brevis* and fibrolytic enzymes on fermentation of switchgrass silages. – Journal of Animal Science 94(5): 320. https://doi.org/10.2527/jam2016-0670.

[102] Loow, Y.-L., Wu, T. Y., Md. Jahim, J., Mohammad, A. W., Teoh, W. H. (2016): Typical conversion of lignocellulosic biomass into reducing sugars using dilute acid hydrolysis and alkaline pretreatment. – Cellulose 23: 1491-1520.

[103] Madakadze, I. C., Stewart, K., Peterson, P. R., Coulman, B. E., Smith, D. L. (1999): Switchgrass biomass and chemical composition for biofuel in eastern Canada. – Agronomy Journal 91: 696-701.

[104] Majtkowski, W. (2006): Biodiversity of energetic crops as a basis for sustainable development. – Problemy Inżynierii Rolniczej 2: 25-36 (in Polish).

http://www.aloki.hu ● ISSN 1589 1623 (Print) ● ISSN 1785 0037 (Online)
DOI: http://dx.doi.org/10.15666/aeer/1605_57155743
© 2018, ALÖKI Kft., Budapest, Hungary

[105] McLaughlin, S. B., Kszos, L. A. (2005): Development of switchgrass (*Panicum virgatum*) as a bioenergy feedstock in the United States. – Biomass and Bioenergy 28: 515-535.
[106] McLaughlin, S. B., De La Torre Ugarte, D. G., Garten, C. T., Lynd, L. R., Sanderson, M. A., Tolbert, V. R., Wolf, D. D. (2002): High-value renewable energy from prairie grasses. – Environmental Science & Technology 36: 2122-2129.
[107] Miesel, J. R., Renz, M. J., Doll, J. E., Jackson, R. D. (2012): Effectiveness of weed management methods in establishment of switchgrass and a native species mixture for biofuels in Wisconsin. – Biomass and Bioenergy 36: 121-131.
[108] Miesel, J. R., Jach-Smith, L. C., Renz, M. J., Jackson, R. D. (2017): Distribution of switchgrass (*Panicum virgatum* L.) aboveground biomass in response to nitrogen addition and across harvest dates. – Biomass and Bioenergy 100: 74-83.
[109] Min, D., Guragain, Y. N., Prasad, V., Vadlani, P. V., Lee, J. (2017): Effects of Different Genotypes of Switchgrass as a Bioenergy Crop on Yield Components and Bioconversion Potential. – Journal of Sustainable Bioenergy Systems 7: 27-35.
[110] Mitchell, R. B., Schmer, M. (2012): Switchgrass Harvest and Storage. – In: Monti, A. (ed.) Switchgrass: A Valuable Biomass Crop for Energy. Springer-Verlag, London.
[111] Mitchell, R. B., Vogel, K. P., Sarath, S. (2008): Managing and enhancing switchgrass as a bioenergy feedstock. – Biofuels, Bioproducts and Biorefining 2: 530-539.
[112] Mitchell, R., Lee, D. K., Casler, M. (2014): Switchgrass. – In: Karlen, D. L. (ed.) Cellulosic Energy Cropping Systems. John Wiley & Sons, Lincoln.
[113] Mitchell, R. B., Vogel, K. P., Schmer, M. (2016): Switchgrass (*Panicum virgatum*) for Biofuel Production. – http://articles.extension.org/pages/26635/switchgrass-panicum-virgatum-for-biofuel-production (accessed in May, 2018).
[114] Mohamed, B. A., Kim, Ch. S., Ellis, N., Bi, X. (2016): Microwave-assisted catalytic pyrolysis of switchgrass for improving bio-oil and biochar properties. – Bioresource Technology 201: 121-132.
[115] Mohammed, T. A., Raun, W., Kakani, G., Zhang, H., Taylor, R., Desta, K. G., Jared, C., Mullock, J., Bushong, J., Sutradhar, A., Ali, M. S., Reinert, M. (2015): Nutrient sources and harvesting frequency on quality biomass production of switchgrass (*Panicum virgatum* L.) for biofuel. – Biomass and Bioenergy 81: 242-248.
[116] Monti, A., Fazio, S., Venturi, G. (2009a): Cradle-to-farm gate life cycle assessment in perennial energy crops. – European Journal of Agronomy 31: 77-84.
[117] Monti, A., Fazio, S., Venturi, G. (2009b): The discrepancy between plot and field yields: Harvest and storage losses of switchgrass. – Biomass and Bioenergy 33: 841-847.
[118] Moser, L. E., Vogel, K. P. (1995): Switchgrass, Big Bluestem, and Indiangrass. – In: Barnes, R. F., Miller, D. A., Nelson, C. J. (eds.) An Introduction to Grassland Agriculture. Forages, 5th ed. Vol.1. Iowa University Press, Ames, IA.
[119] Muir, J. P., Sanderson, P. A., Ocumpaugh, W. R., Jones, R. M., Reed, R. L. (2001): Biomass production of "Alamo" switchgrass in response to nitrogen, phosphorus and row sparing. – Agronomy Journal 93: 896-901.
[120] Papa, G., Rodriguez, S., George, A., Schievano, A., Orzi, V., Sale, K. L., Singh, S., Adani, F., Simmons, B. A. (2015): Comparison of different pretreatments for the production of bioethanol and biomethane from corn stover and switchgrass. – Bioresource Technology 183: 101-110.
[121] Pardo-Planas, O., Atiyeh, H. K., Phillips, J. R., Aichele, C. P., Mohammad, S. (2017): Process simulation of ethanol production from biomass gasification and syngas fermentation. – Bioresource Technology 245: 925-932.
[122] Parrish, D., Fike, J. (2005): The biology and agronomy of switchgrass for biofuels. – Critical Reviews in Plant Sciences 24: 423-459. https://doi.org/10.1080/07352680500316433.
[123] Pasangulapati, V., Ramachandriya, K. D., Kumar, A., Wilkins, M. R., Jones, C. L., Huhnke, R. L. (2012): Effects of cellulose, hemicellulose and lignin on thermochemical

http://www.aloki.hu ● ISSN 1589 1623 (Print) ● ISSN 1785 0037 (Online)
DOI: http://dx.doi.org/10.15666/aeer/1605_57155743
© 2018, ALÖKI Kft., Budapest, Hungary

conversion characteristics of the selected biomass. – Bioresource Technology 114: 663-669.
[124] Piechocki, J., Sołowiej, P., Neugebauer, M. (2010): Gasification of waste biomass from agricultural production. – Agricultural Engineering 5: 219-224 (in Polish).
[125] Pilon, G., Lavoie, J.-M. (2011): Characterization switchgrass char produced in torrefaction and pyrolysis conditions. – BioResources 6: 4824-4839.
[126] Pilon, G., Lavoie, J.-M. (2013): Pyrolysis of switchgrass (*Panicum virgatum* L.) at low temperatures in N_2 and CO_2 environments; a study on chemical composition of chars extracts and bio-oils. – Journal of Analytical and Applied Pyrolysis 101: 122-131.
[127] Pimentel, D., Patzel, T. W. (2005): Ethanol production using corn, switchgrass, and wood; biodiesel production using soybean and sunflower. – Natural Resources Research 14: 65-76.
[128] Prasifka, J. R., Bradshaw, J. D., Boe, A. A., Lee, D., Adamski, D., Gray, M. E. (2010): Symptons, distribution, and abundance of the stem-boring caterpillar, *Blastobasis repartella* (Dietz), in switchgrass. – BioEnergy Research 3: 238-242.
[129] Prieto, G. S., Ernst, O., Bustamante, M. (2017): Impact of harvest frequency on biomass yield and nutrient removal of elephantgrass, giant reed, and switchgrass. – BioEnergy Research 10: 853-863.
[130] Pszczółkowski, A., Romanowska-Duda, Z., Pszczółkowska, A., Grzesik, M., Wysokińska, Z. (2012): Biomass production of selected energy plants: economic analysis and logistic strategies. – Comparative Economic Research. Central and Eastern Europe 15: 77-103.
[131] Qian, K., Kumar, A., Patil, K. N., Bellmer, D. D., Wang, D., Yuan, W., Huhnke, R. L. (2013): Effects of biomass feedstocks and gasification conditions on the physiochemical properties of char. – Energies 6: 3972-3986. DOI: 10.3390/en6083972.
[132] Qin, X., Mohan, T., El-Halwagi, M., Cornforth, G., McCarl, B. A. (2006): Switchgrass as an alternate feedstock for power generation: an integrated environmental, energy and economic life-cycle assessment. – Clean Technologies and Environmental Policy 8: 233-249.
[133] Quinn, L. D., Straker, K. C., Guo, J., Kim, S., Thapa, S., Kling, G., Lee, D., Voigt, T. B. (2015): Stress-tolerant feedstocks for sustainable bioenergy production on marginal land. – BioEnergy Research 8: 1081-1100.
[134] Rajendran, K., Drielak, E., Varma, V. S., Muthusamy, S., Kumar, G. (2018): Updates on the pretreatment of lignocellulosic feedstocks for bioenergy production–a review. – Biomass Conversion and Biorefinery 8(2): 471-483. DOI 10.1007/s13399-017-0269-3.
[135] Rijal, B., Igathinathane, C., Karki, B., Yu, M., Pryor, S. W. (2012): Combined effect of pelleting and pretreatment on enzymatic hydrolysis of switchgrass. – Bioresource Technology 116: 36-41.
[136] Rodriguez, C., Alaswad, A., Benyounis, K. Y., Olabi, A. G. (2017): Pretreatment techniques used in biogas production from grass. – Renewable and Sustainable Energy Reviews 68(2): 1193-1204.
[137] Sadeghpour, A., Gorlitsky, L. E., Hashemi, M., Weis, S. A., Herbert, S. J. (2014a): Response of switchgrass yield and quality to harvest season and nitrogen fertilizer. – Agronomy Journal 106: 290-296.
[138] Sadeghpour, A., Hashemi, M., DaCosta, M., Jahanzad, E., Herbert, S. J. (2014b): Switchgrass establishment influenced by cover crop, tillage systems, and weed control. – BioEnergy Research 7: 1402-1410.
[139] Samson, R. (2007): Switchgrass production in Ontario: A management guide. Resource Efficient Agricultural Production (REAP) – Canada. http://www.reap-canada.com/online_library/grass_pellets/2007%20SG%20production%20guideFINAL.pdf> (accessed in May, 2018).
[140] Sanderson, M. A., Adler, P. R. (2008): perennial forages as second generation bioenergy crops. – International Journal of Molecular Sciences 9: 768-788.

http://www.aloki.hu ● ISSN 1589 1623 (Print) ● ISSN 1785 0037 (Online)
DOI: http://dx.doi.org/10.15666/aeer/1605_57155743
© 2018, ALÖKI Kft., Budapest, Hungary

[141] Sanderson, M. A., Reed, R. L., McLaughlin, S. B., Wullschleger, S. D., Conger, B. V., Parrish, D. J., Wolf, D. D., Taliaferro, C., Hopkins, A. A., Ocumpaugh, W. R., Hussey, M. A., Read, J. C., Tischler, C. R. (1996): Switchgrass as a sustainable bioenergy crop. – Bioresource Technology 56: 83-93.
[142] Sanderson, M. A., Adler, P. R., Boateng, A. A., Casler, M. D., Sarath, G. (2006): Switchgrass as a biofuels feedstock in the USA. – Canadian Journal of Plant Science 86: 1315-1325.
[143] Sanderson, M. A., Schmer, M., Owens, V., Keyser, P., Elbersen, W. (2012): Crop Management of Switchgrass. – In: Monti, A. (ed.) Switchgrass: A Valuable Biomass Crop for Energy. Springer-Verlag, London.
[144] Sarkar, M., Kumar, A., Tumuluru, J. S., Patil, K. N., Bellmer, D. D. (2014): Gasification performance of switchgrass pretreated with torrefaction and densification. – Applied Energy 127: 194-201.
[145] Schmer, M. R., Vogel, K. P., Mitchell, R. B., Moser, L. E., Eskridge, K. M., Perrin, R. K. (2006): Establishment stand thresholds for switchgrass grown as a bioenergy crop. – Crop Science 46: 157-161.
[146] Schmer, M. R., Vogel, K. P., Mitchell, R. B., Perrin, R. K. (2008): Net energy of cellulosic ethanol from switchgrass. – Proceedings of the National Academy of Sciences 105(2): 464-469.
[147] Schmer, M. R., Vogel, K. P., Varvel, G. E., Follett, R. F., Mitchell, R. B., Jin, V. L. (2014): Energy potential and greenhouse gas emissions from bioenergy cropping systems on marginally productive cropland. – PLoS ONE 9(3): e89501. https://doi.org/10.1371/journal.pone.0089501.
[148] Scordia, D., Zanetti, F., Varga, Sz. S., Alexopoulou, E., Cavallaro, V., Monti, A., Copani, V., Cosentino, S. L. (2015): New Insights into the propagation methods of switchgrass, miscanthus and giant reed. – Bioenergy Research 8: 1480-1491.
[149] Sekutowski, T., Rola, J., Kaus, A. (2009): Weed Communities Occurring in Newly Established Plantations of Crops Used for Energy Purposes and Methods for Their Reduction. – In: Skrobacki, A. (ed.) Biomass Production – Selected Problems. Wyd. Wieś Jutra, Warszawa (in Polish).
[150] Serapiglia, M. J., Bruce, S., Dien, B. S., Boateng, A. A., Casler, M. D. (2017): Impact of harvest time and switchgrass cultivar on sugar release through enzymatic hydrolysis. – BioEnergy Research 10: 377-387.
[151] Sharma, S., Sharma, V., Kuila, A. (2016): Cellulase production using natural medium and its application on enzymatic hydrolysis of thermo chemically pretreated biomass. – 3 Biotech 6: 139. DOI 10.1007/s13205-016-0465-z.
[152] Shield, I. F., Barraclough, T. J. P., Riche, A. B., Yates, N. E. (2012): The yield response of the energy crops switchgrass and reed canary grass to fertiliser applications when grown on a low productivity sandy soil. – Biomass and Bioenergy 42: 86-96.
[153] Smeets, E. M. W., Lewandowski, I. M., Faaij, A. P. C. (2009): The economical and environmental performance of miscanthus and switchgrass production and supply chains in a European setting. – Renewable & Sustainable Energy Reviews 13: 1230-1245.
[154] Sokhansanj, S., Mani, S., Turhollow, A., Kumar, A., Bransby, D., Lynd, L., Laser, M. (2009): Large-scale production, harvest and logistics of switchgrass (*Panicum virgatum* L.) – current technology and envisioning a mature technology. – Biofuels, Bioproducts and Biorefining 3: 124-141.
[155] Steward, C. L., Pyle, J. D., Jochum, C. C., Vogel, K. P., Yuen, G. Y., Scholthof, K.-B. G. (2015): Multi-year pathogen survey of biofuel switchgrass breeding plots reveals high prevalence of infections by *Panicum mosaic* virus and its satellite virus. – Phytopathology 105: 1146-1154. http://dx.doi.org/10.1094/PHYTO-03-15-0062-R.
[156] Suryawati, L., Wilkins, M. R., Bellmer, D. D., Huhnke, R. L., Maness, N. O., Banat, I. M. (2008): Simultaneous saccharification and fermentation of Kanlow switchgrass pretreated

http://www.aloki.hu ● ISSN 1589 1623 (Print) ● ISSN 1785 0037 (Online)
DOI: http://dx.doi.org/10.15666/aeer/1605_57155743
© 2018, ALÖKI Kft., Budapest, Hungary

by hydrothermolysis using *Kluyveromyces marxianus* IMB4. – Biotechnology and Bioengineering 101(5): 894-902.

[157] Suryawati, L., Wilkins, M. R., Bellmer, D. D., Huhnke, R. L., Maness, N. O., Banat, I. M. (2009): Effect of hydrothermolysis process conditions on pretreated switchgrass composition and ethanol yield by SSF with *Kluyveromyces marxianus* IMB4. – Process Biochemistry 44: 540-545.

[158] Sykes, V. R., Allen, F. L., Mielenz, J. R., Stewart Jr., C. N., Windham, M. T., Hamilton, Ch. Y., Rodriguez Jr., M., Yee, K. L. (2016): Reduction of ethanol yield from switchgrass infected with rust caused by *Puccinia emaculata*. – BioEnergy Research 9(1): 239-247. DOI 10.1007/s12155-015-9680-4. https://bioenergycenter.org/besc/publications/sykes_reduction_yr9.pdf (accessed in July, 2018).

[159] Tanner, R. S. (2008): Production of Ethanol from Synthesis Gas. – In: Wall, J. D., Harwood, C. S., Demain, A. L. (eds.) Bioenergy. ASM Press, Washington.

[160] Thamsiriroj, T., Nizami, A. S., Murphy, J. D. (2012): Why does mono-digestion of grass silage fail in long term operation? – Applied Energy 95: 64-76.

[161] Thomason, W. E., Raun, W. R., Johnson, G. V., Taliaferro, C. M., Freeman, K. W., Wynnum, K. J., Mullen, R. W. (2004): Switchgrass response to harvest frequency and time and rate of applied nitrogen. – Journal of Plant Nutrition 27: 1199-1226.

[162] Thomsen, P. M., Brummer, E. C., Shriver, J., Munkvold, G. P. (2008): Biomass yield reductions in switchgrass due to smut caused by *Tilletia maclaganii*. – Plant Health Progress. DOI: 10.1094/PHP-2008-0317-01-RS. https://www.plantmanagementnetwork.org/pub/php/research/2008/smut/ (accessed in July, 2018).

[163] Tillman, D. A. (2000): Biomass co-firing: the technology, the experience, the combustion consequences. – Biomass and Bioenergy 19: 365-384.

[164] Torreiro, Y., Pérez, V., Murillo, J. M., Ramos, R., Fernández, M., García, S., Sáncheza, J. M. (2018): Thermochemical assessment of *Nicotiana glauca, Panicum virgatum* and *Elytrigia elongata* as fuels for energy recovery through gasification. – Fuel 225: 71-79.

[165] Umezawa, T. (2018): Lignin modification in planta for valorization. – Phytochemistry Reviews 1-23. https://doi.org/10.1007/s11101-017-9545-x.

[166] Uppalapati, S. R., Serba, D. D., Ishiga, Y., Szabo, L. J., Mittal, S., Bhandari, H. S., Bouton, J. H., Mysore, K. S., Saha, M. C. (2013): Characterization of the rust fungus, *Puccinia emaculata*, and evaluation of genetic variability for rust resistance in switchgrass populations. – BioEnergy Research 6: 458-468.

[167] Vamvuka, D., Topouzi, V., Sfakiotakis, S. (2010): Evaluation of production yield and thermal processing of switchgrass as a bio-energy crop for the Mediterranean region. – Fuel Processing Technology 91: 988-996.

[168] Vogel, K. P. (2004): Switchgrass. – In: Moser, L. E., Burson, B. L., Sollenberger, L. E. (eds.) Warmseason (C4) Grasses. ASA-CSSA-SSSA, Madison.

[169] Vogel, K. P., Brejda, J. J., Walters, D. T., Buxton, D. R. (2002): Switchgrass biomass production in the Midwest USA: harvest and nitrogen management. – Agronomy Journal 94: 413-420.

[170] Vogel, K. P., Sarath, G., Saathoff, A. J., Mitchell, R. B. (2011): "Switchgrass". – Agronomy & Horticulture Faculty Publications 1028. http://digitalcommons.unl.edu/agronomyfacpub/1028 (accessed in May, 2018).

[171] Vu, A. L., Dee, M. M., Gualandi, R. J., Huff, S., Zale, J., Gwinn, K. D., Ownley, B. H. (2011): First report of leaf spot caused by *Bipolaris spicifera* on switchgrass in the United States. – Plant Disease 95: 1191. https://apsjournals.apsnet.org/doi/10.1094/PDIS-10-10-0774 (accessed in July, 2018).

[172] Wang, C., Guo, L., Li, Y., Wang, Z. (2012): Systematic comparison of C3 and C4 plants based on metabolic network analysis. – BMC Systems Biology 6 Suppl. 2: S9. DOI: 10.1186/1752-0509-6-S2-S9.

http://www.aloki.hu ● ISSN 1589 1623 (Print) ● ISSN 1785 0037 (Online)
DOI: http://dx.doi.org/10.15666/aeer/1605_57155743
© 2018, ALÖKI Kft., Budapest, Hungary

[173] Wang, Z., Smyth, T. J., Crozier, C. R., Gehl, R. J., Heitman, A. J. (2018): Yield and nitrogen removal of bioenergy grasses as influenced by nitrogen rate and harvest management in the coastal plain region of North Carolina. – BioEnergy Research 11: 44-53.
[174] Waramit, N., Moore, K. J., Heggenstaller, A. H. (2011): Composition of native warm-season grasses for bioenergy production in response to nitrogen fertilization rate and harvest date. – Agronomy Journal 103: 655-662.
[175] Wayman, S., Bowden, R. D., Mitchell, R. B. (2014): Seasonal changes in shoot and root nitrogen distribution in switchgrass (*Panicum virgatum*). – BioEnergy Research 7: 243-252.
[176] Williams, C. L., Westover, T. L., Emerson, R. M., Tumuluru, J. S., Li, Ch. (2016): Sources of biomass feedstock variability and the potential impact on biofuels production. – BioEnergy Research 9: 1-14.
[177] Withers, K. K. (2010): Establishment, fertility and harvest management for optimizing switchgrass yield and quality as a cellulosic ethanol feedstock in the Great Lakes region. – Crop and Soil Science, M.S. Thesis, Michigan State University.
[178] Wullschleger, S. D., Davis, E. B., Borsul, M. E., Gunderson, C. A., Lynd, L. R. (2010): Biomass production in switchgrass across the United States: Database description and determinants of yield. – Agronomy Journal 102: 1158-1168.
[179] Xu, J., Wang, Z., Sharma-Shivappa, R. R., Cheng, J. J. (2011): Enzymatic hydrolysis of switchgrass and coastal Bermuda grass pretreated using different chemical method. – BioResources 6: 2990-3003.
[180] Yee, K. L., Rodriguez Jr., M., Thompson, O. A., Fu, Ch., Wang, Z.-Y., Davison, B. H., Mielenz, J. R. (2014): Consolidated bioprocessing of transgenic switchgrass by an engineered and evolved *Clostridium thermocellum* strain. – Biotechnology for Biofuels 7: 75. DOI:10.1186/1754-6834-7-75. http://www.biotechnologyforbiofuels.com/content/7/1/75 (accessed in July, 2018)
[181] Young, H. A., Sarath, G., Tobias, C. M. (2012): Karyotype variation is indicative of subgenomic and ecotypic differentiation in switchgrass. – BMC Plant Biology 12: 117. DOI: 10.1186/1471-2229-12-117.
[182] Zabed, H., Sahu, J., Suely, A., Boyce, A., Faruq, G. (2017): Bioethanol production from renewable sources: current perspectives and technological progress. – Renewable & Sustainable Energy Reviews 71: 475-501.
[183] Zale, J., Freshour, L., Agarwal, S., Sorochan, J., Ownley, B. H., Gwinn, K. D., Castlebury, L. A. (2008): First report of rust on switchgrass (*Panicum virgatum*) caused by *Puccinia emaculata* in Tennessee. – Plant Disease 92: 1710-1710.
[184] Zegada-Lizarazu, W. E., Elbersen, W., Cosentino, S. L., Zatta, A., Alexopoulou, E., Monti, A. (2010): Agronomic aspects of future energy crops in Europe. – Biofuels, Bioproducts and Biorefining 4: 674-691.
[185] Zhao, X., Liu, J., Liu, J., Yang, F., Zhu, W., Yuan, X., Hu, Y., Cui, Z., Wang, X. (2017): Effect of ensiling and silage additives on biogas production and microbial community dynamics during anaerobic digestion of switchgrass. – Bioresource Technology 241: 349-359.
[186] Zheng, Z., Liu, J., Yuan, X., Wang, X., Zhu, W., Yang, F., Cui, Z. (2015): Effect of dairy manure to switchgrass co-digestion ratio on methane production and the bacterial community in batch anaerobic digestion. – Applied Energy 151: 249-257.
[187] Zorer Çelebi, Ş., Zorer, Ö. S. (2018): Accumulation and tolerance of Pb in some bioenergy crops. – Polish Journal of Environmental Studies 27: 591-596.
[188] Zuwała, J., Kopczyński, M., Robak, J. (2014): Coupled torrefaction-pelletization process for biomass co-firing, techno-economic issues. – Polityka energetyczna T.17 z.4: 147-158 (in Polish).

http://www.aloki.hu ● ISSN 1589 1623 (Print) ● ISSN 1785 0037 (Online)
DOI: http://dx.doi.org/10.15666/aeer/1605_57155743
© 2018, ALÖKI Kft., Budapest, Hungary

SYNTHESIS ASSISTED BY MICROWAVE OF ZnO/ZnS/CuS HETEROSTRUCTURES AND ITS PHOTOACTIVITY USING VISIBLE LIGHT FOR DYES DEGRADATION

IZQUIERDO DE LA CRUZ, F.[1] – PÉREZ HERNÁNDEZ, G.[1] – RODRÍGUEZ MELGAREJO, F.[2] – RUIZ PERALTA, M. L.[3] – CASTILLO PALOMERA, R.[4] – RAMÍREZ MORALES, E.[1] – ROJAS BLANCO, L.[1*]

[1]*Universidad Juárez Autónoma de Tabasco, Avenida Universidad S/N, Col. Magisterial, C.P 86040, Villahermosa, Tabasco, México*

[2]*Cinvestav, Libramiento Norponiente #2000, Fracc. Real de Juriquilla, C.P. 76230, Santiago de Querétaro, Qro., México*

[3]*Benemérita Universidad Autónoma de Puebla, Facultad de Ingeniería Química, Av. San Claudio y 18 Sur, C.P. 72570 Puebla, Puebla, México*

[4]*Universidad Politécnica de Chiapas, Carr. Tuxtla-Villaflores K.M. 1+500, Las Brisas, C.P. 29150, Suchiapa, Chiapas, Mexico*

**Corresponding author*
e-mail: lizethrb@gmail.com; phone: +52-993-246-8500; fax: +52-914-336-0940

(Received 28th Jun 2018; accepted 14th Aug 2018)

Abstract. In this study ZnO/ZnS/CuS heterostructure have been controllably synthesized through a microwave-assisted synthesis and cation exchange. The compounds ZnO, ZnO/ZnS and ZnO/ZnS/CuS were characterized by X-ray diffraction (XRD), scanning electron microscopy (SEM), ultraviolet-visible (UV-vis) and Raman. It is found that the crystal structures obtained were Hexagonal Wurtzita for ZnO, hexagonal Wurtzita for ZnS, and hexagonal covellina for CuS. In comparison of ZnO and ZnO/ZnS the results show that ZnO/ZnS/CuS heterostructure has a higher photocatalytic activity under visible light, because its photocatalytic properties increase, helping to separate the electron-hole. These ZnO/ZnS/CuS efficiently decompose organic dyes such as methyl orange and methylene blue upon visible light conditions. Degradation rates can reach 31% and 71% during 240 min of treatment, respectively. The experiments revealed that the ZnO/ZnS/CuS decomposes methylene blue much faster than methyl orange.
Keywords: *semiconductors, photocatalysis, water treatment, KOH, pollutant*

Introduction

In recent years, environmental problems have generated a greater concern for society, due to the excessive growth that companies have presented, which means an increase in the number of pollutants they are producing. An exhaustive research of new techniques has been developed for water treatment; that they are no only low cost, but friendly to the planet (Chaudhuri, 2017). In the search for these new techniques, photocatalysis plays a fundamental role mainly due to its different applications, such as environmental remediation (Ahmad et al., 2016) and hydrogen production (Okemoto et al., 2018).

Of the photocatalysts most widely used, it includes TiO_2 (Liu and Li, 2014), ZnO (Liu et al., 2015) and ZnS (Wan et al., 2014). The semiconductor materials, either type p or n-type (Zhang and Jaroniec, 2018), play a fundamental role due to their different properties such as the great potential as a photocatalyst, its low cost, high

http://www.aloki.hu ● ISSN 1589 1623 (Print) ● ISSN 1785 0037 (Online)
DOI: http://dx.doi.org/10.15666/aeer/1605_57455756
© 2018, ALÖKI Kft., Budapest, Hungary

surface area and low toxicity (Park, Kim, et al., Photoinduced charge transfer processes in solar, photocatalysis based on modified TiO_2 2016), because the energy gap is small, An electron can be excited from the valence band to the conduction band, and then an electron-hole pair is generate producing oxidation-reduction reactions, taking advantage of the photocatalytic efficiency of these semiconductor materials.

The ZnO is a wide band gap semiconductor material, with a large surface area, photosensitivity, a high exciton binding energy of (60 mV), and a band gap of 3.37 eV that belong to II-VI group. ZnO is an important photocatalyst due to the rapidity to produce electron-hole pairs, but it has an important disadvantage as a photocatalyst, since it only can be activated in UV light $\lambda < 385$ nm, therefore, several attempts have been made to improve the absorption capacity of the structures based on ZnO.

To improve the photocatalytic performance of ZnO and to be able to accept visible light, heterostructure are fabricated with other semiconductor material for enhanced their photocatalytic activity (Basu et al., 2014) and its advantage is based on the fact that each of its compounds plays an individual role in the absorption of photons (Zhu et al., 2008).

ZnS with a wide band gap is another well-known photocatalytic, that has a band gap of 3.72 eV belongs to II-VI group semiconductor. However, as the ZnO is restricted to the ultraviolet range. To extend the photoresponse of ZnO/ZnS (Li et al., 2014). It has been shown that there is an efficient coupling between the ZnS and the CuS. Cus is capable of activating zinc oxide and zinc sulphide in the visible region, thus improving the separation of electron-hole pairs (Paria and Reiser, 2014).

Thus, in this study the ZnO/ZnS/CuS was synthesized by microwaves, expanding the light absorption range and ZnO/ZnS/CuS can absorb photons from the range of the solar spectrum taking advantage of the main source of renewable energy that counts (sunlight).

Materials and methods

Materials

Zinc di-hydrated acetate ($Zn(O_2CCH_3)2(H_2O)$, 100%, J. T. Baker), potassium hydroxide (KOH, 85%, CIVEQ), thioacetamide (C_2H_5NS, 99%) and cupric nitrate ($Cu(NO_3)_2 \cdot 2.5H_2O$),98%,CIVEQ). The solutions were prepared with deionized water and ethanol (C2H6O, 99.5%, Meyer). For the evaluation of the photocatalytic activity, methyl orange ($C_{14}H_{14}N_3NaO_3S$, Meyer) and methylene blue ($C_{16}H_{18}C_lN_3S$, CIVEQ) were used.

Synthesis of ZnO

In a typical synthesis 4.4506 g of $Zn(O_2CCH_3)2(H_2O)$ and 720 µL of deionized water was dissolved in 50 mL of ethanol, the solution was under constant stirring at 30 RPM. After 5 min of stirring the pH was modified with potassium hydroxide (KOH) to pH 8. The mixture was then transferred to a vial which was sealed and heated to 130 °C by microwave irradiation for 15 min. After cool down the mixture was filtered and washed with deionized water and acetone at least three times, in order to eliminate residual precursors, finally was dried for 24 h at 80 °C in an electric hot air oven.

http://www.aloki.hu ● ISSN 1589 1623 (Print) ● ISSN 1785 0037 (Online)
DOI: http://dx.doi.org/10.15666/aeer/1605_57455756
© 2018, ALÖKI Kft., Budapest, Hungary

Synthesis of ZnO/ZnS

0.050 g of ZnO previously synthesized, and 0.041 g of thioacetamide C_2H_5NS was dissolve in 40 mL of deionized water. The solution was stirred with an ultrasonic bath for 20 min, then the solution was transferred to a vial which was sealed and irradiated with microwaves for 30 min at 650 W. After cool down the mixture was washed with deionized water and acetone for three times, and finally dried in an electric hot air oven for 24 h at 90 °C.

Fabrication of ZnO/ZnS/CuS

The synthesis method of the ZnO/ZnS/CuS heterostructure was similar to that reported by Can Lu (Lu and Otros, 2016). ZnO/ZnS/CuS was synthesized by cation exchange. 0.0139 g of ZnO/ZnS and 0.0317 g of copper nitrate $Cu(NO_3)_2 \cdot 2.5H_2O$ was dissolve in 20 ml of deionized water. The solution was kept under constant stirring in an ultrasonic bath, at 80° C during 4 h. The precipitate obtained was washed and dried for 24 h in an electric hot air oven and then pulverized.

Characterization

In order to know the crystal structure and its phases, the powders were studied using a Rigaku diffractometer (XRD), with Cu-Kα radiation (λ = 1.544 Å) over the range of 2 θ between 20° and 80°. The average crystallite size was calculated using the Scherrer equation (*Eq. 1*), which is described below;

$$\beta = \frac{k \times \lambda}{B \times \cos\theta} \qquad \text{(Eq.1)}$$

where, λ is the wavelength, k is a constant (shape factor of the diffraction peak), β is the average crystal size, θ is the peak position and B is the full width at half maximium intensity (Patterson, 1939).

The Surface morphology of powders was characterized by using a scanning electron microscopy (SEM) JEOL microscope model JSM-7100F with 10 kV acceleration voltage and a working distance WD. of 9.8 mm. The powders of ZnO, ZnO/ZnS and ZnO/ZnS/CuS were adhered to a double-sided carbon tape for the correct taking of micrographs at magnifications of 1500x, 20,000x, 25,000x, 50,000x and 100,000x.

The optical properties were obtained using UV-Visible spectrophotometer SHIMADZU model UV-2600, with a R-928 photomultiplier over the range of 185 to 900 nm. The band gap was calculated by the modified function of Kubelka-Munk (F(R)*hv) 1/2, and the calculation of F (R) (*Eq. 2*).

$$F(R) = \frac{1-R^2}{R \times 2} \qquad \text{(Eq.2)}$$

where R is the diffuse reflectance and $F(R)$ is the absorbance (Choudhury, 2013).

Raman spectra of the samples were recorded with a HORIBA sciencific spectrophotometer model XploRA PLUS in a spectral range of 100 to 800 cm^{-1} with a 532 nm laser.

http://www.aloki.hu ● ISSN 1589 1623 (Print) ● ISSN 1785 0037 (Online)
DOI: http://dx.doi.org/10.15666/aeer/1605_57455756
© 2018, ALÖKI Kft., Budapest, Hungary

Photocatalytic test

The photocatalytic activity of ZnO, ZnO/ZnS and ZnO/ZnS/CuS were evaluated using Methyl Orange (10 mg/l) and Methylene Blue (10 mg/l) as an organic pollutant using a Halogen FTK lamp 120 V, model 54875 placed at 10 cm.

0.0249 g of photocatalyst was added in 60 ml of the dye, and kept in an ultrasonic bath in the dark to establish the absorption-desorption equilibrium. After 30 min, an aliquot were removed and centrifuged at 4000 RPM for 25 min to separate the powders from the solution. The irradiation of visible light was started with the remaining dye in constant agitation at 180 RPM, at 28 °C. Aliquots were taken every 30 min and centrifuged with the same conditions mentioned above. The degradation was monitored by UV-Vis absorption spectroscopy in the range of 340-600 nm for Methyl Orange, and 500-750 nm for Methylene Blue. The measurements were made during 240 min. The degradation efficiency of the dyes was calculated with the degradation efficiency equation (*Eq. 3*).

Degradation efficiency

$$ED(\%) = \frac{A_0 - A_t}{A_0} \text{ x } 100 \qquad \text{(Eq.3)}$$

where A_0 is the initial absorbance of the dye and A_t is the absorbance of the dye at a time t (Alvi et al., 2017).

Results and discussion

The X-ray diffraction pattern was performed for the samples of ZnO, ZnO/ZnS and ZnO/ZnS/CuS (*Fig. 1*).

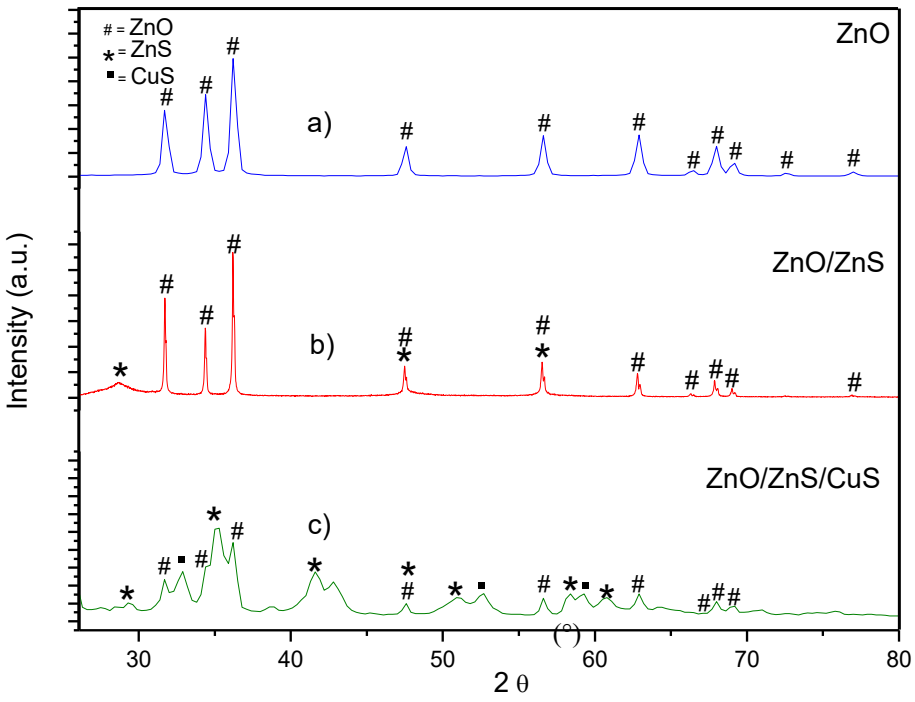

Figure 1. *XRD patterns of the ZnO, ZnO/ZnS and ZnO/ZnS/CuS*

http://www.aloki.hu ● ISSN 1589 1623 (Print) ● ISSN 1785 0037 (Online)
DOI: http://dx.doi.org/10.15666/aeer/1605_57455756
© 2018, ALÖKI Kft., Budapest, Hungary

The ZnO crystallizes in a hexagonal wurtzite phase (JCPDF 89-7102), and the average crystallite size is 21 nm. The compound ZnO/ZnS shows the characteristic peaks of both compounds ZnO and ZnS; checking the obtaining of the hexagonal Wurtzite phase for ZnO (JCPDF 89-7102), and the appearance of zinc sulfide (JCPDF 72-0162) for the Wurtzita Hexagonal phase. Finally, the X-ray diffraction pattern of the heterostructure ZnO/ZnS/CuS is corrobored with the peaks of the coveline phase of CuS (JCPDS 74-1234).

The ZnO powders have an irregular morphology of semi-spherical shape and agglomerations, with particles ranging from 205 to 702 nm in diameter (*Fig. 2*), this morphology is characteristic of the materials prepared by the microwave-assisted method (Kajbafvala et al., 2012; Sooksaen and Chuankrerkkul, 2017).

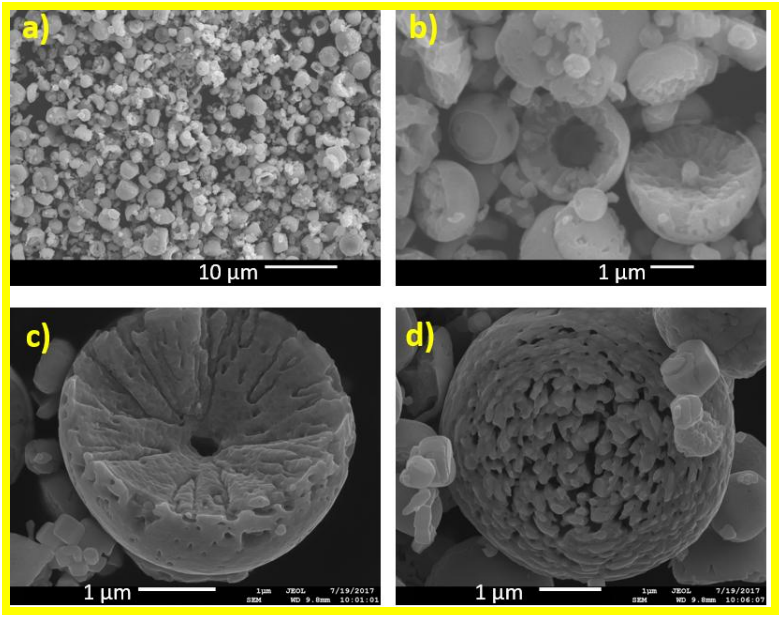

Figure 2. *SEM images of ZnO a) 2 500x b) 15 000x c) 25 000x d) 20 000x*

The SEM images of ZnO/ZnS after adding TAA and do not show variation with respect to the micrographs for ZnO (*Fig. 3*). Semi-spherical forms are presented with the formation of small spherical assembled particles, the size of these particles varies from 677 to 1400 nm in diameter.

Finally, the ZnO/ZnS/CuS heterostructure have a variation in the morphology with respect to the micrographs for ZnO, and ZnO/ZnS in which the circular morphology prevailed, varying for them to elongated forms with 380 nm in length (*Fig. 4*), which coincides with the morphology reported for this compound (Lu et al., 2016).

The optical absorbance was performed for the samples of ZnO, ZnO/ZnS and ZnO/ZnS/CuS (*Fig. 5*). The absorption Edge value of ZnO was obtained at 470 nm wich coinciding with the absorption edge values of the ZnO (3.37 eV). For ZnO/ZnS is possible to observe two edges values of absorption which is associated with the electronic interaction between the ZnO and ZnS with the increase of ZnS in the surface of ZnO (Jia et al., 2013) however no significant changes of the absorption increase above 400 nm are observed. For the ZnO/ZnS/CuS the absorption edges of the heterostructure have been significantly improved allowing the absorption of light in the

http://www.aloki.hu ● ISSN 1589 1623 (Print) ● ISSN 1785 0037 (Online)
DOI: http://dx.doi.org/10.15666/aeer/1605_57455756
© 2018, ALÖKI Kft., Budapest, Hungary

visible region (400-800 nm), which implies that the sample has a good activity photocatalytic in visible light (Lu et al., 2016).

The band gap was calculated with the modified function of Kubelka-Munk (F(R)*hv) 1/2 as a function of the photon energy (hv), It shows the band gap value of the ZnO of 3.18 eV which is similar to the value reported for the ZnO (Munirah et al., 2017). The band gap 3.17 eV of the ZnO/ZnS/CuS is significantly decreased compared with to individual ZnO, so that the increase of the surface of the ZnS over the ZnO produces a decrease in its band gap (Torabi and Staroverov, 2015), in the same way the value obtained from the band gap for the ZnO/ZnS/CuS is 3.09 eV (*Fig. 6*).

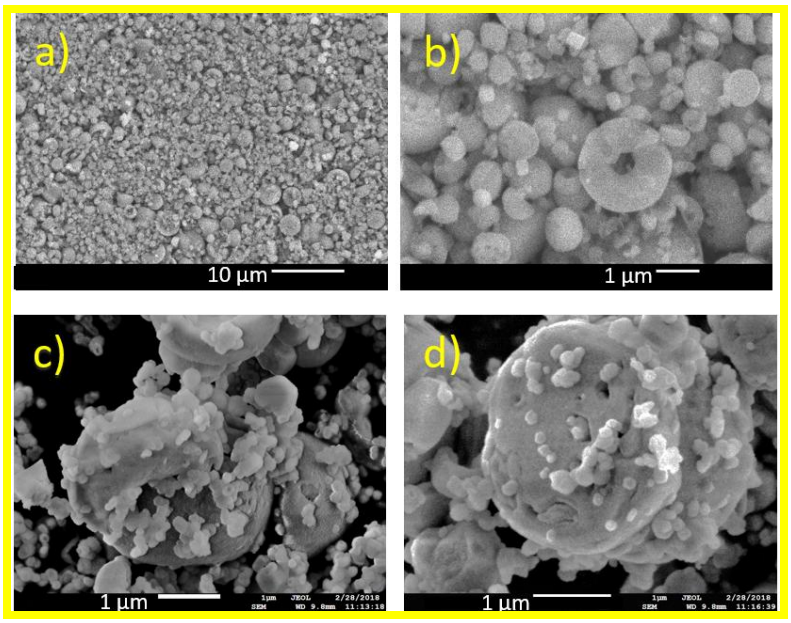

Figure 3. *SEM images of ZnO/ZnS a) 2 500x b) 15 000x c) 25 000x d) 20 000x*

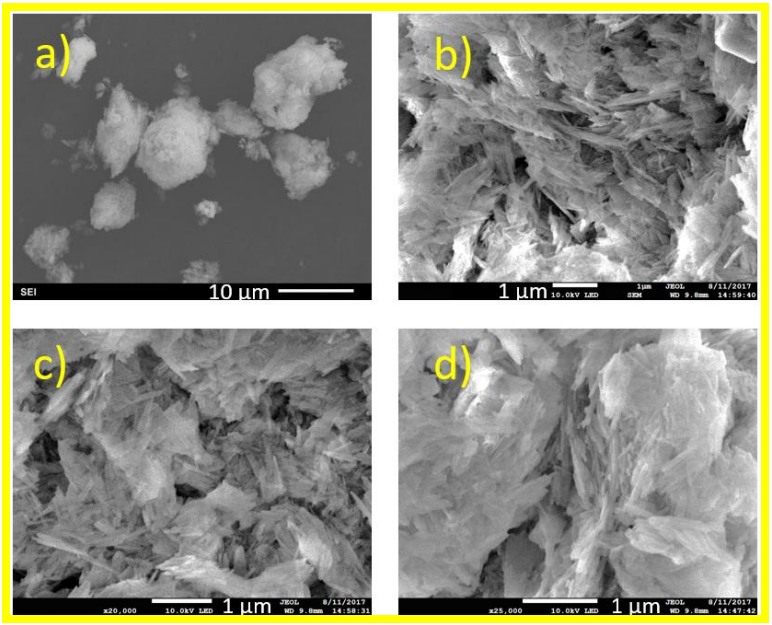

Figure 4. *SEM images of ZnO/ZnS/CuS a) 2 500x b) 15 000x c) 25 000x d) 20 000x*

http://www.aloki.hu ● ISSN 1589 1623 (Print) ● ISSN 1785 0037 (Online)
DOI: http://dx.doi.org/10.15666/aeer/1605_57455756
© 2018, ALÖKI Kft., Budapest, Hungary

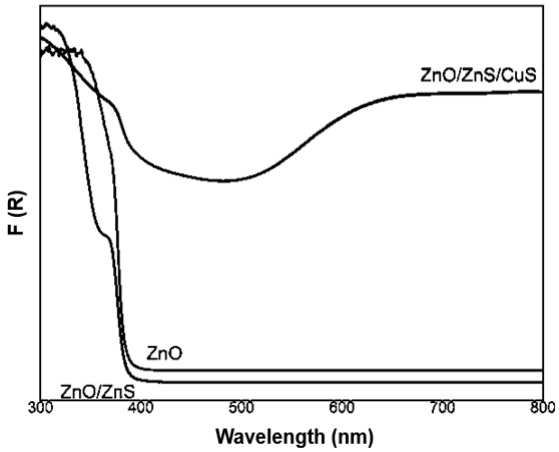

Figure 5. *Plot of absorbance vs wavelength ZnO, ZnO/ZnS and ZnO/ZnS/CuS*

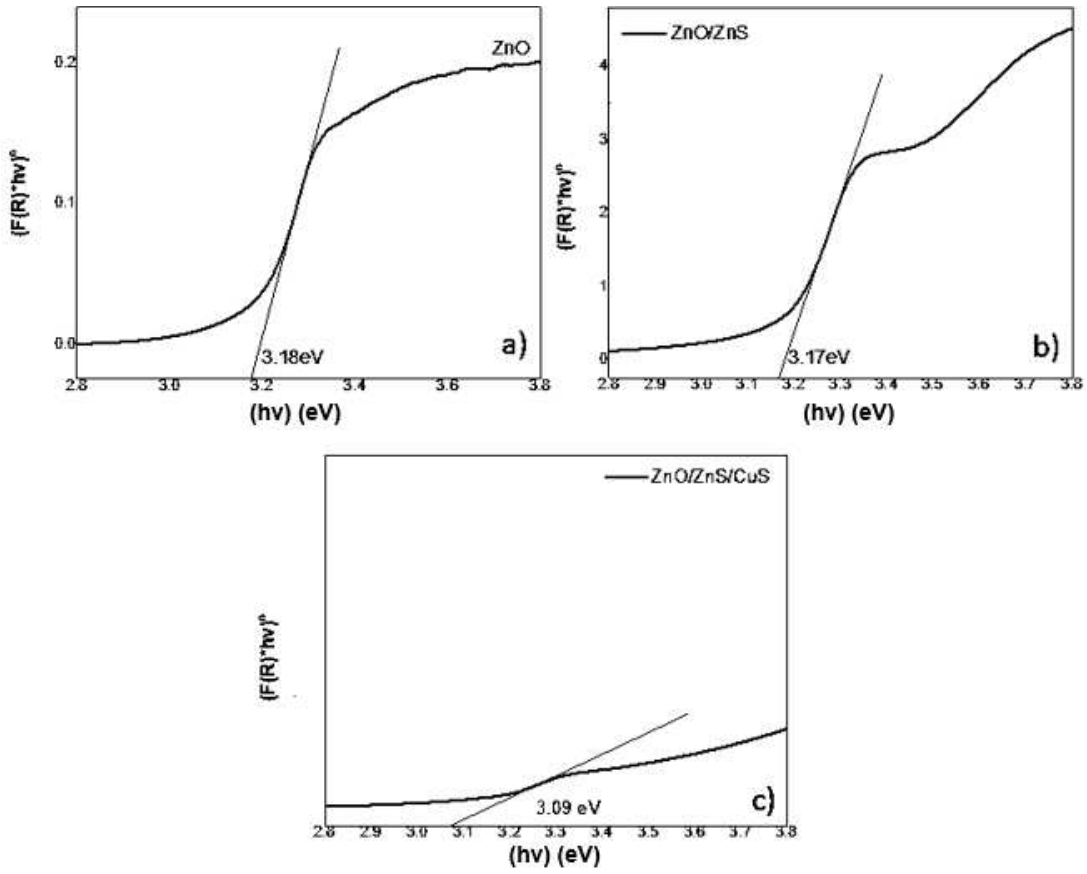

Figure 6. *Band gap of a) ZnO, b) ZnO/ZnS and c) ZnO/ZnS/CuS*

To confirm the formation of the compounds, raman scattering analyzes were performed for the ZnO, ZnO/ZnS and ZnO/ZnS/CuS samples (*Fig. 7*). Zinc Oxide ZnO, where the location of the vibrational modes located at 105, 385, 445, 585 and 663 cm^{-1} are associated with the vibrational active modes of the Wurtzite phase of ZnO (Ruiz et al., 2011) the dominant peak at 445 cm^{-1} is attributed to high-frequency phonons from

http://www.aloki.hu ● ISSN 1589 1623 (Print) ● ISSN 1785 0037 (Online)
DOI: http://dx.doi.org/10.15666/aeer/1605_57455756
© 2018, ALÖKI Kft., Budapest, Hungary

oxygen atoms (Fletcher et al., 2014), and E1 (LO) mode at 585 cm^{-1} is associated with interstitial zinc and oxygen vacancies, the $E2_L$ peak at 105 cm^{-1} is associated with the vibrations of the zinc (Scepanovic et al., 2009), the vibrational mode $E2_{high}$ - $E2_{low}$ at 337 cm^{-1} is associated with multifononic processes (Londoño-Calderón et al., 2012) and finally the vibrational mode A_1TO at 385 cm^{-1} is associated with intrinsic defects (Sundara Venkatesh et al., 2016), for the ZnS the additional presence of two resonant raman lines is observed in 217 and 350 cm^{-1} that correspond to the active vibrational modes of the ZnS, the spectrum shows the dominant peak in 350 cm^{-1} identified as a mode T2 (LO) of first order [20] (Milekhin et al., 2012), the LO mode in 217 cm^{-1} is attributed to the second order of raman scattering (Fairbrother et al., 2014). The heterostructure ZnO/ZnS/CuS locates the characteristic peaks that are associated with the presence of ZnO, ZnS and CuS and the appearance of the new peak that denotes the presence of the coveline phase of CuS at 165 cm^{-1} and 465 cm^{-1} (Baert et al., 2013).

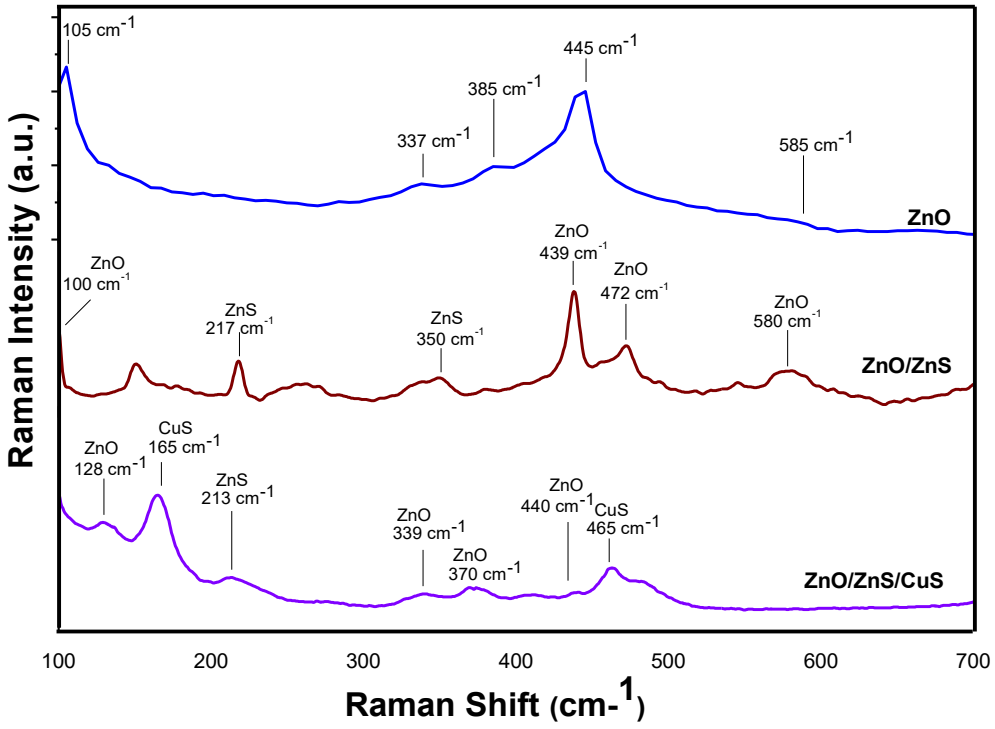

Figure 7. *Raman spectra of ZnO, ZnO/ZnS and ZnO/ZnS/CuS*

The photocatalytic test was performed with the degradation of MB (methylene blue), and MO (methyl orange). The test was prepared with 0.0249 g of photocatalyst and a concentration of 10 ppm of each of the dyes with the use of a lamp in the range of visible light. As mentioned in the methodology aliquots were taken every 30 min to measure its dye concentration during 240 min of reaction.

The UV-Vis absorption spectra show the degradation for the MB and MO dye with the time exposed to visible light radiation for ZnO/ZnS/CuS at a specific wavelength of 464 nm and 664 nm respectively (*Fig. 8*). As seem the aborbance intensity gradually decreased over time, according to what was reported by Lu et al. in 2016 this improvement can be attributed to the formation of the heterostructure constituted by the

http://www.aloki.hu ● ISSN 1589 1623 (Print) ● ISSN 1785 0037 (Online)
DOI: http://dx.doi.org/10.15666/aeer/1605_57455756
© 2018, ALÖKI Kft., Budapest, Hungary

three semiconductors ZnO, ZnS and CuS with which it is possible to reduce the recombination of the electron-hole pair due to the difference of their band gap (Liu et al., 2014).

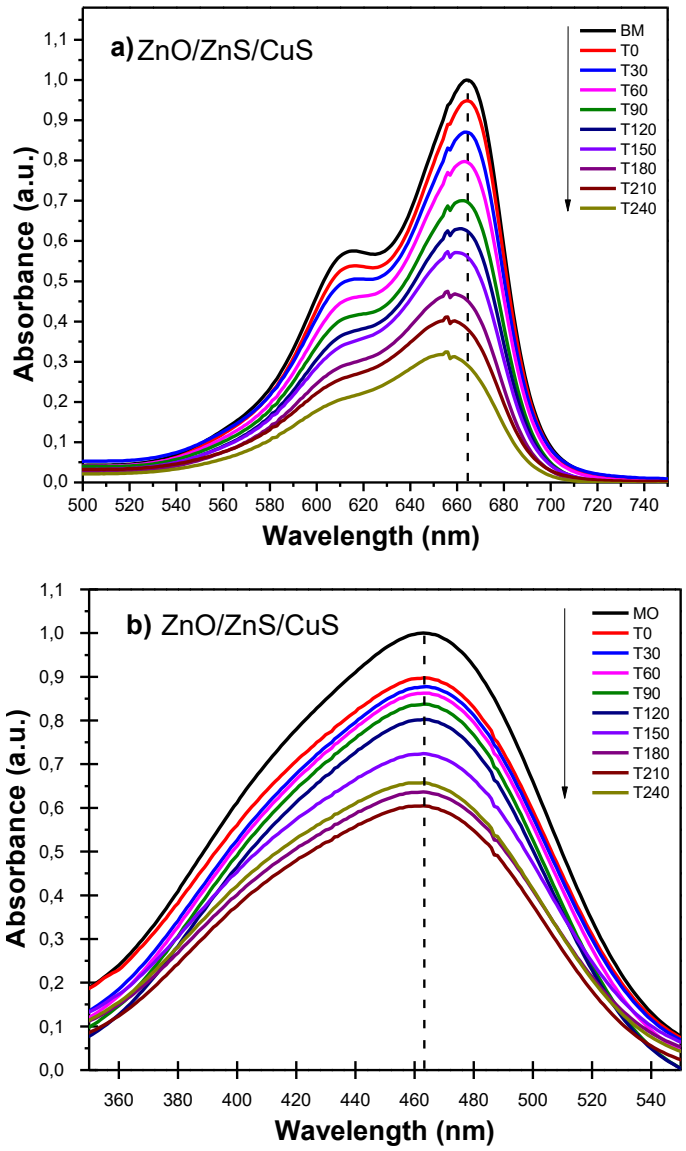

Figure 8. *Photocatalytic decomposition of a) methylene blue and b) methyl orange*

With the data obtained from the UV-Vis and applying the formula of the degradation efficiency (*Eq. 3*) to these values, it is established that the photocatalytic degradation of the MB increased by ~ 57% of its efficiency for the pure ZnO at ~ 61 with ZnO/ZnS and up to ~ 71% for the ZnO/ZnS/CuS heterostructure under visible light irradiation during 240 min of reaction and the photocatalytic degradation efficiency of MO increased from ~ 5% for ZnO to ~ 16% ZnO/ZnS and up to ~ 35% for ZnO/ZnS/CuS under the same conditions.

Figure 9 shows the values of the degradation of methyl orange and methylene blue in terms of $C/C_{0,}$ where C is the concentration of MB/MO at time t and C_0 is the initial concentration of MB/MO.

http://www.aloki.hu ● ISSN 1589 1623 (Print) ● ISSN 1785 0037 (Online)
DOI: http://dx.doi.org/10.15666/aeer/1605_57455756
© 2018, ALÖKI Kft., Budapest, Hungary

All samples of heterostructures exhibit greater photocatalytic activity than pure ZnO. The synthesized ZnO/ZnS/CuS showed high photocatalytic activity in methylene blue MB (~ 71%) unlike orange of methyl NM (~ 35%), this because the hydroxyl radicals play an important role in the breakdown of the anionic anionic dye orange methyl, while in cationic dyes such as methylene blue are involved in controlled reactions on the surface, resulting in the formation of intermediates that generally compete with the degradation of the original dye in solution (Li et al., 2014) than ZnO/ZnS and ZnO powders according to the exposure time (*Fig. 9*).

The difference of efficiencies in the degradation of contaminants is valid since each material is capable of degrading an organic compound efficiently or less efficiently due to the parameters that control the photocatalytic reactions such as temperature and pH (Scuderi et al., 2014).

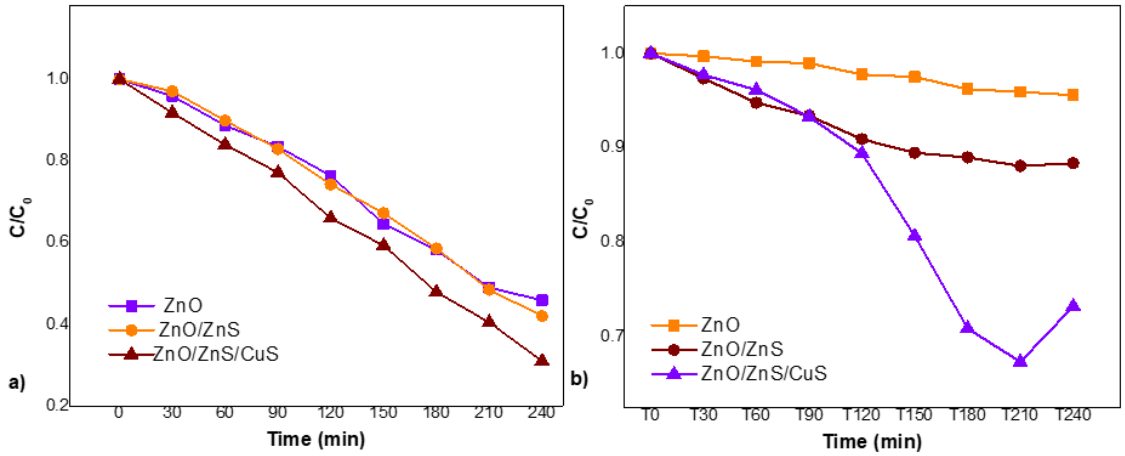

Figure 9. *Photocatalytic decomposition of a) methylene blue and b) methyl orange*

Conclusions

In this work, the ZnO/ZnS/CuS heterostructure was synthesized by microwave-assisted synthesis and cation exchange, which considerably modified its band gap. The ZnO/ZnS/CuS heterostructure can effectively decrease the recombination and exhibit a better photocatalytic activity in visible light compared to ZnO compared to the dyes analyzed in this study. We could also say that the heterostructure has a selective effect on the type and structure of the dye. It is recommended to modify the pH of the initial ZnO to improve the efficiency in the degradation, as well as to perform photocatalytic tests with mixed dyes.

Acknowledgements. The research group appreciates Edith Ponce Recinos for his support in the measures of SEM.

REFERENCES

[1] Ahmad, R., Ahmad, Z., Khan, A. U., Mastoi, N. R., Aslam, M., Kim, J. (2016): Photocatalytic systems as an advanced environmental remediation: Recent developments, limitations and new avenues for applications. – Journal of Environmental Chemical Engineering 4(4): 4143-4164.

http://www.aloki.hu ● ISSN 1589 1623 (Print) ● ISSN 1785 0037 (Online)
DOI: http://dx.doi.org/10.15666/aeer/1605_57455756
© 2018, ALÖKI Kft., Budapest, Hungary

[2] Alvi, M. A., Al-Ghamdi, A. A., ShaheerAkhtar, M. (2017): Synthesis of ZnO nanostructures via low temperature solution process for photocatalytic degradation of rhodamine B dye. – Materials Letters 204: 12-15. DOI: 10.1016/j.matlet.2017.06.005
[3] Baert, K., Breugelmans, T., Buytaert, G., Van Brabant, J., Hubin, A. (2013): The combination of surface enhanced Raman spectroscopy and an ionic liquid as a model system to study the adhesion interface between sulfur and brass. – Journal of Raman Spectroscopy 44: 377-381.
[4] Basu, M., Garg, N., Ganguli, A. K. (2014): A type-II semiconductor (ZnO/CuS heterostructure) for visible light photocatalysis. – Journal of Materials Chemistry A 20: 7517-7525.
[5] Choudhury, B. (2013): Defect generation, d-d transition, and band gap reduction in Cu-doped TiO2 nanoparticles. – International Nano Letters 3: 25.
[6] Fairbrother, A., Izquierdo-Roca, V., Fontané, X., Ibáñez, M., Cabot, A., Saucedo, E., Pérez-Rodríguez, A. (2014): ZnS grain size effects on near-resonant Raman scattering: optical non-destructive grain size estimation. – Cryst Eng Comm 16: 4121-4127.
[7] Fletcher, C., Jiang, Y., Sun, C., Amal, R. (2014): Morphological evolution and electronic alteration of ZnO nanomaterials induced by Ni/Fe co-dopingt. – Nanoscale 6: 7312-7318.
[8] Jia, W., Jia, B., Qu, F., Wu, X. (2013): Towards a highly efficient simulated sunlight driven photocatalyst: a case of heterostructured ZnO/ZnS hybrid structure. – Dalton Tras 42: 14178-14187.
[9] Kajbafvala, A., Ghorbani, H., Paravar, A., Samberg, J. P., Kajbafvala, E., Sadrnezhaad, S. K. (2012): Effects of morphology on photocatalytic performance of Zinc oxide nanostructures synthesized by rapid microwave irradiation methods. – Superlattices and Microstructures 51(4): 512-522.
[10] Li, J.-R., Wang, C.-C., Lv, X.-L., Zhang, Y.-Q. Guo, G. (2014): Photocatalytic organic pollutants degradation in metal–organic frameworks. – Energy Environ. Sci. 7(9): 2831-2867.
[11] Li, Y., Wang, X. Wang, M., Li, W., Chen, M., Zhao, Y. (2014): Synthesis of tunable ZnS–CuS microspheres and visible-light photoactivity for rhodamine B. – New J. Chem. 38(9): 4182.
[12] Liu, C., Wang, Y., Meng, D., Yu, X., Wang, Y., Liu, J., Lu, C., Xu, K. (2014): Enhanced visible light photocatalytic performance of ZnO/ZnS/CuS ternary nanocomposites. – Materials Letters 122: 197-200.
[13] Liu, C., Li, C., Fu, X., Raziq, F., Qua, Y., Jing, L. (2015): Synthesis of silicate-bridged ZnO/g-C3N4 nanocomposites as efficient photocatalysts and mechanism. – The Royal Society of Chemistry 5: 37275-37280.
[14] Liu, L., Li, Y. (2014): Understanding the reaction mechanism of photocatalytic reduction of C02 with H20 on Ti02-based photocatalysts: a review. – Aerosol and Air Quality Research 14: 453-469.
[15] Londoño-Calderón, M, Jurado, J. F., Vargas-Hernández, C. (2012): Estudio vibracional de nanoestructuras de ZnO sinterizadas por reacción en estado sólido. – Revista Colombiana de Física 44(1): 71-75.
[16] Lu, C., Liu, C., Chen, R., Fang, X., Xu, K., Meng, D. (2016): Synthesis and characterization of ZnO/ZnS/CuS ternary nanocomposites as high efficient photocatalyst in visible light. – Journal of Materials Science: Materials in Electronics 27:6947-6954. DOI: 10.1007/s10854-016-4649-4.
[17] Milekhin, A. G., Yeryukov, N. A., Sveshnikova, L. L., Duda, T. A., Himcinschi, C., Zenkevich, E. I., Zahn, D. R. T. (2012): Resonant Raman scattering of ZnS, ZnO, and ZnS/ZnO core/shell quantum dots. – Appl Phys A 107: 275-278.
[18] Munirah, Z. R. K., Aziz, A., Khan, M. S., Khandaker, M. U. (2017): Influence of zinc concentration on band gap and sub-band gap absorption on ZnO nanocrystalline thin films sol-gel grown. – Materials Science-Poland 35(1): 246-253.

http://www.aloki.hu ● ISSN 1589 1623 (Print) ● ISSN 1785 0037 (Online)
DOI: http://dx.doi.org/10.15666/aeer/1605_57455756
© 2018, ALÖKI Kft., Budapest, Hungary

[19] Okemoto, A., Tanaka, K., Kudo, Y., Gohda, S., Koshiba, Y., Ishida, K., Horie, T., Taniya, K., Ichihashi, Y., Nishiyama, S. (2018): Hydrogen production for photocatalytic decomposition of water with urea as a reducing agent. – Catalysis Today 307: 231-236.
[20] Paria, S., Reiser, O. (2014): Copper in photocatalysis. – Chemcatchem Minireviews 6(9): 2477-2483.
[21] Park, H., Kim, H., Moonb, G. Choi, W. (2016): Photoinduced charge transfer processes in solar, photocatalysis based on modified TiO2. – Energy Environ. Sci. 9: 411-436.
[22] Patterson, A. L. (1939): The Scherrer formula for X-ray particle size determination. – Physical Review 56: 978-982.
[23] Ruiz, P., de Lourdes, M., Serrano, J. G., Pal, U. (2011): Morphology defined ZnO nanostructures through microwave assisted chemical synthesis: growth mechanism, defect structure, and emission behaviours. – Advanced Science Letters 4: 1-8.
[24] Scepanovic, M, Grujic-Brojcin, K., Vojisavljevic, K., Bernik, S., Sreckovic, T. (2009): Raman study of structural disorder in ZnO. – Journal of Raman Spectroscopy 41: 914-921.
[25] Scuderi, V., Impellizzeri, G., Romano, L., Scuderi, M., Nicotra, N., Bergum, K., Irrera, A., Svensson, B. G., Privitera, V. (2014): TiO2-coated nanostructures for dye photo-degradation in water. – Nanoscale Research Letters 9(1): 458.
[26] Sooksaen, P., Chuankrerkkul, N. (2017): Morphology-design and semiconducting characteristics of zinc oxide nanostructures under microwave irradiation. – Integrated Ferroelectrics 177(1): 90-102.
[27] Sundara Venkatesh, P., Ramakrishnan, V., Jeganathan, K. (2016): Raman silent modes in vertically aligned undoped ZnO nanorods. – Physica B 481: 204-208.
[28] Torabi, A., Staroverov, V. N. (2015): Band gap reduction in ZnO and ZnS by creating layered ZnO/ZnS heterostructures. – The Journal of Physical Chemistry Letters 6(11): 2075-2080.
[29] Wan, H., Xu, L., Huang, W.-Q. (2014): Band engineering of ZnS by codoping for visible-light. – Appl Phys A 116: 741-750.
[30] Zhang, L., Jaroniec, M. (2018): Toward designing semiconductor-semiconductor heterojunctions for photocatalytic applications. – Applied Surface Science 430: 2-17.
[31] Zhu, Y. F., Fan, D. F., Shen, W. Z. (2008): a general chemical conversion route to synthesize various ZnO-based core/shell structures. – J. Phys. Chem. C 112: 10402-10406.

http://www.aloki.hu ● ISSN 1589 1623 (Print) ● ISSN 1785 0037 (Online)
DOI: http://dx.doi.org/10.15666/aeer/1605_57455756
© 2018, ALÖKI Kft., Budapest, Hungary

TEMPORAL AND SPATIAL VARIATIONS OF NO_2 OVER SAUDI ARABIA AND IDENTIFICATION OF MAJOR HOTSPOT AREAS DURING 2005-2014 BY USING SATELLITE DATA

UL-HAQ, Z.[1*] – BATOOL, S. A.[1] – TARIQ, S.[1] – RANA, A. D.[1] – MAHMOOD, K.[1] – CHAUDHARY, M. N.[2] – NAEEM, M. A.[3]

[1]*Remote Sensing and GIS Group, Department of Space Science, University of the Punjab Lahore, Pakistan*

[2]*College of Earth and Environmental Sciences, University of the Punjab, Lahore, Pakistan*

[3]*Department of Electrical Engineering, University of the Punjab, Lahore, Pakistan*

**Corresponding author*
e-mail: zia.spsc@yahoo.com

(Received 13th Sep 2017; accepted 12th Feb 2018)

Abstract. The present study was designed to analyze the concentration of tropospheric NO_2 over Saudi Arabia for a decade from 2005-2014 based on observations from satellite borne Ozone Monitoring Instrument (OMI). The spatial analysis has identified two hotspots: Jeddah and Riyadh. The result of temporal analysis shows increase of 1.45%, 3.15% and 3.10% per year over Saudi Arabia, Jeddah and Riyadh respectively. The Linear Regression analysis and Analysis of Variance (ANOVA) have been performed to analyze the relationship between meteorological parameters, seasons, years and concentration of NO_2. The results show that temperature and NO_2 are moderately correlated whereas wind and humidity give negative correlation. The major causes of elevated NO_2 over the hotspots are road traffic and the fossil fuel combustion for electrical power generation.
Keywords: *tropospheric NO_2, OMI, spatiotemporal analysis, Saudi Arabia, hotspots*

Introduction

Anthropogenic activities play a very important role in changing the atmospheric composition. It would be very disastrous for the whole ecosystem. Nitrogen dioxide (NO_2) is a very harmful for human beings and their environment. Nitrogen dioxide is an eminent air pollutant due to its strong influence on the chemistry and quality of atmosphere. It helps to normalize the ozone concentration in troposphere and also affects the amount of hydroxyl (OH) ions. The increase in anthropogenic activities especially fossil fuel burning, vehicular traffic and industrial production has enhanced the amount of NO_x in the atmosphere. Identification of the areas rich in this and other pollutants may be the first step to clean the environment. Satellite Remote Sensing (SRS) has now become a useful technique for air pollution monitoring by measuring the pollutants concentration within the study area. This technique helps to assess large scale coverage with uniformity of averaged measurements.

The main objective of the present work was to identify the NO_2 hotspots and analyze their spatial and temporal patterns over Saudi Arabia by using SRS technique. Saudi Arabia is the biggest Arab state in Arabian Peninsula, Western Asia with an area of 2.1 million km^2.

http://www.aloki.hu ● ISSN 1589 1623 (Print) ● ISSN 1785 0037 (Online)
DOI: http://dx.doi.org/10.15666/aeer/1605_57575770
© 2018, ALÖKI Kft., Budapest, Hungary

Review of literature

Satellite data is more appropriate and recent for different emissions. Hence it could be compared with in situ measurements (Zohary and Spiegel-Roy, 1975; Hayn et al., 2009; Kgosiesele, 2010; Lamsal et al., 2010; Sheel et al., 2010; Kloog et al., 2012; Khan, 2012; Khanum et al., 2013a). Satellites provide a high-coverage alternative to ground-based measurements. Many studies (Lennon et al., 2000; Hayn et al., 2009; Kumar and Stohlgren, 2009; Khan et al., 2010) provide useful assessment trends for air pollution especially for NO_2. It is observed that human activities produce approximately 75% NO_x, whereas combustion of fossil fuel contributes about 50% (Leyequien et al., 2007; Jeschke and Strayer, 2008). The tropospheric NO_2 columns derived from satellite have been used to evaluate chemical transport models (Zyrichidou et al., 2013), to study long term changes in anthropogenic emissions of NO_x over developing areas (Khanum et al., 2013b; Yang et al., 2013) and to examine the spatio-temporal patterns of NO_x emissions on global and regional scales (Yuan et al., 2015). In some recent studies these measurements have already been used to provide top down estimates of land surface NO_x emissions via inverse modeling on the global scale (Martin et al., 2003; Jaegle et al., 2005; Lin et al., 2010; Miyazaki et al., 2012). Due to rapid urbanization and industrialization air quality degradation is a serious threat to Saudi Arabia. (Yost et al., 2008; Taheri, 2010; Joly et al., 2004) have provided the temporal and spatial distribution of air pollutants specially NO_x and O_3 for Jeddah using ground based data.

Methodology

Study area and its meteorology

The research has been carried out in Saudi Arabia (16.5 to 32 °N and 35 to 55.6 °E) with population 26.9 million. Its geography is mostly dominated by BSh and BWh (Koppen climate classification types for dry climate, BSh for steppe hot desert and BWh for true hot deserts) There are no water bodies like rivers, ponds or lakes. The central plateau is the major topography from Red Sea to Persian Gulf. Meteorological data have been collected from www.wunderground.com. In general desert climate is dominated in Saudi Arabia with major difference of day and night. The summer temperature is usually found to be >45 °C and winter temperatures do not fall below 0 °C. The precipitation is negligible. The detailed meteorological parameters like maximum and minimum temperature, wind speed and pressure have been taken in account during the analysis of hotspots regarding NO_2.

Satellite data

Tropospheric NO_2 data have been collected from Ozone monitoring instrument (OMI) onboard NASA's satellite Aura. OMI uses spectral range of 270–500 nm (Levelt et al., 2006a, b). Its spectral resolution is about 0.5 nm (Zyrichidou et al., 2013). The data collected is for the past decade (2005-2014). Differential optical absorption spectroscopy (DOAS) analysis has been used to obtain tropospheric NO_2 column with spectral range 405–465 nm spectral range (Yu et al., 2014; Ellis, 2015). NASA's online user's manual for OMI products (Giovanni, 2014) has been consulted for further data analysis and filtering. The collected data of NO_2 column (OMNO2d.003, level–3) is screened for 0–30% cloud cover and binned spatially at 0.25 × 0.25 degrees (Slee and Feliciano, 2015). There is an uncertainty of 0.1×10^{15} molecules/cm^2 in dataset for

http://www.aloki.hu ● ISSN 1589 1623 (Print) ● ISSN 1785 0037 (Online)
DOI: http://dx.doi.org/10.15666/aeer/1605_57575770
© 2018, ALÖKI Kft., Budapest, Hungary

tropospheric NO_2. The tropospheric NO_2 data is compared with in situ data and bottom up emission inventories.

The satellite sensor data is compared with Global Ozone Monitoring Experiment (GOME-2) sensor data from January to December 2013. Both these sensors operate in sun-synchronous orbits, with 13:30 and 10:00 local time crossing at equator, respectively (van Noije et al., 2006). GOME-2 located on board MetOp-A satellite is the first of a series of three identical instruments which will provide more than 15 years of space-borne UV/visible observations of the atmosphere (Munro et al., 2000). The GOME-like nadir viewing spectrometer covers the spectral range between 240 and 790 nm at 0.2–0.4 nm resolution, has a ground pixel size of 80 × 40 km^2 and overpasses the Equator at 09:30 LT in the descending node (Callies et al., 2004). With its large swath of 1920 km, GOME-2 provides near global coverage every day. For this purpose Doha, capital city of Qatar, is considered due to limited data availability over Saudi Arabia. Doha has been considered due to its similarity with Saudi Arabia regarding climate and industrial activities. Both places have hot desert climate with long summers. *Figure 1* shows the time series of both sensors datasets. The time series shows good consistency between mean values of OMI (4.0×10^{15} molecules/cm^2) and GOME-2 (5.04×10^{15} molecules/cm^2) data. It is observed that the both datasets are positively correlated ($r = 0.534$).

Anthropogenic NO_x emissions have been obtained from Emissions of atmospheric Compounds & Compilation of Ancillary Data (ECCAD) web site available at http://eccad.sedoo.fr. These NO_x emissions have been estimated by Monitoring Atmospheric Composition and Climate (MACC) and megaCITY-Zoom for the Environment, CityZEN (Granier et al., 2011; ul-Haq et al., 2017). MACCity anthropogenic NO_x estimates are largely based on emissions from residential, transportation, agricultural, industrial, energy, waste and shipping sectors. Atmospheric Infrared Sounder (AIRS) instrument suite aboard the NASA Earth Observing System satellite Aqua provides the distribution of atmospheric trace gas constituents including ozone (Pagano et al., 2010). We have used monthly averaged and gridded AIRS O_3 product.

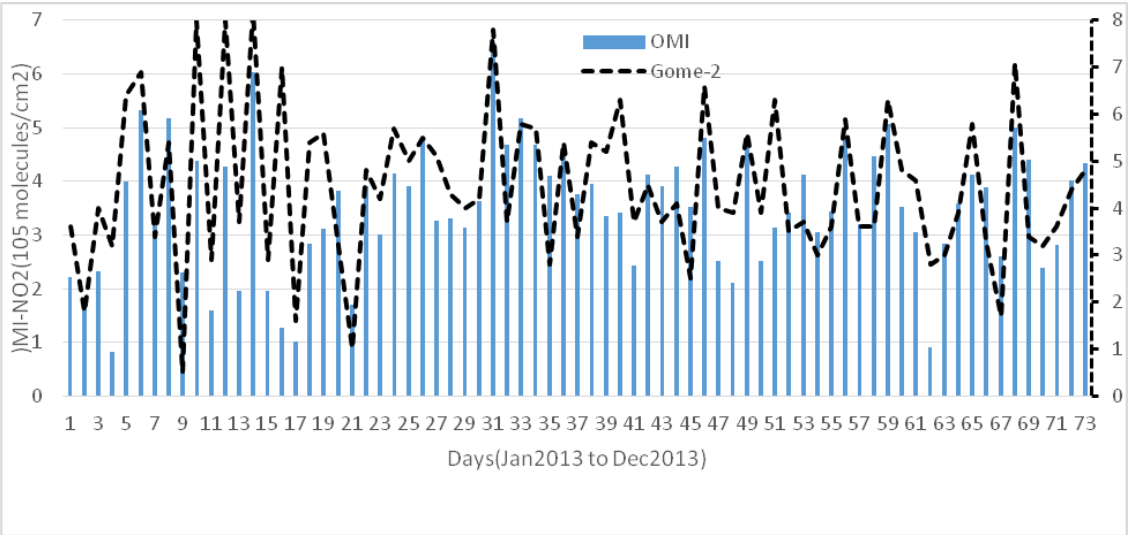

Figure 1. *Time series of OMI-NO_2 ($\times 10^{15}$ molecules/cm^2) and GOME2-NO_2 ($\times 10^{15}$ molecules/cm^2) over Doha during January 2013 to December 2013. Dotted line corresponds to secondary vertical axis*

http://www.aloki.hu ● ISSN 1589 1623 (Print) ● ISSN 1785 0037 (Online)
DOI: http://dx.doi.org/10.15666/aeer/1605_57575770
© 2018, ALÖKI Kft., Budapest, Hungary

Analysis of data

Time series plotting techniques have been used for Data analyses, especially for determining the seasonal and monthly trend of NO_2. These trends over two cities were further explored with Pearson's correlational analysis. Analysis of significant factors associated with concentration of NO_2 was carried out through General Linear Model (ANOVA.). The concentration of NO_2 for two sites has been compared between years, months and seasons. SPSS 20.0 version has been used for this purpose.

Results

The yearly averaged column value of NO_2 is found to be 1.1680×10^{15} molecules/cm^2 with increasing trend of 1.45% per year over Saudi Arabia (*Table 1*).

Table 1. *Descriptive analysis of OMI-NO_2 column ($\times 10^{15}$ molecules/cm^2) over the study area and hotspots during 2005-2014*

	N	Range	Minimum	Maximum	Mean	Std. deviation
Saudi Arabia	3637	2.09	0.28	2.37	1.1680	0.29215
Jeddah	3344	9.99	-0.55	9.43	3.0616	1.18307
Riyadh	3230	11.49	-0.06	11.44	3.0828	1.41565

Two NO_2 hotspots have been identified within the study area as shown in *Figure 2*.

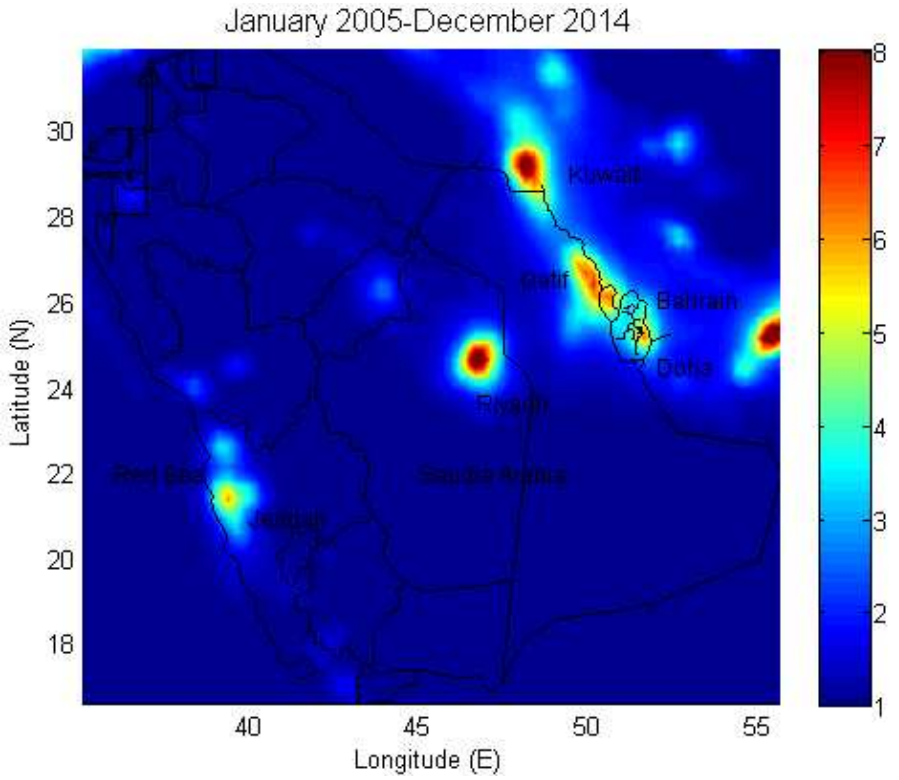

Figure 2. *OMI-NO_2 mean concentration ($\times 10^{15}$ molecules/cm^2) over the study area and two hotspots from 2005 to 2014*

http://www.aloki.hu ● ISSN 1589 1623 (Print) ● ISSN 1785 0037 (Online)
DOI: http://dx.doi.org/10.15666/aeer/1605_57575770
© 2018, ALÖKI Kft., Budapest, Hungary

The yearly averaged column value of NO_2 is found 3.06×10^{15} molecules/cm^2 with increasing trend of 3.15% per year over Jeddah and 3.06×10^{15} molecules/cm^2 with increasing trend of 3.10% per year over Riyadh. These elevated values can be seen throughout the year as shown in *Figure 3*.

The overall trend is found higher in higher percentile. An increasing trend also found year after year both in Jeddah and Riyadh (*Table 2*).

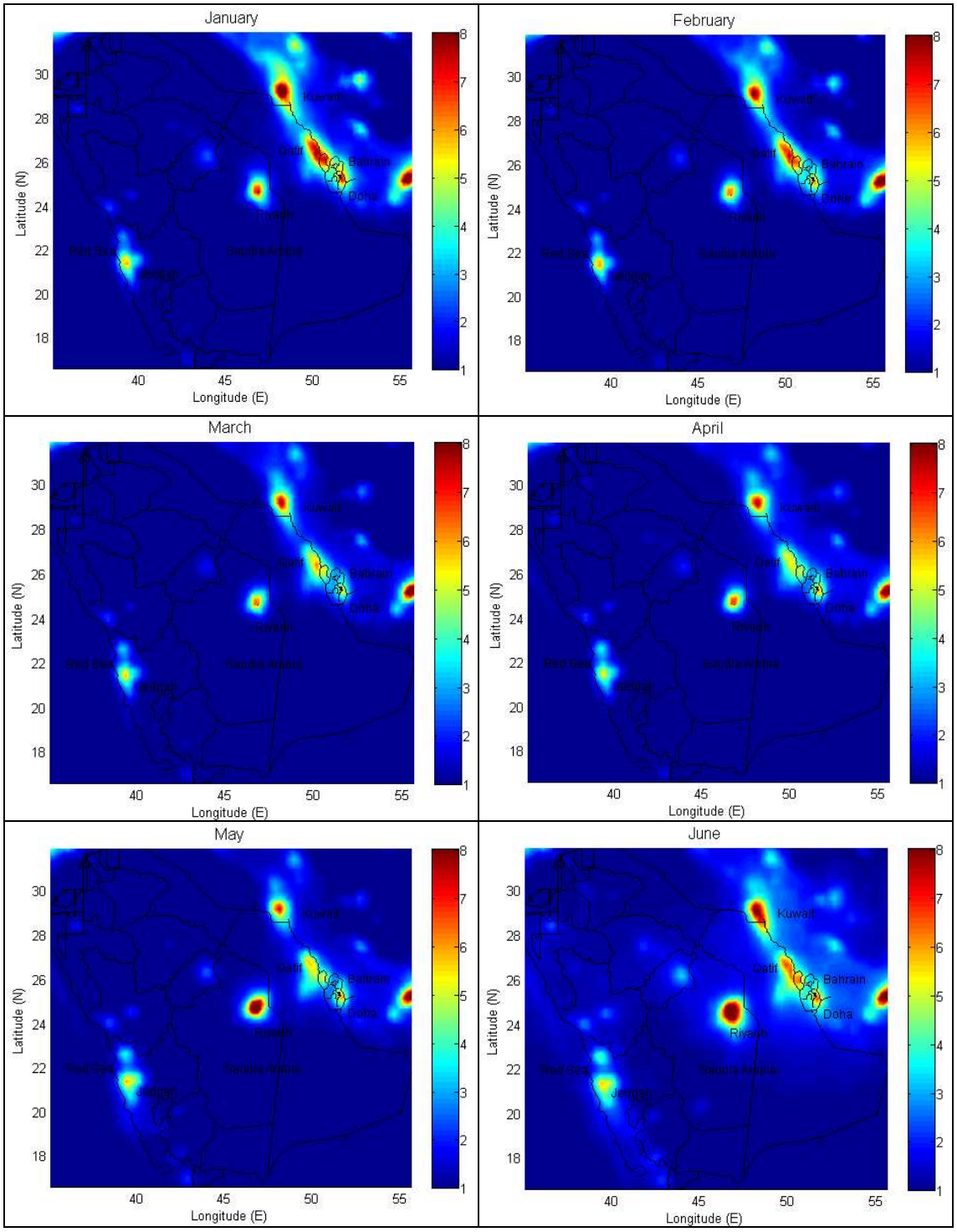

http://www.aloki.hu ● ISSN 1589 1623 (Print) ● ISSN 1785 0037 (Online)
DOI: http://dx.doi.org/10.15666/aeer/1605_57575770
© 2018, ALÖKI Kft., Budapest, Hungary

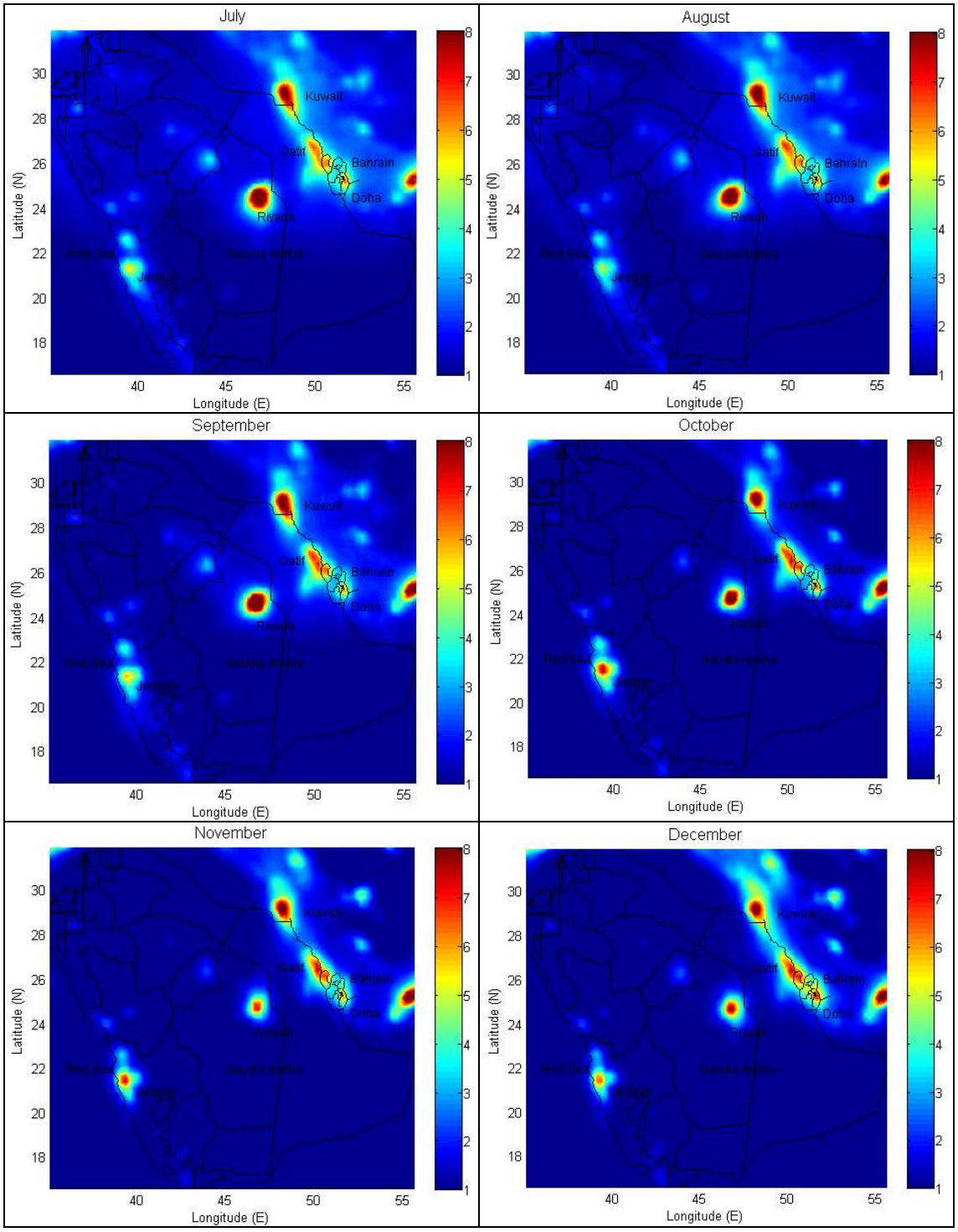

Figure 3. *Monthly spatial distribution of OMI-NO_2 ($\times 10^{15}$ molecules/cm^2) column over the study region during 2005-2014*

The relation between meteorological parameters and tropospheric NO_2 has been found through bivariate correlation analysis and the trends have been found by linear regression (*Table 3*). The mean value of meteorological factors, temperature, wind

http://www.aloki.hu ● ISSN 1589 1623 (Print) ● ISSN 1785 0037 (Online)
DOI: http://dx.doi.org/10.15666/aeer/1605_57575770
© 2018, ALÖKI Kft., Budapest, Hungary

speed, humidity, cloud cover, visibility and sea level pressures has been considered. The meteorological data was collected from www.wunderground.com.

Table 2. *Summary OMI-NO_2 ($\times 10^{15}$ molecules/cm^2) trends statistics over hotspot cities during 2005 to 2014*

	NO2 concentration over Jiddah									
Percentiles	2005	2006	2007	2008	2009	2010	2011	2012	2013	2014
5	1.631	1.468	1.485	1.502	1.510	1.224	0.975	1.138	0.970	1.107
10	1.910	1.734	1.820	1.887	1.811	1.612	1.461	1.677	1.695	1.729
25	2.238	2.114	2.254	2.336	2.321	2.387	2.233	2.335	2.470	2.600
50	2.702	2.552	2.706	2.959	2.889	3.065	2.845	3.154	3.224	3.329
75	3.285	3.149	3.530	3.780	3.668	3.879	3.550	3.950	4.148	4.146
90	4.006	3.848	4.083	4.617	4.437	5.003	4.412	4.979	5.486	5.178
95	4.506	4.367	4.657	5.072	5.113	5.309	5.532	5.739	6.450	5.960
NO2 concentration over Riyadh										
5	1.180	1.058	1.256	1.203	1.216	1.353	1.155	1.114	1.109	1.186
10	1.429	1.284	1.632	1.633	1.583	1.688	1.532	1.478	1.639	1.638
25	1.981	1.906	2.132	2.128	2.249	2.430	2.293	2.110	2.130	2.192
50	2.562	2.442	2.725	2.957	3.026	3.286	3.193	3.008	2.790	2.832
75	3.447	3.189	3.420	3.773	4.225	4.359	4.212	4.107	3.843	3.859
90	4.154	4.075	4.083	4.700	5.376	5.456	5.635	5.688	5.284	4.918
95	4.626	4.632	4.784	5.425	6.118	6.519	6.693	6.588	6.122	5.653

Table 3. *Correlation between concentration of NO_2 over Jeddah, Riyadh and meteorological factors*

		NO_2	**Temperature (^oC)**	**Pressure (hPa)**	**Visibility (km)**	**Humidity (%)**	**Wind speed (km/hr)**	**Cloud cover**
Riyadh	Pearson correlation	1	0.347**	-0.288**	-0.038	-0.342**	-0.319**	-0.166**
	Sig. (1-tailed)		0.000	0.000	0.057	0.000	0.000	0.001
Jeddah	Pearson correlation	1	0.131**	-0.010	-0.123**	-0.004	-0.305**	-0.274**
	Sig. (1-tailed)		0.000	0.278	0.000	0.418	0.000	0.000

**Correlation is significant at the 0.01 level (1-tailed)

Table 4 highlights the effect size of NO_2 concentration for seasons and years over two hotspots Riyadh and Jeddah. Eta square η^2 for both one-way and multiway ANOVA from General Linear Model and then Univariate analysis has been calculated.

Figure 4 shows that Range of NO_2 concentration is higher over Riyadh whereas it found lower for Jeddah for the same reason. The NO_2 Range is high for Riyadh with 7.79×10^{15} molecules/cm^2 than Jeddah with 4.69×10^{15} molecules/cm^2. The seasonal temperature difference of 8 °C and 20 °C has been found for Jeddah and Riyadh respectively. The regression analysis shows that for every one degree increase in temperature tropospheric concentration of NO_2 over Riyadh increased by 0.15, which represent 0.36 standard deviation. F (1, 2388) = 327 had an associated probability level of $p < 0.001$, while for Jeddah increase in one degree in temperature will increase the value of NO_2 by 0.06.

http://www.aloki.hu ● ISSN 1589 1623 (Print) ● ISSN 1785 0037 (Online)
DOI: http://dx.doi.org/10.15666/aeer/1605_57575770
© 2018, ALÖKI Kft., Budapest, Hungary

Table 4. *Comparison between the measured NO_2 values of the sites and years and seasons through ANOVA*

Source	df	Mean square	F	Sig.	Partial eta squared
Season and NO_2_Jeddah	3	60.873	45.217	.000	.039
Year and NO_2_Jeddah	9	19.028	14.073	.000	.037
Season and NO_2_Riyadh	3	191.015	104.477	.000	.089
Year and NO_2_Riyadh	9	29.484	15.298	.000	.041

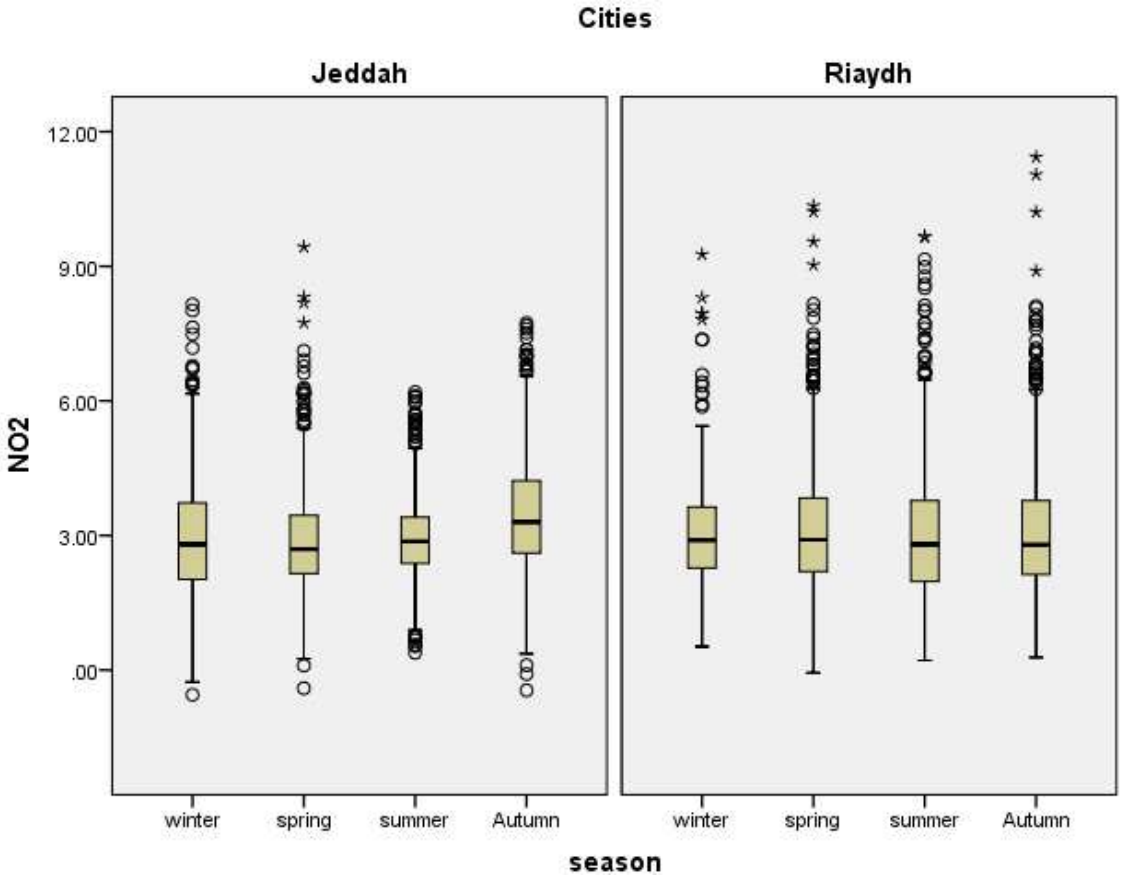

Figure 4. *Concentration of NO_2 ($\times 10^{15}$ molecules/cm^2) in different seasons over hotspots during 2005-2014*

The activities regarding electricity consumption, fossil fuel burning in automobiles and electrical power generators have been noticed at the peak during summer months. Therefore, high concentration of NO_2 has been found both in summer and autumn. The highest value found in Riyadh, i.e. mean 3.41×10^{15} molecules/cm^2 (Std. Dev = 1.25 whereas in Jeddah highest value found in autumn, i.e. mean = 3.39×10^{15} molecules/cm^2 (Std Dev = 1.19) (*Figure 5*).

http://www.aloki.hu ● ISSN 1589 1623 (Print) ● ISSN 1785 0037 (Online)
DOI: http://dx.doi.org/10.15666/aeer/1605_57575770
© 2018, ALÖKI Kft., Budapest, Hungary

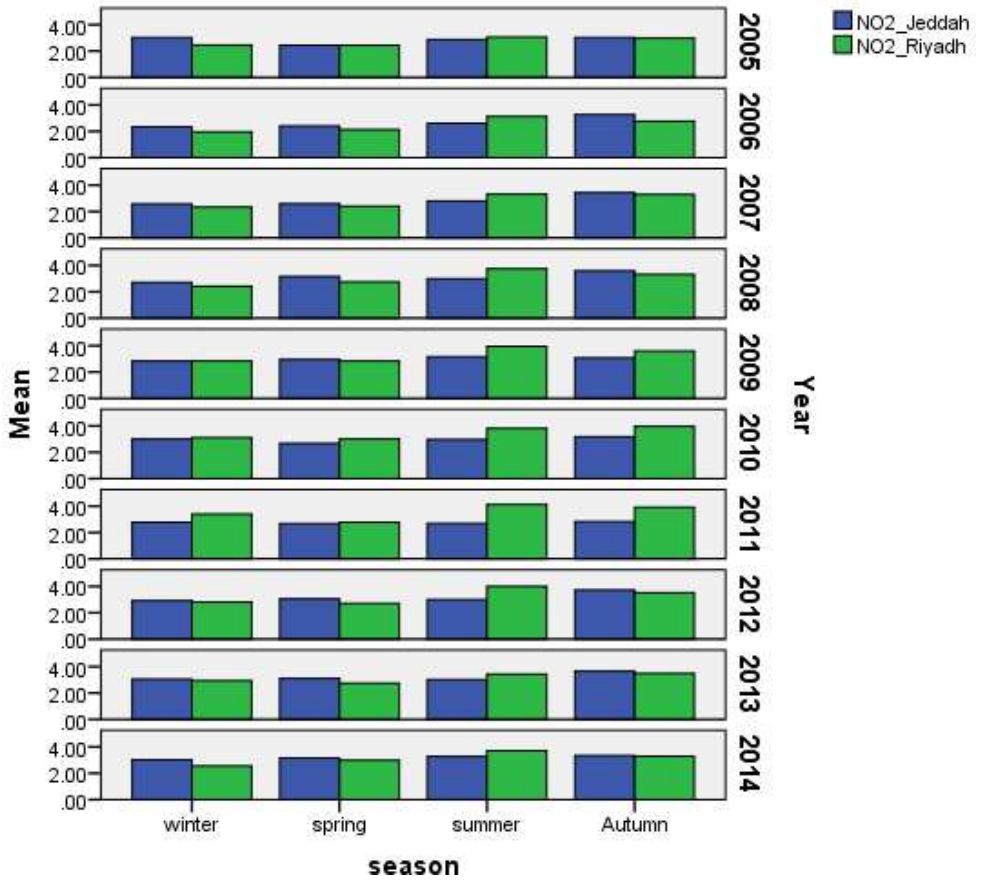

Figure 5. *Seasonal mean variations of NO_2 ($\times 10^{15}$ molecules/cm^2) over hotspots during 2005-2014*

An overall correlation between OMI tropospheric NO_2 and AIRS tropospheric ozone is found $r = 0.21$ during 2005-2014. Also spatial mapping of correlations between OMI tropospheric NO_2 and AIRS tropospheric ozone has been presented in *Figure 6* during 2005-2014. The correlations have been observed to be ranging from $r = 0.6$ to $r = –0.8$. Most of the northern parts of Saudi Arabia are found with higher positive correlations compared to southern parts largely due to more population and economic activities.

Discussion

The results show yearly averaged column value of NO_2 has been increased annually by 1.45%. This increasing trend is in close agreement with previous regional study by (Zohary and Spiegel-Roy, 1975). In Saudi Arabia the consumption of oil (million barrels per day) has increased 60.9% from 1996 to 2006 (EIA, 2008). This increase has contributed to increased levels of NO_2 in the atmosphere. The increase in Saudis' manmade activities contribute significantly to this trend. The most prominent sources of pollution are motor cars, factories and oil refineries. The number of private vehicles was found large because of weak public transportation system in Saudi Arabia (Kaba et al., 2007). According to Arab News (2014) an increase of 6% in motor vehicles from 2012 has been recorded.

http://www.aloki.hu ● ISSN 1589 1623 (Print) ● ISSN 1785 0037 (Online)
DOI: http://dx.doi.org/10.15666/aeer/1605_57575770
© 2018, ALÖKI Kft., Budapest, Hungary

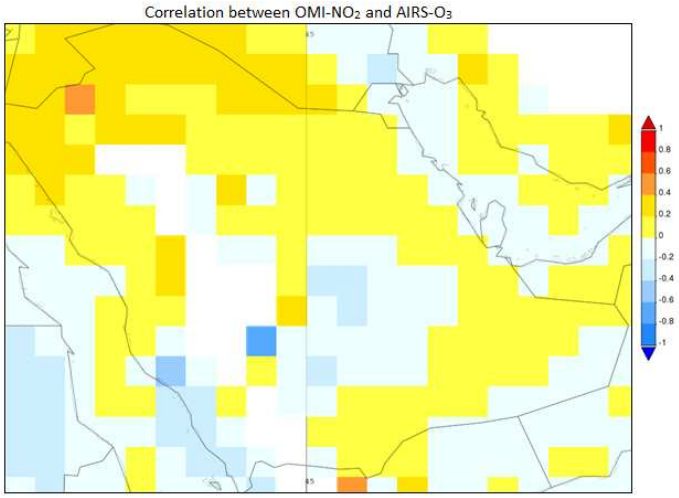

Figure 6. *Spatial map of correlation between OMI observed NO_2 and AIRS retrieved tropospheric ozone over Saudi Arabia during 2005-2014*

EDGAR (Emission Database for Global Atmospheric Research) data has shown 9.4% increase in NO_x emissions in Saudi Arabia (EDGAR, 2010) during 2005–2008 and has identified major sources with significant annual increase in various emission categories, i.e. public electricity and heat production (18.3%), manufacturing industries and construction (15.03%), manure man- agreement (6.93%), direct soil emissions (1.78%). Average oil industrial production growth rate was found 20% from 2010 to 2015 (Arab News, 2014).

Two cities, Jeddah and Riyadh, of Saudi Arabia have been identified with remarkable concentration of NO_2. Many studies have already identified these two cities as important source of NO_2 (Boersma et al., 2004, 2007; Bowler, 2014). Jeddah lat (20.6, 22.1 °N) long (38.9, 40 °E) has comparatively warm and humid climate with mean temperature 29 °C, mean humidity 54%, mean sea level pressure 1008 mb, 57% humidity and 10.9 km/hour wind speed. Precipitation is negligible. Winds blow in north east direction. The winds mostly come from Red Sea. In summers, dust storms blow from the Arabian Peninsula to Jeddah.

Riyadh lat (24.4, 26 °N) long (46.1, 48 °E) is capital city of Saudi Arabia. It has hot desert climate with increased seasonal range of temperature, i.e. 35 °C (mean temp 27.5 °C). The mean sea-level pressure is 1013 mb, and mean humidity value is 25%.

The reason behind higher concentration of NO_2 over Jeddah and Riyadh can be Industrial and vehicular emissions. Their combined effect gives Jeddah a serious air pollution problem. Many old cars cause serious air pollution in the city due to poor maintenance and improper check of regulations and then the industrial area of the city contribute further to environment (Kadi, 2009). Concentrations of heavy metals, gaseous air pollutants and particulate emissions far exceed internationally acceptable standards (Al-Jeelani, 2008; Hassan et al., 2013). Other important reasons of NO_2 emission in both Jeddah and Riyadh are incinerators, oil refineries, cement and electrical power plants. In Riyadh, sand rock quarries and crushers contribute significantly to NO_2 emission (Salama et al., 2011). The sprawling pattern of the cities, such as Riyadh and Jeddah, also contributes to emissions through long trips to work. Al-

http://www.aloki.hu ● ISSN 1589 1623 (Print) ● ISSN 1785 0037 (Online)
DOI: http://dx.doi.org/10.15666/aeer/1605_57575770
© 2018, ALÖKI Kft., Budapest, Hungary

Ahmadi and Al-Zahrani noted that NO_2 concentrations in Jeddah and Riyadh might be caused by vehicle emissions and urban activities (Kaba et al., 2007).

The correlation between OMI NO_2 and MACCity anthropogenic NO_x from sum sectors including residential, transportation, agricultural, industrial, energy, waste and shipping sectors is (r = 0.78 and slope 0.942) over Saudi Arabia during 2005-2014.

The results show positive correlation between temperature and NO_2 and negative correlation with mean humidity, cloud cover and wind speed for both hotspots (*Table 3*). The literature supports these results as life time of NO_2 is 3-10 hours and may be remain for 5 to 10 days only when humidity level is low (Papes, 2007). The tropospheric NO_2 reacts with OH radical and removed from the atmosphere by converting into nitric acid (HNO_3) in day timings (Oindo et al., 2002). The relationship between NO_2 and temperature is discussed by (Moreno-Amat et al., 2015), that with the increase in temperature a significant increase in HNO_3 has been found. However, no significant correlation has been found between these two variables (NO_2 and Humidity) for Jeddah, a coastal city due to higher and constant level of humidity and less temperature variations over coastal city of Jeddah.

As the results showed, seasonal effects are remarkable for both hotspots. Analysis of variance (*Table 4*) showed a main effect of seasons on NO_2 concentration over Riyadh ($p = .000$, $\eta p^2 = 0.08$) and Jeddah ($p = .000$, $\eta p^2 = 0.03$), whereas for years it gives Riyadh ($p = .000$, $\eta p^2 = 0.04$) and Jeddah (($p = .000$, $\eta p^2 = 0.03$). It means seasonal effect is 8% for Riyadh and 3% for Jeddah. The difference in years for NO_2 concentration was found 4% for Riyadh and 3% for Jeddah. Maximum mean values of NO_2 have been found in summer and autumn and comparatively low values are observed in spring and winter. As far as Jeddah is concerned it is one of the major cities of Saudi Arabia and the largest after Mecca. It serves as a major platform for air, road and marine transport. It has also main airport for pilgrims for Hajj (Bowler, 2014). In 2013, 17 million people as tourist enter in Saudi Arabia where its 40.6% approximately 6.9 million were on religious purpose (Ellis, 2015). The highest value of NO_2 found in autumn and early winter reveals the fact that from 2005-2014 the Hajj season came between October and January. *Figure 5* shows a remarkable increase in concentration of NO_2 over Riyadh in summer and autumn 2011. It may be due to heavy transport movement of approximately 1000 Saudi troops (Slee and Feliciano, 2015) to handle the Bahrain uprising and unrest due to the protests in Saudi Arabia especially in Riyadh.

Conclusion

Tropospheric NO_2 has been studied over Saudi Arabia with the help of satellite based OMI data. Two hotspots Jeddah and Riyadh have been identified. The spatiotemporal analysis showed that there was significant increase in NO_2 level from 2005-2014. The NO_2 patterns were also analyzed with the help of meteorological parameters. The results showed positive correlation with temperature and negative correlation with wind speed, humidity and cloud cover. A detailed analysis to assess the relationship of NO_2 with other atmospheric pollutants such as CO, Ozone, SO_2 and aerosols over Saudi Arabia is recommended for future studies with special emphasis on Hajj season.

http://www.aloki.hu ● ISSN 1589 1623 (Print) ● ISSN 1785 0037 (Online)
DOI: http://dx.doi.org/10.15666/aeer/1605_57575770
© 2018, ALÖKI Kft., Budapest, Hungary

REFERENCES

[1] Al-Jeelani, H. A. (2008): Air quality assessment at AlTaneem area in the Holy Makkah City, Saudi Arabia. – Environ. Monit. Assess. 156: 211-222.

[2] Boersma, K. F., Eskes, H. J., Brinksma, E. J. D. (2004): Error analysis for tropospheric NO_2 retrieval from space. – Journal of Geophysical Research 109: D04311.

[3] Boersma, K. F., Eskes, H. J., Veefkind, J. P., Brinksma, E. J., Van Der, A. R. J., Sneep, M., van den Oord, G. H. J., Levelt, P. F., Stammes, P., Gleason, J. F., Bucsela, E. J. (2007): Near-real time retrieval of tropospheric NO_2 from OMI. – Atmospheric Chemistry and Physics 2013-2128.

[4] Bowler, M. G. (2014): Species abundance distributions, statistical mechanics and the priors of MaxEnt. – Theoretical Population Biology 92: 69-77.

[5] Callies, J., Corpaccioli, E., Eisinger, M., Lefebvre, A., Munro, R., Perez-Albinana, A., Ricciarelli, B., Calamai, L., Gironi, G., Veratti, R., Otter, G., Eschen, M., van Riel, L. (2004): GOME-2 Ozone Instrument On-Board the European METOP Satellites. – Weather and Environmental Satellites, Proceedings of SPIE, The International Society for Optical Engineering, Denver, CO, pp. 60-70.

[6] Ellis, C. J. (2015): Ancient woodland indicators signal the climate change risk for dispersal-limited species. – Ecological Indicators 53: 106-114.

[7] Giovanni (2014): Geospatial Interactive Online Visualization and Analysis Infrastructure. – http://disc.sci.gsfc.nasa.gov/giovanni.

[8] Granier, C., Bessagnet, B., Bond, T., D'Angiola, A., van der Gon, H. D., Frost, G. J., Heil, A., Kaiser, J. W., Kinne, S., Klimont, Z., Kloster, S., Lamarque, J.-F., Liousse, C., Masui, T., Meleux, F., Mieville, A., Ohara, T., Raut, J.-C., Riahi, K., Schultz, M. G., Smith, S. J., Thompson, A., van Aardenne, J., van der Werf, G. R., van Vuuren, D. P. (2011): Evolution of anthropogenic and biomass burning emissions of air pollutants at global and regional scales during the 1980–2010 period. – Climatic Change 109: 163.

[9] Hassan, I. A., Basahi, J. M., Ismail, I. M., Haebeebullah, T. M., X, L. (2013): Spatial distribution and temporal variation in ambient ozone and its associated NO in the atmosphere of Jeddah City, Saudi Arabia. – Aerosol and Air Quality Research 13: 1712-1722.

[10] Hayn, M., Beirle, S., Hamprecht, F. A., Platt, U., Menze, B. H., Wagner, T. (2009): Analysing spatio-temporal patterns of the global NO_2-distribution retrieved from GOME satellite observations using a generalized additive model. – Atmospheric Chemistry and Physics 9: 6459-6477.

[11] Jeschke, J., Strayer, D. (2008): Usefulness of bioclimatic models for studying climate change and invasive species. – Annals of the New York Academy of Sciences 1134: 1-24.

[12] Joly, P., Morand, C., COHAS, A. (2004): Habitat fragmentation and amphibian conservation: building a tool for assessing landscape matrix connectivity. – Comptes Rendus Biologies 4: 500-511.

[13] Kaba, E., Ginzler, O., Ogilvie, J., Pinner, L., Patterson, D. (2007): ArcGIS Destop Help 9.2. Determining aspect. – ESRI. http://webhelp.esri.com/arcgisdesktop/9.2/index.cfm?TopicName=Calculating_slope. Accessed on June 21, 2013.

[14] Kadi, M. W. (2009): Soil pollution hazardous to environment: A case study on the chemical composition and correlation to automobile traffic of the roadside soil of Jeddah city, Saudi Arabia. – Journal of Hazardous Materials 168: 1280-1283.

[15] Kgosiesele, E. (2010): Predictive Distribution Modelling of Timon lepida in Spain. – M.Sc. Thesis, ITC, Netherland.

[16] Khan, N. (2012): A community analysis of Quercus baloot Griff, forest District Dir, Upper Pakistan. – African Journal of Plant Science 6: 21-31.

http://www.aloki.hu ● ISSN 1589 1623 (Print) ● ISSN 1785 0037 (Online)
DOI: http://dx.doi.org/10.15666/aeer/1605_57575770
© 2018, ALÖKI Kft., Budapest, Hungary

[17] Khan, N., Ahmed, M., Wahab, M., Ajaib, M., Hussain, S. S. (2010): Studies along an altitudinal Gradient in Monotheca Buxifolia (Faloc.) A. D., Forest, District Lower Dir, Pakistan. – Pakistan Journal of Botany 42: 3029-3038.

[18] Khanum, R., Mumtaz, A. S., Kumar, S. (2013a): Prediciting impact of climate change on medicinal asclepiads of Pakistan using Maxent modeling. – Acta Oecologica 49: 23-31.

[19] Khanum, R., Mumtaz, A. S., Kumar, S. (2013b): Predicting impacts of climate change on medicinal asclepiads of Pakistan using Maxent modeling. – Acta Oecologica 49: 23-31.

[20] Kloog, I., Nordio, F., Coull, B. A., Schwartz, J. (2012): Incorporating local land use regression and satellite aerosol optical depth in a hybrid model of spatiotemporal PM (2.5) exposures in the Mid-Atlantic states. – Environmental Science & Technology 646: 11913-11921.

[21] Kumar, S., Stohlgren, T. J. (2009): Maxent modeling for predicting suitable habitat for threatened and endangered tree Canacomyrica monticola in New Caledonia. – Journal of Ecology and the Natural Environment 1: 094-098.

[22] Lamsal, L. N., Martin, R. V., van Donkelaar, A., Celarier, E. A., Bucsela, E., Boersma, K. F. (2010): Indirect validation of tropospheric nitrogen dioxide retrieved from the OMI satellite instrument: insight into the seasonal variation of nitrogen oxides at northern midlatitudes. – Journal of Geophysical Research: Atmospheres (1984–2012), 115.

[23] Lennon, J. J., Greenwood, J. J. B., Turner, J. R. G. (2000): Bird Diversity and environmental gradients in Britain: A test of the species-energy hypothesis. – Journal of Animal Ecology 69: 581-598.

[24] Levelt, P. F., van den Oord, G. H. J., Dobber, M. R., Malkki, A., Visser, H., De Vries, J., Stammes, P., Lundell, J. O. V., Saari, H. (2006a): The ozone monitoring instrument. – IEEE Transactions on Geoscience and Remote Sensing 44: 1093-1101.

[25] Levelt, P. F., Hilsenrath, E., Leppelmeier, G. W., van den Oord, G. B. J., Bhartia, P. K., Tamminen, J., de Haan, J. F., Veefkind, J. P. (2006b). Science objectives of the Ozone Monitoring Instrument. – IEEE Transactions on Geoscience and Remote Sensing 44: 1199.

[26] Leyequien, E., Verrelst, J., Slot, M., Schaepman-Strub, G., Heitkonig, I., Skidmore, A. K. (2007): Applying remote sensing to terrestrial animal distribution and diversity. – International Journal of Applied Earth Observation and Geoinfomation 9: 1-20.

[27] Moreno-Amat, E., Mateo, R. G., Nieto-Lugilde, D., Morueta-Holme, N., Svenning, J.-C., García-Amorena, I. (2015): Impact of model complexity on cross-temporal transferability in Maxent species distribution models: An assessment using paleobotanical data. – Ecological Modelling 312: 308-317.

[28] Oindo, B., Skidmore, A. K., Rolf, A. (2002): Interannual variability of NDVI and species richness in Kenya. – International Journal of Remote Sensing 23: 285-298.

[29] Pagano, T. S., Chahine, M. T., Fetzer, E. J. Year. The Atmospheric Infrared Sounder (AIRS) on the NASA Aqua Spacecraft: a general remote sensing tool for understanding atmospheric structure, dynamics, and composition. – SPIE Remote Sensing 2010, Songdo Convensia Incheon, Korea, 11–14 October.

[30] Papes, M. G. (2007): Modelling ecological niches from low numbers of occurrences: assessment of the conservation status of poorly known viverrids (Mammalia, Carnivora) across two continents. – Diversity and Distributions 13: 890-902.

[31] Salama, H. M. H., Al-Rumaih, M. M., Al-Dosary, M. A. (2011): Effects of Riyadh cement industry pollutions on some physiological and morphological factors of Datura innoxia Mill. plant. – Saudi Journal of Biological Sciences 18: 227-237.

[32] Sheel, V., Lal, S., Richter, A., Burrows, J. P. (2010): Comparison of satellite observed tropospheric NO_2 over India with model simulations. – Atmospheric Environment 44: 3314-3321.

[33] Slee, B., Feliciano, D. (2015): Challenges in the design of indicators for assessing the impact of the Scotland Rural Development Programme 2007–2013 on climate change mitigation. – Ecological Indicators 59: 94-103.

http://www.aloki.hu ● ISSN 1589 1623 (Print) ● ISSN 1785 0037 (Online)
DOI: http://dx.doi.org/10.15666/aeer/1605_57575770
© 2018, ALÖKI Kft., Budapest, Hungary

[34] Taheri, S. (2010): Hyper temporal NDVI images for modelling and prediction the habitat distribution of Balkan green lizard (Lacerta trilineata) case study: Crete (Greece). – M.Sc. Thesis, ITC Netherlands.

[35] ul-Haq, Z., Tariq, S., Ali, M., Daud Rana, A., Mahmood, K. (2017): Satellite-sensed tropospheric NO_2 patterns and anomalies over Indus, Ganges, Brahmaputra, and Meghna river basins. – International Journal of Remote Sensing 38: 1423-1450.

[36] Van Noije, T. P. C., Eskes, H. J., Dentener, F. J., Stevenson, D. S., Ellingsen, K., Schultz, M. G., Wild, O., Amann, M., Atherton, C. S., Bergmann, D. J., Bey, I., Boersma, K. F., Butler, T., Cofala, J., Drevet, J., Fiore, A. M., Gauss, M., Hauglustaine, D. A., Horowitz, L. W., Isaksen, I. S. A., Krol, M. C., Lamarque, J.-F., Lawrence, M. G., Martin, R. V., Montanaro, V., Müller, J.-F., Pitari, G., Prather, M. J., Pyle, J. A., Richter, A., Rodriguez, J. M., Savage, N. H., Strahan, S. E., Sudo, K., Szopa, S., VAN Roozendael, M. (2006): Multi-model ensemble simulations of tropospheric NO_2 compared with GOME retrievals for the year 2000. – Atmospheric Chemistry and Physics 6: 2943-2979.

[37] Yang, X.-Q., Kushwaha, S. P. S., Saran, S., Xu, J., Roy, P. S. (2013): Maxent modeling for predicting the potential distribution of medicinal plant, Justicia adhatoda L. in Lesser Himalayan foothills. – Ecological Engineering 51: 83-87.

[38] Yost, A. N., Petersen, S. L., Gregg, M., Miller, R. (2008): Predictive modeling and mapping sage grouse (Centrocercus urophasianus) nesting habitat using Maximum Entropy and a long-term dataset from Southern Oregon. – Ecological Informatics 3: 375-386.

[39] Yu, J., Wang, C., Wan, J., Han, S., Wang, Q., Nie, S. (2014): A model-based method to evaluate the ability of nature reserves to protect endangered tree species in the context of climate change. – Forest Ecology and Management 327: 48-54.

[40] Yuan, H.-S., Wei, Y.-L., Wang, X.-G. (2015): Maxent modeling for predicting the potential distribution of Sanghuang, an important group of medicinal fungi in China. – Fungal Ecology 17: 140-145.

[41] Zohary, D., SPIEGEL-ROY (1975): Beginning of fruit growing in the Old World. – Science 187: 319-327.

[42] Zyrichidou, I., Koukouli, M. E., Balis, D. S., Kioutsioukis, I., Poupkou, A., Katragkou, E., Melas, D., Boersma, K. F., van Roozendael, M. (2013): Evaluation of high resolution simulated and OMI retrieved tropospheric NO_2 column densities over Southeastern Europe. – Atmospheric Research 122: 55-66.

http://www.aloki.hu ● ISSN 1589 1623 (Print) ● ISSN 1785 0037 (Online)
DOI: http://dx.doi.org/10.15666/aeer/1605_57575770
© 2018, ALÖKI Kft., Budapest, Hungary

THE IMPACT OF LOW TEMPERATURE ON SEED GERMINATION OF TWO DESERT SPECIES IN JUNGGAR BASIN OF CHINA

PENG, M. W. – WANG, M.* – JIANG, P. – CHANG, Y. L. – CHU, G. M.*

Department of Forestry, Agricultural College, Shihezi University
Road of North 4th, Shihezi City, Xinjiang 832003, China

**Corresponding authors*
e-mail: wangm1205@163.com, chgmxj@163.com

(Received 8th Oct 2017; accepted 27th Feb 2018)

Abstract. Germination behaviour plays an important role for seedling regeneration and the sustainable development of population in arid and semiarid areas. The objectives of the study were to explore germination characteristics of *Anabasis aphylla* and *Haloxylon ammodendron* under low temperature conditions and their ecological significance in Junggar basin of China. We combined the Logistic function and the thermal time equation, and used non-linear regression to estimate the base temperature and the thermal time for germination of both species. Germination experiments were carried out in the illumination incubators with 6 temperature gradients (20/15 °C, 15/10 °C, 10/5 °C, 5/2 °C, 2 °C and 2/-3 °C) for 15 days. Final germination percentages of the two species were not obviously different and were higher than 90% in different temperature treatments, and low temperature only inhibited germination speed. Moreover, germination percentages of the two species surpassed 50% in the eighth day under low temperature conditions. The base temperature and thermal time of *A. aphylla* was 0.54 °C and 9.89 °C, while *H. ammodendron* was 0.79 °C and 7.26 °C, respectively. The results showed that the two desert species adapted to the low temperature habitat and took advantage of humid soil conditions to grow in the snow-melting period.
Keywords: *seed germination, desert plant, snow-melting, base temperature, thermal time model, harsh habitats*

Introduction

Germination is a crucial stage in the life cycle of plants, however, this stage is highly unpredictable over space and time (Tlig et al., 2008). In germination experiments, temperature is an important and determining factor regarding the time of germination (Khan and Ungar, 1998). In general, it is thought that germination starts above 10 °C (Huang et al., 2003; Tobe et al., 2000). However, several researchers suggested that some species could germinate under low temperature conditions (Sun, 2015; Han et al., 2011; Körner, 2003; Shimono and Kudo, 2005; Zhang, 2010). For example, Shimono and Kudo (2005) actually observed that seedlings of *Peucedanum multivittatum* had already emerged at the time of snow-melting in the snow-bed habitat. However, limited information is available for seed germination at low temperature (Huang et al., 2003). So, it is significative for desert seeds to germinate during snowmelt period.

As a result of long-term adaptation to the environment, the majority of plant seeds have a specific requirement of base temperature (T_b) and thermal temperature value for triggering germination (Steadman et al., 2004). When the ambient temperature reaches the base germination temperature, seeds can become receptive to the thermal temperature, once the thermal temperature reaches the specific value for a given species, the seeds can germinate (Steinmaus et al., 2000). Depending on the accumulation process of environmental temperature during seed germination, the thermal time model

http://www.aloki.hu ● ISSN 1589 1623 (Print) ● ISSN 1785 0037 (Online)
DOI: http://dx.doi.org/10.15666/aeer/1605_57715780
© 2018, ALÖKI Kft., Budapest, Hungary

can quantify the influence of external environment on seed germination in a certain degree (Liu et al., 2011). The process of seed germination is related to the accumulation of environment temperature, only the thermal time accumulated to a certain extent can promote seed germination, thermal time is generally considered to be accumulated when the environment temperature exceeds the base temperature of seed germination, and for seeds of the same species the base temperature is constant (Dahal et al., 1990). Thermal time models were derived for germination and shoot emergence using a range of sub-optimal and optimal temperatures (≤ 20 °C) for each provenance, this temperature range was selected as these models assume that there are linear relationships between rate and temperature (Finch-Savage and Whalley, 2006).

Haloxylon ammodendron and *Anabasis aphylla* are two shrubs of Chenopodiaceae, mainly distributed in northwest of China. *H. ammodendron* has many characteristics of adapting to drought, salinity, poor nutrition, strong wind, sand movement, and high light intensity (Huang et al., 2003). As an important component of old Mediterranean flora, it widely spread in Junggar basin, northeast of the Tarim basin and other desert areas on a range of soils and is a representative psammophytic species (Wang et al., 2014). *H. ammodendron* is a precious biological resource in the arid desert region. Besides its ecological value, *H. ammodendron* also has great economic value. *A. aphylla* population mainly distributes in diluvial fan, lowland among dunes, Gobi and hillside, and presents staggered distribution with *H. ammodendron* population in the desert–oasis ecotone (Wang et al., 2015). Several investigations have been conducted on germination and community traits of *H. ammodendron* and *A. aphylla* (Huang et al., 2003; Wang et al., 2014, 2015; Chu et al., 2014a, b). *A. aphylla* plays an important role in saline-alkali land, rehabilitated fissure and windbreak and sand fixation in the desert area, and has a certain significance for maintaining the water and soil safety of the alluvial fan in the foreland. It has a good application for the follow-up industrial development of returning farmland to forestry prospect. In Junggar basin, the habitats are harsh, coupled with improper human exploitation, so the habitats are further destroyed, and the seedlings of various plants are naturally difficult to be regenerated. *H. ammodendron* and *A. aphylla* are the dominant species in this area and can survive in this harsh environment. Studies have shown that temperature of Junggar basin increased in early April, resulting in the rapid drying of the shallow layer of soil, which is not conducive to the growth of *H. ammodendron* seedlings (Huang et al., 2008). In the field, our observations show that a large number of *H. ammodendron* and *A. aphylla* seedlings germinate during the snow-melting period in March. Therefore, studying the adaptability of desert plants at low temperatures is of great significance to ecological construction.

The objective of this study was to explore the characteristics and ecological adaptation of seed germination under low temperature conditions. It is necessary to understand seed germination in adaption to harsh environment, and also to study the evolution of plant life history.

Materials and methods

Experimental materials and habitat conditions

Fresh and matured seeds of *H. ammodendron* and *A. aphylla* were collected in the desert on the southern edge of the Junggar basin in Xinjiang (45°22′43.4″N, 84°50′32.5″E; altitude is 843 m). The annual mean temperature varies from 5 to 9 °C, and minimum winter temperature varies from -30 to -41 °C and maximum summer

http://www.aloki.hu ● ISSN 1589 1623 (Print) ● ISSN 1785 0037 (Online)
DOI: http://dx.doi.org/10.15666/aeer/1605_57715780
© 2018, ALÖKI Kft., Budapest, Hungary

temperatures are 30–40 °C. Snow-melting appears at the end of winter, together with the rainfall that occurs in summer and annual precipitation amounts from 100 mm to 250 mm. Annual potential evaporation is greater than 2000 mm (Wang et al., 2014). In Junggar basin, the snow-melting period is about 10 days in March, the average daytime temperature is higher than 0 °C and the maximum temperature is basically maintained at 7-14 °C, while the minimum temperature is below 0 °C. So, during the snow-melting period, the surface of the soil is repeatedly frozen and thawed (*Fig. 1*).

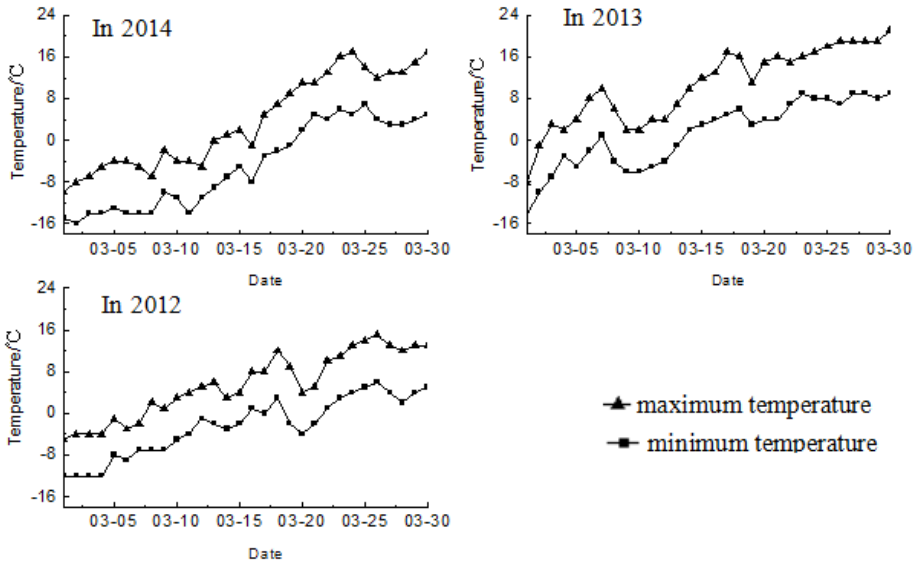

Figure 1. *Temperature conditions of the snow-melting period in the study area*

The seeds of both species are similar in shape and have perianth segments. The seed of *H. ammodendron* is larger than *A. aphylla*, and both seed is gray or black (*Fig. 2*). Its average diameter is 2.13 mm and 1.88 mm, while thousand seed weight is 1.90 g and 1.45 g, respectively. It was found through preliminary experiments that seeds of both species could germinate at 2 °C (*Fig. 3*).

Figure 2. *The pictures of two desert plant seeds morphology (H. ammodendron seed on the left and A. aphylla on the right)*

http://www.aloki.hu ● ISSN 1589 1623 (Print) ● ISSN 1785 0037 (Online)
DOI: http://dx.doi.org/10.15666/aeer/1605_57715780
© 2018, ALÖKI Kft., Budapest, Hungary

Figure 3. *The pictures of two desert plant seeds germinated at 2 °C (H. ammodendron seed on the left and A. aphylla on the right)*

Experimental methods

Experimental design of germination under different temperatures

Germination experiments were carried out in Petri dishes (9 cm in diameter) on two layers of filter paper (GB/T1914-93, Hangzhou Xinhua Paper Ltd., China) moistened with 10 ml of distilled solution. The variable temperatures of day and night were in control of 20/15 °C, 15/10 °C, 10/5 °C, 5/2 °C, 2 °C and 2/-3 °C individually. All Petri dishes were kept in an illumination incubator with 12 h photoperiod (LRH-250-G Illuminating Incubator, Guangdong Medicine Apparatus Manufactory, Guangdong, China) and freeze temperature were conducted in Ronshen Refrigerator (BCD-232YMB/X1). For all treatments (6 temperature gradients), four replicates of 40 seeds each were used in the experiment. Germinated seeds were recorded daily for 15 days. Seed was considered to have germinated with the emergence of the radicle (Chu et al., 2014b).

Experimental design of thermal temperature model

Based on the thermal time model standard, 5 constant temperature gradients were set up experimentally. For all treatments, four replicates of 40 seeds each were used for testing. Germination trials were carried out in Petri dishes with two layers of filter paper, the number of seed germination was recorded every 12 h. In the process of seed germination, the thermal time ($\theta_{T(g)}$) needed for the germination percentage of g is calculated by the following formula (*Eq. 1*):

$$\theta_{T(g)} = (T - T_b)t_g \quad \text{(Eq.1)}$$

T is temperature of the experiment, T_b is the base temperature of seed germination, T_g is the number of days required to accumulate the germination percentage of g.

By using the Logistic function (*Eq. 2*) curve fitting, the relevant parameters m, k, b and the base temperature (T_b) of seed germination can be obtained.

$$g = \frac{m}{1 + e^{-k(T - T_b)t + b}} \quad \text{(Eq.2)}$$

http://www.aloki.hu ● ISSN 1589 1623 (Print) ● ISSN 1785 0037 (Online)
DOI: http://dx.doi.org/10.15666/aeer/1605_57715780
© 2018, ALÖKI Kft., Budapest, Hungary

By using the thermal time to achieve the germination percentage of g to estimate the thermal time value of seed germination, $\theta_{T(50\%)}$ was calculated by *Equation 3* and fitting results *m, k, b* and $g = 50\%$.

$$\theta_{T(g)} = \frac{1}{k}(b + \ln\frac{g}{m-g}) \quad \text{(Eq.3)}$$

Data analysis

Excel 2016 was used to analyze the experimental data. SPSS 19.0 software was used to make significant variance analysis of germination index, and non-linear fitting Logistic function to get the parameters of thermal temperature, and utilize Origin 8.5 to draw the graph.

Results

Seed germination characteristics of two desert species

As a whole, with the decrease of temperature, germination speed of *H. ammodendron* and *A. aphylla* seed increased slowly. Germination periods of high temperatures (20/15 °C and 15/10 °C) were less than 7 days while low temperatures (5/2 °C, 2 °C and 2/-3 °C) were more than 11 days. The experiment ended on the 15th day, the germination percentage of both species tended to be stable at a certain level, and the low temperatures slowed down the seed germination speed (*Fig. 4*). The initial germination time of *H. ammodendron* and *A. aphylla* increased with the decrease of temperature, and the germination index decreased gradually, but the final germination percentage was over 90% with no significant difference (*Table 1*).

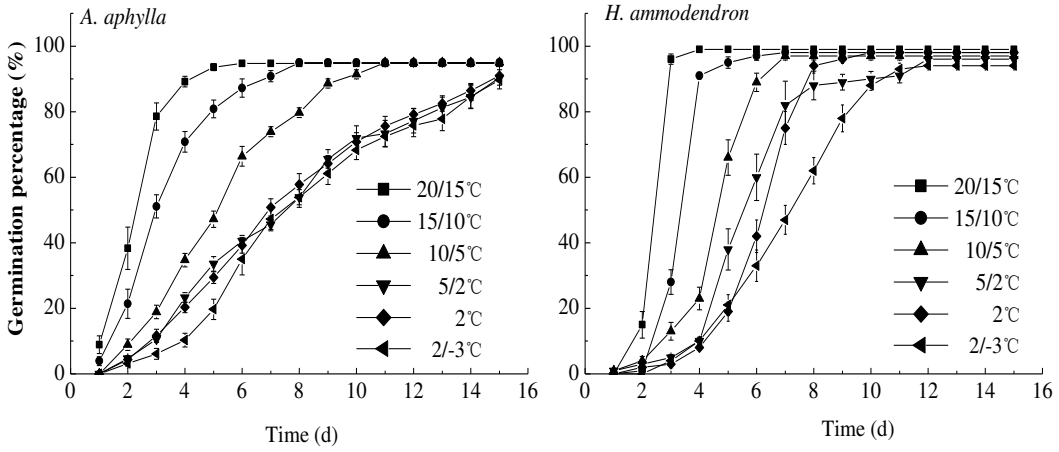

Figure 4. *Seed germination percentages of A. aphylla and H. ammodendron*

Thermal temperature model analysis of two desert species germination

The parameter estimates *m*, *k*, *b*, T_b (±standard error) obtained by fitting the Logistic equation (*Eq. 2*) are shown in *Table 2*. According to the above formula (*Eq. 3*), the relationship between cumulative germination percentage and thermal temperature of *H. ammodendron* was obtained, which is $\theta_{T(g)} = \frac{1}{0.90}(6.18 + \ln\frac{g}{0.85-g})$. *A. aphylla* is

http://www.aloki.hu ● ISSN 1589 1623 (Print) ● ISSN 1785 0037 (Online)
DOI: http://dx.doi.org/10.15666/aeer/1605_57715780
© 2018, ALÖKI Kft., Budapest, Hungary

$\theta_{T(g)} = \frac{1}{0.37}(3.36 + \ln\frac{g}{0.87 - g})$. When the cumulative germination percentage g = 0.5, the thermal temperature of *H. ammodendron* is 7.26 °C, *A. aphylla* is 9.89 °C. The base temperature of both species is low, both at about 0 °C. The determination coefficient R^2 is 0.94 (*Table 2*).

Table 1. *Seed germination characteristics of A. aphylla and H. ammodendron ($p < 0.05$)*

Treatment (°C)	Final germination percentage (%)		Initiate germination time (h)		Germination index	
	Species1	Species2	Species1	Species2	Species1	Species2
20/15 °C	95±2 a	99±2 a	2±1 b	12±1 b	16±3 a	14±1 a
15/10 °C	95±3 a	98±2 a	4±3 b	12±1 b	13±2 b	11±1 b
10/5 °C	95±2 a	97±3 a	26±7 a	24±12 ab	8±1 c	9±1 c
5/2 °C	90±8 a	96±6 a	26±6 a	37±22 a	6±1 d	7±2 d
2 °C	91±5 a	98±3 a	32±14 a	45±17 a	6±1 d	6±1 de
2/-3 °C	90±7 a	95±2 a	38±22 a	48±6 a	5±1 d	6±1 e

Means within a column at each treatment with the same letter are not significantly different. Species1 is A. aphylla and Species2 is H. ammodendron

Table 2. *Non-linear regression analysis results and the average value of thermal time $\theta_T(50\%)$*

Species	*m*±SE	*k*±SE	*b*±SE	T_b±SE (°C)	$\theta_{T(50\%)}$ (°C d)	R^2
H. ammodendron	0.85±0.012	0.90±0.117	6.18±0.775	0.79±0.065	7.26	0.94
A. aphylla	0.87±0.013	0.37±0.040	3.36±0.340	0.54±0.114	9.89	0.94

m, k, b and T_b are the values of parameter estimates. *m:* the approximate final germination percentage; *k:* the rate of increase in germination percentage; *b:* the value related to the lag in germination; T_b: the base or minimum temperature for germination; $\theta_{T(50\%)}$: the median thermal temperature. R^2 and SE are the coefficient of determination and standard error of parameter respectively

Discussion

The research indicates that the majority of seeds germinated optimally in the temperature range of 10–20 °C, in this temperature range, seeds have a high germination percentage, short initial germination time and high germination index (*Table 1*). But soil humidity was not suitable for seed germination of both species when soil surface temperature surpassed 10 °C in the field (Huang et al., 2008). In Junggar basin, the most of desert species can utilize snow-melting water that is available to better germination and seedling survival before the desiccation of early spring (Huang et al., 2009). In the short snow-melting period (12–15 days), air temperature usually is under 15 °C and the soil surface temperature is less than 5 °C (Sun, 2015). Therefore, germination under the low temperature condition has important ecological implications in plant adaptation to drought stress in arid and semi-arid zones. Meanwhile, both species have a lot of seeds germinated in snow-melting period.

In Junggar basin, the research of Han et al. (2011) showed that the snow melted in early spring, during which the maximum air temperature was maintained at 0–15 °C and the relative humidity was 50–60%, and the seeds of *Anabasis elatio* germinated on the

http://www.aloki.hu ● ISSN 1589 1623 (Print) ● ISSN 1785 0037 (Online)
DOI: http://dx.doi.org/10.15666/aeer/1605_57715780
© 2018, ALÖKI Kft., Budapest, Hungary

mother plants and developed into viviparous seedling. Similarly, *Suaeda physophora* can germinate at 10 °C and even at 0 °C from field observation (Li and Zhang, 2007). The phenomenon was consistent with the results from Huang et al. (2003). The results of Zhang et al. (2010) showed germination percentage of *H. ammodendron* and *Haloxylon persicum* was over 80% under 2 °C. In addition, Sun (2015) suggested desert seeds started to germinate only two days when snow melted at the average daily temperature (day/night) of 3.5 °C (6.7/-0.5 °C) and a soil volumetric water content of 24.2%. Therefore, seed germination under low temperatures was a common behaviour for desert plants.

Junggar basin is one of the driest regions of the Eurasian continent. The annual evaporation is 10 times greater than the annual precipitation in the region (Song et al., 2006). The soil may dry up quickly after short periods of rainfall or snowmelt, resulting in a substantial rise in the mortality rate of desert plant seedlings (Huang et al., 2009). So, early germination is of significant importance. Low temperatures only slowed down germination speed in the snow-melting period, and weak salt and high humidity conditions were favourable to desert plant germination in early spring (Chu et al., 2014). Compared with the time of seed germination of different species, seed of early germination was found to provide the advantage for seedling emergency. The seedlings with a longer growth period were as better competitors, gained more nutrition and had a higher precompetitive survival than those with shorter growth period (Körner, 2003; Shimono and Kudo, 2005; Huang et al., 2008; Gornish et al., 2015).

The base temperature of seed germination may be an adaptive feature of plants, and species germinated under low temperatures have a relatively low base temperature (T_b) (Steinmaus et al., 2000). In previous studies, the T_b of temperate species is between 0-4 °C (Angus et al., 1980; Hur and Nelson, 1984; Moot et al., 2000). In this study, *A. aphylla* and *H. ammodendron* are temperate species, and their base temperature was 0.54 °C and 0.79 °C, respectively. This is consistent with previous studies. In the same temperature conditions, species with low base temperature can quickly germinate (Ross and Harper, 1972). Trudgill (2005) showed that germination adapted to low temperature environment requires higher thermal temperature and lower T_b than those adapted to warm environment. Liu et al. (2011) studied the base temperature and thermal temperatures of 12 Compositae species in the Qinghai–Tibet plateau, the base temperatures of the 12 Compositae species ranged from -1.4 to 1.5 °C with an average around 0 °C, and the average thermal temperature was 94.5 °C. Similarly, Larsen (2005) showed that the base temperature for Danish *Festuca rubra* was 2.7 °C and the thermal temperature was 60 °C. In this study, the base temperature of both species was about 0 °C, thermal temperature was 9.89 °C and 7.26 °C, respectively, compared with the previous results. The thermal temperature of the two species was lower than the thermal temperature of other species when the base temperature was similar, indicating that the species in this study not only could germinate at a low temperature, but also thermal temperature was low. In the early spring short snow-melting conditions, plant seeds will quickly germinate and occupy the habitat, with the time and space advantages, this is the result of long-term adaptation to environmental conditions. Therefore, with a consistent water supply in early spring, the seed can tolerate low temperatures to germinate, because of the available water from the melting snow, more heat and nutrients accumulated that are essential for the survival of the seedlings at later stages.

http://www.aloki.hu ● ISSN 1589 1623 (Print) ● ISSN 1785 0037 (Online)
DOI: http://dx.doi.org/10.15666/aeer/1605_57715780
© 2018, ALÖKI Kft., Budapest, Hungary

Conclusions

The final germination percentage of both species had no significant difference in 6 temperature gradients, and low temperature only slowed down germination speed. The base temperature and thermal temperature of both species were low. Therefore, seed germination of *H. ammodendron* and *A. aphylla* requires less energy, and this is conducive to early germinate for desert seed. The two species have opportunistic strategies for germination, and they can germinate quickly with short-term low temperature and snow water conditions.

Prospect

Seed germination is a crucial stage of plant life cycle, which directly determines establishment and regeneration of plant population. In arid and semi-arid areas desert species have formed some peculiar strategies of germination adapted to the harsh habitat. We found that desert species represented by *H. ammodendron* and *A. aphylla* have the characteristic of germination during snowmelt period. At present, there have been a lot of research studies on the physiological and ecological aspects of both species at low temperatures. However, few research studies have been done on the molecular level. Therefore, we are also carrying out molecular study. This study is expected not only to explore the anti-freezing pathway and mechanisms of the two species, but also to find some new anti-freezing substances, which will provide some ideas for gene engineering research of anti-freezing for desert plants.

Acknowledgements. The research was supported by the Program of the National Natural Science Foundation of China (31570595, 31660194), General Financial Grant of the China Postdoctoral Science Foundation (2017M613253) and Scientific Research Foundation of Shihezi University for Advanced Talents (RCZX201518, RCZX201521).

REFERENCES

[1] Angus, J. F., Cunningham, R. B., Moncur, M. W. (1980): Phasic development in field crops I. Thermal response in the seedling phase. – Field Crops Research 3: 365-378.

[2] Chu, G. M., Wang, M., Zhang, S. X. (2014a): Spatial patterns and associations of dominant woody species in desert-oasis ecotone of South Junggar Basin, NW China. – Journal of Plant Interactions 9(1): 738-744.

[3] Chu, G. M., Wang, M., Zhang, S. X. (2014b): Factors influencing seed germination of medicinal plant *Anabasis aphylla L.* in salt desert of Xinjiang. China. – Vegetos 27(1): 123-129.

[4] Dahal, P., Bradford, K. J. (1990): Effects of priming and endosperm integrity on seed germination rates of tomato genotypes. II. Germination at reduced water potential. – Journal of Experimental Botany 41: 1441-1453.

[5] Finch-Savage, W., Whalley, R. (2006): Germination-Field Energence Models. – In: Black, M., Bewley, J. D., Halmer, P. (eds.) The Encyclopedia of Seeds: Science Technology and Uses. Cromwell Press, Trowbridge.

[6] Gornish, E. S., Aanderud, Z. T., Sheley, R. L. (2015): Altered snowfall and soil disturbance influence the early life stage transitions and recruitment of a native and invasive grass in a cold desert. – Oecologia 177(2): 595-606.

[7] Han, J. X., Wei, Y., Yan, C., An, S. Z. (2011): The vivipary characteristic of *Anabasis elatior* and its ecological adaptation. – Chinese Acta Ecologica Sinica 31(10): 2662-2668.

http://www.aloki.hu ● ISSN 1589 1623 (Print) ● ISSN 1785 0037 (Online)
DOI: http://dx.doi.org/10.15666/aeer/1605_57715780
© 2018, ALÖKI Kft., Budapest, Hungary

[8] Huang, Z. Y., Zhang, X. S., Zheng, G. H., Gutterman, Y. (2003): Influence of light, temperature, salinity and storage on seed germination of *Haloxylon ammodendron*. – Journal of Arid Environments 55: 453-464.
[9] Huang, P. Y., Xiang, B., Li, Q. J., Xu, Z. H. (2009): Relationship between *Haloxylon ammodendron* seedling dynamics and habitat before summer. – Chinese Journal of Desert Research 29(1): 87-94.
[10] Huang, P. Y., Li, Q. J., Yuan, S. F. (2008): Effects of climate change on *Haloxylona mmodendron* community in southern edge of Zhunger basin. – Chinese Acta Ecologica Sinica. 28(12): 6051-6059.
[11] Hur, S. N., Nelson, C. J. (1984): Temperature effects on germination of Birdsfoot Trefoil and Seombadi. – Bulletin of the Agricultural College, Chonbuk National University (Korean Republic) 77(4): 557-560.
[12] Khan, M. A., Ungar, I. A. (1998): Germination of the salt tolerant shrub *Suaeda fruticosa* from Pakistan: salinity and temperature responses. – Seed Science and Technology 26: 657-667.
[13] Körner, C. (2003): Alpine Plant Life: Functional Plant Ecology of High Mountain Ecosystems. – Springer-Verlag, Berlin, Heidelberg.
[14] Li, L., Zhang, X. M. (2007): Germination strategies of two halophytes in salt desert of northwestern China. – Science in China Series D-earth Sciences 50: 115-121.
[15] Liu, W., Liu, K., Zhang, C. (2011): Effect of accumulated temperature on seed germination – a case study of 12 Compositae species on the eastern Qinghai-Tibet Plateau of China. – Chinese Journal of Plant Ecology 35(7): 751-758.
[16] Larsen, S. U., Bibby, M. B. (2005): Differences in thermal time requirement for germination of three turfgrass species. – Crop Science 45: 2030-2037.
[17] Moot, D. J., Scott, W. R., Roy, A. M., (2000): Base temperature and thermal time requirements for germination and emergence of temperate pasture species. – New Zealand Journal of Agricultural Research 43(1): 15-25.
[18] Ross, M. A., Harper, J. L. (1972): Occupation of biological space during seedling establishment. – Journal of Ecology 60(1): 77-88.
[19] Scott, S. J., Jones, R. A., Williams, W. A. (1984): Review of data analysis methods for seed germination. Crop Science 24: 1192-1199.
[20] Shimono, Y., Kudo, G. (2005): Comparisons of germination traits of alpine plants between fellfield and snowbed habitats. – Ecological Research 20: 189-197.
[21] Song, J., Feng, G., Zhang, F. S. (2006): Salinity and temperature effects on germination for three salt-resistant halophytes, *Halostachys caspica*, *Kalidium foliatum* and *Halocnemum strobilaceum*. – Plant and Soil 279: 201-207.
[22] Steadman, K. J., Pritchard, H. W. (2004): Germination of Aesculus hippocastanum, seeds following cold-induced dormancy loss can be described in relation to a temperature-dependent reduction in base temperature (T_b) and thermal time. – New Phytologist 161(2): 415-425.
[23] Steinmaus, S. J., Prather, T. S., Holt, J. S. (2000): Estimation of base temperatures for nine weed species. – Journal of Experimental Botany 51(343): 275.
[24] Sun, Y. Y. (2012): Drought adaptation characteristics of plant seedling establishment in Junggar Desert. – Shihezi University, Shihezi (in Chinese).
[25] Tlig, T., Gorai, M., Neffati, M. (2008): Germination responses of *Diplotaxis harra* to temperature and salinity. – Flora 203: 421-428.
[26] Tobe, K., Li, X. M., Omasa, K. (2000): Effects of sodium chloride on seed germination and growth of two Chinese desert shrubs, *Haloxylon ammodendron* and *Haloxylon persicum*. – Australian Journal of Botany 48: 455-460.
[27] Trudgill, D. L., Honek, A., Li. D. (2015): Thermal time--concepts and utility. – Annals of Applied Biology 146(1): 1-14.

http://www.aloki.hu ● ISSN 1589 1623 (Print) ● ISSN 1785 0037 (Online)
DOI: http://dx.doi.org/10.15666/aeer/1605_57715780
© 2018, ALÖKI Kft., Budapest, Hungary

[28] Wang, M., Zhang, S. X., Chu, G. M. (2014): Point pattern analysis of different life stages of *Haloxylon ammodendron* in Desert-oasis ecotone of south Junggar basin. – Polish Journal of Environmental Studies 23(6): 367-373.
[29] Wang, M., Li, Y. Y., Niu, P. X., Chu, G. M. (2015): Spatial pattern formation and intraspecific competition of *Aanbasis aphylla* L. population in the diluvial fan of Junggar basin, NW China. – Pakistan Journal Botany 47(2): 543-550.
[30] Zhang, S. J. (2010): Study on natural cure of main plant species at initialized process in the south marginal zone of the Junggar Basin. – Chinese Arid Environmental Monitoring 24: 89-93.

http://www.aloki.hu ● ISSN 1589 1623 (Print) ● ISSN 1785 0037 (Online)
DOI: http://dx.doi.org/10.15666/aeer/1605_57715780
© 2018, ALÖKI Kft., Budapest, Hungary

EFFECT OF DIFFERENT RESOURCES AND METHODS OF SILICON AND ZINC APPLICATION ON AGRONOMIC TRAITS, NUTRIENT UPTAKE AND GRAIN YIELD OF RICE (*ORYZA SATIVA* L.)

KHEYRI, N.[1] – AJAM NOROUZI, H.[1*] – MOBASSER, H. R.[2] – TORABI, B.[3]

[1]*Department of Agronomy, Gorgan Branch, Islamic Azad University, Gorgan, Iran*

[2]*Department of Agronomy, Ghaemshahr Branch, Islamic Azad University, Ghaemshahr, Iran*

[3]*Department of Agronomy, Gorgan University of Agricultural Sciences and Natural Resources Gorgan, Iran*

**Corresponding author*
e-mail: ajamnorozei@yahoo.com

(Received 16th Feb 2018; accepted 18th May 2018)

Abstract. To evaluate the effect of different resources and methods of silicon (Si) and zinc (Zn) application on agronomic traits, nutrient uptake and grain yield of rice (*Oryza sativa* L.), a field experiment was conducted as a randomized complete block design with 16 treatments and three replications in Noor region, Mazandaran province, Iran in the crop year of 2015-2016. The experimental treatments included the different resources and forms of Si and Zn application as nanoparticles (NPs) foliar application and soil application of the elements. The results indicated that grain and straw yields were increased in response to application of Si and Zn fertilizers. All fertilized treatments had significantly higher yields than the control, although yields did not differ significantly between the fertilized treatments. The experimental treatments significantly affected the yield components, Si, Zn and N concentrations in the plant tissue. The combined application of Si and Zn by both methods, either via NPs foliar application or soil application resulted in an increase in the grain and straw yields, yield components and Si, Zn and N concentrations in rice grain and straw. According to the results of this research, the combined application of Si plus Zn, especially by NPs foliar application, is appropriate for increasing the production of the rice crop in Noor Region of Iran.
Keywords: *crop yield, foliar application, rice, soil application, silicon, zinc*

Introduction

Silicon (Si) and zinc (Zn) as macro and micronutrients, respectively have a key role in improving growth and increasing grain yield of plants, and their deficiency can make a serious problem for crop production, especially in the case of rice. Silicon is the second most abundant mineral in the soil (Kafi and Rahimi, 2011), that is a useful nutrient for healthy growth and sustainable production of rice (Tamai and Ma, 2008). Silicon has a dual effect on the plant and soil system, which, by being absorbed in the plant, makes the plant more resistant to pests, diseases and environmental stresses, and, on the other hand, led to soil fertility by improving water, physicochemical properties of soil and maintaining the nutrients in available form for the plant (Meena et al., 2014). Soil silicon has several benefits for rice including the reduction of the adsorption of heavy metals such as Pb (Jianguo et al., 2015), Cd (Lin et al., 2016), and As (Wu et al., 2015), resistance to salt stress (Mahmoud et al., 2017), increasing the extent of photosynthesis, the improvement of performance, the prevention of lodging (Jeer et al., 2017), as well as the reduction of the negative effects of ultraviolet radiation on the

http://www.aloki.hu ● ISSN 1589 1623 (Print) ● ISSN 1785 0037 (Online)
DOI: http://dx.doi.org/10.15666/aeer/1605_57815798
© 2018, ALÖKI Kft., Budapest, Hungary

physiological processes of photosynthesis and transpiration (Lou et al., 2016). The modern silicon fertilizers (nano-SiO2) easily penetrate into the leaves and create a thick silicate layer on the leaf surface (Meena et al., 2014). Silicon plays an important role in increasing the activity of antioxidant enzymes and enhancing the content of osmolites, in contributing to the resistance of abiotic and biotic stresses in plants (Amiri et al., 2014). Reports indicated that the use of Si increases the grain yield of rice by increasing the number of whole spikelets (Mobasser et al., 2008) and the number of fertile tillers per hill (Ghasemi Mianaei et al., 2011). Other researchers reported that the Si application significantly increased the tiller number and Si concentration in the plant (Zia et al., 2017). Cuong et al. (2017) reported that increase in Si application, increases the Si absorption and other nutrients such as nitrogen, phosphorus and potassium in rice biomass (grain + straw) compared to control.

Zinc, after nitrogen and phosphorus, is the most important nutrient that limits the grain yield of rice (Yakan et al., 2000), and is a global concern for human nutrition (Farooq et al., 2018). Zinc as a cofactor of antioxidant enzymes such as catalase and peroxidase plays an important part in plant protection and ultimately improves yield (Samart et al., 2017). Zinc has an important role in several physiological processes of the plants such as protein synthesis, enzyme activation, gene expression and carbohydrate metabolism (Chang et al., 2005; Qiao et al., 2014). Studies have shown that zinc improves the absorption of other nutrients such as potassium, phosphorus and iron for the plant (Amirjani et al., 2014). It has been reported that the application of nano-ZnO in the rates of 25 and 50 $mg.l^{-1}$ improves the rice growth (Upadhyaya et al., 2014), but in higher concentrations due to the creation of toxicity by the accumulation of this element in the plant lead to reduction in plant growth and biomass (Boonyanitipong et al., 2011; Chen et al., 2015). The improvement of zinc concentration and enhancement of rice grain yield by Zn supply through soil (basal) + 2 foliar applications have been reported in the results of other investigators (Saha et al., 2017). In a study, which the effects of zinc were evaluated by two methods of foliar application and soil application on yield and yield components of rice, reported that the number of fertile tillers, number of grains per panicle, 1000-grain weight, grain yield, harvest index and grain Zn concentration significantly increased compared to control using both methods (Farooq et al., 2018). Sudha and Stalin (2015) found that zinc application in soil with its foliar application significantly increased the agronomic and physiological traits.

The problem of accessibility to nutrients such as Si and Zn by usual methods results in an increase in the attention to the use of modern methods for application of these elements in recent years. Nanotechnology is one of the most modern methods in agricultural practices. The most important of its applications in different aspects of agriculture, that is in the water and soil section are the use of nano-fertilizers for plant nutrition (Mazlomi et al., 2012). Nanofertilizers are more effective in improving plant nutrition, increasing the efficiency of nutrient use, and protecting plants from environmental stresses than conventional fertilizers (Wang et al., 2015). The Maximum use of production sources, especially with the nano-fertilizers application, and enhancing photosynthesis efficiency can reduce the environmental risks associated with the excessive application of chemical fertilizers (Sepehri and Vaziri Amjad, 2015). Although nanotechnology in agriculture is less developed due to lower investment compared to other sectors, nanotechnology is very effective in improving agricultural production (Huang et al., 2015).

http://www.aloki.hu ● ISSN 1589 1623 (Print) ● ISSN 1785 0037 (Online)
DOI: http://dx.doi.org/10.15666/aeer/1605_57815798
© 2018, ALÖKI Kft., Budapest, Hungary

Therefore, the aim of the present study was to evaluate the effects of Si and Zn by applying different resources and methods to improve yield components, nutrient uptake and grain yield of rice.

Materials and methods

Experimental site

The field experiment was conducted during crop year of 2015-2016 in Noor region, Mazandaran province, Iran, located at 36° 46'N latitude, 52° 28'E longitude and 71 m above the sea level (*Fig. 1*). The meteorological data recorded during rice-growing seasons are presented in *Table 1*. The physical and chemical properties of the soil in the experimental site are shown in *Table 2*.

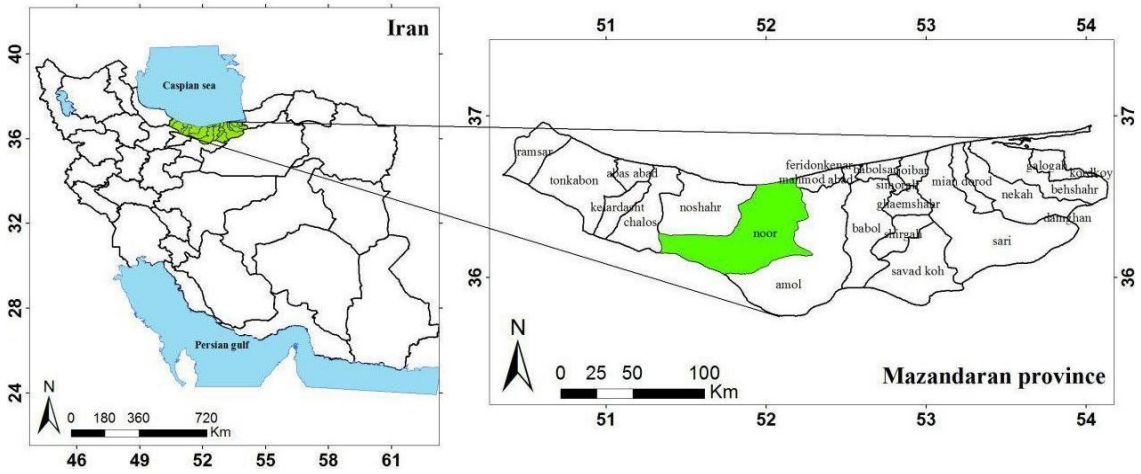

Figure 1. *The study area location in Noor region, Mazandaran province, Iran*

Table 1. *Meteorological data recorded during rice-growing seasons of the experiment*

Month of the year	Average of monthly temperature (°C)		Average of monthly relative humidity (%)		Total monthly rainfall (mm)	Total sunny hours (h)
	Minimum	Maximum	Minimum	Maximum		
March-April	10.4	17.3	67	94	129.8	121.1
April-May	15.5	21.4	73	94	43.0	159.3
May-June	19.4	26.0	67	90	27.7	260.8
June-July	22.6	28.8	67	89	179.9	208.9
July-August	23.2	30.1	68	90	46.1	251.1
August-September	22.0	29.3	66	90	182.6	205.9

Table 2. *Physical and chemical characteristics of the soil in the experimental site in a depth of 0-30 cm*

Soil texture	Silt (%)	Clay (%)	Sand (%)	pH	EC ($ds.m^{-1}$)	SP (%)	O.C (%)	O.M (%)	P ($mg.kg^{-1}$)	K ($mg.kg^{-1}$)	Zn ($mg.kg^{-1}$)	Si (%)
Loam	44	20	36	7.51	3.02	63	1.66	2.86	10.5	116	0.81	0.28

http://www.aloki.hu ● ISSN 1589 1623 (Print) ● ISSN 1785 0037 (Online)
DOI: http://dx.doi.org/10.15666/aeer/1605_57815798
© 2018, ALÖKI Kft., Budapest, Hungary

Experimental layout, design and treatments

This experiment was designed as a randomized complete block design with 16 treatments and 3 replications, thus there were 48 equal plots in size of 10 m^2 (5 m × 2 m). The experimental treatments characteristics are presented in *Table 3*.

Table 3. *The experimental treatments characteristics*

Treatments	Treatments characteristics
T1	Control
T2	Soil application of calcium silicate
T3	Soil application of zinc sulfate
T4	Soil application of calcium silicate + zinc sulfate
T5	Foliar application of nano-SiO_2
T6	Foliar application of nano-SiO_2 + soil application of calcium silicate
T7	Foliar application of nano-SiO_2 + soil application of zinc sulfate
T8	Foliar application of nano-SiO_2 + soil application of calcium silicate + zinc sulfate
T9	Foliar application of nano-ZnO
T10	Foliar application of nano-ZnO + soil application of calcium silicate
T11	Foliar application of nano-ZnO + soil application of zinc sulfate
T12	Foliar application of nano-ZnO + soil application of calcium silicate + zinc sulfate
T13	Foliar application of nano-SiO_2 + nano-ZnO
T14	Foliar application of nano-SiO_2 + nano-ZnO+ soil application of calcium silicate
T15	Foliar application of nano-SiO_2 + nano-ZnO + soil application of zinc sulfate
T16	Foliar application of nano-SiO_2 + nano-ZnO + soil application of calcium silicate + zinc sulfate

The land preparation practices were performed according to the conventional procedure, so that the land was disk-ploughed in late February and the complete practices including puddling and leveling were carried out in mid-May. An indica rice (Oryza sativa L.) cultivar Tarom Hashemi was used as plant material for the present research, which is an early rice cultivar that usually used by farmers in the north of Iran. The seed of rice cultivar Tarom Hashemi was obtained from the Rice Research Institute, Mazandaran, Iran. Rice seedlings were transplanted at a spacing of 20 cm× 20 cm with four seedlings per hill in mid-May, and harvested in mid-August. For all treatments, phosphorus and potassium fertilizers were applied as basal at the rate of 70 kg ha^{-1} as triple superphosphate and 100 kg ha^{-1} as potassium sulfate, respectively. Urea was applied as nitrogen fertilizer uniformly for all the plots at the rate of 150 kg ha^{-1} in three equal splits (one third at the time of transplanting, one third at the tillering stage and one third at the heading stage). For soil application, silicon and zinc fertilizers were applied as basal at the rate of 400 kg ha^{-1} as calcium silicate and 40 kg ha^{-1} as zinc sulfate, respectively. For foliar application, nano-SiO_2 and nano-ZnO in the concentration of 50 mg L^{-1} was applied in four stages of plant growth (early tillering stage, middle tillering, panicle initiation and full heading stage) in plots. Nanofertilizers used in the experiment were products of US Research Nanomaterials, Inc (*Table 4*). In order to control the weeds during growing stages, manual weeding was performed twice on days 14^{th} and 28^{th} after transplanting, and for its chemical control, Butakler's herbicide was applied in the concentration of 3.5 L ha^{-1} a week after transplanting. Furthermore, in order to

http://www.aloki.hu ● ISSN 1589 1623 (Print) ● ISSN 1785 0037 (Online)
DOI: http://dx.doi.org/10.15666/aeer/1605_57815798
© 2018, ALÖKI Kft., Budapest, Hungary

control *Chilo suppressalis,* diazinon insecticide (10% granule) was used at a rate of 15 kg ha^{-1} at the peak of tillering and heading stages (*Fig. 2*). The rice striped stem borer, *Chilo suppressalis*, is one of the most serious sources of damage to rice growth and production in Asia, northern Africa, and southern Europe (He et al., 2014).

Table 4. *Analysis of silicon dioxide (SiO_2) and zinc oxide (ZnO) nanoparticles*

NPs	Purity percentage	Particles size	True density	Color
Sio_2	>99%	20-30 nm	2.4 g/cm^3	white
ZnO	>99%	10-30 nm	5.606 g/cm^3	Milky white

Figure 2. *Photos of experimental field and fertilizer treatments application in growth stages of rice*

Sample preparation and Si, Zn and N analysis

During the flowering stage of the plant, chlorophyll content of flag leaf was measured using chlorophyll meter (SPAD-502, Minolta, Japan). At maturity, determination of plant height and panicle length were performed by measuring 12 plants in each plot. The number of fertile tillers per hill was determined by counting from 12 hill per plot, number of filled and unfilled grains per panicle were determined by counting from 20 panicles per plot and 1000-grain weight was determined by counting and weighing 10 samples of 100 seed. Grain and straw yields were determined by manually harvesting each plot (2 × 2 m^2), separating grains from straw and drying samples in an oven at 70 °C for 48 h. Grain and straw samples were weighed with 14% moisture content and calculated based on kilograms per hectare.

Si concentration in plant samples (grain and straw) was determined by Yoshida method (Yoshida, 1975). Zn concentration in plant tissue was determined by Atomic Absorption Spectrophotometer (AAS) method (Emami, 1996). The N concentration in grain and straw was measured by micro-Kjeldahl method (Emami, 1996). Mobilization efficiency index (MEI) of Si, Zn and N was calculated as *Equations 1, 2* and *3:*

http://www.aloki.hu ● ISSN 1589 1623 (Print) ● ISSN 1785 0037 (Online)
DOI: http://dx.doi.org/10.15666/aeer/1605_57815798
© 2018, ALÖKI Kft., Budapest, Hungary

$$Si\ MEI = \frac{\text{Si concentration in grain (\%)}}{\text{Si concentration in straw (\%)}} \quad \text{(Eq.1)}$$

$$Zn\ MEI = \frac{\text{Zn concentration in grain (mg.kg}^{-1}\text{)}}{\text{Zn concentration in straw (mg.kg}^{-1}\text{)}} \quad \text{(Eq.2)}$$

$$N\ MEI = \frac{\text{N concentration in grain (\%)}}{\text{N concentration in straw (\%)}} \quad \text{(Eq.3)}$$

where Si = silicon, Zn = zinc, N = nitrogen, and MEI = mobilization efficiency index.

The mobilization efficiency index of the elements was calculated to determine the amount of transmission of these elements from straw to grain and their accumulation in grain.

Statistical analysis

The data were statistically analyzed using MSTATC software. Randomized complete block design was used for data analysis. The mean comparison was performed using the least significance difference (LSD) test at 5% probability level. A simple linear regression was used to determine the relationship between the concentrations of Si and Zn in grain and straw with N concentrations in rice plant tissue and its yields.

Results

Grain and straw yields

In this study, grain and straw yields were increased in response to application of Si and Zn fertilizers. All fertilized treatments had significantly higher yield than the control, although its yield did not differ significantly between the fertilized treatments. The maximum grain yield (4502 kg ha^{-1}) and straw yield (5933 kg ha^{-1}) were obtained by the application of T13 (nano-SiO2 + nano-ZnO) and T16 (nano-SiO2 + nano-ZnO + calcium silicate + zinc sulfate) treatments, respectively. However, the combined application of Si and Zn had better effect in increasing grain and straw yields compared to individual application of each element (*Table 5*). There was a positive and significant linear correlation between rice grain and straw yields with the Si and Zn concentration in grain and straw at a probability level of 1%, such that by increasing Si concentration in grain and straw (R^2 = 0.1588 and R^2 = 0.0714, $P < 0.01$, respectively), and Zn concentration in grain and straw (R^2 = 0.1749 and R^2 = 0.2173, $P < 0.01$, respectively), grain and straw yield increased (*Fig. 3*).

Plant height and panicle length

In this research, the plant height did not differ significantly comparing experimental treatments. While, the panicle length was significantly affected by the evaluated treatments. The panicle length was significantly increased by combination of both methods of NPs foliar application and soil application in different treatments, but the maximum panicle length (26 cm) was obtained by the foliar application of nano-SiO_2 + nano-ZnO (T13), while the minimum panicle length (21.67 cm) was obtained in the control or no fertilizer application (*Table 6*).

http://www.aloki.hu ● ISSN 1589 1623 (Print) ● ISSN 1785 0037 (Online)
DOI: http://dx.doi.org/10.15666/aeer/1605_57815798
© 2018, ALÖKI Kft., Budapest, Hungary

Table 5. *Mean comparison of effect the experimental treatments on grain and straw yields of rice (cv. Tarom Hashemi)*

Treatments	Grain yield (kg.ha^{-1})	Straw yield (kg.ha^{-1})
T1	3503b	4845b
T2	3834ab	5316ab
T3	4053ab	5477a
T4	4170ab	5602a
T5	4031ab	5496a
T6	4000ab	5370ab
T7	4210ab	5543a
T8	4358ab	5477a
T9	4133ab	5337ab
T10	4121ab	5389ab
T11	4243a	5692a
T12	4293a	5763a
T13	4502a	5917a
T14	4400a	5827a
T15	4388a	5853a
T16	4423a	5933a
$LSD_{0.05}$	717	626.7

Values followed by different small letters within columns are significantly different ($p < 0.05$) according to the LSD test

Table 6. *Mean comparison of the effects of experimental treatments on agronomic traits of rice (cv. Tarom Hashemi)*

Treatments	Plant height (cm)	Panicle length (cm)	No. of fertile tillers hill^{-1}	No. of filled grain panicle^{-1}	No. of unfilled grain panicle^{-1}	1000-grain weight (g)	Chlorophyll content
T1	135.2a	21.67d	13.13h	81.53f	20.60ab	25.33a	35.03c
T2	137.3a	23.23c	15.03g	88.03b-f	15.93c-f	25.50a	35.43bc
T3	138.4a	24.40bc	16.03efg	87.60c-f	15.30c-f	25.60a	36.20abc
T4	138.3a	25.53ab	16.57b-f	97.07ab	15.43c-f	25.20a	36.07abc
T5	138.9a	25.67ab	15.90efg	85.80def	18.27bc	25.67a	35.70abc
T6	140.1a	25.50ab	15.53fg	100.0a	12.90ef	25.00a	36.40abc
T7	139.0a	25.80ab	16.50c-f	94.10a-d	17.00bcd	25.50a	37.03abc
T8	139.8a	25.93a	16.73b-f	95.00a-d	16.50cde	25.47a	36.90abc
T9	140.1a	25.80ab	16.50c-f	90.93a-e	15.00c-f	25.73a	36.30abc
T10	138.5a	25.70ab	16.37d-g	94.40a-d	13.73def	25.60a	36.70abc
T11	139.2a	25.57ab	17.07a-e	83.50ef	22.80a	25.73a	36.63abc
T12	140.8a	25.77ab	17.13a-e	88.93b-f	17.00bcd	25.50a	37.67ab
T13	138.5a	26.00a	18.47a	93.90a-d	13.37def	25.63a	37.33abc
T14	141.0a	25.93a	17.70a-d	95.50abc	12.60f	25.57a	37.00abc
T15	139.7a	25.83a	17.83abc	90.23b-f	16.37cde	25.77a	37.77ab
T16	143.2a	25.87a	18.00ab	87.37c-f	16.10c-f	25.87a	38.00a
$LSD_{0.05}$	10.24	1.431	1.447	9.307	3.722	1.396	2.343

Values followed by different small letters within columns are significantly different ($p < 0.05$) according to the LSD test

http://www.aloki.hu ● ISSN 1589 1623 (Print) ● ISSN 1785 0037 (Online)
DOI: http://dx.doi.org/10.15666/aeer/1605_57815798
© 2018, ALÖKI Kft., Budapest, Hungary

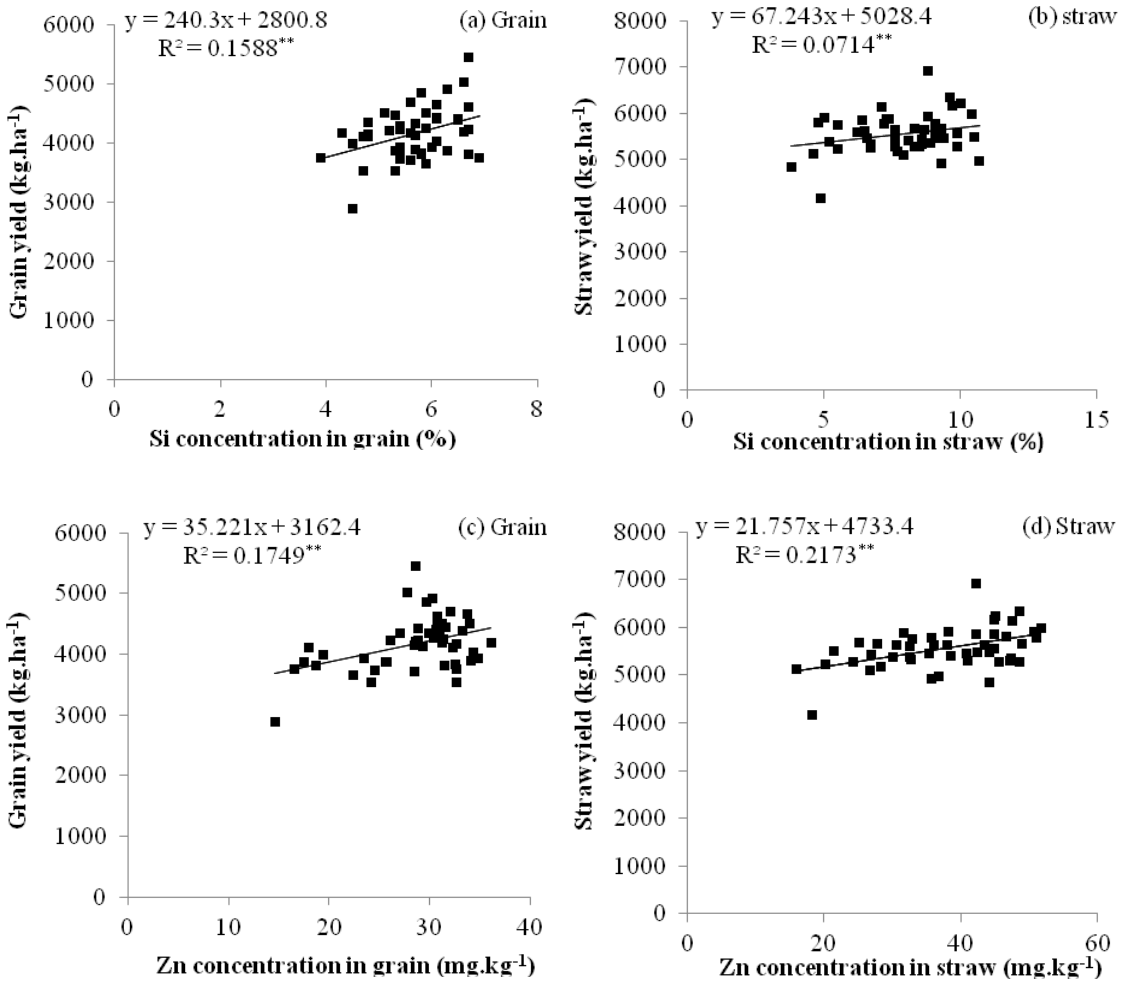

Figure 3. *The relationship of Si concentration in grain (a) and straw (b) with grain and straw yields of rice, correlations of Zn concentration in grain (c) and straw (d) with grain and straw yields of rice under the influence of experimental treatments*

Fertile tiller number per hill

Si and Zn application significantly increased the number of fertile tiller per hill. The maximum fertile tiller number per hill (18.47 tiller) was obtained by simultaneous foliar application of nano-SiO_2 + nano-ZnO (T13), and this trait was reduced under control condition by 28.9% (*Table 6*).

Filled and unfilled grain number, 1000-grain weight

The results of this experiment showed that the number of filled and unfilled grains per panicle were significantly affected by the experimental treatments. The highest number of filled grains per panicle (100 whole grain) was obtained by combined application of nano-SiO_2 foliar spray + calcium silicate soil application (T6), and with no fertilizer application (control), the trait was reduced by 18.4%. Also, the lowest number of unfilled grain per panicle was observed in the treatments of T6 and T14. The effect of experimental treatments was not significant on 1000-grain weight (*Table 6*).

http://www.aloki.hu ● ISSN 1589 1623 (Print) ● ISSN 1785 0037 (Online)
DOI: http://dx.doi.org/10.15666/aeer/1605_57815798
© 2018, ALÖKI Kft., Budapest, Hungary

Chlorophyll content of flag leaf

By Si and Zn application the chlorophyll content of flag leaf improved compared to the control, such that the maximum chlorophyll content (38.00) was obtained by T16 treatment application, whereas without applying Si and Zn, this trait was reduced by 7.8% (*Table 6*).

Si concentration in grain and straw

A significant increase in Si concentration in plant tissue was observed by NPs foliar application and soil application of elements. Mean comparison indicated that the Si concentration in grain (6.40%) and straw (9.80%) of rice was significantly increased by combined application of Si and Zn in both methods of NPs foliar application and soil application (T16). The lowest Si concentration in grain and straw of rice was observed in the control or no fertilizer application (T1). The application of T9 treatment increased the Si mobilization efficiency index (1.01) because of the better transfer of Si from straw to seed and consequently its accumulation in grain (*Table 7*).

Table 7. *Mean comparison of the effects of experimental treatments on Si concentrations in grain and straw of rice (cv. Tarom Hashemi)*

Treatments	Si concentration in grain (%)	Si concentration in straw (%)	Si MEI
T1	4.60e	5.40e	0.85ab
T2	5.36a-e	6.63de	0.81ab
T3	4.93de	6.00e	0.82ab
T4	5.60a-e	7.10b-e	0.79ab
T5	5.83a-d	8.60a-d	0.67b
T6	6.00abc	9.00abc	0.66b
T7	5.90a-d	8.80abc	0.68b
T8	6.30ab	9.40a	0.66b
T9	5.33b-e	5.80e	1.01a
T10	5.46a-e	7.00cde	0.82ab
T11	5.03cde	6.30e	0.85ab
T12	5.70a-d	7.33b-e	0.77ab
T13	6.00abc	9.06ab	0.66b
T14	6.36ab	9.50a	0.66b
T15	6.10ab	8.91abc	0.68b
T16	6.40a	9.80a	0.64b
$LSD_{0.05}$	1.056	2.010	0.2983

Values followed by different small letters within columns are significantly different ($p < 0.05$) according to the LSD test

Zn concentration in grain and straw

The effect of experimental treatments was significant on Zn concentration in rice plant tissue. However, by combined application of Si and Zn in the form of soil and foliar application, Zn concentration was increased in grain and straw. The maximum Zn concentration in grain (32.90 $mg.kg^{-1}$), was obtained by treatments of T16, while the maximum Zn concentration in straw (48.80 and 48.50 $mg.kg^{-1}$) was obtained by

http://www.aloki.hu ● ISSN 1589 1623 (Print) ● ISSN 1785 0037 (Online)
DOI: http://dx.doi.org/10.15666/aeer/1605_57815798
© 2018, ALÖKI Kft., Budapest, Hungary

treatments of T15 and T16, respectively. Zn mobilization efficiency index did not differ significantly in the fertilized treatments (*Table 8*). According to *Figure 4,* the Zn concentration changed by changes in Si concentration, such that by increasing Si concentration in plant tissue, Zn concentration in grain and straw increased ($R^2 = 0.1664$ and $R^2 = 0.1642$, $P < 0.01$, respectively).

Table 8. *Mean comparison of the effects of the experimental treatments on Zn concentrations in grain and straw of rice (cv. Tarom Hashemi)*

Treatments	Zn concentration in grain ($mg.kg^{-1}$)	Zn concentration in straw ($mg.kg^{-1}$)	Zn MEI
T1	16.20e	19.50h	0.84a
T2	21.63d	25.90gh	0.87a
T3	27.80bc	34.50d-g	0.81a
T4	28.40abc	36.30c-f	0.79a
T5	23.70cd	28.20fgh	0.84a
T6	24.20cd	28.70efg	0.89a
T7	30.30ab	37.50b-e	0.82a
T8	30.50ab	38.30bcd	0.79a
T9	30.30ab	38.50bcd	0.79a
T10	30.60ab	40.40a-d	0.76a
T11	31.70ab	42.10a-d	0.75a
T12	31.50ab	43.60abc	0.72a
T13	31.80ab	45.20abc	0.69a
T14	32.00ab	46.20ab	0.69a
T15	32.60ab	48.80a	0.66a
T16	32.90a	48.50a	0.67a
$LSD_{0.05}$	4.944	9.026	0.2529

Values followed by different small letters within columns are significantly different ($p < 0.05$) according to the LSD test

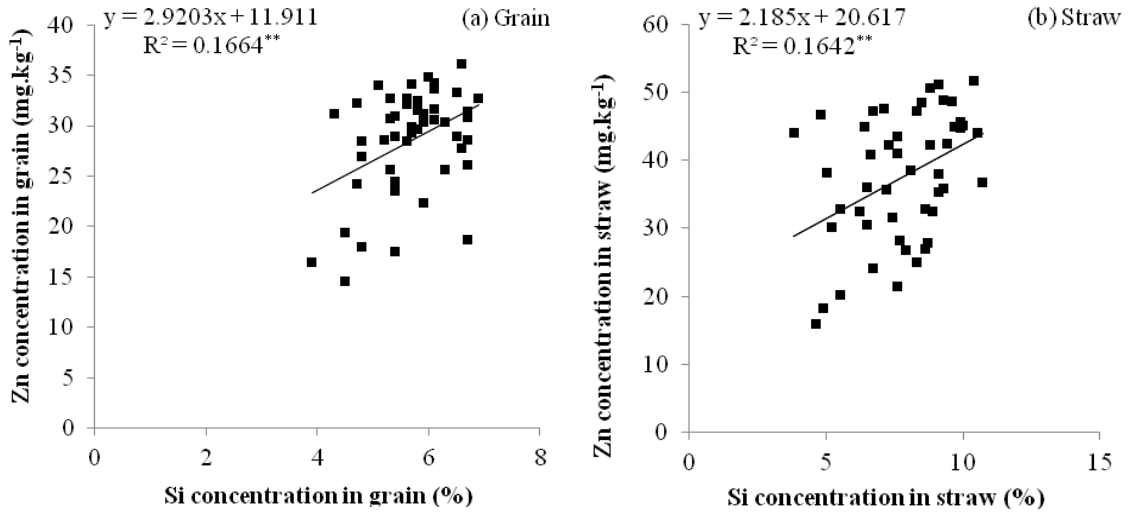

Figure 4. *The relationship of Si concentration in grain (a) and straw (b) and Zn concentration in grain and straw of rice under experimental treatments*

http://www.aloki.hu ● ISSN 1589 1623 (Print) ● ISSN 1785 0037 (Online)
DOI: http://dx.doi.org/10.15666/aeer/1605_57815798
© 2018, ALÖKI Kft., Budapest, Hungary

N concentration in grain and straw

The N concentration in grain and straw was increased by Si and Zn application. The NPs foliar application and soil application of Si and Zn significantly improved the N concentration in plant tissue compared to control. The maximum N concentration in grain was obtained by treatments of T14, T15 and T16. Also, the T15 and T16 treatments had the highest N concentration in rice straw. The maximum N mobilization efficiency index in rice plant was observed by T1 treatment or control (*Table 9*). There was a positive and significant linear correlation between N concentrations in plant tissue with the Si and Zn concentration in grain and straw at a probability level of 1%, such that by increasing Si concentration in grain and straw (R^2 = 0.0655 and R^2 = 0.1859, $P < 0.01$, respectively), and Zn concentration in grain and straw (R^2 = 0.1902 and R^2 = 0.4708, $P < 0.01$, respectively), N concentrations in grain and straw increased (*Fig. 5*).

Table 9. *Mean comparison of the effects of the experimental treatments on N concentrations in grain and straw of rice (cv. Tarom Hashemi)*

Treatments	N concentration in grain (%)	N concentration in straw (%)	N MEI
T1	1.36c	0.569d	2.40a
T2	1.39bc	0.622cd	2.25ab
T3	1.43abc	0.670bcd	2.14ab
T4	1.44abc	0.718abc	2.01ab
T5	1.43abc	0.656bcd	2.18ab
T6	1.43abc	0.668bcd	2.13ab
T7	1.46abc	0.751abc	1.95b
T8	1.47abc	0.767ab	1.97b
T9	1.45abc	0.718abc	2.03ab
T10	1.48abc	0.707abc	2.09ab
T11	1.50abc	0.739abc	2.03ab
T12	1.51abc	0.774ab	1.96b
T13	1.51ab	0.785ab	1.94b
T14	1.54a	0.780ab	1.97b
T15	1.54a	0.823a	1.90b
T16	1.55a	0.816a	1.90b
$LSD_{0.05}$	0.1491	0.1292	0.3981

Values followed by different small letters within columns are significantly different ($p < 0.05$) according to the LSD test

Discussion

The increase of the grain and straw yields with simultaneous application of Si and Zn can be attributed to the positive and synergistic effects between silicon and zinc, which by increasing the Si and Zn uptake, as well as increasing the fertile tiller number per hill lead to an increase in yields. There were synergistic interactions between Si and Zn, which ultimately has contributed to increased absorption of these elements in the plant tissue (Ghasemi et al., 2014). In the present study, in terms of an increase in yields, the NPs foliar application slightly is better than soil application of these elements. The micronutrients in the form of nanoparticles are effective in producing and increasing the

http://www.aloki.hu ● ISSN 1589 1623 (Print) ● ISSN 1785 0037 (Online)
DOI: http://dx.doi.org/10.15666/aeer/1605_57815798
© 2018, ALÖKI Kft., Budapest, Hungary

product yield (Reynolds, 2002). Amrullah et al. (2015) stated that nano-SiO_2 is superior over conventional silicon fertilizer. Gradual release of nutrients during growth stages of the plant by nano-ZnO application increases growth and rice yield (Yuvaraj and Subramanian, 2014). Cuong et al. (2017) reported that by adding silicon, rice grain yield was improved due to increasing growth, yield components, and better absorption of nutrients. Silicon application, especially at reproductive stages increases the chlorophyll content, the number of fertile tiller per hill, percentage of filled spikelets, and finally improves rice grain yield (Tamai and Ma, 2008). Zinc application by both methods foliar application and soil application is suitable for improving grain yield and increasing profitability in various systems of rice production (Farooq et al., 2018). Saha et al. (2017) revealed that zinc supply through soil + 2 foliar application caused the greatest increase in zinc concentration in rice grains by producing optimal grain yield, which confirms the results of the present study.

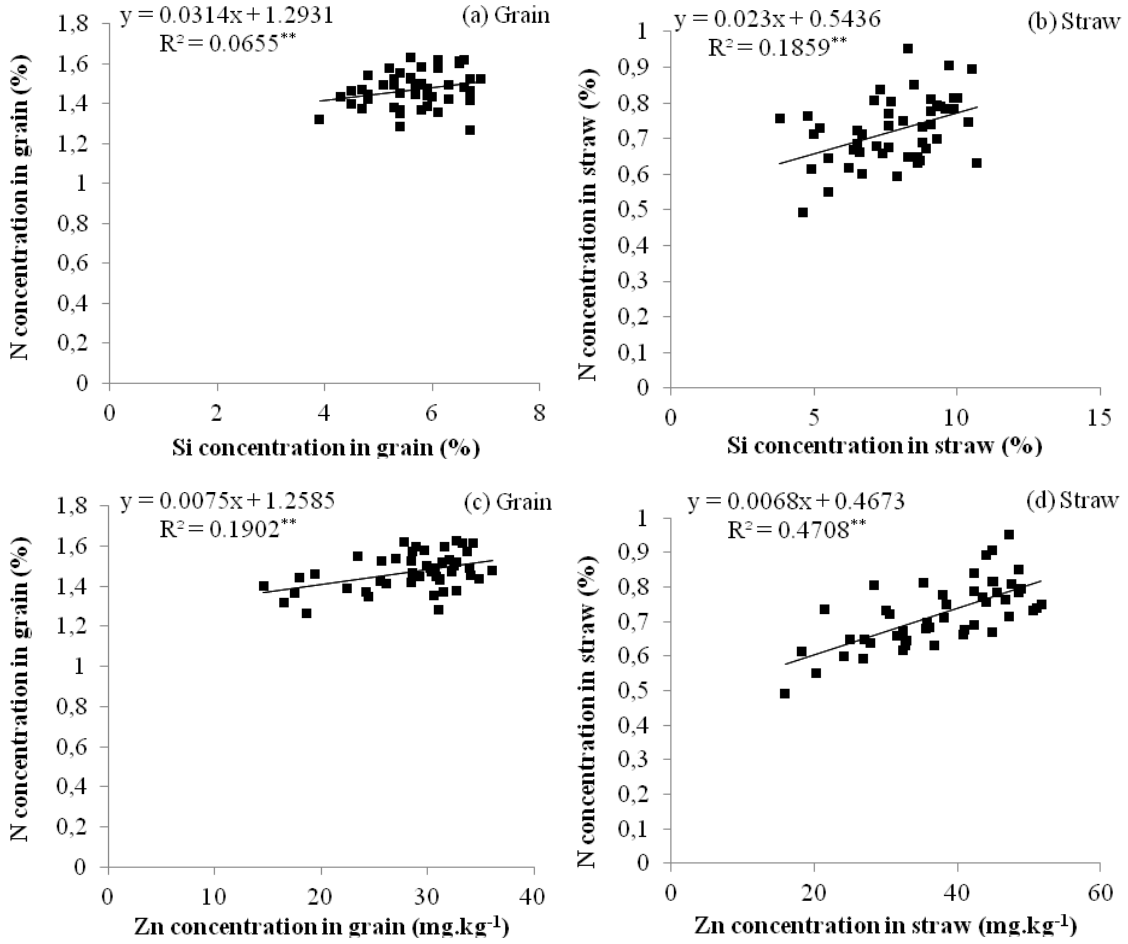

Figure 5. *The relationship of Si concentration in grain (a) and straw (b) and N concentration in grain and straw of rice, correlations of Zn concentration in grain (c) and straw (d) with N concentration in grain and straw of rice under experimental treatments*

It seems that the soil application of Si and Zn was less effective in improving panicle length than NPs foliar application, although it increased the trait compared to control. Although panicle length does not directly have a role in the calculation of grain yield, it

http://www.aloki.hu ● ISSN 1589 1623 (Print) ● ISSN 1785 0037 (Online)
DOI: http://dx.doi.org/10.15666/aeer/1605_57815798
© 2018, ALÖKI Kft., Budapest, Hungary

is considered as one of the yield evaluation attributes (Jalali et al., 2015). Ghasemi Lamraski et al. (2014) reported that foliar application of nano-SiO_2 caused a 1.4% increase in the panicle length compared to non-silicon application. According to Kamari et al. (2014) by foliar application of nano-ZnO significantly increased the panicle length of triticale.

By combined application of Si and Zn in both methods used, the number of fertile tillers per hill significantly increased compared to individual application of Si and Zn. Zia et al. (2017) reported that the proper use of silicon has been effective in increasing the number of rice tillers, such that the application of 3 mM of silicon caused a 19% increase in the number of tiller compared with the control. Application of zinc in both methods of soil and foliar application due to increased zinc concentration in plant leads to an increase in the number of effective tillers per square meter (Farooq et al., 2018). The supply of silicon and zinc by the plant through NPs foliar application increased the number of fertile tillers per hill compared to the soil method. In similar results, the researchers by studying different sources of silicon in the methods of soil and NPs foliar application reported that the maximum fertile tiller number per hill was obtained by nano-SiO_2 foliar application for two crop years (Yazdpour et al., 2014a). The positive effect of zinc on increasing the number of fertile tillers per hill was quite evident over silicon so that in all treatments where zinc fertilizer was used to forms of NPs foliar application and soil application, the fertile tiller number was improved compared to silicon application, although using both elements increased the number of the fertile tiller per hill.

Reduction of the number of filled grains per panicle with no fertilizer application could be due to the lack of availability to nutrients and the reduction of photosynthetic seed distribution, but this trait was increased with the addition of Si and Zn. The result showed that the number of filled grains per panicle significantly increased in treatments where silicon was used. Cuong et al. (2017) reported that the number of grains per panicle was increased by increasing silicon application. The silicon application in the reproductive stages of rice had a very positive effect on the improvement of the number of filled grains per panicle (Lavinsky et al., 2016), which confirms the results of this experiment. According to Tamai and Ma (2008), among the yield components, the percentage of filled spikelets was more affected by silicon fertilizer.

The grain size in rice is controlled by its shell, which shows that why the extent of 1000-grain weight changes is not high (Saha et al., 1998). Reports indicate that the 1000-grain weight was not affected by different concentrations of silicon (Yazdpour et al., 2014a), which is consistent with the results of the present research. In contrast, a piece of research showed that the zinc application from different sources had a significant effect on thousand grain weight of rice (Shivay et al., 2016).

By combined application of Si and Zn in both methods of NPs foliar application and soil application, the chlorophyll meter value increased compared to the separate application of these two element. Nano-Si has an important role in increasing the chlorophyll content of rice leaves (Wang et al., 2015). It was reported that application of nano-Zn oxide did not significantly affect the photosynthetic pigment content of different varieties of rice, but it protected photosynthetic pigments such as chlorophyll a and b in plant cells by improving the antioxidant enzymes activities (Samart et al., 2017). Zinc foliar application at the tillering stage of rice led to an increase in gene expression, carbonic anhydrase enzyme activation, improvement of the photosynthesis process and increase in relative chlorophyll concentration per unit leaf area (Qiao et al.,

http://www.aloki.hu ● ISSN 1589 1623 (Print) ● ISSN 1785 0037 (Online)
DOI: http://dx.doi.org/10.15666/aeer/1605_57815798
© 2018, ALÖKI Kft., Budapest, Hungary

2014). Several reports have been presented by investigators regarding the effects of Si (Ranganathan et al., 2006) and Zn (Kabeya and Shankar, 2013) on increasing the chlorophyll content of plants, which is consistent with the results of this study.

In the present research, Si application increased the Si concentration in grain and straw of rice, and Zn application plus Si led to higher concentrations of Si in rice tissue. Reports indicated that the Zn application in the root increases the Si concentration in root and shoot (Mehrabanjoubani et al., 2015). Zia et al. (2017) found that by increasing silicon consumption from 0 to 3 mM, the Si concentration in root and shoot was increased by about 48 and 42%, respectively. According to Yazdpour et al. (2014b) the highest Si concentration in rice was obtained by nano-Si foliar application in both years of study.

The Zn concentration in grain and straw was improved in all treatments in which Zn fertilizer was used to both methods of soil application and NPs foliar application. It has been reported that the zinc concentration in rice grains increased by 47% compared to control, when zinc fertilizer was applied through soil (basal) + foliar application at maximum tillering and flowering stages (Saha et al., 2017). Zinc application using four different methods (foliar application, soil application, seed priming and seed coating) significantly increased grain zinc concentration in various systems of rice production at two different sites (Farooq et al., 2018). Although the combined application of Si and Zn in soil application method led to an increase in grain and straw Zn, the effect of combined application of elements by NPs foliar application method was greater than soil application. Si application by methods of soil application and NPs foliar application individually or in a combination of two methods could not significantly increase the grain and straw Zn concentration, but the Si application plus Zn significantly increased zinc concentration in rice tissue due to the synergistic interaction of these two elements. Similar to the results of this experiment, in previous studies the increase of Zn concentrations in rice plant tissue by the nano-Si application was reported (Wang et al., 2015).

In this research, it seems that role of Zn in improving N concentration was slightly more than Si, although both elements were effective in improving N concentration. The Zn application increases the accumulation of amino acids and nitrogen metabolism in plant tissue (Sudha and Stalin, 2015). Reports indicate that the N uptake was improved by Zn application in two growing seasons (Kumar Naik and Kumar Das, 2008). The researchers revealed that there was a positive and significant linear relationship between the amount of silicon absorption and the uptake of nitrogen in rice plant (Cuong et al., 2017). According to Yazdpour et al. (2014b) the maximum N concentration and protein content of rice were obtained by the foliar application of nano-Si.

Conclusion

In this research, we investigated the effects of different resources and methods of silicon and zinc application on agronomic and physiological traits, as well as the grain and straw yield of rice in Mazandaran province. The results revealed that the application of Si and Zn in both methods of NPs foliar application and soil application had a positive effect on agronomic traits and seed yield, although the influence of Zn fertilizer on grain and straw yields improvement was slightly more than Si fertilizer. Also, in both methods, the foliar application of nanoparticles had better efficiency than soil application of the elements due to the small size of the particles and the ability to absorb

http://www.aloki.hu ● ISSN 1589 1623 (Print) ● ISSN 1785 0037 (Online)
DOI: http://dx.doi.org/10.15666/aeer/1605_57815798
© 2018, ALÖKI Kft., Budapest, Hungary

more of the elements by the plant. By combined application of Si and Zn, many physiological characteristics such as the Si, Zn and N concentrations in rice plant tissue, yield components and grain and straw yield of rice improved compared to separate application of each elements and control. The main reason for this increase could be synergistic effects between the two elements of silicon and zinc, such that the silicon caused the balance of nutrients in the plant and was a good supplement with zinc in improving the nutrients uptake and increasing grain yield.

Therefore, given that the simultaneous application of silicon and zinc, especially by foliar application of nanoparticles provides the nutrient required for the plant and improves grain production of rice, this fertilizer treatment is recommended for use in soils similar to the one used in this experiment.

Future extensions of this study for future research: It is recommended to investigate the quality of rice produced in the cultivar studied in these treatments. The experimental treatments on late rice varieties can be also studied. Moreover, the germination characteristics of seeds produced in these treatments, as well as the effect of these treatments on the absorption efficiency of the main elements of NPK can be evaluated. Also, the effects of other nano-fertilizers such as nano-MgO and nano-Ag in combination with the nanoparticles used in this experiment, as well as the effects of other fertilizer sources containing silicon and zinc such as potassium silicate and zinc chelate on physiological traits, rice growth and yield can be investigated. Besides, the absorption of other essential nutrients such as P, K, S, Ca, Mg, Fe, Cu, Mn, B, as well as heavy metals such as Cd, As and Pb in rice grains can be measured in order to determine the health status of rice seeds because rice seeds are fed by humans. Finally, the effects of silicon and zinc both in the form of nanoparticles and conventional method on rice grain yield by a foliar application can be studied.

REFERENCES

[1] Amiri, A., Bagheri, A., Khaje, M., Najafabadi Pour, F., Yadollahi, P. (2014): Effect of silicon foliar application on yield and antioxidant enzymes activity of safflower under limited irrigation conditions. – Journal of Agricultural Research 5(4): 361-372.

[2] Amirjani, M. R., Askari, M., Askari, F. (2014): Effect of nano zinc oxide on alkaloids, enzymatic and antienzymatic antioxidant contents and some physiological parameters of *catharantus roseus*. – Journal of Cell and Tissue 5(2): 173-183.

[3] Amrullah, Sopandie, D., Sugianta, Junaedi, A. (2015): Influence of nano-silica on the growth of rice plant (*Oryza sativa* L.). – Asian Journal of Agricultural Research 9(1): 33-37.

[4] Boonyanitipong, P., Kositsup, B., Kumar, P., Baruah, S., Dutta, J. (2011): Toxicity of Zno and Tio2 nanoparticles on germination rice seed *Oryza sativa* L. – International Journal of Bioscience, Biochemistry and Bioinformatics 1(4): 282-285.

[5] Chang, H. B., Win, L., Huang, H. J. (2005): Zinc-induced cell death in rice (*Oryza sativa* L.) roots. – Plant Growth Regulation 46(3): 261-266.

[6] Chen, J., Liu, X., Wang, C., Yin, S. S., Li, X. L., Hu, W. J., Simon, M., Shen, Z. J., Xiao, Q., Chu, C. C., Peng, X. X. (2015): Nitric oxide ameliorates zink oxide nanoparticles-induced phytotoxicity in rice seedlings. – Journal of Hazardous Materials 297: 173-182.

[7] Cuong, T. X., Ullah, H., Datta, A., Hanh, T. C. (2017): Effects of silicon-based fertilizer on growth, yield and nutrient uptake of rice in tropical zone of Vietnam. – Rice Science 24(5): 283-290.

[8] Emami, A. (1996): Methods of Plant Analysis. Vol. 982. – Soil and Water Res. Institute, Tehran.

http://www.aloki.hu ● ISSN 1589 1623 (Print) ● ISSN 1785 0037 (Online)
DOI: http://dx.doi.org/10.15666/aeer/1605_57815798
© 2018, ALÖKI Kft., Budapest, Hungary

[9] Farooq, M., Ullah, A., Rehman, A., Nawaz, A., Nadeem, A., Wakeel, A., Nadeem, F., Siddique, K. H. M. (2018): Application of zinc improves the productivity and biofortification of fine grain aromatic rice grown in dry seeded and puddle transplanted production systems. – Field Crops Research 216: 53-62.

[10] Ghasemi, M., Mobasser, H. R., Asadimanesh, H., Gholizadeh, A. (2014): Investigating the effect of potassium, zinc and silicon on grain yield, yield components and their absorption in grain rice (*Oryza sativa* L.). – Electronic Journal of Soil Management and Sustainable Production 4: 1-24.

[11] Ghasemi Lemraski, M., Normohamadi, G., Madani, H., Heidari Sharifabad, H., Mobasser, H. R. (2014): Effect of silicon and potassium foliar application and nitrogen rates on yield and yield components of Iranian rice cultivars, Tarom Hashemi and Tarom Mahalli. – Journal of New Finding in Agriculture 9(1): 47-66.

[12] Ghasemi Mianaei, A., Mobasser, H. R., Madani, H., Dastan, S. (2011): Silicon and potassium application facts on lodging related characteristics and quantity yield in rice (*Oryza sativa* L.) Tarom Hashemi variety. – Journal of New Finding in Agriculture 5(4): 423-435.

[13] He, Y. P., Zhang, J. F., Chen, J. M. (2014): Effect of synergists on susceptibility to chlorantraniliprole in field populations of *Chilo suppressalis* (Lepidoptera: Pyralidae). – Journal of Economic Entomology 107: 791-796.

[14] Huang, S., Wang, L., Liu, L., Hou, Y., Li, L. (2015): Nanotechnology in agriculture, livestock, and aquaculture in China, A review. – Agronomy for Sustainable Development 35: 369-400.

[15] Jalali, J., Nasiri, M., Habibi, M., Kheyri, N. (2015): Evaluation of possibility of increasing success coefficient of direct seeding of rice genotypes by changing sowing dates. – Crop Physiology Journal 7(26): 85-103.

[16] Jeer, M., Telugu, U. M., Voleti, S. R., Padmakumari, A. P. (2017): Soil application of silicon reduces yellow stem borer, scripophage incertulas (Walker) damage in rice. – Journal of Applied Entomology 141(3): 189-201.

[17] Jianguo, L., Hui, C., Congcong, M., Mingxin, W. (2015): Effects of nano-silicon and common silicon on lead uptake and translocation in two rice cultivars. – Frontiers of Environmental Science and Engineering 1-7.

[18] Kabeya, M. J., Shankar, A. G. (2013): Effect of different levels of zinc on growth and uptake ability in rice zinc contrast lines (*Oryza sativa* L.). – Asian Journal of Plant Science and Research 3(3): 112-116.

[19] Kafi, M., Rahimi, Z. (2011): Effect of salinity and silicon on root characteristics, growth water status, proline content and ion accumulation of purslane (*Portulaca oleracea* L.). – Soil Science and Plant Nutrition 57: 341-347.

[20] Kamari, H., Seyed Sharifi, R., Sedghi, M. (2014): Effect of Nano Zinc oxide foliar application and application of free living nitrogen fixing bacteria on yield and morphophysiological characteristics of Triticale. – Crop Physiology Journal 6(22): 37-52.

[21] Kumar Naik, S., Kumar Das, D. (2008): Relative performance of chelated zink and zink sulfate for lowland rice (*Oryza sativa* L.). – Nutrient Cycling in Agroecosystems 81: 219-227.

[22] Lavinsky, A. O., Detmann, K. C., Reis, J. V., Avila, R. T., Sanglard, M. L., Pereira, L. F., Sanglard, L. M. V. P., Rodrigues, F. A., Araujo, W. L., DaMatta, F. M. (2016): Silicon improves rice grain yield and photosynthesis specifically when supplied during the reproductive growth stage. – Journal of Plant Physiology 206: 125-132.

[23] Lin, H., Fang, C., Li, Y., Lin, W., He, J., Lin, R., Lin, W. (2016): Effect of silicon on grain yield of rice under cadmium-stress. – Acta Physiologiae Plantarum 38-186.

[24] Lou, Y. S., Wu, L., Lixuan, R., Meng, Y., Shidi, Z., Huaiwei, Z. (2016): Effects of silicon application on diurnal variations of physiological properties of rice leaves of plants at the heading stage under elevated UV-B radiation. – International Journal of Biometeorology 60(2): 311-318.

http://www.aloki.hu ● ISSN 1589 1623 (Print) ● ISSN 1785 0037 (Online)
DOI: http://dx.doi.org/10.15666/aeer/1605_57815798
© 2018, ALÖKI Kft., Budapest, Hungary

[25] Mahmoud, E., Abdel-Haliem, F., Hegazy, H. S., Hassan, N. S., Naguib, D. M. (2017): Effect of silica ions and nano silica on rice plants under salinity stress. – Ecological Engineering 99: 282-289.
[26] Mazlomi, M., Pirzad, A., Zardoshti, M. (2012): Allocation ratio of photosynthate to different parts of sugar beet plant affected by nano-iron foliar application at varying growth stages. – International Journal of Plant, Animal and Environmental Sciences 2: 121-128.
[27] Meena, V. D., Dotaniya, M. L., Coumar, V., Rajendiran, S., Ajay, Kundu, S., Rao, A. S. (2014): A case for silicon fertilization to improve crop yields in tropical soils. – Proceedings of the National Academy of Sciences, India Section B: Biological Sciences 84(3): 505-518.
[28] Mehrabanjoubani, P., Abdolzadeh, A., Sadeghipour, H. R., Aghdasi, M. (2015): Impacts of silicon nutrition on growth and nutrient status of rice plants grown under varying zinc regimes. – Theoretical and Experimental Plant Physiology 27(1): 19-29.
[29] Mobasser, H. R., Ghanbari-Malidareh, A., Sedghi, A. H. (2008): Effect of silicon application to nitrogen rate and splitting on agronomical characteristics of rice (*Oryza sativa* L.). – Silicon in Agriculture Conference, Wild Coast Sun, South Africa, 26-31 October.
[30] Qiao, X., He, Y., Wang, Z., Li, X., Zhang, K., Zeng, H. (2014): Effect of foliar spray of zinc on chloroplast β-carbonic anhydrase expression and enzyme activity in rice (*Oryza sativa* L.) leaves. – Acta Physiologiae Plantarum 36: 263-272.
[31] Ranganathan, S., Suvarchala, V., Rajesh, Y. B. R. D., Prasad, M. S., Padmakumari, A. P. and Voleti, S. R. (2006): Effects of silicon sources on its deposition, chlorophyll content, and disease and pest resistance in rice. – Biologia Plantarum 50(4): 713-716.
[32] Reynolds, G. H. (2002): Forward to the future nanotechnology and regulatory policy. – Pacific Research Institute 24: 1-23.
[33] Saha, A., Sarkar, R. K., Yamagishi, Y. (1998): Effect of time of nitrogen application on spikelet differentiation and degeneration of rice. – Botanical Bulletin of Academia Sinica. 39: 119-123.
[34] Saha, S., Chakraborty, M., Padhan, D., Saha, B., Murmu, S., Batabyal, K., Seth, A., Hazra, G. C., Mandal, B., Bell, R. W. (2017): Agronomic biofortification of zinc in rice: influence of cultivars and zinc application methods on grain yield and zinc bioavailability. – Field Crops Research 210: 52-60.
[35] Samart, S., Chutipaijit, S., Phakamas, N. (2017): Evaluating the effect of zinc oxide nanoparticles on the physiological responses of nine non-photoperiod sensitive rice cultivars. – Materials Today: Proceedings 4: 6430-6435.
[36] Sepehri, A., Vaziri Amjad, Z. (2015): The effect of iron and zinc nano fertilizers on quantitative yield of chicory (*Cichorium inyubus* L.) in different crop densities. – Journal of Agricultural Science and Sustainable Production 25(2.1): 61-74.
[37] Shivay, Y. S., Prasad, R., Kaur, R., Pal, M. (2016): Relative efficiency of zinc sulphate and chelated zinc on zinc biofortification of rice grains and zinc use-efficiency in Basmati rice. – Proceedings of the National Academy of Sciences, India Section B, Biological Sciences 86(4): 973-984.
[38] Sudha, S., Stalin, P. (2015): Effect of zinc on yield, quality and grain zinc content of rice genotypes. – International Journal of Farm Sciences 5(3): 17-27.
[39] Tamai, K., Ma, J. F. (2008): Reexamination of silicon effects on rice growth and production under field conditions using a low silicon mutant. – Plant Soil 307: 21-27.
[40] Upadhyaya, H., Shome, S., Tewari, S., Bhattacharya, M. K., Panda, S. K. (2014): Effect of Zn nano-particles on growth responses of rice. – Nano Science Technology Conference pp. 508-512.
[41] Wang, S., Wang, F., Gao, S. (2015): Foliar application with nano-silicon alleviates cd toxicity in rice seedlings. – Environmental Science and Pollution Research 22(4): 2837-2845.

http://www.aloki.hu ● ISSN 1589 1623 (Print) ● ISSN 1785 0037 (Online)
DOI: http://dx.doi.org/10.15666/aeer/1605_57815798
© 2018, ALÖKI Kft., Budapest, Hungary

[42] Wu, C., Zou, Q., Xue, S., Mo, J., Pan, W., Lou, L., Wong, M. H. (2015): Effects of silicon (Si) on arsenic (As) accumulation and speciation in rice (*Oryza sativa* L.) genotypes with different radial oxygen loss (Rol). – Chemosphere 138: 447-453.
[43] Yakan, H., Ali Gurbu, M., Ferzan, A., Halil, S., Necmi, B. (2000): The effect of zinc application on rice yield and some agronomic characters. – http://om.ciheam.org/article.php?IDPDF=3400079.
[44] Yazdpour, H., Noormohamadi, G., Madani, H., Heidari Sharif Abad, H., Mobasser, H. R. (2014a): Role of nano-silicon and other silicon resources with nitrogen and phosphorus application on yield and yield components of rice (*Oryza sativa* L.). – Trends in Life Sciences. An International Peer-Reviewed Journal 3(2): 36-41.
[45] Yazdpour, H., Noormohamadi, G., Madani, H., Heidari Sharif Abad, H., Mobasser, H. R., Oshri, M. (2014b): Role of nano-silicon and other silicon resources on straw and grain protein, phosphorus and silicon contents in Iranian rice cultivar (*Oryza sativa* cv. Tarom). – International Journal of Biosciences 5(12): 449-456.
[46] Yoshida, S. (1975): The physiology of silicon in rice. – Food and Fertilizer Technology Center (FFTC), Technical Bulletin 25: 1-27.
[47] Yuvaraj, M., Subramanian, K. S. (2014): Fabrication of zinc nano fertilizer on growth parameter of rice. – Trends in Biosciences 7: 2564-2565.
[48] Zia, Z., Bakhat, H. F., Saqib, Z. A., Shah, G. M., Fahad, S., Ashraf, M. R., Hammad, H. M., Naseem, W., Shahid, M. (2017): Effect of water management and silicon on germination, growth, phosphorus and arsenic uptake in rice. – Ecotoxicology and Environmental Safety 144: 11-18.

http://www.aloki.hu ● ISSN 1589 1623 (Print) ● ISSN 1785 0037 (Online)
DOI: http://dx.doi.org/10.15666/aeer/1605_57815798
© 2018, ALÖKI Kft., Budapest, Hungary

MULTIVARIATE IMPACT ANALYSIS OF *PARTHENIUM HYSTEROPHORUS* INVASION ON ABOVE-GROUND PLANT DIVERSITY IN POTHWAR REGION OF PAKISTAN

QURESHI, H.[1,2*] – ARSHAD, M.[1] – BIBI, Y.[1] – AHMAD, R.[3] – OSUNKOYA, O. O.[4] – ADKINS, S. W.[2]

[1]*Department of Botany, PMAS-Arid Agriculture University, 46300-Rawalpindi, Pakistan*

[2]*School of Agriculture and Food Science, The University of Queensland St. Lucia-4072 Brisbane, Australia*

[3]*Quality Enhancement Cell, PMAS-Arid Agriculture University- 46300 Rawalpindi, Pakistan*

[4]*Invasive Plant & Animal Science, Biosecurity Unit, Queensland- Department of Agriculture & Fisheries, Brisbane-4001, Australia*

**Corresponding author*
e-mail: huma.qureshi@uq.edu.au, humaqureshi8@gmail.com

(Received 3rd Mar 2018; accepted 10th May 2018)

Abstract. Phytosociological studies help to understand extent of biological invasion. Multiple analyses of ecological parameters at different locations derive general explanations of impact on species diversity in plant communities. Current study assessed the impact of *Parthenium hysterophorus* (an annual weed of great significance in Pakistan and worldwide) invasion on native vegetation in Pothwar region of Pakistan. The approach used for the study was random samplings with two categorical factors: invaded and non-invaded under same habitat conditions. Differences in number of species (S), abundance (N), species richness (R), evenness (J'), Shannon diversity index (H') and Simpson index of dominance (λ) were compared between invaded and control plots by t-test series. Control plots harbored by average of 0.9 more species per 10 m^2. The control category was more diverse (H' = 1.73) than invaded category (H' = 1.53). The higher value of species richness in control plots shows the heterogeneous nature of communities and *vice versa* in invaded plots. The lower value of index of dominance in invaded plots shows less sample diversity than in the control ones. At multivariate scale, ordination (nMDS) and ANOSIM showed significant magnitude of differences between invaded and control plots in all sites. The most effected site by *Parthenium* invasion was Jhelum followed by Attock, Rawalpindi, Chakwal and Islamabad. The decrease in diversity indices in invaded over control sites indicated less productive plant communities due to *Parthenium* invasion. This makes *Parthenium* a candidate of consideration for appropriate control measures.
Keywords: *invasion impacts, diversity indices, multivariate analysis, diversity conservation, PRIMER*

Introduction

There has been a rapid acceleration in the number and rate of plant invasions attributed to increased dispersal of exotics and expansion of disturbed habitats associated with rapid human population growth (Collier and Vankat, 2002). The introduction of invasive plants may change the structure and function of ecosystem, e.g., alterations in succession, species composition, biomass, net primary productivity and nutrient cycling (Charles and Dukes, 2007; Dassonville et al., 2008). Invasive species may also deplete available resources. Other studies have shown changes at population, community and landscape levels (Collier and Vankat, 2002; Qureshi et al., 2014). Consequently, studying the community level impacts of the invader identifies its

http://www.aloki.hu ● ISSN 1589 1623 (Print) ● ISSN 1785 0037 (Online)
DOI: http://dx.doi.org/10.15666/aeer/1605_57995813
© 2018, ALÖKI Kft., Budapest, Hungary

potential effects and provides valued information for management and nature conservation strategies (Hejda et al., 2009).

Plant invasions deplete native species diversity, alter community composition and effect ecosystem processes thus cause ecological and economic imbalance (Kunzi et al., 2015). Exotic plants coexist in relative harmony in native habitat but competitively exclude neighbors in recipient communities. Various studies have provided data on the effects of exotic invasive plants on declining indigenous diversity and altering native community composition. These studies assumed different mechanisms that generate substantial invasion impacts. Among these processes are allelopathy, competition, and alteration of native ecosystem characteristics (Odat et al., 2011). Direct competition with native flora may result in monocultures of exotic species, e.g. *Parthenium hysterophorus* in Pakistan, Australia and India and *Psidium cattleianum* in Mauritius (Dogra et al., 2010). In different parts of the world, 80% of endangered species are threatened by alien invasive species (Pimentel et al., 2005).

Parthenium is an aromatic, annual herb native to Mexico, southern United States and South & Central America. It was inadvertently introduced to many countries and now has become a troublesome rangeland and agricultural weed in parts of Africa, Asia, Australia and the Pacific Islands (*Fig. 1*). Because of its status in the world, it is documented among world's top ten worst weeds (Tamado and Milberg, 2000; Khan et al., 2014). *P. hysterophorus* is assumed to move in to India along food grains trade in from USA. It then has spread to sub-continent (Nath, 1988). It is supposed to enter Pakistan via road links where automobiles cross at many places every day. In Pakistan, *Parthenium* weed was stated in the 1980s from Gujarat, Punjab (Razaq et al., 1994). Since then, it has spread rapidly all through to Islamabad, Punjab Province and parts of Khyber Pukhtunkhwa. *Parthenium* affects biodiversity, crop production and human and animal health (Shabbir, 2013). It grows in a range of habitats. Wide environmental adaptability, drought tolerance, photo and thermo-insensitivity, high seed production, small and light weighted seeds adept of long distance travel via water, wind, birds, animals and vehicles, longevity of seeds in soil seed banks, strong competition and allelopathy contribute to its invasiveness (Khan et al., 2014; Hassan et al., 2012; Shabbir and Bajwa, 2006).

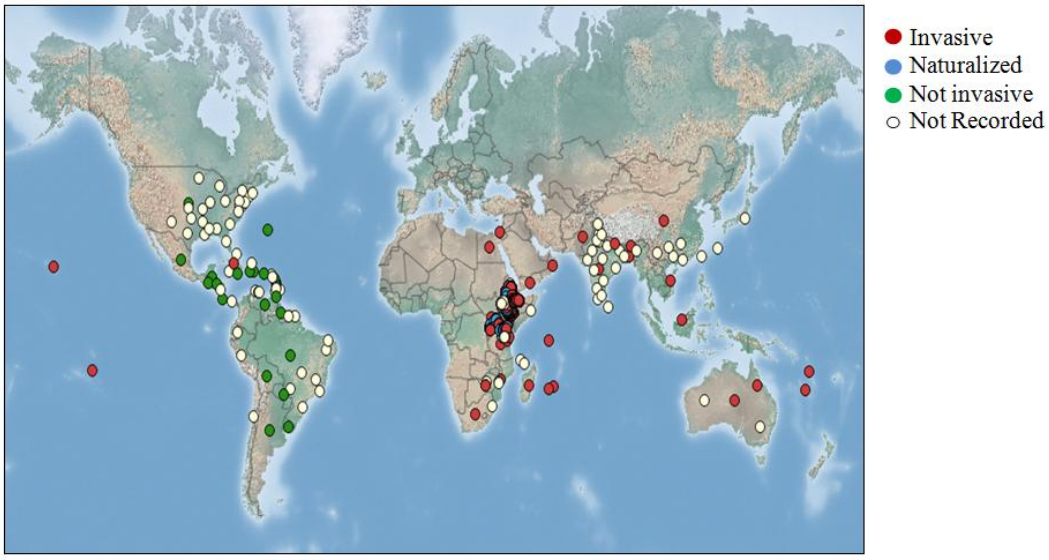

Figure 1. *Distribution map and invasion status of Parthenium weed around the globe*

http://www.aloki.hu ● ISSN 1589 1623 (Print) ● ISSN 1785 0037 (Online)
DOI: http://dx.doi.org/10.15666/aeer/1605_57995813
© 2018, ALÖKI Kft., Budapest, Hungary

Parthenium is one of the worst weeds presently known in Pakistan. No previous study is reported from Pothwar region regarding its ecological impacts. The current study was carried out to find out (1) what is the effect of *Parthenium* weed on ecological diversity indices in different districts of Pothwar region (assuming each district as 'site'); (2) do the effects on diversity differ between different sites (districts) in the area?

Materials and methods

Study area

Pothwar is a north-eastern plateau in Pakistan, making the northern part of Punjab. It edges Azad Kashmir (the western parts) and Khyber Pakhtunkhwa (southern parts). Pothwar Zone extends from 32.5°N to 34.0°N latitude and 72°E to 74°E longitude and lies between the Indus and Jhelum River. The plateau expanses from salt range northward to the foothills of Himalayas. The Pothwar region embraces Jhelum, Islamabad, Attock, Rawalpindi and Chakwal districts (*Table 1*). Total area of Pothwar region is 28488.9 km^2. (Rashid and Rasul, 2011). Pothwar region has an extreme climate with hot summers and cold winters. Weather is divided into four seasons: Cold (December-March); Hot (April-June); Monsoon (July-September) and Post-Monsoon season (October-November). This area gets an average annual rainfall of 812 mm, about half of which occurs in the Monsoon months (July-September). The mean maximum temperature rises till the month of June and then falls appreciably with advent of rains, being coldest in January (14.62-18.7 °C). Average temperatures range from 14 °C in January to 37 °C in June (*Fig. 2*). The region has broadly four types of soil: loess, river alluvium, residual and piedmont alluvium. Due to dynamic climate and combination of hills and plains, Pothwar region is rich in biodiversity. Native vegetation is characterized by open patches of grasses and forb species. *Albizia lebbeck* (L.) Benth., *Acacia modesta* Wall., *Abies pindrow* (Royle ex D. Don) Royle, *Cassia fistula* L., *Cedrela toona* Roxb. ex Rottler, *Dalbergia sissoo* Roxb., *Dodonaea viscosa* Jacq., *Ficus religiosa* L., *Ficus benghalensis* L., *Melia azedarach* L., *Olea cuspidata* Wall. Ex G. Don., *Zizyphus jujuba* Mill. and *Zizyphus nummularia* (Burm. f.) Wight & Arn. are principle species in the region (Shabbir et al., 2012; Ghufran et al., 2013).

Table 1. *Coordinates of study sites*

District	Coordinates
Jhelum	32.94°N, 73.72°E
Islamabad	33.73°N, 73.09°E
Attock	33.76°N, 72.36°E
Rawalpindi	33.59°N, 73.04°E
Chakwal	32.93°N, 72.85°E

Experimental design

Field work was carried out during July-August (being the maximum growth period of plants), 2016. The effect of invasion was studied in each of five districts (Attock, Chakwal, Jhelum, Islamabad and Rawalpindi). Ecological indices for selected invaders

http://www.aloki.hu ● ISSN 1589 1623 (Print) ● ISSN 1785 0037 (Online)
DOI: http://dx.doi.org/10.15666/aeer/1605_57995813
© 2018, ALÖKI Kft., Budapest, Hungary

were calculated and compared at various sites. The sampling technique was random. For each district six invaded and six non-invaded paired vegetation plots (each 3.16 × 3.16 m in size, i.e., 10 m^2 in area) were sampled. Based on visual observations, plot of invaded vegetation ('invaded plot') where the invader showed dominance was considered as 'treatment' and a second vegetation plot, usually 0.5-1 km apart from treatment, where invader has no dominance ('non-invaded plot') was considered as the "control". The estimated density of the weed in the area across locations was 4/m^2. In all, a total of 60 vegetation plots were sampled (consisting of six paired samples per district, and hence 30 treatments; 30 controls for the entire Pothwar region) (*Fig. 3*). Within each randomly chosen plot (10 m^2 in area), all vascular plant species in control and invaded plots were identified to species level.

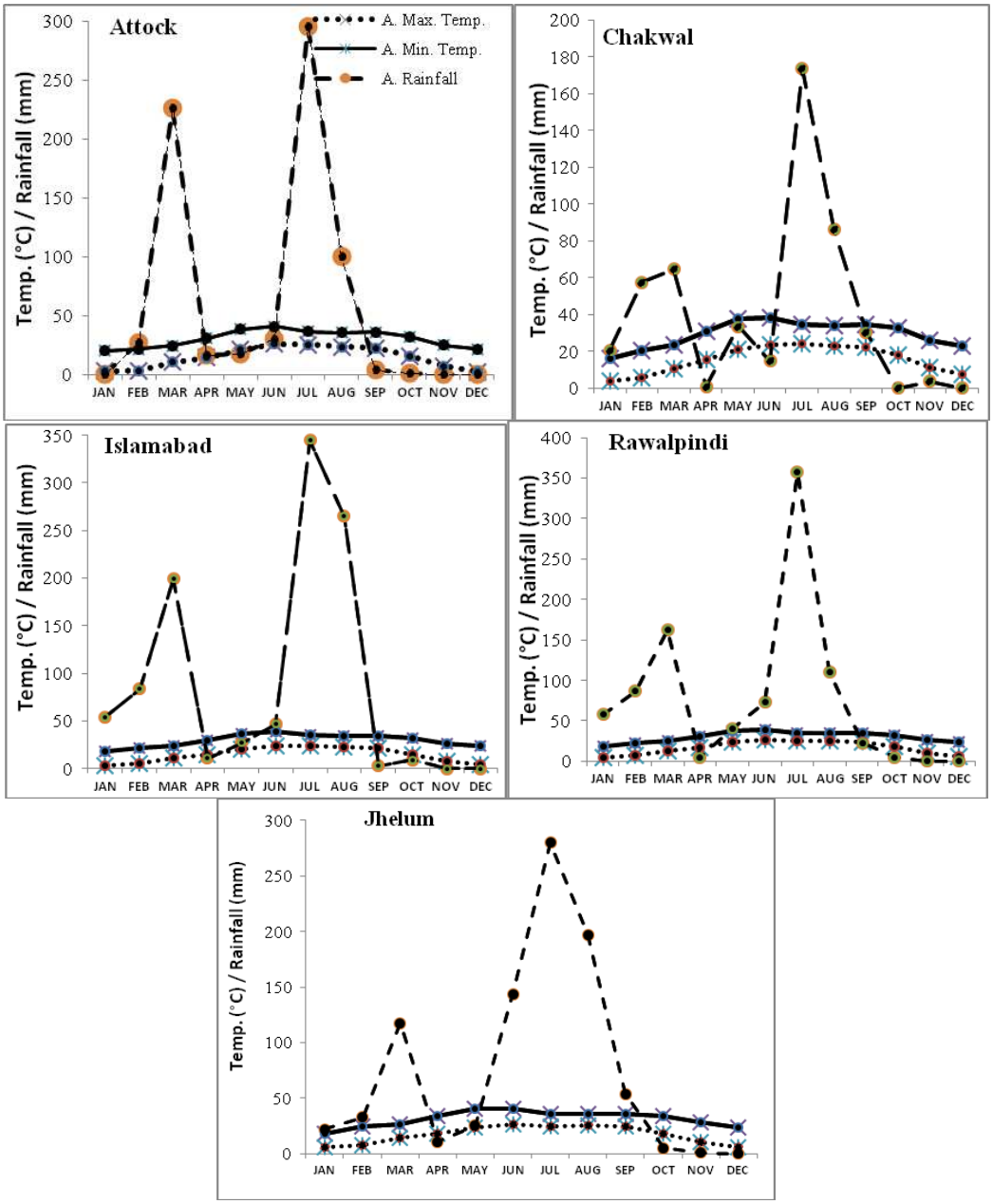

Figure 2. *Mean monthly climate data of Pothwar region, Pakistan for year 2017. (Data sourced from Pakistan Meteorological Department University Road Karachi, Pakistan)*

http://www.aloki.hu ● ISSN 1589 1623 (Print) ● ISSN 1785 0037 (Online)
DOI: http://dx.doi.org/10.15666/aeer/1605_57995813
© 2018, ALÖKI Kft., Budapest, Hungary

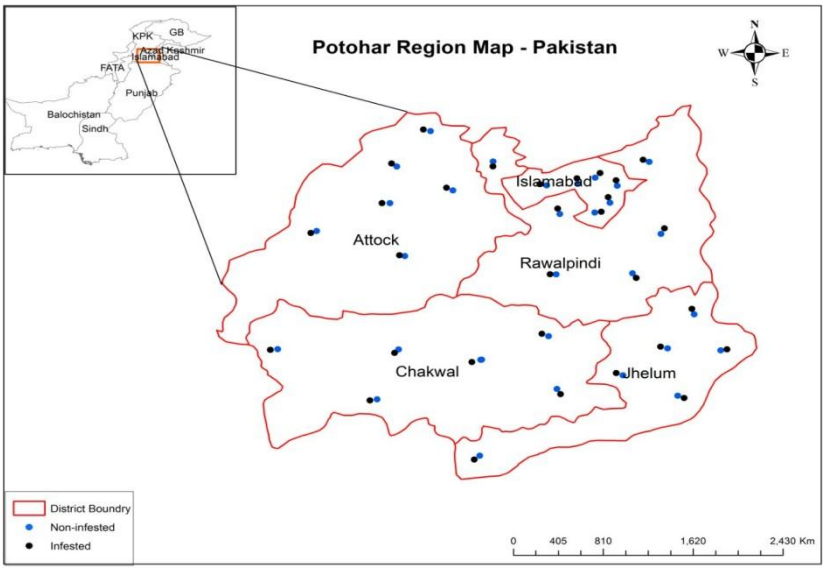

Figure 3. *Distribution of plots for impact analysis of Parthenium hysterophorus in Pothwar region*

Data analyses

Species frequency data were created and invasion impacts of *P. hysterophorus* on local flora were assessed by calculating and comparing ecological indices including Margalef's index of richness, Shannon–Weaver index of diversity, Simpson index of dominance and index of evenness for control and invaded sites (Magurran, 1998). These parameters were calculated as (*Eqs. 1, 2, 3* and *4*):

$$\text{Margalef's index of richness (R)} = \frac{S-1}{\ln N} \quad \text{(Eq.1)}$$

N = Total number of individuals; S = Total number of species.

$$\text{Shannon-Weaver index of diversity } (H') = -\sum_{i=1}^{S}\left(\frac{n_i}{N} \times ln\frac{n_i}{N}\right) \quad \text{(Eq.2)}$$

N = Total number of individuals of all species; n = Actual number of individuals of one species.

$$\text{Simpson index of dominance } (\lambda) = 1 - \frac{\sum_{i=1}^{S} n_i(n_i-1)}{N(N-1)} \quad \text{(Eq.3)}$$

N = Total number of individuals of all species; n = Number of individuals of one species.

$$\text{Index of evenness } (E) = \frac{H'}{lnS} \quad \text{(Eq.4)}$$

H' is Shannon's index; S = Number of species.

http://www.aloki.hu ● ISSN 1589 1623 (Print) ● ISSN 1785 0037 (Online)
DOI: http://dx.doi.org/10.15666/aeer/1605_57995813
© 2018, ALÖKI Kft., Budapest, Hungary

Rarefaction curves were plotted to determine if sampling was adequate in each district using observed, Coleman's, Jackknife, Bootstrap and Chao2 models in PRIMER v. 7 (Clarke and Warwick, 2001). All gave comparable results; consequently only that of real (observed) data are presented. Data were then subjected to univariate and multivariate analyses of non-metric multidimensional scaling procedure (Clarke and Gorley, 2015). Data were log transformed to achieve criteria of normality (evenness and Simpson index of diversity). For invasion impact analysis, diversity indices including total number of species (S), abundance (N), species richness (R), species evenness (J'), Shannon index of diversity (H′) and Simpson index of dominance (λ) were calculated for control as well as for invaded plots. The above ecological indices were subjected to analysis of variance (ANOVA) with invasion status and districts as factors using IBM SPSS v. 21. Differences between ecological indices for five districts were individually tested for significance between invaded and control plots by multiple comparisons tests of t-test. Data were further analyzed for species assemblages by non-metric multidimensional scaling (nMDS) in two-three dimensions with invasion status (control, invaded) as factor using PRIMER V.7 software. nMDS was used to ordinate the similarity of data between site categories (invaded, control) based on Bray-Curtis dissimilarity matrix following log-transformation of species abundance data due to zero species count in some plots. The range of clustering of sites and locations in response to invasion were assessed by analysis of similarity (ANOSIM) and similarity percentage (SIMPER). ANOSIM relates mean difference of ranks between and within groups, generating the Global statistic (R). The values of Global statistic (R) range from -1 to +1. Values near 0 and negative values demonstrate similarity among groups. Values impending +1 indicate a strong dissimilarity among groups (Clarke and Warwick, 2001; Osunkoya et al., 2017). SIMPER identified species contributed most to average dissimilarity between groups (invaded and control plots). This technique calculates average impact of each species contributing to dissimilarity between groups (Clarke and Warwick, 2001). Values of percentage similarity between groups range between 0 to 100, with 100 stating maximum similarity.

Results

To assess sampling completeness, rarefaction curves plotting cumulative number of species as a function of sampling effort were used which indicated that sampling was reasonably complete (*Fig. 4*). A total of 56 plant species from 50 genera were documented during the study (*Table 2*). A total of 56 species were recorded in control plots compared with 37 in infested plots. Mean species diversity and richness/quadrat was higher in control plots (*Fig. 5*).

Table 2. *Plant species found in studied plots, family and life form*

S#	Plant species	Family	Life form
1	*Achyranthes aspera* L.	Amaranthaceae	Herb
2	*Anagallis arvensis* L.	Primulaceae	Herb
3	*Argemone mexicana* L.	Papaveraceae	Herb
4	*Amaranthus viridis* L.	Amaranthaceae	Herb
5	*Astragalus scorplurus* Bunge.	Papilionaceae	Herb
6	*Bellis perennis* L.	Asteraceae	Herb
7	*Broussonetia papyrifera* (L.) L'Herit. ex Vent.	Moraceae	Tree

http://www.aloki.hu ● ISSN 1589 1623 (Print) ● ISSN 1785 0037 (Online)
DOI: http://dx.doi.org/10.15666/aeer/1605_57995813
© 2018, ALÖKI Kft., Budapest, Hungary

S#	Plant species	Family	Life form
8	*Calotropis procera* Br.	Asclepiadaceae	Shrub
9	*Cannabis sativa* L.	Cannabaceae	Herb
10	*Cenchrus biflorus* Roxb.	Poaceae	Grass
11	*Chenopodium ambrosioides* L.	Chenopodiaceae	Herb
12	*Circium arvense* L.	Asteraceae	Herb
13	*Convolvulus arvensis* L.	Convolvulaceae	Herb
14	*Cynodon dactylon* L. (Pers.)	Poaceae	Grass
15	*Datura alba* Nees	Solanaceae	Shrub
16	*Datura innoxia* Miller	Solanaceae	Shrub
17	*Dicanthium annulatum* Stapf.	Poaceae	Grass
18	*Digitaria ciliaris* (Retz.) Koeler	Poaceae	Grass
19	*Erianthus munja* L.	Poaceae	Grass
20	*Fumaria indica* (Hausskn.) Pugsley	Fumariaceae	Herb
21	*Impatiens edgeworthii* Hook. f.	Balsaminaceae	Herb
22	*Lathyrus aphaca* L.	Papilionaceae	Herb
23	*Malvestrum coromandelianum* (L.) Garcke	Malvaceae	Herb
24	*Medicago polymorpha* L.	Papilionaceae	Herb
25	*Poa annua* L.	Poaceae	Grass
26	*Portulaca oleracea* L.	Aizoaceae	Herb
27	*Prosopis cineraria* (Linn.) Druce	Mimosaceae	Tree
28	*Prunella vulgaris* L.	Labiateae	Herb
29	*Ranunculus muricatus* L.	Ranunculaceae	Herb
30	*Ricinus communis* L.	Euphorbiaceae	Shrub
31	*Rosa brunonii* Lindl.	Rosaceae	Shrub
32	*Rosa damascena* Mill.	Rosaceae	Shrub
33	*Rumex hastatus* D. Don	Polygonaceae	Shrub
34	*Rumex dentatus* L.	Polygonaceae	Herb
35	*Saxifragra androsacea* L.	Saxifragaceae	Herb
36	*Silybum marianum* (L.) Gaertn.	Asteraceae	Herb
37	*Solanum incanum* L.	Solanaceae	Shrub
38	*Solanum miniatum* Beruh. ex Willd.	Solanaceae	Herb
39	*Solanum surattense* Burm. F.	Solanaceae	Shrub
40	*Solanum nigrum* L.	Solanaceae	Herb
41	*Sonchus asper* (L.) Hill	Asteraceae	Herb
42	*Sorghum halepense* L.	Poaceae	Grass
43	*Suaeda fruticosa* Forsk.	Amaranthaceae	Shrub
44	*Swertia paniculata* Wall.	Gentianaceae	Herb
45	*Taraxacum officinale* (L.) Weber ex F.H. Wigg	Asteraceae	Herb
46	*Tamarix aphylla* (L.) Karst.	Tamaricaceae	Tree
47	*Tephrosia purpurea* (Linn.) Pers.	Papilionaceae	Herb
48	*Tinospora cordifolia* Miers ex Hook. f	Menispermaceae	Herb
49	*Tribulus terrestris* L.	Zygophyllaceae	Herb
50	*Urtica dioica* L.	Urticaceae	Herb
51	*Withania somnifera* L. (Dunal)	Solanaceae	Shrub
52	*Zizyphus mauritiana* Lamk.	Rhamnaceae	Shrub
53	*Capsella bursa-pestoris* (L.) Medik.	Brassicaceae	Herb
54	*Cyperus rotundus* L.	Cyperaceae	Sedge
55	*Polygonum plabegem* R. Br.	Polygonaceae	Herb
56	*Eclipta prostata* L.	Asteraceae	Herb

http://www.aloki.hu ● ISSN 1589 1623 (Print) ● ISSN 1785 0037 (Online)
DOI: http://dx.doi.org/10.15666/aeer/1605_57995813
© 2018, ALÖKI Kft., Budapest, Hungary

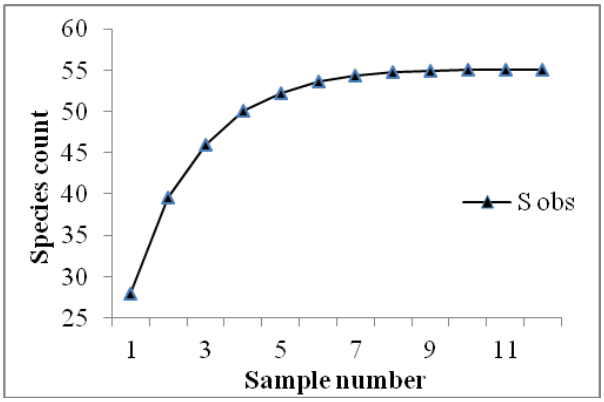

Figure 4. *Rarefaction curve showing cumulative number of species recorded as a function of sampling effort*

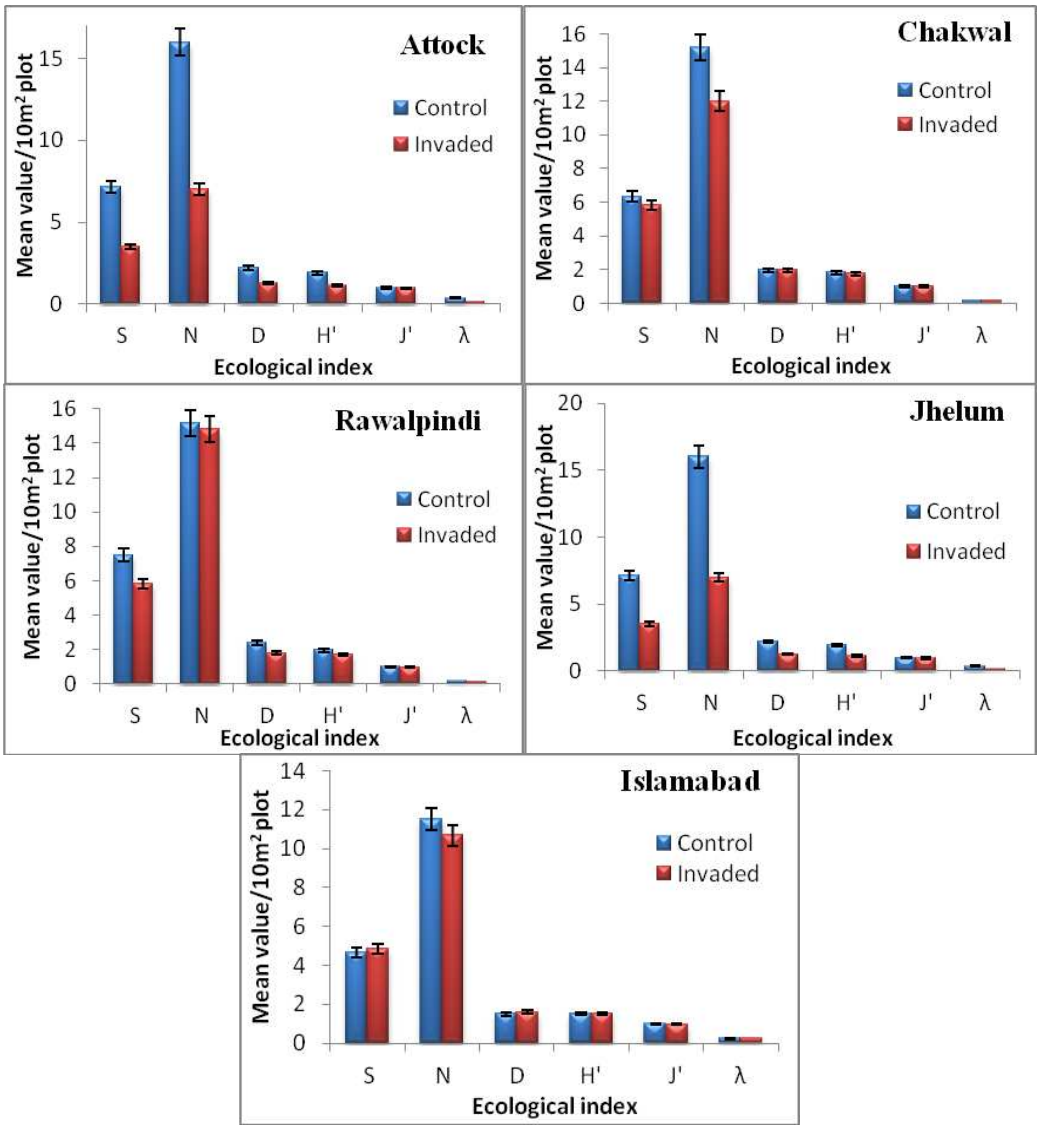

Figure 5. *Mean values/10 m^2 for ecological indices of invaded vs control plots in different sites. (S = Number of species; N = Abundance; D = Species richness; H' = Shannon index of diversity; J' = Species evenness; λ = Simpson index of dominance)*

http://www.aloki.hu ● ISSN 1589 1623 (Print) ● ISSN 1785 0037 (Online)
DOI: http://dx.doi.org/10.15666/aeer/1605_57995813
© 2018, ALÖKI Kft., Budapest, Hungary

Comparisons of ecological indices showed significant difference across districts and invasion status. *Parthenium* invasion exhibited variable impact across five districts by reducing species number per plot (S) and abundance (N) up to a maximum of 40% in Attock. Control plots harbored on average 6.033 ± 1.75 (mean ± SD, n = 30) species. This was greater than that observed in the invaded plots (5.133 ± 1.83) and the difference was statistically significant (t = 2.09, df = 29, p = 0.045). A total of 181 and 154 individuals were recorded in control and invaded plots respectively. Similarly, abundance in control and invaded plots differed by 3.7 ± 3.83 (mean±SD, n = 30) and the difference was significant (t = 4.34, df = 29, p < 0.0001). Control plots also exhibited higher values of species richness by a difference of 0.15 ± 0.51, species evenness by 0.019 ± 0.02; Shannon index of diversity by 0.2 ± 0.34 and Simpson index of dominance by 0.22 ± 0.35 (*Table 3*).

Table 3. *Analysis of variance (ANOVA) of invasion impacts and district on diversity indices of local plant community*

Ecological index	SUMMARY ANOVA			Mean (±SD)	
	District (D)	Invasion status (IS)	D×IS interaction	Control (30)	Invaded (30)
No. of species (S)/10 m^2	**	**	***	6.033±1.75	5.133±1.83
Abundance (N)/10 m^2	**	***	**	14.4±3.81	10.70±3.86
Species richness (R)	**	NS	***	1.87±0.49	1.62±0.53
Species evenness (J')	NS	**	NS	0.028±0.039	0.009±0.006
Shannon index of diversity (H')	**	**	***	1.73±0.29	1.53±0.406
Simpson index of dominance (λ)	**	**	***	1.72±0.29	1.50±0.42

***P ≤ 0.001; **P ≤ 0.02; *P ≤ 0.05; NS (not significant) P > 0.05

For individual district, native flora differed significantly in species density (S), abundance per plot (N), species evenness (J') and Simpson index of dominance (λ) but not in overall species richness (R) and Shannon index of diversity (H'). *Parthenium* invasion had significant impacts on all ecological indices except species richness (R) at site 1 (Attock). For site 2 (Chakwal), only abundance was affected significantly. For site 3 (Islamabad) invasion impacts were not significant only on native species abundance. Species evenness (J') was non-significant for site 4 (Jhelum) while for site 5 (Rawalpindi) the only index significantly affected by *Parthenium* invasion was species evenness (J') (*Table 4*).

Table 4. *Student's t-test for significance of differences between control and invaded plots at different sites*

Site	Number of species (S)	Abundance (N)	Species richness (D)	Species evenness (J')	Shannon index of diversity (H')	Simpson index of dominance (λ)
Attock	*	**	NS	*	**	*
Chakwal	NS	*	NS	NS	NS	NS
Rawalpindi	**	NS	**	**	**	**
Jhelum	***	**	**	NS	**	**
Islamabad	NS	NS	NS	***	NS	NS

***P ≤ 0.001; **P ≤ 0.02; *P ≤ 0.05; NS (not significant) P > 0.05

http://www.aloki.hu ● ISSN 1589 1623 (Print) ● ISSN 1785 0037 (Online)
DOI: http://dx.doi.org/10.15666/aeer/1605_57995813
© 2018, ALÖKI Kft., Budapest, Hungary

The ordination (nMDS) and ANOSIM showed significant magnitude of differences between species composition of invaded and control plots in all sites with global R values of 0.876 (p = 0.002), 0.519 (p = 0.002), 0.598 (p = 0.002), 0.907 (p = 0.002) and 0.759 (p = 0.002) for Attock, Chakwal, Islamabad, Jhelum and Rawalpindi, respectively (*Fig. 6*). The greatest dissimilarity between invaded and control plots was noticed by Jhelum.

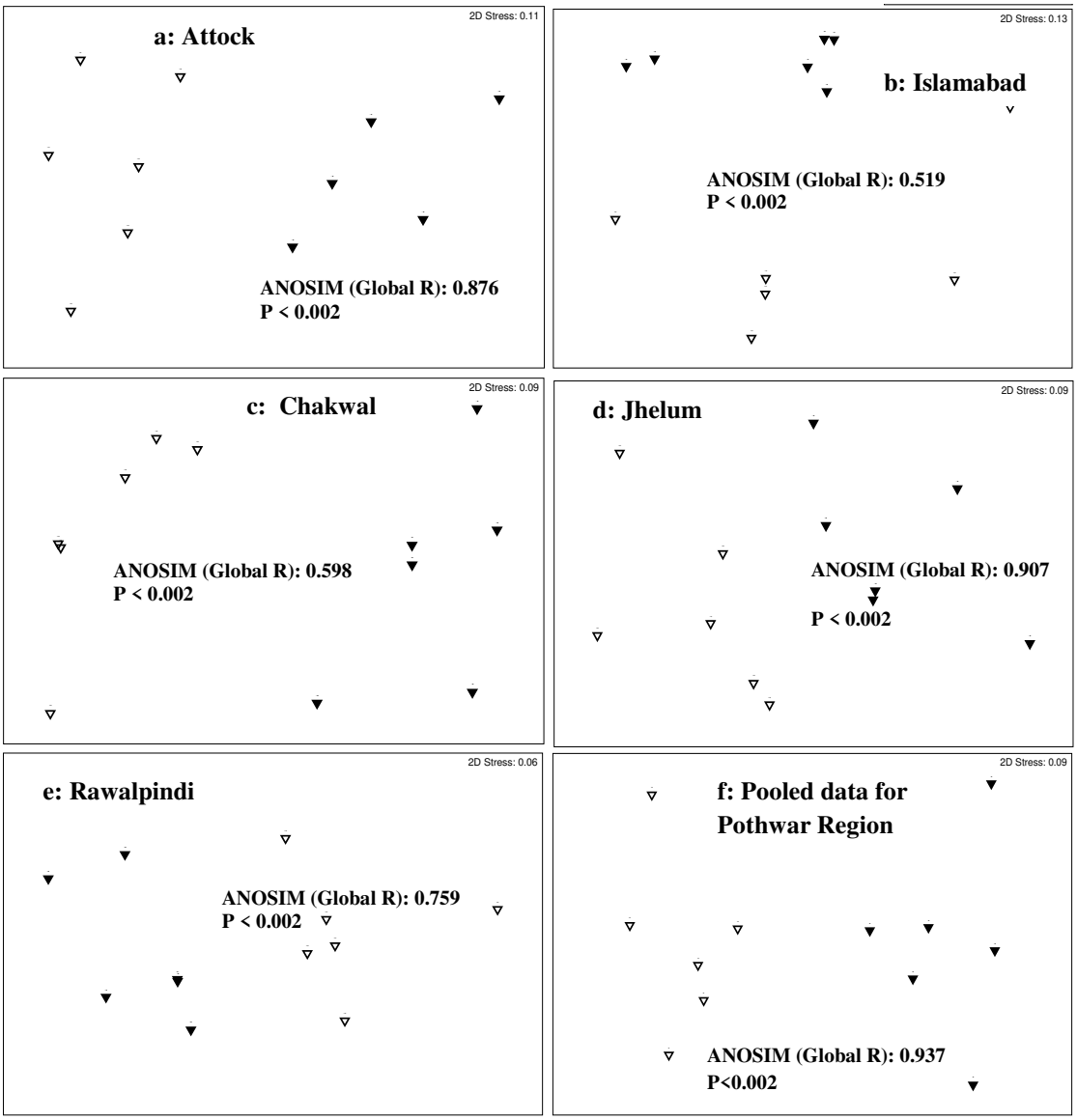

Figure 6. *Multidimensional scaling (MDS) ordination and analyses of similarity (ANOSIM) results of invasion status data for Pothwar region, Pakistan (open symbols are for control, uninvaded plots, and closed symbols are for invaded plots)*

Similarity percentage (SIMPER) analysis of data suggested those species contributing most to average dissimilarity between control and invaded groups. This analysis also computed average contribution of species causing dissimilarity. Few top species separating invaded plots from non-invaded plots (control) for analysis are enlisted in *Table 5*. *Tephrosia purpurea* and *Lathyrus aphaca* were found in control

http://www.aloki.hu ● ISSN 1589 1623 (Print) ● ISSN 1785 0037 (Online)
DOI: http://dx.doi.org/10.15666/aeer/1605_57995813
© 2018, ALÖKI Kft., Budapest, Hungary

plots while they were not observed in invaded plots, whereas a grass species (*Poa annua*), and broad leaf species like *Solanum, Ricinus* and *Taraxacum* were conspicuously displaced in *Parthenium* invaded plots.

Table 5. *SIPMER analysis of Parthenium invaded and control sites in Pothwar region, Pakistan. Data have been pooled prior to analyses across districts*

Average dissimilarity = 60.14%					
	Average abundance				
Species	**Control**	**Invaded**	**Av. Diss.**	**Diss./SD**	**Contribution (%)**
Poa annua L.	2.94	0.00	2.38	8.06	3.95
Lathyrus aphaca L.	0.00	2.69	2.18	5.82	3.63
Solanum miniatum L.	2.47	0.00	2.00	7.85	3.32
Ricinus communis L.	2.19	0.00	1.77	2.05	2.95
Convolvulus arvensis L.	1.80	1.79	1.49	1.32	2.48
Taraxacum officinale (L.) Weber ex F.H. Wigg	1.77	0.00	1.40	2.07	2.32
Rosa *damascena* Mill.	1.82	0.18	1.38	1.41	2.29
Tribulus terrestris L.	1.62	0.00	1.31	2.03	2.18
Fumaria indica (Hausskn.) Pugsley	2.35	1.15	1.31	1.55	2.18
Tephrosia purpurea (L.) Pers.	0.00	1.63	1.29	1.36	2.15
Portulaca oleracea L.	1.94	1.10	1.26	2.37	2.10
Circium arvense L.	1.63	0.00	1.25	1.69	2.08
Saxifragara sndrosacea L.	1.73	0.54	1.24	1.51	2.06
Anagallis arvensis L.	2.67	1.49	1.24	1.24	2.06
Tinospora cordifolia Miers ex Hook. f.	1.52	0.00	1.23	1.90	2.04
Solanum nigrum L.	1.87	0.86	1.21	1.92	2.02
Saxifragra androsacea L.	1.51	0.00	1.19	1.34	1.97
Tamarix aphylla (L.) Karst.	1.39	0.40	1.15	0.96	1.91
Solanum incanum L.	1.74	1.04	1.12	1.56	1.87
Eclipta prostata L.	1.95	1.02	1.12	1.25	1.86

Values are average abundance ranking (1-rare; 2-common; 3-very common; >4-dominant)

Discussion

Parthenium weed exerts significant impact on natural communities by displacement of native species and hence exert discrepancy in natural ecosystems. This discrepancy results in formation of its large monocultures. In present study, comparisons of ecological indices across invaded and control plots indicated significant differences in the study area. These findings are in-line with other studies on this alien invasive weed, in which indicated strong effects of the invader on ecosystem properties, e.g., in grazing and wastelands of district Attock (Riaz and Javaid, 2011), district Hafizabad, (Riaz and Javaid, 2010) and Islamabad, Pakistan (Shabbir and Bajwa, 2007).

The results show modifications in vegetation composition of invaded and control plots. Analysis of variance among invaded and control plots showed significant decrease in ecological indices across site and invasion status. These results are consistent with other studies on invasive species indicating their negative effects on bio-diversity and ecosystem properties (Manchester, 2000; McNeely, 2001; Grice, 2006;

http://www.aloki.hu ● ISSN 1589 1623 (Print) ● ISSN 1785 0037 (Online)
DOI: http://dx.doi.org/10.15666/aeer/1605_57995813
© 2018, ALÖKI Kft., Budapest, Hungary

Borokini et al., 2011; Jeschke et al., 2014; Panetta and Gooden, 2017). In our study, despite the negative effect of *P. hysterophorus* on species composition, species evenness of control and invaded plots was not significantly different. That is contradiction to above-mentioned studies; however, a few studies have shown that invasive species pose little or no effect on species diversity (e.g., Martin, 1999; Hejda and Pysek, 2006; Timsina et al., 2011). It is reported elsewhere that *Parthenium* invasion enriches compositional diversity but may result in extinction of native species (Nigatu and Sharma, 2013).

Wide environmental adaptability, drought tolerance, photo and thermo-insensitivity, high seed production and short life cycle (being an annual), small and light seeds capable of long distance travel via water, wind, birds, animals and vehicles, longevity of seeds in soil seed banks, strong competition and allelopathy contribute to the invasiveness of Parthenium weed (Shabbir and Bajwa, 2006; Hassan et al., 2012; Khan et al., 2014). Allelopathy especially plays important role in the invasion of this weed. The major allelopathic compounds found in *P. hysterophorus* are, gentisic, o-coumaric, p-coumaric, ferulic, vallinic, caffeic, salicylic acid, p-hydroxybenzoic and trans-cinammic acids and sesquiterpene lactone etc. (Borah et al., 2016). These allelochemicals are supposed to reduce native seed germination, allowing the weed to pre-empt space and establish monocultures.

Parthenium invasion exhibited variable impacts in five sites by reducing species number per plot (S), abundance (N), species richness (R), species evenness (J'), Simpson index of dominance (λ) and Shannon index of diversity (H'). The trend of decrease in ecological indices in invaded plots is similar to invasion studies on *P. hysterophorus* from Australia, Ethiopia, Nigeria, Tanzania and India (Grice, 2006; Kilewa and Rashid, 2012; Seta et al., 2013; Borokini et al., 2011; Abdulkerim-Ute and Legesse, 2016). The most effected site by *Parthenium* invasion was Jhelum followed by Attock, Rawalpindi, Chakwal and Islamabad. The lowest invasion impacts in Islamabad compared to other sites are probably because of management practices in the area being its importance as metropolitan region of Pakistan while highest dissimilarity in invaded and control plots in Jhelum is possibly due to the saline soil of the area (Anonymous, 2017).

The ordination (nMDS) and ANOSIM showed significant magnitude of differences between species assemblages of invaded and control plots. The difference was significant for all of five study sites but the greatest dissimilarity between invaded and control plots were noticed by Jhelum. It was reported that the *Parthenium* plant has a higher survival rate in higher level of soil salinity (Upadhyay et al., 2013), a condition inimical to establishment of many native plant species. Consequently the higher invasion impacts in Jhelum are possibly due to its saline soil (Anonymous, 2017).

SIMPER analysis showed dominance of fewer species in invaded plots than in control. These were *Tephrosia purpurea* and *Lathyrus aphaca.* Possible reason for their presence in invaded plot may be due to their aggressive nature as weeds in their own right. Perhaps higher contribution values of Fabaceae weeds is due to competition potential with *Parthenium* as suggested by Belachew and Tessema (2015); Gnanavel (2013). There is an urgent need of appropriate control measures including the use of proven biological control agents for this weed in Pakistan as done elsewhere around the globe/world, e.g., Australia and South Africa (Kaur et al., 2014; Strathie et al., 2011).

http://www.aloki.hu ● ISSN 1589 1623 (Print) ● ISSN 1785 0037 (Online)
DOI: http://dx.doi.org/10.15666/aeer/1605_57995813
© 2018, ALÖKI Kft., Budapest, Hungary

Conclusion

The increased occurrence of invasion around the world poses a major threat to indigenous diversity. Plant invasions in novel areas deplete species diversity, alter indigenous community composition, affect ecosystem processes and thus cause huge ecological and economic imbalance. Invasive species studied in the past revealed that the effects of invasion are complex and can permanently alter the function and structure of communities, cause local annihilations and changes in ecosystem processes. Invasion by alien plant species affect the composition and dynamics of species on a wide scale and have great impact on ecosystem functions. The decrease in ecological diversity indices in invaded over control sites in present study indicated that plant communities become less productive due to *Parthenium* invasion, hence it is a threat to plant diversity of invaded areas. There is an urgent need of appropriate control measures including the use of proven biological control agents for this weed in Pakistan.

Acknowledgements. Pakistan Meteorological Department University Road Karachi, Pakistan is acknowledged for providing climate data of Pothwar region, Pakistan.

REFERENCES

[1] Abdulkerim-Ute, J., Legesse, B. (2016): *Parthenium hysterophorus* L: Distribution, impact, and possible mitigation measures in Ethiopia. – Tropical and Subtropical Agroecosystems 19: 61-72.
[2] Anonymous (2017): https://en.wikipedia.org/wiki/Jhelum_District.
[3] Belachew, K., Tessema, T. (2015): Assessment of weed flora composition in Parthenium (*Parthenium hysterophorus* L.) infested area of East Shewa Zone, Ethiopia. – Malaysian Journal of Medical and Biological Research 2(1): 63-70.
[4] Borah, N., Rabha, D., Athokpam, F. D. (2016): Tree species diversity in tropical forests of Barak valley in Assam, India. – Tropical Plant Research 3(1): 01-09.
[5] Borokini, T. I. (2011): Invasive alien plant species in Nigeria and their effects on biodiversity conservation. – Tropical Conservation Science 4(1): 103-110.
[6] Charles, H., Dukes, J. S. (2007): 13 Impacts of Invasive Species on Ecosystem Services. – Ecological Studies, Ecological Studies 193: 217-237.
[7] Clarke, K. R., Gorley, R. N. (2015): PRIMER V7: user manual/tutorial. – Plymouth Marine Laboratory, Plymouth.
[8] Clarke, K. R., Warwick, R. M. (2001): Change in marine communities: an approach to statistical analyses and interpretation, 2nd ed. – PRIMER-E, Plymouth.
[9] Collier, M. H., Vankat, J. L. (2002): Diminished plant richness and abundance below *Lonicera maackii*, an invasive shrub. – The American Midland Naturalist 147: 60-71.
[10] Dassonville, N., Vanderhoeven, S., Vanparys, V., Hayez, M., Gruber, W., Meerts, P. (2008): Impacts of alien invasive plants on soil nutrients are correlated with initial site conditions in NW Europe. – Oecologia 157: 131-140.
[11] Dogra, K. S., Sood, S. K., Dobhal, P. K., Sharma, S. (2010): Alien plant invasion and their impact on indigenous species diversity at global scale: A review. – Journal of Ecology and the Natural Environment 2: 175-186.
[12] Ghufran, M. A., Hamid, N., Ali, A., Ali, S. M. (2013): Prevalence of allergenic pollen grains in the city of Islamabad, Pakistan and its impact on human health. – Pakistan Journal of Botany 45: 1387-1390.
[13] Gnanavel, I. (2013): *Parthenium hysterophorus* L.: A major threat to natural and agro eco-systems in India. – Science International 1(5): 124-131.

http://www.aloki.hu ● ISSN 1589 1623 (Print) ● ISSN 1785 0037 (Online)
DOI: http://dx.doi.org/10.15666/aeer/1605_57995813
© 2018, ALÖKI Kft., Budapest, Hungary

[14] Grice, A. C. (2006): The impacts of invasive plant species on the biodiversity of Australian rangelands. – The Rangeland Journal 28: 27-35.
[15] Hassan, G., Marwat, K. B., Ali, S., Munir, M., Khaliq, P. (2012): *Parthenium hysterophorus* L. - A predominant weed flora among phytosociology of Islamabad, Pakistan. – Pakistan Journal of Weed Science Research 18: 149-156.
[16] Hejda, M., Pysek, P. (2006): What is the impact of *Impatiens glandulifera* on species diversity of invaded riparian vegetation? – Biological Conservation 132: 143-152.
[17] Hejda, M., Pysek, P., Jarosik, V. (2009): Impact of invasive plants on the species richness, diversity and composition of invaded communities. – Journal of Ecology 97: 393-403.
[18] Jeschke, J. M., Bacher, S., Blackburn, T. M., Dick, J. T. A., Essl, F., Evans, T., Gaertner, M., Hulme, P. E., Kuhn, I., Mrugala, A., Pergl, J., Pysek, P., Rabitsch, W., Ricciardi, A., Richardson, D. M., Sendek, A., Vila, M., Winter, M., Kumschick, S. (2014): Defining the impact of non-native species. – Conservation Biology 28(5): 1188-1194.
[19] Kaur, M., Aggarwal, N. K., Kumar, V., Dhiman, R. (2014): Effects and management of *Parthenium hysterophorus*: A weed of global significance. – International Scholarly Research Notices. http://dx.doi.org/10.1155/2014/368647.
[20] Khan, H., Marwat, K. B., Hassan, G., Khan, M. A., Hashim, S. (2014): Distribution of *Parthenium* weed in Peshawar valley, Khyber Pakhtunkhwa-Pakistan. – Pakistan Journal of Botany 46: 81-90.
[21] Kilewa, R., Rashid, A. (2012): Distribution of invasive weed *Parthenium hysterophorus* in natural and Agro-Ecosystems in Arusha Tanzania. – International Journal of Science and Research 3(12): 1724-1727.
[22] Kunzi, Y., Prati, D., Fischer, M., Bloch, S. (2015): Reduction of native diversity by invasive plants depends on habitat conditions. – American Journal of Plant Sciences 6: 2718-2733.
[23] Manchester, J. S., Bullock, J. M. (2000): The impacts of non-native species on UK biodiversity and the effectiveness of control. – Journal of Applied Ecology 37: 845-864.
[24] Magurran, A. E. (1988): Ecological diversity and its measurement. – Princeton University Press, Princeton, NJ.
[25] Martin, P. H. (1999): Norway maple *Acer platanoides* invasion of a natural forest stand, understory consequence and regeneration pattern. – Biological Invasions 1: 215-222.
[26] McNeely, J. (2001): Invasive species: a costly catastrophe for native biodiversity. – Land Use and Water Resources Research 2: 1-10.
[27] Nath, R. (1988): *Parthenium hysterophorus* L. A review. – Agricultural Reviews 9: 171-179.
[28] Nigatu, L., Sharma, J. J. (2013): *Parthenium* weed invasion and biodiversity loss in Ethiopia: A literature review. – African Crop Science Conference Proceedings 11: 377-381.
[29] Odat, N., Al-Khateeb, W., Muhaidat, R., Al U'datt, M., Irshiad, L. (2011): The effect of exotic *Acacia saligna* tree on plant biodiversity of Northern Jordan. – International Journal of Agriculture and Biology 13: 823-826.
[30] Osunkoya, O. O., Akinsanmi, O. A., Lim, L. S. A., Perrett, C., Callander, J., Dhileepan, K. (2017): *Parthenium hysterophorus* L. (Asteraceae) invasion had limited impact on major soil nutrients and enzyme activity: Is the null effect real or reflects data insensitivity? – Plant Soil. https://doi.org/10.1007/s11104-017-3375-x.
[31] Panetta, F. D., Gooden, B. (2017): Managing for biodiversity: impact and action thresholds for invasive plants in natural ecosystems. – NeoBiota 34: 53-66.
[32] Pimente, L. D., Zuniga, R., Morrison, D. (2005): Update on the environmental and economic costs associated with alien-invasive species in the United States. – Ecological Economics 52: 273- 288.
[33] Qureshi, H., Arshad, M., Bibi, Y. (2014): Invasive flora of Pakistan: A critical analysis. – International Journal of Biosciences 4: 407-424.

http://www.aloki.hu ● ISSN 1589 1623 (Print) ● ISSN 1785 0037 (Online)
DOI: http://dx.doi.org/10.15666/aeer/1605_57995813
© 2018, ALÖKI Kft., Budapest, Hungary

[34] Rashid, K., Rasul, G. (2011): Rainfall variability and Maize production over the Potohar Plateau of Pakistan. – Pakistan Journal of Meteorology 8: 63-74.
[35] Razaq, Z. A., Vahidy, A. A., Ali, S. I. (1994): Chromosome numbers in Compositae from Pakistan. – Annals of the Missouri Botanical Garden 81: 800-808.
[36] Riaz, T., Javaid, A. (2010): Prevalence of invasive *Parthenium* weed in District Hafizabad, Pakistan. – The Journal of Animal and Plant Sciences 20(2): 90-93.
[37] Riaz, T., Javaid, A. (2011): Prevalence of alien weed *Parthenium hysterophorus* L. in grazing and wastelands of district Attock, Pakistan. – The Journal of Animal and Plant Sciences 21(3): 542-545.
[38] Seta, T., Assefa, A., Mesfin, F., Balcha, A. (2013): Distribution status and the impact of Parthenium weed (*Parthenium hysterophorus* L.) at Gedeo Zone (Southern Ethiopia). – African Journal of Agricultural Research 8(4): 386-397.
[39] Shabbir, A. (2013): *Parthenium* invasion in Rawalpindi, Pakistan. – Indian Journal of Weed Science 45: 263-266.
[40] Shabbir, A., Bajwa, R. (2006): Distribution of *Parthenium* weed (*Parthenium hysterophorus* L.): An alien invasive weed species threatening the biodiversity of Islamabad. – Weed Biology and Management 6: 89-95.
[41] Shabbir, A., Bajwa, R. (2007): *Parthenium* invasion in Pakistan. A threat still unrecognized. – Pakistan Journal of Botany 39(7): 2519-2526.
[42] Shabbir, A., Dhileepan, K., Adkins, S. W. (2012): Spread of *Parthenium* weed and its biological control agent in the Punjab, Pakistan. – Pakistan Journal of Weed Science Research 18: 581-588.
[43] Strathie, L. W., McConnachie, A. J., Retief, E. (2011): Initiation of biological control against *Parthenium hysterophorus* L. (Asteraceae) in South Africa. – African Entomology 19(2): 378-392.
[44] Tamado, T., Milberg, P. (2000): Weed flora in arable fields of eastern Ethiopia with emphasis on the occurrence of *Parthenium hysterophorus*. – Weed Research 40: 507-521.
[45] Timsina, B., Shrestha, B. B., Rokaya, M. B., Münzbergová, Z. (2011): Impact of *Parthenium hysterophorus* L. invasion on plant species composition and soil properties of grassland communities in Nepal. – Flora 206(3): 233-240.
[46] Upadhyay, S. K., Ahmad, M., Singh, A. (2013): Ecological impacts of weed (*Parthenium hysterophorus* L.) invasion in saline soil. – International Journal of Scientific and Research Publications 3(4): 1-4.

http://www.aloki.hu ● ISSN 1589 1623 (Print) ● ISSN 1785 0037 (Online)
DOI: http://dx.doi.org/10.15666/aeer/1605_57995813
© 2018, ALÖKI Kft., Budapest, Hungary

THE EFFECT OF LAND TYPES AND CONSEQUENTLY LAND USE ON SOIL ORGANIC CARBON CONTENT – CASE STUDY: DAMAVAND REGION OF IRAN

DADGAR, M.

Department of Soil Sciences, Roudehen Branch, Islamic Azad University, Tehran, Iran
(e-mail: maryam.dadgar2008@gmail.com; phone:+98-912-630-2981)

(Received 29th Apr 2018; accepted 5th Jul 2018)

Abstract. Organic carbon is an important component of soil that influences soil fertility, biological activity, food security, and climate change. One of the important issues in soil science is the establishment of empirical relationships between different soil properties. The objectives of this research were to investigate the influence of different factors on soil organic carbon, such as total nitrogen, clay content, calcium carbonate equivalent and pH, for soils from various geomorphologic settings in the Damavand Region in Northwest Tehran, Iran. Regression models were developed for prediction of the organic carbon content of soils characteristics in this region. Lower SOC concentrations were measured for plateau soils (~4.92 g kg^{-1}), associated with lower plant biomass and reduced temperatures at higher elevations. In contrast, soils from River Alluvial Plain regions, which are currently utilized for gardening, had the highest organic carbon content (~22.05 g kg^{-1}). For all landform types (i.e., alluvial fan (irrigated farming lands), plateau (Rangeland), and River Alluvial Plain soils (garden)), SOC had positive and significant relationship with total nitrogen ($r = 0.962$, $p < 0.01$). Simple linear regression, multiple linear regression, and nonlinear regression models were also developed for describing the relationship between SOC and landforms physical and chemical characteristics.
Keywords: *physiographic characteristics, regression models, soil properties*

Introduction

Current investigation attempted to enhance the amount of organic carbon captured in soils. Organic matter is one of the most important indicators of soil quality. Recent efforts have been made to increase the carbon storage capacity of soils, having a positive effect on biological activity, fertility and productivity (Baldock et al., 2010). The sequestration of carbon in soil has the potential to offset greenhouse gas emissions (i.e., CO_2, CH_4, and N_2O) associated with climate change (Xun et al., 2010). Practical methods to increase carbon sequestration of particular research were developed. This requires an understanding of the influence of different land-management practices (e.g., tillage) on soil organic carbon (SOC) (Gaiser et al., 2008), which is complicated by the fact that SOC is affected by climate, soil type, vegetation type, topography and land drainage, as well as land management practice (Gami et al., 2009).

Zhao et al. (2017) researched the impact of shifts in land use on SOC in an agro-pastoral ecotone of Inner Mongolia. Li et al. (2016) estimated the impact of land use change on SOC sequestration in China from 1985 to 2005. However, the effect of shifts in land use on carbon budget in China's arid and semi-arid regions, such as the Shiyang River Basin, has received little attention, which limits our understanding of the mechanisms by which land use change affects the carbon cycle. Poeplau and Don (2015) showed that planting cover crops during winter and tilling them into the soil as additional carbon input can significantly enhance soil C on croplands.

It is important to identify the relationships between SOC and landscape features and to assess the amount and spatial variability of carbon storage in soils. Physiographic

http://www.aloki.hu ● ISSN 1589 1623 (Print) ● ISSN 1785 0037 (Online)
DOI: http://dx.doi.org/10.15666/aeer/1605_58155824
© 2018, ALÖKI Kft., Budapest, Hungary

characteristics such as altitude, slope and aspect have an influence on the efficiency of carbon sequestration in different regions. Wang et al. (2010) showed that landscape characteristics influenced SOC. They measured lowest organic carbon accumulation in elevated areas and identified a significant negative relationship between SOC and elevation ($r = –0.429^{**}$). The same relationship also found a significant negative correlation between SOC and slope ($r = –0.195^{**}$).

Heidari et al. (2010) suggested that the highest levels of carbon are found in areas that have moderate rainfall and low elevation. These factors are unaffected by human activities (i.e., tillage), and have suitable climatic conditions (i.e., temperature and precipitation) so that the growth period is not limited. While the ability to estimate carbon sequestration in a wide range of environments is essential, this has been limited by the complexities of soil characteristics and environmental conditions (Padilla et al., 2010).

Topography is one of the most important factors affecting the amount of organic carbon in soils, but this is not a simple relationship. For example, Senthilkumar et al. (2009) found that the influence of topography on organic carbon storage varied between different agricultural systems. This was attributed to the accumulation of plant residues that affect SOC content in the uppermost 0–30 cm depth of the soil. Soil organic carbon also varies with slope, due the influence of leaching, soil erosion, vegetation, and other physical properties such as soil texture (Boulal and Macpherson, 2010).

Geostatistical methods provide a way of studying and predicting the spatial variability of SOC based on relationships with other soil properties and landscape characteristics (Zhang and McGrath, 2004). These relationships can be expressed as regression models (Vasques et al., 2010), developed using parameters that measured in the field, or for which data already exist (Sarmadian et al., 2010). Motallebi et al. (2011) also estimated soil hydraulic properties (e.g., bulk density, calcium carbonate content, and sand–silt–clay fractions) for a semi-arid region using similar models. However, few studies have examined the spatial patterns of SOC and its relationship with the physiographic properties in semi-arid regions (Heidari et al., 2010; Parvizi et al., 2010).

The objectives of this research were to: (i) investigate the influence of physical and chemical characteristics (e.g., total nitrogen, equivalent calcium carbonates, clay content and pH) on SOC and (ii) develop regression models between SOC and different landform types in the Damavand Region of Tehran, Iran.

Materials and methods

Study area

The Damavand Region is located in northeast of Tehran in Iran (*Fig. 1*), covers about 6272 ha at 35°35’55”–35°40’37”N and 51°59’11”–52°11’33”E. The climate is predominantly dry and cold, with a mean annual precipitation of 322 mm and a mean annual temperature of 11.6 °C (1999–2010 data) (Climatic Data Center, 2010). Height above sea level varies between 1800 and 2200 m. The main landforms of the region are “alluvial fans, River Alluvial Plains, and plateaus” and soils classified as Entisols and Inceptisols using the USDA soil classification system (Keys to Soil Taxonomy, 2010).

A digital elevation model (DEM) of the region was developed in Arc-GIS from a topographic map (1:25,000 scale). Physiographic characteristics (slope, altitude, and aspect) were classified using the DEM, and landform units were subsequently

http://www.aloki.hu ● ISSN 1589 1623 (Print) ● ISSN 1785 0037 (Online)
DOI: http://dx.doi.org/10.15666/aeer/1605_58155824
© 2018, ALÖKI Kft., Budapest, Hungary

determined. Landform units were determined by overlaying the slope, hypsometric and aspect maps.

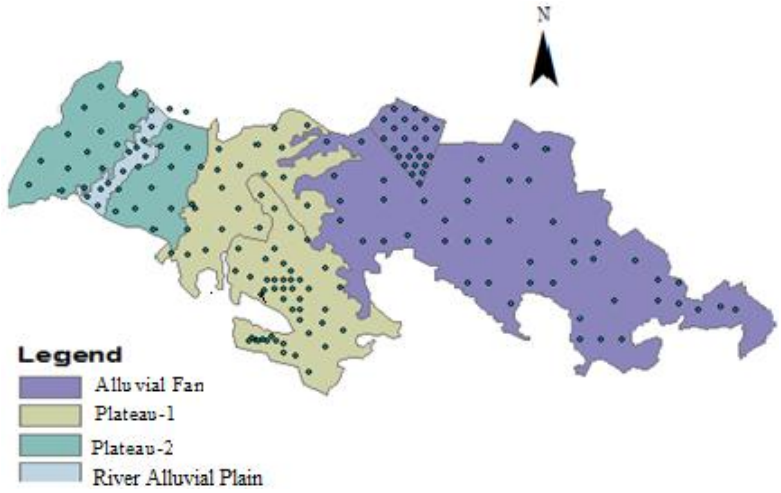

Figure 1. *Landform types and sampling sites in the Damavand Region of Tehran, Iran*

Dividing the slope according to the irrigation management division and determining the height adjustment according to the type of cover and management changes. Nine elevation classes (1820-1900 m, 1900-1950 m, 1950-1985 m, 1985-2020 m, 2020-2045 m, 2045-2075 m, 2075-2110 m, 2110-2150 m, 2150- 2200 m), four slope classes (0-5%, 5-12%, 12-25%, > 25%), and four aspects (north, south, west, east) were defined. ETM+ satellite images (from 2002), Indian Remote Sensing (IRS) satellite images (from 2007), and Moderate Resolution Imaging Spectroradiometer (MODIS) satellite images (from 2010) of the region were analyzed to delineate land type boundary from Rs and using GIS software. The use of remotely sensed data from satellite imagery or aerial photography has become commonplace in soil management studies (Karl and Maurer, 2010).

Soil sampling

Soil samples were collected from 0-25 cm soil depth, for each land unit. Sampling was done with a shovel of about 2 kg. Average slopes of alluvial fan 0-5% and clay loam texture, Plateau 1: average slopes 5-8% and silty clay loam texture, Plateau 2: average slopes 8-12% and sandy loam texture, River Alluvial Plains: average slopes 0-5% and loam texture. They were classified based on the relative area under each soil type, land use, slope, aspect, and elevation class. The plateau was divided into two groups due to the type of cover and management. The total number of 1607 sites was initially classified. According to the Minimum Decision Area (MDA) (*Eq. 1*), areas less than 10 ha were merged with neighbor polygons, reducing the number of sites by 160, as follows:

$$MDA(hac) = 1.6cm^2 \times 10^{-8}(hac.cm^2)(Scalefactor.mm^{-1}) \quad \text{(Eq.1)}$$

Sampling sites were located in the field using GPS in October 2010. At each sampling location, three separate points (approximately 10 m apart) was sampled at 0–

http://www.aloki.hu ● ISSN 1589 1623 (Print) ● ISSN 1785 0037 (Online)
DOI: http://dx.doi.org/10.15666/aeer/1605_58155824
© 2018, ALÖKI Kft., Budapest, Hungary

30 cm soil depth. These three individual samples were combined to form a single bulk sample for each site. Samples were sealed in plastic bags and transported to the laboratory. At each location, recorded the latitude longitude, landscape position, slope class, aspect, elevation, land cover, and land management practice.

Laboratory analysis

Soil samples were air-dried and sieved in the laboratory to retain the <2 mm fraction. Soil pH was measured in a 1:1 suspension of soil and distilled water (McLean, 1982). Soil texture was measured using hydrometer method (Bouyoucos, 1962). Soil organic carbon was determined using the Walkey–Black method (Walkley and Black, 1934). Bulk density (BD) was measured using standard paraffin wax procedures. (USDA, 1995). Total Nitrogen (TN) was determined using the Kjeldahl method (USDA, 1995). Calcium carbonate equivalent (T.N.V), was measured using the Acidimetric method, which involved neutralization of the sample by a titrated acid. Back-titration using a base that used to determine CaCO3 content (USDA, 1995). Particle size distribution was determined using the hydrometer method (Gee and Bauder, 1979).

Statistical analysis

Descriptive statistical parameters for SOC were determined, including the mean, median, skewness, kurtosis, standard deviation, variance, coefficients of variation, maximum and minimum. Pearson correlation coefficients (r) were estimated for all possible paired combinations of the response variables to generate a correlation coefficient matrix. Kolmogorov–Smirnov tests showed that the data were not normally distributed; consequently, non-parametric tests were used. The Kruskal–Wallis test was used to assess differences in SOC between land units (Mills and Cowling, 2010). Simple linear regression, multiple regression, and simple nonlinear regression methods of predicting SOC were assessed. The limiting stepwise regression was applied on the input variables to prevent internal regression.

The performance of the regression models were evaluated by cross validation, where estimated and observed values are compared at each of the observed value location. Reliability of the models evaluated with an independent dataset. Estimated and observed values were compared using two criteria: mean absolute error (MAE) and mean bias error (MBE) (*Eqs. 2* and *3*):

$$MAE = \frac{1}{n}\sum_{i=1}^{n}\left|z^*(x_i) - z(x_i)\right| \quad \text{(Eq.2)}$$

$$\mathrm{MBE} = \frac{1}{\mathrm{n}}\sum_{\mathrm{i}=1}^{\mathrm{n}}\left(\mathrm{z}^*(\mathrm{x_i}) - \mathrm{z}(\mathrm{x_i})\right) \quad \text{(Eq.3)}$$

where z*(xi) is the value to be estimated at the location of xi, z (xi) the known value at the sampling site xi and n is the number of sites.

Geostatistical analysis was also used to infer the spatial variation of SOC at each site. The spatial distribution of SOC was predicted by the IDW method. In this study, the geostatistical analyses were produced with GIS software ArcGIS (version 9.3).

http://www.aloki.hu ● ISSN 1589 1623 (Print) ● ISSN 1785 0037 (Online)
DOI: http://dx.doi.org/10.15666/aeer/1605_58155824
© 2018, ALÖKI Kft., Budapest, Hungary

Results

The results showed that there are significant differences of the Kruskal-Wallis ($p < 0.01$) test between soil organic carbon contents of the four land types (*Table 1*).

Table 1. *Comparing SOC among land forms ranks*

Landform-code	N	Mean rank
Alluvial fan (irrigated farming lands)	54	89.62
Plateau1 (dry farming)	56	66.29
Plateau2 (rangeland)	30	44.12
River alluvial plain (garden)	12	146.08
Total	152	

The highest SOC was measured in River Alluvial Plain soils (mean SOC = 22.04 g kg^{-1}), followed by alluvial fan soils (mean SOC = 7.75 g kg^{-1}), plateau 1 soils (mean SOC = 6.17 g kg^{-1}), and plateau 2 soils (SOC = 4.92 g kg^{-1}). The mean SOC value for the study area was 7.73 g kg^{-1} (*Table 2*).

Table 2. *Descriptive analysis of soil variables*

Parameter	Land type				
	Total area	Alluvial fan	Plateau 1	Plateau 2	River alluvial plain
Mean	7.74	7.750	6.170	4.920	22.05
Median	6.93	6.840	5.830	4.620	22.10
Variance	2.55	6.539	2.710	5.800	20.60
Std. deviation	5.05	2.980	1.650	2.410	4.54
Skewness	2.42	2.282	0.422	0.447	1.22
Kurtosis	6.57	6.539	-0.022	-0.684	2.56
Min	0.91	3.695	2.920	0.914	16.25
Max	33.16	20.222	10.210	9.250	33.16

To explain the spatial variability of SOC, the Inverse Distance Weighting (IDW) method was used. The organic carbon content was low for soils sampled from several sites in the study area, which was the main factor in their low fertility status. The distribution of organic carbon in the upper profile (0–30 cm) of soils is shown in *Figure 2*.

The results showed that soil organic carbon ranged from 0.1% to 3.2% (1–32 g kg^{-1}) in the study area. Organic carbon was very low in the some part of plateau with SOC < 4 g kg^{-1} and higher SOC > 16 g kg^{-1} in the all part of River Alluvial Plain.

The area under each land form had normal distribution (Kolmogorov-Smirnov test). Except total area and alluvial fan, the data distributed abnormal. Based on the result of this table, soil organic carbon was significantly positively correlated with %N ($r = 0.962^{**}$, $P < 0.01$) in total area. In general, the value of N significantly affected SOC for all landform classifications (*Table 3*).

http://www.aloki.hu ● ISSN 1589 1623 (Print) ● ISSN 1785 0037 (Online)
DOI: http://dx.doi.org/10.15666/aeer/1605_58155824
© 2018, ALÖKI Kft., Budapest, Hungary

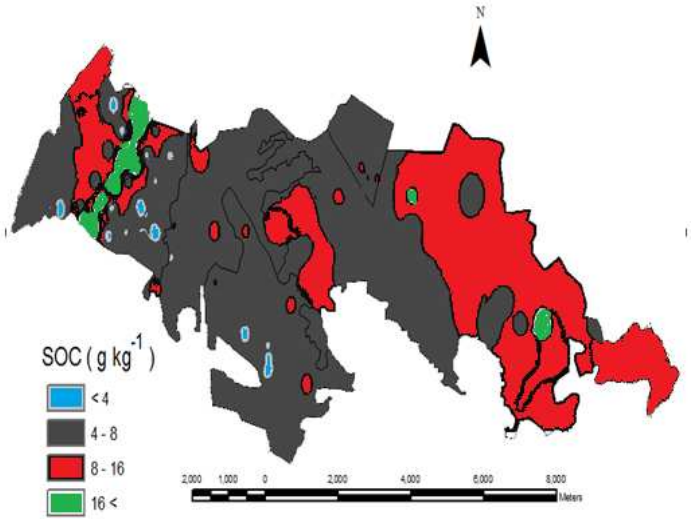

Figure 2. *Distribution of organic carbon in the study area*

Table 3. *Pearson correlations among soil physical, chemical variables and organic carbon in land form classification*

Land type	Total area	Alluvial fan	Plateau 1	Plateau 2	River alluvial plain
Variable	%N %T.N.V pH	%N	%N	%N Clay	%N
r	0.962** 0.407* -0.447*	0.893**	0.609*	0.730** 0.838**	0.960**
n	152	54	56	30	12

**Correlation is significant at the 0.01 level (2-tailed)
*Correlation is significant at the 0.05 level (2-tailed)

Linear and nonlinear regression equations to predict SOC from physiographic variables are shown in *Table 3*. For all landform types, TN had the highest correlation with SOC. There were significant differences between the types of landform ($r = 0.99^{**}$, $p < 0.01$). For each landform, two linear regression model and one nonlinear regression model were developed to predict SOC. In all equations, all or one of the independent variables such as TN, Clay, pH, Bd was used (*Table 4*).

Comparing nonlinear models in all land types, indicate that cubic models has highest coefficient of multiple determination (*Table 4*), and it is fitted for predicting SOC. Estimating regression models in each land type indicated, the models had not any over estimation or under estimation because MBE index was nearly zero (*Table 5*).

MAE value was greater in River Alluvial Plain than any other land types; which means high error in that location. Measured and predicted values were compared using the t-student test. Results showed no significant difference between them in each land type. This means that predicted models is approved and the relationship is reliable.

The significance level of coefficients in each land type for regression models was determined: for River Alluvial Plain, alluvial fan and total area; Correlation coefficient is significant at the 0.01 level. For Plateau 1 and Plateau 2; Correlation is significant at the 0.05 level. Standard Error was calculated 1.01, 0.33, 0.5 and 0.61 for River Alluvial Plain, alluvial fan, Plateau 1 and Plateau 2, respectively.

http://www.aloki.hu ● ISSN 1589 1623 (Print) ● ISSN 1785 0037 (Online)
DOI: http://dx.doi.org/10.15666/aeer/1605_58155824
© 2018, ALÖKI Kft., Budapest, Hungary

Table 4. *Regression models used to estimate SOC*

Land types	Regression	Regression equation	r
Alluvial fan	Linear	$OC(g\ kg^{-1}) = -2.475 + 10.882\ N\ (g\ kg^{-1})$	0.797
		$OC(g\ kg^{-1}) = 17.725+7.488\ N+0.004\ T.N.V-3.082\ pH-0.003$ gravel + 2.615 Bd + 0.001 Clay + 0.003 Sand	0.830
	Nonlinear	$OC(g\ kg^{-1}) = 15.172-26.57\ N+19.458\ N^2$	0.837
Plateau 1	Linear	$OC\ (g\ kg^{-1}) = 4.42+3.21\ N$	0.371
		$OC(g\ kg^{-1}) = 51.941+1.99\ N+ 0.003\ T.N.V-5.656\ pH+0.003$ gravel-0.17 Bd-0.006 Silt-0.009 Sand	0.537
	Nonlinear	$OC(g\ kg^{-1}) = -4.258+27.216\ N-14.27\ N^2$	0.681
Plateau 2	Linear	$OC\ (g\ kg^{-1}) = 1.041+9.34\ N$	0.533
		$OC(g\ kg^{-1}) = -0.467+0.012$ Clay$+6.085\ N$	0.742
	Nonlinear	$OC\ (g\ kg^{-1}) = e^{2.475-0.365/N}$	0.681
River alluvial plain	Linear	$OC(g\ kg^{-1}) = -1.699+11.725N$	0.921
		$OC(g\ kg^{-1}) = -2.837+11.539\ N$ + 0.005 Clay	0.922
	Nonlinear	$OC(g\ kg^{-1}) = 26.582-15.696\ N+6.431\ N^2$	0.948
Total area	Linear	$OC(g\ kg^{-1}) = -0.216+10.061\ N$	0.925
		$OC(g\ kg^{-1}) = 15.5+10.161\ N+0.004$ T.N.V-2.21 pH	0.930
	Nonlinear	$OC(g\ kg^{-1}) = 2.912+2.924\ N+2.935\ N^2$	0.947

Table 5. *Index assessment and significant regression models*

Land types	Model	The correlation coefficient	MBE	MAE
Alluvial fan	Nonlinear	0.84	0.0	0.73
Plateau 1	Nonlinear	0.68	0.0	0.81
Plateau 2	Multiple linear	0.74	0.0	0.8
River alluvial plain	Nonlinear	0.95	0.0	0.9

Discussion

The Pearson's linear correlation analysis revealed a significant positive relationship between SOC and total nitrogen. The highest organic carbon contents measured in soils from the highest storage of N accumulation. It can be assumed that that TN affected SOC status significantly. It assumed that TN has a positive benefit in maintaining and restoring the SOC quality and quantity for cropland in the study area. In similar research, Parvizi (2010) showed that physical variables and land use type can identify carbon sources. In that research, regression models were developed in forestry with a higher coefficient.

In some land types, there was significant correlation between clay and SOC; it is assumed clay protects organic matter from decomposition and runoff. For instance, Kasel et al. (2011) investigated that across north-central Victoria in south-eastern of Australia, mean rates of SOC accumulation in whole soils were greater increase under

http://www.aloki.hu ● ISSN 1589 1623 (Print) ● ISSN 1785 0037 (Online)
DOI: http://dx.doi.org/10.15666/aeer/1605_58155824
© 2018, ALÖKI Kft., Budapest, Hungary

the N-fixing trees. There was poor correlation between SOC and clay content across sites due to the clay mineralogy.

Differences in accumulation of SOC may also be related to physiographic condition such as slope, aspect, elevation, land use, the structure of root systems that could contribute to SOC distribution.

Soil organic carbon originates primarily from plants, thus vegetation and land use history is one of the most important driving factors of SOC (Jafarian and Kavian, 2013; González et al., 2010; Strickland et al., 2010). Accurate and reliable estimates of SOC storage in landscapes and land use are critical to the development of effective policies and strategies to mitigate atmospheric and climate change (Sylvia et al., 2016; Lufafa et al., 2008; Zhao et al., 2010). This research was provided where these findings were used to create a reference of regression models. This information was found to be valuable in supporting the evaluation of SOC field surveys, which are increasingly becoming available. I would also recommend to search on available topographic and management variables to develop models to estimate soil organic carbon.

Conclusion

Soil organic carbon in the land forms of the study area was abnormal, and had an arithmetic mean of 7.7 g kg^{-1}. The highest organic carbon content (22.04 g kg^{-1}) was in River Alluvial Plain region that has lowest elevation, and include river surrounded by river sediment. This fertility area was used for garden utilization. These results explained relationships between organic carbon and land types and land use attributes. In some parts of alluvial fan, including cropland utilization, the level of soil organic carbon (7.75 g kg^{-1}) could be explained by the input of litter, organic manure, decomposition and loss by the soil erosion. Addition of chemical fertilizer and manure could increase SOC in topsoil. Chemical fertilizer can increase root production of crops and products' yield, subsequently increasing organic residue input into the soil.

Acknowledgements. The author would like to thank Islamic Azad University of Roudehen for financial support.

REFERENCES

[1] Baldock, J. A., Sanderman, J., Farquharson, R. (2010): Capturing carbon in Australian soils: Potential and realities. – 19th World Congress of Soil Science, Soil Solutions for a Changing World.

[2] Boulal, H., Gómez-Macpherson, H. (2010): Dynamics of soil organic carbon in an innovative irrigated permanent bed system on sloping land in southern Spain. – Agriculture, Ecosystems & Environment 139: 284-292.

[3] Bouyoucos, G. J. (1962): Hydrometer method improved for making particle size analysis of soils. – Agronomy. J 54: 464-465.

[4] Climatic Data Center (2010): Meteorological Stations of Homand Absard 1999-2010. http://reports.irimo.ir/jasperserver/login.html.

[5] Gaiser, T., Stahr, K., Billen, N., Razek Mohammad, M. A. (2008): Modeling carbon sequestration under zero tillage at the regional scale. I. The effect of soil erosion. – Ecological Modelling 218: 110-1 20.

http://www.aloki.hu ● ISSN 1589 1623 (Print) ● ISSN 1785 0037 (Online)
DOI: http://dx.doi.org/10.15666/aeer/1605_58155824
© 2018, ALÖKI Kft., Budapest, Hungary

[6] Gami, S. K., Lauren, J. G., Duxbury, J. M. (2009): Influence of soil texture and cultivation on carbon and nitrogen levels in soils of the eastern Indo-Gangetic plains. – Geoderma 153: 304-311.
[7] Gee, G. W., Bauder, J. W. (1979): Particle size analysis by hydrometer- a simplified method for routine textural analysis and a sensitivity test of measurement parameters. – Soil Science Society of America Journal 43: 1004-1007.
[8] González, L., Etchevers, J. D., González, J. M., Paz, F. (2010): Soil organic carbon changes at the plot level in hillside systems. – Agriculture, Ecosystems & Environment DOI: 10.1016/j.agee,2010.09.010.
[9] Heidari, A., Faghih, A., Gorji, M. (2010): Carbon sequestration under different physiographic and climatic conditions in north Karaj river basin. – 19th World Congress of Soil Science, Soil Solutions for a Changing World, Brisbane, Australia, 1-6 August, pp. 9-11.
[10] Jafarian, Z., Kavian, A. (2013): Effects of land-use change on soil organic carbon and nitrogen. – Communications in Soil Science and Plant Analysis 44(1-4): 339-346.
[11] Karl, J. W., Maurer, B. A. (2010): Spatial dependence of predictions from image segmentation: A variogram-based method to determine appropriate scales for producing land-management information. – Ecological Informatics 5: 194-202.
[12] Kasel, S., Singh, S., Sanders, G. J., Bennett, L. T. (2011): Species-specific effects of native trees on soil organic carbon in biodiverse plantings across north-central Victoria, Australia. – Geoderma 161: 95-106.
[13] Lufafa, A., Diédhiou, I., Samba, S., Séné, M., Khouma, M., Kizito, F., Dick, R. P., Dossa, E., Noller, J. S. (2008): Carbon stocks and patterns in native shrub communities of Senegal's Peanut Basin. – Geoderma 146: 75-82.
[14] Li, M., Wu, J., Deng, X. (2016): Land use change and soil carbon sequestration in China: Where does it pay to conserve? – Reg. Environ. Chang. 16: 2429-2441.
[15] McLean, E. O. (1982): Soil pH and Lime Requirement. – In: Page, A. L, Miller, R. H., Keeney, D. R. (eds.) Methods of Soil Analysis. Part 2. Chemical and Microbiological Properties. 2nd ed. Agronomy Monograph 9: pp. 199-224. ASA and SSSA, Madison, WI.
[16] Mills, A. J., Cowling, R. M. (2010): Below-ground carbon stocks in intact and transformed subtropical thicket landscapes in semi-arid South Africa. – Journal of Arid Environments 74: 93-100.
[17] Motallebi, E., Homaee, M., Zarei, G., Mahmoudi, S. (2011): The effect of lime on soil moisture characteristics with using pedo transfer function in Garmsar series. – Iranian Journal of Irrigation and Drainage 3(4): 426-439.
[18] Padilla, F. M., Vidal, B., Sanchez, J., Pugnaire, F. I. (2010): Land-use changes and carbon sequestration through the twentieth century in a Mediterranean mountain ecosystem: Implications for land management. – Journal of Environmental Management 91: 2688-2695.
[19] Parvizi, Y. (2010): Zoning spatial variability of soil organic carbon and the effect of physical and managerial factors that analysts use multivariate and artificial neural networks. – PhD. Thesis, Agricultural Engineering and Technology Department, Tehran University, Iran.
[20] Poeplau, C., Don, A. (2015): Carbon sequestration in agricultural soils via cultivation of cover crops – A meta-analysis. – Agr. Ecosyst. Environ. 200: 33-41.
[21] Sarmadian, F., Taghizadeh Mehrjardi, R. (2010): Development of pedotransfer functions to predict soil carbon properties in Golestan Province, Iran. – 19th World Congress of Soil Science, Soil Solutions for a Changing World. Brisbane, Australia.
[22] Senthilkumar, S., Kravchenko, A. N., Robertson, G. P. (2009): Topography Influences management system effects on total soil carbon and nitrogen. – Soil Science Society of America Journal 73: 2059-2067.

http://www.aloki.hu ● ISSN 1589 1623 (Print) ● ISSN 1785 0037 (Online)
DOI: http://dx.doi.org/10.15666/aeer/1605_58155824
© 2018, ALÖKI Kft., Budapest, Hungary

[23] Sylvia, S., Julia, E. M. S, Pongratz, J. (2016): Soil carbon response to land-use change: evaluation of a global vegetation model using observational meta-analyses. – Biogeosciences 13: 5661-5675.
[24] Strickland, M. S., Callaham, Jr. M. H., Davies, C. A., Lauber, C. L., Ramirez, K., Richter, Jr. D. D., Fierer, N., Bradford, M. A. (2010): Rates of in situ carbon mineralization in relation to land-use, microbial community and edaphic characteristics. – Soil Biol Biochem 42: 260-269.
[25] U. S. Department of Agriculture, Natural Resources Conservation Service (USDA-NRCS) (1995): Soil Survey Laboratory Information Manual. – Soil Survey Investigations Report No. 45.
[26] Vasques, G. M., Grunwald, S., Comerford, N. B., Sickman, J. O. (2010): Regional modeling of soil carbon at multiple depths within a subtropical watershed. – Geoderma 156: 326-336.
[27] Walkley, A., Black, I. A. (1934): An examination of the Degtjareff method for determining soil organic matter and a proposed modification of the chromic acid titration method. – Soil Science 37: 29-38.
[28] Wang, Z. M., Zhang, B., Song, K. S., Liu, D. W., Ren, C. Y. (2010): Spatial variability of soil organic carbon under maize monoculture in the Song-Nen Plain, Northeast China. – Pedosphere 20(1): 80-89.
[29] Xun, L., Feng-Min, L., Da-Qian, L., Guo-Jun, S. (2010): Soil organic carbon, carbon fractions and nutrients as affected by land use in semi-arid region of Loess Plateau of China. – Pedosphere 20(2): 146-1 52.
[30] Zhang, C. S., McGrath, D. (2004): Geostatistical and GIS analyses on soil organic carbon concentrations in grassland of southeastern Ireland from two different periods. – Geoderma 119: 261-275.
[31] Zhao, S. Q., Liu, S., Li, Z., Sohl, T. L. (2010): Spatial resolution thresholds of land cover in estimating terrestrial carbon sequestration in four counties in Georgia and Alabama, USA. – Biogeosciences 7: 71-80.
[32] Zhao, W., Hu, Z. M., Li, S. G., Guo, Q., Yang, H., Zhang, T. H. (2017): Impact of land use conversion on soil organic carbon stocks in an agro-pastoral ecotone of Inner Mongolia. – J. Geogr. Sci. 27: 999-1010.

http://www.aloki.hu ● ISSN 1589 1623 (Print) ● ISSN 1785 0037 (Online)
DOI: http://dx.doi.org/10.15666/aeer/1605_58155824
© 2018, ALÖKI Kft., Budapest, Hungary

BIOLOGICAL CONTROL OF *HAEMONCHUS CONTORTUS* BY FUNGAL ANTAGONISTS IN SMALL RUMINANTS

KHATTAK, B.[1*] – SAFI, A. U. R.[1] – SINDHU, Z. U. D.[2]– ATTAULLAH, M.[3] – JAMAL, Q.[1] – KHAN, T. A.[1] – HUSSAIN, M.[1]– ANJUM, S. I.[4] – ISRAR, M.[5] – KHAN, I. A.[6]

[1]*Department of Microbiology, Kohat University of Science and Technology, Pakistan*

[2]*Department of Parasitology, University of Agriculture Faisalabad, Pakistan*

[3]*Department of Zoology, University of Malakand*

[4]*Department of Zoology, Kohat University of Science and Technology, Pakistan*

[5]*Pakistan Science Foundation Islamabad, Pakistan*

[6]*Department of Weed Science, The University of Agriculture Peshawar, Pakistan*

**Corresponding author*
e-mail: baharkk75@gmail.com; phone: +92-33-4907-3552

(Received 10th May 2018; accepted 5th Jul 2018)

Abstract. *Haemonchus contortus* is a highly pathogenic nematode that causes haemonchosis in ruminants. As *H. contortus* is reported to be resistant to anthelmintic drugs, biological control might be the alternative approach. The study was conducted in Pakistan on different parameters to control *H. contortus* biologically by fungi. *Alternaria alternata, Fusarium oxysporum, Aspergillus niger, Trichoderma harzianum* and *Ochroconis gallopava* were isolated from the feces and abomasa of infected domestic sheep (*Ovis aries*) and goats (*Capra aegagrus hircus*). Different concentrations of the extracted spore-free cultures of these fungi were applied on eggs, larvae and adults of *H. contortus* for eggs hatching inhibition assay, larval mortality assay and adult mortality assay. In eggs hatching inhibition assay, the higher concentrations i.e. 100% and 50% of *A. alternata, F. oxysporum, A. niger, T. harzianum* and *O. gallopava* caused 100% inhibition of eggs. In adult mortality assay, all the culture filtrates caused no mortality in the first and second hour while in the third hour of the post treatment mortality varied with concentrations. In larval mortality assay, higher concentrations i.e. 100% and 50% of *T. harzianum* and *A, niger* caused 100% mortality of L_3 larvae of *H. contortus.* All the extracted spore-free cultures significantly caused eggs hatching inhibition. Higher concentrations of *Trichoderma* and *Aspergillus* significantly caused larval mortality (100%) while adult mortality assays were dose and time dependent and insignificantly caused adult mortality of *H. contortus.*
Keywords: *nematode parasite, haemonchosis, biocontrol, fungal extracts, egg hatch assay, adult mortality assay*

Introduction

Livestock plays an important role in the economy of Pakistan. Agriculture contributes 21% in national gross domestic product (GDP) in which share of livestock is 11.9%. The estimated population of domestic sheep (*Ovis aries*) was 29.1 million while domestic goats (*Capra aegagrus hircus*) were 66.6 million during 2013-14. According to a survey in Pakistan, about 45000 tons of meat was obtained from sheep during the year 2013-2014 (Economic Survey of Pakistan 2013-2014). Small ruminant livestock are highly susceptible to gastrointestinal nematodes (GINs). Among GINs, *Haemonchus contortus*, member of the family Trichostrongylidae (Radostits et al., 2006), is a highly pathogenic nematode parasite that causes haemonchosis in sheep and goat, an infection characterized

http://www.aloki.hu ● ISSN 1589 1623 (Print) ● ISSN 1785 0037 (Online)
DOI: http://dx.doi.org/10.15666/aeer/1605_58255835
© 2018, ALÖKI Kft., Budapest, Hungary

by anemia, protein deficiency, bottle jaw and digestive disturbances throughout the world (Getachew et al., 2007; Bowman et al., 2009). It is estimated that an infected sheep with 5000 *H. contortus* worms may lose 250 ml blood/day. Life cycle of *H. contortus* takes about 21 days to complete. *H. contortus'* life cycle is direct i.e. without the involvement of secondary host. Every adult female parasite lays between 5000-10,000 eggs/ day which are passed out in the feces (Hepworth, 2006) as shown in *Figure 1.*

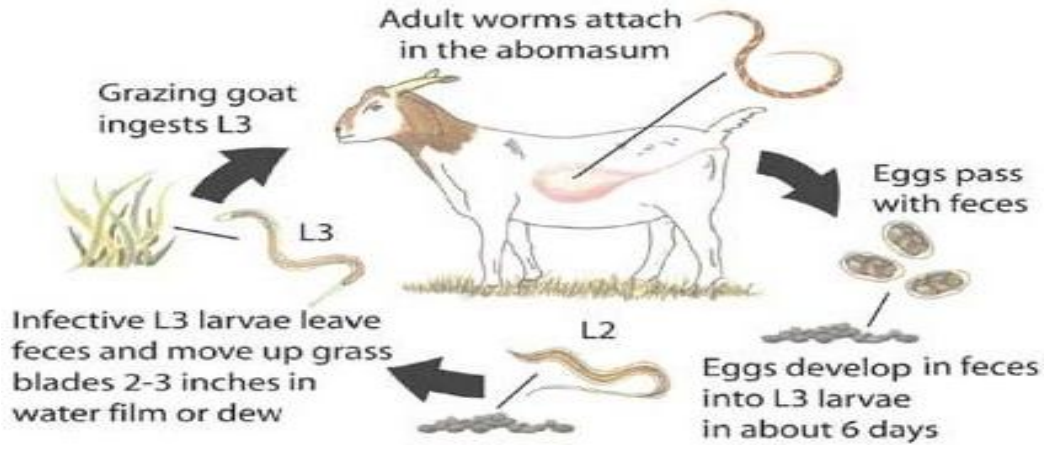

Figure 1. *Life cycle of Haemonchus contortus. (Courtesy: pinterest.com)*

As *H. contortus* is reported to be resistant to anthelmintic drugs (Miller et al., 1987; Sangster, 1999; Jackson and Coop, 2000) biological control might be the alternative approach. Many fungal species have been isolated from nematodes in which *Duddingtonia flagrans* has proven to be the most effective nematode-destroying fungus (Larsen et al., 1997) whose spores are found to survive while passing through the gastro-intestinal tract of grazing livestock (Hertzberg et al., 2001). *Trichoderma, Fusarium* and *Acremonium* have ovicidal effect on *Toxacara canis* ova (Maia Filho et al., 2011).

The present study was carried out in the light of previous work done to isolate and identify fungi from the feces of infected sheep and goats to evaluate the fungal filtrates' abilities of suppression the population of *H. contortus* on eggs hatching level, larval developmental level and adult level. These fungal extracts can be used as biological control against this parasite as a spray on grazing pastures or can be fed to animals in the form suspensions or pellets. Moreover, all fungi investigated in this study are of less toxigenic nature to animals' health so making them more suitable candidates for the purpose of the study.

Materials and methods

This research work carried out in laboratory of the Department of Microbiology, Kohat University of Science and Technology, Kohat, Pakistan.

Sampling

100 fecal samples of rectum from live goats and sheep and 100 abomasa samples from freshly slaughtered goats and sheep were collected from different areas of Kohat-

http://www.aloki.hu ● ISSN 1589 1623 (Print) ● ISSN 1785 0037 (Online)
DOI: http://dx.doi.org/10.15666/aeer/1605_58255835
© 2018, ALÖKI Kft., Budapest, Hungary

Pakistan (33°34'47.1"N 71°26'29.3"E). The samples were analyzed for the detection of eggs (fecal samples) and worms (abomasa samples) of *H. contortus* as shown in *Table 1*. All the samples were processed in the department of Microbiology, Kohat University of Science and Technology Kohat, Pakistan.

Table 1. *Samples collected and analyzed for the detection of eggs and worms of H. contortus*

Ruminants	Fecal samples	Positive (eggs seen)	Negative (no eggs)	Abomasa	Positive (worms seen)	Negative (no worms)
Goats	50	37	13	50	34	16
Sheep	50	31	19	50	41	9
Total	100	68	32	100	75	25

Haemonchus contortus (eggs, adults and larvae)

Eggs of *H. contortus* were identified and concentrated from fecal samples by simple test tube floatation method (Dryden et al., 2005), Mac Master counting chamber (Soulsby, 1968) and isolation of eggs from feces as described by (Hubert and Kerboeuf, 1992). Adult worms were collected from abomasa based on their typical barber pole appearance of female worms in a clean container as shown in *Figure 2*. Collected worms were washed with distilled water and concentrated in a container having freshly prepared phosphate buffer saline (PBS). Third stage larvae (L_3) were cultivated from the eggs recovered from adult female worms following the protocol of (Amarante, 2011) with slight modification. The L_3 were morphologically differentiated and identified as described by (Van Wyk et al., 2004).

Figure 2. *Harvesting worms from abomusam*

Fungi (isolation, identification and extraction)

All positive fecal and abomasa samples were processed for the isolation of fungi. One-gram samples' contents were serially diluted and poured on Sabouraud dextrose agar (SDA) media for fungal growth. After 72 h, the grown colonies were sub cultured to isolate pure cultures. For identification, both colony morphology and microscopic characteristics were deeply compared with the identification keys provided by (Navi et al., 1999) and (Larone and Larone, 1987). Among many other isolates, *Alternaria*

http://www.aloki.hu ● ISSN 1589 1623 (Print) ● ISSN 1785 0037 (Online)
DOI: http://dx.doi.org/10.15666/aeer/1605_58255835
© 2018, ALÖKI Kft., Budapest, Hungary

alternata, Fusarium oxysporum, Aspergillus niger, Trichoderma harzianum and *Ochroconis gallopava* were the main isolates present in all positive samples. So these fungi were selected for fungal extracts.

For extraction, fungi in broth media were incubated in a shaker incubator for 7 days at 25 °C in dark. After 7 days, they were filtered by common Whatman filter papers and the filtrates were again filtered through Millex HA syringe driven filters (0.45 µm). Different concentration i.e. 100%, 50%, 25%, 12.5% and 6.25% were made from each in phosphate buffer saline (PBS) and distilled water separately. Final filtrates were tested on potato dextrose agar (PDA) and SDA media to confirm the absence of fungal spores.

Egg hatch assay (EHA)

EHA was performed in triplicate following the protocol of (Coles et al., 1992) with slight modification. Isolated eggs were dissolved in 15 ml distilled water with concentration adjusted to 100-200 eggs/75 µl. Then 75 µl egg suspension was added to each well of a 24-welled titration plate having 2.5 ml of each concentration. For positive control, 0.025 mg/ml of Oxfendazole (Glaxo-welcome) was prepared in 0.3% dimethyl sulfoxide (DMSO). Wells having egg suspension and 2.5 ml tap water with no extracts were used as negative control. The plate was incubated at 25 °C for 48 h. After 48 h, one drop of Lugol's oil was added to stop the reaction. Then the plate was observed under 10X of inverted microscope as shown in *Figure 3*. The percent hatching inhibition was observed as:

$$\text{Hatching Inhibition } (\%) = \frac{P_{\text{HI}}\text{Test}}{P_{\text{HI}}\text{Total}} \times 100$$

P_{HI}Test = number of unhatched eggs, P_{HI}Total = number of unhatched eggs + number of hatched eggs.

Adult mortality assay (AMA)

In AMA, ten worms were treated in triplicate to each filtrate concentration at room temperature. 25 µg/ml of Closantel was used as positive control. Phosphate buffer saline with worms and no fungal extracts were used as negative control. After each one hour of post treatment, all the plates were observed to check the mortality till all worms were dead in negative control. Because adult worms cannot survive without host longer than 9 h. The percent mortality was calculated as:

$$\text{Adult Mortality}(\%) = \frac{P_{\text{AM}}\text{Test}}{P_{\text{AM}}\text{Total}} \times 100$$

P_{AM}Test = number of dead worms, P_{AM}Total = number of dead worms + number of live worms.

Larval mortality assay (LMA)

One ml of L_3 larval suspension containing 10 larvae were added in triplicate to each well of titration plate having 2.5 ml of fungal filtrates. Negative control well received

http://www.aloki.hu ● ISSN 1589 1623 (Print) ● ISSN 1785 0037 (Online)
DOI: http://dx.doi.org/10.15666/aeer/1605_58255835
© 2018, ALÖKI Kft., Budapest, Hungary

only one ml L_3 suspension and 2.5 ml phosphate buffer saline while positive control well received one ml L_3 suspension and 2.5 ml closantel (25 µg/ml). The plate was incubated at room temperature for 3 h. After 3 h, the plate was observed under 10X of inverted microscope. Percent mortality was calculated as:

$$\text{Larval Mortality}(\%) = \frac{P_{\text{LM}}\text{Test}}{P_{\text{LM}}\text{Total}} \times 100$$

P_{LM}Test = number of dead larvae, P_{LM}Total = number of dead larvae + number of live larvae.

Figure 3. *H. contortus' eggs under inverted microscope*

Statistical analysis

Data obtained from bio-assays i.e. EHA, AMA and LMA were analyzed by ONE Way ANOVA and TWO-Way ANOVA through Statistix version 9 and GraphPad Prism version 5 software. The p values <0.05 was considered significant.

Results

Egg hatch assay

After three days' incubation, the effect of different concentration of all fungal filtrates on eggs, were observed as shown in *Figure 4*. Higher concentrations i.e. 100% and 50% of all filtrates caused 100% inhibition while inhibition by lower concentrations varied from specie to specie. There were 100% and no inhibition (0%) in positive and negative control respectively.

Adult mortality assay

All concentrations of fungal filtrates treated with adult worms caused no mortality in the first three hours of post treatment. After three hours, the results were dose and time dependent and caused insignificant percent mortality as shown in *Figure 5*.

http://www.aloki.hu ● ISSN 1589 1623 (Print) ● ISSN 1785 0037 (Online)
DOI: http://dx.doi.org/10.15666/aeer/1605_58255835
© 2018, ALÖKI Kft., Budapest, Hungary

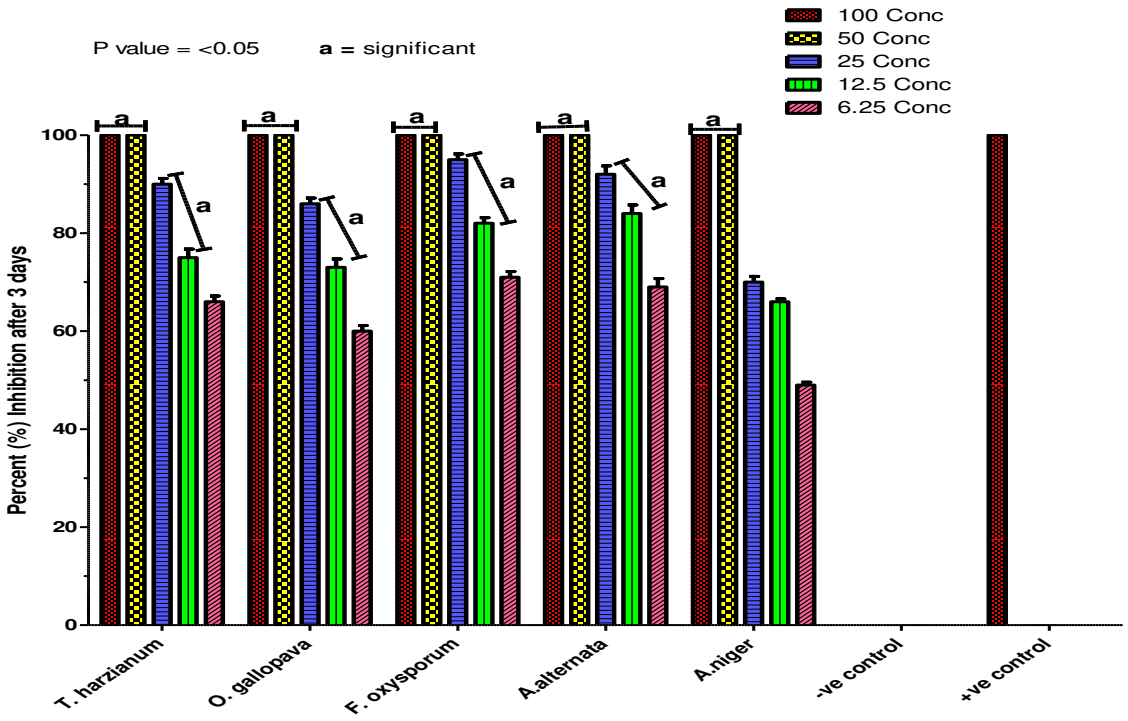

Figure 4. *Percent inhibition of eggs hatching via fungal filtrates*

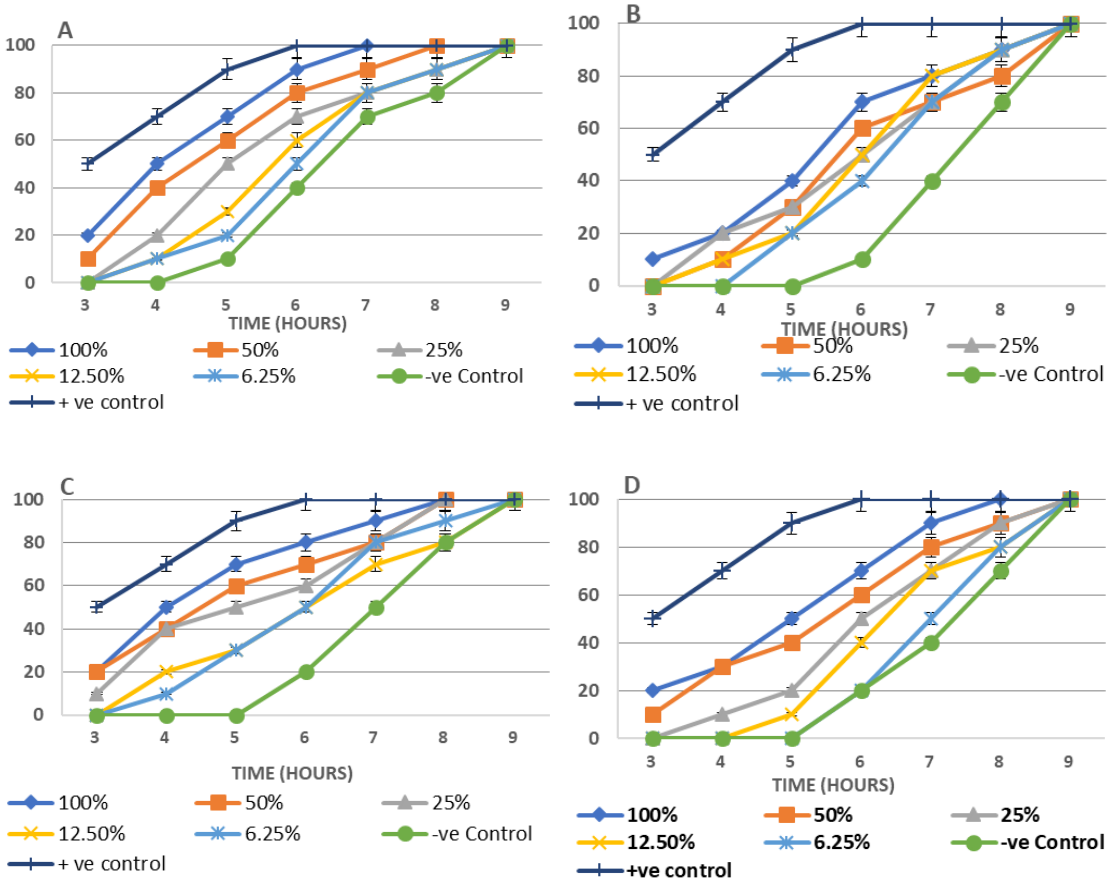

http://www.aloki.hu ● ISSN 1589 1623 (Print) ● ISSN 1785 0037 (Online)
DOI: http://dx.doi.org/10.15666/aeer/1605_58255835
© 2018, ALÖKI Kft., Budapest, Hungary

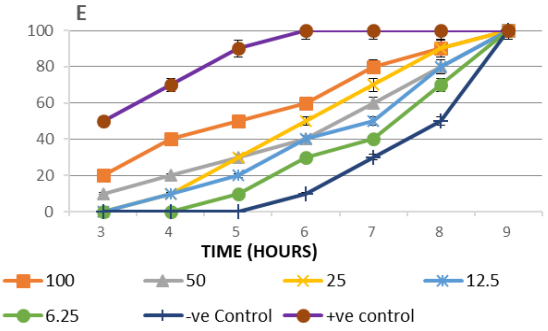

Figure 5. *Adult worms' post-exposure against different concentration of fungal extracts.* ***A.*** *F. Oxysporum.* ***B.*** *A. alternate,* ***C.*** *T. harzianum,* ***D.*** *A. niger,* ***E.*** *O. gallopava*

Larval mortality assay

After 3 h post treatment of L_3 larvae with fungal filtrates, higher concentrations i.e. 100% and 50% of the *Trichoderma harzianum* and *Aspergillus niger* caused 100% mortality while 100% concentrations of *F. oxysporum* and *A. alternata* caused 94% and 91% mortality respectively. Mortality caused by lower concentrations varied from species to species. 100% and no mortality in positive and negative control respectively as shown in *Figure 6*.

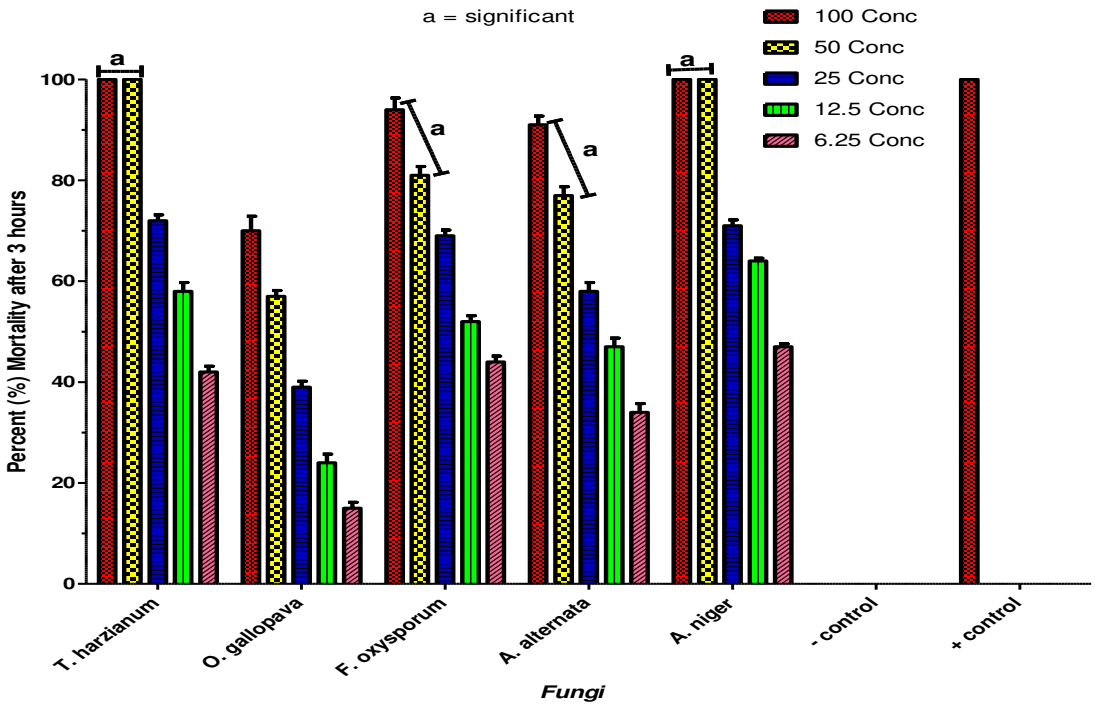

Figure 6. *Percent mortality of L_3 larvae after 3 h post treatment*

Overall effect on Haemonchus contortus

When the averages of all concentrations of each fungal treatment were analyzed by Least Significant Difference (LSD) and All-Pairwise Comparison (APC) tests, the

http://www.aloki.hu ● ISSN 1589 1623 (Print) ● ISSN 1785 0037 (Online)
DOI: http://dx.doi.org/10.15666/aeer/1605_58255835
© 2018, ALÖKI Kft., Budapest, Hungary

results showed that all the tested fungi significantly affected all stages of *H. contortus*. Pairwise comparison of fungi showed that all fungi have equal significant effect on eggs of *H. contortus* while the significance of efficacy on adults and larvae varies from fungal to fungal species as shown in *Figure 7*.

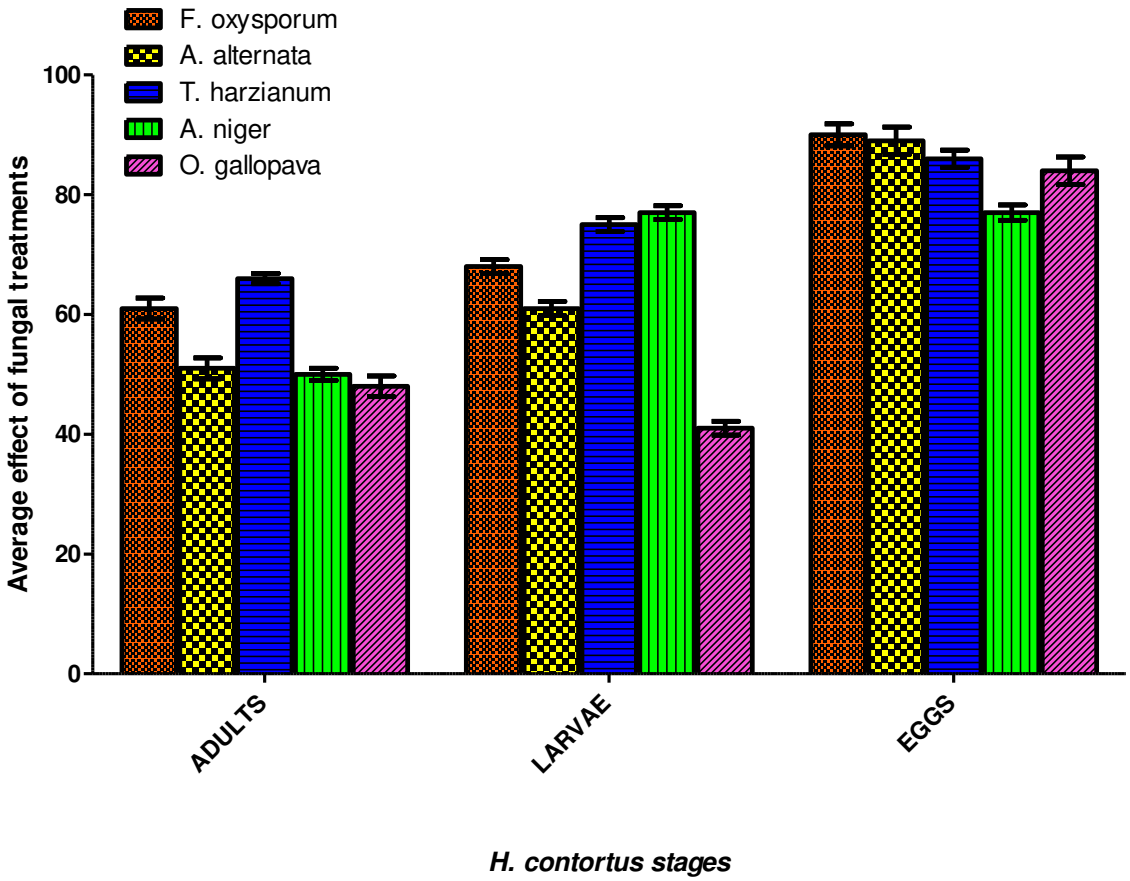

Figure 7. *Average effect of fungal treatments on adults, larvae and eggs of H. contortus*

Discussion

To control *Haemonchus contortus*, common anthelmintics are applied but not enough to erase this parasite completely as it is reported to be resistant to all three broad spectrum families of anthelmintics viz. benzimidazole, lmidazothiazole and ivermectin and against drugs with narrow spectrum of activity such as salicylanilides anthelmintics (Kaplan and Vidyashankar, 2012). Keeping in view the importance of this blood sucker, there is need of alternative methods other than common anthelmintics to prevent sheep and goats from this highly dangerous nematode parasite. Biological control is an environment friendly alternative approach towards these nematodes. Among the microorganisms that parasitize on nematodes, fungi hold an important position in continuously eliminating parasitic nematodes (McSorley et al., 2008). About 70 genera and 200 species of fungi have been investigated that they are associated with nematode parasites. Till now, only a few of them are successful biocontrol agents (Nordbring-Hertz et al., 2011).

In the present study, it was tried to investigate the fungal abilities biologically to suppress the *H. contortus* population on eggs hatching, larval and adult levels. Fungi

http://www.aloki.hu ● ISSN 1589 1623 (Print) ● ISSN 1785 0037 (Online)
DOI: http://dx.doi.org/10.15666/aeer/1605_58255835
© 2018, ALÖKI Kft., Budapest, Hungary

were isolated from the feces of small ruminants and different concentrations of culture extracts were made from the isolated fungi. The spore-free cultures were applied on eggs, L_3 larvae and adult worms of *H. contortus* to find out the percent inhibition and percent mortality. The results demonstrated that the higher concentrations i.e.100% and 50% of all the extracted spore-free cultures of *A. alternata, F. oxysporum, A. niger, T. harzianum* and *O. gallopava* showed 100% eggs hatching inhibition of *H. contortus.* For the first time these fungi were applied on eggs of *H. contortus* although in previous studies many other nematophagous and filamentous fungi such as *Arthrobotrys oligospora, A. musiformis, Cladosporium spp, A, flavus* and *Duddingtonia flagrans* were treated with *H. contortus* eggs and showed similar results (Maia Filho et al., 2011). Also, different plant extracts have been reported previously to affect the biology of the parasitic eggs in the same ratio (Hounzangbe-Adote et al., 2005).

Adult worms of *H. contortus* in this study were treated with different concentrations i.e. 100%, 50%, 25%, 12.5% and 6.25% of the extracted spore-free cultures. The results were dose and time dependent as compared to a similar study conducted on animals grazing on pastures where *D. flagrans* was present which showed 97% efficacy of the fungus against this nematode parasite (Maria et al., 2011). Another study conducted by Chandrawathani and colleagues (Chandrawathani et al., 2003) in which they fed sheep during 24 days with either mineral blocks containing a dose of 500,000 chlamydospores/kg bw/day or pellets with the same fungal dose, and obtained a reduction in adults of *H. contortus* of >95% in the first case and 98% in the second case.

The third stage larvae (L_3) of *H. contortus* in the present study were treated with different concentrations of each extracted spore-free cultures for three hours. After three hours, it was observed that higher concentrations i.e. 100% and 50% of the *Trichoderma harzianum* and *Aspergillus niger* caused 100% mortality in the L_3 larvae while the mortality caused by lower concentrations of extracts varied from species to species. These results resemble a recent study conducted in Iran by Zarrin and colleagues in which they demonstrated that some saprophytic fungi spread in the environment can be effective in reducing the number of third stage larvae of *Trichostrongylidae* family. However, the rate of mortality was different because of the fungal species and isolates. They concluded that there was a considerable decrease in larvae population by *Cladosporium spp.* (98.8%), *Trichoderma spp.* (98.5%), and *Aspergillus spp.* (96.7%) culture. Their results indicated great potential of using appropriate saprophyte fungi for biological control of *H. contortus* larvae in sheep (Zarrin et al., 2015). A similar study conducted on stage 3 larvae of *H. contortus* by Ivonneet al., 2011 investigated that mortality of infective larvae (L_3) by *A. oligospora* was 90.3%, *A. musiformis* was 97%, and *M. thaumasium* was 62.3% (Ivonne et al., 2011). Also, Menduza De Gives and Vazquez-prats investigated that *A. oligospora, Monacrosporium acermatoum* and *A. robusta* caused mortality of the population of *H. contortus* infective L_3 larvae with 93.30%, 95.70% and 10.10%, respectively (Mendoza-De Gives and Vazquez-Prats, 1994).

Conclusion and recommendations

From the study, it is concluded that higher concentrations of all the extracted spore-free culture filtrates from the isolated fungi significantly caused eggs hatching inhibition. Higher concentrations of *Trichoderma harzianum* and *Aspergillus niger* significantly caused larval mortality (100%) while adult mortality assays were dose and

http://www.aloki.hu ● ISSN 1589 1623 (Print) ● ISSN 1785 0037 (Online)
DOI: http://dx.doi.org/10.15666/aeer/1605_58255835
© 2018, ALÖKI Kft., Budapest, Hungary

time dependent and insignificantly caused adult mortality of *Haemonchus contortus*. Keeping in view the importance of this problem and encouraging results obtained from the study, there is need to explore the chemistry of the fungal filtrates to find out their active compounds and their mechanism of actions (both *in vitro* and *in vivo*). The effects of these fungi at molecular level like DNA damage and genetic alterations in *H. contortus* need further explorations.

Acknowledgements. We sincerely acknowledge Pakistan Science Foundation Islamabad for providing us financial support with grant number (PSF/NSLP/KP-KUST-298). Also, thanks go to faculty and staff of Department of Microbiology, Kohat University of Science and Technology Kohat and Department of Parasitology, University of Agriculture Faisalabad for their Technical support.

REFERENCES

[1] Amarante, A. F. (2011): Why is it important to correctly identify *Haemonchus species*? – Revista Brasileira de Parasitologia Veterinária 20(4): 263-268.

[2] Bowman, D. D. (2009): Georgis Parasitology for Veterinarians. 9th ed. – Saunders Elsevier, St; Louis, pp. 161-162.

[3] Chandrawathani, P., Jamnah, O., Waller, P. J., Larsen, M., Gillespie, A. T., Zahari, W. M. (2003): Biological control of nematode parasites of small ruminants in Malaysia using the nematophagous fungus *Duddingtonia flagrans*. – Veterinary Parasitology 117(3): 173-183.

[4] Coles, G. C., Bauer, C., Borgsteede, F. H. M., Geerts, S., Klei, T. R., Taylor, M. A., Waller, P. J. (1992): World Association for the Advancement of Veterinary Parasitology (WAAVP) methods for the detection of anthelmintic resistance in nematodes of veterinary importance. – Veterinary Parasitology 44(1): 35-44.

[5] De Souza, M. F., Vieira, N., Berne, J. A., Stoll, F. E., Nascente, P., Potter, L. (2013): Fungal ovicidal activity on *Toxocara canis* eggs. – Revista Iberoamricana de Micologia 30: 226-30.

[6] Dryden, M. W., Payne, P. A., Ridley, R., Smith, V. (2005): Comparison of common fecal flotation techniques for the recovery of parasite eggs and oocysts. – Veterinary Therapeutics 6(1): 15-28.

[7] Economic Survey of Pakistan (2013-2014): http://www.finance.gov.pk/survey_1314.html.

[8] Getachew, T., Dorchies, P., Jacquiet, P. (2007): Trends and challenges in the effective and sustainable control of *Haemonchus contortus* infection in sheep. – Parasite 14(1): 3-14.

[9] Hepworth, K., Neary, M., Hutchens, T. (2006): Managing Internal Parasitism in Sheep and Goats. – Purdue University Cooperative Extension Service, West Lafayette, IN, pp. 1-10.

[10] Hertzberg, H., Larsen, M., Maurer, V. (2002): Biological control of helminths in grazing animals using nematophagous fungi. – Berliner und Munchener Tierarztliche Wochenschrift 115(7): 278-85.

[11] Hounzangbe-Adote, M. S., Paolini, V., Moutairou, I. K., Hoste, H. (2005): In vitro effects of four tropical plants on three life-cycle stages of the parasitic nematode, *Haemonchus contortus*. – Research in Veterinary Science 78(2): 155-160.

[12] Hubert, J., Kerbouef, D. (1992): A micro larval development assay for the detection of anthelmintic resistance in sheep nematodes. – Veterinary Record 130(20): 442-446.

[13] Ivonne, C. A. G., de Gives, P. M., Hernández, E. L., Arellano, E. L., Valero Coss, R. O., Velázque, M. H. (2011): Nematophagous fungi (*Orbiliales*) capturing, destroying and

http://www.aloki.hu ● ISSN 1589 1623 (Print) ● ISSN 1785 0037 (Online)
DOI: http://dx.doi.org/10.15666/aeer/1605_58255835
© 2018, ALÖKI Kft., Budapest, Hungary

feeding on the histotrophic larvae of *Haemonchus contortus* (Nematoda: *Trichostrongylidae*). – Revista Mexicana De Micología 33: 29-35.

[14] Jackson, F., Coop, R. L. (2000): The development of anthelmintic resistance in sheep nematodes. – Parasitology 120: 95-107.

[15] Kaplan, R. M., Vidyashankar, A. N. (2012): An inconvenient truth: Global warming and anthelmintic resistance. – Veterinary Parasitology 186(1): 70-80.

[16] Larone, D. H. (1987): Medically Important Fungi. A Guide to Identification. – Elsevier Science Ltd., Washington DC.

[17] Larsen, M., Nansen, P., Grønvold, J., Wolstrup, J., Henriksen, S. A. (1997): Biological control of gastro-intestinal nematodes-facts, future, or fiction. – Veterinary Parasitology 72(3): 479-85.

[18] María, F., Sagüés, L. A., Fusé, A., Fernández, S., Lucía, E. I., Fabiana, C. M., Carlos, A. S. (2011): Efficacy of an energy block containing *Duddingtonia flagrans* in the control of gastrointestinal nematodes of sheep. – Parasitology Research 109(3): 707-713.

[19] McSorley, R., Wang, K. H., Church, G. (2008): Suppression of root knot nematodes in natural and agricultural soils. – Applied Soil Ecology 39: 291-298.

[20] Menduza de Gives, P., Vazquez-prats, V. M. (1994): Reduction of *Haemonchus contortus* infective larvae by three nematophagous fungi in sheep faecal cultures. – Veterinary Parasitology 55: 197-203.

[21] Miller, J. E., Hembry, F. G., Kearney, M. T., Williams, J. C., Stag, L. C., Sims, D. (1987): Efficacy of levamisole and netobimin against *Haemonchus contortus* in lambs in Louisiana. – American Journal of Veterinary Research 48(9): 1403-1406.

[22] Navi, S. S., Bandyopadhyay, R., Hall, A. J., Bramel-Cox, P. J. (1999): A pictorial guide for the identification of mold fungi on sorghum grain. – Information Bulletin no. 59 (in En., Summaries in En, Fr). International Crops Research Institute for the Semi-Arid Tropics. Patancheru 502324, Andhra Pradesh, India.

[23] Nordbring-Hertz, B., Jansson, H. B., Tunlid, A. (2011): Nematophagous Fungi. – In: eLS. John Wiley & Sons Ltd, Chichester. http://www.els.net [doi: 10.1002/9780470015902.a0000374.pub3]

[24] Radostits, O. M., Gay, C. C., Hinchcliff, K. W., Constable, P. D. (2007): Veterinary Medicine. A Text Book of the Diseases of Cattle, Horses, Sheep, Pigs and Goats. – Saunders Ltd., Philadelphia, USA pp. 20-65.

[25] Sangster, N. C. (1999): Anthelmintic resistance: past, present, and future. – International Journal for Parasitology 29(1): 115-124.

[26] Soulsby, E. J. (1982): Helminths, Arthropods and Protozoa of Domesticated Animals. – Bailliere Tindall, London, pp. 248-250, 766-770.

[27] Van Wyk, J. A., Cabaret, J., Michael, L. M. (2004): Morphological identification of nematode larvae of small ruminants and cattle simplified. – Veterinary Parasitology 119(4): 277-306.

[28] Zarrin, M., Rahdar, M., Gholamian, A. (2015): Biological control of the nematode infective larvae of *Trichostrongylidae* family with filamentous fungi. – Jundishapur Journal of Microbiology 8(3): e17614.

http://www.aloki.hu ● ISSN 1589 1623 (Print) ● ISSN 1785 0037 (Online)
DOI: http://dx.doi.org/10.15666/aeer/1605_58255835
© 2018, ALÖKI Kft., Budapest, Hungary

PREPARATION OF Bi_2MoO_6/KELP BIOCHAR NANOCOMPOSITE FOR ENHANCING DEGRADABILITY OF METHYLENE BLUE

ZHOU, Y.[1] – CAI, L.[2] – GUO, J.[3] – WANG, Y.[4] – JI, L.[4*] – SONG, W.[5*]

[1]*College of Port and Transportation Engineering, Zhejiang Ocean University*
Haida South Road No.1, Lincheng Street, Dinghai District, 316022 Zhoushan, China

[2]*College of Environmental and Science Technology, Donghua University*
201620 Shanghai, China

[3]*College of Food and Medical, Zhejiang Ocean University, 316022 Zhoushan, China*

[4]*Institute of Innovation & Application, Zhejiang Ocean University, 316022 Zhoushan, China*

[5]*College of Petrochemical and Energy Engineering, Zhejiang Ocean University*
316022 Zhoushan, China

**Corresponding authors*
L. Ji – e-mail: jll-gb@163.com; W. Song – e-mail: swd60@163.com
phone: +86-580-226-2589; fax: +86-580-226-2063

(Received 25th May 2018; accepted 1st Aug 2018)

Abstract. Bi_2MoO_6/kelp biochar (BKB) nanocomposite has been obtained by a combination of pyrolysis and solvothermal method. The synthesized sample was characterized by X-ray diffraction (XRD), scanning electron microscopy (SEM), UV-vis diffuse reflection spectroscopy (DRS) and Fourier transform infrared (FT-IR) spectra. The specific surface area and pore volumes of BKB nanocomposite with the mass ratio of Bi_2MoO_6 to kelp biochar of 0.25 (BKB-0.25) were 210.918 m^2/g and 0.2449 cm^3/g, respectively, indicating that the as-prepared nanocomposite had wide specific surface area and porous structure. Moreover, the photocatalytic tests exhibited that the highest photocatalytic degradation efficiency obtained by BKB-0.25 under visible light irradiation for 60 min was 61.39%, which was up to 13 times higher in comparison with pure Bi_2MoO_6. This showed that the photocatalytic degradation data fitted well with pseudo-first-order model. The unique features of BKB nanocomposite suggested that it may have a great potential for dyes removal from liquid effluents.
Keywords: *kelp biochar, photocatalyst, adsorption activity, nanocomposite, removal efficiency*

Introduction

Methylene blue (MB), a cationic type model dye compound, is widely used in industries such as paper, leather, cosmetics and pharmaceutical industries (Wang et al., 2018; Velanganni et al., 2018). Residues of dye without proper treatment will do harm to both human health and ecological safety (Abdelwahab and Emh, 2018; Liu et al., 2017; Ghosh and Bandyopadhyay, 2017; Fan et al., 2016). The most common methods have been used for wastewater treatment such as chemical oxidation, microbiological degradation, electrochemical treatment, adsorption, etc, but they are limited to some kinds of dyes due to many reasons. Being effective and attractive, the photocatalytic technique is a promising way for the treatment of dyes and organic compounds from aqueous effluents.

Nanostructured photocatalysts have gained worldwide attention currently, due to their potential application in environmental purification and solar energy conversion

http://www.aloki.hu ● ISSN 1589 1623 (Print) ● ISSN 1785 0037 (Online)
DOI: http://dx.doi.org/10.15666/aeer/1605_58375847
© 2018, ALÖKI Kft., Budapest, Hungary

(Zhang et al., 2006; Zhang et al., 2007; Umapathy et al., 2015). Recently, Bi_2MoO_6 has been one of the excellent photocatalysts for the degradation of organic compounds under visible light irradiation, which has excellent intrinsic properties, such as, dielectric nature, catalytic behavior and luminescence with a typical E_g of about 2.6 eV (Zhang et al., 2011). However, the photocatalytic performance of Bi_2Mo_6 is still far from satisfactory due to the high recombination rate of photogenerated electron–hole pairs and potentially poor surface chemistry, which limits the application of Bi_2MoO_6 catalysts (Yan et al., 2015). It has been demonstrated that complex or hierarchical hetero-nano-structures with high performance can be achieved to facilitate the separation of photo-generated electron–hole pairs and further improve the photocatalytic activity (Shang et al., 2010; Li et al., 2016; Chen et al., 2015; Cao et al., 2011). Among them, Bi_2MoO_6-based composites, such as MoS_2/Bi_2MoO_6, $BiOI/Bi_2MoO_6$ and Bi_2MoO_6/TiO_2 have been proved to have higher photocatalytic activity.

Biochar materials obtained from waste biomass (gasification or pyrolysis) show better performance in adsorption of organic pollutants from water owing to their low cost, economically feasible, developed porosity, wide specific surface area and abundant functional groups (Enniya et al., 2018; Jian et al., 2018; Yang et al., 2017). Macroalgae has been promising biomass resources for the production of activated carbon with a high adsorption capacity (Rathinam et al., 2011; Yu et al., 2015; Son et al., 2018; Lee et al., 2018; Ross et al., 2018). However, the present transformation and utilization of seaweed are mainly in the production of fertilizers, industrial gums (phytocolloids), and bio-materials for medical applications, which limits the utilization of this raw material for the production of adsorption and carrier material (Haykiri-Acma et al., 2013; Yu et al., 2017; Joonhyuk et al., 2014).

In this work, a novel Bi_2MoO_6/kelp biochar nanocomposite by using the abundant and available kelp was fabricated by a combination of pyrolysis and solvothermal method, which exhibited an enhanced photocatalytic activity in the visible light irradiation. Therefore, the as-prepared sample may be expected to effectively degrade organic pollutants in water, which could realize the value-added use of kelp biomass.

Materials and methods

Materials

The fresh kelp was collected from a local food market in Zhoushan, Zhejiang. Bi $(NO_3)\cdot 5H_2O$, $Na_2MoO_4\cdot H_2O$, Methylene blue (MB, $C_{16}H_{18}N_3SCl$), glycol, ethanol (>99.7%) and hydrochloric acid were analytical grade and had been obtained from Sinopharm Chemical Reagent Co., Ltd. China.

Preparation of carbon

45 g of dried kelp powder was pyrolyzed in a tubular furnace under nitrogen flow (100 mL min^{-1}) up to 800 °C with a rate of 10 °C/min, and the final temperature lasted for 3 h (Wang et al., 2016; Aravindhan et al., 2007; Aravindhan et al., 2004; Rathinam et al., 2011). The carbonized residue was allowed to cool down to room temperature in a furnace under the same gas flow. Then, it was removed from the furnace and stored in an air-tight sample vessel (Choi et al., 2014; Yu et al., 2017; Afonso et al., 2018).

http://www.aloki.hu ● ISSN 1589 1623 (Print) ● ISSN 1785 0037 (Online)
DOI: http://dx.doi.org/10.15666/aeer/1605_58375847
© 2018, ALÖKI Kft., Budapest, Hungary

The obtained black solid was mixed with KOH powder with the mass ratio of 1:3. Then the mixture was also pyrolyzed in that tubular furnace under nitrogen flow (100 mL min^{-1}) up to 800 °C with a rate of 10 °C/min. The residence time of the final temperature would reduce to 2 h. This cooled sample was immersed in the deionization water and then heated in a water bath at 80 °C. The sample was washed with 0.1 mol/L HCl to neutrality, then filtered and washed with deionization water three times, and finally dried at 73 °C overnight.

Preparation of Bi_2MoO_6–kelp biochar nanocomposite

In a typical case, 0.363 g $Bi(NO_3)_3$•$5H_2O$ and 0.0907 g Na_2MoO_4•$2H_2O$ were dissolved in 7 mL ethylene glycol. Then, 0.1016 g kelp biochar was dispersed into 20 mL ethanol under magnetic stirring for 60 min to form a homogeneous solution, which was slowly added into the $Bi(NO_3)_3$•$5H_2O$ and Na_2MoO_4•$2H_2O$ mixed solution, stirring for 12 h. The resulting mixture was transferred into a 50 mL Teflon-lined stainless steel autoclave, heated to 160 °C and maintained for 24 h. Then, the autoclave was cooled down to room temperature. The obtained sample was washed with deionized water and ethanol to remove any ionic residual, then dried at 73 °C for 12 h. The as-fabricated sample was denoted as BKB-2.25. According to this method, the Bi_2MoO_6/kelp biochar composite with different mass ratios of 0.25, 0.75, 1.25 and 1.75 were synthesized and named as BKB-0.25, BKB-0.75, BKB-1.25 and BKB-1.75, respectively. For comparison, pure Bi_2MoO_6 was prepared by adopting the method in the absence of kelp biochar.

Characterization

Composition and morphology of the samples were investigated by scanning electron microscopy (SEM, Hitachi S-4800, Japan), and X-ray diffraction (Ultima IV X-Ray Diffractometer, Rigaku Corporation, Japan) in the range of 2θ = 10–80°. The surface functional group were analyzed by Fourier transform infrared spectra (FTIR, Nicolet 5700, Thermo Corp., USA). UV–vis spectrophotometer (UV-4100, Shimadzu) was used to analyze the optical properties of the as-fabricated materials in the wavelength range of 200–1000 nm by the diffuse-reflectance spectroscopy (DRS). The specific surface areas of the samples were measured with a Micromeritics ASAP 2010 instrument and analyzed by the BET method.

The removal efficiency of MB

The adsorption experiments of MB were investigated by adding 0.01 g as-fabricated samples to 50 mL MB solutions (80 mg/L) in Erlenmeyer flasks which were stirred in the dark for 4 h to ensure the dye and sample to reach adsorption-desorption equilibrium.

The photocatalytic activity of BKB composite was evaluated by photodegradation of MB solution under visible light (λ > 420 nm) irradiation. To obtain the needed irradiation photo source (14 V, 16 A, 15 cm), a 300 W xenon lamp (FSX-300, NBeT Group Corp. Beijing) was used as a visible light source. Moreover, 2 mL of suspension was collected followed via centrifuging to move the remained photocatalysts at specific illumination intervals. And the obtained clear solution was measured at 665 nm via a UV–vis spectroscopy (UV 2600, Shimadzu). The adsorption

http://www.aloki.hu ● ISSN 1589 1623 (Print) ● ISSN 1785 0037 (Online)
DOI: http://dx.doi.org/10.15666/aeer/1605_58375847
© 2018, ALÖKI Kft., Budapest, Hungary

capacity of BKB composite was calculated according to *Equation 1* as follows (Chen et al., 2016):

$$\text{Adsorption capacity (mg/g)} = (C_0\text{-}C_e) \times (V/m) \quad \text{(Eq.1)}$$

where q_e is equilibrium adsorption capacity of the BKB composite, mg/g; C_e and C_0 are the equilibrium and initial concentration of MB concentration, mg/L; V is the volume of the solution, L; M is the mass of the BKB composite, g.

The photocatalytic degradation of BKB composite was calculated according to *Equation 2* as follows (Geng et al., 2017):

$$\text{Degradation} = [(A_0 - A_1) / A_0] \times 100\% \quad \text{(Eq.2)}$$

where A_0 is an initial photocatalytic degradation of methylene blue, A_1 is an absorbance measured at the irradiation time.

Results and discussion

Characterization of as-prepared samples

The specific surface area and pore volumes of BKB composite are listed in *Table 1*. It can be seen that the specific surface area and pore volumes increase with the decrease of Bi_2MoO_6 content. Particularly, the maximum values BKB-0.25 obtained are 210.918 m^2/g and 0.2449 cm^3/g, respectively, which may be beneficial for the enhancement of sorption capacity. The nitrogen adsorption isotherms for BKB-0.25 suggests the V isotherms with a hysteresis loop at $P/P_0 > 0.4$. Moreover, the slit between adsorption and desorption curves may be due to the presence of stacking holes. The pore size distribution of BKB-0.25 also exhibits the significance of mesopores with pores mainly in the range 2-20 nm (*Fig. 1*).

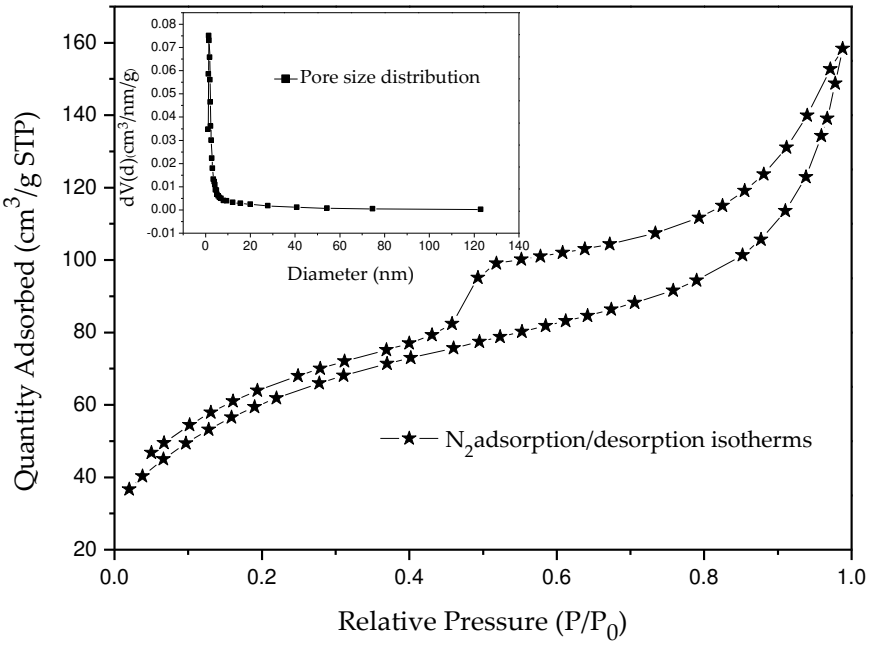

Figure 1. *Nitrogen sorption isotherms of BKB—0.25 with corresponding pore size distribution*

http://www.aloki.hu ● ISSN 1589 1623 (Print) ● ISSN 1785 0037 (Online)
DOI: http://dx.doi.org/10.15666/aeer/1605_58375847
© 2018, ALÖKI Kft., Budapest, Hungary

Table 1. *Specific surface area parameters of BKB composite*

Composites	BET (m^2/g)	Total pore volumes (cm^3/g)	Average pore diameter (nm)
BKB-0.25	210.918	0.2449	4.645
BKB-0.75	168.731	0.2032	4.817
BKB-1.25	105.936	0.1549	5.850
BKB-1.75	41.528	0.1066	10.27
BKB-2.25	35.793	0.1150	12.86

As shown in *Figure 2a,* kelp biochar has a very smooth surface. And surface morphologies of BKB-0.25 (*Fig. 2b*) shows the presence of uneven structure, which suggests that Bi_2MoO_6 nanoparticles successfully grow on the surface of kelp carbon.

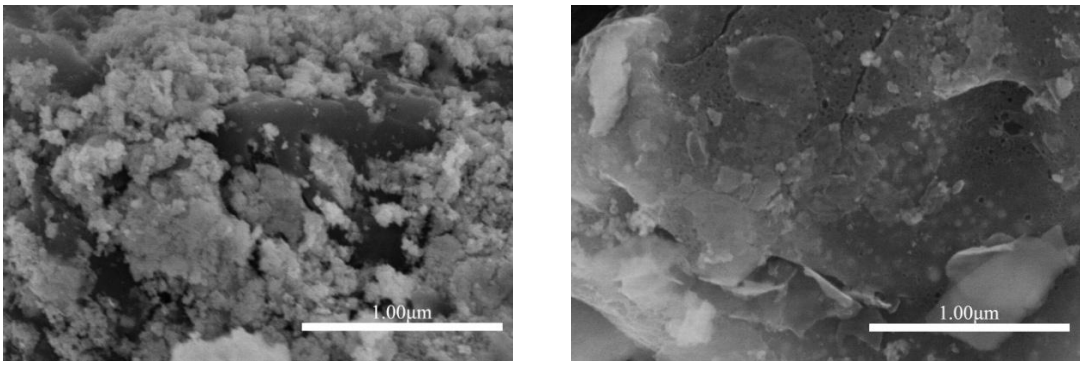

a **b**

Figure 2. *Surface morphologies of (a) kelp biochar, (b) BKB-0.25*

Figure 3 shows the FT-IR spectrum of the kelp biochar and as-prepared Bi_2MoO_6/kelp biochar composite to investigate their chemical structures. The spectrum of pure Bi_2MoO_6 contains some strong characteristic bands such as Mo = O (~ 842 cm^{-1}) stretching vibration and the absorption at 743 cm^{-1} is attributed to the tetrahedral stretching vibration of Mo (VI)—O groups. However, a band at 580 cm^{-1} may be due to the bending mode of the MoO_6. Characteristic absorption bands are all observed on the as-prepared composite, indicating the presence of Bi_2MoO_6 grown on kelp biochar materials.

Information concerning the crystal structure and phase analysis of the as-fabricated materials are shown in *Figure 4*. The XRD patterns of pure Bi_2MoO_6 and BKB composite exhibit that diffraction peaks at about 2θ = 23.3°, 28.1°, 32.3°, 35.8°, 46.7°, 55.3° and 58.2° could be perfectly indexed to the (111), (131), (200), (151), (062), (331) and (191) crystal planes of orthorhombic Bi_2MoO_6 (JCPDS76-2388) respectively. This indicates that BKB composite is successfully synthesized.

A comparison of the UV–vis diffuse reflectance spectra of pure Bi_2MoO_6 and BKB composite are shown in *Figure 5*. The pure Bi_2MoO_6 exhibits a weak absorption in the visible light with range absorption edges located at 478 nm. For the BKB heterostructures, there is an enhanced absorbance in the visible-light region (λ > 400 nm) with different contents of kelp biochar added. The optical absorption edge of composite is gradually red shifted when increasing the content of kelp biochar. The

http://www.aloki.hu ● ISSN 1589 1623 (Print) ● ISSN 1785 0037 (Online)
DOI: http://dx.doi.org/10.15666/aeer/1605_58375847
© 2018, ALÖKI Kft., Budapest, Hungary

formation of the Bi_2MoO_6/Kelp biochar heterostructures could realize a more efficient utilization of the solar energy, which is expected to become an excellent photocatalyst shortly.

A comparison of the UV–vis diffuse reflectance spectra of pure Bi_2MoO_6 and BKB composite are shown in *Figure 5*. The pure Bi_2MoO_6 exhibits a weak absorption in the visible light with range absorption edges located at 478 nm. For the BKB heterostructures, there is an enhanced absorbance in the visible-light region ($\lambda > 400$ nm) with different contents of kelp biochar added. The optical absorption edge of composite is gradually red shifted when increasing the content of kelp biochar. The formation of the Bi_2MoO_6/Kelp biochar heterostructures could realize a more efficient utilization of the solar energy, which is expected to become an excellent photocatalyst shortly.

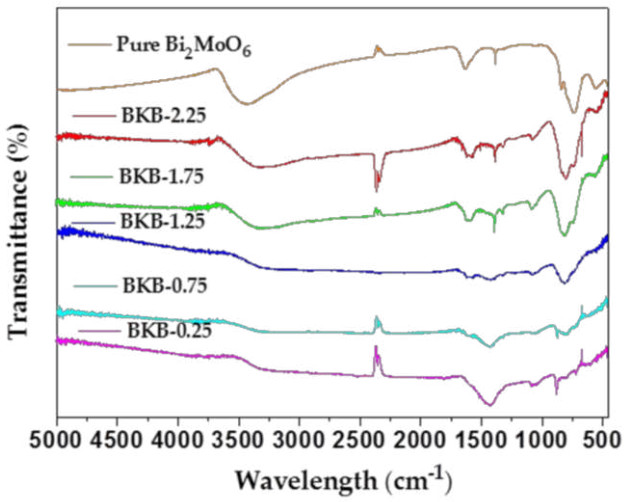

Figure 3. *FTIR spectra of BKB-0.25, BKB-0.75, BKB-1.25, BKB-1.75, BKB-2.25, and pure Bi_2MoO_6*

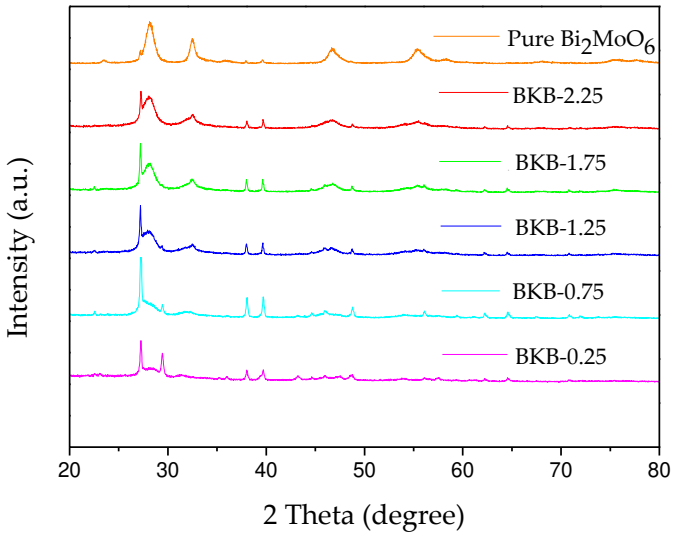

Figure 4. *XRD patterns of BKB-0.25 BKB-0.75, BKB-1.25, BKB-1.75, BKB-2.25, and pure Bi_2MoO_6*

http://www.aloki.hu ● ISSN 1589 1623 (Print) ● ISSN 1785 0037 (Online)
DOI: http://dx.doi.org/10.15666/aeer/1605_58375847
© 2018, ALÖKI Kft., Budapest, Hungary

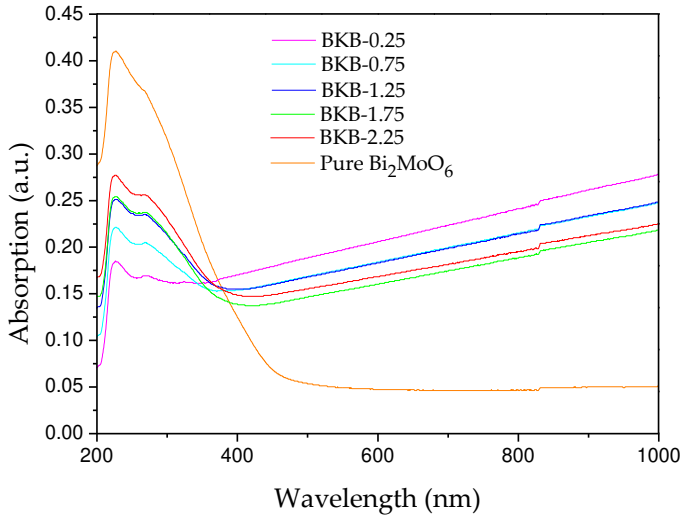

Figure 5. *UV-Vis diffuse reflectance spectra of BKB-0.25, BKB-0.75, BKB-1.25, BKB-1.75, BKB-2.25, and pure Bi_2MoO_6*

The removal efficiency of MB

Adsorption tests

The adsorption of methylene blue on the composite is implemented for 4 h under dark conditions without exposure to visible light illumination, and the results are represented in *Figure 6*. The increased adsorption percentage from 0.6625% to 45.28%, indicated that the adsorption will increase with the decrease of Bi_2MoO_6 content. The equilibrium adsorption capacity of MB on different Bi_2MoO_6/Kelp biochar composite is shown in *Table 2*. It can be seen that the maximum adsorption capacity obtained by BKB-0.25 is consistent with the BET results.

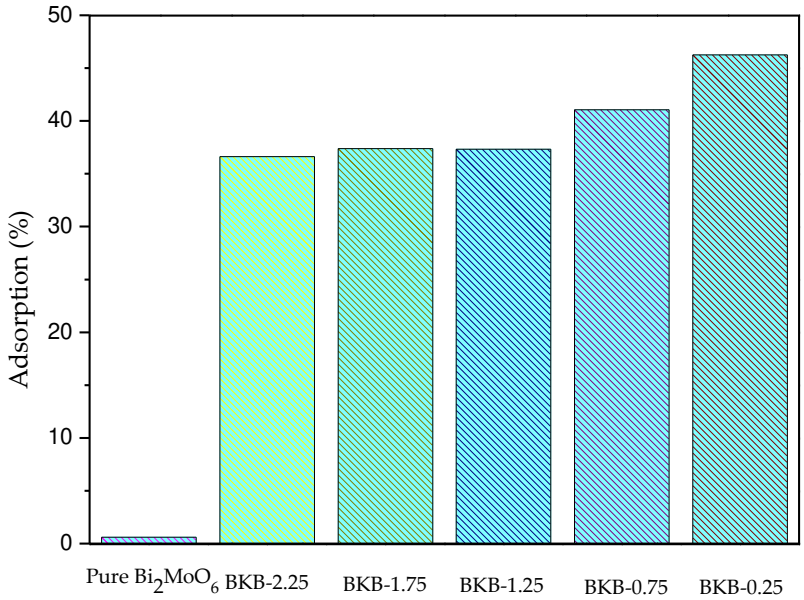

Figure 6. *Adsorption of MB for BKB-0.25, BKB-0.75, BKB-1.25, BKB-1.75, BKB-2.25, and pure Bi_2MoO_6*

http://www.aloki.hu ● ISSN 1589 1623 (Print) ● ISSN 1785 0037 (Online)
DOI: http://dx.doi.org/10.15666/aeer/1605_58375847
© 2018, ALÖKI Kft., Budapest, Hungary

Table 2. *Equilibrium adsorption capacity of MB on samples*

Catalysts	q_e (mg/g)
pure Bi_2MoO_6	2.65
BKB-2.25	143.4
BKB-1.75	146.4
BKB-1.25	146.2
BKB-0.75	160.75
BKB-0.25	181.1

Photodegradation texts

On the other hand, photodegradation texts are implemented to evaluate the photocatalytic efficiency of samples under visible light irradiation. As we can see in *Figure 7,* the Bi_2MoO_6/Kelp biochar composite may have a better photocatalytic performance than pure Bi_2MoO_6. Moreover, the photocatalytic activity of the composite is remarkably enhanced with the increasing of kelp biochar content added. Significantly, BKB-0.25 composite exhibits the best catalytic activity, while the percent of MB degraded (out of total MB) is 16.11%. For comparison, blank tests are carried out at the identical conditions except for the absence of either irradiation or photocatalyst.

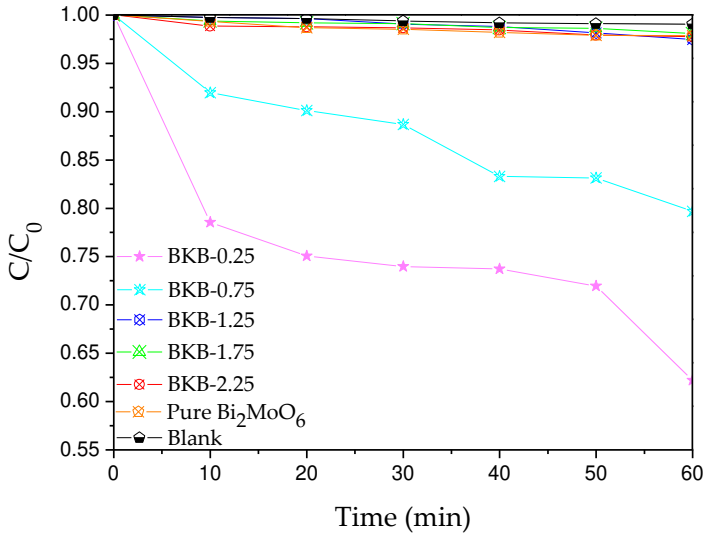

Figure 7. *Degradation efficiency of MB for BKB-0.25, BKB-0.75, BKB-1.25, BKB-1.75, BKB-2.25, and pure* Bi_2MoO_6

The photocatalytic degradation process of MB is studied on the basis of pseudo-first- order kinetic model, which can be expressed by *Equation 3* (Liu et al., 2017):

$$-\ln(C_t / C_0) = kt \qquad \text{(Eq.3)}$$

where k is apparent rate constant; C_0 is initial dye concentration in mg/L; C_t is the concentration of dye in mg/L at different time intervals.

http://www.aloki.hu ● ISSN 1589 1623 (Print) ● ISSN 1785 0037 (Online)
DOI: http://dx.doi.org/10.15666/aeer/1605_58375847
© 2018, ALÖKI Kft., Budapest, Hungary

Figure 8 shows that photocatalytic degradation processes have the good consistency with pseudo-first-order kinetic model. Moreover, pure Bi_2MoO_6 only shows a low degradation rate of 0.00045 min^{-1}. As for the BMB composite, the mass ratio of kelp biochar could greatly influence the degradation rate increasing from 0.0003 min^{-1} to 0.0082 min^{-1}. Moreover, the maximum value is 0.0082 min^{-1} obtained by BKB-0.25, which is up to 18.22 times higher in comparison with pure Bi_2MoO_6. As it is shown in *Figure 7,* the order of the MB removal efficiency is BKB-0.25 > BKB-0.75 > BKB-1.25 ≈ BKB-1.75 ≈ BKB-2.25 > pure Bi_2MoO_6. The enhanced degradation efficiency may be attributed to the synergetic effects of effective absorption as well as the heterojunction constructed between Bi_2MoO_6 and kelp biochar.

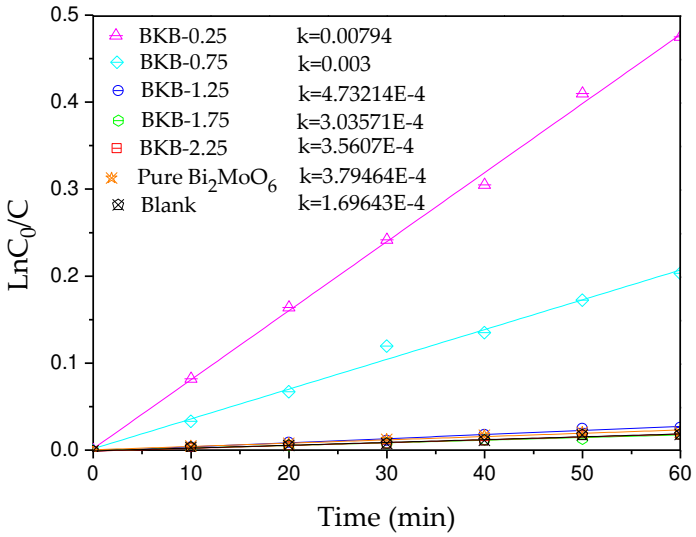

Figure 8. *Kinetic process of MB degradation for BKB-0.25, BKB-0.75, BKB-1.25, BKB-1.75, BKB-2.25, and pure Bi_2MoO_6*

Conclusions

In summary, a novel BKB composite has been successfully prepared via combining the pyrolysis and solvothermal method. As shown in the work, BKB nanocomposite exhibits superior removal efficiency of MB compared with pure Bi_2MoO_6, and the best degradability can be obtained by BMB-0.25 composite the best degradability. The total removal efficiency of MB on BMB-0.25 is 61.39%, which was up to 13 times higher than pure Bi_2MoO_6. Consequently, the novel composite materials with enhanced photocatalytic activity are promising candidate materials for environmental remediation.

Acknowledgements. This study was supported by the Natural Science Foundation of Zhejiang Province of China (No. LQ16D060004), Key Research and Development Projects of Zhejiang Province of China (No. 2018C02043), Demonstration Project of Marine Economic Innovation and Development of Zhoushan City of China, and Demonstration Project of Marine Economic Innovation and Development of Yantai City of China (No. YHCX-SW-L-201705).

http://www.aloki.hu ● ISSN 1589 1623 (Print) ● ISSN 1785 0037 (Online)
DOI: http://dx.doi.org/10.15666/aeer/1605_58375847
© 2018, ALÖKI Kft., Budapest, Hungary

REFERENCES

[1] Abdelwahab, N. A., Emh, M. (2018): Synthesis and characterization of methyl pyrazolone functionalized magnetic chitosan composite for visible light photocatalytic degradation of methylene blue. – International Journal of Biological Macromolecules 108: 1035-1044.

[2] Afonso, C., Cardoso, C., Ripol, A. et al. (2018): Composition and bioaccessibility of elements in green seaweeds from fish pond aquaculture. – Food Research International. DOI: 10.1016/j.foodres.2017.11.015.

[3] Aravindhan, R., Madhan, B., Rao, J. R. et al. (2004): Recovery and reuse of chromium from tannery wastewaters using Turbinaria ornata, seaweed. – Journal of Chemical Technology & Biotechnology 79(11): 1251-1258.

[4] Aravindhan, R., Rao, J. R., Nair, B. U. (2007): Kinetic and equilibrium studies on biosorption of basic blue dye by green macroalgae Caulerpa scalpelliformis. – Journal of Environmental Science & Health Part A Toxic/Hazardous Substances & Environmental Engineering 42(5): 621-631.

[5] Cao, J., Xu, B., Luo, B. et al. (2011): Novel BiOI/BiOBr heterojunction photocatalysts with enhanced visible light photocatalytic properties. – Catalysis Communications 13(1): 63-68.

[6] Chen, Y., Tian, G., Shi, Y. et al. (2015): Hierarchical MoS 2/Bi 2 MoO 6, composites with synergistic effect for enhanced visible photocatalytic activity. – Applied Catalysis B Environmental 164: 40-47.

[7] Chen, Y., Yu, B., Lin, J. et al. (2016): Simultaneous adsorption and biodegradation (SAB) of diesel oil using immobilized Acinetobacter venetianus, on porous material. – Chemical Engineering Journal 289: 463-470.

[8] Choi, J., Choi, J. W., Dong, J. S. et al. (2014): Production of brown algae pyrolysis oils for liquid biofuels depending on the chemical pretreatment methods. – Energy Conversion & Management 86(10): 371-378.

[9] Enniya, I., Rghioui, L., Jourani, A. (2018): Adsorption of hexavalent chromium in aqueous solution on activated carbon prepared from apple peels. – Sustainable Chemistry & Pharmacy 7: 9-16.

[10] Fan, S., Tang, J., Wang, Y. et al. (2016): Biochar prepared from co-pyrolysis of municipal sewage sludge and tea waste for the adsorption of methylene blue from aqueous solutions: Kinetics, isotherm, thermodynamic and mechanism. – Journal of Molecular Liquids 220: 432-441.

[11] Geng, B., Wei, B., Gao, H. et al. (2017): Ag_2O nanoparticles decorated hierarchical Bi2MoO6 microspheres for efficient visible light photocatalysts. – Journal of Alloys & Compounds 699: 783-787.

[12] Ghosh, S. K., Bandyopadhyay, A. (2017): Adsorption of methylene blue onto citric acid treated carbonized bamboo leaves powder: Equilibrium, kinetics, thermodynamics analyses. – Journal of Molecular Liquids 248. DOI: 10.1016/j.molliq.2017.10.086.

[13] Haykiri-Acma, H., Yaman, S., Kucukbayrak, S. (2013): Production of bio briquettes from carbonized brown seaweed. – Fuel Processing Technology 106(2): 33-40.

[14] Jian, X., Zhuang, X., Li, B. et al. (2018) : Comparison of characterization and adsorption of biochars produced from hydrothermal carbonization and pyrolysis. – Environmental Technology & Innovation 10: 27-35.

[15] Joonhyuk, C., Jaewook, C., Dongjin, S. et al. (2014): Production of brown algae pyrolysis oils for liquid biofuels depending on the chemical pretreatment methods. – Energy Conversion & Management 86(10): 371-378.

[16] Lee, D. J., Cheng, Y. L., Wong, R. J. et al. (2018): Adsorption removal of natural organic matters in waters using biochar. – Bioresource Technology 260: 413-416.

http://www.aloki.hu ● ISSN 1589 1623 (Print) ● ISSN 1785 0037 (Online)
DOI: http://dx.doi.org/10.15666/aeer/1605_58375847
© 2018, ALÖKI Kft., Budapest, Hungary

[17] Li, J., Liu, X., Zhuo, S., Pan, L. (2016): Novel Bi_2MoO_6/TiO_2, heterostructure microspheres for degradation of benzene series compound under visible light irradiation. – Journal of Colloid & Interface Science 463: 145-153.
[18] Liu, Y., Yang, Z. H., Song, P. P. et al. (2017): Facile synthesis of $Bi_2MoO_6/ZnSnO_3$, heterojunction with enhanced visible light photocatalytic degradation of methylene blue. – Applied Surface Science 430. DOI: 10.1016/j.apsusc.2017.06.231.
[19] Rathinam, A., Rao, J. R., Nair, B. U. (2011): Adsorption of phenol onto activated carbon from seaweed: Determination of the optimal experimental parameters using factorial design. – Journal of the Taiwan Institute of Chemical Engineers 42(6): 952-956.
[20] Ross, A., Jones, J., Kubacki, M. et al. (2008): Classification of macroalgae as fuel and its thermochemical behaviour. – Bioresour Technol 99(14): 6494-504.
[21] Shang, M., Wang, W., Ren J. et al. (2010): A novel BiVO4 hierarchical nanostructure: Controllable synthesis, growth mechanism, and application in photocatalysis. – Crystengcomm 12(6): 1754-1758.
[22] Son, E. B., Poo, K. M., Chang, J. S., Chae, K. J. (2018): Heavy metal removal from aqueous solutions using engineered magnetic biochars derived from waste marine macro-algal biomass. – Science of the Total Environment 615: 161.
[23] Umapathy, V., Manikandan, A., Antony, S. A. et al. (2015): Structure, morphology and opto-magnetic properties of Bi 2 MoO 6, nano-photocatalyst synthesized by sol–gel method. – Transactions of Nonferrous Metals Society of China 25(10): 3271-3278.
[24] Velanganni, S., Pravinraj, S., Immanuel, P. et al. (2018): Nanostructure CdS/ZnO heterojunction configuration for photocatalytic degradation of Methylene blue. – Physica B Condensed Matter 534(April): 56-62.
[25] Wang, S., Hu, Y., Uzoejinwa, B. B. et al. (2016): Pyrolysis mechanisms of typical seaweed polysaccharides. – Journal of Analytical & Applied Pyrolysis 124. DOI: 10.1016/j.jaap.2016.12.005.
[26] Wang, S., Zhou, Y., Han, S. et al. (2018): Carboxymethyl cellulose stabilized ZnO/biochar nanocomposites: Enhanced adsorption and inhibited photocatalytic degradation of methylene blue. – Chemosphere 197: 20-25.
[27] Yan, T., Sun, M., Liu, H. et al. (2015): Fabrication of hierarchical BiOI/Bi2MoO6, heterojunction for degradation of bisphenol A and dye under visible light irradiation. – Journal of Alloys & Compounds 634(1): 223-231.
[28] Yang, K., Jiang, Y., Yang, J. et al. (2017): Correlations and adsorption mechanisms of aromatic compounds on biochars produced from various biomass at 700 °C. – Environmental Pollution 233: 64.
[29] Yu, K. L., Lau, B. F., Show, P. L. et al. (2017): Recent developments in algal biochar production and characterization. – Bioresource Technology 246: 2-11.
[30] Yu, Y., Wang, C., Guo, X., Paul, C. J. (2015): Modification of carbon derived from sargassum sp. by lanthanum for enhanced adsorption of fluoride. – J Colloid Interface Sci 441: 113-120.
[31] Zhang, M., Shao, C., Mu, J. et al. (2011): One-dimensional Bi2MoO6/TiO2 hierarchical heterostructures with enhanced photocatalytic activity. – Crystengcomm 14(2): 605-612.
[32] Zhang, S., Zhang, C., Man, Y. et al. (2006): Visible-light-driven photocatalyst of Bi_2WO_6, nanoparticles prepared via complex amorphous precursor and photocatalytic properties. – Journal of Solid State Chemistry 179(1): 62-69.
[33] Zhang, S. C., Yao, W. Q., Zhu, Y. F. et al. (2007): Preparation and photoelectrochemical properties of Bi_2WO_6 films with visible light response. – Acta Physico-Chimica Sinica 23(1): 111-115.

http://www.aloki.hu ● ISSN 1589 1623 (Print) ● ISSN 1785 0037 (Online)
DOI: http://dx.doi.org/10.15666/aeer/1605_58375847
© 2018, ALÖKI Kft., Budapest, Hungary

QUATERNARY EQUILIBRIUM LINE ALTITUDE ESTIMATION BY DIFFERENT METHODS IN THE ALVAND MOUNTAIN OF HAMEDAN, IRAN

JAFARI, GH. H.[1*] – BARATI, Z.[2]

[1]*Department of Geography, Faculty of Humanities, University of Zanjan, Zanjan, Iran*
(Phone: +98-24-3305-4176; fax: +98-24-3228-3201)

[2]*Master of Hydrogeomorphology, University of Zanjan, Zanjan, Iran*
(Phone: +98-469-2329)

**Corresponding author*
E-mail: jafarihas@znu.ac.ir

(Received 28th May 2018; accepted 31st Aug 2018)

Abstract. From the early Quaternary, external factors such as climate change have altered the surface of the earth. The climatic changes have led to increase or decrease of glacier in highlands of Iran. The Alvand Mountain with an altitude of 3500 m is one of Iran's highlands, which is located in Hamedan Provence. In order to the equilibrium line altitude (ELA) estimate during the last glacial maximum (LGM) in Alvand Mountain, this paper has used five methodological approaches such as Wright, slope–direction (SD), curvature coefficient (CC), the accumulation-area ratio (AAR), and terminus to head altitude ratio (THAR). After estimating ELA through the aforementioned methods, ELA in the northeast and southwest slopes were compared. According to the ELA estimates require the identification of Quaternary glacier circuses. The cirques in southwest slopes had an altitude between of 1700 to 2900 m and in northeast slopes had an altitude between of 2000 to 3400 m. The estimation of ELA of the whole study area turned out to be 2294 m. In the SD method, the average ELA in the northeast and the southwest slopes was 1960 and 2491 m, respectively. In the CC method, the ELA of the northeast and the southwest slopes was 2167 and 2099 m, respectively. The results of ELA analysis indicate that there are differences between the northeast and southwest slopes. According to Wright and CC methods, ELA in the northeast is higher than the southwest slopes, which is against the natural order of the environment. ELA estimated by AAR and SD methods in the northeast slopes is lower than in the southwest slopes. According to these two methods, there is about 500 m difference between the ELA of the northeast and southwest slopes. In this paper, in addition to the ELA, the water and ice equilibrium line altitude (WIELA) have been estimated. The field observation of the moraines revealed that WIELA during LGM was located at 1680 and 1776 m in the northeast and southwest slopes, respectively.
Keywords: *Alvand, curvature coefficient, glacial Quaternary, slope-direction, Wright*

Introduction

The Quaternary period represents the past 2.58 million years and is officially subdivided into the Pleistocene and Holocene epochs, with the base of the Holocene aging 11,700 calendar years before 2000 AD (Head and Gibbard, 2014). The Quaternary is characterized by repeated cycles of cold-warm climatic oscillations as the Earth alternated between glacial and retreating continental modes. Glacial –interglacial climate changes during the Quaternary were largely controlled by cyclic variations in the amount of solar radiation, or solution received in middle to high latitudes of the northern hemisphere (Bondarenko et al., 2013). The study of glaciers is of great importance for understanding and predicting global environmental changes (Knight, 2006). Climatic cold phases and future changes can be predicted by investigating the glacier advances (Abramowski et al., 2006; Solomina et al., 2004). Due to the different

http://www.aloki.hu ● ISSN 1589 1623 (Print) ● ISSN 1785 0037 (Online)
DOI: http://dx.doi.org/10.15666/aeer/1605_58495868
© 2018, ALÖKI Kft., Budapest, Hungary

nature of glaciers depending on the areas and their physiographic features, the various evidence is remarkable for glacier processes (Stroeven et al., 2013). As glaciers move across the Earth's surface, they erode and transport sediments. Ice sheets and glaciers are, therefore, powerful agents of erosion that are manifested in the grandeur of, e.g., glacial cirques and valleys (Jafari, 2013). Landforms resulted from glacial erosion are mostly detected in an area where the summits are 300-400 m higher than those of the equilibrium line altitudes (ELA) during the Quaternary cold periods (Zomorodian, 2012; JedariEivazi, 2011). The ELAs are the elevation across the glacier where the annual net balance is zero. "The equilibrium line indicates the position where, over a period of one year, accumulation of snow is exactly balanced by ablation" (Benn and Lehmkuhl, 2000). ELA is a statistical concept representing the line dividing the accumulation and ablation zones. The ELA of glaciers is particularly sensitive to changes in summer temperature and winter precipitation (Ohmura et al., 1992; Paterson, 1994; Nesje and Dahl, 2000; Osmaston, 2005). The ELA of a glacier separates the accumulation zone (where the annual mass balance is >0) from the ablation zone (where the annual mass balance is <0). These changes are commonly summarized by the fluctuations in the ELA (the dividing line between a glacier's accumulation and ablation areas). There is substantial controversy regarding the interpretation of changes in mountain glacial extent during the last glacial maximum (LGM). The LGM is in the Quaternary history when world glaciers reaching their maximum integrated volume (Clark et al., 2009). The LGM was the period when the Scandinavian, Irish, British and Laurentide ice sheets were at their maximum extent, coinciding with the period of lower sea level (approximately 130 m relative to the current sea level) (Yokoyama et al., 2000).

Review of literature

Regarding the context of this study, the geographical position of Iran and its climate limited the extension of continental glaciers. In fact, Iran's geographical position, i.e. 25 to 40 N and its arid and semi-arid climate have put a limitation on the formation of glaciers. Vaziri (2003) estimated the ELAs of present glaciers in some high mountains of Iran, including Damavand (5610 m), Alamkouh (4850 m), Sabalan (4811 m), Oshtorankouh (4090 m), and Zardkouh (4221 m). Several researchers have estimated the ELA of the glacier Quaternary, some of them are referred to in *Table 1*.

Many geomorphologists have studied the late Quaternary glaciers of Iran using Wright method. This method affects the topography and altitude of mountain sinusitis (The mountain knick point). In regions which mountain sinusitis is higher than ELA, the recognition of cirques becomes troublesome. This ends with not being able to estimate the exact ELA. In order to solve this problem, various methods have been compared in this article (Slope-direction (SD), curvature coefficient (CC), altitude- ratio (AR), accumulation-area ratio method (THAR) and Wright methods during the LGM to estimate ELA).

Materials and methods

The study area of this research is known as Alvand batholith. It is located in the vicinity of Hamedan province, Iran, with an area of 1375 km^2. This batholith belongs to the Quaternary and has been created by igneous masses. This area is made up of

http://www.aloki.hu ● ISSN 1589 1623 (Print) ● ISSN 1785 0037 (Online)
DOI: http://dx.doi.org/10.15666/aeer/1605_58495868
© 2018, ALÖKI Kft., Budapest, Hungary

intrusive granite rock, shale, siltstone, and schist of the Jurassic. It is surrounded from two directions: from the northwest by Khodabandehlu, Sanandaj, and Chehelcheshmeh Mountains, and from the southeast by Rasund Highlands and Vafs Mountains in the Central Province. The mountain is oriented to NW–SE directions and divides Hamedan Province into northern and southern halves. The Alvand Batholith is located between 48°–48.6°E and 34.5°–34.85°N. The highest and the lowest parts of the study area had 3574 and 1700 m altitude, respectively (*Fig. 1*).

Various methods of reconstructing ELAs have been critically reviewed (Meirding, 1982; Benn and Evans, 1998; Porter, 2001; Kaser and Osmaston, 2002; Osmaston, 2005). In order to reconstruct ELA, Wright, slope- direction (SD), curvature coefficient (CC), altitude- ratio (AR), and accumulation-area ratio method (AAR) methods were employed in this project. To this end, cirques altitude and extent of the glacier tongues were determined in both northern and southern slopes. The topographic 1: 50,000 scale maps were provided, and the study area was also divided into 28 sub-basins. All this information was recorded through direct observations and field surveys. In the next step, the results of the field surveys and Quaternary landform processes were considered together and combined with the geomorphological, topographic, and geological results.

Table 1. *Researchers of glacial geomorphology of Iran*

Researcher	Year	Region
Bobek	1934	Alborz and Kurdistan
Desio	1934	Zardkouh
Bobek	1963	Iran
Yamani	2002	Alamkouh
Tahoni	2005	Talesh
Moghimi	2008	Damavand Mountain
Mahmudi	2008	West of Iran (Kurdistan Province)
Yamani	2007	Zardkouh
Zomorodian	2012	Iran
Ramesht and Shoshtari Zadeh	2007	Salafchegan Mountain
Yamani	2007	Zard-kuh
Yamani et al.	2007	Karkas Mountain
Yamani and Zamani	2007	In the Shahrestanac valley (Alamkouh Mountain)
Ramesht and Kazemi	2007	Bol Mountain
Almodaresi and Ramesht	2007	Shirkouh Mountain
Moayeri et al.	2008	Safashahr Mountain
Nojavan et al.	2009	Shirkouh Mountain
Esfandiari Dur Abadi	2009	Sabalan
Zamani	2009	Jajroud and Karaj Mountain
Amirahmadi et al.	2011	Eghlid Aspas plain
Yamani et al.	2011	Jajroud and Karaj Mountain
Abtahi	2014	Jajroud basin
Parizi et al.	2014	Tangoeye Sirjan
Jafari and Asghari	2014	Zabjanroud
Jafarbiglo et al.	2014	Bidkhun Kerman
Seife et al.	2015	Shirkouh Mountain
Sharifi and Farah Bakhsh	2015	Shirkouh Mountain
Khosravi et al.	2016	Binalud Mountain

http://www.aloki.hu ● ISSN 1589 1623 (Print) ● ISSN 1785 0037 (Online)
DOI: http://dx.doi.org/10.15666/aeer/1605_58495868
© 2018, ALÖKI Kft., Budapest, Hungary

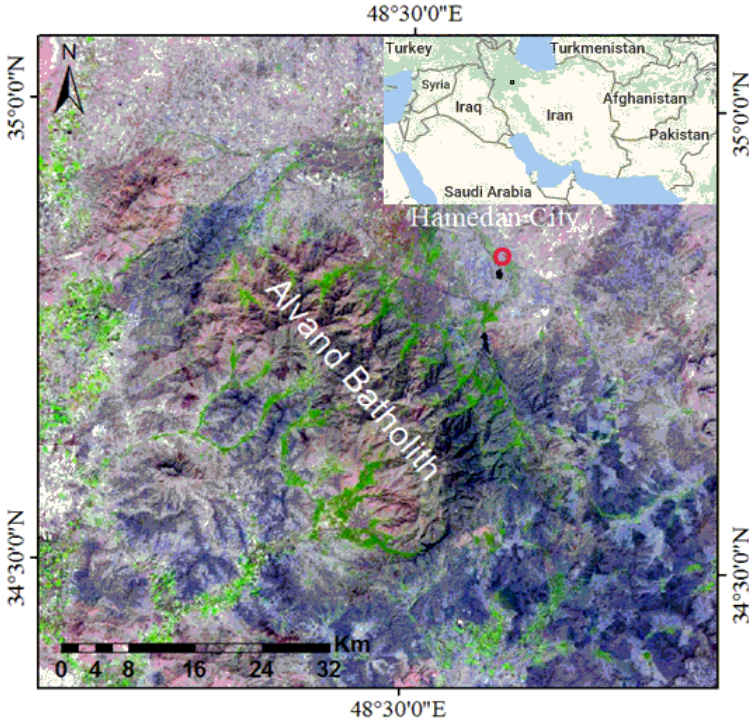

Figure 1. *The position in the study area*

Wright method

This method estimates ELA by determining the location and altitude of 60% of cirques above the line. Above this, the annual snowfall is more than the melting of annual, and below this altitude, the snowfall is less than the melting of annual. For estimating ELA, the altitude of identifying cirques is sorted based on descending order. Then the number of cirques is multiplied to 60% (*Eq. 1*) (Ramesht and Nematollahi, 2005; Ramesht and Shahzeidi, 2011; Ghahroudi Tali et al., 2013; Abtahi, 2014). The gained number represents a numerical line of cirques in which ELA is located. In the following, X shows the number of rows and N is cirques number (Porter, 2001).

$$X = N \times 0.6 \qquad \text{(Eq.1)}$$

The northeast and southwest slopes of sub-basins are separated using topographic maps, and cirques are determined in each slope.

Slope-direction (SD) method

Mountainous topography is constructed through a variety of interacting processes. In addition to other geomorphic processes, in many mountainous region's topography has been affected by glacier erosion (Headley and Ehlers, 2015). Among several factors, which influence ELA location, two important factors are determinate in SD Method. One of these factors is mountains' slope direction. A shady mountain slope will have a lower ELA than the one which receives more solar energy. Wind is another factor because it produces snow drifts on the leeward side of mountain ranges. In the middle latitudes of the Northern Hemisphere, ELA is lower on the north (shaded) and east

http://www.aloki.hu ● ISSN 1589 1623 (Print) ● ISSN 1785 0037 (Online)
DOI: http://dx.doi.org/10.15666/aeer/1605_58495868
© 2018, ALÖKI Kft., Budapest, Hungary

(leeward) slopes. Consequently, the most significant glacier development in this region is on north-facing and east-facing slopes (Petersen et al., 2008).

The principal reason for naming this method as SD is that ELA is estimated based on differences between mountain slope and their directions; besides these two elements, the latitude and longitude of the pikes must be calculated. This method depends on the solar elevation angle which varies according to the direction and slope of the mountains. In order to apply this method in Iran's context, appropriate equation was defined according to the prevailing geographical direction in 16 polygons. Which was determined considering the 16 Iran climate stations, and 8 acquisitions were defined in 16 geographical directions (Jafari, 2013). The reason why 8 equations were used for 16 directions is that the solar elevation angles in symmetric directions were equal. For example, the solar elevation angles are similar to each other in the southwest to southeast or in the northwest to northeast provided that the amount of slope is equal. Slope value is estimated by using 30 m Digital Elevation Mountain (DEM) of the area, and aspect is determined along with the main mountainous region. To this end, the slope maps were prepared separately for the northeast and southwest slopes. Based on slope maps, *Equation 2* was used to estimate the average slope in percent.

$$S = \frac{\Sigma(s.x)}{A} \qquad \text{(Eq.2)}$$

In this equation S is the average slope (%), *s* is the slope of each pixel, x is the area of each pixel in the slope map, and A is the total area. Jafari (2009) has estimated 144 equations in main and secondary directions on the basis of the slope and 16 Polygon Radiometers of Iran (*Table 2a* and *b*) (Moayeri et al., 2011).

Table 2a. *Temperature equations with slope in different directions of Iran (Moayeri et al., 2011)*

City	Station altitude	Latitude	Altitude	Station temperature	SE or SW		SE or SW		NNE or NNW		SSE or SSW	
					T=	R^2	T=	R^2	T=	R^2	T=	R^2
Ahvaz	22.5	48.69	31.32	25	24.94- 0.11s	1	25.33+.08s	.98	25.18-.18s	1	25.56+.09s	.96
Birjand	1491	59.22	32.88	16.4	16.7-.12s	1	17.15+0.9s	.98	16.29-.16s	.99	17.33+.1S	.97
Bakhtaran	1322	47	34.31	14.5	14.41- 0.12s	1	14.79+.09s	.99	14.63-.18s	1	15+.1S	.97
Bujnord	1091	57.32	37.47	13.1	13.12-.11s	.99	13.56+.09s	.99	13.36-.17s	1	13.76+.1S	.98
Esfahan	1600	51.67	32.64	16.1	16.01-.12s	1	16.44+.08s	.98	16.25-.18s	1	16.65+.09S	.96
Hamedan	1749	48.52	34.8	10.98	10.84-.11s	1	11.27+.09s	.99	11.09-.18s	1	11.49+.1s	.97
Kerman	1754	57	30.29	15.6	15.68-.12s	1	16.01+.08s	.98	15.95-.19s	1	16.22+.09s	.95
Mashhad	990	59.6	36.28	13.8	14.8-.11s	1	15.25+.09s	.99	15.05-.18s	1	15.44+.1s	.97
Uromieh	1312	45	37.55	11.4	11.04-.1s	.99	11.46+.08s	.99	11.27-.16s	1	11.64+.09s	.98
Shiraz	1488	52.53	29.61	17.5	17.41-.11s	1	17.81+.07s	.98	17.65-.18s	1	18.01+.08s	.95
Ramsar	20	50.66	36.9	22.3	21.99-.1s	.99	22.42+.09s	.99	22.23-.17s	1	22.62-.1s	.98
Tabas	711	56.92	33.58	21.3	21.84-.12s	1	22.31+.09s	.98	22.11-.2s	1	22.53+.1s	.97
Tabriz	1361	46.4	38.07	12.2	11.79-.11s	.99	12.24+.09s	.99	12.03-.17s	1	12.44+.1s	.98
Tehran	1190	51.41	35.71	17	16.84-.12s	1	17.32+.1s	.99	17.1-.19s	1	17.52+.11s	.97
Yazd	1230	54.35	31.88	18.8	18.74-.11s	1	19.15+.08s	.98	18.37-.16s	.99	19.17+.1s	.98
Zanjan	1663	48.47	36.67	10.9	10.63-.11s	.99	11.1+.1s	.99	10.88-.18s	1	11.31+.11s	.98

http://www.aloki.hu ● ISSN 1589 1623 (Print) ● ISSN 1785 0037 (Online)
DOI: http://dx.doi.org/10.15666/aeer/1605_58495868
© 2018, ALÖKI Kft., Budapest, Hungary

Table 2b. *Temperature equations with slope in different directions of Iran (Moayeri et al., 2011)*

City	North		South		WSW or ENE		ESE or WSW		W or E	
	T=	R^2	T=	R^2	T=	R^2	T=	R^2	T=	R^2
Ahvaz	31.231-.5s	1	25.97+S	.95	24.81-.04s	.96	25.07+.06s	1	24.87.02s	.95
Birjand	16.55-.2S	.99	17.45+.1S	.96	16.6-.04s	.96	16.89+.07s	1	16.56+.03s	.99
Bakhtaran	14.78-.2S	1	15.07+.1S	.96	14.3-.04s	.96	14.55+.07s	1	14.36+.02s	.95
Bujnord	13.52-.2s	1	13.8+.1S	.97	12.02-.03s	.93	13.31+.07s	1	13.11+.03s	.96
Esfahan	16.4-.21S	1	16.74+.09S	.95	15.9-.04s	.96	16.17+.06s	1	15.95+.02s	.95
Hamedan	24.21-.11s	1	11.56+.1S	.96	10.73-.04s	.94	11.02+.07s	1	10.8+.02s	.96
Kerman	16.07-.21s	1	16.49+.09S	.94	15.55-.04s	.97	15.73+.06s	1	15.61+.02s	.95
Mashhad	15.2-.21S	1	15.51+.1S	.97	14.71-.04s	.94	15+.07s	1	14.78+.03s	.96
Uromieh	11.42-.19S	1	11.71+.1S	.97	10.95-.03s	.93	11.22+.06s	1	11.04+.02s	.96
Shiraz	17.78-.2S	1	18.09+.09S	.94	17.29-.04s	.97	17.55+.06s	1	17.34+.02s	.96
Ramsar	22.38-.2S	1	22.68+.1S	.97	21.89-.03s	.93	22.18+.07s	1	21.98+.03s	.96
Tabas	22.26-.23s	1	22.62+.1S	.96	21.73-.04s	.96	22.02+.07s	1	21.79+.02s	.95
Tabriz	12.12-.2S	1	12.52+.11S	.97	11.71-.03s	.92	12+.07s	1	11.79+.03s	.95
Tehran	17.27-22s	1	17.6+.11S	.98	16.73-.04s	.94	17.05+.07s	1	16.82+.03s	.96
Yazd	19.1-.21S	1	19.22+.11S	.98	18.62-.04s	.96	18.88+.06s	1	18.69+.02s	.95
Zanjan	11.06-.22s	1	11.38+.11S	.97	10.52-.04s	.93	10.83+.07s	1	10.62+.03s	.96

For Alvand Mountain, polygonal equations of Hamadan in the northeast and southwest have been used based on the direction of the slopes. Placing the calculated slope of the northeast slopes in *Equation 3* and the southwest slopes in *Equation 4,* the annual average temperature was estimated for the related slope (Moayeri et al., 2011).

$$T = 10.84 - 0.11S \quad \text{(Eq.3)}$$

$$T = 11.27 + 0.09S \quad \text{(Eq.4)}$$

In the above equations, *T* is temperature in degrees Celsius, and *S* is the average slope in percentage. The estimated temperature in a thousand is multiplied, and the result is divided by the lapse rate of the region. Then the altitude of the base station is obtained. The estimated number is the contemporary ELA. According to the ELA estimated by Wright method and assuming zero temperature °C, the contemporary temperature estimated for altitude was deducted from the temperatures estimated for the northeast (*Eq. 3*) and southwest slopes of the relationships (*Eq. 4*), and the result was multiplied in thousand and divided by the lapse rate of the region, resulting in the altitude of the base station. The estimated number is the ELA. Therefore, determining the altitude is necessary where the temperature (slope and specific direction) is equal to zero. *Equation 5* was applied for this purpose.

$$H = \frac{T.1000}{Lr} + hs \quad \text{(Eq.5)}$$

http://www.aloki.hu ● ISSN 1589 1623 (Print) ● ISSN 1785 0037 (Online)
DOI: http://dx.doi.org/10.15666/aeer/1605_58495868
© 2018, ALÖKI Kft., Budapest, Hungary

In this equation, *H* is altitude, *Lr* is the environmental temperature drop per thousand meters, and *hs* is the altitude of the base station.

Curvature coefficient (CC)

Consideration of the contour line as the characteristics of topographic maps is an important step in the study of geomorphologic processes. Extensive glacial landforms related to valley glaciation are found in the study area, including glacial valleys, cirques (*Fig. 2A* and *B*), erratic block (*Fig. 2C*), Drumlin (*Fig. 2D*), and terminal moraines (*Fig. 2E* in southwest and F in northeast slope). Glacial valleys have distinct U-shaped cross-profiles, usually with a distinctive cirque at the valley head (Fu et al., 2013).

Figure 2. *Glacial landforms in the Alvand Mountain*

Steep mountain streams carve valleys in cross section that resemble the letter V (CC closer to zero). Since glaciers are much thicker than streams, they erode the sides as well as the bottom of these valleys, bowing the cross-sectional shape out to a U-shaped glacial trough (Gabler et al., 2017: 391) (CC is closer to one).

http://www.aloki.hu ● ISSN 1589 1623 (Print) ● ISSN 1785 0037 (Online)
DOI: http://dx.doi.org/10.15666/aeer/1605_58495868
© 2018, ALÖKI Kft., Budapest, Hungary

The contour line in different slopes of Alvand Mountain was determined by 30-m DEM. The mountain valleys were divided into 28 sub-basins by drawing a line along the mountain sinuosity on topographical maps 1.50000 (*Fig. 3*).

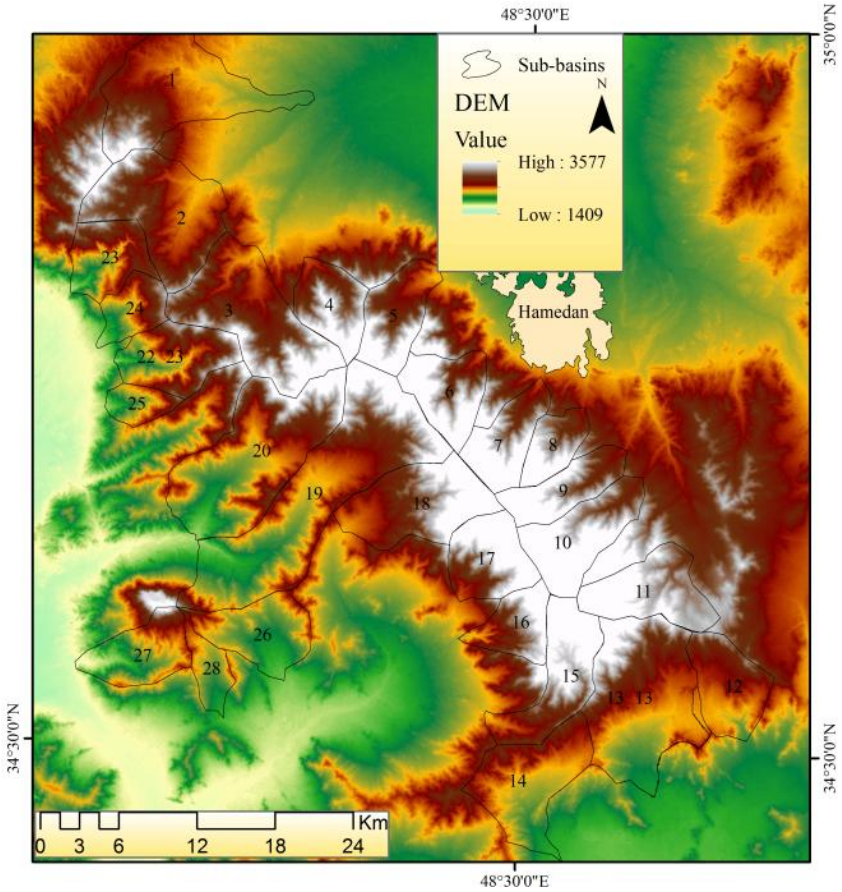

Figure 3. *Sub-basin of Alvand Mountain*

For further analysis, the contour lines with 50 m intervals were selected along the main stream. From the peak toward the lowlands, the first contour line with no straight form was selected, and later the length of the part which were located in the watershed was measured. Then, *Equation 6* was used to estimate CC (Jafari and Rostamkhani, 2015).

$$CC = \frac{a}{b} \qquad \text{(Eq.6)}$$

CC is the ratio between the aerial (a) and the actual distance of a curve (b) within a valley. Estimated values vary between 0 and 1. Thus, the estimated coefficient in a contour with low intensity and frequency in the process during the set time will be closer to 1, and if the processes mostly occur along the thalweg, the estimated coefficient will be closer to 0. Investigation of the linear relationships between the estimated coefficients and altitude implies the ascending and descending distribution of the coefficients with respect to altitude. The altitude of this trend change was considered as the ELA.

http://www.aloki.hu ● ISSN 1589 1623 (Print) ● ISSN 1785 0037 (Online)
DOI: http://dx.doi.org/10.15666/aeer/1605_58495868
© 2018, ALÖKI Kft., Budapest, Hungary

Altitude-ratio (AR) and accumulation-area ratio method (AAR)

In the median-altitude variant of altitude-ratio method, ELA lays midway in the altitude between the head of the glacier (Ah) and the terminus (At). In the terminus-head altitude ratio (THAR) approach, the THAR equals the ratio of the altitude difference between the terminal and the ELA divided by the total altitude range of the glacier. ELA can be estimated by adding the altitude of the terminus to the product of the total altitude range and an assumed THAR. The use of accumulation-area ratio (AAR) method is based on the ratio of the accumulation area (Sc) to the total area of the glacier (where *Sa* is the ablation area). Empirical studies suggest that a steady-state (SS, when the mass balances 0) AAR of 0.65±.15 is appropriate for more temperate, relatively debris-free glaciers. The surface topography of the former glacier is reconstructed based on glacial-geologic data. ELA value is obtained from glacier's area-altitude distribution (here depicted as a cumulative curve) and an assumed AAR (*Fig. 4*).

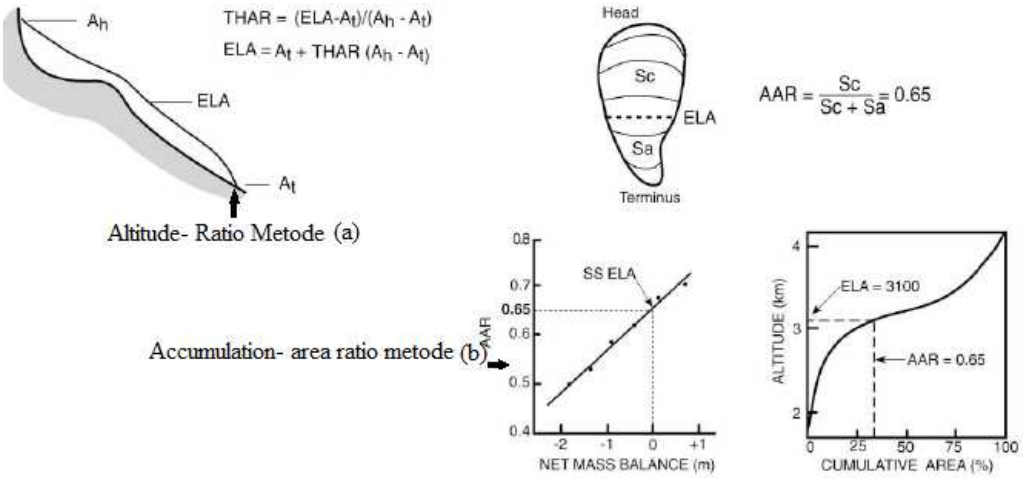

Figure 4. *AR and AAR method used to derive past equilibrium-line altitudes in the tropics. (Adopted from Porter, 2001)*

Results and discussion

ELA estimation of Alvand Mountain by Wright method

Iran's Alvand Mountain, which is above 3500 m and possess different forms of cirques, is one of the ancient glacial cirques in mountainous regions and can be employed for estimating ELA. In the study area of this research by studying the topographical maps the numbers and positions of cirques were determined through the contour lines. Accordingly, ELA for Alvand Mountain were estimated. Then the number of cirques was separately identified in both northeast and southwest slopes and their ELA was estimated. Investigations revealed that cirques in the southwest slope (100 cirques) have been decreasing at an altitude between 1700 to 2900 m, and their number has been decreasing up to 2300 m. Whereas cirques in the northeast slope (162 cirques) have been decreasing at an altitude between 1900 to 3300 m, and their number has been decreasing up to 2200 m. According to Wright Method, ELA was estimated at 2294 m for the entire study area of this research. Also, ELAs of 2404 and 2246 m were estimated for northeast and southwest slopes, respectively (*Fig. 5*).

http://www.aloki.hu ● ISSN 1589 1623 (Print) ● ISSN 1785 0037 (Online)
DOI: http://dx.doi.org/10.15666/aeer/1605_58495868
© 2018, ALÖKI Kft., Budapest, Hungary

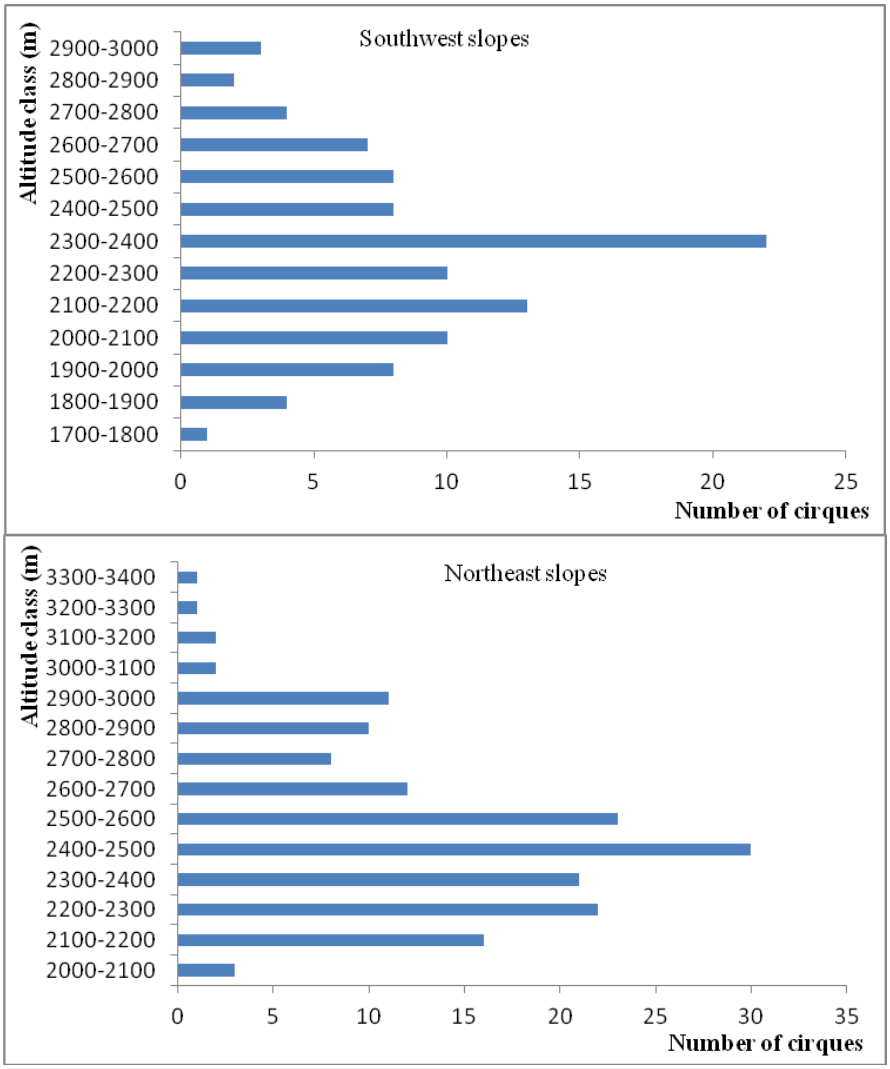

Figure 5. *The distribution of cirques altitude at northeast and southwest slopes*

ELA estimation of Alvand Mountain by slope-direction method

The amount of slope is very important in the Slope-Direction (SD) method. The GIS estimated average slope for northeast and southwest were 10.035% and 13.73%, respectively. The calculated slope was placed in *Equations 3* and *4* and eventually their temperatures were estimated. Estimated temperatures were placed in *Equation 5* and their altitude was obtained.

$$T = 10.84 - 10.035(0.11) \qquad T = 9.74^{0}C$$

$$T = 11.27 + 0.09(13.73) \qquad T = 12.5^{0}C$$

Contemporary ELA in northeast slopes:

$$X = \frac{9.74(1000)}{5.2} = 1873.07 + 1741.5 = 3614$$

http://www.aloki.hu ● ISSN 1589 1623 (Print) ● ISSN 1785 0037 (Online)
DOI: http://dx.doi.org/10.15666/aeer/1605_58495868
© 2018, ALÖKI Kft., Budapest, Hungary

Contemporary ELA in southwest slopes:

$$X = \frac{12.5(1000)}{5.2} = 2403.84 + 1741.5 = 4145$$

ELA in northeast slopes:

$$T = 9.74 - 8.5 = 1.14^0C \; X = \frac{1.14 \times 1000}{5.3} = 219.03 + 1741.5 = 1960$$

ELA in southwest slopes:

$$T = 12.5 - 8.5 = 3.9^0C \; X = \frac{3.9 \times 1000}{5.3} = 735.84 + 1741.5 = 2491.5$$

ELA will be achieved using *Equation 5*. Thus, the average ELA was obtained at 1960 and 2491 m for northeast and southwest slopes, respectively, which were about 530 m higher in southwest slopes.

ELA estimation by CC method

In this method, GIS software was used to draw the mountain sinuosity on topographical maps of 1.50000. The mountain valleys were separated into 28 sub-basins. In all sub-basins, the contour lines with 50 m intervals were selected along the main stream. From the peak toward the lowlands, the first contour with no straight form was selected, and the length of part located in the basin was measured (b). Then, *Equation 6* was used to estimate CC. CC is the ratio between the aerial (a) and the actual (b) distance of a contour in a valley. Fitted values of the linear regression between the estimated coefficients and altitude denote the ascending and the descending distribution of the coefficients with respect to the altitude. The altitude at which this trend change was considered to be the lowest point of the CC, the altitude of which matches ELA. The CC status at low altitude was also examined with respect to the dominant peak in the basin. To evaluate the geomorphologic processes over time, curvature coefficients were compared in all sub-basins using *Equation 6*. Linear regression was fitted between altitude, as an independent variable, and curvature, as a dependent variable. The results show that CC had specific trends in most sub-basins. The estimated CC was close to 1 on the slopes, and it decreased with increasing altitude (*Figs. 6* and *7*). With increasing distance from the basin outlet, first the coefficient reached with minimum and then increased again.

As it is evident in *Figures 6* and *7,* the lowest altitude of CC (0.31) is located at 2500 m altitude (No. 19, Shahrestaneh Valley) and the maximum value of this coefficient (0.8) is located at 3300 m altitude. The amount of this coefficient reduces from the mountain peak up to 2400-2500 m, and it increases again toward the basin outlet (*Table 3*). This process is also affected by the topography of the region. The altitude of these changes was estimated 2400 m in northeast slopes and 2400-2500 m in southwest slopes in most of the sub-basins. As the peak altitude reduces, the lowest amount of the coefficient shifts toward the lower altitudes. *Table 3* indicates the lowest altitude diagrams for each sub-basin. Where the sub-basins' slope direction is inclined north, the lowest altitude in the diagrams is expected to be in sub-basins number 4, 6, 8,

http://www.aloki.hu ● ISSN 1589 1623 (Print) ● ISSN 1785 0037 (Online)
DOI: http://dx.doi.org/10.15666/aeer/1605_58495868
© 2018, ALÖKI Kft., Budapest, Hungary

9, 10, 11, 16, 17, 20, 22, 27, 26, and 28. For example, the minimum altitude located at sub-basin number 26 (1750 m) with estimated weigh value of 96° tends toward the north. The maximum altitude at sub-basin number 7 (2450 m) with estimated weigh value of 179° completely tends toward the south.

Roughness within the basin will be affected by the solar elevation angles. Air masses will also affect the region and precipitation currents in different forms, the outcome of which will be reflected in contour lines. Consequently, Quaternary glacial processes had greater impacts on the northeast slopes. In comparison with the southwest slopes, the lowest altitude was located at a lower altitude.

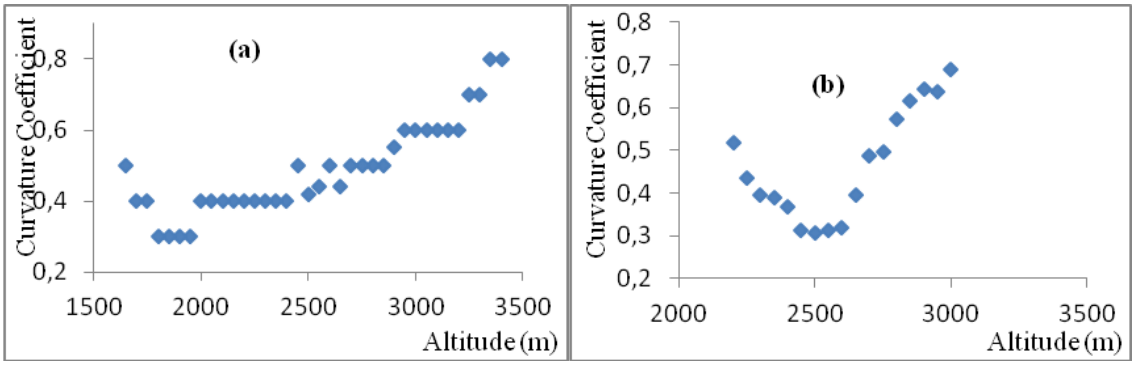

Figure 6. *Distribution of the curvature coefficients with respect to the altitude (a) in all sub-basins (b) sub-basin N 19*

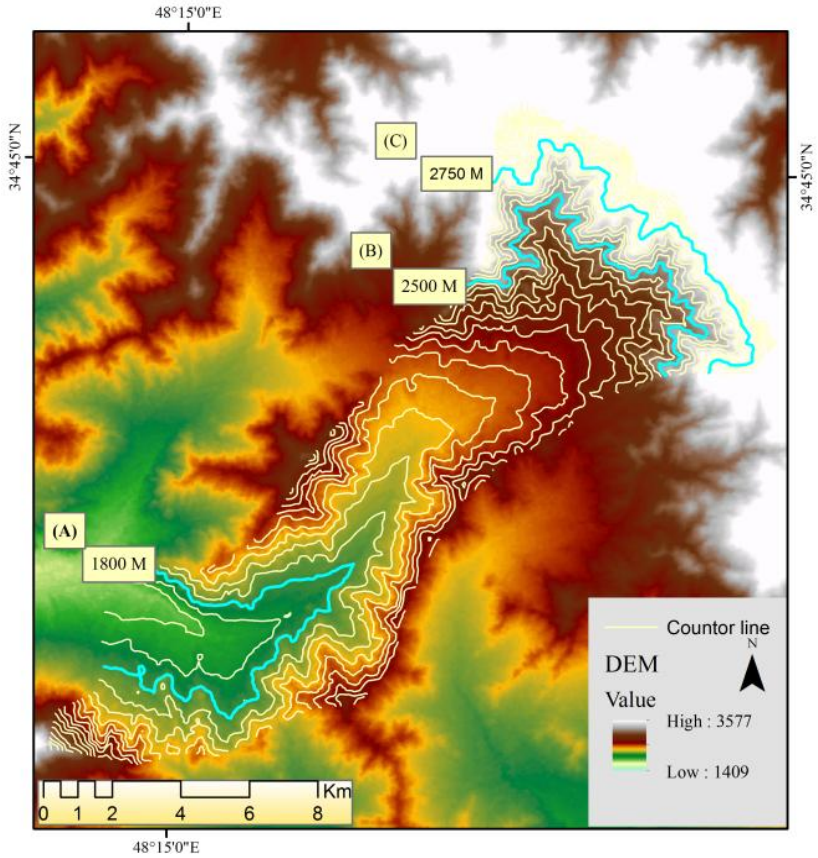

Figure 7. *Contour lines and curvature CC in one of the sub-basins*

http://www.aloki.hu ● ISSN 1589 1623 (Print) ● ISSN 1785 0037 (Online)
DOI: http://dx.doi.org/10.15666/aeer/1605_58495868
© 2018, ALÖKI Kft., Budapest, Hungary

Table 3. *Fitted perigee altitude with CC (Alvand Mountain sub-basins)*

Number of the sub-basin	Altitude range	Lowest altitude	Number of the sub-basin	Altitude range	Lowest altitude
1	1950-2750	2400	15	1950-32300	2150
2	2000-2800	2150	16	2000-3200	1200
3	1950-3000	2100	17	2150-3350	1200
4	2200-3200	2200	18	2450-3350	2400
5	1950-3000	2400	19	2150-3000	2500
6	2050-3100	2050	20	1750-3000	1250
7	2050-3250	2450	21	1600-2600	2150
8	2150-3000	2150	22	1700-2600	1700
9	2150-3250	2150	23	1650-2450	1800
10	2200-3200	2200	24	1800-2400	2050
11	2300-3350	2350	25	1650-2350	1850
12	1900-2450	2150	26	1600-2600	1750
13	1800-3100	2250	27	1850-2050	1850
14	1650-2300	1850	28	1800-2200	1800

In order to estimate the altitude variations, they were classified into four classes of 3500, 3400, 3200, and 2800 m. A linear relationship was fitted between the altitude of the mountain peaks, as an independent variable (X), and the lowest altitude, as a dependent variable (Y) (*Eq. 8*). According to this equation, it can be expressed that the low altitude increases by about 51 m for every 100 m altitude. The sub-basins were classified into seven groups based on the dominant geographical direction in the main valley. Also, the average lowest altitude (the altitude at which the CC varies) and the average CC were estimated in the same directions for each group (*Table 4*). To estimate the relationship between the average geographical direction and the average lowest altitude, *Equation 8* was used and *Equation 9* was applied to estimate the CC and the average lowest altitude.

Table 4. *CC and altitude values according to different geographical directions*

Directions	WSW	SSE	S	NNE	ENE	N	E
Average lowest altitudes	2167	2150	1980	2263	2200	2250	1957
Average CC	.47	.4	.52	.47	.35	.4	.52

$$Y = -1.0968x + 2242 \quad \text{(Eq.8)}$$

$$Y = -0.0004x + 1.227 \quad \text{(Eq.9)}$$

Accordingly, it was revealed that as the sub-basins' geographical direction stretches toward the north, the lowest altitude increases in the curvature coefficients (*Table 3* and *Eqs. 8* and *9*). This altitude was estimated at 2242 and 2044 m for the valleys that completely lean towards the south. This represents the glacial impact on the northeast and southwest slopes, which varies according to the environmental conditions. The

http://www.aloki.hu ● ISSN 1589 1623 (Print) ● ISSN 1785 0037 (Online)
DOI: http://dx.doi.org/10.15666/aeer/1605_58495868
© 2018, ALÖKI Kft., Budapest, Hungary

accumulation of glaciers emanated from the cirques above the ELA indicates a better condition in the topography of southwest slopes. Hence, the lower altitudes move toward the lower altitudes in comparison to the northeast slopes. Although the southwest slopes of Alvand Mountain have lower CC altitude, its CC value is much lower for the glacial processes were less effective on the highlands. Accordingly, the average lowest altitude was 2130 m in the entire area, and 2000 and 2146 m in the northeast and southwest sub-basins, respectively.

The matter and energy distribution have been usually uniform from the Mountain peak down to the slopes. In the V-shaped valleys, the CC became close to zero. In the glacial valleys, although the glacier thickness increases, the concentration of the matter and energy did not occur in the thalweg. By investigating CC in the 28 sub-basins of Alvand Mountain, it was revealed that the descending trend of the CC was expected to the point where matter and energy (glacial ice) are concentrated, and later from that altitude, the CC is increasing. In the sub-basin, where the slopes lengths are considerable (the southwest slopes), the lowest altitude of the CC varies based on the highest peak in the area. In the valleys that the highest peaks are more than 3400 m, the altitude of change CC is between 2400 and 2500 m. As if the tallest peak in the sub-basin is less than 3400, the altitude of change CC decreases.

ELA estimation by AR and AAR Method

For estimating ELA of Alvand Mountain via AR and AAR Method, a profile of cirques' floor was detected by global mapper software. If the profile is a concave, landform is considered as cirque. In field observation, the beginning literate moraines were determined. Their record was positioned by GPS and the data transferred to GIS. Through field observations, cirque number 42 was detected in northeast slope, cirque number 25 was detected in the southwest, and *At* was estimated. To obtain altitude and determine Ah in the profile (*Fig. 8*), ELA was estimated and translated into equations related to THAR and AAR. Based on AAR method, the estimated ELA for northeast slopes is 2297 m and for southwest slopes is 2727 m.

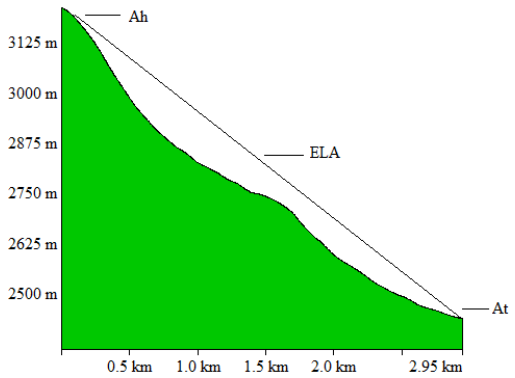

Figure 8. *sample of profile in Alvand Mountain*

Water and ice equilibrium line altitude (WIELA)

Values of erratic block and paleo-climates have been investigated as archive of historic glacial activity and as ice glaciers, respectively (Millar and Westfall, 2008). Large terminal moraines mark the outer limit of the ice sheet. In some places, the

http://www.aloki.hu ● ISSN 1589 1623 (Print) ● ISSN 1785 0037 (Online)
DOI: http://dx.doi.org/10.15666/aeer/1605_58495868
© 2018, ALÖKI Kft., Budapest, Hungary

terminal moraine is a single ridge; in other places, it may be a series of sub parallel ridges. There may be a large sandar (outwash plains) leading away from the terminal moraines wherever sub glacial or supra glacial streams emerge from the ice margin. The terminal moraines can be used to reconstruct the size of the ice sheet at its maximum extent (Bennett and Glasser, 2009: 367). There are moraine terminals around Alvand Mountain that can be used to estimate the WIELA in the longest glacial period in the Quaternary. For this purpose, several major paths of the erratic block were chosen in the northeast and southwest slopes and their expansion was investigated. Field survey revealed that the WIELA in the longest glacial period in the southern slopes was placed at 1680 m, and erratic block evidence has been detected in northeast slopes (1776 m). In the middle latitudes of the Northern Hemisphere (like Iran), the most suitable places for the cirques are topographical hollows facing northeast. The most extensive glacier of the Alamkouh is located on the northeast side and constitutes permanent glacial (Zomorodian, 2012).

In this regard, consideration of environmental gradients and topographical conditions (features that affect the ice flow velocity and moves WIELA to the lowlands) is highly recommended. The greater the slope, the greater the increase in glacier flow velocity is. Thus, it takes more time to achieve a balance between the flows and melt velocity. The second feature is the topography on the front side of the mountain that will accumulate more ice and consequently, be thicker and faster ice flow in favourable conditions. As a result, it limited the lateral extent of ice and prevented melting. These two features indicate the slope of the southwest slopes leads to ice accumulation and valley glacier formation. Although there is no appropriate condition for the glacial formation in the northeast slopes, the valleys come together after the mountain knick. Hamedan topographical similarities with a large cirque (with a radius of 3.3 km) imply that if the glacier tongues were fed well and accumulated, it could not overflow for the low slope gradient. The existence of the erratic block in different parts of Hamedan is an evidence for this claim (*Fig. 9*).

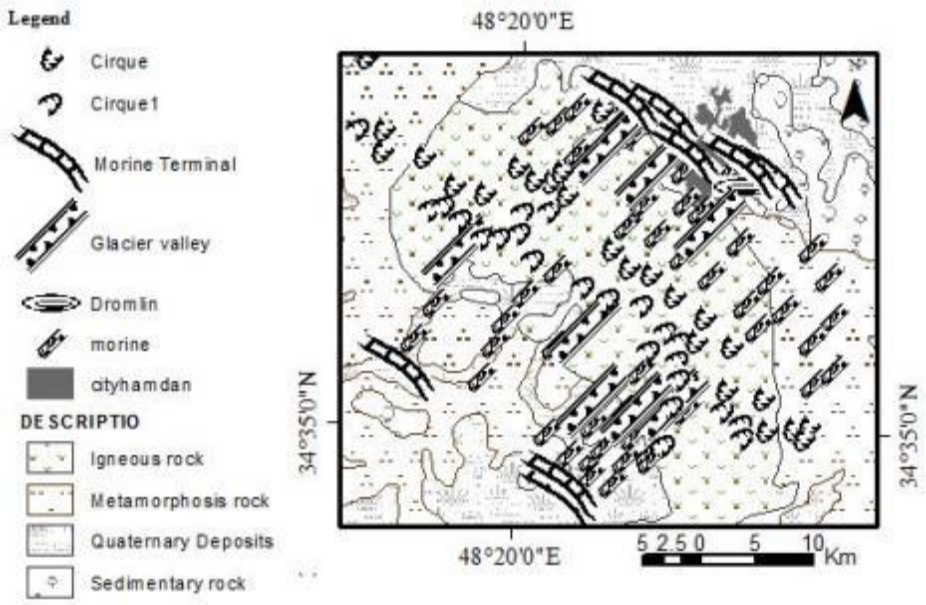

Figure 9. *Geomorphologic map of maximum expansion of Quaternary glaciers in Alvand Mountain*

http://www.aloki.hu ● ISSN 1589 1623 (Print) ● ISSN 1785 0037 (Online)
DOI: http://dx.doi.org/10.15666/aeer/1605_58495868
© 2018, ALÖKI Kft., Budapest, Hungary

Conclusion

Wright method is often used for estimating the Quaternary ELA of the Iranian mountains. Four methods have used to test this method in an Alvand Mountain (SD, CC, AAR and THAR). The ELA of Alvand Mountain estimated using the Write method indicates that the ELA of the northeast slopes is above the ELA of the southwest slopes. While, given the position of Iran in the temperate region of the northern hemisphere, the ELA in the northeast slopes should be in lower heights than the southwest slopes. The ELA estimated using the CC method in the northeast slopes is 68 meters above the southwest slopes, such a difference, like the Wright method, cannot be accepted with regard to environmental conditions. The non-conformance of ELAs estimated using Wright and CC methods with environmental conditions is due to differences in altitude of mountainous sinusitis in two northeast and southwest slopes. The sinusitis elevation in the northeast slopes is 2000 m and 1700 m in the southwest slopes. The 300 m difference of the sinusitis altitude has led to the identification of the cirque up to 1700 m in the southwest slopes and its identification up to 2000 m in the northeast slopes. The identification of the cirques at different heights of the two slopes led to estimate a lower ELA in the northeast slopes compared to the southeast slopes. The beginning of the pediment at an altitude of 2000 m in the northeast slopes in the Cc method has led to a higher ELA estimation of northeast slopes compared to southwest slopes. In the Cc method, the ELA is estimated based on the contour line forms. The result is that these two methods cannot be used for ELA estimation in areas where sinusitis height is above the maximum expansion of the Quaternary glacial. Estimated ELA for northeast slopes by the SD method is 513 m lower than the estimated ELA on the southwest slopes. Such a difference is justifiable with regard to the sun's altitude angle in the northeast slopes. The ELAs Estimated through both AAR and THAR methods were similar. That is why the AAR method is just presented. The ELA estimated using the AAR method in the northeast slopes is 430 m lower than the estimated ELA of southwest slopes (*Fig. 10* and *Table 5*). The results of using SD and AAR methods for ELA estimation are consistent with the findings of Jafari (2013), Moayeri et al. (2011), and Ramesth (2002). Therefore, these two methods can be used to estimate ELA.

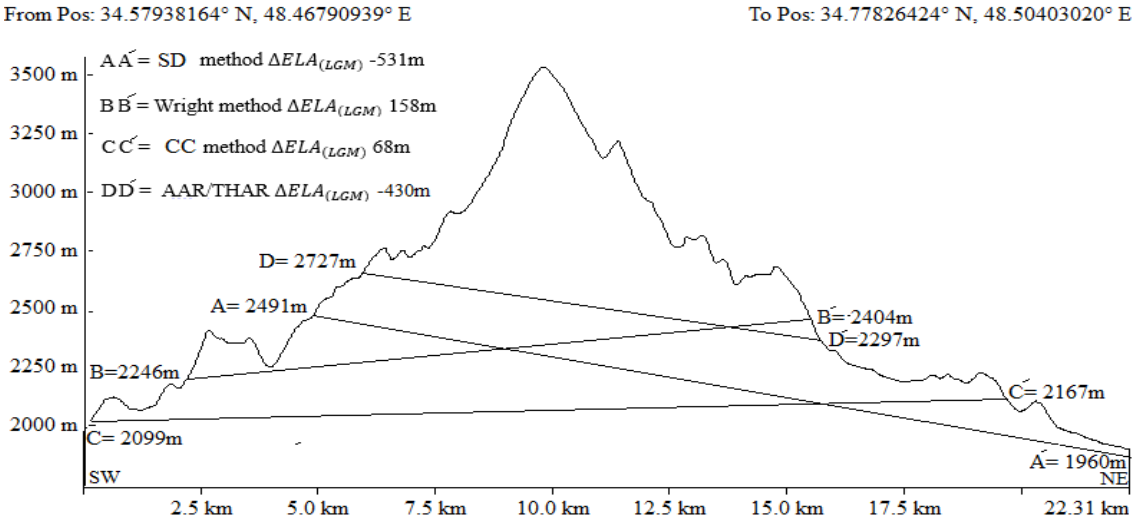

Figure 10. *The past ELA estimated by the Wright, SD, and curvature coefficient methods*

http://www.aloki.hu ● ISSN 1589 1623 (Print) ● ISSN 1785 0037 (Online)
DOI: http://dx.doi.org/10.15666/aeer/1605_58495868
© 2018, ALÖKI Kft., Budapest, Hungary

Table 5. *The comparisons of ELA in Alvand Mountain*

Method	Total	Northeast slope	Southwest slope
CC	2138	2167	2099
Wright	2294	2404	2246
SD	2226	1960	2491.5
AAR	2512	2297	2727

In addition to the ELA, WIEA has been also estimated in the present study. WIEA was detected using erratic blocks. The WIEA estimated in the southwest slopes was 1680 m and on the northeast slopes was 1780 m. Glacial's tongues in the southwest slopes than the northeast slopes have flowed until a lower altitude. The reason is due to the differences between the topography of the pediment of the southwest and northeast slopes. The topography of the southwest slopes causes glacial's tongues to be connected and creates a glacial valley. Whereas, the topographic conditions of the pediments of the northeast slopes have led to the creation of a glacial sheet (ice sheet) instead of a glacial valley. The flow velocity in the glacial sheet is less than the flow velocity of the glacial valley due to the less thickness. As a result, in the maximum expansion of the WIEL, the topographic conditions of the pediment were more effective than the direction of mountain slopes.

REFERENCES

[1] Abramowski, U., Bergau, A., Seebach, D., Zech, R., Glaser, B., Sosin, P., ... Zech, W. (2006): Pleistocene glaciations of Central Asia: results from 10 Be surface exposure ages of erratic boulders from the Pamir (Tajikistan), and the Alay–Turkestan range (Kyrgyzstan). – Quaternary Sci Rev 25(9): 1080-1096.

[2] Abtahi, S. M. (2014): Investigating the Jajroud watershed palaeoclimate by using the glacial evidence. – Geographical Explore in Desert Areas 1(1): 185-201.

[3] Almodaresi, S. A., Ramesht, M. H. (2007): Glacial evidence in Sakhvidi valley of Yazd. – Geography Space 19: 93-107.

[4] Amirahmadi, A., Maghsodi, A., Ahmadi, T. (2011): Evaluating the effects of Quaternary glaciers on the lack of civilization and main urban habitation in Aspas plain. – Urban - Regional Studies and Research Journal 3(10): 61-80.

[5] Benn, D. I., Evans, D. J. A. (2010): Glaciers and Glaciation. – Hodder Education, Abingdon.

[6] Benn, D. I., Lehmkuhl, F. (2000): Mass balance and equilibrium-line altitudes of glaciers in high-mountain environments. – Quaternary International 65: 15-29.

[7] Bennett, M. R., Glasser, F. N. (2009): Glacial Geology, Ice Sheets and Landforms (2nd ed.). – Wiley-Blackwell, Chichester.

[8] Bobek, H. (1934): Reise in Nordwest Persien 1934 (Travel in northwest Persia). – Zeitschrift der Gesellschaft fur Erdkunde zu Berlin 9(10): 359-369.

[9] Bobek, H. (1963): Nature and implications of Quaternary climatic changes in Iran. – Changes of Climate 20: 403-4013.

[10] Bondarenko, O. V., Blokhjna, N. I., Utescher, T. (2013): Quantification of Calabrian climate in southern Primory'e, Far East of Russia. An integrative case study using multiple proxies. – Palaeogeography, Palaeoclimatology, Palaeoecology 386: 445-458.

[11] Clark, P. U., Dyke, A. S., Shakun, J. D., Carlson, A. E., Clark, J., Wohlfarth, B., ... McCabe, A. M. (2009): The last glacial maximum. – Science 325(5941): 710-714.

http://www.aloki.hu ● ISSN 1589 1623 (Print) ● ISSN 1785 0037 (Online)
DOI: http://dx.doi.org/10.15666/aeer/1605_58495868
© 2018, ALÖKI Kft., Budapest, Hungary

[12] Desio, A. 1934. Appunti geografici e geologici sulla catena dello Zardeh Kuh in Persia. – Memorie Geologiche e Geographiche di G. Dainelli 4: 141-167.
[13] Esfandiari Dur Abadi, F. (2009): Geomorphological evidence of Upper Pleistocene climate change in the easterly slope of Sabalan. – Physical Geography Research Quaternary 3: 83-96.
[14] Fu, P., Harbor, J. M., Stroeven, A. P., Hättestrand, C., Heyman, J., Zhou, L. (2013): Glacial geomorphology and paleoglaciation patterns in Shaluli Shan, the southeastern Tibetan Plateau—Evidence for polythermal ice cap glaciation. – Geomorphology 182: 66-78.
[15] Ghahroudi Tali, M., Abdoli, E., Nezammahalleh, M. A. (2013): Geomorphological and Sedimentological evidence of alpine glaciers in the Zagros Mountains, Dinevar, Iran. – Tethys 1(1): 85-95.
[16] Head, M. J., Gibbard, P. L. (2015): Formal subdivision of the Quaternary system/period: Past, present, and future. – Quaternary International 383: 4-35.
[17] Headley, R. M., Ehlers, T. A. (2015): Ice flow models and glacial erosion over multiple glacial-interglacial cycles. – Earth Surf Dyn 3(1): 153.
[18] Jafarbeglu, M., Yamani, M., Abbasnegad, A., Zamznzadeh, M., Zahabnazoury, S. (2014): Reconstruction of Quaternary snow line in Bid Khan mountain (Kerman province). – Geography Quarterly 12(40): 93-107.
[19] Jafari, G. H. (2009): The Effect of the Roughness's on the Quaternary WIELA. – University of Isfehan, Department of Geography.
[20] Jafari, G. H. (2013): Estimating the ELA with Iran. – Geography and Environmental Planning 4(24): 99-115.
[21] Jafari, G. H., Asghari, S. (2014): Analysis the effects Quaternary glacial Zanjanrood. – Quantitative Geomorphological Researches 2(3): 16-30.
[22] Jafari, G. H., Rostamkhani, A. (2015): Quaternary evolutions of mountain valleys by using contour lines case study (Sabalan Mountains). – Geography Research Quarterly 118: 121-138.
[23] JedariEivazi, J. (2011): Geomorphology of Iran. – Payame Noor Press, Iran.
[24] Kaser, G., Osmaston, H. (2002): Tropical Glaciers. – Cambridge University Press, Cambridge.
[25] Khosravi, A., Quorbani Shorestani, A., Nur Mohammadiy, A. M. (2016): Study of Quaternary glacial geomorphological evidence in the highlands of North-East of Iran (Case Study: Mountains Binalud). – Quantities Geomorphology Researches 5: 1-13.
[26] Knight, G. P. (2006): Glacier Science and Environmental Change. – Blackwell Science, Oxford.
[27] Mahmoudi, F. A. (2008): Geomorphology of Iran (Vol. 2). – Tehran University Press, Tehran.
[28] Meierding, T. C. (1982): Late Pleistocene glacial equilibrium-line altitudes in the Colorado Front Range: a comparison of methods. – Quaternary Res 18: 289-310.
[29] Millar, C., Westfall, R. D. (2008): Rock glaciers and related per glacial landforms in the Sierra Nevada, CA, USA; inventory, distribution and climatic relationships. – Quaternary International 188: 90-104.
[30] Moayeri, M. Ramesht, M. H., Taghvaei, M., Naghizadeh, M. M. (2008): Glacial evidences (case study: SafaShahr, Fars Province). – Geography and Environmental Planning 32(4): 109-130.
[31] Moayeri, M., Ramesht, M. H., Saif, A. Yamani, M., Jafari, G. H. (2011): The impact of mountainous skirts direction of Iran on differences in altitude of wither and ice equilibrium line of the Quaternary. – Geography and Environmental Planning 40(4): 1-12.
[32] Moghimi, I. (2008): Geomorphology in the Cold and Glacial Territory. – Tehran University Press, Tehran.
[33] Nesje, A., Dahl, O. (2000): Glaciers and Environmental Change. – Arnold, London.

http://www.aloki.hu ● ISSN 1589 1623 (Print) ● ISSN 1785 0037 (Online)
DOI: http://dx.doi.org/10.15666/aeer/1605_58495868
© 2018, ALÖKI Kft., Budapest, Hungary

[34] Nojavan, M. R., Mir Hossini, A., Ramesht, M. H. (2010): Yazd Geotups and its attractions. – Geography and Development 13: 47-60.
[35] Ohmura, A., Kasser, P., Funk, M. (1992): Climate at the equilibrium line of glaciers. – Glaciology 38: 397-411.
[36] Osmaston, H. (2005): Estimates of glacier equilibrium line altitudes by the Area×Altitude, the Area×Altitude Balance Ratio and the Area×Altitude Balance Index methods and their validation. – Quaternary International 138-139: 22-31.
[37] Parizi, E., Ramesht, M. H., Taghian, A. R. (2014): Glacial evidence of Late Quaternary in the basin Sirjan Tigroeih. – Quantities Geomorphology Researches 3: 111-128.
[38] Paterson, W. S. B. (1994): The Physics of Glaciers (3rd ed.). – Elsevier, Oxford.
[39] Petersen, J. F., Sack, D., Gabler, R. E. (2017): Physical Geography (11th ed.). – Cengage Learning, Brooks Cole, Boston, MA.
[40] Porter, S. C. (2001): Snowline depression in the tropics during the Last Glaciation. – Quaternary Sci Rev 20: 1067-1091.
[41] Ramesht, M. H., Kazemi, M. M. (2002): Glacial evidence (case study: Eghlid, Iran). – Geographical Education, Growth 4(21): 3-11.
[42] Ramesht, M. H., Nematollahi, F. (2005): Glacier evidences in Iran. – Humanities Educations 9(4): 143-162.
[43] Ramesht, M. H., Shahzeidi, S. (2011): Geomorphology Application in National and Regional Planning. – Isfahan University Press, Isfahan.
[44] Ramesht, M. H., Shoshtari Zadeh, N. (2004): Evidence of ice caps and glaciers in Salafchegan. – Geographical Research 19(73): 119-132.
[45] Seife, A., Servati, M. R., Rahdan Monfared, M. (2015): Restructuring of Late Quaternary snowline in within of site Rige. – Geographical Research 116: 193-208.
[46] Sharifi, M., Farahbakhsh, Z. (2015): Investigation about temperature and humidity anomalies between Pleistocene and present times; reconstruction of climate condition using geomorphic evidence (case study: Khezrabad-Yazd). – Physical Geography Quarterly 47(4): 499-675.
[47] Solomina, O., Barry, R., Bodnya, M. (2004): The retreat of Tien Shan glaciers (Kyrgyzstan) since the Little Ice Age estimated from aerial photographs, lichenometric and historical data. – Geografiska Annaler: Series A, Physical Geography 86(2): 205-215.
[48] Stroeven, A. P., Hättestrand, C., Heyman, J., Kleman, J., Morena, B. M. (2013): Glacial geomorphology of the Tian Shan. – Maps 9(4): 505-512.
[49] Tahoni, P. (2005): Geomorphic evidence of Pleistocene glacial erosion in the highlands of Talysh. – Geography Research Quarterly 47: 31-55.
[50] Vaziri, F. (2003): Hydrology in Iran: preliminary identification of the glaciers in Iran (Vol. 2). – Management and Planning Organization Press, Tehran.
[51] Yamani, M. (2002): Geomorphological evidence for glaciers Alamkouh. – Physical Geography Research Quaternary, Tehran University 41: 1-17.
[52] Yamani, M. (2007): Geomorphology of the glaciers in Zardkouh mountain: geomorphologic forms and their extension. – Geographical Research 39(59): 125-139.
[53] Yamani, M., Zamani, H. (2007): Recovery of the Snowline Valley Shahrestanak the last glacial era. – Quarterly Geography 12-13: 99-116.
[54] Yamani, M., Jedari Eyvazi, J., Gorabi, A. (2007): The geomorphological traces of glaciers boundaries in Karkas Mountains. – Spatial Planning 11(1): 207-228.
[55] Yamani, M., Shamsipour, A. A., Jafariaghdam, M. (2011): Reconstruction of the Pleistocene snowline (case study: Jajroud watershed). – Physical Geography Research 43(76): 30-50.
[56] Yokoyama, Y., Lambeck, K., De Deckker, P., Johnston, P., Fifield, L. H. (2000): Timing of the Last Glacial Maximum from observed sea-level minima. – Nature 406: 713-716.

http://www.aloki.hu ● ISSN 1589 1623 (Print) ● ISSN 1785 0037 (Online)
DOI: http://dx.doi.org/10.15666/aeer/1605_58495868
© 2018, ALÖKI Kft., Budapest, Hungary

[57] Zamani, H. (2009): Evidence and Boundaries of Development of the Quaternary Glaciers in Central Alborz. – Doctoral Thesis, Tehran University.
[58] Zomorodian, M. J. (2012): Geomorphology of Iran (Vol. 2). – Mashhad University Press, Mashhad.

http://www.aloki.hu ● ISSN 1589 1623 (Print) ● ISSN 1785 0037 (Online)
DOI: http://dx.doi.org/10.15666/aeer/1605_58495868
© 2018, ALÖKI Kft., Budapest, Hungary

RECONSTRUCTION OF THE QUATERNARY GLACIAL LAKES OF IRAN (QALA'EHCHAI BASIN OF ZANJAN PROVINCE)

JAFARI, GH. H.[1*] – MOHAMMADI, H.[2]

[1]*Department of Geography, Faculty of Humanities, University of Zanjan, Zanjan, Iran*
(Phone: +98-24-3305-4176; fax: +98-24-3228-3201)

[2]*Masters of Hydrogeomorphology, University of Zanjan, Zanjan, Iran*
(Phone: +98-918-647-8944)

**Corresponding author*
E-mail: Jafarihas@znu.ac.ir; phone: +98-917-751-9227

(Received 31st May 2018; accepted 31st Aug 2018)

Abstract. The essence of all external morphogenesis processes depends on the governing climatic conditions of the time. Evidence suggests that the climatic conditions of the world and, consequently, external morphogenesis processes have undergone changes throughout the life of the earth. There are U-shaped valleys, cirques, local names and lake evidence around the Qala'ehchai Basin, which can be a reason for the quaternary glacier process. The glacier process of the region is approved by evidence such as the cirques and snow-line. For identification of glacier cirques, curve of the values extracted from DEM and Pari topographic map of 1: 50,000 scale is used. The quaternary snow-line is obtained using two methods of Wright and Porter. To identify pseudo-cirques, allometric method for the three parameters of length (L), width (W) and height difference (A) of the cirque, linear regression analysis in Excel software, and lithology study of main cirques have been used. Based on the highest snow-line calculated by Porter method (2425 m), all the lakes are situated above the height of the quaternary water and the ice equilibrium line. Field evidence and lithology of the region indicate that glaciers that are originated from high altitudes and well fed enter marl deposits by exiting the igneous area and resistant sediments. Glaciers in marl sediments create U-shaped valleys with a linear flow. After the treatment of glaciers, the necessary conditions for the creation of lakes are provided. The granulometry of the sediment sample suggests that when the location of the sediment is closer to the bank of the lake, its profile is similar to lake sediments and when its location is far from the center or bank of the lake, its profile is somewhat between glacial-lake sediments.
Keywords: *allometry, paleoclimate, granulometry, cirque, Ghezelowzan*

Introduction

The essence of all external morphogenesis processes depends on the governing climatic conditions of the time. Evidence suggests that the climatic conditions of the world and, consequently, external morphogenesis processes have undergone changes throughout the life of the earth. The long-term climatic data of the regions as well as the tracing of geomorphic evidence of climate change have not only been a nodule to many of the problems regarding the how of past lives, but also have raised a radical transformation in sociologists' perception of the evolution of human societies and have called some of their definitive findings for a serious reconsideration (Ramesht, 2001). The morphological effects of very old climatic changes, with the exception of the quaternary, used in various issues of geology and old geography, are either lost or fossilized (Jedari Eyvazi, 2013). Quaternary is the fourth, last, and youngest period that is so short unlike other geological periods. The existence of multiple climatic changes has led to the importance of studying this period (Martin et al., 2008). The emergence of humans and the recurrence of glacial and inter glacial periods are two important features

http://www.aloki.hu ● ISSN 1589 1623 (Print) ● ISSN 1785 0037 (Online)
DOI: http://dx.doi.org/10.15666/aeer/1605_58695891
© 2018, ALÖKI Kft., Budapest, Hungary

of the quaternary period; in this period, two different glaciers and inter glacial climates are dealt with (Seif and Abtahi, 2013). The quaternary period, which began with the advent of continental glaciers from the polar regions, ended with the melting of the continental glaciers. After that, the post-glacial period was replaced. In Iran, the beginning of the post-glacial period has been estimated to be 10,000 years ago (Zomorodiyan, 2012). At the end of the Ice Age, global changes were made in atmospheric conditions with the global retreat of ice-covered plates and glaciers. As a result of the warming of the air and the increase in evaporation in rainfall, most of the lakes, covering many plains and plain areas in the midst of the mountains and current desert areas of the planet were dried up (Klinsley, 2009). Some believe that these lakes are caused by a tensile regime after compression, another group attribute them to the anticline bending of the Mirror toward Masha, and eventually, some other consider non-domesticated births as their cause (Oskooi and Omidian, 2013). The size of the lakes and altitude of aridity and water equilibrium line during the quaternary have been a function of snow-line altitude and ice and water equilibrium line altitude (Ramesht, 2004). The snow line is a linear boundary above which snow does not change, i.e. the snow remains in a cumulative state for a long time and does not turn into water above this line (Chinn and Whitehouse, 1980). Aside from lakes that simultaneously remain with ice until the formation of a part of the coast, there are also lakes that are formed when the glacier or ice field decoys. Thus, water in the ditch creates a lake with the wall of valleys on the iceberg. These lakes are slightly filled up until they flow to the surrounding area from the lowest point (Gresswell, 1958).

During the glacial periods, the lower regions of the water and ice line equilibrium have had high rainfall and lower temperatures than the current conditions. Therefore, this positive equilibrium of water and water, resulting from the melting of upstream ice, caused the formation of lakes whose banks are known as the aridity and water equilibrium line (Abtahi, 2013). Existing evidence in nature show that the conditions governing the past climate differ from today. In addition to the climate, the conditions of dehydration and hydrological cycles in basins depend on the physiographies and geological conditions. River entry or discharge does not depend only on the climate of the region, but the position of the lake relative to the basin makes sense of the increase in the entry because nutrition and energy are meaningful when there is a life (Velayati, 1995). Hollows and lakes are the lowest part of the basin and planar surfaces that are the result of stagnant waters. In other words, lagoons, lakes, reservoirs and sedimentation mechanisms in them lead to the formation of smooth surfaces with fine texture (Ramesht, 2013).

In addition to the presence of U-shaped valleys, cirques and local names of the mountains such as the Gharghalan (Permanent snow) around the Qala'ehchai Zanjan Basin, which are evidence of the sovereignty of the quaternary glacial process, there is a lake called Khandaghlo that still retains its identity. In fact, this lake, with greater water in the past, is another reason for the governance of the morphogenesis system of the quaternary glaciers in the region. In addition to Khandaghlo Lake, the reflection of landforms with simple and sometimes closed contour lines along with convergent drains, single-point elevations and two-way drain in topographic maps with a scale of 1:50,000 was evidence of the abundance of such lakes in the past, which are now largely destroyed and have lost their independence. In addition to the climatic changes in the quaternary, the change in the level of Ghezelowzan, including the Qala'ehchai, and the dominance of backward erosion in the region has played an indelible role in the

http://www.aloki.hu ● ISSN 1589 1623 (Print) ● ISSN 1785 0037 (Online)
DOI: http://dx.doi.org/10.15666/aeer/1605_58695891
© 2018, ALÖKI Kft., Budapest, Hungary

destruction of the lakes in the region. Investigation of this issue can be very important in introducing the region, which is likely to be called the Finland of Iran, and encouraging environmentalists, paleontologists and, in particular, paleoclimatologists for further study of the region.

Literature review

According to the studies of Russell (1889) and Longmore and Heijnis (1999) on the lakes of the past, lunar periods coincided with the ice age. Walter Goldthwait (1908) reconstructed extinct aqueducts and glaciated lakes in the Michigan Lake Basin and used field evidence, and concluded that in Michigan and Wisconsin, rock cuts at the current levels of Michigan lake are severe, but stretch of the old coastline, which was 5 to 25 miles further away from the current surface, is partially or completely destroyed. In a study entitled fluctuations and changes in the cold stages of large lakes, including Larness affected by the Agassis and Barlow ice currents, Lewis and Anderson (1989) concluded that during the second period of frost and after its end, ice currents caused the discharge of the lake from the frozen state and flooded with the flow of the glacier down the lake, increasing the flow velocity. Olvmo and Johansson (2002) evaluated the importance of stone and lithological structure in deep weathering before glaciation and glacial erosion on the landforms of the West Coast of Sweden using satellite imagery, accurate mapping and frequent field observations, and concluded that the direction of ice and pre-glacial landforms is aligned with the forms engraved on the rocks of the area. Glassera and Bennettb (2004) argue that landforms of glacial erosion are the basis of paleo glaciology. Cossart et al. (2008) analyzed the slope instability of the glaciers in the mountainous areas of the Durranz Basin, in southeastern France, using field evidence, geographic information system, and spatial pattern combination, and concluded that large stones in avalanche of rock are related to the stress of the pressure; these avalanches are due to the rock breaking during the glacial period, where rocks become unstable with the slope after the glaciation and appear as avalanches. Bao et al. (2009) studied coverage of surface tensile stresses in the past Neo-Proterozoic 2 ice lake in Svalbard. Sundal et al. (2009) explored the evolution of the ultra-glacial lake across the Greenland plate. Bajracharya and Mool (2009) discovered the behavior of glaciers and the explosion of lagoons in ice lakes in the study of glacial and ice lakes in the Nepalese region of Everest. Askari Chawardi (2009) investigated lake of the Jajrood valley during the quaternary period and concluded that one of the factors causing the formation of lakes is the transfer of glacial deposits in the quaternary period, their density at the margin of Jajrood valley, landslide occurrence during the glacial and tectonic periods. Bolch et al. (2011a) identified a dangerous ice lake in North Shian and concluded that climate change and global warming have the potential to create an increasing number of glacial lakes, and the flooding of these lakes also causes serious damages and risks. In another study, Bolch et al. (2011b) studied the evolution of ice lakes along the Hindu Kush mountain range between 1990 and 2009 using Landsat satellite imagery and concluded that in eastern Nepal, India and Bhutan, lakes are larger and more numerous; however, glacier in the Hindu Kush (50%) and Karakorum (30% contraction) is associated with the loss of ice in the western part of Hindu Kush Himalaya. With a study on the potential volume of the Himalayan lake flood based on satellite imagery, the angle of stagnation on the lake bank, and estimation of the volume of flood on more than 2000 lakes, Fujita et al. (2013) found that there are 794 lakes lacking Steep Lakefront Area; meanwhile, the volume of the lake was identified as

http://www.aloki.hu ● ISSN 1589 1623 (Print) ● ISSN 1785 0037 (Online)
DOI: http://dx.doi.org/10.15666/aeer/1605_58695891
© 2018, ALÖKI Kft., Budapest, Hungary

10 million m^3 of ice. Jananeh, and Rajabi (2016) studied the effects of the quaternary period on Iranian seas and lakes and found evidence that the sea and lake levels had been up and down during glacial quaternary periods. In addition, they asserted that changes in Iran's sea and lake levels during glacial periods are quite similar to changes in the global scale and that there is evidence of existence of lakes in today's deserts, but there are different views on their extent and depth. The glaciers are the origin of the formation of most lakes, and alone contribute to the formation of lakes more than any other factor. These types of lakes are not too deep and are caused by glacial factors. Kiani et al. (2016) assessed the ecological vulnerability of climate change in Abarkuh Basin, concluding that the change in the ratio of environmental parameters occurs during cooler periods and all of the thresholds of transit stability and general state of environmental systems are on the verge of collapse. Ghiyas Abadi et al. (2014) stated that Gohar Lake is the only mountainous lake with glacial Paternoster species in Iran. Entezari et al. (2015) studied the geomorphology of climate change in the Gorganroud Basin during the quaternary period and compared two maps of the current and quaternary periods, showing a temperature difference of 9.4 °C. They also showed that the cool and humid climates are in the fourth quarter. Studies on the Paleolithic in Iran go back to the work of French Democrats (1907); while discovering some rocky devices in the Pleistocene sediments in the Caspian Basin, it is stated that Iran was covered by mountain glaciers and lakes during this period. Some of the Iranian researches on glaciation and glaciers include Ramesht (2004), Tahoni (2004), Yamani et al. (2007), Rezvani et al. (2010), Ghahroudi Tali (2011), Amirahmadi et al. (2011), Abtahi (2013), Parizi et al. (2013), Jafari and Asghari Serkansrudi (2014), and Shamsipour et al. (2015).

Materials and methods

Study area

Several lakes in the quaternary have been created by glaciers or glacial treatment. These lakes have been created by rill erosion or sedimentation of glaciers or due to the creation of a moraine dam. The Ombilics and the Verrous are also places that have spawned in glacier valleys, creating permanent and temporary lakes. Posture, on the one hand, and proper rainfall feeding, on the other hand, have led the glacier cirques to become small and scattered lakes so that the high cirque lakes are the result of the melting of the upstream snow and downstream cirque lakes are due to the overflow of the upper cirque lake (Derruau, 2011). The Qala'ehchai Basin is one of the regions in Iran that has well retained evidence of glacial lakes. The Qala'ehchai is one of the sub-basins of Ghezelowzan Basin, originating from the northeastern slope of Belquis Mountain and joining Ghezelowzan from the western-eastern direction near the village of Moshampa. The Ghezel Owzen joins the Caspian sea through Sefidrud, and pouring into the lake of the Manjil dam. Khandaghlo Lake is one of the lakes alive in Zanjan Province in highlands near Belquis Mountains. Basin area is over 618,400 m^2 and has a length of over 3150 m. Its maximum depth is 5-6 m and its average depth is 1.5 m. The main lithology of deposits is marl. The altitude of Khandaghlo Lake is 1600 m and it is under the influence of the adjacent glacial system. The lithology and climatic conditions of the Qala'ehchai Basin have led to the formation of closed basins, some of which have been ruptured and destroyed. However, they can have water for some times of year through proper management. The geographical area of the Qala'ehchai Basin is located about 47° 15' to 47° 30' east and 36° 45' to 37° north latitude. The total area is 780 km^2

http://www.aloki.hu ● ISSN 1589 1623 (Print) ● ISSN 1785 0037 (Online)
DOI: http://dx.doi.org/10.15666/aeer/1605_58695891
© 2018, ALÖKI Kft., Budapest, Hungary

and its average height is 2220 m above sea level. This basin is limited from the west to Takab Provance, from the east to Hesar-Moshampa Department, from the south of Mahneshan Township, and from the north to Miyaneh Township (*Fig. 1*). This basin is a part of the Khoy–Mahabad Zone (Nabavi, 1976) in terms of geological structure and it is located in the intersection of Sanandaj-Sirjan, Alborz-Azerbaijan and Central Iran zones. This area is composed of metamorphosed rocks of schist, marl, gneiss and amphibole, with the northwest-southeast trend in the middle sections of the Ghezelowzan Basin. The higher altitudes are 3330 m in Belquis Mountain and 3208 m in Ghebleh Dagh Mountain. These rocks are directly covered by non-sorting Oligo-Miocene sediments. It seems that metamorphic rocks of the Precambrian to Paleozoic period from the second to the middle of the terrain constitute high altitudes with no sediments on them, a slight potential deposition may have been demolished due to high altitude and erosion. Generally, the rocks in the studied area are Precambrian metamorphic rocks, Late Precambrian sedimentary rocks, previous Cambrian and Cambrian-Ordovician, Paleozoic metamorphic rocks, Diorite intrusive masses, Granodiorite and Gracie volcanoes, Oligo-Miocene volcanic rocks, Pliocene, and quaternary sediments from below upwards, respectively (The Iran Geological Survey).

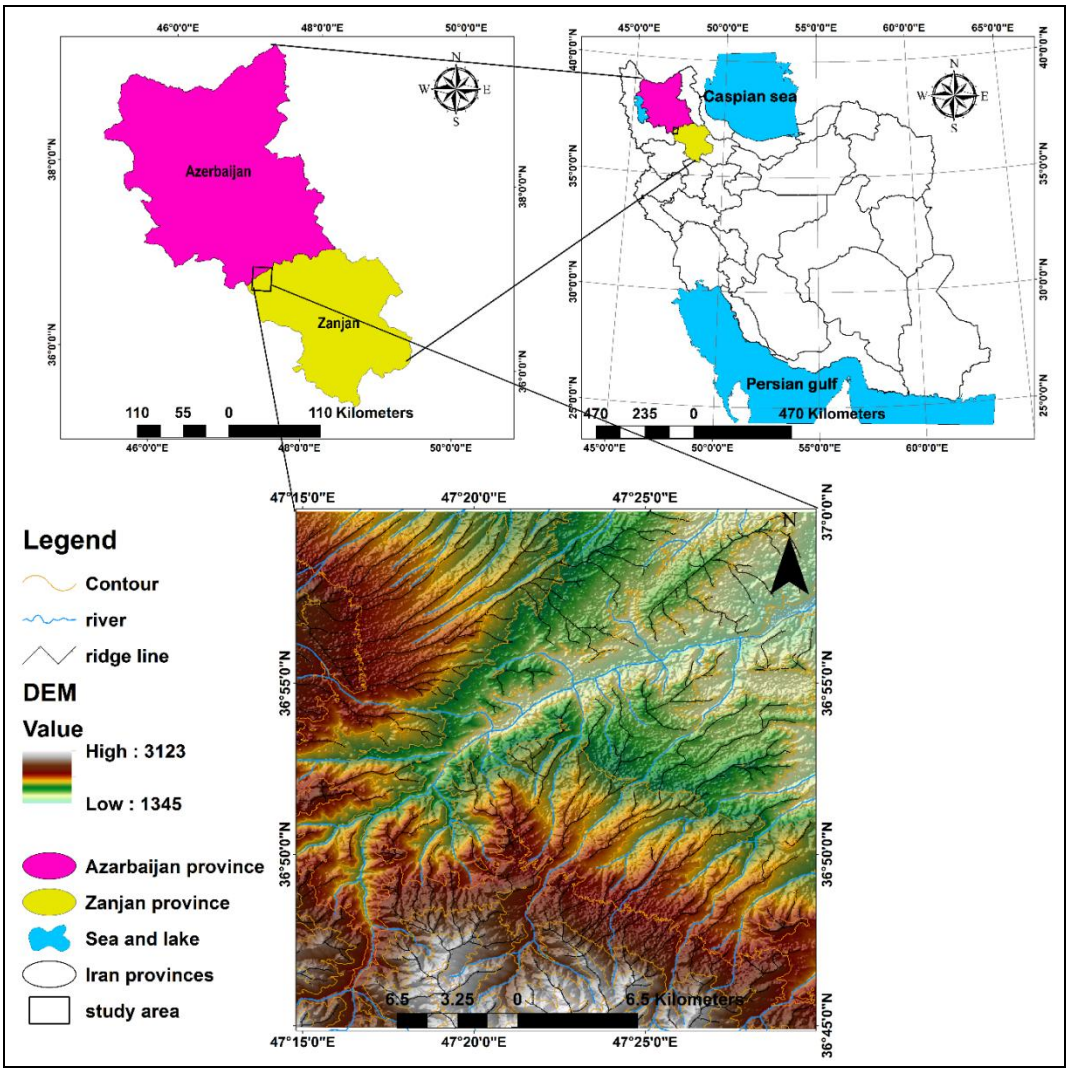

Figure 1. *Map of the study area*

http://www.aloki.hu ● ISSN 1589 1623 (Print) ● ISSN 1785 0037 (Online)
DOI: http://dx.doi.org/10.15666/aeer/1605_58695891
© 2018, ALÖKI Kft., Budapest, Hungary

Extrusive basalt disturbs the region's morphology and is resistant to erosion, which does not easily react to corrosive factors. It is unevenly distributed on the marl and gypsum sandstone, periodic andesite lava of marl, and red sandstone with gypsum, been greatly expanded in the southwest region with layers of the travertine spring deposited horizontally. The sediments of this unit can be considered equivalent to the upper red formations in Qom area. It is also distributed on the periodic conglomerate unit of marl and sandstone with gypsum horizons, being expanded to the west-southwest of the basin. Geomorphologic and hydrological conditions of the area, such as the existence of marl between the sandstone and conglomerate layers in vast areas of the basin, together with the low topographic conditions reflected in topographic maps of 1:50,000 scale farther away from the current river bed indicate that many parts of the region have had more equilibrium conditions during the quaternary. Disturbances of faults and over thrusts are seen in Takht-e-Solayman Mountains and west of Qala'ehchai. These faults are perpendicular to the Qala'ehchai River. The most important fracture in the Ghirgeh-Chahar Tagh fault is in the north west-southeastern trend that crosses the middle sections of the area (*Fig. 2*).

Methods

To study quaternary changes, Digital elevation model (DEM) was extracted from satellite images with resolution 30 m from ASTER of the year 2017. The topography layer was prepared using ARC GIS software. The glacial process of the region was proven by evidence such as cirques and snow-line frontiers. For identification of glacier cirques, curve of the values extracted from DEM and Pari topographic map of 1: 50,000 scales is used. The curved line indicates the glacial process that is reflected as a fan in the impassable valleys. Also, the quaternary snow-line was obtained using Wright and Porter methods. The method of elevation of the cirques floor is one of the five methods Porter has proposed to reconstruct the equilibrium line at low latitudes. The use of this method depends on the number, geographic direction, the altitude classes and the percentage of cirques. Floor altitudes were measured as the single lowest DEM grid cell within each cirque. Latitude and longitude were measured from the centre point of each cirque; and the aspect was measured as the outward direction of each cirque's median axis (Evans, 1977; Evans and Cox, 1995; Barr and Spagnolo, 2015). In Wright's method, by multiplying the number of glacier cirques in 0.6, the number of rows of cirques in descending from in terms of height is obtained. This altitude is the height of the quaternary equilibrium line altitude (ELA). This method estimates ELA by determining the location and altitude of 60% of cirques above the line. For estimating ELA, the altitude of identifying cirques is sorted based on descending order. Then the number of cirques is multiplied to 60% (*Eq.1*). The gained number represents a numerical line of cirques in which ELA is located. In the following, X shows the number of rows and N is cirques number.

$$X = N \times 0.6 \qquad \text{(Eq.1)}$$

The existence of pseudo-cirques led to the determination of the three parameters of length (L), width (W), a height difference of cirque (A) through allometric method and linear regression analysis in Excel software and lithologic study of main cirques in order to determine the correct snow-line.

http://www.aloki.hu ● ISSN 1589 1623 (Print) ● ISSN 1785 0037 (Online)
DOI: http://dx.doi.org/10.15666/aeer/1605_58695891
© 2018, ALÖKI Kft., Budapest, Hungary

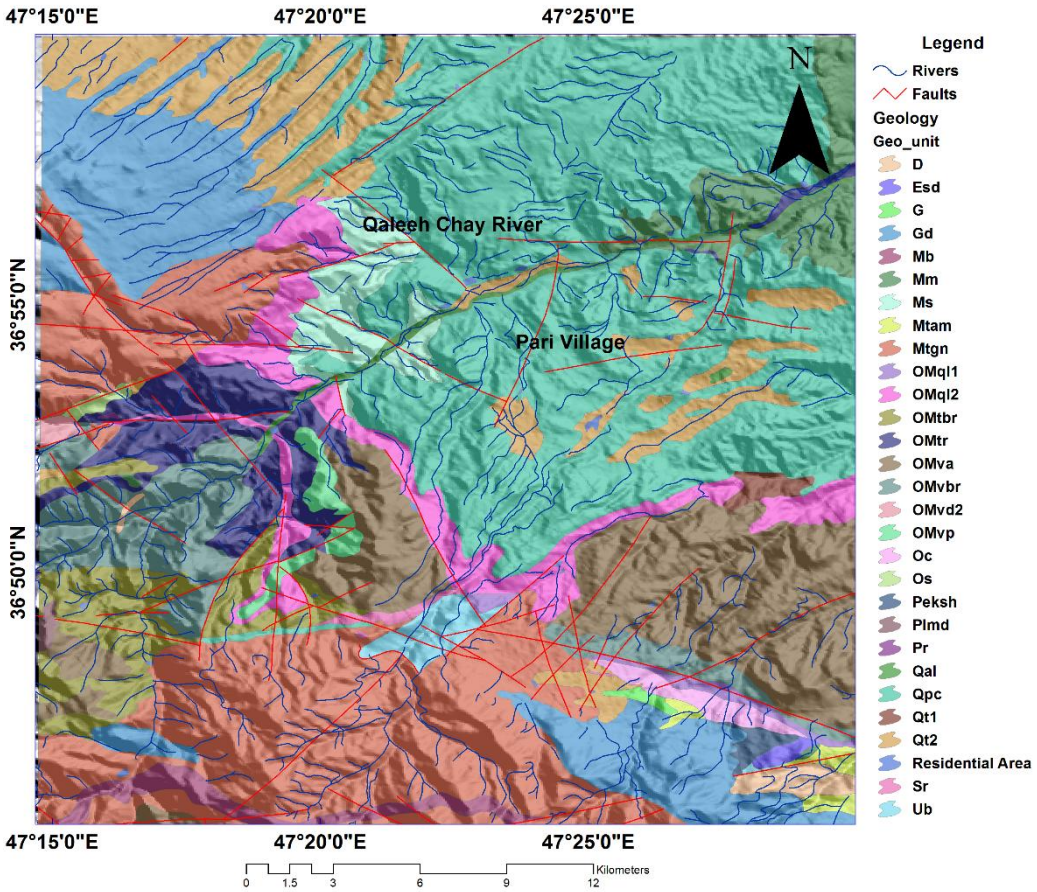

Figure 2. *Geologic maps of Qala'ehchai Basin. D = Quartzdiorite, diorite, gabbro. Esd = Grey dolomite with black landed there. G = Granite. Gd = Grey granodiorite, granodiorite gneiss. Mb = Marble. Mm = Marl and sandstone with gypsum beds. Ms = Alternation of red marl and sandstone. Mtam = Amphibolite with marble intercalations. Mtgn = Alternation of gneiss, marble and amphibolite. Omql1 = Massive limestone, fossiliferous, cream to light grey. Omql2 = Cream, thick bedded to massive limestone (Aquitanian-Burdigalin) with yellowish - green marly intercalations. Omtbr = Hyaloclastic luff breccia, luff and sandy tuff, thick bedded to massive, grey-green. Omtr = White to pink pernicious luff breccia. Omva = Grey brown and violet porphyritic andesitic lava. Omvbr = Andesitic volcanic breccia and conglomerate, hyaloclastic tuff breccia. Omvd2 = Pink dacitic and jgnimbritic lavas and related tuffs. Omvp = Andesitic pillow lava. Oc = Red conglomerate and sandstone. Os = Red sandstone and marl. Peksh = Alternation of micaschist and quartzite grey – green. Plmd = Microdiorite - rnicromonzonite subvolcanic bodies. Diabasic dykes. Pr = Volcanic glass (perlite). Qal = Recent alluvium. Qpc = Loose clay-cemented polygentic conglomerate. Qt1 = Old terraces and high gravel fans (Gravel, sill and clay). Qt2 = young terraces and low gravel fans (sand, ails and clays). Residental area = village and city. Sr = Metamorphosed ultramafic - mafic lava flow (Komatiile). Ub = Metamorphosed ophiolitic rocks (serpentine, diabase and basaltic lava)*

Geologic maps of the Mahneshan at 1: 100,000 scales were used. The topography is reconstructed with respect to the equilibrium environments in the topographic maps. Two-way drains and single-point elevations along with closed contour lines on topographic maps indicate the abundance of lake in the past. Using the pixel to code software, the areas where such evidence was seen were digitalized and the past

http://www.aloki.hu ● ISSN 1589 1623 (Print) ● ISSN 1785 0037 (Online)
DOI: http://dx.doi.org/10.15666/aeer/1605_58695891
© 2018, ALÖKI Kft., Budapest, Hungary

topography of the region was reconstructed with the help of digitalized data in the Surfer software through the Kriging interpolation. The watershed and basins were drawn and lake area was reconstructed with Generate watershed extension in the Global Mapper software. The converging radial drainage channels represent a lake. To verify and document the previous lakes, sediment sampling was implemented in areas where there was the possibility of lake in the simulation of previous topography. In this way, sediment samples were taken from places where there were old terraces. In the laboratory, the granulometry operation was carried out through the following steps: 1- Sample washing; 2- Sample placement in the oven device for 24 h; 3- Detachment of dried sediment after the operation of shiker for 15 min; 4- Weighing each of the remaining samples in each of the sieve's pieces; 5- Plotting the frequency table based on the obtained data; and finally, 6- Drawing the cumulative curve graph in Excel software and matching each of the obtained graphs with the curve of the lake sediment.

Quantitative relationships were applied to the data resulting from the granulometry of the sampled sediments. Using these relationships, sediment status was analyzed in terms of standard deviation (σi), mean size (Mz), skewness (SKi) and kurtosis (KG). The final analysis of the data was done according to the values of *Table 1*. In addition, the final analysis was done by comparing the data of other samples with the data's Peri Lake sediment sample, the only live evidence from past lakes.

Table 1. *Descriptive measures of grain size distribution (Ward, 1957; Obinegbu et al., 2013)*

Parameters	Formulas	Verbal terms
Mean size (Mz)	Q16 + Q50 + Q84/ 3	Mz = -1- -2 granule 0- -1 very coarse sand 0-1: coarse sand 1-2: medium sand 2-3: fine sand
Standard deviation (σi)	Q84 – Q16 / 4 + Q95 – Q5 / 6.6	σi => 0.35: very well sorted 0.35-0.50: well sorted 0.50-1.0: moderately sorted 1.0-2.0: poorly sorted 2.0-4.0: very poorly sorted < 4.0: extremely poorly sorted
Skewness (SKi)	Q16 + Q84 – 2(Q50) / 2 (Q84 – Q16) + Q5 + Q95 – 2(Q50) / 2(Q95 – Q5)	Ski => +1.0-+0.3 very positively skewed 0.3-0.1: positively skewed 0.1-(-0.1): symmetrical skewed -0.1-(-3.0): negatively skewed -0.3-1.0: very negatively skewed
Kurtesis (KG)	Q95-Q5/2.44 (Q75-Q25)	KG=> <0.67 very platykurtic 0.67–0.90 platykurtic 0.90-1.11 mesokurtic 1.11-1.50: lepokurtic 1.50-3.00: very lepokurtic >3.00 extremely lepokurtic

Results and discussion

Many of the lakes that were in the glacial period have been torn apart after being overflowed or absorbing large quantities of water, and have been ruined by the dominance of various erosions. One of the major factors affecting the destruction of

http://www.aloki.hu ● ISSN 1589 1623 (Print) ● ISSN 1785 0037 (Online)
DOI: http://dx.doi.org/10.15666/aeer/1605_58695891
© 2018, ALÖKI Kft., Budapest, Hungary

lakes is the change in the base level that results in the collapse of the river system, causing phenomena such as gullies. These gullies or so-called gully erosion snatches and captures the rivers. There are many other lakes that have not been completely destroyed or eroded. There is evidence around these basins indicating that they were lakes in the quaternary. Among the evidence that can be seen in the field vision is the alluvial terrace left by the lake after passing wet and dry periods. Based on their own characteristics, such as texture, structure, color and thickness, these terraces are of particular features. Existence of other evidence on topographic and geological maps is of great help in identifying the lake. These evidences are as follows (*Fig. 3*): 1. Closed and hole-like contour lines; however, these holes should be detected from the contour line of mountain peaks and volcanoes; 2. Rivers that have been deformed to two-way canals; 3. Single altitude points in the between contour line; 4. To entity material of sediments of past terraces in geological maps.

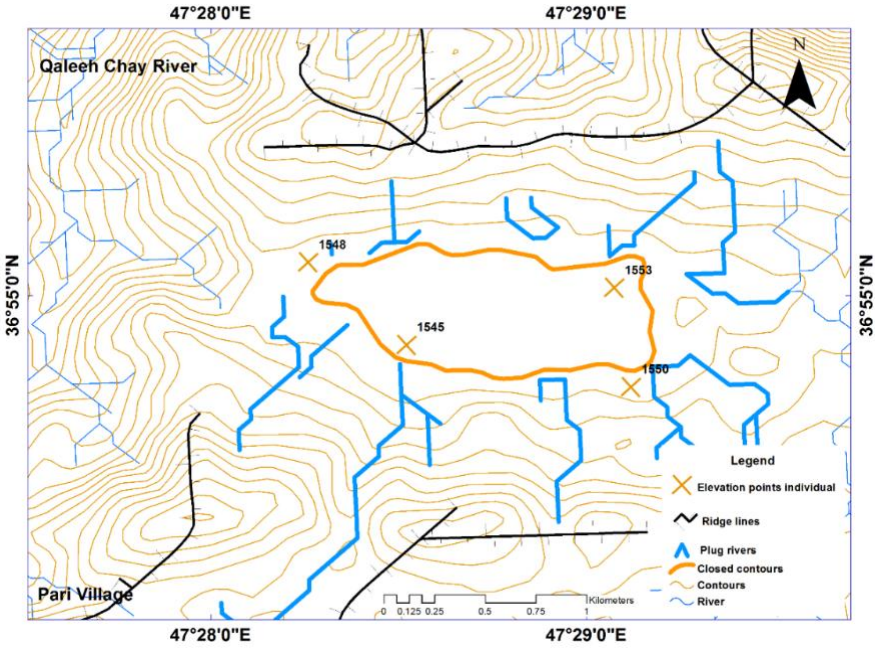

Figure 3. *Evidence of the existence of a lake on a topographic map*

Allometry of the cirques

Detecting glacial effects in mountainous areas is one of the important tasks to be achieved by the remaining evidence. The most important pattern resulting from glacial erosion is the glacial cirques. From a spatial point of view, any hole-like area holds snow and is called a snow house. However, not all holes and amphitheatres are glacial cirques. On the other hand, it is necessary to consider several factors including lithology. Effects of cirques do not remain in loose sediments such as marl, clay and conglomerate for a long time, and they are pseudo-cirques that cannot be attributed to the cirque. For a better study of the cirques and separation from pseudo-cirque, the cirque allometry, i.e. obtaining parameters such as length, width, floor area, height of the peak overlooking the cirques, and slope of the cirque, is done. Usually, in a cirque space, there is a high correlation between the special parameters of the cirque. Otherwise, correlation is reached to higher than 50% by eliminating liars that are

http://www.aloki.hu ● ISSN 1589 1623 (Print) ● ISSN 1785 0037 (Online)
DOI: http://dx.doi.org/10.15666/aeer/1605_58695891
© 2018, ALÖKI Kft., Budapest, Hungary

pseudo-cirques. After finding glacial cirques, their height was accurately calculated. The cirques were sorted by height in a descending order and the total number of cirques was multiplied by 0.6, and the altitude of the number of the row obtained in the descending order was considered as the quaternary snow-line elevation. Accordingly, the snow-line of the study area was 2364 m above sea level. The corrected snow-line after allometry of glacial cirques also averaged 2354.7 m. Snow-line correctly to suit the paper (Seif and Ebrahimi, 2014) was a linear relationship between the length, width and height of the cirques confidence R2 above 90% for solidarity cirques evaluated. Using the cirque floor method of Porter, the frequency of the cirques was determined in geographical directions and snow-line elevation was obtained after performing the necessary analyses. Snow-line elevation was 2354.7 m above the sea level in the Wright method and it was 2425.12 m in Porter's method, with a difference of 70 m (*Table 2*) (*Fig. 4*).

Table 2. *Data Porter's method for determining snow-line*

Elevation classes*	**Cirque abundance**	**Directions**								**Cirque percent**
		North	**North East**	**East**	**South East**	**South**	**South West**	**West**	**North West**	
1600-1200	7	3	1	-	2	-	-	-	1	4.96
2000-1700	11	2	2	4	1	-	-	1	1	7.8
2300-2100	33	4	11	11	3	-	2	1	1	23.40
2600-2400	53	3	18	17	8	2	1	2	2	37.58
3300-2700	37	4	11	15	3	-	1	2	1	26.24
Sum	141	16	43	47	17	2	4	6	5	100
Average height (m)	-	2469.6	2337.9	2290.4	2479.64	2651.75	2724	2473	2369.8	2477.01
Facade (M)	-	2559	2100	2519	1600	2752	2699	2732	2448	2425.12
Opposite poles Cirque					Amounts Facade					2559
Equator opposite cirque					Amounts Facade					2752
ΔELA					The difference between the two domains					193
Snow-line altitude										2425.12

Given the linear relationship of temperature and height, the current temperature of these elevations can be estimated (*Eq. 2*).

$$Y = -0.0045X + 18.06 \qquad R^2 = 0.84 \qquad \text{(Eq.2)}$$

In *Equation 2,* X is the height and Y is the estimated temperature for the current situation. Based on *Equation 2,* the current snow-line temperature is 7.46 using the Wright method and is 7.15 °C using Porter's method. In subsequent calculations, the

http://www.aloki.hu ● ISSN 1589 1623 (Print) ● ISSN 1785 0037 (Online)
DOI: http://dx.doi.org/10.15666/aeer/1605_58695891
© 2018, ALÖKI Kft., Budapest, Hungary

average temperature is considered to be 7.3. In fact, the minimum quaternary temperature reduction is considered to be 7.3 °C.

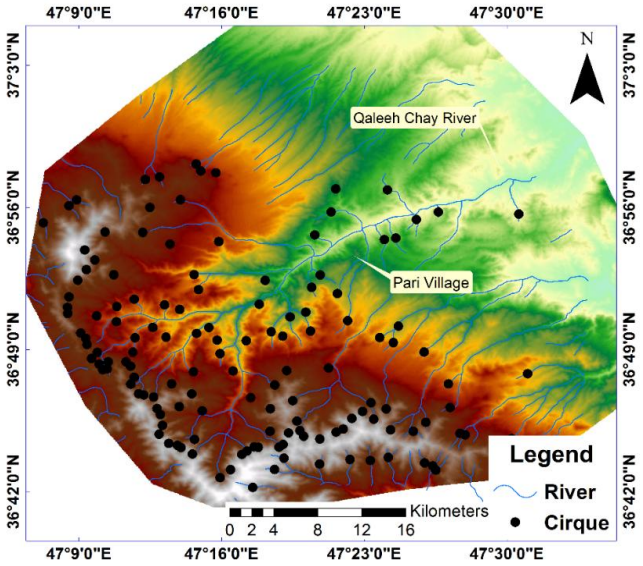

Figure 4. *Scattering of glacial cirques in the study area*

Topographic reconstruction

The base level of Ghezelowzan River Basins and Sub-basins has considerably changed during the quaternary period. The base level changes basically led to the formation of various morphogenesis and processes, such as the capture phenomena. In the capture of a river, the river changes into another direction. Stream capture, river capture, river piracy or stream piracy is a geomorphological phenomenon occurring when a stream or river drainage system or watershed is diverted from its own bed, and flows instead down the bed of a neighbour stream. The changes in the base level of Ghezelowzan River were about 200 m (*Fig. 5*). Base level changes have changed the flow of river processes and the dominance of gully erosion. The domination of gully erosion in the headwaters of the basin changes the alluvial process in pluvial process. In clay and silt lands in stagnant waters, in the case of running water, the form of the contour lines is expressed as the claw sinusoidal. Depending on the degree of erosion of these surfaces, the sinusoidal contour lines tend to be medial and claw-like. On topographic maps, wherever the gradient of the earth is very low, single elevation points are plotted instead of plotting the contour lines. This indicates that the intended level has evolved in the process of functioning of stagnant water. This is because very slow slopes have been developed in the bed of stagnant waters and secondly, the sediments will be fine-grained since the lake's environments and stagnant waters are low-energy and provide conditions for sedimentation with a diameter of less than 0.15 mm. In addition, convergent radial channel lines at these levels suggest the existence of past lakes. Drawing profiles (*Fig. 6*) Perpendicular to Qala-ehchai River on the left and right banks of the river showed that there were terraces of the same height with common ground, common slope and common morphology. Placing the longitudinal and transversal profiles on the region and the probability of existence of lake focuses attention on the terraces of the same height on both sides of the Qala-ehchai River.

http://www.aloki.hu ● ISSN 1589 1623 (Print) ● ISSN 1785 0037 (Online)
DOI: http://dx.doi.org/10.15666/aeer/1605_58695891
© 2018, ALÖKI Kft., Budapest, Hungary

Figure 5. *Drop down to Qala-ehchai River base*

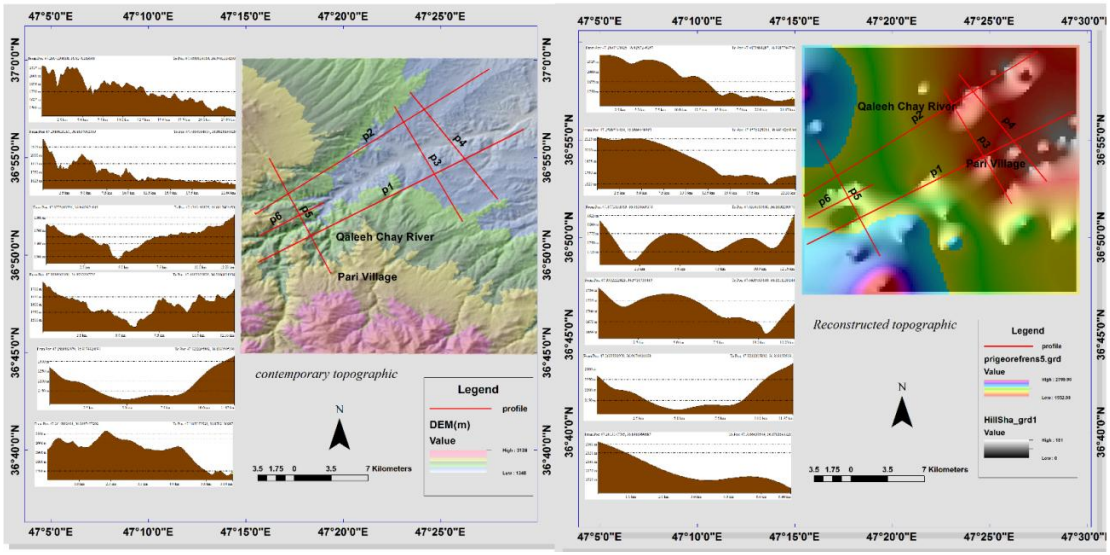

Figure 6. *Location and schematic figure of profiles in the studied area in both quaternary and contemporary conditions*

For further study of the reconstruction of the entire topography of the region, the height of these terraces was the basis of analysis and reconstruction of the total topography was done accordingly (*Figs 7* and 8). An examination of the old terraces of the entire area during the quaternary topographic reconstruction suggests that the lake's conditions and closure of the area still retain their original status. In the drawn profiles, the average depth of erosion in profiles 1 to 6 was 140, 115, 80, 225, 110 and 150 m, respectively. Border of lake was also drawn assigning banks to each river. After simulating the topography of the quaternary, the previous profiles drawn on the topography were drawn on the reconstructed topography in the same direction. In this way, the altitude of eroded land levels was detected and quaternary lakes were reconstructed.

http://www.aloki.hu ● ISSN 1589 1623 (Print) ● ISSN 1785 0037 (Online)
DOI: http://dx.doi.org/10.15666/aeer/1605_58695891
© 2018, ALÖKI Kft., Budapest, Hungary

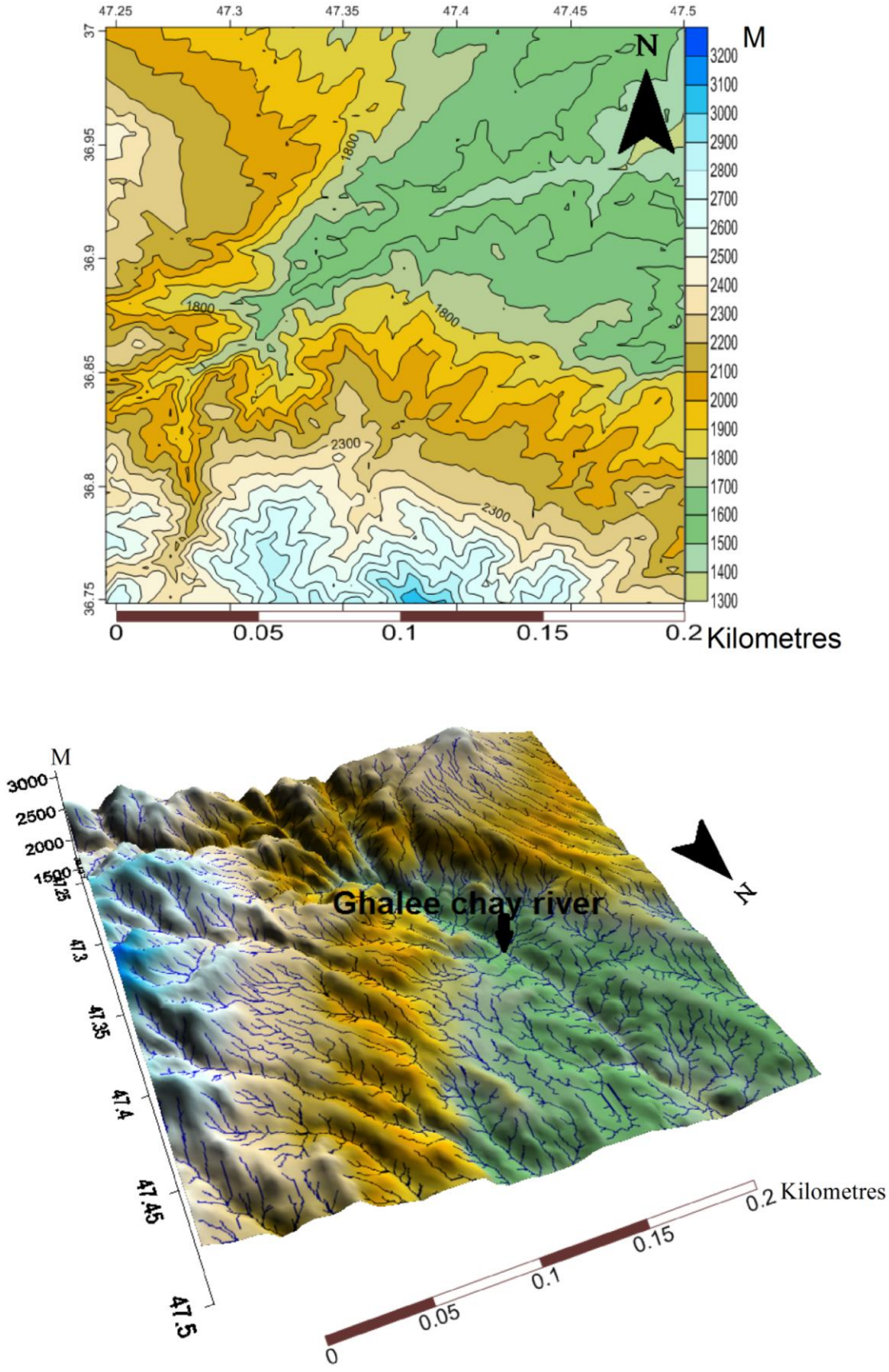

Figure 7. *Contemporary topographic and 3D maps*

http://www.aloki.hu ● ISSN 1589 1623 (Print) ● ISSN 1785 0037 (Online)
DOI: http://dx.doi.org/10.15666/aeer/1605_58695891
© 2018, ALÖKI Kft., Budapest, Hungary

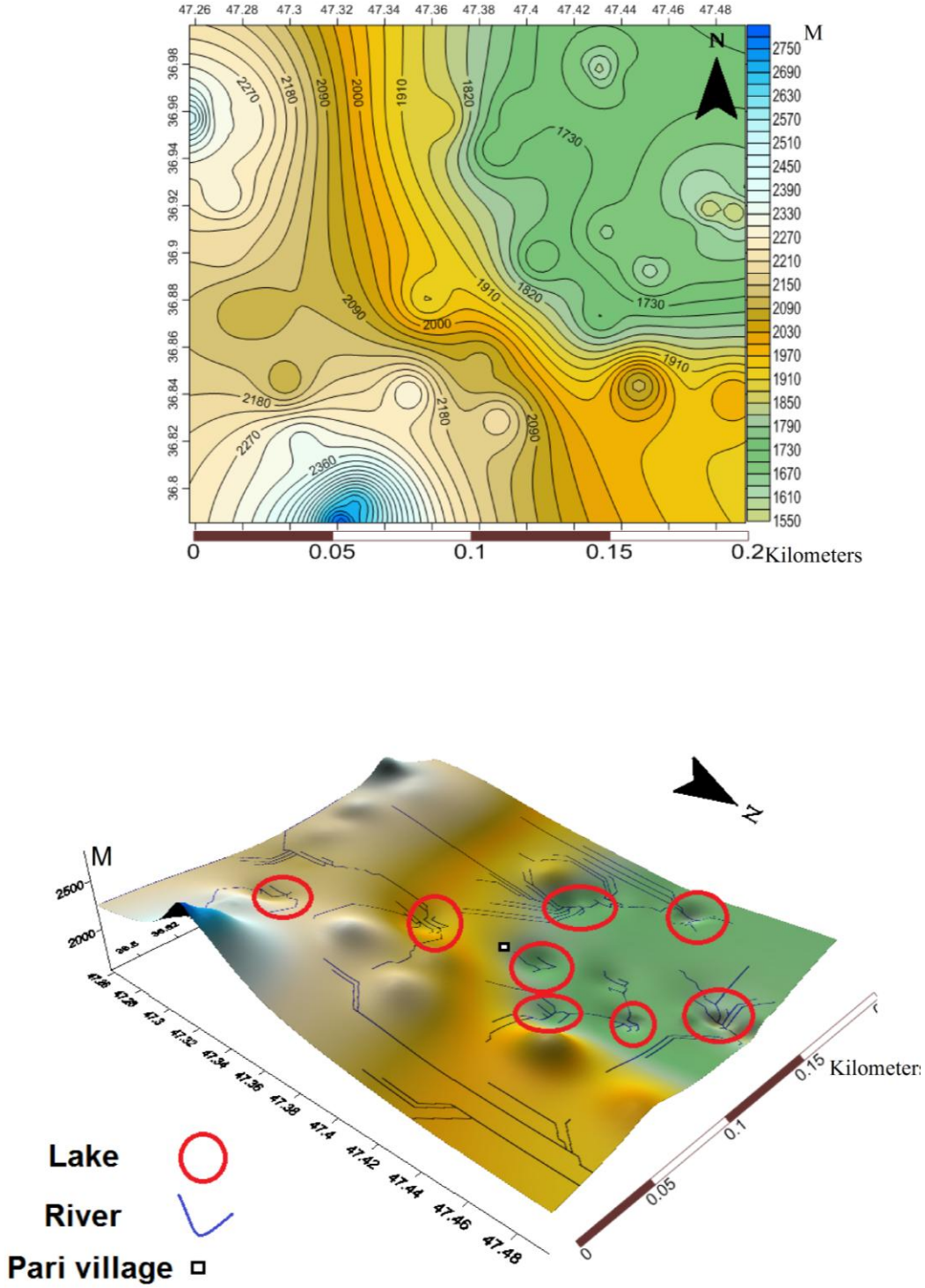

Figure 8. *Reconstructed topographic and 3D maps*

Given that the morphogenesis system in the quaternary was glacial and the study area was dominated by various lakes, it can be said that the glacial plates caused pouring erosion and created a number of lakes in one direction. The lakes have also been torn and drained on their left side. In the profile shown in *Figure 7,* this can be completely seen (*Fig. 9*).

http://www.aloki.hu ● ISSN 1589 1623 (Print) ● ISSN 1785 0037 (Online)
DOI: http://dx.doi.org/10.15666/aeer/1605_58695891
© 2018, ALÖKI Kft., Budapest, Hungary

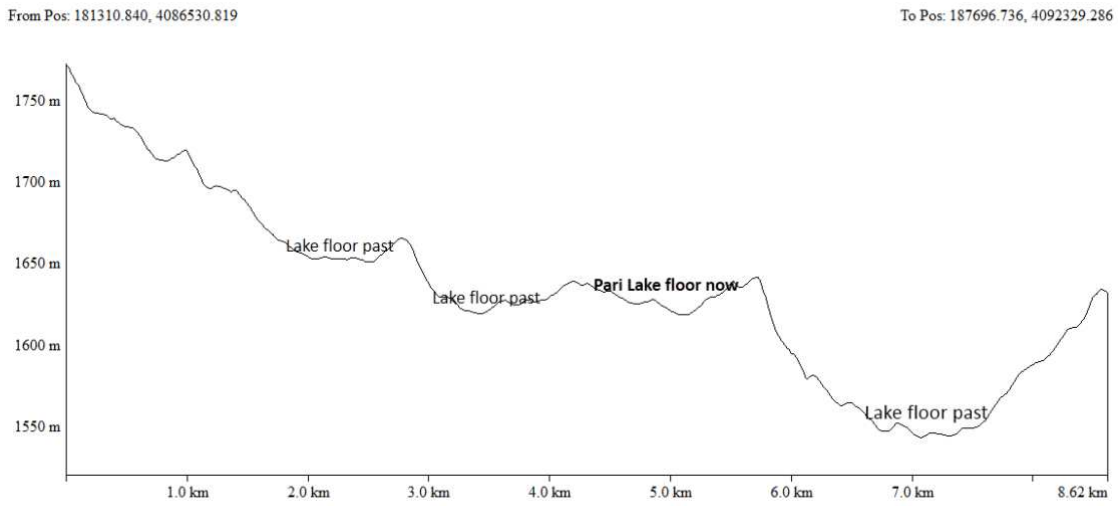

Figure 9. *Transversal profile in the quaternary*

The granulometry of sediments

Controlling slope over a long period of time in the plane causes exposure to air and physical and chemical weathering. The value of slope is also different in different bed rocks. This means that in a resistant formation, the slope undergoes fewer changes. In the study area, using a 30-meter DEM, a gradient map was obtained (*Fig. 10*). It turned out that the slopes of up to 5% are almost smooth and are considered as plain. On the direction map, the slopes of up to 5% are called highlands. However, given that lakes have transformed from hole-like shape into a flat form over time, they indicate past lakes in the quaternary period. In addition to topographic maps, more environmental documentations, the best of which is granulometry of sediments, are required for proving that the area under study was a lake during the quaternary period. For this purpose, 14 specimens of sediment in 9 points with different geographical coordinates were transferred from the profiles to the laboratory environment (*Fig. 11*). After selection and initial washings, a specified amount of each specimen was weighed and granulometry started using a Shaker between sieves number 20 to 230. The remaining sediment in each sieve was weighed and the graph was finally plotted. Based on the location of the sediments, three samples were taken at different depths with respect to the apparent change of sediment type near Khandaghlo Lake, which is currently one of the lakes in the region; although it has become independent due to a change in the base level of Qala'ehchai River and the upstream basin waters are not naturally directed to the lake, part of the water of Qala'ehchai goes to its centre by creating an artificial pond and it is used for agricultural and fish farming purposes. Profiles 1, 2, 3 belong to sediment condition of this part of the basin. These profiles were used as control profiles for the analysis of other profiles because them granulometry indicates lagoon coastal sediments. The change in these three profiles indicates the uniform distribution of grains in different sieves, and more than 60% of the sediments remain in the sieves receiving the finer grains. In other areas, it was not possible to identify the exact river bank due to changes in the use of the rivers and the diversion of the rivers, but it was attempted take samples from the nearest potential bank (*Fig. 12; Table 3*).

http://www.aloki.hu ● ISSN 1589 1623 (Print) ● ISSN 1785 0037 (Online)
DOI: http://dx.doi.org/10.15666/aeer/1605_58695891
© 2018, ALÖKI Kft., Budapest, Hungary

Table 3. *Charts obtained from granulometric sediments*

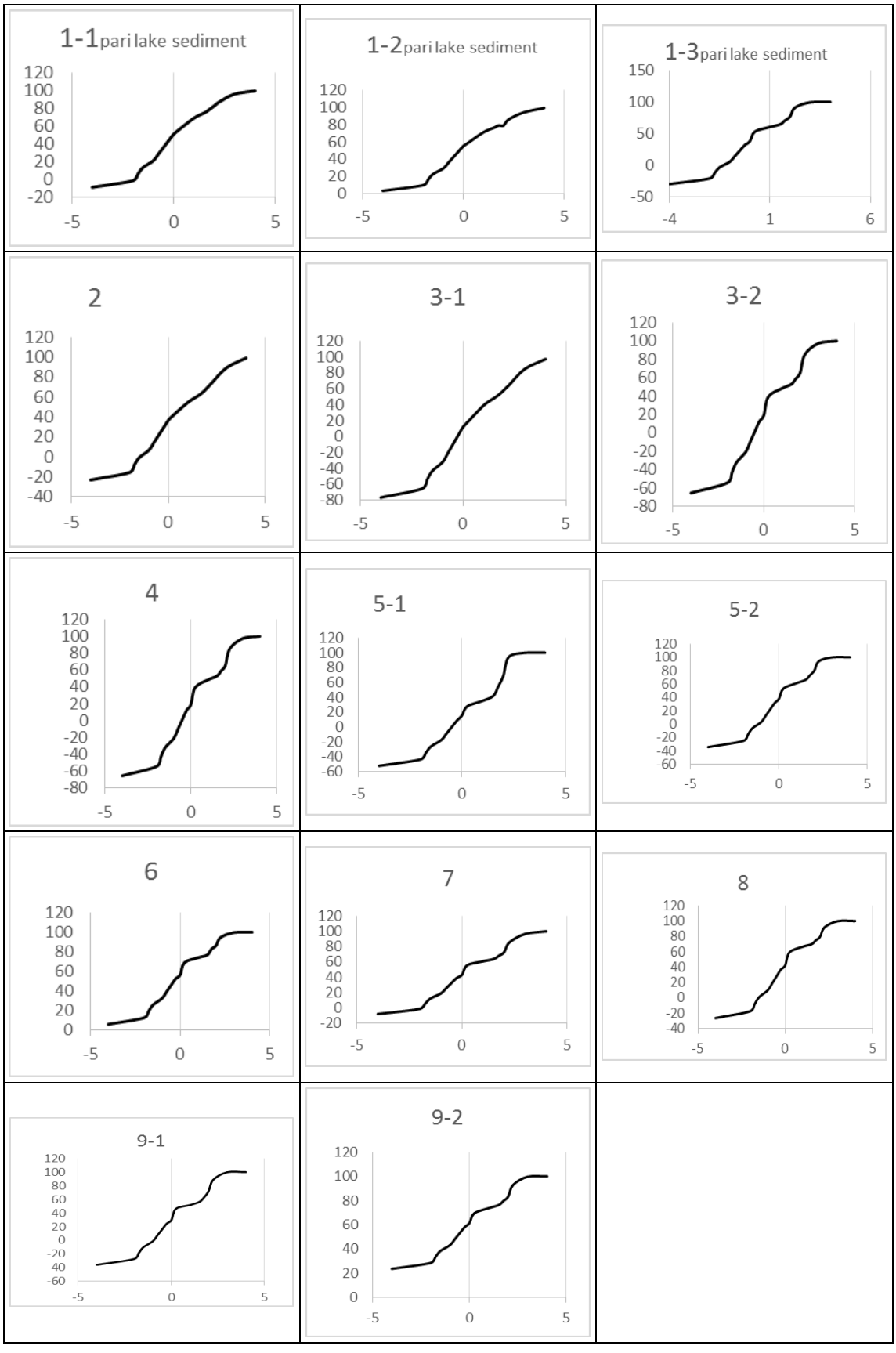

http://www.aloki.hu ● ISSN 1589 1623 (Print) ● ISSN 1785 0037 (Online)
DOI: http://dx.doi.org/10.15666/aeer/1605_58695891
© 2018, ALÖKI Kft., Budapest, Hungary

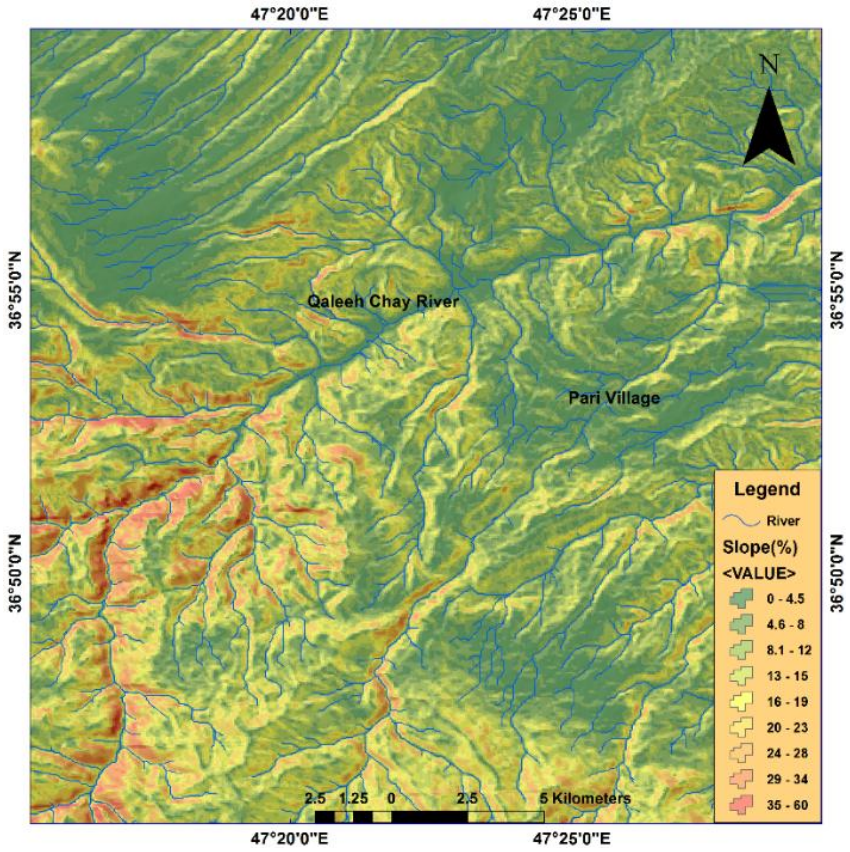

Figure 10. *Slope map of the study area obtained from DEM with 30 m spatial resolution*

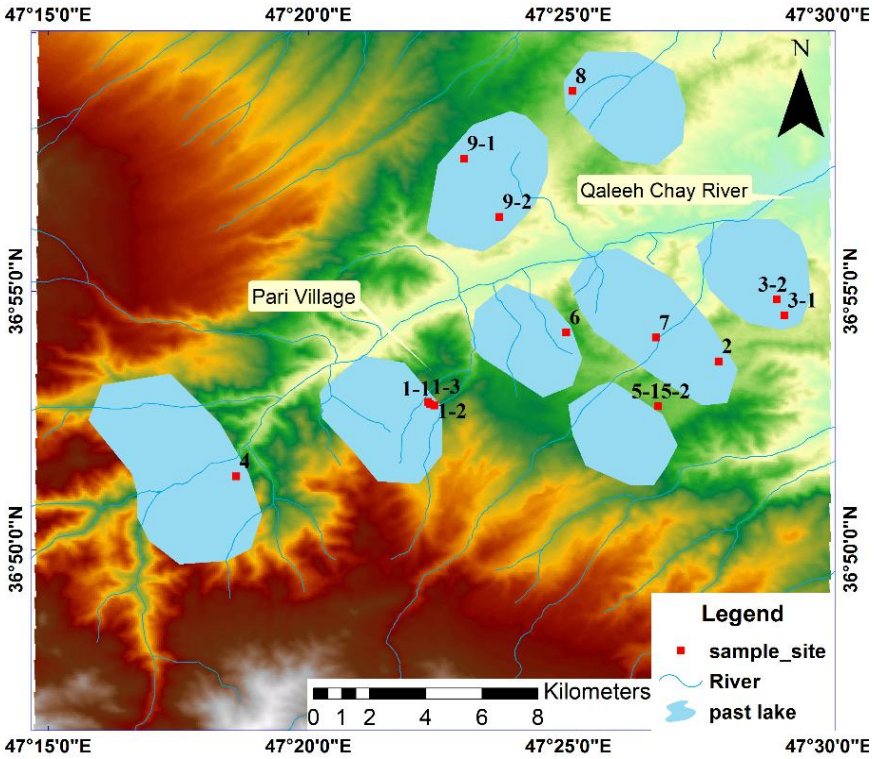

Figure 11. *Location of sampling sites*

http://www.aloki.hu ● ISSN 1589 1623 (Print) ● ISSN 1785 0037 (Online)
DOI: http://dx.doi.org/10.15666/aeer/1605_58695891
© 2018, ALÖKI Kft., Budapest, Hungary

Profiles 1-3 and 2-3, taken from the same location with the farthest distance to the centre, are known as the Polygon of Lake and are very similar to the profiles provided by researchers such as Mahmoudi and Moghimi (2011) for glacier deposits, which is evidence that the area was a glacier during cold quaternary periods. Rest of the profiles (4, 5, 6, 7, 8, and 9) are affected by lake-glacier process, which indicates that the environment is affected by the glacier-lake process and that the polygon of the sediment lake shows a tendency to be glacier when being taken away from the centre.

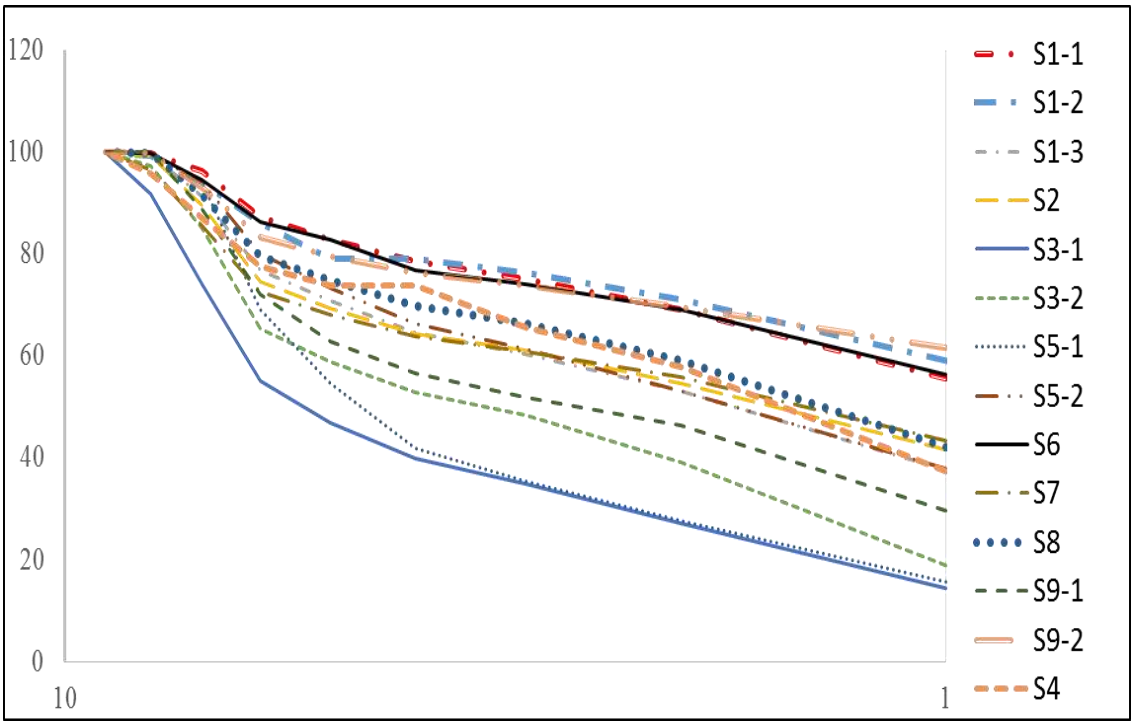

Figure 12. *Plot of different sediment samples*

The granulometric results of the data and the relationships in *Table 1* show that, in terms of the Mz index, all samples are coarse grains and are divided into two groups of medium sand and coarse sand. In terms of Q1 index, the sediments fall into two very poorly sorted and poorly sorted groups, and only one sample has been moderately sorted. The Ski index subdivides the sediment into four groups. Most of the samples are located in the mediums positively skewed group of the fine particles. Two samples of asymmetric sediments are very positively skewed toward coarse particles and granularity. A large asymmetric sample is symmetrically skewed toward fine particles. In the KG index, the whole sediment sample was divided into two very platykurtic and leptokurtic groups. According to the data in *Table 4,* it can be said that most of the collected grains correspond to very slight differences with the precipitates taken from the Peri Lake. Accordingly, the condition of the lake is confirmed by past sampling sites.

The quaternary glacial processes of Iran have been exposed to various geographic and environmental conditions. Until now, moraines, U-shaped valleys, and cirques or mountain snow flats have attracted attention of many glacier researchers. Evidence of the quaternary glacial lakes was less considered. The topographic and geomorphological

http://www.aloki.hu ● ISSN 1589 1623 (Print) ● ISSN 1785 0037 (Online)
DOI: http://dx.doi.org/10.15666/aeer/1605_58695891
© 2018, ALÖKI Kft., Budapest, Hungary

conditions of the Qala'ehchai Basin and the adjacent basins indicate that the streams flow out of the mountains to the plains in the wide and U- shaped valleys. U-shaped valleys were shaped due to the glacier flow in the quaternary cold periods. Investigating Qala'ehchai Basin as a typical basin on the west of the Ghezelowzan river from Mahneshan to Miyaneh shows that there is evidence of geomorphological effects of eight lakes from the quaternary period. Glacier lakes are not caused by the deposition of the terminal moraines or by the exploration of the glacier in the cirques, but rather they are formed by the glacier flow in marl sediments. Glacier flow in the marl sediments has created U-shaped valleys that have become independent basins, creating small and shallow lakes with the withdrawal of the glacier. By changing the base level of the Ghezelowzan River during the quaternary and overcoming the decreasing erosion on its branches, small basins have lost their independence and have been evacuated in Ghezelozen River. Several field surveys in different areas affected by the quaternary glacier in Iran indicate that the areas around the Qala'ehchai Basin are the only area that has kept the effects of glacial lakes. Studies of quaternary climate change in Khandaghlo Lake, as a remaining ecosystem since then, can be a nod to many quaternary issues.

Table 4. *Computed grain size parameters and their verbal terms for outcrops from study areas*

Sample and figure number	Mean size (MZ)	Sorting (Q1)	Skewness (Ski)	Kurtesis (KG)
1-1	0.3 coarse sand	1.5 poorly sorted	2.266 mediums positively skewed	0.2 very platykurtic
1-2	0.17 coarse sand	2.015 very poorly sorted	1.19 mediums positively skewed	0.45 very platykurtic
1-3	0.94 coarse sand	2.48 very poorly sorted	5.15 mediums positively skewed	0.63 very platykurtic
2	0.9 coarse sand	1.57 poorly sorted	0.25 symmetrical skewed	0.65 very platykurtic
3-1	1.43 medium sand	1.14 poorly sorted	-1.1 negatively skewed	0.70 platykurtic
3-2	1.53 medium sand	1.31 poorly sorted	0.657 very positively skewed	0.72 platykurtic
4	1.75 medium sand	1.07 poorly sorted	0.58 very positively skewed	0.69 platykurtic
5-1	1.33 medium sand	0.971 moderately sorted	0.325 very positively skewed	0.69 platykurtic
5-2	0.56 coarse sand	1.125 poorly sorted	5.67 mediums positively skewed	0.43 very platykurtic
6	0.6 coarse sand	1.8 poorly sorted	1.31 mediums positively skewed	0.85 platykurtic
7	0.37 coarse sand	1.51 poorly sorted	2.17 mediums positively skewed	0.61 very platykurtic
8	0.51 coarse sand	2.28 very poorly sorted	2.75 mediums positively skewed	0.68 platykurtic
9-1	0.76 coarse sand	1.22 poorly sorted	1.87 mediums positively skewed	0.59 very platykurtic
9-2	0.83 coarse sand	2.52 very poorly	1.22 mediums	1.33 lepokurtic

http://www.aloki.hu ● ISSN 1589 1623 (Print) ● ISSN 1785 0037 (Online)
DOI: http://dx.doi.org/10.15666/aeer/1605_58695891
© 2018, ALÖKI Kft., Budapest, Hungary

		sorted	positively skewed	

Conclusion

In the east of the western highlands of Zanjan Province, landforms are either closed or semi-closed basins. Their geomorphological evidence at first sight brings a land like the land of thousands of lakes in Finland to mind. Khandaghlo Lake is the only remaining lake in this region. In this area, where the altitude varies from 1600 to 1900 m, there are convergence centres in the waterway network that are sometimes cut off from one side and water has been discharged. In order to have a standard profile, three sediment samples were taken at different depths from the lake bank; Granulometry of sediments indicate their homogeneous distribution. The snow-line height according to Wright, and Porter methods was 2357 and 2425 m. If the highest snow-line height estimated by the Porter method is taken into account, it is noteworthy that all lakes are above the quaternary water and the ice equilibrium line since the height of the water and the ice equilibrium line is 1042 m below the snow-line height based on the findings. On this basis, the quaternary water and ice equilibrium line is less than 1400 m, with the lower lakes with a height of nearly 1600 m above it. Field evidence and lithology of the region indicate that glaciers that are originated from high altitudes and well fed enter marl deposits by exiting the igneous area and resistant sediments. Glaciers in marl sediments create U-shaped valleys with a linear flow. They contribute to the creation of lakes in two ways: Lakes closest to the water and the ice equilibrium line have been established for the glacier valley terminal, such as the glacier and the terminal moraine. The rest of the lake has been created due to explorative erosion in long-tailed valleys as a result of further dredging of the lake bed. The granulometry of taking samples indicates that the profile of the sediments taken from the lake bank or its centre is more similar to the lake sediments, and their profile becomes of lake-glacial sediments by going away from the centre or bank of the lake. Of the 780,000 m^2 of the total area of Qala'ehchai, about 96,000 m^2 (12%) includes the identified 8 lake beds. Khandaghlo Lake, as an evidence of the lakes of the quaternary period, owes its existence to an artificial canal that transfers part of the water of the Qala'ehchai to the lake. With regard to climate change over the last few decades, the study of climate changes and quaternary ecological conditions has an important role to play in environmental planning. A detailed study of the climate change aspects of the region can provide important solutions for managing global warming. On the other hand, given the tourist boom, the introduction of these places is of particular importance in attracting tourists.

REFERENCES

[1] Abtahi, S. M. (2013): Investigation of paleoclimatology of Jajrood Basin in Iran by glacial evidence. – Geological Exploration of Desert Areas 1(1): 185-201.

[2] Amirahmadi, A. Maghsodi, A., Ahmadi, T. (2011): Evaluating the effects of quaternary glaciers on the lack of civilization and main urban habitation in Aspas plain. – Urban-Regional Studies and Research 3(10): 61-80.

[3] Askari Chawardi, H. (2009): Study of Quaternary Mountain Lakes in Jajrood Valley (Case Study: Hajiabad Area). – Master's Thesis, Islamic Azad Tehran University, Faculty of Literature and Humanities.

http://www.aloki.hu ● ISSN 1589 1623 (Print) ● ISSN 1785 0037 (Online)
DOI: http://dx.doi.org/10.15666/aeer/1605_58695891
© 2018, ALÖKI Kft., Budapest, Hungary

[4] Bajracharya, S. R., Mool, P. (2009): Glaciers, glacial lakes and glacial lake outburst floods in the Mount Everest region, Nepal. – Annals of Glaciology 50(53): 81-86.
[5] Bao, H. Fairchild, I. J., Wynn, P. M., Spötl, C. (2009): Stretching the envelope of past surface environments: Neoproterozoic glacial lakes from Svalbard. – Science 2(323): 119-22.
[6] Barr, I. D., Spagnolo, M. (2015): Understanding controls on cirque floor altitudes: insights from Kamchatka. – Geomorphology 248: 1-13.
[7] Bolch, T., Peters, J., Yegorov, A., Pradhan, B., Buchroithner, M., Blagoveshchensky, V. (2011a): Identification of potentially dangerous glacial lakes in the northern Tien Shan. – Nat Hazards 59: 1691-1714.
[8] Bolch, T., Pieczonka, T., Benn, D. I. (2011b): Multi-decadal mass loss of glaciers in the Everest area (Nepal Himalaya) derived from stereo imagery. – The Cryosphere 5(2): 349-358.
[9] Chinn, T. J., Whitehouse, I. E. (1980): Glacier Snow Line Variations in the Southern Alps. – Iahs-Aish Press, New Zealand.
[10] Cossart, E., Braucher, R., Fort, M., Bourlès, D. L., Carcaillet, J. (2008): Slope instability in relation to glacial debuttressing in alpine areas (Upper Durance catchment, southeastern France): evidence from field data and 10Be cosmic ray exposure ages. – Geomorphology 95(1-2): 3-26.
[11] Derruau, M. (2011): Les forms du relief terrestre de geomorphology (translated by Mqsud, K.) – Tabriz University Press, Tabriz.
[12] Entezari, A. Amir Ahmadi, A. Ghandajik, A. Jahanfar, A., Shayan Yeganeh, A. K. (2015): Geomorphologic assessment of climatic changes of Gorganroud Basin in the quaternary. – Quaternary Iran 1(2): 169-180.
[13] Evans, I. S. (1977): World-wide variations in the direction and concentration of cirque and glacier aspects. – Geografiska Annaler: Series A, Physical Geography 59(3-4): 151-175.
[14] Evans, I. S. (1995): The form of glacial cirques in the English Lake District, Cumbria. – Zeitschrift fur Geomorphologie NF 39: 175-202.
[15] Fujita, K. Sakai, A., Takenaka, S. Nuimura, T,. Surazakov, A. B. Sawagaki, T., Easuremen, T. (2013): Potential flood volume of Himalayan glacial lakes. – Hazards Earth Syst Sci (13): 1827-1839.
[16] Ghahroudi Taley, M. (2011): Estimation and comparison of the realm of permanent snow on the glacier and glacier Case study: Haraz Basin. – Geography and Development 9(25): 97-103.
[17] Ghiyas Abadi, M., Mousavi Nadushan, R., Fatemi, M. R., Jozi, S. A. (2014): Assessment of Gahar Lake Trophic Status using TLI Index. – Journal of Marine Science and Technology Research 8(4): 75-88.
[18] Glassera, N. F., Bennettb, M. R. (2004): Glacial erosional landforms: origins and significance for palaeoglaciology. – Progress in Physical Geography 28(11): 43-75.
[19] Gresswell, R. K. (1958): The Physical Geography of Glaciers and Glaciation. – Hulton Educational Publ., London.
[20] Jafari, G. H., Asghari Serkansrudi, S. (2014): The analysis of quaternary glacial effects of Zanjanrood. – Quantitative Geomorphology Researches 3(2): 16-30.
[21] Jananeh, C., Rajabi, M. (2016): The effects of the quaternary period in the seas and lakes of Iran. – 2nd International Congress of Earth Sciences and Urban Development 1-12.
[22] Jedari Eyvazi, J. (2013): Geomorphology of Iran. – Payame Noor University Press, Tehran.
[23] Kiani, T., Ramesht, M. H., Maleki, A., Safakish, F. (2016): Assessment and review the environmental risks resulting from climatic changes in Abarkooh Basin. – Geography and Development, Iranian 14(43): 19-34.
[24] Klinsley, D. B. (2009): The Deserts of Iran and Geomorphological Features and Its Paleoclimatology. – National Geographical Organization, Tehran.

http://www.aloki.hu ● ISSN 1589 1623 (Print) ● ISSN 1785 0037 (Online)
DOI: http://dx.doi.org/10.15666/aeer/1605_58695891
© 2018, ALÖKI Kft., Budapest, Hungary

[25] Koinig, K. A., Shotyk, W., Lotter, A. F., Ohlendorf, C., Sturm, M. (2003): 9000 years of geochemical evolution of lithogenic major and trace elements in the sediment of an alpine lake–the role of climate, vegetation, and land-use history. – Journal of Paleolimnology 30(3): 307-320.
[26] Lewis, C. F. M., Anderson, T. W. (1989): Oscillations of levels and cool phases of the Laurentian Great Lakes caused by inflows from glacial Lakes Agassiz and Barlow-Ojibway. – Journal of Paleolimnology (2): 99-146.
[27] Longmore, M. E., Heijnis, H. (1999): Aridity in Australia: Pleistocene records of palaeo hydrological and palaeoecological change from the perched lake sediments of Fraser Island, Queensland, Australia. – Quaternary International (57): 35-47.
[28] Mahmoudi, F., Moghimi, E. (2011): Research Method in Physical Geography (Geomorphology). – Gomes Press, Tehran.
[29] Martin, J. Head, Ph. G. and Amos, S. (2008): The quaternary: its character and definition. – Episodes 31(2): 234-238.
[30] Nabavi, H. (1976): A Preface to the Geology of Iran. – Atomic Advocates of the Geological Survey, Tehran.
[31] Obinegbu, I. R., Chiaghanam, O. I., Chiadikobi, K. C (2013): Paleoenvironmental indications from textural parameters: a case study of the Paleocene to Eocene sandstones in some parts of Anambra Basin, South-Eastern, Nigeria. – International Journal of Scientific & Technology Research 2(10): 201-213.
[32] Olvmo, M., Johansson, M. (2002): The significance of rock structure, lithology and pre-glacial deep weathering for the shape of intermediate-scale glacial erosional landform. – Earth Surf, Process Landforms (27): 251-268.
[33] Oskooi, B., Omidian, S. (2013): Evaluation of Havir Lake formation causes based on magnetotelluric data. – Earth and Space Physics 39(2): 95-110.
[34] Parizi, I. Taqian, A., Ramsht, M. H. (2013): Evidence of the quaternary glaciers in the Tiguani Basin of Sirjan. – Quantitative Geomorphology Research 2(3): 111-128.
[35] Ramesht, M. H. (2001): Glacier Works in Zefareh, Isfahan. – Research Project No. 800305, Research Council of Isfahan University.
[36] Ramesht, M. H. (2004): The fourth glaciers in the suburbs of Isfahan. – The Growth of Geography Education 19(67): 22-10.
[37] Ramesht, M. H. (2013): Symbols and Images in Geomorphology. – SAMT Press, Tehran.
[38] Rezvani, M. R., Ramezanzadeh, L. M., Mohammadpour, J. M. (2010): The analysis of socio-economic effects of industrial areas on developing rural areas (case study: industrial area of Soleiman Abad, Tonekabon). – Geography and Development, Iranian 8(18): 69-92.
[39] Russell, C. (1889): Quaternary History of Mono Valle. – US Government Printing Office 1889 - Geology, Strati-Graphic, California.
[40] Seif, A., Abtahi, S. M. (2013): A survey of climatic Changes of Namak Lake Basin in the late quaternary. – Geography and Planning 17(46): 91-111.
[41] Seif, A., Ebrahimi, B. (2014): Combined use of GIS and experimental functions for the morphometric study of glacial cirques, Zardkuh Mountain, Iran. – Quaternary International (3): 1-14.
[42] Shamsipour, A,. Bagheri, S. Shokri, S. Jafari Aghdam, M., Salimimanesh, J. (2015): Reconstruction of the last glacial snow lines by the evidences of glacial periods in North West Zagros (Case study: Anticline Qalajeh). – Geography and Development, Iranian 13(39): 61-74.
[43] Sundal, A. V. Shepherd, A. Nienow, P. Hanna, E. Palmer, B., Huybrecht, P. (2009): Evolution of supra-glacial lakes across the Greenland Ice Sheet. – Remote Sensing of Environment (113): 2164-2171.
[44] Tahoni, P. (2004): Geomorphological evidences of Pleistocene glacial erosion in Talesh Mountain. – Geosciences Researches 36(1): 55-31.

http://www.aloki.hu ● ISSN 1589 1623 (Print) ● ISSN 1785 0037 (Online)
DOI: http://dx.doi.org/10.15666/aeer/1605_58695891
© 2018, ALÖKI Kft., Budapest, Hungary

[45] Velayati, S. A. (1995): Geography of Water and Water Resources Management. – Khorasan Press, Mashhad.
[46] Walter Goldthwaite, J. (1908): A reconstruction of water planes of the extinct glacial lakes in the Lake Michigan Basin. – The Journal of Geology 16(5): 459-476.
[47] Ward, W. C. (1957): Brazos River bar: A study in the significance of grain-size parameters. – Journal of Sedimentary Petrology (27): 3-26.
[48] Yamani, M. Jiadari Ayvazi, J., Abolghasem, G. (2007): Geomorphologic evidences of glacier borders in the Karkas Domain. – Modarres of Humanities 11(1): 207-228.
[49] Zomorodiyan, M. J. (2012): Geomorphology of Iran. – Ferdowsi University, Mashhad.

http://www.aloki.hu ● ISSN 1589 1623 (Print) ● ISSN 1785 0037 (Online)
DOI: http://dx.doi.org/10.15666/aeer/1605_58695891
© 2018, ALÖKI Kft., Budapest, Hungary

THE IMPACT OF THE MORPHOLOGY OF MOUNTAIN WATERCOURSES ON THE HABITAT PREFERENCES INDICATED BY ICHTYOFAUNA USING THE IFIM METHODOLOGY

ŠTEFUNKOVÁ, Z.[1*] – BELČÁKOVÁ, I.[2] – MAJOROŠOVÁ, M.[1] – ŠKRINÁR, A.[1] – VASEKOVÁ, B.[1] – NERUDA, M.[3] – MACURA, V.[1]

[1]*Faculty of Civil Engineering, Slovak University of Technology in Bratislava*
Radlinského 11, 810 05 Bratislava, Slovakia
(phone: +421-2-5927-4471; fax: +421-2-5296-7027)

[2]*Faculty of Ecology and Environmental Sciences, Technical University in Zvolen*
T. G. Masaryka 24, 960 53 Zvolen, Slovakia
(phone: +421-455-206-492; fax: +421-455-206-279

[3]*Faculty of Environment, Jan Evangelist Purkkyně University in Ústi nad Labem*
Králova Výšina 3132/7, 400 96 Ústí nad Labem, Czech Republic
(phone: +420-739-335-079; fax: +420-475-284-158)

**Corresponding author*
e-mail: zuzana_stefunkova@stuba.sk; phone: +421-2-5927-4617; fax: +421-2-5292-3575

(Received 4th Jun 2018; accepted 14th Aug 2018)

Abstract. A natural channel differs from a prismatic one by its rich variability. Regulated rivers have a geometrically regular shape that is not suitable for the instream biota. The morphology of a regulated river is the main cause of habitat changes. The article provides the results of research that was focused on assessing the impact of a channel's morphology on the instream habitat preferences by ichthyofauna. In the article the ichthyofauna is represented by brown trout (*Salmo trutta m. fario*). During the years 2015 and 2016, research was carried out for 13 reaches of mountain watercourses in Slovakia. These reaches were geodetically measured, and a hydraulic model was created. The ichthyological survey was focused on the fish's habitat preferences. A set of data was created from the results that was statistically evaluated by cluster analysis, and the correlation relations for the abiotic and biotic characteristics of the watercourses were evaluated. The individual evaluations provide mutually compatible results. It can be concluded from the results that bioindications by fish provide reliable results in relationship to the changes in habitats in regulated rivers. There was an unambiguous statistical correlation in the preferences of brown trout in the regulated and natural rivers.
Keywords: *brown trout, suitability curves, RHABSIM, river regulation effect*

Introduction

In most cases, the regulation of rivers has always been and is still oriented towards flood protection. Often, such implementation has been unilaterally aimed at increasing the capacity of the channel, so that the variability of the channel's morphology was replaced by a prismatic shape. Such modifications significantly altered the natural morphology of the channel. Natural habitats that create favorable conditions for biota during minimum flows have disappeared in regulated rivers. Therefore, a whole set of methodologies that assess the consequences of changes in rivers has been developed.

http://www.aloki.hu ● ISSN 1589 1623 (Print) ● ISSN 1785 0037 (Online)
DOI: http://dx.doi.org/10.15666/aeer/1605_58935907
© 2018, ALÖKI Kft., Budapest, Hungary

Modelling of the biological variables of a stream was used for this purpose. This method enable an assessment of the suitability of the microhabitat of a reach (Copp, 1992; Bockelmann et al., 2004), the organization of aquatic communities (Townsend and Hildrew, 1994) or the anthropogenic impact on a watercourse (Shuler and Nehring, 1994; Shields et al., 1997).

A key aspect of these methodologies is to identify and assess the links between the hydromorphological, physical-chemical and biological states of streams (Conallin et al., 2010; Galie et al., 2017).

Along with the quality of streams and biotic interactions, morphological characteristics form a basis for assessing the availability of a habitat (Carnie et al., 2016; Gibson and Pasternack, 2016). When restoring the regulations that were aimed only on flood protection, it is important to be able to predict the response of the biota to the restoration measures. Therefore, the modelling of the impact of the morphology on a river's ecosystem requires a systematic and repeatable analysis of the impacts of the habitat characteristics of the stream on its suitability (Galbraith et al., 2016; Turner et al., 2016), the organization of aquatic compartments (Piniewski et al., 2016), and any anthropogenic changes in the stream (Santiago et al., 2016). This is the methodological framework for an environmental assessment of the effects of changes in streams (climatic, morphological, quality of water, etc.), on the quality of the aquatic habitat that are based on the Instream Flow Incremental Methodology – IFIM (Bovee, 1982; Bovee et al., 1998).

The impact of changes of the quality of a habitat is determined by bioindications. Research shows that freshwater fish are good indicators of morphological changes in streams and of biotic integrity in freshwater ecosystems (Pont et al., 2006; Cheek et al., 2016; Roni et al., 2014). They also respond sensitively to changes in the temperature and flow (Avery-Gomm et al., 2014). Due to their mobility, which they also have in their old age, and sensitivity to biotope changes, fish are suitable for assessing a river's ecological integrity (Keeley et al., 2015; Booker and Dunbar, 2004).

Information about the impact of channel characteristics on the quality of a habitat is important. This problem was solved by Holm et al. (2001), when he created three different suitability curves of flow velocity at three different flow rates for juvenile Atlantic salmon (*Salmo salar*) under laboratory conditions. Holm's study focused on fish habitat preferences in terms of changes in flow, depth and velocity (see also Marsili-Libelli et al., 2013; Ayllón et al., 2009; Macura et al., 2016).

Intensive discussions are ongoing among water managers, ichthyologists and hydrobiologists. Nowadays, these specialists believe that the success or failure of any restoration project depends on understanding of river biotopes (Zhang et al., 2016) and continuous stream monitoring.

In view of this trend, the results in this article are aimed at assessing the impact of the river regulation on the quality of the aquatic habitat, which is indicated by ichthyofauna.

At present, it can be said that the success or failure of any restoration project does not only depend on continuous river monitoring; it also particularly depends on a design based on a high-quality forecast of the reaction of the biotope to the restoration interventions that will be needed. This procedure minimizes inappropriate restoration measures in a stream. In accordance with this trend, the

http://www.aloki.hu ● ISSN 1589 1623 (Print) ● ISSN 1785 0037 (Online)
DOI: http://dx.doi.org/10.15666/aeer/1605_58935907
© 2018, ALÖKI Kft., Budapest, Hungary

results presented in this article are aimed on the impact of river regulation on the quality of an aquatic habitat that is mainly indicated by brown trout.

Materials and methods

From the point of view of the restoration of a river, it is important to quantify its design parameters. It is important to focus on the summer season. Minimum flows along with high temperatures create the highest load factors for the biota. Therefore, the summer period can be considered as a design condition for assessing the quality of a habitat or for the design of appropriate parameters for restoration measures for a river (Carlson et al., 2015; Macura et al., 2016).

The main objective was to determine the effect of the morphology of a river on the habitat preferences of the ichthyofauna, which in this article is represented by brown trout. The following methodology was selected:

- Selection of the reference reaches
- Ichthyological survey and hydrometric measurements
- Topographic measurements of the reference reaches
- Statistical evaluation of the characteristic parameters of the aquatic habitat
- Modelling of the quality of the aquatic habitat
- Effect of the flow velocity and channel depth on the suitability of the river habitat

Reference reaches of the rivers

For this study smaller mountain and piedmont streams were selected for the following reasons:

- Mountain streams have more characteristics in common, so the negative effects of their regulation are also common in many areas. Therefore, it can be expected that the results obtained could be generalized
- Mountain streams are in the upper sections of a river basin. Their length is relatively short, so the pollution load is low, and the water quality is usually suitable for the full use of the restoring effect on the stream and its surroundings.
- River regulations mainly affect the morphology of a stream. The good water quality of the selected reaches of mountain and piedmont streams does not alter the impact of the morphology on the quality of the aquatic habitat.

The reference reaches with a river basin of a size of 10-100 km^2 were selected from a whole database of reference reaches by a selective method in the environment of ArcView GIS. From the point of view of the rock complexes, a flysch was selected. At this selection stage, the river basin database contained 265 river basins that fulfilled the previous conditions. In the first phase, streams where hydrological stations are located were selected. Based on the ArcView GIS analysis, a physical survey of the streams was performed, and suitable representative reaches for ichthyological and hydrometrical field measurements were selected. The Teplička, Lesnianka, Petrovička, Zázrivka, Veselianka, Kľačianka, Hybica, Lipnik and Kamienka reaches, which are located in the Váh River basin in Slovakia, were selected (*Fig. 1* and *Table 1*).

http://www.aloki.hu ● ISSN 1589 1623 (Print) ● ISSN 1785 0037 (Online)
DOI: http://dx.doi.org/10.15666/aeer/1605_58935907
© 2018, ALÖKI Kft., Budapest, Hungary

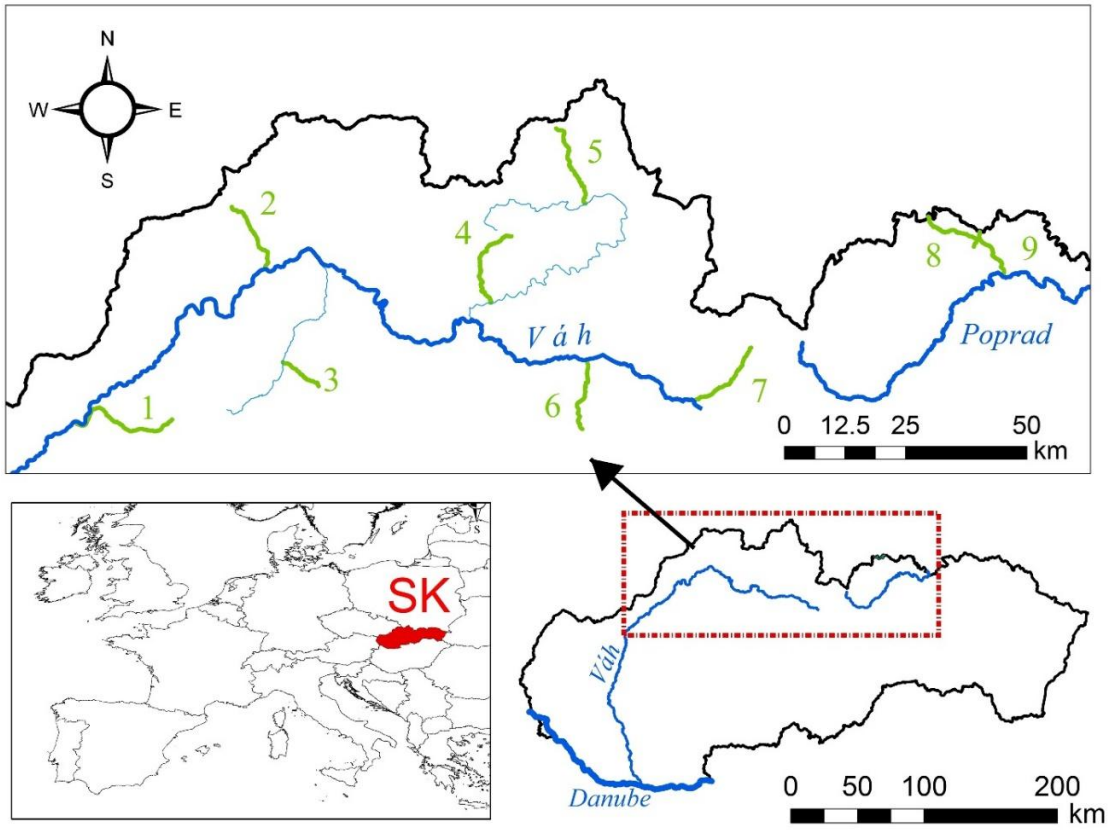

Figure 1. *Localization of the reference reaches of the mountain streams in Slovakia: 1 - Teplička, 2 - Lesnianka, 3 - Petrovička, 4 - Zázrivka, 5 - Veselianka, 6 - Kľačianka, 7 - Hybica, 8 - Lipnik, 9 - Kamienka*

Table 1. *WGS84 coordinates of the reference reaches. Stream condition: N - Natural stream, R - Regulated reach*

Teplička	N	48°55.169'N	18°08.687'E
	R	49°17.364'N	18°47.809'E
Lesnianka	N	49°02.246'N	18°39.422'E
	R	49°02.715'N	18°37.563'E
Petrovička	N	49°14.679'N	18°33.100'E
	R	49°15.366'N	18°31.713'E
Zázrivka	N	49°14.469'N	19°09.328'E
	R	49°11.351'N	19°11.521'E
Veselianka	N	49°26.192'N	19°24.294'E
	R	49°24.867'N	19°25.965'E
Klačianka	N	49°04.611'N	19°28.679'E
Hybica	N	49°02.146'N	19°47.526'E
	R	49°02.654'N	19°49.574'E
Lipník	N	49°22.439'N	20°28.256'E
	R	49°22.883'N	20°26.374'E
Kamienka	N	49°20.745'N	20°36.221'E
	R	49°18.091'N	20°38.314'E

http://www.aloki.hu ● ISSN 1589 1623 (Print) ● ISSN 1785 0037 (Online)
DOI: http://dx.doi.org/10.15666/aeer/1605_58935907
© 2018, ALÖKI Kft., Budapest, Hungary

Ichthyological survey

An ichthyological survey of the selected reaches was oriented towards determining the suitability curves of the individual fish species. The data were obtained by electro fishing, similarly as in Lamouroux et al. (1999). An electrofishing device (Hans-Grassl ELT62IIHI) with the possibility of a choice of electric parameters was used to capture the fish. The parameters of the electrofishing device were determined based on the conductivity of the water and the fish species but were also based on the sensitivity of the fish to the electric current similarly as in Scholten (2003). Each part where the individual species were found has been described (Lambert and Hanson, 1989). At the capture point of each fish, the depth of the flow, the microhabitat characteristics, and the flow rate, which was measured by a set of hydrometric propellers, were recorded; three hydrometric propellers were placed on one rod. The velocities were measured as standard in the following depths of water (d): 0.2d, 0.4d, 0.8d. Using these measured flow velocities, the mean vertical velocity was derived. Based on the mean vertical velocity, the suitability curve was created. The ichthyological survey was carried out in July 2015 and June 2016. *Table 2* shows the number of fish caught in particular reaches.

Topographic measurement of the reference reaches

The topographic measurement of the various reaches was adapted to the requirements of the hydraulic modelling. The cross-section profiles were measured by levelling. The water level was fixed in characteristic profiles to stable points that accelerate the measurement of the water level mode at other flow rates. The topographic and hydrometric measurements were carried out in September 2015 in a period of minimum flow rates.

Modelling of the quality of the aquatic habitat

Based on the technical interventions in the stream, the quality of the aquatic habitat was assessed by the Instream Flow Incremental Methodology (IFIM). This method is used for an analysis of the relationship between the flow rate and biotic components of an environment, while this relationship is a continuous function of the flow rate (Williams, 2001; Lopes et al., 2004). The IFIM methodology (Bovee et al., 1998) is traditionally considered to be state of the art despite persistent criticism (Rosenfeld and Ptolemy, 2012). Based on this methodology, a number of models have been created. The Riverine Habitat Simulation Model (RHABSIM) was used. It is an interdisciplinary decision-making system that helps landscape engineers consider the benefits and consequences of different water management solutions. This model is widely used not only in the region of its creation (Payne, 1998) but also in many European countries (e.g., the U.K., Norway, and France, and often with certain modifications). A very good overview of the overall philosophy, history, development and background of the IFIM, including a comprehensive list of the literature, can be found in Stalnaker et al. (1995). The model contains data from the biotic and abiotic areas. The abiotic parameters are the width, depth and surface area of the channel, the velocity of the flow, and the hydraulic characteristics in relation to the flow and morphology of the channel. The biotic information is mainly represented by bioindicators (fish) in the form of suitability curves. The relationship of the basic characteristics of the channel (depth and flow velocity) was statistically evaluated in the first phase.

http://www.aloki.hu ● ISSN 1589 1623 (Print) ● ISSN 1785 0037 (Online)
DOI: http://dx.doi.org/10.15666/aeer/1605_58935907
© 2018, ALÖKI Kft., Budapest, Hungary

Table 2. *The number of fish caught in particular reaches. Stream condition: N - Natural stream, R - Regulated reach*

	Stream	**Teplička**		**Lesnianka**		**Petrovička**		**Zázrivka**		**Veselianka**		**Kľačianka**	**Hybica**		**Lipník**		**Kamienka**	
	Stream condition	N	R	N	R	N	R	N	R	N	R	N	N	R	N	R	N	R
	Stream length	115	162	118	150	115	136	186	198	100	143	96.3	111	136	88	120	112	146
Common name	***Scientific name***	**the number of fish caught in the ichthyological survey**																
Bleak	*Alburnus alburnus*	1	-	-	-	-	-	-	-	62	15	-	-	-	-	-	-	-
Eurasian minnow	*Phoxinus phoxinus*	18	78	-	1	55	-	-	24	274	33	-	-	-	2	31	171	5
Alpine bullhead	*Cottus poecilopus*	-	-	94	89	1	60	45	253	67	48	-	19	35	1	16	34	10
Gudgeon	*Gobio gobio*	21	29	-	-	-	-	-	-	-	-	-	-	-	-	-	-	-
Chub	*Leuciscus cephalus*	122	154	-	-	-	-	-	-	1	6	-	-	-	-	-	-	-
Common dace	*Leuciscus leuciscus*	-	-	-	-	-	-	-	-	3	-	-	-	-	-	-	-	-
Common carp	*Cyprinus carpio*	2	-	-	-	-	-	-	-	-	-	-	-	-	-	-	-	-
Grayling	*Thymallus thymallus*	-	-	-	-	-	-	11	56	-	1	-	17	4	1	-	9	-
European brook lamprey	*Lampetra planeri*	-	-	-	-	-	-	-	-	-	-	-	1	1	-	-	-	-
European perch	*Perca fluviatilis*	-	-	-	-	-	-	-	-	11	9	-	-	-	-	-	-	-
Roach	*Rutilus rutilus*	15	-	-	-	-	-	-	-	70	2	-	-	-	-	-	-	-
Common nase	*Chondrostoma nasus*	-	-	-	-	-	-	-	2	-	-	-	-	-	-	-	-	-
Rainbow trout	*Oncorhynchus mykiss*	-	-	-	-	-	-	-	27	-	-	-	-	-	-	-	2	-
Brown trout - adult	*Salmo trutta m. fario*	19	14	26	16	27	15	31	16	26	14	22	23	14	18	12	28	18
Brown trout - juvenile	*Salmo trutta m. fario*	18	21	19	21	14	16	13	18	17	42	33	19	16	7	38	9	19
Stone loach	*Barbatula barbatula*	6	5	-	-	162	40	-	1	9	-	-	-	-	5	6	10	4

APPLIED ECOLOGY AND ENVIRONMENTAL RESEARCH 16(5):5893-5907.
http://www.aloki.hu ● ISSN 1589 1623 (Print) ● ISSN 1785 0037 (Online)
DOI: http://dx.doi.org/10.15666/aeer/1605_58935907
© 2018, ALÖKI Kft., Budapest, Hungary

Results

Statistical evaluation of the characteristic parameters of the aquatic habitat

At the point of the capture of each individual fish of the species, the depth and flow velocity were measured. The flow velocity and depth of the stream preferences were indicated by three fish species, i.e., the brown trout (*Salmo trutta m. fario*), Alpine bullhead (*Cottus poecilopus*) and Eurasian minnow (*Phoxinus phoxinus*). A graph of the habitat preferences for the individual fish species (*Fig. 2*) was developed. According to *Figure 2,* there is no significant difference between habitat preferences of individual fish species.

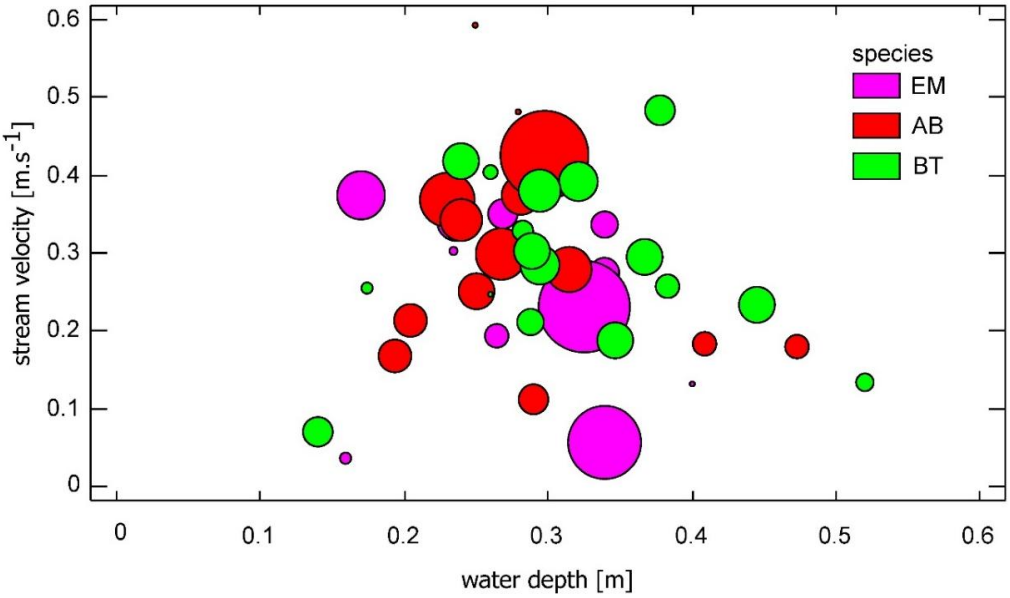

Figure 2. *The graph shows the presence of the Eurasian minnow (EM), Alpine bullhead (AB) and brown trout (BT) at individual depths and flow velocities*

For the next analysis the cluster method of the furthest neighbour was used. (Horváth and Gregušová, 1999).

The file was divided into two subsets, i.e., regulated and natural streams, to verify the cluster analysis results. Data on the depth, flow velocity and number of individual fish species were used as variables. Specifically, the brown trout was singled out. The number of complete cases in the cluster analysis was seventeen for the brown trout. *Figure 3* clearly shows the process of the merging of the objects into clusters. The objects that were joined at the bottom of the chart are similar; those objects that are linked at the top are different. Two clusters were created:

1) Hybica N, Veselianka N, Kamienka N, Lesnianka N, Lipnik N, Teplička N and Kamienka R, which can be described as a cluster of natural (N) reaches.

2) Hybica R, Petrovička R, Petrovička N, Teplička R, Kľačianka R, Zázrivka N, Lesnianka R, Lipník R, Veselianka R and Zázrivka R, which can be described as a cluster of regulated (R) reaches.

On a vertical axis, the distance between the individual objects is displayed where this distance is defined as the centroid distance of the two clusters. Centroid is a vector of diameters (each coordinate is the diameter of the respective coordinate objects in the

http://www.aloki.hu ● ISSN 1589 1623 (Print) ● ISSN 1785 0037 (Online)
DOI: http://dx.doi.org/10.15666/aeer/1605_58935907
© 2018, ALÖKI Kft., Budapest, Hungary

cluster). The method was derived by R. R. Sokal and C. D. Michener (1958) based on the geometric concepts and the degree of disparity of the two clusters was expressed as the Euclidean distance of their drawings.

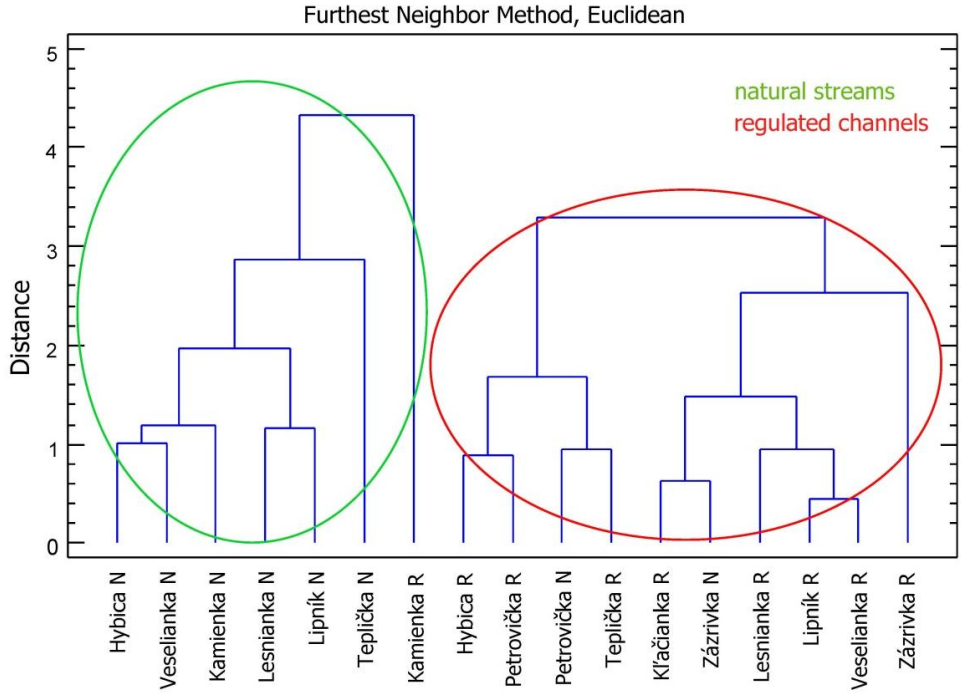

Figure 3. *Dendrogram of brown trout. The vertical axis represents the distance between the individual objects. Stream condition: N - Natural stream, R - Regulated reach*

This division is not perfect because the regulated reach of Kamienka is included in the group of natural reaches, but it is attached at the top of the dendrogram, which shows a certain difference from this group. Also, there are two natural reaches in the cluster of regulated reaches. The reason for this classification is the fact that the morphology of these reaches is poorly variable and therefore little different from the regulated reach.

Figure 4 shows the division of the individual reaches into clusters that focus on the distance between the objects. The objects located at the edge of the cluster are the most remote and therefore the least alike. This difference is evident in the Kamienka flow.

The next analysis will be based on the preference of the brown trout as expressed by the suitability curves that are the basic input to the RHABSIM model.

Derivation of the suitability curves

In the RHABSIM model, the basic parameters of a river habitat are divided into abiotic and biotic parameters. The biotic parameters are represented by fish as a bioindicator of the quality of the habitat of an aquatic flow area. The relation between abiotic and biotic characteristics is represented by the suitability curves of the individual fish species. Specifying the suitability curves is most challenging part of the RHABSIM model. Each species of fish (or other bioindicator) prefers certain combinations of abiotic environmental parameters. These parameters, for example, can be the flow velocity, depth, cover possibilities for the fish, type of bottom substrate, or water

http://www.aloki.hu ● ISSN 1589 1623 (Print) ● ISSN 1785 0037 (Online)
DOI: http://dx.doi.org/10.15666/aeer/1605_58935907
© 2018, ALÖKI Kft., Budapest, Hungary

temperature or quality. The suitability curves for the depth and flow velocity are the most typical and most used curves. These curves are continuous since the parameters of the depth and flow velocity can be interpolated between each computational node of the model. It is necessary to emphasize that a change in flow also changes the suitability curves, similarly as in the work of Jager and Pert (1997). Therefore, during each ichthyological survey, the flow is determined using the hydrometry, and the suitability curve is recalculated to Q_{365}. The suitability curves of all the reference reaches for the depths are shown in *Figure 5* and for the flow velocity in *Figure 6*.

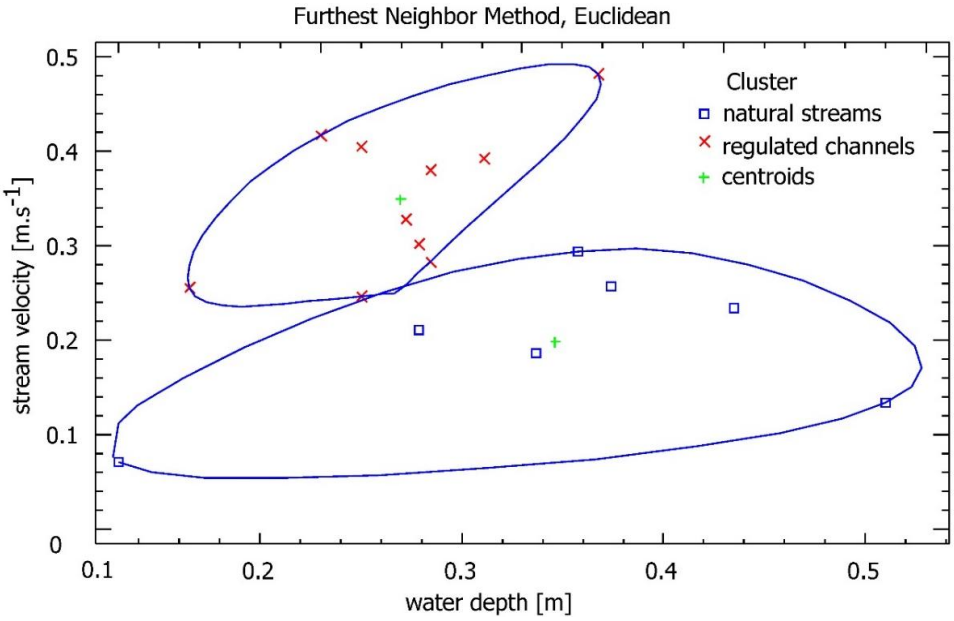

Figure 4. *The occurrence of the brown trout at the individual depths and flow velocities*

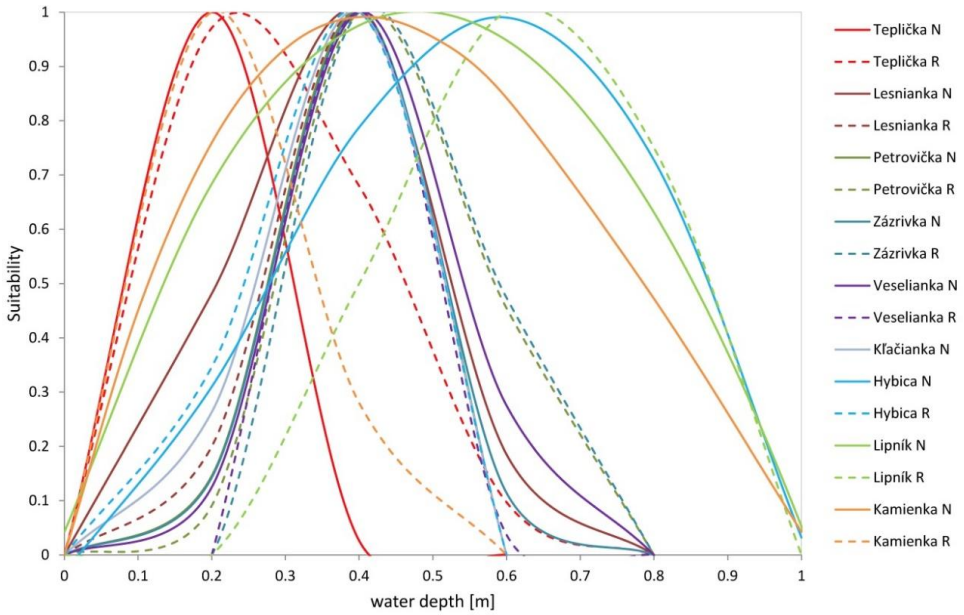

Figure 5. *Suitability curves for the depths for the brown trout in the reference reaches of the stream*

http://www.aloki.hu ● ISSN 1589 1623 (Print) ● ISSN 1785 0037 (Online)
DOI: http://dx.doi.org/10.15666/aeer/1605_58935907
© 2018, ALÖKI Kft., Budapest, Hungary

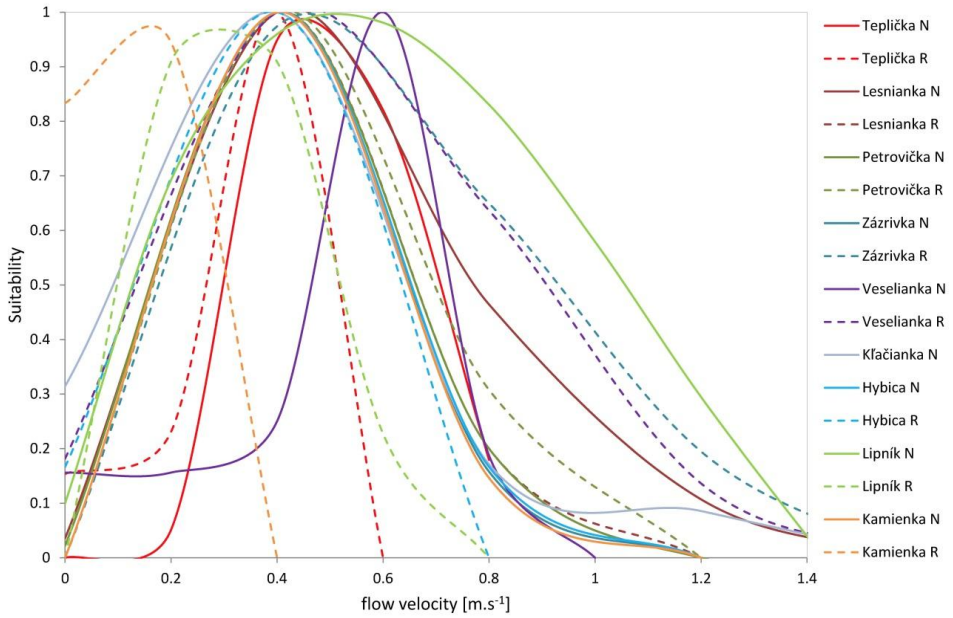

Figure 6. *Suitability curves for the velocity for the brown trout in the reference reaches of the stream*

Relationship between the abiotic and biotic characteristics of the stream

The previous evaluation is only based on the basic characteristics of the stream depth and flow velocity along with the occurrence of the representative fish species. Further, the morphological and hydraulic characteristics of the channel were assessed in relation to the fish preferences of the habitat, which are represented by suitability curves. The morphological and hydraulic characteristics of the channel are represented by the constant of the geometric and dynamic similarity M (*Eq. 1;* Grišanin, 1981):

$$M = \frac{R(g.B)^{\frac{1}{4}}}{Q^{\frac{1}{2}}} \qquad \text{(Eq.1)}$$

where:
R the hydraulic radius [m]
g the gravitational acceleration [$m.s^{-2}$]
B the channel width at the water level [m]
Q the flow [$m^3.s^{-1}$]
M a more detailed description of this parameter (dimensionless) is given in Grišanin (1981).

The peaks of the suitability curves were compared, i.e., the location with the largest occurrence of the given species at a certain depth and flow velocity. These values are listed as the velocity parameter (P_v) and the depth parameter (P_d). An important factor was the selection of a suitable representative fish species. Brown trout, which occurred in all the observed streams, is the most representative, and is very responsive to the morphology of the stream, was selected.

http://www.aloki.hu ● ISSN 1589 1623 (Print) ● ISSN 1785 0037 (Online)
DOI: http://dx.doi.org/10.15666/aeer/1605_58935907
© 2018, ALÖKI Kft., Budapest, Hungary

To evaluate the correlation relationship, the Pearson's correlation coefficient *r* was used. The interpretation of *r* is a very common problem. According to Cohen (1988), the following evaluation of the correlation ratio is stated: A correlation below 0.1 is considered trivial, 0.1 - 0.3 small, 0.3 - 0.5 mean, and above 0.5, large. The correlation of 0.7 - 0.9 is often referred to as very large, and 0.9 - 1 is almost perfect. P_v and P_d were tested to *M* (*Table 3*).

Table 3. *Comparison of the Pearson correlation coefficient (r) for the brown trout between the following variables: velocity parameter (P_v), depth parameter (P_d), the M-factor*

	P_v-*M*	P_d-*M*
r All the watercourses	0.06	0.14
r Regulated channels	0.64	0.28
r Natural channels	0.13	0.52

The correlation coefficient *r* was not confirmed in the case of the file created by all the flows (P_v - M = 0.06 and P_d - M = 0.14). Therefore, the file was divided into two files: regulated streams and natural streams. In both files, the same parameters were correlated (*Table 3*). For the regulated streams the relationship between P_v and *M* equals 0.64, which can be characterized as a large degree of dependence; for the P_d and *M* relationship = 0.28, which indicates an indirect relationship. For natural flows, the relation P_d and M = 0.52, i.e., shows a strong dependence, and for the P_v and *M* relationship = 0.13, which is a small dependence.

Discussion

There is plenty of information about the effect of river regulation on ichthyofauna (Bovee, 1982, 1986; Booker and Dunbar, 2004; Parasiewicz and Walker, 2007). Most fish species prefer certain combinations of water depth, flow velocity, bedding material and hiding possibilities. Information about the influence of water flow rate and depth of water on habitat preference is also sufficient, for example in Macura et al. (2016) or in Wilding et al. (2014) where the authors stated that for several years, eco-hydraulic research has been focused on the effects of velocity and depth on the channel habitats of fish and other aquatic species. Applications of many models, such as IFIM, have shown that the water current can provide a series of speed and depth combinations that support a wide variety of species during their lifetime.

Previous studies have confirmed the correlation between suitability curve characteristics and flow hydraulics, particularly in relation to depth and water velocity (Macura et al., 2012; Davey et al., 2011). The flow velocity and the depth of water are the basic hydraulic characteristics that are interconnected. Therefore, the article analyzes the impact of the hydraulic flow on the quality of the aquatic habitat. Flow Hydraulics is represented by a constant of geometric and dynamic similarity *M* and the preference of the habitat by ichthyofauna is represented by P_d and P_v.

The results presented in *Table 3* can be explained in relation to the morphology of the channel and the habitat preference of the brown trout as follows:

The brown trout does not have a suitable habitat in regulated rivers during small flows. Trout is only present in a regulated river during migration (in the summer it is a

http://www.aloki.hu ● ISSN 1589 1623 (Print) ● ISSN 1785 0037 (Online)
DOI: http://dx.doi.org/10.15666/aeer/1605_58935907
© 2018, ALÖKI Kft., Budapest, Hungary

food migration), when trout is guided by the flow velocity. This responds to the strong correlation of P_v and M.

In natural streams trout prefer cover places with a sufficient depth. The velocity of the flow is not decisive in areas with greater depths, as there is usually a low velocity in these areas. This matches with the significant correlation of P_d and M. The evaluated results directly confirmed the sensitivity of trout as a bioindicator to habitat parameters that are dominant in the characteristic reaches.

The results of the statistical evaluation show a clear division. Overall, it can be said that the basic stream characteristics indicated by the brown trout clearly divided the whole set for the regulated and natural streams.

Even in this case it has been confirmed that trout is a suitable bioindicator of the environment because it responds sensitively to changes in flow rates and flow depths (Hooper, 1973; Shirvell and Dungey, 1983; Reiser and Wesche, 1976; Macura et al., 2012, 2018).

Conclusion

Based on the current research results on the selected reference reaches of mountain watercourses in Slovakia, it follows that the changes caused by the topography of the channel and flow rates are well described by the relationship between the fish population and the characteristics of the habitat. The results from the cluster analysis and correlation analysis show the same trends. In particular, it can be said that the brown trout sensitively responds to abiotic characteristics such as the channel's morphology, flow velocity and depth and the biotic characteristics represented by the suitability curves.

Using these results it is possible to evaluate the impact of the proposed restoration measures. Such a process will greatly contribute to the quality of the restoration of the stream.

Acknowledgements. We thank the Slovak Research and Development Agency for the support of Project no. APVV-16-0253.

REFERENCES

[1] Avery-Gomm, S., Rosenfeld, J. S., Richardson, J. S., Pearson, M. (2014): Hydrological drought and the role of refugia in an endangered riffle-dwelling fish, Nooksack dace (Rhinichthys cataractae ssp.). – Canadian Journal of Fisheries and Aquatic Sciences 71: 1625-1634. DOI: 10.1139/cjfas-2013-0585.

[2] Ayllón, D., Almodóvar, A., Nicola, G. G., Elvira, B. (2009): Interactive effects of cover and hydraulics on brown trout habitat selection patterns. – River Res. Appl. 25(8): 1051-1065. DOI: 10.1002/rra.1215.

[3] Bockelmann, B. N., Fenrich, E. K., Lina, B., Falconer, R. A. (2004): Development of an ecohydraulics model for stream and river restoration. – Ecological Engineering 22: 227-235. DOI: 10.1016/j.ecoleng.2004.04.003.

[4] Booker, D. J., Dunbar, M. J. (2004): Application of physical habitat simulation (PHABSIM) modelling to modified urban river channels. – River Research and Applications 20: 167-183. DOI: 10.1002/rra.742.

http://www.aloki.hu ● ISSN 1589 1623 (Print) ● ISSN 1785 0037 (Online)
DOI: http://dx.doi.org/10.15666/aeer/1605_58935907
© 2018, ALÖKI Kft., Budapest, Hungary

[5] Bovee, K. D. (1982): A Guide to Stream Habitat Analysis Using the Instream Flow Incremental Methodology. – Instream Flow Information Paper 12. FWS ⁄OBS-82 ⁄26. USDI Fish and Wildlife Service, Office of Biology Services: Washington, DC.
[6] Bovee, K. D. (1986): Development and Evaluation of Habitat Suitability Criteria for Use in the Instream Flow Incremental Methodology. – Instream Flow Information Paper 21. FWS/OBS-86/7. USDI Fish and Wildlife Service, Office of Biology Services: Washington, DC.
[7] Bovee, K. D., Lamb, B. L., Bartholow, J. M., Stalnaker, C. B., Taylor, J., Henriksen, J. (1998): Stream Habitat Analysis Using the Instream Flow Incremental Methodology. – Information and Technology Report USGS/BRD/ITR-1998-0004. Geological Survey BRD, Fort Collins, CO.
[8] Carlson, A. K., Taylor, W. W., Schlee, K. M., Zorn, T. G., Infante, D. M. (2015): Projected impacts of climate change on stream salmonids with implications for resilience-based management. – Ecology of Freshwater Fish. DOI: 10.1111/eff.12267.
[9] Carnie, R., Tonina, D., McKean, J. A., Isaak, D. (2016): Habitat connectivity as a metric for aquatic microhabitat quality: application to Chinook salmon spawning habitat. – Ecohydrol. 9: 982-994. DOI: 10.1002/eco.1696.
[10] Cheek, C. A., Taylor, C. M. (2016): Salinity and geomorphology drive long-term changes to local and regional fish assemblage attributes in the lower Pecos River, Texas. – Ecology of Freshwater Fish 25: 340-351. DOI: 10.1111/eff.12214.
[11] Cohen, J. (1988): Statistical power analysis for the behavioral sciences. 2nd ed. – Lawrence Earlbaum Associates, Hillsdate, NJ.
[12] Conallin, J., Boegh, E., Jensen, J. K. (2010): Instream physical habitat modelling types: an analysis as stream hydromorphological modelling tools for EU water resource managers. – Int. J. River Basin Manag. 8(1): 93-107. DOI: 10.1080/15715121003715123.
[13] Copp GH. (1992): Comparative microhabitat use of cyprinid larvae and juveniles in a lotic floodplain channel. – Environmental Biology of Fishes 33: 181-193.
[14] Davey, A. J. H., Booker, D. J., Kelly, D. J. (2011): Diel variation in stream fish habitat suitability criteria: implications for instream flow assessment. – Aquatic Conserv: Mar. Freshw. Ecosyst. 21: 132-145. DOI: 10.1002/aqc.1166.
[15] Galbraith, H. S., Blakeslee, C. J., Cole, J. C., Talbert, C. A., Maloney, K. O. (2016): Evaluating methods to establish habitat suitability criteria: a case study in the Upper Delaware River Basin, USA. – River Res. Applic. 32: 1765-1775. DOI: 10.1002/rra.3025.
[16] Galie, A. C., Moldoveanu, M., Antonaru, O. (2017): Hydromorphological assessment of atypical lowland river –Rromanian litoral basin case study. – Carpathian Journal of Earth and Environmental Sciences 12(1): 161-169.
[17] Gibson, S. A., Pasternack, G. B. (2016): Selecting between one-dimensional and two-dimensional hydrodynamic models for ecohydraulic analysis. – River Res. Applic. 32: 1365-1381. DOI: 10.1002/rra.2972.
[18] Grišanin, K. V. (1981): Riverbed Dynamics (in Russian: Dinamika ruslovych potokov). – Izd. Gidrometeoizdat, Leningrad.
[19] Holm, C. F., Armstrong, J. D., Gilvear, D. J. (2001): Investigating a major assumption of predictive instream habitat models: is water velocity preference of juvenile Atlantic salmon independent of discharge? – Journal of Fish Biology 59: 1653-1666. DOI: 10.1111/j.1095-8649.2001.tb00228.x.
[20] Hooper, D. (1973): Evaluation of the Effects of Flows on Trout Stream Ecology. – Pacific Gas and Electric Company, Dept. Of Engineering Research, Emeryville, California.
[21] Horváth, J., Gregušová, H. (1999): Clustered Analysis and Projective Methods. Mathematical Statistics and Numerical Mathematics and Their Applications. – Faculty of Civil Engineering, Slovak University of Technology, Bratislava, pp. 205-237.

http://www.aloki.hu ● ISSN 1589 1623 (Print) ● ISSN 1785 0037 (Online)
DOI: http://dx.doi.org/10.15666/aeer/1605_58935907
© 2018, ALÖKI Kft., Budapest, Hungary

[22] Jager, H. I., Pert, E. G. (1997): Comment testing the independence of microhabitat preferences and flow (Part 2). – Transaction of the American Fisheries Society 126: 537-540. DOI: 10.1577/1548-8659-126.3.537.
[23] Keeley, E. R., Campbell, S. O., Kohler, A. E. (2015): Bioenergetic calculations evaluate changes to habitat quality for salmonid fishes in streams treated with salmon carcass analog. – Canadian Journal of Fisheries and Aquatic Sciences 73: 819-831. DOI: 10.1139/cjfas-2015-0265.
[24] Lambert, T. R., Hanson, D. F. (1989): Development of habitat suitability criteria for trout in small streams. – Regulated Rivers: Research & Management 3: 291-303. DOI: 10.1002/rrr.3450030128.
[25] Lamouroux, N., Capra, H., Pouilly, M., Souchon, Y. (1999): Fish habitat preferences in large streams of southern France. – Freshwater Biology 42: 673-687. DOI: 10.1046/j.1365-2427.1999.00521.x.
[26] Lopes, L., Do Carmo, J., Cortes, R., Oliveira, D. (2004): Hydrodynamics and water quality modelling in a regulated river segment: application on the instream flow definition. – Ecological Modelling 173: 197-218. DOI: 10.1016/j.ecolmodel.2003.07.009.
[27] Macura, V., Škrinár, A., Kalúz, K., Jalčovíková, M., Škrovinová, M. (2012): Influence of the morphological and hydraulic characteristics of mountain streams on fish habitat suitability curves. – River Research and Applications. DOI: 10.1002/rra.1518.
[28] Macura, V., Štefunková, Z., Škrinár, A. (2016): Determination of the effect of water depth and flow velocity on the quality of an in-stream habitat in terms of of climate change. – Advances in Meteorology 2016: Article ID 4560378. DOI: 10.1155/2016/4560378.
[29] Macura, V., Štefunková, Z., Majorošová, M., Halaj, P., Škrinár, A. (2018): Influence of discharge on fish habitat suitability curves in mountain watercourses in IFIM methodology. – J. Hydrol. Hydromech 66: 12-22. DOI: 10.1515/johh-2017-0044.
[30] Marsili-Libelli, S., Giusti, E., Nocita, A. (2013): A new instream flow assessment method based on fuzzy habitat suitability and large scale river modelling. – Environ. Model. Softw. 41: 27-38. DOI: 10.1016/j.envsoft.2012.10.005.
[31] Parasiewicz, P., Walker, J. D. (2007): Comparison of Meso-HABSIM with two microhabitat models (PHABSIM and HARPHA). – River Res. Applic. 23: 904-923. DOI: 10.1002/rra.1043.
[32] Payne, T. R. (1998): RHABSIM 2.1 for DOS and Windows User's Manual. – Fisheries Biology, Consulting and Software Publishing, Agrata, CA.
[33] Piniewski, M., Prudhomme, C., Acreman, M. C., Tylec, L., Oglęcki, P., Okruszko, T. (2016): Responses of fish and invertebrates to floods and droughts in Europe. – Ecohydrol. DOI: 10.1002/eco.1793.
[34] Pont, D., Hugueny, B., Beier, U., Goffaux, D., Melcher, A., Noble, R., Rogers, C., Roset, N., Schmutz, S. (2006): Assessing river biotic condition at a continental scale: a European approach using functional metrics and fish assemblages. – Journal of Applied Ecology 43: 70-80. DOI: 10.1111/j.1365-2664.2005.01126.x.
[35] Reiser, D. W., Wesche, T. A. (1976): Determination of physical and hydraulic preferences of brown and brook trout in the selection of spawning locations. – University of Wyoming, Water Resources Research Institute. Water Resources Series 64.
[36] Roni, P., Beechie, T., Pess, G., Hanson, K. (2014): Wood placement in river restoration: fact, fiction, and future direction. – Canadian Journal of Fisheries and Aquatic Sciences 72: 466-478. DOI: 10.1139/cjfas-2014-0344.
[37] Rosenfeld, J. S., Ptolemy, R. (2012): Modelling available habitat versus available energy flux: do PHABSIM applications that neglect prey abundance underestimate optimal flows for juvenile salmonids? – Canadian Journal of Fisheries and Aquatic Sciences 69: 1920-1934. DOI: 10.1139/f2012-115.
[38] Santiago, J. M., García de Jalón, D., Alonso, C., Solana, J., Ribalaygua, J., Pórtoles, J., Monjo, R. (2016): Brown trout thermal niche and climate change: expected changes in

http://www.aloki.hu ● ISSN 1589 1623 (Print) ● ISSN 1785 0037 (Online)
DOI: http://dx.doi.org/10.15666/aeer/1605_58935907
© 2018, ALÖKI Kft., Budapest, Hungary

the distribution of cold-water fish in central Spain. – Ecohydrol. 9: 514-528. DOI: 10.1002/eco.1653.

[39] Scholten, M. (2003): Efficiency of point abundance sampling by electro-fishing modified for short fishes. – J. Appl. Ichtyol. 19: 265-244. DOI: 10.1046/j.1439-0426.2003.00505.x.

[40] Shields, F. D., Knight, S. S., Cooper, C. M. (1997): Rehabilitation of warmwater stream ecosystems following channel incision. – Ecological Engineering 8: 93-116.

[41] Shirvell, C. S., Dungey, R. G. (1983): Microhabitats chosen by brown trout for feeding and spawning in rivers. – Transactions of the American Fisheries Society 112(3): 355-367.

[42] Shuler, S. W., Nehring, R. B. (1994): Using the Physical Habitat Simulation Model to evaluate a stream habitat enhancement project. – Rivers 4: 175-193.

[43] Sokal, R. R., Michener, C. D. (1958). A statistical method for evaluating systematic relationships. – Univ. Kansas Sci Bull. 38: 1409-1438.

[44] Stalnaker, C., Lamb, B. L., Henriksen, J., Bovee, K., Bartholow, J. (1995): The Instream Flow Incremental Methodology. A Primer for IFIM. – Biological Science Report 29. National Biological Service, US Dept. of Interior, Washington, DC.

[45] Townsend, C. R., Hildrew, A. G. (1994): Species traits in relation to habitat templet for river systems. – Freshwater Biology 31: 265-275.

[46] Turner, D., Bradford, M. J., Venditti, J. G., Peterman, R. M. (2016): Evaluating uncertainty in physical habitat modelling in a high-gradient mountain stream. – River Res. Applic. 32: 1106-1115. DOI: 10.1002/rra.2915.

[47] Vannote, R. L., Minshall, G. W., Cummins, K. W., Sedell, J. R., Cushing, C. E. (1980): The river continuum concept. – Canadian Journal of Fisheries and Aquatic Sciences 37(1): 130-137.

[48] Wilding, T. K., Bledsoe, B., Poff, N. L., Sanderson, J. (2014): Predicting habitat response to flow using generalized habitat models for trout in Rocky Mountain streams. – River Res. Applic. 30: 805-824. DOI: 10.1002/rra.2678.

[49] Williams, J. G. (2001): Tripping over spatial scales: a comment on Guay et al. 2000. – Canadian Journal of Fisheries and Aquatic Sciences 58: 2105-2107.

[50] Zhang, H., Wang, C. Y., Wu, J. M., Du, H., Wei, Q. W., Kang, M. (2016): Physical habitat assessment of a remaining high-biodiversity reach of the upper Yangtze river, China. – Applied Ecology and Environmental Research 14: 129-143. DOI: http://dx.doi.org/10.15666/aeer/1401_129143.

http://www.aloki.hu ● ISSN 1589 1623 (Print) ● ISSN 1785 0037 (Online)
DOI: http://dx.doi.org/10.15666/aeer/1605_58935907
© 2018, ALÖKI Kft., Budapest, Hungary

EFFECTS OF CULTURE MEDIA ON YIELD, GROWTH, PHOTOSYNTHETIC CAPACITY AND ANTIOXIDANT ENZYME OF DIFFERENT TOMATO (*SOLANUM LYCOPERSICUM* L.) VARIETIES

SHI, L.[1,2,3,#] – LV, N.[1,#] – NIE, J.[2,3] – TAN, D.[2,3] – ZHENG, J.[2] – LUO, G.[2,3] – LI, Y.[2] – XIONG, Y.[2,3] – XIE, Y.[2,3] – WANG, J.[1*]

[1]*Key Laboratory of Agroenvironment in Tropic, Ministry of Agriculture, South China Agricultural University, 510642 Guangzhou, China*

[2]*Agro-innovative Demonstration Base, Guangdong Academy of Agricultural Sciences 510642 Guangzhou, China*

[3]*Key Laboratory of Urban Agriculture in South China, Ministry of Agriculture 510640 Guangzhou, China*

**Corresponding author*
e-mail: wangjw@scau.edu.cn

[#] *These authors contributed equally to this work.*

(Received 15th Jun 2018; accepted 22nd Aug 2018)

Abstract. Culture media affects the yield and quality of tomato. Knowledge about the tomato yield formation in response to culture media is still needed. The purpose of this study was to investigate the effect of culture media on yield, growth, photosynthetic capacity and antioxidant enzyme of different tomato varieties. A greenhouse experiment was conducted at the Baiyun Experimental Base of Guangdong Academy of Agricultural Sciences, Guangdong, China, three culture media treatments viz. soil culture cultivation treatment, substrate cultivation treatment and hydroponics cultivation treatment were applied. Four represented tomato varieties viz. Xinxing 101, Jinbaolai, Kaidi and Xiariyangguang were used as materials. The result showed that, the substrate cultivation and hydroponics produced higher yield than soil culture treatment due to higher dry weight accumulation, fruit weight, and net photosynthetic rate at seedling stage and mature stage. The yield showed significant correlation with individual fruit weight ($R^2 = 0.8205$, $P < 0.01$), net photosynthetic rate in leaves at seedling stage ($R^2 = 0.7189$, $P < 0.05$). The SPAD value and antienzyme activity vary among different planting patterns, cultivars and growth stages. Further study to observe the quality of tomato fruits and nutrition of the tomato plant under different culture media is needed.
Keywords: *antioxidant capacity, culture cultivation, plant growth, photosynthetic ability, tomato, yield formation*

Introduction

Tomato is an important vegetable crop worldwide which ranks next to spuds in terms of the planted area whilst ranks first as a processing crop (Mehdizadeh et al., 2013). It is susceptible to pest and disease while water management and nutrient supply could significantly affect tomato's health (Salokhe et al., 2005). However, this problem could be solved in greenhouse condition which has been known as a protected cultivation (Pires et al., 2011). Recently tomato is suitable for facility cultivation for its high yield and quality requirement and precise management for pest and disease control (Xie et al., 2017). Greenhouse farming, one of the famous agriculture systems, is widely used to create and maintain a stable and suitable environment to optimize the crop production in

http://www.aloki.hu ● ISSN 1589 1623 (Print) ● ISSN 1785 0037 (Online)
DOI: http://dx.doi.org/10.15666/aeer/1605_59095919
© 2018, ALÖKI Kft., Budapest, Hungary

order to maximum profits (Abou-Hadid et al., 1994). For facility cultivation of tomato, the culture media is one of the most important key factors that affecting the yield and quality of tomato for the cultivated culture media are different in physicochemical properties such as water-retaining property, nutrient preserving capability, heat retaining property, gas permeability and so on (Liu et al., 2006).

A previous study revealed that different nitrogen forms in media culture had significant effects on tomato's photosynthetic rate, plant growth, root vigor and leaf water content (Yang, 2003). Previous report demonstrated that silicate application in culture media affected tomato fruits and silicon content (Lee et al., 2002). Furthermore, supplementing the nutrient solution with NaCl was able to decrease the yield of tomato significantly (Korkmaz et al., 2016). Thus, it is commonly recommended to select appropriate cultivated culture media for the tomato growth and to improve plant establishment and enhance yield.

Photosynthesis is the basis of crop yield and has a significant correlation with both the yield and fruit quality of tomato (Xu et al., 2001). Regarding to photosynthetic traits, different growth culture media will have effect on net photosynthetic rate, transpiration rate, stomatal conductance and Intercellular carbon dioxide. A previous report showed that culture on sugar medium enhances photosynthetic capacity and high light resistance of plantlets grown in vitro (Tichá et al., 2010). The study of Chen (Chen et al., 2009) demonstrated that tomato assimilation products were enhanced in organic substrates compared with the soil control while the photosynthetic rate and intracellular CO_2 concentration were higher in organic substrate cultivation. Ghoreishy et al. (2018) found that tomato grown in culture media which using composted wheat residue had better fruit yield, chlorophyll, and vitamin C contents. In addition, Hydroponics is also a modern agriculture technique which uses nutrient solution for crop production and a report demonstrated that hydroponic greenhouse system is only system which could meet the food requirements of our needs (Khan, 2018).

However, effect of culture media on yield, growth, photosynthetic capacity and antioxidant enzyme of different tomato varieties is still unknown. Here, we studied the effect of culture media viz. soil culture cultivation treatment, substrate cultivation treatment and hydroponics cultivation treatment on yield, growth, photosynthetic capacity and antioxidant enzyme of four represented tomato varieties viz. Xinxing 101, Jinbaolai, Kaidi and Xiariyangguang.

Materials and methods

Tomato plant growth condition

A greenhouse experiment was conducted from 2016 to 2017 at the Baiyun Experimental Base of Guangdong Academy of Agricultural Sciences, Guangdong, China. Four popular tomato cultivars were used in this study, two of them were large fruit tomato cultivar (Xinxing 101 and Jinbaolai), the other two were small fruit tomato (Kaidi and Xiariyangguang), these four cultivars can be planted in spring, autumn or winter and is provided by the Modern Demonstration Garden of Guangdong Academy of agricultural Sciences. The seeds of the tomato cultivar were sown at March 15th and the seedlings were transplanted at April 22nd. Two seedlings were transplanted to each foam box, the foam box (Length × Width × Height = 59.5 cm × 36 cm × 45 cm) purchased from Guangzhou Xinyinfa Foam Products co. LTD. The climatic conditions

http://www.aloki.hu ● ISSN 1589 1623 (Print) ● ISSN 1785 0037 (Online)
DOI: http://dx.doi.org/10.15666/aeer/1605_59095919
© 2018, ALÖKI Kft., Budapest, Hungary

applied during plant growth period was 30 ± 5 °C in air temperature and 70 ± 20% in air humidity.

Experimental design

The tomato cultivars were growing under three culture media: I) Soil culture filled the foam box with 80 kg soil. II) Substrate cultivation, filled the foam box with 20 kg substrate (vermiculite: pearlite: ceramsite: turfy earth = 1:1:1.5:3). III) Hydroponics, filled the foam box with 85 L nutrient solution, the nutrient solution containing $Ca(NO_3)_2 \cdot 4H_2O$ 590mg·L^{-1}, KNO_3 404 mg·L^{-1}, KH_2PO_4 136 mg·L^{-1}, $MgSO_4 \cdot 7H_2O$ 246 mg·L^{-1}, $MnSO_4 \cdot H_2O$ 2.13 mg·L^{-1}, H_3BO_3 2.86 mg·L^{-1}, $ZnSO_4 \cdot 7H_2O$ 0.22 mg·L^{-1}, $CuSO_4 \cdot 5H_2O$ 0.08 mg·L^{-1}, and $(NH_4)_6Mo_7O_{24} \cdot 4H_2O$ 0.02 mg·L^{-1} (Lv et al., 2010). For the soil culture and substrate cultivation treatment, each foam box was irrigated with 400 ml of the nutrient solution every two days. For the hydroponics treatment, the nutrient solution kept constant volume.

Sampling and measurements

Fruit weight and yield of tomato

The mature fruit was harvest during November 2016 to February 2017, the fruit numbers per was calculated, the individual fruit weight and yield was investigated.

Dry weight of tomato plants

At harvest stage, three represented plants in each treatment were harvested, the plants were separated into stem and leaves, the different plant parts were oved- dried at 80 °C to constant weight for measurement of dry weight of tomato plant.

SPAD value and net photosynthetic rate (Pn) in leaves

The SPAD value and net photosynthetic rate (Pn) in leaves was measured at seedling stage (2016-08-26), flowering stage (2016-10-21) and mature stage (2017-01-20). Three represented plants in each treatment were selected for the measurement of SPAD value and Pn. For SPAD value, the SPAD value was detected by using the SPAD-502 reading meter (KONICA MINOLTA, Japan). The Pn (μmol·m^{-2}·s^{-1}) was measured using LI-6400 (LI-COR, USA). Measurement was conducted in the morning (9:30 - 11:30) in each stage.

Superoxide dismutase (SOD), peroxidase (POD), catalase (CAT) activity in leaves

The fifth leaf from the top of the seven tomato plants were sampled for the measurement of antienzyme activity. The leaves were immediately put in liquid nitrogen and stored at -80 °C (for biochemical assays).

Fresh leaf samples were crushed in liquid-nitrogen and homogenized in 3 ml of 50 mM sodium phosphate buffer (pH 7.8) and the homogenates were centrifuged at 10,000 g for 15 min at 4 °C and the aliquot of the supernatant was used to investigate the enzymatic activities. The SOD activity was measured by detecting the inhibition of photochemical reduction due to nitro blue tetrazolium (NBT) (Foyer, 1987). The POD activity was measured by using guaiacol method (Foyer, 1987). The CAT activity was investigated according to the procedures of Foyer (1987) by recording the decomposition of H_2O_2 at A240.

http://www.aloki.hu ● ISSN 1589 1623 (Print) ● ISSN 1785 0037 (Online)
DOI: http://dx.doi.org/10.15666/aeer/1605_59095919
© 2018, ALÖKI Kft., Budapest, Hungary

Statistical analysis

Pots were arranged in randomized complete block design (RCBD), the data were analyzed by using a statistical software (SPSS 13.0), the mean value among the different culture media treatments within one variety was separated by LSD method at $P < 0.05$ level. Correlation analyses among yield and other parameters were computed and represented by using Excel 2010.

Result

Yield of different tomato varieties

Compared to control (soil culture treatment), the hydroponics treatment increased fruit number per plant for all the varieties, while the substrate cultivation increased fruit number per plant in Xinxing101, Jinbaolai, and Kaidi. The substrate cultivation and hydroponics treatment remained statistically similar in individual fruit weight in Xinxing 101, whilst significant increase in Jinbaolai was detected as compared with control (soil culture treatment). In addition, the hydroponics treatment dramatically increased individual fruit weight in Kaidi and Xiariyangguang, but substrate cultivation did not differ from soil culture condiction in individual fruit weight. The yield of tomato showed substantial changes in Xinxing101, Jinbaolai and Kaidi with an increase of 64.87, 77.61, and 48.59%, respectively for substrate cultivation treatment as compared with soil culture treatment. Moreover, compared to control, all tomato cultivars showed significant improvement in hydroponic treatment, with a percentage increase of 107.41, 58.28, 73.19, and 120.29% in Xinxing101, Jinbaolai, Kaidi, and Xiariyangguang, respectively (*Table 1*).

Table 1. *Effect of culture media on yield of different tomato varieties*

Varieties	Culture media	Fruit number per plant	Individual fruit weight ($g \cdot fruit^{-1}$)	Yield ($g\ plant^{-1}$)	Yield change relative to soil culture (%)
Xinxing101	Soil culture	199	5.02±0.05ab	1000.68±83.94b	—
	Substrate cultivation	307	5.38±0.10a	1649.83±111.81a	64.87
	Hydroponics	432	4.81±0.19b	2076.02±347.04a	107.41
Jinbaolai	Soil culture	179	4.86±0.02c	870.90±82.66b	—
	Substrate cultivation	282	5.48±0.15b	1546.66±128.18a	77.61
	Hydroponics	213	6.51±0.16a	1378.31±182.97a	58.28
Kaidi	Soil culture	270	1.53±0.03b	413.64±39.85c	—
	Substrate cultivation	401	1.53±0.02b	613.78±20.63b	48.59
	Hydroponics	302	2.37±0.06a	715.76±39.96a	73.19
Xiariyangguang	Soil culture	245	1.38±0.00b	338.59±45.57b	—
	Substrate cultivation	237	1.56±0.02b	369.27±38.91b	9.11
	Hydroponics	351	2.12±0.11a	745.06±139.79a	120.20

Different lowercase letters within one variety represent significant difference at $P < 0.05$ level

Dry weight of different tomato varieties

In response to different culture media, the stem dry weight and leaf dry weight in Xinxing101, Kaidi, and Xiariyangguang was not affected by culture media. The stem

http://www.aloki.hu ● ISSN 1589 1623 (Print) ● ISSN 1785 0037 (Online)
DOI: http://dx.doi.org/10.15666/aeer/1605_59095919
© 2018, ALÖKI Kft., Budapest, Hungary

dry weight in Jinbaolai significantly differed among culture media. The substrate cultivation (63.33%) and hydroponics treatment (128.88%) recorded significant higher stem dry weight than the soil culture treatment. Hydroponics treatment induced a significant improvement in leaf dry weight by 97.89% (*Table 2*).

Table 2. *Effect of culture media on dry weight of different tomato varieties*

Varieties	Culture media	Stem dry weight (g)	Stem dry weight change relative to soil culture (%)	Leaf dry weight (g)	Leaf dry weight change relative to soil culture (%)
Xinxing101	Soil culture	23.03±1.97a		36.78±7.89a	
	Substrate cultivation	32.89±5.63a	42.81	38.05±8.67a	3.45
	Hydroponics	31.05±2.36a	34.80	37.44±4.87a	1.80
Jinbaolai	Soil culture	18.19±1.63c		22.71±4.15b	
	Substrate cultivation	29.71±1.41b	63.35	25.46±2.16b	12.09
	Hydroponics	41.27±5.31a	126.90	44.94±2.30a	97.87
Kaidi	Soil culture	30.72±2.43a		33.83±3.31a	
	Substrate cultivation	33.50±3.80a	9.07	22.24±1.37a	-34.27
	Hydroponics	37.34±7.88a	21.56	31.43±10.02a	-7.08
Xiariyangguang	Soil culture	22.94±2.72a		18.69±3.00a	
	Substrate cultivation	31.90±3.02a	39.05	26.92±3.92a	43.99
	Hydroponics	24.20±4.59a	5.49	29.88±5.82a	59.86

Different lowercase letters within one variety represent significant difference at $P < 0.05$ level

Photosynthetic capacity of different tomato varieties

Compared to CK, the substrate cultivation and hydroponics treatment improved the net photosynthetic rate in leaves in Xinxing 101. The net photosynthetic rate in leaves in Jinbaolai, Kaidi, and Xiariyangguang were increased at seedling and mature stage as compared to CK. At flowering stage, compared with CK, the net photosynthetic rate in leaves was significantly decreased under substrate cultivation treatment, while dramatically increased under hydroponics treatment for Jinbaolai and Xiariyangguang. For Kaidi, the net photosynthetic rate in leaves at flowering stage was significantly decreased. The Pn in the varieties in response to different culture media showed similar trend at seedling stage and mature stage, while vary among culture media at flowering stage (*Table 3*).

The SPAD value in leaves of Xinxing101 was not affected by culture media at seedling stage and mature stage, only hydroponics treatment showed significant reduction in SPAD value at flowering stage as compared to CK. For Jinbaolai, substrate cultivation treatment induced significant reduction in SPAD value at seedling stage, while significant reduction in SPAD value at flowering stage and mature stage was detected for hydroponics treatment. Compared to CK, the culture media (substrate cultivation and hydroponics treatment) did not affected the SPAD value in leaves at seedling stage and mature stage, while significantly decreased SPAD value in leaves at flowering stage (*Table 4*).

http://www.aloki.hu ● ISSN 1589 1623 (Print) ● ISSN 1785 0037 (Online)
DOI: http://dx.doi.org/10.15666/aeer/1605_59095919
© 2018, ALÖKI Kft., Budapest, Hungary

Table 3. *Effect of culture media on net photosynthetic rate in leaves of different tomato varieties ($\mu mol \cdot m^{-2} \cdot s^{-1}$)*

Varieties	Culture media	Seedling stage	Flowering stage	Mature stage
Xinxing101	Soil culture	7.74±0.55b	16.01±0.07b	7.27±0.13b
	Substrate cultivation	9.46±0.12a	18.02±0.28a	8.08±0.10a
	Hydroponics	8.64±0.30ab	17.96±0.42a	8.09±0.34a
Jinbaolai	Soil culture	5.59±0.08b	14.52±0.16b	8.57±0.32c
	Substrate cultivation	6.59±0.39ab	14.06±0.11c	16.34±0.35a
	Hydroponics	7.18±0.47a	18.26±0.12a	10.50±0.60b
Kaidi	Soil culture	4.58±0.31b	19.71±0.13a	11.27±0.30b
	Substrate cultivation	6.17±0.43a	16.66±0.30b	12.24±0.16b
	Hydroponics	6.73±0.63a	16.30±0.12b	17.56±0.85a
Xiariyangguang	Soil culture	4.38±0.38b	14.47±0.13b	7.12±0.58b
	Substrate cultivation	7.31±0.53a	12.58±0.08c	8.33±0.33b
	Hydroponics	4.51±0.21b	16.10±0.14a	10.41±0.62a

Different lowercase letters within one variety represent significant difference at $P < 0.05$ level

Table 4. *Effect of culture media on SPAD value of different tomato varieties*

Varieties	Culture media	Seedling stage	Flowering stage	Mature stage
Xinxing101	Soil culture	35.97±0.33a	39.27±2.49a	46.40±2.51a
	Substrate cultivation	32.63±1.15a	35.60±1.91ab	45.30±1.07a
	Hydroponics	35.93±1.28a	32.27±0.75b	45.03±1.78a
Jinbaolai	Soil culture	40.50±0.26a	42.27±1.60a	54.00±2.03a
	Substrate cultivation	37.00±1.46b	43.20±1.44a	49.60±0.78ab
	Hydroponics	39.63±0.56ab	35.83±0.80b	48.47±0.47b
Kaidi	Soil culture	42.93±1.87a	43.20±1.44a	54.67±1.33a
	Substrate cultivation	40.00±0.45a	44.17±1.11a	55.43±0.97a
	Hydroponics	42.77±1.74a	39.37±1.72a	51.00±0.35b
Xiariyangguang	Soil culture	33.57±0.58ab	36.23±0.58a	40.27±0.98a
	Substrate cultivation	31.73±0.20b	32.23±0.27b	41.47±1.11a
	Hydroponics	36.47±1.88a	31.73±0.93b	40.37±1.17a

Different lowercase letters within one variety represent significant difference at $P < 0.05$ level

Antioxidant enzyme of different tomato varieties.

Compared to CK, the substrate cultivation treatment significantly decreased SOD activity in leaves at mature stage for Xinxing101 and Kaidi, and at seedling stage for Xiariyangguang. Significant enhance in SOD activity in leaves at mature stage for Xiariyanguang was detected as compared to CK. The hydroponics treatment dramatically reduced SOD activity in leaves at all the stage for Xinxing 101 and Kaidi, and at mature for Jinbaolai and Xiariyangguang as compared to CK (*Table 5*).

http://www.aloki.hu ● ISSN 1589 1623 (Print) ● ISSN 1785 0037 (Online)
DOI: http://dx.doi.org/10.15666/aeer/1605_59095919
© 2018, ALÖKI Kft., Budapest, Hungary

Table 5. *Effect of culture media on SOD activity in leaves of different tomato varieties ($U \cdot g^{-1}$)*

Varieties	Culture media	Seedling stage	Flowering stage	Mature stage
Xinxing101	Soil culture	234.94±5.54a	320.16±1.39a	259.34±4.70a
	Substrate cultivation	221.56±15.81a	260.07±20.41ab	193.30±20.89b
	Hydroponics	181.57±9.69b	233.35±23.37b	166.47±16.91b
Jinbaolai	Soil culture	247.56±15.53a	326.06±12.84a	251.09±7.53a
	Substrate cultivation	256.96±9.65a	315.48±3.34a	228.27±8.32a
	Hydroponics	215.69±15.19a	283.04±23.85a	172.44±12.17b
Kaidi	Soil culture	264.07±12.57a	351.54±1.51a	288.39±3.48a
	Substrate cultivation	266.10±9.43a	321.86±1.98ab	222.05±11.25b
	Hydroponics	211.29±14.88b	261.52±34.73b	203.73±19.43b
Xiariyangguang	Soil culture	269.83±12.01a	326.51±11.83a	150.64±4.88b
	Substrate cultivation	213.48±16.66b	304.61±2.11a	193.52±0.34a
	Hydroponics	236.79±13.09ab	316.77±15.77a	144.67±0.79b

Different lowercase letters within one variety represent significant difference at $P < 0.05$ level

For Xinxing101, compared with CK, substrate cultivation treatment significantly reduced POD activity in leaves at seedling stage and mature stage, hydroponics treatment improved POD activity in leaves at seedling stage significantly, but significantly reduced POD activity in leaves at mature stage. For Jinbaolai, compared with CK, significant reduction in POD activity was investigated for substrate cultivation treatment at both seedling stage and mature stage, while hydroponics treatment significantly reduced POD activity at flowering stage and mature stage. Substrate cultivation treatment significantly reduced POD activity in leaves in Kaidi and Xiariyangguang as compared to CK. Compared with CK, significant reduction in POD activity in leaves at flowering stage and mature stage was recorded for hydroponics treatment (*Table 6*).

Table 6. *Effect of culture media on POD activity in leaves of different tomato varieties ($U \cdot g^{-1} \cdot min^{-1}$)*

Varieties	Culture media	Seedling stage	Flowering stage	Mature stage
Xinxing101	Soil culture	55.98±0.23b	382.54±69.21a	640.48±94.33a
	Substrate cultivation	38.62±4.96c	235.29±43.22a	412.40±51.68b
	Hydroponics	88.81±6.51a	333.78±48.99a	226.51±29.46b
Jinbaolai	Soil culture	71.87±7.24a	278.43±9.12a	407.02±15.84a
	Substrate cultivation	9.61±0.63b	249.49±26.02ab	277.01±14.67b
	Hydroponics	67.15±5.79a	193.91±23.22b	197.78±5.94c
Kaidi	Soil culture	87.21±3.44a	242.26±16.87a	391.11±34.00a
	Substrate cultivation	22.82±1.96b	164.74±9.80b	158.47±9.08b
	Hydroponics	85.94±7.98a	116.79±0.73c	138.89±14.54b
Xiariyangguang	Soil culture	74.05±5.78a	231.75±32.71a	457.69±12.32a
	Substrate cultivation	16.27±0.69b	95.17±12.51b	352.42±27.47b
	Hydroponics	85.48±3.53a	87.48±3.14b	201.56±4.06c

Different lowercase letters within one variety represent significant difference at $P < 0.05$ level

http://www.aloki.hu ● ISSN 1589 1623 (Print) ● ISSN 1785 0037 (Online)
DOI: http://dx.doi.org/10.15666/aeer/1605_59095919
© 2018, ALÖKI Kft., Budapest, Hungary

Compared with CK, the substrate cultivation treatment did not affect CAT in leaves for Xinxing101, Jinbaolai, and Xiariyangguang. Significant enhancement in Kaidi at seedling stage was detected. The hydroponics treatment significantly reduced CAT activity in leaves at mature stage for Xinxing 101 and Jinbaolai as compared to CK. Compared with CK, significant improvement in CAT activity in leaves at seedling stage was investigated for Jinbaolai and Xiariyangguang, and at flowering stage for Kaidi and Xiariyangguang (*Table 7*).

Table 7. *Effect of culture media on CAT activity in leaves of different tomato varieties ($U \cdot g^{-1} \cdot min^{-1}$)*

Varieties	Culture media	Seedling stage	Flowering stage	Mature stage
Xinxing101	Soil culture	14.31±3.32a	17.90±4.77a	210.94±8.12a
	Substrate cultivation	19.89±2.76a	11.03±5.11a	208.59±5.41a
	Hydroponics	14.69±0.53a	10.79±4.87a	87.02±4.23b
Jinbaolai	Soil culture	21.57±5.04b	18.38±7.89a	207.98±13.20a
	Substrate cultivation	13.58±3.91b	14.59±6.49a	216.68±2.18a
	Hydroponics	39.39±4.83a	4.82±0.04a	80.10±12.42b
Kaidi	Soil culture	7.61±0.64b	9.68±2.37b	152.13±29.35ab
	Substrate cultivation	42.01±8.54a	17.50±4.82b	198.67±49.19a
	Hydroponics	13.51±3.66b	31.09±2.65a	77.34±1.35b
Xiariyangguang	Soil culture	8.62±0.00b	13.35±2.18b	126.03±3.28a
	Substrate cultivation	15.79±0.00a	19.25±1.44ab	140.52±9.41a
	Hydroponics	15.07±1.22a	21.74±2.80a	139.23±2.16a

Different lowercase letters within one variety represent significant difference at $P < 0.05$ level

Correlation analysis

Significant correlation relationship between yield and yield per plant and fruit weight ($R^2 = 0.8205$, $P < 0.01$), net photosynthetic rate in leaves at seedling stage ($R^2 = 0.7189$, $P < 0.05$) was detected (*Fig. 1*).

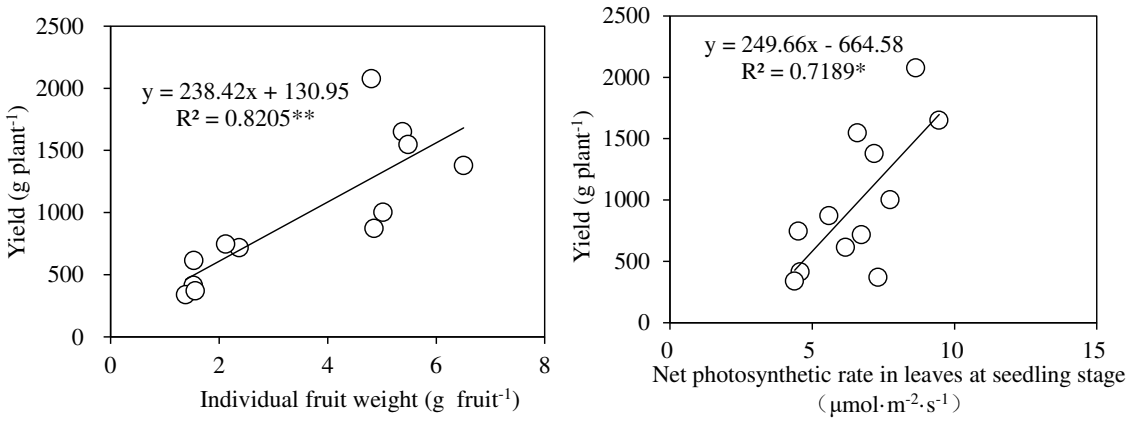

Figure 1. *Correlation relationship between yield per plant and fruit weight, net photosynthetic rate in leaves at seedling stage. ** and * represent significant difference at $P < 0.01$ and $P < 0.05$ level, respectively*

http://www.aloki.hu ● ISSN 1589 1623 (Print) ● ISSN 1785 0037 (Online)
DOI: http://dx.doi.org/10.15666/aeer/1605_59095919
© 2018, ALÖKI Kft., Budapest, Hungary

Discussion

Soilless culture mainly includes water culture, fog culture and substrate culture, among which substrate culture is the most important form of soilless culture. The main function of culture media is to support and fix plants, and provide a stable and coordinated water, gas and fertilizer environment for the crops (Liu et al., 2006). In the traditional sense, soilless cultivation mainly relies on nutrient solution to supply the total value nutrients needed by crops, and the nutrient content of cultivation matrix is often ignored whilst in fact, various organic substrates are rich in nutrients. In this study, we observed higher yield was recorded in both substrate cultivation and hydroponics than soil culture. This result agreed with the study of Tzortzakis (Tzortzakis and Economakis, 2008) which found that tomato grown in special substrate had higher yield and better fruit quality. There are several factors which effected yield and photosynthesis. The researches of Zhu (Zhu et al., 2012) showed that the interaction of water and fertilizer affected photosynthetic capacity and yield significantly in tomato plants. And in our study, the substrate cultivation and hydroponics indeed had some differences in net photosynthetic rate compared with soil culture. Meanwhile, early study proved that the net photosynthetic rate was a limited factor for yield, dry matter and fruit quality (Whitehead and Singh, 1997). Our research evidenced the view again by showing a significant positive correlation between yield and net photosynthetic rate in leaves at seedling stage.

In addition, we also found that the hydroponics treatment and substrate cultivation treatment reduced the activity of SOD or POD in leaves for some tomato cultivars in some stage. SOD and POD anti-oxidative enzymatic which have significant roles in osmo-regulations and often help to quench ROS while maintaining cellular structures and functions (Kong et al., 2017). For example, SOD dismutases superoxide radical when POD involved in scavenging H_2O_2 (Sairam et al., 2000). The changes in activity of SOD and POD might suggest that the environment of substrate cultivation and hydroponics was more stable and less environmental stresses for tomato and thus the tomato could had higher dry weight accumulation, fruit weight, and net photosynthetic rate.

In recent years, with the development of ecological agriculture and sustainable circular agriculture, greenhouse tomato in media culture develops rapidly. We would suggest that the substrate cultivation and hydroponics is benefit for tomato growth because they produced higher yield as a consequences of higher dry weight accumulation, fruit weight, and net photosynthetic rate at seedling stage and mature stage.

Conclusion

The substrate cultivation and hydroponics produced higher yield than soil culture treatment due to higher dry weight accumulation, fruit weight, and net photosynthetic rate at seedling stage and mature stage. The yield showed significant associate to fruit weight ($R^2 = 0.8205$, $P < 0.01$), net photosynthetic rate in leaves at seedling stage ($R^2 = 0.7189$, $P < 0.05$). The SPAD value and antienzyme activity vary from different planting patterns, cultivars and growth stages.

Acknowledgements. This research was supported by the Project of Display of Super Vegetable Cultivation Mode in National Agricultural Science and Technology Park, Guangzhou Guangdong province (2014 **A**070709007), Display of Special Rice and Vegetable Germplasm Collection in National Agricultural Science and Technology Park, Guangzhou Guangdong province (2015A070708010).

http://www.aloki.hu ● ISSN 1589 1623 (Print) ● ISSN 1785 0037 (Online)
DOI: http://dx.doi.org/10.15666/aeer/1605_59095919
© 2018, ALÖKI Kft., Budapest, Hungary

Author contributions. Liangliang Shi, Jinrong Zheng and Jianwu Wang designed the research, Liangliang Shi, Na Lv, Delong Tan and Jun Nie performed the experiments and collected the data, Liangliang Shi and Na Lv analyzed the data and wrote the manuscript, Guoqing Luo, Yuming Xie, Yanhong Li and Yan Xiong edited the manuscript and provided guidance during experimentation.

REFERENCES

[1] Abou-Hadid, A. F., El-Shinawy, M. Z., El-Oksh, I., Gomaa, H., El-Beltagy, A. S. (1993): Studies on water consumption of sweet pepper plant under plastic houses. – II Symposium on Protected Cultivation of Solanacea in Mild Winter Climates 366: 365-372.

[2] Chen, S., Cheng, W., Liu, A., He, C., Zou, Z. (2009): Effect of different organic substrate on leaf photosynthesis and root ATPase activity of tomato. – China Vegetables (14): 23-27.

[3] Foyer, C. H. (1987): The basis for source-sink interaction in leaves. – Plant Physiol Biochem 25(5): 649-657.

[4] Ghoreishy, F., Ghehsareh, A. M., Fallahzade, J. (2018): Using composted wheat residue as a growth medium in culture of tomato. – Journal of Plant Nutrition 41(6): 766-773.

[5] Khan, F. A. A. (2018): A Review on hydroponic greenhouse cultivation for sustainable agriculture. – International Journal of Agriculture, Environment and Food Sciences 2(2): 59-66.

[6] Kong, L., Ashraf, U., Cheng, S., Rao, G., Mo, Z., Tian, H., Pan, S., Tang, X. (2017): Short-term water management at early filling stage improves early-season rice performance under high temperature stress in South China. – European Journal of Agronomy 90: 117-126.

[7] Korkmaz, A., Karagöl, A., Horuz, A. (2016): Effect of NaCI in solid media culture on the yield and fruit quality of tomato plant. – Anadolu Tarım Bilimleri Dergisi 31(1): 127-135.

[8] Lee, J. W., Kim, Y. C., Yun, H. K., Seo, T. C., Park, K. W. (2002): Influence of silicate application on the sucrose synthetic enzyme activity of tomato in perlite media culture. – XXVI International Horticultural Congress: Protected Cultivation 2002: In Search of Structures, Systems and Plant Materials for for Sustainable Greenhouse Production. ISHS Acta Horticulturae 633: 259-262.

[9] Liu, W., Yu, H. J., Jiang, W. J. (2006): Review on research progress and application of growing media for vegetable production in China. – Chinese Journal of Eco-Agriculture 14(3): 4-7.

[10] Lv, J., Sang, P., Li, L., Li, X. (2010): Effect of nutrient solution with different formulas and concentrations on the growth of tomato seedling. – Journal of Shanxi Agricultural University (Natural Science Edition) 2: 8.

[11] Mehdizadeh, M., Darbandi, E. I., Naseri-Rad, H., Tobeh, A. (2013): Growth and yield of tomato (*Lycopersicon esculentum* Mill.) as influenced by different organic fertilizers. – International Journal of Agronomy and Plant Production 4(4): 734-738.

[12] Pires, R. C. D. M., Furlani, P. R., Ribeiro, R. V., Bodine Junior, D., Sakai, E., Lourenção, A. L., Torre Neto, A. (2011): Irrigation frequency and substrate volume effects in the growth and yield of tomato plants under greenhouse conditions. – Scientia Agricola 68(4): 400-405.

[13] Sairam, R. K., Srivastava, G. C., Saxena, D. C. (2000): Increased antioxidant activity under elevated temperatures: a mechanism of heat stress tolerance in wheat genotypes. – Biologia Plantarum 43(2): 245-251.

[14] Salokhe, V. M., Babel, M. S., Tantau, H. J. (2005): Water requirement of drip irrigated tomatoes grown in greenhouse in tropical environment. – Agricultural Water Management 71(3): 225-242.

http://www.aloki.hu ● ISSN 1589 1623 (Print) ● ISSN 1785 0037 (Online)
DOI: http://dx.doi.org/10.15666/aeer/1605_59095919
© 2018, ALÖKI Kft., Budapest, Hungary

[15] Tichá, I., Čáp, F., Pacovská, D., Hofman, P., Haisel, D., Čapková, V., Schäfer, C. (1998): Culture on sugar medium enhances photosynthetic capacity and high light resistance of plantlets grown in vitro. – Physiologia Plantarum 102(2): 155-162.
[16] Tzortzakis, N. G., Economakis, C. D. (2008): Impacts of the substrate medium on tomato yield and fruit quality in soilless cultivation. – Hort. Sci 35(2): 83-89.
[17] Whitehead, W. F., Singh, B. P. (1997): Effect of N source on photosynthesis and plant dry matter yield of tomato. – HortScience 32(3): 518-518.
[18] Xie, J., Yu, J., Chen, B., Feng, Z., Li, J., Zhao, C., Lyu, J., Hu, L., Gan, Y., Siddique, K. (2017): Facility cultivation systems "设施农业": a Chinese model for the Planet. – Advances in Agronomy 145: 1-42.
[19] Xu, H., Wang, R., Mau, M. (2001): Effects of organic fertilizers and a microbial inoculant on leaf photosynthesis and fruit yield and quality of tomato plants. – Journal of Crop Production 1: 173-182.
[20] Yang, Y., Zhang, F., Qiao, X. (2003): Effect of nitrogen forms on growth development, yield and fruit quality of tomato in media culture. – Acta Agriculturae Boreali Sinica 18(1): 86-89.
[21] Zhu, J., Liang, Y., Zhu, Y., Hao, W., Lin, X., Xing, W., Luo, A. (2012): The interactive effects of water and fertilizer on photosynthetic capacity and yield in tomato plants. – Australian Journal of Crop Science 2: 200-209.

http://www.aloki.hu ● ISSN 1589 1623 (Print) ● ISSN 1785 0037 (Online)
DOI: http://dx.doi.org/10.15666/aeer/1605_59095919
© 2018, ALÖKI Kft., Budapest, Hungary

EFFECTS OF N FERTILIZATION ON SOIL MICROBIAL RESPIRATION IN *LARIX GMELINII* PLANTATION

JIA, S. X.[1] – HU, C. Q.[2] – SUN, Y.[2] – HAN, J.[2] – ZHANG, W. L.[1] – CHEN, X. W.[1] – LIANG, A. Z.[1] – ZHANG, S. X.[1*]

[1]*Key Laboratory of Mollisols Agroecology, Northeast Institute of Geography and Agroecology, Chinese Academy of Sciences, 130102 Changchun, China*

[2]*Jilin Provincial Academy of Forestry Sciences, 130033 Changchun, China*

**Corresponding author*
e-mail: zhangshixiu@neigae.ac.cn

(Received 15th Jun 2018; accepted 14th Aug 2018)

Abstract. Soil organic carbon decomposition is regulated by soil physical and chemical properties, such as soil nitrogen (N) and soil substrate quality. In this study, soil samples from both N fertilization and control plots were collected at two depths in a *Larix gmelinii* plantation to determine if N addition elicits consistent responses in microbial respiration in bulk and rhizosphere soil, and to determine the temporal and spatial dynamics of soil organic carbon decomposition. Soil bulk and rhizosphere microbial respiration were determined using the NaOH solution absorption method. Soil microbial biomass was determined by a modified $CHCL_3$ fumigation-extraction method. The greatest soil bulk and rhizosphere microbial respiration occurred in July. Soil rhizosphere microbial respiration was higher than bulk respiration at 0–10 cm and 10–20 cm. The biggest reductions in soil microbial respiration induced by fertilization were 15.0% (bulk) and 19.6% (rhizosphere) at 0–10 cm in July, and 6.4% (bulk) and 7.9% (rhizosphere) at 10–20 cm in September. Fertilization did not influence the rhizosphere priming effect except for at 10–20 cm in May. Structural equation modeling revealed that soil microbial biomass carbon (MBC) and nitrogen (MBN) contributed directly to soil microbial respiration. Moreover, soil total N and organic carbon content were associated with soil microbial respiration through MBC and MBN. These results suggest that N fertilization suppresses soil organic carbon decomposition by decreasing soil microbial biomass, while C input induced by root exudates determined the rhizosphere priming effect, not soil microbes in the rhizosphere.
Keywords: *soil microbe, rhizosphere, soil N availability, soil organic carbon decomposition*

Introduction

Soil is a large organic carbon pool ($1.5 \cdot 10^{18}$ g of C), containing twice the total C in the atmosphere (Schlesinger, 1997). The decomposition of soil organic carbon occurs via the microbial assimilation process known as soil microbial respiration, which is one of the most important processes in global carbon cycling (Schimel and Schaeffer, 2012), response to the primary decomposed ability of new carbon associated to soil by plant (Schlesinger, 1997). Therefore, the decomposition ratio of soil C pools is regulated by soil physical and chemical properties (Xu et al., 2016). Soil nutrient availability, particularly that of nitrogen (N), has been suggested as a key driver of soil organic carbon decomposition (Zhou et al., 2014), such that the soils with a high C:N ratio showing lower decomposition rates (Xu et al., 2016). Recent studies have shown that nitrogen addition reduced soil microbial respiration induced by the negative effects of N application on soil microbial abundance and composition (Zhang et al., 2018), as well as that of soil microbial activity by shifting the metabolic capabilities of soil bacterial communities (Ramirez et al., 2012). These results suggest that N addition slows soil organic carbon decomposition by decelerating microbial mineralization. Therefore, a better

http://www.aloki.hu ● ISSN 1589 1623 (Print) ● ISSN 1785 0037 (Online)
DOI: http://dx.doi.org/10.15666/aeer/1605_59215932
© 2018, ALÖKI Kft., Budapest, Hungary

understanding of soil microbial responses to N addition is critical to predicting soil carbon sequestration in terrestrial ecosystems.

Soil substrate quality controls the soil organic carbon mineralization and efficiency of soil organic carbon microbial assimilation (Manzoni et al., 2008, 2012), with a higher substrate quality leading to higher microbial assimilation, large microbial biomass (Blagodatskaya et al., 2011), and a higher ratio of microbial carbon to soil organic carbon (Xu et al., 2014). Plant root exudates and other labile root-derived rhizodeposit are important substrates for soil microbes (Haichar et al., 2014). For example, the soil adjacent to roots has larger C mineralization rates than bulk soil in undisturbed temperate forest sites (Phillips and Fahey, 2007). A meta-analysis showed that input of labile organic C to the rhizosphere can stimulate soil organic carbon decomposition by 59% (Huo et al., 2017), and this process may be regulated by changes in the size and composition of the microbial community (Dorodnikov et al., 2009; Talbot et al., 2008). This is likely because there is 14–31% higher microbial biomass (Blagodatskaya et al., 2014) and an order of magnitude higher microbial activity and abundance in the rhizosphere than in bulk soil (Kuzyakov and Xu, 2013). However, few studies have investigated the rhizosphere soil microbial activity when there is no more ongoing labile organic C input under N addition.

Therefore, the present study was conducted to determine if N addition elicits consistent responses in microbial respiration in bulk and rhizosphere soil, and to determine the temporal and spatial dynamics of soil organic carbon decomposition. To accomplish this, soils were collected from a larch plantation (*Larix gmelinii*) during the growing season and incubated under laboratory conditions. We expected that soil microbial activity under N fertilization would mitigate any increases in soil organic carbon decomposition induced by rhizosphere microbes. We also hypothesized that changes in microbial biomass would result in concurrent changes in soil microbial respiration.

Materials and methods

Study site

This study was conducted at the Maoershan Experimental Station (127°30'–127°34'E, 45°21'–45°25' N) of Northeast Forestry University, Heilongjiang Province, China (*Fig. 1*).

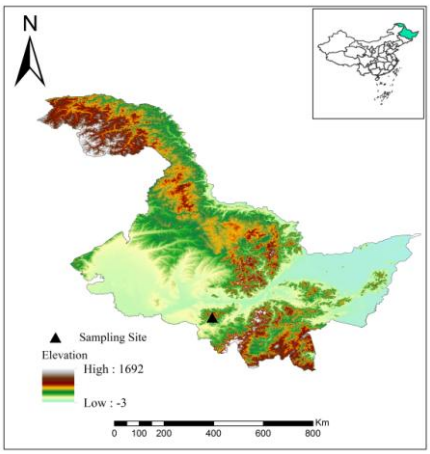

Figure 1. *The sampling site of the experiment*

http://www.aloki.hu ● ISSN 1589 1623 (Print) ● ISSN 1785 0037 (Online)
DOI: http://dx.doi.org/10.15666/aeer/1605_59215932
© 2018, ALÖKI Kft., Budapest, Hungary

This region is characterized by a cold, temperate-zone, continental monsoonal climate. The average annual temperature is 2.8 °C, with average daily air temperatures ranging from -19.6 °C (January) to 20.9 °C (July). The mean annual precipitation is 723 mm, with 66% (477 mm) occurring in June, July and August. Additionally, the mean annual evapotranspiration is 1,094 mm. The soil (Hap-Boric Luvisol) is usually frozen to a depth of 1 m in winter (December–April). More details about the soil in the region are given by Wang et al. (2006).

Experimental design

The experiment was designed to test the fertilization treatment effects on soil and plantations. *L. gmelinii* and *Fraxinus mandshurica* with representing 65% and 10% of conifer and hardwood plantations are both dominant species in natural forests of Northeast China and key commercial plantation specie. Two plantations were established in 1986 by planting 2-year-old seedlings using a 1.5–2.0 m planting grid. The experiment was arranged in a randomized design in each plantation in May of 2002, and all plots were 20 m×30 m. Each stand had two N (NH_4NO_3) fertilization treatments, control plots (0 g $N \cdot m^{-2} \cdot y^{-1}$) and fertilized plots (10 g $N \cdot m^{-2} \cdot y^{-1}$), and each treatment was applied in triplicate. The fertilizer was applied continuously on the 15th of each month from 2003 until sampling year (2014) in amounts set based on soil temperatures (*Table 1*). All measurements were performed after the fertilizer had been applied for two weeks. In the present experiment, only the *L. gmelinii* plantation of the parent experiment was sampled.

Table 1. *Soil temperature at different soil depth of research site*

Season	Soil temperature different depths (°C)			Fertilizer amount (%)
	5 cm	10 cm	20 cm	
May	12.50	9.70	8.70	15.25
June	19.50	17.20	16.30	21.00
July	22.30	20.60	19.90	27.50
August	22.10	21.00	20.80	21.00
September	14.60	16.00	14.60	15.25

Soil sampling

Six soil samples were collected from each plot using soil cores with a 6 cm inner diameter at depths of 0–10 cm and 10–20 cm in May, July, and September of 2014. Samples were separated into bulk and rhizosphere soil. To accomplish this, rhizosphere soil was collected from the soil tightly adhering to fine roots (<2 mm in diameter) as described by Wang and Zabowski (1998). Briefly, the soil not tightly adhering to roots was first removed by gently shaking the roots, then tightly adhered soil was collected by putting the roots into a paper bag and vigorously shaking them. Bulk samples were obtained from pooled soil by mixing thoroughly after fine root and rhizosphere soil removal. Soil samples were transported to the research station in a cooler (~4 °C), then sieved (<2 mm) to remove stones, coarse and fine roots and stored at 4 °C.

http://www.aloki.hu ● ISSN 1589 1623 (Print) ● ISSN 1785 0037 (Online)
DOI: http://dx.doi.org/10.15666/aeer/1605_59215932
© 2018, ALÖKI Kft., Budapest, Hungary

Soil microbial biomass

Soil microbial biomass was determined by a modified $CHCL_3$ fumigation-extraction method (Vance et al., 1987). The C and N content that were K_2SO_4-extracted from the $CHCL_3$-fumigated and unfumigated soils were estimated using a TOC-VCPH analyzer (Shimadzu, Tokyo, Japan), and soil microbial biomass C (MBC) and soil microbial biomass N (MBN) were calculated using extraction factors of 0.45 and 0.54, respectively (Brookes et al., 1985; Vance et al., 1987).

Soil microbial respiration

The microbial (basal) respiration (including bulk and rhizosphere soil) was determined based on the soil CO_2 emissions over a 10 d incubation period. Briefly, 20 g soil samples adjusted to 60% of the water holding capacity were incubated in 1000 cm^3 gas-tight jars at 20 °C ± 2 °C. The CO_2 was then absorbed by NaOH solution (0.05 M) and CO_2 was determined by single end-point titration with HCl following addition of 400 µl of 0.5 M $BaCl_2$, and precipitated as barium carbonate, after which the amount of CO_2 was calculated (Bekku et al., 1997; Phillips and Fahey, 2007).

Soil properties

Soil total C and N were determined using a FlashEA 1112 elemental analyzer (Thermo Finnigan, Italy). Soil pH was measured in a 1:5 soil: water solution using a FiveEasy pH meter (Mettler-Toledo Ltd., Mississauga, Canada). Soil NO^-_3-N and NH^+_4-N were extracted using 2 M KCl and were determined with an 8500 series flow injection autoanalyzer (Hach Company, Loveland, USA).

Data analysis

Repeated measures ANOVA was conducted to assess the effects of fertilization on soil microbial respiration using the SPSS statistical software 11.5 (SPSS Inc., Chicago, USA). When the results of ANOVA demonstrated a statistically significant difference, Tukey's test was conducted to assess the effects of fertilization treatments. A $P < 0.05$ was considered to indicate statistical significance.

Structural equation modeling (SEM) was used to evaluate the general hypothesis that soil microbial biomass (C, N), soil organic carbon, total N, NO_3^--N, NH_4^+-N and pH influence soil microbial respiration in response to fertilizer application. We constructed an a priori model including possible causal relationships among predictors. Those eight predicators in the initial model were treated as observed variables. Mardia's test was then used to estimate the multivariate normality of the dataset, and the model fit was assessed using the χ^2-test, comparative fit index (CFI), and root mean square error of approximation (RMSEA). Analyses were performed with the SPSS AMOS 21.0 software (SPSS Inc., Hong Kong, China) using the robust maximum likelihood estimation procedures.

Results

Soil microbial respiration

Soil bulk and rhizosphere microbial respiration showed similar seasonal dynamics as soil temperature, with the greatest respiration rate occurring in July (*Fig. 2*). Soil

http://www.aloki.hu ● ISSN 1589 1623 (Print) ● ISSN 1785 0037 (Online)
DOI: http://dx.doi.org/10.15666/aeer/1605_59215932
© 2018, ALÖKI Kft., Budapest, Hungary

microbial (bulk and rhizosphere) respiration varied with soil depths. Specifically, the surface (0–10 cm) soil microbial respiration rate was about 4.0 times (bulk: 3.1–4.9) and 3.9 (rhizosphere: 3.1–4.6) greater than that at 10–20 cm ($P < 0.05$). Soil rhizosphere microbial respiration was 6.6% (control) to 6.8% (fertilized) and 10.0% (fertilized) to 11.7% (control) higher than the bulk respiration at 0–10 cm and 10–20 cm ($P > 0.05$), respectively. Additionally, the priming effects were positive, being about 6.7% and 10.9% at 0–10 cm and 10–20 cm (*Fig. 2; Table 2*).

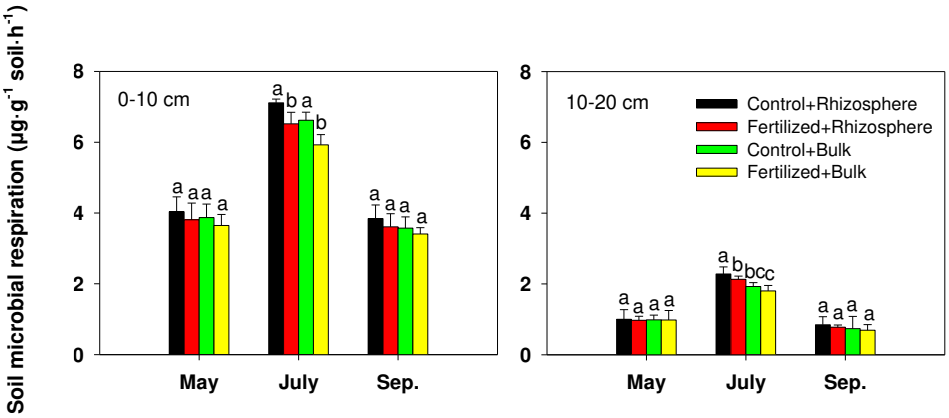

Figure 2. *Seasonal dynamical of soil rhizosphere and bulk respiration at surface and subsurface layer*

Table 2. *Repeated measurement ANOVA of fertilizer and rhizosphere on soil microbial respiration*

Source	df	0-10 cm		10-20 cm	
		F value	*P* value	F value	*P* value
Sampling time (S)	2	235.045	**0.000**	114.102	**0.000**
Fertilized (F)	1	8.371	**0.045**	1.153	0.050
Rhizophere (R)	1	6.544	0.060	5.145	**0.045**
S×F	2	1.372	0.722	0.293	0.238
S×R	2	1.119	0.343	2.347	0.503
S×F×R	2	0.039	0.654	0.001	0.728
Error	8				

Effect of fertilization on soil microbial respiration

Fertilization decreased soil bulk and rhizosphere microbial respiration, while its effects on soil microbial respiration varied with sampling time and soil depth (*Fig. 2; Table 2*). The greatest reductions in soil microbial respiration induced by fertilization of 15.0% (bulk) and 19.6% (rhizosphere) occurred in July at 0–10 cm, and by 6.4% (bulk) and 7.9% (rhizosphere) at 10–20 cm in September (*Fig. 2; Table 2*). Fertilization did not influence the rhizosphere priming effect at 0–10 cm and 10–20 cm during the growing season except during May at 10–20 cm (*Fig. 2*).

http://www.aloki.hu ● ISSN 1589 1623 (Print) ● ISSN 1785 0037 (Online)
DOI: http://dx.doi.org/10.15666/aeer/1605_59215932
© 2018, ALÖKI Kft., Budapest, Hungary

Relationship between soil properties and soil microbial respiration

Structural equation modeling revealed that the predictors explained 88% of the variation in soil microbial respiration (Rmic) (*Fig. 3*). Soil MBC and MBN contributed directly to soil microbial respiration, and the response of soil microbial respiration to MBC and MBN differed. Soil total N (STN) and organic carbon (SOC) content were associated with soil microbial respiration through MBC and MBN. It should be noted that fertilization influenced soil microbial respiration indirectly through soil NO^-_3-N and pH.

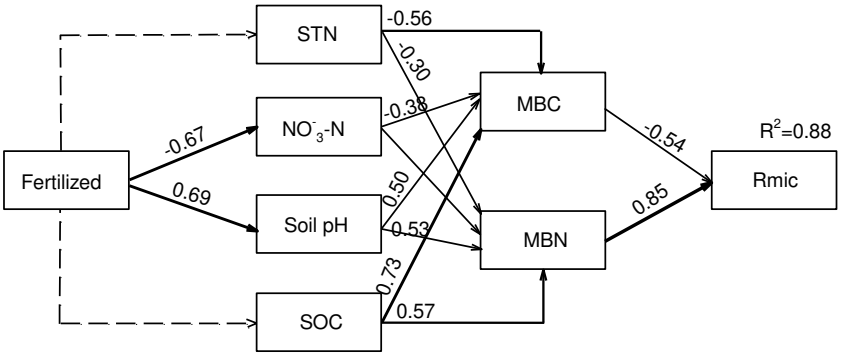

Figure 3. *Structural equation model relating fertilization on soil microbial respiration ($\chi 2$ = 14.385; df = 28; P = 0.695; CFI = 1.000; RMSEA = 0.000). Note: Rectangles represent observed variables; ovals represent latent variables; arrow thickness represents the magnitude of the path coefficient. Solid line arrows represent significant paths (P < 0.05), dot lines represent not significantly different (P > 0.05). STN: Soil total N; SOC Soil organic carbon; MBC: Soil microbial biomass carbon; MBN: Soil microbial biomass nitrogen; Rmic: Soil microbial respiration*

Discussion

Soil microbial respiration

Soil microbial respiration showed significant seasonal and soil depth effects. Specifically, the respiration rate was 2.04–4.87 μgC·g^{-1} soil·h^{-1} and 1.90–4.27 μgC g^{-1} soil·h^{-1} in rhizosphere and bulk soil, respectively, which is consistent with the results of other studies (Ananyeva et al., 2008; Olsson et al., 2005). These seasonal dynamics differed from those of the MBC and MBN (*Table 3*). This likely occurred because of interspecific competition between plants and microbes for nutrients (Kuzyakov and Xu, 2013), especially for N. In July, soil conditions are beneficial to both soil microbes and plant growth. Soil microbes showed higher respiration rate, indicating they were taking more nutrients for their own and plant growth, leading to decreased biomass accumulation (*Fig. 2; Table 3*). Soil microbes might utilize available N more effectively than plants in the short-term, while plants might be more competitive in the long run (Kuzyakov and Xu, 2013). Moreover, temporal dynamics of soil microbial biomass are associated with alternating periods of microbial death and growth, which has important consequences for soil nutrient dynamics and soil microbial biomass turnover (Wardle, 1998). The soil microbial respiration rate decreased with declining soil microbial biomass turnover, leading to the accumulation of soil microbial biomass in September (*Table 3*). Finally, soil microbial biomass and activity determined the soil microbial respiration rates (Xu et al., 2017). A higher soil microbial metabolic quotient (qCO_2),

http://www.aloki.hu ● ISSN 1589 1623 (Print) ● ISSN 1785 0037 (Online)
DOI: http://dx.doi.org/10.15666/aeer/1605_59215932
© 2018, ALÖKI Kft., Budapest, Hungary

which is defined as the microbial respiration per unit of microbial biomass, indicates higher respiration consumption of carbon and lower construction carbon. The results of the present study showed that the qCO_2 value in July was higher than in May and September at depths of both 0–10 and 10–20 cm (*Table 4*). In general, if microbes are more active during that period, cumulative maintenance respiration should be greater, and the population size should be lower (Brown et al., 2004).

Table 3. *Soil microbial biomass C and N (mean ± SE) at surface and subsurface layer*

Soil depths	Sampling time	Treatment	MBC (mg/kg)	MBN (mg/kg)
0-10 cm	May	Control	670.85±77.68	143.16±17.63
		Fertilized	447.34±41.68	78.23±9.38
	July	Control	731.71±32.18	204.67±24.67
		Fertilized	435.01±25.28	95.17±13.16
	September	Control	1106.59±40.36	223.52±4.99
		Fertilized	864.08±47.30	122.28±20.03
10-20 cm	May	Control	406.29±49.79	82.38±6.28
		Fertilized	285.57±5.13	58.88±7.28
	July	Control	450.61±34.71	107.51±12.07
		Fertilized	241.33±31.19	64.47±13.65
	September	Control	732.95±52.50	128.51±9.39
		Fertilized	649.26±37.39	97.94±9.53

Table 4. *Soil microbial respiration metabolic quotient (qCO_2)*

	Month	0-10 cm		10-20 cm		0-20 cm	
		Control	Fertilized	Control	Fertilized	Control	Fertilized
Metabolic quotient (qCO_2) $mgCO_2\text{-}C \cdot g^{-1}(C_{mic}) \cdot h^{-1}$	May	5.77	8.15	2.42	3.44	4.51	6.31
	July	9.05	13.62	4.07	7.47	7.23	11.44
	Sep.	3.23	3.94	1.01	1.06	2.34	2.71

Fertilization effect

Soil nitrogen availability strongly influences the growth and abundance of soil organisms. The addition of N has been shown to affect microbial growth, abundance and composition, as well as soil microbial activity (Bowden et al., 2004; Phillips and Fahey, 2007; Zhang et al., 2018), which is consistent with our finding that fertilization decreased soil microbial respiration (*Fig. 2*). There are several explanations for these results. First, N fertilization decreased the number of colony forming units of bacteria, fungi, and actinomycetes in our research plot by 98%, 63% and 61%, respectively (Jia et al., 2009). Because the number of colony forming units of soil microbes was positively related to soil pH (Compton et al., 2004), which declined from 5.18 (control plot) to 4.35 (fertilized plot) in this larch plantation. Moreover, the SEM results revealed that fertilization influenced soil microbial respiration indirectly through soil pH. Second, N fertilization decreased soil microbial biomass (*Table 3*). Soil MBC and MBN contributed directly to soil microbial respiration (*Fig. 3*). Because soil microbial biomass turnover was fast under lower soil pH, it would be slower under higher pH

http://www.aloki.hu ● ISSN 1589 1623 (Print) ● ISSN 1785 0037 (Online)
DOI: http://dx.doi.org/10.15666/aeer/1605_59215932
© 2018, ALÖKI Kft., Budapest, Hungary

(Wardle, 1998). Third, the soil microbial respiration metabolic quotient (qCO_2) is increasingly being used as an index of ecosystem development and disturbance (Wardle and Ghani, 1995). Nitrogen fertilization increased qCO_2 by 42% (the average of the growing season) at both 0–10 and 10–20 cm. The increasing qCO_2 indicates that microbes invested more in consuming carbon instead of construction carbon. These findings suggested that soil microbes may change their strategy by increasing the function per unit of soil microbial biomass in high nutrient soil. Therefore, N fertilization decreased microbial respiration because of reduced microbial demand for mining of soil organic carbon for N uptake.

Rhizosphere effect

Soil organic carbon is the source of soil microbial respiration. In rhizosphere soil, organic C derived from living roots consists of soluble and insoluble forms of organic C such as sugars, organic acids, mucilage, sloughed cell walls and root hairs, providing a carbon- and energy-rich environment (Haichar et al., 2014). This can suppress soil organic carbon decomposition by 50% or stimulate it by 380% during incubation in soil without plants (Cheng et al., 2014). Therefore, rhizosphere microbial communities, biomass, activity and abundance are distinct from those not affected by living roots (Blagodatskaya et al., 2014; Garland, 1996). The soil microbial community and biomass in the rhizosphere have been shown to be higher than in bulk soil. For example, Gram-negative, Gram-positive and fungal PLFA abundance in rhizosphere were higher by 45.4%, 33.3% and 66.7% than in bulk soil, and the average rhizosphere microbial biomass was 3.5 times more than that of bulk soil in a previous study (Paterson et al., 2007). The root exudates and other rhizodeposits can influence physical, chemical, biological and environmental interactions between plants and soils (Cheng et al., 2014; Kuzyakov and Blagodatskaya, 2015), and it is estimated that the quantity of C released in soil via root exudates ranges from 50 to 1500 μg g^{-1} soil d^{-1} (Cheng, 1996; Jones and Darrah, 1993; Meharg and Kilham, 1991; Trofymow et al., 1987), which may induce higher microbial abundance and diversity and faster microbial growth in rhizosphere soil (Berg and Smalla, 2009; Paterson et al., 2009). Moreover, exudation rates were shown to be positively correlated with organic carbon decomposition in the rhizosphere (Yin et al., 2014). Furthermore, the amount of soil microbial biomass was not closely related to priming (Liu et al., 2017). In the present study, no significant priming effects were observed (*Fig. 4*), even though the average rhizosphere soil respiration was 6.4% (4.0–7.1%) and 11.7% (1.9–18.5%) higher than that of bulk soil at depths of 0–10 and 10–20 cm (*Fig. 2; Table 2*). These findings differ from the previous studies, which showed significantly higher basal respiration in the rhizosphere than root-free soil after glucose addition (Blagodatskaya et al., 2014). Our findings suggest that the C input induced by root exudates determined the occurrence of rhizosphere priming, not soil microbes in the rhizosphere.

The priming effect did not differ significantly between the control and fertilized (except for in May at 10–20 cm) plot in this study (*Fig. 4*). This may have been because there was no ongoing new C input in the present study. Indeed, a previous study showed that N fertilization decreased the decomposition of old and stable soil organic carbon, but did not affect newly deposited C (Zang et al., 2017). However, soil nutrient availability is one of the factors controlling priming effects between soil depths. Greater priming has been observed in low nutrient soils compared with high nutrient soils (Dimassi et al., 2014), which may explain why the rhizosphere effects in July and

http://www.aloki.hu ● ISSN 1589 1623 (Print) ● ISSN 1785 0037 (Online)
DOI: http://dx.doi.org/10.15666/aeer/1605_59215932
© 2018, ALÖKI Kft., Budapest, Hungary

September were higher at 10–20 cm than at 0–10 cm (*Fig. 4*). Another reason may be the lower MBC at 10–20 cm soil, because soils with a higher MBC showed less priming compared to those with a lower MBC (Wang et al., 2015). These results suggest that microbes from deeper soil were less dependent on the C input derived from roots.

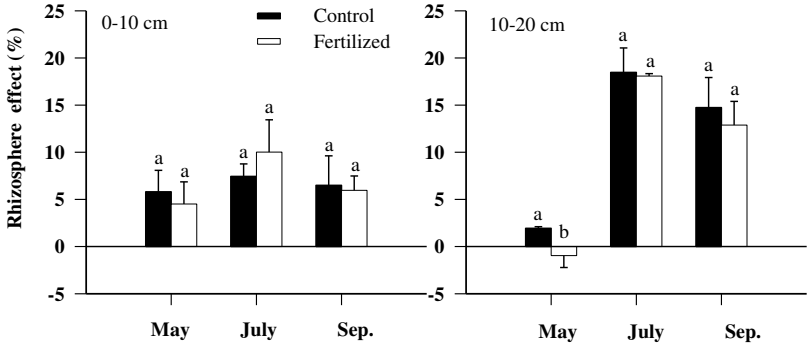

Figure 4. *Effect of N fertilization on rhizosphere effect at surface and subsurface layer*

Conclusion

In summary, there was no significant rhizosphere priming effect when there was no ongoing new C input to soil, even though soil rhizosphere microbial respiration was higher than bulk respiration. Nitrogen fertilization decreased soil bulk and rhizosphere microbial respiration, but did not influence the rhizosphere priming effect. Soil microbial biomass carbon and nitrogen contributed directly to soil microbial respiration. Moreover, soil total N and organic carbon content were associated with soil microbial respiration through soil microbial biomass. These results suggest that it is not the soil microbes in the rhizosphere that determined the occurrence of rhizosphere soil organic carbon decomposition (priming effect). Soil microbes may change their strategy for mining soil organic carbon under higher soil N availability.

Acknowledgements. The project was financially supported by Jilin Province Development Program for Sciences and Technology (20160204024NY).

REFERENCES

[1] Ananyeva, N. D., Susyan, E. A., Chernova, O. V., Wirth, S. (2008): Microbial respiration activities of soil from different climatic regions of European Russia. – European Journal of Soil Biology 44(2): 147-157.

[2] Bekku, Y., Koizumi, H., Oikawa, T., Iwaki, H. (1997): Examination of four methods for measuring soil respiration. – Applied Soil Ecology 5: 247-254.

[3] Berg, G., Smalla, K. (2009): Plant species and soil type cooperatively shape the structure and function of microbial communities in the rhizosphere. – FEMS Microbiology Ecology 68: 1-13.

[4] Blagodatskaya, E., Yuyukina, T., Blagodatsky, S., Kuzyakov, Y. (2011): Turnover of soil organic matter and of microbial biomass under C3-C4 vegetation change: consideration of ^{13}C fractionation and preferential substrate utilization. – Soil Biology and Biochemistry 43: 159-166.

http://www.aloki.hu ● ISSN 1589 1623 (Print) ● ISSN 1785 0037 (Online)
DOI: http://dx.doi.org/10.15666/aeer/1605_59215932
© 2018, ALÖKI Kft., Budapest, Hungary

[5] Blagodatskaya, E., Blagodatsky, S., Anderson, T. H., Kuzyakov, Y. (2014): Microbial growth and carbon use efficiency in the rhizosphere and root-free soil. – PLoS ONE 9(4): e93282.
[6] Bowden, R. D., Davidson, E., Savage, K., Arabia, C., Steudler, P. (2004): Chronic nitrogen additions reduce total soil respiration and microbial respiration in temperate forest soils at the Harvard Forest. – Forest Ecology Management 196: 43-56.
[7] Brookes, P. C., Landman, A., Pruden, G., Jenkinson, D. S. (1985): Chloroform fumigation and the release of soil nitrogen: A rapid direct extraction method to measure microbial biomass nitrogen in Soil. – Soil Biology and Biochemistry 17: 837-842.
[8] Brown, J. H., Gillooly, J. F., Allen, A. P., Savage, V. M., West, G. B. (2004): Toward a metabolic theory of ecology. – Ecology 85: 1771-1789.
[9] Cheng, W. (1996): Measurement of rhizosphere respiration and organic matter decomposition using natural ^{13}C. – Plant and Soil 183: 263-268.
[10] Cheng, W. X., Parton, W. J., Gonzalez-Meler, M. A., Phillips, R., Asao, S., McNickle, G., Brzostek, E., Jastrow, J. (2014): Synthesis and modeling perspectives of rhizosphere priming. – New Phytologist 201: 31-44.
[11] Compton, J. E., Watrud, L. S., Porteous, L. A., Degrood, S. (2004): Response of soil microbial biomass and community composition to chronic nitrogen additions at Harvard Forest. – Forest Ecology Management 196: 143-158.
[12] Dimassi, B., Mary, B., Fontaine, S., Perveen, N., Revaillot, S., Cohan, J. P. (2014): Effect of nutrients availability and long-term tillage on priming effect and soil C mineralization. – Soil Biology and Biochemistry 78: 332-339.
[13] Dorodnikov, M., Blagodatskaya, E., Blagodatsky, S., Fangmeier, A., Kuzyakov, Y. (2009): Stimulation of r- vs. K-selected microorganisms by elevated atmospheric CO_2 depends on soil aggregate size: research article. – FEMS Microbiology Ecology 69: 43-52.
[14] Garland, J. L. (1996): Patterns of potential C source utilization by rhizosphere communities. – Soil Biology and Biochemistry 28(2): 223-230.
[15] Haichar, F. Z., Santaella, C., Heulin, T., Achouak, W. (2014): Root exudates mediated interactions belowground. – Soil Biology and Biochemistry 77: 69-80.
[16] Huo, C. F., Luo, Y. Q., Cheng, W. X. (2017): Rhizosphere priming effect: A meta-analysis. – Soil Biology and Biochemistry 111: 78-84.
[17] ISO 14240-1 (1997): Soil Quality—Determination of Soil Microbial Biomass—Part 1: Substrate-Induced Respiration Method. – International Organisation for Standardisation, Geneva.
[18] Jia, S. X., Wang, Z. Q., Li, X. P., Sun, Y., Zhang, X. P., Liang, A. Z. (2010): N fertilization affects on soil respiration, microbial biomass and root respiration in Larix gmelinii and Fraxinus mandshurica plantations in China. – Plant and Soil 333: 325-336.
[19] Jones, D. L., Darrah, P. R. (1993): Re-sorption of organic compounds by roots of *Zea mays* L. and its consequences in the rhizosphere. II. Experimental and model evidence for simultaneous exudation and re-sorption of soluble C compounds. – Plant and Soil 153: 47-59.
[20] Kuzyakov, Y., Blagodatskaya, E. (2015): Microbial hotspots and hot moments in soil: concept and review. – Soil Biology and Biochemistry 83: 184-199.
[21] Kuzyakov, Y., Xu, X. L. (2013): Competition between roots and microorganisms for nitrogen: mechanisms and ecological relevance. – New Phytologist 198: 656-669.
[22] Liu, X. J., Sun, J. R., Mau, R. L., Finley, B. K., Compson, Z. G., Gestel, N., Brown, J. R., Schwartz, E., Dijkstra, P., Hungate, B. A. (2017): Labile carbon input determines the direction and magnitude of the priming effect. – Applied Soil Ecology 109: 7-13.
[23] Manzoni, S., Jackson, R. B., Trofymow, J. A., Porporato, A. (2008): The global stoichiometry of litter nitrogen mineralization. – Science 321: 684-686.

http://www.aloki.hu ● ISSN 1589 1623 (Print) ● ISSN 1785 0037 (Online)
DOI: http://dx.doi.org/10.15666/aeer/1605_59215932
© 2018, ALÖKI Kft., Budapest, Hungary

[24] Manzoni, S., Taylor, P. G., Richter, A., Porporato, A., Agren, G. I. (2012): Environmental and stoichiometric controls on microbial carbon-use efficiency in soils. – New Phytologist 196: 79-91.
[25] Meharg, A. A., Kilham, K. (1991): A novel method of quantifying root exudation in the presence of soil microflora. – Plant and Soil 113: 111-116.
[26] Olsson, P., Linder, S., Giesler, R., Högberg, P. (2005): Fertilization of boreal forest reduces both autotrophic and heterotrophic soil respiration. – Global Change Biology 11: 1745-1753.
[27] Paterson, E., Gebbing, T., Abel, C., Sim, A., Telfer, G. (2007): Rhizodeposition shapes rhizosphere microbial community structure in organic soil. – New Phytologist 173: 600-610.
[28] Paterson, E., Midwood, A. J., Millard, P. (2009): Through the eye of the needle: a review of isotope approaches to quantify microbial processes mediating soil carbon balance. – New Phytologist 184: 19-33.
[29] Phillips, R. P., Fahey, T. J. (2007): Fertilization effects on fine root biomass, rhizosphere microbes and respiratory fluxes in hardwood forest soils. – New Phytologist 176: 655-664.
[30] Ramirez, K. S., Craine, J. M., Fierer, N. (2012): Consistent effects of nitrogen amendments on soil microbial communities and processes across biomes. – Global Change Biology 18: 1918-1927.
[31] Schimel, J. P., Schaeffer, S. M. (2012): Microbial control over carbon cycling in soil. – Frontiers in Microbiology 3: 1-11.
[32] Schlesinger, W. H. (1997): Biogeochemistry. – Geotimes 42(2): 44.
[33] Talbot, J. M., Allison, S. D., Treseder, K. K. (2008): Decomposers in disguise: mycorrhizal fungi as regulators of soil C dynamics in ecosystems under global change. – Functional Ecology 22: 955-963.
[34] Trofymow, J. A., Coleman, D. C., Cambardella, C. (1987): Rates of rhizodeposition and ammonium depletion in the rhizosphere of axenic oat roots. – Plant and Soil 97: 333-344.
[35] Vance, E. D., Brookes, P. C., Jenkinson, D. S. (1987): An extraction method for measuring soil microbial biomass-C. – Soil Biology and Biochemistry 19: 703-707.
[36] Wang, H., Xu, W., Hu, G., Dai, W., Jiang, P., Bai, E. (2015): The priming effect of soluble carbon inputs in organic and mineral soils from a temperate forest. – Oecologia 178: 1239-1250.
[37] Wang, X. P., Zabowski, D. (1998): Nutrient composition of Douglas-fir rhizosphere and bulk soil solutions. – Plant and Soil 200: 13-20.
[38] Wang, Z. Q., Guo, D. L., Wang, X. R., Gu, J. C., Mei, L. (2006): Fine root architecture, morphology and biomass, of different branch orders of two Chinese temperate tree species. – Plant and Soil 288: 155-171.
[39] Wardle, D. A. (1998): Controls of temporal variability of the soil microbial biomass: a global-scale synthesis. – Soil Biology and Biochemistry 30(13): 1627-1637.
[40] Wardle, D. A., Ghani, A. (1995): A critique of the microbial metabolic quotient (qCO_2) as a bio-indicator of disturbance and ecosystem development. – Soil Biology and Biochemistry 27(12): 1601-1610.
[41] Xu, X., Shi, Z., Li, D. J., Rey, A., Ruan, H. H., Craine, J. M., Liang, J. Y., Zhou, J. Z., Luo, Y. Q. (2016): Soil properties control decomposition of soil organic carbon: Results from data-assimilation analysis. – Geoderma 262: 235-242.
[42] Xu, X. F., Schimel, J. P., Thornton, P. E., Song, X., Yuan, F. M., Goswami, S. (2014): Substrate and environmental controls on microbial assimilation of soil organic carbon: a framework for Earth system models. – Ecology Letter 17: 547-555.
[43] Xu, X. F., Schimel, J. P., Janssens, I. A., Song, X., Song, C. C., Yu, G. R., Sinsabaugh, R. L., Tang, D. D., Zhang, X. C., Thornton, P. E. (2017): Global pattern and controls of soil microbial metabolic quotient. – Ecological Monographs 87(3): 429-441.

http://www.aloki.hu ● ISSN 1589 1623 (Print) ● ISSN 1785 0037 (Online)
DOI: http://dx.doi.org/10.15666/aeer/1605_59215932
© 2018, ALÖKI Kft., Budapest, Hungary

[44] Yin, H. J., Wheeler, E., Phillips, R. P. (2014): Root-induced changes in nutrient cycling in forests depend on exudation rates. – Soil Biology and Biochemistry 78: 213-221.
[45] Zang, H. D., Blagodatskaya, E., Wang, J. Y., Xu, X. L., Kuzyakov, Y. (2017): Nitrogen fertilization increases rhizodeposit incorporation into microbial biomass and reduces soil organic matter losses. – Biology and Fertility of Soils 53(4): 419-429.
[46] Zhang, T. A., Chen, H. Y. H., Ruan, H. H. (2018): Global negative effects of nitrogen deposition on soil microbes. – The ISME Journal. DOI: 10.1038/s41396-018-0096-y.
[47] Zhou, L., Zhou, X., Zhang, B., Lu, M., Luo, Y., Liu, L., Li, B. (2014): Different responses of soil respiration and its components to nitrogen addition among biomes: a meta-analysis. – Global Change Biology 20(7): 2332-2343.

http://www.aloki.hu ● ISSN 1589 1623 (Print) ● ISSN 1785 0037 (Online)
DOI: http://dx.doi.org/10.15666/aeer/1605_59215932
© 2018, ALÖKI Kft., Budapest, Hungary

>ZB05141030(XJ-1)-A1-M13-

TCCTACGGGAGGCAGCAGTCGGGAATTTTGGACAATGGGCGCAAGCCTGATCCAGCCATGCCGCGTGGATGAT
GAAGGCCTTAGGGTTGTAAAATCCTTTCGTCAGGGACGATAATGACGGTACCTGAAGAAGAAGCCCCGGCTAA
CTTCGTGCCAGCAGCCGCGGTAAT

- domain Bacteria (0/20/1459456)
- phylum "Proteobacteria" (0/20/418265)
- class Alphaproteobacteria (0/20/88104)
- order Caulobacterales (0/2/5084)
- family Hyphomonadaceae (0/2/1610)
- unclassified_Alphaproteobacteria (0/15/5054)

S002500928 not_calculated 0.883 1338 uncultured alpha proteobacterium; Ppss_Ma40; JF421149
S002903729 not_calculated 0.883 1298 uncultured alpha proteobacterium; HG-B02221; JN409270
S002904822 not_calculated 0.883 1312 uncultured bacterium; MPB1-64; AB630446
S002904826 not_calculated 0.877 1301 uncultured bacterium; MPB1-68; AB630450
S002972327 not_calculated 0.883 1346 uncultured alpha proteobacterium; E06L-1; HE614839

>ZB05141031(XJ-2)-A1-M13-

TCCTACGGGAGGCAGCAGTGAGGAATATTGGTCAATGGGCGCAAGCCTGAACCAGCCATGCCGCGTGCAGGAT
GACGGTCCTATGGATTGTAAACTGCTTTTGTACGGGAAGAAACACTCCTACGAGTAGGAGCCTGACGGTACCGT
AAGAATAAGGATCGGCTAACTCCGTGCCAGCAGCCGCGGTAAT

- domain Bacteria (0/20/1459456)
- phylum "Bacteroidetes" (0/20/177857)
- class Flavobacteriia (0/20/48280)
- order "Flavobacteriales" (0/20/48280)
- family Flavobacteriaceae (0/20/29549)
- genus Flavobacterium (0/20/4440)

S001098092 not_calculated 0.922 1314 Flavobacterium denitrificans; JS14-1; EU599190
S001327996 not_calculated 0.917 1398 Flavobacterium sp. TISTR 1610; AB465579
S001327997 not_calculated 0.917 1403 Flavobacterium sp. TISTR 1602; AB465580
S002035054 not_calculated 0.933 1395 Flavobacterium phragmitis; BLN_2; GU564236

>ZB05141032(XJ-3)-A1-M13-

TCCTACGGGAGGCAGCAGTAGGGAATTTTGCGCAATGGAGGAAACTCTGACGCAGCAACGCCATGTGTGGGAT
GAAGCATTTCGGTGTGTAAACCACTGTCAGCAGGGAATAAAAGGTCGCCTCGGCGGCACTTGAATGTACCTGC
AAAGGAAGCCCCGGCTAACTTCGTGCCAGCAGCCGCGGTAAT

- domain Bacteria (0/20/1459456)
- unclassified_Bacteria (0/20/34557)

S000933198 not_calculated 0.773 1278 uncultured bacterium; FFCH12636; EU134604
S002195654 not_calculated 0.851 1322 uncultured bacterium; E2006TS6.35; GU983350
S002695007 not_calculated 0.768 1277 uncultured bacterium; ncd2021a05c1; JF175074
S002697389 not_calculated 0.768 1270 uncultured bacterium; ncd2060d08c1; JF177456

S002893909 not_calculated 0.840 1349 uncultured bacterium; TX2_1O21; JN177914

>ZB05141033(XJ-4)-A1-M13-

TATTACCGCGGCTGCTGGCACGTAGTTAGCCGTGGCTTATTCACCGGGTACCTTCAAGTTCCCACGCATGGGATT
TTTATCCCCCGGCAAAAGCAGTTTACAACCCAGAAGGCCTTCTTCCTGCACGCGGCATGGCTGGTTCAGACTTG
CATCCATTGACCAATATTCCCTACTGCTGCCTCCCGTAGG

domain Bacteria (0/20/1459456)
phylum "Bacteroidetes" (0/20/177857)
class "Bacteroidetes"_incertae_sedis (0/20/1617)
genus Ohtaekwangia (0/20/846)

S001266288 - not_calculated 0.923 1299 uncultured Sphingobacteriales bacterium; AMJE10; AM934896
S001266293 - not_calculated 0.929 1293 uncultured Sphingobacteriales bacterium; AMJF3; AM934901
S001266297 - not_calculated 0.923 1299 uncultured Sphingobacteriales bacterium; AMJF8; AM934905
S001266380 - not_calculated 0.923 1294 uncultured Sphingobacteriales bacterium; AMLG11; AM934988
S001267856 - not_calculated 0.929 1275 uncultured Sphingobacteriales bacterium; CM38D11; AM936464

>ZB05141034(XJ-5)-A1-M13-

TCCTACGGGAGGCAGCAGTGGGGAATTTTGCGCAATGGGCTAACGCCTGACGCAGCAACGCCGCGTGGAGGAT
GAAGGTCTTTGGATTGTAAACTCCTGTCAGCAGGGAAAAAGGGAGTGGGCCTAATACGTCCGCAACTTGATTGT
ACCTGCAGAGGAAGCCCCGGCTAACTCTGTGCCAGCAGCCGCGGTAAT

domain Bacteria (0/20/1459456)
phylum "Acidobacteria" (0/20/15997)
class Acidobacteria_Gp7 (0/20/446)
genus Gp7 (0/20/446)

S001407496 not_calculated 0.904 1276 uncultured bacterium; nbw774f12c1; GQ016556
S001598443 not_calculated 0.914 1408 uncultured bacterium; AK4AB1_10F; GQ396911
S002508697 not_calculated 0.909 1352 uncultured Acidobacteria bacterium; QZ-B68; JF776898
S002876698 not_calculated 0.898 1429 uncultured bacterium; 2f05; JF979346
S002887682 not_calculated 0.904 1382 uncultured Acidobacteria bacterium; M-B249; JN038969

>ZB05141035(XJ-6)-A1-M13-

TATTACCGCGGCTGCTGGCACGAAGTTAGCCGGGGCTTCCTTTGCAGGTACATTCAACTGCCTCCGAAGAGACC
ATTTATTCCCTGCTGACAGTGGTTTACACACCGAAATGCTTCATCCCACACATGGCGTTGCTGCGTCAGAGTTTC
CTCCATTGCGCAAAATTCCCTACTGCTGCCTCCCGTAGG

domain Bacteria (0/20/1459456)
unclassified_Bacteria (0/20/34557)

S000933198 - not_calculated 0.821 1278 uncultured bacterium; FFCH12636; EU134604
S002195654 - not_calculated 0.827 1322 uncultured bacterium; E2006TS6.35; GU983350
S002695007 - not_calculated 0.765 1277 uncultured bacterium; ncd2021a05c1; JF175074

S002893909 - not_calculated 0.899 1349 uncultured bacterium; TX2_1O21; JN177914
S002894364 - not_calculated 0.927 1424 uncultured bacterium; TX2_5J03; JN178369

>ZB05141036(XJ-7)-A1-M13-

TATTACCGCGGCTGCTGGCACAGAGTTAGCCGGTGCTTCTTCTGTGAGTAACATCATCCGCCATTGGTATTAACA
ATGGCCTCTTTCTCCCCACTGAAAGTGCTTTACAACCCTCAGGCCTTCTTCACACACGCGGCATTGCTGGATCA
GGCTTGCGCCCACTGTCCAATATTCCCCACTGCTGCCTCCCGTAGG

- domain Bacteria (0/20/1459456)
- phylum "Proteobacteria" (0/20/418265)
- class Gammaproteobacteria (0/20/198197)
- order Legionellales (0/4/1471)
- family Coxiellaceae (0/4/715)
- genus Coxiella (0/4/368)

S000830387 - not_calculated 0.755 1320 uncultured Methylococcaceae bacterium; Elev_16S_1037; EF019533
S002189518 - not_calculated 0.750 1321 uncultured bacterium; Llo_014; FR667312
S003451402 - not_calculated 0.788 1303 uncultured bacterium; T30-An-20C-9; JX105588
S004244955 - not_calculated 0.739 1380 uncultured bacterium; smkt_G-pro_012_002; AB806792

>ZB05141037(XJ-8)-A1-M13-

TATTACCGCGGCTGCTGGCACGGAGTTAGCCGGTGCTTATTCCTAGGGTACCGTCAGTCTCTTTAGAAAAAGAG
GTTTCGTCCCCTATAAAAGAAGTTTACAATCCAGAGGACCTTCATCCTTCACGCGGCATGGCTGGTTCAGACTT
GCGTCCATTGACCAATATTCCTTACTGCTGCCTCCCGTAGG

- domain Bacteria (0/20/1459456)
- phylum "Bacteroidetes" (0/20/177857)
- class Sphingobacteriia (0/20/17689)
- order "Sphingobacteriales" (0/20/17689)
- family Chitinophagaceae (0/20/4875)
- genus Flavisolibacter (0/20/343)

S000544377 - not_calculated 0.978 1380 uncultured bacterium; 21BSF3; AJ863256
S001191728 - not_calculated 0.885 1388 uncultured bacterium; sl1307; EU244045
S001192260 - not_calculated 0.885 1388 uncultured bacterium; sls1324; EU376237
S002083376 - not_calculated 1.000 1288 uncultured bacterium; ncd553f01c1; HM278350
S002134949 - not_calculated 0.874 1283 uncultured bacterium; ncd941e07c1; HM329923

>ZB05141038(XJ-9)-A1-M13-

TCCTACGGGAGGCAGCAGTGGGGAATATTGGACAATGGGGGCAACCCTGATCCAGCAATGCCGCGTGTGTGAA
GAAGGCCTGCGGGTTGTAAAGCACTTTCAGAGGGGAAGAAAAAATTGGAGCTAACACCTCCGATCTTGACGTT
ACCCTTAGAAGAAGCACCGGCTAACTCCGTGCCAGCAGCCGCGGTAAT

- domain Bacteria (0/20/1459456)
- phylum "Proteobacteria" (0/20/418265)
- class Gammaproteobacteria (0/20/198197)
- unclassified_Gammaproteobacteria (0/20/14896)

S000493193 not_calculated 0.930 1310 uncultured gamma proteobacterium; AKYG1556;

AY921959
S000493321 not_calculated 0.930 1312 uncultured gamma proteobacterium; AKYH1000; AY922087
S000493399 not_calculated 0.930 1313 uncultured gamma proteobacterium; AKYH885; AY922165
S000854373 not_calculated 1.000 1378 uncultured soil bacterium; MK6;
S001800395 not_calculated 1.000 1409 uncultured bacterium; 2y-73; FJ444687

>ZB05141039(XJ-10)-A1-M13-

TCCTACGGGAGGCAGCAGTAGGGAATATTGGTCAATGGATGCAAGTCTGAACCAGCCATGCCGCGTGCAGGAA
GAAGGCCCTATGGGTTGTAAACTGCTTTTGCCAGGGGATAAAACGAGCATGCGTGCTTAATTGAAGGTACCTGG
TGAATAAGCCACGGCTAACTACGTGCCAGCAGCCGCGGTAAT

domain Bacteria (0/20/1459456)
phylum "Bacteroidetes" (0/20/177857)
class "Bacteroidetes"_incertae_sedis (0/20/1617)
genus Ohtaekwangia (0/20/846)

S000932249 not_calculated 0.907 1283 uncultured bacterium; FFCH599; EU133655
S000932262 not_calculated 0.880 1230 uncultured bacterium; FFCH10617; EU133668
S000932307 not_calculated 0.913 1334 uncultured bacterium; FFCH12631; EU133713
S000944222 not_calculated 0.880 1362 uncultured bacterium; CK06-06_Mud_MAS4B-12; AB369181

>ZB05141040(XJ-11)-A1-M13-

TCCTACGGGAGGCAGCAGTGGGGAATATTGGACAATGGGGGAAACCCTGATCCAGCGACGCCGCGTGGGTGAT
GAAGGCCTTCGGGTCGTAAAGCCCTGTCTGGGGGGACGAATCCCCTGCCGGTGAACAATCGGCAGGAATGACG
GTACCTTCAAAGGAAGCACCGGCTAACTCTGTGCCAGCAGCCGCGGTAAT

domain Bacteria (0/20/1459456)
phylum "Proteobacteria" (0/20/418265)
class Deltaproteobacteria (0/18/30263)
order Myxococcales (0/1/3299)
unclassified_Deltaproteobacteria (0/17/6433)

S000932930 not_calculated 0.842 1312 uncultured bacterium; FFCH2225; EU134336
S000933293 not_calculated 0.784 1267 uncultured bacterium; FFCH6210; EU134699
S001234328 not_calculated 0.889 1437 uncultured bacterium; p9j07ok; FJ478475
S001234559 not_calculated 0.842 1430 uncultured bacterium; p7p03ok; FJ478706

>ZB05141041(XJ-12)-A1-M13-

TCCTACGGGAGGCAGCAGTGGGGAATATTGCACAATGGGCGCAAGCCTGATGCAGCCATGCCGCGTGTATGAA
GAAGGCCTTCGGGTTGTAAAGTACTTTCAGCGGGGAGGAAGGCGGTGCGGTTAATAACCGCGCCGATTGACGT
TACCCGCAGAAGAAGCACCGGCTAACTCCGTGCCAGCAGCCGCGGTAAT

domain Bacteria (0/20/1459456)
phylum "Proteobacteria" (0/20/418265)
class Gammaproteobacteria (0/20/198197)
order "Enterobacteriales" (0/20/47931)

family Enterobacteriaceae (0/20/47931)
genus Pantoea (0/20/1644)

S000333636 not_calculated 1.000 1397 Pantoea stewartii subsp. stewartii; 0028; AY642383
S000514043 not_calculated 1.000 1406 Pantoea agglomerans; XW131; AY941841
S000691536 not_calculated 1.000 1315 Pantoea sp. BD 639; DQ512489
S000722635 not_calculated 1.000 1288 Pantoea sp. BD 500; DQ849042
S000722636 not_calculated 1.000 1296 Pantoea sp. BD 502; DQ849043

>ZB05141042(XJ-13)-A1-M13-

CCTACGGGAGGCAGCAGTGGGGAATTGTTCGCAATGGGCGCAAGCCTGACGACGCAACGCCGCGTGGAGGAC
GAAGATCTTCGGGTCGTAAACTCCTGTCGAGTGGGAAGAACATCTTTCCGATGAATATTCGGAGAGACTGACGG
TACCACTAAAGGAAGCCCCGGCCAACTCCGTGCCAGCAGCCGCGGTAAT

domain Bacteria (0/20/1459456)
phylum "Acidobacteria" (0/20/15997)
class Acidobacteria_Gp6 (0/20/4463)
genus Gp6 (0/20/4463)

S000144968 not_calculated 0.831 1361 uncultured Acidobacterium sp.; KCM-C-55; AJ581627
S000493217 not_calculated 0.831 1309 uncultured Acidobacteria bacterium; AKYG1751; AY921983
S000493346 not_calculated 0.915 1315 uncultured Acidobacteria bacterium; AKYH1441; AY922112
S000500777 not_calculated 0.847 1461 uncultured Acidobacteria bacterium; 23k22; AY281352

>ZB05141043(XJ-14)-A1-M13-

TATTACCGCGGCTGCTGGCACGTAGTTAGCCGTGGCTTCTTCCTCAGGTACCGTCATTATCGTCCCTGAGAAAAG
AGGTTTACAACCCGAAGGCCTTCATCCCTCACGCGGCGTTGCTGCGTCAGACTTTCGTCCATTGCGCAAAATTC
CCGACTGCTGCCTCCCGTAGG

domain Bacteria (0/20/1459456)
phylum "Chloroflexi" (0/13/22092)
unclassified_"Chloroflexi" (0/13/9347)

S000493143 - not_calculated 0.884 1284 uncultured Chloroflexi bacterium; AKYH943; AY921909
S000829439 - not_calculated 0.902 1282 uncultured bacterium; Amb_16S_854; EF018585
S001565917 - not_calculated 0.909 1352 uncultured bacterium; F2_63X2; GQ263112
S002124329 - not_calculated 0.896 1244 uncultured bacterium; ncd352d01c1; HM319303

>ZB05141044(XJ-15)-A1-M13-

TCCTACGGGAGGCAGCAGTAGGGAATATTGCACAATGGACGAAAGTCTGATGCAGCGACGCCGCGTGAGTGAT
GAAGGCCTTCGGGTCGTAAAACTCTGTGATAGGGGAAGATGATGACGGTACCCTATCAGAAAGGACCGGCTAA
CTACGTGCCAGCAGCCGCGGTAAT

domain Bacteria (0/20/1459456)
phylum "Proteobacteria" (0/15/418265)
class Deltaproteobacteria (0/14/30263)
order Bdellovibrionales (0/10/1804)
family Bdellovibrionaceae (0/10/1139)

genus Bdellovibrio (0/10/274)

S000344657	not_calculated	0.854	1394	Bdellovibrio sp. oral clone CA006; AF385539
S000840660	not_calculated	0.695	1381	uncultured bacterium; FCPT447; EF516218
S002495818	not_calculated	0.701	1382	uncultured bacterium; LJ-J64; JF319240
S002501426	not_calculated	0.701	1416	uncultured bacterium; B55; JF429081
S002648890	not_calculated	0.787	1271	uncultured bacterium; ncd1561c04c1; JF128957

>ZB04031934(ZJ-8)-2-M13-

TGTAGTCATATGCTTGTCTCAAAGATTAAGCCATGCACGTCTAAGTACATGCCGACTTAAGGCGAAACCGCGAAT
GGCTCATTAAATCAGTTACGGTTCACTGTATTCTAACTTCCTACTTGGATAACTGTGGTAATTCTAGAGCTAATAC
ATGCCTCGGGTTCTCAACTGCGTGCCAGGCAACTGGTTGCAGACGAGACGCACTTATTAGACCAAGACCAGCC
CCGTCAGCAATGGCGGGCAATCTGTTGGTGACTCTGGATAATTATCGCATGACCGCATGGCCTCGTGCCGGCGG
CTAGTACATCAAGTGTCTGCCTTATCAACTGTCGATGGTGGGTTATACGCCCACCATGGTTGCAACGGGTAACGG
GGAAT

Description	Max score	Total score	Query cover	E value	Ident	Accession
Uncultured eukaryote partial 18S rRNA gene, clone A2-14	553	553	99%	1e-153	93%	AM409623.1
Paal uncultured eukaryote partial 18S ribosomal RNA, clone RPZ4YC22	540	540	99%	8e-150	93%	FO181430.1
Uncultured eukaryote partial 18S rRNA gene, clone 01DPZ110600090	525	525	99%	2e-145	92%	FN394868.1
Uncultured eukaryote partial 18S rRNA gene, clone 01DPZ110600065	525	525	99%	2e-145	92%	FN394851.1
Derocheilocaris typicus 18S ribosomal RNA gene, complete sequence	316	316	99%	1e-82	82%	L81937.1
Nymphon gracile 18S ribosomal RNA gene, partial sequence	307	307	99%	8e-80	82%	AY446920.1
Nymphon charioti 18S ribosomal RNA gene, partial sequence	305	305	99%	3e-79	82%	AY446931.1
Nymphon stroemi strain C28 18S ribosomal RNA gene, partial sequence	302	302	99%	4e-78	82%	EU420136.1
Austropallene cornigera 18S ribosomal RNA gene, partial sequence	289	289	99%	3e-74	81%	AY446918.1
Nymphon gracile voucher MNHN-JAA25 18S ribosomal RNA gene, partial sequence	285	285	96%	4e-73	81%	FJ862851.1

>ZB04031934(ZJ-8)-3-M13-

TGTAGTCATATGCTTGTCTCAAAGATTAAGCCATGCACGTCTAAGTACATGCCGACTTAAGGCGAAACCGCGAAT
GGCTCATTAAATCAGTTACGGTTCACTGTATTCTAACTTCCTACTTGGATAACTGTGGTAATTCTAGAGCTAATAC
ATGCCTCGGGTTCTCAACTGCGCGCCAGGCAACTGGTTGCAGACGAGACGCACTTATTAGACCAAGACCAGCC
CCGTCAGCAATGGCGGGCAATCTGTTGGTGACTCTGGATAATTATCGCATGACCGCATGGCCTCGTGCCGGCGG
CTAGTACATCAAGTGTCTGCCTTATCAACTGTCGATGGTGGGTTATACGCCCACCATGGTTGCAACGGGTAACGG
GGAAT

Description	Max score	Total score	Query cover	E value	Ident	Accession
Uncultured eukaryote partial 18S rRNA gene, clone A2-14	547	547	99%	4e-152	93%	AM409623.1
Paal uncultured eukaryote partial 18S ribosomal RNA, clone RPZ4YC22	540	540	99%	8e-150	93%	FO181430.1
Uncultured eukaryote partial 18S rRNA gene, clone 01DPZ110600090	525	525	99%	2e-145	92%	FN394868.1
Uncultured eukaryote partial 18S rRNA gene, clone 01DPZ110600065	525	525	99%	2e-145	92%	FN394851.1

Description	Max score	Total score	Query cover	E value	Ident	Accession
Derocheilocaris typicus 18S ribosomal RNA gene, complete sequence	316	316	99%	1e-82	82%	L81937.1
Nymphon gracile 18S ribosomal RNA gene, partial sequence	307	307	99%	8e-80	82%	AY446920.1
Nymphon charioti 18S ribosomal RNA gene, partial sequence	305	305	99%	3e-79	82%	AY446931.1
Nymphon stroemi strain C28 18S ribosomal RNA gene, partial sequence	302	302	99%	4e-78	82%	EU420136.1

>ZB04031935(ZJ-9)-1-M13-

TATTCCCCGTTACCCGTTGGAGCCATGGTAGACACAGATTCTACCATCGACAGTTGATAAGTCAGGCATTTGAAA
GATAAGTCGTCGGTTCTGGGACCATACGATCTGATGTGTTATCTAGGTTCATCAAGCATACGCCCGAACAAGCCG
GGCGAATGGTTTTGATCTAATAAAAGCGCCCTTTCCGTGAAAGTCAGGGCTTTGTTGCATGTATTAGCTCTAGAA
TTACCACAGTTGTCCAAAGACAGTCAAGTTTACTCAAGTGAATCAAAACTGGTTTACTGAGCCTTTTGCGGTTT
CACTTTAATACAGTCTGTACTGAGACTTGCATGGCTTAAGCTTTGAGACAAGCATATGACTAC

Description	Max score	Total score	Query cover	E value	Ident	Accession
Nabis ferus 18S ribosomal RNA gene, partial sequence	593	593	93%	5e-166	98%	EF487300.1
Nabis brevis 18S ribosomal RNA gene, partial sequence	588	588	90%	3e-164	99%	DQ199630.1
Nabis punctatus mimoferus 18S ribosomal RNA gene, partial sequence	582	582	93%	1e-162	98%	EF487315.1
Nabis ferus 18S ribosomal RNA gene, partial sequence	582	582	90%	1e-162	99%	DQ199629.1
Nabis limbatus 18S ribosomal RNA gene, partial sequence	577	577	90%	5e-161	98%	DQ199631.1
Nabis stenoferus 18S ribosomal RNA gene, partial sequence	575	575	89%	2e-160	99%	GQ258426.1
Nabis flavomarginatus 18S ribosomal RNA gene, partial sequence	571	571	90%	3e-159	98%	DQ199628.1
Nabis biformis 18S ribosomal RNA gene, partial sequence	560	560	90%	6e-156	98%	DQ199633.1
Nabis flavomarginatus 18S ribosomal RNA gene, partial sequence	558	558	89%	2e-155	98%	GQ258424.1

>ZB04031936(ZJ-10)-1-M13-

TGTAGTCATATGCTTGTCTCAAAGATTAAGCCATGCATGTCTAAGTACGCACGGCCGGTACAGTGAAACTGCGA
ATGGCTCATTAAATCAGTTATGGTTCCTTTGGTCGCTCGCTCCTCTCCTACTTGGATAACTGTGGTAATTCTAGAG
CTAATACATGCCGACGGGCGCTGACCCCCTTCGCGGGGGGGATGCGTGCATTTATCAGATCAAAACCAACCCGG
TCAGCCTCCTCCCGGCCCCGGCCGGGGGGCGGGCGCCGGCGGCTTTGGTGACTCTAGATAACCTCGGGCCGAT
CGCACGCCCCCCGTGGCGGCGACGACCCATTCGAACGTCTGCCCTATCAACTTTCGATGGTAGTCGCTGTGCCT
ACCATGGTGACAACGGGTAACGGGGAAT

Description	Max score	Total score	Query cover	E value	Ident	Accession
Uncultured eukaryote isolate DGGE gel band 7 18S ribosomal RNA gene, partial sequence	726	726	100%	0.0	99%	KF650051.1
Uncultured eukaryote isolate DGGE gel band JLJ-11-80 18S ribosomal	717	717	99%	0.0	99%	JN846872.1

Description	Max score	Total score	Query cover	E value	Ident	Accession
RNA gene, partial sequence						
Bubalus bubalis 18S ribosomal RNA gene, internal transcribed spacer 1, 5.8S ribosomal RNA gene, internal transcribed spacer 2, and 28S ribosomal RNA gene, complete sequence	717	717	99%	0.0	99%	JN412502.1
Odocoileus virginianus 18S ribosomal RNA gene, partial sequence	717	717	99%	0.0	99%	EU823286.1
Equus caballus 18S ribosomal RNA (RN18S), ribosomal RNA	715	715	98%	0.0	99%	NR_046271.1
PREDICTED: Bos taurus uncharacterized LOC104975904 (LOC104975904), ncRNA	712	712	99%	0.0	99%	XR_815498.1
Bos taurus 18S ribosomal RNA (RN18S1), ribosomal RNA	712	712	99%	0.0	99%	NR_036642.1
Bos taurus 45S ribosomal RNA (RN45S), ribosomal RNA	712	712	99%	0.0	99%	NR_046257.1
Ovis canadensis canadensis isolate 43U chromosome 24 sequence	708	708	99%	0.0	99%	CP011909.1
Budorcas taxicolor 18S ribosomal RNA gene, complete sequence	706	706	99%	0.0	99%	HQ658084.1
Dasypus novemcinctus partial 18S rRNA gene	704	704	98%	0.0	99%	AJ311674.1
Uncultured Chordata clone D0735_45_S small subunit ribosomal RNA gene, partial sequence	702	702	99%	0.0	98%	EU647001.1

>ZB04031937(ZJ-11)-1-M13-

TGTAGTCATATGCTTGTCTCAAAGATTAAGCCATGCATGTGCAAGTATGAACTAATTCGAACTGTGAAACTGCGA
ATGGCTCATTAAATCAGTTATAGTTTGTTTGATGGTACGTGCTACTCGGATAACCGTAGTAATTCTAGAGCTAATA
CGTGCAACAAACCCCGACTTCCGGGAGGGGCGCATTTATTAGATAAAAGGCTGACGCGGGCTCTGCTCGCTGAT
CCGATGATTCATGATAACTTGACGGATCGCACGGCCCTCGTGCCGGCGACACATCATTCAAATTTCTGCCCTATC
AACTTTCGATGGTAGGATAGGGGCCTACCATGGTGGCAACGGGTAACGGGGAAT

Description	Max score	Total score	Query cover	E value	Ident	Accession
Sorghum bicolor hypothetical protein (SORBIDRAFT_1205s002020) mRNA, complete cds	630	630	99%	4e-177	99%	XM_002488912.1
Sorghum bicolor hypothetical protein (SORBIDRAFT_1236s002010) mRNA, complete cds	630	630	99%	4e-177	99%	XM_002488909.1
Sorghum bicolor hypothetical protein (SORBIDRAFT_1506s002010) mRNA, complete cds	630	630	99%	4e-177	99%	XM_002488893.1
Saccharum hybrid cultivar R570 clone BAC 039D18 complete sequence	625	8754	99%	2e-175	99%	KF184927.1
Uncultured eukaryote clone SA27_18S ribosomal RNA gene, partial sequence	614	614	99%	4e-172	98%	KC922256.1
Uncultured eukaryote clone SA23_18S ribosomal RNA gene, partial sequence	614	614	99%	4e-172	98%	KC922252.1
Uncultured eukaryote clone CA79_18S ribosomal RNA gene, partial sequence	614	614	99%	4e-172	98%	KC922228.1

>ZB04031938(ZJ-1)-1-M13-

TGTAGTCATATGCTTGTCTCAAAGATTAAGCCATGCATGTCTAAGTATAAAAGTATTCTATACTTGAAACTGCGAA

TAGCTCATTAAATCAGTTATAGTTTATTTGATGGTGCCTTACTACATGGATACCCGTAGTAATTCTAGAGCTAATAC
ATGCCAAAAAAACCCAACCGCAAGGGCGGGTTGTATTTATTAGATAAAAACCATTACTCGCAAGAGTTTTTGTG
GTGATTCATAATAACTGTTCGAATCGCATGCCGCAAGGCGGCGATAGATCATTCAAATTTCTGCCCTATCAGCTCT
CGACGGTAGTGTAGTGGACTACCGTGGCATCAACGGGTAACGGGGAAT

Description	Max score	Total score	Query cover	E value	Ident	Accession
Uncultured eukaryote clone P3S3-1_e11 isolation-source soil anoxic incubation T70h 18S ribosomal RNA gene, partial sequence	638	638	100%	2e-179	99%	KF356929.1
Uncultured Cercomonas clone EF_C09 18S ribosomal RNA gene, partial sequence	636	636	99%	9e-179	99%	KP686487.1
Paracercomonas sp. HFCC 910 18S ribosomal RNA gene, partial sequence	636	636	99%	9e-179	99%	HM536155.1
Soil flagellate AND3 18S ribosomal RNA gene, partial sequence	636	636	99%	9e-179	99%	AY965859.1
Cercomonas sp. SmallSA 18S ribosomal RNA gene, partial sequence	636	636	99%	9e-179	99%	AF534712.1
Paracercomonas sp. CWPL small subunit ribosomal RNA gene, partial sequence	634	634	99%	3e-178	99%	KF589954.1
Uncultured Cercomonas clone EF_F11 18S ribosomal RNA gene, partial sequence	630	630	99%	4e-177	99%	KP686498.1
Anoplodactylus pycnosoma 18S ribosomal RNA gene, partial sequence	625	625	99%	2e-175	99%	AY446925.1

>ZB04031939(ZJ-2)-1-M13-

TATTCCCCGTTACCCGTTGTAACCATGGCAGGCCAAGACCCTGCCATCGAAAGTTGATAGGGCAGAAATTTGAA
TGAACCATCGCCGGCGCAAGGCCATGCGATTCGAGAAGTTATTATGAATCACCAGAGAGCCCCGAAGGGCATT
GGTTTTTAATCTAATAAATACATCCCTTCGTGAGTCGGGATTTTTAGCATGTATTAGCTCTAGAATTACCACGATTA
TCCAAGTAGTAAGGTACTATCAAATAAACGATAACTGATTTAATGAGCCATTCGCAGTTTCGCTGTATAATTGCTT
ATACTTAGACATGCATGGCTTAATCTTTGAGACAAGCATATGACTAC

Description	Max score	Total score	Query cover	E value	Ident	Accession
Amphisphaeriaceae sp. E00175 18S ribosomal RNA gene, partial sequence	614	614	98%	4e-172	99%	DQ872672.1
Seiridium sp. A9-1 18S ribosomal RNA gene, partial sequence	614	614	98%	4e-172	99%	AF346559.1
Xylariales sp. H15 18S ribosomal RNA gene, partial sequence	612	612	99%	1e-171	99%	DQ310771.1
Xylariales sp. H12 18S ribosomal RNA gene, partial sequence	612	612	99%	1e-171	99%	DQ310768.1
Balen uncultured eukaryote partial 18S ribosomal RNA, clone RBA2YD01	606	606	97%	7e-170	99%	FO181483.1
Pestalosphaeria sp. NK101 18S ribosomal RNA gene, partial sequence	603	603	98%	9e-169	99%	HM130668.1
Pestalotiopsis sp. YN-6 18S ribosomal RNA gene, partial sequence	603	603	98%	9e-169	99%	EU375525.1
Muscodor sp. A10-1 18S ribosomal RNA gene, partial sequence	603	603	98%	9e-169	99%	AY049023.1

>ZB04031940(ZJ-3)-1-M13-

TGTAGTCATATGCTTGTCTCAAAGATTAAGCCATGCATGTCTAAGTACTTGCCGAAATAAGGTGAAACCGCGAAT
GGCTCATTAAATCAGTTACGGTTCTATAGATATTGACTATCTACATGGATAACTGTGGTAATTCTAGAGCTAATACA
TGCACAAAAGCCCTAACCTTGCGGGAGGGGCGCATTTATTAGAACAAGACCAATGGGGCTCCTTGTGGGTCCTT
ACGTTGGTGACTCTGGATAACTTCAGCTGATCGCACGGCCTCCGAGCCGGCGACGAATCTTTCAAGTGTCTGCC
TTATCAACTGTCGATGGTAGGTTATGCGCCTACCATGGTTGCAACGGGTAACGGGGAAT

Description	Max score	Total score	Query cover	E value	Ident	Accession
Alicorhagia environmental sample isolate DGGE gel band 5 18S ribosomal RNA gene, partial sequence	662	662	99%	0.0	100%	KF650049.1
Limulidae environmental sample clone Amb 18S 691 18S ribosomal RNA gene, partial sequence	662	662	99%	0.0	100%	EF023363.1
Uncultured fungus isolate DGGE gel band 10 18S ribosomal RNA gene, partial sequence	658	658	100%	0.0	99%	KF650054.1
Uncultured eukaryote clone 31 isolation-source soil oxic incubation T0h 18S ribosomal RNA gene, partial sequence	658	658	100%	0.0	99%	KF357066.1
Uncultured fungus clone FN4 18S ribosomal RNA gene, partial sequence	658	658	100%	0.0	99%	HQ190186.1
Uncultured eukaryote clone 41 isolation-source soil oxic incubation T0h 18S ribosomal RNA gene, partial sequence	656	656	99%	0.0	99%	KF357077.1
Uncultured fungus clone YSL-F-144 18S ribosomal RNA gene, partial sequence	656	656	99%	0.0	99%	JX003498.1
Uncultured fungus isolate DGGE gel band F36 18S ribosomal RNA gene, partial sequence	656	656	99%	0.0	99%	HM004651.1

>ZB04031941(ZJ-4)-2-M13-

TGTAGTCATATGCTTGTCTCCAGTTGCTAACCTCAAATTTCTCAAAACAGTTTCCATATAACACAAGTTTCATAAA
ATGTTTTGCAACCAAAGGGTTCTATGGTAAAGTAAGTCTCAGAAACACTCTATACACAATGAAATGCAATTACTT
TTGGAGACATTCTCTTGTAAATATTGGCTTATCCCAATGTTTTTCAAACATTTGATTTCAGCACTAATATATGTATC
TATGTGCATATGTATAAATATACTTAAGTGTGTGTATCAGGCGTAGTTCTCCAGAGAAATAGAACCAACGGGTAA
CGGGGAAT

Description	Max score	Total score	Query cover	E value	Ident	Accession
Ovis canadensis canadensis isolate 43U chromosome 15 sequence	436	436	89%	8e-119	95%	CP011900.1

>ZB04031941(ZJ-4)-3-M13-

TGTAGTCATATGCTTGTCTCAAAGATTAAGCCATGCATGTGCAAGTATGAACTAATTCGAACTGTGAAACTGCGA
ATGGCTCATTAAATCAGTTATAGTTTGTTTGATGGTATGTGCTACTCGGATAACCGTAGTAATTCTAGAGCTAATA
CGTGCATCAAACCCCGACTTCCGGGAGGGGCGCATTTATTAGATAAAAGGCTGACGCGGGCTCTGCTCGCTGAT
CCGATGATTCATGATAACTTGACGGATCGCACGGCCCTCGTGCCGGCGACGCATCATTCAAATTTCTGCCCTATC
AACTTTCGATGGTAGGATAGGGGCCTACCATGGTGGCAACGGGTAACGGGGAAT

Description	Max score	Total score	Query cover	E value	Ident	Accession

Description	Max score	Total score	Query cover	E value	Ident	Accession
Saccharum hybrid cultivar R570 clone BAC 039D18 complete sequence	619	8676	99%	9e-174	98%	KF184927.1
Sorghum bicolor hypothetical protein (SORBIDRAFT_1205s002020) mRNA, complete cds	614	614	99%	4e-172	98%	XM_002488912.1
Sorghum bicolor hypothetical protein (SORBIDRAFT_1236s002010) mRNA, complete cds	614	614	99%	4e-172	98%	XM_002488909.1
Sorghum bicolor hypothetical protein (SORBIDRAFT_1506s002010) mRNA, complete cds	614	614	99%	4e-172	98%	XM_002488893.1
Uncultured eukaryote clone SA27 18S ribosomal RNA gene, partial sequence	608	608	99%	2e-170	98%	KC922256.1
Uncultured eukaryote clone SA23 18S ribosomal RNA gene, partial sequence	608	608	99%	2e-170	98%	KC922252.1
Uncultured eukaryote clone CA79 18S ribosomal RNA gene, partial sequence	608	608	99%	2e-170	98%	KC922228.1

>ZB04031942(ZJ-5)-2-M13-

TATTCCCCGTTACCCGTTGCAACCATGGTAGGCGCATAACCGACCATCGACAGTTGATAAGGCAGACACTTGAA
AGATTCATCGCCGGCTCTTAGGCCATGCGATTAGCAAGGTTATTCAGAGTCACCACCGTAAGGAGTTCCGTGAA
GAACCCCATTGGTCTTGGTCTAATAAATGCGCTTCTTCCATTACGGTCGAAGCTTTTGTGCATGTATTAGCTCTAG
AATTACCACAGTTATCCATGTAGATAGTCAACATCTAAGGAACCGTAACTGATTTAATGAGCCATTCGCGGTTTC
GCCTTAATACGGCATGTACTTAGACATGCATGGCTTAATCTTTGAGACAAGCATATGACTAC

Description	Max score	Total score	Query cover	E value	Ident	Accession
Xenillus tegeocranus 18S ribosomal RNA gene, partial sequence	593	593	99%	5e-166	96%	AF022042.1
Euzetes globulosus 18S ribosomal RNA gene, partial sequence	582	582	99%	1e-162	96%	AF022030.1
Parhypochthonius aphidinus 18S ribosomal RNA gene, partial sequence	577	577	99%	5e-161	96%	EU432215.1
Eupelops plicatus 18S ribosomal RNA gene, partial sequence	573	573	100%	7e-160	95%	EF091419.2
Eupelops hirtus isolate 07EH 18S small subunit ribosomal RNA gene, partial sequence	573	573	100%	7e-160	95%	EF093783.1
Eupelops hirtus isolate 08EH 18S small subunit ribosomal RNA gene, partial sequence	573	573	100%	7e-160	95%	EF093782.1
Platynothrus peltifer 18S ribosomal RNA gene, partial sequence	571	571	99%	3e-159	95%	EF091422.2
Achipteria coleoptrata 18S ribosomal RNA gene, partial sequence	571	571	99%	3e-159	95%	EF091418.2
Allonothrus russeolus 18S ribosomal RNA gene, partial sequence	564	564	99%	4e-157	95%	AF022025.1

>ZB04031942(ZJ-5)-3-M13-

TATTCCCCGTTACCCGTTGCAACCATGGTAGGCGCATAACCGACCATCGACAGTTGATAAGGCAGACACTTGAA
AGATTCATCGCCGGCTCTTAGGCCATGCGATTAGCAAAGTTATTCAGAGTCACCACCGTAAGGAGTTCCGTGAA

GAACCCCATTGGTCTTGGTCTAATAAATGCGCTTCTTCCATTACGGTCGAAGCTTTTGTGCATGTATTAGCTCTAG
AATTACCACAGTTATCCATGTAGATAGTCAACATCTAAGGAACCGTAACTGATTTAATGAGCCATTCGCGGTTTC
GCCTTAATACGGCATGTACTTAGACATGCATGGCTTAATCTTTGAGACAAGCATATGACTAC

Description	Max score	Total score	Query cover	E value	Ident	Accession
Xenillus tegeocranus 18S ribosomal RNA gene, partial sequence	599	599	99%	1e-167	97%	AF022042.1
Euzetes globulosus 18S ribosomal RNA gene, partial sequence	588	588	99%	3e-164	96%	AF022030.1
Parhypochthonius aphidinus 18S ribosomal RNA gene, partial sequence	582	582	99%	1e-162	96%	EU432215.1
Eupelops plicatus 18S ribosomal RNA gene, partial sequence	579	579	100%	2e-161	96%	EF091419.2
Eupelops hirtus isolate 07EH 18S small subunit ribosomal RNA gene, partial sequence	579	579	100%	2e-161	96%	EF093783.1
Eupelops hirtus isolate 08EH 18S small subunit ribosomal RNA gene, partial sequence	579	579	100%	2e-161	96%	EF093782.1
Platynothrus peltifer 18S ribosomal RNA gene, partial sequence	577	577	99%	5e-161	96%	EF091422.2
Achipteria coleoptrata 18S ribosomal RNA gene, partial sequence	577	577	99%	5e-161	96%	EF091418.2
Allonothrus russeolus 18S ribosomal RNA gene, partial sequence	569	569	99%	9e-159	95%	AF022025.1

>ZB04031943(ZJ-6)-1-M13-

TGTAGTCATATGCTTGTCTCAAAGATTAAGCCATGCATGTGCAAGTATGAACCAATTTGAACTGTGAAACTGCGA
ATGGCTCATTAAATCAGTTATAGTTTGTTTGATGGTACGTGCTACTCGGATAACCGTAGTAATTCTAGAGCTAATA
CGTGCAACAAACCCCGACTTCTGGGAGGGGCGCATTTATTAGATAAAAGGCTGACGCGGGCTCTGCCCGCTGAT
CCGATGATTCATGATAACTCGACGGATCGCACGGCCCTCGTGCCGGCGACGCATCATTCAAATTTCTGCCCTATC
AACTTTCGATGGTAGGATAGGGGCCTACCATGGTGGCAACGGGTAACGGGGAAT

Description	Max score	Total score	Query cover	E value	Ident	Accession
Balen uncultured eukaryote partial 18S ribosomal RNA, clone RBA1YC19	630	630	99%	4e-177	99%	FO181533.1
Restionaceae environmental sample clone Elev 18S 537 18S ribosomal RNA gene, partial sequence	630	630	99%	4e-177	99%	EF024189.1
Uncultured soil eukaryote clone L 18S ribosomal RNA gene, partial sequence	625	625	99%	2e-175	99%	JX014283.1
Uncultured marine streptophyte partial 18S rRNA gene, clone BS12_C1	625	625	99%	2e-175	99%	FN598332.1
Uncultured streptophyte clone D0810 21 M small subunit ribosomal RNA gene, partial sequence	625	625	99%	2e-175	99%	EU647131.1
Restionaceae environmental sample clone Elev 18S 1302 18S ribosomal RNA gene, partial sequence	625	625	99%	2e-175	99%	EF024795.1
Uncultured eukaryote clone Amb 18S 6891 18S ribosomal RNA gene, partial sequence	625	625	99%	2e-175	99%	EF024091.1
Restionaceae environmental sample clone Elev_18S_715 18S ribosomal RNA gene, partial sequence	625	625	99%	2e-175	99%	EF024309.1
Uncultured eukaryote gene for 18S rRNA, partial sequence, clone:	623	623	99%	7e-175	99%	AB222295.1

Description	Max score	Total score	Query cover	E value	Ident	Accession
d0-Band_L-TrP+B-Lower						
Lolium multiflorum 18S ribosomal RNA gene, partial sequence	623	623	99%	7e-175	99%	AY846367.1

>ZB04031944(ZJ-7)-1-M13

TATTCCCCGTTACCCGTTGCCACCATGGTAAGCATATCACTTACCATCGACAGTTGATAGGGCACACACTTGAAA
GATACGTCGCCGGCACCAGGCCATGCGATCAGCTCGAAGTTATCCAGAGTCACCAAACGTACGGACCCGCGAA
GGCCCGATTGGTTTTGATCTAATAAACGCGCTCTTTCCCAAATCCGGCCGCCACCCGAGAGCAACGACCGGCCG
GGTCGGAGCTTGCTTGCATGTATTAGCTCTAGAATTACCACAGTTATCCAAGTAGGATTGTACAATCTAATAAATC
ATGGGTGGCCTAATGAGCCATTCGCAGCTTCACCGTGTAAAGGTCTGTGCTTAGACATGCATGGCTTAATCTTTG
AGACAAGCATATGACTACA

Description	Max score	Total score	Query cover	E value	Ident	Accession
Uncultured fungus isolate DGGE gel band f19 18S ribosomal RNA gene, partial sequence	704	704	99%	0.0	99%	KJ425571.1
Uncultured fungus isolate DGGE gel band 12 18S ribosomal RNA gene, partial sequence	699	699	99%	0.0	99%	KF650056.1
Uncultured fungus isolate DGGE gel band 1-1 18S ribosomal RNA gene, partial sequence	654	654	95%	0.0	98%	KP059035.1
Uncultured fungus isolate DGGE gel band 16D 18S ribosomal RNA gene, partial sequence	636	636	90%	1e-178	99%	JN583491.1
Uncultured fungus isolate DGGE gel band 49D 18S ribosomal RNA gene, partial sequence	625	625	89%	2e-175	99%	JN583521.1
Uncultured fungus isolate DGGE gel band 5 18S ribosomal RNA gene, partial sequence	562	562	99%	2e-156	93%	FJ608623.1
Enchytraeus environmental sample isolate DGGE gel band S2-10 18S ribosomal RNA gene, partial sequence	551	551	99%	4e-153	92%	GQ995691.1
Enchytraeus albidus 18S ribosomal RNA gene, partial sequence	534	534	99%	4e-148	92%	GU453340.1
Enchytraeus sp. 'Aguinaldo, 1997' 18S ribosomal RNA gene, complete sequence	529	529	99%	2e-146	92%	U95948.1
EnchytraeUs crypticus isolate CE2183 18S ribosomal RNA gene, partial sequence	527	527	99%	6e-146	92%	GU901874.1

>ZB04031945(ZJ-12)-2-M13-

TATTCCCCGTTACCCGTTGTCACCATGGTAGGCACAGCGACTACCATCGAAAGTTGATAGGGCAGACGTTCGAA
TGGGTCGTCGCCGCCACGGGGGGCGTGCGATCGGCCCGAGGTTATCTAGAGTCACCAAAGCCGCCGGCGCCCG
CCCCCCGGCCGGGGCCGGGAGGAGGCTGACCGGGTTGGTTTTGATCTGATAAATGCACGCATCCCCCCCGCGA
AGGGGGTCAGCGCCCGTCGGCATGTATTAGCTCTAGAATTACCACAGTTATCCAAGTAGGAGAGGAGCGAGCG
ACCAAAGGAACCATAACTGATTTAATGAGCCATTCGCAGTTTCACTGTACCGGCCGTGCGTACTTAGACATGCAT
GGCTTAATCTTTGAGACAAGCATATGACTAC

Description	Max score	Total score	Query cover	E value	Ident	Accession
Uncultured eukaryote isolate DGGE gel band 7 18S ribosomal RNA gene, partial sequence	725	725	99%	0.0	99%	KF650051.1
Uncultured eukaryote isolate DGGE gel band JLJ-11-80 18S ribosomal RNA gene, partial sequence	717	717	99%	0.0	99%	JN846872.1
Bubalus bubalis 18S ribosomal RNA gene, internal transcribed spacer 1, 5.8S ribosomal RNA gene, internal transcribed spacer 2, and 28S ribosomal RNA gene, complete sequence	717	717	99%	0.0	99%	JN412502.1
Odocoileus virginianus 18S ribosomal RNA gene, partial sequence	717	717	99%	0.0	99%	EU823286.1
Equus caballus 18S ribosomal RNA (RN18S), ribosomal RNA	715	715	98%	0.0	99%	NR_046271.1
PREDICTED: Bos taurus uncharacterized LOC104975904 (LOC104975904), ncRNA	712	712	99%	0.0	99%	XR_815498.1
Bos taurus 18S ribosomal RNA (RN18S1), ribosomal RNA	712	712	99%	0.0	99%	NR_036642.1
Bos taurus 45S ribosomal RNA (RN45S), ribosomal RNA	712	712	99%	0.0	99%	NR_046257.1

>ZB04031945(ZJ-12)-3-M13-

TATTCCCCGTTACCCGTTGCCACCATGGTAGGCCACTATCCTACCATCGAAAGTTGATAGGGCAGAAATTTGAAT
GAACCATCGCCGGCGCAAGGCCATGCTATTCGAGAAGTTATTATGAATCACCAAGAAGCCCCGAAGGGCATTGG
TTTTTTATCTAATAAATACACCCCTTCCGAAGTCGAGGTTTTTAGCATGTATTAGCTCTAGAATTACCACAGGTAT
CCATGTAGTAAGGTACTATCAAATAAGCGATAACTGATTTAATGAGCCATTCGCAGTTTCACCGTATAGATTGCTT
ATACTCAGACATGCATGGCTTAATCTTTGAGACAAGCATATGACTAC

Description	Max score	Total score	Query cover	E value	Ident	Accession
Malbranchea cinnamomea strain CBS 343.55 small subunit ribosomal RNA gene, partial sequence	614	614	99%	4e-172	99%	JQ067912.1
Malbranchea cinnamomea strain Zhei20 18S ribosomal RNA gene, partial sequence	608	608	99%	2e-170	98%	JX268593.1
Uncultured fungus clone SIP_Fungi_M2_05 18S ribosomal RNA gene, partial sequence	603	603	99%	9e-169	98%	HM475189.1
Neocarpenteles acanthosporus gene for 18S rRNA, partial sequence, strain:IFO9490	603	603	99%	9e-169	98%	AB002075.1
Blastomyces dermatitidis 18S ribosomal RNA	603	603	99%	9e-169	98%	M63096.1
Blastomyces dermatitidis small subunit ribosomal RNA gene sequence	603	603	99%	9e-169	98%	M55624.1
Aphanoascus terreus strain NBRC 32655 18S ribosomal RNA (SSU) gene, partial sequence	599	599	99%	1e-167	98%	JN941596.1

>ZB04031946(ZJ-13)-1-M13-

TGTAGTCATATGCTTGTCTCAAAGATTAAGCCATGCATGTCTAAGTACGCACGGCCGGTACAGTGAAACTGCGA
ATGGCTCATTAAATCAGTTATGGTTCCTTTGGTCGCTCGCTCCTCTCCTACTTGGATAACTGTGGTAATTCTAGAG
CTAATACATGCCGACGGGCGCTGACCCCCTTCGCGGGGGGGATGCGTGCATTTATCAGATCAAAACCAACCCGG
TCAGCCTCCTCCCGGCCCCGGCCGGGGGGCGGGCGCCGGCGGCTTTGGTGACTCTAGATAACCTCGGGCCGAT

CGCACGCCCCCCGTGGCGGCGACGACCCATTCGAACGTCTGCCCTATCAACTTTCGATGGTAGTCGCTGTGCCT
ACCATGGTAACAACGGGTAACGGGGAAT

Description	Max score	Total score	Query cover	E value	Ident	Accession
Uncultured eukaryote isolate DGGE gel band 7 18S ribosomal RNA gene, partial sequence	721	721	100%	0.0	99%	KF650051.1
Uncultured eukaryote isolate DGGE gel band JLJ-11-80 18S ribosomal RNA gene, partial sequence	712	712	99%	0.0	99%	JN846872.1
Bubalus bubalis 18S ribosomal RNA gene, internal transcribed spacer 1, 5.8S ribosomal RNA gene, internal transcribed spacer 2, and 28S ribosomal RNA gene, complete sequence	712	712	99%	0.0	99%	JN412502.1
Odocoileus virginianus 18S ribosomal RNA gene, partial sequence	712	712	99%	0.0	99%	EU823286.1
Equus caballus 18S ribosomal RNA (RN18S), ribosomal RNA	710	710	98%	0.0	99%	NR_046271.1
PREDICTED: Bos taurus uncharacterized LOC104975904 (LOC104975904), ncRNA	706	706	99%	0.0	99%	XR_815498.1
Bos taurus 18S ribosomal RNA (RN18S1), ribosomal RNA	706	706	99%	0.0	99%	NR_036642.1
Bos taurus 45S ribosomal RNA (RN45S), ribosomal RNA	706	706	99%	0.0	99%	NR_046257.1

>ZB04031947(ZJ-14)-1-M13-

TGTAGTCATATGCTTGTCTCAAAGATTAAGCCATGCATGTCTAAGTGCGCACGGCCGGTACAGTGAAACTGCGA
ATGGCTCATTAAATCAGTTATGGTTCCTTTGGTCGCTCGCTCCTCTCCTACTTGGATAACTGTGGTAATTCTAGAG
CTAATACATGCCGACGGGCGCTGACCCCCTTCGCGGGGGGGATGCGTGCATTTATCAGATCAAAACCAACCCGG
TCAGCCTCCTCCCGGCCCCGGCCGGGGGGCGGGCGCCGGCGGCTTTGGTGACTCTAGATAACCTCGGGCCGAT
CGCACGCCCCCCGTGGCGGCGACGACCCATTCGAACGTCTGCCCTATCAACTTTCGATGGTAGTCGCTGTGCCT
ACCATGGTGACAACGGGTAACGGGGAAT

Description	Max score	Total score	Query cover	E value	Ident	Accession
Uncultured eukaryote isolate DGGE gel band 7 18S ribosomal RNA gene, partial sequence	721	721	100%	0.0	99%	KF650051.1
Uncultured eukaryote isolate DGGE gel band JLJ-11-80 18S ribosomal RNA gene, partial sequence	712	712	99%	0.0	99%	JN846872.1
Bubalus bubalis 18S ribosomal RNA gene, internal transcribed spacer 1, 5.8S ribosomal RNA gene, internal transcribed spacer 2, and 28S ribosomal RNA gene, complete sequence	712	712	99%	0.0	99%	JN412502.1
Odocoileus virginianus 18S ribosomal RNA gene, partial sequence	712	712	99%	0.0	99%	EU823286.1
Equus caballus 18S ribosomal RNA (RN18S), ribosomal RNA	710	710	98%	0.0	99%	NR_046271.1
PREDICTED: Bos taurus uncharacterized LOC104975904 (LOC104975904), ncRNA	706	706	99%	0.0	99%	XR_815498.1
Bos taurus 18S ribosomal RNA (RN18S1), ribosomal RNA	706	706	99%	0.0	99%	NR_036642.1
Bos taurus 45S ribosomal RNA (RN45S), ribosomal RNA	706	706	99%	0.0	99%	NR_046257.1

>ZB04031948(ZJ-15)-1-M13-

TATTCCCCGTTACCCGTTGTCACCATGGTAGGCACAGCGACTACCATCGAAAGTTGATAGGGCGGACGTTCGAA

TGGGTCGTCGCCGCCACGGGGGGCGTGCGATCGGCCCGAGGTTATCTAGAGTCACCAAAGCCGCCGGCGCCCG
CCCCCCGGCCGGGGCCGGGAGGAGGCTGACCGGGTTGGTTTTGATCTGATAAATGCACGCATCCCCCCCGCGA
AGGGGGTCAGCGCCCGTCGGCATGTATTAGCTCTAGAATTACCACAGTTATCCAAGTAGGAGAGGAGCGAGCG
ACCAAAGGAACCATAACTGATTTAATGAGCCATTCGCAGTTTCACTGTACCGGCCGTGCGTACTTACACATGCAT
GGCTTAATCTTTGAGACAAGCATATGACTAC

Description	Max score	Total score	Query cover	E value	Ident	Accession
Uncultured eukaryote isolate DGGE gel band 7 18S ribosomal RNA gene, partial sequence	713	713	99%	0.0	99%	KF650051.1
Uncultured eukaryote isolate DGGE gel band JLJ-11-80 18S ribosomal RNA gene, partial sequence	706	706	99%	0.0	99%	JN846872.1
Bubalus bubalis 18S ribosomal RNA gene, internal transcribed spacer 1, 5.8S ribosomal RNA gene, internal transcribed spacer 2, and 28S ribosomal RNA gene, complete sequence	706	706	99%	0.0	99%	JN412502.1
Odocoileus virginianus 18S ribosomal RNA gene, partial sequence	706	706	99%	0.0	99%	EU823286.1
Equus caballus 18S ribosomal RNA (RN18S), ribosomal RNA	704	704	98%	0.0	99%	NR_046271.1
PREDICTED: Bos taurus uncharacterized LOC104975904 (LOC104975904), ncRNA	701	701	99%	0.0	98%	XR_815498.1
Bos taurus 18S ribosomal RNA (RN18S1), ribosomal RNA	701	701	99%	0.0	98%	NR_036642.1
Bos taurus 45S ribosomal RNA (RN45S), ribosomal RNA	701	701	99%	0.0	98%	NR_046257.1
Ovis canadensis canadensis isolate 43U chromosome 24 sequence	697	697	99%	0.0	98%	CP011909.1
Budorcas taxicolor 18S ribosomal RNA gene, complete sequence	695	695	99%	0.0	98%	HQ658084.1

GenBank accession MF673132-MF673161

Bacteria: in turns
BankIt2041003 Seq1 MF673132
BankIt2041003 Seq2 MF673133
BankIt2041003 Seq3 MF673134
BankIt2041003 Seq4 MF673135
BankIt2041003 Seq5 MF673136
BankIt2041003 Seq6 MF673137
BankIt2041003 Seq7 MF673138
BankIt2041003 Seq8 MF673139
BankIt2041003 Seq9 MF673140
BankIt2041003 Seq10 MF673141
BankIt2041003 Seq11 MF673142
BankIt2041003 Seq12 MF673143
BankIt2041003 Seq13 MF673144
BankIt2041003 Seq14 MF673145
BankIt2041003 Seq15 MF673146

Fungi: in turns
BankIt2041022 Seq16 MF673147
BankIt2041022 Seq17 MF673148
BankIt2041022 Seq18 MF673149
BankIt2041022 Seq19 MF673150
BankIt2041022 Seq20 MF673151
BankIt2041022 Seq21 MF673152
BankIt2041022 Seq22 MF673153
BankIt2041022 Seq23 MF673154
BankIt2041022 Seq24 MF673155
BankIt2041022 Seq25 MF673156
BankIt2041022 Seq26 MF673157
BankIt2041022 Seq27 MF673158
BankIt2041022 Seq28 MF673159
BankIt2041022 Seq29 MF673160
BankIt2041022 Seq30 MF673161

EXPLORATION OF SOIL MICROBIAL DIVERSITY IN RHIZOSPHERE OF SOME TRITICEAE SPECIES IN SHANXI, CHINA

YANG, Z. P.[1#*] – YANG, W.[2#] – HAO, J.[3] – SUN, M.[1] – GAO, Z. Q. – KHAN, S.[1] – ANWAR, S.[4] – DU, T.[1] – XUE, N.[1]

[1]*College of Agriculture, Shanxi Agricultural University, Taigu 030801, Shanxi, P. R. China*

[2]*College of Life Science, North China University of Science and Technology Tangshan, P. R. China*

[3]*College of Food Science and Engineering, Shanxi Agricultural University Taigu 030801, Shanxi, P. R. China*

[4]*College of Plant Science and Technology, Huazhong Agricultural University, Wuhan, P. R. China*

[#]*These authors equally contributed to the study.*

**Corresponding author*
e-mail: yangzp.2@163.com

(Received 16th Jun 2018; accepted 22nd Aug 2018)

Abstract. Microbial diversity in rhizospheric soil plays a vital role for sustainable crop production and maintenance of soil quality. The aim of this study was to evaluate microbial diversity in rhizosphere of Triticeae species by denaturing gradient gel electrophoresis (DGGE) and DNA sequencing technique and to select suitable varieties being introduced to Shanxi province to improve soil quality and crop production. In the experiment, there were nine introduced varieties of Triticeae crops and one local breeding winter wheat variety (S1, Shannong 129, white grain, middle-gluten). The nine Triticeae varieties included six common wheat varieties, one durum wheat variety (S8, Yavaros F9), one rye variety (S9, rye 4R) and one triticale variety (S10, taisi 1). The six common wheat varieties were: Yannong 19 (S2, white grain, middle-gluten, winter), Huaimai 18 (S3, white, middle-gluten, half-winter), Yumai 34 (S4, white, high-gluten, spring), Shannong zixiaomai (S5, purple, middle-gluten, winter), Heixiaomai 031244 (S6, black, high-gluten, winter), Wumai 202W22 (S7, black, high-gluten, spring). Results showed that the rhizospheric bacterial and fungal community varied with Triticeae genera and wheat varieties. Huaimai 18 stimulated the increase of uncultured bacterium and *Nabis ferus*, while Shannong 129 stimulated the increase of uncultured *Chloroflexi bacterium*. Bacterial diversity was higher in rhizosphere of Heixiaomai 031244, whereas, fungal diversity was relatively higher in Huaimai 18. Hence, our study implies that, Huaimai 18, Yannong 19, and Heixiaomai 031244 could be planted in Shanxi province to develop high quality wheat variety resources and rye 4R as a feed crop for planting structure adjustment.
Keywords: *bacterial community, rhizobial fungal, common wheat, rye, triticale, durum wheat, DGGE*

Introduction

Soil microbes are an important component of soil fertility and play critical roles in ecosystems and influence many important ecosystem processes such as organic matter mineralization, humus formation and decomposition, carbon-nitrogen cycling, soil formation, plant nutrient acquisition and so on (Li, 1993), although they are very small parts of the soil composition (Jia et al., 2004b). Especially in terrestrial ecosystems, soil microbes make important contributions to plant productivity and diversity. Van der Heijden et al. (2008) showed that mycorrhizal fungi and nitrogen-fixing bacteria were

http://www.aloki.hu ● ISSN 1589 1623 (Print) ● ISSN 1785 0037 (Online)
DOI: http://dx.doi.org/10.15666/aeer/1605_59335954
© 2018, ALÖKI Kft., Budapest, Hungary

responsible for about 5-20% (in grassland and savannah) to 80% (in temperate and boreal forests) of all nitrogen, and up to 75% of phosphorus, that was annually acquired by the vegetation.

Crop roots spread widely in farmland soil, forming special soil microbial habitat and affecting soil fertility and nutrient circulation (Jia et al., 2004a). Guriguis et al. (1969) had divided farmland soil into rhizosphere and non-rhizosphere soil. The bioactivity of rhizosphere soil was significantly higher than that of non-rhizosphere soil during crop growth period (Takuya, 1990). Organic matter of rhizosphere soil came from crop roots, which could account for about 30% of plant photosynthetic products (Martin, 1977). The amount of rhizosphere soil microbial carbon accounted for about 3 percent of the total soil organic carbon (Joergensen, 2000). The ratio of rhizosphere and non-rhizosphere soil microbial biomass (R/S) was in turn bacterial > fungus > actinomycetes (Lou, 1962; Chen, 1990). Rhizospheric microbes can stabilize soil structure, accumulate organic residue, fix nitrogen, and remove toxin (Doran and Zeiss, 2000; Gomes et al., 2003; Sainia et al., 2004; Wakelin et al., 2008). Also, rhizospheric microbial species and their populations can considerably maintain crops healthy and improve crop growth (Acosta-Martínez et al., 2010; Aira et al., 2010). There were a few relevant reports about the effects of these factors, such as soil type and properties, soil nutrition, cropping system, cultivating management practice, varietal differences within a species, plant age, plant species, and plant genotype (Mar et al., 2000; Xu et al., 2009; Buyer et al., 2010; Teaumroong et al., 2010; Piromyou et al., 2011) on rhizospheric soil microbial diversity as one of the most sensitive biological indicators for monitoring soil quality changes (Brock, 1987; Niemi et al., 2001). However, very few reports were published about rhizospheric soils' microbial diversities when a number of wheat resources were introduced into a particular area.

Wheat (*Triticum aestivum* L.) is one of the most important crops due to having the biggest cultivated area and yield as well as having the widest geographical distribution in the world (FAOSTAT, 2017). In China, the planting area and yield of wheat is next to that of rice. Shanxi Province, located at the eastern edge of loess plateau, is one of the main provinces of wheat production in China. According to wheat ecological quality regionalization, Shanxi province belongs to strong-gluten and middle-gluten wheat producing area in China (He et al., 2006).

Grain quality is determined by the environment and interaction between environment and genotype (Kaya and Akcura, 2014). Grain quality of wheat is characterized by a number of physical and compositional properties and threshold requirements are set according to end-use requirements. For instance in wheat whole-grain physical properties such as size and shape, grain protein content and protein composition is also an important quality measure which defines nutritional and end-use properties of dough mixing, dough strength and effect the efficiency of the bread making process and product quality (Nuttall et al., 2017).

Based on wheat quality classification of the National standard of the People's Republic of China (GB/T 17320-2013), the average protein content of wheat grains in Shanxi has reached above 14% which is in accordance with the protein content of strong-gluten quality, but the average wet gluten content is up to 28%-30% which was between the strong-gluten and middle-gluten range and cannot meet the wheat standard for making bread for which wet gluten content should be ≥ 32% (Ma et al., 2016). Therefore, in order to further improve the quality of wheat varieties in Shanxi Province, it is necessary to introduce some high-protein and high-wet gluten varieties from other

http://www.aloki.hu ● ISSN 1589 1623 (Print) ● ISSN 1785 0037 (Online)
DOI: http://dx.doi.org/10.15666/aeer/1605_59335954
© 2018, ALÖKI Kft., Budapest, Hungary

regions (Xiyong et al., 2012). Xia et al. (2014) reported that grain qualities such as protein content and wet gluten content of six wheat varieties from Huanghuai wheat region were improved significantly compared to those of local variety Shannong 129 after late sowing in Jinzhong wheat region, Shanxi province. Ma et al. (2016) showed that Wumai 201W22 and Wumai 203W2 contain high-protein (≥14%) with high-gluten (≥32%) and high-protein (≥14%) with middle-gluten (30%-32%), respectively, while the local Shannong 129 contains middle-protein (13.4%-14%) with lower-gluten (<30%) after late sowing in Jinzhong wheat region. Juanjuan et al. (2016) studied the genetic potential and wheat quality in Jinzhong, Shanxi province and reported that Heixiaomai 031244 was higher-protein and middle-gluten (30-32%), however, Wumai 202W22 was low-yield with middle-protein (13.4-14.0%) and lower-gluten, and there was only Jinmai84 which was middle-yield with lower-protein (≤13.05%) and lower-gluten (≤30%). Shannong129 of the local breeds was higher-yield with middle-protein and lower-gluten. Besides, Shanxi is also an important livestock and poultry production area, such as pig, cattle, sheep, chick, but feed crops are mainly oats and corn. In order to enrich feed crop resources, it is necessary to introduce some other feed crops, such as rye and triticale.

Soil microbes could be a critical factor affecting grain quality because they are important regulators of plant productivity. The cultivar selection can also affect soil microbial diversity (Nelson et al., 2008; Yang et al., 2016). Therefore, rhizosphere soil microbial diversity was hypothesized to be significantly different among different varieties of Triticeae crops. To validate our hypothesis, in our study, we have chosen ten different varieties of Triticeae crops, which are of high quality and variable in chromosome ploidy, grain color, overwintering, gluten, and source. They include four varieties of common winter wheat (Shannong 129, Yannong 19, Shannong zixiaomai and Heixiaomai 031244), one variety of common half-winter wheat (Huaimai 18), one variety of rye (rye 4R), one variety of triticale (taisi 1), two varieties of common spring wheat (Yumai 34 and Wumai 202w22), and one variety of durum wheat (Yavaros F9). Using the method of PCR-denaturing gradient gel electrophoresis (PCR-DGGE) of the V3 region of 16S or the V1-V2 region of 18S ribosomal DNA (rDNA) (Yang et al., 2016), we preliminarily compared the similarity and diversity of rhizosphere soil microbes (bacteria and fungi) in the above Triticeae crops, collected general (occurring in all soils) and specific (occurring in some soils only) bands of their DGGE gel, and then sequenced the 16S or 18S rDNA fragments to examine the microbial species and to determine detailed microbial community changes among rhizospheric soils of ten Triticeae crop varieties.

Materials and methods

Field site description

The experiment was conducted in the experimental field of Shanxi Agricultural University in Taigu County, Shanxi Province, China (*Fig. 1*). The experimental field is located at 37°25' N and 112°35' E and continuously planted with winter wheat many years, one time per year. The winter wheat variety Shannong 129, which was bred by Shanxi Agricultural University in 2009, previously had been planting in the experimental field for many years. The field soil was medium loam; soil samples of cultivated horizon (20 cm) contained total nitrogen of 1.80 g kg^{-1}, organic matter of 12.6 g kg^{-1}, available N 53.6 mg kg^{-1}, available P 9.6 mg kg^{-1} and exchangeable K

http://www.aloki.hu ● ISSN 1589 1623 (Print) ● ISSN 1785 0037 (Online)
DOI: http://dx.doi.org/10.15666/aeer/1605_59335954
© 2018, ALÖKI Kft., Budapest, Hungary

137.5 mg kg^{-1}, which were measured by the methods as previously described (Lü et al., 2002; Yang et al., 2016). The winter wheat in the fall and the spring wheat in the spring are planted one time per year in the field.

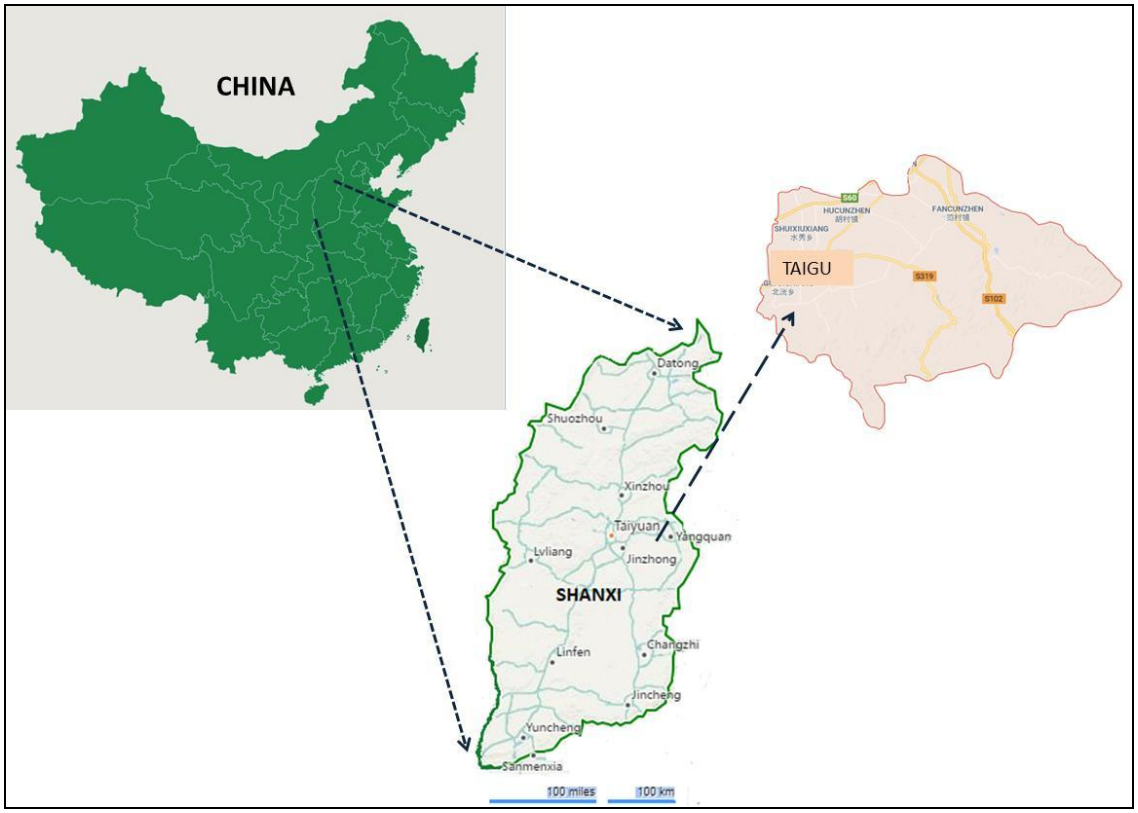

Figure 1. *Map of experimental region in China*

Triticeae species and varieties

Four kinds of Triticeae crops, belonging to common wheat, durum wheat, rye and triticale, respectively, were introduced in the experiment. The characteristics of each variety were summarized in *Table 1*. Common wheat is one of the main food crops planted in Shanxi province and is divided into winter, semi-winter and spring wheat according to vernalization. Winter wheat is often sown in the fall of current year and harvested in the summer of the following year, especially must pass through the vernalization stage (low temperature of 0-5 °C, short-day) and then enter the reproductive growth period (including heading, flowering and grain filling stages). Spring wheat is often sown in spring and harvested in summer this year without overwintering stage. Semi-winter wheat is also sown in fall but its cold resistance is less than winter wheat's. Rye is a feed crop with high yield and high nutritional value, being sown in fall and harvested in summer like winter wheat. Triticale is a new artificial combination species, which is produced by using the sexual hybridization technology and doubling hybrid chromosomes numbers from Triticum and Secale. Durum wheat belongs to Triticum and is usually used for improving wheat grain quality in breeding because both the protein (average 15%) and wet gluten (average 35%) content of its grains are higher than those of common wheat (average 14% and 30%, respectively). Like spring wheat, durum wheat is also sown in spring and harvested in summer. Nine

http://www.aloki.hu ● ISSN 1589 1623 (Print) ● ISSN 1785 0037 (Online)
DOI: http://dx.doi.org/10.15666/aeer/1605_59335954
© 2018, ALÖKI Kft., Budapest, Hungary

different varieties of above the Triticeae crops selected for this study were planted because of their high qualities in the Jinzhong region of Shanxi province, China (Xia et al., 2014; Liu et al., 2015; Ma et al., 2016; Su et al., 2017). The local breeding variety Shannong 129 was chosen as control.

Experimental design

In the experiment, randomized block design was adopted to plant the ten varieties above mentioned. Ten varieties made up a block group in random order, in triplicate, that is to say, in total three block groups, which were named as A, B, and C groups, respectively. The distance between two adjacent blocks was 60 cm, and the distance between two adjacent varieties was 40 cm. Each variety was planted four rows, row-length 5 m, row-space 20 cm, planting area 4 m^2 (4.20 m × 5 m), planting-depth 5 cm and planting density 300 grains per row. The seven of winter and semi-winter varieties (Shanong 129, Yannong 19, Shannong zixiaomai, Heixiaomai 031244, rye 4R, Taisi 1 and Huaimai 18) were sown on September 30, 2012, and the remaining three of spring varieties (Yumai 34, Wumai 202w22 and Yavaros F9) were sown on February 26, 2013. During the entire development period, common field management was used for each variety. At the mature stage (June 30, 2013), rhizospheric soil samples from the 0-20 cm soil layer were taken to complete microbial community diversity analysis for each variety.

Soil sampling

For the ten varieties of Triticeae crops, soil samples were collected at three different sampling sites of three block groups (A, B and C) at the maturity stage (*Fig. 2*).

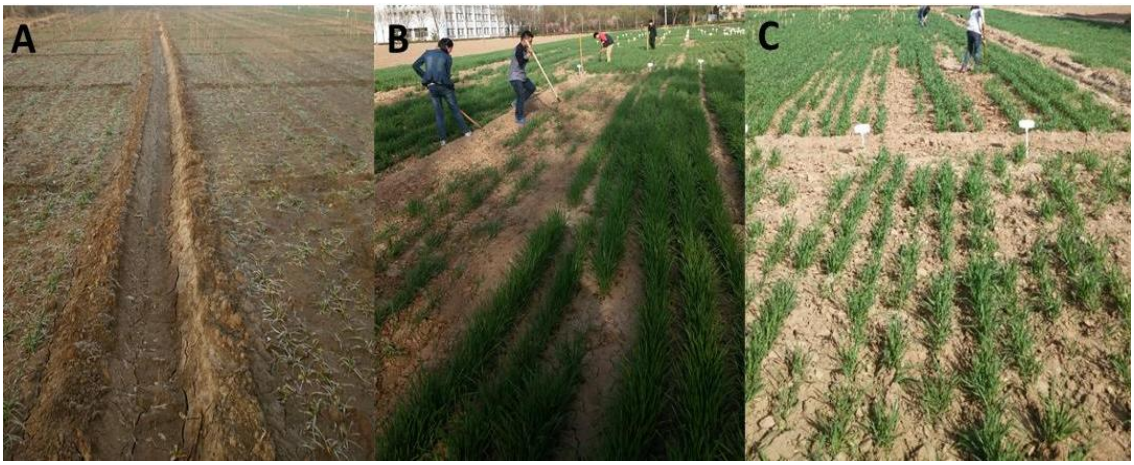

Figure 2. *Sampling sites for soil collection at Shanxi province, China*

The Triticeae crops having different sowing and flowering time but the maturity time was almost consistent, therefore, samples were collected at maturity stage. Considering the effect of the side row, three random sampling points were chosen from two rows in the middle for each sampling site (such as A) with a minimum distance of 2 m between individual sampling points. An 8-cm diameter soil auger was used to drill a suitable hole into the ground around the crop roots for the soil samples from the 0-20 cm layer. In the sterile petri dishes, the roots were taken out and shaken gently to remove non

http://www.aloki.hu ● ISSN 1589 1623 (Print) ● ISSN 1785 0037 (Online)
DOI: http://dx.doi.org/10.15666/aeer/1605_59335954
© 2018, ALÖKI Kft., Budapest, Hungary

rhizospheric soil to collect the soil remaining on the roots as rhizospheric soil. Every variety had nine random single samples of rhizospheric soil. By thoroughly mixed the nine samples to reduce the spatial difference in soil and sieved by a 2 mm sieve, respectively, the composite samples representing each Triticeae crop variety were obtained, collected in sealed individual plastic bags, and stored at -20 °C until DNA extraction was performed in the lab (*Table 1*).

Table 1. *Characteristics and rhizosphere soil samples of ten varieties of several Triticeae crops in the experiment*

Crops	Varieties	Chromosome ploidy	Grain color	Varietal characteristic	Source region	Rhizosphere soil samples
Common wheat	Shannong 129	Hexaploid	Red	Winter	Middle of Shanxi, China	S1
Common wheat	Yannong 19	Hexaploid	White	Winter	Shandong, China	S2
Common wheat	Huaimai 18	Hexaploid	White	Half-winter	Jiangsu, China	S3
Common wheat	Yumai 34	Hexaploid	White	Spring	Henan, China	S4
Common wheat	Shannong zixiaomai	Hexaploid	Purple	Winter	Middle of Shanxi, China	S5
Common wheat	Heixiaomai 031244	Hexaploid	Black	Winter	Middle of Shanxi, China	S6
Common wheat	Wumai 202w22	Hexaploid	Black	Spring	South of Shanxi	S7
Durum wheat	Yavaros F9	Tetraploid	Red	Spring	Canada	S8
Rye	Rye 4R	Diploid	Black	Winter	Canada	S9
Triticale	Taisi 1	Octaploid	Red	Winter	England	S10

PCR-DGGE microbial community analysis

The PCR-DGGE technique, separating the DNA of different sequence by the concentration gradient of the denatured agent of polyacrylamide gel, and providing community composition as well as information about the dominant species in the community by analyzing the sequence of excised bands (Yang et al., 2016), is suitable for investigating the spatiotemporal changes of species population, has the characteristics of repeatability and simple operation, and can be used to analyze multiple samples simultaneously. Therefore, it is feasible to use the PCR-DGGE technique in this experiment. To investigate microbial community diversity in the rhizospheric soil of Triticeae crops, PCR-DGGE) of the V3 region of 16S or the V1-V2 region of 18S ribosomal DNA (rDNA) was performed. Species of the complex microbial community were assayed by a genotypic fingerprinting approach using the PCR-DGGE technique. Each composite soil sample was divided in triplicate, and then total DNA was extracted directly from the soil according to the E.Z.N.A.™ Soil DNA Kit protocol (Omega Bio-Tek).

http://www.aloki.hu ● ISSN 1589 1623 (Print) ● ISSN 1785 0037 (Online)
DOI: http://dx.doi.org/10.15666/aeer/1605_59335954
© 2018, ALÖKI Kft., Budapest, Hungary

PCR amplification of 16S rDNA V3 hypervariable region for bacteria

The PCR amplification of the 16S rDNA V3 hypervariable region for bacteria (about 250 bp PCR product) was performed in 50 μL of reaction mixture by universal bacterial specific primers F338-GC (5'-CGCCCGCCGCGCGCGGCGGGCGGGGCGGGGGCACGGGGGGCCTACGGGAG GCAGCAG-3') and R518 (5'- ATT ACC GCG GCT GCT GG -3') on a C1000-Touch Thermocycler (Gene Amplification PCR System, Bio-Rad, USA) using the touchdown PCR method, which increases specificity of PCR reactions and uses a cycling program in which the annealing temperature is gradually reduced (e.g. decrease 0.5 °C /each cycle). The thermal cycling scheme was as follows: initial denaturation at 94 °C for 5 min, 20 touchdown cycles of denaturation at 94 °C for 1 min, annealing at 65 °C (reduced 0.5 °C per cycle) for 1 min, and extension at 72 °C for 3 min, followed by 10 cycles of denaturation at 94 °C for 1 min, annealing at 55 °C for 1 min, and extension at 72 °C for 3 min, and a final extension period at 72 °C for 10 min. The compositions of the PCR reaction mixture and the examination of the PCR products consulted the reference (Yang et al., 2016) with a minor modification.

PCR amplification of 18S rDNA V1-V2 region for fungus

Similar to bacteria, the target part of the 18S rDNA V1-V2 region (about 450-bp PCR product), which is the most suitable region for detecting fungal diversities in soil using DGGE analysis, was amplified by universal fungal specific primers Fung-GC (5'-CGCCCGCCGCGCCCCGCGCCCGGCCCGCCGCCCCCGCCCCATTCCCCGTTAC CCGTTG-3' and NS1 5'-GTAGTCATATGCTTGTCTC-3'). The PCR mixture compositions were the same as the bacterial fragment amplification above, except for the universal primers (1 μL of Fung-GC (10 μM) and 1 μL of NS1 (10 μM)) and product checks. DNA samples were amplified by PCR using the following thermal cycling scheme: initial denaturation at 94 °C for 3 min, 40 cycles of denaturation at 94 °C for 1 min, annealing at 50 °C for 1 min, and extension at 72 °C for 1 min, followed by a final extension period at 72 °C for 10 min.

DGGE analysis

Gels for the DGGE of PCR products (300 ng) carried out using a D-Code Mutation Detection System instrument (Bio-Rad, USA) were prepared, run for 8.0 h at 120 V and 60 °C in 10% (w/v) polyacrylamide, and visualized by the UVI Gene Genius Bioimaging System (*Figs. 1* and *2*) according to the reference (Yang et al., 2016). Soil samples used in the study were labelled as in *Table 1*.

DGGE gel bands recovery

Some bands in DGGE gel (bands indicated by yellow arrows in (*Figs. 3* and *4*), no matter general (occurring in all soils, such as band No. 13 in *Fig. 2*) or specific (occurring in some soils only, including bands No. 1-15 in (*Fig. 3*) as well as bands No. 1-12 and 14-15 in (*Fig. 4*) bands, were identified using direct sequencing of PCR products recovered from the gel by the SK1135 UNIQ-10 Column Kit (Shanghai Sangon Biological Engineering Technology & Service Co., Ltd., P. R. China). The target genes were re-amplified with the original primer sets (F357 5'-CCTACGGGAGGCAGCAG -3', R518 5'- ATTACCGCGGCTGCTGG -3' for

http://www.aloki.hu ● ISSN 1589 1623 (Print) ● ISSN 1785 0037 (Online)
DOI: http://dx.doi.org/10.15666/aeer/1605_59335954
© 2018, ALÖKI Kft., Budapest, Hungary

bacteria; and fungi; 5'-CATTCCCCGTTACCCGTTG-3', NS1: 5'-GTAGTCATATGCTTGTCTC-3' for fungi), and the expected fragments (about 250 bp for bacteria and about 450 bp for fungi) were obtained. The PCR mixture compositions and reaction conditions were the same as above. The PCR products were recovered using the SK1131 UNIQ-10 Column Kit. All reactions were performed in triplicate.

Cloning and sequencing

The target fragments were TA ligated to Takara pMD®18-T vector. According to the methods of published document (Yang et al., 2016), DNA sequencing of one 16S rDNA or 18S rDNA fragment was performed step by step. In the end, we compared these partial 16S and 18S rDNA sequences with sequences deposited in the GenBank database using Blast (http://blast.ncbi.nlm.nih.gov/). The new DNA sequences had been submitted to GenBank with accession numbers MF673132-MF673161.

The DNA sequence results of bacteria and fungi are given in *Attachments 1* and *2*. The similarity values of BLASTN results are in *Table 3* and accession numbers shown in *Attachment 3*.

Statistical analysis of DGGE patterns

Digitized DGGE images were analyzed by Quantity One software (Bio-Rad, USA). The Shannon diversity index (H) and Simpson's (D) index as mathematical measurements have been commonly used to characterize species diversity in a community (Du et al., 2016). DNA bands in gels were identified by Quantity One software (Bio-Rad, USA). Both Shannon diversity index (H) and Simpson's index (D) were calculated based on the number and relative intensities of DGGE bands. The Shannon (H) and Simpson's (D) index were calculated as follows:

$$H = -\sum(P_i)(\ln P_i),$$

$$D = 1 - \sum P_i^2,$$

where p_i is the proportion of i th phylotype.

To further understand the differentiation among DNA fragments from rhizosphere soil samples, the UPGMA (unweighted pair group method with arithmetic means) dendrograms of DGGE band profiles for bacteria and fungus (*Figs. 5* and *6*) were constructed using the clustering algorithm baseetd on the Dice similarity coefficient (*Tables 3* and *4*). The data of diversity index among ten varieties was statistically analyzed by ANOVA program of SAS9.1.3 software. A probability value (P) of < 0.05 was considered statistically significant.

Results

PCR–DGGE analysis of soil samples for ten varieties

In the DGGE gel, DNA fragments of the same length, but with different base-pair sequences, could be separated (Muyzer et al., 1993). The electrophoresis band pattern provided a profile of microbe diversity in rhizosphere soil samples. It is commonly assumed that these profiles and quantitation of peaks (bands) reflects the structure of the community. Concretely speaking, in each lane of the DGGE gel, the visualized

http://www.aloki.hu ● ISSN 1589 1623 (Print) ● ISSN 1785 0037 (Online)
DOI: http://dx.doi.org/10.15666/aeer/1605_59335954
© 2018, ALÖKI Kft., Budapest, Hungary

intensities of DNA bands could respond to relative microbe biomass, and the number of DNA bands might reflect the genetic diversity of microbe community in rhizosphere soil samples. The greater the band number, the more diverse the microbial community is. These individual bands represented different gene fragments or different stable structural conformations of either the bacterial 16S rDNA V3 hypervariable region or the fungal 18S rDNA V1-V2 region. The relative intensity of each band and its position most likely represent the relative abundance of a particular species in the microbial community. Firstly, PCR-DGGE analysis was performed to investigate the microbe diversity of each Triticeae crop variety. The DGGE profiles indicated different bands' patterns for different soil samples (*Figs. 3* and *4*). As seen from DGGE profiles of PCR products of 16S rDNA V3 region in *Figure 3*, it was different in the bands' patterns from soil samples S1-S10 of different varieties, such as the location, intensity and number. Some strong and unique bands were observed in bacterial DGGE patterns of some varieties, while they were not detected in other varieties (*Fig. 3*). For example, Huaimai 18 soil of S3 had bands shown as code number 7, 8 and 10, while other varieties had no such bands. Bands 14 and 6 were observed in Shannong 129 soil of S1 and Yannong 19 soil of S2, respectively. Band 2 was found in rhizosphere soil samples from all crops except Shannong129 (S1). The bands shown as code number 1, 11 and 15 were found in rhizosphere soil samples of Yannong 19, Huaimai 18, and Yumai 34.

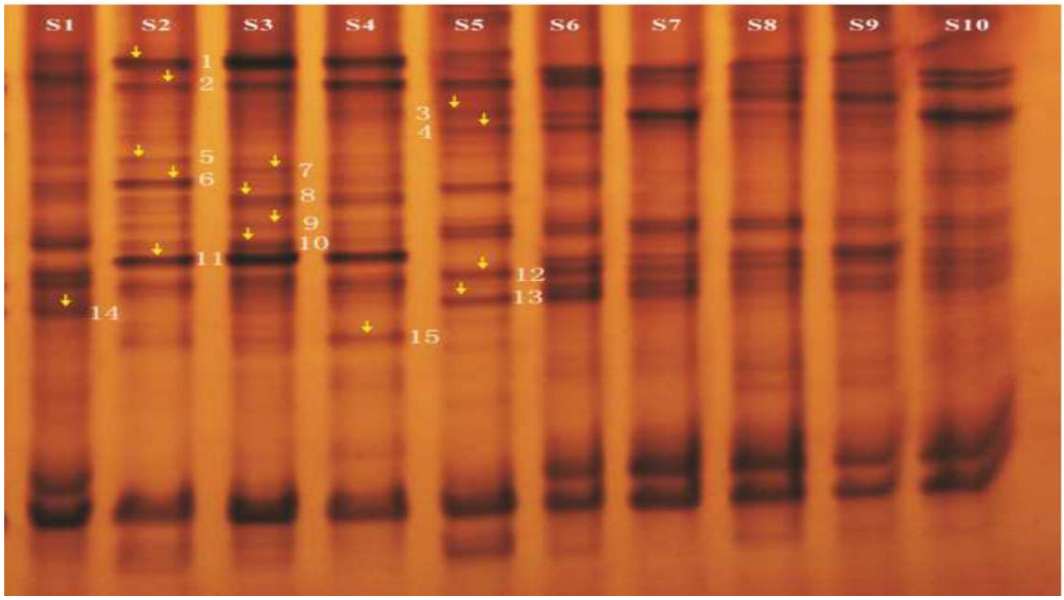

Figure 3. *DGGE analysis of bacterial community profiles of 16S rDNA PCR amplification products of rhizospheric soil samples S1-S10 of 10 different Triticeae crops*

The same situation occurred in fungal DGGE patterns of soil samples of different Triticeae crops. As shown in *Figure 4*, Yumai 34 soil of S4 was observed to show bands 2 and 8 compared to other Triticeae varieties soil; only Shannong zixiaomai soil of S5 was observed to show bands 1 and 3; band 9 was specific to the rhizosphere soil sample of Huaimai 18; band 13 was observed in all rhizosphere soil samples; Shannong 129 and Yumai 34 did not contain the band labeled as code number 15 (*Fig. 4*). The results revealed that the compositions of rhizospheric soil microbial communities including both bacteria and fungi were different among the ten varieties of Triticeae crops.

http://www.aloki.hu ● ISSN 1589 1623 (Print) ● ISSN 1785 0037 (Online)
DOI: http://dx.doi.org/10.15666/aeer/1605_59335954
© 2018, ALÖKI Kft., Budapest, Hungary

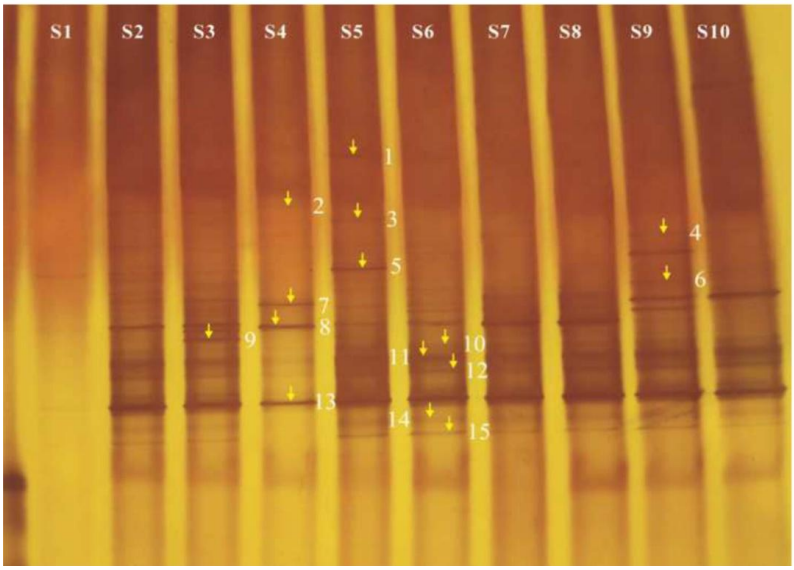

Figure 4. *DGGE analysis of fungal community profiles of 18S rDNA PCR amplification products of rhizospheric soil samples S1-S10 of 10 different Triticeae crops*

Genetic diversity of rhizospheric soil bacterial and fungal communities in soil samples S1-S10 of different Triticeae crop varieties

To investigate the level of microbial diversity, we used the cluster analysis generated by a UPGMA dendrogram to calculate the diversity indices (*Table 2*).

Table 2. *Bacterial and fungi Simpson's and Shannon's method/ Log base of rhizospheric soil samples S1-S10 of different varieties for Triticeae crops*

Varieties for Triticeae crops	Rhizosphere soil samples	Bacteria		Fungus	
		Simpson's Index	Shannon's Index	Simpson's index	Shannon's index
Shannong 129	S1	0.665±0.011 b	3.59±0.06 c	0.663±0.009 e	1.29±0.04 i
Yannong 19	S2	0.574±0.004 cd	2.04±0.06 e	0.779±0.008 b	4.46±0.07 b
Huaimai 18	S3	0.587±0.005 c	2.85±0.09 d	0.796±0.003 a	4.82±0.02 a
Yumai 34	S4	0.570±0.006 de	2.00±0.12 e	0.772±0.007 b	4.25±0.08 c
Shannong zixiaomai	S5	0.562±0.008 e	1.69±0.07 g	0.684±0.001 d	3.70±0.07 e
Heixiaomai 031244	S6	0.676±0.017 a	3.84±0.06 a	0.733±0.010 c	4.06±0.05 d
Wumai 202w22	S7	0.563±0.005 de	1.52±0.04 gh	0.696±0.007 d	2.25±0.09 g
Yavaros F9	S8	0.552±0.009 e	1.45±0.04 h	0.690±0.006 d	2.07±0.06 h
rye 4R	S9	0.669±0.014 a	3.70±0.06 b	0.725±0.005 c	3.39±0.10 f
Taisi 1	S10	0.573±0.004c de	1.78±0.06 f	0.722±0.009 c	3.31±0.13 f

The indices of all soil samples were represented by the mean values with standard deviation and were compared by Duncan's multiple comparison. Different lowercase letters in the same column indicate significant difference ($P < 0.05$)

Diversity indices of the soil bacterial and fungal communities were significantly different among the varieties of soil samples S1-S10 ($P < 0.05$) of Triticeae crops. These findings were mostly consistent with band patterns observed in the DGGE profiles (*Figs. 3* and *4*) and revealed that the diversity of rhizospheric soil bacterial and

http://www.aloki.hu ● ISSN 1589 1623 (Print) ● ISSN 1785 0037 (Online)
DOI: http://dx.doi.org/10.15666/aeer/1605_59335954
© 2018, ALÖKI Kft., Budapest, Hungary

fungal communities was significantly affected by different varieties of Triticeae crops ($P < 0.05$). Reports have that 'interband' regions were considered as a potential source for less dominant members of natural microbial communities, and indicate that including such members might be a better fit for the use of Shannon index. Our study results showed that the Shannon index of a variety was high and its Simpson index was also high, and the differences of Shannon index between the varieties were greater than those of Simpson index (*Table 2*).

The Shannon index was more suitable than the Simpson index for reflecting microbial community diversity. Among the ten soil samples in this experiment, Heixiaomai 031244 (S6) had the highest bacterial diversity indices, followed by rye 4R (S9) and Shannong 129 (S1). The lowest diversity was shown in Yavaros F9 (S8) (*Table 2*). However, in terms of fungal community diversity, Huaimai 18 (S3) had the highest diversity indices, followed by Yannong 19 (S2), Yumai 34 (S4), Heixiaomai 031244 (S6), rye 4R (S9) and Taisi 1 (S10). The lowest level of diversity was exhibited in Shannong 129 (S1). To further understand the differences among microbial community structures of each sample, we constructed a UPGMA dendrogram with the 16S rDNA and 18S rDNA fragments (about 250 bp and 450 bp, respectively) and community Dice Coefficient for samples S1-S10 (*Figs. 5* and *6*, *Tables 3* and *4*).

Table 3. *The Dice coefficient calculated by DGGE profiles of bacterial 16S rDNA PCR amplification products from rhizospheric soil samples S1-S10 from different varieties of several Triticeae crops*

Lane	S1	S2	S3	S4	S5	S6	S7	S8	S9	S10
S1	1.000									
S2	0.544	1.000								
S3	0.443	0.666	1.000							
S4	0.489	0.691	0.645	1.000						
S5	0.442	0.329	0.254	0.342	1.000					
S6	0.534	0.645	0.461	0.601	0.536	1.000				
S7	0.415	0.499	0.412	0.567	0.433	0.776	1.000			
S8	0.424	0.329	0.278	0.339	0.388	0.462	0.543	1.000		
S9	0.299	0.353	0.390	0.284	0.301	0.277	0.260	0.455	1.000	
S10	0.355	0.436	0.404	0.474	0.343	0.447	0.582	0.602	0.363	1.000

Table 4. *The Dice coefficient calculated by DGGE profiles of bacterial 18S rDNA PCR amplification products from rhizosphere soil samples S1-S10 from different varieties of several Triticeae crops.*

Lane	S1	S2	S3	S4	S5	S6	S7	S8	S9	S10
S1	1.000									
S2	0.159	1.000								
S3	0.337	0.558	1.000							
S4	0.000	0.352	0.186	1.000						
S5	0.248	0.418	0.562	0.265	1.000					
S6	0.065	0.342	0.498	0.349	0.519	1.000				
S7	0.000	0.151	0.299	0.247	0.200	0.453	1.000			
S8	0.245	0.255	0.445	0.065	0.328	0.331	0.461	1.000		
S9	0.220	0.358	0.417	0.118	0.365	0.332	0.547	0.480	1.000	
S10	0.219	0.217	0.191	0.081	0.222	0.128	0.205	0.561	0.415	1.000

http://www.aloki.hu ● ISSN 1589 1623 (Print) ● ISSN 1785 0037 (Online)
DOI: http://dx.doi.org/10.15666/aeer/1605_59335954
© 2018, ALÖKI Kft., Budapest, Hungary

Even though the diversity indices of microbial communities in some rhizospheric soil samples such as S9 and S10 in the fungus community were similar to each other, as seen in *Table 2,* the population structures of microorganisms in these soil samples were different as indicated in *Figure 5* or *Figure 6*. In the bacterial community of rhizospheric soil samples, five main clusters were detected in the condition of a Dice Coefficient of 0.53 (*Fig. 5*). in the condition of a Dice Coefficient of 0.78, only S6 (Heixiaom 031244) and S7 (Wumai 202W22) were clustered into a group (*Fig. 5*). The two varieties were black and high-gluten common wheat, but S6 is winter wheat but S7 is spring wheat. In the condition of a Dice Coefficient of 0.69, S2 (Yannong 19) and S4 (Yumai 34) were also clustered into a group. The two varieties were white and high-gluten common wheat, but S2 is winter wheat but S4 is spring wheat. In the condition of a Dice Coefficient of 0.66, S2, S4 and S3 (Huaimai 18) were further clustered into a group. Huaimai 18 was a white, middle-gluten and half-winter common wheat variety. In the same manner, in the condition of a Dice Coefficient of 0.53, the above-mentioned five varieties were clustered a group. The control of Shannong 129 (red and middle-gluten) was significant different with above-mentioned five varieties in the bacteria community structure. It inferred that bacteria community structure of wheat varieties could be related with grain color as well as grain quality. Besides, in the condition of a Dice Coefficient of 0.60, the durum wheat S8 (Yavaros F9) and triticle S10 (Taisi 1) were clustered into a group.

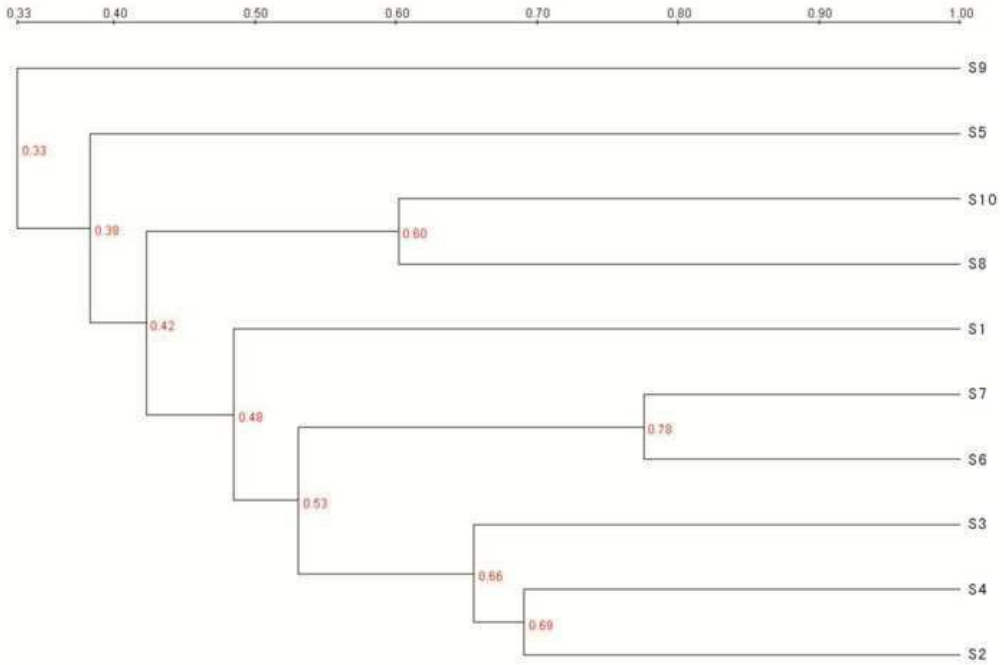

Figure 5. *UPGMA dendrogram constructed with DGGE profiles of bacterial 16S rDNA PCR amplification products from rhizospheric soil samples S1-S10 from different varieties of several Triticeae crops*

So, in the similarity level of 0.53, five main clusters were detected. One cluster was found in S3, S2, S4, S6 and S7. Another cluster was observed in S8 and S10. Besides, S9 (rye 4R), S5 (Shannong zixiaomai) and S1 (Shannong 129) stood in three clusters,

http://www.aloki.hu ● ISSN 1589 1623 (Print) ● ISSN 1785 0037 (Online)
DOI: http://dx.doi.org/10.15666/aeer/1605_59335954
© 2018, ALÖKI Kft., Budapest, Hungary

respectively. However, in terms of a Dice Coefficient of 0.48, S1, S2, S3, S4, S6 with S7 could form a new cluster. If the Dice Coefficient was 0.42, the above-mentioned new cluster and S8 as well as S10 furthermore composed a bigger cluster. Till a Dice Coefficient of 0.33, all of ten varieties stood in only one cluster. On the contrary, when the Dice Coefficient was greater than 0.78, ten varieties had 10 clusters. Similarly, in the condition of a Dice Coefficient of 0.51, six main clusters were found in the fungal community of rhizospheric soil samples (*Fig. 6*). These included a cluster formed by S6 and S5 with S3, a cluster shared by S9 and S7, a cluster containing S8 and S10, and else three clusters formed by S1, S2 and S4, respectively. The larger the Dice coefficient, the more clusters. In contrast, the smaller the Dice coefficient, the less clusters. When the Dice Coefficient was 0.44, S2, S3, S5 & S6 formed a cluster. When the Dice Coefficient was 0.39, S7, S8, S9 & S10 form a cluster. When the Dice Coefficient was 0.29, above mentioned the two clusters formed a new cluster. Ten varieties were clustered into 10 classes when the Dice Coefficient was greater than 0.56 (*Fig. 6*). Just the opposite, ten varieties were clustered into one class when the Dice Coefficient was less than 0.17. Therefore, the changes in bacterial and fungal community structure were distinct in different varieties of Triticeae crops.

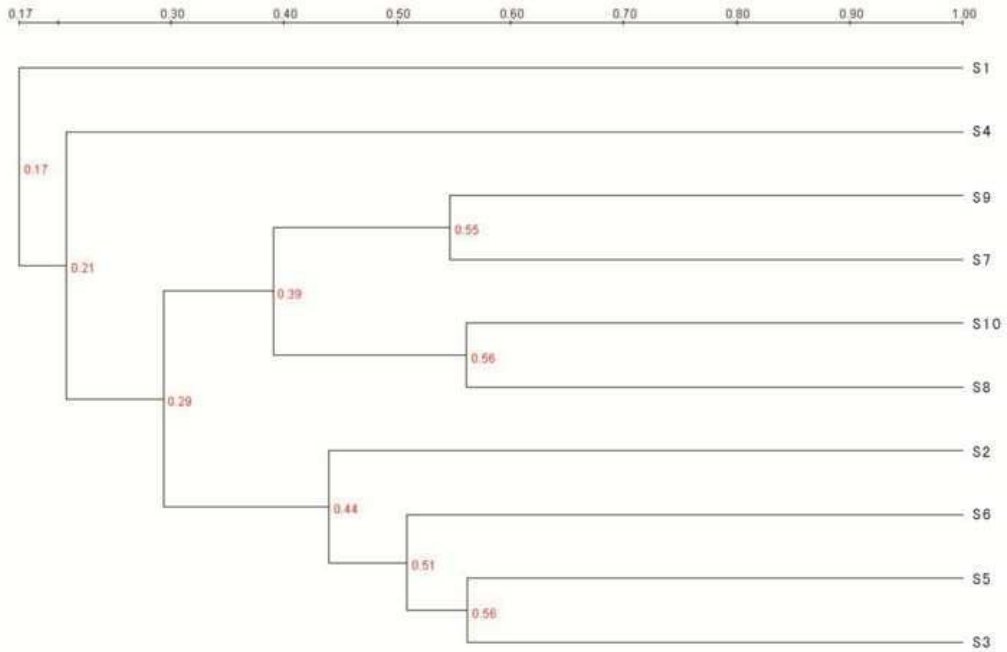

Figure 6. *UPGMA dendrogram constructed with DGGE profiles of bacterial 18S rDNA PCR amplification products from rhizosphere soil samples S1-S10 from different varieties of several Triticeae crops*

Bacterial and fungal community changes in different rhizospheric soil samples

To identify the microbial species in each sample, 15 common and specific excised bands were selected from bacterial and fungi DGGE gels of rhizosphere soil samples, respectively (*Figs. 3* and *4*). The PCR product was recovered from each excised band. Following the sequencing of all PCR products, the sequences obtained were compared with public DNA database sequences by BLASTN on the NCBI web server. The results of sequence comparisons were shown in *Tables 5* and *6*.

http://www.aloki.hu ● ISSN 1589 1623 (Print) ● ISSN 1785 0037 (Online)
DOI: http://dx.doi.org/10.15666/aeer/1605_59335954
© 2018, ALÖKI Kft., Budapest, Hungary

Table 5. *Identification of bacteria species for fifteen bands sequenced from rhizosphere soil samples S1-S10 of different varieties -from several Triticeae crops*

Code number of bands in *Fig. 3*	Accession number in NCBI	V3 Region	Similarity (%)	Bacterium identification
1	MF673132	170bp	88.3	Uncultured *alpha proteobacterium*
2	MF673133	190bp	93.3	*Flavobacterium phragmitis*
3	MF673134	188bp	85.1	Uncultured bacterium
4	MF673135	189bp	92.3	Uncultured *Sphingobacteriales* bacterium
5	MF673136	195bp	90.4	Uncultured *Acidobacteria* bacterium
6	MF673137	188bp	92.7	Uncultured bacterium
7	MF673138	195bp	78.8	Uncultured bacterium
8	MF673139	189bp	97.8	Uncultured bacterium
9	MF673140	194bp	93	Uncultured *gamma proteobacterium*
10	MF673141	189bp	91.3	Uncultured bacterium
11	MF673142	196bp	88.9	Uncultured bacterium
12	MF673143	195bp	100	*Pantoea* sp.
13	MF673144	195bp	91.5	Uncultured *Acidobacteria* bacterium
14	MF673145	170bp	88.4	Uncultured *Chloroflexi* bacterium
15	MF673146	170bp	85.4	*Bdellovibrio* sp.

Table 6. *Identification of fungus for fifteen bands sequenced from rhizospheric soil samples S1-S10 of different varieties from several Triticeae crops*

Code number of bands in *Fig. 4*	Accession number in NCBI	V1-V2 Region	Similarity (%)	Fungal identification
1	MF673147	351bp	99	Uncultured *Eukaryote clone*
2	MF673148	347bp	99	*Xylariales* sp.
3	MF673149	359bp	99	Uncultured fungus
4	MF673150	354bp	98	Uncultured Eukaryote
5	MF673151	361bp	97	*Xenillus tegeocranus*
6	MF673152	354bp	99	Balen uncultured Eukaryote
7	MF673153	392bp	99	Uncultured fungus
8	MF673154	378bp	93	Uncultured *Eukaryote*
9	MF673155	362bp	98	*Nabis ferus*
10	MF673156	399bp	99	Uncultured *Eukaryote*
11	MF673157	354bp	98	Uncultured *Eukaryote*
12	MF673158	348bp	99	*Malbranchea cinnamomea*
13	MF673159	399bp	99	Uncultured Eukaryote
14	MF673160	399bp	99	Uncultured Eukaryote
15	MF673161	399bp	99	Uncultured Eukaryote

Digitized DGGE images were analyzed by Quantity One software (Bio-Rad, USA). The software can detect the presence or absence of individual bands in all lanes by binary matrix. In total, 30 detectable microbial species were identified, each band representing a different microbial species. The results indicated that some bacteria or

http://www.aloki.hu ● ISSN 1589 1623 (Print) ● ISSN 1785 0037 (Online)
DOI: http://dx.doi.org/10.15666/aeer/1605_59335954
© 2018, ALÖKI Kft., Budapest, Hungary

fungi were detected only in certain crops. For example, uncultured *Chloroflexi* bacterium was detected in Shannong 129 (S1), while uncultured *Sphingobacteriales* bacterium was detected in Shannong zixiaomai (S5) and Heixiaomai 031244 (S6) only. *Nabis ferus* and *Xylariales* sp. were detected only in the rhizosphere soils of Huaimai 18 (S3) and Yumai 34 (S4), respectively. *Xenillus tegeocranus* was detected in Shannong 129 (S1), Yannong 19 (S2), Huaimai 18 (S3), and Shannong zixiaomai (S5), but not detected in the rhizosphere soils of other samples. By identifying the microbial species from different samples, our research demonstrated that the effects of different Triticeae crops on bacterial and fungal community diversity in rhizospheric soils were obvious.

In addition, we found some common bands in soil samples of some different varieties, which indicated there were similarities among the populations of microorganisms that existed in these rhizospheric soils. In the bacterial community, there was one common band coded the number of 2 (*Flavobacterium phragmitis*) in other nine varieties except Shannong 129 (*Fig. 3*). The else bands were specific in some varieties. For example, the uncultured *alpha proteobacterium* (band code 1 in *Fig. 3*), *Flavobacterium phragmitis* (band code 2 in *Fig. 3*), uncultured bacterium (band code 11 in *Fig. 3*), and *Bdellovibrio* sp. (band code 15 in *Fig. 3*) were commonly found in rhizospheric soil samples of common wheat crops, including Yannong 19, Huaimai 18 and Yumai 34 (S2, S3 and S4 in *Fig. 3,* respectively). As for the fungal community, there was only one common band coded the number of 13 (uncultured *Eukaryote*) in all soil samples (*Fig. 4*). The uncultured *Eukaryote* (band code 15 in *Fig. 4*) was common across all crops except Shannong 129 and Yumai 34 samples (S1 and S4 in *Fig. 4,* respectively). *Xenillus tegeocranus* (band code 5 in *Fig. 4*) was found in rhizospheric soil samples of common wheat crops, including Shannong 129, Yannong 19, Huaimai 18 and Shannong zixiaomai (S1, S2, S3 and S5 in *Fig. 4,* respectively). These common microorganisms indicated that there were some shared characteristics among wheat varieties.

Discussion

The climate features of Shanxi province provide natural and long-standing advantages such as adequate sunlight, moderate mean temperature, large temperature difference between day and night and abundant seed resources for wheat production (Tian et al., 2013). However, drought, a major Shanxi's climate characteristic, on the one hand is beneficial to accumulate protein during grain filing period, and on the other hand is responsible to limit the growth and development of wheat and has resulted in a continuously decreasing planting area of wheat in recent years. The planting area of wheat is currently about 720,000 hectares in Shanxi province, which is not enough to meet market demand. In addition, Shanxi wheat is supposed to contain the protein content of more than 14% on the average, however its wet-gluten content (28%-30% on the average) is lower than that of a large quantity of high quality wheat flour (more than 30%) for processing bread or dumpling. Therefore, it is necessary to introduce high-quality wheat varieties and improve local wheat variety quality for meeting consumer demand. In addition, the Shanxi provincial government has proposed to adjust the agricultural planting structure, which is to reduce the planting area of corn and increase that of feed crops to develop livestock and poultry production.

Previous evidence has shown that wheat cultivars were involved in shaping the rhizosphere by differentially altering the bacterial community (Aaron et al., 2017). The

http://www.aloki.hu ● ISSN 1589 1623 (Print) ● ISSN 1785 0037 (Online)
DOI: http://dx.doi.org/10.15666/aeer/1605_59335954
© 2018, ALÖKI Kft., Budapest, Hungary

differences in microbial communities observed on different wheat lines showed that wheat breeding could affect rhizospheric communities (Aaron et al., 2017). Yang ZP (one of the authors) had studied the number of rhizosphere soil microbial populations (including bacterial, fungi and actinomycetes) with that of non-rhizosphere soil of 24 crops in north China using the plate culture method. The results revealed that the microbial population of rhizosphere soil was significantly higher than that of non-rhizosphere soil, which was consistent with previous studies (Lou, 1962; Chen, 1990; Takuya, 1990). Besides, in the previous studies by author, 120 varieties from different wheat areas were introduced and planted to Jinzhong wheat area of Shanxi province. Some of the varieties, which were suitable for local ecological climatic conditions and of higher yield-quality than others were selected. For reasons mentioned above, in this experiment, rhizosphere soil was regarded as research object to compare the differences between the introduced varieties from other wheat region and local varieties of Shanxi in rhizosphere soil microbial diversity. Triticeae varieties including nine introduced high-quality wheat / rye / triticale varieties and one local variety (Shannong 129 as control) were selected for preliminarily investigating rhizospheric soil bacterial and fungal community diversity in the Jinzhong region. This study was also conducted for providing theoretical basis for further analyzing the correlation of these indices with grain protein as well as wet-gluten contents to evaluate whether rhizospheric soil microbial community diversity can be used as an accessory ecological indicator on the basis of grain yield and quality for screening varieties. Shannong 129 is a local breeding late maturity winter wheat variety belongs to the northern area of China, and planted widely in the Shanxi wheat region region and fit to the local ecological environment conditions. The other varieties were introduced from other different wheat production regions. In order to expand Triticeae crop resources in Shanxi province, these high quality Triticeae crops were introduced and further investigated their microbial community structures compared with Shannong 129.

Rhizospheric soil is of great importance to plant health and soil fertility. The plant can affect its rhizospheric microbial communities by releasing root exudates (Glick, 1995; Kourtev et al., 2003; Andersen and Winding, 2004;), which are made up of saccharides, organic acid, amino acid, phenolic compound etc (Xiong et al., 2002). The amount and types of root exudates as well as allelopathy differ between crop species. Root exudates could provide a large amount of nutritional energy, stimulate species-specific shifts in the soil microbial community, and make changes to microbial community distribution (Xiong et al., 2002; Welbaum et al., 2004; Singh et al., 2007; Xu et al., 2009; van Dam and Bouwmeester, 2016). A general role for root exudates is becoming evident in repelling or attracting pathogenic or beneficial organisms, inhibiting growth of competing plant species, and altering soil properties (Bais et al., 2006; Weston et al., 2012). For instance, in terms of three hydroponic plants including *Ipomoea aquatica, Chlorophytum comosum* and *Oenanthe javanica,* the effects of organic acid in their root exudates on bacteria were not different, a positive effect on some bacteria, such as ammonifying and denitrifying bacteria and an inhibitory effect on others such as nitrobacteria and nitrosobacteria (Zhu and Cheng, 2011).

Previous studies have showed that plants could “shape” the microbial communities in their rhizosphere by attracting beneficial microorganisms that in turn could suppress the growth of pathogenic microbes either through direct competition or by priming the plant’s own defenses (Marschner et al., 2004; Miao et al., 2004; Doornbos et al., 2012; Aaron et al., 2017; Schlemper et al., 2017). In our study, it was founded that there were

http://www.aloki.hu ● ISSN 1589 1623 (Print) ● ISSN 1785 0037 (Online)
DOI: http://dx.doi.org/10.15666/aeer/1605_59335954
© 2018, ALÖKI Kft., Budapest, Hungary

differences in the community structures of rhizospheric soil organisms (*Figs. 3* and *4*) and the diversity indices (*Table 2*) among wheat varieties, indicating that different varieties of wheat could obviously cause shifts in the composition of dominant populations about rhizospheric microbial communities through DGGE profiles. This conclusion is consistent with previous research (Miao et al., 2004), which showed that numbers of three main species of rhizospheric microbes were much more different after planting different crops on unused soil 2 m below ground.

Generally thought is that the larger the Shannon's index, the more diverse will be the components of microbial population. Similarly, the larger the Simpson's index, the richer will be the number of microbial population. Our results indicated that the Shannon's index and Simpson's index of Heixiaomai 031244 were highest among the bacterial communities in rhizospheric soils of ten varieties ($P < 0.05$). This suggested that Heixiaomai 031244 was the most beneficial variety for improving the diversity and abundance of bacterial communities in rhizospheric soils. The second variety was rye 4R. Similarly, the Shannon's index and Simpson's index of Huaimai 18 the highest among the fungal communities in rhizospheric soils of ten varieties ($P < 0.05$). Huaimai 18 was the most beneficial variety for increasing the diversity and abundance of fungal communities in rhizospheric soils, followed by Yannong 19 and Yumai 34. This suggests that Heixaomai 031244 and Huaimai 18 could be the two best species of seven common wheat varieties introduced into the Jinzhong region of Shanxi province according to Shannon's and Simpson's indexes. The rye 4R was second only to Heixiaomai 031244 in terms of bacterial community diversity. Yannong 19 and Yumai 34 were just behind Huaimai 18 in terms of fungal community diversity. It could be introduced to the Jinzhong region as a feed crop in planting structure adjustment.

Microbial species recognition by cloning and sequencing 16S rDNA or 18S rDNA fragments showed that crop species could stimulate specific microbial species while also causing the loss of others, thereby affecting rhizospheric soil microbial communities (Yang et al., 2016). Our study observed significant stimulation of uncultured bacterium (code No. 8, 7 and 10 in *Table 5,* respectively) and *Nabis ferus* (code No. 9 in *Table 6*), as well as the loss of uncultured *Sphingobacteriales* bacterium (code No. 4 in *Table 5*) and *Xylariales* sp. (code No. 2 in *Table 6*) in Huaimai 18. In addition, our studies hinted a relatively strong species-specific pattern on rhizospheric soil microbial community structure. Uncultured *Chloroflexi* bacterium was only found in the rhizosphere soil growing Shannong 129. Uncultured *alpha proteobacterium, Flavobacterium phragmitis,* uncultured bacterium, and *Bdellovibrio* sp. were observed in common wheat including Yannong 19, Huaimai 18 and Yumai 34. Uncultured eukaryote (code No. 13 in *Table 6*) was found in all experimental samples. The wheat cultivar-associated microbes identified in this work could provide beneficial services to their hosts, such as the utilization of organic matter, the degradation of hydrocarbons, and the cycling of respiratory sulfur and nitrogen (Chen et al., 2016; Dombrowski et al., 2017). Observable differences in microbial species of Triticeae crops in the present work could be related to root exudates which select and increase microbes associated with mineral mobilization and nutrient responsive metabolisms, such as nitrogen, sulfur and phosphorus (Aaron et al., 2017). Root exudates are intrinsic factors of rhizospheric effects. There is evidence to suggest that microbes are recruited through root exudates, and the greatest release may occur during the reproductive stages (Zhang et al., 2009; Lakshmanan et al., 2013). For example, Neal et al. (2012) demonstrated a central role in root exudates of maize, as a semiochemical below ground for recruitment of plant-

http://www.aloki.hu ● ISSN 1589 1623 (Print) ● ISSN 1785 0037 (Online)
DOI: http://dx.doi.org/10.15666/aeer/1605_59335954
© 2018, ALÖKI Kft., Budapest, Hungary

beneficial rhizobacteria during the relatively young and vulnerable growth stages of maize. Plant hosts could benefit from these microbes with improved growth, drought and salt tolerance, and protection against soilborne pathogens (Kasim et al., 2013; Glick et al., 2014; de Boer et al., 2015). More interestingly, many uncultured organisms were observed when these Triticeae crop varieties were introduced into the Jinzhong region. In that way, in the course of wheat production, what might be the material cycle process that these specific microbial species or uncultured organisms could be mainly involved in? What would be dominant microbial populations? These issues will be further discussed in the future.

It is worth mentioning that the rhizospheric bacterial diversity of Shannong 129 was higher than that of Huaimai 18 (S3) or Yannong 19 (S2), while fungal diversity was much lower as above mentioned (*Table 2*). However, our previous studies showed that the grain qualities of Shannong 129 were lower, but its grain yield was higher than that of Yannong 19, whereas both the grain yield and qualities of Shannong 129 were higher than those of Huaimai 18. Considering Huaimai 18 and Yannong 19 have more than 60% similarity in bacterial community structure and a similar quality of grain, we speculate that various dominant and functional organisms enhanced in these two varieties (Uncultured *alpha proteobacterium, Flavobacterium phragmitis,* uncultured bacterium, *Pantoea* sp., *Bdellovibrio* sp., *Xenillus tegeocranus,* and uncultured eukaryote) imply a potential relationship between the yield increase of crops and microbial diversity.

Conclusion

Our study highlighted that variation of rhizospheric soil microbial community diversity is related to different Triticeae varieties. Among the ten experimental varieties, Heixiaomai 031244 was the most beneficial to improving the diversity and abundance of bacterial communities in rhizospheric soils, and Huaimai 18 was the most beneficial to increasing the diversity and abundance of fungal communities in rhizospheric soils. Different wheat varieties across wheat regions could induce an increase in some functional and uncultured rhizospheric soil organisms, such as uncultured *alpha proteobacterium, Flavobacterium phragmitis,* uncultured bacterium, *Bdellovibrio* sp., uncultured *Sphingobacteriales* bacterium, uncultured *Acidobacteria* bacterium, *Nabis ferus* and uncultured *Eukaryote,* suggesting some potential relationship between crop yield increase and microbes in new wheat varieties when compared with local original wheat variety. Our study strongly suggested that Huaimai 18, Yannong 19, and Heixiaomai 031244 could be considered for introduction to the Jinzhong region to develop high quality wheat variety resources for Shanxi. Additionally, rye 4R could be introduced to the Jinzhong region as a feed crop in planting structure adjustment. Further studies should be conducted to examine the exact mechanisms of these uncultured rhizospheric organisms and their interactions with specific crop species. Further to find whether these microorganisms affect grain quality formation and accumulation will be discussed in a follow-up study.

Acknowledgements. This study was supported by the National Key Technology R&D Program of China (2015BAD23B04-2), National Natural Science Foundation of China (31101113), Special Funds for Scientific Research on Public Causes (201503120), Research Project Supported by Shanxi Scholarship Council of China (2015-Key 4), fund for Shanxi "1331 Project", Earmarked Fund for Modern Agro-industry Technology Research System (CARS-03-01-24), Shanxi Youth Fund (20031047), and Shanxi Agricultural University Post-doctoral Fund (No. 112124).

http://www.aloki.hu ● ISSN 1589 1623 (Print) ● ISSN 1785 0037 (Online)
DOI: http://dx.doi.org/10.15666/aeer/1605_59335954
© 2018, ALÖKI Kft., Budapest, Hungary

REFERENCES

[1] Aaron, K. M., Chuntao, Y., Scot, H. H. (2017): Community structure, species Variation, and potential functions of rhizosphere-associated bacteria of different winter wheat (*Triticum aestivum*) cultivars. – Frontiers in Plant Science 8: 132.
[2] Acosta-Martínez, V., Burow, G., Zobeck, T. M., Allen, V. G. (2010): Soil microbial communities and function in alternative systems to continuous cotton. – Soil Science Society of America Journal 74: 1181-1192.
[3] Aira, M., Gomez-Brandon, M., Lazcano, C., Bååth, E., Domínguez, O. (2010): Plant geno-type strongly modifies the structure and growth of maize rhizosphere microbial communities. – Soil Biology and Biochemistry 42: 2276-2280.
[4] Andersen, K. S., Winding, A. (2004): Non-target effects of bacterial biological control agents on soil Protozoa. – Biology and Fertility of Soils 40: 230-236.
[5] Bais, H. P., Weir, T. L., Perry, L. G., Gilroy, S., Vivanco, J. M. (2006): The role of root exudates in rhizosphere interations with plants and other organisms. – Annual Review of Plant Biology 57: 233-266.
[6] Brock, T. D. (1987): The study of microorganisms in situ: progress and problems. – Symposium of the Society for General Microbiology 41: 1-17.
[7] Buyer, J. S., Teasdale, J. R., Roberts, D. P., Zasada, I. A., Maul, J. E. (2010): Factors affecting soil microbial community structure in tomato cropping systems. – Soil Biology and Biochemistry 42: 831-841.
[8] Chen, J., Han, Y., Wang, Y., Gong, B., Zhou, J., Qing, X. (2016): Start-up and microbial communities of a simultaneous nitrogen removal system for high salinity and high nitrogen organic wastewater via heterotrophic nitrification. – Bioresource Technology 216: 196-202.
[9] Chen, W. X. (1990): Soil and Environment Microbiology (1st ed.). – Beijing Agricultural University Press, Beijing, pp. 202-204 (in Chinese).
[10] de Boer, W., Hundscheid, M. P., Klein, G. P. J., de Ridder-Duine, A. S., Thion, C., van Veen, J. A., et al. (2015): Antifungal rhizosphere bacteria can increase as response to the presence of saprotrophic fungi. – PLos One 10(9): e0137988.
[11] Dombrowski, N., Seitz, K. W., Teske, A. P., Baker, B. J. (2017): Genomic insights into potential interdependencies in microbial hydrocarbon and nutrient cycling in hydrothermal sediments. – Microbiome 5(1): 106.
[12] Doornbos, R. F., van Loon, L. C., Bakker, P. A. (2012): Impact of root exudates and plant defense signaling on bacterial communities in the rhizosphere. A review. – Agronomy for Sustainable Development 32(1): 227-243.
[13] Doran, J. W., Zeiss, M. R. (2000): Soil health and sustainability: managing the biotic component of soil quality. – Applied Soil Ecology 15: 3-11.
[14] Du, Y. X., Xie, B. M., Cai, H. S., Tang, L., Guo, C. H. (2016): Structural and functional diversity of rhizosphere microbial community of nine plant species in the Daqing Saline-alkali soil region. – Acta Ecologica Sinica 3: 740-747.
[15] FAOSTAT (2017): http://www.fao.org/faostat.
[16] Glick, B. R. (1995): The enhancement of plant growth by free-living bacteria. – Canadian Journal of Microbiology 41: 109-117.
[17] Glick, B. R. (2014): Bacteria with ACC deaminase can promote plant growth and help to feed the world. – Microbiological Research 169: 30-39.
[18] Gomes, N. C., Fagbola, O., Costa, R., Rumjanek, N. G., Buchner, A., Mendona-Hagler, L. (2003): Dynamics of fungal communities in bulk and maize rhizosphere soil in the tropics. – Applied and Environmental Microbiology 69: 3758-3766.
[19] Guriguis, M. A., Kunc, F., Vancura, V. (1969): Presence and oxidation of amino acids in rhizosphere and nonrhizosphere soil. – Folia Microbiology 14: 1-12.
[20] He, W., Miao, G., Zhang, Y. (2006): Study on wheat quality zone in Shanxi province. – Journal of Shanxi Normal University (Natural Science Edition) 20(2): 82-83.

http://www.aloki.hu ● ISSN 1589 1623 (Print) ● ISSN 1785 0037 (Online)
DOI: http://dx.doi.org/10.15666/aeer/1605_59335954
© 2018, ALÖKI Kft., Budapest, Hungary

[21] Jia, Z. H., Sun, M., Yang, Z. P. (2004a): Influence of different fertilizers to crop rhizosphere microorganisms. – Acta Agronomica Sinica 30(5): 491-495 (in Chinese).
[22] Jia, Z. H., Yang, Z. P., Zhang, Y. Q. (2004b): Study on the quantity of three main molony of soil microbe in wheat farmland. – Journal of Triticeae Crops 24(3): 53-56 (in Chinese).
[23] Joergensen, R. G. (2000): Ergosterol and microbial biomass in the rhizosphere of grassland soils. – Soil Biology and Biochemistry 32: 647-652.
[24] Kasim, W. A., Osman, M. E., Omar, M. N., El-Daim, I. A. A., Bejai, S., Meijer, J. (2013): Control of drought stress in wheat using plant-growth-promoting bacteria. – Journal of Plant Growth Regulation 32: 122-130.
[25] Kaya, Y., Akcura, M. (2014): Effects of genotype and environment on grain yield and quality traits in bread wheat (*T. aestivum* L.). – Food Science and Technology 34(2): 386-393.
[26] Kourtev, P., Ehrenfeld, J., Häggblom, M. (2003): Experimental analysis of the effect of exotic and native plant species on the structure and function of soil microbial communities. – Soil Biology and Biochemistry 35: 895-905.
[27] Lakshmanan, V., Castaneda, R., Rudrappa, T., Bais, H. P. (2013): Root transcriptome analysis of *Arabidopsis thaliana* exposed to beneficial *Bacillus subtilis FB17* rhizobacteria revealed genes for bacterial recruitment and plant defense independent of *malate efflux*. – Planta 238: 657-668.
[28] Li, F. D. (1993): Prosperous areas of current soil microbiology. – Acta Pedologica Sinica 30(3): 229-235 (in Chinese).
[29] Liu, T. T., Wang, B. Q., Yang, Z. P., Sun, M., Hao, J. M., Du, T. Q. (2015): Development Behavior and quality properties of nine winter wheat varieties from the Yellow-Huai River and Yangtse River middle-downstream winter wheat zone in Jinzhong. – Journal of Triticeae Crops 2: 182-191 (in Chinese).
[30] Lou, L. H. (1962): Roles of Soil Microbial on the Change of Soil Nutrient (1st ed.). – Science Press, Beijing, pp. 283-287 (in Chinese).
[31] Lü, Y. H., Qin, S. Y. (2002): Soil Measure and Fertilization. – Chinese Agricultural Press, Beijing, pp. 48-84.
[32] Ma, J. J., Yang, Z. P., Xia, Q., Wang, B. Q., Sun, M., Gao, Z. Q. (2016): Study on yield and quality traits of color wheat varieties in Jinzhong wheat area. – Journal of Shanxi Agricultural Sciences 11: 1615-1618, 1668.
[33] Marschner, P., Crowley, D., Yang, C. H. (2004): Development of specific rhizosphere bacterial communities in relation to plant species, nutrition and soil type. – Plant and Soil 261: 199-208.
[34] Martin, J. K. (1977): Factors influencing the loss of organic carbon from wheat roots. – Soil Biology and Biochemistry 9: 1-7.
[35] Miao, G. Y., Jia, Z. H., Yang, Z. P., Zhang, Y. Q. (2004): Quantity difference of rhizosphere microbe of different crops. – Journal of Shanxi Agricultural University 24(2): 93-96 (in Chinese).
[36] Muyzer, G., De Waal, E. C., Uitterlinden, A. G. (1993): Uitterlinden. Profiling of complex microbial populations by denaturing gradient gel electrophoresis analysis of polymerase chain reaction-amplified genes coding for 16S rRNA. – Applied and Environmental Microbiology 59(3): 695-700.
[37] Neal, A. L., Ahmad, S., Gordon-weeks, R., Ton, J. (2012): Benzoxazinoids in root exudates of maize attract *Pseudomonas putida* to the rhizosphere. – PLos One 7: e35498.
[38] Nelson, A., Frick, B., Clapperton, J., Quideau, S., Spaner, D. (2008): Does wheat cultivar choice affect crop quality and soil microbial communities in cropping systems? – 16th IFOAM Organic World Congress, Modena, Italy, June 16-20, 2008.
[39] Niemi, R. M., Heiskanen, I., Wallenius, K., Lindström, K. (2001): Extraction and purification of DNA in rhizosphere soil samples for PCR-DGGE analysis of bacterial consortia. – Journal of Microbiological Methods 45: 155-165.

http://www.aloki.hu ● ISSN 1589 1623 (Print) ● ISSN 1785 0037 (Online)
DOI: http://dx.doi.org/10.15666/aeer/1605_59335954
© 2018, ALÖKI Kft., Budapest, Hungary

[40] Nuttall, J. G., O'Leary, G. J., Panozzo, J. F., Walker, C. K., Barlow, K. M., Fitzgerald, G. J. (2017): Models of grain quality in wheat—A review. – Field Crops Research 202: 136-145.
[41] Piromyou, P., Buranabanyat, B., Tantasawat, P., Tittabutr, P., Boonkerd, N., Teaumroong, N. (2011): Effect of plant growth promoting rhizobacteria (PGPR) inoculation on microbial community structure in rhizosphere of forage corn cultivated in Thailand. – European Journal of Soil Biology 47: 44-54.
[42] Sainia, V. K., Bhandarib, S. C., Tarafdar, J. C. (2004): Comparison of crop yield, soil microbial C, N and P, N-fixation, nodulation and mycorrhizal infection in inoculated and non-inoculated sorghum and chickpea crops. – Field Crops Research 89: 39-47.
[43] Schlemper, T. R., Leite, M. F., Lucheta, A. R., Shimels, M., Bouwmeester, H. J., van Veen, J. A., Kuramae, E. E., Bouwmeester, J. A. van Veen, et al. (2017): Rhizobacterial community structure differences among sorghum cultivars in different growth stages and soils. – Federation of European Microbiology Ecology 93(8).
[44] Singh, B. K., Munro, S., Potts, J. M., Millard, P. (2007): Influence of grass species and soil type on rhizosphere microbial community structure in grassland soils. – Applied Soil Ecology 36: 147-155.
[45] Su, L., Yang, Z., Xia, Q. (2017): Grain yield and quality traits research of Canada durum wheat in Jinzhong region. – Journal of Shanxi Agricultural University (Natural Science Edition) 37(3): 158-163 (in Chinese).
[46] Takuya, M. (1990): Turnover of microbial biomass nitrogen in rhizosphere soil of upland crops. – Plant and Soil 116: 179-188.
[47] Teaumroong, N., Wanapu, C., Chankum, Y., Arjharn, W., Sang-Arthit, S., Teaimthaisong, K. (2010): Production and Application of Bioorganic Fertilizers for Organic Farming Systems in Thailand: A Case Study. – In: Insam H, Franke-Whittle I, Goberna, M. (eds.) Microbes at Work. Springer, Berlin, Heidelberg; pp. 293-312.
[48] Tian, Z. G., Gao, T., Yang, G. (2013): Situation and existing problems of wheat production in Shanxi province. – Sci-Tech information Development & Economy 23(17): 139-141 (in Chinese).
[49] van Dam, N. M., Bouwmeester, H. J. (2016): Metabolomics in the rhizosphere: tapping into belowground chemical communication. – Trends in Plant Science 21(3): 256-265.
[50] van der Heijden, M. G. A., Bardgett, R. D., van Straalen, N. M. (2008): The unseen majority: soil microbes as drivers of plant diversity and productivity in terrestrial ecosystems. – Ecology Letters 11(3): 296-310.
[51] Vázquez, M. M., César, S., Azcón, R., Barea, J. M. (2000): Interactions between arbuscular mycorrhizal fungi and other microbial inoculants (Azospirillum, Pseudomonas, Trichoderma) and their effects on microbial population and enzyme activities in the rhizosphere of maize plants. – Applied Soil Ecology 15(3): 261-272.
[52] Wakelin, S. A., Macdonald, L. M., Rogers, S. L., Gregg, A. L., Bolger, T. P., Baldock, J. A. (2008): Habitat selective factors influencing the structural composition and functional capacity of microbial communities in agricultural soils. – Soil Biology and Biochemistry 40: 803-813.
[53] Welbaum, G. E., Sturz, A. V., Dong, Z., Nowak, J. (2004): Managing soil microorganisms to improve productivity of agro-ecosystems. – Critical Reviews in Plant Sciences 23: 175-193.
[54] Weston, L. A., Ryan, P. R., Watt, M. (2012): Mechanisms for cellular transport and release of allelochemicals from plant root into the rhizosphere. – Journal of Experimental Botany 63(9): 3445-3454.
[55] Xia, Q., Yang, Z. P., Xi, J. F., Li, N., Sun, M., Gao, Z. Q. (2014): A study on yields and qualities traits of six wheat varieties (from Huanghuai wheat region) late-sowed in Jinzhong region. – Acta Laser Biology Sinica 23(2): 170-177.

http://www.aloki.hu ● ISSN 1589 1623 (Print) ● ISSN 1785 0037 (Online)
DOI: http://dx.doi.org/10.15666/aeer/1605_59335954
© 2018, ALÖKI Kft., Budapest, Hungary

[56] Xiong, M. B., He, J. P., Song, G. Y. (2002): Effect of root exudations on ecological distribution of rhizospheric microorganisms. – Chinese Journal of Soil Science 33(2): 145-148 (in Chinese).
[57] Xiyong, C., Haixia, X., Zhongdong, D. O. N. G., Feng, C. H. E. N., Kehui, Z. H. A. N., Dangqun, C. (2012): Genetic evolution and utilization of wheat germplasm resources in Huanghuai winter wheat region of China. – Pakistan Journal of Botany 44(1): 281-288.
[58] Xu, Y., Wang, G., Jin, J., Liu, J., Zhang, Q., Liu, X. (2009): Bacterial communities in soybean rhizosphere in response to soil type, soybean genotype, and their growth stage. – Soil Biology and Biochemistry 41: 919-925.
[59] Yang, Z., Yang, W., Li, S., Hao, J., Su, Z., Sun, M. (2016): Variation of bacterial community diversity in rhizosphere soil of sole-cropped versus intercropped wheat field after harvest. – PLoS One 11(3): e0150618.
[60] Zhang, J., Subramanian, S., Stacey, G., Yu, O. (2009): Flavones and flavonols play distinct critical roles during nodulation of *Medicago t*runcatula by *Sinorhizobium meliloti*. – The Plant Journal for Cell and Molecular Biology 57(1): 171-183.
[61] Zhu, J. P., Cheng, K. (2011): Effect of organic acids exuded from hydroponic plants roots on nitrogen cycling bacteria. – Chinese Journal of Environmental Engineering 5(9): 2139-2143 (in Chinese).

ELECTRONIC APPENDICES

Attachment 1: Sequences of bacteria
Attachment 2: Sequences of fungi
Attachment 3: Accession numbers

http://www.aloki.hu ● ISSN 1589 1623 (Print) ● ISSN 1785 0037 (Online)
DOI: http://dx.doi.org/10.15666/aeer/1605_59335954
© 2018, ALÖKI Kft., Budapest, Hungary

A STUDY ON THE INFLUENCE MECHANISM OF VANDALISM INTENTION OF OUTBOUND TOURISTS BASED ON EXTENDED THEORY OF PLANNED BEHAVIOR MODEL

LIN, M. S.[1,2] – YU, H.[2] – ZENG, Y. F.[1] – XIAO, X. N.[1*] – WANG, K. Y.[2]

[1]*College of Tourism, Fujian Normal University*
1 Science and Technology Road50117 Fuzhou, P. R. China

[2]*Institute of Geographic Sciences and Natural Resources Research, Chinese Academy of Sciences, 11 A Datun Road, 100101 Beijing, P. R. China*

**Corresponding author*
e-mail: xinni4@hotmail.com; phone: +86-591-2286-8726

(Received 17th Jun 2018; accepted 22nd Aug 2018)

Abstract. Tourist vandalism has been a common phenomenon in different countries and regions with the rapid development of tourism industry. It is deteriorating the quality of recreational environment, and hazarding the safety. Current researches implied that the unified understanding of the concept of vandalism had not yet formed, basic theoretical framework research was still weak and the antecedent factors of vandalism and its generating mechanism had not been paid enough attention to, which greatly affected the management of tourist vandalism. Therefore, adopting the extended Theory of Planned Behavior (TPB) perspective, this paper constructs the theoretical model of tourist vandalism. Then, using Structural Equation Models (SEM), taking tourists from Mainland to Taiwan as the case study, combined with questionnaire data, the study seeks to examine the influence factors of vandalism and its generating mechanism. The study found out that: (1) past behavior has significant positive effects on behavior intention, while subjective norm and perceived behavioral control have no significant positive effect on behavior intention; (2) past behavior has a significant positive effect on behavior intention, while subjective norm and perceived behavioral control have no significant positive effects on behavioral attitude; (3) environmental awareness has a significant positive effect on behavioral attitude, subjective norm, past behavior, while has no significant positive effect on perceived behavioral control. To conclude, environmental awareness and past behavior are applied to understand tourist vandalism and makes contribution to the tourist vandalism literature. Consequently, the paper suggests that family, schools and the educational institution should provide targeted training to outbound tourists to guide their attitude and clarify the concept of tourist vandalism and its negative influences through establishment of vandalism list to help tourists recognize and avoid vandalism in the future.
Keywords: *environmental awareness, Mainland, Taiwan, structural equation models*

Introduction

With the rapid development of tourism, Tourist vandalism has become widely discussed in various countries and regions (Bhati and Pearce, 2016). Whether vandalism is caused by independent tourists or group tourists, intentional or unintentional, accidental or repeated acts, it damages the surrounding environment and resources quality, public or private property, recreational safety, etc. Tourist vandalism greatly increases the management costs of tourism destinations. The annual repair costs due to tourist vandalism were up to 79.2 million US dollars in National Parks of USA and the cleaning and maintenance reached the amount of 18.8 million US dollars (Johnson et al., 1996); 10% of the annual budget for recreation forest in Beth, Canada is used to recover the damages caused by tourists; 9% of the total annual budget accounts for cleaning and maintenance for Yangmingshan Park in Taiwan area (Yang et al., 2013).

http://www.aloki.hu ● ISSN 1589 1623 (Print) ● ISSN 1785 0037 (Online)
DOI: http://dx.doi.org/10.15666/aeer/1605_59555969
© 2018, ALÖKI Kft., Budapest, Hungary

Obviously, tourist vandalism has always been one of the main factors to worsen the quality of recreational environment and safety (Chang et al., 1995).

Different disciplines have different understanding of tourist vandalism. Social behavioral studies mainly recognize tourist vandalism from the perspective of social behavior standards, legal provisions, and moral deviations; Environmental Psychology perceives the message of vandalism from the surrounding environment and personal psychological attitudes; Environmental Ethology focuses on the interaction between environmental information and vandalism from the emotions and attitudes of tourists response to the environment; Recreational behavior theory emphasizes the influence of physical and psychological needs and external human, social, and natural factors, and determines the intention to vandalism through the cognitive process of the surrounding environment (Kaplan, 1983). Based on the definition of different disciplines, the concepts similar to tourist vandalism include tourist deviant behavior (Mills et al., 1978), dysfunctional behavior (Daunt et al., 2012), depreciative behavior (Ibitayo et al., 1996), misbehavior (Fullerton et al., 2004), uncivilized behavior (Li et al., 2002), etc. These similar concepts have, to a certain extent, outlined the current state of negative impact of tourist behavior on the natural and humanistic social environment of tourism destinations. However, these concepts have not reflected the degree of harm caused by tourist negative behavior, and whether it constitutes a crime or not. This is not conducive to tourists' understanding and control of their negative behaviors.

Some scholars have pointed out that tourist behavior is a comprehensive manifestation of a series of psychological and physical behaviors formed by interaction between tourists and the new environment. It can be expressed by the equation $B = f(P,E)$, that is, tourist behavior is shaped by personal and environmental factors (Lewin, 1951). Based on the above equation, this paper defines tourist vandalism as tourists' improper behavior that violated social norms resulted from inadequate or excessive stress on the changes when tourists engaged in recreational activities, in an unconventional context. Although the behavior may not necessarily constitute a crime, it does harm the natural and human social environment of the tourist destination (Bhati and Pearce, 2016) Typical tourist vandalism includes graffiti, littering, throwing food to animals, damaging the vegetation, snapping off coral, noise making, improper dressing code, damaging recreational property, etc. (Chang et al., 1995).

After reviewing the relevant domestic and foreign literatures of tourist vandalism, it has been found out that academic attention focused on vandalism behaviors of tourists (Weaver, 2006), theoretical basis (Bhati, 2014), influential factors (McCaghy, 2008), motivation (Crotts, 2003), behavioral control (Cohen, 1973), etc. Foreign researchers and researchers form Hongkong and Taiwan have made fruitful achievements on the characteristics of tourist vandalism (Chang et al., 1995), macro (social, economic and environmental design) and micro (physiological, developmental, psychological) influential factors (Chang et al., 2003; Hou et al., 1998; Huang et al., 2016), Environment design ecological explanations of vandalism, Human ecological explanations of vandalism, Behavioral ecological explanations of vandalism, Integrative ecological explanations to vandalism, Cohen typology, situational crime, environmental design, technical and non-technical preventive approaches (Bhati and Pearce, 2016) etc. But Chinese scholars have not yet reached uniformed understanding on the concept and research subject of tourist vandalism (Li, 2012). Due to the sensitive topics of tourist vandalism, the complexity of classification, and the difficulties in obtaining survey data, researchers are more likely to adopt obscure words like uncivilized behaviors,

http://www.aloki.hu ● ISSN 1589 1623 (Print) ● ISSN 1785 0037 (Online)
DOI: http://dx.doi.org/10.15666/aeer/1605_59555969
© 2018, ALÖKI Kft., Budapest, Hungary

inappropriate behaviors to replace the word vandalism, which leads to weak basic of theoretical researches. The current research mainly focuses on the influential factors and motivations of uncivilized behavior, with the research achievements scattered in areas such as outbound tourism (Qiu, 2016) and ecotourism (Gao, 2003), which indicates the huge gap with foreign researches. It is urgently necessary to unify conceptual understanding of tourist vandalism and construct psychological and environmental science research paradigms, so as to promote the breadth and depth of the research.

Based on Theory of Planned Behavior (TPB) in psychology, this study expands the model to construct a framework of tourist vandalism. Taking the tourists visiting Taiwan as an example, the Structural Equation Models (SEM) is adopted to verify the influencing factors and mechanisms of vandalism. Furthermore, the study proposes counter measures to promote the in-depth study of tourist vandalism in theory and practice.

Literature review and research hypothesis

Theory of planned behavior

Theory of Planned Behavior (TPB), a derivative theory of Reasoned Action (TRA), was proposed by Ajzen to explain the process of individual decision-making (Ajzen, 1991). TPB holds the idea that human behavior is the result of deliberate planning, which can explain how people change their behavior patterns. TPB also can be used to predicate human behavior. In the 185 studies of Armitage and Conner (2001), TPB can explain 39% of behavior intention and 27% of behavior variance, so it is often used in the study of tourist behavior, such as tourist low-carbon travel decisions (Bamberg et al., 2003), ecological choices (Greaves et al., 2013; Kaiser, 2003), intention to participate in low-carbon tourism (Hu, 2014), green hotel consumption options (Xie, 2016), and pro-environmental behavior (López-Mosquera, 2016), etc. TPB has a better explanation for tourist behavior intention (Lin et al., 2016; Qiu, 2016).

In TPB, Attitude toward the behavior (AT) is a determinant factor of behavioral intention (BI). Salient Beliefs are cognitive and emotional foundations of attitude toward the behavior (AT), Subjective norm (SN), and Perceived behavioral control (PBC) (Ajzen, 1991). TPB assumes that behavioral intention covers the motivation for behavior. It reflects people's willingness to try or plan to work hard for something, that is, the stronger a person's intention to act, the more likely the action will happen (Duan, 2008). TPB further assumes that behavioral intention is mainly determined by AT, SN, and PBC (Cui, 2010). Lin et al. (2016) constructed a conceptual framework of tourist civilized behavioral intention and civilized behavior attitude based on TPB. It was found that there was a significant positive correlation between tourists' attitudes, travel times and tourist civilized behavioral intention; and there was a significant positive correlation between tourists' jobs, educational background, travel times and tourists' civilized behavior attitude.

Based on above description, the following hypothesis is proposed:

H1. The behavioral attitude has a positive effect on tourist's intention of vandalism.

Xie (2016) studied the decision-making mechanism of consumers choosing to stay in a green hotel based on TPB. The study proposed that behavioral attitude is the most important factor. Subjective norms not only directly affect behavioral intentions, but also indirectly influence behavioral intentions through behavioral attitudes and perceived behavioral control. Qiu (2017, 2016) introduced moral norms and local

http://www.aloki.hu ● ISSN 1589 1623 (Print) ● ISSN 1785 0037 (Online)
DOI: http://dx.doi.org/10.15666/aeer/1605_59555969
© 2018, ALÖKI Kft., Budapest, Hungary

attachment based on TPB, and constructed a model of outbound tourists civilized behavior intention mechanism. It is confirmed that subjective norms, perceived behavior control, moral norms, and local attachment all indirectly affect the intentions of outbound tourists civilized behavior through behavioral attitudes. Meanwhile, subjective norms not only directly affect behavioral attitudes, but also indirectly affect behavioral attitudes through moral norms; behavioral attitudes are the most important factor in driving intentions of outbound tourists' civilized behaviors. Based on the above discussion, the following hypotheses can be proposed:

H2. Subjective norms have a positive effect on tourist's intention of vandalism.

H3. Perceived behavioral control has a positive effect on tourist's intention of vandalism.

H4. Subjective norms have a positive effect on tourist's attitude toward vandalism.

H5. Perceived behavioral control has a positive effect on tourist's attitude toward vandalism.

H6. Perceived behavioral control has a positive effect on subjective norms of tourist's vandalism.

Past behavior and behavioral intentions

"More than 90% of people's daily activities are habitual behaviors" (Li, 2007). Ajzen (1991) suggested adding past behaviors to perceived behavioral control of TFB which could better predict behavior. Ouellette and Wood (1998) pointed out that past behaviors had an impact on future behaviors in two phases. Good behaviors repeatedly occur in a specific behavioral context. The frequency of past behaviors reflects the habit strength and has direct influence on future performance (Ouellette and Wood, 1998). Christina et al. (2004), after studying the tourist littering behavior, pointed out that there was a very significant relationship between past behavior and behavioral intentions for those who did not have recycling habits. Compared with behavioral attitudes, subjective norms, and perceived behavioral control variables, past behaviors can better explain behavioral variances, and people's past behaviors mainly influence their behaviors through intermediary variables such as behavioral attitudes and behavioral intentions (Ajzen, 2005). Therefore, it is necessary to include tourists' past vandalism into the theoretical framework of tourist vandalism and put forward the following hypothesis:

H7. Past behaviors have a positive effect on tourist's intention of vandalism.

H8. Past behaviors have a positive effect on tourist's attitude toward vandalism.

H9. Past behaviors have a positive effect on the subjective norms of tourist's vandalism.

H10. Past behaviors have a positive effect on perceived behavioral control of tourist's vandalism.

Environmental awareness and behavioral intention

Environmental Awareness (EA), also known as "Ecological Awareness", "Environmental/ Ecological Literacy" or "Environmental/Ecological Concern" (Dunlap et al., 1978). Though there is no uniformed definition at home and abroad (Roth, 1992), a common sense still exits that EA reflects relationship between man and nature (Hwang, 2000). According to the B = f(P,E) formula, environmental awareness is one important factor influencing tourist vandalism. Many tourists may think their vandalism reasonable, and make excuses for their behavior, or they are completely unaware of

http://www.aloki.hu ● ISSN 1589 1623 (Print) ● ISSN 1785 0037 (Online)
DOI: http://dx.doi.org/10.15666/aeer/1605_59555969
© 2018, ALÖKI Kft., Budapest, Hungary

their mistakes (Chang et al., 2003). Studies have shown that tourists with better environmental awareness would have incentives to protect the environment (Hwang et al., 2000). Wang (2010) applied TPB to the study of the relationship between environmental awareness and environmental behavior of tourists, and found out that there was a significant correlation between environmental awareness and environmental behavior of tourists. The key factors of environmental awareness influencing environmental behavior had been identified. Lin et al. (2014) surveyed that there was a significant positive correlation between the environmental awareness and tourists' behavior. Based on Widegren (Bamberg, 2003), Corral-Verdugo et al. (2008) and other related research results, the following research hypotheses are proposed:

H11. Environmental awareness has a positive effect on tourist's attitude toward vandalism.

H12. Environmental awareness has a positive effect on tourist's past vandalism.

H13. Environmental awareness has a positive effect on subjective norms of tourist's vandalism.

H14. Environmental awareness has a positive effect on perceived behavioral control of tourist's vandalism (*Fig. 1*).

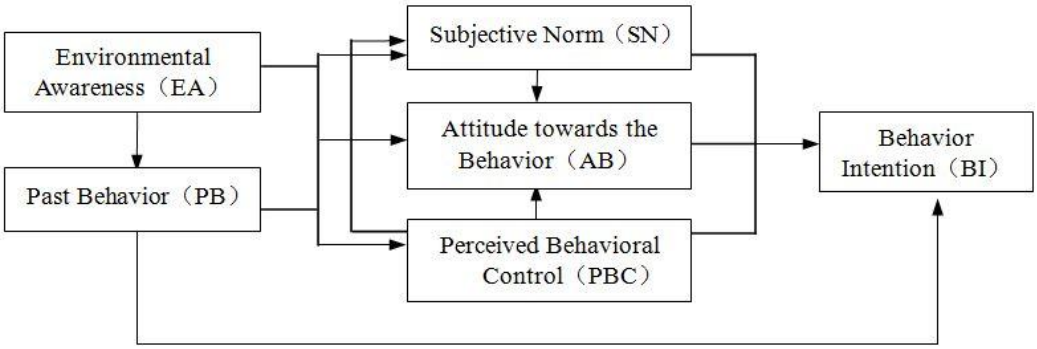

Figure1. *Conceptual framework of vandalism intention*

Methodology

Research methods

Based on the tourist vandalism and environmental awareness scale, the questionnaire was divided into two parts: the demographic characteristics of tourists and the main body of the questionnaire. The demographic characteristics of tourists include the tourist's place of residence, age, gender, monthly income, occupation, educational background, and travel times. Tourist vandalism includes "graffiti, littering, throwing food to animals, damaging the vegetation, snapping off coral, noise making, improper dressing code, damaging recreational property" (Xu, 2014). Questionnaire topics cover tourists' attitude toward vandalism, subjective norms, perceived behavioral control, past vandalism, environmental awareness, and vandalism intentions. The questions refer to Bamberg and Ajzen (2003), Gao (2003), Li (2007), Dunlap (1978, 2008), Luo (2007) in TPB and environmental awareness measurement (*Table 1*). The questionnaire was measured by 5-points Likert-type scale, and the respondents were asked about their level of agreement. In order to avoid hurried responses from the visitors, the fuzzy options of "don't know" and "general" were removed and respondents were required to make choices, with actual scores ranging from 1 to 4 points.

http://www.aloki.hu ● ISSN 1589 1623 (Print) ● ISSN 1785 0037 (Online)
DOI: http://dx.doi.org/10.15666/aeer/1605_59555969
© 2018, ALÖKI Kft., Budapest, Hungary

Table1. *Questionnaire of vandalism*

Variable	Measurement index	Mean	Standard deviation
Attitude towards the behavior (AB)	AB1 It's fine to have vandalism in Taiwan	3.03	0.883
	AB2 It's allowed to have vandalism in Taiwan	2.93	0.965
	AB3 It's reasonable to have vandalism in Taiwan	3.11	0.919
Subjective norm (SN)	SN1 My family and relatives believe that I can have vandalism in Taiwan	2.96	0.972
	SN2 My friends believe that I can have vandalism in Taiwan	2.85	0.882
	SN3 My relatives and family believe that I can have vandalism in Taiwan	2.88	0.880
Perceived behavioral control (PBC)	PBC1 It is entirely up to me to make vandalism in Taiwan	2.84	0.981
	PBC2 There is no control to make vandalism in Taiwan	2.91	0.962
	PBC3 I could behave like a vandalist anytime in Taiwan	2.76	0.983
Behavior intention (BI)	BI1 How likely does vandalism occur in Taiwan?	2.80	0.874
	BI2 How willful does vandalism occur in Taiwan?	2.87	0.884
	BI3 At what probability does the vandalism occur in Taiwan?	2.80	0.873
Past behavior (PB)	PB1 Vandalism happened last time I visited Taiwan	2.93	0.950
	PB2 Vandalism happened a lot last time I visited Taiwan	3.01	0.898
Environmental awareness (EA)	EA1 Natural self-regulation is strong enough to withstand the effects of modern industrial society	2.24	0.905
	EA2 Humans can develop and change the natural environment in order to meet their own needs	2.32	0.859
	EA3 Humans will eventually understand natural laws to fully control the natural world	2.28	0.876

Descriptive statistics of the questionnaires were collected by SPSS22.0 software to obtain the mean scores and standard deviations of each test topic. Correlation analysis was carried out on each test topic to obtain the correlation coefficient. Based on this, factor analysis was conducted to obtain the KMO value of the questionnaire and the factor loadings of each item. Reliability analysis was conducted to obtain the Cronbach's α coefficient of each variable and each item.

This study investigated the influence mechanism of tourist vandalism. To test the proposed model, the statistical tool Amos22.0 was used to conduct Structural Equation Models (SEM) analysis. Combined with the questionnaire data, the hypothetical model was fitted and tested, and was modified by removing insignificant path links.

Composite reliability was assessed by *Equation 1,* and the average variance extracted (AVE) values were acquired by *Equation 2*.

http://www.aloki.hu ● ISSN 1589 1623 (Print) ● ISSN 1785 0037 (Online)
DOI: http://dx.doi.org/10.15666/aeer/1605_59555969
© 2018, ALÖKI Kft., Budapest, Hungary

$$CR = \frac{\left(\sum_{i=1}^{k} \lambda_i\right)^2}{\left(\sum_{i=1}^{k} \lambda_i\right)^2 + \sum_{i=1}^{k} e_i} \quad \text{(Eq.1)}$$

$$AVE = \frac{\sum_{i=1}^{k} \lambda_i^2}{\sum_{i=1}^{k} \lambda_i^2 + \sum_{i=1}^{k} e_i} \quad \text{(Eq.2)}$$

In *Equations 1* and *2, k* means the number of measured corresponding factors, λ_k means the true variance, and e_k means error variance.

Data collection

Considering the diversity of tourists, representativeness of tourist vandalism, and availability of data, this study takes Chinese tourists who are visiting Taiwan as an example (*Table 1*). Taiwan could make a typical case. Chinese traditional culture is deeply penetrated into the society of Taiwan. On the other hand, Taiwan had been under Japan's rule for 50 years, and it is also westernized. Due to the political and historical reasons, Chinese visitors visiting Taiwan can be regarded as domestic tourism in theory, but it is actually viewed as outbound tourism in practice. Therefore, it is meaningful to take Chinese visitors visiting Taiwan as an example to study the influence factors and mechanism of tourist vandalism, which will contribute a lot to the prevention of tourist vandalism in domestic and outbound tourism.

This study chose to cooperate with the Hong Kong, Macao and Taiwan Affairs Offices of the Fujian Provincial Tourism Administration from September to October of 2017, peak time of mid-autumn holiday, to conduct a questionnaire survey at Fuzhou Changle International Airport and Pingtan cruise to Taiwan. A simple random sampling method was adopted. 200 questionnaires were issued each month. 5 copies had been sent to each Taiwan tour each time. 400 questionnaires were distributed to backpack tourists, 367 were returned and with a final example of 316 (79% response rate).

Data analysis and research results

Demographic characteristics description

This study measured 17 items and the 400 sample size estimate by Cochran method. Also, structural equation analysis is used to assess the overall fitness of the model and examine the statistical significant of each hypothesis (Wu, 2009). 316 respondents were mainly from Fujian Province, only 27.53% respondents were non-Fujian Province tourists. 51.90% were female. They are predominately young, with 37.97% in their 20s and 52.53% in their 30s. Most respondents received bachelor degree (44.93%) or got education to senior middle/professional college (35.44%). 58.86% of respondents monthly earned 2000-3999 yuan. In terms of the occupation of tourists, most of them work for public institutions (41.14%), corporate staff (33.23%) and civil service (14.87%); 77.22% of respondents visited Taiwan for the first time, and 22.15% tourists visited Taiwan for the second time; 84.18% of respondents visited Taiwan by group

http://www.aloki.hu ● ISSN 1589 1623 (Print) ● ISSN 1785 0037 (Online)
DOI: http://dx.doi.org/10.15666/aeer/1605_59555969
© 2018, ALÖKI Kft., Budapest, Hungary

tour, only 15.82% chose independent travel. The sample data satisfy the assumption of normal distribution as each indicator's skewness are between -0.60 and 0.842, the corresponding the absolute value is less than 3; the kurtosis are between -0.127 and 1.002, the corresponding absolute value is less than 8 (Wu, 2009).

Common method variance

Harman's single-factor test was used to perform exploratory factor analysis on the variables of interest. The results showed that the variance interpretation ratio of the first unrotated factor was only 39.79% and less than 50%, indicating that CMV was Acceptable range; the maximum correlation coefficient of all variables is 0.85, less than 0.90, the CMV of the displayed data is not obvious. Therefore, the common method bias of survey data is not a pervasive issue.

Reliability and validity test

Using SPSS22.0, we scrutinized the overall reliability was 0.923, and the Cronbach's alpha value of each latent variable was between 0.783 and 0.923 (*Table 2*), which exceeded acceptable thresholds of 0.7, thus indicating that the scale was reliable.

Table 2. *Reliability and validity test of the scale*

Latent variables	Measurement index	Factor loading	t-value	Cronbach's α	C.R.	AVE
Attitude towards the behavior (AB)	AB1	0.931	-	0.906	0.914	0.780
	AB2	0.777	18.705			
	AB3	0.933	27.542			
Subjective norm (SN)	SN1	0.806	-	0.889	0.896	0.742
	SN2	0.879	18.055			
	SN3	0.896	18.486			
Perceived behavioral control (PBC)	PBC1	0.946	-	0.932	0.913	0.778
	PBC2	0.798	19.827			
	PBC3	0.895	25.463			
Behavior intention (BI)	BI1	0.955	-	0.911	0.934	0.825
	BI2	0.863	24.351			
	BI3	0.904	27.374			
Past behavior (PB)	PB1	0.876	-	0.853	0.854	0.746
	PB2	0.851	17.321			
Environmental awareness (EA)	EA1	0.747	-	0.783		
	EA2	0.689	10.579		0.783	0.547
	EA3	0.780	11.336			

In terms of construct validity, first, we completed the reviews of literature to gain each construct. Second, we employed the pilot studies and the factor analysis method was adopted. For structural validity, the factor with the eigenvalue greater than 1 was retained. The cumulative variance contribution rate was 75.32%, the KMO was 0.885, and the Bartlett's sphere test had a significance of 0.000. The normalized load values

http://www.aloki.hu ● ISSN 1589 1623 (Print) ● ISSN 1785 0037 (Online)
DOI: http://dx.doi.org/10.15666/aeer/1605_59555969
© 2018, ALÖKI Kft., Budapest, Hungary

corresponding with each latent variable are between 0.689-0.946, all loadings and corresponding t-value is between 10.579 to 27.542, the composite reliability is between 0.783-0.934, and the average variance extracted (AVE) for each scale is between 0.547-0.825. Each AVE exceeded Fornell and Larcker's (1981) suggested minimum value of .50, which indicates convergence validity was good.

Analysis of the goodness fit indexes suggested good model fit(X^2/df = 2.473, Root Mean Square Residual [RMR] = 0.041, Root mean square error of approximation [RMSEA] = 0.068, goodness-of-fit indexes [GFI] = 0.914, TLI = 0.952, normed fit index [NFI] = 0.940, Incremental Fit Index [IFI] = 0.963, comparative fit index [CFI] = 0.963). The fit statistics shows that the overall research model provides a good fit with the data (Wu, 2009).

Structural equation models analysis

Using Amos22.0, The fit index met the corresponding requirement (X2/df = 2.456, RMR = 0.041, RMSEA = 0.068, GFI = 0.914, TLI = 0.952, NFI = 0.940, IFI = 0.963, CFI = 0.963), and supported nine hypotheses (H1, H4, H6, H7, H9, H10, H11, H12, H13), while H2, H3, H5, H8, H14 have been rejected (*Table 3*).

Table 3. *Result of hypothesis test*

Hypothesis path			Path coefficient	t value	Result
H1 : AB	→	BI	0.259**	2.636	Support
H2 : SN	→	BI	-0.003	-0.028	Denial
H3 : PBC	→	BI	-0.03	-0.035	Denial
H4 : SN	→	AB	0.607***	7.111	Support
H5 : PB	→	AB	0.052	0.757	Denial
H6 : PBC	→	SN	0.178*	2.451	Support
H7 : PB	→	BI	0.405**	2.999	Support
H8 : PB	→	AB	0.013	0.137	Denial
H9 : PB	→	SN	0.553***	9.124	Support
H10 : PB	→	PBC	0.762***	8.837	Support
H11 : EA	→	AB	0.216**	2.730	Support
H12 : EA	→	PB	0.470***	5.474	Support
H13 : EA	→	SN	0.444***	5.917	Support
H14 : EA	→	PBC	-0.064	-0.736	Denial

***P < 0.001, **P < 0.01, *P < 0.05. AB: Attitude towards the behavior, SN: Subjective norm, PBC: Perceived behavioral control, BI: Behavior intention, PB: Past behavior, EA: Environmental awareness

The model has been modified by removing insignificant path links (Wu,2009). The corrected fit index was: X2/df = 2.358, RMR = 0.043, RMSEA = 0.066, GFI = 0.914, TLI = 0.955, NFI = 0.939, IFI value = 0.964, CFI = 0.964. Meanwhile, the post-correction fit index was good and the initial model has been improved. The revised model was more concise than the initial model (*Fig. 2*).

http://www.aloki.hu ● ISSN 1589 1623 (Print) ● ISSN 1785 0037 (Online)
DOI: http://dx.doi.org/10.15666/aeer/1605_59555969
© 2018, ALÖKI Kft., Budapest, Hungary

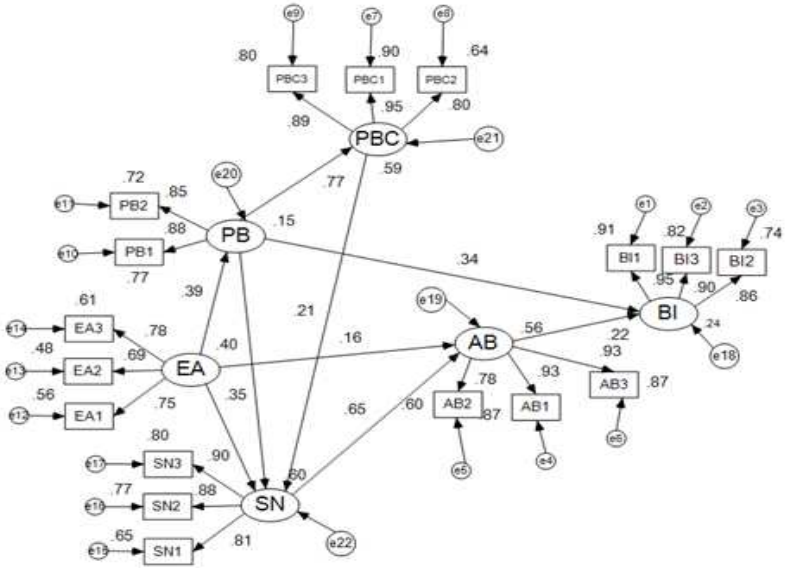

Figure 2. *Map of vandalism intention of tourists from Mainland to Taiwan. (AB: Attitude towards the behavior, SN: Subjective norm, PBC: Perceived behavioral control, BI: Behavior intention, PB: Past behavior, EA: Environmental awareness)*

Conclusions and discussions

Conclusions

First, tourist's attitudes toward vandalism and past vandalism have a significant positive effect on behavioral intentions, which is consistent with the original assumptions of theoretical models of planned behaviors. The results also reflect in Lin's (2016) research on the formation mechanism of the tourists to Taiwan civilized behaviors intention and the findings of Qiu (2017) on the influencing mechanism of civilized tourists behavior intentions. The coefficient of influence on the behavioral intention of the past behavior (0.34) was significantly higher than that of the behavioral attitude on the behavioral intention (0.22). It shows that tourists past vandalism would significantly influence their intention to repeat their vandalism.

Second, the subjective norms of tourist vandalism and perceived behavioral control have no direct positive influence on behavior intentions, which explains that the attitude of peers and the willingness of tourists to act vandalism have not directly positive affected their vandalism intention, while they indirectly influence behavioral intentions through behavioral attitudes. This proves Qiu's (2017) study on perceived behavior control of the civilized tourists' behaviors indirectly affecting behavioral intentions through behavioral attitudes. When the subject of the study is macroscopic, vague, and does not have much to do with tourists' own interests, such as ecotourism behaviors, civilized tourist behavior, and green purchasing behavior, the approval attitude of the peers has a direct positive effect on tourists' behavior intentions. On the opposite, when the subject of the study is quite sensitive and more related to the interests of tourists, like, graffiti, littering, throwing food to animals, snapping off the vegetation and coral, noise making, improper dressing, damaging recreational property and other vandalism, then the attitudes of the peers do not have a direct positive effect on the tourist behavior intentions. And the approval attitude of the local residents of the tourism destination may become an important factor that directly affects tourist vandalism intention. The

http://www.aloki.hu ● ISSN 1589 1623 (Print) ● ISSN 1785 0037 (Online)
DOI: http://dx.doi.org/10.15666/aeer/1605_59555969
© 2018, ALÖKI Kft., Budapest, Hungary

positive effects of perceived behavioral control on behavioral attitudes are not significant, but they indirectly affect behavioral attitudes through subjective norms. This is different from the results of Qiu (2017) research that these two variables are multi-influenced. It shows that the attitudes of the peers have a positive impact on the tourist vandalism, furthermore affects the behavioral attitudes and behavioral intentions.

Third, past behavior has positively influenced behavioral intentions, subjective norms and perceived behavioral control, but the positive impact on behavioral attitudes is not significant. The findings are basically consistent with Ajzen's (1991) expansion research on the TPB, while are not consistent with the findings of Li (2007). Past behavior has a significant positive effect on behavioral intentions, but the impact on behavioral attitudes is not significant, possibly due to the Face issues. Tourist vandalism are kinds of sensitive and negative behaviors, although tourists respond positively. However, in decision-making process of specific behavioral intentions, they are deeply influenced by past behaviors, and may deliberately avoid the choice of true behavioral intentions.

Fourth, environmental awareness has positive influence on past behaviors, subjective norms, and behavioral attitudes, but the impact on perceived behavioral control is not significant. This is consistent with Lin's (2014) findings of significant correlation with environmental awareness and tourism behavior, and has deepened the research on the mechanism of environmental awareness affecting tourism behavior. There are mainly two ways how environmental awareness influences behavior intentions: one is indirect influence on behavioral intentions by past behavior; the other is indirect influence on behavioral intentions through subjective norms and behavioral attitudes. Thus, environmental awareness is an important latent variable for outbound tourist vandalism. In addition, the direct impact of environmental awareness on perceived behavioral control is not significant. The reason is that environmental awareness reflects the tourists' opinions on the relationship between people and nature, which can directly affect behavior intentions and the behavior itself. Therefore, through the direct influence on the past behavior, it will indirectly affect the perceived behavioral control.

In conclusion, based on the conceptual formula $B = f(P, E)$, this study further defines the connotation and extension of tourist vandalism, and provides a theoretical basis for the study of vandalism behaviors of domestic and foreign tourists. Furthermore, variables such as environmental awareness and past behaviors are introduced into the modified tourist vandalism intention model, which further verifies the reliability of the planned behavior theory to explain the mechanism of tourist vandalism, and further clarifies the influence mechanism of environmental awareness on past behaviors, subjective norms, and behavioral attitudes. This study has important reference significance for the study of the mechanism of tourist vandalism. It also promotes the perfection of the theory and application of planned behavior theory in Chinese context.

Discussions

In 2016, the number of Chinese outbound tourists reached 122 million, and the tourists spent 109.8 billion US$ while traveling abroad (Qiu, 2017). The huge outbound tourism market is not only for tourist's personal leisure and holiday activities, but also bears its social awareness and responsibility. Based on the above research, we can unify the individual consumption behavior of outbound tourists and social responsibility from the following three aspects. Such managerial implications foster broader implications for public policy makers. That is, while it may be beneficial for service companies to

http://www.aloki.hu ● ISSN 1589 1623 (Print) ● ISSN 1785 0037 (Online)
DOI: http://dx.doi.org/10.15666/aeer/1605_59555969
© 2018, ALÖKI Kft., Budapest, Hungary

train employees in methods of misbehavior management and deterrence, from a public policy perspective it would appear fruitful to educate customers.

(1) Face the urgent needs of scientific research on tourist vandalism. Tourist vandalism is not a unique phenomenon to China's outbound tourists. The developed countries have experienced various degrees of vandalism during the rapid development of tourism. The key is how to propose appropriate governance programs through scientific research to change the personal vandalism of a few tourists as soon as possible to avoid the formation of group phenomenon. The best reference is Japan's approach to vandalism of outbound tourists in the 1980's. Therefore, there is an urgent need to clarify the concept and characteristics of tourist vandalism in the Chinese context, and establish a black list of outbound tourist behaviors for different tourist destinations. According to the government notices of "20 uncivilized behaviors of domestic and outbound tourists", based on the content and nature of tourism activities, it can be broadly divided into three categories: illegal acts, violations of social moral acts, and uncivilized acts. Among them, violations of social morality and uncivilized behavior are the main body of tourist vandalism.

(2) Correct attitude towards tourist vandalism. Attitude consists of three dimensions: perception (belief, knowledge and understanding), emotion (likes and dislikes), and behavior (participation). Attitude is an important factor affecting the behavioral intention (Zhang, 2018). In recent years, the publicity and education of the media and governments made a significant drop of outbound and domestic uncivilized behavior. This study found that behavioral attitudes are significantly affected by environmental awareness and subjective norms. In addition to the publicity and education of the media, knowledge of correct attitudes towards tourist vandalism should be incorporated into the education of family and schools, so that the society can understand the contents and harms of the vandalism, and make tourists ashamed of vandalism.

(3) Avoid repetition of past vandalism. People always act specific behaviors in a certain way, and as long as such behaviors have occurred in the past, the possibility of repetition is very high (Chang, 2003). The study realizes that past behavior is one of the important factors that influence behavioral intentions. Besides establishing a negative list of vandalism of outbound tourist destinations, we must know the occurrence probability of vandalism and how to make outbound tourists avoid those behaviors. It was reported by "United Daily News" that in the past ten years illegal touching and throwing food to animals, littering, and urination anywhere were the typical tourist vandalism in Taiwan. These behaviors should be targeted and educated before trip.

In addition, the study also found out that past behavior was significantly affected by environmental awareness. Under the economic reform, China is undergoing a structural adjustment of industries, and people's environmental awareness is changing from the mainstream social paradigm (DSP) to the new ecological paradigm (NEP). That is to say, Chinese has changed from simply pursuit of GDP and economic benefits to integration sustainable development of economic, environmental and social benefits. Although tourists' environmental awareness at this stage is weak in human exceptionalism (Lin et al., 2014), they can be trained and educated.

Acknowledgements. This work was supported by the project of China Postdoctoral Science Foundation (grant No. 2017M610976), Natural Science Foundation of China (grant No. 41871146, No. 4187208, No. 41601590).

http://www.aloki.hu ● ISSN 1589 1623 (Print) ● ISSN 1785 0037 (Online)
DOI: http://dx.doi.org/10.15666/aeer/1605_59555969
© 2018, ALÖKI Kft., Budapest, Hungary

REFERENCES

[1] Ajzen, I. (1991): The theory of planned behavior. – Organizational Behavior and Human Decision Processes 50: 179-211.
[2] Ajzen, I., Fishbein, M. (2005): The Influence of Attitudes on Behavior. The Handbook of Attitudes. – Erlbaum, Ahwah, NJ, pp. 173-221.
[3] Armitage, C. J., Conner, M. (2001): Efficacy of the theory of planned behavior: A meta-analytic review. – British Journal of Social Psychology 40: 471-499.
[4] Bamberg, S. (2003): How does environmental concern influence specific environmentally related behaviors? A new answer to an old question. – Journal of Environmental Psychology 23: 21-32.
[5] Bamberg, S., Ajzen, I., Schmidt, P. (2003): Choice of travel mode in the theory of planned behavior: the roles of past behavior, habit, and reasoned action. – Basic and Applied Social Psychology 25(3): 175-187.
[6] Bhati, A. D. S. (2014): Stakeholder responses to vandalism at visitor attractions: A Singapore and Bangkok comparison. – Dissertation/Thesis, James Cook University Australia, pp. 9-21.
[7] Bhati, A., Pearce, P. (2016): Vandalism and tourism settings: An integrative review. – Tourism Management 57: 91-105.
[8] Chang, C. Y., Cai, C. S., Weng, S. Y. (1995): An environmental cognition approach to the analysis of visitors' vandalism: A case study of Chung-Shan Park in the Taichung city. – Journal of Outdoor Recreation 8: 67-89.
[9] Chang, L., C, Sung, B. M. (2003): Why are recreational areas vandalized? A synthetic perspective from five theories. – Journal of Criminology 6: 283-300.
[10] Christina, K., MacKenzie, J., Wells, M. et al. (2004): An analysis of intentions to recycle household waste: the roles of past behavior, perceived habit, and perceived lack of facilities. – Journal of Environmental Psychology 24: 237-246.
[11] Cohen, S. (1973): Property Destruction: Motives and Meanings. – Architectural Press, London, pp. 23-53.
[12] Corral-Verdugo, V., Carrus, G., Bonnes, M. et al. (2008): Environmental beliefs and endorsement of sustainable development principles in water conservation. Toward a new human interdependence paradigm scale. – Environment and Behavior 40: 703-725.
[13] Crotts, J. C. (2003): Theoretical perspectives on tourist criminal victimisation. – The Journal of Tourism Studies 14: 92-98.
[14] Daunt, K. L., Harris, L. C. (2012): Exploring the forms of dysfunctional customer behaviour: a study of differences in servicescape and customer disaffection with service. – Journal of Marketing Management 28: 129-153.
[15] Duan, W. T., Jiang, G. R. (2008): A review of the theory of planned behavior. – Advances in Psychological Science 16: 315-320.
[16] Dunlap, R. E. (2008): The new environmental paradigm scale: From marginality to worldwide use. – Journal of Environmental Education 40: 3-18.
[17] Dunlap, R. E., Van Liere, K. D. (1978): The "New Environmental Paradigm": A proposed measuring instrument and preliminary results. – The Journal of Environmental Education 9: 10-19.
[18] Fornell, C., Larcker, D. F. (1981): Structural equation models with unobservable variables and measurement error: algebra and statistics. – Journal of Marketing Research 18: 382-388.
[19] Fullerton, R. A., Punj, G. (2004): Repercussions of promoting an ideology of consumption: consumer misbehavior. – Journal of Business Research 57: 1239-1249.
[20] Gao, M. D., Hung, C. C., Huang, C. C. (2003): The ecotourism behavioral model. – Journal of Outdoor Recreation 16: 23-48.

http://www.aloki.hu ● ISSN 1589 1623 (Print) ● ISSN 1785 0037 (Online)
DOI: http://dx.doi.org/10.15666/aeer/1605_59555969
© 2018, ALÖKI Kft., Budapest, Hungary

[21] Greaves, M., Zibarras, L. D., Stride, C. (2013): Using the theory of planned behavior to explore environmental behavioral intentions in the workplace. – Journal of Environmental Psychology 34: 109-120.
[22] Hou, J. X., Guo, Z. R. (1998): Study on the relationship between environmental attitudes of park visitors' inappropriate behavior management strategies and identity. – Journal of Outdoor Recreation 11: 17-42.
[23] Hu, B., Fu, Y. X., Xiong, Y. B. (2014): The driving factors and the formation mechanism of tourists' intention participating in low-carbon tourism: Based on theory of planned behavior. – Journal of Business Economics 8: 64-72.
[24] Huang, X, T., Liu, C. (2016): Companion constraints on tourist behavior: A case study of Hongkong ocean park. – Human Geography 31: 128-135.
[25] Hwang, Y. H., Kim, S. I., Jeng J M. (2000): Examining the causal relationships among selected antecedents of responsible environmental behavior. – Journal of Environmental Education 31: 19-25.
[26] Ibitayo, O. O., Virden, R. J. (1996): Visitor and manager perception of depreciative behavior in urban park setting. – Journal of Park and Recreation Administration 14: 36-51.
[27] Johnson, D. R., Kamp, M. E. V. (1996): Extent and control of resource damage due to noncompliant visitor behavior: A case study from the U. S. national parks. – Natural Areas Journal 16: 134-141.
[28] Kaiser, F. G., Gutscher, H. (2003): The proposition of a general version of the theory of planned behavior: predicting ecological behavior. – Journal of Applied Social Psychology 33: 586-603.
[29] Kaplan, S. (1983): A model of person-environment compatibility. – Environment and Behavior 15: 311-332.
[30] Lewin, K. (1951): Field Theory in Social Science. – Harper, New York, pp. 15-27.
[31] Li, H. M. (2007): Study on the Formation Mechanism of Rural Tourism Behavioral Intention Based on an Extended Theory of Planned Behavior Model. – Zhejiang University, Hang Zhou, pp. 48-58.
[32] Li, J. (2012): Review of research on uncivilized behavior of domestic tourists. – Journal of Management 25: 80-85.
[33] Li, M., He, C. P. (2002): Research on tourist uncivilized behavior. – Journal Beijing International Studies University 107: 26-28.
[34] Lin, M. S., Gong, F. H, Yuan, S. Q. (2014): Study on the relationship between environmental awareness and tourism behavior of tourists from Mainland to Taiwan. – Fujian Tribune (Humanities and Social Science Edition) 5: 136-141.
[35] Lin, M. S., Zhao, D. X, Liu, L. H. (2016): Improved paths of tourists uncivilized behavior—based on the perspective of the theory of planned behavior. – Journal of Fujian Normal University (Natural Science Edition) 32: 152-159.
[36] López-Mosquera, N. (2016): Gender differences, theory of planned behavior and willingness to pay. – Journal of Environmental Psychology 45: 165-175.
[37] Luo, Y. J., Deng, J. Y. (2007): The new environmental paradigm and nature-based tourism motivation. – Journal of Travel Research 46: 392-402.
[38] McCaghy, C. H. (2008): Deviant Behavior: Crime, Conflict, and Interest Groups. – Pearson/Allyn and Bacon, Boston, pp. 32-55.
[39] Mills, M. K., Bonoma, T. V. (1978): Deviant consumer behavior: a different view. – Advances in Consumer Research 6: 347-352.
[40] Ouellette, J. A., Wood, W. (1998): Habit and intention in everyday life: the multiple processes by which past behavior predicts future behavior. – Psychological Bulletin 124: 54-74.
[41] Qiu, H. L. (2016): Study on the relationship moral norm and tourists' civilization tourism behavioral intention: An extended theory of planned behavior model. – Zhejiang Social Sciences 3: 96-103.

http://www.aloki.hu ● ISSN 1589 1623 (Print) ● ISSN 1785 0037 (Online)
DOI: http://dx.doi.org/10.15666/aeer/1605_59555969
© 2018, ALÖKI Kft., Budapest, Hungary

[42] Qiu, H. L. (2017): Developing an Extended theory of planned behavior model to predict outbound tourists' civilization tourism behavioral intention. – Tourism Tribune 32: 75-86.
[43] Roth, C. E. (1992): Environmental Literacy: Its Roots, Evolution, and Directions in the 1990s. – ERIC/CSMEE Environmental Education, Columbus, Ohio, pp. 3-17.
[44] Wang, N. (2010): A research on Relationship between Tourists' Environmental Awareness and Environmental Behavior. – Tianjin University of Finance and Economics, Tianjin, pp. 22-31.
[45] Weaver, D. (2006): Sustainable Tourism: Theory and Practice. – Butterworth Heinemann, Oxford, pp. 31-47.
[46] Wu, M. L. (2009): Structural Equation Modeling. Operation and Application of AMOS. – Chongqing University Press, Chongqing, pp. 95-121.
[47] Xie, T. (2016): Consumers' intention to visit green hotels: based on TPB perspective. – Tourism Tribune 31: 94-103.
[48] Xu, C. (2014): Study on the tourist image of mainland in Taiwan media: "United Daily News" reported as an example. – Southeast Propagation 121: 24-28.
[49] Yang, T. H., Cheng, Y. Y. (2013): The influences of visitors' environmental attitude and situational factors on the occurrence of vandalism: A case study of littering in Yang-Ming-Shan National Park. – Journal of Outdoor Recreation 26: 83-98.
[50] Zhang, C. J., Bai, K. (2015): A Study on the effect of face need on tourist inappropriate behavior. – Tourism Tribune 30: 55-65.
[51] Zheng, Q. J., Xu, A. X., Kong, D. Y. et al. (2018): Correlation between the environmental knowledge, environmental attitude, and behavioral intention of tourists for ecotourism in china. – Applied Ecology and Environmental Research 16(1): 51-62.

http://www.aloki.hu ● ISSN 1589 1623 (Print) ● ISSN 1785 0037 (Online)
DOI: http://dx.doi.org/10.15666/aeer/1605_59555969
© 2018, ALÖKI Kft., Budapest, Hungary

DETERMINATION OF SEDIMENT PHOSPHATE SORPTION CHARACTERISTICS IN SHALLOW MOGAN LAKE, TURKEY

TOPÇU, A.[1*] – ULUSOY, U.[2] – PULATSÜ, S.[1]

[1]*Department of Fisheries and Aquaculture Engineering, Agricultural Faculty, Ankara University, Ankara, Turkey*
(e-mail: spulatsu@agri.ankara.edu.tr)

[2]*Department of Chemistry, Faculty of Science, Cumhuriyet University, Sivas, Turkey*
(e-mail: ulusoy@cumhuriyet.edu.tr)

**Corresponding author*
e-mail: atopcu@.ankara.edu.tr; phone:+90-312-596-1648, fax: +90-312-318-5298

(Received 20th Jun 2018; accepted 22nd Aug 2018)

Abstract. This study was conducted on sediment and overlying water samples from Mogan Lake, an important recreational area, in April, July and October 2015 and January 2016. The noteworthy data for this study were presented as follows: a) Sediment adsorption/desorption characteristics dependent on phosphate concentration, temperature and time were determined using models, and the relevant parameters were derived. b) Sediment equilibrium phosphate concentrations (EPC_0) and the critical dissolved phosphorus in the overlyingwater were estimated. Presentation of the research data is as follows: a) Phosphorous adsorption in the sediment samples was theoretically between 421 mgP kg^{-1} and 1,001 mgP kg^{-1}, and phosphorus sorption efficiency was estimated at 0.21-1.92 L mg^{-1}. Based on the Langmuir Model, the mean maximum adsorption capacity obtained for the July samples was significantly higher than that obtained for October ($p < 0.05$). Moreover, regarding the very low degree of sediment phosphorus desorption (<1%), it can be concluded that sediment does not behave as a desorbant material for phosphorus. b) Considering the EPC_0 values (5.5×10^{-3} and 46.6×10^{-3} mg L^{-1}), when the overlying water SRP concentrations fall below 0.008 mg L^{-1} in October and 0.046 mg L^{-1} in July, there will be a risk of phosphorus flux from the sediment to the lake water. Considering the overlying water SRP values reported for Lake Mogan, monitoring them in the months of October and July will prove to be decisive in predicting the internal phosphorus load of the lake.
Keywords: *adsorption, desorption, Freundlich model, Langmuir model, phosphorus, sediment*

Introduction

Phosphate sorption (adsorbtion/desorbtion) between the sediment and the sediment porewater is one of the mechanisms controlling phosphate exchange between the sediment and the overlying water in aquatic ecosystems. In determining the sediment's role as either a trap or a source of phosphorus, sediment phosphate adsorption is recognized as one of the most important components of long-term phosphate retention mechanisms especially in shallow lakes (Wang and Li, 2010; Zhang et al., 2012). Long-term estimates of sediment phosphate adsorption are important in determining phosphate pollution and suitable restoration techniques in lakes. The measurement of the most recent phosphate concentration in lake water is not restricted to the lake's phosphate intake and the measures taken to reduce its phosphate level; it can also be determined using the phosphate sorption rate. Kinetic models of sediment phosphate adsorption are defined by Langmuir isotherm (a rational basis) and Freundlich isotherm (an empirical equation) these are generally used in determining the rate of the chemical reaction and the effective factors following the calculation of the equilibrium phosphate concentration (Huang et al., 2011). The above models are often excellent at describing

http://www.aloki.hu ● ISSN 1589 1623 (Print) ● ISSN 1785 0037 (Online)
DOI: http://dx.doi.org/10.15666/aeer/1605_59715985
© 2018, ALÖKI Kft., Budapest, Hungary

adsorption, which are simply numerical relationships used to curve-fit data. Langmuir and Freundlich equations, widely and well used to explain the K adsorption, took into account the quantity, intensity and capacity factors which are important for estimating the sediment nutrient amounts (Wang et al., 2017).

The equilibrium phosphate concentration (EPC_0) is the state of aquatic systems in which adsorption and desorption values between the sediment and the overlying water are equal. It is an important parameter used for determining internal phosphate loading potential following a reduction in external phosphate loading or for measuring the level of phosphorus release and/or retention (Palmer-Felgate et al., 2011; Zhijian et al., 2012). If the equilibrium phosphate concentration is greater than the SRP value of the overlying water, phosphate release from the sediment into the overlying water occurs (Wang and Li, 2010; Wang et al., 2012; Jin et al., 2013; Tang et al., 2014).

Lake Mogan is an important recreational area for metropolitan Ankara, Turkey. It is under environmentally protected status as the 'Golbasi Specially Protected Area' since the major source of phosphorus in the area is wastewater containing detergents and fertilizers applied in the surrounding agricultural areas. Lake Mogan is an important recreational area due to its proximity to the city of Ankara, and studies have been conducted on the interaction between eutrophication and sediment in the lake (Pulatsü et al., 2008; Topçu and Pulatsü, 2008; Pulatsü and Topçu, 2009).

This study, being the pioneer one regarding the determination of sediment phosphate sorption characteristics, was conducted in Lake Mogan in April, July, and October 2015 and January 2016 with the aims of: a) deriving parameters for the use of kinetic and thermodynamic models for adsorption/desorption features of sediment phosphates in terms of concentration, temperature and time, and b) estimating the critical total dissolved phosphate concentration for the overlying water by calculating the sediment's equilibrium phosphate concentration (EPC_0).

Materials and methods

Study area

Lake Mogan is located 20 km south of Ankara on the Ankara-Konya road. It is an alluvial lake fed in large part by rain and also by more than five large and small streams (Boşgelmez et al., 2005). Detailed locations of the sampling stations in Mogan Lake are shown in *Figure 1*. Because the eastern littoral area's lakebed is covered with stones, the two stations were placed near the lake's western shore, where the lakebed is more suitable for collecting sediment samples. The area surrounding the sampling stations is covered with rooted aquatic macrophytes and is under the effects of intense negative development and pollution from anthropogenic sources.

Sediment sampling and analyses

All sediment samples were collected from the surface sediment (0-20 cm) in April, July, October 2015 and January 2016 with Van Veen Grab. Prior to mixing and splitting the sediment samples, they were taken to the laboratory in sealed plastic bags, which were put in iceboxes. After that these samples were air-dried, homogenized by grinding, and finally passed through a 0.5 mm sieve. The overlying water was grained by siphoning from the water located 10 cm above the sediment sampling locations. The mean depth of the sampling stations vary between 2.20 and 2.80 m. The supernatants of

http://www.aloki.hu ● ISSN 1589 1623 (Print) ● ISSN 1785 0037 (Online)
DOI: http://dx.doi.org/10.15666/aeer/1605_59715985
© 2018, ALÖKI Kft., Budapest, Hungary

overlying water were filtered through Whatman GF/C filters and then analyzed for SRP as ascorbic acid method according to standard analytical procedures (APHA, 2005). Two samples were obtained from each station and dublicate sub-samples were used for every sample in all analyses.

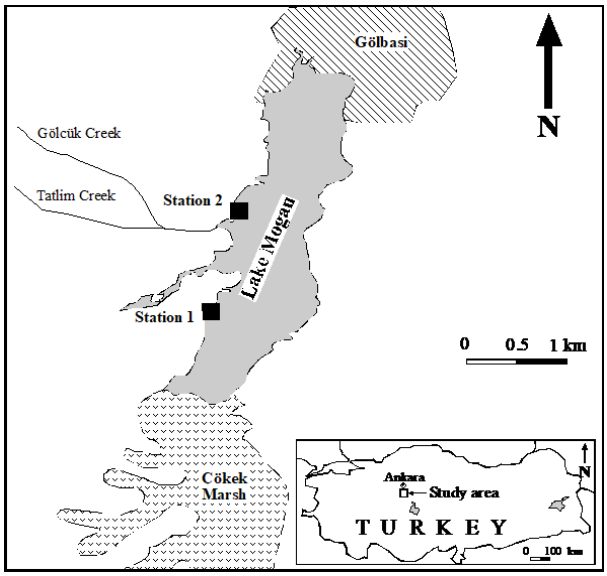

Figure1. *Study site and sampling stations (■: Station 1: 39°46'07" N 32°47'03" E; Station 2: 39°45'33" N 32°47'05" E) in Mogan Lake*

Adsorption procedures

Phosphorous adsorption studies were performed for various temperatures (277, 289, 295 and 300 K). The change of adsorption by phosphorous concentration was investigated for the range of 0.1-10 mg L^{-1} by considering previous investigations related to the seasonal change of phosphorous release in Mogan Lake by Pulatsu et al. (2008) at 277, 289, 295 and 300 K. 0.2 g fractions of sediment samples exemplified for July and October were added in screw-cap centrifuge tubes containing 20 mL of 0.1-10 mg L^{-1} phosphorous equivalent KH_2PO_4 (Ca ≈ 0.4-40 mg L^{-1}) solutions at studied temperatures. Two drops of 0.1% chloroform to inhibit bacterial activity. The samples were let to equilibrate for 24 h in temperature controlled water bath with gentle agitations. The solution and solid phases were separated by centrifugation at 4000 rpm for 15 min. Solutions were filtered and the phosphorous contents were determined by the APHA procedures (2005). This prescription was also applied for investigations enquiring the effect of time (kinetics) at 277 and 300 K and temperature (thermodynamics) at 289, 295 and 300 K on phosphorous adsorption at constant phosphorous concentration (2 mg L^{-1}). The solid and solution interaction was 24 h for the temperature effect whilst that was variable from 10 min to 36 h for the kinetics.

Calculation of phosphate desorption

The experimental processes of desorption measurement (change of desorption with concentration, thermodynamic, and kinetic), the 'desorbant (sediment)–phosphorus equilibrium solution' balance in the system, the 'phosphorus' concentrations were measured with spectrophotometric methods.

http://www.aloki.hu ● ISSN 1589 1623 (Print) ● ISSN 1785 0037 (Online)
DOI: http://dx.doi.org/10.15666/aeer/1605_59715985
© 2018, ALÖKI Kft., Budapest, Hungary

Data evaluation

The adsorbed amounts 'Q' (mg kg^{-1}) were calculated by *Equation 1* where 'C_0 and C_e' were phosphorous concentrations (mg L^{-1}), 'V' was solution volume (L), and 'm' was the mass of adsorbent (kg).

$$Q = \frac{(C_0 - C_e)xV}{m} \quad \text{(Eq.1)}$$

The concentration dependence of adsorption was evaluated with reference to the compatibility of experimental data (Q vs. C_e) to Langmuir, Freundlich and Sips models (*Eqs. 2–4*) in which X_L (mg kg^{-1}) and K_L (L mg^{-1}) were monolayer adsorption capacity and a constant energetically related to the adsorbate affinity to adsorbent. According to Langmuir model the active adsorptive centers were homogeneously distributed over the surface; the amount of adsorbate filling of these centers completely was X_L.

$$Q = \frac{X_L K_L C_e}{1 + K_L C_e} \quad \text{(Eq.2)}$$

Freundlich model was description of adsorption exponentially related to the surface heterogeneity '$0 < \beta < 1$' where 'a' was Freunlich capacity constant associated with adsorption intensity.

$$Q = aC_e^{\beta} \quad \text{(Eq.3)}$$

'K_s' and 'a_s' were the model constants and 'β_s' was known to be Sips exponent. This model explained that the isotherm was compatible to Freundlich model at low adsorbate concentrations, the compatibility shifted to Langmuir at high concentrations. The equation defines Langmuir model at $\beta_s = 1$ (Foo and Hameed, 2010; Baybaş and Ulusoy, 2011).

$$Q = \frac{K_s C_e^{\beta_s}}{1 + a_s C_e^{\beta_s}} \quad \text{(Eq.4)}$$

These models were commonly considered in obtaining adsorption characteristics of any sorbents and of sorption processes. The obtained parameters were used as references for comparison of e.g. adsorption dependence on sorbents and/or processes. According to Wang et al. (2012), Langmuir model should be further evaluated by taking into account of the contribution natively adsorbed exchangeable phosphorous (NAP) to adsorption process (*Eq. 5,* where C^0_e denotes equilibrium concentration of exchangeable phosphorous i.e. the concentration in desorption equilibrium by fresh water). EPC_0 (zero phosphorous concentration) as the threshold concentration referring the release of phosphorous from the reservoir sediment back into the water when 'EPC_0 > Soluble Reactive Phosphorous (SRP)' can be foreseen after NAP by *Equation 6*.

$$NAP = \frac{X_L K_L C_e^0}{1 + K_L C_e^0} + C_e^0 \frac{V}{m} \quad \text{(Eq.5)}$$

http://www.aloki.hu ● ISSN 1589 1623 (Print) ● ISSN 1785 0037 (Online)
DOI: http://dx.doi.org/10.15666/aeer/1605_59715985
© 2018, ALÖKI Kft., Budapest, Hungary

$$EPC_0 = \frac{NAP}{K_L(X_L - NAP)} \quad \text{(Eq.6)}$$

The adsorbed amounts calculated by *Equation 1* with reference to the phosphorous contents of solutions taken by time intervals were evaluated in view of the compatibility of adsorption to pseudo-first and -second order models (*Eqs. 7* and 8) where 'Q_t' (mg kg^{-1}) defines the adsorbed amounts at time 't (h)', 'Q_1 and Q_2' are the theoretical adsorptions obtained from the compatibilities. The adsorption rate constants are referred by 'k_1 (h^{-1}) and k_2 (mg^{-1}.kg h^{-1})' for first and second order kinetics (Ho and McKay, 1999).

$$Q_t = Q_1(1 - e^{-k_1 t}) \quad \text{(Eq.7)}$$

$$\frac{t}{Q_t} = \frac{1}{k_2 Q_2^2} + \frac{t}{Q_2} \quad \text{(Eq.8)}$$

Time required reducing initial phosphorous concentration to its half i.e. the time passed reaching half of the maximum adsorption 't1/2 (h)' and the initial adsorption rate 'H ($mg.kg^{-1}.st^{-1}$)' are given by *Equations 9–12* for pseudo first and second-order kinetics models.

$$t_{1/2} = 0.693/k_1 \quad \text{(Eq.9)}$$

$$H_1 = k_1 Q_1 \quad \text{(Eq.10)}$$

$$t_{1/2} = 1/k_2 Q_2 \quad \text{(Eq.11)}$$

$$H_2 = k_2 Q_2^2 \quad \text{(Eq.12)}$$

Adsorption activation energy, EA (J mol^{-1}) is calculated by Arrhenius equation (*Eq. 13*) rearranged for rate constants (k_{T1} and K_{T2}) obtained for two different temperatures where 'T' and 'R' are temperature in Kelvin scale (K) and ideal gas constant (8.314 J mol^{-1} K^{-1}) respectively (Winzor and Jackson, 2006).

$$\ln \frac{k_{T2}}{k_{T1}} = -\frac{E_a}{R}\left(\frac{1}{T_2} - \frac{1}{T_1}\right) \quad \text{(Eq.13)}$$

Further evaluation of the kinetics by Weber-Morris Model (*Eq. 14;* k_i is the rate constant for the model) provides information for the nature of adsorption, i.e., the process most effective on adsorption and its kinetics amongst mass transfer/diffusion, adsorption by surface precipitation or electrostatic attraction between adsorbent and adsorbate, and intrapartical diffusion could be proposed.

$$Q_t = k_i \sqrt{t} \quad \text{(Eq.14)}$$

Adsorption thermodynamics is evaluated by Gibbs-Helmotz and van t'Hoff equations (*Eqs. 15* and *16*) for which the values 'ln K_T' (distribution coefficient

http://www.aloki.hu ● ISSN 1589 1623 (Print) ● ISSN 1785 0037 (Online)
DOI: http://dx.doi.org/10.15666/aeer/1605_59715985
© 2018, ALÖKI Kft., Budapest, Hungary

obtained from the ratio of the amount adsorbed to equilibrium concentration after the solid-solution interaction is ceased, $K_T = Q_T/C_T$) vs. '1/T' for the studied temperatures is firstly depicted to figure out the changes in adsorption entropy (ΔS, J $mol^{-1}K^{-1}$) from the intercept and enthalpy (ΔH, J mol^{-1}) and from the slope. Adsorption free energy (ΔG, J mol^{-1}) is then calculated.

$$\ln K_T = -\frac{\Delta H}{R}\frac{1}{T} + \frac{\Delta S}{R} \quad \text{(Eq.15)}$$

$$\Delta G = \Delta H - T\Delta S \quad \text{(Eq.16)}$$

Results

The experimental isotherms and adsorption parameters

Figures 2 and *3* show the compatibility of concentration dependence of phosphorous adsorption to Langmuir and Freundlich models. Sips models is not provided in the figures to avoid chaotic view. The parameters derived from the compatibilities to all three models considered are presented in *Table 1*.

Table 1. *The adsorption parameters for various temperatures for adsorption of phosphorous on Lake Mogan sediment collected in July and October (C_0 = 0.1-10 mg L^{-1}, m/V = 0.25g/20 mL)*

	Langmuir			Freundlich			Sips			
	^1X_L	^2K_L	R^2	a	β	R^2	K_s	a_s	β_s	R^2
July-277K	1001	0.47	0.975	300	0.65	0.972	431	0.37	0.92	0.975
July-289K	655	2.87	0.947	434	0.44	0.936	1109	1.35	0.76	0.952
July-295K	711	0.46	0.983	217	0.56	0.985	259	0.17	0.68	0.986
July-300K	907	0.21	0.954	167	0.66	0.971	85	-0.43	0.34	0.981
***Mean±SEM**	**819±81**									
Oct-277K	421	1.92	0.955	229	0.4	0.942	488	0.88	0.7	0.967
Oct-289K	654	1.17	0.942	308	0.52	0.962	316	0.02	0.53	0.962
Oct-295K	513	1.71	0.941	262	0.47	0.95	380	0.35	0.6	0.952
Oct-300K	531	0.8	0.944	223	0.43	0.914	486	1.05	1.35	0.947
***Mean±SEM**	**530±48**									

[1]mg kg^{-1}
[2]L mg^{-1}
*Means are significantly different

Although the results of compatibility of experimental isotherms to all adsorption models considered were significant with coefficient of variations of $R^2 \geq 0.936$ ($p < 0.05$) the best fits were obtained for the Sips (*Table 1*). This could be attributed to the theoretical considerations of the model which is combination of both Langmuir and Freundlich models. The mean of maximum adsorption values obtained for the defined temperatures for samples collected in July was 819 ± 81 mg kg^{-1} as it is significantly different ($p < 0.05$) from those collected in October (530 ± 48 mg kg^{-1}). This should be attributed to the heat activation of the sediment as depending on the weathering, i.e., the sediment of Mogan is subjected to heat a prolonged period of time in summer. In fact

http://www.aloki.hu ● ISSN 1589 1623 (Print) ● ISSN 1785 0037 (Online)
DOI: http://dx.doi.org/10.15666/aeer/1605_59715985
© 2018, ALÖKI Kft., Budapest, Hungary

the mean of temperatures reached were 25.25 ± 0.03 °C in July and 10.23±0.05 °C in October. The significance of the adsorption mean values also imply that the studying of adsorption at changing temperatures is not much effect on adsorption capacities because of the interaction time of solution and sediment in batch experiments is not enough (24 h) to change temperature associated sediment feature. The experiments to recover the phosphorous adsorbed on the sediments samples by distilled water proved that the adsorption is not reversible so that the corresponding amounts with phosphorous concentrations in recovery solutions were <1% of the adsorbed quantities.

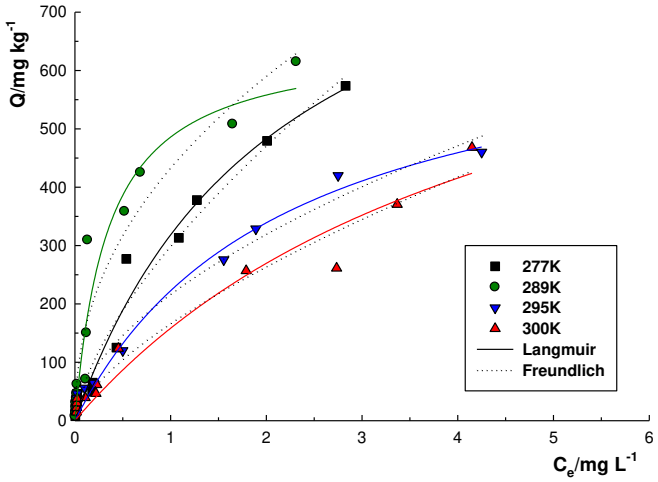

Figure 2. *The experimental isotherms for various temperatures obtained for adsorption of phosphorous on sediments sampled in July and its compatibility to Langmuir and Freundlich models. [For each experimental data, Q is the adsorbed amount of phosphorous on to sediment sample calculated from the phosphorous concentrations at initial (C_0) and equilibrium (C_e) by using Equation 1, please see section "Data Evaluation" for details] (C_0 = 0.1-10 mg L^{-1}, m/V = 0.25 g/20 mL)*

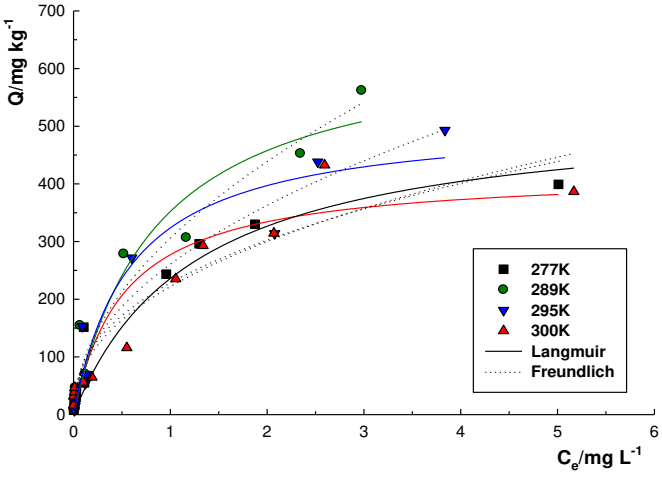

Figure 3. *The experimental isotherms for various temperatures obtained for adsorption of phosphorous on sediments sampled in October and its compatibility to Langmuir and Freundlich models. [For each experimental data, Q is the adsorbed amount of phosphorous on to sediment sample calculated from the phosphorous concentrations at initial (C_0) and equilibrium (C_e) by using Equation 1, please see section "Data evaluation" for details] (C_0 = 0.1-10 mg L^{-1}, m/V = 0.25 g/20 mL)*

http://www.aloki.hu ● ISSN 1589 1623 (Print) ● ISSN 1785 0037 (Online)
DOI: http://dx.doi.org/10.15666/aeer/1605_59715985
© 2018, ALÖKI Kft., Budapest, Hungary

Table 2 provides results relevant to NAP and EPC_0. The comparison of the magnitudes of NAP with that of X_L values predicated that contribution of NAP to adsorption process is not considerable for any of the studied conditions. The values of EPC_0 were in the range of 0.004-0.012 mg L^{-1} for the sediments sampled in both seasons which is less than the values of SRP 0.018 ± 0.009 and 0.039 ± 0.003 mg L^{-1} for July and October sediments respectively.

Table 2. *NAP (natively adsorbed exchangeable phosphorous) and zero phosphorous concentration (EPC_0; the threshold concentration referring the release of phosphorous from the reservoir sediment back into the water) values for Lake Mogan sediment calculated by using Langmuir parameters (X_L and K_L) and the equilibrium concentrations (Ce^0) for various temperatures*

	[1]X_L	[2]K_L	[3]$C_e^0 x10^3$	[1]NAP	[3]$EPC_0 x10^3$	[4](NAP/EPC_0)
July-277K	1001	0.47	3.8	2.1	4.4	477
July-289K	655	2.87	3.8	7.4	4	1850
July-295K	513	1.71	4.2	1.9	5.8	328
July-300K	907	0.21	8.9	2.4	12.6	190
Oct-277K	421	1.92	3.7	3.2	4.0	800
Oct-289K	654	1.17	4.1	3.4	4.5	755
Oct-295K	711	0.46	4.6	4	4.6	870
Oct-300K	531	0.8	9.6	4.8	11.4	421

[1]mg kg^{-1}
[2]L mg^{-1}
[3]mg L^{-1}
[4]L kg^{-1}

Adsorption kinetics

Time dependence of phosphorous adsorption on sediment samples were investigated to evaluate the adsorption with reference to pseudo first and second order models of the kinetics for sediments sampled in July and October for two different temperatures. The compatibility of experimental data to the models from which the parameters were obtained are presented in *Figure 4*, and *Table 3*.

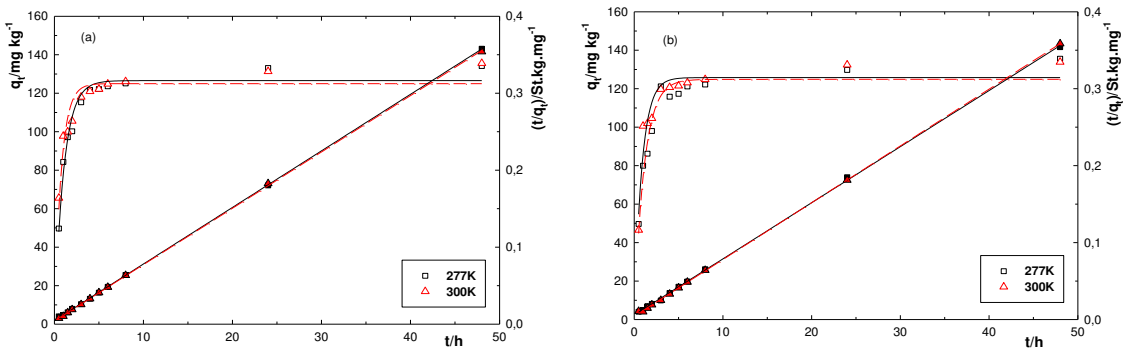

Figure 4. *The compatibility of experimental data for July (a) and October samples (b) at 277 and 300 K to pseudo-first (i vs. qt) and second order (t vs. t/qt) kinetic models;' t' and 'qt' refer the time elapsed after the solid-solution contact as hour and adsorbed amounts calculated for time 't' as mol kg-1 (C0 = 2 mg L-1, m/V = 0.25g/20 mL)*

http://www.aloki.hu ● ISSN 1589 1623 (Print) ● ISSN 1785 0037 (Online)
DOI: http://dx.doi.org/10.15666/aeer/1605_59715985
© 2018, ALÖKI Kft., Budapest, Hungary

Table 3. *Kinetic parameters derived from the compatibility of time dependence of phosphorous adsorption to pseudo first and second order models*

	Pseudo first order						Pseudo second order		
	$^1Q_{exp}$ (6-48)^2		$^1Q_1$	$^3k_1$	R^2	$^4t_{1/2}$	$^1Q_2$	$^5k_2x10^3$ R^2	$^4t_{1/2}$
July-277K	124-134	127	0.95	0.962	0.7(89)[6]	136	11.7	0.999	0.6(216)[6]
July-300K	125-136	125	1.3	0.894	0.5 (63)	137	12.9	0.999	0.6(242)
Oct-277K	121-136	125	0.89	0.943	0.8(111)	137	9.00	0.999	0.8(169)[6]
Oct-300K	123-133	126	1.14	0.914	0.6 (76)	135	13.00	0.999	0.6(237)

[1]mg kg^{-1}
[2]The adsorbed amounts experimentally determined 6 and 48 h after adsorbent–adsorbate contact
[3]h^{-1}
[4]h
[5]$mg^{-1}.kg.h^{-1}$
[6]Initial adsorption rates as $mg.kg^{-1}$ h^{-1}

As seen from the table that the phosphorous adsorption kinetics obeyed more significantly to second order model ($R^2 \geq 0.999$) than that to the first order model. This was also consistent with closeness of the values for Q_2 (the adsorbed amounts found from second order model) and Q_{exp} (the adsorbed amounts after experimental equilibrium). Adsorption rate constants proved that the increasing temperatures increase the adsorption rates k_2 (300 K)>k_2 (277 K), although this was not significant for P adsorption on the Mogan Sediments at the studied conditions. From the comparison of Q_{max} and Q_2 values, it was obvious that P adsorption completed in a few hours after adsorbent-adsorbate contact. In fact that the values of $t_{1/2}$ (time elapsed up to half of the completion of adsorption) showed that half lives were about 0.6-0.8 h with high initial adsorption rates ranging between 169 mg kg^{-1} h^{-1} and 242 mg kg^{-1} h^{-1}. Similar trends were also seen from the parameters derived from first order model. The adsorption activation energy was calculated and evaluated under thermodynamics section because of energetically relevance of the subjects.

The adsorption kinetics of P was further evaluated with reference to Weber-Morris model to figure out the physicochemical nature of adsorption for which the graph of Q vs. $t^{0.5}$ was obtained by using all the data obtained from the adsorption kinetics to signify the figure's pattern which could be considered with two parts (*Fig. 5*). The profile of graph was typical for adsorption of species to an adsorbent with chemical feature; otherwise, the pattern is with a straight linearity passing through the origin for adsorptions with physical nature.

Adsorption thermodynamics

Temperature dependence of P adsorption on Lake Mogan sediments studied for 289, 295 and 300 K for both sediment samples of the July and October. The obtained data were evaluated with reference to Gibbs-Helmotz and van t'Hoff equations for which the linearity of 'ln K vs. 1/T' depiction was considered (*Fig. 6*). The values acquired from slop and intercept of the linear relation ($R^2 \geq 0.974$) were used to calculate Gibbs free enthalpy of the adsorption. The results were exhibited in *Table 4*. Because of its energetical relevance, the activation energy of the adsorption derived from the kinetics studies was also represented in the table.

http://www.aloki.hu ● ISSN 1589 1623 (Print) ● ISSN 1785 0037 (Online)
DOI: http://dx.doi.org/10.15666/aeer/1605_59715985
© 2018, ALÖKI Kft., Budapest, Hungary

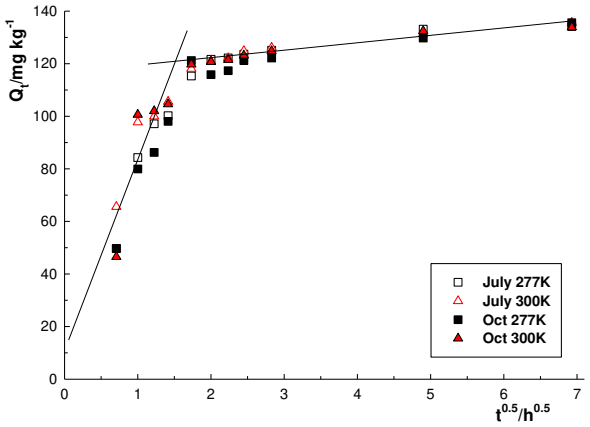

Figure 5. *The compatibility of experimentally obtained data from the kinetics of P adsorption to Weber-Morris Model*

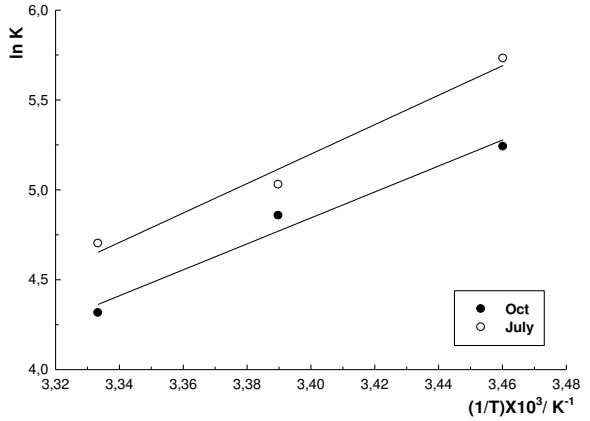

Figure 6. *Compatibility of the temperature dependence of P adsorption to linearity (C_0 = 10 mg L^{-1}, m/V = 0.25 g/20 mL)*

Table 4. *Thermodynamic parameters for adsorption of P to sediment samples*

	ΔH (kJ mol^{-1})	ΔS J mol^{-1}K^{-1}	ΔG_{298K} (kJ mol^{-1})	R^2	E_a (kJ mol^{-1})
July	-68.1	-188	-12.1	0.979	2.9
Oct	-60	-164	-11.1	0.974	11

ΔH, ΔS and ΔG are of the state functions and represent the energetically changing overall adsorption process which here refers to the changes in not only P adsorption alone but also in the contributions made by all other interactions in adsorption medium (such as P hydrolysis/hydration of P ions, water and sediment contents interaction, and many others) to the process. The results demonstrated that overall adsorption process was exothermic (ΔH < 0) with decreasing entropy (ΔS < 0), and spontaneous (ΔG < 0) under enthalpy influence (ΔH-ΔS <0). The energy released after adsorption is not big enough to form a covalent bonding (ΔH ≈ 200 kJ mol^{-1}) but it is sufficient to identify the presence of highly strong interactions between P species and sediment surface via electrostatic attractions This should also further evidence for the occurrence of

http://www.aloki.hu ● ISSN 1589 1623 (Print) ● ISSN 1785 0037 (Online)
DOI: http://dx.doi.org/10.15666/aeer/1605_59715985
© 2018, ALÖKI Kft., Budapest, Hungary

adsorption is via surface precipitation. Activation energy, the threshold to be overcome for the adsorption did not have considerable impact opposing to the adsorption at studied temperatures. However the value of Ea for July samples significantly lower than that for October samples because of the heat activation of the sediment during summer season as discussed above, as concordant with the results of ΔH found for the same seasonal sediments.

The phosphorus desorption for all the sediment samples under different temperature applications in both months were all calculated at less than 1%, these values were not taken into consideration.

Discussion

Langmuir and Freundlich's equations were used in order to estimate the phosphate adsorption in the sediment of Lake Mogan. The equilibrium phosphate concentration was determined using the mentioned kinetic models, and the rate of the chemical reaction during the adsorption process was measured. During the research, the effects of four different temperatures (277 K, 289 K, 295 K, 300 K) reflecting the natural conditions of phosphate sorption in the sediment of Lake Mogan were taken into account, and thus, measurements were taken during the months of October and July.

As reported by Huang et al. (2011), since shallow lakes are often isothermal, their sediments are sensitive to temperature changes, and the initial rates of sediment phosphorus adsorption are in direct proportion to the temperature. The constant values for the phosphorus adsorption rate in Lake Mogan for October and July were estimated at between 169-277 mg kg^{-1} h^{-1} and 216-242 mg kg^{-1} h^{-1} at temperatures of (k) 277 K and 300 K, respectively. The fact that these values for the lake sediment increased in direct proportion to the increase in temperature was in accordance with the above-mentioned research findings.

According to Wang et al. (2009) in a study on Three-Gorges Reservoir (China), the phosphate adsorption rate from the sediment reached its peak within six hours, and the maximum phosphate adsorption amount was 0.15-0.402 mgP g^{-1}. The kinetic characteristic of P-sorption in sediment is described by the Elovich model in sediment of Dongting Lake (Zhu and Yang, 2018). The rapid stage of P adsorption occurs within 60 min, and then, slow P sorption appears between 60 and 240 min. The P-sorption amount of sediment changes smaller after 240 min. The phosphate adsorption rate in Lake Mogan was at 90% within six hours that takes longer than Zhu and Yang (2018) and the maximum phosphate adsorption amount was estimated at 421-1001 mgP kg^{-1}. While the phosphate adsorption rate in this study resembles that reported in Wang et al. (2009), the extremely high maximum phosphate adsorption amounts in the Three-Gorges Reservoir were found to be lower (137.79-1975.50 mg kg^{-1}) in another study undertaken in the same reservoir by Zhang et al. (2012). In that study, the phosphate sorption activity in the sediment was determined to be 47.341-230.88 L kg^{-1} (Zhang et al., 2012). Lake Mogan's sediment phosphate sorption activity (0.21-1.92 L mg^{-1}) is higher than the findings of the above study.

Lai and Lam (2008) revealed sediment phosphate adsorption/release and the factors affecting this mechanism in Hong Kong's eutrophic Mai Po Marshes. The study's estimated EPC_0 values were lower than the overlying water's SRP concentrations, and the sediment phosphate release level under aerobic conditions was found to be, on average, 9.4 mg m^{-2} day^{-1}. The EPC_0 values in Lake Mogan were similar to the findings

http://www.aloki.hu ● ISSN 1589 1623 (Print) ● ISSN 1785 0037 (Online)
DOI: http://dx.doi.org/10.15666/aeer/1605_59715985
© 2018, ALÖKI Kft., Budapest, Hungary

of Lai and Lam (2008) in that they were found to be lower than the overlying water SRP concentrations. When the EPC_0 and the overlying water SRP concentrations were examined in the present study, it was suggested that internal phosphate loading from the sediment has a lower effect on the current nutrient level of the lake than the external phosphate load.

In Cry et al.'s (2009) study of oligomesotrophic Opeongo Lake (Canada), when the highest estimated EPC_0 values in the sediment (5 $\mu gP\ L^{-1}$) and the unmeasurable level of SRP values in the overlying water were considered, it was dertermined that there was a phosphate reserve in the sediment. In Nansi Lake (China), kinetic and adsorption/desorption isotherms were detected in the sediment and the equilibrium phosphate concentration and phosphate release potential were estimated, and it was determined that EPC_0 < SRP (Li et al., 2012). The fact that the estimated EPC_0 values in Lake Mogan were found to be lower than the SRP concentrations measured in the overlying water shows agreement with the reports of the above researchers.

In a study examining the details of phosphate adsorption at the sediment-water interface in Fushi Reservoir (China), sorption isothermic experiments were defined using the Langmuir and Freundlich models. When comparing the EPC_0 values with the overlying water SRP values, it was emphasized that the higher EPC_0 values facilitated phosphate release from the sediment, and that the sediment played a role as a phosphate source (Wang et al., 2012). Shoja et al. (2017), in their study of Ekbatan Reservoir (Iran), found that the EPC_0 value was much higher than the SRP concentration and that, despite the high adsorption capacity of the sediment, phosphate release from the sediment could occur. The fact that the estimated EPC_0 values in Lake Mogan are lower than the SRP concentrations found in the overlying water, unlike the findings of Wang et al. (2012) and Shoja et al. (2017), points to phosphorus adsorption in the sediment.

According to Fang et al. (2017) the role of particle morphology of clay minerals in P adsorption were studied. They revealed that Sips model can provide a better prediction than the Langmuir model, especially for kaolinite and hematite minerals and performs improvements as compared to the Langmuir model. This better performance could be attributed to the consideration of particle morphology reflected in the heterogeneity coefficient γ and adsorption capacity Q_m. The fact that the correlation coefficients calculated for the Sips model in Lake Mogan were greater than the values found for the Langmuir and Freundlich models shows the heterogenous behavior of the low phosphorus concentrations on the sediment surface in line with the researchers below. This finding supports the case for high adsorption levels in the lake. Moreover, during the research period, the low phosphorus concentration in the overlying water and the phosphorus fractions undergoing irregular changes in the sediment (Topçu and Pulatsu, 2017) concur with the finding that the sediment's phosphorus adsorption mechanism behaves heterogeneously.

Wang and Li (2010) studied the phosphorus adsorption and desorption mechanism in sediment samples obtained from six different sources in America (canal, ocean, coastal, river, marsh and lake). The estimated NAP and EPC_0 values in the canal and lake sediments were found to be higher than in the other sources. The phosphorus adsorption values in the sediment were calculated in order as Coastal>Marsh>Ocean. In the scope of the research it was reported that the desorption potential of the coastal and marsh sediment samples was extremely low. The fact that the phosphorus desorption value in Lake Mogan, one of Turkey's important wetlands, was found to be lower than 1% supports the high phosphorus adsorption value (907 mg kg^{-1}) and the low NAP (4.8-

http://www.aloki.hu ● ISSN 1589 1623 (Print) ● ISSN 1785 0037 (Online)
DOI: http://dx.doi.org/10.15666/aeer/1605_59715985
© 2018, ALÖKI Kft., Budapest, Hungary

11.7 mg kg^{-1}) and EPC_0 (5.5×10^{-3}-46.6×10^{-3} mg L^{-1}) values determined for the sediment. Our findings concur with Wang and Li's (2010) report stating that high values for adsorption in the sediment are effective at keeping desorption at low levels.

Tang et al. (2014) reported that the values for the energy released through phosphorus adsorption (Ea) are in inverse proportion to the calculated phosphorus adsorption in the sediment. The fact that the phosphorus adsorption energy (Ea) values reported in Lake Mogan were lower for the samples taken in July than those taken in October supports the finding that phosphate adsorption values were calculated to be at a maximum in July. Prevalence of ΔH with a high magnitude is generally evidence for the high adsorption energy affinity of P to the sediment. The results of the thermodynamics experiments demonstrated that overall, the adsorption process was exothermic ($\Delta H < 0$) with decreasing entropy ($\Delta S < 0$), and spontaneous ($\Delta G < 0$) under the influence of enthalphy (ΔH-$\Delta S < 0$). The high-magnitude values of ΔH signal strong interactions between phosphorus species and the sediment surface via electrostatic attraction. Adsorption activation energy did not have a significant impact on adsorption resistance at the temperatures in this study.

Experimentally obtained isotherms for phosphorus adsorption onto Lake Mogan sediments were well compatible to all three adsorption models considered ($R^2 \geq 0.936$; $p < 0.05$). Based on Langmuir the Model, the mean of maximum adsorption capacity obtained for July samples was significantly higher than that obtained for October samples ($p < 0.05$). This was attributed to heat activation of July samples due to the exposure of sunlight. The adsorbed phosphorous was not recoverable by distilled water. The comparison of EPC_0 and SRP values signified that the soluble phosphorous do not release from the sediment into the lake water.

The adsorption kinetics comply with the second order model with a high significance ($R^2 \geq 0.999$). Phosphorous adsorption completed in a few hours after adsorbent-adsorbate contact with a period of 0.6-0.8 h with high initial adsorption rates (169-242 mg kg^{-1} h^{-1}). The overall adsorption process was surface precipitation with a high mass transfer to the boundary layer after evaluation of the kinetics with reference to Weber-Morris model.

Conclusions

The sediment's equilibrium phosphate concentration value is used in estimating the phosphorus concentration in the overlying water, which may negatively affect the nutrient value of a lake. With this study, it has been scientifically proven through laboratory research that there may be a risk of phosphorus release from the sediment when the overlying water SRP concentration for October of 0.008 mg L^{-1} falls below the July value of 0.046 mg L^{-1}. Accordingly, considering the overlying water SRP values reported above for Lake Mogan, monitoring them especially in the months of October and July will prove to be decisive in predicting the internal phosphorus load of the lake.

Acknowledgements. This research is supported by Turkish Scientific and Technological Research Council TUBITAK Project No. TOVAG :115Y375).

Conflicts of interest. The authors declare that they have no conflicts of interest.

http://www.aloki.hu ● ISSN 1589 1623 (Print) ● ISSN 1785 0037 (Online)
DOI: http://dx.doi.org/10.15666/aeer/1605_59715985
© 2018, ALÖKI Kft., Budapest, Hungary

REFERENCES

[1] APHA (2005): Standard Methods for the Examination of Water and Waste Water. 21st edn. – American Public Health Association, Washington, DC.

[2] Baybaş, D., Ulusoy, U. (2011): Polyacrylamide–clinoptilolite/Y-zeolite composites: Characterization and adsorptive features for terbium. – Journal of Hazardous Materials 187: 241-249.

[3] Boşgelmez, A., Boşgelmez, İ. İ., Savcı, A. E., Aldemir, A., Gürpınar, E., Mutlu, B., Topaloğlu, S., Ege M, Çiçek N (2005): Ankara-Gölbaşı and *Centaurea tchihatcheffii*. – Centaurea tchihatcheffii Ankara-Gölbaşı Sevgi Çiçeği, Ankara, pp. 131-178.

[4] Cry, H., McCabe, S. K., Nurnberg, G. K. (2009): Phosphorus sorption experiments and the potential for internal phosphorus loading in littoral areas of a stratified lake. – Water Research 43: 1654-1666.

[5] Fang, H., Cui, Z., He, G., Huang, L., Chen, M. (2017): Phosphorus adsorption onto clay minerals and iron oxide with consideration of heterogeneous particle morphology. – Science of the Total Environment 605-606: 357-367.

[6] Foo, K. Y., Hameed, B. H. (2010): Insights into the modeling of adsorption isotherm systems. – Chemical Engineering Journal 156: 2-10.

[7] Ho, Y. S., McKay, G. (1999): Pseudo-second order model for sorption processes. – Process Biochemistry 34: 451-465.

[8] Huang, L., Fu, L., Jin, C., Gielen, G., Lin, X., Wang, H., Zhang, Y. (2011): Effect of temperature on phosphorus sorption to sediments from shallow eutrophic lakes. – Ecological Engineering 37: 1515-1522.

[9] Jin, X., He, Y., Kirumba, G., Hassan, Y., Li, J. (2013): Phosphorus frations and phosphate sorption-release characteristics of the sediment in the Yangtze River estuary reservoir. – Ecological Engineering 55: 62-66.

[10] Lai, D. Y. F., Lam, K. C. (2008): Phosphorus sorption by sediments in a subtropical constructed wetland receiving stormwater runoff. – Ecological Engineering 35: 735-743.

[11] Li, Z., Yue, Q., Gao, B., Wang, Y., Liu, Q. (2012): Phosphorus release potential and pollution characteristics of sediment in downstream Nansi Lake, China. – Front. Environ. Sci. Engin. 6(2): 162-170.

[12] Palmer-Felgate, E. J., Bowes, M. J., Stratford, C., Neal, C., MacKenzie, S. (2011): Phosphorus release from sediments in a treatment wetland: contrast between DET and EPC_o methodologies. – Ecological Engineering 37: 826-832.

[13] Pulatsü, S., Topcu, A. (2009): Seasonal and vertical distributions of porewater phosphorus and iron concentrations in a macrophyte-dominated eutrophic lake. – Journal of Environmental Biology 30(5): 801-806.

[14] Pulatsü, S., Topçu, A., Kırkağaç, M., Köksal, G. (2008): Sediment phosphorus characteristics in the clearwater state of Lake Mogan, Turkey. – Lakes and Reservoirs: Research and Management 13: 197-205.

[15] Shoja, H., Rahimi, G., Fallah, M., Ebrahimi, E. (2017): Investigation of phosphorus fractions and isotherm equation on the lake sediments in Ekbatan Dam (Iran). – Environmental Earth Sciences 76: 235. DOI 10.1007/s12665-017-6548-2.

[16] Tang, X., Wu, M., Dai, X., Chai, P. (2014): Phosphorus storage dynamics and adsorption characteristics for sediment from a drinking water source reservoir and its relation with sediment compositions. – Ecological Engineering 64: 276-284.

[17] Topçu, A., Pulatsü, S. (2008). Phosphorus fractions in sediment profiles of the eutrophic Lake Mogan, Turkey. – Fresenius Environmental Bulletin 17(2): 164-172.

[18] Topçu, A., Pulatsü, S. (2017): Evaluation of some management strategies in eutrophic Mogan Lake, Turkey: Phosphorus mobility in the sediment-water interface. – Applied Ecology and Environmental Research 15(4): 705-717. DOI: http://dx.doi.org/10.15666/aeer/ 1504_705717.

http://www.aloki.hu ● ISSN 1589 1623 (Print) ● ISSN 1785 0037 (Online)
DOI: http://dx.doi.org/10.15666/aeer/1605_59715985
© 2018, ALÖKI Kft., Budapest, Hungary

[19] Wang, C., Boithias, L., Ning, Z., Han, Y., Sauvage, S., Perez, J. M. S., Kuramochi, K., Hatano, R. (2017): Comparison of Langmuir and Freundlich adsorption equations within the SWAT-K model for assessing potassium environmental losses at basin scale. – Agricultural Water Management 180(B): 205-211.
[20] Wang, Q., Li, Y. (2010): Phosphorus adsorption and desorption behavior on sediments of different origins. – J. Soils Sediments 10: 1159-1173.
[21] Wang, X., Zhang, L., Zhang, H., Wu, X., Mei, D. (2012): Phosphorus adsorption characteristics at the sediment-water interface and relationship with sediment properties in Fushi Reservoir, China. – Environ. Earth Science 67: 15-22.
[22] Wang, Y., Shen, Z., Niu, J., Liu, R. (2009): Adsorption of phosphorus on sediments from the Three-Gorges Reservoir (China) and the relation with sediment compositions. – Journal of Hazardous Materials 162: 92-98.
[23] Winzor, D. J., Jackson, C. M. (2006): Interpretation of the temperature dependence of equilibrium and rate constants. – J. Mol. Recognit. 19: 389-407.
[24] Zhang, B., Fang, F., Guo, J., Chen, Y., Li, Z., Guo, S. (2012): Phosphorus fractions and phosphate sorption-release characteristics relevant to the soil composition of water-level-fluctuating zone of Three Gorges Reservoir. – Ecological Engineering 40: 153-159.
[25] Zhhijian, L., Yue, Q., Gao, B., Wang, Y., Liu, Q. (2012): Phosphorus release potential and pollution characteristics of sediment in downstream Nanski Lake, China. – Front. Environ. Sci. Engin. 6(2): 162-170.
[26] Zhu, G., Yang, Y. (2018): Variation laws and release characteristics of phosphorus on surface sediment of Dongting Lake. – Environmental Science and Pollution Research 25(13): 12342-12351.

http://www.aloki.hu ● ISSN 1589 1623 (Print) ● ISSN 1785 0037 (Online)
DOI: http://dx.doi.org/10.15666/aeer/1605_59715985
© 2018, ALÖKI Kft., Budapest, Hungary

ENHANCEMENT IN ARSENIC REMEDIATION BY MAIZE (*ZEA MAYS* L.) USING EDTA IN COMBINATION WITH ARBUSCULAR MYCORRHIZAL FUNGI

WANG, S.[1] – PAN, S.[1] – SHAH, G. M.[1,2] – ZHANG, Z.[1] – YANG, L.[1] – YANG, S.[1*]

[1]*Yantai Institute, China Agricultural University, 264670 Yantai, Shandong Province, China*

[2]*Department of Environmental Sciences, COMSATS University Islamabad, Vehari-Campus 61100 Vehari, Pakistan*

**Corresponding author*
e-mail: sjyang-2008@163.com

(Received 26th Jun 2018; accepted 31st Aug 2018)

Abstract. This study was conducted to evaluate the effects of combination of ethylene diamine tetra acetic acid (EDTA) with arbuscular mycorrhizal fungi (AMF) on arsenic (As) phytoremediation using maize plants in pot experiment with four treatments (Control, EDTA, AMF, and EDTA+AMF). The results showed that lone addition of EDTA significantly increased exchangeable As concentration in the rhizosphere soil, and thus, enhanced plant uptake of As in shoots and roots. However, it markedly inhibited the root colonization, plant growth, and antioxidant enzyme activity. Consequently, As biological enrichment factor was the lowest because of reduced plant dry weight, although the plants possessed the highest As extraction efficiency. Unlike EDTA, AMF alone had a positive effect on root colonization, dry matter accumulation, and antioxidant enzyme activity, whereas negative effects of AMF on exchangeable As content in the rhizosphere soil and As uptake in shoots and roots were observed. However, using EDTA-AMF combination, maize plants simultaneously exhibited significantly higher exchangeable As extraction efficiency and biological enrichment factor, which were beneficial for the remediation of heavy metal-contaminated soil. Therefore, it is concluded that the EDTA-AMF combination could be regarded a promising choice for phytoremediation of heavy metal-polluted soil.
Keywords: *EDTA, AMF, heavy metal, hyperaccumulator, phytoremediation, soil remediation*

Introduction

Soil becomes polluted when potentially toxic substances are released in amounts exceeding their permissible levels, and reaching prohibitively high concentrations, which affect normal ecosystem functions (Meier et al., 2012). According to most legislative schemes, soil may require remediation if the concentration of one or more metals exceeds the specified threshold level in the soil profile (Meier et al., 2012). Regarding the increasing need to combat heavy-metal pollution, various strategies for soil remediation, mainly mechanical or physicochemical methods, including soil washing, vitrification, thermal treatment, excavation and confinement of soil, and so on, have been used to treat contaminated soil in recent decades (Bhargava et al., 2012; Sarwar et al., 2017). These techniques are usually expensive, require technical expertise and disturb the soil, occasionally rendering the land useless as a medium for further events such as plant growth (Marques et al., 2009). Therefore, mechanical and physicochemical treatments are not applicable on a large scale.

In contrast, phytoremediation is proposed to be efficient, cost-effective, with greater public acceptance, environmental-friendly and sustainable technology from remediation of metal contaminated soils (Pandey, 2012; Sinha et al., 2013; Shabir et al., 2018). In these techniques, plant roots absorb metals from the soil and accumulate them into their

http://www.aloki.hu ● ISSN 1589 1623 (Print) ● ISSN 1785 0037 (Online)
DOI: http://dx.doi.org/10.15666/aeer/1605_59875999
© 2018, ALÖKI Kft., Budapest, Hungary

vegetative parts which are then harvested, and thereby metal is removed from the site of contamination (Shabir et al., 2018). The prerequisite for phytoremediation is that the plants must be genetically capable of growing in soils with high concentrations of metals, and have ability to accumulate metals in their shoots and roots without toxicity to their metabolic processes (Seth, 2011; Tang et al., 2012). The known plants meeting these requirements are called hyperaccumulators. However, growth and biomass production of hyperaccumulators are slow, and consequently, phytoremediation requires several years to reduce soil metal concentrations to an acceptable levels (McGrath and Zhao, 2003). This long duration is a drawback of metal-polluted soil remediation. Nevertheless, owing to preferred occurrence in residual forms, and strong binding with non-biotic or biotic ligands in soil, or inclusion within the crystal lattices of primary or secondary soil minerals, heavy metal bioavailability in soils is actually reduced (Charriau et al., 2011; Echevarria et al., 2006; Shahid et al., 2012). Additionally, the relatively low solubility and phytoavailability of heavy metals in soil is unfavorable for phytoremediation.

To compensate for the relatively small biomass of hyperaccumulators and low metal availability in soil, one alternative scenario has been hypothesized, wherein the plant selected for remediation can have large biomass production, and a chelating agent combined with soil amendment is used. This hypothesis is infact based on the concepts that (1) high plant biomass can enhance metal extraction from polluted soil, (2) chelating agents are used to improve the mobility, solubility, and bioavailability of heavy metals in the soil solution phase, and (3) amendment is applied to increase plant tolerance to heavy metal stress.

Actually, ethylene diamine tetra acetic acid (EDTA) is widely used as the most efficient and effective chelating agent to extract metals from contaminated soil. After soil application, EDTA transfers the metal sorption and precipitation equilibrium toward the enhanced dissolution of heavy metals owing to metal-EDTA complex formation (Goel and Gautam, 2010; Hadi et al., 2010). However, certain researchers reported that there was no significant effect of EDTA on metal uptake by plants, and in certain cases, even negative effects of EDTA application were observed (De La Rosa et al., 2007; Tomé et al., 2009). These contradictory findings indicate that the effect of EDTA on heavy-metal uptake varies with soil type, plant variety, heavy metal concentration and soil pH.

Arbuscular mycorrhizal (AM) fungi (AMF) can develop extensive extraradical hyphal networks, which explore the soil to a greater extent, absorb nutrients from a large vacinity, and translocate them to the roots of host plants. Therefore, they are considered intermediary between soil nutrients and host plants. Moreover, AMF shows great potential for use in phytoremediation due to (i) their ubiquity in the soil environments, and (ii) the development of several strategies enabling host plants to tolerate high metal concentrations in the soil (Hildebrandt et al., 1999; Janousková et al., 2005). Nevertheless, the role of AMF in phytoremediation is still not completely understood. Many studies have demonstrated that AMF promote phytoextraction, causing an increase in metal translocation to shoots (Davies et al., 2001; Trotta et al., 2006). However, other researchers have showed that AMF develop mechanisms that only enable metal accumulation within plant roots, and prevent metal translocation to the shoots (Citterio, 2005; Giasson et al., 2005). To the best of our knowledge, research investigating role of EDTA or AMF in phytoremediation of metal contaminated soils

http://www.aloki.hu ● ISSN 1589 1623 (Print) ● ISSN 1785 0037 (Online)
DOI: http://dx.doi.org/10.15666/aeer/1605_59875999
© 2018, ALÖKI Kft., Budapest, Hungary

are scarce, whereas no solid data set exists regarding their combined application for the aforementioned purpose.

With growing concern about remediation techniques for heavy metal-polluted soil, Knowledge of the processes and factors behind the combination of EDTA and AMF for enhancing the phytoremediation of heavy metal-polluted soil is crucial to evaluate and manage the outcomes of this technique. Therefore, this study aimed to highlight the role of the combination of EDTA and AMF in the phytoremediation of soil contaminated with arsenic (As), and additionally, to possibly provide new insight into the remediation of heavy metal-polluted soil.

Material and methods

Experimental design

The experiment was based on a randomized complete block design with three replications, and included four treatments. (i) Control: no EDTA and no AMF, (ii) EDTA: EDTA alone, (iii) AMF: AMF alone, and (iv) EDTA + AMF: EDTA-AMF combination.

AMF inoculum and domestication

The AMF inoculum *Glomus versiforme* was isolated from uncontaminated fluvo-aquic soil at the Yantai Institute, China Agricultural University, Thereafter, a pot culture was prepared with *Trifolium repens* L. grown in a sterilized soil-sand mixture at 1:9 contaminated with arsenic (As) at 50 mg kg^{-1}. After 90 days, chopped root pieces of *T. repens* along with soil were defined as the inoculum, containing a mixture of AM spores, colonized root pieces, AM mycelia, and 700–750 spores per 100 g of inoculum.

Pot culture experiment

To explore the objective as outlined above, an indoor pot experiment was conducted under controlled conditions in a greenhouse at the Yantai Institute, China Agricultural University. For this purpose, plastic pots were used with height and surface diameter of 30 and 23 cm, respectively. Soil used in this study had 6.44 pH (soil:water, 1:2.5), 2.1% organic matter, 140 mg kg^{-1} available nitrogen, 58 mg kg^{-1} Olsen phosphorus, 158 mg kg^{-1} available potassium, and 5.2 mg kg^{-1} total As. After collection from the field soil was air-dried, and then sterilized at 121 °C for 25 min. Required amounts of $Na_2HAsO_4 \cdot 7H_2O$ (50 mg kg^{-1} of soil) were dissolved in 1000 ml of distilled water, and then sprayed onto the soil. Subsequently, the soil was mixed thoroughly, and each pot was filled with 25 kg of the soil. The pots were incubated for 60 days to improve the balance of As in the contaminated soil. During incubation, moisture in the pots was maintained roughly at pot capacity. As was allowed to penetrate deep into the pots via watering, and then, transferred to the soil surface by volatilization, and thereby, was distributed uniformly in the soil. Regarding the AMF, 100 g of inoculum was uniformly introduced at a depth of 3 cm. Thereafter, 5 seeds of maize (*Zea mays* L. 'Denghai-3622') were sown in each pot. Before sowing the seeds were surface-sterilized with 0.5% NaClO solution, subsequently washed several times with distilled water, and allowed to germinate at 28 °C for 48 h. Seven days after emergence, maize were thinned to 3 plants per pot. In each pot, soil moisture was maintained daily at 70% of the pot capacity with distilled water based on weight, and amount of nutrients were added

http://www.aloki.hu ● ISSN 1589 1623 (Print) ● ISSN 1785 0037 (Online)
DOI: http://dx.doi.org/10.15666/aeer/1605_59875999
© 2018, ALÖKI Kft., Budapest, Hungary

according to chemical analysis and plant requirements. Fifty days after emergence EDTA (5 mmol kg^{-1}), prepared in distilled-deionized water, was sprayed on the soil surface as per treatment plan

Data collection and analytical methods

From each pot, maize plants were harvested at 65 days after germination to estimate shoot and root biomass. Shoots were clipped with a pair of scissor at ground level (Shah et al., 2016). To harvest the roots, the whole soil clump from the pot was taken out and placed in a container filled with cold water. After 2 h of soaking, the clump was manually divided into 6 pieces. These pieces were taken out of the container one by one and placed on a 0.5 mm mesh frame to separate roots from soil with a jet of tap water and then, with deionized water as described by Shah et al. (2013). Percentage root colonization by AMF was calculated using the gridline intersect method after staining the roots with trypan blue (Koske and Gemma, 1989). The activities of superoxide dismutase (SOD) and catalase (CAT) in fresh shoots and roots were measured as described by Beauchamo and Fridovich (1971) and Aebi (1974), respectively. The remaining parts were dried in an oven at 80 °C for 48 h, and then weighed to obtain dry matter of shoots and roots. As concentrations in the dried plant materials were determined by inductively coupled plasma atomic emission spectrometry (ICP-AES) (Yang, 1986). Rhizosphere soil was collected following the procedures described by Wang and Zabowski (1998). Classification of the heavy metal species in the dried soil was performed using continuous extraction (Yang et al., 2003). The extraction efficiency of the heavy metal and biological enrichment factor were calculated using *Equations 1* and *2,* respectively.

$$\text{Extraction efficiency } (mg\ g^{-1}) = \frac{\text{shoot heavy metal uptake}}{\text{root dry weight}} \quad \text{(Eq.1)}$$

$$\text{Biological enrichment factor} = \frac{\text{amount of heavy metal in plant}}{\text{amount of heavy metal in soil}} \quad \text{(Eq.2)}$$

Statistical analysis

Values of the collected data are expressed as means of the three replicates. Effects of EDTA, AMF and their combinations were tested using analysis of variance (ANOVA). Means were compared among the treatments using the LSD (least significant difference) test at the 0.05 probability level.

Results

Percentage root colonization

Results revealed the significant effects of AMF on the extent of root colonization (*Fig. 1*). Mycorrhizal colonization was not observed in the control and EDTA treatments, due to the lack of mycorrhizal inoculation. However, plants treated with AMF alone and EDTA-AMF combination showed high colonization rates. In the former case, percentage root colonization was 1.6 folds higher than in case of EDTA-AMF combination.

http://www.aloki.hu ● ISSN 1589 1623 (Print) ● ISSN 1785 0037 (Online)
DOI: http://dx.doi.org/10.15666/aeer/1605_59875999
© 2018, ALÖKI Kft., Budapest, Hungary

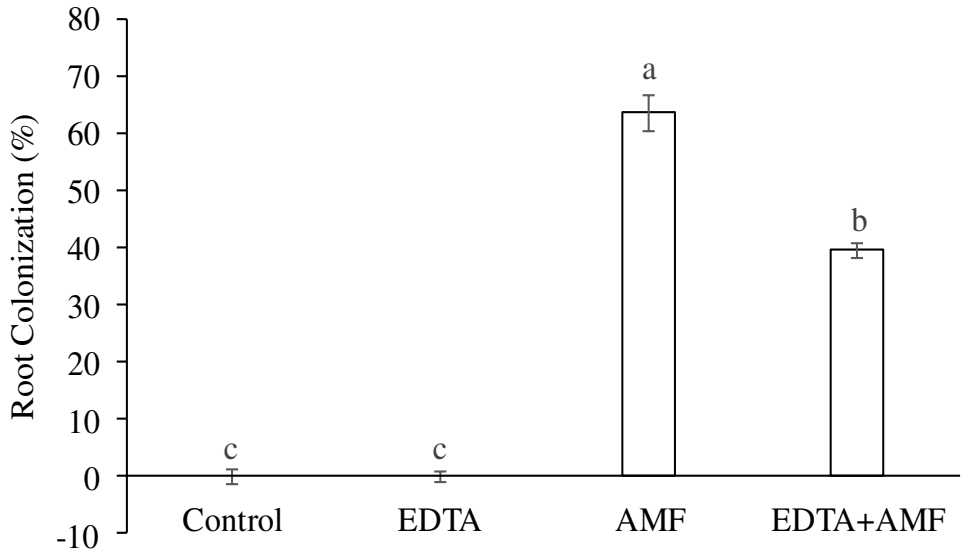

Figure 1. *Root colonization percentage affected by AMF and EDTA application. All the values are the mean of triplications. Different letters above columns indicate significant differences between means by LSD at 5% level*

Dry weights of maize shoots and roots

Dry weight of maize shoots and root are shown in *Figure 2*. Dry weights of both shoots and roots were significantly influenced by application of AMF and/or EDTA. The highest dry weights of both shoots and roots were observed in AMF and least in case of EDTA. Results revealed 53, 119, and 21% higher shoot dry matter yield from AMF treatment as compared to Control, EDTA, and EDTA-AMF, respectively. The respective increased fractions in case of roots dry matter were 63, 122, and 27%. Furthermore, the results indicated that EDTA application seriously inhibited dry matter accumulation in shoots as well as roots and the values were even lower than the control.

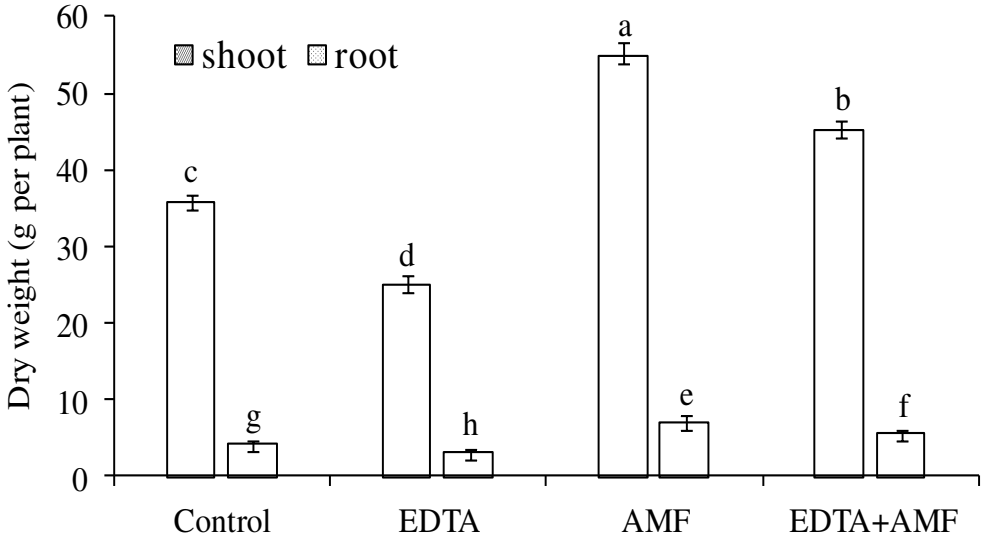

Figure 2. *Dry weight in shoot and root affected by AMF and EDTA application. All the values are the mean of triplications. Different letters above columns indicate significant differences between means by LSD at 5% level*

http://www.aloki.hu ● ISSN 1589 1623 (Print) ● ISSN 1785 0037 (Online)
DOI: http://dx.doi.org/10.15666/aeer/1605_59875999
© 2018, ALÖKI Kft., Budapest, Hungary

As concentrations in maize shoots and roots

Results revealed greater total plant As accumulation from AMF, EDTA and their combination as compared to the control (*Table 1*). Among these treatments total As accumulation followed the order EDTA> EDTA-AMF>AMF>Control. Out of the total As accumulation, greater fractions ended up in roots irrespective to the treatments. For the shoots, the highest value was observed in the plants treated with EDTA alone, and the lowest value was observed in the AMF-inoculated plants. Compared with EDTA alone, there was a decrease in As concentration in the plants treated with the EDTA-AMF combination; however, statistical analysis revealed no difference. For the roots, the highest value was similarly observed in the plants treated with EDTA alone; however, the lowest value was observed in the control plants. Moreover, the results indicated that increase in As concentration was larger in the roots than in the shoots, and there were significant differences between them.

Table 1. *Changes in average As concentration (n = 3) in shoot and root of maize plants. Different letters following the means indicate significant differences between means by LSD at 5% level*

Treatment	As concentration (mg kg^{-1})		
	Shoot	**Root**	**Total**
Control	4.16 b	92.07 d	96 d
EDTA	7.58 a	258.72 a	266 a
AMF	3.88 c	168.49 c	172 c
EDTA+AMF	7.25 a	220.93 b	228 b

Enzyme activity

Results revealed a significant effect of AMF, EDTA, and their combination on SOD and CAT activities as compared to the control (*Fig. 3*). SOD and CAT activities in the shoots and roots were significantly improved after AMF application and respectively increased by 37 and 30%, as compared to the control plants. This increased fractions in case of AMF-EDTA combination was 29 and 16%. In contrast, sharp inhibition of both these enzymes was observed in plants receiving EDTA only (*Fig. 3*). Consequently, SOD and CAT activities in the shoots decreased by 17% and 30% respectively, as compared with the control plants. Similar trend was observed for the roots; however, the increase in CAT activity was evidently larger than that in SOD activity (*Fig. 3*).

Relative change in As in different species

Figure 4 shows the relative changes if As speciation as affected by the addition of AMF, EDTA and their combination. We found that the ratio of different species to total As exhibited different changes in the rhizosphere soil. When EDTA was added alone, exchangeable As content increased to 13%, which was 1.72 times greater than control, 2.7 times that AMF alone, and 1.8 times than the EDTA-AMF combination. However, the contents of all the other As forms in the EDTA treatment decreased as compared to the other treatments. Although the exchangeable As content in the rhizosphere soil treated with AMF alone was the lowest, the contents of carbonate As, Fe-Mn-bound As, and organic-bound As increased by 71%, 63%, and 16% as compared to the control.

http://www.aloki.hu ● ISSN 1589 1623 (Print) ● ISSN 1785 0037 (Online)
DOI: http://dx.doi.org/10.15666/aeer/1605_59875999
© 2018, ALÖKI Kft., Budapest, Hungary

Whereas the respective increased fraction was 212, 160, and 31% than EDTA alone, and 15, 26 and 9%, as compared with EDTA-AMF combination. Compared with AMF alone, the EDTA-AMF combination caused slight decreases in the contents of carbonate As, Fe-Mn-bound As, organic-bound As, and residual As, equivalent to the increase in exchangeable As content. The residual As was the greatest among all the As species, irrespective to the treatment.

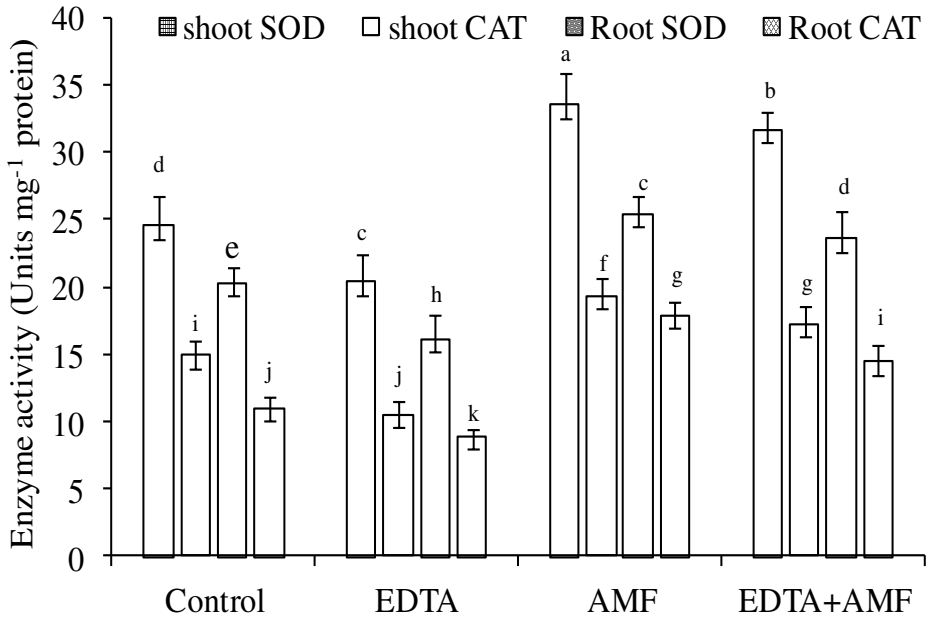

Figure 3. *Enzyme activities of SOD and CAT in shoot and root affected by AMF and EDTA application. All the values are the mean of triplications. Different letters above columns indicate significant differences between means by LSD at 5% level*

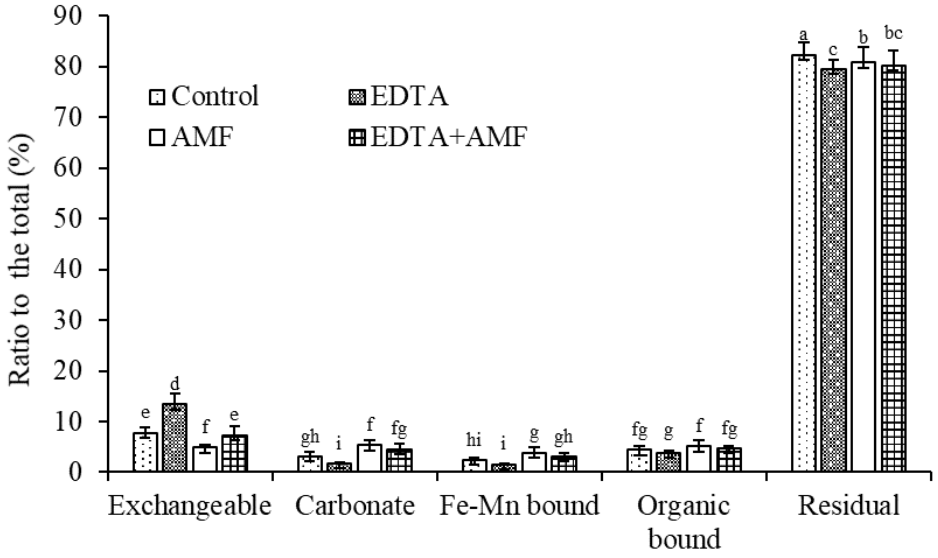

Figure 4. *Relative change of As in different speciations as affected by AMF and EDTA application. All the values are the mean of triplications. Different letters above columns indicate significant differences between means by LSD at 5% level*

http://www.aloki.hu ● ISSN 1589 1623 (Print) ● ISSN 1785 0037 (Online)
DOI: http://dx.doi.org/10.15666/aeer/1605_59875999
© 2018, ALÖKI Kft., Budapest, Hungary

As extraction efficiency and biological enrichment factor

As extraction efficiency is shown in *Table 2* and followed the order EDTA ≥ EDTA + AMF > Control > AMF ($P < 0.05$). The order of As biological enrichment factor was EDTA + AMF > AMF > EDTA > Control. The As extraction efficiency of maize plants treated with the EDTA-AMF combination was 1.71, and 1.95 folds greater that of the control, and AMF-treated plants, respectively, whereas the values were almost similar to that of EDTA Similarly, As biological enrichment factor was 2.84, 1.54, and 1.11 times greater than that of the control, EDTA-treated, and AMF-treated plants, respectively.

Table 2. *Average As extraction efficiency and biological enrichment factor (n = 3) in maize plants. Different letters following the means indicate significant differences between means by LSD at 5% level*

Treatment	As extraction efficiency (mg g^{-1})	As biological enrichment factor (%)
Control	0.0347 b	0.0403 d
EDTA	0.0600 a	0.0743 c
AMF	0.0304 c	0.1029 b
EDTA+AMF	0.0593 a	0.1145 a

Discussion

Mycorrhizal colonization

Percentage root colonization is an important factor indicating the establishment of mycorrhizal associations by plants. This study showed that AMF application alone was favorable for mycorrhizal colonization, whereas the EDTA-AMF combination was observed to exert inhibitory effects to AMF survival (*Fig. 1*). These results were in line with some earlier studies who reported that EDTA addition to soil decreases the viability and number of AMF in the rhizosphere soil, although it is not lethal to the fungus (Marques et al., 2008; Tanwar et al., 2013).

Plant dry weight

Figure 2 shows that the order of the dry weights of both shoots and roots was AMF > EDTA + AMF > Control > EDTA. EDTA treatment alone considerably decreased dry weight, probably because of the added phytotoxicity of EDTA and the heavy metal. Moreover, *Figure 2* indicates that biomass accumulation in the mycorrhizal plants with and without EDTA treatment tended to increase. Various mechanisms have been reported to demonstrate that mycorrhizae can help plant species colonize metal-contaminated sites by improving P uptake by the plant, and thus, well-nourished plants show better growth (Lin et al., 2007; Tabrizi et al., 2015). Furthermore, AMF can effectively bind As to their cell walls, immobilize As in the fungal biomass, and subsequently improve plant tolerance to the metal-contaminated environment (Garg and Chandel, 2010; Joner et al., 2000). The positive effect of mycorrhizae on dry matter accumulation was partly offset by EDTA; the dry weight of plants treated with the EDTA-AMF combination was lower than that of the AMF-treated plants, yet significantly higher than that of the EDTA-treated plants.

http://www.aloki.hu ● ISSN 1589 1623 (Print) ● ISSN 1785 0037 (Online)
DOI: http://dx.doi.org/10.15666/aeer/1605_59875999
© 2018, ALÖKI Kft., Budapest, Hungary

As uptake and transport

Roots are the first organs to be exposed to metal toxicity, and therefore, greater As accumulation was observed in the roots than in the shoots for all treatments. This might be regarded a strategy for preventing further metal translocation to the shoots and evidence of the operation of a potential tolerance mechanism in the root cells (Khudsar, 2008). It is well known that EDTA addition to contaminated soil can bring metals into solution through desorption of sorbed species and dissolution of precipitated compounds, thus maintaining their bioavailability for plant uptake (Marques, 2009; Norwell, 1984). Moreover, because of their neutral charge, metal-EDTA complexes are not blocked or bound by carboxyl groups or polysaccharides on the rhizodermal cell surface (Shahid et al., 2012). Therefore, root As concentration was the highest with the EDTA treatment (*Table 1*).

Xu et al. (2009) indicated that metal-EDTA complexes are transported through the apoplastic pathway, causing several-fold-stimulated metal translocation from roots to aerial plant parts, in agreement with our finding that, shoot As concentration was higher with the EDTA treatment than with other treatments. Extraradical hyphae of AMF can restrict heavy metal transport from soil to aboveground plant organs, and thus, may serve as a filter/biological barrier against heavy metal transport to plant shoots (Gaur and Adholeya, 2004; Schutzendubel and Polle, 2002). Therefore, shoot As concentration was observed to be minimum when AMF was applied alone. Although As was mainly retained in the root through immobilization by efficient mycorrhizal symbiosis, root As concentration with AMF alone was significantly lower than those with EDTA alone and EDTA-AMF combination, because of improved As uptake by EDTA.

Relative change in different As species

When EDTA was added to the soil, the ratios of the carbonate, Fe-Mn-bound, and organic-bound forms to total As were the lowest in the rhizosphere soil among all treatments, and the following mechanisms were mainly highlighted to explain this decrease caused by EDTA: (1) EDTA can decrease soil pH (Chen et al., 2004). Carbonates are sensitive to pH, and decrease in pH triggers As release from carbonate minerals; (2) EDTA destabilizes the weak bond between metal ions and Fe-Mn oxides and organic matter, and releases the metal ions from these substances (Luciano et al., 2013). EDTA generally increases the exchangeable fractions of heavy metals in soil by forming soluble complexes with them, and this organic molecule is capable of releasing metals linked with different soil particles (Jean-Soro et al., 2012; Udovic and Lestan, 2009). These may be the reasons for the increase in exchangeable As content and decrease in residual As content in the rhizosphere soil after EDTA application alone.

Figure 4 indicates that AMF application had a negative impact on exchangeable As content in the rhizosphere soil; however, it had a positive impact on the contents of carbonate-bound As, Fe-Mn-bound As, organic-bound As, and residual As. The decrease in exchangeable As content and increase in bound As contents were beneficial to maize growth under As stress. The benefits conferred by the mycorrhizosphere for plant growth are: (1) metal ions are bound to extraradical mycelia, which form a dense network of up to several meters of hyphae, and have an unusually high metal sorption capacity (Janoušková and Pavlíková, 2010); (2) binding of metal ions to chitin in the fungal cell wall reduces metal concentration in the mycorrhizosphere soil (Göhre and

http://www.aloki.hu ● ISSN 1589 1623 (Print) ● ISSN 1785 0037 (Online)
DOI: http://dx.doi.org/10.15666/aeer/1605_59875999
© 2018, ALÖKI Kft., Budapest, Hungary

Paszkowski, 2006); (3) AMF have high affinity for heavy metals, and are particularly suitable for fixing metal in the rhizosphere soil (Göhre and Paszkowski, 2006). These phenomena clearly explain the decrease in exchangeable As content and increase in bound As contents after AMF application alone. The ratio of exchangeable As to total As with the EDTA-AMF combination was evidently higher than that with the control and AMF alone, yet lower than that with EDTA alone, which was mainly because of mycorrhizal inhibition and EDTA promotion of EDTA-As chelation.

Enzyme activity

Under stress induced by As at 50 mg kg^{-1}, the activities of both SOD and CAT increased significantly with AMF alone and EDTA-AMF combination; however, activities of both enzymes decreased with EDTA alone, in both shoots and roots, compared with the control (*Fig. 3*). Increase in enzyme activity is actually a defense mechanism activated by the AMF relationship wherein the metal-induced production of reactive oxygen species increases under metal stress, and activated SOD and CAT are responsible for scavenging the excessively accumulated reactive oxygen species to reduce oxidative stress (Saraswat and Rai, 2011). Concerning EDTA alone, the decrease in enzyme activity might be related to the increase in As bioavailability promoted by EDTA, which may result in enzyme inactivation.

As extraction efficiency and biological enrichment factor

Different responses of As extraction efficiency and biological enrichment factor are presented in *Table 2*. The decrease in extraction efficiency with AMF alone and EDTA-AMF combination indicated that the growth dilution effect was likely to be an important protective mechanism provided by AMF (Zhang et al., 2005). However, the significant increase in biological enrichment factor with AMF alone and EDTA-AMF combination may be attributed to higher dry weight conferred by AMF and higher metal bioavailability facilitated by EDTA. Although EDTA application alone showed the highest extraction efficiency among all the treatments, biological enrichment factor was lower, excluding the control, because of growth inhibition caused by higher metal bioavailability.

Conclusions

We found that lone application EDTA significantly increased As extraction efficiency. However, it reduced plant yield, root colonization and antioxidant enzymatic activity. On the other hand, sole use of AMF, increased root colonization, maize dry matter yield and antioxidant enzyme activities, whereas decreased As extraction efficiency. Combine application of EDTA and AMF utilized the advantages of both EDTA and AMF to enhance As desorption from soil, improve the tolerance of maize plants to As stress, and increase As accumulation in shoots and roots. Thus, it showed a promising option for the remediation of heavy metal-polluted soil. This study warrants further investigations to optimize proportion of combination between AMF and EDTA. Moreover, the time and cost required for the phytoremediation of metal-polluted soil using maize should be considered.

http://www.aloki.hu ● ISSN 1589 1623 (Print) ● ISSN 1785 0037 (Online)
DOI: http://dx.doi.org/10.15666/aeer/1605_59875999
© 2018, ALÖKI Kft., Budapest, Hungary

Acknowledgements. This work was supported by the (i) National Key Research and Development Program, Shandong Province (project No. 2016ZDJS11A07 and GG201709210196) and (ii) Key Research and Development Program, Yantai (Project No. 2017ZH097), Shandong China. We are equally indebted to Yantai Institute, China Agriculture University for providing research facilities.

REFERENCES

[1] Aebi, H. (1974): Catalase. – In: Bergmeyer, H. U. (eds.) Methods of Enzymatic Analysis. Academic Press Inc, New York, pp. 674-684.

[2] Audet, P., Charest, C. (2006): Effects of AM colonization on 'wild tobacco' plantsgrown in zinc-contaminated soil. – Mycorrhiza 16: 277-283.

[3] Beauchamp, C., Cridovich, F. (1971): Superoxide dismutase: improved assays and an assay application to acrylamide gels. – Annals of Biochemestry 44: 276-287.

[4] Bhargava, A., Carmona, F. F., Bhargava, M., Srivastava, S. (2012): Approaches for enhanced phytoextraction of heavy metals. – Journal of Environmental. Management 105: 103-120.

[5] Charriau, A., Lesven, L., Gao, Y., Leermakers, M., Baeyems, W., Ouddane, B., Billon, G. (2011): Trance metal behavior in riverine sediments: Role of organic matter and sulfides. – Appl. Geochemistry 26: 80-90.

[6] Chen, Y., Li, X,. Shen, Z. (2004): Leaching and uptake of heavy metals by tem different species of plants during an EDTA-assisted phytoextraction process. – Chemosphere 57: 187-196.

[7] Citterio, S., Prato, N., Fumagalli, P., Santagostino, A., Sgorbati, S., Berta, G. (2005): The arbuscular mycorrhizal fungus *Glomus mosseae* induces growth and metal accumulation changes in *Cannabis sativa* L. – Chemosphere 59: 21-29.

[8] Davies, F. T., Puryear, J. D., Newton, R. J., Egilla, J. N., Saraiva Grossi, J. A. (2001): Mycorrhhizal fungi enhance accumulation and tolerance of chromium in sunflower (*Heliantbus ammuus*). – Journal of Plant Physiology 158: 777-786.

[9] De la Rosa, G., Peralta-Videa, J. R., Cruz-Jimenez, G., Duarte-Gardea, M., Martinez-Martinez, A., Cano-Aguilera, I., Sharma, N. C., Sahi, S. V., and Gardea-Torresdey, J. L. (2007): Role of ethylene diamine tetraacetic acid on lead uptake and translocation by tumbleweed (*Salsola kali* L.). – Environmental Toxicology and Chemistry 26: 1033-1039.

[10] Echevarri, G., Massoura, S., Sterckeman, T., Becquer, T., Schwartz, C., Morel, J. L. (2006): Assessment and control of the bioavailability of Ni in soils. – Environmental Toxicology and Chemistry 25: 643-651.

[11] Garg, N. Chandel, S. (2010): Arbuscular mycorrhizal networks: Process and functions. A review. – Agronomy for Sustainable Development 30: 581-599.

[12] Gaur, A., Adholeya, A. (2004): Prospect of arbuscular mycorrhizal fungi in phytoremediation of heavy metal contaminated soils. – Current Science 86: 528-534.

[13] Giasson, P., Jaouich, A., Gagné, S., Moutoglis, P. (2005): Arbuscular mycorrhizal fungi involvement in zinc and cadmium speciation change and phytoaccumulation. – Remediation 15: 75-81.

[14] Goel, S., Gautam, A. (2010): Effect of chelating agents on mobilization of metal from waste catalyst. – Hydrometallurgy 101: 120-125.

[15] Göhre, V., Paszkowski, U. (2006): Contribution of the arbuscular mycorrhizal symbiosis to heavy metal phytoremediation. – Planta 223: 1115-1122.

[16] Hadi, F., Bano, A., Fuller, M. P. (2010): The improved phytoextraction of lead (Pb) and the growth of maize (Zea mays, L.): The role of plant growth regulators (GA_3 and IAA) and EDTA alone and in combinations. – Chemosphere 80: 457-462.

[17] Hildebrandt, U., Kaldorf, M., Bothe, H. (1999): The zinc violer and its colonization by arbuscular mycorrhizal fungi. – Journal of Plant Physiology 154: 709-717.

http://www.aloki.hu ● ISSN 1589 1623 (Print) ● ISSN 1785 0037 (Online)
DOI: http://dx.doi.org/10.15666/aeer/1605_59875999
© 2018, ALÖKI Kft., Budapest, Hungary

[18] Janoušková, M., Pavlíková, D. (2010): Cadmium immobilization in the rhizosphere of arbuscular mycorrhizal plants by fungal extra radical mycelium. – Plant and Soil 332: 511-520.
[19] Janousková, M., Pavlíková, D., Macek, T., Vosátka, M. (2005): Arbuscular mycorrhiza decreases cadmium phytoextraction by transgenic tobacco with inserted metallothionein. – Plant and Soil 272: 29-40.
[20] Jean-Soro, L., Bordas, F., Bollinger, J. C. (2012): Column leaching of chromium and nickel from a contaminated soil using EDTA and citric acid. – Environmental Pollution 164: 175-181.
[21] Joner, E. J., Briones, R., Leyval, C. (2000): Metal-binding capacity of arbuscular-myccorhizal mycelium. – Plant and Soil 226(2), 227-234.
[22] Khudsar, T., Arshi, A., Siddiqi, T. O., Mahmooduzzafar, Iqbal, M. (2008): Zinc-induced changes in growth characters, foliar properties, and Zn-accumulation capacity of pigeon pea at different stages of plant growth. – Journal of Plant Nutrition 31: 281-306.
[23] Koske, R. E., Gemma, J. N. (1989): A modified procedure for staining roots to detect VA mycorrhizae. – Mycological Research 92: 486-505.
[24] Lin, A., Zhang, X., Wong, M., Ye, Z., Lau, L., Wang, Y., Zhu, Y. (2007): Increase of mutimetal tolerance of three leguminous plants by arbuscular mycorrhizal fungi colonization. – Environmental Geochemistry and Health 29: 473-481.
[25] Luciano, A., Viotti, P., Torretta, V., Mancini, G. (2013): Numerical approach to modeling pulse-mode soil flushing on Pb-contaminated soil. – Journal of Soil and Sediments 13: 43-45.
[26] Marques, A. P. G. C., Oliveira, R. S., Sam-Ardjieva, K. A., Pissarra, J., Rangel, A. O. S. S., Pissarra, J., Castro, P. M. L. (2008): EDDS and EDTA-enhanced zinc accumulation by *Solanum nigrum* inoculated with arbuscular mycorrhizal fungi grown in contaminated soil. – Chemosphere 70: 1002-1014.
[27] Marques, A. P. G. C., Rangel, A. O. S. S., Castro, P. M. L. (2009): Remediation of heavy metal contaminated soils: phytoremediation as a potentially promising clean-up technology. – Critical Reviews in Environmental Science and Technology 39: 622-654.
[28] McGrath, S. P., Zhao, F. J. (2003): Phytoextraction of metals and metalloids from contaminated soils. – Current Opinion in Biotechnology 14: 227-282.
[29] Meier, S., Borie, F., Bolan, N., Cornejo, P. (2012): Phytoremediation of metal-polluted soils by arbuscular mycorrhizal fungi. – Critical Reviews in Environmental Science and Technology 42(7): 741-775.
[30] Norwell, W. A. (1984): Comparison of chelating agents as extractants for metals in diverse soil materials. – Soil Science Society of America Journal 48: 1285-1292.
[31] Pandey, V. C. (2012): Phytoremediation of heavy metals from fly ash pound by Azolla caroliniana. – Ecotoxicology and Environmental Safety 82: 8-12.
[32] Saraswat, S., Rai, J. P. N. (2011): Mechanism of Metal Tolerance and Detoxification in Mycorrhizal Fungi. – In: Khan, M. S., Zaidi, A. (eds.) Biomanagement of Metal-Contaminated Soil, Springer, The Netherlands, pp. 225-240.
[33] Sarwar, N., Imran, M., Shaheen, M. R., Ishaque, W., Kamran, M. A., Matloob, A., Rehim, A., Hussain, S. (2017): Phytoremediation strategies for soils contaminated with heavy metals: Modifications and future perspectives. – Chemosphere 171: 710-721.
[34] Schutzendubel, A., Polle, A. (2002): Plant responses to abiotic stresses: heavy metal oxidative stress and protection by mycorrhhization. – Journal of Experimental Botany 53: 1351-1365.
[35] Seth, C. S. (2011): A review on mechanisms of plant tolerance and role of transgenic plants in environmental clean-up. – The Botanical Review 78: 32-62.
[36] Shabir, R., Abbas, G., Saqib, M., Shahid, M., Shah, G. M., Akram, M., Ashraf, F. (2018): Phytoremediation of Cd by Acacia nilotica L. as affected by NaCl salinity. – International Journal of Phytoremediation 7: 739-746.

http://www.aloki.hu ● ISSN 1589 1623 (Print) ● ISSN 1785 0037 (Online)
DOI: http://dx.doi.org/10.15666/aeer/1605_59875999
© 2018, ALÖKI Kft., Budapest, Hungary

[37] Shah, G. M., Rashid, M. I., Shah, G. A., Groot, J. C. J., Lantinga, E. A. (2013): Mineralization and herbage recovery of animal manure nitrogen after application to various soil types. – Plant and Soil 365(1-2): 69-79.
[38] Shah, G. M., Shah, G. A., Groot, J. C. J., Raza, M. A. S., Shahid, N., Lantinga, E. A. (2016): Nitrogen recovery and dry matter production of silage maize as affected by the application of solid cattle manure stored under different conditions. – Journal of Soil Science and Plant Nutrition 16(3): 591-603.
[39] Shahid, M., Pinelli, E., and Dumat, C. (2012): Review of Pb availability and toxicity to plant in relation with metal speciation: role of synthetic and natural organic ligands. – Journal of Hazardous Material 219-220: 1-12.
[40] Sinha, S., Mishra, R. K., Sinam, G., Mallick, S., Gupta, A. K. (2013): Comparative evaluation of metal phytoremediation potential of trees, grass, and flowering with the hyperaccumulator plants from tannery-wastewater-contaminated soil in relation with physicochemical properties. – Soil Sediment Contamination 22: 958-983.
[41] Tabrizi, L., Mohammadi, S., Delshad, M., Zadeh, B. M. (2015): Effect of arbuscular mycorrhizal fungi on yield and phytoremediation performance of pot marigold (*Calendula officinalis* L.) under heavy metals stress. – International Journal of Phytoremediation 17: 1244-1252.
[42] Tang, Y. T., Deng, T., Wu, Q. H., Wang, S. Z., Qiu, R. L., Wei, Z. B., Guo, X. F., Lei, M., Chen, T. B., Echevarria, G., Sterckeman, T., Simonnot, M. O., Morel, J. L. (2012): Designing cropping system for metal-contaminated sites: A review. – Pedosphere 22: 470-488.
[43] Tanwar, A., Aggarwal, A., Charaya, M. U., Kumar, P. (2013): Enhancement of lead uptake by fenugreek using EDTA and glomus mosseae. – Communication in Soil Science and Plant Analysis 44: 3431-3443.
[44] Tomé, V. F., Blanco, R. P., Lozano, J. C. (2009): The ability of *Helianthus annuus* L. and *Brassica juncea* to uptake and translocate natural uranium and 226Ra under different milieu conditions. – Chemosphere: 74: 293-300.
[45] Trotta, A., Falaschi, P., Cornara, L., Minganti, V., Fusconi, A., Drava, G., Berta, G. (2006): Arbuscular mycorrhizae increase the arsenic translocation factor in the As hyperaccumulating fern *Pteris vittata* L. – Chemosphere: 65: 74-81.
[46] Udovic, M., Lestan, D. (2009): Pb, Zn and Cd mobility, availability and fractionation in aged soil remediated by EDTA leaching. – Chemosphere 74: 1367-1373.
[47] Wang, X. P., Zabowski, D. (1998): Nutrient composition of Douglas-fir rhizosphere and bulk soil solutions. – Plant and Soil 200: 13-20.
[48] Xu, W., Li, W., He, J., Balwant, S., and Xiong, Z. (2009): Effects of insoluble Zn, Cd, and EDTA on the growth, activities of antioxidant enzymes and uptake of Zn and Cd in *Vetiveria zizanioides*. – Journal of Environmental Science 21: 186-192.
[49] Yang, G. Y., Li, F. B., Wan, H. F. (2003): Changes in the contents of heavy metals in pig manure compositing (in Chinese). – Ecology and Environment 12(4): 412-414.
[50] Yang, J. R., Che, Y. H. (1986): Ecological impact assessment for opencut coal mine. – Acta Scientiae Circumstantiae 6(1): 1-7.
[51] Zhang, X. H., Zhu, Y. U., Chen, B. D., Lin, A. J., Smith, S. E., Smith, F. A. (2005): Arbuscular mycorrhizal fungi contribute to resistance of upland rice to combined metal contamination of soil. – Journal of Plant Nutrition 28: 2065-2077.

http://www.aloki.hu ● ISSN 1589 1623 (Print) ● ISSN 1785 0037 (Online)
DOI: http://dx.doi.org/10.15666/aeer/1605_59875999
© 2018, ALÖKI Kft., Budapest, Hungary

THE REPELLENCY EFFECTS OF THREE PLANT ESSENTIAL OILS AGAINST THE TWO-SPOTTED SPIDER MITE *TETRANYCHUS URTICAE*

YEŞILAYER, A.

Plant Protection Department, Agricultural Faculty, Gaziosmanpasa University
60216 Tokat, Turkey
(e-mail: ayse.yesilayer@gop.edu.tr)

(Received 26th Jun 2018; accepted 31st Aug 2018)

Abstract. Many spider mite species are polyphagous and live together. They are significantly harmful pests for agricultural crops. Acaricides and insecticides are commonly used to control *T. urticae*. Spider mites can rapidly develop resistance to pesticides. Organic control may be considered as an alternative and environment-friendly approach. Three native plants essential oils were isolated by hydrodistillation technique hydro distillation in a Clevenger type apparatus. In this study, *Thymbra spicat*a L. (Labiatae), *Laurus nobilis* L. (Lauraceae) and *Myrtus communis* L. (Myrtaceae) plants have been tested for their essential oil's repellency effect. Essential oils of these three plants were compared for 48 h at four different doses (0.1, 0.5, 1 and 2 ml/l). We observed repellency effect all does and for all essential oils, whereas *M. communis* was proven to be a stronger repellent compared to *L. nobilis* at 2 ml/l.
Keywords: *control, essential oil, repellency effect, Tetranychus urticae, Tokat, Turkey*

Introduction

The two-spotted spider mites, *Tetranychus urticae* Koch. (Acarina: Tetranychidae), are about 0.5 mm in size, with reddish or greenish body color. The adult female body bears 12 pairs of dorsal seta. Two-spotted spider mites (TSSM) were initially described as a European species by Tuttle and Baker in 1968. *T. urticae* is a significant proliferous polyphagous pest, commonly controlled by pesticides in Turkey and other countries. This mite has more than 1200 known host plants (Zhang, 2003). Pesticides pose serious risks for the environment, non-target-organisms and also human life. Tetranychidae has developed resistance against 80 different acaricides to date (Darp, 2004; Miresmailli et al., 2006; Vanpottelberge et al., 2009). *T. urticae* has developed resistance to many insecticides and acaricides (Ay and Gürkan, 2005; Dermauw et al., 2013). Eventually, its control has become problematic in many regions of the world. Several researchers have focused on alternative methods to overcome the negative impacts of conventional pesticides. Essential oils and plant extracts are among the alternative methods against pests and spider mites. Plant essential oils have toxic effects on pests through contact, ingestion and fumigation; in addition, plant essential oils or their constituents have significant behavioral effects on pests, especially as repellents (Akhtar et al., 2010). Another study investigated repellency effects of plant extracts obtained from weeds and essential oils of 53 different plants on *T. urticae* (Kawka and Tomczyk, 2002). The use of plant extracts and essential oils in pest control could be an effective alternative compared to pesticides. Essential oils and their contents such as terpenoids, alkaloids and flavonoids are effective in pest control (Grodnitzky and Coats, 2002). EOs are used antibacterial, antifungal and insecticidal (Chang and Cheng, 2002). Furthermore, plant essential oils have minimal direct and/or indirect effect on predators or the ecosystem (Isman, 2006). Black thyme (*Tthymus spicata*) grows wild in some Eastern

http://www.aloki.hu ● ISSN 1589 1623 (Print) ● ISSN 1785 0037 (Online)
DOI: http://dx.doi.org/10.15666/aeer/1605_60016006
© 2018, ALÖKI Kft., Budapest, Hungary

Mediterranean countries and Turkey (Kizil, 2010); its essential oil contains 60-80% of carvacrole. It is belongs to the Lamiaceae family. Thyme has been studied as repellents (Rajkumar and Jebanesan, 2005). *Laurus nobilis* is also a major source of essential oil and its leaf essential oil was reported to be rich in 1.8-cineole (Baydar, 2009). *L. nobilis* is a important plant of used in foods, drugs, and cosmetics. Laurus leaves and essential oils are used for antimicrobial and insecticidal activities (Patrakar et al., 2012). *Myrtus communis* (myrtle) is grows wild and cultivated. It is widespread throughout the Mediterrian region of Anatoloia-Turkey. *Myrtus* leaves and fruit of the plant contain mirtenol, cineol and terpenes. The main constituents of *M. communis* oil are 1.8-cineole, myrtenyl acetate, myrtenol and limonene (Traveset et al., 2001). The myrtle essential oil observed toxicity fumigation of lepidoptera and coleoptera species (Ayvaz et al., 2010; Tayoub et al., 2012).

This article reports repellency effects of essential oils obtained from flowers, stems and leaves of *T. spicata*, *L. nobilis* and *M. communis* against two-spotted spider mites, and positions them as an alternative to pesticides.

Material and methods

Mites culture

Two-spotted spider mites were obtained from a colony maintained at the Plant Protection Department, Tokat Gaziosmanpaşa University (GOP), Turkey. Mites were grown in a climate chamber at 26 ± 1 °C, 60-80% of relative humidity (RH) and 16 h of light and 8 h of dark (LD) photoperiod.

Material collection and processing

T. spicata, L. nobilis and *M. communis* were collected from around the campus area of GOP University during the summer season in June-August 2016 (Location 40.3339, 36.4769). Fresh plant parts were air-dried in the shade at room temperature and then grounded. Essential oils were extracted from a 100 g mixture of stems, flowers and leaves using a Clevenger-type apparatus within 2 h. The essential oils were later stored in sealed vials at 4 °C until the time of analyses (as previously performed by Cosimi et al., 2009).

Repellency effect

During the trial, same age ten adult female mites were transferred into 3 cm bean leaf disks as nutriment and then placed in 9 cm Petri dishes. We tested four different concentrations (0.1, 0.5, 1 and 2 ml/l) of essential oils of *T. spicata*, *L. nobilis* and *M. communis*. They were dissolved in water containing 0.3% Tween 20 and were diluted to the targeted doses. Leaf discs (30 mm diameter) were cut from *P. vulgaris* leaves. In the repellency assay, half of leaf discs were immersed in water containing 0.3% Tween 20, which served as control and the other half of the leaf discs were immersed in each essential oil solution for 20 s before drying in room temperature for 30 s. Afterwards, leaf discs were put in Petri dishes; ten adult females (1-2 day old) of *T. urticae* were placed on the center of each leaf disc. Cotton saturated with water was added in the Petri dishes in order to maintain the leaf turgor and avoid escape of mites.

Plates were then sealed with parafilm to prevent any loss of essential oils. Each treatment was repeated for three times. The number of mites on treated leaves (half of

http://www.aloki.hu ● ISSN 1589 1623 (Print) ● ISSN 1785 0037 (Online)
DOI: http://dx.doi.org/10.15666/aeer/1605_60016006
© 2018, ALÖKI Kft., Budapest, Hungary

the leaf) and untreated leaves (the other half of the leaf) were counted at 2, 24 and 48 h post treatment respectively and repellency index was calculated by RI = (C – T / C + T) × 100 (Pascual-Villalobos and Robledo, 1998). In this formula RI stands for repellency index, T is the number of mites in treatment group and C is the number of mites in the control group.

Phytotoxicty test

Based on a study by Miresmailli and Isman (2006), essential oils of three test plants were tested on rose shoots (*Rosa damascena* Mill) using 1% solution (300 ml) consisting of essential oil, distilled water and Triton X. Each plant's essential oil (30 ml solution) was sprayed on rose shoots by using a handle sprayer, while control rose shoots remained unsprayed. Shoots were prepared in a glass flask filled with tap water (500 ml) under laboratory condition maintained at 26 ± 1 °C and 16 h of light and 8 h of dark (LD) photoperiod. Results were recorded after a treatment 24 using a scale between 0 to 4. Each treatment was replicated three times.

Data analysis

The repellency effects were analyzed by one-way analysis of variance (ANOVA) and significant differences between mean values were found by Tukey test using SPSS version 19.0. P-value < 0.05 was regarded as a significant difference.

Results and discussion

The repellent activity of three different plant essential oils tested at various concentrations after 2, 24 and 48 h post exposure period are presented in *Table 1*. *T. spicata* was found to have the lowest repellency effect at 49.9% in 2 h and 45.8% after 24 and 48 h. We also observed that the repellency effects of essential oils on adult mites would increase with time regardless of the concentration level.

Table 1. *Repellency effects of three plants' essential oil on Tetranychus urticae*

Time (h)	Concentration (ml/l)	Repellency effect (% ± SE)		
		Laurus nobilis	*Myrtus communis*	*Thymbra spicata*
2	0.1	76.9±11.98a	79.16±12.50a	49.99±08.90a
	0.5	75.00±10.44a	79.16±16.59a	70.83±11.67 a
	1	80.95±12.29a	83.33±06.29a	79.16±10.79a
	2	87.50±8.76a	95.83±04.16b	83.33±08.90a
24	0.1	58.33±08.33a	79.16±12.50a	45.83±06.09a
	0.5	66.66±08.90a	75.00±12.19ab	75.01±10.44ab
	1	70.83±07.55a	83.33±06.29a	79.16±08.76b
	2	79.16±08.76b	91.66±05.45 b	83.33±06.29a
48	0.1	50.00±06.29a	66.66±08.90a	45.83±06.09a
	0.5	58.33±08.33ab	70.83±13.26a	75.00±10.44ab
	1	66.66±06.29ab	79.16±06.09a	79.16±08.76ab
	2	75.00±04.35a	95.83±11.78 b	91.66±05.45 b

Different letters within the same rows and columns indicate significant differences between essential oils and treatment concentrations, respectively ($p \leq 0.05$) (Tukey test)

http://www.aloki.hu ● ISSN 1589 1623 (Print) ● ISSN 1785 0037 (Online)
DOI: http://dx.doi.org/10.15666/aeer/1605_60016006
© 2018, ALÖKI Kft., Budapest, Hungary

24-h repellency effects of *L. nobilis* and *M. communis* at 0.5 ml/l concentration on adult females of two-spotted spider mites were recorded as 66.6% and 75% respectively, which was statically significant ($P < 0.05$). The repellency effect of *T. spicata* at the lowest concentration (0.1 ml/l) was found to be lower than *L. nobilis* and *M. communis* at the end of 2, 24 and 48 h and there is no difference statistically. In addition, no significant difference was found between the repellency effects at 2 h and 48 h, when applying 0.1 ml/l concentration. At 2 h, in all three plant essential oil treatments, the effect of 0.1 and 2 ml/l concentrations were statistically within the same range. The highest repellency effects were observed at the and of 48 h with *M. communis* and *T. spicata* essential oil on *T. urticae* adults as 95.8% and 91.6% respectively. Furthermore, the highest repellency effect on adult mites identified as 95.8% with 2 ml/l concentration of *M. communis* at the 48 was found to be statistically different from other groups ($F = 01.50$, d.f. = 3, $P < 0.05$). Regardless of duration, the repellency effects of all three tested essential oils on *T. urticae* adults changed with the changing concentration. Eventually, *M. communis* essential oil was observed to have highest repellency effects as compared to other test plant essential oils on *T. urticae* in 24 and 48 h exposure ($P < 0.05$).

Essential oils contain several biochemicals including acids, alcohols, aldehydes, ketones, esters, phenols, terpenes and sesquiter penes. Essential oils are used as antifeedant, antiviral, acaricidal, antimicrobial, antioxidant, antifungal, contact and repellent (Isman, 2000, 2006). In this study, we demonstrated repellency effects of essential oils from three plants belonging to Lamiaceae family against two-spotted spider mite. There is no observed any phytotoxic effect on bean plants.

Previously, different concentrations of essential oils from 14 species of Lamiaceae were shown to cause mortality and induce repellency in adult females of the carmine spider mite, *T. cinnabarinus*. (Mansour et al., 1986). Other studies also confirm repellency effect of *M. communis* essential oil against two spotted spider mites (El-Zemmity et al., 2006). In another repellency effect study, four different concentrations of rose essential oil, geraniol and citronellol were applied to *T. urticae* and results confirmed repellency effects of essential oils on the mites (Yorulmaz-Salman and Erbaş, 2014). In a repellency trial on *T. urticae* with essential oils of *Origanum vulgare* L, *Micromeria fruticosa* L. And *Nepeta racemosa* L. of the Lamiacea (mint) family, highest motalily rate was observed at 2 µl/l concetration, and it also increased with time. (Çalmaşur et al., 2006). Another study in greenhouse conditions with essential oils obtained from *Cuminum cyminum* and *Origanum syriacum* var *bevanii* revelaed fumigant effects on *T. cinnabarinus* and *Aphis gossypii* (Tuni and Sahinkaya, 1998).

Conclusion

In conclusion *M. communis* essential oil showed stronger repellency effect on TSSM adults at the highest concentration (2 ml/l) in comparison to *L. nobilis* and *T. spicata* essential oils. We concluded that all three plant essential oils can be used to control *T. urticae*. The repellency effects of *T. spicata*, *L. nobilis* and *M. communis* essential oils on TSSM adults in all concentrations increased with time. However, it is necessary to perform experiments with these three plant essential oils under the greenhouse conditions and compare results with laboratory results. As a final note, at given concentrations, the tested essential oils were not detected to have any phytotoxic effect on the plants.

http://www.aloki.hu ● ISSN 1589 1623 (Print) ● ISSN 1785 0037 (Online)
DOI: http://dx.doi.org/10.15666/aeer/1605_60016006
© 2018, ALÖKI Kft., Budapest, Hungary

Acknowledgements. We are grateful to Prof. Dr. İzzet Kadıoğlu (Tokat GOP Univ., Agricultural Fac. of Plant Protection Dept. Turkey) for providing us with the plant specimens.

REFERENCES

[1] Akhtar, Y., Yu, Y., Isman, M. B., Plettner, E. (2010): Dialkoxybenzene and dialkoxyallylbenzene feeding and oviposition deterrents against the cabbage looper, Trichoplusia ni: potential insect behavior control agents. – Journal of Agricultural Food and Chemistry 58(8): 4983-4991.

[2] Ay, R., Gürkan, M. O. (2005): Resistance to bifenthrin and resistance mechanisms of different strains of the two-spotted spider mite (*Tetranychus urticae*) from Turkey. – Phytoparasitica 33(3): 237-244.

[3] Ayvaz, A., Sagdıç, O., Karaborklu, S., Özturk, I. (2010): Insecticidal activity of the essential oils from different plants against three stored-product insects. – Journal of Insect Science 10(21): 13.

[4] Baydar, H. (2009): Tıbbi ve Aromatik Bitkiler Bilmi ve Teknolojisi. – Süleyman Demirel Üniversitesi Ziraat Fakültesi Yayınları Isparta 51: 234-235.

[5] Çalmaşur, O., Aslan, I., Sahin, F. (2006): Insecticidal and acaricidal effect of three Lamiaceae plant essential oils against Tetranychus urticae Koch and Bemisia tabaci Genn. – Indian Crops Production 23: 140-146.

[6] Chang, S. T., Cheng, S. S. (2002): Anitermitic activity of leaf essential oils and components from Cinnamonum osmophleum. – Journal of Agricultural Food Chemistry 50(5): 1389-1392.

[7] Cosimi, S., Rossi, E., Cioni, P. L., Canale, A. (2009): Bioactivity and quallitative analysis of some essential oil from Mediterrian plants against stored-product pests. Evaluation of repellency against *Sitophilus zeamais* Motschulsky, *Cryptolestes ferrugineus* Stephens and *Tenebrio molitor* L. – Journal of Stored Product Research 45: 125-132.

[8] DARP (2004): Database of arthropods resistance to pesticides. – http://www.pesticideresistance.org/DB/index.html. Accessed on 25.05.2016.

[9] Dermauw, W., Wybouw, N., Rombauts, S., Menten, B., Vontas, J., Grbi, M., Clark, R. M., René Feyereisen, R., Van Leeuwen, T. (2013): A link between host plant adaptation and pesticide resistance in the polyphagous spider *mite Tetranychus urticae*. – PNAS 110(2): 113-122. www.pnas.org/cgi/doi/10.1073/pnas.1213214110.

[10] El-Zemity, S., Hussien, R., Saher, F., Ahmed, Z. (2006): Acaricidal activities of some essential oils and their monoterpenoidal constituents against house dust mite, *Dermatophagoides pteronyssinus* (Acari: Pyroglyphidae). – Journal of Zhejiang University Science B. 7: 957-962.

[11] Grotnitzky, J. A., Coats, J. R. (2002): QSAR evaluation of monoterpenoids insecticidal activity. – Journal of Agricultural Food Chemistry 50: 4576-4580.

[12] Isman, M. B. (2000): Plant essential oils for pest and disease management. – Crop Protection 19: 603-608.

[13] Isman, M. B. (2006): Botanical insecticides, deterrents, and repellents in modern agriculture and increasingly regulated world. – Annual Review Entomology 51: 45-56.

[14] Kawka, B., Tomczyk, A. (2002): Influence of extract from sage (*Salvia officinalis*) on some biological parameters of *Tetranychusurticae* Koch feeding on Algerian Ivy (*Hederahelix variegate* L.). – IOBC Bulletin 22: 96-100.

[15] Kizil, S. (2010): Determination of essential oil variations of *Thymbra spicata* var. *spicata* L. naturally growing in the wild flora of East Mediterranean and Southeastern Anatolia regions of Turkey. – Industrial Crops and Products 32: 593-600.

[16] Mansour, F., Ravid, U., Putievsky, E. (1986): Studies on the effects of essential oils isolated from 14 species of labiatae on the carmine spider mite, *Tetranychus cinnabarinus*. – Phytoparasitica 14: 137-142.

http://www.aloki.hu ● ISSN 1589 1623 (Print) ● ISSN 1785 0037 (Online)
DOI: http://dx.doi.org/10.15666/aeer/1605_60016006
© 2018, ALÖKI Kft., Budapest, Hungary

[17] Miresmailli, S., Bradbury, R., Isman, M. B. (2006): Comparative toxicity of *Rosmarinus officinalis* L. essential oil and blends of its major constituents against *Tetranychus urticae* Koch (Acari: Tetranychidae) on two different host plants. – Pest Management Science 62: 366-371.
[18] Pascual-Villalobos, M. J., Robledo, A. (1998): Anti-insect activity of plant extracts from the Wild Flora in Southern Spain. Biochem. – Systematic Ecology 27: 1-10.
[19] Patrakar, R., Mansuriya, M., Priyanka, P. (2012): Phytochemical and pharmacological review on *Laurus nobilis*. – International Journal of Pharmaceutical and Chemical Sciences 1(2): 595-602.
[20] Rajkumar, S., Jebanesan, A. (2005): Oviposition deterrent and skin repellent activities of Solanum trilobatum leaf extract against the malarial vector Anopheles stephensi. – Journal of Insect Science 5(15): 1-3.
[21] Tayoub, G., Abu Alnaser, A., Ghanem, I. (2012): Fumigant activity of leaf essential oil from *Myrtus communis* L. against the Khapra Beetle. – International Journal of Medicinal Aromatic Plants 2(11): 207-213.
[22] Tomczyk, A., Szymanska, M. (1995): Possibility of reduction of spider mite population by spraying with selected herb extracts. – Proceeding of 35th Scientific Session IOR, Part II, pp. 125-128.
[23] Traveset, A., Riera, N. R. E. (2001): Ecology of fruit-colour polymorphism in *Myrtus communis* and differential effects of birds and mammals on seed germination and seedling growth. – Journal of Ecology 89: 749-760.
[24] Tuni, I., Sahinkaya, S. (1998): Sensivity of two greenhouse pest to vapors essential oils. – Experimental and Applied Entomology 86: 312-324.
[25] Tuttle, D. M., Baker, E. W. (1968): Spider Mites of Southwestern United States and a Revision of the Family Tetranychidae. – University of Arizona Press, Tucson, AZ.
[26] Van Pottelbelge, S., Van Leeuwen, T., Khajehali, J., Tirry, L. (2009): Genetic and biochemical anlysis of a laboratory-selected spirodiclofen-resistant strain of Tetranychus urticae Koch (Acari: Tetranychidae). – Pest Management Science 65: 358-366.
[27] Yorulmaz-Salman, S., Erbaş, S. (2014): Contact and repellency effects of Rosa damascena Mill. essential oil and its two major constituents against Tetranychus urticae Koch (Acari: Tetranychidae). – Türkiye Entomoloji Dergisi 38(4): 365-376.
[28] Zhang, Z. (2003): Mites of Greenhouses: Identification, Biology and Control. – CABI Publishing, Wallingford.

http://www.aloki.hu ● ISSN 1589 1623 (Print) ● ISSN 1785 0037 (Online)
DOI: http://dx.doi.org/10.15666/aeer/1605_60016006
© 2018, ALÖKI Kft., Budapest, Hungary

TILLAGE TIME AFFECTS SOIL HYDRO-THERMAL PROPERTIES, SEEDLING GROWTH AND YIELD OF MAIZE (*ZEA MAYS* L.)

WANG, X. – YUE, Y. – NOOR, M. A. – HOU, H. – ZHOU, B. – MA, W.* – ZHAO, M.*

Institute of Crop Sciences, Chinese Academy of Agricultural Sciences, Key Laboratory of Crop Physiology and Ecology, Ministry of Agriculture, 100081 Beijing, P. R. China

**Corresponding authors*
e-mail: mawei02@caas.cn, zhaoming@caas.cn; phone/fax: +86-10-8210-8752

(Received 9th May 2018; accepted 11th Jul 2018)

Abstract. Two-year experiments were conducted to determine optimum tillage time to improve soil compaction and hydro-thermal properties for maize growth. Two tillage treatments: no-tillage (NT), and subsoiling (SS) were performed in correspondence to eight tillage times from March 25 to July 20 (I: March 25, II: April 10, III: April 25, IV: May 10, V: May 25, VI: June 10, VII: July 5, and VIII: July 20) at 15 days interval, synchronously with eight sowing times. SS significantly decreased soil bulk density (0-30 cm) by about 0.13 g cm^{-3} at times of I–V, and about 0.08 g cm^{-3} at VI–VIII. Increment in total soil porosity due to SS was about 3.88% during I–V and about 2.27% at VI–VIII. SS significantly increased soil moisture content by 1.60% in 10-30 cm soil profile. Soil minimum temperature significantly increased by about 0.58 °C (0-20 cm) for I–V, while an increase of 1.06 °C (0-10 cm) was seen for maximum soil temperature due to SS. Greater seedling dry matter coupled with higher growth, and yield improvement was achieved with SS. Dry matter accumulation and grain yield was maximum for May 25 to June 10 sowing as compared to early (22%, 43.5%) and late (60%, 41%, respectively) sowing due to SS versus NT. Initial SS intervals could alleviate soil compaction and low temperature stress for spring maize, with improved soil hydrothermal properties.
Keywords: *subsoiling time, soil bulk density, soil moisture, soil temperature, maize growth*

Introduction

No-tillage in maize (*Zea mays* L.) is the dominant agricultural practice in Huang-Huai-Hai (HHH) maize growing region in China, and the long-term no-tillage is often unfavorable for the growth of maize. Soil compaction has been a major limiting factor for soil environment and plant growth (Zheng and Yan, 2006). To improve soil environment and health, subsoiling tillage as an effective measure is getting popular for maize growth (Ji et al., 2013). Normally, soil tillage and seed sowing are always conducted in June with low precipitation and high temperature in HHH region. Although, no-tillage is practiced for maize sowing in HHH region, except a little soil disturbance at the time of sowing, under winter-wheat and summer-maize cropping system. However, intensive tillage could cause serious soil surface water evaporation during this period, especially with high temperature (Yu and Zhang, 2005), and intensive tillage over longer periods also alters the chemical and physical properties of soil (Lozano-García and Parras-Alcántara, 2014; Jabro et al., 2009). This could lead to a severe drought stress for maize seedling growth (Zhou et al., 2009). Especially under the recent scenario of climate change, in which air temperature is increasing and causing irregular rainfall flashes in northern China (Zafar et al., 2018; Piao et al., 2010; Guo et al., 2010). To avoid the negative effects of soil problems and external micro and macro climate on maize growth and development, the time of soil tillage and sowing date considering the external environment should be given greater attentions (Noor,

http://www.aloki.hu ● ISSN 1589 1623 (Print) ● ISSN 1785 0037 (Online)
DOI: http://dx.doi.org/10.15666/aeer/1605_60076023
© 2018, ALÖKI Kft., Budapest, Hungary

2017; Yin et al., 2017). Therefore, identifying an effective tillage time to decrease soil compaction level and improving soil hydro-thermal properties is very important for the maize seedling growth (Nath and Lal, 2017; Lu et al., 2016).

Recently, great progress has been made through soil tillage management in reducing soil bulk density and increasing soil moisture storage. Subsoiling tillage is reported as conservation tillage practice, by improvement of soil characteristics for maize sowing and seedling growth (Liu et al., 2009; Hou et al., 2012; Hoffmann and Kismányoky, 2001). Many studies indicated that subsoil deep tillage could break the soil plough pan and reduces soil bulk density to a proper soil compaction in northeast China (Wang et al., 2014). Soil structure and hydro-thermal characteristics are not only influenced by soil tillage management, but also highly sensitive to the external environmental conditions such as temperature and precipitation (Karandish and Shahnazari, 2016; Hartmann et al., 2012; Bhaduri et al., 2017).

Therefore, studying the effects of subsoiling tillage implemented at different time intervals has practical guiding value for selecting optimal soil tillage management in maize. Our objectives in present study were, in the process of soil improvement, (1) to find the differential effects of subsoiling tillage on soil compaction and hydro-thermal properties at different subsoiling tillage times; (2) to evaluate the specific subsoiling tillage time alleviating the soil compaction stress at maize seedling growth; (3) to identify optimum time for subsoiling tillage for improving soil compaction problem and minimizing drought stress effects encountered by maize at the seedling stage in HHH region.

Materials and methods

Site description

The field experiments were conducted in Xinxiang Experiment Station of Chinese Academy of Agricultural Sciences, Henan Province, China (35°18áN, 113°54áE). Soil textural class for studied site is classified as clay loam (ISSS Classification, International Soil Science Society), with percentage composition of sand, silt and clay as 32.95, 34.2 and 32.85%, respectively (saturation: 38.5%). Soil bulk density was 1.29 g cm^{-3}, 1.34 g cm^{-3}, 1.55 g cm^{-3} and 1.52 g cm^{-3} at 0-10 cm, 10-20 cm, 20-30 cm and 30-40 cm soil depth, respectively. Major soil nutrient contents analyzed were: organic matter 12.55 g kg^{-1}, total nitrogen 1.13 g kg^{-1}, available phosphorus 16.15 mg kg^{-1}, and 109.95 mg kg^{-1} available potassium (pH = 8.21, EC = 1.2 dSm^{-1}, slope gradient with negligible risk of soil erosion). Usual crop rotation for this area is double cropping system with winter-wheat and summer-maize, in that rotary tillage (15-20 cm) is practiced for wheat and no-tillage farming for maize crop is followed usually.

Annual mean temperature and accumulated precipitation conditions from March to July during 1990 to 2012 are shown in *Figure 1*. From year 1990 to 2012, annual accumulated precipitation had a decline trend, whereas annual mean temperature gradually increased.

Experimental design and soil tillage management

The experiment was conducted from 2011 to 2012. Randomized complete block design was used with split plot arrangement and three replications. Main plots were assigned to tillage times correspondingly with eight sowing intervals starting from

http://www.aloki.hu ● ISSN 1589 1623 (Print) ● ISSN 1785 0037 (Online)
DOI: http://dx.doi.org/10.15666/aeer/1605_60076023
© 2018, ALÖKI Kft., Budapest, Hungary

March 25 to July 20 (I: March 25, II: April 10, III: April 25, IV: May 10, V: May 25, VI: June 10, VII: July 5, and VIII: July 20). Whereas, in subplots two soil tillage treatments just before the maize sowing were conducted viz. SS: subsoiling tillage management involved complete soil inversion and burial of crop residues to a depth of 30 cm using a stripe deep loosening machine (Hehuinong machine Co. Ltd., Beijing, China)., NT: no tillage for two consecutive years. The experimental plots were 30 m long and 3.6 m wide and consisted of 6 rows. Maize sowing and soil tillage were conducted at the same day, so the experiment had eight sowing dates correspondingly. There was no deep soil tillage management for the rotational crops and the plough pan lies at the depth of 20-30 cm of soil profile. The maize variety Zhengdan-958 was planted at the density of 67500 plants ha^{-1} with an 80-40 cm wide/narrow row spacing pattern. N fertilizers at 225 kg N ha^{-1} (Urea: 46% N) were applied in two split applications: 1/3 as basal application before planting, and the remaining 2/3 as side-dressing at the V8-V9 growth stage. Phosphate (P_2O_5) and Potassium (K_2O) fertilizers were applied at 75 kg/ha and 150 kg/ha before sowing, respectively.

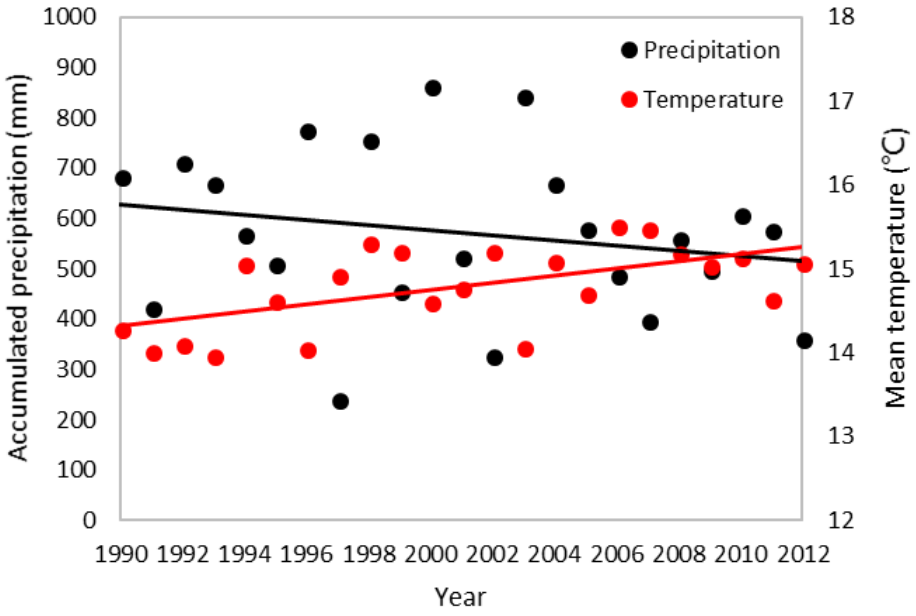

Figure 1. *Changes of annual mean temperature and accumulated precipitation from 1990 to 2012*

Sampling and measurement

Soil samples were collected from four soil depths (0-10 cm, 10-20 cm, 20-30 cm, and 30-40 cm) for each tillage treatment 20 days after soil tillage implementation. In each plot, soil sample was obtained to determine soil bulk density, soil porosity, soil moisture content and soil temperature. For plant samples plant shoots were cut manually at the ground level to determine the shoot dry weight, and plant roots were dug out from soil profile of 40 cm depth to determine the root dry weight for 3 plants per plot at 20 days after soil tillage management.

Soil bulk density was determined by weighing method (*Eq. 1*) with cutting-ring which had a fixed volume of 100 cm^3 to sample the soil maintaining the soil physical structure at the same time. Then weighing the soil fresh weight and dry weight:

http://www.aloki.hu ● ISSN 1589 1623 (Print) ● ISSN 1785 0037 (Online)
DOI: http://dx.doi.org/10.15666/aeer/1605_60076023
© 2018, ALÖKI Kft., Budapest, Hungary

$$\text{Soil bulk density (g/cm}^3) = \frac{\text{soil dry weight (g)}}{\text{cutting-ring volume (cm}^3)} \quad \text{(Eq.1)}$$

The measurement was made at four depths of soil (0-10, 10-20, 20-30, and 30-40 cm) at seedling stage of maize. The measurement was repeated three times in each plot. Total soil porosity was calculated (*Eq. 2*) from soil bulk density as follows:

$$\text{Total soil porosity (100\%)} = \frac{(\text{soil density} - \text{soil bulk density})}{\text{soil density}} \quad \text{(Eq.2)}$$

where soil density is 2.65 g cm^{-3}. For soil moisture content (*Eq. 3*), soil samples were taken from the 0-40 cm soil profile at 10 cm intervals and oven-dried to constant weight in an aluminum container.

$$\text{Soil moisture content (100\%)} = \frac{(\text{fresh soil weight} - \text{dry soil weight})}{\text{dry soil weight}} \quad \text{(Eq.3)}$$

The measurement was repeated three times in each plot at 20 days after sowing of maize. For soil temperature measurement, thermistor temperature probes were buried at three points in each plot and four depths in the 0-20 cm soil profile (0-5, 5-10, 10-15, and 15-20 cm). Daily soil minimum and maximum temperatures were measured at consecutive 20 days after sowing of maize.

Sampling was done from each plot by cutting three adjacent plants in a row at ground level to determine leaf area and dry matter accumulation at V3, V6, VT and R3 growth stages. Leaf area index (LAI) was calculated by multiplying leaf area with plant density per m^2. Already sampled three plants were oven dried at 105 °C for one hour initially and then at 71 ± 1 °C to measure dry matter accumulation. Twenty days after sowing of maize, five whole plants were randomly sampled from each sub-plot and then plant shoot and roots were separated and dry matter was determined. At harvest stage, maize ears were hand harvested in the two central rows (the length of each row was 20 m) of each plot, dried and shelled. Dry matter and yields were obtained according to standard procedures. The maize yield potential (YP) in HHH area was obtained by the Hybrid-Maize simulation model (Yang et al., 2004).

The effect of soil tillage time on all analyzed parameters was tested using a one-way analysis of variance (ANOVA) (SPSS 13.0 for Windows; SPSS Inc., Chicago, USA). Tukey's HSD method was used as post hoc test for multiple comparisons of means. Mean data was presented for both years (2011 and 2012) for all the studied parameters except for some growth attributes (LAI, dry matter accumulation), due to non-significant year effect for the studied period.

Results

Soil and external environment before soil tillage

The values of soil temperature and soil moisture were significantly lower at initial soil tillage time intervals than later tillage intervals (*Table 1*). Soil mean temperature at different soil tillage times were recorded as the sequence of I<II<III<IV<V<VI<VII<VIII.

http://www.aloki.hu ● ISSN 1589 1623 (Print) ● ISSN 1785 0037 (Online)
DOI: http://dx.doi.org/10.15666/aeer/1605_60076023
© 2018, ALÖKI Kft., Budapest, Hungary

Table 1. *Soil hydrothermal properties before soil tillage in 0-40 cm soil depth*

Soil tillage time	I	II	III	IV	V	VI	VII	VIII
Soil mean temperature (°C)	16.53	17.23	18.52	22.39	24.60	25.63	29.53	30.00
Soil mean moisture content (%)	14.14	14.47	15.15	15.84	16.56	16.66	15.87	17.14
Soil mean bulk density (g cm^{-3})	1.36	1.35	1.36	1.32	1.39	1.31	1.37	1.37

I: March 25, II: April 10, III: April 25, IV: May 10, V: May 25, VI: June 10, VII: July 5, VIII: July 20

The values of soil mean moisture content at different soil tillage times were recorded in the sequence of I<II<III<IV<VII<V<VI<VIII. The values of effective accumulated temperature for different soil tillage times were as the sequence of IV>III>V>II>VI>VII>I>VIII during whole crop growth period (*Fig. 2*).

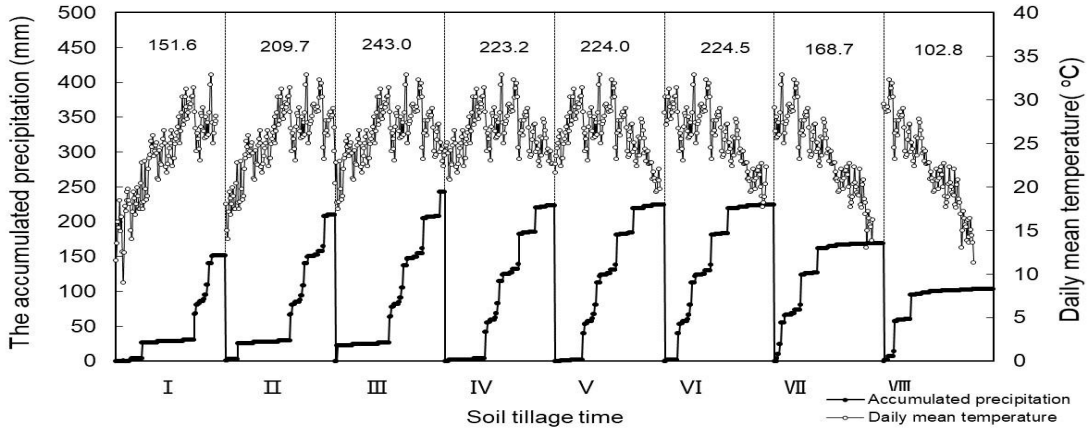

Figure 2. *Effective accumulated temperature (top word in figure), daily mean temperature (center line in figure) and accumulated precipitation (bottom line in figure) during growth cycle of maize at different soil tillage time. I: March 25, II: April 10, III: April 25, IV: May 10, V: May 25, VI: June 10, VII: July 5, and VIII: July 20*

Soil bulk density

In 0-10 cm soil layer, SS significantly decreased soil bulk density by about 0.13 g cm^{-3} ($P < 0.01$) at former tillage time of I–V, and the decrease was about 0.04 g cm^{-3} ($P < 0.05$) at later soil tillage intervals of VI–VIII, compared to NT (*Fig. 3*). In 10-20 cm soil layer, soil bulk density significantly decreased by about 0.07 g cm^{-3} ($P < 0.05$) at each soil tillage time under SS treatment compared to NT. Because of the destruction of soil hard plough pan, SS significantly decreased soil bulk density by about 0.15 g cm^{-3} ($P < 0.01$) at each soil tillage time compared to NT in 20-30 cm soil layer.

Soil porosity

Because of the decrease in soil bulk density, soil total porosity was therefore increased significantly (*Fig. 4*). In 0-10 cm soil layer, SS significantly increased soil total porosity by 4.18% ($P < 0.01$) at initial tillage intervals of I–V, and the increment was 2.38% ($P < 0.05$) at later soil tillage time of VI–VIII compared to NT. SS significantly increased soil porosity with average of 3.75% ($P < 0.01$) in top (0-30 cm) soil layer at initial tillage intervals of I–V, while the increment was 2.26% ($P < 0.05$) at tillage intervals VI–VIII, as compared to NT.

http://www.aloki.hu ● ISSN 1589 1623 (Print) ● ISSN 1785 0037 (Online)
DOI: http://dx.doi.org/10.15666/aeer/1605_60076023
© 2018, ALÖKI Kft., Budapest, Hungary

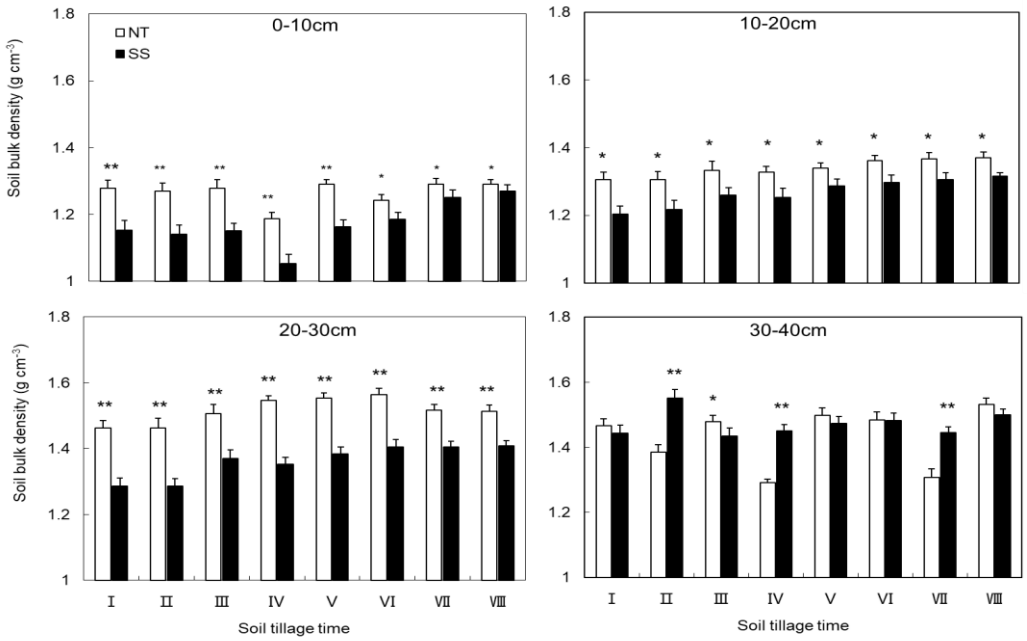

Figure 3. *Soil bulk density in 0–40 cm depth at different soil tillage time. NT: no tillage, SS: subsoiling tillage; I: March 25, II: April 10, III: April 25, IV: May 10, V: May 25, VI: June 10, VII: July 5, and VIII: July 20; ** above the column indicate statistical significance at the P = 0.01 level within the same soil tillage time; * above the column indicate statistical significance at the P = 0.05 level within the same soil tillage time*

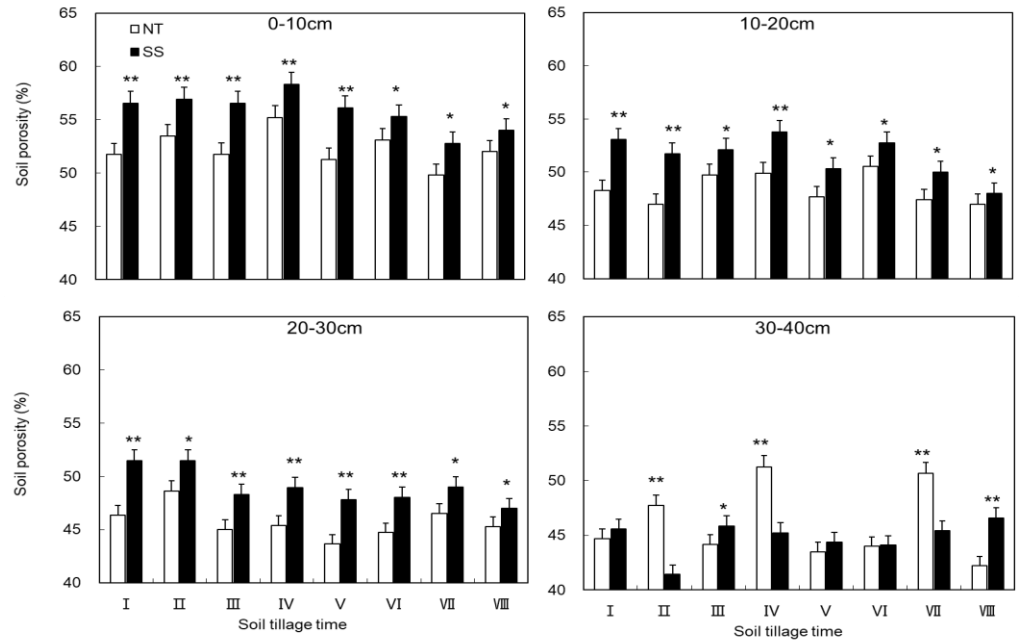

Figure 4. *Soil porosity in 0-40 cm depth at different soil tillage times. NT: no tillage, SS: subsoiling tillage; I: March 25, II: April 10, III: April 25, IV: May 10, V: May 25, VI: June 10, VII: July 5, and VIII: July 20; ** above the column indicate statistical significance at the P = 0.01 level within the same soil tillage time; * above the column indicate statistical significance at the P = 0.05 level within the same soil tillage time*

http://www.aloki.hu ● ISSN 1589 1623 (Print) ● ISSN 1785 0037 (Online)
DOI: http://dx.doi.org/10.15666/aeer/1605_60076023
© 2018, ALÖKI Kft., Budapest, Hungary

Soil moisture content

In 0-10 cm soil layer, SS significantly decreased soil moisture content by 2.06% ($P < 0.01$) at later soil tillage time of VI–VIII, because of the soil disturbance coincidence with high soil evaporation (*Fig. 5*). In 10-20 cm soil layer, SS significantly increased soil moisture content by 2.24% ($P < 0.01$) at intervals I, II, III, V, and the increment was 1.13% ($P < 0.05$) at later intervals of IV, VI, VII, VIII. In 20-30 cm soil layer, soil moisture content significantly increased by 2.26% ($P < 0.01$) at I, II, V, VI intervals, and the increment was about 1.13% ($P < 0.05$) at later intervals of III, IV, VII, VIII.

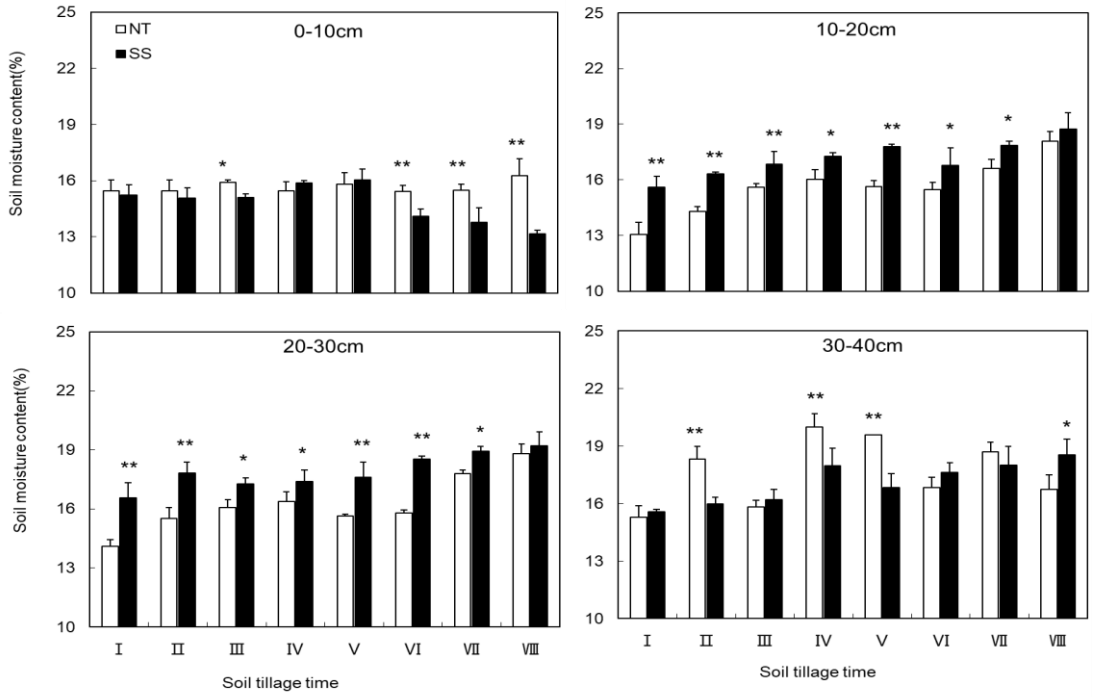

Figure 5. *Soil moisture content in 0–40 cm depth at different soil tillage. NT: no tillage, SS: subsoiling tillage; I: March 25, II: April 10, III: April 25, IV: May 10, V: May 25, VI: June 10, VII: July 5, and VIII: July 20; ** above the column indicate statistical significance at the P = 0.01 level within the same soil tillage time; * above the column indicate statistical significance at the P = 0.05 level within the same soil tillage time*

Soil temperature

In 0-10 cm soil layer, SS was able to increase soil minimum, maximum and mean temperatures as compared to NT (*Table 2*). For soil lowest temperature, the significant increment was 1.29 °C ($P < 0.05$) at tillage time of I, II, while it was 0.51 °C at intervals III, IV, V, VI. For soil maximum temperature, the increment was about 1.06 °C ($P < 0.05$) at each soil tillage time. For soil mean temperature, the increment recorded was 1.12 °C ($P < 0.05$) at former soil tillage intervals of I, II, while it was 0.65 °C at intervals III, IV, V, VI, VII, VIII. In 10-20 cm soil layer, SS just increased soil lowest temperature compared to NT, the increment was 0.43 °C for tillage intervals of I–V, while it was -0.28 °C at later soil tillage time of VI–VIII, as compared to NT.

http://www.aloki.hu ● ISSN 1589 1623 (Print) ● ISSN 1785 0037 (Online)
DOI: http://dx.doi.org/10.15666/aeer/1605_60076023
© 2018, ALÖKI Kft., Budapest, Hungary

Table 2. *Soil minimum, maximum and mean temperature in 0–20 cm soil depth at 20 days after sowing of maize*

Soil depth (cm)	Soil temperature (°C)	Soil tillage method	Soil tillage time							
			I	II	III	IV	V	VI	VII	VIII
0–5	Minimum	NT	14.71b	15.48b	18.80b	21.10a	22.00a	25.24a	27.00a	26.75a
		SS	15.95a	16.62a	19.65a	21.65a	22.50a	25.86a	26.47a	25.75b
	Maximum	NT	22.52b	24.71b	29.15b	30.95b	30.95a	36.69a	35.95b	33.00b
		SS	23.43a	25.62a	29.95a	32.10a	31.70a	37.24a	37.69a	34.00a
	Mean	NT	18.62b	20.06b	23.98b	26.00b	26.45a	30.97a	31.47a	29.88a
		SS	19.69a	21.11a	24.80a	26.88a	27.10a	31.55a	32.08a	29.88a
5–10	Minimum	NT	11.76b	14.66b	18.65b	21.50a	22.40a	25.62a	26.84a	26.65a
		SS	13.33a	15.78a	19.35a	22.00a	22.65a	25.76a	26.32a	25.90a
	Maximum	NT	19.19b	21.09b	26.65a	27.60b	29.15b	34.24a	33.95b	31.75b
		SS	22.14a	21.91a	27.05a	29.40a	30.10a	34.71a	35.42a	33.00a
	Mean	NT	15.48b	17.86b	22.33b	24.55b	25.78a	29.93a	30.40a	29.20a
		SS	16.87a	18.84a	23.20a	25.70a	26.38a	30.24a	30.87a	29.45a
10–15	Minimum	NT	15.33a	16.26a	19.50a	22.00a	22.80a	26.09a	26.74a	27.18a
		SS	15.95a	16.75a	20.20a	22.35a	23.20a	25.81a	26.05a	26.55a
	Maximum	NT	21.59a	22.10a	24.65a	26.90a	27.95a	31.19a	32.16a	30.90a
		SS	20.67b	21.19b	24.25a	26.05a	28.45a	31.14a	30.68b	30.20a
	Mean	NT	18.46a	19.13a	22.43a	24.45a	25.38a	28.64a	29.17a	29.04a
		SS	18.31a	18.97a	21.90a	24.20a	25.83a	28.48a	28.49a	28.35a
15–20	Minimum	NT	15.66a	16.29a	19.26a	22.50a	23.35a	27.14a	27.16a	27.05a
		SS	16.10a	16.71a	19.65a	23.00a	23.65a	27.00a	26.79a	27.55a
	Maximum	NT	18.95a	19.18a	23.25a	26.05a	26.35a	30.05a	30.11a	29.85a
		SS	18.00b	18.62a	22.75a	25.15b	25.95a	30.00a	30.79a	29.30a
	Mean	NT	17.10a	17.73a	21.26a	24.28a	24.85a	28.60a	28.63a	28.45a
		SS	17.05a	17.67a	21.20a	24.08a	24.80a	28.52a	28.79a	28.43a

NT: no tillage, SS: subsoiling tillage; I: March 25, II: April 10, III: April 25, IV: May 10, V: May 25, VI: June 10, VII: July 5, and VIII: July 20. Values between NT and SS for each tillage date followed by different letters are significantly different at $P < 0.05$

Relationship of soil temperature and soil moisture content

Soil moisture content influences the range of soil temperature under different tillage treatments. For the soil lowest temperature, it showed increasing trend with the soil moisture content increasing at tillage time of I, II, III, IV, and V when the soil temperature was low (*Fig. 6*). For soil maximum temperature and daily mean temperature, it showed decreased tendency with the soil moisture content increasing at tillage time of IV, V, VI, VII, and VIII. Hence, the soil lowest temperature was easily affected by soil moisture when the soil temperature was very low.

Growth

Among tillage treatments, SS performed better in improving LAI over the all soil tillage intervals as compared to NT, for both the years (*Table 3*). During 2012 year, an increasing trend for LAI was recorded for the intervals I–V, whilst a decrease was

http://www.aloki.hu ● ISSN 1589 1623 (Print) ● ISSN 1785 0037 (Online)
DOI: http://dx.doi.org/10.15666/aeer/1605_60076023
© 2018, ALÖKI Kft., Budapest, Hungary

observed after that for the intervals VI–VIII. This decreasing trend is significantly visible for both the years during VT and R3 growth stages, because of delayed sowing time as compared to initial sowing intervals of I–V.

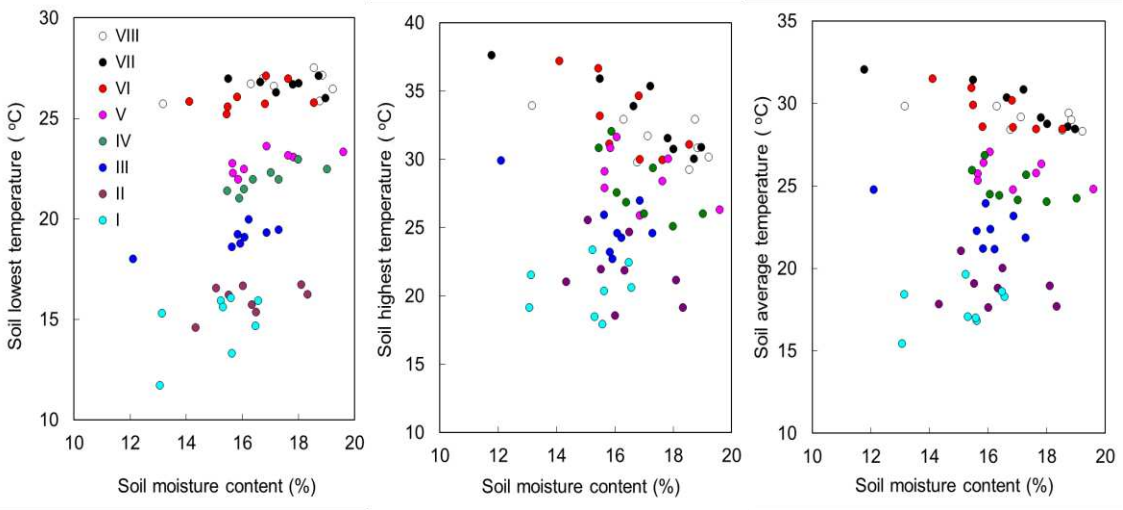

Figure 6. *Relationship of soil temperature and soil moisture content at different soil tillage time. I: March 25, II: April 10, III: April 25, IV: May 10, V: May 25, VI: June 10, VII: July 5, and VIII: July 20*

Table 3. *LAI of maize during crop growth period of maize at eight soil tillage times*

Year	Growth stage	Soil tillage	Soil tillage time							
			I	II	III	IV	V	VI	VII	VIII
2011	V3	NT	0.05b	0.06b	0.06b	0.07b	0.07b	0.08b	0.10b	0.11b
		SS	0.06a	0.07a	0.07a	0.08a	0.09a	0.09a	0.11a	0.12a
	V6	NT	0.43a	0.46b	0.49b	0.58b	0.64b	0.65a	0.65b	0.75b
		SS	0.43a	0.48a	0.51a	0.61a	0.65a	0.65a	0.67a	0.77a
	VT	NT	4.14b	4.33b	4.50b	4.58b	4.91b	4.77b	3.49b	3.74b
		SS	4.41a	4.69a	4.79a	4.84a	5.16a	5.07a	3.74a	4.03a
	R3	NT	3.14b	3.14b	3.68b	3.88b	4.46b	4.49b	3.82b	3.61b
		SS	3.37a	3.37a	3.82a	4.06a	4.59a	4.57a	3.95a	3.72a
2012	V3	NT	0.05b	0.06b	0.06b	0.07b	0.07b	0.08b	0.10b	0.11b
		SS	0.06a	0.07a	0.07a	0.08a	0.09a	0.09a	0.11a	0.12a
	V6	NT	0.38b	0.47b	0.58b	0.55b	0.63b	0.42b	0.45b	0.41b
		SS	0.43a	0.52a	0.63a	0.57a	0.67a	0.46a	0.50a	0.44a
	VT	NT	4.41a	4.92a	4.29b	3.68b	4.56b	4.35b	4.20a	3.09b
		SS	4.27b	4.71b	4.36a	3.85a	4.97a	4.69a	4.05b	3.33a
	R3	NT	3.91a	4.02b	3.89b	3.69a	4.15b	4.23a	3.52b	2.99a
		SS	3.90a	3.98a	3.96a	3.42b	4.51a	4.13b	3.92a	3.00a

NT: no tillage, SS: subsoiling tillage; I: March 25, II: April 10, III: April 25, IV: May 10, V: May 25, VI: June 10, VII: July 5, and VIII: July 20; Values between NT and SS for each tillage date followed by different letters are significantly different at $P < 0.05$

http://www.aloki.hu ● ISSN 1589 1623 (Print) ● ISSN 1785 0037 (Online)
DOI: http://dx.doi.org/10.15666/aeer/1605_60076023
© 2018, ALÖKI Kft., Budapest, Hungary

From *Figure 7,* we could see that SS caused a significant increase in dry weight of shoot and root at 20 days after sowing of maize. For shoot dry weight, the highest value was obtained at soil tillage time of VIII, while the highest increment was obtained at soil tillage time of I under SS (*Fig. 7*). SS significantly increased shoot dry weight by 13.85% ($P < 0.01$) at initial tillage intervals of I–IV, and by 7.83% ($P < 0.05$) at later soil tillage time of V– VIII compared to NT. For root dry weight, the highest value was obtained at soil tillage time of VI, while the highest increment was obtained at soil tillage time of I under SS. Similar to LAI, dry matter accumulation varied across different sowing intervals as well as sampling stages of crop growth period (V3–R3) (*Table 4*). Maximum value for dry matter was found for SS during sowing interval VI (2011) and V (2012) at R3 sampling stage.

Table 4. *Dry matter accumulation of maize during crop growth stages of maize for eight soil tillage times*

Year	Growth stage	Soil tillage	Soil tillage time							
			I	II	III	IV	V	VI	VII	VIII
2011	V3	NT	0.34b	0.47b	0.61b	0.66b	0.91b	1.16b	1.48b	1.64b
		SS	0.39a	0.53a	0.69a	0.75a	0.98a	1.25a	1.60a	1.75a
	V6	NT	6.43b	6.87b	6.40a	8.20a	8.45b	10.47b	11.08b	12.90a
		SS	8.13a	9.10a	6.97a	8.83a	9.62a	11.03a	12.49a	12.97a
	VT	NT	90.03b	100.80b	116.67b	116.80b	134.53a	129.81b	121.87b	116.85b
		SS	103.20a	113.40a	133.10a	132.99a	137.67a	139.40a	137.57a	132.99a
	R3	NT	177.37b	171.60b	186.40b	210.23b	214.22b	238.47b	186.40b	136.65b
		SS	186.67a	186.03a	198.60a	227.07a	228.45a	252.73a	198.60a	153.70a
2012	V3	NT	0.34b	0.45b	0.55b	0.58b	0.98b	1.07b	1.42b	1.75a
		SS	0.41a	0.51a	0.66a	0.67a	1.07a	1.18a	1.53a	1.79a
	V6	NT	4.10b	4.53b	5.47a	5.23a	6.36b	6.60b	8.42a	8.75a
		SS	5.17a	5.25a	5.67a	5.67a	7.35a	8.30a	8.53a	9.31a
	VT	NT	98.53b	98.53b	98.13b	102.53b	110.63b	120.10a	94.23b	86.00a
		SS	105.97a	102.00a	107.97a	108.17a	115.20a	120.83a	105.30a	86.20a
	R3	NT	194.53b	192.53b	193.97b	198.10b	214.42b	201.10b	170.20b	145.37a
		SS	198.77a	194.87a	196.80a	203.27a	219.82a	204.97a	176.63a	146.13a

NT: no tillage, SS: subsoiling tillage; I: March 25, II: April 10, III: April 25, IV: May 10, V: May 25, VI: June 10, VII: July 5, and VIII: July 20; Values between NT and SS for each tillage date followed by different letters are significantly different at $P < 0.05$

Regardless of soil tillage time, the grain yield of maize was significantly higher under the SS management than no-tillage treatment (*Fig. 8*). In terms of tillage intervals, the yield of maize was highest in the SS tillage management implemented at VI, but the highest increment of yield was recorded at SS tillage implemented at I. The highest yield potential (YP) of maize was recorded at soil tillage time of V. The potential equivalent was in the range of 71.89–85.10% at SS, while it was 67.08-81.78% (range) at NT for tillage times I, II, III, IV, V, VI, and VII, respectively.

http://www.aloki.hu ● ISSN 1589 1623 (Print) ● ISSN 1785 0037 (Online)
DOI: http://dx.doi.org/10.15666/aeer/1605_60076023
© 2018, ALÖKI Kft., Budapest, Hungary

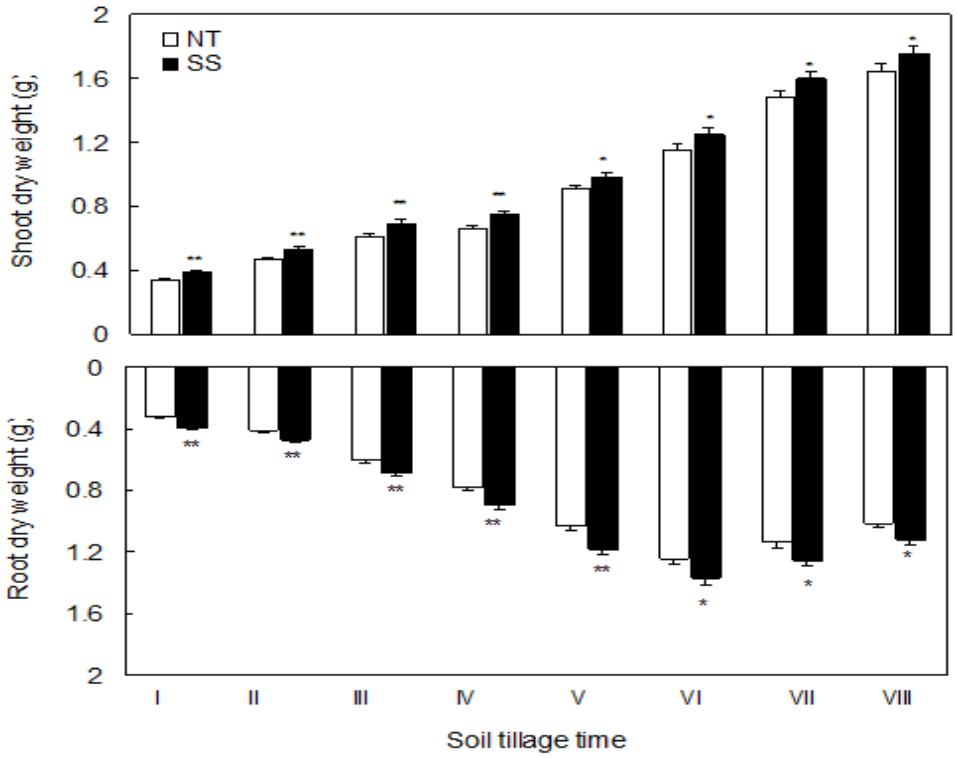

Figure 7. *Shoot and root dry matter at 20 days after sowing of maize. NT: no tillage, SS: subsoiling tillage; I: March 25, II: April 10, III: April 25, IV: May 10, V: May 25, VI: June 10, VII: July 5, and VIII: July 20; ** above the column indicate statistical significance at the P = 0.01 level within the same soil tillage time; * above the column indicate statistical significance at the P = 0.05 level within the same soil tillage time*

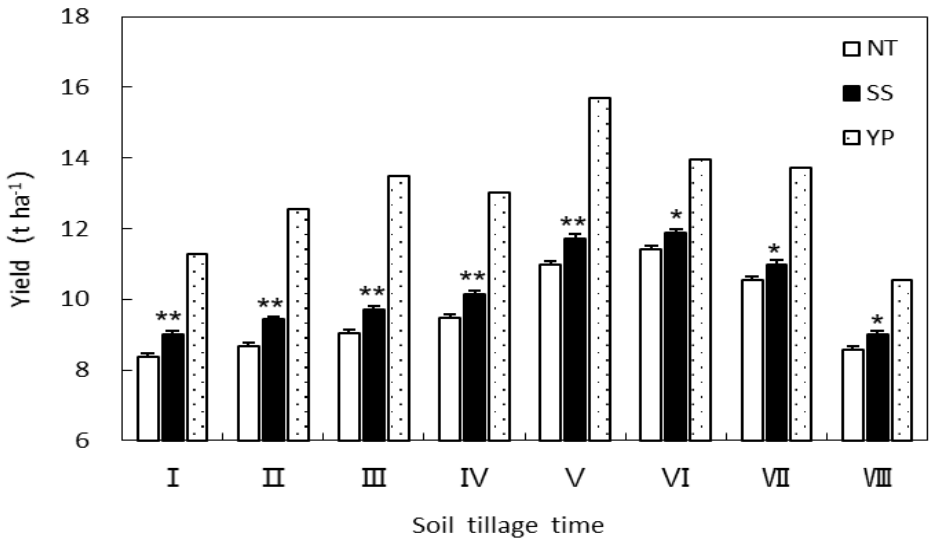

Figure 8. *Final grain yield of maize at different soil tillage time. NT: no tillage, SS: subsoiling tillage, YP: yield potential; I: March 25, II: April 10, III: April 25, IV: May 10, V: May 25, VI: June 10, VII: July 5, and VIII: July 20; ** above the column indicate statistical significance at the P = 0.01 level within the same soil tillage time; * above the column indicate statistical significance at the P = 0.05 level within the same soil tillage time*

http://www.aloki.hu ● ISSN 1589 1623 (Print) ● ISSN 1785 0037 (Online)
DOI: http://dx.doi.org/10.15666/aeer/1605_60076023
© 2018, ALÖKI Kft., Budapest, Hungary

Discussion

Soil bulk density is an important indicator for soil stiffness (Carter, 1990). Liang et al. (2010) and Liu et al. (2010) found that subsoiling tillage could break the soil hard plough pan and loosen the compacted soil, thereby reducing soil bulk density. Meanwhile because of the dryness and reduced soil viscosity with low soil moisture and temperature, the soil structure could easily be altered (Yang et al., 2013). Our results indicated that SS significantly reduced soil bulk density in 0-30 cm soil layer, especially at the former soil tillage time of I–V, when compared to no-tillage treatment (*Fig. 3*). These results are in disagreement with that of Gürsoy et al. (2011). Whereas, Ozpinar and Ozpinar (2015) found a significant decrease in soil bulk density, confirming our results, in top soil due to tillage practices in a five-year experiment at enhancing maize productivity. In 20-30 cm soil layer, because of the destruction of hard plough layer, soil bulk density showed a much significant decrease in present case, promising for sustainable field maize production in China.

Assouline (2006) suggested that, soil can be significantly loosened and the proportion of large pores can be increased significantly under SS tillage. The level of soil porosity is related to intensity of soil tillage (Chen et al., 2009). In present study, the implementation of SS tillage significantly increased soil total porosity in 0-30 cm soil depth compared with no-tillage treatment (*Fig. 4*). This improvement can be attributed to the reason that the level and distribution of soil total porosity were significantly affected by the soil bulk density (Raczkowski et al., 2012; Wang et al., 2017).

Soil moisture content is a basic characteristic required for optimum crop growth. Appropriate soil moisture contents could support uptake of crop root and can regulate the dynamics of soil temperature and heat (Karandish and Shahnazari, 2016; Tsironi and Taoukis, 2017). Assouline (2006) showed that SS could improve soil moisture infiltration and storage attributed to the decrease in soil bulk density and increased soil total porosity. Meanwhile the SS tillage could break the continuity of soil pores to prevent the evaporation and reduction of deep soil moisture (Osunbitan, 2005), thereby significantly increasing deep-layer soil moisture contents. However, the SS tillage involves excessive soil ploughing, resulting in relatively higher surface soil moisture evaporation due to more exposure to sunshine (Debaeke and Aboudrare, 2004). And the high soil and air temperature accelerate the surface soil moisture evaporation (Wang et al., 2007). Our study showed the same results that SS significantly increased soil moisture content in 10-30 cm soil depth, while the soil moisture content decreased in 0-10 cm soil depth compared with no-tillage (*Fig. 5*). In 10-20 cm soil depth, soil moisture content showed a much significant increase at soil tillage intervals of I, II, III, V, and VI because of the relevant decrease in soil bulk density and increase in soil total porosity due to SS, compared to NT.

In field, seed germination and seedling growth of maize are closely related to soil temperature (Ahmad et al., 2016; Lopushinsky and Max, 1990). Fu et al. (2005) suggested that SS tillage could balance and improve the status of soil temperature through the function of heat preservation on minimum soil temperature conditions and may cause decrease in maximum soil temperature and it could keep the stability of soil temperature, beneficial for the crop growth. In this study, SS tillage increased soil minimum temperature in 0-20 cm soil depth at soil tillage time of I–VI. For soil maximum temperature and daily mean temperature, the increments were only occurred in 0-10 cm soil depth at each tillage time (*Table 2*). Soil temperature jointly determined

http://www.aloki.hu ● ISSN 1589 1623 (Print) ● ISSN 1785 0037 (Online)
DOI: http://dx.doi.org/10.15666/aeer/1605_60076023
© 2018, ALÖKI Kft., Budapest, Hungary

with atmospheric temperature and soil heat conditions are reported to be regulated by soil moisture content and soil porosity (Lakshmi, 2003). Higher soil porosity and moisture content could contribute to heat transfer and storage (Zhang et al., 2009; Wu et al., 2017). For these reasons, the soil minimum temperature showed an increased tendency with increase in soil moisture content, especially at intervals III, IV and V. While the soil maximum and daily mean temperature showed an decreased tendency with increasing soil moisture at later soil tillage time of V, VI, VII and VIII (*Fig. 6*).

Anand et al. (2012) reported that the decrease in soil penetration resistance, increase in soil moisture and temperature could improve the seedling emergence and growth during early spring under low temperature conditions. Tolon-Becerra et al. (2011) showed that better seedling emergence and growth were achieved under soil with lower compaction, and the relationship between root dry matter and maize yields was strongly positive. In our study, SS significantly increased shoot and root dry matter of maize seedling. Though the highest maize seedling dry matter was obtained at SS tillage time of VI, VII and VIII, which are contrary to the findings of Ge et al. (2013). The reason can be described by effective accumulated temperature, daily mean temperature and accumulated precipitation at respective growth stage of maize (*Fig. 2*), the maximum increase in maize seedling matter was obtained at tillage intervals of I, II, III, IV and V (*Fig. 7*). The decrease during former tillage intervals plausibly because of the soil high compaction and low temperature, which may be attributed as main limits for maize seedling growth at March, April, and May (*Fig. 1*). The improvement in soil compaction and temperature significantly enhanced the maize seedling growth, corroborating the findings of Hoffmann and Kismányoky (2001). The increase in maize yield was significantly improved at SS tillage compared with no-tillage management, which is against the results reported earlier by Mohammadi et al. (2013), and SS also decreased the yield gap between yield and yield potential in our case. Though the highest maize yield was harvested at SS tillage time of V, VI and VII, whilst the highest increment in maize yield was harvested at subsoiling tillage time of I, II, III and IV (*Fig. 8*), which are contrary to the results of Zhang et al. (2009). Recently, Moinoddini et al. (2017) also found significant positive effects of deep tillage on maize grain yields as compared to no-tillage during the evaluation of different tillage practices and N application rates under corn-based rotation system. In present case, SS tillage significantly increased soil moisture storage and soil temperature, and improved seedling growth of maize at subsoiling tillage time of I, II, III and IV, as compared no tillage.

Our results indicate that in no-tillage maize growing areas of HHH, soil hydro-thermal properties can be improved by implementing the SS in the month of May and June. This improvement reflects in terms of increased soil temperature, moisture content, porosity and the significant decrease in soil bulk density, which in turn is attributed to better seedling growth and early stand establishment with higher shoot/root parameters, and the succeeding plant growth and final dry matter accumulation. The reason can be explained through the maximum accumulated temperature, precipitation (*Fig. 2*) and the sunshine hours during these months (May, June), which were favorable to improve soil environment and the plant growth under SS tillage implementation, as compared to no-tillage.

http://www.aloki.hu ● ISSN 1589 1623 (Print) ● ISSN 1785 0037 (Online)
DOI: http://dx.doi.org/10.15666/aeer/1605_60076023
© 2018, ALÖKI Kft., Budapest, Hungary

Conclusion

In Huang-Huai-Hai area of China, SS tillage proved effective in improving soil physical and hydro-thermal properties, and improving maize seedling growth and grain yield, especially when implemented at early time (March, April and May). Compared with no-tillage, subsoiling tillage significantly decreased soil bulk density, and greatly increased soil porosity. SS tillage at early time (especially for May and June) significantly increased the soil moisture storage in 10-30 cm soil depth. Soil minimum temperature (0-20 cm) and soil maximum temperature (0-10 cm) significantly increased at SS tillage time of March, April and May. The SS tillage produced maximum dry seedling matter in maize and grain yields compared to no-tillage management, especially when implemented at early time. Because at early sowing of maize, low soil temperature and Spring seasonal drought cause serious hindrance for early stand establishment in HHH. We can conclude that SS tillage could alleviate the soil high compaction and low temperature stress for spring maize, and can alleviate the soil high compaction stress for summer maize. Dry matter accumulation and grain yield was maximum for sowing from May 25 to June 10. It will be of great significance in improving soil environment, seedling growth and grain yield of maize at early sowing with low precipitation and temperature.

Acknowledgements. The research was supported by the National Natural Science Fund 31401952, National Key R&D Program of China (2018YFD0200601), Key National Research and Development Programs (2016YFD0300207).

REFERENCES

[1] Ahmad, W., Noor, M. A., Afzal, I., Bakhtavar, M. A., Nawaz, M. M., Sun, X., Zhou, B., Ma, W., Zhao, M. (2016): Improvement of sorghum crop through exogenous application of natural growth-promoting substances under a changing climate. – Sustainability 8: 1330. http://dx.doi.org/10.3390/su8121330.

[2] Anand, A., Nagarajan, S., Verma, A. P. S., Joshi, D. K., Pathak, P. C., Bhardwaj, J. (2012): Pre-treatment of seeds with static field ameliorates soil water stress in seedlings of maize (*Zea mays* L.). – Indian J Biochem Biophys. 49: 63-70.

[3] Assouline, S. (2006): Modeling the relationship between soil bulk density and the water retention curve. – Vadose Zone J. 5: 554-563.

[4] Bhaduri, D., Purakayastha, T. J., Chakraborty, D., Chakraborty, K., Singh, M. (2017): Integrated tillage-water-nutrient management effects on selected soil physical properties in a rice-wheat system in the Indian subcontinent. – Arch Agron Soil Sci. DOI: 10.1080/03650340.2017.1332407.

[5] Certer, M. R. (1990): Relative measures of soil bulk density to characterize compaction in tillage studies on fine sandy loams. – Can J Soil Sci. 70: 425-433.

[6] Chen, J. K., Li, S. J., Zhang, Y., Chen, F., Zhang, H. L. (2009): Characteristics of soil temperature and response to air temperature under different tillage systems — diurnal dynamic of soil temperature and its response to air temperature. – Sci Agric Sinica 42(7): 2592-2600 (in Chinese).

[7] Debaeke, P., Aboudrare, A. (2004): Adaptation of crop management to water-limited environments. – Eur J Agron. 21: 433-446.

[8] Fu, G. Z., Li, C. H., Wang, J. Z., Wang, Z. L., Cao, H. M., Jiao, N. Y., Chen, M. C. (2005): Effects of stubble mulch and tillage managements on soil physical properties and

http://www.aloki.hu ● ISSN 1589 1623 (Print) ● ISSN 1785 0037 (Online)
DOI: http://dx.doi.org/10.15666/aeer/1605_60076023
© 2018, ALÖKI Kft., Budapest, Hungary

water use efficiency of summer maize. – Transactions of the CSAE 21(1): 52-56 (in Chinese).
[9] Ge, C., Jing, X. Q., Xu, E., Zhao, C. H., Gao, H. M. (2013): Correlation analysis between corn yield and soil physical properties by different subsoiling time and different depth result. – Soil Fert Sci China 3: 15-18 (in Chinese).
[10] Guo, R. P., Lin, Z. H., Mo, X. G., Yang, C. L. (2010): Responses of crop yield and water use efficiency to climate change in the North China Plain. – Agric Water Manag. 97: 1185-1194.
[11] Gürsoy, S., Sessiz, A., Kiliç, H., Bayram, N. (2011): Tillage system and cotton residue management effects on soil physical and chemical properties of an Anatolian clay loam sown within a wheat-cotton sequence. – Arch Agron Soil Sci. 57(4): 391-400.
[12] Hartmann, P., Zink, A., Fleige, H., Horn, R. (2012): Effect of compaction, tillage and climate change on soil water balance of Arable Luvisols in Northwest Germany. – Soil Tillage Res. 124: 211-218.
[13] Hoffmann, S., Kismányoky, T. (2001): Soil fertility in a long-term fertilizer trial with different tillage systems. – Arch Agron Soil Sci. 46(3-4): 239-250.
[14] Hou, X. Q., Li, R., Jia, Z. K., Han, Q. F., Yang, B. P., Nie, J. F. (2012): Effects of rotational tillage practices on soil structure, organic carbon concentration and crop yields in semi-arid areas of northwest China. – Soil Use Manag. 28: 551-558.
[15] Jabro, J. D., Sainju, U. M., Stevens, W. B., Lenssen, A. W., Evans, R. G. (2009): Long-term tillage influences on soil physical properties under dryland conditions in northeastern Montana. – Arch Agron Soil Sci. 55(6): 633-640.
[16] Ji, B., ZhaoY., Mu, X., Liu, K., Li, C. (2013): Effects of tillage on soil physical properties and root growth of maize in loam and clay in central China. – Plant Soil Environ. 59(7): 295-302.
[17] Karandish, F., Shahnazari, A. (2016): Soil temperature and maize nitrogen uptake improvement under partial root-zone drying irrigation. – Pedosphere 26(6): 872-886.
[18] Lakshmi, V., Jackson, T. J., Zehrfuhs, D. (2003): Soil moisture–temperature relationships: results from two field experiments. – Hydrological Processes 17(15): 3041-3057.
[19] Liang, J. F., Qi, Q. Z., Jia, X. H., Gong, S. J., Huang, Y. F. (2010): Effects of different tillage managements on soil properties and corn growth. – Ecol Environ Sci. 19(4): 945-950 (in Chinese).
[20] Liu, S., He, W. Q., Yan, C. R., Liu, Q. (2010): Effects of different tillage managements on soil physical properties in dryland. – Agri Res Arid Area 28(2): 65-70 (in Chinese).
[21] Liu, X. J., Rong, J. D. (2009): Effects of deep tillage on the properties of soil structure. – The Application Technology of Soil and Water Conservation 1: 9-11 (in Chinese).
[22] Lopushinsky, W., Max, T. A. (1990): Effect of soil temperature on root and shoot growth and on budburst timing in conifer seedling transplants. – New For. 4: 107-124.
[23] Lozano-García, B., Parras-Alcántara, L. (2014): Changes in soil properties and soil solution nutrients due to conservation versus conventional tillage in Vertisols. – Arch Agron Soil Sci. 60(10): 1429-1444.
[24] Lu, X., Lu, X., Liao, Y. (2016): Soil CO_2 emission and its relationship to soil properties under different tillage systems. – Arch Agron Soil Sci. 62(7): 1021-1032.
[25] Moinoddini, S. S., Koocheki, A., Mahalati, M. N., Borzooei, A. (2017): Tillage and N application effects on crop yield, N uptake and soil properties in a corn-based rotation. – Arch Agron Soil Sci. 63(8): 1150-1162.
[26] Mohammadi, K., Rokhzadi, A., Saberali, S. F., Byzedi, M., Nezhad, M. T. K. (2013): Tillage effects on soil properties and wheat cultivars traits. – Arch Agron Soil Sci. 59(12): 1625-1641.
[27] Nath, A. J., Lal, R. (2017): Effects of tillage practices and land use management on soil aggregates and soil organic carbon in the north Appalachian region, USA. – Pedosphere 27(1): 172-176.

http://www.aloki.hu ● ISSN 1589 1623 (Print) ● ISSN 1785 0037 (Online)
DOI: http://dx.doi.org/10.15666/aeer/1605_60076023
© 2018, ALÖKI Kft., Budapest, Hungary

[28] Noor, M. A. (2017): Nitrogen management and regulation for optimum NUE in maize–A mini review. – Cogent Food & Agriculture 3(1): 1348214.
[29] Osunbitan, J. A., Oyedele, D. J., Adekalu, K. O. (2005): Tillage effects on bulk density, hydraulic conductivity and strength of a loamy sand soil in southwestern Nigeria. – Soil Tillage Res. 82: 57-64.
[30] Ozpinar, S., Ozpinar, A., (2015): Tillage effects on soil properties and maize productivity in western Turkey. – Arch Agron Soil Sci. 61(7): 1029-1040.
[31] Piao, S. L., Ciais, P., Huang, Y., Shen, Z. H., Peng, S. S., Li, J. S., Zhou, L. P., Liu, H. Y., Ma, Y. C., Ding, Y. H. et al. (2010): The impacts of climate change on water resources and agriculture in China. – Nature 467: 43-51.
[32] Raczkowski, C. W., Mueller, J. P., Busscher, W. J., Bell, M. C., McGraw, M. L. (2012): Soil physical properties of agricultural systems in a large-scale study. – Soil Tillage Re. 119: 50-59.
[33] Tolon-Becerra, A., Tourn, M., Botta, G. F., Lastra-Bravo, X. (2011): Effects of different tillage regimes on soil compaction, maize (*Zea mays,* L.) seedling emergence and yields in the eastern Argentinean Pampas region. – Soil Tillage Res. 117: 184-190.
[34] Tsironi, T. N., Taoukis, P. S. (2017): Effect of storage temperature and osmotic pre-treatment with alternative solutes on the shelf-life of gilthead seabream (*Sparus aurata*) fillets. – Aquaculture and Fisheries 2: 39-47.
[35] Wang, J., Cai, H. J., Kang, Y. X., Chen, F. (2007): Ratio of soil evaporation to the evapotranspiration for summer maize field. – Transactions of the CSAE 23(4): 17-22 (in Chinese).
[36] Wang, Q. J., Lu, C. Y., Li, H. W., He, J., Khokan, K. S., Rabi, G. R., Liang, Z. H., Qiao, X. D., Li, H., Allen, D. J. M. (2014): The effects of no-tillage with subsoiling on soil properties and maize yield: 12-Year experiment on alkaline soils of Northeast China. – Soil Tillage Res. 137: 43-49.
[37] Wang, S., Wang, Z., Gu, J. (2017): Variation patterns of fine root biomass, production and turnover in Chinese forests. – J. Fores. Res. 28: 1185-1194.
[38] Wu, H., Chen, C., Wang, Q., Lin, J., Xue, J. (2017): The biological content of ballast water in China: a review. – Aquaculture and Fisheries 2: 241-246.
[39] Yang, H. S., Dobermann, A., Lindquist, J. L., Walters, D. T., Arkebauer, T. J., Cassman, K. G. (2004): Hybrid-maize: A maize simulation model that combines two crop modeling approaches. – Field Crops Res. 87: 131-154.
[40] Yang, X., Pang, H. C., Li, Y. B., Ren, T. Z., Dong, G. H., Guo, Z. H., Wang, X. J. (2013): Effects of deep rotary subsoiling tillage on the physical properties and crop growth of the Sticky Loamy Soil in north China. – Sci Agric Sinica 46(16): 3401-3412 (in Chinese).
[41] Yin, Y., Gao, J., Liu, Y. (2017): Influence of industrial organizational structure on farming performance of large yellow croaker farmers. – Aquaculture and Fisheries 2: 134-139.
[42] Yu, T. Y., Zhang, X. Y. (2006): Effect of different tillage treatment on black soil water dynamic at tillage layer. – Construction of Modern Agriculture and Farming System 4(1): 511-514 (in Chinese).
[43] Zafar, S. A., Noor, M. A., Waqas, M. A., Wang, X., Shaheen, T., Raza, M., Rahman, M. U. (2018): Temperature Extremes in Cotton Production and Mitigation Strategies. – In: Rahman, M. U., Zafar, Y. (eds.) Past, Present and Future Trends in Cotton Breeding. InTech, Rijeka, Croatia, pp. 65-91 (Chapter 4). dx.doi.org/10.5772/intechopen.74648.
[44] Zhang, S. L., Lars, L., Harald, G., Tong, Y. N., Yang, X. Y., Wang, Q. J. (2009): Effects of mulching and catch cropping on soil temperature, soil moisture and wheat yield on the Loess Plateau of China. – Soil Tillage Res. 102: 78-86.
[45] Zhang, Y. X., Luo, A., Qi, Q. Q., Jiang, Y. M., Cui, H. Q., Cai, Y. (2009): Effect of different cultivation measures on soil temperature in dry areas of west Heilongjiang. – Agri Res Arid Areas 27(5): 93-96 (in Chinese).

http://www.aloki.hu ● ISSN 1589 1623 (Print) ● ISSN 1785 0037 (Online)
DOI: http://dx.doi.org/10.15666/aeer/1605_60076023
© 2018, ALÖKI Kft., Budapest, Hungary

[46] Zheng, S. H., Yan, C. R. (2006): The ecophysiological and morphological characteristics of maize in seedling stage under water stress. – Acta Ecol Sinica 26(4): 1138-1143 (in Chinese).
[47] Zhou, L. M., Li, F. M., Jin, S. L., Song, Y. J. (2009): How two ridges and the furrow mulched with plastic film affect soil water, soil temperature and yield of maize on the semiarid Loess Plateau of China. – Field Crops Res. 113: 41-47.

http://www.aloki.hu ● ISSN 1589 1623 (Print) ● ISSN 1785 0037 (Online)
DOI: http://dx.doi.org/10.15666/aeer/1605_60076023
© 2018, ALÖKI Kft., Budapest, Hungary

EFFECT OF FERMENTED EXTRUDED CORN STOVER ON NUTRIENT DIGESTIBILITY AND MILK COMPOSITION IN COLOSTRUM OF PREGNANT SOWS

NGALAVU, A.[1] – JIANG, H. L.[1*] – YANG, Y.[1] – TYASI, T. L.[2]

[1]*Department of Animal Nutrition, College of Animal Science and Technology, Jilin Agricultural University, Xincheng Avenue 2888, Changchun City of Jilin Province, 130118 P. R. China*

[2]*Department of Animal Genetics, Breeding and Reproduction, College of Animal Science and Technology, Jilin Agricultural University, Xincheng Avenue 2888, Changchun City of Jilin Province, 130118 P. R. China*

**Corresponding author*
e-mail: hljiang@jlau.edu.cn; phone: +86-186-0446-5676

(Received 3rd Jun 2018; accepted 2nd Aug 2018)

Abstract. The study was conducted to determine the effect of fermented extruded corn stover on nutrient digestibility and milk composition in colostrum of pregnant sows. A total of 48 pregnant sows (24 Landrace and 24 Yorkshire) were randomly assigned into four experimental treatment groups (0, 10%, 15%, 20% fermented extruded corn stover). The results of nutrient digestibility (*Table 2*) showed that in crude protein and neutral detergent fibre, there were no significant differences between the control group and 10% fermented extruded stover ($P > 0.05$). However, these results in energy and acid detergent fibre showed a significant differences between control group and all the experimental groups ($P > 0.05$), respectively. In fat, lactose and non-fat solids, there were no significant differences between control group and experimental groups ($P > 0.05$), respectively. There was a significant difference in protein between control group and experimental group ($P < 0.05$). Our findings suggest that with the increase of fiber content in feed, protein and lactose content are increased in colostrum of pregnant sows and there is little effect on digestibility.
Keywords: *dietary fiber, corn stover, pregnant sows performance, digestibility, lactation*

Introduction

Dietary fiber is well recognized to affect digestive functions in the small intestines with result of digestion and absorption of nutrients, also in pigs it is the main substrate for bacteria in the gastro-intestinal tract and its inclusion has shown to promote bacterial growth resulting in higher fecal excretion (Metzler and Mosenthin, 2008). The high interest to use dietary fiber in pig's diets is an economical point and animal welfare perspective, also feedstuff with high content of dietary fiber could be supplied as cheap by products as roughage (Banino, 2012). Kim et al. (2018) stated that during pregnancy, sow feed intake is not adequate to meet the nutrient requirements for maintenance, fetal growth and lactation which leads to mobilization of body reserves. According to Krogh et al. (2015) high fiber diets that are greater than 7% crude fiber, during sow's gestation period have increased growth performance of new born piglets, also increased sow feed intake during lactation and reduced constipation. Sows performance has been improved over the last decades by which energy and nutrients intake has become critical and nutritional factors such as metabolic status, energy supply during lactation may affect the milk production while feed intake and dietary fibre content may affect heat energy of reproductive sows (Theil et al., 2004). Ngalavu et al. (2018) recommended that supplementation is required for feeding during sow's gestation period to improve

http://www.aloki.hu ● ISSN 1589 1623 (Print) ● ISSN 1785 0037 (Online)
DOI: http://dx.doi.org/10.15666/aeer/1605_60256031
© 2018, ALÖKI Kft., Budapest, Hungary

performance. There is little information on dietary fiber supplementation on milk composition in colostrums of pregnant sows. Hence, we hypothesized that the dietary fiber supplementation such as fermented corn stover might be the supplement to improve nutrient digestibility and milk composition of pregnant sows.

The objective of the present study was to investigate the effects of dietary fiber supplementation on nutrient digestibility and milk composition in colostrums of pregnant sows. This study will provide basic scientific knowledge of dietary fiber such as fermented corn stover as supplement during the pregnant stage of sows.

Materials and methods

Study site

This experiment was conducted in a research area of Jilin Agricultural University, Changchun city of the People's Republic of China. Jilin Province is located at latitude 43° 42' N and longitude 126° 12' E whereas Changchun city is found at latitude 43° 88' N and longitude 125° 35' E. The average annual rainfall ranges between 350-1000 mm during rainy seasons between March and August, while the dry season is between September and February. Average daily temperatures in winter (Nov- Mar), ranges between -8 °C (17 ºF) to -20 °C (-4.6 °F, and in summer (May-July) between 16 °C (61.4 °F) and 28 °C (81.2 °F) respectively.

Corn stover preparation and fermentation

Corn stover leaves were removed and dried at a temperature of 70 °C until the constant weight was achieved. Corn stover was completely dried and further cut into 10 cm, thereafter crushed into fine powder to allow passing through a 3.5 mm mesh mini laboratory sieve to determine the level of dry matter. Corn stover fermentation for the current study was prepared using the method indicated by Chang et al. (2012) and Ngalavu et al. (2018). In the current study, the Commercial baking yeast was used as *Saccharomyces cerevisie* for the microbial fermentation process. The yeast was then inoculated into medium, containing glucose 50 gL^{-1}, peptone 5 gL^{-1}, MgSO4.7H2O 1 gL^{-1}, K2HPO2 and 5gL^{-1} of yeast. The medium was autoclaved at 121 °C (249 °F) for 15 min. After autoclaved, the yeast was inoculated on the orbital shaker for a period of 18 h at 30 °C, 50 rmp.

Experimental design and sows feeding management

Experiment was conducted in completely randomized design; forty eight pregnant sows (24 Landrace and 24 Yorkshire) were randomly assigned into 4 experimental treatment groups (0%, 10%, 15% and 20% fermented extruded corn stover) for with 12 replicates per group and were selected on the basis of genetics, weight and parity similar to binary hybrid sow (long x large). In addition, pigs live body weights were ranged between 17.5-20.5 kg (average 19 kg). Daily feed intakes, health conditions of pigs and free access to drinking water were carefully checked and recorded. The duration of the trial included 3 days of pre-feeding; from mating to sow delivery 114 days, sows 7 days after delivery to 28 days after weaning, up to a to a total number of 145 days. Pigs' immunization and disinfection of piggery and experiments were according the conventional method of pigs.

http://www.aloki.hu ● ISSN 1589 1623 (Print) ● ISSN 1785 0037 (Online)
DOI: http://dx.doi.org/10.15666/aeer/1605_60256031
© 2018, ALÖKI Kft., Budapest, Hungary

Table 1 shows the experimental diets contained corn and soybean meal as raw material were prepared according the NRC (1998) pig's nutritional requirements. All the procedures involved pigs were approved by Animal Research Ethics Committee of the Jilin Agricultural University, China.

Table 1. *Fodder during pregnancy and lactation formula*

Experimental diet				
Ingredients	**Percentage per group**			
	(Control)	10%	15%	20%
Corn	76	67	62	59
Soybean meal	14	15	15	16
Wheat bran	5.2	3.2	3.2	0.2
$CaHPO_4$	2	2	2	2
Limestone	1	1	1	1
NaCl	0.2	0.2	0.2	0.2
Fermentation puffed straw	0	10	15	20
$NaHCO_3$	0.6	0.6	0.6	0.6
Premix	1	1	1	1
Total	100	100	100	100
Nutrient levels	**Percentage**			
DE/(MJ/kg)	13.75	13.42	13.21	13.13
CP	12.91	12.92	12.81	12.87
NDF	10.50	15.75	18.58	20.76
ADF	3.40	8.55	11.20	13.63
Ca	0.88	0.88	0.88	0.88
P	0.71	0.70	0.66	0.63
Na	0.15	0.15	0.15	0.15
Cl	0.12	0.12	0.12	0.12

$CaHPO_4$: Calcium Hydrogen Phosphate; NaCl: Sodium Chloride; $NaHCO_3$: Sodium bicarbonate; DE: Digestible Energy; CP: Crude Protein; NDF: Neutral Detergent Fibre; ADF: Acid Detergent Fibre; Ca: Calcium; P: Phosphorus; Na: Sodium; Cl: Chloride

Nutrient digestibility and milk composition analysis

Total of 300 g fecal samples were collected from each pen every morning (9:00 am) for seven days and stored at -20 °C immediately after collection. Frozen dried samples of feces were ground through 1 mm screen in a Wiley Mill model 4; Thomas Scientific, Swedesboro, NJ. The chromium concentration in fecal samples was determined using an ICP procedure (Method 990.08, AOAC Int., 2007). Samples were prepared using nitric acid. Colostrum samples were collected in a 50 ml centrifuge tube immediately after sows had delivered, and the stored at -40 °C refrigerator for cryopreservation tests. The samples were analysed using FOSS multi-functional milk composition analyzer for milk fat, milk protein and non-fat solids.

http://www.aloki.hu ● ISSN 1589 1623 (Print) ● ISSN 1785 0037 (Online)
DOI: http://dx.doi.org/10.15666/aeer/1605_60256031
© 2018, ALÖKI Kft., Budapest, Hungary

Chemical analysis and statistical analysis

The procedure of AOAC (2005) was used to analyze the digestible energy (DE) and crude protein (CP). Van Soest (1994) method was followed to analyze the acid detergent fibre (ADF) and neutral detergent fibre (NDF). All the experimental diets including Calcium (Ca), phosphorus (P), Sodium (Na) and Chloride (Cl) were analyzed according the procedure explained by Chang et al. (2015). One-way analysis of variance (ANOVA) was used for data analysis with Duncan multiply range test for comparing difference among the means using statistical package for social sciences (Version 10.0 for windows, SPSS Inc., Chicago, IL). All the results were expressed as mean ± standard deviation (mean ± SD). Alpha 0.05 was the significance level of the study.

Results and discussion

Effects of fermented extruded corn stover on digestibility

The results of nutrient digestibility (*Table 2*) showed that in crude protein and neutral detergent fibre, there were no significant differences between the control group and 10% fermented extruded stover ($P > 0.05$). However, these results in energy and acid detergent fibre showed a significant differences between control group and all the experimental groups ($P > 0.05$), respectively. It can be seen that with the increase of fiber content in diets, the apparent digestibility of fiber level showed a significant decrease trend. The apparent digestibility of energy and the apparent digestibility of protein decreased with the increase of fiber content. Through the results of this experiment, it can be seen that the addition of fermented extruded stover during pregnancy to improve the level of fiber in sow diets will reduce the apparent digestibility of its energy without affecting the sow during pregnancy. Digestibility, apparent digestibility of acidic detergent fibers, and apparent digestibility of neutral detergent fibers were negatively correlated with increased fiber levels in diets. Sows have high utilization capacity for high fiber diets, mainly because adult sows have a relatively complete intestinal digestion environment. The fiber can be in the intestine through the role of micro-organisms, resulting in short-chain fatty acids (acetic acid, propionic acid, butyric acid) and other volatile fatty acids to supply energy for the sow and other energy needs (Jha and Berrocoso, 2015). The energy digestibility of the test group was not significant, mainly due to the longer metabolic time of the fiber, due to the structural characteristics of the fiber, resulting in sow satiety, thereby reducing the sow physical activity so as to reduce the need to maintain the purpose. The mechanism of protein digestion and absorption in the sow is mainly due to the physical properties of the fiber, to prevent the digestive enzymes in the intestine as well as to digest the nutrient, so that parts of the nutrients are not absorbed by the fiber composition of a membrane and material, which is wrapped up by the sow through the form of feces discharged. Johnston et al. (2003) stated that fibrous feed typically have not been used for non-ruminants due to the reported depression of digestibility, however, some type of fiber do not apply such negative effects on nutrient digestibility. Recent study (Jiang et al., 2016) on Acid Detergent Fibre (ADF) and Neutral Detergent Fibre (NDF) digestibility was improved and Gross Energy (GE) digestibility was improved, which may be the reason for an improved Average Daily Feed Intake (ADFI) compared with pigs fed control diets. Declining Metabolic Energy (ME) intake plus observation that dietary fibre decrease digestibility of energy and other nutrient (Renteria-Flores et al., 2015).

http://www.aloki.hu ● ISSN 1589 1623 (Print) ● ISSN 1785 0037 (Online)
DOI: http://dx.doi.org/10.15666/aeer/1605_60256031
© 2018, ALÖKI Kft., Budapest, Hungary

Table 2. *Effects of fermented extruded corn stover on digestibility in sows*

Digestibility parameters	Experimental groups			
	Control	**10% fermented extruded straw**	**15% fermented extruded straw**	**20% fermented extruded straw**
Crude protein	85.03±0.02[a]	83.12±1.00[a]	81.18±0.80[b]	80.52±0.36[b]
Energy	87.42±1.33[a]	84.26±0.05[b]	83.46±1.31[b]	83.14±2.35[b]
Acid detergent fibre	82.42±0.76[a]	76.77±1.51[b]	61.70±1.62[c]	54.58±1.24[d]
Neutral detergent fibre	87.04±0.24[a]	84.94±1.86[a]	78.30±2.50[b]	68.09±4.53[c]

[a, b, c, d]Means in rows with different superscripts differ significantly ($p \leq 0.05$)

Effects of fermented extruded stover on milk components and composition in sows' colostrum

Effect of corn stover on pregnant sow's colostrum ingredients is portrayed on *Table 3*. The results discovered that in fat, lactose and non-fat solids, there were no significant differences between control group and experimental groups ($P > 0.05$). There was a significant difference in protein between control group and experimental group ($P < 0.05$), respectively. In addition, Devillers et al. (2004) indicated that piglet body weight gain increases concurrently with colostrum intake during the first 24 h after birth and a weight gain of 50 g during the weaning on average is allowed by 250 g of colostrum ingested.

Table 3. *Effects of fermented extruded corn stover on milk components in sows' colostrum*

Milk components	Experimental groups			
	Control	**10% fermented extruded straw**	**15% fermented extruded straw**	**20% fermented extruded straw**
Protein	16.73±0.55[c]	17.79±1.12[ab]	18.53±0.07[ab]	16.38±0.03[a]
Fat	5.18±0.96[a]	5.29±0.56[a]	4.98±0.06[a]	5.37±0.06[a]
Lactose	2.53±0.01[a]	2.61±0.04[a]	2.55±0.06[a]	2.80±0.01[b]
Non-fat solids	21.35±1.43[a]	22.37±0.97[a]	22.41±0.46[a]	20.53±0.54[a]

[a, b]Means in rows with same superscripts are the same significantly ($p \leq 0.05$)

As shown in *Table 4,* there was no significant difference in the total solid content between the control group and the colostrum ($P > 0.05$). There was significant difference between the control group and the experimental groups in colostrum composition ($P < 0.05$). There was no significant difference between the control group and the 20% fermented extruded stover group ($P > 0.05$). The control group and 10% fermented extruded stover group had no significant difference ($P > 0.05$). The results has shown that the amount of protein and lactose in the milk composition of the colostrum of each group increased with the increase of the fiber content in the sow diets, and the difference was significant. Similar results were also reported by Kim et al. (2018), who found that sows fed high energy diet had higher concentration of lactose in milk. The content of free fatty acid (FFT), non-fat solid (NFS), freezing point (FP) and total solid (TS) were not significantly different; however, there was a difference in the decrease free fatty acids. Studies have shown that feeding high-fiber diets can increase the content of volatile fatty acids in sows, while some of the volatile fatty acids play an

http://www.aloki.hu ● ISSN 1589 1623 (Print) ● ISSN 1785 0037 (Online)
DOI: http://dx.doi.org/10.15666/aeer/1605_60256031
© 2018, ALÖKI Kft., Budapest, Hungary

important role in the milk production of sows, and therefore have a higher effect on milk fat content in milk. Quesnel et al. (2009) study have shown that high-fiber diet than the control group increased milk production, but the difference was not significant, no significant difference in milk composition, which is slightly different from the current study results, which may be related to the type of feeding fiber inconsistencies. According to Quesnel et al. (2009), the great appetite of lactating sows fed a high fiber diet during gestation may be slightly indicated by decreased secretion of leptin and does not seem to have connection with change in glucose and insulin metabolism. The reduction in part of the milk composition in the 20% fermented puffed straw group may be related to excessive fiber intake. This also shows that the fiber cannot rely too much on the low energy use effect. Feed ingredients, such as fermented liquid and yeast extracts has shown to cause change in colostrum composition (Farmer and Quesnel, 2009).

Table 4. *Effects of fermented extruded corn stover on milk composition in sows' colostrum*

Milk composition	Experimental groups			
	Control	**10% fermented extruded straw**	**15% fermented extruded straw**	**20% fermented extruded straw**
Total solids	30.43±0.15[a]	28.96±0.08[a]	27.35±0.12[a]	27.10±0.17[a]
Freezing point	1.50±0.03[a]	1.24±0.12[ab]	1.24±0.11[b]	1.26±0.01[b]
Acidity	63.41±4.01[a]	55.15±5.10[b]	54.19±4.62[b]	51.95±0.23[b]
Free fatty acid	71.84±2.59[a]	68.14±4.76[a]	66.27±4.28[a]	66.11±0.30[a]

[a, b]Means in rows with different superscripts differ significantly ($p \leq 0.05$)

Conclusion

Fermented extruded corn stover which is a dietary fiber supplement can be used to slightly improve performance of pregnant sows. Our findings suggest that with the increase of fiber content in feed, protein and lactose content are increased in colostrum of pregnant sows and there is little effect on digestibility. There is great potential to develop different methods of feed processing that will increase the effect of fiber supplementation in pig's performance.

REFERENCES

[1] AOAC (2005): Official Methods of Analysis. 18th ed. – Association of Analytical Chemist, Washington, DC.

[2] AOAC International (2007): Official Methods of Analysis of AOAC Int. 18th ed. Rev. 2. (edited by Hortwitz, W., Latimer, G. W. Jr.) – AOAC Int, Gaithersburg, MD.

[3] Banino, A. (2012): Effect of fiber on physiochemical properties of digesta and fecal microbial composition in pigs. – MSc Thesis, Swedish University of Agricultural Science, Uppsala, Sweden.

[4] Chang, J., Cheng, W., Yin, Q. Q., Zuo, R. Y., Song, A. D., Zheng, Q. H., Wang, X. (2012): Effect of steam explosion and microbial fermentation on cellulose and lignin degradation of corn stover. – Bio-resource Technology 104: 587-592.

[5] Chang, J., Zhang, Q. G., Yang, H. J., Yin, Q. Q., Wang, P., Wang, Q. W. (2015): Effect biological corn stover replacing partial corn meal on production performance, nutrient

http://www.aloki.hu ● ISSN 1589 1623 (Print) ● ISSN 1785 0037 (Online)
DOI: http://dx.doi.org/10.15666/aeer/1605_60256031
© 2018, ALÖKI Kft., Budapest, Hungary

metabolic rates and carcass characteristics of broilers. – Indian Journal of Animal Research 49: 474-481.

[6] Devillers, N., van Milgen, J., Prunier, A., Le Dividich, J. (2004): Estimation of colostrum intake in the neonatal pig. – Animal Science 78: 305-313.

[7] Farmer, C., Quesnel, H. (2009): Nutritional, hormonal and environmental effects on colostrum in sows. – Journal of Animal Science 87: 56-65.

[8] Jha, R., Berrocoso, J. D. (2015): Dietary fiber utilization and its effects on physiological functions and gut health. – Animal 9: 1441-1445.

[9] Jiang, H. L., Cai, W. B., Mokgawa, D. L., Thomas, R. S., Nesengani, L. T., Tlabela, C. P. (2016): Impact of fermented corn straw on growth performance, digestibility and cecal microflora of growing pigs. – Asian Journal of Animal and Veterinary Advances 11(18): 461-468.

[10] Johnston, L. J., Noll, S., Renteria, A., Shurson, J. (2003): Feeding by products high in concentration of fiber to non-ruminants. – National Symposium on Alternative Feeds for Livestock and Poultry 3: 169-186.

[11] Kim, J. S., Hosseindoust, A., Ju, I. K., Yang, X., Lee, S. H., Noh, H. S., Lee, J. H., Chae, B. J. (2018): Effect of dietary energy levels and β- mannanase supplementation in high mannan based diet during lactation on reproductive performance, apparent total tract digestibility and milk composition in multiparous sows. – Italian Journal of Animal Science 17: 128-134.

[12] Krogh, U., Bruun, T. S., Amdi, C., Flummer, C., Poulsen, J., Theil, P. K. (2015): Colostrum production in sows fed different sources of fiber and fat during late gestation. – Canadian Journal of Animal Science 95: 211-223.

[13] Metzler, B. U., Mosenthin, R. (2008): A review of interaction between dietary fiber and gastro-intestinal microbiota and their consequences on intestinal phosphorus metabolism in growing pigs. – Asian Australian Journal of Animal Science 21(4): 603-615.

[14] Ngalavu, A., Jiang, H., Che, D., Han, R., Tyasi, T. L. (2018): Effect of feeding fermented extruded corn stover on reproductive performance of pregnant sows. – Indian Journal of Animal Research, DOI: 10.18805/ijar.B-824.

[15] NRC (1998): Nutrient Requirements of Swine 10th edition. – National Academy Press, Washington, DC.

[16] Quesnel, H., Meunier- Salaun, M. C., Hamard, A., Gullimet, R., Etienne, M., Farmer, C., Dourmad, J. Y., Pere, M. C. (2009): Dietary fiber for pregnant sows: Influence on sow physiology and performance during lactation. – Journal of Animal Science 87: 532-543.

[17] Renteria-Flores, J. A., Johnston, L. T., Shurson, G. C., Gallaher, D. D. (2015): Effect of soluble and insoluble fiber on energy digestibility, nitrogen retention and fiber digestibility of diets fed to gestating sows. – Journal of Animal Science 86: 2568-2575.

[18] Theil, P. K., Jorgensen, H., Jakobsen, K. (2004): Energy and protein metabolism in lactating sows fed two levels of dietary fat. – Livestock Production Science 89: 265-276.

[19] Van Soest, P. (1994): Nutritional Ecology of The Ruminant: 2nd edition. – Cornell University Press, London.

http://www.aloki.hu ● ISSN 1589 1623 (Print) ● ISSN 1785 0037 (Online)
DOI: http://dx.doi.org/10.15666/aeer/1605_60256031
© 2018, ALÖKI Kft., Budapest, Hungary

EVALUATION OF *ALOE VERA* L. AS PHYTOREMEDIATOR OF HEAVY METALS CONTAMINATED SOILS IN ARID ENVIRONMENTS

ELHAG, M.[1*] – AL-GHAMDI, A. A. M.[2] – GALAL, H. K.[2] – DAHLAN, A.[2]

[1]*Department of Hydrology and Water Resources Management, Meteorology, Environment and Arid Land Agriculture, King Abdulaziz University, 21589 Jeddah, Saudi Arabia*

[2]*Department of Botany, Environment Program, Faculty of Biological Science, King Abdulaziz University, P.O. Box 35009, Jeddah 21488, Saudi Arabia*

**Corresponding author*
e-mail: melhag@kau.edu.sa

(Received 5th Jun 2018; accepted 31st Aug 2018)

Abstract. Decontamination of heavy metal polluted soil and water by plants is called phytoremediation. Succulent plant species such as *Aloe vera* (L.) are considered for the current study to investigate their ability to accumulate heavy metals and their uptake rate of different heavy metals are tested. This study aimed to measure the concentration of toxic heavy metals (As, Cd, Cr, Cu, Pb, Hg, and Ni) in arid contaminated soils of Saudi Arabia. The soil was contaminated with 1500 ppm of each element. During a year of the experiment, 4 samples were taken on a trimester basis. All samples were digested to measure heavy metal content in soil and plant. Metal Transfer Factor (MTF) and Translocation Factor (TF) were calculated from the examined data. This study showed that the *A. vera* has the ability to decontaminate heavy metals from polluted soil. The greatest accumulation was detected from As but the accumulation was declined after 9 months. Hg accumulation showed no significant results of heavy metal uptake by *A. vera*. The greatest MTF was of Cd elements and counted for 1.3404 and the lowest was of Cr and counted for 0.1292. Cd TF was the maximum (2.8538) but Pb TF was the minimum (1.2191).
Keywords: *accumulation ability, metal transfer factor, succulent plant, soil treatment, translocation factor*

Introduction

The medium for plant root growth and waste disposal is the soil. Moreover, it is a transmitter of different contaminants in water, air, and food. Soil pollution has effects on the natural quality of agricultural crops and water resources. Subsequently, it may menace human health and may affect the quality of the atmosphere. Some attention has gone to soil pollution linked to crops in the past (Wong, 1996). Also, the polluted soil affecting the functions of soil and the environment has been gradually confirmed by environmentalist (Tiller, 1992).

Heavy metals are physical constituents of the soil's profile. Human industrial activities, as well as extensive agricultural practices, have hardly changed the stability and biological cycles of many heavy metals (Elhag and Bahrawi, 2016; Elhag et al., 2017a). An assessment of the ecological danger due to the polluted soil is of importance for agricultural zones, because of heavy metals that are potentially harmful to all organisms not only human, persist in soils for many years (Grzebisz et al., 2001).

The riskiest hazards affecting both rich and poor countries are heavy metal pollution. Industrialization, fossil fuel consumption and the production of a variety of chemical compounds has led to the worldwide deterioration of the quality of the environment (Chakravarty et al., 2010). All trace elements at the high level of concentrations have

http://www.aloki.hu ● ISSN 1589 1623 (Print) ● ISSN 1785 0037 (Online)
DOI: http://dx.doi.org/10.15666/aeer/1605_60336045
© 2018, ALÖKI Kft., Budapest, Hungary

intense poisonous effects and are viewed as pollutants of the environment (Rashed and Niyazi, 2017).

Phytoremediation is a sustainable, cost-effective, green technique to decontaminate the environment from pollutants such as heavy metals, insecticides, thinners, explosive material, petroleum, polycyclic aromatic hydrocarbons, and landfill leachate in the soil, water, and sediments. It involves the use of plants to take off, move out, balance and control pollutants in soil and water (Hughes et al., 1996). It is a weak entered approach depending on biological attenuation by biodegradation and physiochemical devices that decrease the concentration of the contaminant (Parrish et al., 2005; Schwab and Banks, 1993).

The implementation of phytoremediation approach in arid regions requires special plant selection and is anticipated to be less feasible than in humid regions with more favorable climate for plant growth. The arid climate considered by low annual rainfall and high wind make the phytoremediation research challenging in the Middle East. For phytoremediation in arid and semiarid areas, it is necessary to set up a varied phytocoenosis, including plants that can accumulate, stabilize or degrade contaminants (Piha et al., 1995). Phytoremediation is very hopeful for the removal of pollutants from the soil and water (Garbisu and Alkorta, 2003).

Phytoremediation of metal contaminants falls within four different phytoremediation strategies, each of which includes several techniques of actions for remediating heavy metal pollution: Phytostabilization is the restraint of pollutants in the soil by plants, through uptake by roots, adsorption onto roots or precipitation within the root of the plant grows under soil and maintain the physical balance of soils (Padmavathiamma and Li, 2007), Phytofiltration means that plants use roots or seedlings to accumulate contaminants, heavy metals, from water and aqueous waste streams (Prasad and Freitas, 2003), During the process of phytovolatilization plants absorb these heavy metals in elemental forms from the polluted soil, and their biologically convert them into gaseous forms that are finally emitted into the air (Thangavel and Subbhuraam, 2004). Phytoextraction is the uptake of heavy metals from the polluted soil by plants and their translocation to harvestable green parts of the plant where they accumulate (Padmavathiamma and Li, 2007).

Phytoremediation can involve grasses, shrubs as well as trees. Grasses can run a groundcover and limit wind dispersion which plants provide a wide canopy and develop a deep network of plant root to prevent soil erosion. (Williams and Twine, 1960). The roots of plants in the soil play a chief role in metal removal by purification, uptake and cation exchange, and plant induced chemical changes in the narrow region of soil (Dunbabin and Bowmer, 1992). A heavy metal will only become toxic if its concentration in the plants exceeds the allowable threshold. Plants have been divided into three groups based on their acceptance to accumulate metals: Excluders are plants insensitive for absorption and accumulation of heavy metals, Indicators are plants that content of heavy metal linearly responds to increasing availability of heavy metals in contaminated soil and Accumulators are plants accumulating higher contents of heavy metals in their tissues per their rise in the soil than others (Peer et al., 2005).

Some plants in the group of accumulators called hyperaccumulators, which it can accumulate 100 times higher levels of a specific heavy metal in their shoot tissues compared with regular, non-accumulator plants (Reeves and Baker, 2000). A hyperaccumulator is a plant that can grow in polluted soil with very high concentrations of heavy metals, and uptake these heavy metals through their roots, and accommodate

http://www.aloki.hu ● ISSN 1589 1623 (Print) ● ISSN 1785 0037 (Online)
DOI: http://dx.doi.org/10.15666/aeer/1605_60336045
© 2018, ALÖKI Kft., Budapest, Hungary

very high levels of metals in their tissues. The ability to hyperaccumulate toxic heavy metals compared to other plant species has been exposed to be due to several gene expressions and regulations of the same genes in different plants. (Ali et al., 2013).

There are 41 species of Aloe recorded from the Arab region which encompass the countries of Saudi Arabia (Newton, 2001), Yemen (including Socotra) and Oman. The aloes are principally restricted to the areas in the west and south-west of the peninsula (Walker, 2005).

The main objective of the current study is to investigate the ability of *A. vera* in phytoremediation practice of soils polluted with heavy metals in Saudi Arabia. Metal Transfer Factor and Translocation Factor are the evaluation criteria which used to conduct the designated research study.

Materials and methods

Study area description

The Kingdom of Saudi Arabia is influenced by several natural factors, the most important of which is the Astronomical Observatory. The Kingdom is located between 16 degrees and 33 degrees North and 34 and 56 East longitudes, making it the largest part of the dry tropical desert region in South Asia (Sen et al., 2017). The climate of the Kingdom is characterized by drought throughout the year and by high temperatures especially in the summer (Elhag and Bahrawi, 2014a). The geographic location of Saudi Arabia and its varied geological composition and different surface and climatic features from one region to another led to the existence of many natural environments that differ in the components of the vegetation cover (Elhag et al., 2015) from one place to another. Most of the Kingdom's regions are located in dry areas except the Empty Quarter and the Sarawat Mountains within the semi-arid regions. Much of the Kingdom's soil is calcareous because of insufficient rainfall to wash calcium carbonate. Because of these conditions, the Kingdom's environment is fragile and sensitive (Elhag and Bahrawi, 2014b). Saudi Arabia is located in a geographical area lacking fresh water and has no natural resources such as springs, rivers, and lakes with scarcity or lack of rainfall in some areas. Natural resources in the Kingdom are limited to some wells, rainwater pools, and floods that have not been sufficient to meet the essential needs (Elhag et al., 2017b).

Experimental design

The experiment was designed in a tinplate tank with dimensions of 100 × 50 × 75 cm, length, width, and height, respectively. Four tanks were prepared to implant *A. vera* juveniles in PittMoss soils. *A. vera* is a stemless plant growing to 50 Inch, spreading by offsets. The leaves look thick and pulpy, different shades of green, with some species showing white flecks on their upper and lower stem surfaces. The margin of the leaf is serrated and has short and small thorns. The flowers are produced from June to September on a spike up to 120 cm, and each yellow tubular corolla flowers are droopy. Healthy and intact plants were collected with equal in length of 24 cm which is considered to be the optimum plant condition to be examined (Yates, 2002). Prior to the experiment, the juveniles of *A. vera* were planted in tanks for 3 months to adapt to the experimental environment.

http://www.aloki.hu ● ISSN 1589 1623 (Print) ● ISSN 1785 0037 (Online)
DOI: http://dx.doi.org/10.15666/aeer/1605_60336045
© 2018, ALÖKI Kft., Budapest, Hungary

Experimental process

Aloe vera was selected for this study because it is not part of the food chain of humans or animals, it can grow in dry arid climates and it is naturally occurring in Saudi Arabia. The growing juveniles of *A. vera* were irrigated with a solution containing inorganic compounds of heavy metals. Aqueous solutions of 15 g/l were prepared from the soluble form of each heavy metal. The polluted solution was prepared according to O'Connell et al. (2008). Consequently, the juveniles were irrigated once a month with one liter of clean water in each experimental tank.

The samples were taken from one tank at a time 4 times on a trimester basis. Leaves area was calculated for all samples. Shoots and roots were weighed before air drying. Root and shoot samples were dried in the air than dried in an oven at 60 °C for two days. Mixed acid digestion procedure was used for preparing the extracts of plant materials. $HClO_4$ (60%), concentrated HNO_3 and H_2SO_4 were mixed in 1:3:1 ratio by volumes. 5 ml was used for the digestion of 0.2 g of fine powdered dry root and shoot. After digestion on a hot plate is completed as indicated white fumes developed and the solutions became colorless, the volume was completed to 50 ml with distilled water (Allen, 1989; Wade et al., 1984). Experimental design and experimental process are illustrated in *Figure 1*.

Figure 1. *Experimental design and experimental process*

MTF and TF calculation

Metal Transfer Factor (MTF) and Translocation Factor (TF) were calculated from the sample's analysis' data. The calculations of using heavy metal concentration in the extracts of samples were carried out according to the following formulae (Cluis, 2004; Barman et al., 2000; Gupta et al., 2008):

$$MTF = \frac{metal\ concentration\ in\ plant}{metal\ concentration\ in\ soil}$$

http://www.aloki.hu ● ISSN 1589 1623 (Print) ● ISSN 1785 0037 (Online)
DOI: http://dx.doi.org/10.15666/aeer/1605_60336045
© 2018, ALÖKI Kft., Budapest, Hungary

$$TF = \frac{metal\ concentration\ in\ shoot}{metal\ concentration\ in\ root}$$

Heavy metals analysis

20 g of plant materials were dried in the air than dried in the oven at 100 °C for two days. 5 ml of acids were used for digestion of 0.2 g of plant material (Krumbein and Pettijohn, 1938). In atomic absorption spectroscopy, a liquid sample is aspirated and mixed as an aerosol with combustible gasses (acetylene and air). The mixture is ignited in a flame of temperature ranging from 2100 to 2800 °C. During combustion, atoms of the element of interest in the sample are reduced to the atomic state. A light beam from a lamp, that cathode is made of the element being determined, is passed through the flame into a monochronometer and detector. Free, unexcited ground state atoms of the element absorb light at characteristic wavelengths; this reduction of the light energy at the analytical wavelength is a measure of the amount of the element in the sample (Lindsay and Norvell, 1978).

Results and discussion

Different heavy metals absorption by *A. vera* showed a different accumulation behavior along with the experimental time demonstrated in *Figure 2*. Cd accumulation decreased by the time. The highest accumulation of Cu was after 6 months but it was dropping off after 9 months. Cr, Ni, Pb and Hg accumulation increased but it dropped after 9 months. The least heavy metal accumulation was detected in the case of Hg. The highest accumulation was As accumulation but it decreased after 9 months.

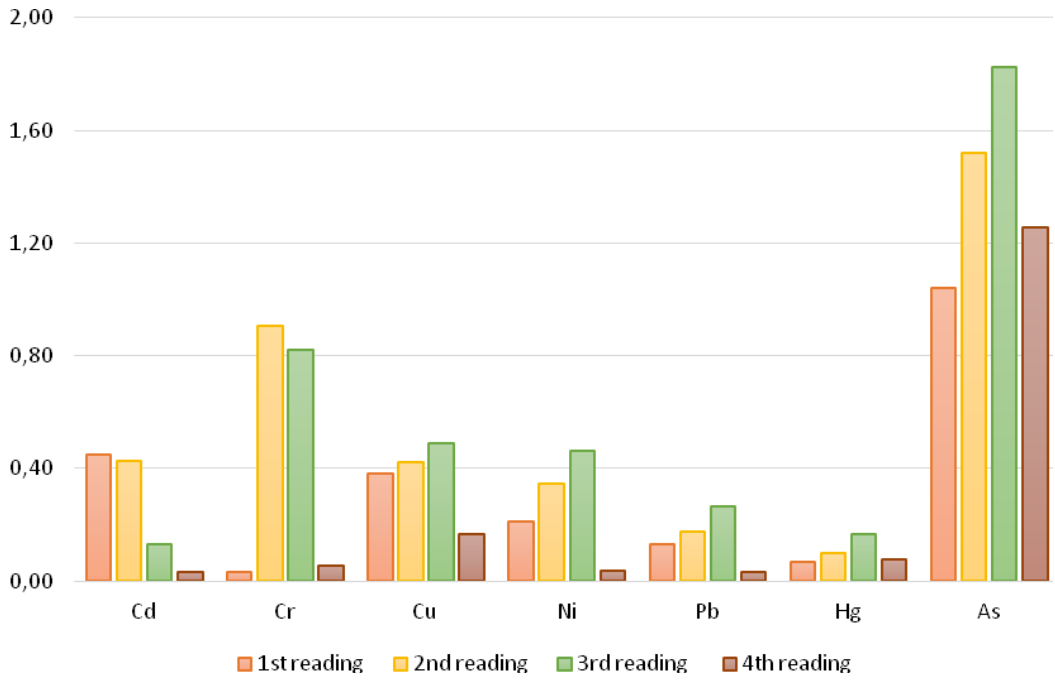

Figure 2. *Heavy metal accumulations in the root (mg/l)*

http://www.aloki.hu ● ISSN 1589 1623 (Print) ● ISSN 1785 0037 (Online)
DOI: http://dx.doi.org/10.15666/aeer/1605_60336045
© 2018, ALÖKI Kft., Budapest, Hungary

Meanwhile, the heavy metal accumulations in the shoot system of *A. vera* showed fewer accumulation rates in general but with less significant behavior in particular with the case of Cr and Cu heavy metal accumulation (*Fig. 3*). Cd accumulation decreased by the time. The highest accumulation of Cr was after 3 months but it was retreating after that and continued decreasing till the end of the experimental period. Cu, Ni, Pb, and Hg accumulation increased by the time. The least accumulation was detected in the case of Hg. The highest accumulation was As accumulation but it decreased after 9 months.

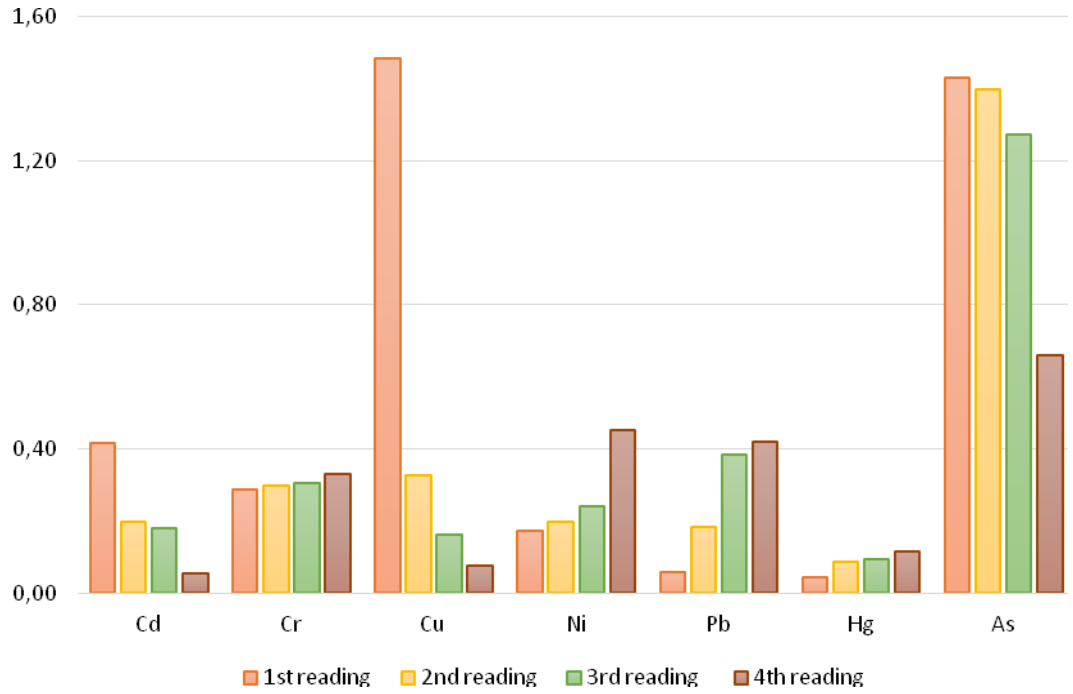

Figure 3. *Heavy metal accumulations in the shoot (mg/l)*

Heavy metal accumulations in both roots and shoots are demonstrated in *Figure 4*. Cd accumulation decreased over time. The least accumulation was Hg accumulation. The highest accumulation was As accumulation but it decreased after 9 months. As, Cu, Ni, Pb and Hg accumulation decreased after 9 months. The concentrations of all heavy metals decreased after 9 months.

The plants for phytoremediation should be rather indigenous to the zones where the contaminants are found, as they have developed adaptation and survival strategies suitable to the hard climate in arid and semiarid areas (Piha et al., 1995). Environmental concerns about the use of exotic species and their threat to the indigenous plant communities are of great importance.

For phytoremediation practices, attention should be given to the use of nonpalatable species before efforts are made to grow these plants. This should contain discussions with concerned regulatory agencies and common organizations about the suitability of the plant species as well. However, non-native species may be an acceptable option provided the climatic conditions are the same and the introduced species do not build a new ecological risk (Radwan et al., 1998).

http://www.aloki.hu ● ISSN 1589 1623 (Print) ● ISSN 1785 0037 (Online)
DOI: http://dx.doi.org/10.15666/aeer/1605_60336045
© 2018, ALÖKI Kft., Budapest, Hungary

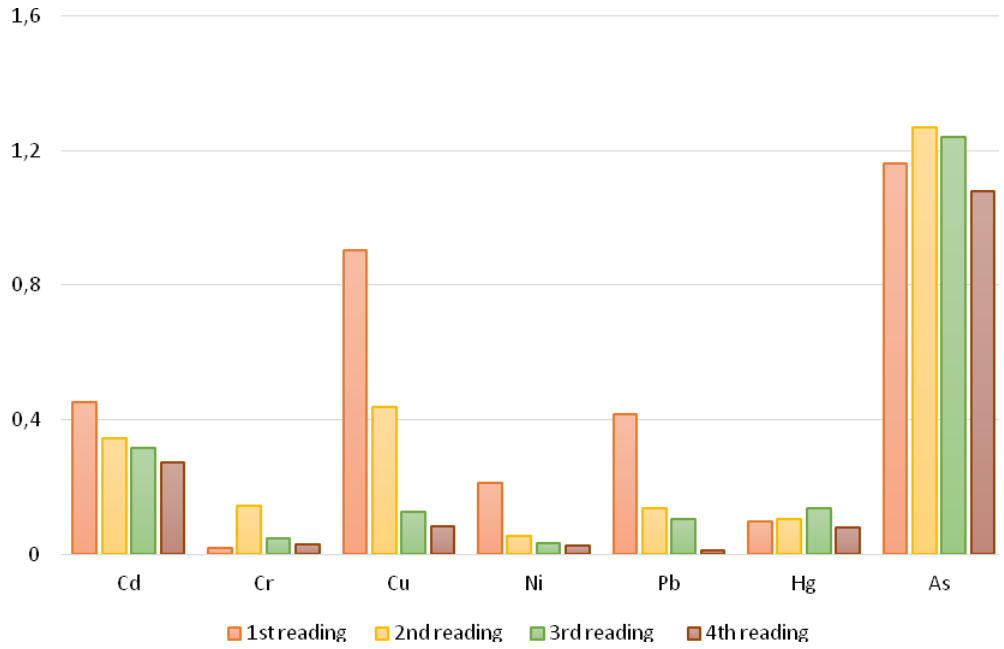

Figure 4. *Heavy metal accumulations in Aloe vera (mg/l).*

The allocation of heavy metals in plant tissues is demonstrated in *Figure 5a–g*. The concentration of Cu and Pb are more in shoot than in root. The concentration of Cd, Cr, Hg and As are more in shoot than in root. The concentration of Ni in root and in the shoot is equal.

The biological effects of heavy metals in plants depend on many ecological factors: the absorptions in the environment, biotic and abiotic factors, exposure time, plant growth, uptake techniques, the affinity of heavy metals for the uptake sites and metals speciation (Mazej and Germ, 2009). Although phytoremediation of contaminated sites in arid and semiarid areas has been attempted by many organizations, the remediation technologies are not properly documented and appear in published literature occasionally. In this study, the current information on phytoremediation for organic and inorganic contaminants in arid and semiarid areas, as well as the potential problems that have an impact on the longstanding practice, are investigated.

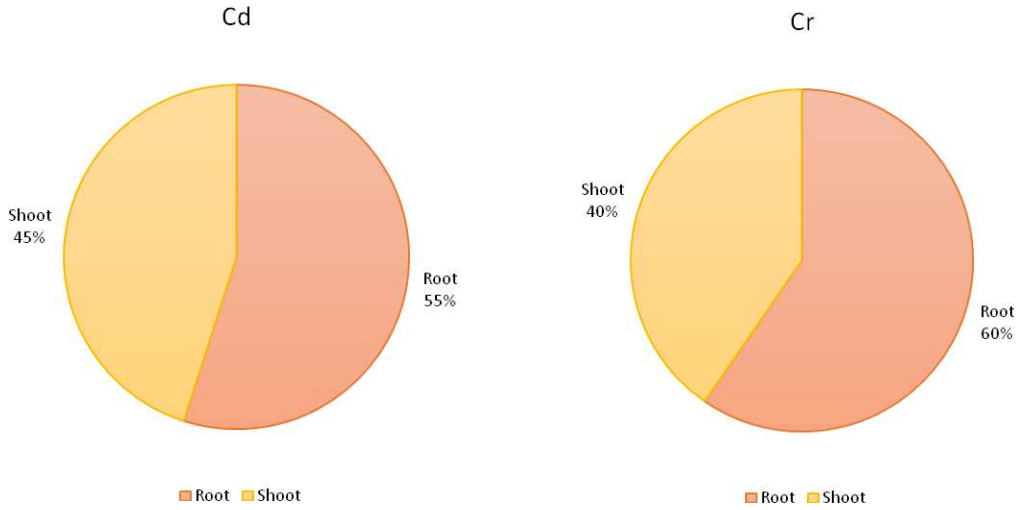

http://www.aloki.hu ● ISSN 1589 1623 (Print) ● ISSN 1785 0037 (Online)
DOI: http://dx.doi.org/10.15666/aeer/1605_60336045
© 2018, ALÖKI Kft., Budapest, Hungary

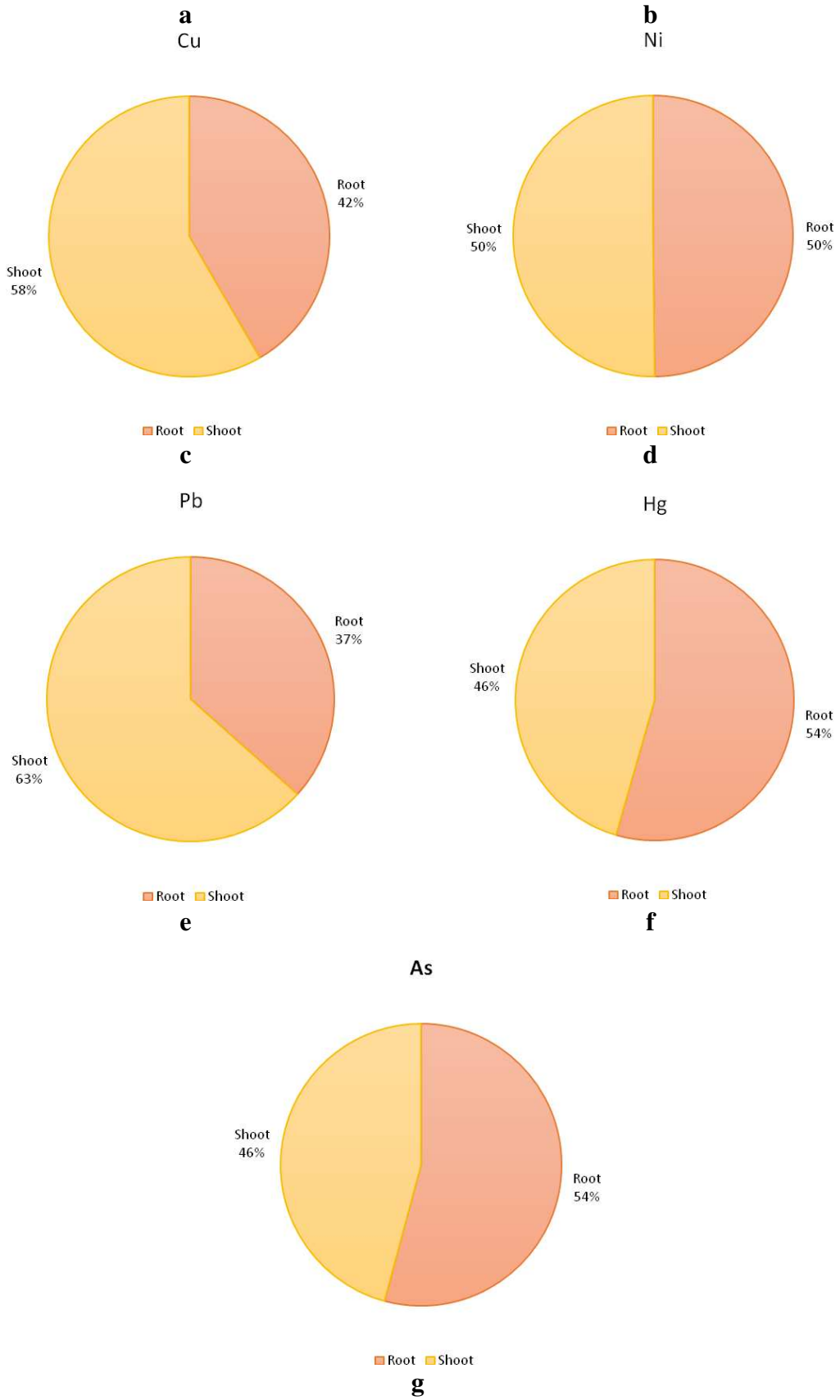

Figure 5. a. *Cadmium accumulation.* ***b.*** *Chromium accumulation.* ***c.*** *Copper accumulation.* ***d.*** *Nickel accumulation.* ***e.*** *Lead accumulation.* ***f.*** *Mercury accumulation.* ***g.*** *Arsenic accumulation*

http://www.aloki.hu ● ISSN 1589 1623 (Print) ● ISSN 1785 0037 (Online)
DOI: http://dx.doi.org/10.15666/aeer/1605_60336045
© 2018, ALÖKI Kft., Budapest, Hungary

According to Deng and Wong (2004), Aloe vera can be considered to have a normal accumulation ability according to its Translocation Factor mentioned in *Table 1*. Different plant species have different TF values based on their affinity to accumulate heavy metals in plant tissues. According to the accumulation ability, phytoremediation plants are categorized into three groups. The first group involves plants with high accumulation ability, like *Typha angustifolia* and *Leersia hexandra*. The second group involves plants with normal accumulation ability, like *Acorus calamus* and *Eleocharis valleculosa*. The third group involves plants with low accumulation ability, like *Neyraudia reynaudiana* and *Phragmites australis* (Deng et al., 2004).

TF and MTF values are demonstrated in *Table 1*. Cu, Ni and Pb concentrations are higher in shoot than in root. Cd, Cr, Hg and As concentrations are higher in root than in shoot. *A. vera* has a high ability to As accumulation, a normal ability to the accumulation of Cd, Cr, Cu, Ni and Pb, and low abilities to accumulate Hg (*Fig. 6*).

Table 1. *Translocation factor and metal transfer factor*

	TF	MTF
Cd	0.820116	2.21934
Cr	0.676804	2.477533
Cu	1.402193	1.713169
Ni	1.00759	1.992467
Pb	1.728856	1.578417
Hg	0.835766	2.196508
As	0.844858	2.183631

TF of Cd, Cr, Hg and As < 1
TF of Cu, Ni and Pb ≥ 1
MTF of Cd, Cr, Hg and As > 2
MTF of Cu, Ni and Pb < 2

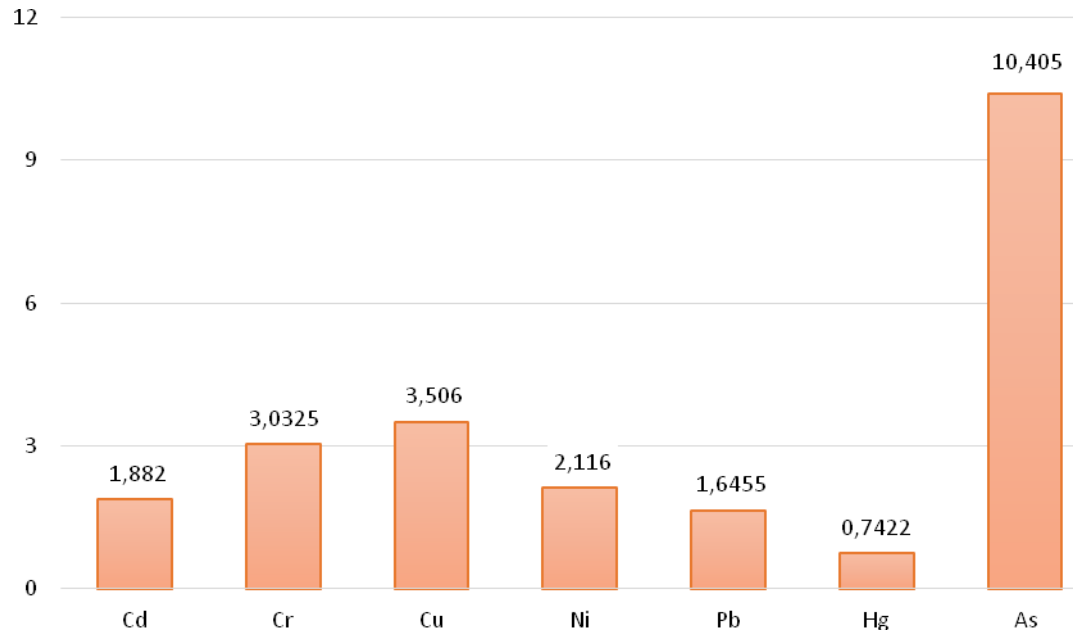

Figure 6. *Total heavy metal accumulation (mg/l)/year*

http://www.aloki.hu ● ISSN 1589 1623 (Print) ● ISSN 1785 0037 (Online)
DOI: http://dx.doi.org/10.15666/aeer/1605_60336045
© 2018, ALÖKI Kft., Budapest, Hungary

In plants, succulence is defined as the presence of thickened tissues in plant organs that the primary function is water-storage and, consequently, drought avoidance (Gibson, 1982; Gibson and Nobel, 1990; Willert, 1992). Because they store water, organs with succulent tissues tend to have a large volume to surface area ratios compared with non-succulent organs in the same plant (Gibson and Nobel, 1990; Rowley, 1987). Such increases in volume result in surface areas with relatively large cross-sectional areas, which leads to greater resistance of bending stresses (Niklas, 1992).

Phytoremediation can be used along with other cleanup techniques. (Padmavathiamma et al., 2014). In general, the use of phytoremediation is confined to sites with low to medium contaminant concentrations, and contamination in the top profile of soils, where phytotoxicity does not occur and the root of the plant can readily access the contaminants (Pivetz, 2001).

Conclusion

This study showed that the *Aloe vera* has the abilities to be a phytoremediators to heavy metals from contaminated soil polluted with metals such as (As, Cd, Cr, Cu, Pb, Hg, and Ni) due to the great reduction of these metals in the contaminated soils which demonstrates a significant level of affinity to these metals. The results confirm that the cultivation of *A. vera* is favorable in soils contaminated with Arsenic (As). Moreover, the optimum lifespan of *A. vera* is nine months after its plantation before its affinity to accumulate heavy metals declines. However, *A. vera* is not recommended for soil polluted with Mercury (Hg). Soil nutrients and soil moisture content among other climatic factors shall be considered in future utilization of *Aloe vera* in phytoremediation. Further investigation needs to be directed towards using *A. vera* under several drought conditions instead of regular irrigation to compare the accumulation ability of *A. vera* in different irrigation schedules.

Acknowledgements. This project was funded by the Deanship of Scientific Research (DSR), King Abdulaziz University, Jeddah, under grant no. 184-155-1439-G. The authors, therefore, acknowledge with thanks to DSR's technical and financial support.

REFERENCES

[1] Ali, H., Khan, E., Sajad, M. A. (2013): Phytoremediation of heavy metals—concepts and applications. – Chemosphere 91: 869-881.
[2] Allen, E. B. (1989): The restoration of disturbed arid landscapes with special reference to mycorrhizal fungi. – Journal of Arid Environments 17: 279-286.
[3] Barman, S., Sahu, R., Bhargava, S., Chaterjee, C. (2000): Distribution of heavy metals in wheat, mustard, and weed grown in field irrigated with industrial effluents. – Bulletin of Environmental Contamination and Toxicology 64: 489-496.
[4] Chakravarty, P., Sarma, N. S., Sarma, H. (2010): Biosorption of cadmium (II) from aqueous solution using heartwood powder of Areca catechu. – Chemical Engineering Journal 162: 949-955.
[5] Cluis, C. (2004): Junk-greedy greens: phytoremediation as a new option for soil decontamination. – BioTeach Journal 2: l-67.

http://www.aloki.hu ● ISSN 1589 1623 (Print) ● ISSN 1785 0037 (Online)
DOI: http://dx.doi.org/10.15666/aeer/1605_60336045
© 2018, ALÖKI Kft., Budapest, Hungary

[6] Deng, H., Ye, Z., Wong, M. (2004): Accumulation of lead, zinc, copper and cadmium by 12 wetland plant species thriving in metal-contaminated sites in China. – Environmental Pollution 132: 29-40.
[7] Dunbabin, J. S., Bowmer, K. H. (1992): Potential use of constructed wetlands for treatment of industrial wastewaters containing metals. – Science of the Total Environment 111: 151-168.
[8] Elhag, M., Bahrawi, J. (2014a): Cloud coverage disruption for groundwater recharge improvement using remote sensing techniques in Asir Region Saudi Arabia. – Life Science Journal 11: 192-200.
[9] Elhag, M., Bahrawi, J. A. (2014b): Conservational use of remote sensing techniques for a novel rainwater harvesting in arid environment. – Environmental Earth Sciences 72: 4995-5005.
[10] Elhag, M., Bahrawi, J. A. (2016): Consideration of geo-statistical analysis in soil pollution assessment caused by leachate breakout in the municipality of Thermi, Greece. – Desalination and Water Treatment 57: 27879-27889.
[11] Elhag, M., Hegazy, A. K., Alatar, A. A., Faisal, M., El-Bana, M., Bahrawi, J. A., Al-Ghamdi, A. A. M. (2015): Population demography and global sensitivity analysis of Avicennia marina on the eastern and western coasts of Saudi Arabia. – Koedoe 57: 1-9.
[12] Elhag, M., Bahrawi, J. A., Galal, H. K., Aldhebiani, A., Al-Ghamdi, A. A. (2017a): Stream network pollution by olive oil wastewater risk assessment in Crete, Greece. – Environmental Earth Sciences 76: 278.
[13] Elhag, M., Galal, H. K., Alsubaie, H. (2017b): Understanding of morphometric features for adequate water resource management in arid environments. – Geoscientific Instrumentation, Methods and Data Systems 6: 293.
[14] Garbisu, C., Alkorta, I. (2003): Basic concepts on heavy metal soil bioremediation. – ejmp & ep (European Journal of Mineral Processing and Environmental Protection) 3: 58-66.
[15] Gibson, A. C. (1982): Phylogenetic Relationships of Pachycereeae. – In: Barker, J. S. F., Starmer, W. T. (eds.) Ecological Genetics and Evolution: The Cactus-Yeast-Drosophila Model System. Academic Press, New York.
[16] Gibson, A. C., Nobel, P. S. (1990): The Cactus Primer. – Harvard University Press, Cambridge, MA.
[17] Grzebisz, W., Ciesla, L., Diatta, J. (2001): Spatial distribution of copper in arable soils and in non-consumable crops (flax, oil-seed rape) cultivated near a copper smelter. – Polish Journal of Environmental Studies 10: 269-274.
[18] Gupta, S., Nayek, S., Saha, R., Satpati, S. (2008): Assessment of heavy metal accumulation in macrophyte, agricultural soil, and crop plants adjacent to discharge zone of sponge iron factory. – Environmental Geology 55: 731-739.
[19] Hughes, J. B., Shanks, J., Vanderford, M., Lauritzen, J., Bhadra, R. (1996): Transformation of TNT by aquatic plants and plant tissue cultures. – Environmental Science & Technology 31: 266-271.
[20] Krumbein, W. C., Pettijohn, F. J. (1938): Manual of Sedimentary Petrography. – Appleton Century Crofts, New York.
[21] Lindsay, W. L., Norvell, W. A. (1978): Development of a DTPA soil test for zinc, iron, manganese, and copper. – Soil Science Society of America Journal 42: 421-428.
[22] Mazej, Z., Germ, M. (2009): Trace element accumulation and distribution in four aquatic macrophytes. – Chemosphere 74: 642-647.
[23] Newton, L. (2001): Sansevieria. – In: Eggli, U. (ed.) Illustrated Handbook of Succulent Plants: Monocotyledons. Springer, New York, pp. 261-272.
[24] Niklas, K. J. (1992): Petiole mechanics, light interception by lamina, and "economy in design". – Oecologia 90: 518-526.

http://www.aloki.hu ● ISSN 1589 1623 (Print) ● ISSN 1785 0037 (Online)
DOI: http://dx.doi.org/10.15666/aeer/1605_60336045
© 2018, ALÖKI Kft., Budapest, Hungary

[25] O'connell, D. W., Birkinshaw, C., O'dwyer, T. F. (2008): Heavy metal adsorbents prepared from the modification of cellulose: A review. – Bioresource Technology 99: 6709-6724.
[26] Padmavathiamma, P. K., Li, L. Y. (2007): Phytoremediation technology: hyper-accumulation metals in plants. – Water, Air, and Soil Pollution 184: 105-126.
[27] Padmavathiamma, P. K., Ahmed, M., Rahman, H. A. (2014): Phytoremediation-A sustainable approach for contaminant remediation in arid and semi-arid regions-a review. – Emirates Journal of Food and Agriculture 26: 757.
[28] Parrish, Z. D., Banks, M. K., Schwab, A. P. (2005): Effect of root death and decay on dissipation of polycyclic aromatic hydrocarbons in the rhizosphere of yellow sweet clover and tall fescue. – Journal of Environmental Quality 34: 207-216.
[29] Peer, W. A., Baxter, I. R., Richards, E. L., Freeman, J. L., Murphy, A. S. (2005): Phytoremediation and Hyperaccumulator Plants. – In: Tamás, M. J., Martinoia, E. (eds.) Molecular Biology of Metal Homeostasis and Detoxification. Springer, Berlin.
[30] Piha, M., Vallack, H., Reeler, B., Michael, N. (1995): A low input approach to vegetation establishment on mine and coal ash wastes in semi-arid regions. I. Tin mine tailings in Zimbabwe. – Journal of Applied Ecology: 372-381.
[31] Pivetz, B. E. (2001): Ground Water Issue: Phytoremediation of Contaminated Soil and Ground Water at Hazardous Waste Sites. – National Risk Management Research Lab, Ada OK.
[32] Prasad, V. M. N., Freitas, D. O. H. M. (2003): Metal hyperaccumulation in plants: biodiversity prospecting for phytoremediation technology. – Electronic Journal of Biotechnology 6: 285-321.
[33] Radwan, S., Al-Awadhi, H., Sorkhoh, N., El-Nemr, I. (1998): Rhizospheric hydrocarbon-utilizing microorganisms as potential contributors to phytoremediation for the oil Kuwaiti desert. – Microbiological Research 153: 247-251.
[34] Reeves, R. D., Baker, A. J. M. (2000): Metal-Accumulating Plants. – In: Raskin, I., Ensley, B. D. (eds.) Phytoremediation of Toxic Metals: Using Plants to Clean Up the Environment. Wiley, New York.
[35] Rashed, M., Niyazi, B. (2017): Environmental impact assessment of the former Al-Musk Lake wastewater dumpsite using electromagnetic induction technique. – Earth Systems and Environment 1: 1-10.
[36] Rowley, G. D. (1987): The Duchess of Beaufort's succulent plants. – Bradleya 5: 1-16.
[37] Şen, Z., Al-Harithy, S., As-Sefry, S., Almazroui, M. (2017): Aridity and risk calculations in Saudi Arabian wadis: Wadi Fatimah case. – Earth Systems and Environment, 1: 26-37.
[38] Schwab, A., Banks, M. (1993): Biologically Mediated Dissipation of Polyaromatic Hydrocarbons in the Root Zone. – In: Anderson, T. A., Coates, J. R. (eds.) Bioremediation through Rhizosphere Technology. ACS Publications, Washington.
[39] Thangavel, P., Subbhuraam, C. (2004): Phytoextraction: role of hyperaccumulators in metal contaminated soils. – Proceedings-Indian National Science Academy Part B, 70: 109-130.
[40] Tiller, K. (1992): Urban soil contamination in Australia. – Soil Research 30: 937-957.
[41] Wade, T., Brooks, J., Kennicutt, L., Mcdonald, J., Sericano, J., Jackson, T. (1984): GERG trace organics contaminant analytical techniques. – Sampling and Analytical Methods of the National Status and Trends Program, National Benthic Surveillance and Mussel Watch Projects 1992: 121-139.
[42] Walker, C. (2005): A tale of two Arabian aloes. – British Cactus & Succulent Journal 23: 175-179.
[43] Willert, D. J. V. (1992): Life Strategies of Succulents in Deserts: With Special Reference to the Namib Desert. – Cambridge University Press, Cambridge.
[44] Williams, V., Twine, S. (1960): Flame photometric method for sodium, potassium and calcium. – Modern Methods of Plant Analysis 5: 3-5.

http://www.aloki.hu ● ISSN 1589 1623 (Print) ● ISSN 1785 0037 (Online)
DOI: http://dx.doi.org/10.15666/aeer/1605_60336045
© 2018, ALÖKI Kft., Budapest, Hungary

[45] Wong, J. (1996): Heavy metal contents in vegetables and market garden soils in Hong Kong. – Environmental Technology 17: 407-414.
[46] Yates, A. (2002): Yates Garden Guide. – Harper Collins, Australia.

http://www.aloki.hu ● ISSN 1589 1623 (Print) ● ISSN 1785 0037 (Online)
DOI: http://dx.doi.org/10.15666/aeer/1605_60336045
© 2018, ALÖKI Kft., Budapest, Hungary

DESIGNING A GREEN MARKETING BEHAVIORAL PATTERN FOCUSING ON POULTRY PRODUCTS

TALEBI, P. – OMIDI-NAJAFABADI, M.* – LASHGARARA, F.

Department of Agricultural Extension and Education, Science and Research Branch, Islamic Azad University, Tehran, Iran

**Corresponding author*
e-mail: m.omidi@srbiau.ac.ir

(Received 17th Jun 2018; accepted 22nd Aug 2018)

Abstract. Green marketing has rapidly emerged as a global phenomenon around the world .As a result, some companies have responded to environmental challenges by applying green marketing strategies. However, with the increasing importance of environmental and health issues and the concept of social responsibility among consumers, recognizing behavior by actors and companies related to green products marketing is necessary. Therefore, this study helps to improve the understanding of green marketing behavior, which plays an important role in improving community health and economic growth. This study aims to design a green marketing behavioral pattern focusing on poultry products. The statistical population of this study is 145 actors who are involved in the production, distribution, promotion and pricing of green poultry products in Iran (Gilan Province). The findings indicate that attitudes toward green marketing (β: 0/94), subjective norms in relation to green marketing (β: 0/90) and feasibility (β: 0/67) had significant positive influences on intention toward green marketing. In addition, the results of green marketing behavior revealed that intention toward green marketing (β: 0/48), feasibility (β: 0.28) and government support (β = 0.56) were the three variables that influenced green marketing behavior, with government support having the greatest impact.
Keywords: *attitudes, subjective norms, feasibility, self-efficacy, decomposed theory of planned behavior, planned behavior theory, green products*

Introduction

In conventional marketing, the needs of customers are identified and satisfied (Kotler, 2003) in the most profitable manner (CIM, 2011) without accounting for social welfare and environmental issues .In other words, conventional marketing focuses on the economic desires of the company and the direct benefits of the products (Khan and Rafat, 2015). In Iran, conventional marketing methods for agricultural production are associated with high costs and are incompatible with sustainable development goals. Among the major problems that Iranian traditional marketing faces in relation to agricultural products are price instability, the high cost and inadequacy of transportation, lack of producer knowledge of market situations due to the inadequacy of the market information system, lack of facilities such as warehouses, high cost of production and waste during the various stages of production, the existence of brokers and the inadequacy of government support in market development and marketing policies. In addition to the lack of green marketing options, information and targeted advertising, the lack of public interest in environmental programs is another challenge in Iran (based on interviews with experts from the Jahad Agricultural Organization).

Since traditional marketing techniques no longer address all of the issues of modern markets, the implementation of green marketing is expected to improve marketing strategies not only by providing long-term financial performance for companies, but also by improving their environmental performance (Kotler et al., 2010; Luchs et al.,

http://www.aloki.hu ● ISSN 1589 1623 (Print) ● ISSN 1785 0037 (Online)
DOI: http://dx.doi.org/10.15666/aeer/1605_60476061
© 2018, ALÖKI Kft., Budapest, Hungary

2010; Liu et al., 2012; Malhotra et al., 2012). Thus, green marketing incorporates a wide range of activities, including product modifications, changes to the production process and, packaging changes, and also modifies the advertising approach (AMA, 2015; Polonsky, 2007). Additionally, Pride and Ferrell (1993) and Grove et al. (1996) noted that the term "green marketing" refers to an organization's efforts to design, promote, price and distribute goods that will not cause damage to the environment. Polonsky (1994) identified several reasons for companies to adopt alternative marketing: (1) social responsibility, i.e., a company understands that it is a members of a wider community and therefore should behave in an environmentally friendly manner and achieve both environmental and profit-related objectives; (2) opportunity, i.e., as people become increasingly concerned about the environment, the benefits of adopting alternative marketing strategies increase, and companies that have incorporated green marketing into their corporate strategy may enjoy a sustainable competitive advantage over companies that have not; and (3) governmental pressure, i.e., governments are attempting to establish regulations that control the amount of dangerous waste produced by companies and are issuing environmental licenses to control those wastes.

Ottman (2011) believes that the companies' product marketing function may be useful for two reasons. First, when a company adopts a program of environmentally friendly products, its distribution, pricing and promotion of the company image and reputation among customers can improve. Second, implementation of a green marketing plan may increase sales by giving a company access to new market segments.

In organic poultry production, the number of birds, nutritional factors, lighting, environmental conditions and even labor force prices and packaging are involved in the quality of the product. In general, the entire production cycle from corn and millet to the final ring of the slaughterhouse should be conducted without chemical interference. Due to the complexity of the production process, organic poultry production in Iran requires a suitable foundation that may take several years to establish. However, the first step in organic poultry in Iran is producing poultry without the use of antibiotics, meaning that during the breeding period, no antibiotic agent is injected into or consumed by poultry that are labeled as green. The northern provinces of Iran, due to their geographical location and the availability of appropriate physical resources, are potentially suitable for the poultry industry (Suri, 2014). Therefore, Gilan province was selected as a northern province in Iran with a high safety factor in the production of green poultry. Research in this field indicates that producers and actors in Gilan province have undergone a positive trend toward green marketing and organic farming because of the competitive and health advantages of such products. However, in recent years, early efforts at green marketing in Iran have focused only on the production; due to the lack of information, no serious efforts have yet been made in the areas of packaging, distribution and pricing. In addition, because of the high cost of organic production and the lack of specialized staff and government policies, this tendency has not led to the associated behavior. Therefore, this study aimed to examine green marketing behavior (GMB) predictors by designing a behavioral pattern.

According to market researcher Mintel, approximately 12% of the U.S. population can be identified as true greens, that is, consumers who seek out and regularly buy so-called green products. Another 68% can be classified as light greens, consumers who sometimes buy green products (Hanas, 2007). Research has also shown that the market grew by approximately 41% from 2004 to 2009 (Mintel, 2010). According to a new survey, most Europeans would be prepared to change their purchasing habits and buy

http://www.aloki.hu ● ISSN 1589 1623 (Print) ● ISSN 1785 0037 (Online)
DOI: http://dx.doi.org/10.15666/aeer/1605_60476061
© 2018, ALÖKI Kft., Budapest, Hungary

more environmentally friendly products, but many feel that they lack information and distrust manufacturers' environmental claims (European Commission, 2013).

A change in agricultural practices is equivalent to changing the culture and mindset of farmers, which can be achieved only by prolonged interaction. Nongovernmental organizations (NGOs) have demonstrated capabilities to this effect (Shenoy, 2003). In Iran, due to the dispersion of active actors in the field of green production and green marketing as well as the lack of government support, official and accurate statistics regarding those who are engaged in green marketing are not available. With the emergence of the phenomena of social responsibility and green marketing, the private sector and NGOs play an important role in promoting and advertising organic farming activities; however, there is still little consumer participation in these activities (Sabori, 2009).

Academic studies on green marketing began in the 1990s and focused on concepts and approaches (Polonsky, 1994; Peattie, 2001; Peattie and Crane, 2005; Rex and Baumann, 2007), the evaluation of green marketing strategies (Polonsky and Rosenberger, 2001; Rivera Camino, 2007), the relationship between green marketing and consumers (Laroche et al., 2001; Ginsberg and Bloom, 2004; D'Souza et al., 2006; Lee, 2008) and the application of green marketing (Johri and Sahasakmontri, 1998; Teisl et al., 2002; Gurau and Ranchhod, 2005). Other researchers reported that there is a significant relationship between green product features, promotion, pricing and distribution and consumers' green behavior (Shahlaee Bagheri, 2014; Boztepe, 2012). Therefore, higher levels of green consciousness lead to greater influence by the mediating factors of attitude, subjective norm, and behavioral control on behavioral intention and the consequent actual behavior. Many studies applied the theory of planned behavior (TPB) to explore consumers' attitude, intention and actual buying behavior with regard to green products (Arvola et al., 2008; Smith and Paladino, 2010; Tanner and Wölfing Kast, 2003; Tarkiainen and Sundqvist, 2005).

The theoretical model of GMB is a set of factors. To better understand these factors, the most important are described in *Table 1*.

Table 1. *Constructing the research model factors*

Factors	Definition	
Attitude	H1	The degree to which the individual favors the behavior being examined (Ajzen, 1991)
Perceived risk	H2	An actor's perceptions of the uncertainty and adverse consequences of engaging in an activity (Bauer, 1960; Taylor, 1974)
Perceived usefulness	H3	The degree to which the individual believes that a technology would improve his or her job performance (Davis, 1989)
Ease of use	H4	The degree to which an innovation is easy to understand and operate (Rogers, 2003)
Subjective norms	H5	An individual's perception of social normative pressures, or relevant others' beliefs that he or she should or should not perform a behavior (Ajzen, 1991). Subjective norms are decomposed into injunctive norms and descriptive norms
Injunctive norms	H6	People's beliefs about what ought to be done (Cialdini et al., 1990; Lapinski and Rimal, 2005)
Descriptive norms	H7	Beliefs about what is actually done by most others in one's social group (Cialdini et al., 1990; Lapinski and Rimal, 2005)

http://www.aloki.hu ● ISSN 1589 1623 (Print) ● ISSN 1785 0037 (Online)
DOI: http://dx.doi.org/10.15666/aeer/1605_60476061
© 2018, ALÖKI Kft., Budapest, Hungary

Feasibility (PBC)	H8	Beliefs regarding access to the resources and opportunities needed to perform a behavior or, alternatively, the internal and external factors that may impede the performance of the behavior (Ajzen, 1985, 1991; Ajzen and Driver, 1992; Ajzen and Madden, 1986; Madden et al., 1992)
Self-efficacy	H9	An individual's self-confidence in his/her ability to perform a behavior (Bandura, 1977)
Facilitating conditions	H10	The availability of resources needed to engage in a behavior, such as time, money or other specialized resources (Taylor and Todd, 1995). In other words, the person believes that this behavior is in his or her control
GMI	H11	An indication of an individual's readiness to perform a given behavior. It is assumed to be an immediate antecedent of behavior (Ajzen, 2002)
GMB	H12	The actors offer an environmentally friendly product that is not deleterious to health, the environment and society (based on qualitative research). Therefore, the term "behavior" is calculated with a mixture of green marketing aspects, including green product, green price, green promotion and green location

Surprisingly, there are few studies on Iranian agriculture in general, and none specific to green marketing that provides a behavioral pattern. For this study, a green marketing behavioral pattern was designed for actors in green poultry production in Gilan province. The author of this article had the following aims:

1. Describe certain personal and professional characteristics of actors in green poultry production.
2. Determine the effects of attitude, subjective norms, feasibility (perceived behavioral control), governmental support, and knowledge and intention toward green marketing (GMI) in green poultry production on GMB.
3. Provide a path analysis model of the green marketing behavioral pattern of actors in green poultry production.

Materials and methods

This is an applied study based on quantitative research, and the method of analysis used is correlation. This study focused on Gilan province, which has the potential capacity to serve as a poultry production zone in northern Iran .Due to the lack of sufficient facilities, most Iranian poultry farms are not used to produce green poultry. The production and marketing of this product are controlled by private companies that are responsible simultaneously for production, monitoring and marketing; therefore, accurate statistics regarding the amount of green poultry production and those engaged in it in Gilan were not available. However, information was informally obtained from experts. The sample in this study is 145 people who are involved in the production, distribution, promotion and pricing of green poultry in Gilan province; they are referred to as the actors (n = 145). The study was conducted as a census study because of the small size of the population of experts, and 128 usable questionnaires were obtained from interviews with the actors.

The main instrument used for data collection was a questionnaire, which was developed from a review of the related literature, in 8 sections (present status of GMB, intention toward green marketing (GMI), attitude toward green marketing, review of the actor's subjective norms, green marketing feasibility, review of government support, assessment of the actor's knowledge and description of the actor's personal and

http://www.aloki.hu ● ISSN 1589 1623 (Print) ● ISSN 1785 0037 (Online)
DOI: http://dx.doi.org/10.15666/aeer/1605_60476061
© 2018, ALÖKI Kft., Budapest, Hungary

professional characteristics). The evaluations were based on two 5-point Likert scales ranging from 1 (strongly disagree) to 5 (strongly agree).

The content and validity of the questionnaire were established and revised with the help of experts, including faculty members and a few specialists in green marketing. A pretest study was conducted with 20 experts randomly chosen from these populations; the reliability of the questionnaire was verified (calculated Cronbach's alpha was 87.3 and ordinal theta coefficients were 81-94%), confirming the suitability of the items.

This study contained two types of variable: 1) GMB (Y2) as the final dependent variable, which was measured by the respondents' answers to 19 items, and 2) GMI as an intermediate dependent variable, which was measured by 5 items on the Likert scale. Independent variables included governmental support, actors' knowledge of green marketing, actors' attitude, actors' subjective norms and feasibility of green marketing.

The hypotheses were measured by studying the relationships between the variables and their direct and indirect effects. Structural equation modeling (SEM) is a general approach to data analysis that can accommodate either observable or latent variables (or factors) within structural models. This study used descriptive statistics and SEM. Following data mining, descriptive statistics and SEM analysis were conducted with SPSS20 and AMOS20 software, respectively.

Although some authors support the TPB model, whether it can predict all the determinants of human behavior has been questioned (Ajzen, 1991). Therefore, many researchers have proposed revised models to predict behavior accurately (Bond et al., 2009; He, 2012; Läpple and Kelley, 2010; McCarthy, 2007; Wauters and Mathijs, 2010). Many studies have applied the TPB to explore attitude, intention and actual behavior with regard to green products (Arvola et al., 2008; Smith and Paladino, 2010; Tanner and Wölfing Kast, 2003; Tarkiainen and Sundqvist, 2005). Additionally, influential studies have focused on green purchasing and green consumers, but none have provided an exhaustive study integrating all the effective elements from several viewpoints in the form of an individual study. In this study, the theoretical basis of the model is the planned behavior theory by Icek Ajzen and the decomposed theory of planned behavior described by Taylor and Todd. To better predict the green marketing behavioral pattern of actors in green poultry production and to evaluate the model performance, related variables used by other authors were also used to develop this model (*Fig. 1*).

Results

Personal characteristics

The results showed that of the 128 respondents, 4 (3.1%) were female and 124 (96.9%) were male; the average age and average work experience of the respondents were 40 and 9 years, respectively. Of the actors, 35.2% had an associate's degree. The actors' knowledge of green marketing was measured by a test (correct or wrong answers); the results indicated that their average level of green marketing knowledge was 65%.

Significance test

SEM was used to verify the research model. As shown in *Table 2,* some paths are significant and others are not significant.

http://www.aloki.hu ● ISSN 1589 1623 (Print) ● ISSN 1785 0037 (Online)
DOI: http://dx.doi.org/10.15666/aeer/1605_60476061
© 2018, ALÖKI Kft., Budapest, Hungary

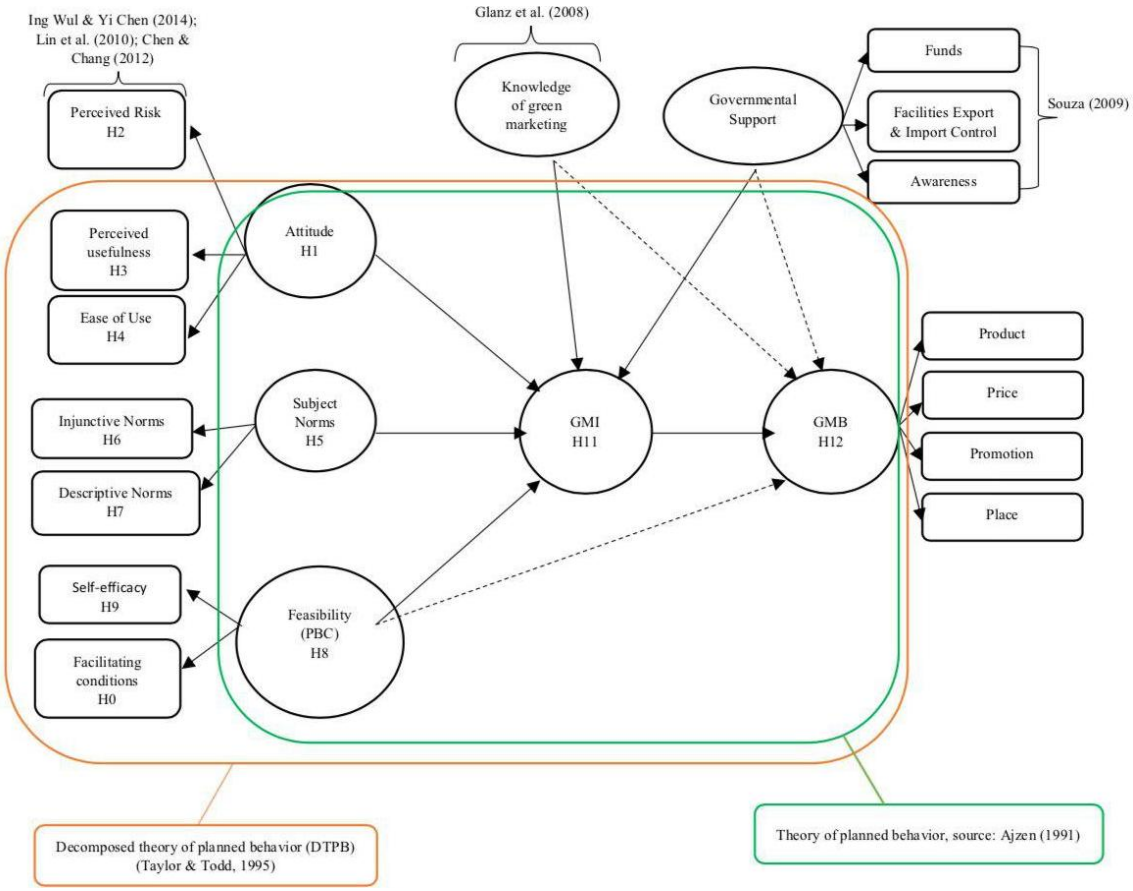

Figure 1. *Theoretical model*

Table 2. *Regression weight and significance test of paths*

Path	Estimate	S.E.	C.R.	*P* value
Attitude → intention	0.939	0.053	17.679	***
Subjective norms → intention	0.899	0.077	11.700	***
Feasibility → intention	0.657	0.070	9.354	***
Feasibility → behavior	0.161	0.062	2.594	0/009**
Governmental support → intention	0.146	0.194	0.752	0/452 n.s.
Governmental support → behavior	0.619	0.122	5.060	***
Knowledge → intention	-0.009	0.042	-0.207	0/836 n.s.
Knowledge → behavior	-0.044	0.045	-0.967	0/334 n.s.
Intention → behavior	0.422	0.097	4.342	***
Knowledge → self-efficacy	0.051	0.018	2.780	0.005**

*P < 0.05, **P < 0.01, ***P < 0.001

As shown in *Table 3,* the variable attitude at 0.94 has the greatest effect on GMI, and the variable governmental support at 0.56 has the greatest effect on the dependent variable (GMB).

http://www.aloki.hu ● ISSN 1589 1623 (Print) ● ISSN 1785 0037 (Online)
DOI: http://dx.doi.org/10.15666/aeer/1605_60476061
© 2018, ALÖKI Kft., Budapest, Hungary

Table 3. *Standardized regression weights of significant paths*

Path	Estimate
Attitude of actors ⟶ GMI	0.94
Subjective norms of actors ⟶ GMI	0.90
Feasibility ⟶ GMI	0.67
Feasibility ⟶ GMB	0.28
Governmental support ⟶ GMB	0.56
GMI ⟶ GMB	0.48
Knowledge of actors ⟶ self-efficacy	0.12

Structural analysis and measures of fit

Model evaluation is one of the most unsettled and difficult issues of structural modeling. SEM was used to verify the research model with a covariance relationship among antecedents. The following goodness-of-fit measures were used to confirm the appropriateness of the research model for this study: P = 0.213, CMIN/DF = 1.431, GFI = 0.830, AGFI = 0.820, CFI = 0.980 and RMSEA = 0.037. These indices suggest a good model approximation to the sample data, and regression models are shown below:

1. GMB = 0.28 × feasibility + 0.48 × GMI + 0.56 × governmental support
2. GMI = 0.94 × attitude + 0.9 × subjective norms + 0.67 × feasibility

Figure 2 shows latent variables that influence GMB and GMI. The effect of knowledge of green marketing and government support on intention is not significant. The final model of the green marketing behavioral pattern of actors in green poultry production in Gilan province is shown in *Figure 3*.

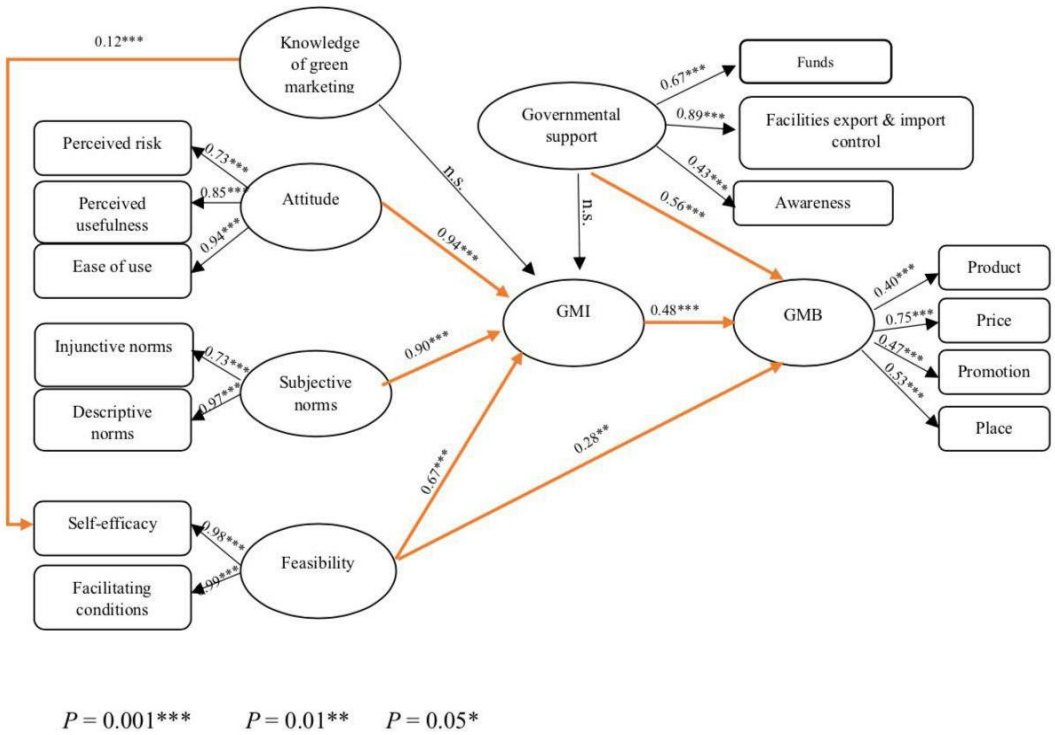

http://www.aloki.hu ● ISSN 1589 1623 (Print) ● ISSN 1785 0037 (Online)
DOI: http://dx.doi.org/10.15666/aeer/1605_60476061
© 2018, ALÖKI Kft., Budapest, Hungary

Figure 2. *Model of latent variables*

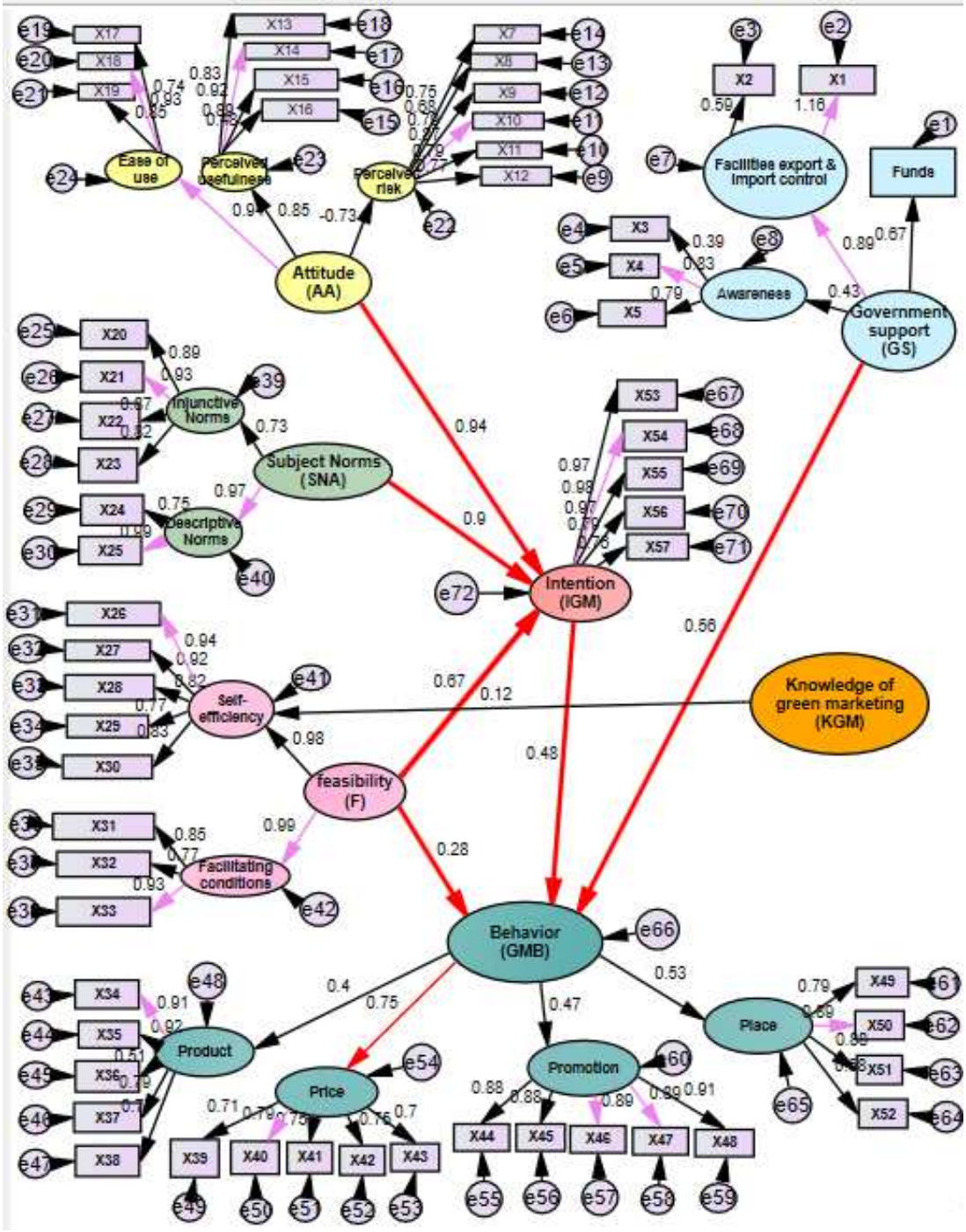

Figure 3. *Structural equation model for estimated standard coefficients*

Discussion

The purpose of this study was to design a green marketing behavioral pattern focusing on poultry products. It was predicted that certain elements would affect GMB. The results show how the TPB can increase our understanding of the factors that influence and determine GMB. In this regard, political (government support) and

http://www.aloki.hu ● ISSN 1589 1623 (Print) ● ISSN 1785 0037 (Online)
DOI: http://dx.doi.org/10.15666/aeer/1605_60476061
© 2018, ALÖKI Kft., Budapest, Hungary

educational (knowledge of green marketing) elements were also used to better predict the results of this model.

According to the analysis of the results, it can be deduced that:

- The attitude of the actors has a significant positive effect on their GMI. Our finding is consistent with the findings of Ing Wul and Yi Chen (2014), Knabe (2012), Lin et al. (2010), Arvola et al. (2008), Smith and Paladino (2010), Tarkiainen and Sundqvist (2005) and Asadollahpour et al. (2016).
- The subjective norms of the actors have a significant positive effect on their GMI. This finding is in accordance with the findings of Ing Wul and Yi Chen (2014), Knabe (2012), Lin et al. (2010), Arvola et al. (2008), Smith and Paladino (2010), Tarkiainen and Sundqvist (2005), Soonthensmai (2001) and Asadollahpour et al. (2016).
- Feasibility has a significant positive effect on the actors' GMI. This finding supports the findings of Ing Wul and Yi Chen (2014), Knabe (2012) and Asadollahpour et al. (2016).
- Feasibility has a significant positive effect on the actors' GMB. This finding supports the findings of Ing Wul and Yi Chen (2014) and Asadollahpour et al. (2016).
- Governmental support has a significant effect on the actors' GMB. This finding is consistent with the findings of Chen and Chai (2010), Mei et al. (2012), Diekmeyer (2008) and Punitha and Rahman (2011).
- GMI has a significant positive effect on the actors' GMB. This finding is in accordance with the findings of Ing Wul and Yi Chen (2014), Knabe (2012), Lin et al. (2010), Arvola et al. (2008), Smith and Paladino (2010), Tarkiainen and Sundqvist (2005), Asadollahpour et al. (2016), Soonthensmai (2001) and Che Hsu et al. (2016).
- The knowledge of the actors has a positive effect on their self-efficacy.
- The effect of the actors' knowledge on their GMI is not significant. This finding confirms the results of Maichum et al. (2016).

The results indicated that first, the three components of intention, actors' attitude (0.94), actors' subjective norms (0.90), and feasibility (0.67), had significant positive effects on GMI. Additionally, the three variables GMI (0.48), governmental support (0.56) and feasibility (0.28) each contributed to the prediction of perceptions of GMB and were found to have significant positive effects on GMB. Attitude (0.94) had the most significant influence on GMI and thus was the strongest predictor of GMI, followed by subjective norms (0.90) and feasibility (0.67). Additionally, governmental support (0.56) had the greatest effect on GMB. The overall results confirmed that the TPB model and its measures were suitable for the studied group.

The reason that knowledge of green marketing was not a strong predictor of GMB and GMI in this study may be that most of the actors had no education in green marketing. The results indicated that knowledge of green marketing had a small effect on self-efficacy (0.12) and an indirect effect on feasibility. These findings are consistent with those of Ing Wul and Yi Chen (2014), Asadollahpour et al. (2016), Chen and Deng (2016) and Maichum et al. (2016).

http://www.aloki.hu ● ISSN 1589 1623 (Print) ● ISSN 1785 0037 (Online)
DOI: http://dx.doi.org/10.15666/aeer/1605_60476061
© 2018, ALÖKI Kft., Budapest, Hungary

Conclusion

Although levels of analysis are not necessarily mutually exclusive, there are three general levels into which social science research may fall: microlevel; mesolevel, or middle range; and macrolevel (Blalock, 1970). Based on the results of this study, the following recommendations are presented at these three levels:

Macrolevel: The macrolevel is the national policy governing these activities in the country, including legislation and regulations. The analysis focuses on how these national policies influence activities in an institution or organization or at the field level. International influences on laws and policies may also be examined (ITCILO, 2009).

Among the variables constructing the GMB factor, governmental support was identified as the most important. In Iran, due to the lack of specific government policies related to organic products, there is little potential for organic poultry production; thus, government agencies and policy makers should consider specific policies such as:

- Allocating funds to develop organic production infrastructures
- Preparations and government support to attract foreign investors
- Allocating targeted funds to the construction of modern slaughterhouses in accordance with European standards
- Increasing government support to increase the ability of actors to produce organic products

Mesolevel: At the mesolevel, the focus is on how institutions such as NGOs and development organizations operate in terms of service provision and implementation and how they influence national policy. At this level, the focus is on education services, the role of the public and private sectors, the level of decentralization and the level of expertise in the institutions (ITCILO, 2009).

The importance of the variable subjective norms among the variables that construct the GMB factor has been explained by Montaño and Kasprzyk (2008). Montaño and Kasprzyk (2008) believe that if a person realizes that the result is a positive behavior, he or she will have a positive attitude toward performing that behavior; in addition, if others are positive about the behavior and the individual is motivated to satisfy others' expectations, a positive subjective norm is expected. Studies have shown that individuals' subjective norms affect GMI, and the results of this study confirmed the positive relationship between these two variables. As a result, it is recommended that institutions and service organizations use modern methods of information and advertisement, such as social media and the Internet, to develop green marketing campaigns to create positive subjective norms.

Microlevel: At the microlevel, the focus is on female and male consumers. The analysis should focus on how to identify the contexts-related specific needs and priorities of consumers and examine the extent to which gender roles, relationships and cultural issues are key (ITCILO, 2009).

Among the variables that construct the GMI factor, attitude was identified as the most important. Montaño and Kasprzyk (2008, p. 71) believe that "Attitude is determined by the individual's beliefs about outcomes or attributes of performing the behavior weighted by evaluations of those outcomes or attributes." In Iran, green marketing is related mostly to production, and no serious action has been taken for green packaging, distribution and pricing. Due to high production costs and the risk of customer distrust of green products, there is the possibility of financial losses for the

http://www.aloki.hu ● ISSN 1589 1623 (Print) ● ISSN 1785 0037 (Online)
DOI: http://dx.doi.org/10.15666/aeer/1605_60476061
© 2018, ALÖKI Kft., Budapest, Hungary

actors. As a result, there is no positive attitude toward green marketing, and the impact of this variable on GMI is known to be the most important. Therefore, justifying the profitability of green products due to increased consumption of these products in the coming years and managing production, pricing, promotion and distribution plans in the framework of export standards may be fruitful for companies.

In sum, the results of this study showed that positive attitudes, appropriate subjective norms, and the feasibility of green marketing improve actors' GMI, and this positive intention will have an impact on GMB for organic production. In addition, government policies and support for the development of organic agriculture will significantly influence the process of GMB. Therefore, with a view to highlighting the financial and commercial aspects of organic agriculture, the agricultural extension as an educational institution can play an important role in this field with facilities and activities for educational and cultural promotion and the implementation of incentive policies.

The novelty of this study is its consideration of political, social, cultural, economic and educational dimensions in the hope that the results will be useful to managers, researchers, practitioners, and policy makers and contribute to future research as a reference. Also in this study, the theoretical basis of the model is combination of the planned behavior theory by Icek Ajzen and the decomposed theory of planned behavior described by Taylor and Todd, on the other hand to better predict the green marketing behavioral pattern of actors in green poultry production and to evaluate the model performance, related variables (governmental support, knowledge of green marketing and perceive risk) were also used to develop this model based on interviews with actors and the researchers' view.

There are some recommendations for future studies in this area. First, other aspects of the marketing mix that are considered substitutes for the 4 Ps, such as the 4 Cs (consumer, cost, communication, and convenience), and are more customer-oriented should be studied. Additionally, the limitations of the present study include the small size; therefore, future research should include a more comprehensive sample. In this study, based on some interviews and literature review, a questionnaire was developed. For further studies, using Delphi technique and grounded theory, will be suggested.

Acknowledgements. Thanks are expressed to Gilan Veterinary Organization and Jahad Agricultural Organization for their constructive comments.

REFERENCES

[1] Ajzen, I. (1985): From Intentions to Actions: A Theory of Planned Behavior. – In: Kuhl, J., Beckmann, J. (eds.) Action-Control: From Cognition to Behavior. Springer, Heidelberg, pp. 11-39.

[2] Ajzen, I. (1991): The theory of planned behavior. – Organizational Behavior and Human Decision Processes 50: 179-211.

[3] Ajzen, I. (2002): Perceived behavioral control, self-efficacy, locus of control, and the theory of planned behavior. – Journal of Applied Social Psychology 32(4): 665-683. http://dx.doi.org/10.1111/j.1559-1816.2002.tb00236.

[4] Ajzen, I., Driver, B. L. (1992): Application of the theory of planned behavior to leisure choice. – Journal of Leisure Research 24: 207-224.

http://www.aloki.hu ● ISSN 1589 1623 (Print) ● ISSN 1785 0037 (Online)
DOI: http://dx.doi.org/10.15666/aeer/1605_60476061
© 2018, ALÖKI Kft., Budapest, Hungary

[5] Ajzen, I., Madden, T. J. (1986): Prediction of goal-directed behavior: Attitudes, intentions, and perceived behavioral control. – Journal of Experimental Social Psychology 22: 453-474.
[6] AMA (2015): https://www.ama.org/resources/Pages/Dictionary.aspx?dLetter=G. – American Marketing Association, Chicago, IL.
[7] Arvola, A., Vassallo, M., Dean, M., Lampila, P., Saba, A., Lhteenmki, L. et al. (2008): Predicting intentions to purchase organic food: The role of affective and moral attitudes in the theory of planned behaviour. – Appetite 50: 443-454.
[8] Asadollahpour, A., Omidi Najaf Abadi, M., Hosseini, S. J. (2016): Modeling behavior pattern of Iranian organic paddy farmers. – Paddy Water Environ. 14: 221-229.
[9] Bandura, A. (1977): Self-efficacy: Toward a unifying theory of behavioral change. – Psychological Review 84(2): 191-215.
[10] Bauer, R. A. (1960): Consumer Behavior as Risk Taking. – In: Hancock, R. S. (ed.) Dynamix Marketing for a Changing World, American Marketing Association, Chicago, IL, pp. 389-98.
[11] Blalock, H. M. (1979): Social Statistics. – McGraw-Hill, New York.
[12] Bond, J. L., Kriesemer, S. K., Emborg, J. E., and Chadha, M. L. (2009): Understanding farmers' pesticide use in Jharkhand India. – Extension Farming Systems Journal 5(1): 53-61.
[13] Boztepe, A. (2012): Green marketing and its impact on consumer buying behavior. – European Journal of Economic and Political Studies 5(1): 5-21.
[14] Camino, J. R. (2007): Re-evaluating green marketing strategy: A stakeholder perspective. – European Journal of Marketing 41(11/12): 1328-1358.
[15] Chartered Institute of Marketing (2011): http://www.cim.co.uk/. – CIM, UK.
[16] Che Hsu, W., I Huang, K., Ming Hsu, S., Hsuan Huang, C. (2016): A study of behavioral model on green consumption. – Journal of Economics, Business and Management 4(5). DOI: 10.18178/joebm.2016.4.5.420.
[17] Chen, K., Deng, T. (2016): Research on the green purchase intentions from the perspective of product knowledge. – Sustainability 8: 943.
[18] Chen, T. B., Chai, L. T. (2010): Attitude towards the environment and green products: consumers' perspective. – Management Science and Engineering 4: 27 39.
[19] Chen, Y.-Sh., Chang, Ch. H. (2012): Enhance green purchase intentions: The roles of green perceived value, green perceived risk, and green trust. – Management Decision 50(3): 502-520.
[20] Cialdini, R. B., Reno, R. R., Kallgren, C. A. (1990): A focus theory of normative conduct: Recycling the concept of norms to reduce littering in public places. – Journal of Personality and Social Psychology 58: 1015-1026.
[21] Davis, F. D. (1989): Perceived usefulness, perceived ease of use, and user acceptance of information technology. – MIS Quarterly 13(3): 319-340.
[22] Diekmeyer, P. (2008): Bribery in Public Procurement: Protecting Your Company from Corruption. – OECD, Paris.
[23] D'Souza, C., Taghian, M., Lamb, P. (2006): An empirical study on the influence of environmental labels on consumers. – Corporate Communication: An International Journal 11(2): 162-173.
[24] European Commission. (2013): 80% of Europeans are concerned about the environmental impact of products. – http://europa.eu/rapid/press-release_IP-13-653_en.htm.
[25] Ginsberg, J. M., Bloom, P. N. (2004): Choosing the right green marketing strategy. – MIT Sloan Management Review 46(1):79-84.
[26] Glanz, K., Rimer, B. K., Viswanath, K. (2008): Health Behavior and Health Education: Theory, Research, and Practice (4th ed.). – Jossey-Bass, San Francisco.
[27] Grove, S. J., Fisk, R. P., Pickett, G. M., Kangun, N. (1996): Going green in the service sector social responsibility issues, implications and implementation. – European Journal of Marketing 30(5): 56-66.

http://www.aloki.hu ● ISSN 1589 1623 (Print) ● ISSN 1785 0037 (Online)
DOI: http://dx.doi.org/10.15666/aeer/1605_60476061
© 2018, ALÖKI Kft., Budapest, Hungary

[28] Gurau, C., Ranchhod, A. (2005): International green marketing: a comparative study of British and Romanian firms. – International Marketing Review 22(5): 547-561.
[29] Hanas, J. (2007): Environmental awareness has not only tipped in the media – it's hit corporate boardrooms as well. Advertising age. – http://adage.com/article/special-report-ecomarketing/a-world-green/117113/.
[30] He, C. (2012): Assessment of the impact of organic school meals to improve the school food environment and children's awareness of healthy eating habits. – Department of Planning Faculty of Engineering and Science Aalborg University, PhD Dissertation.
[31] Ing Wul, S., Yi Chen, J. (2014): A model of green consumption behavior constructed by the theory of planned behavior. – International Journal of Marketing Studies 6(5): 119-132. DOI: 10.5539/ijms.v6n5p119.
[32] International Training Centre of the International Labour Organisation (2009): Introduction to Gender Analysis and Gender-Sensitive Indicators. – Gender Campus. www.focusintl.com/GD124a-%20Gender%20Campus%20-%20Tools.pdf.
[33] Johri, L. M., Sahasakmontri, K. (1998): Green marketing of cosmetics and toiletries in Thailand. – Journal of Consumer Marketing 15: 265-281.
[34] Khan, M. S., Rafat, A. (2015): Conventional marketing v/s green marketing: myth and reality. – International Journal of Pure and Applied Researches 1(1): 97-104.
[35] Knabe, A. (2012): Applying Ajzen's Theory of Planned Behavior to a Study of Online Course Adoption in Public Relations Education. – Dissertations (2009): Paper 186. http://epublications.marquette.edu/dissertations_mu/186/.
[36] Kotler, P. (2003): Marketing Management. 11th International Edition. – Prentice Hall, Upper Saddle River, NJ.
[37] Kotler, P., Kartajaya, H., Setiawan, I. (2010): Marketing 3.0: From products to customers to the human spirit. Wiley InterScience (Online service). – Wiley, Hoboken, NJ.
[38] Laroche, M., Bergeron, J., Barbaro-Forleo, G. (2001): Targeting consumers who are willing to pay more for environmentally-friendly products. – Journal of Consumer Marketing 18(6): 503-520.
[39] Lapinski, M. K., Rimal, R. N. (2005): An explication of social norms. – Communication Theory 15: 127-147.
[40] Lapple, D., Kelley, H. (2010): Understanding farmers' uptake of organic farming. An application of the theory of planned behavior. – The 84th Annual Conference of the Agricultural Economics Society Edinburgh, 29th to 31st March 2010.
[41] Lee, K. (2008): Opportunities for green marketing: young consumers. – Marketing Intelligence & Planning 26(6): 573-586. http://dx.doi.org/10.1108/02634500810902839.
[42] Lin, W. B., Wang, M. K., Hwang, K. P. (2010): The combined model of influencing on-line consumer behavior. – Expert Systems with Applications 37: 3236-3247.
[43] Liu, S., Kasturiratne, D., Moizer, J. (2012): A hub-and-spoke model for multi-dimensional integration of green marketing and sustainable supply chain management. – Industrial Marketing Management 41: 581-588. DOI: 10.1016/j.indemarman.2012.04.005.
[44] Luchs, M. G., Naylor, R. W., Irwin, J. R., Raghunathan, R. (2010): The sustainability liability: potential negative effects of ethicality on product preference. – Journal of Marketing 74: 18-31. DOI: 10.1509/jmkg.74.5.18.
[45] Madden, T. J., Ellen, P. S., Ajzen, I. (1992): A comparison of the theory of planned behavior and the theory of reasoned action. – Personality and Social Psychology Bulletin 18(3): 3-9.
[46] Maichum, K., Parichatnon, S., Peng, K. C. (2016): Application of the extended theory of planned behavior model to investigate purchase intention of green products among Thai consumers. – Sustainability 8: 1077. DOI: 10.3390/su8101077.
[47] Malhotra, N. K., Lee, O. F., Uslay, C. (2012): Mind the gap: The mediating role of mindful marketing between market and quality orientations, their interaction, and

http://www.aloki.hu ● ISSN 1589 1623 (Print) ● ISSN 1785 0037 (Online)
DOI: http://dx.doi.org/10.15666/aeer/1605_60476061
© 2018, ALÖKI Kft., Budapest, Hungary

consequences. – International Journal of Quality & Reliability Management 29(6): 607-626. DOI: 10.1108/02656711211245629.
[48] Mei, O. J., Ling, K. C., Piew, T. H. (2012): The antecedents of green purchase intention among Malaysian consumers. – Asian Social Science 8(13): 248-264. DOI: 10.5539/ass.v8n13p248.
[49] McCarthy, M., O'Reilly, S., O'Sullivan, A., Guerin, P. (2007): An investigation into the determinants of commitment to organic farming in Ireland. – Journal of Farm Management 13(2): 135-152.
[50] Mintel (2010): Green Living_USA. – Mintel, London.
[51] Montaño, D. E., Kasprzyk, D. (2008): Theory of Reasoned Action, Theory of Planned Behavior, and the Integrated Behavioral Model. – In: Glanz, K., Rimer, B. K., Viswanath, K. (eds.) Health Behavior and Health Education: Theory, Research, and Practice. Jossey-Bass, San Francisco, CA, pp. 67-96.
[52] Ottman, J. A. (2011): The New Rules of Green Marketing: Strategies Tools, and Inspiration for Sustainable Branding. – Greenleaf Publishing, Sheffield, UK.
[53] Peattie, K. (2001): Towards sustainability: the third age of green marketing. – Marketing Review 2(2): 129.
[54] Peattie, K., Crane, A. (2005): Green marketing: legend, myth, farce or prophesy? – An International Journal 8(4): 357-370.
[55] Polonsky, M. J. (1994): An introduction to green marketing. – Electronic Green Journal 1(2). https://escholarship.org/uc/item/49n325b7.
[56] Polonsky, M. J. (2007): An introduction to green marketing. – Electronic Green Journal 1(2): 1-10.
[57] Polonsky, M. J., Rosenberger, P. J. (2001): Reevaluating green marketing: a strategic approach. – Business Horizons 44(5): 21-30.
[58] Pride, W. M., Ferrell, O. C. (1995): Marketing: Concepts and Strategies. – Houghton Mifflin, Boston.
[59] Punitha, S., Rahman, A. A. (2011): Antecedents of green purchasing behavior among Malaysian consumers. – International Business Management 5(3): 129-139.
[60] Rex, E., Baumann, H. (2007): Beyond Ecolab Les: what green marketing can learn from conventional marketing. – Journal of Cleaner Production 15: 567-576.
[61] Rivera-Camino, J. (2007): Re-evaluating green marketing strategy: A stakeholder perspective. – European Journal of Marketing 41(11): 1328-1358.
[62] Rogers, E. M. (2003): Diffusion of Innovations (5th ed.). – Free Press, New York.
[63] Sabori, SH. (2009): Green Marketing in Iran: Potentials and Challenges. The First Green Marketing Conference in Iran. – http://www.mgtsolution.com/olib/473594249.aspx.
[64] Shahlaee Bagheri, J. (2014): Green marketing and its impacts on consumer behavior in sports shops. – Annals of Applied Sport Science 2(2): 75-82.
[65] Shenoy Devananda, N. A. (2003): Organic Farming Role of NGOs. – Spice India, Cochin, Kerala (India).
[66] Smith, S., Paladino, A. (2010): Eating clean and green? Investigating consumer motivations towards the purchase of organic food. – Australasian Marketing Journal 18(2): 93-104.a.
[67] Soonthensmai, V. (2001): Predicting Intention and Behavior to Purchase Environmentally Sound or Green Products among Thai Consumers: An Application of the Theory of Reasoned Action. – The Wayne Huizenga Graduate School of Business and Entrepreneurship, Nova Southeastern University, DBA.
[68] Soza, F. (2009): Nota Fiscal Paulista: Proposition of a Theoretical Model in Social Marketing. – http://www.procurandorespostas.com/artigos/notafiscalpaulista/.
[69] Suri, M. R. (2014): Non-antibiotic hen. – Javan Online News. http://javanonline.ir/fa/print/688456.
[70] Tanner, C., Kast, S. W. (2003): Promoting sustainable consumption: Determinants of green purchases by Swiss consumers. – Psychology & Marketing 22(10): 883-902.

http://www.aloki.hu ● ISSN 1589 1623 (Print) ● ISSN 1785 0037 (Online)
DOI: http://dx.doi.org/10.15666/aeer/1605_60476061
© 2018, ALÖKI Kft., Budapest, Hungary

[71] Tarkiainen, A., Sundqvist, S. (2005): Subjective norms, attitudes and intentions of Finnish consumers in buying organic food. – British Food Journal 107(11): 808-822.
[72] Taylor, J. W. (1974): The role of risk in consumer behavior. – The Journal of Marketing 38(2): 54-60.
[73] Taylor, S., Todd, P. (1995): Understanding information technology usage: A test of competing models. – Information Systems Research 6(2): 144-176.
[74] Teisl, M. F., Roe, B., Hicks, R. L. (2002): Can eco-labels tune a market? Evidence from dolphin-safe labeling. – Journal of Environmental Economics and Management 43(3): 339-359.
[75] Wauters, E., Mathijs, E. (2010): A Behavioral Model for the Adoption of Soil Conservation Practices. – Institute for Agricultural and Fisheries Research, Social Sciences Unit, Merelbeke, Belgium.

http://www.aloki.hu ● ISSN 1589 1623 (Print) ● ISSN 1785 0037 (Online)
DOI: http://dx.doi.org/10.15666/aeer/1605_60476061
© 2018, ALÖKI Kft., Budapest, Hungary

STRUCTURAL AND MORPHOMETRIC STUDY OF SCALES IN PETZEA RUDD (*SCARDINIUS RACOVITZAI* MÜLLER 1958)

ȘERBAN, C.[1,2*] – GRIGORAȘ, G.[2]

[1]*Cross-Border Faculty of Humanities, Economics and Engineering (Cahul - Republic of Moldova), "Dunărea de Jos" University, Galați, România*

[2] *"Răsvan Angheluță" Museum Complex of Natural Sciences*
Str. Regiment 11 Siret nr. 6A, 800 340 Galați, Romania
(phone: +40-236-311-898; fax: +40-236-414-475)

**Corresponding author*
e-mail: cecilia.serban@ugal.ro

(Received 22nd Jun 2018; accepted 22nd Aug 2018)

Abstract. The present study reveals preliminary lepidological results in a critically endangered species, Petzea rudd (*Scardinius racovitzai* Müller 1958) from Petea Spring Natural Reservation, Bihor county, Romania. Study of scales morphology in Petzea rudd was performed by use of light microscopy. This is the first attempt to reveal some scale features such as: scale type, shape, arrangement and number of radii and position of focus on scale on Petzea rudd. The geometric morphometric analysis has been applied in order to identify the characteristics for a reliable discrimination between Petzea rudd and its related species from Romanian inland waters, common rudd, *Scardinius erythropthalmus* (Linnaeus, 1758). The comparative analysis of scales shape in *S. racovitzai* and *S. erythrophthalmus* highlighted the statistically significant discrimination among two sets of observations and the significant variation of focus position and shape of scales among these two species.
Keywords: *Petzea rudd, scales, morphology, geometric morphometrics, light microscopy*

Introduction

Petzea rudd, *Scardinius racovitzai* Müller 1958, is a critically endangered fish species (Freyhof and Kottelat, 2008) that is endemic in Ochiul Mare Thermal Lake from the Petea Spring Natural Reservation, Bihor county, from Western part of Romania (Müller, 1958; Bănărescu; 1964; Kottelat and Freyhof, 2007). The present-day status of thermal ecosystem is strongly deteriorated and exposed to extinction because the over exploitation of the thermo-mineral underwater springs and decreasing of thermal water flow (Telcean an Cupșa, 2013; Grigoras et al., 2014; Müller et al., 2014b).

The taxonomic status of *S. racovitzai* was differently approached by ichthyologists, after first description as specific taxon by Müller (1958). Thus, *S. racovitzai* was described as subspecies of the cosmopolite common rudd, *S. erythrophthalmus* (Linnaeus, 1758) by Bănărescu (1964) while further studies revealed specific morphological, physiological and ethological patterns of Petzea rudd (Crăciun, 1998, unpublished PhD dissertation quoted by Bănărescu, 2002; Crăciun, 1997; Müller et al., 2014a; Grigoras et al., 2014, 2015). The species is indexed with specific rank, as *S. racovitzai* by Kottelat and Freyhof in 2007. Bănărescu (2002) supposed *S. racovitzai* could be a recent isolated species from Central European common rudd and he considered that molecular techniques are necessary for clarifying the taxonomic status of Petzea rudd.

http://www.aloki.hu ● ISSN 1589 1623 (Print) ● ISSN 1785 0037 (Online)
DOI: http://dx.doi.org/10.15666/aeer/1605_60636076
© 2018, ALÖKI Kft., Budapest, Hungary

The present study provides preliminary results regarding morphology of the *S. racovizai* scales. To the best of our knowledge, this is the first attempt to study the scales morphology in thermal rudd from Natural Reserve of Petea Spring.

A second objective of the paper is to assess the scales morphometric patterns that can be used for discrimination of Petzea rudd from its congener species from Romanian inland waters, *S. erythrophthalmus*. The disruption of the thermal barrier which separated in the past the Petzea rudd from the related species (Telcean and Cupșa, 2013) raises the question of continuity for thermal population under the conditions of cohabitation with a more opportunistic species with hybridisation potential (Nico et al., 2015). We have applied principal components analysis for examination the particularities of shape variation in scales samples (Klingenberg, 2011). Canonical variate analysis (CVA) provides information that maximizes the separation of species (Klingenberg, 2011). We also used the discriminant analysis (DA) for reliability testing of groups dissimilarity (Klingenberg, 2011).

Literature review

Research of fish scales represents a useful tool for identifying the fish at genus or species levels and also in studies of fish phylogeny, sexual dimorphism, age determination, evaluation of the habitats impact on development etc. (Cărăușu, 1952; Esmaeili et al., 2007, 2009; Esmaeili and Gholami, 2011; Ibáñez et al., 2007, 2016; Jawad, 2005a, 2005b; Jawad and Al-Jufaili, 2007; Masood et al., 2015; Miranda and Escala, 2000; Poulet et al., 2005; Renjith et al., 2014).

Shape, size and number of scales are characters used in the taxonomy of fish (Bănărescu, 1964). Since the beginning of the 19th century, Agassiz used a classification system of the fish into four groups, based upon scale morphology (Esmaeili et al., 2009; Renjith et al., 2014). Likewise, the presence or absence of the denticles as well as their shape, size and the distances between them can be utilised as taxonomy analysis criteria in various fish species (Esmaeili et al., 2007, 2009; Jawad, 2005a, b; Delmater et al., 1974; Lippitsch, 1990; Jawad et al., 2007 cited by Esmaeili and Gholami, 2011).

Scale morphology is frequently applied as an instrument of analysis of the differentiation between populations, species or assessment of the phenotypic plasticity of fishes in relation with the habitat conditions and effect of toxic chemicals (Cărăușu, 1952; Jindal and Jha, 2005; Pillay, 1950; Taylor, 2012).

Deviation from pattern of circuli disposal or discontinuities of circuli, breakage or loss of interradial denticles, deformations or losses of tubercles provide conclusions regarding the past environment under which were exposed the fish, including the effect of pollutants on organism during its development and growth (Esmaeili and Gholami, 2011). Lippitisch (1990) and Pou and Gallego (1990), both quoted by Jawad (2005a) show different environment factors may have an effect on some scales morphological characters. Taylor (2012) mentions the fish populations display different growing characteristics in relation with various external factors, e.g. seasonal or habitat variability, availability of feeding resources etc. and therefore, the scales, that also are the first contact barrier with surrounding environment, represent an important phenotypic particularity in relation with all these factors.

In the same, way, the researches of Cadrin (2000) cited by Taylor (2012) pointed out the geographical isolation may lead to occurrence of some morphological patterns of

http://www.aloki.hu ● ISSN 1589 1623 (Print) ● ISSN 1785 0037 (Online)
DOI: http://dx.doi.org/10.15666/aeer/1605_60636076
© 2018, ALÖKI Kft., Budapest, Hungary

fish scales at population level as a result of environment influence or selection over ontogenetic development, inducing morphometric differentiation between species.

There are studies that highlight the influence of intrinsic factors on the intraspecific differences of scale characters in fish. The lepidological researches of Sire (1986) quoted by Mekkawy et al. (2011) in cichlids as well as the studies of Mekkawy et al. (2011), Mahmoud et al. (2005) and Harabawy et al. (2007) in various wide-spread fresh water and marine species, sustain the genetic determinism of scales morphology, invalidating environment control.

In the research of Müller et al. (2014a), on morphology of scales in *S. racovitzai,* authors discriminate Petzea rudd population from its congeneric species, common rudd, *S. erythrophthalmus,* by using geometric morphometrics of scales. Several references regarding the lepidological studies in various cyprinids have been used in the interpretation of our results; Gursoy et al. (2005) in *Scardinius erythrophthalmus,* Miranda and Escala (2000) and Jawad (2005a) in species of *Barbus* genus, Poulet et al. (2005) in *Leuciscus burdigalensis* Valenciennes, 1844, Jindal and Jha (2005) in *Cyprinus carpio* var. *communis* Linnaeus, 1758, Esmaeili et al. (2007) in *Capoeta damascina* (Valenciennes, 1842), Esmaeili and Gholami (2011) in *Rutilus frisii kutum* Kamenskii 1901, Staszny et al. (2012) in *Carassius gibelio* (Bloch, 1782).

Statistical tools used in our study for shape variability analysis with the help of shape coordinates (geometric morphometrics) is largely applied in biology researches (Ibáñez et al., 2007; Klingenberg, 2011; Miranda and Escala, 2000; Moneva et al., 2012; Poulet et al., 2005; Staszny et al., 2012).

Materials and methods

The *S. racovitzai* specimens have been sampled in August and September, 2013 from the "Ochiul Mare" Lake, Natural Reserve Petea Spring, Bihor county, North-Western Romania (*Fig. 1 left)*. The fish sampling was approved by Order no. 1231/2013 of the Environment and Climate Changes Ministry. Different methods have been used for fish capture: a cast-net and a fishing net with 10–16 mm mesh sizes *(Fig. 1 right)*.

Figure 1. *"Ochiul Mare" Lake, Natural Reservation Petea Spring, Bihor county, Romania. The natural habitat of Petzea rudd (left). Fish sampling with fishing net (right)*

The scales were removed from the left side of the body, in the area between the dorsal fin insertion and the lateral line (*Fig. 2*) from thirteen specimens. The small

http://www.aloki.hu ● ISSN 1589 1623 (Print) ● ISSN 1785 0037 (Online)
DOI: http://dx.doi.org/10.15666/aeer/1605_60636076
© 2018, ALÖKI Kft., Budapest, Hungary

number of fish used for this study is linked to the special conservation status of the species and special law of exemption for capture. Around 3–5 scales taken from each specimen have been preserved in dry state and pressed in paper envelopes, after the removal of the epithelium cells and mucus.

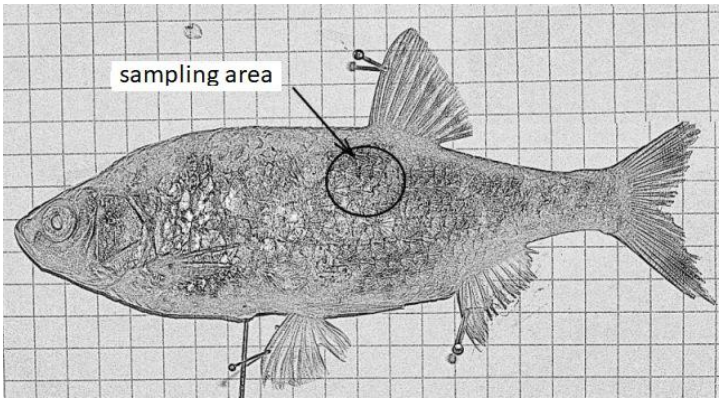

Figure 2. *S. racovitzai and the emphasised area of the scales sampling from the fish body*

The analysis of scales morphology was carried out between 2 microscope glass slides, under microscope (Olympus CH2), magnification up to 1500x, for the identification of the structure details.

Scales morphometric patterns (shape and size variation) were used for discrimination between *S. racovitzai* and its congener species from Romanian inland waters. Similar operations of sampling/processing scales where applied in the case of common rudd, *S. erythrophthalmus*. Atotal of fourteen specimens of common rudd have been captured from Lower Danube River in the confluence area with Prut and Siret rivers (Mm80).

A stereo-microscope (Olympus SZ 40-CTV), 10x ocular and 4x maximum focus has been used for images collecting of scales from both species. The images of the scales enlarged through stereomicroscopy where digitised with the camera (Canon A590 IS).

Seven markers were attached on every digital image of the scales using the TPS Digitize (Rohlf, 2016a) (*Fig. 3*).

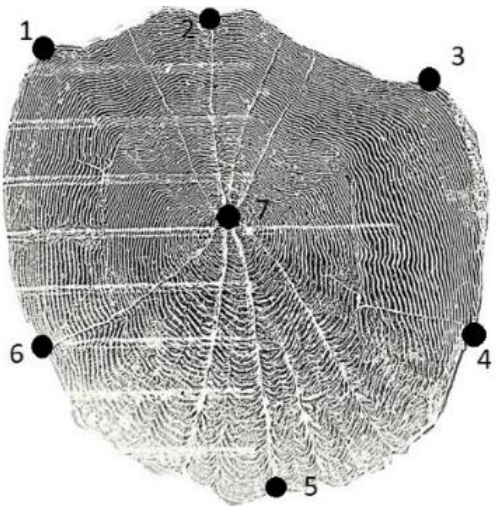

Figure 3. *Landmarks data collection on Petzea rudd scale*

http://www.aloki.hu ● ISSN 1589 1623 (Print) ● ISSN 1785 0037 (Online)
DOI: http://dx.doi.org/10.15666/aeer/1605_60636076
© 2018, ALÖKI Kft., Budapest, Hungary

The digital images were processed with and TPS Utility (Rohlf, 2016b) software before statistical analyses.

The geometric morphometric analysis of the scales of two congener species where processed with MORFOJ 1.05f software (Klingenberg, 2011). Data regarding the scales shape was obtained by Procrustes superimposition that excludes the variation of size, position and orientation of landmarks. Several statistical tools: the principal component analysis (PCA), discriminant analysis (DA) and canonical variate analysis (CVA) were applied in order to draw conclusions regarding the two groups separation.

Results and discussions

Preliminary results regarding the scales morphology in S. racovitzai.

The type of scales from the lateral side is elasmoid cycloid, with general particularities of a cycloid scale (*Fig. 4*): anterior field (rostral), posterior field (caudal), the focus, radii, circuli, denticles of circuli, tubercles in posterior zone of the scale.

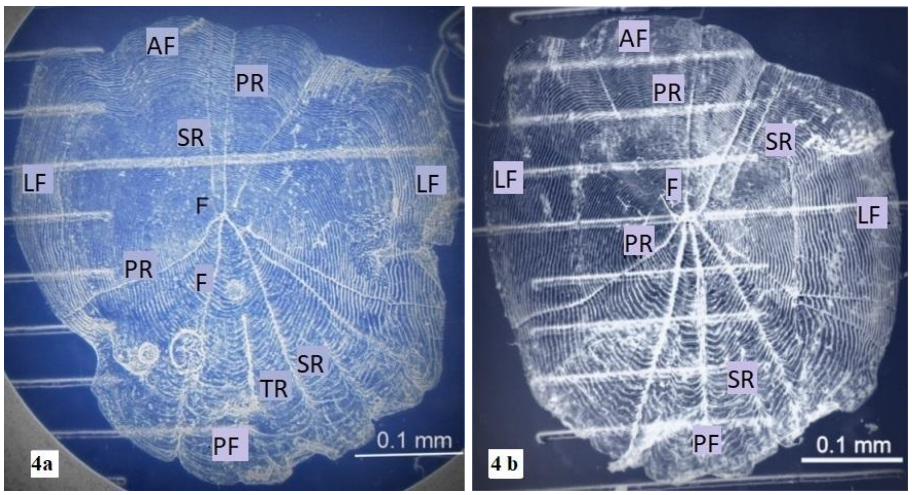

Figure 4. *Stereomicroscope images of normal scales from the lateral side of Petzea rudd (10 x 3). a – scale with all three radii types, b – scale with primary and secondary radii. AF – anterior field, PF – posterior field; LF – lateral field, PR – primary radii, SR – secondary, TR – tertiary radii; F – focus (nucleus)*

The focus or nucleus of the scale (*Fig 4, 5a*), that occurs during ontogenetic development of fish, can represent a taxonomic criterion (Jawad, 2005a). In *S. racovitzai*, the focus is slightly displaced to front of the scale and divides the scale in anterior field (cephalic towards focus) and the posterior one (caudal towards focus). The focus area appears as a reticulate structure, with a not clear shape delimitation, with or without pore mucus. This aspect is recorded in other fish species scales. Jawad (2005a) mentions similar focus characteristics in another cyprinid, *B. arabicus* (Trewavas, 1941).

There are interspecific differences regarding the position and shape of scale focus. A pointed shape is observed by Esmaeili et al. (2011) in *Rutilus frisii* (Nordmann, 1840), a round shape focus in *Labeo niloticus* (Linnaeus, 1758) by Jawad (2005a), translucent or with mucus pores in *Capoeta damascina* according to Esmaeili et al. (2007).

http://www.aloki.hu ● ISSN 1589 1623 (Print) ● ISSN 1785 0037 (Online)
DOI: http://dx.doi.org/10.15666/aeer/1605_60636076
© 2018, ALÖKI Kft., Budapest, Hungary

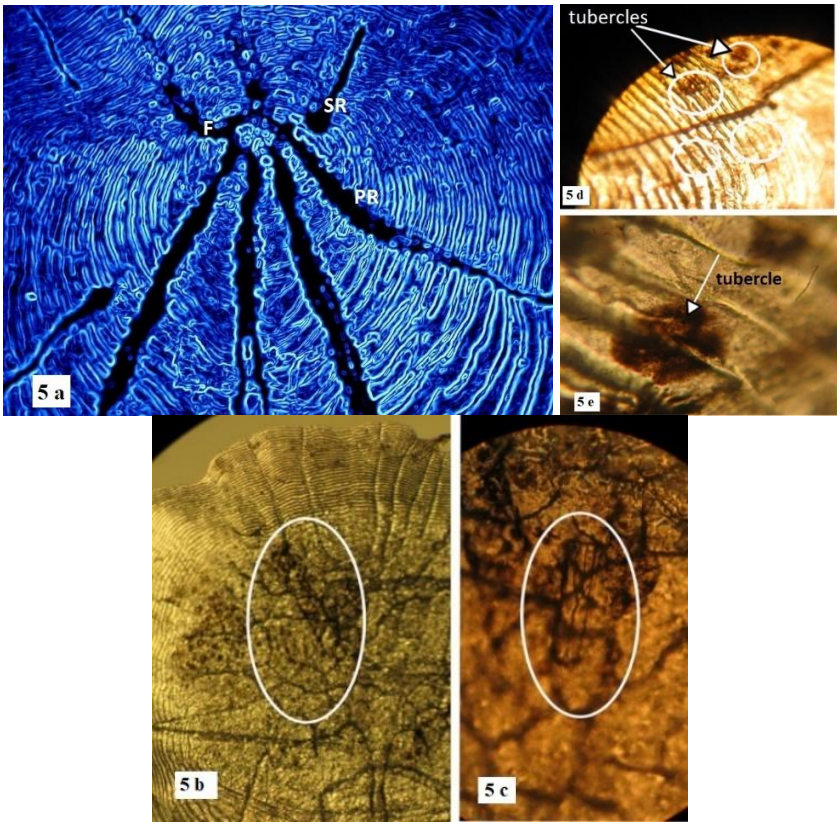

Figure 5. *Microscope images of normal scales and lateral lines scales. a – normal scale with reticulate focus (nucleus) and radii that cross the focus and circuli (15 x 40), b – lateral lines scale image revealing the lack of focus and the disposal of lateral line canal along the anterior – posterior axis (10 x 3.5), c – the lateral lines channel with previous pore and posterior pore (15 x 10), d – normal scale with tubercles, e – normal scale with tubercle with circular shape from the posterior field (15 x 40)*

The scales from the vicinity of the lateral line have the focus slightly outlined and covered by reticular structures shaped like honeycomb. Hagerman (1952) noted the scale focus of some fish species may gain a diffused appearance as the age increasing.

The same reticulate structures of the focus of scales from the vicinity of the lateral line in Petzea rudd is revealed by Esmaeili et al. (2007) for other cyprinids as *Catla catla* (Hamilton–Buchanan, 1822) and *Tor putitora* (Hamilton–Buchanan, 1822).

Microscopic observation in Petzea rudd scales from lateral line revealed the lack of focus (*Fig. 5b, c*). The same feature is mentioned by Esmaeili et al. (2007) in cyprinid *C. damascina*. Conversely, other species display the focus in the lateral line scales as is highlighted by Masood et al. (2015) on some mugilid species.

The lateral line canal (*Fig. 5b, c*) is positioned on the anterior-posterior axis of the scale, slightly oblique and crossing about a half from the anterior scale field, with two pores, the anterior one in a „V" shape and the posterior pore in a „C" shape. The electronic microscopy studies regarding the lateral line scales of various teleost species reveal an increased structural variability of the lateral line canal, which can take different form as straight or oblique simple perforations (Delmater et al., 1973 quoted by Esmaeili et al., 2007) till the wide canals protected by complex structures covering

http://www.aloki.hu ● ISSN 1589 1623 (Print) ● ISSN 1785 0037 (Online)
DOI: http://dx.doi.org/10.15666/aeer/1605_60636076
© 2018, ALÖKI Kft., Budapest, Hungary

two-thirds of the scale on which focus is present (e.g. in *Barbus arabicus, Lates niloticus*, according to researches of Jawad, 2005a).

Primary radii (*Figs. 4, 5a*) reach the focus and there are 1–4 radii in the anterior field and 1–4 radii in the posterior field. The similar results have been reported in other species such as genus *Barbus* studied by Jawad (2005a). These radii type can converge to the nucleus without crossing it, e.g. in Tripterygiidae as it is shown by Jawad study (2005b). Lateral body scales also have secondary radii, more numerous than the primary ones (0–2 secondary radii in the anterior field of scale, 1–8 secondary radii in the posterior field) and even less tertiary radii (0–1 tertiary radii in the posterior field of scale) (*Figs. 4, 5a*). We have not identified a significant relationship between the scales size and the number of radii. The studies of Esmaeili et al. (2007, 2009), Esmaeili and Gholami (2011) reveal the number of radii depends upon the location of scales in different body areas and represents a line of scale flexibility. According to these authors as well as Jawad (2007) quoted by Esmaeili et al. (2007), in some teleost fish, there is a proportional relation between the radii number and body length, the radii number could being used as a taxonomic tool for a reliable species identification.

The presence of primary, secondary and tertiary radii could also provide information regarding the growing conditions of fish (environment factors, feeding resources) (Lippitsch, 1990 quoted by Esmaeili and Gholami, 2011). This scale pattern is considered as being linked to quantity and quality of trophic resources, available during development and growing period (Johal et al., 1984 and Tandon and Johal, 1996 cited by Esmaeili et al., 2007; Esmaeili and Gholami, 2011).

Concentric circuli (*Figs. 4, 5* and *6*) start near the focus area, being interrupted by radii and represent concentric distinctive growth lines, formed through sclerite sedimentation and separation through inter circular space (*Fig. 6*).

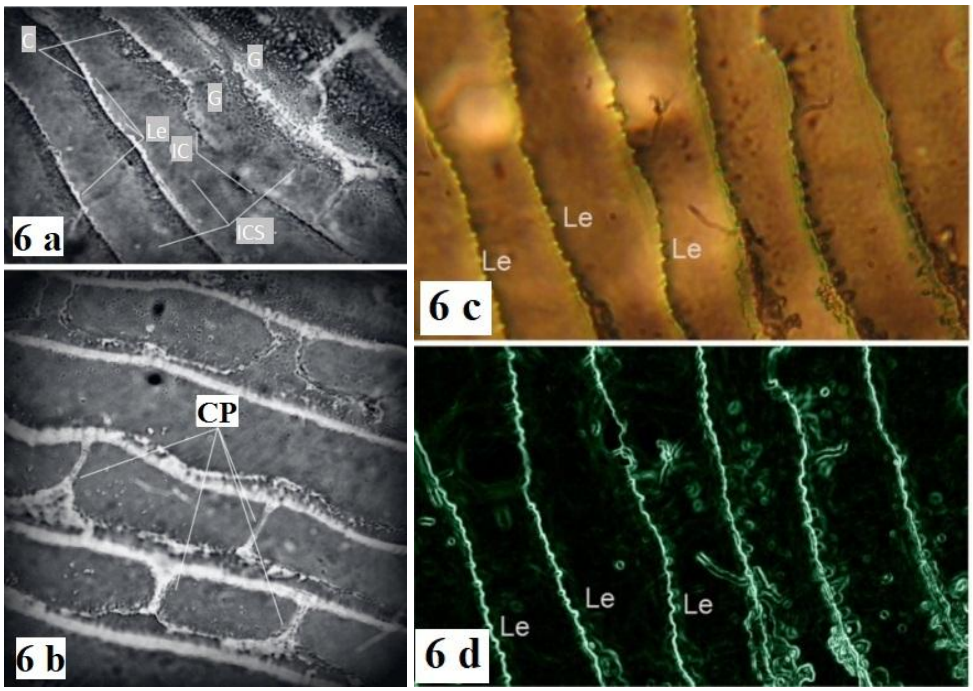

Figure 6. *Microscope images of the scales from the lateral side in S. racovitzai (15 x 40). a – scale with circuli (C), hyaline intercircular spaces (ICS), interrupted circuli (IC) and inter circular granulations (G); b – scales with calcium projections (CP); c, d – scales with denticles or lepidonts on the interradial circuli (Le)*

http://www.aloki.hu ● ISSN 1589 1623 (Print) ● ISSN 1785 0037 (Online)
DOI: http://dx.doi.org/10.15666/aeer/1605_60636076
© 2018, ALÖKI Kft., Budapest, Hungary

Inter circular spaces are in general really narrow in the anterior field of scale as a result of the focus position, and wider in the lateral and posterior fields. Similar observations are mentioned by Esmaeili (2011) at Rutilus frisii kutum, the posterior circuli could being less distinctive (Moneva et al., 2012), covered by tubercles or missing in other species such as a cyprinid fish, Capoeta damascina (Esmaeili et al., 2007).

The anterior and lateral interradial circuli are almost rectilinear while these structures are convex in the posterior field. According to Lippitsch (1990) cited by Esmaeili et al. (2007), the shape of the first interradial circuli (rectilinear, convex or concave) could be used in the determination of some cichlid species and can suffer changes under environment factors influence.

The concentric annuli formed around the nucleus, typical for the fish species from temperate zones (Bănărescu, 1964; Cărăușu, 1952; Hagerman, 1952; Ilieș et al., 2014) are difficult to detect in the Petzea rudd, which is not subjected to the same seasonal temperature variation. Appearance false annuli in some observed scales could be linked to other extrinsic or intrinsic factors that can can lead to a variable growing rhythm, e.g. reproduction period (Hagerman, 1952; Gursoy et al., 2005), but this aspect should be further investigated.

The circuli have calcium projections (*Fig. 6b*), radii bifurcations and specific structures called denticles (lepidonts) (*Figs. 5c, d*), the last ones being identified in the lateral field of scale and oriented towards the focus. The presence or absence of the denticles, their shape, size and the distances between them can be utilised as taxonomy analysis criteria in various fish species (Esmaeili et al., 2005, 2009; Jawad, 2005a, b; Delmater et al., 1974; Lippitsch, 1990; Jawad et al., 2007 cited by Esmaeili and Gholami, 2011).

The posterior field of the scales possesses pigmentary granules (tubercles) with regular shape or formless contour (*Figs. 5d, e*). The tubercles are formed by crowding of the epithelial cells of epiderma. According to researches of Esmaeili et al. (2007), Esmaeili and Gholami (2011), Ibáñez et al. (2007), these tubercles contribute to the rigour of the scales and represent a useful tool for taxonomic research as well as habitat condition assessment. We noted a poor distribution of the tubercles on the scales. This aspect must be further investigated in order to verify the origin of this observed particularity (genetical or medial effect).

Geometric morphometric analysis of scales in S. racovitzai

The principal components analysis (PCA) has enabled conclusions regarding the shape variation between fish samples. and was performed by use of the covariance matrix of Procrustes coordinates (Klingenberg, 2011) for each group of the two congener species, *S. racovitzai* and *S. erythrophthalmus*. The data of the landmarks were superimposed through a full Procrustes fit.

According to PCA analysis, the first three components sum 70.459% from total variance (*Fig. 7*) that reveal significant variation in shape of scales sampled from two rudd groups.

The shape changes of lateral body scales in both species are illustrated in *Figure 7*. The focus position (represented trough the L7 landmark, *Fig. 8*) in S. racovitzai, is displaced prior from the centre of the scale compared with the S. erythrophthalmus focus disposal and the entire shape is more elongated in Petzea rudd (*Fig. 8*). One the other hand, the axis represented by the L4–L6 landmarks (which delineates the field

http://www.aloki.hu ● ISSN 1589 1623 (Print) ● ISSN 1785 0037 (Online)
DOI: http://dx.doi.org/10.15666/aeer/1605_60636076
© 2018, ALÖKI Kft., Budapest, Hungary

with tubercles) does not show significant variation of position, being connected with the adaptive phenotypic response of the two related species to similar hydrodynamic feature (Ibáñez et al., 2007; Sudo et al., 2002 cited by Ibáñez et al., 2007).

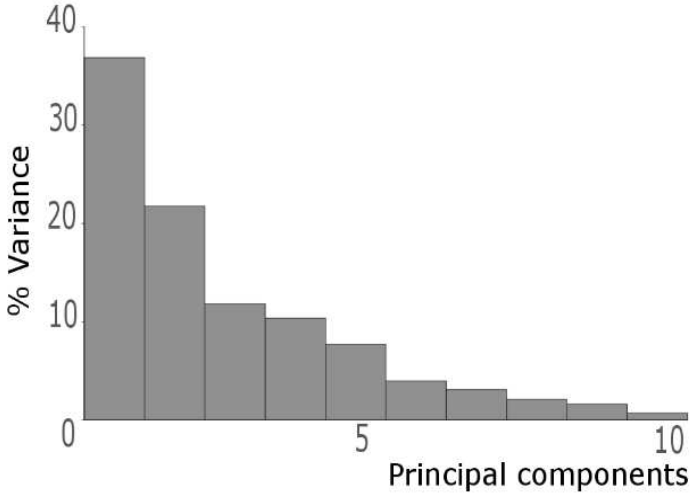

Figure 7. *The percentage of total variance for each principal component (PC) of the fish scales analysis of S. racovitzai and S. erythrophthalmus*

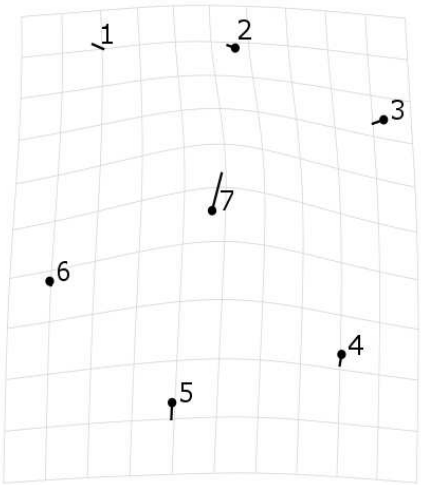

Figure 8. *Transformation grid illustrating the scale shape changes associated with PC, between the S. racovitzai and S. erythrophthalmus. The lines point in the direction of the shape change for each landmark*

The relationships between observations carried out on scales geometric morphometric analysis and the disposal of the specimens of two species in the multivariate analysis morphospace is shown in *Figure 9*. The scatter plot of PC scores reveals the two clear groups separated by PC1.

CVA provides extra information in data interpretation that maximise the separation between groups (species/ecotypes, Klingenberg, 2011). The histogram of canonical variate scores covers the shapes particularities which denote the dissimilarities between the two species (*Fig. 10*).

http://www.aloki.hu ● ISSN 1589 1623 (Print) ● ISSN 1785 0037 (Online)
DOI: http://dx.doi.org/10.15666/aeer/1605_60636076
© 2018, ALÖKI Kft., Budapest, Hungary

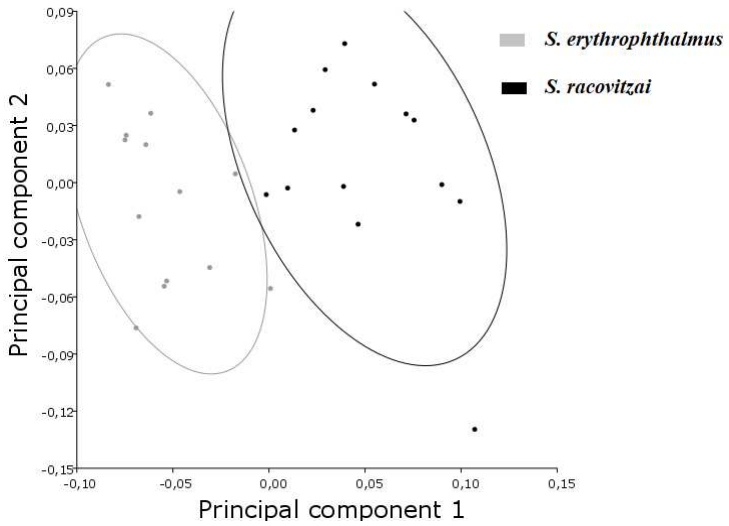

Figure 9. *The tolerance limits (90% confidence level) of the scores distribution of the first two principal components (PC) of the scales shape analysis of fish from two groups. The species disposal in the morphospace of the multivariate analysis (PC1 36.865%, PC2 21.766%)*

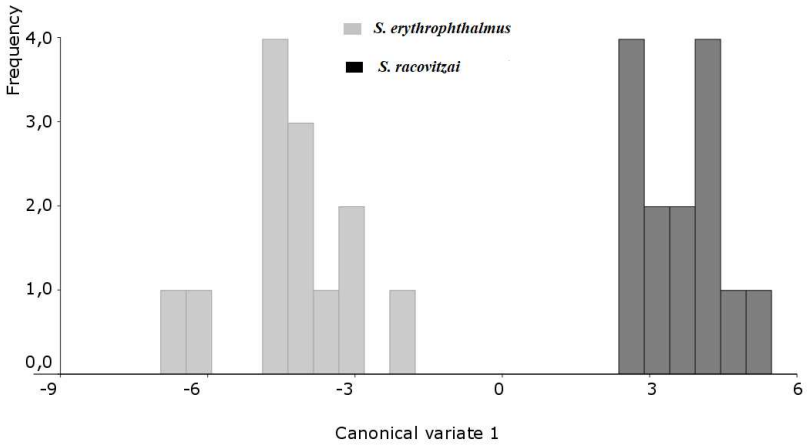

Figure 10. *Scatter plot of CV scores for scales shape of two congener species (S. racovitzai and S. erythrophthalmus)*

Mahalanobis distance (7.5872) reveals a significant separation between groups ($P < 0.0001$ from 10 000 permutation tests). The same result is obtained by permutation test for Procrustes distances ($P = 0.1067$, $P < 0.0001$).

The discriminant analysis (DA) of scales shape of fish from the two groups allows the examination of reliability of separation between groups.

The histogram of distribution of eigenvalues discriminant scores highlighted the separation among the two congener species (*Fig. 11*).

The parametric P-value (<0.0001) for null hypothesis test of similarity between means of observations groups sustains the reliable distinguish between the rudd species. The results for Procrustes distance (0.10672500), Mahalanobis distance (7.5872) and associated parametric P-values could also be in connection with anisotropy of scales samples (Klingenberg, 2011).

http://www.aloki.hu ● ISSN 1589 1623 (Print) ● ISSN 1785 0037 (Online)
DOI: http://dx.doi.org/10.15666/aeer/1605_60636076
© 2018, ALÖKI Kft., Budapest, Hungary

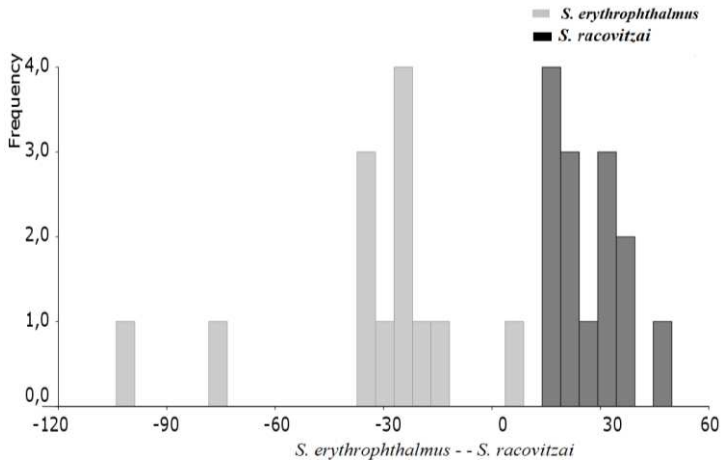

Figure 11. *Discriminant analysis of two rudd species using fish scales. Frequencies of discriminant scores predicted by a Mahalanobis distance (leave-one-out) cross-validation are shown using histogram bars*

Conclusions

The microscopic analysis of scale morphology reveals that lateral scales in *S. racovitzai* are of elasmoid cycloid type, with following particularities: anterior field (rostral) and posterior field (caudal), focus, radii, circuli, denticles on the circular radii and tubercles.

Some scale features on Petzea rudd as: the reticulate structure of the normal scale focus, the lack of the focus on lateral line scale, the primary radii crossing the focus, the presence of toward oriented denticles in the lateral fields of scale, displaying of tubercles with regular or formless shape in the posterior field of scale are common with other cyprinids species.

The focus position, slightly displaced to front of scale represents a reliable criterion that discriminate the *S. racovitzai* from the congener species, *S. erythrophthalmus.*

Taking into consideration our preliminary results regarding the morphology of Petzea rudd scales and the pattern that discriminate *S. racovitzai* from *S. erythrophthalmus*, futur comparative works will develop in order to define which scale features clearly distinguish Petzea rudd from other related cyprinids species.

Acknowledgements. The present study was supported by The Mohamed bin Zayed Species Conservation Fund, Abu Dhabi (project no. 13255722 "Captive breeding and maintaining ex situ populations of *Scardinius racovitzai* and *Melanopsis parreyssii*"). The authors gratefully acknowledge the following individuals for their support: the anonymous reviewers and the editors of Applied Ecology and Environmental Research for the valuable, critical and helpful comments on the manuscript.

REFERENCES

[1] Bănărescu, P. (1964): Pisces - Osteichthyes (peşti ganoizi şi osoşi). Vol. XIII. – Fauna R.P.R., Edit. Academiei, București, pp. 53-55 (in Romanian).

[2] Bănărescu, P. (2002): Species and subspecies of fish fauna and lampreys andemic or almost endemic to the drainage area of the river. – TISCIA Monograph Series, Ecological Aspect of the Tisa River Basin, 21-24 March, 2002, 6: 167-172.

http://www.aloki.hu ● ISSN 1589 1623 (Print) ● ISSN 1785 0037 (Online)
DOI: http://dx.doi.org/10.15666/aeer/1605_60636076
© 2018, ALÖKI Kft., Budapest, Hungary

[3] Cadrin, S. X. (2000): Advances in morphometric identification of fishery stocks. – Reviews in Fish Biology and Fisheries 10: 91-112.
[4] Cărăuşu, S. (1952): Tratat de ihtiologie. – Ed. Acad. RPR, Bucureşti, pp. 36-46 (in Romanian).
[5] Crăciun, N. (1997): Ethological researches on *Scardinius racovitzai* from the Thermal Lake 1 Mai, Oradea. – St şi Cercet 2: 79-88.
[6] Crăciun, N. (1998)**:** Cercetări de etologie comparată a unor peşti marini şi dulcicoli din fauna României. – Teză de doctorat, Institutul de Biologie al Academiei Române, Bucureşti (in Romanian).
[7] Delmater, E. D., Courtenay, W. R. (1973): Variations in structure of the lateral line canal on the scales of Teleostean fishes. – Z. Morph. Tiere 75: 259-266.
[8] Delmater, E. D., Courtenay, W. R. (1974): Fish scale as seen by scanning electron microscopey. – Biological Sciences 37: 141-149.
[9] Esmaeili H R, Gholami, Z. (2011): Scanning electron microscopy of the scale morphology in Cyprinid fish, *Rutilus frisii kutum* Kamenskii, 1901 (Actinopterygii: Cyprinidae), Iran. – J Fish Sci 10(1): 155-166.
[10] Esmaeili, H. R., Hojat, A. T., Teimory, A. (2007): Scale structure of a cyprinid fish, *Capoeta damascina* (Valenciennes in Cuvier and Valenciennes, 1842) using scanning electron microscope (SEM). – Iranian J Sci Tech 31: 255-262.
[11] Esmaeili, H. R., Somayeh, B., Halimeh, Z., Fatemeh, S. (2009): Scales morphology of thank goby *Glossogobius giuris* (Hamilton–Buchanan, 1822) (Perciformes, Gobiidae) using scanning electron microscope. – J Biol Sci 9: 899-903.
[12] Freyhof, J., Kottelat, M. (2008): *Scardinius racovitzai.* The IUCN Red List of Threatened Species. Version 2017-3. – www.iucnredlist.org. Accessed on 12 January 2018.
[13] Grigoras, G., Müller, T., Gagiu, A., Bontas, I., Serban, C., Rosca, M. (2014): Ex situ conservation of the thermal rudd (*Scardinius racovitzai*): a general review of work and results. – Nymphaea (Folia naturae Bihariae) 41: 103-134.
[14] Grigoraș, G., Müller, T., Gagiu, A., Bontaș, I. (2015): Preliminary results regarding the present morphometric characters of *Scardinius racovitzai* Müller 1958 from Petea Spring Natural Reserve. – Transylv Rev Syst Ecol Res: 79-95.
[15] Gursoy, C., Tarkan, A. S., Acipina, H., Gaygusuz, O. (2005): Validation of the scales age determination in a cyprinid, *Scardinius erythrophthalmus* (L., 1758). – Int J Zool Res 1(1): 33-36.
[16] Hagerman, F. B. (1952): The biology of the Dover sole, *Microstomus pacificus* (Lockington). – Fish Bulletin, No. 85, UC San Diego.
[17] Harabawy, A. S. A., Mekkawy, I. A. A., Mahmoud, U. M. (2007): A comparative study on scale characteristics and their functional morphology of four Goatfishes (Family Mullidae) from the Red Sea. – J. Egypt. Soc. Biotech. Environ. Soc. 9: 123-163.
[18] Ibáñez, A. L., Cowx, I, G., O'Higgins, P. (2007): Geometric morphometrics analysis of fish scales for identifying genera, species and local populations within Mugilidae. – J Fish Aquat Sci 64: 1091-1100.
[19] Ibáñez, A. L., Jawad, L. A., Sadighzadeh, Z. (2016): Morphometric variation of fish scales among some species of the family Lutjanidae from Iranian waters. – Cah Biol Mar 57: 289-295.
[20] Ilieş, I., Traniello, I. M., Sîrbulescu, R. F., Zupanc, G. K. H. (2014): Determination of relative age using growth increments of scales as a minimally invasive method in the tropical freshwater *Apteronotus leptorhynchus*. – J Fish Biol 84: 1312-1325.
[21] Jawad, L. A. (2005a): Comparative morphology of scales of four teleost fishes from Sudan and Yemen. – Journal of Natural History 39(28): 2643-2660.
[22] Jawad, L. A. (2005b): Comparative scale morphology and squamation patterns in triplefins (Pisces: Teleostei: Perciformes: Tripterygiidae). – Tuhinga 16: 137-167.
[23] Jawad, L. A., Al-Jufaili, S. M. (2007): Scale morphology of greater lizardfish *Saurida tumbil* (Bloch, 1795) (Pisces: Synodontidae). – Journal of Fish Biology 70: 1185-1212.

http://www.aloki.hu ● ISSN 1589 1623 (Print) ● ISSN 1785 0037 (Online)
DOI: http://dx.doi.org/10.15666/aeer/1605_60636076
© 2018, ALÖKI Kft., Budapest, Hungary

[24] Jindal, R., Jha, S. K. (2005): Lepidological and toxicological studies of monocrotophos: An organophosphate pesticide on the scales of *Cyprinus carpio* var. *communis* Linnaeus 1758. – Aquacult 6(1): 39-44.
[25] Johal, M. S., Novak, J., Oliva, O. (1984): Notes on the growth of the common carp *Cyprinius carpio* in Northen India and middle Europe. – Vest. Cs. Spolec. Zool. 48: 24-38.
[26] Klingenberg, C. P. (2011): MorphoJ: an integrated software package for geometric morphometrics. – Mol Ecol Resour 11: 353-357.
[27] Kottelat, M., Freyhof, J. (2007): Handbook of European Freshwater Fish. – Kottelat, Cornol and Freyhof, Berlin.
[28] Lippitsch, E. (1990): Scale morphology and squamation patterns in cichlids (Teleostei, Perciformes): a comparative study. – Journal of Fish Biology 37: 265-291.
[29] Mahmoud, U. M., Makkawy, I. A. A., Harabawy, A. S. A. (2005): Scales characyeristics of seven species of genus *Lethrinus* (Family Lethrinidae) from Red Sea, Egypt. – J. Zool. 44: 545-580.
[30] Masood, Z., Yasmeen, R., Haider, M. S., Lakht-e-Zehra, Tarar, O. M., Mussarat-Ul-Ain, Hameed-Ur-Rehaman, Ullah, U., Ihsan-Ul-Haq, B. M., Hossain, Y. (2015): Comparative studies of the scale characters in four mugilid species (Family Mugilidae; Order Mugiliformes) from Karachi Coast, Pakistan. – Biological Forum - An International Journal 7(1): 410-418.
[31] Mekkawy, I. A. A., Wassi, E. T., Basmidi, A. M. (2011): Scales characteristics of three *Lutjanus* species (Fam. Lutjanidae) from the Red Sea, Egypt. – J Fish Aquat Sci 6(5): 506-522.
[32] Miranda, R., Escala, C. (2000): Morphological and biometric comparison of the scales of the barbels (*Barbus* Cuvier) of Spain. – J Morphol. 245: 196-205.
[33] Moneva, C. S. O., Torres, M. A. J., Tabugo, S. R., Demayo, C. G. (2012): Qualitative and geometric morphometric description of the shapes of scales of viridescent parrotfish, *Calotomus viridescens* (Rüppell, 1835). – The Second International Congress on Interdisciplinary Research and Development, 31 May-1 June 2012, Thailand.
[34] Müller, G.-J. (1958): *Scardinius racovitzai* n. sp. (Pisces, Cyprinidae), eine reliktäre Rotfeder aus Westrumänien. – Senckenbergiana Biologica 39(3/4): 165-168.
[35] Müller, T., Várkonyi, L., Gagiu, A., Kovács, B., Buza, E., Majoros, G., Staszny, Á., Horváth, Á., Bernáth, G., Tóth, G., Tatár, S., Urbányi, B., Fehér, Z., Grigoras, G., Serban, C., Müllerné, T. M. (2014a): Attempts on ex situ conservation of *Melanopsis parreyssii* and *S. racovitzai.* – Book of Abstracts II. Sustainable Development in the Carpathian Basin International Conference, 11-12 December, 2014, Budapest. Szent Istvan University Press, pp. 35-36.
[36] Müller, T., Várkonyi, L., Gagiu, A., Balázs, K., Buza, E., Majoros, G., Staszny, Á., Horváth, Á., Bernáth, G., Tóth, G., Tatár, S., Urbányi, B., Fehér, Z., Grigoras, G., Serban, C., Müllerné, T. M. (2014b): Kísérlet a váradi maradványcsiga (*Melanopsis parreysi*) és a Racovitza-kele (*Scardinius racovitzai*) megmentésére. – Book of Abstracts II. Sustainable Development in the Carpathian Basin International Conference, 11-12 December, 2014, Budapest. Szent Istvan University Press, pp. 36-37.
[37] Nico, L., Fuller, P., Jacobs, G., Larson, J., Makled, T. H., Fusaro, A., Neilson, M. (2015): *Scardinius erythrophthalmus* (Linnaeus, 1758). – U.S. Geological Survey, Nonindigenous Aquatic Species Database, Gainesville, FL. https://nas.er.usgs.gov/queries/FactSheet.aspx?speciesID=648. Accessed on 2/13/2018.
[38] Pillay, T. V. R. (1950): Structure and development of the scales of five species of grey mullets of Bengal. – Proceedings of the National Institute of Sciences of India 17: 413-424.
[39] Pou, M. N., Gallego, L. (1990): Metodo para el estudio anatomico de las escamas de los osteichthyes. – Revista Cientifica (IEB) 7: 79-84 (in Spanish).

http://www.aloki.hu ● ISSN 1589 1623 (Print) ● ISSN 1785 0037 (Online)
DOI: http://dx.doi.org/10.15666/aeer/1605_60636076
© 2018, ALÖKI Kft., Budapest, Hungary

[40] Poulet, N., Reyjol, Y., Collier, H., Lek, S. (2005): Does fish scale morphology allow the identification of populations at a local scale? A case study for rostrum dace *Leuciscus leuciscus burdigalensis* in River Viaur (S W France). – Aquat Sci 67: 122-127.
[41] Renjith, R. K., Jaiswar, A. K., Chakraborty, S. K., Sreekanth, G. B. (2014): Application of scale shape variation in fish systematics - an illustration using six species of the family Nemipteridae (Teleostei: Perciformes). – Indian J Fish 61(4): 88-92.
[42] Rohlf, F. J. (2016a): TpsDig2 version 2.26 (Tps_Digitize). – http://life.bio.sunysb.edu/morph/.
[43] Rohlf, F. J. (2016b): TpsUtil version 1.70 (Tps_Utility program). – http://life.bio.sunysb.edu/morph/.
[44] Sire, J. Y. (1986): Ontogenetic development of surface ornamentation in the scale of *Hemichromis bimaculatus (Cichlidae)* J. – Fish Biol. 28: 713-724.
[45] Staszny, Á., Ferincz, Á., Weiperth, A., Havas, E., Urbányi, B., Paulovits, G. (2012): Scale-morphometry study to discriminate gibel carp (*Carassius gibelio*) populations in the Balaton-catchment (Hungary). – Acta Zool Hung 58(Suppl.): 19-27.
[46] Sudo, S., Tsuyuki, K., Ito, Y., Ikohagi, T. (2002): A study on the surface shape of fish scales. – SME Int. J. Ser. C. 45: 1100-1105.
[47] Tandon, K. K., Johal, M. S. (1996): Age and Growth in Indian Freshwater Fishes. – Narendra Publishing House, New Delhi.
[48] Taylor, R. J. (2012): Applications of Fish Scale Analysis to Understand Growth Dynamics of Fish Populations. – PhD Thesis, University of Hull, Hull, UK.
[49] Telcean, C. I., Cupșa, D. (2013): The drastic decline of fish fauna in the thermal lake of Baile 1 Mai (Băile Episcopale, Bihor County, Romania). – Pisces Hungarici 7: 141-142.

http://www.aloki.hu ● ISSN 1589 1623 (Print) ● ISSN 1785 0037 (Online)
DOI: http://dx.doi.org/10.15666/aeer/1605_60636076
© 2018, ALÖKI Kft., Budapest, Hungary

EFFICIENCY OF TWO DIFFERENT ENTOMOPATHOGEN FUNGI *BEAUVERIA BASSIANA* AND *PURPUREOCILLIUM LILACINUM* TR1 AGAINST *TETRANYCHUS URTICAE*

YEŞILAYER, A.

Department of Plant Protection, Faculty of Agriculture, Gaziosmanpasa University, 60216 Tokat, Turkey
(e-mail: ayse.yesilayer@gop.edu.tr; phone: +90-356-256-1616)

(Received 26th Jun 2018; accepted 31st Aug 2018)

Abstract. Two-spotted red spider/red spider mite is an important pest of cultivated crops. Resistance is one of the most important problems in the intensive chemical control used in traditional management methods. Therefore, researchers have been using alternative control methods in pest management to overcome resistance problem. This study was conducted between 2015 and 2017 to investigate the effects of entomopathogenic fungi (EPF) *Beauveria bassiana* and *Purpureocillium lilacinum* TR1 on *Tetranychus urticae* (Koch) (Acarina: *Tetranychidae*). The doses used for *P. lilacinum* were 10^4, 10^5, 10^6, 10^7, 10^8 and 1.6 10^8 conidia ml^{-1} and for *B. bassiana* 10^4, 10^5, 10^6, 10^7, 10^8, 10^9 and 3.7×10^9 conidia ml^{-1}. After five days the results showed that mortality of *T. urticae* adults were started with 10^5 conidia ml^{-1} concentration of *B. bassiana* and after seven days 10^4 conidia ml^{-1} concentration of *P. lilacinus.* At the end of the trial, the mortality rate recorded by the highest doses, 10^8 conidia/ml, of both EPFs were 28.3 and 66.6% with *P. Lilacinus and B. bassiana*. Since many EPF fungi are thought to be epizootic, *B. bassiana* and *P. lilacinum* can be effectively used against *T. urticae* control as biological agents.
Keywords: *two spotted spider mites, entomopathogenic fungi, control, Turkey*

Introduction

The polyphagous pests are among the most harmful pest groups of agricultural products (Vacante, 2016). *Tetranychus urticae* is also an important pest of cultivated crops. Hatched two-spotted spider mites ((TSSM) mostly fed on the lower surface of leaves. The TSSM causes destruction in leaves by feeding in approximately 18-22 plant cells in a minute. After inserting the stylet like mouthparts into leaf cells, secretes the enzyme and absorbs the cell contents. Consequently, leaves are turned on pale, yellowish, gray or bronze-colored spots and causing drying and defoliation. In addition, adults cause damage by spinning tight and silk webs on the plants (Anonymous, 2008). Approximately 4000 different host plant species of *T. urticae* have been identified in worldwide (Migeon and Dorkeld, 2010, 2017) as well as in different studies conducted in Turkey (Yabaş and Ulubilir, 1995; Bulut, E., 1999; Yeşilayer, 2009).

The most preferred method in TSSM management is chemical control which is inexpensive and easy to adapt. However, one of the most important disadvantages of continuous use of chemical control is the resistance of *T. urticae* to the pesticides over time (Keena and Granett, 1987; Herron and Rophail, 1998; Van Leeuwen et al., 2004). New methods which can be alternative or complementary to chemical control of pests have recently been studied and especially importance of biological control is increasing as a suitable alternate method. Biological control is an appropriate method to sustainable agricultural techniques and sensible to human and animal health. The main components of this method used in pest control are parasitoids, predators and entomopathogens (Kılınçer et al., 2010; Dermauw et al., 2013). Studies conducted to date have reported approximately 500 fungi species as pathogenic in insects The

http://www.aloki.hu ● ISSN 1589 1623 (Print) ● ISSN 1785 0037 (Online)
DOI: http://dx.doi.org/10.15666/aeer/1605_60776086
© 2018, ALÖKI Kft., Budapest, Hungary

entomopathogenic fungi species of *Lagenidium, Entomophaga, Neozygites, Entomophytora, Erynia, Aschersonia, Lecanicillium, Nomuraea, Hirsutella, Metarhizium, Beauveria* and *Isaria* have gained importance in the field of plant protection (Erkılıç and Uygun, 1993; Kılıç and Yıldırım, 2008). *P. lilacinus* is known as a nematophagus fungi and used to control mites and insects. In addition, EPN activity of entomopatogen fungus *B. bassiana* against *T. urticae* and insects has also been demostrated (Örtücü and Albayrak İskender, 2017).

Thee fungi do not develop resistance in mites, insects and like other pesticides, have absence of any toxic effects on ecology and have potential for future biotechnological developments. The longtime control, infecting the development period of their hosts, applicability with many insecticides and easiness in for mass production are also other advantages of these fungi (Demirbag, 2008). Fungi directly enter from the cell wall. The spores on cuticle settle here and germinate. The germinating spores enter due to the appressorium (penetration peg). The hyphae in epidermis and hypodermic grow, continue to proliferation in the insect body and blood cells and cause the death of insect (Ortiz-Urquiza, 2013). Commercial preparation of some entomopathogenic fungi as mycoinsecticides (*B. bassiana*, *Metarhiz anisopliae, Hirsutell thompsoni*) are available in the world and Turkey (Kılınçer et al., 2010). Recent studies have recorded the efficiency of some EPFs such as B. *bassiana*, *Verticillium lecanii* and *M. anisoplia* against two spotted spider mites (Chandler et al., 2005). The aim of this study was to evaluate the efficiency of two different entomopathogenic fungi, *Purpureocillium lilacinum* and *Beauveria bassiana* against *Tetranychus urticae*.

Material and methods

Plant and mites culture

Bean used as host plant *Phaseolus vulgaris* L. (Fabaceae) was grown in production cabinets at 25 ± 2 °C, 65 ± 5% relative humidity and 16 h lights: 8 h darkness photoperiod in the Plant Protection Department of Faculty of Agriculture, Gaziosmanpaşa University in Tokat-Turkey. The plants, at 5-6 leaves stage were transferred to the production cabin to be used in the production of two-spotted red spiders. Cultures of *Tetranychus urticae* were reared in climate chambers of Plant Protection Department, Faculty of Agriculture, Gaziosmanpasa University. The infected bean plant leaves with mites were cut and placed on non-infected plants to infect.

Cultures of entomopathogenic fungus

The EPFs used in the study, *Purpureocillium lilacinum* (syn: *Paecilomyces lilacinus* (Thom) Samson) TR1 and *Beauveria bassiana* (Balsamo) Vuillemin were obtained from the stock cultures of Prof. Dr İlker KEPENEKÇİ (Department of Plant Protection, Faculty of Agriculture, Gaziosmanpasa University) and from Prof. Dr. Fikret DEMİRCİ (Department of Plant Protection, Faculty of Agriculture, Ankara University), respectively. The fungus was produced at the PDA medium to obtain sufficient spore suspension. Pure entomopathogenic isolates were planted using with glass hokey stick. After 4 weeks, 5 ml of 0.02% Tween 80 solution was added to the petri dishes containing the cultures and homogenous mixing of fungi spores was achieved by spreading with glass hokey stick. The resulting suspension was then filtered through a sterile material to remove particulates, and transferred to 15 ml and 50 ml centrifuge

http://www.aloki.hu ● ISSN 1589 1623 (Print) ● ISSN 1785 0037 (Online)
DOI: http://dx.doi.org/10.15666/aeer/1605_60776086
© 2018, ALÖKI Kft., Budapest, Hungary

tubes. The centrifuge tubes were shaken for 5 min on a Vortex shaker to separate the clustered fungi spores in the fungi suspensions. The spore intensity was determined using Thoma slide and light microscopy (Gabarty et al., 2014). Afterwards, each fungi isolate was diluted and the number of spores was adjusted.

Bioassay

Total of 13 different conidial concentrations were prepared to study the efficiency of entomopathogenic fungi on *T. urticae*. The conidial concentrations included 7 different doses of *B. bassiana* (1×10^4, 1×10^5, 1×10^6, 1×10^7, 1×10^8, 1×10^9 and 3.7×10^9 conidia ml^{-1}) and 6 different intensities of *P. lilacinum* (1×10^4, 1×10^5, 1×10^6, 1×10^7, 1×10^8 and $1 \times 1.6\ 10^8$ conidia ml^{-1}). For each application, 10 ml suspensions of different spore-density solutions were shaken for 2-3 min on the Vortex shaker. The EFPs, then, were sprayed to the leaves using a hand sprayer (2.5 ml). For each application, 10 *T. urticae* adults were used. Fungi solutions were sprayed to the down side of bean leaf disc and placed on a moist cotton in Petri dishes. Adult mites were transferred with a fine brush to the surface of leaf disc. Sterile distilled water (dH_2O) containing 0.02% Tween 80 was sprayed onto the leaves in the control. Mortality values were counted on days 1, 3, 5, 7 and 9 after the application, and mycosis rates observed on days 7, 11 and 19 were recorded. Mites, mortality in mycosis experiment were placed on a moist filter paper in 9 cm sterile glass petri dishes and fungal development was observed.

Daily maintenance and humidity control were carried out during the experiments. The experiment was set up with three replicates and repeated twice.

Statistical analyses

Data was subjected to the one-way analysis of variance (One-Way ANOVA), and mean values were compared by Tukey's test at P = 0.05 significance level (SPSS, 2011).

Results

Total of 13 concentrations of two different entomopathogenic fungi were applied to the adults of *T. urticae* under the laboratory conditions. Mortality using single dose of 10^5 started to occur on days 3 and 5 after applications of *P. lilacinum* and *B. bassiana*, respectively. Mortality of *T. urticae* adults among the application of other concentrations after the single dose experiment, were observed from day 5 at 10^6 concentration of *P. lilacinum*. The mortality rate at 10^6, 10^7 and 10^8 conidia ml^{-1} doses on day 9 was 28.3% and the mortality rate at the highest concentration ($1 \times 1.6\ 10^8$ conidia ml^{-1}) on day 11 was 76.6%. The mortality rates were linearly increased with increasing the doses and days (*Table 1*). The counting results in day 3 of *P. lilacinum* application in controlling the adult mites was not significantly different ($P > 0.05$). The mortality rates counted on days 5, 7 and 9 at 10^7 conidia/ml dose were statistically significant ($P < 0.05$) and the mortality rate ranged from 20 to 61.6% (*Table 1*).

The deaths of two-spotted adult mites at the highest concentration (3.7×10^9 conidia ml^{-1}) of *B. bassiana,* the second EPF used in the study, started on day 3 and mortality rate reached to 20%. The mortality rate was recorded as 91% on the last day (*Table 2*).

The mortality rates on days 5 (13.3%) and 7 (16.6%) at 10^7 and 10^8 conidia ml^{-1} concentrations of *B. bassiana* were statistically significant ($P < 0.05$). In contrast to *B.*

http://www.aloki.hu ● ISSN 1589 1623 (Print) ● ISSN 1785 0037 (Online)
DOI: http://dx.doi.org/10.15666/aeer/1605_60776086
© 2018, ALÖKI Kft., Budapest, Hungary

bassiana, the difference between mortality rates obtained with *P. lilacinum* starting from 10^8 conidia ml^{-1} concentration on day 3 was significant ($P < 0.05$). The differences between mortality rates on days 5 and 7 were similar, though statistically significant ($P < 0.05$). Mortality has not been observed after 3 days treatment with 10^4 but mortality was 48.3% at end of the day 9.

Table 1. *Effect of P. lilacinum on T. urticae (% mortality rate±SE)*

Concentration (conidia ml^{-1})	3th	5th	7th	9th
Control	0.00±0.00a	0.00±0.00a	1.66±1.66a	1.66±1.66a
10^4	0.00±0.00a	0.00±0.00a	10.00±0.00a	20.00±0.00a
10^5	0.00±0.00a	0.00±0.00a	11.66±1.66a	21.66±0.18 a
10^6	0.00±0.00a	1.66±2.43a	11.66±1.66a	28.33±1.23a
10^7	0.00±0.00a	3.33±2.10b	15.00±2.23ab	28.33±1.23a
10^8	0.00±0.00a	10.00±1.56b	20.00±1.45b	28.33±1.23a
$1 \times 1.6\ 10^8$	0.00±0.00a	28.33±1.33c	38.33±1.66c	61.66±2.32b

Means followed in the same column by different letters are significantly different $P < 0.05$, Tukey test

Table 2. *Effects of B. bassiana on T. urticae adults (% mortality rate ± SE)*

Concentration (conidia ml^{-1})	3th	5th	7th	9th
Control	1.66±1.66a	1.66±1.66a	1.66±1.66a	13.33±2.10a
10^4	0.00±0.00a	1.66±2.43a	1.66±2.43a	48.33±12.75abc
10^5	0.00±0.00a	8.33±3.01ab	8.33±3.01ab	31.66±2.56a
10^6	0.00±0.00a	11.66±1.66ab	11.66±1.66ab	41.66±3.06ab
10^7	0.00±0.00a	13.33±2.10ab	13.33±2.10ab	58.33±2.86bc
10^8	10.00±0.00b	16.66±2.10b	16.66±2.10b	66.66±2.10cd
10^9	16.66±2.10c	45.00±6.70c	45.00±6.70c	88.33±3.42de
3.7×10^9	20.00±2.58c	45.00±2.23c	45.00±2.23c	91.38±0.45e

Means followed in the same column by different letters are significantly different $P < 0.05$, Tukey test

Mycosis study with EPF fungus

Mycosis observations were conducted on days 7, 11 and 19 within the efficiency study against *T. urticae* adults included the different concentrations of the two EPF fungi. The mycosis rate on the end of day 7 at the lowest concentration (10^4 conidia ml^{-1}) was 10% and it was 51.6% at the end of the 19th day. The mycosis development rates of six different *P. lilacinum* concentrations on various days showed mycosis development on day 7 at 1×10^5, 1×10^6 and 1×10^7 conidia/ml concentrations, but the difference was not statistically significant ($P > 0.05$). The rate of mycosis development at 1×10^8 and $1 \times 1.6\ 10^8$ conidia ml^{-1} concentrations on day 7 was statistically significant ($P < 0.05$) (*Table 3*).

Similar to *P. lilacinum* (*P. lilacinus*), the mycosis development rates conducted at different concentrations of *B. bassiana* started to be observed from the day 7. The mycosis development rate at the highest concentrations of 1×10^7, 1×10^8 and $1 \times 1.6\ 10^8$ conidia ml^{-1} ranged from 20 to 45% and it was statistically significant ($P < 0.05$). The rate of mycosis development, which increased to over 50% at the highest

http://www.aloki.hu ● ISSN 1589 1623 (Print) ● ISSN 1785 0037 (Online)
DOI: http://dx.doi.org/10.15666/aeer/1605_60776086
© 2018, ALÖKI Kft., Budapest, Hungary

concentrations from the day 11, linearly increased. The minimum mycosis development rate at 10^4 conidia ml^{-1} concentration on the end of day 19 which was the last day was 58.3%. The mycosis development rate at 1×10^8, 1×10^9 and 3.7×10^9 conidia ml^{-1} concentrations was 100% and the difference was statistically significant ($P < 0.05$) (*Table 4*).

Table 3. *P. lilacinus of mycosis rate (%)*

Concentration (conidia ml^{-1})	7th	11th	19th
Control	0.00±0.00a	0.00±0.00a	0.00±0.00a
1×10^4	10.00±0.00a	21.66±1.66b	51.66±3.45b
1×10^5	13.33±2.10b	28.33±1.66b	65.00±2.23c
1×10^6	13.33±2.10b	38.33±1.66c	81.66±3.07d
1×10^7	20.00±2.52b	45.00±2.23c	100.00±0.00e
1×10^8	31.66±1.66c	55.00±3.42d	100.00±0.00e
$1 \times 1.6\ 10^8$	45.00±5.00d	60.00±2.58d	100.00±0.00e

Means followed in the same column by different letters are significantly different $P < 0.05$, Tukey test)

Table 4. *B. bassiana of mycosis rate (%)*

Concentration (conidia ml^{-1})	7th	11th	19th
Control	0.00±0.00a	0.00±0.00a	0.00±0.00a
1×10^4	11.66±1.66b	28.33±1.66b	58.33±3.66b
1×10^5	15.00±2.23b	40.00±2.06c	71.66±1.66c
1×10^6	16.66±2.10b	43.33±2.10c	81.66±1.66d
1×10^7	21.66±1.66b	53.33±3.21d	86.66±2.10d
1×10^8	36.66±2.10c	66.66±2.10e	100.00±0.00e
1×10^9	50.00±4.47d	78.33±3.44f	100.00±0.00e
3.7×10^9	70.00±3.16e	78.00±3.00f	100.00±0.00e

Means followed in the same column by different letters are significantly different $P < 0.05$, Tukey test

The difference between observed mycosis rates of both EPF applications was statistically significant ($P < 0.05$). The mycosis development rate at the lowest concentration on the day 11 varied from 21 to 60% for *P. lilacinum* and from 28 to 78% for *B. bassiana*. The mycosis development rates of two different EPFs at different concentrations on days 7, 11 and 19 are presented in *Figure 1a-d*.

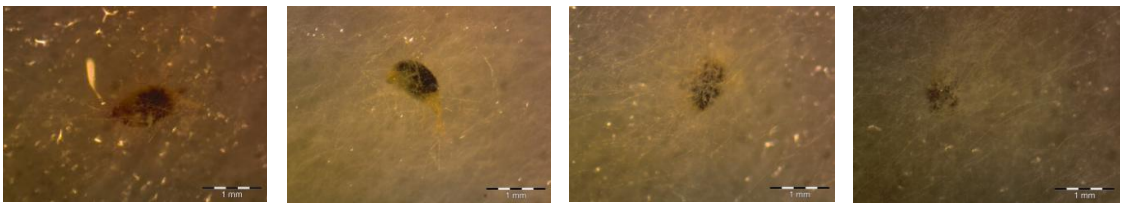

a **b** **c** **d**

Figure 1. *The mycosis development rates a- P. lilacinus 10^5, b- P. lilacnius 10^7, c- B. bassiana 10^5, d- B. bassiana 10^7 micosis*

http://www.aloki.hu ● ISSN 1589 1623 (Print) ● ISSN 1785 0037 (Online)
DOI: http://dx.doi.org/10.15666/aeer/1605_60776086
© 2018, ALÖKI Kft., Budapest, Hungary

The mycosis rates at 10^4 conidia ml^{-1} concentration of *B. bassiana* and *P. lilacinum* were recorded on days 7, 11 and 19. The mycosis development at 10^4 conidia ml^{-1} concentration in both fungi application was similar at the end of day 19 day. The lowest mycosis rates at 10^4 conidia ml^{-1} concentration on day 7 were 13.3 and 15% for *P. lilacinum* and *B. bassiana*, respectively. The mycosis rate on day 19 was lower in *P. lilacinum* than in *B. bassiana*. The lowest mycosis rates at 10^6 conidia ml^{-1} concentration on day 7 were 13.3 and 16% for *P. lilacinum* and *B. bassiana*, respectively. The mycosis rate of *P. lilacinum* from day 11 at 10^7 conidia ml^{-1} concentration was 45% while that of *B. bassiana* was over 50%. The mycosis rate at the highest common concentration (10^8 conidia ml^{-1}) on day 11 was recorded over 50% for both fungi while a mycosis rate of 100% was recorded on day 19.

Discussion

The lowest mortality rate for both fungi, *P. lilacinum* and *B. bassiana*, used in the study at the lowest concentration of 10^4 conidia ml^{-1} on day 9 was 20% and 48.3%, respectively. The mortality rate at the highest concentration on day 5 was found to be 28.3% for *P. lilacinum* and 45% for B. *bassiana*. The mortality and mycosis rates in the *B. bassiana* treatment were higher than that of *P. lilacinum* and the mortality rate of *T. urticae* at 7 different concentrations ranged from 10 to 100% between days 3 and 9. Similarly, Shi et al. (2008b) reported that *B. bassiana* application caused 31.9 to 87.7% mortalities of *Tetranychus cinnabarinus*, a red spider, in a study with three different EPFs. In laboratory conditions, application of two different isolates of *B. bassiana* caused mortality between 22.1 and 82.6 of adult females of *T. evansi* mites (Wekesa et al., 2005). In another study conducted with four different EPFs, *M. anisopliae* V275 and *M. anisopliae* led to quite high mortality on adult stages of *T. urticae*. In the same study, *M. flavoviride*, *L. lecanii* and *B. bassiana* were found effective in the adult stage by 57.8, 50 and 45.8%, respectively, and the differences in adult mortality rates caused by entomopathogenic fungi were statistically significant (Doğan, 2016). Shi and Feng (2009) and Wekesa et al. (2006) reported that entomopathogenic fungus applications resulted in deaths in *T. urticae* mites and also reduced their reproductive potentials. Tamai et al. (2002) investigated the effects of 45 isolates belonging to *Aschersonia aleyrodis* (1), *Beauveria bassiana* (32), *Metarhizium anisopliae* (10), *Hirsutella* sp. (1) and *Paecilomyces farinosus* on *T. urticae*. The concentration of entomopathogenic fungi were 5×10^7 conidia ml^{-1} except for *Hirsutella* sp. which was 1.7×10^7 conidia ml^{-1}. *B. bassiana, Hirsutella sp*. and *M. anisopliae* were found more pathogenic than other fungi used in the study, and these fungi have been reported causing mortalities of mites from the third day after inoculation. Similar to the findings of others, the mortality of mites in this study started after the third day of 10^8 and 10^9 conidia ml^{-1}. *B. bassiana* application.

The highest mortality rate of *B. bassiana* at 1×10^7 conidia ml^{-1} concentration in this study was 58.3%, while Doğan et al. (2017) reported 80% mortality on *T. urticae* at 1×10^7 concentration of the same fungus. Wu et al. (2016) reported 37 to 49% adult mortality at 1×10^7 concentration of different *B. bassiana* strains, and fungal virulence was attributed not only to strains but also to the concentration, frequency of application and formulation. Therefore, 80% mortality was reported from *T. evansi* and *T. cinnabarinus* strains of *B. bassiana* (Wekasa et al., 2005; Shi et al., 2008a). Bugeme et al. (2014) found that 1×10^7 conidia ml^{-1} concentration of *B. bassiana* and *M.*

http://www.aloki.hu ● ISSN 1589 1623 (Print) ● ISSN 1785 0037 (Online)
DOI: http://dx.doi.org/10.15666/aeer/1605_60776086
© 2018, ALÖKI Kft., Budapest, Hungary

anisopliae increased the mortality rates of *T. urticae* nymphs and adults and both EPFs were found effective.

The *P. lilacinum*, in the experiment, was very effective in two-spotted spider mites. The mortality rate linearly increased with the increase in concentrations. The mortality rate at 1×10^6, 1×10^7 and 1×10^8 conidia ml^{-1} concentrations ranged from 80 to 100%. Amjad et al. (2012) applied three different doses (1×10^6, 1×10^7 and 1×10^8 conidia ml^{-1}) of *Metarhizium anisopliae*, *Paecilomycis fumosoroseus* (Wize) and *Verticillium lecanii* against *T. urticae* and reported 90% mortality with *P. fumoroseus* application. In this experiment, the mortality rate at $1 \times 1.6\ 10^8$ conidia ml^{-1} *P. lilacinum* application was %66.3. In addition, development of mycosis was observed on day 7 of *P. lilacinum* applications against mites tested. Amjad et al. (2012) have also observed mycosis development on adult female mites from day 7 of *P. lilacinus* application against *Tetranychus kanzawai*.

The results of efficacy study conducted in Tokat province of Turkey revealed that *B. bassiana* and *P. lilacinum,* entomopathogenic fungi, caused effective mortality of mites at the end of 72 h (3 days) and 120 h (5 days), respectively. The development of mycosis has been intense from the day 7 at both fungi application. The *B. bassiana*, comparing the mortality and mycosis rates, was more effective against red spider mites than *P. lilacinum*.

In conclusion, we may conclude from the laboratory results that *B. bassiana* and *P. lilacinus* can be successfully used in controlling *T. urticae*. However, greenhouse and field trials are needed to support the findings of this study and to obtain more effective control against *T. urticae*. The use of entomopathogens in management of two-spotted red spiders has more advantageous to practice in terms of human, environment, benefices and predators. In addition, mass production, formulation development, licensing and further research efforts are required on entomopathogens fungi.

Acknowledgements. The authors thank Prof. Dr. İlker Kepenekci (Gaziosmanpaşa University, Turkey) and *B. bassiana* Prof. Dr Fikret Demirci (Ankara University, Turkey) for providing *P. lilacinum*. This study was funded by Research Foundation (BAP-2015-137) of Gaziosmanpaşa University

REFERENCES

[1] Amjad, M., Bashir, M. H., Afzal, M., Sabri, M. A., Javed, N. (2012): Synergistic effects of some entomopathogenic fungi and synthetic pesticides, against two spotted spider mite, *Tetranychus urticae* Koch (Acarina: Tetranychidae). – Pakistan Journal of Zoology 44(4): 977-984.

[2] Anonymous (2008): Zirai Mücadele Teknik Talimatları. – T. C. Tarım ve Köyişleri Bakanlığı Koruma ve Kontrol Genel Müdürlüğü 3,183-268-276, 332 ss.

[3] Bugeme, D. M., Knapp, M., Boga, H. I., Ekesi, S., Maniania, N. K. (2014): Susceptibility of developmental stages of *Tetranychus urticae* (Acari: Tetranychidae) to infection by *Beauveria bassiana* and *Metarhizium anisopliae* (Hypocreales: Clavicipitaceae). – International Journal of Tropic. Insect Science 34: 190-196.

[4] Bulut, E. (1999): Antalya ve Çevresinde sebze seralarında bulunan zararlılar ve doğal düşmanlarının saptanması. – Akdeniz Üniversitesi, Bitki Koruma Anabilim Dalı, Antalya.

[5] Chandler, D., Davidson, G., Jacobson, R. J. (2005): Laboratory and glasshouse evaluation of entomopathogenic fungi against the two-spotted spider mite, *Tetranychus urticae*

http://www.aloki.hu ● ISSN 1589 1623 (Print) ● ISSN 1785 0037 (Online)
DOI: http://dx.doi.org/10.15666/aeer/1605_60776086
© 2018, ALÖKI Kft., Budapest, Hungary

(Acari: Tetranychidae), on tomato, *Lycopersicon esculentum*. – Biocontrol Science Techonology 15: 37-54.
[6] Demirbağ, Z. (2008): Entomopatojenler ve biyolojik mücadele. – Esen Ofset Matbaacılık, Istanbul.
[7] Dermauw, W., Wybouw, N., Rombauts, S., Menten, B., Vontas, J., Grbic, M. (2013): A link between host plant adaptation and pesticide resistance in the polyphagous spider mite *Tetranychus urticae*. – Proceedings of the National Academy of Sciences of the USA 110: E113-E122.
[8] Doğan, Ö. Y. (2016): Entomopatpjen fungusların *Tetranychus urticae*'ye karşı etkinliklerinin belirlenmesi. – Yüksek lisans tezi. Fen Bilimleri Enstitüsü, Adnan Menderes Üniversitesi.
[9] Doğan, Ö. Y., Hazır, S., Yıldız, A., Butt, T. M., Çakmak, İ. (2017): Evaluation of entomopathogenic fungi for the control of *Tetranychus urticae* (Acari: Tetranychidae) and the effect of *Metarhizium brunneum* on the predatory mites (Acari: Phytoseiidae). – Biological Control 111: 6-12.
[10] Erkılıç, L., Uygun, N. (1993): Entomopatojen fungusların biyolojik mücadelede kullanılma olanakları. – Türkiye Entomoloji Dergisi 17(2): 117-128.
[11] Gabarty, A., Salem, H. M., Fouda, M. A., Abas, A. A., Ibrahim, A. A. (2014): Pathogencity induced by the entomopathogenic fungi *Beauveria bassiana* and *Metarhizium anisopliae* in *Agrotis ipsilon* (Hufn.). – Journal of Radiation Research and Applied Sciences 7: 95-100.
[12] Herron, G. A., J., Rophail, J. (1998): Tebufenpyrad (pyranica$^{(R)}$) resistance detected in two-spotted spider mite *Tetranychus urticae* Koch (Acarina: Tetranychidae) from Apples in Western Australia. – Experimental and Applied Acorology 22: 633-641.
[13] Keena, M, A., Granett, J. (1987): Cyhexatin and propargite resistance in populations of spider mites (Acari: Tetranychidae) from california almonds. – Journal of Economic Entomology 80: 560-564.
[14] Kılıç, E., Yıldırım, E. (2008): Beyazsineklerin (Homoptera: Aleyrodidae) mücadelesinde entomopatojen fungusların kullanım imkanları. – Atatürk Üniversitesi Ziraat Fakültesi Dergisi 39(2): 249-254.
[15] Kılınçer, N., Yiğit, A., Kazak, C., Er, M. K., Kurtuluş, A., Uygun, N. (2010): Teoriden Pratiğe Zararlılarla Biyolojik Mücadele. – Türkiye Bioloji Mücadele Dergisi 1: 15-59.
[16] Migeon, A., Dorkeld, F. (2016): Spider Mites Web: a Comprehensive Database for the Tetranychidae. – http://www.montpellier.inra.fr/CBGP/spmweb. Accessed 3 July 2017.
[17] Migeon, A., Nouguier, E., Dorkeld, F. (2010): Trends in Acarology. Spider Mites Web: A Comprehensive Database for the Tetranychidae. – Springer, Amsterdam, pp. 557-560.
[18] Ortiz-Urquiza, A., Keyhani, N. (2013): Action on the surface: entomopathogenic fungi versus the insect cuticle. – Insects 4(3): 357-374.
[19] Örtücü, S., Albayrak, N. (2017): Determination of control potentials and enzyme activities of *Beauveria bassiana* (Bals.) Vull. isolates against *Tetranychus urticae* Koch (Acari: Tetranychidae). – Trakya University Journal of Natural Sciences 18(1): 33-38.
[20] Shi, W. B., Feng, M. G. (2009): Effect of fungal infection on reproductive potential and survival time of *Tetranychus urticae* (Acari: Tetranychidae). – Experimental and Applied Acarology 48: 229-237.
[21] Shi, W. B., Zhang, L. L., Feng, M. G. (2008a): Field trials of four formulations of *Beauveria bassiana* and *Metarhizium anisopliae* for control of cotton spider mites (Acari: Tetranychidae) in the Tarim Basin of China. – Biological Control 45: 48-55.
[22] Shi, W. B., Zhang, L. L., Feng, M. G. (2008b): Time-concentration-mortality responses of Carmine spider mite (Acari: Tetranychidae) females to three hypocrealean fungi as biocontrol agents. – Biological Control 46: 495-501.
[23] Tamai, M. A., Alves, S. B., Almedia, J. E. M., de Faion, M. (2002): Evaluation of entomopathogenic fungi for control of *Tetranychus urticae* koch (Acari: Tetranychidae).

http://www.aloki.hu ● ISSN 1589 1623 (Print) ● ISSN 1785 0037 (Online)
DOI: http://dx.doi.org/10.15666/aeer/1605_60776086
© 2018, ALÖKI Kft., Budapest, Hungary

– Centro de Pesquisa e Desenvolvimento de Sanidad Vegetal, Inst. Biology, Campinas, SP, Brasil.

[24] Vacante, V. (2016): The Handbook of Mites of Economic Plants. – CABI Publishing, Wallingford.

[25] Van Leeuwen, Stillatus, T., Tirry, L. (2004): Genetic analysis and cross-resistance spectrum of a laboratory-selected chlorfenapyr resistant of two spotted spider mite (Acari: Tetranychidae). – Experimental and Applied Acarology 32: 249-261.

[26] Wan, H. (2003): Molecular biology of the entomopathogenic fungus *beauveria bassiana*: insect-cuticle degrading enzymes and development of a new selection marker for fungal transformation. – Unpublished Ph. D. Thesis, Combined Faculties for the Natural Sciences and for Mathematics of the Ruperto-Carola University of Heidelberg, Germany.

[27] Wekesa, V. W., Maniania, N. K., Knapp, M., Boga, H. I. (2005): Pathogenicity of *Beauveria bassiana* and *Metarhizium anisopliae* to the tobacco spider mite *Tetranychus evansi*. – Experimental and Applied Acarology 36(1-2): 41-50.

[28] Wekesa, V. W., Knapp, M., Maniania, N. K., Boga, H. I. (2006): Effects of *Beauveria bassiana* and *Metarhizium anisopliae* on mortality, fecundity and egg fertility of *Tetranychus evans*i. – Journal of Applied Entomology 130: 155-159.

[29] Wu, S., Xie, H., Li, M., Xu, X., Lei, Z. (2016): Highly virulent *Beauveria bassiana* strains against the two-spotted spider mite, *Tetranychus urticae*, show no pathogenicity against five phytoseiid mite species. – Experimental and Applied Acarology 435.

[30] Yabaş, C., Ulubilir, A. (1995): Akdeniz Bölgesi'nde biberde yeni saptanan bir zararlı *Polyphagotarsonemus latus* (Banks) (Acarina, Tarsonemidae). – Türkiye Entomoloji Dergisi 19(1): 43-46.

[31] Yeşilayer, A. (2009): İstanbul ili yeşil alanlarında zararlı akar (acarina) türlerinin tanımı, yayılışı, önemli türün populasyon yoğunluğu ve doğal düşmanları üzerinde araştırmalar. – Ankara Üniversitesi Fen Bilimleri Enstitüsü Doktora Tezi.

APPENDIX

ANOVA (BB)

		Sum of Squares	df	Mean Square	F	Sig.
day1	Between Groups	.000	7	.000	.	.
	Within Groups	.000	40	.000		
	Total	.000	47			
day3	Between Groups	2014.583	7	287.798	18.668	.000
	Within Groups	616.667	40	15.417		
	Total	2631.250	47			
day5	Between Groups	10997.917	7	1571.131	96.685	.000
	Within Groups	650.000	40	16.250		
	Total	11647.917	47			
day7	Between Groups	7247.917	7	1035.417	55.222	.000
	Within Groups	750.000	40	18.750		
	Total	7997.917	47			
day9	Between Groups	26349.479	7	3764.211	179.783	.000
	Within Groups	837.500	40	20.938		
	Total	27186.979	47			

http://www.aloki.hu ● ISSN 1589 1623 (Print) ● ISSN 1785 0037 (Online)
DOI: http://dx.doi.org/10.15666/aeer/1605_60776086
© 2018, ALÖKI Kft., Budapest, Hungary

ANOVA (PTR)

		Sum of Squares	df	Mean Square	F	Sig.
day1	Between Groups	.000	6	.000	.	.
	Within Groups	.000	35	.000		
	Total	.000	41			
day3	Between Groups	61.905	6	10.317	.867	.529
	Within Groups	416.667	35	11.905		
	Total	478.571	41			
day5	Between Groups	3661.905	6	610.317	42.722	.000
	Within Groups	500.000	35	14.286		
	Total	4161.905	41			
day7	Between Groups	3447.619	6	574,603	33,519	.000
	Within Groups	600.000	35	17,143		
	Total	4047.619	41			
day9	Between Groups	7223.810	6	1203.968	54.964	.000
	Within Groups	766.667	35	21.905		
	Total	7990.476	41			

http://www.aloki.hu ● ISSN 1589 1623 (Print) ● ISSN 1785 0037 (Online)
DOI: http://dx.doi.org/10.15666/aeer/1605_60776086
© 2018, ALÖKI Kft., Budapest, Hungary

THE EFFECTS OF CHEMICAL AND ORGANIC FERTILIZER APPLICATIONS ON FORAGE YIELD AND QUALITY OF SMOOTH BROME (*BROMUS INERMIS* L.) UNDER IRRIGATED AND NON-IRRIGATED CONDITIONS

GENC LERMI, A.[1*] – ERDOGDU, İ.[2] – ALTINOK, S.[3]

[1]*Department of Crop and Animal Production, Vocational School, University of Bartın Bartın, Turkey*

[2]*Eskisehir Transitional Zone Agricultural Research Institute, Eskisehir, Turkey*

[3]*Department of Field Crops, Faculty of Agriculture, Ankara University, Ankara, Turkey*

**Corresponding author*
e-mail: aysegenclermi@gmail.com; phone: +90-505-815-3474; fax: +90-378-227-8875

(Received 26th Jun 2018; accepted 31st Aug 2018)

Abstract. The aim of this research is to examine the effects of chemical and organic fertilizer applications on the forage yield and quality of smooth brome. The research was conducted in two separate experiments under irrigated and non-irrigated conditions in a randomized complete blocks design with three replications. Ammonium sulphate was used as chemical fertilizer, manure and poultry manure as organic fertilizer and *Vicia sativa* L as green manure. Under irrigated and non-irrigated conditions, the impacts of different fertilizer applications on the smooth brome's height of plant, crude protein rate, crude protein yield, green grass yield and dry matter yield were evaluated. According to the results of the research, while the average dry matter yield was obtained to be 3.94 t ha^{-1} under irrigated conditions, it was obtained as 1.70 t ha^{-1} under non-irrigated conditions. The peak values under irrigated conditions were obtained from chemical fertilizer application. However, under non-irrigated conditions the highest values were obtained from organic fertilizer applications. Consequently, considering the impacts of using organic fertilizers on the ecological properties of the soil in the long term, it was concluded that the yield difference between chemical fertilizer and organic fertilizer under irrigated conditions was at tolerable level.
Keywords: *manure, poultry manure, chemical fertilizer, dry matter yield, organic forage*

Introduction

Plant production methods not damaging the natural resources and ecosystem should be preferred, while it is aimed to obtain maximum yield in unit area from plant production. One of the most frequently used methods in increasing productivity is fertilization. Especially, with the use of chemical fertilizers, the importance and value of organic fertilizers were ignored. The most applied method in improving the physical properties of soil and maintaining its sustainability is the addition of organic matters (Bender et al., 1998). Organic fertilizer improved the physical, chemical and biological properties of the soil (Shiralipour et al, 1992; Carpenter-Boggs et al., 2000; Marinari et al., 2000) as well as increasing the plant yield and quality Yolcu (2011). Sonmez et al. (2008) emphasized that the use of chemical fertilizer was essential in agricultural production despite some of its adverse effects, but that the arising problems could be reduced by paying attention to the amount and time of application and by supporting with organic fertilizer. The sustainability and profitability of plant production shall only be achieved by increasing chemical fertilization and organic fertilization made

http://www.aloki.hu ● ISSN 1589 1623 (Print) ● ISSN 1785 0037 (Online)
DOI: http://dx.doi.org/10.15666/aeer/1605_60876094
© 2018, ALÖKI Kft., Budapest, Hungary

according to the available nutrient content of our soil that was exposed to intensive chemical fertilizer use. With the use of organic fertilizer, organic matter of the soil increases, and thus the physical, chemical and biological properties of the soil improve. Manure, poultry manure, compost and green fertilizer are used for organic fertilization purpose.

According to the researches, it is seen that the effects of chemical fertilizers on the increase of forage yield are higher, whereas the advantages of organic fertilizers in terms of productivity, cost and ecology decrease the attractiveness of chemical fertilizers. Nazli et al. (2014) found that the use of organic fertilizers and chemical fertilizers met the forage need, while at the same time it could reduce the dependence on inorganic fertilizers in agricultural areas. Thus, it was reported that it had positive impact on both the soil productivity and the environment. Bulluck et al. (2002) examined of the effects of the organic and synthetic fertility amendments on the soil in organic and conventional farm. The researchers reported that the yield is not affected by the fertilizer applications within the first year, but the organic production yield is higher than the conventional production yield within the second year. Furthermore, the researchers emphasized that the useful microorganisms in the soil increase, the pathogen population decrease, the soil organic substance, the total carbon and the cation exchange capacity (CEC) increase and thus the soil quality is improved with the alternative fertilizer applications. Emerenciano Neto et al. (2016) concluded that manure was lower than chemical fertilizer as a nitrogen source but that manure was available to be used in order to reduce cost and environmental impacts. Razec et al. (2009) stated that through fertilization made with manure, more economic efficiency was obtained, the yield increased by 75-123% and vegetation density and seed formation capacity increased.

Among the forage legumes, the smooth brome is one of the plants that can be included in the planting pattern under arid and semi-arid conditions due its temperature-tolerance and drought-tolerance. In addition, smooth brome is the leading forage plant that can be used alone or in mixtures with legumes under irrigated and arid conditions (Serin et al., 1998).

In the last decade, organic animal production has been rapidly increasing in many countries around the world. In fourteen countries of the European Union, Cereals and forage crops are cultivated on more than 80% of arable under organic farming (Golijan, 2017). The most important need for organic livestock farming is the production of organic forage plants (Yolcu, 2011). The production of organic forage crops plays an important role in organic livestock farming especially in terms of the ecological and economic sustainability of the farms (Will, 2012). As in conventional agriculture, the forage plant cultivation constitutes about 70% of production costs in organic livestock farming. Organic meadow-pasture areas constitute 62% of total organic agricultural areas in the world and organic forage plants production areas constitute 5%. In total, organic roughage production areas constitute 67% of the world's organic agricultural production areas. Organic roughage production in our country is 44206 tonnes in organic meadows and 315 053 tonnes in organic forage plants (Yolcu et al., 2014). Moreno-Resendez et al. (2017) reported that in the organic forage crops production, organic fertilizer increases the forage yield and quality of corn.

Smooth brome can be considered as alternative forage plant especially in the regions where stiff winters are dominant due to its resistance to cold and semi-arid ecologies. Researchers conducted in different locations on yield and quality of smooth brome.

http://www.aloki.hu ● ISSN 1589 1623 (Print) ● ISSN 1785 0037 (Online)
DOI: http://dx.doi.org/10.15666/aeer/1605_60876094
© 2018, ALÖKI Kft., Budapest, Hungary

Albayrak and Ekiz (2005) obtained the dry matter and crude protein yields of smooth brome under arid conditions as 1.28 t ha^{-1} and 0.142 t ha^{-1}, respectively. Karakurt and Ekiz (2000) obtained the highest dry matter and crude protein yields of smooth brome, which was subjected to nitrogen fertilizer and manure under arid conditions, from 120 kg ha^{-1} of nitrogenous fertilizer 3 t ha^{-1} applications. Serin et al. (1998) stated that the highest dry matter yield of smooth brome was obtained in the first year and that the yield decreased in the 2nd and 3rd years. Hongrong et al. (2000) reported that the smooth brome aboveground yield increases with the sewage-sludge application.

The aim of this research is to determine the effects of chemical and organic fertilizer applications on the forage yield and quality of smooth brome. In addition, the effectiveness of different fertilizer applications under irrigated and dried conditions were also determined. The data obtained shall be of importance in terms of applications that have gained importance in recent years such as sustainable agriculture, low-input agriculture, good agricultural practices and organic agriculture.

Materials and methods

Locations, soil and climate

This research was conducted in 2003 and 2004 in the smooth brome experiment field that was established in 2002 in Field Crops Department of Faculty of Agriculture, Ankara University, Turkey. The geographical coordinates of the experiment field are within 39° 57' northern latitude, 32° 52' eastern longitude and 860 m altitude. The soil properties of the experimental field have clayed-loamy texture, with pH = 7.88, 1.15% of organic matter, 0.061% of total salt, 10% of lime and with phosphorus and potassium of 6.6 and 140 kg/ha, respectively. The long-term average of total precipitation was determined as 384.9 mm, 308 mm in 2003 and 272.4 mm in 2004 (*Fig. 1*). The average temperature in the experimental years was high in 2003, but it was similar to the long-term average in 2004.

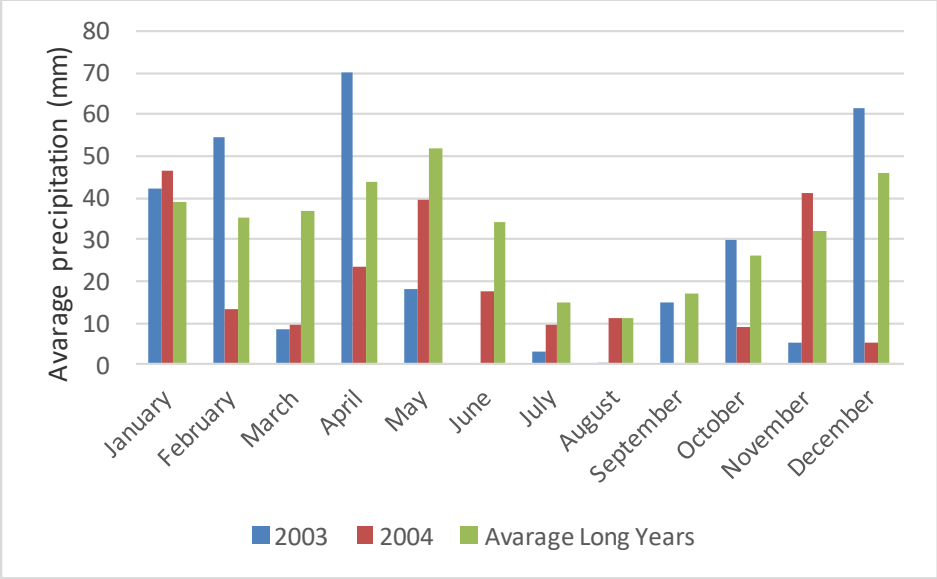

Figure 1. *Monthly precipitation for the years of 2003 and 2004 and long-term average in Ankara*

http://www.aloki.hu ● ISSN 1589 1623 (Print) ● ISSN 1785 0037 (Online)
DOI: http://dx.doi.org/10.15666/aeer/1605_60876094
© 2018, ALÖKI Kft., Budapest, Hungary

Materials and treatments

The experiment was conducted complete blocks design with three replications in 2003-2004 years. Within the second and third year of the experiment established in 2002, the effects of the fertilizer applications applied to smooth brome plant were examined within the following years. This research was conducted in two separate experiments under irrigated and non-irrigated conditions. Smooth brome (*Bromus inermis L.*) (15 kg ha^{-1}) seed populations characteristic was used as seed material. Ammonium sulphate, manure, poultry manure and as a green manure common vetch (*Vicia sativa* L.) were used as fertilizer materials in the experiment. The applications were determined as smooth brome (control), smooth brome + ammonium sulphate, smooth brome + barnyard manure, smooth brome + poultry manure, smooth brome + green manure. In the experiment, the parcels were at the length of 4 × 2.4 m and smooth brome and vetch were planted as 12 rows at the row interval of 20 cm in alternative orders in the parcels where vetch is planted (100 kg ha^{-1}) for the purpose of green manure to 6 rows at the row interval of 40 cm. The vetch was mixed into the soil by being harvested from the surface of the soil when it reached to 50% blooming period (Karatas, 2004). In the fertilizer applications, barnyard manure of 20 tons ha^{-1} and poultry manure of 10 tons ha^{-1} were mixed into the depth of 0-20 cm of the soil in the spring ploughing. Ammonium sulphate manure was applied as 100 kg ha^{-1} within the seedling period after planting. In the experiment conducted under irrigated conditions, the decision was taken according to the precipitation condition of traditional flood irrigation. Traditional flood irrigation was made for once in March 2003 and for twice in March and April due to the precipitation decrease in March and April 2004.

In the irrigated and non-irrigated plots, harvesting was performed at the beginning of flowering. The harvested plant samples were dried until reaching a constant mass to obtain dry matter yields at 70 °C (Martin et al.,1990). After the weed samples were ground, the nitrogen ratio was determined by the Kjeldahl method. The determined nitrogen ratios were multiplied by a coefficient of 6.25 and the crude protein ratio was calculated in the dry weeds. The crude protein yields were determined by proportioning the crude protein ratios obtained with dry matter yields.

Statistics

Variation analyses of the obtained data were conducted separately according to significance levels of 5% and 1% based on the General Linear Model of Statistical Analysis Systems (SAS) program. LSD test was used to compare treatment means at a 5% significance level, when differences emerged between fertilizer applications.

Results and discussion

The mean values and variance analysis results of effects of chemical and organic fertilizer on the examined properties in the smooth brome cultivated under irrigated and non-irrigated conditions are given in *Table 1*. The height of the plant was not affected by the application during the years when the research was conducted. Considering the two-year average, the highest plant height was obtained by application of ammonium sulphate and manure under irrigated conditions. Under the non-irrigated conditions, the highest plant height was obtained from green fertilizer application with 70 cm. Karakurt

http://www.aloki.hu ● ISSN 1589 1623 (Print) ● ISSN 1785 0037 (Online)
DOI: http://dx.doi.org/10.15666/aeer/1605_60876094
© 2018, ALÖKI Kft., Budapest, Hungary

and Ekiz (2000) reported that different nitrogen and manure applications in Ankara conditions did not affect the plant height of the smooth brome.

In statistical evaluation regarding the crude protein ratio, the difference between the applications in 2003 and 2004 was found to be significant at a level of 1% under irrigated conditions and 5% under non-irrigated conditions (*Table 1*). Under irrigated conditions, the highest crude protein ratios in 2003 and 2004 were obtained from ammonium sulphate with 13.93 and 14.16%, respectively. The values we obtained regarding the crude protein ratio under irrigated conditions are similar to those of Serin (1996b). The crude protein ratio values in the non-irrigated conditions according to the two years average were obtained between the ranges of 11.8-14.2%. The values obtained by Serin (1996a) and Karakurt and Ekiz (2000) are similar to the values of crude protein ratio we obtained from our research. Albayrak et al. (2011) and Albayrak and Ekiz (2005) obtained crude protein ratio in smooth brome as 10.79% and 10.30%, respectively. It was determined that while the crude protein ratio values were affected by different fertilizer applications in both years, they were not affected by irrigation.

Table 1. *The means of the effects of different fertilizer applications on the properties of smooth brome under irrigated and non-irrigated conditions on plant height (PH), crude protein ratio (CPR), crude protein yield (CPY) and dry matter yield (DMY)*

Applications	Irrigated conditions				Nonirrigated conditions			
	PH (cm)	CPR (%)	CPY (t ha^{-1})	DMY (t ha^{-1})	PH (cm)	CPR (%)	CPY (t ha^{-1})	DMY (t ha^{-1})
	2003				2003			
Control	95	13.4ab**	0.59cb**	4.41b**	67	13.2ab*	0.18dc**	1.38c**
Ammonium Sulphat	100	13.9a	0.93a	6.70a	65	13.9a	0.22bc	1.58c
Manure	101	12.4c	0.65b	5.26b	71	12.0b	0.31a	2.57a
Poultry manure	99	12.7bc	0.65b	5.06b	70	12.8ab	0.27ab	2.08b
Green manure	95	11.3d	0.49c	4.34b	70	12.0b	0.16d	1.31c
Mean	97.8	12.7	0.66A**	5.15A*	68.7	12.8	0.23	1.78
LSD	8.72	0.90	0.151	11.11	11.13	1.35	0.056	0.374
	2004				2004			
Control	96	12.6bc**	0.35bc**	2.76ab*	68	13.0b*	0.23a*	1.75ab*
Ammonium Sulphat	103	14.1a	0.45a	3.17a	62	14.5a	0.21a	1.42ab
Manure	100	11.6dc	0.28c	2.39b	64	11.6b	0.13b	1.14b
Poultry manure	96	13.6ab	0.39ab	2.92ab	66	12.5b	0.25a	1.99a
Green manure	99	11.0d	0.27c	2.42b	70	12.0b	0.22a	1.85a
Mean	98.7	12.6	0.35B	2.73B	65.8	12.7	0.207	1.63
LSD	9.10	1.39	0.086	0.535	10.52	1.54	0.071	0.641
	Two years average				Two years average			
Control	96	13b**	0.47b**	3.58bc**	68	13.1b**	0.21b*	1.57bc*
Ammonium Sulphat	101	14a	0.69a	4.93a	64	14.2a	0.21b	1.50c
Manure	100	12c	0.47b	3.83bc	68	11.8c	0.22ab	1.85ab
Poultry manure	97	13.1b	0.52b	3.99b	68	12.6cb	0.26a	2.03a
Green manure	97	11.1d	0.38c	3.38c	70	12c	0.18b	1.58bc
Mean	98.2	12.7	0.51	3.94	67.26	12.8	0.21	1.71
LSD	3.63	0.45	0.048	0.566	4.28	0.55	0.026	0.341

**$p < 0.01$, *$p < 0.05$. Means within the same column followed by the same letter are not significantly different

http://www.aloki.hu ● ISSN 1589 1623 (Print) ● ISSN 1785 0037 (Online)
DOI: http://dx.doi.org/10.15666/aeer/1605_60876094
© 2018, ALÖKI Kft., Budapest, Hungary

In the first year of the research, the highest crude protein yield was obtained from the ammonium sulphate application under irrigated conditions and this was followed by manure and poultry manure applications. The highest average crude protein yield was obtained from the application of chemical fertilizer with 0.69 t ha^{-1} and this was followed by poultry manure application with 0.52 t ha^{-1}. Yolcu (2011) reported that the highest crude protein yield was obtained from manure and chemical fertilizer applications. In the second year of the research, yields of crude protein decreased significantly due to the decrease in dry matter yields. Ozaslan et al. (2011) stated that there was an increase in the amount of sod-boinding by the increase in precipitation and that the same problem was encountered again 3-4 years after the year of establishment. The crude protein yields of smooth brome decreased in the research due to irrigation and the fact that it was the 3rd year of establishment.

Under non-irrigated conditions, it was found that there was a significant decrease only in the application of manure in the second year, but there was no significant decrease in other applications and accordingly the difference between the years was not significant (*Table 1*). In the first year, the highest crude protein yield was obtained from manure application with 0.31 t ha^{-1}. In the second year, values close to each other were obtained from all other applications except manure. Considering the two-year general average, the highest value was obtained from the application of poultry manure with 0.26 t ha^{-1}. Karakurt and Ekiz (2000) obtained the highest crude protein yield from 120 kg ha^{-1} of nitrogen application and this was followed by manure application with 3 t ha^{-1}. The difference between applications and years may be caused by the amount of precipitation of that year, and thus the fertilizer efficiencies (*Fig. 1*).

Irrigation improves the effectiveness of chemical fertilizers. The highest dry matter yield in smooth brome was obtained from ammonium sulphate application in both years under irrigated conditions. In organic fertilizers, values close to each other were obtained in manure and poultry manure and values close to the control value were obtained in green fertilizer. The highest dry matter yield was obtained from chemical fertilizer application with 4.93 t ha^{-1}. This application was followed by poultry manure application with 3.99 t ha^{-1}. The dry matter yield values obtained in 2003 decreased by half in 2004, the third year of the research (*Table 1*). The decrease in yield may be caused by the sod-boinding occurred in the smooth brome due to irrigation and the fact that the field was in its third year. The values we obtained in our research for the dry matter yield of smooth brome cultivated under irrigated conditions are consistent with the values obtained by Serin (1996b) and Tukel et al. (2001). Serin et al. (1998) reported that and that smooth brome yield decreased in the 2nd and 3rd years compared to the first year under irrigated conditions.

The highest dry matter yield of smooth brome cultivated under non-irrigated conditions was obtained from the manure in the first year of the research, from poultry manure and green fertilizer in the second year and from poultry manure in the two-year average. These results show that organic fertilizers have more effect on plant yields in arid and semi-arid conditions. According to the consolidated years average, the highest dry matter yield was obtained from the application of poultry manure with 2.03 t ha^{-1}. The lowest dry matter yield was obtained from control and chemical fertilizer applications.

http://www.aloki.hu ● ISSN 1589 1623 (Print) ● ISSN 1785 0037 (Online)
DOI: http://dx.doi.org/10.15666/aeer/1605_60876094
© 2018, ALÖKI Kft., Budapest, Hungary

Conclusion

According to the research results, it was determined that crude protein ratio, crude protein yield and dry matter yield were affected by different fertilizer applications under both irrigated and non-irrigated conditions. It was found that the efficiency of chemical fertilization was higher under irrigated conditions, but that the sod-boinding problem observed in smooth brome was higher due to the effect of irrigation. This situation significantly decreased the dry matter yields. It was determined that organic fertilizers were more efficient than chemical fertilizers under arid and semi-arid conditions. This result is of importance for producers carrying out conventional agriculture. Also, it is a known fact that the use of organic fertilizer is more profitable in the long term, despite the fact that there is a difference between chemical fertilization applications and organic fertilizers in irrigated agricultural lands.

Acknowledgements. This study was presented as a poster at the 10th National Field Crops Congress.

REFERENCES

[1] Albayrak, S., Ekiz, H. (2005): An investigation on the establishment of artificial pasture under Ankara's ecological conditions. – Turkish Journal of Agriculture and Forestry 29(1): 69-74.

[2] Albayrak, S., Türk, M., Yuksel, O., Yilmaz, M. (2011): Forage yield and the quality of perennial legume-grass mixtures under rainfed conditions. – Notulae Botanicae Horti Agrobotanici Cluj-Napoca 39(1): 114.

[3] Alçiçek A, Kılıç A, Ayhan V, Özdoğan, M. (2010): Forage Production and Problems in Turkey. – Turkey Agricultural Engineer VII. Technical Congress, 11-15 January 2010, Ankara.

[4] Bender, D., Erdal, İ., Dengiz, O., Gürbüz, M., Tarakçıoğlu, C. (1998): The Effects of Some Organic Materials on Some Physical Properties of a Clay Soil. International Symposium on Arid Region Soil. – International Agrohydrology Research and Training Center, Menemen, İzmir, pp. 506-510.

[5] Bulluck Iii, L. R., Brosius, M., Evanylo, G. K., Ristaino, J. B. (2002): Organic and synthetic fertility amendments influence soil microbial, physical and chemical properties on organic and conventional farms. – Applied Soil Ecology 19(2): 147-160.

[6] Çakmakçı, S., Aydınoğlu, B., Arslan, M., Özyiğit, Y., Tetik, M., Bilgen, M. (2004): Determination of optimum fall sowing date for some forage species in terms of forage yield of rangelands in the continental climate zones. – Mediterranean Agricultural Sciences 17(1): 43-47.

[7] Carpenter-Boggs, L., Kennedy, A. C., Reganold, J. P. (2000): Organic and biodynamic management effects on soil biology. – Soil Science Society of America Journal 64(5): 1651-1659.

[8] Emerenciano Neto, J. V., Pereira, G. F., Difante, G. D. S., Oliveira, L., Santos, W., Gurgel, M. (2016): Production and structure of massai grass pastures fertilized with animal manures. – Boletim de Indústria Animal 73(2): 111-117.

[9] Golijan, J., Popović, A., Dimitrijević, B., Kolarić, L., Živanović, L. (2017): The status of the forage organic production in the Republic of Serbia. – Agriculture & Forestry/Poljoprivreda i Sumarstvo 63(3): 177-187.

[10] Hongrong, Z. Z. F. H. Z., Xuerui, Z. X. L. (2000): Effect of Sludge Utilization on Smooth Brome Growth. – Acta Agrestia Sinica 2: 010.

http://www.aloki.hu ● ISSN 1589 1623 (Print) ● ISSN 1785 0037 (Online)
DOI: http://dx.doi.org/10.15666/aeer/1605_60876094
© 2018, ALÖKI Kft., Budapest, Hungary

[11] Karakurt, E., Ekiz, H. (2000): Effects of nitrogen fertilizer doses on important agronomic characters in some forage grasses. – Journal of Central Research Institute for Field Crops 9: 1-11.
[12] Karataş, N. (2004): The effect of some fertilizer application in smooth bromegrass (Bromus inermis Leyss.) to plant development under irrigated and nonirrigated conditions. – Master Thesis, University of Ankara Institute of Science.
[13] Marinari, S., Masciandaro, G., Ceccanti, B., Grego, S. (2000): Influence of organic and mineral fertilisers on soil biological and physical properties. – Bioresource Technology 72(1): 9-17.
[14] Martin, R.C., Harvey, H.D. ve Smith, D.L. (1990): Intercropping corn and soybean for silage in a cool temperate region; yield, protein and economic effects. - Field Crops Research, 23: 295-310.
[15] Moreno-Reséndez, A., Cantú Brito, J. E., Reyes-Carrillo, J. L., Contreras-Villarreal, V. (2017): Forage maize nutritional quality according to organic and inorganic fertilization. – Scientia Agropecuaria 8(2): 127-135.
[16] Nazlı, R. I., Kuşvuran, A., Inal, I., Demirbaş, A., Tansi, V. (2014): Effects of different organic materials on forage yield and quality of silage maize (Zea mays L.). – Turkish Journal of Agriculture and Forestry 38(1): 23-31.
[17] Özaslan Parlak, A., Ekiz, H. (2011): Effects of Pitting and Nitrogenous Fertilizer Aplications on Elemination of Sod-Boinding in Smooth brom grass (*Bromus inermis leyss*.). – 10th Turkey Field Crops Congress, 12-15 September 2011, Bursa.
[18] Razec, I., Razec, M., Noaghea, M., Ujupan, G. (2009): Forage productivity and soil fertility under organic fertilizer conditions on Agrostis capillaries pastures. – Scientific Papers Animal Science and Biotechnologies 42(1): 205-209.
[19] Serin, Y. (1996a): Research on the effects of different row space and fertilizers applied on smooth brome (Bromus inermis Leyss.) grown on erzurum dried conditions on hay and and crude protein ratio. – Turkey 3rd Meadow and Pasture Congress, 17-19 June, Erzurum.
[20] Serin, Y. (1996b): Research on the effects of different row space and fertilizers applied on smooth brome (Bromus inermis Leyss.) grown on erzurum irrigated conditions on hay and crude protein ratio. – Turkey 3rd Meadow and Pasture Congress, 17-19 June, Erzurum.
[21] Serin, Y., Gökkuş, A., Tan, M., Koç, A., Çomaklı, B. (1998): Determination of suitable forage crop species and their mixtures for meadow establishment. – Turkish Journal of Agriculture and Forestry 22(1): 13-20.
[22] Shiralipour, A., McConnell, D. B., Smith, W. H. (1992): Physical and chemical properties of soils as affected by municipal solid waste compost application. – Biomass and Bioenergy 3(3-4): 261-266.
[23] Sönmez, İ., Kaplan, M., Sönmez, S. (2008): Effect of chemical fertilizers on environmental pollution and its prevention methods. – Batı Akdeniz Agricultural Research Institute DERİM Journal 25(2): 24-34.
[24] Tükel, T., Hatipoglu, R., Polat, T., Can, E., Yılmaz, Ş., Çeliktaş, N., Kökten, K. (2001): Research on the Forage Yields of Some Perennial, Grasses and Legumes Under Irrigated Conditions of Çukurova and Southesthern Regions. – GAP II. Agricultural Congress, 24-26 October, Şanlıurfa.
[25] Will, J. (2012): Organic Forage: A Strategy for Planning Future Cropping. – https://businesswales.gov.wales (accessed March 21, 2017).
[26] Yolcu, H. (2011): The effects of some organic and chemical fertilizer applications on yield, morphology, quality and mineral content of common vetch (Vicia sativa L.). – Turkish Journal of Field Crops 16(2): 197-202.
[27] Yolcu, H., Okçu, M., Tan, M. (2014): Current situation of organic roughage production in Turkey. – Yuzuncu Yıl University Journal of Agricultural Science 24(2): 201-209.

http://www.aloki.hu ● ISSN 1589 1623 (Print) ● ISSN 1785 0037 (Online)
DOI: http://dx.doi.org/10.15666/aeer/1605_60876094
© 2018, ALÖKI Kft., Budapest, Hungary

THE PERFORMANCE AND EXTRACELLULAR POLYMERIC SUBSTANCES VARIATIONS OF AN ANAEROBIC-ANOXIC-OXIC WASTEWATER TREATMENT PROCESS SUBJECTED TO ORGANIC CARBON AND AMMONIA NITROGEN SHOCK LOADINGS

ZHANG, L. H.[1*] – ZHANG, M. S.[1] – GUO, J. B.[2] – CHEN, Z. C.[1] – LING, L. X.[1]

[1]*School of Chemical Engineering, Northeast Electric Power University, 132012 Jilin, China (phone/fax: +86-432-6480-6371)*

[2]*School of Civil and Architecture Engineering, Northeast Electric Power University 132012 Jilin, China (phone/fax: +86-432-6480-6371)*

**Corresponding author e-mail: zhanglanhe@163.com*

(Received 29th Jun 2018; accepted 22nd Aug 2018)

Abstract. Sudden changes in influent organic carbon (OC) and ammonia nitrogen (AN) concentrations were performed to evaluate the resistance of A^2O process against shock loadings. The influent organic loading rate was increased from 11 gCOD/(gMLSS·d) to 48 gCOD/(gMLSS·d) with low OC shocking loading and to 125 g COD/(gMLSS·d) with high OC shock loading. The influent NH_4^+-N was increased from 55 mg/L to 110 mg/L as AN shock loading. The results showed that the augmented OC concentration was beneficial for nitrogen removal and high AN concentration had slight influences on COD removal, but was detrimental to nitrogen removal in the A^2O system. The performance of the A^2O system restored rapidly from the shock loadings once the normal influent conditions were provided. The loosely bound extracellular polymeric substances (LB-EPS) and total extracellular polymeric substances (EPS) increased at the initial stage of shock loadings and then declined with the prolonged shock loading, whereas the tightly bound EPS (TB-EPS) experienced smaller variations. The SVI value varied in a similar trend with LB-EPS and total EPS and their low values indicated a good settleability of the activated sludge. In conclusion, the A^2O process produced high-quality effluents once the shock loading ceased.

Keywords: *activated sludge, denitrification rate, nitrification rate, flocculation, settleability, dissolved oxygen*

Abbreviations: A^2O: Anaerobic-anoxic-oxic, OLR: Organic loading rate, EPS: Extracellular polymeric substances, LB-EPS: Loosely bound EPS, TB-EPS: Tightly bound EPS, DO: Dissolved oxygen, ORP: Oxidation-reduction potential, COD: Chemical oxygen demand, BOD: Biochemical oxygen demand, MLSS: Mixed liquid suspended solids, NH_4^+-N: Ammonia-nitrogen, NO_2^--N: Nitrite nitrogen, NO_3^--N: Nitrate nitrogen, TN: Total nitrogen, HRT: Hydraulic retention time, SVI: Sludge volume index

Introduction

Excessive nitrogen inflow from industrial and municipal wastewater is strictly controlled due to severe eutrophication and environmental pollution (Chang et al., 2006; Yang et al., 2008; Chen et al., 2011). A variety of nitrogen removal processes had been developed and extensive researches have been conducted on the nitrogen removal mechanisms. Over the past several decades, biological nitrification-denitrification processes have been widely applied for their cost-effective and eco-friendly features compared with chemical treatment methods (Guo et al., 2005; Bassin et al., 2012; Seifi

http://www.aloki.hu ● ISSN 1589 1623 (Print) ● ISSN 1785 0037 (Online)
DOI: http://dx.doi.org/10.15666/aeer/1605_60956112
© 2018, ALÖKI Kft., Budapest, Hungary

and Fazaelipoor, 2012; Tanabene et al., 2018). The biological nitrogen removal processes developed include the five-stage Bardenpho process, the University of Cape Town (UCT) process, the sequencing batch reactor (SBR) and the anaerobic–anoxic–oxic (A^2O) process, etc. (Peng et al., 2006; Chen et al., 2011). Based on these biological processes, strategies for realizing short-cut nitrification denitrification, anaerobic ammonium oxidation (ANAMMOX) and simultaneous nitrification and denitrification (SND) were widely investigated in order to lower the construction investment and energy requirements (Zhang et al., 2008; Walters et al., 2009; Park et al., 2010; Yong et al., 2017). The most commonly used process was the anaerobic-anoxic-oxic process (A^2O process) due to its convenient operation and management and high biological nitrogen removal efficiency (Pai et al., 2010). The A^2O process is a sludge suspended growth system incorporating separate anaerobic, anoxic and aerobic stages in sequence to satisfy the requirement of oxygen in the nitrification and the absence of oxygen in the denitrification. Under aerobic stages, NH_4^+-N was oxidized, first to NO_2^--N and then, to NO_3^--N. Furthermore, the residual NO_2^--N and NO_3^--N in the reflux were then denitrified to gaseous nitrogen compounds under the anaerobic and anoxic conditions.

The nitrogen removal performances of the A^2O process under various environmental conditions were widely investigated in the previous literature. Ma et al. (2006) indicated that the nitrogen removal efficiency increased when the dissolved oxygen (DO) concentration in the aerobic stage rose from 2 mg/L to 3 mg/L, and almost no improvement was observed when the DO was further enhanced to 4 mg/L. The reflux ratio of the mixed liquid and carbon source type could also influence the performance of A^2O process (Xu et al., 2009; Zhu et al., 2014). However, a very limited number of investigations were reported in terms of the performances of the A^2O process under shock loadings. The sudden changes of influent constituents or shock loading could eventually destabilize the performance of the biological treatment system (Wang et al., 2006). As the biological systems were frequently under shock loadings as a result of wastewater quantity and quality fluctuations, it is necessary to understand the performance of the A^2O process under shock loadings.

In the biological wastewater treatment reactors, the bio-flocculated microbial aggregates, known as activated sludge flocs, are the essential components of the process. It is, therefore, an undisputed fact that the physicochemical characteristics of activated sludge flocs play an important role in the performance of the process (Ye et al., 2011). Indeed, almost all the performances of the activated sludge process are related to or dependent on the physicochemical properties of the flocs, including flocculation, sludge settling and sludge dewatering. Extracellular polymeric substances (EPS) are one of the representative components of the flocs and are considered to have significant influences on the physicochemical properties of microbial aggregates, including structure, surface charge, flocculation, settling properties, dewatering properties, and adsorption ability (Sheng et al., 2008; Shou et al., 2018). They came from molecules in wastewater or from cell lyses, which consisted of various organic substances mainly including polysaccharides, proteins, and nucleic acid, etc. (Li et al., 2008). EPS in sludge flocs could be stratified into loosely bound EPS (LB–EPS) and tightly bound EPS (TB–EPS) based on the extraction methodology (Zhang and Wang, 2014). LB-EPS could diffuse into mixed liquid and had a loose structure at the outer layer of EPS. However, TB-EPS had a stable structure between LB-EPS and cell. And TB-EPS could be tightly combined with the cell surface and stick to the cell wall (Sheng et al., 2008). EPS are involved in the formation of microbial aggregates and are

http://www.aloki.hu ● ISSN 1589 1623 (Print) ● ISSN 1785 0037 (Online)
DOI: http://dx.doi.org/10.15666/aeer/1605_60956112
© 2018, ALÖKI Kft., Budapest, Hungary

closely connected to their mass transfer, surface charge, adhesion ability, flocculation ability, settleability and stability (Sheng et al., 2010). The nature and content of EPS are sensitive to the operational and environmental conditions (Ye et al., 2011). However, few data were available concerning the effects of the organic loading rate (OLR) on the EPS. The resistant ability to shock loading and nitrogen removal properties can be comprehensively understood when the characterization of EPS was comprehended under different OLRs in the activated sludge of the A^2O process.

The shock loadings were carried out by varying the influent sodium acetate as the carbon source and the influent ammonia chloride as the nitrogen source in synthetic municipal wastewater of the A^2O process. The carbon and nitrogen removal efficiency were evaluated under organic carbon (OC) and ammonia nitrogen (AN) shock loadings. Meanwhile, the variations of EPS and sludge volume index (SVI) were also investigated under various levels of OC and AN shock loadings. The objective of this study is to investigate the ability of the A^2O process to withstand the shock loadings that were applied to the reactors and to evaluate the corresponding characteristics of the activated sludge represented by EPS amount and SVI value. The results obtained in this study could provide guidance for the operation of the A^2O process encountering shock loadings; for example, whether the system could survive the shock loadings without additional installations or measures should be performed to alleviate the passive influences of the shock loadings.

Materials and methods

Operation of the reactor

A bench-scale anaerobic-anoxic-oxic (A^2O) reactor with a working volume of 60 L was used in this study (*Fig. 1*) and it was constructed refer to the reference (Zeng et al., 2010; Li et al., 2014; Zhang et al., 2017). A^2O reactor was operated from April 2016 to November 2017 in the waste treatment lab of Northeast Electric Power University, Jilin, China. There were eight zones in the reactor, separated by baffles to achieve anaerobic/anoxic and aerobic conditions. The first two zones were typically operated as anaerobic reactors, and the following two zones as anoxic reactors, while the remaining four as aerobic zones with separate aeration facilities. The raw wastewater and the recycled sludge flowed into the first zone of the anaerobic reactor and the mixed nitrate liquid was recycled from the last zone of the aerobic reactor to the first zone of the anoxic reactor. The flow rates of the influent, recycled sludge and nitrate recirculation were controlled together by peristaltic pump and regulating valve and the regulating valve was located at the outlet of the influent water tank. Internal recycle was the recycle of nitrification liquid to anoxic stage and external recycle was the recycle of sludge to anaerobic stage.

Recycle ratios of internal recycle and external recycle were 100% and 80%, respectively, with an influent flow rate of 43.44 L/d. Stirrers provided the mixture of sludge in the anaerobic and anoxic zones and kept the biomass in suspension. Aeration was provided in each aerobic zone when the pressurized air passed through long stone diffusers. The diffusers used in the lab-scale A^2O system were stone material with micro pores that could transfer the compressed air into the mixed liquid. The treated wastewater was settled in a vertical sedimentation basin with a total volume of 5 L. The design and operational parameters of the A^2O configuration are listed in *Table 1*.

http://www.aloki.hu ● ISSN 1589 1623 (Print) ● ISSN 1785 0037 (Online)
DOI: http://dx.doi.org/10.15666/aeer/1605_60956112
© 2018, ALÖKI Kft., Budapest, Hungary

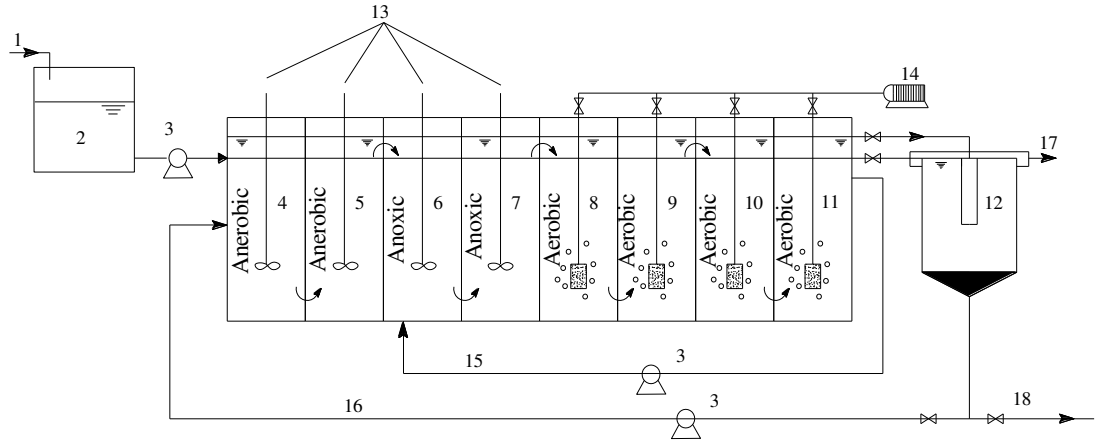

Figure 1. *Schematic diagram of the A^2O process. 1-Feed; 2-Tank; 3-Peristaltic pump; 4-Anerobic 1; 5-Anerobic 2; 6-Anoxic 1; 7-Anoxic 2; 8-Aerobic 1; 9-Aerobic 2; 10-Aerobic 3; 11-Aerobic 4; 12-Settling tank; 13-Stirrer; 14-Air compressor; 15-Internal recycle; 16-Sludge recycle; 17-Effluent; 18-Excess sludge*

Table 1. *The design and operational parameters of A^2O reactor*

Design parameters			
Stage	**Number**	**Volume (L)**	**HRT (h)**
Anaerobic zone	2	15	4.34
Anoxic zone	2	15	4.34
Aerobic zone	4	30	8.70
Total	8	60	17.38
Settler	1	5	2.48
Operational parameters			
$Q_{Influent}$ (L/d)		43.44	
Internal recycling ratio (%)		80	
External recycling ratio (%)		100	
DO (mg/L)	Anoxic reactor	≤1	
	Oxic reactor	5–7	
ORP in the anaerobic reactor		≤–100 mv	
T (°C)		15±2	
pH		7.0–8.0	
MLSS (mg/L)		1500±200	

During the start-up period, the system was operated and fed with the synthetic wastewater with chemical oxygen demand (COD) of approximately 400 mg/L and NH_4^+-N of approximately 55 mg/L. Samples were collected regularly from the influent and different zones of the reactor in order to analyze NH_4^+-N, NO_2^--N, NO_3^--N, total nitrogen (TN), COD and mixed liquid suspended solids (MLSS), respectively. Temperature, DO, ORP and pH were measured online. After two-month operation, the removal efficiency of COD, NH_4^+-N and TN were respectively higher than 95%, 95% and 85%, which could indicate the successful start-up of the A^2O system and

http://www.aloki.hu ● ISSN 1589 1623 (Print) ● ISSN 1785 0037 (Online)
DOI: http://dx.doi.org/10.15666/aeer/1605_60956112
© 2018, ALÖKI Kft., Budapest, Hungary

achievement of the steady-state as the effluent water quality meet the Level I (B) criteria of the Discharge Standard of Pollutants for Municipal Wastewater Treatment Plant (GB18918-2002) of China. COD, NH_4^+-N and TN were lower than 60 mg/L, 15 mg/L and 20 mg/L, respectively, in the Discharge Standard of Pollutants for Municipal Wastewater Treatment Plant (GB18918-2002). And then the operation of the A^2O process was divided into four different phases to investigate the influences of the OC and AN shock loadings on the performance of the system and the variations of the EPS and SVI. The arrangement of the organic and nitrogen shock loading experiment was illustrated in *Table 2*.

Table 2. *The arrangement of the shock loading experiments*

Operation	Influent conditions	Days
Phase I (Normal operation)	Organic loading rate of 11 gCOD/(gMLSS·d); NH_4^+-N concentration of 55 mg/L	0–60
Phase II (Low OC shock loading)	Organic loading rate increased from 11 gCOD/(gMLSS·d) (3 days) to 48 gCOD/(gMLSS·d) (7 days) and then recovered to 11 gCOD/(gMLSS·d) influent (5 days); NH_4^+-N concentration of 55 mg/L	61–75
Phase III (High OC shock loading)	Organic loading rate increased from 11 gCOD/(gMLSS·d) (3 days) to 125 gCOD/(gMLSS·d) (7 days) and then recovered to 11 gCOD/(gMLSS·d) (5 days); NH_4^+-N concentration of 55 mg/L	76–90
Phase IV (High AN shock loading)	Organic loading rate is 11 gCOD/(gMLSS·d); NH_4^+-N concentration increased from 55 mg/L to 110 mg/L (10 days) and then recovered to 55 mg/L (10 days)	91–110

Synthetic wastewater and sludge

The bench-scale A^2O reactor was fed with synthetic wastewater when sodium acetate was used as carbon source. The synthetic wastewater was prepared as follows (per liter): CH_3COONa, 0.48–4.8 g; NH_4Cl, 0.2±0.02 g; K_2HPO_4, 0.03 g; $MgSO_4 \cdot 7H_2O$, 0.05 g; $CaCl_2 \cdot 2H_2O$, 0.01 g. The pH was controlled at 7.0–8.0 by adding $NaHCO_3$ and HCl solution. Excess sludge, which collected from the secondary settling tank of a municipal wastewater plant located in Jilin, China, was used as inoculum. The major influent characteristics are shown in *Table 3*.

Table 3. *The major characteristics of the influent*

Parameters (mg/L)	Min/Max
COD	360–4300
NH_4^+-N	55–110
NO_2^--N	0-2
NO_3^--N	0
TN	53–59

http://www.aloki.hu ● ISSN 1589 1623 (Print) ● ISSN 1785 0037 (Online)
DOI: http://dx.doi.org/10.15666/aeer/1605_60956112
© 2018, ALÖKI Kft., Budapest, Hungary

Analytical methods

COD, BOD, MLSS, NH_4^+-N, NO_2^--N, NO_3^--N and TN were measured according to the Standard Methods for the Examination of Water and Wastewater (APHA, 1998). Temperature, pH, ORP and DO were analyzed online with a WTW pH/ORP sensor (WTW, pH 3310) and a DO sensor (WTW, OXi340i). 50 mL of activated sludge collected from Aerobic 4 of the A^2O reactor was used to analyze the EPS amount. The extraction and quantification of LB-EPS and TB-EPS were performed according to the protocol described by Liang et al. (2010).

Results

The influences of OC shock loading on COD removal performance

Unexpected industrial wastewater was often discharged into the sewage and resulted in the high COD surge of the municipal wastewater treatment plant. In addition, the biological wastewater system often experienced higher pollutants surge when there was an equipment failure. In order to investigate the effects of high COD surge on the performance of the municipal wastewater treatment plant, high OLRs of 48 gCOD/(gMLSS·d) and 125 gCOD/(gMLSS·d) were applied.

The COD removal performances under OC shock loading were shown in *Figure 2*. The effluent COD was below 60 mg/L and more than 95% of COD was removed in the first 3 days when the influent OLR was elevated from 11 gCOD/(gMLSS·d) to 48 gCOD/(gMLSS·d). The effluent COD was higher than 100 mg/L when the low OC shock loading continued. An average of 95% COD removal efficiency was achieved though the effluent COD concentration was higher than 100 mg/L, which indicated that the A^2O system could remove more organic carbon at higher OLR. When the influent OLR returned to 11 gCOD/(gMLSS·d) on the 71th day, the effluent COD concentration was stable and below 30 mg/L. It is suggested that the A^2O process had strong resistant ability to low organic shock loading and the system could restore rapidly when the organic shock loading stopped.

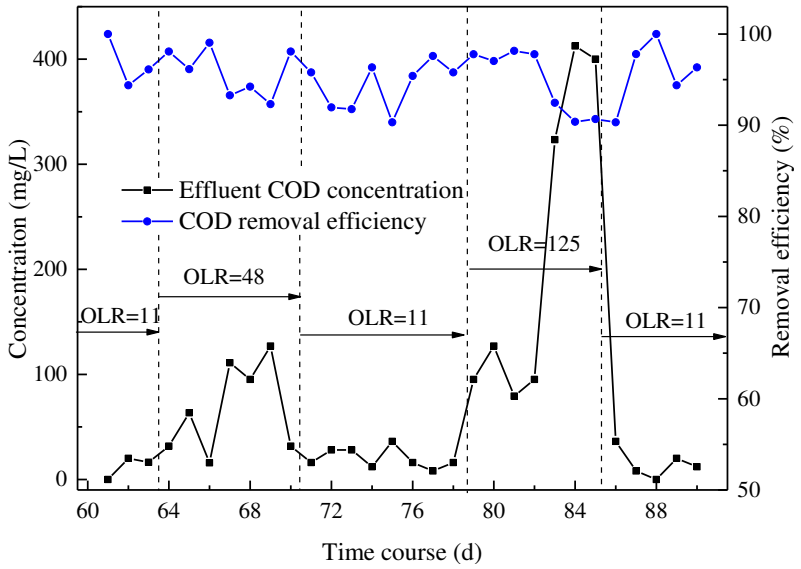

Figure 2. *The COD removal under OC shock loadings*

http://www.aloki.hu ● ISSN 1589 1623 (Print) ● ISSN 1785 0037 (Online)
DOI: http://dx.doi.org/10.15666/aeer/1605_60956112
© 2018, ALÖKI Kft., Budapest, Hungary

The effluent COD concentration was greater than 100 mg/L and then increased to more than 500 mg/L when there was a sudden increase of OLR from 11 gCOD/(gMLSS·d) to 125 gCOD/(gMLSS·d). However, when the influent OLR declined to 11 gCOD/(gMLSS·d), the effluent COD concentration dropped rapidly and restored to the original level, which demonstrated that the A^2O system could remove high loads of carbon and recover low carbon concentration in the effluent after high shock loading.

The influences of OC shock loading on nitrogen removal performance

The nitrogen removal performances of the A^2O process under organic shock loading were plotted in *Figure 3*. As the influent OLR increased sharply from 11 gCOD/(gMLSS·d) to 48 gCOD/(gMLSS·d), negligible variations of the NH_4^+-N removal efficiency and the effluent NH_4^+-N concentration were detected and their average values were 96.57% and 1.93 mg/L, respectively. Satisfactory TN removal was also achieved when the influent OLR increased. And meanwhile, NO_3^--N concentration in the effluent reduced compared with that under normal OC feeding condition. The effluent NO_3^- was between 14.50 mg/L and 15.45 mg/L and the average value was 14.86 mg/L under normal OC feeding condition, however, the effluent NO_3^--N was between 11.13 mg/L and 13.15 mg/L and the average value was 12.19 mg/L when influent OLR increased. In the aerobic zones, NH_4^+-N was converted into NO_3^--N by nitrifiers with the presence of DO. Nitrifiers are autotrophic microorganisms and efficient nitrogen removal could be achieved if there is enough hydraulic retention time and sufficient DO. The total nitrogen (TN) removal efficiency was up to 91% with an effluent TN concentration of 4.6 mg/L, which was improved when the A^2O system encountered low organic shock loading. The TN removal efficiency declined with an effluent concentration of 10 mg/L when the influent OLR was recovered from 48 gCOD/(gMLSS·d) to 11 gCOD/(gMLSS·d). Since variations of effluent NH_4^+-N and the corresponding NH_4^+-N removal efficiency under low organic carbon surge were small under low organic carbon surge when compared with that of the TN, the improved TN removal efficiency was thus attributed to the instantaneous improvement of denitrification rate when the system encountered OC surges.

During the high OC shock loading, the NH_4^+-N concentration in effluent ranged from 1.68 mg/L to 3.87 mg/L with an average value of 2.53 mg/L, which was comparable to that before shock loading. The removal efficiencies of TN exceeded 85% with an average effluent TN concentration of 10.5 mg/L. The removal efficiencies of TN decreased when the OLR returned from high value to low value because of the absence of carbon sources.

Nitrification and denitrification rate were two key indexes for the evaluation of the nitrogen removal efficiency. The variation of NH_4^+-N concentration between influent and effluent was used to calculate the nitrification rate (Mino et al., 1995; Li and Irvin, 2007). The equation was as follows (*Eq. 1*):

$$r_N = \frac{dc_{NH_4^+-N}}{dt}\left(\frac{mg \cdot N}{L.h}\right) \quad \text{(Eq.1)}$$

http://www.aloki.hu ● ISSN 1589 1623 (Print) ● ISSN 1785 0037 (Online)
DOI: http://dx.doi.org/10.15666/aeer/1605_60956112
© 2018, ALÖKI Kft., Budapest, Hungary

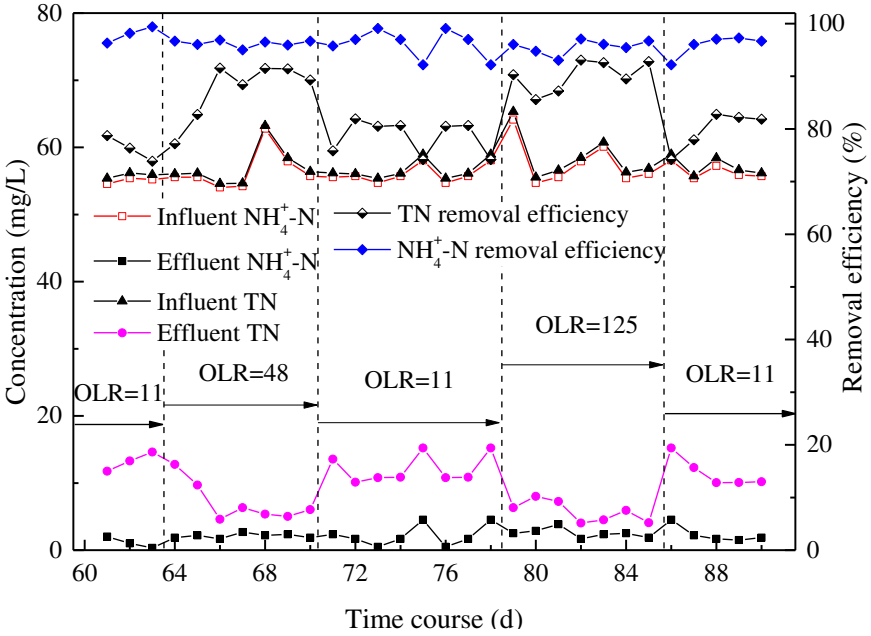

Figure 3. *Nitrogen removal under OC shock loadings*

The variations of nitrification rate under different OLR were shown in *Figure 4*. Initially, the nitrification rate showed an arising trend when the OLR of influent increased from 11 gCOD/(gMLSS·d) to 48 gCOD/(gMLSS·d) and then declined as the shock loading continued. The figure increased to the original level at the end of the shock loading. The nitrification rate increased from 1.20 mg/(L·h) to 1.26 mg/(L·h) and then slightly reduced to 1.25 mg/(L·h) when the A^2O system was subjected to a OLR of 125 gCOD/(gMLSS·d). The variation of the nitrification rate was small when the A^2O system suffered high OLR.

Two steps are involved in the denitrification process, of which NO_3^--N is reduced to NO_2^--N and then NO_2^--N is further reduced to N_2. The difference between the sum of influent NH_4^+-N, NO_2^--N and NO_3^--N in the anoxic zones and the sum of effluent NH_4^+-N, NO_2^--N and NO_3^--N was utilized to calculate the denitrification rate (Liu et al., 2014; Shen et al., 2016). The calculation equation was as follows (*Eq. 2*):

$$r_N = \frac{d(c_{NH_4^+-N} + c_{NO_2^--N} + c_{NO_3^--N})}{dt}(\frac{mg \cdot N}{L.h}) \quad \text{(Eq.2)}$$

As shown in *Figure 4*, the denitrification rate was improved with the increase of influent COD concentration. The denitrification rate increased from 1.17 mg·N/(L·h) to 2.11 mg·N/(L·h) when the influent OLR ascended from 11 gCOD/(gMLSS·d) to 125 gCOD/(gMLSS·d). Consequently, OLR increases were beneficial for the denitrification process by providing sufficient carbon source.

The influences of AN shock loading on the COD removal performance

As shown in *Figure 5*, the effluent COD concentration was below 30 mg/L and the corresponding removal efficiency was greater than 95% when high influent AN concentration (110 mg/L) was provided. The COD removal performance of the A^2O

http://www.aloki.hu ● ISSN 1589 1623 (Print) ● ISSN 1785 0037 (Online)
DOI: http://dx.doi.org/10.15666/aeer/1605_60956112
© 2018, ALÖKI Kft., Budapest, Hungary

system was not influenced by the increase of influent NH_4^+-N concentration as sufficient HRT was provided and the influent OLR was 11 gCOD/(gMLSS·d). It is indicated that in the biological system, the removal of organic pollutants was started ahead of the nitrification process as the nitrification reaction was slower and more sensitive to environmental conditions than carbon oxidation by heterotrophs in the biological system (Liang et al., 2010). Hence, the influence of NH_4^+-N concentration variation on the COD removal of the A^2O process was very small and could be neglected under the condition of a relative high AN concentration in the A^2O process.

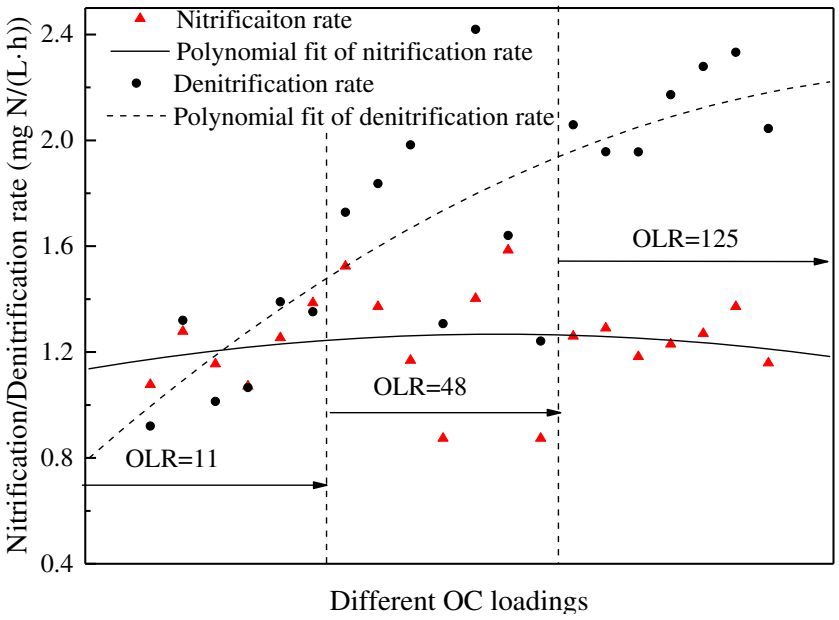

Figure 4. *Variations of nitrification and denitrification rate under OC shock loadings*

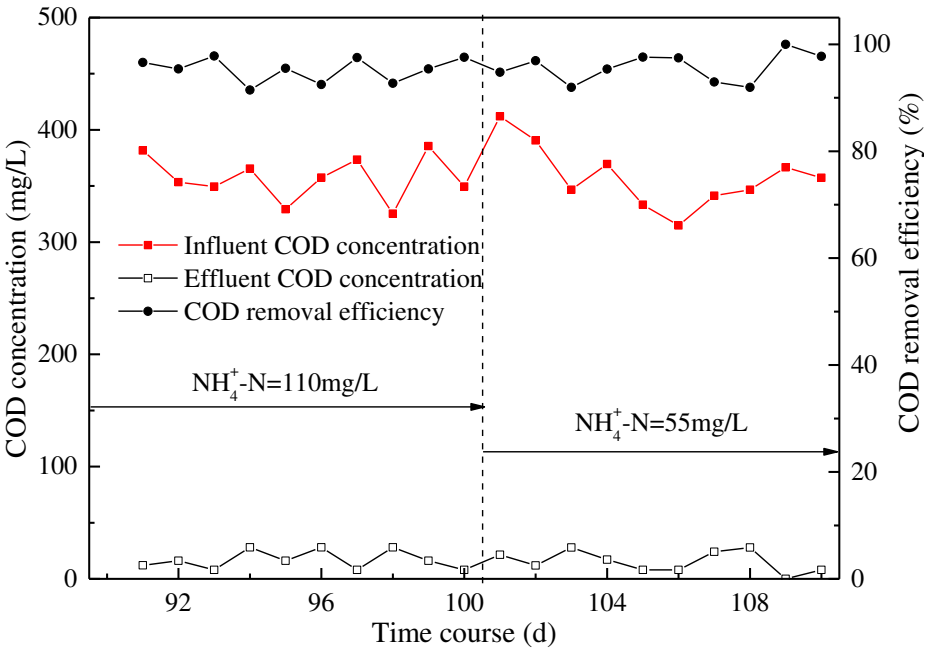

Figure 5. *COD removal performance under AN shock loading*

http://www.aloki.hu ● ISSN 1589 1623 (Print) ● ISSN 1785 0037 (Online)
DOI: http://dx.doi.org/10.15666/aeer/1605_60956112
© 2018, ALÖKI Kft., Budapest, Hungary

The influences of AN shock loading on the nitrogen removal performance

As shown in *Figure 6*, the nitrogen removal efficiency of the A^2O process under high influent NH_4^+-N concentration (110 mg/L) was evaluated by the removal performance of NH_4^+-N and TN. The effluent NH_4^+-N concentration was below 5 mg/L with a removal efficiency of 95% on the first day. The effluent NH_4^+-N concentration began to increase along with the duration of the AN shock loading and was higher than 60 mg/L at the end of the AN shock loading. It was assumed that at the initial stage of the AN surge, high NH_4^+-N concentration was buffered by the remaining reactor contents within the range that the nitrifiers could effectively convert NH_4^+-N to NO_2^--N and NO_3^--N. Gradually, the effluent NH_4^+-N concentration increased as the continuous feed of excessive NH_4^+-N exceeded the nitrifying ability of the microorganisms in the A^2O process. The effluent NH_4^+-N concentration declined to 29 mg/L when the AN shock loading ceased. Then the effluent NH_4^+-N concentration gradually returned to the original level before the occurrence of AN shock loading.

The removal performance of TN was similar to that of NH_4^+-N. The effluent TN was 8 mg/L and 90% removal efficiency was obtained on the first day of the AN shock loading. The effluent TN concentration increased to more than 70 mg/L at the end of the AN shock loading possibly due to the accumulation of nitrite and nitrate.

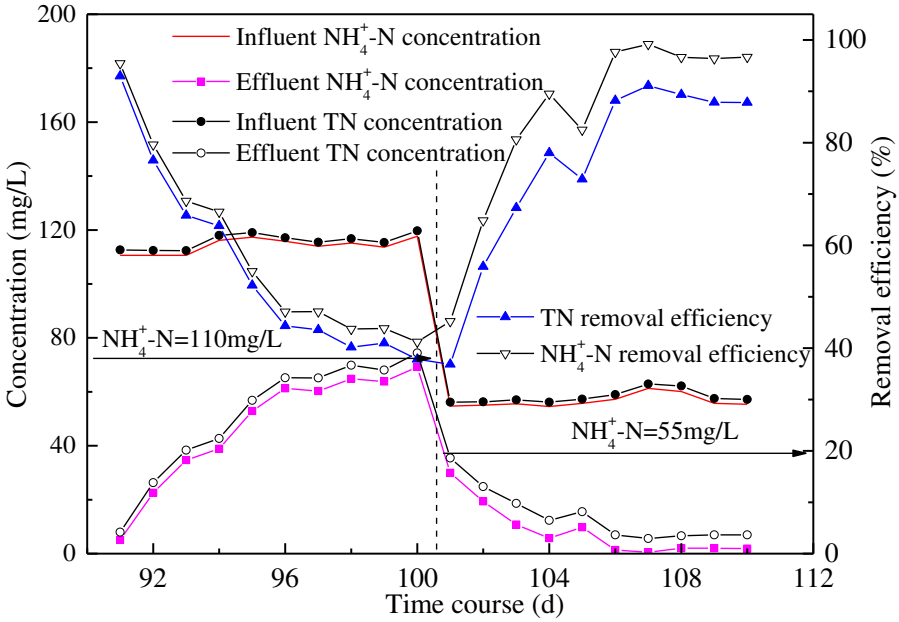

Figure 6. *Nitrogen removal performance under AN shock loading*

As shown in *Figure 7*, the nitrification rate ranged from 1.36 mg·N/(L·h) to 0.58 mg·N/(L·h) under the AN shock loading, whereas the denitrification rate varied in a range between 0.57 mg·N/(L·h) and 2.46 mg·N/(L·h). It was demonstrated that high nitrogen-loading rate can provoke the inhibition of nitrification and consequently the BNR instability (Jubany et al., 2008; Torà et al., 2011). In the present study, the variation of the denitrification rate were more remarkable than that of the nitrification rate, indicating that the AN shock loading interference with the nitrification process and the denitrification process was further influenced as the former provided the reaction source for the latter.

http://www.aloki.hu ● ISSN 1589 1623 (Print) ● ISSN 1785 0037 (Online)
DOI: http://dx.doi.org/10.15666/aeer/1605_60956112
© 2018, ALÖKI Kft., Budapest, Hungary

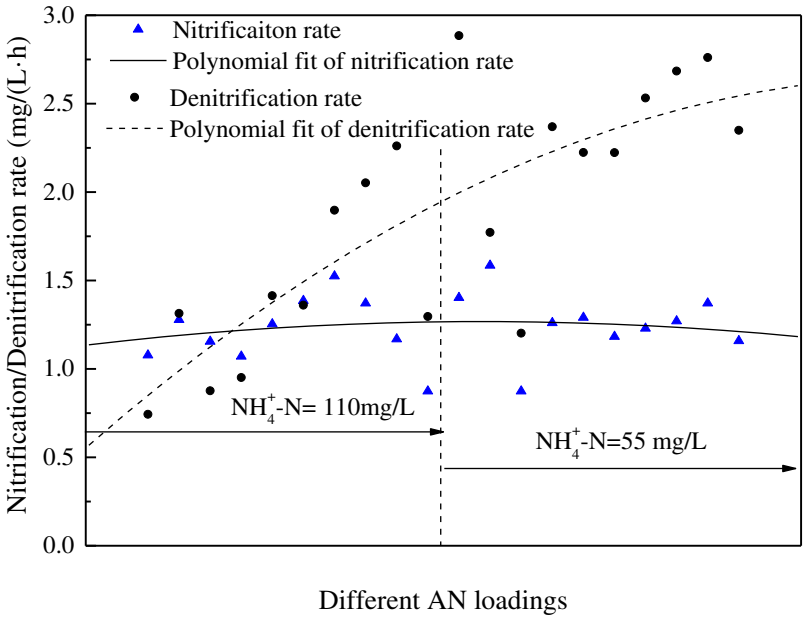

Figure 7. *Variations of nitrification and denitrification rate under AN shock loadings*

The influences of shock loading on EPS amount and SVI value

The daily variations of LB-EPS, TB-EPS, the total EPS amounts and effluent COD were observed during OC and AN surges in the discharged mixed liquid from the last aerobic zone (shown in *Fig. 8*). The average values of different types of EPS, VSS (Volatile Suspended Solids) and SVI were summarized in *Table 4*.

Table 4. *EPS amounts and SVI values during different shock loadings*

Experiment	LB (mg/L)	TB (mg/L)	EPS (mg/L)	SVI (mL/g)	VSS (mg/L)	Effluent appearance
Phase I	161.8	252.1	413.9	100	1210	Clean
Phase II	99.4	297.9	397.3	87	1176	Clean
Phase III	194.5	278.7	473.2	200	1290	Turbid
Phase IV	83.4	231.0	314.5	80	1105	Clean

During the low OC shock loading, the LB-EPS amount showed a dramatic reduction and then stabilized at approximately 60 mg/L, whereas the variations of TB-EPS amount fluctuated at a range of 265.1–343.2 mg/L with an average value of 297.9 mg/L. The amount of total EPS increased in the first 3 days and then dropped in the following days. Meanwhile, the effluent COD increased when there was an influent OC shock loading at the initial stage and then decreased with prolonged shock loading, which might be due to the acclimation of microorganisms to shock loadings. VSS was decreased from 1201 mg/L to 1176 mg/L, and furthermore, the sludge volume index (SVI) descended from 100 mL/g to 87 mL/g and the effluent quality was affected as indicated by the variations of effluent NH_4^+-N, TN and COD concentrations. Gentle variations of the LB-EPS amount were observed when the influent OLR increased sharply from 11 gCOD/(gMLSS·d) to 125 gCOD/(gMLSS·d). The TB-EPS amount

http://www.aloki.hu ● ISSN 1589 1623 (Print) ● ISSN 1785 0037 (Online)
DOI: http://dx.doi.org/10.15666/aeer/1605_60956112
© 2018, ALÖKI Kft., Budapest, Hungary

increased to an average value of 297.9 mg/L and then became constant with the proceeding of high OC shock loading. The total EPS amount and VSS were up to 473.2 mg/L and 1290 mg/L, respectively, which were much higher than situation without shock loading. An average SVI value of 200 mL/g was obtained when the A^2O system suffered high OC shock loading. During AN shock loading, the LB-EPS amount increased to 167.2 mg/L and then showed a sharp reduction from the 3rd day. The TB-EPS and LB-EPS amounts showed a similar trend. The average SVI value and VSS were 80 mL/g and 1105 mg/L, respectively, and the effluent had a clean appearance.

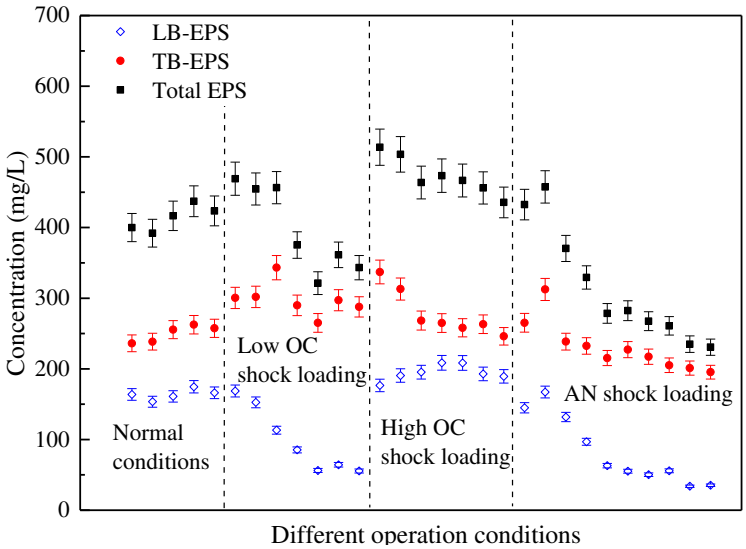

Figure 8. *Variations of LB-EPS, TB-EPS and the total EPS amounts*

It is indicated that low OC shock loading could lead to the temporary increase of the EPS amount, whereas the LB-EPS amount and VSS declined when the low OC shock loading continued. When the A^2O process was subjected to high OC shock loading, the amount of LB-EPS and VSS showed a milder variation compared with TB-EPS. The total EPS amount and VSS during high OC shock loading were the highest among all operational conditions. All types of EPS amount and VSS declined in the long-term operation when the A^2O process experienced the AN shock loading.

In this work, the SVI values were in good agreement with the LB-EPS (or total EPS) concentration and VSS. It is indicated that the LB-EPS had a negative effect on sludge flocculation and excessive EPS in the form of LB-EPS could weaken cell attachment and result in poor flocculation (Xu et al., 2016). Along with the increase of LB-EPS concentration and VSS, the presence of a large number of fine flocs significantly reduced the effluent quality and the activated sludge settleability. Zhang and Yang (2015) also found that LB-EPS had a negative effect on the sludge settleability as an increase in LB-EPS content might bring more bound water into the aggregates, and therefore produced highly porous flocs with a low density.

Discussion

As a widely applied biological wastewater treatment process, the A^2O process was resistant to all the shock loadings and produced high quality effluents once the shock

http://www.aloki.hu ● ISSN 1589 1623 (Print) ● ISSN 1785 0037 (Online)
DOI: http://dx.doi.org/10.15666/aeer/1605_60956112
© 2018, ALÖKI Kft., Budapest, Hungary

loading ceased. However, the effluent deteriorated when the system was subjected to high-strength or prolonged shock loadings. The use of real-time control systems were thus proposed to optimize processes under various effluent and environmental conditions (Li et al., 2016). The A^2O system was capable of removing more organic carbon at higher OLR and the elevated carbon source supply was beneficial for the removal of nitrogen compounds.

The heterotrophic microorganisms showed fast proliferation and became dominant in the anaerobic zones owing to the sufficient organic compounds in the influent. In the anoxic zones, heterotrophic facultative denitrifying bacteria could utilize the NO_x^--N as the electron acceptor and the denitrification rate was higher under a relative high influent OC. In the aerobic zones, the growth of heterotrophic microorganisms was restricted due to the low organic compounds from the anoxic zones and nitrifying bacteria became the dominant bacteria under sufficient DO. The COD in aerobic and anoxic zones was lower than 50 mg/L when the influent COD was 414 mg/L. The difference between effluent COD in aerobic zone and effluent COD in anoxic zone was slight. Therefore, a large portion of the organic substrate was consumed in the anaerobic and anoxic reactors of the A^2O process. Low concentration of organic compounds could not meet the demand of the growth of heterotrophic microorganisms in the aerobic zones. Previous literature indicated that the increase of COD concentration would induce the competition of the heterotrophic microorganisms and the nitrifiers for DO, nutrients, space or other ecological factors (Zhu and Chen, 2001; Tsuno et al., 2002). Ling and Chen (2005) also reported that the decrease of nitrification rate with the addition of OC and the nitrification rate was lower when the OC was higher. In this study, a large portion of organic substrate was already consumed in the anaerobic and anoxic zones of the multistage A^2O process. The level of COD in the aerobic zones was thus below the concentration to induce the competition between the heterotrophic microorganisms and the nitrifiers since sufficient HRT and DO concentration were provided for the growth and reproduction of heterotrophs and nitrifiers.

On the contrary, the denitrifiers in the anoxic zones demand external carbon source for denitrification. The denitrification step reduces nitrate to nitrogen gas by many species of heterotrophic facultative bacteria and require biodegradable organic carbon to perform metabolic processes. Enough carbon must be available for the complete denitrification of nitrate formed during the nitrification (Wunderlich et al., 2012; Xie et al., 2012; Xu et al., 2018). In our study, similar results were obtained and denitrification efficiency was improved in the anaerobic zones under high influent OLR. However, compared with high OLR shock loading, denitrification efficiency was lower in the anaerobic zones under the low OLR shock loading. An external carbon source addition was proposed to raise the denitrification rate when needed to compensate for high nitrogen loads or low seasonal temperatures (Han et al., 2010). The external COD addition was known as a feasible and flexible strategy to increase the denitrification rate when the COD concentration was low and could not cope with the current nitrogen load (Majumder et al., 2008). However, at a high C/N ratio, Michaud (Michaud et al., 2006) reported that heterotrophic bacteria outcompeted nitrifiers for available oxygen and space in the biofilter media, which deteriorated the nitrification process and led to nitrate deficiency for the denitrification. The present study showed that the majority of organic compounds were consumed in the anaerobic and anoxic zones. Therefore, the COD concentration was relative low in the aerobic zones, which resulted in low

http://www.aloki.hu ● ISSN 1589 1623 (Print) ● ISSN 1785 0037 (Online)
DOI: http://dx.doi.org/10.15666/aeer/1605_60956112
© 2018, ALÖKI Kft., Budapest, Hungary

multiplication rate of heterotrophic bacteria and high multiplication rate of nitrifiers in the aerobic zones. Consequently, the nitrification rate was high in the aerobic zones.

High AN concentration had slight influences on COD removal, but was detrimental to the removal of nitrogen compounds. Greater fluctuations were observed on the denitrification rate than the nitrification rate when the A^2O was subjected to shock loadings. It was reported that the COD/N ratio of 5–15 in the bioreactor was suitable for nitrification and denitrification reaction (Ding et al., 2011). The deficiency of carbon substrate resulted in the unbalance of nitrification and denitrification reactions and finally led to low overall nitrogen removal.

The nature and content of EPS are sensitive to the operational and environmental conditions. The LB-EPS, TB-EPS and total EPS amount showed an increase at the initial stage of the shock loadings and then declined with the prolonged shock loading. The characteristics of EPS in the activated sludge were closely connected with its resistant ability to shock loading and pollutants removal properties. SVI was widely used for characterizing sludge settleability and SVI values below 100 mL/g were considered as an indication of good settling properties of the sludge (Satyawalia and Balakrishnan, 2009). The SVI value was changed in a similar trend with the variation of average LB-EPS and total EPS amounts. The amount of LB-EPS had great influences on the SVI value and VSS, and SVI increased with the increasing content of LB-EPS and VSS because LB-EPS was not bound tightly to the cell. Meanwhile, LB-EPS had open and loose structure, high moisture content, low density and large volume around the cell, which could result in the larger volume and smaller density of sludge flocs and furthermore weaken the compressibility of sludge flocs. On the contrary, the effect of the change of TB-EPS on the volume of sludge flocs was relative small because TB-EPS was bound tightly to the cell and had tight structure, low moisture content and high density (Ruan et al., 2013). A long-term high shock loading leads to high LB-EPS and total EPS, which could influence the settleability of sludge and SVI increased. Substrate type and concentration, bacterial growth phase, the presence of toxic substances, shear rate of the bioreactor and other external conditions could influence the quantity and nature of EPS (Badireddy et al., 2008; Janus and Ulanicki, 2010; Li et al., 2015). At the initial state of each shock loading, the amounts of all types of EPS were elevated to a different level and SVI was increased with the increasing EPS. The temporary increase of EPS could be consequence of the necessity to acclimate to the new conditions. Moreover, a decline tendency was observed with the prolonged shock loadings. On the one hand, the bacterial cells tended to produce more EPS to protect themselves against unfavorable conditions (Sheng et al., 2008), which could be a possible reason for the temporary increase of EPS at the initial stage of the shock loading (Laspidou and Rittmann, 2002). On the other hand, the microorganisms could not adapt to the prolonged high organic loadings. The activity of microorganisms decreased and their cells could not autolyze when there was high substrate concentration. Therefore, less EPS was released when the system was under long-term high organic loadings (Shao et al., 2017). However, the EPS production rate is not necessary proportional to the substrate consumption rate. Laspidou and Rittmann (2002) demonstrated that the relationship between EPS production and substrate consumption rate depended on the kind of microorganisms involved and the system conditions. Consequently, the EPS variation could be an indication of the flocculation in microbial community of the A^2O system. The LB-EPS amount declined dramatically during the low OC and AN shock loading, which was in accordance with the previous literatures that LB-EPS functioned

http://www.aloki.hu ● ISSN 1589 1623 (Print) ● ISSN 1785 0037 (Online)
DOI: http://dx.doi.org/10.15666/aeer/1605_60956112
© 2018, ALÖKI Kft., Budapest, Hungary

as the primary surface for cell interaction and attachment (Sheng et al., 2008). The LB-EPS increased initially when the biological system was under high OC loading and then its amount decreased. The temporarily increased LB-EPS may cover the surface or fill the interior of the activated sludge flocs. As a result, the mass transfer of the substrates and the export of metabolic products were significantly prevented as described in the previous literature (Mu et al., 2006; Zheng and Yu, 2007). Consequently, a high level of EPS was not beneficial for biodegradation, which could be the reason for the effluent deterioration during the high OC shock loading. The highest EPS amount was accompanied by elevated effluent COD concentration and turbidity. Therefore, the composition of the activated sludge flocs changed, followed by the alteration of the physiochemical characteristics of the activated sludge as a result of shock loading.

Conclusion

The A^2O process successfully withstood all the shock loadings and restored its performance once the shock loading ceased. The enhanced carbon source concentration was beneficial for the removal of nitrogen compounds in the A^2O system. High AN concentration had slight influences on COD removal, but was detrimental to the removal of nitrogen compounds. Greater fluctuations were observed on the denitrification rate than the nitrification rate when the A^2O was subjected to shock loadings. The LB-EPS, TB-EPS and total EPS amount showed an increase at the initial stage of the shock loadings and then declined with the prolonged shock loading. The SVI value varied in a similar trend with the variation of average LB-EPS and total EPS amounts. Smaller concentrations of LB-EPS and total EPS indicated a good settleability of the activated sludge.

Acknowledgements. The authors want to express their gratitude to the National Natural Science Foundation of China (grant numbers 51678119 and 51508073), and the Science and Technology Development Program of Jilin Province (grant numbers 20180201016SF, 20180101309JC and 20170519013JH) for their financial supports.

REFERENCES

[1] APHA (1998): Standard Methods for the Examination of Water and Wastewater, 20th ed. – American Public Health Association, Washington, DC.

[2] Badireddy, A. R., Chellam, S., Yanina, S., Gassman, P., Rosso, K. M. (2008): Bismuth dimercaptopropanol (BisBAL) inhibits the expression of extracellular polysaccharides and proteins by Brevundimonas diminuta: implications for membrane microfiltration. – Biotechnology and Bioengineering 99(3): 634-643.

[3] Bassin, J. P., Kleerebezem, R., Dezotti, M., van Loosdrecht, M. C. M. (2012): Simultaneous nitrogen and phosphate removal in aerobic granular sludge reactors operated at different temperatures. – Water Research 46(12): 3805-3816.

[4] Chang, H., Yang, X., Fang, Y., Pu, P., Li, Z., Rengel, Z. (2006): In-situ nitrogen removal from the eutrophic water by microbial-plant integrated system. – Journal of Zhejiang University Science B 7(7): 521-531.

[5] Chen, B., Kim, Y., Westerhoff, P. (2011): Occurrence and treatment of wastewater-derived organic nitrogen. – Water Research 45(15): 4641-4650.

http://www.aloki.hu ● ISSN 1589 1623 (Print) ● ISSN 1785 0037 (Online)
DOI: http://dx.doi.org/10.15666/aeer/1605_60956112
© 2018, ALÖKI Kft., Budapest, Hungary

[6] Ding, D. H., Feng, C. P., Jin, Y. X., Hao, C. B., Zhao, Y. X., Suemura, T. (2011): Domestic sewage treatment in a sequencing batch biofilm reactor (SBBR) with an intelligent controlling system. – Desalination 276(1-3): 260-265.
[7] Guo, H., Zhou, J., Su, J., Zhang, Z. (2005): Integration of nitrification and denitrification in airlift bioreactor. – Biochemical Engineering Journal 23(1): 57-62.
[8] Han, H., Li, Y., Hu, H., Wang, B. (2010): Effect of external carbon source on denitrification in biofilter at low temperature. – Advanced Materials Research 113-116: 1358-1362.
[9] Janus, T., Ulanicki, B. (2010): Modelling SMP and EPS formation and degradation kinetics with an extended ASM3 model. – Desalination 261(1-2): 117-125.
[10] Jubany, I., Carrera, J., Lafuente, J., and Baeza, J. A. (2008): Start-up of a nitrification system with automatic control to treat highly concentrated ammonium wastewater: experimental results and modelling. – Chemical Engineering Journal 144(3): 407-419.
[11] Laspidou, C. S., Rittmann, B. E. (2002): A unified theory for extracellular polymeric substances, soluble microbial products, and active and inert biomass. – Water Research 36(11): 2711-2720.
[12] Li, B., Irvin, S. (2007): The comparison of alkalinity and ORP as indicators for nitrification and denitrification in a sequencing batch reactor (SBR). – Biochemical Engineering Journal 34(3): 248-255.
[13] Li, D., Wu, Q., Liang, Y. H., Su, Q. L., Zhang, J. K., Wei, J. J., Zhang, J. (2015): Effect of substrate concentration and type on the content of extracellular polymeric substances in the nitrification sludge. – Journal of Harbin Institute of Technology 47(4): 81-86 (in Chinese).
[14] Li, G. R., Li, Q., Cao, S. S., Su, J. P., Fan, R. C. (2016): Effect of carbon source on nitrogen and phosphorus removal efficiency of an A^2/O system. – Environmental Engineering 9(6): 22-25 (in Chinese).
[15] Li, X., Li, Y., Liu, H., Hua, Z., Du, G., Chen, J. (2008): Correlation between extracellular polymeric substances and aerobic biogranulation in membrane bioreactor. – Separation and Purification Technology 59(1): 26-33.
[16] Li, X. L., Wei, L. L., Zhao, Q. L., Chen, Z. Q. (2014): Effects and mechanisms of polymeric aluminum-iron (PAFC) added of aeration tank in A^2O systems for phosphorus and nitrogen removal. – Research of Environmental Sciences 27(10): 1212-1218 (in Chinese).
[17] Liang, Z., Li, W., Yang, S., Du, P. (2010): Extraction and structural characteristics of extracellular polymeric substances (EPS), pellets in autotrophic nitrifying biofilm and activated sludge. – Chemosphere 81(5): 626-632.
[18] Ling, J., Chen, S. L. (2005): Impact of organic carbon on nitrification performance of different biofilters. – Aquacultural Engineering 33(2): 150-162.
[19] Liu, X. Y., Lin, H., Ma, Z. R., Wang, L., Liu, J. W., Guo, C., Jiang, Y. H. (2014): Characteristics of nitrification and denitrification for simultaneous nitrogen and phosphorus remova. – Environmental Science 35(01): 214-220 (in Chinese).
[20] Ma, J., Zhang, Y., Liu, L., Fu, B. (2006): Nitrogen removal effect of A2/O process. – Journal of Harbin University (Natural Sciences Edition) 22(1): 28-31 (in Chinese).
[21] Majumder, P. S., Gupta, S. K. (2008): Effect of carbon sources and shock loading on the removal of chlorophenols in sequential anaerobic-aerobic reactors. – Bioresource Technology 99(8): 2930-2937.
[22] Michaud, L., Blancheton, J. P., Bruni, V., Piedrahita, R. (2006): Effect of particulate organic carbon on heterotrophic bacterial populations and nitrification efficiency in biological filters. – Aquacultural Engineering 34(3): 224-233.
[23] Mino, T., Liu, W. T., Kurisu, F., Matsuo, T. (1995): Modeling glycogen-storage and denitrification capability of microorganisms in enhanced biological phosphate removal processes. – Water Science and Technology 31(2): 25-34.

http://www.aloki.hu ● ISSN 1589 1623 (Print) ● ISSN 1785 0037 (Online)
DOI: http://dx.doi.org/10.15666/aeer/1605_60956112
© 2018, ALÖKI Kft., Budapest, Hungary

[24] Mu, Y., Yu, H., Wang, G. (2006): Permeabilities of anaerobic CH_4-producing granules. – Water Research 40(9): 1811-1815.
[25] Pai, T. Y., Chiou, R. J., Tzeng, C. J., Lin, T. S., Yeh, S. C., Sung, P. J., Tseng, C. H., Tsai, C. H., Tai, Y. S., Hsu, W. J., Wei, Y. L. (2010): Variation of biomass and kinetic parameters for nitrifying species in the TNCU3 process at different aerobic hydraulic retention times. – World Journal of Microbiology and Biotechnology 26(4): 589-597.
[26] Park, S., Bae, W., Rittmann, B. E., Kim, S., Chung, J. (2010): Operation of suspended-growth shortcut biological nitrogen removal (SSBNR) based on the minimum/maximum substrate concentration. – Water Research 44(5): 1419-1428.
[27] Peng, Y. Z., Wang, X. L., Li, B. K. (2006): Anoxic biological phosphorus uptake and the effect of excessive aeration on biological phosphorus removal in the A^2O process. – Desalination 189(1-3): 155-164.
[28] Ruan, X. D. (2013): Flocculation characteristics of flocs formed by tightly bound extracellular polymeric substances (TB-EPS)-the formation, breakup and regrowth of flocs. – Acta Scientiae Circumstantiae 33(3): 655-663 (in Chinese).
[29] Satyawali, Y., Balakrishnan, M. (2009): Effect of PAC addition on sludge properties in an MBR treating high strength wastewater. – Water Research 43(6): 1577-1588.
[30] Seifi, M., Fazaelipoor, M. H. (2012): Modeling simultaneous nitrification and denitrification (SND) in a fluidized bed biofilm reactor. – Applied Mathematical Modelling 36(11): 5603-5613.
[31] Shao, Y. X., Shi, Y. J., Mohammed, A., Liu, Y. (2017): Wastewater ammonia removal using an integrated fixed-film activated sludge-sequencing batch biofilm reactor (IFAS-SBR): comparison of suspended flocs and attached biofilm. – International Biodeterioration and Biodegradation 116: 38-47.
[32] Shen, Y. J., Wu, Y., Zhang, X. X. (2016): Influence of the different test methods on the determination of activated sludge denitrification rate. – Shandong Chemical 45(05): 7-11 (in Chinese).
[33] Sheng, G. P., Zhang, M. L., Yu, H. Q. (2008): Characterization of adsorption properties of extracellular polymeric substances (EPS) extracted from sludge. – Colloids and Surfaces B: Biointerfaces 62(1): 83-90.
[34] Sheng, G. P., Yu, H. Q., Li, X. Y. (2010): Extracellular polymeric substances (EPS) of microbial aggregates in biological wastewater treatment systems: A review. – Biotechnology Advances 28(6): 882-894.
[35] Shou, W. J., Kang, F. X., Lu, J. H. (2018): Nature and value of freely dissolved eps ecosystem services: insight into molecular coupling mechanisms for regulating metal toxicity. – Environmental Science and Technology 52(2): 457-466.
[36] Tanabene, R., Genty, T., Carolina, G. M., Bruno, B., Potvin, R., Neculita, C. M. (2018): Nitrification-denitrification of thiocyanate, ammonia, and nitrates in highly contaminated gold mine effluents using methanol as energy source. – Journal of Environmental Engineering 144(5): 1-6.
[37] Torà, J. A., Baeza, J. A., Carrera, J., Oleszkiewicz, J. A. (2011): Denitritation of a high-strength nitrite wastewater in a sequencing batch reactor using different organic carbon sources. – Chemical Engineering Journal 172(2-3): 994-998.
[38] Tsuno, H., Hidaka, T., Nishimura, F. (2002): A simple biofilm model of bacterial competition for attached surface. – Water Research 36(4): 996-1006.
[39] Walters, E., Hille, A., He, M., Ochmann, C., Horn, H. (2009): Simultaneous nitrification/denitrification in a biofilm airlift suspension (BAS) reactor with biodegradable carrier material. – Water Research 43(18): 4461-4468.
[40] Wang, X. L., Peng, Y. Z., Wang, S. Y., Fan, J., Cao, X. M. (2006): Influence of wastewater composition on nitrogen and phosphorus removal and process control in A^2O process. – Bioprocess and Biosystems Engineering 28(6): 397-404.

http://www.aloki.hu ● ISSN 1589 1623 (Print) ● ISSN 1785 0037 (Online)
DOI: http://dx.doi.org/10.15666/aeer/1605_60956112
© 2018, ALÖKI Kft., Budapest, Hungary

[41] Wunderlich, A., Meckenstock, R., Einsiedl, F. (2012): Effect of different carbon substrates on nitrate stable isotope fractionation during microbial denitrification. – Environmental Science and Technology 46(9): 4861-4868.
[42] Xie, L., Chen, J. R., Wang, R., Zhou, Q. (2012): Effect of carbon source and COD/NO_3^--N ratio on anaerobic simultaneous denitrification and methanogenesis for high-strength wastewater treatment. – Journal of Bioscience and Bioengineering 113(6): 759-764.
[43] Xu, F., Li, Y., Huang, Y. (2009): Effect of inner circumfluence rate on the performance of continuous-flow improved A^2/O reactor. – Technology of Water Treatment 35(8): 59-62 (in Chinese).
[44] Xu, J., Yu, H. Q., Li, X. Y. (2016): Probing the contribution of extracellular polymeric substance fractions to activated-sludge bioflocculation using particle image velocimetry in combination with extended DLVO analysis. – Chemical Engineering Journal 303: 627-635.
[45] Xu, Z. S., Dai, X. H., Chai, X. L. (2018): Effect of different carbon sources on denitrification performance, microbial community structure and denitrification genes. – Science of the Total Environment 634: 195-204.
[46] Yang, X., Wu, X., Hao, H. L., He, Z. L. (2008): Mechanisms and assessment of water eutrophication. – Journal of Zhejiang University Science B 9(3): 197-209.
[47] Ye, F., Ye, Y., Li, Y. (2011): Effect of C/N ratio on extracellular polymeric substances (EPS) and physicochemical properties of activated sludge flocs. – Journal of Hazardous Materials 188(1-3): 37-43.
[48] Yong, Z. J., Mjk, B., Ng, C. A., Sethupathi, S., Lim, J. W. (2017): A sequential treatment of intermediate tropical landfill leachate using a sequencing batch reactor (SBR) and coagulation. – Journal of Environmental Management 205: 244-252.
[49] Zeng, W., Li, L., Yang, Y. Y., Zhang, Y., Wang, S. Y. (2010): Short-cut nitrification and denitrification in A^2O process treating domestic wastewater. – China Environmental Science 30(5): 625-632 (in Chinese).
[50] Zhang, H. F., Wang, Z. P., Zhang, L. H., Song, L. F. (2014): Impact of sludge cation distribution pattern on its filterability in membrane bioreactor. – Bioresource Technology 171: 16-21.
[51] Zhang, L., Zheng, P., Tang, C., Jin, R. (2008): Anaerobic ammonium oxidation for treatment of ammonium-rich wastewaters. – Journal of Zhejiang University Science B 9(5): 426-426.
[52] Zhang, M., Zhang, Y., Huang, P. L., He, C. D., Peng, Y. Z., Wu, J. (2017): Migration and transformation and utilization of organic matter in A^2/O-MBBR denitrifying phosphorus removal process. – China Environmental Science 37(11): 4132-4139 (in Chinese).
[53] Zhang, W. J., Yang, P., Xiao, P., Xu, S. W., Liu, Y. Y., Liu, F., Wang, D. S. (2015): Dynamic variation in physicochemical properties of activated sludge floc from different wwtps and its influence on sludge dewaterability and settleability. – Colloids and Surfaces A: Physicochemical and Engineering Aspects 467: 124-134.
[54] Zheng, Y. M., Yu, H. Q. (2007): Determination of the pore size distribution and porosity of aerobic granules using size-exclusion chromatograph. – Water Research 41(1): 39-46.
[55] Zhu, S., Chen, S. (2001): Effects of organic carbon on nitrification rate in fixed film biofilters. – Aquacultural Engineering 25(1): 1-11.
[56] Zhu, Z., Chang, L., Deng, D. (2014): Regulation of mixture liquid reflux ratio for effect of an improved A^2O process. – Chinese Journal of Environmental Engineering 8(11): 4762-4766 (in Chinese).

http://www.aloki.hu ● ISSN 1589 1623 (Print) ● ISSN 1785 0037 (Online)
DOI: http://dx.doi.org/10.15666/aeer/1605_60956112
© 2018, ALÖKI Kft., Budapest, Hungary

PHYSICAL PROPERTIES OF THREE SONGKHLA LAGOON FISH SPECIES IN THE LOWER GULF OF THAILAND DURING AND AFTER THE MONSOON SEASON

HUE, H. T. T.[1,2,3*] – PRADIT, S.[1,3*] – JARUNEE, C.[1,3] – LIM, A.[4] – NITIRATSUWAN, T.[5] – GONCALO, C.[6]

[1]*Marine and Coastal Resources Institute (MACORIN), Prince of Songkla University, Hat Yai, Songkhla 90112, Thailand*

[2]*Central Institute for Natural Resources and Environmental Studies, Vietnam National University, Ha Noi, Vietnam*

[3]*Coastal Oceanography and Climate Change Research Center, Prince of Songkla University, Hatyai, Thailand*

[4]*Faculty of Science and Technology, Prince of Songkla University, Pattani, Thailand*

[5]*Rajamangala University of Technology, Srivijaya, Trang, Thailand*

[6]*Swedish Agency for Marine and Water Management, Stockholm, Sweden*

**Corresponding authors*
e-mail: hathithuhue2001@yahoo.com; spradit22@gmail.com; phone: +66-910-495-786; +84-98-726-1294

(Received 3rd Jul 2018; accepted 31st Aug 2018)

Abstract. Length–weight relationships (LWR) were estimated for three main Songkhla Lagoon fish species occurring in the lower gulf of Thailand. Samples were collected monthly during monsoon and after monsoon season (September 2017 to April 2018). Fishes were captured by three methods: fishing gear, crab gear and shrimp gear. This study is the first reference on LWR equation parameters of *Pellona ditchella* (Valenciennes, 1847), *Sardinella gibbosa* (Bleeker, 1849) and *Alepes vari* (G. Cuvier, 1833) in the lower gulf of Thailand, this good document would be used to compare these fish condition with many coastal areas in the world. This work provides the important information of fish migration between lagoon and lower gulf of Thailand as well as for two species from which we present a wider size range in FishBase, *Pellona ditchella* (Valenciennes, 1847) and *Sardinella gibbosa* (Bleeker, 1849).
Keywords: *length–weight relationship, Pellona ditchella, Sardinella gibbosa, Alepes vari, fish migration, fish well-being*

Introduction

Songkhla Lagoon is one of the two lagoons in the world that has Irrawaddy dolphins (*Orcaella brevirostris*), which are endangered species. The lagoon is located in the southern part of Thailand and is divided into three distinct parts. The southern part of the lagoon is connected to the Gulf of Thailand through a 380 m wide strait Songkhla Lagoon. It is very rich regarding biodiversity and provides resources and livelihoods for local fishermen all year around. The livelihood of more than 1.9 million people of the 25 districts located in the three provinces of Southern Thailand rely on the lagoon's fishery resources. However, as in many other similar ecosystems elsewhere (Martínez et al., 2007; Satumanatpan and Pollnac, 2017), those resources have been declining sharply over recent decades. Many fishermen of Songkhla Lagoon are wondering

http://www.aloki.hu ● ISSN 1589 1623 (Print) ● ISSN 1785 0037 (Online)
DOI: http://dx.doi.org/10.15666/aeer/1605_61136127
© 2018, ALÖKI Kft., Budapest, Hungary

whether they can sustain themselves through fishing or if they must convert to another occupation. Many of them have already moved to other fishing areas or changed profession.

As part of the efforts to create policies for sustainable fishing in Songkhla Lagoon and improve the livelihoods of fishing communities dependent on the lagoon's resources, numerous studies were conducted in the past two decades on Songkhla Lagoon, focusing mostly on models of fish catch landing (e.g. Chesoh and Lim, 2008; Chesoh, 2009; Chesoh and Choonpradub, 2011; Hue et al., 2018) or the effects of chemical contamination (e.g. Pradit et al., 2013). Other research has dealt with the government-led shrimp restocking program (Xu et al., 1997; Davenport et al., 1999; Wang et al., 2006; Hamasaki and Kitada, 2013; Niamaimandi and Zarshenas, 2015).

Fish condition can be a very important parameter to the managers of fisheries. Plump fish may be an indicator of favorable environmental conditions (e.g., habitat, food availability), whereas thin fish may indicate a less favorable environment. Thus, monitoring fish well-being can be extremely useful for the biologists of fisheries to make management recommendations concerning fish populations and their management. There is evidence that length–weight relationships (LWR) plays an important role in estimating fish biomass based on length. These parameters can be compared between seasons, years or different areas using standardized sampling procedures (Correia et al., 2017), and data on the length and weight of fish are currently two of the most common and standardized parameters about the biology of fish (Le Cren, 1951).

Pellona ditchella (Valenciennes, 1847), *Sardinella gibbosa* (Bleeker, 1849) and *Alepes vari* (G. Cuvier, 1833) are present in most of the markets in Southeast Asia. Their current known distribution extends across the Indo-West Pacific: from Madagascar, and Durban, South Africa to the Gulf of Oman and the coasts of India; from the Andaman Sea to Indonesia and the Philippines, southeast to the Arafura Sea, northern and western Australia and Papua New Guinea (Russell et al., 1989). During the period 2003-2017, they were found frequently in the lower Gulf of Thailand, including Songkhla Lagoon. *P. ditchella* is found most often in coastal, marine waters, but also enters mangroves and river estuaries, and tolerates brackish water and freshwater. *S. gibbosa* is commonly found in marine, pelagic-neritic habitats, and forms schools in coastal waters. Alepes scads are marine, coastal predatory fish not found in the open oceans (Pauly et al., 1996; Riede, 2004; Fricke et al., 2011).

Information about the health of these fishes is important in all countries along their range of distribution where they are fished commercially. Previous research on these fishes focuses on *S. gibbosa* and includes a study on the genetics and morphology of cryptic species of *S. gibbosa* (Thomas et al., 2014); the confirmation of presence of *S. gibbosa* in the Red sea and documenting its introduction into the Eastern Mediterranean Sea (Stern et al., 2015); heavy metal contamination in *S. gibbosa* in the coast of Balochistan, Pakistan (Ahmed et al., 2015); and stock assessment of *S. gibbosa* in the Gulf of Thailand (Boonjorn et al., 2012). No studies are known of the ecology or the living conditions of these fishes, let alone of monthly or seasonal changes in those two aspects. This paper addresses this gap by studying monthly and seasonal changes in the length–weight relationship of the two species and one genus of fish. It provides an account of investigations carried out in both Songkhla Lagoon and Sathing Pra, in a context of sharp decline in fish catches in Songkhla Lagoon. This study concentrates primarily on the populations and general biology of those fishes, in particular growth

http://www.aloki.hu ● ISSN 1589 1623 (Print) ● ISSN 1785 0037 (Online)
DOI: http://dx.doi.org/10.15666/aeer/1605_61136127
© 2018, ALÖKI Kft., Budapest, Hungary

and related aspects, thereby providing early findings to inform further research on measures to enhance fish populations in Songkhla Lagoon.

Material and methods

Study site

This study was conducted in the lower Gulf of Thailand, in the coastal area of Sathing Pra District, Thailand (*Fig. 1*). The climate of the lower Gulf of Thailand is governed by two monsoons the southwest monsoon from May to September, and the northeast monsoon between October and March. There are two seasons: (a) the rainy season, usually covering the period May to January, with the heaviest rains typically in November; and (b) the dry season, from February to April. April is normally the hottest month (ONEP, 2005).

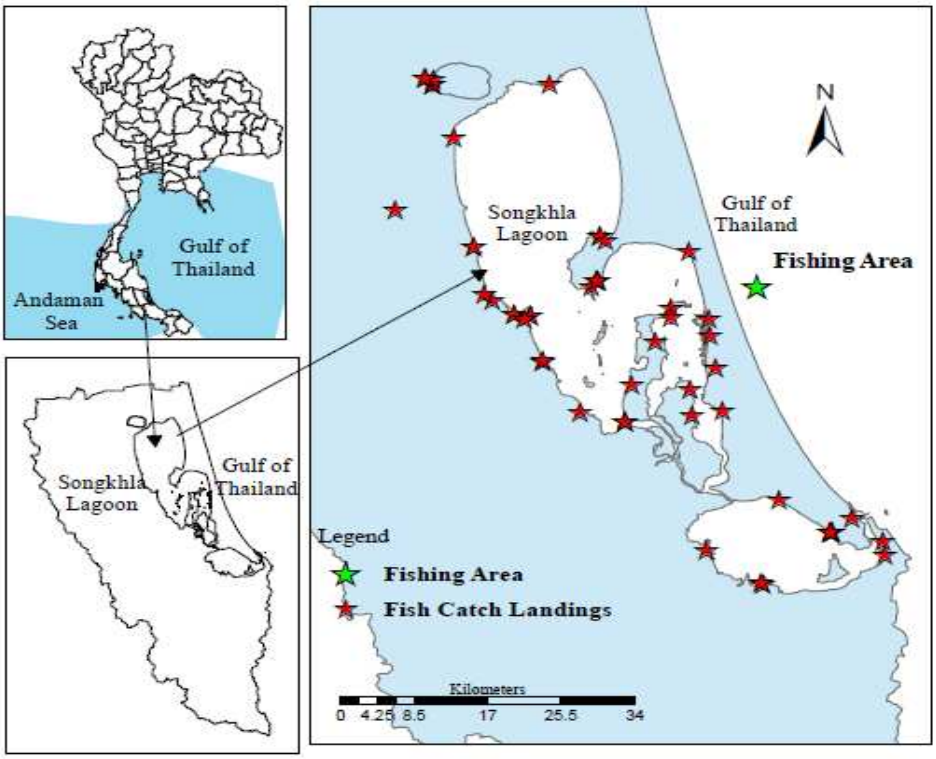

Figure 1. *The locations of sampling*

Data collection

Specimens used in this study were collected on a monthly basis from fishermen fishing in the coastal district of Sathing Pra during the period of September 2017 to April 2018, at the sampling sites indicated in *Figure 1* (07°31'24" N; 100°27'46" E). A list of 185 fish species found in Songkhla Lagoon during 2003-2017 issued by the Thai National Institute of Coastal Aquaculture (NICA) was used to identify the caught fish species. The list was first given to the head of Fisherman Association in Sathing Pra, through whom it was distributed to the fishermen contributing to the study, who did the first species identification themselves.

http://www.aloki.hu ● ISSN 1589 1623 (Print) ● ISSN 1785 0037 (Online)
DOI: http://dx.doi.org/10.15666/aeer/1605_61136127
© 2018, ALÖKI Kft., Budapest, Hungary

The fishing grounds where the specimens were caught are located approximately 3 km from the shores of the lagoon. Number Fish specimens were captured with two main fishing gears: fish nets (length: 180 m, mesh size: 4.5 × 4.5 cm) and shrimp nets (length: 30 m, mesh size: 3 × 3 cm), the only one fish specimen Sardinella gibbosa was caught with crab nets (length: 180 m, mesh size: 11 × 11 cm), at depths of approximately 80, 15 and 20 m, respectively. Fishing usually took place between 3 and 6 am, with some variation between months and seasons. The fishing boats in this coastal area are usually small boats with a length of 7-10 m length and a width of 1.8-2 m.

All specimens were bought from the fishermen, iced and transferred to the laboratory of the Marine and Coastal Resources Institute, Prince of Songkla University (MACORIN), where a verification of the species was carried out, followed by the measurement of the total length and weight. Total length of fish was measured from the tip of the premaxilla to the tip of the longest caudal fin ray stretched out posteriorly. Millimeter was used to be length measurements (Society, 2017). The total weight of fish specimens was recorded with an accuracy of 0.1 g using an Ohaus digital weighing balance (Ajani et al., 2013).

Data analysis

The purpose of this study is to assess the condition of commercially important fish found in Songhkla Lagoon by investigating their length–weight relationship, and monthly and seasonal changes in this parameter. The monthly data on length and weight was separated into two periods: the monsoon season (from September 2017 to January 2018) and after the monsoon season (dry season) (from February to April 2018).

Length–weight relationship analysis

Linear transformation of fish length and weight was made by using natural logarithm at the observed lengths and weights. The length–weight relationship (LWR) was calculated following Pauly (1983) and used to calculate the regression coefficient (slope of regression line of weight and length). The parameter "β" of the LWR was estimated using *Equation 1:*

$$W = aL^{\beta} \quad \text{(Eq.1)}$$

Here: W = the weight of the fish in grams, L = the total length of the fish in millimeters, a = constant, β = growth exponent.

A logarithmic transformation was used to make the relationship linear (*Eq. 2;* Le Cren, 1951):

$$\text{Log } W = \beta \log L + \log a \quad \text{(Eq.2)}$$

The LWR parameters *a* and β as well as the coefficient of determination (R^2) were derived by least squares regression (Ricker, 1973). The slope (β) also known as the allometry coefficient, has an important biological meaning, indicating the rate of weight gain relative to growth in length or the rate at which weight increases for a given increase in length.

http://www.aloki.hu ● ISSN 1589 1623 (Print) ● ISSN 1785 0037 (Online)
DOI: http://dx.doi.org/10.15666/aeer/1605_61136127
© 2018, ALÖKI Kft., Budapest, Hungary

Inferences about slope (β)

If a fish grows without changing its shape or density, then it is said to exhibit isometric growth. In this case, the volume of the fish is proportional to any linear measure of its size and β = 3. Isometric growth in fish is rare (Bolger and Connolly, 1989; McGurk, 1985). If β > 3 the fish tends to become "plumper" with an increase in length, a situation called positive allometric growth (Blackwell et al., 2000). If β < 3 the fish tends to become "thinner" with a decrease in length, a situation called negative allometric growth (Froese, 2006).

A test of whether the fish from the lower Gulf of Thailand exhibits allometric growth or not and confidence interval for β can be obtained by fitting the transformed length–weight model. The slope is generically labeled with beta (β) such that the test for allometry can be translated into the following statistical hypotheses:

$$H_0 : \beta = 3 \text{ ("Isometric growth")}$$

$$H_1 : \beta \neq 3 \text{ ("Allometric growth")}$$

Regarding model parameters can be obtained with a t-test using *Equation 3:*

$$t = \frac{\hat{\beta} - \beta_0}{SE_{\hat{\beta}}} \quad \text{(Eq.3)}$$

where β, SE_β are from the linear regression result and β_0 is the specified value in the H_0. In this study, the hypothesis test that a linear model parameter is equal to a specific value. To test a parameter is equal to a value other than 0, hoCoef meets all the requires and was used to efficiently compute the t and corresponding P-value for non-default hypothesis (for H_0: $\beta = 0$ by default).

Predictions of fish original scale

The study used the result from the length–weight regression to predict the weight of the fishes at the mean length. The result was back – transformed to the original scale by exponentiation. Due to the fact that the geometric mean is always less than the arithmetic means and, thus, the back-transformed mean always underestimates the arithmetic mean from the original scale (Ogle and College, 2013), the final original scale was multiplied with a correction factor derived from analysis of normal and log – normal distribution theory, using *Equation 4:*

$$e^{\frac{(\delta_{Y/X})^2}{2}} \quad \text{(Eq.4)}$$

where $\delta_{Y/X}$ is calculated from summarizing model length–weight regression of fish.

Comparing length–weight regressions (between seasons)

Inter-seasonal variation in the LWR of the fish included in this study was assessed by means of an analysis of variance (ANOVA) of the regression models using the factor season. The statistical significance for the study was set at a P value < 0.05. The full

http://www.aloki.hu ● ISSN 1589 1623 (Print) ● ISSN 1785 0037 (Online)
DOI: http://dx.doi.org/10.15666/aeer/1605_61136127
© 2018, ALÖKI Kft., Budapest, Hungary

model with indicator and interaction terms was then fit and stored in an object with the ANOVA table. All statistical analysis was performed using the FSA package (Ogle, 2018) from the R software (R Core Team, 2018).

Results

During the study period, 20 different Songkhla Lagoon species were captured in the coastal area of Sathing Pra, of which two species were crabs, three species were shrimps and 15 species were fish. The number of species varied markedly between months, but the fish species Indian pellona (*Pellona ditchella*), goldstripe sardinella (*Sardinella gibbosa*) and genus alepes (*Alepes vari*) appeared regularly, with sample sizes of 537, 162 and 49, respectively *(Table 1).* Among the samples, the total length of *P. ditchella* ranged from 103 to 183 mm, *S. gibbosa* from 102 to 175 mm, and *Alepes vari* from 122 to 216 (*Table 1*), whereas the ranges of the total body weight were 9 to 59 g, 6 to 43 g, and 11 to 93 g, respectively (*Table 1*).

Table 1. *Total length and weight for Pellona ditchella, Alepes vari and Sardineela gibbosa*

Common name	Scientific name	Sample size	Total length (mm)		Total weight (g)	
			Range	Mean	Range	Mean
Pellona ditchella	*Pellona ditchella* (Valenciennes, 1847)	537	103-187	143.9	9-59	30.81
Alepes vari	*Alepes vari* (G. Cuvier, 1833)	49	112-216	162.9	11-93	47.71
Sardinella gibbosa	*Sardinella gibbosa* (Bleeker, 1849)	162	102-175	130.8	6-43	19.93

Length–weight model

Figure 2 depicts the natural log-transformed total length and weight of *P. ditchella*, Alepes and *S. gibbosa* captured in the lower gulf of Thailand between September 2017 and April 2018, with the best fit regression line superimposed. *Table 2* gives the equations and other parameters of the length weight models for the three fish included in the study by using *Equation 2,* derived from those regression lines.

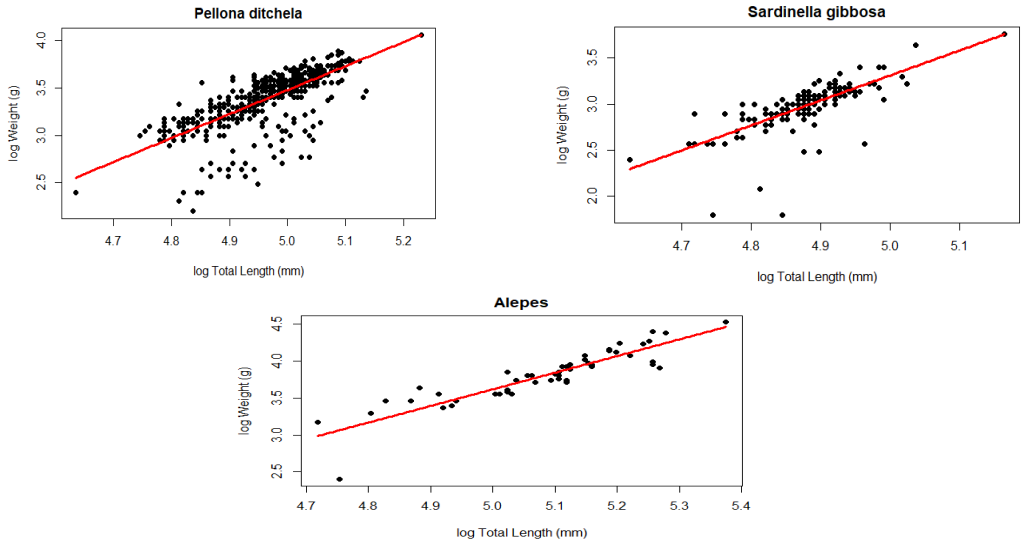

Figure 2. *Plot of natural log total length and weight of the three sampled fish*

http://www.aloki.hu ● ISSN 1589 1623 (Print) ● ISSN 1785 0037 (Online)
DOI: http://dx.doi.org/10.15666/aeer/1605_61136127
© 2018, ALÖKI Kft., Budapest, Hungary

Table 2. *Equation of the length weight models for P. ditchella, Alepes vari. and S. gibbosa*

Fish species	Equation (on the transformed scale)	Equation (on the original scale)	R^2	b range (95% confidence)	P value
P. ditchella	log(W) = -9.19+2.53log(L)	$W = 0.000102*L^{2.53}$	0.51	2.32 - 2.75	P = 0.00002
Alepes vari	Log(W) = -7.64+2.25log(L)	Log(W) = -7.64+2.25log(L)	0.81	1.93 - 1.93	P = 2.538096e-05
S. gibbosa	Log(W) = -10.25 + 2.71*log(L)	$W = 0.000035*L^{2.71}$	0.55	2.33 - 3.1	P = 0.1432605

With a value of R^2 between 0.5 and 0.6 the models for *P. ditchella* and *S. gibbosa* have a weaker fit to the data than the model for Alepes vari, with a value of R^2 of 0.81. The results for the slopes of the equations show that, according to the model, *S. gibbosa* exhibits isometric growth ($p > 0.05$) with an exponent parameter (β) between 2.33 and 3.1, with 95% confidence. The results for the other two fish show that, according to the respective models, both *P. ditchella* and Alepes vari exhibit allometric growth ($p < 0.05$) with values of β between 2.32 and 2.75 for *P. ditchella* and 1.93 and 2.27 for Alepes vari.

Predictions based on original scale

Table 3 presents the results for the predicted mean weight of the three fish included in the study, using the length–weight models presented in *Table 2* and *Equation 4*. With a mean length of 150 mm, *P. ditchella* was estimated to have a weight between 33.4 and 34.6 g. For *Alepes vari,* with the mean length is 160 mm, the weight predicted lies between 18.6 to 19.7, whereas for *S. gibbosa* the figures are 130 mm and 42.2 to 46.3 g.

Table 3. *Prediction of weight of P. ditchella, Alepes vari and S. gibbosa based on the mean length*

Fish species	Bias correction factor	Predicted weight (g)	Mean length (mm)
P. ditchella	1.097	33.4 - 34.6	150
Alepes vari	1.01	18.6 - 19.7	160
S. gibbosa	1.015	42.2 – 46.3	130

Monthly variation of length–weight relationship of the fish

Monthly length–weight relationship of the fish was calculated by using *Equation 1.*, where a = constant, β = slope (or allometry coefficient or growth exponent), n = number of fish sampled, R^2 = Coefficient of determination. The results are shown in *Table 4*.

Table 4 presents the monthly data for the length and weight of the three fish, for the entire study period (September 2017 to April 2018), and the parameters for the respective length–weight relationships. The value of β could not be determined for certain fish in the months of November 2017 and January, March and April 2018 due to the small size of the sample. No sampling was carried out in December 2017, as the heavy weather prevented all fishing activities.

There is a slight variation in the value of β (slope) between months for the three fish included in the study, with the majority exhibiting negative allometric growth ($\beta < 3$), and only Alepes vari exhibiting positive allometric growth during the month of October

http://www.aloki.hu ● ISSN 1589 1623 (Print) ● ISSN 1785 0037 (Online)
DOI: http://dx.doi.org/10.15666/aeer/1605_61136127
© 2018, ALÖKI Kft., Budapest, Hungary

2017 (β = 3.14). This suggests that the majority of the fish sampled experiences poor growth and living conditions. Carlander (1969) showed that the coefficient β in the LWR of fish usually ranged from 2.5 to 3.5. In this study, there were 10 instances in which the value of β was outside this range, as depicted in *Table 4* and *Figure 3*. The same table and figure also show that the lowest value of β was obtained for *S. gibbosa* in October 2017, whereas the highest was for Alepes vari in October 2017 (β = 3.14), followed by that for *S. gibbosa* in January 2018 (*b* = 2.94).

In the majority of instances (76.9%) the value of the coefficient of determination (R^2) was equal or greater than 0.60, which indicates a moderately significant relationship between length and weight of the fish examined in the period of this study *(Fig. 4)*.

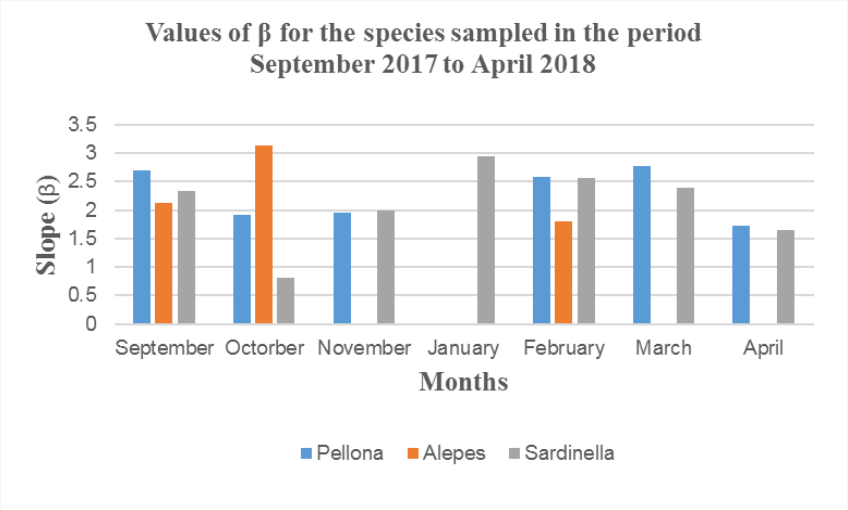

Figure 3. *Values of β for the species sampled in the period September 2017 to April 2018*

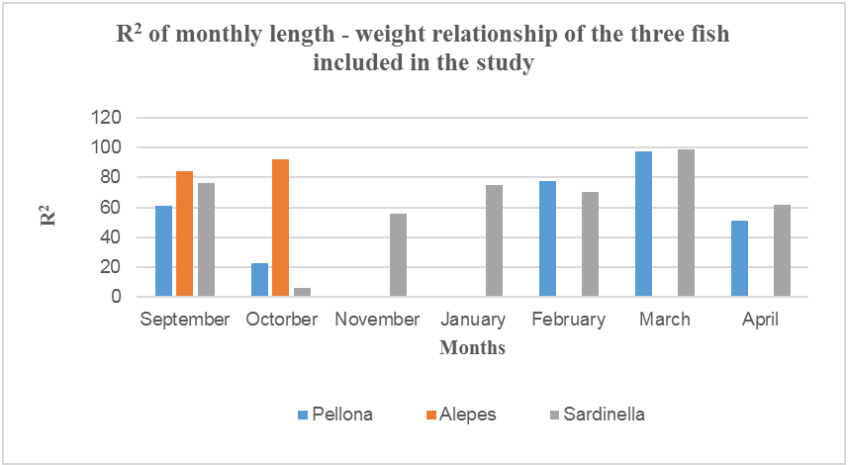

Figure 4. *R^2 of monthly length–weight relationship of the three fish included in the study*

Comparing length–weight regressions during and after the monsoon season

Table 5 presents the values of the ANOVA of the length–weight relationship for the three fish in two distinct periods, namely during and after the monsoon season.

http://www.aloki.hu ● ISSN 1589 1623 (Print) ● ISSN 1785 0037 (Online)
DOI: http://dx.doi.org/10.15666/aeer/1605_61136127
© 2018, ALÖKI Kft., Budapest, Hungary

Table 4. *Monthly values of length and weight for P. ditchella, Alepes vari. and S. gibbosa, and respective length–weight model parameters, September 2017–April 2018*

Month	P. ditchella							Alepes vari							S. gibbosa					
	n	LWR			Length			n	LWR			Length			n	LWR			Length		
		a	β	R^2	Min	Max	Mean		a	β	R^2	Min	Max	Mean		a	β	R^2	Min	Max	Mean
September	9	0.000099	2.69	61**	147	165	154.8	42	0.000942	2.13	84.15***	122	196	162.4	16	0.000232	2.33	76.53***	117	147	132.4
Octerber	189	0.00197	1.92	23***	115	169	137.4	3	0.0000041	3.14	92.02***	167	216	191.7	18	0.25	0.81	6.12	102	152	120.4
November	2	0.00181	1.96		132	142	137	1				116	116	116	9	0.00119	1.995	55.53**	124	138	132.7
January	1				147	147	147								23	0.0000122	2.94	74.89***	112	154	131.7
February	305	0.0000808	2.59	77.93**	130	170	147.4	2	0.00416	1.802		167	192	179.5	75	0.0000727	2.57	70.4***	119	175	132
March	16	0.0000302	2.78	97.46***											3	0.000169	2.4	99.14*	128	144	137.3
April	15	0.0059	1.72	51.39**	134	160	144.3	1				112	112	112	18	0.0066609	1.65	62.06***	122	146	131.6

*P-value < 0.1; **P-value < 0.05; ***P-value much less than 0.01

Table 5. *ANOVA of fish species in monsoon and after monsoon season*

Variables	Df	SS	MS	F value	P value	Confidence interval (2.5 And 97.5%)		
						Intercept	Log (L)	fSeason Monsoon
P. ditchella								
Log (L)	1	21.4152	21.4152	576.7773	< 2.2e-16 ***	-3.3-(-2.1)	2.08-2.53	-0.12-(-0.055)
fSeason	1	0.8866	0.8866	23.8779	1.36e-06 ***			
Log(L)$fSeason	1	0.1973	0.1973	5.3127	0.02155 *			
Alepes vari								
Log (L)	1	5.0864	5.0864	210.0341	<2e-16 ***	-9.30-(-9.30)	1.92-2.57	-0.13-0.25
fSeason	1	0.0098	0.0098	0.4032	0.5286			
Log(L)$fSeason	1	0.1078	0.1078	4.4501	0.0405 *			
S. gibbosa								
Log (L)	1	5.9244	5.9244	205.2222	< 2e-16 ***	-11.53-(-7.82)	2.22 - 2.98	-0.14- (-0.033)
fSeason	1	0.2904	0.2904	10.0608	0.00182 **			
Log(L)$fSeason	1	0.0110	0.0110	0.3808	0.53806			

*P-value < 0.1; **P-value < 0.05; ***P-value much less than 0.01

http://www.aloki.hu ● ISSN 1589 1623 (Print) ● ISSN 1785 0037 (Online)
DOI: http://dx.doi.org/10.15666/aeer/1605_61136127
© 2018, ALÖKI Kft., Budapest, Hungary

These results show that for *P. ditchella* the interaction terms are significant (p = 0.02), which indicates that there is enough evidence of the difference in the slope in the length–weight relationship between the monsoon and after monsoon seasons. The p-value for the indicator variable also suggests that there is a difference in the intercepts between seasons (p < 0.05). There are statistically significant differences between the slopes and intercepts of the regressions for the two different seasons, and there is a constant difference between the log-transformed weights of fish from the two seasons regardless of the log-transformed lengths of the fish. This is confirmed by the plots *(Fig. 5)* and confidence intervals. This result states that, the growth of *P. ditchella* during monsoon and after monsoon seasons is different.

For *S. gibbosa Table 5* shows that the difference in the length–weight regression between seasons is not significant (p = 0.538), hence there is not enough evidence to draw any conclusions about inter seasonal differences in the length–weight relationship of this fish species. The p-value for the indicator variable suggests that there is a difference in the intercepts between the two seasons (p < 0.05).

The interaction term for Alepes vari is slightly significant (p = 0.04), suggesting that there is enough evidence to conclude that there is difference in the slopes in the length–weight relationship between the monsoon and after monsoon seasons. The p-value for the indicator variable suggests that there is no difference in the intercepts of the regressions for each of the two seasons (p = 0.53).

These results also show that *P. ditchella* and *S. gibbosa* captured during the monsoon season are smaller than those captured after the monsoon (dry) season, with differences in weight of 0.05 - 0.13 g and 0.03 - 0.14 g, respectively. The opposite was found for Alepes vari, in which case fish captured during the monsoon season was 0.14 to 0.25 g larger than the fish captured during the dry season. *Figure 5* portrays the final models for the length–weight regressions for the monsoon and dry seasons for the three fish, with the respective fit plots.

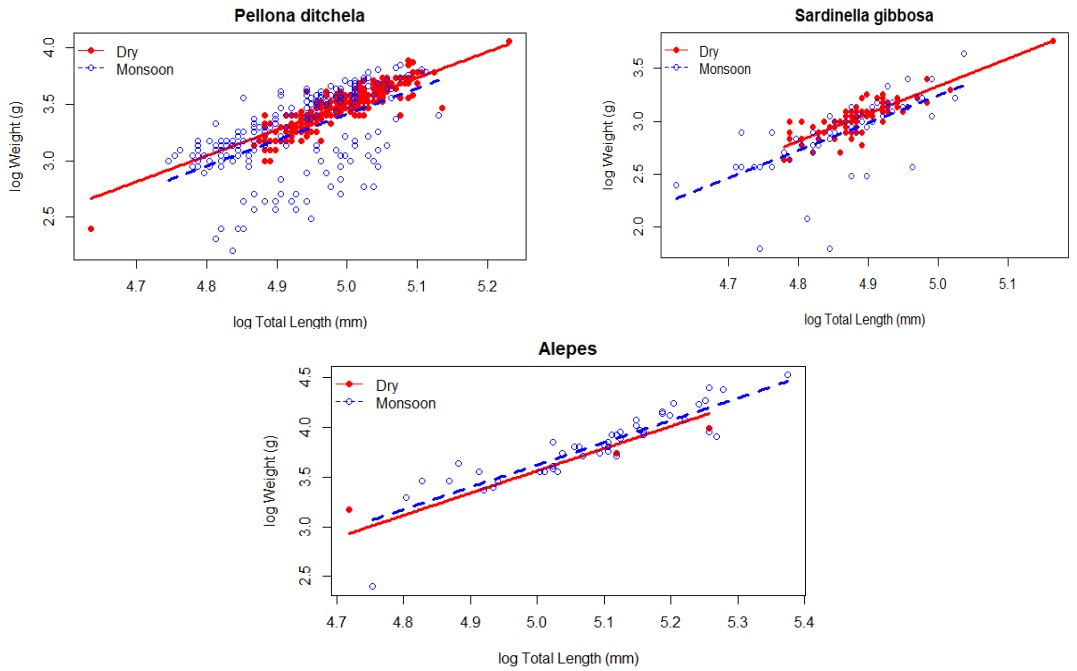

Figure 5. *Fit plot of the length–weight relationship for the three fish during the monsoon and after monsoon (dry) seasons*

http://www.aloki.hu ● ISSN 1589 1623 (Print) ● ISSN 1785 0037 (Online)
DOI: http://dx.doi.org/10.15666/aeer/1605_61136127
© 2018, ALÖKI Kft., Budapest, Hungary

Discussion

This paper provides the first monthly values for the length–weight relationship of three commercially important fish commonly found in Songkhla Lagoon and captured in the coastal areas of the lower Gulf of Thailand. It also contributes with revised values for the maximum length of two of the species studied in the online database FishBase (Froese and Pauly, 2018, *Table 1*): the maximum recorded length for *P. ditchella* (Valenciennes, 1847) and *S. gibbosa* (Bleeker, 1849) was previously 160 mm and 170 mm length (Whitehead, 1985), and this study determined new maximums at 187 mm and 175 mm, respectively.

With respect to the LWR, a value of 3 (three) for the slope of the regression (β) corresponds to the ideal growth of fish. However, such situation is seldom found (Allen, 1938) due to changes in the shape of fish during the growth period (Martin, 1949). That coefficient can be affected by factors such as the length and shape of the fish itself and the time of spawning; the fishing gear used (Farran, 1936; Deason and Hile, 1947); or environmental factors such as food supply and season changes in environmental parameters (Brosset et al., 2015). In this study, the average of the monthly values of β for the three fish studied fall below the standard interval of 2.5 to 3.5 as determined by Carlander (1969). The average values from this study are 2.277, 2.357 and 2.099 for *P. ditchella,* Alepes vari and *S. gibbosa*, respectively. This indicates that all three fish have negative allometry, which is interpreted as a sign of poor body condition. This is in line with the views of fishermen contacted for this study, most of whom were of the view that the amount and size of fish has decreased in the coastal area of the southern Gulf of Thailand, which they attribute to the oil drilling activities taking place offshore and the illegal fishing gear, such as: sai nang (sitting cage). 14.29% of the fishermen interviewed in this area said they are using sai nang, they knew that this fishing gear catches all small fishes, but they still have to use because the number of fishes are decreasing sharply (Source: Author). The results from this study are insufficient to establish such a causal relationship though, and a broader investigation would be needed to determine the effects of coastal water quality on the condition of fish in the lower Gulf of Thailand.

The study also found that two of the fish captured after the monsoon season (dry season), namely *P. ditchella* and *S. gibbosa* were on average fatter than when captured during the monsoon season. This is in line with the result from the author, only 13.6% amount of fish was caught during monsoon season, 39.98% was before monsoon season and 46.42% was after monsoon season (Source: Author). This may be due to the biology of these two species, as both migrate to the mangroves in the estuarine and freshwater environments of the lagoon (Hue et al., 2018), which affects their growth negatively compared to life in the marine environment of the coastal waters. Eventhough, Alepes was found thinner in the dry season, but due to its small sample size (N = 3), it is not appropriate for a correct statistical evaluation, to conclude about Alepes, it requires further study.

The main limitation of this study is the relatively short study period of seven months, which is insufficient for studying the biology of the fish included in the assessment. Despite this limitation, it has unveiled statistically significant differences in selected growth parameters between two seasons in the lower Gulf of Thailand. The fish studied are all of high commercial importance, yet are subject to increasing anthropogenic pressure from fishing, including the use of illegal gear such as sitting cage (Source: Author), offshore drilling for oil and habitat destruction (Satumanatpan and Pollnac,

http://www.aloki.hu ● ISSN 1589 1623 (Print) ● ISSN 1785 0037 (Online)
DOI: http://dx.doi.org/10.15666/aeer/1605_61136127
© 2018, ALÖKI Kft., Budapest, Hungary

2017). In view of these pressures and the need to improve the management of commercial fish stocks, the findings of this study are potentially very useful for current and future stock estimation and evaluation studies. Moreover, these findings could be useful for comparing the body condition of fish over time and between different regions. Further studies of similar nature and involving some elements of the biology of commercially important species are necessary to support the formulation of policies for the sustainable utilization and appropriate management of fisheries resources in the southern Gulf of Thailand and in the whole the country.

Conclusion

Seven months for studying the biology of fish may not be a long time but this is enough time to see the difference of growth parameters between two typical seasons in the lower gulf of Thailand for some fish species. In the investigated area, these species have high commercial value, however, high pressure on population caused by fishing, illegal fishing gear (trawl), oil drilling from human activities are destroying fish habitat. Findings of present research are very important for stock estimation and evaluation studies in the future. Moreover, they will give an opportunity to compare fish conditional living over the time and between regions.

Further studies of similar nature and involving some biological aspects of commercially important species are necessary to support the formulation of policies for sustainable utilization and appropriate management of fisheries resources in the country.

Acknowledgements. This paper has been partly prepared with the support of the Higher Education Research Promotion and the Thailand's Education Hub for the Southern Region of ASEAN Countries Project Office of the Higher Education Commission. Financial support was granted by the Graduate School, Prince of Songkla University, Thailand. The authors would like to thank the Fishermen Association in Sathing Pra district for giving us the chance to go fishing with, thanks to the MACORIN research team for helping authors to do the lab works. Thanks NICA for agreeing authors to use the data.

Conflict of interest. The authors confirm that this article content has no conflict of interest.

REFERENCES

[1] Ahmed, Q., Benzer, S., Elahi, N., Ali, Q. M. (2015): Concentrations of heavy metals in Sardinella gibbosa (Bleeker, 1849) from the coast of Balochistan, Pakistan. – Bulletin of Environmental Contamination and Toxicology 95(2): 221-225. DOI: 10.1007/s00128-015-1572-y.

[2] Ajani, E. G., Beatrice, B. O., Olufemi, O. (2013): Comparative condition factor of two Penaeid shrimps, Peneaus notialis (Pink shrimp) and Peneaus monodon (Tiger shrimp) in a coastal state, Lagos, South West Nigeria. – Nature and Science 11(4). http://www.sciencepub.net/nature/ns1104/001_16157ns1104_1_3.pdf.

[3] Allen, K. R. (1938): Some observations on the biology of the trout (Salmo trutta) in Windermere. – Journal of Animal Ecology 7(2): 333-349. DOI: 10.2307/1168.

[4] Blackwell, B. G., Brown, M. L., Willis, D. W. (2000): Relative weight (Wr) status and current use in fisheries assessment and management. – Reviews in Fisheries Science 8(1): 1-44. DOI: 10.1080/10641260091129161.

[5] Boonjorn, N., Noranarttragoon, P., Sanitmajjaro, W., Pankaew, K. (2012): Stock assessment of Goldstripe sardinella, Sardinella gibbosa (Bleeker, 1849) resources in the

http://www.aloki.hu ● ISSN 1589 1623 (Print) ● ISSN 1785 0037 (Online)
DOI: http://dx.doi.org/10.15666/aeer/1605_61136127
© 2018, ALÖKI Kft., Budapest, Hungary

Gulf of Thailand. – Department of Fisheries, Thailand (in Thai). https://www.fisheries.go.th/marine/research/files/en/abs%201_56%20eng.pdf.

[6] Bolger, T., Connolly, P. L. (1989): The selection of suitable indices for the measurement and analysis of fish condition. – Journal of Fish Biology 34: 171-182. DOI: 10.1111/j.1095-8649.1989.tb03300.x.

[7] Brosset, P., Menard, F., Fromentin, J, M., Bonhommeau, S., Ulses, C., Bourdeix, J, H., Bigot, J, L., Van, B, E., Roos, D., Saraux, C. (2015): Influence of environmental variability and age on the body condition of small pelagic fish in the Gulf of Lions. – Marine Ecology Progress Series 529: 219-231. DOI: 10.3354/meps11275.

[8] Carlander, K. D. (1969): Handbook of Freshwater Fishery Biology. – The Iowa State University Press, Ames, Iowa.

[9] Chesoh, S., Choonpradub, C. (2009): Method for analyzing fish assemblage distribution with application to fishery landings of tropical shallow lake as Songkhla Lake, Thailand. – Modern Applied Science 3(5): 179-192. DOI: 10.5539/mas.v3n5p179.

[10] Chesoh. S., Choonpradub, C. (2011): A model for clustering fish community structure with application to Songkhla Lake bi-monthly catches 2003-2006. – Turkish Journal of Fisheries and Aquatic Sciences 11(2): 177-184. DOI: 10.4194/trjfas.2011.0201.

[11] Chesoh, S., Lim, A. (2008): Forecasting fish catches in the Songkhla Lake basin. – ScienceAsia 34(3): 335-340. DOI: 10.2306/scienceasia1513-1874.2008.34.335.

[12] Correia, E., Granadeiro, J. P., Regalla, A., Catry, P. (2017): Weight relationship of fish species from the Bijagós Archipelago, Guinea-Bissau. – Journal of Applied Ichthology 2017: 1-3. DOI: 10.1111/jai.13522.

[13] Davenport, J., Ekaratne, S. U. K., Walgama, S. A., Lee, D., Hills, J. M. (1999): Successful stock enhancement of a lagoon prawn fishery at Rekawa, Sri Lanka using cultured post-larvae of penaeid shrimp. – Aquaculture 180(1-2): 65-78. DOI: 10.1016/S0044-8486(99)00141-6.

[14] Deason, H. J., Hile, R. (1947): Age and growth of the kiyi, Leucichthys kiyi Koelz, in Lake Michigan. – Transactions of the American Fisheries Society 74(1): 88-142. DOI: 10.1577/1548-8659(1944)74[88:AAGOTK]2.0.CO;2.

[15] Farran, G. P. (1936): On the mesh of herring drift- nets in relation to the condition factor of the fish. – ICES Journal of Marine Science 11(1): 43-52. DOI: 10.1093/icesjms/11.1.43.

[16] Fricke, R., Kulbicki, M., Wantiez, L. (2011): Checklist of the fishes of New Caledonia, and their distribution in the Southwest Pacific Ocean (Pisces). – Stuttgarter Beiträge zur Naturkunde A, Neue Serie 4: 341-463.

[17] Froese, R. (2006): Cube law, condition factor and weight-length relationships: History, meta-analysis and recommendations. – Journal of Applied Ichthyology 22(4): 241-253. DOI: 10.1111/j.1439-0426.2006.00805.x.

[18] Froese, R., Pauly, D. (2018): FishBase. World Wide Web Electronic Publication. – www.fishbase.org (accessed on 02/2018).

[19] Hamasaki, K., Kitada, S. (2013): Catch fluctuation of Kuruma prawn, Penaeus japonicus in Japan relative to ocean climate variability and a stock enhancement program. – Reviews in Fisheries Science 21(3-4): 454-468. DOI: 10.1080/10641262.2013.800781.

[20] Hue, H. T. T., Pradit, S., Lim, A., Goncalo, C., Nitiratsuwan, T. (2018): Shrimp and fish catch landing trends in Songkhla lagoon, Thailand during 2003-2016. – Applied Ecology and Environmental Research 16(3): 3061-3078. DOI: 10.15666/aeer.

[21] ONEP (Office of Nature and Environmental Policy and Planning) (2005): Master plan for Songkhla Lake Basin Development Project (Final Report). – Ministry of Natural Resources and Environment, Bangkok, Thailand.

[22] Martin, W. R. (1949): The Mechanics of Environmental Control of Body Form in Fishes. – The University of Toronto Press, Publication of the Ontario Fisheries Research Laboratory, No. 70, South Part, ON.

http://www.aloki.hu ● ISSN 1589 1623 (Print) ● ISSN 1785 0037 (Online)
DOI: http://dx.doi.org/10.15666/aeer/1605_61136127
© 2018, ALÖKI Kft., Budapest, Hungary

[23] Martínez, M. L., Intralawana, A., Vázquezb, G., Pérez-Maqueoa, O., Suttond, P., Landgrave, R. (2007): The coasts of our world: Ecological, economic and social importance. – Ecological Economics 63(2-3): 254-272. DOI: 10.1016/j.ecolecon.2006.10.022.
[24] Le Cren, E. D. (1951): The length-weight relationship and seasonal cycle in gonad weight and condition in the perch (*Perca fluviatilis*). – Journal of Animal Ecology 20: 201-219.
[25] Mc Gurk, M. D. (1985): Effects of net capture on the post preservation morphometry, dry weight, and condition factor of Pacific herring larvae. – Transactions of the American Fisheries Society 114(3): 348-355. DOI: 10.1577/1548-8659(1985)114<348: EONCOT>2.0.CO;2.
[26] Niamaimandi, N., Zarshenas, G. A. (2015): Economic valuation of stock enhancement of banana prawn (Fenneropenaeus merguiensis) in the Strait of Hormuz. – Fishery Bulletin 113(1): 40-46. DOI: 10.7755/FB.113.1.4.
[27] Ogle, D., College, N. (2013): fishR Vignette - Length-Weight Relationships. – http://derekogle.com/fishR/examples/oldFishRVignettes/LengthWeight.pdf.
[28] Ogle, D. H. (2018): FSA: Fisheries Stock Analysis. – R package version 0.8.20.
[29] Pauly, D. (1983): Some simple methods for the assessment of tropical fish stocks. – FAO Fisheries Technical Paper No. 234. https://s3-us-west-2.amazonaws.com/legacy.seaaroundus/doc/Researcher+Publications/dpauly/PDF/1983/Books+and+Chapters/SomeSimpleMethodsAssessmentTropicalFishStocks.pdf.
[30] Pauly, D., Cabanban, A., Torres, F. S. B. Jr. (1996): Fishery biology of 40 trawl-caught teleosts of western Indonesia. – ICLARM Studies and Reviews 23: 135-216. http://www.reefbase.org/resource_center/publication/pub_6864.aspx.
[31] Pradit, S., Pattarathomrong, M. S., Panutrakul, S. (2013): Arsenic cadmium and lead concentrations in sediment and biota from Songkhla Lake: a review. – Procedia Social and Behavioral Sciences 91: 573-580. http://linkinghub.elsevier.com/retrieve/pii/S1877042813025871.
[32] R Core Team. (2018): R: A Language and Environment for Statistical Computing. – R Foundation for Statistical Computing, Vienna, Austria. https://www.R-project.org/.
[33] Ricker, W. E. (1973): Linear regressions in fisheries research. – Journal of Fisheries Research Board of Canada 30(3): 409-434. DOI: 10.1139/f73-072.
[34] Riede, K. (2004): Global register of migratory species - from global to regional scales. Final Report of the R&D-Projekt 808 05 081. – Federal Agency for Nature Conservation. https://www.researchgate.net/publication/235225727_Global_register_of_migratory_species_from_global_to_regional_scales_final_report_of_the_RD-Projekt_808_05_081.
[35] Russell, B. C., Houston, W. (1989): Offshore fishes of the Arafura Sea. – Beagle: Records of the Museums and Art Galleries of the Northern Territory 6(1): 69-84. https://search.informit.com.au/documentSummary;dn=941910625031493;res=IELHSS.
[36] Satumanatpan, S., Pollnac, R. (2017): Factors influencing the well-being of small-scale fishers in the Gulf of Thailand. – Ocean and Coastal Management 142: 37-48. DOI: 10.1016/j.ocecoaman.2017.03.023.
[37] Stern, N., Rinkevich, B., Goren, M. (2015): First record of the Goldstripe sardinella - Sardinella gibbosa (Bleeker, 1849) in the Mediterranean Sea and confirmation for its presence in the Red Sea. – BioInvasions Records 4(1): 47-51. DOI: 10.3391/bir.2015.4.1.08.
[38] Thomas, R. C, Jr., Willette, D. A., Carpenter, K. E., Santos, M. D. (2014): Hidden Diversity in Sardines: genetic and morphological evidence for cryptic species in the goldstripe sardinella, *Sardinella gibbosa* (Bleeker, 1849). – PLoS ONE 9(1): e84719. DOI: 10.1371/journal.pone.0084719.
[39] Wang, Q., Zhuang, Z., Deng, J., Ye, Y. (2006): Stock enhancement and translocation of the shrimp Penaeus chinensis in China. – Fisheries Research 80(2006): 67-79. DOI: 10.1016/j.fishres.2006.03.015.

http://www.aloki.hu ● ISSN 1589 1623 (Print) ● ISSN 1785 0037 (Online)
DOI: http://dx.doi.org/10.15666/aeer/1605_61136127
© 2018, ALÖKI Kft., Budapest, Hungary

[40] Whitehead, P. J. P. (1985): FAO Species Catalogue. Vol. 7. Clupeoid fishes of the world (suborder Clupeoidei). An annotated and illustrated catalogue of the herrings, sardines, pilchards, sprats, shads, anchovies and wolf-herrings. – FAO Fish Synopsis 125(7/1): 1-303. http://www.fao.org/3/a-ac482e.pdf.

[41] Xu, J., Xia, M., Ning, X., Mathews, C. P. (1997): Stocking, enhancement, and mariculture of Penaeus orientalis and other species in Shanghai and Zhejiang Provinces, China. – Marine Fisheries Review 59(4): 8-14. http://aquaticcommons.org/9811/1/mfr5942.pdf.

http://www.aloki.hu ● ISSN 1589 1623 (Print) ● ISSN 1785 0037 (Online)
DOI: http://dx.doi.org/10.15666/aeer/1605_61136127
© 2018, ALÖKI Kft., Budapest, Hungary

PARASITOFAUNA OF ALLOCHTHONOUS FISH SPECIES IN THE OPEN WATERS OF THE DANUBE RIVER BASIN (SERBIAN PART) – IMPACT ON THE NATIVE FISH FAUNA

DJIKANOVIĆ, V.[1*] – SIMONOVIĆ, P.[2] – CAKIĆ, P.[1] – NIKOLIĆ, V.[2]

[1]*Institute for Biological Research "Sinisa Stankovic", University of Belgrade*
142 Bulevar Despot Stefan, 11060 Belgrade, Serbia
(e-mail: djiki@ibiss.bg.ac.rs; cakic@ibiss.bg.ac.rs)

[2]*Institute for Zoology, Faculty of Biology, University of Belgrade*
Studentski trg 16, 11000 Belgrade, Serbia
(e-mail: pedja@bio.bg.ac.rs; vera@bio.bg.ac.rs)

**Corresponding author*
e-mail: djiki@ibiss.bg.ac.rs; phone: +381-11-207-8357

(Received 4th Jul 2018; accepted 14th Aug 2018)

Abstract. In this review data on parasitofauna of allochthonous fish species in the Danube River Basin in Serbia is presented. Up to now, 33 ecto- and endoparasites of seven examined allochthonous invasive fish species have been reported. Some of the identified parasitic species are new for fish parasitofauna in the Serbian waters (*Trichodina nobilis, Balantidium sp., Philometroides cyprini, Philometroides parasiluri, Eustrongylides* sp., *Ergasilus sieboldi, Lernaea cyprinacea, Sinergasilus polycolpus)*. In the open waters of Serbia (the Danube River Basin) a total of 26 non-indigenous fish species were recorded, of which 16 were the allochthonous invasive fishes. The major means of introductions and translocations were found to be the aquaculture, fish stocking and transportation. Habitat modification was found to be the factor that largely contributes to the capability of the water bodies to become a suitable recipient area. The large presence of alien fish species (27.66%) and its parasites creates a serious threat to the stability of freshwater ecosystems and the survival of the native ichthyofauna. The main environmental consequences of alien fish spreading are related to the alteration in fish community structure and function, as well as the introduction of the alien parasite species.
Keywords: *parasites, alien fish, alteration in fish community, Danube, Serbia*

Introduction

The introduction of fish specimens into aquatic ecosystems is common around the world. The main purpose of these introductions over the past three decades is for aquaculture, reinforcement of natural populations, biological control or recreation activities (exotic fish aquaria, angling, etc.) (Welcomme, 1981, 1988; Stewart, 1991). Ballast water of ships, deliberate fish stocking and introduction into aquaculture were pointed as prospective agents of dispersal of non-indigenous fish species in aquatic ecosystems (Gherardi et al., 2009).

Alien fishes have been introduced for many reasons in Europe: ornament, sport, improvement of wild stocks, aquaculture, biological control and accident (Elvira, 2001).

Aquatic introductions are made possible by a range of factors, including species-specific traits as well as by human activities such as river regulation, the connection of bordering basins by canals or ballast transport (Grigorovich et al., 2003). The success of introduction depends on the capability of species to avoid predators and parasites (Torchin et al., 2003). According to that, introduced species attain higher population densities and greater individual sizes in the recipient areas as compared to nonspecific

http://www.aloki.hu ● ISSN 1589 1623 (Print) ● ISSN 1785 0037 (Online)
DOI: http://dx.doi.org/10.15666/aeer/1605_61296142
© 2018, ALÖKI Kft., Budapest, Hungary

in their native range (Torchin et al., 2001). Non-indigenous species may affect indigenous species by competing for resources, transferring pathogens, or significantly altering the habitat. The introduction of non-indigenous species may work synergistically with some factors, such as water pollution, to alter the population and distribution of indigenous species (Elvira, 2001). The main environmental consequences of alien fish spreading are related to the alteration in fish community structure and function, as well as the introduction of the non-indigenous parasite fauna. Despite the importance of host manipulation by parasites for ecosystems and health, the effects of environmental changes on their ecological roles are largely ignored (Labaude et al., 2015). In contrast to other ecological effects, the importation of parasites, pathogens and diseases can be made via alien fish never intended to be released into the wild. Many diseases of salmonids that infect hatchery-reared fish and also occur in wild populations have been imported. Rainbow trout *Oncorhynchus mykiss* (Walbaum, 1792) from the western part of North America has carried furunculosis to Europe (Borno and Colquhoun, 2009). The importation of pathogens that are not group specific is a great risk associated with the introduction of exotic species (Elvira, 2001).

The consequences of biotic invasions are diverse and interconnected, since invaders can alter fundamental ecological properties such as dominant species in a community, productivity, nutrient cycling and thus can alter the structure and function of the ecosystem (Mack et al., 2000). Also, when present in sympatry, invasive species have the potential to amplify or diminish their ecological impacts through their trophic interactions, like it is tested for *Cyprinus carpio* and *Pseudorasbora parva* (Jackson and Britton, 2014).

Aquatic ecosystems in Serbia, especially those settled in north, lowland district, are influenced by biological invasion and contamination. The Danube River is an important invasion corridor, so called "Southern Invasion Corridor" (Galil et al., 2007) highly suitable for introduction of invasive fish species in Serbian waters (Jankovic et al., 1987; Hegedis et al., 1991; Cakic et al., 1996, 2004; Maletin et al., 1997; Simonovic and Nikolic, 1997; Simonovic et al., 1998, 2001). Also, the role of hydro-morphological alterations in aquatic invasions in this region has already been shown in the case of introduction and acclimation of invertebrate and fish species (Jankovic et al., 1987; Lenhardt et al., 2011). Thus, the Iron Gate area, downstream stretches of the main tributaries of the Danube River (the Sava, the Tisa and the Velika Morava River), that are under the influence of hydro-morphological changes, as well as artificial channel network Danube-Tisa-Danube, seemed to be suitable recipient areas for introduction and population establishment of non-native taxa.

Non-native ichthyofauna in Serbia has mostly been investigated as the part of ecological or taxonomical studies of particular areas. The data on alien fish fauna within the Serbian part of the Danube River originated from a number of studies and monitoring programs (Cakic and Hristic, 1987; Maletin et al., 1997; Jankovic, 1998; Simonovic et al., 1998, 2001; Lenhardt et al., 2011; Zorić et al., 2014). Introduction of allochthonous species into Serbian waters were made primarily in order to increase ichthyoproduction for weed control, sport fishing purposes and also accidentally (Lenhardt et al., 2011).

The aim of the present study is to report parasitic species of allochthonous fish species in the Serbian waters in the period of the last 31 years, and to investigate their contribution to diversity of fish parasitofauna.

http://www.aloki.hu ● ISSN 1589 1623 (Print) ● ISSN 1785 0037 (Online)
DOI: http://dx.doi.org/10.15666/aeer/1605_61296142
© 2018, ALÖKI Kft., Budapest, Hungary

Materials and methods

The study comprehends the data derived from several long-term investigations of freshwater fish species in the surface waters of the Danube River Basin in Serbia. During these studies, many allochthonous fish species have been identified and processed. Fish samples were collected using multi-mesh nets with mesh size of 10-60 mm, as well as by electrofishing (HONDA 1.2 kW, 6 A). After sampling, fish specimens were anesthetized in clove solution and sacrificed with a quick blow to the head. Fish species were identified according to Simonović (2006). The material of non-native freshwater fishes was analyzed for ecto- and endoparasites using standard parasitological procedure. Squash slides were taken from the skin and gills and observed under a light microscope (400 x magnitudes) within two hours. The slides were impregnated with silver-nitrate according to the modified Klein-Feussner method. The collected parasites were preserved in 4% formaldehyde (Acantocephala, Digenea/Trematoda, Cestoda, Bivalvia), in a mixture of ammonium picrate and glycerin (Monogenea) or in a mixture of glycerin and alcohol (Nematoda). Metazoan parasites were bleached, stained, prepared and fixed for determination and collection. Isolation, sorting and identification of parasite fauna have been done in the laboratory. Appropriate identification keys were used for the determination of parasite fauna representatives to the lowest taxonomic level (Bykhovskaya-Pavlovskaya et al., 1962; Banina, 1984; Shulman and Jankovsky, 1984; Stein, 1984; Bauer, 1987; Lom and Dikova, 1992; Moravec, 1994).

Results

In total, 26 non-indigenous fish species from nine different families have been reported from the Serbian part of the Danube River basin area (*Table 1*), contributing to the total species richness of ichthyofauna of Serbia 27.66%. Their parasitic species have been investigated and identified. In this paper, a total of 33 parasites (ecto- and endo-) are reported. The impact of those aliens on native fish is the topic for further research.

The list of allochthonous fish species, their status and occurrence in recipient area, pathway of introduction in our waters as well as their origin are presented (*Table 1*).

Table 1. *Non-indigenous fish species (26) within the Danube River Basin in Serbia*

Taxa	ST	OC	MI	OR
Fam. Polyodontidae				
Polyodon spathula (Walbaum, 1792)	NN	R	AC	NA
Fam. Coregonidae				
Coregonus peled (Gmelin, 1789)	U	R	FS	E
Fam. Salmonidae				
Salvelinus fontinalis (Mitchill, 1815)	NN	R	AC	NA
Salvelinus alpinus (Linnaeus, 1758)	NN	R	AC	E
Oncorhynchus mykiss (Walbaum, 1792)	NN	F	AC	NA
Salmo letnica (Karaman, 1924)	N	R	FS	E
Fam. Cyprinidae				
Pseudorasbora parva (Schlaegel, 1842)	N	FA	AC	A
Ctenopheryngodon idella (Valenciennes, 1844)	N	FA	AC	A
Hypophthalamichthys molitrix (Valenciennes, 1844)	N	FA	AC	A

http://www.aloki.hu ● ISSN 1589 1623 (Print) ● ISSN 1785 0037 (Online)
DOI: http://dx.doi.org/10.15666/aeer/1605_61296142
© 2018, ALÖKI Kft., Budapest, Hungary

Hypophthalamichthys nobilis (Richardson, 1844)	N	FA	AC	A
Carassius gibelio (Bloch, 1783)	N	FA	FS	A
Alburnus albidus (Costa, 1838)	N	FA	FS	E
Pachychilon macedonicus (Steindachner, 1892)	U	R	UC	E
Rutilus basak (Heckel, 1843)	U	R	FS	E
Scardinius graecus Stephanidis, 1937	U	R	UC	E
Fam. Ictaluridae				
Ameiurus nebulosus (Le Sueur, 1819)	N	FA	AC	NA
Ameiurus melas (Rafinesque, 1820)	N	FA	AC	NA
Fam. Centrarchidae				
Lepomis gibbosus (Linnaeus, 1758)	N	FA	AC	NA
Micropterus salmonides (Lacepede, 1802)	N	FA	FS	NA
Fam. Gobiidae				
Neogobius melanostomus (Pallas 1811)	N	FA	S	PC
Neogobius fluviatilis (Pallas, 1811)	N	FA	UC	PC
Ponticola kessleri (Gunther, 1861)	N	F	S	PC
Babka gymnotrachelus (Kessler, 1857)	N	F	S	PC
Proterorhinus semilunaris (Heckel, 1837)	N	F	UC	PC
Odontobutidae				
Perccottus glenii (Dybowsky, 1877)	N	R	UC	A
Fam. Syngnathidae				
Syngnathus abaster (Risso, 1826)	N	FA	S	PC

Status **(ST)** – N-Naturalized, NN-not naturalized, U-unknown. Occurrence **(OC)** – FA-frequent and abundant, F-frequent, R-rare or single findings. Means of Introduction **(MI)** – AC-aquaculture, FS-fish stocking, S-shipping, UC-unclear. Origin **(OR)** – PC-Ponto-Caspian, A-Asia, NA-North America, E-Europe out of Ponto-Caspian Area

In *Table 2* the list of parasitic species (14 ecto- and 19 endoparasites) are presented, in seven allochthonous invasive fish species from the Serbian part of the Danube River Basin. Among them, some of the identified parasitic species are new for fish parasitofauna in the Serbian waters (*Trichodina nobilis, Balantidium sp., Philometroides cyprini, Philometroides parasiluri, Eustrongylides* sp., *Ergasilus sieboldi, Lernaea cyprinacea, Sinergasilus polycolpus)* (marked *, see *Table 2*).

Table 2. *Parasitic species (ecto-and endoparasitic species) of seven allochthonous invasive fish species, Danube River in Serbia*

Taxonomy group	Parasitic species	Fish host	Reference
Eumycota	*Saprolegnia sp*	*Oncorhynchus mykiss*	Nikolic et al., 2010
Myxosporidia	*Myxobolus sp.*	*Oncorhynchus mykiss*	Cakic, 2002
Ciliophora	*Ichthyophthirius multifilis* (Fouquet, 1876)	*Carassius gibelio*	Nikolic and Simonovic, 1998a
		Oncorhynchus mykiss	Cakic, 2002
		Ameiurus nebulosus	Nikolic and Simonovic, 1998b
	Chilodonella cyprini (Moroff, 1902)	*Carassius gibelio*	Nikolic and Simonovic, 1998b
		Ameiurus nebulosus	Nikolic and Simonovic, 1999a

http://www.aloki.hu ● ISSN 1589 1623 (Print) ● ISSN 1785 0037 (Online)
DOI: http://dx.doi.org/10.15666/aeer/1605_61296142
© 2018, ALÖKI Kft., Budapest, Hungary

	Chilodonella hexasticha (Kiernik, 1909)	*Carassius gibelio* *Oncorhynchus mykiss*	Nikolic et al., 2006 Nikolic et al., 2006
	Trichodina nigra (Lom, 1960)	*Carassius gibelio* *Ameiurus nebulosus*	Nikolic et al., 2003 Nikolic et al., 2003
	Trichodina nobilis (Chen, 1963)*	*Ctenopharyngodon idella* *Hypophthalmichthys molitrix*	Nikolic and Simonovic, 1998a Nikolic and Simonovic, 1998a
	Trichodina acuta (Lom, 1961)	*Ameiurus nebulosus*	Nikolic et al., 2003
	Trichodina sp.	*Carassius gibelio* *Oncorhynchus mykiss*	Nikolic et al., 2003 Cakic, 2002
	Trichodinella epizootica (Raabe, 1950)	*Lepomis gibbosus* *Ameiurus nebulosus*	Nikolic and Simonovic, 1999a,b Nikolic and Simonovic, 1999a,b
	Trichodinella subtilis (Lom, 1959)	*Ameiurus nebulosus*	Nikolic and Simonovic, 1999a,b
	Balantidium sp. (Claparède & Lachmann, 1858)*	*Carassius gibelio*	Cakic and Hristic, 1987
	Apiosoma piscicola var. *minor* (Blanchard, 1885)	*Oncorhynchus mykiss*	Nikolic and Simonovic, 1999a
	Apiosoma piscicola piscicola (Blanchard, 1885)	*Ameiurus nebulosus*	Nikolic and Simonovic, 1999b
Monogenea	*Gyrodactylus derjavini* (Mikailov, 1975)	*Oncorhynchus mykiss*	Nikolic and Simonovic, 1999b
	Urocleidus similis (Mueller, 1936)	*Lepomis gibbosus*	Kiskaroly and Tafro, 1988
Digenea	*Diplostomum spathaceum* (Nordmann, 1832)	*Oncorhynchus mykiss*	Nikolic and Simonovic, 1999b
	Posthodiplostomum cuticula (Nordmann,, 1832)	*Carassius gibelio*	Cakic et al., 1998
Cestoda	*Triaenophorus nodulosus* (Pallas, 1781)	*Ctenopharyngodon idella*	Cakic and Hristic, 1987
Nematoda	*Philometroides cyprini* (Ishii, 1931)*	*Carassius gibelio*	Cakic et al., 1998
	Philometroides parasiluri (Yamaguti, 1935)*	*Percottus glenii*	Nikolic et al., 2007
	Schulmanela petruschewskii (Schulman, 1948)	*Lepomis gibbosus*	Peric, 1994
	Eustrongylides sp. (Jägerskiöld, 1909)*	*Percotus glenii*	Moravec, 2008 (Nikolic et al., 2007)
Acanthocephala	*Acanthocephalus anqullae* (Müller, 1780)	*Oncorhynchus mykiss* *Ameiurus nebulosus*	Cakic, 2002
	Neoechinorhynchus rutili (Müller, 1780)	*Oncorhynchus mykiss*	Cakic and Hristic, 1987
	Pomphorhynchus laevis (Müller, 1776)		Babic, 1935
	Pomphorhynchus bosniacus (Kiskarolj & Cankovic, 1969)		Cakic, 2002
	Metechinorhynchus salmonis (Muller, 1780)		Cakic, 2002
	Pseudoechinorhynchus borealis (Linstow, 1901		Cakic, 2002
Hirudinea	*Piscicola geometra* (Linnaeus, 1758)	*Carassius gibelio*	Cakic et al., 1998
Crustacea	*Ergasilus sieboldi* (von Nordmann, 1832)*	*Ctenopharyngodon idella* *Lepomis gibbosus*	Cakic and Hristic, 1987
	Lernaea cyprinacea (Linnaeus, 1758)*	*Hypophthalmichthys molitrix* *Lepomis gibbosus*	Cakic and Hristic, 1987 Cakic and Hristic, 1987
	Sinergasilus polycolpus (Markevich, 1940)*	*Hypophthalmichthys molitrix*	Cakic, 1986 Cakic et al., 1998

*A new parasite species in the ichthyoparasitofauna in Serbian open waters

http://www.aloki.hu ● ISSN 1589 1623 (Print) ● ISSN 1785 0037 (Online)
DOI: http://dx.doi.org/10.15666/aeer/1605_61296142
© 2018, ALÖKI Kft., Budapest, Hungary

Detailed data of parasite species records from seven examined invasive allochthonous fish species from Serbian open waters are presented in *Table 3*. Sampling localities are marked in *Figure 1*.

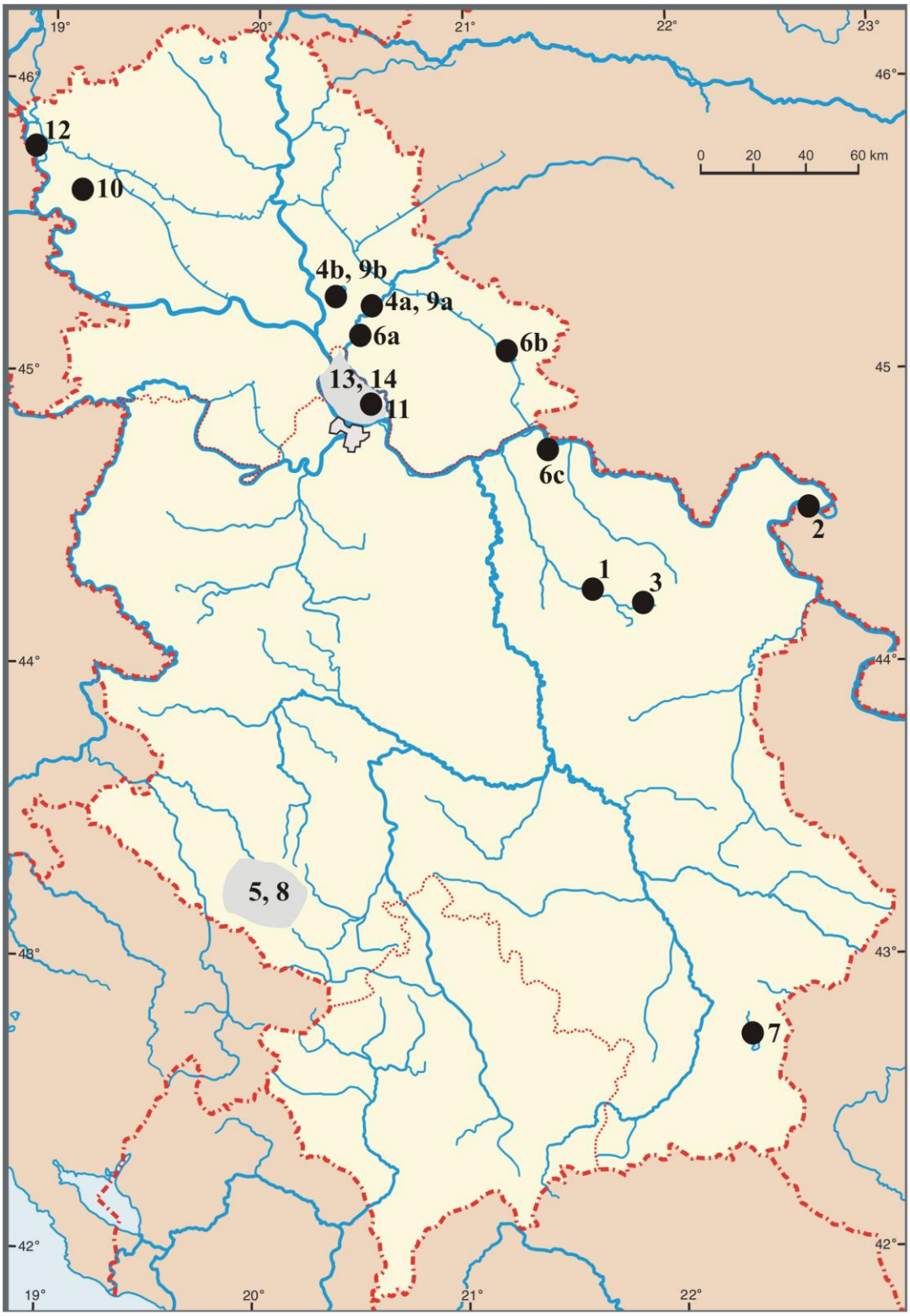

Figure 1. *Map of sampling localities on Serbian surface waters. (Numbers in map are given in Table 3)*

http://www.aloki.hu ● ISSN 1589 1623 (Print) ● ISSN 1785 0037 (Online)
DOI: http://dx.doi.org/10.15666/aeer/1605_61296142
© 2018, ALÖKI Kft., Budapest, Hungary

Table 3. *Details about sampling of invasive fish species and their parasites*

Cited reference	Sampling date and location	Symbol	GPS coordinates
Nikolic et al., 2010	1998, Krepoljin	1	N 44°16' 0", E 21°37' 0"E
Nikolic et al., 2007	2003, Vajuga near Kladovo	2	N 44°33'15.84", E 22°37'58.08"
Nikolic et al., 2006	1998, Žagubica	3	N 44°12'0", E 21°48'0"
Nikolic et al., 2003	1994, (a)Uzdin and (b)Ečka	4	N 45°12'10", E 20°37'7' N 45°19'4", E 20°26'20"
Cakic, 2002	October 1986 - May 1989, Uvac river basin on Sjenica-Pešter plateau	5	N 43°-43°30', E 19° 45'-20° 15'
Nikolic and Simonovic, 1999a	1991-1998, (a)Baranda (b)Vršački ritovi (c)Silver lake	6	N 45°5'4", E 20°26'22" N 45°9'23", E 21°10'11" N 44°45'36", E 21°27'0"
Nikolic and Simonovic, 1999b	1993, Vlasina lake	7	N 42°42', E 22°20'
Cakic et al., 1998	October 1986 - May 1989, waters of Sjenica-Pešter plateau	8	N 43°-43°30', E 19° 45'-20°15'
Nikolic and Simonovic, 1998a	1994, (a)Uzdin and (b)Ečka	9	N 45°12'10", E 20°37'7" N 45°19'4", E 20°26'20"
Nikolic and Simonovic, 1998b	1995, Svilojevo	10	N 45°39', E 19°4'
Peric, 1994	1993, Sibnica channel (Pancevacki rit wetland)	11	N 41°4'12", E 30° 8'59.99"
Kiskaroly and Tafro, 1988	1985-1987, Danube river (Channel system DTD)	12	N 45°45'27.24", E 19°0'35.96"
Cakic and Hristic, 1987	1984-1985, lowland channels of Pancevacki rit wetland	13	N 45° 2'46.91" - 44°52'19.25" E 20°22'33.80"- 20°35'0.82"
Cakic, 1986	1984-1985, waters of Pancevacki rit channels	14	N 45° 2'46.91" - 44°52'19.25" E 20°22'33.80"- 20°35'0.82"
Babic, 1935	Serbian part of Danube and Sava rivers		

Discussion

The Danube River is one of the main target areas for invasive fish species, as well as one of the most convenient ways for their dispersal. In the Danube River drainage area in Serbia 26 non-indigenous fishes have been recorded (Maletin et al., 1997; Simonovic and Nikolic, 1997; Simonovic, 2006).

One of the most adverse effects of the introduction of non-indigenous fish species on the native ones is associated with the introduction of exotic parasitic species. The unfavorable consequences of parasitism related with introduction of non-native fish species and spreading of parasites to native taxa have already been reported in Serbia (Cakic and Hristic, 1987; Cakic et al., 1998, 2001, 2004; Nikolic and Simonovic, 1998a,b, 1999a,b; Nikolic et al., 2003, 2006, 2007, 2010).

According to previous investigations in Serbia, the fish parasite fauna was supplemented by *Trichodina nobilis (*Ciliata*), Triaenophorus nodulosus* (Pallas, 1781) (Cestoda) and *Philometroides cyprini* (Nematoda) after the deliberate introduction of Asian fish species, such as Grass carp *Ctenopharyngodon idella*, Bighead carp *Hypophthalmichthys nobilis (*Richardson, 1845), silver carp *Hypophthalmichthys*

http://www.aloki.hu ● ISSN 1589 1623 (Print) ● ISSN 1785 0037 (Online)
DOI: http://dx.doi.org/10.15666/aeer/1605_61296142
© 2018, ALÖKI Kft., Budapest, Hungary

mollitrix (Valenciennes, 1844) into fish farms (Nikolic and Simonovic, 1998a) and invasion by *Philometroides parasiluri* (Yamaguti, 1935) *and Eustrongylides* sp. (Jägerskiöld, 1909) from *P. glenii* (Nikolic et al., 2007). Comparing with the results reported for the last 70 years (Djikanovic et al., 2012), eight parasitic species found in allochthonous fish are new for parasitofauna in the Serbian open water.

Ectoparasites of allochthonous fish species in Serbian open waters are examined. They can be detected as an outcome of fish juveniles' introduction or together with alien fish species. With fish juveniles several Asiatic ectoparasitic species were imported from the family of *Trichodinidae*, as a consequence of fish introduction in fishponds without previous health condition control (Nikolic and Simonovic, 1998a,b; Nikolic et al., 2007).

Endoparasites of allochthonous fish species in Serbian open waters have been the subject of a few hydrobiological investigations (Cakic et al., 1998, 2001, 2004). In relation to the growing concern about biological invasions in the Serbian section of the Danube River and interconnected ecosystems (Cakic et al., 1998, 2001, 2004; Simonovic et al., 1998, 2001; Simonovic, 2006) this work provides worthy information on the parasitofauna of non-indigenous fish species.

Metazoan parasites of *Neogobius* fishes (monkey goby *Neogobius fluviatilis* (Pallas, 1814), bighead goby *Ponticola kessleri* (Günther, 1861) and round goby *Neogobius melanostomus* (Pallas, 1814)) have been investigated in the Slovak section of the Danube River. Thirteen parasite species were identified, and the most prevalent parasites were *Pomphorhynchus laevis* (Acanthocephala) and glochidia of *Anodonta anatine*. The maximum parasite diversity was found in *N. fluviatilis* (Ondračkova et al., 2005). These founds are common to parasites in the Middle Danube basin. Gobiid fish (*Neogobius melanostomus* and *N. fluviatilis*) from the north-western Black Sea were analysed for presence of helminth species, and representatives from Cestoda (1), Trematoda (6), Nematoda (6) and Acanthocephala (3) have been reported (Kvach, 2005). In Serbian open waters no parasites for *Neogobius* fishes were observed. Parasitofauna of gobiid species in the Serbian part of the Danube River has not been investigated yet.

In the brown bullhead *Ameiurus nebulosus* some Trematodes from family Allocreadiinae and a few helminth parasites were found in the USA (Arnold, 1934; Krueger, 1954), while in the Serbian section of the Danube ectoparasites from the group Cliophora and *Acanthocephalus anguillae* (Acanthocephala) (Cakic and Hristic, 1987; Kiskaroly and Tafro, 1988; Nikolic and Simonovic, 1998b, 1999a,b; Nikolic et al., 2003) have been recorded. *Piscicola geometra* (Hirudinea) was recorded in Prussian carp *Carassius gibelio* (Bloch, 1782) from a lake in Turkey (Arslan and Emiroglu, 2011). Prussian carp from the Srebarna Biosphere Reserve was infected with two trematode species (*Posthodiplostomum cuticola* and *Diplostomum rutili)* and two nematode species (*Contracaecum microcephalum* and *Raphidascaris acus*) (Shukerova, 2005). In the Serbian open waters, Prussian carp have been infected by *Posthodiplostomum cuticula* and *Philometroides cyprinid* and some ectoparasites (Ciliophora) (Cakic and Hristic, 1987; Nikolic and Simonovic, 1998a,b; Cakic et al., 2001; Nikolic et al., 2003, 2006).

Some Monogenean parasites (*Dactylogyrus suchengtai, D. hypophthalmichthys* and *D. scrjabini*) were recovered from the silver carp at a fish farm in Hungary (Molnar, 1984). In our study, one Ciliophora and two crustaceans were found for this fish (Cakic and Hristic, 1987; Cakic et al., 1998; Nikolic and Simonovic, 1998a). Intestinal lesions

http://www.aloki.hu ● ISSN 1589 1623 (Print) ● ISSN 1785 0037 (Online)
DOI: http://dx.doi.org/10.15666/aeer/1605_61296142
© 2018, ALÖKI Kft., Budapest, Hungary

in the Grass carp caused by infection of *Balantidium ctenopharyngodonis* (Protozoa: Ciliophora) were reported by Molnar and Reinhardt (1978). Species *Trichodina nobilis, Ergasilus sieboldi* and *Triaenophorus nodulosus* have been detected in this alien fish species in the Serbian section of the Danube River Basin (Nikolic and Simonovic, 1998a).

During the survey in Denmark, the Rainbow trout *Oncorhynchus mykiss* has been examined and 12 protozoans and 10 metazoan species were found (Buchmann and Bresciani, 1997). In Serbian surface waters, a diverse parasitofauna of rainbow trout has been detected (Babic, 1935; Cakic, 1992; Nikolic and Simonovic, 1999a,b; Nikolic et al., 2006, 2010). Helminth fauna of the Chinese sleeper (*Nippotaenia mogurndae*, *Asymphylodora* sp.) and *Lepomis gibbosus* (*Triaenophorus nodulosus, Proteocephalus percae*, Echinorhynchidae) have been reported (Košuthová et al., 2009). Two monogenean parasites were found on the gill filaments of the pumpkinseed *Lepomis gibbosus* (Linnaeus, 1758) (Sterud and Jorgensen, 2006). Some monogenean parasites of pumpkinseed from the Slovak part of the Danube River Basin have been collected (*Gyrodactylus sp., Onchocleidus similis, O. dispar* and *Actinocleidus recurvatus*) (Ondračková et al., 2011). Monogenea *Urocleidus similes,* Nematoda *Schulmanela petruschewskii,* two crustaceans *(Ergasilus sieboldi*, *Lernaea cyprinacea*) as well as one species from Ciliophora (*Trichodinella epizootica)* were identified for *Lepomis gibbosus* in our study (Cakic and Hristic, 1987; Kiskaroly and Tafro, 1988; Cakic et al., 1998; Nikolic and Simonovic, 1999a).

The cestode *Nippotaenia mogurndae* is reported for the Chinese sleeper *Perccottus glenii* (Perciformes: Odontobutidae) (Košuthová et al., 2004; Reshetnikov et al., 2011). Except this cestoda species, the parasite community consisted of *Trichodina domerguei* and of 3 species, *Diplostomum spathaceum* (metacercaria), *Echinochasmus spinosus* (met.), and *Eustrongylides excisus* (larvae) (Mierzejewska et al., 2012). The parasites of the *Perccottus glenii* were studied in different parts of Ukraine and 15 taxa of parasites were registered; among them were 1 species of Microsporidia, 5 species of ciliates, 2 species of cestodes, 2 species of trematodes, 2 species of nematodes, 1 species of acanthocephalan, 1 species of parasitic crustacean and 1 mollusk (glochidia) (Kvach et al., 2013). For this alien fish, two Nematodes have been recorded in Serbian open waters (*Philometroides parasiluri, Eustrongylides* sp.) (Nikolic et al., 2007; Moravec, 2008).

Generally, the helminth fauna of invasive fish species reported from the new territories is less rich than their native areas (Drake, 2003; Torchin et al., 2003).

The consequences of introducing pathogens or hosts into new geographical zones where certain parasites exist can affect the healthiness of native fish population (Blanc, 2001; Pegg et al., 2015). The impacts of alien fish introduction on the fish populations in open waters are several: Demographic impacts (the impacts on the survival of fish populations are rarely quantified, except in the particular case of lake ecosystems, or populations targeted for fishing or long-term scientific studies); Genetic impacts (genetic differences of the hosts could play a critical role in the nature and outcome of helminthiasis – Wakelin (1978, 1992), hybridization was also considered with introgression of the resistance character or selective rearing of the survivors of a given population (Blanc, 2001). One of the negative impacts of alien species on freshwater ecosystems is the introduction of alien infectious agents, representing one of the greatest risks associated with ecological implications of introduction of species (Britton, 2013; Britton et al., 2011). As such, topmouth gudgeon in Europe is a carrier of several

http://www.aloki.hu ● ISSN 1589 1623 (Print) ● ISSN 1785 0037 (Online)
DOI: http://dx.doi.org/10.15666/aeer/1605_61296142
© 2018, ALÖKI Kft., Budapest, Hungary

pathogens (Gozlan et al., 2005), posing a risk not only to freshwater aquatic species, as this threat has also expanded to marine fishes.

Usually, invasive species have less parasite richness than in their native habitats (Torchin et al., 2003). The release of parasites and pathogens is one of the conditions of successful invasion (Kvach et al., 2013).

Conclusion

The large presence of alien fish species and its parasites creates a serious threat for the stability of freshwater ecosystems and the survival of the native ichthyofauna. In the Serbian surface waters contribution of allochthonous fish species to the total species richness of ichthyofauna is 27.66%. Invasive species are often superior competitors in relation to the evolutionary isolated native species populations (Mills et al., 2004). Negative impacts on native species include predation, trophic competition, behavioural interference, hybridization, spread of novel parasites and diseases, alteration of food webs and modification of biochemical cycles (Mills et al., 2004; Cucherousset and Olden, 2011; Kalogianni et al., 2014).

Invasion of allochthonous fishes in the Danube River Basin in Serbia caused important changes in the native fish fauna composition and also enriched the fish parasite fauna.

Acknowledgements. This work is supported by Ministry of Education, Science and Technological Development of the Republic of Serbia, Projects No. 173045 and No. 173025.

REFERENCES

[1] Arnold, G. J. (1934): Some trematodes of the common bullhead *Ameiurus nebulosus* (Le Sueur). – Transactions of the American Microscopical Society 53(3): 267-276.

[2] Arslan, N., Emiroglu, Ö. (2011): First record of parasitic Annelida-Hirudinea (*Piscicola geometra* Linnaeus, 1761) on *Carassius gibelio* (Bloch, 1782) in Lake Uluabat (Turkey). – Kafkas Universitesi Veteriner Fakultesi Dergisi 17(1): 131-133.

[3] Babic, I. (1935): Records of endoparasites in freshwater fishes. – Veterinary Archiv 5(8): 356-367.

[4] Banina, N. N. (1984): Order: Peritrichida. Suborder: Sessilina. – In: Shulman, S. S. (ed.) Key to Parasites of Freshwater Fish of USSR. Zoologicheskij Institut, Leningrad, pp. 281-321.

[5] Bauer, O. N. (1987): The Guide for Identification of Parasites of Freshwater. Fish Fauna of SSSR, Tom III. – Akademiya Nauk SSSR, Zoologicheskij Institut, Leningrad.

[6] Blanc, G. (2001): Introduction of Pathogens in European Aquatic Ecosystems: Attempt of Evaluation and Realities. – In: Uriarte, A., Basurco, B. (eds.) Environmental Impact Assessment of Mediterranean Aquaculture Farms. CIHEAM, Zaragoza, Spain, pp. 37-56.

[7] Bornø, G., Colquhoun, D. (2009): Classical Furunculosis (in Norwegian). Fact Sheet. – Norwegian Veterinary Institute. http://www.vetinst.no/nor/Faktabank/Allefaktaark/Furunkulose-klassisk.

[8] Britton, J. R. (2013): Introduced parasites in food webs: new species, shifting structures? – Trends Ecol. Evol. 28: 93-99.

[9] Britton, J. R., Pegg, J., Williams, C. F. (2011): Pathological and ecological host consequences of infection by an introduced fish parasite. – PLoS One 6(10): e26365.

http://www.aloki.hu ● ISSN 1589 1623 (Print) ● ISSN 1785 0037 (Online)
DOI: http://dx.doi.org/10.15666/aeer/1605_61296142
© 2018, ALÖKI Kft., Budapest, Hungary

[10] Buchmann, K., Bresciani, J. (1997): Parasitic infections in pond-reared rainbow trout *Oncorhynchus mykiss* in Denmark. – Diseases of Aquatic Organisms 28: 125-138.
[11] Bykhovskaya-Pavlovskaya, I. E., Gusev, A. V., Dubinina, M. N. et al. (1962): The guide for Determination of Parasites of Fresh Water Fish of SSSR. – Akademiya Nauk SSSR. Zoologicheskij Institut, Leningrad.
[12] Cakic, P. (1992): Fish parasites in waters of Sjenicko-Pesterska plateau and possibilities of their decrease. – Dissertation, University of Belgrade.
[13] Cakic, P., Hristic, D. J. (1987): Ichthyofauna of Pancevacki rit channels with regard to alochthonous species. – Natural Museum B42: 103-118.
[14] Cakic, P., Kataranovski, D., Milutinovic, M. (1996): *Ancyrocephalus paradoxus* Creplin, 1839 (Monogenea), a new species for ichthyoparasitofauna of Yugoslavia. – Proceedings of 7th International Congress on the Zoogeography and Ecology of Greece and Adjacent Regions, Book of abstracts, Athens, Greece.
[15] Cakic, P., Petrovic, Z., Kataranovski, D., Fister, S. (1998): Detection of parasitic copepods *Lamproglena pulcella* (Nordmann, 1983) and *Lernaea cyprinacea* (Linnaeus, 1758) on the gills of fish from Yugoslav waters. – Acta Veterinaria Belgrade 48(2-3): 131-138.
[16] Cakic, P., Stojanovski, S., Kataranovsk, I. D., Fister, S. (2001): The first finding of the nematode *Philometroides cyprini* (Ishii, 1931) on *Carassius auratus gibelio* from the Danube River, Yugoslavia. – Proceedings of the Scientific Meeting "Tissue Helminthoses of Men and Animals", Belgrade, pp. 65-70.
[17] Cakic, P., Lenhardt, M., Kolarevic, J. (2004): *Sinergasilus polyclopus*, a new copepod species in the ichthyoparasitofauna of Serbia and Montenegro. – Diseases of Aquatic Organisms 58: 265-266.
[18] Djikanovic, V., Paunovic, M., Nikolic, V., Simonovic, P., Cakic, P. (2012): Parasitofauna of freshwater fishes in the Serbian open waters: a checklist of parasites of freshwater fishes in Serbian open waters. – Reviews in Fish Biology and Fisheries 22(1): 297-324.
[19] Drake, J. M. (2003): The paradox of the parasites: implications for biological invasion. – Proceeding of the Royal society of London Series B, Biological Sciences 270: S133-S135.
[20] Elvira, B. (2001): Identification of non-native freshwater fishes established in Europe and assessment of their potential threats to the biological diversity. – Document on the 21st Meeting of the Standing Committee of the Convention of the Conservation of European Wildlife and Natural Habitats. Strasbourg, pp. 1-35.
[21] Galil, B. S., Nehring, S., Panov, V. E. (2007): Waterways as Invasion Highways. Impact of Climate Change and Globalization. – In: Nentwig, W. (ed.) Ecological Studies, Biological Invasions No 193. Springer, Berlin, pp. 59-74.
[22] Gherardi, F., Gollasch, S., Minchin, D., Olenin, S., Panov, V. (2009): Alien Invertebrates and Fish in European Inland Waters. – In: Drake. J. A. (ed.) DAISIE. Handbook of Alien Species in Europe. Springer, Knoxville, pp. 81-92.
[23] Grigorovich, I. A., Colautti, R. I., Mills, E. L., Holeck, K., Ballert, A. G., MacIsaac, H. J. (2003): Ballast-mediated animal introductions in the Laurentian Great Lakes: retrospective and prospective analyses. – Canadian Journal of Fish Aquatic Science 60: 740-756.
[24] Hegedis, A., Nikcevic, M., Mickovic, B., Jankovic, D., Andjus, R. K. (1991): Discovery of the goby *Neogobius gymnotrachelus* in Yugoslav fresh waters. – Archives of Biological Sciences 43: 39-40.
[25] Hoffman, G. L., Schubert, G. (1984): Some Parasites of Exotic Fishes. – In: Courtney, W. R. Jr., Stauffer, J. R. Jr. (eds.) Distribution, Biology and Management of Exotic Fishes. Johns Hopkins University Press, Baltimore, pp 233-261.
[26] Jackson, M. C., Britton, J. R. (2014): Divergence in the trophic niche of sympatric freshwater invaders. – Biological Invasions 16(5): 1095-1103.

http://www.aloki.hu ● ISSN 1589 1623 (Print) ● ISSN 1785 0037 (Online)
DOI: http://dx.doi.org/10.15666/aeer/1605_61296142
© 2018, ALÖKI Kft., Budapest, Hungary

[27] Jankovic, D. (1998): Natural reproduction by Asiatic herbivorous fishes in the Yugoslav section of the River Danube. – Italian Journal of Zoology 65: 227-228.
[28] Jankovic, D., Hegedis, A., Krpo, J. (1987): Taxonomische und Okologosche Charakteristiken des *Gobius* (*Neogobius*) *fluviatils* Pallas (1811) im Jugoslawischen Donauteil. – Proceedings of 26. Arbeitstagung der IAD, Passau, Deutschland, pp. 266-269.
[29] Kiskaroly, M., Tafro, A. (1988): The contribution of knowledge of helminthofauna of some fishes in one part of the Danube River. – Veterinaria 37(2-3): 211-221.
[30] Košuthová, L., Letková, V., Koščo, J., Košuth, P. (2004): First record of *Nippotaenia mogurndae* Yamaguti and Miyata, 1940 (Cestoda: Nippotaeniidae), a parasite of *Perccottus glenii* Dybowski, 1877, from Europe. – Helminthologia 4: 55-57.
[31] Košuthová, L., Koščo, J., Letkova, V., Košuth, P., Manko, P. (2009): New records of endoparasitic helminths in alien invasive fishes from the Carpathian region. – Biologia 64(4): 776-780.
[32] Krueger, R. F. (1954): A survey of the helminth parasites of fishes from Van Buren lake and rocky ford Greek. – The Ohio Journal of Science 54(4): 277-279.
[33] Kvach, Y. (2005): A comparative analysis of helminth faunas. And infection parameters of ten species of gobiid fishes (Actinipterygii: Gobiidae) from the north-western Black Sea. – Acta Ichthyologica et Piscatoria 35(2): 103-110.
[34] Kvach, Y., Drobiniak, O., Kutsokon, Y., Hoch, I. (2013): The parasites of the invasive Chinese sleeper *Perccottus glenii* (Fam. Odontobutidae), with the first report of *Nippotaenia mogurndae* in Ukraine. – Knowledge and Management in Aquatic Ecosystems 409(05): 1-11.
[35] Labaude, S., Rigaud, T., Cézilly, F. (2015): Host manipulation in the face of environmental changes: Ecological consequences. – International Journal for Parasitology: Parasites and Wildlife 4: 442-451.
[36] Lenhardt, M., Markovic, G., Hegedis, A., Maletin, S., Cirkovic, M., Markovic, Z. (2011): Non-native and translocated fish species in Serbia and their impact on the native ichthyofauna. – Reviews in Fish Biology and Fisheries 21: 407-421.
[37] Lom, J., Dykova, I. (1992): Protozoan parasites of fishes. Developments in Aquaculture and Fisheries Science 26. – Elsevier Science Publishers B. V., Amsterdam.
[38] Mack, R. N., Simberloff, D, Lonsdale, W. M., Evans, H., Clout, M., Bazzaz, F. A. (2000): Biotic invasions: causes, epidemiology, global consequences, and control. – Ecological Applications 10: 689-710.
[39] Maletin, S., Djukic, N., Miljanovic, B., Ivanc, A. (1997): Status of allochthonous ichthyofauna of Panonian Basin in Yugoslavia. – Acta Biologica Iugoslavica – Ecology 32(2): 87-98.
[40] Mierzejewska, K., Kvach, Y., Woźniak, M., Kosowska, A., Dziekońska-Rynko, J. (2012): Parasites of an Asian fish, the Chinese sleeper *Perccottus glenii*, in the Włocławek Reservoir on the lower Vistula River, Poland: Search of the key species in the host expansion process. – Comparative Parasitology 79(1): 23-29.
[41] Molnar, K. (1984): Occurrence of new monogeneans of Far-East origin on the gills of fishes in Hungary. – Acta Veterinaria Hungarica 32(3/4): 153-157.
[42] Molnar, K., Reinhardt, M. (1978): Intestinal lesions in grass carp *Ctenopharyngodon idella* (Valenciennes) infected with *Balantidium ctenopharyngodonis* Chen. – Journal of Fish Diseases 1(2): 151-156.
[43] Moravec, F. (1994): Parasitic Nematodes of Freshwater Fishes of Europe. – Kluwer Acad. Publ., Dordrecht, pp. 172-173, 195-198, 377-380, 396-399.
[44] Moravec, F. (2008): Misidentification of nematodes from the Chinese sleeper in Europe. – Bulletin of the European Association of Fish Pathologists 28(2): 86-87.
[45] Nikolic, P. V., Simonovic, P. D. (1998a): Seasonal dynamics of carp infestation by *Trichodina nobilis* Chen, 1963 (Peritrichia, Ciliata) in two fish-ponds in Banat. – Tiscia Szeged 31: 59-61.

http://www.aloki.hu ● ISSN 1589 1623 (Print) ● ISSN 1785 0037 (Online)
DOI: http://dx.doi.org/10.15666/aeer/1605_61296142
© 2018, ALÖKI Kft., Budapest, Hungary

[46] Nikolic, P. V., Simonovic, D. P. (1998b): *Trichodinella epizootica* (Raabe, 1950) (Protozoa: Ciliata) – a new species for the Yugoslav fish-parasite fauna. – Ichthyologia 30(1): 39-41.
[47] Nikolic, P. V., Simonovic, D. P. (1999a): A survey of ciliate fish-parasite fauna of Yugoslavia. – Ichthyologia 31(1): 37-41.
[48] Nikolic, P. V., Simonovic, P. (1999b): Ciliata parasitofauna of fish in fishponds and open waters of Yugoslavia. – Proceedings of the Environmental Protection in Intensive Fish farming Workshop '97, Novi Sad, pp. 96-101.
[49] Nikolic, P. V., Simonovic, P., Poleksic, V. (2003): Preference of trichodinids (Ciliata, Peritrichia) occuring on fish-pond carp for particular organs and some morphological implications. – Acta Veterinaria Belgrade 53(1): 41-46.
[50] Nikolic, P. V., Simonovic, P. D., Maric, S. P. (2006): Occurrence of *Chilodonella hexasticha* (Ciliophora, Protista) on the farmed rainbow trout *Oncorhynchus mykiss* through the season. – Acta Veterinaria Belgrade 56(1): 55-61.
[51] Nikolic, P. V., Simonovic, P., Karan Znidarsic, T. (2007): First record in Europe of a nematode parasite in Amur sleeper *Perccottus glenii* Dybowski 1877 (Perciformes, Odontobutidae). – Bulletin of the European Association of Fish Pathologists 27: 36-38.
[52] Nikolic, P. V., Djikanovic, V., Paunovic, M., Maric, S., Simonovic, P. (2010): Parasitic infections in pond-reared rainbow trout *Oncorhynchus mykiss* in eastern Serbia. – Proceedings of the 1st International Symposium of Fisheries and Fishing Tourism, June 2010. Center for Fisheries "Neretva" Konjic, Boracko Lake, Bosnia and Herzegovina, pp. 245-247.
[53] Ondračková, M., Dávidová, M., Pečínková, M. et al. (2005): Metazoan parasites of Neogobius fishes in the Slovak section of the River Danube. – Journal of Applied Ichthyology 21: 345-349.
[54] Ondračková, M., Dávidová, M., Přikrylová, I., Pečínková, M. (2011): Monogenean parasites of introduced pumpkinseed *Lepomis gibbosus* (Centrarchidae) in the Danube River Basin. – Journal of Helminthology 85(4): 435-441.
[55] Pegg, J., Andreou, D., Williams, C. F., Britton, J. R. (2015): Temporal changes in growth, condition and trophic niche in juvenile *Cyprinus carpio* infected with a non-native parasite. – Parasitology 142(13): 1579-1587.
[56] Peric Z (1994): Dynamic of fish endoparasites appearance in open waters, as well as criterions for their repression. – Msc Thesis, Faculty of Veterinary Medicine, University of Belgrade.
[57] Reshetnikov, A. N., Protasova, E. N., Sokolov, S. G., Pelgunov, A. N., Voropaeva, E. L. (2011): Infection of *Perccottus Glenii* Dybowski, 1877 (Odontobutidae, Pisces) by parasite *Nippotaenia Mogurndae* Yamaguti et Miyata, 1940 (Nippotaeniidae, Cestoda) through cannibalism. – Russian Journal of Biological Invasions 2(1): 46-48.
[58] Shukerova, S. (2005): Helminth fauna of the Prussian carp, *Carassius gibelio* (Bloch, 1782), from the Srebarna Biosphere reserve. – Trakia Journal of Sciences 3(6): 36-40.
[59] Shulman, S. S., Jankovsky, A. V. (1984): Phylum Ciliophora. – In: Shulman, S. S. (ed.) Key to Parasites of Freshwater Fish of USSR. Zoologicheskij Institut, Leningrad, pp. 225-280.
[60] Simonovic, P. (2006): The Fishes in Serbia. 2nd edition. – NNK International, Faculty of Biology & Agency for Environment Protection, Belgrade, Serbia.
[61] Simonovic, P., Nikolic, V. (1997): Freshwater fish of Serbia: an annotated check list with some faunistic and zoogeographic considerations. – Bios Thessaloniki 4: 137-156.
[62] Simonovic, P., Valkovic, B., Paunovic, M. (1998): Round goby *Neogobius melanostomus*, a new Ponto-Caspian element for Yugoslavia. – Folia Zoologica 47(4): 305-312.
[63] Simonovic, P., Paunovic, M., Popovic, S. (2001): Morphology, feeding and reproduction of the round goby, *Neogobius melanostomus* (Pallas), in the Danube River basin, Yugoslavia. – Journal of Great Lakes Research 27(3): 281-289.

http://www.aloki.hu ● ISSN 1589 1623 (Print) ● ISSN 1785 0037 (Online)
DOI: http://dx.doi.org/10.15666/aeer/1605_61296142
© 2018, ALÖKI Kft., Budapest, Hungary

[64] Stein, G. A. (1984): Order Peritrichida. Suborder Mobilina. – In: Shulman, S. S. (ed.) Key to Parasites of Freshwater Fishes of the USSR. Zoologicheskij Institut, Leningrad, pp. 321-389.
[65] Sterud, E., Jorgensen, A. (2006): Pumpkinseed *Lepomis gibbosus* (Linnaeus, 1758) (Centrarchidae) and associated parasites introduced to Norway. – Aquatic Invasions 1(4): 278-280.
[66] Stewart, J. E. (1991): Introductions as factors in diseases of fish and aquatic invertebrates. – Canadian Journal of Fisheries and Aquatic Sciences 48: 110-117.
[67] Torchin, M. E., Lafferty, K. D., Kuris, A. M. (2001): Release from parasites as natural enemies: increased performance of a globally introduced marine crab. – Biology Invasions 3: 333-345.
[68] Torchin, M. E., Lafferty, K. D., Dobson, A. P., McKenzie, V. J., Kuris, A. M. (2003): Introduced species and their missing parasites. – Nature 421: 628-630.
[69] Wakelin, D. (1978): Genetic control of susceptibility and resistance to parasitic infections. – Advances in Parasitology 16: 219-308.
[70] Wakelin, D. (1992): Genetic variation in resistance to parasitic infection: experimental approaches and practical applications. – Research in Veterinary Science 53: 139-147.
[71] Welcomme, R. L. (1981): Register of International Transfers of Inland Fish Species. – FAO Fisheries Technical Paper, Rome.
[72] Welcomme, R. L. (1988): International Introductions of Inland Aquatic Species. – FAO Fish. Tech. Pap. 294: 318, Rome.
[73] Zorić, K., Simonović, P., Djikanović, V., Marković, V., Nikolić, V., Simić, V., Paunović, M. (2014): Checklist of non-indigenous fish species of the River Danube. – Archives of Biological Sciences 66(2): 629-639.

http://www.aloki.hu ● ISSN 1589 1623 (Print) ● ISSN 1785 0037 (Online)
DOI: http://dx.doi.org/10.15666/aeer/1605_61296142
© 2018, ALÖKI Kft., Budapest, Hungary

IMPACTS OF KHAPRA BEETLE (*T. GRANARIUM* EVERTS) ONTO MARKETING PRICE AND RELEVANT TRAITS IN BREAD WHEAT (*T. AESTIVUM* L.)

ÖZBERK, F.

Akcakale Vocational College, The University of Harran, Sanliurfa, Turkey
(e-mail: fethiye@harran.edu.tr; phone:+90-505-527-5003)

(Received 4th Jul 2018; accepted 3rd Sep 2018)

Abstract. This research aimed to inspect the influence of khapra beetle (*T. granarium* Everts, 1898) onto marketing price and relevant traits in the controlled conditions in the laboratory of department of field crops of Faculty of Agriculture in the University of Harran in the south-east Anatolia. Laboratory experiment including larvae production was carried out employing 10 bread wheat advanced lines derived from CIMMYT (International Wheat and Corn Improvement Center) from 22 November 2017 and 29 April 2018. A split plot experimental design where the larval infestation levels are main plots and entries as sup plots with 3 replications was employed. Various physical, grain quality characteristics and marketing prices were scored initially and at nearly 40, 80 and 120 days after starting date. The results revealed that quality parameters declined significantly at the end of study. Geometric mean of weight loss was 8 kg ton^{-1}. This was 32.7 kg ton^{-1} at the end of study. Comparing ceiling prices at the local commodity market, marketing price loss of khapra damaging grains excluding parity loss of Turkish Lira against US dollar for 120 days was 30.8 USD ton^{-1}. It was concluded that there were response differences to khapra beetle among the entries regarding quality characteristics and marketing prices. Entry number of 9, 6 and 10 were the least weight loosing genotypes and 9, 1, and 10 were the least affected genotypes from marketing price declines due to khapra damaging.
Keywords: *khapra damage, common wheat, weight and quality losses, economical loss*

Introduction and literature review

Khapra beetle, *Trogoderma granarium* Everts (Coleoptera: Dermestidae) is one the worst pest of cereals and many other stored products (Ahmedani et al., 2011, 2009, 2007). Its undeniable economic importance relies on its ability to cause huge physical and quality losses in the stored grains by feeding and increasing temperature of storage environment making them liable to be invaded by some other pests including fungi and bacteria (Sayed et al., 2006; Ahmedani et al., 2009, 2007). It has tough larval ability to withstand starvation as long as three years under very low relative humidity (Ahmedani et al., 2009). Larvae feed from embryo initially and later consume the whole grain. This results in a hollow in the grain and only the seed coat remains (Ahmedani et al., 2009). The youngest larvae cannot feed on whole grain and is able to survive utilizing from deteriorated grains. Elderly larvae cannot eat whole grains. Rate of population increase may reach to 12.5 times in a month at 37 °C (Anonymous, 2005). Adults have no long life span and do not result in significant damage in grains (Ahmedani et al., 2007).

Parameters of grain quality reduce due to ending up of nutrients such as, total carbohydrates, crude fat, sugars, real protein content and sedimentation. Contrary, damaging khapra beetle increases grain moisture, total protein and crude fiber (Jood et al., 1993, 1996; Jood and Kapoor, 1993). Moreover anti nutrient polyphenol and phytic acid increase significantly (Kumar and Srivastava, 2017). Khapra beetle occurs in large scale in Northern hemisphere including Europe, Middle East, Central and Southern Asia (Ahmedani et al., 2007).

http://www.aloki.hu ● ISSN 1589 1623 (Print) ● ISSN 1785 0037 (Online)
DOI: http://dx.doi.org/10.15666/aeer/1605_61436153
© 2018, ALÖKI Kft., Budapest, Hungary

Post-harvest losses due to the storage pests were guessed to be up to 9% in developed countries whereas it could reached up to 20% in developing countries (Yadav et al., 2018). Post-harvest losses for grains in India were 7-10% of total production from field to purchasers and 4-5% at marketing (Yadav et al., 2018). In Pakistan, estimated storage loss for food grains due to pests was 4-10% (Hugue et al., 1969), 5.08% (Chaudhry, 1980), 5% (Ahmad, 1984), and 3.5-25.5% (Irshad and Baloch, 1985). Varietal differences were also detected in response to khapra beetle damage (Ahmedani et al., 2011, 2009). Average weight loss at 36 °C and 15% infestation level may reach to 2.6% with a 24% viability loss (Prasad et al., 1977). Weight loss may rise to 16.36% in wheat (Girish et al., 1975). Turkey is an important grain producer among top-ten countries in the world (FAO Stat, 2009) and host for many storage pests (Ekmekçi and Ferizli, 2000). Citing the last ten year average, wheat acreage varies from 7.5 to 8.5 mil ha and the annual production varies from 17.2 to 22.6 mil tons (TMO, 2016). 14.3% of total bread wheat production was met by southeastern Anatolia in 2016. Khapra beetle damage can reach high infestation levels in the region (Işıkber et al., 2014) and may vary from 10% (Ekmekçi and Ferizli, 2000) to 25-35% (Kalkan,1963). Weight loss in durum wheat for an 8 months storage period was 4.075% with a 103 USD ton^{-1} marketing price loss (Özberk et al., 2017). Downgrading factors mostly referred by purchasers in local commodity market are the presence of sunn pest damaged grains (%), barley grain contaminations (%), protein (%), energy value (Joule) and sedimentation (ml), thousands kernel weight (g) and hectoliter weight (kg) (Macca and Özberk, 2012; Özberk et al., 2005). Impact of khapra beetle deteriorated grains onto marketing price has not been assessed systematically in bread wheat. This study aimed to assess some physical traits, quality and marketing price of khapra beetle damaged grains under increasing larval infestations and various genotypes.

Material and methods

This laboratory experiment was carried out between 22 November 2017 and 29 April 2018 in the laboratory of department of field crops of Faculty of Agriculture in the University of Harran in Sanliurfa in Turkey. Ten advanced lines (Entry numbers of 2, 3, 4, 5, 6, 7, 8, 9, 10 and 13) from 35 th ESWYT (Elite Selection Wheat Yield Trial) 2014-15 (*Table 4*) were tested employing a split plot experimental design with three replications where larval infestation rates, i.e. 5, 10 and 15 and entries were assigned as main and subplots respectively. Losses in TKWs (g) (Uluoz, 1965), hectoliter weight (kg), sample weight (g) and marketing prices (cents kg^{-1}) were scored at 11.01.2018, 16.02.2018 and 29.03.2018 respectively. Except for marketing price scoring, all rest of experimental material (90 jars) was subjected to above analysis. At above given dates, first replication of experiment (30 jars) were presented to randomly selected 4 purchasers in local commodity market (as replications) for marketing price estimations holding on split plot experimental design. Initial marketing price estimations of all entries with non-damage grains were scored by presenting randomly selected 4 purchasers at the same commodity market employing randomized complete block design with 4 replications (purchasers). Some of grain quality analysis of entries at the beginning such as TKW (g) (Uluoz,1965), HLW (kg) (AACC 2000 method 55-10), protein (%) (AACC 2000 method 46-10.01), wet gluten (%) (AACC 2000 method 38-12.02), dry gluten (g) (AACC 2000 method 38-12.02), gluten index (%) (AACC 2000 method 38-12.02), grain hardness (kg m^{-2}) (AGW) and sedimentation (ml) (AACC 2000

http://www.aloki.hu ● ISSN 1589 1623 (Print) ● ISSN 1785 0037 (Online)
DOI: http://dx.doi.org/10.15666/aeer/1605_61436153
© 2018, ALÖKI Kft., Budapest, Hungary

method 38-10.01) were both scored at the beginning and at the end of study and a paired 't' test was performed for statistical significance. Geometric means of weight loss and marketing price reductions due to increasing khapra beetle damage were calculated and rank stability performance of entries for weight loss and marketing price punishments were scored and graphical illustrations were drawn (Huen, 1990). JMP-5 statistical software was used for all types of analyses including graphics.

Implementations for laboratory trial

Larvae were grown in corn a month prior to study start day. Grain samples were subjected to high temperature (5 hours at 45 °C) to omit the possibility of early infestations. Relative humidity (RH) (%) after heat treatment was 10% for all experimental material. Nine samples (100 g grain in each) of healthy grains from each entry were placed into 250 mL glass jars. Then jars were covered by muslin cloth with rubber bunds. 5, 10 and 15 neonate khapra beetle larvae were put into 3 jars of each entry (replications). Jars were placed into incubator calibrated to 32±2 °C and 55±5% RH for 120 days. Damaging grains in each jar were subjected to sieving to isolate the grains dust and other residues prior to scoring for various traits. All larvae and pupae in jars were kept alive and returned to jars after scoring traits.

Results

Thousands kernel weights, hectoliter weights, sample weights and marketing prices

Above given characteristics for all entries were scored at the three consecutive dates of study. A split plot ANOVA for all traits was performed individually and the statistically significant components of variation excluding larval intensity x entries interactions were grouped through LSD (Least significant differences). Joint effects of major factors may result in complications in interpretations. Therefore this was avoided. Grain samples of all entries free from Khapra damage were presented to local purchasers for initial marketing price estimates and purchasers (replications) were non-significant ($F = 3.13^{ns}$ $p > 0.05$). Entries were found to be significant ($F = 3.38^{**}$ $p < 0.01$). Entries 8, 3 and 2 were at top three ranks giving 30.893, 30.806 and 30.675 cents kg^{-1} respectively. Average marketing price of all entries was 30.50 cents kg^{-1}.

First scoring date (10.01.2018)

Individual analysis of variance revealed that the response of entries against khapra beetle infestation for TKW, sample weights and marketing price were statistically significant giving $F = 77.36^{***}$ ($p < 0.001$), $F = 3.829^{**}$ ($p < 0.01$), $F = 16.97^{**}$ ($p < 0.01$) respectively (*Table 1*). No significant differences were found among larval infestation levels for TKW, HLW and sample weights. But this turned out to be significant for marketing price ($F = 46.05^{***}$, $p < 0.001$). Except HLW, CV's (%) for above given characteristics seemed to be reliable giving low values. A 13.28% CV for HLW was found to be higher than expected one. The means of statistically significant entries for TKW, sample weights and marketing price were grouped by LSD test. Entry number of 6, 8 and 7 ranked at top three giving 49.238, 44.988 and 44.539 g of TKW values. Entry numbers of 6, 8 and 10 for sample weight ranked at first three presenting none weight losses. Entry numbers of 3, 9, and 4 for marketing price placed at the first

http://www.aloki.hu ● ISSN 1589 1623 (Print) ● ISSN 1785 0037 (Online)
DOI: http://dx.doi.org/10.15666/aeer/1605_61436153
© 2018, ALÖKI Kft., Budapest, Hungary

three ranks giving 27.530, 27.504 and 27.496 cents kg^{-1} respectively. Larval infestations of 5, 10 and 15 for same characteristics gave 27.632, 26.965 and 26.376 cents kg^{-1}as expected.

Table 1. *Means and LSD groups of varieties and larval infestation levels for the TKW, HLW, weight loss and marketing price from 100 g of initial sample weight in first scoring date (10.01.2018)*

Entry number	TKW (g/groups)	Entry number	HLW (kg/groups)	Entry number	Sample weight (g/groups)	Entry number	Marketing price (cent/kg/groups)
6	49.238a	3	82.40	6	100.0	3	27.530a
8	44.988b	7	81.97	8	100.0	9	27.504a
7	44.537b	9	81.08	10	100.0	4	27.496a
9	44.228bc	1	80.51	9	99.99	1	27.268a
10	43.498c	4	80.37	5	99.98	6	27.236ab
3	42.096d	10	80.25	4	99.95	10	27.235ab
4	40.874e	2	79.87	3	99.88	7	27.197ab
2	40.341ef	6	79.10	2	99.84	5	26.885b
5	39.674fg	8	78.75	7	99.84	8	26.375c
1	38.993g	5	75.05	1	99.66	2	25.847d
Larval intensity							
5	43.133	10	81.27	5	99.99	5	27.632a
15	42.763	5	81.11	10	99.89	10	26.965b
10	42.645	15	77.44	15	99.85	15	26.576c
Statistical significances for some sources of variation and some descriptive statistics							
F entries	77.36**		0.57^{ns}		3.829**		16.97**
F larval intensity	1.74^{ns}		2.14^{ns}		0.07^{ns}		46.05**
Grand mean	42.84		79.94		99.917		27.057
Std. deviation	1.056		8.118		0.168		0.46
LSD entries	1.728		13.28		0.278		0.644
LSD larval intensity	na		na		na		0.324
CV%	2.46		10.01		0.168		1.70

na: not available, ns: not significant, *p < 0.05, **p < 0.01

Second scoring date (16.02.2018)

Individual analyses of variances (*Table 2*) were also performed for same traits given above. $F_{entries}$ turned out to be significant for all characteristics giving F = 53.57*** (p < 0.001), F = 5.87** (p < 0.01), F = 3.02** (p < 0.01) and F = 19.98** (p < 0.01) respectively. F values for larval infestation levels for all traits also turned out to be significant giving F = 20.94** (p < 0.01), F = 45.75*** (p < 0.001), F = 28.55** (p < 0.01) and F = 102.53*** (p < 0.001) respectively. CV's (%) for all traits under study were also quite low presenting reliability of the results. Entry numbers of 6, 8 and 9 for TKW ranked at top three giving 48.24, 43.53 and 43.50 g respectively. For HLW, entry numbers of 9, 5 and 4 placed at the first three ranks with 81.12, 81.06 and 80.95 kg respectively. For the sample weight, entry numbers of 10, 9 and 6 were the first three ranking entries with 99.08, 99.06 and 98.53 g presenting to be the least

http://www.aloki.hu ● ISSN 1589 1623 (Print) ● ISSN 1785 0037 (Online)
DOI: http://dx.doi.org/10.15666/aeer/1605_61436153
© 2018, ALÖKI Kft., Budapest, Hungary

affected genotypes from khapra beetle infestation. For the marketing price estimates, entry numbers of 1, 9 and 3 were the higher marketing price offer receiving genotypes with 26.910, 26.779 and 26.354 cents Kg^{-1} respectively. When the larval intensity increased from 5 to 15, TKW declined from 42.47 to 40.10 g, HLW from 81.62 to 78.25 kg, sample weight from 98.97 to 96.918 g and marketing price from 26.918 to 25.389 cents kg^{-1}.

Table 2. *Means and LS D groups of varieties and larval infestation levels for the TKW, HLW, weight loss and marketing price from 100 g of initial sample weight in second scoring date (16.02.2018)*

Entry number	TKW (g/groups)	Entry number	HLW (kg/groups)	Entry number	Sample weight (g/groups)	Entry number	Marketing price (cent/kg/groups)
6	48.24a	9	81.12a	10	99.08a	1	26.910a
8	43.53b	5	81.06a	9	99.06a	9	26.779a
9	43.50b	4	80.95a	6	98.53ab	3	26.354b
7	43.46b	1	80.94a	8	98.35ab	6	26.215bc
10	40.44c	3	80.43ab	2	98.06abc	10	26.177bc
3	40.18c	10	80.34ab	4	97.87bc	4	26.154bc
4	39.55cd	2	80.13ab	5	97.81bc	2	26.000c
5	38.67de	7	80.05ab	3	97.66bc	7	25.687d
2	37.89e	6	79.40b	7	97.51bc	8	25.667d
1	36.38f	8	77.35c	1	97.18c	5	25.380e
Larval intensity							
5	42.47a	5	81.62a	5	98.97a	5	26.918a
10	4098b	10	80.66a	10	98.45a	10	26.095b
15	40.10c	15	78.25b	15	96.91b	15	25.389c
Statistical significances for some sources of variation and some descriptive statistics							
F entries	53.57**		5.87**		3.02**		19.98**
F larval intention	20.94**		45.75**		28.55**		102.53**
G. mean	41.188		80.18		98.11		26.134
Std. deviation	1.43		1.40		1.098		0.37
LSD entries	2.34		2.26		1.79		0.626
LSD larval int.	na		3.18		2.49		0.510
CV%	3.47		1.74		1.11		1.41

na: not available, ns: not significant, *p < 0.05, **p < 0.01

Third scoring date (29.03.2018)

Analysis of variance for each traits was performed (*Table 3*) and $F_{entries}$ and $F_{larval\ intensities}$ were all found to be significant giving either $p < 0.01$ or $p < 0.001$ significance. CV's (%) obtained from ANOVA's ranging from 1.307 to 3.47% indicated the reliability of the results. Entry numbers of 6, 9 and 8 were the first three ranking genotypes giving 46.66, 43.59 and 43.31 g of TKW's respectively. For the hectoliter weight, entries 5, 6 and 9 were the highest ranking entries giving 81.72, 81.19 and 80.03 kg respectively. For the sample weight, entry numbers of 9, 6 and 10 were the top ranking and least affected genotypes with 98.30, 98.28 and 97.86 g respectively. Finally

http://www.aloki.hu ● ISSN 1589 1623 (Print) ● ISSN 1785 0037 (Online)
DOI: http://dx.doi.org/10.15666/aeer/1605_61436153
© 2018, ALÖKI Kft., Budapest, Hungary

in marketing price, entries 9, 1 and 10 were found to be less affected genotypes from khapra beetle infestation giving 25.755, 24.792 and 24.450 cents kg^{-1} respectively. As the larval intensity increased from 5 to 15, TKW decreased from 42.95 to 39.43 g, HLW from 81.14 to 77.26 kg, sample weight from 98.68 to 94.18 g and marketing price from 25.542 to 22.803 cents kg^{-1} respectively.

Table 3. *Means and LS D groups of varieties and larval infestation levels for the TKW, HLW, weight loss and marketing price from 100 g of initial sample weight in second scoring date (29.03.2018)*

Entry number	TKW (g/groups)	Entry number	HLW (kg/groups)	Entry number	Sample weight (g/groups)	Entry number	Marketing price (cent/kg/groups)
6	46.66a	5	81.72a	9	98.30a	9	25.755a
9	43.59b	6	81.19ab	6	98.28a	1	24.792b
8	43.31b	9	80.03ab	10	97.86ab	10	24.450c
7	42.75b	1	79.89ab	2	97.08abc	7	24.039d
10	41.31c	3	79.77ab	5	96.57bcd	4	23.950de
3	39.38cd	2	79.57ab	8	96.23cd	6	23.948de
2	39.55de	7	79.53ab	3	96.06cd	3	23.804de
4	39.47de	4	78.88b	4	95.93cd	2	23.762e
5	38.42e	10	78.83b	7	95.76cd	8	23.447f
1	37.39f	8	77.08c	1	95.19d	5	22.960g
Larval intensity							
5	42.95a		81.14a		98.68a		25.542a
10	41.34b		79.95a		97.32b		23.927b
15	39.43c		77.26b		94.18c		22.803c
Statistical significances for some sources of variation and some descriptive statistics							
F entries	34.99**		2.71**		3.80**		71.00**
F larval ıntensity	45.45**		35.49**		55.41**		387.9**
G. mean	41.246		79.45		96.73		24.09
Std. deviation	1.432		1.83		1.697		0.315
LSD entries	2.345		2.995		2.778		0.442
LSD larval int.	3.247		4.148		3.848		0.534
CV%	3.47		2.30		1.75		1.307

na: not available, ns: not significant, *p < 0.05, **p < 0.01

Comparison of initial and final quality parameters

Some of the major quality traits of all entries scored as the average of three reads at the beginning and at the end of study were given in *Table 4*. For the final quality analysis, all three replicates of each infestation level were joined prior to analyzing quality. Statistical significance between grand means of various characteristics at the beginning and at the end of study was investigated through paired 't' test. Except grain hardness, grand mean differences for all scored traits were found to be significant. Final means were always lower than those of initials. In grain hardness, non-damaged kernels were employed for scoring both at the beginning and at the end of study. Final grand means for TKW (g), HLW (kg), protein content (%), wet gluten (%), dry gluten (g), gluten index (5) and sedimentation (ml) were significantly lower than those of initials.

http://www.aloki.hu ● ISSN 1589 1623 (Print) ● ISSN 1785 0037 (Online)
DOI: http://dx.doi.org/10.15666/aeer/1605_61436153
© 2018, ALÖKI Kft., Budapest, Hungary

Table 4. *Comparison of some of quality characteristics scored initially and at the end of study*

Entry number (initial)	Orijin ESWYT 2014-15	TKW (g)	HLW (kg)	Protein (%)	Wet gluten (%)	Dry gluten (g)	Gluten index (%)	Grain hardness (kg)	Sedimentation (ml)
1	Prl/2**Pastor	38.48	80.94	12.40	37.9	1.23	89.0	12.62	43
2	Kachu#1	44.63	81.69	12.60	34.5	1.15	95.2	13.51	39
3	Mısr 1	41.86	82.30	12.90	38.3	1.29	94.1	12.88	46
4	Munal#1	41.51	80.63	11.00	32.2	1.08	97.0	10.91	49
5	Bekard#1/5/Kritati/4/..	41.20	81.99	10.50	31.0	1.06	92.1	10.34	34
6	Becard/Chyak	48.97	80.67	12.10	38.2	1.24	8105	10.70	39
7	Taita	45.55	80.88	11.40	30.7	1.08	98.4	10.67	37
8	Kachu//Kritati/2*TRCH	44.59	77.22	11.60	25.4	0.91	98.2	8.39	35
9	Kachu/Chonte	40.47	81.97	12.70	35.2	1.19	97.6	9.36	44
10	Kritati/Huw234+LR34/Prinia..	40.64	80.33	12.40	37.8	1.24	96.0	10.88	49
Entry number (final)	**Orijin ESWYT 2014-15**	**TKW (g)**	**HLW (Kg)**	**Protein (%)**	**Wet gluten (%)**	**Dry gluten (g)**	**Gluten index (%)**	**Grain hardness (Kg)**	**Sedimentation (ml)**
1	Prl/2**Pastor	37.70	79.90	13.24	36.8	1.22	85.0	10.51	37
2	Kachu#1	39.55	79.48	12.28	31.9	1.10	95.5	10.95	37
3	Mısr 1	39.98	79.77	13.40	37.8	1.05	87.4	11.57	40
4	Munal#1	39.27	78.88	11.65	29.6	1.05	98.3	11.82	42
5	Bekard#1/5/Kritati/4/..	38.42	80.72	10.60	30.8	1.01	87.2	10.35	32
6	Becard/Chyak	46.66	80.19	13.08	35.4	1.23	76.5	10.42	36
7	Taita	41.74	79.53	11.00	32.3	1.04	88.1	10.85	36
8	Kachu//Kritati/2*TRCH	43.31	77.55	10.20	26.4	0.86	98.8	9.79	31
9	Kachu/Chonte	40.49	80.03	12.20	32.5	1.14	95.1	7.77	41
10	Kritati/Huw234+LR34/Prinia..	41.31	78.83	11.80	32.1	1.08	77.8	10.81	47
Mean (initial)		**42.79**	**80.91**	**11.96**	**34.12**	**1.147**	**93.86**	**11.026**	**41.5**
Mean (final)		**40.85**	**79.56**	**11.94**	**32.56**	**1.078**	**88.97**	**10.48**	**37.9**
Paired student t /significance		**3.08***	**5.04****	**0.083^{ns}**	**2.75***	**3.00***	**2.60***	**1.903^{ns}**	**5.523****

na: not available, ns: not significant, *p < 0.05, **p < 0.01

Ranks stability analysis for sample weight and marketing price

A rank stability analysis for sample weight (*Fig. 1*) and marketing price (*Fig. 2*) was performed employing average rank and rank standard deviations of all entries. Entry numbers of 6, 10, 9 and 8 were the least weight loosing genotypes. Especially entry number of 6 had also lower standard deviation than grand mean of all standard deviations. Entry numbers of 9, 1, 3 and 10 were the highest marketing price offer receiving genotypes respectively. Entry numbers of 9, 1 and 10 were also found to be more stable than that of 3 with relatively lower standard deviation than that of grand mean of all entries. Geometric mean of weight loss during 120 days was 8 kg ton^{-1} and the loss was 32.7 kg ton^{-1} at the final scoring date. Ceiling marketing prices and grands mean of marketing prices of all entries at the scoring dates were given in *Figure 3*. Taking into account initial and final marketing prices and excluding parity loss of Turkish Lira against US Dollar, a 30.08 USD ton^{-1} genuine marketing price loss was detected for 120 days.

http://www.aloki.hu ● ISSN 1589 1623 (Print) ● ISSN 1785 0037 (Online)
DOI: http://dx.doi.org/10.15666/aeer/1605_61436153
© 2018, ALÖKI Kft., Budapest, Hungary

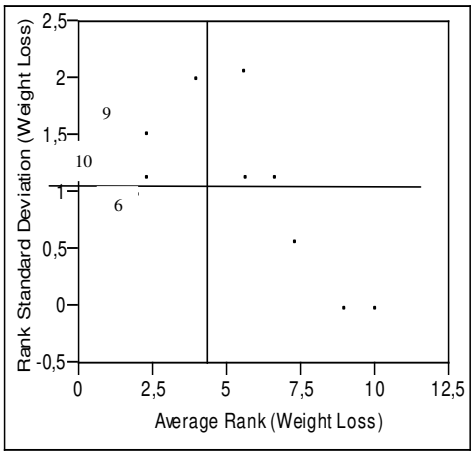

Figure 1. *Rank stability analysis for weight loss of entries*

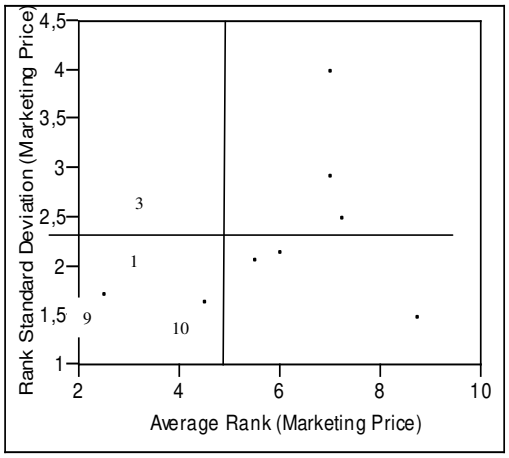

Figure 2. *Rank stability analysis for marketing price of entries*

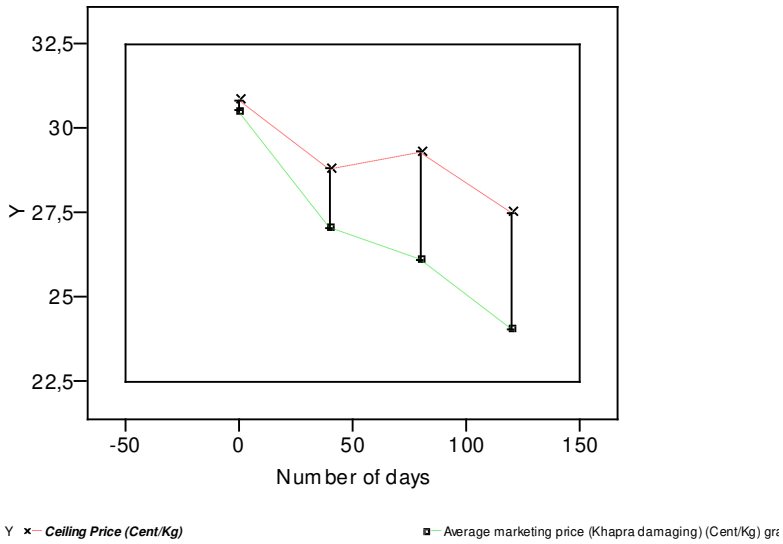

Figure 3. *Differences between ceiling prices and current marketing prices of entries at the beginning and at the consecutive dates of scoring (0, 40, 80 and 120 days)*

http://www.aloki.hu ● ISSN 1589 1623 (Print) ● ISSN 1785 0037 (Online)
DOI: http://dx.doi.org/10.15666/aeer/1605_61436153
© 2018, ALÖKI Kft., Budapest, Hungary

Discussion

Apart from initial and final scoring, TKW and HLW were scored regularly during the course of study. There was only 1.544 g reduction between grand means of all entries at the beginning (42.79 g) and that of at the end (41.246 g). Same trend was detected for HLW. There was only 1.46 kg decline at the beginning (80.96 kg) and at the end of study (79.45 kg). Özberk et al. (2017) obtained a 3.96 g reduction in TKW for 8 months in durum wheat. Weight loss of jars with 100 g of grain sample initially increased during the course of a 120 day period. Geometric mean of weight loss for study period was 8 kg ton^{-1} whereas at the final date, weight loss was 32.7 kg ton^{-1} (3.27%). Grand mean of weight loss in durum wheat was 4.075% in 8 months (Özberk et al., 2017). Varietal differences to khapra beetle infestation were detected for above given characteristics. Entry number of 6, 7, 8 and 9 for TKW and entry numbers of 6, 9 and 10 for HLW were the least affected genotypes. These results matched those of Ahmedani et al. (2009, 2011), Sayed et al. (2006) and Khattak et al. (2000). In which Mehran-89 and Wafaq-2001 were the least affected cultivars against khapra beetle infestation. Physio- chemical and biochemical structure of grains were proved to be properties for resistance mechanism (Warchalewski et al.,1993; Dobbie, 1991; Baker, 1986). The effects of larval intensities for all traits given above were significant. When the larval intensity increased, TKW, HLW and initial weight decreased confirming the results of Özberk et al. (2017), Ahmedani et al. (2011), Khattak et al. (2000) and Navarro et al. (1978). They proved the presence of high degree positive and significant correlations between progeny development vs. damage ratio and weight loss. Some of quality analysis such as wet (%), dry gluten (g), gluten index (%) and sedimentation (ml) at initial stage vs. final resulted in lower values for latter significantly. For the final analysis, all replications were joined to avoid any biased estimation. Non-significant grain hardness may be due to employment of only healthy grains for both scoring. Non-significant protein content (%) between initial vs. final seemed to be insect inclusion to flour and this results in some increase in protein (%). Marketing price estimations were received from randomly selected 4 purchasers (replications) at the local commodity market employing first replication of laboratory experiment. As shown by *Figure 3,* ceiling prices decreased gradually toward end of study due to the parity loss of Turkish Lira against US dollar (30.84 - 27.51 = 3.33 cents kg^{-1}). Whereas marketing price of khapra beetle infested grains reduced from 30.50 to 24.09 cents kg^{-1} for 120 days. A 6.41 cents kg^{-1} marketing price loss can be attributed to khapra infestation and parity loss. A 3.08 cents kg^{-1} marketing price loss (6.41- 3.33 cents kg^{-1}) was genuine due to khapra damage. This means a 30.8 USD ton^{-1} marketing price loss for 120 days. This was a 103 USD ton^{-1} for durum wheat in 8 months (Özberk et al., 2017).

Varietal differences to khapra beetle attack were genuine and entry numbers of 9, 1, 3 and 10 were the least marketing price loosing and stable genotypes. Increasing larval intensity reduced marketing price as detected by Özberk et al. (2017) in durum wheat. Economic loss of grain grower countries suffering Khapra beetle damage seem to be huge (Sayed et al., 2006; Ahmedani et al., 2007; Özberk et al., 2017). Hence, taking into account for zero tolerance trends of some countries such as Canada (Canada Grain Act, 1975) to stored grain insects, control measures and resistance mechanism of grains against Khapra beetle must be the focused of such researches.

http://www.aloki.hu ● ISSN 1589 1623 (Print) ● ISSN 1785 0037 (Online)
DOI: http://dx.doi.org/10.15666/aeer/1605_61436153
© 2018, ALÖKI Kft., Budapest, Hungary

Conclusions

It was concluded that even a short duration of storage such as 120 days, khapra beetle affected all quality parameters negatively and resulted in as much as 3.27% weight loss and a 30.8 USD ton^{-1} marketing price loss. The presence of varietal response to khapra beetle attack should also be stressed.

Acknowledgements. Many thanks for the purchasers (M. Satıs, B. Koc, H. Aslan, O. Gok, H. Salgu) in local commodity market for their help in marketing price estimates, K. Ayıkgoz for quality analysis and marketing price scoring, H. Ayhan for grain hardness analysis, D. Izol for larvae development, incubation and scoring. I declare my deep respects to I. Ozberk for his encouragement, comments, critics and helps for statistical analysis and M/s preparation.

REFERENCES

[1] AACC (2000): Approved methods of the American Association of Cereal Chemists.10th ed. – The American Association of Cereal Chemists, Approved Methods Committee, St. Paul, MN, USA.
[2] Ahmad, H. (1984): Storage of wheat in Pakistan. – Progressive Farming (Pakistan) 4(4): 36-40.
[3] Ahmad, M., Khan, M. R., Iqbal, A., Hassan, M. (1986): Farm level storage loss of wheat by insect pests in Samundri Tehsil. – Pakistan Entomology 8: 41-44.
[4] Ahmedani, M. S., Khaliq, A., Tarıq, M., Anwar, M., Naz, S. (2007): Khapra beetle (Tragoderma granarium Everts): A serious threat to food security and safety. – Pakistan Journal of Agricultural Science 44(3): 481-487.
[5] Ahmedani, M. S., Haque, M. I., Afzal, S. N., Aslam, M., Naz, S. (2009): Varietal changes in nutritional composition of wheat kernel (Triticum aestivum L.) caused by Khapra beetle infestation. – Pakistan Journal of Botany 41(3): 1511-1519.
[6] Ahmedani, M. S., Haque, M. I., Afzal, S. N., Naeem, M., Hussain, T., Naz, S. (2011): Quantitative losses and physical damage caused to wheat kernel (Triticum aestivum L.) by khapra beetle infestation. – Pakistan Journal of Botany 43(1): 659-668.
[7] Anonymous (2005): Industry Biosecurity Plan for the Grains Industry. Threat-Specific Contingency Plan 2005. – Department of Agriculture, Bentley Delivery Centre, WA, Australia.
[8] Baker, J. E. (1986): Amylase/proteinase ratios in larval midgets of ten stored product insects. – Entomol. Exp. Appl. 40: 41-46.
[9] Canada Grain Act. (1975): Canada grain regulations. – Canada Gazette, Part II 109(14): 1708-1839.
[10] Chaudhry, M. A. (1980): Aggregate Post-harvest Food Grain Losses in Pakistan, Vol. VI. – Dept. Agric. Marketing, UAF., Faisalabad.
[11] Dobie, P. (1991): Host-Plant Resistance to Insects in Stored Cereals and Legumes. – In: Gorham, J. R., Arlington, V. A. (eds.) Ecology and Management of Food-Industry Pests. AOAC, Rochville, Maryland, pp. 373-383.
[12] Ekmekçi, M. A., Ferizli, G. (2000): Current status of stored products protection in Turkey. – Integrated Protection of Stored Products IOBC Bulletin 23: 39-46.
[13] FAO Stat (2009): http://faostat.fao.org. – Accessed on 08.10.2014.
[14] Girish, G. K., Kumar, A., Jain, S. K. (1975): Assessment of the quality loss in wheat damaged by Tragorderma granarium Everts during storage. – Bulletin of Grain Technology 13(1): 26-32.

http://www.aloki.hu ● ISSN 1589 1623 (Print) ● ISSN 1785 0037 (Online)
DOI: http://dx.doi.org/10.15666/aeer/1605_61436153
© 2018, ALÖKI Kft., Budapest, Hungary

[15] Huehn, M. (1990): Non-parametric Estimation and Testing of g x e Interactions by Rank. – In: Manjit, S. K. (ed). Genotype and Environment Interactions and Plant Breeding. Dept. of Agriculture, Lousiana State Univ., USA, pp. 69-94.
[16] Huque, H., Anwar, M. S., Anisa, B. (1969): Control of khapra beetle in larval stage by the use of Malathion. – Agriculture Pakistan 20: 279-286.
[17] Irshad, M., Baloch, U. K. (1985): Losses in wheat during storage and their prevention. – Progressive Farming (Pakistan) 5(2): 17-79.
[18] Işıkber, A. A., Er, M. K., Tunaz. H., Bozkurt, H., Aydın, Z., Eroğlu, S. (2014): The occurrence and abundance of insect pests infesting stored wheat grains in different climatic zones of Turkey. – Proceedings of the 11th International Working Conference on Stored Product Protection (24-28 November 2014, Chiang Mai, Thailand), pp. 626-630.
[19] Jood, S., Kapoor, A. C. (1993): Protein and uric acid contents of cereal grains as affected by insect infestation. – Food Chemistry 46: 143-146.
[20] Jood, S., Kapoor, A. C., Singh, R. (1993): Available carbohydrates of cereal grains as affected by storage and insect infestation. – Plant Foods and Human Nutrition 43: 45-54.
[21] Jood, S., Kapoor, A. C., Singh, R. (1996): Effect of insect infestation and storage on lipids of cereal grains. – Journal of Agriculture and Food Chemistry 44: 1502-1506.
[22] Kalkan, M. (1963): Türkiye'de Trogederma Türleri, Trogoderma granarium (Everst)' in Laboratuvarda Kısa Biyolojisi ve Mücadelesi Üzerine İncelemeler. – Tarım Bakanlığı Zirai Mücadele Enstitüsü, Ankara.
[23] Khattak, S. U., Kamal, S., Ullah, K., Ahmad, S. Khan, A. U., Jabbar, A. (2000): Appraisal of rainfed wheat lines against Khapra beetle (Trogoderma granarium Everts). – Pakistan Journal of Zoology 32: 131-134.
[24] Kumar, S. K., Srivastava, C. (2017): Effect of temperature and food on the biology of Khapra beetle, tragoderma granarium Everts. – Journal of Entomology and Zoology Studies 5(3): 1015-1019.
[25] Macca, I., Özberk, I. (2012): Adıyaman ürün borsasında ekmeklik buğday fiyatlarını etkileyen faktörler. – Harran Üniversitesi Ziraat Fakültesi Dergisi 16(3): 49-59.
[26] Navarro, S., Kashanchi, Y., Green, M., Frandji, H. (1978): Causes of Loss in Stored Grain in Israel. – Progress Report, Israel Ministry of Agriculture, Israel Research Organization 1976/77.
[27] Özberk, I., Atlı, A., Pfeiffer, W., Özberk, F., Coşkun, Y. (2005): The effect of sunn pest (Eurigaster integriceps) damage on durum wheat: Impact in the market place. – Crop Protection 24(3): 267-274.
[28] Özberk, F., Özberk, I., Yücel, A. Atlı, A., Izol, D. (2017): Khapra beetle (Trogoderma granarium Everts, 1898) in durum wheat (Triticum durum Desf): Impacts on some seed characteristics and marketing price. – Turkish Journal of Entomology 41(2): 207-218.
[29] Prasad, H., Bhatia, P., Sethi, G. R. (1977): Estimation of feeding losses by Tragoderma granarium Everts in wheat. – Indian Journal of Entomology 39: 377-378.
[30] Sayed, T. S., Hirad, F. Y., Abro, G., H. (2006): Resistance of different wheat varieties to Khapra beetle, Trogoderma granarium Everts and lesser grain borer, Rhizopertha dominica (Fabricius). – Pakistan Journal of Biological Science 9: 1567-1571.
[31] TMO (2016): 2016 Yılı hububat raporu. – http://www.tmo.gov.tr. Accessed on 10.10.2017.
[32] Uluöz, M. (1965): Wheat Flour and Bread Analysis. – EUZF Pub. No: 57, Izmir, Turkey.
[33] Warchalewski, J. R., Nawrot, J. (1993): Insect infestation versus some properties of wheat grain. – Roczniki Nauk Rolniczych, Seria E. 23: 85-92.
[34] Yadav, J., Yadav, J. L., Saini, R. K., Devi, M. (2018): Stored grain pests incidence in wheat with particular reference to Khapra beetle, Tragoderma granarium Everts in southern Haryana, India. – International Journal of Current Microbiology and Applied Sciences 7(3): 2179-2186.

http://www.aloki.hu ● ISSN 1589 1623 (Print) ● ISSN 1785 0037 (Online)
DOI: http://dx.doi.org/10.15666/aeer/1605_61436153
© 2018, ALÖKI Kft., Budapest, Hungary

TETRACONAZOLE LEADS TO ALTERATIONS IN *FUSARIUM GRAMINEARUM* AT DIFFERENT MOLECULAR LEVELS

YÖRÜK, E.

Department of Molecular Biology and Genetics, Istanbul Yeni Yuzyıl University
Istanbul, Cevizlibag, Turkey
(e-mail: emre.yoruk@yeniyuzyil.edu.tr; phone: +90-532-599-3325; fax: +90-212-481-4058)

(Received 6th Jul 2018; accepted 31st Aug 2018)

Abstract. The alterations in *F. graminearum* due to tetraconazole (TCZ) have been investigated in this study. The minimum inhibitory concentration (MIC), and inhibitory concentrations 50% and 25% (IC_{50} and IC_{25}) were obtained by adding different concentrations of TCZ to potato dextrose agar (PDA). MIC, IC_{50} and IC_{25} values were detected as 32, 16 and 8 µg/mL TCZ. Epigenetic changes have been evaluated via genomic template stability (GTS) by the RAPD and CRED-RA methods. GTS values were recorded as 86.73% and 85.71% in IC_{50} and IC_{25} sets. A total of 157 bands were obtained via RAPD. The average % polymorphism values of *HapII* and *MspI* digested samples were detected as 5.72 and 5.37 with 4.68 and 2.6% for IC_{25} and IC_{50} groups, respectively. The expression levels of genes related to apoptosis (*Hog1*), cell stability (*Mgv1*), oxidative stress (*POD*) and deoxynivalenol production (*tri5*) in the control and the experiment sets were investigated by qPCR. Increased concentrations of TCZ lead to upregulation in *Hog1, Mgv1* and *POD* genes whereas down regulation was recorded in *tri5* expression. The late apoptosis and oxidative stress were detected via the acridine orange-ethidium bromide (AoEb) and the DCF-DA staining assays. The findings showed that TCZ could lead to damage on phytopathogenic fungi at genomic, epigenetics, transcriptomics and apoptotic levels.
Keywords: *apoptosis, epigenetics, fungicide, genomic stability, oxidative stress*

Introduction

Fusarium graminearum species complex is a worldwide important phytopathogenic species. *F. graminearum* is predominating causal agent of fusarium head blight (FHB) disease in humid and semi-humid areas. The FHB results in destructive affects in fields related to economically important cereals such as wheat, barley and maize (Goswami and Kistler, 2005; Miedaner et al., 2008). Annual economic losses reach up to millions of dollars only in the USA and China (Lori et al., 2009; Matny, 2015). Epidemics result in products with reduced quality and quantity. Also, deoxynivalenol, zearalenone and some other minor mycotoxins contamination of cereals have been detected in the fields related to FHB worldwide (Miedaner et al., 2008; Pasquali et al., 2016). FHB and the related mycotoxins lead to several kinds of negative effects on human health and struggle with major agent of FHB*, F. graminearum,* is a preliminary step in disease management.

F. graminearum is a homothallic fungus with asexual (*F. graminearum*) and sexual (*Gibberella zeae*) stages (Kerényi et al., 2004). High levels of genotypic and morphological diversity have been reported for *F. graminearum*. 16 members for this species complex have been identified by the morphological and multiloci genotyping analysis (Aoki and O'Donnell, 1999; O'Donnell et al., 2004; Miedaner et al., 2008; Sarver et al., 2011; Przemieniecki et al., 2015). The species also shows high levels of variation in host, chemotype and aggressiveness worldwide (Pasquali and Migheli, 2014). These and some features of *F. graminearum* make it popular phytopathogen and also allow it to become a model organism in molecular plant pathology research area.

http://www.aloki.hu ● ISSN 1589 1623 (Print) ● ISSN 1785 0037 (Online)
DOI: http://dx.doi.org/10.15666/aeer/1605_61556167
© 2018, ALÖKI Kft., Budapest, Hungary

The genome of *F. graminearum* PH-1 strain has been sequenced and annotated. Up to 14.000 genes are identified by bioinformatics analysis and comparative data for ESTs, DNA markers, gene clusters related to mycotoxin production or genes associated with secondary metabolite biosynthesis pathways have been well characterized (King et al., 2017). The knowledge on genome structure of *F. graminearum* shows that it would facilitate further molecular genetics studies about FHB.

Struggle with FHB and *F. graminearum* have been maintained by different approaches worldwide. The development of disease-resistant plant cultivars or genetically modified plants, the antagonistic microorganisms' usage and the fungicide treatment are currently the most popular strategies. However, the development of resistant plants or antagonistic microorganism usage have some possible disadvantages such as prolonged periods, laborious assays, non-cost-effective processes, low agronomic traits and poor results (Dal-Bello et al., 2002; Anand et al., 2003; Bai and Shaner, 2004; Bernardo et al., 2007). However, the usage of fungicides has become the most popular and the most effective strategy in fighting with FHB worldwide. Several common types of fungicides including benzimidazole class and demethylation inhibitors have been used in disease management worldwide. However, the fungicide application does not present successful results in the fields, where they have been used. Particularly, the antifungal resistant development has been reported for those chemical compounds in many regions of the world. The logic behind the poor results in disease management and fungicide resistance development have been related to high level of genetic diversity among the populations of *F. graminearum* species complex. The failure in fungicide application and fungicide resistance have been shown by genetic and phenotypic analysis. Isolates with MIC values higher than 10 µg/mL for azole derivatives have been detected in *F. graminearum* species complex isolates by the agar dilution technique. The point mutations in *β-tubulin* and *cyp51* genes leading to the fungicide resistance have been detected. Time management and climatic changes in agro-ecological regions where FHB present have also become related to failure related to fungucide application (Chung et al., 2008; Talas and McDonald, 2015; Qian et al., 2018; Yang et al., 2018). However, investigations associated with alterations in molecular levels in fungicide treated fungi could provide additional and extra point of view for disease management. In this study, it was aimed to detect the effects of tetraconazole (TCZ; one of the most common azole derivative used in disease management worldwide) on *F. graminearum* have been evaluated at epigenetics, transcriptomics and cellular levels by different approaches..

Materials and methods

Fungal material and phenotypic tests

F. graminearum H-11 strain which is isolated from the diseased rice sample was provided from Dr. Theresa Lee from Seoul National University (Lee et al., 2001). The experimental steps of this study were carried out in Turkey. The fungal control sets were grown on potato dextrose agar/broth (PDA/PDB) for 7 days at 26 ± 2 °C (PDA: Hi-Media, India) at controlled growth chamber (Nüve, Turkey). Experimental groups were grown on PDA/PDB amended with different concentrations of TCZ (2, 4, 8, 16 and 32 µg/mL) (Sigma, U.S.A.). The 0.25 cm^2 mycelial plugs were used for obtaining fresh cultures. Minimum inhibitory concentration (MIC), inhibitory concentration 50% and 25% (IC_{50} and IC_{25}) values were detected by the agar dilution technique and the

http://www.aloki.hu ● ISSN 1589 1623 (Print) ● ISSN 1785 0037 (Online)
DOI: http://dx.doi.org/10.15666/aeer/1605_61556167
© 2018, ALÖKI Kft., Budapest, Hungary

linear growth rates (LGR) were calculated by the measurement of radial growth of fungal cultures as mm day^{-1} at 4th and 7th days of incubation.

Genomic DNA (gDNA) extraction, RAPD (random amplified polymorphic DNA) and CRED-RA (coupled restriction enzyme digestion-random amplification) analysis

gDNA was extracted from the 7-day-old *F. graminearum* cultures of experiment sets. 100 mg mycelia was homogenized with liquid nitrogen, sterile pestle and mortar. 500 µL of lysis buffer (100 mM Tris HCl, 100 mM EDTA, 1 M NaCl, 1% SDS and 1/500: v/v: β-mercaptaethanol) was added and the homogenization was completed. Then, the sodium dodecyl sulphate-based protocol was followed (Niu et al., 2008; Yörük et al., 2016). Qualitative and quantitative analyses were performed via 1% agarose gels and spectrophotometer (Thermo, U.S.A.).

RAPD and CRED-RA methods were used in the genomic template stability and epigenetic profiling of TCZ treated and non-treated *F. graminearum*. A routine RAPD protocol (Yörük and Albayrak, 2013) was used in GTS assays of non-digested control, *MspI*-digested, *HapII*-digested experiment sets by using thermal cycler (Hi-Media, India). The total of 20 RAPD primers were used in this study (*Table 1*).

Table 1. *RAPD primers used in this study and total band numbers obtained in RAPD analysis*

Primer	Sequence (5´-3´)	% GC	Total band no
OPA-03	AGTCAGCCAC	60%	11
OPA-04	AATCGGGCTG	60%	-
OPA-05	AGGGGTCTTG	60%	-
OPA-07	GAAACGGGTG	60%	13
OPA-08	GTGACGTAGG	60%	12
OPA-01	CAGGCCCTTC	70%	12
OPA-02	TGCCGAGCTG	70%	8
OPA-06	GGTCCCTGAC	70%	-
OPA-09	GGGTAACGCC	70%	8
OPA-13	CAGCACCCAC	70%	10
OPB-06	TGCTCTGCCC	70%	9
OPB-07	GGTGACGCAG	70%	10
OPB-10	CTGCTGGGAC	70%	10
OPB-13	TTCCCCCGCT	70%	11
OPC-5	GATGACCGCC	70%	9
OPC-4	CCGCATCTAC	60%	9
OPB-19	ACCCCCGAAG	70%	7
OPB-14	TCCGCTCTGG	70%	8
OPC-07	GTCCCGACGA	70%	10

gDNA digestion was carried out in 20 µL mixture including: 1X digestion buffer, 20 U of digestion enzyme (Takara, Japan) and 250 ng/µL gDNA. The incubation for digestion was carried out at 37 °C for 1 h in the thermal cycler. The digested (and also non-digested) samples were used in CRED-RA assays. PCR bands were

http://www.aloki.hu ● ISSN 1589 1623 (Print) ● ISSN 1785 0037 (Online)
DOI: http://dx.doi.org/10.15666/aeer/1605_61556167
© 2018, ALÖKI Kft., Budapest, Hungary

electrophoresed on 1.7% agarose gels and captured via UV light using a transilluminator (Hi-Media, India). The genomic template stability (GTS %) and the polymorphisms % for methylation was calculated as reported previously (Nardemir et al., 2015). The amplified bands were scored according to their presence (1) or absence (0). A similarity matrix and dendrogram were obtained from Nei-Li's coefficient (Nei and Li, 1979) and the unweighted pair group method with arithmetic average algorithm (UPGMA) by using MVSP 3.1 software, respectively.

Total RNA extraction and cDNA synthesis

Total RNA molecules were extracted using Tri-Pure reagent (Roche, Switzerland) from seven days old culture. 50 mg of mycelium was homogenized with 0.5 mL Tri-Prure reagent by using sterile mortar and pestle. The manufacturer's recommendations were then followed in the binding, washing and elution steps (Thermo, USA). The RNAs were evaluated as described as in gDNA analysis.

After RNA isolation, total RNAs were immediately converted to cDNA molecules. 2 µg total RNA was used as starting amount. cDNAs were obtained by using one step commercial kit (Takara, Japan) by using the thermal cycler. The manufacturer's recommendations about thermal cycling and reaction mixtures were used in cDNA synthesis. cDNA molecules cDNAs were diluted as ¼ for gene expression analysis and used in the qPCR (quantitative polymerase chain reaction; real time PCR) analysis.

Gene expression assays

qPCR assays were used in the expression analysis of the *Hog1* (apoptosis related putative MAP kinase; DQ065608.1), *Mgv1* (MAP kinase; AF492766.1), *POD* (peroxidase; XM_011329011.1) and *tri5* (Trichodiene synthase; EF661664.1) genes. The housekeeping gene was the *β-tubulin* (AY303689.1). Primers (*Table 2*) were designed via Primer 3 software and checked via the olygoanalyzer tool of the Integrated DNA Technologies.

Table 2. *Primers related to gene expression analysis used in this study*

Primer	Primer sequence (5'-3')	Band size (bp)
betaF/betaR	agggtcattacaccgagggt / gtaccaccaccaagagagtgg	121
MgvRTF/MgvRTR	aggttcaacgattccgacag / gaccattaccctgaggcaga	100
FusHog1F/FusHog1R	cctggcaaaaatacgacgtt / tgatggagaattggttgacg	117
FusPodrtF/FusPodrtR	tggatcaaggacattggtga / gttggtagcatcctgctggt	117
tri5fullF/tri5fullR	atggagaactttcccaccgagtatt / agtccatagtgctacggataaggttcaa	469

In qPCR assays, the target gene expressions were normalized according to the housekeeping gene expression by using the $2^{-\Delta\Delta CT}$ formula (Livak and Schmittgen, 2001). The Cp (crossing point), ΔCT, ΔΔCT, $2^{-\Delta\Delta CT}$ values were recorded and calculated using the software provided by Roche LightCycler 480 II system (Roche, Switzerland). The one step Sybr Green I master mix kit (Takara, Japan) was used in qPCR assays. qPCRs were carried out in 12 µL reaction volume with 1X Sybr Green I mix, 0.5 pmol primers and 2 µL of cDNA corresponding to 0.5 µg total RNA. Cycling

http://www.aloki.hu ● ISSN 1589 1623 (Print) ● ISSN 1785 0037 (Online)
DOI: http://dx.doi.org/10.15666/aeer/1605_61556167
© 2018, ALÖKI Kft., Budapest, Hungary

conditions, standard dilutions of 4 log phases and the melting curve analysis were carried out as described by Yörük et al. (2018a). Experiments were replicated at least three times. Statistical analyses were performed via One Way ANOVA Analysis with Tukey's post-hoc test (GraphPad Prism 5.0, USA).

Acridine orange/ethidium bromide (AO/EB) fluorescent staining

The apoptotic and oxidative stress stemming from alteration in *F. graminearum* which is related to the TCZ treatment was evaluated via fluorescent microscopy. The determination early and/or late apoptosis and potential oxidative stress/reactive oxygen species (ROS) were investigated using Acridine Orange/Ethidium Bromide (AO/EB) and 2′,7′-Dichlorofluorescin diacetate (DCF-DA) staining, respectively. *F. graminearum* cultivated on PDB supplemented with TCZ (IC_{50} and IC_{25} concentrations) were used in the fluorescence detection.

In AO/EB dual staining assays, mycelia were obtained in 1X Phosphate buffered saline buffer (PBS) of 2 mL (Leiter et al., 2005). The mycelia were then fixed with 4% paraformaldehyde and 0.1% Triton X-100 at least 30 min at 25 °C. The cells were centrifuged at 14.000 rpm for 5 min. The cells were washed with 1.5 mL 1X PBS twice. 5 µL AO/EB (60 µg mL^{-1} / 100µg mL^{-1}) was added onto cells. The mixture was incubated at 25 °C for 5 min. After staining, the cells were washed with 1 mL of 1X PBS twice and then the cells were solved in 100 µL 1X PBS. Dual staining was managed with fluorescence microscope (Carl Zeiss, Germany) with green fluorescent protein (GFP; AO 502ex/526em nm, EB 510ex/595em nm) and Texas RED (595ex/613em nm).

In ROS detection assays, TCZ treated and non-treated cells were suspended in PDB including 5 µg/mL DCF-DA for 15 min. The cells were washed with 1X PBS and the fluorophore was excluded as mentioned above. ROS detection was carried out via the FITC filter (494ex/518em nm). The significant differences for fluorescence analysis were evaluated as described in qPCR assays.

Results

TCZ resistance

F. graminearum H-11 showed both mycelial and also conidial growth in PDA media supplemented with 2, 4, 8 and 16 µg/mL TCZ. MIC concentration was detected as 32 µg mL^{-1} TCZ. The IC_{50} and IC_{25} values were detected as 16 and 8 µg/mL TCZ. These concentrations of TCZ were used in the further analysis.

GTS and epigenetics profiles

The total of 20 primers were used in both RAPD and CRED-RA analysis. Three of these primers (OPA-04, OPA-05 and OPA-06) yielded no amplicon. Remaining 17 primer gave PCR bands in nine experiment sets comprising non-digested, *HapII*-digested and *MspI*-digested groups of TCZ untreated, TCZ treated with IC_{25} and TCZ treated with IC_{50} sets.

In GTS analysis, 108 bands were obtained from the non-digested sets of IC_{50}, IC_{25} and control groups by using 17 primers. The minimum and maximum band numbers were obtained from OPB19 with 3 bands and OPA07 with 13 bands (*Fig. 1*). The GTS values were detected as 86.73% and 85.71% for the IC_{25} and IC_{50} groups. These data

http://www.aloki.hu ● ISSN 1589 1623 (Print) ● ISSN 1785 0037 (Online)
DOI: http://dx.doi.org/10.15666/aeer/1605_61556167
© 2018, ALÖKI Kft., Budapest, Hungary

showed that the TCZ treatment (with increased concentrations) lead to a potential decrease in genomic stability.

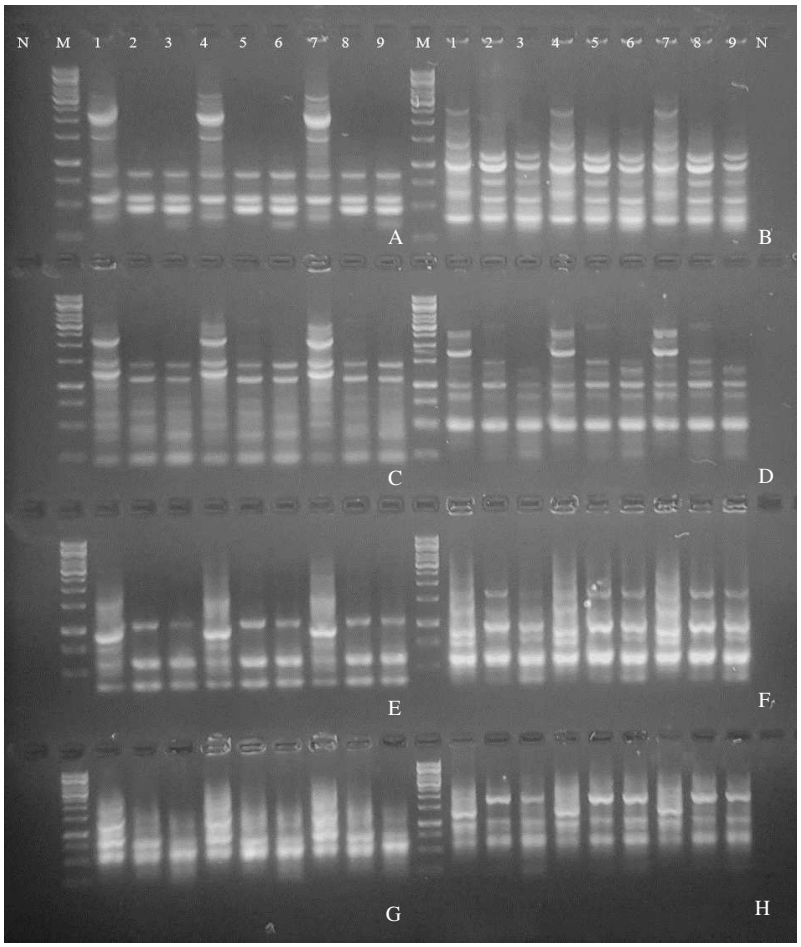

Figure 1. *RAPD and CRED-RA profiles obtained from primers OPA01 (A), OPA03 (B), OPA07 (C), OPA08 (D), OPA09 (E), OPA02 (F), OPA13 (G), and OPAC7 (H), M: 1 kb DNA ladder (Genemark, Taiwan), 1: control non-digested, 2: control HapII digested, 3: control MspI digested, 4: IC25 TCZ-treated non-digested, 5: IC25 TCZ-treated HapII digested, 6: IC25 TCZ-treated MspI digested, 7: IC50 TCZ-treated non-digested, 8: IC50 TCZ-treated HapII digested, 9: IC50 TCZ-treated MspI digested samples. N: no template control*

As well as in GTS analysis, 17 RAPD primers gave amplicon from each experiment set in CRED-RA analysis. Results showed that there were Type II and Type III epigenetics alterations due to TCZ treatment. The epigenetic alterations related to *HapII* and *MspI* digestion profiles of IC*50* and IC*25* groups were given in *Table 3*.

The average polymorphisms for epigenetic alterations were ranged from 2.6 to 5.72% for *HapII* and *MspI* analysis. Polymorphic changes based on epigenetics alterations were characterized by the band intensity and the loss or addition of a band. Additionally, the conventional band presence/absence analysis of Nei & Li's coefficient showed that the minimum and the maximum genetic similarity values were as 40.86% and 97.98% in nine experimental groups. Genetically the most similar samples were belonged to the same enzyme digestion or the non-digestion sets for each experimental sets (*Table 4*).

http://www.aloki.hu ● ISSN 1589 1623 (Print) ● ISSN 1785 0037 (Online)
DOI: http://dx.doi.org/10.15666/aeer/1605_61556167
© 2018, ALÖKI Kft., Budapest, Hungary

Table 3. *Bands profiling obtained from CRED-RA analysis*

Primer	Control		Experiment total band number				Experiment total polymorphic band number				Polymorphism (%)			
			IC25		IC50		IC25		IC50		IC25		IC50	
	HapII	***MspI***	***HapII***	***MspI***	***HapII***	***MspI***	***HapII***	***MspI***	***HapII***	***MspI***	***HapII***	***MspI***	***HapII***	***MspI***
OPA1	3	5	3	5	3	5	0	0	0	0	0	0	0	0
OPA3	6	6	6	6	6	6	0	0	0	0	0	0	0	0
OPA7	6	6	6	6	6	7	1	0	1	0	16.67	0	16.67	0
OPA8	6	5	6	7	5	6	0	2	0	1	0	28.5	0	16.7
OPA9	3	3	3	3	3	3	0	0	0	0	0	0	0	0
OPA13	3	6	3	6	4	6	0	0	1	0	0	0	25	0
OPA2	4	3	4	4	4	4	0	1	0	1	25	25	0	25
OPC7	5	5	4	5	4	5	0	0	0	0	0	0	0	0
OPB6	5	5	5	5	5	5	0	0	0	0	0	0	0	0
OPB7	5	4	5	4	5	4	0	0	0	0	0	0	0	0
OPB10	6	5	6	5	6	5	0	0	0	0	0	0	0	0
OPB13	4	4	4	5	4	4	0	1	0	0	0	20	0	0
OPC5	7	7	7	6	7	6	0	0	0	0	0	0	0	0
OPC4	2	7	4	8	3	7	2	1	1	0	50	12.5	33.3	0
OPB19	4	5	4	4	4	4	0	0	0	0	0	0	0	0
OPB14	4	7	4	7	3	5	0	0	0	0	0	0	0	0
Mean	4.56	5.19	4.625	5.38	4.5	5.13	0.1875	0.3125	0.1875	0.13	5.729	5.375	4.685625	2.6

Table 4. *Genetic similarity values related to non-digested, HapII digested or MspI digested control, IC_{25} and IC_{50} experiment sets*

	Control	**Control/*HapII***	**Control/*MspI***	**EC_{25}**	**EC_{25}/ *HapII***	**EC_{25}/*MspI***	**EC_{50}**	**EC_{50}/ *HapII***	**EC_{50}/*MspI***
Control	100								
Control/*HapII*	54.971	100							
Control/*MspI*	46.409	76.923	100						
EC_{25}	92.929	50.867	42.623	100					
EC_{25}/*HapII*	53.179	97.297	77.215	49.143	100				
EC_{25}/*MspI*	44.565	77.987	95.858	40.86	79.503	100			
EC_{50}	93	51.429	45.405	97.03	50.847	43.617	100		
EC_{50}/*HapII*	52.326	96.599	77.707	49.425	97.987	78.75	51.136	100	
EC_{50}/*MspI*	45.556	78.71	95.758	41.758	78.981	96.429	44.565	79.487	100

Gene expression analysis

cDNA molecules were converted from total RNAs of high quality and quantity and then used in qPCR. In qPCR analysis, mean E values and melting scores (important markers for efficient qPCR experiments) were in the ranges of 2 ± 0.2 and $90 \pm 10\%$,

http://www.aloki.hu ● ISSN 1589 1623 (Print) ● ISSN 1785 0037 (Online)
DOI: http://dx.doi.org/10.15666/aeer/1605_61556167
© 2018, ALÖKI Kft., Budapest, Hungary

respectively. Minimum and maximum Cp values for the control and the experiment sets of *b-tubulin, Hog1*, *Mgv1, POD,* and *tri5* genes were as 19.86 and 26.174, 19.53 and 24.7, 21.61 and 27.1, 20.19 and 24.8 with 21.58 and 26.74, respectively. Fold changes in *Hog1*, *Mgv1, POD, tri5* expressions were recorded as 1.57 ± 0.13 ($p > 0.05$), 1.44 ± 0.28 ($p > 0.05$), 1.56 ± 0.27 ($p > 0.05$) and 0.32 ± 0.09 ($p < 0.001$) for IC_{25} set, respectively (*Fig. 2*). Similarly, these values for *Hog1*, *Mgv1, POD* and *tri5* genes were as 2.31 ± 0.55 ($p < 0.001$), 2.08 ± 0.33 ($p < 0.01$), 2.08 ± 0.33 ($p < 0.01$) and 0.033 ± 0.01 ($p < 0.001$) for IC_{50} set (*Fig. 2*). Significant changes in gene expression was found in each gene for IC_{50} sets where as only in *tri5* expression showed significant differences in IC_{25} set.

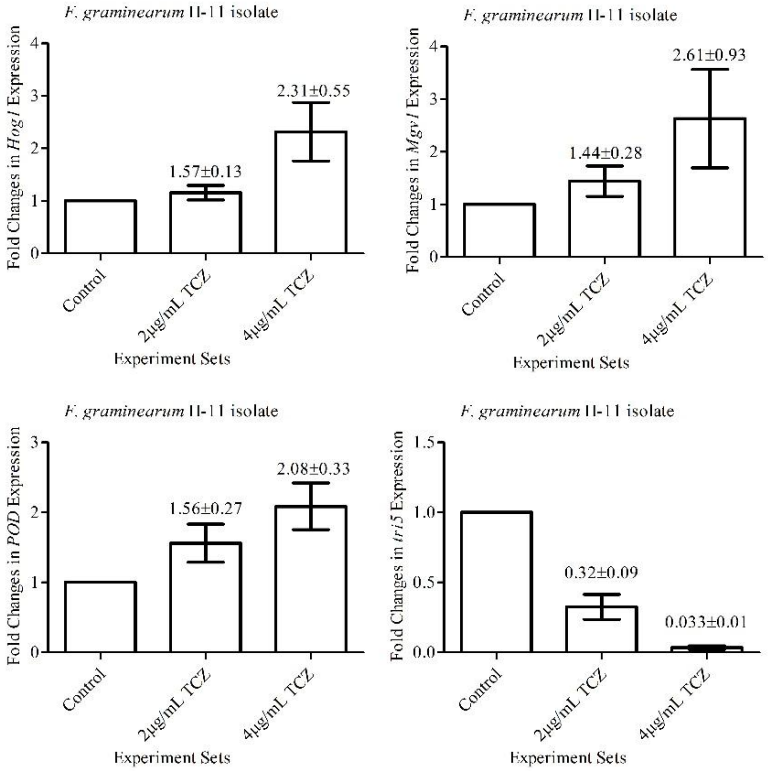

Figure 2. *qRTPCR data of four target genes in the control and two experiment sets*

Fluorescence staining analysis

The late apoptotic cells and the presence of oxidative stress were evaluated via the AoEb dual staining and the DCF-DA staining. In AoEb staining, both experiment sets showed apoptotic profiles while no yellow or orange painted cells were present in the control set. The fluorescence intensity of EB was higher (%50) than AO in the experiment sets. The healthy cell percentages in IC_{25} and IC_{50} groups were 86.38 ± 5.54 and 77.19 ± 9.91, respectively (*Fig. 3A, B*). Significant differences in apoptotic cell levels were detected for IC_{25} ($p < 0.05$) and IC_{50} ($p < 0.01$) experimental sets.

Similarly, control set showed no fluorescent dye effect whereas the ROS activity was detected in the IC_{25} and IC_{50} groups via the DCF-DA staining (*Fig. 3C, D*). The healthy cell percentages were detected as 79.25 ± 5.13 ($p < 0.01$) and 72.2 ± 3.81 ($p < 0.001$) in IC_{25} and IC_{50} experimental sets, respectively.

http://www.aloki.hu ● ISSN 1589 1623 (Print) ● ISSN 1785 0037 (Online)
DOI: http://dx.doi.org/10.15666/aeer/1605_61556167
© 2018, ALÖKI Kft., Budapest, Hungary

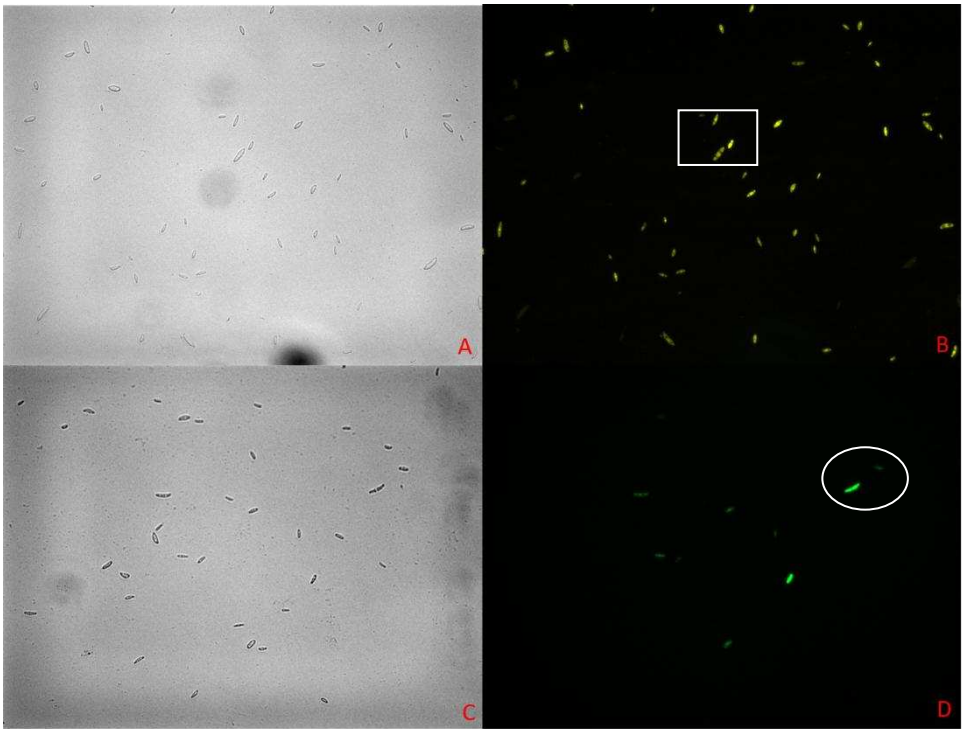

Figure 3. *AoEb (A and B) and DCF-DA (C and D) staining profiles of IC_{50} experiment set at 20X magnification. A and C are of DIC filter photographs. B and D are belonging to AoEB with FITC filters, respectively. Cells in the square show the late apoptosis and cells with circle show the oxidative stress presence*

Discussion

The alterations due to the TCZ on *F. graminearum* was investigated at different molecular levels in this study. TCZ is one of the major fungicide worldwide for many phytopathogenic species (Cools and Hammond-Kosack, 2013). MIC value for *F. graminearum* was recorded as 32 µg/mL. It can be easily said that this level of fungicide could provide a powerful strategy to overcome the *F. graminearum* infections in the fields. Especially, if and when the MIC value is compared to the potential antifungal agents, the MIC values which could reach up to 1 mg/mL (Sefer et al., 2017; Yörük et al., 2018a), TCZ could be considered as a strong antimicrobial agent.

The common and powerful fungicides could lead to an antifungal resistance in the fields where they have been applied (Chung et al., 2008; Arif et al., 2009; Cools and Hammond-Kosack, 2013). The resistance to the common fungicides has been generally related to the genotypic variation, crop rotation, climatic conditions and some other characteristics related to the fungus and the host. However, the molecular basis has not been explained clearly and comprehensively. Responses of several phytopathogens to the specific antifungals have been investigated by several molecular genetics approaches such as the gene expression analysis, the oxidative stress and the apoptosis determination (Agus et al., 2018; Yörük et al., 2018a). However, those investigations present only limited data for antifungal resistance. In this study, the responses of *F. graminearum* to TCZ (which is harmful to the human health indirectly by feeding and drinking water supplies) have been evaluated at different molecular levels. The GTS and the CRED-RA analysis showed that this common antifungal could lead to

http://www.aloki.hu ● ISSN 1589 1623 (Print) ● ISSN 1785 0037 (Online)
DOI: http://dx.doi.org/10.15666/aeer/1605_61556167
© 2018, ALÖKI Kft., Budapest, Hungary

alterations at the genomic and epigenomics levels. The long-term usage of TCZ could lead to more changes in GTS which can be a sign of genotypic diversity. Additionally, the transposable elements movement could be triggered by TCZ usage. GTS changes could result in high level of genomic variations, might lead to differentiation of novel species complex members. However, this kind of a suggestion needs further investigation. Epigenetics alterations have also been detected in this study. These results could serve as the turn on/off genes which could have a critical role in the fungal life cycle. Genetic engineering based tools such as the gene silencing and the gene replacement analysis could be used in further studies to support these findings.

TCZ usage led to the significantly important changes in the gene expression in *F. graminearum*. Upregulation of *Hog1*, *Mgv1* and *POD* genes in TCZ treated experiment set showed that the TCZ application could result in apoptosis like cell death and oxidative stress. Similarly, significant decrease in *tri5* expression was detected in TCZ treated groups. Findings showed that TCZ could inhibit mycotoxin biosynthesis in addition to decrease in the fungal radial growth capacity. These genes or homologues have been used in different studies related to the apoptosis mechanism, downregulation of mycotoxin synthesis and the novel antifungal resistance etc. (Ponts et al., 2007; Sharon et al., 2009; Shlezinger, Goldfinger and Sharon, 2012; Sefer et al., 2017; Yörük et al., 2018b). However, in this study, it was claimed that the alterations in *Hog1*, *Mgv1*, *POD* and *tri5* genes could be used as markers in revealing the detailed antifungal effects of any specific chemical compound. These antifungal effects could include a programmed cell death, oxidative stress, toxin inhibition, an abiotic stress response etc. Oxidative stress and programmed cell death like processes were also verified by the fluorescence microscopy analysis. Ethidium bromide penetrates into the cells with lost integrity and stains the cell as orange to red (McGahon et al., 1995). Similarly, the cells subjected to oxidative stress turn into green since DCF-DA is rapidly oxidized with ROS, and turn into the fluorescent DCF dye (Jou et al., 2004). The TCZ treated experimental sets showed that yellow-tan and green colored profiles with AoEb and DCF-DA, respectively. Both gene expression analysis and cellular display assays showed that TCZ is a potential abiotic stress factor for *F. graminearum* at different molecular levels.

The investigation of the effects of this TCZ on *F. graminearum* at molecular levels would provide useful data for the studies related to phytopathology. *F. graminearum* is hemi-biotrophic fungus with an asexual and a sexual reproduction. The species is accepted as major causal agent of head blight and crown rot of some economically important cereals worldwide (Miedaner et al., 2008; Matny, 2015). This popular enemy of field crops seem to be lose the against TCZ or some other common fungicides in many regions of the world. However, since resistance to common antifungals could be improved in the coming years, molecular responses of phytopathogens to antifungals should be clearly investigated. In this study, it was shown that TCZ could lead to alterations in *F. graminearum* at different molecular processes. However, the effects of TCZ on plant tissue cultures and the mammalian cell cultures should also be investigated in further studies.

Conclusion

The struggle with *F. graminearum* diseases have different approaches including the fungicide treatment as the most common protocol. The resistance to common

http://www.aloki.hu ● ISSN 1589 1623 (Print) ● ISSN 1785 0037 (Online)
DOI: http://dx.doi.org/10.15666/aeer/1605_61556167
© 2018, ALÖKI Kft., Budapest, Hungary

antimicrobials has been known for many different microorganisms so far. In this study, it was shown that TCZ lead to mycelial growth inhibition, GTS changes, methylation alterations, oxidative stress and apoptosis like process. These changes at molecular processes could be responsible for the development of a resistance against common or specific antifungal compounds. However, further studies could include necrotrophic species, the plant tissue culture test, the mammalian cell culture tests, and genetic engineering confirmation etc. which also provide additional and supportive data related to plant pathology research area.

REFERENCES

[1] Agus, H. H., Sarp, C., Cemiloglu, M. (2018): Oxidative stress and mitochondrial impairment mediated apoptotic cell death induced by terpinolene in *Schizosaccharomyces pombe*. – Toxicology Research. DOI: 10.1039/c8tx00100f.

[2] Anand, A., Zhou, T., Trick, H. N,. Gill, B. S., Bockus, W. W., Muthukrishnan, S. (2003): Greenhouse and field testing of transgenic wheat plants stably expressing genes for thaumatin-like protein, chitinase and glucanase against *Fusarium graminearum*. – Journal of Experimental Botany 54(384): 1101-1111.

[3] Aoki, T., O'Donnell, K. (1999): Morphological and molecular characterization of *Fusarium pseudograminearum* sp. nov., formerly recognized as the Group 1 population of *F. graminearum*. – Mycologia: 597-609.

[4] Arif, T., Bhosale, J. D., Kumar, N., Mandal, T. K., Bendre, R. S., Lavekar, G. S., Dabur, R. (2009): Natural products–antifungal agents derived from plants. – Journal of Asian Natural Products Research 11(7): 621-638.

[5] Bai, G., Shaner, G. (2004): Management and resistance in wheat and barley to Fusarium head blight. – Annual Review of Phytopathology 42: 135-161.

[6] Bernardo, A., Bai, G., Guo, P., Xiao, K., Guenzi, A. C., Ayoubi, P. (2007): *Fusarium graminearum*-induced changes in gene expression between Fusarium head blight-resistant and susceptible wheat cultivars. – Functional & integrative Genomics 7(1): 69-77.

[7] Chung, W. H., Ishii, H., Nishimura, K., Ohshima, M., Iwama, T., Yoshimatsu, H. (2008): Genetic analysis and PCR-based identification of major *Fusarium* species causing head blight on wheat in Japan. – Journal of General Plant Pathology 74(5): 364-374.

[8] Cools, H. J., Hammond-Kosack, K. E. (2013): Exploitation of genomics in fungicide research: current status and future perspectives. – Molecular Plant Pathology 14(2): 197-210.

[9] Dal Bello, G. M., Monaco, C. I., Simon, M. R. (2002): Biological control of seedling blight of wheat caused by *Fusarium graminearum* with beneficial *rhizosphere* microorganisms. – World Journal of Microbiology and Biotechnology 18(7): 627-636.

[10] Goswami, R. S., Kistler, H. C. (2005): Pathogenicity and in planta mycotoxin accumulation among members of the *Fusarium graminearum* species complex on wheat and rice. – Phytopathology 95(12): 1397-1404.

[11] Jou, M-J., Peng, T-I., Reiter, RJ., Jou, S-B., Wu, H-Y., Wen, S-T. (2004): Visualization of the antioxidative effects of melatonin at the mitochondrial level during oxidative stress-induced apoptosis of rat brain astrocytes. – Journal of Pineal Research 37(1): 55-70.

[12] Kerényi, Z., Moretti, A., Waalwijk, C., Oláh, B., Hornok, L. (2004): Mating type sequences in asexually reproducing *Fusarium* species. – Applied and Environmental Microbiology 70(8): 4419-4423.

[13] King, R., Urban, M., Hammond-Kosack, K. E. (2017): Annotation of *Fusarium graminearum* (PH-1) version 5.0. – Genome Announcements 5(2): e01479-16.

http://www.aloki.hu ● ISSN 1589 1623 (Print) ● ISSN 1785 0037 (Online)
DOI: http://dx.doi.org/10.15666/aeer/1605_61556167
© 2018, ALÖKI Kft., Budapest, Hungary

[14] Lee, T., Oh, D. W., Kim, H. S., Lee, J., Kim, Y. H., Yun, S. H., Lee, Y. W. (2001): Identification of deoxynivalenol-and nivalenol-producing chemotypes of *Gibberella zeae* by using PCR. – Applied and Environmental Microbiology 67(7): 2966-2972.

[15] Leiter, É., Szappanos, H., Oberparleiter, C., Kaiserer, L., Csernoch, L., Pusztahelyi, T., Emri, T., Pocsi, I., Salvenmoser, W., Marx, F. (2005): Antifungal protein PAF severely affects the integrity of the plasma membrane of *Aspergillus nidulans* and induces an apoptosis-like phenotype. – Antimicrobial Agents and Chemotherapy 49(6): 2445-2453.

[16] Livak, K. J., Schmittgen, T. D. (2001): Analysis of relative gene expression data using real-time quantitative PCR and the $2^{-\Delta\Delta CT}$ method. – Methods 25(4): 402-408.

[17] Lori, G. A., Sisterna, M. N., Sarandón, S. J., Rizzo, I., Chidichimo, H. (2009): Fusarium head blight in wheat: impact of tillage and other agronomic practices under natural infection. – Crop Protection 28(6): 495-502.

[18] Matny, O. N. (2015): Fusarium head blight and crown rot on wheat & barley: losses and health risks. – Advances in Plants & Agricultural Research 2(39): 10-15406.

[19] McGahon, A. J., Martin, S. J., Bissonnette, R. P., Mahboubi, A., Shi, Y., Mogil, R. J., Nishioka, W. K., Green, D. R. (1995): The End of the (Cell) Line: Methods for the Study of Apoptosis in Vitro. – In: Prescott, D. M. (ed.) Methods in Cell Biology Vol. 46. Academic Press, Cambridge, MA, pp. 153-185.

[20] Miedaner, T., Cumagun, C. J. R., Chakraborty, S. (2008): Population genetics of three important head blight pathogens *Fusarium graminearum, F. pseudograminearum* and *F. culmorum*. – Journal of Phytopathology 156(3): 129-139.

[21] Nardemir, G., Agar, G., Arslan, E., Erturk, F. A. (2015): Determination of genetic and epigenetic effects of glyphosate on *Triticum aestivum* with RAPD and CRED-RA techniques. – Theoretical and Experimental Plant Physiology 27(2): 131-139.

[22] Nei, M., Li, W. H. (1979): Mathematical model for studying genetic variation in terms of restriction endonucleases. – Proceedings of the National Academy of Sciences 76(10): 5269-5273.

[23] Niu, C., Kebede, H., Auld, D. L., Woodward, J. E., Burow, G., Wright, R. J. (2008): A safe inexpensive method to isolate high quality plant and fungal DNA in an open laboratory environment. – African Journal of Biotechnology 7(16).

[24] O'Donnell, K., Ward, T. J., Geiser, D. M., Kistler, H. C., Aoki, T. (2004): Genealogical concordance between the mating type locus and seven other nuclear genes supports formal recognition of nine phylogenetically distinct species within the *Fusarium graminearum* clade. – Fungal Genetics and Biology 41(6): 600-623.

[25] Pasquali, M., Migheli, Q. (2014): Genetic approaches to chemotype determination in type B-trichothecene producing Fusaria. – International Journal of Food Microbiology 189: 164-182.

[26] Pasquali, M., Cocco, E., Guignard, C., Hoffmann, L. (2016): The effect of agmatine on trichothecene type B and zearalenone production in *Fusarium graminearum*, *F. culmorum* and *F. poae*. – PeerJ 4: e1672. DOI: 10.7717/peerj.1672.

[27] Ponts, N., Pinson-gadais, L., Barreau, C., Richard-forget, F. (2007): Exogenous H_2O_2 and catalase treatments interfere with *Tri* genes expression in liquid cultures of *Fusarium graminearum*. – FEBS Letter 581: 443-447.

[28] Przemieniecki, S. W., Kurowski, T. P., Korzekwa, K. (2015): Chemotypes and geographic distribution of the *Fusarium graminearum* species complex. – Environmental Biotechnology 10(2): 45-59.

[29] Qian, H., Du, J., Chi, M., Sun, X., Liang, W., Huang, J., Li, B. (2018): The Y137H mutation in the cytochrome P450 FgCYP51B protein confers reduced sensitivity to tebuconazole in *Fusarium graminearum*. – Pest Management Science 74(6): 1472-1477.

[30] Sarver, B. A. J., Ward, T. J., Gale, L. R., Broz, K., Kistler, H. C., Aoki, T., Nicholson, P., Carter, J., Donnell, K. O. (2011): Novel Fusarium head blight pathogens from Nepal and Louisiana revealed by multilocus genealogical concordance. – Fungal Genetics and Biology 48: 1096-1107.

http://www.aloki.hu ● ISSN 1589 1623 (Print) ● ISSN 1785 0037 (Online)
DOI: http://dx.doi.org/10.15666/aeer/1605_61556167
© 2018, ALÖKI Kft., Budapest, Hungary

[31] Sefer, Ö., Yörük, E., Develi, E. S., Sezer, A. S., Konukcu, Z. (2017): Investigation of the effects of 2, 4-Dimethylpyrrole on *Fusarium culmorum* causal agent of head blight disease. – International Journal of Secondary Metabolite 4(2): 103-113. DOI: 10.21448/ijsm.307943.

[32] Sharon, A., Finkelstein, A., Shlezinger, N., Hatam, I. (2009): Fungal apoptosis: Function, genes and gene function. – FEMS Microbiology Reviews 33: 833-854.

[33] Shlezinger, N., Goldfinger, N., Sharon, A. (2012): Apoptotic-like programmed cell death in fungi: the benefits in filamentous species. – Frontiers in Oncology 2: 1-8.

[34] Talas, F., McDonald, B. A. (2015): Genome-wide analysis of *Fusarium graminearum* field populations reveals hotspots of recombination. – BMC Genomics 16: 1-13.

[35] Yang, Y., Li, M., Duan, Y., Li, T., Shi, Y., Zhao, D., Zhou, Z. (2018): A new point mutation in *β2 – tubulin* confers resistance to carbendazim in *Fusarium asiaticum*. – Pesticide Biochemistry and Physiology 145: 15-21. DOI: 10.1016/j.pestbp.2017.12.006.

[36] Yörük, E., Albayrak, G. (2013): Genetic characterization of *Fusarium graminearum* and *F. culmorum* isolates from Turkey by using random-amplified polymorphic DNA. – Genetic Molecular Research 12(2): 1360-72.

[37] Yörük, E., Tunali, B., Kansu, B., Ölmez, F., Uz, G., Zümrüt, I. M., Sarıkaya, A., Meyva, G. (2016): Characterization of high-level deoxynivalenol producer *Fusarium graminearum* and *F. culmorum* isolates caused head blight and crown rot diseases in Turkey. – Journal of Plant Diseases and Protection 123(4): 177-186. DOI: 10.1007/s41348-016-0027-y.

[38] Yörük, E., Sefer, Ö., Sezer, A. S., Konukcu, Z., Develi, E. S. (2018a): Investigation of the Effects of Eugenol on *Fusarium culmorum.* – Iğdır University Journal of Institute of Science and Technology 8(2): 215-221.

[39] Yörük, E., Sefer, Ö., Tunali, B., Kansu, B., Sharifnabi, B., Yli-mattila, T. (2018b): Thiophanate methyl susceptibility and alterations in *tri5*, *Mgv1* and *StuA* expression among *Fusarium graminearum* and *F. culmorum* isolates. – Journal of Plant Pathology 1(9). DOI: 10.1007/s42161-018-0094-y.

http://www.aloki.hu ● ISSN 1589 1623 (Print) ● ISSN 1785 0037 (Online)
DOI: http://dx.doi.org/10.15666/aeer/1605_61556167
© 2018, ALÖKI Kft., Budapest, Hungary

FUNCTIONAL STRATEGIES FOR CERTAIN GROWTH STAGES OF CORN IN RESPONSE TO ENVIRONMENTAL FACTORS: IRRIGATION AND PLANTING DATE MANAGEMENT

MIRSHEKARNEZHAD, B.[1] – PAKNEJAD, F.[1*] – AMIRI, E.[2] – ARDAKANI, M. R.[1] – ILKAEE, M. N.[1]

[1]*Department of Agronomy, Karaj Branch, Islamic Azad University, Karaj, Iran*
(e-mails: bob_mirshekar@yahoo.com; farzadpaknejad@yahoo.com; mreza.ardakani@gmail.com; mn64_ilkaee@yahoo.com)

[2]*Department of Agriculture, Lahijan Branch, Islamic Azad University, Lahijan, Iran*
(e-mail: eamiri57@yahoo.com)

**Corresponding author*
e-mail: farzadpaknejad@yahoo.com; phone: +98-263-418-3942; fax: +98-263-418-3928

(Received 7th Jul 2018; accepted 31st Aug 2018)

Abstract. Agriculture in arid areas with inadequate water supply enquires the right cognition of evapotranspiration related to water application. In this research a single-cross hybrid of maize (S.C. 704), under the split plot experiment based on randomized complete block design was selected for cultivation in 2015 and 2016 years. The experimental treatments were set up in three planting dates: 21st April, 11th May and 31st May, and four irrigation regimes: I_{100} (100%), I_{80} (80%), I_{60} (60%) and I_{40} (40%) of the estimated evapotranspiration (ET). The results showed a drastic reduction by 44 to 49% in grain yield under low irrigation regime (I_{40}) compared with full irrigation regime (I_{100}), respectively. Irrigation water use efficiency based on grain yield (1.39 and 1.20 kg/m^3) and biological yield (4.79 and 4.53 kg/m^3) was the highest in I_{40} for each year, respectively. Corns planted earlier fulfilled silking-maturity duration faster than corns planted at the end of planting window as a result of reducing final yield potential. Under drought stress situation of this experiment it was shown that with long season hybrid, grain yield and irrigation efficiency can be improved by timely applications of planting dates and irrigation levels.
Keywords: *drought stress, evapotranspiration, grain yield, silking-maturity duration, water use efficiency*

Introduction

In many parts of the world where agriculture is important, crops usually encounter a large variation in water supply during their growing seasons. Thus water deficit is a major constraint to crop production, even in humid environments (Soltani and Sinclair, 2012). Corn biomass can be reduced with deficit irrigation and any loss in biomass can result in the final yield reduction. When water for irrigation is limited the goal should be integrated to maximize net income per unit water used rather than per land unit. Thus, the limited irrigation strategy meets this concept by establishing water economy as well as achieving efficiencies (Fereres and Soriano, 2007).

Many crops have lower yield in response to water stress at vegetative and reproductive stages. Deficit irrigation involves an appropriate scheduling of irrigation because crop sensitivity to water deficit changes with the phenological stages (Istanbulluoglu, 2009). Water stress affects crop growth and productivity in many ways. Most of the responses have negative effect on production but crops have different and often complex mechanisms against water scarcity (Kirda et al., 1999). Many results implied that crop water use efficiency was an intrinsic system sensitive to climate change. These findings indicated that crops had the resilience by adjusting water use

http://www.aloki.hu ● ISSN 1589 1623 (Print) ● ISSN 1785 0037 (Online)
DOI: http://dx.doi.org/10.15666/aeer/1605_61696180
© 2018, ALÖKI Kft., Budapest, Hungary

efficiency (Zhang et al., 2015). Planting date analysis showed that a delayed planting date caused a decrease in average yield of 55% for the rainfed and 21% for the irrigated conditions for all hybrids (Soler et al., 2007).

Weather conditions that are optimal for maize production are likely to be less predictable in future due to variability in weather conditions and may have infrastructural effects on the stage of maturity at harvest (Blignaut et al., 2009). Manipulations that increase carbohydrate supply to developing grains during drought stress not only decrease abortion but can also increase grain yield (Morison et al., 2008). Anthesis-silking interval is a predictor of seed set in many maize cultivars when affected by stresses at flowering (Edmeades et al., 2000). Grain yield can be reduced by decreasing yield components like ear size, number of kernel per ear and kernel weight. Claassen and Shaw (1970) observed that water stress at silking stage and pollination process resulted in kernel number reduction, while stress during or after silking reduced kernel weight.

Whether or not, one of the confrontational challenges for us is how we can adapt the crop system processes to the future environmental changes. However the challenge still remains of low crop yield and sometimes crop failure due to poor choice of planting date. Thus with the aim of optimizing water and corn productivities in relevant to optimum ET maintenance, this research explores the key agronomic practices such as taking right planting dates and well-apprised water requirements at critical stages of corn growth cycle.

Materials and methods

Study area

The arid and semi-arid region of Karaj in Alborz province, Iran (35° 50’ N, 51° 0’ E, 1312 m a.s.l.) is demarcated as one of the most important area for both food and forage crops cultivation. Maize production is possible only under irrigated condition (*Fig. 1*). The average rainfall of this site is less than 250 mm per annum. Such diversity of geographical features plays a dominant role in determining the topography, climate and plant species present in the region.

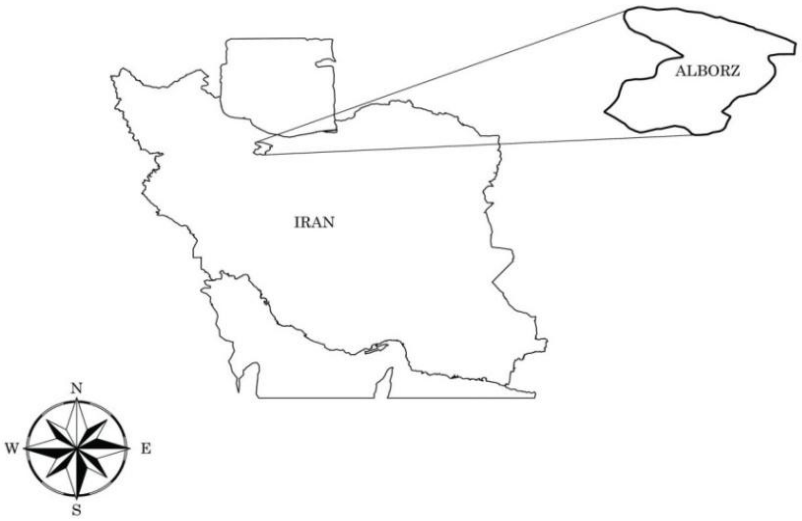

Figure 1. *Geographical location of Alborz province in Iran map*

http://www.aloki.hu ● ISSN 1589 1623 (Print) ● ISSN 1785 0037 (Online)
DOI: http://dx.doi.org/10.15666/aeer/1605_61696180
© 2018, ALÖKI Kft., Budapest, Hungary

Soil characteristics and agronomic management

Primarily the research field plowed and disked regularly to pulverize the clods. Thereafter, a Hiller-Furrower was employed to create planting furrows in the seedbed. According to the United States Department of Agriculture classification (USDA), the territory soil of the site is classified as a Typic Haplocambid (Mirkhani et al., 2010). The soil samples were tested for some physical and chemical compositions in both successive years (*Table 1*). The soil texture was determined as clay loam throughout the experiment.

Table 1. *Some physical and chemical compositions of soil in the experimental site*

Year	Soil depth	EC (ds/m)	Sp (%)	pH	N (%)	P (mg/kg)	K (mg/kg)	O.C. (%)
2015-16	0-30	2.53	39.8	8.3	0.08	6.3	203	0.71
2016-17	0-30	1.58	38.2	8.5	0.09	7.0	207	0.75

The field of research site was arranged in three blocks of 12 plots each, with an even space between them so that each plot involved six rows of 5 m in length and 75 cm spacing apart. After testing the seeds with fungicide (Tebuconazole), applying dry method, three-four seeds spaced in created grooves on the top of the furrows. The plots were kept weed-free by hand weeding and Rotavator applying between rows. Nitrogen application in the form of urea at a rate of 150 kg/ha, top-dressed at two stages of corn life cycle. Ultimately, thinning at five-leaf stage of seedlings was down up to a final density of 8 plants per square meter.

Experimental layout and crop assessment

The field experiments took place in the research farm of the College of Agriculture and Natural Resources, University of Tehran, located in Karaj, Iran (35° 48' N, 50° 57' E, 1293 m a.s.l.). The split-plot experiment based on a randomized complete block design with three replicates carried out in 2015-16 and 2016-17 cropping seasons. The experimental treatments in three planting dates in main plots were scheduled for 21st April, 11th May and 31st May, and four irrigation levels consisting of 100%, 80%, 60% and 40% of (ET) in sub plots were summarized as I_{100}, I_{80}, I_{60} and I_{40}. The amount of evaporated water through transpiration was estimated by *Equation 1* (FAO, 1977).

$$ET_c = K_c \times ET_o \quad \text{(Eq.1)}$$

where, ET_c is crop evapotranspiration (mm/d), ET_0 is reference evapotranspiration (mm/d) and K_c is crop coefficient. The calculation of ET_0 was determined in mm by recording weekly evaporation data obtained from the class A evaporation pan, located in synoptic weather station of Karaj. The amount of water evaporated during a period corresponds with the decrease in water depth of the pan in that period. On the basis of FAO Penman-Monteith Method, K_c values (0.3, 1.2 and 0.3-0.6) for three corn growth stages were defined as $K_{c\ ini}$, $K_{c\ mid}$, and $K_{c\ end}$, under the given condition (Allen et al., 1998). Water requirements for individual plots measured in gallon weekly then converted to liter per week. The final volume of water application for irrigating each plot was computed using *Equation 2:*

http://www.aloki.hu ● ISSN 1589 1623 (Print) ● ISSN 1785 0037 (Online)
DOI: http://dx.doi.org/10.15666/aeer/1605_61696180
© 2018, ALÖKI Kft., Budapest, Hungary

$$In = \frac{0.623 \times A \times Kc \times ET0}{IE} \quad \text{(Eq.2)}$$

where, I_n denotes the volume of irrigation water in gallons per week, 0.623 is the equation constant, A stands for plot area (sq. ft.), Kc represents crop coefficient, ET_0 is the reference evapotranspiration in (mm) per day. IE at the rate of 80 percent is the indicator of irrigation efficiency that finally expressed in decimal i.e. (0.80) (Howell, 2003). The total of irrigation volumes that computed for two consecutive years are presented in the following timetable (*Table 2*). All plots were irrigated uniformly until the plants were completely established. The irrigation treatments started when the plants were at the 6-7 leaf growth stage using water flow meter.

Table 2. *The weekly reference evapotranspiration (ET_o) and water volumes applied after starting irrigation regimes*

Year	Total weekly ET_0 (mm)	Number of irrigations	Total water volume applied for irrigation regimes (m^3/ha)			
			I_{100}	I_{80}	I_{60}	I_{40}
2015-16	27.1	7	7482	5986	4489	2993
2016-17	29.5	8	7490	5992	4494	2996

When the ears were at full physiological maturity stage with an evident black layer of the grains, whole plants from two adjacent rows in each plot including ears were harvested near the ground level to determine total dry matter. The plants separated into leaf, stem and ear fractions. Then leaf and stem samples separately put into a labeled paper bag and were placed in a dehydrator to dry at 75 °C until constant mass. For grain yield, 10 plants from the remaining half-plot were harvested and measured for weight of ears per plant and number of grains per ear. Finally, irrigation water use efficiency (IWUE) based either on grain yield (GY) or biological yield (BY) was calculated by *Equations 3* and *4:*

$$IWUE = (GY/I) \quad \text{(Eq.3)}$$

$$IWUE = (BY/I) \quad \text{(Eq.4)}$$

where, GY is grain yield (kg/ha), BY is biological yield (kg/ha), and I is the amount of applied irrigation water (m^3). It is important to emphasize, in the case of precipitation the amount of added water to the evaporation pan was measured daily during pan readings to account for estimating reference evapotranspiration. Also harvest index (HI) estimated by the ratio of harvested grains to total shoot dry matter by *Equation 5:*

$$HI = (GY/BY) \times 100 \quad \text{(Eq.5)}$$

Statistical analysis

Analysis of variance (ANOVA) employed for two years datasets using PROC GLM in SAS program (V., 9.1). Growing degree days (GDDs) accumulation measured by summing the number of daily accumulated heat degrees in a day, obtained by the

http://www.aloki.hu ● ISSN 1589 1623 (Print) ● ISSN 1785 0037 (Online)
DOI: http://dx.doi.org/10.15666/aeer/1605_61696180
© 2018, ALÖKI Kft., Budapest, Hungary

average of the maximum (T-Max) and minimum (T-Min) temperatures (°C) for the day, minus the base temperature (T-Base) which is established as 10 °C for corn development. T-Max and T-Min are limited to 30 °C and 10 °C, respectively. All tables and graphs were designed by excel software. Significant differences among means were compared by Duncan's multiple range test.

Results

Weather conditions during corn life cycle

The maximum and minimum air temperatures, rainfall and relative humidity data were prepared based on Karaj auto weather station reports in the vicinity of the research site. The seasonal maximum and minimum air temperatures were approximately the same for both cropping seasons (*Fig. 2*). The total rainfall of 12.1 mm in 2016-17, was remarkably less than of 33.5 mm which mainly occurred in April during 2015-16. Therefore, due to more rainfall and wetter condition in 2015-16, the number of irrigations and the rates of estimated water volume in various irrigation regimes in 2016-17 were slightly greater than in 2015-16.

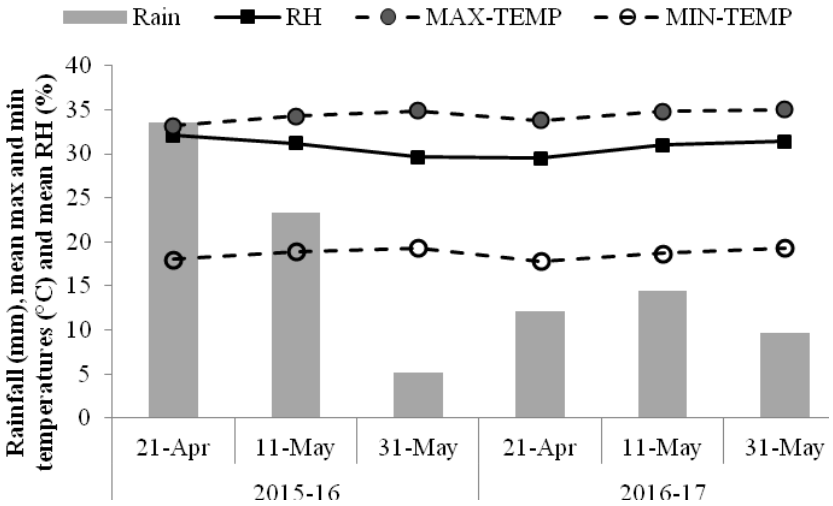

Figure 2. *Seasonal average of climatic data during corn maturity in 2015-16 and 2016-17*

Silking-maturity interval across various planting dates

Silking-maturity interval varies when crops are planted either early or late. Grain yield is in direct contact with kernel weight and GDD requirements. As planting delays, temperature and radiation levels become increasingly critical for yield determination. Hence, if corn is stressed during silking to maturity period, inadequate GDD levels can form prematurely preventing additional dry matter accumulation (*Table 3*).

Corn growth stage development can vary according to planting date. An early-planting corn may develop through growth stages slower than a late-planting corn. However, apart from early or late planting date, there is a transition between silking to physiological maturity time during which kernels are filled. In addressing the results of *Table 3,* silking to maturity duration by late-planted corns occurred at a slower pace (42 and 43 days) after the accumulation of 684 and 621 GDDs in each year, respectively

http://www.aloki.hu ● ISSN 1589 1623 (Print) ● ISSN 1785 0037 (Online)
DOI: http://dx.doi.org/10.15666/aeer/1605_61696180
© 2018, ALÖKI Kft., Budapest, Hungary

(*Fig. 3*). In contrast, early-planted corns with longer vegetative growth stage fulfilled silking to maturity period rapidly (40 and 39 days) after the accumulation of 739 and 711 GDDs in both years, respectively (*Fig. 4*).

Table 3. *Some growth and climate data during silking-maturity interval in corn*

Year	Reproductive stage	Planting date (PD)	Mean temp (°C)	Radiation ($MJ/m^2/day$)	ET_c (mm)	GDDs (°C-day)
2015-16	Silking to maturity	PD_1	28.0	30	425	739
		PD_2	28.8	26	454	734
		PD_3	29.6	23	493	684
2016-17	Silking to maturity	PD_1	28.3	28	396	711
		PD_2	28.4	27	441	697
		PD_3	29.1	24	507	621

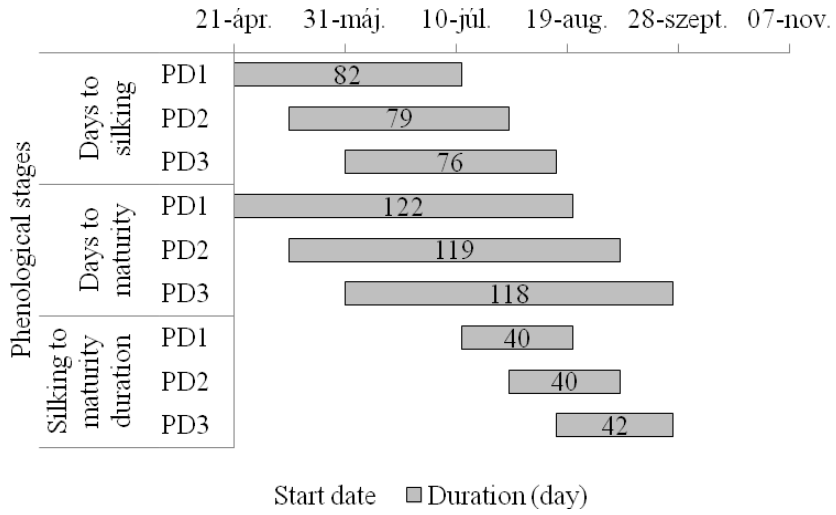

Figure 3. *Days from silking to maturity completion in three planting dates (2015-16)*

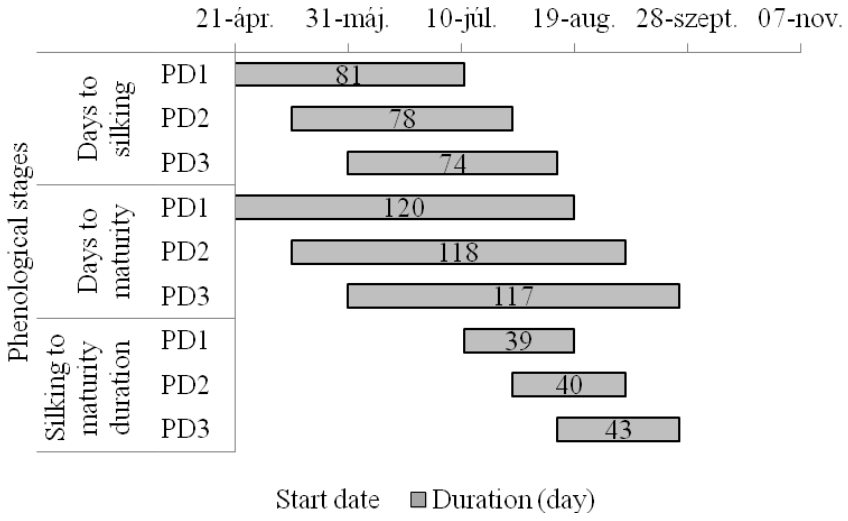

Figure 4. *Days from silking to maturity completion in three planting dates (2016-17)*

http://www.aloki.hu ● ISSN 1589 1623 (Print) ● ISSN 1785 0037 (Online)
DOI: http://dx.doi.org/10.15666/aeer/1605_61696180
© 2018, ALÖKI Kft., Budapest, Hungary

Mean comparisons and significance level of interactions

As planting date (PD) delayed and water amount restricted from non-stress treatment (I_{100}) to full-stress treatment (I_{40}), there was a drastic reduction by 44 and 49% in GY during both 2015-16 and 2016-17, respectively (*Tables 4* and *5*). However the reduction of GY in response to late-planting date was more evident in the second year. Incidentally, the same tragedy occurred with BY which made a reduction by 17 and 22% in I_{40} compared to I_{100} in both years, respectively. There was also a decrement in the range of 32 to 35% for harvest index (HI) against irrigation levels in both years, respectively.

Table 4. *Means comparison of main traits and significance level of interactions in corn for 2015-16*

Corn Traits		Grain yield (kg/ha)	Biological yield (kg/ha)	Ear weight (kg/ha)	Kernel abortion (%)	1000-KW (gr)	Harvest index (%)	$IWUE_{GY}$ (kg/m^3)	$IWUE_{BY}$ (kg/m^3)
Irrigation levels	I_{40}	4150.3^{d}	14354.6^{d}	5177.7^{d}	18.00^{a}	165.55^{c}	28.76^{d}	1.39^{a}	4.79^{a}
	I_{60}	5038.6^{c}	14885.7^{c}	5773.9^{c}	15.44^{b}	180.33^{c}	33.76^{c}	1.12^{b}	3.31^{b}
	I_{80}	6446.1^{b}	16643.8^{b}	7873.1^{b}	13.66^{b}	203.78^{b}	38.53^{b}	1.08^{b}	2.78^{c}
	I_{100}	7364.4^{a}	17398.2^{a}	8613.7^{a}	10.55^{c}	239.44^{a}	42.16^{a}	0.98^{c}	2.32^{d}
Planting dates	PD_1	6613.6^{a}	16724.6^{a}	7599.6^{a}	13.83^{a}	211.50^{a}	39.02^{a}	1.32^{a}	3.49^{a}
	PD_2	5484.2^{b}	15853.3^{b}	6547.6^{b}	13.50^{a}	212.67^{a}	34.20^{b}	1.09^{b}	3.31^{b}
	PD_3	5151.8^{b}	14883.8^{c}	6431.6^{b}	15.91^{a}	167.67^{b}	34.19^{b}	1.02^{b}	3.10^{c}
PD × IR (DMRT< 0.05)		ns	ns	*	ns	ns	ns	ns	ns

Means within the same column followed by the same letters are not significantly different ($p < 0.05$). KW = Kernel weight; $IWUE_{GY}/IWUE_{BY}$ = Irrigation water use efficiency of grain yield/biological yield; PD = Planting Date; IR = Irrigation

Table 5. *Means comparison of main traits and significance level of interactions in corn for 2016-17*

Corn traits		Grain yield (kg/ha)	Biological yield (kg/ha)	Ear weight (kg/ha)	Kernel abortion (%)	1000-KW (gr)	Harvest index (%)	$IWUE_{GY}$ (kg/m^3)	$IWUE_{BY}$ (kg/m^3)
Irrigation levels	I_{40}	3589.60^{d}	13563.90^{d}	4849.00^{d}	28.44^{a}	151.4^{d}	26.34^{d}	1.20^{a}	4.53^{a}
	I_{60}	4597.20^{c}	14689.70^{c}	5808.20^{c}	22.44^{b}	171.4^{c}	31.25^{c}	1.02^{b}	3.27^{b}
	I_{80}	5860.00^{b}	15851.00^{b}	6936.00^{b}	15.22^{c}	197.4^{b}	37.00^{b}	0.98^{bc}	2.64^{c}
	I_{100}	7099.10^{a}	17317.80^{a}	7927.60^{a}	11.11^{c}	245.3^{a}	40.96^{a}	0.95^{c}	2.31^{d}
Planting dates	PD_1	5770.30^{a}	15628.30^{a}	6617.40^{a}	18.00^{a}	203.58^{a}	36.28^{a}	1.13^{a}	3.25^{a}
	PD_2	5168.00^{b}	15601.20^{a}	6399.10^{ab}	18.42^{a}	188.50^{b}	32.70^{b}	1.01^{b}	3.21^{ab}
	PD_3	4921.10^{b}	14837.30^{b}	6124.10^{b}	21.50^{a}	182.16^{b}	32.69^{b}	0.95^{b}	3.09^{b}
PD × IR (DMRT < 0.05)		**	ns	ns	ns	*	*	ns	ns

Means within the same column followed by the same letters are not significantly different ($p < 0.05$). KW = Kernel weight; $IWUE_{GY}/IWUE_{BY}$ = Irrigation water use efficiency of grain yield/biological yield; PD = Planting Date; IR = Irrigation

http://www.aloki.hu ● ISSN 1589 1623 (Print) ● ISSN 1785 0037 (Online)
DOI: http://dx.doi.org/10.15666/aeer/1605_61696180
© 2018, ALÖKI Kft., Budapest, Hungary

Irrigation water use efficiency (IWUE) at high irrigation level (I_{100}), was the lowest and at low irrigation level (I_{40}), was the highest. In consequence, the highest values of $IWUE_{GY}$ (1.39 and 1.20 kg/m^3) and the greatest values of $IWUE_{BY}$ (4.79 and 4.53 kg/m^3) were recorded at I_{40} compared with I_{100} in both years, respectively. Early-planting date was prominent for holding the highest values of each trait except kernel abortion.

Effect of water variability and planting date on grain yield

Planting dates and irrigation levels interaction (PD × IR) had significant effect ($p < 0.01$) on grain yield (GY) in 2016-17 (*Fig. 5*). Corns that planted later under effect of limiting factors such as drought stress, poor levels of radiation as well as irrepressible changes in temperature and assimilate supply, formed kernels poor in size and quality. Whereas, early-planting corns (PD_1), produced more nutrient levels than PD_2 or PD_3 in exchange of full water application of 100% ET_c. Consequential effects of these responses can find in bigger kernels which have been set during grain-fill stage as a result of grater final yield potential.

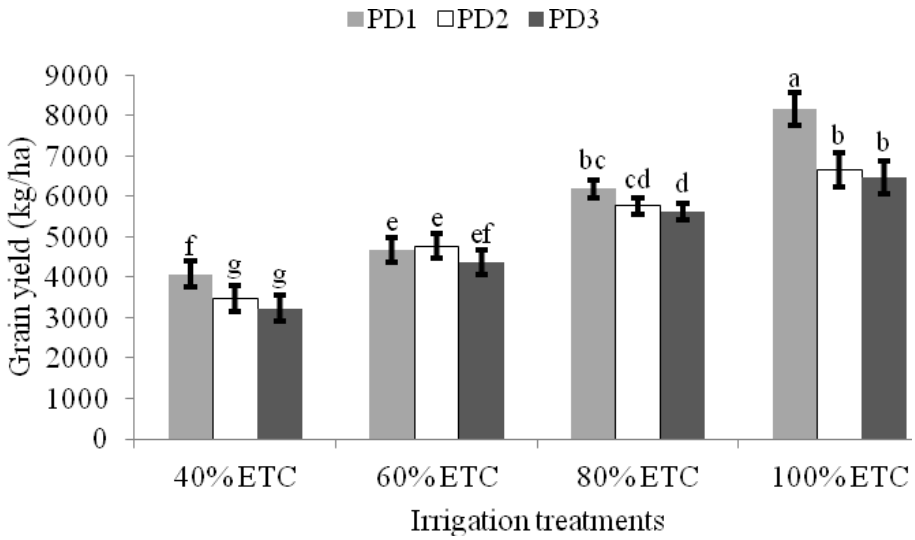

***Figure 5**. The interaction of planting dates and irrigation levels on grain yield in 2016-17. Different letters indicate significant difference ($p < 0.01$) based on DMRT test*

ET- function and management considerations of relevance

The effects of the various weather conditions are incorporated into the reference evapotranspiration (ET_0) estimates. ET_0 represents an index of climate demand and K_c varies, predominately with the specific crop characteristics and only to a limited extends with climate (Allen et al., 1998). In particular, crop ET demand can vary according to the location, time of planting, soil texture and corn growth period. The values of ET_0 and ET_c were quite low at the initial period due to the less evaporation from the soil and plant surfaces and subsequently from transpiration through stomata in the early of the corn life cycle. Initially, the ET_c values virtually followed constant trend at low fixed rates of K_c (0.3), then peaked at 70-80 days after planting at the higher K_c ranges (1.2 and 0.6) in mid and last terms of corn life cycle, respectively (*Fig. 6*).

http://www.aloki.hu ● ISSN 1589 1623 (Print) ● ISSN 1785 0037 (Online)
DOI: http://dx.doi.org/10.15666/aeer/1605_61696180
© 2018, ALÖKI Kft., Budapest, Hungary

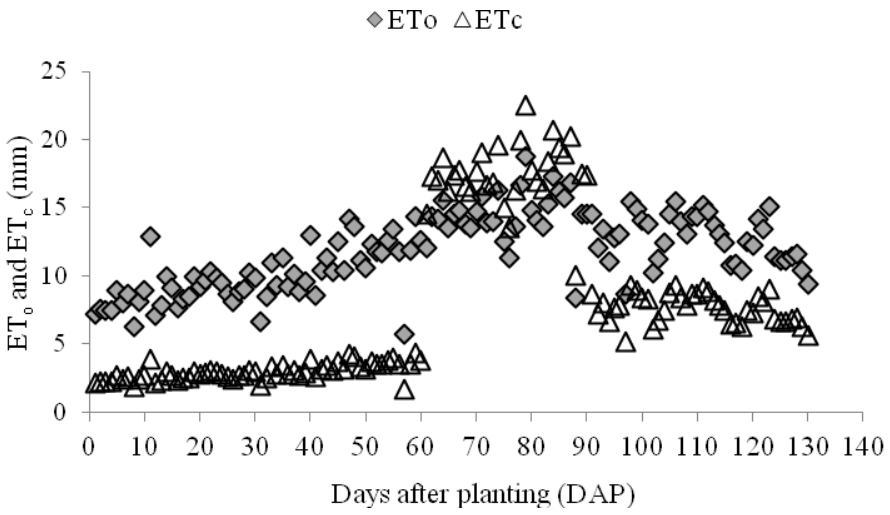

Figure 6. *Reference and crop ET estimations based on FAO (K_c) during corn maturity as a function of days after planting. ET_0 is a climatic parameter expressing the evaporation power of the atmosphere; ET_c refers to the evaporative demand from crops that are grown under the given climatic conditions*

Crop ET-value was the highest at silking stage (R1) which occurred around 80-82 days after planting (*Fig. 7*).

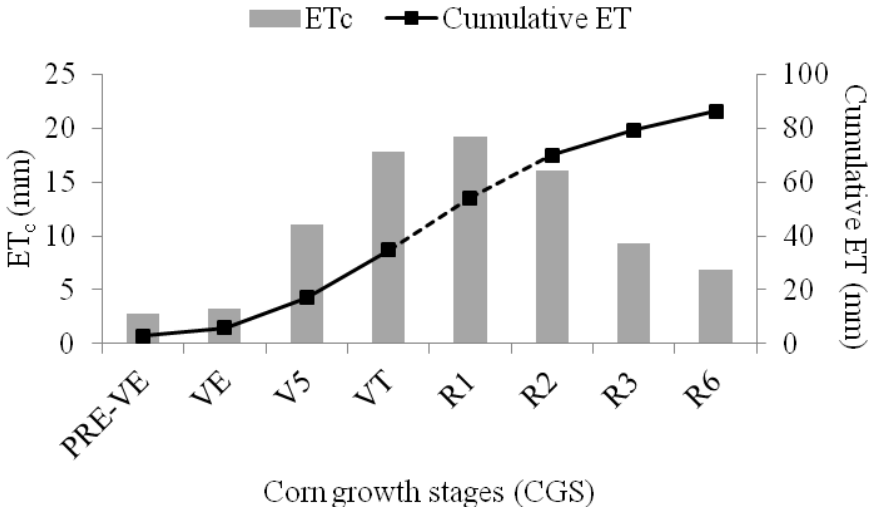

Figure 7. *Crop ET and cumulative ET (mm) variations in different corn growth stages, the dotted part represents the most critical time to water stress. PRE-VE = Pre emergence, VE = Emergence, V5 = Fifth leaf visibility, VT = Tasseling stage, R1 = Silking stage, R2 = Beginning grain fill, R3 = Milk stage and R6 = Physiological maturity*

Regionally when irrigation applied in the common rate of ET demand, grain yield reduction is not directly related to ET and biomass reduction. When ET demand cumulatively increases from what is needed for crop longevity and substantially deficit irrigation occurs below the optimum ET level, it can be more devastating at tassel to grain-fill stage (VT to R2). Although overall grain yield will decline as biomass

http://www.aloki.hu ● ISSN 1589 1623 (Print) ● ISSN 1785 0037 (Online)
DOI: http://dx.doi.org/10.15666/aeer/1605_61696180
© 2018, ALÖKI Kft., Budapest, Hungary

declines, effective deficit irrigation management can allow corn water stress to be managed so that HI does not decline. For this reason, planting corn early in the season with sufficient water supply in the soil and less water loss by evaporation can avoid irrigations which are surplus to requirements. In this experiment, irrigation efficiency based on GY was improved by 23% and 16% in PD_1 compared to PD_3 for both years, respectively. These results underlined the advantage of water management at certain growth stages to minimize corn negative physiological responses.

Discussion

Based on the findings, the effect of deficit irrigation on GY was greater than on total biomass, as reflected in low HI under deficit irrigation treatments. Our observation corroborated by those of (Payero et al., 2009; Chaichi et al., 2015). According to Fereres and Soriano (2007), as biomass production is tightly associated with ET, it represents that in the case of deficit irrigation plant capability in converting per unit of water to biomass will be improved through transpiration due to the proximity of wetter condition and cooler temperatures in the early of the growing season. Early-planted corns via earlier shading of soil surface with unrestricted accessibility to water resources have higher irrigation efficiency. In contrast late-planted corns due to loss of moisture increasingly below the optimum ET level and less demand for assimilate; produce smaller grains in relation to per mm of water application. Lower GYs were largely occurred as total biomass and harvest index decreased with delayed plantings (Tsimba et al., 2013). Instead, in cereals it may also result in beneficial redistribution of assimilate from storage to developing grains to increase HI under scarcer water condition (Yang et al., 2002). In spite of improving irrigation efficiency with water deficit in this experiment, AL-Kaisi and Xinhua (2003) reported that drought stress reduced the water use efficiency for the production of biological yield but somewhat increased it for the production of economical yield in maize. In general, there is not inordinate demand for water during corn developmental stages due to proximity of rainy season and minimal weed competition in the early stage of corn life cycle. As plant population increase, an early-planting date becomes more important. Thus in a water-limited situation, planting long duration hybrids early in the season when the cumulative seasonal ET demand is low induced less yield penalty (Tsimba et al., 2013). Based on the soil type and ET demand, avoiding water stress around two weeks prior to pollination entering into two weeks after silking, can assure economical yields as a result of better seed set and less barren tips. The results obtained are in agreement with the ex-reports (Doorenbos and Kassam, 1979; Hatfield et al., 2015). Vegetative growth is strongly affected by water stress at different developmental stages. Short-duration irrigations during the rapid vegetative growth period caused 28 to 32% loss of final dry matter weight (Cakir, 2004). Fundamentally, GDDs are used to account for corn growth relative to temperature. Normally, corn requires approximately 600 to 800 GDDs to accomplish silking to maturity period. If unfavorable conditions exist it may take more time for late-planted corns to achieve this period with less GDDs accumulation than early-planted corns. Additionally, as planting delayed, radiation abatement and low GDDs accumulation became increasingly critical for kernels setting. Water stress during this time can delay silking, reduce pollination and lead to kernel abortion. These remarks compared with those who addressed silking to pollen shed or anthesis-silking

http://www.aloki.hu ● ISSN 1589 1623 (Print) ● ISSN 1785 0037 (Online)
DOI: http://dx.doi.org/10.15666/aeer/1605_61696180
© 2018, ALÖKI Kft., Budapest, Hungary

interval responses to water stress (Herrero and Johnson, 1981; Westgate, 1994; Bolaños and Edmeades, 1996).

Conclusion

In conclusion, when corn planting occurs later in the season the source-sink limitations can avert loading and substantially grain yield losses in response to drought stress. Instead, corns that are planted earlier in the season tend to develop more gradually under more abundant of water supplies with definite number of GDDs accumulation. Reasons for this can help greater overall productivity with early-planting date. In the case of being in trouble for water supply, early planting date via holding optimum ET level and accelerating silking to maturity interval can avoid irrigations that are surplus to requirements. The irrigation water use efficiency and overall productivity of corn in this research improved through the assignment of early-planting date and deficit irrigation to the environmental and crop physiological limitations. Consequently, shifting planting date from common-planting date (PD_2) to an earlier date as well as deficit irrigation were integrated as the best adaptive strategies for Iran climate and other regions in the world with high evaporative ranges. Other adaptation strategy can prioritize by producer to select diverse hybrids of maize with high drought tolerance ratings.

REFERENCES

[1] Al-Kaisi, M. M., Xinhua, Y. (2003): Effects of nitrogen rate, irrigation rate and plant population on corn yield and water use efficiency. – Agronomy Journal 95: 1475-1482.
[2] Allen, R. G., Pereira, L. S., Raes, D., Smith, M. (1998): Crop Evapotranspiration Guidelines for Computing Crop Water Requirements. – FAO Irrigation and Drainage Paper 56. FAO, Rome.
[3] Blignaut, J., Urckermann, L., Aronson, J. (2009): Agriculture production's sensitivity to changes in climate in South Africa. – Journal of Science 105: 61-71.
[4] Bolaños, J., Edmeades, G. O. (1996): The importance of the anthesis-silking interval inbreeding for drought tolerance in tropical maize. – Field Crops Research 48: 65-80.
[5] Cakir, R. (2004): Effect of water stress at different development stages on vegetative and reproductive growth of corn. – Field Crops Research 89: 1-16.
[6] Chaichi, M. R., Nurre, P., Slaven, J., Rostamza, M. (2015): Surfactant application on yield and irrigation water use efficiency in corn under limited irrigation. – Crop Science 55: 386-393.
[7] Claassen, M. M., Shaw, R. H. (1970): Water deficit effects on corn. II. Grain components. – Agronomy Journal 62: 652-655.
[8] Doorenbos, J., Kassam, A. H. (1979): Yield Response to Water. – In: Johl, S. S. (ed.) Irrigation and Agricultural Development: Based on an International Expert Consultation, Baghdad Iraq. Pergamon Press, New York.
[9] Edmeades, G. O., Bolaños, J., Elings, A., Ribaut, J. M., Bänziger, M., Westgate, M. E. (2000): The Role and Regulation of the Anthesis-Silking Interval in Maize. – In: Westgate, M. E., Boote, K. (eds.) Physiology and Modeling Kernel Set in Maize. CSSA, Madison, WI, pp. 43-73.
[10] FAO (1977): Crop Water Requirement. – Irrigation and Drainage Paper No. 24. FAO, Rome.
[11] Fereres, E., Soriano, M. A. (2007): Deficit irrigation for reducing agricultural water use. – Journal of Experimental Botany 58: 147-59.

http://www.aloki.hu ● ISSN 1589 1623 (Print) ● ISSN 1785 0037 (Online)
DOI: http://dx.doi.org/10.15666/aeer/1605_61696180
© 2018, ALÖKI Kft., Budapest, Hungary

[12] Hatfield, J., Prueger, L., John, H. (2015): Temperature extremes: Effect on plant growth and development. – Weather and Climate Extremes 10: 4-10.
[13] Herrero, M. P., Johnson, R. R. (1981): Drought stress and its effects on maize reproductive systems. – Crop Science 21: 105-110.
[14] Howell, T. A. (2003): Irrigation Efficiency. – In: Stewart, B. A., Howell, T. A. (eds.) Encyclopedia of Water Science. Marcel Dekker, New York, pp. 467-472.
[15] Istanbulluoglu, A. (2009): Effects of irrigation regimes on yield and water productivity of safflower (*Carthamus tinctorius* L.) under Mediterranean climatic conditions. – Agricultural Water Management 96: 1792-1798.
[16] Kirda, C., Moutonnet, P., Hera, C., Nielsen, D. R. (1999): Crop Yield Response to Deficit Irrigation. – Water Reports 22. FAO, Rome.
[17] Mirkhani, R., Roozitalab, N., Khaleghpanah, N., Rezaei, S. (2010): Physico-chemical characteristics and clay mineralogy composition of selected soils in arid and semiarid regions of Iran. – In: Extended Abstracts 21st, Australian Clay Minerals Conference, Brisbane, QLD, Australia, 5-8 Aug. 2010.
[18] Morison, J. I. L., Baker, N. R., Mullineaux, P. M., Davies, W. J. (2008): Improving water use in crop production phil. – Transactions of the Royal Society B 363: 639-658.
[19] Payero, J. O., Tarkalson, D. D., Irmak, S., Davison, D., Petersen, J. L. (2009): Effect of timing of a deficit-irrigation allocation on corn evapotranspiration, yield, water use efficiency and dry mass. – Agricultural Water Management 96: 1387-1397.
[20] Soler, C. M. T., Sentelhas, P. C., Hoogenboom, G. (2007): Application of the CSM-CERES-Maize model for planting date evaluation and yield forecasting for maize grown off-season in a subtropical environment. – European Journal of Agronomy 27: 165-177.
[21] Soltani, A., Sinclair, T. R. (2012): Modeling Physiology of Crop Development, Growth and Yield. – CABI, Wallingford, UK.
[22] Tsimba, R., Edmeades, G. O., Millner, J. P., Kemp, P. D. (2013): The effect of planting date on maize: Phenology, thermal time durations and growth rates in a cool temperate climate. – Field Crops Research 150: 145-155.
[23] Westgate, M. E. (1994): Water status and development of the maize endosperm and embryo during drought. – Crop Science 34: 76-83.
[24] Yang, J. C., Zhang, J. H., Liu, L. J., Wang, Z. Q., Zhu, Q. S. (2002): Carbon remobilization and grain filling in Japonica/Indica hybrid rice subjected to post anthesis water deficit. – Agronomy Journal 94: 102-109.
[25] Zhang, J., et al. (2015): Responses of crop water use efficiency to climate change and agronomic measures in the semiarid area of Northern China. – PLoS ONE 10(9): e0137409. DOI: 10.1371/journal.pone.0137409.

http://www.aloki.hu ● ISSN 1589 1623 (Print) ● ISSN 1785 0037 (Online)
DOI: http://dx.doi.org/10.15666/aeer/1605_61696180
© 2018, ALÖKI Kft., Budapest, Hungary

GENOME-WIDE IDENTIFICATION AND CHARACTERIZATION OF THE SBP GENE FAMILY IN *EUCALYPTUS GRANDIS*

BUYUK, I.

Department of Biology, Faculty of Science, Ankara University, Ankara, Turkey
(e-mail: buyuki@ankara.edu.tr; phone: +90-312-212-6720 (1390); fax: +90-312-223-2395)

(Received 9th Jul 2018; accepted 6th Sep 2018)

Abstract. SQUAMOSA promoter binding proteins (SBP) are a group of plant transcription factor (TF) families that play an important role in plant development and defence response. Genome-wide investigations of *SBP* genes have been carried out in many plant species, however this is the first comprehensive report on the identification and characterization of *SBP* genes in *Eucalyptus grandis* (*E. grandis*). According to the results herein, 16 *SBP* genes from *E. grandis* were identified and SBP proteins were clustered in eight clades. 16 *SBP* genes were presented to distribute 7 out of 11 chromosomes and three segmental duplicated gene couple were found throughout the entire genome of *E. grandis*. A total of 15 conserved motifs were described and 3 out of 15 were found to be conserved among all Egrandis_SBP proteins, due to forming of SBP domain which is essential for the function of SBP proteins. Gene structures of all *Egrandis_SBP* genes were investigated and the estimated number of exons among all genes extended from 2 to 11. According to the synteny analysis, it was seen that homologs of *E. grandis* genes were found in corresponding syntenic blocks of *Arabidopsis thaliana* and *Vitis vinifera*. Digital gene expression analyses showed that most of the *Egrandis_SBP* genes were highly expressed in shoot tips, young leaf, xylem, mature leaf, immature xylem and phloem tissues of *E. grandis*. Taken all together, the results of this study will provide an important source for literature and further works.
Keywords: *bioinformatic approach, phylogeny, RNAseq, digital gene expression*

Introduction

Squamosa promotor binding proteins (SBPs) are transcription factor (TF) genes that are only found in plants, their presence have not been verified in animals and prokaryotic organisms thus far (Klein et al., 1996; Hou et al., 2013). One common feature in members of the SBP TF family is the presence of 76 aa DNA-binding domain which have been called: SBP domain containing two zinc fingers (Cys-Cys-His-Cys and Cys-Cys-Cys-His) (Klein et al., 1996; Yamasaki et al., 2004; Pan et al., 2017).

They were first discovered in *Antirrhinum majus* (Klein et al., 1996) and their first comprehensive characterization was performed in *A. thaliana* (Cardon et al., 1997) in order to explore their exact function in plants. Like all TFs that have been discovered up to date, SBP proteins were indicated to play crucial roles in the expressional regulation of genes that are involved in many important processes related to plant development and defence response (Unte et al., 2003; Zhang et al., 2007; Wu and Poethig, 2006).

Genome-wide characterization and expression studies of *SBP* genes have been conducted on a number of plant species including *Betula pendula, Chlamydomonas, Oryza sativa, Zea mays, Populus trichocarpa, Lycopersicon esculentum* L.*, Malus* × *domestica* Borkh., *Salvia miltiorrhiza, Gossypium hirsutum, Arachis hypogaea* L., *Petunia*, *Capsicum annuum* L., and *Phyllostachys edulis* (Chuck et al., 2010; Kropat et al., 2005; Lannenpaa et al., 2004; Li et al., 2013, 2016; Lu et al., 2011; Pan et al., 2017; Preston et al., 2016; Salinas et al., 2012; Xie et al., 2006; Zhang et al., 2016, 2014; Zhang et al., 2015). Nonetheless, the SBP proteins in *Eucalyptus grandis,* a tall forest tree in the *Myrtaceae* known as the flooded gum or rose gum, have not been identified and characterized despite the fact its genome was sequenced in 2014 (Myburg et al., 2014).

http://www.aloki.hu ● ISSN 1589 1623 (Print) ● ISSN 1785 0037 (Online)
DOI: http://dx.doi.org/10.15666/aeer/1605_61816193
© 2018, ALÖKI Kft., Budapest, Hungary

Eucalyptus grandis (*E. grandis*) is a plantation crop which spreads widely in tropics and subtropics areas. It is commonly found in nature in Australia, and it is considered an important plant for plant scientist because, of its extreme ability to adapt to both climate and soil (Robinson et al., 2006). Moreover, there is a wide range of uses for *E. grandis* in farm; specialty products (flowers generate nectar for honey production), urban (used for ornamental purposes), wildlife value (its flowers attracts birds) and wood products including: pulpwood, boat building, boxes, flooring, heavy construction, fuelwood, industrial charcoal, panelling and timber for furniture etc (dos Santos et al., 2004; Nautiyal and Couto, 1984; Hardie and Wood, 1973; Dye, 2013).

Due to its importance in a wide range of use for the industry, and its ability to adapt to extreme soil and climate conditions, our aim was to identify and characterize SBP proteins in *E. grandis* which are important TF family for the plant developmental processes. Accordingly, 16 Egrandis_SBP members were identified and comprehensive analyses of the sequence phylogeny, genomic organization, exon-intron region of gene, conserved protein motifs, gene duplication events, and expression analysis were performed.

Materials and methods

Identification of SBP genes in E. grandis genome

E. grandis of SBP protein sequences were retrieved from Phytozome database v12.1 (www.phytozome.net) using keywords in the search with Pfam Accession Number (PF03110) obtained from Pfam Database (http://pfam.xfam.org). BLASTP and BLASTX searches (National Center for Biotechnology Information [NCBI]: http://www.ncbi.nlm.nih.gov) were used to confirm Egrandis_SBP proteins. Non-redundant sequences were obtained using decrease redundancy tool (http://web.expasy.org/decrease_redundancy/). SBP domains in non-redundant sequences were checked by HMMER (http://www.ebi.ac.uk). The solid and chemical traits of SBP proteins in *E. grandis* were identified using the ProtParam tools (http://web.expasy.org/protparam/) such as: the theoretical isoelectric point (pI), number of amino acids, and molecular weight (Da).

Phylogenetic analysis, physical location, conserved motifs of Egrandis_SBP genes, gene structure and gene duplication events

Chromosomal locations and CDS sizes (bp) were identified by using Phytozome database v12.1. The *Egrandis_SBP* genes were mapped with MapChart (Voorrips, 2002). Multiple sequence alignment of aminoacid sequences of Egrandis_SBP proteins was conducted with ClustalW Phylogenetic analysis were performed using MEGA v7 (Tamura et al., 2013; Buyuk and Aras, 2016) and Neighbor-joining (NJ) algorithm with 1000 replicated-bootstrap value.

Egrandis_SBP protein sequences of the conserved motifs were identified using MEME (Multiple Expectation Maximization for Motif Elucidation; http://meme-suite.org/) (Bailey et al., 2006; Buyuk et al., 2016; Inal et al., 2017; Ilhan et al., 2018). The limits for maximum number of motifs and minimum/maximum width were adjusted to; 20 and 2, 50, respectively. Motif sites were among 2 and 300. Site distribution was set as any number of repetitions. The described conserved motifs were examined in InterProscan with default adjusting (Quevillon et al., 2005).

http://www.aloki.hu ● ISSN 1589 1623 (Print) ● ISSN 1785 0037 (Online)
DOI: http://dx.doi.org/10.15666/aeer/1605_61816193
© 2018, ALÖKI Kft., Budapest, Hungary

Gene Structure Display Server program tool (GSDS; http://gsds.cbi.pku.edu.cn/) was used (Guo et al., 2007) to predict the exon/intron organization of the *Egrandis_SBP* genes. Genomic DNA sequences and coding sequences of *Egrandis_SBP* genes were utilized.

Segmental duplicate gene pairs were examined on the Plant Genome Duplication Database server (http://chibba.agtec.uga.edu/duplication/index/locus), with a display range of 100 kb. The nonsynonymous rates (Ka), synonymous rates (Ks) and developmental constraints (Ka/Ks) with the duplicated pairs of *Egrandis_SBP*s were evaluated using CODEML program in PAML (Yang, 2007).

Synteny analysis

E. grandis and *A. thaliana*, *E. grandis* and *V. vinifera* of orthologue *SBP* genes were identified with Plant Genome Duplication Database (PGDD; http://chibba.agtec.uga.edu/duplication/) (Lee et al., 2013). Then, the protein sequences of orthologue were retrieved from Phytozome v12.1. The obtained synteny map was created using iTAK - Plant Transcription factor & Protein Kinase Identifier and Classifier (http://itak.feilab.net/cgi-bin/itak/index.cgi) (Zheng et al., 2016).

Gene expression analysis in silico

The expression levels of *Egrandis_SBP* genes were examined in special tissue libraries of plants at different stages of; shoot tips, young leaf, xylem, mature leaf, immature xylem and phloem. They were retrieved from Phytozome Database v12.1 (http://phytozome.jgi.doe.gov/pz/portal.html#!info?alias=Org_Pvulgaris). FPKM (expected number of fragments per kilobase of transcript sequence per millions base pairs sequenced) units were used for the expression levels in silico. FPKM values were log2 transformed and the heatmap was produced with the algorithm CIMMiner (http://discover.nci.nih.gov/cimminer).

Results and discussion

Identification of SBP gene family in E. grandis

Sequences of *SBP* proteins in the *E. grandis* genome were downloaded from Phytozome database v12.1 (www.phytozome.net) using keywords in the search with Pfam Accession Number (PF03110) retrieved from Pfam Database (http://pfam.xfam.org/). Subsequently, SBP domains were analyzed by performing a search in the HMMER and Pfam databases in candidate Egrandis_SBP proteins, and the redundant sequences were discarded after obtaining confirmation. A total of 16 candidate *SBP* genes in *E. grandis* genome were discovered and given in *Table 1* which includes information about chromosomal location, amino acid (length), molecular weight, number of isoelectric point (pI) and instability index.

As shown in *Table 1* and *Figure 1*, all of the non-redundant *Egrandis_SBP* genes were distributed on 7 out of 11 chromosomes of *E. grandis*. While the lowest number of *Egrandis_SBP* genes was observed on chromosome 4 (one *Egrandis_SBP* gene), the highest number was found on chromosome 11 (4 *Egrandis_SBP* genes) (*Fig. 1*). The length of Egrandis_SBP proteins extended from 147 (Egrandis_SBP_8) to 1078 (Egrandis_SBP_10) amino acids (aa). PI values of Egrandis_SBP proteins were among 5.77 (Egrandis_SBP_9) and 9.50 (Egrandis_SBP_5) ranging from acidic to alkaline

http://www.aloki.hu ● ISSN 1589 1623 (Print) ● ISSN 1785 0037 (Online)
DOI: http://dx.doi.org/10.15666/aeer/1605_61816193
© 2018, ALÖKI Kft., Budapest, Hungary

while the molecular weight of Egrandis_SBPs was between 21.277 kDa (Egrandis_SBP_11) and 119.285 kDa (Egrandis_SBP_10) (*Table 1*). SBP, which is a plant specific transcription gene family, was detected and classified in various species thus far, such species include: *A. thaliana* (Rhoades et al., 2002), *Orzya sativa* (Xie et al., 2006), *Lycopersicon esculentum L.* (Salinas et al., 2012), *V. vinifera* (Hou et al., 2013), *Citrus* (Shalom et al., 2015), *Triticum L.* (Wang et al., 2015), *Zea mays* (Mao et al., 2016), *Gossypium raimondii* (Ali et al., 2017), *Petunia* (Zhou et al., 2018), *Fragaria vesca*, *Pyrus bretschneideri*, *Prunus persica* and *Prunus mume* (Abdullah et al., 2018). Nevertheless, this is the first comprehensive report on identification and characterization of *SBP* genes in *E. grandis.*

Table 1. *Information of 16 Egrandis_SBP proteins*

Gene ID	Gene name	Locations	aa	mw (kDa)	pI	Instability index	Classifies
Egrandis_SBP_1	Eucgr.A01019	Chr01:30283917..30289641 forward	984	109.125	5.79	56.75	Unstable
Egrandis_SBP_2	Eucgr.A02441	Chr01:39752248..39757521 reverse	390	41.273	9.12	54.92	Unstable
Egrandis_SBP_3	Eucgr.B00631	Chr02:6573009..6576407 reverse	524	57.179	8.74	55.34	Unstable
Egrandis_SBP_4	Eucgr.B03500	Chr02:54998894..55003285 reverse	488	53.532	8.67	53.61	Unstable
Egrandis_SBP_5	Eucgr.B03518	Chr02:55118387..55120136 reverse	318	34.533	9.50	53.22	Unstable
Egrandis_SBP_6	Eucgr.D02505	Chr04:39040236..39042737 forward	348	38.354	8.45	64.98	Unstable
Egrandis_SBP_7	Eucgr.E01600	Chr05:18228156..18230663 forward	367	38.759	9.07	72.79	Unstable
Egrandis_SBP_8	Eucgr.E03260	Chr05:53739864..53743190 reverse	147	16.977	6.00	88.37	Unstable
Egrandis_SBP_9	Eucgr.B01228	Chr06:24482430..24488179 forward	821	91.221	5.77	55.35	Unstable
Egrandis_SBP_10	Eucgr.F01828	Chr06:24482430..24488179 forward	1078	119.285	7.11	58.38	Unstable
Egrandis_SBP_11	Eucgr.F03303	Chr06:44594386..44595751 reverse	186	21.277	8.86	69.09	Unstable
Egrandis_SBP_12	Eucgr.H04114	Chr08:55717528..55724988 reverse	1005	112.303	6.39	49.39	Unstable
Egrandis_SBP_13	Eucgr.K01046	Chr11:13456169..13458136 forward	236	26.056	8.66	64.51	Unstable
Egrandis_SBP_14	Eucgr.K01828	Chr11:23807022..23809835 reverse	376	39.879	9.12	59.39	Unstable
Egrandis_SBP_15	Eucgr.K02545	Chr11:33320448..33325312 reverse	551	59.583	6.83	50.07	Unstable
Egrandis_SBP_16	Eucgr.K02708	Chr11:34626111..34629250 forward	363	39.804	8.96	55.21	Unstable

Based on the importance of gene duplications in the evolution of gene families in plants, the gene duplication events of putative *SBP* genes in *E. grandis* genome have been examined in this study. Our analysis identified three duplicated gene couple (Egrandis_SBP_2/ Egrandis_SBP_4, Egrandis_SBP_8/ Egrandis_SBP_13, Egrandis_SBP_11/ Egrandis_SBP_13 and Egrandis_SBP_3/ Egrandis_SBP_15) among eight identified *Egrandis_SBP* genes (*Fig. 1*). The Ka/Ks ratios between these duplication gene couples were found to be lower than '1' which suggests that: natural selection has occurred during segmental duplication events (Juretic et al., 2005).

Likewise, many segmental duplications of SBP genes have been detected in *A. thaliana* (*AtSPL10*/*AtSPL11*, *AtSPL4*/*AtSPL5*, *AtSPL1*/*AtSPL12*) and *O. sativa* (*OsSBP10*/*OsSBP5*, *OsSBP11*/*OsSBP4*, *OsSBP12*/*OsSBP3*) (Blanc and Wolfe, 2004; Bowers et al., 2003; Paterson et al., 2004; Wang et al., 2005). Besides segmental duplication events, some plant species including *Malus* × *domestica Borkh* (Li et al., 2013), *V. vinifera* (Hou et al., 2013), *F. vesca, Pyrus bretschneideri, P. persica* and *P. mume* (Abdullah et al., 2018) have demonstrated to have tandem duplication events either.

http://www.aloki.hu ● ISSN 1589 1623 (Print) ● ISSN 1785 0037 (Online)
DOI: http://dx.doi.org/10.15666/aeer/1605_61816193
© 2018, ALÖKI Kft., Budapest, Hungary

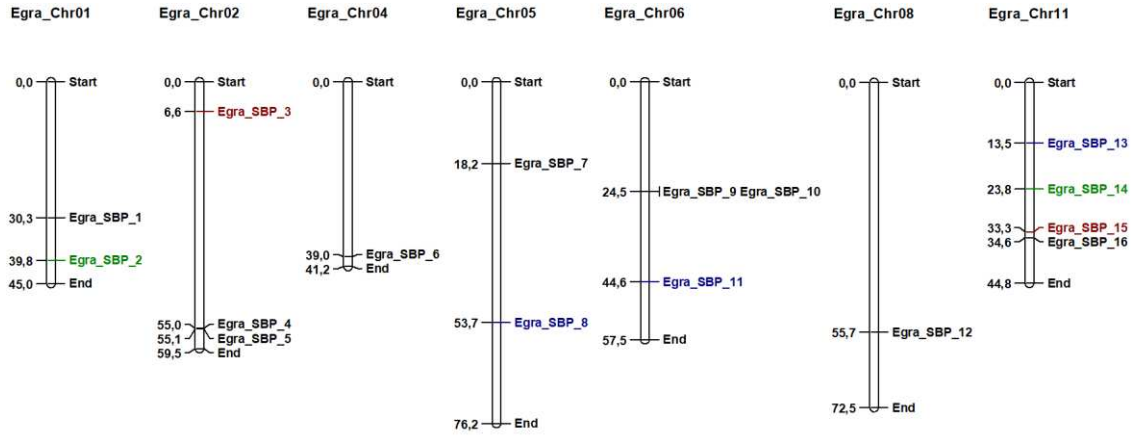

Figure 1. *Distribution of Egrandis_SBP genes on chromosomes of Eucalyptus grandis*

Phylogenetic analysis, gene structure and conserved motifs of Egrandis_SBPs

To discover the relationships between Egrandis_SBP proteins, a phylogenetic tree of SBP proteins in *E. grandis*, *A. thaliana* and *V. vinifera* was constructed using neighbor-joining (NJ) method with bootstrapping 1000 times (*Fig. 2*). Egrandis_SBPs were clustered into eight groups from A to D4 (*Fig. 2*). Group C2 was the largest group containing 18 SBP members, that is almost 34% of the total SBP proteins in the tree. And a minimum of one member of Egrandis_SBP proteins have made a contribution to each group, except for the Group A which has only one SBP protein from *V. vinifera* (*Fig. 2*). Egrandis_SBP proteins were clustered with the same number (7 from each) of *A. thaliana* and *V. vinifera* SBP proteins in Group C2. In contrast, any of *A. thaliana* were clustered with SBP proteins of *E. grandis* and *V. vinifera* in Group C1 suggesting that these genes may have been lost during evolution in *A. thaliana.* As previously declared by Abdullah et al. (2018), this kind of loss and birth of SBP genes which are specific to species might cause divergence in these genes in terms of functionality (Abdullah et al., 2018). In addition, similar coding and exon-intron sequences were observed in *SBP* genes which were found in the same subgroup of the phylogenetic tree (*Fig. 2*).

Similarly, phylogenetic trees of SBP proteins from several plant species including rice (Xie et al., 2006), *A. thaliana* (Guo et al., 2008), *Z. mays* (Chuck et al., 2010), *L. esculentum* (Salinas et al., 2012), *Malus slyvestris* (Li et al., 2013) and *Phyllostachys edulis* (Pan et al., 2017) were also divided into eight groups in accordance with the phylogenetic tree of SBP proteins from *E. grandis.*

To investigate conserved motifs in Egrandis_SBP proteins, MEME (v4.12.0) were used, and a total of 15 conserved motifs were described (*Fig. 3* and *Table A1* in the *Appendix*). The lengths of identified motifs were between 11 and 50 amino acids and all identified Egrandis_SBP proteins were found to have Motif 1, 2 and 3, which constitute the SBP domain (*Fig. 3*). Some of the other SBP motifs were only found in some Egrandis_SBP proteins, suggesting that these motifs may be provide by a specific function of these proteins (*Fig. 3*).

http://www.aloki.hu ● ISSN 1589 1623 (Print) ● ISSN 1785 0037 (Online)
DOI: http://dx.doi.org/10.15666/aeer/1605_61816193
© 2018, ALÖKI Kft., Budapest, Hungary

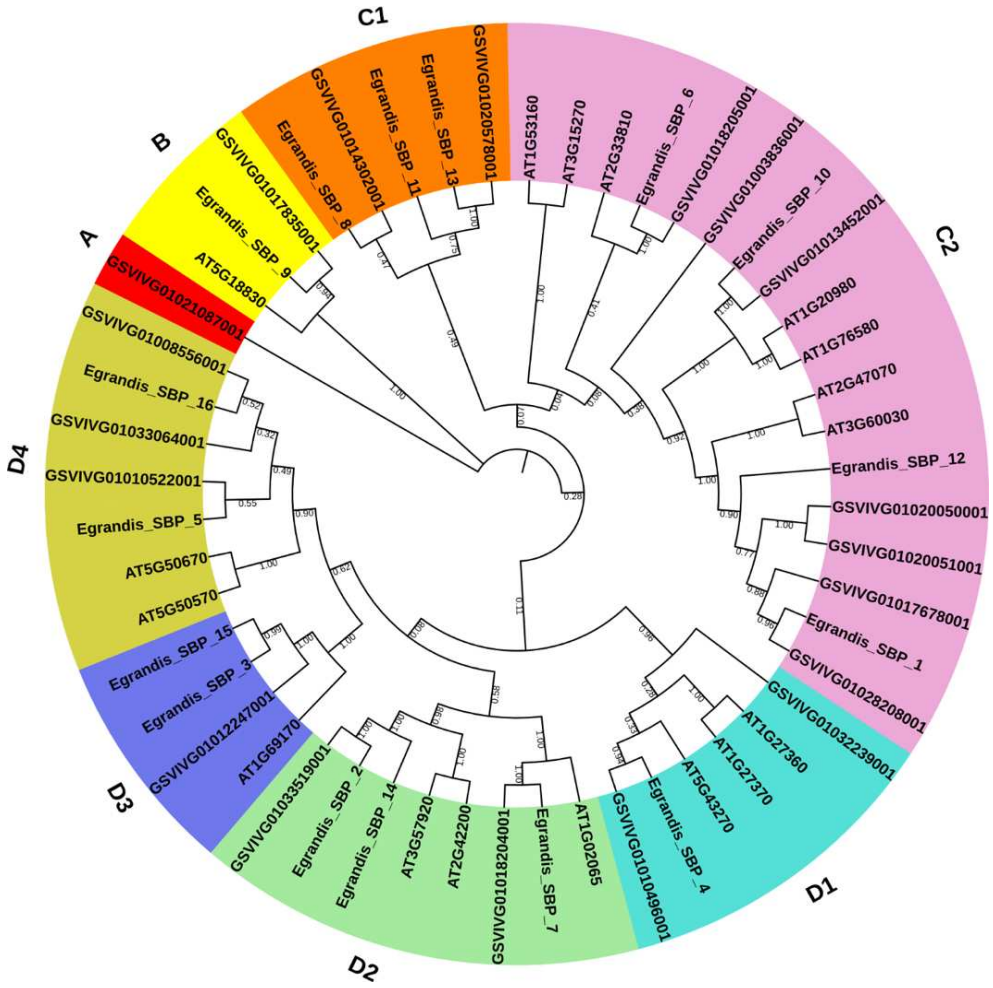

Figure 2. *Phylogenetic tree based on the conserved SBP domains alignment of 16 Egrandis_SBP predicted proteins, 17 A. thaliana SBP proteins and 19 Vitis vinifera SBP proteins, respectively. The tree was generated with MEGA v7.0 software, using the Neighbor-joining (NJ) method, and bootstrap values were calculated with 1000 replicates. Identified groups are shown on the outside of the circle*

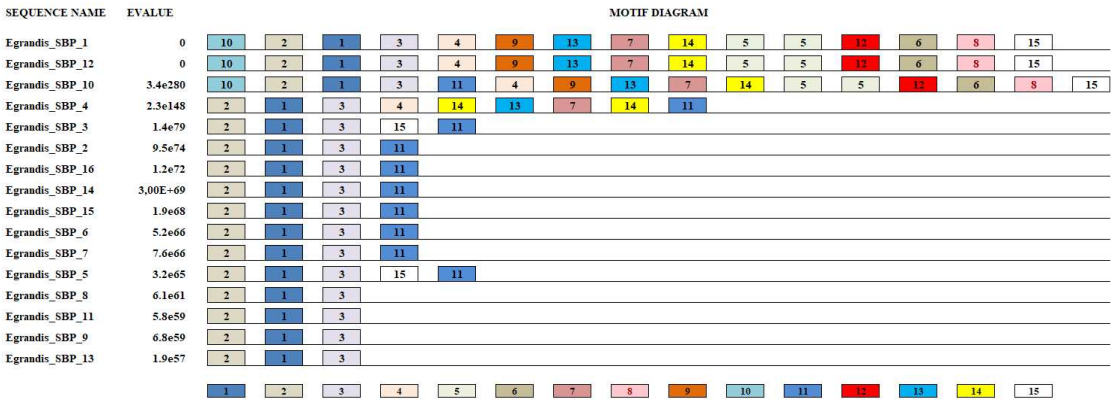

Figure 3. *Distribution of conserved motif of SBP genes in E. grandis. Full explanation of the motifs were given as seen in Table A1 in the Appendix*

http://www.aloki.hu ● ISSN 1589 1623 (Print) ● ISSN 1785 0037 (Online)
DOI: http://dx.doi.org/10.15666/aeer/1605_61816193
© 2018, ALÖKI Kft., Budapest, Hungary

The SBP domain were shown to form two zinc fingers in all *Egrandis_SBP* proteins and zinc finger 1 (Cys-Cys-His-Cys) was composed of Motif 1 while Motif 2 and 3 were involved in the construction of zinc finger 2 (Cys-Cys-Cys-His) as shown in *Figure 4*. These zinc binding sites were shown to be essential for SBP domain however they have been reported as having different structures than other zinc binding structures by Yamasaki et al. (2004) and thus, they are known as a novel zinc-binding motif (Yamasaki et al., 2004).

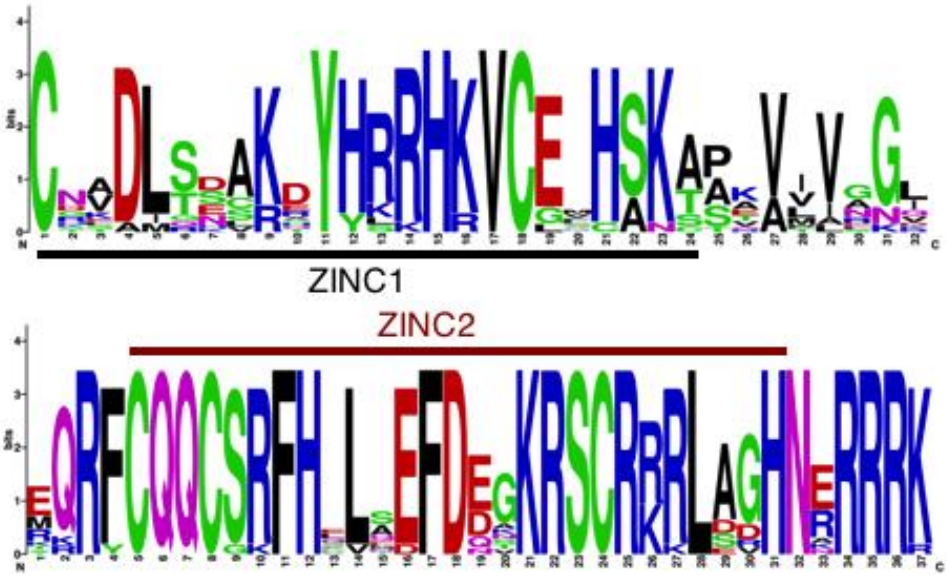

Figure 4. *Domain compositions of Egrandis_SBP genes. Thirteen Egrandis_SBP genes have both the characteristics of ZINC1 (Cys-Cys-His-Cys) and ZINC2 (Cys-Cys-Cys-His). The bit score represents the information content for each position in the sequence*

Gene structures of 16 *E. grandis* SBP gene were investigated and the estimated number of exons among all genes extended from 2 (*Egrandis_ SBP_8*) to 11 (*Egrandis_ SBP_1*) (*Fig. 5*). This varied numbers of exons in *E. grandis SBP* family genes by gain or loss of exon(s)/intron(s) might have occurred during evolution of *Egrandis_SBP* genes.

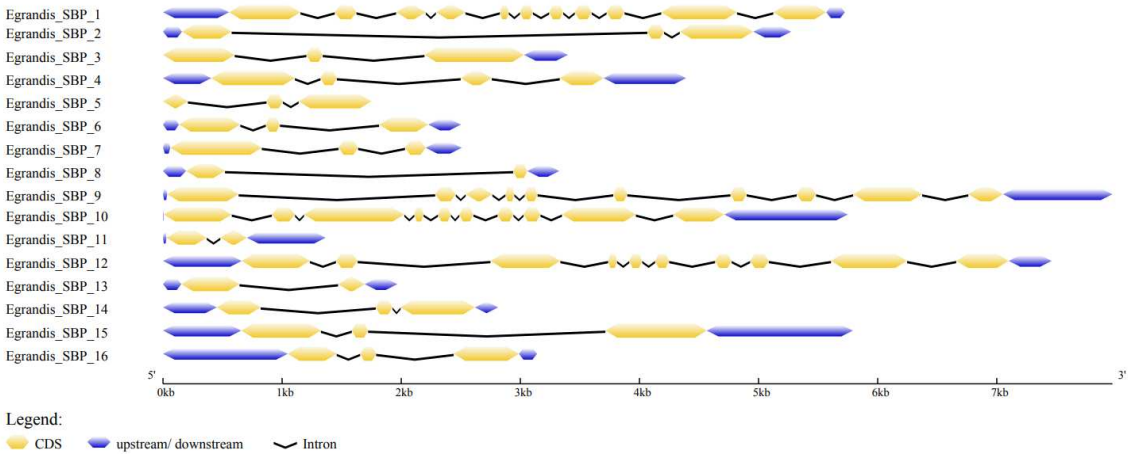

Figure 5. *Gene structure of SBP genes in E. grandis*

http://www.aloki.hu ● ISSN 1589 1623 (Print) ● ISSN 1785 0037 (Online)
DOI: http://dx.doi.org/10.15666/aeer/1605_61816193
© 2018, ALÖKI Kft., Budapest, Hungary

Comparative and synteny events among SBP genes of E. grandis, A. thaliana and V. vinifera

SBP protein sequences from *E. grandis*, *A. thaliana* and *Vitis vinifera* were subjected to comparative synteny analysis, to calculate evolutionary relationship of the SBP gene family between these species (*Fig. 6*). A total of 16 SBP proteins from *E. grandis*, 12 from *A. thaliana,* and 10 from *V. vinifera* was used to perform the synteny analysis. According to the synteny analysis results, homologs of *E. grandis* genes were found in corresponding syntenic blocks of *A. thaliana* and *V. vinifera* (*Fig. 6*). In terms of co-evaluation of gene duplications and synteny analyses of *Egrandis_SBP* genes, we can conclude from here, that both of these events might contribute to the evolutionary expansion of SBP genes in *E. grandis* genome (*Figs. 1* and *6*).

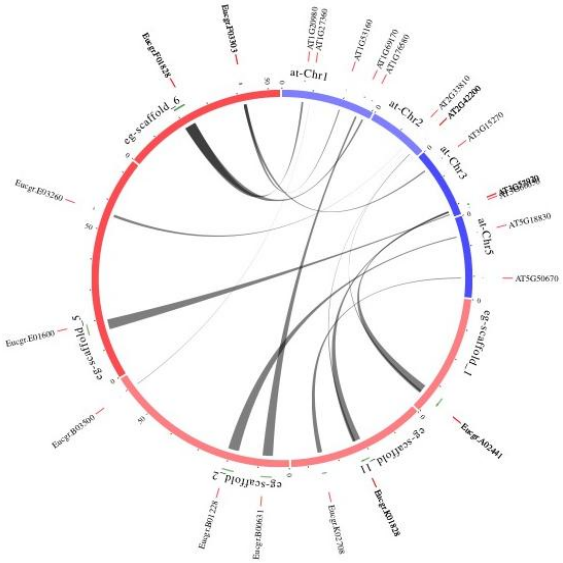

A

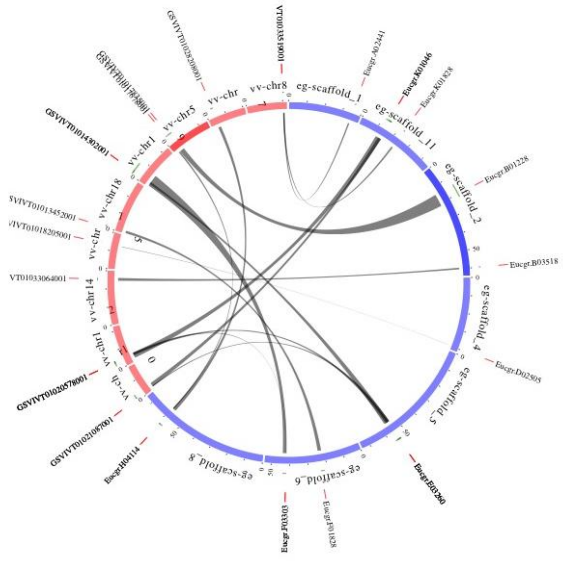

B

Figure 6. *Genome wide synteny analysis of SBP genes.* ***A.*** *Comparative map between E. grandis and A. thaliana.* ***B.*** *Comparative map between E. grandis and V. vinifera*

http://www.aloki.hu ● ISSN 1589 1623 (Print) ● ISSN 1785 0037 (Online)
DOI: http://dx.doi.org/10.15666/aeer/1605_61816193
© 2018, ALÖKI Kft., Budapest, Hungary

Expression profiles of Egrandis_SBPs in different tissues

In this study, a common mRNA analysis of *Egrandis_SBP* genes were performed via publicly available expression data in Phytozome v12.1 online plant genomics resource (https://phytozome.jgi.doe.gov). The heatmap shows the expression variance of identified 16 *Egrandis_SBP* genes in different plant tissues (*Fig. 7*).

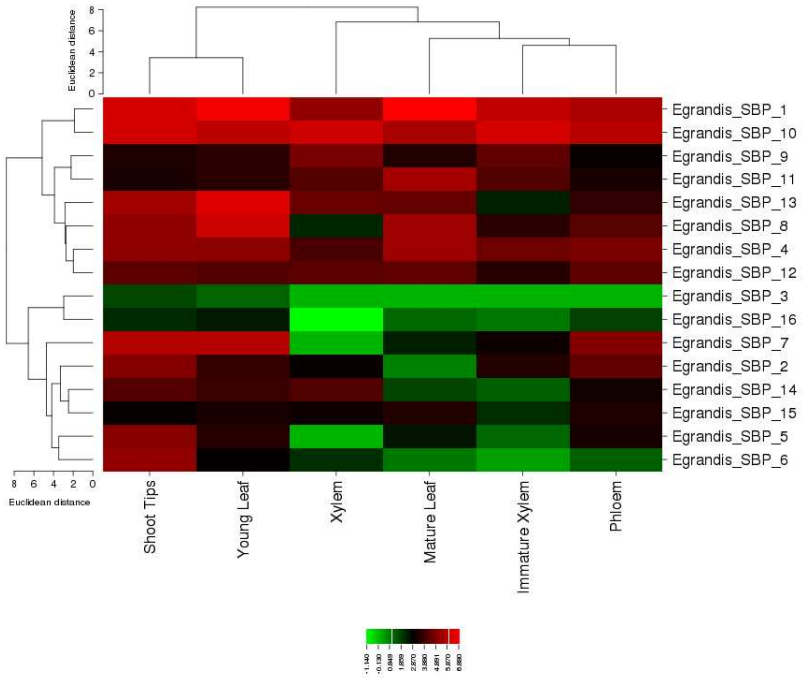

Figure 7. *Expression profiling of E. grandis SBP genes in shoot tips, young leaf, xylem, mature leaf, immature leaf and phloem tissues. Green and red colors indicate low-expression and high-expression, respectively*

As seen in the *Figure 7, Egrandis_SBP_1, -10, -9, -11, -13, -8, -4* and *-12* genes revealed relatively high expression levels in almost all tissues including shoot tips, young leaf, xylem, mature leaf, immature xylem and phloem. However, *Egrandis_SBP_2, -3, -5, -6, -7, -14, -15* and *-16* genes constituted relatively low expression levels in all tissues except for: shoot tips and young leaf (*Fig. 7*). In short, a conclusion can be drawn from the heatmap, that most of the *Egrandis_SBP* genes were highly expressed in all examined tissues of *E. grandis.*

Conclusions

The study herein, provides a comprehensive genome-wide identification of SBP genes in *E. grandis.* A total of 16 SBP genes were identified and were labelled as: *Egrandis_1* to *Egrandis_16*. They were sorted based on their chromosomal locations. To get insight into their biological functions in the genome of *E. grandis,* several analyses were conducted using many online and offline bioinformatic tools and genome databases. This study being the first study regarding the identification of SBP genes in *E. grandis*, it can be considered as a useful resource for the future studies regarding SBP genes in either in *E. grandis* or comparative different plant species.

http://www.aloki.hu ● ISSN 1589 1623 (Print) ● ISSN 1785 0037 (Online)
DOI: http://dx.doi.org/10.15666/aeer/1605_61816193
© 2018, ALÖKI Kft., Budapest, Hungary

REFERENCES

[1] Abdullah, M., Cao, Y., Cheng, X., Shakoor, A., Su, X., Gao, J., Cai, Y. (2018): Genome-wide analysis characterization and evolution of SBP genes in Fragaria vesca, Pyrus bretschneideri, Prunus persica and Prunus mume. – Frontiers in Genetics 9: 64. DOI: 10.3389/fgene.2018.00064.

[2] Ali, M. A., Alia, K. B., Atif, R. M., Rasul, I., Nadeem, H. U., Shahid, A., Azeem, F. (2017): Genome-wide identification and comparative analysis of squamosa-promoter binding proteins (Sbp) transcription factor family in *Gossypium raimondii* and *Arabidopsis thaliana*. – Pakistan Journal of Botany 49: 1113-1126.

[3] Bailey, T. L., Williams, N., Misleh, C., Li, W. W. (2006): MEME: discovering and analyzing DNA and protein sequence motifs. – Nucleic Acids Research 34: W369-W373.

[4] Blanc, G., Wolfe, K. H. (2004): Widespread paleopolyploidy in model plant species inferred from age distributions of duplicate genes. – The Plant Cell 16(7): 1667-1678.

[5] Bowers, J. E., Chapman, B. A., Rong, J., Paterson, A. H. (2003): Unravelling angiosperm genome evolution by phylogenetic analysis of chromosomal duplication events. – Nature 422(6930): 433-438.

[6] Buyuk, I., Aras, S. (2016): Genome-wide in silico identification, characterization and transcriptional analysis of the family of growth-regulating factors in common bean (Phaseolus vulgaris L.) subjected to PEG-induced drought stress. – Archives of Biological Science 69(1): 5-14.

[7] Buyuk, I., Inal, B., Ilhan, E., Tanrıseven, M., Aras, S., Erayman, M. (2016): Genome-wide identification of salinity responsive HSP70s in common bean. – Molecular Biology Reports 43(11): 1251-1266.

[8] Cardon, G. H., Hohmann, S., Nettesheim, K., Saedler, H., Huijser, P. (1997): Functional analysis of the Arabidopsis thaliana SBP-box gene SPL3: a novel gene involved in the floral transition. – Plant J 12(2): 367-377.

[9] Chuck, G., Whipple, C., Jackson, D., Hake, S. (2010): The maize SBP-box transcription factor encoded by tasselsheath4 regulates bract development and the establishment of meristem boundaries. – Development 137: 1585-1585.

[10] Dos Santos, P. E. T., Geraldi, I. O., Garcia, J. N. (2004): Estimates of genetic parameters of wood traits for sawn timber production in Eucalyptus grandis. – Genet Mol Biol 27(4): 567-573.

[11] Dye, P. (2013): A review of changing perspectives on Eucalyptus water-use in South Africa. – Forest Ecol Manag 301: 51-57.

[12] Guo, A., Zhu, Q., Chen, X., Luo, J. (2007): GSDS: a gene structure display server. – Yi chuan = Hereditas 29: 1023-1026.

[13] Guo, A. Y., Zhu, Q. H., Gu, X., Ge, S., Yang, J., Luo, J. (2008): Genome-wide identification and evolutionary analysis of the plant specific SBP-box transcription factor family. – Gene 418(1-2): 1-8.

[14] Hardie, A. D. K., Wood, A. A. (1973): Eucalyptus grandis timber from plantations in Zambia. – Commonw Forest Rev 52(152): 153-159.

[15] Hou, H. M., Li, J., Gao, M., Singer, S. D., Wang, H., Mao, L. Y., Fei, Z. J., Wang, X. P. (2013): Genomic organization, phylogenetic comparison and differential expression of the SBP-box family genes in grape. – Plos One 8.

[16] Inal, B., Buyuk, I., Ilhan, E., Aras, S. (2017): Genome wide analysis of Phaseolus vulgaris C2C2-YABBY transcription factors under salt stress conditions. – 3Biotech 7(5): 302.

[17] Ilhan, E., Buyuk, I., Inal, B. (2018): Transcriptome-scale characterization of salt responsive bean TCP transcription factors. – Gene 5(642): 64-73.

[18] Juretic, N., Hoen, D. R., Huynh, M. L., Harrison, P. M., Bureau, T. E. (2005): The evolutionary fate of MULE-mediated duplications of host gene fragments in rice. – Genome Research 15: 1292-1297.

http://www.aloki.hu ● ISSN 1589 1623 (Print) ● ISSN 1785 0037 (Online)
DOI: http://dx.doi.org/10.15666/aeer/1605_61816193
© 2018, ALÖKI Kft., Budapest, Hungary

[19] Klein, J., Saedler, H., Huijser, P. (1996): A new family of DNA binding proteins includes putative transcriptional regulators of the Antirrhinum majus floral meristem identity gene SQUAMOSA. – Mol Gen Genet 250(1): 7-16.
[20] Kropat, J., Tottey, S., Birkenbihl, R. P., Depege, N., Huijser, P., Merchant, S. (2005): A regulator of nutritional copper signaling in Chlamydomonas is an SBP domain protein that recognizes the GTAC core of copper response element. – Proceedings of the National Academy of Sciences of the United States of America 102: 18730-18735.
[21] Lannenpaa, M., Janonen, I., Holtta-Vuori, M., Gardemeister, M., Porali, I. and Sopanen, T. (2004): A new SBP-box gene BpSPL1 in silver birch (*Betula pendula*). – Physiologia Plantarum 120: 491-500.
[22] Lee, T. H., Tang, H. B., Wang, X. Y., Paterson, A. H. (2013): PGDD: a database of gene and genome duplication in plants. – Nucleic Acids Research 41: D1152-D1158.
[23] Li, J., Hou, H. M., Li, X. Q., Xiang, J., Yin, X. J., Gao, H., Zheng, Y., Bassett, C. L., Wang, X. P. (2013): Genome-wide identification and analysis of the SBP-box family genes in apple (*Malus* × *domestica* Borkh.). – Plant Physiology and Biochemistry 70: 100-114.
[24] Li, M., Zhao, S. Z., Zhao, C. Z., Zhang, Y., Xia, H., Lopez-Baltazar, J., Wan, S. B., Wang, X. J. (2016): Cloning and characterization of SPL-family genes in the peanut (*Arachis hypogaea* L.). – Genetics and Molecular Research 15. DOI: 10.4238/gmr.15017344.
[25] Lu, S. F., Yang, C. M., Chiang, V. L. (2011): Conservation and diversity of MicroRNA-associated copper-regulatory networks in Populus trichocarpa. – Journal of Integrative Plant Biology 53: 879-891.
[26] Mao, H. D., Yu, L. J., Li, Z. J., Yan, Y., Han, R., Liu, H., Ma, M. (2016): Genome-wide analysis of the SPL family transcription factors and their responses to abiotic stresses in maize. – Plant Gene 6: 1-12.
[27] Myburg, A. A., Grattapaglia, D., Tuskan, G. A., Hellsten, U., Hayes, R. D., Grimwood, J., Jenkins, J., Lindquist, E. et al. (2014): The genome of Eucalyptus grandis. – Nature 510(7505): 356-362.
[28] Nautiyal, J. C., Couto, L. (1984): The nature and uses of the timber production function Eucalyptus grandis in Brazil. – Forest Sci 30(3): 761-773.
[29] Pan, F., Wang, Y., Liu, H. L., Wu, M., Chu, W. Y., Chen, D. M., Xiang, Y. (2017): Genome-wide identification and expression analysis of SBP-like transcription factor genes in Moso Bamboo (*Phyllostachys edulis*). – BMC Genomics 18.
[30] Paterson, A. H., Bowers, J. E., Chapman, B. A. (2004): Ancient polyploidization predating divergence of the cereals, and its consequences for comparative genomics. – Proceedings of the National Academy of Sciences of the United States of America 101(26): 903-9908.
[31] Preston, J. C., Jorgensen, S. A., Orozco, R., Hileman, L. C. (2016): Paralogous SQUAMOSA PROMOTER BINDING PROTEIN-LIKE (SPL) genes differentially regulate leaf initiation and reproductive phase change in petunia. – Planta 243: 429-440.
[32] Quevillon, E., Silventoinen, V., Pillai, S., Harte, N., Mulder, N., Apweiler, R., Lopez, R. (2005): InterProScan: protein domains identifier. – Nucleic Acids Research 33: W116-W120.
[33] Rhoades, M. W., Reinhart, B. J., Lim, L. P., Burge, C. B., Bartel, B., Bartel, D. P. (2002): Prediction of plant microRNA targets. – Cell 110: 513-520.
[34] Robinson, N., Harper, R. J., Smettem, K. R. J. (2006): Soil water depletion by Eucalyptus spp. integrated into dryland agricultural systems. – Plant and Soil 286(1): 41-151.
[35] Salinas, M., Xing, S. P., Hohmann, S., Berndtgen, R., Huijser, P. (2012): Genomic organization, phylogenetic comparison and differential expression of the SBP-box family of transcription factors in tomato. – Planta 235: 1171-1184.
[36] Shalom, L., Shlizerman, L., Zur, N., Doron-Faigenboim, A., Blumwald, E., Sadka, A. (2015): Molecular characterization of SQUAMOSA PROMOTER BINDING PROTEIN-

http://www.aloki.hu ● ISSN 1589 1623 (Print) ● ISSN 1785 0037 (Online)
DOI: http://dx.doi.org/10.15666/aeer/1605_61816193
© 2018, ALÖKI Kft., Budapest, Hungary

LIKE (SPL) gene family from Citrus and the effect of fruit load on their expression. – Frontiers in Plant Science 6.

[37] Tamura, K., Stecher, G., Peterson, D., Filipski, A., Kumar, S. (2013): MEGA6: Molecular Evolutionary Genetics Analysis Version 6.0. – Molecular Biology and Evolution 30: 2725-2729.

[38] Unte, U. S., Sorensen, A. M., Pesaresi, P., Gandikota, M., Leister, D., Saedler, H., Huijser, P. (2003): SPL8, an SBP-Box gene that affects pollen sac development in *Arabidopsis.* – Plant Cell 15: 1009-1019.

[39] Voorrips, R. E. (2002): MapChart: Software for the graphical presentation of linkage maps and QTLs. – Journal of Heredity 93: 77-78.

[40] Wang, B. N., Geng, S. F., Wang, D., Feng, N., Zhang, D. D., Wu, L., Hao, C. Y., Zhang, X. Y., Li, A. L., Mao, L. (2015): Characterization of SQUAMOSA PROMOTER BINDING PROTEIN-LIKE genes in wheat. – Journal of Plant Biology 58: 220-229.

[41] Wang, X., Shi, X., Hao, B., Ge, S., Luo, J. (2005): Duplication and DNA segmental loss in the rice genome: implications for diploidization. – The New Phytologist 165(3): 37-946.

[42] Wu, G., Poethig, R. S. (2006): Temporal regulation of shoot development in Arabidopsis thaliana by miR156 and its target SPL3. – Development 133(18): 539-3547.

[43] Xie, K. B., Wu, C. Q., Xiong, L. Z. (2006): Genomic organization, differential expression, and interaction of SQUAMOSA promoter-binding-like transcription factors and microRNA156 in rice. – Plant Physiology 142: 280-293.

[44] Yamasaki, K., Kigawa, T., Inoue, M., Tateno, M., Yamasaki, T., Yabuki, T., Aoki, M., Seki, E., Matsuda, T., Nunokawa, E., Ishizuka, Y., Terada, T., Shirouzu, M., Osanai, T., Tanaka, A., Seki, M., Shinozaki, K., Yokoyama, S. (2004): A novel zinc-binding motif revealed by solution structures of DNA-binding domains of Arabidopsis SBP-family transcription factors. – Journal of Molecular Biology 337(1): 9-63.

[45] Yang, Z. H. (2007): PAML 4: Phylogenetic analysis by maximum likelihood. – Molecular Biology and Evolution 24: 1586-1591.

[46] Zhang, H. X., Jin, J. H., He, Y. M., Lu, B. Y., Li, D. W., Chai, W. G., Khan, A., Gong, Z. H. (2016): Genome-wide identification and analysis of the SBP-Box family genes under Phytophthora capsici stress in pepper (*Capsicum annuum* L.). – Frontiers in Plant Science 7. DOI: 10.3389/fpls.2016.00504.

[47] Zhang, L. S., Wu, B., Zhao, D. G., Li, C. L., Shao, F. J., Lu, S. F. (2014): Genome-wide analysis and molecular dissection of the SPL gene family in *Salvia miltiorrhiza.* – Journal of Integrative Plant Biology 56: 38-50.

[48] Zhang, X. H., Dou, L. L., Pang, C. Y., Song, M. Z., Wei, H. L., Fan, S. L., Wang, C. S., Yu, S. X. (2015): Genomic organization, differential expression, and functional analysis of the SPL gene family in *Gossypium hirsutum.* – Molecular Genetics and Genomics 290: 115-126.

[49] Zhang, Y., Schwarz, S., Saedler, H., Huijser, P. (2007): SPL8, a local regulator in a subset of gibberellin-mediated developmental processes in *Arabidopsis.* – Plant Molecular Biology 63: 429-439.

[50] Zheng, Y., Jiao, C., Sun, H. H., Rosli, H. G., Pombo, M. A., Zhang, P. F., Banf, M., Dai, X. B., Martin, G. B., Giovannoni, J. J., Zhao, P. X., Rhee, S. Y., Fei, Z. J. (2016): iTAK: a program for genome-wide prediction and classification of plant transcription factors, transcriptional regulators, and protein kinases. – Molecular Plant 9: 1667-1670.

[51] Zhou, Q., Zhang, S., Chen, F., Liu, B., Wu, L., Li, F., Zhang, J., Bao, M., Liu, G. (2018): Genome-wide identification and characterization of the SBP-box gene family in *Petunia.* – BMC Genomics 19: 193.

http://www.aloki.hu ● ISSN 1589 1623 (Print) ● ISSN 1785 0037 (Online)
DOI: http://dx.doi.org/10.15666/aeer/1605_61816193
© 2018, ALÖKI Kft., Budapest, Hungary

APPENDIX

Table A1. *Sequence information of predicted motifs in Egrandis_SBP proteins*

Motif #	Width	Best possible match
#1	50	YHRRHKVCEVHSKAPKVIVGGLEQRFCQQCSRFHELSEFDEGKRSCRRRL
#2	21	GAQPPRCQVEGCNADLSDAKD
#3	13	AGHNERRRKPPPE
#4	50	RTGRIVFKLFGKDPNDFPLALRTQIFNWLSHSPTEMESYIRPGCIILTVY
#5	24	KWLLHFAVERDCRALVKKLLDYJF
#6	41	NDPQLVGIEAWKSARDASGQTPEDYAVLRGHYSYIHLVQKK
#7	50	DELQFLKFPCSIPKVCGRGFIEVENQGLPGSFFPFIVAEEEVCSEIRMLE
#8	28	YRPAMLSMVAIAAVCVCVALLFKSLPEV
#9	50	AWEELHGNLGSSLRKLLDVSDDDFWRTGWIYVRVQDKLAFVYNGQIVLGT
#10	21	VEWDPNDWKWDGDLFVAKPLN
#11	19	VSESSRALSLLSSQSQDSS
#12	21	NFLFKPNAVGPAGLTPLHIAA
#13	48	HNSPRJLSIRPIAISAGQSTEFVVKGFNLFQPATRLLCALEGKYLAQE
#14	11	FINEIGWLLKR
#15	14	GCLQPFRWEALDYG

http://www.aloki.hu ● ISSN 1589 1623 (Print) ● ISSN 1785 0037 (Online)
DOI: http://dx.doi.org/10.15666/aeer/1605_61816193
© 2018, ALÖKI Kft., Budapest, Hungary

ASSESSMENT OF RELATIONSHIP BETWEEN LOCATIONS AND DISTANCES TO ROADSIDE OF FOREST FIRES IN ISTANBUL, TURKEY

SENTURK, N.

Department of Forest Construction and Transportation, Faculty of Forestry, Istanbul University-Cerrahpasa, 34473 Bahcekoy, Istanbul, Turkey
(e-mail: nsenturk@istanbul.edu.tr)

(Received 16th Jul 2018; accepted 22nd Aug 2018)

Abstract. Forest fires have negative effects on human health, ecosystems and climate change. One way to fight and prevent forest fires is formation of risk maps based on Geographical Information Systems (GIS). This study created a GIS-based database that contains information on forest fires that took place in Istanbul, Turkey in the period of 2013-2016 such as location, reason, burned area, etc. According to the spatial analysis maps that were obtained based on the initial location of the fires in 2013-2016, a large part of the fires took place in the zone in the south of the city between forests and settlement areas. It was also aimed in this study to reveal the relationship between the initial locations of forest fires and their distance to forest roads. For this purpose, spatial and temporal distribution maps were crated for the fires that took place in 2013-2016 with buffer zones that were created in distances of 0-25 m, 25-50 m, 50-75 m and 75-100 m from forest roads. According to the results of this analysis, among the total of 427 forest fires that took place within 0-100 m from forest roads, 186 (43%) took place within 0-25 m, 99 (23.19%) took place within 25-50 m, 90 (21.08%) took place within 50-75 m and 52 (12.18%) took place within 75-100 m. As it may be understood from the analysis results, numbers of fires decrease when the distance from forest roads increases.
Keywords: *forest road, forest fire, spatial analysis*

Introduction

Forest fires occur due to natural and anthropogenic effects (Adab et al., 2013; Demir et al., 2009) and affect human health, ecosystems and climates negatively (Sukitpaneenit and Oanh, 2014; Arganaraz et al., 2015). In a time less than the last 200 years, about six million square kilometers (600,000,000 ha) of the forests in the world were damaged due to forest fires (Dimopoulou and Giannikos, 2004).

Reducing the severity of losses related to forest fires is largely dependent on precautions such as fire prevention, detection and elimination (Kucuk et al., 2017). One of the most important precautions in question is formation of fire risk maps. Fire risk maps, which are created for determining areas with high fire risk, are a significant prevention tool that will help plan firefighting and fire prevention work (Aricak et al., 2014).

In forming fire risk maps, GIS-based spatial analysis results provide significant basis in fighting fire (Jaiswal et al., 2002; Erten et al., 2004).

Based on their cause of occurrence, forest fires may be divided into six groups as natural fires, fires with no known cause, accident fires, deliberate fires, voluntary fires and rekindle fires (San-Miguel-Ayanz et al., 2012). The FAO report dated 1998 stated that the vast majority of the fires in Turkey were anthropogenic. While the ratio of anthropogenic fires in Turkey is 97%, only 3% occurred due to lightning. Among anthropogenic fires, 23% occur due to arson and deliberation, 27% occur due to neglect

http://www.aloki.hu ● ISSN 1589 1623 (Print) ● ISSN 1785 0037 (Online)
DOI: http://dx.doi.org/10.15666/aeer/1605_61956204
© 2018, ALÖKI Kft., Budapest, Hungary

and carelessness, and 50% occur without a known cause (Mol and Kucukosmanoglu, 1997; FAO, 1998).

As Mol and Kucukosmanoglu stated in 1997, people cause the majority of forest fires in Turkey. Again, a significant part of these occurs due to fires that are lit during picnics with recreational purposes. There are areas for building controlled fires in recreational areas.

However, especially in large metropolitan cities where there is intense anthropogenic pressure on forests such as Istanbul, recreational areas may be insufficient, and people may build picnic fires in forests outside controlled picnic areas. The majority of the places where these fires in question are built are near forest roads as they are easily accessed. In addition to all forestry operations, forest roads are also used for recreational needs (Akgul et al., 2016).

In the scope of the study, GIS-based spatial analyses were used to map the fires that took place in the forest areas within the border of the province of Istanbul in the period of 2013-2016 based on the causes of fires and the distances of the fires to forest roads, and the initial locations and intensities of the fires were analyzed.

Material and methods

Study area

The research area was selected as Istanbul city which is located in the north-west Marmara region of Turkey, in the coordinates of 28°10’ and 29°40’ East longitudes and 40°50’ and 41°30’ North latitudes (*Fig. 1*).

Figure 1. *Location map of the study area*

About 46.6 (251,716 ha.) of Istanbul is covered with forests, and these areas are distributed in the north of the city. Within the forest areas, there is a total of 4414-km-long forest roads. There are also 36 recreational areas with different sizes within the forest areas in Istanbul. These areas are popular among the citizens (*Fig. 2*).

http://www.aloki.hu ● ISSN 1589 1623 (Print) ● ISSN 1785 0037 (Online)
DOI: http://dx.doi.org/10.15666/aeer/1605_61956204
© 2018, ALÖKI Kft., Budapest, Hungary

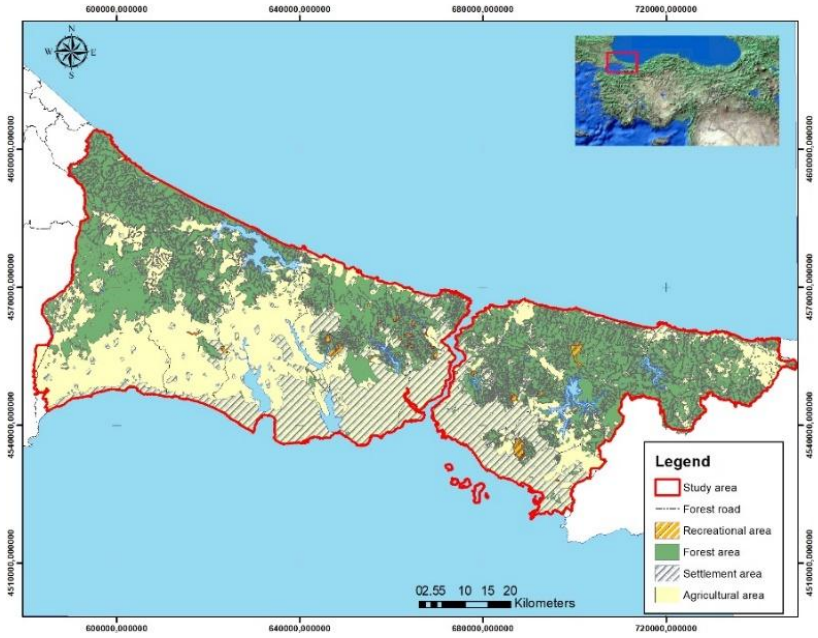

Figure 2. *Location map of the study area*

Methods

This study investigated the fires that took place in 2013-2016 in forests within the provincial borders of Istanbul according to General Directorate of Forestry Turkey (GDF, 2017). Where these fires mostly occurred and the distances of these fires were determined. For this, a database was created using the ArcGIS 10.3 GIS software to analyze the locations of these fires. In the database, the date of the forest fires, forest fire occurrence locations (in the ITRF 96 coordinate system), total burnt areas (ha) were defined.

Forest fire density analysis was conducted with the database that was create within the scope of the study. In addition to the density analysis, spatial analysis of the fires that took place in 2013-2016 was carried out using the Kernel Density method. Kernel density method is commonly used in several engineering disciplines it provides to calculates the density of features in a neighborhood around the features.

Within the main purpose of the study buffer zones were defined in distances of 0-25 m, 25-50 m, 50-75 m and 75-100 m from forest roads. This is how the zone where the fires mostly occurred was determined. The buffer zones were overlapped with the forest fire locations in the ArcGIS 10.3 software. The overlapping process was carried out based on the years.

Results and discussion

Numerical and spatial distribution of forest fires according to main reason of fires

In the study, according to fire reasons, forest fires were investigated in five groups as lightning, carelessness, sabotage, electrical fault and unknown cases. In order to determine the relationship between the locations of fire and numbers of fire with fire reasons, the number of fire over the years is also shown in *Table 1* depending on the fire reasons. According to spatial distribution analysis results for 2013 it was calculated that

http://www.aloki.hu ● ISSN 1589 1623 (Print) ● ISSN 1785 0037 (Online)
DOI: http://dx.doi.org/10.15666/aeer/1605_61956204
© 2018, ALÖKI Kft., Budapest, Hungary

the minimum number of fire occurred by lightning as one while maximum number of fire caused carelessness was calculated as one.

According to the distribution analysis of main reason of fires (*Table 1*);

Considering the total of 243 fires that took place in 2013;

- Most (87) of the fires occurred due to carelessness,
- Following this, 78 fires occurred without a known cause,
- The least of the fires (1) occurred due to lightning.

Considering the total of 100 fires that took place in 2014;

- Most (46) of the fires occurred due to carelessness,
- Following this, 28 fires occurred without a known cause,
- The least of the fires (2) occurred due to lightning.

Considering the total of 121 fires that took place in 2015;

- Most (53) of the fires occurred due to carelessness,
- Following this, 45 fires occurred without a known cause,
- The least of the fires (2) occurred due to electrical fault.

Considering the total of 196 fires that took place in 2016;

- Most (141) of the fires occurred due to unknown causes,
- Following this, 38 fires occurred due to carelessness,
- The least of the fires (17) occurred due sabotage.

As understood from the results of the spatial distribution analysis and seen in *Figure 4,* a large part of the fires took place in the zone in the south of the city between forests and settlement areas. It is also seen that the forest areas and northern parts where forest fires took place the least frequently had high numbers of recreational areas (*Fig. 3*).

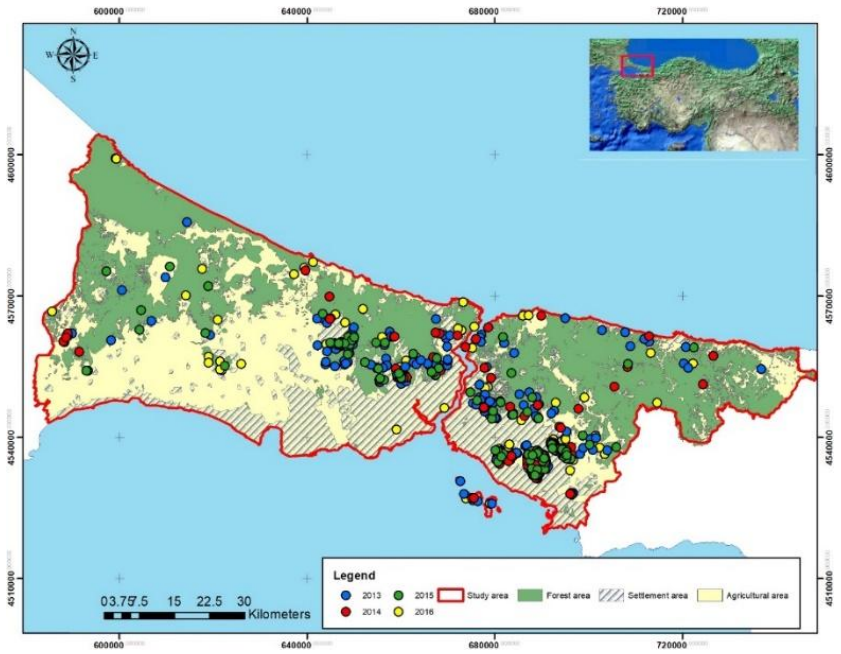

Figure 3. *Fire locations by year*

http://www.aloki.hu ● ISSN 1589 1623 (Print) ● ISSN 1785 0037 (Online)
DOI: http://dx.doi.org/10.15666/aeer/1605_61956204
© 2018, ALÖKI Kft., Budapest, Hungary

Table 1. *Distribution of fires according to main reason of fires*

Fire reason	2013	2014	2015	2016	Total
Lightning	1	2	0	0	3
Carelessness	87	46	53	38	224
Sabotage	72	24	21	17	134
Electrical fault etc.	5	0	2	0	7
Unknown cases	78	28	45	141	292
Total	**243**	**100**	**121**	**196**	**660**

According to the results of the spatial distribution analysis on the causes of fires;
Within the total of 50.46 ha of burnt areas in 2013;

- The smallest area (0.02 ha) was burnt due to lightning,
- The largest area (26.05 ha) was burnt due to sabotage.

Within the total of 14.13 ha of burnt areas in 2014;

- The smallest area (0.03 ha) was burnt due to lightning,
- The largest area (6.60 ha) was burnt due to carelessness.

Within the total of 24.20 ha of burnt areas in 2015;

- The smallest area (0.09 ha) was burnt due to electrical fault,
- The largest area (9.52 ha) was burnt due to sabotage.

Within the total of 33.78 ha of burnt areas in 2016;

- The smallest area (1.77 ha) was burnt due to sabotage,
- The largest area (28.83 ha) was burnt due to unknown reasons (*Table 2, Fig. 4*).

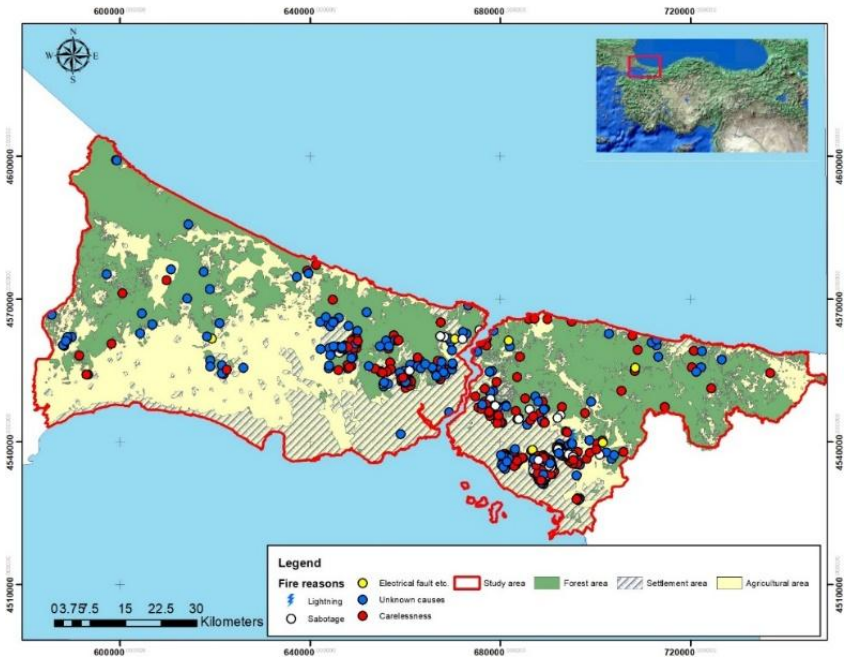

Figure 4. *Spatial distribution of forest fires according to fire causes*

http://www.aloki.hu ● ISSN 1589 1623 (Print) ● ISSN 1785 0037 (Online)
DOI: http://dx.doi.org/10.15666/aeer/1605_61956204
© 2018, ALÖKI Kft., Budapest, Hungary

Table 2. *Distribution of burning areas according to main causes of fires*

Fire reason	2013	2014	2015	2016	Total
Lightning	0.02	0.03	0	0	0.05
Carelessness	8.15	6.60	9.6	3.18	27.53
Sabotage	26.05	4.46	9.52	1.77	41.80
Electrical fault etc.	1.33	0	0.09	0	1.42
Unknown cases	14.91	3.044	4.99	28.83	51.77
Total area (ha)	**50.46**	**14.13**	**24.20**	**33.78**	**122.57**

Spatial distribution of forest fires by distance to road

It was aimed to reveal the relationship between the initial locations of the fires and their distance to forest roads. For this purpose, spatial and temporal distribution maps were crated for the fires that took place in 2013-2016 with buffer zones that were created in distances of 0-25 m, 25-50 m, 50-75 m and 75-100 m from forest roads (*Fig. 5*).

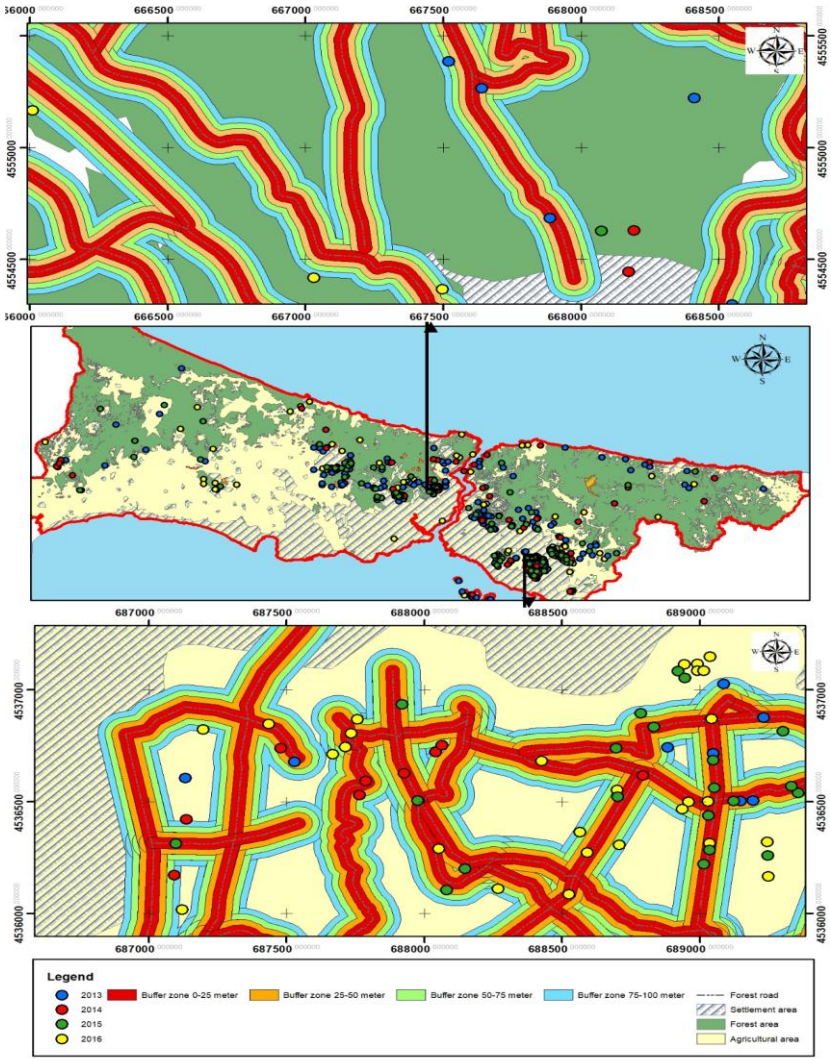

Figure 5. *Spatial distribution of forest fires by distance to forest road*

http://www.aloki.hu ● ISSN 1589 1623 (Print) ● ISSN 1785 0037 (Online)
DOI: http://dx.doi.org/10.15666/aeer/1605_61956204
© 2018, ALÖKI Kft., Budapest, Hungary

According to the spatial and temporal distribution analysis results, within 100 m from forest roads, there were

- 197 fires in 2013,
- 42 fires in 2014,
- 76 fires in 2015,
- 112 fires in 2016,

constituting a total of 427 fires. This number represents 64.6% of the total number of fires that took place in Istanbul in 2013-2016 (*Table 3, Fig. 6*).

Additionally, considering the distances of the fires that occurred in 2013-2016, 186 (43%) took place within 0-25 m, 99 (23.19%) took place within 25-50 m, 90 (21.08%) took place within 50-75 m and 52 (12.18%) took place within 75-100 m.

In the study by Eskandari (2017) that aimed to reveal forest fire risk using the fuzzy Analytic Hierarchy Process (AHP) and GIS methods, it was found that the distance from the road and the distance from settlements were the most important risk factors among anthropogenic risk factors. Moreover, Narayanaraj and Wimberly (2012) determined that reduction of closure near the roads, increase of wind and temperature and forest management activities impact burning. It was also emphasized by several authors that proximity to roads increases risk of fire (Pourtaghi et al. 2016; Vinod et al., 2016; Ajin et al., 2016).

Table 3. *Distribution of forest fires by distance to road*

Years	Buffer zone (m)								Total
	0-25 m		25-50 m		50-75 m		75-100 m		
	Number	%	Number	%	Number	%	Number	%	
2013	81	41.12	48	24.37	43	21.83	25	12.69	**197**
2014	21	50.00	6	14.29	8	19.05	7	16.67	**42**
2015	39	51.32	18	23.68	11	14.47	8	10.53	**76**
2016	45	40.18	27	24.11	28	25.00	12	10.71	**112**
Total	**186**	**43.56**	**99**	**23.19**	**90**	**21.08**	**52**	**12.18**	**427**

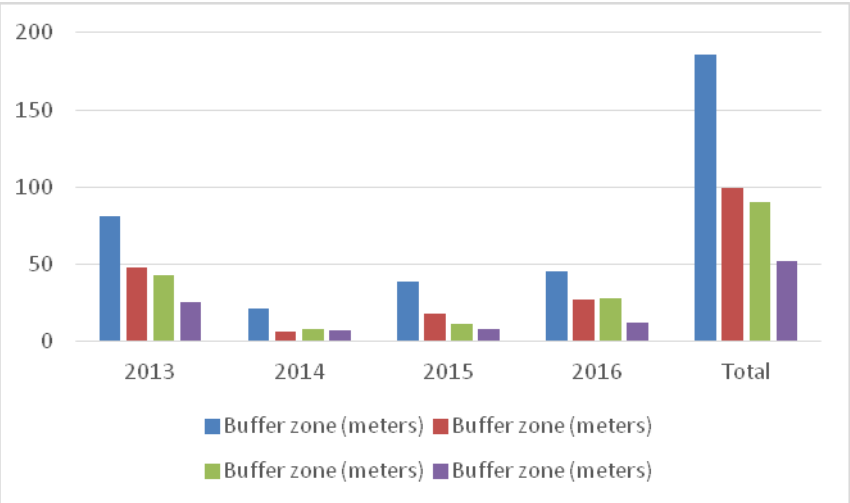

Figure 6. *Forest fires by distance to forest road*

http://www.aloki.hu ● ISSN 1589 1623 (Print) ● ISSN 1785 0037 (Online)
DOI: http://dx.doi.org/10.15666/aeer/1605_61956204
© 2018, ALÖKI Kft., Budapest, Hungary

As it may be understood from the analysis results, numbers of fires decrease when the distance from forest roads increases. Furthermore, when the ratios of the locations of the fires are considered, it is seen that 97.13% of the fires in Istanbul occurred in the southern parts of the city. It is understood that most of the fires were found near the settlement areas as can be seen from *Figure 4*.

This may be interpreted as the following. When the recreational purposes of the citizens in large metropolitan cities like Istanbul and the distance of residential areas to green spaces are considered, the numbers of forest fires are higher in the southern parts of Istanbul where green spaces are lacking. The fire density analysis based on the initial locations of forest fires that is shown in *Figure 7a* and the area size and fire density analysis that is shown in *Figure 7b* which were carried out to test this hypothesis also confirmed that the highest density of the forest fires was in the southern parts.

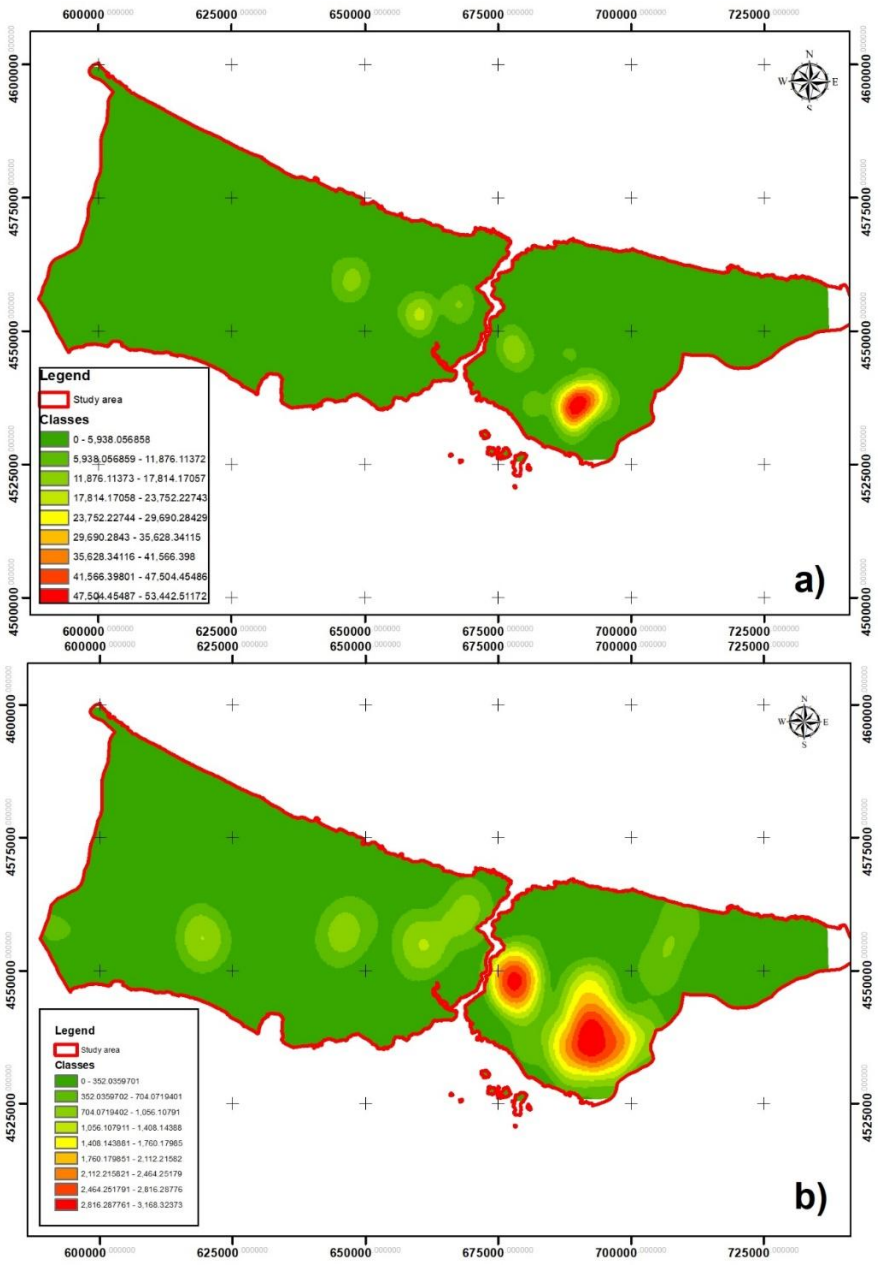

Figure 7. *Results of intensity and area fire intensity analysis according to fire exit points*

http://www.aloki.hu ● ISSN 1589 1623 (Print) ● ISSN 1785 0037 (Online)
DOI: http://dx.doi.org/10.15666/aeer/1605_61956204
© 2018, ALÖKI Kft., Budapest, Hungary

In agreement with this situation, Dong et al. (2005) stated that as the distance from roads, residential areas and agricultural lands increases, risk of fire would decrease. Moreover, other studies by Suryabgavan et al. (2016) and Matin et al. (2017) observed that forest fires are more frequent in relation to anthropogenic factors in places that are close to residential areas.

Furthermore, considering the distances of the fires from forest roads, in the southern parts of Istanbul where there is a dearth of recreational spaces, it is seen that people park their vehicles on the side of roads and take part in picnic activities with fire due to lacking and/or uncontrolled picnic and recreational needs.

Additionally, the reason for reduced numbers of fires as one gets further away from forest roads may be that people carry out picnic activities with fire at locations close to their vehicles to keep a line of sight for security.

Conclusions

With this study, the relationship between the locations of fires and their distances to roads and other areas (residential and agricultural land) was determined with the help of GIS. Based on the analyses that were carried out within the scope of the study, it was found that proximity to such locations increased the number of fire. Accordingly, proximity to these places should be kept in mind and planning should involve information on this within the scope of fighting and taking precautions against forest fires. The results of the study are important especially in terms of reducing forest fires that occur due to anthropogenic reasons as people access recreational areas with these roads in large metropolitan cities.

Moreover, it is believed that this study will allow determination of priority and importance of firefighting and precautions against fires, as well as detection and ranking of risk zones. In addition to all these precautions, protective activities in forests and zones between forests and settlements where anthropogenic pressure is high should be carried out intensely, and green spaces (picnic areas and parks) that will reduce the pressure of the citizens on the forest should be planned and built in suitable locations and with suitable space.

REFERENCES

[1] Adab, H., Kanniah, K. D., Solaimani, K. (2013): Modeling forest fire risk in the northeast of Iran using remote sensing and GIS techniques. – Natural Hazards 65(3): 1723-1743.

[2] Ajin, R. S., Loghin, A. M., Vinod, P. G., Jacob, M. K. (2016): RS and GIS based forest fire risk zone mapping in Periyar Tiger Reserve, Kerala, India. – J. Wetl. Biodivers 6: 175-84.

[3] Akgul, M., Demir, M., Ozturk, T., Topatan, H., Budak, Y. E. (2016): Investigation of recreational vehicles maneuverability on forest roads by computer-aided driving analysis. – Baltic Journal of Road & Bridge Engineering 11(2): 111-119.

[4] Argañaraz, J. P., Pizarro, G. G., Zak, M., Landi, M. A., Bellis, L. M. (2015): Human and biophysical drivers of fires in Semiarid Chaco mountains of Central Argentina. – Science of the Total Environment 520: 1-12.

[5] Aricak, B., Kucuk, O., Enez, K. (2014): Determination of pumper truck intervention ratios in zones with high fire potential by using geographical information system. – Journal of Applied Remote Sensing 8(1): 1-9.

http://www.aloki.hu ● ISSN 1589 1623 (Print) ● ISSN 1785 0037 (Online)
DOI: http://dx.doi.org/10.15666/aeer/1605_61956204
© 2018, ALÖKI Kft., Budapest, Hungary

[6] Demir, M., Küçüksmanoglu, A., Hasdemir, M., Öztürk, T., Acar, H. H. (2009): Assessment of forest roads and firebreaks in Turkey. – African Journal of Biotechnology 8(18): 4553-4561.
[7] Dimopoulou, M., Giannikos, I. (2004): Towards an integrated framework for forest fire control. – European Journal of Operational Research 152(2): 476-486.
[8] Dong, X. U., Li-min, D., Guo-fan, S., Lei, T., Hui, W. (2005): Forest fire risk zone mapping from satellite images and GIS for Baihe Forestry Bureau, Jilin, China. – Journal of Forestry Research 16(3): 169-174.
[9] Erten, E., Kurgun, V., Musaoglu, N. (2004): Forest fire risk zone mapping from satellite imagery and GIS: a case study. – XXth Congress of the International Society for Photogrammetry and Remote Sensing, Istanbul, Turkey, pp. 222-230.
[10] Eskandari, S. (2017): A new approach for forest fire risk modeling using fuzzy AHP and GIS in Hyrcanian forests of Iran. – Arabian Journal of Geosciences 10(8): 190.
[11] FAO (1998): FAO Meeting on Public Policies Affecting Forest Fires. – Proceedings, Rome, 28-30 October 1998.
[12] GDF (2017): Orman yanginlari ile mucadele faaliyet raporu. – Orman Genel Mudurlugu yayinlari, Ankara (in Turkish).
[13] Jaiswal, R. K., Mukherjee, S., Raju, K. D., Saxena, R. (2002): Forest fire risk zone mapping from satellite imagery and GIS. – International Journal of Applied Earth Observation and Geoinformation 4(1): 1-10.
[14] Kucuk, O., Topaloglu, O., Altunel, A. O., Cetin, M. (2017): Visibility analysis of fire lookout towers in the Boyabat State Forest Enterprise in Turkey. – Environmental Monitoring and Assessment 189(7): 329.
[15] Matin, M. A., Chitale, V. S., Murthy, M. S., Uddin, K., Bajracharya, B., Pradhan, S. (2017): Understanding forest fire patterns and risk in Nepal using remote sensing, geographic information system and historical fire data. – International Journal of Wildland Fire 26(4): 276-286.
[16] Mol, T., Kucukosmanoglu, A. (1997): Forest fires in Turkey. – Proceedings of the XIth World Forestry Congress, Antalya.
[17] Narayanaraj, G., Wimberly, M. C. (2012): Influences of forest roads on the spatial patterns of human- and lightning-caused wildfire ignitions. – Applied Geography 32(2): 878-888.
[18] Pourtaghi, Z. S., Pourghasemi, H. R., Aretano, R., Semeraro, T. (2016): Investigation of general indicators influencing on forest fire and its susceptibility modeling using different data mining techniques. – Ecological Indicators 64: 72-84.
[19] San-Miguel-Ayanz, J., Schulte, E., Schmuck, G., Camia, A., Strobl, P., Liberta, G., McInerney, D. (2012): Comprehensive Monitoring of Wildfires in Europe: The European Forest Fire Information System (EFFIS). – In: Tiefenbacher, J. (ed.) Approaches to Managing Disaster. Assessing Hazards, Emergencies and Disaster Impacts. IntechOpen, London.
[20] Sukitpaneenit, M., Oanh, N. T. K. (2014): Satellite monitoring for carbon monoxide and particulate matter during forest fire episodes in Northern Thailand. – Environmental Monitoring and Assessment 186(4): 2495-2504.
[21] Suryabhagavan, K. V., Alemu, M., Balakrishnan, M. (2016): GIS-based multi-criteria decision analysis for forest fire susceptibility mapping: a case study in Harenna forest, southwestern Ethiopia. – Tropical Ecology 57(1): 33-43.
[22] Vinod, P. G., Ajin, R. S., Jacob, M. K. (2016): RS and GIS based spatial mapping of forest fires in Wayanad Wildlife Sanctuary, Wayanad, North Kerala, India. – Int. J. Earth Sci. Eng. 9: 498-502.

http://www.aloki.hu ● ISSN 1589 1623 (Print) ● ISSN 1785 0037 (Online)
DOI: http://dx.doi.org/10.15666/aeer/1605_61956204
© 2018, ALÖKI Kft., Budapest, Hungary

INFLUENCE OF GIRDLING ON THE SEASONAL LEAF NUTRITION STATUS AND FRUIT SIZE OF ROBINSON MANDARIN (*CITRUS RETICULATA* BLANCO)

YILMAZ, B.[1] – CIMEN, B.[1*] – INCESU, M.[1] – YESILOGLU, T.[1] – YILMAZ, M.[2]

[1]*Department of Horticulture, Faculty of Agriculture, Cukurova University*
01330 Adana, Turkey

[2]*Department of Horticulture, Faculty of Agriculture, Ordu University*
52200 Ordu, Turkey

**Corresponding author*
e-mail: bcimen@cu.edu.tr; phone/fax: +90-322-338-6388

(Received 18th Jul 2018; accepted 22nd Aug 2018)

Abstract. This study was undertaken to investigate the effects of single and double girdling applications on the fruit yield, commercial size, quality, photosystem II (PSII), leaf chlorophyll and leaf nutrition content of 22-year-old Robinson mandarin (*Citrus reticulata*). Girdling treatments were performed at anthesis (when 60% of the flowers were opened) with approximately 5 mm trunk diameter in 2014. The fruit was harvested in 2014 at the optimum harvest time (in December) for fruit yield, properties and size. Evaluations of leaf mineral content, chlorophyll concentration and fluorescence measurements were performed at monthly intervals. Leaf samples were taken in eight periods for analysis of plant nutri-elements. It was determined that double girdling was the best application in terms of fruit yield and percentage of marketable fruit. The treatments did not significantly affect fruit internal quality. Girdling reduced PSII and leaf chlorophyll concentration but did not affect leaf mineral content. However, we observed a tendency toward a decrease in nitrogen levels in the girdled trees. According to the results of the present study, girdling treatments significantly affected fruit yield and size together with several macro-micro plant nutri-elements.
Keywords: *citrus, chlorophyll concentration, fruit yield, cultural practices, plant nutri-elements*

Introduction

Due to the steady increase in citrus production in Turkey, 3,781,359 million tons of citrus fruits were produced in 2014. Of the citrus produced in Turkey, 1,779,675 tons were oranges (FAO, 2015). The main varieties of mandarin (*Citrus reticulata*) grown in Turkey are satsumas, such as 'Okitsu Wase',' Owari' and 'Dobashi Beni'; the rest include 'Nova', 'Robinson', 'Fremont', Clementine 'Murcott' and 'Minneola' (Tuzcu et al., 2001). Robinson is an early-ripening mandarin cultivar with high fruit quality; this variety is also productive and has low tendency for alternate bearing. However, fruit size in the citrus fruit market is very important, and small fruit size is one of the main factors limiting the sales of citrus fruit; large fruits bring higher prices in the export market. Consumers prefer large fruits; thus, there is a significant price difference between large and small fruits (Agustí et al., 1994; Guardiola and García Luis, 2000; Erner et al., 2004). In terms of determining profitability, the size of citrus fruit has become as important as the yield. This phenomenon is readily apparent for small mandarin fruits as well as lemons, sweet oranges and large grapefruit species (Guardiola and García Luis, 2000). Fruit size is affected by many factors, including irrigation management, soil type, rootstock, as well as ecological variables that cannot be controlled by the producer. Moreover, fruit size is inversely proportional to yield and fruit number (Guardiola, 1997). Bevington (2003) demonstrated that region, cultivar, rootstock, soil type, microecology

http://www.aloki.hu ● ISSN 1589 1623 (Print) ● ISSN 1785 0037 (Online)
DOI: http://dx.doi.org/10.15666/aeer/1605_62056218
© 2018, ALÖKI Kft., Budapest, Hungary

and plant age all affect fruit size. The availability of carbohydrates (increases fruit size), flower intensity (decreases fruit size), competition between flowers/fruitlets (decreases fruit size) and abiotic stressors (decrease fruit size) are the most important factors affecting the final size of citrus fruits (Guardiola et al., 1982; Patrick, 1993; Agustí et al., 1995; Goldschmidt and Koch et al., 1996; El-Otmani et al., 2000). Cultural treatments such as pruning, irrigation and fertilization can be optimized to increase fruit size. For instance, techniques such as girdling (Cohen, 1984) and thinning (Hirose, 1981; Wheaton, 1981; Zaragoza et al., 1992; Guardiola and García Luis, 2000) are used in citrus production to increase fruit size.

Girdling applications are important and have been used worldwide for centuries in citrus and other fruit tree crops, especially to increase flowering, fruit set and fruit size (Tuzcu et al., 1992; Mostafa and Saleh, 2006). Girdling consists of the removal of a strip of bark from the trunk or major limbs of a fruit tree, which blocks the downward translocation of photosynthates and metabolites through the phloem, thus reducing fruit drop and enhancing fruit growth and yield (Zhao et al., 2013; Raveh, 2013; Mostafa and Saleh, 2006). Girdling applications at different times are used to increase the yield of fruit in some varieties, such as Robinson, Nova, Dancy, Osceola, Klemantin, Minneola, Orlando and Ortanique, which are self-sterile. The fruit set process is complex because photosynthetic activity and, thus, the production of photosynthetic compounds, can be altered by sink demand. Girdling effect has been related to the accumulation of photoassimilates in the canopy as a result of the interruption of the downward transport of soluble sugars resulting increases in fruit set in Citrus (Rivas et al., 2007). It has been reported that girdling treatments increased yield by 125% in mandarins (Rivas et al., 2006).

Girdling has also been shown to alter the partitioning of photosynthates, mineral nutrients and plant growth regulators in the tree (Rivas et al., 2006). On the upper line of girdling, leaf nitrogen (N) content and Carbon (C)/N ratio are improved, and as a result, flowering and fruit set are increased (Mostafa and Saleh, 2006). However, the effects of girdling on the translocation of various mineral nutrients in leaves are still unclear (Wang et al., 2010). Exactly how girdling functions in this way is still unknown, but the immediate effect of this technique is to break the phloematic flow toward the roots, thereby modifying the nutritional and hormonal balance of the plant (Vaio et al., 2001). In addition to single girdling, double girdling had, in most cases, a much greater effect than a single girdle. The greater efficiency of the double girdling may be due to this treat- ment keeping the girdling wound open for longer than with single girdles (Cohen, 1984).

The aim of this work was to study the effects of girdling on yield, fruit size and quality in the Robinson mandarin. Another objective was to determine the effects of trunk girdling on the quantum yield efficiency of PS II and the mobility of the mineral elements in Robinson mandarin leaves.

Materials and methods

Plant materials

The experiments were conducted on 22-year-old Robinson mandarin trees planted on sour orange rootstock at 6 × 6 m intervals at the Research Station of Cukurova University, Agricultural Faculty Citrus Experiment Station, Adana, Turkey (latitude 35° 23' N; longitude 36° 50' E; altitude 27 m) in 2016. The trees were managed and selected for uniformity and crop load. In the experimental area, the soil was clay loam (55% clay, 22% silt and 23% sand containing 11% $CaCO_3$), and the soil pH was between 7.20 and

http://www.aloki.hu ● ISSN 1589 1623 (Print) ● ISSN 1785 0037 (Online)
DOI: http://dx.doi.org/10.15666/aeer/1605_62056218
© 2018, ALÖKI Kft., Budapest, Hungary

7.29 at a depth of 0-90 cm. The area has mean maximum and minimum temperatures of 26 and 14.5 °C, respectively, and an average annual rainfall of 465 mm (*Fig. 1*). The trees were irrigated weekly from May to October using drip irrigation. Nitrogen (N) was applied at a rate of 1.5 kg N/tree (2/3 in mid-February and 1/3 in mid-May), phosphorus (P) was applied at a rate of 1 kg P/tree (December), and potassium (K) was applied at a rate of 1 kg K/tree (January).

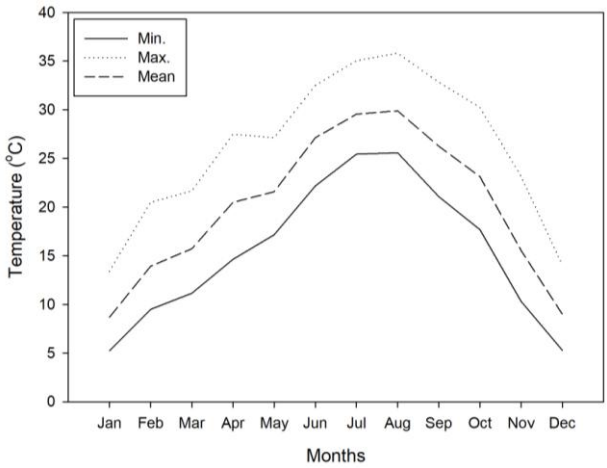

Figure 1. *Minimum, maximum and mean temperature data of the experimental field in 2016*

Girdling treatments

Girdling treatments were performed at anthesis (when 60% of the flowers were opened) with an approximately 5 mm diameter trunk using a girdling knife without injuring the wood layers. The experiment utilized a randomized complete block design with ten replicates for each treatment. Ten trees of each treatment were selected for similarity in size, vigor and flowering intensity. The girdling treatments were conducted on three plots with single girdling (SG), double girdling (DG) or without girdling (control). Single girdling (SG) was undertaken at 15 cm under the scaffold branch junction level. In the double girdling (DG) treatment, the first girdling was taken at 15 cm under the scaffold branch junction level and the second girdling at 5 cm above it (*Fig. 2*).

Figure 2. *Single (left) and double (right) girdled 'Robinson' trees from examined orchard*

http://www.aloki.hu ● ISSN 1589 1623 (Print) ● ISSN 1785 0037 (Online)
DOI: http://dx.doi.org/10.15666/aeer/1605_62056218
© 2018, ALÖKI Kft., Budapest, Hungary

Leaf chlorophyll concentration and photosystem II efficiency

The leaf chlorophyll concentration was estimated using a portable SPAD meter (Minolta, Japan), and the chlorophyll fluorescence parameter ((*Fv' / Fm'*) = quantum yield in light-adapted leaves) was measured with a portable fluorometer (FluorPen FP100, Photon System Instruments Ltd, Drasov, Czech Republic). The evaluations of the chlorophyll concentration and fluorescence measurements were taken in six periods between 2015 and 2016. The same leaves were used to estimate the leaf chlorophyll (Chl) concentrations and PSII efficiency, based on the quantum yield of light-adapted leaves (*Fv' / Fm'*), The chlorophyll concentration and maximum chlorophyll fluorescence efficiency readings for the light-adapted leaves were measured on 10 fully expanded young leaves (third and fourth leaves from the shoot apex) of each replicate at the four chosen time points. Measurements were performed before midday (08.00-11.00).

Fruit yield, properties and size measurements

The fruit was harvested in 2014 at the optimum harvest time (in December) from each plot. The yield per tree (kg/tree) was obtained by weighing the harvested fruit. A random sample of 25 grapefruits was evaluated for rind thickness, percent juice, juice soluble solids (SSC), acidity and soluble solid/acid ratio. Fruits from each of the plots were measured at the fruit equatorial diameter and graded according to commercial categories as follows: >78 mm (extra), 71-78 mm (class 1), 65-70 mm (class 2), 59-64 mm (class 3), 53-58 mm (class 4), 47-52 mm (class 5) and <47 (discard). The 25 fruits were weighed and juiced using a standard juicer; then, the juice was weighed and expressed as a percentage of the total fruit weight. The fruit rind thickness was measured with a digital caliper (Mitutoyo CD-15CPX, Mitutoyo America Corporation, USA). Soluble solids were determined with a portable refractometer (FG-103/113) using a few drops of juice. The total acidity of the juice was determined by titrating 5 ml of the juice sample with 0.1 N sodium hydroxide (NaOH) using phenolphthalein as the indicator.

Leaf chlorophyll concentration and fluorescence measurements

The leaf chlorophyll concentration was estimated using a portable SPAD meter (Minolta, Japan), and the chlorophyll fluorescence parameter ((*Fv' / Fm'*) = quantum yield in light adapted leaves) was measured with a portable fluorometer (FluorPen FP100, Photon System Instruments Ltd, Drasov, Czech Republic). Evaluations of leaf mineral content, chlorophyll concentration and fluorescence measurements were initiated 15 d before girdling (in April) to ensure that there were no differences among trees at the beginning of the trial. Subsequent measurements were performed at monthly intervals as follows: 30 d after girdling (d.a.g) (in May), 60 d.a.g (in June), 90 d.a.g (in July), 120 d.a.g (in August), 150 d.a.g (in September), 180 d.a.g (in October), and 210 d.a.g (in November). Readings of chlorophyll concentration and maximum chlorophyll fluorescence efficiency in the light-adapted stage were measured on 10 fully expanded young leaves (third and fourth leaves from the shoot apex) of each replicate at the eight chosen time points. Measurements were performed before midday (08.00-11.00).

Leaf mineral concentrations

Leaf samples were taken at each of the eight time points for analysis of plant nutri-elements in 2014 according to Chapman (1960). The leaves were washed in a detergent

http://www.aloki.hu ● ISSN 1589 1623 (Print) ● ISSN 1785 0037 (Online)
DOI: http://dx.doi.org/10.15666/aeer/1605_62056218
© 2018, ALÖKI Kft., Budapest, Hungary

solution, rinsed several times in distilled water, and then dried at 70 °C for 48 h using a thermo-ventilated oven. The dried leaves were ground (<0.5 mm) and ashed in a muffle furnace at 550 °C for 8 h. The ash samples were digested in HNO_3-$HClO_4$ (3:1 v/v) and filtered through a blue band paper filter (Kacar, 1972). In the extract solutions, sodium (Na), potassium (K), magnesium (Mg), iron (Fe), manganese (Mn) and copper (Cu) concentrations were determined by inductively coupled plasma-atomic emission spectrometry (ICP-AES, Varian Liberty Series II), and the concentrations of phosphorus (P) were determined by UV-VIS spectrophotometry (Barton, 1948). Leaf total nitrogen (N) content was determined by the semi-micro-Kjeldahl method (Less, 1971).

Statistical analysis

Data were subjected to two-way analysis of variance (ANOVA), and significant differences between means were evaluated using Tukey's multiple range test at $p \leq 0.05$ and $p \leq 0.01$. All statistical analyses were performed by using SAS v9.00 statistics software procedures (SAS, 2006), and SigmaPlot® version 11.00 was used for the data presentation.

Results

Effects of girdling on fruit yield and fruit size

The effects of girdling treatment on the distribution of the crop within the commercial fruit size classes were presented in *Figure 3A*.

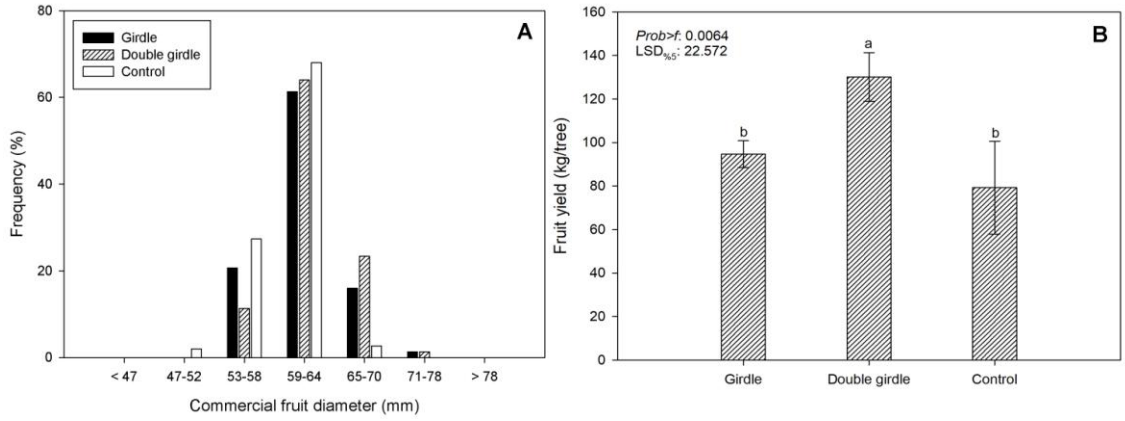

Figure 3. *Effects of girdling treatments on the frequency distribution of the diameter (A) and fruit yield (B) of the Robinson mandarin*

The results indicated that the frequency distribution of the fruit shifted toward larger sizes when the trees were girdled. The highest percentage of large, commercially valuable Robinson fruits (71.00-78.00 mm and 65.00-70.00 mm; classes 1 and 2, respectively) was obtained from trees with DG followed by those with SG. The control trees yielded no commercially valuable Robinson fruits (71.00-78.00 mm) and had the lowest percentage of large fruits (fruit sizes 65.00-70.00 mm). Moreover, compared with trees that were girdled, control trees produced a higher percentage of class 3 (59.00-64.00 mm) and class 4 (53.00-58.00 mm) fruits. Alternatively, the highest

http://www.aloki.hu ● ISSN 1589 1623 (Print) ● ISSN 1785 0037 (Online)
DOI: http://dx.doi.org/10.15666/aeer/1605_62056218
© 2018, ALÖKI Kft., Budapest, Hungary

percentage of commercially unacceptable fruits (47.00-52.00 mm) was obtained from the control trees, even though in the girdled trees, there were no commercially unacceptable fruit sizes (47.00-52.00 mm and <47 mm). Girdling treatments had a significant effect on the yield of Robinson mandarin (*Fig. 3B*). Compared with the controls, the girdling treatment led to an increase in the fruit yield. As shown in *Figure 3B,* the highest fruit yield per tree was obtained in the DG treatment followed by SG. Control trees produced a low yield compared with the treatment trees.

Fruit internal quality

Data in *Table 1* show the effect of the girdling treatments on fruit internal quality in the Robinson mandarin. Girdling did not affect fruit internal quality, and no significant differences in the rind thickness, SSC content, acidity, SSC/acid ratio and juice content were observed. The girdling treatments decreased the rind thickness, although not significantly compared to the control. There were no trends observed for internal fruit quality due to girdling.

Table 1. *Effects of girdling treatment on the rind thickness, total soluble solids (TSS), total acidity (TA), juice content and TSS/TA ratio*

Treatment	Rind thickness (mm)	TSS (%)	TA (%)	Juice content (%)	TSS/TA
SG	4.37	11.27	0.96	49.42	11.92
DG	4.25	11.87	1.14	48.70	10.49
Control	4.60	11.87	1.01	47.74	11.72
Prob>f	*0.6953*	*0.2014*	*0.2226*	*0.8058*	*0.2334*

Leaf chlorophyll concentration and fluorescence measurements

Girdling significantly affected the leaf chlorophyll (Chl) concentration. A two-way ANOVA indicated a significant main effect of girdling and sample date and of their interaction ($P \leq 0.01$) on Chl concentration (*Table 2*).

Table 2. *Results of two-way analysis of variance (ANOVA) testing for effects of sampling date (SD) and girdling (G) and their interaction (SD×G) on the dependent variables*

Dependent variable	Independent variable		
	SD	G	SD × G
N	15.44**[1]	1.31	2.06*
Fe	14.82**	2.91	5.96**
Cu	1.97	1.58	1.80
Mn	3.96**	0.65	1.71
Mg	12.47**	0.83	2.90**
Na	4.45**	0.39	2.12*
K	5.42**	2.01	1.51
P	7.16**	1.13	2.50**
PSII	16.09**	5.11**	0.90
SPAD	14.58**	29.25**	3.34**

[1]Numbers represent *F* values. *$p \leq 0.05$, **$p \leq 0.01$

http://www.aloki.hu ● ISSN 1589 1623 (Print) ● ISSN 1785 0037 (Online)
DOI: http://dx.doi.org/10.15666/aeer/1605_62056218
© 2018, ALÖKI Kft., Budapest, Hungary

Leaf chlorophyll concentrations ranged between 52.13 and 68.84 (*Fig. 4A*). The highest Chl concentration was obtained from the leaves of control plants, whereas the lowest was obtained from trees with SG followed by DG. In terms of Chl measurements, statistically significant differences were found between the sample time points. The lowest Chl was observed in June (60 d.a.g) and 15 d before girdling (in April). The highest Chl was found at 150 d.a.g (in September) (*Fig. 4A*). Girdling significantly affected on PSII efficiency in the Robinson mandarin (*Table 2*). A two-way ANOVA indicated a significant main effect of girdling and sampling time point ($P \leq 0.01$). However, interactions were not observed between girdling treatment sampling points. In the present study, there was a tendency toward a decrease in PSII in girdled trees, especially in the DG treatment in comparison with controls. In terms of the PSII measurements, statistically significant differences were found between time points (*Fig. 4B*). The lowest chlorophyll fluorescence was observed in July (90 d.a.g) followed by 15 d before girdling (in April) and 30 d.a.g. (in May). The highest chlorophyll fluorescence levels were observed in October (180 d.a.g) and November (210 d.a.g).

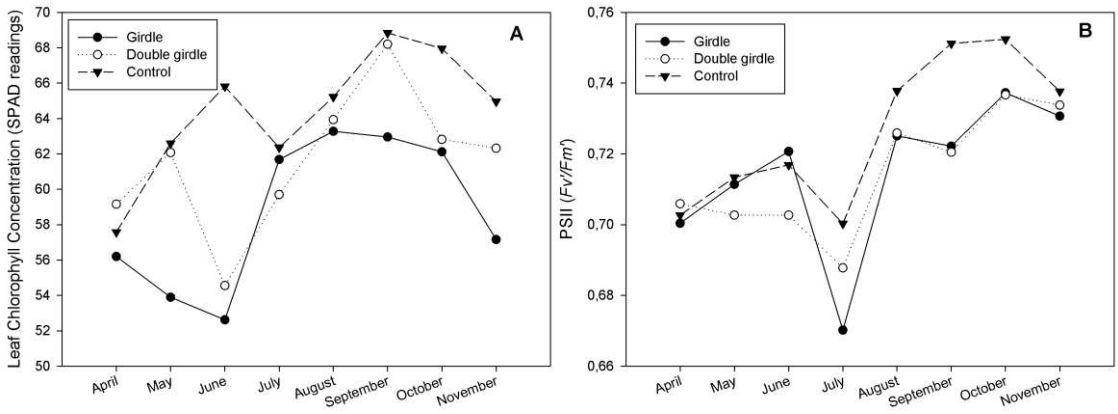

Figure 4. *Effects of girdling treatments on the leaf chlorophyll concentration (A) and PSII efficiency (B) in Robinson mandarins*

Leaf mineral concentrations

In the present study, leaf mineral content was not affected by girdling treatment (*Table 2*). A two-way ANOVA indicated a significant effect of sample date and the interaction on the concentrations of some leaf minerals (N, P, Na, Mg, Fe) (*Table 2*). It can be argued that the significant differences among sample dates in mineral elements are a natural result because plant nutrients are used at different rates in different periods. Although not significantly, the leaf N levels were reduced in the girdled trees compared with non-girdled trees. There was a decrease in leaf N content until 30 d.a.g (in May) in girdled trees, while an increase was observed in untreated trees (*Fig. 5A*). In all treatments, a rapid increase was observed in the 60 d.a.g (June), but it was lower in girdled trees, especially after double girdling. The values of the control and girdled trees (except double girdling) showed a similar tendency after 120 d.a.g. (August) and remained more or less constant throughout the measurement periods. The potassium (K) percentage in the leaves was not affected by any treatment (*Fig. 5C*).

http://www.aloki.hu ● ISSN 1589 1623 (Print) ● ISSN 1785 0037 (Online)
DOI: http://dx.doi.org/10.15666/aeer/1605_62056218
© 2018, ALÖKI Kft., Budapest, Hungary

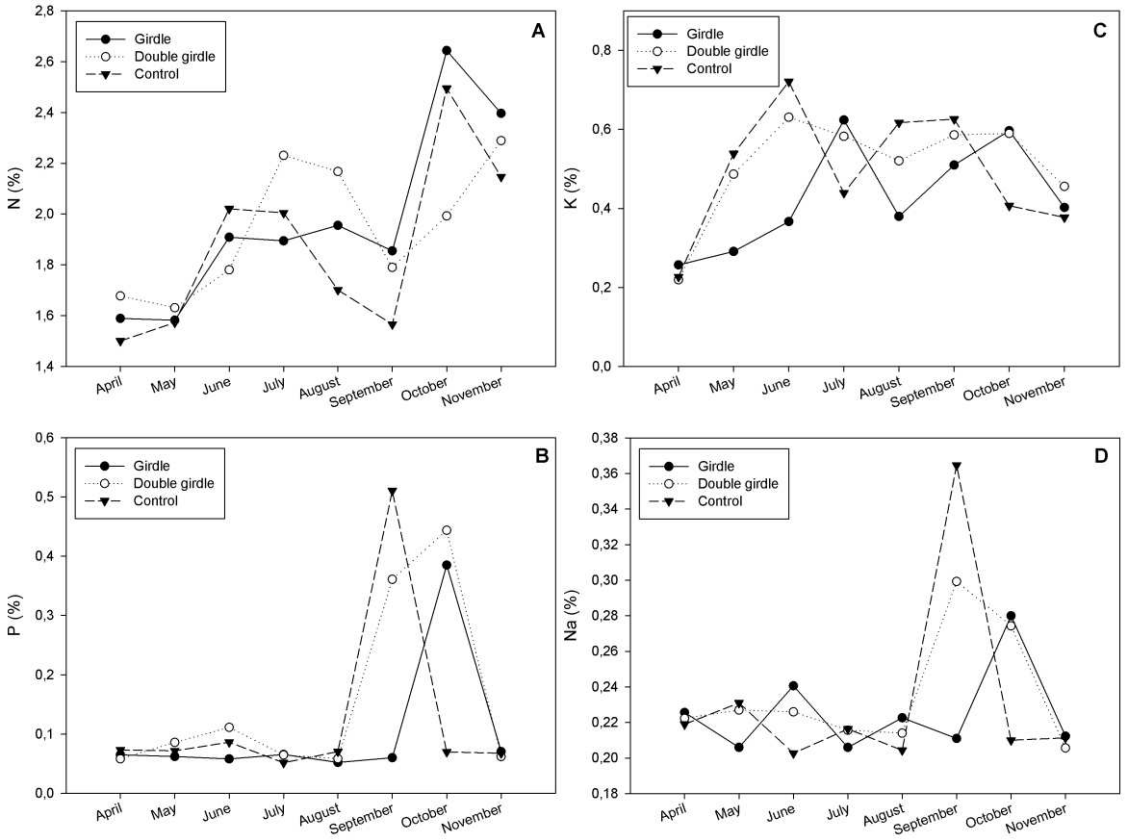

Figure 5. *Effects of girdling treatments on the leaf N (A), P (B), K (C) and Na (D) concentrations in Robinson mandarins*

The K value in the DG trees increased up to the 60 d.a.g (June) in all applications, though not as much as in the control trees. Similar trends were observed in other measurement periods in all treatments. Leaf P, Na and Mg contents we not affected by the treatments and no trend was determined among the treatment in the different sample periods (*Figs. 5B-D* and *6A*). However, in terms of these values (P, Na and Mg), a significant increase was observed in both control and girdled trees from the 120 d.a.g. (August), and these increases were more prominent in the control trees than in girdled trees. For all the measured micronutrients, similar trends were found (*Fig. 6 A-D*).

Discussion

According to the results obtained in this study, girdling application significantly affected fruit set, and the most effective treatment was DG followed by SG. The most favorable effect of girdling was the improvement of fruit set and growth, especially after DG treatment. In previous studies, a significant increase in the fruit yield of the Balady mandarin was obtained when a girdling treatment was applied before blossoming (Mostafa and Saleh, 2006). Additionally, according to Rivas et al. (2007), girdling delayed fruitlet abscission in all shoot types and leafy flowering shoots had increased fruit set in Loretina and Nova mandarin cultivars. According to Rivas et al. (2006), the productivity of Fortune and Clausellina mandarins can be improved by girdling. Moreover, Tuzcu et al. (1992) found that the application of double girdling at

http://www.aloki.hu ● ISSN 1589 1623 (Print) ● ISSN 1785 0037 (Online)
DOI: http://dx.doi.org/10.15666/aeer/1605_62056218
© 2018, ALÖKI Kft., Budapest, Hungary

the beginning of flowering increases the yield of the Algerian tangerine (clementine/mandarin) compared to the control. Similarly, trunk girdling has been shown to increase fruit set in many crops, including apple (*Malus domestica* Borkh.) (Hoying and Robinson, 1992), lychee (*Litchi chinensis* Sonn.) (Roe et al., 1997), kiwifruit (*Actinidia chinensis* Planch.) (Boyd and Barnett, 2011) and Fuyu persimmon (*Diospyros kaki* L.) (Choi et al., 2010).

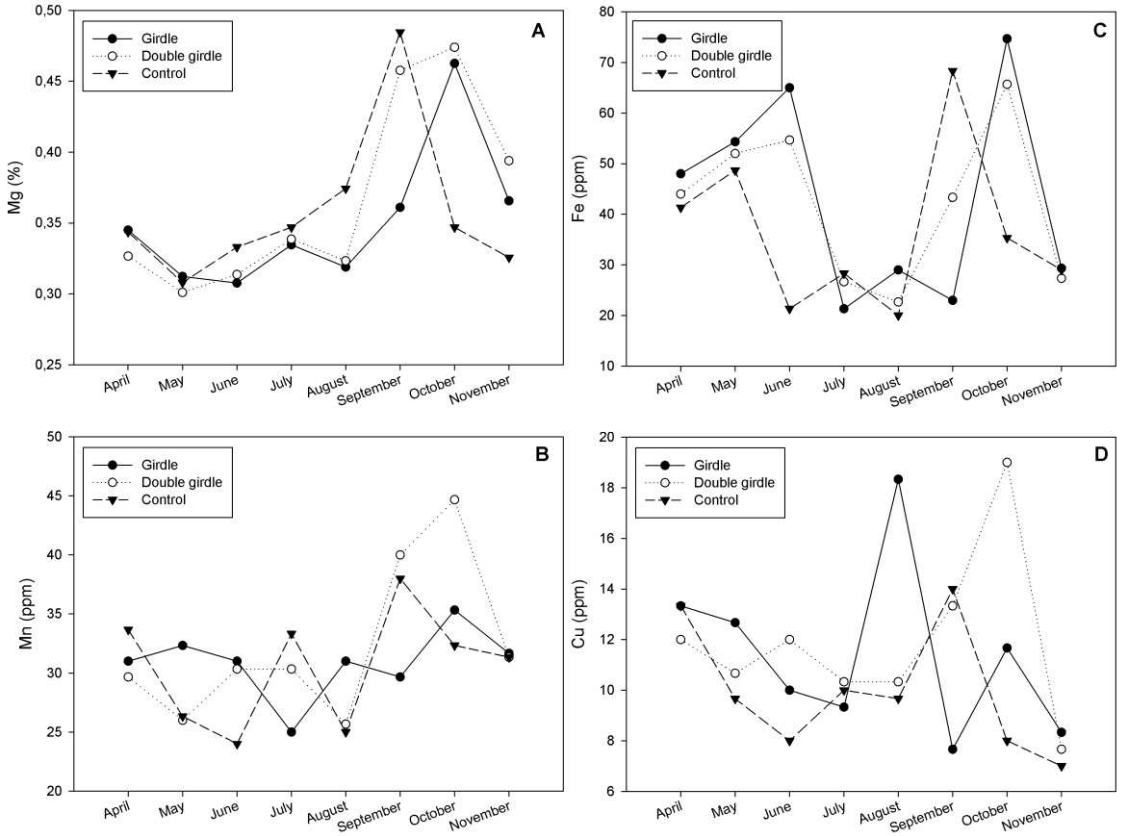

Figure 6. *Effects of girdling treatments on the leaf Mg (A), Mn (B), Fe (C) and Cu (D) concentrations in Robinson mandarins*

Fruit size is one of the most important factors affecting the marketing of fresh citrus fruits. Thus, techniques such as girdling, thinning and synthetic auxin application are commonly used to increase the size of fruit for fresh consumption. Girdling applications often promote fruit set and increase the size of fruit. In addition, Agustí et al. (2002) demonstrated that girdling can be used to increase final fruit size. In the present study, fruit diameter was significantly affected by the application of girdling treatments. Specifically, treatment with girdling increased the number of large fruits and reduced the number of fruits with a diameter <65 mm. In previous studies, fruits harvested from trees treated with girdling were significantly larger than fruits from control trees, which indicated that the application of girdling increased fruit size (Tuzcu et al., 1992; Mostafa and Saleh, 2006; Rivas et al., 2007). Moreover, Cohen (1984) found that the application of summer girdling increased fruit size of the Marsh seedless grapefruit. Similarly, Khandaker et al. (2011) indicated that fruit size of wax jambu was

http://www.aloki.hu ● ISSN 1589 1623 (Print) ● ISSN 1785 0037 (Online)
DOI: http://dx.doi.org/10.15666/aeer/1605_62056218
© 2018, ALÖKI Kft., Budapest, Hungary

significantly influenced by different girdling treatments and that girdled branches produced the highest fruit length and diameter compared to the control branches.

Girdling treatments resulted in no marked effects upon the fruit quality. The results obtained in the present study are in concordance with those of previous studies that reported that girdling increases SSC in navels (Church, 1993) and satsumas (Peng and Rabe, 1996). However, the increased SSC due to girdling was not always significant. The results obtained in the present study are in agreement with those described in a previous report by Verreynne et al. (2001), who studied the effects of trunk girdling on the internal fruit quality of the "Marisol" clementine and found no significant differences in fruit quality due to girdling. According to Peng and Rabe (1996), girdling did not have any significant effect on juice volume; however, Mostafa and Saleh (2006) reported lower juice volume after girdling. In addition, Roussos and Tassis (2011) demonstrated that the titratable acidity, pH and maturity index of the Nova mandarin were not significantly affected by girdling.

Our results demonstrate that girdling has a significant effect on the quantum yield of PSII (*Fv/Fm*), especially with DG. In addition, the differences in PSII between girdled trees tended to decrease in comparison with controls. The results obtained in the present study are in agreement with those described in a previous report by Rivas et al. (2007), who studied the effects of girdling on fruit set and quantum yield efficiency of PSII in two *Citrus* cultivars and indicated that girdling reduced the quantum yield efficiency of PSII in the leaves of vegetative shoots. Similar results were reported in mango (Urban et al., 2004), and *P. canariensis* (López et al., 2015). Additionally, according to Quentin et al. (2013), leaves on girdled trees had a reduction of A_{net} compared to leaves on control trees. Similar results have also been reported for wet tropical rainforest trees (Asao and Ryan, 2015). Similarly, no significant differences in photosynthetic activity between the control and girdled shoots were observed until the day after girdling. However, the photosynthesis activity of the control tree then increased until harvest, while the girdled shoots showed a significant reduction (Vaio et al., 2001). The most well-known effect of girdling is the increase in carbohydrates above the girdle (Fishler et al., 1983; Mataa et al., 1998; Urban et al., 2004). However, girdling reduces leaf net photosynthesis in numerous fruit trees (Inglesias et al., 2002; Zou and Quebedeaux, 2003; Urban et al., 2004; Frank et al., 2006). According to Quentin et al. (2013), the photosynthetic activity of leaves might be restricted by feedback control in the absence of adequate sinks or upregulated where sink demand is increased. Recent studies have shown that the decline in leaf net photosynthesis due to sink demand is independent of a direct feedback effect of the end products (DaMatta et al., 2008; Cheng et al., 2008). In addition, López et al. (2015) demonstrated that the accumulation of carbohydrate can explain the reduction in the quantum yield efficiency of photosystem II through feedback loops.

Regarding chlorophyll concentration in the leaves, we found that chlorophyll concentrations decreased in girdled plants. The values of the control trees increased continuously until 60 d.a.g (in June), while the girdled trees showed a marked decrease. The values of control and girdled trees showed a similar tendency after 90 d.a.g (July) and remained more or less constant throughout the measurement periods. The results obtained in the present study are in agreement with those described in a previous report by López et al. (2015), who studied the effects of stem girdling on photosynthesis and chlorophyll in *P. canariensis* and found that they progressively decreased in girdled plants but that the effect was rapidly reversed when the phloem was reconnected. Rivas et al. (2007) demonstrated that girdling had no effect on foliar Chl concentrations

http://www.aloki.hu ● ISSN 1589 1623 (Print) ● ISSN 1785 0037 (Online)
DOI: http://dx.doi.org/10.15666/aeer/1605_62056218
© 2018, ALÖKI Kft., Budapest, Hungary

between control and girdled trees in two *Citrus* cultivars. In addition, Mostafa and Saleh (2006) indicated that all treatments significantly increased both total chlorophyll and Ch_a compared to untreated trees, but no significant differences in leaf Ch_b were detected among the treatments.

Our results showed that girdling did not affect leaf mineral content. However,, we observed a tendency toward decrease in nitrogen level in the girdled trees. Similar trends were observed in the other measurement periods in all treatments. According to Cimó et al. (2013), girdling treatments decreased N, P, K, Ca and Mg concentrations in the leaves of citrus and reduced the levels of all measured micronutrients. Davies et al. (1995) reported that N, K and Ca levels were lower in avocado leaves in girdled branches compared with those of control branches. Similarly, trunk girdling decreased N levels in the leaves of several crops, including lychee (*Litchi chinensis* Sonn.) (Wang et al., 2010) and pistachio (*Pistacia vera L.*) (Vemmos, 2005). Mostafa and Saleh (2006) also demonstrated that the P percentage in the leaves of the Balady mandarin was not affect by girdling. Moreover, Jasrotia et al. (2014) found that leaf N and P in olive were not affected by girdling.

Conclusion

In conclusion, girdling significantly increased fruit set; especially when girdling was performed at the onset of cell enlargement stage, it increased the final fruit size and improved the commercial fruit size distribution. According to our results, girdling treatments increased the yield and commercial fruit size of the Robinson mandarin variety so that the girdling as one of the cultural practices can be applied for higher fruit size and fruit yield. We determined that girdling has a significant effect on both the PSII and leaf chlorophyll concentration as both decreased in girdled trees. This decrease may be related to carbohydrate accumulation in upper site of the girdling zone as reported in previous studies.

REFERENCES

[1] Agustí, M., Almela, V., Juan, M., Primo-Millo, E., Trenor, I., Zaragoza, S. (1994): Effects of 3,5,6-trichloro-2-pyridyloxyacetic acid on fruit size and yield of clausellina mandarin (Citrus unshiu Marc.). – Jour. of Hort. Sci. 69(2): 219-223.

[2] Agustí, M., El-Otmani, M., Aznar, M., Juan, M., Almela, V. (1995): Effect of 3,5,6-trichloro-2-pyridyloxyacetic acid on Clementine early fruitlet development and on fruit size at maturity. – J. of Hort. Sci. 70(6): 955-962.

[3] Agustí, M., Martinez-Fuentes, A., Mesejo, C. (2002): Citrus fruit quality. Physiological basis and techniques of improvement. – Agrociencia 2: 1-16.

[4] Asao, S., Ryan, M. G. (2015): Carbohydrate regulation of photosynthesis and respiration from branch girdling in four species of wet tropical rain forest trees. – Tree Physiology 35: 608-620.

[5] Barton, C. J. (1948): Photometric analysis on phosphate rock. – Ind. and Eng. Chem. Anal. Ed. 20: 1068-1073.

[6] Bevington, K. (2003): Optimisation of Citrus Production and Fruit Size: An Interactive Management Model. Fruit Size Management Guide Part I. – Australian Citrus Growers Publication, Mildura.

http://www.aloki.hu ● ISSN 1589 1623 (Print) ● ISSN 1785 0037 (Online)
DOI: http://dx.doi.org/10.15666/aeer/1605_62056218
© 2018, ALÖKI Kft., Budapest, Hungary

[7] Boyd, L. M., Barnett, A. M. (2011): Manipulation of whole-vine carbon allocation using girdling, pruning, and fruit thinning affects fruit numbers and quality in kiwifruit. – Hortscience 46: 590-595.
[8] Chapman, H. D. (1960): Leaf and Soil Analysis in Citrus Orchards, Criteria and Diagnosis of Management Practice. – Manuel Berkeley, California University of California Division of Agricultural Science, Berkeley.
[9] Cheng, Y., Arakawa, O., Kasai, M., Sawada, S. (2008): Analysis of reduced photosynthesis in the apple leaf under sink-limited conditions due to girdling. – J Jpn Soc Hortic Sci. 77: 115-121.
[10] Choi, S. T., Song, W. D., Park, D. S., Kang, S. M. (2010): Effect of different girdling dates on tree growth, fruit characteristics and reserve accumulation in a late-maturing persimmon. – Scientia Horticulturae 126: 152-155.
[11] Church, C. G. (1933): Composition of juice of oranges from girdled and normal trees. – Calif. Citrogr. 18: 348-349.
[12] Cimò, G., Bianco, R. L., Gonzalez, P., Bandaranayake, W., Etxeberria, E., Syvertsen, J. P. (2013): Carbohydrate and nutritional responses to stem girdling and drought stress with respect to understanding symptoms of Huanglongbing in Citrus. – HortScience 48(7): 920-928.
[13] Cohen, A. (1984): Citrus fruit enlargement by means of summer girdling. – J. Hortic. Sci. 59: 119-125.
[14] Da Matta, F. M., Cunha, R. I., Antunes, W. C., Martins, S. C. V., Araujo, W. I., Fernie, A. R., Moraes, G. A. B. K. (2008): In field-grown coffee trees source-sink manipulation alters photosynthetic rates, independently of carbon metabolism, via alterations in stomatal function. – New Phytol. 178: 348-357.
[15] Davies, S. J., Stassen, P. J. C., Martie, W. (1995): Girdling for increased Hass fruit size and its effect on carbohydrate production and storage. – Proc. World Avocado Congress 3: 25-28.
[16] El-Otmani, M., Coggins, C. W., Agustí, M., Lovatt, C. (2000): Plant growth regulators in citriculture: World current uses. – Critical Reviews in Plant Sciences 19: 395-447.
[17] Erner, Y., Tagari, E., Hamou, M., Katzir, I. (2004): Enhancing citrus fruit size: An overview of opportunities and achievements in Israel. – Proc. Int. Soc. Citriculture 2: 495-501.
[18] FAO (2015): Food and Agriculture Organization. The Database of Annual Production. – FAOSTAT. Statistical database. http://faostat.fao.org.
[19] Fishler, M., Goldschmidt, E. E., Monselise, S. P. (1983): Leaf area and fruit size on girdled grapefruit branches. – J. Amer. Soc. Hort. Sci. 108(2): 218-221.
[20] Frank, N., Vaast, P., Génard, M., Dauzat, J. (2006): Soluble sugars mediate sink feedback down-regulation of leaf photosynthesis in field-grown Coffea Arabica. – Tree Physiol. 26: 517-525.
[21] Goldschmidt, E. E., Koch, K. E. (1996): Citrus. – In: Zamski, E., Schafer, A. A. (eds.) Photoassimilate Distribution in Plants and Crops. Source-Sink Relationships. Marcel Dekker, Inc., NewYork, pp.797-823.
[22] Guardiola, J. L. (1997): Increasing Citrus Fruit Size with Synthetic Auxins. – In: Futch, S. H., Kender, W. J. (eds.) Citrus Flowering and Fruiting Short Course. – Univ. of Florida, Lake Alfred, FL, pp. 79-86.
[23] Guardiola, J. L., Agustí, M., García-Marí, F., Almela, V. (1982): The regulation of fruit size in citrus by tree factors. – XXIst Int. Hortic. Congress 1: 1363.
[24] Guardiola, J. L., García-Luis, A. (2000): Increasing fruit size in Citrus. Thinning and stimulation of fruit growth. – Plant Growth Regulation 31: 121-132.
[25] Hirose, K. (1981): Development of chemical thinners for commercial use for satsuma mandarin in Japan. – Proc. of Int. Soc. of Citriculture 1: 256-260.
[26] Hoying, S. A., Robinson, T. L. (1992): Effects of chain saw girdling and root pruning of apple trees. – Acta Hortic. 322: 167-172.

http://www.aloki.hu ● ISSN 1589 1623 (Print) ● ISSN 1785 0037 (Online)
DOI: http://dx.doi.org/10.15666/aeer/1605_62056218
© 2018, ALÖKI Kft., Budapest, Hungary

[27] Inglesias, D. J., Llsio, I., Tadeo, F. R., Talon, M. (2002): Regulation of photosynthesis through source: sink imbalance in citrus is mediated by carbohydrate content in leaves. – Physiol. Plant. 116: 563-572.
[28] Jasrotia, A., Bakshi, P., Wali, V. K., Bhushan, B., Ji Bhat, D. (2014): Influence of girdling and zinc and boron application on growth, quality and leaf nutrient status of olive cv. Frontoio. – African J. of Agric. Res. 9(18): 1354-1361.
[29] Kacar, B. (1972): Chemical Analysis of Soil and Plant. – Ankara Univertisty Press, Ankara, Turkey.
[30] Khandaker, M. M., Hossain, A. B. M. S., Osman, N., Boyce, A. N. (2011): Application of girdling for improved fruit retention, yield and fruit quality in *Syzygium samarangense* under field conditions. – Int J of Agric & Bio. 13: 18-24.
[31] Less, H. (1971): Laboratory Handbook of Methods of Food Analysis. – Leonard Hill Books, London.
[32] López, R., Brossa, R., Gil, L., Pita, P. (2015): Stem girdling evidences a trade-off between cambial activity and sprouting and dramatically reduces plant transpiration due to feedback inhibition of photosynthesis and hormone signaling. – Frontiers in Plant Sci. 6: 1-11.
[33] Mataa, M., Tominaga, S., Kozaki, I. (1998): The effect of time of girdling on carbohydrate contents and fruiting in Ponkan mandarin (*Citrus reticulata* Blanco). – Sci Hortic. 73: 203-211.
[34] Mostafa, E. A. M., Salah, M. M. S. (2006): Response of Balady mandarin trees to girdling and potassium sprays under sandy soil conditions. –Research J of Agric and Bio Sci 2(3): 137-141.
[35] Patrick, J. W. (1993): Sink strength: whole plant considerations. – Plant Cell and Environment 16: 1019-1020.
[36] Peng, Y. H., Rabe, E. (1996): Effect of summer trunk girdling on fruit quality, maturation, yield, fruit size and tree performance in Mihowase satsumas. – J. Hortic. Sci. 71: 581-589.
[37] Quentin, A. G., Close, D. C., Hennen, L. M. H. P., Pinkard, E. A. (2013): Down-regulation of photosynthesis following girdling, but contrasting effects on fruit set and retention, in two sweet cherry cultivars. – Plant Physiology and Biochemistry. 73: 359-367.
[38] Raveh, E. (2013): Girdling for Crop Regulation. – Citrus Growers Technical Conference & Workshop, Dareton.
[39] Rivas, F., Erner, Y., Alós, E., Juan, M., Almela, V., Agustí, M. (2006): Girdling increases carbohydrate availability and fruit set in citrus cultivars irrespective of parthenocarpic ability. – Journal of Hort. Sci. & Biotechnology 81(2): 289-295.
[40] Rivas, F., Gravina, A., Agustí, M. (2007): Girdling effects on fruit set and quantum yield efficiency of PSII in two Citrus cultivars. – Tree Physiol. 27: 527-535.
[41] Roe, D. J., Menzel, C. M., Oosthuizen, J. H., Doogan, V. J. (1997): Effects of current CO2 assimilation and stored reserves on lychee fruit growth. – J. Hortic. Sci. 72: 397-405.
[42] Roussos, P. A., Tassis, A. (2011): Effects of girdling, nitrogen, zinc and auxin foliar spray applications on mandarin fruit Nova quality characteristics. – Emir J Food Agric 23(5): 431-439.
[43] Tuzcu, O., Kaplankıran, M., Yeşiloğlu, T. (1992): Effects of girdling applications on fruit yield and fruit size in Clementine mandarin. – Proc. Int. Soc. Citriculture 2: 735-739.
[44] Tuzcu, Ö., Yeşiloğlu, T., Yıldırım, B. (2001): Citrus 2001 Reports: Turkey. – Florida Grower Annual Edition, Mid-August 2001, pp. 25-26.
[45] Urban, L., Lechaudel, M., Lu, P. (2004): Effect of fruit load and girdling on leaf photosynthesis in *Magnifera indica* L. – J. of Experimental Botany 55(405): 2075-2085.
[46] Vaio, C. D., Petito, A., Buccheri, M. (2001): Effect of girdling on gas exchanges and leaf mineral content in the independence nectarine. – J of Plant Nutrition 24(7): 1047-1060.

http://www.aloki.hu ● ISSN 1589 1623 (Print) ● ISSN 1785 0037 (Online)
DOI: http://dx.doi.org/10.15666/aeer/1605_62056218
© 2018, ALÖKI Kft., Budapest, Hungary

[47] Vemmos, S. N. (2005): Effects of shoot girdling on bud abscission, carbohydrate and nutrient concentrations in pistachio (*Pistacia vera* L.). – The Journal of Hort. Sci. and Biotech. 80(5): 529-536.
[48] Verreynne, J. S., Rabe, E., Theron, K. I. (2001): The effect of combined deficit irrigation and summer trunk girdling on the internal fruit quality of Marisol Clementines. – Scientia Horticulturae 91: 25-37.
[49] Wang, L., Wang, H., Li, J., Huang, X. (2010): Effects of branch girdling on shoot growth and mineral nutrients in Litchi. – Journal of Fruit Sci. 27: 2.
[50] Wheaton, T. A. (1981): Fruit thinning of Florida mandarins using plant growth regulators. – Proc. Int. Soc. Citriculture 1: 263-268.
[51] Zaragoza, S., Tenor, I., Alonso, E., Primo Millo, E., Agustí, M. (1992): Treatments to increase the final fruit size on Satsuma Clausellina. – Proc. Int. Soc. Citriculture 2: 725-728.
[52] Zhao, Y., Zhang, L., Gao, M., Tian, L., Zheng, P., Wang, K., Zhang, L., Li, B., Han, M., Alva, A. K. (2013): Influence of girdling and foliar applied urea on apple (Malus domestica L.) fruit quality. – Pak. J. Bot. 45(5): 1609-1615.
[53] Zou, R., Quebedeaux, B. (2003): Changes in photosynthesis and carbohydrate metabolism in mature apple leaves in response to whole plant source-sink manipulation. – J. Ame. Soc. Hortic. Soc. 128: 113-119.

http://www.aloki.hu ● ISSN 1589 1623 (Print) ● ISSN 1785 0037 (Online)
DOI: http://dx.doi.org/10.15666/aeer/1605_62056218
© 2018, ALÖKI Kft., Budapest, Hungary

SPATIO-TEMPORAL PATTERN EVOLUTION OF NON-POINT SOURCE PHOSPHORUS LOADS IN CHAOHU LAKE BASIN (ANHUI PROVINCE, CHINA) UNDER DIFFERENT LAND USE PATTERNS

XIONG, J. F.[1,2] – LIN, C.[1*] – MIN, M.[1] – MA, R. H.[1] – WU, Z. P.[3] – JIA, J. J.[4]

[1]*Key Laboratory of Watershed Geographic Sciences, Nanjing Institute of Geography and Limnology, Chinese Academy of Sciences, Nanjing 210008, China*

[2]*School of Geography and Remote Sensing, Nanjing University of Information Science & Technology, Nanjing 210044, China*
(e-mail: xjfpanda@163.com; phone: +86-25-8688-2169)

[3]*Ministry of Education Key Laboratory of Protection and Development Utilization of Tropical Crop Germplasm Resources, Hainan University, Haikou 570228, China*

[4]*Enterprise Innovation Center, Jiangsu Academy of Science and Technology for Development, Nanjing 210042, China*

**Corresponding author*
e-mail: clin@niglas.ac.cn

(Received 2nd Sep 2017; accepted 6th Sep 2018)

Abstract. Non-point source (NPS) pollution is an important source of lake eutrophication, the phosphorus (P) is one of the main elements of NPS pollution, and land use change has an important influence on NPS pollution load. Most previous studies focused on a single phase and did not analyze the internal structure of land use. In this study, six natural river basins such as the Hangbu River Basin were selected as the study area in Chaohu Basin, China. Based on the Sediment Delivery Distributed (SEDD) model, the NPS P load was simulated from 2000 to 2015, and the characteristics of land use change were depth analyzed at the same time to discuss the mechanism of land use pattern on NPS P load under long-term sequence. The main result are as follow: the NPS P load intensity was positively correlated with FL (forest land) area, in the whole study area, the correlation coefficient between NPS load intensity and FL area was 0.67, and the NPS P load intensity was negatively correlated with arable land (AL), construction land (CL) and wetland (WL) area, and the correlation coefficients were 0.56, 0.26 and 0.14 respectively. On the other hand, the internal structure of land use is also affecting NPS P load, the Fractal Dimension Index Mean (FRAC) was positively correlated with NPS P loss intensity, and the correlation coefficient is 0.56. Compared to the AL, FL and CL are more easily affected by FRAC. The optimization of land use spatial layout plays an important role in alleviating NPS pollution particle state.
Keywords: *sediment delivery distributed model, landscape index, long-term sequence, wetland, arable land, construction land, forest land*

Introduction

Phosphorus (P) is one of the main nutrients in inland lakes (Naramngam and Tong, 2013; Norton et al., 2012). As the main reason of eutrophication, Non-point source (NPS) P has been proven to be an important cause of bloom (Delpla et al., 2011; Dong et al., 2014; Hoffmann et al., 2009). The surface P is mainly lost by soil erosion in the adsorbed state (Wang et al., 2012). Under the influence of the dramatic change of land use, the ground surface conditions changed significantly, leading to changes in surface runoff characteristics and soil erosion (Hollis, 1975; Hundecha and Bardossy, 2004),

http://www.aloki.hu ● ISSN 1589 1623 (Print) ● ISSN 1785 0037 (Online)
DOI: http://dx.doi.org/10.15666/aeer/1605_62196238
© 2018, ALÖKI Kft., Budapest, Hungary

Furthermore, the temporal and spatial evolution of NPS pollution loads is influenced (Ahearn et al., 2005). Therefore land use change is an important factor of NPS pollution and lake nutrient enrichment (El-Khoury et al., 2015; Haggard et al., 2001). It can be seen that the improvement of lake water environment must be based on optimizing the spatial distribution of the river basin and reducing the NPS pollution. And exploring the internal relation and the influence mechanism between them has become the hot spot in the academic circles together with river basin environmental management department (Ouyang et al., 2013; Recanatesi et al., 2013; Wu et al., 2012b).

There are two types of estimation models for NPS pollution. The first is physical model, such as the Soil Water Assessment Tool (SWAT) and the Annualized Agricultural Non-Point Source model (AnnAGNPS). This kind of model can accurately simulate NPS P loads (Bingner et al., 2003; Kim et al., 2013; Wilson and Weng, 2011), but the model parameters are complicated, and strongly depending on the plot experiment and observation. Therefore, this model is not suitable for large space scale and long time series, and unfavorable to the comparative analysis between different watershed (Bechmann et al., 2009; Yang et al., 2012). Another kind is empirical model, such as the Sediment Delivery Distributed (SEDD) model and the Pollution Loads (PLOADS) model. Empirical model, by contrast, have characteristics of simple data acquisition, wide applicable scope, strong operability and easy to operate. Therefore, it is very suitable for assessing and simulating NPS P loads in the large space scale and long time series (Borrelli et al., 2014; Bu et al., 2008; Lin et al., 2016).

There have been some studies on the relationship between land use and NPS P loads. In the early stage, Garnier et al. (1998) overlaid USLE model and land use type, results show that, compared to other areas, the NPS pollution loads is significantly higher than other area in the animal husbandry and agriculture concentration areas. Later, urban construction land surface runoff is considered to be one of the important reasons to the NPS pollution (Li et al., 2008; Tang et al., 2005). In addition, some scholar's studies found that the bare surface type, like cultivated land and plantation, is an important source of NPS P loads (Ahearn et al., 2005; Catherine et al., 2013). Recently, with the further research, there are different conclusions about the influence of forest land, construction land, and cultivated land on NPS P loads. Jiang et al. (2014) found NPS P loads was negatively correlated with cultivated land and construction land, while it was positively correlated with forest land. However Tasdighi et al. (2017) suggested that phosphorus loads was positively correlated with construction land, was negatively correlated with agricultural land. Kim et al. (2016) found that the phosphorus loads intensity of cultivated land is highest, followed by forest land.

There are many conclusions which have shown that the change of land use caused by human activities affects NPS P loads. However, previous studies have focused on a single phase and did not analyse the internal structure of land use. This leads to differences between the various scholars, particularly, there is a disagreement about the effects of cultivated land, forest land, and construction land on NPS P loads. Therefore, in this paper, the Chaohu Lake Basin, which has the most serious NPS P loads in China, is selected as the study area (Jiang et al., 2014; Kong et al., 2015), and 6 regions were determined according to the main natural rivers into the lake. The SEDD model (Fu et al., 2006; Lin et al., 2016; Taguas et al., 2011) was used to estimate the NPS P loads in Chaohu Lake Basin from 2000 to 2015, and the spatial analysis methods and indicators, which focus on the diversity of spatial and temporal changes of land use and internal structure, are used in the study to analyze the changes of NPS P loads and land use

http://www.aloki.hu ● ISSN 1589 1623 (Print) ● ISSN 1785 0037 (Online)
DOI: http://dx.doi.org/10.15666/aeer/1605_62196238
© 2018, ALÖKI Kft., Budapest, Hungary

pattern under long-term sequence, and then reveals the mechanism of land use mode on the NPS P loads. First, we confirmed the main land types that affect the NPS P loads, and then discussed the effects of different land use types on NPS P loads. Finally the response mechanism of different land use change patterns to NPS P loads is determined, and it can be used to provide scientific and technical support, and data base for spatial optimization of land use for NPS pollution control.

Materials and methods

Study sites

Chaohu Lake is one of China's five major fresh water lake, the lake area is 769 km^2, normal hydrological year average water depth is 2.69 m, the maximum water depth of 3.77 m (Wang and Dou, 1998). Chaohu Lake basin is located in central Anhui Province and north of the Yangtze River Delta, the area is 13350 km^2, the terrain is mainly plain, mountain is located in the southwest of the basin. Average annual rainfall is 1215 mm, which flood season for 5 ~ 8 month, precipitation accounts for 51% of annual precipitation. The agricultural economy is developed in Chaohu Lank basin, which is the main commodity grain production base in China, agricultural land area accounted for 60% of the basin area, and the agricultural NPS pollution is serious (Yan and Wang, 1998; Zhou and Gao, 2011). According to remote sensing inversion results and river water quality monitoring data, the west lake area water quality serious pollution (Pan et al., 2011; Shang and Shang, 2007), Nanfei River and Pai River total phosphorus input accounted for 60% of the total pollution loads of rivers into the lake (Wang et al., 2011).

Natural river basin mainly based on the terrain, and the artificial river is less affected by the terrain, so the main six natural rivers into the lake were selected: ①Zhegao River, ②Tongyang River, ③Nanfei River, ④Pai River, ⑤Hangbu River, ⑥Baishitian River. Six river basin range preliminarily determined through the analysis of the hydrological Arc SWAT function, counterclockwise number R1 ~ R6 from east to west, and further subdivided is 55 sub-basins (*Fig. 1*), the study area partition and its basic information such as shown in *Table 1*.

The land use data source and land use indices

Land use is divided into six types: ① forest land (FL); ② construction land (CL); ③ grass land (GL); ④ wetland (WL); ⑤ arable land (AL); ⑥ unutilized land (UL). According to 55 sub-basin, the area and spatial distribution of six land types were analyzed respectively. In order to evaluate the change of landscape characteristics of each sub-basin with time, four landscape indices that can reflect the spatial structure characteristics are selected, included: ① Contagion index (CONTAG); ② Fractal Dimension Index Mean, (FRAC); ③ Shannon`s Diversity Index (SHDI); ④ Shannon`s Evenness Index (SHEI). CONTAG is used to measures the degree of aggregation of the same type of patches and is influenced by the number of landscape homogeneity and type. High value shows that the greater the landscape connectivity of the advantages of plaque type exist. FRAC is a fractal pattern index, is obtained by calculation complexity area ratio, the greater the value the more complex landscape shape. SHDI is used to measure the diversity of land use in a given area. The SHDI value increases with the increase of land use type. SHEI indicates the uniformity of the land use type distribution in the area, the closer the value 1, and distribution more uniform. All landscape indices

http://www.aloki.hu ● ISSN 1589 1623 (Print) ● ISSN 1785 0037 (Online)
DOI: http://dx.doi.org/10.15666/aeer/1605_62196238
© 2018, ALÖKI Kft., Budapest, Hungary

are calculated in Fragstats3.3 (Lin et al., 2015; McGarigal and Marks, 1995). To show the change of land use structure and distribution in sub-basin, according to the landscape index changes over time to classify it into five types: ① gradually increased (GI); ② gradually decreased (GD)); ③ first increased and then decreased (ID); ④ first decreased and then increased (DI); ⑤ fluctuation type (FT).

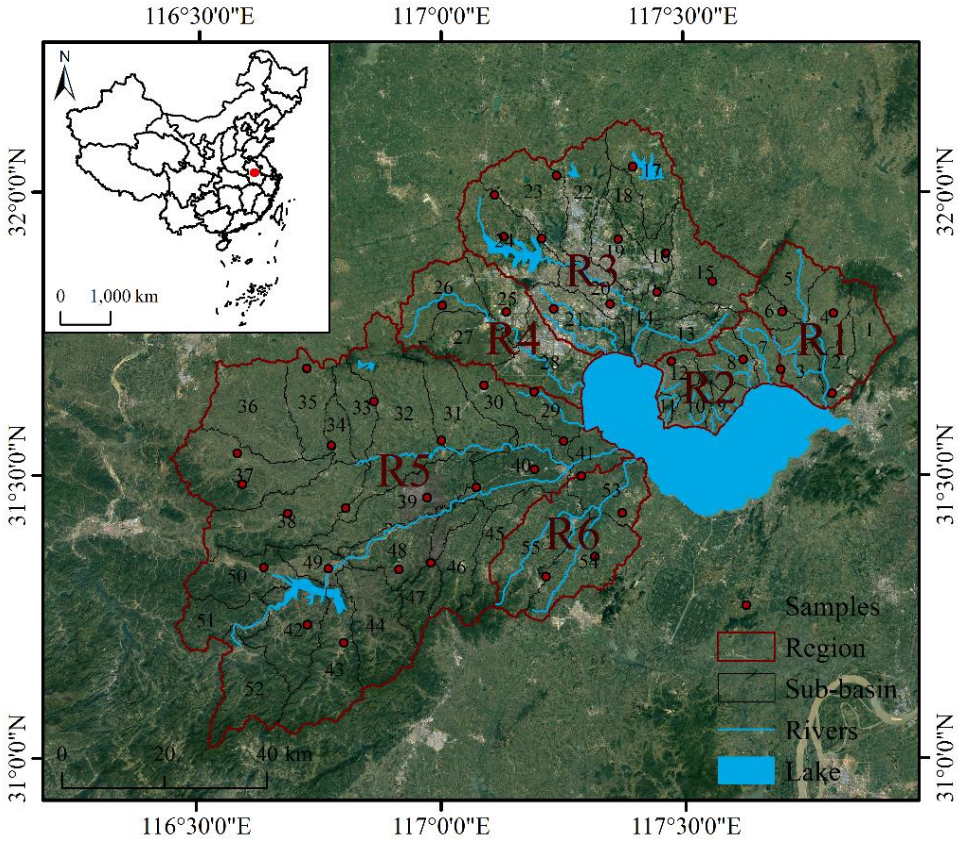

Figure 1. *Location of study site and sampling plots*

Table 1. *Watershed situation of study area*

Regions	Stream	Sub-basin	Area (km^2)	Administrative unit
R1	Zhegao River	1~6	546	Chaohu City
R2	Tongyang River	7~12	350	Chaohu City, Feidong
R3	Nanfei River	13~24	1680	Hefei City, Feidong
R4	Pai River	25~28	603	Feixi
R5	Hangbu River	29~52	4154	Lu'an City, Feixi, Shucheng, Yuexi
R6	Baishitian River	53~55	581	Lujiang

Quantitative evaluation of NPS P loads

The calculation method of surface phosphorus loads is based on the fundamental form of Revised Universal Soil Loss Equation (RUSLE), the sediment delivery ratio (SDR) and the phosphorus content in the soil, to estimate watershed NPS P loads (*Eq. 1;* Lin et al., 2016; Yang et al., 2012).

http://www.aloki.hu ● ISSN 1589 1623 (Print) ● ISSN 1785 0037 (Online)
DOI: http://dx.doi.org/10.15666/aeer/1605_62196238
© 2018, ALÖKI Kft., Budapest, Hungary

$$W = A_i \times P \times SDR_i \quad \text{(Eq.1)}$$

where W is the surface loads of the nutrient substance per unit area per unit area ($kg \cdot km^{-2} \cdot yr^{-1}$); A_i is the soil erosion amount; P is the soil phosphorus content ($g \cdot kg^{-1}$); SDR_i is the sediment delivery ratio of the grid i (Stefano and Ferro, 2007; Yang et al., 2012; Zhou and Wu, 2008), the equation is (*Eq. 2*):

$$SDR_i = \exp(-\beta t_i) \quad \text{(Eq.2)}$$

where t_i is the time required for the loss from the grid i point to the nearest water system, and β is a constant. The soil erosion estimation model uses RUSLE as the prototype, and uses the satellite remote sensing technology to provide the data for the model. Therefore, the model calculates the spatial resolution consistent with the satellite remote sensing image, with a 30 * 30 m grid as the minimum evaluation unit. The model equation is expressed as (*Eq. 3*):

$$A_i = R_i \times LS_i \times P_i \times C_i \times K_i \quad \text{(Eq.3)}$$

where R_i is rainfall erosivity factor ($MJ\ mm \cdot (ha\ h\ yr)^{-1}$); LS_i is slope length and steepness factor; P_i is conservation support practice factor based on land use; C_i is cover management factor; K_i is soil erodibility factor. R_i is based on the monthly rainfall calculation, the calculation method is (*Eq. 4*):

$$R_i = \sum_{n=1}^{12} 1.735 \times 10^{(1.5 \times \lg(\frac{P_i^2}{P}) - 0.8188)} \quad \text{(Eq.4)}$$

P_i is the average monthly rainfall (mm), and P is the average annual rainfall (mm). LS_i reflects the topographic factors on the driving force of soil erosion, according to the related literature (Onyando et al., 2005), the calculation method is (*Eqs. 5–7*):

$$L = (\lambda/22.13)^m \quad \text{(Eq.5)}$$

$$m = \begin{cases} m = 0.2 & \theta < 0.5° \\ m = 0.3 & 0.5° \le \theta < 1.5° \\ m = 0.4 & 1.5° \le \theta < 3° \\ m = 0.5 & \theta \ge 3° \end{cases} \quad \text{(Eq.6)}$$

$$S = \begin{cases} 10.8\,sin(\theta) + 0.03 & \theta \le 5° \\ 16.8\,sin(\theta) - 0.5 & 5° < \theta < 10° \\ 21.9\,sin(\theta) - 0.96 & \theta \ge 10° \end{cases} \quad \text{(Eq.7)}$$

where θ is the slope (°) of the grid I and λ is the slope length (m) of the grid in. P_i reflects the influence of regional soil and water conservation measures on soil erosion, and its assignment is determined by different land use patterns. The P was taken on Xu et al. (2013).

http://www.aloki.hu ● ISSN 1589 1623 (Print) ● ISSN 1785 0037 (Online)
DOI: http://dx.doi.org/10.15666/aeer/1605_62196238
© 2018, ALÖKI Kft., Budapest, Hungary

C_i reflects the effect of vegetation on soil erosion, according to Cai et al. (2000) and (Wu et al., 2012a), the calculation method is (*Eq. 8*):

$$C = \begin{cases} 1, & c = 0 \\ 0.6508 - 0.3436\ lgc, & 0 < c \leq 78.3\% \\ 0, & c > 78.3\% \end{cases} \quad \text{(Eq.8)}$$

where c is plant coverage (%), K_i is the soil erodibility, many of the research on the literature research in the study area, assignment of each soil type, interal (0, 1). Because the soil types will not change with the passage of time, so we cannot reflect the change characteristics of soil erodibility. In order to reflect the temporal and spatial variability of soil erodibility, the K_i values were directly assigned by literature research in 2000 and 2005 (Bu et al., 2002; Zhang et al., 2007), The K_i values for 2010 and 2015 are calculated using the initial measurement method specified in the RUSLE equation guide (*Eq. 9;* Sharpley and Williams, 1990):

$$K = \left\{0.2 + 0.3 \times \exp\left[-0.0256 \times Sd \times \left(1 - \frac{Sl}{100}\right)\right]\right\} \times \left[\frac{Sl}{Cl + Sl}\right]^{0.3} \times \left\{1.0 - 0.25 \times \frac{Coc}{Coc + \exp\left(3.72 - 2.95 \times Coc\right)}\right\} \times \left\{1.0 - \frac{0.7 \times \left(1 - Sd/100\right)}{1 - Sd/100 + exp - 5.51 + 22.9 \times \left(1 - Sd/100\right)}\right\} \quad \text{(Eq.9)}$$

The model is a function of soil organic matter and mechanical composition, where Sd, Sl, Cl, and Coc correspond to the percentage of soil sand, granule and clay and soil organic carbon.

Sample collection and data acquisition

Land use classification data sets in 2000, 2005, 2010 and 2015, are provided by the Lake-Watershed Science Data Center, National Earth System Science Data Sharing Infrastructure, National Science & Technology Infrastructure of China (http://lake.geodata.cn). Land use data supported by the "Strategic Priority Research Program - Climate Change: Carbon Budget and Related Issues" of the Chinese Academy of Sciences, Grant No. XDA05050106.

The soil's physical and chemical properties data were obtained from the laboratory testing which were collected in field (*Fig. 1*). Surface soil samples (0~10 cm depth) were collected from July 22 to 24, 2016, using four points method according to different land use types: FL, CL and AL. A total of 43 samples were collected and brought back to the laboratory to analyze the physical and chemical properties of the critical soil. The soil total phosphorus (TP), soil organic matter (SOM) and soil particle composition (sand (0.05~2 mm), silt (0.002~0.05 mm) and clay (0~0.002 mm)) were analyzed after air drying and grinding. TP were measure with inductively coupled plasma-atomic emission spectrometry (ICP-AES). SOM measure with potassium dichromate method.

http://www.aloki.hu ● ISSN 1589 1623 (Print) ● ISSN 1785 0037 (Online)
DOI: http://dx.doi.org/10.15666/aeer/1605_62196238
© 2018, ALÖKI Kft., Budapest, Hungary

The contents of soil particle composition were measured with the pipette method (Lin et al., 2008; Lin et al., 2016). The test results are shown in *Table 2*.

Table 2. *Statistic of soil properties*

	Min	Max	Mean	Std	CV/%
TP (g/kg)	0.25	2.95	0.76	0.53	70.76
SOM (g/kg)	7.41	128.77	36.08	21.94	60.80
Clay (%)	10.63	29.88	19.43	3.76	19.34
Silt (%)	42.39	81.91	72.14	7.94	11.00
Sand (%)	0.41	45.15	8.43	9.80	116.19

The spatial representation of each factor of the SEDD model depends on the plot test and the data extraction of the satellite remote sensing image. The basic data needed for each factor are shown in the *Table 3*.

Table 3. *The data source for NPS P loads calculation*

Data type	Data source	Description
Precipitation data	Meteorological monitoring stations in Chaohu Basin	The Chaohu Lake Basin has a total of 14 meteorological monitoring stations, which can get the monthly rainfall data from 1970 to the present. After the monthly average and spatial interpolation, the spatial and temporal distribution of rainfall erosivity is estimated
Digital elevation model (DEM)	ASTER global DEM	Downloads the 30 m spatial resolution DEM data from the USGS site, to calculate the slope length, steepness factor and SDR
Soil physical and chemical properties	Laboratory test	All chemical tests are done in the Key Laboratory of Watershed Geographic Sciences, Institute of Geography and Limnology, Chinese Academy of Sciences
Vegetation coverage	Landsat 5/8 Satellite imagery	Data were downloaded from the USGS website to obtain 30 m spatial resolution remote sensing images in four years, and extract the corresponding year vegetation index
Soil types	National soil type distribution map	After digitizing the national soil type distribution map, according to the soil type, assigned the soil erodibility factor

Results

Characteristics of land use change

According to the time series, six typical types of land use in the study area were classified. The spatial distribution characteristics of each land use type were shown in *Figure 2*. The main land use type in the whole basin is the arable land. Forest land is mainly distributed in the southwest mountainous area. The forest land area increased rapidly during 2010~2015 in R4 and R5. In 2000, the most of construction land was distributed in R3. Construction land expanded rapidly over time, constantly occupying arable land, gradually covered the entire R3 and expanding to the R4 in 2015.

http://www.aloki.hu ● ISSN 1589 1623 (Print) ● ISSN 1785 0037 (Online)
DOI: http://dx.doi.org/10.15666/aeer/1605_62196238
© 2018, ALÖKI Kft., Budapest, Hungary

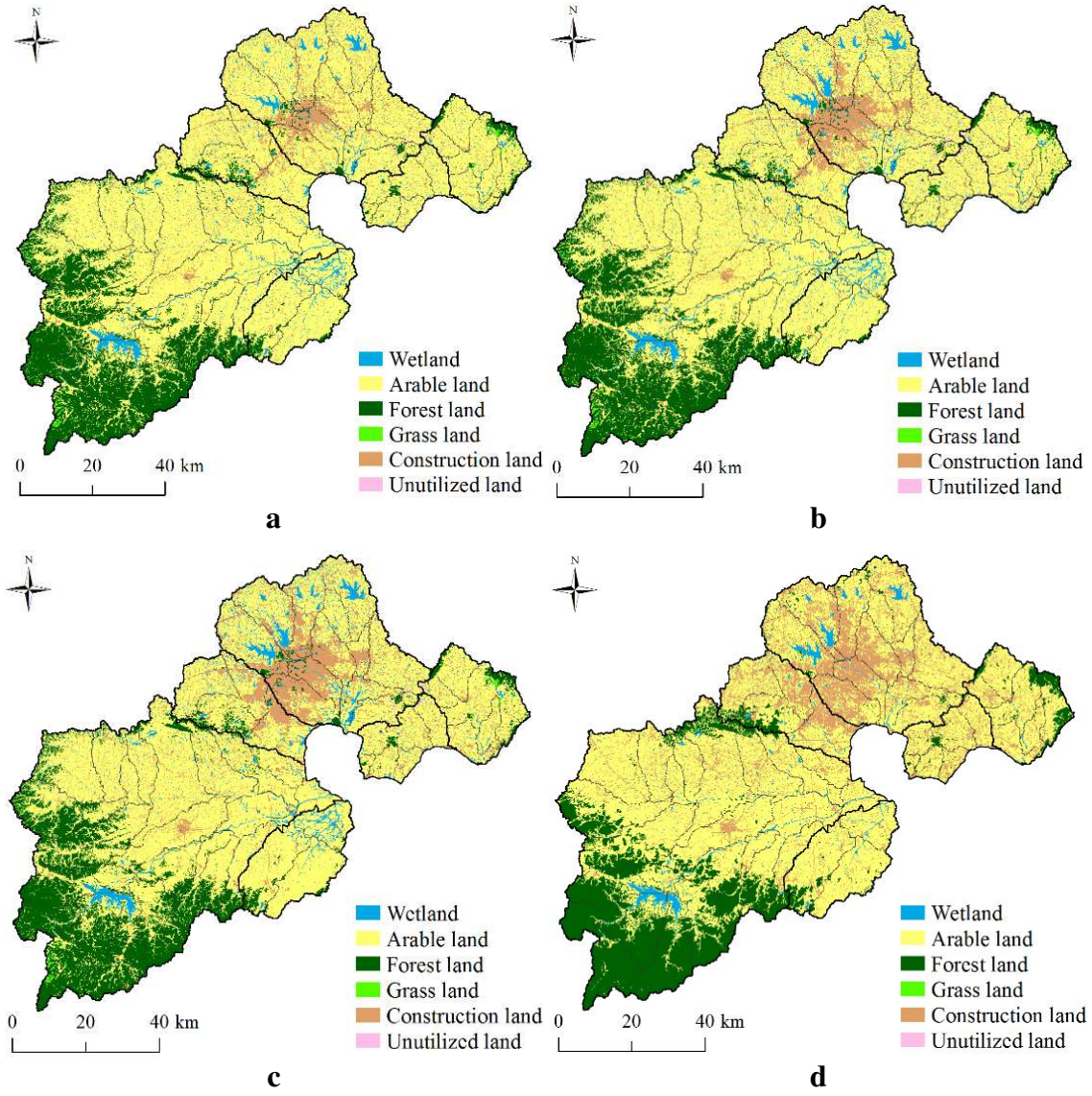

Figure 2. *The tendency of land use/cover change (LUCC) over of each sub-basins.* ***a.*** *2000;* ***b.*** *2005;* ***c.*** *2010;* ***d.*** *2015*

In addition to the spatial distribution characteristics of different land use types, the spatial structure and landscape characteristics also changed significantly with time. To show the change of land use structure and distribution in sub-basin, according to the landscape index changes over time to classify it into five types: ① gradually increased (GI); ② gradually decreased (GD)); ③ first increased and then decreased (ID); ④ first decreased and then increased (DI); ⑤ fluctuation type (FT). As shown in *Figure 3,* the land use patterns of most sub-basins were regular, and the sub-watersheds with exponential fluctuation are few.

The mainly type of change in CONTAG is GD. Except the sub-basin 20 is GI, the other sub-basins show the DI and FT characteristics, because the 20th sub-basin is the city center of Hefei, the land use types are mainly composed of construction land. In the latest decade, the construction land expands rapidly with urbanization process, so CONTAG showed a gradual increased trend. It is notable that half of the sub-basins in

http://www.aloki.hu ● ISSN 1589 1623 (Print) ● ISSN 1785 0037 (Online)
DOI: http://dx.doi.org/10.15666/aeer/1605_62196238
© 2018, ALÖKI Kft., Budapest, Hungary

R3 show a trend of DI, because these sub-basins construction land expanded rapidly, the occupation of cultivated land has led to the decline of connectivity and advantage of cultivated land, so CONTAG decrease. In the later period, the cultivated land became the main land use type in the sub-basin, and the connectivity of construction land increased, so do the CONTAG increase.

The main types of FRAC are GI and DI. The land use pattern in the study area showed a tendency of fragmentation over time. In the six regions, all the sub-basins in R1, R2 and R4 showed a trend of DI, and the GI is mainly in the R5 region.

The trends of SHDI in each sub-basin were different. The sub-basins in the R1, R2 and R3 show the trend of ID, and the other sub-basins are GI and FT. Only 20 and 52 sub-basin are GD, because the 20 sub-basin is the city center of Hefei, construction land gradually replaced the other land use types, so SHDI showed a trend of GD, and 52th sub-basin forest area gradually increased to replace other land types, resulting in SHDI decreased.

The main change of SHEI was GI, few sub-basins showed the ID and FT characteristics. The distribution of different land use types in the study area were more uniform over time, and the dominant position of cultivated land was decreasing gradually.

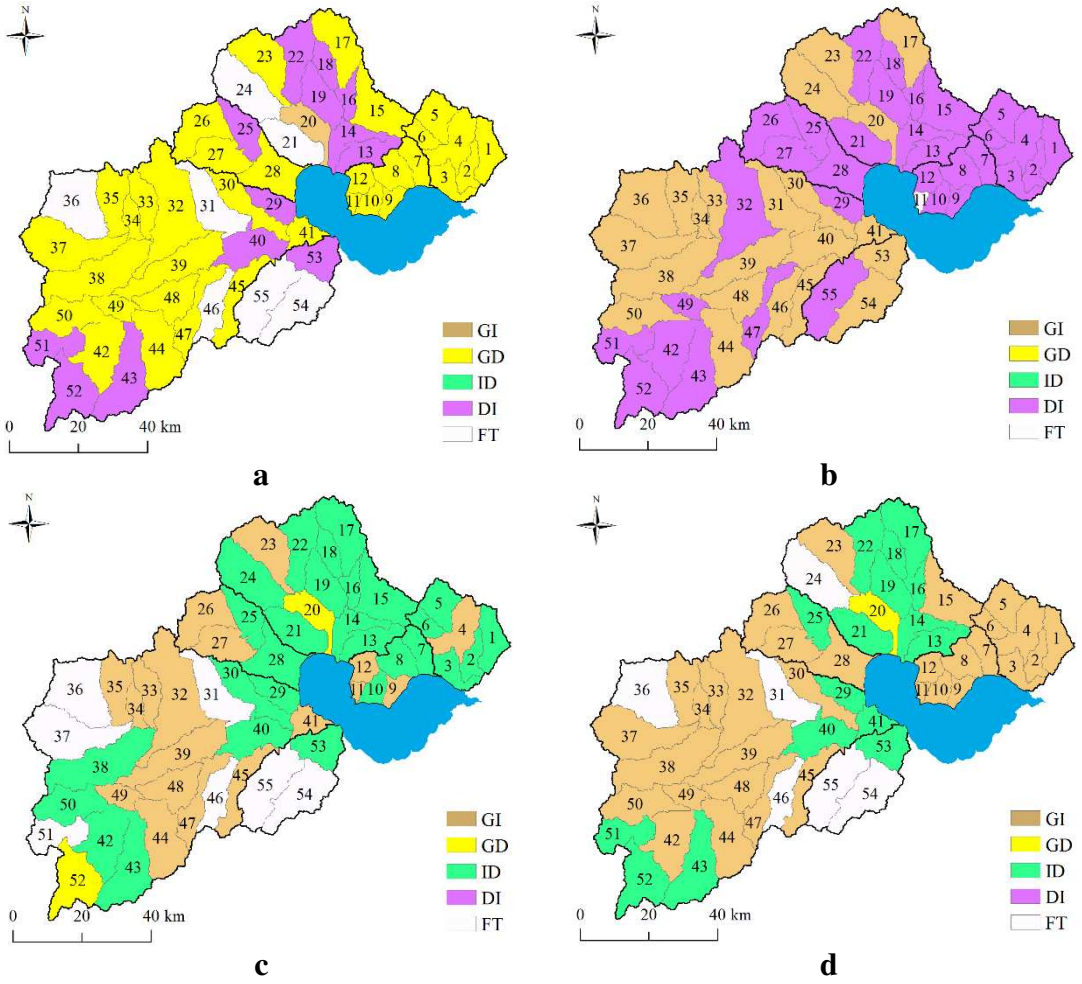

Figure 3. *Landscape index changes in each sub-basin.* ***a.*** *CONTAG;* ***b.*** *FRAC;* ***c.*** *SHDI;* ***d.*** *SHEI*

http://www.aloki.hu ● ISSN 1589 1623 (Print) ● ISSN 1785 0037 (Online)
DOI: http://dx.doi.org/10.15666/aeer/1605_62196238
© 2018, ALÖKI Kft., Budapest, Hungary

The main land use types in Chaohu Lake Basin was AL, and the area of CL increased rapidly. The CONTAG was decreasing, and the FRAC and SHEI show an increasing trend.

Characteristics of NPS P loads change

According to SEDD model, 2000, 2005, 2010 and 2015 NPS P loads estimated. In order to analysis the NPS P loads intensity in each sub-basin, the 55 sub-basins NPS P loads intensity was divided into seven grades (*Fig. 4*). On the whole, the change of NPS P loads changes was not obvious from 2000 to 2005, part of sub-basins showed an increasing trend during 2005~2010, all sub-basins showed a rapid increase trend during 2010~2015. The most obvious change area is R5, the spatial distribution characteristics are obvious that the high loads area is concentrated in the southwest mountain area. In 2000, the NPS P loads was low, the highest value was 1.11 $t \cdot km^{-2} \cdot yr^{-1}$, and all the sub-basins NPS P loads were below 40 $kg \cdot km^{-2} \cdot yr^{-1}$, and nearly half of the sub-basins NPS P loads is less than 5 $kg \cdot km^{-2} \cdot yr^{-1}$. In 2005, the highest value is 1.67 $t \cdot km^{-2} \cdot yr^{-1}$, shows a slow increasing trend, most of the sub-basins NPS P loads change is not obvious, except No. 1, No. 3 and No. 4 sub-basin NPS P loads decreased in R1, No. 38, No. 47 and No. 50 sub-basin NPS P loads increased in R5. In 2010, the NPS P loads showed a rapid increase trend, the highest value reached 11.66 $t \cdot km^{-2} \cdot yr^{-1}$, NPS P loads changes is different in different sub-basins, 22th sub-basin is the only sub-basin with descending trend, nearly half of the sub-basins NPS P loads showed an increasing trend. In particular, No. 43, No. 44, No. 51 and No. 52 sub-basins NPS P loading in R5 showed a rapid upward trend, more than 100 $kg \cdot km^{-2} \cdot yr^{-1}$. In 2015, the highest value of the NPS P loads decreases to 5.42 $t \cdot km^{-2} \cdot yr^{-1}$, but most of the sub-basins NPS P loads present increased. A total of 22 sub-basins NPS P loads is higher than 20 $kg \cdot km^{-2} \cdot yr^{-1}$. In addition, it is necessary to note that, when the most of the sub-basins in R5 are showing an increasing trend, especially after 2010 sub-basins NPS P loads is more than 100 $kg \cdot km^{-2} \cdot yr^{-1}$ in the southwest, the No. 40 and No. 41 sub-basins NPS P loads remained below 5 $kg \cdot km^{-2} \cdot yr^{-1}$.

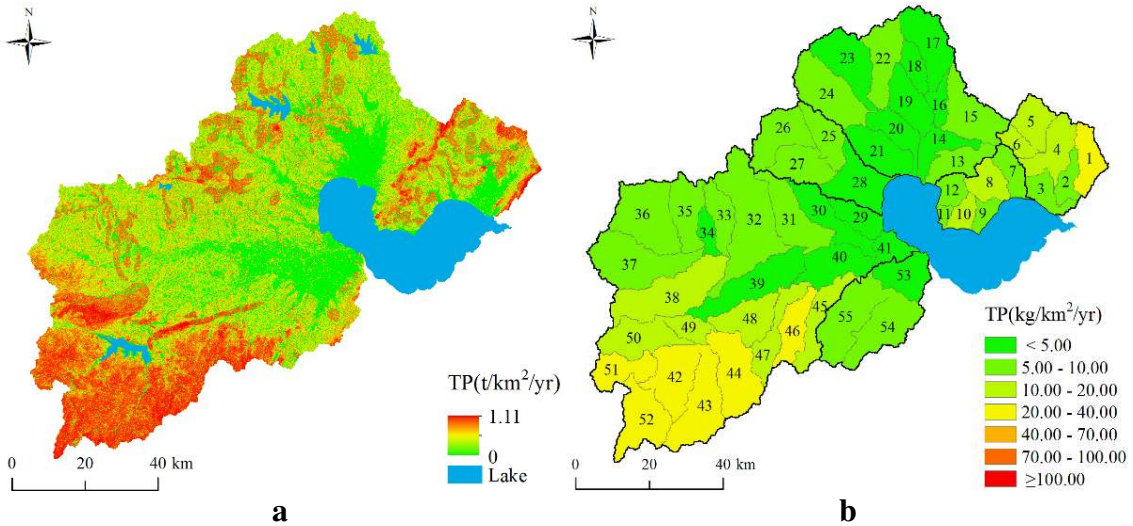

http://www.aloki.hu ● ISSN 1589 1623 (Print) ● ISSN 1785 0037 (Online)
DOI: http://dx.doi.org/10.15666/aeer/1605_62196238
© 2018, ALÖKI Kft., Budapest, Hungary

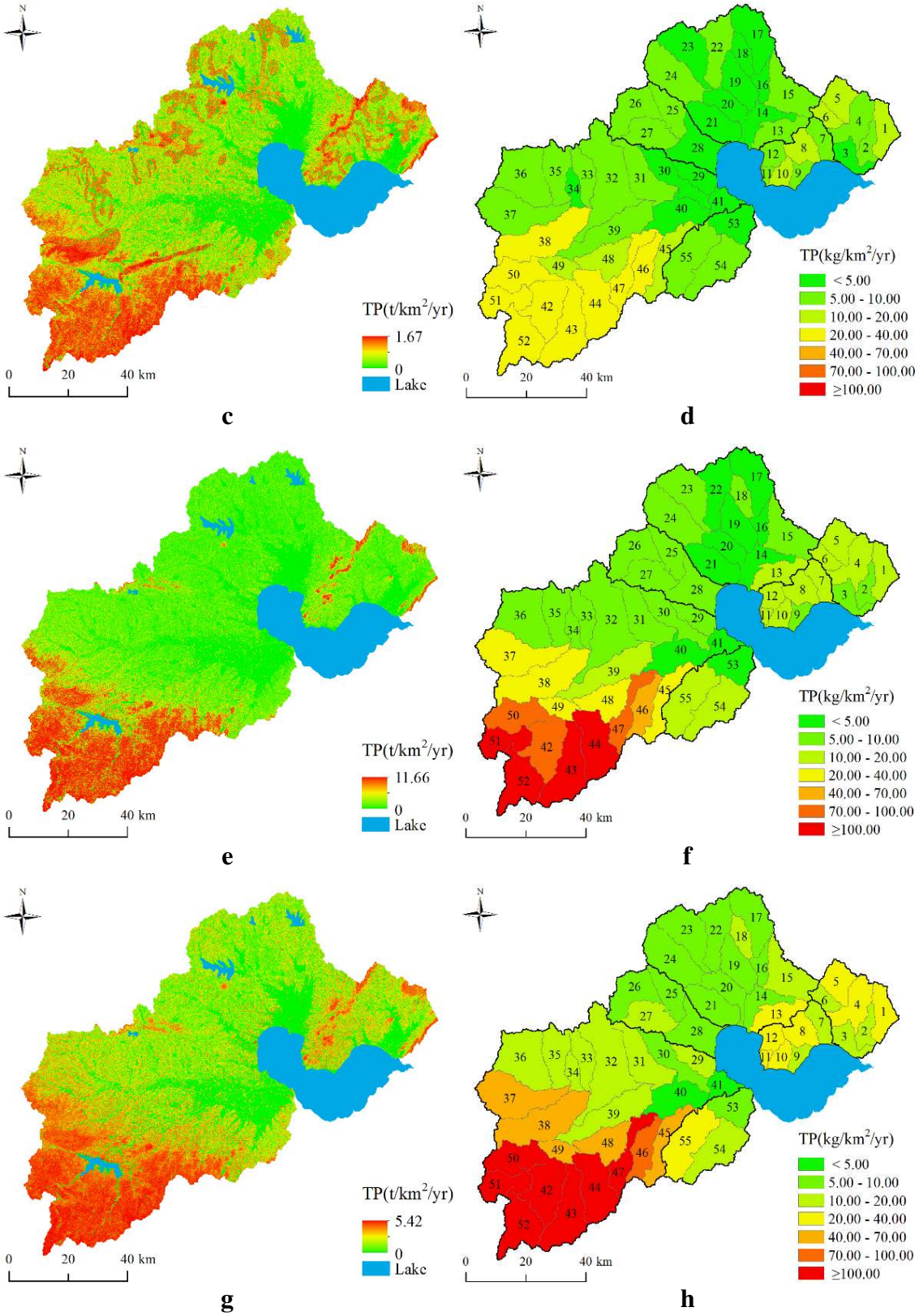

Figure 4. *The spatial distribution of NPS P loads.* ***a.*** *NPS P loads intensity in 2000;* ***b.*** *each basin NPS P loads intensity in 2000;* ***c.*** *NPS P loads intensity in 2005;* ***d.*** *each basin NPS P loads intensity in 2005;* ***e.*** *NPS P loads intensity in 2010;* ***f.*** *each basin NPS P loads intensity in 2010;* ***g.*** *NPS P loads intensity in 2015;* ***h.*** *each basin NPS P loads intensity in 2015*

http://www.aloki.hu ● ISSN 1589 1623 (Print) ● ISSN 1785 0037 (Online)
DOI: http://dx.doi.org/10.15666/aeer/1605_62196238
© 2018, ALÖKI Kft., Budapest, Hungary

In summary, NPS P loads did not change significantly before 2005, and increased rapidly after 2005. The spatial distribution of the high loads zone was closely related to the terrain, so it concentrated in the southwest mountainous area.

Relationship between NPS P loads and land use change

The correlation coefficients between the NPS P loads and the different land use area and land use index in the whole study area and the six region are shown in *Table 4*.

On the whole, NPS P loads intensity was positively correlated with FL area and FRAC, negatively correlated with AL, CL and WL area. Verify the Jiang et al. (2014) conclusions on the cultivated land, construction land and forest land. The correlation coefficient of the whole study area was clear, but the correlation coefficients in each region were different. For example: (1) Although the NPS P loads was significantly positive correlated construction land area, but only in R5 was significantly positive correlated, and it was opposite in R2 and R6; (2) Although, on the whole, CONTAG, SHDI and SHEI were not significantly correlated with NPS P loads, there was a significant correlation in both R1 and R2.

Table 4. *Correlation coefficients (r) between NPS P loads intensity and LUCC area and indices*

	FL	CL	GL	AL	WL	UL	CONTAG	FRAC	SHDI	SHEI
All	0.67**	-0.26**	0.09	-0.14*	-0.56**	-0.09	0.13	0.56**	-0.11	-0.09
R1	0.80**	0.04	-0.09	-0.82**	-0.78**	-0.31	-0.76**	0.53**	0.53**	0.80*
R2	0.47*	0.60**	-0.18	-0.68**	-0.15	-0.26	-0.60**	0.66**	0.52**	0.57*
R3	0.19	-0.12	.[b]	0.18	-0.30*	0.27	0.10	0.38**	-0.12	-0.15
R4	0.40	-0.04	-0.77**	-0.19	-0.72**	0.19	-0.46	0.29	0.16	0.38
R5	0.63**	-0.39**	0.09	-0.63**	-0.07	-0.10	0.06	0.69**	-0.04	0.00
R6	0.69*	0.64*	-0.17	-0.14	-0.63*	.[b]	-0.24	0.49	0.26	0.26

*Correlation is significant at the 0.05 level (2-tailed)
**Correlation is significant at the 0.01 level (2-tailed)
.[b] indicates that there is no such land use type in this region

Some conclusions can be drawn from the simple correlation coefficient, but the relationship between the NPS P loads and the land use pattern cannot be generalized. There were differences in different regions, especially the relationship, in particular the relationship between the land area and NPS P loads.

Discussion

Effects of land use change on NPS P loads in different regions

The land use change statistics for the six regions are shown in *Figure 5,* AL was a major land use type in Chaohu Lake basin, and the second was followed by construction land. Except the R5, the region includes the Dabie Mountain, the FL area was larger than the CL area, become the second largest land area after cultivated land. Land. CL area showed an increasing trend in all basins, especially in R2, R3 and R4, CL area increased rapidly, AL area decreased rapidly, indicated that the expansion of construction land is based on the occupation of cultivated land. During 2000~2010, the

http://www.aloki.hu ● ISSN 1589 1623 (Print) ● ISSN 1785 0037 (Online)
DOI: http://dx.doi.org/10.15666/aeer/1605_62196238
© 2018, ALÖKI Kft., Budapest, Hungary

wetlands in the six regions had different trends, such as R3 increased, while the R6 decreased, but during 2010~2015, WL area decreased in all regions. GL and UL area were small, almost replaced by other land in 2015

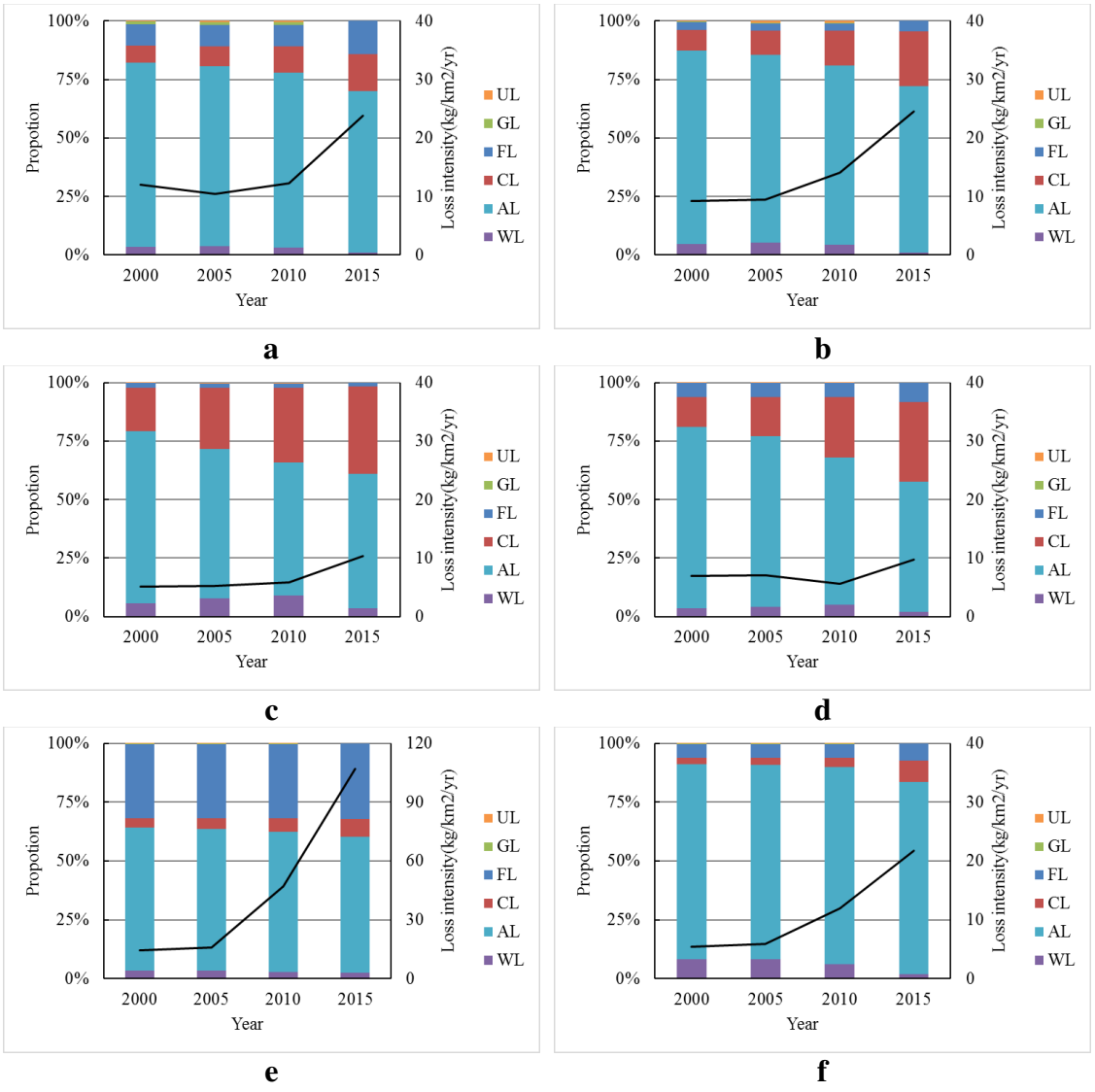

Figure 5. *Statistical data of each land use proportion and NPS P loss intensity in different region.* ***a.*** *R1;* ***b.*** *R2;* ***c.*** *R3;* ***d.*** *R4;* ***e.*** *R5;* ***f.*** *R6*

NPS P loss intensity showed an increasing trend, the highest intensity areas in R5. During 2000~2005, NPS P loss intensity growth slowly. During 2005~2010, loss intensity increased rapidly, but the change is different in different regions, for example, in R5, NPS P loss intensity have trebled, while R4 is decreased. During 2010~2015, NPS P increased rapidly, the loss intensity in all regions have doubled. Chaohu Lake Basin NPS P loads estimation results are comparable with other scholars. On the spatial distribution, Jiang et al. (2014), calculated the three periods of Chaohu Lake Basin NPS P loads, the results of 2001 to 2008 show that the high value of NPS P is concentrated in the southwest mountainous area, and there is a small amount in the northeast, which is consistent with the results of this study. Wang et al. (2015) simulated the spatial

http://www.aloki.hu ● ISSN 1589 1623 (Print) ● ISSN 1785 0037 (Online)
DOI: http://dx.doi.org/10.15666/aeer/1605_62196238
© 2018, ALÖKI Kft., Budapest, Hungary

distribution of NPS pollution in the Chaohu Lake Basin in 2010, and the spatial distribution of the NPS P loads was also the same. Kong et al. (2015) estimated the surface loads of the Chaohu basin from 1953 to 2012, NPS P loads are showing an increasing trend in 2000, 2000 and 2010 three periods, consistent with the trend of this research. Therefore, this study of NPS P loads estimation has a certain credibility.

During 2005~2010, R1 and R3 NPS P loads changed not obviously, R5 and R6 increased quickly, because the proportion of CL in R1 and R3 was significantly higher than that in R5 and R6, indicating that the CL can slow down the growth rate of the NPS P loads. During 2000~2010, NPS P loads intensity was not increasing in all regions, but during 2010~2015, all regions NPS P increased rapidly. During this period, the most obvious change of land use was the WL area decreased dramatically, illustrate the WL area was small, but played an important role in NPS P loads. This was consistent with the findings of Chescheir et al. (1992) and Braskerud (2002).

In summary, the WL and CL area had an important influence on the NPS P loads, WL area decreasing lead to NPS P loads intensity increase rapidly, the increase of CL area can slow down the growth rate of NPS P loads. On the other hand, FL and AL were not only the main land use types in the study area, but also the land classes that many scholars have paid attention to over the years. Therefore, we are going to discuss the effect of land use change on NPS P loads in WL, CL, FL and AL.

Effects of land use change on NPS P loads in different land use types

Because the proportion of WL area was small, and it had a very important impact on NPS P loads, so the WL was discussed separately. And the influence of WL area on the basin NPS P loads, as well as to the three main land use types NPS P loads. In recent years, many scholars have different opinions about the influence of AL, CL and FL on the NPS P loads (Jiang et al., 2014; Kim et al., 2016; Tasdighi et al., 2017). These three land use types are not only the main land use types in basin, but also would influence each other between the three land use types, so these three land use types are discussed together.

Wetland

According to *Table 4*, sub-basin was the evaluation unit, the correlation coefficient between WL area and NPS P loads is only 0.14, and not all regions have significant correlation. Taking the region as the evaluation unit, the NPS P loads intensity and WL area of 6 regions in 4 years were shown in *Figure 6*. The results showed that the WL area was negatively correlated with the NPS P loads intensity, R^2 was only 0.17, and the highest point of the loads intensity belongs to the R5. When the 4 points in the R5 area were removed (*Fig. 6b*), R2 reached 0.55. It indicated that there was a strong negative correlation between WL area and NPS P loads intensity, the change of WL area had a significant effect on the NPS P loads. In the R5, compared with other regions, the influence of WL area on the NPS P loads was different. As the area was affected by the mountain, the surface phosphorus loads intensity was significantly higher than other regions, causing the regional NPS P loads intensity beyond the adjustment ability of WL. On the other hand, it indicated that in different spatial scales, the WL area influence on NPS P loads approach was different, it still need further study in the future.

Table 5 is the correlation coefficient between WL area and the NPS P loads intensity of the three main land types. In the whole study area, the wetland area was negatively

http://www.aloki.hu ● ISSN 1589 1623 (Print) ● ISSN 1785 0037 (Online)
DOI: http://dx.doi.org/10.15666/aeer/1605_62196238
© 2018, ALÖKI Kft., Budapest, Hungary

correlated with the NPS P loads intensity in AL, and there was no significant correlation with the other two land use types. However, there were differences in different areas and land use types. For example, in R1 and R6, WL area was significantly negative correlated with NPS P loads intensity in three land use types, but in R2 and R5, there was no significant correlation between WL area and NPS P in three land use types. It indicated that the change of WL area plays a role in the NPS P loads intensity in the whole area.

The WL area played an important role in NPS P loads intensity of the entire study area, and it was significantly negatively correlation with NPS P in AL, but the adjustment ability of the WL to NPS P loads was limited.

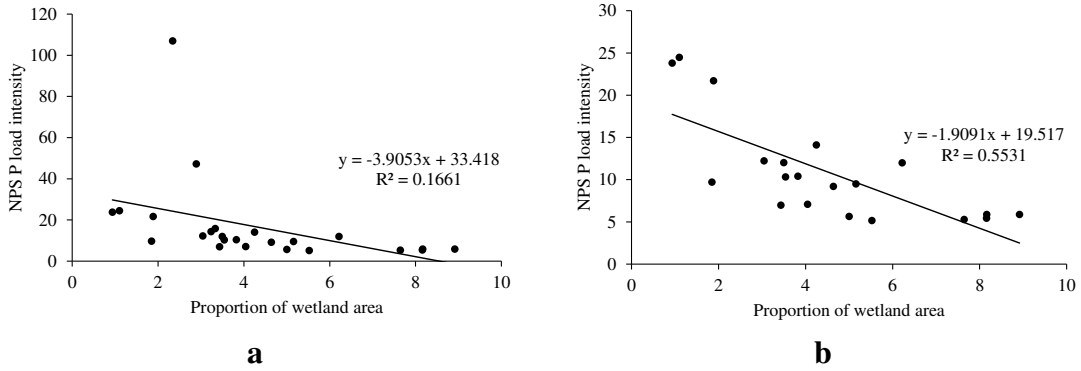

Figure 6. *Relation between wetland area and NPS P loads intensity.* ***a.*** *All regions and years;* ***b.*** *remove R5*

Table 5. *Correlation coefficient between the wetland area and different land NPS P loads intensity*

	Whole area	R1	R2	R3	R4	R5	R6
Al	-0.52**	-0.85**	-0.17	-0.27	-0.74**	-0.07	-0.67*
Cl	-0.28	-0.78**	-0.33	-0.3*	-0.53*	0.02	-0.66*
Fl	-0.34	-0.68**	0.03	-0.27	-0.05	-0.05	-0.69*

*Correlation is significant at the 0.05 level (2-tailed)
**Correlation is significant at the 0.01 level (2-tailed)

Arable land, construction land and forest land

The correlation coefficients between the NPS P loads intensity and the land area and landscape index were calculated for each of the three land use types (*Table 6*). It can be seen that the effect of land use change on the NPS P loads in different land use types was very complicated.

(1) The NPS P loads intensity in different land use types were affected by FRAC in different degrees, and FRAC impact on NPS P loads intensity in AL is minimal. There were only three regions that the NPS P loads intensity in AL were significantly correlated with FRAC, and there were five regions that the NPS P loads intensity in FL were significant correlated with FRAC. And the correlation coefficient of FRAC and the loads intensity in R2 was the highest, reaching 0.83. (2) Among the three types of land use, the NPS P loads intensity in CL was most affected by its own area. Except R4,

http://www.aloki.hu ● ISSN 1589 1623 (Print) ● ISSN 1785 0037 (Online)
DOI: http://dx.doi.org/10.15666/aeer/1605_62196238
© 2018, ALÖKI Kft., Budapest, Hungary

CL NPS P loads intensity in all regions were significantly correlated with its area, the highest correlation coefficient was 0.75. (3) Overall, three kinds of land NPS P loads intensities were positively correlated with FRAC, negatively correlated with CONTAG, which indicates that when the land use fragmentation was higher and the contagion was lower, the NPS P loads intensity was higher.

Table 6. *Correlation coefficient of NPS P loads intensity and landscape index in three land use type*

Land use type	Region	Area	CONTAG	FRAC	SHDI	SHEI
Al	R1	-0.04	-0.67**	0.73**	-0.01	0.59**
	R2	-0.23	-0.55**	0.55**	0.5*	0.54**
	R3	0.23	0.38*	0.11	-0.33*	-0.4**
	R4	-0.41	0.18	-0.29	-0.47	-0.23
	R5	-0.39**	-0.08	0.74**	0.09	0.15
	R6	0.48	-0.5	0.17	0.66*	0.55
Cl	R1	0.58**	-0.69**	0.59**	-0.02	0.6**
	R2	0.53**	-0.51*	0.83**	0.32	0.45*
	R3	0.33*	-0.2	0.52**	0.06	0.15
	R4	0.25	-0.31	0.28	-0.07	0.23
	R5	-0.32**	-0.1	0.64**	0.15	0.16
	R6	0.75**	-0.32	0.24	0.47	0.36
Fl	R1	0.02	-0.8**	0.62**	0.34	0.76**
	R2	0.27	-0.64**	0.78**	0.49*	0.6**
	R3	0.02	-0.04	0.43**	-0.08	-0.03
	R4	-0.14	-0.46	0.53*	0.1	0.35
	R5	0.52**	0	0.68**	0.03	0.06
	R6	0.67*	-0.42	0.19	0.58*	0.46

*Correlation is significant at the 0.05 level (2-tailed)
**Correlation is significant at the 0.01 level (2-tailed)

In R5, three land use types NPS P loads intensities were significantly correlated with the corresponding land area. Moreover, only in R5, the CL area negatively correlated with its NPS P loads intensity, and the NPS P loads intensity of the R5 region was hardly affected by the WL area (*Table 5*). This indicated that the NPS P load in mountainous area was mainly affected by terrain. In this case, the change of human activities on soil properties, and the blocking effect of artificial surface on rainfall erosion can lead to the decrease of NPS P load. Therefore, the effect of land use on NPS P load in mountainous and plain was different. In the future research, it is necessary to explore the mechanism of phosphorus loss in different slope conditions. In contrast to previous scholars' conclusions (Catherine et al., 2013; Tang et al., 2005), human activity does not only exacerbate the NPS P loads. In plain areas, human activities lead to NPS P loads intensity increased, while in mountainous areas, terrain plays a dominant role in NPS P loads intensity, human activities can reduce the NPS P loads.

In conclusion, three land use types, NPS P loads intensity in AL was the least affected by FRAC, NPS P loads intensity in CL was affected by its own area change most significantly. Human activities in the mountains may reduce the NPS P loads intensity.

http://www.aloki.hu ● ISSN 1589 1623 (Print) ● ISSN 1785 0037 (Online)
DOI: http://dx.doi.org/10.15666/aeer/1605_62196238
© 2018, ALÖKI Kft., Budapest, Hungary

Conclusion

In this study, six main natural rivers basin into the Chaohu Lake were chosen as the study area. The SEDD model was used to estimate the NPS P loads from 2000 to 2015, and a variety of typical land use types were selected to analyze the relationship between NPS P loads and land use change pattern, in order to explore the impact mechanism of land use on NPS P loads. The conclusions are:

(1) The NPS P loads intensity was positively correlated with FL area, and negatively correlated with AL, CL and WL area, and positively correlated with FRAC.

(2) Although the WL area was small, it played an important role in the NPS P loads in the basin, the WL area was significantly negative correlated with the NPS P loads intensity in AL. But its ability to adjust the NPS P loads was limited.

(3) Compared with AL, NPS P loads intensities of FL and CL were more susceptible to FRAC. The NPS P loads intensity of CL was more susceptible to its own area.

Land use patterns have an important impact on lake water quality through the impact of NPS pollution. Combining the basin and lake as a whole and analyzing the mechanism between land use, NPS pollution and lake water quality will be the focus of future research.

Acknowledgements. This work was funded by the National Natural Science Foundation of China (41671284). Acknowledgement for the data support from "Lake-Watershed Science Data Center, National Earth System Science Data Sharing Infrastructure, National Science & Technology Infrastructure of China. (http://lake.geodata.cn)". Land use data supported by the "Strategic Priority Research Program - Climate Change: Carbon Budget and Related Issues" of the Chinese Academy of Sciences, Grant No. XDA05050106.

REFERENCES

[1] Ahearn, D. S., Sheibley, R. W., Dahlgren, R. A., Anderson, M., Johnson, J., Tate, K. W. (2005): Land use and land cover influence on water quality in the last free-flowing river draining the western Sierra Nevada, California. – J Hydrol 313(3-4): 234-247.

[2] Bechmann, M., Stalnacke, P., Kvoerno, S., Eggestad, H. O., Oygarden, L. (2009): Integrated tool for risk assessment in agricultural management of soil erosion and losses of phosphorus and nitrogen. – Sci Total Environ 407(2): 749-759.

[3] Bingner, R. L., Theurer, F. D., Yuan, Y. (2003): AnnAGNPS Technical Processes. – USDA-ARS. National Sedimentation Laboratory, Oxford, MS.

[4] Borrelli, P., Marker, M., Panagos, P., Schutt, B. (2014): Modeling soil erosion and river sediment yield for an intermountain drainage basin of the Central Apennines, Italy. – Catena 114: 45-58.

[5] Braskerud, B. C. (2002): Factors affecting nitrogen retention in small constructed wetlands treating agricultural non-point source pollution. – Ecol Eng 18(3): 351-370.

[6] Bu, K., Zhang, S. W., Yan, Y. C., Wang, W. J., Zhang, Y. B. (2008): Soil erosion change characteristic of different watersheds of Sanjiang Plain during the past 50 years. – Scientia Geographica Sinica 28(3): 361-368.

[7] Bu, Z., Yang, L., Bu, Y., Wu, J. (2002): Soil erodibility (K) value and its application in Taihu lake catchment. – Acta Pedologica Sinica 39(3): 296-300.

[8] Cai, C., Ding, S., Shi, Z., Huang, L., Zhang, G. (2000): Study of applying USLE and geographical information system IDRISI to predict soil erosion in small watershed. – Journal of Soil and Water Conservation 14(2): 19-24.

http://www.aloki.hu ● ISSN 1589 1623 (Print) ● ISSN 1785 0037 (Online)
DOI: http://dx.doi.org/10.15666/aeer/1605_62196238
© 2018, ALÖKI Kft., Budapest, Hungary

[9] Catherine, A., Mouillot, D., Maloufi, S., Troussellier, M., Bernard, C. (2013): Projecting the impact of regional land-use change and water management policies on lake water quality: an application to periurban lakes and reservoirs. – Plos One 8(8).
[10] Chescheir, G. M., Skaggs, R. W., Gilliam, J. W. (1992): Evaluation of wetland buffer areas for treatment of pumped agricultural drainage water. – T Asae 35(1): 175-182.
[11] Delpla, I., Baures, E., Jung, A. V., Thomas, O. (2011): Impacts of rainfall events on runoff water quality in an agricultural environment in temperate areas. – Sci Total Environ 409(9): 1683-1688.
[12] Dong, G., Yang, S., Gao, Y., Bai, J., Wang, X., Zheng, D. (2014): Spatial evaluation of phosphorus retention in riparian zones using remote sensing data. – Environ Earth Sci 72(5): 1643-1657.
[13] El-Khoury, A., Seidou, O., Lapen, D. R., Que, Z., Mohammadian, M., Sunohara, M., Bahram, D. (2015): Combined impacts of future climate and land use changes on discharge, nitrogen and phosphorus loads for a Canadian river basin. – J Environ Manage 151: 76-86.
[14] Fu, G., Chen, S., McCool, D. K. (2006): Modeling the impacts of no-till practice on soil erosion and sediment yield with RUSLE, SEDD, and ArcView GIS. – Soil and Tillage Research 85(1): 38-49.
[15] Garnier, M., Lo Porto, A., Marini, R., Leone, A. (1998): Integrated use of GLEAMS and GIS to prevent groundwater pollution caused by agricultural disposal of animal waste. – Environ Manage 22(5): 747-756.
[16] Haggard, B. E., Storm, D. E., Tejral, R. D., Popova, Y. A., Keyworth, V. G., Stanley, E. H. (2001): Stream nutrient retention in three Northeastern Oklahoma agricultural catchments. – T Asae 44(3): 597-605.
[17] Hoffmann, C. C., Kjaergaard, C., Uusi-Kamppa, J., Hansen, H. C. B., Kronvang, B. (2009): Phosphorus retention in Riparian buffers: review of their efficiency. – J Environ Qual 38(5): 1942-1955.
[18] Hollis, G. (1975): The effect of urbanization on floods of different recurrence interval. – Water Resources Research 11(3): 431-435.
[19] Hundecha, Y., Bardossy, A. (2004): Modeling of the effect of land use changes on the runoff generation of a river basin through parameter regionalization of a watershed model. – J Hydrol 292(1): 281-295.
[20] Jiang, T., Huo, S., Xi, B., Su, J., Hou, H., Yu, H., Li, X. (2014): The influences of land-use changes on the absorbed nitrogen and phosphorus loadings in the drainage basin of Lake Chaohu, China. – Environ Earth Sci 71(9): 4165-4176.
[21] Kim, D. K., Kaluskar, S., Mugalingam, S., Arhonditsis, G. B. (2016): Evaluating the relationships between watershed physiography, land use patterns, and phosphorus loading in the bay of Quinte basin, Ontario, Canada. – J Great Lakes Res 42(5): 972-984.
[22] Kim, J., Choi, J., Choi, C., Park, S. (2013): Impacts of changes in climate and land use/land cover under IPCC RCP scenarios on streamflow in the Hoeya River Basin, Korea. – Sci Total Environ 452: 181-195.
[23] Kong, X., Dong, L., He, W., Wang, Q., Mooij, W. M., Xu, F. (2015): Estimation of the long-term nutrient budget and thresholds of regime shift for a large shallow lake in China. – Ecol Indic 52: 231-244.
[24] Li, H., Yang, G., Liu, X., Li, J. (2008): Response of non-point pollution output to landuse change and management strategy in Lihe River watershed of Taihu Lake Basin. – Journal of Natural Disasters 1: 027.
[25] Lin, C., He, M., Zhou, Y., Guo, W., Yang, Z. (2008): Distribution and contamination assessment of heavy metals in sediment of the Second Songhua River, China. – Environ Monit Assess 137(1): 329-342.
[26] Lin, C., Ma, R., Su, Z., Zhu, Q. (2015): Detection of critical LUCC indices and sensitive watershed regions related to lake algal blooms: a case study of Taihu Lake. – Int J Env Res Pub He 12(2): 1629-1648.

http://www.aloki.hu ● ISSN 1589 1623 (Print) ● ISSN 1785 0037 (Online)
DOI: http://dx.doi.org/10.15666/aeer/1605_62196238
© 2018, ALÖKI Kft., Budapest, Hungary

[27] Lin, C., Wu, Z., Ma, R., Su, Z. (2016): Detection of sensitive soil properties related to non-point phosphorus pollution by integrated models of SEDD and PLOAD. – Ecol Indic 60: 483-494.
[28] McGarigal, K., Marks, B. J. (1995): FRAGSTATS: Spatial Pattern Analysis Program for Quantifying Landscape Structure. General Technical Report PNW-GTR-351. – U.S. Department of Agriculture, Forest Service, Pacific Northwest Research Station, Portland, OR.
[29] Naramngam, S., Tong, S. T. Y. (2013): Environmental and economic implications of various conservative agricultural practices in the Upper Little Miami River basin. – Agr Water Manage 119: 65-79.
[30] Norton, L., Elliott, J. A., Maberly, S. C., May, L. (2012): Using models to bridge the gap between land use and algal blooms: An example from the Loweswater catchment, UK. – Environ Modell Softw 36: 64-75.
[31] Onyando, J. O., Kisoyan, P., Chemelil, M. C. (2005): Estimation of potential soil erosion for River Perkerra catchment in Kenya. – Water Resour Manag 19(2): 133-143.
[32] Ouyang, W., Huang, H., Hao, F., Guo, B. (2013): Synergistic impacts of land-use change and soil property variation on non-point source nitrogen pollution in a freeze-thaw area. – J Hydrol 495: 126-134.
[33] Pan, B., Yi, W., Wang, X., Qin, H., Wang, J., Qiao, Y. (2011): Inversion of the lake total nitrogen concentration by multiple regression kriging model based on hyperspectral data of HJ-1A. – Spectrosc Spect Anal 31(7): 1884-1888.
[34] Recanatesi, F., Ripa, M. N., Leone, A., Luigi, P., Luca, S. (2013): Land use, climate and transport of nutrients: evidence emerging from the lake vicocase study. – Environ Manage 52(2): 503-513.
[35] Shang, G., Shang, J. (2007): Spatial and temporal variations of eutrophication in western Chaohu Lake, China. – Environ Monit Assess 130(1): 99-109.
[36] Sharpley, A. N., Williams, J. R. (1990): EPIC, Erosion/Productivity Impact Calculator. – Technical Bulletin, USDA, Washington, DC.
[37] Stefano, C. D., Ferro, V. (2007): Evaluation of the SEDD model for predicting sediment yield at the Sicilian experimental SPA2 basin. – Earth Surface Processes and Landforms 32(7): 1094-1109.
[38] Taguas, E. V., Moral, C., Ayuso, J. L., Perez, R., Gomez, J. A. (2011): Modeling the spatial distribution of water erosion within a Spanish olive orchard microcatchment using the SEDD model. – Geomorphology 133(1-2): 47-56.
[39] Tang, Z., Engel, B. A., Pijanowski, B. C., Lim, K. J. (2005): Forecasting land use change and its environmental impact at a watershed scale. – J Environ Manage 76(1): 35-45.
[40] Tasdighi, A., Arabi, M., Osmond, D. L. (2017): The relationship between land use and vulnerability to nitrogen and phosphorus pollution in an urban watershed. – J Environ Qual 46(1): 113-122.
[41] Wang, S., Dou, H. (1998): Chinese Lakes. – Science Press, Beijing.
[42] Wang, S., Jiang, X., Jin, X. (2011): Classification and pollution characteristic analysis for inflow rivers of Chaohu Lake. – Environmental Science 32(10): 2834-2839.
[43] Wang, X., Wang, Q., Wu, C., Liang, T., Zheng, D., Wei, X. (2012): A method coupled with remote sensing data to evaluate non-point source pollution in the Xin'anjiang catchment of China. – Sci Total Environ 430: 132-143.
[44] Wang, X., Wang, X., Zhu, L., Ma, Y., Wu, C., Wang, Q., Feng, A., Chen, M. (2015): Spatial analysis on diffuse pollution and algal bloom characteristic with remote sensing in Chao Lake Basin. – China Environmental Science 35(5): 1511-1519.
[45] Wilson, C. O., Weng, Q. (2011): Simulating the impacts of future land use and climate changes on surface water quality in the Des Plaines River watershed, Chicago Metropolitan Statistical Area, Illinois. – Sci Total Environ 409(20): 4387-4405.

http://www.aloki.hu ● ISSN 1589 1623 (Print) ● ISSN 1785 0037 (Online)
DOI: http://dx.doi.org/10.15666/aeer/1605_62196238
© 2018, ALÖKI Kft., Budapest, Hungary

[46] Wu, C., Li, S., Ren, H., Yao, X., Huang, Z. (2012a): Quantitative estimation of vegetation cover and management factor in USLE and RUSLE models by using remote sensing data: a review. – The Journal of Applied Ecology 23(6): 1728-1732.
[47] Wu, L., Long, T., Liu, X., Guo, J. (2012b): Impacts of climate and land-use changes on the migration of non-point source nitrogen and phosphorus during rainfall-runoff in the Jialing River Watershed, China. – J Hydrol 475: 26-41.
[48] Xu, L., Xu, X., Meng, X. (2013): Risk assessment of soil erosion in different rainfall scenarios by RUSLE model coupled with Information Diffusion Model: A case study of Bohai Rim, China. – Catena 100: 74-82.
[49] Yan, W., Wang, X. (1998): Preliminary study on non3point sources pollution in the Chaohu Lake drainage basin. – Scientia Geographica Sinica 18(3): 263r267.
[50] Yang, M., Li, X., Hu, Y., He, X. (2012): Assessing effects of landscape pattern on sediment yield using sediment delivery distributed model and a landscape indicator. – Ecol Indic 22: 38-52.
[51] Zhang, K., Peng, W., Yang, H. (2007): Soil erodibility and its estimation for agricultural soils in China. – Acta Pedologica Sinica 44(1): 7-13.
[52] Zhou, H., Gao, C. (2011): Assessing the risk of phosphorus loss and identifying critical source areas in the Chaohu Lake watershed, China. – Environ Manage 48(5): 1033-1043.
[53] Zhou, W., Wu, B. (2008): Assessment of soil erosion and sediment delivery ratio using remote sensing and GIS: a case study of upstream Chaobaihe River catchment, north China. – Int J Sediment Res 23(2): 167-173.

http://www.aloki.hu ● ISSN 1589 1623 (Print) ● ISSN 1785 0037 (Online)
DOI: http://dx.doi.org/10.15666/aeer/1605_62196238
© 2018, ALÖKI Kft., Budapest, Hungary

BIOMASS, CARBON STOCKS AND CO_2 SEQUESTRATION IN THREE DIFFERENT AGED IRRIGATED *POPULUS DELTOIDES* BARTR. EX MARSH. BUND PLANTING AGROFORESTRY SYSTEMS

YASIN, G.[1*] – NAWAZ, M. F.[1] – SIDDIQUI, M. T.[1] – NIAZI, N. K.[2,3]

[1]*Department of Forestry and Range Management, University of Agriculture Faisalabad, Pakistan*

[2]*Institute of Soil and Environmental Sciences, University of Agriculture Faisalabad, Pakistan*

[3]*Southern Cross GeoScience, Southern Cross University, Lismore, NSW 2480, Australia*

**Corresponding author*
e-mail: yasin_2486@yahoo.com; phone: +92-344-855-5970

(Received 23rd May 2018; accepted 14th Aug 2018)

Abstract. Carbon sequestration needs to be accompanied by socio-economic enhancements, especially, in developing countries like Pakistan. Agroforestry has been considered as an ancient practice throughout the country but the knowledge about its impacts on tree and soil carbon storage is minimal. Growth, biomass, carbon stocks and CO_2 sequestration rate in three different age classes of *Populus deltoides* Bartr. Ex Marsh. planted in linear patterns along boundaries (bund planting) were estimated in three subdivisions (Tehsils) of district Chiniot (Bhawana, Chiniot and Lalian) of Punjab, Pakistan. For estimating tree biomass and carbon stocks, allometric equation was used and soil organic carbon (SOC) was assessed at two depths (0-15 and 15-30 cm). The diameter at breast height (DBH) and height of trees were higher at 4-6 years as compared to 2-4 years and the plant biomass was found the maximum (90.55 Mg ha^{-1}) in Tehsil Lalian at 6 years. Total carbon stocks and CO_2 sequestration rate varied from 0.89 Mg ha^{-1} and 1.63 Mg ha^{-1} yr^{-1} at 2 years to 43.54 Mg ha^{-1} and 26.58 Mg ha^{-1} yr^{-1} at 6 years, respectively, across all Tehsils. Total SOC stocks were maximum (43.73 Mg ha^{-1}) at 6 years in Tehsil Lalian while minimum 27.92 Mg ha^{-1} in Tehsil Bhawana at 2 years. Overall, soil + tree carbon stocks increased with age and was maximum at 6 years: 61.54 Mg ha^{-1}, 80.76 Mg ha^{-1}, and 87.27 Mg ha^{-1} in Tehsil Bhawana, Chiniot, and Lalian, respectively. The above results encouraged the establishment of *P. deltoides* planting along farm crops as an important possibility for increased carbon storage and mitigation of atmospheric accumulation of CO_2.
Keywords: *agroforestry, climate change, tree biomass, carbon capture, agriculture, environment*

Introduction

The agriculture sector of Pakistan is at risk and facing diverse challenges such as diminution of natural resources (agriculture, forests and water) and severe climatic changes due to increasing population pressure and growing needs of food, feed, fodder, pulp, fuel wood and timber (Saifullha, 2017). Being a less developed country, Pakistan is ranked 7th among the most vulnerable countries in the world (Kreft et al., 2017). Therefore, to ensure sustainability in agriculture and to fulfill the food requirements of the enormous population, suitable methods of climate change mitigation have to be adapted by the country (Nawaz et al., 2017b).

The contribution of agriculture in the anthropogenic emissions of greenhouse gases (GHGs) ranges from 10-12% around the globe (Smith et al., 2008). However, tree crop combination (agroforestry) has been documented by UNFCCC (United Nations

http://www.aloki.hu ● ISSN 1589 1623 (Print) ● ISSN 1785 0037 (Online)
DOI: http://dx.doi.org/10.15666/aeer/1605_62396252
© 2018, ALÖKI Kft., Budapest, Hungary

Framework Convention on Climate Change) as GHG mitigation opportunity because of its high carbon sequestering potential and fast growth rate of farm trees (Watson et al., 2000; Updegraff et al., 2004; Chauhan et al., 2009). Planting of trees and shrubs along crops or on grazed pastures on the same land area is known as agroforestry (Nair et al., 2009). In developing countries, like Pakistan, agroforestry has recently attained growing attention for mitigating GHG emissions. Agroforestry systems can store the higher amount of carbon as compared to conventional plantations (Hergoualc'h et al., 2012).

In recent years, agroforestry has got attention as a portion climate-smart-agriculture and is repeatedly declared as a prospective source to mitigate the adverse climatic conditions (Ajit et al., 2014). In Pakistan, agroforestry provides fuelwood, timber, fodder, fertilizer, fiber and contribute in the provision of food, maintain livelihoods, cope to overcome poverty and promotes the prolific and irrepressible cropping and agricultural environment, thus playing a vital role in the daily life of rural population of the country (Nawaz et al., 2016). Moreover, agroforestry has been getting noteworthy considerations by the researchers as well as by policymakers for its apparent ability to sequester carbon, alleviation of poverty, economic growth (DAC, 2014) and considered as an important part of 'Green Pakistan' movement in the country.

Poplar (*Populus deltoides* Bartr. Ex Marsh.) based agroforestry system has received a wide recognition throughout the globe, covering an area of 1.5 million ha (Kutsokon et al., 2015). The area is supposed to increase up to many folds in near future by planting the poplar in marginal agricultural lands to fullfil the needs of fuel and timber in developing regions of the world (Nielsen et al., 2014; Jha, 2018). Because of its fast growth rate, compatibility with crops and high industrial demand, poplar has got a wide acceptance by the farmers of Pakistan, especially, in Punjab during the last two decades. The branches, leaves and sometimes roots are used as fuelwood by the local dwellers while timber of the tree is used in plywood industries of the country. The tree has an enormous potential to store carbon and sequester CO_2 owing to its fast growth habit and wider adaptability throughout the country (Arora et al., 2014; Qureshi, 2005).

A number of studies have been documented on biomass, productivity, functioning, structure and carbon stocks of Poplar throughout the world (Das and Chaturvdi, 2005; Fang et al., 2007; Rizvi et al., 2011; Arora et al., 2014). Most of these studies were carried out in plantations and/or under different agroforestry systems, however, the studies in bund planting based agroforestry system under semiarid climate are rare. Moreover, in Pakistan, the information regarding biomass, productivity, carbon stock and rate of CO_2 sequestration of bund planted poplar based agroforestry by age under the set of local environmental conditions is scanty. Keeping in mind the above situation, the study was formulated to investigate the hypothesis that *P. deltoides* (poplar) planted linearly along field bunds (bund planting) store significant amount of carbon and thus mitigate CO_2 from the environment. The second hypothesis was that site factor can play a significant role in c sequestration owing to minor climatic differences and/or different agroforestry practices. The study was performed in three Tehsils of District Chiniot: Bhawana, Chiniot, and Lalian, with the major objective to estimate the growth, biomass, carbon storage and its dissemination in the various carbon pools (above ground biomass and belowground biomass + soil) among three different age classes of *P. deltoides*.

http://www.aloki.hu ● ISSN 1589 1623 (Print) ● ISSN 1785 0037 (Online)
DOI: http://dx.doi.org/10.15666/aeer/1605_62396252
© 2018, ALÖKI Kft., Budapest, Hungary

Materials and methods

Ethics statement

The current study was carried out in three administrative subdivisions (Tehsils) of District Chiniot (*Fig. 1*). Tree inventory and soil sampling were carried out in rural areas of these Tehsils with special permission from the farmers. It is confirmed that during sampling no harm was done to the farm crops and/or farm trees (*P. deltoides*).

Site description

The studied district shared boundary with four districts: Faisalabad on the south-east, Hafizabad on the north, Jhang on the south and Sargodha on the west. The whole district was comprised of three subdivisions (Tehsils): Bhawana, Chiniot, and Lalian, with a total area of 1,020 square miles. Geographically, this region is divided into two surface levels, i.e. low-level river valley in the center along river Chenab and old Sandal Bar area present along the extreme east. Areas near River Chenab experience severe floods during monsoon season. The region experiences very long summers and short severe winters. The dry period starts from early October and lasts until mid-July (Nawaz et al., 2016). The annual rainfall ranges from 345 mm (Tehsil Lalian) to 324 mm (Tehsil Bhawana). The mean annual temperature ranges from 24 to 24.3 °C with an average June high of 34.3 °C and January low of 11.8 °C among all three Tehsils of District Chiniot. (https://en.climate-data.org).

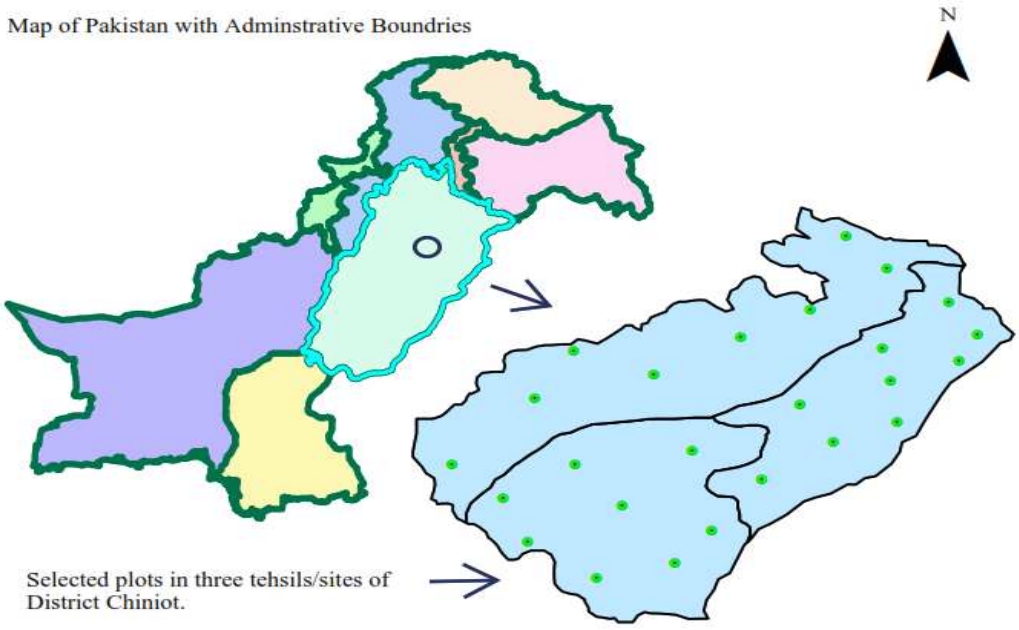

Figure 1. *Map of Pakistan with administrative boundaries and study area map showing the distribution of sampled plots in three Tehsils of District Chiniot*

Biomass sampling, carbon stocks, and CO_2 sequestration

A nondestructive approach was used to estimate the tree above and belowground biomass. Inventory data was collected from selected villages of each Tehsil. For that purpose, field visits were carried out during April 2016 and 2 plots of 0.405 ha (1 acre)

http://www.aloki.hu ● ISSN 1589 1623 (Print) ● ISSN 1785 0037 (Online)
DOI: http://dx.doi.org/10.15666/aeer/1605_62396252
© 2018, ALÖKI Kft., Budapest, Hungary

for each age group, which have *P. deltoides* planted linearly along croplands were randomly selected from each village (Nawaz et al., 2018; Murthy et al., 2013). The height and diameter at breast height (DBH) of all the *P. deltoides* trees planted by farmers on each plot were measured. The aboveground biomass was measured by using species-specific allometric equation from the literature (Arora et al., 2014). The belowground biomass was assumed to be 26% of the aboveground biomass (Cairns et al., 1997). Inventory parameters: DBH and height were then used to calculate the individual tree biomass of each age group which was then converted to biomass per plot. Carbon stock for each age group was calculated by assuming that the dry mass is 48.1% carbon of biomass (Thomas and Martin, 2012). The calculated weight of carbon content was then converted to CO_2 sequestered by trees of each age group by multiplying with 3.6663 (Afzal and Aqeela, 2013).

Soil sampling and soil carbon stocks

Soil sampling was done randomly at 5 places for each age group of *P. deltoides* at two depths (0-15 cm and 15-30 cm). Samples were collected in cardinal directions under the tree canopy as well as outside the tree canopy. To get a composite sample, these collected samples were then mixed together for each depth. Overall, 90 samples (3 ages × 3 Tehsils × 2 depths × 5 replicates), 10 for each age class and 30 from each Tehsil were collected. All of the soil samples within the same soil depth were pooled together and air dried. The Walkley Black method was used to calculate the soil organic carbon (Walkley and Black, 1934). Metal core having a height of 4 cm and an internal diameter of 5 cm was used to determine the bulk density at two depths (0-15 cm and 15-30 cm) by a procedure described by (Arora et al., 2014). Soil carbon per hectare was calculated by multiplying the values of bulk density, soil depth and %age of organic carbon content (Joa Carlos et al., 2001).

Statistical analysis

Descriptive statistics and the data regarding soil carbon and bulk density was analyzed for each age group by using two-way analysis of variance (ANOVA). The mean comparison was carried out by least significant difference test (LSD) at ($p \leq 0.05$) by using SAS 9.4 & Statistica 10 statistical softwares.

Results

Tree growth and biomass

The growth parameters indicated the increasing trend with increased age, a steady increase in DBH and height was noted among all three Tehsils of District Chiniot (*Table 1*). The DBH and height of *P. deltoides* increased from 1.98 cm and 1.83 m at the 2 years to 24.57 cm and 20.89 m at the 6 years, respectively. Among all the Tehsils, the maximum mean DBH (6.84 ± 1.58 cm, 12.46 ± 2.20 cm, and 20.43 ± 4.08 cm) was noted in Tehsil Lalian at the 2, 4 and 6 years, respectively. Whereas, for 2-year-old age, maximum mean height (5.52 ± 1.23 m) was calculated in Tehsil Bhawana and for 4 and 6 years, maximum mean height (9.28 ± 1.85 m and 13.45 ± 1.86 m) was estimated in Tehsil Lalian. Positive and significant relationship between tree age and DBH ($r = 0.92$, $p < 0.001$), tree age and Height ($r = 0.60$, $p < 0.001$) illustrate that both the parameters were responsible for biomass increment of *P. deltoides*. The AGB (aboveground

http://www.aloki.hu ● ISSN 1589 1623 (Print) ● ISSN 1785 0037 (Online)
DOI: http://dx.doi.org/10.15666/aeer/1605_62396252
© 2018, ALÖKI Kft., Budapest, Hungary

biomass), BGB (belowground biomass), and PB (plant biomass) recorded for different age classes of the *P. deltoides* viewed in the order: 6 > 4 > 2. Across all the three age classes of the *P. deltoides* bund agroforestry plantation, higher biomass proportion was noted in stem biomass as compared to the other parts. The AGB and BGB of the *P. deltoides* was increased with increasing age among all three Tehsils with maximum in Tehsil Lalian: 1.89 Mg ha^{-1} and 0.49 Mg ha^{-1} (2 years), 17.67 Mg ha^{-1} and 4.60 Mg ha^{-1} (4 years), and 71.85 Mg ha^{-1} and 18.68 Mg ha^{-1} (6 years), while minimum in Tehsil Bhawana 1.47 Mg ha^{-1} and 0.38 Mg ha^{-1} (2 years), 9.15 Mg ha^{-1} and 2.38 Mg ha^{-1} (4 years), and 37.80 Mg ha^{-1} and 9.85 Mg ha^{-1} (6 years), respectively. The plant biomass of the *P. deltoides* in the study district increased from 1.86 Mg ha^{-1} at the 2 years age to 90.55 Mg ha^{-1} at the 6 years plots, with the maximum increase found in the 4-6 years age (*Table 2*).

Table 1. *The general status of three age classes of Populus deltoides planted linearly along crops among three Tehsils of District Chiniot (mean ± SD)*

Tree age (years)	Measured parameters	Tehsils/sites								
		Bhawana			Chiniot			Lalian		
		Mean±SD	Mini.	Max.	Mean±SD	Mini.	Max.	Mean±SD	Mini.	Max
2	DBH (cm)	5.50±1.44	2	8.66	4.45±1.26	1.98	8	6.84±1.58	4.45	10.11
	Height (m)	5.52±1.23	1.98	7.86	4.71±1.34	1.83	8.56	5.16±1.52	1.88	9.29
	Tree density ha^{-1}	28.01±9.59	17.32	39.54	66.23±23.14	34.60	88.96	23.6±7.67	14.83	39.53
4	DBH (cm)	11.85±1.72	6.38	15.87	11.50±2.16	5.98	18.11	12.46±2.20	6.98	19.02
	Height (m)	8.27±1.48	4.94	12.19	8.87±1.91	4.96	12.77	9.28±1.85	5.88	13.83
	Tree density ha^{-1}	25.77±15.15	9.88	54.36	46.6±31.27	21.47	77.87	49.24±20.30	17.30	79.19
6	DBH (cm)	15.45±2.49	15.76	21.51	17.44±3.70	16	22.67	20.43±4.08	17.98	24.57
	Height (m)	13.05±1.86	7.4	17.03	12.86±2.18	8.68	18.5	13.45±1.86	9.44	20.89
	Tree density ha^{-1}	26.19±3.74	22.24	32.12	36.71±12.05	19.77	56.84	41.48±16.70	24.71	67.19

DBH: Diameter at breast height. Mini: Minimum. Max: Maximum

Table 2. *Biomass (Mg ha^{-1}) distribution in P. deltoides by age among three Tehsils of District Chiniot*

Age (years)	Biomass (Mg ha^{-1})								
	Tehsils/sites								
	Bhawana			Chiniot			Lalian		
	AGB	BGB	PB	AGB	BGB	PB	AGB	BGB	PB
2	1.47	0.38	1.86	1.65	0.43	2.08	1.89	0.49	2.38
4	9.15	2.38	11.53	15.70	4.08	19.79	17.67	4.60	22.27
6	37.89	9.85	47.75	64.27	16.71	80.98	71.85	18.68	90.55

AGB, BGB and PB refer to aboveground biomass, belowground biomass and plant biomass, respectively

Tree carbon stocks and CO_2 sequestration

Tree carbon stocks and CO_2 sequestration was estimated at Tehsil level in three different age classes of the *P. deltoides* planted along the farm crops on bunds by farmers. Across all age groups, the aboveground carbon stocks (AGCS), belowground carbon stock (BGCS), total plant carbon stock (TPCS), CO_2 sequestration and CO_2

http://www.aloki.hu ● ISSN 1589 1623 (Print) ● ISSN 1785 0037 (Online)
DOI: http://dx.doi.org/10.15666/aeer/1605_62396252
© 2018, ALÖKI Kft., Budapest, Hungary

sequestration rate were highest at the 6-year-old plots and the lowest at the 2-year-old plots given in *Table 3*. A positive and significant linear relationship was found between plot-level tree carbon stock and tree basal area with R^2 = 0.98 as represented in *Figure 2*.

Table 3. *Carbon stock (Mg ha^{-1}), CO_2 sequestration (Mg ha^{-1}) and CO_2 sequestration rate ha^{-1} yr^{-1} in P. deltoides by age among three Tehsils of Distirct Chiniot*

Carbon stock (Mg ha^{-1}), CO_2 sequestration (Mg ha^{-1}) and CO_2 sequestration rate ha^{-1}yr^{-1}															
Age (years)	Tehsils/sites														
	Bhawana					Chiniot					Lalian				
	AGCS	BGCS	TPCS	CO_2 Seq.	CO_2 Seq. rate	AGCS	BGCS	TPCS	CO_2 Seq.	CO_2 Seq. rate	AGCS	BGCS	TPCS	CO_2 Seq.	CO_2 Seq. rate
2	0.71	0.18	0.89	3.27	1.63	0.80	0.21	1	3.67	1.83	0.91	0.24	1.14	4.19	2.09
4	4.40	1.14	5.55	20.31	5.08	7.44	1.96	9.52	34.86	8.72	8.50	2.21	10.71	39.24	9.81
6	18.23	4.74	22.97	84.13	14.02	30.91	8.04	38.95	142.68	23.78	34.56	8.99	43.54	159.50	26.58

AGCS, BGCS and TPCS refer to aboveground carbon stock, belowground carbon stock and total plant carbon stock, respectively

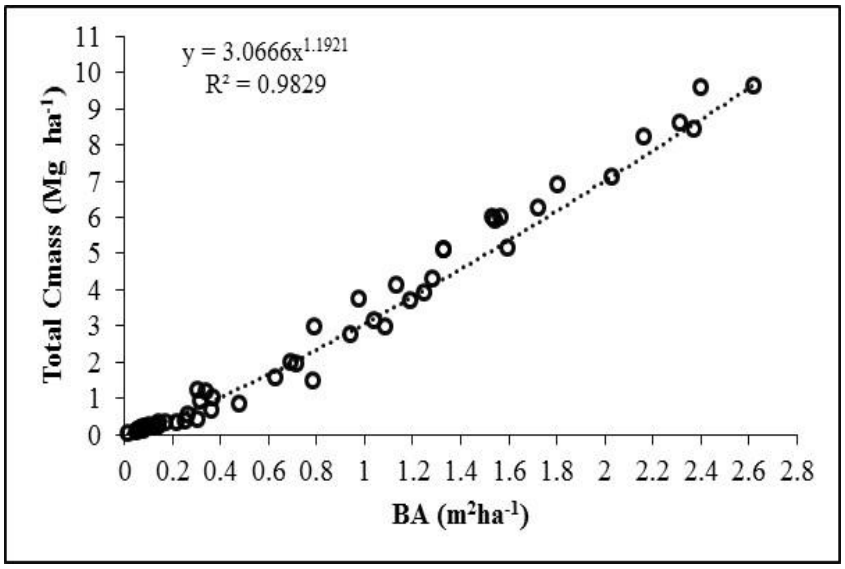

Figure 2. *Allometric model representing relationship between total carbon mass (Mg ha^{-1}) and tree basal area (BA m^2 ha^{-1}) for inventory plots of P. deltoides planted linearly along farm crops in District Chiniot*

Across all three Tehsils, the above and belowground carbon stocks at the 2-year-old plots were increased from 0.71 Mg ha^{-1} and 0.18 Mg ha^{-1} to 0.91 Mg ha^{-1} and 0.24 Mg ha^{-1}, with minimum values in Tehsil Bhawana and maximum in Tehsil Lalian. Similar trends were noted about the above and belowground distribution of carbon contents at the 4 and 6-year-old plots, maximum values accounted for Tehsil Lalian (8.50 Mg ha^{-1}, 2.21 Mg ha^{-1} and 34.56 Mg ha^{-1}, 8.99 Mg ha^{-1}), followed by Chinot (7.44 Mg ha^{-1}, 1.96 Mg ha^{-1} and 30.91 Mg ha^{-1}, 8.04 Mg ha^{-1}), while minimum carbon stocks were estimated in Tehsil Bhawana (4.40 Mg ha^{-1}, 1.14 Mg ha^{-1} and 18.23 Mg ha^{-1}, 4.74 Mg

http://www.aloki.hu ● ISSN 1589 1623 (Print) ● ISSN 1785 0037 (Online)
DOI: http://dx.doi.org/10.15666/aeer/1605_62396252
© 2018, ALÖKI Kft., Budapest, Hungary

ha^{-1}), respectively. The total plant carbon stocks increased from 0.89 Mg ha^{-1} at the 2 years age class (Tehsil Bhawana) to 43.54 Mg ha^{-1} at the 6 years (Tehsil Lalian) with a maximum increase occurred in the 4-6 years age class. There was a positive and significant correlation was observed between biomass carbon and tree age ($r = 0.42$, $p < 0.001$). The CO_2 sequestration and CO_2 sequestration rate was increased from 84.13 Mg ha^{-1} and 14.02 Mg ha^{-1} yr^{-1} at 2 years of and reached up to a maximum of 159.50 Mg ha^{-1} and 26.58 Mg ha^{-1} yr^{-1} at 6 years in this study.

Soil organic carbon and carbon stocks

Soil organic carbon (SOC %) revealed a decreasing trend with the increase of soil depth across all age classes in the three Tehsils: SOC was higher in upper soil (0-15 cm) as compared to the sub-soil (15-30 cm). The difference in soil organic carbon because of age was significant (*Table 4*). SOC, in upper soil, was 36.97% greater in Tehsil Bhawana, 32.52% in Tehsil Chiniot and 38.28% in Tehsil Lalian in the 6 years as compared to the 2 years of *P. deltoides*. Bulk density (BD) showed antagonistic results as compared to SOC. However, BD increased with tree age across all the Tehsils. For all age classes, bulk density was more in the subsoil as compared to the upper soil surface (*Table 4*). It decreased from 1.50 g cm^{-3} at 2 years to 1.28 g cm^{-3} at 6 years in surface soil (0-15 cm).

Table 4. *Organic carbon (%) and bulk density (g cm^{-3}) in P. deltoides by age planted linearly among three Tehsils of District Chiniot*

Age (years)	Tehsils/sites	Organic carbon %		Bulk density (g cm^{-3})	
		0-15 cm	15-30 cm	0-15 cm	15-30 cm
2	Bhawana	0.75±0.07^{f}	0.51±0.03 ^{f}	1.47±0.02 ^{ab}	1.48±0.03 ^{bc}
	Chiniot	0.83±0.05^{e}	0.57±0.04 ^{def}	1.43±0.04 ^{bc}	1.51±0.02 ^{ab}
	Lalian	0.79±0.07^{ef}	0.53±0.06 ^{ef}	1.50±0.07 ^{a}	1.53±0.06 ^{a}
4	Bhawana	0.91±0.04^{cd}	0.59±0.03 ^{de}	1.31±0.04 ^{efg}	1.44±0.06 ^{cd}
	Chiniot	0.86±0.05^{de}	0.62±0.06 ^{cd}	1.40±0.04 ^{cd}	1.41±0.02 ^{cde}
	Lalian	0.95±0.06^{c}	0.66±0.05 ^{c}	1.37±0.05 ^{cde}	1.44±0.05 ^{cd}
6	Bhawana	1.19±0.04^{b}	0.78±0.06 ^{b}	1.28±0.04 ^{g}	1.34±0.06 ^{f}
	Chiniot	1.23±0.03^{ab}	0.86±0.05 ^{a}	1.31±0.03 ^{fg}	1.36±0.02 ^{ef}
	Lalian	1.28±0.03^{a}	0.85±0.06 ^{a}	1.35±0.03 ^{def}	1.39±0.03 ^{def}

n = 5 for each age class and values are mean with standard deviation. Means having same letters are not significantly different at a probability level of 5%

With the increase in tree age soil organic carbon stocks (SOCS) increased, regardless of soil depth across three Tehsils of District Chiniot (*Table 5*). In surface soil, SOCS were increased maximum 36.33% in Tehsil Chiniot while minimum 28.01% in Tehsil Bhawana at 6 years than in 2-year-old trees. At 15-30 cm depth, SOCS were decreased from 11.37 Mg ha^{-1} at the 2-year-old trees (Tehsil Bhawana) to 17.76 Mg ha^{-1} at 6-year-old trees. Tree age and SOC indicate a positive and significant correlation at both soil depths ($r = 0.86$ and $r = 0.80$, $p < 0.001$). The carbon sequestration rate (CSR) at 0-30 cm soil was greater in Tehsil Lalian (2.27 Mg ha^{-1} yr^{-1}) as compared to other two Tehsils at 6-year-old trees.

http://www.aloki.hu ● ISSN 1589 1623 (Print) ● ISSN 1785 0037 (Online)
DOI: http://dx.doi.org/10.15666/aeer/1605_62396252
© 2018, ALÖKI Kft., Budapest, Hungary

Table 5. *Effect of three age classes of P. deltoides on soil organic carbon stock among three Tehsils of District Chiniot*

Age (years)	Tehsils/sites	Soil organic carbon stock (Mg ha^{-1})	
		0-15 cm	15-30 cm
2	Bhawana	16.55±1.88 ^{e}	11.37±0.66 ^{e}
	Chiniot	17.78±1.39 ^{de}	13.01±1.09 ^{d}
	Lalian	17.87±1.59 ^{de}	12.22±1.53 ^{de}
4	Bhawana	19.20±0.66 ^{cd}	12.67±0.79 ^{de}
	Chiniot	18.19±1.27 ^{cd}	13.29±1.43 ^{cd}
	Lalian	19.58±1 ^{c}	14.49±1.28 ^{bc}
6	Bhawana	22.99±0.9 ^{b}	15.58±1.28 ^{b}
	Chiniot	24.24±0.88 ^{b}	17.57±1.20 ^{a}
	Lalian	25.97±0.74 ^{a}	17.76±1.20 ^{a}

Total carbon stocks

Keeping in mind the guidelines of Intergovernmental Panel on Climate Change (IPCC), total carbon stock was (biomass + soil) calculated by considering the soil C up to 30 cm soil depth. The amount of total carbon increased with an increase of tree age in all three Tehsils (*Table 6*). The maximum total carbon stock at 2-year-old trees was estimated in Tehsil Chiniot (31.98 Mg ha^{-1} whereas at 4 and 6-year-old age trees higher total carbon stocks (44.75 Mg ha^{-1} and 87.27 Mg ha^{-1}) were estimated in Tehsil Lalian. Overall the total carbon stock increased from 28.81 Mg ha^{-1} at 2 years of age to 87.27 Mg ha^{-1} at 6 years of age among all three Tehsils. A significant and positive correlation was studied between total carbon stock and age of the *P. deltoides* trees ($r = 0.90$, $p < 0.001$).

Table 6. *Total carbon stock (tree + soil) in P. deltoides by age among three Tehsils of District Chiniot*

Age (years)	Tehsils/sites	Total carbon stock (Mg ha^{-1})		
		Total biomass carbon	Soil organic carbon (0-15 cm + 15-30 cm)	Total carbon
2	Bhawana	0.89	27.92	28.81
	Chiniot	1	30.98	31.98
	Lalian	1.14	30.09	31.23
4	Bhawana	5.55	31.87	37.42
	Chiniot	9.52	31.48	41
	Lalian	10.71	34.04	44.75
6	Bhawana	22.97	38.57	61.54
	Chiniot	38.95	41.81	80.76
	Lalian	43.54	43.73	87.27

Discussion

The present study supports our hypothesis that biomass and carbon stocks in *P. deltoides* increased markedly in both above and belowground parts with tree age among

http://www.aloki.hu ● ISSN 1589 1623 (Print) ● ISSN 1785 0037 (Online)
DOI: http://dx.doi.org/10.15666/aeer/1605_62396252
© 2018, ALÖKI Kft., Budapest, Hungary

three Tehsils of District Chiniot. For example, Tehsil Lalian has the highest biomass than other two Tehsils because of higher tree density and greater DBH of all age classes. This can be attributed to better climatic conditions: slightly higher rainfall (345 mm annually) as compared to Tehsil Chiniot and Bhawana or there may be other factors such as agroforestry awareness and agroforestry practices. Similar trends of growth of *P. deltoides* planted in agroforestry and plantations have been reported in various studies (Jain et al., 2017; Chauhan et al., 2011; Kanime et al., 2013). Moreover, *P. deltoides* at 6 years age, accumulate more biomass in all Tehsils (47.75 Mg ha-1 to 90.55 Mg ha-1) than a 7 years old *E. camaldulensis* (62.35 Mg ha^{-1}) and 6 years old *S. siamea* (45.39 Mg ha^{-1}) described by Harmand et al. (2004). Though, the results of our study concerning aboveground biomass fall in line to those described by Rizvi et al. (2011) for *P. deltoides* in agroforestry systems. Overall, the findings of the biomass of the present study are comparable to other agroforestry trees such as *E. camaldulensis* hybrid, 95 Mg ha^{-1} at 7 years and *D. sissoo*, 50.3 to 122.7 Mg ha^{-1} (Negi and Sharma, 1985; Lodhiyal and Lodhiyal, 2003). The findings of the present study different as compared to previous studies might be because of climatic conditions, growth pattern, site quality, species density, age and cultural plus management practices.

In the present study we have quantified the above and belowground carbon stock in bund planted *P. deltoides* based agroforestry system at early growth stages. The findings of present study are based on bund planted agroforestry system while the previous studies were mostly carried out in different plantations and agroforetsry systems under different climatic conditions. For instance, mean carbon stock in a *P. deltoides* based agroforestry system in temperate region has been reported 15.1 t C ha^{-1} at 111 trees ha^{-1} (Peichl et al., 2006). The amount of carbon found by Fang et al. (2010) in 5 years old *P. deltoides* trees was only 7.8 t C ha^{-1}, far lesser as compared with our findings. The present estimates of total carbon stocks were maximum at 6 years of age across all Tehsils (22.7 Mg ha^{-1} to 43.54 Mg ha^{-1}), much higher as compared to the findings of Chauhan et al. (2010) for *P. deltoides*, Nawaz et al. (2017a) for *E. camaldulensis*. The potential of agroforestry systems to stock and sequester CO_2 are extremely inconsistent (0.29 to 15.21 t C ha^{-1} yr^{-1}) relying on several aspects including site characteristics, type of species, land use type, the age of trees and cultural practices (Nair et al., 2009). Traditional tree crop combination in Africa stock more carbon because of their greater DBH and height than the abandoned land and improved agroforestry systems which were comparatively young (Takimoto et al., 2008). Gera (2012) recommended that differences among carbon stocks can be credited to mean annual increment of trees which differed with nature of planting stock, site, age and tree density. In the present study, largest carbon amount was accounted for stem (about half) from above tree biomass, which is identical with different results for distinctive species (Redondo, 2007; Fonseca et al., 2012).

In agroforestry systems, the soil is considered as an important subsystem for lowering CO_2 levels in the atmosphere. Nair et al. (2009) compare SOC contents among different land use practices and found the trend in the order of forests > agroforestry > plantations > arable crops. A few studies from Africa demonstrated that tree carbon sequestration will not quickly hold soil carbon equivalent to the baseline level (Kaya and Nair, 2001). In the current study, higher organic carbon concentrations and SOC stocks were noted with increase in tree age at both depths. The higher SOC stocks in the upper soil surface are credited to more noteworthy carbon input from tree litter, dead roots, and root exudates (Kaushal et al., 2012; Nawaz et al., 2014; Yasin et al., 2016).

http://www.aloki.hu ● ISSN 1589 1623 (Print) ● ISSN 1785 0037 (Online)
DOI: http://dx.doi.org/10.15666/aeer/1605_62396252
© 2018, ALÖKI Kft., Budapest, Hungary

Poplar trees in agroforestry systems by and large increase 3.5 Mg ha^{-1} of litter fall each year (Kaushal et al., 2012). Higher SOC was observed with increase in tree age in upper soil layer 0-15 cm and was 18% higher under 3-year-old tree stand when compared with 1-year-old tree stand and it further increases by 18.5% at 0-15 cm layer of soil under 6-year-old tree stand (Gupta et al., 2009). The CSR (Carbon sequestration rate) in the soil across all Tehsils varied from 1.77 Mg ha^{-1} yr^{-1} to 2.27 Mg ha^{-1} yr^{-1} in 6-year-old trees which is slightly higher to the findings (1.18 Mg ha^{-1} yr^{-1} to 1.81 Mg ha^{-1} yr^{-1}) of Arora et al. (2014).

Conclusions

Carbon sequestration through woody vegetation is a sustainable and efficient approach. In the present study, it was found that the carbon sequestration ability of *P deltoides* increases with age and, when planted as bund planting in agroforestry systems, it differs from other patterns of tree planting such as compact plantations. The species is sequestering the exceptional amount of carbon in the limited span of time, thus creating an option for farmers to get extra revenue in terms of carbon credits. Moreover, *P deltoides* fulfill the demand of plywood industry and fuel because of its fast growth and higher biomass accretion of the country. Therefore, our study suggests planting *P. deltoides* in various agroforestry systems act as a feasible alternative for higher biomass production and carbon stocks to mitigate climate change. Along with carbon capturing and sequestration these systems could develop into technological alternative to reduce deforestation rates in the country. Therefore, further studies should be carried out to explore the potential impact of various bund planted tree based agroforestry systems in climate change mitigation through carbon sequestration.

Acknowledgements. The authors of the study are highly grateful to Higher Education Commission (HEC), Pakistan for providing necessary facilities and funds for the completion of current research under the NRPU Project No. 2459.

REFERENCES

[1] Afzal, M., Aqeela, M. A. (2013): Factors affecting carbon sequestration in trees. – Journal of Agricultural Research 51: 61-68.

[2] Ajit., Dhyani, S. K., Handa, A. K., Newaj, R., Chavan, S. B., Alam, B., Prasad, R., Ram, A., Rizvi, R. H., Arora, G. S., Chaturvedi, R., Kaushal, A., Nain, S., Tewari, N., Alam, M., Chaturvedi, O. P. (2014): Growth, biomass, carbon stocks, and sequestration in an age series of *Populus deltoides* plantations in Tarai region of central Himalaya. – Turkish Journal of Agriculture and Forestry 38: 550-560.

[3] Arora, G. S., Chaturvedi, R., Kaushal, A., Nain, S., Tewari, N., Alam, M., Chaturvedi, O. P. (2014): Growth, biomass, carbon stocks, and sequestration in an age series of Populus deltoides plantations in Tarai region of central Himalaya. – Turkish Journal of Agriculture and Forestry, 38: 550-560.

[4] Cairns, M. A., Brown, S., Helmer, E. H., Baumgardner, G. A. (1997): Root biomass allocation in the world's upland forests. – Oecologia 111: 1-11.

[5] Chauhan, S. K., Gupta, N., Ritu, Y. S., Chauhan, R. (2009): Biomass and carbon allocation in different parts of agroforestry tree species. – Indian Forester 135: 981-993.

http://www.aloki.hu ● ISSN 1589 1623 (Print) ● ISSN 1785 0037 (Online)
DOI: http://dx.doi.org/10.15666/aeer/1605_62396252
© 2018, ALÖKI Kft., Budapest, Hungary

[6] Chauhan, S. K., Sharma, S. C., Beri, V., Ritu, Y. S., Gupta, N. (2010): Yield and carbon sequestration potential of wheat (*Triticum aestivum*) and poplar (*Populus deltoides*) based agri-silvicultural system. – Indian Journal of Agricultural Sciences 80: 129-135.

[7] Chauhan, S. K., Gupta, N., Walia, R., Yadav, S., Chauhan, R., Mangat, P. S. (2011): Biomass and carbon sequestration potential of poplar wheat inter-cropping system in irrigated agro-ecosystem in India. – Journal of Agricultural Science and Technology 1: 575-586.

[8] DAC (2014): National Agroforestry Policy-2014. – DAC, Ministry of Agriculture, GOI, New Delhi. http://agricoop.nic. in/imagedefault/whatsnew/Agroforestry.pdf. Accessed on 18th June, 2015.

[9] Das, D. K., Chaturvedi, O. P. (2005): Structure and function of *Populus deltoides* agroforestry systems in eastern India: Dry matter dynamics. – Agroforestry Systems 65: 215-221.

[10] Fang, S., Xue, J., Tang, L. (2007): Biomass production and carbon sequestration potential of poplar plantations with different management patterns. – Journal of Environment Management 85: 672-679.

[11] Fang, S. Z., Li, H. L., Sun, Q. X., Chen, L. B. (2010): Biomass production and carbon stocks in poplar-crop intercropping systems: a case study in northwestern Jiangsu, China. – Agroforestry Systems 79: 213-222.

[12] Fonseca, W., Alice, F. E., Rey-Benayas, J. M. (2012): Carbon accumulation in aboveground and belowground biomass and soil of different age native forest plantations in the humid tropical lowlands of Costa Rica. – New Forests 43: 197-211.

[13] Gera, M. (2012): Poplar culture for speedy carbon sequestration in India: a case study from Terai region of Uttarakhand. – Envis Forestry Bulletin 12: 75-83.

[14] Gupta, N., Kukal, S. S., Bawa, S. S., Dhaliwal, G. S. (2009): Soil organic carbon and aggregation under poplar based agroforestry system in relation to tree age and soil type. – Agroforestry System 76: 27-35.

[15] Harmand, J. M., Njiti, C. F., Bernhard-Reversat, F., Puig, H. (2004): Aboveground and belowground biomass, productivity and nutrient accumulation in tree improved fallows in the dry tropics of Cameroon. – Forest Ecology and Management 188: 249-265.

[16] Hergoualc'h, K., Blanchart, E., Skiba, U., Henault, C., Harmand, J. M. (2012): Changes in carbon stock and greenhouse gas balance in a coffee (*Coffea arabica*) monoculture versus an agroforestry system with *Inga densiflora*, in Costa Rica. – Agriculture, Ecosystems and Environment 148: 102-110.

[17] Jain, A. K., Tripathi, D., Shakhela, R. R., Patel, A. G., Dalvi, V. V., Saxena, A. K., Parihar, A. K. S., Backiyavathy, M. R., Sudhagar, R. J., Bandeswaran, C., Gunasekaran, S. (2017): Estimating carbon sequestration potential of existing agroforestry systems in India. – Agroforestry systems 91: 101-118.

[18] Jha, K. k. (2018): Root Carbon Sequestration and Its Efficacy in Forestry and Agroforestry Systems: A Case of *Populus euramericana* I-214 Cultivated in Mediterranean condition. – Notulae Scientia Biologicae 10: 68-78.

[19] Joa Carlos de, M. S., Carlos, C. C., Warren, A. D., Lal, R., Filho, S. P. V., Piccolo, M. C., Feigl, B. E. (2001): Organic matter dynamics and carbon sequestration rates for a tillage Chrono sequence in a Brazilian Oxisol. – Soil Science Society of America Journal 65: 1486-1499.

[20] Kanime, N., Kaushal, R., Tewari, S. K., Raverkar, K. P., Chaturvedi, S., Chaturvedi, O. P. (2013): Biomass production and carbon sequestration in different tree-based systems of Central Himalayan Tarai region. – Forests Trees and Livelihoods 22: 38-50.

[21] Kaushal, R., Verma, K. S., Chaturvedi, O. P., Alam, N. M. (2012): Leaf litter decomposition and nutrient dynamics in four important multiple tree species. – Range Management and Agroforestry 33: 20-27.

[22] Kaya, B., Nair, P. K. R. (2001): Soil fertility and crop yields under improved fallow systems in southern Mali. – Agroforestry Systems 52: 1-11.

http://www.aloki.hu ● ISSN 1589 1623 (Print) ● ISSN 1785 0037 (Online)
DOI: http://dx.doi.org/10.15666/aeer/1605_62396252
© 2018, ALÖKI Kft., Budapest, Hungary

[23] Kreft, S., David, E., Inga, M. (2017): Who suffers most from extreme weather events? Global Climate Risk Index. – Germanwatch, p. 32. www.germanwatch.org/en/cri.
[24] Kutsokon, N. K., Jose, S., Holzmueller, E. (2015): A global analysis of temperature effects on populus plantation production potential. – American Journal of Plant Science 6: 23-33.
[25] Lodhiyal, N., Lodhiyal, L. S. (2003): Biomass and net primary productivity of Bhabar Shisham forests in central Himalaya, India. – Forest Ecology and Management 176: 217-235.
[26] Murthy, I. K., Gupta, M., Tomar, S., Munsi, M., Tiwari, R., Hegde, G. T. (2013): Carbon sequestration potential of agroforestry systems in India. – Journal of Earth Science and Climate Change 4: 1-7
[27] Nair, P. K. R., Kumar, B. M., Nair, V. D. (2009): Agroforestry as a strategy for carbon sequestration. – Journal of Plant Nutrition and Soil Science 172: 10-23.
[28] Nawaz, M., Gul, S., Farooq, T., Siddiqui, M. T., Asif, M., Ahmad, I., Niazi, N. K. (2016): Assessing the actual status and farmer's attitude towards agroforestry in Chiniot, Pakistan. – International Journal of Bioliogy, Biomolecular, Agriculture, Food, Biotechnological Engineering 10: 465-469.
[29] Nawaz, M. F., Bourrie, G., Gul, S., Trolard, F., Mouret, J. C., Tanvir, M. A. (2014): Effects of postharvest management practices on the stability of iron minerals in rice culture. – Pakistan Journal of Agricultural Sciences 51: 861-866.
[30] Nawaz, M. F., Mazhar, K., Gul, S., Ahmad, I., Yasin, G., Asif, M., Tanvir, M. (2017a): Comparing the early stage carbon sequestration rates and effects on soil physico-chemical properties after two years of planting agroforestry trees. – Journal of Basic and Applied Sciences 13: 527-533.
[31] Nawaz, M. F., Shah, S. A. A., Gul, S., Afzal, S., Ahmad, I., Ghaffar, A. (2017b): Carbon sequestration and production of Eucalyptus camaldulensis plantations on marginal sandy agricultural lands. – Pakistan Journal of Agricultural Sciences 54: 335-342.
[32] Nawaz, M. F., Yousaf, M. T. B., Yasin, G., Gul, S., Ahmed, I., Abdullah, M., Rafay, M., Tanvir, M. A.1., Asif, M., Afzal, S. (2018): Agroforestry status and its role to sequester atmospheric CO_2 under semi-arid climatic conditions in Pakistan. – Applied Ecology and Environmental Research 16: 645-661.
[33] Negi, J. D. S., Sharma, S. C. (1985): Biomass production and nutrient distribution in an age series of Eucalyptus hybrid plantation in Tamil Nadu. – Indian Forester 111: 1111-1122.
[34] Nielsen, U. B., Madsen, P., Hansen, J. K., Nord-Larsen, T., Nielsen, A. T. (2014): Production potential of 36 poplar clones grown at medium length rotation in Denmark. – Biomass and Bioenergy 64: 99-109.
[35] Peichl, M., Thevathasan, N. V., Gordon, A. M., Huss, J., Abohassan, R. A. (2006): Carbon sequestration potentials in temperate tree based intercropping systems, southern Ontario, Canada. – Agroforestry Systems 66: 243-257.
[36] Qureshi, M. A. A. (2005): Basics of Forestry and Allied Sciences. – A. One Publishers Lahore, Pakistan, pp. 145-149.
[37] Redondo, A. (2007): Growth, carbon sequestration, and management of native tree plantations in humid regions of Costa Rica. – New Forests 34: 253-268.
[38] Rizvi, R. H., Dhyani, S. K., Yadav, R. S., Singh, R. (2011): Biomass production and carbon stock of popular agroforestry systems in Yamunanagar and Saharanpur districts of northwestern India. – Current Science 100: 736-742.
[39] Saifullha (2017): Climate change impact on agriculture of Pakistan, a leading agent to food security. – International Journal of Environmental Sciences and Natural Resources 6: 1-4.
[40] Smith, P., Martino, D., Cai, Z. (2008): Greenhouse gas mitigation in agriculture. – Philosophical Transactions of the Royal Society Series B 363: 789-813.

http://www.aloki.hu ● ISSN 1589 1623 (Print) ● ISSN 1785 0037 (Online)
DOI: http://dx.doi.org/10.15666/aeer/1605_62396252
© 2018, ALÖKI Kft., Budapest, Hungary

[41] Takimoto, A., Nair, P. K., Nair, V. D. (2008): Carbon stock and sequestration potential of traditional and improved agroforestry systems in the West African Sahel. – Agriculture, Ecosystems and Environment 125: 159-166.
[42] Thomas., Martin, A. R. (2012): Carbon content of tree tissues: – A Synthesis Sean C. Forests 3: 332-352.
[43] Updegraff, K., Baughman, M. J., Taff, S. J. (2004): Environmental benefits of cropland conversion to hybrid poplar: economic and policy considerations. – Biomass and Bioenergy 27: 411-428.
[44] Walkley, A. J., Black, I. A. (1934): An examination of the Degtjareff method for determining soil organic matter and a proposed modification of the chromic acid titration method. – Soil Science 37: 29-38.
[45] Watson, R. T., Noble, I. R., Bolin, B., Ravindranath, N. H., Verarado, D. J., Dokken, D. J. (eds.) (2000): Land Use, Land Use Changes and Forestry: A Special Report of the IPCC. – Cambridge University Press, New York.
[46] Yasin, G., Nawaz, M. F., Rasool, F., Yousaf, M. T. B., Nazir, M. Q., Javed, A. (2016): Effect of canopy cover of Capparis decidua Forsk. on soil conditions in Thal Desert. – Journal of Bioresource Management 3: 17-26.

APPENDIX

ANOVA table of bulk density at 0-15 cm depth

Source	DF	SS	MS	F	P
Age	2	0.17472	0.08736	44.57	0.0000
Tehsil	2	0.02192	0.01096	5.59	0.0077
Age*Tehsil	4	0.02289	0.00572	2.92	0.0344
Error	36	0.07056	0.00196		
Total	44	0.29010			

ANOVA table of bulk density at 15-30 cm depth

Source	DF	SS	MS	F	P
Age	2	0.17330	0.08665	51.75	0.0000
Tehsil	2	0.00995	0.00498	2.97	0.0639
Age*Tehsil	4	0.01804	0.00451	2.69	0.0463
Error	36	0.06028	0.00167		
Total	44	0.26156			

ANOVA table of soil organic carbon at 0-15 cm depth

Source	DF	SS	MS	F	P
Age	2	418.368	209.184	157.07	0.0000
Tehsil	2	22994	11.497	8.63	0.0009
Age*Tehsil	4	16.788	4.197	3.15	0.0255
Error	36	47.943	1.332		
Total	44	506.093			

http://www.aloki.hu ● ISSN 1589 1623 (Print) ● ISSN 1785 0037 (Online)
DOI: http://dx.doi.org/10.15666/aeer/1605_62396252
© 2018, ALÖKI Kft., Budapest, Hungary

ANOVA table of soil organic carbon at 15-30 cm depth

Source	DF	SS	MS	F	P
Age	2	168.401	84.2005	89.82	0.0000
Tehsil	2	27.036	13.5179	14.42	0.0000
Age*Tehsil	4	9.909	2.4771	2.64	0.0494
Error	36	33.748	0.9374		
Total	44	239.093			

ANOVA table of organic carbon at 0-15 cm depth

Source	DF	SS	MS	F	P
Age	2	1.57667	0.78834	307.41	0.0000
Tehsil	2	0.01995	0.00998	3.89	0.0295
Age*Tehsil	4	0.03889	0.00972	3.79	0.0113
Error	36	0.09232	0.00256		
Total	44	1.72783			

ANOVA table of organic carbon at 15-30 cm depth

Source	DF	SS	MS	F	P
Age	2	0.65154	0.32577	147.93	0.0000
Tehsil	2	0.03127	0.01564	7.10	0.0025
Age*Tehsil	4	0.02304	0.00576	2.62	0.0512
Error	36	0.07928	0.00220		
Total	44	0.78512			

http://www.aloki.hu ● ISSN 1589 1623 (Print) ● ISSN 1785 0037 (Online)
DOI: http://dx.doi.org/10.15666/aeer/1605_62396252
© 2018, ALÖKI Kft., Budapest, Hungary

PRESSURE ANALYSIS AND SPATIAL QUANTITATIVE ASSESSMENT OF IMPACT OF HUMAN ACTIVITIES ON LAGOON ECOSYSTEM: A CASE STUDY IN XINCUN AND LI'AN LAGOONS, HAINAN, CHINA

FANG, X.[1,2] – HAO, C. L.[1] – CHENG, C. G.[1] – NI, W.[1] – WANG, J. C.[1] – ZHANG, Y. F.[1*]

[1]*The Second Institute of Oceanography, State Oceanic Administration*
36 BaochubeiLu Rd., Hangzhou 310012, P. R. China
(phone: +86-571-8196-3336; fax: +86-571-8805-4750)

[2]*Nanjing University, No. 22 Hankou Rd., Gulou District, Nanjing, Jiangsu 210093, P. R. China*

**Corresponding author*
e-mail: zhangyf123@163.com

(Received 25th May 2018; accepted 31st Aug 2018)

Abstract. Compared to bays, coastal lagoons are more vulnerable to the effects of human activities. The continued deterioration of the Xincun and Li'an Lagoon ecosystems has affected habitat health in the region; therefore, the State Oceanic Administration has proposed the "Blue Bay Remediation Action Plan". To formulate a comprehensive, evidence-based remediation plan, a comprehensive assessment of ecosystem pressure that includes a quantitative spatial study of the cumulative impact intensity of human activities was conducted in the study region. The results showed that the Xincun Lagoon ecosystem pressure composite values have gradually decreased since 2012. Additionally, the area of extremely strong human activities accounted for only 6.67% of the sea area, most of which was distributed at the mouth of the lagoon. However, the ecosystem pressure composite value of the Li'an Lagoon continued to grow until 2014, at which time the area of extremely strong human activities accounted for 13.53% of the sea area, primarily in the Li'an town center region.
Keywords: *human activities, eco-environmental stress, impact assessment, spatial quantization, P-S-R model, coastal lagoons ecosystem*

Introduction

Coastal lagoons occupy 13% of the world coastline (Ana et al., 2018). Compared with bays, coastal lagoons are more actively affected by interactions between land, marine, and atmospheric processes and their environments and ecosystems are more prone to the dual effects of land and sea. Coastal lagoons are also more sensitive to fluctuations caused by changes in various natural processes and human activities, and their ecosystems are particularly vulnerable.

The deterioration of the ecosystems of the Xincun and Li'an Lagoons has affected many habitats (including coral reefs, mangrove forests, and seagrass beds) in the region. According to relevant data and preliminary surveys, large patches of coral reefs are no longer alive, and mangrove habitats are fragmented in the study site. Seagrass beds in the region have also exhibited reduced area and abundance and increased pollutants attached to seagrass.

In 2016, the State Oceanic Administration proposed the "Blue Bay Remediation Action Plan" to improve marine environmental quality, as well as coastal, marine and island ecosystem functions, and to protect marine ecological security. To formulate a scientific and comprehensive remediation plan, it is necessary to conduct a preliminary

http://www.aloki.hu ● ISSN 1589 1623 (Print) ● ISSN 1785 0037 (Online)
DOI: http://dx.doi.org/10.15666/aeer/1605_62536266
© 2018, ALÖKI Kft., Budapest, Hungary

survey and analysis of relevant pressure factors of the Xincun Lagoon ecosystem, diagnose the impact of pressure factors on the lagoon ecosystem, and propose a comprehensive remediation target system and measures for ecosystem conservation and utilization.

The academic community has conducted research into and put forward some indicators and methods for quantitative evaluation of ecosystem pressure. These include ecological footprint analysis (Leo et al., 2014), the green accounting method (Bartelmus, 1999), energy analysis (Brown and Ulgiat, 1991), the environment quality index (Cui and Li, 2014), pollutant emissions indicators, system dynamics (Château et al., 2015), input-output methods, and multivariate statistical analysis. These methods have made positive contributions to efforts to assess the power of economic development to the ecosystem, but there are still some problems. For example, the ecological footprint analysis method describes very little about the pressure from environmental pollution. The environmental quality method and the pollutant emission indicator method cannot describe the pressure caused by ecological damage, so they are not sufficiently comprehensive; the green nuclear algorithm and the energy (value) analysis method represent environmental pollution and ecological damage in the form of currency and energy, respectively, but they are not sufficiently reliable in terms of quantification; the system dynamics, input-output, and multivariate statistical methods are reasonably comprehensive and take into account more factors, but their calculation processes are more complicated than those of other methods, and the results are not intuitive.

In addition, the study of the cumulative impact of human activities has proceeded tortuously. Since the 1970s, the academic community has used environmental sensitivity indicators to identify marine areas sensitive and susceptible to human activities (Gundlach et al., 1978). In the late 1990s, scholars began to evaluate the cumulative effects of multiple pressures (Wiegers et al., 1998). But it was not until 2008 when Halpern et al. selected 17 human activities for the global marine ecosystem, quantified their cumulative impact on global marine ecosystem, and mapped out cumulative impact increments (Halpern et al., 2008), that related studies began to spring up like bamboo shoots after rain. Since then, the field has rapidly developed and gradually become one of the hotspots of basic research in marine spatial planning (MSP). According to a literature review analysis (Korpinen et al., 2016), the research method reported by Halpern et al. was used directly or indirectly in more than half of the papers in the relevant field (Micheli et al., 2013; Marcotte et al., 2015). Compared with the earlier methods, Halpern et al. combined and quantified human activity pressure with ecosystem state (simplified to a linear relationship), so that the research method forms a standardized model, and the results can be compared globally.

Preparation

Conceptual framework

This study aimed to combine data describing the current status of human activities (pressure) and ecosystem condition (state) in the study site and propose corresponding remediation measures (response). This process meets the definition of the pressure-state-response (PSR) framework.

The PSR framework was first proposed by Friends and Rapport (Friends and Rapport, 1979) to analyze the relationship between pressure, current state, and response

http://www.aloki.hu ● ISSN 1589 1623 (Print) ● ISSN 1785 0037 (Online)
DOI: http://dx.doi.org/10.15666/aeer/1605_62536266
© 2018, ALÖKI Kft., Budapest, Hungary

in natural environments (Xu et al., 2017). In the 1970s, the Organization for Economic Co-operation and Development revised the PSR model and applied it to environmental studies. In the early 1990s, the OECD conducted applicability and efficacy analysis of the PSR model when used in analysis and studies of important ecosystem-associated indicators. Because the PSR model has an extremely clear causal relationship, it is widely used in studies of marine ecosystems and evaluation of wetland and lake resources.

Study region and area

The study site is located in the southeast portion of Lingshui Li Autonomous County, which is located on the southeast coast of Hainan Island, China (N18°22'-18°47', E109°45'-110°08'). This site is a classical tide-controlled natural lagoon composed of two lakes separated by a shoal in the middle. The southern portion of the study site is bounded by Nanwan Monkey Island and Niubai Mountain as natural barriers to the South China Sea. The waves are gentle in the lake, and the twin lakes are connected by the South China Sea through narrow mouths (*Fig. 1*).

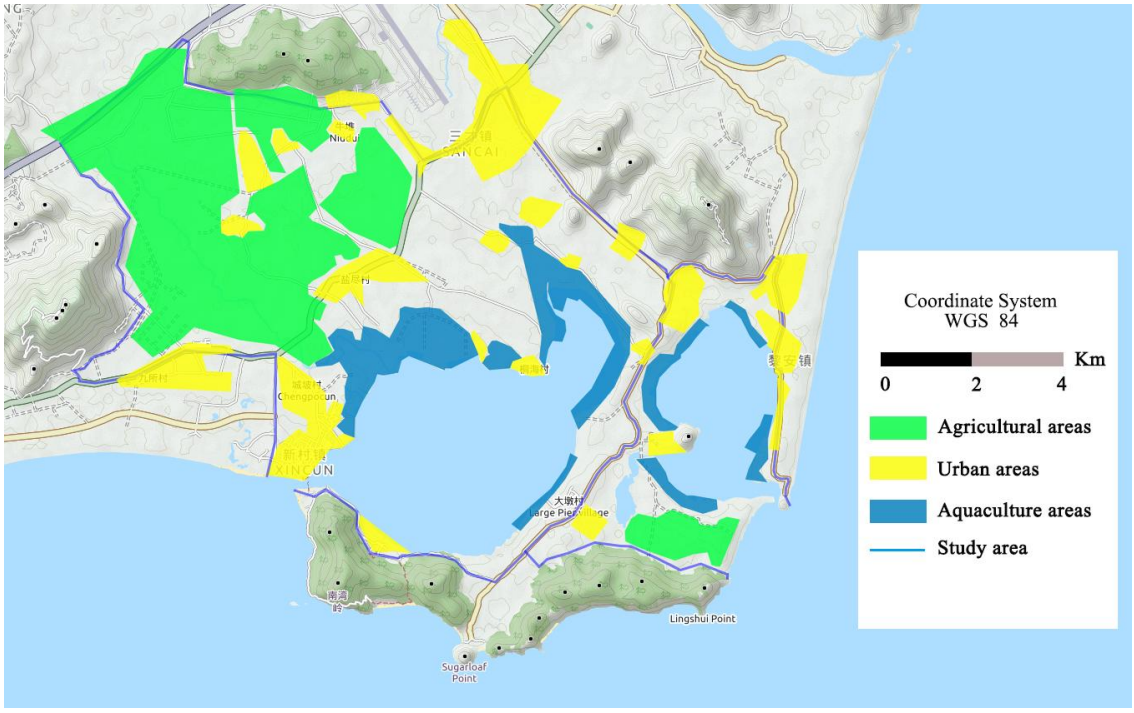

Figure 1. *Map of study region and area*

Lagoon pollution originates from water bodies, but land is also a major pollution source; therefore, water and land regions were included when determining the study site. The water region refers to regions that are formed by the water that curves inwards. The delineation of the land region boundary was based on an enclosed area formed by the watershed in the lagoon and the coastline of the lagoon.

However, for a large drainage basin, if the entire basin cannot be traced during estimation, tracing can be conducted to the part which is below the controlled section of the basin (i.e., the drainage basin only includes the region below the controlled section),

http://www.aloki.hu ● ISSN 1589 1623 (Print) ● ISSN 1785 0037 (Online)
DOI: http://dx.doi.org/10.15666/aeer/1605_62536266
© 2018, ALÖKI Kft., Budapest, Hungary

while that in upstream region will be estimated by using monitoring data for the controlled section. Therefore, the study area for this investigation was the water catchment area of the Qugang and Qugou rivers and their tributaries, which are bound by the G98 Hainan Island Ring Expressway, the China National Highway 223 and the surrounding mountains (region enclosed by the blue line in *Figure 1*.

Methods

Comprehensive assessment of lagoon ecosystem pressure

So far, there have been few studies on the evaluation of lagoon ecosystem pressure, and there is currently no standard evaluation indicator or method. We here report an optimized method on the basis of the Eco-environmental Stress Index (ESI) method proposed by Xu et al. (2004) of Peking University, rendering it able to adapt to the actual situation of the lagoon. This method has been validated in terrestrial areas (Hao et al., 2012; Song et al., 2014) and is a relatively new method that can intuitively indicate the pressure of socio-economic development on ecosystems and the change trend of the pressure.

This study analyzed the major stress factors of lagoon ecosystems to design an evaluation indicator system and then applied this system to the evaluation of the lagoon ecosystem. The specific evaluation steps were as follows: (i) determination of evaluation indicators and selection of year limit for evaluation; (ii) data standardization; (iii) determination of weight values; (iv) calculation of ecosystem pressure index.

Step i: We selected representative indicators (*Table 1*) based on the current status of the ecosystem in the study site for an evaluation period of 2011 to 2015.

Table 1. *Pressure evaluation indicator system for Xincun and Li'an Lagoon ecosystems*

Layer A		Layer B		Layer C		Layer D	
Population pressure	A_1	Population density	B_1				
		Population growth rate	B_2				
Economic pressure	A_2	GDP per capita	B_3				
		GDP growth rate	B_4				
Human activity pressure	A_3	Land activity pressure	B_5	Land-based pollution	C_1	Domestic wastewater discharge volume	D_1
						High and low aquaculture pond area	D_2
						Nitrogen and phosphorus content in chemical fertilizers	D_3
				Reclamation	C_2	Area of cultivated land	D_4
				Animal husbandry	C_3	Total number of livestock at year end	D_5
		Marine activity pressure	B_7	Mariculture	C_5	Aquaculture raft farming area	D_6
				Marine fishing	C_6	Fixed fishing area	D_7
				Shipping pollution	C_7	Number of fishing vessels	D_8

http://www.aloki.hu ● ISSN 1589 1623 (Print) ● ISSN 1785 0037 (Online)
DOI: http://dx.doi.org/10.15666/aeer/1605_62536266
© 2018, ALÖKI Kft., Budapest, Hungary

Step ii: As the evaluation indicators are not unified (*Tables 2* and *3*), a differential method was used for standardization of the ecosystem pressure indicators x_{ij} (*Tables 4* and *5*).

Table 2. *Annual representative Xincun Lagoon ecosystem pressure values*

	2011	2012	2013	2014	2015
Population density (people/km^2)	586	600	590	574	558
Population growth rate (%)	2.2	2.4	0	0	0
GDP per capita (RMB)	20,378	26,775	30,472	34,000	36,857
GDP growth rate (%)	6	8	13	8.5	8.4
Domestic wastewater discharge volume (tons)	1,909,940	1,889,292	1,858,320	1,806,700	1,755,080
High and low aquaculture pond area (km^2)	5.879	6.542	7.667	7.667	7.667
Nitrogen and phosphorus content in chemical fertilizers (kg)	192,733	192,658	205,939	210,812	195,486
Area of cultivated land (hectares)	5181	5179	5536	5667	5255
Total amount of livestock at year end (number of animals)	19,245	21,458	18,565	19,982	20,382
Aquaculture raft farming area (km^2)	2.489	2.632	2.769	2.836	3.219
Fixed fishing area (km^2)	1.974	2.103	2.256	2.383	2.989
Total number of fishing vessels	2257	2054	1896	1736	1932

Data source description: the domestic wastewater discharge volume was calculated according to the sewage discharge coefficient method in the First Pollution Source Survey: Urban sub-volume. The aquaculture pond area, cultivated land area, aquaculture raft farming area, and fixed fishing area were based on satellite image analysis, and the rest of the data were obtained from the *Lingshui Statistical Yearbook* and the *Hainan Statistical Yearbook*

Table 3. *Annual representative Li'an Lagoon ecosystem pressure values*

	2011	2012	2013	2014	2015
Population density (people/km^2)	397	406	408	467	443
Population growth rate (%)	2.6	2.2	0.5	14.46	0
GDP per capita (RMB)	8824	9253	9654	10,087	12,542
GDP growth rate (%)	7	13.2	13	12.5	12
Domestic wastewater discharge volume (tons)	877,540	898,188	903,350	1,032,400	980,780
High and low aquaculture pond area (km^2)	2.77	2.65	2.43	2.25	2.4
Nitrogen and phosphorus content in chemical fertilizers (kg)	38,948	38,390	37,014	36,716	16,330
Area of cultivated land (hectares)	1047	1032	995	987	439
Total number of livestock at year end (number of animals)	19,864	31,855	22,737	21,487	22,737
Aquaculture raft farming area (km^2)	1.946	1.974	1.996	2.002	2.420
Fixed fishing area (km^2)	0.41	0.45	0.49	0.53	0.83
Total number of fishing vessels	325	300	335	312	335

Data source description: the domestic wastewater discharge volume was calculated according to the sewage discharge coefficient method in the First Pollution Source Survey: Urban sub-volume. The aquaculture pond area, cultivated land area, aquaculture raft farming area, and fixed fishing area were based on satellite image analysis, and the rest of the data were obtained from the *Lingshui Statistical Yearbook* and the *Hainan Statistical Yearbook*

http://www.aloki.hu ● ISSN 1589 1623 (Print) ● ISSN 1785 0037 (Online)
DOI: http://dx.doi.org/10.15666/aeer/1605_62536266
© 2018, ALÖKI Kft., Budapest, Hungary

Table 4. *Annual representative Xincun Lagoon ecosystem pressure standardization values*

	2011	**2012**	**2013**	**2014**	**2015**
Population density (people/km^2)	0.51	0.52	0.51	0.50	0.48
Population growth rate (%)	0.92	1.00	0.00	0.00	0.00
GDP per capita (RMB)	0.36	0.47	0.53	0.59	0.64
GDP growth rate (%)	0.32	0.42	0.68	0.45	0.44
Domestic wastewater discharge volume (tons)	0.52	0.52	0.51	0.49	0.48
High and low aquaculture pond area (km^2)	0.43	0.48	0.57	0.56	0.57
Nitrogen and phosphorus content in chemical fertilizers (kg)	0.48	0.48	0.51	0.52	0.48
Area of cultivated land (hectares)	0.48	0.48	0.51	0.52	0.48
Total amount of livestock at year end (number of animals)	0.48	0.54	0.46	0.50	0.51
Aquaculture raft farming area (km^2)	0.44	0.46	0.49	0.50	0.56
Fixed fishing area (km^2)	0.40	0.42	0.45	0.48	0.60
Total number of fishing vessels	0.57	0.51	0.47	0.43	0.48

Considering that the amount of evaluation indicators for ecosystem pressure assessment is generally large, the difference method was used to standardize the ecosystem pressure index. The specific calculation process is as described in *Equations 1* and *2*

Table 5. *Annual representative Li'an Lagoon ecosystem pressure standardization values*

	2011	**2012**	**2013**	**2014**	**2015**
Population density (people/km^2)	0.46	0.47	0.47	0.54	0.51
Population growth rate (%)	0.18	0.15	0.03	1.00	0.00
GDP per capita (RMB)	0.41	0.43	0.45	0.47	0.59
GDP growth rate (%)	0.37	0.69	0.68	0.66	0.63
Domestic wastewater discharge volume (tons)	0.46	0.47	0.47	0.54	0.51
High and low aquaculture pond area (km^2)	0.55	0.53	0.48	0.45	0.48
Nitrogen and phosphorus content in chemical fertilizers (kg)	0.70	0.69	0.67	0.66	0.30
Area of cultivated land (hectares)	0.70	0.69	0.67	0.66	0.30
Total number of livestock at year end (number of animals)	0.38	0.62	0.44	0.42	0.44
Aquaculture raft farming area (km^2)	0.45	0.45	0.46	0.46	0.55
Fixed fishing area (km^2)	0.33	0.36	0.40	0.43	0.67
Total number of fishing vessels	0.51	0.47	0.53	0.49	0.53

Considering that the amount of evaluation indicators for ecosystem pressure assessment is generally large, the difference method was used to standardize the ecosystem pressure index. The specific calculation process is as described in *Equations 1* and *2*

The formula used for positive pressure indicators was (*Eq. 1*)

$$x_{ij}^{'} = \frac{x_{ij}}{\max(x_{ij}) + \min(x_{ij})}. \quad \text{(Eq.1)}$$

The formula used for negative pressure indicators was (*Eq. 2*)

$$x_{ij}^{'} = 1 - \frac{x_{ij}}{\max(x_{ij}) + \min(x_{ij})} \quad \text{(Eq.2)}$$

http://www.aloki.hu ● ISSN 1589 1623 (Print) ● ISSN 1785 0037 (Online)
DOI: http://dx.doi.org/10.15666/aeer/1605_62536266
© 2018, ALÖKI Kft., Budapest, Hungary

Negative pressure is mainly targeted against economic pressure. This is because, under a specific environmental policy intervention, the overall environmental quality of a country or region will exhibit an initial deterioration followed by a subsequent improvement when economic strength increases.

Step iii: The analytic hierarchy process was used to determine weight values.

Step iv: Based on the determination of the weights (relative importance) at the corresponding layers of various single indicators and the total sorted weight (integrated importance) of the system layers, linear weighting was used to obtain the ecosystem pressure index further to evaluate pressure levels as follows (*Eq. 3*):

$$ESI = \sum_{i=1}^{m} W_i X_i \quad \text{(Eq.3)}$$

where ESI is the ecosystem pressure index; W_i is the indicator weight; and X_i is the standardized value of the indicator.

Spatial quantitative assessment of the impact of human activities on lagoon ecosystem

This study employed spatial quantization to investigate the relationship between human activities and marine ecosystems as described to evaluate the effects of human activities on the lagoon ecosystem and spatial visualization of the evaluation results was conducted (Li et al., 2015). The specific evaluation process for the model was as follows: (i) Determination of the study site, including the spatial range and rational layout of unit points; (ii) Identification of seas with human activities, i.e. determination of effect points, including spatial positions, effect strength, and maximum effect distance; (iii) Calculation of the effects of various human activities on the lagoon ecosystem; (iv) Superimposition of the aforementioned processes in (3) (e.g., comprehensive evaluation).

Step i: The study site consisted of the maritime areas of Xincun and Li'an Lagoons. If human land activities were present, they were represented by unit points concentrated in the coastal region. Estimation results from papers above were used as data. The grid was divided into 100 m×100 m (*Fig. 2*).

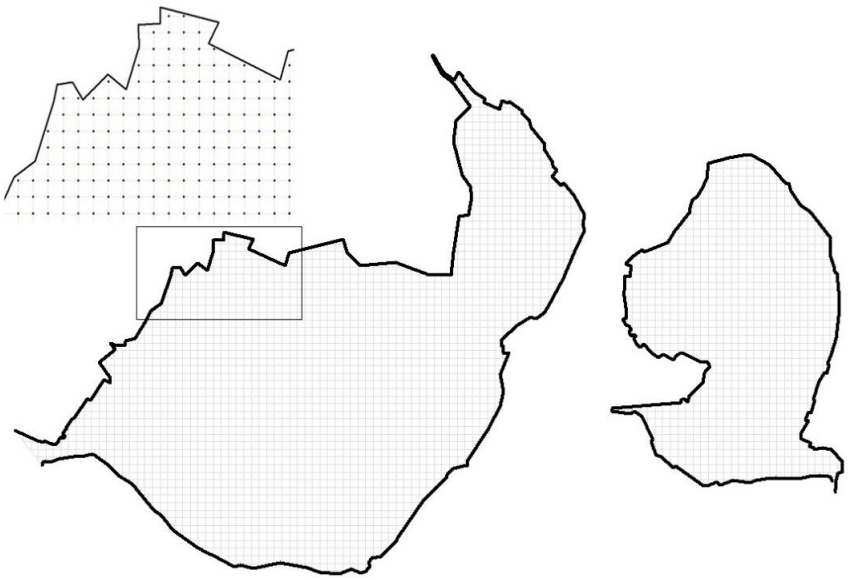

Figure 2. *Map of study region and spatial unit points*

http://www.aloki.hu ● ISSN 1589 1623 (Print) ● ISSN 1785 0037 (Online)
DOI: http://dx.doi.org/10.15666/aeer/1605_62536266
© 2018, ALÖKI Kft., Budapest, Hungary

Step ii: In this study, eight human activities were selected according to the characteristics of the studied sea and actual utilization status to construct an evaluation indicator system that was subsequently used to summarize various seascape human activities comprehensively.

A) Effect strength

Effect strength was expressed from 0 to 1, with 1 indicating the strongest impact and 0 indicating that the effect was negligible. The effect strength (F) of various effect points of human activities was directly assigned values according to the grade of the actual survey value in the standard range (Halpern et al., 2008).

B) Effect distance

Parravicini (Parravicini et al., 2012) used a geospatial model to evaluate the pressure status of eight seascape human activities on marine ecosystems. Their results showed that the effect of each type of human activity on marine ecosystems was about 50%. Therefore, this paper assumes that half the distance between any effect point and the furthest unit point is the maximum effective distance of that effect point (D).

C) Indicator weight

The indicator weights (W) of various human activities were determined according to the analytic hierarchy process. *Table 6* shows the calculated weights.

Table 6. *Evaluation indicator system and effect strength criteria for quantitative model*

Target layer	Factor layer	Indicator layer	Effect strength assigned value table					Weight
			1	0.75	<0.5	0.25	0	
Impact of human activities on marine ecosystems	Land-based human activities	Domestic wastewater discharge volume (10^4 tons)	>5	3–5	1–3	0–1	-	0.1787
		High and low aquaculture pond area (km^2)	>0.3	0.15–0.3	0.1–0.15	0–0.1	-	0.2148
		Nitrogen and phosphorus content in chemical fertilizers used (tons)	>5	3–5	1–3	0–1	-	0.0837
		Area of cultivated land (hectares)	>30	15–30	5–15	0–5	-	0.0837
		Total number of livestock at year end (number of animals)	>60	40–60	20–40	0–20	-	0.0837
	Marine human activities	Farming area of aquaculture raft (km^2)	>0.6	0.4–0.6	0.2–0.4	0–0.2	-	0.2148
		Fixed fishing area (km^2)	>0.3	0.2–0.3	0.1–0.2	0–0.1	-	0.0481
		Total number of fishing vessels	>75	50–75	25–50	0–25	-	0.0925

Step iii: The formula for calculation of the effects of certain human activities on unit points was as follows (*Eq. 4*):

http://www.aloki.hu ● ISSN 1589 1623 (Print) ● ISSN 1785 0037 (Online)
DOI: http://dx.doi.org/10.15666/aeer/1605_62536266
© 2018, ALÖKI Kft., Budapest, Hungary

$$I = \sum_{i=1}^{m} F_i \times \frac{D_i - d_i}{D_i} \quad \text{(Eq.4)}$$

In *Equation 4, I* represents the effects of a certain human activity on a unit point. Human activity is present in *m* effect points; *i* represents the *i*th effect point; F_i is the intensity of the *i*th effect point of that human activity; D_i is the maximum effect distance of the *i*th effect point of that human activity; d_i is the distance between the unit point and the *i*th effect point of that human activity.

Step iv: The calculation formula for the integrated effects of various human activities on unit points was as follows (*Eq. 5*):

$$I_{Total} = \sum_{j=1}^{n} I_j \times W_j \quad \text{(Eq.5)}$$

where I_{Total} represents the integrated effects of various human activities on that unit point and there are *n* types of human activities; *j* represents the *j*th human activity; and I_j is the effect of the *j*th human activity on the unit point. W_j is the weight of the *j*th human activity in the comprehensive evaluation.

Results

Comprehensive assessment of lagoon ecosystem pressure

A) Xincun Lagoon

Table 7 shows the ecosystem pressure composite values for Xincun Lagoon, which peaked in 2012 before gradually decreasing. This occurred because population pressure is gradually decreasing, during which time growth has been negative. Also, economic pressure has been stable since 2014. This is because, although GDP is growing, the growth rate is decreasing significantly. However, human activity pressure is increasing annually because, although the number of aquaculture ponds is generally unchanged (due to aquaculture pond management policies), the quantity and area of aquaculture rafts are increasing.

Table 7. *Annual Xincun Lagoon ecosystem pressure composite values*

	2011	**2012**	**2013**	**2014**	**2015**
Pressure composite value	0.492	0.533	0.476	0.459	0.472
Population pressure	0.142	0.152	0.051	0.050	0.048
Economic pressure	0.067	0.089	0.122	0.104	0.109
Human activity pressure	0.283	0.293	0.304	0.305	0.315

Calculation explanation: On the basis of determining the weight (relative importance) of each individual indicator at its respective level and its total ranking weight (integrated importance) to the overall level of the system, the ecosystem pressure index can be further determined by the linear weighting method to evaluate the pressure level

B) Li'an Lagoon

Table 8 shows that the ecosystem pressure composite value for Li'an Lagoon increased continuously until 2014. This occurred because population pressure showed a sudden increase in 2014 because it increased from 408 people in 2013 to 467 people.

http://www.aloki.hu ● ISSN 1589 1623 (Print) ● ISSN 1785 0037 (Online)
DOI: http://dx.doi.org/10.15666/aeer/1605_62536266
© 2018, ALÖKI Kft., Budapest, Hungary

When compared with Xincun Lagoon, the GDP of Li'an Lagoon continued to increase, as did the rate of increase. Thus, economic pressure is still continuously increasing. However, human activity pressure started to decrease in 2012. Although the area of aquaculture rafts is increasing, and the area of high and low aquaculture ponds was generally unchanged (due to aquaculture pond management policies) the area of cultivated land shows an annual decreasing trend.

Table 8. *Annual Li'an Lagoon ecosystem pressure composite values*

	2011	**2012**	**2013**	**2014**	**2015**
Pressure composite value	0.448	0.489	0.466	0.569	0.462
Population pressure	0.064	0.062	0.051	0.154	0.051
Economic pressure	0.078	0.113	0.114	0.113	0.122
Human activity pressure	0.306	0.314	0.302	0.302	0.288

Calculation explanation: On the basis of determining the weight (relative importance) of each individual indicator at its respective level and its total ranking weight (integrated importance) to the overall level of the system, the ecosystem pressure index can be further determined by the linear weighting method to evaluate the pressure level

Cumulative impact intensity because of human activities

Based on the research results of Halpern et al. (2008) and Li et al. (2015), we combine the actual situation of the research area to conduct research and analysis. For the specific calculation process, see Step i-Step iv of spatial quantitative assessment of the impact of human activities on lagoon ecosystem in the Methods section above.

Spatial data analysis of the effects of human activities on the Xincun and Li'an Lagoon ecosystems was conducted using the ArcGIS10.2 software, with Kriging interpolation employed to process the effect values of human activities. *Figures 3* and *4* show the spatial quantitation results.

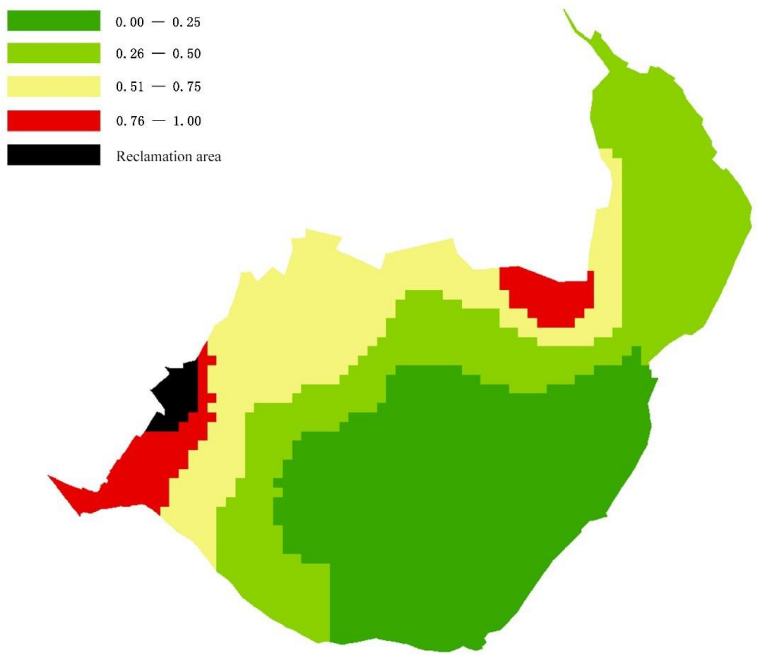

Figure 3. *Map of cumulative impact intensity due to human activities in Xincun Lagoon*

http://www.aloki.hu ● ISSN 1589 1623 (Print) ● ISSN 1785 0037 (Online)
DOI: http://dx.doi.org/10.15666/aeer/1605_62536266
© 2018, ALÖKI Kft., Budapest, Hungary

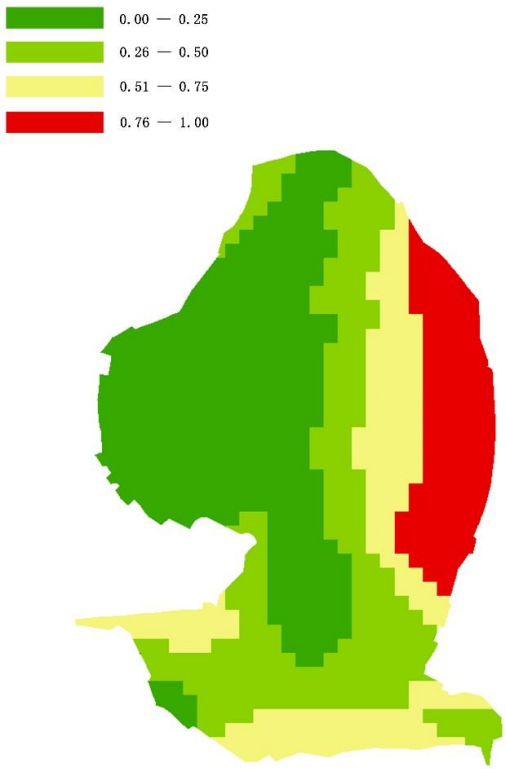

Figure 4. *Map of cumulative impact intensity due to human activities in Li'an Lagoon*

In Xincun Lagoon, extremely strong effect regions (effect values of 0.75–1.00) accounted for 6.67% of the entire sea space, while strong effect regions (effect values of 0.50–0.75) accounted for 21.63% of the entire sea space; moderate effect regions (effect values of 0.25–0.50) accounted for 32.32% of the entire sea space, and weak effect regions (effect values of 0.00–0.25) accounted for 37.75% of the entire sea space. Also, some reclamation sites were located outside the managed coastline (black lines in the figure). As shown in *Figure 3,* the area with the strongest human activity in Xincun Lagoon is located at the mouth of the lagoon and around Tonghai Village inside the lagoon, while the human activity in the southern sea of the lagoon is almost negligible. Therefore, the effect value for that region is less than 0.25.

In Li'an Lagoon, extremely strong effect regions (effect values of 0.75-1.00) accounted for 13.53% of the entire sea space; strong effect regions (effect values of 0.50-0.75) accounted for 19.74% of the entire sea space; moderate effect regions (effect values of 0.25-0.50) accounted for 26.75% of the entire sea space, and weak effect regions (effect values of 0.00-0.25) accounted for 39.98% of the entire sea space. As shown in *Figure 4,* the area with the strongest human activity in Li'an Lagoon is located in Li'an Village. Conversely, the human activity in the western sea of the lagoon is almost negligible; therefore, the effect value for that region is less than 0.25.

Analysis of remediation measures

According to the P-S-R model, after clarifying the pressure and status of Xincun and Li'an Lagoons, it will be necessary to combine the results of the studies above for analysis to effectively remediate the two lagoons. Generally, the response measures

http://www.aloki.hu ● ISSN 1589 1623 (Print) ● ISSN 1785 0037 (Online)
DOI: http://dx.doi.org/10.15666/aeer/1605_62536266
© 2018, ALÖKI Kft., Budapest, Hungary

should be targeted against different aspects of pressure and status. Generally, the response measures should be targeted toward different aspects of pressure and status, as described below.

Pressure reduction measures

A) Optimization of aquaculture raft farming. The aquaculture capacity should be determined rationally. The specific measures are as follows. Aquaculture density should be controlled within the carrying capacity of the water body so that aquaculture pollutants do not exceed the self-cleaning capability of the water body. According to relevant studies (Hu et al., 2007), the presence of aquaculture raft farming causes the flow speed of some sea regions to significantly decrease, resulting in the reduced self-cleaning capability of the water body. Optimization of aquaculture raft layout should be conducted according to the unique hydrodynamic model of the study site. Adjustment and optimization of aquaculture structure should be conducted to develop the aquaculture of benthic economic species actively. Improvement of baitcasting techniques and improvement of feed quality will also greatly reduce water pollution.

B) Remediation of land-based pollution. According to the onsite survey and pollution calculations, domestic wastewater from the surrounding villages and towns of Xincun and Li'an Lagoons is an important source of land-based pollution. The specific measures to reduce this include the following. Sewage interception and treatment of domestic wastewater and solid waste of coastal villages and towns. Low aquaculture ponds, which are mariculture ponds that are below the surveyed coastline (State Oceanic Administration, 2012), not only occupy large amounts of valuable wetland but are usually accompanied by many mangrove forests. However, long-term immersion in aquaculture wastewater will threaten these habitats. Therefore, rapid pond reclamation and reforestation should be conducted to form a complete mangrove forest corridor. High aquaculture ponds are mariculture ponds that are above the surveyed coastline (State Oceanic Administration, 2012). Because it is difficult to remove these ponds completely, a wastewater treatment system of high aquaculture pond should be developed for centralized processing of the discharged wastewater.

Ecological improvement measures

A) Dismantlement of illegal facilities and garbage removal. The facilities to be dismantled and garbage to be removed include fixed fishing facilities and night-time fishing illumination equipment, utility poles that provide electricity for fishing and aquaculture rafts, and other fishing facilities that occupy and segment the sea. Also, floating public toilets and restaurants, as well as other fixed buildings that directly discharge excreta and solid waste into the sea should be removed. Finally, garbage thrown into the lagoons by tourists and villagers should be removed.

B) Sediment dredging. In the marine ecosystem, sediments are sinks and sources of nutrients, heavy metals, and persistent organic pollutants. Under conditions in which extrinsic pollutant sources are effectively controlled, biological or physical factors will promote the release of sediments. This can still result in maintenance of eutrophication in water bodies or deterioration of water quality for long periods of time. Sediment dredging can permanently remove contaminated sediment from aquatic systems and is widely used in the remediation of lakes, rivers, and bays (Zhong et al., 2007).

http://www.aloki.hu ● ISSN 1589 1623 (Print) ● ISSN 1785 0037 (Online)
DOI: http://dx.doi.org/10.15666/aeer/1605_62536266
© 2018, ALÖKI Kft., Budapest, Hungary

C) Bottom culturing and release of shellfish. Relevant studies have shown that shellfish are commonly used for ecological restoration and remediation of water bodies. Shellfish can decrease the concentration of particulate organic matter (seaweeds and organic debris) in the water body, indirectly control the concentration of nitrogen and phosphorus salts, couple with the aquatic benthic environment, and protect biodiversity and create biological habitats. Also, shellfish play an important role in carbon fixation in the oceans. Specifically, shellfish can remove particulate carbon in the sea by filter feeding, absorb carbon during formation of calcium carbonate shells and sequester large amounts of marine carbon.

Conclusion

This study not only identifies the pressure categories of human activities on the lagoon but can also be used to determine the ecosystem pressure index; it is also possible to spatially quantify the cumulative impact intensity.

The calculation model introduced in the paper is suitable for coastal lagoons that are little affected by the outer seas, have relatively weak water exchange capacity, and have relatively flat seabed topography. The model not only quantifies the impact results to a value of 0–1 in order to indicate the impact degree, but also displays the distribution of the impact results in the sea space. The findings can coordinate the entire research area for management but can also manage according to the different partitions of the affected areas in different regions.

The findings of this work allow us to draw the following conclusions:

(1) The results of the study showed that the intensity of human activities experienced by Xincun Lagoon decreased annually from 2011 to 2015 and the intensity of human activity was greatest at the mouth of the lagoon. Conversely, the intensity of human activities that Li'an Lagoon was subject to is still growing, although intensity was greatest at the Li'an town center.

(2) Generally, remediation measures are proposed based on pressure and state aspects. With regards to decreasing human activity pressure, optimization of aquaculture raft farming and remediation of land-based pollution are major methods proposed in the study. Also, dismantlement of illegal facilities and garbage removal, sediment dredging, bottom culturing and release of shellfish could improve the ecosystem status.

REFERENCES

[1] Ana, M. V., Angel, P. R., José, M. M., et al. (2018): Ecosystem services and main environmental risks in a coastal lagoon (MarMenor, Murcia, SE Spain). – Journal for Nature Conservation 43: 180-189.

[2] Bartelmus, P. (1999): Green accounting for a sustainable economy: Policy use and analysis of environmental accounts in the Philippines. – Ecological Economics 29(1): 155-170.

[3] Borja, A., Elliot, M., Andersen, J. H., et al. (2016): Overview of integrative assessment of marine systems: the ecosystem approach in practice. – Frontiers in Marine Science 3(55): 1-20.

[4] Brown, M. T., Ulgiati, S. (1991): Energy-based indices and ratios to evaluate sustainability: monitoring economies and technology toward environmentally sound innovation. – Ecological Engineering 9(1-2): 51-69.

http://www.aloki.hu ● ISSN 1589 1623 (Print) ● ISSN 1785 0037 (Online)
DOI: http://dx.doi.org/10.15666/aeer/1605_62536266
© 2018, ALÖKI Kft., Budapest, Hungary

[5] Château, P. A., Huang, Y. C. A., Chen, C. A., et al. (2015): Integrated assessment of sustainable marine cage culture through system dynamics modeling. – Ecological Modelling 299: 140-146.
[6] Cui, L. T., Li, Z. W. (2014): Assessment of ecological environment effects of coastal development in Hebei Province, China. – Chinese Journal of Applied Ecology 25(7): 2063-2070.
[7] Friends, A., Raport, D. (1979): Towards a Comprehensive Framework for Environment Statistics Stress-Response Approach. – Statistics Canada, Ottawa, Canada.
[8] Gundlach, E. R., Ruby, C. H., Hayes, M. O., et al. (1978): Theurquiola oil spill, La Coruña, Spain: impact and reaction on beaches and rocky coasts. – Environmental Geology 2(3): 131-143.
[9] Halpern, B. S., Walbridge S, Selkoe, K. A. et al. (2008): A global map f human impact on marine ecosystems. – Science 319(5865): 948-952.
[10] Hao C G, Shan W, G. (2012): Study on eco-environmental stress trend of Inner Mongolia based on ecological stress index. – Journal of Anhui Agricultural Sciences 40(15): 8684-8686.
[11] Hu, W. J., Yang, S. Y. (2007): The impact of mariculture on the marine ecosystem and studies on bioremediation. – Journal of Xiamen University (Natural Science) 8: 197-202.
[12] Leo, F. D., Miglietta, P. P., Pavlinović, S. (2014): Marine ecological footprint of Italian Mediterranean fisheries. – Sustainability 6(11): 7482-7495.
[13] Li, Y. F., Zhu, X. D., Zou, X. Q. et al. (2004): Resource-environmental pressure analysis and ecological cybernetics response: a case study of coastal wetlands in Yancheng, Jiangsu province. – Journal of Natural Resources 19(6): 754-760.
[14] Li, Y. F., Song, X. X., Wu, Z. X. et al. (2015): An integrated methodology for quantitative assessment on the impact of human activities on marine ecosystems: a case study in Laizhou Bay, China. – Oceanologia et Limnologia Sinica 1: 133-139.
[15] Marcotte, D., Hung, S. K., Caquard, S. (2015): Mapping cumulative impacts on Hong Kong's pink dolphin population. – Ocean & Coastal Management 109: 51-63.
[16] Micheli, F., Halpern, B. S., Walbridge, S., et al. (2013): Cumulative human impacts on Mediterranean and black sea marine ecosystems: assessing current pressures and opportunities. – Plos One 8(12): e79889-e79889.
[17] Parravicini, V., Rovere, A., Vassallo, P. et al. (2012): Understanding relationships between conflicting human uses and coastal ecosystems status: A geospatial modelling approach. – Ecological Indicators 19: 253-263.
[18] Song, J., Wang, H. X., Liu, S. Y. (2014): Quantitative assessment of stress of economic development to environment using ecological stress index. – Chinese Journal of Eco-Agriculture 22(3): 368-374.
[19] Wiegers, J. K., Feder, H. M., Mortensen, L. S., et al. (1998): A regional multiple-stressor rank-based ecological risk assessment for the fjord of Port Valdez, Alaska. – Human & Ecological Risk Assessment An International Journal 4(5): 1125-1173.
[20] Xu F L, Zhao, S. S., Du, T. T., et al. (2004): Quantitative assessment for economic development stress status and trends of eco-environment. – China Population, Resources and Environment 14(4): 30-36.
[21] Xu, H. T., Zhou, L. F., Cheng, Q.(2017): Study on ecosystem health evaluation and risk assessment for Linghekou wetlands based on a PSR model. – Acta Ecologica Sinica 37(24): 8264-8274.
[22] Zhong, J. C., Fan, C. X. (2007): Advance in the study on the effectiveness and environmental impact of sediment dredging. – Journal of Lake Sciences 1: 1-10.

http://www.aloki.hu ● ISSN 1589 1623 (Print) ● ISSN 1785 0037 (Online)
DOI: http://dx.doi.org/10.15666/aeer/1605_62536266
© 2018, ALÖKI Kft., Budapest, Hungary

ANTI-BACTERIAL, ANTI-BIOFILM AND ANTI-SWARMING EFFECTS OF EUCALYPT AND ORIENTAL SWEET GUM BARK EXTRACTIVES

DÖNMEZ, İ. E.[1*] – ÖNEM, E.[2]

[1]*Department of Forest Products Engineering, Faculty of Forestry, Isparta University of Applied Sciences, 32100 Isparta, Turkey*

[2]*Department of Main Pharmaceutical Sciences, Faculty of Pharmacy, Süleyman Demirel University, 32100 Isparta, Turkey*

**Corresponding author*
e-mail: emrahdonmez@isparta.edu.tr; phone: +90-246-211-3968; fax: +90-246-211-3948

(Received 29th May 2018; accepted 31st Jul 2018)

Abstract. Current study focused on two phases; in the first the composition and the amount of extractives were determined. Thus, hexane and acetone:water (95:5, v:v) extracts of *Eucalyptus camaldulensis* and *Liquidamber orientalis* bark were analysed by GC-MS to determine lipophilic and hydrophilic extractive composition of these species. The second phase was to identify anti-bacterial, anti-biofilm and anti-swarming effects of the gathered extractives. Total amount of lipophilic extractives was found 3.90 mg/g in *E. camaldulensis* whereas it was determined as 7.67 mg/g in *L. orientalis* bark. However, total amount of hydrophilic extractives in *E. camaldulensis* bark (55.51 mg/g) had almost 1.5 times more than *L. orientalis* bark (39.19 mg/g). Fatty acids and sugar groups were the dominant groups as lipophilic and hydrophilic, respectively, in both species. Anti-bacterial test was carried out by using three Gram-positive (*Staphylococcus aureus*, *Methicillin Resistant Staphylococcus aureus*, *Bacillus cereus*) and three Gram-negative (*Pseudomonas aeruginosa*, *Escherichia coli* and *Pseudomonas aeruginos*a PA01) strains with agar well diffusion method. In addition, the minimum inhibitory concentrations (MICs) of the extracts were also determined using the micro-dilution method. When hexane and acetone:water (95:5, v:v) extracts of *E. camaldulensis* and the acetone:water (95:5, v:v) extract of *L. orientalis* have anti-bacterial effect on Gram-positive bacteria but they do not have anti-bacterial effect on the tested Gram-negative bacteria. Whereas the hexane extract of *L. orientalis* did not show anti-bacterial activity on any tested strains. The minimum inhibitory concentration of these extracts ranged from 0.52 to 51.5 mg/ml. It was also found that hexane extract of *E. camaldulensis* inhibited biofilm formation and acetone extract of *L. orientalis* and *E. camaldulensis* indicated anti-swarming activity on P. aeruginosa PA01.
Keywords: *Eucalyptus camaldulensis, Liquidamber orientalis, extractives, anti-bacterial activity, quorum sensing*

Introduction

Extractives affect such functions in a tree as texture, odor, taste and color. They compose 5-10% of a tree's chemical substances by weight. In general terms, extractives are lipophilic and hydrophilic substances that are soluble in neutral solvents (Fengel and Wegener, 1989; Sjöström, 1993; Holmbom, 1999). Lipophilic extractives mostly consist of fats, fatty acids, resin acids and sterols and they are chemical substances that are soluble in dichloromethane, ether and some hydrocarbon solvents. Moreover, hydrophilic extractives are substances like carbohydrates, lignans, phenols, stilbens and chalkones that are soluble in such polar solvents as water, alcohol and acetone (Holmbom, 1999).

http://www.aloki.hu ● ISSN 1589 1623 (Print) ● ISSN 1785 0037 (Online)
DOI: http://dx.doi.org/10.15666/aeer/1605_62676279
© 2018, ALÖKI Kft., Budapest, Hungary

Although wood and bark of a tree have similar chemical composition, there are big differences regarding the amount of extractives in the bark. The essential chemicals for the plant, like cellulose and hemicelluloses, have lower amount in the bark but the amount of lignin and especially extractives is always higher in the bark than in its wood.

Oriental sweet gum (*Liquidamber orientalis*) is classified in *Hammalidaceae* family in the plant kingdom and it occurs as tree or a bush. It has thick branches and balsam cells in its wood. *L. orientalis* can only be seen in Muğla, Turkey (south Aegean part of Turkey) and can grow up to 15-20 m height (Anşin and Özkan, 1993). The oil, gathering from its stem, is used in the production of soap, perfumery and medicine and also in incenses because of its nice odor. Since most of the studies have been focused on sweetgum oil there are limited knowledge about wood and bark of this species. Istek and Hafizoğlu (2005) investigated main chemical composition and the solubility values of wood and bark of *L. orientalis*.

Eucalypt *(Eucalyptus camaldulensis)* is a fast growing woody taxon in the form of a tall-tree. It usually occurs in coastal areas having warmer weather and it can grow up to 90 m. *E. camaldulensis* has dark-colored heartwood and light yellow sapwood. It has valuable wood that can be evaluated in such industries as mine poles, packaging, pulp and paper. In addition, eucalyptol is produced from the leaves of *E. camaldulensis* and it is used in pharmacy and soap industry. Thus, it is called as "malaria tree" because they dry marshes causing malaria disease in tropical areas (Anşin and Özkan, 1993).

Plant bark is considered as the source of energy by burning it in many industries (Hemingway, 1981). However, in recent years, it is known by the studying of the chemical composition of bark that it is a rich source of chemical substances like lipophilic and other phenolic compounds (Kahkonen et al., 1999; Freire et al., 2002a, b; Pietarinen et al., 2006; Ferreira et al., 2013).

Using plants as a treatment of some illness is common all over the world since ancient times. Besides, plants are also being used for combating bacterial infections. Inappropriate consumption of antibiotics causes the development of resistant bacteria and after a while causes the antibiotics to become inefficient (Chitemerere and Mukanganyama, 2011). All these problems made it necessary to develop new strategies in combating with bacteria. After the discovery of cell to cell communication system in bacteria it has been thought that this is a new way to combat with bacteria and studies have focused on inhibition of this system. This communication known as the quorum sensing (QS), and it is responsible for regulating production of some virulence factors such as elastase, alkaline protease, pyocyanin, phospholipase and exotoxin A, biofilm formation and swarming motility in some bacteria (Lee and Zhang, 2015). *P. aeruginosa* is a major cause of hospital-acquired bacterial infections, especially isolated from patients with cystic fibrosis (Overhage et al., 2008). It is now known that *P. aeruginosa* regulate biofilm formation and swarming motility processes through a QS. Given its importance as a virulence, treatment of bacterial biofilm with antibiotics is more difficult than infections caused by planktonic bacteria (Bjarnsholt et al., 2010; Lee and Zhang, 2015).

For this purposes most researchers focus on plant extracts or essential oils of plants. Therefore, in the present study, it was aimed to determine anti-bacterial properties and anti-quorum sensing effect of bark extractives from *E. camaldulensis* and *L. orientalis* and also the amount and the composition of extractives gathered from different solvents.

http://www.aloki.hu ● ISSN 1589 1623 (Print) ● ISSN 1785 0037 (Online)
DOI: http://dx.doi.org/10.15666/aeer/1605_62676279
© 2018, ALÖKI Kft., Budapest, Hungary

Material and method

Material

L. orientalis and *E. camaldulensis* were taken from Köyceğiz, Muğla, Turkey and Tarsus, Mersin, Turkey where the altitude was 100 m and 85 m respectively. Bark samples were supplied from living trees by the aid of sharp knives in April 2017. All samples were stored at -24 °C until analyses. Barks were broken into small pieces, which were freeze-dried and ground by a Wiley mill to 1 mm (Ekman, 1983). To remove volatile compounds, the ground samples were treated with a second drying procedure.

Extraction

Approximately 10 g of ground bark from each sample was successively extracted with n-hexane to get lipophilic extractives and then with acetone:water (95:5, v:v) to obtain hydrophilic extractives by using Soxhlet apparatus. After extraction, aliquots of extractives were removed by using rotary evaporator to 100 ml and gravimetric analyses were carried out (Kilic et al., 2011; Dönmez et al., 2016). For gravimetric analyses, 10 ml of the aliquot was evaporated to dryness, i.e, constant weight, leaving a film of extractives in the solvent container. The containers were weighed before and after extraction to determine the extractive yield. Gravimetric analyzes were performed in 3 replicates. All results, given in mg/g are calculated for freeze-dried samples. The appropriate amount of mixture was evaporated under nitrogen prior to silylation. Hexane and acetone:water (95:5, v:v) extracts were injected to GC-MS for identifying lipophilics and hydrophilics.

Chromatographic analyses

GC-MS analyses were performed using a Shimadzu GC-2010 gas chromatograph equipped with an MS-QP 2010 plus a mass spectrometer (Shimadzu Corporation, Kyoto, Japan). The analyses conditions are as follows: column, Rxi-5Sil MS (30 m × 0.25 mm i.d. × 0.25 μm film thickness; Restek, Bellefonte, PA, USA); temperature program, from 60 °C (1 min) to 280 °C at 2 °C/min; injection temperature, 280 °C; carrier gas, He flow 1 mL/min; injection mode, split (10:1); MS temperature, 280 °C.

Test microorganisms and anti-bacterial activity test

The organisms included in this study were *S. aureus* ATCC 25923 *MRSA* ATCC 43300, *B. cereus* ATCC 11778, *P. aeruginosa* ATCC 27853, *E. coli* 25922, *P. aeruginosa* PA01.

Anti-bacterial activities of tree extracts were carried out by agar well diffusion assay Holder and Boyce (1994). According to assay, 1.5% agar medium as bottom layer and soft agar as an overlay layer was prepared in which 100 μl indicator microorganisms were inoculated (0.5 McFarland turbidity). Then, a hole with a diameter of 6 mm was punched aseptically with a sterile cork borer and 100 μL of the extracts were introduced into the well.

The plates were incubated for 18–24 h at 30/37 °C. Antibacterial activity was determined by the diameter of inhibition zones (mm) around the wells. DMSO was used as a negative control because extraction yields dissolve in it and Gentamicin was used as a positive control. All tests were repeated 3 times.

http://www.aloki.hu ● ISSN 1589 1623 (Print) ● ISSN 1785 0037 (Online)
DOI: http://dx.doi.org/10.15666/aeer/1605_62676279
© 2018, ALÖKI Kft., Budapest, Hungary

Minimum inhibitory concentration (MIC)

To determine the minimum inhibitory concentration (MIC) of the plant extracts serial dilution technique using 96-well microliter plates was performed (Andrews, 2001). 100 µl of bark extracts were added to the wells containing 100 µl of the medium and each well was diluted by serial two-fold dilutions. Finally, 10 µl of bacterial culture (0.5 McFarland standard) was added and plates were incubated at 37 °C for 24 h. The MIC was determined at the lowest concentration of the extracts where no visible growth of microorganisms was observed. Dimethyl sulfoxide was used as a control because of bark extracts dissolved in it and Mueller Hinton broth was used as a negative control by adding well without bacteria. Gentamicin was used as a positive control. The experiments were reproduced three times.

Biofilm formation assay

Inhibition effect of extracts on biofilm formation in standard strain *P. aeruginosa* PA01 was evaluated by crystal violet (CV) assay (O'Toole, 2011). For each treatment 3-6 replicate wells were used in a 96-well polystyrene plate. *P. aeruginosa* PA01 and different concentrations of extracts added to the wells and incubated for 48 h. After 48 h of incubation at 36 °C content of each well were dumped out and washed three times with distilled water to remove planktonic cells. Plate let to dry about 15 min. 250 µl 0.1% of crystal violet was added to each well and again left to dry for 15 min. Following staining for 15 min at room temperature all tubes were washed three times with distilled water. 250 µl of 95% ethanol was added each well after 15 min. The optical density of each well was measured at 570 nm by using Epoch Microplate Spectrofotometer. The experiments were reproduced three times and data were expressed as mean ±SD.

Swarming motility assay

For swarming assay prepared medium which contained 8 g/l nutrient broth, 5 g/l bacto agar and 0.5% glucose and 100 µl of bark extracts was added to each 20 ml medium. After poured swarm medium, 5 µl each supernatant of bacteria cultures was inoculated at the centre of the medium and the plates were incubated overnight at 37 °C. The ability to swarm was assessed by the distance of swarming from the central inoculation site (Lee and Zhang, 2015).

Statistical analysis

This study was designed according to Randomized Plot Design. Each treatment had three replications. Data were subjected to analysis of variance ANOVA with JUMP software and the differences among treatments were compared by LSD test.

Results and discussion

L. orientalis and *E. camaldulensis* barks were analysed by GC-MS to determine lipophilics and hydrophilics after extraction with different solvents. The amount of soluble substances in the solvents was calculated gravimetrically and shown in *Table 1*. The extent of solubility in hexane in *L. orientalis* bark (7.67 mg/g) was found two-times higher than *E. camaldulensis* bark (3.90 mg/g). However, the extent of solubility in acetone:water (95:5, v:v) was determined higher in *E. camaldulensis* bark (55.51 mg/g)

http://www.aloki.hu ● ISSN 1589 1623 (Print) ● ISSN 1785 0037 (Online)
DOI: http://dx.doi.org/10.15666/aeer/1605_62676279
© 2018, ALÖKI Kft., Budapest, Hungary

than *L. orientalis* bark (39.19 mg/g). Bark gravimetric analyses results is usually more concentrated when the bark is extracted by some polar solvents like acetone (Dönmez et al., 2016). Bark extractives and the amount can be seen in *Table 2*.

Table 1. *Gravimetric amount of extractives from L. orientalis and E. camaldulensis bark (mg/g of dry weight)*

Species	Hexane extracts	Acetone:water extracts
L. orientalis	7.67±0.02	39.19±0.41
E. camaldulensis	3.90±0.10	55.51±0.49

Fatty alcohols, fatty acids and sterols were detected as lipophilic extractives both in *L. orientalis* and in *E. camaldulensis* after extraction with n-hexane and injection to GC-MS. Total identified amount of fatty acids in *L. orientalis* bark was 72.46% and 51.22% in *E. camaldulensis* bark. Total amount of identified phytosterols (39.88%) and fatty alcohols (8.90%) was found higher in *E. camaldulensis* bark compared to *L. orientalis* bark 25.44% and 2.10%, respectively. Alcohol 18:0 was detected as the dominant fatty alcohol both in *L. orientalis* (1.19%) and in *E. camaldulensis* bark (3.14%).

The major fatty acid was Acid 24:0 in both samples. It was determined two-fold higher in *L. orientalis* bark (20.09%) than in *E. camaldulensis* bark (10.28%). Acid 24:0 was also detected in Turkish scots pine bark suberin monomers within the range of 0.52-1.70 mg/g (Dönmez et al., 2012).

Only three sterols were determined from the phytosterol group in both bark samples. While stigmasterol had the highest amount in *L. orientalis* bark (13.03%), stigmastenol was the major component with 27.74% in *E. camaldulensis* bark.

Table 2. *Extractive composition of L. orientalis and E. camaldulensis bark (%)*

Compound	*L. orientalis*		*E. camaldulensis*	
	Hexane	**Acetone:water**	**Hexane**	**Acetone:water**
Fatty alcohol	**2.10**		**8.90**	
Alcohol 11-12:1			0.30	
Alcohol 14:0	0.21		0.40	
Alcohol 16:0	0.37		2.82	
Alcohol 18:0	1.19		3.14	
Alcohol 9-18:1	0.33			
Alcohol 20:0			2.24	
Fatty acids	**72.46**	**4.16**	**51.22**	
Acid 10:0	1.29			
Acid 1.12-12:2	1.89			
Acid 14:0			0.54	
Acid 16:0	4.47	0.32	9.45	
Acid 9-16:1			2.64	
Acid 17:0	0.14		0.23	
Acid 9.12-18:2	8.17	1.20	5.84	
Acid 9-18:1	6.52	1.47	7.04	

http://www.aloki.hu ● ISSN 1589 1623 (Print) ● ISSN 1785 0037 (Online)
DOI: http://dx.doi.org/10.15666/aeer/1605_62676279
© 2018, ALÖKI Kft., Budapest, Hungary

Acid 18:0	3.34		3.36	
Acid 20:0	16.40		8.43	
Acid 22:0	6.21	1.17	3.41	
Acid 24:0	20.09		10.28	
Acid 26:0	3.94			
Sugar group		**67.56**		**86.96**
Xylitol		3.32		0.08
Inositol				0.11
Myo-Inositol				0.30
2-monooleglycerol				0.12
D-ribose		0.48		0.81
D-fructose		8.30		22.67
D-galactose		0.12		
D-turanose		19.79		0.10
D-galactofuranose		0.20		
Arabinose		1.24		0.10
Melibiose		1.03		
Allose		0.23		
Fucose		0.12		
Sucrose		3.16		3.30
Mannose				6.32
Maltose				0.11
Gulose		0.51		
α-D-galactopyranose				0.75
β-D-arabinopyranose				0.19
β-D-glucopyranose		13.37		21.79
α-D-glucopyranose		2.20		
β -L-mannofuranose		0.68		
β-D-mannopyranoside		0.30		
α-D-galactoside		0.25		0.13
α-L-galactofuranose,		1.14		
β-D-galactofuranose				0.10
Arabinofuranose				8.67
L-altrose				0.97
2-deoxy ribose		2.93		
D-glucitol		8.19		20.34
Phytosterols	**25.44**		**39.88**	
β-sitosterol	4.34		5.35	
Stigmasterol	13.03		6.79	
Stigmastenol	8.07		27.74	
Hydrocarbons		**6.56**		**5.50**
Tetradecane		0.98		0.75
Hexadecane		1.61		1.14

http://www.aloki.hu ● ISSN 1589 1623 (Print) ● ISSN 1785 0037 (Online)
DOI: http://dx.doi.org/10.15666/aeer/1605_62676279
© 2018, ALÖKI Kft., Budapest, Hungary

Eicosane		1.22		1.26
Docosane		1.49		1.32
Tetracosane		1.26		1.03
Phenolics		**21.72**		**7.54**
Gallic acid		11.04		1.34
1,2-benzenedicarboxylic acid		2.26		1.50
Benzoic acid		3.22		3.95
Ferulic acid		0.62		0.75
Cinnamyl cinnamate		2.47		
Glycerol		2.11		

Hydrophilic extractives was determined by the extraction of bark samples with acetone:water (95:5, v:v) and then injected to GC-MS just after n-hexane. Sugar group was seen as the major hydrophilics both in *L. orientalis* and in *E. camaldulensis* bark. Glucose, xylose, arabinose and galactose were determined as dominant monomeric components of some barks (Miranda et al., 2016, 2013; Ruiz-Aquinon et al., 2015). However, the dominant monosaccharides were D-turanose (19.79%), D-glucopyranose (13.37%) and D-fructose (8.30%) in *L. orientalis* bark and D-fructose (22.67%), D-glucopyranose (21.79%) and D-glucitol (20.34%) in *E. camaldulensis* bark.

Total amount of identified phenolics was 21.72% in *L. orientalis* bark and 7.54% in *E. camaldulensis* bark. In the phenolics group, gallic acid (11.04%) and benzoic acid (3.95%) had the highest amount in *L. orientalis* and *E. camaldulensis* bark, respectively.

According to the anti-bacterial test results of the extracts; it was observed that acetone and hexane extracts of *E. camaldulensis* and acetone extract of *L. orientalis* showed anti-bacterial effect on Gram-positive bacteria (*S. aureus*, *MRSA*, *B. cereus*) at different rates whereas no inhibition effect was observed on other Gram-negative bacteria. Unlike these results, it was not observed anti-bacterial effect of hexane extract of *L. orientalis* on both Gram-positive and Gram-negative bacteria. Results obtained from anti-bacterial activity tests can be seen in *Table 3*. Except hexane extract of *L. orientalis* other extracts showed similar inhibition results on the tested bacteria. In acetone extract of *E. camaldulensis*, the highest inhibition zone was found 18.3 mm on MRSA and 17.7 mm, 15.3 mm *B. cereus* and *S. aureus,* respectively. When acetone extract of *E. camaldulensis* with hexane extract were compared similar results were detected. The average MIC value of the plant extracts against *S. aureus* was 12.5 mg/ml to 51.5 mg/ml. All three extracts showed efficient inhibition at the lowest MIC values in *B. cereus* (*Table 4*).

Table 3. *Inhibition zone (mm) of E. camaldulensis and L. orientalis bark extracts (acetone, hexane)*

	E. Cml. **(acetone)**	***E. Cml.*** **(hexane)**	***L. Ori.*** **(acetone)**	***L. Ori.*** **(hexane)**	**Gentamicin**	**DMSO**
S. aureus	15.3±0.58	16.00±0.00	13.7±1.15	NI	19.00±0.00	NI
MRSA	18.3±0.58	18.7±0.58	13.7±0.58	NI	19.33±0.58	NI
B. cereus	17.7±0.58	13.00±1.00	15.00±1.00	NI	19.66±0.58	NI

NI: No inhibition, E. Cml: *Eucalyptus camaldulensis,* L. Ori: *Liquidamber orientalis*

http://www.aloki.hu ● ISSN 1589 1623 (Print) ● ISSN 1785 0037 (Online)
DOI: http://dx.doi.org/10.15666/aeer/1605_62676279
© 2018, ALÖKI Kft., Budapest, Hungary

Table 4. *MIC value of E. camaldulensis and L. orientalis bark extracts (mg/ml)*

	E. camaldulensis **(acetone)**	***E. camaldulensis*** **(hexane)**	***L. orientalis*** **(acetone)**
S. aureus ATCC 25923	16.7	12.5	51.5
MRSA ATCC 43300	8.35	12.5	51.5
B. cereus ATCC 11778	0.52	0.78	1.61

Inhibition effect of plant extracts on *S. aureus* compared with antibiotic, three different groups were formed (**P < 0.01), hexane and acetone extracts of *E. camaldulensis* (16 mm, 15.3 mm) showed similar effects to antibiotics in the second group. Acetone extract of *L. orientalis* (13.7 mm), however, has been the lowest effective extract for *S. aureus*. In addition to *S. aureus* test results, according to statistical evolution results of MRSA hexane and acetone extracts of *E. camaldulensis* (18.7 mm, 18.3 mm) were significant (**P < 0.01) compared with antibiotic (19.3 mm) (*Fig. 1*).

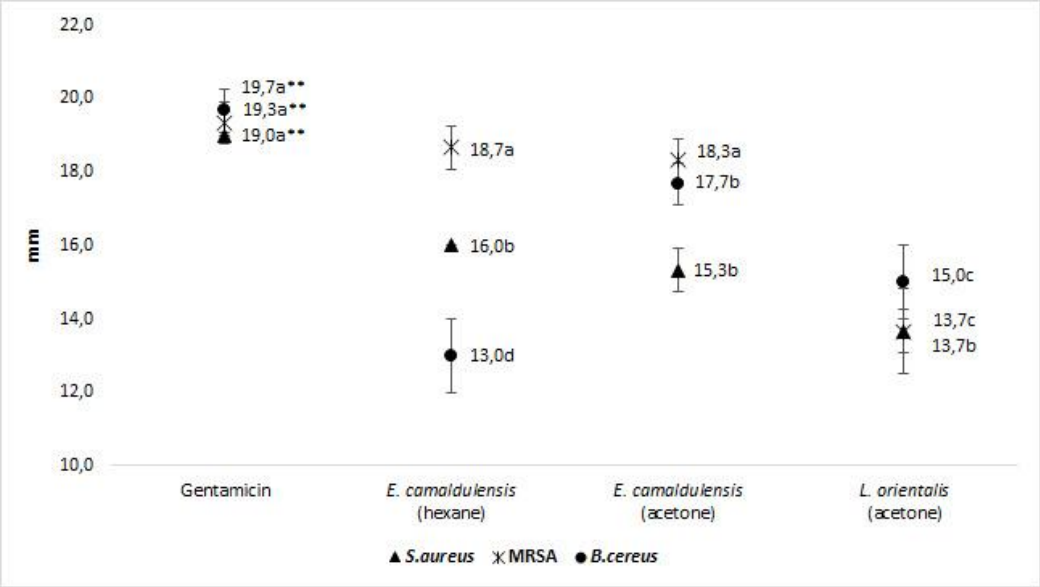

Figure 1. *Antibacterial effects of plant extracts. **Differences between mean values followed by different letters of plant extracts in the same bacteria are statistically significant at P < 0.01. Bars = Sd±*

Anti-biofilm assay results showed that only hexane extract of *E. camaldulensis* had inhibition effect on biofilm formation at 25 mg/ml concentration and 52% inhibition rate on *P. aeruginosa* PA01 (*Fig. 2*). According to statistical analysis of biofilm formation results, acetone extracts of *E. camaldulensis* (1.02) and *L. orientalis* (1.23) showed similar effect by entering the same statistical group as control (1.03) (*Table 5*).

Previous studies showed that some natural compounds from plants had a great potential to inhibit biofilm formation. In a study, gallic and ferulic acids were investigated and the two phenolic acids demonstrated the potential to inhibit swarming

http://www.aloki.hu ● ISSN 1589 1623 (Print) ● ISSN 1785 0037 (Online)
DOI: http://dx.doi.org/10.15666/aeer/1605_62676279
© 2018, ALÖKI Kft., Budapest, Hungary

motility and to prevent biofilm in *P. aeruginosa* (Borges et al., 2012). Our results also showed that acetone extracts of plants include different amount of ferulic and gallic acids.

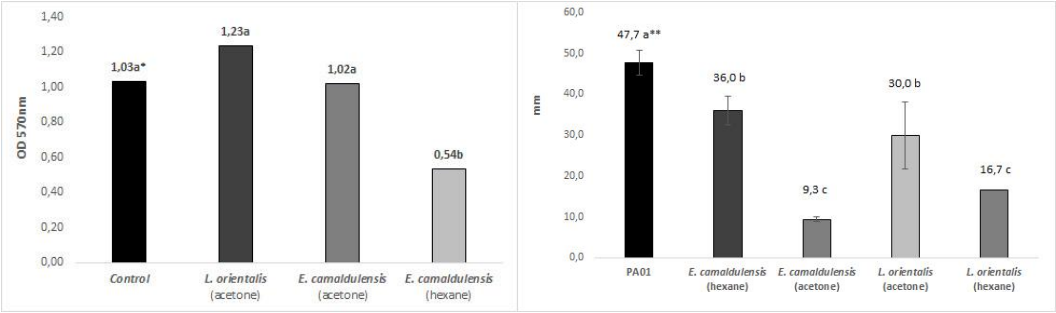

Figure 2. *Anti-biofilm (left) and anti-swarming (right) effect of plant extracts. *Differences between mean values followed by different letters of plant extracts are statistically significant at $p < 0.05$*

Table 5. *Variance analysis of biofilm formation*

Source	DF	Sum of squares	Mean square	F Ratio
Model	3	0.7877409	0.262580	5.0347
Error	8	0.4172300	0.052154	**Prob > F**
C. Total	11	1.2049709		0.0301*

Gram-positive bacteria were more sensitive than Gram-negative bacteria to most plant material. It is thought to be due to the lipopolysaccharide layer that the Gram-negative bacteria have. As a result, it might have a role as a barrier to the phytochemical substances that are responsible for anti-bacterial activity (Nazzaro et al., 2013). Results from this study also showed that Gram-positive bacteria were more susceptible to extracts than Gram-negative bacteria. It was also observed that there was not any anti-bacterial activity detected in Gram-negative (*P. aeruginosa*, *E. coli* and *P. aeruginosa* PA01) bacteria in the studied concentration.

QS inhibitory compounds that do not kill or inhibit microbial growth are less likely to impose a selective pressure for the development of resistant bacteria (Uğurlu et al., 2016). In the present study, plant extracts showed no anti-bacterial effect on *P. aeruginosa* PA01. In order to detect anti-biofilm effect of extracts CV assay were done. Anti-biofilm assay results showed that only hexane extract of *E. camaldulensis* had inhibition effect on biofilm formation on *P. aeruginosa* PA01. In a similar study with some Gram-positive and Gram-negative bacteria anti-biofilm effect of bark extract of *E. camaldulensis* were investigated and results showed that there was significant inhibition in biofilm formation on tested bacteria (Sidkey and Omran, 2017). In a study with anti-biofilm activity of eucalypt oil has been evaluated in urinary tract pathogen *Proteus mirabilis* was ascertained (Mathur et al., 2013, 2014). Swarming motility is one of the major virulence factors that is known to play a role in early biofilm development (Uğurlu et al., 2016). As can be seen from *Figure 3* the greatest inhibition of swarming motility was examined by acetone extract of *E. camaldulensis* (81%) and *L. orientalis* (65%).

http://www.aloki.hu ● ISSN 1589 1623 (Print) ● ISSN 1785 0037 (Online)
DOI: http://dx.doi.org/10.15666/aeer/1605_62676279
© 2018, ALÖKI Kft., Budapest, Hungary

Figure 3. *Effect of plant extracts on swarming motility (Scale bar = 30 mm)*

For swarming motility assay, the control (PA01; 47.7 mm) received the highest value and the other applications were statistically separated from the control. The lowest swarm diameters of acetone extracts of *E. camaldulensis* (9.3 mm) and hexane extracts of *L. orientalis* (16.7 mm) were included in the third statistical group ($P < 0.01$ **) (*Table 6*). Many studies were reported about inhibition effects of essensial oils of *E. camaldulensis* and *L. orientalis* on swarming motility but this is the first report with bark extracts.

Table 6. *Variance analysis of swarming motility*

Source	DF	Sum of Squares	Mean Square	F Ratio
Model	6	2801.4667	466.911	20.1399
Error	8	185.4667	23.183	**Prob > F**
C. Total	14	2986.9333		0.0002*

Mostafa et al. (2014) found the anti-bacterial effects of hexane extract of *E. camaldulensis* against *S. aureus* and *B. cereus* 12 mm and 11 mm zone diameter respectively. There was no inhibition effect on *P. aeruginosa* like in our results.

Although there are some anti-bacterial activity studies with leaf extracts of *L. orientalis*, antibacterial activity of *L. orientalis* bark extracts is out of our knowledge. In a study with leaf extracts of *L. orientalis*, anti-bacterial activity was observed on *S. aureus* with 15.3 mm diameter. Contrary to our work they also detected anti-bacterial activity on Gram-negative *E. coli* and *P. aeruginosa* on leaf extracts (Köse et al., 2016). The differences in results might be the concentration of the extracts or synergistic reactions of the various phytochemicals in different part of plants (Onuh et al., 2017). On the other hand, solvent variation effects diversity of phytochemical compounds via polarity features (Shagal et al., 2012). Most of the anti-microbial active compounds were soluble in polar solvent such as alcohol and water (Parekh et al., 2006; Yazdi et al., 2015). Thus, different results might be revealed in studies. According to our results of bark extracts of *L. orientalis*, the diameter of inhibition zones ranging from 13.7 mm to 15 mm was observed. The highest inhibition activity was found in *B. cereus* with 15 mm and there were other results with the same range (13.7 mm) against *S. aureus* and MRSA.

Conclusions

Hexane and acetone:water (95:5, v:v) extracts of *L. orientalis and E. camaldulensis* bark were analysed by GC-MS to get lipophilic and hydrophilic extractives. It was observed that in the total amount of acetone:water (95:5, v:v) extracts hydrophilics had

http://www.aloki.hu ● ISSN 1589 1623 (Print) ● ISSN 1785 0037 (Online)
DOI: http://dx.doi.org/10.15666/aeer/1605_62676279
© 2018, ALÖKI Kft., Budapest, Hungary

higher value in both species. Fatty acids were the most abundant group as lipophilics in hexane extracts and Acid 24:0 was detected with the highest concentration both in *L. orientalis* (20.09%) and in *E. camaldulensis* bark (10.28%). While D-turanose had the highest value in *L. orientalis* bark (19.79%), β-D-glucopyranose was detected as the major component in *E. camaldulensis* bark (21.79%).

Acetone, hexane extracts of *E. camaldulensis* and acetone extract of *L. orientalis* had anti-bacterial activity against some Gram-positive bacteria. But none of those extracts showed anti-bacterial activity on Gram-negative bacteria. Besides these results, hexane extracts of *E. camaldulensis* bark showed anti-biofilm activity against *P. aeruginosa* PA01 and acetone extract of *E. camaldulensis* and *L. orientalis* showed anti-swarming activity. Antibiotic resistance is a crucial problem in the treatment of infectious diseases, so new strategies must be tried and developed. Thus, *E. camaldulensis*, *L. orientalis* can be good resources to fight against pathogen bacteria and active components of these plants might be tried in further studies. Not only anti-bacterial features but also inhibition effects of bark extracts in QS-regulated virulence are thought to be potential sources to struggle with infectious diseases.

REFERENCES

[1] Andrews, J. M. (2001): Determination of minimum inhibitory concentrations. – Journal of Antimicrobial Chemotherapy 48: 1 5-16.

[2] Anşin, R., Özkan, Z. C. (1993): Seed Plants (Spermatophyta) Woody Taxa (in Turkish: Tohumlu Bitkiler (Spermatophyta) Odunsu Taksonlar). – Black Sea Technical University Faculty of Forestry Publications, Trabzon, Turkey.

[3] Bjarnsholt, T., Gennip, M. V., Jakobsen, T. H., Christensen, L. D., Jensen, P. Ø., Givskov, M. (2010): In vitro screens for quorum sensing inhibitors and in vivo confirmation of their effect. – Nature Publishing Group 5: 2 282-293.

[4] Borges, A., Saavedra, M. J., Simoes, M. (2012): The activity of ferulic and gallic acids in biofilm prevention and control of pathogenic bacteria. – Biofouling 28: 7 755-767.

[5] Chitemerere, T. A., Mukanganyama, S. (2011): In-vitro antibacterial activity of selected medicinal plants from Zimbabwe. – African Journal of Plant Science and Biotechnology 5: 1-7.

[6] Dönmez, I. E., Hafızoğlu, H., Kılıç, A., Hemming, J., Eckerman, C. (2012): Effect of altitude on the composition of suberin monomers in the outer bark of Scots pine (*Pinus sylvestris* L.). – Industrial Crops and Products 37: 441-444.

[7] Dönmez, İ. E., Hemming, J., Willför, S. (2016): Bark extractives and suberin monomers from *Arbutus andrachne* and *Platanus orientalis*. – BioResources 11(1): 2809-2819.

[8] Ekman, R. (1983): The suberin monomers and triterpenoids from the outer bark of *Betula verrucosa* (Ehrh.). – Holzforschung 37: 4 205-211.

[9] Fengel, D., Wegener, G. (1989): Wood Chemistry. Ultrastructure, Reactions. – Walter de Gruyter, Berlin.

[10] Ferreira, R., Garcia, H., Sousa, A. F., Freire, C. S. R., Silvestre, A. J. D., Rebelo, L. P. N., Pereira, C. S. (2013): Isolation of suberin from birch outer bark and cork using ionic liquids: A new source of macromonomers. – Industrial Crops and Products 44: 520-527.

[11] Freire, C. S. R., Silvestre, A. J. D., Neto, C. P. (2002a): Identification of new hydroxy fatty acids and ferulic acid esters in the wood of *Eucalyptus globulus.* – Holzforschung 56: 143-149.

[12] Freire, C. S. R., Silvestre, A. J. D., Neto, C. P., Cavaleiro, J. A. S. (2002b): Lipophilic extractives of the inner and outer barks of *Eucalyptus globulus*. – Holzforschung 56: 372-379.

http://www.aloki.hu ● ISSN 1589 1623 (Print) ● ISSN 1785 0037 (Online)
DOI: http://dx.doi.org/10.15666/aeer/1605_62676279
© 2018, ALÖKI Kft., Budapest, Hungary

[13] Hemingway, R. W. (1981): Bark: its Chemistry and Prospects for Chemical Utilization. – In: Goldstein, I. S. (ed.) Organic Chemicals from Biomass. CRC Press, Boca Raton.
[14] Holder, I. A., Boyce, S. T. (1994): Agar well diffusion assay testing of bacterial susceptibility to various antimicrobials in concentrations non-toxic for human cells in culture. – Burns 20(5): 426-429.
[15] Holmbom, B. (1999): Extractives. – In: Sjöström, E., and Alén, R. (eds.) Analytical Methods in Wood Chemistry, Pulping, and Papermaking. Springer-Verlag, Berlin.
[16] İstek, A., Hafızoğlu, H., (2005): The Chemical Components in Wood and Bark Of Sweetgum (*Liquidambar orientalis* Mill.). – Journal of Forestry Faculty, Gazi Uni.-Kastamonu 5(1): 1-6.
[17] Kähkönen, M. P., Hopia, A. I., Vuorela, H. J., Rauha, J. P., Pihlaja, K., Kujala, T. S., Heinonen, M. (1999): Antioxidant activity of plant extracts containing phenolic compounds. – Journal of Agricultural and Food Chemistry 47: 3954-3962.
[18] Kilic, A., Hafızoğlu, H., Dönmez, İ. E., Tümen, İ., Sivrikaya, H., Reunanen, M., Hemming, J. (2011): Extractives in the cones of *Pinus* species. – European Journal of Wood and Wood Products. 69: 37-40.
[19] Köse, M. D, Bayraktar, O., Balta, A. B. (2016): Antioxidant and antimicrobial activities of extracts from some selected Mediterranean plant species. – International Journal of New Technology and Research (IJNTR) 2(5): 113-118.
[20] Lee, J., Zhang, L. (2015): The hierarchy quorum sensing network in *Pseudomonas aeruginosa*. – Protein Cell 6(1): 26-41.
[21] Mathur, S., Udgire, M., Khambhapati, A. (2013): Effect of essential oils on biofilm formation by Proteus mirabilis. – International Journal of Pharma and Bio Sciences 4(4): 1282-1289.
[22] Mathur, S., Udgire, M., Khambhapati, A., Paul, D. (2014): Anti-biofilm activity and bioactive component analysis of eucalyptus oil against urinary tract pathogen. – International Journal of Current Microbiology and Applied Sciences (IJCMAS) 3(5): 912-918.
[23] Miranda, I., Gominho, J., Mirra, I., Pereira, H. (2013): Fractioning and chemical characterization of barks of *Betula pendula* and *Eucalyptus globulus*. – Industrial Crops and Products 41: 299-305.
[24] Miranda, I., Lima, L., Quilhó, T., Knapic, S., Pereira, H. (2016): The bark of *Eucalyptus sideroxylon* as a source of phenolic extracts with anti-oxidant properties. – Industrial Crops and Products 82: 81-87.
[25] Mostafa, M., Hossain, H., Hasan, M. M., Hossain, M. A., Parveen, S. (2014): Antibacterial activity of six medicinal plants used in traditional medicine growing in Bangladesh. – International Journal of Pharmaceutical Sciences and Research 5(6): 2210-2215.
[26] Nazzaro, F., Fratianni, F., De Martino, L., Coppola, R., De Feo, V. (2013): Effect of essential oils on pathogenic bacteria. – Pharmaceuticals 6: 1451-1474.
[27] Onuh, J. O., Idoko, G., Yusufu, P., Onuh, F. (2017): Comparative studies of the phytochemical, antioxidant and antimicrobial properties of cashew leaf, bark and fruits extracts. – American Journal of Food and Nutrition 5: 115-120.
[28] O'Toole, G. A. (2011): Microtiter dish biofilm formation assay. – Journal of Visualized Experiments 47: 2437.
[29] Overhage, J., Bains, M., Brazas, M. D., Hancock, R. E. (2008): Swarming of *Pseudomonas aeruginosa* is a complex adaptation leading to increased production of virulence factors and antibiotic resistance. – Journal of Bacteriology 190: 2671-2679.
[30] Parekh, J., Karathia, N., Chanda, S. (2006): Evaluation of antibacterial activity and phytochemical analysis of *Bauhinia variegata* L. bark. – African Journal of Biomedical Research 9: 53-56.

http://www.aloki.hu ● ISSN 1589 1623 (Print) ● ISSN 1785 0037 (Online)
DOI: http://dx.doi.org/10.15666/aeer/1605_62676279
© 2018, ALÖKI Kft., Budapest, Hungary

[31] Pietarinen, S. P., Willför, S. M., Athotupa, M. O., Hemming, J. E., Holmbom, B. R. (2006): Knotwoods and bark extracts: Strong antioxidants from waste materials. – Journal of Wood Science 52: 436-444.
[32] Ruiz-Aquino, F., Gonzalez-Pena, M. M., Valdez-Hernandez, J. I., Revilla, U. S., Romero-Manzanares, A. (2015): Chemical characterization and fuel properties of wood and bark of two oaks from Oaxaca, Mexico. – Industrial Crops and Products 65: 90-95.
[33] Shagal, M. H., Kubmarawa, D., Tadzabia, K., Dennis, K. I. (2012): Evaluation of phytochemical and antimicrobial potentials of roots, stem-bark and leaves extracts of *Eucalyptus camaldulensis*. – African Journal of Pure and Applied Chemistry 6: 74-77.
[34] Sidkey, B., A., J., Omran, A., H. (2017): Evaluation of the antibacterial effects of *Eucalyptus camaldulensis* L., *Glycyrrhiza glabra* L. and *Morus nigra* L. extracts against some pathogenic bacteria in vitro. – Iraqi Journal of Science 58: 1371-1380.
[35] Sjöström, E. (1993): Wood Chemistry Fundamentals and Applications (2nd edition). – Academic Press, San Diego.
[36] Uğurlu, A., Karahasa, A., Ulusoy, S., Aksu, B., Tınaz, B. G. (2016): Phenolic compounds affect production of pyocyanin, swarming motility and biofilm formation of *Pseudomonas aeruginosa*. – Asian Pacific Journal of Tropical Biomedicine 6: 698-701.
[37] Yazdi, F. T., Behbahani, B. A., Zanganeh, H. (2015): The comparison among antibacterial activity of *Mespilus germanica* extracts and number of common therapeutic antibiotics "in vitro". – Zahedan Journal of Research in Medical Sciences 7: 5190.

http://www.aloki.hu ● ISSN 1589 1623 (Print) ● ISSN 1785 0037 (Online)
DOI: http://dx.doi.org/10.15666/aeer/1605_62676279
© 2018, ALÖKI Kft., Budapest, Hungary

REMOTE SENSING-BASED EXTRACTION OF SUMMER SNOWLINE AND ANALYSIS OF ITS VARIATION CHARACTERISTICS IN XINJIANG, CHINA

HU, L. Q.[2] – ZHANG, L. C.[1*] – LI, S.[3] – LI, H. J.[4] – ZHANG, T. W.[3] – HOU, X. G.[2]

[1]*Xinjiang Climate Center, Urumqi 830002, China*

[2]*Xinjiang Meteorological Service Center, Urumqi 830002, China*

[3]*Institute of Desert Meteorology, China Meteorological Administration, Urumqi 830002, China*

[4]*College of Geography Science and Tourism, Xinjiang Normal University Urumqi, Xinjiang 830054, China*

**Corresponding author*
e-mail: 524480929@qq.com

(Received 31st May 2018; accepted 2nd Aug 2018)

Abstract. As a zero-balance line, lying between snow-covered and snow-free land areas, the snowline reflects the melting and retreating of snow and ice, which also mirrors the basic situation of climate and environment on mountain plateaus and in polar regions where there is a lack of ground meteorological stations. Thus, it is important to accurately extract and assess the distribution characteristics of the snow-line from hydrological, climatological, and geological aspects. This study extracted summer snowline data from the Xinjiang region in China using the snow cover duration ratio (SCDR) method with MODIS daily snow cover products (MOD10A1 and MYD10A1), IMS and Landsat data, and temperature and precipitation observations from 2001–2015. The variation and distribution characteristics of the summer snowline elevation were analyzed comparatively for the Xinjiang region and its different subareas. The results showed that snowline elevation data extracted using the SCDR method passed the accuracy test and therefore, it was considered suitable for the Xinjiang region. During 2001–2015, the average snowline elevation remained at about 3950 m within a 250-m range of fluctuation. However, linear trend analysis revealed an annual increasing trend of average snowline elevation with a tendency rate of 160.38 m/decade. The minimum snowline elevation exhibited a fluctuating upward trend, whereas the maximum snowline elevation showed a slight downward trend. Comparative analysis of snowline elevation in different areas of the Xinjiang region revealed a fluctuating upward trend in the Kunlun, Tianshan, and Altai Mountains. The Altai Mountains showed the most stable variation of snowline elevation, followed by the Kunlun Mountains and then the Tianshan Mountains. Spatially, the distribution of snowline elevation in the Xinjiang region was characterized by a decline from south to north with longitudinal zonation.
Keywords: *Xinjiang, summer snowline, snow cover duration ratio method*

Introduction

Traditionally, snowline elevation has been determined mainly by artificial means (Jiang, 1987; Wang et al., 2003; Hangel and Maurer, 2011; Liu et al., 2015). For example, ground stations for field observations would be established and devices used to perform the measurements. However, such methods are time consuming, costly, and provide only limited numbers of samples (Li et al., 2013). Subsequently, the Hess method was introduced to measure snowline altitude (ELAh) indirectly (Deng et al., 2006; Wang et al., 2010; Nie et al., 2013). Although this method overcame some of the disadvantages of direct measurement, the ELAh measured was primarily confined to large glaciers. Additionally, this method could only acquire static ELAh and it could not

http://www.aloki.hu ● ISSN 1589 1623 (Print) ● ISSN 1785 0037 (Online)
DOI: http://dx.doi.org/10.15666/aeer/1605_62816298
© 2018, ALÖKI Kft., Budapest, Hungary

rapidly reflect the state of snowline variation. With the development of remote sensing technology, McFadden et al. (2011) identified snowline spatial distribution using Landsat TM and ETM+ satellite images. Furthermore, based on ASTEG–DEM, this research group also extracted the range of ELAh in the area of glacier coverage in the Peruvian Andes. Using LISS III and AWIFS data from the United States, Brahmbhatt et al. (2012) calculated the glacier mass balance and extracted the glacier snowline in the Warwan and Bhut Basins in northern India during 2005–2007. Moreover, Xiao et al. (2010) introduced an analysis of water flow path into the extraction of snowline information based on remote sensing data.

Complex topography makes access difficult to mountainous glacier areas, and therefore, to meet the requirements for macroscopic, comprehensive, and rapid monitoring of snowline variation, remote sensing-based snowline extraction methods remain the focus of future development. Several different types of snowline have been proposed as a consequence of snowline research (Jiang et al., 2004), e.g., the theoretical snowline, local snowline, glacier equilibrium line, permanent snowline, and seasonal snowline. Presently, no research is available in the literature regarding the snowline in the Xinjiang region of China. Recently, the area of snow cover in the Xinjiang region has shown increasing variability with a downward trend (Sa et al., 2013). From the perspective of seasonal variation, a study of summer snowline is most informative regarding snow cover stability and snow water resources. Therefore, in this study of the Xinjiang region, we adopted the term snowline to mean the summer snowline. Using MODIS daily snow cover products (MOD10A1 and MYD10A1) after cloud removal for 2001–2015, we extracted snowline data using the snow cover duration ratio (SCDR) method, and we analyzed the dynamic variation characteristics of snowline elevation.

Materials and methods

Study area

Xinjiang is located in the center of the Eurasian continent (33°86'–48°50'N, 73°18'–96°69'E) (*Fig. 1*). It is part of China's northwest frontier and it covers an area of 1,664,900 km^2, accounting for 1/6 of the total land area of China (Sa et al., 2013). The topography can be described broadly as two basins between three mountain ranges. To the south are the Kunlun Mountains, which extend eastward from Pamirs, bordering the Tarim and Qaidam deserts. They have a warm temperate climate with little precipitation; however, with increasing elevation, the warm temperate climate shifts to alpine desert and the amount of precipitation increases accordingly. To the north are the Altai Mountains, which have a continental climate with warm and rainy summers and cold winters. While there is little snow in the valleys, heavy snowfall occurs in the high mountains. The Tianshan Mountains cross central Xinjiang, dividing the region into two parts. The northern slopes of the Tianshan Mountains have a humid to semiarid climate, with an average annual temperature of 0.9 °C and average annual precipitation of 450–800 mm (Zhang et al., 2015b). The foothills of the southern slopes of the Tianshan Mountains extend southward and connect with the Tarim Basin. Because of the influence of the Tarim Basin desert, the southern slopes have higher temperatures than the northern slopes and they receive little precipitation.

Considering the Xinjiang region as an entity, it is far from the sea and it is surrounded by high mountains. It has a typical temperate continental arid climate, with large variation of temperature, long duration of sunshine hours (average annual

http://www.aloki.hu ● ISSN 1589 1623 (Print) ● ISSN 1785 0037 (Online)
DOI: http://dx.doi.org/10.15666/aeer/1605_62816298
© 2018, ALÖKI Kft., Budapest, Hungary

sunshine duration: 2500–3500 h), and dry air. The average annual precipitation is ~150 mm, but this varies considerably in the different subareas. The average annual surface water resources of the Xinjiang region are 789 × 108 m^3, accounting for only 3% of China's total surface water resources, and in the ranking of water production per unit area in China, Xinjiang is third from bottom (Gao et al., 2010). For a province covering 1/6 of China's total land area, this shortage of water resources is particularly serious (Lu et al., 2007). However, the Xinjiang region has abundant snow cover resources that account for ~1/3 of the total snow cover in China (Wang and Che, 2012). Snow cover water resources provide a lifeline to the arid areas of the Xinjiang region; where there is snow cover on the mountains, there is often an associated oasis development on the piedmont plain. In recent years, the reserves of snow and ice in this region have begun to decrease as temperatures have risen. Furthermore, the snowline elevation has become increasingly unstable, and both the regulation capability and the storage capacity of the solid reservoirs in the mountains have deteriorated (Lu et al., 2007). Therefore, the study of the dynamic variation of snowline in this region is of great significance to the protection and utilization of local water resources and ecological construction.

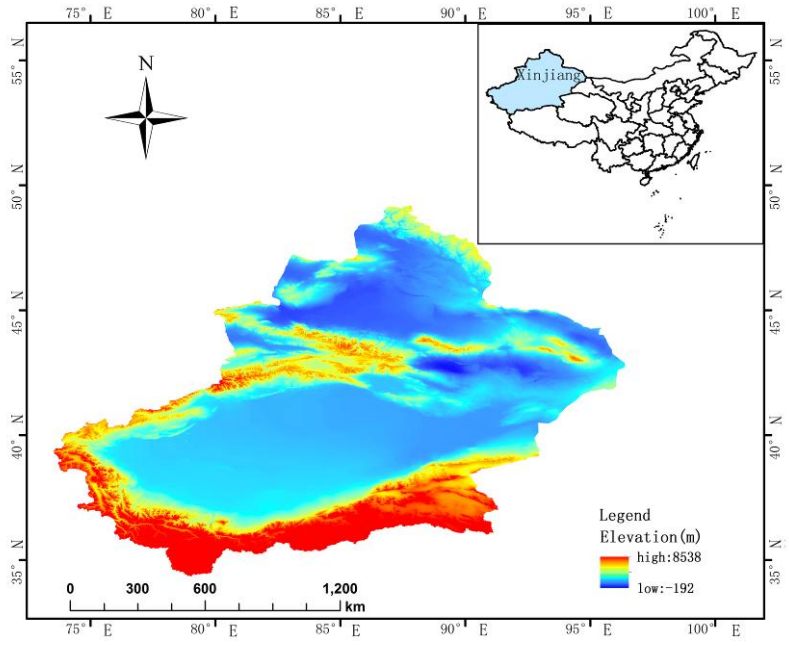

Figure 1. *Location of the study area*

Study data

The data used in this study comprised the following:

(1) MODIS daily snow cover products (MOD10A1 and MYD10A1) covering the Xinjiang region were acquired for 2001–2015 from the NASA Data Center, and 4-km IMS data for 2001–2015 were acquired from the NSIDC website. Cloud removal was accomplished using a combination of temporal and spatial filtering on the MOD10A1 and MYD10A1 data, with the IMS data as reference. Thus, the snowline elevation in the study area was extracted for 2001–2015.

http://www.aloki.hu ● ISSN 1589 1623 (Print) ● ISSN 1785 0037 (Online)
DOI: http://dx.doi.org/10.15666/aeer/1605_62816298
© 2018, ALÖKI Kft., Budapest, Hungary

(2) Cloudless 30-m Landsat data of the Xinjiang region for June–August of 2005, 2010, 2014, and 2015 (downloaded from the official USGS website). These data were used as the "true value" to determine the threshold for snowline extraction when using the SCDR method, and to evaluate the accuracy of the extracted snowline elevation.

(3) SRTM DEM data (derived from the International Scientific Data Services Platform, 90-m resolution). These data were used for extracting snowline elevation within the study area.

Study methods

(1) SCDR method

In this study, we extracted snowline elevation within the study area using the SCDR method. After cloud removal, MODIS daily snow cover products were used to calculate the probability of snow cover occurrence within specific pixels on the study date. Snowline elevation was then extracted at different probabilities and the 30-m Landsat data were used as the "true value" for error analysis. The probability of snow cover occurrence with the minimum error was taken as the threshold for snowline extraction. The extraction of snowlines using this threshold was regarded as the SCDR method (Zhang et al., 2015a).

(2) Statistical methods

1. Statistical methods were used to calculate the daily snow cover area within the study area and to determine the range of the study date.

We used the MOD10A1/MYD10A1 snow cover product data for 2001–2015 to calculate the daily snow cover area for June–August of each studied year. The data of minimum snow cover area in each year was obtained, based on which the date range of the minimum snow cover area over the past 15 years was obtained. This range was determined as the study date. Given the vast area of the Xinjiang region, to be able extract the snowline using the SCDR method with greater accuracy, we divided the study area into three parts for the statistical analysis: the Tianshan Mountains, Altai Mountains, and Kunlun Mountains.

2. Statistical methods were used in two schemes to evaluate the accuracy of the extracted snowline.

The first scheme examined the accuracy difference of planar snow cover area. High-resolution (30 m) Landsat satellite images were used to evaluate the 500-m MOD10A1/MYD10A1 snow cover area image based on the Kappa coefficient (*Eq. 1*). Given the large difference in the spatial resolutions of the two image types, we counted the number of pixels at 500-m resolution in the area extracted by the Landsat satellite snow cover image after the extraction of the snow cover area by visual interpretation. This was performed to keep the pixel size consistent for calculation of the Kappa coefficient:

$$K = (P_o - P_c)/(1 - p_c) \quad \text{(Eq.1)}$$

where Po is the observed consistency rate and Pc is the expected consistency rate. Here, Pc = (a1 × b1 + ao × bo) and Po = s / n, where n is the total number of pixels in the image, a1 and ao represent the number of pixels with snow cover in the remote sensing image representing the actual snow cover conditions on the ground and the number of

http://www.aloki.hu ● ISSN 1589 1623 (Print) ● ISSN 1785 0037 (Online)
DOI: http://dx.doi.org/10.15666/aeer/1605_62816298
© 2018, ALÖKI Kft., Budapest, Hungary

remaining pixels, respectively, b1 and bo represent the number of pixels with snow cover in the validation image and the number of remaining pixels, respectively, and s is the number of pixels with equal values in the corresponding raster of the two images.

The second scheme obtained the snowline elevation extracted from the Landsat satellite imagery as the "true value" through visual interpretation. The accuracy of snowlines extracted using the SCDR method was evaluated through calculation of the mean error (Pa), positive and negative errors (Pc and Pb), mean absolute error (Pd), and root mean square error (RMSE) (*Eqs. 2–6*) between the snowline elevation extracted using the SCDR method and the "true value," as well as the correlation between the above two factors (Yu et al., 2009; Zhang et al., 2013).

$$Pa=\frac{1}{n}\sum_{i=1}^{n}(y_i-\hat{y}_i) \quad \text{(Eq.2)}$$

$$Pc=\frac{1}{r}\sum_{k=1}^{r}(y_k-\hat{y}_k)(y_k>\hat{y}_k) \quad \text{(Eq.3)}$$

$$Pb=\frac{1}{m}\sum_{j=1}^{m}(y_j-\hat{y}_j)(y_j<\hat{y}_j) \quad \text{(Eq.4)}$$

$$Pd=\frac{1}{n}\sum_{i=1}^{n}(|y_i-\hat{y}_i|) \quad \text{(Eq.5)}$$

$$RMSE=\sqrt{\frac{\sum_{i=n}^{n}(Z_{ai}-Z_{ei})^2}{n}} \quad \text{(Eq.6)}$$

where y_i, y_j, y_k, and $\hat{y}_i$, $\hat{y}_j$, $\hat{y}_k$ are the true values and their corresponding snowline elevations to be validated, respectively; n, m, and r are the total number of samples, number of samples with a measured value lower than the estimated value, and the number of samples with a measured value higher than the estimated value, respectively; Z_{ai} is the true value of the i-th sample point; Z_{ei} is the estimated value.

(3) Linear trend method

The linear trend method was used to calculate the trend of snowline variation and to establish the linear regression equation (*Eq. 7*) between y_t and time t:

$$y_t = a + bt \quad \text{(Eq.7)}$$

Where a is the regression constant and b is the regression coefficient, i.e., the variation trend; when b is higher (lower) than zero, it indicates an upward (downward) trend. Here, $b \times 10$ (unit: m/decade) is the tendency rate of the snowline (Tang et al., 2012).

http://www.aloki.hu ● ISSN 1589 1623 (Print) ● ISSN 1785 0037 (Online)
DOI: http://dx.doi.org/10.15666/aeer/1605_62816298
© 2018, ALÖKI Kft., Budapest, Hungary

Results and discussion

Determination of study dates

Figure 2 shows the dates of minimum snow cover area in the Tianshan, Kunlun, and Altai mountains for each year. To reduce statistical error, we removed the values at two endpoints of anomalies. The results showed that day 206 was the earliest date of minimum snow cover area in the Tianshan Mountains, whereas the corresponding date was day 203 and 216 in the Kunlun and Altai mountains, respectively. The latest date of minimum snow cover area was day 236 in both the Tianshan and Kunlun mountains, whereas it was day 239 in the Altai Mountains. Based on the above, we obtained the study dates for the three major mountain areas of the Xinjiang region: July 25–August 24 (days 206–236) of each year in the Tianshan Mountains (total: 31 days); July 22–August 24 (days 203–236) of each year in the Kunlun Mountains (total: 34 days); and August 4–August 27 (days 216–239) of each year in the Altai Mountains (total: 24 days).

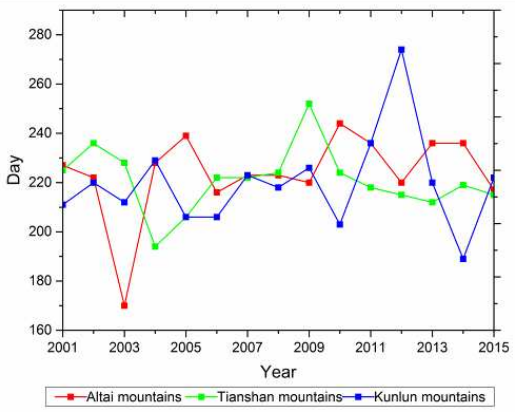

Figure 2. *Dates of minimum snow cover area in three mountain areas of the Xinjiang region for each year*

3.2 Snowline extraction in the Xinjiang region

Threshold determination for the SCDR method

After cloud removal, we overlaid the MOD10A1/MYD10A1 snow cover product data from the Tianshan, Kunlun, and Altai mountains for the study dates of 2005, 2010, and 2014, respectively (*Fig. 3*). Then, we calculated the probability of snow cover occurrence in specific pixels within 31 days (Tianshan Mountains), 34 days (Kunlun Mountains), and 24 days (Altai Mountains). In the Tianshan Mountains, we extracted snowline elevation with 3.2%, 6.4%, 9.6%, and up to 100.0% probability of snow cover occurrence. In the Kunlun Mountains, we extracted snowline elevation with 2.9%, 5.9%, 8.8%, and up to 100.0% probability of snow cover occurrence. In the Altai Mountains, we extracted snowline elevation with 4.2%, 8.3%, 12.5%, and up to 100.0% probability of snow cover occurrence. Then, 30-m Landsat data were used as the "true value" for error analysis. The smaller the difference, the smaller the error, and the probability of snow cover occurrence with the smallest error was determined as the minimum error ratio. Based on the minimum error ratio, we extracted the snowline threshold using the SCDR method when overlaying data for 31, 34, and 24 days in the

http://www.aloki.hu ● ISSN 1589 1623 (Print) ● ISSN 1785 0037 (Online)
DOI: http://dx.doi.org/10.15666/aeer/1605_62816298
© 2018, ALÖKI Kft., Budapest, Hungary

Tianshan, Kunlun, and Altai mountains, respectively. *Figure 4* shows the error curves of different ratios in 2005, 2010, and 2014. The minimum error ratios for the Tianshan Mountains were 83.2%, 70.4%, and 70.4%; for the Kunlun Mountains, they were 67.7%, 79.4%, and 85.3%, and for the Altai Mountains, they were 83.3%, 83.3%, and 87.5%. The average of the minimum error ratios of the three years was obtained as the threshold for the SCDR method when overlaying data for 31, 34, and 24 days in the Tianshan, Kunlun, and Altai mountains, respectively. In the Tianshan Mountains, the average ratio was estimated to be 74.7%, closest to the true ratio of 74.2%, i.e., the lower edge of snow cover that appeared in each pixel for 23 days was taken as the snowline in the Tianshan Mountains. In the Kunlun Mountains, the average ratio was 77.5%, closest to the true ratio of 76.5%, i.e., the lower edge of snow cover that appeared in each pixel for 26 days was taken as the snowline in the Kunlun Mountains. In the Altai Mountains, the average ratio was 84.7%, closest to the true ratio of 83.3%, i.e., the lower edge of snow cover that appeared in each pixel for 20 days was taken as the snowline in the Altai Mountains. In summary, when extracting the snowline elevation in the three mountainous areas using the SCDR method, the threshold values were 74.2%, 76.5%, and 83.3% for the Tianshan Mountains (overlaying data for 31 days), Kunlun Mountains (overlaying data for 34 days), Altai Mountains (overlaying data for 24 days), respectively.

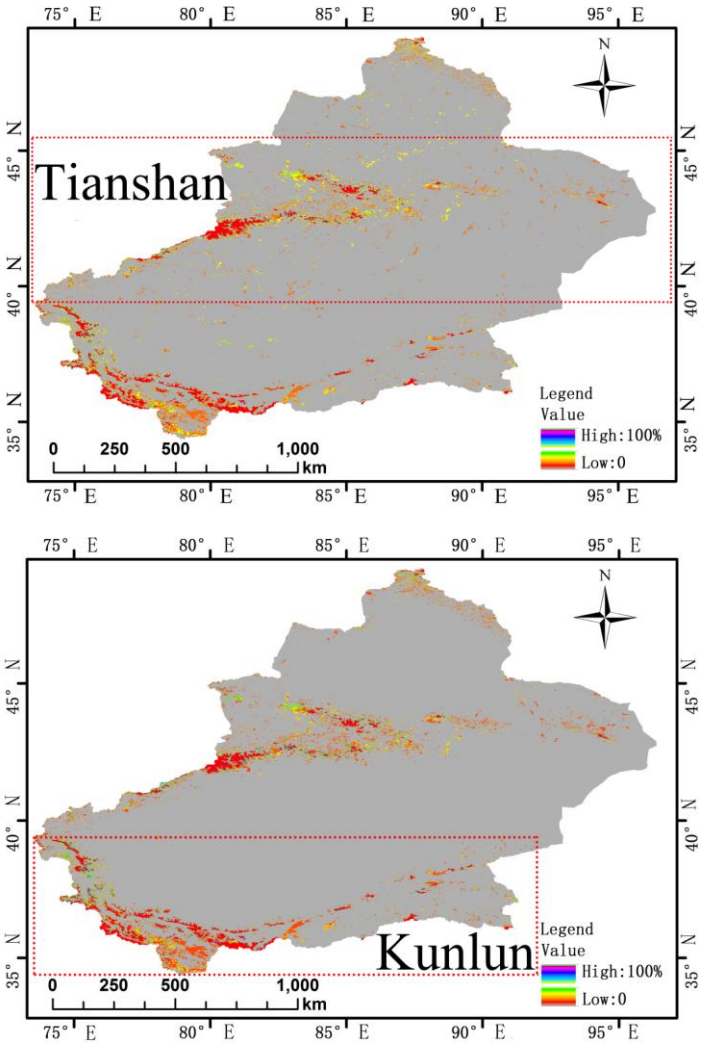

http://www.aloki.hu ● ISSN 1589 1623 (Print) ● ISSN 1785 0037 (Online)
DOI: http://dx.doi.org/10.15666/aeer/1605_62816298
© 2018, ALÖKI Kft., Budapest, Hungary

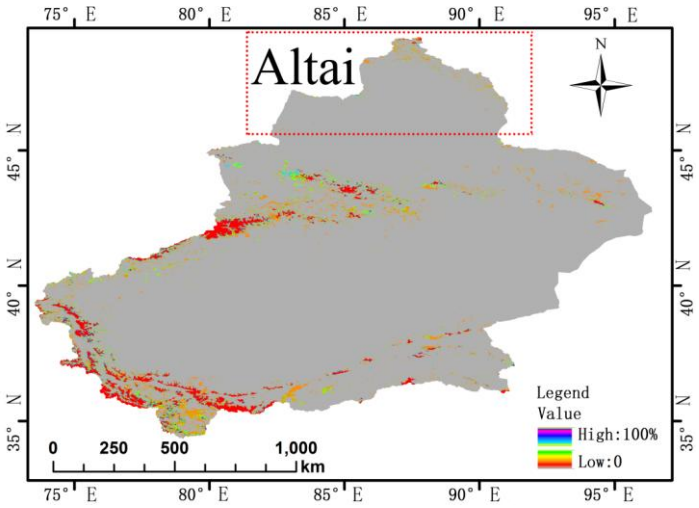

Figure 3. *Overlaid maps of snow cover with different ratios for days 206–236 in the Tianshan Mountains (top), days 203–236 in the Kunlun Mountains (middle), and days 216–239 in the Altai Mountains (bottom), 2014*

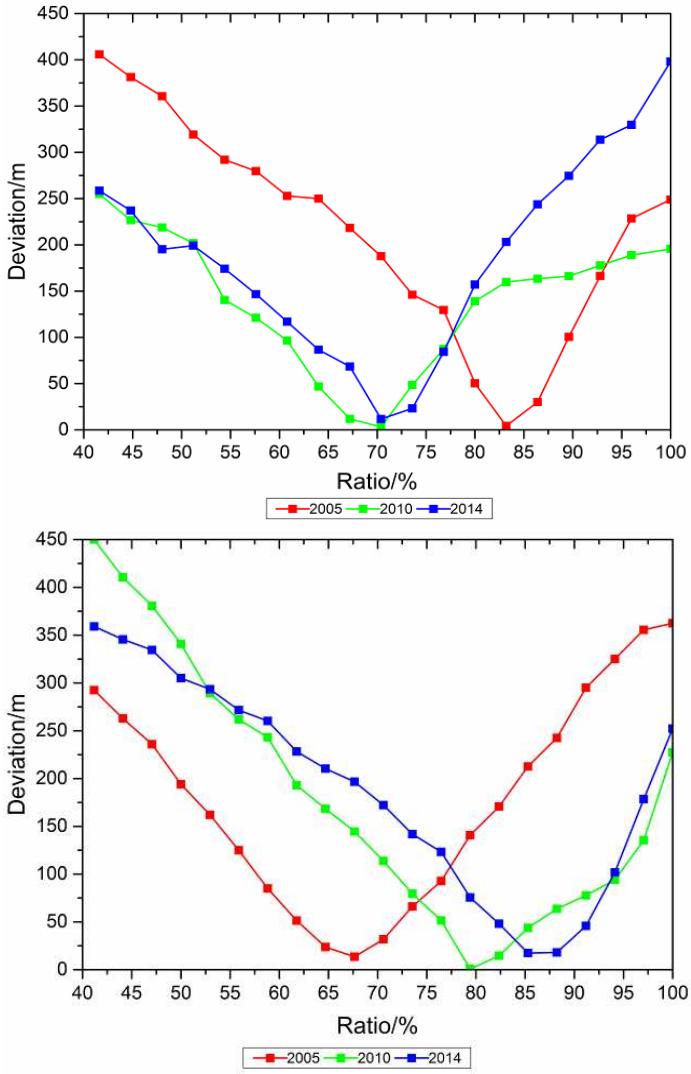

http://www.aloki.hu ● ISSN 1589 1623 (Print) ● ISSN 1785 0037 (Online)
DOI: http://dx.doi.org/10.15666/aeer/1605_62816298
© 2018, ALÖKI Kft., Budapest, Hungary

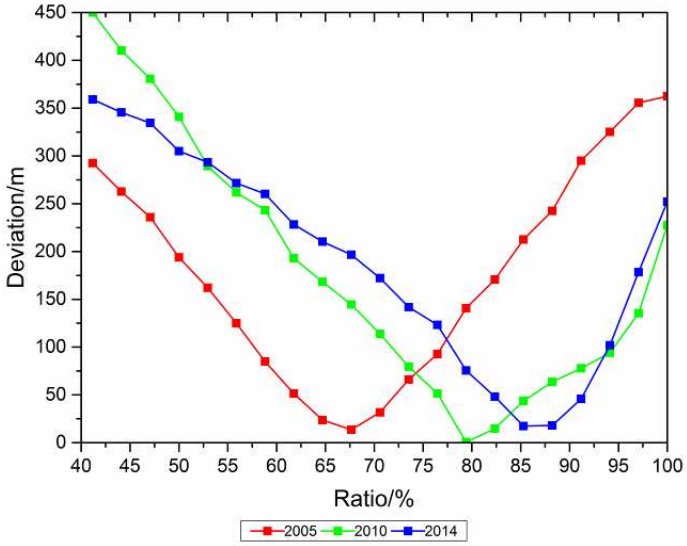

Figure 4. *Deviation of snowline elevation with different ratios from "true value" in the Tianshan Mountains (top), Kunlun Mountains (middle), and Altai Mountains (bottom) over different years*

Accuracy evaluation of snowline

(1) Accuracy evaluation of snow cover area

Local areas were selected from the three major mountainous areas in 2015 (*Fig. 5*). The evaluation was accomplished in different areas using the Kappa coefficient, based on the consistency between the snow cover area obtained using the SCDR method and the "true value" of snow cover area based on the MOD10A1/MYD10A1 snow cover classification map. *Table 1* shows that the Kappa coefficients were 0.92, 0.82, and 0.87 for the Tianshan, Kunlun, and Altai mountains, respectively. A study (Klein and Barnett, 2003) has shown that with 0.81 < Kappa < l.00, two images can be considered highly consistent. In summary, relatively high consistency was obtained with the "true value" when extracting the snow cover area, based on the MOD10A1/MYD10A1 daily snow cover image, using the SCDR method with thresholds of 74.2%, 76.5%, and 83.3% for the Tianshan Mountains (overlaying data for 31 days), Kunlun Mountains (overlaying data for 34 days), and Altai Mountains (overlaying data for 24 days), respectively.

Table 1. *Kappa coefficients for snow cover area extracted using snow cover duration ratio method*

	Tianshan Mountains	**Kunlun Mountains**	**Altai Mountains**
	Number of pixels with snow cover		
Landsat-OLI	4562	522	176
MOYD10A1	4315	484	157
Number of shared pixels	4213	435	149
Number of total pixels	11775	2275	716
Kappa coefficient	0.92	0.82	0.87

http://www.aloki.hu ● ISSN 1589 1623 (Print) ● ISSN 1785 0037 (Online)
DOI: http://dx.doi.org/10.15666/aeer/1605_62816298
© 2018, ALÖKI Kft., Budapest, Hungary

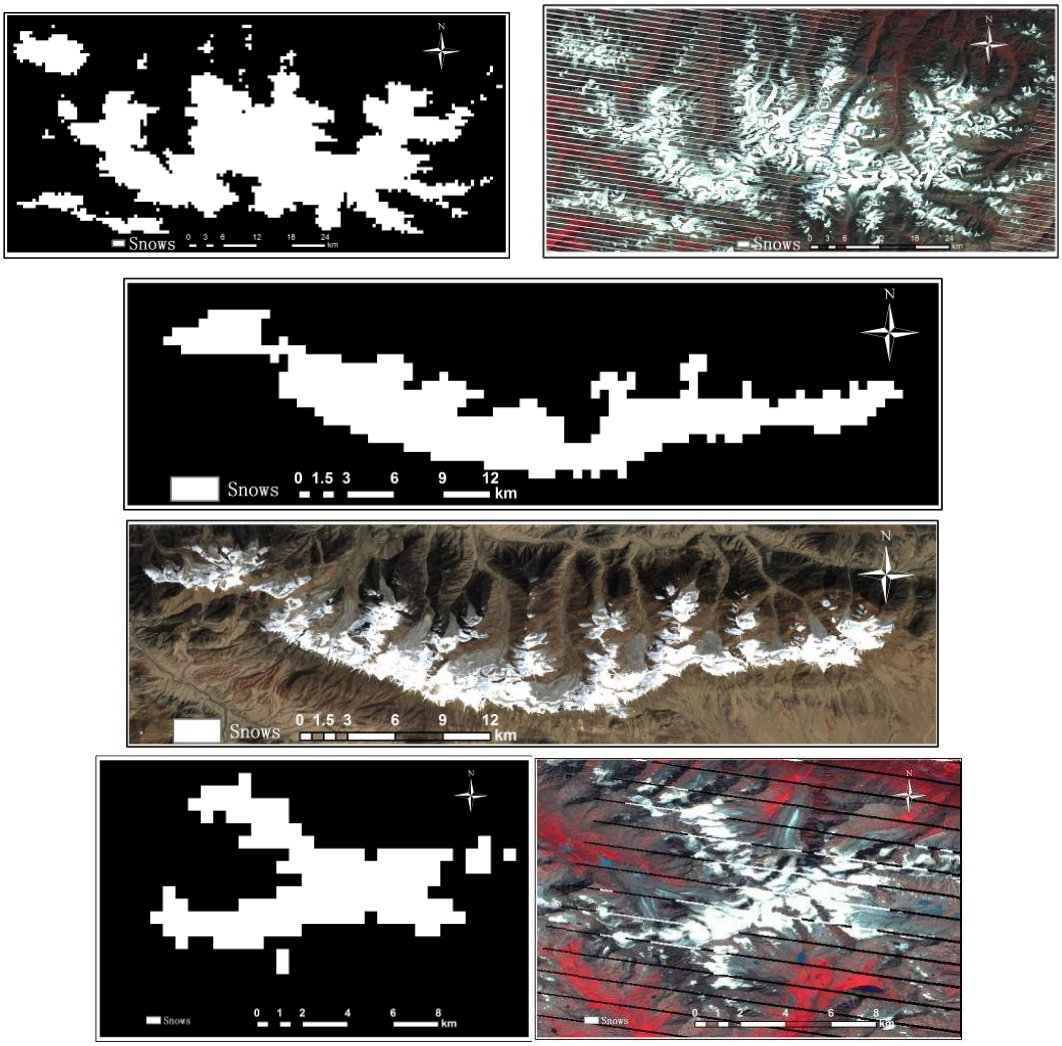

Figure 5. *MOD10A1/MYD10A1 and Landsat-OLI snow cover maps in the same areas of the Tianshan Mountains (top), Kunlun Mountains (middle), and Altai Mountains (bottom)*

(2) Accuracy evaluation of snowline elevation

Local areas were selected from the three major mountain areas of the Xinjiang region in 2015. The accuracy of snowline extracted using the SCDR method was analyzed statistically based on Pa, Pc, Pb, Pd, RMSE, and the correlation with the "true value." As shown in *Table 2,* the value of Pa = –8.15 m for the Kunlun Mountains was the smallest, and the values for the Tianshan and Altai mountains were similar to each other (19.07 and 19.12 m, respectively). The Tianshan Mountains ranked highest for Pc and Pb (93.13 and –85.55 m, respectively); the values for the Kunlun Mountains were 52.41 and –70.38 m, respectively, and those for the Altai Mountains were 71.67 and –53.92 m, respectively. The Kunlun Mountains had the smallest value of Pd (61.81 m), followed by the Altai Mountains (65.88 m) and the Tianshan Mountains (90.63 m). The RMSEs of the Altai and Kunlun mountains were similar to each other (77.01 and 76.32 m, respectively), whereas that of the Tianshan Mountains was relatively large (97.93 m). The above analysis shows that all the errors for the three mountain areas were within the range of 100 m, meeting the accuracy requirement of the study.

http://www.aloki.hu ● ISSN 1589 1623 (Print) ● ISSN 1785 0037 (Online)
DOI: http://dx.doi.org/10.15666/aeer/1605_62816298
© 2018, ALÖKI Kft., Budapest, Hungary

Table 2. *Errors in snowline elevations obtained using the snow cover duration ratio method*

	Mean error (Pa)/m	**Negative error (Pb)/m**	**Positive error (Pc)/m**	**Mean absolute error (Pd)/m**	**Root mean square error (RMSE)/m**
Tianshan Mountains	19.07	-85.55	93.13	90.63	97.93
Kunlun Mountains	-8.15	-70.38	52.41	61.81	76.32
Altai Mountains	19.12	-53.92	71.67	65.88	77.01

Table 3 summarizes the average snowline elevations extracted using the SCDR method and the "true value," together with their correlation coefficients. The average snowline elevations for the Tianshan, Kunlun, and Altai mountains, extracted using the SCDR method, were 4030.12, 5458.15, and 3114.59 m, respectively, whereas the "true value" snowlines were 4046.12, 5449.99, and 3133.71 m, respectively. The correlation between the snowlines extracted using the SCDR method and the "true value" was highest for the Altai Mountains (0.943); the coefficients were 0.843 and 0.887 for Tianshan and Kunlun mountains, respectively. *Table 4* shows that the correlation coefficients of snowline elevations extracted using the SCDR method and the "true value" ranged from 0.8 to 1.0 in the three mountain areas, indicating a relatively high degree of correlation. *Figure 6* shows scatter plots of snowline elevation in the three mountain areas extracted using the SCDR method versus the "true value," which reflects their correlation with the "true value" more directly.

Table 3. *Correlations between snowline elevation extracted using the snow cover duration ratio (SCDR) method and the "true value"*

	Average elevation of snowlines extracted by SCDR/m	**Average elevation of "true-value" snowlines/m**	**Correlation coefficient**
Tianshan Mountains	4030.13	4046.12	0.843
Kunlun Mountains	5458.15	5449.99	0.887
Altai Mountains	3114.59	3133.71	0.943

In summary, the SCDR method achieved high accuracy for snowline extraction in the Tianshan, Kunlun, and Altai mountains with thresholds of 74.2%, 76.5%, and 83.3%, respectively. This method was therefore considered suitable for extracting snowlines in the Xinjiang region.

Table 4. *Degree of correlation for correlation coefficients*

Correlation coefficients	**Degree of correlation**
$0.8 < \|r\| < 1$	High correlation
$0.5 < \|r\| \leq 0.8$	Moderate correlation
$0.3 < \|r\| \leq 0.5$	Low correlation
$0.8 < \|r\| < 0.3$	Extremely low correlation

http://www.aloki.hu ● ISSN 1589 1623 (Print) ● ISSN 1785 0037 (Online)
DOI: http://dx.doi.org/10.15666/aeer/1605_62816298
© 2018, ALÖKI Kft., Budapest, Hungary

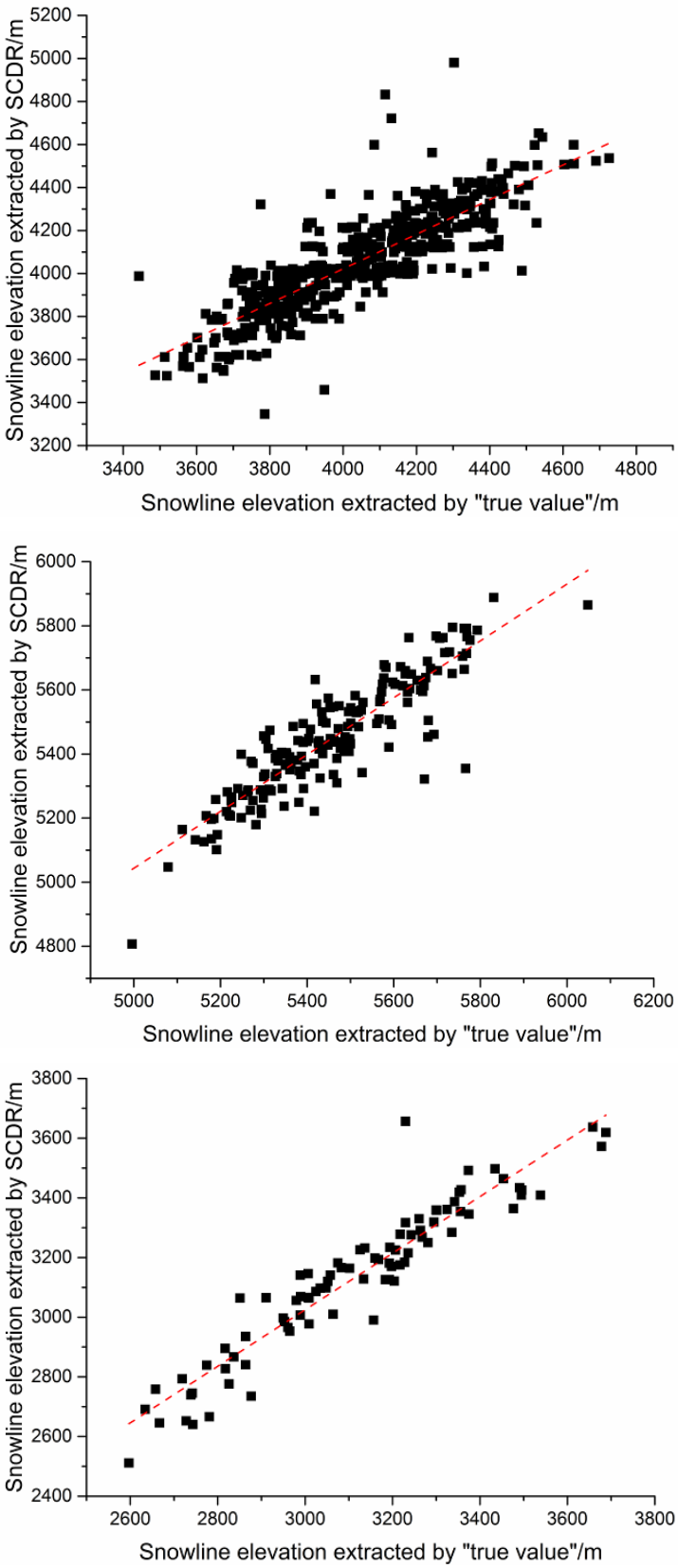

Figure 6. *Scatter plots of snowline elevation extracted using the snow cover duration ratio (SCDR) method versus the "true value" in the Tianshan Mountains (top), Kunlun Mountains (middle), and Altai Mountains (bottom)*

http://www.aloki.hu ● ISSN 1589 1623 (Print) ● ISSN 1785 0037 (Online)
DOI: http://dx.doi.org/10.15666/aeer/1605_62816298
© 2018, ALÖKI Kft., Budapest, Hungary

Dynamic variation characteristics of snowline in Xinjiang

Dynamic variation analysis of snowline elevation in the entire Xinjiang region

Figure 7 shows that the variation of average snowline elevation in the Xinjiang (2001–2005) was within the range of 250 m, while the snowline elevation was maintained at approximately 3950 m. Through linear fitting (*Table 5*), we found that the average snowline elevation increased annually, with a tendency rate of 160.38 m/decade. The lowest average elevation occurred in 2001 (3828.06 m) and the highest occurred in 2015 (4085.00 m). Here, the result of snowline change in the middle of Qilian Mountains and Western Nyainqentanglha are compared with Zhao et al. (2015) and Zhang et al. (2016). Generally, the mean snowline elevation increases. Although the average elevation in Xinjiang, less than that inWestern Nyainqentanglha Range and the Middle of Qilian Mountains, the increase trend in Xinjiang is the fastest. The annually increasing snowline elevation in the Xinjiang region is a consequence of the considerable influence of global warming. A study has shown that global warming poses a profound threat to the ecological environment, and that it is the primary cause of the reductions of permafrost, snow cover area, and glaciers in China. The decrease of ice and the decline in snow cover area lead to the rise of snowline elevation.

Based on linear fitting, we found that the maximum snowline elevation had a weak downward trend, with a tendency rate of 25.14 m/decade. Conversely, the minimum snowline elevation showed a slow upward trend, with a tendency rate of 128.68 m/decade. Compared with the average annual snowline elevation in the Xinjiang region, the minimum and maximum snowline elevations have changed significantly, and the extents of their variations have been larger than the change in average snowline elevation. For different years, the maxima and minima snowline elevations have appeared in different locations within the study area. Compared with the Tibetan Plateau, the minimum snowline elevation is on the rise, but the maximum snowline elevation trend is the opposite. This is because of the vast area of the Xinjiang region and the complex distribution of topography. In addition to climatic factors that have affected the constant variation of minimum and maximum snowline elevations, localized topography, geomorphology, and occurrence of extreme disasters have also had an effect. In some marginal areas of the Xinjiang region with complex topography and geomorphology, even small variations of precipitation and temperature can cause an increase in disastrous weather events because of the impact of aspect, slope, or human factors. For example, were the temperature to increase sharply and precipitation to decrease during summer, the snowline elevation would show correspondingly large variation. This is why the minimum, maximum, and average snowline elevations varied with significant differences.

Table 5. *Linear regression models between snowline elevation and time in different areas*

	Linear regression model
Average snowline elevation in Xinjiang region	y = 16.038t – 28237
Maximum snowline elevation in Xinjiang region	y = –2.5143t + 12221
Minimum snowline elevation in Xinjiang region	y = 12.868t – 23152
Average snowline elevation in Tianshan Mountains	y = 27.563t – 51659
Average snowline elevation in Kunlun Mountains	y = 14.287x – 23612
Average snowline elevation in Altai Mountains	y = 5.5493x – 7999

http://www.aloki.hu ● ISSN 1589 1623 (Print) ● ISSN 1785 0037 (Online)
DOI: http://dx.doi.org/10.15666/aeer/1605_62816298
© 2018, ALÖKI Kft., Budapest, Hungary

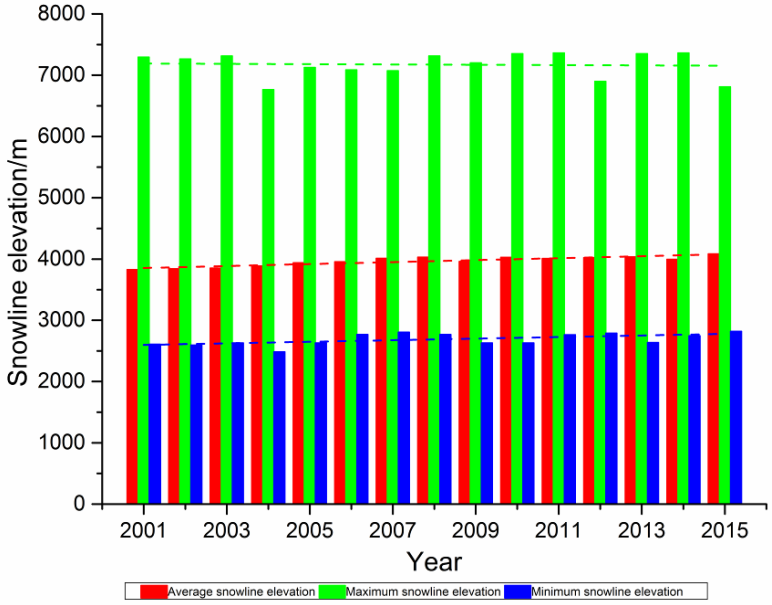

Figure 7. *Dynamic variation of snow elevation in the Xinjiang region (2001–2015)*

Comparative analysis of dynamic variation of snowline elevation in the three mountain areas

To study the dynamic variation of snowline elevation in the different mountain areas of the Xinjiang region, and with consideration of the spatial heterogeneity of the region, we divided the Xinjiang region into the three mountain areas (Kunlun, Tianshan, and Altai mountains) and analyzed their respective snowline elevations comparatively.

Figure 8 depicts fluctuating upward trends of snowline elevation in the Kunlun, Tianshan, and Altai mountains during 2001–2015, consistent with the trend of average snowline elevation across the entire Xinjiang region.

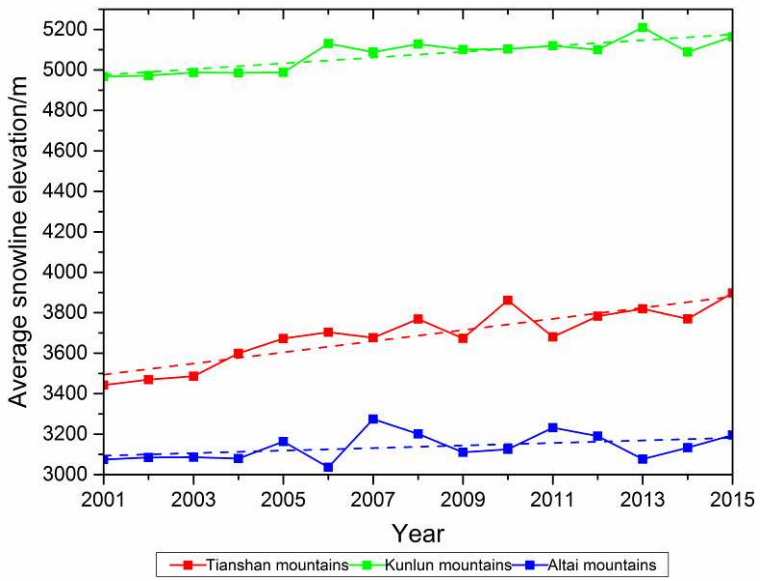

Figure 8. *Dynamic variation of snowline elevation in the three mountain areas of the Xinjiang region (2001-2015)*

http://www.aloki.hu ● ISSN 1589 1623 (Print) ● ISSN 1785 0037 (Online)
DOI: http://dx.doi.org/10.15666/aeer/1605_62816298
© 2018, ALÖKI Kft., Budapest, Hungary

Figure 9 illustrates the dynamic variation of air temperature and precipitation in the three mountain areas. During 2001–2015, temperature showed an upward trend in all three areas, whereas precipitation showed a downward trend. The temperature rise and decline of precipitation led to the upward trend of snowline elevation in the three mountain areas. *Table 5* shows that the tendency rates and amplitude fluctuations of snowline elevation were 142.87, 275.63, and 55.29 m/decade and 242.81, 454.65, and 200.34 m in the Kunlun Tianshan, and Altai mountains, respectively. The above analysis revealed upward trends of snowline elevation in the three mountain areas of the Xinjiang region during 2001–2015. The Altai Mountains showed the most stable variation of snowline elevation, followed by the Kunlun Mountains, and the Tianshan Mountains.

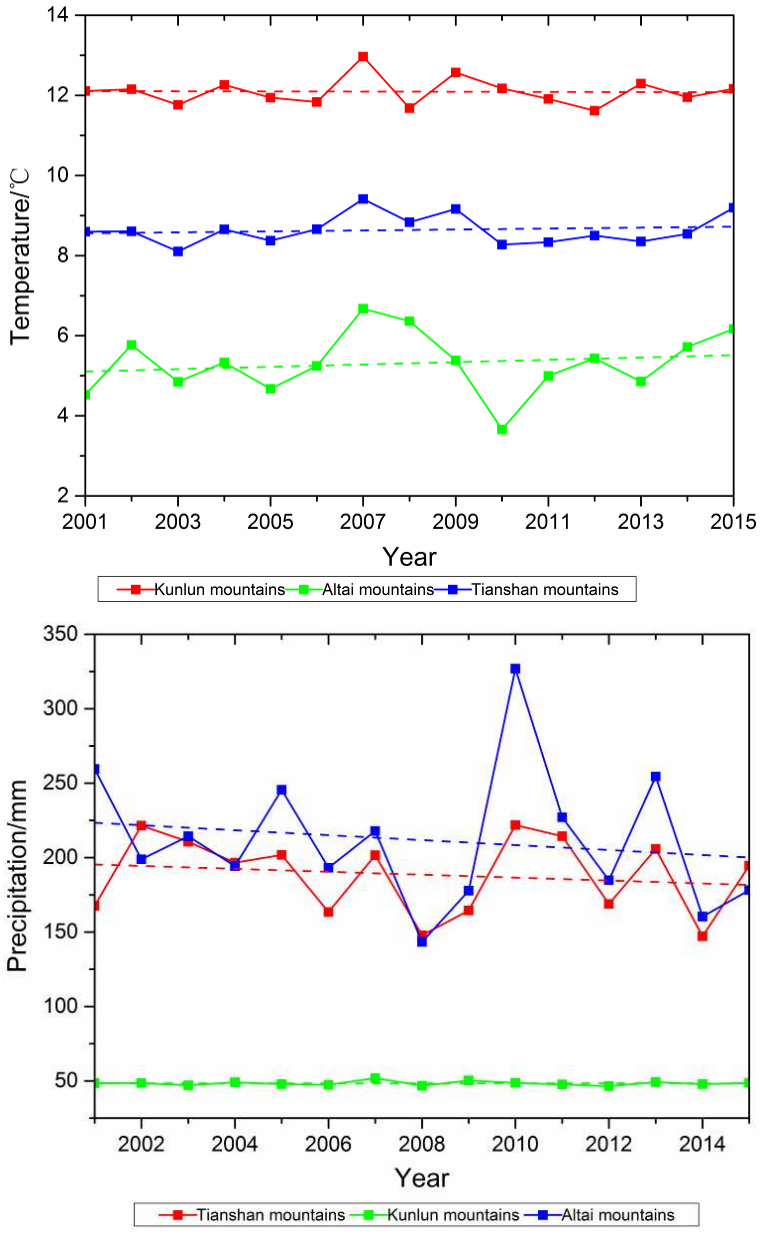

Figure 9. *Variations of temperature (top) and precipitation (bottom) in the three mountain areas of the Xinjiang region (2001–2015)*

http://www.aloki.hu ● ISSN 1589 1623 (Print) ● ISSN 1785 0037 (Online)
DOI: http://dx.doi.org/10.15666/aeer/1605_62816298
© 2018, ALÖKI Kft., Budapest, Hungary

As shown by the distribution of average snowline elevation in the three mountain areas (2001–2015), the annual snowline elevation of the Kunlun Mountains was highest, followed by the Tianshan Mountains, and the Altai Mountains. This indicates that the snowline elevation decreased from south to north across the Xinjiang region, and that the distribution was characterized by longitudinal zonation. This is mainly because the Indian monsoon weakens as it passes across the Tibetan Plateau (with elevation of 5000 m), and thus, it produces only small amounts of precipitation on the northern slopes of the Kunlun Mountains. Only a strong Pacific monsoon can reach the eastern edge of the Kunlun Mountains during June–August, which can produce some precipitation; however, its impact on the middle section of the Kunlun Mountains is weak. Additionally, the movement of moist air masses from the Atlantic Ocean is prevented by the Pamirs, and thus, they have little effect on the mid-section of the Kunlun Mountains. The southern section of the Tianshan Mountains is relatively sheltered, blocked by high mountain ranges that prevent access by Atlantic water vapour (Gao et al., 2010). Furthermore, this area faces China's largest desert (Taklimakan Desert) and thus, the effect of reduced atmospheric moisture results in decreased precipitation and high temperatures. However, the Ili River Valley is surrounded by mountains on three sides, which trap water vapor from the Atlantic Ocean, resulting in abundant precipitation and low temperatures on the windward slopes in this area. The Altai Mountains are located on the moist westerly windward side, making the area rich in precipitation, particularly solid precipitation in the winter. *Figure 9* shows that the Kunlun Mountains had higher average annual temperature and much lower precipitation than the other two areas during 2001–2015. The highest precipitation and lowest temperature were found in the Altai Mountains every year. The above analysis showed that the snowline elevation decreased from south to north in the Xinjiang region and that the distribution was characterized by longitudinal zonation.

Conclusions

(1) For the SCDR method, the extracted snowline elevations passed the accuracy test and thus, the method was considered suitable for the Xinjiang region.

(2) During 2001–2015, the average snowline elevation remained at about 3950 m within a 250-m range of fluctuation. However, linear trend analysis revealed an annual increasing trend of average snowline elevation in the Xinjiang region, with a tendency rate of 160.38 m/decade. The minimum snowline elevation showed a fluctuating upward trend, while the maximum snowline elevation exhibited a weak downward trend. However, both the minimum and maximum snowline elevations showed larger fluctuations compared with the change of the average snowline elevation.

(3) Comparative analysis of different areas of the Xinjiang region revealed that the snowline elevation showed a fluctuating rising trend in the Kunlun, Tianshan, and Altai mountains during 2001–2015. Of the three areas, the Altai Mountains showed the most stable variation of snowline elevation, followed by the Kunlun Mountains, and the Tianshan Mountains.

(4) According to the distribution of snowline elevation in three mountain areas (2001–2015), the snowline elevation of the Kunlun Mountains in each year was the highest, followed by the Tianshan Mountains and the Altai Mountains. Thus, the snowline elevation has decreased from south to north in the Xinjiang region and its distribution is characterized by longitudinal zonation.

http://www.aloki.hu ● ISSN 1589 1623 (Print) ● ISSN 1785 0037 (Online)
DOI: http://dx.doi.org/10.15666/aeer/1605_62816298
© 2018, ALÖKI Kft., Budapest, Hungary

Acknowledgements. This research was supported by the National Natural Science Foundation of China (41471358) and the National Science Foundation of China (41505077).

REFERENCES

[1] Brahmbhatt, R. M., Bahuguna, I., Rathore, B. P. et al. (2012): Variation of snowline and mass balance of glaciers of Warwan and Bhut Basins of Western Himalaya using remote sensing technique. – Journal of the Indian Society of Remote Sensing 40(4): 629-637.
[2] Deng, Y. W., Xie, Z. C., Qin, J. X. et al. (2006): The field equilibrium line altitude in the Ganga Yarlung Zangbo rivers system: Establishment and its environmental significance. – Journal of Glaciology and Geocryology 28(6): 865-872.
[3] Gao, P., Wei, W. S., Liu, M. Z. et al. (2010): Snow density and Liquid water content within the seasonal snow cover in the Western Tianshan mountains. – Journal of Glaciology and Geocryology 32(4): 786-790.
[4] Hantel, M., Maurer, C. (2011): The median winter snowline in the Alps. – Meteorologische Zeitschrift 20(3): 267-276.
[5] Jiang, F. C., Wu, X. H., Wang, S. B. et al. (2004): Features of space distribution of the forest line and relations between the forest line and climatic limit of permafrost and climatic snowline in china. – Journal of Geomechanics 10(4): 289-298.
[6] Jiang, Z. X. (1987): Trend surface analysis of the existent snowline in west China. – Scientia Geographica Sinica 7(1): 1-8.
[7] Klein, A.-G., Barnett, A. C. (2003): Validation of daily MODIS snow cover maps of the Upper Rio Grande River Basin for the 2000-2001 snow year. – Remote Sensing of Environment 86(2): 162-176.
[8] Li, G. H., Wang, C., Xi, X. H. et al. (2013): Extraction of glacier snowline based on airborne LiDAR and hyperspectral data fusion. – Remote Sensing for Land & Resources 29(3): 79-84.
[9] Liu, J., Chen, R., Wang, G. (2015): Snowline and snow cover monitoring at high spatial resolution in a mountainous river basin based on a time-lapse camera at a daily scale. – Journal of Mountain Science 12(1): 60-69.
[10] Lu, Z., Liu, Z. H., Yan, Y. (2007): Features of snowmelt flood and control measures in Xinjiang. – Research of Soil and Water Conservation 14(6): 216-219.
[11] McFadden, E. M., Ramage, J., Rodbell, D. T. (2011): Landsat TM and ETM+ derived snowline altitudes in the Cordillera Huayhuash and Cordillera Raura. – The Cryosphere 5(2): 419-430.
[12] Nie, N., Zhang, Z. J., Zhang, W. C. et al. (2013): Analysis of the characteristics of the glacier system and typical glacier change based on remote sensing in the Yarlung Zangbo River basin during the past 30 years. – Journal of Glaciology and Geocryology 35(3): 541-552.
[13] Sa, C. L., Liu, G. X., Bao, G. et al. (2013): Spatial-temporal changes of snow cover in Xinjiang in recent 10 years. – Science of Surveying and Mapping 38(1): 72-74.
[14] Tang, X. N., Yan, X. L., Ni, M. J. et al. (2012): Changes of the snow cover days on Tibet Plateau in last 40 years. – Acta Geographica Sinica 67(7): 951-959.
[15] Wang, L. P., Xie, Z. C., Ding, L. F. et al. (2010): Establishing the field of equilibrium line altitude of the glacier system in the Chiangtang Plateau based on geographic information system and its distribution characteristics. – Arid Land Geography 33(5): 692-702.
[16] Wang, X., Xie, Z. S., Feng, Q. H. (2003): The calculated ELA and its distribution characteristics of the glacier system in the Tarim River basin. – Journal of Glaciology and Geocryology 25(4): 380-388.
[17] Wang, Z. Y., Che, T. (2012): Validation and assessment of cloud obscuration reduction of snow cover products in arid areas in China. – Arid Zone Research 29(2): 312-315.

http://www.aloki.hu ● ISSN 1589 1623 (Print) ● ISSN 1785 0037 (Online)
DOI: http://dx.doi.org/10.15666/aeer/1605_62816298
© 2018, ALÖKI Kft., Budapest, Hungary

[18] Xiao, F., Du, Y., Ling, F. et al. (2010): Digital extraction of snowline based on flow path analysis. – Journal of Remote Sensing 14(1): 62-67.
[19] Yu, H., Feng, Q. S., Zhang, X. T. et al. (2009): An approach for monitoring snow depth based on AMSR-E data in the pastoral area of Northern Xinjiang. – Acta Prataculturae Sinica 18(4): 210-216.
[20] Zhang, L. C., Hu, L. Q., Li, S. et al. (2015a): GIS-Based analysis on the snowline distributional characteristics of south and North slopes of Tianshan mountain and their influencing factors. – Research of Soil and Water Conservation 22(3): 259-263.
[21] Zhang, L. C., Hu, L. Q., Li, S. et al. (2015b): Contrastive analysis based on remote sensing image snow line elevation extraction method—on the north slope of Tianshan Mountains as an example. – Arid Land Geography 38(4): 788-796.
[22] Zhang, Q. B., Kang, S. C., Zhang, G. S. (2016): Changes of snow line altitude for glaciers on Western Nyainqentanglha range observed by remote sensing. – Scientia Geographica Sinica 36(2): 1937-1943.
[23] Zhang, Y., Huang, X. D., Wang, W. et al. (2013): Validation and algorithm redevelopment of MODIS daily fractional snow cover products. – Arid Zone Research 30(5): 808-814.
[24] Zhao, J., Huang, Y. S., Shi, Y. F. et al. (2015): Relationship between snow line change and climate change in the middle of Qilian Mountains during 2000-2012. – Mountain Research 33(3): 683-689.

http://www.aloki.hu ● ISSN 1589 1623 (Print) ● ISSN 1785 0037 (Online)
DOI: http://dx.doi.org/10.15666/aeer/1605_62816298
© 2018, ALÖKI Kft., Budapest, Hungary

ANALYSIS OF VARIATION CHARACTERISTICS OF EXTREME PRECIPITATION EVENTS IN HETAO AREA, CHINA BASED ON FUZZY CLUSTERING CLIMATE ZONING

FENG, K.[1,2,3*] – TIAN, J.[1,2,3]

[1]*School of Civil and Hydraulic Engineering, Ningxia University, Yinchuan, China*

[2]*Engineering Research Center for Efficient Utilization of Water Resources in Modern Agriculture in Arid Regions, Yinchuan, China*

[3]*Ningxia Research Center of Technology on Water-saving Irrigation and Water Resources Regulation, Yinchuan, China*

**Corresponding author*
e-mail: feng_kp@163.com

(Received 31st May 2018; accepted 2nd Aug 2018)

Abstract. This paper adopts the meteorological data from 1951 to 2014 provided by 73 national ordinary stations in Hetao area, China, combines Kendall-tau non-parametric test method and Sen's slope estimation method based on sub-regions divided by fuzzy clustering method and analyses the variation trend of extreme precipitation indexes in the area. The results show that: (1) In the arid and semi-arid sub-region (located in the upper reaches of the Yellow River) and humid and semi-humid sub-region (located in the middle and lower reaches of the Yellow River) in Hetao area, extreme precipitation events have different variation trends, and the spatial distribution of precipitation is unbalanced. (2) Except the precipitation of extreme wet days has significantly increased (R99p is 32.01 mm /10a), other indexes do not increase significantly in the arid and semi-arid sub-region of Hetao area. (3) In the humid and semi-humid sub-region of Hetao area, the variation trends of the other 9 indexes are negative except the indexes consecutive days with rain (CWD) which showed upward trend (0.03d/10a). (4) There is an upward trend of extreme precipitation events in Bayinmaodao, but other regions in Hetao area have not increased.
Keywords: *fuzzy C-means, climate division, Kendall-tau, extreme precipitation*

Introduction

In more than half a century in the past, Scholars all over the world have conducted a lot of research work on extreme climate events in different regions of the world and have achieved research results of different depths. In early 2014, Science published 7 papers in a row to discuss the "the Challenge of Climate Science" and elaborate on some core issues of current climate and hydrology sciences, including the issue of "regional climate and extreme events". The paper believes that an important trend of warming research is to reflect global warming in the research on regional climate and extreme events, but the research needs to be further developed, where also exists great difficulties (Wang et al., 2014). At present, domestic and international researches focus mainly on the observational facts of extreme climate. The assessment report (IPCC-AR4) of the UN Intergovernmental Panel on Climate Change (IPCC) has summed up the observations and research findings of extreme temperature and precipitation events in full length, pointing out that extreme precipitation events are very sensitive to the global climate change, and minor changes in the climate may cause greater changes in

http://www.aloki.hu ● ISSN 1589 1623 (Print) ● ISSN 1785 0037 (Online)
DOI: http://dx.doi.org/10.15666/aeer/1605_62996316
© 2018, ALÖKI Kft., Budapest, Hungary

the frequency and intensity of extreme climate (Zhai et al., 2003; Zhou et al., 2010; Wang et al., 2013; Shen et al., 2012).

Scholars all over the world have done a lot of research work on extreme precipitation events on different spatial and temporal scales in different regions, which mainly includes four aspects: determination of representative values of extreme precipitation, characteristics of temporal and spatial distribution and evolution trend of extreme precipitation, factor of influence of extreme precipitation and simulation and prediction of extreme precipitation based on the climate change mode. With regard to the arid area in northwestern China and even the entire country, the research findings are given that the variation of extreme precipitation events in China is extremely complex with obvious regional and local characteristics. The micro-precipitation in the North significantly decreased, the drought continued in North China and the summer monsoon precipitation in the basin of the Yangtze and Huaihe Rivers increased significantly; heavy precipitation decreased significantly in North China, extreme precipitation events showed a significant upward trend in most parts of Northwest China and western part of Northeast China, but that showed a significant downward trend in the eastern part of Northeast China (Wang et al., 2012). the temperature in the northwestern region has shown an overall upward trend in the past 50 years, during which extreme high temperature events have increased and extreme low temperature events decreased; precipitation has shown a slight increase and extreme precipitation events was on the rise (Qi et al., 2015). The precipitation in the Yellow River basin showed a downward trend year by year, while extreme precipitation events in winter showed an upward trend, which mainly centralized in the upper reaches, while the downward trend was mainly seen in the middle and lower reaches, and spatial differences can be found in the Yellow River Basin in terms of precipitation and precipitation variation trend (Zhao et al., 2015). The precipitation in Xinjiang increased, extreme precipitation also showed an upward trend and continuous drying index dropped under the impact of climate warming (Li et al., 2015). The extreme precipitation indexes in the semi-arid region in the north such as maximum precipitation of 5 days, heavy precipitation, precipitation intensity, consecutive wet days, consecutive dry days, heavy rain days and annual total precipitation have shown a downward trend (Wang et al., 2016).

From previous research findings, it can be seen that extreme precipitation events on different scales have different rules or characteristics. The research area in this paper is Hetao area in China, which refers to the “T-shaped” bend of the Yellow River and its surrounding river basins. The whole area is located in the confluence of the Loess Plateau, Ordos Plateau and Inner Mongolia Plateau and the transitional zone of China’s arid, semi-arid and semi-humid regions, where plains, deserts, mountains, platforms, lakes and wetlands are intertwined, topography and landform are complex, terrain changes greatly and the structure of the underlying surface is complex. They have a temperate continental climate with low precipitation, strong evaporation and sensitivity to climate change. At the same time, the area relies on the irrigation of the Yellow River passing through, which is known as the major producing area of grain and cash crops in China and an emerging industrial cluster. It thus can be seen that the economic development in the area requires the sound development of precipitation resources and even extreme precipitation events. If extreme precipitation events occur frequently, it will have an adverse impact on the industrial and agricultural production and urban development in the area. Therefore, it is of both scientific and practical significance to

http://www.aloki.hu ● ISSN 1589 1623 (Print) ● ISSN 1785 0037 (Online)
DOI: http://dx.doi.org/10.15666/aeer/1605_62996316
© 2018, ALÖKI Kft., Budapest, Hungary

study the characteristics and evolution trend of extreme precipitation events in Hetao area.

Predecessors have already conducted some researches on extreme precipitation events in Hetao area. The precipitation within the year in Hetao area was unevenly distributed with about 80% of the precipitation concentrated in the period from June to September, while the precipitation was less in winter. The annual total precipitation in Hetao area has shown an upward trend in the past 50 years, but the trend is not obvious, which is less than 10 mm (Tao et al., 2011). The extreme precipitation threshold in summer in northern Hetao area showed an upward trend from northwest to southeast, and the extreme precipitation events in summer showed a slight upward trend in the past 45 years (Huang et al., 2013). The rainstorm days in Hetao area showed an insignificant downward trend. In addition, the rainstorm is characterized by less rainy day, heavy precipitation, more local rainstorm and less regional rainstorm in terms of distribution (Cai et al., 2014; Zhang et al., 2014). At present, the variation trend and characteristics of extreme precipitation events in Hetao area still need to be further studied to enhance systematic understanding.

Therefore, this paper, based on the daily precipitation data of 73 meteorological stations in Hetao area from 1951 to 2014, uses the extreme precipitation event index recommended by ETCCDMI and the climate change reference period and reference value of 30 years (1981-2010) recently recommended by WMO, and divides the sub-regions for study using fuzzy clustering method (FCM) to conduct an in-depth research on the variation of extreme precipitation events in Hetao area from differential temporal and spatial scales, reveal the variation characteristics and trend and answer the key issue that if the extreme precipitation events tend to increase in the area, hoping to provide a reference for water resource management, ecological vulnerability assessment and hydrogeological hazard warning in the area.

Data and methodology

Data information

When it comes to the research on the variation of extreme precipitation events, this paper usually uses the observed values of precipitation provided by meteorological stations distributed in the research area as data information. This paper adopts the daily precipitation data from 1951 to 2014 of 73 national ordinary stations in Hetao area provided by China Meteorological Data Network (http://data.cma.cn/). Prior to research, the meteorological data selected in this paper has been pretreated, including homogenization inspection; inspection of climate threshold and abnormal value; inspection of station extremum; internal consistency inspection of set value, daily average and daily extremum; temporal and spatial consistency inspection and so on, and the data has been corrected based on the inspection results. In addition, the distribution of meteorological stations is shown in *Figure 1*.

Research method

Fuzzy clustering analysis

Clustering analysis is a multivariate statistical analysis method, which classifies individuals based on their several characteristics, so that individuals of the same category have a higher homogeneity while individuals of different categories have a

http://www.aloki.hu ● ISSN 1589 1623 (Print) ● ISSN 1785 0037 (Online)
DOI: http://dx.doi.org/10.15666/aeer/1605_62996316
© 2018, ALÖKI Kft., Budapest, Hungary

higher heterogeneity. Since the boundaries of individual categories are not always clear and exact, varying degrees of fuzziness is always seen in practical classification problems. When clustering involves fuzzy boundaries between individuals, a fuzzy clustering analysis method is usually used, which is established on fuzzy mathematics. The commonly used fuzzy clustering analysis method is Fuzzy C-Means (FCM for short), which was proposed by Bezkek in 1981. The impact of different number of categories *c* on classification results is highly significant. To evaluate the classification effect under different *c* values in a scientific way, the predecessors have done a lot of research work and defined a number of evaluation indexes to guide the specific classification process. Assuming that different *c* values are determined according to those indexes, the smaller *c* value shall prevail if different *c* values have similar classification effect (Qi et al., 2015).

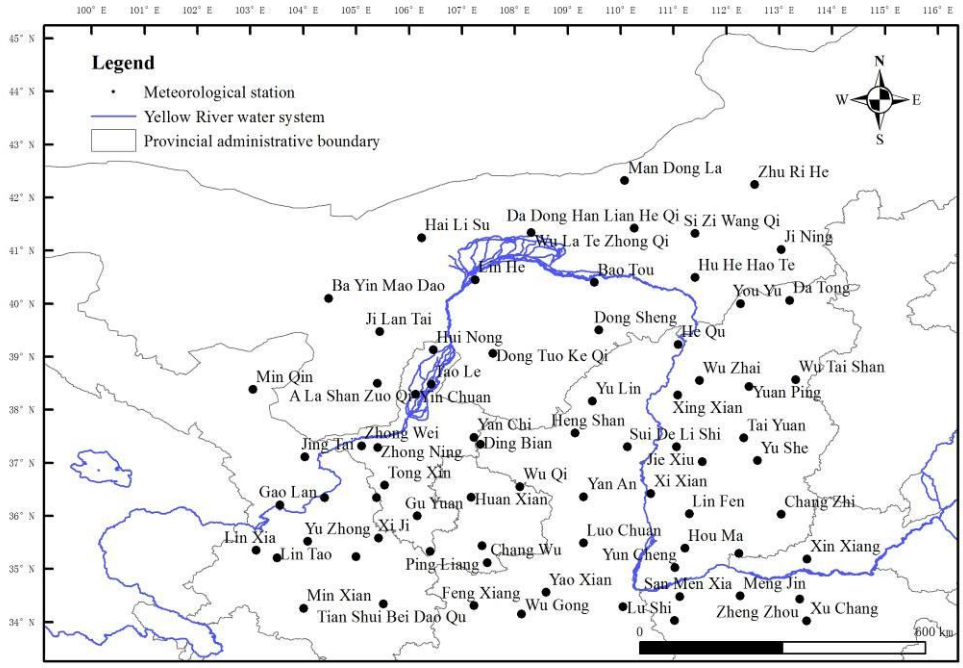

Figure 1. *Diagram of distribution of meteorological stations in Hetao area*

Definition and calculation of extreme precipitation indexes

The extreme precipitation indexes used in the research are "climate change detection and indexes" defined and recommended by CCI, WCRP, CLIVAR and ETCCDMI. These indexes and their calculation methods have been widely used in the world, and the research results also reflect that these indexes in this series are characterized by good regional adaptability, and low noise (Zhao et al., 2015; Li et al., 2012).

There are 29 indexes in this series, including temperature and precipitation. This paper selects 11 indexes of precipitation to analyze the extreme precipitation events in Hetao area, and specific indexes and meanings are shown in *Table 1*. The indexes are calculated using RClimDex1.1 software. In the process of calculation, quality inspection and control is conducted on the said meteorological data including outliers and error

http://www.aloki.hu ● ISSN 1589 1623 (Print) ● ISSN 1785 0037 (Online)
DOI: http://dx.doi.org/10.15666/aeer/1605_62996316
© 2018, ALÖKI Kft., Budapest, Hungary

values. Meanwhile, this paper also adopts the climate change reference period and value of 30 years (1981-2010) recently recommended by WMO (Zhang et al., 2014).

Table 1. *Definitions of extreme precipitation indexes*

S.N.	Abbreviation of index	Index name	Index definition	Index unit
1	CWD	Continuous moisture index (consecutive days with rain)	Maximum stay with daily precipitation greater than or equal to 1 mm	d
2	R10mm	Heavy precipitation days	Total days with annual daily precipitation greater than or equal to 10 mm	d
3	R20mm	Very heavy precipitation days	Total days with annual daily precipitation greater than or equal to 20 mm	d
4	R25mm	Strong precipitation days	Total days with annual daily precipitation greater than or equal to 25 mm	d
5	PRCPTOT	Annual total precipitation	Daily cumulant with precipitation greater than or equal to 1 mm	mm
6	R99p	Precipitation of extremely wet days	Sum of heavy precipitation with the tantile greater than 99%	mm
7	Rx5day	5-day maximum precipitation	Annual/quarterly/monthly/daily maximum precipitation in 5 days in a row	mm
8	SDII	Ordinary daily precipitation intensity (daily precipitation intensity)	Ratio of total precipitation greater than or equal to 1 mm and number of days	mm/d

Analysis method of variation trend of extreme precipitation indexes

Meteorological data belong to time series. For the trend analysis of time series, a linear regression method is usually used, but such method directly calculates the slope based on the actual data value, which is greatly affected by the abnormal value. Sen's slope estimation algorithm has strong anti-noise performance, but it cannot be used to make a significant judgement of sequence trend. The Kendall-tau non-parametric test method does not require the sample to follow a certain distribution, allows the existence of missing values and can achieve significant judgments, but it cannot be used to obtain the slope of the sequence (Zhai et al., 2003). Therefore, Kendall-tau non-parametric test method and Sen's slope estimation method are combined in this paper to analyze the variation trend of extreme precipitation indexes, and since they are subject to no abnormal value, they are more suitable for the time sequence trend analysis in the research of extreme climate changes. In addition, the area weighted average method shall be adopted for zone leveling.

Homogeneity test method for meteorological data

Data quality is the primary condition for drawing the correct conclusion in research and is also one of the decisive conditions. Affected by factors such as the replacement of observation instrument, changes in station position, changes in observation procedures and subjective biases of observers, meteorological data is found to have problems such skewness, lack of observation and outliers, thereby resulting in inhomogeneity of the sequence of meteorological data, which shall be homogenized. In

http://www.aloki.hu ● ISSN 1589 1623 (Print) ● ISSN 1785 0037 (Online)
DOI: http://dx.doi.org/10.15666/aeer/1605_62996316
© 2018, ALÖKI Kft., Budapest, Hungary

this paper, the RHtest method is used to carry out homogenization and correction of the meteorological data sequence in Hetao area. The method was established by Wang et al. from Climate Research Center of Environment Canada to test the entire sequence of meteorological data based on a two-stage linear regression model (Wang et al., 2007; Zhang et al., 2005), whose feasibility and rationality has been widely verified (Zhang et al., 2012; Zhang, 2012).

Results and discussion

FCM-based climate division

Combined with the natural conditions of the geographical location of the research area, latitude and longitude, altitude, average temperature and maximum and minimum temperature of the meteorological stations are regarded as characteristic values to perform clustering analysis on 73 meteorological stations in Hetao area. The number of divisions is preliminarily estimated to be c = 2 or c = 3. By selecting different c values, FCM can obtain corresponding membership matrix. According to the relationship reflected in the matrix, the classification results shall be plotted when c = 2 or c = 3 (see *Fig. 2a, b*). On this basis, the most reasonable number of divisions shall be analyzed. In addition, it can be seen from *Figure 2* that more stations are not classified in Hetao area when c = 3; while the classification shows good results when c = 2.

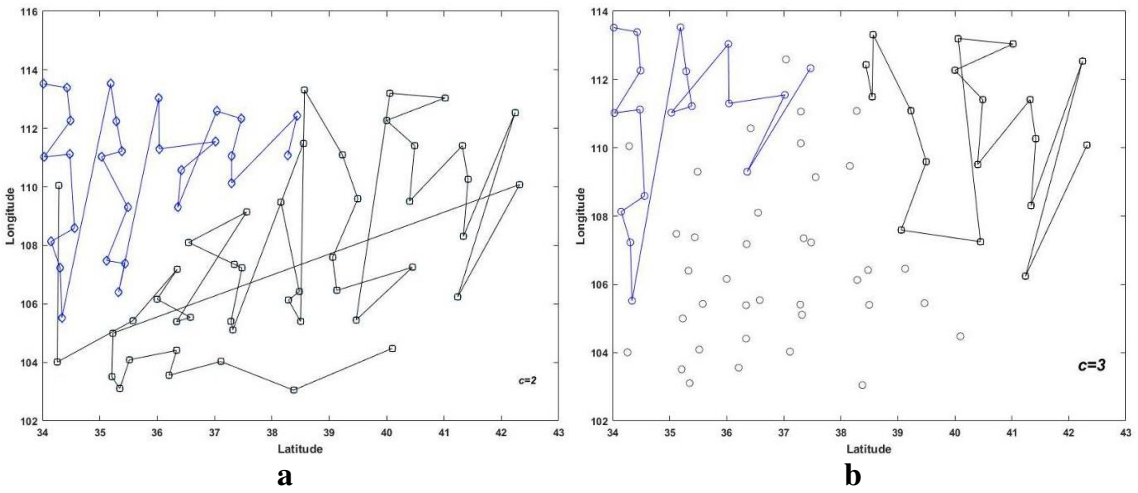

Figure 2. *FCM analysis of meteorological stations in Hetao area: c = 2 (a) and c = 3 (b)*

To more intuitively express the FCM climate divisions in Hetao area, the classification results are represented in a map (see *Fig. 3*). It can be clearly observed that 73 stations are classified into 2 different climate divisions along the line of "Yuanping—Xing County—Suide—Yan'an—Pingliang—Tianshui", and the line is very close to China's 400 mm equivalent precipitation line, which also fully indicates that it is reliable and reasonable to apply the fuzzy clustering algorithm to climate division in this paper. By referring to the significance of the 400 mm equivalent precipitation line, this paper defines 2 different climate divisions in Hetao area obtained by FCM clustering analysis as "arid and semi-arid sub-region" and "humid and semi-humid sub-region", respectively.

http://www.aloki.hu ● ISSN 1589 1623 (Print) ● ISSN 1785 0037 (Online)
DOI: http://dx.doi.org/10.15666/aeer/1605_62996316
© 2018, ALÖKI Kft., Budapest, Hungary

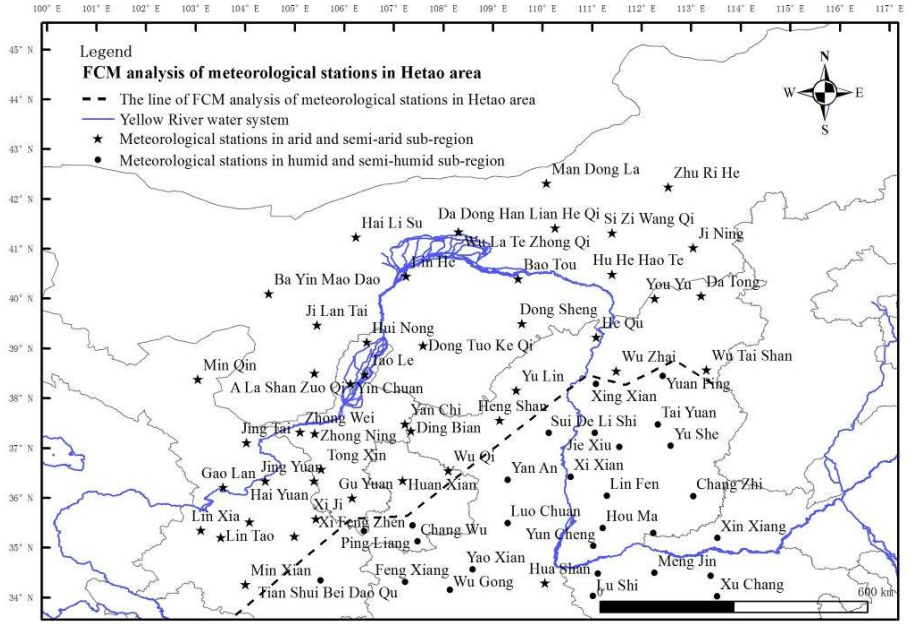

Figure 3. *FCM analysis results of meteorological stations in Hetao area*

Variation characteristics of extreme precipitation indexes in Hetao area

Variation of CWD, R10mm, R20mm and R25mm indexes

There is no station with significant upward trend of CWD; stations with significant downward trend include Linhe, Taiyuan, Wutaishan, Yan'an and Lushi (see *Fig. 4, Table 2*). In addition, the interannual change process of CWD in the entire Hetao area, CWD index have shown an upward trend whether in arid and semi-arid sub-region or humid and semi-humid sub-region (see *Table 2* and *Fig. 5*), but this upward trend is not significant.

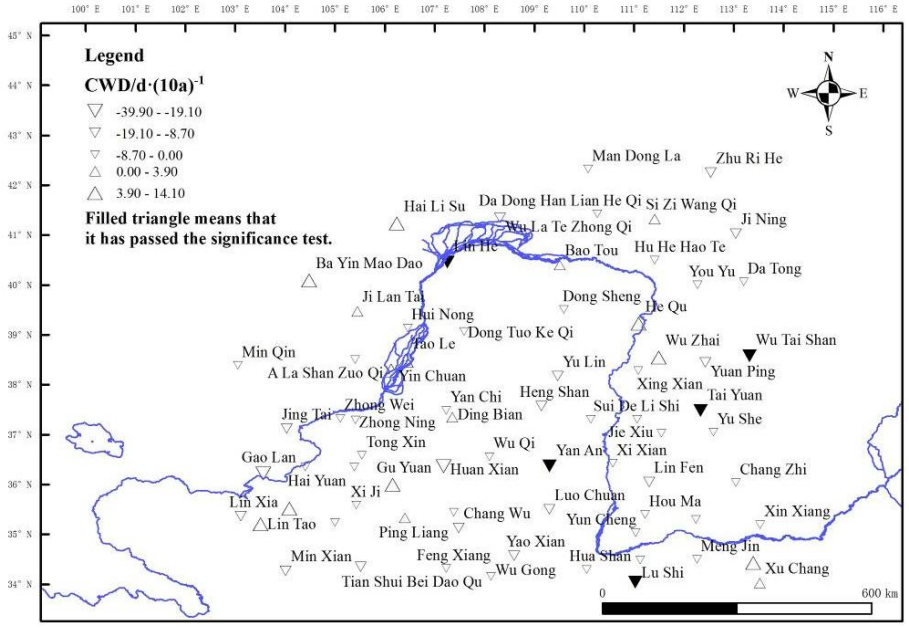

Figure 4. *Space variation of CWD index in Hetao area*

http://www.aloki.hu ● ISSN 1589 1623 (Print) ● ISSN 1785 0037 (Online)
DOI: http://dx.doi.org/10.15666/aeer/1605_62996316
© 2018, ALÖKI Kft., Budapest, Hungary

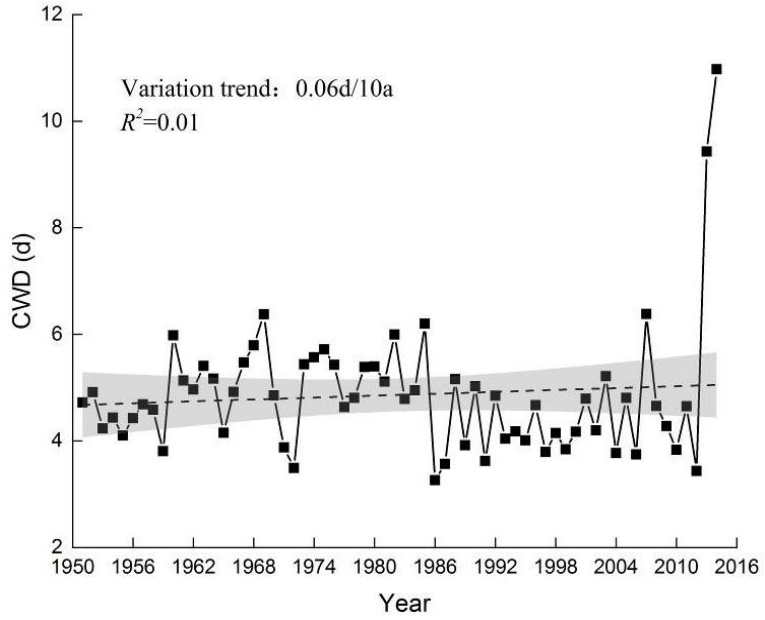

Figure 5. *Interannual variation of CWD index in Hetao area (73 stations involved)*

Stations with significant upward trend of R10mm include Bayinmaodao and Zhongwei; those with significant downward trend include Linhe, Wutaishan and Huashan (see *Fig. 6; Table 2*). Stations with significant upward trend of R20mm include Bayinmaodao and those with significant downward trend include Linhe, Wutaishan and Huashan (see *Fig. 7; Table 2*). There is no station with insignificant upward trend of R25mm; those with significant downward trend include Gaolan, Linhe and Wutaishan (see *Fig. 8; Table 2*).

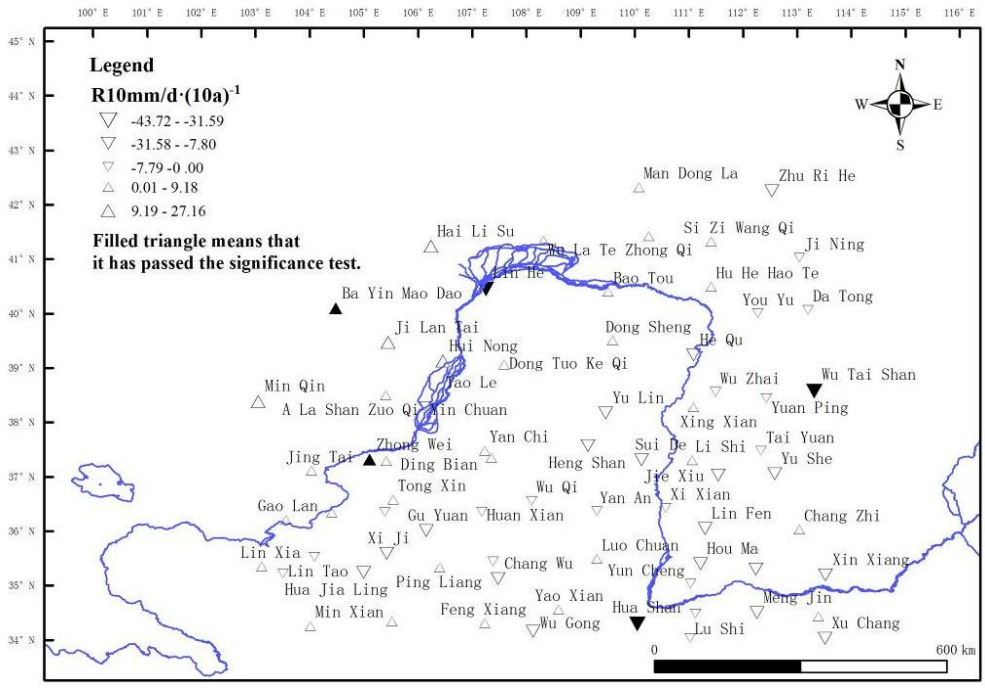

Figure 6. *Space variation of R10mm index in Hetao area*

http://www.aloki.hu ● ISSN 1589 1623 (Print) ● ISSN 1785 0037 (Online)
DOI: http://dx.doi.org/10.15666/aeer/1605_62996316
© 2018, ALÖKI Kft., Budapest, Hungary

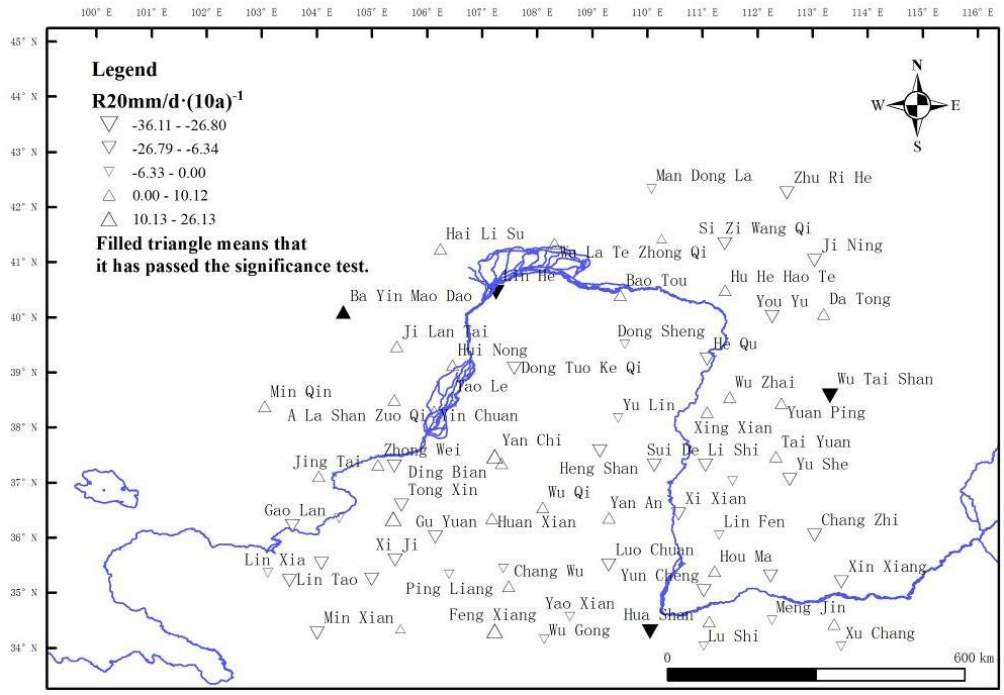

Figure 7. *Space variation of R20mm index in Hetao area*

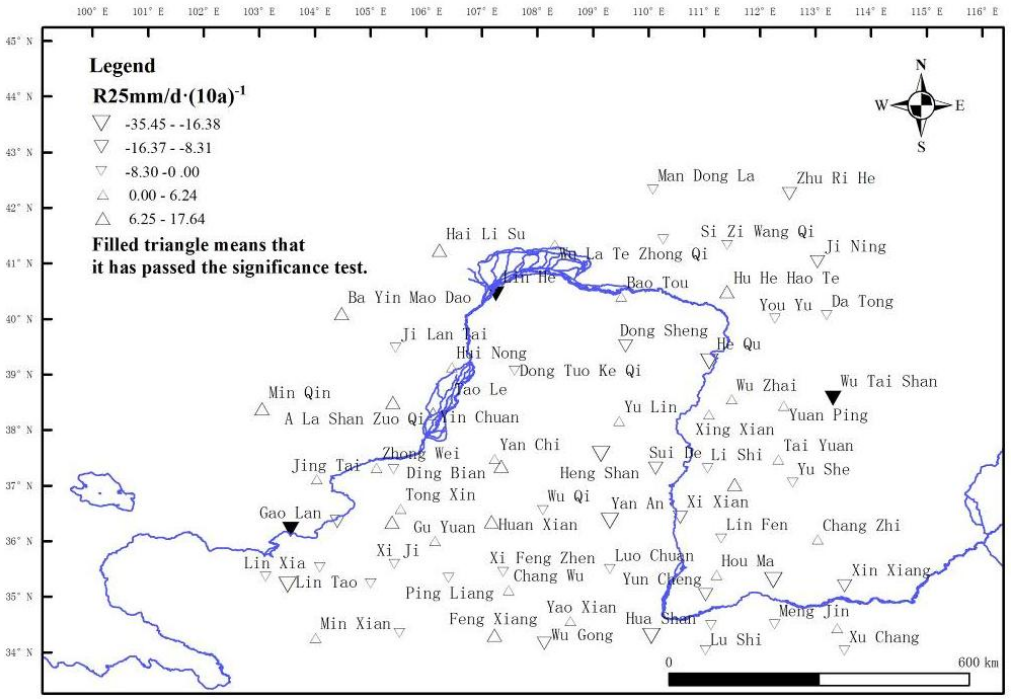

Figure 8. *Space variation of R25mm index in Hetao area*

There is an upward trend in interannual variation of the following indexes in the entire Hetao area, such as heavy precipitation days (R10mm), very heavy precipitation days (R20mm) and strong precipitation days (R25mm) (see *Figs. 9, 10* and *11*), but the

http://www.aloki.hu ● ISSN 1589 1623 (Print) ● ISSN 1785 0037 (Online)
DOI: http://dx.doi.org/10.15666/aeer/1605_62996316
© 2018, ALÖKI Kft., Budapest, Hungary

upward trend is not significant. On the scale of sub-regions, the variation trend is quite different in two sub-regions. The arid and semi-arid sub-region is positive while humid and semi-humid sub-region is negative (see *Table 3*).

Table 2. *Meteorological site with significant variation trend in extreme precipitation indexes*

Extreme precipitation index	Meteorological station	Variation trend (d/10a)
CWD	Lin He	-39.90*
CWD	Wu Tai Shan	-29.50*
CWD	Tai Yuan	-20.20*
CWD	Yan An	-20.10*
CWD	Lu Shi	-22.00*
R10mm	Ba Yin Mao Dao	27.16*
R10mm	Lin He	-31.59*
R10mm	Wu Tai Shan	-43.72*
R10mm	Zhong Wei	22.36*
R10mm	Hua Shan	-31.61*
R20mm	Ba Yin Mao Dao	26.13*
R20mm	Lin He	-36.11*
R20mm	Wu Tai Shan	-26.80*
R20mm	Hua Shan	-28.88*
R25mm	Gao Lan	-22.43*
R25mm	Lin He	-35.45*
R25mm	Wu Tai Shan	-21.89*

* means that it passed the 95% confidence level test

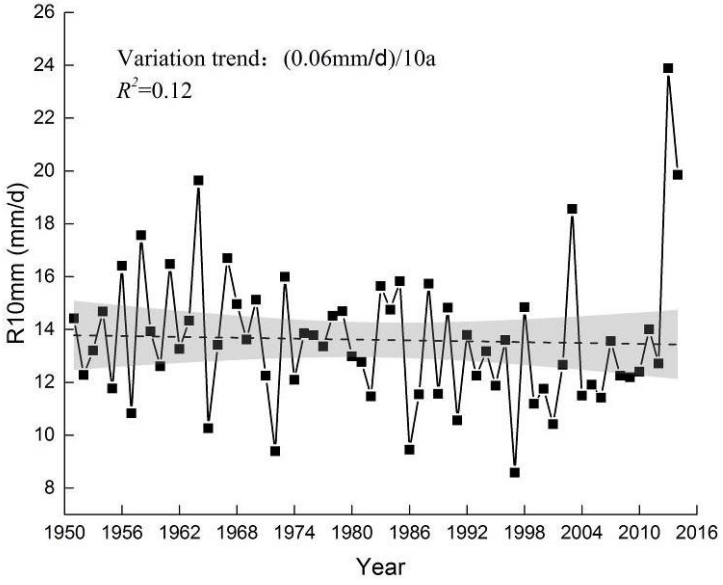

Figure 9. *Interannual variation of R10mm index in Hetao area (73 stations involved)*

http://www.aloki.hu ● ISSN 1589 1623 (Print) ● ISSN 1785 0037 (Online)
DOI: http://dx.doi.org/10.15666/aeer/1605_62996316
© 2018, ALÖKI Kft., Budapest, Hungary

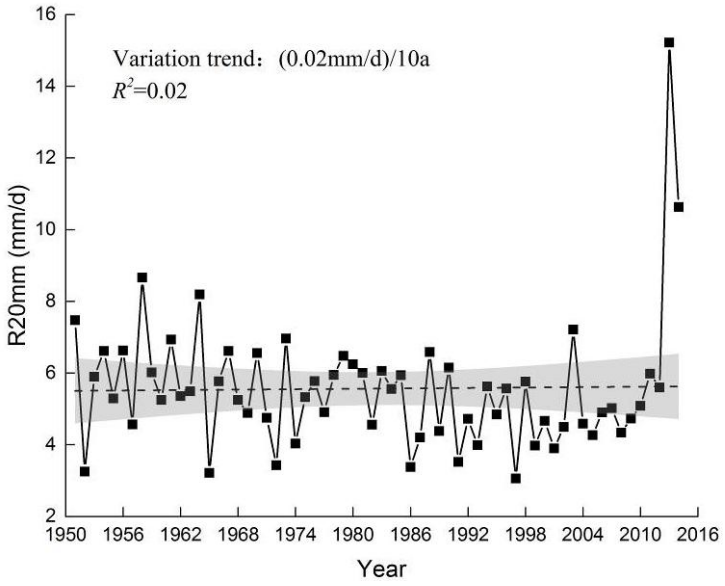

Figure 10. *Interannual variation of R20mm index in Hetao area (73 stations involved)*

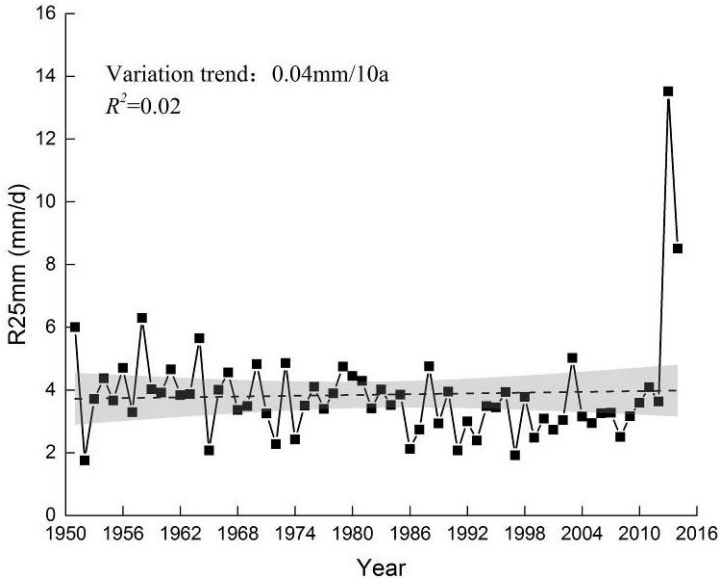

Figure 11. *Interannual variation of R25mm index in Hetao area (73 stations involved)*

Table 3. *Variation trend of extreme precipitation indexes in Hetao area from 1951 to 2014*

Extreme precipitation index	Arid and semi-arid sub-region			Humid and semi-arid sub-region		
	F-statistics	Significance	Variation trend (d/10a)	F-statistics	Significance	Variation trend (d/10a)
CWD	1.45	n.s.	0.18	0.20	n.s.	0.03
R10mm	0.04	n.s.	0.05	0.63	n.s.	-0.16
R20mm	0.77	n.s.	0.16	1.03	n.s.	-0.12
R25mm	1.18	n.s.	0.19	1.24	n.s.	-0.11

n.s. means that the variation trend is not significant

http://www.aloki.hu ● ISSN 1589 1623 (Print) ● ISSN 1785 0037 (Online)
DOI: http://dx.doi.org/10.15666/aeer/1605_62996316
© 2018, ALÖKI Kft., Budapest, Hungary

It is analyzed in this paper that there is a significant upward trend in heavy precipitation days in Bayinmaodao, Inner Mongolia. According to the records and related literature of the local meteorological department, heavy precipitation occurred in the area in 2010, 2013, 2014, 2015 and 2016 (Sun et al., 2013; Song et al., 2015; Ma, 2016; Lv, 2015; Man, 2015; Sun, 2018; Song, 2016). In order to detect whether there is extreme precipitation event at this station, this paper analyses the decades average precipitation and dynamic precipitation averages of Bayinmaodao meteorological station (see *Tables 4* and *5*).

Table 4. *Decades precipitation averages of Bayinmaodao meteorological station*

S.N.	Decades	Average precipitation (mm/year)
1	1957-1960	91.15
2	1961-1970	80.78
3	1971-1980	114.57
4	1981-1990	96.32
5	1991-2000	112.21
6	2001-2010	123.18
7	2011-2014	131.225

Table 5. *Dynamic precipitation averages of Bayinmaodao meteorological station*

S.N.	Periods of time	Average precipitation (mm/30 years)
1	1957-1980（24 years）	95.5
2	1961-1990（30 years）	97.22
3	1971-2000（30 years）	98.99
4	1981-2010（30 years）	107.7
5	1991-2014（24 years）	122.21

Based on statistical evaluation, the upward trend of decades precipitation averages and dynamic precipitation averages passed the 95% confidence level test in Bayinmaodao.

The above four indexes illustrate the extreme precipitation events from the perspective of time duration. Based on comprehensive analysis of the variation trend of the said indexes, this paper believes that the imbalance of precipitation in Hetao area is prominent, there is an extreme trend in Bayinmaodao, but extreme precipitation events in other regions have not increased.

Variation of PRCTOT, R99p, Rx5day and SDII indexes

Stations with significant upward trend of PRCTOT include Hailinsu and Bayinmaodao; those with significant downward trend include Linhe, Wutaishan and Huashan (see *Fig. 12*). There is no station with significant upward trend of R99p, while stations with significant downward trend include Sanmenxia and Gaolan (see *Fig. 13*). Stations with significant upward trend of Rx5day include Bayinmaodao; those with

http://www.aloki.hu ● ISSN 1589 1623 (Print) ● ISSN 1785 0037 (Online)
DOI: http://dx.doi.org/10.15666/aeer/1605_62996316
© 2018, ALÖKI Kft., Budapest, Hungary

significant downward trend include Linhe and Wutaishan (see *Fig. 14*). In addition, stations with significant upward trend of SDII include Bayinmaodao and Luochuan; station with significant downward trend is Linhe (see *Fig. 15*). Based on the comprehensive analysis of the information, it also reinforces the conclusion drawn in the preceding part of this paper that the extreme precipitation events in Bayinmaodao.

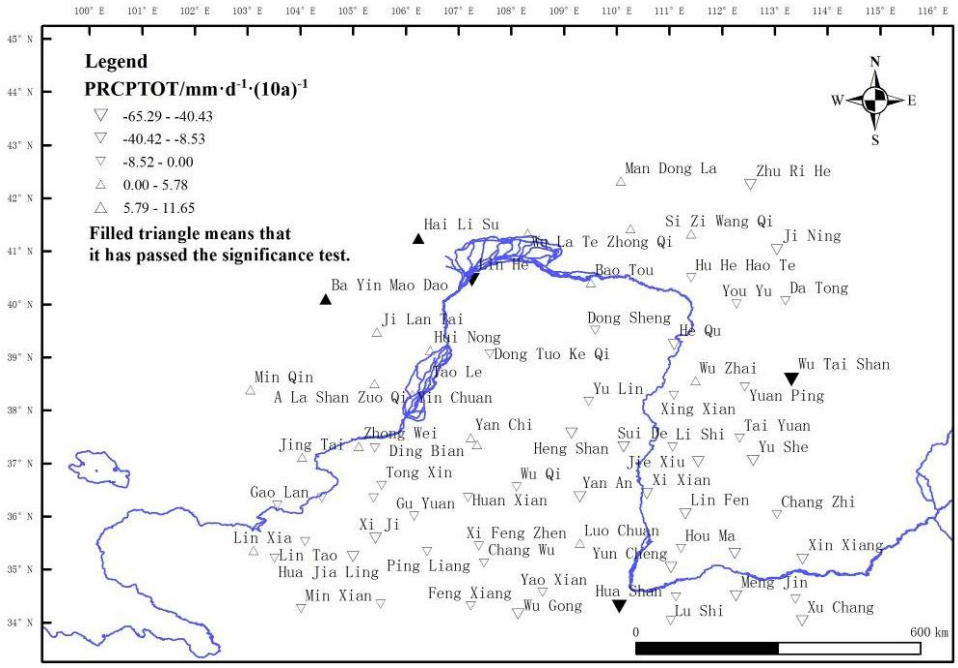

Figure 12. *Space variation of PROCTOT index in Hetao area*

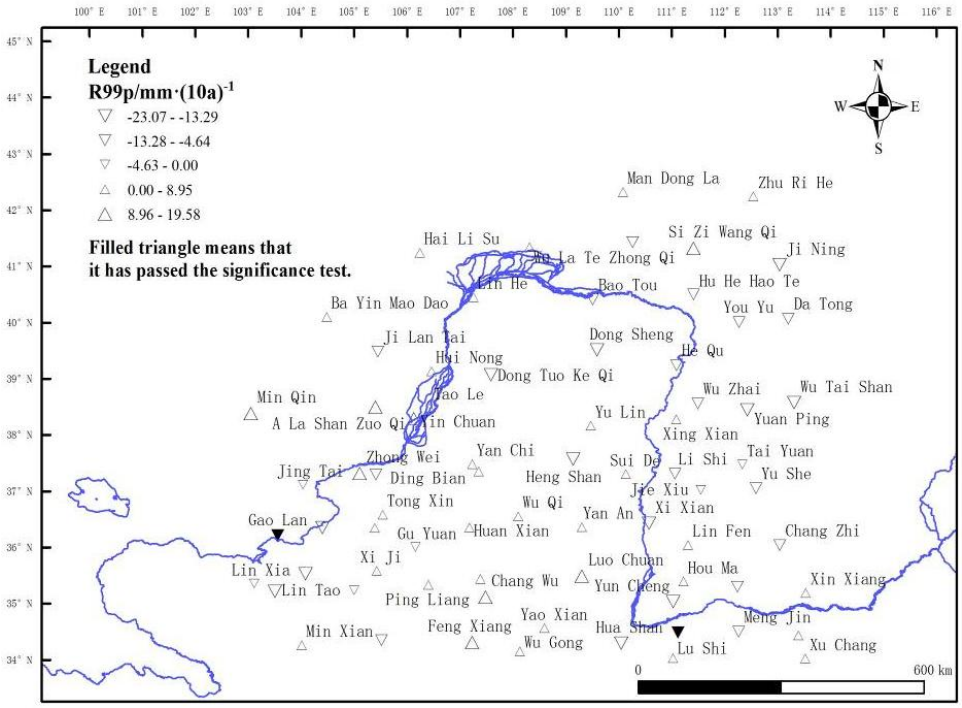

Figure 13. *Space variation of R99p index in Hetao area*

http://www.aloki.hu ● ISSN 1589 1623 (Print) ● ISSN 1785 0037 (Online)
DOI: http://dx.doi.org/10.15666/aeer/1605_62996316
© 2018, ALÖKI Kft., Budapest, Hungary

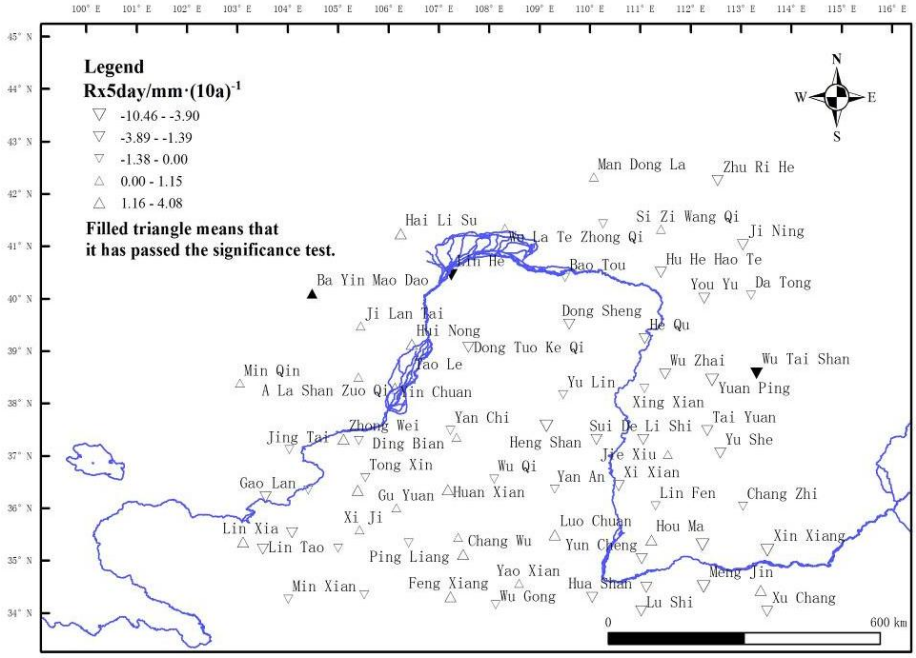

Figure 14. *Space variation of Rx5day index in Hetao area*

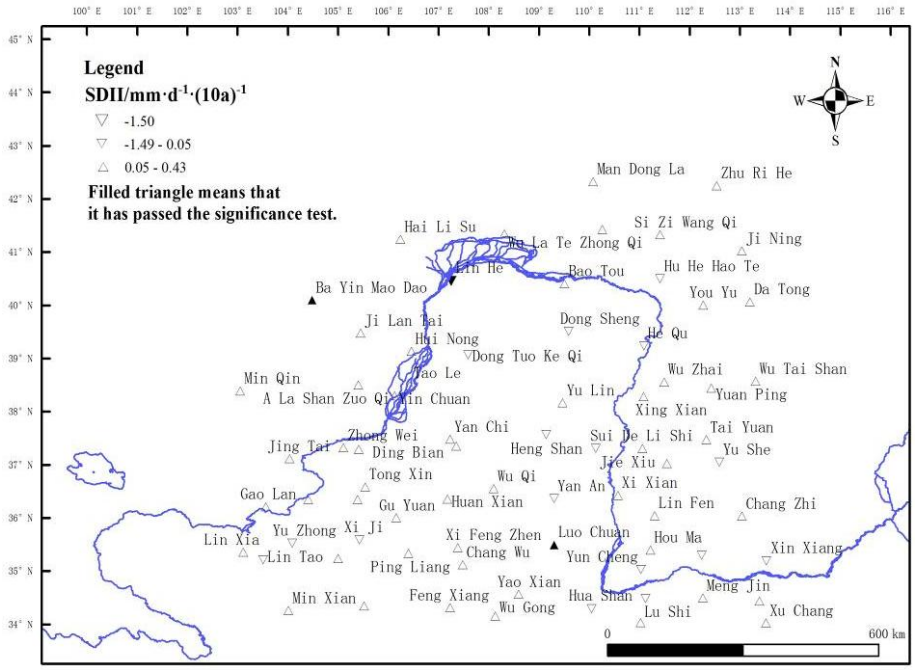

Figure 15. *Space variation of SDII index in Hetao area*

Viewed from interannual variation, the extreme precipitation events in the entire Hetao area have shown an upward trend, but it is not significant (see *Figs. 16, 17, 18, 19* and *Table 6*). However, the variation trend is different on sub-regions scale. The 4 indexes above in arid and semi-arid sub-region are positive, especially the index R99p (32.01 mm/10a) trend is significant; while the 4 indexes above in humid and semi-

http://www.aloki.hu ● ISSN 1589 1623 (Print) ● ISSN 1785 0037 (Online)
DOI: http://dx.doi.org/10.15666/aeer/1605_62996316
© 2018, ALÖKI Kft., Budapest, Hungary

humid sub-region are negative (see *Table 6*). This highlighting that the precipitation in the entire Hetao area is spatially unbalanced.

Table 6. *Variation trend of extreme precipitation indexes in Hetao area from 1951 to 2014*

Extreme precipitation index	Arid and semi-arid sub-region			Humid and semi-humid sub-region		
	F-statistics	Significance	Variation trend (/10a)	F-statistics	Significance	Variation trend (/10a)
PRCPTOT	1.07	n.s.	18.28 mm	2.88	n.s.	-12.24 mm
R99p	4.37	*	32.01 mm	1.45	n.s.	-5.94 mm
Rx5day	0.37	n.s.	1.04 mm	0.63	n.s.	-0.43 mm
SDII	2.01	n.s.	0.26 mm/d	0.15	n.s.	-0.03 mm/d

* means that it passed the 95% confidence level test; n.s. means that the variation trend is not significant

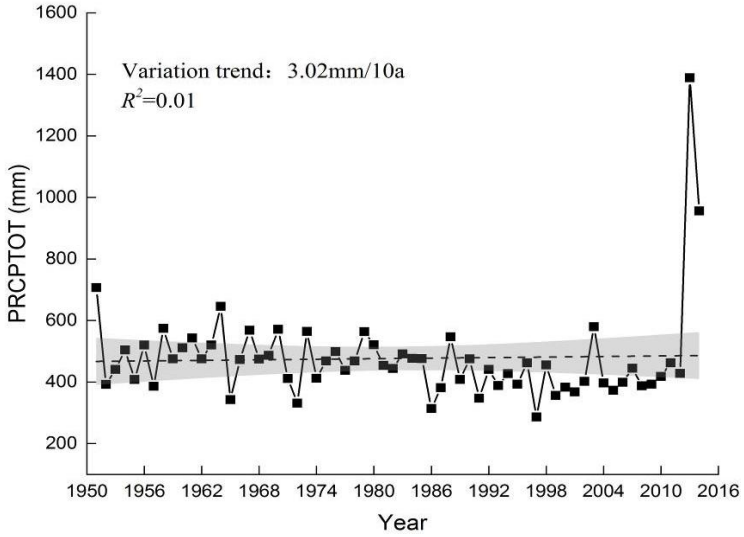

Figure 16. *Interannual variation of PROCTOT index in Hetao area (73 stations involved)*

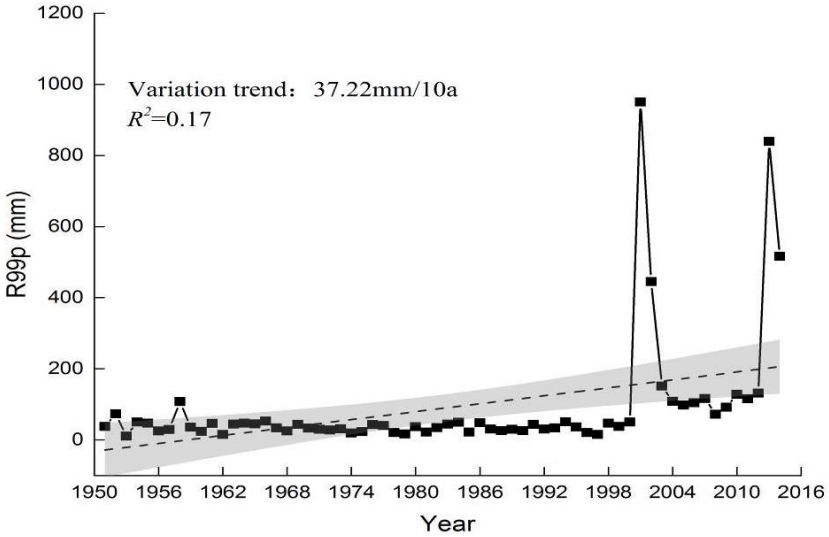

Figure 17. *Interannual variation of R99p index in Hetao area (73 stations involved)*

http://www.aloki.hu ● ISSN 1589 1623 (Print) ● ISSN 1785 0037 (Online)
DOI: http://dx.doi.org/10.15666/aeer/1605_62996316
© 2018, ALÖKI Kft., Budapest, Hungary

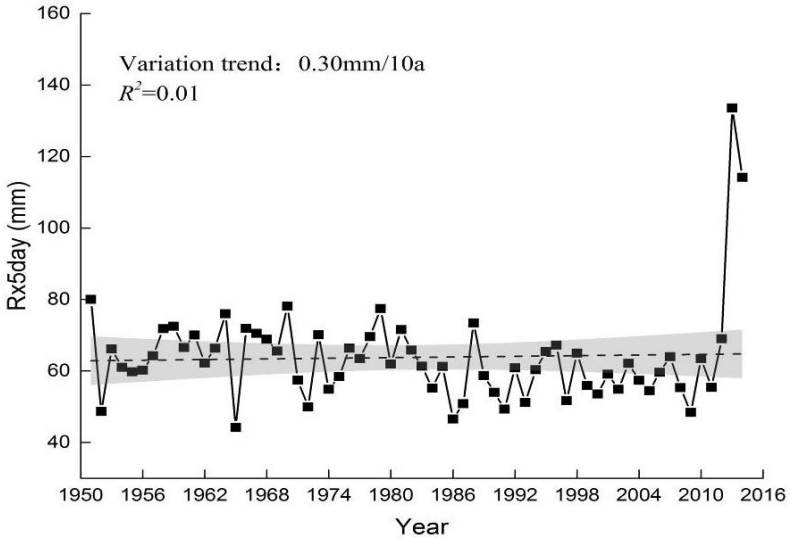

Figure 18. *Interannual variation of Rx5day index in Hetao area (73 stations involved)*

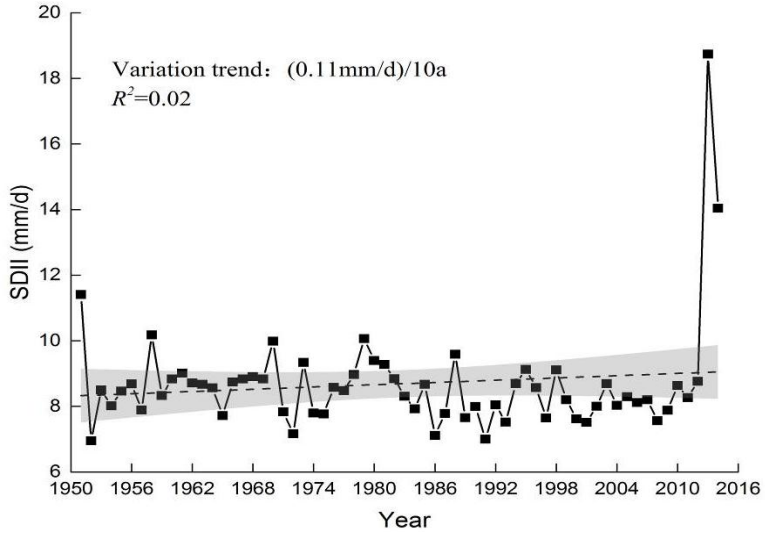

Figure 19. *Interannual variation of SDII index in Hetao area (73 stations involved)*

Conclusion

It is a focused issue for many scholars to probe into the evolution rule and its reasons of extreme precipitation events. Other studies have shown an increasing trend in extreme precipitation in China. The trend of annual precipitation changes in northwestern China showed a slight upward trend, but extreme precipitation did not increase significantly. Hetao area is located in the transitional zone of arid, semi-arid and semi-humid regions in China and is sensitive to climate change. This paper analyzes 8 extreme precipitation indexes from a temporal-spatial perspective in Hetao area China from 1951 to 2014, and comes to the following conclusions:

(1) Hetao area is located in the transitional zone of arid and semi-arid climate and humid and semi-humid climate, so the variation trend of extreme precipitation events is different in arid and semi-arid sub-region (located in the upper reaches of the Yellow

http://www.aloki.hu ● ISSN 1589 1623 (Print) ● ISSN 1785 0037 (Online)
DOI: http://dx.doi.org/10.15666/aeer/1605_62996316
© 2018, ALÖKI Kft., Budapest, Hungary

River) and humid and semi-humid sub-region (located in the middle and lower reaches of the Yellow River), and precipitation is spatially unbalanced.

(2) Although the R99p index is a significant upward trend, the trend of other indicators is not significant. Except for the Bayinmaodao, the extreme precipitation events in Hetao area has not an obvious trend

(3) In the humid and semi-humid sub-region of Hetao area, only the variation trend of CWD index is positive, the variation trend of other 7 indices are negative. Whether this situation indicates that precipitation is decreasing is yet to be further studied.

Based on the research above, this paper draws the conclusion that the extreme precipitation events in Hetao area has not an obvious trend in the past half a century. In addition, the trend has no spatial consistency due to the trend is quite different in sub-regions. The reasons for this situation is extremely complex, and reasons for such phenomenon still need to be further studied.

Acknowledgements. This study was supported mostly by the university first-class discipline construction project of Ningxia, China (Grant No. NXYLXK2017A03).

REFERENCES

[1] Cai, M. (2014): A Study on Climatic Characteristics and Causes of the Rainstorm over Hetao Region and Their Relation with Atmospheric circulation anomaly. – Lanzhou University, China.

[2] Cai, M., Zhang, Z. (2014): Characteristic analysis on climatological variation of precipitation days with heavy and above rain intensities over Hetao region. – Torrential Rain and Disasters 4: 401-406.

[3] Huang, P., Tan, Z., Liao, X. (2013): Statistical analysis of summer extreme precipitation events in Hetao. – Journal of Anhui Agricultural Sciences 6: 2594-2596.

[4] Li, J., Du, C.-L, Du, S. et al. (2015): Temporal-spatial variation and trend prediction of extreme precipitation events in Xinjiang. – Arid Zone Research 06: 1103-1112.

[5] Li, Y., He, D., Hu, J. et al. (2012): Spatial and temporal variations of extreme precipitation events in the Red River basin during 1960-2007. – Journal of Natural Resources 11: 1908-1917.

[6] Lv, N. (2015): Cause analysis on heavy precipitation weather in spring of 2014. – Meteorology Journal of Inner Mongolia 06: 7-10.

[7] Ma, S. (2016): Diagnosis analysis of extreme rainstorm process in Hetao region of Inner Mongolia in July 14, 2013. – Meteorology Journal of Inner Mongolia 03: 8-12+43.

[8] Man, D. (2015): April 1, 2015 Bayannaoer City, Dengkou County spring rare rain weather forecast technical summary. – Science and Technology Economic Market 11: 193-194.

[9] Qi, T., Zhang, Q., Wang, Y. et al. (2015): Spatiotemporal patterns of pan evaporation in 1960-2005 in China: Changing properties and possible causes. – Scientia Geographica Sinica 12: 1599-1606.

[10] Qi, Y., Chen, H., Fang, S. et al. (2015): Variation characteristics of extreme climate events in Northwest China during 1961–2010. – Journal of Arid Meteorology 6: 963-969.

[11] Shen, H., Ma, M., Wang, J. et al. (2012): Variation characteristics of extreme air temperature events in Qinghai Province. – Journal of Glaciology and Geocryology 06: 1371-1379.

[12] Song, G., Li, X., Jiang, J. et al. (2015): Procession and causes of the extreme rainstorm event in Inner Mongolia in July 2012. – Plateau Meteorology 01: 163-172.

http://www.aloki.hu ● ISSN 1589 1623 (Print) ● ISSN 1785 0037 (Online)
DOI: http://dx.doi.org/10.15666/aeer/1605_62996316
© 2018, ALÖKI Kft., Budapest, Hungary

[13] Song, G.-Y., Li, X.-Z., Jiang, J. et al. (2016): Two extreme rainstorms in the arid-semiarid zone of Inner Mongolia in summer 2013. – Arid Zone Research 04: 747-757.
[14] Sun, L., Wang, Y., Liang, F. et al. (2013): Diagnostic analysis of a heavy rainfall in Bayannur, Inner Mongolia. – Meteorological and Environmental Sciences 03: 34-38.
[15] Sun, S. (2018): Analysis of rainfall process in Bayannaoer City from August 16th to 18th. – Modern Agricultural Science and Technology 10: 234+242.
[16] Tao, N., Wang, B., Zhang, L. et al. (2011): Analysis on climatic characteristics of air temperature and precipitation in Hetao region. – Meteorology Journal of Inner Mongolia 01: 19-21.
[17] Wang, B., Jiang, Y., Dong, M. Y. et al. (2016): Spatiotemporal variations of extreme precipitation in the semiarid region in North China during the period of 1961-2010. – Arid Zone Research 05: 913-920.
[18] Wang, M., Guo, P., Wu, Y. et al. (2012): Progresses in researches on extreme precipitation over China. – Meteorological Science and Technology 6: 914-921.
[19] Wang, Q., Zhang, M., Wang, S. et al. (2013): Extreme temperature events in Yangtze River basin during 1962-2011. – Acta Geographica Sinica 05: 611-625.
[20] Wang, S., Luo, Y., Zhao, Z. et al. (2014): Climate science challenges. – Advances in Climate Change Research 04: 306-309.
[21] Wang, X. L., Wen, Q. H., Wu, Y. (2007): Penalized maximal t-test for detecting undocumented mean change in climate data series. – Journal of Applied Meteorology & Climatology 6: 916-931.
[22] Zhai, P., Pan, X. (2003): Change in extreme temperature and precipitation over Northern China during the second half of the 20th century. – Acta Geographica Sinica S1: 1-10.
[23] Zhang, G. (2012): Homogeneity study of the temperature and precipitation data over China using multi-methods. – Nanjing University of Information Science & Technology, Nanjing.
[24] Zhang, G., He, J., Zhou, Z. et al. (2012): Homogeneity study of precipitation data over china using RHtest method. – Meteorological Science and Technology 6: 914-921.
[25] Zhang, S. (2015): A new international climate change benchmark was officially opened in 2015. – Advances in Earth Science 08: 967.
[26] Zhang, X., Aguilar, E., Sensoy, S. et al. (2005): Trends in Middle East climate extreme indices from 1950 to 2003. – Journal of Geophysical Research Atmospheres D22: 3159-3172.
[27] Zhang, Z., Cai, M. (2014): Regional characteristics and disaster analysis on rainstorms in Hetao. – Journal of Catastrophology 1: 81-86.
[28] Zhao, C., Chen, Y., Wang, W. et al. (2015): Temporal and spatial variation of extreme precipitation indexes of the Yellow River basin in recent 50 years. – Yellow River 01: 18-22.
[29] Zhou, Y., Ren, G. (2010): Variation characteristics of extreme temperature indices in Mainland China during 1956-2008. – Climatic and Environmental Research 4: 405-417.

http://www.aloki.hu ● ISSN 1589 1623 (Print) ● ISSN 1785 0037 (Online)
DOI: http://dx.doi.org/10.15666/aeer/1605_62996316
© 2018, ALÖKI Kft., Budapest, Hungary

THE RELATIONSHIPS AMONG INTERPRETIVE SERVICE QUALITY, SATISFACTION, PLACE ATTACHMENT AND ENVIRONMENTALLY RESPONSIBLE BEHAVIOR AT THE CULTURAL HERITAGE SITES IN XI'AN, CHINA

CHENG, T. E.[1,2] – WANG, J.[3] – CAO, M. M.[2*] – ZHANG, D. J.[3] – BAI, H. X.[1]

[1]*School of Foreign Languages, Northwest University, Xi'an, China*
(e-mail: 958632991@qq.com – T.E. Cheng, 374220178@qq.com – H.X. Bai)

[2]*College of Urban and Environmental Sciences, Northwest University, Xi'an, China*

[3]*College of Geography Sciences, Shanxi Normal University, Linfen, China*
(e-mail: 1565612766@qq.com – J. Wang, 112936666@qq.com – D.J. Zhang)

**Corresponding author*
e-mail: chengshi@nwu.edu.cn

(Received 31st May 2018; accepted 2nd Aug 2018)

Abstract. The present study investigated the causal relationships among interpretive service quality, satisfaction, place attachment and environmentally responsible behavior. 1800 tourists visiting five historic heritage sites in Xi'an, China were surveyed and 1408 valid questionnaires were collected. The validity and reliability of the data were analyzed by using SPSS 22.0 and the structural equation model (SEM) was tested using AMOS 24. The findings of the study showed that interpretive service quality has direct and positive effect on satisfaction and satisfaction directly impacts place attachment and environmentally responsible behavior respectively. In addition, interpretive service quality exerts indirect influence on place attachment and environmentally responsible behavior respectively through satisfaction, indicating the mediating role of satisfaction in the relationship between interpretive service quality and place attachment as well as that in the relationship between interpretive service quality and environmentally responsible behavior. Moreover, the study demonstrated that place attachment influences environmentally responsible behavior directly. In the end, management implications about the improvements in interpretive services at cultural heritage sites are suggested in order to sustain sustainable development of heritage tourism.
Keywords: *interpretation outcome, behavioral intention, heritage tourism, structural equation modeling*

Introduction

Xi'an (34°N, 108°E), the capital city of Shaanxi province, China, has a history of around 3100 years and 13 dynasties in Chinese history established their capitals in this city. As a result, it boasts a wealth of historical relics left by past dynasties and enjoys a reputable Natural History Museum in China (Ma, 2007, p. 139). An overwhelming majority of these historical relics have been preserved and developed into tourist attractions. Reflecting the economic, social and cultural development in history, these sites carry the heritage creators' values, aesthetical standards and spiritual needs (Hall and McArthur, 1998). The meaning ascribed to the sites mean more to tourists than what the physical artifacts do to them (Graham, 2007). Unfortunately, many tourists cannot understand the profound meaning carried by such sites (Risk, 1982, p. 195). Heritage tourism management agencies provide interpretive services to help visitors understand values inherent in the heritages to enrich their experiences (Knudson et al., 2003). It is claimed that the enhanced experiences enable tourists to increase

http://www.aloki.hu ● ISSN 1589 1623 (Print) ● ISSN 1785 0037 (Online)
DOI: http://dx.doi.org/10.15666/aeer/1605_63176339
© 2018, ALÖKI Kft., Budapest, Hungary

knowledge, which results in their behavioral change (Moscardo, 2014). Previous studies examined the influence of interpretation on environmentally responsible behavior (ERB) and found the former could help elicit the latter (Powell and Ham, 2008). Some researchers believed that interpretation also affected tourists' emotional attachments to visited place. Carr (2004) as well as Knudson, Cable and Beck (2003) viewed that emotional attachments to natural and cultural resources were meaningful for tourists to understand the essence of a place**.** Unfortunately, very limited empirical studies explored the relationship between interpretation and emotional attachment.

Past ERB literature indicated place attachment (Ramkissoon et al., 2013; Lee, 2011) and satisfaction (Lee and Moscarbo, 2005) predicted ERB. However, the relationships among satisfaction, place attachment and ERB have not been tested in the field of interpretation. Since interpretation is demonstrated to influence tourists' behaviors, there might be causal relationships among the above 4 variables. Besides, although some researchers held that quality interpretation could enable tourists to exhibit ERB (Powell and Ham, 2008), few quantitative studies have been conducted to examine the outcomes of it. Most of the existing studies were conducted in community-based (Lee et al., 2013b) and natured-based tourism destinations (Kim, 2011; Lee, 2009). Very limited such studies have been conducted at cultural heritage sites. Skibins et al. (2011) argued that it was very necessary to fully study interpretation outcomes if long-term management of tourism resource relied on sustainable use by visitors.

Therefore, the purposes of this study are:

1. To explore the relationship between interpretive service and place attachment.
2. To investigate the causal relationship between interpretive service and ERB.
3. To examine whether interpretive service influences satisfaction.
4. To study whether satisfaction affects place attachment.
5. To explore the relationship between satisfaction and ERB.
6. To test whether place attachment impacts ERB at cultural heritage site.

Selecting 5 heritage sites in Xi'an area as study sites, this empirical study will not only contribute to conceptual models related to interpretation outcomes but will benefit the sustainable development of heritage tourism in Xi'an in the long run.

Literature review

Interpretation service

Interpretive services at heritage sites include personal interpretation given by tour guides and on-site interpreters as well as non-personal interpretive services delivered through various media such as signage, on-site panels, brochures, exhibits, visitor centre etc. (Skibins, 2010). Tourists often depend on interpretation to understand the inherent meaning and value of heritage sites, which helps them experience a worthwhile and enjoyable trip. From the perspective of tourism management, they provide interpretive services to help tourists understand the embodied meaning in heritages resources (Knudson et al., 2003), express their requirements for tourists and inspire them to protect heritage. Obviously, interpretation serves as a communication bridge between tourists and tourism management.

Tilden (2007) defined interpretation as "an educational activity which aims to reveal meanings and relationships through the use of original objects, by firsthand experience, and by illustrative media, rather than simply to communicate factual information". His

http://www.aloki.hu ● ISSN 1589 1623 (Print) ● ISSN 1785 0037 (Online)
DOI: http://dx.doi.org/10.15666/aeer/1605_63176339
© 2018, ALÖKI Kft., Budapest, Hungary

ideas about interpretation had enormous influence on the researchers of later generations. Although researchers after Tilden modified the definition of interpretation (Moscardo, 2014; Poria et al., 2009), the core part of educational function emphasized by Tilden remains. This can be seen from the research focus of some researchers. Munro et al. (2008) and Skibins et al. (2011) found most of studies concerning focused on evaluating knowledge increase of tourists after they experienced interpretive services and these studies also reported knowledge increase (Mace, 2013; Morgan and Hwang, 2014; Powell and Ham, 2008). However, besides educational functions, interpretation has more functions like enhancing tourists' experiences, fostering positive attitudes and behaviors among tourists (Ham and Weiler, 2006), providing them with opportunities to form emotional link to the visited site (Larsen, 2003) etc. Some studies showed that contemporary tourists hoped to gain some emotional experience through interpretation rather than just getting an educational experience (Poria et al., 2009). It is argued that the emotional link between the tourist and the place should be explored to understand and manage historic settings (Poria, 2006). Unfortunately, the affective outcome of interpretation is usually ignored. In addition, effective interpretation was believed to prompt more environmentally responsible behavior among tourists (Ballantyne et al., 2011), which is one of the core goals of interpretation (Ward and Wilkinson, 2006). For instance, the study conducted by Tubb (2003) found that interpretation provided in Dartmoor National Park in the UK encouraged tourists to behave more respectfully towards the local environment. The findings of Powell and Ham (2008) also showed that quality interpretation during the ecotourism experience could help tourists show general environmental behavioral intentions. In short, previous literature showed that interpretation impacted ERB, but such studies mainly used national parks or other nature-based settings.

Tourist satisfaction

In the field of tourism industry, many studies examined the antecedents of tourist satisfaction and its outcomes. According to past literature, the antecedents contributing to overall tourist satisfaction involve leisure service of destination attributes (Bernini et al., 2014), positive destination attributes (Battour et al., 2014; Zabkar et al., 2010), service quality (Song et al., 2010), place attachment (Yuksel et al., 2010). The consequences of satisfaction involved in the past studies mainly include its positive influence on destination loyalty (Yuksel et al., 2010), place attachment (Ramkissoon et al., 2015; Su et al., 2011), behavioral intention (Chen, 2010) and ERB (Davis et al., 2011).

Studies examining the link between interpretive services and satisfaction found the former had direct and positive effect on the latter (Huang et al., 2015; Ham and Weiler, 2007; Lee, 2009). However, these studies mainly focused on personal interpretation and very limited studies examined the impact of both personal and non-personal interpretive services on satisfaction. Although interpretation provided by tour guide is proved to be more effective than non-personal ones (Hughes, 2004), it is still important to study the outcome of non-personal ones since most of the tourists at cultural heritage sites in China depend on them to understand the inherent meaning of visited sites. Besides, past research mainly studied the relationship between interpretive service and satisfaction in nature-based context and that in historic heritage context is usually ignored. What is more, the above studies failed to assess the quality of interpretation, which may affect the accuracy of their research findings.

http://www.aloki.hu ● ISSN 1589 1623 (Print) ● ISSN 1785 0037 (Online)
DOI: http://dx.doi.org/10.15666/aeer/1605_63176339
© 2018, ALÖKI Kft., Budapest, Hungary

The findings of previous literature showed inconsistent or opposite results about the relationship between satisfaction and place attachment. Some studies demonstrated that satisfaction affected place attachment (George and George, 2004), while other studies indicated opposite results. (Prayag and Ryan, 2012; Yuksel and Bilim, 2010). Research of the relationship between the two mainly examined satisfaction with service quality (Su et al., 2011), satisfaction with attractiveness of a destination (Hou et al., 2005) and overall level of satisfaction (Petrick et al., 1999). Very limited studies were conducted to study the relationship between interpretive service satisfaction and place attachment and no relative studies have ever been conducted at cultural heritage settings.

Satisfaction was shown to influence customers' behavioral responses in the field of marketing (Baker and Crompton, 2000) and in the field of recreation and tourism satisfaction was viewed as a factor influencing ERB (Lopez-Mosquera and Sanchez, 2011; Powell and Ham, 2008) at national parks or other nature-based settings. For instance, Ramkissoon et al. (2013) surveyed tourists visiting the Dandenong Ranges National Park, Australia to explore the relationships among place attachment, place satisfaction and pro-environmental behavioral intentions and found that visitors' satisfaction with the visited site influenced their on-site behaviors. The existing literature concerning the relationship between the two variables mainly focused on satisfaction with travel experience or with the visited sites at natured-based settings. No study has ever been conducted to examine the relationship between satisfaction with interpretive service quality and ERB at historic heritage sites.

Place attachment

Place attachment is an affective and emotional bond that people develop with a place (Low and Altman, 1992) and the term "place attachment" highlights a positive bond between the two (Trentelman, 2009). Researchers in different fields view it as a multi-dimensional construct including place dependence, place identity, place social bonding (Ramkissoon et al., 2013) and place affect (Hinds and Sparks, 2008). Among these dimensions, the most widely accepted and frequently studied ones are the former two. Place dependence emphasizes functional attachment to a place because the place can provide necessary resources or facilities to meet the individual's specific activity needs (Williams and Roggenbuck, 1989). Place identity reflects the symbolic importance of a place to a person (Williams and Vaske, 2003). In the field of tourism, researchers have studied factors predicting place attachment as well as effects of it. According to past literature, some factors like service quality (Alexandris et al., 2006), attractiveness of a destination (Xu and Zhang, 2016), environmental sensitivity (Cheng and Wu, 2013), activity involvement (Xu and Zhang, 2016), satisfaction with service quality (Su et al., 2011) etc. predict place attachment.

Lee et al. (1997) emphasized that psychological attachment was important in understanding tourist behavior in explaining behavioral phenomena. Several researchers have found that place attachment was a positive predictor of ERB (Halpenny, 2010; Lee, 2011). According to the findings of previous studies, when tourists were highly attached to tourist destinations, they were more likely to exhibit their ERB (Cheng et al., 2013; Ramkissoon et al., 2013). For example, Cheng et al. (2013) examined the causal relationships among place attachment, destination attractiveness and ERB and the study results showed that place attachment was positively associated with stronger ERB.

http://www.aloki.hu ● ISSN 1589 1623 (Print) ● ISSN 1785 0037 (Online)
DOI: http://dx.doi.org/10.15666/aeer/1605_63176339
© 2018, ALÖKI Kft., Budapest, Hungary

Past studies mainly focused on place attachment elicited by destination attractiveness (Cheng et al., 2013), environmental sensitivity (Cheng et al., 2013) and satisfaction with service quality of the resort (Su et al., 2011). To date, no research has ever explored whether satisfaction with interpretive service will affect place attachment. In addition, studies of place attachment are extremely limited in interpretation literature (Goldman et al., 2001). For further understanding the nature of human place bonding, it is necessary to study the relationship between place attachment and ERB in the field of interpretation. Research into place attachment is classified into three contexts: personal context, natural environment context and community context (Raymond et al., 2010), but very limited research has been conducted to investigate the relationship between place attachment and ERB in the context of historic heritage site. Evidence shows that sustainability practices in national parks and other natural areas can be improved by fostering place attachment (Halpenny, 2010) and by encouraging ERB among visitors (Ballantyne et al., 2009) and such an inference may also apply to sustainable development of cultural heritage tourism.

Environmentally responsible behavior

Environmentally responsible behavior (ERB) is defined as an intentional action of an individual or group to directly or indirectly benefit the environment (Stern, 2000) and such action contributes to tourism resource protection and conservation (Lee, 2011). Many studies of ERB borrowed the definition given by Sivek and Hungerford (1990) which limits ERB to nature-based settings. In studying ERB at various settings, the attitude-behavior model is frequently employed. According to the theory of reasoned action (Fishbein and Ajzen, 1975) and the theory of planned behavior (Ajzen, 1991), attitude significantly affects an individual's behavior and it is an important predictive variable of behavior (Lee et al., 2013a). According to the theory of reasoned action, the best predictor of behavior is the intention to adopt the behavior (Halpenny, 2005). In empirical studies, it is rather difficult to measure the actual ERB of tourists. Based on the above theory, most studies measured behavioral intentions of visitors instead of their actual behaviors. Smith-Sebasto and D'Costa (1995) classified ERB into six categories including civic action, educational action, financial action, legal action, physical action as well as persuasive action. Compared with measurement scales developed by other scholars for ERB, the construct of ERB developed by Smith-Sebasto (1995) seemed to be more holistic (Lee et al., 2013b) and his categories of environmental action are widely used by tourism scholars to evaluate personal ERB (Ballantyne et al., 2011). ERBs are usually measured from two dimensions: general ERBs and specific ERBs (Lee et al., 2013b).

ERB has been widely studied in the field of tourism. Past research found that factors predicting ERB included place attachment (Lee, 2011; Ramkissoon et al., 2013), environmental attitudes (Schultz et al., 2004), commitment to the natural environment and tourist motivations (Lee, 2011), perceived value, satisfaction and activity involvement (Davis et al., 2011; Ramkissoon et al., 2014), environmental knowledge and environmental sensitivity etc. (Cheng and Wu, 2013). The studies of ERB that involved satisfaction mainly focused on visitors' satisfaction with the global setting at tourism destinations or their travel experience. To date, no study has ever examined whether satisfaction with interpretive service may lead to visitor's adoption of ERB. Some scholars argued that interpretive services helped facilitate tourists' ERB (Ballantyne et al., 2011). Marion and Reid (2007) reviewed the theoretical and empirical

http://www.aloki.hu ● ISSN 1589 1623 (Print) ● ISSN 1785 0037 (Online)
DOI: http://dx.doi.org/10.15666/aeer/1605_63176339
© 2018, ALÖKI Kft., Budapest, Hungary

studies concerning interpretation outcomes in the US and found that most of the interpretation services could effectively modify visitors' behaviors. However, most of the past research of ERB indicated that interpretive services had impacts on ERB mainly as a result of visitors' knowledge increase. Since satisfaction is considered one of the antecedents of ERB, the present study views that satisfaction with interpretive services may impact visitors' ERB. In addition, past studies only studied ERB at nature-based settings and very limited research has ever assessed ERB at historic heritage settings. In addition, the relationship between place attachment and ERB is frequently studied in the field of recreation and tourism, but no study has ever been conducted to evaluate such a relationship in interpretation literature. This research attempts to study whether satisfaction with interpretive service affects tourists' ERB and the relationship between place attachment and ERB in the field of interpretation in historic heritage context in order to enrich the literature of ERB.

Based on the above literature review, the following hypotheses and theoretical model (*Fig. 1*) are proposed:

H_1: Interpretive service quality directly and positively influences place attachment;
H_2: Interpretive service quality directly and positively influences ERB.
H_3: Interpretive services directly and significantly influence tourist satisfaction;
H_4: Satisfaction directly and positively affects place attachment;
H_5: Satisfaction directly influences ERB.
H_6: Place attachment directly and significantly influences ERB

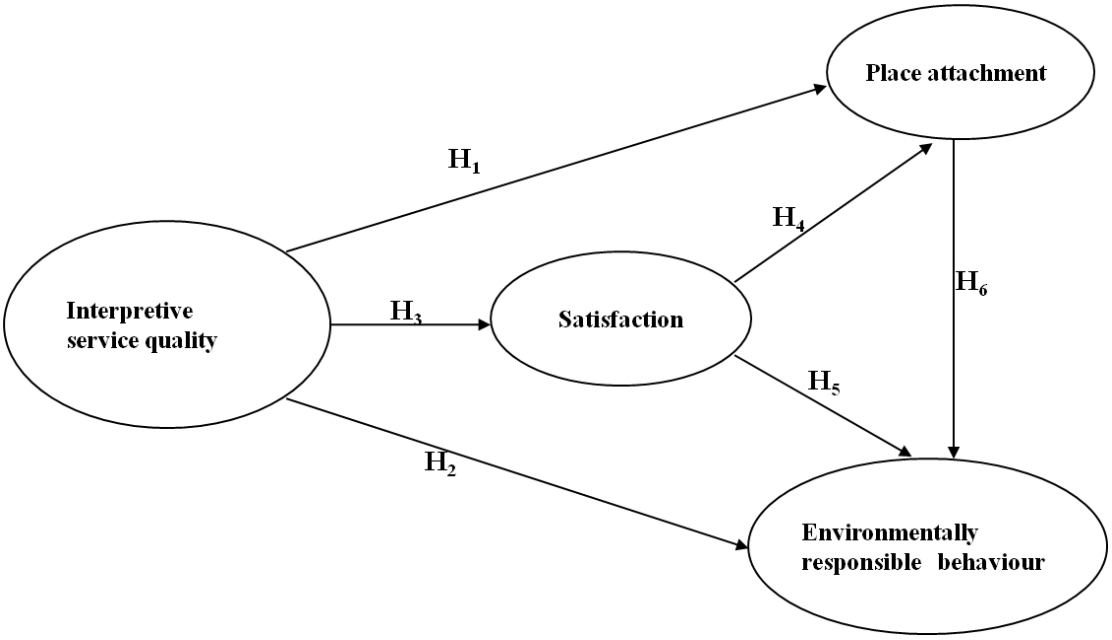

Figure 1. *The theoretical model of heritage site tourists*

Research methods

Study sites

The study sites include the following five historic heritage sites in Xi'an, China (*Fig. 2*). (1) Emperor Qinshihuang's Mausoleum Site Museum is the only cultural historic heritage in Shaanxi province inscribed on the World Heritage List. It is China's

http://www.aloki.hu ● ISSN 1589 1623 (Print) ● ISSN 1785 0037 (Online)
DOI: http://dx.doi.org/10.15666/aeer/1605_63176339
© 2018, ALÖKI Kft., Budapest, Hungary

largest ancient military museum representing an epitome of the powerful army in the Qin dynasty (221B.C.-207B.C.). (2) Huaqing Palace which characterizes culture of the Tang dynasty (618A.D.-907A.D.) is famous for hot springs, imperial palaces, imperial gardens and historical events in the Tang dynasty. (3) Dayan Pagoda and Tang Paradise are two neighboring historic sites located in Xi'an city. Dayan Pagoda enjoys a history of over 1300 years and is famous for storing Buddhist scriptures. Tang Paradise is a historic site featuring culture of the Tang dynasty. (4) Mausoleum of Yellow Emperor is a holy land to worship the Chinese ancestor—Xuanyuan Emperor and it is claimed No. 1 Mausoleum in China. (5) Honored as royal temple, Famen Temple has a history of 1700 years and is a holy land of Buddhism for storing Sakyamuni's finger bone.

Figure 2. *The map of study location*

Data collection

The questionnaire consists of 3 sections. The first section introduces interpretive services and programs at the heritage sites and one question is designed to investigate the interpretive services used by tourists. The second section consists of 47 items devised to examine tourists' evaluation of interpretive service quality, satisfaction, place attachment and ERB. The third section is the profile of respondents. The pretest of 180 questionnaire surveys was conducted and data analysis was valid and all the items were kept. Based on the suggestions given by some respondents and staff of management agencies, the wording was revised in order to help tourists better understand each item. The final formal questionnaire was established based on the pretest results.

The graduates who were trained how to hand out questionnaires went to the heritage sites to conduct the survey. Convenience sampling was used to survey respondent

http://www.aloki.hu ● ISSN 1589 1623 (Print) ● ISSN 1785 0037 (Online)
DOI: http://dx.doi.org/10.15666/aeer/1605_63176339
© 2018, ALÖKI Kft., Budapest, Hungary

tourists at the exits of the historic sites between May and September 2015. It took about 10 min for each respondent to answer all the questions on the questionnaire. A total of 1800 questionnaires were distributed and 1408 valid ones were collected (*Table 1*).

Table 1. *Survey sample at each heritage site*

Heritage sites	Total surveys	Valid sample	Sampling dates
1. Emperor Qinshihuang's Mausoleum Site Museum	200	154	May 1-3, 2015
2. Huaqing Palace	193	143	June 23-24, 2015
3. Dayan Pagoda and Tang Paradise	1007	841	July 2015 (8 days)
4. Mausoleum of Yellow Emperor	200	139	August 11-12, 2015
5. Famen Temple	200	131	September 19-20, 2015
Total	1800	140	

Measurement of constructs

This study adopted SERVPERF model to assess interpretative service quality including five dimensions like tangibles, empathy, assurance, responsiveness and reliability. 22 items were borrowed and adapted from Cronin and Taylor's (1994) research findings. Satisfaction was evaluated from a holistic perspective and 4 items borrowed and adapted from the research results of Oliver (1980) and Ramkisoon et al. (2013) were used to measure tourists' global satisfaction with interpretive services. The construct of place attachment consisted of two dimensions: place dependence and place identity. 13 items borrowed and adapted from Williams and Roggenbuck's (1989) as well as Morgan's (2009) research findings were used to measure place attachment. Two dimensions were included in ERB. 8 items adapted from Smith-Sebasto and D' Costa's work (1995) were used to measure ERB. All the above-mentioned items were scored on a 7-point Likert scale (7 = strongly agree; 1 = strongly disagree). Demographic variables of the questionnaire included gender, age, marital status, education, city of residence, companion, number of visiting times, visit duration and purposes of visiting the sites.

Results of the study

Respondent profiles

There were more female respondents (54.4%) than male ones (45.6%). 85.6% were between 18 and 50 years old. 50.6% were married and 62.2% received college education. More than half of the respondents (58.7%) came from outside of Shaanxi and 38.9% were locals. Only 1.6% came from Hong Kong, Macao and Taiwan. 76.6% were accompanied by friends or family members and 12.6% were with group tour. Most of the respondents (68.5%) visited the destinations for the first time. It took most of them (76.7%) 2–3 h to visit the sites. The motivation of 58.9% was to seek nostalgic experience and 55.1% went to relax themselves. 41.4% went to broaden their horizon and 36.4% visited the places due to the site reputation. Various interpretive services

http://www.aloki.hu ● ISSN 1589 1623 (Print) ● ISSN 1785 0037 (Online)
DOI: http://dx.doi.org/10.15666/aeer/1605_63176339
© 2018, ALÖKI Kft., Budapest, Hungary

were used by the tourists: personal interpretation (51.3%), signage (41.4%), digital interpretation (11.6%), printed materials (12.8%), visitor center (10.4%), films (6.6%), projects participation (7.3%) and websites (7.2%) (*Fig. 3*).

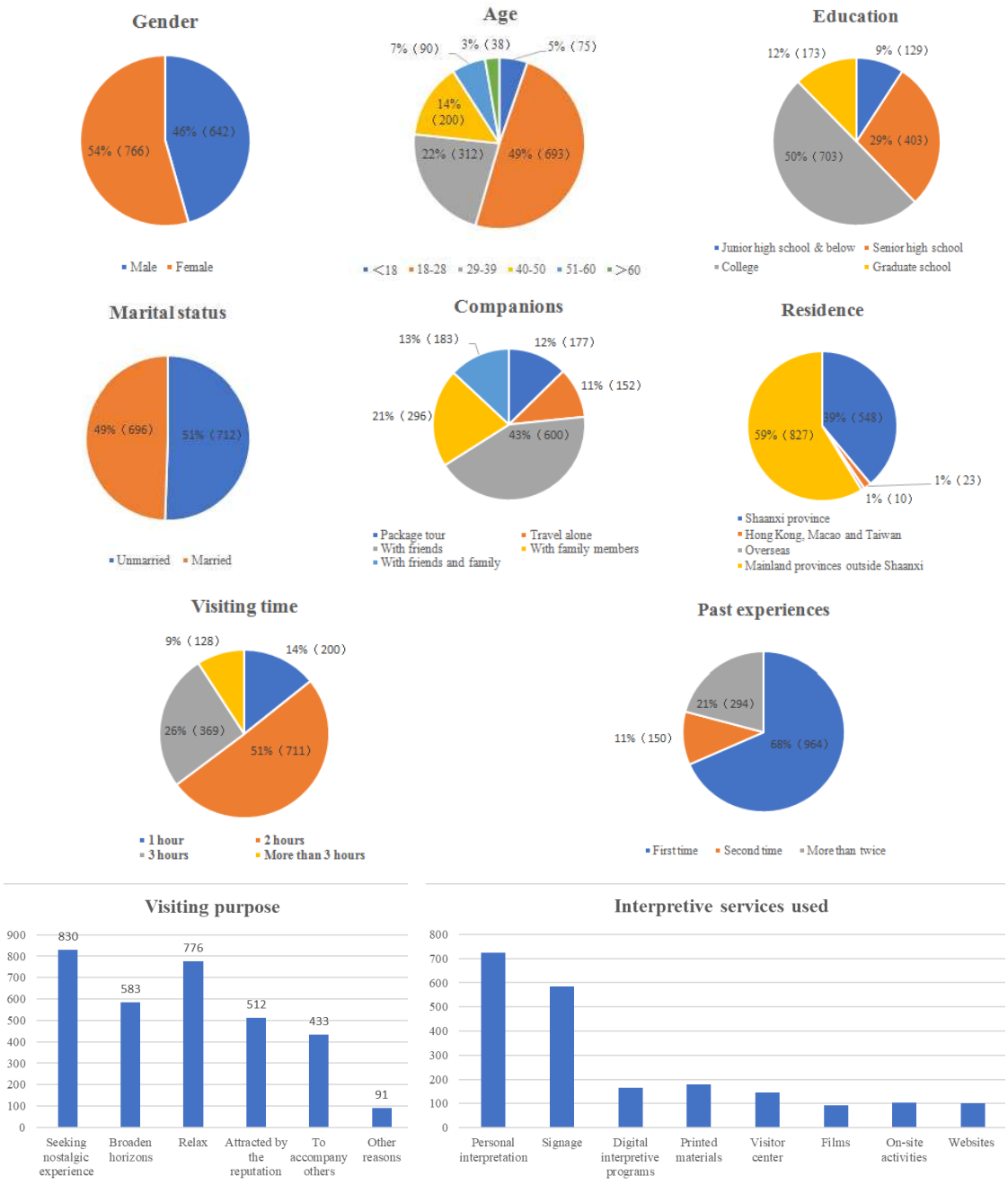

Figure 3. *Demographics of the respondents*

Data analysis

SPSS 22.0 was used to analyze the collected data. The reliability and validity were tested to find whether the instrument had good internal consistency. Principal component analysis and varimax rotation were used for factor analysis and convergent factors extraction and all the items were kept. In the end, the extracted common factors

http://www.aloki.hu ● ISSN 1589 1623 (Print) ● ISSN 1785 0037 (Online)
DOI: http://dx.doi.org/10.15666/aeer/1605_63176339
© 2018, ALÖKI Kft., Budapest, Hungary

as well as the corresponding factor loadings were obtained (*Table 2*). The Cronbach's alpha (between 0.72 and 0.99) exceeded the threshold value of 0.7, indicating a good level of internal of consistency of all the constructs in the study. In addition, factor loadings (between 0.57 and 0.87) of all the variables were significant ($p < 0.001$). Composite reliability (CR) exceeded 0.60, indicating all the constructs in the research had good reliability (*Table 2*).

Table 2. *The results of reliability and validity analysis*

Measured variables and dimensions	Cronbach Alpha	Factor loadings	CR	AVE
Interpretive service quality				
Tangibles	0.77		0.82	0.53
The digital interpretive programs at the heritage site provide effective interpretation	0.74	0.78		
The signage and tour route signs are easily spotted	0.79	0.70		
Tour guide, interpreters and the staff at visitor center are properly dressed	0.75	0.71		
The design, color and character size of the signage are in harmony with the environment	0.75	0.71		
Empathy	0.87		0.87	0.57
The interpretive services meet visitors' needs	0.85	0.71		
The staff at visitor center serve visitors with patience	0.84	0.73		
Interpreters provide appropriate interpretation for visitors	0.84	0.74		
Personal interpretation satisfies visitors	0.85	0.78		
The interpretive programs are rich in variety and sufficient in quantity	0.84	0.82		
Assurance	0.83		0.83	0.55
The interpreter's expertise is trustworthy	0.80	0.72		
The information on signage and printed materials is completely correct	0.80	0.69		
Interpreters and the staff at visitor center serve visitors with courtesy	0.78	0.77		
Interpreters are competent for their job	0.77	0.79		
Responsiveness	0.86		0.86	0.61
Visitors can get information about interpretive services at visitor center	0.85	0.71		
The heritage site provides visitors with the interpretive services that satisfy them	0.82	0.78		
The staff at visitor center are ready to serve visitors	0.81	0.83		
Interpreters can answer visitors' questions precisely	0.82	0.81		
Reliability	0.90		0.90	0.65
The visitor center can provide timely consultative service for visitors	0.89	0.79		
The staff at visitor center value the need of visitors	0.88	0.80		
The interpretive services are reliable	0.88	0.81		

http://www.aloki.hu ● ISSN 1589 1623 (Print) ● ISSN 1785 0037 (Online)
DOI: http://dx.doi.org/10.15666/aeer/1605_63176339
© 2018, ALÖKI Kft., Budapest, Hungary

The interpretive programs are used to the best advantage	0.99	0.82		
The heritage site provides quality interpretation services for visitors	0.88	0.82		
Satisfaction	0.88		0.88	0.65
I think my decision to use the interpretive services when visiting the heritage site is correct	0.86	0.78		
I'm pleased to use the interpretive services when visiting the heritage site	0.83	0.85		
Using interpretive services makes my visit here very pleasant	0.84	0.82		
I'm satisfied with the interpretive services here	0.86	0.77		
Place attachment				
Place dependence	0.89		0.89	0.63
This is the best choice for historic heritage tourism	0.88	0.62		
Visiting this place satisfies me more than other places	0.86	0.79		
Other heritage sites cannot replace my visit here	0.85	0.83		
No other heritage site is comparative to this place	0.85	0.86		
My visit here is more important than visit to other places	0.86	0.83		
Place identity	0.91		0.91	0.57
I always want to come here	0.90	0.79		
I like the heritage site very much	0.90	0.82		
I think this heritage site fits me well	0.89	0.83		
This heritage site is very special to me	0.90	0.75		
I'm willing to spend more time visiting the heritage site	0.89	0.80		
Visiting this heritage site is of great significance to me	0.90	0.74		
I think visiting this place is part of my life	0.90	0.69		
I'm proud of the heritage resources at the site	0.90	0.58		
Environmentally responsible behavior				
On-site behavior	0.88		0.89	0.68
Seeing others damage heritage items and the environment, I'll stop them or report their behaviors to the staff	0.87	0.67		
I don't litter at the heritage site	0.82	0.87		
I'll protect the heritage resources and the environment here	0.83	0.86		
I'll obey the rules of heritage and environment protection	0.84	0.87		
Off-site behavior	0.81		0.83	0.56
I'm willing to learn how to protect the heritage and environment here	0.79	0.77		
I'm willing to talk about heritage and environmental protection here with others	0.73	0.83		
I'm willing to learn about the heritage and environment protection via Internet, news etc.	0.72	0.79		
I'm willing to donate money to protect the historic heritage and the environment	0.80	0.57		

http://www.aloki.hu ● ISSN 1589 1623 (Print) ● ISSN 1785 0037 (Online)
DOI: http://dx.doi.org/10.15666/aeer/1605_63176339
© 2018, ALÖKI Kft., Budapest, Hungary

Average variance extracted (AVE) was used to assess the validity of the scale. AVE exceeding 0.5 indicates good convergent validity. If the square root of the AVE is greater than the correlation coefficient of other variables, the discriminant validity is good. The result of the data analysis showed that the AVEs of all the dimensions were above 0.5. The square root of the AVE was between 0.73 and 0.82, which was greater than the corresponding correlation coefficient, indicating better convergent validity and discriminant validity (*Table 3*).

Table 3. *Correlation matrix of the latent variables*

Dimensions of variables	Means	SD	1	2	3	4	5	6	7	8	9	10
Tangibles	4.40	0.94	0.73									
Empathy	4.17	1.04	0.62	0.75								
Assurance	4.29	0.97	0.65	0.61	0.74							
Responsiveness	4.26	1.03	0.54	0.65	0.62	0.78						
Reliability	3.23	1.08	0.51	0.53	0.59	0.63	0.81					
Global satisfaction	3.35	1.05	0.67	0.53	0.52	0.54	0.60	0.81				
Place dependence	4.97	1.24	0.42	0.52	0.53	0.53	0.53	0.56	0.79			
Place identity	4.00	1.14	0.39	0.42	0.47	0.46	0.50	0.56	0.54	0.75		
On-site behavior	5.89	0.91	0.29	0.22	0.32	0.23	0.18	0.34	0.23	0.26	0.82	
Off-site behavior	5.64	0.99	0.33	0.36	0.45	0.39	0.34	0.45	0.40	0.44	0.69	0.75

Using AMOS 24, the proposed model was tested by utilizing the Structural Equation Modeling (SEM) to measure the causal relationships within the model and the overall fitness of the model. The maximum likelihood estimation was applied to estimate all the parameters. Since a large size of samples may affect Chi-square (x^2) value, several other measurement model fit indices were used to determine whether the model fit was good. Model fit indicators include absolute fit indices and relative indices. Absolute fit indices include x^2/df (1-3), GFI (≥0.9), AGFI (≥0.9), RMR (<0.05), RMSEA (<0.08). The relative fit indices include NFI (≥0.9), RFI (≥0.9), CFI (≥0.9) and IFI (≥0.9).

The testing results of hypothesis 1 and hypothesis 2

The proposed model (Model l) (*Fig. 4*) was created to test whether interpretive service quality positively and significantly impacted on place attachment and ERB respectively. The test on goodness of fit indicated that all the indices were satisfying (RMR = 0.06, RMSEA = 0.08; GFI = 0.94; AGFI = 0.90; NFI = 0.95; RFI = 0.93; CFI = 0.96; IFI = 0.96). GFI, AGFI, NFI, RFI, CFI and IFI were within 0.90 and 1.00. RMSEA was 0.08 and RMA was greater than 0.05, a little bit higher than the threshold value of 0.05, but it still indicated a good model fitness. In short, the above analysis result demonstrated a good model fitness (*Table 4*). According to the calculated path coefficient, interpretive service quality had direct and significant effect on place

http://www.aloki.hu ● ISSN 1589 1623 (Print) ● ISSN 1785 0037 (Online)
DOI: http://dx.doi.org/10.15666/aeer/1605_63176339
© 2018, ALÖKI Kft., Budapest, Hungary

attachment ($\alpha 1 = 0.58$) ($p < 0.001$). It proves that the higher interpretive service quality is, the stronger place attachment will be. Meanwhile, interpretive service affected ERB directly and significantly ($\alpha 2 = 0.45$)($p < 0.001$), which means that higher quality of interpretation elicits stronger intention of exhibiting ERB (*Fig. 4*).

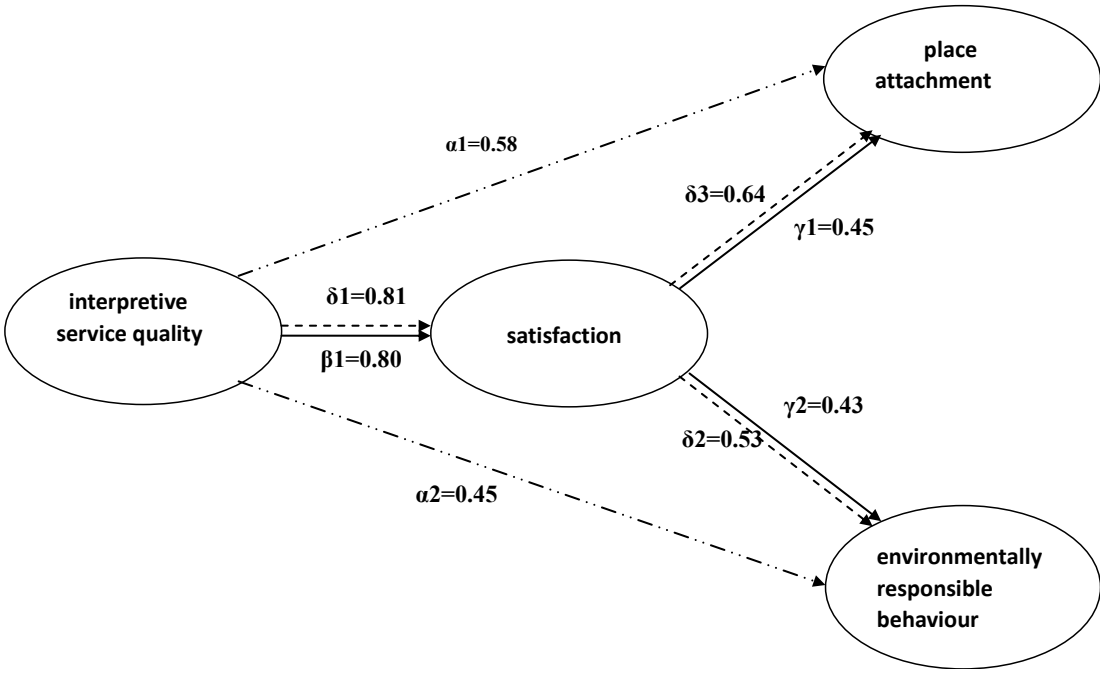

Figure 4. *The model of satisfaction mediating effect*

The testing results of hypothesis H_3, hypothesis H_4 and hypothesis H_5

After confirming the positive direct effect of interpretive service quality on place attachment and ERB, the study further explored whether interpretive service quality impacted on satisfaction and whether satisfaction influenced place attachment and ERB respectively. The authors therefore established a model (Model 2) to test the above-mentioned relationships. The goodness-of-fit indicators were as follows: RMR = 0.04; RMSEA = 0.07; GFI = 0.94; AGFI = 0.90; NFI = 0.95; RFI = 0.93; CFI = 0.96; IFI = 0.96. GFI, AGFI, NFI, RFI, CFI and IFI were between 0.90 and 1.00, while RMSEA (0.07) was a little bit lower than the cut-off point of 0.08 and RMR (0.04) was lower than 0.05. Therefore, the proposed model (Model 2) had a good fitness (*Table 4*). The path analysis results demonstrated that the direct effect of interpretive service quality on satisfaction was significant ($\beta 1 = 0.80$) ($p < 0.001$), indicating that higher quality of interpretation makes tourists feel satisfied with the visited place. Furthermore, satisfaction affected place attachment ($\gamma 1 = 0.45$) ($p < 0.001$) and ERB ($\gamma 2 = 0.43$) ($p < 0.001$) directly and significantly, showing that the more satisfied the tourists are with the destination, the stronger their emotional attachment to it and they are more willing to exhibit pro-environmental behavior. Thus, hypothesis3, hypothesis4 and hypothesis5 are supported (*Fig. 4*). However, after entering satisfaction into the proposed model, the direct effect of interpretive service quality on place attachment and ERB were 0.22 ($p < 0.05$) and 0.12 ($p < 0.05$) respectively. It demonstrated that the direct effect of interpretive service quality on place attachment and ERB were much

http://www.aloki.hu ● ISSN 1589 1623 (Print) ● ISSN 1785 0037 (Online)
DOI: http://dx.doi.org/10.15666/aeer/1605_63176339
© 2018, ALÖKI Kft., Budapest, Hungary

lower after entering the variable of satisfaction, indicating that the effect of interpretive service quality on place attachment and ERB were indirect, with the path coefficients being 0.36 (0.80×0.45) ($p < 0.01$) and 0.34 (0.80×0.43) ($p < 0.01$) respectively.

Based on the above analysis, satisfaction might mediate the relationship between interpretive service quality and place attachment as well as the relationship between interpretive service quality and ERB. Interpretation quality may not have direct causal relationship with place attachment and ERB. In other words, the original causal relationship might be influenced by a mediating variable. Therefore, the real causal relationship between interpretive service quality and place attachment as well as the causal relationship between interpretive service quality and ERB should be further explored.

To further explore the function of satisfaction in depth, the proposed model (Model 3) was created for path analysis. The results of the path analysis demonstrated that the proposed model had good fit indicators: RMR = 0.04; RMSEA = 0.07; GFI = 0.94; AGFI = 0.91; NFI = 0.95; RFI = 0.94; CFI = 0.97; IFI = 0.97. GFI, AGFI, NFI, RFI, CFI and IFI fell within 0.90 and 1.0. RMR was lower than the cut-off point of 0.05 and RMSEA was below the threshold value of 0.08. Such analysis results indicated that the mediating model had good model fitness (*Table 4*). Further path analysis demonstrated that interpretive service influenced satisfaction positively ($\delta 1 = 0.81$)($p < 0.001$), establishing the causal relationship between the two. What is more, satisfaction exerted positive and significant influence on place attachment ($\delta 3 = 0.64$) ($p < 0.001$) and ERB ($\delta 2 = 0.53$) ($p < 0.001$) respectively. It indicates that the more satisfied the tourists are, the stronger their place attachment will be and they are more willing to show ERB. Path analysis also showed that interpretive service quality impacted place attachment 0.52 (0.81×0.64) ($p < 0.01$) and ERB0.43 (0.81×0.53) ($p < 0.01$) indirectly through the mediating role of satisfaction. The results demonstrated that satisfaction had a full mediating effect on the relationship between interpretive service quality and place attachment and the relationship between interpretive service quality and ERB (*Fig. 4*). Such a finding is consistent with the study result about the mediating function of satisfaction between the relationship of service quality and behavioral outcomes by Fullerton and Taylor (2002).

Table 4. *Fit indices for measurement model*

Fit indices	Criteria	Model 1	Model2	Model 3	Model4
Absolute fit indices					
GFI	≥0.9	0.94	0.94	0.94	0.94
AGFI	≥0.9	0.90	0.90	0.91	0.91
RMR	<0.05	0.06	0.04	0.04	0.04
RMSEA	<0.08	0.08	0.07	0.07	0.07
Comparative fit indices					
NFI	≥0.9	0.95	0.95	0.95	0.95
RFI	≥0.9	0.93	0.93	0.94	0.94
CFI	≥0.9	0.96	0.96	0.97	0.97
IFI	≥0.9	0.96	0.96	0.97	0.97

http://www.aloki.hu ● ISSN 1589 1623 (Print) ● ISSN 1785 0037 (Online)
DOI: http://dx.doi.org/10.15666/aeer/1605_63176339
© 2018, ALÖKI Kft., Budapest, Hungary

The analysis results of hypothesis H_6

To examine the direct effect of place attachment on ERB, the path analysis of place attachment to ERB was added to establish the final structural model (Model 4) for this empirical study. The results showed a good model fitness: RMR = 0.04; RMSEA = 0.07; GFI = 0.94; AGFI = 0.91; NFI = 0.95; RFI = 0.94; CFI = 0.97; IFI = 0.97. GFI, AGFI, NFI, RFI, CFI and IFI ranged from0.90 to1.00. RMR was lower than the benchmark value of 0.05 and RMSEA was below the cut-off point of 0.08. All the figures demonstrated a good model fitness (*Table 4*). The path analysis indicated that place attachment influenced ERB positively and significantly 0.34 ($p < 0.001$). Therefore, stronger place attachment can facilitate stronger ERB. The effect of interpretive service on satisfaction was direct and positive 0.81 ($p < 0.001$), showing that quality interpretation will satisfy the tourists. Path analysis also indicated that satisfaction affected place attachment 0.63 ($p < 0.001$) and ERB 0.29 ($p < 0.001$) directly and significantly. Namely, the more satisfied the tourists with the visited site, the stronger their emotional attachment and ERB will be.

Thus hypothesis 6 is supported. Meanwhile, satisfaction played a role of complete mediation in the relationship between interpretive service quality and place attachment and in the relationship between interpretive quality and ERB. As a result, interpretive service quality had indirect effect on place attachment through satisfaction, with a path coefficient of 0.51 ($p < 0.01$) and interpretive service quality impacted on ERB indirectly and significantly through satisfaction, with a path coefficient of 0.23 ($p < 0.01$) (*Fig. 5*).

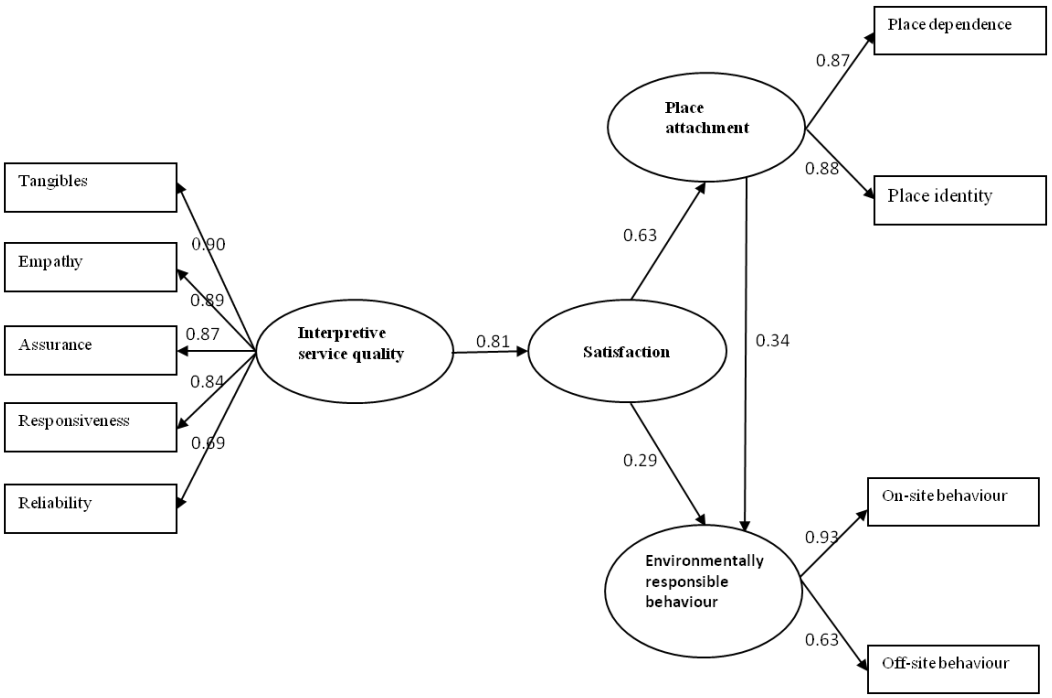

Figure 5. *The structural model*

Discussion

This study investigated the causal relationships among interpretive service quality, satisfaction, place attachment and ERB at five cultural heritage sites in Xi'an. It is the

http://www.aloki.hu ● ISSN 1589 1623 (Print) ● ISSN 1785 0037 (Online)
DOI: http://dx.doi.org/10.15666/aeer/1605_63176339
© 2018, ALÖKI Kft., Budapest, Hungary

first time in literature to simultaneously examine the structural relationships among these four variables in the same model. The findings showed that the causal relationship does exist between interpretive service quality and place attachment. Meanwhile, it is found that satisfaction plays a mediating role in the relationship between interpretive service quality and place attachment, which indicates that satisfaction with high quality of interpretive services will help tourists foster place attachment. The more satisfied tourists are with interpretive services, the stronger their place attachment to the visited sites will be. Second, the results also show that satisfaction mediates the relationship between interpretive service quality and ERB. Previous research showed that knowledge gain as a result of experiencing interpretation would elicit ERB among visitors, while this research demonstrates that satisfaction with interpretive service also helps visitors exhibit ERB. Third, the present study indicates that interpretive service affects satisfaction directly and significantly.

The results also demonstrate that tourists' satisfaction positively and significantly influences place attachment. Moreover, the present study shows that satisfaction with interpretive service helps facilitate visitors to demonstrate ERB at heritage sites, which supports the study results found by Moscardo (1996) and Powell and Ham (2008), indicating the importance of high quality of interpretive service at heritage sites. In addition, the young age of the respondents indicates that tourism management departments should strive to provide more vitalized interpretive programs such as well designed signage, movies using modern technology like 5D or 6D, the live programs that young visitors may get involved in to satisfy them. In addition, very few visitors using web sites of the destination to obtain information about the visited sites indicates that tourism management agency should design fantastic web sites with amazing pictures as well as convincing descriptions, which is very informative, attractive and at the same time easy to access, to attract more visitors from outside of Shaanxi province. What is more, larger number of respondents relying on personal interpretation to help them understand the visited heritage sites implies that tour guides should be trained to do their work more efficiently in order to meet the needs of the visitors. Since nearly half of the respondents turn to various signs for getting the information about the destination, well designed and properly located signage are very important to serve the visitors.

Conclusions

Based on the results of this study, the following conclusions can be reached: (1) relationship between interpretive service and place attachment does exist and the former affects the latter indirectly and significantly, with satisfaction playing a mediating role between them. (2) interpretive service influences ERB indirectly and satisfaction plays a mediating role in the relationship between the two. (3) The direct effect of interpretive service on satisfaction is positive. Meanwhile, satisfaction exerts direct influence on place attachment and ERB respectively; (4) place attachment impacts ERB directly.

The findings of this study demonstrate the importance of interpretive service quality in facilitating place attachment and ERB among tourists. High quality of interpretive services is beneficial to satisfying tourists and enriching their travel experience, which leads to their place attachment to the destination. In addition, satisfaction with high quality of interpretive services and place attachment will elicit ERB among tourists and such pro-environmental behavior will contribute to the tourist management as well as

http://www.aloki.hu ● ISSN 1589 1623 (Print) ● ISSN 1785 0037 (Online)
DOI: http://dx.doi.org/10.15666/aeer/1605_63176339
© 2018, ALÖKI Kft., Budapest, Hungary

heritage resource management. Ultimately, sustainable use of heritage resources and sustainable development of heritage tourism will be achieved. Therefore, it is very necessary for tourism management agency to improve interpretive service quality.

Limitations

The research limitations are as follows: First, the authors of this study did not analyze how each dimension of interpretive service affected satisfaction respectively. Second, the study did not examine the mediating role of place attachment in the relationship between satisfaction and ERB. Third, the historic sites selected for the study were of higher ranking sites and those of lower ranking were not included. To test the universality of the proposed model, historic sites of different ranking should be investigated. Future research may avoid the above limitations and further explore the outcomes of interpretation in depth.

Acknowledgements. 1. A Study of Optimization of Interpretive System in Tourist Destinations in Shaanxi (2013JK0301), funded by Shaanxi Education Department. 2. A Study of Affective and Behavioral Outcomes of Interpretive Services in Cultural Heritage Sites in Shaanxi (2017S006), funded by Shaanxi Social Science Academy.

REFERENCES

[1] Alexandris, K., Kouthouris, C., Melogdis, A. (2006): Increasing customers' loyalty in a skiing resort: The contribution of place attachment and service quality. – International Journal of Contemporary Hospitality Management 18: 414-425.
[2] Ajzen, I. (1991): The theory of planned behavior. – Organizational Behavior and Human Decision Processes 50: 179-211.
[3] Baker, D. A., Crompton, J. L. (2000): Quality, satisfaction and behavioral intentions. – Annals of Tourism Research 27(3): 785-804.
[4] Ballantyne, R., Packer, J. (2011): Using tourism free-choice learning experiences to promote environmentally sustainable behavior: The role of post-visit "action resources". – Environmental Education Research 17(2): 201-215.
[5] Ballantyne, R., Packer, J., Hughes, K. (2009): Tourists' support for conservation messages, and sustainable management practices in wildlife experiences. – Tourism Management 30(5): 658-664.
[6] Ballantyne, R., Packer, J., Falk, J. (2011): Visitors' learning for environmental sustainability: testing short-and long-term impacts of wildlife tourism experiences using structural equation modelling. – Tourism Management 32(6): 1243-1252.
[7] Battour, M., Battor, M., Bhatti, M. A. (2014): Islamic attributes of destination: construct development and measurement validation, and their impact on tourist satisfaction. – International Journal of Tourism Research 16(6): 556-564.
[8] Bernini, C., Cagnone, S. (2014): Analysing tourist satisfaction at a mature and multi-product destination. – Current Issues in Tourism 17(1): 1-20.
[9] Carr, A. (2004): Mountain places, cultural spaces: The interpretation of culturally significant landscapes. – International Journal of Heritage Studies 12(5): 432-459.
[10] Chen, C. F., Chen, F. S. (2010): Experience quality, perceived value, satisfaction and behavioral intentions for heritage tourists. – Tourism Management, (31): 29-35.
[11] Cheng, T. M., Wu, H. C., Huang, L. M. (2013): The influence of place attachment on the relationship between destination attractiveness and environmentally responsible behavior

http://www.aloki.hu ● ISSN 1589 1623 (Print) ● ISSN 1785 0037 (Online)
DOI: http://dx.doi.org/10.15666/aeer/1605_63176339
© 2018, ALÖKI Kft., Budapest, Hungary

for island tourism in Penghu, Taiwan. – Journal of Sustainable Tourism 21(8): 1166-1187.
[12] Cronin Jr, J. J., Taylor, S. A. (1994): SERVPERF versus SERVQUAL: Reconciling performance-based and perceptions-minus-expectations measurement of service quality. – Journal of Marketing 58(1): 125-131.
[13] Davis, J. L., Le, B., Coy, A. E. (2011): Building a model of commitment to the environment to predict ecological behavior and willingness to sacrifice. – Journal of Environmental Psychology 31: 257-265.
[14] Fishbein, M. A., Ajzen, I. (1975): Belief, attitude, intention, and behavior: An introduction to theory and research. – Addison-Wesley, Reading, MA.
[15] George, B. P., George, B. P. (2004): Past visit and the intention to revisit a destination: Place attachment as a mediator and novelty seeking as the moderator. – The Journal of Tourism Studies 15(2): 51-66.
[16] Goldman, T., Chen, J., Larsen, D. (2001): Clicking the icon: Exploring the meanings visitors attach to three national capital memorials. – Journal of Interpretation Research 6(1): 3-30.
[17] Graham, B. (2007) Heritage as Knowledge: Capital or Culture? – In: Smith, L. (ed.) Cultural Heritage: Critical Concepts in Media and Cultural Studies. Routledge, London pp. 249-268.
[18] Hall, C. M., Mcarthur, S. (1998): Integrated Heritage Management: Principles and Practice. – The Stationary Office, London.
[19] Halpenny, E. A. (2005): Pro-environment intentions: Examining the affect of place attachment, environmental attitudes toward pro-environmental behavior. – Paper presented at the Eleventh Canadian Congress on Leisure Research, May 17-25, 2005, Department of Recreation and Tourism Management, Malaspina University-College, Nanaimo, B.C.
[20] Halpenny, E. A. (2010): Pro-environmental behaviors and park visitors: The effect of place attachment. – Journal of Environmental Psychology 30: 409-421.
[21] Ham, S., Weiler, B. (2006): Development of a Research-based Tool for Evaluating Interpretation. – CRC for Sustainable Tourism, Gold Coast, Qld.
[22] Ham, S., Weiler, B. (2007): Isolating the role of on-site interpretation in a satisfying experience. – Journal of Interpretation Research 12(2): 5-24.
[23] Hinds, J., Sparks, P. (2008): Engaging with the natural environment: The role of affective connection and identity. – Journal of Environmental Psychology 28(2): 109-120.
[24] Hou, J. S., Lin, C. H., Morais, D. B. (2005): Antecedents of attachment to a cultural tourism destination: The case of Hakka and non-Hakka Taiwanese visitors to Pei-Pu, Taiwan. – Journal of Travel Research 44: 221-223.
[25] Huang, S., Weiler, B., Assaker, G. (2015): Effects of interpretive guiding outcomes on tourist satisfaction and behavioral intention. – Journal of Travel Research 54(3): 344-358.
[26] Hughes, M. (2004): Influence of varying intensities of natural area on-site interpretation on attitudes and knowledge. – PhD Thesis, Murdoch University, Australia.
[27] Kim, A., Airey, D., Szivas, E. (2011): The multiple assessment of interpretation effectiveness: promoting visitors' environmental attitudes and behavior. – Journal of Travel Research 50(3): 321-334.
[28] Knudson, D., Cable, T., Beck, L. (2003): Interpretation of Cultural and Natural Resources. – Venture Publishing, State College, PA.
[29] Larsen, D. L. (ed.) (2003): Meaningful Interpretation: How to Connect Hearts and Minds to Places, Objects, and Other Resources. – Eastern National, Fort washing, PA.
[30] Lee, C., Backman, K., Backman, S. (1997): Understanding Antecedents of Repeat Visitation and Tourists' Loyalty to a Resort Destination. – In: Proceedings of the 1997 Travel and Tourism Research Association Annual Conference. TTRA, Boulder, CO.

http://www.aloki.hu ● ISSN 1589 1623 (Print) ● ISSN 1785 0037 (Online)
DOI: http://dx.doi.org/10.15666/aeer/1605_63176339
© 2018, ALÖKI Kft., Budapest, Hungary

[31] Lee, T. H. (2009): A structural model for examining how destination image and interpretation services affect future visitation behavior: a case study of Taiwan's Taomi eco-village. – Journal of Sustainable Tourism 17(6): 727-745.
[32] Lee, T. H. (2011): How recreation involvement, place attachment and conservation commitment affect environmentally responsible behavior. – Journal of Sustainable Tourism 19(7): 895-915.
[33] Lee, T. H., Jan, F. H., Yang, C. C. (2013a): Environmentally responsible behavior of nature-based tourists: A review. – International Journal of Development and Sustainability 2(1):100-115.
[34] Lee, T. H., Jan, F. H., Yang, C. C. (2013b): Conceptualizing and measuring environmentally responsible behaviors from the perspective of community-based tourists. – Tourism Management 36: 454-468.
[35] Lee, W. H., Moscardo, G. (2005): Understanding the impact of ecotourism resort experiencing on tourists' environmental attitudes and behavioral intentions. – Journal of Sustainable Tourism 13(6): 546-565.
[36] Lopez-Mosquera, N., Sanchez, M. (2011): Emotional and satisfaction benefits to visitors as explanatory factors in the monetary evaluation of environmental goods. An application to periurban green spaces. – Land Use Policy 28(1): 151-166.
[37] Low, S., Altman, I. (1992): Place Attachment: A conceptual Inquiry. – In: Althman, I., Low, S. (eds.) Place Attachment. Plenum, New York.
[38] Ma, Y. F., Song, B. P., Zhao, Z. B. (2007): Research and Evaluation of Tourism Resources in Shaanxi Province. – Science Publishing House, Beijing.
[39] Mace, B. L., McDaniel, J. (2013): Visitor evaluation of night sky interpretation in Bryce Canyon National Park and Cedar Breaks National Monument. – Journal of Interpretation Research 18(1): 39-57.
[40] Marion, J., Reid, S. (2007): Minimizing visitor impacts to protected areas: the efficacy of low impact education programs. – Journal of Sustainable Tourism 15(1): 5-27.
[41] Morgan, M. (2009): Interpretation and place attachment: implications for cognitive map theory. – Journal of Interpretation Research 14(1):47-59.
[42] Morgan, M., Hwang, G. (2014): Perception of thematic-based interpretation at the Jefferson National Expansion Memorial - A study of Korean visitors. – Journal of Interpretation Research 19(2): 25-37.
[43] Moscardo, G. (1996): Mindful visitors: heritage and tourism. – Annals of Tourism Research 23(2):376-397.
[44] Moscardo, G. (2014): Interpretation and tourism: holy grail or emperor's robes? International Journal of Culture. – Tourism and Hospitality Research 8(4): 462 - 476.
[45] Munro, J. K., Morrison-Saunders, A., Hughes, M. (2008): Environmental interpretation evaluation in natural areas. – Journal of Ecotourism 7(1): 1-15.
[46] Oliver, R. L. (1980): A cognitive model of the antecedents and consequences of satisfaction decisions. – Journal of Marketing Research 17: 460-469.
[47] Petrick, J. F., Backman, S. J., Bixler, R. (1999): An investigation of selected factors' impact on golfer satisfaction and perceived value. – Journal of Park and Recreation Administration 17(1): 40-59.
[48] Poria, Y., Reichel, A., Biran, A. (2006): Heritage site management: motivations and expectations. – Annals of Tourism Research 33(1): 162-178.
[49] Poria, Y., Biran, A., Reichel, A. (2009): Visitors' preferences for interpretation at heritage sites. – Journal of Travel Research 48(1): 92-105.
[50] Powell, R. B., Ham, S. H. (2008): Can ecotourism interpretation really lead to pro-conservation knowledge, attitudes and behavior? Evidence from the Galapagos Islands. – Journal of Sustainable Tourism 16(4): 467-489.
[51] Prayag, G., Ryan, C. (2012): Antecedents of tourists' loyalty to Mauritius: the role and influence of destination image, place attachment, personal involvement, and satisfaction. – Journal of Travel Research 51(3): 342-356.

http://www.aloki.hu ● ISSN 1589 1623 (Print) ● ISSN 1785 0037 (Online)
DOI: http://dx.doi.org/10.15666/aeer/1605_63176339
© 2018, ALÖKI Kft., Budapest, Hungary

[52] Ramkissoon, H., Mavondo, F. (2014): Pro-environmental behavior: The link between place attachment and place satisfaction. – Tourism Analysis 19: 673-688.
[53] Ramkissoon, H., Mavondo, F. (2015): The satisfaction–place attachment relationship: Potential mediators and moderators. – Journal of Business Research 68: 2593-2602.
[54] Ramkissoon, H., Weiler, B., Smith, LDG. (2013): Place attachment, place satisfaction and pro-environmental behavior: a comparative assessment of multiple regression and structural equation modelling, – Journal of Policy Research in Tourism, Leisure and Events 5(3): 215-232.
[55] Raymond, C., Brown, G., Weber, D. (2010): The measurement of place attachment: Personal, community, and environmental Connections. – Journal of Environmental Psychology 30: 422-434.
[56] Risk, P. (1982): The Interpretive Talk. – In: Sharpe, G. (ed.) Interpreting the Environment. John Wiley & Sons, New York, NY (pp. 194-213).
[57] Schultz, P. W., Shriver, C., Tabanico, J. J., Khazian, A. M. (2004): Implicit connections with nature. – Journal of Environmental Psychology 24(1): 31-42.
[58] Sivek, D., Hungerford, H. R. (1990): Predictors of responsible environmental behavior in members of three Wisconsin conservation organizations. – Journal of Environmental Education 21: 35-40.
[59] Skibins, J. C., Powell, R. B., Stern, M. J. (2011) Exploring empirical support for interpretation's best practices. – Journal of Interpretation Research 17(1): 25-44.
[60] Smith-Sebasto, N. J., D'Costa, A. (1995): Designing a Likert-type scale to predict environmentally responsible behavior in undergraduate students: a multistep process. – The Journal of Environmental Education 27(1):14-20.
[61] Song, H. Q., Cheung, C. (2010): Factors affecting tourist satisfaction with theatrical performances: a case study of the romance of the Song Dynasty in Hangzhou, China. – Journal of Travel & Tourism Marketing 27(7): 708-722.
[62] Stern, P. C. (2000): Toward a coherent theory of environmentally significant behavior. – Journal of Social Issues 56(3): 407-424.
[63] Su, H. J., Cheng, K. F., Huang, H. H. (2011): Empirical study of destination loyalty and its antecedent: the perspective of place attachment. – The Service Industries Journal 31(16): 2721-2739.
[64] Tilden, F. (2007): Interpreting Our Heritage (Fourth Ed.) – The University of North Carolina Press, Chapel Hill, NC.
[65] Trentelman, C. K. (2009): Place attachment and community attachment: A primer grounded in the lived experience of a community sociologist. – Society and Natural Resources 22: 191-210.
[66] Tubb, K. N. (2003): An evaluation of the effectiveness of interpretation within Dartmoor National Park in reaching the goals of sustainable tourism development. – Journal of Sustainable Tourism 11(6): 476-498.
[67] Ward, C., Wilkinson, A. (2006): Personal Interpretation – a Field Guide for Success. – Fulcrum Applied Communication Series, Fulcrum Books, Golden, Colorado.
[68] Williams, D. R., Roggenbuck, J. W. (1989): Measuring place attachment: Some preliminary results. – Paper presented at the Symposium on Outdoor Recreation Planning and Management, National Recreation and Park Association Research Symposium on Leisure Research, San Antonio, TX.
[69] Williams, D. R., Vaske, J. (2003): The measurement of place attachment: Validity and generalizability of a psychometric approach. – Forest Science 49: 830-840.
[70] Xu, Z. X., Zhang, J. (2016) Antecedents and consequences of place attachment: A comparison of Chinese and Western urban tourists in Hangzhou, China. – Journal of Destination Marketing & Management 5(2):86-96.
[71] Yuksel, A., Yuksel, F., Bilim, Y. (2010): Destination attachment: Effects on customer satisfaction and cognitive, affective and connative loyalty. – Tourism Management 31(2): 274-284.

http://www.aloki.hu ● ISSN 1589 1623 (Print) ● ISSN 1785 0037 (Online)
DOI: http://dx.doi.org/10.15666/aeer/1605_63176339
© 2018, ALÖKI Kft., Budapest, Hungary

[72] Zabkar, V., Brencic, M. M., Dmitrovic, T. (2010): Modeling perceived quality, visitor satisfaction and behavioral intentions at the destination level. – Tourism Management 31: 537-546.

APPENDIX

VISITOR SURVEY

In this survey we would like to ask you some questions about the place you visited today. Your cooperation will help us make some important management suggestions about the service quality of this place. Your honest, personal opinions are important. It will take you about 10 minutes to complete it. Thanks for your time!

Northwest University

Your evaluations of the interpretive service quality

How would you evaluate the service quality of this place? Please score each item. "1" represents" Strongly Disagree "(SD), "4 " for "Neutral"(N) and "7" for "Strongly Agree" (SA).

Statements	SD			N			SA
1. The digital interpretive programs at the heritage site provide effective interpretation.	1	2	3	4	5	6	7
2. The signage and tour route signs are easily spotted.	1	2	3	4	5	6	7
3. Tour guide, interpreters and the staff at visitor center are properly dressed.	1	2	3	4	5	6	7
4. The design, color and character size of the signage are in harmony with the environment.	1	2	3	4	5	6	7
5. The interpretive services meet visitors' needs.	1	2	3	4	5	6	7
6. The staff at visitor center serve visitors with patience.	1	2	3	4	5	6	7
7. Interpreters provide appropriate interpretation for visitors.	1	2	3	4	5	6	7
8. Personal interpretation satisfies visitors.	1	2	3	4	5	6	7
9. The interpretive programs are rich in variety and sufficient in quantity.	1	2	3	4	5	6	7
10. The interpreter's expertise is trustworthy.	1	2	3	4	5	6	7
11. The information on signage and printed materials is completely correct.	1	2	3	4	5	6	7
12. Interpreters and the staff at visitor center serve visitors with courtesy.	1	2	3	4	5	6	7
13. Interpreters are competent for their job.	1	2	3	4	5	6	7
14. Visitors can get information about interpretive services at visitor center.	1	2	3	4	5	6	7
15. The heritage site provides visitors with the interpretive services that satisfy them.	1	2	3	4	5	6	7
16. The staff at visitor center are ready to serve visitors.	1	2	3	4	5	6	7
17. Interpreters can answer visitors' questions precisely.	1	2	3	4	5	6	7
18. The visitor center can provide timely consultative service for visitors.	1	2	3	4	5	6	7
19. The staff at visitor center value the need of visitors.	1	2	3	4	5	6	7
20. The interpretive services are reliable.	1	2	3	4	5	6	7
21. The interpretive programs are used to the best advantage.	1	2	3	4	5	6	7
22. The heritage site provides quality interpretation services for visitors.	1	2	3	4	5	6	7

http://www.aloki.hu ● ISSN 1589 1623 (Print) ● ISSN 1785 0037 (Online)
DOI: http://dx.doi.org/10.15666/aeer/1605_63176339
© 2018, ALÖKI Kft., Budapest, Hungary

Your satisfaction with the visited place

How much are you emotionally attached to this tourist attraction? Please score each item by circling the number. "1" represents "Strongly Disagree"(SD), "4 " for "Neutral"(N) and "7" for "Strongly Agree" (SA)

Statements	SD			N			SA
23. I think my decision to use the interpretive services when Visiting the heritage site is correct.	1	2	3	4	5	6	7
24. I'm pleased to use the interpretive services when visiting the heritage site.	1	2	3	4	5	6	7
25. Using interpretive services makes my visit here very pleasant.	1	2	3	4	5	6	7
26. I'm satisfied with the interpretive services here.	1	2	3	4	5	6	7

Your emotional attachment to the visited site

How much are you emotionally attached to this tourist attraction? Please score each item. "1" represents" Strongly Disagree"(SD), "4 " for "Neutral"(N) and "7" for "Strongly Agree" (SA)

Statements	SD			N			SA
27. This is the best choice for historic heritage tourism.	1	2	3	4	5	6	7
28. Visiting this place satisfies me more than other places.	1	2	3	4	5	6	7
29. Other heritage sites cannot replace my visit here.	1	2	3	4	5	6	7
30. No other heritage site is comparative to this place.	1	2	3	4	5	6	7
31. My visit here is more important than visit to other places.	1	2	3	4	5	6	7
32. I always want to come here.	1	2	3	4	5	6	7
33. I like the heritage site very much.	1	2	3	4	5	6	7
34. I think this heritage site fits me well.	1	2	3	4	5	6	7
35. This heritage site is very special to me.	1	2	3	4	5	6	7
36. I'm willing to spend more time visiting the heritage site.	1	2	3	4	5	6	7
37. Visiting this heritage site is of great significance to me.	1	2	3	4	5	6	7
38. I think visiting this place is part of my life.	1	2	3	4	5	6	7
39. I'm proud of the heritage resources at the site.	1	2	3	4	5	6	7

Your behaviors exhibited on and off the visited site

What were or would be your behaviors exhibited on and off the visited site? Please score each item. "1" represents" Strongly Disagree "(SD), "4" for "Neutral"(N) and "7" for "Strongly Agree" (SA)

Statements	SD			N			SA
40. Seeing others damage heritage items and the environment, I'll stop them or report their behaviors to the staff.	1	2	3	4	5	6	7
41. I don't litter at the heritage site.	1	2	3	4	5	6	7
42. I'll protect the heritage resources and the environment here.	1	2	3	4	5	6	7
43. I'll obey the rules of heritage and environment protection.	1	2	3	4	5	6	7
44. I'm willing to learn how to protect the heritage and environment here.	1	2	3	4	5	6	7
45. I'm willing to talk about heritage and environmental protection here with others.	1	2	3	4	5	6	7
46. I'm willing to learn about the heritage and environment protection via Internet, news etc.	1	2	3	4	5	6	7
47. I'm willing to donate money to protect the historic heritage and the environment.	1	2	3	4	5	6	7

http://www.aloki.hu ● ISSN 1589 1623 (Print) ● ISSN 1785 0037 (Online)
DOI: http://dx.doi.org/10.15666/aeer/1605_63176339
© 2018, ALÖKI Kft., Budapest, Hungary

Demographic traits

Your gender: □male □female

Age: □<18 □18-28 □29-39 □40-50 □51-60 □>60

Marital status: □unmarried □ married

Education: □junior high school & below □senior high school
□college □graduate school

Companions: □package tour □travel alone □with friends
□with families □with friends and families

Residence: □Shaanxi province □Mainland province outside Shaanxi
□Hong Kong, Maocao and Taiwan □Overseas

Past experiences: □ First time □ Second time □Third time

Visiting time: □1hour □2 hours □3 hours □ 4hours

Visiting purpose (you may choose more than one answer):

□seeking nostalgia experience □broaden horizons □relax and relieve pressure □attracted by the reputation □To accompany others □other reasons

Interpretive services used

□ personal interpretation □signage □digital interpretive programs □printed materials
□visitor center □films □ on-site activities □ websites

THANKS FOR YOUR COOPERATION!

http://www.aloki.hu ● ISSN 1589 1623 (Print) ● ISSN 1785 0037 (Online)
DOI: http://dx.doi.org/10.15666/aeer/1605_63176339
© 2018, ALÖKI Kft., Budapest, Hungary

SEX-TYPING OF BLUE-CROWNED LAUGHINGTHRUSH (*GARRLUAX COURTOISI*) USING *CHD1*-BASED POLYMERASE CHAIN REACTION

HUANG, J.[1,2#] – MAO, H.[3#] – XU, H.[1] – TANG, J.[1] – OUYANG, J.[1] – WU, Z.[4] – LIU, D.[4*] – YAN, X.[1,2*]

[1]*College of Life Sciences, Jiangxi Science and Technology Normal University, Nanchang, Jiangxi Province, China*

[2]*Jiangxi Key Laboratory of Bioprocess Engineering, Jiangxi Science and Technology Normal University, Nanchang, Jiangxi Province, China*

[3]*College of Animal Sciences, Jiangxi Agricultural University, Nanchang, Jiangxi Province, China*

[4]*Nanchang Zoo, Nanchang, Jiangxi Province, China*

**Corresponding author*
e-mail: liudaoqiang@foxmail.com, xuemingyan@hotmail.com

[#]*These authors contributed equally to this work*

(Received 31st May 2018; accepted 2nd Aug 2018)

Abstract. Blue-crowned laughingthrush (*Garrluax courtoisi*), an endemic species in China, is a critically endangered and sexually monomorphic bird. It is difficult to identify the gender of this species through the observation of its external morphology. To solve this problem, we herein established a *CHD1*-based PCR method for sex-typing of *Garrluax courtoisi*. We first collected blood samples from six Blue-crowned laughingthrush raised in Nanchang Zoo, and then extracted high-quality genomic DNA from blood clots using an optimized phenol/chloroform method. We designed a degenerate primer pair to amplify fragments of the *CHD1* gene, resulting an amplicon of 700 bp for males and an extra PCR product of 600 bp for females. We also performed extensive behavioral observations of these six birds and the obtained data allowed us to deduce the sexes of these birds. The sex-typing results are generally consistent with the behavior-deduced results. This study sheds light on the sex determination of other endangered birds, and also paves a road to further test the reproduction mechanism, taxonomic classification and population relationships of *Garrluax courtoisi*.
Keywords: *blue-crowned laughingthrush, sex identification, CHD1, endangered species*

Introduction

Blue-crowned laughingthrush (*Garrulax courtoisi*, *Fig. 1*) is currently classified as a critically endangered bird by BirdLife International (2017). The only known wild population of approximately 300 birds currently lives in Wuyuan County, Jiangxi Provence, China (He et al., 2017). Its emergence and re-emergence after a long period of disappearance is really a mystery to people. Also its status in taxonomy has changed several times. Thus it is regarded as a legend in birds.

Currently a total of slightly more than 200 birds are kept captive in several zoos located in Asia, Europe, and North America (Liu et al., 2017). We started a captive breeding program for this species in 2010 in the Nanchang Zoo at Nanchang City, Jiangxi Province of China, and joined the Global Species Management Plan (GSMP) (WAZA, n. d.) in 2012. One of the major obstacles we have been facing is the sex-typing of these sexually monomorphic birds, as the birds do not have any external

http://www.aloki.hu ● ISSN 1589 1623 (Print) ● ISSN 1785 0037 (Online)
DOI: http://dx.doi.org/10.15666/aeer/1605_63416347
© 2018, ALÖKI Kft., Budapest, Hungary

genitalia. Traditional sexing methods involve physical examination of the cloacae or the use of a laparoscope, both are invasive to such small birds and may cause anaphylaxis or death during the procedures. As sexing is inevitable as a management requirement, we decided to evaluate the feasibility of using a relatively safer molecular sex-typing method.

Figure 1. *The blue-crowned laughingthrush in Nanchang Zoo*

There have been several useful molecular sex-typing protocols established for birds over the past decades (Griffiths et al., 1998; Lessells and Mateman, 1996), among which the amplification of an intron of the *CHD1* gene has been successfully used for a range of avian species (Fridolfsson and Ellegren, 1999, 2000). The *CHD1* gene is located on sex chromosomes and is highly conserved in non-ratite birds. Chromosomes W and Z carry nearly identical exons but different sizes of introns of this gene. The *CHD1*-specific primer pair can be used to generate different amplicons representing *ZW* (female) and *WW* (male) individuals. In this study, we sought to test whether this method can be used for sex-typing of *Garrluax courtoisi*, and discussed its correlation with behavioral characteristics of the birds.

Materials and methods

Animals

Seven *Garrluax courtoisi* birds (numbered 1-7) were kept captives in the Nanchang Zoo, Nanchang City in Jiangxi Provence. Color-coded foot bands were placed to facilitate visual identification of the birds from distance. A total of 40 µl blood was drawn from the brachial vein and dropped into tubes containing 75% ethanol and saved in -20 °C until used for DNA isolation. We were unable to capture bird #5, thus blood sample for this bird was not collected.

Behavioral observations

Extensive behavioral observations of these birds were documented from 2014 to 2016, especially during the breeding seasons. These birds are small in size and move swiftly. It was still quite difficult to trace every individual bird, especially when visibility was low, even though they wore color-coded foot-bands. In order to establish

http://www.aloki.hu ● ISSN 1589 1623 (Print) ● ISSN 1785 0037 (Online)
DOI: http://dx.doi.org/10.15666/aeer/1605_63416347
© 2018, ALÖKI Kft., Budapest, Hungary

correlations between behavioral characteristics and molecular sexing results, we put our efforts to the following observations: 1) the presence of prelaying behaviors, including preening, elaborate display, or chasing of females; 2) documentation of nesting and egg-laying in varying grouping strategies to identify the reproducing females; and 3) observation of brooding behavior to identify the egg-laying female, and, ideally, the pairing male. It has been known that the breeding bird during the night is predominately the egg-laying female (Reul-Schneider and Schneider, 2006).

Genomic DNA isolation

Genomic DNA was isolated from blood clots using a commercial genomic DNA isolation kit CW2298 (Kang Wei, China), a standard phenol/chloroform method and an optimized phenol/chloroform method by testing different volumes of lysis buffer, concentrations of Proteinase K and digestion time (*Table 1*). DNA concentration and quality were measured using a NanoDrop 2000 spectrophotometer (Thermo Fisher Scientific, USA) and 0.8% agarose gel electrophoresis.

Table 1. *Optimization parameters of DNA extraction*

Lysis buffer (ul)	Digestion time (h)	Proteinase K (ul)
400	2	2
450	4	4
500	6	6
500	8	8
500	10	10
500	15	15

PCR sex-typing

Primers 2550F/2718R (Forward: 5'-GTTACTGATTCGTCTACGAGA-3'; Reverse: 5'-ATTGAAAT GATCCAGTGCTTG-3') were designed based on a conservative intronic region within the *CHD* gene (Fridolfsson and Ellegren, 2000). PCR was conducted in 25 μl reactions containing 40 ng genomic DNA, 2.5 μM 10×buffer, 25 mM MgCl2, 2.5 mM dNTP, 0.2 μM each of primers and 2.5 units Taq polymerase (Tiangen, China). The PCR reaction profile was as follows: 94 °C for 5 min, 29 cycles of 94 °C for 30 s, 65 °C (decreasing 0.5 °C every cycle) for 20 s, 72 °C for 40 s; then followed by 14 cycles of 94 °C for 30 s, 50 °C for 20 s, 72 °C for 40 s; reaction was ended after a final extension of 10 min at 72 °C. Eight μl of the PCR product was loaded to a 2.5% agarose gel (containing ethidium bromide) for electrophoresis. A 50-bp ladder (Tiangen, China) was used to indicate the sizes of the PCR products. DNA bands were visualized under UV light and pictures taken. PCR products were purified from agarose gel using a gel purification kit (Qiagen, Germany) and sent for sequencing using primers 2550F and 2718R (BGI, China).

Results

Behavioral observations indicate the gender of Garrluax courtoisi birds

From 2014 to 2016, eight blue-crowned laughingthrushes including seven birds tested in this study were separated into different groups (*Table 2*). These birds were

http://www.aloki.hu ● ISSN 1589 1623 (Print) ● ISSN 1785 0037 (Online)
DOI: http://dx.doi.org/10.15666/aeer/1605_63416347
© 2018, ALÖKI Kft., Budapest, Hungary

painstakingly inspected for nest building, egg laying and hatching. Both male and female birds have existed in this flock, as one brood of chicks was hatched each year in 2014 through 2016 (*Table 2*). One extra nest was built, into which no egg was laid, both in year 2014 and year 2016. There had been no obvious courtship displays or aggressiveness observed during the last three mating seasons. However, flocked chasing was frequently seen among blue-crowned laughingthrushes, similar to that seen in Darwin's finches on the Galápagos Islands. It has been believed that chasing of the female by the male promotes sexual synchronization between the two sexes, leading to successful copulation and insemination. Chasing of bird #2, mostly led by bird #6, has been frequently observed during the mating seasons in years 2015 and 2016, although pairing could not be confirmed. Bird #4 also showed chasing activity to a lesser extent in these two mating seasons. In addition, the birds were divided into two groups during the breeding seasons in year 2014 and year 2016, and the broody group included bird #2 in both years (*Table 2*). This suggests that bird #2 was the breeding female in these three years while bird #6 was the dominant male in the same period.

Table 2. *Reproduction record of blue-crowned laughingthrush (Garrluax courtoisi) in Nanchang Zoo from year 2014 through 2016*

Year	Groups	Birds in group	Nests built	Eggs laid	Chicks hatched
2014	A	#2, #5, #8*	Yes	Yes	Yes
	B	#1, #3, #4, #6, #7	Yes	No	No
2015	C	#1~7 (no division)	Yes	Yes	Yes
2016	D	#1, #2, #4, #6,	Yes	Yes	Yes
	E	#3, #5, #7	Yes	No	No

*Bird #8 died for unknown reason at the end of 2014; this bird was male by autopsy

Both male and female blue-crowned laughingthrushes can be broody (Liu et al., 2016), but it is not clear how they cooperate or what specific roles they take. In this study, as the birds are loosely confined in a large wire mesh aviary, it is not clear whether there had been indeed a broody male. Previous captive breeding of this avian species suggests that the females are usually the brooding birds at night [8]. In the breeding season in year 2014, there was an attack by a snake (*Dinodon rufozonatum*) on the hatching nest, and the brooding female bird (bird #2) was thought to be the last to abandon the nest. Birds have weak visions at night, but are sensitive to vibrations of the tree branches and hence the approaching snake. In addition, during the breeding seasons in year 2015 and year 2016, we took daily close-up checks of the hatching nest, and bird #2 was nearly always perching nearby. This further suggests that bird #2 was the only egg-laying female bird in these two years.

An optimized method for isolation of genomic DNA of Garrluax courtoisi birds

In this study, a commercial kit was first used to isolate genomic DNA of *Garrluax courtoisi birds*. However, the isolated DNA was of poor quality as the electrophoresis bands showed uneven brightness and a severe pollution of protein residue (*Fig. 2*). A standard phenol /chloroform method was then explored for DNA isolation, also resulting in poor-quality DNA. To solve this problem, we optimized this phenol /chloroform method by testing three parameters including the volume of lysis buffer, the concentration of Proteinase K and the digestion time. Finally, 500 μl lysis buffer,10 μl

http://www.aloki.hu ● ISSN 1589 1623 (Print) ● ISSN 1785 0037 (Online)
DOI: http://dx.doi.org/10.15666/aeer/1605_63416347
© 2018, ALÖKI Kft., Budapest, Hungary

Proteinase K and a digestion time of 8 hours were used in the extraction protocol, which allowed us to obtain high-quality genomic DNA from each blood clot (*Fig. 2*).

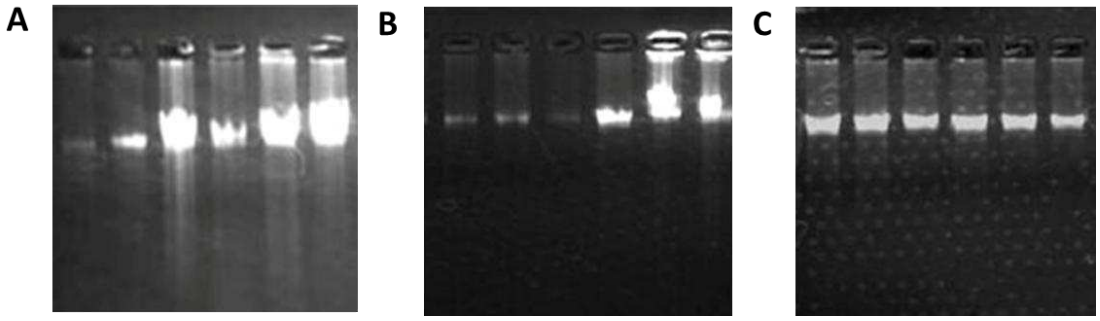

Figure 2. *Electrophoresis patterns of genomic DNA isolated by three approaches. (A) A commercial kit. (B) A routine phenol chloroform method. (C) An optimized phenol chloroform method*

PCR sex typing

The *CHD1*-based PCR generated one or two amplicons representing the two sexes (*Fig. 3*). Sequencing of the two PCR products confirmed that the 700 bp product was from Z chromosome, while the 600 bp product was from the W chromosome. Thus, PCR with primers 2550F/2718R will generate only one band of 700 bp for a male *(ZZ)* blue-crowned laughingthrush, and generate two bands (700 bp and 600 bp) for a female (*ZW*). The two bands can be easily separated in a 2.5% agarose gel, and there was no amplicon other than the two alternative fragments. According to the PCR sex typing results, Birds #2, 3 and 4 are female, and Birds#1, 6 and 7 are males.

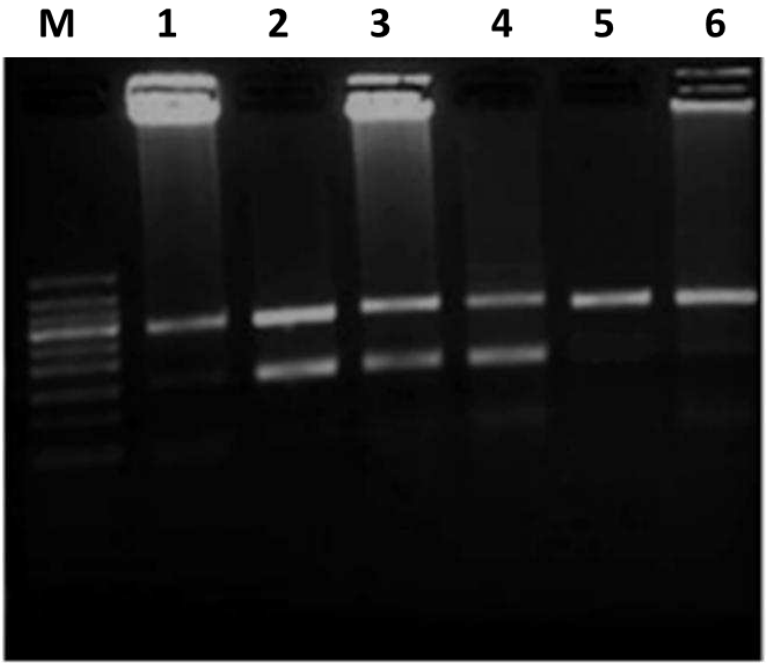

Figure 3. *CHD1-based PCR sex-typing of blue-crowned laughingthrush (Garrulax courtoisi). A gel image of PCR products by primer pair 2550F/2718R. M, molecular marker; lines 1,5 and 6, ZZ (male) individuals; lines 2, 3 and 4, ZW (female) individuals*

http://www.aloki.hu ● ISSN 1589 1623 (Print) ● ISSN 1785 0037 (Online)
DOI: http://dx.doi.org/10.15666/aeer/1605_63416347
© 2018, ALÖKI Kft., Budapest, Hungary

Discussion

Blue-crowned laughingthrush is the critically endangered bird and the endemic species in China, it distributed in Simao, Yunnan and Wuyuan, Jiangxi in history. The existing wild blue-crowned laughingthrush is only in Wuyuan, and their population is more than 300. In 1980's and 1990's, blue-crowned laughingthrush were exported to Hong Kong, Europe and North America through wildlife trade. Presently, there are above 200 individuals in zoos or feeding units around the world including Nanchang Zoo. However, as a sexually monomorphic species, it is hard to determine their sex by body, voice or behaviour (Liu et al., 2016).

Bird #2 had demonstrated apparent female behaviors and this is confirmed by PCR sex-typing; on the contrary, bird #6 showed active chasing behavior and is indeed sex-typed by PCR as male. Because there had been more than one nest built during two of the three breeding seasons from year 2014 to 2016, there were likely multiple female birds in the flock. PCR results revealed that birds #2, #3, and #4 were females, while #1, #6 and #7 were males. This represents a 1:1 male/female sex ratio in this small population. Birds #3 and #4 were both captured from the wild in year 2011 without knowledge of their ages or gender. The reasons for the absence of egg-laying from these two female birds could be complex. A sudden environmental change from the wild to the captive status may have affected their breeding behaviors, and the possibility cannot be excluded that they might have been carrying unnoticed diseases that affected reproduction; or they might simply have lost their reproductive ability due to aging. Our study suggests that behavioral characteristics can be used for gender identification with caution, as some of them are weak and sometimes misleading. For example, though bird #4 showed chasing inclination during the two mating seasons in years 2015 and 2016, it was clearly demonstrated by PCR to be a female.

Itoh et al.(2001) have successfully identified the gender of flamingo using two pairs of primers in EE0.6 gene, which was then verified by the CHD1 gene-based method. The unambiguous and easily separable two PCR products from the CHD1 genes on the Z and the W chromosomes make this molecular sexing method a simple and reliable way for sex determination of blue-crowned laughingthrushes, avoiding the risk of severe physical injuries to the bird or death from traditional sex examination methods. It should be noted that DNA isolation from feathers should make this method even safer for the birds (Bello et al., 2001). As successful as in many other avian species, the accuracy of sex-typing brought by this non-invasive method is very helpful for the management of and research on populations of this critically endangered species.

Conclusion

In summary, blue-crowned laughingthrush is a critically endangered avian species. We used CDH1-specific primers for PCR sex-typing of this sexually monomorphic bird, and compared the PCR-typing results with the deduced gender of this bird on the basis of extensive behavioral observations. We believed that the method is reliable and non-invasive to the birds, thus it is an ideal tool for the management and study of this critically endangered species under captivity.

Acknowledgements. We thank Professor Jun Ren at the Jiangxi Agricultural University for his kind assistance in experimental design, data interpretation, and manuscript writing. This work was supported

http://www.aloki.hu ● ISSN 1589 1623 (Print) ● ISSN 1785 0037 (Online)
DOI: http://dx.doi.org/10.15666/aeer/1605_63416347
© 2018, ALÖKI Kft., Budapest, Hungary

by these projects in China (2013-CXTD002, Co-Innovation Center for In Vitro Diagnostic Reagents and Devices of Jiangxi Province; National Natural Science Foundation of China (31460591;31401047;31660302;31760625); Natural Science Foundation of Jiangxi Province (20143ACB21006;20142BCB23028);Science and technology research project of Jiangxi Provincial Education Department(14571).

REFERENCES

[1] Bello, N., Francino, O., Sanchez, A. (2001): Isolation of genomic DNA from feathers. – J. Vet. Diagn. Invest. 13(2): 162-164.
[2] BirdLife International (2017): Species factsheet: Garrulax courtoisi. – http://www.birdlife.org. Accessed on 23/04/2017.
[3] Fridolfsson A. K., Ellegren, H. (1999): A simple and universal method for molecular sexing of nonratite birds. – J. Avian. Biol. 30: 116-121.
[4] Fridolfsson, A. K., Ellegren, H. (2000): Molecular evolution of the avian – CHD1 genes on the Z and W sex chromosomes. – Genetics 155(4): 1903-1912.
[5] Griffiths, R., Double, M. C., Orr, K., Dawson, R. J. G. (1998): A DNA test to sex most birds. – Mol. Ecol. 7(8): 1071-1075.
[6] He, F. Q., Lin, J. S., Wen, C., Lin, Z., Shi, Q. H., Huang, H. Q., Cheng, S. L., Xiao, H. (2017): Prelim of biology of the blue-crowned laughingthrush Garrulax courtoisi in Wuyuan of NE Jiangxi, SE China. – Chin. J. Zool. 52(1): 167-175.
[7] Itoh, Y., Suzuki, M., Ogawa, A. (2001): Identification of the sex of a wide range of Carinatae birds by PCR using primer sets selected from chicken EE0.6 and its related sequences. – J. Hered. 92: 315-321.
[8] Lessells, K., Mateman, C. (1996): Molecular sexing of birds. – Nature 383: 761-762.
[9] Liu, D. Q., Wu, Z. Y., Wang, X. H., Huang, H. L., Li, D. T. (2016): Cooperative breeding behaviour of captive blue-crowned laughingthrush (Garrulax courtoisi) . – Chin. J. Wildl. 37(3): 228-233.
[10] Liu, D. Q., Wang, X. H., Fu W.K., Lin J.S., Wu, Z. Y. (2017): Observation of Blue-Crowned Laughingthrush Nestling Behaviors in Wuyuan, Hong Kong and Nanchang. – Chin. J. Wildl. 38 (2):249-253.
[11] Reul-Schneider, M., Schneider, H. (2006): Some notes on our experiences of keeping and breeding the yellow-throated laughingthrush Garrulax galbanus courtoisi. – Avicul. Mag. 112(2): 53-56.
[12] WAZA (n. d.): Global Species Management Plan [EB/OL] – http://www.waza.org/en/site/conservation/conservation-breeding-programmes/gsmp. Access date: 3/10/2012.

http://www.aloki.hu ● ISSN 1589 1623 (Print) ● ISSN 1785 0037 (Online)
DOI: http://dx.doi.org/10.15666/aeer/1605_63416347
© 2018, ALÖKI Kft., Budapest, Hungary

LIGHTNING ACTIVITY CHARACTERISTICS UNDER COMPLEX TOPOGRAPHY IN LOW LATITUDE PLATEAU OF CHINA

YIN, L. Y.[1,2] – WANG, H. Y.[1,3] – JIN, W. J.[2] – ZHANG, S. D.[1] – WANG, W. G.[1*] – MEI, H.[2]

[1]*Department of Atmospheric Sciences, Yunnan University, Kunming 650500, P. R. China*

[2]*Weather Modification Center of Yunnan Province, Kunming 650034, P. R. China*

[3]*Department of Environmental Science & Engineering, Shanghai Key Laboratory of Atmospheric Particle Pollution and Prevention, Fudan University 220 Handan Road, Shanghai 200433, P. R. China*

**Corresponding author*
e-mail: wangwg@ynu.edu.cn

(Received 31st May 2018; accepted 2nd Aug 2018)

Abstract. Comparison analysis was performed for the characteristics of cloud-to-ground (CG) lightning and topography in low latitude plateau of China and showed that CG lightning activity was characterized Gaussian distribution along the variation of elevation centered at approximately 2000 m above sea level and decreased on both sides; it was also linearly inversely correlated with variations in terrain slope. CG lightning activity was showed a typical positive dipole distribution of electric charges in the thunderstorm clouds. The average current intensity of negative CG lightning located in the lower layers was obviously weaker than that of the positive CG lightning located in the upper layers, and decreased initially and subsequently increased as the elevation increased, whereas the positive CG lightning had no significant variation. The CG lightning current intensity increased linearly with terrain slope, and the variation slope of positive CG lightning was smaller than that of negative CG lightning, variation of current intensity with latitude was inversely correlated with the variation of CG lightning densities. The CG lightning activity and variation of current intensity had the same characteristics in specific regions and in zonal and meridional cross-sections, but it was significantly affected by the topography in the low/high regions where elevation was <600 />3500 m.
Keywords: *cloud-to-ground (CG) lightning, elevation, terrain slope, effect of topography*

Introduction

Terrain topography can greatly affect the movement and development of the general circulation of the atmosphere, particularly convergence systems, fronts, and typhoons (Egger et al., 1992; Smith, 1979). Smith (1979) proposed using linear regression to describe the correlation between annual average precipitation and altitude; studies have used linear regression to describe the linear correlation between lightning and precipitation (Ezcurra et al., 2002; Jayaratne and Kuleshov, 2006; Soula and Chauzy, 2001). Without considering the formation mechanisms of lightning, precipitation, and other factors, topography has an obvious influence on precipitation and lightning activity. Topography can directly or indirectly affect the direction of the local prevailing wind, and in appropriate conditions, different elevations and terrain slopes can directly affect updrafts, resulting in strong weather, such as barrier jets and thunderstorms, which are usually accompanied by obvious precipitation and lightning activity. Researchers have also employed numerical model simulations to find that topography has a great influence on lightning activity (Smith, 1979).

http://www.aloki.hu ● ISSN 1589 1623 (Print) ● ISSN 1785 0037 (Online)
DOI: http://dx.doi.org/10.15666/aeer/1605_63496367
© 2018, ALÖKI Kft., Budapest, Hungary

Researchers have found that topography can affect the spatial and temporal distributions of lightning. Pinto Jr. et al. (1999) analyzed the spatial distribution of lightning in southern Brazil and found a favorable correlation between topography and lightning activity, and Schulz and Diendorfer (1999) revealed a nonlinear correlation between topography and lightning activity: cloud-to-ground (CG) lightning activity increased linearly as elevation increased, whereas the CG lightning decreased linearly as elevation increased for elevation >1300 m. Wagner et al. (2006) found a favorable correlation between topography, wind direction, and CG lightning flash count in the United States, and Zajac and Rutledge (2001) analyzed the relationships between CG lightning flash density, thunderstorm days, topography, and other meteorological parameters, which showed favorable correlations between the topography, CG lightning flash density, and thunderstorm days in the United States. Bourscheidt (2009) analyzed data on lightning records from 2005 to 2007 in Brazil and found that terrain slope had a highly significant influence on lightning flash distribution. In China, Ma et al. (2004) analyzed 6 years of lightning data recorded using a satellite-equipped optical transient detector (May 1995–March 2000) and lightning imaging sensors (December 1997–March 2003) and obtained the distribution of lightning density in this area with a grid format of 0.5° × 0.5°, which showed significant regional differences in lightning density in mainland China: as with different geographic environments, the high lightning density areas (centers) have different relationships to mesoscale topography. Tong et al. (2008) analyzed the characteristics of lightning activity in Zhejiang Province by using a map of CG lightning density as measured by a lightning coordination system from 2004 to 2007; their study showed a correlation between topography, seasonal climate, and lightning activity. Qie et al. (2003) compared the lightning activity of typical topographies globally using lightning coordination data measured by the lightning detection system on the Tropical Rainfall Measuring Mission satellite, and the results showed significant differences in lightning activities both in lightning flash count and lightning intensity in different topographic regions. Qie et al. (2009) analyzed the electrical characteristics of thunderstorms in different elevations and found that the special-type thunderstorm was positively related to the elevation of the region, in the Chinese Inland Plateau, the height of the charge region neutralized by negative CG flashes ranges from 3 km to 5 km above the ground, corresponding to an ambient temperature between -2 and -15 °C. For the two positive CG flashes, the neutralized charge regions are located at a height of about 5.5 km and the ambient temperature is about -18 °C, indicating the existence of upper positive charge in the thunderstorm. Qie et al. (2013), Wang et al. (2016) analyzed the lightning activity in northeastern China, and the results showed lightning events mainly occurred in regions with a large gradient of CAPE. Comparisons between lightning and non-lightning regions indicated that lightning regions featured more intense ascending motion than non-lightning regions.

Yunnan Province is in the southwestern border region of China, and it has the typical geographic characteristics of a low latitude plateau with the terrain descending from the northwest to the southeast; it has unusually great elevational differences; the maximum elevation difference can be more than 6000 m. Yunnan has frequent CG lightning activity throughout the year, with uneven temporal and spatial distributions (Xie et al., 2013). In the present study, Lightning activity characteristics under complex topography in low latitude plateau was analyzed using 10 years of CG lightning records from 2007 to 2016 and detailed geographic elevation data from Yunnan Province of China.

http://www.aloki.hu ● ISSN 1589 1623 (Print) ● ISSN 1785 0037 (Online)
DOI: http://dx.doi.org/10.15666/aeer/1605_63496367
© 2018, ALÖKI Kft., Budapest, Hungary

Data and methods

The CG lightning data were recorded by the Lightning Detection and Coordination Network based on 22 ADTD (ADvanced TOA and Direction) lightning locators and a central data processing station that provided information on each lightning flash, including time, location, intensity, and polarity, with theoretical coordinating accuracy and detection efficiency of approximately 500 m and 95%, respectively. The CG lightning data were not corrected for efficiency.

The topography data comprised a Digital Elevation Model (DEM) measured by the Shuttle Radar Topography Mission (SRTM), with two datasets, SRTM1 and SRTM3, with precisions of 1 arcsecond and 3 arcseconds, respectively. Of these datasets, SRTM3 can cover the globe and is the most widely used topographic dataset. The spatial resolution of the SRTM3 data discussed in this article was 3 s. Its elevation datum was the EGM96 geoid with an accuracy of ±16 m, and the horizontal datum was the WGS84 with a horizontal accuracy of ±20 m. Positive CG lightning whose intensity was less than 20 kA was expelled as cloud-to-cloud lightning (Biagi et al., 2007).

Terrain slope is the degree of inclination compared with the horizontal plane of a point on the ground that can be calculated from the value of the elevation of two adjacent points using DEM data. It is defined as the angle between the tangential plane and the horizontal ground at this point (Monmonier, 1982); the exact calculation formula is

$$slp = \sqrt{\left(\frac{right - left}{res * 2}\right)^2 + \left(\frac{top - bottom}{res * 2}\right)^2}.$$

Within this formula, *top*, *bottom*, *right*, and *left* represent the elevations of the adjacent points, respectively, to the top, bottom, right, and left; *res* represents the distance between two adjacent points, and the units of all these parameters are, m. $tan^{-1}(slp)$ is used in this article to describe the inclination to the horizontal plane as the terrain slope.

The latitude and longitude in the present study ranged from 20.5°N to 29.5°N and from 95.5°E to 106.6°E, and the CG lightning data were integrated into the statistics as a grid with an accuracy of 0.01°, and the average elevation was taken as the elevation value of the grid to analyze the CG lightning activity characteristics.

Results

Topographic variation and lightning density characteristics

Figure 1a is the map of elevation with an accuracy of 0.01° × 0.01°. Yunnan of China is located in the junction region of the southeastern margin of the Tibetan Plateau and the Yunnan–Guizhou Plateau, a region which is mainly mountains and plateaus with low latitude and high elevation. The terrain is highest in the northwest and descends toward the southeast and stretches toward the east, southeast, south, southwest, and west in a fingerlike fashion. In northwestern Yunnan, the terrain is an obvious fold mountain area with sharp rises and drops in elevation because the elevations of the valleys of the Three Parallel Rivers are lower than 1500 m, whereas those of the snow mountains exceed 5000 m; the Kawakarpo Peak of the Meili Snow

http://www.aloki.hu ● ISSN 1589 1623 (Print) ● ISSN 1785 0037 (Online)
DOI: http://dx.doi.org/10.15666/aeer/1605_63496367
© 2018, ALÖKI Kft., Budapest, Hungary

Mountain is the highest point in Yunnan Province, ascending to 6740 m. Except for the northwestern part, the terrain of Yunnan Province can be divided into two major regions with the fault area of the Ailao Mountains as the boundary; to the west are the highlands with moderate- and high-elevation mountains as the main terrain. This highland region contains a high concentration of mountains; to the north of the Wuliang Mountain, all the mountaintops are higher than 2500 m, whereas the heights gradually decrease to the south. In the region to the east of the Ailao Mountains, the Honghe Valley and Yuanjiang Valley stretch alongside the Ailao Mountains; the elevation declines rapidly as the valleys stretch southward, and the lowest point is only 76.4 m high. The elevation is relatively high further east and it declines gradually to the southeastern part of Wenshan Autonomous Prefecture. Further north is an area of plateaus and hills whose elevations are relatively high, fluctuating from 1800 to 3000 m; this area stretches northeast to the northern part of Zhaotong City where the elevation declines rapidly. The slope features of terrain in Yunnan Province are also divided by the Ailao Mountains (see *Fig. 1b*); the east is the flattest area in Yunnan, dominated by basins and hills, and corresponding to the mid-altitude regions, mostly with an elevation of 1500–3000 m. To the southwest of the Ailao Mountains is the second region of mild terrain slope. The elevation of this region varies to a greater extent than do theentral and eastern areas of Yunnan, which have elevations between 1000 and 2000 m. The terrain slope of the rest of the region is more complicated and follows the trend of the mountains, and the deviation to the Hengduan Mountains in the northwestern Yunnan is severe. Affected by this topography, the CG lightning density has a typical spatial distribution along the mountains' trends (see *Fig. 1c*).

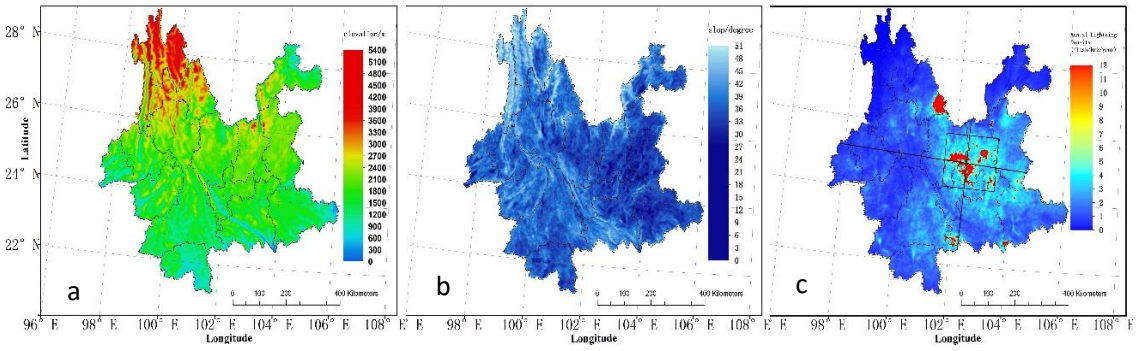

Figure 1. *Map of elevation and annual average CG lightning density distribution of Yunnan Province. a: elevation (m); b: terrain slope (degree); c: CG lightning density (time/year•km^2)*

The area with the highest CG lightning density was in the central region of Yunnan, northeast of the Ailao Mountains, which features relatively flat and unobvious folded topography with elevations of 1800–2500 m. Synoptic analysis showed that this region was mainly affected by cold front shear, convergence shear, and other synoptic systems. The frequent convergence of cold and warm air made this region suitable for forming large-scale strong convective weather systems (Li, 2011; Xu et al., 2011). The second-highest CG lightning density area was in Huaping County, Lijiang City, northwestern Yunnan, which is surrounded by mountains higher than 3100 m to the north, west, and south, whereas the elevation of the high density area is lower than 2000 m. Furthermore, to the east of this area lie the Hengduan Mountains at the Yunnan–Sichuan border, which the plateau trough and southwestern vortex cross when moving southeastward

http://www.aloki.hu ● ISSN 1589 1623 (Print) ● ISSN 1785 0037 (Online)
DOI: http://dx.doi.org/10.15666/aeer/1605_63496367
© 2018, ALÖKI Kft., Budapest, Hungary

into northwestern Yunnan; consequently, an obvious upward stream was formed, thus creating this high CG lightning density area (Li, 2011; Xu et al., 2011). The third-highest CG lightning density area was located in southeastern Pu'er City, which is on the southwestern side of the Ailao Mountains. This area was dominated by warm and humid air flow that could form an upward stream due to the topographic uplift effect. The blockading effect of the Ailao Mountains weakens the effect of cold air in this area; thus, the lightning activity is relatively weak (Li, 2011; Xu et al., 2011). In the valley regions to the western side of the Ailao Mountains and in the low-elevation regions in northeastern and eastern Yunnan (elevation <1000 m, flat topography, and with no mountains higher than 3000 m), the CG lightning activity is relatively weak. The high-elevation regions (elevation >3500 m with obvious folded topography) and northeastern Yunnan, where the effects of warm and humid airstreams are minimal, are nearly zero-zones for CG lightning activity.

Distribution of topographic variation and lightning density

The distribution of CG lightning at different elevations was determined by analyzing the statistics on CG lightning flashes from 2007 to 2016, with 100 m as the elevation increment unit. The result (see *Fig. 2a*) showed that total CG lightning flashes were normally distributed with elevation and mainly appeared in the area between 800 and 3300 m. Within this range of elevation, the area of the corresponding regions accounts for 90.6% of the land area of Yunnan Province, where 96% of the total CG lightning occurred; in particular, in the regions with elevations between 1900 and 2100 m, the number of CG lightning flashes reached 1.56 million.

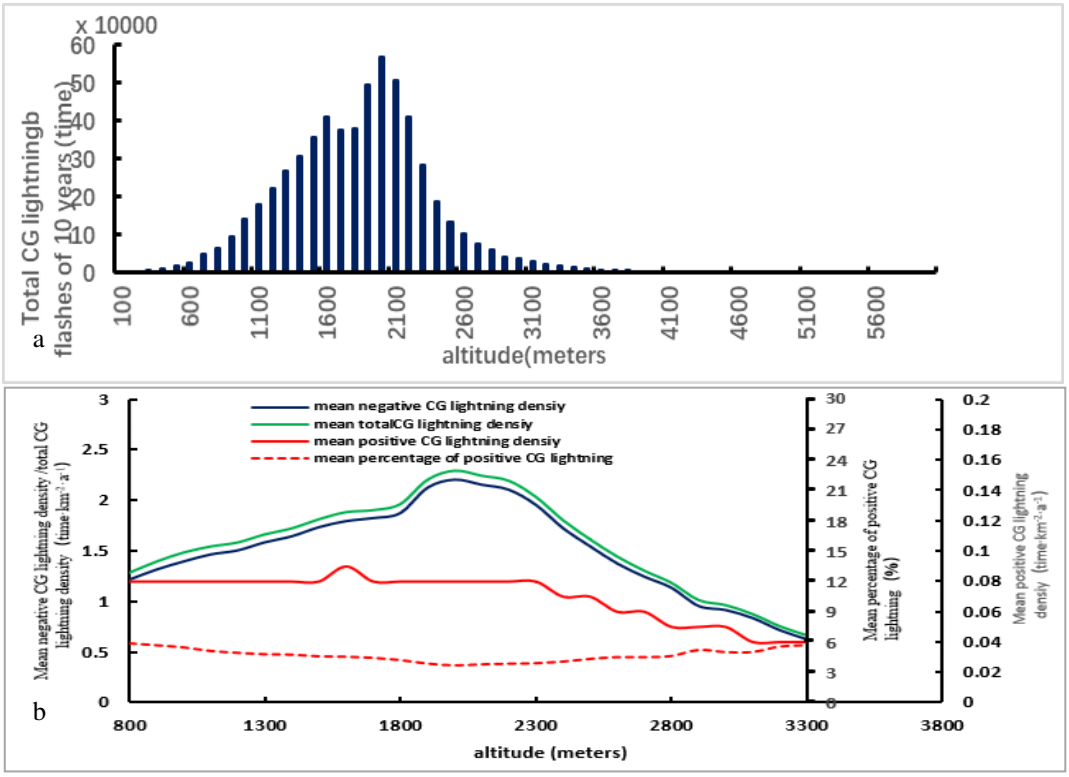

Figure 2. *distribution of elevation variation and total CG lightning counts, average CG lightning density and the proportion of positive CG lightning (a: variation of total CG lightning counts; b: variation of CG lightning density and proportion of positive CG lightning)*

http://www.aloki.hu ● ISSN 1589 1623 (Print) ● ISSN 1785 0037 (Online)
DOI: http://dx.doi.org/10.15666/aeer/1605_63496367
© 2018, ALÖKI Kft., Budapest, Hungary

The regions with elevation <800 m account for 3.7% of the land area of Yunnan Province, and only 3% of the CG lightning flashes were recorded in these regions, whereas regions with elevation >3300 m account for 5.7% of the land area, and only 1% of the CG lightning flashes were recorded in these regions. Therefore, the CG lightning activity in regions <800 m or >3300 m was unrepresentative; thus, only the effect of elevation within the range of 800 to 3300 m on CG lightning activity was analyzed (see *Fig. 2b*). The average total CG lightning density and average negative CG lightning density corresponded to the trend of elevation, which exhibited unimodal variation with the peak in the 1900–2000-m range where the average total CG lightning density peaked at 2.29 events·km^{-2}·a^{-1} and the average negative CG lightning density peaked at 2.2 events·km^{-2}·a^{-1}, whereas the average positive CG lightning density was stable at 0.08–2.2 events·km^{-2}·a^{-1} from 800 to 2000 m. As the elevation increased, the average total/negative CG lightning density decreased linearly, the average positive CG lightning density fluctuated between 0.06 and 0.08 events·km^{-2}·a^{-1}, and the average total/negative (positive) CG lightning densities exhibited fluctuating reduction when elevation >2300 m. Land area increased linearly as elevation increased when elevation <1600 m, fluctuated at approximately 1800 m, and peaked between 1900 and 2000 m. This phase corresponded to the peak value of average negative/total CG lightning densities, and the average positive CG lightning density was stable in this area, exhibiting frequent CG lightning activity at the elevation band of 1900–2000 m, where the convergence of cold and warm air frequently occurs.

As can be seen from the variation characteristics of positive CG lightning and elevation, the average percentage of positive CG lightning was only approximately 5%, there was bipolar structural characteristics of thunderstorms in Yunnan Province because the center of negative charge is close to the ground and the center of positive charge is located at high layers. Positive CG lightning exhibited slow fluctuating reductions as the elevation increased from 800 to 2000 m, and the proportion of them was at a minimum of 3.69% at approximately 2000 m, which corresponded to the peak value of negative CG lightning activity. This indicated that the negative charge of the thunderstorm cloud was abnormally active in the area of cold and warm air interaction. In the range of 2000–3300 m above sea level, the proportion of positive CG lightning flashes fluctuating increased as the elevation increased, indicating a significant difference between the excitation conditions of positive/negative CG lightning flashes in the high- and low-altitude regions and the excitation conditions in the mid-altitude (1900–2000 m) regions where negative CG lightning flashes were concentrated.

Distribution of terrain slope and CG lightning density

The terrain slope has a promoting effect on airflow uplift and convection. Statistics on average CG lightning density for each slope section of 1° were analyzed (see *Fig. 3*), and the results showed that CG lightning activity increased rapidly and decreased linearly after peaking as the terrain slope increased, and the total CG lightning count significantly decreased when the tendency declined as the terrain slope continued to steepen more than 20°. CG lightning was mainly concentrated in the slope sections between 0° and 30°, where 98.6% of the total CG lightning occurred; these sections contained 97.7% of the total land area of Yunnan Province, particularly the sections between 0° and 5° where CG lightning was most active and where the 10-year total count reached 2.75 million, approximately 46% of the total CG lightning count. These sections contained approximately 37% of the total land area. Only 3% of total CG

http://www.aloki.hu ● ISSN 1589 1623 (Print) ● ISSN 1785 0037 (Online)
DOI: http://dx.doi.org/10.15666/aeer/1605_63496367
© 2018, ALÖKI Kft., Budapest, Hungary

lightning occurred within the slope sections steeper than 30°, which constituted only 1.3% of the total land area, indicating that within the range of 1 km^2, regions with terrain slope >30° were few and the CG lightning in these regions was too infrequent to be further analyzed. Thus, the analysis of the effects of terrain slope on CG lightning density and the proportion of the positive lightning in *Figure 3b* consisted only of the sections less than 30°.

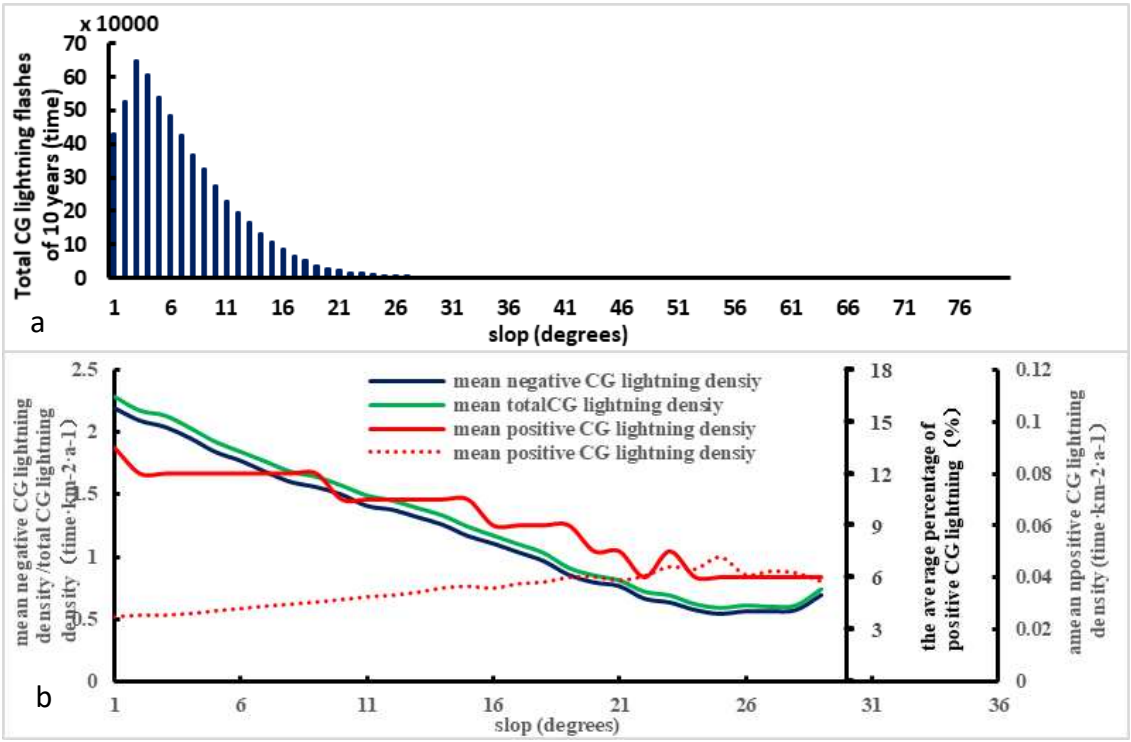

Figure 3. *Variations in total CG lightning counts, average CG lightning densities, and the proportion of positive CG lightning over terrain slope of 2007–(2016). a: Variation of total CG lightning counts over terrain slope; b: variations of average CG lightning densities and the proportion of positive CG lightning over terrain slope*

The average total/negative CG lightning density peaked (2.28 events·km^{-2}·a^{-1} and 0.57 events·km^{-2}·a^{-1}) at a slope of 1° and declined linearly as slope steepened and reached a minimum (0.6 events·km^{-2}·a^{-1} and 0.57 events·km^{-2}·a^{-1}) at a slope of 27°. As the terrain slope steepened, the average total/negative CG lightning density increased again. These findings, as well as the topographic characteristics of Yunnan Province, indicated that 90% of the land was undulating plateau with many south-northward mountains and that the synoptic systems of the strong convection in Yunnan come mainly from the east to the west and create thunderstorms because of the uplift airflow affected by the terrain slope, causing an increase in CG lightning activity in regions of slope >27°. Overall, the average positive CG lightning density declined in the performance of the staircase-like trend as the slope increased. At a slope of 1°, the average positive CG lightning peaked (0.9 events·km^{-2}·a^{-1}) and subsequently dropped at 10°, 16°, and 20°, and after a slight increase at a slope of approximately 23°, it remained at approximately 0.04 events·km^{-2}·a^{-1}. The downward trend in CG lightning density indicated the smaller decline for positive CG lightning density and an obvious positive correlation between the

http://www.aloki.hu ● ISSN 1589 1623 (Print) ● ISSN 1785 0037 (Online)
DOI: http://dx.doi.org/10.15666/aeer/1605_63496367
© 2018, ALÖKI Kft., Budapest, Hungary

proportion of positive CG lightning and the terrain slope. Furthermore, a comparison between elevation and terrain slope in Yunnan Province indicated that regions with slope >27° and elevation >3000 m corresponded favorably. The uplift airflow caused by the windward slope of the mountains accelerated convection development, and this, combined with the rate of precipitation, reduced negative charges in the lower part of the cloud during the falling process (Biagi, 2007). This resulted in precipitation current formation, thereby reducing the frequency of low-level negative CG lightning and indirectly resulting in an increase in positive CG lightning in regions of high elevation and terrain slope.

Variation in CG lightning densities and terrain slope at different elevations

Bourscheidt's (2009) research on the variation in CG lightning density as terrain slope changed in Brazil was limited to elevations <1000 m, with the result that the CG lightning density increased linearly with increases in terrain slope, which was contrary to the conclusion reached in this paper. To further analyze the relationship between CG lightning density and terrain slope at different elevations, elevation was divided into four bands: 0–1500 m, 1500–2300 m, 2300–4000 m and >4000 m, and the variations in the CG lightning density with terrain slope were analyzed for the four bands (see *Fig. 4*).

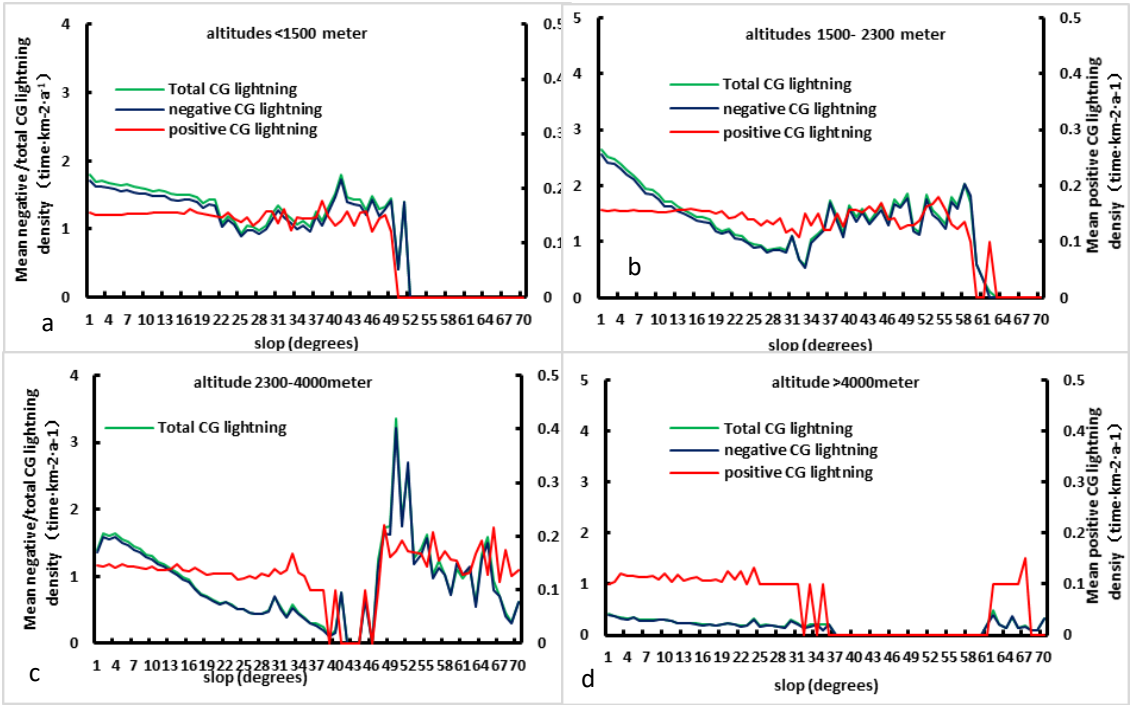

Figure 4. *Variations in average total/negative and positive CG lightning densities over terrain slope at different elevations. a: <1500 m; b: 1500-2300 m; c: 2300-4000 m; c: >4000 m*

In the <1500 m band, the average total/negative CG lightning densities decreased linearly as the terrain slope increased from 0°–25° and peaked at 1.79/1.7 events·km^{-2}·a^{-1} at a slope of 1°. It subsequently reached a minimum of 0.93/0.9 events·km^{-2}·a^{-1} at a slope of 25°. Subsequently, as the terrain slope steepened, the average total/negative CG

http://www.aloki.hu ● ISSN 1589 1623 (Print) ● ISSN 1785 0037 (Online)
DOI: http://dx.doi.org/10.15666/aeer/1605_63496367
© 2018, ALÖKI Kft., Budapest, Hungary

lightning densities also increased, fluctuating between slopes of 25° and 50°; within this range, the average total/negative CG lightning densities exceeded 1 events·km^{-2}·a^{-1} and exhibited many peaks, with terrain slope having a strengthened uplift effect on airflow. Subsequently, the average total/negative CG lightning densities dropped rapidly for slopes of >52°. The trend of average positive CG lightning density was consistent with the trend of average total/negative CG lightning densities because average positive CG lightning decreased slowly and linearly as terrain slope increased in flat (slopes <25°) regions and fluctuated between 25°–50°. Additionally, CG lightning activities tended to decrease for slopes >45°. Within the 1500–2300 m band, which constitutes the largest proportion of land area (total 58% of land area and 49% of land area), the tendency of average CG lightning was consistent with the lower elevation band. The average total/negative CG lightning densities peaked (3.64/0.9 events·km^{-2}·a^{-1}, 2.55/0.9 events·km^{-2}·a^{-1}) where the terrain slope was 1° and reached a minimum (0.57/0.9 events·km^{-2}·a^{-1}, 0.52/0.9 events·km^{-2}·a^{-1}) where the terrain slope was 33°. Additionally, they fluctuated between the terrain slope range of 34°–59° and tended to decrease when terrain slope >60°. The average positive CG lightning density was consistent with the trend of total/negative CG lightning density, except for fluctuation in flat terrain (0°–30°), where the positive CG lightning density remained approximately 0.15 events·km^{-2}·a^{-1}. The topographic distribution in the 2300–4000 m elevation band exhibited two-stage differentiation, and the variation in the average CG lightning density showed consistent characteristics of a linear decrease for slopes of 1°–20°. The variation in the average CG lightning density land area (where terrain slope ranged from 20° to 36°) decreased rapidly, but the lightning activity remained stable, resulting in peaks in the average CG lightning density. No land had a slope in the range from 37° to 45°, and regions with terrain slope >45° comprised just 1% of the land area and total CG lightning count. Additionally, the small sample size resulted in larger average total/negative and positive CG lightning densities, indicating that greater terrain slope was favorable for updraft uplift and formation of local lightning activity and convection. The CG lightning density was less than 0.4 where the elevation >4000 m, and topography and lightning activity also exhibited two-stage differentiation.

The CG lightning activity and elevation in Yunnan Province were normally distributed but inversely correlated with the slope. Within all the elevation bands, when slopes were less steep, the CG lightning activity was relatively dense as long as the terrain slope remained smaller than 30°. In regions with elevation <2300 m and slope of 30°–59°, a small peak occurred due to the topographic uplift effect of airflow, and almost no CG lightning activity was recorded in the mountain regions where slope >60°. Regions whose elevation >2300 m comprised gentle basins and high mountains, causing a blank zone of CG lightning activity between the terrain slope range of 40°–55°. Scattered CG lightning activity occurred in greater terrain slopes, further indicating the importance of topography on CG lightning activity in Yunnan Province.

Latitude and lightning density distribution

Studies have determined that the total lightning density gradually decreases from low latitudes to high latitudes, and the proportion of CG lightning within the total lightning also decreases gradually from low latitudes to high latitudes (Chen, 2003). At a given elevation, the convective clouds in low latitudes are more active, resulting in higher CG lightning densities than in the high latitudes. *Figure 5a* shows the distribution of average CG lightning density by latitude with a resolution of 0.01° for Yunnan Province

http://www.aloki.hu ● ISSN 1589 1623 (Print) ● ISSN 1785 0037 (Online)
DOI: http://dx.doi.org/10.15666/aeer/1605_63496367
© 2018, ALÖKI Kft., Budapest, Hungary

from 2007 to 2016, showing that the average total/negative CG lightning densities tended to increase first and subsequently decrease with multiple peaks as latitude increased. The first peak appeared at 22.8°N, and the average total/negative CG lightning density was 1.72/1.66 events·km^{-2}·a^{-1}. The two regions with CG lightning densities larger than 12 events·km^{-2}·a^{-1} within this latitude band were located to the west of the Ailao Mountains and to the east of Honghe Valley where the elevation rises from the west to the east. Subsequently, the average total/negative CG lightning density dropped rapidly within the mountainous region of the Ailao Mountains and the lower regions where elevation <1800 m. The second peak in average total/negative CG lightning density appeared between 24°N–25.2°N with density sustained at 1.6–1.8 events·km^{-2}·a^{-1}; these regions corresponded to the convergence area of cold and warm air to the east of the Ailao Mountains, where the low 0 °C layer, sufficient moisture, and strong uplift airflow caused a high negative lightning density. The third peak in average total/negative CG lightning densities appeared at approximately 26.5°N, located near the Hengduan Mountains by the Yunnan–Sichuan boundary, which was also one pathway for the intruding cold air. Subsequently, the average total/negative CG lightning density dropped rapidly as the latitude increased. Compared with the average total/negative CG lightning density, the average positive CG lightning density was approximately one order of magnitude less, and the trend of variation almost corresponded to the average total/negative CG lightning except that the third peak was obviously southward. To further analyze the relationship between the CG lightning densities and latitude of the dense CG lightning area (1900–2100 m), the variation in CG lightning density by latitude in this elevation band is shown in *Figure 5b*.

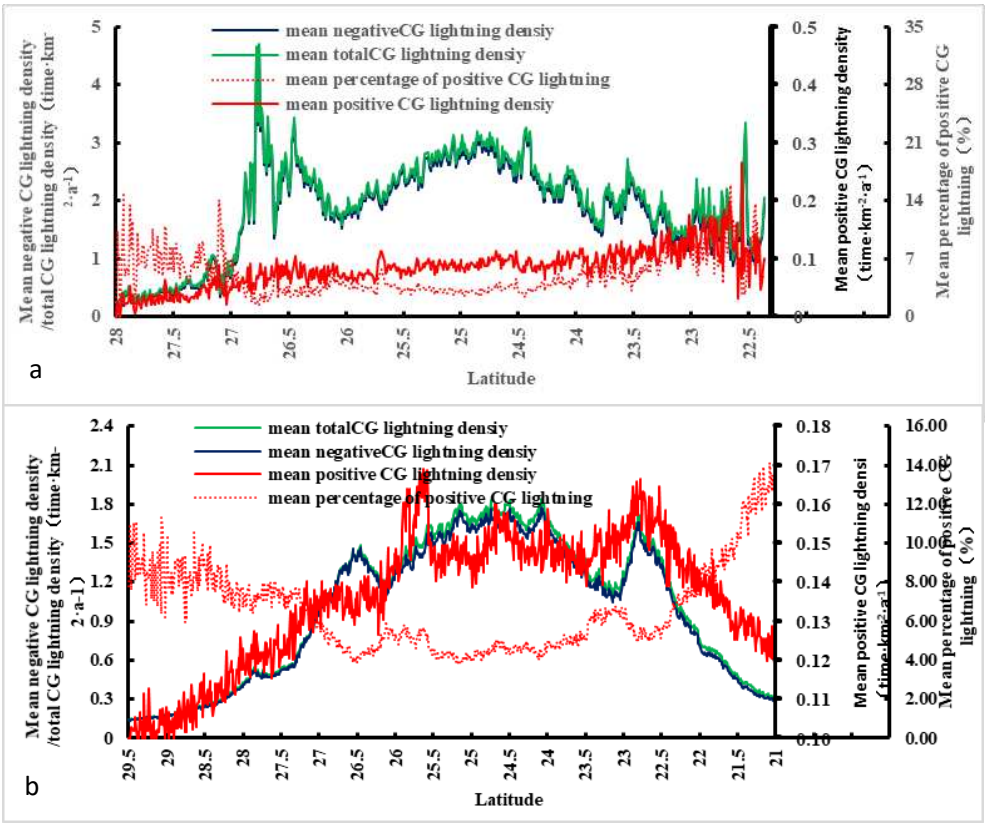

Figure 5. *Variations in CG lightning densities and proportion of positive CG lightning over latitude in Yunnan Province. a: Entire province; b: Elevations between 1900 and 2100 m*

http://www.aloki.hu ● ISSN 1589 1623 (Print) ● ISSN 1785 0037 (Online)
DOI: http://dx.doi.org/10.15666/aeer/1605_63496367
© 2018, ALÖKI Kft., Budapest, Hungary

South of 26.7°N, the average total/negative CG lightning density tended to increase with latitude, albeit with fluctuations, and three peaks were observed, essentially as already described, with the maximum density, 4.65 events·km^{-2}·a^{-1}, appearing at 26.7°N. The average positive CG lightning density decreased with latitude with fluctuations. The variation in the proportion of positive CG lightning for latitudes between 1900–2100 m of elevation was consistent with the variation of the entire province.

Topographic variation and the current intensity of CG lightning

To determine the differences in CG lightning activity in the complex topography in Yunnan Province, the average intensity of positive/negative CG lightning of different elevations, terrain slope, and latitude were analyzed and are described as follows.

Distribution of terrain and the current intensity of CG lightning

Because the CG lightning activities in Yunnan mainly occurred between 800 and 3300 m above sea level, analysis on the effect of elevation on CG lightning intensity was limited in this range. *Figure 6a* shows that the average current intensity of positive CG lightning was significantly greater than that of negative CG lightning. The average current intensity of positive CG lightning fluctuated within the range of 60–63 kA as the elevation increased except for the abrupt increase at 1000 m above sea level. The current intensity of negative CG lightning initially decreased and subsequently increased with elevation and was negatively correlated with the variation in negative CG lightning density by elevation, with the minimum value (33.3 kA) appearing between 1900 and 2000 m where the peak value of negative CG lightning density appeared. The CG lightning activity in Yunnan Province was dominated by negative CG lightning, and the distribution of electrical charges in the thunderstorm cloud was negative–positive from the lower to the upper layers. The typical plateau topography facilitated rapid accumulation of the energy of low-layer negative electric charge and rapid formation of the CG lightning channel, causing the discharge process to occur when current intensity was still weak. This finding is basically consistent with Li (2011), who concluded that the variation in the current intensity of negative CG lightning and elevation tended to be stable at approximately 40 kA. In regions whose elevation >2000 m, as the elevation increased, the average current intensity of negative CG lightning increased slowly and linearly. CG lightning activity in high-elevation regions mainly occurred from local convection caused by solar radiation. As the elevation increased, water vapor content continuously decreased, and the energy required for accumulating electric charge in the cloud to form the CG lightning channel was high relative to that of the low-elevation regions, resulting in the linear increase of current intensity with elevation in high-elevation regions. In lower regions with elevation <1000 m, compared with the special topography in Yunnan Province, descending motion dominated the airflow. Because of the higher elevation differences between the troposphere and ground level, thunderstorms could release their energy after fully maturing, causing the relatively strong current intensity of negative CG lightning in low-elevation regions.

Distribution of terrain slope and the current intensity of CG lightning

The topography of Yunnan Province has five major characteristics: plateau waviness, mountains speckled with valleys, staircase-like decreases, fault basins, and rivers and lakes dividing the region. Relatively large fluctuations in terrain slope are present in

http://www.aloki.hu ● ISSN 1589 1623 (Print) ● ISSN 1785 0037 (Online)
DOI: http://dx.doi.org/10.15666/aeer/1605_63496367
© 2018, ALÖKI Kft., Budapest, Hungary

regions with different elevations, and *Figure 6b* shows the variation in the average current intensity of CG lightning over terrain slope.

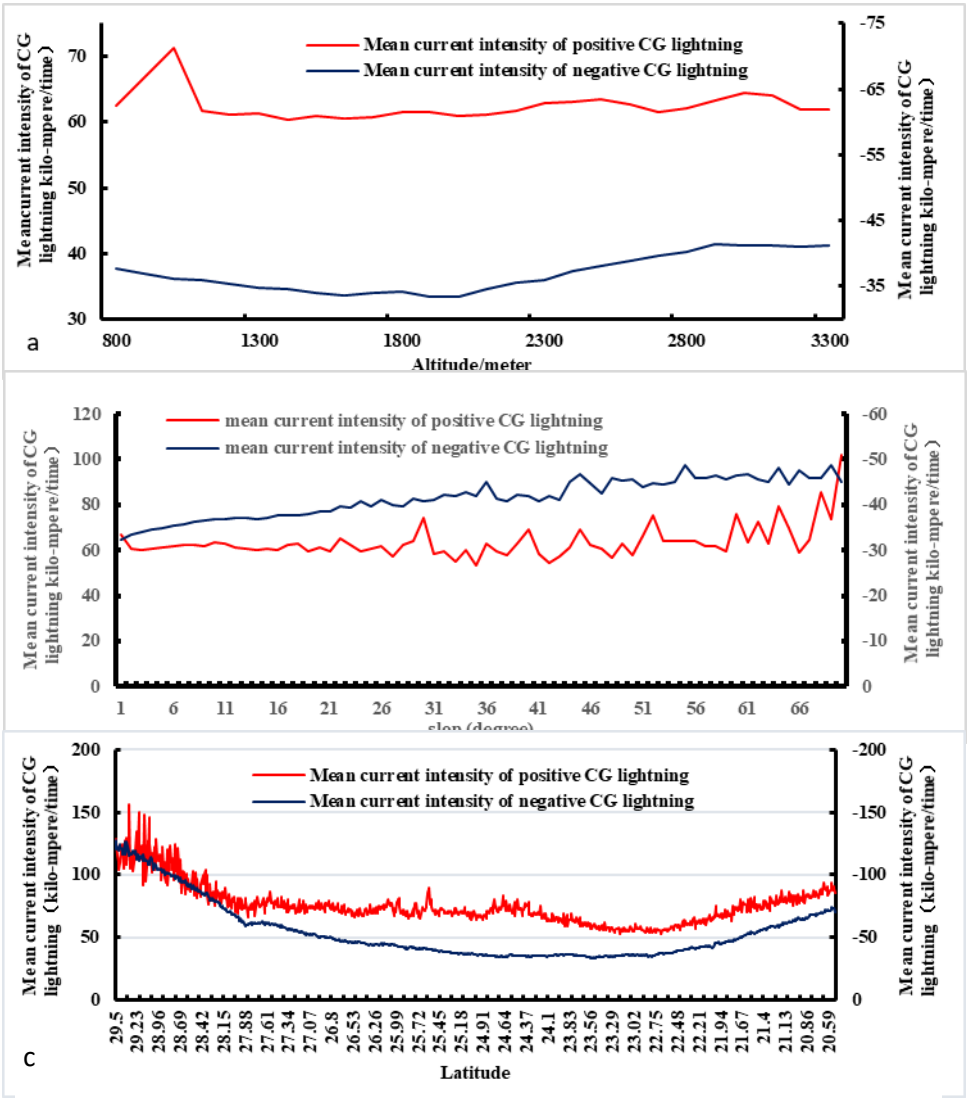

Figure 6. *Variation in average current intensity of CG lightning with elevation and terrain slope from 2017–2016. a: variation in average current intensity of negative/positive CG lightning with elevation; b: variation in average current intensity of negative/positive CG lightning with terrain slope; c: variation in average current intensity of negative/positive CG lightning with latitude*

The average current intensity of negative CG lightning increased linearly with terrain slope, and in the basins and smooth regions with terrain slope <20°, the average current intensity of negative CG lightning was <40 kA. However, the average current intensity of negative CG lightning in regions with terrain slope >20° exhibited fluctuating increases, further indicating the dipolar characteristics of the electric charge distribution of thunderstorms of Yunnan Province, which means that the lower layers were mostly negatively charged, and as the terrain slope increased, the water vapor carried in the ascending airflow gradually decreased. Furthermore, negative electric charge

http://www.aloki.hu ● ISSN 1589 1623 (Print) ● ISSN 1785 0037 (Online)
DOI: http://dx.doi.org/10.15666/aeer/1605_63496367
© 2018, ALÖKI Kft., Budapest, Hungary

accumulation increased the energy of CG lightning discharge, resulting in the linear increase of current intensity of negative CG lightning in regions with steep terrain slope. Additionally, the larger mountains in Yunnan Province are mostly distributed in the high-elevation regions. Generally, the current intensity of positive CG lightning was 20 kA stronger than that of the negative CG lightning, whereas the linear variation slope of average current intensity was less than that of negative CG lightning, indicating an obvious stronger energy requirement for positive lightning discharge in the upper troposphere. In areas of flat terrain with slopes of <30°, the average current intensity of positive CG lightning fluctuated slightly between 60 and 63 kA. Although the average current intensity of positive CG lightning fluctuated between 53 and 75 kA in regions where the terrain slope was between 30° and 60°, which was related to the drastic change in elevation in these regions. The average current intensity of positive CG lightning in regions with terrain slope >60° increased significantly. Both the current intensities of positive and negative CG lightning showed a significant linear positive change with variation in terrain slope. Where slopes are steeper, more energy is required to generate CG lightning, resulting in more infrequent CG lightning but with stronger current intensity on steep slopes. The current intensity of positive CG lightning was larger than that of negative CG lightning but the variable slope was smaller. The center of negative electric charge was located in the lower layer of the thunderstorm cloud, and negative CG lightning was more easily affected by topography.

Distribution of latitude and the current intensity of CG lightning

The distribution of electric charge in cumulonimbus cloud was as follows: the lower layer between 0 and -20 °C was the negative charge accumulation area, and the higher layer between -20 and -50 °C was the positive accumulation area. For a given amount of electric charge, a pilot stroke with a small distance to the ground could reach the ground to form a CG lightning bolt easily; the energy requirement was small, and the chance of CG lightning formation was small if the distance to the ground was large and the energy required for CG lightning discharge was relatively large. The current intensity of positive CG lightning in Yunnan Province was significantly larger than that of the negative CG lightning because the number of return stroke of positive CG lightning was significantly less than that of the negative CG lightning. The current intensity decreases rapidly due to multiple discharges caused by multiple flashbacks (Xie, 2013). The average current intensity of positive/negative CG lightning initially decreased and subsequently increased as latitude increased. In the low latitude regions south of 23°N, the average current intensity of positive CG lightning decreased from 85 kA to 55 kA as latitude increased. Regions between 23°N and 27°N in Yunnan are areas of frequent intense convection, which significantly increased the development of positively charged particles in the cloud and caused the average current intensity of positive CG lightning to increase with fluctuations. The regions north of 27.8°N in Yunnan Province include the snow mountains in the northwest with elevations >3000 m and the river valleys with elevations <1000 m, where the terrain slope was steeper and the amount of CG lightning was lower; thus, the current intensity of CG lightning increased linearly with latitude. The variation in average current intensity of negative CG lightning with latitude fluctuated less. In the low latitude regions, the 0 °C level height was relatively high, and the average current intensity was stronger. Additionally, within the range 23°N–27°N, the convergence of the cold and warm air caused severe convection, reducing the 0 °C level height; therefore, the average current intensity weakened obviously to

http://www.aloki.hu ● ISSN 1589 1623 (Print) ● ISSN 1785 0037 (Online)
DOI: http://dx.doi.org/10.15666/aeer/1605_63496367
© 2018, ALÖKI Kft., Budapest, Hungary

approximately -35 kA, and the negative CG lightning current intensity increased linearly to 100 kA where latitude >27°N.

The current intensity of CG lightning in Yunnan Province was obviously affected by the combination of topography, terrain slope, and latitude. South of 23°N, the topography was mainly basins, river valleys, and hills with steep terrain slope, low elevation, and high 0 °C level height; thus, the current intensity of CG lightning was relatively strong. Regions between 23°N and 27°N were mainly basins and hills with less steep terrain slope and elevation of approximately 1900–2100 m; because of the decrease in 0 °C level height caused by more active cold air, the current intensity of CG lightning was relatively weak. North of 27°N were the snowy mountains with high elevation and steep terrain slope and river valleys with low elevation and steep terrain slope where forming convection currents was more difficult; therefore, the current intensity of CG lightning was obviously stronger.

Relationship between CG lightning activity and topography in the central Yunnan region

Previous analysis revealed that CG lightning activity was highly concentrated in basins and placid hills whose elevation was between 1500 and 2300 m with terrain slope <30°. Of these areas, the central Yunnan region was the most active for CG lightning activity. In this study, CG lightning data on more than 20,000 grids with a definition of 0.01° × 0.01° ranging within 101.6°N–103.6°E and 24.5°N–25.5°N were chosen and analyzed.

Figure 7a shows the variation in CG lightning density over elevation in central Yunnan and reveals that within the elevation range of 1100–2700 m, the average CG lightning density was positively linearly correlated with elevation ($R = 0.65$) because as elevation increased, the CG lightning density increased.

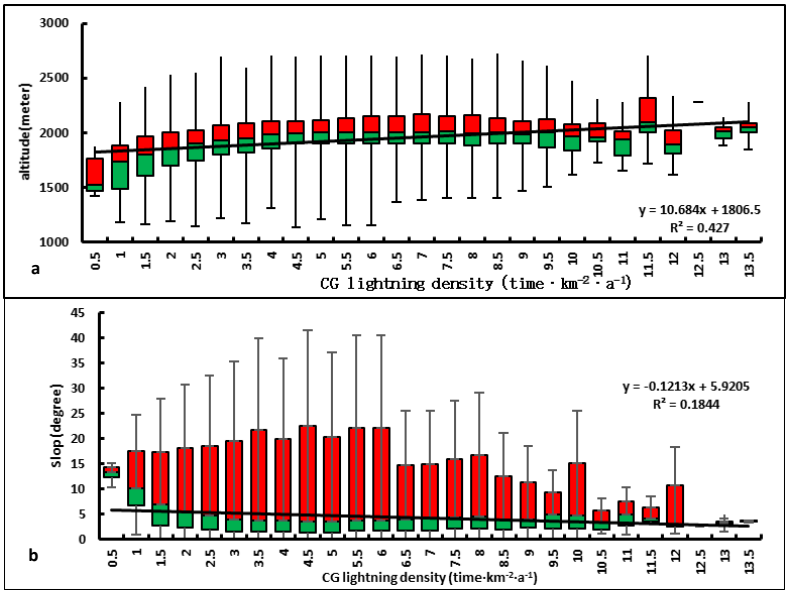

Figure 7. *Correlation between CG lightning densities with elevation and terrain slope in grid of 0.01°× 0.01° and using 0.5 time·km^{-2}·a^{-1} as intervals in central Yunnan. The variation range of CG lightning densities was 0.5-13.5 time·km^{-2}·a^{-1}; a: the correlation parameter of average CG lightning densities and elevation was 0.65; b: the correlation parameter of CG lightning densities and terrain slope was 0.43*

http://www.aloki.hu ● ISSN 1589 1623 (Print) ● ISSN 1785 0037 (Online)
DOI: http://dx.doi.org/10.15666/aeer/1605_63496367
© 2018, ALÖKI Kft., Budapest, Hungary

Furthermore, areas with a lower CG lightning density were mainly concentrated within the elevation range of 1400–1800 m, whereas areas with a higher CG lightning density were mainly concentrated within the elevation range of 1800–2000 m. However, the CG lightning density was inversely correlated with the change in the terrain slope (R = *0.43*). CG lightning activity with a density <6 events·km^{-2}·a^{-1} was vastly spread between terrain with slope ranging 3°–24°, whereas CG lightning activity with density >10 events·km^{-2}·a^{-1} was mainly distributed over the terrain with slope ranging 2°–12°.

The variation characteristics of current intensity of CG lightning over elevation in this region were generally the same as the variation characteristics of the entire province (see *Fig. 7b*); the current intensity of negative CG lightning was weaker, and the positive current intensity was approximately twice the negative current intensity. Additionally, as the elevation increased, the current intensity increased slowly. The variation in current intensity of CG lightning over terrain slope in this region was relatively complicated because the average negative current intensity initially increased and subsequently decreased, whereas the current intensity of positive CG lightning stabilized at 53–56 kA with terrain slope <20° and fluctuated violently with terrain slope >20° (*Fig. 8*).

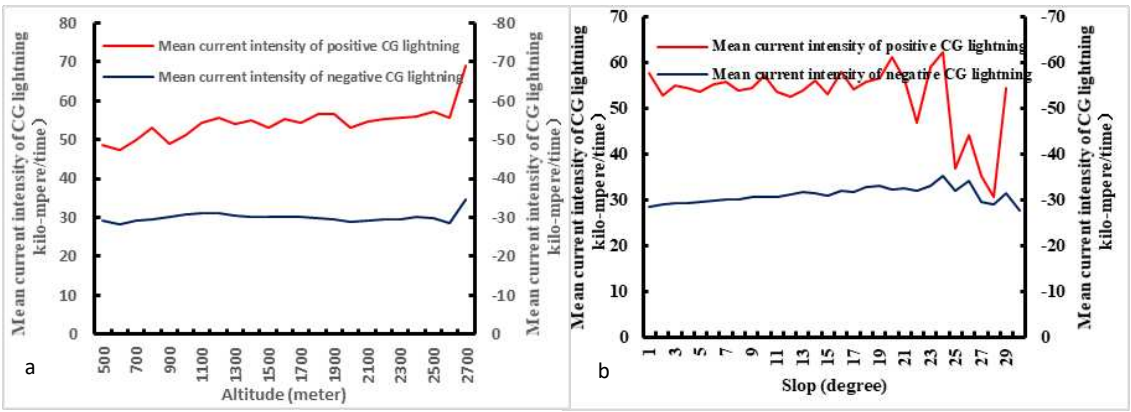

Figure 8. *Correlations between average current intensity of CG lightning, elevation, and terrain slope in 0.01°× 0.01° intervals in the central Yunnan region. a: Variation in current intensity with elevation; b: Variation in current intensity with terrain slope*

Relationship between CG lightning activity and topography in specific regions

CG lightning data, topography, and terrain slope of fixed zonal and meridional cross-sections along the central Yunnan region where CG lightning activity was dense were selected for further analysis. The east-west cross-section of 25.2°N was chosen for analysis of the synoptic systems and CG lightning activity, whereas the influence of the greater elevation and slope difference was analyzed using the north-south cross-section of 102.5°E. In *Figure 9a,* from east to west in the zonal cross-section, the elevation remained stable at approximately 2000 m and the CG lightning density in 101.6°E–103.6°E exhibited clear peaks, indicating that the main synoptic systems and the CG lightning densities exhibited a positive correlation within this longitude range. The CG lightning densities and terrain slope of the corresponding area exhibited a significant inverse correlation (see *Fig. 9c*) as the CG lightning densities increased and the terrain slope decreased, and vice versa. From the south to the north in the meridional cross-

http://www.aloki.hu ● ISSN 1589 1623 (Print) ● ISSN 1785 0037 (Online)
DOI: http://dx.doi.org/10.15666/aeer/1605_63496367
© 2018, ALÖKI Kft., Budapest, Hungary

section, the elevation fluctuated and increased from 23.4°N–25.5°N (see *Fig. 9b*) and exhibited a positive correlation with the corresponding CG lightning densities; however, the terrain slope initially increased and subsequently decreased within this area (see *Fig. 9d*) and was inversely correlated with the CG lightning densities. In summary, the CG lightning activity in Yunnan had a favorable correlation with the topography and terrain slope, particularly in the area between 101.6°E–103.6°E and 24°N–25.5°N because the CG lightning densities were correlated with elevation and inversely correlated with terrain slope. Furthermore, the effect of the large-scale strong convective synoptic systems was most significant in this same area.

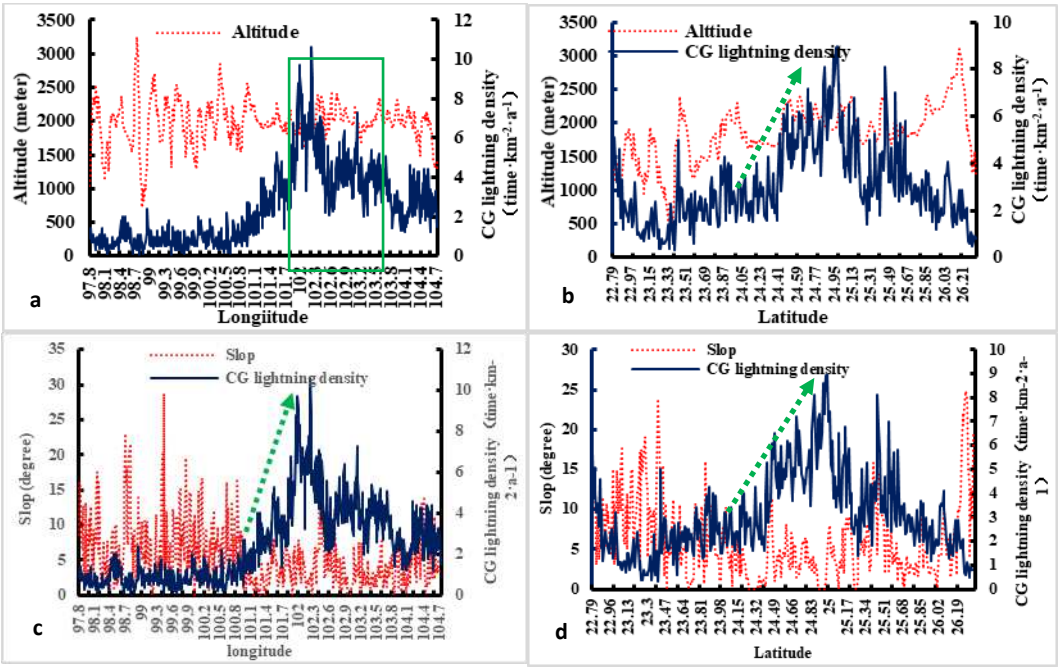

Figure 9. *Relationship between CG lightning densities and elevation and terrain slope along the zonal cross-section of 25.2°N and the meridional cross-section of 102.5°E. a: CG lightning densities and elevation in cross-section of 25.2°N; b: CG lightning densities and elevation in cross-section of 102.5°E; c: CG lightning densities and terrain slope in cross-section of 25.2°N; d: CG lightning densities and terrain slope in cross-section of 102.5°E*

Hourly variation characteristics of CG lightning activity at different elevations

Figure 10 shows the diurnal variation in the average CG lightning frequency in Yunnan from 2007 to 2016 with 100-m increments of elevation to further elucidate the contributions of the topography. The dense area of CG lightning is an elliptical shape 600–3500 m above sea level, indicating that as the elevation increases, the effect of the large-scale convection systems decreases. Low-elevation areas dominated by topography (<600 m) were night thunderstorm hotspots and generally occurred between 21:00 and dawn on the subsequent day. Affected by the topography, terrain slope, and elevation, the main forming and enhancement period of large-scale strong convective systems in Yunnan Province was between afternoon and midnight, which corresponded to the period of enhancement of convection caused by solar radiation (Xu et al., 2011; Zhang et al., 2013). The double influence of topography and large-scale strong convection system aggravated the CG lightning activity, resulting in the consistent

http://www.aloki.hu ● ISSN 1589 1623 (Print) ● ISSN 1785 0037 (Online)
DOI: http://dx.doi.org/10.15666/aeer/1605_63496367
© 2018, ALÖKI Kft., Budapest, Hungary

large-amplitude variation characteristics of CG lightning in Yunnan Province at 600–3500 m above sea level, and in low (high) elevation areas where elevation was lower than 600 m (higher than 3500 m), the effect of topography on CG lightning activity was more significant.

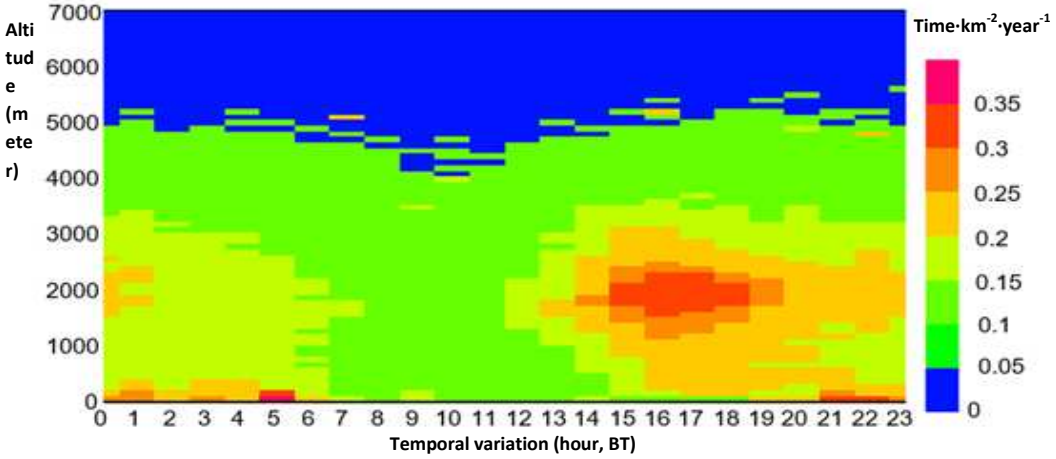

Figure 10. *Diurnal variation of the average CG lightning frequency (with elevation range from 0–7000 m and using 100 m as intervals)*

Discussion and conclusion

CG lightning activity was normally distributed along the variation in elevation, which centered on 2000 m above sea level and decreased on both sides and which exhibited linear inverse correlation characteristics between terrain slopes because when the terrain slope is less steep, the CG lightning activity is relatively dense. Regions of elevation <2300 m were generally basins, river valleys, or hills, and their corresponding CG lightning densities were approximately twice as high as those in regions whose elevation >2300 m. Within these regions, the uplift effect in areas with terrain slope from 30° to 59° could cause smaller peaks of CG lightning activity, and no significant CG lightning activity was observed in areas with terrain slope >60°. However, in regions where elevation >2300 m, the topography was mainly basins and large mountains. Furthermore, a blank zone was observed in areas with terrain slope 40°–50°, and only sporadic CG lightning activity was observed on the windward side of mountain areas with terrain slope >60°, indicating the substantial influence of topography on CG lightning activity. Furthermore, the results showed that the CG lightning activity in Yunnan Province initially increased and subsequently decreased with the increase of latitude, indicating that the influence of topography and large-scale synoptic systems was larger than the influence of variations in solar radiation along latitude.

The electric charge distribution in thunderstorms in Yunnan exhibited a typical positive dipole characteristic, and the average current intensity of positive CG lightning was significantly greater than that of negative CG lightning. Furthermore, the positive charge was located in the upper layers of the thunderstorm cloud; thus, the average current intensity fluctuated stably within a small range, 60–63 kA, as the elevation varied and the current intensity of negative CG lightning initially decreased and subsequently increased with the change in elevation and was inversely correlated with

http://www.aloki.hu ● ISSN 1589 1623 (Print) ● ISSN 1785 0037 (Online)
DOI: http://dx.doi.org/10.15666/aeer/1605_63496367
© 2018, ALÖKI Kft., Budapest, Hungary

CG lightning densities. The current intensity of CG lightning increased linearly with the increase of terrain slope, and the slope of variation of positive CG lightning was less than that of negative CG lightning, indicating that the effect of topography on the current intensity of negative CG lightning was more significant than that of the positive CG lightning in lower layers. The variation in intensity of CG lightning with latitude was inversely correlated with the variation in CG lightning density. South of 23°N, the current intensity was strongly affected by solar radiation and the relatively high 0 °C level height and greatly affected by the uplift effect of the large mountains. The current intensity was relatively strong north of 27°N. Within 23°N–27°N, affected by the impact of the large-scale synoptic systems and the low 0 °C level height, the current intensity was relatively weak.

The present study on the relationship between CG lightning activity and topography in central Yunnan, which is greatly influenced by large-scale synoptic systems, found a favorable positive correlation between the CG lightning density and elevation in the range 1100–2700 m; it was inversely correlated with the variation in terrain slope steeper than 40°. The variation in current intensity was essentially the same as reported in previous studies.

Analysis of CG lightning activity and topography in zonal and meridional cross-sections revealed that the CG lightning activity was positively correlated with elevation less than 2500 m, but was inversely correlated with terrain slope less than <15°.

Acknowledgements. Funded by the National Natural Science Foundation of China (41641044) and Technological and Planning Project of Yunnan Province (2015FB166, 2016RA096).

REFERENCES

[1] Biagi, C. J., Cummins, K. L., Kehoe, K. E., Krider, E. P. (2007): National Lightning Detection Network (NLDN) performance in southern Arizona, Texas and Oklahoma in 2003–2004. – J. Geophys. Res. 112: D05208.

[2] Bourscheidt, V. Pinto Junior, O., Naccarato, K. P., Pinto, I. R. C. A. (2009): The influence of topography on the cloud-to-ground lightning density in South Brazil. – Atmospheric Research 91(2009) 508–513.

[3] Chen, W. M. (2003): Theory of Lightning. – China Meteorological Press, Beijing.

[4] Egger, J., Hoinka, K. P. (1992): Fronts and orography. – Meteor. Atmos. Phys. 48: 3–36.

[5] Ezcurra, A., Areitio, J., Herrero, I., (2002): Relationships between cloud-to-ground lightning and surface rainfall during 1992–1996 in the Spanish Basque Country area. – Atmos. Res. 61(3): 239–250.

[6] Jayaratne, E. R., Kuleshov, Y. (2006): Geographical and seasonal characteristics of the relationship between lightning ground flash density and rainfall within the continent of Australia. – Atmos. Res. 79: 1–14.

[7] Li, W. L., Qie, X. S., Fu, S. M. (2016): Simulation of quasi-linear mesoscale convective systems in northern China: Lightning activities and storm structure. – Advances in Atmospheric Sciences 33(1): 85–100.

[8] Li, Z. (2011): Characteristics of Lightning Activity in Chongqing Affected by The Analysis of Underlying Surface. – Master of Science Thesis, Nanjing University of Information Engineering.

[9] Ma, M., Tao, S. C., Zhu, B. Y., Lv, W. T. (2004): The climate distribution of lightning density in China and surrounding areas observed by satellites. – Science in China Ser. D Earth Sciences 34(4): 298–306.

http://www.aloki.hu ● ISSN 1589 1623 (Print) ● ISSN 1785 0037 (Online)
DOI: http://dx.doi.org/10.15666/aeer/1605_63496367
© 2018, ALÖKI Kft., Budapest, Hungary

[10] Monmonier, M. S. (1982): Computer-Assisted Cartography. – Prentice-Hall, Englewood Cliffs, NJ.
[11] Pinto Jr., O., Pinto, I. R. C. A., Gomes, M. A. S. S., Vitorello, I., Padilha, A. L., Diniz, J. H., Carvalho, A. M., Cazetta Filho, A. (1999): Cloud-to-ground lightning in Southeastern Brazil in 1993. - 1. Geographical distribution. – J. Geophys. Res. 104(D24): 31369–31379.
[12] Qie, X. S., Zhang, T. L., Zhang, G. S. (2009): Electrical characteristics of thunderstorms in different plateau regions of China. – Atmospheric Research 91(2–4): 244–249.
[13] Qie, X. S., Zhou, D., Tie, Y. (2003): Global lightning activities and their regional differences observed from the satellite. – Chinese Journal of Geophysics 46(6): 743–751.
[14] Qie, X. S., Wang, Z. C., Wang, D. F. (2013): Characteristics of positive cloud-to-ground lightning in Da Hinggan Ling forest region at relatively high latitude, northeastern China. – Journal of Geophysical Research-Atmospheres 118(24): 13393–13404.
[15] Schulz, W., Diendorfer, G., (1999): Lightning characteristics as a function of altitude evaluated from lightning location network data. – Proceedings of the International Conference on Lightning and Static Electricity (ICOLSE). Society of Automotive Engineers, Toulouse, France.
[16] SEMC (2002): Rio Grande do Sul: atlas eólico. – Secretaria de Energia, Minas e Comunicações, Brasil.
[17] Smith, R. B., (1979): The Influence of Mountains on the Atmosphere. – In: Saltzman, B. (ed.) Advances in Geophysics. Academic Press Inc., New York, pp. 87–230.
[18] Soula, S., Chauzy, S., (2001): Some aspects of the correlation between lightning and rain activities in thunderstorms. – Atmos. Res. 56: 355–373.
[19] Tong, H. W., Fan, G. W., Wang, H. T. (2008): The characteristics of the lightning activity and its relationship with topography and climate in Zhejiang province. – Power System Technology 6: 9–100.
[20] Wagner, G., Fuelberg, H. E., Kann, D., Wynne, R., Cobb, S., (2006): A GIS-based approach to lightning studies for West Texas and New Mexico. – Proceedings of the Second Conference on Meteorological Applications of Lightning Data. American Meteorological Society, Atlanta.
[21] Wang, L. L., Qie, X. S., Shen, M. F. (2016): Simulation of quasi-linear mesoscale convective systems in northern China: lightning activities and storm structure. – Advances in Atmospheric Sciences 33(1): 85–100.
[22] Xie, Y. R., Xu, K., Zhang, T. F., Liu, X. T. (2013): Five-year study of cloud-to-ground lightning activity in Yunnan province, China. – Atmospheric Research 129–130: 49–57.
[23] Xu, M. L., Duan, X., Qi, M. H. (2011): Yunnan Weather Forecaster Handbook. – China Meteorological Press, Beijing.
[24] Zajac, B. A., Rutledge, S. A., (2001): Cloud-to-ground lightning activity in the contiguous United States from 1995 to 1999. – Mon. Wea. Rev. 129 5): 999–1019.
[25] Zhang, T. F., Yin, L. Y., Xie, Y. R. (2013): Study and application of lightning monitoring and warning method in low latitude plateau area. – China Meteorological Press, Beijing.

http://www.aloki.hu ● ISSN 1589 1623 (Print) ● ISSN 1785 0037 (Online)
DOI: http://dx.doi.org/10.15666/aeer/1605_63496367
© 2018, ALÖKI Kft., Budapest, Hungary

ACTIVITY CHARACTERISTICS OF SULFATE REDUCING BACTERIA AND FORMATION MECHANISM OF HYDROGEN SULFIDE

DENG, Q.[1,2,3*] – WU, X.[2] – WANG, Y.[2] – LIU, M.[1,2]

[1]*State Key Laboratory Cultivation Base for Gas Geology and Gas Control, Henan Polytechnic University, 454003 Jiaozuo, P. R. China*

[2]*School of Safety Science and Engineering, Henan Polytechnic University 454003 Jiaozuo, P. R. China*

[3]*Collaborative Innovation Center of Coal Safety Production of Henan Province 454003 Jiaozuo, P. R. China*

**Corresponding author*
e-mail: dengqigen@hpu.edu.cn; phone: +86-391-398-6252; fax: +81-391-398-7881

(Received 31st May 2018; accepted 13th Sep 2018)

Abstract. Various anaerobic environments exist in the Earth's ecosystem, which can produce a great deal of organic matter each year. In anaerobic habitats, bacterial sulfate reduction may occur due to the action of sulfate-reducing bacteria. As a result, hydrogen sulfide (H_2S) is formed. This paper focuses on sulfate-reducing bacteria and the revision of the activity characteristics of these bacteria in the reducing environment. It discusses the metabolic process of sulfate-reducing bacteria using sulphate and organo-sulfur compounds as sulfur source, the mechanism of bacterial sulfate reduction and H_2S formation mechanism. There are two main ways of H_2S formation in sulfate-reducing bacteria, the production of metabolic sulphate and the metabolic organo-sulfur compounds (mainly cysteine). The paper, combined with the activity characteristics of sulfate-reducing bacteria and the pathway of metabolic formation of H_2S, also discusses the circulation of sulfur in the environmental system of the Earth due to the action of sulfate-reducing bacteria, concerning the redox zone division in submarine sedimentary strata and landfills, the biogas formation phase of sulfate-reducing bacteria metabolism in sedimentary formations, and the bacterial sulfate reduction action in salt lakes (seawater) systems. Moreover, the production of hydrogen sulfide and the formation model of dolomite are both presented here. The findings support that sulfate-reducing bacteria are the most important biological source of H_2S production. The study of the physiological characteristics of sulfate-reducing bacteria and the formation mechanism of H_2S due to bacterial sulfate reduction can provide useful reference for the exploration of the laws of sulfur geochemical cycle and the rules of the ecological environment, which is essential for the protection of the natural environment and the restoration of polluted ecosystems, and can also provide a useful reference for the control of aerobic microorganisms.
Keywords: *microorganism, hydrogen sulfide (H_2S), bacterial sulfate reduction, formation mechanism*

Introduction

Hydrogen sulfide is mostly the product of the decomposition of organic matter under the microorganisms' action, the action of bacterial sulfate reduction (BSR), or the chemical process byproducts (Deng, 2017). The sulfate-reducing bacteria absorbs sulfate without the participation of oxygen, obtains energy from the oxidation of organic compound and discharges H_2S produced by the reduction of sulfate, which metabolic process is defined as bacterial sulfate reduction (Machel, 2001; Orr, 1974). The gaseous pollutant of H_2S mainly comes from man-made pollution and natural pollution. Man-made pollution mainly includes exploitation of petroleum, coal-bed methane, shale gas

http://www.aloki.hu ● ISSN 1589 1623 (Print) ● ISSN 1785 0037 (Online)
DOI: http://dx.doi.org/10.15666/aeer/1605_63696383
© 2018, ALÖKI Kft., Budapest, Hungary

etc, mining and non-ferrous metal smelting, low-temperature coking of coal, extraction of sulfur-containing substances, rubber, leather, dyes and other industrial production. Natural pollution often exists in many anaerobic environments in the Earth's ecosystems, such as underground pipeline, rice fields, industrial effluent, mud, swamps, lake bottom sediments, oil and gas wells, hot springs, landfills, and farm excretion, deposits and other venues (Martins et al., 2009).

The hazards of H_2S are mainly manifested in the following two aspects:

(1) Hazards to health. H_2S, a polar molecule, is highly toxic and flammable. It is colorless, smelly and prone to explosion. A small amount of H_2S in high concentration inhaled can be fatal to a person in a short time (Wei et al., 2014; Deng et al., 2018). And H_2S in low concentration affects the eye, respiratory and central nervous system badly. The physiological effects of H_2S concentration and contact time on human body are shown in *Figure 1* (Wei et al., 2014).

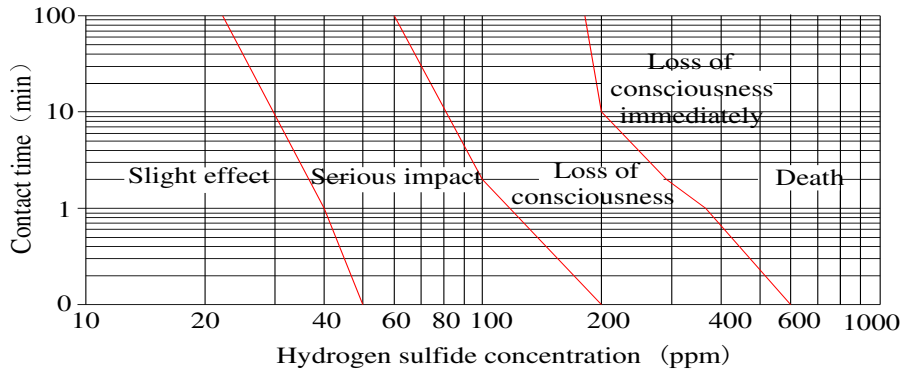

Figure 1. *Physiological influence to human of H_2S*

(2) Pollution to the environment. In the combustion process or in the atmosphere, H_2S will be quickly oxidized to sulfur dioxide, which will increase the concentration of SO_2 in the atmosphere to damage the plants and animals. Furthermore, it is also the main reason for the formation of acid rain (smog). Sulfate-reducing bacteria (SRB) is considered to be one of the main causes of corrosion of industrial equipment (Wei et al., 2014). H_2S in the water and air has a strong corrosion effect on concrete, electrical equipment, pipe networks, metals and plastics. When the H_2S content in the water exceeds 0.5 to 1.0 mg/L, it will cause great harm to the aquaculture (Ren et al., 2009).

H_2S is estimated to account for 100 million tons into the atmosphere per year in the world, of which about 3 million tons are produced annually by humans. The majority of the remaining H_2S produce naturally, mainly derived from the metabolic activities of producing H_2S sulfate-reducing bacteria. Therefore, SRB is the most important biological source for H_2S production. Therefore, the study on the physiological characteristics of SRB and the formation mechanism of H_2S under BSR can provide reference for revealing the laws of sulfur geochemical cycling and ecological environment.

Activity characteristics of SRB

The group SRB is heterotrophic and mixed that can utilise sulfates, sulfites, thiosulfates, sulfur, or other oxidized sulfides as electron acceptors to catabolize organic

http://www.aloki.hu ● ISSN 1589 1623 (Print) ● ISSN 1785 0037 (Online)
DOI: http://dx.doi.org/10.15666/aeer/1605_63696383
© 2018, ALÖKI Kft., Budapest, Hungary

materials and form H_2S (Gibson, 1990; Xiao et al., 2011). 18 genera and more than 40 species of SRB have been studied respectively. The names and characteristics of some genera are shown in *Table 1* (Ren et al., 2009; Liao, 2004). The common 9 genera mainly involve Desulfovibrio which does not produce spores and Desulfotomaculum which produce spores. The former is generally medium or low temperature, and it is likely to die when the temperature exceeds 43 °C. The latter is generally medium temperature or high temperature (Luptakova et al., 2005).

Table 1. *Characteristics of SRB*

Name	Features	Exercisability	Growth T (°C)
Desulfovibrio	No spores, curved rods	+	25-40
Desulfomicrobium	Rod-shaped, no spores	+/-	25-40
Desulfobollus	curved	+/-	
Desulfotomaculum	Straight or curved rod	+	25-40, 40-65
Desulfobacter	Round, rod-shaped, without spores	+/-	20-23
Desulfococcus	Spheroidal, no spores	-/+	28-35
Desulfosarcina	Stacking, without spores	+/-	33
Desulfoarculus	curved	+/-	
Desulfomonile	Rod-shaped, spheroidal	-	37
Desulfobulbus	Oval, shape of Lemon, No spores	-/+	25-40
Desulfacinum	Spheroidal or oval type		
Thermodesul fobocterium	Small shape, arc, rod		65-70
Desulfobacula	Oval		
Desul fonema	Screw shape, no spores	slide	28-32
Desulfobacterium	Round, rod-shaped	+/-	20-35

The group SRB is heterotrophic and mixed, and it survives in facultative anaerobic environment. The suitable grow temperature is between -5 and 75 °C. Some strains can grow below -5 °C, and some with spore species can withstand high temperatures of 80 °C. The optimum growth temperature for most mesophilic SRB is 28 ~ 38 °C, and some can grow in the condition of 45 °C (Larry, 1995). The surviving pH value of SRB is 4 to 9.5. Most SRBs are neutrophils. The most suitable pH is 6.5 ~ 7.8 (Vallero et al., 2005). SRB can survive in salinity greater than 1 g/L water. The best growth salinity is 100 g/L, and the upper limit reaches to 240 g/L. Some SRBs are halophilic, and they can be detected in some high-salt (such as salt lakes, the Dead Sea) ecosystems. Most of the halophilic bacteria isolated in the laboratory are mild halophilic bacteria (suitable salinity ranged from 1 to 4%), and rarely isolated moderately halophilic bacteria (Zhao et al., 1995). The growth of SRB is generally lower than -150 mV in Eh (Barton et al., 1995). Fe^{2+} is the active component of various enzymes in SRB cells. Decreasing the concentration of Fe^{2+} ions can reduce the growth rate of SRB.

The carbon sources used by different strains of SRB are different. The carbon source not only increases the amount of bioenergy required, but also acts as an electron donor to reduction and dissimilation sulfates. The most common source is the use of C_3, C_4 fatty acids. In addition, the sources as some volatile fatty acids and easily fermented substances are also applied. Stephenson et al. (Stephensonl et al., 1931) presented that

http://www.aloki.hu ● ISSN 1589 1623 (Print) ● ISSN 1785 0037 (Online)
DOI: http://dx.doi.org/10.15666/aeer/1605_63696383
© 2018, ALÖKI Kft., Budapest, Hungary

hydrogenases contained in SRBs and (Jannasch, 1988) illustrated that 33 out of 39 SRBs can absorb hydrogen at 28 °C.

Formation mechanism of H_2S by SRB

SRB can produce H_2S by assimilation of sulfates, or degradation of sulfur-containing organics (mainly cysteine). The former has a small yield and is quickly assimilated into organic sulfur compounds. The latter, with a larger yield, is the main formation of H_2S (Luhachack et al., 2014).

The metabolic mechanism of sulfate as a sulfur source

The metabolic process of SRB with sulfate as sulfur source can be divided into three stages. Decomposition, electron transfer, and oxidation, as shown in *Figure 2* (Xu et al., 2009).

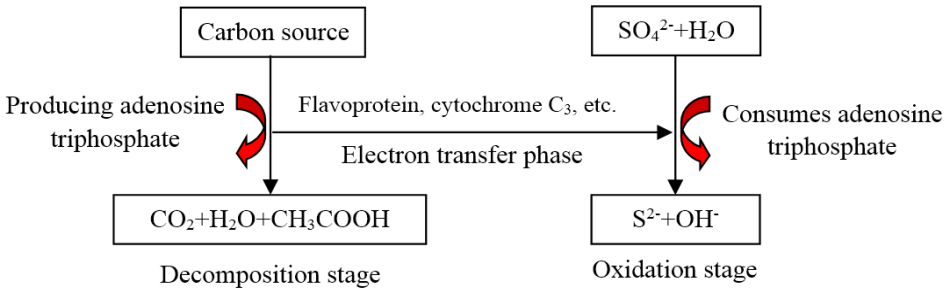

Figure 2. *The metabolic process of SRB with sulfate as a sulfur source*

(1) Decomposition stage. Sulfates are highly thermostable. Under anaerobic conditions, the sulfate ion (SO_4^{2-}) first accumulates out of cell and then enters the cell of SRB, while organics produce adenosine triphosphate (ATP) and energetic electrons through substrate level phosphorlation. Thereafter, SO_4^{2-} is activated by ATP sulfurylase to produce pyrophosphoric acid (PPi) and adenosine-5'-phosphosulfate (APS), PPi quickly decomposed into inorganic phosphate (Pi) (Zhao et al., 1997), stepwise reaction formulas are shown *Equation 1* and *2*, and total reaction formula is shown in *Equation 3*.

$$SO_4^{2-} + ATP + 2H^+ \xrightarrow{\text{ATP sulfurylase}} APS + PPi \quad \text{(Eq.1)}$$

$$PPi + H_2O \xrightarrow{\text{Pyrophosphatase}} 2Pi \quad \text{(Eq.2)}$$

$$SO_4^{2-} + ATP + 2H^+ + H_2O \rightarrow APS + 2Pi \quad \text{(Eq.3)}$$

(2) Electron transfer stage. In the previous stage, the energetic electrons released by energy are transferred step by step through SRB-specific electron transport chains (such as flavoprotein, cytochrome C_3, etc.). Affected by APS reductase, APS is continuously decomposed to sulfite and adenosine monophosphate (AMP). Sulfite is dehydrated into pyrosulfite ($S_2O_5^{2-}$). $S_2O_5^{2-}$ is extremely unstable and then would be converted to the intermediate dithionite ($S_2O_4^{2-}$). Afterwards, $S_2O_4^{2-}$ is rapidly reducted to trithionate

http://www.aloki.hu ● ISSN 1589 1623 (Print) ● ISSN 1785 0037 (Online)
DOI: http://dx.doi.org/10.15666/aeer/1605_63696383
© 2018, ALÖKI Kft., Budapest, Hungary

($S_3O_6^{2-}$), and $S_3O_6^{2-}$ is broken down to thiosulfate ($S_2O_3^{2-}$) and sulphite (SO_3^{2-}). The reaction formula is shown in *Equations 4–6,* and the electron transfer is shown in *Figure 3* (Bradley et al., 2011).

$$\text{E-FAD} + \text{Electronic carrier (RED)} \leftrightarrow \text{Electronic carrier (OX)} + \text{E-FADH}_2 \quad \text{(Eq.4)}$$

$$\text{E-FADH}_2 + \text{APS} \leftrightarrow \text{E-FADH}_2(SO_3^{2-}) + \text{AMP} \quad \text{(Eq.5)}$$

$$\text{E-ADH}_2(SO_3) \leftrightarrow \text{E-FAD} + SO_3^{2-} \quad \text{(Eq.6)}$$

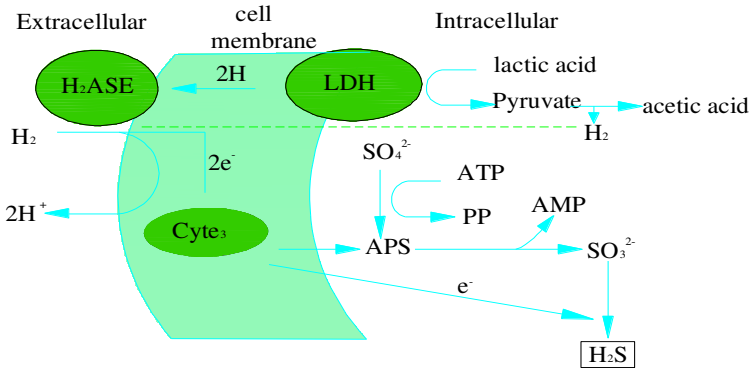

Figure 3. *Electron transfer process of SRB. ATP - adenosine triphosphate; PP - Polypyrrole; APS - adenosine-5'-phosphosulfate; AMP - adenosine monophosphate; LDH-lactate dehydrogenase*

(3) Oxidation stage. The electrons are transferred to the oxidized sulfur elements ($S_2O_3^{2-}$, SO_4^{2-}, SO_3^{2-}), which consume a lot of ATP. From SO_4^{2-} to S^{2-}, there are 8 electron transfers. ATP thiokinase catalyzes the adsorption of SO_4^{2-} to ATP phosphatase, which in turn forms APS. The sulfated portion of APS is directly reduced to sulfite and releases AMP. The initial product of sulfate reduction is sulfite. Once the sulfite is formed, the reaction process shown in *Figure 4* can be proceed (Bradley et al., 2011), finally producing H_2S, H_2S and the reaction formula is shown in *Equation 7*.

$$SO_4^{2-} + 8e^- + 10H^+ \rightarrow H_2S\uparrow + 4H_2O \quad \text{(Eq.7)}$$

The followings may be the reaction pathway from SO_3^{2-} to H_2S formation (Cai et al., 2009). (1) 3 consecutive two-electron transfer, forming $S_3O_6^{2-}$ and thiosulfate ($SO_3^{2-} \rightarrow S_3O_6^{2-} \rightarrow S_2O_3^{2-} \rightarrow S^{2-} \rightarrow H_2S$). (2) SO_3^{2-} directly lose 6 electrons, the above-mentioned intermediate product is not formed and is referred to as coordinated 6-electron reaction, namely $SO_3^{2-} + 6e^- + 8H^+ \rightarrow H_2S + 3H_2O$. (3) In the continuous two-electron transfer process, the reverse reaction may also occur. The reaction formula is shown in *Equation 8*.

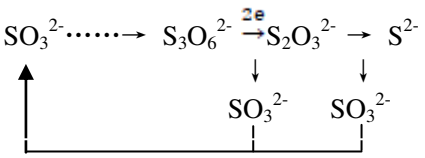

(Eq.8)

http://www.aloki.hu ● ISSN 1589 1623 (Print) ● ISSN 1785 0037 (Online)
DOI: http://dx.doi.org/10.15666/aeer/1605_63696383
© 2018, ALÖKI Kft., Budapest, Hungary

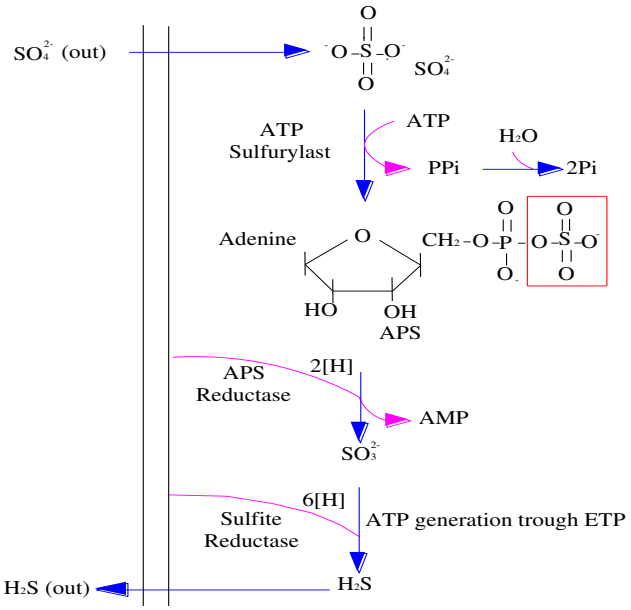

Figure 4. *Diagram of dissimilatory sulfate reduction. ATP - adenosine triphosphate; PPi - pyrophosphoric acid; Pi - inorganic phosphate; APS - adenosine-5'-phosphosulfate; AMP - adenosine monophosphate; ETP - electron transport particles*

SRB utilizes lactate as an electron donor and SO_4^{2-} as an electron acceptor for BSR action. There are three enzymes involved in the sulfite reduction process during the reduction of SO_3^{2-} to S^{2-}, namely $S_3O_6^{2-}$ forming enzyme, $S_3O_6^{2-}$ reductase or thiosulfate-forming enzyme and thiosulfate reductase. In BSR, SRB produces and accumulates large amounts of S^{2-} or HS^- in the cells. When the concentration of S^{2-} or HS^- in the cell reaches to a certain value, it will be released into the solution through the cell membrane, increasing the concentration of S^{2-} in the surroundings, which leads to the change in the redox potential of the environment and the concentration of related ions (Ren et al., 2009; Pérez et al., 2001). SRB metabolic H_2S formation process is shown in *Figure 5* (Peck et al., 1982).

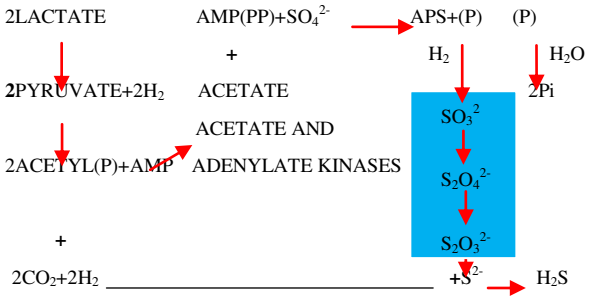

Figure 5. *Flowchart of SRB metabolism forming H_2S. Pi - inorganic phosphate; APS - adenosine-5'-phosphosulfate; P - Phosphorum*

The carbon of dibenzothiophene (DBT) as metabolic material is reacted with SRB to decompose the aromatic ring structure and form a sulfur-containing compound. The Kodama pathway is shown in *Figure 6* (Kodama et al., 2008).

http://www.aloki.hu ● ISSN 1589 1623 (Print) ● ISSN 1785 0037 (Online)
DOI: http://dx.doi.org/10.15666/aeer/1605_63696383
© 2018, ALÖKI Kft., Budapest, Hungary

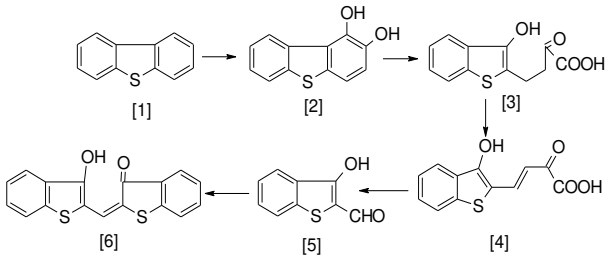

Figure 6. *Kodama pathway of metabolic mechanism of SRB use the carbon*

The metabolic mechanism of organo-sulfur compounds as a sulfur source

SRB is degraded by sulfur-containing organic substances (such as sulfur amino acids, cysteine, cysteine, sulfanilic acid, methionine, sulfonate, glutathione, etc.) as sulfur sources to produce H_2S. The degradation process differs depending on the types of SRB. Usually some SRBs will completely degrade some polymer-containing organic compounds to produce H_2S. Some will only degrade them into relatively low-molecular-weight sulfur-containing organic compounds such as mercaptans, and then other species. The SRB degrades it to the end product such as H_2S (Ren et al., 2001). The sulphur-containing organic degradation reaction can be summarized as shown in *Equation 9.*

$$\begin{array}{l} \text{R-SCH}_2\text{CHCOOH} \rightarrow \text{H}_2\text{S}\uparrow + \text{NH}_3\uparrow + \text{R-CH}_2\text{COOH} \\ \quad\quad | \\ \quad\quad \text{NH}_2 \end{array} \qquad \text{(Eq.9)}$$

The 4S pathway of sulfur metabolism (sulphoxide/sulphone/sulponate/sulphate) (Isbister et al., 1998). For different strains, the 4S pathway is not exactly the same, all of which have a common role in the C-S bond. For example, Rhodococcus sp. strain IGTS8 bacteria are considered to have two desulfurization pathways (Ma et al., 2000), as shown in *Figure 7.*

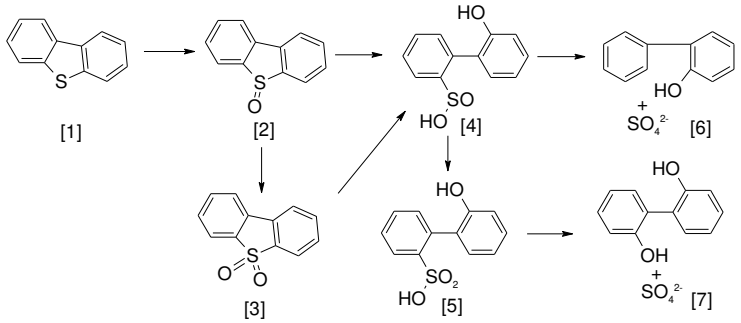

Figure 7. *The 4S pathway of Rhodococcus sp. strain IGTS8 bacterium*

The sulfur in DBT will generate SO_4^{2-}, SO_3^{2-} and 2, 2'- 2- Dihydroxybiphenyl or 2-hydroxybiphenyl and sulphur containing compounds after 4 steps.

http://www.aloki.hu ● ISSN 1589 1623 (Print) ● ISSN 1785 0037 (Online)
DOI: http://dx.doi.org/10.15666/aeer/1605_63696383
© 2018, ALÖKI Kft., Budapest, Hungary

Metabolic pathway of SRB

The sulfur cycle is an important geochemical cycle in the Earth's environmental system, and SRB plays an indispensable role in this system. The basic process can be described as the following (Rasch et al., 2000): when the onshore volcanic eruptions, sulfur in the earth's crust and magma is released into the atmosphere in the form of H_2S, sulfate and SO_2. Some of the sulfur emitted from the volcanic eruption of the submarine is dissolved in sea water and some of it is released into the atmosphere by gaseous sulfides. Sulfur in the atmosphere circulates through sulfuric acid or sulphate aerosols into the biosphere, pedosphere and hydrospheres. These sulphur compounds are then passively absorbed and assimilated by plants and animals. The absorbed sulfur forms the body of plants and animals. Animal and plant residues are decomposed by microorganisms, and sulfur becomes H_2S escaped into the atmosphere or deposited into peat. The reduction of sulphate in water is accomplished by reverse sulfidation of various sulfate-reducing bacteria. In the absence of oxygen, sulfates are produced into H_2S as hydrogen acceptors. Sulfate, H_2S and sulfur is mineralized under the common action of aqueous medium and organic matter to generate organic sulfide or inorganic sulfide. The sulfur cycle in global ecosystem is shown in *Figure 8* (Deng et al., 2013).

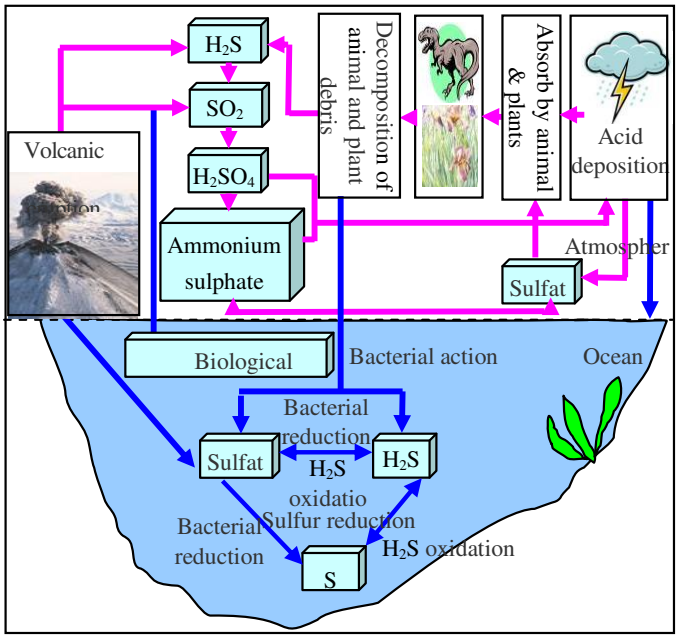

Figure 8. *Sulfur cycle in the Earth's environmental systems*

It has been known that due to the action of microorganisms, there are obvious redox zone from the top down of shallow sediment layers in the seabed, which can be divided into oxidation zone, weak oxidation zone, reduction zone and methanogenic zone in turn. The SRB is mainly distributed in the reduction zone in *Figure 9,* where it plays a dominant role and produces H_2S (Berner, 1981; Froelich et al., 1979).

There are also four sequential redox zones in the sulfate reduction zone, iron reduction zone, nitrate reduction zone and oxidation zone in landfill leachate sites, as shown in *Figure 10* (Zhou et al., 2008). The biocenosis structure in each zone has obvious bacterial species properties. Accordingly, sulfate-reducing bacteria, iron-

http://www.aloki.hu ● ISSN 1589 1623 (Print) ● ISSN 1785 0037 (Online)
DOI: http://dx.doi.org/10.15666/aeer/1605_63696383
© 2018, ALÖKI Kft., Budapest, Hungary

reducing bacteria (IRB) and denitrifying bacteria (NRB) are the dominant bacterial groups. The distribution of redox zone and microbial flora indicates that there is a certain overlap between the redox zones, where the sulfate reduction zone is the main zone where malodorous gas (H_2S) is generated.

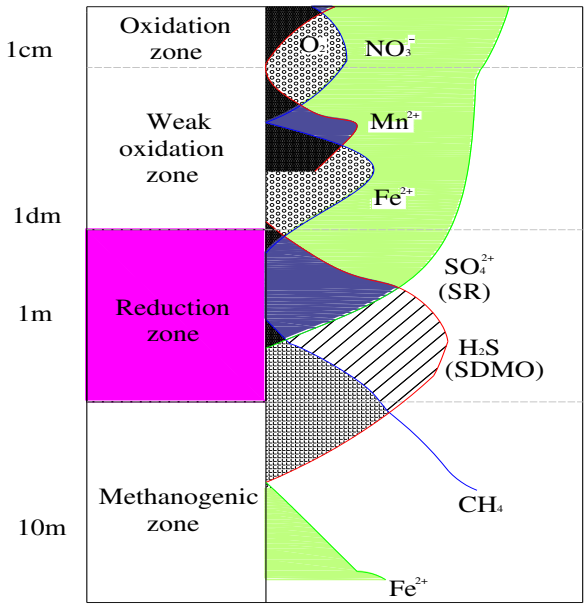

Figure 9. *SRB and redox zone division in submarine deposits*

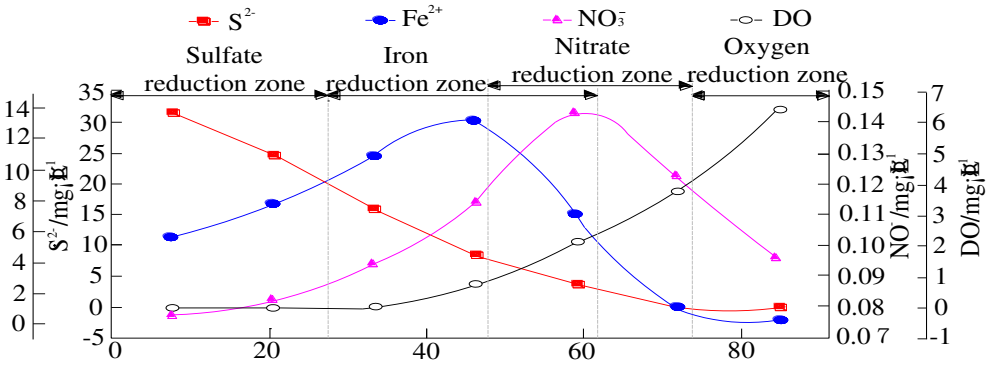

Figure 10. *Distribution of redox zones in landfills*

Organic sulfur compounds are produced mainly in humification stage. H_2S, CH_3SH, and (CH_3) S, S^0, or polysulfide compounds generated by the bacteria dissociation are oxidized to sulfates in an oxygen-rich environment. When the interface between the aqueous medium and the sediment exists in anoxic environment and the sulphate solubility reaches a certain value, SRB is metabolized by SO_4^{2-} as a sulphur source, and BSR works after decomposition, electron transfer and oxidation. The metabolic activity of SRB reduces the solubility of SO_4^{2-} and releases H_2S, HS^-, or S^0. HS^- or S^0 can react with organic matter to form organic sulfur, which can also react with iron ions to form pyrite. If the active iron ion is absent in the system and the SO_4^{2-} content is relatively

http://www.aloki.hu ● ISSN 1589 1623 (Print) ● ISSN 1785 0037 (Online)
DOI: http://dx.doi.org/10.15666/aeer/1605_63696383
© 2018, ALÖKI Kft., Budapest, Hungary

sufficient, a large amount of secondary organic sulfur compounds may be produced under suitable conditions, which is shown in *Figure 11* (Dai et al., 1996).

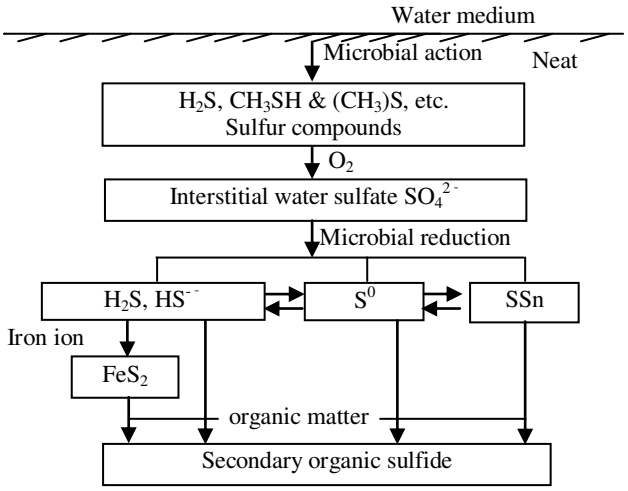

Figure 11. *The evolution of organic sulfur*

In sedimentary formations, due to the interaction between sedimentary factors and ecological factors, three different biological systems are formed, each of which is dominated by different microbial populations, namely the Aerobic microbial zones, sulfate reduction zones and organisms Methane generation zone. In the sulfate reduction zone, H_2S may be generated as shown in *Figure 12* (Lin et al., 2015).

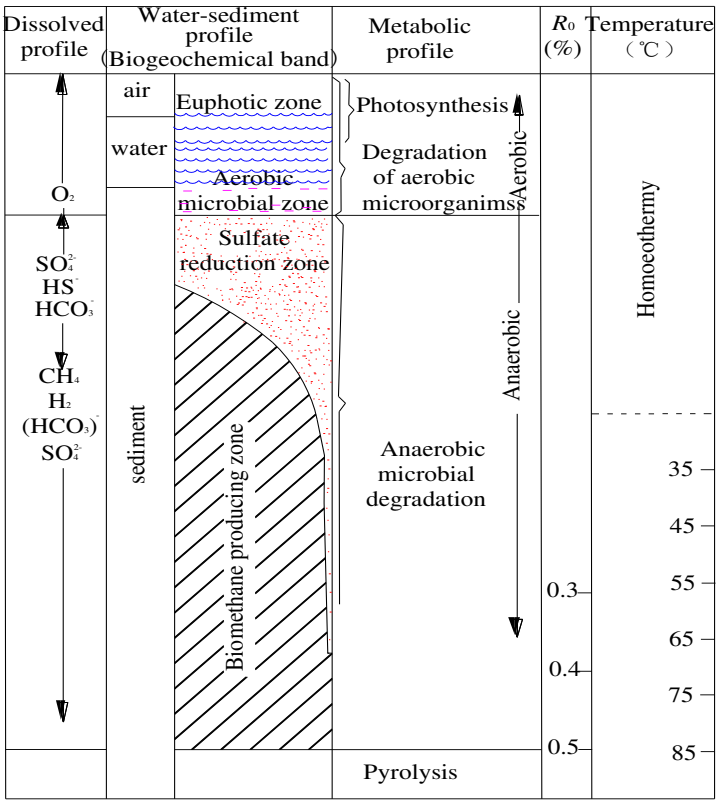

Figure 12. *Schematic diagram of biogenic gas phase in sedimentary strata*

APPLIED ECOLOGY AND ENVIRONMENTAL RESEARCH 16(5):6369-6383.
http://www.aloki.hu ● ISSN 1589 1623 (Print) ● ISSN 1785 0037 (Online)
DOI: http://dx.doi.org/10.15666/aeer/1605_63696383
© 2018, ALÖKI Kft., Budapest, Hungary

(1) In a reducing environment, anaerobic sulfate-reducing bacteria reduce the sulfate in the water to form H_2S (*Eq. 10*).

$$SO_4^{2-}+2C+H_2O \xrightarrow{BSR} {}_2S\uparrow+4HCO_3^- \quad \text{(Eq.10)}$$

(2) In the oxygen-enriched oxidizing environment, biosulfur and sulfuric acid are formed under the action of sulfur oxidizing bacteria (*Eq. 11*).

$$2H_2S+O_2\rightarrow 2H_2O+2S,\ 2S+3O_2+2H_2O\rightarrow 2H_2SO_4 \quad \text{(Eq.11)}$$

(3) If the solution contains Fe^{2+}, native pyrite framboids and microbial dolomite will be appeared. The principle is that Fe^{2+} reacts with H_2S to produce pyrite (*Eq. 12*).

$$Fe^{2+} + S^{2-} \rightarrow FeS\downarrow \quad \text{(Eq.12)}$$

SRB has become an active participant in the early diagenesis process (Brüchert et al., 2001; Krause et al., 2012). Krause et al. found that in anoxic, low-temperature (21 °C) modern seawater (normal salinity and Mg^{2+}/Ca^{2+} values), BSR action occurs under the action of SRB, which can lead to the formation of H_2S and precipitation of dolomite. Its formation model is shown in *Figure 13*. The possible reaction formulas are shown in *Equations 13* and *14* (Glud et al., 1998).

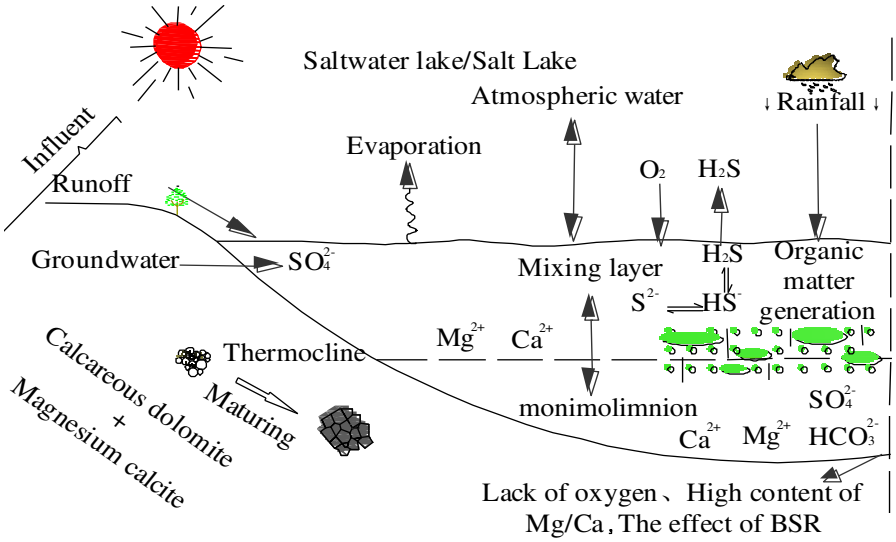

Figure 13. *Microbial mechanism model of primary dolomite in lake system*

$$2CH_2O + SO_4^{2-} \xrightarrow{SRB} S\uparrow + 2HCO_3^- \quad \text{(Eq.13)}$$

$$2HCO^{3-} + Mg^{2+} + Ca^{2+} \rightarrow CaMg(CO_3)_2 + 2H^+ \quad \text{(Eq.14)}$$

In the formation of dolomite and H_2S under the action of BSR in the salt lake (seawater) system, the SRB metabolic activity and intracellular reaction processes can be described as shown in *Figure 14* and *Equations 15–18* (Corzo et al., 2005).

http://www.aloki.hu ● ISSN 1589 1623 (Print) ● ISSN 1785 0037 (Online)
DOI: http://dx.doi.org/10.15666/aeer/1605_63696383
© 2018, ALÖKI Kft., Budapest, Hungary

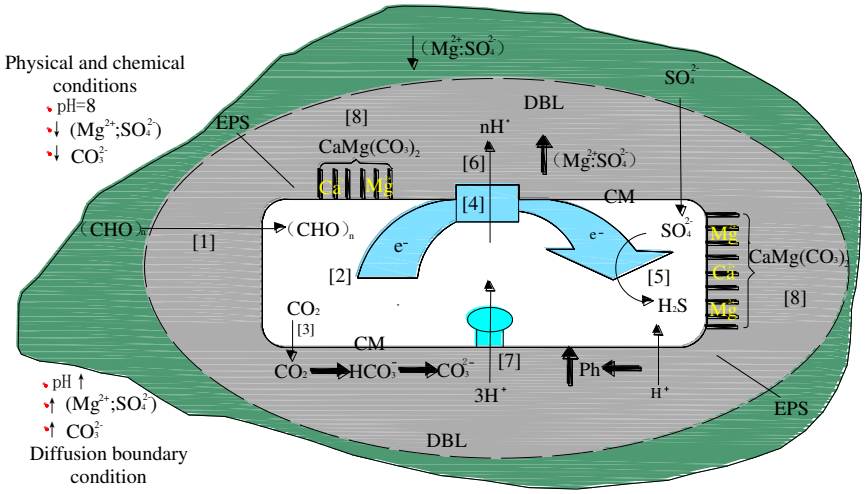

Figure 14. *SRB metabolic activity and intracellular reaction process. DBL - diffusion boundary layer; EPS - cell membrane and outer polymer matrix; CM - cell membranes*

$$2CH_2O + 2H_2O \rightarrow 2CO_2 + 4H_2 \quad \text{(Eq.15)}$$

$$CO_2 + H_2O \rightarrow HCO_3^- + H^+,\ HCO_3^- \rightarrow CO_3^{2-} + H^+ \quad \text{(Eq.16)}$$

$$SO_4^{2-} + 8e^- + 10H^+ \rightarrow H_2S + 4H_2O\ \text{(BSR)} \quad \text{(Eq.17)}$$

$$2CO_3^{2-} + Mg^{2+} + Ca^{2+} \rightarrow CaMg(CO_3)_2 \quad \text{(Eq.18)}$$

In the process of degrading organic matter, SRB in solution can reduce the SO_4^{2-} solubility, increase the concentration of Mg^{2+}/SO_4^{2-}, pH value, HCO_3^- concentration and dolomite saturation, and generate H_2S, which will produce a micro-environment conducive to the precipitation of dolomite. SRB cells, which are in the dark green area, are surrounded by the effective diffusion boundary layer (DBL) in the colour of the dark gray. The low-molecular-weight organic compounds in surroundings enter the cells [1], which are oxidized to CO_2 [2, e.g. (*Eq. 16*)] and released to DBL [3, e.g. (*Eq. 16*)]. The ions formed by the oxidation of organic matter pass through cell-electron-transporting cell membranes (CM) [4] to SO_4^{2-} and undergo a reduction to generate H_2S [5, e.g. (*Eq. 17*)]. The electron flow (H^+) migrates to the DBL[6] through the anaerobic respiratory chain, forming an electrochemical gradient across the cell membrane and stimulating H^+ entry via ATP synthetase. Hence, under fully constrained stoichiometry ($3H^+$. ATP), the H+ ion flux in these cells is coupled to ATP synthase [7]. Since these processes cause the cells to be negatively charged, Ca^{2+} and Mg^{2+} are adsorbed to the cell membrane and outer polymer matrix [8, e.g. *(Eq. 18)*] (Lith et al., 2010, 2003). Therefore, near the cell membrane and DBL, H_2S is formed and dolomite is produced and precipitated [8, e.g. (*Eq. 18*)].

Conclusion

In anaerobic (reduced) habitats, sulfate-reducing bacteria have a unique sulfate-reducing activity. The physiological characteristics and mechanism of H_2S formation not only provide a basis for revealing the biogeochemical cycle of sulfur elements,

http://www.aloki.hu ● ISSN 1589 1623 (Print) ● ISSN 1785 0037 (Online)
DOI: http://dx.doi.org/10.15666/aeer/1605_63696383
© 2018, ALÖKI Kft., Budapest, Hungary

which is conducive to the protection of the natural environment and the restoration of polluted ecosystems, and also provide a useful reference for the control of aerobic microorganisms.

The metabolic reduction process of SRB, using sulfate and sulfur-containing organic material as sulfur source, is not only related to sulfate-reducing bacteria, but also closely related to non-sulfate-reducing microorganisms. A large number of sulfur sources metabolized by SRB are converted into soluble intermediate organic products that can be used by non-SRBs in the metabolic system.

In the earth system, there are many places of metabolism of sulfate-reducing bacteria. And under the metabolism of SRB, BSR may occur to form H_2S. The metabolites in various places are closely related to their micro-environment.

It finds that SRB is the most important biological source for H_2S production. The study on the formation mechanism of H_2S under BSR can provide meaningful reference for the disclosure of the geochemical cycle law of sulfur and the rules of the ecological environment, and supply with a helpful reference for the control of aerobic microorganisms.

Acknowledgements. This work was supported by "National Natural Science Foundation of China (51774116, U1504403)", "Scientific and Technological Project of Department of Science & Technology of Henan Province (182102210320)" and "Postdoctoral Research Fund of Henan Province (2017)". In the study process, the authors are also grateful to Professor Mingju Liu of Henan Polytechnic University for his ardent guidance and help.

REFERENCES

[1] Barton, L. L. (1995): Sulfate-Reducing Bacteria. – Plenum Press, New York.
[2] Barton, L. L., Tomei, F. A. (1995): Characteristics and Activities of Sulfate-Reducing Bacteria. – Springer, New York, pp. 1-32.
[3] Berner, R. A. (1981): A new geochemical classification of sedimentary environments. – Journal of Sedimentary Research 51(2): 359-365.
[4] Bradley, A. S., Leavitt, W. D., Johnston, D. T. (2011): Revisiting the dissimilatory sulfate reduction pathway. – Journal of Geobiology 9(5): 446-457.
[5] Brüchert, V., Knoblauch, C., Bo, B. J. (2001): Controls on stable sulfur isotope fractionation during bacterial sulfate reduction in Arctic sediments. – Journal of Geochimica Et Cosmochimica Acta 65(5): 763-776.
[6] Cai, J., Zheng, P., Zhang, L. (2009): Sulfate-reducing bacteria and their metabolic pathway. – Bulletin of Science and Technology 25(4): 427-431.
[7] Corzo, A. Luzon, M. J., Mayayo, M. et al. (2005): Carbonate mineralogy along a biogeochemical gradient in recent lacustrine sediments of gallocanta lake (Spain). – Journal of Geomicrobiology Journal 22(6): 283-298.
[8] Dai, S., Liu, Y., Ren, D. (1996): The formation of sulphur in coal and its control factors. – Journal of Shandong Mining Institute 15(4): 7-11.
[9] Deng, Q., Liu, M., Zhao, F. et al. (2013): Geochemistry characteristics of sulfur in coals. – Journal of Disaster Advances 6: 234-240.
[10] Deng, Q., Liu, M., Cui, X. et al. (2017): A study of hydrogen sulfide genesis in coal mine of southeastern margin of Junggar Basin. – Journal of Earth Science Frontiers 24(5): 395-401.
[11] Deng, Q., Wang, Y., Wu, X. et al. (2018): Research progress of prevention and control technology of hydrogen sulfide in coal mines. – Journal of Science Technology Review 36(2): 1-7.

http://www.aloki.hu ● ISSN 1589 1623 (Print) ● ISSN 1785 0037 (Online)
DOI: http://dx.doi.org/10.15666/aeer/1605_63696383
© 2018, ALÖKI Kft., Budapest, Hungary

[12] Froelich, P. N., Klinkhammer, G. P., Bender, M. L. et al. (1979): Early oxidation of organic matter in pelagic sediments of the eastern equatorial Atlantic suboxic diagenesis. – Journal of Geochimica et Cosmochimica Acta 43(7): 1075-1090.
[13] Gibson, G. R. (1990): Physiology and ecology of the sulfate-reducing bacteria. – Journal of Applied Bacteriology 69: 767-797.
[14] Glud, R. N., Holby, O., Hoffmann, F. et al. (1998): Benthic mineralization and exchange in Arctic sediments (Svalbard, Norway). – Journal of Marine Ecology Progress 173(8): 237-251.
[15] Isbister, J. D., Wyza, R. E., Lippold, J. et al. (1988): Bioprocessing of Coal. – In: Omenn, G. S. (ed.) Environmental Biotechnology, Reducing Risks from Environmental Chemicals through Biotechnology. Plenum Press, New York, pp. 281-293.
[16] Jannasch, H. W. (1988): Marine microbiology. – Journal of Bioscience 38(10): 711-712.
[17] Kodama, K., Umehara, K., Shimizu, K. et al. (2008): Identification of microbial products from dibenzothiophene and its proposed oxidation pathway. – Journal of the Agricultural Chemical Society of Japan 37(1): 45-50.
[18] Krause, S., Liebetrau, V., Gorb, S. et al. (2012): Microbial nucleation of Mg-rich dolomite in exopolymeric substances under anoxic modern seawater salinity. New insight into an old enigma. – Journal of Geology 40(7): 987-990.
[19] Liao, Y. (2004): Mechanism and Technology of Biological Desulfurization of Waste Water. – Chemical Industry Press, Beijing.
[20] Lin, X., Gao, G., Xu, Y. et al. (2015): Discussion on generation and evolution mode of biogenetic gas. – Journal of Special Oil and Gas Reservoirs 22(1): 1-7.
[21] Lith, Y. V., Warthmann, R., Vasconcelos, C. et al. (2003): Sulphate-reducing bacteria induce low-temperature Ca-dolomite and high Mg-calcite formation. – Journal of Geobiology 1(1): 71-79.
[22] Lith, Y. V., Warthmann, R., Vasconcelos, C. et al. (2010): Microbial fossilization in carbonate sediments. a result of the bacterial surface involvement in dolomite precipitation. – Journal of Sedimentology 50(2): 237-245.
[23] Luhachack, L., Nudler, E. (2014): Bacterial gasotransmitters. An innate defense against antibiotics. – Journal of Current Opinion in Microbiology 21: 13-17.
[24] Luptakova, A., Kusnierova, M. (2005): Bioremediation of acid mine drainage contaminated by SRB. – Journal of Hydrometallurgy 77(1-2): 97-102.
[25] Ma, C., Xu, P., Yu, J. (2000): Progress of microbial organo-desulfurization in fossil fuel. – Journal of Acta Biochimica et Biophysica Sinica 20(3): 55-59.
[26] Machel, H. G. (2001): Bacterial and thermochemical sulfate reduction in diagenetic settings – old and new insights. – Sedimentary Geology 140: 143-175.
[27] Martins, M., Faleiro, M. L., Barros, R. J. et al. (2009): Characterization and activity studies of highly heavy metal resistant sulphate reducing bacteria to be used in acid mine drain age decontamination. – Journal of Hazardous Materials 166(2-3): 706-713.
[28] Orr, W. L. (1974): Changes in sulfur content and isotopic ratios of sulfur during petroleum maturation - Study of Big Horn Basin Palaeozoic oils. – American Association of Petroleum Geologists Bulletin 58(11): 2295-2318.
[29] Peck, H. D. Jr., Legall, J. (1982): Biochemistry of dissimilatory sulphate reduction. – Philosophical Transactions of the Royal Society of London 298(1093): 443-466.
[30] Pérez-Jiménez, J. R., Young, L. Y., Kerkhof, L. J. (2001): Molecular characterization of sulfate-reducing bacteria in anaerobic hydrocarbon-degrading consortia and pure cultures using the dissimilatory sulfite reductase (dsrAB) genes. – Fems Microbiology Ecology 35(2): 145-150.
[31] Rasch, P. J., Barth, M. C., Kiehl, J. T. et al. (2000): A description of the global sulfur cycle and its controlling processes in the NCAR CCM3. – J. Geophys. Re. 105: 1367-1385.
[32] Ren, N., Wang, A., Zhen, W. (2001): Ecology of SRB in anaerobic bio-treatment reactor. – Journal of Harbin University of C. E. & Architecture 34(1): 39-44.

http://www.aloki.hu ● ISSN 1589 1623 (Print) ● ISSN 1785 0037 (Online)
DOI: http://dx.doi.org/10.15666/aeer/1605_63696383
© 2018, ALÖKI Kft., Budapest, Hungary

[33] Ren, N., Wang, A., Zhao, Y. (2009): Ecology of Sulfate-Reducing Bacteria in Anaerobic Biotreatment Processes. – Science Press, Beijing.
[34] Stephensonl, M., Stickland, L. H. (1931): Hydrogenase. The reduction of sulphate to sulfide by molecular hydrogen. – Journal of Biochemical Journal (25): 215-220.
[35] Vallero, M. V. G., Lettinga, G., Lens, P. N. L. (2005) High rate sulfate reduction in a submerged anaerobic membrane bioreactor (SAMBaR) at high salinity. – Journal of Membrane Science 253(1-2): 217-232.
[36] Wei, J., Deng, Q., Liu, M. (2014): Hazards of hydrogen sulfide and control measures in Coal Mines. – Journal of Coal Technology 33(10): 269-272.
[37] Xiao, L., Zhang, L., Li, Y. (2011): Application of sulfate-reducing bacteria to anaerobic wastewater treatment. – Journal of Water Resources & Water Engineering 22(1): 45-49.
[38] Xu, W., Liu, Y., Zeng, G.et al. (2009): Sulfate-reducing bacteria and research progress of Cr(VI) reduction by sulfate-reducing bacteria. – Microbiology 36(7): 1040-1045.
[39] Zhao, H., Li, A., Wan, B. et al. (1995): Isolation and physiology of a moderate halophilic sulfate-reducing bacterium. – Chinese Journal of Applied & Environmental Biology 1(1): 61-67.
[40] Zhao, Y., Ye, Y., Liu, X. (1997): sulfate reducing bacteria and its influencing factors. – Journal of Environmental Pollution & Control 19(5): 41-43.
[41] Zhou, R., Zhao, Y., Zhu, Z. et al. (2008): Redox zones and its functional bacteria in a contaminated landfill site. – Journal of Environmental Science (11): 3270-3274.

http://www.aloki.hu ● ISSN 1589 1623 (Print) ● ISSN 1785 0037 (Online)
DOI: http://dx.doi.org/10.15666/aeer/1605_63696383
© 2018, ALÖKI Kft., Budapest, Hungary

MEDIUM AND LONG-TERM INFLUENCES OF TYPICAL PLANTATIONS ON SURFACE SOIL NUTRIENTS IN THE TEMPERATE ZONE OF MOUNT MENG, CHINA

GAO, Y.[1,2*] – WANG, Y.[1]

[1]*Shandong Provincial Key Laboratory of Water and Soil Conservation and Environmental Protection, College of Resources and Environment, Linyi University, Linyi 276005, China (e-mail: wangyunsd@163.com)*

[2]*Linyi Scientific Exploration Laboratory, Linyi 276037, China*

**Corresponding author*
e-mail: gaoyuan1182@tom.com, gaoy@lyu.edu.cn

(Received 31st May 2018; accepted 2nd Aug 2018)

Abstract. Very few studies are concerned with the medium and long-term soil nutrients of plantations, which often have inconsistent research results. This paper studied the characteristics of the surface soil nutrient changes in two types of plantations with different stand age: 30 years and 60 years. They are needle-leaved plantations (*Pinus thunbergii* plantation and *Pinus densiflora* plantation) and broad-leaved plantations (*Quercus variabilis* plantation). Research results showed: 1) When the stand age is 30 years, the content of organic matters and the nitrogen of the surface soil was presented as follows: *Pinus thunbergii* plantation>*Quercus variabilis* plantation>*Pinus densiflora* plantation, and the content of organic carbon, available phosphate and rapidly available potassium of the surface soil was presented as follows: *Quercus variabilis* plantation>*Pinus thunbergii* plantation>*Pinus densiflora* plantation. Significant differences were found in the content of active organic carbon in the surface soil. 2) When the stand age is 60 years, the content of organic matters, the total nitrogen and rapidly available potassium in the surface soil was presented as follows: *Pinus densiflora* plantation>*Quercus variabilis* plantation> *Pinus thunbergii* plantation and significant differences were found in the content of organic matters and total nitrogen of the surface soil. The content of active organic carbon in the surface soil was ranked as follows: *Pinus thunbergii* plantation>*Pinus densiflora* plantation>*Quercus variabilis* plantation. 3) Among the plantations with 60-year stand age, the content of five nutrients all increased in the surface soil of the *Pinus densiflora* plantation, namely, organic matters, active organic carbon, total nitrogen, available phosphorus and rapidly available potassium. The content of organic matters, total nitrogen and available phosphorus significantly increased in the surface soil, but no significant differences were found in the surface soil nutrient content of *Quercus variabilis* plantation and *Pinus thunbergii* plantation.
Keywords: *plantation, soil nutrient, organic matter, active organic carbon, total nitrogen, available phosphorus, available potassium*

Introduction

At the Asia-Pacific Regional Conference on Forest Restoration on March 26, 2018, Peng Y. D., deputy director of the State Forestry Administration, pointed out that as of 2017, China's plantation forest area was 693,300 km^2, ranking first in the world. Forest plantation is a major measure to recover the degraded ecosystem and conserve the ecosystem service functions (Togonidze and Akhalkatsi, 2015; Wei et al., 2017; Yin et al., 2018). In the forest ecosystem, the vegetation of plantations influences a lot of ecological processes above and below the ground, and plays a crucial role in maintaining the stability and diversification of the forest ecological system (Nilsson and Wardle, 2005). In the ecological restoration of the forest, the changes of soil nutrients have been a focus of the modern ecological research. Soil, an important component of

http://www.aloki.hu ● ISSN 1589 1623 (Print) ● ISSN 1785 0037 (Online)
DOI: http://dx.doi.org/10.15666/aeer/1605_63856393
© 2018, ALÖKI Kft., Budapest, Hungary

the forest ecosystem, provides necessary nutrients for the growth and propagation of plants as well as serves as carriers to the multiple ecological processes in the ecosystem (Trumbore and Czimczik, 2008). The status of forest soil nutrients is influenced by factors like climate, soil types and vegetation types together (Roy et al., 2010; Schmidt et al., 2015; Hedwall et al., 2015). Soil nutrients are important quantitative indexes of soil fertility, and they are crucial to the species composition and structural changes of vegetation. Moreover, they directly influence the productivity level of the ecosystem (Xu et al., 2008; Schmidt et al., 2015). The forest succession and the compound afforestation pattern obviously influence the soil fertility (Rutigliano et al., 2004; Hedwall et al., 2015). Vegetation influences the characteristics and development of the soil because the changes accompanying the vegetation succession, plant litters and root exudates directly influence the quantity of the input soil nutrients (Jia et al., 2005). Different development stages of plantations are throughout the whole life cycle of the forest growth. Therefore, it is of great ecological significance to understand the soil fertility of different development stages and the fertilizer requirement characteristics of forests in the plantation management. It could provide the scientific basis for the operation and management of the local plantations and evaluate the ecological consequences of the introduced exotic tree species.

The existing experimental research shows that broad-leaved species could immobilize more nutrients than coniferous species in the restoration of the forest the stand age of which is less than 30 years (Laganière et al., 2010; Li et al., 2012; Nave et al., 2013). However, the research ignores the changes of the soil nutrient storage in the restoration of the forest the stand age of which is over 30 years (Wang et al., 2016). Coniferous species are more difficult to resolve than broad-leaved species. Theoretically, the former is higher than the latter in the quantity of the immobilized soil nutrients (Vesterdal et al., 2008; Wang et al., 2016). These research inconsistencies reflect that: the soil nutrient data of the medium and long term plantations (trees whose stand age is over 30 years) are required for the research, especially those plantations with over 50 years of stand age because of their scarcity and preciousness (Bai et al., 2008; Gao et al., 2013).

Mount Meng is located in the low hilly areas of the central-south Shandong Province of China, and it is one of the two major ecological reserves in Shandong. Meanwhile, it is also a typical representative of the rocky mountain areas in northern China as well as one of the earliest areas to develop plantations in China. Typical plantations are *Pinus thunbergii* (black pine) plantation, *Pinus densiflora* (red pine) plantation and *Quercus variabilis* (cork oak) plantation (Gao et al., 2009, 2011, 2013). According to different forest types, studies relevant to surface soil nutrients and their dynamics are conducted, which helps to understand the surface soil nutrient supply of the forest ecosystem. This study will explore the soil surface nutrient changes of needle plantations (*Pinus thunbergii* plantation and *Pinus densiflora* plantation) and broad-leaf plantations (*Quercus variabilis* plantation) in terms of the stand age: 30 years and 60 years. The presupposed scientific hypotheses of the study are as follows: 1) Litters of coniferous species are more difficult to resolve than those of broad-leaf species. If the stand age of plantations are the same, more surface soil nutrients should be accumulated, namely, needle plantations are higher than broad-leaf plantations in the content of soil surface nutrients when their stand age are both 60 years. 2) The content of soil surface nutrients of plantations increases progressively along with the time, namely, the 60-year plantations have more soil surface nutrients than the 30-year plantations.

http://www.aloki.hu ● ISSN 1589 1623 (Print) ● ISSN 1785 0037 (Online)
DOI: http://dx.doi.org/10.15666/aeer/1605_63856393
© 2018, ALÖKI Kft., Budapest, Hungary

Materials and methods

Research sample plot

The research was conducted in typical areas of Mount Meng. Located in the warm temperate zone of the southeastern hilly areas in Shandong Province, Mount Meng covers an area of 1,125 square kilometers, and its soil is the brown forest soil. The research selected *Pinus thunbergii* plantation, *Pinus densiflora* plantation and *Quercus variabilis* plantation with two types of stand age—30a and 60a as research plots by investigating the community structure of wild plants and interviewing the technicians of the forest station in order to carry out the soil sampling. Forest in this area has been damaged by man-made for a long time. In 1949, only about 25 km^2 of forest was left, the forest coverage rate was less than 2%, and there were less than 300 plant species. The government has successively established 7 forest farms in Tashan, Wanshou Palace, Tianma, Mingguang Temple, Datun, Hailuo Temple and Tianbao Mountain to restore and reconstruct Mengshan vegetation from the 1950s to the 1980s.

Research methods

The sample plots were selected as follows: 12 sample plots of *Pinus thunbergii* plantation (6 sample plots with 30 years of stand age and 6 sample plots with 60 years of stand age), 12 sample plots of *Pinus densiflora* plantation (6 sample plots with 30 years of stand age and 6 sample plots with 60 years of stand age), and 16 sample plots of *Quercus variabilis* plantation (8 sample plots with 30 years of stand age and 8 sample plots with 60 years of stand age). The sampling area coordinates were 35°10'~36°00'N, 117°35'~118°20' E. The plot spacing is more than 1 km. There was no garbage in the plot, and the roots of the plant were dried when the soil sample was treated.

1 quadrat of 20 m × 30 m was selected in each sample plot, and the five-point sampling method was used to drill 5 repeated soil samples. The diameter of the earth boring auger was 3.5 cm and the sampling depth was 10 cm (Wang et al., 2017). Then, the repeated soil samples were mixed into one soil sample and taken to the lab. Sampling was conducted in August, 2016, and the lab was responsible for the assay determination of organic matters, active organic carbon, total nitrogen, available phosphorus and rapidly available potassium of the soil samples. According to the LY/T1237-1999 standard for the organic matters of forest soil, the external heating method of potassium dichromate was used for measuring the organic matters of soil, and the potassium permanganate oxidation method was adopted for measuring the content of active organic matters. According to the LY/T 1228-2015 standard of nitrogen measurement for the forest soil, the Kjeldahl nitrogen method was used to measure the content of total nitrogen. According to the LY/T 1232-2015 standard of phosphorous measurement for the forest soil, the colorimetric method was used for measuring the phosphorous content. According to the LY/T 1234-2015 standard of potassium measurement for the forest soil, the atomic absorption spectrophotometer was used for the rapidly available potassium measurement.

Statistical analysis

The single factor statistical method was used to analyze the soil nutrient differences of the forest type, and T test was applied to measure the soil nutrient differences of the

http://www.aloki.hu ● ISSN 1589 1623 (Print) ● ISSN 1785 0037 (Online)
DOI: http://dx.doi.org/10.15666/aeer/1605_63856393
© 2018, ALÖKI Kft., Budapest, Hungary

plantations with different stand age. SPSS 17.0 and Excel 2003 were used for the data analysis and table introduction.

Results and analysis

Organic matters of surface soil

In plantations with the same stand age but different forest types, the organic matter content was as follows: 1) when the stand age of plantations is 30 years, *Pinus thunbergii* plantations (33.03 ± 8.86 g·kg^{-1})>*Quercus variabilis* plantation (28.78 ± 5.33 g·kg^{-1})>*Pinus densiflora* plantation (24.40 ± 11.26 g·kg^{-1}). 2) when the stand age of plantations is 60 years, *Pinus densiflora* plantation (64.02 ± 11.06 g·kg^{-1})>*Quercus variabilis* plantation (46.6 ± 11.48 g·kg^{-1})>*Pinus thunbergii* plantations (29.20 ± 4.95 g·kg^{-1}). And *Pinus densiflora* plantation was significantly higher than the other two types of plantations in terms of the organic matter content (*Fig. 1A*).

In plantations with the same forest type but different stand age, the organic matter content of the surface soil was as follows: three plantations with 60 years of stand age had more organic matters than those with 30 years of stand age, where the *Pinus densiflora* plantation with 60 years of stand age is significantly higher than that with 30 years of stand age in terms of the organic matter content (*Fig. 1A*).

Active organic carbon of surface soil

In plantations with the same stand age but different forest types, the content of active organic carbon of surface soil was as follows: 1) when the stand age of plantations is 30 years, *Quercus variabilis* plantation (22.80 ± 1.87 g·kg^{-1})>*Pinus thunbergii* plantation (14.21 ± 2.22 g·kg^{-1})>*Pinus densiflora* plantation (12.06 ± 3.66 g·kg^{-1}), where *Quercus variabilis* plantation was significantly higher than the other two types of plantations in terms of the content of active organic carbon. 2) When the stand age of plantations is 60 years, *Pinus thunbergii* plantation (20.39 ± 0.34 g·kg^{-1})>*Quercus variabilis* plantation (20.30 ± 0.41 g·kg^{-1})>*Pinus densiflora* plantation (19.87 ± 0.34 g·kg^{-1}) (*Fig. 1B*).

In plantations with the same forest type but different stand age, the content of active organic carbon of surface soil was as follows: 1) the group of *Pinus thunbergii* plantation and *Pinus densiflora* plantation with 60 years of stand age were higher than the group with 30 years of stand age, while the *Quercus variabilis* plantation group with 60 years of stand age was lower than the group with 30 years of stand age in terms of the active organic carbon content (*Fig. 1B*).

Total nitrogen of surface soil

In plantations with the same stand age but different forest types, the content of total nitrogen of surface soil was as follows: 1) When the stand age of plantations is 30 years, *Pinus thunbergii* plantation (1.54 ± 0.44 g·kg^{-1})>*Quercus variabilis* plantation (1.43 ± 0.37 g·kg^{-1})>*Pinus densiflora* plantation (1.14 ± 0.32 g·kg^{-1}). 2) When the stand age of plantations is 30 years, *Pinus densiflora* plantation (2.56 ± 0.50 g·kg^{-1})>*Quercus variabilis* plantation (1.65 ± 0.34 g·kg^{-1})>*Pinus thunbergii* plantation (1.22 ± 0.23 g·kg^{-1}), where *Pinus densiflora* plantation was significantly higher than the other two types of plantations in terms of the total nitrogen content of surface soil (*Fig. 1C*).

http://www.aloki.hu ● ISSN 1589 1623 (Print) ● ISSN 1785 0037 (Online)
DOI: http://dx.doi.org/10.15666/aeer/1605_63856393
© 2018, ALÖKI Kft., Budapest, Hungary

In plantations with the same forest type but different stand age, the total nitrogen content of surface soil was as follows: the *Pinus densiflora* plantation group with 60 years of stand age was significantly higher than the group with 30 years of stand age in terms of the total nitrogen content, but the *Pinus thunbergii* plantation group with 60 years of stand age was lower than the group with 30 years of stand age. Contrarily, the *Quercus variabilis* plantation group with 60 years of stand age was higher than the group with 30 years of stand age in terms of the total nitrogen content of surface soil.

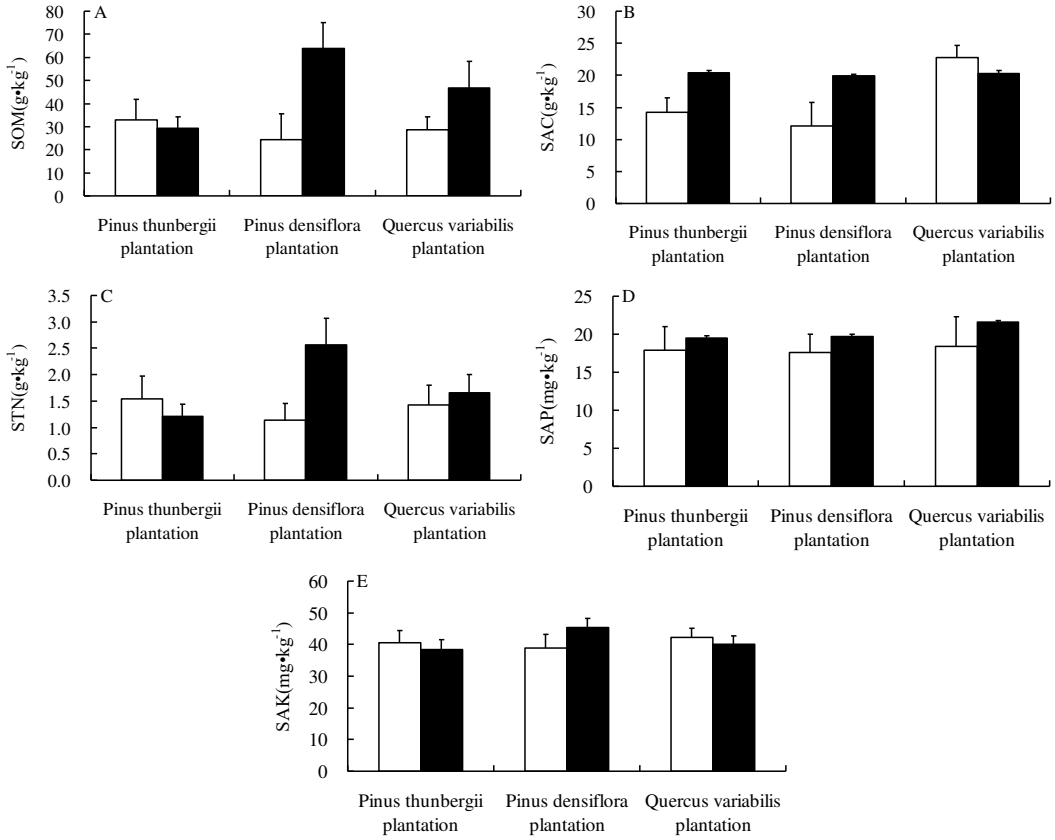

Figure 1. *Content difference of soil organic matter (SAM, A), soil active organic carbon (SAC, B), soil total nitrogen (STN, C), soil available phosphorus (SAP, D) and soil available potassium (SAK, E) of Pinus thunbergii plantation, Pinus densiflora plantation and Quercus variabilis plantation in 30 years of age and 60 years of age in Mount Meng (average + standard error). □ 30 years of age; ■ 60 years of age*

Available phosphorus of surface soil

In plantations with the same stand age but different forest types, the available phosphorus content of surface soil was as follows: 1) When the stand age of plantation is 30 years, *Quercus variabilis* plantation (18.43 ± 3.85 mg·kg^{-1})>*Pinus thunbergii* plantation (17.85 ± 3.15 mg·kg^{-1})>*Pinus densiflora* plantation (17.64 ± 2.38 mg·kg^{-1}). 2) When the stand age of plantation is 60 years, *Quercus variabilis* plantation (21.65 ± 0.18 mg·kg^{-1})>*Pinus densiflora* plantation (19.74 ± 0.21 mg·kg^{-1})>*Pinus thunbergii* plantation (19.55 ± 0.26 mg·kg^{-1}) (*Fig. 1D*).

http://www.aloki.hu ● ISSN 1589 1623 (Print) ● ISSN 1785 0037 (Online)
DOI: http://dx.doi.org/10.15666/aeer/1605_63856393
© 2018, ALÖKI Kft., Budapest, Hungary

In plantations with the same forest type but different stand age, the available phosphorus content of surface soil was as follows: 1) The three types of plantations with 60 years of stand age were higher than those with 30 years of stand age in terms of the available phosphorus content of surface soil, where the *Pinus densiflora* plantation group with 60 years of stand age had significantly more available phosphorus than the group with 30 years of stand age (*Fig. 1D*).

Rapidly available potassium of surface soil

In plantations with the same stand age but different forest types, the rapidly available potassium content of surface soil was as follows: 1) When the stand age of plantation is 30 years, *Quercus variabilis* plantation (42.20 ± 2.86 $mg \cdot kg^{-1}$)>*Pinus thunbergii* plantation (40.53 ± 3.93 $mg \cdot kg^{-1}$)>*Pinus densiflora* plantation (45.37 ± 2.77 $mg \cdot kg^{-1}$). 2) When the stand age of plantation is 60 years, *Pinus densiflora* plantation (45.37 ± 2.77 $mg \cdot kg^{-1}$)>*Quercus variabilis* plantation (40.09 ± 2.64 $mg \cdot kg^{-1}$)>*Pinus thunbergii* plantation (38.43 ± 3.15 $mg \cdot kg^{-1}$) (*Fig. 1E*).

In plantations with the same forest type but different stand age, the rapidly available potassium content of surface soil was as follows: 1) in terms of the rapidly available potassium content, the *Pinus densiflora* plantation group with 60 years of stand age was higher than the group with 30 years of stand age, while the other two types of plantations with 60 years of stand age were lower than those with 30 years of stand age (*Fig. 1E*).

Principal component analysis of soil nutrients

The accumulative variance contribution rates of the first and second principal components respectively reached 81.05% and 80.81% in Mount Meng's plantations with 30 years and 60 years of stand age as shown in *Tables 1* and *2,* which revealed the majority of information. In Mount Meng's plantations with 30 years and 60 years of stand age, the first principal component was closely relevant to organic matters, total nitrogen, available phosphorus and rapidly available potassium, with the accumulative variance contribution rates being 59.85% and 59.05% as shown in *Table 1* and *Figure 2A*. In Mount Meng's plantations with 30 years and 60 years of stand age, the second principal component was closely relevant to the active organic carbon of the soil with the accumulative variance contribution rates being 21.20% and 21.76% as shown in *Table 2* and *Figure 2B*.

Table 1. *Soil nutrients of 30a plantation in principal component analysis in Mount Meng, China*

	SAM	**SAC**	**STN**	**SAP**	**SAK**
Main component 1	0.95	–0.11	0.91	0.88	0.70
Main component 2	0.05	0.98	–0.09	0.28	–0.15

The total explanatory power of two principal components was 81.05%, where principal component 1 and principal component 2 were 59.85% and 21.20%, respectively
SAM: soil organic matter; SAC: soil active organic carbon; STN: soil total nitrogen; SAP: soil available phosphorus; SAK: soil available potassium

http://www.aloki.hu ● ISSN 1589 1623 (Print) ● ISSN 1785 0037 (Online)
DOI: http://dx.doi.org/10.15666/aeer/1605_63856393
© 2018, ALÖKI Kft., Budapest, Hungary

Table 2. *Soil nutrients of 60a plantation in principal component analysis in Mount Meng, China*

	SAM	SAC	STN	SAP	SAK
Main component 1	0.94	0.09	0.89	0.91	0.67
Main component 2	0.19	0.96	0.12	–0.27	–0.18

The total explanatory power of two principal components was 80.81%, where principal component 1 and principal component 2 were 59.05% and 21.76%, respectively
SAM: soil organic matter; SAC: soil active organic carbon; STN: soil total nitrogen; SAP: soil available phosphorus; SAK: soil available potassium

Discussion

The differences of the surface soil nutrients in the forest are largely influenced by the types of vegetation. They are mainly reflected like this: plant litters and root exudates keep supplementing the surface soil nutrients and energy substances (Hedwall et al., 2015; Jia et al., 2005). Litter is an important structure and functional unit of material circulation and energy flow in the forest ecosystem (Jia et al., 2016). As the folia of needle-leaved trees have more lignin content (Wang et al., 2009) and relatively less leaf area than broad-leaved trees (Wang et al., 2004; Guo et al., 2006), the litter decomposition rate gets limited, thus influencing the nutrient return rate of litters. Some research shows that: when the stand age is the same, the soil of broad-leaved threes has more nitrogen than that of needle-leaved trees. It is thought that a large quantity of deciduous input and quicker litter decomposition rates could be used to explain why broadleaved trees are higher than needle leaved trees in terms of the topsoil fertility in the broadleaved deciduous forest (Jiang and Xu, 2006; Laganière et al., 2010). We suggest that for plantations with similar environmental backgrounds, *Pinus densiflora* are more suitable than *Pinus thunbergii* and *Quercus variabilis* in terms of maintaining soil nutrients when selecting tool species.

Conclusion

The research found that: when the stand age is 60 years, the content of organic matters, total nitrogen and rapidly available potassium was presented in a descending order: *Pinus densiflora* plantation>*Quercus variabilis* plantation>*Pinus thunbergii* plantation, and the content of active organic carbon was as follows: *Quercus variabilis* plantation>*Pinus densiflora* plantation>*Pinus thunbergii* plantation. The content of available phosphorus was as follows: *Quercus variabilis* plantation>*Pinus densiflora* plantation>*Pinus thunbergii* plantation. The research result relevant to *Pinus densiflora* plantation and *Quercus variabilis* plantation supported the first research hypothesis.

When the stand age of *Pinus densiflora* plantation changes from 30 years to 60 years, the content of surface soil nutrients all increased, including organic matters, active organic carbon, total nitrogen, available phosphorus and rapidly available potassium, where the content of organic matters, active organic carbon, total nitrogen, available phosphorus significantly increased. The research result relevant to *Pinus densiflora* plantation basically supported the second research hypothesis.

http://www.aloki.hu ● ISSN 1589 1623 (Print) ● ISSN 1785 0037 (Online)
DOI: http://dx.doi.org/10.15666/aeer/1605_63856393
© 2018, ALÖKI Kft., Budapest, Hungary

Acknowledgements. Funded by the National Natural Science Foundation of China, NO. 41401329 and Fund of Shandong Provincial Key Laboratory of Water and Soil Conservation and Environmental Protection, Linyi University, NO. STKF201603.

REFERENCES

[1] Bai, F., Sang, W. G., Li, G. Q., Liu, R. G., Chen, L. Z., Wang, K. (2008): Long-term protection effects of national reserve to forest vegetation in 4 decades: biodiversity change analysis of major forest types in Changbai Mountain Nature Reserve, China. – Science in China Series C: Life Sciences 51: 948-958.

[2] Gao, Y., Ci, H. X., Qiu, Z. L., Chen, Y. F. (2009): Plant diversity and its elevational gradient patterns in Mengshan Mountain, Shandong, China. – Acta Ecologica Sinica 29: 6377-6384 (in Chinese).

[3] Gao, Y., Chen, Y. F., Dong, H., Hao, J. C., Ci, H. X. (2011): Vegetation and species diversity change analysis in 50 years in Tashan Mountain, Shandong Province, China. – Acta Ecologica Sinica 31: 5984-5991 (in Chinese).

[4] Gao, Y., Zhu, K, S., Hao, J. C., Xu, L. S. (2013): An evaluation of the afforestation outcome of six tree species in more than 40 years in Mengshan mountain, Shandong province, China. – Chinese Journal of Plant Ecology 37: 728-738 (in Chinese).

[5] Guo, Z. L., Zheng, J. P., Ma, Y. D., Li, Q. K., Yu, G. R., Han, S. J., Fan, C. N., Liu, W. D. (2006): Researches on litterfall decomposition rates and model simulating of main species in various forest vegetations of Changbai Mountains, China. – Acta Ecologica Sinica 26: 1037-1046 (in Chinese).

[6] Hedwall, P. O., Skoglund, J., Linder, S. (2015): Interactions with successional stage and nutrient status determines the life-form-specific effects of increased soil temperature on boreal forest floor vegetation. – Ecology and Evolution 5: 948-960.

[7] Jia, B. R., Zhou, G. S., Liu, Y. Z., Jiang, Y. L. (2016): Spatial pattern and environmental controls of annual litterfall production in natural forest ecosystems in China. – Scientia Sinica Vitae 46: 1304-1311 (in Chinese).

[8] Jia, G. M., Cao, J., Wang, C. Y., Wang, G. (2005): Microbial biomass and nutrients in soil at the different stages of secondary forest succession in Ziwulin, northwest China. – Forest Ecology and Management 217: 117-125.

[9] Jiang, P. K., Xu, Q. F. (2006): Abundance and dynamics of soil labile carbon pools under different types of forest vegetation. – Pedosphere 16: 505-511.

[10] Laganière, J., Angers, D., Paré, D. (2010): Carbon accumulation in agricultural soils after afforestation: a meta-analysis. – Global Change Biology 16: 439-453.

[11] Li, D. J., Niu, S. L., Luo, Y. Q. (2012): Global patterns of the dynamics of soil carbon and nitrogen stocks following afforestation: a meta-analysis. – New Phytologist 195: 172-181.

[12] Nave, L. E., Swanston, C. W., Mishra, U., Nadelhoffer, K. J. (2013): Afforestation effects on soil carbon storage in the United States: a synthesis. – Soil Science Society of America Journal 77: 1035-1047.

[13] Nilsson, M. C., Wardle, D. A. (2005): Understory vegetation as a forest ecosystem driver: Evidence from the northern Swedish boreal forest. – Frontiers in Ecology and the Environment 3: 421-428.

[14] Roy, P. K., Samal, N. R., Roy, M. B., Mazumdar, A. (2010): Soil carbon and nutrient accumulation under forest plantations in Jharkhand State of India. – Clean-Soil Air Water 38: 706-712.

[15] Rutigliano, F. A., Ascoli, R. D., De Santo, A. V. (2004): Soil microbial metabolism and nutrient status in a Mediterranean area as affected by plant cover. – Soil Biology and Biochemistry 36: 1719-1729.

http://www.aloki.hu ● ISSN 1589 1623 (Print) ● ISSN 1785 0037 (Online)
DOI: http://dx.doi.org/10.15666/aeer/1605_63856393
© 2018, ALÖKI Kft., Budapest, Hungary

[16] Schmidt, M., Veldkamp, E., Corre, M. D. (2015): Tree species diversity effects on productivity, soil nutrient availability and nutrient response efficiency in a temperate deciduous forest. – Forest Ecology and Management 338: 114-123.
[17] Togonidze, N., Akhalkatsi, M. (2015): Variability of plant species diversity during the natural restoration of the subalpine birch forest in the Central Great Caucasus. – Turkish Journal of Botany 39: 458-471.
[18] Trumbore, S. E., Czimczik, C. I. (2008): An uncertain future for soil carbon. – Science 321: 1455-1456.
[19] Vesterdal, L., Schmidt, I. K., Callesen, I., Nilsson, L. O., Gundersen, Per. (2008): Carbon and nitrogen in forest floor and mineral soil under six common European tree species. – Forest Ecology and Management 255: 35-48.
[20] Wang, F. M., Zhu, W. X., Chen, H. (2016): Changes of soil C stocks and stability after 70-year afforestation in the northeast USA. – Plant and Soil 401: 319-329.
[21] Wang, H., Chen, L., Song, M., Song, T. Q., Zeng, Y. P., Peng, X. X., Du, H., Su, L. (2017): Spatial heterogeneity of soil phosphorus and potassium in a mixed evergreen and deciduous broad-leaved forest in karst region of southwest China. – Acta Ecologica Sinica 37: 8285-8293 (in Chinese).
[22] Wang, X. E., Xue, L., Xie, T. F. (2009): A review on litter decomposition. – Chinese Journal of Soil Science 40: 1473-1478 (in Chinese).
[23] Wang, X. H., Huang, J. J., Yan, E. R. (2004): Leaf litter decomposition of commen trees in Tiantongwang. – Chinese Journal of Plant Ecology 28: 457-467 (in Chinese).
[24] Wei, J. J., Gao, Y., Zhao, W. G., Liu, J. (2017): Hillside topographic pattern of shrub and herb diversity of forest in Mount Tai of China. – Journal of Environmental Protection and Ecology 18: 571-580.
[25] Xu, Z. H., Ward, S., Chen, C. R., Blumfield, T., Prasolova, N., Liu, J. X. (2008): Soil carbon and nutrient pools, microbial properties and gross nitrogen transformations in adjacent natural forest and hoop pine plantations of subtropical Australia. – Journal of Soils and Sediments 8(2): 99-105.
[26] Yin, W. D., Gao, Y., Liu, J., Zhao, W. G. (2018): Influence of scenic road corridor to plant diversity in Kunyu Mountain, China. – Applied Ecology and Environmental Research 16: 1461-1469.

http://www.aloki.hu ● ISSN 1589 1623 (Print) ● ISSN 1785 0037 (Online)
DOI: http://dx.doi.org/10.15666/aeer/1605_63856393
© 2018, ALÖKI Kft., Budapest, Hungary

THE EVOLUTION CHARACTERISTICS OF DROUGHT AND THE ANALYSIS OF RAINFALL INTENSITY PROBABILITY DURING ALTERNATING DRY-WET CHANGE IN THE HAIHE RIVER BASIN

ZHANG, X.[1*] – HUA, Y.[1] – FENG, J.[1*] – YAN, D.[2] – LIU, J.[2] – LI, C.[2] – CHENG, Y.[1] – REN, Q.[3]

[1]*Institute of Environmental Economics, Tianjin Polytechnic University, Tianjin 300387, China*
(e-mail: yonsionh@163.com – Y. Hua; fanxing07@126.com – Y. Cheng)

[2]*State Key Laboratory of Simulation and Regulation of Water Cycle in River Basin, China*
Institute of Water Resources and Hydropower Research, 100038 Beijing, China
(e-mail: yandh@iwhr.com – D. Yan; hettyliu@126.com – J. Liu; azhe051@163.com – C. Li)

[3]*State Key Laboratory of Soil Erosion and Dryland Farming on the Loess Plateau, Northwest A&F University, 712100 Yangling Shaanxi, China*
(e-mail: wxws.2008@163.com)

**Corresponding authors*
e-mail: xuehua671231@163.com – X. Zhang; jingfengwater@126.com – J. Feng

(Received 31st May 2018; accepted 13th Sep 2018)

Abstract. Under the impact of climate change, extreme events occur frequently and the speed of alternation of drought and flood gets faster. Based on the daily rainfall data of 42 meteorological stations for the years 1963-2013, Haihe River basin in China was divided into four sub-regions (region A, region B, region C, region D) by means of cluster analysis of the meteorological stations using the self-organizing map (SOM) neural network method. The drought index of the number of consecutive days without rainfall was used to identify the drought magnitudes and the first rainfall intensity and the maximum daily rainfall after a drought period was analyzed with the Pearson-III frequency curve, then the relationship between rainfall intensity and different drought magnitudes was observed. The results indicated that: (1) Annual rainfall reduced significantly and the drought number increased in the Haihe River basin, meanwhile the occurrence frequency of different drought level showed an overall increasing trend. This region was dominated by light drought, with the probability as 76%, while the probability of moderate drought was about 20%. The spatial difference was significant. The occurrence frequencies of moderate drought and severe drought were higher in region A. The frequency of extraordinary drought was the most in region B as 0.35%. (2) As the drought level increased, the probability of the first effective rainfall reaching heavy rain decreased in region A, region B and region C, while the probability increased in region D. With the increase of the drought number, rainfall frequency decreased and rainfall intensity enhanced obviously.
Keywords: *frequency analysis, evolution characteristics, drought, rainfall, climatic change, Haihe River basin, semi-arid area*

Introduction

Under the impact of climate change, the occurrence frequency and strength of extreme climate events, such as heavy rain, flood and drought has shown an increasing trend as a result of atmospheric circulation anomaly (Burke et al., 2001). Meanwhile, extreme drought and flood events have occurred frequently and widely in the Haihe River basin in China in recent years (Yan et al., 2013). These disasters can create the huge economic loss and the society affects, creating a new challenge for disaster risk management. Rain is a key factor in the occurrence of droughts and floods, as the

http://www.aloki.hu ● ISSN 1589 1623 (Print) ● ISSN 1785 0037 (Online)
DOI: http://dx.doi.org/10.15666/aeer/1605_63956407
© 2018, ALÖKI Kft., Budapest, Hungary

variation of rainfall intensity determines the intensity and range of droughts and floods (Zavareh, 1997). With the speeding alternating drought and flood (Feng et al., 2012), there is an intensive and concentrated rainfall after a long duration of drought (Yan et al., 2013; Feng, 2014). The change of rainfall intensity after drought is the most important for water resources management.

A large number of scholars have studied the temporal and spatial evolution characteristic and driving mechanism of drought events and higher rainfall, such as the drought evaluation method based on the long series of observational rainfall data (Cancelliere et al., 2007; Łabędzki, 2010; Palmer, 1965) and hydrological frequency analysis method based on Pearson-III frequency curve (Narasimhan and Srinivasan, 2005) used to scale the drought severity. Based on the components of water cycle, drought is characterized by meteorological drought, soil moisture drought, hydrological drought, socio-economic drought and ecological drought (Tallaksen, 2009; Huijgevoort, 2012). As such a complex phenomenon, it requires multiple climatological and hydrological parameters to calculate (Mishra and Singh, 2010). Moreover, due to the arid conditions and low precipitation patterns, Haihe River basin is susceptible to drought in crop growing season. Therefore, this paper used consecutive rain-less days as the standard to identify the start and end day of drought released by the Ministry of Water Resources of the People's Republic of China. In a wide range of frequency analysis method, the Pearson-III frequency curve is the most used curve, which is widely applied in hydrological frequency analysis in China. Most studies focused on the analysis of the spatial-temporal distribution of floods and droughts, while little analysis regarding the rainfall intensity change patterns following the drought exists. Thus, this article selected the daily rainfall data of 42 representative meteorological sites in Haihe River from 1963 to 2013, and the basin was divided into four sub-regions by SOM neural network method. The drought index of continuous rain-less day was used to determine the drought degree. The first effective daily rainfall and the maximum daily rainfall following the drought were analyzed with the Pearson-III frequency curve, and then the relationship between rainfall and drought magnitudes was shown.

Materials and methods

Description of the study area

The Haihe River basin includes Beijing, Tianjin, Hebei, Shanxi, Shandong, Henan, Inner Mongolia, Liaoning provinces and is located within the geographic coordinates of 112°-120°E and 35°-43°N. The total area of the basin is 318,000 km^2, including the mountainous area of 189,000 km^2 and the plain area of 129,000 km^2. This basin belongs to the temperate zone and semi-humid continental climate. Annual rainfall is 536 mm and it shows a negative trend. It suffers from drought risk frequently in China. Annual rain is mainly concentrated in the summer monsoon season and average monthly rainfall between June and August accounts for 50-75% of annual rainfall. In particular, heavy rain mostly occurs in July and August, leading to flood as one of the most water logging areas. The flood frequency between 1970 and 1994 is more than 45 times in the basin. The frequent drought and flood disasters are attributed to uneven seasonal distribution of rainfall and its inter-annual variability, which directly affects the sustainable development and property safety.

In this paper, the rainfall data for 42 meteorological stations with continuous observation series in and around the Haihe River basin for the years 1963 to 2013

http://www.aloki.hu ● ISSN 1589 1623 (Print) ● ISSN 1785 0037 (Online)
DOI: http://dx.doi.org/10.15666/aeer/1605_63956407
© 2018, ALÖKI Kft., Budapest, Hungary

provided by China National Climate Center were selected to analyze the drought and higher rainfall. The numbers of consecutive days without rainfall for both inter-annual and inter-decadal periods were determined.

Clustering methods of SOM and division

Due to the geographical position of the meteorological stations, the altitude and rainy features differ throughout the basin. Thus, meteorological stations within the basin with similar features require the clustering analysis. In this paper, the longitude and latitude of each meteorological station, as well as their respective altitudes and annual mean rainfall were selected for the cluster analysis by the SOM (self-organizing map) neural network algorithm.

A homogeneous area refers to the rainy characteristics of various meteorological sites in the area that are similar and their spatial distribution is even (Gwo-Fong and Lu-Hsien, 2006). The result of regional frequency analysis is representative and credible if the stations in the region belong to a homogeneous area. Using rainfall data for meteorological stations in the homogenous area is more accurate than using rainfall data at single station to analyze regional frequency. Therefore, the SOM neural network algorithm was selected to process the rainy data of 42 meteorological sites and Haihe River basin was divided according to the clustering results.

This article selected the longitude (m), latitude (m), the average annual rainfall (mm), 5-9 monthly rainfall (mm) as eight variables on behalf of regional rainy characteristics, and carried on the normalized processing. Training steps directly influence the performance of the SOM neural network clustering. The greater the training steps are, the more precise classifications are. This article carried on the classification of 42 meteorological sites in the basin and the basin was divided into four regions based on the cluster result with training steps as 2. The results of spatial classification were shown in *Table 1* and the locations of these stations were shown in *Figure 1*.

Drought magnitude standards

Less rain or no rain for a long time lead to drought and no effective continuous rainfall days are used to characterize the drought magnitude in crop growing season. Consecutive rainless days refer to the number of consecutive days without rainfall. Based on the standard of the classification for drought severity released by the Ministry of Water Resources of the People's Republic of China, the drought evaluation criteria are shown in *Table 2* as follows: If consecutive rain-less days last for 15 to 30 days, it belongs to the light drought; If consecutive rain-less days last for 31 to 50 days in a row, it belongs to the moderate drought; If consecutive rain-less days last for 51 to 75 days, it belongs to severe drought; If consecutive rain-less days exceed 75 days, it belongs to the extraordinary drought.

Table 1. *Cluster results of meteorological stations in and around Haihe River Basin*

Subarea	Meteorological stations
Region A	53399, 53478, 53487, 53593, 53663, 53673, 54208, 54308, 54311, 54401, 54405, 54423, 54511, 54518, 54527, 54602, 54606, 54618
Region B	53588, 53698, 53782, 53787, 53798, 53898, 53986, 54705, 54808, 54823, 54906, 57083
Region C	54416, 54429, 54436, 54449, 54534, 54539, 54616, 54623, 54624
Region D	54714, 54715, 54725

http://www.aloki.hu ● ISSN 1589 1623 (Print) ● ISSN 1785 0037 (Online)
DOI: http://dx.doi.org/10.15666/aeer/1605_63956407
© 2018, ALÖKI Kft., Budapest, Hungary

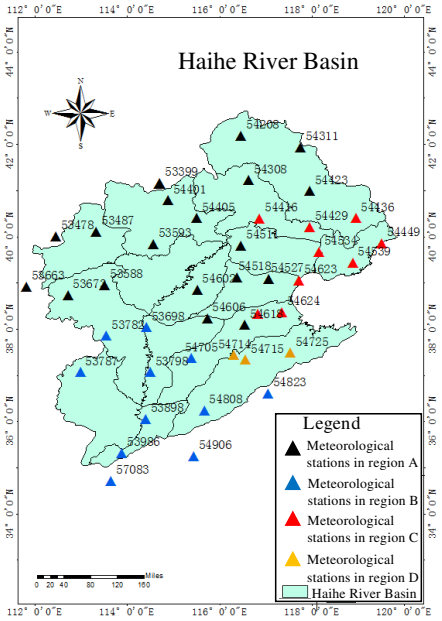

Figure 1. *Locations of meteorological stations in and around Haihe River Basin*

Table 2. *Drought classifications derived from continuous non-effective rainy days*

Drought classification	Continuous non-effective rainy days (d)
No drought	<15
Mild drought	15~30
Moderate drought	31~50
Severe drought	51~75
Extreme drought	>75

Pearson-III frequency curve

Pearson-III frequency distribution model has been widely applied in the field of hydrology and meteorology. This distribution is the third of 13 types of distribution curves which is put forward by the British biologist Pearson. Pearson-III frequency curve is asymmetric unmoral and skew normal distribution curve which one end is limited and the other end is unlimited. It refers to gamma distribution and the probability density function is as follows (*Eq. 1*):

$$f(x)=\frac{\beta^{\alpha}}{\Gamma(\alpha)}(x-b)^{\alpha-1}e^{-\beta(x-b)}(b\le x<\infty) \quad \text{(Eq.1)}$$

Where $\Gamma(\alpha)$ is gamma function, $\Gamma(\alpha)=\int_0^{\infty}x^{\alpha-1}e^{-x}dx;\alpha,\beta>0$. Three original parameters *α, β, b* can be converted appropriately, and can be shown as three statistical parameters $\bar{x}$, C_v, C_s (*Eqs. 2, 3* and *4*):

$$\alpha=\frac{4}{C_s^2} \quad \text{(Eq.2)}$$

http://www.aloki.hu ● ISSN 1589 1623 (Print) ● ISSN 1785 0037 (Online)
DOI: http://dx.doi.org/10.15666/aeer/1605_63956407
© 2018, ALÖKI Kft., Budapest, Hungary

$$\beta = \frac{2}{\bar{x} C_V C_S} \quad \text{(Eq.3)}$$

$$b = \bar{x}(1 - \frac{2C_v}{C_S}) \quad \text{(Eq.4)}$$

where C_v is dispersion coefficient; C_S is deviation factor; $\bar{x}$ is the average. The three statistical parameters can be determined primarily by the moment's method. Moment method is used to calculate the three statistical parameters of the formula which is as follows (*Eqs. 5, 6* and *7*):

$$\bar{x} = 1/n \sum x_i \quad \text{(Eq.5)}$$

$$C_V = \sqrt{\frac{\sum (k_i - 1)^2}{n-1}} \quad \text{(Eq.6)}$$

$$C_s = \frac{\sum (k_i - 1)^3}{(n-3) C_v^3} \quad \text{(Eq.7)}$$

Adding these undetermined parameters into the equations of Pearson-III type curve, the equation is written as (*Eq. 8*):

$$y = f(\bar{x}, C_v, C_s, x) \quad \text{(Eq.8)}$$

The division of rainy intensity

According to the national 24-h rainfall standard, rainfall is divided into light rain, moderate rain, heavy rain, rainstorm, heavy rainstorm and extraordinary rainstorm. If total rainfall during 24 h is less than 10.0 mm, it is light rain; if between 10.0 and 24.9 mm, it is moderate rain; if between 25.0 and 49.9 mm, it is heavy rain; if between 50.0 and 99.9 mm, it is rainstorm; if between 100.0 and 249.0 mm, it is heavy rainstorm; if more than 250.0 mm, it is extraordinary rainstorm. Considering water availability, light rain and heavy rainstorm are not effectively used for crops and sometimes cause natural disasters. Thus, in the paper, only effective rainfall (including moderate rain, heavy rain, rainstorm) was use to analyze its relationship between drought.

Results and discussion

The analysis of drought in the Haihe River basin

Time evolution characteristic of droughts

According to no effective rainy days in a row, the sum of the drought frequency in different regions in the Haihe River basin was calculated. The results indicated that drought frequency showed an increasing trend in the Haihe River basin from 1963 to 2013. The total drought frequency increased at a rate of 2.23% per year in 18 meteorological stations of region A, the total drought frequency increased at a rate of

http://www.aloki.hu ● ISSN 1589 1623 (Print) ● ISSN 1785 0037 (Online)
DOI: http://dx.doi.org/10.15666/aeer/1605_63956407
© 2018, ALÖKI Kft., Budapest, Hungary

about 7.8% per year in 12 meteorological stations, 8.9% per year in 9 meteorological stations, 2.5% per year in 3 meteorological stations, respectively in region B, region C and region D. Drought frequency increased notably in region A, while it increased more slowly in region D. Region A was the economic society center of the basin, and the increase of no-rainfall day seriously affected the crop growth and the social and economic development.

Space evolution characteristic of droughts

According to no effective rainy days, the drought frequency in four areas under different drought degree was calculated between 1963 and 2013 as shown in *Table 3*. It could be seen that region A, region B, region C and region D were all given priority to light drought which accounted for about 75% of the total number of drought, the second was moderate drought, and the probability of extraordinary drought occurred least. The probability of moderate drought and severe drought in region A was higher than that of region B, C and D, and the probability of extraordinary drought was the largest in region B with 0.35%.

Table 3. *The proportion of different drought numbers of regional total numbers during 1963 to 2013*

Drought degree	Region A		Region B		Region C		Region D	
	Frequency	Proportion (%)	Frequency	Proportion (%)	Frequency	Proportion (%)	Frequency	Proportion (%)
Light drought	2468	74.70%	1748	76.23%	1277	78.15%	464	76.07%
Moderate drought	692	20.94%	452	19.71%	300	18.36%	125	20.49%
Severe drought	133	4.03%	85	3.71%	55	3.37%	21	3.44%
Extraordinary drought	11	0.33%	8	0.35%	2	0.12%	0	0

The analysis of rainfall frequency after drought in Haihe River basin

The frequency of multi-yearly mean effective rainfall

Only effective rainfall is available for crops. Thus, the paper used the Pearson-III curve to only analyze the frequency of multi-yearly mean effective rainfall in each subarea of the Haihe River basin, and the probability of the moderate rain to heavy rain was calculated but probably sum of rainfall percentage within a region was less than 100%. According to Pearson-III frequency curve, the probability of the multi-yearly mean effective rainfall was different and the results were illustrated in *Table 4*.

Table 4. *The frequency of multi-yearly mean effective rainfall in different areas*

Subarea	Moderate rain (%)	Heavy rain (%)	Rainstorm (%)	Heavy rainstorm (%)
Region A	9.65	2.24	0.2	0
Region B	12.57	3.78	0.54	0.02
Region C	15.3	5.54	1.1	0.06
Region D	13.99	4.82	0.88	0.04

http://www.aloki.hu ● ISSN 1589 1623 (Print) ● ISSN 1785 0037 (Online)
DOI: http://dx.doi.org/10.15666/aeer/1605_63956407
© 2018, ALÖKI Kft., Budapest, Hungary

The probability of moderate rain, heavy rain, rainstorm and heavy rainstorm was 9.65%, 2.24%, 0.2% and 0 for region A, 12.57%, 3.78%, 0.54% and 0.02% for region B, 15.3%, 5.54%, 1.1% and 0.06 for region C, 13.99%, 4.82%, 0.88% and 0.04% for region D, respectively.

The frequency of the first effective rainfall after different drought degrees

This paper used consecutive rain-less days as drought standard and the first effective rainfall after drought period to represent the rainfall intensity at the end of the drought. The crop growing season in Haihe River basin was from May to September and in the periods the droughts and floods occurred frequently, causing disasters for the most important cash crop of summer corn growing. Thus, the first effective rainfall after different drought degrees during the growing season of crops was calculated. For further analysis, Pearson-III was used to analyze the frequency of the first effective rainfall after drought with different magnitudes in each subarea.

This paper only took region A as an example to analyze the first effective rain frequency after different drought degrees. *Figure 2* listed the Pearson-III curve after different droughts for region A. The results were as follows: The probability of moderate rain, heavy rain, rainstorm and heavy rainstorm after light drought were 39.02%, 9.65%, 1.26% and 0.33%, respectively shown in *Figure 2a*. From the Pearson-III curve for moderate drought in *Figure 2b,* it illustrated that the respective probabilities of moderate rain, heavy rain, rainstorm and heavy rainstorm were 40.85%, 8.28%, 0.7% and 0.13%. As shown in *Figure 2c* of the Pearson-III curve for severe drought, the respective probabilities of moderate rain, heavy rain, rainstorm and heavy rainstorm were 38.06%, 9.28%, 1.17% and 0.3%. From the Pearson-III curve of extraordinary drought in *Figure 2d,* the respective probabilities of moderate rain, heavy rain, rainstorm and heavy rainstorm were 50.25%, 7.97%, 0.12% and 0.

The rainfall frequencies after drought with different magnitudes in the other subareas for the years 1963-2013 were shown in *Table 3*. We presented the frequency of first effective rainfall after a drought period in sub-areas in *Table 5*. The effective rainfall did not include light rain (total rainfall during 24 h is less than 10.0 mm) and extraordinary rainstorm (total rainfall during 24 h is more than 250.0 mm), which could not been used and managed effectively for crops in growing seasons. Thus, the sum of frequency in different clusters was less than 100% within one region in case of all drought degrees.

From *Table 3* it was concluded that in region A, for the light and moderate drought, the occurrence frequency of moderate rain increased, then reduced and finally increased. The probability of moderate rain was the maximum after extraordinary drought at 50.25%, while the frequency for heavy rain first reduced, then increased and finally reduced, and the frequency for heavy rain was the least after extraordinary drought. In region B, for the light and moderate drought, the frequency for moderate rain decreased continuously, while the probability of rainfall after drought was higher than region A. In region C, for the the light and moderate drought, the occurrence frequency for moderate rain increased, while for the extraordinary drought, the occurrence frequency for moderate rain increased obviously. In region D, for the light and moderate drought, occurrence frequency of moderate rain increased significantly and the occurrence frequency for heavy rain first reduced, then increased and finally reduced. The probability of flood disaster of the first effective rainfall after severe drought was the most in region D.

http://www.aloki.hu ● ISSN 1589 1623 (Print) ● ISSN 1785 0037 (Online)
DOI: http://dx.doi.org/10.15666/aeer/1605_63956407
© 2018, ALÖKI Kft., Budapest, Hungary

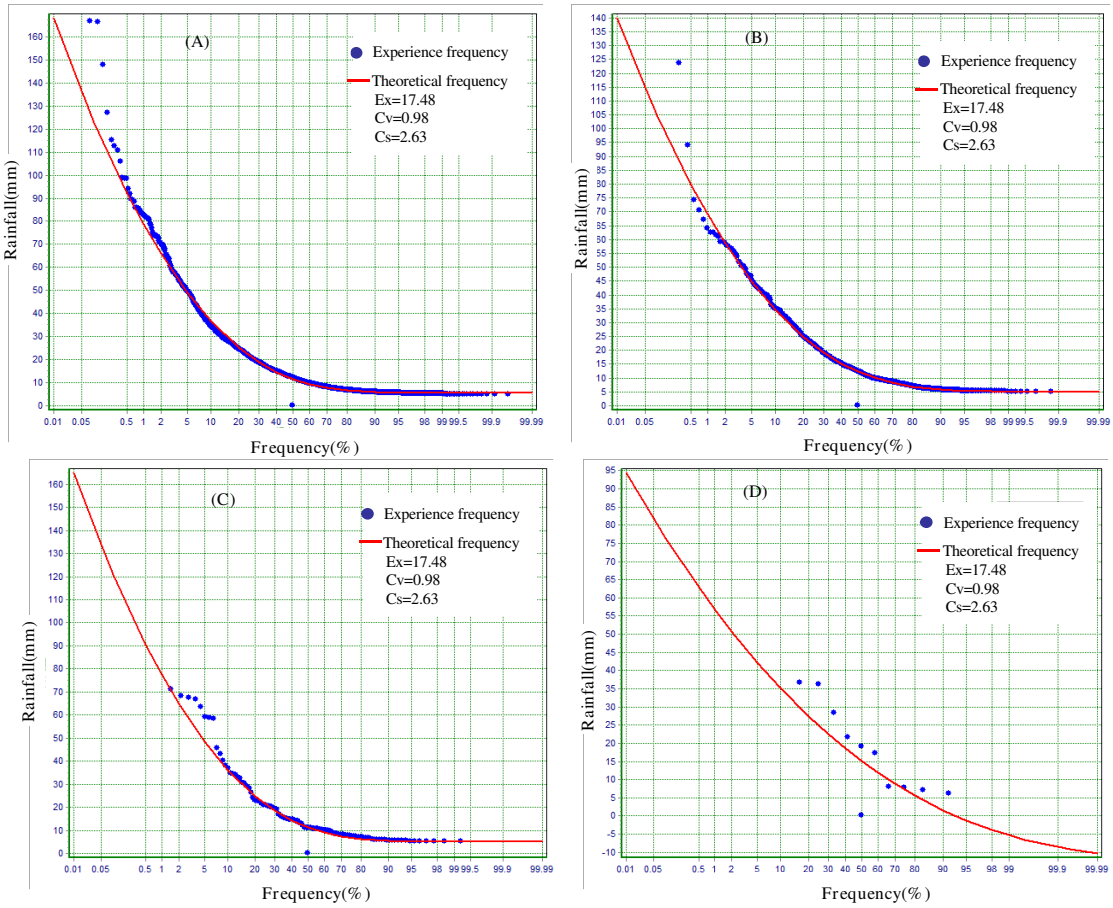

Figure 2. *Frequency of the first effective rainfall after different droughts in region A (a: light drought; b: moderate drought; c: severe drought; d: extraordinary drought)*

Table 5. *The frequency of the first effective rainfall after drought in subareas*

Subarea	Drought degree	Moderate rain (%)	Heavy rain (%)	Rainstorm (%)	Heavy rainstorm (%)
Region A	Light drought	39.02	9.65	1.26	0.33
	Moderate drought	40.85	8.28	0.7	0.13
	Heavy drought	38.06	9.28	1.17	0.3
	Extraordinary drought	50.25	7.97	0.12	0
Region B	Light drought	49.44	19	3.6	1.29
	Moderate drought	49.11	15.27	2.62	0.8
	Heavy drought	43.63	8.33	0.53	0.08
	Extraordinary drought	35.09	0.5	0	0
Region C	Light drought	46.91	15.1	2.94	1
	Moderate drought	39.38	9.32	1.1	0.27
	Heavy drought	60.69	17.24	1.4	0.22
Region D	Light drought	52.09	17.33	3.27	1.07
	Moderate drought	54.24	12.99	1.17	0.22
	Heavy drought	66.01	28.47	5.32	1.51

http://www.aloki.hu ● ISSN 1589 1623 (Print) ● ISSN 1785 0037 (Online)
DOI: http://dx.doi.org/10.15666/aeer/1605_63956407
© 2018, ALÖKI Kft., Budapest, Hungary

In summary, from the analysis of the probability of the first effective rainfall after the different degrees of drought, it was concluded that with the increase in drought magnitude, the probability of extraordinary rainstorm, in the Haihe River basin became lower in region A, region B and region C, however, the probability of extraordinary rainstorm increased in region D. With the increase in drought magnitude, the probability of different degrees of rainfall in different areas showed different trends. In region A, for the light and moderate drought, the occurrence frequency for moderate rain first reduced, then increased and finally reduced. In contrary, for region B, it showed a continuously decreasing trend. In region C and D, for the light drought and moderate drought, the occurrence frequency for moderate rain first reduced and then increased.

Compared with the probability of multi-yearly mean effective rainfall, it presented that the probabilities of moderate rain, heavy rain, rainstorm, heavy rainstorm were 9.65%, 2.24%, 0.2% and 0, respectively in region A. However, the respective probabilities of moderate rain, heavy rain, rainstorm, heavy rainstorm of the first effective rainy after light drought were 39.02%, 9.65%, 1.26% and 0.33%, the respective probabilities of moderate rain, heavy rain, rainstorm, heavy rainstorm of the first effective rainfall after moderate drought were 40.85%, 8.28%, 0.7% and 0.13%, those of the first effective rainfall after severe drought were 38.06%, 9.28%, 1.17% and 0.3% and after extraordinary drought were 50.25%, 7.97%, 0.12% and 0. The probability of the first effective rainy after drought was relatively higher than that of multi-yearly mean effective rainfall in region B, region C and region D. The results showed that the probability of heavy rain for the first effective rainfall after drought was strongly higher and it was easy to suffer flood disaster after droughts.

The frequency of maximum daily rainfall after different drought degrees

Pearson-III curve was used to analyze the frequency of the maximum daily rainfall after droughts with different magnitudes in each subarea of the Haihe River basin. The results of the frequency of maximum daily rainfall after droughts in region A were presented in *Figure 3*. Based on the Pearson-III curve of light drought, the probability of moderate rain was 62.47%, that of heavy rain was 23.96%, that of rainstorm was 5.19% and that of heavy rainstorm was 1.83%, respectively. For the moderate drought, the respective probabilities of moderate rain, heavy rain, rainstorm and heavy rainstorm reached 58.2%, 23.73%, 6.48% and 2.76%. For the Pearson-III curve of severe drought, the respective probabilities of moderate rain, heavy rain, rainstorm and heavy rainstorm were 72.02%, 35.61%, 10.17% and 4.17%. Moreover, for the Pearson-III curve of extraordinary drought, the respective probabilities of moderate rain, heavy rain, rainstorm and heavy rainstorm were 81.75%, 60.46%, 23.64% and 8.81%, respectively.

The rainfall frequencies after drought with different magnitudes in the other subareas for the years 1963-2013 were listed in *Table 6*. In this table, it was concluded that in region A, for the light drought and moderate drought, the occurrence frequency for moderate rain first reduced then increased and the frequency for rainstorm increased continuously. In region B, for the light drought, moderate drought and severe drought, the occurrence frequency for moderate rain decreased continuously. On the contrary, the occurrence frequency for rainstorm increased obviously after moderate drought. With the increase of drought degree, the occurrence frequency for heavy rain increased significantly. In region C, for the light drought magnitude, the occurrence frequency for heavy rain decreased continuously. With the increase of drought degree, the occurrence frequency for moderate rain increased significantly. Region D showed the same trend as region C.

http://www.aloki.hu ● ISSN 1589 1623 (Print) ● ISSN 1785 0037 (Online)
DOI: http://dx.doi.org/10.15666/aeer/1605_63956407
© 2018, ALÖKI Kft., Budapest, Hungary

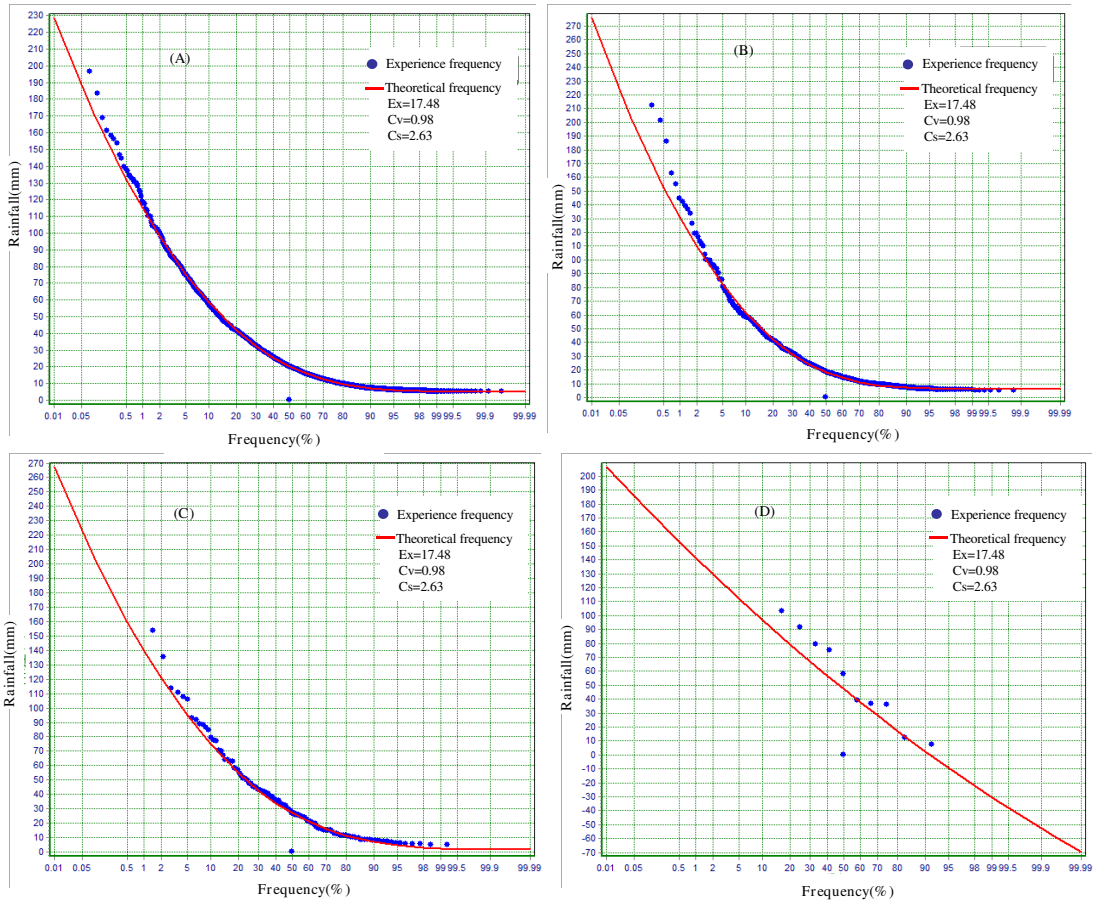

Figure 3. *Frequency of maximum daily rainfall after different droughts in region A (a: light drought; b: moderate drought; c: severe drought; d: extraordinary drought)*

Table 6. *The frequency of the maximum daily rainfall after different drought magnitude in subareas*

Subarea	Drought degree	Moderate rain (%)	Heavy rain (%)	Rainstorm (%)	Heavy rainstorm (%)
Region A	Light drought	62.47	23.96	5.19	1.83
	Moderate drought	58.2	23.73	6.48	2.76
	Heavy drought	72.02	35.61	10.17	4.17
	Extraordinary drought	81.75	60.46	23.64	8.81
Region B	Light drought	71.66	35.43	11.13	5.01
	Moderate drought	67.56	34.29	12.49	6.4
	Heavy drought	66.47	31.94	8.77	3.5
	Extraordinary drought	77.01	47.16	17.39	8.15
Region C	Light drought	70.52	38.91	15.78	8.64
	Moderate drought	60.66	30.61	12.08	6.67
	Heavy drought	77.02	46.26	17.84	8.91
Region D	Light drought	72.08	37.39	12.31	5.67
	Moderate drought	66.1	31.21	10.15	4.81
	Heavy drought	81.45	54.03	22.39	11.25

http://www.aloki.hu ● ISSN 1589 1623 (Print) ● ISSN 1785 0037 (Online)
DOI: http://dx.doi.org/10.15666/aeer/1605_63956407
© 2018, ALÖKI Kft., Budapest, Hungary

Generally, from the analysis of the probability of the maximum daily rainfall after different droughts, it was concluded that with the increase in drought magnitude, the probability of heavy rainstorm after drought increased. However, with the increase in drought magnitude, the probability of different degrees of rainfall in different areas showed different characteristics. The whole trend showed that for the light and moderate drought magnitude, the occurrence frequency for moderate rain first reduced and then increased in the four subareas for region A, region B, region C and region D generally. The probability of rainfall after moderate drought was lower than other degree of drought in region A, region C and region D, while the probability of rainfall after severe drought was notably lower than other degree of drought in region B.

Compared with the probability of multi-yearly mean effective rainfall in *Table 2,* the results indicated that the respective probabilities of moderate rain, heavy rain, rainstorm, heavy rainstorm were 9.65%, 2.24%, 0.2% and 0 in region A for the multi-yearly average. However, the respective probabilities of moderate rain, heavy rain, rainstorm, heavy rainstorm of the maximum daily rainfall after light drought could reach up to 62.47%, 23.96%, 5.19% and 1.83%, those after moderate drought 58.2%, 23.73%, 6.48% and 2.76%, those after severe drought 72.02%, 35.61%, 10.17% and 4.17% and those after extraordinary drought 81.75%, 60.46%, 23.64% and 8.81%, respectively, in *Table 4*. Furthermore, in the same way, the probability of the maximum daily rainfall after drought was significantly higher than multi-yearly mean effective rainfall in region B, region C and region D. The results showed that the probability of heavy rain for the maximum daily rainfall after drought was higher and the region there was more vulnerable to suffer flood disaster after drought.

Conclusions

In recent years, extreme climatic events such as alternating droughts and floods, sharp transitions between droughts and floods, and floods following extreme droughts, have been a research hotspot. This paper analyzed the relationship between drought and rainfall intensity through the rainfall frequency after different drought magnitudes based on the daily rainfall data from 42 stations for the years 1963-2013 in the Haihe River basin in northern China. The conclusions were as follows:

(1) Annual rainfall showed a dramatical reduction trend in the Haihe River basin and drought frequency increased. The result was consistent with the finding that the mean values of daily precipitation declined, and its fluctuation became weak with years by Sang (2014). Drought numbers for region A increased the most at a rate of about 0.223 times per year. The region was dominated by light drought. The probability of light drought and moderate drought were 76% and 20%, while that of extraordinary drought was the least.

(2) With the increase in drought magnitude, the probability of extraordinary rainstorm of the first effective rainfall became lower in region A, region B and region C, however, the probability of extraordinary rainstorm increased in region D. And with the increase of drought degree, the probability of extraordinary rainstorm of the maximum rainfall in A, B, C, D four regions increased significantly. Compared with the probability of multi-yearly mean effective rainfall, the probability of heavy rain to heavy rainstorm of the first effective rainfall was 4 to 5 times than the multi-yearly mean effective rainfall and the probability of heavy rain to heavy rainstorm of the maximum rainfall was 9 to 10 times than the multi-yearly mean effective rainfall.

http://www.aloki.hu ● ISSN 1589 1623 (Print) ● ISSN 1785 0037 (Online)
DOI: http://dx.doi.org/10.15666/aeer/1605_63956407
© 2018, ALÖKI Kft., Budapest, Hungary

Based on the frequency levels of different rainfall after different droughts in the region, we evaluated that more rainfall happened after higher drought and a dry-wet alternation happened frequently. With the increase of the drought numbers, rainfall frequency decreased and the rainfall intensity enhanced obviously. This result was consistent with the findings of Zhang (2014) that the frequency of extreme precipitation was decreasing, but the intensity of extreme precipitation was increasing in the Huang-Huai-Hai River basin, and moreover, the probability distribution functions of simple daily intensity index and consecutive dry days were positively shifted while the rest of the indices were negatively shifted. Because the flood in the basin was primarily caused by the intensive heavy rainstorm, the Haihe River basin was in higher frequency of simultaneous flood and drought disasters and more vulnerable to the impact of climatic change.

Acknowledgments. The authors acknowledge the National Social Science Fund of China (18BJY079) and the Training Plan for Innovation Teams in Tianjin Colleges and Universities (TD13-5038).

REFERENCES

[1] Burke, E. J., Brown, S. J., Christidis, N. (2001): Modeling the recent evolution of global drought and projections for the twenty-first century with the Hadley centre climate model. – J. Hydrometeorol. 7(5): 1113.
[2] Cancelliere, A., Mauro, G. D., Bonaccorso, B. G. et al. (2007): Drought forecasting using the 15 standardized precipitation index. – Water Resour. Manage. 21: 801-819.
[3] Feng, J., Yan, D., Li, C. (2012): General framework and key issues concerning integrated strategies for coping with drought and flood in China in a changing environment. – Natural Hazards 64(1): 577-592.
[4] Feng, J., Yan, D., Li, C., Gao, Y., Liu, J. (2014): Regional frequency analysis of extreme precipitation after drought events in the Haihe River basin, Northwest China. – J. Hydrol. Eng. 19(6): 1101-1112.
[5] Gwo-Fong, L., Lu-Hsien, C. (2006): Identification of homogeneous regions for regional frequency analysis using the self-organizing map. – J. Hydrol. 324: 1-9.
[6] Huijgevoort, M. H. J. V., Hazenberg, P., Lanen, H. A. J. V. et al. (2012): A generic method for hydrological drought identification across different climate regions. – Hydrol. Earth Syst. Sci. 16(8): 2437-2451.
[7] Łabędzki, L. (2010): Estimation of local drought frequency in central Poland using the standardized precipitation index SPI. – Irrigat. Drain. 56(1): 67-77.
[8] Mishra, A. K., Singh, V. P. (2010): A review of drought concepts. – J. Hydrol. 391: 202-216.
[9] Narasimhan, B., Srinivasan, R. (2005): Development and evaluation of soil moisture deficit index (SMDI) and evapotranspiration deficit index (ETDI) for agricultural drought monitoring. – Agric. Forest Meteorol. 133(1): 69-88.
[10] Palmer, W. C. (1965): Meteorological Drought. – Research Paper No. 45. U. S. Weather Bureau, Washington, DC, pp. 45-58.
[11] Sang, Y. F., Wang, Z., Liu, C. (2014): Spatial and temporal variability of precipitation extrema in the Haihe River basin, China. – Hydrol. Processes 28(3): 926-932.
[12] Tallaksen, L. M., Hisdal, H., van Lanen, H. A. J. (2009): Space-time modelling of catchment scale drought characteristics. – J. Hydrol. 375: 363-372.
[13] Yan, D. H., Wu, D., Huang, R., Wang, L. N. (2013): Drought evolution characteristics and precipitation intensity changes during alternating dry-wet

http://www.aloki.hu ● ISSN 1589 1623 (Print) ● ISSN 1785 0037 (Online)
DOI: http://dx.doi.org/10.15666/aeer/1605_63956407
© 2018, ALÖKI Kft., Budapest, Hungary

changes in the Huang-Huai-Hai River basin. – Hydrol. Earth Syst. Sci. Discuss. 17(7): 2859-2871.

[14] Zavareh, K. (1997): Extreme precipitation events and the applicability of global climate models to the study of floods and droughts. – Mathematics and Computers in Simulation (43): 261-268.

http://www.aloki.hu ● ISSN 1589 1623 (Print) ● ISSN 1785 0037 (Online)
DOI: http://dx.doi.org/10.15666/aeer/1605_63956407
© 2018, ALÖKI Kft., Budapest, Hungary

STUDY ON ALLELOPATHY OF THREE SPECIES OF *PINUS* IN NORTH CHINA

ZHANG, Z. X.[1,2] – GAO, Y.[1,3*] – ZHAO, Y. J.[4]

[1]*Shandong Provincial Key Laboratory of Water and Soil Conservation and Environmental Protection, College of Resources and Environment, Linyi University, 276005 Linyi, China*

[2]*Linyi No. 4 High School of Shandong Province, 276000 Linyi, China*
(e-mail: 1431873619@qq.com)

[3]*Linyi Scientific Exploration Laboratory, 276037 Linyi, China*

[4]*College of Agriculture and Forestry, Linyi University, 276005 Linyi, China*
(e-mail: zhaoyanjie1882@126.com)

**Corresponding author*
e-mail: gaoyuan1182@tom.com, gaoy@lyu.edu.cn

(Received 31st May 2018; accepted 13th Sep 2018)

Abstract. Two-year-old seedlings of *Pinus* species typical in North China (*Pinus thunbergii*, *Pinus tabuliformis* and *Pinus koraiensis*) were selected as the research object. The water extracted from the litter of *P. thunbergii*, *P. tabuliformis* and *P. koraiensis* were used to test the changes of photosynthetic pigment Chl. a, Chl. b and allelochemicals. The results were as follows: aqueous extract of *P. thunbergii* needle litter had significantly low inhibition on *P. thunbergii* while strongly inhibited *P. tabuliformis* and *P. koraiensis*. It also showed a markedly low inhibition on *P. thunbergii*, a moderate inhibition on *P. tabuliformis*, and a greatly strong inhibition on *P. koraiensis*. Obviously strong inhibition on *P. thunbergii*, *P. tabuliformis* and *P. koraiensis* were observed as well. Our study showed that pine needle water leaching solutions, such as *P. tabuliformis*, *P. thunbergii* and *P. koraiensis*, significantly inhibit their Chl. a and Chl. b, and will be a norm, which provides a new explanation for the decline in the coniferous forests of northern China.
Keywords: *Pinus thunbergii, Pinus tabuliformis, Pinus koraiensis, allelopathy, Chl. a, Chl. b*

Introduction

Allelopathy refers to the process that those chemical substances produced by plants, which can have beneficial or detrimental effects on the growth of the plants themselves or other plants around, are released into the environment through leaching, volatilization, stubble degradation and root excretion, (Peng and Shao, 2001; Kong et al., 2002; Zhou et al., 2004). Studies on allelopathy have dramatically increased since the 1970s and have undergone rapid development since the 1990s. In recent years, the research has become a hot topic in the fields of botany, ecology, agronomy and soil science (Albuquerque et al., 2011; Cheng and Cheng, 2015). At present, allelochemicals mean basically secondary metabolites. The most common allelochemicals are organic acids, phenols and terpenoids (Yan et al., 2000; Chen et al., 2015).

Allelopathy exists widely in nature and significantly affects forest community succession, vegetation restoration and forestry production (Li et al., 2010; Albuquerque et al., 2011; Cheng and Cheng, 2015). Conifers are important timber and afforestation species in China. In recent years, many coniferous plantations have faced such problems as productivity decline, soil degradation and natural regeneration obstacles. The traditional view is that this phenomenon is caused by rotation, inappropriate harvesting

http://www.aloki.hu ● ISSN 1589 1623 (Print) ● ISSN 1785 0037 (Online)
DOI: http://dx.doi.org/10.15666/aeer/1605_64096417
© 2018, ALÖKI Kft., Budapest, Hungary

methods, harvesting residues, tillage and land preparation (Chen et al., 2003; Wang et al., 2007). However, in recent years, convincing evidence has showed that allelopathy may be the key factor affecting the natural regeneration of coniferous forests. Allelochemicals can be transported to the ground through pine needles and litters (Kimura et al., 2015), which will limit the growth of seedlings and herbaceous plants (Kil and Yang, 1983; Kato-Noguchi et al., 2011) and will impede the regeneration of the stands (Pan et al., 2009; Wang et al., 2007). Researches on the allelopathy of the main afforestation species in northern China can provide important theoretical and practical guidance for the management and survival of regional man-made forests.

The type and dose of allelochemicals released by plants to the environment are decided by combined effects, namely the plant itself and environmental factors. Environmental stress can increase the release of allelochemicals (Albuquerque et al., 2011). Therefore, both the environment and the plant itself must be taken into consideration in the study of allelopathy. *P. thunbergii*, *P. tabuliformis* and *P. koraiensis* are the main afforestation species in northern China (Wei et al., 2017; Yin et al., 2018). At present, only few studies focus on the allelopathic effects of *P. thunbergii* tissue and understory extracts on Brassica rapa pekinensis (Zhang et al., 2012), litter leaf and soil extract on seed germination and seedling growth of *P. koraiensis* (Chen et al., 2016), Allelopathic effects on the growth and photosynthesis of *P. tabuliformis* seedlings (Jia et al., 2003), the autotoxicity of *P. tabuliformis* (Li et al., 2010), the allelopathic effect of *P. tabuliformis* soil in the Loess Plateau (Zhu et al., 2014), and the allelopathic effect of *P. tabuliformis* root in Hilly Loess Plateau (Wang et al., 2015), etc. There is no study focusing on the interaction between *P. thunbergii*, *P. tabuliformis* and *P. koraiensis*. In this research, 2-year-old seedlings of *P. thunbergii*, *P. tabuliformis* and *P. koraiensis* were selected for the pot experiment to study the effects of water and aqueous solution of *P. thunbergii* pine needles, *P. tabuliformis* pine needles and *P. koraiensis* pine needles. Changes of Chl. a, Ch. b, allelochemicals, also total triterpenes in seedlings were examined after 30 days.

Materials and methods

Testing materials

The pine needle litter of *P. thunbergii* and *P. tabuliformis* was collected from Tianmeng area of Mountain Meng, China. All target trees grew in a natural environment, with a height of about 10 m, and a diameter of about 15 cm. The pine needle litter of *P. koraiensis* was purchased from Hunchun seedling breeding base in Jilin, China. *P. thunbergii* and *P. tabuliformis* seedlings were purchased from the seedling breeding base of Junan County in Linyi city, China, the seedlings were about 0.5 m in height and 1.5 cm in diameter. *P. koraiensis* seedlings were purchased from Hunchun seedling breeding base in Jilin, China, the seedlings were about 0.5 m in height and 1.5 cm in diameter. The pot experiment was conducted at the science exploration laboratory base in Linyi, China.

Testing method

1) Five 600 m^2 *P. thunbergii* and *P. tabuliformis* sample plots were set up, and a 1 m^2 litter box was placed in each plot; 2) From January 2017 to July 2017, pine needles in the collection boxes of *P. thunbergii* and *P. tabuliformis* were packaged and transferred to the laboratory and summarized for natural drying; 3) From July 25 to August 25, 2017, pine needle litters of *P. thunbergii*, *P. tabuliformis* and *P. koraiensis* were soaked; 4) From July

http://www.aloki.hu ● ISSN 1589 1623 (Print) ● ISSN 1785 0037 (Online)
DOI: http://dx.doi.org/10.15666/aeer/1605_64096417
© 2018, ALÖKI Kft., Budapest, Hungary

20 to August 25, 2017, *P. thunbergii*, *P. tabuliformis* and *P. koraiensis* seedlings were potted; 5) From August 25 to September 25, 2017, the seedlings of *P. thunbergii*, *P. tabuliformis* and *P. koraiensis* were inoculated in pots. Four treatments (clean water control group, *P. thunbergii* needle water leaching solution treatment group, *P. tabuliformis* needle water leaching solution treatment group and *P. koraiensis* needle water leaching solution treatment group) were set for each of the three young pine trees. Five plants were cultivated in parallel. 100 mL water or pine needles water leachate was added to the young pine trees every 5 days for 6 times, a total volume of 600 mL was used; 5) On September 25, all pine needles were sampled and sealed in bags for inspection.

Determination method

Determination of Chl. a and Chl. b content

0.1 g pine needles were weighed, cut and placed into the mortar. More than 15 mL absolute ethanol was added to the mortar until the total volume of the liquid was 25 mL. These solutions were stored in the dark for 24 h and then were filtered. The pigment's optical density was measured by a spectrophotometer 721 at a wavelength of 665 nm and 649 nm, and the content Chl. a and Chl. b were calculated.

Determination of total triterpene content

After extraction and centrifugation of the pine needles the sample solution was filtered through a 0.3 μm membrane filter. The residue was separated on a C_{18} column by high performance liquid chromatography. The mobile phase was $(NH_4)_2HPO_4$-H_3PO_4 buffer solution (pH = 2.7). For detection a UV detector at 210 nm was used. External standard method was performed for the determination of total triterpene content. The test was completed in the Environment Laboratory of Scistd Testing Qingdao Branch, China.

Data processing

Excel 2003 and SPSS 17.0 Chinese version were used for processing, and one-way analysis of variance was performed.

Results

Effects of 4 kinds of treatment on the Chl. a content in 3 kinds of seedlings

Groups of *P. thunbergii* seedlings for Chl. a content test: clean water control group> *P. thunbergii* needle water leaching solution treatment group> *P. tabuliformis* needle water leaching solution treatment group> *P. koraiensis* needle water leaching solution treatment group. *P. thunbergii* needle water leaching solution treatment group, *P. tabuliformis* needle water leaching solution treatment group and *P. koraiensis* needle water leaching solution treatment group showed significantly lower results than clean water control group ($P < 0.01$, $P < 0.01$, $P < 0.01$), and *P. koraiensis* needle water leaching solution treatment group showed significantly lower results than *P. thunbergii* needle water leaching solution treatment group and *P. tabuliformis* needle water leaching solution treatment group ($P < 0.01$, $P < 0.01$) (Fig. 1A).

Groups of *P. tabuliformis* seedlings for Chl. a content test: clean water control group> *P. thunbergii* needle water leaching solution treatment group> *P. tabuliformis*

http://www.aloki.hu ● ISSN 1589 1623 (Print) ● ISSN 1785 0037 (Online)
DOI: http://dx.doi.org/10.15666/aeer/1605_64096417
© 2018, ALÖKI Kft., Budapest, Hungary

needle water leaching solution treatment group> *P. koraiensis* needle water leaching solution treatment group. *P. thunbergii* needle water leaching solution treatment group, *P. tabuliformis* needle water leaching solution treatment group and *P. koraiensis* needle water leaching solution treatment group showed significantly lower results than clean water control group ($P < 0.05$, $P < 0.01$, $P < 0.01$), and *P. koraiensis* needle water leaching solution treatment group showed significantly lower results than *P. thunbergii* needle water leaching solution treatment group and *P. tabuliformis* needle water leaching solution treatment group ($P < 0.01$, $P < 0.01$) (Fig. 1A).

Groups of *P. koraiensis* seedlings for Chl. a content test: clean water control group> *P. thunbergii* needle water leaching solution treatment group> *P. tabuliformis* needle water leaching solution treatment group> *P. koraiensis* needle water leaching solution treatment group. *P. thunbergii* needle water leaching solution treatment group, *P. tabuliformis* needle water leaching solution treatment group and *P. koraiensis* needle water leaching solution treatment group showed significantly lower results than clean water control group ($P < 0.05$, $P < 0.01$, $P < 0.01$), and *P. koraiensis* needle water leaching solution treatment group showed significantly lower results than *P. thunbergii* needle water leaching solution treatment group ($P < 0.01$, $P < 0.05$) and *P. tabuliformis* needle water leaching solution treatment group, *P. tabuliformis* needle water leaching solution treatment group showed significantly lower results than *P. thunbergii* needle water leaching solution treatment group ($P < 0.01$) (Fig. 1A).

Effects of 4 kinds of treatment on the Chl. b content in 3 kinds of seedlings

Groups of *P. thunbergii* seedlings for Chl. b content test: clean water control group> *P. thunbergii* needle water leaching solution treatment group> *P. tabuliformis* needle water leaching solution treatment group> *P. koraiensis* needle water leaching solution treatment group. *P. koraiensis* needle water leaching solution treatment group showed significantly lower results than clean water control group, *P. thunbergii* needle water leaching solution treatment group and *P. tabuliformis* needle water leaching solution treatment group ($P < 0.01$, $P < 0.01$, $P < 0.05$) (Fig. 1B).

Groups of *P. tabuliformis* seedlings for Chl. b content test: clean water control group> *P. thunbergii* needle water leaching solution treatment group> *P. tabuliformis* needle water leaching solution treatment group> *P. koraiensis* needle water leaching solution treatment group. *P. thunbergii* needle water leaching solution treatment group, *P. tabuliformis* needle water leaching solution treatment group and *P. koraiensis* needle water leaching solution treatment group showed significantly lower results than clean water control group ($P < 0.01$, $P < 0.01$, $P < 0.01$), and *P. koraiensis* needle water leaching solution treatment group showed significantly lower results than *P. thunbergii* needle water leaching solution treatment group and *P. tabuliformis* needle water leaching solution treatment group ($P < 0.01$, $P < 0.01$) (Fig. 1B).

Groups of *P. koraiensis* seedlings for Chl. b content test: clean water control group> *P. thunbergii* needle water leaching solution treatment group> *P. tabuliformis* needle water leaching solution treatment group> *P. koraiensis* needle water leaching solution treatment group. *P. thunbergii* needle water leaching solution treatment group, *P. tabuliformis* needle water leaching solution treatment group and *P. koraiensis* needle water leaching solution treatment group showed significantly lower results than clean water control group ($P < 0.01$, $P < 0.01$, $P < 0.01$), and *P. koraiensis* needle water leaching solution treatment group showed significantly lower results than *P. thunbergii* needle water leaching solution treatment group and *P. tabuliformis* needle water

http://www.aloki.hu ● ISSN 1589 1623 (Print) ● ISSN 1785 0037 (Online)
DOI: http://dx.doi.org/10.15666/aeer/1605_64096417
© 2018, ALÖKI Kft., Budapest, Hungary

leaching solution treatment group ($P < 0.01$, $P < 0.05$), *P. tabuliformis* needle water leaching solution treatment group was significantly lower than *P. thunbergii* needle water leaching solution treatment group ($P < 0.01$) (Fig. 1B).

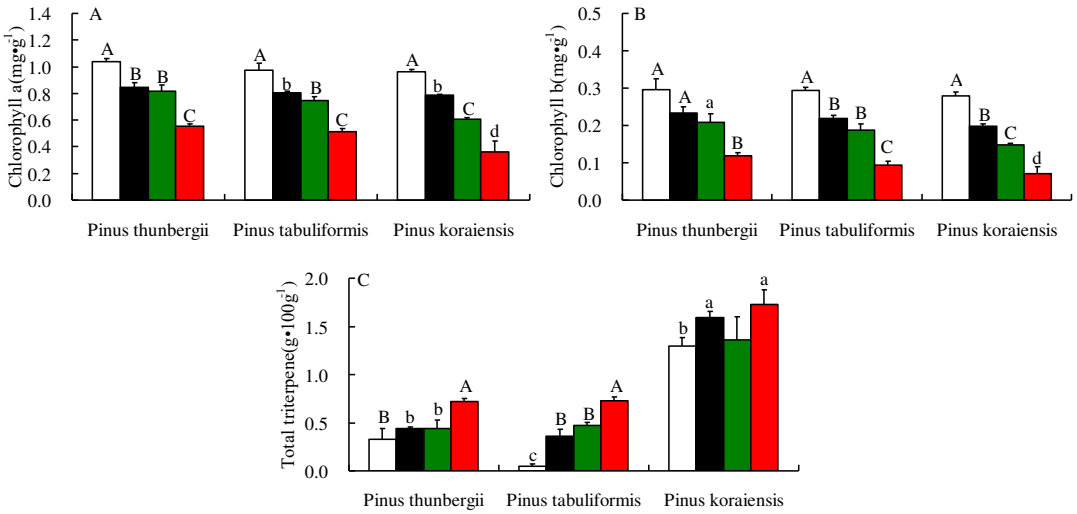

Figure 1. *Effects of 4 kinds of treatment on Chl. a (A), Chl. b (B) and total triterpene (C) in 3 kinds of seedlings (average + standard error). □ Clean water control group; ■ P. thunbergii needle water leaching solution treatment group; ■ P. tabuliformis needle water leaching solution treatment group; ■ P. koraiensis needle water leaching solution treatment group The difference between the adjacent letters is significant, capitalized letters P < 0.01, and lowercase letters P < 0.05*

Effects of 4 kinds of treatment on the total triterpene content in 3 kinds of seedlings

Groups of *P. thunbergii* seedlings for total triterpene content test: *P. koraiensis* needle water leaching solution treatment group> *P. thunbergii* needle water leaching solution treatment group> *P. tabuliformis* needle water leaching solution treatment group>clean water control group. *P. koraiensis* needle water leaching solution treatment group showed significantly higher results than *P. thunbergii* needle water leaching solution treatment group, *P. tabuliformis* needle water leaching solution treatment group and clean water control group, while *P. thunbergii* needle water leaching solution treatment group, *P. tabuliformis* needle water leaching solution treatment group and clean water control group had no significant difference ($P < 0.01$, $P < 0.01$, $P < 0.05$) (Fig. 1C). *P. koraiensis* needle water leaching solution had a significant allelopathic effect on *P. thunbergii* seedlings.

Groups of *P. tabuliformis* seedlings for total triterpene content test: *P. koraiensis* needle water leaching solution treatment group> *P. tabuliformis* needle water leaching solution treatment group> *P. thunbergii* needle water leaching solution treatment group>clean water control group. *P. koraiensis* needle water leaching solution treatment group, *P. tabuliformis* needle water leaching solution treatment group and *P. thunbergii* needle water leaching solution treatment group showed significantly higher results than clean water control group ($P < 0.01$, $P < 0.01$, $P < 0.05$), and *P. koraiensis* needle water leaching solution treatment group showed significantly higher results than *P. tabuliformis* needle water leaching solution treatment group and *P. thunbergii* needle water leaching solution treatment group ($P < 0.01$, $P < 0.01$), while *P. tabuliformis*

http://www.aloki.hu ● ISSN 1589 1623 (Print) ● ISSN 1785 0037 (Online)
DOI: http://dx.doi.org/10.15666/aeer/1605_64096417
© 2018, ALÖKI Kft., Budapest, Hungary

needle water leaching solution treatment group and *P. thunbergii* needle water leaching solution treatment group had no significant difference (Fig. 1C). *P. koraiensis* needle water leaching solution, *P. tabuliformis* needle water leaching solution and *P. thunbergii* needle water leaching solution had a significant allelopathic effect on *P. tabuliformis* seedlings.

Groups of *P. koraiensis* seedlings for total triterpene content test: *P. koraiensis* needle water leaching solution treatment group> *P. thunbergii* needle water leaching solution treatment group> *P. tabuliformis* needle water leaching solution treatment group>clean water control group. *P. koraiensis* needle water leaching solution treatment group and *P. thunbergii* needle water leaching solution treatment group showed significantly higher results than clean water control group ($P < 0.05$, $P < 0.05$), while *P. tabuliformis* needle water leaching solution treatment group and clean water control group had no significant difference (Fig. 1C). *P. koraiensis* needle water leaching solution and *P. thunbergii* needle water leaching solution had a significant allelopathic effect on *P. koraiensis* seedlings.

Relevance of Chl. a, Chl. b and total triterpene

Analysis indicated significant positive linear correlation between Chl. a and Chl. b in 3 kinds of seedlings, such as *P. tabuliformis*, *P. thunbergii* and *P. koraiensis* ($y = 0.3976 x - 0.1056$, $R^2 = 0.9435$, $P < 0.01$, $n = 58$) (Fig. 2A). Relevance of Chl. a and total triterpene is significant in 3 kinds of seedlings ($y = -0.1303 x^3 + 0.4627 x^2 - 0.4896 x + 0.3312$, $R^2 = 0.37$, $P < 0.01$, $n = 58$) (Fig. 2B). Relevance of Chl. b and total triterpene is significant in 3 kinds of seedlings ($y = -0.3161 x^3 + 1.1339 x^2 - 1.2147 x + 1.0971$, $R^2 = 0.3815$, $P < 0.01$, $n = 58$) (Fig. 2C).

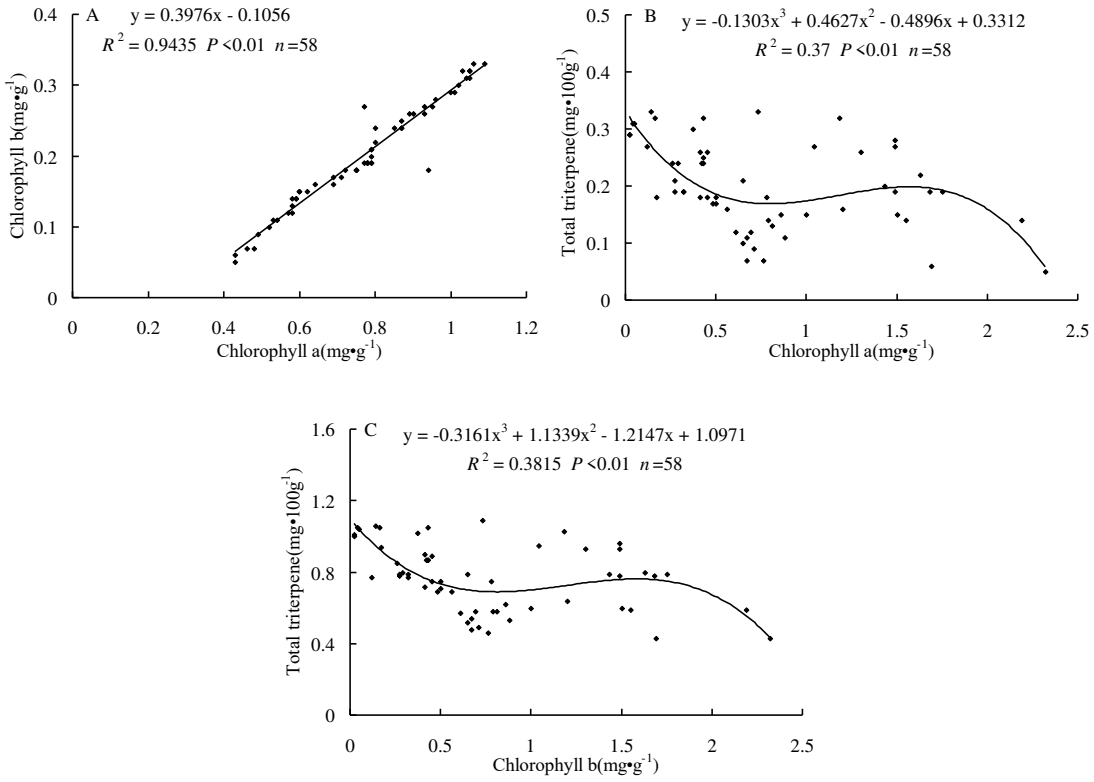

Figure 2. *Relevance of Chl. a, Chl. b and total triterpene in 3 kinds of seedlings (A, B, C)*

http://www.aloki.hu ● ISSN 1589 1623 (Print) ● ISSN 1785 0037 (Online)
DOI: http://dx.doi.org/10.15666/aeer/1605_64096417
© 2018, ALÖKI Kft., Budapest, Hungary

Discussion

In recent years, it has been found that allelochemicals can inhibit the absorption and transport of amino acids, and can interfere with the protein synthesis (Li et al., 2010), inhibit or damage the synthesis of photosynthetic pigments and accelerate the decomposition of photosynthetic pigments (Poonpaiboonpipat et al., 2013). It also affects the shape and structure of plant cells, and change the transport of nutrients and nutrient accumulation efficiency (Singh et al., 2009; Sunar et al., 2013; Grana et al., 2013), eventually causing a strong change in plant cells and growth of plants. The soil leaching liquor in *P. koraiensis* plantation had suppressive effects on the 7 measured indices, such as germination percentage, germination potential, hypocotyl and radicle length, seedling height, root length and dry mass (Chen et al., 2016). The leaf litter, semi-decomposed litter and surface soil infiltration solution of *P. tabulaeformis* significantly inhibited the growth, chlorophyll content (especially Chl. a content) and net photosynthetic rate of *P. tabulaeformis* seedlings (Jia et al., 2003). Japanese red pine (*P. koraiensis*) produces resin acids, such as abscisic acid-β-d-glucopyranosyl ester (Kato-Noguchi et al., 2011), 9α,13β-epidioxyabeit-8(14)en-18-oic acid and abscisic acid-β-Dglucopyranosyl ester (Kimura et al., 2015), 15-hydroxy-7-oxodehydroabietate and 7-oxodehydroabietic acid (Kato-Noguchi et al., 2017), which are transported to the surface soil through fallen leaves, inhibiting the growth of roots and shoots of other plants, resulting in sparse understory vegetation. The cedar (*Cedrus deodara*) leaves volatiles have a strong allelopathic effect, and its main components are terpenoids (Li et al., 2015). Their leaf water leaching liquid affects root length, shoot length and chlorophyll content, and reduce seed germination and plant dry weight (Talukdar and Talukdar, 2012; Uddin and Robinson, 2017). Allelochemicals reduce plant absorption and increase the availability of soil nutrients (Aslam et al., 2017; Mohammadkhani and Servati, 2018). Our study showed that pine needle water leaching solutions, such as *P. tabuliformis*, *P. thunbergii* and *P. koraiensis*, significantly inhibit their Chl. a and Chl. b, and will be a norm, which provides a new explanation for the decline in the coniferous forests of northern China. We propose to carry on research in this direction, such as dividing the concentration of the pine needle litter water extract, separating and identifying more new allelochemicals, thus revealing the plant physiological and biochemical reactions and countermeasures of the three major *Pinus* species in northern China.

Conclusions

P. thunbergii needle water leaching solution treatment significantly reduced chl. a and chl. b contents in *P. thunbergii* seedlings. It greatly reduced the total triterpene content in *P. tabuliformis* seedlings while enhanced the total triterpene content in *P. tabuliformis.* In addition, it significantly reduced the total triterpene content in *P. koraiensis* seedlings while enhanced the total triterpene content in *P. koraiensis* seedlings.

P. tabuliformis needle water leaching solution treatment significantly reduced Chl. a and Chl. b contents in *P. thunbergii* seedlings and Chl. a and Chl. b contents in *P. tabuliformis* seedlings as well. However, it strengthened the total triterpene content in *P. tabuliformis* seedlings, with the decrease of Chl. a and Chl. b contents in *P. koraiensis* seedlings.

http://www.aloki.hu ● ISSN 1589 1623 (Print) ● ISSN 1785 0037 (Online)
DOI: http://dx.doi.org/10.15666/aeer/1605_64096417
© 2018, ALÖKI Kft., Budapest, Hungary

Although *P. koraiensis* needle water leaching solution treatment significantly reduced Chl. a and Chl. b contents in *P. thunbergii* seedlings, it dramatically increased total triterpene content in *P. thunbergii* seedlings. And it also caused the total triterpene content in *P. tabuliformis* seedlings to decrease and the total triterpene content in *P. tabuliformis* seedlings to increase. Moreover, it decreased the total triterpene content in *P. koraiensis* seedlings while it increased the total triterpene content in *P. koraiensis* seedlings.

Comprehensive assessment showed that *P. thunbergii* needle litter water leaching solution had a significantly low inhibition on *P. thunbergii* while a significantly strong inhibition on *P. tabuliformis* and *P. koraiensis*. It also showed a significantly low inhibition on *P. thunbergii*, a moderate inhibition on *P. tabuliformis* and a significantly strong inhibition on *P. koraiensis*. *P. koraiensis* needle litter water leaching solution had a significantly strong inhibition on *P. thunbergii*, *P. tabuliformis* and *P. koraiensis*.

Acknowledgements. Funded by the Fund of Shandong Provincial Key Laboratory of Water and Soil Conservation and Environmental Protection, Linyi University, NO. STKF201603.

REFERENCES

[1] Albuquerque, M. B. D., Santos, R. C. D., Lima, L. M., Câmara, C. A. G. D., Ramos, A. D. R. (2011): Allelopathy, an alternative tool to improve cropping systems. – Agron Sustain Dev 31: 379-395.

[2] Aslam, F., Khaliq, A., Matloob, A., Tanveer, A., Hussain, S., Zahir, Z. A. (2017): Allelopathy in agro-ecosystems: a critical review of wheat allelopathy-concepts and implications. – Chemoecology 27: 1-24.

[3] Chen, L., Zhang, M., Xin, M., Li, J. D. (2015): Effects of exogenous phenolic acids on allelopathy of potted soybean seedlings. – Agr Sci Tech 16: 1151.

[4] Chen, L. C., Wang, S. L., Chen, C. Y. (2003): Degradation mechanism of Chinese fir plantation. – Chin J Appl Ecol 15: 1953-1957 [in Chinese].

[5] Chen, L. X., Li, S. B., Qiao, L., Bu, F., Duan, W. B. (2016): Influence of leaf litter and soil leaching liquor on seed germination and seedling growth of Pinus koraiensis. – Journal of Nanjing Forestry University (Natural Science) 40(2): 81-87 [in Chinese].

[6] Cheng, F., Cheng, Z. H. (2015): Research progress on the use of plant allelopathy in agriculture and the physiological and ecological mechanisms of allelopathy. – Front Plant Sci 1020.

[7] Graña, E., Sotelo, T., Díaz-Tielas, C., Araniti, F., Krasuska, U., Bogatek, R., Reigosa, M. J., Sánchez-Moreiras, A. M. (2013): Citral induces auxin and ethylene-mediated malformations and arrests cell division in *Arabidopsis thaliana* roots. – J Chem Ecol 39: 271-282.

[8] Jia, L. M., Zhai, M. P., Feng, C. H. (2003): Effects of allelopathic substances on the growth and photosynthesis of *Pinus tabulaeformis* Seedlings. – J Beijing Fore Univ 25(4): 6-10 [in Chinese].

[9] Kato-Noguchi, H., Fushimi, Y., Tanaka, Y., Teruya, T., Suenaga, K. (2011): Allelopathy of red pine: isolation and identification of an allelopathic substance in red pine needles. – Plant Growth Regul 65: 299-304.

[10] Kato-Noguchi, H., Kimura, F., Ohno, O., Suenaga, K. (2017): Involvement of allelopathy in inhibition of understory growth in red pine forests. – J Plant Biol 218: 66-73.

[11] Kil, B. S., Yang, J. Y. (1983): Allelopathic effects of *Pinus densiflora* on undergrowth of red pine forest. – J Chem Ecol 9: 1135-1151.

http://www.aloki.hu ● ISSN 1589 1623 (Print) ● ISSN 1785 0037 (Online)
DOI: http://dx.doi.org/10.15666/aeer/1605_64096417
© 2018, ALÖKI Kft., Budapest, Hungary

[12] Kimura, F., Sato, M., Kato-Noguchi, H. (2015): Allelopathy of pine litter: delivery of allelopathic substances into forest floor. – J Plant Biol 58: 61-67.
[13] Kong, C. H. (2002): Frontier fields of plant chemical ecology in the 21st century. – Chin J Appl Ecol 13: 349-353 [in Chinese].
[14] Li, D. W., Wang, D. M., Yao, W. X. (2010): Autotoxicity of *Pinus tabulaeformisand* its ecology significance. – Sci Silva Sin 46(11): 174-178 [in Chinese].
[15] Li, X. F., Jiao, H., Yuan, Y., Tian, S. N. (2015): Allelopathic effects and chemincal components of the volatiles from *Cedrus deodara* leaves and branches. – Ecol Environ 24: 263-269.
[16] Li, Z. H., Wang, Q., Ruan, X., Pan, C. D., Jiang, D. A. (2010): Phenolics and plant allelopathy. – Molecules 15: 8933-8952.
[17] Mohammadkhani, N., Servati, M. (2018): Nutrient concentration in wheat and soil under allelopathy treatments. – J Plant Res 131: 143-155.
[18] Pan, C. D., Wang, Q., Ruan, X., Li, Z. H. (2009): Biological activity and quantification of potential autotoxins from the leaves of *Picea Schrenkiana*. – Chin J Plant Ecol 33: 183-196 [in Chinese].
[19] Peng, S. L., Shao, H. (2001): Research significance and foreground of allelopathy. – Chin J Appl Ecol 12: 780-785 [in Chinese].
[20] Poonpaiboonpipat, T., Pangnakorn, U., Suvunnamek, U., Teerarak, M., Charoenying, P., Laosinwattana, C. (2013): Phytotoxic effects of essential oil from *Cymbopogon citratus* and its physiological mechanisms on barnyardgrass (*Echinochloa crus-galli*). – Ind Crop Prod 41: 403-407.
[21] Singh, A., Singh, D., Singh, N. B. (2009): Allelochemical stress produced by aqueous leachate of Nicotiana plumbaginifolia Viv. – Plant Growth Regul 58: 163-171.
[22] Sunar, S., Yildirim, N., Aksakal, O., Agar, G. (2013): Determination of the genotoxic effects of *Convolvulus arvensis* extracts on corn (*Zea mays* L.) seeds. – Toxicol Ind Health 29: 449-459.
[23] Talukdar, D., Talukdar, T. (2012): Alien invasive legumes and allelopathy: a case study at Gangetic West Bengal, India. – Int J Energ Res 4(4): 32-40.
[24] Uddin, M. N., Robinson, R. W. (2017): Allelopathy and resource competition: the effects of Phragmites australis invasion in plant communities. – Bot Stud 58: 29-40.
[25] Wang, Q., Ruan, X., Li, Z. H., Pan, C. D. (2007): Autotoxicity of plants and research of coniferous forest autotoxicity. – Sci Sin 43(6): 134-142 [in Chinese].
[26] Wang, X., Wei, T. X., Zhu, J. Z., Zhao, X. K., Liu, H. Y. (2015): Allelopathic effect of *Pinus tabulaeformis* root in on loess hilly area. – J Beijing Fore Univ 37(4): 82-89 [in Chinese].
[27] Wei, J. J., Gao, Y., Zhao, W. G., Liu, J. (2017): Hillside topographic pattern of shrub and herb diversity of forest in Mount Tai of China. – J Environ Prot Ecol 18: 571-580.
[28] Yan, F., Yang, Z. M., Han, L. M. (2000): Review on research methods for allelopathy and allelochemicals in plants. – Acta Ecol Sin 20: 692-696 [in Chinese].
[29] Yin, X. D., Gao, Y., Liu, J., Zhao, W. G. (2018): influence of scenic road corridor to plant diversity in Kunyu Mountain, China. – Appl Ecol Env Res 16: 1461-1469.
[30] Zhang, J., Wang, G. M., Qu, Z. Q., Yang, L., Wang, L. H., Sun, J. G., Zhang, X. N., Xing, H. J. (2012): Preliminary study on allelopathy of *Pinus thunbergii*. – Shandong Agric Sci 44(7): 37-40 [in Chinese].
[31] Zhou, K., Guo, W. M., Xu, Y. C. (2004): Advances of research on allelopathic potential in compositae. – Acta Ecol Sin 24: 1776-1784 [in Chinese].
[32] Zhu, B. C., Liu, Z. W., Huang, L. J., Bing, Y. H., Zhang, X. X., Lv, C. (2014): Allelopathic effects of humus soil from *Pinus tabulaeformis* forest on 10 plant species in the loess plateau. – Acta Agrect Sin 22: 1014-1020 [in Chinese].

http://www.aloki.hu ● ISSN 1589 1623 (Print) ● ISSN 1785 0037 (Online)
DOI: http://dx.doi.org/10.15666/aeer/1605_64096417
© 2018, ALÖKI Kft., Budapest, Hungary

DEGRADATION OF POLYCYCLIC AROMATIC HYDROCARBONS: A REVIEW

PENG, X.* – XU, P.-F. – DU, H. – TANG, Y. – MENG, Y. – YUAN, L. – SHENG, L.-P.

National and Local United Engineering Laboratory for New Petrochemical Materials and Fine Utilization of Resources; Key Laboratory of Resource Fine-Processing and Advanced Materials of Hunan Province; Key Laboratory of Chemical Biology and Traditional Chinese Medicine Research (Hunan Normal University), Ministry of Education; College of Chemistry and Chemical Engineering, Hunan Normal University, Changsha 410081, China

**Corresponding author*
e-mail: xinp@hunnu.edu.cn

(Received 8th Jun 2018; accepted 13th Sep 2018)

Abstract. Polycyclic aromatic hydrocarbons (PAHs) are hydrocarbons composed of two or more benzene rings, and they are widely found in nature. The degradation of PAHs remains in a dynamic equilibrium, which has suffered from the increasing PAHs emissions under the continuous development of society. Therefore, the environmental pollution is getting increasingly serious. Many scholars have conducted researches on the degradation of PAHs. In this paper, the origin and properties of PAHs are introduced. Besides, the physical, chemical and biological methods for the degradation of PAHs were reviewed. Among them the biodegradation of PAHs has been especially analyzed. Meanwhile, the advantages and disadvantages of each method were described through comparison.
Keywords: *PAHs, remove, physical methods, chemical methods, biological methods, characteristics*

Introduction

Polycyclic aromatic hydrocarbons (PAHs) are organic compounds that consist of either at least two condensed benzene rings or pentad molecules that are arranged in various chemical configurations. PAHs are categorized as low molecular weight (LMW) and high molecular weight (HMW) PAHs based on molecular structure. The structures of LMW PAHs include two-rings structure and three-rings structure while those of HMW PAHs include at least four rings. The aqueous solubility of PAHs decreases almost linearly with the increase in molecular mass (Mahler et al., 2012).

PAHs feature high melting points, high boiling points, and the low aqueous solubility, which gradually decreases with the increase of molecular weight. At the same time, the high fat solubility enables PAHs to dissolve in organic solvents easily. PAHs are widely available as they can be released into the environment by nature or by human activities. Bio-combustion, such as the combustion of forest and grassland, is the main source of PAHs. In addition, the emission of PAHs is also caused by the combustion of gasoline and coal, as well as the combustion of industrial waste (Liu et al., 2008; Tiwari et al., 2013). Moreover, in urban areas, street dust and sewage contain not only PAHs but also heavy metals such as lead and copper. In areas abounded with coal mines, the formation of PAHs caused by incomplete combustion of bituminous coal leads to soil and air pollution (Brown and Peake, 2006; Sprovieri et al., 2007). When the PAHs are released into the air, it can be deposited in the soil or water. Road traffic emissions are related not only to vehicles exhaust but also to problems concerning tire, brake wear and re-suspended dust. Traffic re-suspended particles contain road dust accumulated from vehicle track-out from construction sites, water or

http://www.aloki.hu ● ISSN 1589 1623 (Print) ● ISSN 1785 0037 (Online)
DOI: http://dx.doi.org/10.15666/aeer/1605_64196440
© 2018, ALÖKI Kft., Budapest, Hungary

wind erosion from nearby areas, tire and brake wear, oil leaks and spills, street repair materials and atmospheric deposition (Ravindra and Grieken, 2008). When humans eat plants that have been irrigated by the water, PAHs are transmitted to human through the food chain, and therefore harm humans. The toxicity of PAH compounds was noticed by many researchers. Researchers found that only a low concentration of PAHs could cause tissue mutations or cancer (Ruge et al., 2015). The U.S. Environmental Protection Agency has included 16 of them in the list of priority pollutants (naphthalene, acenaphtalene, acenaphtene, fluorene, phenanthrene, anthracene, fluoranthene, pyrene, benzo (*a*) anthracene, chrysene, benzo (*b*) fluoranthene, benzo (*k*) fluoranthene, benzo (*a*) pyrene, indeno (1,2,3-*cd*) pyrene, dibenzo (*a*,*h*) anthracene, benzo (*g*,*h*,*i*) perylene) (Llobet et al., 2006).

The degradation of PAHs in nature is in a dynamic equilibrium. With the current industrial development, more and more PAHs are released, which has serious adverse effect on the environment and human health (Debajyoti et al., 2016). Therefore, more and more researchers pay their attention to PAHs and their degradation methods, including physical, chemical, biological methods and other methods (Cerniglia, 1992; Kalmykova and Moona, 2014). In this paper, the methods for the degradation of PAHs are reviewed and their advantages and disadvantages are summarized in turn.

Physical methods

Most PAHs are colorless or pale-yellow crystals, There are also some PAHs which are dark crystals. Besides, they feature high melting points and boiling points, while their vapor pressure is very small. In addition, they are mostly insoluble in water but soluble in benzene aromatic solvents, and slightly soluble in other organic with high adsorption affinity for solid media (Lamichhane et al., 2016). Therefore, the use of suitable adsorption and extraction materials can effectively degrade the PAHs in water, soil and sludge. Due to these properties, many researchers use adsorption, extraction and other physical methods to remove PAHs (Belo et al., 2017; Li et al., 2017).

Sorption

Sorption is one of the widely used methods of PAHs degradation, as PAHs possess low aqueous solubility and great sorptive ability for solid media. When the fluid is contacted with the porous solid, at least one type of component of the fluid accumulate on the solid surface. This process is called adsorption, which includes absorption, adsorption and ion exchange (Khattri and Singh, 2009; Lamichhane et al., 2016; Yuan et al., 2011). Several kinds of adsorbent media such as activated carbon, biochar and modified clay minerals have been largely used to remove PAHs from aqueous solution and to immobilise PAHs in the contaminated soils (Luna et al., 2016).

According to the functions of different kinds of adsorbent and adsorbed substance, there two types of adsorption: physical adsorption and chemical adsorption. In general, physical adsorption is a reversible process, while chemical adsorption is irreversible. Compared to other methods, adsorption is regarded as a good method to remove PAHs for its simple design, low cost and no secondary pollution. Therefore, choosing suitable adsorbent can solve the problems concerning the pollution of PAHs in water, soil and sludge (Yuan et al., 2010).

The choice of adsorbent material plays an important role in the degradation of PAHs. Pyrene, benzo (b) fluoranthene, benzo (k) fluoranthene, benzo (a) anthracene, indene

http://www.aloki.hu ● ISSN 1589 1623 (Print) ● ISSN 1785 0037 (Online)
DOI: http://dx.doi.org/10.15666/aeer/1605_64196440
© 2018, ALÖKI Kft., Budapest, Hungary

(1,2,3) pyrene, dibenzo (a, h) anthracene, benzene (g, h, i) perylene were studied by adsorption experiments. It was found that activated carbon was an excellent adsorbent and could effectively remove PAHs (Lamichhane et al., 2016). Some scholars applied activated carbon to the absorption of PAHs pollutants in soil and sludge, and the removal rate reached 95%. However, they did not take into account the fact that the metal ions in the sludge has effect on the adsorbent, which need to be noticed in actual operations (Oleszczuk et al., 2012). In fixed-bed column experiments, activated carbon is uesd by Luna et al. to carry out continuous adsorption and desorption experiments on PAHs in heavy naphthenic oil. It was found that the PAHs content in samples decreased from 8% to 3% (Luna et al., 2016).

Biochar is a kind of solid product produced by the pyrolysis of biomass in an anaerobic environment. Because of its porous structure and high surface area, bio-carbon is conducive to the removal of PAHs in water and soil. The biochar can be produced by the pyrolysis of the coniferous, corn stover, peanut shell, wheat residue that occurs under the hypoxia condition and at the temperature ranging from 500 to 600 °C (Yongwoon et al., 2013). Black carbon, a kind of bio-carbon, does not function solely in the adsorption degradation of PAHs and other organic pollutants, but completes the process together with soil constituents. Rhodes et al. added black carbon to the soil, resulting in a significant reduction in the content of phenanthrene, which may be caused by the decrease in the concentration of aqueous solution containing phenanthrene owing to the adsorption of black carbon (Rhodes et al., 2008). Oleszczuk et al. added the biochar prepared at 600 °C to sludge containing napthalene, phenanthrene, anthracene, fluoranthene, pyrene, benzo (a) anthracene, chrysene, benzo (b) fluoranthene, benzo (k) fluoranthene, benzo (a) pyrene, indeno (1,2,3cd) pyrene, benzo (g, h, i) perylene and so on, and the dosage of biochar ranged from 0.5% to 10%. It was found that biochar could reduce 57% of the PAHs in sludge (Oleszczuk et al., 2012). There are scholars who use charcoal in adsorption experiments on the pyrene and phenanthrene in the water, and the results show that the conversion rate of PAHs is more than 60% (Yuan et al., 2010). The above studies show that the biochar has a good adsorption effect on most PAHs. It is worth mentioning that the biochar has better PAH adsorption effect on the PAHs with five- or six-ringed structures, than on those with two- to four-ringed structures. Besides, only few types of PAHs can achieve good adsorption effect, and biochar needs a very high temperature to convert from peanut shell and other materials. Maybe the more lowering conversion temperature is a key element to the future research direction for the researchers.

Magnetic nanomaterial is a kind of magnet containing hematite core and silica mesoporous material (Ríos and Zougagh, 2016). They can be used as adsorbent to remove PAHs. Yuxiong Huang et al. used this kind of material to adsorb acenaphthene in industrial wastewater. The results show that in 30 min, the capture rate of acenaphthene reached 85% and the adsorption capacity reached 1060 mg/kg. It was proved that the removal rate of magnetic nanometal ions is very high. Besides, the adsorption capacity of magnetic nanomaterial increases with the increasing pH and magnetic nanomaterial has excellent regeneration performance (Huang et al., 2016).

In addition to the abovementioned materials, grapheme oxide, electro spun nanofibers; laccase carrying electric fiber membrane can also be used for the adsorption of PAHs in the degradation (Feng et al., 2013; Niu et al., 2013). Through a large number of experiments, researchers have demonstrated that these materials can effectively adsorb and degrade PAHs. Moreover, in recent years, a combination of

http://www.aloki.hu ● ISSN 1589 1623 (Print) ● ISSN 1785 0037 (Online)
DOI: http://dx.doi.org/10.15666/aeer/1605_64196440
© 2018, ALÖKI Kft., Budapest, Hungary

adsorbent materials and enzymes can not only achieve the physical adsorption, but also completely degrade the PAHs. Of course, there are many factors that affect the adsorption, such as temperature, pH value, humidity and so on. The removal rate of PAHs may vary under different conditions. Zhang et al. used black carbon to study the adsorption of pyrene in the soil. It was found that the adsorption capacity of pyrene was stronger when the soil moisture was higher, especially when the pyrene concentration was low. The adsorption of pyrene varies with different soil organic compounds. Compared with the black soil, the paddy soil has much higher polarity, therefore the adsorption capacity of black carbon to pyrene decreased more obviously (Zhang et al., 2013). By using plant residues to remove the PAHs in water, Xi et al. found that the higher the polarity of the aqueous solution, the more detrimental to the removal of PAHs. They removed the polar components by acid hydrolysis and the results show that the adsorption rate of phenanthrene increased by 6 to 18 times, and the adsorption rate of naphthalene, acenaphthene and pyrene increased by 6 to 8 times. It was also found that deodorized pine has the best adsorption capacity due to its lowest polarity (Zeledón-Toruño et al., 2007). Hiller et al. experimentally investigated the effect of temperature on the adsorption of naphthalene, phenanthrene and pyrene. When the temperature ranges from 4 to 27 °C, with the increase of temperature, the adsorption rate of naphthalene decreased by 27.3%, and the adsorption rate of phenanthrene decreased by 17% while the adsorption rate of pyrene decreased by 27.4% (Hiller et al., 2008). It can be concluded that with the increase of temperature, the adsorption rate of PAHs decreased gradually. Some scholars prepared activated carbon by using orange peels and then conducted an adsorption test. They found that orange peel activated carbon can effectively remove the phenanthrene in the water (Chen et al., 2011). At the same time, they also investigated the factors affecting the adsorption. It was found than the adsorption rate of phenanthrene increased with the increase of the absorbent dose. When the absorbent dose was 18 mg, the phenanthrene was completely absorbed, therefore this adsorption dose was also found to be the best value. The experiments on the adsorption of phenanthrene at different pH values showed that the adsorption rate of the adsorbent decreased with the increasing pH value. Of course, some scholars pointed out that the pH value has little effect on the adsorption of some PAHs., Zeledon et al. (2007) used weathered lignite as an adsorbent to remove PAHs (fluorene, pyrene, benzo (k) fluoranthene, benzo (a) pyrene and benzo (g, h, i) perylene) in water. There was no significant difference in the adsorption rate of other contaminants at different pH levels except for that of fluorene, which is higher when pH value is small. When the pH value was 2, the adsorption rate of fluorene was 86%. As the pH value increased to 6, the adsorption rate of fluorene dropped to 63%. Therefore, we drew a conclusion that the results vary due to different conditions, which have different effects on different adsorbent materials. No matter what kind of material, we need to find the best conditions to achieve the best results.

Extraction

Extraction is also a commonly used method for treating PAHs in water and soil. The extraction agents include acetone, methanol, n-hexane and dimethyl ether (Lambropoulou, 2010; Noordkamp et al., 1997; Szulejko et al., 2014). Some scholars have demonstrated that these extractants can extract PAHs successfully. However, these solvents may cause re-contamination for the environment. Thus, more and more

http://www.aloki.hu ● ISSN 1589 1623 (Print) ● ISSN 1785 0037 (Online)
DOI: http://dx.doi.org/10.15666/aeer/1605_64196440
© 2018, ALÖKI Kft., Budapest, Hungary

researchers are looking for other solvents or comprehensive methods to improve the extraction process and extraction rate.

Song et al. (2012) were studied the removal of phenanthrene in soil by combining ultrasound with soil cleaning. It was also found that increasing the ultrasonic time and the concentration of phenanthrene can be of great help to the removal of phenanthrene. According to the results, the removal rate of phenanthrene reached to 69.5% after 20 min of sonication. The investigation provides a viable method for the modification of highly contaminated soils. Sliva et al. used non-in situ extraction techniques to treat hydrocarbons contaminated soils. The contaminated soils was treated by a ethanol-acetone-water ternary miscible systems, and a kinetic equilibrium was achieved after 10 min. The extraction rate of the compound reached 85% and it increased by 8% with the increase of solid-liquid ratio from 1: 2 to 1: 8 (Silva et al., 2005).

More and more scholars use vegetable oils as extractants in the extraction of PAHs, because they are naturally non-toxic, cheap and feasible to be used for biodegradation. Lau et al. (2014) found that peanut oil is an excellent extractant to remove PAHs. They used peanut oil whose concentration ranges from 2.5% to 20% to extract the anthracene from garden soil, and the extraction rate reached higher than 90%. At the same time, through experiment, they found that the optimum pH was 6-7. In addition, the extraction rate of PAHs increased from 51.5% to 81.4% when the temperature rose from 20 to 60 °C, which indicated that when peanut oil is the extractant, the extraction rate of PAHs increased with the increase of temperature. Some scholars used sunflower oil to extract PAHs so as to repair the soil (Gong et al., 2005). The results show that sunflower oil has excellent ability to remove PAHs, especially for soil with a high concentration of PAHs, and the removal rate was close to 100%. Different vegetable oils have different If the vegetable oils that used for extraction are different, the extraction rates of the same PAH as different as well. Lau et al. extracted the fluoranthene and phenanthrene with palm kernel oil and soybean oil. It was demonstrated that using palm kernel oil for extracting PAHs can achieve a higher extraction rate compared with using soybean oil. Besides, with these two vegetable oils being used as extractant, the extraction rates of PAHs was lower when gravel was highly polluted, compared with that of PAHs when gravel was low-polluted (Lau et al., 2014). The investigation also indicated that the difference of temperature affects the extraction rates of fluoranthene and phenanthrene. Especially at a high temperature, the extraction rate of fluoranthene is higher than that of phenanthrene. When the soybean oil was utilized to extract, PAHs, the extraction rate of fluoranthene was 0.7% and 4.75% higher than that of the phenanthrene at the temperature of 30 °C and 70 °C respectively. When the palm kernel oil was used as extractant, the extraction rate of anthracene was 3.35% and 1.35% higher than that of fluoranthene at the temperature of 30 °C and 70 °C respectively (Von et al., 2012). Sanchez-Trujillo et al. studied the biodegradation of PAHs contaminated soils by using cyclodextrin as an extractant (Sáncheztrujillo et al., 2013). It is proved that cyclodextrin has a good degradation effect on PAHs. They studied the PAHs composed of three benzene rings (anthracene, phenanthrene, fluorene, acenaphthene, etc.) with chemically modified cyclodextrin, $Ca(NO_3)_2$ electrolyte solution and natural cyclodextrin utilized as extractants. It was found that the chemically modified cyclodextrin achieved the highest extraction rate of PAHs, about 10% higher than those achieved by the other two extractants.

http://www.aloki.hu ● ISSN 1589 1623 (Print) ● ISSN 1785 0037 (Online)
DOI: http://dx.doi.org/10.15666/aeer/1605_64196440
© 2018, ALÖKI Kft., Budapest, Hungary

Chemistry methods

In summary, the two physical methods of adsorption and extraction have significant effects on the removal of PAHs. However, there is no chemical change in these physical processes. These materials simply transfer PAHs from water or soil, and the PAHs cannot be completely removed. Therefore, chemical methods have been used to degrade PAHs.

Physical adsorption and extraction have a significant effect on the degradation of PAHs, but these physical processes are time-consuming and inefficient. Therefore, many researchers have paid their attention to chemical methods. At present, the most important approaches to the PAHs degradation are oxidation and photocatalysis (Rubio-Clemente et al., 2014).

Oxidation

It is well known that potassium permanganate is highly oxidizing, therefore some researchers used it to deal with PAHs contaminated soil. Brown et al. utilized potassium permanganate to deal with potassium the benzo (a) pyrene, chrysene, fluoranthene, phenanthrene, and pyrene in the soil. After 30 min, the content of benzo (a) pyrene, pyrene, phenanthrene and anthracene were decreased 72.1%, 64.2%, 56.2% and 53.8%, respectively. Under the same conditions, fluoranthene and chrysene were reduced by at least 13.4% and 7.8%, respectively. According to the investigation, the order of the oxidation degradation rates of potassium permanganate for these six kinds of PAHs can be listed as: benzo (a) pyrene> pyrene> phenanthrene> anthracene> fluoranthene> chrysene (Brown et al., 2003). The results show that the effect of potassium permanganate on the degradation of low molecular weight PAHs is obvious. However, the adverse effects of potassium permanganate on aquatic plant are severe.

Ozone has a strong oxidizing power and it is mostly used in the degradation of PAHs. However, many researchers found that the shortcomings of ozone will be revealed if ozone is used alone. Many studies show that the degradation efficiency of the combination of ozone and certain reagents is better than that of ozone (Bouzid et al., 2017; Ji et al., 2018).

Bernal-Martinez et al. used ozone to conduct anaerobic digestion experiments on 12 kinds of PAHs such as anthracene, phenanthrene and pyrene, so as to study the efficiency of ozone degradation of PAHs in sludge (Bernalmartinez et al., 2007). They conducted three comparative experiments. In the first experiment, oxidant was not added to the samples. On the contrary, the oxidant was the only thing that had been added to the samples of the second experiment. Moreover, samples of the third experiment contained not only oxidant but also tetrabutyl phenol. Under the same experimental conditions, the comparison of the three experiments showed that the oxidant had the most obvious degradation effect on PAHs. The other two groups of sample also showed the degradation of PAHs, but the effect was not obvious. At the same time, the amount of added oxidant is also critical factor. Through anaerobic digestion experiments, they found that the optimum ozone dose is of 0.11 g per gram of sludge.

Oxidative degradation of PAHs has proven to be an effective means by many researchers, but some scholars have suggested that relying on ozone oxidation alone is less efficient. Brown also proposed to use ultraviolet radiation or the addition of other oxidants such as hydrogen peroxide to improve ozone oxidation rate (Brown et al.,

http://www.aloki.hu ● ISSN 1589 1623 (Print) ● ISSN 1785 0037 (Online)
DOI: http://dx.doi.org/10.15666/aeer/1605_64196440
© 2018, ALÖKI Kft., Budapest, Hungary

2003). Beltran et al. improved the ozonation of fluorene, phenanthrene and acenaphthene by UV radiation and the addition of hydrogen peroxide. Experiments show that the use of ultraviolet radiation and the addition of hydrogen peroxide do not always play a role in the degradation of PAHs. These method can only improved the efficiency of fluorene degradation and phenanthrene degradation, and there is almost no effect on acenaphthene (Beltrán et al., 1996).

With a method combining UV radiation and ozone, Ledakowicz et al. (2014) also conducted degradation experiments on benzo (a) pyrene, chrysene and fluorene in water. The mechanism of this process is listed as follows (*Eqs. 1–7*):

$$O_3 + h\nu \longrightarrow O_2 + O(1D) \quad \text{(Eq.1)}$$

$$O(1D) + H_2O \longrightarrow H_2O_2 \quad \text{(Eq.2)}$$

$$H_2O_2 + h\nu \longrightarrow 2\ {\bullet}OH \quad \text{(Eq.3)}$$

$$H_2O_2 \rightarrow HO_2^- + H^+ \quad \text{(Eq.4)}$$

$$O_3 + OH^- \longrightarrow HO_2^- + O_2 \quad \text{(Eq.5)}$$

$$O_3 + HO_2^- \longrightarrow HO_2{\bullet} + O_3{\bullet}^- \quad \text{(Eq.6)}$$

$$PAH + O_3 + h\nu + {\bullet}OH \longrightarrow products \quad \text{(Eq.7)}$$

Among them, • OH, HO^{2-}, O_3 • achieved a major oxidation. The results show that the degradation rate of benzo (a) pyrene reached 85% with ultraviolet radiation and ozone, and the degradation rate of chrysene and that of fluorene reached 90%. As for the method that using ozone alone, the degradation rates of benzo (a) pyrene, chrysene and fluorene were 10%, 70% and 50%, respectively. As for the method that using UV radiation alone, the degradation rates of benzo (a) pyrene, chrysene and fluorene were 80%, 40% and 55%, respectively. Because of the hydrogen ions emerging in the reaction process, the pH value has a certain effect on the oxidation process, and this effect needs to be further investigated. In contrast, combining UV radiation with ozone is more effective for the degradation of PAHs. Eberius et al. studied the aromatic core structures by using the mass-spectra. They found that the final product of pyrene is benzene with the possible functional groups such as carboxyl (Eberius et al., 1997). Fenton (Fe_2 + / H_2O_2) has been widely used in the treatment of organic pollutants (Pérez et al., 2002). The reaction of divalent iron ions in Fenton and hydrogen peroxide generates oxidative hydroxyl radicals and lead to the formation of ferric ions (*Eq. 8*). The main oxidative component of the Fenton reagent is hydroxyl radicals.

$$Fe^{2+} + H_2O_2 \rightarrow Fe^{3+} + OH^- + OH \quad \text{(Eq.8)}$$

Homem et al. demonstrated the feasibility of removing benzo (a) pyrene (BaP) in water with Fenton reagent (Homem et al., 2014). They also researched the effect of temperature, pH value, divalent iron ion concentration and the concentration of hydrogen peroxide on the removal efficiency of BaP. As the temperature increased from 30 to 70 °C, the removal rate of BaP increased from 90 to 100%. But pH value has little

http://www.aloki.hu ● ISSN 1589 1623 (Print) ● ISSN 1785 0037 (Online)
DOI: http://dx.doi.org/10.15666/aeer/1605_64196440
© 2018, ALÖKI Kft., Budapest, Hungary

effect on the removal rate of BaP. The effect of divalent iron ion concentration is similar to that of temperature, as the removal rate of BaP increased with the increase of divalent iron ion concentration. The increase in the concentration of hydrogen peroxide will improve the removal rate, but an excessive concentration will contrarily reduce the removal rate. Homem proved that Fenton had a good effect on the removal of PAHs. With an initial concentration of 50 mg L^{-1}, 90% removal was achieved, while with the concentration of 150 mg L^{-1}, only 80% BaP was eliminated. Therefore, it can be concluded that advanced oxidation technology is more helpful to PAHs degradation than conventional oxidation technology.

Photocatalytic

Photocatalysis is also an important way to remove organic matter such as PAHs and other pollutants. Photocatalytic materials consist of titanium dioxide, zinc oxide, silicon dioxide and so on. Among them, titanium dioxide is extensively applied because of its high degree of oxidability and stability (Jiang et al., 2018, 2017; Woo et al., 2009).

Veréb et al. used UV lamps as light sources to perform degradation experiments on phenanthrene in water. Titanium dioxide absorbs the energy produced by ultraviolet light so as to produce electrons. Besides, the reaction of positive charge and water produces hydroxyl radicals and hydrogen ions, while the negative charge reacts with oxygen and hydrogen ions to form a peroxy radical (Veréb et al., 2012). Hydroxy radicals and peroxygen have strong oxidizing properties, which play an important role in photocatalytic degradation of phenanthrene. The results show that titanium dioxide photocatalytic materials were the most effective for the removal of phenanthrene. Besides, the final oxidation product of phenanthrene is carbon dioxide and so on (Wen et al., 2002).

Different experimental conditions may have an effect on photocatalytic efficiency. Lair et al. (2008) used titanium dioxide as the photocatalytic material for naphthalene degradation experiments. At the same time, they studied the impact of the photoelectron flux, temperature, pH value and inorganic ions on the photocatalytic efficiency. When the received photoelectron flux rises from 0 to 10^{16} photons per second, the degradation rate also increases. When this range is exceeded, the amount of photoelectron flux has no effect on the degradation rate. When the temperature increases from 10 to 4 °C, since the photoactivation is independent of the thermal activation, the temperature has no effect on the photocatalytic rate. Under the strong acid or strong alkaline conditions, the degradation rate will be reduced. The study also pointed out that carbonates and carbonates will inhibit photocatalysis.

Similar to titanium dioxide, zinc oxide is also a kind of semiconductor material., Currently, in the field of photocatalysis, titanium dioxide materials are widely the most widely used materials, while people have little knowledge of Zinc Oxide materials. Zinc oxide is a kind of wide band gap semiconductor material with a 3.37 eV, and its exciton binding energy at room temperature is 60 eV (Ramasamy et al., 2013). In the degradation of PAHs, using oxidation alone and using photocatalysis alone can improve the efficiency. Therefore, combining these two methods may have a better effect. It has been experimentally demonstrated by Vela et al. that zinc oxide and titanium dioxide have excellent effects on removing PAHs in water. They applied a method concerning the combined use of ZnO and $Na_2S_2O_8$ to the degradation of PAHs in groundwater. After comparison, it was found that compared to utilizing photocatalytic method alone, the use of the combined method improved the total organic carbon reduction by 21%

http://www.aloki.hu ● ISSN 1589 1623 (Print) ● ISSN 1785 0037 (Online)
DOI: http://dx.doi.org/10.15666/aeer/1605_64196440
© 2018, ALÖKI Kft., Budapest, Hungary

(Vela et al., 2012). The combination of photocatalysis and oxidation seems to have a better effect.

From the above results, it is not difficult to conclude that the chemical method has a significant improvement in the degradation rate of PAHs compared to physical methods. However, when use photocatalysis alone or use ozone alone, the efficiency of PAHs degradation is lower than that of adding other oxidants together. Moreover, it is necessary to pay attention to the secondary pollution caused by intermediate products.

Biodegradation

In recent years, with the improvement of environmental awareness, the concern of many researchers has gradually shifted from physical and chemical degradation methods to biodegradable methods. Because of no secondary pollution, low cost and simple operation and so on, biodegradation methods are considered as the best ways to deal with PAHs. Fungi, bacteria, and plants have good abilities to degrade PAHs (Haritash and Kaushik, 2009; Kronenberg et al.; 2017; Nzila, 2018).

Plant

Plants belong to autotrophic organisms that features using light and carbon dioxide for photosynthesis. Because the roots of plants can absorb some toxic compounds, plants function as natural cleaning systems. Therefore, for the purpose of repairing PAHs contaminated soils plants can be applied to the degradation of PAHs (Alagić et al., 2015; Chen et al., 2011). Alagić et al. demonstrated that plant has the ability to degrade BaP, which is mainly due to a series of biotransformation of the enzyme system in plant roots (Alagić et al., 2016). Chen et al. labeled pyrene with ^{14}C, and evaluated the degradation abilities of tall fescue (Festuca arundinacea) and switchgrass (Panicum virgatum L.) (Yenchih Chen et al., 2003). After 190 days, 37.7% and 30.4% of pyrene were mineralized in the soil where tall fescue (*Festuca arundinacea*) was planted and where switchgrass (Panicum virgatum L.) was planted, respectively. Only 4.3% of the pyrene in the soil without the two plants was mineralized. At the end of the experiment, the residual quantity of pyrene in the two kinds of soil was only 7.6 and 8.7%, respectively. Somtrakoon et al. studied the degradation of anthracene and fluorene that affected by sweet corn, cucumber, and winged bean. They transplanted these three plants to the soil that contained containing 138.9 mg/kg of anthracene and 95.9 mg/kg of fluorene (Somtrakoon et al., 2014). After 15 to 30 days, the plant elongation, plant weight, chlorophyll content, and PAHs content in soil and plant tissue were determined. The results show that winged bean achieved the best degradation rate of anthracene and fluorene, which were degraded by 92.2% and 75.8%, respectively. Besides, 91.2% and 95.9% of the anthracene and fluorene degraded in the soil mixed with corn and four ribbean. Corn and cucumber grown in soil After 15 days, 14% of fluorene remained in the corn-planted, and 17.3% of fluorene remained in the cucumber-planted soil. The degradation of fluoranthene, pyrene, and a mixture of fluoranthene and pyrene affected by Scenedesmus platydiscus, Scenedesmus quadricauda, Chlorella vulgaris, and Selenastrum capricornutum has been studied by scholars. In the experiment, the concentrations of fluoranthene, pyrene, and a mixture of fluoranthene and pyrene were all 1 mg/L. The results show that Selenastrum capricornutum achieved the highest conversion efficiency, and the removal rate of PAHs reached 78% in 7 days. However,

http://www.aloki.hu ● ISSN 1589 1623 (Print) ● ISSN 1785 0037 (Online)
DOI: http://dx.doi.org/10.15666/aeer/1605_64196440
© 2018, ALÖKI Kft., Budapest, Hungary

among these four kinds of algae, vulgaris achieved the lowest efficiency of, the removal rate was only 48% (Lei et al., 2007).

Bacteria

Bacteria are microorganisms that are critical to the degradation of organic pollutants. It is well known that many bacteria can accelerate the degradation of PAHs with a very high efficiency (Kuppusamy et al., 2016; Mohanrasu et al., 2018). Bacteria can produce dioxygenase, which enable bacteria to facilitate PAHs degradation through the enzyme catalysis. Subsequently, the oxygen is added to the benzene ring, and the formation of the C-O bond is achieved. Moreover, after hydrogenation and dehydration, the benzene ring is eliminated, and the degradation is completed (Cerniglia, 1992). Xia et al. found that *Pseudomonas aeruginosa WJ6* can produce surface active agents, fermudamycin and lichen proteins. It was concluded that *Pseudomonas sp. WJ6* excels in facilitating the degradation of PAHs. During the 20-day period, the fluorene, naphthalene and phenanthrene in the culture dish were decreased significantly by 39.45%, 23.14% and 21.93%, respectively. The degradation rate of pyrene affected by *Pseudomonas sp. WJ6* to was only 19.50% for two-ring PAHs and three-ring- PAHs (Xia et al., 2014). Romero et al. isolated yeast strains from contaminated rivers and studied their ability to facilitating the degradation of tricyclic PAHs. Phenanthrene is the only carbon source, while red yeast and Pseudomonas aeruginosa are the main microbes. The researchers added different amounts of phenanthrene to the mineral medium containing ethanol. At a temperature of 3 °C, the samples were irradiated with ultraviolet light for 40 min so that the ethanol volatilized subsequently. They found that the medium phenanthrene underwent an almost complete degradation after one-month incubation period (Romero et al., 1998). Some scholars conducted the same experiments, and they drew the conclusion that the culture of the phenanthrene is not completely degraded and the degradation rate was only about 60%, which is different from Romero's finding. Rahman et al. studied the ability of immobilized bacteria to degrade hydrocarbons (Rahman et al., 2006). Rahman et al. planted hydrocarbon-degrading bacterial strains in alginate and are cultured in contaminated artificial seawater. After 30 days, it was found that the pollutants contaminated by petroleum hydrocarbons were removed effectively. Evidently, the immobilized bacteria in the alginate could be used to degrade the hydrocarbons effectively. As PAHs are hydrocarbons, it can be concluded that immobilized bacteria can be of great help to the degradation of PAHs. For the degradation of PAHs, Rehmann et al. proposed a method concerning the use of the mycobacterium strain *KR2*. Using *Mycobacterium strain KR2*, they investigated the degradation ability of pyrene-contaminated soils. Pyrene was the sole carbon source, and the *mycobacterial strain KR2* was the only strain (Rehmann et al., 1998). The experiment was carried out at a temperature of 20 °C. After 8 days of incubation, the degradation rate of pyrene reached 60%. The degradation products of pyrene are cis-4,5-pyrene diethylene glycol, 4,5-phenylene dicarboxylic acid, 1-hydroxy-2-naphthoic acid, 2-carboxybenzaldehyde, phthalic acid and the original Catechins, etc., and these products are easy to remove. It can be concluded that the use of mycobacteria is also effective to degrade PAHs.

Dean-Ross et al. used the *mycobacterial strain* to determine the ability of bacteria through the mineralization of PAHs (Dean-Ross et al., 2002). The mineralization rate of pyrene was 0.044 mg/L, and the mineralization rate of anthracene was 0.470 ug/L. At the same time, they also found a degradation method of fluoranthene. Among the two

http://www.aloki.hu ● ISSN 1589 1623 (Print) ● ISSN 1785 0037 (Online)
DOI: http://dx.doi.org/10.15666/aeer/1605_64196440
© 2018, ALÖKI Kft., Budapest, Hungary

strains, the metabolism of fluoranthene occurred on the fused ring of fluoranthene molecules. The degradation products of fluorinated anthracene mineralized by *mycobacteria* were 9-fluorenone-1- carboxylic acid, and the degradation product of fluoranthene mineralized by *Rhodococcus* is α-(carboxymethylene) fluorene-1-carboxylic acid. Muangchinda et al. studied the degradation of PAHs in river sediments of the Chao Phraya River Basin (Muangchinda et al., 2017). They isolated two *actinomycetes* in the river sediments: *Arthrobacter* and *Rhodococcus*. These two bacteria showed a high degradation activity in the culture medium. The concentration of fluorene, phenanthrene and pyrene in the medium was initially 300 mg/kg, and the concentration of acenaphthene was 600 mg/kg. After 70 days of incubation, fluorene and phenanthrene were all degraded and the degradation rates of pyrene and acenaphthene reached 50%. It was proved that *Agrobacterium* and *Rhodococcus sp.* play important roles in the degradation of PAHs with high concentration. Jin et al. selected two strains (*JB1* and *JB2*) from the contaminated wetland sediments and fixed them on the cinder, which means the bacterial cells is immobilized (Jin et al., 2017a). The degradation rate of benzo (a) pyrene reached 71.9% after 40 days in the medium, while the degradation rate of free cells was only 47.7%. The reason is that the cinder has a large specific surface area and pore size, which is conducive to the aerobic degradation of strains. It also indicates that the carrier material plays an important role in the degradation of PAHs. Tetracyclic pyrene has a low biological activity and a strong biological resistance. *Strain F14* was constructed by protoplast fusion of *Sphingomonas GY2B* and *Pseudomonas sp. GP3A*. Lu et al. studied the degradation of pyrene with F14 (Lu et al., 2014). When the concentration of pyrene was 15 mg/L, the degradation rate of pyrene was 40.4% in F14 medium, while only 9.8% of the pyrene in the GP3A was degraded. When the concentration of pyrene was 50 mg/L, the degradation rates of pyrene was 37.1% and 22.3%, respectively. Experiments showed that the F14 strain constructed by protoplast fusion has better ability to degrade than the original strain. While GY2B is inefficient to degrade pyrene. They also found that when several kinds PAHs were mixed together, the degradation velocity and degradation rate has improved. When naphthalene and phenanthrene were simultaneously added to the medium, 42% of the pyrene degraded in 120 h. After 240 h, 79% of the pyrene degraded. Contaminated soil, sludge and water generally contain metal ions, which are likely to affect the degradation of PAHs. Chen et al. studied the role of copper ions in the degradation of PAHs by the utilization of bacteria (Chen et al., 2013). The degradation of BaP was studied by using BaP as the carbon source and using matrix of coexisting maltose and copper ion. The initial BaP concentration was 1 mg L^{-1}, subsequentlly, after 3 days at a temperature of 30 °C and natural pH, 45% of BaP was degraded. When the temperature rose to 35 °C, the degradation rate was 48% after two days. The different contents of copper ions also affect the degradation of BaP. When the concentration of copper ions is 2 mg L^{-1}, the degradation rate of BaP can be improved slightly. When the concentration of copper ions is 100 mg L^{-1}, only 5% of BaP is degraded and the removal rate of copper ions is 70%. Because a portion of the copper ions converted to copper hydroxide precipitation, which inhibited the activity of bacteria, therefore the degradation rate of BaP decreased. Doping some sucrose as a carbon source can make *Maltobacter* function better, which facilitates PAHs degradation. Some plants contain bacteria, and they are called endophytic plants. When the soil is contaminated by PAHs, these bacteria can improve soil quality. For example, *Aims Endophytic* bacteria that are widely found in plants. Sun et al. extracted

http://www.aloki.hu ● ISSN 1589 1623 (Print) ● ISSN 1785 0037 (Online)
DOI: http://dx.doi.org/10.15666/aeer/1605_64196440
© 2018, ALÖKI Kft., Budapest, Hungary

Staphylococcus BJ06 from plants, and the concentration of pyrene in the medium was 50 mg/L (Sun et al., 2014). After 15 days, 56% of the pyrene was degraded in the medium. Ryegrass and bamboo shoots are endophytic plants from which BJ06 can be extracted. It is found that the content of pyrene in the ryegrass-planted soil and bamboo shoots-planted soil is 31.01% and 44.22% lower than that planting non - endemic plants. Evidently, *Staphylococcus BJ06* can remove the PAHs in the soil effectively, which is an efficient way to reduce PAHs from the beginning of the food chain. Some scholars have found *Leclercia adecarboxylata PS4040*, which is isolated from oil and contaminated soil. When pyrene is used as a carbon source and affected by *Leclercia adecarboxylata PS4040*, 61.5% of the pyrene in the culture medium was degraded after 20 days of observation. After 5 days, the metabolites of pyrene were 1-hydroxypyrene. Besides, through high performance liquid chromatography and magnetic resonance, it was found that the 1-hydroxypyrene could also be used as a carbon source and can produce acid or aldehyde by being further mineralized by *Leclercia adecarboxylata PS4040* (Sarma et al., 2010).

Fungi

At present, it is found that several kinds of fungi help to maintain the sustainable degradation of PAHs contaminants. In recent years, the study of fungal degradation of PAHs has been further improved (Cutright, 1995; Shi et al., 2018; Szczepaniak et al., 2015). *Aspergillussp, Trichocladium canadense* and *Fusarium oxysporum* are widely used to degrade low-molecular-weight PAHs, while *Verticillium sp.,* and *Areremonium sp.* are used to degrade high-molecular-weight PAHs (Silva et al., 2009). Fungi can produce enzymes, which facilitates the degradation of PAHs. Kristanti et al. found that enzymes are a key factor in the degradation of polycyclic aromatic hydrocarbons affected by fungi (Kristanti and Hadibarata, 2015). They used *Pestalotiopsis sp. W15* to carry out a degradation experiments on fluorene. *Pestalotiopsis sp. W15* could produce laccase. After 23 days of experiment, fluorene was completely degraded and the degradation products were salicylic acid and indanone. In order to facilitate the production of laccase, Tween 80 and Brij35 were added to the culture medium. The results show that the addition of Tween 80 could facilitate the production of laccase. When, Waszak et al. studied BaP degradation by using the mixtures of several kinds of bacterial and fungal to achieve the degradation of pollutants. The mixtures contained *Pseudomonas aeruginosa*, *Candida albicans, Aspergillus flavus, and Fusarium sp.* (Waszak et al., 2015). With BaP as carbon source and its concentration of 16 μL/g, the degradation rate of BaP was about 65.51% after 42 days of incubation in an oven at a temperature of 35 °C. Hadibarata et al. used white-rot fungus *Armillaria sp. F022* in the study of fluoranthene (Hadibarata and Kristanti, 2014). The genus Armillaria is produced in the process of degradation of ligninolytic enzymes, namely laccase and 1,2-dioxygenase. These two enzymes play key roles in the degradation process. In the experiment, different concentrations of *Armillaria sp. F022* were added to culture medium. After 30 days of incubation, when F022 concentration is 10 mg/L, the fluoranthene was completely degraded. The degradation rate decreased with the increase of F022 concentration. When the concentration of F022 was 20 mg/L and 30 mg/L, the degradation rate of fluoranthene was 79.2% and 61.6%, respectively.

Zhang et al. investigated the degradation rates of different PAHs affected by the same kind of fungus under the same conditions (Zhang et al., 2015). They studied the metabolic transformation of anthracene and pyrene affected by *Pangnoporus*

http://www.aloki.hu ● ISSN 1589 1623 (Print) ● ISSN 1785 0037 (Online)
DOI: http://dx.doi.org/10.15666/aeer/1605_64196440
© 2018, ALÖKI Kft., Budapest, Hungary

sanguineus H1. Under the vivo conditions, the degradation rate of anthracene reached 67.5% and the degradation rate of pyrene was 31.1%. When the tert-butyl ether was added to the samples, it enhanced the activity of laccase. Therefore, the degradation rate of anthracene increased to 73.1% while the degradation rate of pyrene declined, accurately, only 5.3%. In the in vitro conditions, 59.9% of the anthracene was degraded in the extracellular fluid. Subsequently, after adding 2, 2' -azabis (3-ethylbenzothiazoline-6-sulfonate) to the anthracene sample, the degradation rate increased to 92%, but pyrene cannot degrade in the extracellular fluid. It can be concluded that the ability of *Pangnoporus sanguineus H1* to facilitate the degradation of anthracene is better than that to facilitate the degradation of pyrene. There was no laccase in the extracellular fluid, which demonstrates that laccase is critical to the degradation of PAHs. This study has fully demonstrated that fungi can produce laccase and degrade PAHs due to the oxidative catalytic ability of laccase, and therefore provides a good basis for researchers to study the degradation of PAHs utilizing laccase. Garonet et al. studied the degradation of maltosyl-cyclodextrin-modified fluorine (Garon et al., 2004). They screened 47 strains from the fungus to find the most effective strains to be used in the process of biological proliferation, and they finally selected *Trichoderma* spore bacteria. With the presence of *Trichoderma sp.*, more than 90% of the fluorene was degraded after 288 h. However, it takes 576 h for fluorene degradation rate to reach 90% without the fungal proliferation process. Hilton et al. isolated 146 filamentous fungal strain in the separation of contaminants from the Amazon region and named them from S1 to S146 (Souza et al., 2016). The results show that only *Megasporoporia sp. S47* and *Sordariales S69* showed the highest activity of laccase and manganese peroxidase during BaP degradation. Besides, *Megasporoporia sp. S47* achieved the best results, and it enabled the degradation rate of BaP to reach 54%. While the other strains reached only about 23%. The fungal strain *Aspergillus BAP14* was isolated from coastal sediments by Wu et al. and it was used in the degradation of BaP (Wu et al., 2009). In the experiment, the initial concentration of BaP was 10 mg /L. After 3 days of incubation, 30% of BaP was degraded. After 9 days, BaP was degraded by 60%. When sugar and other carbon compounds are added to the culture medium, especially lactose and naphthalene, the degradation rate increases significantly. The changes in pH value in the culture medium has little effect on the degradation rate. *Monascus* is a kind of white rot fungus, which can be easily isolated from the rotting woods. Hadibarata et al., investigated the degradation of naphthalene by *Monascus* and tested the metabolites (Hadibarata et al., 2013). *Monascus* and naphthalene was added to the culture medium for 14 days, and naphthalene was the only carbon source. Subsequently, naphthalene metabolites were tested by the use of ultraviolet, thin layer chromatography and gas chromatography-mass spectrometry, and the metabolites included 1,4-naphthoquinone, benzoic acid and catechol. At the same time they also detected enzyme, which plays an important role in the degradation, including manganese peroxidase, lignin peroxidase, laccase, 1,2-dioxygenase and 2,3-dioxygenase. Oil spill is also a source of PAHs that pollutes the oceans. Michel et al., extracted eight fungi from the oceans to study their influence on the degradation of PAHs (Passarini et al., 2011b). In the experiment, pyrene and benzo (a) pyrene were carbon sources. With the use of *Aspergillus sclerotiorum CBMAI 849*, the degradation rate of pyrene was up to 99.7% after eight days. After a 16-day use of *Aspergillus sclerotiorum CBMAI 849*, the optimum degradation rate of benzo (a) pyrene was achieved, and the degradation rate was 76.6%. The degradation rate of benzo (a) pyrene

http://www.aloki.hu ● ISSN 1589 1623 (Print) ● ISSN 1785 0037 (Online)
DOI: http://dx.doi.org/10.15666/aeer/1605_64196440
© 2018, ALÖKI Kft., Budapest, Hungary

achieved by *Mucor racemosus CBMAI 847* was more than 50%. The metabolites of pyrene and BaP being dealt with these fungi are pyrenyl sulfate and benzo (a) pyrenyl sulfate, respectively. This study provides an effective remedy for the PAHs pollution of marine. Arun et al., found that *Pseudomonas sp.* is the most potent fungus that degrades pyrene, and the degradation rate of pyrene is 42% (Arun et al., 2008). In the subsequent experiment, they added C. versicolor and P. ostreatus active agents to the culture medium. The results show that the degradation rate of pyrene reached 93.7%, which indicated that the surfactant was important for improving the ability of fungi to facilitate PAHs degration. The degradation rate is not only related to surfactant, but also related to the role of enzymes. The degradation of pyrene was positively correlated with the potential of lignin peroxidase (Lip), manganese peroxidase (MnP) and laccase, but it was not related to the activity of the enzyme. Da et al. screened *Cyclothyrium sp.*, which has a positive impact on the degradation of pyrene. In medium mixed with PAHs, *Cyclothyrium sp.* also exhibited good ability to improve degradation efficiency. Da selected four kinds of fungi, including *Cyclothyrium sp.; Penicillium simplicissimum; Psilocybe sp.* and *a sterile mycelium*, the degradation rate and metabolites of pyrene in culture medium were studied by applying HPLC and UV. In the culture medium, 48% pyrene was converted to trans-4,5-dihydrogenated diol, pyrene-1,6-quinone, pyrene-1,8-quinone and 1-hydroxypyrene. After 192 h of incubation, influenced by Cyclothyrium sp., the degradation rates of phenanthrene, pyrene, anthracene and benzo (a) pyrene are 70%, 74%, 59% and 38%, respectively(Da et al. 2004).

In recent years, many non-white rot fungi strains have been observed to be highly resistant to adverse environment. Many non-white rot fungi have been proved to have the ability to degrade PAHs (Marcourrea and Aranda, 2015; Veignie et al., 2004). *Fusarium sp.'s* (Strain E033) excellent ability to degrade BaP has been demonstrated by Chulalaksananukul et al. (2006). According to the investigation, the initial concentration of BaP in the medium was 100 mg/L, and 65% to 70% of the BaP was degraded after 30 days of culture at a temperature of 32 °C. In addition, there were two degradation products: dihydroxybenzo (a) pyrene and benzo (a) pyrene quinone. Increasing air and carbohydrates can improve degradation efficiency of PAHs. Anaisell et al., isolated nine natural non-lignin-decomposing fungal strains in crude oil-contaminated soils, including *Fusarium, Neurospora, Aspergillus, Scedosporium, Penicillium, Neosartorya* and *Talaromyces* (Reyes-César et al., 2014). Researchers selected *Aspergillusterreus, Talaromyces spectabilis*, and *Fusarium sp.* to conduct an experiment on the degradation of naphthalene and pyrene, and the concentration of mixed PAHs was 2,000 mg/kg. After 14 days, about 21% of the PAH mixture was degraded.

In summary, there are two mechanisms for fungi to impact on the degradation of PAHs, one is the lignin degrading enzyme system, and the other is the single oxygenase degradation system. Lignin degrading enzymes are lignin peroxidase, manganese peroxidase and laccase. These enzymes can convert PAHs into quinone, and subsequently achieve the PAHs degradation with the help of hydrogenation and dehydration (Ryu et al., 2003). As for monooxygenase degradation system, the initial process is adding oxygen to benzene ring to achieve the formation of epoxy compounds based on the catalysis of *cytochrome P-450*. Then phenol derivatives are generated and combined and rearranged with sulfate, glucose, xylose and glucuronic acid, so as to obtained degradation intermediates with high water solubility and low toxicity (Haritash and Kaushik, 2009; Shoun et al., 1989). No matter which mechanism is used, the

http://www.aloki.hu ● ISSN 1589 1623 (Print) ● ISSN 1785 0037 (Online)
DOI: http://dx.doi.org/10.15666/aeer/1605_64196440
© 2018, ALÖKI Kft., Budapest, Hungary

purpose is to achieve the best results by ensuring the best external conditions to maintain the activity of the enzyme.

In general, biodegradation process is environmentally friendly and is able to remove PAHs completely. More and more scholars are paying attention to it and are working to improve the degradation rate. In addition, the vital role of enzymes can help us better study the biodegradation process of PAHs.

Each method has a significant effect on the degradation of PAHs, but each method has its own characteristics. As shown in *Table 1*, the advantages and disadvantages of each method are compared, and the average degradation rates that each method can achieve are summarized.

Table 1. *The characteristics of different methods*

Methods		Advantages	Shortages	Possible efficiency
Physical	Sorption Extraction	The material is easy to obtain. It is cost-effective and environmental friendly. The resource can be reused, which has obvious effects on the degradation of PAHs.	Although PAHs can be transferred, they cannot be completely decomposed. The temperature required to prepare materials such as biochar is too high.	60%
Chemical	Oxidation Photocatalytic	The degradation rate is extremely high and the time taken for degradation is short.	The intermediate produced by degradation is likely to cause secondary pollution.	85%
Biological	Plants Bacteria Fungi	It is environmentally friendly and it can degrade PAHs rather than transfer them. Intermediates do not cause secondary pollution.	The degradation rate is lower than the chemical method and the cycle is too long.	65%

Conclusion

Concerning the PAHs pollution, more and more scholars are committed to finding the most effective way to degrade PAHs. Currently, physical, chemical and biological methods have been used to control it. Physical degradation is related to the utilization of activated carbon, bio-carbon, mesoporous silicon and other materials. These materials all feature high specific surface area which is conducive to adsorb polycyclic aromatic hydrocarbon. An appropriate selection of extraction agent is critical to the extraction of PAHs in sludge or water, and external environmental factors such as temperature, pH value, etc. will influence the extraction efficiency. Compared with physical methods and biodegradation, chemical methods excel in the removal of PAHs. Photocatalysis and oxidation have been proved to facilitate high degradation efficiency. Among the chemical methods, the advanced oxidation technology is the most effective. Its mechanism is about generating lively oxygen which can destroy toxic organic compounds. There is an oxidation reaction between •OH and PAHs till carbon dioxide and water are generated. In advanced oxidation, active oxygen production requires external conditions such as ultraviolet light, divalent iron ions, ultrasound, etc. Scientific studies show that the external environment has an obvious influence on the

http://www.aloki.hu ● ISSN 1589 1623 (Print) ● ISSN 1785 0037 (Online)
DOI: http://dx.doi.org/10.15666/aeer/1605_64196440
© 2018, ALÖKI Kft., Budapest, Hungary

oxidation degradation efficiency. For instance, the higher the temperature is, the higher oxidation efficiency will be. Certainly, the combination of photocatalytic and advanced oxidation techniques can also greatly improve the degradation efficiency with the utilization of synergistic effects. The bioremediation efficiency of PAHs depends on the number, type and chemical structure of the microorganisms. The degradation efficiency of various PAHs affected by bacteria or fungi isolated from diverse environments also varies. At present, in PAHs bioremediation, white rot fungi is used the most widely, which can produce a series of enzyme lignin peroxidase, manganese peroxidase and laccase. These enzymes play crucial roles in the PAHs repair and degradation by converting PAHs into simple and less harmful compounds. Mostly, the degradation of PAHs impacted by bacteria and plants is also dependent on their own enzymes.

Physical, chemical and biological methods have their own advantages and disadvantages. The physical method is a good way for PAHs degradation owing to its simplicity, availability and low cost. However, it cannot completely solve the problem by moving PAH pollutants from one place to another. Chemical method can achieve a high degradation rate of PAHs, especially the advanced oxidation technology. But chemical materials may cause secondary pollution to the environment. Biological method is the most environmentally friendly way and it can completely remove PAHs, but it takes at least 15 to 20 days to remove the PAHs. At the same time, the external environment greatly impacts the enzyme activity, and there are many destabilizing factors in the environment.

To sum up, among the three types of methods, the best method is biological method. As for biological methods, the plants, bacteria and fungi are used to produce enzymes to degrade PAHs. Therefore, protecting the activity of enzymes is the key to improve the degradation rate. Storing enzymes in a certain environment can protect their activity and reduce the harm from the outside world. In recent years, metal organic frameworks (MOFs) have been developed rapidly and used in many fields. This kind of material is porous and has large surface area and other characteristics. Therefore, it functions as a kind of adsorption material for the adsorption of polycyclic aromatic hydrocarbon molecules. Combining MOFs and enzyme molecules can fix the enzyme molecule on the material and give full play to its catalysis. The reverse micelle system can provide a suitable place for enzymes, and effectively prevent the destruction of enzymes from external factors. Therefore, it is necessary to explore more effective ways that combine the advantages of physical, chemical and biological methods.

Acknowledgements. The authors acknowledge the financial support from the National Natural Science Foundation of China (51608194), Natural Science Foundation of Hunan (2015JJ3091), and Opening Fund of Key Laboratory of Chemical Biology and Traditional Chinese Medicine Research (Hunan Normal University), Ministry of Education.

REFERENCES

[1] Alagić, S. Č., Maluckov, B. S., Radojičić, V. B. (2015): How can plants manage polycyclic aromatic hydrocarbons? May these effects represent a useful tool for an effective soil remediation? A Review. – Clean Technologies & Environmental Policy 17(3): 597-614.

[2] Alagić, S. Č., Jovanović, V. P., Mitić, V. D., Cvetković, J. S., Petrović, G. M., Stojanović, G. S. (2016): Bioaccumulation of HMW PAHs in the roots of wild blackberry

http://www.aloki.hu ● ISSN 1589 1623 (Print) ● ISSN 1785 0037 (Online)
DOI: http://dx.doi.org/10.15666/aeer/1605_64196440
© 2018, ALÖKI Kft., Budapest, Hungary

from the Bor region (Serbia): Phytoremediation and Biomonitoring Aspects. – Science of the Total Environment 562(562): 561-570.

[3] Arun, A., Raja, P. P., Arthi, R., Ananthi, M., Kumar, K. S., Eyini, M. (2008): Polycyclic aromatic hydrocarbons (Pahs) biodegradation by Basidiomycetes fungi, Pseudomonas isolate, and their cocultures: comparative in vivo and in silico approach. – Applied Biochemistry & Biotechnology 151(2-3): 132-142.

[4] Belo, R. F. C., Figueiredo, J. P., Nunes, C. M., Pissinatti, R., Junqueira, R. G. (2017): Accelerated solvent extraction method for the quantification of polycyclic aromatic hydrocarbons in cocoa beans by gas chromatography–mass spectrometry. – J Chromatogr B Analyt Technol Biomed Life Sci 1053: 87-100.

[5] Beltrán, F. J., Ovejero, G., A., Rivas, J. (1996): Oxidation of polynuclear aromatic hydrocarbons in water. 4. ozone combined with hydrogen peroxide. – Industrial & Engineering Chemistry Research 35(3): 883-890.

[6] Bernalmartinez, A., Carrère, H., Patureau, D., Delgenès, J. P. (2007): Ozone pre-treatment as improver of PAH removal during anaerobic digestion of urban sludge. – Chemosphere 68(6): 1013-9.

[7] Bouzid, I., Maire, J., Brunol, E., Caradec, S., Fatin-Rouge, N. (2017): Compatibility of surfactants with activated-persulfate for the selective oxidation of PAH in groundwater remediation. – Journal of Environmental Chemical Engineering 5(6).

[8] Brown, G. S., Barton, L. L., Thomson, B. M. (2003): Permanganate Oxidation of sorbed polycyclic aromatic hydrocarbons. – Waste Management 23(8): 737-740.

[9] Brown, J. N., Peake, B. M. (2006): Sources of heavy metals and polycyclic aromatic hydrocarbons in urban stormwater runoff. – Science of the Total Environment 359(1): 145-155.

[10] Cerniglia, C. E. (1992): Biodegradation of polycyclic aromatic hydrocarbons. – Current Opinion in Biotechnology 3(2-3): 351-368.

[11] Chen, B., Yuan, M., Hao, L. (2011): Removal of polycyclic aromatic hydrocarbons from aqueous solution using plant residue materials as a biosorbent. – Journal of Hazardous Materials 188(1): 436-442.

[12] Chen, S., Yin, H., Ye, J., Peng, H., Zhang, N., He, B. (2013): Effect of copper (II) on biodegradation of benzo[a]pyrene by Stenotrophomonas maltophilia. – Chemosphere 90(6): 1811-20.

[13] Chulalaksananukul, S., Gadd, G. M., Sangvanich, P., Sihanonth, P., Piapukiew, J., Vangnai, A. S. (2006): Biodegradation of benzo(a)pyrene by a newly isolated fusarium sp. – Fems Microbiology Letters 262(1): 99-106.

[14] Cutright, T. J. (1995): Polycyclic aromatic hydrocarbon biodegradation and kinetics using Cunninghamella echinulata var. Elegans. – International Biodeterioration & Biodegradation 35(4): 397-408.

[15] Da, S. M., E. Esposito, J. D. Moody, V. P. Canhos & C. E. Cerniglia (2004) Metabolism of aromatic hydrocarbons by the filamentous fungus Cyclothyrium sp. *Chemosphere,* 57**,** 943-952.

[16] Dean-Ross, D., Moody, J., Cerniglia, C. E. (2002): Utilization of mixtures of polycyclic aromatic hydrocarbons by bacteria isolated from contaminated sediment. – Fems Microbiology Ecology 41(1): 1-7.

[17] Debajyoti, G., Shreya, G., Dutta, T. K., Youngho, A. (2016): Current state of knowledge in microbial degradation of polycyclic aromatic hydrocarbons (PAHs): a review. – Frontiers in Microbiology 7(386): 1369.

[18] Eberius, M., Berns, A., Schuphan, I. (1997): Ozonation of pyrene and benzo[a]pyrene in silica and soil – 14C-Mass balances and chemical analysis of oxidation products as a first step to ecotoxicological evaluation. – Fresenius Journal of Analytical Chemistry 359(3): 274-279.

http://www.aloki.hu ● ISSN 1589 1623 (Print) ● ISSN 1785 0037 (Online)
DOI: http://dx.doi.org/10.15666/aeer/1605_64196440
© 2018, ALÖKI Kft., Budapest, Hungary

[19] Feng, C., Khulbe, K. C., Matsuura, T., Tabe, S., Ismail, A. F. (2013): Preparation and characterization of electro-spun nanofiber membranes and their possible applications in water treatment. – Separation & Purification Technology 102(1): 118-135.
[20] Garon, D., Sage, L., Wouessidjewe, D., Seigle-Murandi, F. (2004): Enhanced degradation of fluorene in soil slurry by Absidia cylindrospora and maltosyl-cyclodextrin. – Chemosphere 56(2): 159-166.
[21] Gong, Z., Alef, K., Wilke, B. M., Li, P. (2005): Dissolution and removal of PAHs from a contaminated soil using sunflower oil. – Chemosphere 58(3): 291.
[22] Hadibarata, T., Kristanti, R. A. (2014): Fluorene biodegradation and identification of transformation products by white-rot fungus Armillaria sp. F022. – Biodegradation 25(3): 373-382.
[23] Hadibarata, T., Teh, Z. C., Rubiyatno, Zubir, M. M., Khudhair, A. B., Yusoff, A. R., Salim, M. R., Hidayat, T. (2013): Identification of naphthalene metabolism by white rot fungus Pleurotus eryngii. – Bioprocess & Biosystems Engineering 36(10): 1455-1461.
[24] Haritash, A. K., Kaushik, C. P. (2009): Biodegradation aspects of polycyclic aromatic hydrocarbons (PAHs): a review. – Journal of Hazardous Materials 169(1-3): 1.
[25] Hiller, E., Jurkovič, L., Bartal, M. (2008): Effect of temperature on the distribution of polycyclic aromatic hydrocarbons in soil and sediment. – Soil & Water Research 3(4): 231-240.
[26] Homem, V., Dias, Z., Santos, L., Alves, A. (2014): Preliminary feasibility study of benzo(a)pyrene oxidative degradation by fenton treatment. – Journal of Environmental & Public Health 2009(2009):: 149034.
[27] Huang, Y., Fulton, A. N., Keller, A. A. (2016): Simultaneous removal of PAHs and metal contaminants from water using magnetic nanoparticle adsorbents. – Science of the Total Environment 571: 1029-1036.
[28] Ji, H., Gong, Y., Duan, J., Zhao, D., Liu, W. (2018): Degradation of petroleum hydrocarbons in seawater by simulated surface-level atmospheric ozone: reaction kinetics and effect of oil dispersant. – Marine Pollution Bulletin 135: 427-440.
[29] Jiang, L., Yuan, X., Zeng, G., Wu, Z., Liang, J., Chen, X., Leng, L., Wang, H., Wang, H. (2017): Metal-free efficient photocatalyst for stable visible-light photocatalytic degradation of refractory pollutant. – Applied Catalysis B Environmental 221.
[30] Jiang, L., Yuan, X., Zeng, G., Liang, J., Chen, X., Yu, H., Wang, H., Wu, Z., Zhang, J., Xiong, T. (2018): In-situ synthesis of direct solid-state dual Z-scheme WO_3/g-C_3 N_4 /Bi_2 O_3 photocatalyst for the degradation of refractory pollutant. – Applied Catalysis B Environmental 227.
[31] Jin, X., Tian, W., Liu, Q., Qiao, K., Zhao, J., Gong, X. (2017): Biodegradation of the benzo[A]pyrene-contaminated sediment of the Jiaozhou bay wetland using Pseudomonas sp. immobilization. – Marine Pollution Bulletin 117(1-2): 283.
[32] Kalmykova, Y., Moona, N. (2014): Sorption and degradation of petroleum hydrocarbons, polycyclic aromatic hydrocarbons, alkylphenols, bisphenol A and phthalates in landfill leachate using sand, activated carbon and peat filters. – Water Research 56(3): 246-257.
[33] Khattri, S. D., Singh, M. K. (2009): Removal of malachite green from dye wastewater using neem sawdust by adsorption. – Journal of Hazardous Materials 167(1-3): 1089-1094.
[34] Kristanti, R. A., Hadibarata, T. (2015): Biodegradation and identification of transformation products of fluorene by Ascomycete fungi. – Water Air & Soil Pollution 226(12): 1-6.
[35] Kronenberg, M., Trably, E., Bernet, N., Patureau, D. (2017): Biodegradation of polycyclic aromatic hydrocarbons: using microbial bioelectrochemical systems to overcome an impasse. – Environmental Pollution 231(Pt 1): 509.
[36] Kuppusamy, S., Thavamani, P., Megharaj, M., Naidu, R. (2016): Biodegradation of polycyclic aromatic hydrocarbons (PAHs) by novel bacterial consortia tolerant to diverse

http://www.aloki.hu ● ISSN 1589 1623 (Print) ● ISSN 1785 0037 (Online)
DOI: http://dx.doi.org/10.15666/aeer/1605_64196440
© 2018, ALÖKI Kft., Budapest, Hungary

physical settings - assessments in liquid-and slurry-phase systems. – International Biodeterioration & Biodegradation 108: 149-157.

[37] Lair, A., Ferronato, C., Chovelon, J. M., Herrmann, J. M. (2008): Naphthalene degradation in water by heterogeneous photocatalysis: An investigation of the influence of inorganic anions. – Journal of Photochemistry & Photobiology A Chemistry 193(2-3): 193-203.

[38] Lambropoulou, D. A. (2010): An overview of modern extraction techniques for the determination of organic pollutants in environmental matrices: a review. – Current Organic Chemistry 14(19): -.

[39] Lamichhane, S., Krishna, K. C. B., Sarukkalige, R. (2016): Polycyclic aromatic hydrocarbons (PAHs) removal by sorption: a review. – Chemosphere 148: 336-353.

[40] Lau, E. V., Gan, S., Ng, H. K., Poh, P. E. (2014): Extraction agents for the removal of polycyclic aromatic hydrocarbons (PAHs) from soil in soil washing technologies. – Environmental Pollution 184(1): 640.

[41] Ledakowicz, S. A., Miller, J. S., Olejnik, D. (2014): Oxidation of PAHs in water solution by ozone combined with ultraviolet radiation. – International Journal of Photoenergy 3(1): 95-101.

[42] Lei, A. P., Hu, Z. L., Wong, Y. S., Tam, N. F. (2007): Removal of fluoranthene and pyrene by different microalgal species. – Bioresource Technology 98(2): 273-80.

[43] Li, Z., Liu, Y., Yang, X., Xing, Y., Yang, Q., Yang, R. T. (2017): Adsorption thermodynamics and desorption properties of gaseous polycyclic aromatic hydrocarbons on mesoporous adsorbents. – Adsorption-journal of the International Adsorption Society 23(2-3): 361-371.

[44] Liu, G., Niu, Z., Niekerk, D. V., Xue, J., Zheng, L. (2008): Polycyclic aromatic hydrocarbons (PAHs) from coal combustion: emissions, analysis, and toxicology. – Reviews of Environmental Contamination & Toxicology 192: 1.

[45] Llobet, J. M., Falcó, G., Bocio, A., Domingo, J. L. (2006): Exposure to polycyclic aromatic hydrocarbons through consumption of edible marine species in Catalonia, Spain. – J Food Prot 69(10): 2493-2499.

[46] Lu, J., Guo, C., Zhang, M., Lu, G., Dang, Z. (2014): Biodegradation of single pyrene and mixtures of pyrene by a fusant bacterial strain F14. – International Biodeterioration & Biodegradation 87: 75-80.

[47] Luna, F. M. T., Filho, A. N. O., Araújo, C. C. B., Azevedo, D. C. S., Jr, C. L. C. (2016): Adsorption of polycyclic aromatic hydrocarbons from heavy naphthenic oil using commercial activated carbons. 2. column adsorption studies. – Industrial & Engineering Chemistry Research 55(29).

[48] Mahler, B. J., Metre, P. C. V., Crane, J. L., Watts, A., Scoggins, M., Williams, E. S. (2012): Coal-tar-based pavement seal coat and PAHs: Implications for the environment, human health, and stormwater management. – Environmental Science & Technology 46(6): 3039-45.

[49] Marcourrea, E., Aranda, E. (2015): Potential of non-ligninolytic fungi in bioremediation of chlorinated and polycyclic aromatic hydrocarbons. – New Biotechnology 32(6): 620-628.

[50] Mohanrasu, K., Premnath, N., Siva Prakash, G., Sudhakar, M., Boobalan, T., Arun, A. (2018): Exploring multi potential uses of marine bacteria; an integrated approach for PHB production, PAHs and polyethylene biodegradation. – Journal of Photochemistry and Photobiology B: Biology 185: 55-65.

[51] Muangchinda, C., Yamazoe, A., Polrit, D., Thoetkiattikul, H., Mhuantong, W., Champreda, V., Pinyakong, O. (2016): Biodegradation of high concentrations of mixed polycyclic aromatic hydrocarbons by indigenous bacteria from a river sediment: a microcosm study and bacterial community analysis. – Environmental Science and Pollution Research 24(5): 4591-4602.

http://www.aloki.hu ● ISSN 1589 1623 (Print) ● ISSN 1785 0037 (Online)
DOI: http://dx.doi.org/10.15666/aeer/1605_64196440
© 2018, ALÖKI Kft., Budapest, Hungary

[52] Niu, J., Dai, Y., Guo, H., Xu, J., Shen, Z. (2013): Adsorption and transformation of PAHs from water by a laccase-loading spider-type reactor. – Journal of Hazardous Materials 248-249C(6): 254.
[53] Noordkamp, E. R., Grotenhuis, J. T. C., Rulkens, W. H. (1997): Selection of an efficient extraction method for the determination of polycyclic aromatic hydrocarbons in contaminated soil and sediment. – Chemosphere 35(9): 1907-1917.
[54] Nzila, A. (2018): Biodegradation of high-molecular-weight polycyclic aromatic hydrocarbons under anaerobic conditions: overview of studies, proposed pathways and future perspectives. – Environ Pollut 239: 788-802.
[55] Oleszczuk, P., Hale, S. E., Lehmann, J., Cornelissen, G. (2012): Activated carbon and biochar amendments decrease pore-water concentrations of polycyclic aromatic hydrocarbons (PAHs) in sewage sludge. – Bioresource Technology 111(111): 84-91.
[56] Pérez, M., Torrades, F., Domènech, X., Peral, J. (2002): Fenton and photo-fenton oxidation of textile effluents. – Water Research 36(11): 2703.
[57] Passarini, M. R., Rodrigues, M. V., da Silva, M., Sette, L. D. (2011): Marine-derived filamentous fungi and their Potential application for polycyclic aromatic hydrocarbon bioremediation. – Mar Pollut Bull 62(2): 364-70.
[58] Ríos, Á., Zougagh, M. (2016): Recent advances in magnetic nanomaterials for improving analytical processes. – Trac Trends in Analytical Chemistry 84: 72-83.
[59] Rahman, R. N., Ghaza, F. M., Salleh, A. B., Basri, M. (2006): Biodegradation of hydrocarbon contamination by immobilized bacterial cells. – Journal of Microbiology 44(3): 354-359.
[60] Ramasamy, V., Anandan, C., Murugadoss, G. (2013): Structural, morphological and photoluminescence studies of multi shells coated ZnO nanocomposites. – Superlattices & Microstructures 61(9): 106-114.
[61] Ravindra, K., Grieken, S. R. V. (2008): Atmospheric polycyclic aromatic hydrocarbons: source attribution, emission factors and regulation. – Atmospheric Environment 42(13): 2895-2921.
[62] Rehmann, K., Noll, H. P., Steinberg, C. E., Kettrup, A. A. (1998): Pyrene degradation by Mycobacterium sp. Strain KR2. – Chemosphere 36(14): 2977-2992.
[63] Reyes-César, A., Absalón, Á. E., Fernández, F. J., González, J. M., Cortés-Espinosa, D. V. (2013): Biodegradation of a mixture of PAHs by non-ligninolytic fungal strains isolated from crude oil-contaminated soil. – World Journal of Microbiology and Biotechnology 30(3): 999-1009.
[64] Rhodes, A. H., Carlin, A., Semple, K. T. (2008): Impact of black carbon in the extraction and mineralization of phenanthrene in soil. – Environmental Science & Technology 42(3): 740.
[65] Romero, M. C., Cazau, M. C., Giorgieri, S., Arambarri, A. M. (1998): Phenanthrene degradation by microorganisms isolated from a contaminated stream. – Environmental Pollution 101(3): 355-359.
[66] Rubio-Clemente, A., Torres-Palma, R. A., Peñuela, G. A. (2014): Removal of polycyclic aromatic hydrocarbons in aqueous environment by chemical treatments: a review. – Science of the Total Environment 478(8): 201-225.
[67] Ruge, Z., Muir, D., Helm, P., Lohmann, R. (2015): Concentrations, trends, and air–water exchange of PAHs and PBDEs derived from passive samplers in lake superior in 2011. – Environmental Science & Technology 49(23): 13777-13786.
[68] Ryu, W. Y., Jang, M. Y., Cho, M. H. (2003): The selective visualization of lignin peroxidase, manganese peroxidase and laccase, produced by white rot fungi on solid media. – Biotechnology & Bioprocess Engineering 8(2): 130-134.
[69] Sáncheztrujillo, M. A., Morillo, E., Villaverde, J., Lacorte, S. (2013): Comparative effects of several cyclodextrins on the extraction of PAHs from an aged contaminated soil. – Environmental Pollution 178: 52-58.

http://www.aloki.hu ● ISSN 1589 1623 (Print) ● ISSN 1785 0037 (Online)
DOI: http://dx.doi.org/10.15666/aeer/1605_64196440
© 2018, ALÖKI Kft., Budapest, Hungary

[70] Sarma, P. M., Duraja, P., Deshpande, S., Lal, B. (2010): Degradation of pyrene by an enteric bacterium, Leclercia adecarboxylata PS4040. – Biodegradation 21(1): 59.
[71] Shi, W., Guo, Y., Ning, G., Li, C., Li, Y., Ren, Y., Zhao, O., Yang, Z. (2018): Remediation of soil polluted with HMW-PAHs by alfalfa or brome in combination with fungi and starch. – Journal of Hazardous Materials 360: 115-121.
[72] Shoun, H., Sudo, Y., Sato, K. I., Beppu, T. (1989): Components of the cytochrome P-450 monooxygenase system of the fungus, Fusarium oxysporum: conditions for induction and isolation of cytochrome b5. – Journal of the Agricultural Chemical Society of Japan 53(8): 2153-2161.
[73] Silva, A., Delerue-Matos, C., Fiúza, A. (2005): Use of solvent extraction to remediate soils contaminated with hydrocarbons. – Journal of Hazardous Materials 124(1-3): 224-229.
[74] Silva, I. S., Grossman, M., Durrant, L. R. (2009): Degradation of polycyclic aromatic hydrocarbons (2-7 rings) under microaerobic and very-low-oxygen conditions by soil fungi. – International Biodeterioration & Biodegradation 63(2): 224-229.
[75] Silva, M. D. (2002): Fungos filamentosos isolados de sedimentos estuarinos que metabolizam hidrocarbonetos aromaticos policiclicos. – Tese (doutorado), Universidade Estadual de Campinas, Faculdade de Engenharia de Alimentos, Campinas, SP.
[76] Somtrakoon, K., Chouychai, W., Lee, H. (2014): Comparing anthracene and fluorene degradation in anthracene and fluorene-contaminated soil by single and mixed plant cultivation. – Int J Phytoremediation 16(4): 415-428.
[77] Song, W., Li, J., Zhang, W., Hu, X., Wang, L. (2012): An experimental study on the remediation of phenanthrene in soil using ultrasound and soil washing. – Environmental Earth Sciences 66(5): 1487-1496.
[78] Souza, H. M. D. L., Sette, L. D., Mota, A. J. D., Rodrigues, A., Oliveira, T. B. D., Oliveira, F. M. D., Oliveira, L. A. D., Barroso, H. D. S., Zanotto, S. P. (2016): Filamentous fungi isolates of contaminated sediment in the Amazon region with the potential for benzo(a)pyrene degradation. – Water Air & Soil Pollution 227(12): 431.
[79] Sprovieri, M., Feo, M. L., Prevedello, L., Manta, D. S., Sammartino, S., Tamburrino, S., Marsella, E. (2007): Heavy metals, polycyclic aromatic hydrocarbons and polychlorinated biphenyls in surface sediments of the Naples harbour (southern Italy). – Chemosphere 67(5): 998-1009.
[80] Sun, K., Liu, J., Jin, L., Gao, Y. (2014): Utilizing pyrene-degrading endophytic bacteria to reduce the risk of plant pyrene contamination. – Plant & Soil 374(1-2): 251-262.
[81] Szczepaniak, Z., Cyplik, P., Juzwa, W., Czarny, J., Staninska, J., Piotrowska-Cyplik, A. (2015): Antibacterial effect of the Trichoderma viride Fungi on soil microbiome during PAH's biodegradation. – International Biodeterioration & Biodegradation 104: 170-177.
[82] Szulejko, J. E., Kim, K. H., Brown, R. J. C., Bae, M. S. (2014): Review of progress in solvent-extraction techniques for the determination of polyaromatic hydrocarbons as airborne pollutants. – Trends in Analytical Chemistry 61(5): 40-48.
[83] Tiwari, M., Sahu, S. K., Bhangare, R. C., Ajmal, P. Y., Pandit, G. G. (2013): Estimation of polycyclic aromatic hydrocarbons associated with size segregated combustion aerosols generated from household fuels. – Microchemical Journal 106(1): 79-86.
[84] Veignie, E., Rafin, C., Woisel, P., Cazier, F. (2004): Preliminary evidence of the role of hydrogen peroxide in the degradation of benzo[a]pyrene by a non-white rot fungus Fusarium solani. – Environmental Pollution 129(1): 1-4.
[85] Vela, N., Martínez-Menchón, M., Navarro, G., Pérez-Lucas, G., Navarro, S. (2012): Removal of polycyclic aromatic hydrocarbons (PAHs) from groundwater by heterogeneous photocatalysis under natural sunlight. – Journal of Photochemistry & Photobiology A Chemistry 232(5): 32-40.
[86] Veréb, G., Ambrus, Z., Pap, Z., Kmetykó, Á., Dombi, A., Danciu, V., Cheesman, A., Mogyorósi, K. (2012): Comparative study on UV and visible light sensitive bare and

http://www.aloki.hu ● ISSN 1589 1623 (Print) ● ISSN 1785 0037 (Online)
DOI: http://dx.doi.org/10.15666/aeer/1605_64196440
© 2018, ALÖKI Kft., Budapest, Hungary

doped titanium dioxide photocatalysts for the decomposition of environmental pollutants in water. – Applied Catalysis A General 417-418(1): 26-36.

[87] Von, L. E., Gan, S., Ng, H. K. (2012): Extraction of phenanthrene and fluoranthene from contaminated sand using palm kernel and soybean oils. – Journal of Environmental Management 107(107): 124-130.

[88] Waszak, D. Q., Cunha, A. C. B. D., Agarrallua, M. R. A., Goebel, C. S., Sampaio, C. H. (2015): Bioremediation of a benzo[a]pyrene-contaminated soil using a microbial consortium with Pseudomonas aeruginosa, Candida albicans, Aspergillus flavus, and Fusarium sp. – Water Air & Soil Pollution 226(9): 1-11.

[89] Wen, S., Zhao, J., Sheng, G., Fu, J., Peng, P. (2002): Photocatalytic reactions of pyrene at TiO_2/water interfaces. – Chemosphere 46(6): 871-7.

[90] Woo, O. T., Chung, W. K., Wong, K. H., Chow, A. T., Wong, P. K. (2009): Photocatalytic oxidation of polycyclic aromatic hydrocarbons: intermediates identification and toxicity testing. – Journal of Hazardous Materials 168(2): 1192-1199.

[91] Wu, Y.-R., He, T.-T., Lun, J.-S., Maskaoui, K., Huang, T.-W., Hu, Z. (2009): Removal of benzo[a]pyrene by a fungus Aspergillus sp. BAP14. – World Journal of Microbiology and Biotechnology 25(8): 1395-1401.

[92] Xia, W., Du, Z., Cui, Q., Dong, H., Wang, F., He, P., Tang, Y. (2014): Biosurfactant produced by novel pseudomonas sp. WJ6 with biodegradation of N-alkanes and polycyclic aromatic hydrocarbons. – Journal of Hazardous Materials 276(5): 489-498.

[93] Yenchih Chen, And, M. K. B., Schwab, A. P. (2003): Pyrene degradation in the rhizosphere of tall fescue (Festuca arundinacea) and switchgrass (Panicum virgatum L.). – Environmental Science & Technology 37(24): 5778-82.

[94] Yongwoon, L., Jinje, P., Gang, K. S., Changkook, R., Yang, W., Jinho, J., Seunghun, H. (2013): Production and characterization of biochar from various biomass materials by slow pyrolysis. – Technical Bulletin (Asian and Pacific Council, Food & Fertilizer Technology Center) no. 197.

[95] Yuan, M., Tong, S., Zhao, S., Jia, C. Q. (2010): Adsorption of polycyclic aromatic hydrocarbons from water using petroleum coke-derived porous carbon. – Journal of Hazardous Materials 181(1-3): 1115.

[96] Yuan, Q., Posch, T., Schmidt, T. C. (2011): Sorption of polycyclic aromatic hydrocarbons (PAHs) on glass surfaces. – Chemosphere 82(6): 859-865.

[97] Zeledón-Toruño, Z. C., Lao-Luque, C., Heras, F. X. C. D. L., Sole-Sardans, M. (2007): Removal of PAHs from water using an immature coal (leonardite). – Chemosphere 67(3): 505-512.

[98] Zhang, S., Ning, Y., Zhang, X., Zhao, Y., Yang, X., Wu, K., Yang, S., La, G., Sun, X., Li, X. (2015): Contrasting characteristics of anthracene and pyrene degradation by wood rot fungus Pycnoporus sanguineus H1. – International Biodeterioration & Biodegradation 105: 228-232.

[99] Zhang, W., Sun, H., Wang, L. (2013): Influence of the interactions between black carbon and soil constituents on the sorption of pyrene. – Journal of Soil Contamination 22(4): 469-482.

http://www.aloki.hu ● ISSN 1589 1623 (Print) ● ISSN 1785 0037 (Online)
DOI: http://dx.doi.org/10.15666/aeer/1605_64196440
© 2018, ALÖKI Kft., Budapest, Hungary

ASSESSMENT OF ECONOMIC CONSIDERATIONS FOR AIR POLLUTION CONTROL TECHNOLOGIES

MORIDI, F.[1] – YARAHMADI, R.[2*] – ABDOLI-SENJANI, M.[1] – MARJANI, A.[1]

[1]*Department of Chemistry, Arak Branch, Islamic Azad University, Arak, Iran*

[2]*Air Pollution Research Center, school of public health, Iran University of Medical Sciences, Tehran, Iran*

**Corresponding author*
e-mail: yarahmadi.r@iums.ac.ir; phone: +98-21-8889-7613

(Received 9th Jun 2018; accepted 14th Aug 2018)

Abstract. Today, advances in technology help humans to overcome emissions to some extent. Environmental researchers have attempted in recent years to find low-cost and effective approaches to pollutants control. It is important to consider the economic sphere in the approaches of dealing with pollution, as it has merits that should not be ignored, because of the existence of inefficient and expensive rules. To control air pollution, effective and long-term strategies should be identified and implemented. Among the components of air pollution control systems, pollution remediation equipment is of high importance. The present study aimed to assess air filtration systems, with emphasis on hybrid and new technologies, economic evaluation and prioritization of particle control technologies using a cost-benefit analysis method. According to the results, the research Cost-benefit analysis of particles control technologies based on research aspect had different weights. Wet ESP, Nano fiber beds, and ESP Bag Filter respectively were identified as the most appropriate particulates control techniques.
Keywords: *particle filtration, priority, equipment, new technology, air pollution*

Introduction

Industrial and technological developments and increasing energy consumption have led to renewable sources pollution (Zhang et al., 2015; Zeng et al., 2017). Given operating costs of different methods of pollution control and lack of return on investment have become air pollution control into an unprofitable economic burden (Robert and Erson, 1983; Moridi et al., 2017; Yarahmadi et al., 2010). To control air pollution, effective and long-term strategies should be identified and implemented (Vlachokostas et al., 2011; Yarahmadi et al., 2010; Lei, 2005; Vanoye and Mendoza, 2014; Chen et al., 2018). However, most decision-makers are not able to properly assess and reduce the costs of environmental degradation and the expenditure necessary to comply with the standard rules of air pollution reduction. For this reason, in many cases managers have had to use methods that are either expensive and unaffordable, or inexpensive but unreliable. Engineering Economics is a specialized field in economics that uses analysis methods to estimate costs (Zhao et al., 2016) and determine the value of industrial projects. This field has many roles, including the evaluation of industrial project usefulness, estimating values, and evaluating them in terms of technical and engineering issues (Salehi and Tavakkoli-Moghaddam, 2008). General methods used to particles are settling chamber, cyclone, bag house, scrubber, ESP and extra. The final composition is applying control measures and using technical equipment based on economic aspects (Boardman et al., 2017; Jin et al., 2018; Min et al., 2017). The absence of relevant studies can lead to health, safety, economic, energy, environmental (HSE_3) and social losses; this research was the first to prioritize and select the most

http://www.aloki.hu ● ISSN 1589 1623 (Print) ● ISSN 1785 0037 (Online)
DOI: http://dx.doi.org/10.15666/aeer/1605_64416451
© 2018, ALÖKI Kft., Budapest, Hungary

appropriate particles control hybrid and new technologies based on cost benefit analysis. Effective and affordable control measures are an optimal solution for administrative-managerial considerations (Murty et al., 2006; Nath and Cholakov, 2009; Yarahmadi and Sadoughi, 2012; Spiegel and Maystre, 1998). Previous studies indicate that, the high initial and operative costs of common filtration methods and lack of return on investment have turned air pollution control into an unprofitable economic burden. Based on these concern policy makers have hence made numerous efforts to develop cost-effective methods and optimized techniques to manage air pollution based on all economic, environmental, and social considerations. Therefore, selection of air pollution new technologies have been proposed to prioritize and chosen by seeking an option which provides maximum benefit based on all mention criteria (Moridi et al., 2017).

These also include the cost of raw materials, design costs, consulting costs, personnel costs and maintenance costs. A study entitled cost analysis framework project was published; it used cost-benefit analysis as a practical tool for evaluating different types of projects. This study aimed to analyze costs and benefits, assess money value, and offer the highest quality of results in order to optimize the use of valuable resources (Qld, 2011). The most common method for assessing the beneficial effects of environmental policies is cost-benefit analysis (CBA) (Voorhees et al., 2001; Gao et al., 2016; Bollen et al., 2009; Huang et al., 2017; Sen, 2000).

Robert et al. (1983) considered the economic sphere in the approaches of dealing with pollution to have merits that should not be ignored, as inefficient and expensive rules exist (Robert and Erson, 1983). Studies show that in most cases, the most cost-effective pollution control program is the cheapest one (Yarahmadi et al., 2012). The aim of research is assessment of new technologies with economic, environmental, social consideration for particulate control technologies using a cost-benefit method.

Methods

The cost-benefit analysis (CBA) method is often used as an efficient tool for estimating environmental costs and benefits. This method is used in decision-making relating to development projects as well as the evaluation of policies (Voorhees et al., 2001; Quah, 2007).

This method, which uses the simple cost-benefit approach tool (SCBAT), selects the best option in regard to economic-executive considerations that help project managers in managerial decision-making. This method was used for optimized air filtration technologies selection with the cost-benefit aspects include of Financial, Personnel, Service and maintenance, Environmental-social, Production and HSE risks for the first. Using this method in our study, the procedure is as follow (Cellini and Kee, 2010):

1. A list of innovative technologies in the field of particles control was collected.
2. Experts assessed the initial survey list. Determination the aspects of cost-benefits associated for key selected technologies were done by expert panel groups (brainstorm).
3. Criteria for the costs and benefits and their elements associated with each option of the investigated technologies in *Table 1* were identified (Treasury, 2006; Campbell and Brown, 2003).

http://www.aloki.hu ● ISSN 1589 1623 (Print) ● ISSN 1785 0037 (Online)
DOI: http://dx.doi.org/10.15666/aeer/1605_64416451
© 2018, ALÖKI Kft., Budapest, Hungary

4. According to the method, the criteria of cost benefit were scored through linguistic variables (scores: 1–3 Scale Rating: Low = 1, Moderate = 2, High = 3).
5. The benefit-to-cost ratings ratio and the ranking by the outcome of technology from benefit-cost standards were determined (Svensson, 2016).
6. If the resulting number is greater than one, it means there is more profit than cost and high priority will be given. If the number is one, the benefit is equal to the cost, and priority will be given with caution. If the benefit ratio is less than the cost and the obtained value is smaller than one, the action will be in completion. Cost-benefit in this case does not have any benefit, and this option will not be given priority.
7. Setting priorities based on larger concessions will be a top consideration.

According to the method, a list of hybrid and new control equipment for particle air pollutants was given to the experts to be indexed**.** In this study, an expert panel of six technicians with high experience in the fields of air pollution, environmental sciences, occupational health and industrial safety was used. The present study expert panel of was selected of four company in Iran with the ability of design, manufacture, install, and maintenance. The criteria of each cost-benefit exercise and their constituent elements associated with each option were scored by experts and specialists from design and manufacturing companies. Then, the benefit-to-cost ratio was calculated and ranked.

Table 1. *Aspects of costs and benefits associated with each action*

The cost-benefit aspects	More description
Financial	Investment - required equipments to build and launch
Personnel	Training - internships - internal, external period - absence from work
Service and maintenance	Operating period - services - operational energy - maintenance and service
Environmental-social	Release of toxic substances - waste management - the rule of law - efficiency
Customer orientation	Investment - new products - the need of new information
Production	Development - efficiency - replacing equipment and entrance fees
HSE risks	Personnel's safety - fires - the damage to the production network

Results

Initial and selected list of particulate control technologies were shown in *Table 2*. Information collected in the *Tables 3–7* for rating particle-filtering technologies after the preliminary analysis:

Table 2. *Initial and selected final particulate air pollution control*

Initial list			Key selected technologies by expert panel
Bag house	Wet ESP	Fabric filters	ULPA Filter
Settling chamber	Nano fibers bed	HEPA Filter	Wet ESP
ULPA filter	Scrubber	Wet cyclone	Nano fibers bed
Cyclone	ESP bag filter	Multicyclone	ESP Bag filter

http://www.aloki.hu ● ISSN 1589 1623 (Print) ● ISSN 1785 0037 (Online)
DOI: http://dx.doi.org/10.15666/aeer/1605_64416451
© 2018, ALÖKI Kft., Budapest, Hungary

Table 3. *Results of cost-benefit criteria and elements evaluation for ULPA Filter*

Cost-Benefit criteria	Elements of cost-benefit criteria	Benefit elements examples	Average benefit rate	Examples of cost elements	Average cost rate
Financial	Investment, required equipments to build and launch	✓ Construction with composite of a valuable materials internal ✓ Construction and design of structural frames	1.66	✓ Assembled and the possibility changes in the original design ✓ The need for special compounds against heat high	2.33
Personnel	Training, internships, internal, external period, absence from work	✓ Need to launch scientific education course	1.66	✓ Training of technicians for technical changes in the structure	2.33
Service and maintenance	operating period, Services, Operational Energy, Maintenance service	✓ Reuse the filter after cleaning ✓ Very low energy consumption	2	✓ High level maintenance service ✓ Blocked pores through time ✓ Damage Due to heat	1.66
Environmental -social	Release of toxic substances, Waste Management, the rule of law, efficiency	✓ High purification efficiency	2.33	✓ toxic gas emissions ✓ Blocked pores through time and quality loss	1.33
Customer orientation	Investment, new products, the need of new information	✓ This technology is native ✓ In plaster and cement factories are part of a high quality product	1.33	✓ Require a regenerator needed for recycling ✓ Require a pulse jet of high pressure	2.33
Production	Development, efficiency, replacing equipment and entrance fees	✓ Low explosive hazard	1.33	✓ Possibility of reusing the filter after cleaning ✓ High cost raw material	2.33
HSE risks	Personnel's safety, fires, the damage to the production network	✓ Minimum risk fire and explosion	1.66	✓ Unavailability of testing technology ✓ Environmental hazards caused by waste production from changing period ✓ Exposure to particles and fibers released during the changing and maintenance	1.66
Arithmetic mean and standard deviation of benefit- cost rating			X=1.7 SD=0.36	Arithmetic mean and standard deviation of cost rating	X=2 SD=0.43

http://www.aloki.hu ● ISSN 1589 1623 (Print) ● ISSN 1785 0037 (Online)
DOI: http://dx.doi.org/10.15666/aeer/1605_64416451
© 2018, ALÖKI Kft., Budapest, Hungary

Table 4. *Results of cost-benefit criteria and elements evaluation for wet ESP*

Cost-benefit criteria	Elements of cost-benefit criteria	Benefit elements examples	Average benefit rate	Examples of cost elements	Average cost rate
Financial	Investment, required equipments to build and launch	✓ Low operating costs except in the high efficiency ✓ Low operating costs ✓ Collectors fewer plate compared to dry type	2.33	✓ Complicated design ✓ Chemical base particles ✓ Assembly and the possibility of changes to the original design ✓ The need to large physical space	1.33
Personnel	Training, internships, internal, external period, absence from work	✓ Short-term training courses	2.33	✓ Training of technicians for technical changes in the structure	1.33
Service and maintenance	Operating period, services, operational energy, maintenance and service	✓ Reuse the filter after cleaning ✓ Energy consumption depends on the size of the particles that not exist in other devices ✓ Low operating costs except in the high range	1.66	✓ Maintenance service ✓ Low rate of efficiency with incorrect design	1.33
Environmental -social	Release of toxic substances, waste management, the rule of law, efficiency	✓ High purification efficiency ✓ ACCEPTANCE acidic and corrosive gases ✓ Ability to collect the gas and particles at the same time	2.33	✓ Disposal of leachate from ash ✓ Malfunctions the system due to changes psychometrics' conditions (temperature, speed, ...) ✓ Produce byproducts same as mist ✓ Removal efficiency change due to the properties of the particle or droplet	1.66
Customer orientation	Investment, new products, the need of new information	✓ This technology is native ✓ Unexpected products in plaster and cement factories are part of a high quality product	2	✓ Materials do not separated of the size ✓ Corrosion in the pages due to sludge production	1.33
Production	Development, efficiency, replacing equipment and entrance fees	✓ Acceptance of a wide range of gas and dust high volume ✓ The electromechanical equipment in the existing	1.66	✓ Integration electrical - mechanical function simultaneous is problem	1.33
HSE risks	Personnel's safety, fires, the damage to the production network	✓ Impossibility of release of captured dust ✓ Minimal risk of fire and explosion	1.66	✓ Recycling problems ✓ The possibility to respiratory exposure ✓ Generated waste and contamination soil, etc. ✓ Generated noise and vibration ✓ The creation of high-frequency waves	1.33
Arithmetic mean and standard deviation of benefit- cost rating			X=1.42 SD=0.16	Arithmetic mean and standard deviation of cost rating	X=1.954 SD=0.4

http://www.aloki.hu ● ISSN 1589 1623 (Print) ● ISSN 1785 0037 (Online)
DOI: http://dx.doi.org/10.15666/aeer/1605_64416451
© 2018, ALÖKI Kft., Budapest, Hungary

Table 5. *Results of cost-benefit criteria and elements evaluation for ESP bag filter*

Cost-benefit criteria	Elements of Cost-benefit criteria	Benefit elements examples	Average benefit rate	Examples of cost elements	Average cost rate
Financial	Investment, required equipments to build and launch	✓ High-efficiency filter is not necessary ✓ Plate cost is less compared with Wet ESP	2.33	✓ Power supply ✓ High pressure loss ✓ ESP plate	2.66
Personnel	Training, internships, internal, external period, absence from work	✓ Initial training for commissioning	2	✓ Training of technicians for technical changes in the structure ✓ More specialized training for multiple functions (mechanical -electrical)	1.66
Service and maintenance	Operating period, services, operational energy, maintenance and service	✓ Reuse the filter after cleaning ✓ Control at the time charged and neutral particles	1.66	✓ Special maintenance - high cost	2.66
Environmental -social	Release of toxic substances, waste management, the rule of law, efficiency	✓ High filtration efficiency for a wide range of particles	2	✓ High energy consumption ✓ Particles hunk into the bag ✓ Influence of gases and active radicals ✓ Services of This technology is a combination of ESP and bag filter	2
Customer orientation	Investment, new products, the need of new information	✓ This technology is native ✓ A wide range of particles are extraction able	2	✓ Reuse the filter after cleaning	1.33
Production	Development, efficiency, replacing equipment and entrance fees	✓ Large systems needed to the large-scale due to the production	2	✓ The creation of return Corona into the reactor	2
HSE risks	Personnel's safety, fires, the damage to the production network	✓ Fire risk is low due to low load on the bag filter ✓ Bag Filter is the pre-treatment	2.33	✓ Waste production ✓ The possibility of electrocution ✓ Produce noise and vibration ✓ Need to earth system	2.33
Arithmetic mean and standard deviation of benefit- cost rating			X=2.1 SD=0.5	Arithmetic mean and standard deviation of cost rating	X=2.1 SD=0.23

http://www.aloki.hu ● ISSN 1589 1623 (Print) ● ISSN 1785 0037 (Online)
DOI: http://dx.doi.org/10.15666/aeer/1605_64416451
© 2018, ALÖKI Kft., Budapest, Hungary

Table 6. *Results of cost-benefit criteria and elements evaluation for Nano fibers beds*

Cost-benefit criteria	Elements of cost-benefit criteria	Benefit elements examples	Average benefit rate	Examples of cost elements	Average cost rate
Financial	Investment, required equipments to build and launch	✓ The use of polymer salt for making nanofibers ✓ Access to the production of polymer composite within	2	✓ Electrospinning device is essential for nanofibers production ✓ Power supply with high voltage (25 kV)	2.33
Personnel	Training, internships, internal, external period, absence from work	✓ Initial training to operate machines	2.33	✓ The experts are allowed to work with nanofibers platforms	2.66
Service and maintenance	operating period, Services, Operational Energy, Maintenance and Service	✓ Low energy operation ✓ Simple mechanical function	1.66	✓ The need for technicians highly skilled ✓ Training course performance of every machine for 1-2 years ✓ Large particles caused the pressure loss ✓ The need for monitoring temperature and pressure	1
Environmental -social	Release of toxic substances, Waste Management, the rule of law, efficiency	✓ Ability to filtration simultaneously of gases - particles and acid mist ✓ Elimination of odors ✓ High quality factor filter	2	✓ Residual production ✓ High pressure loss ✓ Quality factor fall at high temperatures	2.33
Customer orientation	Investment, new products, the need of new information	✓ Elimination of active radicals organic and inorganic ✓ Simultaneous elimination of particles and gases	2.33	✓ Reuse the filter after cleaning	2.33
Production	Development, efficiency, replacing equipment and entrance fees	✓ Easily used for treating gaseous pollutants at the nanoscale ✓ Composite polymer could be replaced with material available	2.33	✓ Costly recycling technology	2.33
HSE risks	Personnel's safety, fires, the damage to the production network	✓ Ability to fire ✓ High pressure loss	2	✓ Skin and respiratory exposure to nano materials ✓ Generated noise and vibration ✓ Replaceable fiber is waste material	1.66
Arithmetic mean and standard deviation of benefit- cost rating			X=2.1 SD=0. 57	Arithmetic mean and standard deviation of cost rating	X=2.14 SD=0.32

http://www.aloki.hu ● ISSN 1589 1623 (Print) ● ISSN 1785 0037 (Online)
DOI: http://dx.doi.org/10.15666/aeer/1605_64416451
© 2018, ALÖKI Kft., Budapest, Hungary

Table 7. *Average and coefficient of variation in cost-benefit of particle control technologies*

Controlling technology	Average benefit rate	Average cost rate	Benefit coefficient of variation	Cost coefficient of variation	Benefit-cost ratio	Rating
ULPA filter	1.7±0.36	2±0.43	21%	21%	0.85	*
Wet ESP	1.954±0.4	1.42±0.16	20%	11%	1.37	1
ESP bag filter	2.10±0.5	2.10±0.23	10%	23%	1	3
Nano fibers beds	2.14±0.32	2. 1±0.57	14%	27%	1.01	2

Discussion

ULPA filter technology

The results in *Table 3* show more costs in the financial, personnel, customer service, and production areas. Possible changes to the original design, heat-resistant compounds, maintenance and service, blocked pores and vulnerability to high temperatures, and recycling are the costs of using this technology. High efficiency, information localization, least risk of fire and explosion, and the re-use of filters after cleaning are the benefits of using this technology. The results of previous research study showed that the filtration efficiency of ULPA filter is over 99.999% with a particle diameter of 0.12–0.17-μm Along with significant costs in maintenance and operations (Liu et al., 2017).

Wet ESP technology

According to the results *Table 4,* the financial, personnel, environmental, social, and customer benefits are a result of lower operating costs, short-term training, low power consumption, high temperature tolerance, and high filtration efficiency stemming from the use of this technology. The simultaneous collection of gas and particle is also an advantage of using this technology. The costs of this technology include those incurred in changes to the original design, the need for more physical space, maintenance and servicing, and corrosion caused by the generated sludge. According to the results, the obtained benefits of this technology outweigh the costs. Brandley (2005) announced that ESPs are a common means of reducing PM emissions from boilers, kilns and engines. Collection efficiencies was various, depending on the size and quality of the ESP, but in some cases have reached to upwards of 99% levels. The economic impact was found to be $5,430/tpy (Brandley, 2005).

Wet ESP technology provides with many features and benefits including low operating and maintenance costs, ultra low particulate emissions, compatibility with wet flue gas desulfurization (wet FGD) technology, and an optimized system design for sorbent injection technologies. For manufacturers with existing air pollution control equipment, wet ESP upgrades draw praise from customers who are eliminating carryover and costly maintenance. Improvements to water treatment, gas flow distribution and mist elimination enhance performance, reduce operating costs and protect downstream equipment (http://www.babcock.com/technology/pollution-control/particulate).

ESP bag filter technology

According to the results in *Table 5* the benefits of this technology include the removal of environmental emissions and social benefits resulting from the simultaneous

http://www.aloki.hu ● ISSN 1589 1623 (Print) ● ISSN 1785 0037 (Online)
DOI: http://dx.doi.org/10.15666/aeer/1605_64416451
© 2018, ALÖKI Kft., Budapest, Hungary

control of ESP Bag filter and neutral chargeable particles, as well as high profits from pre-filtering bags. The technology however has high financial and design costs, as well as investment-related costs such as the need for supply source, ES pages, and the need for lightning protection systems. Research and education, especially for service and maintenance, have been allocated a big budget. Localization and the reuse of filters after cleaning are the advantages of using this technology. The combination of electrostatic precipitator (ESP) with bag filter technologies, which can filter smaller particles but fail to work effectively on larger particles, were selected as the proper alternative (closeness coefficient = 0.867) (Moridi et al., 2017).

Nano fibers beds technology

Results in *Table 6* show that the removal of particles (10 microns and smaller) in nano-technology fibers platform leads to social consequences and damage control, and is therefore beneficial. Recycling is however costly with this technology. Removal of organic and non-organic radicals, simultaneous extraction of particles and gases, odor elimination, low power operation, and access to raw materials and polymer composites are the advantages of using this technology. On the basis of the results captured in *Table 7* and T-test (one-sample-test) with a significance level of 5%, one can relatively have a realistic judgment in estimating the approximate financial, human, environmental costs.

Bennett (2016) announced that nanofiber coatings Plus filter cartridges are another development from Freudenberg. According to Freudenberg, high initial efficiency can be guaranteed because, unlike conventional filters, these filters do not need pre-coating with dust. The corrugated filter medium ensures constant low resistance, reducing power and compressed air consumption, potentially extending the product lifetime. Nanofiber coated filter cartridges are straight for-ward to handle and require minimal maintenance (Bennett, 2016).

Conclusion

In this study, the problem of choosing the effectively technical and economic for particulate control technologies, were addressed based on the cost benefit analysis method, which is a reliable scientific method for decision-makers. The methodology developed in this work in term of weighting the seven aspects of cost and benefits (financial, personnel, service and maintenance, environmental-social, customer orientation, production, HSE risks) for selected effectively technical and economic particulate control technologies. Furthermore, decision-makers could use the results obtained via this method to better assess their performance in particulate control. The use of hybrid technologies, including Wet-ESP, has been a top priority for research, but it is feasible to use emission sources with limitations that require extensive research.

REFERENCES

[1] Bennett, A. (2016): Developments in air & gas filtration technology. – Filtration + Separation 53: 30-35.

[2] Boardman, A. E., Greenberg, D. H., Vining, A. R., Weimer, D. L. (2017): Cost-Benefit Analysis: Concepts and Practice. – Cambridge University Press, Cambridge, UK.

http://www.aloki.hu ● ISSN 1589 1623 (Print) ● ISSN 1785 0037 (Online)
DOI: http://dx.doi.org/10.15666/aeer/1605_64416451
© 2018, ALÖKI Kft., Budapest, Hungary

[3] Bollen, J., van der Zwaan, B., Brink, C., Eerens, H. (2009): Local air pollution and global climate change: A combined cost-benefit analysis. – Resource and Energy Economics31: 161-81.
[4] Brandley, M. (2005): Best Available Technology for Air Pollution Control: Analysis Guidance and Case Studies for North America. – Commission for Environmental Cooperation (CEC) of North America, Montréal, QC.
[5] Campbell, H. R., Brown, R. P. C. (2010): Benefit-Cost Analysis: Financial and Economic Appraisal using Spreadsheets. – Cambridge University Press, Cambridge, UK.
[6] Cellini, S. R., Kee, J. E. (2010): Cost-Effectiveness and Cost-Benefit Analysis. – Handbook of Practical Program Evaluation 3. Jossey-Bass Wiley, San Francisco, CA.
[7] Chen, X., Zhao, L., Özdemir, M. S., Liang, H. (2018): Mixed strategy to allocate resources with air pollution treatment in China: based on the analytic network process and large-group decision-making method. – Environmental Science and Pollution Research: 1-15.
[8] Gao, J., Yuan, Z., Liu, X., Xia, X., Huang, X., Dong, Z. (2016): Improving air pollution control policy in China A perspective based on cost–benefit analysis. – Science of the Total Environment 543: 307-14.
[9] Huang, C., Moran, A. E., Coxson, P. G., Yang, X., Liu, F., Cao, J., Chen, K., Wang, M., He, J., Goldman, L., Zhao, D. (2017): Potential cardiovascular and total mortality benefits of air pollution control in urban China. – Circulation 136: 1575-84.
[10] Jin, J., Cheon, S., Lee, J., Lee, S. Kim, J. (2018): Economic impact of overseas coal bed methane development project on Korean economy. – Energy & Environment: 2: 0958305X18762153. https://doi.org/10.1177/0958305X18762153.
[11] Lei, J. A. (2005): Fuzzy Multi-Criteria Decision Analysis for Assessing Technologies of air Pollution Abatement at Coal-Fired Power Plants. – M. S. Thesis Engineering in Environment, University of Regina, Regina, Canada.
[12] Liu, G., Xiao, M., Zhang, X., Gal, C., Chen, X., Liu, L., Clements-Croome, D. (2017): A review of air filtration technologies for sustainable and healthy building ventilation. Sustainable Cities and Society. – 32: 375-396.
[13] Min, S. H., Lim, S. Y., Yoo, S. H. (2017): The environmental benefits of reducing thermal discharge from nuclear power generation. – Energy & Environmental Science 28: 885-894.
[14] Moridi, P., Atabi, F., Nouri, J., Yarahmadi, R. (2017): Selection of optimized air pollutant filtration technologies for petrochemical industries through multiple-attribute decision-making. – Journal of Environmental Management 197: 456-63.
[15] Murty, M. N., Dhavala, K. K., Ghosh, M., Singh, R. (2006): Social Cost-Benefit Analysis of Delhi Metro. – Institute of Economic Growth, Delhi.
[16] Nath, B., Cholakov, G. S. (2009): Pollution Control Technologies. – EOLSS Publications, London.
[17] Qld, D. I. (2011): Project Assurance Framework: Cost Benefit Analysis. Analysis. – Queensland Department of Infrastructure and Planning, Queensland.
[18] Quah, E. (2007): Cost-Benefit Analysis. – Routledge, London.
[19] Robert, J., Erson, J. R. (1983): An empirical analysis of economic strategies for controlling air pollution. – Journal of Environmental Economics and Management 10: 112-124.
[20] Salehi, M., Tavakkoli-Moghaddam, R. (2008): Project selection by using a fuzzy TOPSIS technique. – International Journal of Mechanical, Aerospace, Industrial, Mechatronic and Manufacturing Engineering 2: 375-380.
[21] Sen, A. (2000): The discipline of cost-benefit analysis. – The Journal of Legal Studies 29: 931-52.
[22] Spiegel, J., Maystre, L. Y. (1998): Environmental Pollution Control and Prevention. – In: Stellman, J. M. (ed.) Encyclopedia of Occupational Health and Safety (4th ed.) International Labour Office, Switzerland, Geneva.

http://www.aloki.hu ● ISSN 1589 1623 (Print) ● ISSN 1785 0037 (Online)
DOI: http://dx.doi.org/10.15666/aeer/1605_64416451
© 2018, ALÖKI Kft., Budapest, Hungary

[23] Svensson, L. E. (2016): A Simple Cost-Benefit Analysis of Using Monetary Policy for Financial Stability Purposes. – In: Blanchard, O. J. et al. (eds.) Progress and Confusion: The State of Macroeconomic Policy. MIT Press, Cambridge.
[24] Treasury, Q. (2006): Cost-Benefit Analysis Guidelines Achieving Value for Money in Public Infrastructure and Service Delivery. – Project Assurance Framework Supplementary Guidance Material, Brisbane, Australia.
[25] Vanoye, A. Y., Mendoza, A. (2014): Application of direct regularization techniques and bounded-variable least squares for inverse modeling of an urban emissions inventory. – Environmental Science and Pollution Research International 5: 219-25.
[26] Vlachokostas, C. h., Achillas, C. h., Moussiopoulon, N., Banias, G. (2011): Multicriteria Methodological approach to manage urban air pollution. – Atmospheric Environment 41: 4160-4169.
[27] Voorhees, A. S., Sakai, R., Araki, S. h., Sato, H., Otsu, A. (2001): Cost-benefit analysis methods for assessing air pollution control program in urban environments. – Environmental Health and Preventive Medicine 6: 63-73.
[28] Yarahmadi, R., Sadoughi, S. H. (2012): Evaluating and prioritizing of performance indices of environment using fuzzy TOPSIS. – Indian Journal of Science and Technology 5: 2713-2719.
[29] Yarahmadi, R., Mortazavi, S. B., Omidkha, M. R., Asilian, H., Khavanin, A., Moridi, P. (2010): Examination of optimized conditions for the conversion of NOx pollution DBD Plasma reactor. – Iranian Journal of Chemistry and Chemical Engineering 29: 133-140.
[30] Yarahmadi, R., Mortazavi, S. B., Moridi, P. (2012): Development of Air Treatment Technology Using Plasma Method. – International Journal of Occupational Hygiene 4: 27-35.
[31] Zeng, X. T., Tong, Y. F., Cui, L., Kong, X. M., Sheng, Y. N., Chen, L., Li, Y. P. (2017): Population-production-pollution nexus based air pollution management model for alleviating the atmospheric crisis in Beijing, China. – Journal of Environmental Management 197: 507-521.
[32] Zhang, Q., Qiu, M., Lai, K., Zhong, N. (2015): Cough and environmental air pollution in China. – Journal of Pulmonary Pharmacology and Therapeutics 35: 132-136.
[33] Zhao, X., Yu, X., Wang, Y., Fan, C. (2016): Economic evaluation of health losses from air pollution in Beijing, China. – Environmental Science and Pollution Research 23: 11716-11728.

http://www.aloki.hu ● ISSN 1589 1623 (Print) ● ISSN 1785 0037 (Online)
DOI: http://dx.doi.org/10.15666/aeer/1605_64416451
© 2018, ALÖKI Kft., Budapest, Hungary

REDUCTION POSSIBILITY OF PHOSPHORUS USING WITH THE APPLICATION OF MYCORRHIZA IN *PURPLE CONEFLOWER* (*ECHINACEA PURPUREA* L.) THROUGH PHYSIOLOGICAL TRAITS AND ESSENCE YIELD UNDER DIFFERENT IRRIGATION LEVELS

RAFAT, N.[1] – YARNIA, M.[2*] – MIRSHEKARI, B.[1] – RASHIDI, V.[1] – MOGHADAM, A. M. D.[3]

[1]*Department of Agriculture, Tabriz Branch, Islamic Azad University, Tabriz, Iran*

[2]*Department of Agronomy, Faculty of Agriculture, Tabriz Branch, Islamic Azad University, Tabriz, Iran*

[3]*Department of Agriculture, Shabestar Branch, Islamic Azad University, Shabestar, Iran*

**Corresponding author*
e-mail: m.yarnia@yahoo.com

(Received 11th Jun 2018; accepted 2nd Aug 2018)

Abstract. The aim of this study was to investigate the effects of irrigation levels (irrigation after 70, 110 and 150 mm of pan evaporation), phosphorus fertilizer levels (non-application of phosphorus fertilizer and application of 25 and 50% of recommended doses) and different species of Mycorrhiza (non-application of mycorrhiza, application of *Glomus intraradices*, *Glomus mossae*, *Glomus hoei* and co-application of the three species) on growth, essential oil production and physiological characteristics of medicinal plant, purple coneflower, in two crop years of 2015 and 2016. The study was performed in the form of split-split plot based on random block design. In most of the studied traits, decrease in water content for irrigation after 70 to 110 mm had no significant effect on vegetative traits and essential oil yield of purple coneflower. In irrigation after 150 mm of pan evaporation, despite a significant reduction of 44% in vegetative traits such as plant yield, the use of a number of fertilizer treatments, such as 50% of phosphorus application, combined with the application of mycorrhizal species and *G. hoei* species without phosphorus fertilizer, completely prevented the depressant effect of dehydration. In most of the traits, including wet and biological function per unit area, percentage of colonization, relative water content and aperture length, application of phosphorous fertilizer alone in full irrigation conditions (irrigation after 70 mm of pan evaporation), moderate dehydration (irrigation after 110 mm of pan evaporation) and severe dehydration (irrigation after 150 mm of pan evaporation), had no effect. The combined application of phosphorus and mycorrhiza fertilizer in irrigation after 70 and 150 mm of pan evaporation had no effect on the traits; however, at irrigation after 110 mm of pan evaporation, most of the treatment of combined application of phosphorus fertilizer and mycorrhiza increased significantly, especially in vegetative traits. Therefore, increase in the growth characteristics of purple coneflower at irrigation after 110 mm of pan evaporation with most fertilizer treatments did not affect these traits. The highest and lowest essential oil yields were obtained as 27.4 and 25.5 g in *G. intraradices* treatment with irrigation after 150 mm of pan evaporation and non-application of fertilizer with irrigation after 70 mm of pan evaporation. Considering the economic importance of the essential oil of purple coneflower, planting of this plant even in severe dehydration with the application of mycorrhiza may appear possible without reducing the essential oil yield, even though growth is negatively affected by dehydration.
Keywords: *bio fertilizer, chemical fertilizer, drought, essential oil, physiological characteristic*

Introduction

The purple coneflower (*Echinacea purpurea* L.), is an herbaceous and perennial plant. The active ingredients in the root and vegetative body of the various species of purple coneflower have anti-fungal, antibacterial and anti-viral properties. Medications

http://www.aloki.hu ● ISSN 1589 1623 (Print) ● ISSN 1785 0037 (Online)
DOI: http://dx.doi.org/10.15666/aeer/1605_64536468
© 2018, ALÖKI Kft., Budapest, Hungary

for prevention and also treating cold and respiratory illnesses are prepared from this plant (Chevallier, 1996). Chemical fertilizers increase the growth and production of active ingredients in medicinal and crop plants. However, the excessive use of these fertilizers without soil degradation, combined with severe crop agronomic practices and adverse management, leads to instability in agriculture and serious threats to the health of underground resources, the destruction of microorganisms and insects, soil degradation and soil organic matter reduction (Pajooheshgar et al., 2015). Phosphorus is the essential food ingredient of plants which plays an important role in maximizing production in crops. The efficiency of phosphorus application in crops is between 10 and 30% (Arshad et al., 2016). Reduction of inorganic phosphorus uptake is an appropriate strategy for reducing production cost. The application of mycorrhizal fungi is one of the suitable methods for reducing the amount of phosphorus consumed. The hypha massive fungi network effectively increases the absorption rate of the roots, allowing the plant to have more access to phosphorus. Phosphate ions are released into the heifers more rapidly than the roots, because they have a high tendency to absorb phosphorus in the hyphas and reduce threshold concentrations for absorption into the hyphas (Elbon and Valen, 2014). The results of several studies reveal the importance of mycorrhiza in helping plants with drought stress. One of the reasons for increasing resistance to stress is that, root colonization with mycorrhizal fungi in different plant species results in increased adsorption and proline production in drought stress conditions (Rapparini et al., 2013). Studies have shown that the effects of mycorrhizal fungi vary depending on the species of fungus. Das (2015) examined the type of mycorrhizal fungus in 12 herbal medicines and observed that, the type and intensity of fungal coexistence varied in different plants. Robinson et al. (2014) examined the effect of mycorrhiza on physiological growth and response of sesame. The application of mycorrhizal fungus enhanced the number of leaves, number of roots, the length of the aerial organ, the root biomass and chemical parameters. Total chlorophyll, chlorophyll a, chlorophyll b and carotenoids also increased with the use of mycorrhizal fungi. Mohseni et al. (2015) investigated the effect of inoculation with mycorrhizal fungi on cumin, and showed that the application of mycorrhizal fungus increased the number of branches, shoot dry weight, root length, root fresh weight, root volume, root diameter, root dry weight, root length density and root surface. Considering the importance of less water consumption and increasing plant tolerance to it and the role of mycorrhiza in these conditions on one hand, and reduction of the use of phosphorus fertilizer in line with sustainable agricultural goals on the other hand, the aim of this study was to investigate the effects of mycorrhiza species on the reduction of phosphorus in low irrigation conditions and response of some of physiological traits and yield and yield components of essence in Purple Coneflower (*Echinacea purpurea* L.) to these factors.

Materials and methods

In order to evaluate the effect of different species of mycorrhiza at different levels of phosphorus fertilizer application on some morpho-physiological traits of purple coneflower in dehydration conditions, an experiment was performed at Agricultural Station of Islamic Azad University, Tabriz, Iran during two crop years of 2015 and 2016. This area is located 5 km from Tabriz, at longitude 46° and 17’ E, latitude 38° and 5’ N, and 1360 m above sea level. Based on the cluster classification of Dumontron, the region has a semi-arid cold climate. The average annual temperature is 10 °C, the average annual temperature is 16 °C and the mean annual temperature is 2.2 °C. The

http://www.aloki.hu ● ISSN 1589 1623 (Print) ● ISSN 1785 0037 (Online)
DOI: http://dx.doi.org/10.15666/aeer/1605_64536468
© 2018, ALÖKI Kft., Budapest, Hungary

average annual precipitation in this area is 271.3 mm (Khalilvand and Yarnia, 2016). The soil pH of the region is in the weak alkaline range (*Table 1*).

Table 1. *The results of physical and chemical analysis of the test site soil*

Organic carbon percent	Organic matter percent	Sand	Silt	Clay	Conductivity (ds/m)	pH	P (ppm)	K (ppm)	Potassium solution (mg/l)
1.7	2.9	76	13	11	1.56	7.53	25.7	7.7	45

The experiment was carried out as split-split plot in a completely randomized block design with three replications in two crop years of 2014 and 2015. The test factors include:

Different levels of dehydration as the main factor in three levels: Irrigation after 70 mm of evaporation from class A pan (control), irrigation after 110 mm of evaporation from class A pan (medium stress) and irrigation after 150 mm of evaporation from class A pan (severe stress). Phosphorus at three levels as a sub-factor: Non use of phosphorus, 25% and 50% recommended**.** The application rate of phosphorous fertilizer for treatment of 0 and 50% of the recommended dose was 25 and 50 kg of phosphorus fertilizer per hectare, respectively. Different species of mycorrhiza in five levels as sub-factor including: Non-use (control), Rhizophagus intraradices species (*G. intraradices*), Funneliformis mosseae (*G. mossae*), *G. hoci* species, and mixture of the three species.

For the test, land acquisition operations were performed in March 2014, with appropriate climatic conditions. After leveling the land, dimensions of 1.5 × 2 m was applied on the plot. Each plot has three rows of irrigated crops and a stack of 45 cm in east-west direction. The spacing of the subplots was one-to-one plot, the main plots were 1.5 m and the distance between the two blocks was 2 m. In early spring, after preparation of the land, different levels of phosphorus were applied based on the planting plan in the experimental plots. After the purple coneflower straws were prepared in mid-May, they were transported to the main land during the second to third leaf stages. Before planting, different strains of mycorrhiza (prepared from the Institute of Water and Soil) were based on the experimental map and 9 g were added to each straw. In the case of each mixed strain, 3 g were added to the planting site, and then transplantation was carried out. The straws were planted 30 cm apart from each other and in hot water stacks. Irrigation was done immediately after seedling. Irrigation was done every three to one day for the nesting. To combat weed, manual weeding was done at the required time. To supply nitrogen, 200 kg/ha of urea was applied in two steps: half of the recommended amount was applied after nesting, and the other half was applied at the 8-10 leaf stage and before application of the aqueous treatments. After the first flowers emerged, dehydration stress was applied on the basis of irrigation after evaporation from class A pan. Each irrigation was done after 70 ± 5, 110 ± 5 and 150 ± 5 mm of evaporation from class A pan. The daily evaporation rate of the pan, after reaching the desired amount for each treatment (70, 110 and 150 mm), indicated irrigation time.

The amount of irrigated water was calculated for each treatment based on the total water requirement, and by random sampling from three different parts of each plot and determining the percentage of soil water content; the amount was calculated at about

http://www.aloki.hu ● ISSN 1589 1623 (Print) ● ISSN 1785 0037 (Online)
DOI: http://dx.doi.org/10.15666/aeer/1605_64536468
© 2018, ALÖKI Kft., Budapest, Hungary

24 h before irrigation. To measure vegetative traits, 5 samples from each plot were harvested. To determine the vegetation factor, *Equation 1* was used:

$$ET_c = K_c \times ET_{0;} \text{ and } ET_0 = K_{pan} \times E_p \quad \text{(Eq.1)}$$

where, ETC and ETO are the plant and reference evapotranspirations, Kpan and Ep are the pan coefficient, respectively (Allen et al., 1998; Fazeli Rostampour et al., 2013).

Total volumes of irrigation water applied in the control treatment (Irrigation after 70 mm of evaporation) were 4885.7 and 5026.4 m^3 in 2015 and 2016, respectively. The volume of water used in other treatments (irrigation after 110 and 150 mm of evaporation) were 3574.6, 3685.4, 2169.8 and 2344.1 m^3, respectively; so the lowest volume of water used in the irrigation after 150 mm of evaporation in 2015.

Relative water content (RWC) was obtained after determining fresh weight (FW), saturation weight (TW) and dry weight (DW) of the 10 end leaves of the plant using the following formula (*Eq.2;* Levitt, 1980):

$$RWC = \left(\frac{FW - DW}{TW - DW}\right) * 100 \quad \text{(Eq.2)}$$

To determine the biological yield, the specimens were kept in ventilated condition under shade conditions at room temperature for one month (25 °C) and after that, they were weighted with a weighing scale of 0.01 g and their average in grams was used in the study. Fresh weight of total organs of shoot (stem, leaf and flower) known shoot fresh weight. Flower shoots together with dried leaves in shade conditions were powdered using the mill and the essential oil was extracted by water distillation with Clevenger. A sample of 25 g of herbal powder was selected and it was put inside a balloon together with 5.00 ml of distilled water. It was then heated by a Clevenger device for three hours. The yellow-colored essence was collected and the dehydration rate and essential oil percentage were determined using sodium water-free sodium sulfate and diethyl ether. The essential oil yield was obtained by multiplying dry matter yield by essential oil percentage.

The Arnon method (1949) was used to determine the amount of chlorophyll a, b and total chlorophyll, and carotenoids content in mg per grams of fresh leaf weight (*Eq. 3*). For this purpose, 0.5 g of fresh leaves was washed with 5 ml of acetone 80% (*W/V*). After 15 min of centrifugation at 1000 rpm per minute and 4 °C, it reached 10 ml. The absorbance of the extract was read by spectrophotometer at 663, 645, 510 and 480 nm wavelengths and the following relationships were used to measure the parameters. In these relationships, C is chlorophyll, A is the wavelength, V is the volume of solution, and W is the leaf sample weight.

$$\begin{aligned} C_a &= 12.7\ (A_{663}) - 2.69\ (A_{645}) \times V/P50\%M0W \\ C_b &= 22.9\ (A_{645}) - 2.69\ (A_{663}) \times V/P50\%M0W \\ C_T &= 20.2\ (A_{645}) + 8.02\ (A_{663}) \times V/P50\%M0W \\ \text{Carotenoid} &= 7.6\ (A_{480}) - 14.9\ (A_{510}) \times V/P50\%M0W \end{aligned} \quad \text{(Eq.3)}$$

http://www.aloki.hu ● ISSN 1589 1623 (Print) ● ISSN 1785 0037 (Online)
DOI: http://dx.doi.org/10.15666/aeer/1605_64536468
© 2018, ALÖKI Kft., Budapest, Hungary

For assessment of the stability of cytoplasmic membrane, ion leakage measurement method was employed using a conductivity meter.

Statistical data analysis was performed based on statistical model of split-split plot test using SAS 9.1 software and the mean of the treatments was compared by Duncan's multi-range test method at 5% level. Diagrams were obtained with Excel software.

Results and discussion

The effects of experimental factors and compounds on the traits evaluated are presented in *Table 2*.

Number of flowering branches

In this study, interaction between the levels of irrigation and phosphorus fertilizers and interaction between levels of phosphorus fertilizer and mycorrhizal fertilizer treatment with regards to the number of flowering branches were significant (*Table 2*). Under irrigation conditions, change in irrigation water after 70 to 150 mm of pan evaporation had no significant effect on the number of flowering branches in the purple coneflower. Nevertheless, consumption of 25% of the recommended dose of phosphorus fertilizer with irrigation after 150 mm pan evaporation, the number of flowering branches as compared to irrigation after 70 mm pan evaporation was higher by 31.4%; this reaction appears to be due to an incremental effect of 25% of recommended dose of phosphorus fertilizer. In this study, number of flowering branches increased in consumption of 25 and 50% of the recommended dose of phosphorus with reduced water irrigation after 70 and 150 mm of pan evaporation (*Fig. 1*). Research has shown that dehydration reduces the number of branches produced; one of the main reasons is decrease in the amount and activity of the hormone, cytokine (DaCosta and Huang, 2007). The cytokine hormone plays an important role in the formation of side stems (Miyawaki et al., 2004). According to Evers et al. (2011), the branching depends on the presence of assimilates. While dryness reduces assimilate content in the plant (Ash et al., 2001), phosphorus that plays an important role in photosynthesis, production of photosynthetic materials and their transfer to various parts of plants, reduces the effects of dryness reduction (Khan et al., 2013; Hammond and White, 2008). Kotoky et al. (2015) also observed that application of phosphorus fertilizer significantly increases the number of branches produced in *Aristolochia indica* plant.

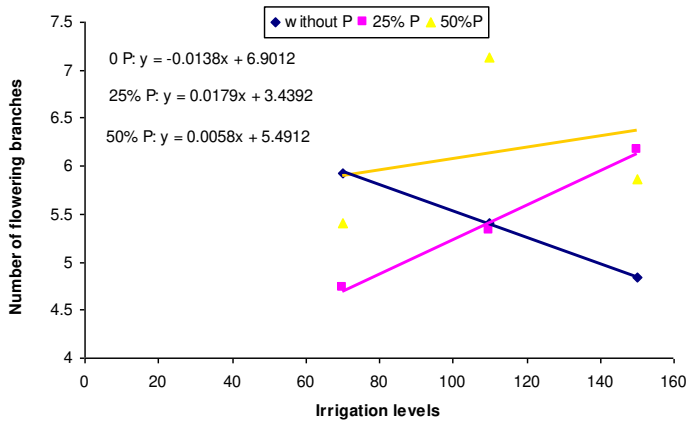

Figure 1. *Effect of phosphorous on number of flowering branches under irrigation levels*

http://www.aloki.hu ● ISSN 1589 1623 (Print) ● ISSN 1785 0037 (Online)
DOI: http://dx.doi.org/10.15666/aeer/1605_64536468
© 2018, ALÖKI Kft., Budapest, Hungary

Table 2a. *Combined variance analysis of studied traits in purple coneflower*

S.O.V.	DF	Number of flowering branches	Biological yield	Shoot fresh weight	Leaf area index	Essence percent	Essence yield	Chlorophyll a content	Chlorophyll b content
Year (y)	1	274.01**	8122.57	3719.05	28.42**	0.99*	6.57	4.92	1253501
Error 1	4	5.94	4047.67	767.84	0.36	0.1	15.53**	18.43**	579642**
Irrigation levels (A)	2	16.14	106103.**	199331**	0.22	0.08	13.91*	22.3	89628.04
Y * A	2	5.62	1074.56	77.73	0.09	0.2	0.18	0.141	87870.36
Error 2	8	12.401*	1627.03	1155.09	0.14	0.1	2.31	9.77**	71788**
Phosphorus fertilizer levels (B)	2	8.133	5626.17	5140.49*	0.1	0.42*	4.09	8.866*	1985.786
Mycorrhizal specie (C)	4	12.58	10092**	9438.85**	0.02	0.04	4.36	4.97	5709*
A * B	4	20.311**	7775.09**	39542**	0.39*	0.31	4.42	10.469**	2309.149
A * C	8	10.153	5762.5*	12513.2**	0.13	0.11	9.38**	1.77	1283.794
B * C	8	11.75*	5722.01*	4390.61**	0.38*	0.31*	2.66	3.8	2491.6
A * B * C	16	6.36	5313**	4604.74**	0.2	0.17	3.35	3.062	2799.168
Y * B	2	6.45	1389.646	36.2	0.002	0.17	0.22	0.022	1690.288
Y * c	4	1.24	1660.921	33.89	0.29	0.03	0.39	0.11	4323.631
Y * B * C	8	1.2	1508.031	2.65	0.21	0.06	0.38	0.19	1871.82
Y * A * B	4	2.3	1410.989	13.41	0.1	0.01	0.2	0.0796	1528.395
Y * A * C	8	1.35	1366.123	7.89	0.1	0.1	0.3	0.249	1022.415
Y * A * B * C	16	0.81	1420.476	21.83	0.05	0.035	0.43	0.24	1833.318
Error 3	168	5.34	2221.842	1104.86	0.15	0.13	3.48	2.78	2099.487
CV (%)		40.95	32.97306	17.18	11.68	7.89	7.04	8.8	44.607

*and **, respectively, represent significance at the probability level of 1 and 5%

Table 2b. *Combined variance analysis of studied traits in purple coneflower (continued)*

S.O.V.	DF	Carotenoid content	Plasma membrane stability	Root colonization	Stoma length	Stoma width	Relative water content	Stoma resistance
Year (y)	1	4.802667	152.62	1737.87	34.13	2.314	54.8	25.42
Error 1	4	6.12**	39.67**	722.11**	11.4**	13.56**	56.86	11.08**
Irrigation levels (A)	2	7.67	8.55	47.11	1.35	2.8	99.27	45.08
Y * A	2	0.0008	4.58	41.55	2.01	0.72	9.05	1.8
Error 2	8	5 **	18.64*	37.09	1.12	5.25**	50.1	12.89**
Phosphorus fertilizer levels (B)	2	3.29	18.69	294.81	0.1	2.23	3.23	13.03*
Mycorrhizal specie (C)	4	4.5*	4.53	758.96**	3.24*	2.45*	525.61**	3.2
A * B	4	5.39*	5.34	713.84**	1.32	3.76*	311.86**	6.09
A * C	8	2.975	7.18	176.7	3.34**	3.32**	191.93*	4.1
B * C	8	4.101*	13.42	608.15**	1.02	3.29**	157.9	5.18
A * B * C	16	4.18**	27.27**	575.35**	2.16*	2.76**	347.78**	3.83
Y * B	2	0.016	3.803704	1.48	0.17	0.27	2.72	2.19
Y * c	4	0.015	1.41	5.25	0.23	0.16	2.37	1.97
Y * B * C	8	0.009	0.88	7.78	0.80	0.4	2.37	1.19
Y * A * B	4	0.06	2.47	10.9537	0.32	0.11	2.75	1.25
Y * A * C	8	0.052	2.88	1.61	0.72	0.14	2.76	1.84
Y * A * B * C	16	0.054	1.36	8.75	1.62	0.23	2.01	1.41
Error 3	168	1.609	7.96	109.32	1.21	1.24	89.91	2.85
CV (%)		25.361	12.51	28.1	17.12	27.96	23.64	51.12

*and **, respectively, represent significance at the probability level of 1 and 5%

http://www.aloki.hu ● ISSN 1589 1623 (Print) ● ISSN 1785 0037 (Online)
DOI: http://dx.doi.org/10.15666/aeer/1605_64536468
© 2018, ALÖKI Kft., Budapest, Hungary

In this study, among the fertilizer treatment combinations, the highest number of flowering branches with 7.3% was obtained in the treatment of 25% recommended phosphorus dose combined with the mixture of all mycorrhiza species; the lowest was 4.1 which was associated with *G. hoei* application without phosphorus fertilizer application. In the present study, with 25% of recommended phosphorus fertilizer dose, the application of mycorrhiza fertilizer, and also in mixture, a significant increase of 48.9% in the number of purple coneflower branches was observed (*Table 3*). The most important role of mycorrhizal fungi is in increasing phosphorus absorption (Yadav and Aggarwal, 2015). Application of mycorrhiza increases phosphorus effect on plant branching by increasing plant access to phosphorus. Increasing phosphorus absorption via the use of fungi can increase the number of side flowering branches by increasing the production of assimilates. On the other hand, these microorganisms play an important role in the morphology of plants by releasing growth stimulants such as auxin and cytokine (Salvucci et al., 2010).

Table 3. *Comparison of the mean of studied traits under the influence of phosphorous fertilizer levels and mycorrhizal fungi species*

Phosphorus fertilizer levels (% of desired dose)	Mycorrhiza specie	Number of flowering branches	Leaf area index	Essential oil percentage	Essential oil yield
Non-use of phosphorus	Control	6.722 ab	3.444 abc	4.867 a	25.24 b
Non-use of phosphorus	*G. intraradices*	5.056 bcd	3.432 abc	4.733 abc	26.12 ab
Non-use of phosphorus	*G. mossae*	5.500 bcd	3.251 abc	4.729 abc	27.38 a
Non-use of phosphorus	*G. hoei*	4.167 d	3.326 abc	4.623 abc	27.03 ab
Non-use of phosphorus	Mixture of three species	5.333 bcd	3.524 ab	4.600 abc	25.35 b
25	Control	4.944 bcd	3.419 abc	4.689 abc	26.82 ab
25	*G. intraradices*	6.167 abc	3.369 abc	4.533 bc	26.36 ab
25	*G. mossae*	5.444 bcd	3.271 abc	4.778 ab	26.52 ab
25	*G. hoei*	5.889 abcd	3.229 bc	4.878 a	26.31 ab
25	Mixture of three species	7.333 a	3.348 abc	4.689 abc	25.76 ab
50	Control	6.444 abc	3.163 c	4.467 c	27.26 a
50	*G. intraradices*	5.611 abcd	3.277 abc	4.611 abc	27.45 a
50	*G. mossae*	5.389 bcd	3.544 a	4.543 bc	26.27 ab
50	*G. hoei*	4.833 cd	3.532 ab	4.611 abc	26.80 ab
50	Mixture of three species	5.833 abcd	3.335 abc	4.733 abc	27.03 ab

Means with different letters in each column have significant difference at 5% probability level.

Leaf area index

In this study, the highest leaf area index (3.5) was related to non-use of phosphorus fertilizer with irrigation after 70 mm of pan evaporation, and the lowest (3.1) was associated with non-use of phosphorus chemical fertilizer and irrigation after 150 of the pan evaporation. Dehydration at levels of 25 and 50% of recommended phosphorus fertilizer dose did not have a significant effect on leaf area index of purple coneflower leaves. In the case of non-application of phosphorus fertilizer, water reduction with irrigation after 70 to 150 mm of pan evaporation reduced the leaf area index to 11.4% (*Fig. 2*). According to the results of this study, application of phosphorus prevented the reduction of leaf areas in low-irrigation conditions. The positive effect of phosphorus fertilizer application on the increase of plant tolerance to dehydration in terms of leaf growth has been also reported by Jamali (2013) in *Coriandrum sativum* herb. Phosphorus

http://www.aloki.hu ● ISSN 1589 1623 (Print) ● ISSN 1785 0037 (Online)
DOI: http://dx.doi.org/10.15666/aeer/1605_64536468
© 2018, ALÖKI Kft., Budapest, Hungary

is an essential nutrient for leaf growth, which plays an important role in the production of new leaves and increase of the area of each leaf in plants (Fletcher et al., 2004; Trindade et al., 2010). Anatomical studies have revealed that, using phosphorus fertilizer increases the length of leaf cells which increases leaf growth (Esmail et al., 2014).

In the present study, the maximum leaf area index was 3.5% for 50% of recommended dose of phosphorus fertilizer with *G. mossae*, and the lowest was associated with the application of 25% of recommended dose of phosphorus fertilizer without mycorrhiza application. At phosphorus fertilizer level of 25% and non-application of phosphorus fertilizer, none of the mycorrhizal treatments had a significant effect on leaf area index of purple coneflower. Nevertheless, in application of 50% of recommended phosphorus fertilizer dose, the application of *G. mossae* increased the leaf area index of purple coneflower by 7.8% (*Table 3*). The positive effect of mycorrhiza on the growth of plant leaves has been also reported by other researchers. In a study conducted on *Coriaria nepalensis*, Bargali and Bargali (2009) observed that, the application of mycorrhiza causes a 17% increase in the leaf area of *C. nepalensis*. In the present study, differences were observed between the studied species of mycorrhiza in terms of effectiveness on leaf area index. Kumar et al. (2009) in a study, evaluated the effects of two types of mycorrhizal fungi on *Salvia officinalis* growth and there was a significant difference between the species of mycorrhizal fungi in terms of leaf area. Thus, one of the species increased leaf area of *S. officinalis* by 45%, and *G. mossae* increased the leaf area of peppermint by 85%.

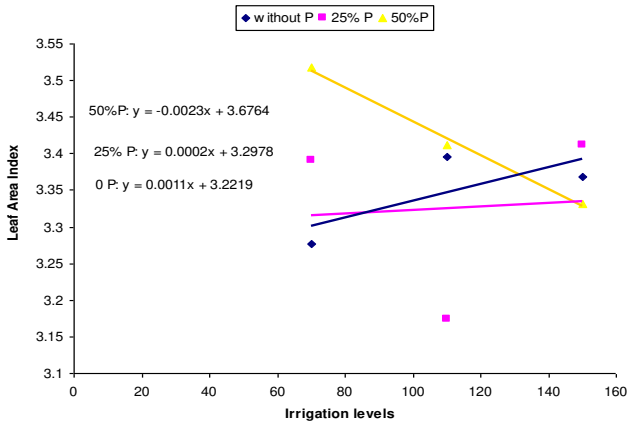

Figure 2. *Effect of phosphorous on leaf area index under irrigation levels*

Essential oil yield and percentage

In this study, the highest percentage of essential oil was related 25% of recommended dose of phosphorus fertilizer and *G. hoei*, and the lowest value was associated with 50% of recommended dose of phosphorus fertilizer alone. In this study, in the case of non-application of mycorrhiza, 50% of the recommended dose decreased the percentage of purple coneflower essential oil by 8.3%; however, with the use of mycorrhiza, no reduction was found in the percentage of essential oil due to the application of phosphorous fertilizer (*Fig. 3*). Similar results have been obtained by Hosseini Valiki et al. (2015) for Rosemary plant and Le et al. (2013) for *Salvia miltiorrhiza*. Lo et al. (2013) stated that probably, under conditions of increased phosphorus fertilizer levels, growth and early metabolism of the plant were more

http://www.aloki.hu ● ISSN 1589 1623 (Print) ● ISSN 1785 0037 (Online)
DOI: http://dx.doi.org/10.15666/aeer/1605_64536468
© 2018, ALÖKI Kft., Budapest, Hungary

affected by phosphorus fertilization and consequently, the production of essential oils in medicinal herbs reduced.

The highest and lowest essential oil yield per unit area was 27.4 and 25.5 g in *G. intraradices* treatments with irrigation after 150 mm of pan evaporation and non-application of the fertilizer after 70 mm of pan evaporation. In this study, an increase of 7.9% was observed in essential oil yield per square meter in only non-application of mycorrhiza with reduced water irrigation after 70 and 150 mm of pan evaporation (*Fig. 3*). In addition, among the fertilizer treatments, *G. mossae* fertilizer treatment alone, 50% recommended phosphorus fertilizer alone and 50% of recommended dose of phosphorus fertilizer with *G. intraradices* significantly increased the essential oil yield; however, other fertilizer compounds did not have a significant effect on the yield of essential oil. Therefore, the effect of application of fertilizer on essential oil yield depends on mycorrhiza species and phosphorus level. Habibzadeh (2015) reported that the degree of coexistence of different mycorrhiza species with plants is different at different levels of phosphorus fertilizer; this is due to structural and secretion changes of the roots at different levels of chemical phosphorus fertilization. In the present study, high levels of phosphorus fertilizer with application of mycorrhiza species alone reduced essential oil content. At high levels of phosphorus fertilizer application, the amount of carbohydrate secretion from plant roots decreased and the thickness of the epidermis layer of the root increased which reduced the coexistence of fungi with plants (Habibzadeh, 2015).

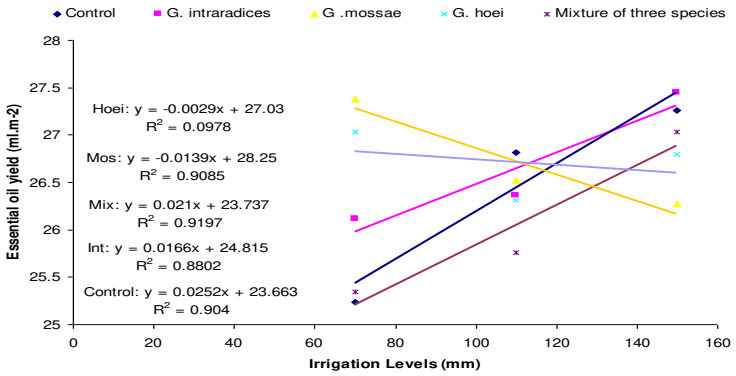

Figure 3. *Effect of mycorhiza on essential oil yield under irrigation levels*

Percentage of colonization

The highest percentage of root colonization of 58.6% was observed in the treatment of *G. intraradices* alone and with irrigation after 110 mm of pan evaporation and the lowest (21.33%) in the application of 25% of recommended dose of phosphorus fertilizer with *G. hoei* was obtained for irrigation after 150 mm of pan evaporation. According to the results obtained from this study, dehydration had a significant effect on the percentage of root colonization in *G. mossae* treatment alone. In the application of *G. mossae* alone, by decreasing irrigation water, 32.5% of root colonization was reduced (*Table 3*). At irrigation level after 150 mm of evaporation, fertilizer treatment had no significant effect on the root colonization percentage. At irrigation level after 110 mm of pan evaporation of some fertilizer treatments, a significant increase was observed in percentage of root colonization. At irrigation level after evaporation of 110 mm from the evaporation pan, application of *G. intraradices* and *G. mossae*

http://www.aloki.hu ● ISSN 1589 1623 (Print) ● ISSN 1785 0037 (Online)
DOI: http://dx.doi.org/10.15666/aeer/1605_64536468
© 2018, ALÖKI Kft., Budapest, Hungary

treatments alone and 25% of recommended dose of phosphorus fertilizer in addition to *G. hoei*, increased this trait by 93.4, 87.9 and 74.2%, respectively. According to the results, the *G. intraradices* species can be considered as a superior species in the establishment of coexistence with purple coneflower.

Biological yield and shoot fresh weight

In this study, the highest wet and biological yields were obtained as 303.6 and 235 g in 50% of recommended dose of phosphorus fertilizer with *G. mossae* and irrigation after 70 mm of pan evaporation. The lowest wet and biological yields were observed as 108 and 65.4 g, respectively, in treatments with 50% of recommended dose of phosphorus fertilizer together with *G. hoei* and 50% of recommended dose of phosphorus fertilizer with a mixture of mycorrhizal fertilizers at irrigation after 150 mm of pan evaporation. From the results, irrigation water reduction had negative effect on wet and biological yields per square meter. With decrease in irrigation water from after 70 to 150 mm of pan evaporation, the highest reduction of 62.4% was achieved in the application of 25% of recommended dose of phosphorus fertilizer alone. Nevertheless, in the fertilizer mixture of *G. intraradices*, *G. hoei* and a mixture of fertilizers alone and 25% of recommended dose of phosphorus fertilizer with *G. intraradices*, dehydration did not affect the wet and biological yields (*Table 4*). Research has shown that by decreasing irrigation water, the accumulation of dry matter and the rate of water absorption reduces (Nazarli and Zardashti, 2010). The absorption of water and food in the plant is dependent on the activity of the roots, and in the case of dehydration, root growth and absorption activity of the roots will be reduced (Boomsma and Wyn, 2008). On the other hand, decrease in dry weight due to dehydration can be as a result of reduced assimilate production and the capacity to absorb assimilates for growth (Yardanova and Popova, 2007).

Table 4. *Comparison of the mean of studied traits under the influence of irrigation levels, phosphorus fertilizer levels and mycorrhizal fungal species*

Irrigation levels (mm of pan	Phosphorus fertilizer levels (% of optimal dose)	Mycorrhiza specie	Root colonization (%)	Plasma membrane stability	Shoot fresh weight (g/plant)	Biological yield (g/m^2)	Carotenoid (mg/g)	RWC (%)	Stoma length (mm)	Stoma width (mm)
		Control	47.50 a-e	17.83 c	258.4 a-d	162.1 a-h	3.417 e	48.49 abc	5.833 cd	4.000 a-e
		G. intradices	54.33 abc	22.33 abc	201.1 d-i	141.0 b-k	3.665 de	48.09 a-d	6.167 bcd	4.333 a-e
	0	G. mossae	28.00 e-i	25.17 ab	277.7 ab	169.7 a-h	3.783 cde	34.82 b-g	7.000 abc	4.333 a-e
		G. hoei	22.00 hi	25.50 a	212.8 c-h	164.1 a-h	5.160 a-e	37.59 b-g	6.167 bcd	5.167 abc
		Mix	28.67 e-i	22.83 abc	170.2 g-m	156.3 a-i	5.347 a-e	42.59 a-f	6.833 abc	5.667 a
		Control	30.67 e-i	22.17 abc	257.5 a-d	169.1 a-h	6.060 abc	41.59 a-g	5.667 cd	3.667 a-e
		G. intradices	26.17 f-i	20.67 abc	185.5 f-l	139.5 b-k	4.648 a-e	41.96 a-g	4.833 d	3.167 cde
70	25	G. mossae	44.50 a-f	20.83 abc	267.3 abc	180.1 a-f	5.493 a-e	40.81 a-g	7.500 ab	4.500 a-d
		G. hoei	52.33 a-d	23.17 ab	216.3 c-h	172.4 a-g	4.600 a-e	28.16 fg	6.833 abc	5.333 ab
		Mix	31.00 e-i	23.67 ab	203.2 d-i	141.5 b-k	4.362 a-e	43.99 a-f	5.667 cd	4.000 a-e
		Control	28.00 e-	24.00 ab	268.8 abc	199.5 abc	5.813 a-d	43.72 a-f	6.667 abc	3.667 a-e
		G. intradices	41.50 a-g	24.17 ab	188.4 e-k	149.6 a-k	6.093 abc	32.56 c-g	7.167 abc	4.500 a-d
	50	G .mossae	35.50 c-i	21.00 abc	303.6 a	235.8 a	3.273 e	32.26 c-g	7.000 abc	5.167 abc
		G. hoei	41.00 a-h	20.00 bc	193.6 e-j	142.3 b-k	4.925 a-e	38.60 b-g	5.667 cd	3.000 de
		Mix	45.17 a-f	20.00 bc	263.5 abc	111.3 d-k	4.320 a-e	44.66 a-f	5.833 cd	2.333 e
		Control	30.33 e-i	21.33 abc	129.2 lmn	90.48 g-k	6.255 ab	51.59 ab	6.500 abc	3.833 a-e
		G. intradices	58.67 a	23.83 ab	114.3 mn	97.14 e-k	5.907 a-d	43.60 a-f	6.500 abc	3.333 b-e
	0	G. mossae	57.00 ab	23.00 abc	132.2 k-n	119.1 c-k	4.755 a-e	33.68 c-g	6.500 abc	4.000 a-e
		G. hoei	36.50 c-i	21.33 abc	202.0 d-i	159.9 a-h	6.255 ab	34.77 b-g	6.167 bcd	3.667 a-e
		Mix	37.50 c-i	23.17 ab	211.8 c-h	163.1 a-h	4.900 a-e	40.38 a-g	6.000 bcd	3.333 b-e

http://www.aloki.hu ● ISSN 1589 1623 (Print) ● ISSN 1785 0037 (Online)
DOI: http://dx.doi.org/10.15666/aeer/1605_64536468
© 2018, ALÖKI Kft., Budapest, Hungary

		Control	38.50 b-i	22.67 abc	257.6 a-d	224.8 ab	5.907 a-d	40.96 a-g	7.000 abc	3.667 a-e
		G. intradices	42.33 a-g	23.83 ab	220.0 b-g	211.3 ab	6.602 a	28.20 fg	6.667 abc	3.333 b-e
110	25	G. mossae	29.67 e-i	23.83 ab	247.0 a-e	142.2 b-k	4.178 b-e	38.89 b-g	7.000 abc	4.667 a-d
		G. hoei	52.83 a-d	22.83 abc	231.9 b-f	194.9 abcd	4.897 a-e	43.50 a-f	6.167 bcd	4.167 a-e
		Mix	30.17 e-i	21.17 abc	237.6 b-f	152.6 a-j	4.975 a-e	36.76 b-g	6.500 abc	4.833 a-d
		Control	27.50 f-i	20.67 abc	213.9 c-h	181.5 a-e	5.112 a-e	48.78 abc	7.167 abc	4.667 a-d
		G. intradices	41.83 a-g	21.50 abc	246.0 a-e	169.3 a-h	5.800 a-d	45.93 a-f	6.000 bcd	3.667 a-e
	50	G. mossae	36.50 c-i	21.17 abc	212.9 c-h	196.1 a-d	5.447 a-e	37.22 b-g	5.833 cd	3.333 b-e
		G. hoei	23.00 ghi	24.00 ab	245.1 b-f	166.4 a-h	4.178 b-e	24.68 g	5.833 cd	3.667 a-e
		Mix	27.33 f-i	24.67 ab	224.1 b-g	180.2 a-f	4.505 a-e	37.90 b-g	6.500 abc	4.667 a-d
		Control	38.50 b-i	23.83 ab	140.4 j-n	97.57 e-k	4.302 a-e	45.05 a-f	6.500 abc	4.333 a-e
		G. intradices	42.33 a-g	24.67 ab	157.7 h-n	85.55 g-k	3.825 cde	29.26 efg	6.500 abc	3.667 a-e
	0	G. mossae	41.50 a-g	23.50 ab	194.0 e-j	159.2 a-h	4.213 b-e	34.38 b-g	6.333 bcd	4.333 a-e
		G. hoei	32.50 e-i	22.50 abc	233.7 b-f	157.4 a-i	5.140 a-e	45.71 a-f	6.833 abc	4.000 a-e
		Mix	33.83 d-i	22.50 abc	134.9 k-n	98.00 e-k	4.830 a-e	30.33 d-g	6.167 bcd	3.667 a-e
		Control	38.17 b-i	25.83 a	112.4 mn	92.71 f-k	5.495 a-e	39.63 a-g	6.167 bcd	4.333 a-e
		G. intradices	39.17 b-i	23.00 abc	138.9 j-n	98.82 e-k	5.867 a-d	56.49 a	8.000 a	4.000 a-e
150	25	G. mossae	33.83 d-i	23.17 ab	147.8 i-n	100.1 e-k	4.310 a-e	39.99 a-g	6.667 abc	4.000 a-e
		G. hoei	21.33 i	21.17 abc	122.5 mn	69.88 jk	4.555 a-e	37.68 b-g	6.500 abc	4.000 a-e
		Mix	28.50 e-i	23.00 abc	120.2 mn	65.41 k	5.082 a-e	46.28 a-e	5.833 cd	3.000 de
		Control	32.83 e-i	20.83 abc	132.1 k-n	83.18 h-k	5.572 a-e	41.45 a-g	6.167 bcd	4.167 a-e
		G. intradices	42.33 a-g	22.33 abc	117.9 mn	72.63 ijk	4.218 a-e	48.52 abc	7.167 abc	4.333 a-e
	50	G. mossae	38.50 b-i	22.00 abc	114.3 mn	99.33 e-k	5.585 a-e	46.66 a-e	7.167 abc	4.333 a-e
		G. hoei	42.33 a-g	23.00 abc	108.1 n	182.4 a-e	5.033 a-e	41.25 a-g	6.667 abc	3.333 b-e
		Mix	42.50 a-g	21.17 abc	135.4 k-n	87.47 g-k	6.477 ab	35.53 b-g	5.833 cd	2.333 e

Means with different letters in each column have significant difference at 5% probability level.

In this study, application of fertilizers, especially in dehydration, has a moderate effect on resistance to dehydration in plants. In irrigation after 110 mm of pan evaporation, most fertilizer combinations cause a significant increase in wet and biological yields. The most desirable fertilizer compounds with irrigation after 110 mm of pan evaporation in terms of wet and biological yields, were 25% of recommended dose of phosphorus fertilizer alone, 25% of recommended dose of phosphorus fertilizer combined with *G. mossae*, 50% recommended phosphorus fertilizer dose with *G. intraradices* and 50% of recommended dose of phosphorus with *G. hoei*. Various studies have shown that phosphorus fertilizers can play an important role in increase in the resistance of plants to dehydration (Mirabello et al., 2013). On the other hand, mycorrhizal fertilizers can increase the water access of plants by increasing the absorption rate of the roots and reducing the impact of dehydration on plants (Sharma et al., 2015). It seems that in environmental conditions, moderate dehydration enhances the efficiency of phosphorous and mycorrhizal fertilizers in the growth of purple coneflower. The application of phosphorous fertilizer in moderate dehydration conditions increased biological yield of purple coneflower, which is probably due to reduced plant access to phosphorus in dehydrated conditions. Studies have shown that by reducing irrigation water, plant access to soil phosphorus decreases linearly; therefore, increase in the amount of phosphorus available in the soil through fertilization can play an effective role in increasing plant growth in dehydration conditions (Mirabello et al., 2013). Mycorrhizal fertilizers have also shown little impact in full irrigation conditions in different studies, while more effectiveness of this group of microorganisms has been obtained in dehydration conditions (Krishnakumar et al., 2013). This is because in dehydration conditions, the role of mycorrhizae becomes more pronounced by restricting plant access to growth resources such as fertilizers and water (Krishnakumar et al., 2013). In dehydrated conditions, mycorrhizae increase the

http://www.aloki.hu ● ISSN 1589 1623 (Print) ● ISSN 1785 0037 (Online)
DOI: http://dx.doi.org/10.15666/aeer/1605_64536468
© 2018, ALÖKI Kft., Budapest, Hungary

absorption level and the amount of water absorbed by the plant (Sharma et al., 2015). However, researchers believe that in severe dehydration, the growth and activity of mycorrhizal can be reduced (Krishnakumar et al., 2013) and thus, these fertilizers cannot have a positive effect on plants in severe dehydration. In a study, Khalili et al. (2014) examined the effects of different levels of phosphorus fertilizer on *Lepidium sativum* herb. Based on the results of that study, application of phosphorous fertilizer increased the wet yield of peppermint significantly. However, in this study, there was a difference in the effectiveness of different species of mycorrhizal fungi in plant growth. Hedayati Mahdi Abadi et al. (2015) examined the effect of *G. mossae* and *G. intraradices* species on Caraway plant and observed that *G. intraradices* species did not have a significant effect on Caraway biomass, but *G. mossae* caused a significant increase in the biomass.

Photosynthetic pigments

The highest leaf carotenoid content of 6.6 mg per gram of shoot fresh weight was obtained with the treatment of 25% of recommended dose of phosphorus fertilizer combined with *G. intraradices* in irrigation after 110 mm of pan evaporation and the lowest values of 3.4 and 3.2 mg per gram were obtained in two treatment combination of 25% recommended phosphorus fertilizer. The dose was combined with a mixture of mycorrhizal fertilizers and 50% of recommended dose of phosphorus fertilizer combined with *G. mossae* with irrigation after 70 mm of pan evaporation. At irrigation after 70 mm of pan evaporation, fertilizer treatment including 25% of recommended dose of phosphorus fertilizer alone, 50% of recommended dose of phosphorus fertilizer alone and 50% of recommended dose of phosphorus fertilizer combined with *G. intraradices* increased leaf carotenoid content by 77.3, 70.1 and 78.3%, respectively (*Table 4*). Chlorophyll content decreased under the influence of dehydration. At 25% of the recommended phosphorus fertilizer dose, by decreasing irrigation water from 70 to 150 mm pan evaporation, a decrease of 8.2% was observed in chlorophyll a content. In this study, a non significant increase was observed in chlorophyll content in only 25% of the recommended phosphorus fertilizer dose with reduced water irrigation after 70 to 150 mm of pan evaporation (*Fig. 4*). Dehydration reduces chlorophyll content by reducing the amount of chlorophyll produced and increasing its degradation (Rapparini et al., 2013). Chlorophyll a and carotenoid content were not affected by mycorrhiza but chlorophyll b content was only affected by mycorrhiza which decreased it. Robinson et al. (2014) showed that the application of mycorrhiza increases the chlorophyll b content in sesame.

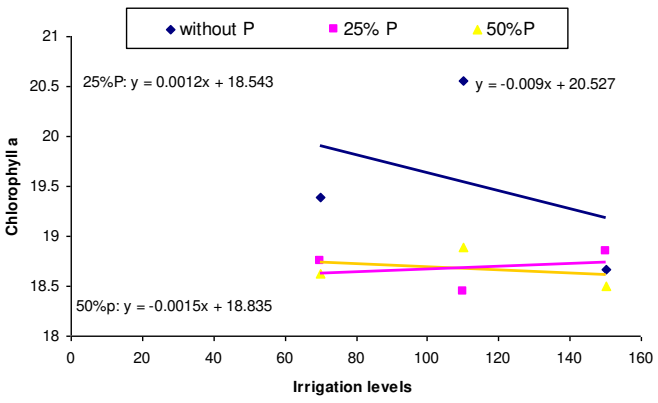

Figure 4. *Effect of phosphorous on Chlorophyll a under irrigation levels*

http://www.aloki.hu ● ISSN 1589 1623 (Print) ● ISSN 1785 0037 (Online)
DOI: http://dx.doi.org/10.15666/aeer/1605_64536468
© 2018, ALÖKI Kft., Budapest, Hungary

Plasma membrane stability

In this study, in all the combinations of phosphorus fertilizer and mycorrhiza species, dehydration had no significant effect on plasma membrane stability and only in non-application of fertilizer, did reduction in irrigation water after 70 to 150 mm of evaporation caused a decrease of 33.7% in plasma membrane stability. In this study, in irrigation after 70 mm of pan evaporation, a number of combinations of phosphorus fertilizer and mycorrhiza had a significant effect on the stability of the plasma membrane. At this irrigation level, the treatments of *G. mossae* and *G. hoei* application alone, 25% of recommended dose of phosphorus fertilizer with *G. hoei*, 25% of recommended dose of phosphorus fertilizer with a mixture of fertilizers, 50% of recommended dose of phosphorus fertilizer alone and 50% of recommended dose of phosphorus fertilizer with *G. intraradices* increased the plasma membrane stability by 29.2, 41.7, 41.6, 30.6 and 28.7%, respectively (*Table 4*).

Stoma properties and relative water content

According to the ANOVA results, traits of interactions between irrigation levels, phosphorous fertilizer levels and mycorrhiza species had a significant effect on aperture length and width (*Table 2*). In this study, the maximum aperture length of 8 μm in the treatment combination was observed for 25% of recommended dose of phosphorus fertilizer with *G. intraradices* and irrigation after 150 mm of pan evaporation. The minimum (4.8 μm) was associated with the application of 25% of recommended dose of phosphorus fertilizer with *G. intraradices* and irrigation after 70 mm of pan evaporation. In addition, the maximum aperture width of 5.6 μm was observed in the mixture of mycorrhizal fertilizers alone with irrigation after 70 mm of pan evaporation and the lowest (2.3 μm) was associated with the treatment of 50% recommended phosphorus fertilizer with a mixture of mycorrhizal fertilizers and irrigation after 150 mm of pan evaporation. In this study, a significant increase of 65% for the aperture length was observed only at 25% of recommended dose of phosphorus fertilizer with *G. intraradices* and reduced irrigation water at irrigation after 70 to 150 mm of pan evaporation. Moreover, except for the application of mixture of fertilizers alone or with 50% of recommended dose of phosphorus fertilizer, there was no significant difference between the irrigation levels in terms of aperture width in the fertilizer treatments. In the mixture of fertilizers alone, reducing irrigation water after 70 to 110 mm of pan evaporation decreased the aperture width by 2.4%. In the treatment of a mixture of fertilizers with 50% of the recommended dose of phosphorus fertilizer in irrigation treatment after 150 mm of pan evaporation, the aperture width was 50% lower than the case of irrigation after 110 mm of pan evaporation (*Table 4*). Thus, in this plant, in the presence of mycorrhiza and conditions of dehydration, the aperture length increases and their width decreases, this will lead to higher carbon dioxide input and a decrease in transpiration.

In this study, except for *G. intraradice*s application alone, relative water content was not affected by irrigation levels in the fertilizer treatments. In the application of *G. intraradices* alone, by reducing irrigation after 70 and 150 mm of pan evaporation, a decrease of 39.2% in relative water content was observed (*Table 3*).

http://www.aloki.hu ● ISSN 1589 1623 (Print) ● ISSN 1785 0037 (Online)
DOI: http://dx.doi.org/10.15666/aeer/1605_64536468
© 2018, ALÖKI Kft., Budapest, Hungary

Conclusion

The results of this experiment prove that the application of mycorrhiza prevented a significant change in plant production due to dehydration by increasing leaf area and the production of flowering shoots, even under the conditions of less phosphorus fertilizer application. Changes in physiological traits, especially, the plasma membrane stability and aperture movements with the application of mycorrhiza, led to an increase in plant cellular power in the continuation of metabolic reactions and the production of essential oils also increased with mycorrhizal application even under extreme stress conditions. Reduction to at least, 50% of phosphorus consumption without significantly reducing the production of purple coneflower in terms of mycorrhiza application is more important in sustainable agriculture, even in the case of dehydration.

REFERENCES

[1] Allen, R. G., Pereira, L. S., Raes, D., Smith, M. (1998): Crop Evapotranspiration. Guidelines for Computing Crop Water Requirements. – FAO Irrigation and Drainage Paper 56. FAO, Rome.

[2] Arnon, D. I. (1949): Determination of chlorophyll concentration in leaf tissues of plants. – Plant Physiol. 24: 1.

[3] Arshad, M., Adnan, M., Ahmed, S., Karim Khan, A., Ali, I., Ali, M., Ali, A., Khan, A., Anwar Kamal, M., Gul, F., Ayaz Khan, M. (2016): Integrated effect of phosphorus and zinc on wheat crop. – American-Eurasian J. Agric. & Environ. Sci. 16(3): 455-459.

[4] Asch, F., Andersen, M. N., Jensen, C. R., Mogensen, V. O. (2001): Ovary abscisic acid concentration does not induce kernel abortion in field-grown maize subjected to drought. – European Journal of Agronomy 15: 119-129.

[5] Bargali, K., Bargali, S. S. (2009): Effect of phosphorus nutrition on growth and mycorrhizal dependency of *Coriaria nepalensis* seedlings. – Nature and Science 7(6): 19-24.

[6] Boomsma, C. R., Vyn, T. J. (2008): Maize drought tolerance: Potential improvements through arbuscular mycorrhizal symbiosis? – Field Crops Research 108: 14-31.

[7] Chevallier, A. (1996): The Encyclopedia of Medicinal Plants. – Dorling Kindersley Ltd. Publ., London.

[8] DaCosta, M., Huang, B. (2007): Drought survival and recuperative ability of bentgrass species associated with changes in abscisic acid and cytokinin production. – JASHS 132: 60-66.

[9] Das, D. (2015): A Contribution to the vesicular arbuscular mycorrhizal fungal status on twenty selected medicinal plants of Pandam forest in Darjeeling Himalaya, West Bengal, India. – Journal of Environmental Science, Toxicology and Food Technology 9: 61-71.

[10] Elbon, A., Whalen, J. K. (2014): Phosphorus supply to vegetable crops from arbuscular mycorrhizal fungi: a review. – Biological Agriculture & Horticulture: An International Journal for Sustainable Production Systems 31(2): 73-90.

[11] Esmail, A. O., Sediq Yasin, H., Jalal Mahmood, B. (2014): Effect of levels phosphorus and iron on growth, yield and quality of flax. – Journal of Agriculture and Veterinary Science 7: 7-11.

[12] Evers, J. B., van der Krol, A. R., Vos, J., Struik, P. C. (2011): Understanding shoot branching by modelling form and function. – Trends in Plant Science 16: 464-467.

[13] Fazeli Rostampour, M., Yarnia, M. Rahimzadeh Khoee, F. Seghatoleslami, M. J., Moosavi, G. R. (2013): Physiological response of forage sorghum to polymer under water deficit conditions. – Agronomy Journal 105(4): 951-959.

http://www.aloki.hu ● ISSN 1589 1623 (Print) ● ISSN 1785 0037 (Online)
DOI: http://dx.doi.org/10.15666/aeer/1605_64536468
© 2018, ALÖKI Kft., Budapest, Hungary

[14] Fletcher, A. L., Mooe, D. J., Scott, W. R. (2004): Leaf appearance and primordia initiation of 'Challenger' sweet corn in response to phosphorus. – Agronomy 4: 84-91.
[15] Habibzadeh, Y. (2015): Effects of phosphorus levels on dry matter production and root traits of chickpea plants in presence or absence of Arbuscular mycorrhizal fungi. – Journal of Agricultural Science and Food Technology 1(1): 1-6.
[16] Hammond, J. P., White, P. J. (2008): Sucrose transport in the phloem: integrating root responses to phosphorus starvation. – Journal of Experimental Botany 59: 93-109.
[17] Hedayati Mahdi Abadi, B., Ganjali, H. R., Mobasser, H. R. (2015): Effect of mycorrhiza and phosphorus fertilizer on some characteristics of black cumin. – Biological Forum - An International Journal 7(1): 1115-1120.
[18] Hosseini Valiki, S. R., Ghanbari, S., Akbarzadeh, M., Ghasempor Alamdari, M., Golmohammadzadeh, S. (2015): Effect of organic and chemical fertilizers on dry yield, essential oil and compounds on rosemary (*Rosemarinus officinalis* L.). – Biological Forum - An International Journal 7(1): 773-782.
[19] Khalil, S. E., Yousef, R. M. M. (2014): Interaction effects of different soil moisture levels, arbuscular mycorrhizal fungi and three phosphate levels on: i- growth, yield and photosynthetic activity of garden cress (*Lepidium sativum* L.) plant. – International Journal of Advanced Research 2: 723-737.
[20] Khan, M. S., Ahmad, E., Zaidi, A., Oves, M. (2013): Functional Aspect of Phosphate-Solubilizing Bacteria: Importance in Crop Production. – In: Maheshwari, D. K., Aeron, A., Saraf, M. (eds.) Bacteria in Agrobiology: Crop Productivity. Springer, Berlin, pp. 237-263.
[21] Kotoky, R., Rabha, A., Kanjilal, P. B. (2015): Root yield and yield attributes of *Aristolochia indica* L. (Piperales: Aristolochiaceae) as effected by different spacing and fertilizer treatments in the North-East India. – Brazilian Journal of Biological Sciences 2: 235-243.
[22] Khalilvand, E., Yarnia, M. (2016): Effect of methanol foliar application on nutrient content and RWC of sugar beet under water deficit stress. – Bangladesh Journal of Botany 45(5): 1069-1074.
[23] Krishnakumar, S., Balakrishnan, N., Muthukrishnan, R., Ramesh Kumar, S. (2013): Myth and mystery of soil mycorrhiza: A review. – African Journal of Agricultural Research 8(38): 4706-4717.
[24] Kumar, R., Chandra, R. (2009): Influence of PGPR and PSB on rhizobium leguminosarum bv. viciae strain competition and symbiotic performance in Lentil. – World Journal of Agricultural Sciences. 4(3): 297-301.
[25] Levitt, J. (1980): Response of plants to environmental stresses. Vol. II. – Academic Press. Inc., New York, pp. 279.
[26] Lu, L., He, C., Jin, Y. (2013): Effects off the applications of phosphorous and potasium fertilizers at different growth stages on the root growth and bioactive componds of Salvia militiorrhiza Bunge. – Ausralian Journal of Crop Science 7: 1533-1543.
[27] Mirabello, M. J., Yavitt, J. B., Garcia, B. A. D. M., Harms, K. E., Turner, B. C. B. L., Wright, S. J. (2013): Soil phosphorus responses to chronic nutrient fertilisation and seasonal drought in a humid lowland forest, Panama. – Soil Research 51: 215-221.
[28] Miyawaki, K., Matsumoto-Kitano, M., Kakimoto, T. (2004): Expression of cytokinin biosynthetic isopentenyltransferase genes in Arabidopsis: tissue specificity and regulation by auxin, cytokinin, and nitrate. – The Plant Journal 37: 128-138.
[29] Mohseni, M., Ardekani, M. R., Vazan, S., Paknezhad, F. (2015): The effect of mycorrhiza inoculation and *azotobacter* strains on the characteristics of the root of *Cuminum Cyminum* in agroecosystem without chemical materials. – J. Appl. Environ. Biol. Sci. 5(6): 96-104.
[30] Nazarli, H., Zardashti, M. R. (2010): The effect of drought stress and super absorbent polymer (a200) on agronomical traits of sunflower (*Helianthus annuus* L.) under field condition. – Cercetări Agronomice în Moldova 3(12): 5-14.

http://www.aloki.hu ● ISSN 1589 1623 (Print) ● ISSN 1785 0037 (Online)
DOI: http://dx.doi.org/10.15666/aeer/1605_64536468
© 2018, ALÖKI Kft., Budapest, Hungary

[31] Pajooheshgar, R., Azizi, M., Nemati, H., Khorasani, R. (2015): Effect of organic substrate and phosphorus fertilization on seed, oil yields and composition of medicinal pumpkin (*Cucurbita pepo* var. styriaca). – Biological Forum - An International Journal 7(1): 593-601.

[32] Rapparini, F., Penuelas, J. (2013): Mycorrhizal Fungi to Alleviate Drought Stress on Plant Growth, Use of Microbes for the Alleviation of Soil Stresses. – In: Egamberdieva, D., Lugtenberg, B. (eds.) Use of Plant Growth-Promoting Rhizobacteria to Alleviate Salinity Stress in Plants. Vol. 1, pp. 21-42. Springer, New York.

[33] Robinson, J., Nithya, K., Ramya, R., Karthikbalan, B., Kripa, K. (2014): Effect of vesicular arbuscular mycorrhiza *Glomus fasiculatum* on the growth and physiological response in *Sesamum indicum* L. – International Letters of Natural Sciences 23: 47-62.

[34] Salvucci, M. E., Bartaa, C., Byersa, J. A., Canarini, A. (2010): Photosynthesis and assimilate partitioning between carbohydrates and isoprenoid products in vegetatively active and dormant guayule: physiological and environmental constraints on rubber accumulation in a semiarid shrub. – Physiologia Plantarum 140: 368-379.

[35] Sharma, N., Yadav, K., Cheema, J., Badda, N. and Aggarwal, A. (2015): Arbuscular mycorrhizal symbiosis and water stress: a critical review. – Pertanika J. Trop. Agric. Sci. 38(4): 427-453.

[36] Trindade, R. S., Paulo Araújo, A., Grandi Teixeira, M. (2010): Leaf area of common bean genotypes during early pod filling as related to plant adaptation to limited phosphorus supply. – R. Bras. Ci. Solo 34: 115-124.

[37] Yadav, A., Aggarwal, A. (2015): The associative effect of arbuscular mycorrhizae with *Trichoderma viride* and *Pseudomonas fluorescens* in promoting growth, nutrient uptake and yield of *Arachis hypogaea* L. – New York Science Journal 8(1): 101-108.

[38] Yordanova, R., Popova, L. (2007): Effect of exogenous treatment with salicylic acid on photosynthetic activity and antioxidant capacity of chilled wheat plants. – Gen. Appl. Plant Physiology 33(3-4): 155-170.

http://www.aloki.hu ● ISSN 1589 1623 (Print) ● ISSN 1785 0037 (Online)
DOI: http://dx.doi.org/10.15666/aeer/1605_64536468
© 2018, ALÖKI Kft., Budapest, Hungary

CALIBRATION AND EVALUATION OF CERES-RICE MODEL UNDER DIFFERENT DENSITY AND WATER MANAGEMENTS

EBRAHIMIRAD, H.[1] – AMIRI, E.[2*] – BABAZADEH, H.[1] – SEDGHI, H.[1]

[1]Department of Water Science and Engineering, Science and Research Branch, Islamic Azad University, Tehran, Iran
(phone: +98-911-337-7497 – H. E. R., +98-912-699-0105 – H. B., +98-912-348-6557 – H. S.)

[2]Department of Water Engineering, Lahijan Branch, Islamic Azad University, Lahijan, Iran
(phone: +98-911-651-6300)

**Corresponding author*
e-mail: eamiri57@yahoo.com; phone: +98-911-651-6300

(Received 13th Jun 2018; accepted 2nd Aug 2018)

Abstract. The objective of this study was the evaluation of the Ceres-Rice model under different density and water management options in Semi-Mediterranean climate condition. An experiment was conducted in a randomized complete block design (RCBD) with three replications in north of Iran during cropping seasons of 2014 and 2015. There were 5 levels of irrigation treatments in this research including: I_1: Flood irrigation, I_2: Saturation, I_3: Irrigation with 8 days alternative before anthesis, I_4: Irrigation with 8 days alternative after anthesis, I_5: Irrigation with 8 days alternative whole growth season) and there were three plant spacing including: $D_1 = 15 \times 15$, $D_2 = 20 \times 20$, $D_3 = 25 \times 25$cm. Evaluation simulated and measured grain yield, total crop biomass, and crop biomass by adjusted coefficient of correlation and by absolute and normalized root mean square errors (RMSE). Grain yield of D_2 was predicted the most accurate than other density treatments (RMSE = 439 and RMSEn = 11%). Biomass of D_2 was predicted the most accurate than other density treatments (RMSE = 873 and RMSEn = 9%). Observed and predicted planting densities by rice showed good agreement in both calibration and evaluation steps. The Ceres-Rice model can be applied to research purposes (irrigation and planting densities) under northern Iranian conditions.
Keywords: *Semi-Mediterranean, Ceres-Rice, Irrigation, Crop Model, Water Productivity*

Introduction

Rice is a main food for majority of the world's population, raised on about 146.5 million ha of the agricultural fields of the world. So it is necessary to optimize usage of available resources due to shortage of water resources in rice fields (Thakur et al., 2014; Gill et al., 2014; Murumkar et al., 2014). Water necessity is more for this plant than other grains and the amount of it is affected by the rice cultivar, stage of growth, length of growth stage, plant density and even method of cultivation and weather conditions. Iran is an area with an annual rainfall of 240 mm and 0.57 million ha paddy field. Most rainfalls occur out of rice growth stages. Water allocation is not sufficient for low efficient irrigation in Iran, and surface water storage will be increased by construction of dams (Amiri et al., 2011).

Agricultural water productivity directly affects crop production; therefore, various water saving techniques and managements have been developed for rice producers to minimize water use and maintain optimum yield (Pascual, 2016). For instance, observed yield and simulated water balance, the calculated average WP_{ET} was significantly lower than the average WP_T: 37%. The average WP_I, WP_{ET}, WP_T and WP_{ETQ} were 1.01, 0.89, 1.41 and 0.65 kgm^{-3} (Amiri and Rezaei, 2013).

http://www.aloki.hu ● ISSN 1589 1623 (Print) ● ISSN 1785 0037 (Online)
DOI: http://dx.doi.org/10.15666/aeer/1605_64696482
© 2018, ALÖKI Kft., Budapest, Hungary

Severe drought stress at mid-tillering delayed flowering, and caused substantial yield losses by large percentage of unfilled grains (Davatgar et al., 2009). This finding has been confirmed by Pirdashti et al. (2009) who pointed out that water shortage in the vegetative growth stage extended the number of days for flowering in different rice cultivars. It has been documented that dry matter is more affected under vegetative stage stress whereas severe effects on sink size (spikelet fertility, 1000 grain weight and seed yield) under reproductive stage stress would be resulted (Guan et al., 2010).

Roderick et al. (2011) concluded in a research that alternate wet and drying irrigation deficit method has reduced about 38% of irrigation water usage, with the same yields and farmers profits.

High densities of rice cultivation reduce plant yield and yield components (Chamara et al., 2016). Some researchers have reported increased yield per unit area as a result of increasing density per unit area (Clerget et al., 2016). Other researchers have also reported declined yield and biomass per unit area due to increasing density (Awan et al., 2014). In addition, high densities are recommended to suppress weeds and increase yield in rice (Chauhan et al., 2011).

In order to detect the effect of planting density on the water productivity of rice product, an experiment was conducted in a split plot design with three plant-distance (20 × 20, 15 × 15, 20 × 10 cm) as a sub plots and four different irrigation regimes (permanent flooding treatment as a control group and 100%, 75% and 50% evaporation from the pan) as the main factors. The best yield in irrigation was reported for 75% evaporation from the pan and the plant-density of (20 × 20 cm) (Amiri et al., 2011).

In recent years, there has been an increasing amount of literature on simulation and modeling application on rice production (Amiri et al., 2014; Vijayalaxmi et al., 2016)

Until now, the most conducted researches have been about the method of irrigation management based on fixed round of irrigation from the first to the end of growing season. Fewer researches have been conducted about the method of irrigation management regarding cultivation density. At present, information required for the rice production improvement with suitable management practices is a need of hour. The generation of new data through agronomic research methods is insufficient and time consuming to meet these needs. So crop simulation models are considered as potentially useful tools in agricultural decision making. The major objectives of this study were to investigate: (i) Modeling response of Hashemi rice variety to change in planting densities and irrigation managements (ii) Calibrate and validate the DSSAT v 4.5. model based on experimental data; (iii) To explore on-farm strategies which result in higher economic gains and water productivity.

Materials and methods

Experimental design, crop establishment, and crop management

The experiment was conducted as split plot based on randomized complete block design with three replications on rice Hashemi cultivar during growing season of 2014 and 2015 in Koosal-Lahijan region located in north of Iran. The height of the site is 3 m from the sea level and it is located at 14”3’37° of north latitude and14”1’50° of east length. Irrigation treatments were at five levels: full irrigation = I_1 saturated = I_2 irrigation with 8 days alternative until anthesis = I_3, irrigation with 8 days alternative after anthesis = I_4, irrigation with 8 days alternative during the whole period of growth = I_5 and density was at 3 levels: 15 × 15 = D_1, 20 × 20 = D_2, 25 × 25 = D_3 cm

http://www.aloki.hu ● ISSN 1589 1623 (Print) ● ISSN 1785 0037 (Online)
DOI: http://dx.doi.org/10.15666/aeer/1605_64696482
© 2018, ALÖKI Kft., Budapest, Hungary

(444000, 250000, 160000 plants per hectare, respectively). Each experimental plot was 9.2 m long and 3 m wide. After transplanting the markers to the main land, the plots were kept for 10 days in permanent flooding until the markers were settled. After that, irrigation management was applied in the plots based on the program. I_1 was often flooding and I_2 was often saturated. I_3 was irrigated every 8 days before anthesis and then was flooded. The treatments I_4 was irrigated every two to three days before anthesis and then irrigated every 8 days. I_5 was completely irrigated every 8 days. It should be noted that the management of irrigation with frequency of 8 days (Amiri and Rezaei, 2013) was performed based on the alternation according to the growth of rice, using optimal water management in drought stress condition and in order to cope with damages caused by water stress on Hashemi cultivar.

According to the *Table 1,* soil of the experiment site is suitable for rice. *Table 2* also shows crop information and *Figures 1* and *2* shows the meteorological characteristics of the site. The first 20 days were irrigated by flooding. Urea, potassium and phosphate fertilizers were each used at baseline of 60 $kg.ha^{-1}$. 60 kg urea fertilizer was also consumed one month after the baseline stage. Graining was carried out at the end of April in the treasury environment and transplantation of the treatments was done at the end of May. After handling and harvesting, the clusters were placed in an oven for drying for 72 h at 70 °C.

Table 1. *Soil physical and chemical characteristics of the experimental site before sowing the rice crop*

Soil characteristics	Depth (cm)				40–50
	0–10	10–20	20–30	30–40	
Texture					
Sand (%)	18	14	17	9	11
Silt (%)	39	39	39	44	42
Clay (%)	47	47	44	47	47
Bulk density (g cm^{-3})	1.45	1.4	1.4	1.42	1.41
Water content at saturation	0.392	0.392	0.39	0.39	0.39
Water content at FC (0.01 MPa)	0.204	0.204	0.209	0.209	0.209
Water content at PWP (1.5 MPa)	0.34	0.34	0.345	0.345	0.345
KSAT (cm day^{-1})	57.54	57.54	30.79	0.40	11.79
pH	7.05	7.15	7.23	7.26	7.08
CEC (meq 100 g^{-1})	33	33	32	31	31
Organic carbon (%)	2.30	2.72	2.54	2.25	2.76
Total N (%)	0.19	0.16	0.14	0.074	0.074
Extractable P (ppm)	8.7	10.1	7.3	5.2	3.2
Extractable K (ppm)	225	195	176	185	161

Table 2. *Crop information in two different years of experiment*

Crop year	Date of plowing	Date of plotting	Date of fertilizing	Date of transplantation	Date of anthesis	Date of excess fertilizing	Date of harvesting	Total period of growth-day
2014	27 May	30 May	4 Jun.	2 Jun.	5 Aug.	6 Jul.	5 Sep.	95
2015	27 May	31 May	4 Jun.	3 Jun.	6 Aug.	6 Jul.	10 Sep.	99

http://www.aloki.hu ● ISSN 1589 1623 (Print) ● ISSN 1785 0037 (Online)
DOI: http://dx.doi.org/10.15666/aeer/1605_64696482
© 2018, ALÖKI Kft., Budapest, Hungary

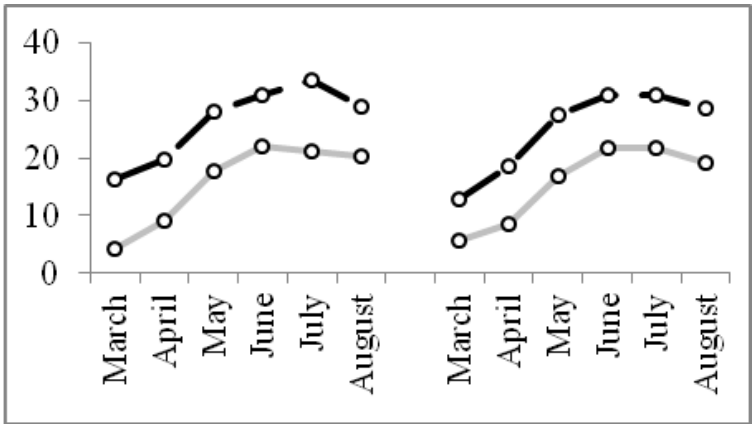

Figure 1. *Monthly minimum and maximum air temperatures (°C) during the growing periods of rice in 2014 and 2015 growing seasons (left to right, respectively)*

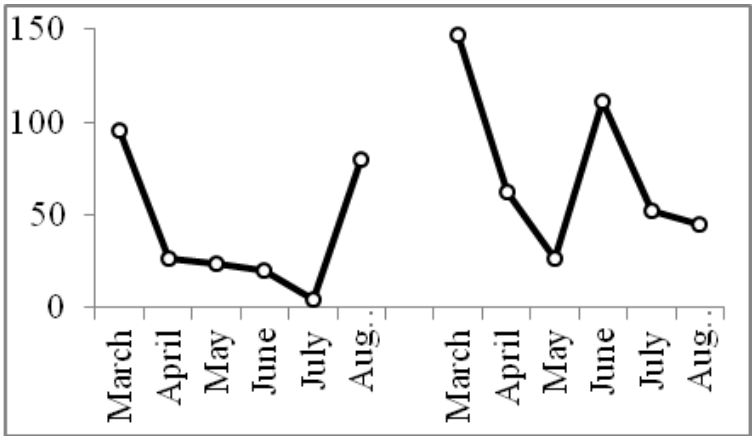

Figure 2. *Monthly rainfall during the growing periods of rice in 2014 and 2015 growing seasons (left to right, respectively)*

Ceres-Rice description

Ceres-Rice model was selected as a tool for simulating growth and yield of rice under different environment and management strategies. The Ceres-Rice model simulates rice crop growth and development from either planting or transplanting to physiological maturity and is based on the physiological processes that describe the response of rice to local soil and weather conditions. Potential growth is mainly dependent upon photosynthetically active radiation (PAR), light interception and the light conversion efficiency, while actual growth is a constraint of crop management, soil and weather interactions.

The input data required to run the DSSAT models include daily weather data, i.e. maximum and minimum temperature, rainfall, and solar radiation; soil characterization data, genetic coefficients and crop management information, such as date of planting, age of seedlings, row and plant spacing, rates and dates and amount of fertilizer and irrigation applied. Input data files of Ceres-Rice model are as per IBSNAT standard input/output formats and file structure described in DSSAT v 4.5 (Hoogenboom et al., 2003).

http://www.aloki.hu ● ISSN 1589 1623 (Print) ● ISSN 1785 0037 (Online)
DOI: http://dx.doi.org/10.15666/aeer/1605_64696482
© 2018, ALÖKI Kft., Budapest, Hungary

Model inputs

The DSSAT models require the minimum data set for model operation. They encompass data on the site where the model is to be operated, on the daily weather data, on the soil properties, and on the all aspects management of the crop growth. Important crop management factors include planting date, planting depth, row spacing and direction, plant population, fertilization, irrigation, inoculation, residue applications, tillage, and harvest date.

Calibration of Ceres-Rice model

The calibration of the Ceres-Rice model was based on data from measured data of grain yield, total biomass in 2014-2015 field experiment. The genetic coefficients of the rice cv. Hashemi that affect the occurrence of phonological stages in the Ceres-Rice models were derived using the GLUE Estimator of DSSAT v 4.6. This program estimates the coefficients for a genotype by iteratively running the crop model with an approximate value of the coefficients concerned.

One would expect to have, for good model performance, values of RMSE as close as possible to 0. A model produces experimental data perfectly when α is close to 1, β is close to 0, R^2 is close to 1, RMSEa is similar to the SD of measured values, and RMSEn is similar to the coefficient of variation (CV) of measured values.

Model evaluation

Summary measures used in the present study were the mean of measured and simulated values, the standard deviations (SD) of the observations and simulations, the slope α, intercept β, and coefficient of determination (R^2) of the linear regression line between simulated and measured values. The different measures were based on the analysis of residual errors, that is, the difference between simulated and measured values. We computed the absolute and normalized root mean square errors (RMSE and RMSEn, respectively). Also, based on the measured data and relationship data and statistical estimation of the model were done through the root mean square error (RMSE), normalized root mean square error (RMSEn), relative error of the model (ME). When the RMSE and RMSEn values are closer to zero, it indicates that the prediction has been done better by relations (*Eqs. 1–3*).

$$RMSE = \sqrt{\frac{\sum_{i=1}^{n}(P_i - O_i)^2}{n}} \quad \text{(Eq.1)}$$

$$RMSE_n = 100\ (\sum_{i=1}^{n}(P_i - O_i)^2 / n)^{0.5}) \Big/ \overline{O} \quad \text{(Eq.2)}$$

$$RMSE = 100\ (\frac{P_i - O_i}{O_i}) \quad \text{(Eq.3)}$$

In the first two relations (*Eq. 1* and *2*), S_i and O_i are respectively the values of relative and observed performance equations. $\overline{O}$ is the mean of observed values and n is the number of observations (Amiri et al., 2011).

http://www.aloki.hu ● ISSN 1589 1623 (Print) ● ISSN 1785 0037 (Online)
DOI: http://dx.doi.org/10.15666/aeer/1605_64696482
© 2018, ALÖKI Kft., Budapest, Hungary

Water balance components

The water balance of lowland rice model includes (*Eq. 4*):

$$dW = I + R + C - E - T - S - Q - D \quad \text{(Eq.4)}$$

where dW is the change in stored water, I is irrigation supply, R is rainfall, C is capillary rise, E is evaporation, T is transpiration, S is seepage, Q is percolation, and D is surface drainage/runoff (all units are mm) (Bouman et al., 2001).

Water productivity

WP indices express the profit derived from the consumption of water and can be used for assessing the impact of on-farm strategies under water scarce situations. They provide a proper vision of where and when water could be conserved. The following equations (*Eqs. 5–9*) were used to calculate the water productivity components (Singh et al., 2006).

$$WP_T = \frac{Y_g}{T} \quad \text{(Eq.5)}$$

$$WP_{ET} = \frac{Y_g}{E+T} \quad \text{(Eq.6)}$$

$$WP_I = \frac{Y_g}{I} \quad \text{(Eq.7)}$$

$$WP_{I+R} = \frac{Y_g}{I+R} \quad \text{(Eq.8)}$$

$$WP_{ETQ} = \frac{Y_g}{E+T+Q} \quad \text{(Eq.9)}$$

where Yg (Kg) is the crop grain yield, T (mm) is the actual transpiration, E (mm) is the actual soil evaporation, I (mm) is irrigation, R (mm) is rainfall and Q (mm) is the percolation. WP_I (kg/m^3), WP_{I+R} (kg/m^3), WP_{ET} (kg/m^3), WP_T (kg/m^3) and WP_{ETQ} (kg/m^3) are expressed in crop grain yield (Yg) per unit amount of I, I+R, ET, T and ETQ respectively.

Results and discussion

Model calibration

The calibrated genetic coefficients (cv. Hashemi) as derived by Gencalc for Ceres-Rice are given in *Table 3*.

Table 4 shows the goodness-of-fit parameters for grain yield and aboveground biomass at harvest of the whole data set. The model simulated aboveground biomass

http://www.aloki.hu ● ISSN 1589 1623 (Print) ● ISSN 1785 0037 (Online)
DOI: http://dx.doi.org/10.15666/aeer/1605_64696482
© 2018, ALÖKI Kft., Budapest, Hungary

and Grain yield quite well, with the absolute and normalized RMSE values greater than the error in the measured value (*Table 4*). For biomass, the slope was close to 1, and the intercept ß was high, indicating general overestimation of simulated values. Almost the same pattern was observed for grain yield. The model simulated grain yield and biomass generally good. The slope in validation was a little bit greater than that of calibration while the intercept ß was less than that of calibration. The relatively high R^2 reflects the low spread of the data. The error value in validation step has decreased, which is a reason to accept the results of the model. Also, the mean square error should be less than the standard deviation of the actual values that the results of the evaluation of Ceres-Rice model accuracy in irrigation management and different crop distances indicate that.

Table 3. *Genetic coefficients of the rice cv. Hashemi as derived by GENCALC of DSSAT model*

Genetic parameters	Description	Coefficient for Hashemi
P1	Time period (expressed as growing degree days (GDD) in °C above a base temperature of 9 °C from seedling emergence during which the rice plant is not responsive to changes in photoperiod	320.0
P20	Critical photoperiod or the longest day length (in h) at which the development occurs at a maximum rate	5.0
P2R	Extent to which phasic development leading to panicle initiation is delayed (expressed as GDD in °C) for each hour increase in photoperiod above P20	13.5
P5	Time period in GDD °C) from beginning of grain filling (3 to 4 days after flowering) to physiological maturity with a base temperature of 9 °C	240.0
G1	Potential spikelet number coefficient as estimated from the number of spikelets per g of main culm dry weight (less lead blades and sheaths plus spikes) at anthesis	55.2
G2	Single grain weight (g) under ideal growing conditions, i.e., nonlimiting light, water, and nutrients and absence of pests and diseases	0.0200
G3	Tillering coefficient (scaler value) relative to IR64 cultivar under ideal conditions	1.00
G4	Temperature tolerance coefficient. Usually 1.0 for varieties grown in normal environments	1.00

Model evaluation

Grain yield the graphical comparison between simulated and measured grain yield is presented in *Figure 3*. The Ceres-Rice model simulated grain yield in 2015 quite well. Grain yield of D_2 was predicted the most accurate than other density treatments ($R^2 = 0.85$).

The graphical performance of the Ceres-Rice model in simulating total crop biomass at harvest is presented in *Figure 4*. Similar to the simulation results of the grain yield, the best performance of the model in simulating total crop biomass was obtained in

http://www.aloki.hu ● ISSN 1589 1623 (Print) ● ISSN 1785 0037 (Online)
DOI: http://dx.doi.org/10.15666/aeer/1605_64696482
© 2018, ALÖKI Kft., Budapest, Hungary

2015. Biomass of D_2 was predicted the most accurate than other density treatments ($R^2 = 0.89$).

Table 4. *Evaluation results for Ceres-Rice simulations of final aboveground biomass and yield, for the calibration and validation conditions*

Year	Crop variables		N	X_{obs}	X_{sim}	Sd_{obs}	α	ß	R^2	RMSE (kg.ha^1)	RMSEn (%)
2014 Calibration	D_1	Biomass (kg.ha^{-1})	5	9648	10027	2254	0.40	6168	0.72	1363	14.13
		Yield (kg.ha^{-1})	5	3736	4042	919	0.79	1093	0.78	491	13.15
	D_2	Biomass (kg.ha^{-1})	5	9944	9930	2069	052	4719	0.87	955	9.60
		Yield (kg.ha^{-1})	5	3818	3971	1212	070.	1314	0.83	499	13.06
	D_3	Biomass (kg.ha^{-1})	5	9379	9720	1449	0.54	4682	0.57	917	9.78
		Yield (kg.ha^{-1})	5	3741	3907	874	0.77	1045	0.63	521	13.92
2015 Validation	D_1	Biomass (kg.ha^{-1})	5	9093	9638	1678	0.58	4364	0.77	958	10.53
		Yield (kg.ha^{-1})	5	3837	4188	814	0.81	1082	0.81	473	12.32
	D_2	Biomass (kg.ha^{-1})	5	9858	9563	1783	0.59	3750	0.89	790	8.02
		Yield (kg.ha^{-1})	5	3926	4095	937	0.74	1191	0.85	379	9.66
	D_3	Biomass (kg.ha^{-1})	5	9269	9343	1098	0.55	4231	0.64	872	9.41
		Yield (kg.ha^{-1})	5	3842	4000	852	0.76	1073	0.69	457	11.90

N: number of treatments, X_{obs}: mean of observed value; X_{sim}: mean of simulated value; Sd_{obs}: standard deviation of observed value; α: slope of linear relation between simulated and measured values; ß: intercept of linear relation between simulated and measured values; R^2: adjusted linear correlation coefficient between simulated and measured values; RMSEn: normalized root mean square error (%); RMSE: absolute, absolute root mean square error

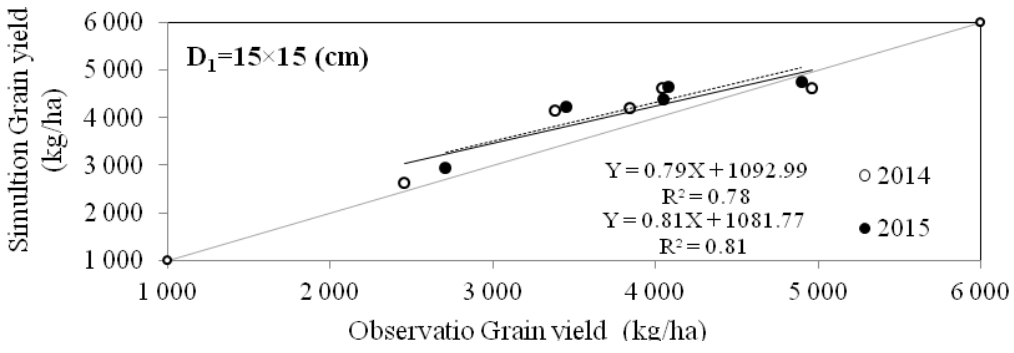

http://www.aloki.hu ● ISSN 1589 1623 (Print) ● ISSN 1785 0037 (Online)
DOI: http://dx.doi.org/10.15666/aeer/1605_64696482
© 2018, ALÖKI Kft., Budapest, Hungary

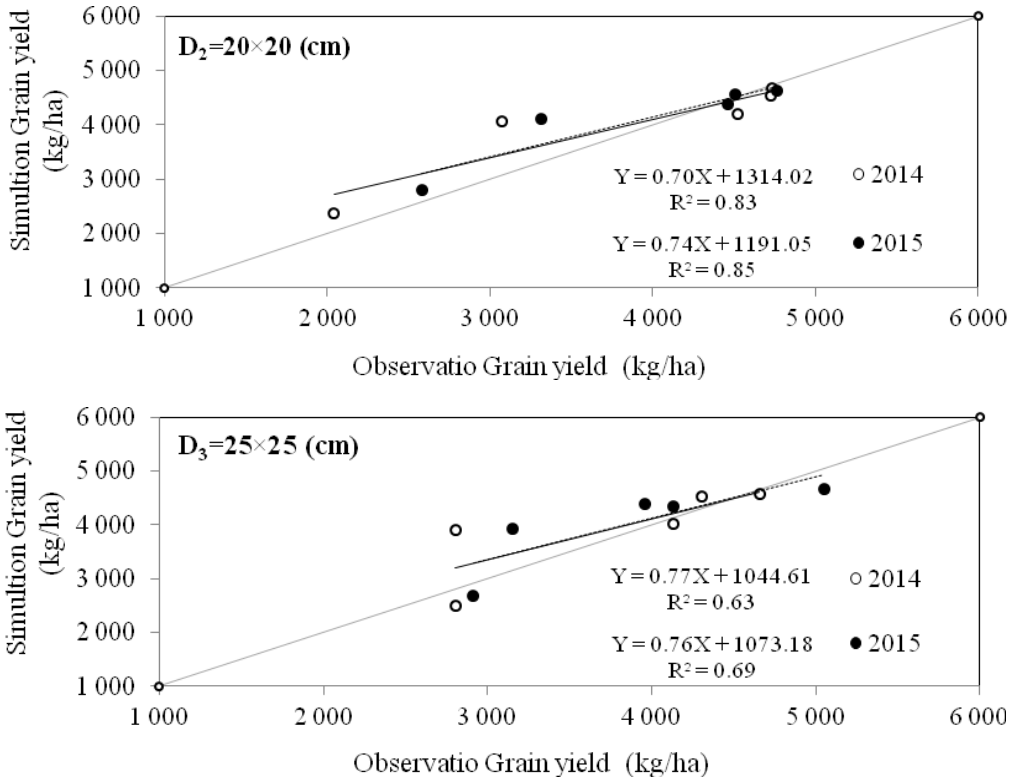

Figure 3. *Evaluation of Ceres-Rice model for grain yield under different density and water management*

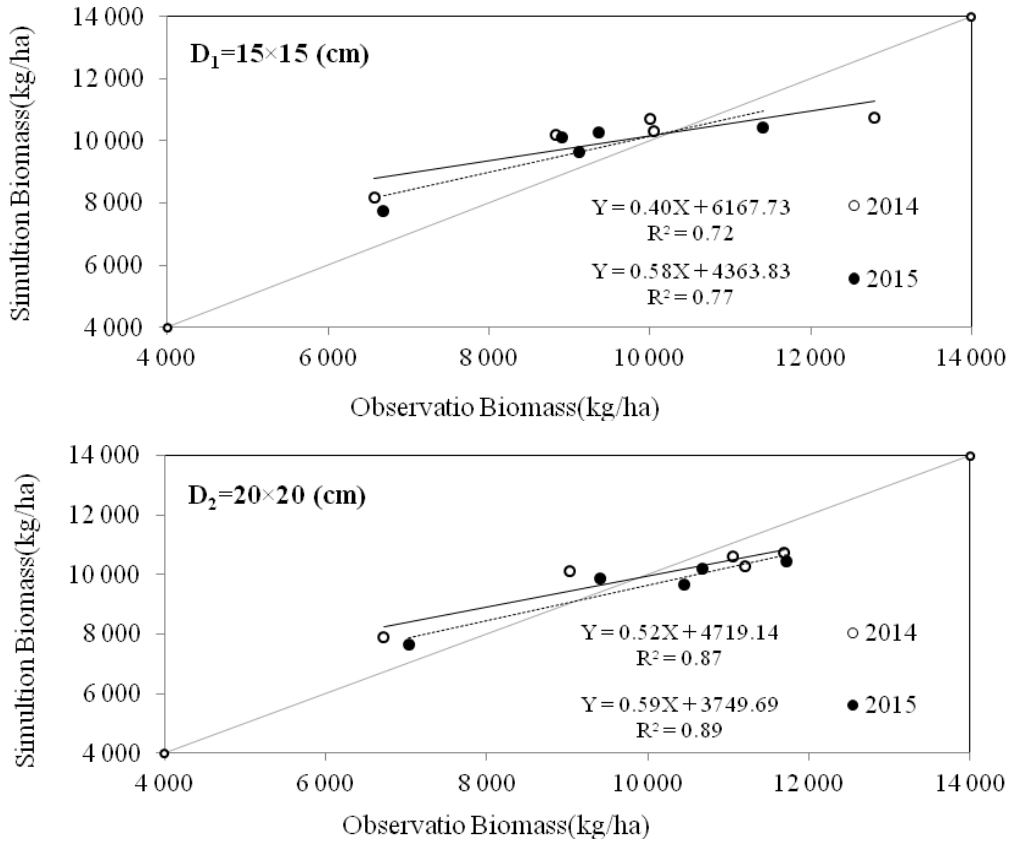

http://www.aloki.hu ● ISSN 1589 1623 (Print) ● ISSN 1785 0037 (Online)
DOI: http://dx.doi.org/10.15666/aeer/1605_64696482
© 2018, ALÖKI Kft., Budapest, Hungary

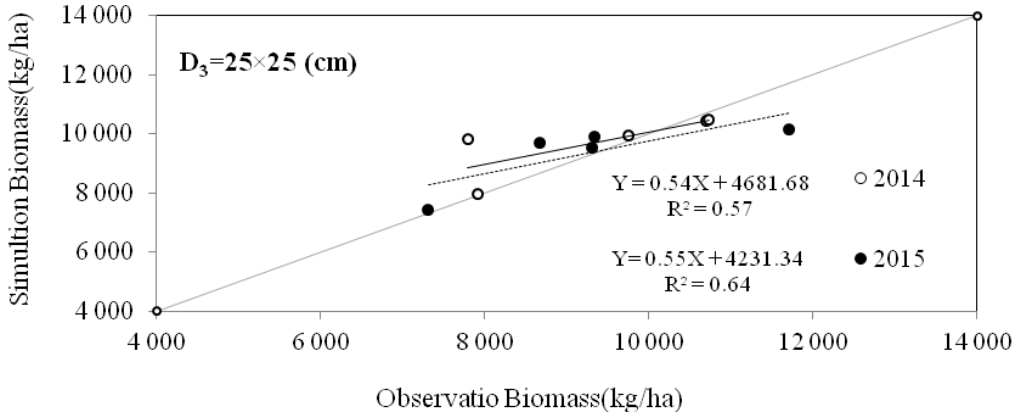

Figure 4. *Evaluation of Ceres-Rice model for final above ground biomass under different density and water management*

The use of Ceres-Rice model in different years to simulate rice yield in irrigation management and different densities is shown in *Figure 5*. The ability of the Ceres-Rice model to simulate the total biomass of rice in different years under irrigation management and different densities is shown in *Figure 6.* In the second year, the plant was exposed to warmer days and the rice plant was subjected to more severe drought stress, which caused the plant to close its stomata more than the first year, and the yield and total biomass decreased compared to the first year.

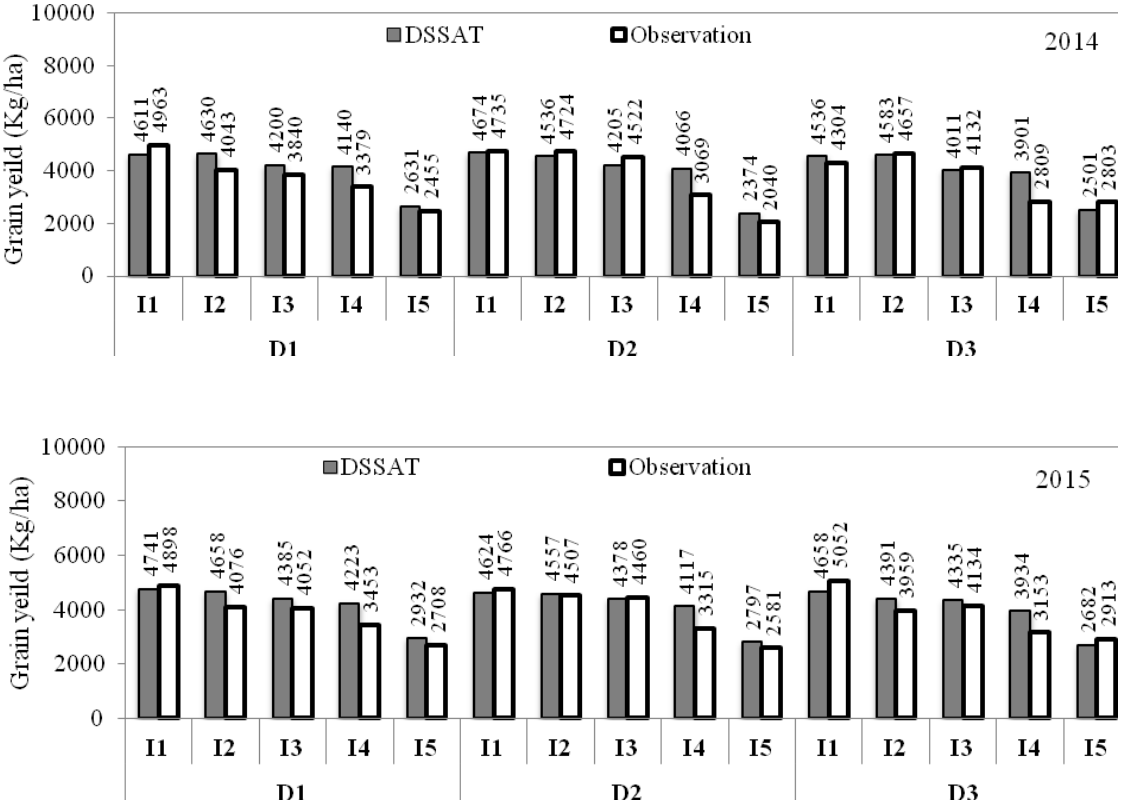

Figure 5. *Performance of Ceres-Rice model for simulating grain Yield of rice under water management and plant density situations (15 × 15 = D_1, 20 × 20 = D_2, 25 × 25 = D_3 cm)*

http://www.aloki.hu ● ISSN 1589 1623 (Print) ● ISSN 1785 0037 (Online)
DOI: http://dx.doi.org/10.15666/aeer/1605_64696482
© 2018, ALÖKI Kft., Budapest, Hungary

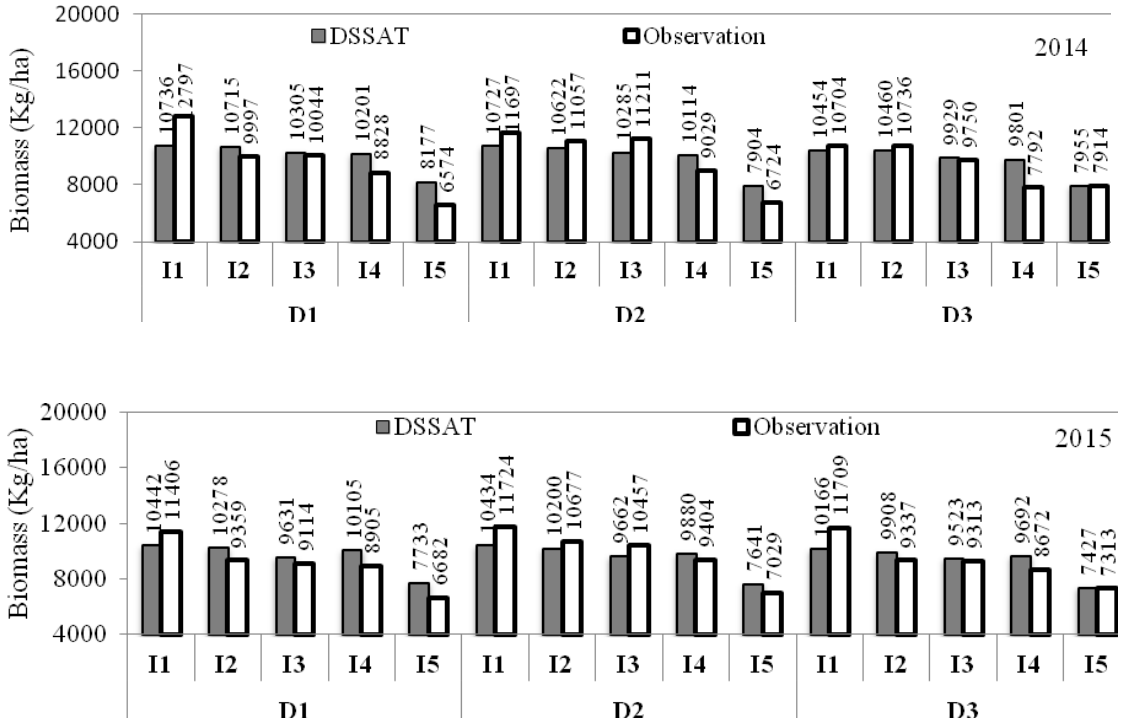

Figure 6. *Performance of Ceres-Rice model for simulating Biomass of rice water management and plant density situations (15 × 15 = D_1, 20 × 20 = D_2, 25 × 25 = D_3 cm)*

Water balance components

An examination of simulated components of water balance under different density and water management reveals interesting facts (*Fig. 7*).

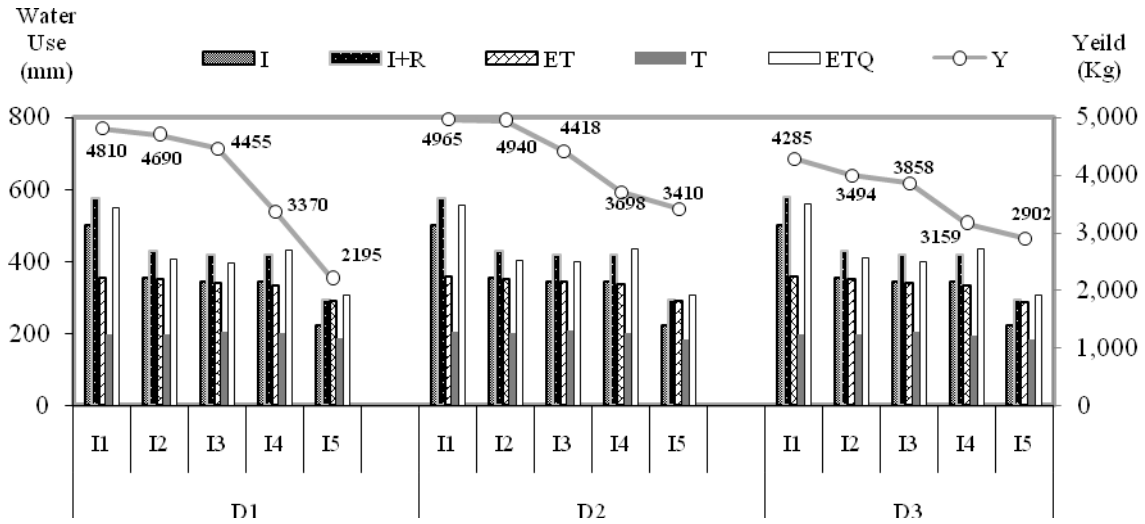

Figure 7. *Water productivity values at different irrigation and crop distance treatments*

The seasonal evaporation varied from 103 to 159 mm and showed a significant reduction with a decrease in plant spacing and applied water amount. The results of the

http://www.aloki.hu ● ISSN 1589 1623 (Print) ● ISSN 1785 0037 (Online)
DOI: http://dx.doi.org/10.15666/aeer/1605_64696482
© 2018, ALÖKI Kft., Budapest, Hungary

model showed that the amount of evaporation (E) is 36-44% of evapotranspiration (ET). The variability of physiological function of rice plant in irrigation management and different intervals of cultivation and changing environmental conditions leads to different transpirational requirements and consequently the amount of transpiration (T) in the plant. Changing the irrigation method from floodwaters to non-floodwaters results in increased transpiration (T). Investigation of transpiration amount in irrigation management and planting distance showed that transpiration values varied in the range of 187-217 mm; the highest transpiration (T) was observed in I_3: Irrigation with 8 days alternative before anthesis for irrigation and crop distance $D_2 = 20 \times 20$ cm was observed at 209 mm. Estimation of depth of penetration (ETQ) in irrigation and planting intervals showed that depth of penetration (ETQ) varies in the range of 534-295 mm; the results of deep penetration in the study period showed that the maximum amount of water loss Through deep penetration (ETQ) was observed in flood management. Amounts of rainfall from transplanting to harvest stage were 38 mm for 2014 and 169 mm for 2015. The amount of irrigation water applied varied between 221 mm to 502 mm. As the spacing increased, the depth of penetration (ETQ) increased. Irrigation with 8 days alternative before anthesis with only 4% reduction in yield (Y) compared to the usual method of flooding reduced water consumption and savings of 16% in irrigation water + precipitation (I + R).

Water productivity components

The water productivity for rice was analyzed using the Ceres-Ricesimulation model. We calculated the water productivity rates using the simulated water balance components of T and ET by Ceres-Rice and the actual (observed) grain yield (*Table 5*).

Table 5. *Water productivity values at different irrigation and crop distance treatments*

Treatment		Year									
		2014					2015				
		WP_I	WP_{I+R}	WP_{ET}	WP_T	WP_{ETQ}	WP_I	WP_{I+R}	WP_{ET}	WP_T	WP_{ETQ}
D_1	I_1	0.92	0.86	1.30	2.30	0.86	0.94	0.77	1.34	2.40	0.85
	I_2	1.31	1.19	1.30	2.33	1.18	1.32	1.00	1.36	2.35	1.12
	I_3	1.22	1.11	1.20	1.97	1.09	1.27	0.96	1.33	2.22	1.08
	I_4	1.20	1.09	1.24	2.08	0.99	1.23	0.92	1.26	2.11	0.95
	I_5	1.19	1.03	0.90	1.39	0.89	1.33	0.87	1.03	1.59	0.92
D_2	I_1	0.93	0.87	1.28	2.23	0.85	0.92	0.75	1.32	2.32	0.83
	I_2	1.28	1.17	1.28	2.26	1.16	1.29	0.97	1.32	2.27	1.09
	I_3	1.22	1.11	1.19	1.93	1.08	1.27	0.96	1.32	2.19	1.07
	I_4	1.18	1.08	1.21	2.01	0.96	1.20	0.90	1.23	2.06	0.93
	I_5	1.07	0.93	0.81	1.26	0.81	1.26	0.83	0.98	1.53	0.87
D_3	I_1	0.90	0.85	1.25	2.24	0.83	0.93	0.76	1.32	2.39	0.82
	I_2	1.30	1.18	1.26	2.27	1.14	1.24	0.94	1.29	2.27	1.05
	I_3	1.17	1.06	1.14	1.90	1.03	1.26	0.95	1.32	2.18	1.06
	I_4	1.13	1.03	1.17	1.99	0.93	1.14	0.86	1.19	2.02	0.88
	I_5	1.13	0.98	0.86	1.34	0.85	1.21	0.80	0.95	1.50	0.84

http://www.aloki.hu ● ISSN 1589 1623 (Print) ● ISSN 1785 0037 (Online)
DOI: http://dx.doi.org/10.15666/aeer/1605_64696482
© 2018, ALÖKI Kft., Budapest, Hungary

Table 5 shows the WP values at different irrigation and crop distance treatments in the experiment. Water productivity values for irrigation management and different densities are shown in *Table 5*. Water productivity is based on the amount of mechanism secretion in the plant and depends on the type of plant. As a result, WP_T for a rice plant is a measurable variable that depends on eco-hydrological conditions. The results of this study indicate that the WP_T value varies between 1.6 and 2.46 kg/cm^3. Water productivity is discussed based on the amount of evapotranspiration on soil and plant matter and shading, depending on the type of soil and climate and plant. The inevitable water shortage due to evaporation from the surface water and saturated soil (E) leads to a reduction in water productivity from WP_T to WP_{ET}; on average, WP_{ET} is 41% lower than WP_T. By changing the irrigation management from flood to non-waterlogging, water productivity (WP_I) increases, so that the lowest water productivity (WP_I) in flood treatment is I_1 = 0.92 kg/m^3 and The highest water productivity (WP_I) was observed in saturated treatment of I_2 = 1.27 kg/m^3. The average amount of water-based components of irrigation, evapotranspiration, transpiration and total evapotranspiration and deep penetration (WP_I, WP_{I+R}, WP_{ET}, WP_T and WP_{ETQ}) were 1.13, 0.94, 16.1, 1.97 and 0.49 kg/m^3 respectively. In general, I_3D_3 treatment has reduced water consumption while maintaining optimum performance and water productivity. Continuously surface water flooded method result in high soil evaporation in Hashemi rice planting. Reducing water allocation from continuous flooded methods to soil saturation or alternative irrigation methods will slightly decrease the rice yields but will substantially increase the water productivity (Amiri and Rezaei, 2013).

Conclusion

The results from this study showed that the Ceres-Rice model generally predicted biomass and grain yield, fairly satisfactorily across a range of data sets covering varying levels of water- and density management during 2 years. Results showed that predicted grain yields agreed well with observed yields (RMSEa = 382 and RMSEn = 10%). Also total biomass also were simulated well (RMSEa = 975 and RMSEn = 10%). High evaporation rate at initial stages of crop growth due to traditional irrigation method, has decreased WP_{ET} by 41% compared to WP_T. The results showed that I_3: Irrigation with 8 days alternative before anthesis and D_2 = 20 × 20 cm plant density is the optimum irrigation method and crop density management. The Ceres-Rice model is calibrated and validated using field experimental data, and can be used to predict the experimental results of irrigation and different densities conditions in northern Iran, thus helping to identify target domains and irrigation and density management recommendations for farmers.

REFERENCES

[1] Amiri, E., Rezaei, M. (2013): Evaluation of water balance components and water productivity of rice under interval irrigation and nitrogen fertilizer conditions. – Iranian Journal of Irrigation and Drainage 4(6): 306-315.

[2] Amiri, E., Razavipour, T., Farid, A., Bannayan, M. (2011): Effects of crop density and irrigation management on water productivity of rice production in Northern Iran: field and modeling approach. – Communications in Soil Science and Plant Analysis 42(17): 2085-2099.

http://www.aloki.hu ● ISSN 1589 1623 (Print) ● ISSN 1785 0037 (Online)
DOI: http://dx.doi.org/10.15666/aeer/1605_64696482
© 2018, ALÖKI Kft., Budapest, Hungary

[3] Amiri, E., Rezaei, M., Rezaei, E. E., Bannayan, M. (2014): Evaluation of Ceres-Rice, Aquacrop and Oryza2000 models in simulation of rice yield response to different irrigation and nitrogen management strategies. – Journal of Plant Nutrition 37: 1749-1769.
[4] Awan, T. H., Cruz Sta, P. C., Chauhan, B. S. (2014): Ecological significance of rice (Oryza sativa L.) planting density and nitrogen rates in managing the growth and competitive ability of itchgrass (Rottboelliacochinchinensis) in direct-seeded rice systems. – Journal of Pest Science 88(2): 427-438.
[5] Bouman, B. A. M., Kropff, M. J., Tuong, T. P., Wopereis, M. C. S., ten Berge, H. F. M., Van Laar, H. H. (2001): ORYZA2000: Modeling Lowland Rice. – International Rice Research Institute and Wageningen University and Research Centre, Los Baños, Philippines, and Wageningen, The Netherlands.
[6] Chamara, B. S., Marambe, B., Bhagirath, S. (2016): Management of Cleome rutidosperma DC. using high crop density in dry-seeded rice. – Crop Protect 95: 120-128.
[7] Chauhan, B. S., Johnson, D. E. (2011): Ecological studies on Echinochloa crus-galli and the implications for weed management in direct-seeded rice. – Crop Protect 30: 1385-1391.
[8] Clerget, B., Buenob, C., Domingob, A. J., Layaoenb, H. L., Vialb, L. (2016): Leaf emergence, tillering, plant growth, and yield in response to plant density in a high-yielding aerobic rice crop. – Field Crops Researches 199: 52-64.
[9] Davatgar, N., Neishabouri, M. R., Sepaskhah, A. R., Soltani, A. (2009): Physiological and morphological responses of rice (Oryza sativa L.) to varying water stress management strategies. – International Journal of Plant Production 3: 19-32.
[10] Gill, J. S., Walia, S. S., Gill, R. S. (2014): Direct seeded rice: An alternative rice establishment technique in north-west India - A review. – International Journal of Advanced Research 2(3): 375-386.
[11] Guan, Y. S., Serraj, R., Liu, S. H., Xu, J. L, Ali, J., Wang, W. S. (2010): Simultaneously improving yield under drought stress and non-stress conditions: a case study of rice (Oryza sativa L.). – Journal of Experimental Botany 61: 4145-4156.
[12] Hoogenboom, G., Jones, J. W., Porter, C. H., Wilkens, P. W., Boote, K. J, Batchelor, W. D, Hunt, L. A., Tsuji, G. Y. (2003): Decision Support System for Agrotechnology Transfer Version 4.0. Volume 1: Overview. – University of Hawaii, Honolulu.
[13] Murumkar, R. P., Dongarwar, U. R., Phad, D. S., Borkar, B. Y., Pisalkar, P. S. (2014): Performance testing of four row self propelled paddy transplanter. – International Journal of Science, Environment and Technology 3(6): 2015-2019.
[14] Pascual, V. J., Wang, Y. M. (2016): Utilizing rainfall and alternate wetting and drying irrigation for high water productivity in irrigated lowland paddy rice in southern Taiwan. – Plant Production Science 19: 1-12.
[15] Pirdashti, H., Sarvestani, Z. T., Bahmanyar, M. A. (2009): Comparison of physiological responses among four contrast rice cultivars under drought stress conditions. – World Acad. Sci. Eng. Technol. 25: 52-53.
[16] Roderick, M., Florencia, G. R., Rodriguez, G. D. P., Lampayan, R. M., Bouman, B. A. M. (2011): Impact of the alternate wetting and drying (AWD) water-saving irrigation technique: Evidence from rice producers in the Philippines. – Food Policy 36(2): 280-288.
[17] Singh, R., Van Dam, J. C., Feddes, R. A. (2006): Water productivity analysis of irrigated crops in Sirsa district, India. – Agriculture Water Management 82: 253-278.
[18] Thakur, A. K., Mohanty, R. K., Patil, D. U., Kumar, A. (2014): Impact of water management on yield and water productivity with system of rice intensification (SRI) and conventional transplanting system in rice. – Paddy Water Environ 12: 413-424.
[19] Vijayalaxmi, G., Sreenivas, G., Leela Rani, P. (2016): Evaluation of Ceres-Rice model under various plant densities and age of seedlings in transplanted rice in Southern Telangana Zone of Telangana State. – International Journal of Current Microbiology and Applied Sciences 5(4): 667-674.

http://www.aloki.hu ● ISSN 1589 1623 (Print) ● ISSN 1785 0037 (Online)
DOI: http://dx.doi.org/10.15666/aeer/1605_64696482
© 2018, ALÖKI Kft., Budapest, Hungary

IMPACT OF SURROUNDINGS LANDSCAPE STRUCTURE ON FORMATION OF PLANT SPECIES IN AFFORESTRATED MANOR PARKS

FORNAL-PIENIAK, B.[1] – OLLIK, M.[2] – SCHWERK, A.[3*]

[1]*Faculty of Horticulture, Biotechnology and Landscape Architecture, Department of Environmental Protection, Warsaw University of Life Sciences – SGGW*
Nowoursynowska Street 166, 02-787 Warsaw, Poland
(phone: +48-22-59-32066; fax: +48-22-853-0944)

[2]*Faculty of Agriculture and Biology, Department of Experimental Design and Bioinformatics, Warsaw University of Life Sciences – SGGW*
Nowoursynowska Street 166, 02-787 Warsaw, Poland
(phone: +48-22-59-32727; fax: +48-22-59-32722)

[3]*Faculty of Horticulture, Biotechnology and Landscape Architecture, Laboratory of Evaluation and Assessment of Natural Resources, Warsaw University of Life Sciences – SGGW*
Nowoursynowska Street 166, 02-787 Warsaw, Poland
(phone: +48-22-59-32224; fax: +48-22-59-32227)

**Corresponding author*
e-mail: aschwerk@yahoo.de

(Received 13th Jun 2018; accepted 2nd Aug 2018)

Abstract. Manor parks established on oak-hornbeam habitat (*Tilio-Carpinetum*) are very characteristic elements of agricultural landscapes in Poland. In light of the loss of old growth oak-hornbeam forests because of deforestations, these habitats have the potential to become refuges. Thus, the aim of the study was to determine the influence of surroundings landscape structure on the development of the plant species composition on the herb layer in selected manor parks in the southern part of Poland. The study was conducted in 60 manor parks located in southern Poland characterized by differences in land use of the surroundings. Manor parks located close to forest were characterized by higher numbers of forest plant species in the herb layer. Both the percentage share of the *Tilio-Carpinetum* species and the percentage share of ancient forest species were increased in parks adjacent to forests. However, forest size seems to be of minor importance. Indicator plant species for manor parks adjacent to villages as well as indicator species for parks nearby forests could be identified. The results of the study are important for landscape planners and landscape ecologists in order to formulate directions of shaping and management of rural landscapes including manor parks.
Keywords: *Forest species, Ancient species, Tilio-Carpinetum, Landscape ecology, Poland*

Introduction

The impact of anthropogenic and natural factors is important for shaping the species composition of the forest herbaceous layer (Verheyen et al., 2003; Hale et al., 2006; Verheyen et al., 2012; Hofmeister et al., 2013). The diversity of the forest herb layer constitutes the largest fraction of the total plant diversity in deciduous forests (Gilliam, 2007; Alberdi et al., 2010). The distribution of forest species in human-dominated forests and agroforests varies as a function of the species traits that are vulnerable to disturbance and fragmentation (Carreneo-Rocabado et al., 2012). Characteristics of a habitat patch and its surrounding matrix and the degree of fragmentation are important determinants of plant species composition (Honnay et al., 2005; Moxham and Turner,

http://www.aloki.hu ● ISSN 1589 1623 (Print) ● ISSN 1785 0037 (Online)
DOI: http://dx.doi.org/10.15666/aeer/1605_64836497
© 2018, ALÖKI Kft., Budapest, Hungary

2011; Aggemyr and Cousins, 2012; Amici et al., 2015, Ojoyi et al., 2015; Pao and Upadhaya, 2017). Therefore, the floristic diversity and forest plant species composition of isolated patches is limited (Ewers and Didham, 2006; Tscharntke et al., 2012), based on the relative importance of the landscape and habitat factors.

Herbaceous plants are very dynamic so they are suitable indicators of changes of habitats in short time (Alberdi et al., 2010; Del Vecchio et al., 2016). Among them, a special role can be attached to ancient forest plant species. Ancient forest plant species are plants that are characteristic of ancient woodlands (older than 200 years) and old woodlands (200-100 years old) according to Wulf (2003). The list of ancient forests indicator species for Central and Western Europe was proposed by Hermy et al. (1999). Then, for Polish conditions it was complemented by Dzwonko and Loster (2001). In this context the role of the forest islands in the agricultural landscape was determined as the places of forest flora refuges (Wojcik, 1991; Dzwonko and Loster, 1992; Dzwonko and Gawroński, 1994; Braun and Koch, 2016). Ancient plants are proper indicators of long term continuity of the habitat (Hermy et al., 1999; Nordén and Appelqvist, 2001; Verheyen et al., 2003; Kolb and Diekmann, 2004; Stefanska-Krzaczek et al., 2016; Lalechère et al., 2017; Webb and Goodenough, 2018). The degree of naturalness of forests is one of the attributes for the assessment of the ecological stability of forests (Macků, 2012).

Many of the vascular species that grow in these forests have slow dispersal mechanisms and/or rely heavily upon the forest structure for survival (Webb and Goodenough, 2018). Secondary forests located close to an ancient forest are often distinguished by a high abundance of "ancient forest species" (Brunet and von Oheimb, 1998; Hermy and Verheyen, 2007), despite colonization by "ancient forest species" (Hermy et al., 1999) demands a lot of time (e.g. Dupouey et al., 2002). Mixed-oak–hornbeam forests are one of the potentially dominant forest vegetations in Eastern Europe (Matuszkiewicz et al., 2013). Mixed forests provide with habitat for a rich biodiversity and their decline in abundance has endangered a large number of species (Berg et al., 1994). The herbaceous understory plays a key role during restoration of the biodiversity of forest plantations (Gilliam, 2007). Agricultural landscape fragmentation in central Europe has resulted in decreased species richness in the forest herbaceous layer (Honnay et al., 1999; Mortelliti et al., 2010). Deforestation and forest management have resulted in a negligible share of the oak–hornbeam forests in the total forest area in Poland (Matuszkiewicz et al., 2013). Manor parks are an essential part of the Polish countryside. Most of the manor parks were established on oak-hornbeam habitat (*Tilio-Carpinetum*), and they were abandoned and uncultivated after World War II (Fornal-Pieniak and Wysocki, 2009b). In light of the loss of old growth oak-hornbeam forests because of deforestations, manor park habitats have the potential to become refuges (Glendell and Vaughan, 2002; Jonsell, 2012; Liira et al., 2012). Forest plants of oak-hornbeam forest (*Tilio-Carpinetum*) are very important for keeping the biodiversity of rural landscapes.

Therefore, it is important to analyze the impact of the surroundings forest landscape structure on the flora of the manor parks. However, studies dealing with the effects of the surroundings landscape structure on the development of the composition of plant species in herbaceous layer in manor parks in Poland are rare (Lirra et al., 2008; Fornal-Pieniak and Wysocki, 2009a).

The aim of the study was to determine the influence of surroundings landscape structure on the development of the species composition of the herbaceous layer in four

http://www.aloki.hu ● ISSN 1589 1623 (Print) ● ISSN 1785 0037 (Online)
DOI: http://dx.doi.org/10.15666/aeer/1605_64836497
© 2018, ALÖKI Kft., Budapest, Hungary

types of manor parks differing with respect to their surrounding in the Sandomierska Basin Region in Poland. It was tested, (1) whether the neighborhood of a forest influences the species composition and frequency of forest species in the herbaceous layer of manor parks, and (2) if there are existing characteristic / diagnostic species for different types of manor parks depending on the surroundings landscape structures. Since many forest species are sensitive to habitat fragmentation (Brunet et al., 2011), a special focus was set on forest plants from *Tilio-Carpinetum* as well as ancient forest plants.

Materials and Methods

Study area and field methods

The study was carried out in the area of the Sandomierz Basin (*Fig. 1*). 166 manor parks of the landscape style registered as historical monuments are located in this area. According to geobotanical division (Lencerewicz and Kondracki, 1959) the Sandomierz Basin belongs to the South Uplands area with a surface of about 14.5 thousand km^2. It is situated between the Carpathian foothills, Miechów Upland, Sandomierz Upland and Roztocze and is a foreground of Carpathians (Starkel, 1999). Potential vegetation is represented by a mosaic of diverse habitats in the area of the Sandomierz Basin. The largest area of the Sadomierska Basin is occupied by forests represented by: *Quercoroboris Pinetum*, *Serratulo-Pinetum*, *Tilio-Carpinetum*, *Lecobryo-Pinetum*, *Cladonio-Pinetum* and *Molinio-Pinetum*. Along watercourses especially the Vistula, San and Wisłoka habitats are lowland riverine riparian elm-ash forests (*Ficario-Ulmetum minoris*).

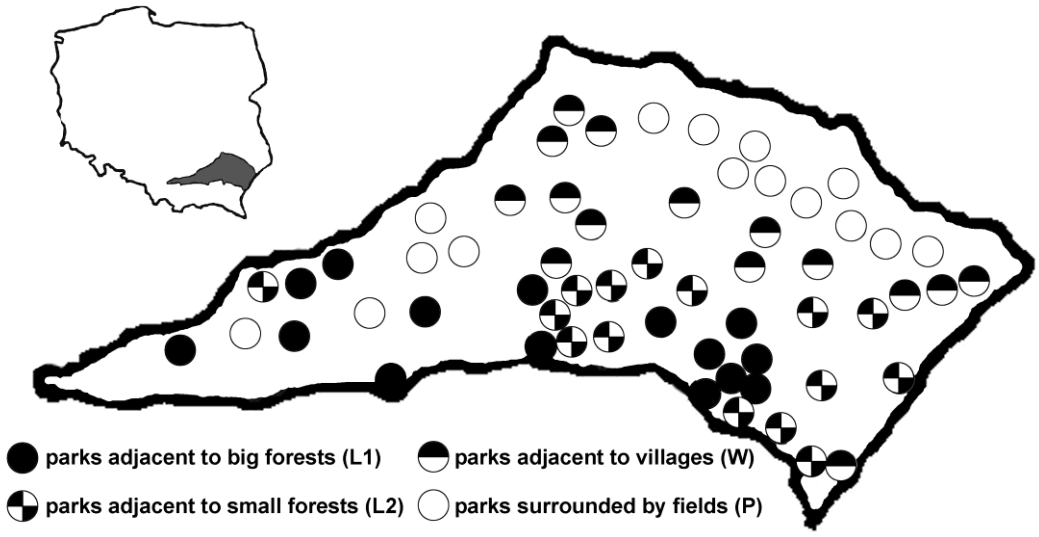

Figure 1. *Location of the Sandomierz Basin area in Poland and location of the manor parks in the area*

The manor parks were subjected to the following evaluation criteria: the same type of habitat, size of afforestrated areas, and landscape structures in the surrounding (size of the forests, fields, villages). Based on these criteria, 60 manor parks located in the

http://www.aloki.hu ● ISSN 1589 1623 (Print) ● ISSN 1785 0037 (Online)
DOI: http://dx.doi.org/10.15666/aeer/1605_64836497
© 2018, ALÖKI Kft., Budapest, Hungary

Sandomierz Basin with 3 to 5 ha of afforestrated areas were selected for the study (*Fig. 1*). All these manor parks were established on oak-hornbeam habitat. Based on their specific localization the study objects were divided into four types of manor parks: 15 parks adjacent to big forests (L1), 15 parks adjacent to small forests (L2), 15 parks surrounded by fields (P), and 15 parks adjacent to villages (W). The surrounding forests were growing on the same oak-hornbeam habitats as the manor parks. As big forests (L1) those with a size of 15 to 20 ha were defined and small forests (L2) had a size range from 2 to 4 ha. The studied parks surrounded by fields were located in a distance of at least 2 km from the nearest villages.

In the herbaceous layer of each manor park 10 phytosociological records using the Braun-Blanquet method (1951) were carried out during the spring and summer time in the years 2016-2017. Syntaxonomic division was made according to Matuszkiewicz (2008) and plant species were named according to Mirek et. al. (1995). Existing plant species were grouped according to naturalness of vegetation (Keddy, 2016). The degree of naturalness is often assessed by the similarity of a biocoenosis to the presumed natural state before it was affected by man (Reif and Walentowski, 2008). We distinguished according to Matuszkiewicz (2008) between plants of natural (forest plants), seminatural (meadows, pasture plants), and synantropical (segetal and ruderal plants) vegetation as well as companion species.

Statistical methods

In order to determine the influence of the surroundings on the species composition in the manor parks, it was first compared the share of the distinguished species groups based on the criteria of naturalness of vegetation (Keddy, 2016) between the four types of parks. It was calculated the percentage of species of the relevant groups on the whole species number for each plot (phytosociological record). The resulting values were averaged for each park type.

Next, it was studied a more detailed impact on the forest species in order to determine the degree of long term continuity of the habitat. For that purpose the influence of the park's neighborhood on two parameters was analyzed: the percentage share of *Tilio-Carpinetum* class species and the percentage share of ancient forest species on the whole number of species in the individual phytosociological records. The average share of both parameters and the significance of their differences for parks and park types was studied by two identical analyses, using a Generalized Linear Model with two categorical factors in a nested design. The main factor was park surrounding type (four types) and the nested factor was park (60 parks, 15 for each type). Each single record was a repetition (10 per each park). Because share of species (dependent variable) is a typical ratio variable (varying between 0 and 1) the beta distribution was chosen as model distribution and as a link function identity was selected (Song and Tan, 2000). Based on the adopted model, it is possible to assess not only the differences in the average share of forest species depending on the character of the park's neighborhood, but also to determine the magnitude of this difference to the variability between individual parks (of the same type). The statistical analyses were carried out using STATISTICA v. 10.5.

In order to detect characteristic / diagnostic species whose presence or absence depends on the forms of land use in the surrounding of the parks, the Classification And Regression Trees (CART) method was used (Breiman et al., 1984). As dependent variable park type was chosen. This is a categorical (qualitative) variable, determining a

http://www.aloki.hu ● ISSN 1589 1623 (Print) ● ISSN 1785 0037 (Online)
DOI: http://dx.doi.org/10.15666/aeer/1605_64836497
© 2018, ALÖKI Kft., Budapest, Hungary

classification algorithm of CART. As independent variable the abundances of each species denominated in Braun-Blanquet scale were used. Single phytosociological records were used as repetitions, without considering their origin from a specific park, but considering their origin from a given group of parks.

Since the abundances were encoded as categorical variables, it was possible to evaluate the quality of the analysis. Splits consistent with an abundance gradient, i.e. lower values for one side compared to the other one, should be interpreted as real effect, whereas those with mixed low and high values for both sides should be interpreted as errors. Additionally, it was analyzed the secondary splits (near optimal variables) in order to detect all diagnostic species. Finally, it was checked the allocation of the records to the end nodes of the CART tree in order to discover any regularities. It especially focused on records causing inhomogeneities in the end nodes.

The CART analysis were carried out using R 3.4.1 (R Development Core Team, 2013) with *rpart* and *rpart.plot* libraries.

Results

In the herb layer of parks adjacent to the forest (L1 and L2 types) the forest species (natural vegetation) distinctly dominated, constituting approximately 85% of all species supplemented with associated companion species (*Fig. 2*). Other species representing seminatural and synantropical vegetation occurred only occasionally. In parks neighboring with villages or surrounded only by crop fields, an increase share of species which are no indicators of long term continuity of the habitat was noticeable, i.e. species representing synantropical and seminatural vegetation, which represented 20% and 10% of the species composition in village-adjacent parks (W) and 21% and 9% of the species composition in field-adjacent parks (P) respectively.

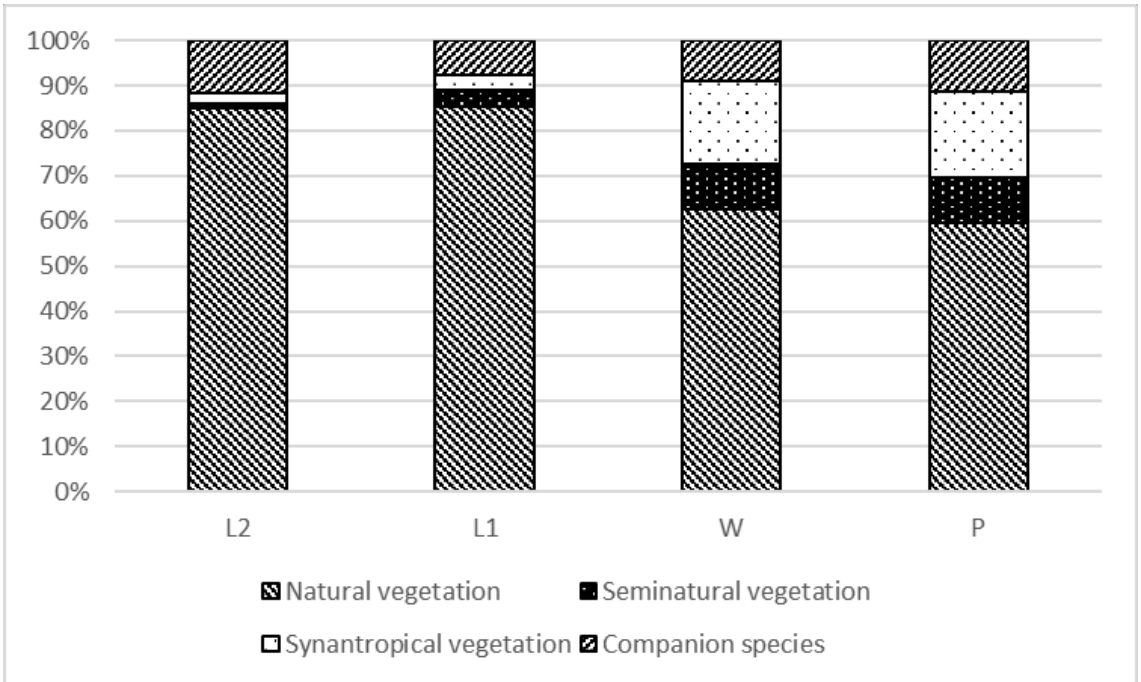

Figure 2. *Mean percentage share of species belonging to different types of naturalness of vegetation for the four types of manor parks (L1, L2, W, P)*

http://www.aloki.hu ● ISSN 1589 1623 (Print) ● ISSN 1785 0037 (Online)
DOI: http://dx.doi.org/10.15666/aeer/1605_64836497
© 2018, ALÖKI Kft., Budapest, Hungary

The mean share of *Tilio-Carpinetum* species differed significantly ($p<0.001$) by type of park neighborhood (*Fig. 3*, *Table 1*). In forest-adjacent parks it reached 78% (L1) and 75% (L2) but in village-adjacent parks only 50% and in field-adjacent parks 47%. The mean share of *Tilio-Carpinetum* species for single parks varied ($p<0.001$). However, for both types of forest-adjacent parks it fluctuated between 60% and 90 % and for parks of type W and P between 40% and 60%.

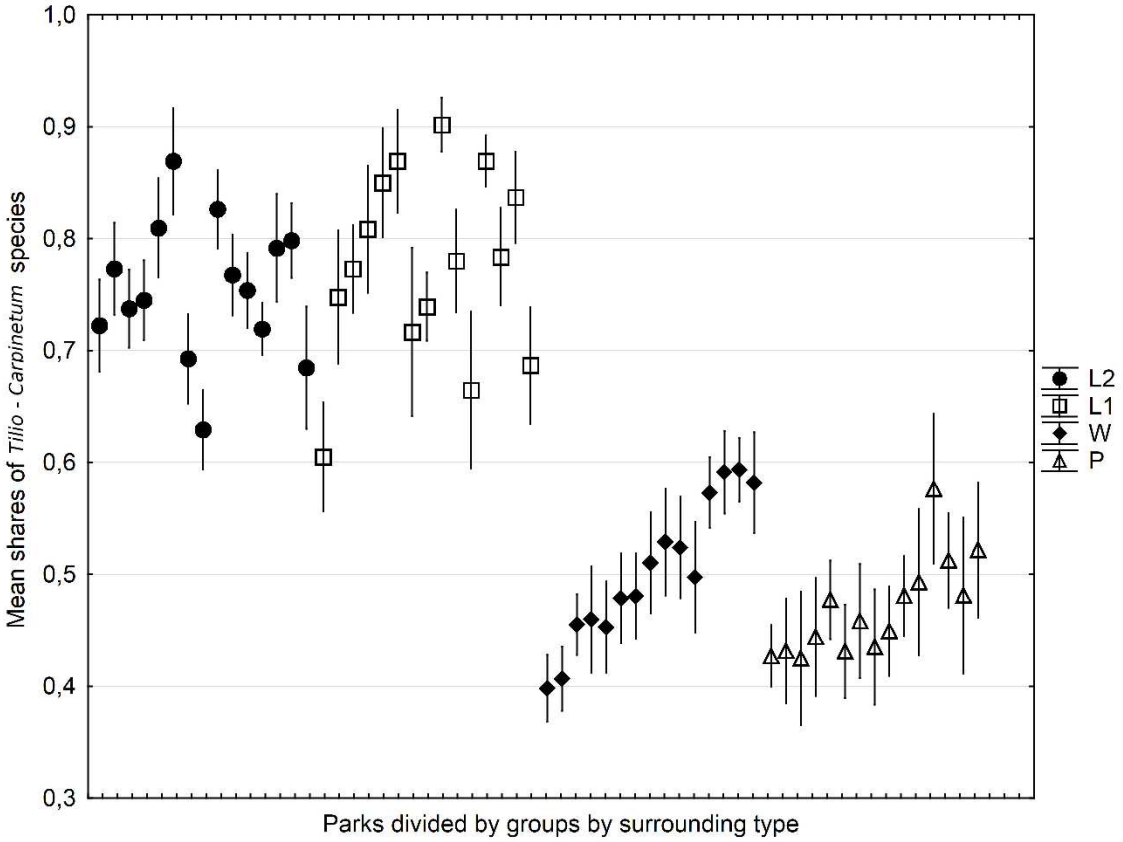

Figure 3. *Mean percentage shares of Tilio-Carpinetum species per record in parks apportioned to type of surroundings (L2, L1, W, P). Bars show 95% confidence intervals*

Table 1. *GLM results of the effects of surrounding type and park on mean shares of Tilio-Carpinetum species per record*

Factor	SS	df	MS	F	p
Intercept	234.9391	1	234.9391	58509.41	0.00
Surrounding type	11.8540	3	3.9513	984.05	0.00
Park	2.3582	56	0.0421	10.49	0.00
Error	2.1683	540	0.0040	-	-

The share of ancient forest species showed a pattern similar to the shares of the *Tilio-Carpinetum* species (*Fig. 4*, *Table 2*). It was also significantly ($p<0.001$) higher for forest-adjacent parks (63% for L1 and 70% for L2) than others (38% for W and P). Similarly, we were able to observe a clear border between the average shares in

http://www.aloki.hu ● ISSN 1589 1623 (Print) ● ISSN 1785 0037 (Online)
DOI: http://dx.doi.org/10.15666/aeer/1605_64836497
© 2018, ALÖKI Kft., Budapest, Hungary

individual parks. On all forest-adjacent parks it was above 42% and in the other below 42%. The mean share of species for single parks varied too ($p<0.001$).

Two of the first splits of the CART analysis (*Fig. 5*) divided most of the records into more or less homogenous groups. An almost homogenous group containing 93 (out of 150) records from parks adjacent to villages (type W) with a small infusion of other types was extracted by the first node. The division criterion was the presence of *Oxalis fontana* (common yellow woodsorrel). The near optimal variables were the presence of *Geranium sylvaticum* (wood cranesbill), *Convolvulus arvensis* (field bindweed), and *Chelidonium majus* (greater celendine) and the absence of *Melica nutans* (mountain melick). The power of the alternative variables was not distinctly lower than that of the main variable. The second node was split on two descendants. The left (node 4) contained most of records from parks adjacent to forests (type L1 and L2), and the right (node 5) encompassed almost all records from parks surrounded only by agricultural land (type P). The left node (node 4) was distinguished by the presence of *Melica nutans*. The alternative criteria were the absence of *Geranium sylvaticum*, *Allium ursinum* (buckrams), *Chelidonium majus* and *Lysimachia nummularia* (moneywort). Practically, after the two first splits we obtained three groupings of nodes that correctly classified most of the records, but nodes 4 and 5 were not homogenous. The further splits represented purging efforts. Twenty-five type W parks were separated from node 4 based on the presence of *Convolvulus arvensis*, a higher abundance of *Urtica dioica* (common nettle) (more than 1 on the Braun-Blanquet scale) and a lower abundance of *Lathyrus vernus* (spring vetchling) as criteria.

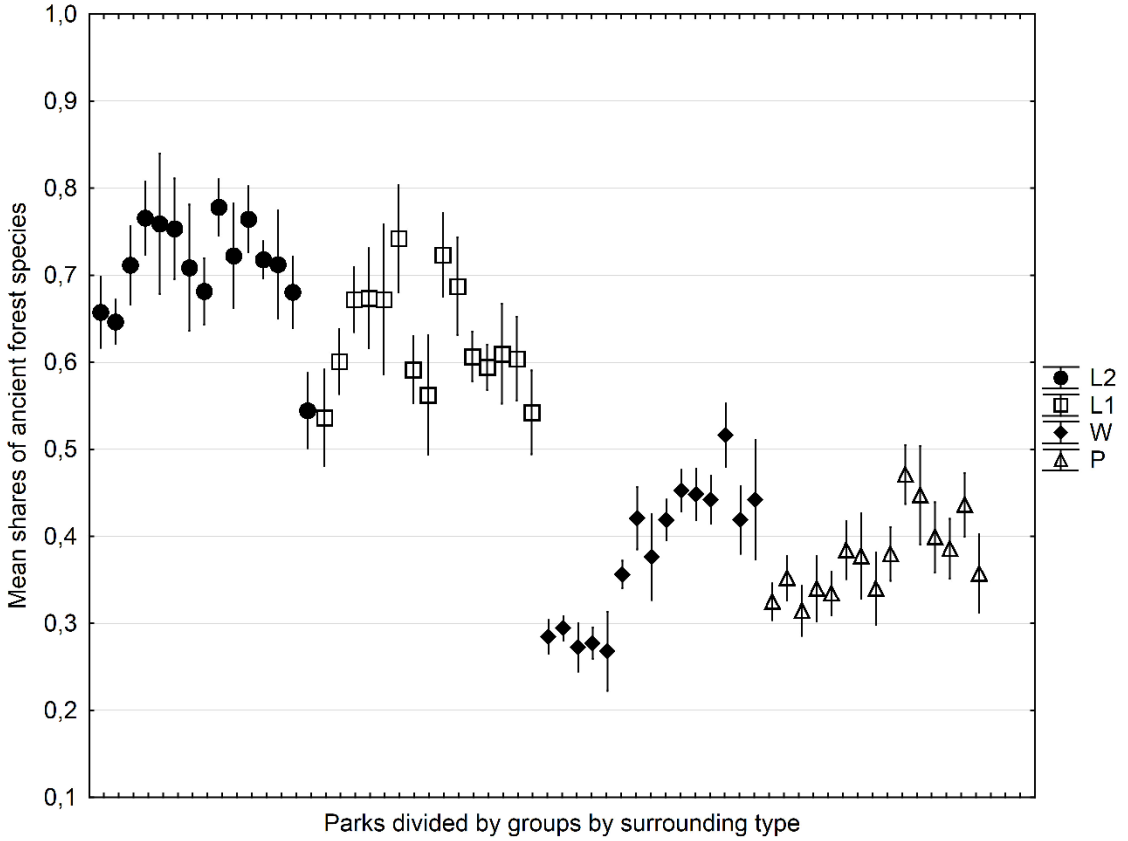

Figure 4. *Mean shares of ancient forest species per record in parks apportioned to type of surroundings. Bars show 95% confidence intervals*

http://www.aloki.hu ● ISSN 1589 1623 (Print) ● ISSN 1785 0037 (Online)
DOI: http://dx.doi.org/10.15666/aeer/1605_64836497
© 2018, ALÖKI Kft., Budapest, Hungary

Table 2. *GLM results of the effects of surrounding type and park on mean shares of Tilio-Carpinetum species per record*

Factor	SS	df	MS	F	p
Intercept	163.8228	1	163.8228	43051.16	0.00
Surrounding type	13.0589	3	4.3530	1143.92	0.00
Park	2.2990	56	0.0411	10.7910.79	0.00
Error	2.0549	540	0.0038	-	-

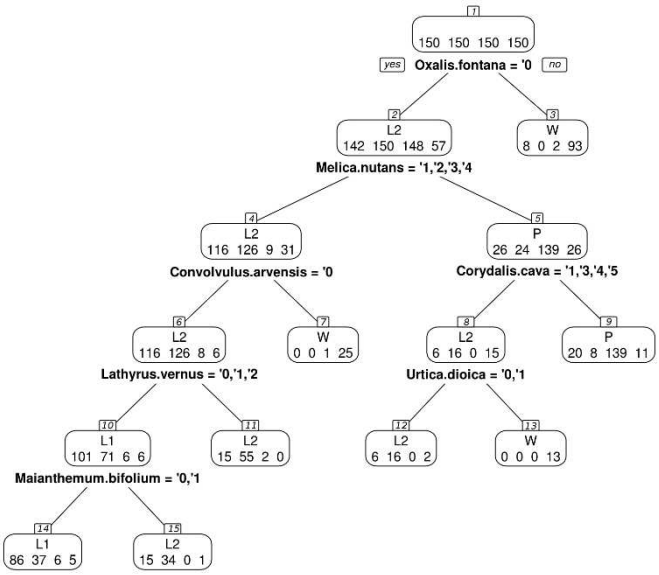

Figure 5. *CART tree. The little squares above the nodes contain the node numbers. The type of extracted records and the quantities of records of each type, from left: L1, L2 P and W, are plotted in the node. Under the nodes are the names of the species that provide the criterion for division and the respective abundances denominated in Braun-Blanquet scale for the left descendant node*

The CART analysis treated all records separately, but after the analysis, we checked the association between individual parks. We looked for patterns between records of type L1 and L2 from nodes 3 and 5 and between records of type P and W from node 4. Moreover, it was checked the association of records of type L1 and L2 with nodes 11, 14 and 15. In most cases, misclassification concerned single records from different parks, which could be considered as elements of statistical noise. Only two forest parks (L1, numbers 22 and 23) showed some distinctness. Most of the records were classified with W (in node 3) and P (in node 5) types.

Discussion

The study confirmed that the surroundings landscape structure influences the species composition and frequency of forest species in the herbaceous layer of manor parks (research question 1). Both the percentage share of *Tilio-Carpinetum* species and the percentage share of ancient forest species were increased in parks adjacent to forests. However, forest size seems to be of minor importance. Some species could be identified as characteristics for some of the studied park types (research question 2).

http://www.aloki.hu ● ISSN 1589 1623 (Print) ● ISSN 1785 0037 (Online)
DOI: http://dx.doi.org/10.15666/aeer/1605_64836497
© 2018, ALÖKI Kft., Budapest, Hungary

The results are in agreement with other studies, which show that different management and human activities modify the species composition (Jamoneau et al., 2011), also in manor parks. Studies have shown that rural areas surrounding the parks, such as fields and built-up areas, have an impact on the appearance of non-forest plant species. Changes in habitat conditions have a strong impact on the occurrence of many ruderal plant species (Gawenda-Kempczyńska et al., 2017). An increased number of grasses and synantropical plants was observed in manor parks located nearby fields and village. According to Dzwonko and Gawroński (1994) and Bossuyt (2001) forest patches are very important for forests and ancient plants colonization. Forests patches have also positive effects with respect to natural regeneration of the herbaceous layer (Hill and Curran, 2003). Authors like LaPaix and Freedman (2010) and Liira et al. (2012) argue that forest stands, as well as the studied parks adjacent to the forests, can be suitable habitats for some forest species.

Large patches may be more important for maintaining the stability of populations (Ewers and Didham, 2006; Økland et al., 2003; Honnay et al., 2005; Naaf and Kolk, 2015). According to Erikson (1996) many plants species characteristic for the herb layer of old forests have the ability to adapt to the new fragmented small and isolated forests in the agricultural landscape. However, the minimum size of forest islands in order to retain optimum conditions for forest species is an open question. Vestal and Heermans (1945) mention that the forest patches of an area of 1.6 ha and over retain forest plant species, but according to Levenson (1981) the critical value is 2.3 ha. Oostermeijer et al. (2003), stated that the reduction of the forest surface by fragmentation leads to reduction of the population of forest species. In addition, the size of the forest is obligatorily more important for plants that can grow only in forest communities (Kolb and Diekmann, 2004; Brunet et al. 2011). Higher species richness of plants was observed in bigger forest patches than in small ones (MacArthur and Wilson, 1967; Forman and Godron, 1986; Connor and McCoy, 1979, 2001; Saunders et al., 1991; Hill and Curran, 2001, 2003; Graae and Oakland, 2004). Some of the studied manor parks in the Sandomierz Basin area are adjacent to big forests, which might allow for a higher chance of the migration of forest plants into the parks. However, in this study we did not detect a clear influence of the size of the neighboring forests.

Size and management of the respective manor park is also of importance. A higher frequency and diversity of oak-hornbeam species in forests was observed in manor parks with a minimum area of 5 hectares (Fornal-Pieniak and Ollik, 2013). Studies by Fornal-Pieniak and Wysocki (2009a,b) on the vegetation of manor parks (2003-2007 and 2011-2012) allowed to confirm that mowing and the size of the forested timberland have an influence on the formation of the species composition of parks' undergrowth. In our study we observed a higher number of forest plants and ancient plants in manor parks, which were adjacent to forests. However, we analyzed only manor parks with afforestrated parts up to 5 ha. We can suppose that bigger afforestrated parts of manor parks could keep higher numbers of ancient and forest plant species. Yet, this is only an hypothesis which has to be verified by future research.

Another important factor affecting the number of forest species in the forest patches is their distance from forests with the same type of forest community (Dzwonko and Loster, 1988; Baker et al., 2013; Naaf and Kolk, 2015). Forest ecosystem fragmentation and habitat loss change spatial landscape features; consequently, fragmented and isolated habitats may vary more in terms of species composition than more connected habitats. The existence of forests adjacent to our studied manor parks facilitate the

http://www.aloki.hu ● ISSN 1589 1623 (Print) ● ISSN 1785 0037 (Online)
DOI: http://dx.doi.org/10.15666/aeer/1605_64836497
© 2018, ALÖKI Kft., Budapest, Hungary

colonization of forests plants in these objects. In the agricultural landscape many forest species can survive only due to the presence of small residues of formerly large forest complexes, because they are quite vulnerable to anthropogenic pressure caused by humans (Wójcik, 1991; Anderson et al., 2007). Many of the vascular species that grow in these forests have slow dispersal mechanisms and/or rely heavily upon the forest structure for survival. Protection of these forest settings is essential for keeping biodiversity of rural environments (Webb and Goodenough, 2018).

Forest communities have a vertical structure which determines ecological conditions specific to each type of forest for plant species in the herbaceous layer. The CART analysis detected *Oxalis fontana* as the indicator plant species in parks adjacent to villages, where it was observed as a component of human activities or in their immediate surroundings. Alien species are indicators in a given area whose presence is due to human pressure, regardless of whether these activities are intentional or unintentional (Pysek et al., 2004). *Oxalis fontana* is an alien species which is classified as an agriophyte. Agriophytes are neophytes that penetrate natural habitats (Zając at el., 1998). According to Dajdak and Wuczyński (2008), Rzymowska and Skrajna (2015) and Kolářová et al. (2017) *Oxalis fontana* was found more frequently in cultivated fields (segetal habitats). In our study, *Oxalis fontana* occurred in manor parks adjacent to villages but also in two parks adjacent to forest (L1 numbers 22 and 23). However, these two parks were located near to small forests (approximately 3 ha) with high anthropogenic pressure. As source of the anthropogenic pressure the respective village located behind the forest, as seen from the park, may be assumed. Many footpaths were discovered, which were caused by local people crossing the forest when walking to the village. Therefore, *Oxalis fontana* was very common in two types of manor parks (W, P). According to Chmura (2004) and Kolářová et al. (2017) *Oxalis fontana* mostly occurs close to roads, footpaths and forest margins. Other indicators of anthropogenic pressure in our study were *Geranium sylvaticum*, *Convolvulus arvensis*, *Chelidonium majus* and *Lysimachia nummularia*.

Parks which are adjacent to forests were characterized by a higher share of forest and ancient plant species than the other manor parks. The CART method identified *Melica nutans* as indicator species for manor parks adjacent to forests (L1, L2). According to Zielewicz and Kozłowski (2011) the stand structure constitutes important ecological factors, especially the amount of light reaching to the bottom of the forest determines the changing participation of grass species. Grass species need large amounts of solar energy for initiation of their development. At the beginning of spring a higher proportion of coverage with grasses was observed, followed by a decrease with increasing density of tree canopies. Such conditions allow the occurrence of *Melica nutans* in the forests (Slezák et al., 2011). In our study we did not analyze the light factor and density of tree canopies in the manor parks, but it can be assumed that proper ecological conditions allowed the growing of Melica nutans in their herbaceous layer. Another species associated with forest in our study was *Lathyrus vernus*. Distinguishing the species composition of parks adjacent to larger (L1) and smaller (L2) forest was impossible. The splits after node 6 (group of most of L1 and L2 records) reflected the character of the park habitat (humidity or fertility) rather than the type of surroundings. Thus, it can be assumed that some species (e.g. *Melica nutans*) require natural forests in the surroundings and do not survive in isolated manor parks.

The results indicated that manor parks are important as “forest islands” in the agriculture landscape, because they contain ancient and forest plant species typical for

http://www.aloki.hu ● ISSN 1589 1623 (Print) ● ISSN 1785 0037 (Online)
DOI: http://dx.doi.org/10.15666/aeer/1605_64836497
© 2018, ALÖKI Kft., Budapest, Hungary

Tilio-Carpinetum habitats. Because of their values, manor parks should be considered as important refuges in the ecological structure of the Sandomierz Basin. To formulate directions of shaping and management of rural landscapes including manor parks is a challenging task for landscape planners and landscape ecologists. In this context it is also recommended to monitor the impact of land-use practices, which are of particular importance with regard to biodiversity hotspots (Braun and Koch, 2016; Alphan, 2017) as *Tilio-Carpinetum* forests and manor parks.

Conclusions

Manor parks constitute a suitable habitat for survival of many forest species characteristic for oak-hornbeam forests and therefore are important ecological islands in the rural landscape. The surrounding of the parks decides to a large extent about the herb layer composition. Isolated parks are settled by a distinct lower number of forest species and numerous synantropical species. Some species (*Melica nutans*) cannot survive in isolated parks and occur only in those close to natural forest. However, forest size seems to be of minor importance. The results of the study are important for landscape planners and landscape ecologists in order to formulate directions of shaping and management of rural landscapes including manor parks.

Acknowledgements. The authors are grateful to Professor Czesław Wysocki for his valuable methodical remarks. This paper is communication no. 497 of the Laboratory of Evaluation and Assessment of Natural Resources, Warsaw University of Life Sciences – SGGW.

REFERENCES

[1] Aggemyr, E., Cousins, S. A. O. (2012): Landscape structure and land use history influence changes in island plant composition after 100 years. – Journal of Biogeography 39: 1645-1656.

[2] Alberdi, I. S., Condés, S., Martínez-Millán, J. (2010): Review of monitoring and assessing ground vegetation biodiversity in national forest inventories. – Environmental Monitoring and Assessment 164: 649–676.

[3] Alphan, H. (2017): Analysis of landscape changes as an indicator for environmental monitoring. – Environmental Monitoring and Assessment 189: 24.

[4] Amici, V., Rocchini, D., Filibeck, G., Bacaro, G., Santi, E., Geri, F., Landi, S., Scoppola, A., Chiarucci, A. (2015): Landscape structure effects on forest plant diversity of local scale: Exploring the role of spatial extent. – Ecological Complexity 21: 44-52.

[5] Anderson, J., Rowcliffe, J., M., Cowlishaw, G. (2007): Does the matrix matter? A forest primate in a complex agricultural landscape. – Biological Conservation 135: 212-222.

[6] Baker, S. C., Spies, T. A., Wardlaw, T. J., Balmer, J., Franlin, J. F., Jordan, G. J. (2013): The harvested side of edges: Effect of retained forests on the re-establishment of biodiversity in adjacent harvested areas. – Forest Ecology and Management 302: 107-121.

[7] Berg, A., Ehnstrom, B., Gustafsson, L., Hallingback, T., Jonsell, M., Weslien, J. (1994): Threatened plant, animal, and fungus species in Swedish forests: distribution and habitat associations. – Conservation Biology 8: 718–731.

[8] Bossuyt, B. (2001): Plant species and soil dynamics across ancient-recent forest ecotones: consequences for ecological restoration. – Ph.D. thesis, Catholic University of Leuven, Leuven.

http://www.aloki.hu ● ISSN 1589 1623 (Print) ● ISSN 1785 0037 (Online)
DOI: http://dx.doi.org/10.15666/aeer/1605_64836497
© 2018, ALÖKI Kft., Budapest, Hungary

[9] Braun-Blanquet, J. (1951): Pflanzensoziologie, 2 Aufl. – Springer Verlag, Wien.
[10] Braun, A. Ch., Koch, B. (2016): Estimating impacts of plantation forestry on plant biodiversity in southern Chile—a spatially explicit modelling approach. – Environmental Monitoring and Assessment 188: 564.
[11] Breiman, L., Friedman, J. H., Olshen, R. A., Stone, C. J., (1984): Classification and Regression Trees. – Chapman & Hall, Boca Raton.
[12] Brunet, J., von Oheimb, G. (1998): Migration of vascular plants to secondary woodlands in southern Sweden. – Journal of Ecology 86: 429-438.
[13] Brunet, J., Valtinat, K., Mayr, M. L., Felton, A., Lindbladh, M., Bruun, H. H. (2011): Understory succession in post-agricultural oak forests: Habitat fragmentation affects forest specialists and generalists differently. – Forest Ecology and Management 262: 1863–1871.
[14] Chmura, D. (2004): Penetration and naturalisation of invasive alien plant species (neophytes) in woodlands of the Silesian Uplands (Southern Poland). – Nature Conservation 60: 3-11.
[15] Carreno-Rocabado, G., Pena-Claros, M., Bongers, F., Alarcon, A., Licona, J., Poorter L. (2012): Effects of disturbance intensity on species and functional diversity in a tropical forest. – Journal of Ecology 100: 1453-1463.
[16] Connor, E. F., McCoy, E. D. (1979): The statistics of the species area relationship. – The American Naturalist 113: 791-833.
[17] Connor, E. F., McCoy, E. D. (2001): Species-area relationships. – In: Levin, S. A. (ed.) Encyclopedia of Biodiversity 5, Academic Press, New York.
[18] Dajdak, Z., Wuczyński, A. (2008): Alien plants in field margins and fields of southwestern Poland. – Biodiversity Research and Conservation 9-10, 19-33.
[19] Del Vecchio, S., Slaviero, A., Fantinato, E., Buffa G. (2016): The use of plant community attributes to detect habitat quality in coastal environments. – AoB Plants 8: 1-14.
[20] Dupouey, J. L., Dambrine, E., Laffite, J. D., Moares, C. (2002): Irreversible impact of past land use on forest soils and biodiversity. – Ecology 83: 2978-2984.
[21] Dzwonko, Z., Loster, S. (2001): Wskaźnikowe gatunki roślin starych lasów i ich znaczenie dla ochrony przyrody i kartografii roślinności. Typologia zbiorowisk i kartografia roślinności w Polsce. – Prace Geograficzne 178: 119–132.
[22] Dzwonko, Z., Loster, S. (1988): The number and distribution of vascular plant species in islands forest communities in the norther part the west Carpathian Foothills. – Folia Geobotanica et Phytotaxonomica 23: 1-16.
[23] Dzwonko, Z., Gawroński, S. (1994): The role woodlands fragments, soil types, and dominant species in secondary succession on the western Carpatian foothills. – Vegetatio 111: 149-160.
[24] Dzwonko, Z., Loster, S. (1992): Species richness and seed dispersal to secondary woods in southern Poland. – Journal of Biogeography 19: 195-204.
[25] Eriksson, O. (1996): Regional dynamics of plants: a review of evidence of remnant, source-sink, and metapopulations. – Oikos 77: 248-258.
[26] Ewers, R. M., Didham, R. K. (2006): Confounding factors in the detection of species responses to habitat fragmentation. – Biological Reviews 81: 117-142.
[27] Forman, R. T. T., Godron, M. (1986): Landscape Ecology. J. – Wiley and Sons, New York.
[28] Fornal-Pieniak, B., Ollik, M. (2013): Diversity of flora in the undergrowth of park afforestations, rural plantings and oak-hornbeam forests. – Folia Forestalia Polonica A 55: 132–136.
[29] Fornal-Pieniak, B., Wysocki, Cz. (2009a): Typy parków wiejskich w krajobrazie rolniczym na przykładzie Krainy Kotlina Sandomierska. – Woda-Środowisko-Obszary Wiejskie 9: 51-57.

http://www.aloki.hu ● ISSN 1589 1623 (Print) ● ISSN 1785 0037 (Online)
DOI: http://dx.doi.org/10.15666/aeer/1605_64836497
© 2018, ALÖKI Kft., Budapest, Hungary

[30] Fornal-Pieniak, B., Wysocki, Cz. (2009b): Diversity of ancient forest plant species in country parks. – Annals of Warsaw University of Life Sciences - SGGW, Horticulture and Landscape Architecture 30: 201-205.
[31] Gawenda-Kempczyńska, D., Iwona Paszek, I., Załuski, T. (2017): Regeneration of vegetation in manor park in Laskowice (Dąbrowa Forest District). – Ecological Questions 27: 39-52.
[32] Gilliam, F. S. (2007): The ecological significance of the herbaceous layer in temperate forest ecosystems. – Bioscience 57: 845–858.
[33] Glendell, M.,Vaughan, N. (2002): Foraging activity of bats in historic landscape parks in relation to habitat composition and park management. – Animal Conservation 5: 309–316.
[34] Graae, B. J., Oakland, R. H. (2004): Influence of historical, geographical and environmental variables on understory composition and richness in Danish forest. – Journal of Vegetation Science 15: 465-474.
[35] Hale, C. M., Frelich, L. E., Reich, P. B. (2006): Changes in hardwood forest understorey communities in response to European earthworm invasions. – Ecology 87: 1637-1649.
[36] Hermy, M., Verheyen, K. (2007): Legacies of the past in the present-day forest biodiversity: a review of past land-use effects on forest plant species composition and diversity. – Ecological Research 22: 361-371.
[37] Hermy, M., Honnay, O., Firbank, L., Grashof-Bokdam, C., Lawesson, J. E. (1999): An ecological comparison between ancient and other forest plant species of Europe and the implications for forest conservation. – Biological Conservation 91: 9–22.
[38] Hill, J. L., Curran, P. J. (2001): Species composition in fragmented forest: conservation implications of changing forest area. – Applied Geography 21: 157-174.
[39] Hill, J. L., Curran, P. J. (2003): Area, shape, and isolation of tropical forest fragments: effects on tree species diversity and implications for conservations. – Journal of Biogeography 30: 1391-1403.
[40] Hofmeister, J., Hosek, J., Brabec, M., Hédl, R., Modry, M. (2013): Strong influence of long-distance edge effect on herb-layer vegetation In forest fragments in an agricultural landscape. – Perspectives in Plant Ecology, Evolution and Systematics 15: 293– 303.
[41] Honnay, O., Hermy, M., Coppin, P. (1999): Effects of area, age and diversity of forest patches in Belgium on plant species richness, and implications for conservation and reforestation. – Biological Conservation 87: 73-84.
[42] Honnay, O., Jacquemyn, H., Bossuyt, B., Hermy, M. (2005): Forest fragmentation effects on patch occupancy and population viability of herbaceous plant species. – New Phytosociologist 166: 723-736.
[43] Jamoneau, A., Sonnier, G., Chabrerie, O., Closset-Kopp, D., Saguez, R., Gallet-Moron, E., Decocq, G. (2011): Drivers of plant species assemblages in forest patches among contrasted dynamic agricultural landscapes. – Journal of Ecology 99: 1152–1161.
[44] Jonsell, M. (2012): Old park trees as habitat for saproxylic beetle species. – Biodiversity and Conservation 2: 619–642.
[45] Keddy, P. A. (2016): Plant ecology. Origins. Processes. Consequences. – Cambrige University Press, Cambridge.
[46] Kolářová M., Tyšer, L., Krähmer, H. (2017): Occurrence of neophytes in agrophytocoenoses – field survey in the Czech Rebublic. – Acta Universitatis Agriculturae et Silviculturae Mendelianae Brunensis 65: 661-668.
[47] Kolb, A., Diekmann, M. (2004): Effects of environment, habitat configuration, and forest continuity on the distribution of forest plant species. – Journal of Vegetation Science 15: 199-208.
[48] Lalechère, E., Jabot, F., Archaux, F., Deffuant, G. (2017): Non-equilibrium Plant metapopulation dynamics challenge the concept of ancient/recent forest species. – Ecological Modelling 366: 48–57.

http://www.aloki.hu ● ISSN 1589 1623 (Print) ● ISSN 1785 0037 (Online)
DOI: http://dx.doi.org/10.15666/aeer/1605_64836497
© 2018, ALÖKI Kft., Budapest, Hungary

[49] LaPaix, R., Freedman, B. (2010): Vegetation structure and composition within urban parks of Halifax Regional Municipality Nova Scotia Canada. – Landscape and Urban Planning 98: 124-135.
[50] Lencewicz, S., Kondracki, J. (1959): Geografia fizyczna Polski. – Wydawnictwo PWN, Warszawa.
[51] Levenson, J. B. (1981): Woodlots as biogeographic islands in south landscapes. – In: Burgess R. L., Sharpe D. M. (ed.) Forest island dynamics in man-dominated landscapes, Springer-Verlag, New York, Heidelberg, Berlin.
[52] Liira, J., Lõhmus, K., Tuisk, E. (2012): Old manor parks as potential habitats for forest flora in agricultural landscape of Estonia. – Biological Conservation 146: 144-154.
[53] Lirra, J., Schmidt, T., Aavik, T., Arens, P., Augenstein, J., Bailey, D., Billeter, R., Bukáček, R., Burel, F., De Blust, G., De Cock, R., Dirksen, J., Edwards, P. J., Hamerský, R., Herzog, F., Klotz, S., Kühn, I., Le Coeur, D., Miklová, P., Roubalova, M., Schweiger, O., Smulders, M. J. M., van Wingerden, W. K. R. E., Bugter, R., Zobel, M. (2008): Plant functional group composition and large scale species richness in European agricultural landscape. – Journal of Vegetation Science 19: 3-14.
[54] Macků, J. (2012): Methodology for establishing the degree of naturalness of forest stands. – Acta Universitatis Agriculturae et Silviculturae Menselianae Brunensis 5: 161-165.
[55] MacArthur, R. H., Wilson, E. D. (1967). The theory of islands biogeography. – Princeton Univ. Press, Princeton.
[56] Matuszkiewicz, W. (2008): Przewodnik do oznaczania zbiorowisko roślinnych Polski. – Wydawnictwo Naukowe PWN, Warszawa.
[57] Matuszkiewicz, J., M., Kowalska, A., Solon, J., Degórski, M., Kozłowska, A., Roo-Zielińska, E., Zawiska, I., Wolski, J. (2013): Long-term evolution models of post-agricultural forests. – IGiPZ PAN, Warsaw.
[58] Mirek, Z., Zając, M., Zając, A., Piękoś-Mirkowa, H. (1995): Vascular plants of Poland. A checklist. – W. Szafer Institue of Botany, Polish Academy of Sciences, Cracow.
[59] Mortelliti, A., Amori G., L. Boitani L. (2010): The role of habitat quality in fragmented landscapes: a conceptual overview and prospectus for future research. – Oecologia 163: 535-547.
[60] Moxham, C., Turner, V. (2011): The effect of fragmentation on the threatened plant community Coastal Moonah Woodland in Victoria, Australia. – Urban Ecosystems 14: 569-593.
[61] Naff, T., Kolk, J. (2015): Colonization credit of post-agricultural forest patches in NE Germany. – Biological Conservation 182: 155-163.
[62] Nordén, B., Appelqvist, T. (2001): Conceptual problems of ecological continuity and its bioindicators. – Biodiversity Conservation 10: 779-791.
[63] Ojoyi, M. Mutanga, O., Odindi, J. Aynekulu E., Abdel Rahman, E. (2015): The effect of forest fragmentation on tree species abundance and diversity in the eastern Arc Mountains of Tanzania. – Applied Ecology and Environmental Research 13: 307-324.
[64] Oostermeijer, J. G. B., Luijten, S. H., den Nijs, J. C. M. (2003): Integrating demographic and genetic approaches in plant conservation. – Biological Conservation 113: 389-398.
[65] Ókland, R. H., Rydgren, K., Ókland, T. (2003): Plant species composition of boreal spruce swamp forests: closed doors and windows of opportunity. – Ecology 84: 1909-1919.
[66] Pao, N.T., Upadhaya, K. (2017): Effect of fragmentation and anthropogenic disturbances on floristic composition and structure of subtropical broad leaved humid forest in Meghalaya, northeast India. – Applied Ecology and Environmental Research 15: 385-407.
[67] Pysek, P., Richardson, D., M., Rejmanek, M., Webster, G., L., Williamson, M., Kirschner, J. (2004): Alien plants in checklists and floras: towards better communication between taxonomists and ecologists. – Taxon 53: 131-143.

http://www.aloki.hu ● ISSN 1589 1623 (Print) ● ISSN 1785 0037 (Online)
DOI: http://dx.doi.org/10.15666/aeer/1605_64836497
© 2018, ALÖKI Kft., Budapest, Hungary

[68] R Development Core Team (2013): R: A Language and Environment for Statistical Computing. – R Foundation for Statistical Computing, Vienna.
[69] Reif, A., Walentowski, H. (2008): The assessment of naturalness and its role for nature conservation and forestry in Europe. – Waldökologie, Landschaftsforschung und Naturschutz 6: 63-76.
[70] Rzymowska, Z., Skrajna, T. (2015): Associations and communities of cereal crops of the Łuków Plain. Part III. Intermediate and impoverished communities. – Acta Agrobotanica 68: 17-22.
[71] Saunders, D. A, Hobbs, R. J., Margules, C. R. (1991): Biological consequences of ecosystem fragmentation: A review. – Biological Conservation 5: 18-32.
[72] Slezák, M., Hegedušová, K., Senko, D. (2011): Syntaxonomy and ecology of forest vegetation in the Štiavnickě Vrchymts (Central Slovakia). – Acta Societatis Botanicorum Poloniae 80: 115-127.
[73] Song, P. X. K., Tan, M. (2000): Marginal models for longitudinal continuous proportional data. – Biometrics 56: 496–502.
[74] Starkel, L. (1999): Geografia Polski. Środowisko Przyrodnicze. – Wydawnictwo PWN, Warszawa.
[75] Stefańska-Krzaczek, E., Kacki, Z., Szypuła, B. (2016): Coexistence of ancient forest species as an indicator of high species richness. – Forest Ecology and Management 365: 12-21.
[76] Tscharntke, T., Clough, Y., Wanger, T. C., Jackson, L., Motzke, I., Perfecto I., Vandermeer, J., Whitbread, A., (2012): Global food security, biodiversity conservation and the future of agricultural intensification. – Biological Conservation 151: 53–59.
[77] Verheyen, K., Baeten, L., De Frenne, P., Bernhardt-Römermann, M., Brunet, J., Cornelis, J., Decocq, G., Dierschke, H., Eriksson, O., Hédl, R., Heinken, T., Hermy, M., Hommel, P., Kirby, K., Naaf, T., Peterken, G., Petřík, P., Pfadenhauer, J., Van Calster, H., Walther, G., R., Wulf, M., Verstraeten, G. (2012): Driving factors behind the eutrophication signal in understory plant communities of deciduous temperate forests. – Journal of Ecology 100: 352-365.
[78] Verheyen, K., Honnay, O., Motzkin, G., Hermy, M., Foster, D. R. (2003): Response of forest plant species to land-use change: a life-history trait-based approach. – Journal of Ecology 91: 563–577.
[79] Vestal, A. G., Heermans, M. F. (1945): Size requirements for reference areas in mixed forest. – Ecology 26: 122-134.
[80] Webb, J. C., Goodenough, A. E. (2018): Questioning the reliability of "ancient" woodland indicators: Resilience to interruptions and persistence following deforestation. – Ecological Indicators 84: 354-363
[81] Wójcik, Z. (1991). The vegetation of forest islands in the agricultural landscape of the Jorka river reception basin in Masurian Lakeland (north-east part of Poland). – Ekologia Polska 39: 437-479.
[82] Wulf, M. (2003): Preference of plant species for woodlands with differing habitat continuities. – Flora 198: 444-460.
[83] Zając, A., Zając, M., Tokarska-Guzik, B. (1998): Kenophytes in the flora of Poland: list, status and origin. – Phytocoenosis 10 (N.S.) Supplement of Cartography and Geobotany 9: 107-116.
[84] Zielewicz, W., Kozłowski, S. (2011): Występowanie barwników chlorofilowych i karotenowych w trawach leśnych. – Łąkarstwo w Polsce 14: 161-170.

http://www.aloki.hu ● ISSN 1589 1623 (Print) ● ISSN 1785 0037 (Online)
DOI: http://dx.doi.org/10.15666/aeer/1605_64836497
© 2018, ALÖKI Kft., Budapest, Hungary

AN OVERVIEW OF ENERGY PRODUCTION FROM ANIMAL WASTE DURING IRAN'S ENERGY TRANSITION: IMPLICATION OF MANURE CHEMICAL COMPOSITION

DARYABEIGI ZAND, A.[1*] – RABIEE ABYANEH, M.[1] – KHODAEI, H. R.[2]

[1]*School of Environment, College of Engineering, University of Tehran, Tehran, Iran*

[2]*Department of Animal Science, Islamic Azad University, Golpayegan Branch, Isfahan, Iran*

**Corresponding author*
e-mail: adzand@ut.ac.ir

(Received 15th Jun 2018; accepted 7th Aug 2018)

Abstract. Biogas is a renewable energy source that is generated by the decomposition of organic waste in anaerobic process. The theoretical biogas potential is defined as the possible amount of gas production from biomass. This potential can be evaluated using various calculation methods each of which considers different parameters. The objective of this study was therefore to compare the potential of biogas energy generation from the livestock waste produced from the animal husbandry in Iran using different calculation methods. Using 4 methods of calculation indicated that the amount of 11.82, 5.25, 16.05 and 2.1 million ton of animal waste could be produced in Iran in 2016 with a biogas generation potential of 886.57, 173.36, 745.37 and 565.85 million m^3, energy equivalent of 5.14, 1, 4.32 and 3.28 thousand GWh and electricity generation of 1.59, 0.31, 1.34 and 1.02 thousand GWh. These amounts of electricity generation could provide 2.03%, 1.71%, 0.39% and 1.3% of the electrical energy consumed in household sector in 2016 in Iran, respectively. Furthermore the methane yield potential from the livestock manure with considering the different types of substrate (lipid, lignin, dry matter and cellulose) was evaluated. The highest methane yield was obtained from biochemical methane potential (BMP) value based on lipid and lignin content at 5.27E + 10 NL CH_4 $digester^{-1}$ day^{-1}. The results showed that livestock waste is a low-cost and extensive source of renewable energy in Iran that can be used optimally for biogas energy and electricity generation. Also the treatment of huge amount of livestock manure in anaerobic digestion is helpful for reducing its polluting effects on the environment.
Keywords: *renewable energy, biogas, anaerobic digestion, organic waste, manure livestock*

Introduction

Global demand for energy is increasing rapidly, because of population growth and technological advancements. Use of renewable energy sources is essential due to the limitation of fossil fuel sources and negative environmental effects (International Energy Agency, 2015; United Nations Environment Programme, 2014; Achinas and Euverink, 2016; Abdeshahian et al., 2016; Santos et al., 2018; Chandekar and Debnath, 2018). Biogas is one of the important renewable energy sources which is produced through decomposing organic waste under anaerobic conditions by microorganisms (Travnicek et al., 2018; Scarlat et al., 2018a; Angelidaki et al., 2018). Biogas is mainly composed of CH_4 (60%) and CO_2 (35–40%) (Ilaboya et al., 2010; Sahota et al., 2018). Organic materials such as animal, human and plant wastes are biodegradable and can be converted into biogas (Zareei, 2018; Cu et al., 2015; Ozer, 2017; Yazan et al., 2018). Manure waste obtained from livestock industries are the largest and cheapest source for biogas production in anaerobic process (Comparetti et al., 2012; Ch'ng et al., 2014; Plume et al., 2012; Than, 2005; Cu et al., 2012; Yildirim et al., 2017; Mohammadi Maghanaki et al., 2013). Manure livestock is a type of organic waste which will be

http://www.aloki.hu ● ISSN 1589 1623 (Print) ● ISSN 1785 0037 (Online)
DOI: http://dx.doi.org/10.15666/aeer/1605_64996523
© 2018, ALÖKI Kft., Budapest, Hungary

hazardous to environment if it is not managed suitably. Livestock manure contains residues of some harmful substances such as growth hormones, antibiotics and heavy metals. So, disposal of them contaminates air, soil and water sources and prevalence of the human diseases (Abdeshahian et al., 2016; Pessuto et al., 2016). Anaerobic treatment of manure has the beneficial outcomes of reducing environmental pollution through proper waste management, reduction of unpleasant odors and microbial pathogens with a sustainable production of energy source as biogas (Wyman and Goodman, 1993; Mata-alvarez, 2000; Gebrezgabher et al., 2010; Holm-Nielsen et al., 2009; Wang et al., 2018; Samun et al., 2017; Neshat et al., 2017). Also it can be used for the production of a rich fertilizer which is favorable for the improvement of agricultural lands (De-Vries, 2012; Meyer et al., 2018; Eze and Agbo, 2010).

Considering the importance of animal waste as the enormous raw substances for energy production, many studies have been carried out on assessing the potential of biogas production from livestock waste. For instance, the potential of biogas production from livestock waste was studied in Turkey. The results showed that the amount of 2177.55 million m^3 of biogas can be produced annually in Turkey (Onurbas-Avcioglu and Turker, 2012). Similar studies have also been performed in Finland, Sweden and Denmark to estimate the potential of energy production from livestock waste as evaluated in Turkey. These studies showed that the potential of biogas production is 332.97, 352.09 and 402.1 million m^3 yr^{-1} in mentioned countries, respectively (Abdeshahian et al., 2016; Luostarinen, 2013).

In recent years, the animal husbandry is drastically grown in Iran (Hamzeh et al., 2011; Government of Islamic Republic of Iran and Food and Agriculture Organization, 2012; Tehran Chamber of Commerce, Industries, Mines and Agriculture, 2016; Beldman et al., 2017). Number of industrial cattle farms in Iran based on capacity from 1990-2016 is shown in *Figure 1*.

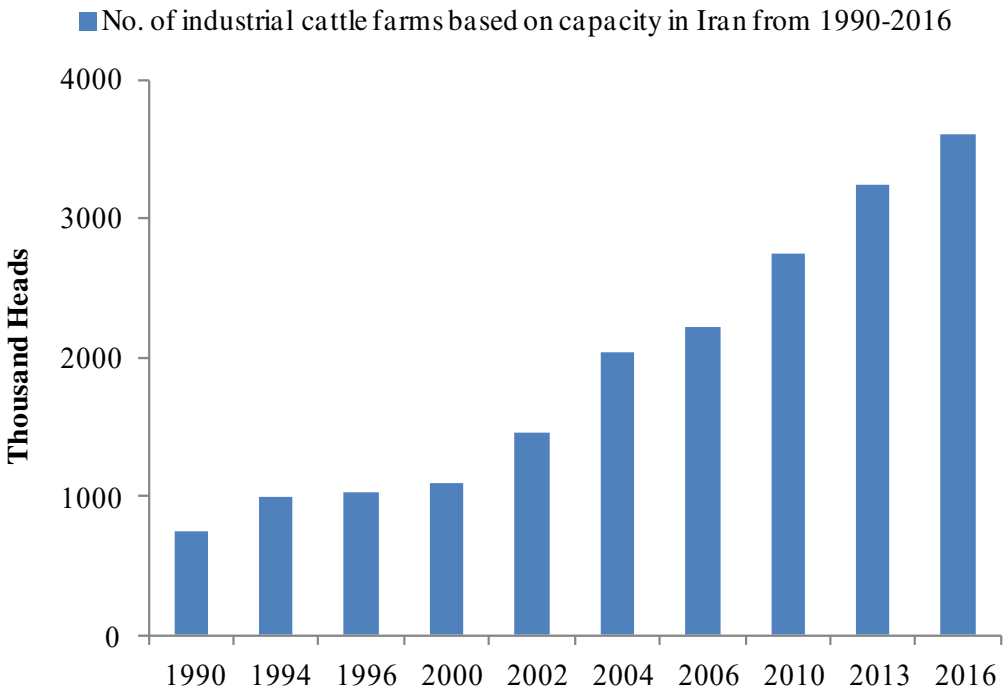

Figure 1. *The increasing capacity of industrial cattle farms in Iran from 1990-2016 (Tehran Chamber of Commerce, Industries, Mines and Agriculture, 2016)*

http://www.aloki.hu ● ISSN 1589 1623 (Print) ● ISSN 1785 0037 (Online)
DOI: http://dx.doi.org/10.15666/aeer/1605_64996523
© 2018, ALÖKI Kft., Budapest, Hungary

As can be seen, industrial cattle farms capacity in Iran has revealed an increasing trend from 1990-2016. The increase population of the livestock has caused an elevated production of livestock waste, resulting in the difficulty with the disposal of a large amount of manure. Unsafe disposal of livestock waste and its accumulation in environment has caused unfavorable conditions due to creating a favorable environment for growth and spread of microbes, in addition to intolerable odor and insects (Zareei, 2018), but could instead be used as a tremendous source for generating biogas energy. A wide variety of calculations exist to evaluate the potential of biogas generation from livestock waste, each of them considers different parameters such as pH, temperature, type, concentration and composition of raw materials and the time remaining in digester (Costa et al., 2016; Abdeshahian et al., 2016; Boysan et al., 2015; Cu et al., 2015; Burg et al., 2018; Zareei, 2018).

A wide variety of calculations exist to evaluate the potential of biogas generation from livestock waste. Some studies provide information about the factors that affect the biogas production such as pH, temperature, type, concentration and composition of raw materials and the time remaining in digester (Costa et al., 2016; Abdeshahian et al., 2016; Boysan et al., 2015; Cu et al., 2015; Burg et al., 2018; Zareei, 2018). But variation of quantity of biogas generated from different evaluation methods has rarely been studied in a distinct study. The current study aims to compare the potential of biogas energy generation from the livestock waste produced from the animal husbandry in Iran using different calculation methods.

Materials and methods

Livestock population in Iran

In order to calculate the potential of biogas generation from the livestock manure, initial data was collected from the Statistical Centre of Iran (SCI) (Statistical Centre of Iran, 2017). According to the data reported by SCI, in 2016, Iran had a total of 26061 industrial cattle farms with a capacity of 3619696 heads. In this year 18547 cattle farms were active and the rest were inactive. The total number of cattle was 1439391 heads in Iran in 2016. *Table 1* shows the number of specified groups of cattle population in each province of Iran.

Table 1. *Number of specified groups of cattle population in Iran (Thousand Heads) (Statistical Centre of Iran, 2017)*

Province	Original		Crossbred		Native	Total
	Holstein	Other races	Holstein	Other races		
Azerbaijan, West	21.98	0.52	3.13	2.26	0.45	28.36
Azerbaijan, East	10.83	0.88	0.78	0.16	0.55	13.21
Ardabil	21.48	0	2.99	0.41	0.06	24.95
Isfahan	125.94	1.24	72.95	6.6	0.12	206.87
Alborz	66.77	0.27	3.30	1.19	0.76	72.31
Ilam	5.61	0.10	0.43	0	0	6.15
Bushehr	0.44	0.03	1.88	5.14	2.02	9.52
Tehran	223.55	5.84	14.81	38.31	38.88	321.42
ChaharMahaal and Bakhtiari	28.98	0.10	0.32	0.01	0	29.42
Khorasan, South	8.93	0.03	2.10	0.41	0	11.49

http://www.aloki.hu ● ISSN 1589 1623 (Print) ● ISSN 1785 0037 (Online)
DOI: http://dx.doi.org/10.15666/aeer/1605_64996523
© 2018, ALÖKI Kft., Budapest, Hungary

Table 1 (continued). *Number of specified groups of cattle population in Iran (Thousand Heads) (Statistical Centre of Iran, 2017)*

Province	Original		Crossbred		Native	Total
	Holstein	Other races	Holstein	Other races		
Khorasan, Razavi	92.64	2.75	16.01	1.17	0.03	112.62
Khorasan, North	4.75	0.23	2.46	0.03	0.14	7.62
Khuzestan	4.75	0.37	15.35	2.28	0.43	23.19
Zanjan	14.19	0	2.63	0.04	0.14	17.02
Semnan	16.84	4.06	12.56	23.38	0.78	57.64
Sistan and Baluchestan	2.19	0.23	0.29	0.58	0.79	4.11
Fars	75.65	0.37	17.86	8.21	3.00	105.12
Qazvin	65.59	0.10	5.84	1.05	0	72.59
Qom	28.73	1.13	5.56	16.75	12.65	64.84
Kurdistan	1.85	0.47	0.38	0.31	0.40	3.42
Kerman	29.28	0.26	2.35	0.53	0.75	33.19
Kermanshah	14.74	1.14	0.33	0.06	0.25	16.54
Kohgiluyeh and Boyer-Ahmad	3.13	0	1.28	0.02	0	4.43
Golestan	15.35	1.56	0.98	0.35	0.01	18.26
Gilan	2.31	0.22	0.41	0.10	0.70	3.76
Lorestan	6.35	0	2.21	0.30	1.01	9.89
Mazandaran	10.87	0.82	2.90	6.39	0.66	21.65
Markazi	10.62	0	15.13	33.95	0.34	60.05
Hormozgan	0.24	0.01	0.14	0.52	0.34	1.27
Hamadan	15.34	0.25	1.62	0.29	0	17.52
Yazd	18.35	0.37	38.89	2.96	0.24	60.83
Iran	948.42	23.48	248.02	153.85	65.6	1439.39

Livestock manure production

Livestock waste is composed of the organic matter that can be treated as the potential raw substance for the production of bioenergy (Afazeli et al., 2014; Mathias, 2014). The amount of livestock manure can vary based on the type of animal, feeding methods, animal body size, the type of breeding and keeping time at day or night (Onurbas-Avcioglu and Turker, 2012; Omrani, 1996). Abdeshahian et al., (2016) categorized cattle into the large ruminants and calculated the amount of livestock manure based on the live body weight. The amount of the manure was calculated based on the 9% of body weight for large ruminants. The average live body weight accounted 250 kg for the large ruminants. Accordingly, the average amount of the manure was calculated based on 22.5 kg/day for the large ruminants. This is while that Boysan et al. (2015) calculated the amount of livestock manure production based on 10 kg/day for one cattle. On the other hand, Plume et al. (2012) calculated the manure output from livestock in a year using *Equation 1*.

$$M = \sum_{n=1}^{i} N_i * M_i \qquad \text{(Eq.1)}$$

http://www.aloki.hu ● ISSN 1589 1623 (Print) ● ISSN 1785 0037 (Online)
DOI: http://dx.doi.org/10.15666/aeer/1605_64996523
© 2018, ALÖKI Kft., Budapest, Hungary

where:
M- Livestock manure produced in region (t),
n- Number of specified groups of livestock population in region,
N_i- Average number of livestock present year-round within i^{th} group of livestock,
m_i- Manure produced per one head in a year in the i^{th} group of livestock (t).

Furthermore Zareei (2018) denoted that the livestock manure production can be calculated using parameters including livestock weight and the ratio of the annual manure generation to livestock weight as shown in *Table 2*.

Table 2. *Coefficient for calculation of manure production from livestock (Zareei, 2018)*

Material type	Livestock weight	The ratio of the annual livestock manure to livestock weight
Cow manure	500-620	2.6

The average weight of livestock was estimated according to the dominant races of the area. As stated in *Table 2,* livestock weight was considered in the range of 500 to 620. The total amount of livestock waste can be calculated by multiplying the waste mass by the population number (Zareei, 2018).

The potential of biogas production from the livestock manure

The biogas produced from the livestock waste is affected by the different factors such as feeding regime, animal type, body weight, the proportion of total solids and the waste availability (United Nations Environment Programme, 2014; Than, 2005). Abdeshahian et al. (2016) considered the total solids of the waste as an important factor for the production of biogas from the livestock waste. They considered the total solids value of livestock manure as 25% for the large ruminants with the quantity of estimated biogas produced per kilogram of the total solids as 0.6 (0.6 m3/kg TS). Also they have pointed that the collection of the manure cannot always be carried out efficiently for the production of biogas and the availability of the manure is varied. Hence, for the calculating of biogas production from the livestock manure the availability coefficient was considered as 50% for large ruminants (Onurbas-Avcioglu and Turker, 2012; Afazeli et al., 2014). By taking into account the mentioned assumptions, the theoretical potential of biogas production from the livestock manure and the potential of electricity generation from the biogas was calculated as shown in *Equations 2* and *3* (Abdeshahian et al., 2016).

$$TPB = M * TS * AC * EB_{TS} \quad \text{(Eq.2)}$$

where:
TPB- Theoretical potential of biogas (m^3 yr^{-1}),
M- Total amount of the manure produced for each region (kg yr^{-1}),
TS- Ratio of the total solids of the animal manure,
AC- Availability coefficient,
EBTS- Quantity of estimated biogas produced per kilogram of the total solids (m^3 kg^{-1} TS).

$$e_{biogas} = E_{biogas} * n \quad \text{(Eq.3)}$$

http://www.aloki.hu ● ISSN 1589 1623 (Print) ● ISSN 1785 0037 (Online)
DOI: http://dx.doi.org/10.15666/aeer/1605_64996523
© 2018, ALÖKI Kft., Budapest, Hungary

where:
e_{biogas}- Quantity of generated electricity (kWh yr^{-1}),
E_{biogas}- Unconverted raw energy in the biogas (kWh yr^{-1}),
n- Overall efficiency of the conversion of biogas to electricity (%). The amount of *n* is varied depending on the power generation plants. The *n* value is considered 35-42% and 25% in the power plants with large turbine system and small generators, respectively (Hosseini and Wahid, 2014; Benito et al., 2015). In this study, the *n* value was assumed as 30%based on Iran power plants characterization (Iran Energy Ministry, 2017).

The quantity of E_{biogas} is calculated using *Equation 4* (Abdeshahian, 2016).

$$E_{biogas} = Energycontent_{biogas} * m_{biogas} \quad \text{(Eq.4)}$$

where:
Energy $content_{biogas}$- Calorific value of biogas (kWh m^{-3}). The quantity of the Energy $content_{biogas}$ is assumed as 6 kWh m^{-3} by considering the biogas calorific value as 21.5 MJ per m^3 biogas (1 kWh = 3.6 MJ) (Hosseini and Wahid, 2014; Garcia, 2014).
m_{biogas}- Amount of biogas produced per year (m^3 yr^{-1}).

On the other hand, Boysan et al. (2015) calculated the potential of biogas production from livestock manure based on 0.33 m^3/cattle with considering assumptions including fermenter temperature as 37 °C, 20% mass in manure and waiting time as 30 days. It is while that in the study conducted by Zareei (2018) the biogas production potential per kilogram of cow manure was considered as 0.28-0.28 m^3. Furthermore, Plume et al. (2012) proposed *Equation 5* for calculating the potential of biogas production from livestock manure.

$$V_B = \sum_{n}^{i} N_i * m_i * K_{DMi} * K_{OMi} * v_{Bi} \quad \text{(Eq.5)}$$

where:
V_B- Biogas volume, potentially obtainable from manure biomass in region in a year (m^3),
K_{DMi}- Dry matter content in manure produced by i^{th} group of animals in region,
K_{Omi}- Organic matter content in dry matter of manure produced by i^{th} group of animals in region,
v_{Bi}- Specific biogas output from manure organic matter for i^{th} group of animals in region (m^3 t^{-1}).

The energy of biogas obtainable from manure biomass in region then was calculated according to *Equation 6* (Plume et al., 2012).

$$E_B = \sum_{n=1}^{i} N_i * m_i * K_{DMi} * K_{OMi} * v_{Bi} * e_{Bi} \quad \text{(Eq.6)}$$

where:
E_B- Energy potential obtainable from biogas produced from manure (kWh),
e_{Bi}- Specific heat energy content of biogas obtained from manure produced by i^{th} group of animals (kWh m^{-3}).

http://www.aloki.hu ● ISSN 1589 1623 (Print) ● ISSN 1785 0037 (Online)
DOI: http://dx.doi.org/10.15666/aeer/1605_64996523
© 2018, ALÖKI Kft., Budapest, Hungary

Calculation of methane (CH_4) content of biogas

The biogas obtained from the anaerobic digestion process of livestock manure is composed of 50-70% of methane (Omar et al., 2009; Nasir et al., 2012; Ounnar et al., 2012; Nasir et al., 2013). The methane yield can be calculated based on the original Hashimoto equation (*Eq. 7* below) (Chen and Hashimoto, 1978; Hashimoto et al., 1981).

$$\gamma = \frac{\beta_0 * S_0}{HRT}\left(1 - \frac{K}{HRT * \mu m - 1 + K}\right) \quad \text{(Eq.7)}$$

where:
γ- Methane yield (NL CH_4 digester^{-1} day^{-1}),
β_o- Biochemical methane production (BMP) value of specific substrate (NL CH_4 kg VS^{-1}),
S_o- VS concentration (g kg^{-1}),
HRT- Hydraulic retention time (days),
K- Kinetic constant (K = 0.6 + 0.0206.EXP[0.051.S_0],
μm- Maximum specific growth rate (day^{-1}). μm = 0.013 T – 0.129, for temperature (T) between 20 and 60 °C.

Rennuit and Sommer (2013) extended the Hashimoto equation to calculate the methane yield for a biogas digester. The extended equation takes into account the difference in lowland and highland temperature regimes. It is assumed that the mean monthly air temperature represents the mean monthly digester temperature (Perrigault et al., 2012). Hence, the methane yield for a biogas digester for an air temperature between 15 to 30 °C and 20 to 60 °C is calculated based on *Equations 8* and *9,* respectively (Rennuit and Sommer, 2013).

$$\gamma_{winter}(HRT, \mu m, TD) = \beta_0 * \left[1 - \frac{K}{\mu m(TD) * \left(HRT + \frac{1}{\mu m(TD)}\right) - 1 + K}\right] \quad \text{(Eq.8)}$$

$$\gamma_{summer}(HRT, \mu m, TD) = \beta_0 * \left[1 - \frac{K}{\mu m(TD) * HRT - 1 + K}\right] \quad \text{(Eq.9)}$$

where:
μm(Td)- maximum specific growth rate of the microorganisms at the digester temperature in the temperature interval from 10 to 30 °C (μm[Td] = 0.0039 $e^{0.1188 \cdot (Td)}$ (day^{-1}) and (Td) is the digester temperature which is set to be equal to the average monthly air temperature (°C) represented by region.

In line with this, Cu et al. (2015) suggested that the BMP value (β_0 in the Hashimoto equation) from different types of substrate can be predicted based on their chemical composition. Biogas production is related to the chemical composition of the substrate. Low concentrations of organic matter such as lipids and protein will lead to a low biogas production. However, the high concentration of organic matter in substrates will have a negative effect on biogas production, causing foaming and inhibition if not co-fermented with biomasses low in protein and lipids (Cu et al., 2015; Kougias et al.,

http://www.aloki.hu ● ISSN 1589 1623 (Print) ● ISSN 1785 0037 (Online)
DOI: http://dx.doi.org/10.15666/aeer/1605_64996523
© 2018, ALÖKI Kft., Budapest, Hungary

2013). There is a clear relationship between lipid content of the biomass and biochemical methane potential. Lipid content is the most important factor for biochemical methane potential compared to other components. However, in a biogas technology every component in the substrates affects biogas production. It was found that lipid, lignin, protein, and cellulose contents were the main chemical components of substrates contributing to the variation in the BMP (Cu et al., 2015). Equations to predict BMP are shown in *Table 3*.

Table 3. *Equations to predict BMP for livestock manure (Cu et al., 2015)*

Variables	Equations for BMP
Lipid	57.9+35×lipid
Lipid, lignin	186+30.6×lipid–5.13×lignin
Lipid, lignin, dry matter	167+30.1×lipid–5.43×lignin+1.15×dry matter
Lipid, lignin, cellulose	201+31.5×lipid–3.85×lignin–1.88×cellulose

Results and discussion

Calculation of livestock manure production in Iran

The amount of livestock manure production was calculated for all provinces of Iran based on Abdeshahian, Boysan and Zareei methods. The results are shown in *Table 4*.

Table 4. *The estimated values of livestock manure of different provinces in Iran in 2016 based on different methods*

	Manure production (t yr^{-1})						
Province	**Abdeshahian**	**Boysan**	**Zareei**	**Province**	**Abdeshahian**	**Boysan**	**Zareei**
Azerbaijan, West	2.33E+05	1.04E+05	4.13E+04	Fars	8.63E+05	3.84E+05	1.53E+05
Azerbaijan, East	1.08E+05	4.82E+04	1.92E+04	Qazvin	5.96E+05	2.65E+05	1.06E+05
Ardabil	2.05E+05	9.11E+04	3.63E+04	Qom	5.33E+05	2.37E+05	9.44E+04
Isfahan	1.70E+06	7.55E+05	3.01E+05	Kurdistan	2.82E+04	1.25E+04	4.99E+03
Alborz	5.94E+05	2.64E+05	1.05E+05	Kerman	2.73E+05	1.21E+05	4.83E+04
Ilam	5.05E+04	2.25E+04	8.96E+03	Kermanshah	1.36E+05	6.04E+04	2.41E+04
Bushehr	7.82E+04	3.48E+04	1.39E+04	Kohgiluyeh and Boyer-Ahmad	3.64E+04	1.62E+04	6.46E+03
Tehran	2.64E+06	1.17E+06	4.68E+05	Golestan	1.50E+05	6.67E+04	2.66E+04
ChaharMahaal and Bakhtiari	2.42E+05	1.07E+05	4.28E+04	Gilan	3.10E+04	1.38E+04	5.49E+03
Khorasan, South	9.44E+04	4.19E+04	1.67E+04	Lorestan	8.12E+04	3.61E+04	1.44E+04
Khorasan, Razavi	9.25E+05	4.11E+05	1.64E+05	Mazandaran	1.78E+05	7.90E+04	3.15E+04
Khorasan, North	6.26E+04	2.78E+04	1.11E+04	Markazi	4.93E+05	2.19E+05	8.74E+04
Khuzestan	1.90E+05	8.46E+04	3.38E+04	Hormozgan	1.04E+04	4.64E+03	1.85E+03
Zanjan	1.40E+05	6.21E+04	2.48E+04	Hamadan	1.44E+05	6.40E+04	2.55E+04

http://www.aloki.hu ● ISSN 1589 1623 (Print) ● ISSN 1785 0037 (Online)
DOI: http://dx.doi.org/10.15666/aeer/1605_64996523
© 2018, ALÖKI Kft., Budapest, Hungary

Table 4 (continued). *The estimated values of livestock manure of different provinces in Iran in 2016 based on different methods*

Manure production (t yr^{-1})							
Province	**Abdeshahian**	**Boysan**	**Zareei**	**Province**	**Abdeshahian**	**Boysan**	**Zareei**
Semnan	4.73E+05	2.10E+05	8.39E+04	Yazd	5.00E+05	2.22E+05	8.86E+04
Sistan and Baluchestan	3.38E+04	1.50E+04	5.99E+03	Iran	1.18E+07	5.25E+06	2.10E+06

Manure production by livestock in different groups based on Plume et al. (2012) is presented in *Table 5*.

Table 5. *Manure production by livestock in different groups based on Plume et al. (2012)*

Group characteristics	Manure production per head t yr^{-1})
Dairy cows	$0.0024Y_D+0.447$
Heifers	8
Calves	2.6
Cattle	12

Average values of manure production per one head in a year for all groups of livestock, except dairy cows, are given in *Table 5*. Average manure production per one dairy cow is dependent on cow's milk yield and calculates help by regression *Equation 10* (Plume et al., 2012).

$$m_1 = 0.0024 * Y_d + 0.447 \quad \text{(Eq.10)}$$

where:
m_1- Average manure production per dairy cow in region in a year (t yr^{-1}),
Y_d- Average milk yield per dairy cow in region in a year (kg yr^{-1}).

Aiming to improve accuracy of manure resources evaluation, all the animals was divided in 4 groups (dairy cows, heifers, calves and cattle) according to its manure production capability per one head. The number of livestock within specified groups in each province of Iran in 2016 is presented in *Table 6*.

Table 6. *Number of livestock within specified groups in each province of Iran in 2016*

Province	**Dairy cow**			**Heifers**		**Calves**		**Cattle**	
	Lactating cow	**Dry cow**		**Pregnant**	**Unpregnant**	**Bull**	**Cow**	**Breeding cattle**	**Other**
		Pregnant	**Unpregnant**						
Azerbaijan, West	9085	2197	748	3175	2461	4016	2881	1478	2322
Azerbaijan, East	3804	1069	560	1154	971	2629	1600	940	482
Ardabil	7977	1964	396	2184	1841	4231	4286	389	1688
Isfahan	85333	18747	6047	25458	16938	22081	25890	1615	4766
Alborz	28921	6951	2041	7956	6450	5529	11199	915	2350
Ilam	1552	853	704	315	322	1340	344	438	285

http://www.aloki.hu ● ISSN 1589 1623 (Print) ● ISSN 1785 0037 (Online)
DOI: http://dx.doi.org/10.15666/aeer/1605_64996523
© 2018, ALÖKI Kft., Budapest, Hungary

Table 6 (continued). *Number of livestock within specified groups in each province of Iran in 2016*

Province	Dairy cow			Heifers		Calves		Cattle	
	Lactating cow	Dry cow		Pregnant	Unpregnant	Bull	Cow	Breeding cattle	Other
		Pregnant	Unpregnant						
Bushehr	1026	609	381	346	308	6335	151	53	316
Tehran	93015	25956	10066	25284	24227	104542	28958	6220	3152
ChaharMahaal and Bakhtiari	10136	3738	2031	3230	2535	2896	3848	972	41
Khorasan, South	3451	1109	746	1027	1226	1573	1552	437	371
Khorasan, Razavi	42617	10634	3539	10815	11499	13083	14029	931	5475
Khorasan, North	2290	618	173	691	546	1707	945	592	66
Khuzestan	3881	1480	362	576	1021	11323	1106	676	2767
Zanjan	5984	1752	282	2081	2004	1391	2074	1284	174
Semnan	17947	3811	1592	4081	3311	10407	3722	6540	6233
Sistan and Baluchestan	627	404	136	177	107	1322	256	290	794
Fars	33313	9111	2447	10681	11417	18293	11255	3097	5514
Qazvin	26322	6201	658	7380	5975	11451	10288	596	3722
Qom	9559	2301	745	2928	2470	36488	3770	745	5835
Kurdistan	1090	206	32	278	242	1069	281	130	100
Kerman	10349	3422	1581	3723	2867	4525	3462	2925	338
Kermanshah	5915	1134	978	1785	1701	1445	1973	644	971
Kohgiluyeh and Boyer-Ahmad	1301	358	17	438	471	1243	576	32	0
Golestan	5635	2287	733	2333	2213	2361	2213	393	96
Gilan	1204	310	235	575	241	390	547	250	19
Lorestan	2848	818	116	958	598	2800	1573	29	153
Mazandaran	7544	2354	689	2174	1922	2667	2348	195	1759
Markazi	9822	2133	997	2387	1894	33381	5686	1367	2390
Hormozgan	227	76	32	43	15	298	90	397	92
Hamadan	5878	1999	922	1351	1197	3323	2248	606	0
Yazd	21136	7208	1154	7487	5981	6754	7605	1526	1985
Iran	459789	121810	41140	133071	114971	320893	156756	36702	54256

In line with this, the amount of livestock manure production in different provinces of Iran was calculated based on Plume et al. (2012) and is presented in *Table 7*.

http://www.aloki.hu ● ISSN 1589 1623 (Print) ● ISSN 1785 0037 (Online)
DOI: http://dx.doi.org/10.15666/aeer/1605_64996523
© 2018, ALÖKI Kft., Budapest, Hungary

Table 7. *The estimated values of livestock manure of different provinces in Iran in 2016 based on Plume et al. (2012)*

Manure production (t yr^{-1})						
Province	**Dairy cows**		**Heifers**	**Calves**	**Cattle**	**Total**
	Lactating cow	**Dry cow**				
Azerbaijan, West	199870	35340	45088	17932	45600	343830
Azerbaijan, East	72276	19548	17000	10995	17064	136883
Ardabil	127632	28320	32200	22144	24924	235220
Isfahan	2218658	297528	339168	124724	76572	3056650
Alborz	607341	107904	115248	43492	39180	913165
Ilam	27936	18684	5096	4378	8676	64770
Bushehr	4104	11880	5232	16863	4428	42507
Tehran	1581255	432264	396088	347100	112464	2869171
ChaharMahaal and Bakhtiari	233128	69228	46120	17534	12156	378166
Khorasan, South	72471	22260	18024	8125	9696	130576
Khorasan, Razavi	980191	170076	178512	70491	76872	1476142
Khorasan, North	48090	9492	9896	6895	7896	82269
Khuzestan	62096	22104	12776	32315	41316	170607
Zanjan	155584	24408	32680	9009	17496	239177
Semnan	287152	64836	59136	36735	153276	601135
Sistan and Baluchestan	8151	6480	2272	4102	13008	34013
Fars	732886	138696	176784	76824	103332	1228522
Qazvin	605406	82308	106840	56521	51816	902891
Qom	248534	36552	43184	104670	78960	511900
Kurdistan	22890	2856	4160	3510	2760	36176
Kerman	196631	60036	52720	20766	39156	369309
Kermanshah	159705	25344	27888	8886	19380	241203
Kohgiluyeh and Boyer-Ahmad	33826	4500	7272	4729	384	50711
Golestan	118335	36240	36368	11892	5868	208703
Gilan	20468	6540	6528	2436	3228	39200
Lorestan	48416	11208	12448	11369	2184	85625
Mazandaran	181056	36516	32768	13039	23448	286827
Markazi	157152	37560	34248	101574	45084	375618
Hormozgan	2043	1296	464	1008	5868	10679
Hamadan	141072	35052	20384	14484	7272	218264
Yazd	422720	100344	107744	37333	42132	710273
Iran	9777075	1955400	1984336	1241875	1091496	16050182

Calculation of the potential of biogas production from the livestock manure in Iran

The biogas production potential from the livestock manure in all provinces of Iran was calculated based on Abdeshahian, Boysan and Zareei methods and is presented in *Table 8.*

http://www.aloki.hu ● ISSN 1589 1623 (Print) ● ISSN 1785 0037 (Online)
DOI: http://dx.doi.org/10.15666/aeer/1605_64996523
© 2018, ALÖKI Kft., Budapest, Hungary

Table 8. *The estimated values of biogas production in all provinces in Iran in 2016 based on different methods*

Biogas production potential (million m^3 yr^{-1})							
Province	**Abdeshahian**	**Boysan**	**Zareei**	**Province**	**Abdeshahian**	**Boysan**	**Zareei**
Azerbaijan, West	17.46	3.41	11.15	Fars	64.75	12.66	41.32
Azerbaijan, East	8.13	1.59	5.19	Qazvin	44.71	8.74	28.53
Ardabil	15.37	3.00	9.81	Qom	39.93	7.80	25.49
Isfahan	127.42	24.91	81.32	Kurdistan	2.11	0.41	1.34
Alborz	44.53	8.70	28.4269	Kerman	20.44	3.99	13.04
Ilam	3.78	0.74	2.41	Kermanshah	10.19	1.99	6.50
Bushehr	5.86	1.14	3.74	Kohgiluyeh and Boyer-Ahmad	2.73	0.53	1.74
Tehran	197.97	38.71	126.35	Golestan	11.24	2.19	7.17
ChaharMahaal and Bakhtiari	18.12	3.54	11.56	Gilan	2.32	0.45	1.48
Khorasan, South	7.07	1.38	4.51	Lorestan	6.09	1.19	3.88
Khorasan, Razavi	69.36	13.56	44.27	Mazandaran	13.33	2.60	8.51
Khorasan, North	4.69	0.91	2.99	Markazi	36.99	7.23	23.60
Khuzestan	14.28	2.79	9.11	Hormozgan	0.78	0.15	0.49
Zanjan	10.48	2.05	6.69	Hamadan	10.79	2.11	6.88
Semnan	35.50	6.94	22.66	Yazd	37.47	7.32	23.91
Sistan and Baluchestan	2.53	0.49	1.61	Iran	886.57	173.36	565.85

The manure and biogas characteristics for calculating the potential of biogas production from the livestock manure based on Plume et al. (2012) such as dry matter content, organic matter content in dry matter, biogas output from manure and heat energy of biogas are shown in *Table 9.*

Table 9. *Manure and biogas characteristics in different groups of livestock based on Plume et al. (2012)*

Groups of livestock	**Dairy cows, heifers, calves, cattle**
Dry matter content	0.18
Organic matter content in dry matter	0.86
Biogas output from manure (m^3 t^{-1})	300
Heat energy of biogas (kWh m^{-3})	5.8

The biogas production potential of livestock manure from the different groups of livestock in Iran was calculated based on Plume et al. (2012) using *Equation 5* and is presented in *Table 10.*

http://www.aloki.hu ● ISSN 1589 1623 (Print) ● ISSN 1785 0037 (Online)
DOI: http://dx.doi.org/10.15666/aeer/1605_64996523
© 2018, ALÖKI Kft., Budapest, Hungary

Table 10. *The estimated values of biogas production of different provinces in Iran in 2016 based on Plume et al. (2012)*

Biogas production (million m^3 yr^{-1})						
Province	**Dairy cows**		**Heifers**	**Calves**	**Cattle**	**Total**
	Lactating cow	**Dry cow**				
Azerbaijan, West	9.28	1.64	2.09	0.83	2.11	15.96
Azerbaijan, East	3.35	0.90	0.78	0.51	0.79	6.35
Ardabil	5.92	1.31	1.49	1.02	1.15	10.92
Isfahan	103.03	13.81	15.75	5.79	3.55	141.95
Alborz	28.20	5.01	5.35	2.01	1.81	42.40
Ilam	1.29	0.86	0.23	0.20	0.40	3.00
Bushehr	0.19	0.55	0.24	0.78	0.20	1.97
Tehran	73.43	20.07	18.39	16.11	5.22	133.24
ChaharMahaal and Bakhtiari	10.82	3.21	2.14	0.81	0.56	17.56
Khorasan, South	3.36	1.03	0.83	0.37	0.45	6.06
Khorasan, Razavi	45.52	7.89	8.29	3.27	3.56	68.55
Khorasan, North	2.23	0.44	0.45	0.32	0.36	3.82
Khuzestan	2.88	1.02	0.59	1.50	1.91	7.92
Zanjan	7.22	1.13	1.51	0.41	0.81	11.10
Semnan	13.33	3.01	2.74	1.70	7.11	27.91
Sistan and Baluchestan	0.37	0.30	0.10	0.19	0.60	1.57
Fars	34.03	6.44	8.20	3.56	4.79	57.05
Qazvin	28.11	3.82	4.96	2.62	2.40	41.93
Qom	11.54	1.69	2.00	4.86	3.66	23.77
Kurdistan	1.06	0.13	0.19	0.16	0.12	1.68
Kerman	9.13	2.78	2.44	0.96	1.81	17.15
Kermanshah	7.41	1.17	1.29	0.41	0.90	11.20
Kohgiluyeh and Boyer-Ahmad	1.57	0.20	0.33	0.21	0.01	2.35
Golestan	5.49	1.68	1.68	0.55	0.27	9.69
Gilan	0.95	0.30	0.30	0.11	0.14	1.82
Lorestan	2.24	0.52	0.57	0.52	0.10	3.97
Mazandaran	8.40	1.69	1.52	0.60	1.08	13.32
Markazi	7.29	1.74	1.59	4.71	2.09	17.44
Hormozgan	0.09	0.06	0.02	0.04	0.27	0.49
Hamadan	6.55	1.62	0.94	0.67	0.33	10.13
Yazd	19.63	4.65	5.00	1.73	1.95	32.981
Iran	454.04	90.80	92.15	57.67	50.68	745.37

Calculation of the potential of electricity generation from the livestock manure in Iran

The potential of electricity generation from the biogas obtainable from livestock manure calculated based on Abdeshahian, Boysan, Zareei and Plume methods was estimated for all provinces of Iran according to *Equations 3* and *4* and is presented in *Table 11.*

http://www.aloki.hu ● ISSN 1589 1623 (Print) ● ISSN 1785 0037 (Online)
DOI: http://dx.doi.org/10.15666/aeer/1605_64996523
© 2018, ALÖKI Kft., Budapest, Hungary

Table 11. *The estimated values of the potential of electricity generation from livestock manure based on different methods in all provinces of Iran in 2016*

Electricity generation potential (kWh yr^{-1})									
Province	**Abdeshahian**	**Boysan**	**Zareei**	**Plume**	**Province**	**Abdeshahian**	**Boysan**	**Zareei**	**Plume**
Azerbaijan, West	3.14E+07	6.15E+06	2.01E+07	2.87E+07	Fars	1.17E+08	2.28E+07	7.44E+07	1.03E+08
Azerbaijan, East	1.46E+07	2.86E+06	9.35E+06	1.14E+07	Qazvin	8.05E+07	1.57E+07	5.14E+07	7.55E+07
Ardabil	2.77E+07	5.41E+06	1.77E+07	1.97E+07	Qom	7.19E+07	1.41E+07	4.59E+07	4.28E+07
Isfahan	2.29E+08	4.49E+07	1.46E+08	2.56E+08	Kurdistan	3.80E+06	7.43E+05	2.43E+06	3.02E+06
Alborz	8.02E+07	1.57E+07	5.12E+07	7.63E+07	Kerman	3.68E+07	7.20E+06	2.35E+07	3.09E+07
Ilam	6.82E+06	1.33E+06	4.35E+06	5.41E+06	Kermanshah	1.83E+07	3.59E+06	1.17E+07	2.02E+07
Bushehr	1.06E+07	2.06E+06	6.74E+06	3.55E+06	Kohgiluyeh and Boyer-Ahmad	4.92E+06	9.61E+05	3.14E+06	4.24E+06
Tehran	3.56E+08	6.97E+07	2.27E+08	2.40E+08	Golestan	2.02E+07	3.96E+06	1.29E+07	1.74E+07
ChaharMahaal and Bakhtiari	3.26E+07	6.38E+06	2.08E+07	3.16E+07	Gilan	4.18E+06	8.17E+05	2.67E+06	3.28E+06
Khorasan, South	1.27E+07	2.49E+06	8.13E+06	1.09E+07	Lorestan	1.10E+07	2.14E+06	7.00E+06	7.16E+06
Khorasan, Razavi	1.25E+08	2.44E+07	7.97E+07	1.23E+08	Mazandaran	2.40E+07	4.69E+06	1.53E+07	2.40E+07
Khorasan, North	8.46E+06	1.65E+06	5.40E+06	6.88E+06	Markazi	6.66E+07	1.30E+07	4.25E+07	3.14E+07
Khuzestan	2.57E+07	5.03E+06	1.64E+07	1.43E+07	Hormozgan	1.41E+06	2.75E+05	8.99E+05	8.93E+05
Zanjan	1.89E+07	3.69E+06	1.20E+07	2.00E+07	Hamadan	1.94E+07	3.80E+06	1.24E+07	1.82E+07
Semnan	6.39E+07	1.25E+07	4.08E+07	5.03E+07	Yazd	6.74E+07	1.32E+07	4.30E+07	5.94E+07
Sistan and Baluchestan	4.56E+06	8.92E+05	2.91E+06	2.84E+06	Iran	1.60E+09	3.12E+08	1.02E+09	1.34E+09

Calculation of the potential of energy of biogas from the livestock manure in Iran

The potential of energy of biogas obtainable from manure biomass calculated based on Abdeshahina, Boysan, Zareei and Plume Methods in all provinces of Iran was estimated using *Equation 6* and is presented in *Table 12*.

Table 12. *The estimated values of the biogas energy obtainable from manure biomass based on different methods in all provinces of Iran in 2016*

The potential of biogas energy obtainable from manure (kWh)									
Province	**Abdeshahian**	**Boysan**	**Zareei**	**Plume**	**Province**	**Abdeshahian**	**Boysan**	**Zareei**	**Plume**
Azerbaijan, West	1.01E+08	1.98E+07	6.47E+07	9.26E+07	Fars	3.76E+08	7.34E+07	2.40E+08	3.31E+08
Azerbaijan, East	4.72E+07	9.23E+06	3.01E+07	3.69E+07	Qazvin	2.59E+08	5.07E+07	1.65E+08	2.43E+08
Ardabil	8.92E+07	1.74E+07	5.69E+07	6.34E+07	Qom	2.32E+08	4.53E+07	1.48E+08	1.38E+08
Isfahan	7.39E+08	1.45E+08	4.72E+08	8.23E+08	Kurdistan	1.22E+07	2.39E+06	7.77E+06	9.74E+06
Alborz	2.58E+08	5.05E+07	1.65E+08	2.46E+08	Kerman	1.19E+08	2.32E+07	7.56E+07	9.95E+07
Ilam	2.20E+07	4.30E+06	1.40E+07	1.74E+07	Kermanshah	5.91E+07	1.16E+07	3.77E+07	6.50E+07

http://www.aloki.hu ● ISSN 1589 1623 (Print) ● ISSN 1785 0037 (Online)
DOI: http://dx.doi.org/10.15666/aeer/1605_64996523
© 2018, ALÖKI Kft., Budapest, Hungary

Table 12 (continued). *The estimated values of the biogas energy obtainable from manure biomass based on different methods in all provinces of Iran in 2016*

The potential of biogas energy obtainable from manure (kWh)									
Province	**Abdeshahian**	**Boysan**	**Zareei**	**Plume**	**Province**	**Abdeshahian**	**Boysan**	**Zareei**	**Plume**
Bushehr	3.40E+07	6.65E+06	2.17E+07	1.14E+07	Kohgiluyeh and Boyer-Ahmad	1.58E+07	3.10E+06	1.01E+07	1.37E+07
Tehran	1.15E+09	2.25E+08	7.33E+08	7.73E+08	Golestan	6.52E+07	1.28E+07	4.16E+07	5.62E+07
ChaharMahaal and Bakhtiari	1.05E+08	2.06E+07	6.70E+07	1.02E+08	Gilan	1.35E+07	2.63E+06	8.58E+06	1.06E+07
Khorasan, South	4.11E+07	8.03E+06	2.62E+07	3.52E+07	Lorestan	3.53E+07	6.91E+06	2.25E+07	2.31E+07
Khorasan, Razavi	4.02E+08	7.87E+07	2.57E+08	3.98E+08	Mazandaran	7.73E+07	1.51E+07	4.94E+07	7.73E+07
Khorasan, North	2.72E+07	5.33E+06	1.73E+07	2.22E+07	Markazi	2.15E+08	4.20E+07	1.37E+08	1.01E+08
Khuzestan	8.28E+07	1.62E+07	5.28E+07	4.60E+07	Hormozgan	4.54E+06	8.87E+05	2.84E+06	2.88E+06
Zanjan	6.08E+07	1.19E+07	3.88E+07	6.44E+07	Hamadan	6.26E+07	1.22E+07	3.99E+07	5.88E+07
Semnan	2.06E+08	4.03E+07	1.31E+08	1.62E+08	Yazd	2.17E+08	4.25E+07	1.39E+08	1.91E+08
Sistan and Baluchestan	1.47E+07	2.87E+06	9.34E+06	9.16E+06	Iran	5.14E+09	1.01E+09	3.28E+09	4.32E+09

Calculation of methane (CH_4) content of biogas from manure livestock in Iran

The chemical composition of the livestock manure which is required to calculate the biochemical methane potential based on Cu et al. (2015) including dry matter, volatile solid, protein, lipid, cellulose and lignin are shown in *Table 13*.

Table 13. *Chemical composition of livestock manure based on Cu et al. (2015)*

Substrates	Animal manure group
Dry matter	10.94
Volatile solid[1]	73.01
Protein[1]	7.55
Lipid[1]	3.63
Cellulose[1]	17.59
Lignin[1]	10.41

[1]% in dry matter

The BMP value based on chemical composition of the substrate was calculated according to chemical composition of the livestock manure (*Table 13*) and equations to predict BMP (*Table 3*) and is presented in *Table 14*.

Table 14. *The estimated values of BMP based on chemical composition of the substrate*

Variables	BMP
Lipid	184.95
Lipid, lignin	243.67
Lipid, lignin, dry matter	232.31
Lipid, lignin, cellulose	242.34

http://www.aloki.hu ● ISSN 1589 1623 (Print) ● ISSN 1785 0037 (Online)
DOI: http://dx.doi.org/10.15666/aeer/1605_64996523
© 2018, ALÖKI Kft., Budapest, Hungary

The methane yield was calculated in different provinces of Iran according to the BMP value (β_o in the extended Hashimoto equation by Rennuit and Sommer (2013)) from different types of substrate based on chemical composition (*Table 14*) and is presented in *Tables 15–18*.

Table 15. *The estimated values of methane yield (NL CH_4 digester^{-1} day^{-1}) based on the BMP value of specific substrate (lipid)*

Province	Methane yield	Province	Methane yield	Province	Methane yield	Province	Methane yield
Azerbaijan, West	5.64E+08	ChaharMahaal and Bakhtiari	3.13E+08	Fars	3.19E+09	Gilan	7.90E+07
Azerbaijan, East	1.72E+08	Khorasan, South	2.89E+08	Qazvin	1.45E+09	Lorestan	2.60E+08
Ardabil	1.41E+08	Khorasan, Razavi	2.65E+09	Qom	2.20E+09	Mazandaran	5.53E+08
Isfahan	5.94E+09	Khorasan, North	1.33E+08	Kurdistan	7.02E+07	Markazi	1.29E+09
Alborz	1.70E+09	Khuzestan	1.24E+09	Kerman	8.38E+08	Hormozgan	7.31E+07
Ilam	1.52E+08	Zanjan	2.33E+08	Kermanshah	3.73E+08	Hamadan	2.67E+08
Bushehr	4.98E+08	Semnan	2.00E+09	Kohgiluyeh and Boyer-Ahmad	7.68E+07	Yazd	2.28E+09
Tehran	1.05E+10	Sistan and Baluchestan	1.32E+08	Golestan	4.71E+08	Iran	4.01E+10

Table 16. *The estimated values of methane yield (NL CH_4 digester^{-1} day^{-1}) based on the BMP value of specific substrate (lipid and lignin)*

Province	Methane yield	Province	Methane yield	Province	Methane yield	Province	Methane yield
Azerbaijan, West	7.42E+08	ChaharMahaal and Bakhtiari	4.12E+08	Fars	4.2E+09	Gilan	1.04E+08
Azerbaijan, East	2.26E+08	Khorasan, South	3.81E+08	Qazvin	1.9E+09	Lorestan	3.43E+08
Ardabil	1.85E+08	Khorasan, Razavi	3.49E+09	Qom	2.9E+09	Mazandaran	7.27E+08
Isfahan	7.82E+09	Khorasan, North	1.75E+08	Kurdistan	92446950	Markazi	1.7E+09
Alborz	2.23E+09	Khuzestan	1.64E+09	Kerman	1.1E+09	Hormozgan	97949190
Ilam	1.99E+08	Zanjan	3.07E+08	Kermanshah	4.9E+08	Hamadan	3.51E+08
Bushehr	6.57E+08	Semnan	2.63E+09	Kohgiluyeh and Boyer-Ahmad	1.02E+08	Yazd	3E+09
Tehran	1.38E+10	Sistan and Baluchestan	1.74E+08	Golestan	6.2E+08	Iran	5.27E+10

http://www.aloki.hu ● ISSN 1589 1623 (Print) ● ISSN 1785 0037 (Online)
DOI: http://dx.doi.org/10.15666/aeer/1605_64996523
© 2018, ALÖKI Kft., Budapest, Hungary

Table 17. *The estimated values of methane yield (NL CH_4 $digester^{-1}$ day^{-1}) based on the BMP value of specific substrate (lipid, lignin and dry matter)*

Province	Methane yield	Province	Methane yield	Province	Methane yield	Province	Methane yield
Azerbaijan, West	7.08E+08	ChaharMahaal and Bakhtiari	3.93E+08	Fars	4.01E+09	Gilan	9.90E+07
Azerbaijan, East	2.15E+08	Khorasan, South	3.63E+08	Qazvin	1.81E+09	Lorestan	3.27E+08
Ardabil	1.77E+08	Khorasan, Razavi	3.33E+09	Qom	2.77E+09	Mazandaran	6.93E+08
Isfahan	7.46E+09	Khorasan, North	1.66E+08	Kurdistan	8.81E+07	Markazi	1.62E+09
Alborz	2.13E+09	Khuzestan	1.56E+09	Kerman	1.05E+09	Hormozgan	9.17E+07
Ilam	1.9E+08	Zanjan	2.93E+08	Kermanshah	4.68E+08	Hamadan	3.34E+08
Bushehr	6.26E+08	Semnan	2.5E+09	Kohgiluyeh and Boyer-Ahmad	9.71E+07	Yazd	2.86E+09
Tehran	1.31E+10	Sistan and Baluchestan	1.66E+08	Golestan	5.91E+08	Iran	5.03E+10

Table 18. *The estimated values of methane yield (NL CH_4 $digester^{-1}$ day^{-1}) based on the BMP value of specific substrate (lipid, lignin and cellulose)*

Province	Methane yield	Province	Methane yield	Province	Methane yield	Province	Methane yield
Azerbaijan, West	7.38E+08	ChaharMahaal and Bakhtiari	4.09E+08	Fars	4.18E+09	Gilan	1.03E+08
Azerbaijan, East	2.25E+08	Khorasan, South	3.79E+08	Qazvin	1.89E+09	Lorestan	3.41E+08
Ardabil	1.84E+08	Khorasan, Razavi	3.47E+09	Qom	2.89E+09	Mazandaran	7.23E+08
Isfahan	7.78E+09	Khorasan, North	1.74E+08	Kurdistan	91942230	Markazi	1.69E+09
Alborz	2.22E+09	Khuzestan	1.63E+09	Kerman	1.1E+09	Hormozgan	95695200
Ilam	1.98E+08	Zanjan	3.05E+08	Kermanshah	4.88E+08	Hamadan	3.49E+08
Bushehr	6.53E+08	Semnan	2.61E+09	Kohgiluyeh and Boyer-Ahmad	1.01E+08	Yazd	2.98E+09
Tehran	1.37E+10	Sistan and Baluchestan	1.73E+08	Golestan	6.16E+08	Iran	5.25E+10

The potential of livestock manure production, biogas, electricity and energy obtainable from livestock manure and methane yield of biogas were calculated for all provinces in Iran in order to compare the results between provinces and determine which of them has the least and most potential. The amount of livestock manure production in different provinces in Iran based on Abdeshahian, Boysan and Zareei methods (*Table 4*), shows that the higher amount of the manure was produced in Tehran while the lowest amount of the manure is related to Hormozgan and it is because of this

http://www.aloki.hu ● ISSN 1589 1623 (Print) ● ISSN 1785 0037 (Online)
DOI: http://dx.doi.org/10.15666/aeer/1605_64996523
© 2018, ALÖKI Kft., Budapest, Hungary

that Tehran and Hormozgan have the highest and the lowest number of livestock, respectively, compared to that other provinces of Iran. On the other hand, the amount of livestock manure based on Plume method (*Table 7*) shows that the higher amount of the manure was produced in Isfahan. This is due to considering the different manure production for each group of livestock (dairy cows, heifers, calves and cattle) in this method. The lowest amount of manure production still belongs to Hormozgan.

Figure 2 shows the potential of livestock manure production in Iran according to 4 different methods. It is shown that the higher amount of the manure was produced in Plume method with the annual manure production of 16.05 million ton followed by Abdeshahian, Boysan and Zareei methods with a manure production of 11.82, 5.25 and 2.1 tons, respectively. As can be seen, the amount of livestock manure produced using Zareei method was much less compared to that from Plume, Abdeshahian and Boysan methods. This is due to the fact that the lowest coefficient of manure production was considered in this method (the ratio of the annual livestock manure to livestock weight = 2.6).

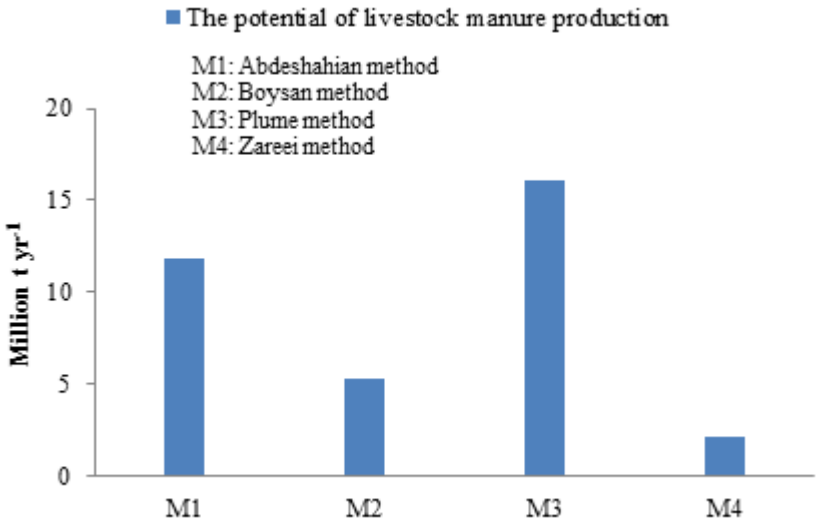

Figure 2. *Comparison the estimated values of the manure production potential in Iran using 4 different calculation methods*

The comparison of the biogas production potential in different provinces of Iran (*Tables 8* and *10*) revealed that Tehran had the highest potential of biogas evolution based on Abdeshahian, Zareei and Boysan methods, while Isfahan had the highest potential of biogas evolution based on Plume method. Hormozgan had the lowest amount of biogas production potential in each method.

The biogas production potential from the livestock manure based on 4 mentioned methods is shown in *Figure 3*. It is found that the highest potential of biogas from the manure is obtained from Abdeshahian method with the biogas production potential of 886.57 million m^3 yr^{-1}, followed by Plume, Zareei and Boysan methods with a biogas generation potential of 745.37, 565.85 and 173.36 million m^3 yr^{-1}, respectively.

This study showed that the cattle manure can be considered as the good source for the generation of biogas in an AD process. Similar observations were reported by other studies. For instance, it has been reported that Vietnam has the potential of generation

http://www.aloki.hu ● ISSN 1589 1623 (Print) ● ISSN 1785 0037 (Online)
DOI: http://dx.doi.org/10.15666/aeer/1605_64996523
© 2018, ALÖKI Kft., Budapest, Hungary

of 16878 TJ y^{-1} biogas in 2014 from the cattle manure (Roubik et al., 2017). The study on the Nigeria biogas potential has revealed that Nigeria biogas potential from livestock manure represents a minimum of 1.62×109 m^3 of biogas per annum (Adeoti et al., 2014).

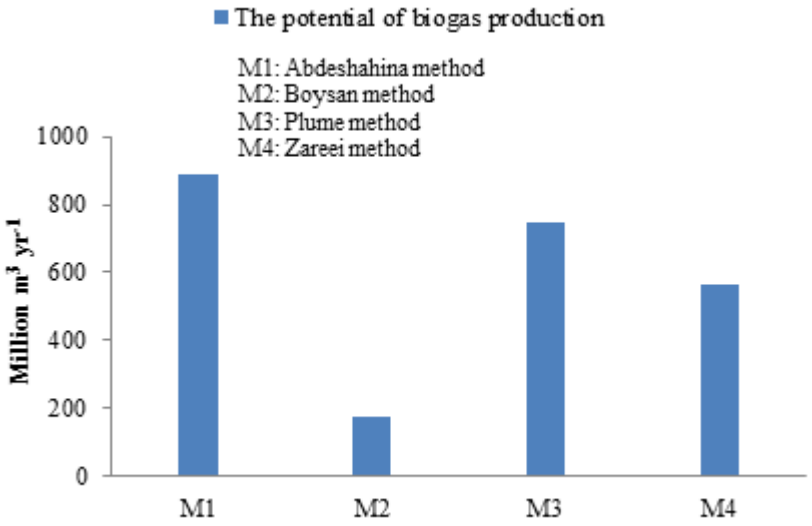

Figure 3. *Comparison the estimated values of the biogas production potential in Iran using 4 different calculation methods*

Figure 4 depicts the energy and electricity potential from livestock manure in Iran based on 4 calculation methods. As can be seen, the biogas produced from the livestock manure based on Abdeshahian, Boysan, Plume and Zareei methods was potentially able to provide the heat energy with the value of 5.14, 1, 4.32 and 3.28 thousand GWh yr^{-1}, respectively. The results shown in *Figure 4* also indicated that the total amount of electricity generation estimated in Iran based on Abdeshahian, Boysan, Plume and Zareei methods was 1.59, 0.31, 1.34 and 1.02 thousand GWh yr^{-1}, respectively. These estimated values could provide the 0.67%, 0.56%, 0.13% and 0.42% of the total electrical energy consumed in Iran in 2016 with the total electricity consumption of 237.4 billion kWh (Iran Energy Ministry, 2017). It should be noted that the electricity consumption with the value of 237.4 billion kWh was related to household, public, agricultural, industrial and other uses of the electrical energy consumed. The share of electrical energy consumption in household sector in Iran in 2016 was mainly for lightning, electrical household appliances and cooling systems with amount of 33% of the total electricity consumption. Hence, the electricity generation from livestock manure based on Abdeshahian, Plume, Boysan and Zareei methods could provide the 2.03%, 1.71%, 0.39% and 1.3% of the total electrical energy consumed in household sector in Iran in 2016, respectively, with the total electricity consumption of 78378 million kWh.

In this regard, the investigation on the potential of electricity generation from livestock manure in Malaysia showed that the total amount of electricity generation was 6.85E + 09 kWh yr^{-1} (Abdeshahian et al., 2016). Also the study on the potential for electricity generation from biogas in South Africa showed that the potential of electricity production from cattle manure was 2098553 MWh (Laks, 2017).

http://www.aloki.hu ● ISSN 1589 1623 (Print) ● ISSN 1785 0037 (Online)
DOI: http://dx.doi.org/10.15666/aeer/1605_64996523
© 2018, ALÖKI Kft., Budapest, Hungary

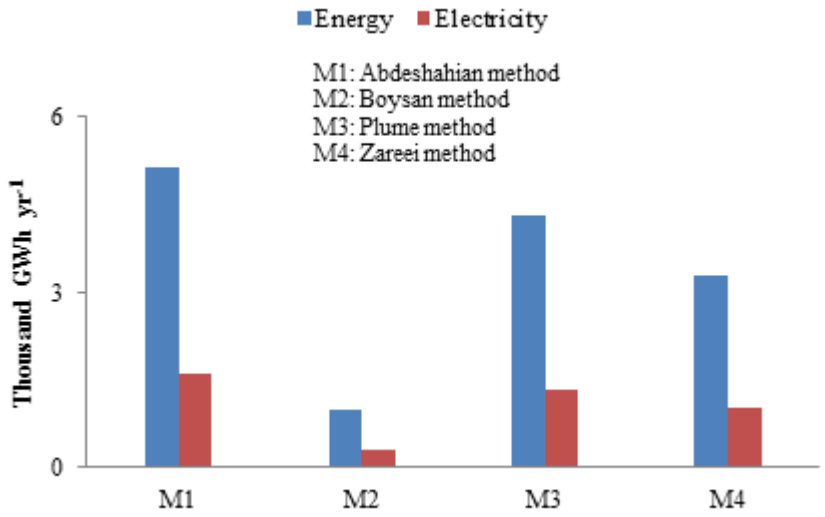

Figure 4. *Comparison the estimated values of the energy and electricity potential from livestock manure in Iran using 4 different calculation methods*

The methane production potential from the livestock manure in Iran with considering the different types of substrate (lipid, lignin, dry matter and cellulose) is shown in *Figure 5.* As can be observed, the highest potential of methane yield is related to the BMP value of lipid and lignin content at 5.27E + 10 NL CH_4 digester^{-1} day^{-1} followed by BMP value of lipid, lignin and cellulose, BMP value of lipid, lignin and dry matter and BPM value of lipid, at, respectively, 5.25E + 10, 5.03E + 10 and 4.01E + 10 NL CH_4 digester^{-1} day^{-1}.

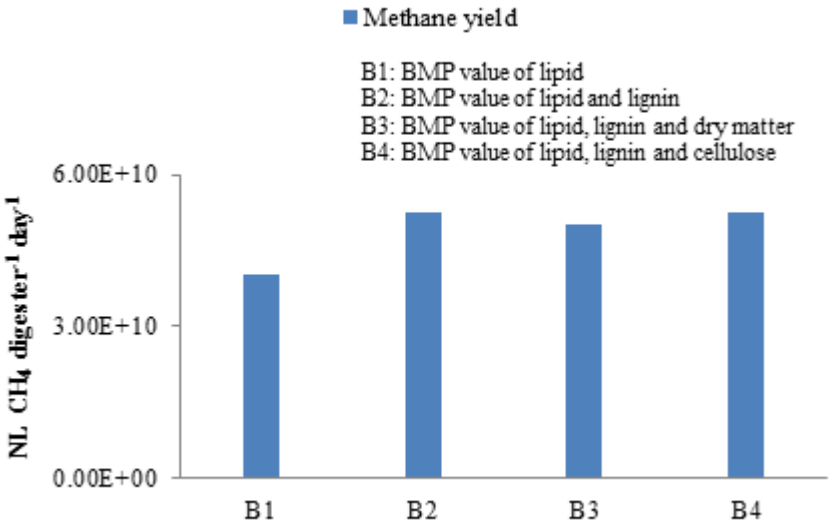

Figure 5. *Comparison the estimated values of the methane production potential from livestock manure in Iran considering the BMP value of specific substrate*

http://www.aloki.hu ● ISSN 1589 1623 (Print) ● ISSN 1785 0037 (Online)
DOI: http://dx.doi.org/10.15666/aeer/1605_64996523
© 2018, ALÖKI Kft., Budapest, Hungary

Study fulfilled by Scarlat et al. (2018b) revealed that the potential of methane production from livestock manure in Belgium, Germany, Ireland, Spain and France is 556, 2907, 893, 2298, 3952 million m^3, respectively. These results reflect the lower methane potential in mentioned countries than Iran. This discrepancy could be related to the variation in the biotransformation rate of manure into methane and different amount of the livestock waste produced.

Conclusion

Present study focuses on the evaluation of the different methods for estimating biogas production potential from livestock manure in Iran. Biogas generation from animal wastes has rarely been assessed based on their chemical structure and the findings of this research reveal the significance of manure chemical properties to be considered or the estimation of biogas production in husbandry industry. As a result of the calculations made, the manure production was estimated as 11.82, 5.25, 16.05 and 2.1 million ton yr^{-1} based on Abdeshahin, Boysan, Plume and Zareei methods with a biogas generation potential of 886.57, 173.36, 745.37 and 565.85 million m^3 yr^{-1}, energy equivalent of 5.14, 1, 4.32 and 3.28 thousand GWh yr^{-1}, and electricity generation potential of 1.59, 0.31, 1.34 and 1.02 thousand GWh yr^{-1}, respectively. The electrical energy values could provide the 2.03%, 1.71%, 0.39% and 1.3% of the total electrical energy consumed in household sector in Iran in 2016, respectively. Furthermore the methane yield potential from the livestock manure with considering the different types of substrate (lipid, lignin, dry matter and cellulose) was evaluated. The highest methane yield was obtained from BMP value based on lipid and lignin content at 5.27E + 10 NL CH_4 $digester^{-1}$ day^{-1}. This study shows that the treatment of the livestock manure by the anaerobic digestion process is helpful for producing the huge amounts of renewable energy as biogas. In addition, anaerobic digestion of livestock waste reduces their deleterious impacts on the environment and the treated organic matters could be used for the improvement of crops growth in the agriculture land. For future studies it is recommended to develop new applicable models based on chemical composition of animal wastes to further reveal the contribution of animal waste composition in generation of biochar and precisely estimate biogas production potential from such wastes.

REFERENCES

[1] Abdeshahian, P., Lim, J. S., Ho, W. S., Hashim, H., Lee. C. T. (2016): Potential of biogas production from farm animal waste in Malaysia. – Renewable and Sustainable Energy Reviews 60: 714-723.

[2] Achinas, S., Euverink, G. J. W. (2016): Theoretical analysis of biogas potential prediction from agricultural waste. – Resource-Efficient Technologies 2: 143-147.

[3] Adeoti, O., Ayelegun, T. A., Osho, S. O. (2014): Nigeria biogas potential from livestock manure and its estimated climate value. – Renewable and Sustainable Energy Reviews 37: 243-248.

[4] Afazeli, H., Jafari, A., Rafiee, S., Nosrati, M. (2014): An investigation of biogas production potential from livestock and slaughter house wastes. – Renewable and Sustainable Energy Reviews 34: 380-386.

http://www.aloki.hu ● ISSN 1589 1623 (Print) ● ISSN 1785 0037 (Online)
DOI: http://dx.doi.org/10.15666/aeer/1605_64996523
© 2018, ALÖKI Kft., Budapest, Hungary

[5] Angelidaki, I., Treu, L., Tsapekos, P., Luo, G., Campanaro, S., Wenzel, H., Kougias, P. G. (2018): Biogas upgrading and utilization: Current status and perspectives. – Biotechnology Advances 36: 452-466.
[6] Beldman, A., van Berkum, S., Kortstee, H., Zijlstra, J. (2017): Dairy farming and dairy industry in Iran. – Wageningen University &Research.
[7] Benito, M., Ortiz, I., Rodriguez, L., Munoz, G. (2015): Ni–Co bimetallic catalyst for hydrogen production in sewage treatment plants: biogas reforming and tars removal. – International Journal of Hydrogen Energy 40(42): 14456-14468.
[8] Boysan, F., Ozer, C, Bakkaloglu, K., Borekci, M. T. (2015): Biogas production from animal manure. – Procedia Earth and Planetary Science 15: 908-911.
[9] Burg, V., Bowman, G., Haubensak, M., Baier, U., Thees, O. (2018): Valorization of an untapped resource: Energy and greenhouse gas emissions benefits of converting manure to biogas through anaerobic digestion. – Resources, Conservation & Recycling 136: 53-62.
[10] Chandekar, A. C., Debnath, B. K. (2018): Computational investigation of air-biogas mixing device for different biogas substitutions and engine load variations. – Renewable Energy 127: 811-824.
[11] Chen, Y. R., Hashimoto, A. G. (1978): Kinetics of Methane Fermentation. Biotechnology and Bioengineering Symposium. – Wiley, New York, USA.
[12] Ch'ng, H. Y., Ahmed, O. H., Kassim, S., Majid, N. M. A. (2014): Recycling of sago (Metroxylon sagu) bagasse with chicken manure slurry through co-composting. – J. Agr. Sci. Tech. 16: 1441-1454.
[13] Comparetti, A., Greco, C., Navickas, K., Venslauskas, K. (2012): Evaluation of potential biogas production in Sicily. – 11th International Scientific Conference: Engineering for Rural Development, Jelgava, Latvia.
[14] Costa, M. S. S. D. M., Jr, J. D. L., Costa, L. A. D. M., Orrico, A. C. A. (2016): A highly concentrated diet increases biogas production and the agronomic value of young bull's manure. – Waste Management 48: 521-527.
[15] Cu, T. T. T., Pham, H. C., Le, T. H., Nguyen, V. C., Le, X. A., Nguyen, X. T., Sven, G. C. (2012): Manure management practices on biogas and non-biogas pig farms in developing countries using livestock farms in Vietnam as an example. – Journal of Cleaner Production 27: 64-71.
[16] Cu, T. T. T., Nguyen, T. X., Triolo, J. M., Pedersen, L., Le, V. D., Le, P. D., Sommer. S. G. (2015): Biogas production from Vietnamese animal manure, plant residues and organic waste: influence of biomass composition on methane yield. – Asian Australas. J. Anim. Sci. 28(2): 280-289.
[17] De-Vries, J. W., Vinken, T. M. W. J., Hamelin, L., De-Boer, I. J. M. (2012): Comparing environmental consequences of anaerobic mono- and co-digestion of pig manure to produce bio-energy - a life cycle perspective. – Bioresource Technology 125: 239-248.
[18] Eze, J. I., Agbo, K. E. (2010): Studies on the microbial spectrum in an aerobic bio-methanization of cow dung in 10 m^3 fixed dome biogas digester. – International Journal of the Physical Sciences 5(8): 1331-1337.
[19] Garcia, A. P. (2014): Techno-economic feasibility study of a small-scale biogas plant for treating market waste in the city of El Alto. – Master of Science Thesis, KTH School of Industrial Engineering and Management, Division of Energy and Climate, Stockholm.
[20] Gebrezgabher, S. A., Meuwissen, M. P. M., Prins, B. A. M., Lansink, A. G. J. M. O. (2010): Economic analysis of anaerobic digestion - a case of Green power biogas plant in The Netherlands. – NJAS - Wageningen Journal of Life Sciences 57(2): 109-115.
[21] Government of Islamic Republic of Iran (GOI)/Ministry of Jihad-e-Agriculture (MOJA), Food and Agriculture Organization (FAO) of the United Nations (2012): Country Programming Framework (CPF) 2012-2016 for Iran's Agriculture Sector. – GOI, MOJA, FAO, Tehran, Rome.

http://www.aloki.hu ● ISSN 1589 1623 (Print) ● ISSN 1785 0037 (Online)
DOI: http://dx.doi.org/10.15666/aeer/1605_64996523
© 2018, ALÖKI Kft., Budapest, Hungary

[22] Hamzeh, Y., Ashori, A., Mirzaei, B., Abdulkhani, A., Molaei, M. (2011): Current and potential capabilities of biomass for green energy in Iran. – Renewable and Sustainable Energy Reviews 15: 4934-4938.
[23] Hashimoto, A. G., Chen, Y. R., Varel, V. H. (1981): Theoretical aspects of methane production: State-of-the-art. – Livestock Wastes: A Renewable Resource - 4th International Symposium on Livestock Wastes, ASAE, pp. 86-91.
[24] Holm-Nielsen, J. B., Seadi, T. A., Oleskowicz-Popiel, P. (2009): The future of anaerobic digestion and biogas utilization. – Bioresource Technology 100(22): 5478-4584.
[25] Hosseini, S. E., Wahid, M. A. (2014): Development of biogas combustion in combined heat and power generation. – Renewable and Sustainable Energy Reviews 40: 868-875.
[26] Ilaboya, I. R., Asekhame, F. F., Ezugwu, M. O., Erameh, A. A., Omofuma, F. E. (2010): Studies on biogas generation from agricultural waste; analysis of the effects of alkaline on gas generation. – World Appl. Sci. J. 9(5): 537-545.
[27] International Energy Agency (2015): Energy and Climate Change. – World Energy Outlook Special Report, OECD/IEA, Paris.
[28] Iran Energy Ministry (2017): Iran Power Industry 2016. – Tavanir Holding Company, Iran (Persian).
[29] Kougias, P. G., Boe, K., Angelidaki, I. (2013): Effect of organic loading rate and feedstock composition on foaming in manure-based biogas reactors. – Bioresource Technology 144: 1-7.
[30] Laks, R (2017): The Potential for Electricity Generation from Biogas in South Africa. – ECN-E--17-001. ECN, Petten, Netherlands
[31] Luostarinen, S. (2013): Energy Potential of Manure in the Baltic Sea Region: Biogas Potential & Incentives and Barriers for Implementation. – Knowledge Report, Baltic Forum for Innovative Technologies for Sustainable Manure Management.
[32] Mata-alvarez, J., Mace, S., Llabres, P. (2000): Anaerobic digestion of organic solid wastes - an overview of research achievements and perspectives. – Bioresource Technology 74(1): 3-16.
[33] Mathias, J. F. C. M. (2014): Manure as a resource: livestock waste management from anaerobic digestion, opportunities and challenges for Brazil. – International Food and Agribusiness Management Review 17: 87-110.
[34] Meyer, A. K. P., Ehimern. E. A., Holm-Nielsen, J. B. (2018): Future European biogas: Animal manure, straw and grass potentials for a sustainable European biogas production. – Biomass and Bioenergy 111: 154-164.
[35] Mohammadi Maghanaki, M., Ghobadian, B., Najaf, G., Janzadeh Galogah, R. (2013): Potential of biogas production in Iran. – Renewable and Sustainable Energy Reviews 28: 702-714.
[36] Nasir, I. M., Ghazi, T. I. M., Omar, R. (2012): Anaerobic digestion technology in livestock manure treatment for biogas production: a review. – Engineering in Life Sciences 12: 258-269.
[37] Nasir, I. M., Ghazi, T. I. M., Omar, R., Idris, A. (2013): Anaerobic digestion of cattle manure: influence of inoculums concentration. – International Journal of Engineering Technology 10(1): 22-26.
[38] Neshat, S. A., Mohammadi, M., Najafpour, G. D., Lahijani, P. (2017): Anaerobic co-digestion of animal manures and lignocellulosic residues as a potent approach for sustainable biogas production. – Renewable and Sustainable Energy Reviews 79: 308-322.
[39] Omar, R., Harun, R. M., Ghazi, T. I. M., Wan-Azlina, W. A. K. G., Idris, A., Yunus, R. (2009): Anaerobic treatment of cattle manure for biogas production. – Proceedings of the annual meeting of American Institute of Chemical Engineers, Philadelphia, USA.
[40] Omrani, GH. (1996): Basics Biogas Production from Urban and Rural Waste. – University of Tehran Publication, Iran.

http://www.aloki.hu ● ISSN 1589 1623 (Print) ● ISSN 1785 0037 (Online)
DOI: http://dx.doi.org/10.15666/aeer/1605_64996523
© 2018, ALÖKI Kft., Budapest, Hungary

[41] Onurbas-Avcioglu, A., Turker, U. (2012): Status and potential of biogas energy from animal wastes in Turkey. – Renewable Sustainable Energy Reviews 16(3): 1557-1561.
[42] Ounnar, A., Benhabyles, L., Igoud, S. (2012): Energetic valorization of biomethane produced from cow-dung. – Procedia Engineering 33: 330-334.
[43] Ozer, B. (2017): Biogas energy opportunity of Ardahan city of Turkey. – Energy 139: 1144-1152.
[44] Perrigault, T., Weatherford, V., Marti-Herrero, J., Poggio, D. (2012): Towards thermal design optimization of tubular digesters in cold climates: A heat transfer model. – Bioresource Technology 124: 259-268.
[45] Pessuto, J., Scopel, B. S., Perondi, D., Godinho, M., Dettmer, A. (2016): Enhancement of biogas and methane production by anaerobic digestion of swine manure with addition of microorganisms isolated from sewage sludge. – Process Safety and Environmental Protection 104: 233-239.
[46] Plume, I., Dubrovskis, V., Plume, B. (2012): Specified evaluation of manure resources for production of biogas in planning region Latgale. – International Scientific Conference of Renewable Energy and Energy Efficiency, Latvia University of Agriculture.
[47] Rennuit, C., Sommer, S. G. (2013): Decision support for the construction of farm-scale biogas digesters in developing countries with cold seasons. – Energies 6(10): 5314-5332.
[48] Roubik, H., Mazancova, J., Phung, L. D., Dung. D. V. (2017): Quantification of biogas potential from livestock waste in Vietnam. – Agronomy Research 15: 540-552.
[49] Sahota, S., Shah, G., Ghosh, P., Kapoor, R., Sengupta, S., Singh, P., Vijay, V., Sahay, A., Vijay, V. K., Thakur, I. S. (2018): Review of trends in biogas upgradation technologies and future perspectives. – Bioresource Technology Reports 1: 79-88.
[50] Samun, I., Saeed, R., Abbas, M., Rehan, M., Nimazi, A. S., Asam, Z. U. Z. (2017): Assessment of bioenergy production from solid waste. – Energy Procedia 142: 655-660.
[51] Santos, R. O. D., Santos, L. D. S., Prata, D. M. (2018): Simulation and optimization of a methanol synthesis process from different biogas sources. – Journal of Cleaner Production 186: 821-830.
[52] Scarlat, N., Dallemand, J-F., Fahl, F. (2018): Biogas: developments and perspectives in Europe. – Renewable Energy. DOI: 10.1016/ j.renene.2018.03.006.
[53] Scarlet, N., Fahl, F., Dallemand, J. F., Monforti, F., Motola, V. (2018): A spatial analysis of biogas potential from manure in Europe. – Renewable and Sustainable Energy Reviews 94: 915-930.
[54] Statistical Centre of Iran (2017): Statistical Surveys of Dairy Industry in Iran, 2016. – Statistical Centre of Iran. Office of the Head, Public Relations and International Cooperation, Tehran (Persian).
[55] Tehran Chamber of Commerce, Industries, Mines and Agriculture, Deputy of Economic Research (2016): Raw Milk Production from Industrial Cattle Farms in Tehran in 2016. – Tehran Chamber of Commerce, Tehran (Persian).
[56] Than, T. M. M. (2005): Myanmar's energy sector: banking on natural gas. – Southeast Asian Affairs 257-289.
[57] Travnicek, P., Kotek, L., Junga, P., Vítez, T., Drapela, K., Chovanec, J. (2018): Quantitative analyses of biogas plant accidents in Europe. – Renewable Energy 122: 89-97.
[58] United Nations Environment Programme (2014): The Emissions Gap Report. – A UNEP Synthesis Report, UNEP, Nairobi.
[59] Wang, Y., Wu, X., Tong, X., Li, T., Wu, F. (2018): Life cycle assessment of large-scale and household biogas plants in northwest China. – Journal of Cleaner Production 192: 221-235.
[60] Wyman, C. E., Goodman, B. J. (1993): Biotechnology for production of fuels, chemicals and materials from biomass. – Applied Biochemistry and Biotechnology 39: 41-59.

http://www.aloki.hu ● ISSN 1589 1623 (Print) ● ISSN 1785 0037 (Online)
DOI: http://dx.doi.org/10.15666/aeer/1605_64996523
© 2018, ALÖKI Kft., Budapest, Hungary

[61] Yazan, D. M., Fraccascia, L., Mes, M., Zijm, H. (2018): Cooperation in manure-based biogas production networks: An agent-based modeling approach. – Applied Energy 212: 820-833.
[62] Yildirim, E., Ince, O., Aydin, S., Ince, B. (2017): Improvement of biogas potential of anaerobic digesters using rumen fungi. – Renewable Energy 109: 346-353.
[63] Zareei, S. (2018): Evaluation of biogas potential from livestock manures and rural wastes using GIS in Iran. – Renewable Energy 118: 351-356.

http://www.aloki.hu ● ISSN 1589 1623 (Print) ● ISSN 1785 0037 (Online)
DOI: http://dx.doi.org/10.15666/aeer/1605_64996523
© 2018, ALÖKI Kft., Budapest, Hungary

BIO-SYSTEM IN HIGH CONCENTRATION ORGANIC WASTEWATER TREATMENT

CHENG, X.-X. – LI, G.-C.* – PIAO, C.-X.*

Department of Agricultural Resources and Environment, Agricultural College of Yanbian University, Yanji, P. R. China

**Corresponding authors*
e-mail: gcli@ybu.edu.cn, cxpiao@ybu.edu.cn

(Received 21st Jun 2018; accepted 3rd Sep 2018)

Abstract. In this paper we studied a bio-system which could be applied to the treatment of high concentration organic wastewater and aimed at increasing its efficiency by laboratory scale wastewater treatment reactors. The reactors were divided into control reactor, reactor one (Adding Pellet bacteria and pumice) and reactor two (Adding Pellet and pumice). The reactors had two patterns of long aeration, and intermittent aeration which could be divided into four stages. The COD, NH_3-N, NO_3-N, Total Nitrogen (TN), Total Phosphorus (TP) were measured. The experimental results showed that the removal abilities of COD, NH_3-N, NO_3-N, TN and TP of reactor one and two were better than those of the control reactor in two modes. Above all, the reactor one and two increased the removal efficiency of high concentration organic wastewater. The reactor two achieved the best removal efficiency of high concentration organic wastewater. The best effect was reached when the operating condition was 1 h 20 min/1 h 20 min (Aeration / Stopping aeration), and the average removal rates were enhanced by 3%, 21%, 54%, 21%, 25% respectively.
Keywords: *pellet, pumice, reactor, intermittent aeration, water quality analysis*

Introduction

China is a country with serious water shortage, and the per capita water consumption is very low, accounting for only 1/4 of the world's per capita level (Chen et al., 2002):. In addition, serious problems such as serious waste and serious pollution in China's water resources still exist. For a long time, water pollution had been the most prominent problem in the national environmental safety (Zhang, 2014). According to the national environmental statistics bulletin, the total amount of wastewater discharge in 2015 was 735.3 million tons, including 199.5 tons of industrial wastewater and 535.2 million tons of urban sewage discharge. It can be seen that industrial wastewater accounts for about 27% of the national wastewater discharge, and industrial wastewater was mainly organic wastewater with high concentration. Additionally, the slaughterhouse wastewater and livestock wastewater have been high concentration organic wastewater and therefore the treatment of high concentration organic wastewater was very significant in the process of sewage treatment.

High concentration organic wastewater generally refers to the wastewater whose COD was more than 2000 mg/L (Wang and Liao, 2011), which was mainly discharged from papermaking, leather, food and slaughterhouse. As the high concentration, organic wastewater contains a large number of organic compounds such as carbohydrates, fat, protein, cellulose and many organic pollutants which were extremely difficult to decompose and contained high levels of toxicity, it would cause serious water environmental pollution (Chen et al., 2008), even endangering human health if they were not treated properly and discharged directly. It has been one of the most difficult

http://www.aloki.hu ● ISSN 1589 1623 (Print) ● ISSN 1785 0037 (Online)
DOI: http://dx.doi.org/10.15666/aeer/1605_65256547
© 2018, ALÖKI Kft., Budapest, Hungary

problems in the field of environmental protection research in China and abroad because it caused wide range and high degree of pollution (Huang et al., 2004).

Currently, there have been mainly three kinds of technologies commonly used for high concentration organic wastewater treatment, which were chemical treatment, physicochemical treatment and biological treatment. At present, the two which commonly used chemical treatment technologies were Incineration (Bie et al., 2000) and Catalytic wet oxidation (Sun et al., 1999; Du et al., 1997a, b) respectively. The two widely used physical extraction technologies included complexation extraction (Yang and Dai, 1997; Rousseau, 1987) and Pulsed extraction (He et al., 2002; Zhu et al., 2001). Biological treatment technology mainly uses the decomposition of microbes, which means that the microorganism decomposes the polluted material in the wastewater as its own nutrition and energy, and finally realizes sewage purification (Zhao et al., 2003). In recent years, biological treatment technology has played an extremely important role in the treatment of high concentration organic wastewater, because it accorded with the idea of sustainable development (Ren, 2000). At present, the activated sludge process has become the main treatment technology of various organic wastewaters (Li and Yang, 2002; Lu et al., 2001). Complete Mixing Activated Sludge Process was one of the most common wastewater treatment processes in an aerobic activated sludge process. It has many advantages. First of all, it can resist a high sludge load. Secondly, the automatic reflux of sludge can be realized. Thirdly, it is easy to manage and the delayed aeration can be reached by prolonging the age of sludge. Last but not least, the primary sedimentation tank can be saved (Wang and Sun, 1995). However, when to use the activated sludge process, especially the traditional activated sludge process to treat high concentration organic wastewater, the phenomenon that the water quality of the effluent was poor such as the high content of N and P will always happen. The Sequencing Batch Reactor Activated Sludge Process (SBR) was developed later and it greatly made up the deficiency of the activated sludge process. Therefore, it was widely used in the treatment of high concentration organic wastewater (Ganigué et al., 2012; Liu et al., 2015; Jena et al., 2016). The technology of SBR has expressed many strengths. First of all, the most prominent feature of SBR is the realization of intermittent aeration. Secondly, the precipitation performance of SBR is great and the push flow state is ideal. Thirdly, it can efficiently remove organic matter, there is no need to increase the performance to involve more reactors (Wu, 2017). Additionally, it can also provide anaerobic, anoxic and aerobic living environment for microorganism and this kind of environment was beneficial to improve the treatment efficiency of refractory wastewater including the removal of N and P. Finally, due to the large gradient of substrate concentration in the SBR system and the alternating between aerobic and anoxic (or anaerobic); the breeding of filamentous bacteria can be inhibited effectively, and the sludge bulking was controlled (Liu and Meng, 2008).

In addition to these traditional biological processes, there are also some derived processes such as the Reactor-Bio-System (RBS). RBS system was a relatively advanced high concentration organic wastewater treatment technology developed in Japan (Jiang et al., 2008; Zhai, 2014). RBS technology imitates nature and achieves the artificial induction and screening of microorganisms in the soil in the soil reaction by adding many small particles filled with humic precursors and some silica, for which the soil reaction can provide a large number of soil dominant bacteria and highly active nutrients for the whole sewage treatment system and then enhance the efficiency of sewage treatment. Therefore, RBS technology was also named “natural purification.”

http://www.aloki.hu ● ISSN 1589 1623 (Print) ● ISSN 1785 0037 (Online)
DOI: http://dx.doi.org/10.15666/aeer/1605_65256547
© 2018, ALÖKI Kft., Budapest, Hungary

RBS technology uses the biochemical effect of highly active facultative soil bacteria to purify sewage, and it embodies many advantages when compared with the traditional activated sludge process. It has six major advantages (Jiang et al., 2008). Firstly, it can be directly used to treat high concentration organic wastewater and the influent does not need to be diluted. Secondly, it can ensure SS concentration in the sewage treatment system. Thirdly, it has a high efficiency. Fourthly, it performs well in removing N and P. Fifthly, it has a good sludge characteristic. Lastly, it can effectively inhibit odor. The COD in the sewage discharged from the original field of Anshan's Tianyi pig farm was 2000 mg/L, and the BOD_5 reached 500 mg/L. The sewage was one kind of high concentration organic wastewater, and it would cause serious pollution to the receiving water. Tianyi pig farm introduced RBS technology from Japan to discharge sewage and formally put it into using in June 2001. The operation results showed that after the application of this technology, the concentrations of COD and BOD_5 in the sewage were obviously reduced, and the water quality of the effluent reached the standard of sewage discharge (Zhao, 2002). Above all, the application of RBS in Tianyi pig farm achieved good results.

This experiment applied laboratory scale wastewater biological treatment reactor to the treatment of high concentration organic wastewater with a bio-system, which was used with pellet and pumice.

Materials and methods

Materials

Pellet and Pellet (bacteria) for bio-system were columnar materials made in the laboratory. Pumice was purchased from the Tianhe pumice factory in Songjiang River town of Fusong county.

Production method of Pellet: Mix peat soil (pH 5.47) 40 g, bentonite 20 g, calcium alginate 0.6 g and cement 15 g in a beaker, then spray a certain amount of distilled water into the beaker. The cultivation (*Bacillus* CGMCC13429: CICC23692: CICC20666 = 1: 1: 1) for production pellet （bacteria） was sprayed in distilled water ($\geq 10^8$ cfu/ml).

Production of artificial wastewater

The artificial wastewater was made from glucose, NH_4Cl, KNO_3, urea, KH_2PO_4 and deionized water. The concentration range of COD was 2000 ~ 3000 mg/L; NH_3-N was 30 ~ 70 mg/L; NO_3-N was 10 ~ 15 mg/L; TN was 100 ~ 140 mg/L; TP was 30 ~ 40 mg/L. 1 ml trace element solution was added to 25 L artificial wastewater in order to provide microelement for microorganism.

Trace element solution (Li et al., 2007): MoO_3 1.0 mg, $ZnSO_4 \cdot 7H_2O$ 7.0 mg, $CuSO_4 \cdot 5H_2O$ 0.5 mg, H_3BO_3 1.0 mg, $MnSO_4 \cdot 5H_2O$ 1.0 mg, $CoCl_2 \cdot 6H_2O$ 1.0 mg, $NiSO_4 \cdot 7H_2O$ 1.0 mg, 1 L deionized water.

Experimental reactor

The laboratory scale bioreactor was made of organic glass (*Figure 1*). It consisted of three parts including aeration tank, sedimentation tank and reaction tank (consist of the bio-system with pellet and pumice). The effective volumes of the aeration tank, the sedimentation tank and the reaction tank were 48 L, 11 L, 15 L respectively. Water

http://www.aloki.hu ● ISSN 1589 1623 (Print) ● ISSN 1785 0037 (Online)
DOI: http://dx.doi.org/10.15666/aeer/1605_65256547
© 2018, ALÖKI Kft., Budapest, Hungary

distribution bucket was used to fill the artificial wastewater with a total volume of 25 L. The mechanical agitator was used to mix. The peristaltic pump was used to control influent and sludge reflux and the air lift pump was used to control sludge return. The electromagnetic air pump was used to offer aeration for aeration tank and reaction tank. The quantity of influent, sludge return was 8 L/d, 3 L/d and the overall HRT of reactor was 6 days.

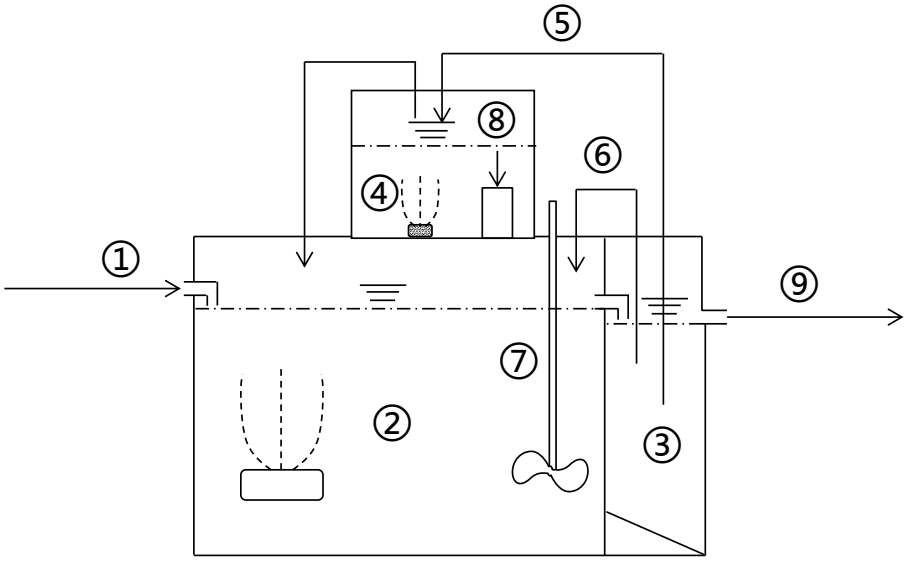

Figure 1. *Laboratory scale wastewater treatment reactor. ① influent, ② aeration tank, ③ sedimentation tank, ④ reaction tank, ⑤ sludge reflux, ⑥ sludge return, ⑦ mechanical agitator, ⑧ pellet + pumice, ⑨ effluent*

There were three reactors, which were controlled reactor, reactor one and reactor two. Six Pellet bacteria (about 363.72 g) and 727.44 g pumice were added to the reaction tank of reactor one and six Pellet (about 363.72 g), and 727.44 g pumice were added to the reaction tank of reactor two. The reaction tank of three reactors continued to be aerated. The reactor operation included two modes, which were long-term aeration and intermittent aeration. The intermittent aeration was divided into four stages, which were 1 h/1 h (the first stage), 1 h 20 min/1 h (the second stage), 1 h 20 min/1 h 20 min (the third stage), 1 h/1 h min (the fourth stage).

Water quality analysis

The researchers were analyzed the amount of COD, NH_3-N and NO_3-N with APHA Standard Method (Gilcreas, 1998). The GB (GB 11901, 1989) was used to the analysis of SS. The pretreatment of TN and TP analysis was carried out by digestion with persulfate (Qualls, 1989) and the subsequent treatment followed the APHA Standard Method.

SiO_2 determination

In the long-term aeration of 120 days, the concentration of SiO_2 was measured from the aeration tank and the reaction tank. SiO_2 was determined by citric acid extraction and silicon molybdenum blue colorimetric method (Bao, 2000).

http://www.aloki.hu ● ISSN 1589 1623 (Print) ● ISSN 1785 0037 (Online)
DOI: http://dx.doi.org/10.15666/aeer/1605_65256547
© 2018, ALÖKI Kft., Budapest, Hungary

Results and discussion

COD analysis

Figure 2 shows that the influent COD concentration was from 2000 to 3000 mg/L. For the control reactor, the effluent COD remained stable after running 113 days. The concentration range was stable from 189 mg/L to 237 mg/L and the average concentration was 208 mg/L. *Figure 3* shows that the average COD removal rate was from 91% to 94%, and the average removal rate reached 93%. For the reactor one, the effluent COD remains stable after running 99 days. The concentration is stable from 91 mg/L to 117 mg/L and the average concentration is 101 mg/L. The removal rate of COD is from 96% to 98% and the average removal rate reached 97%. For the reactor two, the effluent COD remains stable after 106 days. and the concentration was stable from 91 mg/L to 128 mg/L and the average concentration was 110 mg/L. The removal rate of COD was from 95% to 98% and the average removal rate reached 96%. The effluent COD of the reactors one and two was less than 150 mg/L. After the reactor operation was stable, the COD concentrations of the reactor one and two were lower than those of the control reactor and the reactor one was the lowest. It was shown that the removal effect for COD of reactor one was better than reactor two and both of them were better than the control reactor under the long-term aeration condition, which could be attributed with the creation of the bio-system which was similar to RBS in the reaction tanks of reactor one and two.

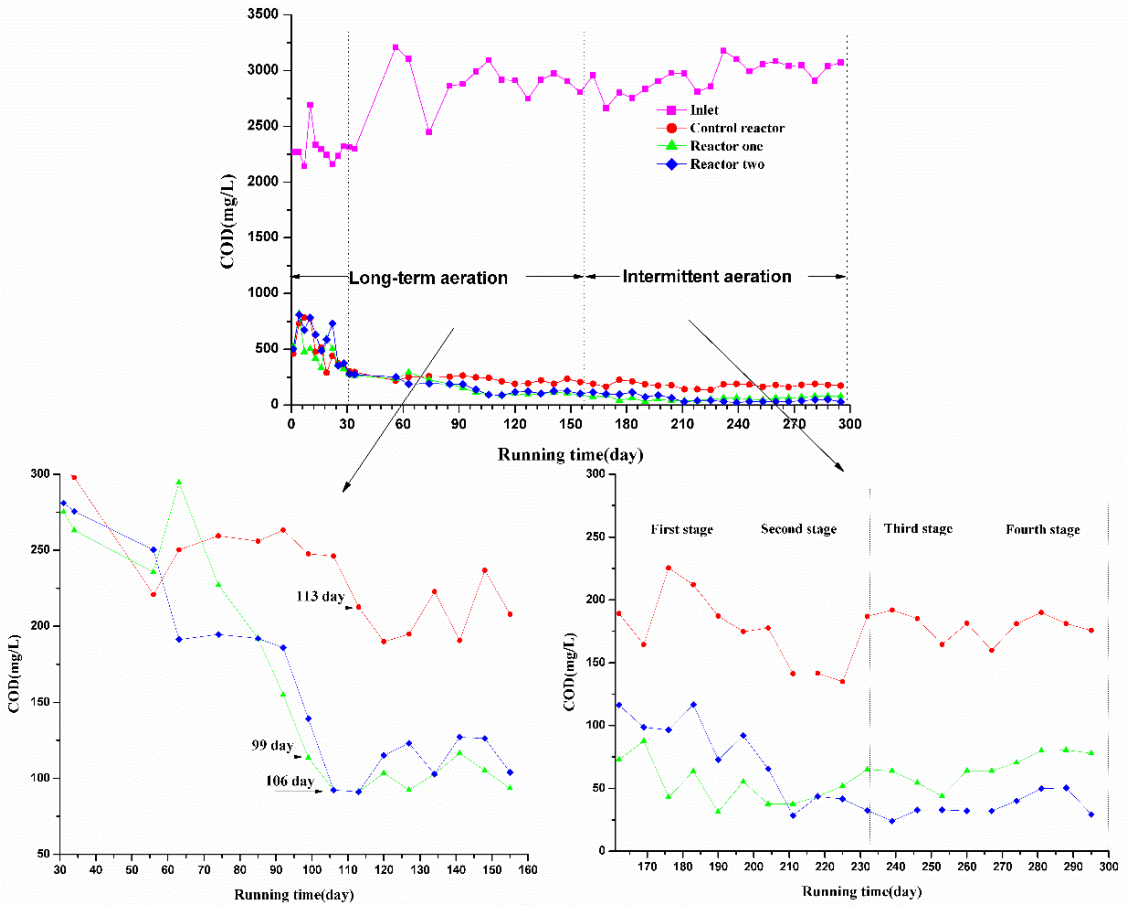

Figure 2. *Changes of COD concentration in the influent and effluent*

http://www.aloki.hu ● ISSN 1589 1623 (Print) ● ISSN 1785 0037 (Online)
DOI: http://dx.doi.org/10.15666/aeer/1605_65256547
© 2018, ALÖKI Kft., Budapest, Hungary

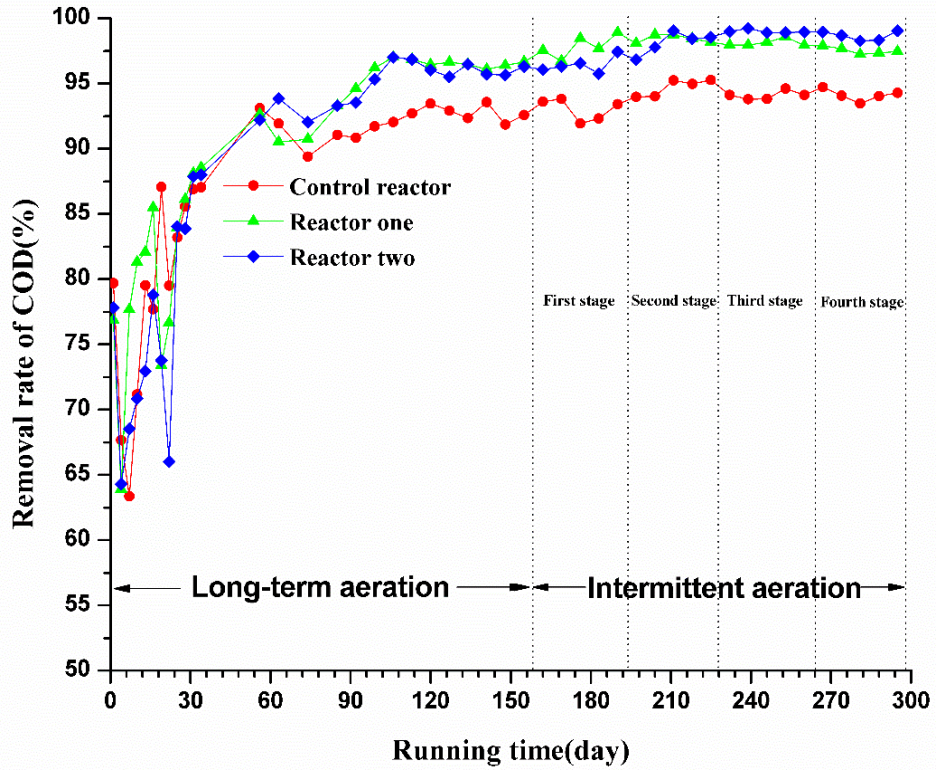

Figure 3. *Changes of COD removal rate*

During the four stages of intermittent aeration, the effluent COD concentration ranges as shown in *Table 1*. The average concentrations of four stages were 195.58 mg/L, 154.05 mg/L, 181.91 mg/L, 177.57 mg/L in control reactor. The average concentrations of four stages were 59.62 mg/L, 43.47 mg/L, 58.25 mg/L, 74.60 mg/L in reactor one. The average concentrations of four stages were 100.18 mg/L, 47.00 mg/L, 30.80 mg/L, 40.37 mg/L in reactor two. Therefore, the lowest effluent COD concentration of control reactor appeared in the second stage. The removal rate of COD was from 92% to 96% and the average removal rate was 95%. The lowest effluent COD concentration of reactor one appeared in the second stage. The removal rate of COD was from 98% to 99% and the average removal rate was 98%. The lowest effluent COD concentration of reactor two appeared in the third stage. The removal rate of COD was from 98% to 100% and the average removal rate was 99%. Therefore, for the removal of COD, the most suitable aeration conditions for control reactor, reactor one, reactor two were 1 h 20 min/1 h, 1 h 20 min/1 h, 1 h 20 min/1 h 20 min. During the four stages of intermittent aeration, the effluent COD of reactors one and two was less than 150 mg/L.

Table 1. *Effluent COD concentration ranges*

Stage	Control	Reactor one	Reactor two
1	164.38 ~ 225.50 mg/L	31.17 ~ 87.67 mg/L	72.73 ~ 116.56 mg/L
2	135.06 ~ 177.78 mg/L	37.43 ~ 55.17 mg/L	28.24 ~ 91.95 mg/L
3	164.38 ~ 192.00 mg/L	43.84 ~ 64.97 mg/L	24.00 ~ 32.88 mg/L
4	160.00 ~ 190.00 mg/L	64.00 ~ 80.50 mg/L	29.27 ~ 50.31 mg/L

http://www.aloki.hu ● ISSN 1589 1623 (Print) ● ISSN 1785 0037 (Online)
DOI: http://dx.doi.org/10.15666/aeer/1605_65256547
© 2018, ALÖKI Kft., Budapest, Hungary

Figure 4 shows that the COD concentrations in the aeration tank were stable after a long period of aeration of three reactors. The concentration of COD in the aeration tank of control reactor was reduced from 2000 ~ 3000 mg/L to 1000 mg/L while that of reactor one and reactor two was reduced to 800 mg/L. After the intermittent aeration mode was converted to intermittent aeration, the COD concentrations in the aeration tank reduced. In the third stage of intermittent aeration, the COD concentrations in the aeration tank of three reactors were minimum and those of control reactor, reactor one, reactor two were 493.15 mg/L, 482.19 mg/L, 405.48 mg/L. It was indicated that the aeration tank played an important role in the removal of COD in the long-term aeration stage and the intermittent aeration stage. Since the operating modes of three reactors were changed from long-term aeration to intermittent aeration, the COD removal efficiency has been increased.

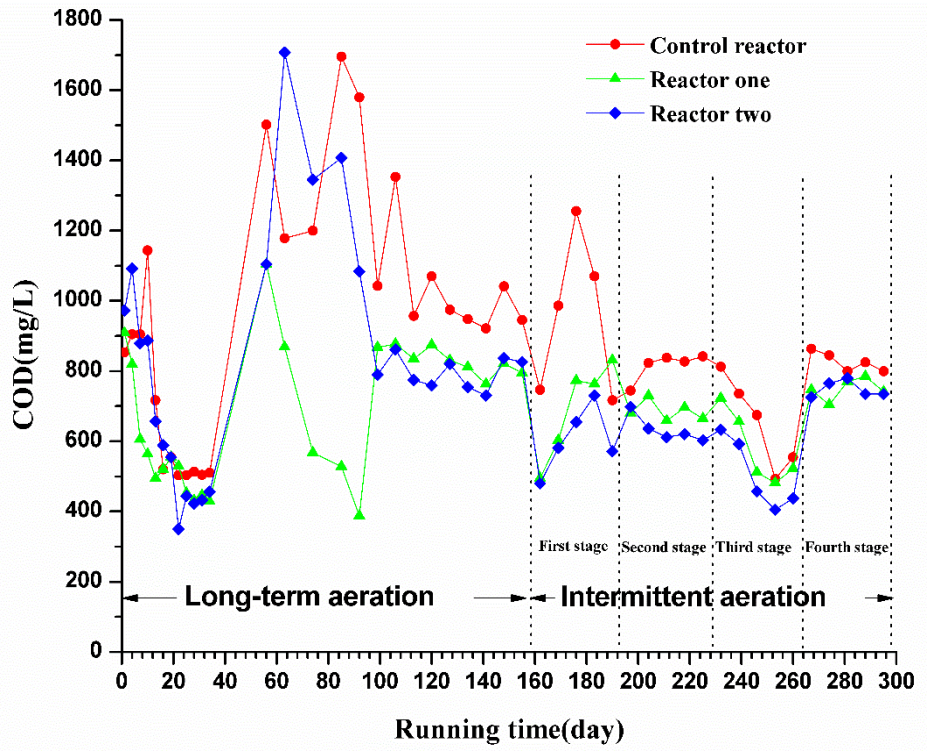

Figure 4. *Changes of COD concentration in the aeration tank*

NH_3-N analysis

Figure 5 shows that the influent NH_3-N concentration was from 35 to 70 mg/L. For the control reactor, the effluent NH_3-N remained stable after running 120 days. The concentration was stable from 26 mg/L to 32 mg/L and the average concentration was 30 mg/L. *Figure 6* shows that the average removal rate of NH_3-N was from 10% to 24% and the average removal rate reached 16%. For the reactor one, the effluent NH_3-N remained stable after running 120 days. The concentration was stable from 22 mg/L to 27 mg/L and the average concentration was 24 mg/L. The removal rate of NH_3-N was from 25% to 40% and the average removal rate reached 33%. For the reactor two, the effluent NH_3-N remains stable after 120 days. The concentration was stable from 19 mg/L to 26 mg/L and the average concentration was 22 mg/L. The removal rate of NH_3-

http://www.aloki.hu ● ISSN 1589 1623 (Print) ● ISSN 1785 0037 (Online)
DOI: http://dx.doi.org/10.15666/aeer/1605_65256547
© 2018, ALÖKI Kft., Budapest, Hungary

N was from 29% to 46% and the average removal rate reached 38%. The effluent NH_3-N of the reactor one and two were less than 25 mg/L. When the reactor operation was stable, the NH_3-N concentrations of the reactor one and two were lower than those of the control reactor and the reactor two was the lowest. It was shown that the removal effect for NH_3-N of reactor two was better than that of reactor one and both of them were better than that of the control reactor under the long-term aeration condition, which could be attributed to the creation of the bio-system which was similar to RBS in the reaction tanks of reactor one and two.

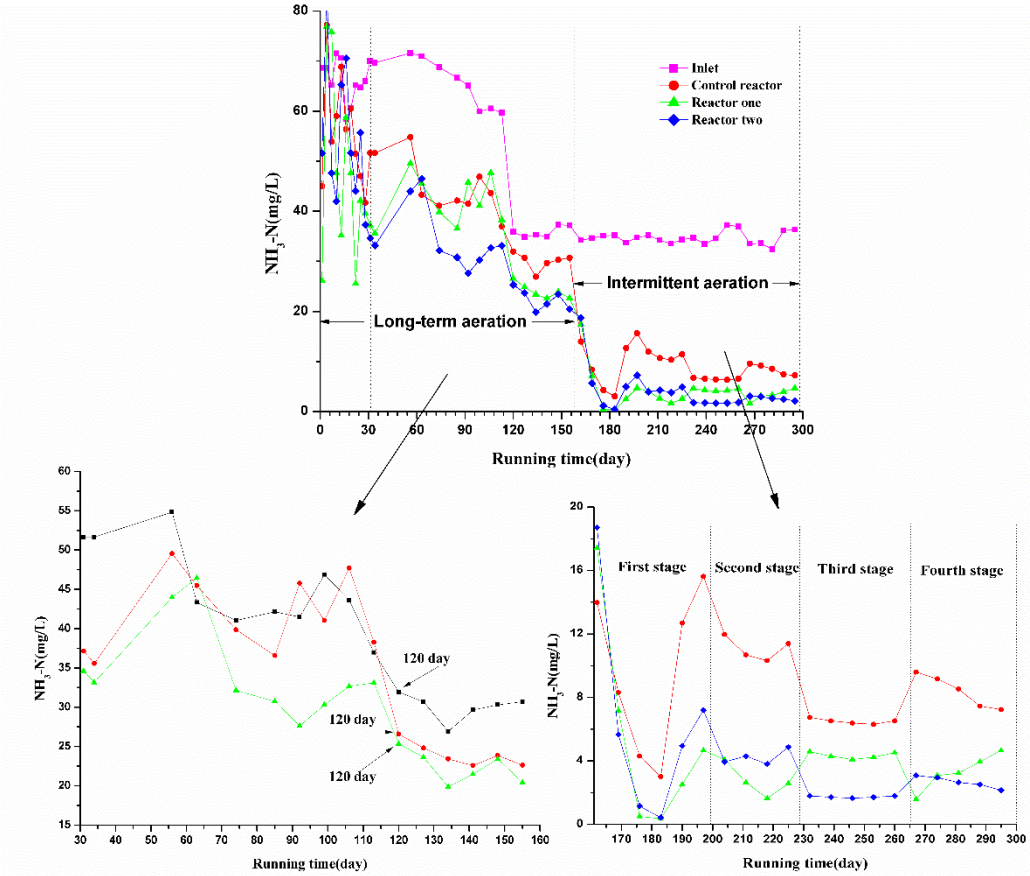

Figure 5. *Changes of NH_3-N concentration in the influent and effluent*

During the four stages of intermittent aeration, the effluent NH_3-N concentration ranges as shown in *Table 2*. The average concentrations of four stages were 8.46 mg/L, 12.00 mg/L, 6.49 mg/L, 8.4 mg/L in control reactor. The average concentrations of four stages were 5.59 mg/L, 3.13 mg/L, 4.34 mg/L, 3.30 mg/L in reactor one. The average concentration of four stages were 6.18 mg/L, 4.82 mg/L, 1.73 mg/L, 2.67 mg/L in reactor two. Therefore, the lowest effluent NH_3-N concentration of control reactor appeared in the third stage. The removal rate of NH_3-N was from 71% to 81% and the average removal rate was 75%. The lowest effluent NH_3-N concentration of reactor one appeared in the second stage. The removal rate of NH_3-N was from 82% to 96% and the average removal rate was 90%. The lowest effluent NH_3-N concentration of reactor two appeared in the third stage. The removal rate of NH_3-N was from 90% to 95% and the average removal rate was 92%. Therefore, for the removal of NH_3-N, the most suitable

http://www.aloki.hu ● ISSN 1589 1623 (Print) ● ISSN 1785 0037 (Online)
DOI: http://dx.doi.org/10.15666/aeer/1605_65256547
© 2018, ALÖKI Kft., Budapest, Hungary

aeration conditions for control reactor, reactor one, reactor two were 1 h 20 min/1 h 20 min, 1 h 20 min/1 h, 1 h 20 min/1 h 20 min. During the four stages of intermittent aeration, the effluent NH_3-N of reactor one and two was less than 25 mg/L.

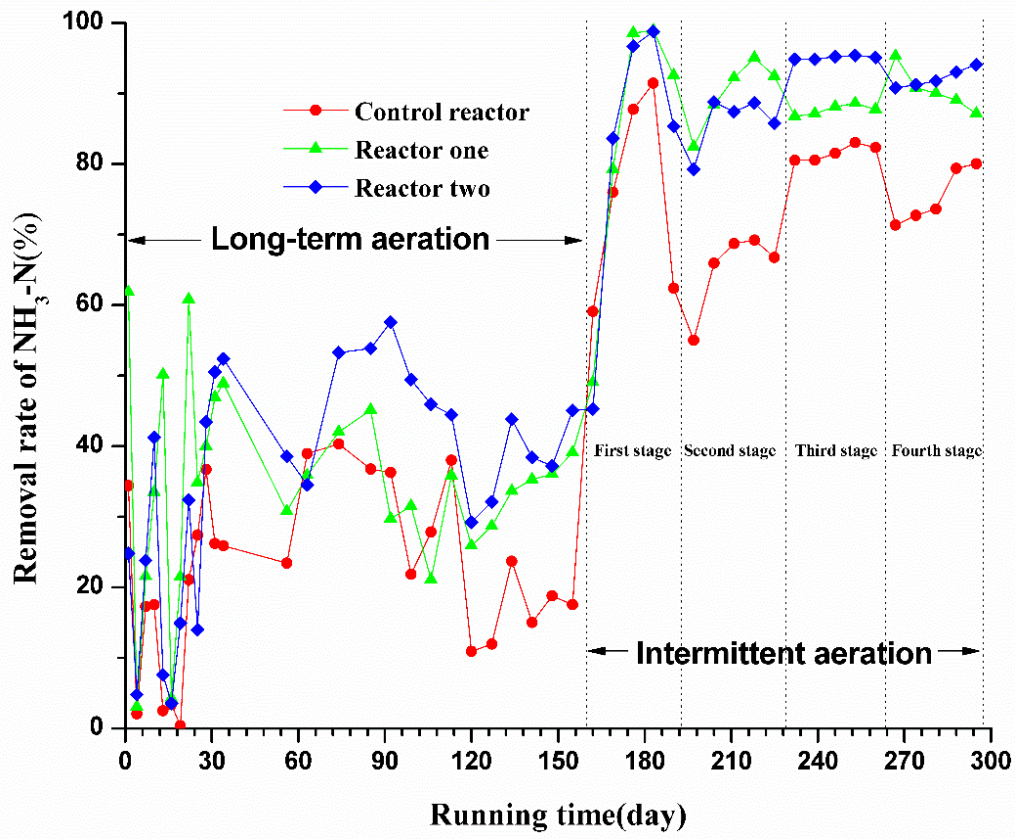

Figure 6. *Changes of NH_3-N removal rate*

Table 2. *Effluent NH_3-N concentration ranges*

Stage	Control	Reactor one	Reactor two
1	3.01 ~ 13.98 mg/L	0.36 ~ 17.42 mg/L	0.43 ~ 18.71 mg/L
2	10.32 ~ 15.63 mg/L	1.65 ~ 6.09 mg/L	3.80 ~ 7.20 mg/L
3	6.31 ~ 6.74 mg/L	4.09 ~ 4.58 mg/L	1.65 ~ 1.79 mg/L
4	7.24 ~ 9.60 mg/L	1.58 ~ 4.66 mg/L	2.15 ~ 3.08 mg/L

Figure 7 shows that the NH_3-N concentrations in the aeration tank were stable after a long period of aeration of three reactors. The concentration of NH_3-N in the aeration tank of control reactor was reduced from 30 ~ 70 mg/L to 28 mg/L while that of reactor one and reactor two was reduced to 22 mg/L and 21 mg/L. After the intermittent aeration mode was converted to intermittent aeration, the NH_3-N concentrations in the aeration tank of three reactors were reduced. In the third stage of intermittent aeration, the NH_3-N concentrations in the aeration tank of three reactors were minimum and that of control reactor, reactor one, reactor two were 2.29 mg/L, 0.22 mg/L, 0.57 mg/L. It was indicated that the aeration tank played an important role in the removal of NH_3-N in

http://www.aloki.hu ● ISSN 1589 1623 (Print) ● ISSN 1785 0037 (Online)
DOI: http://dx.doi.org/10.15666/aeer/1605_65256547
© 2018, ALÖKI Kft., Budapest, Hungary

the long-term aeration stage and the intermittent aeration stage. Since the operating modes of three reactors were changed from long-term aeration to intermittent aeration, the COD removal efficiency increased.

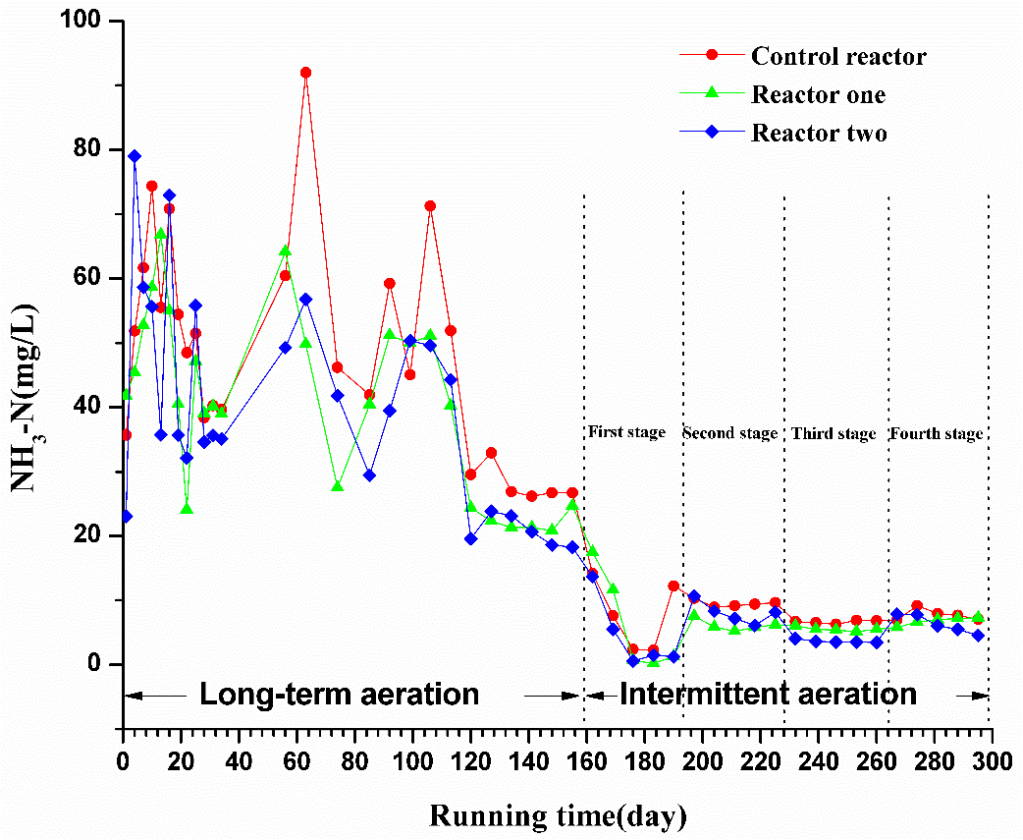

Figure 7. *Changes of NH_3-N concentration in the aeration tank*

NO_3-N analysis

Figure 8 shows that the influent NO_3-N concentration was from 10 to 15 mg/L. For the control reactor, the effluent NO_3-N remained stable after running 120 days. The concentration was stable from 8 mg/L to 13 mg/L and the average concentration was 11 mg/L. *Figure 9* shows that the average removal rate of NO_3-N was lower than 24% and the average removal rate reached 13%. For the reactor one, the effluent NO_3-N remains stable after running 106 days. The concentration was stable from 7 mg/L to 11 mg/L and the average concentration reached 8 mg/L. The removal rate of NO_3-N was from 10% to 41% and the average removal rate reached 30%. For the reactor two, the effluent NO_3-N remains stable after running 99 days, and the concentration was stable from 7 mg/L to 9 mg/L and the average concentration was 8 mg/L. The removal rate of NO_3-N was from 7% to 40% and the average removal rate reached 30%. When the reactor operation was stable, the NO_3-N concentrations of the reactor one and two were lower than that of the control reactor. It was shown that the removal effect of reactor one and reactor two on NO_3-N was better than the control reactor under the long-term aeration condition, which could be attributed to the creation of the bio-system which was similar to RBS in the reaction tanks of reactor one and two.

http://www.aloki.hu ● ISSN 1589 1623 (Print) ● ISSN 1785 0037 (Online)
DOI: http://dx.doi.org/10.15666/aeer/1605_65256547
© 2018, ALÖKI Kft., Budapest, Hungary

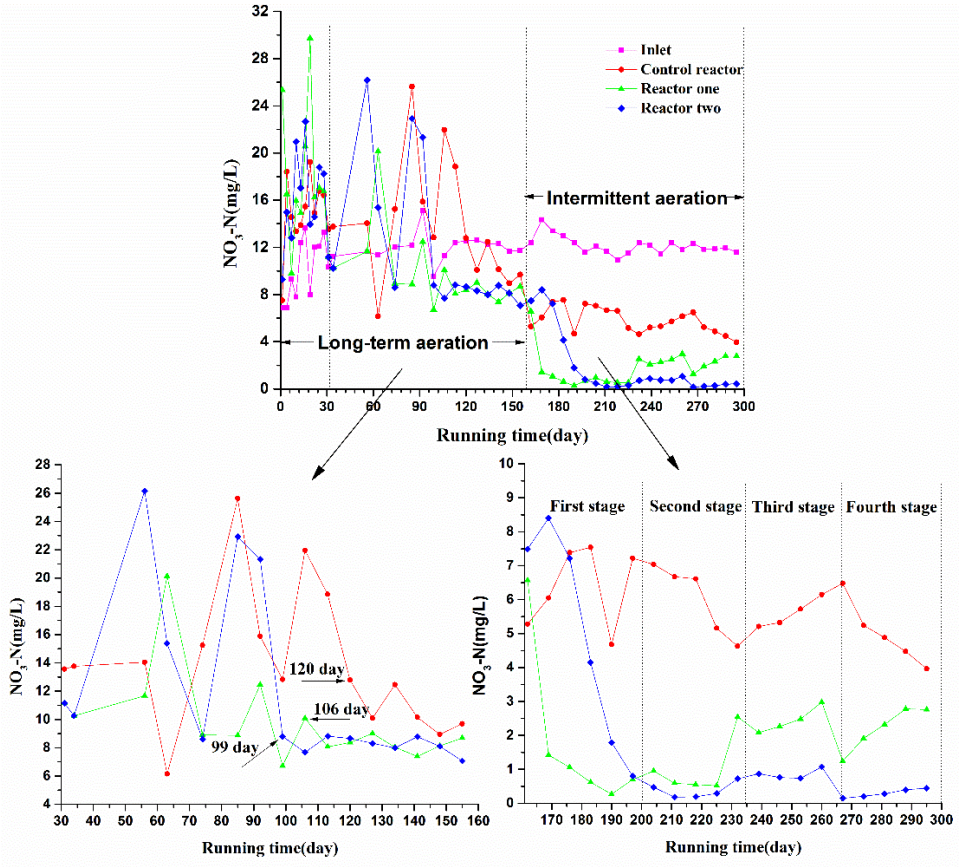

Figure 8. *Changes of NO_3-N concentration in the influent and effluent*

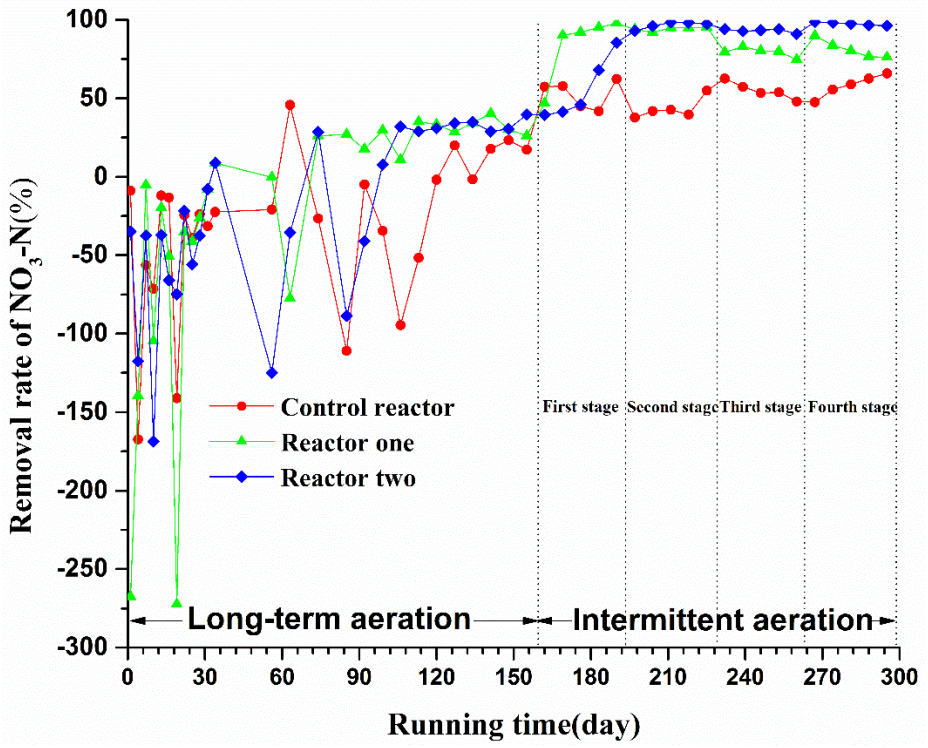

Figure 9. *Changes of NO_3-N removal rate*

http://www.aloki.hu ● ISSN 1589 1623 (Print) ● ISSN 1785 0037 (Online)
DOI: http://dx.doi.org/10.15666/aeer/1605_65256547
© 2018, ALÖKI Kft., Budapest, Hungary

During the four stages of intermittent aeration, the effluent NO_3-N concentration ranges as shown in *Table 3*. The average concentrations of four stages were 6.19 mg/L, 6.54 mg/L, 5.41 mg/L, 5.01 mg/L in control reactor. The average concentrations of four stages were 1.99 mg/L, 0.66 mg/L, 2.47 mg/L, 2.20 mg/L in reactor one. The average concentrations of four stages were 0.39 mg/L, 0.39 mg/L, 0.83 mg/L, 0.30 mg/L in reactor two. Evidently, among the effluent NO_3-N concentrations of the four stages, the lowest was one of the last stage. The removal rate of NO_3-N was from 47% to 63%, and the average removal rate was 55%. The lowest effluent NO_3-N concentration of reactor one was the one of the second stage. The removal rate of NO_3-N was from 92% to 96%, and the average removal rate was 94%. The lowest effluent NO_3-N concentration of reactor two was the one of the fourth stage. The removal rate of NO_3-N was from 90% to 95%, and the average removal rate was 93%. Obviously, for the removal of NO_3-N, the most suitable aeration conditions for control reactor, reactor one, reactor two were 1 h/1 h 20 min, 1 h 20 min/1 h, 1 h/1 h 20 min.

Figure 10 shows that the NO_3-N concentrations of three reactors in the aeration tank were stable after a long period of aeration while the concentration of NO_3-N was higher than the influent. After the intermittent aeration mode was converted to intermittent aeration, the NO_3-N concentrations in aeration tank has reduced. In the fourth stage of intermittent aeration, the NO_3-N concentrations in the aeration tank of the three reactors were minimum and those of control reactor, reactor one, reactor two were 7.19 mg/L, 0.45 mg/L, 0.34 mg/L. It was indicated that the aeration tank played an important role in the removal of NO_3-N in the long-term aeration stage and the intermittent aeration stage. Since the operating modes of three reactors were changed from long-term aeration to intermittent aeration, the COD removal efficiency increased.

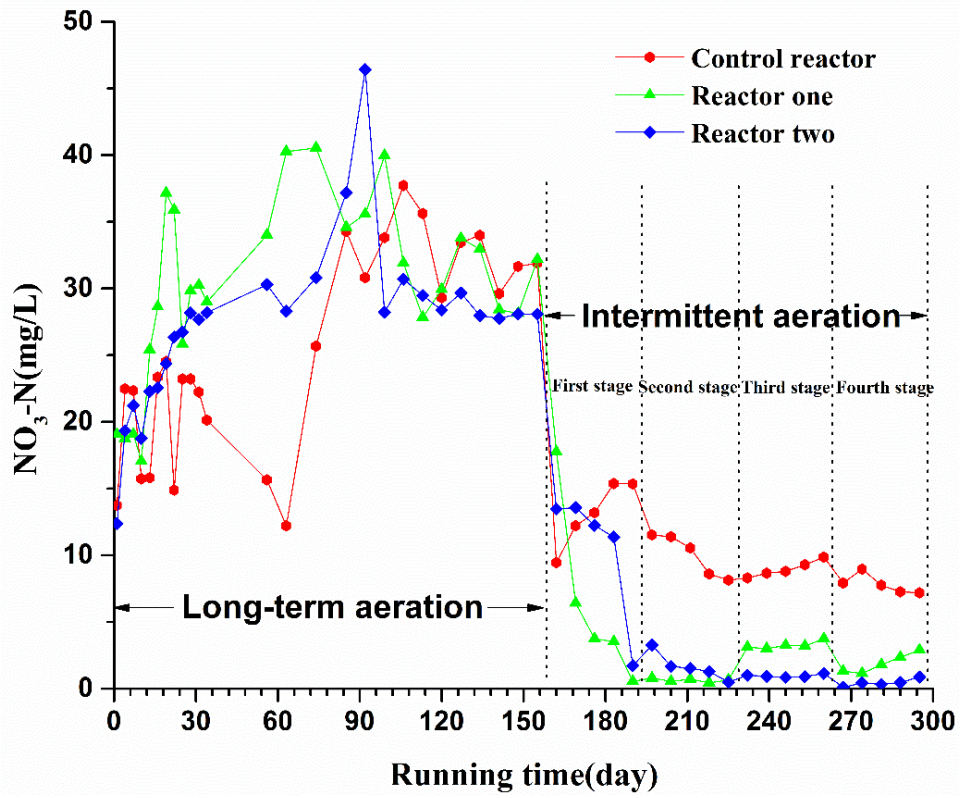

Figure 10. *Changes of NO_3-N concentration in the aeration tank*

http://www.aloki.hu ● ISSN 1589 1623 (Print) ● ISSN 1785 0037 (Online)
DOI: http://dx.doi.org/10.15666/aeer/1605_65256547
© 2018, ALÖKI Kft., Budapest, Hungary

Table 3. *effluent NO_3-N concentration ranges*

Stage	Control	Reactor one	Reactor two
1	5.28 ~ 7.54 mg/L	0.27 ~ 6.57 mg/L	1.79 ~ 8.40 mg/L
2	5.16 ~ 7.22 mg/L	0.52 ~ 0.95 mg/L	0.18 ~ 0.80 mg/L
3	4.63 ~ 6.15 mg/L	2.08 ~ 2.98 mg/L	0.72 ~ 1.07 mg/L
4	3.96 ~ 6.48 mg/L	1.24 ~ 2.78 mg/L	0.15 ~ 0.44 mg/L

TN analysis

Figure 11 shows that the influent TN concentration was from 10 to 15 mg/L. For the control reactor, the effluent TN remained stable after running 113 days. The concentration was stable from 60 mg/L to 64 mg/L and the average concentration was 62 mg/L.

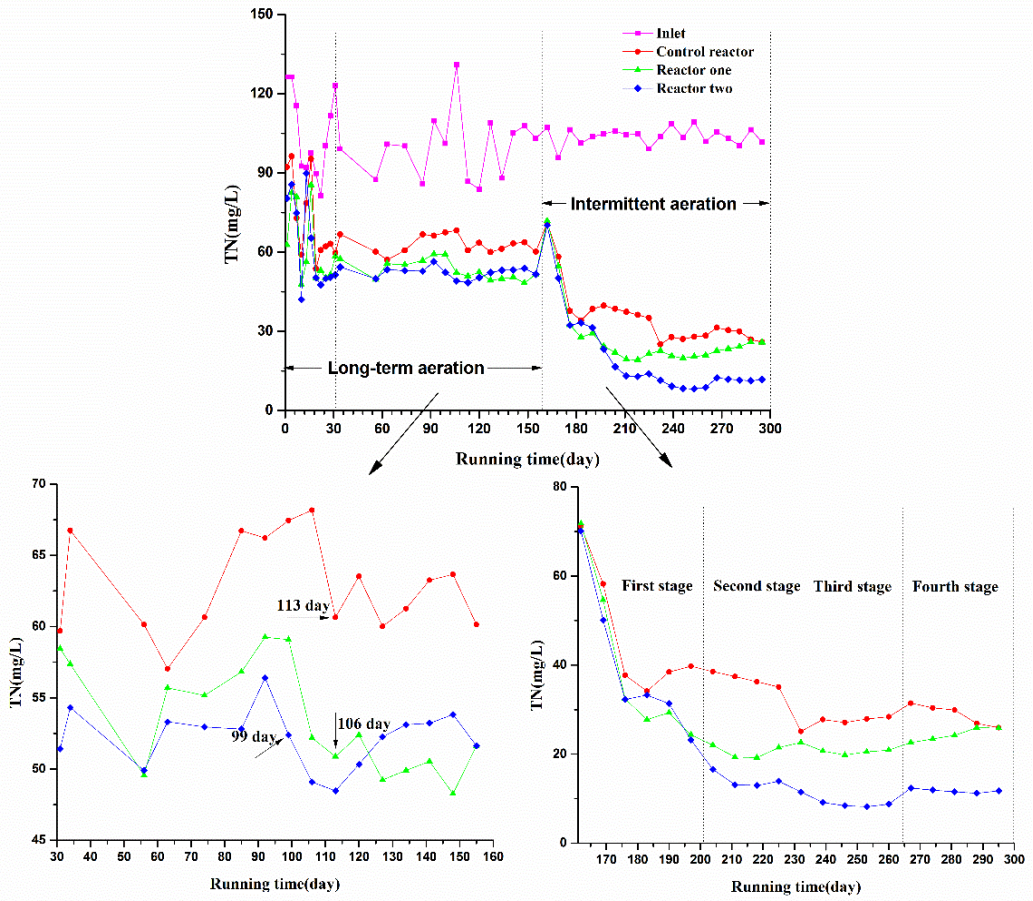

Figure 11. *Changes of TN concentration in the influent and effluent*

Figure 12 shows that the average removal rate of TN was from 39% to 54% and the average removal rate reached 43%. For the reactor one, the effluent TN remained stable after running 106 days. The concentration was stable from 48 mg/L to 53 mg/L and the average concentration was 50 mg/L. The removal rate of TN was from 49% to 62% and the average removal rate reached 54%. For the reactor two, the effluent TN remains

http://www.aloki.hu ● ISSN 1589 1623 (Print) ● ISSN 1785 0037 (Online)
DOI: http://dx.doi.org/10.15666/aeer/1605_65256547
© 2018, ALÖKI Kft., Budapest, Hungary

stable after running 99 days. The concentration was stable from 48 mg/L to 54 mg/L and the average concentration was 51 mg/L. The removal rate of TN was from 48% to 64% and the average removal rate reached 54%. When the reactor operation was stable, the TN concentrations of the reactor one and two were lower than those of the control reactor and the reactor one was the lowest. It was shown that the removal effect for TN of reactor one was better than reactor two and both of them were better than the control reactor under the long-term aeration condition, which could be attributed to the creation of the bio-system which was similar to RBS in the reaction tanks of reactor one and two.

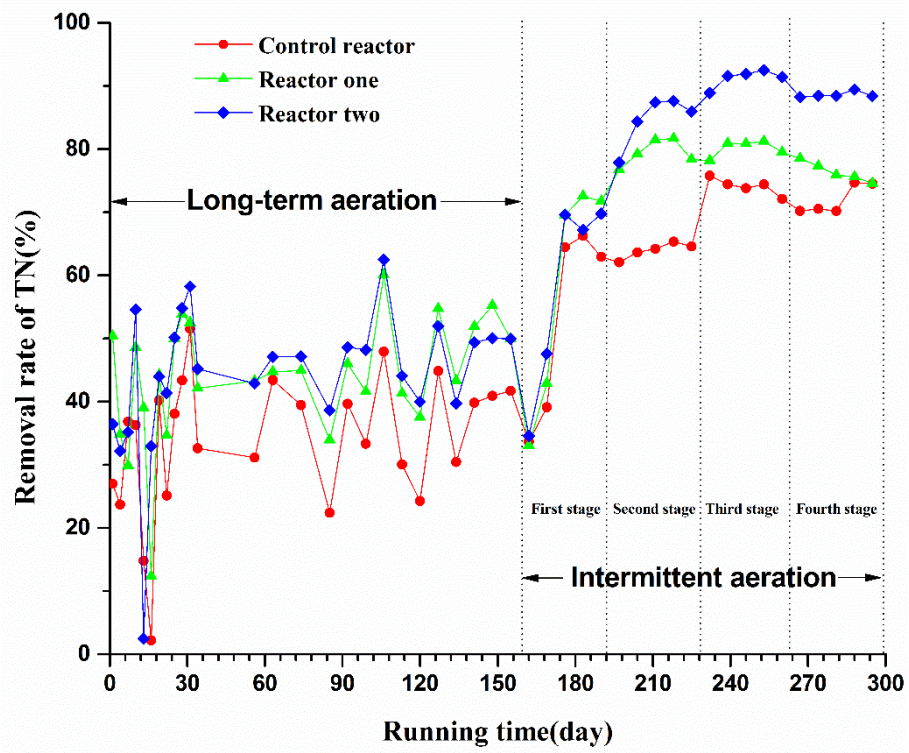

Figure 12. *Changes of TN removal rate*

During the four stages of intermittent aeration, the effluent TN concentration ranges as shown in *Table 4*. The average concentrations of four stages were 47.94 mg/L, 37.39 mg/L, 27.25 mg/L, 28.90 mg/L in control reactor. The average concentrations of four stages were 43.16 mg/L, 20.90 mg/L, 21.26 mg/L, 24.39 mg/L in reactor one. The average concentration of four stages are 43.42 mg/L, 15.94 mg/L, 9.18 mg/L, 11.76 mg/L in reactor two. It can be observed that the lowest effluent TN concentration of control reactor was the one of the third stage. The removal rate of TN was from 70% to 75% and the average removal rate was 72%. The lowest effluent TN concentration of reactor was the one of the second stage. The removal rate of TN was from 76% to 82% and the average removal rate was 80%. The lowest effluent TN concentration of reactor two was the one of the fourth stage. The removal rate of TN was from 88% to 90% and the average removal rate was 89%. Therefore, for the removal of TN, the most suitable aeration conditions for control reactor, reactor one and reactor two were 1 h 20 min/1 h 20 min, 1 h 20 min/1 h, 1 h 20 min/1 h 20 min.

http://www.aloki.hu ● ISSN 1589 1623 (Print) ● ISSN 1785 0037 (Online)
DOI: http://dx.doi.org/10.15666/aeer/1605_65256547
© 2018, ALÖKI Kft., Budapest, Hungary

Table 4. *Effluent TN concentration ranges*

Stage	Control	Reactor one	Reactor two
1	34.14 ~ 74.16 mg/L	27.78 ~ 71.78 mg/L	31.35 ~ 70.13 mg/L
2	35.06 ~ 39.74 mg/L	19.18 ~ 24.34 mg/L	12.93 ~ 23.17 mg/L
3	25.09 ~ 28.39 mg/L	19.80 ~ 22.62 mg/L	8.18 ~ 11.48 mg/L
4	25.92 ~ 31.42 mg/L	22.62 ~ 25.92 mg/L	11.21 ~ 12.38 mg/L

Figure 13 shows that the TN concentrations of three reactors in the aeration tank were stable after a long period of aeration. The TN concentration of control reactor was higher than the influent concentration while that of reactor one and reactor two reduced to 97 mg/L and 95 mg/L. After the intermittent aeration mode was converted to intermittent aeration, the TN concentrations in the aeration tank have reduced. In the first stage of intermittent aeration, the TN concentration in the aeration tank of control reactor was minimum and that of control reactor was 54.04 mg/L. In the first stage of intermittent aeration, the TN concentration in the aeration tank of reactor one was minimum and that of reactor one was 45.38 mg/L. In the third stage of intermittent aeration, the TN concentration in aeration tank of reactor two was minimum and that of reactor two was 34.1 mg/L. It was indicated that the aeration tank played an important role in the removal of TN in the long-term aeration stage and the intermittent aeration stage. Since the operating modes of three reactors were changed from long-term aeration to intermittent aeration, the COD removal efficiency increased.

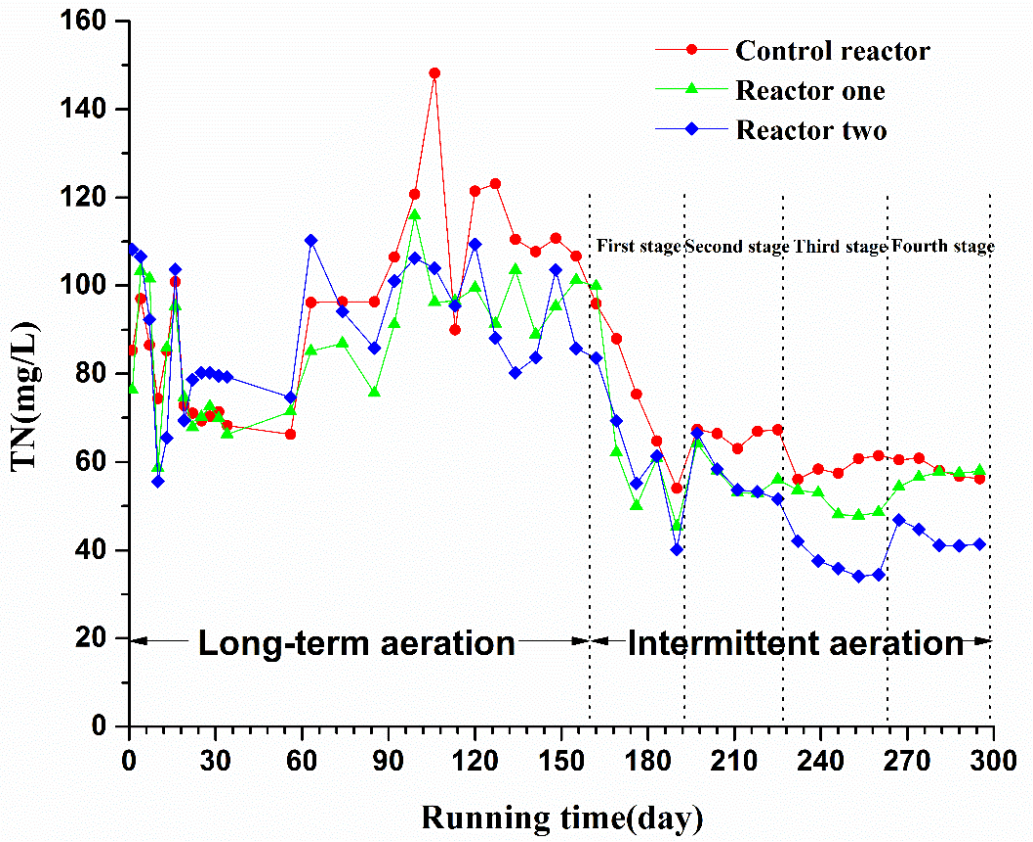

Figure 13. *Changes of TN concentration in the aeration tank*

http://www.aloki.hu ● ISSN 1589 1623 (Print) ● ISSN 1785 0037 (Online)
DOI: http://dx.doi.org/10.15666/aeer/1605_65256547
© 2018, ALÖKI Kft., Budapest, Hungary

TP analysis

Figure 14 shows that the influent TP concentration was from 30 to 40 mg/L. For the control reactor, the effluent TP remained stable after running 120 days. The concentration was stable from 25 mg/L to 29 mg/L and the average concentration was 27 mg/L. *Figure 15* shows that the average removal rate of TP was from 8% to 18% and the average removal rate reached 12%. For the reactor one, the effluent TP remained stable after running 113 days. The concentration was stable from 20 mg/L to 24 mg/L and the average concentration was 22 mg/L. The removal rate of TP was from 22% to 33% and the average removal rate reached 28%. For the reactor two, the effluent TP remains stable after running 113 days. The concentration was stable from 20 mg/L to 24 mg/L and the average concentration was 21 mg/L. The removal rate of TP was from 26% to 34% and the average removal rate reached 30%. After the reactor operation was stable, the TP concentrations of the reactor one and two were lower than those of the control reactor, and the reactor two was the lowest. It was shown that the removal effect on TP of reactor two was better than reactor one and both of them were better than the control reactor under the long-term aeration condition, which could be attributed to the creation of the bio-system which was similar to RBS in the reaction tanks of reactor one and two.

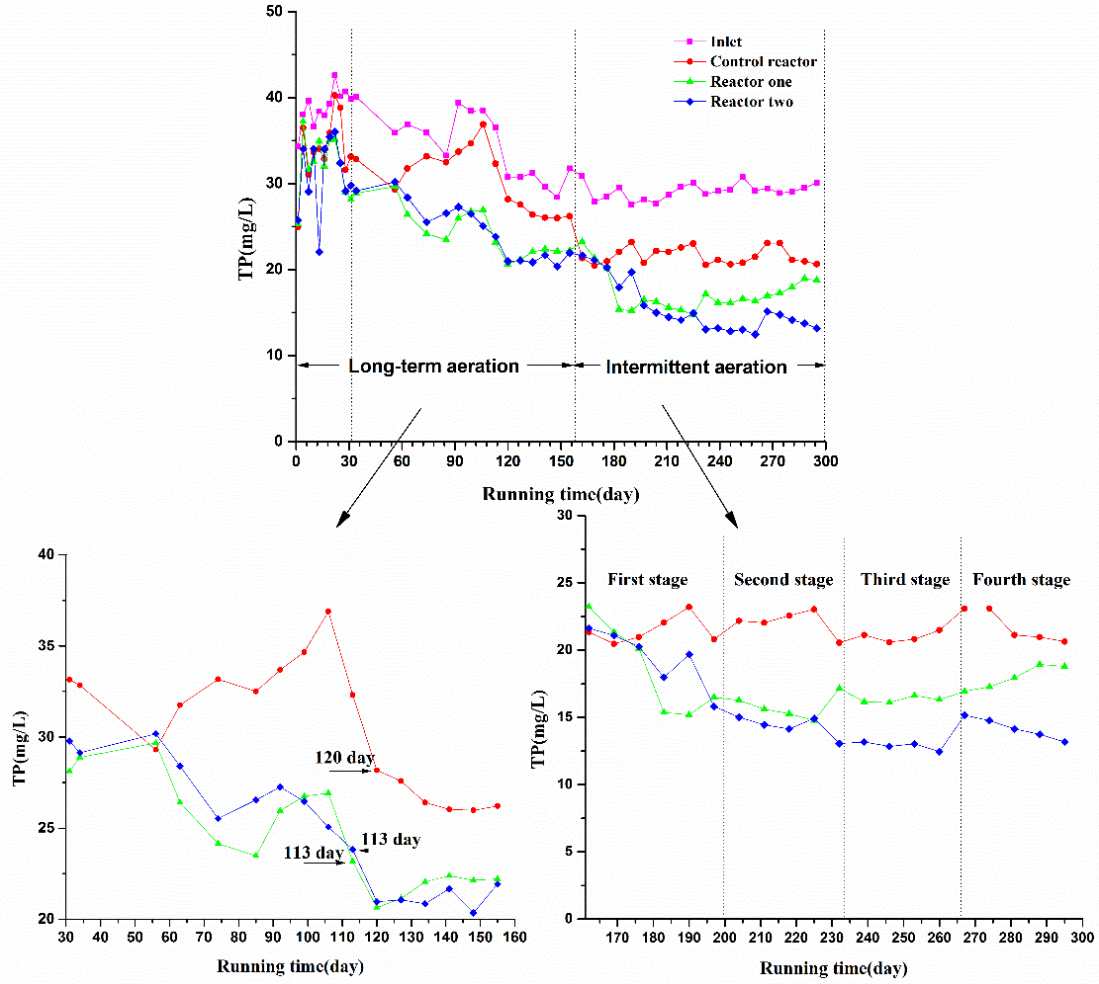

Figure 14. *Changes of TP concentration in the influent and effluent*

http://www.aloki.hu ● ISSN 1589 1623 (Print) ● ISSN 1785 0037 (Online)
DOI: http://dx.doi.org/10.15666/aeer/1605_65256547
© 2018, ALÖKI Kft., Budapest, Hungary

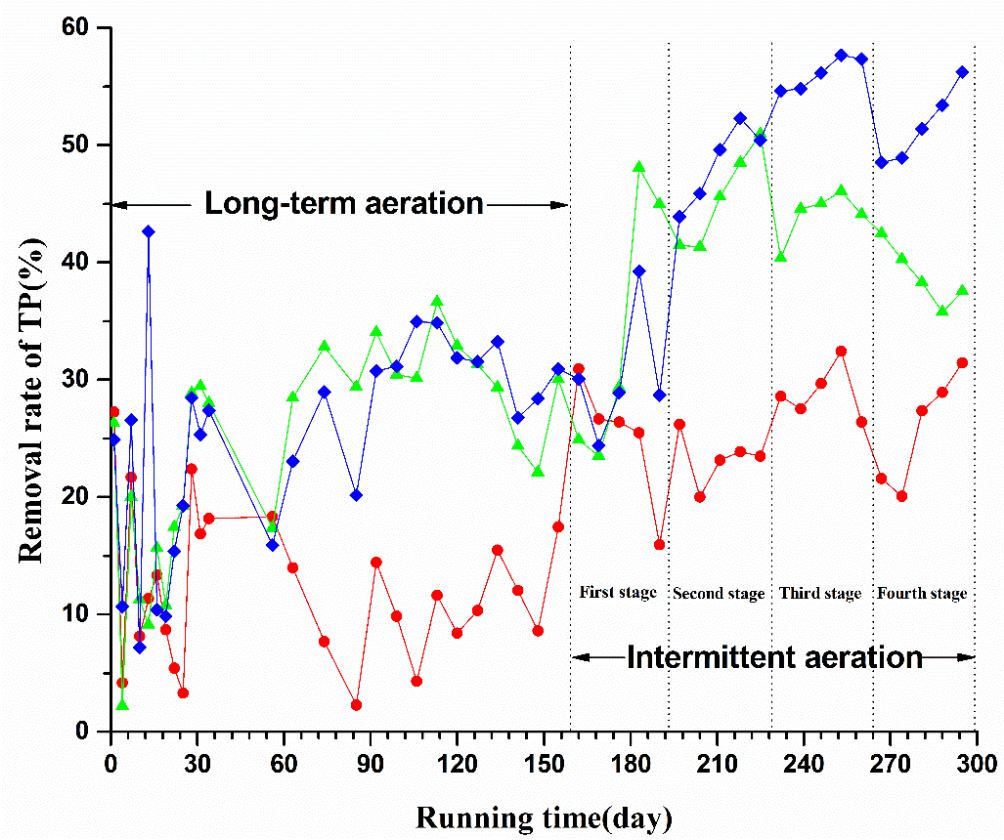

Figure 15. *Changes of TP removal rate*

During the four stages of intermittent aeration, the effluent TP concentration ranges as shown in *Table 5*. The average concentrations of four stages were 21.60 mg/L, 22.12 mg/L, 20.91 mg/L, 21.78 mg/L in control reactor. The average concentrations of four stages were 19.04 mg/L, 15.67 mg/L, 16.46 mg/L, 17.97 mg/L in reactor one. The average concentrations of four stages were 20.12 mg/L, 14.86 mg/L, 12.91 mg/L, 14.19 mg/L in reactor two. Therefore, the lowest effluent TP concentration of control reactor was the one of the third stage. The removal rate of TP was from 20% to 32% and the average removal rate was 26%. The lowest effluent TP concentration of reactor one was the one of the second stage. The removal rate of TP was from 41% to 51% and the average removal rate was 46%. The lowest effluent TP concentration of reactor two was one of the fourth stage. The removal rate of TP was from 48% to 57% and the average removal rate was 52%. It can be concluded that for the removal of TP, the most suitable aeration conditions for control reactor, reactor one, reactor two were 1 h 20 min/1 h 20 min, 1 h 20 min/1 h, 1 h 20 min/1 h 20 min.

Table 5. *Effluent TP concentration ranges*

Stage	Control	Reactor one	Reactor two
1	20.46 ~ 23.19 mg/L	15.18 ~ 23.22 mg/L	17.96 ~ 21.62 mg/L
2	20.80 ~ 23.03 mg/L	14.76 ~ 16.49 mg/L	14.13 ~ 15.81 mg/L
3	20.54 ~ 21.48 mg/L	16.10 ~ 17.15 mg/L	12.45 ~ 13.16 mg/L
4	20.62 ~ 23.09 mg/L	16.94 ~ 18.94 mg/L	13.16 ~ 15.15 mg/L

http://www.aloki.hu ● ISSN 1589 1623 (Print) ● ISSN 1785 0037 (Online)
DOI: http://dx.doi.org/10.15666/aeer/1605_65256547
© 2018, ALÖKI Kft., Budapest, Hungary

Figure 16 shows that the TP concentrations of three reactors in the aeration tank appeared stable after a long period of aeration of three reactors. The concentration of TP in the aeration tank of control reactor reduced from 30 ~ 40 mg/L to 29 mg/L while that of reactor one and reactor two reduced to 26 mg/L and 27 mg/L. After the intermittent aeration mode was converted to intermittent aeration, the TP concentration in the aeration tank reduced. In the third stage of intermittent aeration, the TP concentrations in the aeration tank of three reactors were minimum and those of control reactor, reactor one, reactor two were 24.53 mg/L, 20.33 mg/L, 12.00 mg/L. It was indicated that the aeration tank played an important role in the removal of TP of the long-term aeration stage and the intermittent aeration stage. Since the operating modes of three reactors were changed from long-term aeration to intermittent aeration, the COD removal efficiency increased.

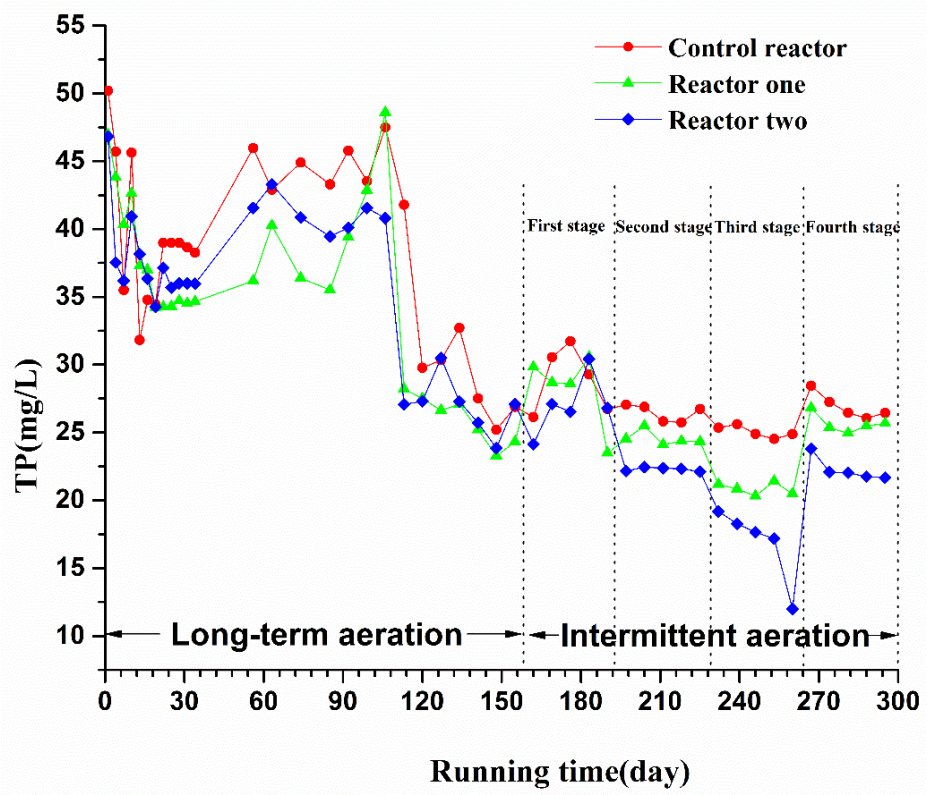

Figure 16. *Changes of TP concentration in the aeration tank*

Above all, after 120 days of long-term aeration, three reactors became a stable state. The removal of COD, NH_3-N, NO_3-N, TN, TP of reactor one and two were better than those of control reactor, especially the removal of COD. In terms of the removal of COD, the capacity of reactor one was better than reactor two. In terms of the removal of NH_3-N, NO_3-N, TN, TP, the capacities of reactor one and two were basically alike. In the intermittent aeration mode, the most optimum aeration condition for reactor one was 1 h 20 min/1 h; reactor two was 1 h 20 min/1 h 20 min. Under the optimum conditions of three reactors, reactor two achieved the highest removal efficiency of COD, NH_3-N, NO_3-N, TN, TP, which were better those of reactor one, and both of them were better than that of control reactor.

http://www.aloki.hu ● ISSN 1589 1623 (Print) ● ISSN 1785 0037 (Online)
DOI: http://dx.doi.org/10.15666/aeer/1605_65256547
© 2018, ALÖKI Kft., Budapest, Hungary

SS analysis

Figure 17 shows that for the reactor one, the concentration of SS in the aeration tank reached the maximum of 2084 mg/L in the second stage of intermittent aeration. In this stage, the highest removal efficiency of COD, NH_3-N, NO_3-N, TN, TP was achieved. For the reactor two, the concentration of SS in the aeration tank reached the maximum of 1946 mg/L in the third stage. The highest removal efficiency of COD, NH_3-N, TN, TP was achieved in this stage.

As shown in *Figure 17*, the control always showed a steady trend from the beginning to the fourth stage, while the reactor one and reactor two showed an upward trend and tended to be gentle in the third to fourth stages. In the operating, the SS concentration reached a maximum in the second stage, at which stage the highest removal efficiency of COD, NH_3-N, NO_3-N, TN, TP were achieved. In the long-term aeration mode, the SS concentration from large to small was the control reactor, reactor two, reactor one, and the three reactors had significant differences ($P < 0.05$); in the first phase and the second phase the concentration of reactor one were significantly higher than those of the control and reactor two ($P < 0.05$). In the third stage, the SS concentration of the reactor two was the highest, and there was significant difference between the two reactors and the control and reactor one ($P < 0.05$); The fourth stage was basically the same as the third stage. The reactor two had the highest concentration, the reactor one was the second, and the control was the lowest.

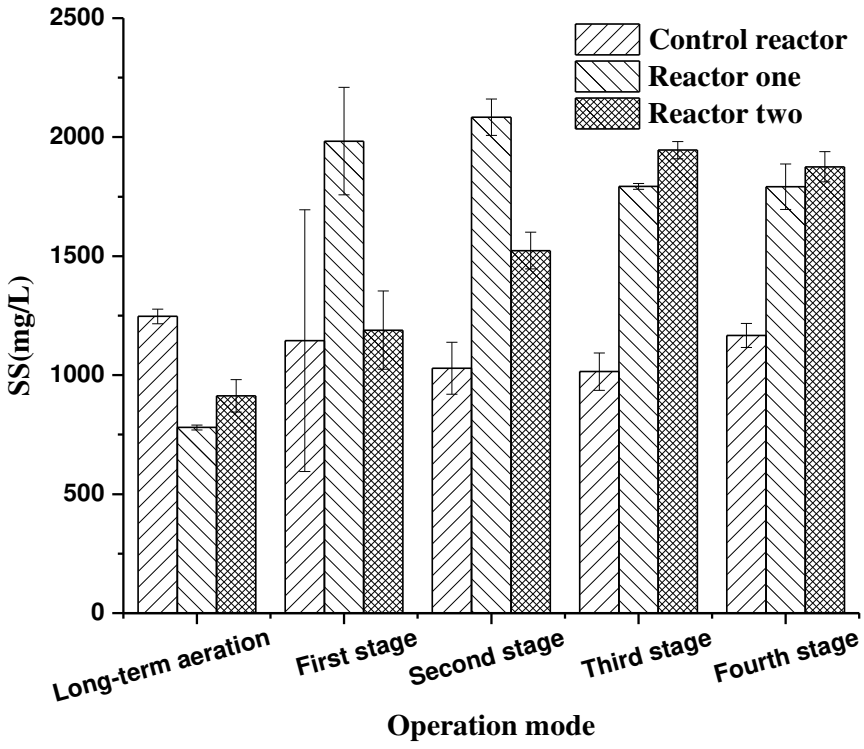

Figure 17. *Changes of SS concentration in the aeration tank*

SiO_2 analysis

Figure 18 shows that the concentrations of SiO_2 in reactor one's and reactor two's aeration tanks and reaction tanks were higher than those of control reactor. The reactor

http://www.aloki.hu ● ISSN 1589 1623 (Print) ● ISSN 1785 0037 (Online)
DOI: http://dx.doi.org/10.15666/aeer/1605_65256547
© 2018, ALÖKI Kft., Budapest, Hungary

one achieved the highest SiO_2 concentrations in its aeration tank and reaction tank, which were 0.218 mg/L and 0.310 mg/L. It shows that silicates in reactor one and two were decomposed into SiO_2. However, the SiO_2 concentration in reactor one was the highest, which indicated that three kinds of silicate bacteria inoculated in Pellet (bacteria) played roles in the process of silicate decomposition.

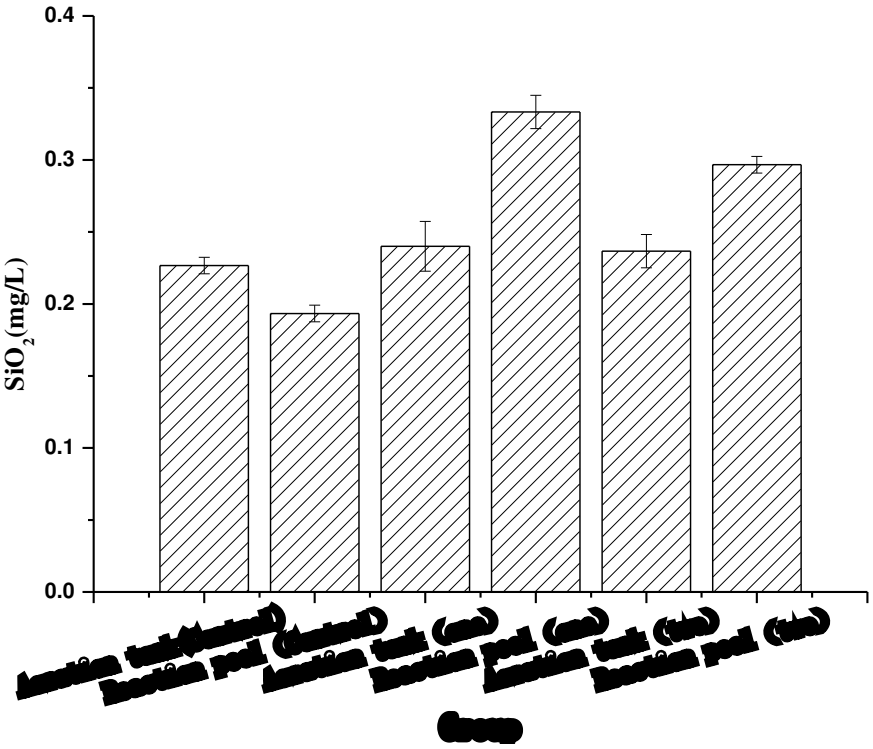

Figure 18. *SiO_2 concentration in the aeration tank and reactor in the 120th day*

For the operation of three reactors, the removal efficiencies of reactor one and two on COD, NH_3-N, NO_3-N, TN, TP were better than those of control reactor under long aeration and intermittent aeration, which indicated that the removal efficiency of the high concentration organic wastewater is enhanced. Pellet (bacteria), Pellet and pumice have been aerated in the reaction tank of reactor one and reactor two for a long time. The main component of Pellet was peat soil and the content of organic matter in the peat soil was 70 ~ 80%. The peat soil contains a large amount of water and incompletely decomposed plant residues, humus and a part of mineral matter and therefore there are a lot of humic precursors in Pellet. *Figure 18* shows that the SiO_2 concentrations in the reactor one and reactor two were higher than that of control reactor and thus the humic precursor and SiO_2 existed in the reaction tank of reactor one and reactor two, which satisfies the condition of the soil bacteria culture system (Jiang et al., 2008) in the RBS system. The reaction tank of reactor one and two created a good environment for inducing, domesticating and screening the soil bacteria. Therefore, a large number of dominant soil bacteria are found throughout the whole reactor. In addition, *Figure 18* shows that a decomposition process happens in the reaction tank of reactor one or reactor two. Silicate bacteria can decompose and oxidize the soil aluminosilicate minerals and release the elements such as K, Al, Si and some other

http://www.aloki.hu ● ISSN 1589 1623 (Print) ● ISSN 1785 0037 (Online)
DOI: http://dx.doi.org/10.15666/aeer/1605_65256547
© 2018, ALÖKI Kft., Budapest, Hungary

elements (Zhang, 2000), which were the constant or trace elements for the growth of microbes. In this way, the reaction tanks of reactor one and two were provided a large amount of soil dominant bacteria and nutrients for the whole wastewater treatment system, so that the removal efficiency of the wastewater was enhanced.

He Wenyuan (He, 2008) has studied the effect of pumice in the process of bioactive water. The results of his study showed that the pumice had a large specific surface area and a lot of pores. It offers microorganism a place to live and can absorb organic compounds at the same time. It could release minerals, which can stimulate the growth of microbes. Therefore, it was possible because the minerals released from pumice in reactor one and two stimulate the growth of microbes which the treatment effects of reactor one and two were enhanced.

The removal capacity of three reactors for COD, NH_3-N, NO_3-N, TN, TP was improved after the operation mode was transferred from long-time aeration to intermittent aeration, especially removal capacity of NH_3-N. Therefore, the intermittent aeration is better than long-term aeration for three reactors. In the process of intermittent aeration, the maximum SS concentration of reactor one appears in the second stage of intermittent aeration, which corresponds to the best removal capacity of COD, NH_3-N, NO_3-N, TN, TP in this stage. The maximum SS concentration of reactor two appears in the third stage, which corresponds to the best removal capacity of COD, NH_3-N, TN, TP in this stage.

After 120 days' long-term aeration, three reactors were reached the stable state. The effluents of COD, NH_3-N, NO_3-N, TN, TP concentrations in reactor one and two had little difference, especially the TN concentration and TP concentration, indicating that three kinds of silicate bacteria inoculated in the reactor pellet were less effective than the system itself in the removals of COD, NH_3-N, NO_3-N, TN, TP, but played a role in the process of silicate decomposition.

Conclusions

By analyzing the water quality of COD, TN and TP, compared with DW, BW and BW (bacteria), two bioactive waters increased the removal rates of COD, TN and TP. And the main function of bioactive water was its own, including the structure of biologically active water. Bioactive water increased the decomposition of silicates and releases mineral elements that stimulate microbial activity. In the process of production of bioactive water, the structure of water molecules' changes, that is, the number of water molecules of the water clusters was reduced; the solubility of salt was increased, and the metabolic activity of microorganisms was enhanced. The bioactive water itself (including its own structure) enhanced the activity of the microorganisms, thereby enhancing the removal ability of the high-concentration organic wastewater.

Laboratory scale wastewater treatment reactor one and reactor two enhanced the removal efficiency of high concentration organic wastewater. The reactor had realized its own optimization after the operating mode transfers from long-time aeration to intermittent aeration. The most suitable aeration condition for reactor one was 1 h 20 min/1 h while the most suitable aeration condition for reactor two was 1 h 20 min/1 h 20 min. According to our comprehensive analysis, reactor two achieved the best removal efficiency for high concentration organic wastewater. The optimum intermittent aeration condition of reactor two was 1 h 20 min/1 h 20 min and the average removal rates of COD, NH_3-N, NO_3-N, TN, TP were increased by 3%, 21%,

http://www.aloki.hu ● ISSN 1589 1623 (Print) ● ISSN 1785 0037 (Online)
DOI: http://dx.doi.org/10.15666/aeer/1605_65256547
© 2018, ALÖKI Kft., Budapest, Hungary

54%, 21% and 25% at this stage. The results show that bio-system was able to improve the treatment efficiency of high concentration organic wastewater and played an important role in the treatment reactor.

Acknowledgements. This work was supported by School Enterprise Cooperation Foundation of Yanbian University (project No. [2015]-7); National Natural Science Foundation of China (project No. 51368061).

REFERENCES

[1] Bao, S. D. (2000): Soil Agro Chemical Analysis (3rd ed.). – China Agriculture Press, Beijing.
[2] Bie, R. S., Li, B. X., Lu, H. L. et al. (2000): Deal with high concentration organic wastewater fluidized bed incinerator. – Boiler Manufacturing 1: 40-44.
[3] Chen, J. Q., Wang, H., Yang, X. L. (2002): Water Resources. – Science Press, Beijing.
[4] Chen, X. D., Li, Z. X., Meng, L. Y. (2008): Research progress of high concentration organic wastewater treatment technology. – Hebei Chemical Industry 31(12): 71-73.
[5] Du, H. Z., Fang, L. Q., Jiang, Y. et al. (1997a): Catalytic wet oxidation purification technology for refractory high concentration organic wastewater I. Development of wet oxidation catalyst with high activity and high stability. – Water Treatment Technology 23(2): 23-27.
[6] Du, H. Z., Fang, L. Q., Jiang, Y. et al. (1997b): Study on the catalytic wet oxidation purification technology of refractory high concentration organic wastewater II reaction process conditions. – Water Treatment Technology 23(3): 38-42.
[7] Ganigué, R., Volcke, E. I. P., Puig, S. et al. (2012): Impact of influent characteristics on a partial nitritation SBR treating high nitrogen loaded wastewater. – Bioresource Technology 111: 62-69.
[8] GB 11901 (1989): Water Quality Determination of Suspended Solids Weight Method. – Standards Press of China, Beijing.
[9] Gilcreas, F. W. (1998): Standard Methods for the Examination of Waste and Wastewater. – APHA, Washington, DC.
[10] He, C. H., Zhu, M. Q., Liu, J. Q. et al. (2002): Extraction of caprolactam from aqueous ammonium sulfate solution in pulsed packed column using 250Y Mellapak packings. – Chinese Journal of Chemical Engineering 10(6): 677-680.
[11] He, W. Y. (2008): Research on the Mechanism and Application of Bioactive Water. – Tongji University, Shanghai.
[12] Huang, M., Zhu, Y., Xiao, J. et al. (2004): Evaluation of high concentration refractory organic industrial wastewater treatment technology. – Industrial Water Treatment 24(4): 1-5.
[13] Jena, J., Kumar, R., Saifuddin, M. et al. (2016): Anoxic–aerobic SBR system for nitrate, phosphate and COD removal from high-strength wastewater and diversity study of microbial communities. – Biochemical Engineering Journal 105: 80-89.
[14] Jiang, Z. W., Lian, T. J., Hei, M. X. et al. (2008): Using natural purification RBS technology to treat high concentration organic sewage. – Exhibition and Seminar on Earth Saving of Practical Technology for Water Pollution Control, Fujian.
[15] Li, G. C., Zheng, X. Y., Piao, Z. X. et al: (2007): BTEX decomposition compound bacteria's separation and a decomposition characteristic. – Korea Institute of Industrial Waste 24(8): 689-695.
[16] Li, X. D., Yang, Y. (2002): New technology of wastewater biological treatment. – Fine and Specialty Chemicals 17: 19-21+6.
[17] Liu, F. R., Meng, L. H. (2008): SBR process characteristics and application development. – Science and Technology Information (Science Teaching and Research) 2: 29-30.

http://www.aloki.hu ● ISSN 1589 1623 (Print) ● ISSN 1785 0037 (Online)
DOI: http://dx.doi.org/10.15666/aeer/1605_65256547
© 2018, ALÖKI Kft., Budapest, Hungary

[18] Liu, X. D., Chen, Y., Zhang, X. et al. (2015): Aerobic granulation strategy for bioaugmentation of a sequencing batch reactor (SBR) treating high strength pyridine wastewater. – Journal of Hazardous Materials 295(15): 153-160.
[19] Lu, J., Xu, G. T., Zhang, L. et al. (2001): Pharmaceutical industry wastewater treatment technology. – Industrial Water Treatment 21(10): 1-5.
[20] Qualls (1989): Persulfate Digest for Water Total N and Total P. – http://sisbl.uga.edu/qualls.html.
[21] Ren, A. (2000): Wastewater biological treatment technology and its research progress. – Environment and Sustainable Development 4: 19-24.
[22] Rousseau, R. W. (1987): Handbook of Separation Technology. – John Wiley & Sons, New York.
[23] Sun, P. S., Harada, Y., Yamazaki, K. (1999): Experimental study on catalytic wet air oxidation of high concentration organic wastewater. – Environmental Pollution and Prevention 21(1): 4-6.
[24] Wang, M. X., Liao, C. J. (2011): Biological treatment technology of high concentration organic wastewater. – Contemporary Chemical Industry 40(8): 820-823.
[25] Wang, Z. H., Sun, Y. H. (1995): Biotreatment technology for high concentration organic wastewater. – Jiangsu Environmental Technology 4: 29-32.
[26] Wu, Y. J. (2017): SBR sewage treatment technology application and development prospect. – Resource Conservation and Environmental Protection 5: 88-91.
[27] Yang, Y. Y., Dai, Y. Y. (1997): Complexation extraction method for the treatment of high concentration organic wastewater. – Modern Chemical Industry 3(3): 10-14.
[28] Zhai, H. W. (2014): Experimental Study on Treatment of Domestic Sewage by RBS. – Changchun University of Science and Technology, Changchun.
[29] Zhang, J. S. (2000): Application technology of biological potassium fertilizer. – Heilongjiang Science and Technology Information 2: 22.
[30] Zhang, X. (2014): Trend and governance system of water pollution in China. – Soft Science of China 10: 11-24.
[31] Zhao, Y. (2002): RBS technology for treatment of high concentration pig wastewater. – Liaoning Urban and Rural Environmental Technology 22(1): 28-29.
[32] Zhao, Y., Zhu, F. H., Pang, G. L. et al. (2003): High concentration organic wastewater treatment technology. – Electric Power Environmental Protection 19(3): 46-48.
[33] Zhu, M. Q., Liu, J. Q., He, C. H. et al. (2001): Scale-up effect of pulsed sieve-plate column for recovering caprolactam from wastewater. – Proceedings of CKCSST01, Hangzhou.

http://www.aloki.hu ● ISSN 1589 1623 (Print) ● ISSN 1785 0037 (Online)
DOI: http://dx.doi.org/10.15666/aeer/1605_65256547
© 2018, ALÖKI Kft., Budapest, Hungary

HARNESSING THE POTENTIAL OF MEDICINAL PLANTS USED FOR THE TREATMENT OF DIABETES IN RURAL AREAS OF AZAD JAMMU AND KASHMIR, PAKISTAN

BEGUM, S.[1] – HUSSAIN, S.[2] – MEHMOOD, A.[2*] – AHMAD, K. S.[2] – HAMID, A.[3]

[1]*Department of Botany, Government College (GC) University, Lahore, Pakistan*

[2]*Department of Botany, University of the Poonch Rawalakot (UPR), Azad Kashmir 12350, Pakistan*

[3]*Department of Horticulture, University of the Poonch Rawalakot, Azad Kashmir 12350, Pakistan (phone: +92-34-6538-7843; fax: +92-58-3496-0073)*

**Corresponding author*
e-mail: ansar.mehmood321@gmail.com

(Received 22nd Jun 2018; accepted 14th Aug 2018)

Abstract. This study was aimed to highlight the significance of medicinal plants, used for the treatment of diabetes from Azad Jammu and Kashmir, Pakistan. A total of 340 informants including 171 males and 169 females were interviewed through questionnaire. For reliability of medicinal knowledge, relative frequency of citation (RFC) and family importance value (FIV) were calculated. Novelty of the work was found out with the help of Jaccard index (JI). RFC and FIV were further analysed by multivariate cluster analysis. A total of 42 plant species belonging to 41 genera and 30 families were recorded during the survey. Leaves were the most commonly used plant part and decoction was the most recommended remedy preparation method. *Momodica charantia, Berberis lycium, Syzygium cumini* and *Oxalis corniculata* were the most cited species with relative frequency of citation 0.81, 0.72, 0.59 and 0.55 respectively. The highest consensus between informants and indigenous uses of family was shown by Lamiaceae with 97.44 FIV followed by Fabaceae (87.05) and Myrtaceae (85.88). Novelty index showed that *Berberis lycium*, *Beta vulgaris, Coriandrum sativum* and *Oxalis corniculata* were the newly documented species against diabetes. The results of present study could play vital role in conservation of traditional knowledge of study area.
Keywords: *medicinal knowledge, cluster analysis, traditional knowledge, Jaccard index, Berberis lycium*

Introduction

Diabetes is a major public health problem currently affecting 284.6 million people worldwide and according to the latest International Diabetes Federation estimates it is expected to affect 438.4 million adults by 2030 becoming one of the world's main disabler and killer (IDF, 2010). It disturbs the function of heart, eyes, kidneys and overall body. It is a major health problem that results in reduced life quality and increased illness (Wei et al., 2010). Diabetes is usually managed by diet, exercise, oral hypoglycemic agents and insulin (Ayodhya et al., 2013).

In addition to modern allopathic treatments, plants have also been used for the treatment of diabetes throughout the world in traditional systems of medicines (Donga et al., 2015). Many plants have the potential to lower the blood glucose level and to manage diabetes mellitus like *Morinda citrifolia* (Goodman and Ghafoor, 1992), *Musa sapientum* (Jain et al., 1998)), *Allium cepa* (Mossa, 1999), *Brassica juncea* (Yokozawa, 2003), *Herichrysum odoratissimum*, *Herichrysum petiolare*, *Hypoxis hemerocallidea* and *Hypoxis colchicifolia* (Masika and Afoloayan, 2003). The rural inhabitants of Azad Jammu and Kashmir are mostly depend on traditional medicines and traditional health

http://www.aloki.hu ● ISSN 1589 1623 (Print) ● ISSN 1785 0037 (Online)
DOI: http://dx.doi.org/10.15666/aeer/1605_65496566
© 2018, ALÖKI Kft., Budapest, Hungary

practitioners as the primary source of health care. There are several reports of ethnobotanical surveys in Azad Jammu and Kashmir (Ajaib et al., 2015; Ajaib and Khan, 2014; Mahmood et al., 2011) concerning use of medicinal plants for the management and treatment of diseases including diabetes mellitus. However, in Azad Jammu and Kashmir, the traditional medicinal plants that are used for the treatment of diabetes are not studied in great detail.

Pakistan is ranked 7th in the world for the diabetes prevalence. A recent diabetes prevalence survey has revealed staggering 16.98 percent prevalence of diabetes as 35.3 million people among the adult population are found diabetic in Pakistan. If awareness programs and proper treatment are not adopted, Pakistan may have double of diabetic patients by 2040 (WHO, 2016). Such high prevalence of diabetes calls for continued efforts to improve public awareness regarding the disease. Keeping in view the current scenario of diabetes, the present study was designed to document plant knowledge used exclusively for the treatment of diabetes in rural areas of Azad Jammu and Kashmir, Pakistan.

Materials and methods

Study area

The Himalaya, the emporium of biodiversity, have been variously divided into Western Himalaya, Central Himalaya and Eastern Himalaya. Azad Kashmir (34.22°N 73.28°E) is located in foothills of Western Himalaya with an area of 13,269 km^2 which is divided into two distinct geographical zones. North and East are mostly hilly and mountainous while South and West are valleys and plains (*Fig. 1*). Due to extensive topographical variations, the area supports a variety of plant species (Afshan et al., 2011). In Himalaya, about 70% of flora have medicinal value and rural population largely depends on these plants for medicines (Shaheen et al., 2012). These plants based on traditional medicine system, continue to play an essential role in health care, with about 80% of the world's inhabitants relying mainly on traditional medicines for their primary health care (Franz, 1985). Till date, 6000 species are identified from different parts of Pakistan and Azad Kashmir, and off these, more than 400 species are only dwelling only in Azad Kashmir region with high medicinal values (Shinwari and Shinwari, 2010). In remote areas about 60% of the local population is engaged in collection and processing of different medicinal herbs (Qamar et al., 2010).

Field study

A wide-ranging survey in rural and remote areas was carried out during 2013-15. Information was gathered using open and close ended questioners. A sum of 340 informants including 171 males and 169 females were interviewed after initial survey and many group discussions with the native people. Selection criteria of choosing informants were based on the individual's expertise in the collection and utilization of medicinal plants for diabetes. Prior Informed Consent was obtained from informants involved in interviews and plant collection walks. Ethical approval was not required for this study as research participants were only interviewed on knowledge of plant species used for medicinal purposes. Participants were not subjected to any treatment, were not part of any clinical trials, and no information is presented here that could identify individual participants. Plant samples were collected, pressed with the help of plant

http://www.aloki.hu ● ISSN 1589 1623 (Print) ● ISSN 1785 0037 (Online)
DOI: http://dx.doi.org/10.15666/aeer/1605_65496566
© 2018, ALÖKI Kft., Budapest, Hungary

presser and dried at room temperature. Completely dried plant specimens were mounted on the herbarium sheets. For long term preservation and to avoid fungal attack, each mounted sample was treated with 1% $HgCl_2$ preservative. Plants were identified by the plant taxonomist at The Department of Botany and further clarification was done through herbaria comparison and available taxonomic literature. The International Plant Name Index (IPNI), Scopus, Web of Science and Google Scholar, Catalog of vascular plants of West Pakistan and Kashmir (Ali and Nasir, 1970-2002) were also consulted to obtain correct botanical names. Plant specimens with voucher number were deposited in Herbarium of University of the Poonch Rawalakot.

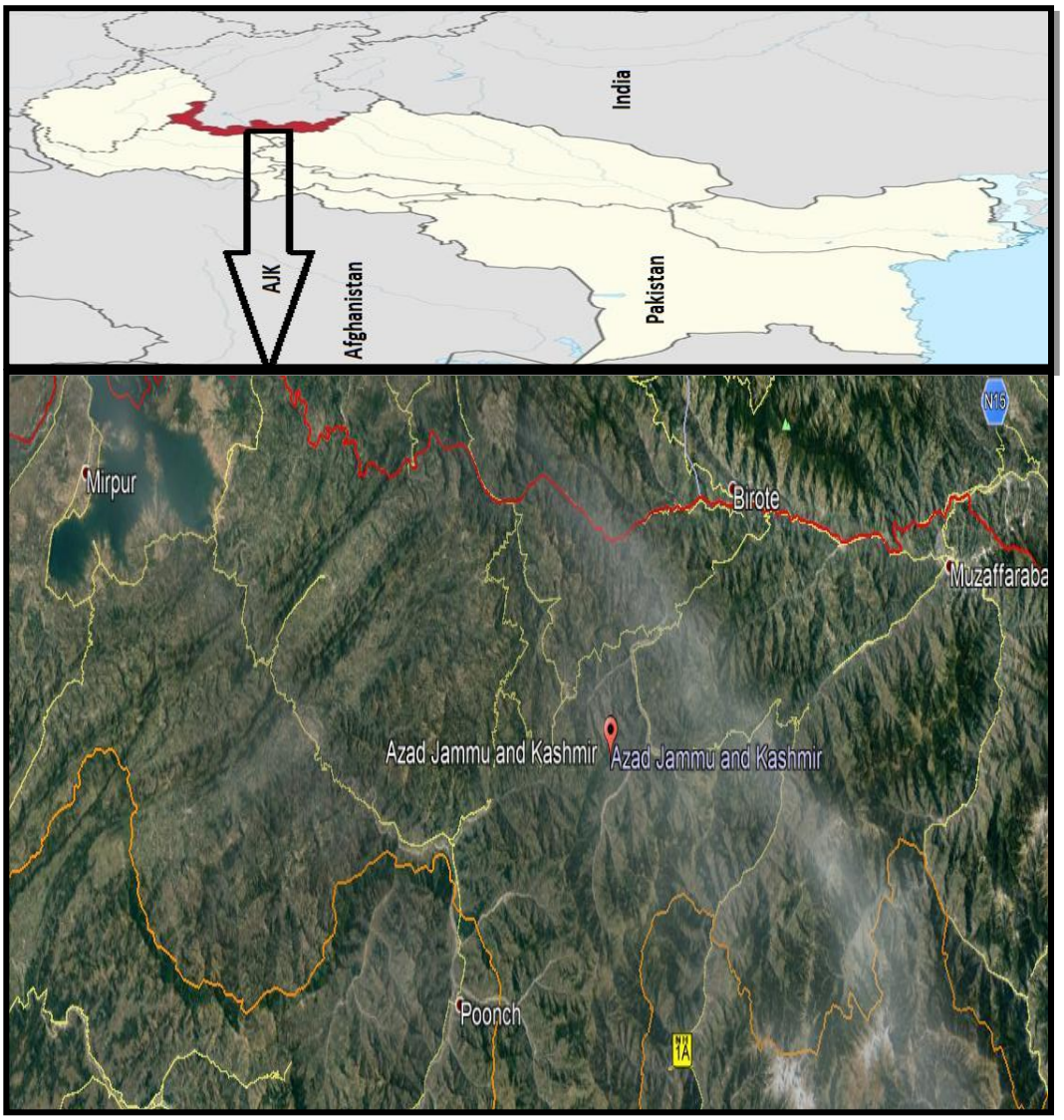

Figure 1. *Map of the study area (AJK)*

Data collection

Data was collected from people of different age groups belonging to different professions (formers, shopkeepers, teachers, herbal practitioners, wood sellers, students etc.) by using semi structured questionnaire (see *Appendix*), developed by using the

http://www.aloki.hu ● ISSN 1589 1623 (Print) ● ISSN 1785 0037 (Online)
DOI: http://dx.doi.org/10.15666/aeer/1605_65496566
© 2018, ALÖKI Kft., Budapest, Hungary

method of Edwards et al. (2005). The collected data comprised of local names of the plants, the parts of plant, recipe and usage method, quantity of dose and duration of treatment.

Relative frequency of citation

The frequency of citation was calculated to assess the incidence of one particular plant species used for the treatment of diabetes in relation to the overall citations for all plants. The relative frequency of citation for a plant species was calculated as *Equation 1* (Tardio and Pardo-de-Santayana, 2008).

$$RFC = \frac{FC}{N} \quad (0 < RFC < 1) \qquad \text{(Eq.1)}$$

Where FC is the number of informants who mentioned the use of plant and N is the total number of informants.

Family importance value

The consensus between informants and indigenous use of family was evaluated by formula in *Equation 2* (Molares and Ladio, 2009)

$$FIV = FC_{Family} / N \times 100 \qquad \text{(Eq.2)}$$

Where FC = Number of informants mentioned indigenous use of family for particular disease and N= total number of informants mentioning all family for particular disease.

Jaccard index

JI was used to find the resemblance in indigenous data among various ethnic groups and geographical areas by comparing present study with published works from the neighboring areas as in *Equation 3* (Gonza et al., 2008).

$$JI = \frac{c \times 100}{(a+b) - c} \qquad \text{(Eq. 3)}$$

where a is the species present in our area only, b is the species present in neighboring area only and c is the species found in both areas.

Data analysis

Measuring the importance of plants and vegetation to people is a central concern in quantitative ethnobotany. Quantitative indices help to obtain quality information on medicinal plant usage which in turn contributes conservation of natural resources. Furthermore, such indices helped to establish consensus on which species are effective to cure diabetes, as well as the species' relative importance and enabled us to understand the extent of the potential utilization of each species. In this study, data ethnobotanical data was tested using quantitative indices namely: RFC, FIV, and JI. Multivariate cluster analysis was done on RFC and FIV.

http://www.aloki.hu ● ISSN 1589 1623 (Print) ● ISSN 1785 0037 (Online)
DOI: http://dx.doi.org/10.15666/aeer/1605_65496566
© 2018, ALÖKI Kft., Budapest, Hungary

Results

Demographic profile

The present study was conducted in rural areas of Azad Jammu and Kashmir, Pakistan. A total of 340 informants have been interviewed (*Table 1*). The demographic profile of the area showed that there were 51% male and 49% female respondents. All the informants were classified into 3 age groups viz. Below 30 years (20%), 30 to 50 years (27%) and above 50 years (56%). It was observed that indigenous knowledge was more confined to older people.

Table 1. *Demographic data of the informants*

Variable	Categories	Total	%
Gender	Male	175	51
	Female	165	49
Age groups	Below 30	69	20
	30-50	91	27
	Above 50	190	56

Documentation of plants

The ethnobotanical data showed that inhabitants of Azad Jammu and Kashmir use 42 plant species belonging to 41 genera and 30 families for the treatment of diabetes. Most of them were angiosperms while gymnosperms and pteridophytes are represented by only one species each. All the recorded plant species are arranged in alphabetical order with their families, voucher specimen, local name, part used and recipes (*Table 2*).

Table 2. *Documentation of medicinal plants used for the treatment of diabetes mellitus in Azad Jammu and Kashmir, Pakistan with scientific names, local names, parts used, recipe, FC and RFC*

S. No.	Taxon	Local name	Part used	Recipe	FC	RFC
1	*Acacia arabica* Willd. **(Fabaceae)**	Keeker	Pods, leaves, gum	Decoction	13	0.03
2	*Aconitum heterophyllum* Wall. **(Ranunculaceae)**	Patrees	Underground stem and roots	Decoction, powder	21	0.06
3	*Ajuga bracteosa* Wall. **(Lamiaceae)**	Kori booti	Whole plant	Decoction	113	0.33
4	*Ajuga parviflora* L. **(Lamiaceae)**	Adamjan	Whole plant	Decoction	70	0.20
5	*Aloe barbadensis* Mill **(Liliaceae)**.	Kanwar gandal	Fresh leaves	Leaf juice	57	0.16
6	*Anethum graveolens* L. **(Apiaceae)**	Saunf	Leaves, stem, fruit	Juice of all fresh parts	103	0.30

http://www.aloki.hu ● ISSN 1589 1623 (Print) ● ISSN 1785 0037 (Online)
DOI: http://dx.doi.org/10.15666/aeer/1605_65496566
© 2018, ALÖKI Kft., Budapest, Hungary

7	*Avena sativa* L. **(Poaceae)**	Jei	Seeds, roots	Extracts of straws and roots, seeds as powder	12	0.03
8	*Bauhinia variegata* L. **(Fabaceae)**	Kachnar	Leaves, flower, bark	Decoction	80	0.23
9	*Berberis lycium* L. **(Berberidaceae)**	Simloo	Root bark	Dried root, bark powder and Juice	257	0.75
10	*Beta vulgaris* L. **(Chenopodiaceae)**	Chuqander	Tap root, leaves, seeds	Juice and decoction	136	0.40
11	*Caltha palustris* L. **(Ranunculaceae)**	Marsh marigold	Aerial parts	Decoction	45	0.13
12	*Catharanthus roseus* L.**(Apocynaceae)**	Madaguscar	Leaves, roots	Decoction and extract	33	0.09
13	*Cedrus deodara* Roxb. **(Pinaceae)**	Deodar	Leaves extract, heart wood oil	Heart wood and dried leaves decoction	88	0.25
14	*Chenopodium album* L **(Chenopodiaceae)**.	Bathuwa	Leaves, seeds	Leaves as vegetable and dry seeds orally with water	29	0.08
15	*Coriandrum sativum* L. **(Apiaceae)**	Dhaniyan	Leaves, fruit	Leaves as salad and fruits are taken with water	139	0.40
16	*Cuscuta reflexa* Roxb.**(Convolvulaceae)**	Neeladhari	Whole plant	Decoction of dry and fresh plant	32	0.09
17	*Equisetum hyemale* L. **(Equistaceae)**	Commen horsetail	Whole plant	Decoction of dried plant	10	0.02
18	*Eriobotrya japonica* Thumb. **(Rosaceae)**	Loquat	Leaves, flower, fruit	Dry leaves extracts and decoction	10	0.02
19	*Fragaria vesca* L. **(Rosaceae)**	Kanachi	Roots, leave	Decoction of dried and fresh roots and leaves	18	0.05
20	*Hedra helix* L. **(Araliaceae)**	Herbambel	Leaves	Powder and decoction of shade dried leaves	136	0.40
21	*Juglans regia* L. **(Juglandaceae)**	Akhore	Leaves, bark, fruit	Decoction of dried leaves and bark, fruit oil	32	0.09
22	*Lycium barbarum* L. **(Solanaceae)**	Kankoli	Ripe fruit	Ripe fruit	111	0.32
23	*Marrubiam vulgare* L. **(Lamiaceae)**	White horehound	Leaves, roots	Extracts of dry leaves and roots	63	0.18
24	*Mentha arvensis* L. **(Lamiaceae)**	Podina	Aerial parts	Decoction and sauce of fresh or dry leaves	87	0.25

http://www.aloki.hu ● ISSN 1589 1623 (Print) ● ISSN 1785 0037 (Online)
DOI: http://dx.doi.org/10.15666/aeer/1605_65496566
© 2018, ALÖKI Kft., Budapest, Hungary

25	*Momordica charantia* L. **(Cucurbitaceae)**	Karela	Fruit, seeds, leaves	Seed oil and leaves decoction	277	0.81
26	*Nasturtium officinale* L. **(Brassicaceae)**	Chow	Aerial parts	Used as vegetable	123	0.36
27	*Olea europaea* L. **(Oleaceae)**	Zeytoon	Leaves, seeds	Decoction of dried leaves and seeds	153	0.45
28	*Oxalis corniculata* L. **(Oxalidaceae)**	Khatkoira	Whole plant	Juice and decoction of fresh leaves and roots	189	0.55
29	*Phaseulus vulgaris* L. **(Fabaceae)**	Lobia	Beans	Pods and bean sauce vegetable	113	0.33
30	*Plantago lanceolata* L. **(Plantaginaceae)**	Chamch-e-Pattar	Whole plant, seeds	Seeds decoction, leaves as vegetable	151	0.44
31	*Polygonum aviculare* L.**(Polygonaceae)**	Masloon	Whole plant	Decoction of fresh or dried plant	109	0.32
32	*Psidium guajava* L. **(Myrtaceae)**	Amrood	Fruit, leaves, roots	Fresh leaves juice and dry leaves extract	91	0.26
33	*Quercus dilatata* Thumb. **(Fagaceae)**	Burri	Bark	Bark decoction	10	0.02
34	*Rehmannia glutinosa* Gaertn. **(Scrophulariaceae)**	Chandal booty	Roots	Decoction	49	0.14
35	*Solanum nigrum* L. **(Solanaceae)**	Kach Maach	Whole plant, fruit	Decoction and extract	29	0.08
36	*Syzygium cumini* L. **(Myrtaceae)**	Jaman	Leaves, seeds, fruit	Powder orally with water	201	0.59
37	*Taraxacum officinale* L. (**Asteraceae)**	Hund	Whole plant	Leaves as vegetable, decoction of dried plant	139	0.40
38	*Trigonella foenum-gracum* L. **(Fabaceae)**	Methi	Leaves and seeds	Leaves fresh as vegetable and seed decoction or extract	80	0.23
39	*Urtica dioica* L. **(Urticaceae)**	Bichhu booty	Roots	Hot water extracts of dried roots	17	0.05
40	*Woodfordia fruticosa* L. **(Lythraceae)**	Bela, Davi	Flowers	Dried flower extract	10	0.02
41	*Zanthoxylum alatum* Roxb. **(Rutaceae)**	Timber	Bark, fruits and leaves	Extracts of all dried parts	38	0.11
42	*Zizpiphus mauritiana* Lam. (**Rhamnaceae)**	Beri.	Fruits and leaves	Mixture of dried fruit and leaves extracts	76	0.22

http://www.aloki.hu ● ISSN 1589 1623 (Print) ● ISSN 1785 0037 (Online)
DOI: http://dx.doi.org/10.15666/aeer/1605_65496566
© 2018, ALÖKI Kft., Budapest, Hungary

Family participation

It was found that most dominant families with respect to species number were Fabaceae and Lamiaceae with 4 species each followed by Apiaceae, Chenopodiaceae, Ranunculaceae, Rosaceae and Solanaceae with 2 species each (*Fig. 2*). All other families were represented with one species. The dominance of the families is corresponded to the fact that these are well known among the people and easy to access.

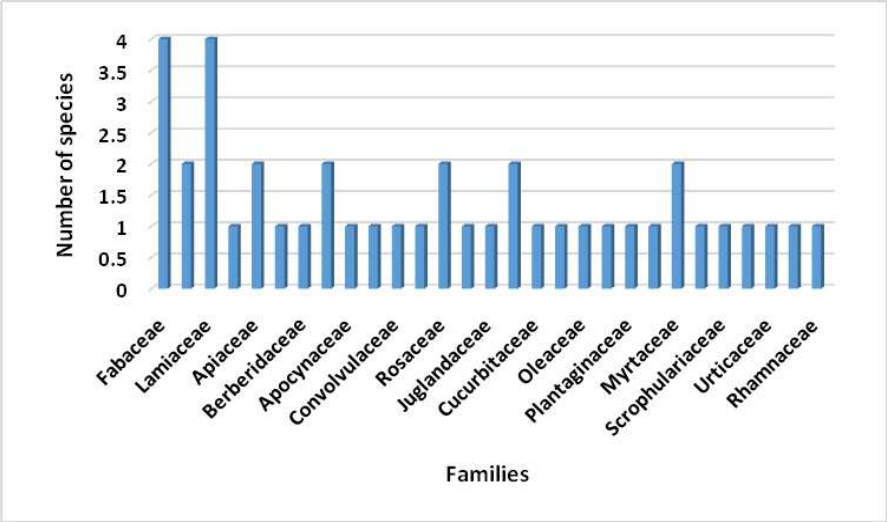

Figure 2. *Number of species per family*

Parts used and methods of administration

Most frequently used plant parts were the leaves (28%) and fruits (16%) followed by whole plant (13%), seeds (12%), roots (10%), bark (7%), flowers (4%) and aerial parts (3%) as shown in *Figure 3*. Herbal medicines were prepared by using different preparation methods, i.e. decoction, powder, juice, extract and vegetable (*Fig. 4*). Most frequent used method was decoction (48%) followed by extract (21%), juice and vegetable (11% each) and powder (9%) as presented in *Figure 4*.

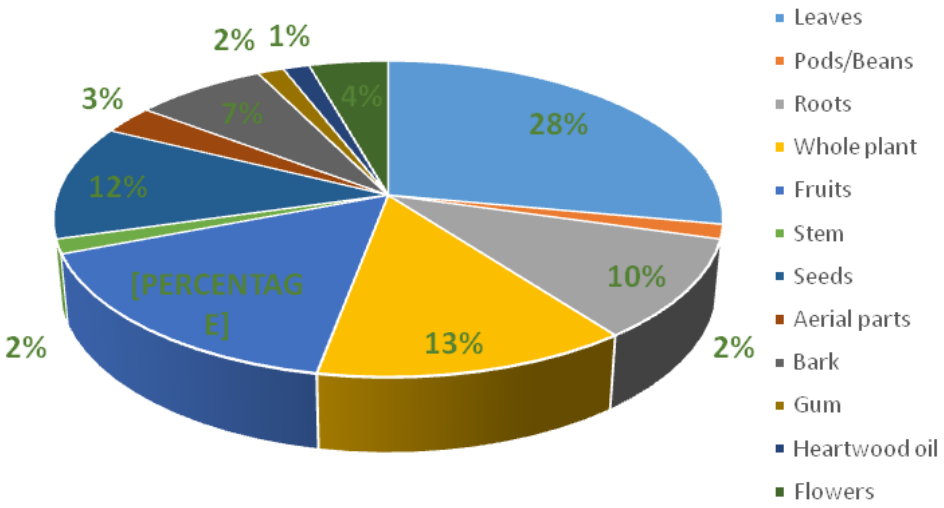

Figure 3. *Plant parts used to treat diabetes*

http://www.aloki.hu ● ISSN 1589 1623 (Print) ● ISSN 1785 0037 (Online)
DOI: http://dx.doi.org/10.15666/aeer/1605_65496566
© 2018, ALÖKI Kft., Budapest, Hungary

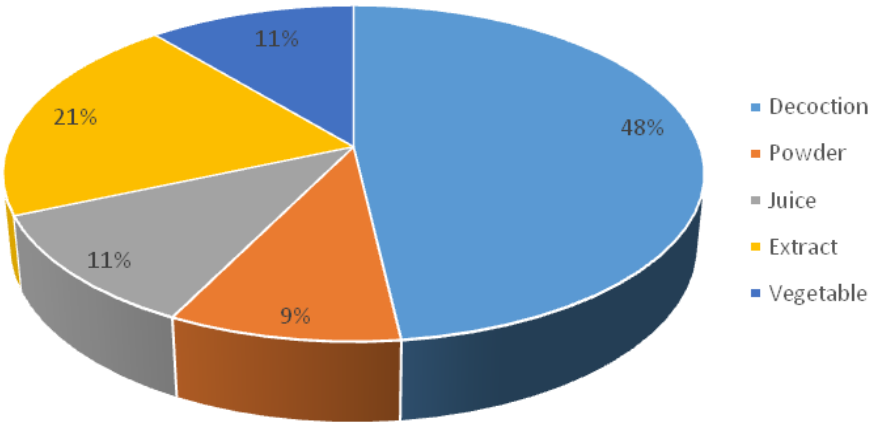

Figure 4. *Methods of herbal drug preparation*

Relative frequency of citation

Most common plants used to treat diabetes as mention by informants were determined by calculating RFC. The RFC values were shown in *Table 2,* which ranged from 0.09 to 0.95. The highest RFC was found for *Berberis lycium* (0.95) followed by *Momordica charantia* (0.91) and *Beta vulgaris* (0.80).

Family importance value

The results of FIV are shown in *Table 3*. The highest consensus between informants and indigenous uses of family was shown by Lamiaceae with 97.44 FIV followed by Fabaceae (87.05), Myrtaceae (85.88), Cucurbitaceae (81.47), Berberidaceae (75.58) and Apiaceae (71.17).

Table 3. *Family importance value*

Family	FC	FIV
Equitaceae	10	2.94
Lythraceae	10	2.94
Polygonaceae	109	32.05
Poaceae	12	3.52
Brassicaceae	123	36.17
Araliaceae	136	40
Asteraceae	139	40.88
Solanaceae	140	41.17
Plantaginaceae	151	44.41
Oleaceae	153	45.00
Chenopodiaceae	165	48.52
Urticaceae	17	50.00
oxalidaceae	189	55.58
Apiaceae	242	71.17
Berberidaceae	257	75.58

http://www.aloki.hu ● ISSN 1589 1623 (Print) ● ISSN 1785 0037 (Online)
DOI: http://dx.doi.org/10.15666/aeer/1605_65496566
© 2018, ALÖKI Kft., Budapest, Hungary

Cucurbitaceae	277	81.47
Rosaceae	28	8.23
Myrtaceae	292	85.88
Fabaceae	296	87.05
Convolvulaceae	32	9.41
Juglandaceae	32	9.41
Apocynaceae	33	9.70
Lamiaceae	333	97.94
Rutaceae	38	11.17
Scrophulariaceae	49	14.41
Liliaceae	57	16.76
Ranunculaceae	66	19.41
Rhamnaceae	76	22.35
Pinaceae	88	25.88

Jaccard index

It was used to compare the indigenous knowledge use to treat diabetes among different communities as the ethnobotanical knowledge greatly vary among the communities because of different origins, geography, culture and social behavior. This comparison of knowledge may result in discovery of many new drugs (Leonti, 2011). The present study was compared with 9 other studies from Pakistan, India, Bangladesh, Iran (*Table 4*). The maximum degree of parallel index was found with studies by Bahmani et al., (Bahmoni et al., 2014) from Uramia, Northwest Iran, Ahmad et al. (2009) Attock Pakistan and Kumari et al. (2011) Uttarakhand, India.

Table 4. *Jaccard index comparing present study with previous studies*

Area	Study year	Number of recorded plant species	Total species common in both area	Species enlisted only in aligned areas	Species enlisted only in study area	JI	Citation
Attock, Pakistan	2009	37	5	32	37	7.81	Ahmad et al., 2009
Tamil Nadu, India	2017	65	5	60	37	5.43	Aadhan and Anand, 2017
Uttarakhand, India	2011	16	3	13	39	6.12	Kumari et al., 2011
Dhaka, Bangladesh	2013	37	3	34	39	4.29	Ocvirk et al., 2013
Madhya Pradesh, India	2012	28	1	27	41	1.49	Yadav et al., 2012
Taroudant Province, Morocco	2017	39	4	35	38	5.80	Katiri et al., 2017
Tamilnadu, Southern India	2012	16	2	14	40	3.85	Elavarasi and Saravanan, 2012
Urmia, Northwest Iran	2014	30	5	25	37	8.77	Bahmani et al., 2014

http://www.aloki.hu ● ISSN 1589 1623 (Print) ● ISSN 1785 0037 (Online)
DOI: http://dx.doi.org/10.15666/aeer/1605_65496566
© 2018, ALÖKI Kft., Budapest, Hungary

Novelty and future impact

The novelty index was determined by comparing present study with previous studies conducted in Pakistan, India, Bangladesh and Iran as shown in *Table 3*. In Azad Jammu and Kashmir, no previous study was found on anti-diabetes uses of medicinal plants. In Pakistan only few studies were found. There was very little resemblance with previous studies in uses of plants to treat diabetes. Some of the newly documented medicinal plants used to treat diabetes were *Berberis lycium*, *Beta vulgaris, Coriandrum sativum, Oxalis corniculata, Phaseulus vulgaris, Psidium guajava, Zizpiphus mauritiana, Mentha arvensis, Hedra helix, Bauhinia variegata, Taraxacum officinale and Zanthoxylum alatum.*

Multivariate cluster analysis

Based upon RFC values, multivariate cluster analysis results reveal significant relationship among plant species. There were two main clusters (*Fig. 5*).

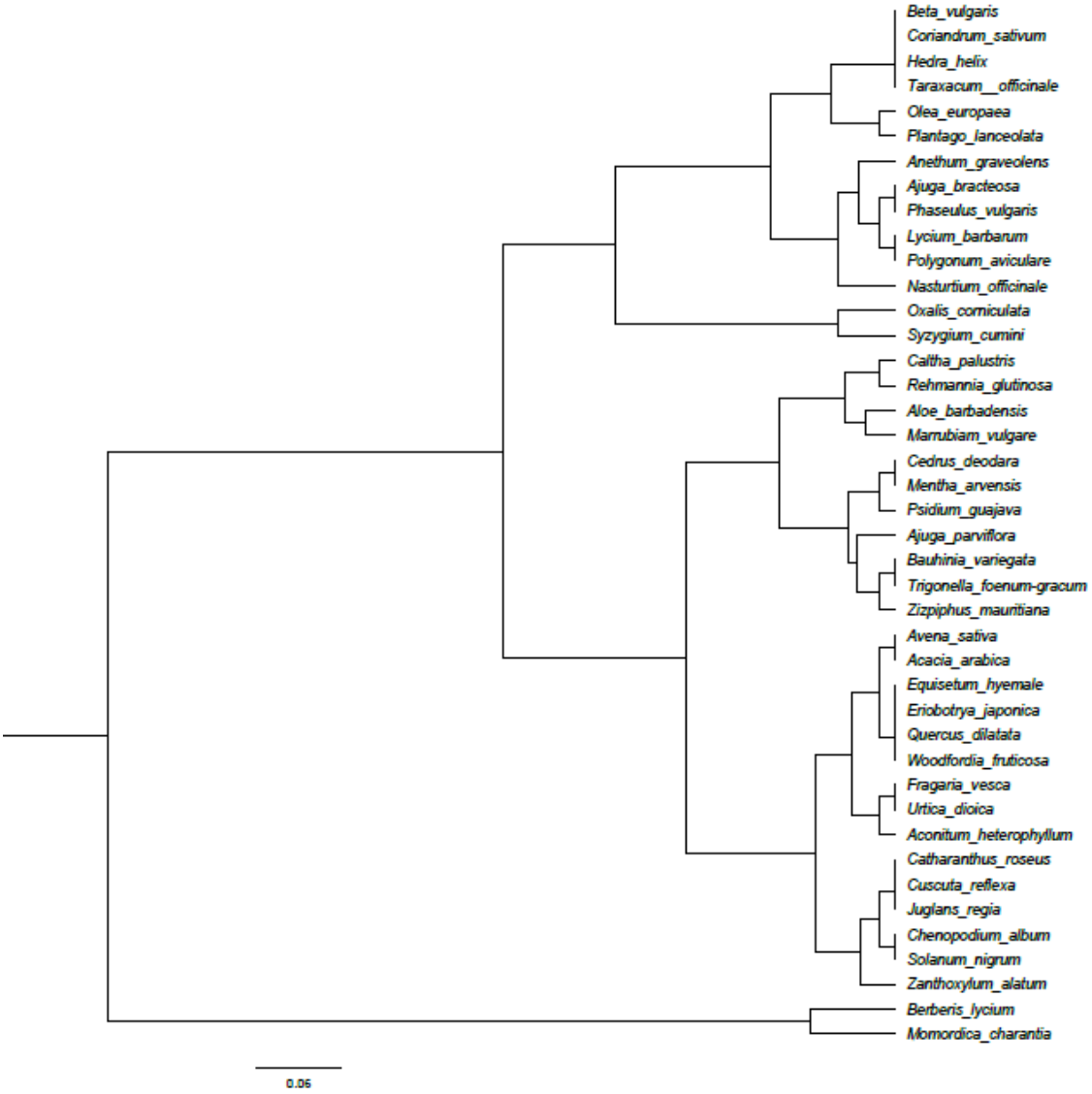

Figure 5. *Cluster analysis based on RIF values of plants*

http://www.aloki.hu ● ISSN 1589 1623 (Print) ● ISSN 1785 0037 (Online)
DOI: http://dx.doi.org/10.15666/aeer/1605_65496566
© 2018, ALÖKI Kft., Budapest, Hungary

Cluster one comprised of *Berberis lycium* and *momordica charantia*. Both species showed close relationship based upon RFC. Cluster two received 41 species, it was the largest group. Cluster two was further divided into 4 sub clades. *Beta vulgaris*, *Coriandrum sativum*, *Hedra helix* and *Taraxacum officinale* showed closed RFC values. *Olea europea* and *Plantago lanceolata* were sister species, showing close association. *Anethum graveolens* and *Nasturtium officinale* showed weak association with rest of the species in the clade, i.e. *Ajuga bracteosa*, *Lycium barbarum* and *Polygonum aviculare*. *Oxalis corniculata* and *S. cumini* were closely associated based on RFC values. *C. palustris* was closely related to *R. glutinosa*. *F. vesca*, *A. dioca* and *A. hydrophyllum* were closely related species. In the next cluster, *C. reflexa*, *J. regia*, *C. album* and *S. nigrum* were more closely related plant species. In the cluster, *B. variegata* was more closely related *T. foenum-gracum* and *Z. mauritiana* than *A. parviflora*. Whereas *C. deodara* was more closely related to *M. arvensis* than *S. guajava*.

Multivariate cluster analysis, on the basis of FIV, suggested a close relationship among the families. It is divided into two main clusters (*Fig. 6*). Cluster 1 showed the association of Rosaceae, Equitaceae, Lythraceae and Poaceae. Cluster 2 is further divided into 3 sub clusters. Brassicaceae was most closely related to Polygonaceae. Chenopodiaceae was closed to Urticaceae than Oxalidaceae. Apiaceae and Berberidaceae were more close to each other on the basis of FIV.

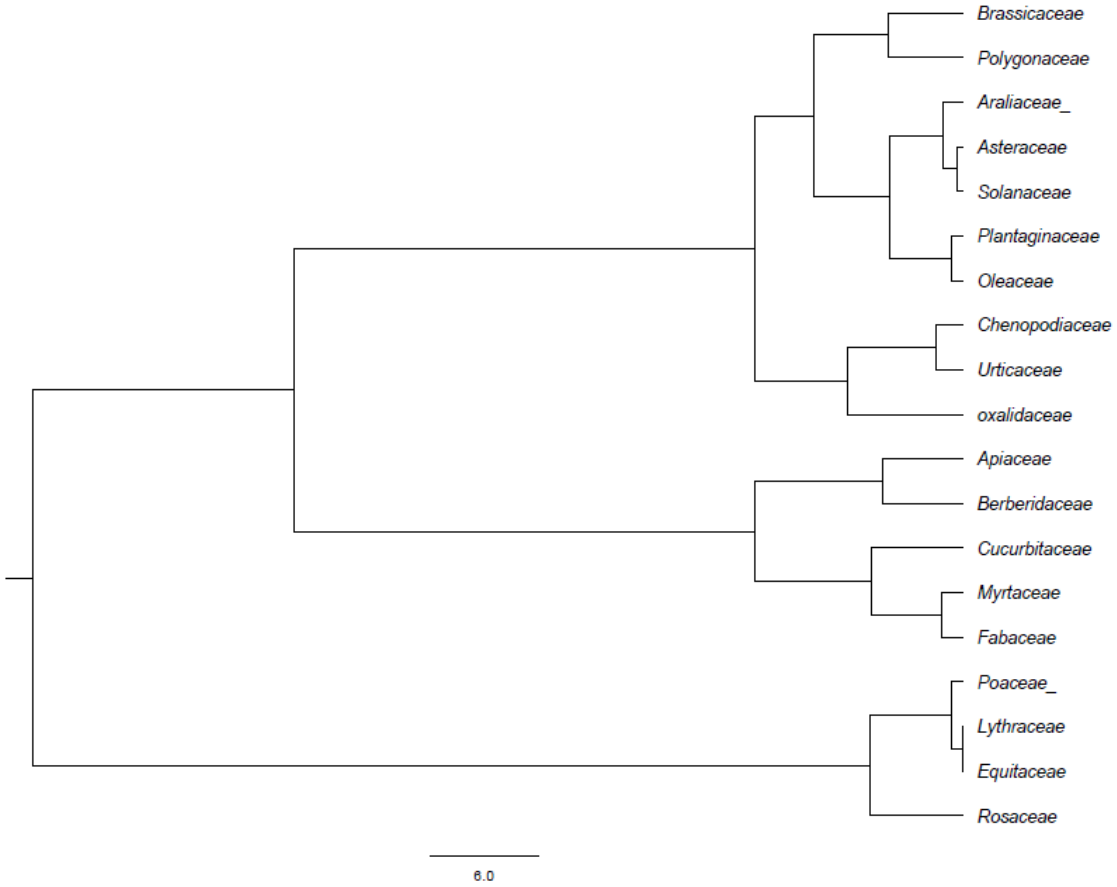

Figure 6. *Cluster analysis of families based on FIV*

http://www.aloki.hu ● ISSN 1589 1623 (Print) ● ISSN 1785 0037 (Online)
DOI: http://dx.doi.org/10.15666/aeer/1605_65496566
© 2018, ALÖKI Kft., Budapest, Hungary

Discussion

The present investigation was confined in rural areas of Azad Jammu and Kashmir, Pakistan. The objective was to document the medicinal flora of the area traditionally used for the treatment of diabetes and to explore the constituents of these medicinal plants. To collect the ethnobotanical information, 340 informants were interviewed. There had been tendency of increasing ethnobotanical knowledge with the age of informants. The ethnobotanical data showed that 42 plant species belonging to 41 genera and 30 families were used for the treatment of Diabetes. The reason is that older people are more familiar with the use of medicinal plants and are involving in ethnomedicinal practicing and traditional knowledge. However younger people have less interest in older traditional knowledge regarding the use of plants for treatment of diseases. Previous studies also show that elder people have more ethnomedicinal knowledge (Kpodar et al., 2015; Abouri et al., 2012).

Fabaceae and Lamiaceae were the dominant families in the study area with 4 species each followed by Apiaceae, Chenopodiaceae, Ranunculaceae, Rosaceae and Solanaceae with 2 species each. The dominance of the families is corresponded to the fact that these are well known among the people and easy to access. Furthermore, locals have more knowledge about these families and used these plants for generations to generations. Frequent use of these families also suggests that important secondary metabolites are present in the member of these families. In previous study, it was found that members of Fabaceae and Lamiaceae are used for the treatment of diabetes (Aadhan and Anand, 2017).

Most frequent used plant parts were the leaves, followed by fruits, whole plant, seeds, roots, bark, flowers and aerial parts Leaves are mostly used parts because of the fact that leaves are the main photosynthetic organs and they are the part of the plants which is most easily reachable and accessible throughout the year (Fezon et al., 2008). Leaves are also valuable in phytotherapy because they contain more effortlessly extractable phyto-compounds, crude drugs and several additional mixtures (Bano et al., 2014a, b). Moreover, leaves are easy to collect and process and their collection does not harm the plant considerably in contrast to collection of bark, roots and whole plant (Telefo et al., 2011; Zheng and Xing, 2009). Leaves are most frequent plant parts used as ethnopharmacology as reported in previous studies (Amjad et al., 2017; Khan et al., 2015).

Most frequent used method was decoction followed by extract, juice, vegetable and powder. In ethnobotanical practices, the major forms of herbal drug preparation are the decoction (mixing plant part with water, tea or soup (Amjad et al., 2017). The other reason of the use of decoction is that it is prepared by heating which may hasten the biological reactions resultant in the increased accessibility of many bioactive compounds (Han et al., 2007; Zhang et al., 2005).

The RFC values were from 0.09 to 0.95. The highest RFC was found for *Berberis lycium* and *Momordica charantia* reflected that these species were very famous and familiar among the local inhabitants of the study area and these species could be further investigated for their pharmacological and phytochemical properties (Mukherjee and Wahile, 2006). Number of studies suggests that *Momordica charantia* has higher potential as antidiabetic (Chaturvedi, 2012; Nama et al., 2011; Shibib et al., 1993; Ali et al., 1993).

Jaccard index results showed ethnobotanical knowledge varied greatly among the communities because of different origins, geography, culture and social behavior. This

http://www.aloki.hu ● ISSN 1589 1623 (Print) ● ISSN 1785 0037 (Online)
DOI: http://dx.doi.org/10.15666/aeer/1605_65496566
© 2018, ALÖKI Kft., Budapest, Hungary

comparison of knowledge may result in discovery of many new drugs (Leonti, 2011). The maximum degree of parallel index was found with studies by Bahmani et al. (2014) from Uramia, Northwest Iran, Ahmad et al. (2009) Attock Pakistan and Kumari et al. (2011) Uttarakhand, India. The highest similarity index corresponds to same type of vegetation and geographical conditions or same ethnic values. Most common species were the *Momordica charantia*, *Trigonella foenum-gracum* and *Syzygium cumini*. These species are found in almost all compared areas, which demonstrate their importance for the treatment of diabetes. The lowest JI was found for the study of Yadav et al. (2012) from Madhya Pradesh, India. This difference is might be due to geographical barriers and different type of vegetation and habitat (Leonti, 2011). Strong positive correlation between UV and RFC showed that increase in number of informants also increases the knowledge of the uses of species (Ishtiaq et al., 2007; Ahmed et al., 2017). This suggested that this study is a significant contribution towards the documentation of plants used for the treatment of diabetes.

Conclusions

This ethnobotanical study documented the ethnophytotherapeutic management of diabetes mellitus and support of traditional healers in Azad Jammu and Kashmir. The indigenous population still relies to a great extent on traditional healers and medicinal plants to meet their healthcare needs because of the perceived effectiveness, presumed safety with minimal side effects and affordability. In conclusion, this article presented a list of anti-diabetic plants used in the treatment of diabetes mellitus. Medicinal plants are good alternative to synthetic drugs due to biocompatibility, cost effective and less or no side effects. Further studies are needed to be carried out to explore the exact mechanism of these medicinal plants' antidiabetic activity. The documented plants should also be further screening for their phyctochemical constituents, pharmacognostic characters and biochemical assays for their sustainable and effective uses.

Acknowledgements. This study was not funded by any organization. We thank local inhabitants of the study area for their hospitality and cooperation.

REFERENCES

[1] Aadhan, K., Anand, S. P. (2017): Survey of medicinal plants used for the treatment of diabetes by the Paliyar's Tribe in Sadhuragiri hills, Tamil Nadu, India. – International Journal of Herbal Medicine 5: 17-25.

[2] Abouri, M., El-Mousadik, A., Msanda, F., Boubaker, H., Saadi, B., Askarne, L. (2012): An ethnobotanical survey of medicinal plants used in the Tata Province, Morocco. – Journal of Medicinal Plants Research 1: 99-123.

[3] Afshan, N. S., Iqbal, S. H., Khalid, A. N., Niazi, A. R. (2011): Some additions to the Uredinales of Azad Jammu and Kashmir, Pakistan. – Pakistan Journal of Botany 43: 1373-1379.

[4] Ahmad, K. S., Hamid, A., Nawaz, F., Hameed, M., Ahmad, F., Deng, J., Akhtar, N., Wazarat, A., Mahroof, S. (2017): Ethnopharmacological studies of indigenous plants in Kel village, Neelum Valley, Azad Kashmir, Pakistan. – Journal of Ethnobiology and Ethnomedicine 13: 68. DOI: 10.1186/s13002-017-0196-1.

http://www.aloki.hu ● ISSN 1589 1623 (Print) ● ISSN 1785 0037 (Online)
DOI: http://dx.doi.org/10.15666/aeer/1605_65496566
© 2018, ALÖKI Kft., Budapest, Hungary

[5] Ahmad, M., Qureshi, R., Arshad, M., Khan, M. A., Zafar, M. (2009): Traditional herbal remedies used for the treatment of diabetes from District Attock (Pakistan). – Pakistan Journal of Botany 4: 2777-2782.
[6] Ajaib, M., Khan, Z. D. (2014): Ethnobotanical studies of useful trees of District Kotli, Azad Jammu and Kashmir. – Biologia (Pakistan) 60: 63-71.
[7] Ajaib, M., Anjum, M., Malik, N. Z., Siddiqui, M. F. (2015): Ethnobotanical study of some plants of Darguti, tehsil Khuiratta, Azad Jammu and Kashmir. – International Journal of Biological Research 3: 101-107.
[8] Ali, L., Khan, A. K., Mamun, M. I., Mosihuzzaman, M., Nahar, N., Nur-e-Alam, M., Rokeya, B. (1993): Studies on hypoglycemic effects of fruit pulp, seed, and whole plant of *Momordica charantia* on normal and diabetic model rats. – Planta Medica 59: 408-412.
[9] Ali, S. I., Nasir, E. (1970–2002): Flora of Pakistan, National Herbarium, NARC. – Islamabad and Department of Botany, University of Karachi, Karachi (Fasc. No. 1-207).
[10] Amjad, M. S., Qaeem, M. F., Ahmad, I., Khan, S. U., Chaudhari, S. K., Malik, N. Z., Shaheen, H., Khan, A. M. (2017): Descriptive study of plant resources in the context of the ethnomedicinal relevance of indigenous flora: A case study from Toli Peer National Park, Azad Jammu and Kashmir, Pakistan. – PLoS ONE 12: e0171896.
[11] Ayodhya, S., Kusum, S., Saxena. Hypoglycaemic activity of different extracts of various herbal plants, – International Journal of Research in Ayurveda and Pharmacy 1: 212-224.
[12] Bahmani, M. I., Zargaran, A., Rafieian-Kopaei, M., Saki, K. (2014): Ethnobotanical study of medicinal plants used in the management of diabetes mellitus in the Urmia, Northwest Iran. – Asian Pacific Journal of Tropical Medicine 71: 348-54.
[13] Bano, A., Ahmad, M., Hadda, T. B., Saboor, A., Sultana, S., Zafar, M., Khan, M. P., Arshad, M., Ashraf, M. A. (2014a): Quantitative ethnomedicinal study of plants used in the skardu valley at high altitude of Karakoram-Himalayan range, Pakistan. – Journal of Ethnobiology and Ethnomedicine 10: 43. DOI: 10.1186/1746-4269-10-4.3 PMID: 24885937.
[14] Bano, A., Ahmad, M., Zafar, M., Sultana, S., Rashid, S., Khan, M. A. (2014b): Ethnomedicinal knowledge of the most commonly used plants from Deosai Plateau, Western Himalayas, Gilgit Baltistan, Pakistan. – Journal of Ethnopharmacology 155: 1046-1052.
[15] Chaturvedi, P. (2012): Antidiabetic potentials of *Momordica* charantia: multiple mechanisms behind the effects. – Journal of Medicinal Food 15: 101-107.
[16] Donga, J. J., Surani, V. S., Sailor, G. U., Chauhan, S. P., Seth, A. K. (2011): A systematic review on natural medicine used for therapy of diabetes mellitus of some Indian medicinal plants. – Pharma Science Monitor 2: 36-72.
[17] Edwards, S., Nebel, S., Heinrich, M. (2005): Questionnaire surveys: methodological and epistemological problems for field-based ethnopharmacologists. – Journal of Ethnopharmacology 100: 30-36.
[18] Elavarasi, S., Saravanan, K. (2012): Ethnobotanical study of plants used to treat diabetes by tribal people of Kolli Hills, Namakkal District, Tamilnadu, Southern India. – International Journal of PharmTech Research 4: 404-411.
[19] Fezan, H. T., Guy, M. I., Kohue, C. C., Mahou, C. H. B. (2008): Etudes de quelques plantes thérapeutiques utilisées dans le traitement de l'hypertension artérielle et du diabète: deux maladies émergentes en Côte d'Ivoire. – Science and Nature 5: 39-48.
[20] Franz, H. (1985): Inhaltsstoffe der Mistel (*Viscum album*) als potentielle Arzneimittel. – Pharmazie 40: 97-104.
[21] Gonza, T. M. R., Casares, P. M., Sanchez, R. C. P., Ramiro, G. J. M., Molero, M. J., Pieroni, A., Giusti, M. E., Censorii, E., De-Pasquale, C., Della, A., Paraskeva-Hadijchambi, D., Hadjichambis, A., El-Demerdash, M., El-zayat, M., Hmamouchi, M., ElJohrig, S. (2008): Medicinal plants in the Mediterranean area: synthesis of the results of the project RUBIA. – Journal of Ethnopharmacology 116: 341-57.

http://www.aloki.hu ● ISSN 1589 1623 (Print) ● ISSN 1785 0037 (Online)
DOI: http://dx.doi.org/10.15666/aeer/1605_65496566
© 2018, ALÖKI Kft., Budapest, Hungary

[22] Goodman, S. M., Ghafoor, A. (1992): The ethnobotany of southern Balochistan, Pakistan, with particular reference to medicinal plants. – Fieldiana Botany New Series 31: 84.
[23] Han, J., Ye, M., Guo, H., Yang, M., Wang, B. R., Guo, D. A. (2007): Analysis of multiple constituents in a Chinese herbal preparation Shuang-Huang-Lian oral liquid by HPLC-DAD-ESI-MS. – Journal of Pharmaceutical and Biomedical Analysis 44: 430-438.
[24] I. D. F. (2010): The Diabetes Atlas (4th ed). – International Diabetes Federation, Brussels. http://www.diabetesatlas.org.
[25] Ishtiaq, M., Hanif, W., Khan, M. A., Ashraf, M., Butt, A. M. (2007): An ethnomedicinal survey and documentation of important medicinal folklore food phytonyms of flora of Samahni Valley, (Azad Kashmir) Pakistan. – Pakistan Journal of Biological Sciences 10: 2241-56.
[26] Jain, S. P., Singh, S. C., Puri, H. S. (1998): Medicinal plants of Neterhat, Bihar India. – International Journal of Pharmacognosy 32: 44-50.
[27] Katiri, A., Barkaoui, M., Msanda, F., Boubaker, H. (2017): Ethnobotanical survey of medicinal plants used for the treatment of diabetes in the Tizi n' Test Region (Taroudant Province, Morocco). – Journal of Pharmacognosy and Natural Products 3: 130.
[28] Khan, M. P. Z., Ahmad, M., Zafar, M., Sultana, S., Ali, M. I., Sun, H. (2015): Ethnomedicinal uses of Edible Wild Fruits (EWFs) in Swat Valley, Northern Pakistan. – Journal of Ethnopharmacology 173: 191-203.
[29] Kpodar, M. S., Lawson-Evi, P., Bakoma, B., Eklu-Gadegbeku, K., Agbonon, A., Aklikokou, K., Gbeassor, M. (2015): Ethnopharmacological survey of plants used in the treatment of diabetes mellitus in south of Togo (Maritime Region). – Journal of Herbal Medicine 5: 147-152.
[30] Kumari, P., Joshi, G. C., Tewari, L. M. (2011): Contribution of indigenous anti-diabetic flora in Almora district, Uttarakhand, India. – Current Botany 2: 01-07.
[31] Leonti, M. (2011): The future is written: impact of scripts on the cognition, selection, knowledge and transmission of medicinal plant use and its implications for ethnobotany and ethnopharmacology. – Journal of Ethnopharmacology 134: 542-55.
[32] Mahmood, A., Mahmood, A., Shaheen, H., Qureshi, R. A., Sangi, Y., Gilani, S. A. (2011): Ethno-medicinal survey of plants from district Bhimber Azad Jammu and Kashmir, Pakistan. – Journal of Medicinal Plants Research 5: 2348-2360.
[33] Masika, P. J., Afoloayan, A. J. (2003): An ethnobotanical study of plants used for the treatment of livestock diseases in the Eastern Cape Province South Africa – Journal of Pharmaceutical Biology 41: 16-21.
[34] Molares, S., Ladio, A. (2009): Ethnobotanical review of the Mapuche medicinal flora: Use patterns on aregional scale. – Journal of Ethnopharmacology 122: 251-260.
[35] Mossa, J. S. (1999): A study on Arabian folk medicine. – International Journal of Crude Drugs Research 23: 137-145.
[36] Mukherjee, P. K., Wahile, A. (2006): Integrated approaches towards drug development from Ayurveda and other Indian system of medicines. – Journal of Ethnopharmacol 103: 25-35.
[37] Namsa, N. D., Mandal, M., Tangjang, S., Mandal, S. C. (2011): Ethnobotany of the Monpa ethnic group at Arunachal Pradesh, India. – Journal of Ethnobiology and Ethnomedicine 7: 31. DOI: 10.1186/1746-4269-7-31.
[38] Ocvirk, S., Kistler, M., Khan, S., Talukder, S. H., Hauner, H. (2013): Traditional medicinal plants used for the treatment of diabetes in rural and urban areas of Dhaka, Bangladesh – an ethnobotanical survey. – Journal of Ethnobiology and Ethnomedicines 9: 43.
[39] Qamar, Z. Q., Anwar, M., Dar, N. I., Ali, U. (2010): Ethno-botanical study of wild medicinal plants of Neelum Valley, Azad Jammu and Kashmir, Pakistan. – Pakistan Journal of Wildlife 1: 25-30.

http://www.aloki.hu ● ISSN 1589 1623 (Print) ● ISSN 1785 0037 (Online)
DOI: http://dx.doi.org/10.15666/aeer/1605_65496566
© 2018, ALÖKI Kft., Budapest, Hungary

[40] Shaheen, H., Shinwari, Z. K., Qureshi, R. A., Zahidullah (2012): Indigenous plant resources and their utilization practices in village population of Kashmir Himalayas. – Pakistan Journal of Botany 44: 739-745.
[41] Shibib, B. A., Khan, L. A., Rahman, R. (1993): Hypoglycaemic activity of *Coccinia indica* and *Momordica charantia* in diabetic rats: depression of the hepatic gluconeogenic enzymes glucose-6-phosphatase and fructose-1,6-bisphosphatase and elevation of both liver and red-cell shunt enzyme glucose-6-phosphate dehydrogenase. – Biochemical Journal 292: 267-270.
[42] Shinwari, M. I., Shinwari, M. I. (2010): Botanical Diversity in Pakistan; Past, Present and Future. – Proc. Workshop World Environment Day, Lahore.
[43] Tardio, J., Pardo-de-Santayana, M. (2008): Cultural importance indicates: a comparative analysis based on the useful wild plants of Southern Cantabria (Northern Spain). – Economic Botany 62: 24-39.
[44] Telefo, P. B., Lienou, L. L., Yemele, M. D., Lemfack, M. C., Mouokeu, C., Goka, C. S., Tagne, S. R., Moundipa, F. P. (2011): Ethnopharmacological survey of plants used for the treatment of female infertility in Baham, Cameroon. – Journal of Ethnopharmacology 136: 178-187.
[45] Wei, M., Gibbons, L., Mitchell, T., Kampert, J., Blair, S. (2010): Alcohol intake and incidence of type 2 diabetes in men. – Diabetes Care 23: 18-22.
[46] World Health Organization (2016): Global Report on Diabetes. – WHO, Geneva, Switzerland.
[47] Yadav, M., Khan, K. K., Beg, M. Z. (2012): Medicinal plants used for the treatment of diabetes by the Baiga tribe living in Rewa District M. P. Ind. – Journal of Life Science 2: 99-102.
[48] Yokozawa, T., Kim, H. Y., Cho, E. J., Yamabi, N., Choi, J. S. (2003): Protective effects of mustard leaf (Brassica juncea) against diabetic oxidative stress. – Journal of Nutritional Science and Vitaminology 49: 87-93.
[49] Zhang, J. L., Cui, M., He, Y., Yu, H. L., Guo, D. A. (2005): Chemical fingerprint and metabolic fingerprint analysis of Danshen injection by HPLC±UV and HPLC±MS methods. – Journal of Pharmaceutical and Biomedical Analysis 36: 1029-1035.
[50] Zheng, X. L., Xing, F. W. (2009): Ethnobotanical study on medicinal plants around Mt. Yinggeling, Hainan Island, China. – Journal of Ethnopharmacology 124: 197-210.

http://www.aloki.hu ● ISSN 1589 1623 (Print) ● ISSN 1785 0037 (Online)
DOI: http://dx.doi.org/10.15666/aeer/1605_65496566
© 2018, ALÖKI Kft., Budapest, Hungary

APPENDIX

Questionnaire for collecting ethnomedicinal data during Ethnobotanical Study

Questionnaire:

Informants' consent for the participation in the study:

I..... (name of informant) hereby give my full consent and conscious to participate in this study and declare that to the best of my knowledge the information that I have provided are true, accurate and complete.

Date..... (Signature/Thumb impression of Informant)

Informants' details:

Name.....
Gender.....
Age.....
Occupation.....
Education.....
Location/Residence.....

Data about medicinal plant and its use:

Plant (Local name).....
Habit (Tree/Herb/Shrub/Climber/…...)
Plant part used.....
Cultivated/Wild.....
If cultivated, cultivated for…….....
If wild, availability in natural resources (easy/difficulty/very difficult)
Conservation needs.....
Conservation efforts made by Government and local residents……..…
Method of collection and storage…….....
Name of disease(s) treated…….....
Method of crude drug preparation.....
Mode of administration.....
Dosage.....
Other uses (if any)…….....…….....

Remarks:

Plant identified as …… (Botanical name and family)

Information provided by informants will be used for research purposes only

Signature of Researcher

http://www.aloki.hu ● ISSN 1589 1623 (Print) ● ISSN 1785 0037 (Online)
DOI: http://dx.doi.org/10.15666/aeer/1605_65496566
© 2018, ALÖKI Kft., Budapest, Hungary

RESEARCH ON THE SUITABILITY EVALUATION OF CONSTRUCTION LAND IN SOUTHWEST MOUNTAINOUS AREAS OF CHINA: A CASE STUDY OF BAOXING COUNTY, SICHUAN PROVINCE, CHINA

CAO, M.[1,2*] – ZHAO, J.[1] – ZHANG, S.[1]

[1]*School of Tourism management, South China Normal University, Panyu district, No. 378 Waihuan West Road, Guangzhou 510000, Guangdong, P. R. China*

[2]*Institute of Mountain Hazards and Environment, Chinese Academy of Sciences & Ministry of Water Conservancy, #9, Block 4. Renminnan Road, Chengdu 610041 Sichuan, P. R. China*

**Corresponding author*
e-mail: caomt@m.scnu.edu.cn; phone: +86-131-2825-1580; fax:+86-20-8521-7757

(Received 27th Jun 2018; accepted 6th Sep 2018)

Abstract. Currently, the threats of mountain disasters are continuously increasing due to the highly vulnerable feedback mechanism of mountain ecosystems, and the construction land use type is most strongly affected by human activities. This study uses multiple index coupling models to evaluate the suitability of construction land. The evaluation uses mountain disaster risk, topographic and geomorphic environments, hydrogeological environments, human activity factors and socio-economic factors as the suitability standards. We use geographic information system (GIS) technology to improve the evaluation model and establish a suitability map of construction land for Baoxing County, Sichuan province, China. This study indicates that the mountain disaster risk is the core factor of the suitability zoning of construction land in Baoxing County, wherein, the development suitability of construction land in the central sectors is relatively high while the mountain disaster risk is relatively high due to the high socio-economic value of the disaster-bearing areas in the central sectors. The development suitability of construction land near the fracture zones and the natural reserves is relatively low.
Keywords: *construction land, suitability assessment, mountain disasters, vulnerability, risk assessment*

Introduction

Mountainous areas account for approximately 25% of the global land area, and the feedback mechanisms in mountain ecosystems are highly vulnerable; therefore, disasters occur frequently (Peng et al., 2016). The characteristics of the limited, easily destroyed and unrestored land resources are obvious, and these characteristics restrict the development, economic value and social benefit of construction land in mountainous areas. At the same time, the international disasters reduction strategy has gradually shifted the "hard" measures of a project to "soft" land planning measures, and land planning limits the development of land in areas where there are disaster potentials (Leroi et al., 2005). All countries and regions throughout the world have combined construction land suitability planning in mountainous areas with research on mountain disasters and have taken the corresponding measures to contribute to the sustainable development of mountainous areas (Hemingway and Gunawan, 2018). For example, the United Nations issued the "Hyogo framework for action 2005-2015: building the resilience of nations and communities to disasters." (ISDR, 2005). Italy has combined hazard risk assessments with land use planning and has applied this theory to actual urban construction. The Advisory Committee, the Planning Association and the United

http://www.aloki.hu ● ISSN 1589 1623 (Print) ● ISSN 1785 0037 (Online)
DOI: http://dx.doi.org/10.15666/aeer/1605_65676587
© 2018, ALÖKI Kft., Budapest, Hungary

States Geological Survey released the "Landslide disasters and Planning: Incorporating Geological disasters Planning into the Planning Process," which notes that land use planning should be focused on reducing the risks of disasters (Lovell, 2010). A series of urban land use plans and natural disaster risk evaluations have become an essential component in the sustainable development of mountainous areas in China. Mountain disaster risk is the most prominent factor in mountain cities and towns, as discussed in., "The National Comprehensive Disaster Prevention and Mitigation Plan (Year 2016-2020)" and "Outline of National Territorial Planning (Year 2016-2030)," for example (The State Council of China, 2017).

In China, mountainous areas cover 6.66 million km^2, accounting for 69.4% of the territorial areas of China, and the population in mountainous areas is more than 1/3 of the total population (Chen et al., 2010). The mountainous areas are vulnerable to landslides, collapses, mudslides and other mountain disasters, which seriously threaten the safety of lives, property and engineering construction and limit the utilization of land resources and economic development. Therefore, the original resource-rich mountainous areas in China have become the "topographic uplift areas and the economic valley areas" (Cui, 2014).

With the rapid development of urbanization, tremendous changes have taken place in China's mountain towns in terms of construction spatial patterns, population structure and living standards (Liu et al., 2016). Mountain disasters pose a serious threat to people's lives and property (Zhang et al., 2009; Deuskar et al., 2015). Construction land is different from other land types as it is relatively irreversible, and once a piece of land is converted into construction land, it is difficult to restore that land to other land use types. Construction land development that is affected by the mountainous environment and disasters induces and intensifies mountain disasters (Wang, 2012). Additionally, the disaster risk is increasing due to the high economic value of various disaster-bearing areas in the central sections of the mountain towns, which seriously restricts the development suitability of construction land. However, disaster risks are often ignored during construction in mountain towns in China, and scientific evaluations are often not conducted (Jiao et al., 2017). These high-intensity land use development and engineering construction activities may lead to a decline in the environmental carrying capacity and exacerbate the problem of larger population and less land. Many scholars and the Chinese government are aware of the need to correctly understand the correlations among mountainous environment, mountain disasters and construction land development. Moreover, the degree of stress related to mountain disasters needs to be measured, and a suitability evaluation of construction land development needs to be conducted, which would fundamentally guarantee the sustainable utilization of land resources in mountainous areas.

The frameworks of the suitability evaluation for construction land at home and abroad mainly include: 1) Pressure-Status-Response (P-S-R) proposed by Organization for Economic Co-operation and Development (OECD). It mainly illustrates the interrelationship among human activities, social development and ecological environment (Ying et al., 2009; Guo et al., 2003). The advantage of P-S-R framework system is that it can be used for reference to evaluate the suitability of construction land in mountainous areas with fragile natural environment and frequent mountain disasters. However, there is no inevitable logical correlation between the driving force indicator and the state indicator, so it is difficult to quantify the specific indicator, and regional promotion and application are also relatively difficult. 2) Goal-Estimate-Consequence

http://www.aloki.hu ● ISSN 1589 1623 (Print) ● ISSN 1785 0037 (Online)
DOI: http://dx.doi.org/10.15666/aeer/1605_65676587
© 2018, ALÖKI Kft., Budapest, Hungary

(G-E-C) from "The Outline of Land Evaluation" and "The Outline of Sustainable Land Management Evaluation". The goals, types and methods of land use need to be identified first, and on this basis, the judgment results are analyzed (FAO, 1993). The advantage of G-E-C is that the indicators are easily quantified, and the empirical significance is greater. The disadvantage is that the location and social factors of land use are not taken into account, and the economic value and benefit efficiency of land use cannot be fully reflected. As a result, the tracking monitoring and efficiency of economic, environmental and social benefits cannot be comprehensively analyzed and compared, and the optimal layout of land use cannot be determined. 3) Nature-Economy-Society (N-E-S), which is to resolve the land use system to natural, economic and social subsystems under the premise of the comprehensive research on the land use system. This multi-subsystem method can measure the integrity of the system and realize the dimensionality reduction of complex systems (Wang and Bao, 2011). The N-E-S framework focuses on the research on other subsystems, rarely discussing the driving mechanism among the ancillary systems. The advantage of this framework is that it can comprehensively and systematically form the unified evaluation of construction land use in the three-dimensional view of nature, economy and society, but there are difficulties in the typicality and regional promotion of some factors in the evaluation system.

Construction land suitability research and evaluation in mountainous areas has mainly focused on the suitability of land for specific uses and the ecological suitability of the land use type. For example, urban construction land has been classified to determine the quality of the land that is suitable for construction at different levels and the areas that are suitable for construction land. The existing soil information system has been utilized to interpret satellite remote sensing images and obtain digital elevation model (DEM) data and map data. An ArcGIS spatial database that includes soil erosion risk data in high-risk areas, land use types, use strength and other land parcel information has been established to combine these layers with the relevant socio-economic information (Akinci et al., 2013). The superposition slope, flood inundation line, public facilities and other factors have been comprehensively considered to analyze and identify suitable construction land parcels and provide basic data for land use suitability evaluations in mountainous areas (Montanarella and Nègre, 2001; Rusdi et al., 2015).

Statistical and econometric model analysis methods have been used in previous research, and there is an obvious shortage of spatial information processing during simple modeling and quantification. For instance, multifactor comprehensive evaluation models, Markov models, neighborhood algorithms, generalized regression neural network (GRNN) models and fuzzy comprehensive evaluation methods have been used to conduct suitability evaluations of on construction land (Zhou, 2010; Liu et al., 2014; Wei et al., 2014; Qiu et al., 2017).

The advancement of computer-aided superposition mapping methods has resulted in the wide use of technical methods to evaluate construction land suitability in mountainous areas based on ArcGIS. Domestic and foreign researchers have used ArcGIS technology to further the processing of previous econometric models (Nan, 2009; Ambarwulan et al., 2016). Integrated superposition analysis methods, multi-indicator decision models, artificial intelligence methods, and mixed data models for vector and raster analysis have been widely used to conduct comprehensive suitability

http://www.aloki.hu ● ISSN 1589 1623 (Print) ● ISSN 1785 0037 (Online)
DOI: http://dx.doi.org/10.15666/aeer/1605_65676587
© 2018, ALÖKI Kft., Budapest, Hungary

judgments for construction land in mountainous areas (Gimblett and Ball, 1994; Malczewski, 2006; Chandio, 2014; Promper et al., 2014).

From the perspective of stress related to mountain disasters, this study combines the unique hazard risks of mountainous areas with the development of construction land suitability based on the actual needs of social and economic development regulations. Baoxing County is a typical mountainous county in Southwest China and is used as an example in this study. After Baoxing County experienced the "5 • 12 Wenchuan Earthquake (Ms 8.0)" in 2008 and the "4 • 20 Lushan Earthquake (Ms 7.0)" in 2013, the number of disaster sites drastically increased, and the hidden dangers of construction land have become more serious (Wu et al., 2016). This study builds multiple coupling models and introduces the risk factors of mountain disasters to evaluates the suitability of construction land in mountain towns. It makes the evaluation results more accurate and reasonable. For the research methods, the weight of other indicators is assessed weight in the suitability evaluation of construction land in mountainous areas in addition to mountain disaster risk factors. The hypermatrix method of the analytic network process (ANP) is adopted so that the correlations among all factors can be fully considered. This study is different from previous research that evaluated the conditions while considering only the relative independence of each factor.

Study area and data sources

Study area

Baoxing County (102°28 - 103°02′E, 30°09′ - 30°56′N) is located in Sichuan province of China, on the western edge of the Sichuan Basin and north of Ya'an City. Baoxing County borders Wenchuan County and Xiaojin County to the north, Tianquan County to the south, Kangding County to the west and Lushan County in the east. The transportation is mainly based on highways, and provincial highway No. 210 runs throughout the territory. The county is 61 km wide from east to west and 81 km long from south to north, and the jurisdiction area is approximately 3114 km^2 (*Fig. 1*).

Data sources

Statistics used in this study is originated from field investigations of Land use of Baoxing county, Sichuan province China in 2016-2017 of institute of Mountain Hazards and Environment, Chinese Academy of Sciences & Ministry of Water Conservancy. The main types of mountain disasters in the county are collapses, landslides and mudslides. At present, there are a total of 337 disaster sites, including 153 landslides, 144 collapses and 40 mudslides. The density of dangerous areas is 8.49 m^2/km^2, and the hazard volume density is 105.4110^4 m^3/km^2. The threatened population is 15,750, accounting for 26.71% of the total population in the county. The total area of construction land in the county is 2,456.67 hm^2. The urban and rural land for industry and mining, land for highways and water and land for water conservation facilities (including reservoir water and hydraulic construction land) constitute areas of 1714.66 hm^2, 219.88 hm^2 and 522.12 hm^2, respectively, accounting for 69.80%, 8.95% and 21.25% of the total construction land area in the county, respectively.

The latest DEM (1:50000 data), administrative division maps, present land use map, river system map, fracture structure map, traffic roadmaps, and population and related socio-economic data were obtained in accordance with the mountain disasters tracking

http://www.aloki.hu ● ISSN 1589 1623 (Print) ● ISSN 1785 0037 (Online)
DOI: http://dx.doi.org/10.15666/aeer/1605_65676587
© 2018, ALÖKI Kft., Budapest, Hungary

survey and construction land development in Baoxing County from research groups between 2014 and 2016. The data originate from the Statistical Bureau, Meteorological Bureau, Land Bureau, archives, geological environment monitoring stations and other relevant government departments of Baoxing County.

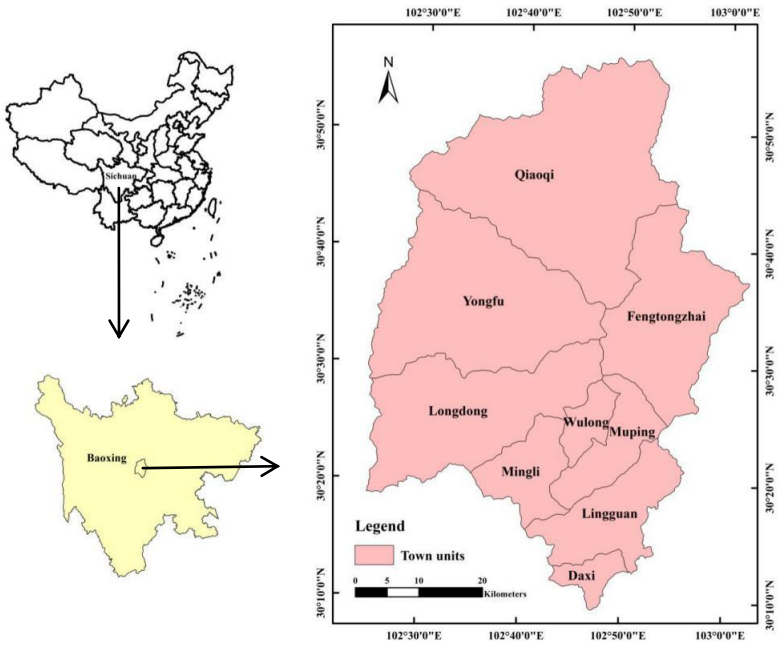

Figure 1. *Title of the given figure, graph or image included in the document*

To facilitate the matching of the vector and raster data, this study first utilized ArcGIS to process the evaluation units of the study area into a square 25 m × 25 m grid. Administrative units were then utilized to perform the regional calculations and evaluate the results of the previous grid unit and obtain the data for each grid unit in each administrative unit. The grid format is convenient for the subsequent comprehensive comparison and analysis. The grid unit is more precise than the land use patches, land types and soil units that have been used previously. Moreover, the land use evaluation attributes are more homogeneous in a grid unit, which improves the accuracy of the evaluation results. The grid unit format is consistent with that of ArcGIS raster data, and the use of computer processing is relatively simple. Additionally, the research results are conducive to the ultimate implementation by the relevant departments of the Chinese government.

Model methods

Mountain disaster risk evaluation models

The analysis of mountain disasters risks, the degree of mountain disasters influence and the degree of vulnerability of hazard-bearing areas are comprehensively studied based on the analysis of mountain disaster risks. To balance the process of the differences in the influencing degree, this study mainly determined the models for hazard risk evaluations in the study area according to the hazard degree and the degree of mountain disaster vulnerability.

http://www.aloki.hu ● ISSN 1589 1623 (Print) ● ISSN 1785 0037 (Online)
DOI: http://dx.doi.org/10.15666/aeer/1605_65676587
© 2018, ALÖKI Kft., Budapest, Hungary

The degree of mountain disasters is closely related to the density of disasters in an environment, and the relative surface structure and tectonic environment indicators were selected. The number, area and volume of 337 disaster sites in Baoxing County were used to determine the contribution rate of each indicator to the development of mountain disasters (Change, 2007). The weight of each indicator and the mutual weight between various indicators were obtained to establish the formula for the degree of mountain disasters, which can be presented as follows (*Eq. 1*):

$$H_j = w_i w_{ij} X_i \quad \text{(Eq.1)}$$

where H_j refers to the degree of mountain disasters; w_i indicates the self-weight; w_{ij} indicates the mutual weight; and X_i denotes the independent variable of the indicator.

The degree of mountain disaster vulnerability is correlated with the possibility for hazard damage and the difficulty level of repairing the damage to the hazard-bearing areas in the county (UNDP, 2004; ADRC,2005; Cardona, 2005; Smith, 2013). The relevant indicators are selected according to the actual situation, and the indicator weight can be represented as a multiplicative summation of the individual and mutual weight of each indicator and the indicator weight value to establish the formula for the degree of mountain disaster vulnerability, which can be determined using *Equation 2:*

$$V_S = \sum_{t=1}^{n} W_z W_h y \quad \text{(Eq.2)}$$

where V_S represents the degree of mountain disasters vulnerability; W_z indicates the individual weight; W_h means the mutual weight; and y refers to the independent variable of the indicator.

Based on *Equations 1* and *2,* the formula for the comprehensive degree of mountain disaster risk (R_I) is obtained as follows (*Eq. 3*):

$$R_I = H_j \cdot V_S = w_i w_{ij} X_i \cdot \sum_{t=1}^{n} W_z W_h y \quad \text{(Eq.3)}$$

Models to evaluate the suitability of construction land development under the stress of mountain disasters

The present land use patterns and the layout of construction land in the study area were taken into account, and the prohibited development areas (areas with slopes greater than 25°, areas within 100 m of fracture zones and core-protected areas) were excluded. The important factors that affect the suitability of construction land in mountainous areas were analyzed, and an evaluation indicator system was established. The weights of the ANP evaluation indicators were obtained by using Super Decisions software, and the comprehensive scores of various indicators were calculated on the grid unit. The ANP uses the hypermatrix method to quantify the degree of influence between indicators and can more objectively and effectively express the complex practical problems than the analytic hierarchy process (AHP). Many decision-making problems cannot be simply expressed as hierarchical structures, and the various levels of elements are interactional and interdependent. The formula to model the suitability of construction land development can be expressed as follows (*Eq. 4*):

http://www.aloki.hu ● ISSN 1589 1623 (Print) ● ISSN 1785 0037 (Online)
DOI: http://dx.doi.org/10.15666/aeer/1605_65676587
© 2018, ALÖKI Kft., Budapest, Hungary

$$L_s = \sum_{i=1}^{n} Z_{j,i}(f, w) \quad \text{(Eq.4)}$$

where, L_S indicates the total score; j refers to the j^{th} evaluation unit; i denotes the i^{th} indicator; n represents the number of indicators; f means the score of the indicator; and w stands for the weight of the indicator. When the calculated value of L_S is high, it indicates that the level of the suitability of construction land will be higher.

Based on *Equations 3* and *4,* the calculation formula for the suitability of construction land under the stress of mountain disasters is determined as follows (*Eq. 5*):

$$O_H = K_i \cdot R_I \cdot L_s \quad \text{(Eq.5)}$$

where, O_H refers to the suitability of construction land under the disaster stress; R_I denotes the comprehensive risk degree of mountain disasters; L_S indicates the suitability of construction land under the non-disaster stress; and K_i means the coefficient of variation, with a value range of 0~1. The value of K_i, the coefficient of variation, is mainly based on the different types of the present situation of construction land in the study area.

Analysis of mountain disaster risk and design of evaluation indicators

Analysis of hazard classification of mountain disasters

The degree of mountain disasters is closely related to various factors of the hazard-prone environment, including surface structure and hydrological structure conditions. Based on the evaluation methods and factor selection used in previous studies, this study focuses on selecting indicators that play a leading role in the degree of mountain disasters in Baoxing County and are convenient for the collection of spatial data. The surface structure factors can be extracted directly from the digital elevation data of the 1:50000 DEM for Baoxing County using ArcGIS software. These factors include the relative height difference, slope, slope aspect and slope shape. The influence on the development of mountain disasters becomes more significant as the relative height increases. It is easier for disaster sites to develop as the steepness of the slope increases. The slope aspect has a remarkable influence on mountain disasters. The south slope typically has the highest solar radiation, and the north slope has the lowest. The light, temperature, precipitation, wind speed and soil vegetation all differ between the windward and leeward slopes. A concave slope is a mature stage that is more stable and has fewer developed disaster sites. A convex slope is in a period of intense evolution, and there are more developed disaster sites. The number of disaster sites on a straight slope is between that of a convex slope and a concave slope. The tectonic environmental factors are extracted using the Proximity Analysis tools in ArcGIS. The distance from rivers and the distance from fracture zones are determined using a buffer analysis. Rivers have a significant influence on the formation and development of disaster sites, and the instability of the geological conditions and the susceptibility of the area is to developing disaster sites increase for areas closer to a fracture zone.

The spatial analyst function in ArcGIS was used to import the classification layers of various indicators, and the Raster calculator was adopted to superimpose the hazard

http://www.aloki.hu ● ISSN 1589 1623 (Print) ● ISSN 1785 0037 (Online)
DOI: http://dx.doi.org/10.15666/aeer/1605_65676587
© 2018, ALÖKI Kft., Budapest, Hungary

degree indicators to obtain the value of the comprehensive mountain disaster risk for each evaluation unit according to the previously described formula. The continuous hazard degree partition was divided into equal intervals and reclassified. Identical cells were merged, and the degree partition of mountain disasters was conducted. A higher degree of mountain disasters is associated with the higher contribution of each indicator to the occurrence of mountain disasters.

As seen from *Table 1* and *Figure 2,* the area of the region in Baoxing County with the lowest degree of mountain disasters (the low-hazard region) is 55,000 km^2, accounting for 17.65% of the total county area.

Table 1. *The distribution of mountainous disasters hazard classification*

Type/level	Area		Disaster spots		
	Number/hm^2	Percentage/%	Number	Percentage/%	Density/hm^2
Low-hazard region	55,000	17.65	55	16.32	0.10
Medium-hazard region	155,400	49.87	193	57.27	0.12
High-hazard region	101,189	32.48	89	26.41	0.09

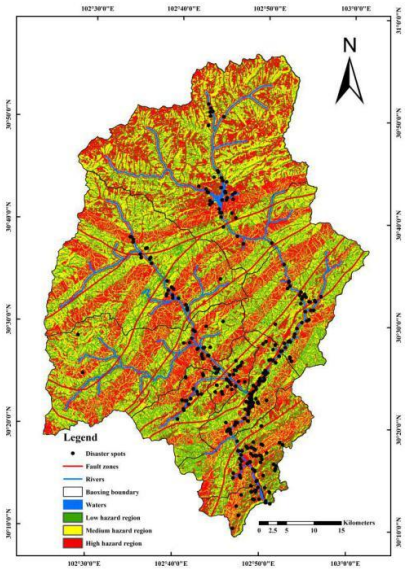

Figure 2. *The distribution map of mountain disasters hazard in Baoxing*

Within this region, 55 disaster sites, which account for 16.32% of the total disaster sites, are distributed in Fengtongzhai Township and Mingli Township, and the density is 0.10/hm^2. The area of the region with a medium degree of mountain disasters (the medium-hazard region) is 155,400 km^2, accounting for 49.87% of the total county area. Within this region, 193 disaster sites that account for 57.27% of the total number of disaster sites, are located in Muping Town, Lingguan Town, Longdong Town and Yongfu Township, and the density is 0.12/hm^2. The area of the region with a high degree of mountain disasters (the high-hazard region) is 101,189 km^2, accounting for 32.48% of the total county area. Within this region, 89 disaster sites that account for 26.41% of the total number of disaster sites are distributed along rivers and near fracture

http://www.aloki.hu ● ISSN 1589 1623 (Print) ● ISSN 1785 0037 (Online)
DOI: http://dx.doi.org/10.15666/aeer/1605_65676587
© 2018, ALÖKI Kft., Budapest, Hungary

zones in Qiaoqi Tibetan Township, Wulong Township and Daxi Township, with the density of 0.09/hm^2.

Analysis of mountainous disasters vulnerability classification

The degree of mountain disaster vulnerability is affected by socio-economic conditions and the conditions of hazard-affected areas. The socio-economic conditions include the spatial distribution of the population, land resources, water resources, transport facilities, large enterprises and other factors. The conditions of hazard-affected areas contain the type, quantity, and value of hazard-affected areas. In socio-economically developed regions, there is a dense population, intensive urbanization, highly concentrated industrial activities, numerous dense hazard-affected areas with high economic value, and the probability of damage from a wide range of mountain disasters is great, leading to the corresponding increase in casualties and economic losses. In view of this, this study selects six indicators for analysis, namely, population density, gross domestic product (GDP) density, fixed asset density, threatened property density, road density and land resource abundance for analysis.

The spatial analyst function in ArcGIS was used to import the classification layers of various indicators. According to the above formula, the Raster calculator was adopted to superimpose the vulnerability indicators to obtain the degree of hazard vulnerability value for each evaluation unit. The raster was reclassified. Identical cells were merged, and the vulnerability degree partition of mountain disasters was conducted. A higher vulnerability degree value indicates a higher degree of mountain disasters vulnerability. The study area is divided into three regions according to the degree of vulnerability, namely, the high-vulnerability region, the medium-vulnerability region, and the low-vulnerability region.

As seen from *Table 2* and *Figure 3,* the degree of vulnerability is higher where the density of disaster sites is greater. In Baoxing County, the area of the low-vulnerability region accounts for 83.22% of the total county area.

Table 2. *The distribution of mountain disasters vulnerability region degree level disaster spots*

Type/vulnerability degree level	Area		Disaster spots		
	Number/hm^2	Percentage/%	Number	Percentage /%	Density/hm^2
Low-vulnerability region	259289	83.22	141	41.84	0.05
Medium-vulnerability region	40000	12.84	149	44.21	0.37
High-vulnerability region	12300	3.95	47	13.95	0.38

Within this region, 141 disaster sites account for 41.84% of the total disaster sites in the county, and these sites are mainly distributed in Qiaoqi Tibetan Township, Yongfu Township, Fengtongzhai Township and Mingli Township, with the density of 0.05/hm^2. The area of the medium-vulnerability region accounts for 12.84% of the total county area. Within this region, 149 disaster sites, 44.21% of the total disaster sites in the county, are located in Muping Town and Lingguan Town, and the density is 0.37/hm^2. The area of the high-vulnerability region accounts for 3.95% of the total county area. Within this region, 47 disaster sites, accounting for 13.95% of the total in the county, are in Wulong Township and Daxi Township, and the density is 0.38/hm^2.

http://www.aloki.hu ● ISSN 1589 1623 (Print) ● ISSN 1785 0037 (Online)
DOI: http://dx.doi.org/10.15666/aeer/1605_65676587
© 2018, ALÖKI Kft., Budapest, Hungary

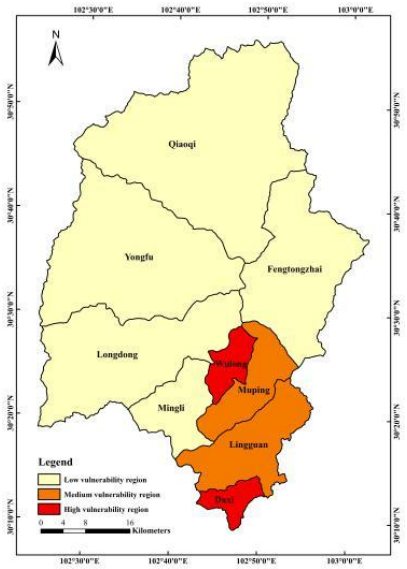

Figure 3. *The distribution map of mountain disasters in Baoxing*

Interpretation of the comprehensive risk degree partition of mountain disasters

Based on the above mentioned results of the hazard degree and partitions of hazard vulnerability degree, the value of the comprehensive degree of mountain disasters risk of each evaluation unit is calculated in accordance with the formula. ArcGIS is used to reclassify the raster. Identical cells are merged, and the comprehensive degree partition of mountain disasters risks is obtained.

As shown in *Table 3* and *Figure 4,* the low-risk region in Baoxing County is located in Fengtongzhai Township and Mingli Township, covering an area of 55,000 hm^2, which accounts for 17.65% of the total county area. The medium-risk region is distributed in Yongfu Township and Longdong Town, covering an area of 115,400 hm^2, which accounts for 37.04% of the total county area. The high-risk region is located in Qiaoqi Tibetan Township, Wulong Township, Muping Town, Lingguan Town and Daxi Township and is mainly on the periphery of the buffered areas of rivers and fracture zones. The high-risk region covers an area of 141,189 hm^2, accounting for 45.31% of the total county area. In general, there are more disaster sites in the areas near fracture zones and rivers, but there are fewer hazard-affected areas in these regions. However, in the peripheral regions, there are more hazard-affected areas and the economic value is higher. Therefore, the potential losses are greater, and the risks are higher in the peripheral regions.

Table 3. *Mountain disasters comprehensive risk degree partition results*

Type/risk degree level	Area		disaster spots		
	Number/hm^2	Percentage /%	Number	Percentage /%	Density/hm^2
Low-risk region	55000	17.65	55	16.32	0.10
Medium-risk region	115400	37.04	44	13.06	0.04
High-risk region	141189	45.31	238	70.62	0.17

http://www.aloki.hu ● ISSN 1589 1623 (Print) ● ISSN 1785 0037 (Online)
DOI: http://dx.doi.org/10.15666/aeer/1605_65676587
© 2018, ALÖKI Kft., Budapest, Hungary

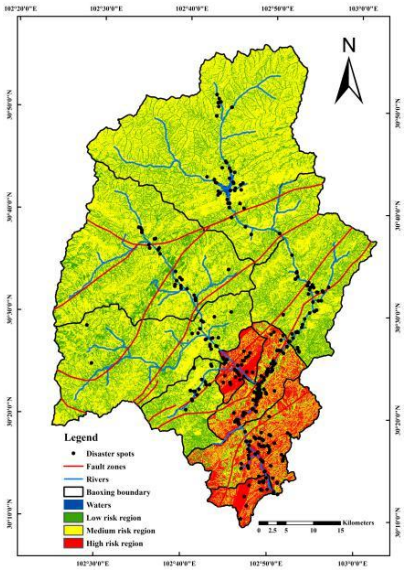

Figure 4. *The distribution map of mountain disasters risk in Baoxing*

Design of evaluation indicators for construction land development suitability

The surface structure factors

Baoxing County is a typical mountainous county, and the layout of its construction land, which is mainly segmented by mountains, rivers and gullies, is scattered. This layout is not conducive to construction land sustainability or infrastructure construction. Areas with slopes greater than 25° are directly classified as prohibited construction areas by the relevant land regulations in China, So the score is 0. Altitude, slope aspect and relief amplitude also play key roles in the stability and safety of buildings, the difficulty of construction and the costs of construction, and these factors directly restrict the layout of land use, the choices of roads and the spatial distribution patterns of buildings.

As can be seen from *Table 4,* we classify and assign values based on the proportion of the number of disaster sites in the developing mountains. The slope is within the 0-5° range, and the proportion of developed mountain disaster points accounts for 3.56% of the total, and within the 5-8° range, 5.90%, 8-15°, 7.67%; 15-25°, 25.82%, greater than 25°, 56.97%, it can be seen that the smaller the slope, the less likely the development disaster point, so the higher the score, the higher the suitability of the construction land. Less than 800 m above altitude, the proportion of mountain disaster sites is 14.24%, 800-1200 m, 15.13%, 1200-1600 m, 19.58%, 800-1600 m, 16.32%, greater than 2000 m, 34.72%. The higher the altitude, the greater the probability of developing disaster points, the lower the score, and the lower the suitability of the construction land. Similarly, the greater the topography fluctuation, the greater the relative height difference, the less suitable for construction. From the slope aspect of view, the proportion of mountain disaster sites developed on the southern slope is 5.93%. The Northern slope is 9.50%, the Northwest slope is 10.09%, the Eastern slope is 10.68%, the Southwest slope is 13.06%, the Northwest slope is 13.06%, the southeast slope is 18.69%, the Western slope is 18.99%. The more disaster points developed up each slope, the lower the score, the less suitable it is to build.

http://www.aloki.hu ● ISSN 1589 1623 (Print) ● ISSN 1785 0037 (Online)
DOI: http://dx.doi.org/10.15666/aeer/1605_65676587
© 2018, ALÖKI Kft., Budapest, Hungary

Table 4. *The surface structure factors' class interval, assign and layer*

Indicators name	Class interval	Score	Layer
Slope (°)	<5	5	
	5-8	4	
	8-15	3	
	15-25	2	
	>25	0	
Altitude (m)	<800	5	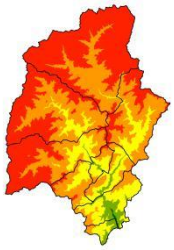
	800-1200	4	
	1200-1600	3	
	1600-2000	2	
	>2000	1	
Relief amplitude (m)	<100	5	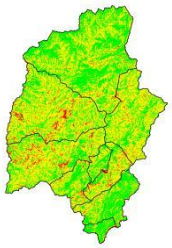
	100-200	4	
	200-300	3	
	300-400	2	
	>400	1	
Slope aspect	Southern slope/Northern slope	5	
	Northwest slope/Eastern slope	4	
	Southwest slope/Northwest slope	3	
	Southeast slope/Western slope	2	

Hydrogeological factors

Due to the constant movements of geological structures in mountainous areas and the long-term effects of river water erosion, the complex hydrogeological environment greatly hinders the development of construction land. The drainage conditions have an important influence on the development of construction land and the construction of a project, and good drainage conditions can reduce construction costs. The cumulative amount of running water was used to measure the displacement of land in the study area, and the drainage conditions were considered to be worse if the cumulative amount of running water was large.

As shown in *Table 5,* the rock formations in mountainous areas are complex, and generally speaking, areas that are farther away from fault zones are more suitable for

http://www.aloki.hu ● ISSN 1589 1623 (Print) ● ISSN 1785 0037 (Online)
DOI: http://dx.doi.org/10.15666/aeer/1605_65676587
© 2018, ALÖKI Kft., Budapest, Hungary

construction due to the higher stability and safety. In terms of the number of disaster sites, the proportion of mountain disaster sites is 33.23% within 500 m of the fault zone. The 500-1000 m range is 24.63%, 1000-2000 m is 13.35%, 2000-4000 m is 17.51%, greater than 4000 m is 11.28%. It can be seen that the farther the distance from the fault zone, the higher the construction score, the more suitable construction.

Table 5. *Hydrogeological factors' class interval, assign and layer*

Indicators name	Unit	Class interval	Score	Layer
Drainage condition	(m^3)	>25	5	
		15-25	4	
		8-15	3	
		5-8	2	
		<5	1	
Distance from the fault zones	(m)	>4000	5	
		2000-4000	4	
		1000-2000	3	
		500-1000	2	
		100-500	1	
Distance from the rivers	(m)	<500	5	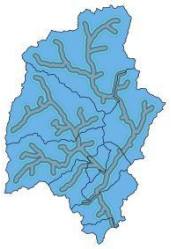
		500-1000	4	
		1000-1500	3	
		1500-2000	2	
		>2000	1	
Distance from the water area (lakes, reservoirs, etc.)	(m)	>3000	5	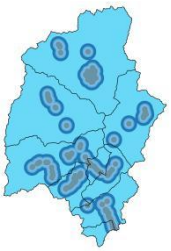
		2000-3000	4	
		1500-2000	3	
		1000-1500	2	
		<1000	1	

The fluvial action of rivers has a significant effect on the formation of landform types, and the distance from rivers is directly related to the guarantee for water supply in urban construction. The water supply conditions for construction land near rivers are better, which increases the suitability. In addition, the distance from water (lakes, reservoirs, etc.) can reflect the degree of water pollution, especially the pollution from

http://www.aloki.hu ● ISSN 1589 1623 (Print) ● ISSN 1785 0037 (Online)
DOI: http://dx.doi.org/10.15666/aeer/1605_65676587
© 2018, ALÖKI Kft., Budapest, Hungary

domestic waste and industrial wastewater. Among them, the water conditions within 500 m are the best, so the score is 5. According to field survey studies, for each additional 500 m, the water level is reduced by one level, and when the water conditions after the distance is greater than 2,000 m do not have a significant impact, so, We divide each classification according to such a rule.

The water area in this study refer to the planar distributed areas except for rivers, lakes and reservoirs. Residential areas, factories and other related public production and living facilities should be located far away from the safe distance range of waters to reduce the influence of water pollution sources. The ecology of the water area is fragile, and the closer it is to the water area, the less suitable it is for construction. Therefore, we follow the distance from far to near, and the score is from high to low.

Human activity factors

Human activities have a remarkable impact on the development of construction land in mountainous areas (Bucała, 2014; Chen et al., 2016). In this study, the current land use conditions were selected as an indicator, which can reflect the land use types. As shown in *Table 6,* industrial and mining lands and Waterworks construction land have large number of construction projects, so the suitability for construction land is higher, that is why we scored highest in our classification. The suitability of dry land and other land is lower than the land mentioned above, but it is higher than forest land, grassland, etc., so the score is second. Moreover, forest land and grassland are highly vulnerable ecologically, and the development and construction costs are high there, so the suitability is lower. Paddy fields and water area (lakes, reservoirs, etc.) can hardly be used for construction. The distance from the built-up areas is also selected as an indicator. Here, built-up areas refer to the tracts where construction has been completed throughout the county, and these areas are the economic growth point, with strong agglomeration and radiation effects. In general, areas closer to built-up areas are more suitable for construction land development due to lower construction costs. The distance from the roads is selected as another indicator that can reflect the accessibility of the regional roads, and the conditions of these roads affect the cost of construction and the development of urban construction land. The suitability of construction land will be higher when the distances between roads are shorter. Finally, the core areas and the periphery of protected areas were selected as indicators. Protected areas have high ecological sensitivity and are banned as construction areas, whereas the areas outside the core-protected areas are more suitable for construction.

Table 6. *Human activities factors and indicators' class interval, assign and layer*

Indicators name	Class	Score	Layer
The present situation of land use	Industrial and mining land in city, waterworks construction land	5	
	Dry land, other land	4	
	Forest land	3	
	Garden land, grassland	2	
	Paddy fields, water area (lakes, reservoirs, etc.)	1	

http://www.aloki.hu ● ISSN 1589 1623 (Print) ● ISSN 1785 0037 (Online)
DOI: http://dx.doi.org/10.15666/aeer/1605_65676587
© 2018, ALÖKI Kft., Budapest, Hungary

Distance from the built-up areas (m)	<1000	5	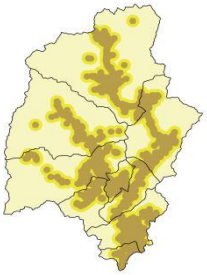
	1000-2000	3	
	>2000	1	
Distance from the roads (m)	<1000	5	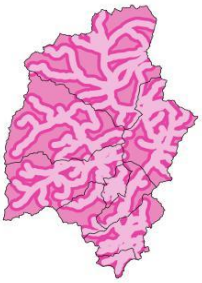
	1000-2000	3	
	>2000	1	
Protected areas	Core areas	0	
	Outside the core areas	1	

Analysis of the assessment of construction land evaluation results

Analysis of evaluation indicator weight

An evaluation indicator system was established using ANP, and the weight of each indicator was calculated using Super Decisions software based on the evaluation indicator selection described above (*Table 7*).

Table 7. *Evaluation indicator weight for construction land development suitability*

Evaluation indicator	Weight	Evaluation indicator	Weight
Slope	0.1547	Distance from the rivers	0.0881
Altitude	0.1404	Distance from the waters (reservoirs)	0.0610
Relief amplitude	0.0468	The present situation of land use	0.2074
Slope aspect	0.0213	Distance from the built-up areas	0.0397
Drainage condition	0.0662	Distance from the roads	0.1110
Distance from the fracture zones	0.0475	Protected areas	0.0159

The Raster calculator function from the spatial analyst tools for ArcGIS10.1 software was used to calculate various evaluation indicators according to the formula, and obtain

http://www.aloki.hu ● ISSN 1589 1623 (Print) ● ISSN 1785 0037 (Online)
DOI: http://dx.doi.org/10.15666/aeer/1605_65676587
© 2018, ALÖKI Kft., Budapest, Hungary

the suitability partition of construction land development in Baoxing County. The construction land suitability level was divided into four categories based on natural breaks classification, and then the regional mean value was used to calculate the spatial distribution of construction land suitability in various townships and towns of the county.

Analysis of evaluation construction land suitability level results

Based on the above results of the mountain disaster risk partitioning and the evaluation indicator weight for construction land development suitability, the coupling model formula was used with the Raster calculator function from the in spatial analyst tools for in ArcGIS. To visually show the analysis results, the spatial analyst reclassification was used to classify the suitability levels into 4 categories according to natural breaks classification. We then determined the construction land suitability levels under the stress of mountain disasters (*Table 8*).

Table 8. *Construction land suitability level results under the stress of mountain disasters*

Suitability degree level	Number of grid cells	Area (hm^2)	Percentage (%)
High-suitability region	451	28.318	0.009
Medium-suitability region	6516	409.136	0.131
Low-suitability region	52028	3266.806	1.048
Unsuitability region	4903453	307884.741	98.811

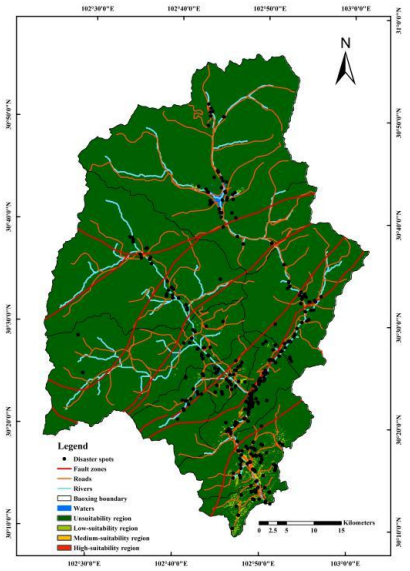

Figure 5. *Construction land suitability degree level in Baoxing*

As shown in *Table 6* and *Figure 5,* the high-suitability region is the smallest area of the four land types and covers an area of 28.318 hm^2, which accounts for 0.009% of the total county area. The high-suitability region is mainly located southwest of Baoxing County, mostly in Wulong Township, Muping Town, Lingguan Town and Daxi Township. The highway mileage in this region is 286.7 km, and the traffic conditions

http://www.aloki.hu ● ISSN 1589 1623 (Print) ● ISSN 1785 0037 (Online)
DOI: http://dx.doi.org/10.15666/aeer/1605_65676587
© 2018, ALÖKI Kft., Budapest, Hungary

and the hazard emergency rescue and response conditions are good. For example, in this region, there are 7 hospitals and health centers, 107 practicing (assistant) physicians and 197 medical beds, which account for 58.33%, 75.89% and 79.76% of the county's total for each of these services, respectively. Most areas of the regions are built-up areas with good infrastructure. There are 16 villages with broadband networks, 26 villages with cable TV, 27 villages with tap water and 20 villages with centralized waste disposal, accounting for 72.73%, 50.00%, 49.09% and 52.63% of the county's total for each of these services, respectively. In addition, the region has high economic value for construction land, and high suitability for construction land development. Nevertheless, these conditions are also associated with higher economic density, land value and construction costs. Moreover, if a disaster occurs, there will be substantial losses will be caused, and the hazard risks will be high.

The medium-suitability region covers an area of 409.136 hm^2, which accounts for 0.131% of the total county area, and the region is located mainly on the periphery of the high-suitability land. Most parts of this region are cultivated land and rural residential areas, with better land drainage conditions, longer highways, better traffic accessibility conditions, higher population densities and higher per capita GDP. In general, compared with the high-suitability region, the conditions of this region are worse, and it is closer to built-up areas.

The low-suitability region covers an area of 3266.806 hm^2, which accounts for 1.048% of the total county area. Generally, the conditions here are worse than those of the medium-suitability region. Specifically, its hazard rescue and response capabilities are weaker, and there are only 3 hospitals, 11 practicing (assistant) physicians and 25 medical beds, which account for 25.00%, 7.80% and 10.12% of the county's total for each of these services, respectively.

Located on the periphery of the low-suitability land, the region that is unsuitable for construction land development covers an area of 307884.741 hm^2, which accounts for 98.811% of the total county area. It covers the largest area in the county, mainly because the Fengtongzhai Nature Reserve, a giant panda protection base is sited there. In addition, the region has a better natural ecological environment, higher vegetation coverage and is far away from the town center, suggesting that there is less interference by human production and living activities. Moreover, this region is regarded as a nature conservation area and development is prohibited there.

Conclusions and discussion

Conclusions

Based on the results indicate that the disaster spots have a significant impact on the suitability of construction land and are directly related to the future development and construction of land resources. At the same time, the built-up areas are smaller than those in the suitable land in Baoxing County, meaning potential for future construction land development in the county. With the continuous improvement of technology, the construction of hazard prevention and mitigation project and the further reduction of hazard stress degrees, more land will likely be available for construction. We also find that the mountain disaster risk is the core factor for the suitability evaluation of the urban construction land in mountainous areas. And the central areas of the mountain towns are the high-risk and high-suitability areas for the development of construction land.

http://www.aloki.hu ● ISSN 1589 1623 (Print) ● ISSN 1785 0037 (Online)
DOI: http://dx.doi.org/10.15666/aeer/1605_65676587
© 2018, ALÖKI Kft., Budapest, Hungary

Discussion

In view of the above evaluation results, this study proposes construction land development paths in Baoxing County, which mainly include the following aspects:

There is a need to establish a planning system that combines construction land with mountain disasters, and the planning and design must comply with the relevant laws and regulations to ensure the standardized development of construction land. All projects under construction in the county must strictly conduct an mountain disasters risk evaluation, especially during the planning and site selection for town relocation and major projects.

Hazard monitoring and construction should be carried out simultaneously in the high-risk high-suitability construction regions. In the county, the high-suitability construction region is also the high-risk region. There are good regional land use conditions, complete public infrastructure, high value-added land use benefits, good traffic accessibility and high vulnerability and high risks of mountain disasters. It is necessary to conduct real-time monitoring and provide early warning for schools, hospitals, industrial and mining enterprises, scenic spots, special land and other hazard-bearing bodies with weak hazard resistance abilities in the region. Moreover, targeted measures must be taken, especially for industrial and mining land, which has a serious hidden danger of mountain disasters and poses a threat to the safety of residents during production, life and travel. It is necessary to combine the regional industrial bases, consider the land function orientation and develop corresponding supporting facilities, so as to improve value and transfer the benefits of construction land assets and achieve better development of the high-risk high-suitability region.

Construction land in rural residential areas should be integrated into the medium-suitability construction region. In this region, new rural construction will be achieved mainly by integrating construction land in rural residential areas. It is necessary to dismantle and merge villages, renovate hollow villages and construct center villages according to local conditions and improve the utilization efficiency of rural homesteads. There is a small amount of urban industrial and mining land in this region, so it is necessary to rely on the county to integrate regional space, promote the division of labor and cooperation between the villages and towns and realize the complementary advantages. In this way, the comprehensive carrying capacity of the county can be improved to fully enhance the overall land use efficiency.

The low-suitability construction region is mainly remote and poverty-stricken areas, which are dominated by agricultural land and bare land. It has a large proportion of idle land, and low per capita net income of farmers. Most of its population belongs to the left-behind elderly, left-behind children and the disabled, and these result in the high vulnerability of this region. Therefore, there is a need to ease the burden on farmers, reduce the prices of agricultural chemical fertilizers and other production materials, develop and utilize the idle land resources and implement precise poverty alleviation measures. Sustainable land use can also be promoted by arranging the idle land and changing the land use patterns. For instance, idle old factories can be converted into a breeding base for farmers, and old rural homesteads can be changed into new housing land.

A protected land network system should be constructed in the unsuitable construction area. The core area of the protected land in this region is habitat for the giant panda. The construction of the protected land network has restricted the sustainable livelihoods of the surrounding farmers to a certain extent. Due to their sole reliance on the fiscal

http://www.aloki.hu ● ISSN 1589 1623 (Print) ● ISSN 1785 0037 (Online)
DOI: http://dx.doi.org/10.15666/aeer/1605_65676587
© 2018, ALÖKI Kft., Budapest, Hungary

transfer payments and ecological compensation from the government, the transformation of the livelihoods of farmers will be faced with challenges.

As a result, when the Chinese government establishes and manages a protected land network, the connection between resource management and the needs of community residents should be considered, and corresponding supportive strategies should be implemented. For instance, the characteristic industry of Baoxing County and a labor export strategy, as well as an ecotourism strategy, can bring a more diversified selection of livelihood strategies for local farmers.

Acknowledgements. We thank all funding support from the science and technology program in Guangdong province of China (Grant No.: 2017A020220009), the 61st batch of Chinese postdoctoral program (Grant No.: 2017M612683), the south China normal university youth teacher scientific research cultivating fund program (Grant No.: 2016JK102). Our Special thanks to Prof. Shaoquan Liu and A/Prof. Li Peng for their help.

REFERENCES

[1] Akinci, H., Ozalp, A. Y., Turgut, B. (2013): Agricultural land use suitability analysis using GIS and AHP technique. – Computers and electronics in agriculture 97: 71-82.
[2] Ambarwulan, W., Santoso, P. B., Sabiham, S., Hikmat, M. (2016): Remote sensing and land suitability analysis to establish local specific inputs for paddy fields in Subang, West Java. – Procedia Environmental Sciences 33: 94-107.
[3] Bucała, A. (2014): The impact of human activities on land use and land cover changes and environmental processes in the Gorce Mountains (Western Polish Carpathians) in the past 50 years. – Journal of Environmental Management 138: 4-14.
[4] Cardona, O. D. (2005): Indicators of Hazard Risk and Risk Management: Program for Latin America and the Caribbean: Summary Report. – Inter-American Development Bank, Washington, DC.
[5] Center, A. D. R. (2005): Total Hazard Risk Management: Good Practices. – Handbook for the UN World Conference on hazard Reduction, Kobe.
[6] Chandio, I. A., Matori, A. N., Yusof, K., Talpur, M. H., Aminu, M. (2014): GIS-based land suitability analysis of sustainable hillside development. – Procedia Engineering 77: 87-94.
[7] Change, I. C. (2007): Climate change impacts, adaptation and vulnerability–summary for policy makers. – Contribution of Working Group I to the Fourth Assessment Report of the Intergovernmental Panel on Climate Change, Paris 12: 171-175.
[8] Chen, G., Fang, Y. et al. (2010): Development Report of Mountainous Area in China. – China Commerce and Trade Press, Beijing (in Chinese).
[9] Chen, M., Qin, X., Zeng, G., Li, J. (2016): Impacts of human activity modes and climate on heavy metal "spread" in groundwater are biased. – Chemosphere 152: 439-445.
[10] Cui, P. (2014): Progress and prospects in research on mountain hazards in China. – Progress in Geography 33(2): 145-152 (in Chinese).
[11] Dang, L., Xu, Y., Tang, Q. (2015): The pattern of available construction land along the Xijiang River in Guangxi, China. – Land Use Policy 42: 102-112.
[12] Deuskar, C., Baker, J. L., Mason, D. (eds.) (2015): East Asia's Changing Urban Landscape: Measuring a Decade of Spatial Growth. – World Bank Group, Washington, DC. FAO (1993): An international framework for evaluating sustainable land management. – World Soil Resources Report 73.
[13] Gimblett, R. H., Ball, G. L., Guisse, A. W. (1994): Autonomous rule generation and assessment for complex spatial modeling. – Landscape and Urban Planning 30(1-2): 13-26.

http://www.aloki.hu ● ISSN 1589 1623 (Print) ● ISSN 1785 0037 (Online)
DOI: http://dx.doi.org/10.15666/aeer/1605_65676587
© 2018, ALÖKI Kft., Budapest, Hungary

[14] Guo, X., Qiu, Y., Lian, G. et al. (2003): The progress and prospect of land quality indicators based on 'Press-State-Response' framework. – Progress in Geography 5: 479-489 (in Chinese).
[15] Hemingway, R., Gunawan, O. (2018): The Natural Hazards Partnership: a public-sector collaboration across the UK for natural hazard disaster risk reduction. – International Journal of Disaster Risk Reduction 27: 499-511.
[16] ISDR (2005): Hyogo framework for action 2005-2015: building the resilience of nations and communities to disasters. – In: Extract from the final report of the World Conference on Disaster Reduction (A/CONF. 206/6, Vol. 380).
[17] Jiao, S., Zhang, X., Xu, Y. (2017): A review of Chinese land suitability assessment from the rainfall-waterlogging perspective: Evidence from the Su Yu Yuan area. – Journal of Cleaner Production 144: 100-106.
[18] Leroi, E., Bonnard, C., Fell, R., McInnes, R. (2005): Risk assessment and management. – Landslide Risk Management 159-198.
[19] Liu, Y., Peng, J., Han, Y., Wei, H., Du, Y. (2014): Suitability assessment for building land consolidation on gentle hillside based on OWA operator: a case in Dali Bai Nationality Borough in Yunnan. – Acta Ecologica Sinica 34(12): 3188-3197 (in Chinese).
[20] Liu, Y., Peng, J., Zhang, T., Zhao, M. (2016): Assessing landscape eco-risk associated with hilly construction land exploitation in the southwest of China: Trade-off and adaptation. – Ecological Indicators 62: 289-297.
[21] Lovell, S. T. (2010): Multifunctional urban agriculture for sustainable land use planning in the United States. – Sustainability 2(8): 2499-2522.
[22] Malczewski, J. (2006): Ordered weighted averaging with fuzzy quantifiers: GIS-based multicriteria evaluation for land-use suitability analysis. – International Journal of Applied Earth Observation and Geoinformation 8(4): 270-277.
[23] Montanarella, L., Nègre, T. (2001): The development of the Alpine soil information system. – International Journal of Applied Earth Observation and Geoinformation 3(1): 18-24.
[24] Nan, X. (2009). Study on suitability evaluation of mountainous city construction land supported by GIS. – Northwest University (in Chinese).
[25] Peng, J., Ma, J., Du, Y., Zhang, L., Hu, X. (2016): Ecological suitability evaluation for mountainous area development based on conceptual model of landscape structure, function, and dynamics. – Ecological Indicators 61: 500-511.
[26] Promper, C., Puissant, A., Malet, J. P., Glade, T. (2014): Analysis of land cover changes in the past and the future as contribution to landslide risk scenarios. – Applied Geography 53: 11-19.
[27] Qiu, L., Zhu, J., Pan, Y., Hu, W., Amable, G. S. (2017): Multi-criteria land use suitability analysis for livestock development planning in Hangzhou metropolitan area, China. – Journal of Cleaner Production 161: 1011-1019.
[28] Rusdi, M., Roosli, R., Ahamad, M. S. S. (2015): Land evaluation suitability for settlement based on soil permeability, topography and geology ten years after tsunami in Banda Aceh, Indonesia. – The Egyptian Journal of Remote Sensing and Space Science 18(2): 207-215.
[29] Smith, K. (2013): Environmental Hazards: Assessing Risk and Reducing Hazard. – Routledge, New York.
[30] The State Council of China (2017): The National Comprehensive Disaster Prevention and Mitigation Plan (Year 2016-2020). – http://www.gov.cn/xinwen/2017-01/13/content_5159563.htm.
[31] United Nations Development Programme (UNDP) (2004): Bureau for Crisis Prevention, Recovery. Reducing Hazard Risk: A Challenge for Development. – A Global Report, United Nations.

http://www.aloki.hu ● ISSN 1589 1623 (Print) ● ISSN 1785 0037 (Online)
DOI: http://dx.doi.org/10.15666/aeer/1605_65676587
© 2018, ALÖKI Kft., Budapest, Hungary

[32] Wang, H. (2012): Study on the suitability evaluation of urban construction land in southwest China: A case study of Yunnan Rili. – Yunnan University Finance and Economics, Yunnan (in Chinese).
[33] Wang, X., Bao, Y. (2011): Study on the methods of land use dynamic change research. – Progress in Geography 18: 81-87 (in Chinese).
[34] Wei, H., Qin, B., Peng, J., Jin, X. (2014): Evaluation on comprehensive exploitation suitability of low-slope hilly land based on GRNN model and neighborhood calculation: A case study of Wumeng Mountain continuous poverty-stricken region. – Geographical Research 33(5): 831-841 (in Chinese).
[35] Wu, M., Zhang, C., Fan, T. (2016): Stress state of the Baoxing segment of the southwestern Longmenshan Fault Zone before and after the M s 7.0 Lushan earthquake. – Journal of Asian Earth Sciences 121: 9-19.
[36] Ying, J., Yin, Z., Xu, S. et al. (2009): Disaster risk theory and risk management method. – Journal of Catastrophology 24: 7-15 (in Chinese).
[37] Zhang, G. P., Xu, J., Bi, B. G. (2009): Relations of landslide and debris flow hazards to environmental factors. – The Journal of Applied Ecology 20(3): 653-658.
[38] Zhou, Q., Su, W. Chen, S. (2010): LUCC analysis of Tongliang County based on the landscape pattern indices and the Markov model. – Resources and Environment in the Yangtze Basin 19(7): 770-775 (in Chinese).

http://www.aloki.hu ● ISSN 1589 1623 (Print) ● ISSN 1785 0037 (Online)
DOI: http://dx.doi.org/10.15666/aeer/1605_65676587
© 2018, ALÖKI Kft., Budapest, Hungary

USE OF MEDICINAL PLANTS BY LIVESTOCK FARMERS IN A LOCAL MUNICIPALITY IN VHEMBE DISTRICT, SOUTH AFRICA

CHITURA, T.[1*] – MUVHALI, P. T.[1] – SHAI, K.[1] – MUSHONGA, B.[2] – KANDIWA, E.[2]

[1]*Department of Agricultural Economics and Animal Production, University of Limpopo Private Bag X1106, Sovenga 0727, South Africa*

[2]*Department of Biomedical Sciences, School of Veterinary Medicine, Faculty of Agriculture and Natural Resources, University of Namibia Private bag X 13301, Mandume Ndemufayo Avenue, Pioneers Park, Windhoek, Namibia*

**Corresponding author*
e-mail: teedzai.chitura@ul.ac.za

(Received 27th Jun 2018; accepted 14th Aug 2018)

Abstract. Respondents (n = 180) from Mutale municipality, Limpopo Province, South Africa, were interviewed so as to assess the factors affecting the use of medicinal herbs in treatment of livestock diseases. A significantly greater proportion of males (79.8%) than females (52.7%) preferred a combination of treatment methods ($P < 0.05$). A significantly greater proportion of females (36.8%) than males (10.6%) preferred using medicinal herbs only ($P < 0.05$). There was no significant difference in the proportions of males and females using conventional drugs only ($P > 0.05$). Overall, a significantly greater proportion of respondents between 20-40years old (83.1%) preferred to use a combination of treatment methods ($P < 0.05$). A significantly greater proportion of the unschooled respondents (46.6%) preferred to use medicinal herbs only ($P < 0.05$). A significantly greater proportion of the tertiary-schooled respondents (50%), however, preferred to use conventional drugs only ($P < 0.05$). Parts from Cassia abbreviata and Cissus quadrangularis were the preferred oral treatments for retained placenta, Pterocarpus angolensis and Combretum collinum were the preferred oral treatments for constipation in cattle. Cissus quadrangularis, Dichrostachys cinerea and Ximenia americana were preferred for topical treatment of wounds, Synadenium cupulare for arthritis, Ziziphus mucronata for mastitis, Maytanus eduncularis for fractures and Gossypium herbaceum for blindness in cattle, sheep and goats.
Keywords: *herbal, ethno-veterinary, practices, Cassia abbreviata, South Africa*

Introduction

Mutale is a rural Municipality in the Vhembe District of the Limpopo Province of South Africa. The municipality, like other places in Limpopo Province, is affected by climate change and receives minimal rainfall. Its poor human population depends mostly on livestock production. Viability of livestock production in Mutale is under threat of diseases which appear to be on the increase, in recent times, due to climate change. However, farmers cannot afford to buy modern drugs for treatment of livestock diseases. To keep their animals alive and healthy, farmers have resorted to the time-honoured approach of using plant remedies (ethno-veterinary or ethno-botanical) to treat the diseases affecting their animals.

The demographics of the farmers using ethno-veterinary medicine, their reasons for doing so, the species of plants used, the parts of plants used, and the specific diseases so treated, though documented elsewhere in South Africa and other developing countries, have, hitherto, not been documented in Mutale Municipality. The objective of this study was to document the demographics of farmers using plant and conventional drugs and the species of plants thus used in the treatment of common animal diseases in Mutale

http://www.aloki.hu ● ISSN 1589 1623 (Print) ● ISSN 1785 0037 (Online)
DOI: http://dx.doi.org/10.15666/aeer/1605_65896605
© 2018, ALÖKI Kft., Budapest, Hungary

Municipality. The overarching aim of this study was to highlight the use of locally available natural resources (plant remedies) by resource constrained rural farmers as a sustainable way of combating climate change.

Literature review

Food security and opportunity for gainful employment has been a challenge with increasing population pressure the world over and is continually threatened by the effects of global warming. It is estimated that demand for animal products will be doubled by 2050. There is an urgent need for innovative sustainable production that also improves livelihood and food security (Notenbaert et al., 2017). Such production initiatives must harness knowledge from the informal sector that possibly helps protect the environment (Munda et al., 2016). Livestock production is one such solution to global food shortage contributing up to 80% of agricultural GDP in developing countries, including those in Africa. In addition, 600 million rural poor people rely on livestock for their livelihoods. Moreover, livestock and derived products act as a buffer against climatic unpredictability, greatly contributing to food security especially in periods of scarce agricultural resources. Livestock diseases and poor management practices are a major threat to sustainable livelihoods of resource-poor rural communities (Marandure et al., 2016). The livestock sector in Mutale local municipality sustains the livelihoods of the majority of inhabitants who are mainly small-scale livestock producers. In this area, the main vegetation type is the *Mopane* woodland, a type of savanna woodland ecosystem dominated by the tree *Colophospermum mopane* (also called *mopane* in local languages) (Makhado et al., 2012, 2014). Due to dry climate and poor soil conditions, land cultivation is difficult and livestock production is the only viable option to farmers and is thus their main and often sole means of survival and source of income. However, successful livestock production has been challenged by changing rural contexts such as limited or lack of grazing land (Doumbia et al., 2012), lack of medications (Usha et al., 2016), increased costs (Ritter et al., 2012) and drug resistance (Raot et al., 2016). In light of the foregoing, resource-limited farmers resort to using locally available resources to control livestock diseases, ectoparasites and other related vectors (Mutibvu et al., 2012).

Over the years, rural farmers have used indigenous methods as an alternative solution for coping with disease constraints in both humans and animals (Ahmad et al., 2016; Paindla et al., 2013). These methods of treatment of animals using indigenous knowledge are broadly referred to as ethno-veterinary medicine (EVM) (Shen et al., 2010; Bartha et al., 2015; Usha et al., 2016; Caudell et al., 2017). The pharmacopeia usually used includes animal products, plant products as well as minerals for treating animals (Bartha et al., 2015; Raikwar and Maurya, 2015). According to Ahmad et al. (2016), the role of EVM in livestock production is beyond dispute. The knowledge is owned communally, under the custody of older members of the population depending on the community, ethnicity, sex, age and caste and is passed down through generations by oral tradition (Ahmad et al., 2016). It is clear from literature that EVM is usually practiced alongside or as an alternative to allopathic (modern western style) veterinary medicine (Shen et al., 2010; Claudell et al., 2017). It has been observed that, in nature, animals consume certain plants in order to derive treatment of various ailments afflicting them (Huffman, 2016). Raikwar and Maurya (2015) pointed out that availability and accessibility of such products at little or no cost are the major selling points for EVM to poor rural communities. In addition, EVM has gained popularity in recent times, in the face of an increasing demand for

http://www.aloki.hu ● ISSN 1589 1623 (Print) ● ISSN 1785 0037 (Online)
DOI: http://dx.doi.org/10.15666/aeer/1605_65896605
© 2018, ALÖKI Kft., Budapest, Hungary

organically raised meat traceable to farms of origin; and the rise of a modern-day consumer willing to pay a higher premium for meat arising from organic farms that strictly adhere to animal welfare guidelines (Lans et al., 2012; Adedeji et al., 2013; Mayer et al., 2014).

There has been an interesting explosion of publications in the last decade from various sub regions of the world including North America (Lans et al., 2012), Australia (Vogl et al., 2016), China (Shen et al., 2010), Europe (Mayer, 2014; Bartha et al., 2015) the Indian subcontinent (Vijayagiri et al., 2012; Mamidala, 2013; Raikwar and Maurya, 2015; Ahmad et al., 2016; Usha et al., 2016) and Africa (McGaw and Eloff, 2008; Marandure, 2016; Caudell et al., 2017; Teklehaymanot, 2017) on EVM. Literature from India outnumbers that arising from any other part of the world, an indication of the strength of the link between India's tribal communities and nature (Paindla et al., 2009). The World Health Organization estimates that nearly 80% of the world's poor depend on EVM (Raikwar and Maurya, 2015). However, it is disappointing to note that, of the recent publications, only a few demonstrate the efficacy of EVM (Luseba et al., 2007; Ndhlala et al., 2009; Adamu et al., 2014; Sserunkuma et al., 2017). The majority of recent publications are EVM surveys documenting which diseases are treated by which plants (McGaw and Eloff, 2008; Shen et al., 2010; Lans et al., 2012; Vijayagiri et al., 2012; Mamidala, 2013; Mayer, 2014; Bartha et al., 2015; Raikwar and Maurya, 2015; Ahmad, et al., 2016; Marandure, 2016; Usha et al., 2016; Vogl et al., 2016; Caudell et al., 2017; Teklehaymanot, 2017) Studies in Africa and elsewhere indicated inadequate veterinary services and lack of low cost alternative technologies as impediments in overcoming livestock diseases (Getachew et al., 2015; Raikwar and Maurya, 2015; Shamim et al., 2015). There is a need to look for environment-friendly technologies in support of livestock welfare and health. Evidence gathered from previous research indicated that there is a scope for the use of EVM within the Southern African Sub region (Gabanakgosi et al., 2012; Maroyi, 2012; Chinsembu et al., 2014; Marandure, 2016) and particularly in South Africa (Luseba and Van der Merwe; 2006; McGaw et al., 2007; Moyo et al., 2009; Ndhlala et al., 2009; Maphosa, 2010; Moyo et al., 2013; Chauke et al., 2015; Tyasi and Nkohla, 2015). Documentation of ethno-veterinary practices is critically urgent so that the knowledge can be preserved, plants conserved and sustainably managed for the control of livestock diseases (Vijayagiri et al., 2012).

Some recent studies have shown that people living in the Venda area still hold a valuable knowledge on food and medicinal plants and that some of these plants can act as crucial factors in livelihood strategies of indigenous communities. *Mopane* woodlands are also believed to host a high diversity of plants with potential ethno-veterinary applications (Luseba and van der Merwe, 2006; Luseba and Tshisikhawe, 2013; Chinsembu et al., 2014). However, to date no systematic information has been gathered on plants locally used in maintaining livestock health and welfare in Mutale municipality. The aim of this study was to record and analyze traditional ethnobotanical knowledge concerning EVM and fodder plants in some communities living in *Mopane* woodlands surrounding the municipality of Mutale.

Materials and methods

The study was conducted in selected villages of Mutale local municipality, Vhembe district, Limpopo Province of the Republic of South Africa, over a period of three months (January-March 2014). Mutale local municipality is situated far north of the

http://www.aloki.hu ● ISSN 1589 1623 (Print) ● ISSN 1785 0037 (Online)
DOI: http://dx.doi.org/10.15666/aeer/1605_65896605
© 2018, ALÖKI Kft., Budapest, Hungary

Limpopo Province largely inhabited by the Venda speaking people. The coordinates of the study area are 22° 35' 0" S, 30° 40' 0" E (*Fig. 1*). The geographical outlook of the area is dominated by the Soutpansberg Mountains and sandy soils. The natural vegetation around the study area was identified as the savannah biome of the Mopane units (*Colophospermum mopane*) and central bushveld (Mucina and Rutherford, 2006). The area receives about 681 mm of rain per year with high rainfall of about 137 mm in summer and about 2 mm of rain experienced in winter (S. A. Explorer, 2014). The average midday temperature in the study area ranges from 29.2 °C in summer to 22.1°C in winter. Small scale livestock production compliments crop production to provide food security and income for the households of the Mutale local municipality. Participation by the respondents in this study was voluntary and under no circumstances were the authors handling or applying any medication to animals during data collection of this study.

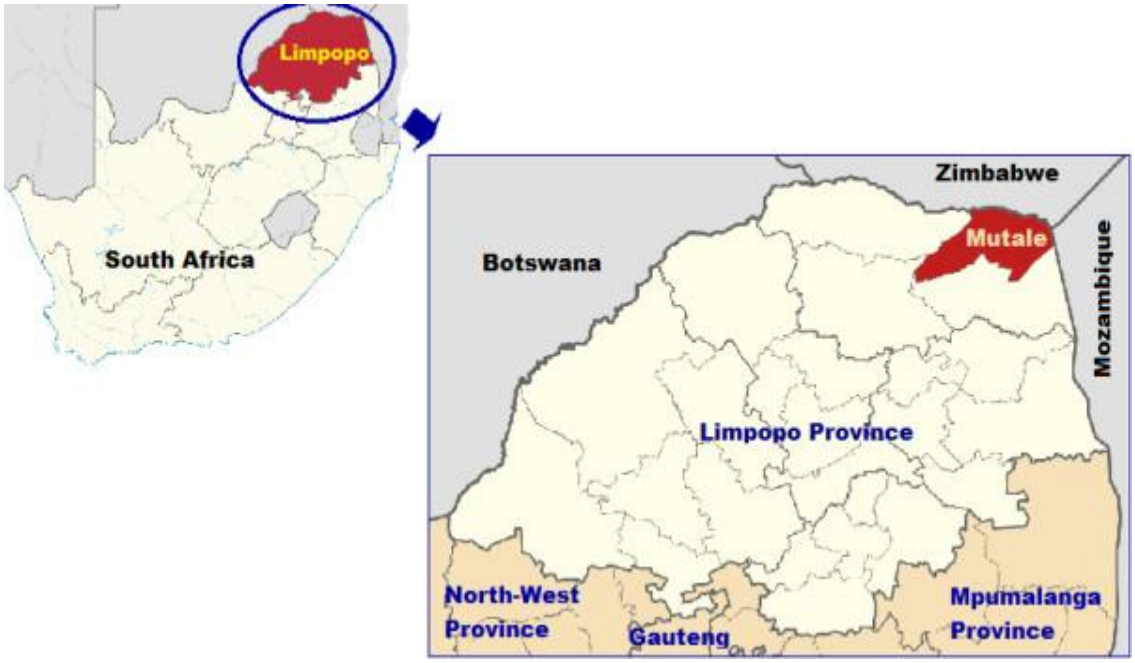

Figure 1. *Map of Mutale local municipality, Vhembe District, South Africa*

One hundred and eighty farmers (104 males and 76 females) were purposely selected and interviewed on their knowledge of livestock diseases and plants used for treatment of identified animal diseases. A structured questionnaire was used to gather information on the demographic characteristics (gender, age and level of education) of the respondents, livestock species kept and ability to identify common livestock diseases based on presenting symptoms. Additionally, the questionnaire captured data on the respondent's knowledge of the history of medicinal plants found in the study area. A majority of the respondents were not keen on stating their exact age thus leading to age being divided into three categories for this study; youth (less than 20 years old), medium aged (between 20 and 40 years old) and seniors (above 40 years of age). Identified plants were collected from their location during field trips within the study area and were further subjected to scientific identification at the University of Limpopo Larry Leach herbarium. Plant parts used, methods of preparation and the conditions for

http://www.aloki.hu ● ISSN 1589 1623 (Print) ● ISSN 1785 0037 (Online)
DOI: http://dx.doi.org/10.15666/aeer/1605_65896605
© 2018, ALÖKI Kft., Budapest, Hungary

which the plants were used were recorded. For the interest of this study, a bark was referred to as the outermost layers of the stem in woody plants while layers covering the roots and branches were referred to as root bark and branches respectively. The data of this study was captured in Microsoft Excel 2013 and statistically analysed using the Statistical Package for Social Sciences (SPSS Inc. 2012). The Z test for comparison of proportions was also used to ascertain statistical significance and $p < 0.05$ was considered significant.

Results

The demographic distribution of the respondents is presented in *Table 1*. The majority of the respondents (57.8%) were males. Almost half of the respondents (49.4%) were in the >40year old age category and the least (17.8%) were in the <20year old category.

Table 1. *Proportional distribution of respondents according to category*

Category	Number of respondents	Proportion (%)
Gender		
Male	104	57.8
Female	76	42.2
Age		
<20years old	32	17.8
20-40years old	59	32.8
>40years old	89	49.4
Education		
None	60	33.3
Primary	29	16.1
Secondary	63	35.0
Tertiary	28	15.6
Main livestock reared		
Cattle	89	49.4
Poultry	52	28.9
Goats	34	18.9
Sheep	5	2.8
Method of animal treatment		
Conventional drugs only	18	10.0
Medicinal herbs only	39	21.7
Combination	123	68.3
Conditions frequently encountered		
Retained placenta	115	63.9
Mastitis	103	57.2
Wounds	97	53.9
Unthriftiness	84	46.7
Fractures	48	26.7
Arthritis	27	15.0
Constipation	19	10.6
Blindness	6	3.3
Overall	180	100

A third of the respondents had no education and yet another third had secondary level education. Of the remaining third, almost equal proportions of respondents had primary (16.1%) and tertiary (15.6%) education. Most of the respondents reared cattle (49.4%)

http://www.aloki.hu ● ISSN 1589 1623 (Print) ● ISSN 1785 0037 (Online)
DOI: http://dx.doi.org/10.15666/aeer/1605_65896605
© 2018, ALÖKI Kft., Budapest, Hungary

followed by poultry (28.9%) and goats (18.9%) whilst very few respondents (2.8%) reared sheep. The majority of the respondents (68.3%) preferred to use a combination of conventional drugs and the least proportion preferred conventional drugs only (10%). The proportion of respondents that preferred medicinal herbs only (21.7%) was significantly smaller than those using a combination and significantly greater than those using conventional drugs only ($P < 0.05$). The conditions that respondents most frequently encountered in livestock were retained placenta (63.9%) followed by mastitis (57.2%), wounds (53.9%), unthriftiness (46.7%), fractures (26.7%), arthritis (15%), constipation (10.6%) and blindness (3.3%).

Gender

Statistical analysis of the results in *Table 2* using the Z test for comparison of proportions showed that the proportion of males using a combination of treatment methods (79.8%) was significantly greater than that of the females (52.7%) ($P < 0.05$). The proportion of females using medicinal herbs (36.8%) only was significantly greater than that of the males (10.6%) ($P < 0.05$). There was no significant difference in the proportions of males and females using conventional drugs only ($P > 0.05$).

Table 2. *Proportional preference of treatment method according to gender, age and educational level*

Category	Conventional drugs only (%)	Medicinal herbs only (%)	Combination (%)	Total (%)
Gender				
Male	9.6	10.6	79.8	100
Female	10.5	36.8	52.7	100
Age				
<20years old	37.5	12.5	50	100
20-40years old	6.7	10.2	83.1	100
>40years old	2.2	32.6	65.2	100
Educational level*				
None	1.7	46.6	51.7	100
Primary	3.4	17.3	79.3	100
Secondary	3.2	6.3	90.5	100
Tertiary	50	7.1	42.9	100
Overall (%)	10	21.7	68.3	100

*The structure of the South Africa education system. Kindergarten is known as 'grade 0' in South Africa, and primary schools are generally divided into junior preparatory schools (grades 0-3) and senior preparatory schools (grades 4-7) before children attend high school (otherwise known as college) from grades 8-12.
https://www.google.com.na/search?q=primary+and+secondary+school+in+south+africa&rlz=1C1CHZL_enNA719NA719&oq=Primary+and+secondary+school+in+South&aqs=chrome.1.69i57j33l5.21755j1j7&sourceid=chrome&ie=UTF-8

Age

Table 2 also showed that a significantly greater proportion of respondents in the 20-40-year-old category (83.1%) preferred to use a combination of treatment methods than in the <20 years old (50%) and the >40 years old category (65.1%) ($P < 0.05$). There was no significant difference between the preferred use of a combination of treatment methods between the <20years old and the >40years old categories ($P > 0.05$). A

http://www.aloki.hu ● ISSN 1589 1623 (Print) ● ISSN 1785 0037 (Online)
DOI: http://dx.doi.org/10.15666/aeer/1605_65896605
© 2018, ALÖKI Kft., Budapest, Hungary

significantly greater proportion of respondents in the >40years old category (32.6%) preferred to use medicinal herbs only ($P < 0.05$). There was no significant difference in the preference of medicinal herbs between the <20 years old and the 20-40 years old categories ($P > 0.05$). A significantly greater proportion of respondents in the <20 years old category (37.5%) preferred to use conventional drugs only ($P < 0.05$). A significantly greater proportion of respondents in the >40years old category (32.6%) preferred to use medicinal herbs only ($P < 0.05$).

Educational level

Table 2 also showed that greater proportions of both primary (79.3%) and secondary-schooled respondents (90.5%) significantly preferred to use a combination of medicinal herbs and conventional drugs for treatment of their livestock ($P < 0.05$). There was, however, no significant difference in the proportions of these two groups ($P > 0.05$). A significantly greater proportion of the unschooled respondents (46.6%) preferred to use medicinal herbs only ($P < 0.05$). There was no significant difference in the proportions of primary (17.3%), secondary (6.3%) and tertiary-schooled respondents (7.1%) that preferred only medicinal herbs as a method of treatment ($P > 0.05$). A significantly greater proportion of the tertiary-schooled respondents (50%) preferred to use conventional drugs only ($P < 0.05$). There was no significant difference in the proportions of primary (3.4%), secondary (3.2%) and unschooled respondents (1.7%) that preferred only conventional drugs as a method of treatment ($P > 0.05$).

As shown in *Table 3* below, *C. abbreviata* (stem bark) and *C. quadrangularis* (branch infusion) were the preferred oral treatments for retained placenta in cattle by the respondents. *P. angolensis* (stem bark) and *C. collinum* (stem bark) were the preferred oral treatments for constipation in cattle by the respondents. *A. crytopoda* (leaf infusion) was the only preferred oral treatment of unthriftness in poultry. The rest of the plants were used topically for treatment of wounds in cattle, sheep and goats (*C. quadrangularis, D. cinerea* and *X. Americana*), arthritis (*S. cupulare*), mastitis (*Z. mucronata*), fractures (*M. eduncularis*) and blindness (*G. herbaceum*) in cattle, sheep and goats.

Discussion

This study has shed some light on the dynamics of use of EVM in Mutale municipality of Vhembe district of South Africa. The study showed that EVM is used more by the older (more than 40 years old) members of the community (49%) than by younger generation (*Table 1*). These results are in agreement with several previous workers who reported that knowledge of medicinal plants use is mostly limited to older people in the communities (Shen et al., 2010; Bartha et al., 2015; Nyahangare et al., 2015; Ahmad et al., 2016; Usha et al., 2016). According to Bartha et al. (2015), the older members of the population have a tendency to choose EVM over allopathic veterinary medicine. This scenario where the aged population is the custodian of EVM and vanguard of its use presents a real risk of permanent loss of this treasure of knowledge that has been gathered over generations. Ahmad et al. (2016) contends that vesting the EVM in older members of the community is vulnerable to and may be undermined by mortality. Consequently, urgent documentation of EVM in rural communities such as Mutale is required so as to conserve such knowledge before this biocultural heritage disappears altogether.

http://www.aloki.hu ● ISSN 1589 1623 (Print) ● ISSN 1785 0037 (Online)
DOI: http://dx.doi.org/10.15666/aeer/1605_65896605
© 2018, ALÖKI Kft., Budapest, Hungary

Table 3. *Plants and plant parts used by respondents for treatment of livestock conditions*

Botanical name	English/local name	Indications	Preparation used	Route of administration
Caesalpiniaceae Cassia abbreviate	Long pod cassia Muboma	Retained placenta in cattle	Stem bark infusion	Oral
Vitaceae Cissus quadrangularis	Devil's backbone Malongakanya	Retained placenta in cattle Wounds in cattle	Branch infusion Branch infusion	Oral Topical
Asphodelaceae Aloe cryptopoda	Dr Kirk's aloe Tshikhopha	Unthriftiness in poultry	Leaf infusion	Oral
Fabaceae Pterocarpus angolensis	Bloodwoood/wild teak Mutondo	Constipation in cattle	Stem bark infusion	Oral
Euphorbiaceae Synadenium cupulare	Dead-man's tree Muswoswo	Arthritis in cattle, sheep and goats	Resin	Topical
Combretaceae Combretum collinum	Bicoloured bushwillow Muvuvha	Constipation in cattle	Stem Bark	Oral
Olacaceae Ximenia americana	Tallow wood/Sour plum Muthanzwa	Wounds in cattle sheep and goats	Root bark powder	Topical
Celastraceae Maytenus eduncularis	Silkybarks Mukwatukwatu	Fractures in cattle	Root bark paste	Topical
Mimosaceae Dichrostachys cinerea	Sicklebush/ Kalahari Christmas tree Murenzhe	Wounds in sheep and goats	Fried fruit powder	Topical
Rhamnaceae Ziziphus mucronata	Buffalo thorn tree Mutshetshete	Mastitis in cattle	Leaf paste	Topical
Malvaceae Gossypium herbaceum	Levant cotton Muluvha	Blindness in cattle, sheep and goats	Seed powder	Topical

According to our results, more males (57.8%) than females (42.2%) responded to our questionnaire. The majority of them reared cattle compared to other livestock species (*Table 1*). In spite of there being more male that female respondents, the results show that EVM is made use of mainly by females (*Table 2*) in the more than 40-year age group (*Table 3*). These findings are similar to those reported by Mwale and Masika (2009) in the Eastern Cape and Luseba and Van der Merwe (2006) in Limpopo Province of South Africa. Elsewhere in Ethiopia, Teklehaymanot (2017) reported that more males than females were involved in EVM. Similarly, Taliq et al. (2014) reported that, in the Kohat region of Pakistan, women and younger generations were not

http://www.aloki.hu ● ISSN 1589 1623 (Print) ● ISSN 1785 0037 (Online)
DOI: http://dx.doi.org/10.15666/aeer/1605_65896605
© 2018, ALÖKI Kft., Budapest, Hungary

involved in the use of EVM. Taliq et al. (2014) reported that men had better knowledge regarding ethno veterinary practices as compared to women. The reason advanced for this observation was that men are mostly favoured in shift of knowledge while women in the majority of the cultures are relegated to family care. The noticeable gender bias observed in our study suggests limited involvement of men in cattle production and herd health in the Mutale local municipality.

The study also shows that EMV is embraced more by the members of the society with no education (46.6%) or with primary education (17.3%) (*Table 4*). This scenario is not sustainable, and the literate section of the society must begin to embrace and document the use of such practices. The fact that the majority (78.3%) of the farmers use EVM in one way or another (conventional and allopathic veterinary medicine 68.3% and EVM alone 10%) is encouraging. This means that only 21% of the farmers in Mutale municipality have not yet adopted the use of EVM. Use of a combination of EVM and allopathic medicine is not unique to South Africa and has been reported elsewhere (Claudell et al., 2017). However, it is not clear from our results if the trend towards adoption of EVM is increasing or decreasing. Given that in South Africa, as in other African countries, many veterinarians and decision makers have not critically examined and incorporated the potential of EVM into primary animal healthcare, the future of EVM appears to be bleak. The fact that EVM has not yet been incorporated into technical and undergraduate veterinary training curricula does not bode well for the future of this practise either. Empirical evidence suggests that many in positions of veterinary authority tend to ignore or ridicule EVM paints a gloomy picture on the adoption of EVM in South Africa. There is need for the documentation, validation and incorporation of EVM in primary animal healthcare in South Africa to the benefit of future generations. Enhancement of this approach is most likely to spur research and development of EVM and undoubtedly enable it to make immense strides in the development of the livestock industry.

Rural farmers rely economically on small scale livestock production which may be complemented by seasonal crop production. Particularly in tropical areas, animal husbandry plays a key role in rural economies as a source of cash income and employment (Herrero et al., 2013). In rural communities where livestock theft is a challenge, farmers keep their livestock in the kraals at night and provide them access to grazing during daylight hours, thus, keeping themselves updated on their livestock's health status. When abnormal health conditions are identified, farmers with little or no access to the modern veterinary services resort to indigenous methods of treating identified diseases. Results of the present study complement the previous findings that wild fodder plants and traditional EVM practices based on medicinal plants can help local communities to cope with environmental and socioeconomic disturbances within livestock systems. As pointed out by several studies (Gómez-Baggethum et al., 2012), transmission of this biocultural heritage is at the base of human adaptive strategies and can play a critical role in minimizing the impact of disturbances on livelihood of local communities, especially those living in highly unpredictable systems like *Mopane* woodlands. On the other hand, these biological resources could be expected to play an increasingly critical role in securing feed and health for livestock in the near future. Furthermore, results from the present study supported the view that initiatives to conserve indigenous knowledge is paramount as loss of this vital knowledge system affects rural communities (Dwebaa and Mearns, 2011). Recognizing problems at community level is an essential step for supporting any interventional activities

http://www.aloki.hu ● ISSN 1589 1623 (Print) ● ISSN 1785 0037 (Online)
DOI: http://dx.doi.org/10.15666/aeer/1605_65896605
© 2018, ALÖKI Kft., Budapest, Hungary

(Ravikumar et al., 2016). Local communities need to be in forefront towards knowledge creation, distribution and sharing system (Lwoga et al., 2010). Creative expressions of informal society can provide solutions and accessibility to appropriate technology (Kumar et al., 2013).

Previous research results revealed several plants that can be used reliably and safely to treat livestock. Legal registration of these botanical products is usually not required for their promotion. This approach offers sustainable strategies directed towards developing sound and appropriate animal health care systems suitable and relevant to rural communities in improving livestock performance and production and, hence, livelihood (Stevenson et al., 2010). The current study identified nine livestock conditions which were treated by 11 plants belonging to 10 families. Among the livestock conditions reported mastitis, retained placenta and wounds were frequently mentioned to occur in cattle. These livestock conditions were similar to the ones reported elsewhere in literature and treated by the use of medicinal plants (Dilshad et al., 2010; Gebrezgabiher et al., 2013; Luseba and Tshisikhawe, 2013). Retained placenta was found to be most common in domestic animals and two plant families were used against this condition (*Table 1*). This contradicts with Taliq et al. (2014) who reported gastrointestinal infections to be most common in domestic animals. Similar to previous studies, farmers in Mutale municipality reported that they were able to define diseases using clinical signs. However, the use of clinical signs only for diagnosis of diseases is not effective as it reduces the accuracy of the diagnosis thereby resulting in incorrect dosages and reduced effectiveness of herbal remedies.

Although livestock conditions in this study are similar to the ones reported previously, different medicinal plants, methods of preparation and to a certain extent administering methods were used. Lack of knowledge or prior experience with alternative therapies can influence willingness of farmers to use plants in treatment of ailments (Richert et al., 2013). Furthermore, different production systems influence decision by farmers to implement disease control strategies (Jemberu et al., 2015). Fabaceae family was only mentioned for the treatment of constipation in cattle. This observation is different from that of Appidi et al. (2008) who in an ethno veterinary survey reported Fabaceae family as the most commonly used plant by livestock farmers. Luseba and Tshisikhawe (2013) reported the use of *Bolusanthus speciosus* (Fabaceae) as a remedy for retained placenta when orally supplied in cattle after crushing and immersing the roots in water for 12 h. In this study when retained placenta was identified two plants (*Cassia abbreviata* and *Cissus quadrangularis*) from two different families (Caesalpiniaceae and Vitaceae) were used respectively. The bark of *Cassia abbreviata* when crushed and infused in water for more than 30 minutes (or less if shaking is done to facilitate quicker extraction of the chemicals) was reportedly used for treatment of retained placenta in the current study. The solution was reported to be administered orally until the complete discharge of placental membranes (*Table 2*). The difference among studies might be related to the differences in the dominant vegetation of the areas or might be associated with traditional beliefs of different cultures in traditional use of specific plants. Plants from the Asteraceae family were reportedly popular among traditional healers in Pakistan for the preparation of traditional medicines used in treatment of different livestock and human ailments (Khan et al., 2014; Akhtar et al., 2013). The fleshy branches of *Cissus quadrangularis* were crushed and infused in water; the solution was then used to clean the wound area. These results are in line with the findings of Gebrezgabiher et al. (2013) who reported that wound

http://www.aloki.hu ● ISSN 1589 1623 (Print) ● ISSN 1785 0037 (Online)
DOI: http://dx.doi.org/10.15666/aeer/1605_65896605
© 2018, ALÖKI Kft., Budapest, Hungary

treatment was done by topical application of the medication. Previous studies reported that *Cissus quadrangularis* exhibits strong antioxidant and free radical scavenging ability due to the presence of β-carotene (Mallik and Shymala Devi, 2005).

A high tannin-containing plant species *Ziziphus mucronata* was frequently mentioned by the respondents for treating mastitis in cattle. These results are in agreement with the findings of Dilshad et al. (2010) who reported the use of tannin containing plants for treating mastitis in dairy cows. *Combcv xbretum collium* was used in ruminants as a remedy to relieve constipation. According to Edwards et al. (1995), leaves and bark of *Combretum collium* are widely used in local medicine to treat various intestinal disorders including diarrhea, colic and jaundice. Interestingly, in the present study the bark of the same plant species was reportedly used for treating constipation. *Pterocarpus angolensis*, well known for its high tannin content, was also mentioned with respect to constipation (Luseba et al., 2007). Tannins occur naturally in plants and have been reported to have a wide range of medicinal uses due to their anti-inflammatory, anti-fungal, mucoprotectant, antioxidant, enzyme inhibition and anti-bacterial properties (McGaw et al., 2007). Swollen joints were reportedly treated by topical application of the latex-like sap from the branches of *Synadenium cupulare*. The roots of this plant have been reported to possess medicinal properties (Chauke et al., 2015). Respondents reported the use of *Aloe* species for treating poultry conditions. The findings are similar to those from previous studies where *Aloe* species were commonly used for treating poultry diseases including Newcastle disease (Mwale et al., 2005; Adedeji et al., 2013). Patterns in the ethnographic literature indicate that widespread, common *Aloe* species in Southern Africa are more likely to be popular, multi-use ethno medicines than rare species with narrow ranges (Glen and Hardy, 2006). Aerial parts of the plants were frequently reportedly used instead of beneath ground parts (*Table 5*). These results are in line with those of Ul Hassan et al. (2014); Luseba and Tshisikhawe (2013) who reported the frequent use of aerial plant parts containing medicinal properties in a plant instead of parts beneath the ground.

The present results are in agreement with other studies where roots were also used in ethno veterinary practices (Cheikhyoussef et al., 2011). However, the use of roots in preparation of herbal remedies is not advisable, as this results in loss of plants from their natural habitats. In the present study, leaves were only mentioned for the family Rhamnaceae (*Table 3*) in contradiction with previous findings which reported a more frequent use of leaves followed by whole plant (Tariq et al., 2014; Gebrezgabiher et al., 2013; Maphosa and Masika, 2010; Setlalekgomo and Setlalekgomo, 2013; Bhatt, 2013). The use of leaves in preparation of herbal remedies is considered a sustainable type of harvesting as it reduces loss of plants from the natural habitats. Farmers in Mutale municipality ought to use aerial plant parts such as leaves rather than the whole plant or roots to prevent plants from becoming extinct (Maroyi, 2012). Furthermore, leaves are the main site of the photosynthetic apparatus and are involved in a variety of physiological processes of plants and produce numerous secondary metabolites that could be a possible reason for their effectiveness and efficacy against different livestock diseases (Bhatt, 2013).

In the current study, few plants possessed medicinal properties in their fruits. Hassan et al. (2013) reported the use of a whole plant for medicinal purposes. In our study there was no case where respondents cited the use of a whole plant for medicinal purposes. This is a good indication since the use of whole plants could lead to a very destructive type of harvesting especially for rare and slow-growing plants from a conservation point

http://www.aloki.hu ● ISSN 1589 1623 (Print) ● ISSN 1785 0037 (Online)
DOI: http://dx.doi.org/10.15666/aeer/1605_65896605
© 2018, ALÖKI Kft., Budapest, Hungary

of view (Tariq et al., 2014). Furthermore, a majority of the medicinal plants cited in this study were not cultivated by the respondents. However, one farmer reported to have planted a shrub (*Synadenium cupulare*) specifically for medicinal purposes. A study conducted in Pakistan by Dilshad et al. (2010), reported the use of cultivated plants (*Oryza sativa* and *Triticum aestivum*) for treating mastitis in dairy cows. A majority of the Mutale farmers interviewed collected the medicinal herbs from their natural habitats. This is a good indication since it is advisable to use wild plants that grow under stress conditions and competition, as they possess secondary metabolites which improve their medicinal properties (Schippmann et al., 2003). In addition, banana roots (*Musa paradisiacal*) were reported to treat internal parasites (worms) in animals when crushed and administered orally after infusion in water. Most plant parts were crushed and infused in water to influence easier extraction of the chemicals within. The methods of application used by local farmers in the current study did not differ from the methods reported by Sindhu et al. (2010) among Pakistan local farmers. Crushing of plant parts and mixing with water were common when medication was administered orally. This is in agreement with Maphosa and Masika (2010) and (Djoueche et al., 2011). Deeba (2009) indicated that powdering or boiling is the most common method of drugs extraction. These findings are in line with a study conducted in the Malakand valley of Pakistan (Ul Hassan et al., 2014). The difference in application methods are in agreement with the findings of McCorkle and Mathias-Mundy (1992) who reported that the mode of preparation of the medication depends on active ingredient to be extracted, and the method of administration.

Oral and topical routes were the only mentioned routes of administration in the present study. This agrees with the findings from previous studies (Tariq et al., 2014). Similar to what was reported in other studies, the ethno veterinary practices of livestock farmers in Mutale municipality are not extensively documented and are mostly passed orally from elders (Farooq et al., 2009). It is important to document ethno-veterinary knowledge so that it will not be lost and to increase the use of common plants.

Conclusion

The present study revealed that EVM is an important part of the livelihood of local farmers residing in the Mutale local municipality. The concept of EVM is highly appreciated and embraced mostly by old farmers who indicated to have acquired the knowledge from their elders' earlier. At present the transfer of this valuable knowledge to younger generations is a challenge considering the substantial development and education system limited to modernized drugs. EVM should not be neglected since it is the only hope for resource limited livestock farmers. However, further studies are still needed to educate farmers on sustainable utilization of indigenous natural resources and evaluation of the chemical composition of medicinal plants reported in this study. Gaining knowledge on the chemical composition of medicinal plants may be beneficial in drug development. It is expected that the situation regarding the use of plants to treat livestock in Mutale Municipality has most probably remained the same or, better still, improved.

Acknowledgements. The authors wish to express their gratitude to the livestock farmers of Mutale local municipality for their cooperation and University of Limpopo's Department of Agricultural Economics and Animal Production for allowing us to carry out this study.

http://www.aloki.hu ● ISSN 1589 1623 (Print) ● ISSN 1785 0037 (Online)
DOI: http://dx.doi.org/10.15666/aeer/1605_65896605
© 2018, ALÖKI Kft., Budapest, Hungary

Author contributions. Teedzai Chitura contributed to the supervision, funding acquisition and execution of the study, writing and editing of the final manuscript. Borden Mushonga contributed to the project planning, implementation, writing of the original draft and editing the final manuscript. Pfunzo Tonny Muvhali contributed to the study design and investigation. Erick Kandiwa contributed to planning, implementation, data curation, writing and editing of the manuscript. Kamogelo Shai contributed to the review and editing of the manuscript.

REFERENCES

[1] Adamu, M., Naidoo, V., Eloff, J. N. (2014): The antibacterial activity, antioxidant activity and selectivity index of leaf extracts of thirteen South African tree species used in ethnoveterinary medicine to treat helminth infections. – BMC Veterinary Research 10(1): 52.

[2] Adedeji, O. S., Ogunsina, T. K., Akinwumi, A. O., Ameen, S. A., Ojebiyi, O. O., Akinlade, J. A. (2013): Ethno veterinary medicine in African organic poultry production. – International Food Research Journal 20: 527-532.

[3] Ahmad, S., Gangoo, S. A., Sultan, S. M., Dar, M. D. (2016): Ethnoveterinary practices and use of herbal medicine by pastoralists of Himalaya: a review. – Annals of Biology 32(2): 260-268.

[4] Akhtar, N., Rashid, A., Murad, W., Bergmeier, E. (2013): Diversity and use of ethno-medicinal plants in the region of Swat, North Pakistan. – Journal of Ethnobiology and Ethnomedicine 9: 9-25.

[5] Appidi, J. R., Grierson, D. S., Afolayan, A. J. (2008): Ethnobotanical study of plants used for the treatment of diarrhoea in the Eastern Cape, South Africa. – Pakistan Journal of Biological Sciences 11(15): 1961-1963.

[6] Bartha, S. G., Quave, C. L., Balogh, L., Papp, N. (2015): Ethnoveterinary practices of Covasna County, Transylvania, Romania. – Journal of Ethnobiology and Ethnomedicine 11(1): 35.

[7] Bhatt, A., Singh, P., Kumar, V., Baunthiya, M. (2013): Documentation of ethno - veterinary practices used for treatments of different ailments in Garhwal Himalayan Region. – Journal of Environmental Nanotechnology 2: 22-29.

[8] Caudell, M. A., Quinlan, M. B., Quinlan, R. J., Call, D. R. (2017): Medical pluralism and livestock health: ethnomedical and biomedical veterinary knowledge among East African agropastoralists. – Journal of Ethnobiology and Ethnomedicine 13(1): 7.

[9] Chauke, M. A., Shai, L. J., Mogale, M. A., Tshisikhawe, M. P., Mokgotho, M. P. (2015): Medicinal plant use of villagers in the Mopani district, Limpopo Province, South Africa. – African Journal of Traditional, Complementary and Alternative Medicines 12: 9-26.

[10] Cheikhyoussef, A., Shapi, M., Matengu, K., Ashekele, H. M. (2011): Ethnobotanical study of indigenous knowledge on medicinal plant use by traditional healers in Oshikoto region, Namibia. – Journal of Ethnobiology and Ethnomedicine 7(10): 1-11.

[11] Chinsembu, K. C., Negumbo, J., Likando, M., Mbangu, A. (2014): An ethnobotanical study of medicinal plants used to treat livestock diseases in Onayena and Katima Mulilo, Namibia. – South African Journal of Botany 94: 101-107.

[12] Deeba, F. (2009): Documentation of ethno veterinary practices in urban and periurban areas of Faisalabad, Pakistan. – PhD Thesis, University of Agriculture, Faisalabad Pakistan.

[13] Dilshad, S. M. R., Rehman, N. U., Ahmad, N., Iqbal, A. (2010): Documentation of ethnoveterinary practices for mastitis in dairy animals in Pakistan. – Pakistan Veterinary Journal 30: 167-171.

[14] Djoueche, C. M., Azebaze, A. B., Dongmo, A. B. (2011): Investigation of plants used for the ethno veterinary control of gastro-intestinal parasites in Benoue Region, Cameroon. – Tropicultura 29(4): 205-211.

http://www.aloki.hu ● ISSN 1589 1623 (Print) ● ISSN 1785 0037 (Online)
DOI: http://dx.doi.org/10.15666/aeer/1605_65896605
© 2018, ALÖKI Kft., Budapest, Hungary

[15] Doumbia, D., Van Paassen, A., Oosting, S. J., Van der Zijpp, A. J. (2012): Livestock in the rice based economy of Office du Niger: The development potential for increased croplivestock integration through multi-actor processes. – Wageningen Journal of Life Sciences 60(63): 101-114.
[16] Dwebaa, T. P., Mearns, M. A. (2011): Conserving indigenous knowledge as the key to the current and future use of traditional vegetables. – International Journal of Information Management 31(6): 564-571.
[17] Edwards, S., Tadesse, M., Hedberg, I. (1995): Flora of Ethiopia and Eritrea, Volume 2, Part 2. Canellaceae to Euphorbiaceae. Review by: Mike Lock. – Royal Botanic Garden Kew 53: 758-760.
[18] Farooq, M., Wahid, A., Kobayash, N., Fujita, D., Basra, S. M. A. (2009): Plant drought stress: effects, mechanisms and management. – Agronomy for Sustainable Development 29(1): 185-212.
[19] Gabanakgosi, K., Moreki, J. C., Nsoso, S. J., Tsopito, C. (2012): Ethnoveterinary medicine usage in family chickens in the selected four villages of Botswana. – Journal of Veterinary Advances 2(12): 586-594.
[20] Gebrezgabiher, G., Kalayou, S., Sahle, S. (2013): An ethno-veterinary survey of medicinal plants in Woredas of Tigray region, Northern Ethiopia. – Internal Journal of Biodiversity and Conservation 5: 89-97.
[21] Getachew, T., Kebede, E., Ameha, N., Terefe, T. A. (2015): Village chicken husbandry practice, marketing and constraints in Eastern Ethiopia. – Journal of Animal and Poultry Sciences 5(4): 104-108.
[22] Glen, H. F., Hardy, D. S. (2006): Aloaceae (First part): Aloe. – In: Germishuizen, G. (ed.) Flora of Southern Africa. 5, Fascicle. National Botanical Institute, South Africa.
[23] Gómez-Baggethum, E., Reyes-Gacia, V., Olson, P., Montes, C. (2012): Traditional ecological knowledge and community resilience to environmental extremes: A case study in Doñana, SW Spain. – Global Environmental Change 22(3): 640-650.
[24] Hassan, S. H. A., Fry, J. R., AbuBakar, M. F. (2013): Phytochemicals content, antioxidant activity and acetylcholinesterase inhibition properties of indigenous Garcinia parvifolia fruit. – Biomedical Research International 7: 201.
[25] Herrero, M., Grace, D., Njuki, J., Johnson, N., Enahoro, D., Silvestri, S., Rufino, M. C. (2013): The roles of livestock in developing countries. – Animal 7: 3-18.
[26] Jemberu, W. T., Mourits, M. C. M., Hogeveen, H. (2015): Farmers' intentions to implement foot and mouth disease control measures in Ethiopia. – PLoS One. 10(9): e0138363. http:// dx.doi.org/10.1371/journal.pone.0138363.
[27] Khan, I., AbdElsalam, N. M., Fouad, H. et al. (2014): Application of ethnobotanical indices on the use of traditional medicines against common diseases. – Evidence Based Complementary and Alternative Medicine. http://dx.doi.org/10.1155/2014/635371.
[28] Kumar, V., Chand, V. S., Zhang, L., Hoppers, C. A. O., Zhang, W., Esders, M., Gupta, A. K. (2013): Grassroots innovations for inclusive development: need for a paradigmatic shift. – Vikalpa 38(3): 103-122.
[29] Lans, C., Bevan, J., Turner, N. (2012): Plants used in rearing locally-grown organic small-scale poultry and rabbits in British Columbia, Canada. – Current Nutrition and Food Science 8(3): 220-234.
[30] Luseba, D., Tshisikhawe, M. P. (2013): Medicinal plants used in the treatment of livestock disease in Vhembe region, Limpopo Province, South Africa. – Journal of Medicinal Plant Research 7: 593-601.
[31] Luseba, D., Van der Merwe, D. (2006): Ethnoveterinary medicine practices among Tsonga speaking people of South Africa. – Onderstepoort Journal of Veterinary Research 73: 115-122.
[32] Luseba, D., Elgorashi, E. E., Ntloedibe, D. T., Staden, J. V. (2007): Antibacterial, anti-inflammatory and mutagenic effects of some herbal plants used in South Africa for the

http://www.aloki.hu ● ISSN 1589 1623 (Print) ● ISSN 1785 0037 (Online)
DOI: http://dx.doi.org/10.15666/aeer/1605_65896605
© 2018, ALÖKI Kft., Budapest, Hungary

treatment of wounds and retained placenta in livestock. – South African Journal of Botany 73: 378-383.

[33] Lwoga, E. T., Ngulube, P., Stilwell, C. (2010): Understanding indigenous knowledge: Bridging the knowledge gap through a knowledge creation model for agricultural development. – South African Journal of Information Management 12(1): 436.

[34] Makhado, R. A., Potgieter, M. J., Wessels, D. C. J., Saidi, A. T., Masehela, K. L. (2012): Use of Mopane woodland resources and associated woodland management challenges in rural areas of South Africa. – Journal of Applied Ethnobotanical Research 10: 369-380.

[35] Makhado, R. A., Potgieter, M. J., Timberlake, J., Gumbo, D. (2014): A review of the significance of Mopane products to rural people's livelihoods in Southern Africa. – Trans. Royal Soc. South Africa 69(2): 117-122.

[36] Mallik, J., Shyamala Devi, C. S. (2005): In vitro and in vivo evaluation of free radical scavenging potential of Cissus quadrangularis. – African Journal of Biomedical Research 8: 95-99.

[37] Mamidala, E. (2013): Ethnobotanical survey in different mandals of Adilabad district, Andhra Pradesh, India. – International Journal of Science 2: 77-83.

[38] Maphosa, V., Masika, P. J. (2010): Ethnoveterinary uses of medicinal plants: A survey of plants used in the ethnoveterinary control of gastrointestinal parasites of goats in the Eastern Cape Province, South Africa. – Pharmaceutical Biology 48(6): 697-702.

[39] Maphosa, V., Tshisikhawe, M. P., Thembo, K., Masika, P. J. (2010): Ethnoveterinary Medicine in Southern Africa. – In: Katerere, D. R., Luseba, D. (eds.) Ethnoveterinary Botanical Medicine Herbal Medicines for Animal Health. CRC Press, Boca Raton.

[40] Marandure, T. (2016): Concepts and key issues of ethnoveterinary medicine in Africa: A review of its application in Zimbabwe. – African Journal of Agricultural Research 11(20): 1836-1841.

[41] Maroyi, A. (2012): Use of traditional veterinary medicine in Nhema communal area of the Midlands Province, Zimbabwe. – African Journal of Traditional, Complementary and Alternative Medicines 9(3): 315-322.

[42] Mayer, M., Vogl, C. R., Amorena, M., Hamburger, M., Walkenhorst, M. (2014): Treatment of organic livestock with medicinal plants: a systematic review of European ethnoveterinary research. – Complementary Medicine Research 21(6): 375-386.

[43] McCorkle, C. M., Mathias-Mundy, E. (1992): Ethno veterinary medicine in Africa. – Journal of International African Institute 62: 59-93.

[44] McGaw, L. J., Eloff, J. N. (2008): Ethnoveterinary use of southern African plants and scientific evaluation of their medicinal properties. – Journal of Ethnopharmacology 119(3): 559-574.

[45] McGaw, L. J., Van der Merwe, D., Eloff, J. N. (2007): In vitro anthelmintic, antibacterial and cytotoxic effects of extracts from plants used in South African ethno veterinary medicine. – Veterinary Journal 173: 366-372.

[46] Moyo, B., Masika, P. J., Dube, S., Maphosa, V. (2009): An in-vivo study of the efficacy and safety of ethnoveterinary remedies used to control cattle ticks by rural farmers in the Eastern Cape Province of South Africa. – Tropical Animal Health and Production 41: 1569-1576.

[47] Moyo, B., Ndlovu, L., Moyo, S., Masika, P. J., Muchenje, V., Ndhlovu, D. N., Maphosa, V. (2013): Alternative remedies and approaches used by resource challenged farmers in the management of black leg disease in cattle in Umzingwane district of Matebeleland South. – Internal Journal of Livestock Production 6: 77-102.

[48] Mucina, L., Rutherford, M. C. (2006): The Vegetation of South Africa, Lesotho and Swaziland. Strelitzia 19. – South African National Biodiversity Institute, Pretoria.

[49] Munda, S., Pandey, R., Bhojne, G. R., Dakshinkar, N., Kinhekar, A. S., Kumar, V., Ravikumar, R. K., Kumar, V. (2016): Indigenous Knowledge Research System (IKRS) for treatment of bloat and its significance towards greenhouse gas emission: Jharkhand, India. – Advances in Animal and Veterinary Sciences 4(5): 241-249.

http://www.aloki.hu ● ISSN 1589 1623 (Print) ● ISSN 1785 0037 (Online)
DOI: http://dx.doi.org/10.15666/aeer/1605_65896605
© 2018, ALÖKI Kft., Budapest, Hungary

[50] Mutibvu, T., Maburutse, B. E., Mbiriri, D. T., Kashangura, M. T. (2012): Constraints and opportunities for increased livestock production in communal areas: A case study of Simbe, Zimbabwe. – Livestock Research and Rural Development 24: 9.
[51] Mwale, M., Masika, P. J. (2009): Ethnoveterinary control of parasites, management and role of village chickens in rural households of Centane district in the Eastern Cape, South Africa. – Tropical Animal Health and Production 41(8): 1685-1693.
[52] Mwale, M., Bhebhe, E., Chimoyo, M., Halimani, T. E. (2005): Use of herbal plants in poultry health management in the Mushagashe small-scale commercial farming area in Zimbabwe. – International Journal of Applied Research in Veterinary Medicine 3: 163-170.
[53] Ndhlala, A. R., Amoo, S. O., Stafford, G. I., Finnie, J. F., Van Staden, J. (2009): Antimicrobial, anti-inflammatory and mutagenic investigation of the South African tree aloe (Aloe barberae). – Journal of Ethnopharmacology 124(3): 404-408.
[54] Notenbaert, A., Pfeifer, C., Silvestri, S., Herrero, M. (2017): Targeting, out-scaling and prioritising climate-smart interventions in agricultural systems: Lessons from applying a generic framework to the livestock sector in sub-Saharan Africa. – Agricultural Systems 151: 153-162.
[55] Nyahangare, E. T., Mvumi, B. M., Mutibvu, T. (2015): Ethno veterinary plants and practices used for ecto parasites control in semi-arid small holder farming areas of Zimbabwe. – Journal of Ethnobiology and Ethno Medicine 11: 30.
[56] Paindla, P., Vijayagiri, R. C., Mamid, E. (2013): Ethno survey in different madals of Adilabad District, Andhra Pradesh, India. – International Journal of Science 2: 77-83.
[57] Raikwar, A., Maurya, P. – (2015): Ethnoveterinary medicine: in present perspective. International Journal of Agricultural Sciences and Veterinary Medicine 3(1): 44-49.
[58] Raot, U. S., Parmar, M., Patel, P., Patel, R., Gogoi, D. M., Patel, J., Sivapregasam, V., Kumar, V., Ravikumar, R. K., Kumar, V. (2016): Value addition of novel herbal livestock medication Mastiherb in treatment of mastitis sustained by creative communities from the regions of Dang, Gujarat. – International Journal of Bio-resource and Stress Management 7(3): 501-507.
[59] Ravikumar, R. K., Dutta, L., Kinhekar, A. S., Kumar, V. (2016): People's knowledge for addressing societal needs: Lessons learnt while engaging farming communities as a part of research system. – Advances in Animal and Veterinary Sciences 4(1): 1-8.
[60] Richert, R. M., Cicconi, K. M., Gamroth, M. J., Schukken, Y. H., Stiglbauer, K. E., Ruegg, P. L. (2013): Risk factors for clinical mastitis, ketosis, and pneumonia in dairy cattle on organic and small conventional farms in the United States. – Journal of Dairy Science 96: 1-17.
[61] Ritter, R. A., Monteiro, M. V. B., Monteiro, F. O. B., Rodrigues, S. T., Soares, M. L., Silva, J. C. R., Palha, M. D. C., Biondi, G. F., Rahal, S. C.,. Tourinho, M. M. (2012): Ethnoveterinary knowledge and practices at Colaresisland, Para State, eastern Amazon, Brazil. – Brazilian Journal of Pharmacognosy 144: 346-352.
[62] S. A. Explorer (2014): Mutale climate. – http://www.saexplorer.co.za/south-africa/climate/mutale_climate.asp (accessed on 23 April 2014).
[63] Setlalekgomo, M., Setlalekgomo, T. (2013): The use of ethnoveterinary medicine in goats in Lentsweletau Village in Kweneng District of Botswana. – Journal of Veterinary Advances 7: 197-202.
[64] Shamim, A., Hassan, M. U., Yousaf, A., Iqbal, M. F., Zafar, M. A., Siddique, R. M., Abubakar, M. (2015): Occurrence and identification of Emeria species in broiler rearing under traditional system. – Journal of Agricultural Science and Technology 57: 41.
[65] Shen, S., Qian, J., Ren, J. (2010): Ethnoveterinary plant remedies used by Nu people in NW Yunnan of China. – Journal of Ethnobiology and Ethnomedicine 6(1): 24.
[66] Sindhu, Z., Iqbal, Z., Khan, M. N., Jonsson, N. N., Siddique, M. (2010): Documentation of ethnoveterinary practices used for treatment of different ailments in a selected hilly area of Pakistan. – International Journal of Agriculture and Biology 12: 353-358.

http://www.aloki.hu ● ISSN 1589 1623 (Print) ● ISSN 1785 0037 (Online)
DOI: http://dx.doi.org/10.15666/aeer/1605_65896605
© 2018, ALÖKI Kft., Budapest, Hungary

[67] Sserunkuma, P., McGaw, L. J., Nsahlai, I. V., Van Staden, J. (2017): Selected southern African medicinal plants with low cytotoxicity and good activity against bovine mastitis pathogens. – South African Journal of Botany 111: 242-247.
[68] Stevenson, P., Simmonds, M., Belmain, S. (2010): Caesalpinioid Woodlands of Southern Africa: Optimising the Use of Pesticidal Plants. Chatham: Southern African Pesticidal Plants (SAPP) Project. Final Technical Report. – Natural Resources Institute, University of Greenwich.
[69] Tariq, A., Hassan, U. H., Murad, W. et al. (2014): Ethnoveterinary study of medicinal plants in Malakand Valley, District Dir (Lower), Khyber Pakhtunkhwa, Pakistan. – Irish Veterinary Journal 67: 6.
[70] Teklehaymanot, T. (2017): An ethnobotanical survey of medicinal and edible plants of Yalo Woreda in Afar regional state, Ethiopia. – Journal of Ethnobiology and Ethno Medicine 13(1): 40.
[71] Tyasi, T. L., Nkohla, M. B. (2015): In-vivo validation of the Elephantorrhiza elephantina's efficacy as alternative in the control of coccidia infections in goats. – African Journal of Environmental Sciences and Technology 3: 225-229.
[72] Ul Hassan, H., Murad, W., Akash Tariq, A., Ahmad, A. (2014): Ethnoveterinary study of medicinal plants in Malakand Valley, District Dir (Lower), Khyber Pakhtunkhwa, Pakistan. – Irish Veterinary Journal 67: 1-6.
[73] Usha, S., Rajasekaran, C., Siva, R. (2016): Ethnoveterinary medicine of the Shervaroy Hills of Eastern Ghats, India as alternative medicine for animals. – Journal of Traditional and Complementary Medicine 6(1): 118-125.
[74] Vijayagiri, R. C., Mamidala, E. (2012): Ethnobotanical investigations among traditional healers in Warangal district of Andhra Pradesh, India. – Pharmacognosy Journal 4(34): 13-17.

http://www.aloki.hu ● ISSN 1589 1623 (Print) ● ISSN 1785 0037 (Online)
DOI: http://dx.doi.org/10.15666/aeer/1605_65896605
© 2018, ALÖKI Kft., Budapest, Hungary

SOCIO-ENVIRONMENTAL IMPACTS OF LAND USE/COVER CHANGE IN ETHIOPIAN CENTRAL RIFT VALLEY LAKES REGION, EAST AFRICA

BEKELE, B.[1,2] – WU, W.[1,3*] – LEGESSE, A.[4] – TEMESGEN, H.[5] – YIRSAW, E.[5]

[1]*College of Land Management, Nanjing Agricultural University, Nanjing 210095, China*
(e-mail: B. Bekele – belewbekele@yahoo.com)

[2]*Department of Natural Resources Management, Assosa ATVET College, Assosa 242, Ethiopia*

[3]*National and Local Joint Engineering Research Center for Rural Land Resources Use and Consolidation, Nanjing 210095, China*

[4]*Department of Geography and Environmental Studies, Dilla University, Dilla 419, Ethiopia*
(e-mail: A. Legesse – abiyottura@gmail.com)

[5]*Department of Natural Resources Management, Dilla University, Dilla 419, Ethiopia*
(e-mail: H. Temesgen – habte023@yahoo.com, E. Yirsaw – eshetu.yirsaw@yahoo.com)

**Corresponding author*
e-mail: ww@njau.edu.cn; phone: +86-137-7065-1675

(Received 27th Jun 2018; accepted 13th Sep 2018)

Abstract. Unregulated land use/cover change (LUCC) has imposed significant local, regional and global impacts on livelihood and environment, particularly in sub-Saharan Africa. Previous studies well documented the extent and drivers of such spectacular LUCC in East Africa. However, data on regional/local impacts particularly that combine its socioeconomic and environmental effects are very scanty currently. Hence, this study is aimed to assess the socio-environmental impacts of LUCC in more dynamic and fragile landscapes of the Ethiopian Central Rift Valley lakes region. We used a combination of data from Remote Sensing, GIS-based processing, household survey and meteorological stations to quantify and analyze LUCC impacts. Results indicated that a rapid LUCC has occurred in the region over the last three decades which imposed a number of socioeconomic and environment-related impacts. Based on the percentage of respondent farmers, climate change (95%), soil productivity decline (94%), land degradation (92%), shortage of wood (91%), shortage of grazing land (89%), soil erosion (88%), loss of biodiversity (81%) and lake water retreat (74%), are the principal impacts of LUCC perceived. Such perceived impacts of LUCC are in line with the observed results obtained from comprehensive measured data analysis. Future land use policies need to consider management options that work on reducing anthropogenic-induced pressures on the environment and encouraging livelihood diversification in order to minimize the adverse socio-environmental impacts of spectacular LUCC in the region.
Keywords: *anthropogenic, climate change, household, land degradation, perception*

Introduction

Anthropogenic activities have altered the planet Earth at unprecedented rates, magnitude and spatial scales since the beginning of human life on Earth (Turner et al., 1994) which made land change science to emerge as one fundamental component of global environmental change and sustainability research (Turner et al., 2007). These changes are complex in nature in space and time (Lambin et al., 2003). For instance, the changes could be land modification, subtle alterations in the attributes of a land cover or land conversion, the complete replacement of one cover type by another (e.g., forest

http://www.aloki.hu ● ISSN 1589 1623 (Print) ● ISSN 1785 0037 (Online)
DOI: http://dx.doi.org/10.15666/aeer/1605_66076632
© 2018, ALÖKI Kft., Budapest, Hungary

land to cropland) (Lambin et al., 2003); or it could be land restoration, human intervention in the form of land cover maintenance and restoration (e.g. degraded land rehabilitation by area closure) (Wortley et al., 2013). Depending on the speed of change, other scientists also consider land changes as gradual or abrupt changes (Geist et al., 2006). Depending on the nature of these changes, the impact they imposed and the subsequent driver for the changes also varies in space and time.

Unregulated land use/cover change (LUCC) has multiple socio-environmental impacts that can significantly affect key aspects of Earth System functioning as well as human life on Earth (Chhabra et al., 2006). For instance, LUCC directly impacts biodiversity loss worldwide (Haines-Young, 2009; Carpio et al., 2016); it affects the carbon balance of terrestrial environments (Houghton and Goodale, 2004; Maharjan and Joshi, 2013); and is the primary source of land and land resources degradation (Meshesha et al., 2012; Matano et al., 2015). By altering ecosystem services (Polasky et al., 2011; Yirsaw et al., 2016), LUCC also affects the ability of biological systems to support human needs and hence affects livelihood systems (Mutoko et al., 2014). Furthermore, LUCC affects spatial landscape pattern and configuration (Pang et al., 2013; Wan et al., 2015). Such impacts of LUCC are more noticeable in developing countries where the livelihood of the majority of the population is directly dependent on natural resources and hence the environment is highly vulnerable to such changes (Lambin and Meyfroidt, 2011).

The other principal impact of anthropogenic-induced LUCC that has been well recognized in recent decades, and also given emphasis in this study, is its effect on local and regional climate change (Dirmeyer et al., 2010; Mutiibwa et al., 2014; Fan et al., 2015) as well as on global warming (Vitousek, 1994; Brovkin et al., 2004). It is known that LUCC affects climate mainly through an accumulation of greenhouse gases (GHG) (Houghton et al., 2012) which is partly originated from intensive agriculture and deforestation (Maharjan and Joshi, 2013). Studies show that LUCC also affects land surface temperature and surface moisture (Jiang et al., 2015; Pal and Ziaul, 2017), carbon balance of terrestrial ecosystems (Houghton and Goodale, 2004), and precipitation and evapotranspiration rates and hence the sustainability of hydrological and climatological systems (Liu et al., 2008). This indicates that in addition to natural factors, LUCC also plays a significant role in world climate change in general.

Natural variability and human activities are the main causes of climate change (Maharjan and Joshi, 2013). However, the contribution of human activities (e.g. LUCC) to climate change has increased from time to time. The increase in atmospheric concentration of GHGs is the major factor contributing to climate change caused by the human activities. For instance, according to Maharjan and Joshi (2013), energy sector, agriculture, land use change and forestry, and industrial process contribute to 68%, 15%, 13% and 4% of global GHG emission respectively. This indicates next to energy sector emission, the carbon emission from the agricultural sector and land use change (e.g., deforestation and forest degradation) (Pacheco-Angulo et al., 2017) is about 28%. Under increased deforestation, not only the amount of GHGs added to the atmosphere increase, but also the capacity of the remaining forest to serve as a sink to such gases is decreasing.

Although LUCC impacts were recognized globally, the degrees of such impacts are markedly different in various time, landscapes and regions. Hence, in sub-Saharan Africa, particularly East Africa, where both LUCC and climate change are the major environmental and livelihood concerns in recent decades (Lambin and Ehrlich, 1997;

http://www.aloki.hu ● ISSN 1589 1623 (Print) ● ISSN 1785 0037 (Online)
DOI: http://dx.doi.org/10.15666/aeer/1605_66076632
© 2018, ALÖKI Kft., Budapest, Hungary

Houghton and Hackler, 2006), detail analysis of the socio-environmental impacts of LUCC has a paramount importance in contributing to future policy and management strategies. This is particularly true for the Central Rift Valley (CRV) lakes region of Ethiopia where a tremendous LUCC has occurred over the last three decades (Temesgen et al., 2013; Ariti et al., 2015). In Ethiopia, previous studies documented the extent and drivers of LUCC in different parts of the country (Tsegaye et al., 2010; Kindu et al., 2015; Bekele et al., 2018a; Temesgen et al., 2018). However, the studies on impacts of LUCC, particularly that combine socioeconomic and environmental effects, by comparing farmers' perceived results with the observed result from measured data analysis is very scarce currently. In this study, it is assumed that the perceived impact of LUCC by farmers is in line with the observed results from measured data analysis.

Hence, this study is intended to examine the socio-environmental impacts of LUCC by integrating Remote Sensing, GIS, socioeconomic and climatic datasets, using the fragile and most dynamic landscapes of the Ethiopian CRV lakes region as an ideal case study site. Such a combined study of socioeconomic, ecological and environmental impacts of LUCC helps to reduce the adverse effects and to devise appropriate policy intervention that works on the root drivers of spectacular LUCC.

Materials and methods

The study area

The Central Rift Valley Lakes Region is located about 170 km south of the capital city, Addis Ababa, Ethiopia which is specifically found in the limits of 38°20'-38°50' east longitude and 7°20'-8°00'north latitude (*Fig. 1*). It is situated in the current administrative regions of Oromia and Southern Nations, Nationalities and Peoples Region, and covers approximately an area of 13,401 km^2. The area is topographically characterized by a depression zone with steep marginal faults along its edges and bounded by eastern and western highlands. The geological and geomorphologic features of the region are the results of Cenozoic volcano-tectonic and sedimentation processes (Ayenew, 2007; Macgregor, 2015). The Ethiopian CRV is part of the Great East African Rift Valley, that originates from Aden Junction (Arabian Plate) in the Middle East and continues in the direction of south-west, traversing longitudinally eastern African countries such as Djibouti, Eritrea, Ethiopia, Kenya, Uganda and Tanzania, and reaches to Mozambique (Hengsdijk and Jansen, 2006; Ayenew, 2007).

The climate of the CRV varies markedly with altitude and season (Jansen et al., 2007). It is humid to sub-humid in the highland portion and semiarid in the rift floor which is characterized by warm and wet summer, and dry, cold and windy winter. The study area receives a bimodal rainfall distribution pattern. The small rainy season (Belg) occurs between February and May (FMAM), which is followed by the main rainy season (Kirmet) that occurs from June to September (JJAS). Based on long-term data from four meteorological stations in CRV namely: Arsi Negele, Bulbula, Meki and Ziway, the mean rainfall is 252 and 386 mm for Belg and Kirmet season respectively, and the overall mean annual rainfall is about 740 mm. The coefficient of variation for rainfall is higher for Belg season (31%) than for Kirmet season (22%). On the other hand, the minimum temperature of the study area ranges from its lower mean value (11.5 °C) for winter season (October to January) to its higher mean value (14.2 °C) for Kirmet season, while the maximum temperature ranges from its lower mean value

http://www.aloki.hu ● ISSN 1589 1623 (Print) ● ISSN 1785 0037 (Online)
DOI: http://dx.doi.org/10.15666/aeer/1605_66076632
© 2018, ALÖKI Kft., Budapest, Hungary

(25.9 °C) for summer season to its higher mean value (28.5 °C) for Belg season. Rainfall in CRV is generally highly erratic which is one of the main constraints to rain-fed agriculture in the region (Jansen et al., 2007).

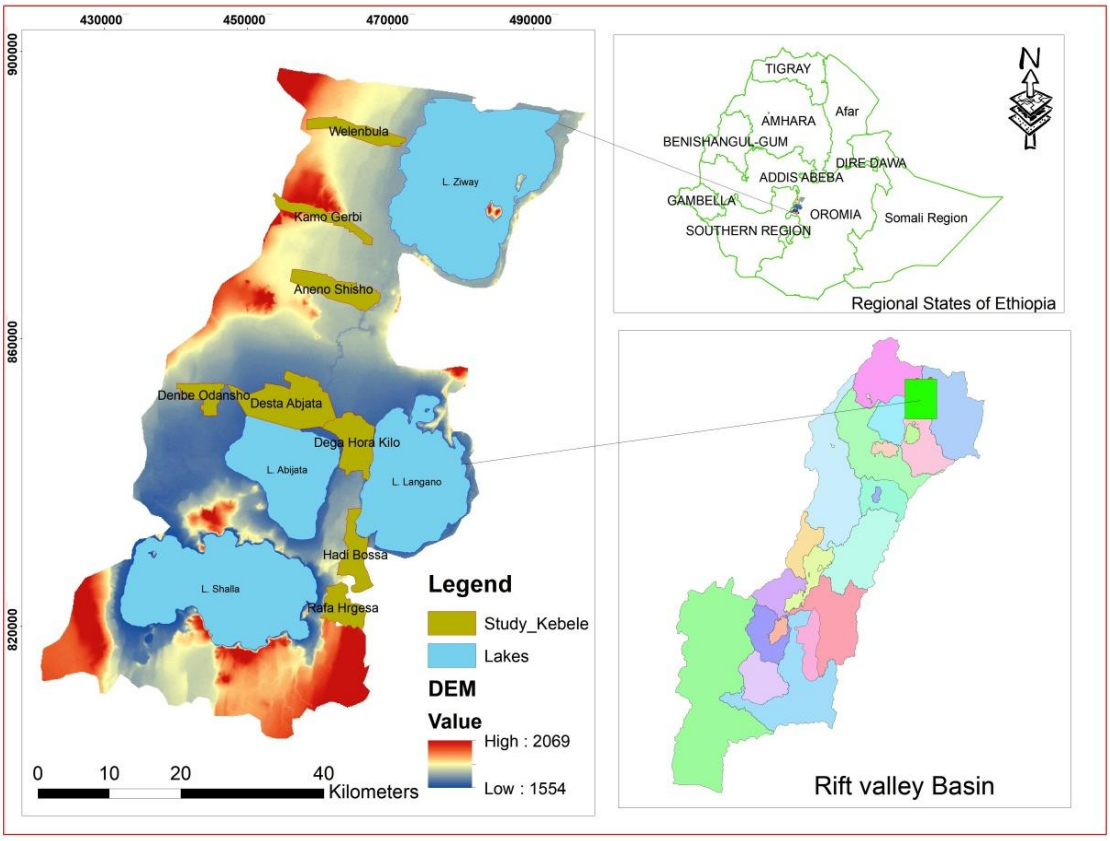

Figure 1. *Location map of the study landscape with agroclimatic areas*

The major land use/cover (LUC) types include agricultural land, dense and open acacia woodlands, water body, bush/shrubland, grazing land, swampy/marshy land and bare land (Bekele et al., 2018a). Acacia woodland is the dominant vegetation type in the region. The Rift Valley Lakes Basin is known for its huge water resource potential in the country which consists of four sub-basins namely: Ziway-Shalla, Awassa, Abaya-Chamo and Chew Bahir basins (*Table 1*). Shalla is the deepest lake (266 m) while Abaya is the largest (1160 km^2) in terms of size in the basin. The study site, Ziway-Shalla sub-basin, encompasses four major interconnected lakes on its rift floor namely: Ziway, Langano, Abijata and Shalla (*Table 1* and *Fig. 1*). These lakes together form one closed basin and a unique hydrological habitat in the region. Lake Abijata receives water from Lake Ziway via Bulbula River and from Lake Langano via Horakalo River. Lake Abijata and Shalla are terminal lakes (i.e. no outflow from such lakes) and hence known for their salty water.

The environment and the natural resources of the study area are currently under enormous pressure due to increased population pressure, agricultural investment expansion, urban expansion, mismanagement of land resources, and natural factors like recurrent drought (Jansen et al., 2007). Studies show that the woodland vegetation of the region has been declined in the expense of agricultural land expansion and continual deforestation over the last half century (Garedew et al., 2009; Biazin and Sterk, 2013;

http://www.aloki.hu ● ISSN 1589 1623 (Print) ● ISSN 1785 0037 (Online)
DOI: http://dx.doi.org/10.15666/aeer/1605_66076632
© 2018, ALÖKI Kft., Budapest, Hungary

Temesgen et al., 2013; Ariti et al., 2015). The lakes and their feeding rivers are intensively used for domestic water use, irrigation, soda ash extraction, fishery, and recreation, while the lakes and their surrounding wetlands supported a wide variety of endemic birds (Hengsdijk and Jansen, 2006; Ayenew and Legesse, 2007). As a result of such anthropogenic pressures, land degradation became a serious threat to natural resources, environment, and livelihood in CRV area in recent decades (Ayenew and Legesse, 2007; Meshesha et al., 2012).

Table 1. *Major lakes of Rift Valley Lakes Basin. (Data from JICA, 2012)*

Sub-basin	Lake	Altitude (m.a.s.l)	Surface area (km^2)	Maximum depth (m)	Average depth (m)	Volume (km^3)
Ziway-Shalla	Ziway	1636	440	8.95	2.5	1.1
	Langano	1582	230	47.9	17	5.3
	Abijata	1578	205	14.2	7.6	1.61
	Shalla	1558	409	266	87	36.7
Awassa	Awassa	1697	129	22	11	1.3
Abaya-Chamo	Abaya	1285	1160	13	7	8.2
	Chamo	1235	551	13	6	3.3
Chew Bahir	Chew Bahir	nd	nd	nd	nd	nd

nd = no data

The population in CRV has shown an accelerated growth over the last three decades with an average growth rate of about 3%, and average family size of 7. For example, the total population for three districts in CRV, namely Dugda, Adami Tulu-Jido Kombolcha and Arsi Negele, has grown from 383 608 in 1994 to 546 444 in 2007, and 659 177 in 2016 (CSA, 1994, 2007), which indicates a sharp increase in population growth in the region. About 85% of the population of the study area is still living in a rural area (CSA, 2007), and unpublished reports indicate that rural-urban migration in search of employment has increased both at the local and national level in recent years.

Subsistence farming, the smallholder mixed rain-fed production system (*Table 2*), is the main economic activity for the vast majority (85%) of the population in the region (Scholten, 2007; Melka et al., 2015). One of the developments reported in the past decades is the introduction and rapid expansion of irrigated agriculture into the region. Smallholder farming irrigation schemes, large-scale private and state domestic farms and foreign investment, particularly in horticulture and floriculture, have been established during the last decades (Hengsdijk and Jansen, 2006). Due to these major agricultural developments, high competition for available water resource becomes a major threat to lake ecosystems in the region (Hengsdijk and Jansen, 2006). In the agro-pastoral areas and areas with no access to irrigation, food insecurity is a major problem and a significant portion of the rural population is still relying on relief assistance from government and external agencies (Bekele et al., 2018a). This is evident from the low household yearly income generated from farming (*Table 2*). As confirmed by farmers and experts during discussion, one of the main causes of poverty in the CRV among others is the low level of agricultural productivity as a result of erratic rainfall and recurrent drought occurrence over the recent decades.

http://www.aloki.hu ● ISSN 1589 1623 (Print) ● ISSN 1785 0037 (Online)
DOI: http://dx.doi.org/10.15666/aeer/1605_66076632
© 2018, ALÖKI Kft., Budapest, Hungary

Table 2. *Summary of household characteristics in CRV lakes region of Ethiopia*

Household characteristics	Mean
Gender (male,%)	81.82
Age (years)	42.18
Education (literate, %)	61.72
Family size (number)	7.43
Source of income (farming, %)	89.90
Land holding size (ha)	2.40
Number of farm plots	2.53
Income (Birr*/year)	29 276.77
Distance to nearest market centre (km)	7.70

*Ethiopian currency at the time of the study, 1 USD = 22.8121 Birr

Data used and sources

The data required for this study was generated through both primary and secondary sources. 1986, 2000 and 2016 LUCC area statistics data was partly adopted from previous work of Bekele et al. (2018a). Primary data on household characteristics, socioeconomic background, historical LUCC extent, drivers and its impacts were gathered by an in-situ formal household survey (see *Appendix*), focus group discussion, field observations, and informal discussion with key informants, and experts working at the study site. A questionnaire with semi-structured type was designed to assess rural farmers' perception of LUC dynamics and its impacts. The survey questions covered a wide range of issues regarding socioeconomic characteristics of households, perception on LUCC extent and drivers, its livelihood and environmental impacts, and adaptation strategies to cope up with such changes. The first fieldwork was conducted in April to June 2017 and the second in September to October 2017. Important secondary socioeconomic and biophysical data was obtained from concerned governmental organizations like: Rift Valley Lakes Basin Authority, Kebele (Village) Administrative Offices (the lowest administrative unit in Ethiopia), and Woreda (District) Agricultural Offices. In addition, population data were obtained from the Central Statistical Agency (CSA, 1994, 2007). The long-term rainfall (1981-2016) and temperature (1988-2017) data for selected sites in CRV namely: Arsi Negele, Bulbula, Meki, and Ziway were taken from the National Meteorological Agency (NMA).

Household survey and sampling

The household survey was conducted in two consecutive districts found in CRV lakes region namely: Adami Tulu-Jido Kombolcha and Arsi Negele Districts which were selected based on agroecology and vulnerability to drought and LUCC in recent decades. From these Districts, representative Villages were purposively selected based on access to market and infrastructure (e.g., road), drought vulnerability (e.g., relief aid dependency in last ten years) and experience in using adaptation measures like small-scale irrigation to cope up with LUCC and drought impacts. Such basic socioeconomic and biophysical background information of the sample Villages were gathered with the help of experts who have been worked in the Districts for a long time. Accordingly, five Villages from Adami Tulu-Jido Kombolcha District namely: Welenbula, Kamo Gerbi,

http://www.aloki.hu ● ISSN 1589 1623 (Print) ● ISSN 1785 0037 (Online)
DOI: http://dx.doi.org/10.15666/aeer/1605_66076632
© 2018, ALÖKI Kft., Budapest, Hungary

Aneno Shisho, Desta Abjata and Deneba Odansho, and three Villages from Arsi Negele District namely: Dega Hora kilo, Hadi Bossa and Rafa Hargesa, were selected for household interview and focus group discussion (*Fig. 1*). The households interviewed were selected randomly from each Village considering age, sex, wealth status, and literacy. The list of the households was obtained from each Village Administration Office. A total of 297 households were interviewed with an average of 37 households from each Village. In addition, at least one focus group discussion (five to ten people per group) and an interview with one key informant (elder), age at least 60, were conducted in each Village. A checklist of questions of interest was used to guide the group discussion which availed information that could not be picked up by using structured questionnaires. Additional discussion was also made with Development Agents (medium level experts assisting farmers in adoption of modern agricultural practices), at Village level and experts working at District level.

Data analysis

A combination of techniques, including Remote Sensing, GIS-based data processing and descriptive statistics were employed for data analysis. The LUC classification was done by employing a supervised maximum likelihood algorithm classification approach (Booth and Oldfield, 1989; Hogland et al., 2013; Richards, 2013) for the reference years of 1986, 2000 and 2016 using Landsat5 Thematic Mapper (TM), Landsat7 Enhanced Thematic Mapper Plus (ETM^{+}) and Landsat8 Operational Land Imager (OLI) imageries respectively with an overall accuracies of at least 90% for each year. Accordingly, the LUC of the study area was classified in to agricultural land, dense and scattered acacia woodlands, grass/grazing land, bush/shrub land, water body, marsh/swampy area and bare land (Bekele et al., 2018a).

Data on socioeconomic characteristics of households and their perceived responses on impacts of LUCC and climate data on rainfall and temperature were coded, summarized and analyzed using descriptive statistics. Data collected through group discussions, key informants interview and field observation was analyzed qualitatively and used in the elaboration of discussion part.

Mean, standard deviation, a coefficient of variations and standardized rainfall anomalies were employed to evaluate inter-annual rainfall fluctuations and temperature variations. The standard deviation for temperature and rainfall variability was calculated using the formula in *Equation 1*. The coefficient of variation (*Eq. 2*) is used as a statistical descriptor of rainfall and temperature variability and calculated as the ratio of the standard deviation to the mean in a given period. Standardized anomalies of rainfall of the crop growing season were calculated using the formula given in *Equation 3* and used to assess the frequency of droughts as in Agnew and Chappell (1999) and Bewket and Conway (2007).

$$SD = \sqrt{\left[\sum_{i=1}^{n} \frac{(x_i - X)^2}{n}\right]} \quad \text{(Eq.1)}$$

$$CV = \frac{SD}{X} * 100 \quad \text{(Eq.2)}$$

http://www.aloki.hu ● ISSN 1589 1623 (Print) ● ISSN 1785 0037 (Online)
DOI: http://dx.doi.org/10.15666/aeer/1605_66076632
© 2018, ALÖKI Kft., Budapest, Hungary

$$SRA = \frac{P_t - P_m}{SD} \quad \text{(Eq.3)}$$

where, SD = standard deviation, CV = coefficient of variation, x_i = individual temperature/rainfall observation, X = mean rainfall/temperature, n = number of years considered, SRA = standardized rainfall anomaly, P_t = annual rainfall in year t, P_m = long term mean annual rainfall over a period of observation (1981-2016).

Results

Major land use/cover changes

The spatiotemporal trend of LUCC in the study area for 1986, 2000 and 2016 is shown in *Figure 2* for each LUC class.

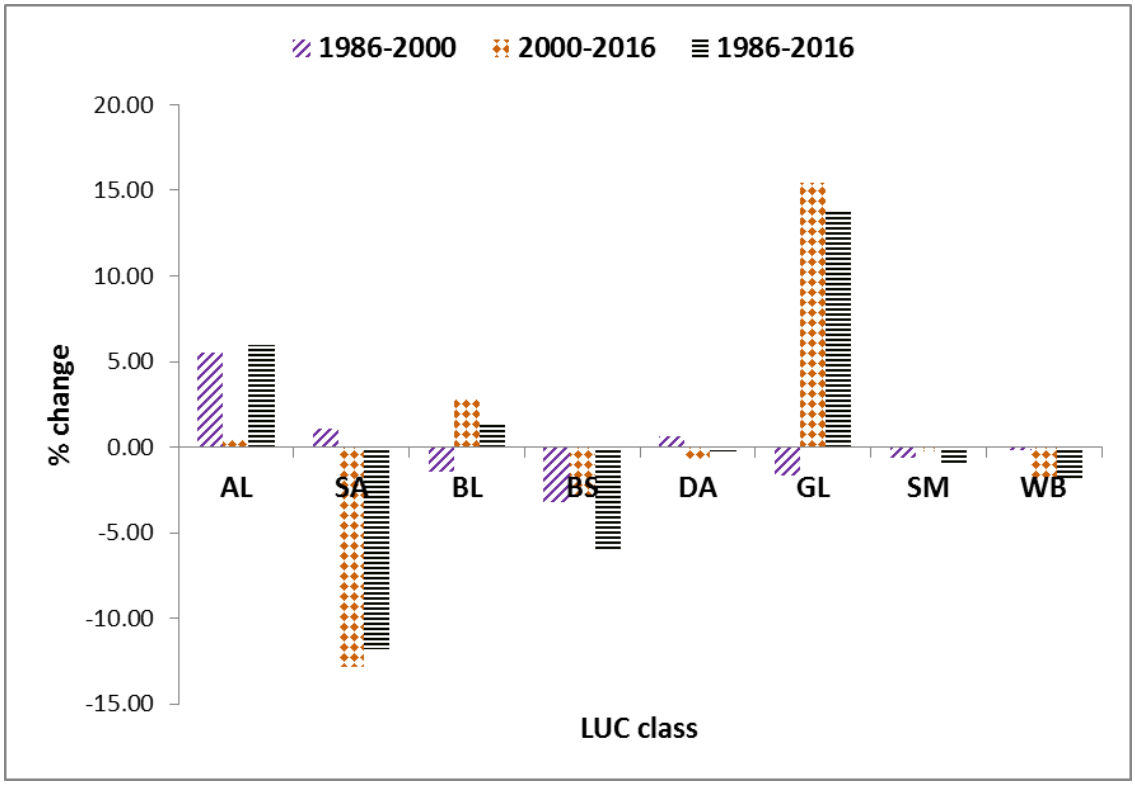

Figure 2. *LUCC (%) in CRV lakes region, adopted partly from Bekele et al. (2018a). AL = Agricultural land, SA = Scattered acacia woodland, BL = Bare land, BS = Bush/shrubland, DA = Dense acacia woodland, GL = Grass/grazing land, SM = Swampy/marshy land, WB = Water body*

Our result indicated that a tremendous LUCC has occurred in CRV lakes region over the last three decades. For instance, during the first phase of the study period (1986-2000), agricultural land and dense acacia woodland have increased by 39% and 23%, whereas bare land and bush/shrub land have declined by 39% and 27%, respectively. On the other hand, during the second phase of the study period (2000-2016), grazing land and bare land have increased by 164% and 121%, while scattered acacia woodland,

http://www.aloki.hu ● ISSN 1589 1623 (Print) ● ISSN 1785 0037 (Online)
DOI: http://dx.doi.org/10.15666/aeer/1605_66076632
© 2018, ALÖKI Kft., Budapest, Hungary

bush/shrubland and dense acacia woodland have declined by 54%, 32% and 27%, respectively. This implies bush/shrubland has declined throughout both study periods. Waterbody and its associated swampy/marshy lands also declined during both study periods. Agricultural land on the other side had increased with a substantial rate until 2000, after which it showed only slight increment. During the overall study period (1986-2016), grass/grazing land, agricultural land and bare land have increased by 124%, 42% and 34%, whereas scattered acacia woodland, bush/shrubland and swampy/marshy land have declined by 52%, 50% and 31%, in that order.

Socio-environmental impacts of land use/cover changes

Climate change and food insecurity

Results show that LUCC has imposed a number of significant socio-environmental impacts in CRV lakes region of Ethiopia during the last three decades. This was confirmed by a number of impacts perceived by rural farmers of the study area and observed evidences from field survey (*Fig. 3*). About 95% of respondent farmers mentioned climate change, particularly rainfall variability and frequent drought, as the main impact of LUCC in the region. They accused LUCC, particularly the rapid decline in vegetation coverage, as a main reason for erratic and shortage of rainfall, and an increased diurnal temperature in recent years in the study area. According to open discussion witness by focus groups, key informants, and experts, this change in climate, in turn, has directly affected the rain-fed agriculture and contributed to high food insecurity problem in the region in recent decades.

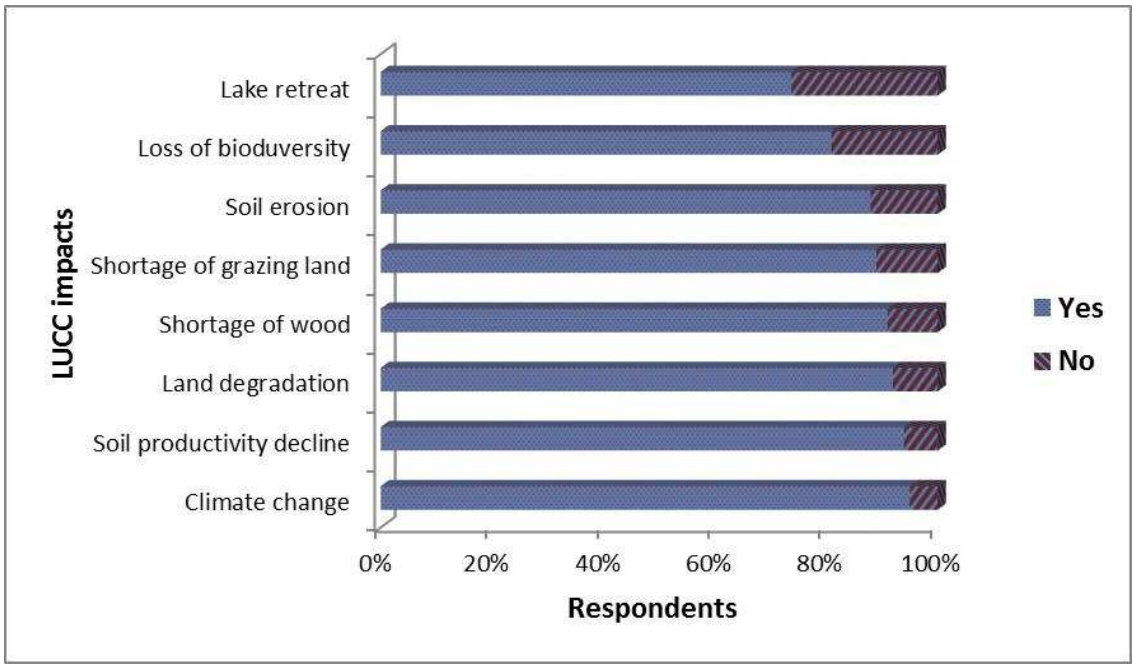

Figure 3. *Impacts of LUCC as perceived by rural households (%) in CRV lakes region of Ethiopia (N = 297)*

Table 3 summarizes rainfall and temperature statistics while *Figure 4* shows the standardized rainfall anomaly of the study area. In line with household perceived

http://www.aloki.hu ● ISSN 1589 1623 (Print) ● ISSN 1785 0037 (Online)
DOI: http://dx.doi.org/10.15666/aeer/1605_66076632
© 2018, ALÖKI Kft., Budapest, Hungary

results, the standardized rainfall anomaly of the growing season showed high inter-annual and inter-seasonal variability and a general decreasing trend (*Fig. 4*) for both Belg (CV = 31%, mean = 252 mm±78) and Kirmet (CV = 22%, mean = 386 mm ± 86) (*Table 3*). Of the 36 years of observation, 20 years (56%) for Belg season and 18 years (50%) for Kirmet season had negative anomalies, implying dry years, which is a risk for rain-fed agricultural production in the region. The coefficient of variation of rainfall is higher during the Belg season (31%) than during Kirmet season (22%). However, average minimum and maximum temperatures did not show significant inter-annual and inter-seasonal variation over the last three decades, though the trend line in *Figure 5* indicates that it is generally hotter in recent years than in earlier years, and it is evident that an increased temperature, in turn, will increase evapotranspiration rate. The mean minimum temperature ranged from 11.5 °C for winter season to to 14.2 °C for Kirmet season, while the mean maximum temperature ranged from 25.9 °C for Kirmet season to 28.5 °C for Belg season. In general, the temperature has shown considerable variability during the last 30 years.

Table 3. *Mean, standard deviation and coefficient of variation (%) for long-term rainfall (1981-2016) and temperature (1988-2017) at CRV lakes region. (Data from NMA)*

Variable	Season	Mean	Standard deviation	Coefficient of variation
Rainfall	FMAM	251.69	78.17	31.06
	JJAS	385.89	85.58	22.18
	ONDJ	102.41	45.91	44.83
	Overall	739.99	140.01	18.92
Minimum temperature	FMAM	14.00	1.34	9.58
	JJAS	14.20	1.23	8.66
	ONDJ	11.51	1.48	12.85
	Overall	13.24	1.26	9.51
Maximum temperature	FMAM	28.52	0.72	2.53
	JJAS	25.87	0.85	3.28
	ONDJ	26.96	0.51	1.90
	Overall	27.12	0.55	2.03

FMAM = February to May, JJAS = June to September, ONDJ = October to January

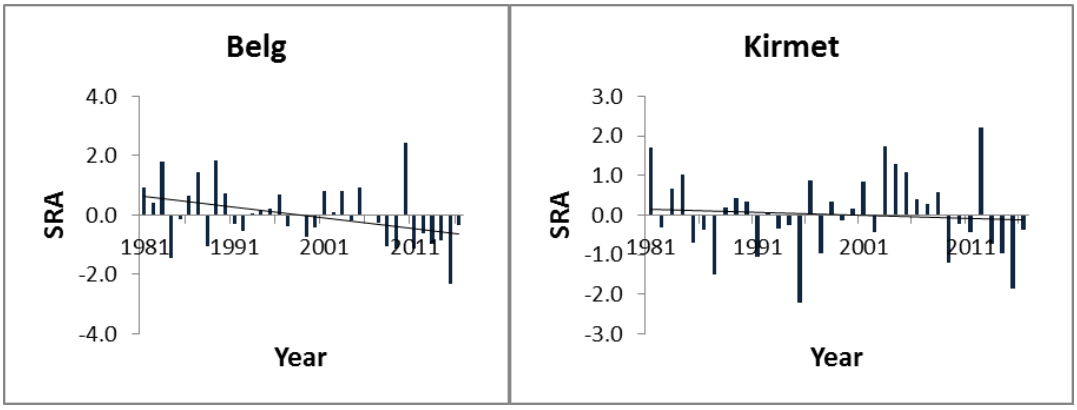

Figure 4. *Standardized rainfall anomaly of the growing season (SRA) at CRV lakes region. (Data from NMA)*

http://www.aloki.hu ● ISSN 1589 1623 (Print) ● ISSN 1785 0037 (Online)
DOI: http://dx.doi.org/10.15666/aeer/1605_66076632
© 2018, ALÖKI Kft., Budapest, Hungary

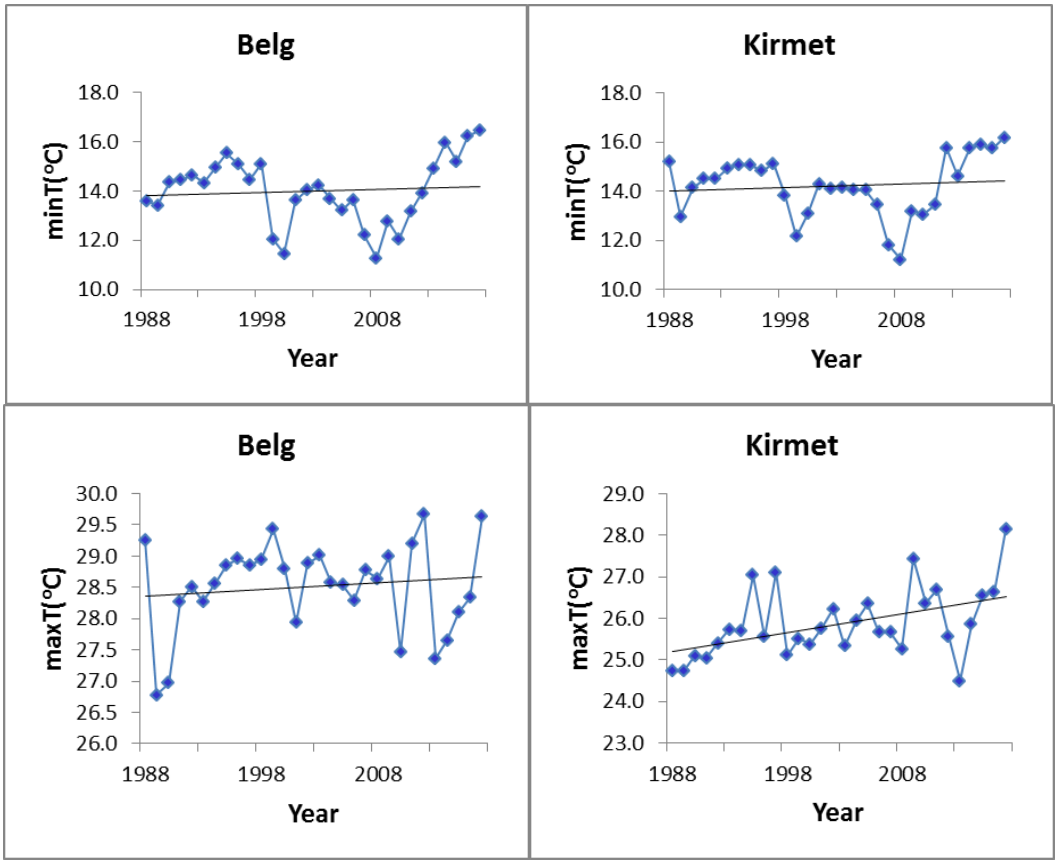

Figure 5. *Trend of seasonal mean minimum (minT) and maximum (maxT) temperatures (1988-2017) at CRV lakes region. (Data from NMA)*

Land degradation

Soil productivity decline, land degradation, and soil erosion are other major impacts of LUCC perceived by 94%, 92% and 88% of respondent farmers respectively (*Fig. 3*). Development Agents and District agricultural experts also confirmed that severe soil erosion and subsequent decline in agricultural productivity are mainly attributed to rapid LUCC in the study area over the last three decades. As observed during the field survey, indicators of land degradation (*Fig. 6*), specifically serious gulley erosion, expansion of bare lands, and decline/drying of streams, rivers, and lakes are among the high threats to the environment and rural livelihood in CRV lakes region. It is common to see severe gulley erosion like the one in *Figure 6a*, in cultivated lands, along a roadside, and in grazing lands. In addition to water erosion, wind erosion is also a common phenomenon observed in CRV area during the dry season. Extensive bare lands are mainly found along the shore of Lake Abijata (*Fig. 6d*) due to its fast retreat and water loss in recent decades. The Bulbula River was already dried due to decline in the level of Lake Ziway (its source), high water consumption for irrigation, drought and catchment degradation in general (*Fig. 6c*).

Shortage of wood and grazing land

Other major important impacts of LUCC mentioned by more than 89% of respondents were a shortage of wood and grazing land (*Fig. 3*). During the discussion,

http://www.aloki.hu ● ISSN 1589 1623 (Print) ● ISSN 1785 0037 (Online)
DOI: http://dx.doi.org/10.15666/aeer/1605_66076632
© 2018, ALÖKI Kft., Budapest, Hungary

focus groups pointed that due to firewood shortage and lack of access to electricity and alternative energy sources, currently they were forced to use either crop residues or cow dung, or buy firewood with expensive price from nearby markets, which had been otherwise accessed from nearby woodlands/forests three decades ago. In addition, respondent households mentioned that due to a shortage of cropland and productivity decline from time to time, they were forced to change part of their previous grazing land to croplands, which contributed to a shortage of grazing land. Hence, coupled with recurrent drought, shortage of grass/grazing land has made cattle rearing the most difficult rural livelihood option, and hence most farmers have been forced to limit the number of their cattle holding in recent decades.

Figure 6. *Indicators of land degradation in CRV lakes region of Ethiopia: (**a**) active gulley head; (**b**) bare and eroded land; (**c**) drying of Bulbula River which flow from Lake Ziway to Lake Abijata; and (**d**) retreat of Lake Abijata. (Photo by B. Bekele)*

Water resources degradation and biodiversity loss

Last but very important impacts of LUCC perceived by about 81% and 74% of interviewees respectively were the loss of biodiversity and lake water retreat (*Fig. 3*). Drying of rivers and streams specifically of Bulbula River (*Fig. 6c*) and lake water loss, particularly of Lake Abijata (*Fig. 6d*) and Lake Ziway, was strongly emphasized by survey participants (individual households, key informants, focus groups and experts) during the discussion. Key informants (elders) confirmed that Lake Abijata now lost at least one-fourth of the area coverage it has 20 years ago.

In agreement with perceived results, the observed trend (*Table 4a*) and projected trend (*Table 4b*) indicate high water resources degradation in CRV lakes region. During 34 years period, Lake Abijata lost about 51% of its area in 1973 (*Table 4*a). The rate of loss is faster in recent years than in earlier years. For example, as shown in *Table 4a,*

http://www.aloki.hu ● ISSN 1589 1623 (Print) ● ISSN 1785 0037 (Online)
DOI: http://dx.doi.org/10.15666/aeer/1605_66076632
© 2018, ALÖKI Kft., Budapest, Hungary

during 1999-2006, eight years alone, Lake Abijata lost about 42% of its area in 1999. The projected change (*Table 4b*) also shows that Lake Abijata will continue to lose about 17% of its area and 1.28 m of its level until 2034 followed by Lake Ziway, which will be expected to lose 10.7% area and 0.57 m level. Such high degradation on lakes, in turn, is a major threat to biodiversity loss particularly bird and fish species inhabiting these lakes.

Table 4. *Observed changes in size of Lake Abijata (1973-2006) (**a**) and long term projected change in level and area of four CRV lakes (2005-2034) (**b**). (Data from Jansen et al., 2007 and Raventós Vilalta, 2010)*

(a) Lake Abijata observed change		**(b) Projected change**		
Year	**Area (km^2)**	**Lake**	**Level (m)**	**Area (%)**
1973	194.00	Ziway	-0.57	-10.70
1986	162.00	Abijata	-1.28	-17.00
1999	163.00	Langano	-1.08	-3.10
2006	95.00	Shala	-1.74	-0.60

Discussion

In their previous studies, the authors reported the systematic and random LUCC transitions (Bekele et al., 2018a) and its principal drivers (Bekele et al., 2018b submitted) in CRV lakes region of Ethiopia. The results of these studies show that a rapid LUCC has occurred in CRV lakes region of Ethiopia in recent three decades and these changes are driven by population growth, fuelwood extraction, agricultural land expansion, charcoal making, recurrent drought and overgrazing. This unregulated change in LUC has imposed a number of socioeconomic and environmental related impacts, according to farmers' perception, experts' opinion and authors' field observation. The impacts are highly interrelated and hence further aggravate each other. These include climate change and subsequent food insecurity, land degradation, shortage of wood and grazing land, degradation of water resources and loss of biodiversity.

Climate change, particularly rainfall variability (late onset, early set-off, accidental flood, frequent drought) as confirmed by respondents and analysis of meteorological dataset, is a major problem in CRV lakes region in recent years, which is also consistent with previous studies (Biazin and Sterk, 2013; Kassie et al., 2013). This unpredictable and erratic rainfall, in turn, increased the vulnerability of rain-fed agriculture to climate change (Gizachew and Shimelis, 2014) which resulted in food insecurity and relief aid dependency of thousands of farmers in the region. Frequent drought is the main challenge to food security in East African countries in recent decades (Pricope et al., 2013; Masih et al., 2014). For instance, historical records showed that Ethiopia has experienced a repeated dry-spells hit over the last half century (Jury, 2010; Fazzini et al., 2015). One causative factor of this variability in rainfall in Ethiopia among others is believed to be the rapid change in LUC of the country, particularly massive deforestation (Gurmessa, 2015). This agrees with our starting assumption that LUCC is one potential contributor that increases climate change vulnerability in the country. It is known that LUCC has local and regional climate change effects especially through the accumulation of GHGs (Pielke, 2005; Houghton et al., 2012). In addition to increasing

http://www.aloki.hu ● ISSN 1589 1623 (Print) ● ISSN 1785 0037 (Online)
DOI: http://dx.doi.org/10.15666/aeer/1605_66076632
© 2018, ALÖKI Kft., Budapest, Hungary

the atmospheric concentration of GHGs and therefore influencing global climate, LUCC, particularly deforestation could also affect the regional or local climate by altering the water and energy budget at the Earth's surface via changing albedo, Bowen ratio and surface moisture (Hagos et al., 2014; Ahmed et al., 2016). Studies also show that LUCC affects land surface temperature and surface moisture (Jiang et al., 2015; Pal and Ziaul, 2017), carbon balance of terrestrial environments (Houghton and Goodale, 2004), and precipitation and evapotranspiration rates and hence influencing the hydrological and climatological systems (Liu et al., 2008).

Land degradation in CRV lakes region, particularly decrease in soil productivity, severe soil erosion, expansion of bare lands and abandon lands are consequences directly linked to unregulated LUCC (e.g. deforestation) and mismanagement of land, for example, overgrazing in the region. It is known that expansion of bare lands further exposes the soil to water and wind erosion, and soil erosion, in turn, is the primary cause for deterioration in soil fertility, and productivity decline (Lal, 2001). Previous studies also reported severe land degradation and subsequent soil productivity decline in CRV region (Meshesha et al., 2012; Adimassu et al., 2013) and in other parts of Ethiopia (Taddese, 2001; Teketay, 2001; Zeleke and Hurni, 2001; Amsalu et al., 2007) which are directly or indirectly related to the rapid LUCC in the country. Studies show that LUCC, particularly extensive vegetation removal and mismanagement of croplands could accelerate soil erosion (Teketay, 2001; Nunes et al., 2011). For instance, keeping other factors constant, soil erosion is expected to be more severe on bare lands and croplands, than on forest lands (Nunes et al., 2011). Some unpublished government reports claim for an increased productivity per hectare of land in recent years in Ethiopia; but as confirmed by farmers and experts during discussion, this could be possible only for good rainy years and at the expense of high inputs (fertilizer, pesticide, herbicide, and labour) which is unaffordable by poor farming households due to high price inflation of such inputs in the country in recent years.

High shortage of wood and wood products is another critical problem faced in Ethiopia following massive deforestation in the country in general and the study site in particular. The wood shortage crisis is evident from the high price of wood products on the local market currently. The demand on wood and wood products, on the other hand, is highly increased in Ethiopia from time to time following population growth, as wood is the basic material required for construction, house furniture, energy supply, and an alternative source of income in the country (Gurmessa, 2015). The demand for wood for firewood is further exacerbated by lack of access to primary energy sources, like rare rural electrification in Ethiopia currently. On the other hand, the domestic supply base for wood products is already in its critical stage in Ethiopia in recent years. This is because the natural forest resource of the country was already lost as a result of rapid deforestation over the last half century (Teketay, 2001; Guta, 2014), whereas efforts made to fill the gap with the expansion of plantation forest is too low to supply the demand and is constrained by several management problems (Lemenih and Kassa, 2014). Such wood shortage crisis is also evident from common usage of crop residues and cow dung as firewood in both urban and rural areas of the country (Guta, 2014) which also further contribute to soil fertility and productivity decline.

The CRV lakes region is known for its huge water resource in the country; because with the exception of Lake Tana, all principal Ethiopian lakes are found within the catchment of Rift Valley Lakes Basin. These lakes are interconnected to each other and together form a closed sub-basin. However, currently there exists a high competing

http://www.aloki.hu ● ISSN 1589 1623 (Print) ● ISSN 1785 0037 (Online)
DOI: http://dx.doi.org/10.15666/aeer/1605_66076632
© 2018, ALÖKI Kft., Budapest, Hungary

claim for land and water resources by different stakeholders in this basin, and managing these different claims to achieve sustainable development remained the most challenging and an issue of environmental and economic debate currently (Jansen et al., 2007). In CRV, land, and water resources are highly interrelated and hence any change in LUC directly affects the water and its habitats. Anthropogenic-induced activities, for example, rapid LUCC and natural processes like climate change in the region imposed a number of critical impacts on lake water resources, their associated wetlands and biodiversity (Seyoum et al., 2015). For instance, the rapid retreat of lakes' volume (e.g., Lake Abijata and Lake Ziway), drying/decline of streams and rivers (e.g., Bulbula River), and water pollution due to chemical-intensified farming (e.g., Laka Ziway) are indicators of severe lakes' degradation in the region. With current rate of retreat studies projected that Lake Abijata will totally dry within the coming 50 years (Jansen et al., 2007; Temesgen et al., 2013; Seyoum et al., 2015), and unless urgent measures are taken, Lake Ziway will be the second to share a similar fate in the coming near future. For example, the drying of Bulbula River, which discharges water from Lake Ziway to Lake Abijata, is a signal of warning for a significant decline in the level of Lake Ziway currently. The average level of Lake Ziway has decreased by approximately 0.5 m since 2002 which is equivalent to a loss of about 200 million m^3 of water (Jansen et al., 2007). High water abstraction for irrigation, climate change, rapid LUCC and land degradation are the major factors for such severe consequences on CRV lakes (Legesse and Ayenew, 2006; Getnet et al., 2014). For instance, the irrigated land has increased from almost zero ha in 1973 to about 10 000 ha in 2006 (Jansen et al., 2007), and an estimated 285 Mm^3 yr^{-1} of water was abstracted for irrigation in 2009 alone (Getnet et al., 2014). Most of these irrigation development activities are situated in the downstream catchments of Lake Zway, which makes it the most vulnerable lake to such pressures. In addition, though the CRV lakes are endowed for tourism potential and they are being home for different migratory species of birds and fish, this biodiversity is currently highly threatened and became extremely vulnerable by such high human-induced pressures on the habitats of these lakes (Jansen et al., 2007).

Conclusions

Based on the results obtained from comprehensive analysis, we can conclude that there has been a rapid and tremendous LUC dynamics occurred in CRV lakes region of Ethiopia. This change, in turn, has imposed adverse socioeconomic and environmental impacts during the study period. Climate change, soil productivity decline, land degradation, shortage of wood and grazing land, soil erosion, loss of biodiversity and lake retreat were the principal impacts of LUCC claimed by respondent farmers in decreasing order of percentage of respondents. The perceived impacts are in line with the results obtained from physical data analysis and eyewitness from in-situ field verification.

Previous studies in CRV and elsewhere mainly focused on spatiotemporal analysis of the extent and drivers of LUCC with little emphasis to its prolonged impacts. Apart from these studies, this study tried to integrate Remote Sensing, GIS, climatic data and socioeconomic survey to investigate LUC dynamics for the last three decades and its wider livelihood as well as environmental impacts in the CRV lakes region of Ethiopia. In addition, this study also tried to compare observed impacts of LUCC with that of farmers' perceived results which will hope to increase the scientific knowledge of the

http://www.aloki.hu ● ISSN 1589 1623 (Print) ● ISSN 1785 0037 (Online)
DOI: http://dx.doi.org/10.15666/aeer/1605_66076632
© 2018, ALÖKI Kft., Budapest, Hungary

study area. It is also believed that the result of this study will serve as one of the information inputs to be used in formulating future policies and management plans for a rapidly changing CRV lakes region. However, this study might have limitations and hence further studies are important. For example, for a better understanding of climate change trends, it needs further research that addresses detail analysis on the extent of meteorological drought and how these could be affected by LUCC by incorporating data from wider meteorological stations in CRV lakes region. In addition, it is better to investigate the LUCC effect on environment and ecosystem functioning, for example, its effect on ecosystem services and human-wellbeing. Furthermore, it is important to assess the adaptation strategies and the constraints of farmers to overcome the impact of LUCC.

The study result implicated that LUCC has still continued in developing countries like East Africa, where the majority of the economy is directly dependent on natural resources. These rapid and extensive LUC dynamics is mainly driven by human-induced pressures and climate change vulnerability, which has imposed significant socioeconomic and environmental impacts at the local, national and regional level. The natural resources of the study area are currently under enormous pressure, and hence the adverse impacts of LUCC observed for this study calls for urgent measures that work on the drivers, particularly population growth and options that help strengthen the adaptation capacity of farmers to cope up with climate change. High land degradation in the region needs integrated and sustainable environmental conservation activities by all stakeholders. The high demand for wood products, especially for firewood, needs strong action on plantation forest establishment and expansion of rural electrification, and improving access to alternative energy sources and efficient energy utilization technologies. Lake water and associated aquatic ecosystems degradation require immediate practice on integrated water resource management and formulation of policies that govern sustainable and efficient water use for irrigation. In general, future land use policies at local, national and regional level needs to address such rapid LUCC and the principal drivers, in order to reduce the adverse impacts and maintain the fragile ecosystems of the CRV lakes region while diversifying alternative livelihood options to feed the ever-growing population of the region.

Acknowledgements. The authors are indebted to thank the National Natural Sciences Foundation of China (Fund No. 41571176), International Cooperation and Cultivation Project of Nanjing Agricultural University (Fund No. 2018-AF-22), and The 111 Project (Fund No. B17024) by State Administration of Foreign Experts Affairs and Ministry of Education of China for financial support and encouragement in conducting this study. We are grateful to thank the Chinese Government Scholarship Council (CSC) for giving the first author a chance to pursue his Ph.D. study in China. Special thanks also go to all the staff members of Agricultural Office of the Dugda, Adami Tulu-Jido Kombolcha and Arsi Negele Districts who helped during field data collection and all the rural farmers of the three Districts who took part during the field survey. We are also pleased to acknowledge the anonymous reviewers for their helpful comments and opinions on the earlier draft of this manuscript.

REFERENCES

[1] Adimassu, Z., Kessler, A., Yirga, C., Stroosnijder, L. (2013): Farmers' perceptions of land degradation and their investments in land management: A case study in the central Rift Valley of Ethiopia. – Environmental Management 51: 989-998.
[2] Agnew, C., Chappell, A. (1999): Drought in the Sahel. – GeoJournal 48: 299-311.

http://www.aloki.hu ● ISSN 1589 1623 (Print) ● ISSN 1785 0037 (Online)
DOI: http://dx.doi.org/10.15666/aeer/1605_66076632
© 2018, ALÖKI Kft., Budapest, Hungary

[3] Ahmed, K. F., Wang, G., You, L., Yu, M. (2016): Potential impact of climate and socioeconomic changes on future agricultural land use in West Africa. – Earth System Dynamics 7: 151-165.
[4] Amsalu, A., Stroosnijder, L., De Graaff, J. (2007): Long-term dynamics in land resource use and the driving forces in the Beressa watershed, highlands of Ethiopia. – Journal of Environmental Management 83: 448-459.
[5] Ariti, A. T., van Vliet, J., Verburg, P. H. (2015): Land-use and land-cover changes in the Central Rift Valley of Ethiopia: Assessment of perception and adaptation of stakeholders. – Applied Geography 65: 28-37.
[6] Ayenew, T. (2007): Water management problems in the Ethiopian rift: Challenges for development. – Journal of African Earth Sciences 48: 222-236.
[7] Ayenew, T., Legesse, D. (2007): The changing face of the Ethiopian rift lakes and their environs: call of the time. – Lakes & Reservoirs: Research & Management 12: 149-165.
[8] Bekele, B., Wu, W., Legesse, A., Temesgen, H., Yirsaw, E. (2018a): Random and systematic land use/land cover transitions in semi-arid landscapes of Ethiopian Central Rift Valley Lakes Region (East Africa). – Applied Ecology and Environmental Research 16: 3993-4014.
[9] Bekele, B., Wu, W., Legesse, A., Temesgen, H., Yirsaw, E. (2018b): Drivers of land use-land cover changes in Ethiopian Central Rift Valley lakes region (East Africa). – Journal of Integrative Environmental Sciences (in press).
[10] Bewket, W., Conway, D. (2007): A note on the temporal and spatial variability of rainfall in the drought-prone Amhara region of Ethiopia. – International Journal of Climatology 27: 1467-1477.
[11] Biazin, B., Sterk, G. (2013): Drought vulnerability drives land-use and land cover changes in the Rift Valley dry lands of Ethiopia. – Agriculture, Ecosystems and Environment 164: 100-113.
[12] Booth, D., Oldfield, R. (1989): A comparison of classification algorithms in terms of speed and accuracy after the application of a post-classification modal filter. – Remote Sensing 10: 1271-1276.
[13] Brovkin, V., Sitch, S., Von bloh, W., Claussen, M., Bauer, E., Cramer, W. (2004): Role of land cover changes for atmospheric CO_2 increase and climate change during the last 150 years. – Global Change Biology 10: 1253-1266.
[14] Carpio, A. J., Oteros, J., Tortosa, F. S., Guerrero-Casado, J. (2016): Land use and biodiversity patterns of the herpetofauna: The role of olive groves. – Acta Oecologica 70: 103-111.
[15] Chhabra, A., Geist, H., Houghton, R. A., Haberl, H., Braimoh, A. K., Vlek, P. L., Patz, J., Xu, J., Ramankutty, N., Coomes, O. (2006): Multiple Impacts of Land-Use/Cover Change. – In: Lambin, E. F., Geist, H. (ed.) Land-Use and Land-Cover Change: Local Process and Global Impacts. Springer-Verlag, Berlin Heidelberg, pp. 71-116.
[16] CSA (1994): The 1994 Population and Housing Census Results for Oromiya Region. – Central Statistical Agency, Addis Ababa, Ethiopia.
[17] CSA (2007): The 2007 Population and Housing Census Results for Oromiya Region. – Central Statistical Agency, Addis Ababa, Ethiopia.
[18] Dirmeyer, P. A., Niyogi, D., De Noblet-Ducoudré, N., Dickinson, R. E., Snyder, P. K. (2010): Impacts of land use change on climate. – International Journal of Climatology 30: 1905-1907.
[19] Fan, X., Ma, Z., Yang, Q., Han, Y., Mahmood, R. (2015): Land use/land cover changes and regional climate over the Loess Plateau during 2001–2009. Part II: interrelationship from observations. – Climatic Change 129: 441-455.
[20] Fazzini, M., Bisci, C., Billi, P. (2015): The Climate of Ethiopia. – In: Bliip, P. (ed.) Landscapes and Landforms of Ethiopia. Springer, Dordrecht, pp. 65-87.

http://www.aloki.hu ● ISSN 1589 1623 (Print) ● ISSN 1785 0037 (Online)
DOI: http://dx.doi.org/10.15666/aeer/1605_66076632
© 2018, ALÖKI Kft., Budapest, Hungary

[21] Garedew, E., Sandewall, M., Soderberg, U., Campbell, B. M. (2009): Land-use and land-cover dynamics in the central rift valley of Ethiopia. – Environmental Management 44: 683-94.
[22] Geist, H., Mcconnell, W., Lambin, E. F., Moran, E., Alves, D., Rudel, T. (2006): Causes and Trajectories of Land-Use/Cover Change. – In: Lambin, E. F., Geist, H. (ed.) Land-Use and Land-Cover Change: Local Process and Global Impacts. Springer-Verlag, Berlin Heidelberg, pp. 41-70.
[23] Getnet, M., Hengsdijk, H., van Ittersum, M. (2014): Disentangling the impacts of climate change, land use change and irrigation on the Central Rift Valley water system of Ethiopia. – Agricultural Water Management 137: 104-115.
[24] Gizachew, L., Shimelis, A. (2014): Analysis and mapping of climate change risk and vulnerability in Central Rift Valley of Ethiopia. – African Crop Science Journal 22: 807-818.
[25] Gurmessa, F. (2015): Forest loss and climate change in Ethiopia. – Research Journal of Agriculture and Environmental Management 4: 216-224.
[26] Guta, D. D. (2014): Effect of fuelwood scarcity and socio-economic factors on household bio-based energy use and energy substitution in rural Ethiopia. – Energy Policy 75: 217-227.
[27] Hagos, S., Leung, L. R., Xue, Y., Boone, A., de Sales, F., Neupane, N., Huang, M., Yoon, J.-H. (2014): Assessment of uncertainties in the response of the African monsoon precipitation to land use change simulated by a regional model. – Climate Dynamics 43: 2765-2775.
[28] Haines-Young, R. (2009): Land use and biodiversity relationships. – Land Use Policy 26: S178-S186.
[29] Hengsdijk, H., Jansen, H. (2006): Agricultural Development in the Central Ethiopian Rift Valley: A Desk-Study on Water-Related Issues and Knowledge to Support a Policy Dialogue. Note 375. – Plant Research International BV, Wageningen.
[30] Hogland, J., Billor, N., Anderson, N. (2013): Comparison of standard maximum likelihood classification and polytomous logistic regression used in remote sensing. European Journal of – Remote Sensing 46: 623-640.
[31] Houghton, R., Goodale, C. (2004): Effects of Land-Use Change on the Carbon Balance of Terrestrial Ecosystems. – In: Defries, R. S., Asner, G. P., Houghton, R. A. (eds.) Ecosystems and land use change. Geophysical Monograph Series 153. American Geophysical Union, Washington, DC, pp. 85-98.
[32] Houghton, R., Hackler, J. (2006): Emissions of carbon from land use change in sub-Saharan Africa. – Journal of Geophysical Research: Biogeosciences 111.
[33] Houghton, R. A., House, J., Pongratz, J., Van Der Werf, G., Defries, R., Hansen, M., Quéré, C. L., Ramankutty, N. (2012): Carbon emissions from land use and land-cover change. – Biogeosciences 9: 5125-5142.
[34] Jansen, H., Hengsdijk, H., Legesse, D., Ayenew, T., Hellegers, P., Spliethoff, P. (2007): Land and Water Resources Assessment in the Ethiopian Central Rift Valley: Project: Ecosystems for Water, Food and Economic Development in the Ethiopian Central Rift Valley. Alterra-Rapport 1587. – Alterra, Wageningen.
[35] Jiang, Y., Fu, P., Weng, Q. (2015): Assessing the impacts of urbanization-associated land use/cover change on land surface temperature and surface moisture: a case study in the Midwestern United States. – Remote Sensing 7: 4880-4898.
[36] JICA (2012): The Study on Groundwater Resources Assessment in the Rift-Valley Lakes Basin in the Federal Democratic Republic of Ethiopia (Main and Final Report). – Japan International Cooperation Agency (Kokusai Kogyo CO., LTD). Ministry of Water and Energy (MoWE), The Federal Democratic Republic of Ethiopia, Addis Ababa.
[37] Jury, M. R. (2010): Ethiopian decadal climate variability. – Theoretical and Applied Climatology 101: 29-40.

http://www.aloki.hu ● ISSN 1589 1623 (Print) ● ISSN 1785 0037 (Online)
DOI: http://dx.doi.org/10.15666/aeer/1605_66076632
© 2018, ALÖKI Kft., Budapest, Hungary

[38] Kassie, B. T., Hengsdijk, H., Rotter, R., Kahiluoto, H., Asseng, S., Van Ittersum, M. (2013): Adapting to climate variability and change: experiences from cereal-based farming in the central rift and Kobo Valleys, Ethiopia. – Environmental Management 52: 1115-31.
[39] Kindu, M., Schneider, T., Teketay, D., Knoke, T. (2015): Drivers of land use/land cover changes in Munessa-Shashemene landscape of the south-central highlands of Ethiopia. – Environmental Monitoring and Assessment 187: 452.
[40] Lal, R. (2001): Soil degradation by erosion. – Land Degradation & Development 12: 519-539.
[41] Lambin, E. F., Ehrlich, D. (1997): Land-cover changes in sub-Saharan Africa (1982–1991): Application of a change index based on remotely sensed surface temperature and vegetation indices at a continental scale. – Remote Sensing of Environment 61: 181-200.
[42] Lambin, E. F., Meyfroidt, P. (2011): Global land use change, economic globalization, and the looming land scarcity. – Proceedings of the National Academy of Sciences 108: 3465-3472.
[43] Lambin, E. F., Geist, H. J., Lepers, E. (2003): Dynamics of land-use and land-cover change in tropical regions. – Annual Review of Environment and Resources 28: 205-241.
[44] Legesse, D., Ayenew, T. (2006): Effect of improper water and land resource utilization on the central Main Ethiopian Rift lakes. – Quaternary International 148: 8-18.
[45] Lemenih, M., Kassa, H. (2014): Re-greening Ethiopia: history, challenges and lessons. – Forests 5: 1896-1909.
[46] Liu, M., Tian, H., Chen, G., Ren, W., Zhang, C., Liu, J. (2008): Effects of land-use and land-cover change on evapotranspiration and water yield in China during 1900-2000. – Journal of the American Water Resources Association 44: 1193-1207.
[47] Macgregor, D. (2015): History of the development of the East African Rift System: a series of interpreted maps through time. – Journal of African Earth Sciences 101: 232-252.
[48] Maharjan, K. L., Joshi, N. P. (2013): Climate Change, Agriculture and Rural Livelihoods in Developing Countries. – Springer, Japan, pp. 1-23.
[49] Masih, I., Maskey, S., Mussá, F., Trambauer, P. (2014): A review of droughts on the African continent: a geospatial and long-term perspective. – Hydrology and Earth System Sciences 18: 3635.
[50] Matano, A.-S., Kanangire, C. K., Anyona, D. N., Abuom, P. O., Gelder, F. B., Dida, G. O., Owuor, P. O., Ofulla, A. V. (2015): Effects of land use change on land degradation reflected by soil properties along Mara River, Kenya and Tanzania. – Open Journal of Soil Science 5: 20.
[51] Melka, Y., Kassa, H., Ketema, M., Abebaw, D., Schmiedel, U. (2015): The effect of drought risk perception on local people coping decisions in the Central Rift Valley of Ethiopia. – Journal of Development and Agricultural Economics 7: 292-302.
[52] Meshesha, D. T., Tsunekawa, A., Tsubo, M. (2012): Continuing land degradation: cause–effect in Ethiopia's Central Rift Valley. – Land Degradation & Development 23: 130-143.
[53] Mutiibwa, D., Kilic, A., Irmak, S. (2014): The effect of land cover/land use changes on the regional climate of the USA high plains. – Climate 2: 153-167.
[54] Mutoko, M. C., Hein, L., Bartholomeus, H. (2014): Integrated analysis of land use changes and their impacts on agrarian livelihoods in the western highlands of Kenya. – Agricultural Systems 128: 1-12.
[55] Nunes, A. N., De Almeida, A. C., Coelho, C. O. (2011): Impacts of land use and cover type on runoff and soil erosion in a marginal area of Portugal. – Applied Geography 31: 687-699.
[56] Pacheco-Angulo, C., Vilanova, E., Aguado, I., Monjardin, S., Martinez, S. (2017): Carbon emissions from deforestation and degradation in a forest reserve in Venezuela between 1990 and 2015. – Forests 8: 291.

http://www.aloki.hu ● ISSN 1589 1623 (Print) ● ISSN 1785 0037 (Online)
DOI: http://dx.doi.org/10.15666/aeer/1605_66076632
© 2018, ALÖKI Kft., Budapest, Hungary

[57] Pal, S., Ziaul, S. (2017): Detection of land use and land cover change and land surface temperature in English Bazar urban centre. – The Egyptian Journal of Remote Sensing and Space Science 20: 125-145.
[58] Pang, C., Yu, H., He, J., Xu, J. (2013): Deforestation and changes in landscape patterns from 1979 to 2006 in Suan County, DPR Korea. – Forests 4: 968-983.
[59] Pielke, R. A. (2005): Land use and climate change. – Science 310: 1625-1626.
[60] Polasky, S., Nelson, E., Pennington, D., Johnson, K. A. (2011): The impact of land-use change on ecosystem services, biodiversity and returns to landowners: a case study in the state of Minnesota. – Environmental and Resource Economics 48: 219-242.
[61] Pricope, N. G., HUsak, G., Lopez-Carr, D., Funk, C., Michaelsen, J. (2013): The climate-population nexus in the East African Horn: Emerging degradation trends in rangeland and pastoral livelihood zones. – Global Environmental Change 23: 1525-1541.
[62] Raventós Vilalta, E. (2010): Water Resources Management in the Central Rift Valley in Ethiopia. – MSc Thesis. Universitat Politecnica Catalunya, Spain.
[63] Richards, J. A. (2013): Supervised Classification Techniques. – In: Richards, J. A. (ed.) Remote Sensing Digital Image Analysis. Springer-Verlag, Berlin, Heidelberg, pp 247-318.
[64] Scholten, W. (2007): Agricultural Development and Water Use in the Central Rift Valley of Ethiopia: A Rapid Appraisal. – Internship Report. University of Twente, Enshde, The Netherlands.
[65] Seyoum, W. M., Milewski, A. M., Durham, M. C. (2015): Understanding the relative impacts of natural processes and human activities on the hydrology of the Central Rift Valley lakes, East Africa. – Hydrological Processes 29: 4312-4324.
[66] Taddese, G. (2001): Land degradation: a challenge to Ethiopia. – Environmental Management 27: 815-824.
[67] Teketay, D. (2001): Deforestation, wood famine, and environmental degradation in Ethiopia's highland ecosystems: urgent need for action. – Northeast African Studies 8: 53-76.
[68] Temesgen, H., Nyssen, J., Zenebe, A., Haregeweyn, N., Kindu, M., Lemenih, M., Haile, M. (2013): Ecological succession and land use changes in a lake retreat area (Main Ethiopian Rift Valley). – Journal of Arid Environments 91: 53-60.
[69] Temesgen, H., Wu, W., Legesse, A., Yirsaw, E., Bekele, B. (2018): Landscape-based upstream-downstream prevalence of land-use/cover change drivers in southeastern rift escarpment of Ethiopia. – Environmental Monitoring and Assessment 190: 166.
[70] Tsegaye, D., Moe, S. R., Vedeld, P., Aynekulu, E. (2010): Land-use/cover dynamics in Northern Afar rangelands, Ethiopia. – Agriculture Ecosystems & Environment 139: 174-180.
[71] Turner, B., Meyer, W. B., Skole, D. L. (1994): Global land-use/land-cover change: towards an integrated study. – Ambio 23: 91-95.
[72] Turner, B. L., Lambin, E. F., Reenberg, A. (2007): The emergence of land change science for global environmental change and sustainability. – Proceedings of the National Academy of Sciences 104: 20666-20671.
[73] Vitousek, P. M. (1994): Beyond global warming: ecology and global change. – Ecology 75: 1861-1876.
[74] Wan, L., Zhang, Y., Zhang, X., Qi, S., Na, X. (2015): Comparison of land use/land cover change and landscape patterns in Honghe National Nature Reserve and the surrounding Jiansanjiang Region, China. – Ecological Indicators 51: 205-214.
[75] Wortley, L., Hero, J. M., Howes, M. (2013): Evaluating ecological restoration success: a review of the literature. – Restoration Ecology 21: 537-543.
[76] Yirsaw, E., Wu, W., Temesgen, H., Bekele, B. (2016): Effect of temporal land use/land cover changes on ecosystem services value in coastal area of China: The case of Su-Xi-Chang region. – Applied Ecology and Environmental Research 14: 409-422.

http://www.aloki.hu ● ISSN 1589 1623 (Print) ● ISSN 1785 0037 (Online)
DOI: http://dx.doi.org/10.15666/aeer/1605_66076632
© 2018, ALÖKI Kft., Budapest, Hungary

[77] Zeleke, G., Hurni, H. (2001): Implications of land use and land cover dynamics for mountain resource degradation in the Northwestern Ethiopian highlands. – Mountain Research and Development 21: 184-191.

APPENDIX

Household survey questionnaire

Name of respondent (Household Head): _____ PA Name: _____

Woreda (District) Name: _____ Date of interview: _____

Name and signature of enumerator: _____

I. Household characteristics

1. Wealth category of a household: a) Poor [] b) Medium [] c) Relatively better-off []
2. Household head sex, age, marital status, family size, education level and occupation

Name	Sex	Age	Marital Status	No. of family members	Level of education	Occupation	
						Primary	Secondary

3. Years of experience as a farmer: a) 5-10 [] b) 11- 15 [] c) 16-20 [] d) 21-25 []
   e) 26-30 [] f) 31-35 [] g) 36- 40 []
4. Main livelihood activity you engaged in:
   - before certain years:

   a) Mixed farming [] b) Pastoralist [] c) Agro-pastoralist [] d) Off-farm income []
   e) Others (specify) _____
   - Currently:

   a) Mixed farming [] b) Pastoralist [] c) Agro-pastoralist [] d) Off-farm income []
   e) Others (specify) _____

II. Land tenure and land holding size

5. Means of land acquisition (tenure): a) Distribution [] b) Inheritance []
   c) Gift [] d) Share cropping [] e) Renting []
6. No of plots of land you own? a) One [] b) Two [] c) Three [] d) Four []
   e) Five or more []
7. The total size of all your land in 'Timad'/hectares: _____
8. Your land holding is currently: a) Certified [] b) Not certified []

III. Income sources

9. Main source of household subsistence income and cash: a) Farm (crops consumed & sold, livestock consumed and sold, and others, specify) _____ b) Non-farm (petty trading: sale of fire wood, charcoal, bole soil, sand, vegetable, grain and others, labor outside the local area, remittance, fishing, private or government job e.g. teaching, health service) [] c) Others (Specify) _____

http://www.aloki.hu ● ISSN 1589 1623 (Print) ● ISSN 1785 0037 (Online)
DOI: http://dx.doi.org/10.15666/aeer/1605_66076632
© 2018, ALÖKI Kft., Budapest, Hungary

10. If your main source of income is non-farm activities, does it enable you to buy all your household basic necessities? a) Yes [] b) No []
    Specify the amount of non-farm income you get per year (Birr)._____
11. Your farm income: a) during 'good' year (Birr/Quintal): _____ b) during 'moderate' year (Birr/Quintal): _____ c) during 'bad' year (Birr/Quintal): _____
12. Do you have saving in 'good' year?: a) Yes [specify amount] _____ b) No []
13. Your household major expenditures: a) Purchase of grain [] b) Buy food ingredients (salt, food oil, etc.) [] c) Buy seeds (local/improved) [] d) Buy fertilizer []
    e) School fees [] f) Government tax [] g) Social affairs ('edir', 'serg', etc.) []
    h) Others (specify) _____

IV. Energy sources

14. Main sources of fuel for cooking & heating: a) Firewood [] b) Charcoal []
    c) Crop residues [] d) Kerosene [] e) Animal dung [] f) Others (specify) []
15. The main source of your fire wood: a) Own farm [] b) Others' farm []
    c) Communal woodland [] d) Market [] e) Others (specify) _____

V. Crop production

16. Area of your crop land during the last 30 years:
    a) Decrease [] b) Increase [] c) No change []
17. Crop yield per hectare of your major crops during specified periods (quintal):

	Crop Type							
Yield/hectare	Maize	'Teff'	Wheat	Sorghum	Potato			
20 years before								
10 years before								
5 years before								
Currently								

18. If crop yield per hectare of your land decreased from time to time, in your opinion, mention major causes of this yield reduction. a) Erratic rainfall [] b) Improved seed scarcity and high price []
    c) Unaffordable price of fertilizer [] d) Shortage of plowing oxen []
    e) Soil degradation (erosion, low fertility) [] f) Prevalence of pests, diseases and weeds []
    g) Lack of credit [] h) Others (specify) _____

VI. Livestock production

19. In case you own livestock, what is your major source of fodder for your animals?
    a) Grazing land b) Crop residues [] c) Forest reserve areas []
    d) Market [] e) Others (specify) _____
20. Did you observed any reduction or disappearance of palatable herbs, grass and trees in the grazing areas during last ten years? a) Yes[] b) No []
21. In which season/s of the year you face more shortage of livestock feed and how do you overcome this problem? _____

http://www.aloki.hu ● ISSN 1589 1623 (Print) ● ISSN 1785 0037 (Online)
DOI: http://dx.doi.org/10.15666/aeer/1605_66076632
© 2018, ALÖKI Kft., Budapest, Hungary

22. The types and number of livestock you own:

a) Cattle (Cows, Oxen, Heifer, Bulls, calves) [] b) Goat [] c) Sheep []

d) Chicken [] e) Donkey [] f) Horse [] g) Mule []

23. What is the trend of the livestock you own in terms of their number and type over the past 30 years?

a) Decreasing [] b) Increasing [] c) No change []

24. If decreasing, what are the major reasons, in the order of importance?

a) Lack of fodder [] b) Shortage of grazing land [] c) Disease prevalence and lack of veterinary services [] d) Drought & shortage of water [] e) Others (specify) _____

VII. Land use/cover change (LUCC) perception

25. Did you observed any LUCC over the last three decades? a) Yes [] b) No []

26. How do you see the trend of LUCC over the last 30 years?

No	LUC type	Change observed		
		Increase	Decrease	No change
1	Dense wood land (forest)			
2	Scattered wood land			
4	Grazing land			
5	Cultivated land			
6	Water bodies			
7	Bare land			
8	Settlement areas			

27. What do you think are the major causes/drivers for LUCC in the last three decades?

a) Population pressure [] b) Agricultural expansion [] c) Over grazing []

d) Fuel wood extraction [] e) Charcoal making [] f) Settlement [] g) Drought (climate change) []

h) Agricultural investment [] i) Livelihood change [] j) Government policy & institutional changes []

k) Social unrest [] l) Market & infrastructure access m) Others (specify) _____

28. What major impacts of LUCC you observed on your livelihood/environment?

a) Soil fertility/productivity decline [] b) Soil erosion [] c) Land degradation []

d) Lake retreat [] e) Climate change/drought [] f) Loss of biodiversity []

g) Shortage of wood [] h) Shortage of grazing land [] i) Others (specify) _____

VIII. Climate change perception

29. Did you observed any climate change over the last three decades? a) Yes [] b) No [].

If your answer to question 29 is 'Yes', answer questions 30-43.

30. Trend of rainfall amount during main rainy season (Kirmet) over the last one decade:

a) Decreased [] b) Increased [] c) No change []

31. Trend of rainfall amount during small rainy season (Belg) over the last one decade:

a) Decreased [] b) Increased [] c) No change []

32. Trend of rainfall of Kirmet season over the last one decade:

a) Coming late [] b) Coming early [] c) Early set-off [] d) Frequent dry spells []

e) Increased intensity in few period [] f) More erratic [] g) No change observed []

http://www.aloki.hu ● ISSN 1589 1623 (Print) ● ISSN 1785 0037 (Online)
DOI: http://dx.doi.org/10.15666/aeer/1605_66076632
© 2018, ALÖKI Kft., Budapest, Hungary

33. Trend of rainfall of Belg season over the last one decade:
    a) Coming late [] b) Coming early [] c) no rain in some years [] d) Normal []
34. Temperature trend over the last one decade:
    a) Increased [] b) Decreased [] c) No change []
35. Have you observed any drought occurrence over the last three decades?
    a) Yes [] b) No []. If yes, how frequent does it occurred? a) Once 2-5 years []
    b) Once 5-10 years [] c) Once 10 years []
36. The most disastrous drought you ever observed occurred in the year/s: _____
37. Have you observed any flood occurrence over the last three decades? a) Yes [] b) No []
    If yes, how frequent it has occurred? a) Every year [] b) Every two year []
38. The most disastrous flood you ever observed occurred in the year/s: _____
39. What do you think is the causes for climate change?
    a) Deforestation [] b) Overgrazing [] c) Agricultural expansion []
    d) Urbanization [] e) Industrial wastes [] f) Others (specify) _____
40. What are the major impacts of climate change on your livelihood and environment?
    a) Total crop failure [] b) Yield decrease [] c) Pest and disease prevalence[]
    d) Decrease in streams and lakes volume [] e) Flood and soil erosion []
    f) LUCC [] g) Others (specify) _____
41. Which adaptation measures did you take to cope up with climate change? Answer by (Yes/No)
    a) Planting trees [] b) Soil and water conservation [] c) Changing crop/animal variety []
    d) Changing planting date [] e) Changing crop type [] f) Using irrigation [] g) Crop diversification [] h) Off-farm employment [] i) Destocking livestock [] j) Asking for disaster relief [] k) Seasonal migration [] l) Storing livestock feed for dry periods []
    m) Others (specify) _____ n) Doing nothing []
42. What are the barriers that hinder you from using adaptation measures?
    a) Lack of early warning/information [] b) Lack of access to irrigation []
    c) Shortage of labor [] d) Lack of resources (money, input) []
    e) Lack of external support [] f) Shortage of land [] g) Others (specify) _____
43. Which of the following livelihood/ land use type you prefer to better cope up with climate change in the future?
    a) Mixed farming b) Agro pastoralist C) Pastoralist

IX. Perception on environmental degradation and conservation

44. Have you ever experienced soil degradation incidence on your farm? a) Yes[] b) No[]
45. If you answered "Yes", mention the indicators. a) Decreased crop productivity[]
    b) Loss of topsoil [] c) Other (specify) _____
46. Soil fertility status of your land currently: a) Poor[] b) Moderate[] c) Relatively fertile[]
47. Traditional land rehabilitation measures used for mitigating soil fertility problems:
    a) Addition of compost [] b) Crop rotation [] c) Fallowing [] d) Ploughing once []
    e) Repeated tillage [] f) Others (specify) _____

http://www.aloki.hu ● ISSN 1589 1623 (Print) ● ISSN 1785 0037 (Online)
DOI: http://dx.doi.org/10.15666/aeer/1605_66076632
© 2018, ALÖKI Kft., Budapest, Hungary

48. The major causes of forest decline in your area?
    a) Expansion of cropland [] b) Illegal cutting of wood [] c) Over-grazing []
    d) Government weak forest law enforcement [] e) Others (specify) _____
49. What type of aquatic habitats (rivers, wetlands, lakes) degradation problem you observed?
    a) Drying/decreasing of water volume [] b) Pollution []
    c) Excessive water withdraws for irrigation [] d) Introduction of invasive species []
    e) Others specify _____

X. Market and infrastructural access, and institutional support

50. Distance to the nearest market center (Km): _____ and distance to the nearest main road (Km): ____
51. Transport type used to sell your produce: a) Public transport [] b) Donkey back []
    c) Donkey cart [] d) Others (specify) _____
52. Do you have any access to the following supports? (Answer by saying Yes/No)
    a) Credit [] b) Inputs (seed, fertilizer) [] c) Training [] d) Extension on field support []
    e) Farmer-to-farmer skill exchange [] f) Weather broadcast [] g) One-to-five social network []
    h) Infrastructures (Tele, road, health center, water supply etc.).

Open-ended questions for key informants, focus groups and local experts

1. How you observed the LUC type and change:
    - Before the 'Derg' regime (before 1974)
    - During 'Derg' regime (1974-1990)
    - During the current government (since 1991 to the present)

---

2. What do you think are the major causes of LUCC?

---

3. What impacts does LUCC brought on people's livelihood and environment of the area?

---

4. How you observed the trend of climate variability (temperature, rainfall) and extremes (drought, flood, disease prevalence etc.) occurrence during the last three decades?

---

5. What do you think are the major causes of climate change in the area?

---

6. What impacts does climate change brought on peoples livelihood and environment?

---

http://www.aloki.hu ● ISSN 1589 1623 (Print) ● ISSN 1785 0037 (Online)
DOI: http://dx.doi.org/10.15666/aeer/1605_66076632
© 2018, ALÖKI Kft., Budapest, Hungary

7. What impacts does climate change brought on peoples livelihood and environment?

---

8. What measures you and other farmers took to cope up with the impacts of climate change?

---

9. What are the barriers to climate change adaptation in the area?

---

10. What are the extent, cause and impact of aquatic habitats (rivers, lakes, wetlands) degradation you observed in this area?

---

11. What measures you expect from the government and community to safeguard degraded aquatic habitats?

Thank you for your cooperation!

http://www.aloki.hu ● ISSN 1589 1623 (Print) ● ISSN 1785 0037 (Online)
DOI: http://dx.doi.org/10.15666/aeer/1605_66076632
© 2018, ALÖKI Kft., Budapest, Hungary

THE CONTENT OF IRON AND MANGANESE IN POTATO TUBERS TREATED WITH BIOSTIMULATORS AND THEIR NUTRITIONAL VALUE

MYSTKOWSKA, I.

State School of Higher Education, Biała Podlaska
Sidorska 95/97, 21-500 Biała Podlaska, Poland
(e-mail: imystkowska@op.pl)

(Received 30th Jun 2018; accepted 6th Sep 2018)

Abstract. The aim of the study was to evaluate the content and nutritional value of iron and manganese in edible potato tubers. Field experiments were carried out in 2015-2017 with the use of biostimulators on the individual farm in Międzyrzec Podlaski, Poland. The experiment was based on the random split-plot method. The influence of two factors was examined. The first row factor included three varieties of edible potato: Honorata, Jelly, Tajfun, and the second row – five methods of using biostimulators: Kelpak SL, Titanit, GreenOk, BrunatneBio Złoto Cytokininy, potato plants sprayed with distilled water were the control object. Potato plants were treated three times with biostimulators (at the beginning of flowering, at full flowering and after plant flowering). The high amount of rainfall in 2017 contributed to the increase of iron and manganese content in potato tubers. Plant tubers treated with the BrunatneBio Złoto Cytokiny preparation were characterized by the highest content of iron and manganese in comparison to plants from the control object. Titanite reduced the content of manganese and iron in tubers. The content of micronutrients in tubers was significantly differentiated by the genotype of the variety. The highest Mn concentration was found in the Jelly tubers, Fe in the Honorata variety. The average content of manganese was 4.4 $mg \cdot kg^{-1}$, and iron 43.5 $mg \cdot kg^{-1}$, which covers the demands in 1.7 and 5.5% per day, respectively.
Keywords: *edible potato, minerals, nutritional value, bioregulators*

Introduction

Nutritionists encourage an increase in the consumption of potato (*Solanum tuberosum* L.) tubers due to low caloric value and high nutritional and dietary values. The calories cooked potato (50-90 kcal per 100 g) slightly exceeds the energy value of apples (54 kcal per 100 g) or milk (62 kcal per 100 g), it is also three times smaller than wheat bread's (275 kcal per 100 g) and seven times smaller than chcolate's (540 kcal per 100 g) (Kunachowicz et al., 2010). This plant also provides a number of valuable nutrients, such as: carbohydrates, proteins, vitamins (C, B_1, B_2, PP, B_6), minerals (K, Mg, Fe, Cu, Mn, J), dietary fibre (Lutaladio and Castaidi, 2009).

The nutritional value of potato tubers, in addition to protein, carbohydrates and vitamins, is also determined by the content of minerals that after digestion and absorption into the blood are used by the body as a building block or a factor regulating life processes (Żechałko-Czajkowska, 1992; Spiak, 2000; LAW ON food and Nutrition Safety, 2009). Potato tubers contain 1-1.2% of minerals. Minerals are those components which remain in the form of ash after burning. In order for the human body to function properly, it must receive all necessary nutrients from outside, including minerals. Microelements control enzymatic processes, the largest amount (73-79%) comes from manure (Kaniuczak et al., 2009). In modern agriculture, more and more attention is paid not only to the amount of harvested crop, but also to its quality. According to Czuba (2000), the content of micronutrients in the crop yields is

http://www.aloki.hu ● ISSN 1589 1623 (Print) ● ISSN 1785 0037 (Online)
DOI: http://dx.doi.org/10.15666/aeer/1605_66336641
© 2018, ALÖKI Kft., Budapest, Hungary

an important agrotechnical issue, as well as an important quality feature assessed according to consumption and feed criteria. For this purpose, in addition to pesticides, a number of preparations are used as plant development regulators or biostimulators (Maciejewski et al., 2007). Biostimulators control mineral metabolism, increase the plant's resistance to stressful environmental conditions (Sawicka and Mikos-Bielak, 2002; Wierzbowska et al., 2015; Papenfus et al., 2013; Panda el al., 2012), as well as increase resistance to attacks of diseases and pests (Grzyś, 2012). Several authors have demonstrated the effect of acid pH < 5.5 on increasing the availability of manganese and iron in it (Prośba-Białczyk and Mydlarski, 2000; Rogóż, 2009). Iron participates in the process of photosynthesis and nucleic acid metabolism, stimulates the formation of chlorophyll, participates in the reduction of nitrates and the binding of free nitrogen, and regulates oxidation-reduction reactions. Manganese is involved in oxidation-reduction processes, photosynthesis, decarboxylation and binding of free nitrogen (Kabata-Pendias and Pendias, 1993; Zarzecka, 2004). The aim of the article is to examine the effect of biostimulators on the content of manganese and iron in potato tubers and to assess the nutritional value of the selected minerals.

Materials and methods

The experimental site

Potato tubers from a field experiment carried out in 2015–2017 in an individual farm in Międzyrzec Podlaski, Poland were the material for testing. The experiment was established in triplicate using the random split-plot method, on the soil included in the very good rye complex, class IVA. In individual years of research, soils differed in the content of organic matter and absorbable macro-elements. In 2015 and 2016, the soil was characterized by slightly acidic reaction, and in the last year of research, alkaline. The content of organic matter ranged from 15.0 to 18.7 g/kg. The content of absorbable phosphorus (P) was from high to very high, potassium (K) from medium to very high, and magnesium (Mg) was high. The first factor was three moderately early varieties of edible potato: Honorata, Jelly and Tajfun, and the second one, four types of biostimulators used in three dates (beginning of flowering, fully flowering and after flowering of plants):

1. Control object – without the use of biostimulators spraying with distilled water
2. Biostimulator Kelpak®SL (active substance – *Ecklonia maxima* algae extract) containing plant hormones: auxin – 11 mg/l and cytokinin – 0.031 mg·l, at a dose of 0.20 $L \cdot ha^{-1}$
3. Biostimulator Tytanit® (active substance – titanium) at a dose of 0.20 $L \cdot ha^{-1}$,
4. Biostimulator GreenOk® (active substance – humus substances 20 g/l) at a dose of 0.20 $L \cdot ha^{-1}$
5. Biostimulator BrunatneBio Złoto (active substances – plant hormones: auxin – 0.06 mg·l and cytokinin – 12 mg·l,) at a dose of 0.20 $L \cdot ha^{-1}$

The forecrop for potato in particular years of research was winter wheat. After harvesting the forecrop, a team of post-harvest crops was made. In autumn, each year preceding planting, natural fertilization in the form of manure in the amount of 25.0 $t \cdot ha^{-1}$ and mineral fertilization with phosphorus-potassium in the amount of P – 44.0 (100 $P_2O_5 \cdot 0.44$) kg/ha (lubofos for potatoes 7%) and K – 124.5 (150 $K_2O \cdot 0.83$)

http://www.aloki.hu ● ISSN 1589 1623 (Print) ● ISSN 1785 0037 (Online)
DOI: http://dx.doi.org/10.15666/aeer/1605_66336641
© 2018, ALÖKI Kft., Budapest, Hungary

$kg \cdot ha^{-1}$ (lubofos for potatoes 25%) was applied. These fertilizers were plowed pre-season plowing. Nitrogen fertilizers were sown in the spring in an amount of N 100 kg/ha (nitro-chalk 27%) and mixed with the soil using a cultivator. Potatoes were planted manually under the marker at a spacing of 67.5 × 37 cm, in the third decade of April (2015, 2016, 2017). Each plot consisted of five ridges. Cultivation and care treatments were carried out in accordance with the requirements of correct agrotechnics and methodological assumptions of the experiment. Prior to harvest, random samples of tubers were collected from each plot and used for chemical analysis and assessment of consumption-related characteristics of the tubers.

Chemical analysis methods

Weight of about 0.2–0.3 g of sample was transferred to the PTFE vessel and HNO_3 and HCL was added, 3:1 respectively. The vessels were placed in the rotor and loaded to the microwave. The following digestion program has been used:

Step 1 – 10' at 350 W

Step 2 – 35' at 650 W

Step 3 – cooling and ventilation

Mineralized samples were transferred to the 50 ml flasks through filtering paper and diluted with ultra-pure water.

Samples were examined with SpectroBlue ICP OES spectrometer at the Regional Research Center for Environment, Agricultural and Innovative Technologies, Pope John II State School of Higher Education in Biała Podlaska. Analytical curves were built by diluting Bernd Kraft Der Standard Spectro Genesis ICAL Solutions and VHG SM68-1-500 Element Multi Standard 1 in 5% HNO_3. Operating parameters for ICP OES instrument: coolant flow: 12 l/min; auxiliary flow: 0.90 l/min; nebulizer flow: 0.78 l/min; pump speed: 30 Rpm; number of measurements: 3.

Meteorological conditions

The weather conditions in the potato growing years were shown by precipitation sums and average air temperatures in *Table 1*.

Table 1. *Weather conditions during of potato vegetation*

Years	Months						April-September
	April	May	June	July	August	September	
Air temperature (°C)							
2015	8.2	12.3	16.5	18.7	21.0	14.5	15.2
2016	9.1	15.1	18.4	19.1	18.0	14.9	15.8
2017	6.9	13.9	17.8	16.9	18.4	13.9	14.6
Multiyear mean 1996-2010	8.0	13.5	17.0	19.7	18.5	13.5	15.0
Rainfall (mm)							
2015	30.0	100.2	43.3	62.6	11.9	47.1	295.1
2016	28.7	54.8	36.9	35.2	31.7	13.6	200.9
2017	59.6	49.5	57.9	23.6	54.7	80.1	325.4
Multiyear sum (1996-2010)	33.6	58.3	59.6	57.5	59.9	42.3	335.4

http://www.aloki.hu ● ISSN 1589 1623 (Print) ● ISSN 1785 0037 (Online)
DOI: http://dx.doi.org/10.15666/aeer/1605_66336641
© 2018, ALÖKI Kft., Budapest, Hungary

The growing season of 2015 proved to be an average air temperature of 15.2 °C, 0.2 °C higher than the long-term average and precipitation at 295.1 mm. The highest average air temperature was recorded in 2016 and amounted to 15.8 °C, it was higher than the long-term average by 0.8 °C, while this year was characterized by the lowest amount of precipitation – 200.9 mm, lower by 134.5 mm from the long-term sum. The highest number of rainfall was recorded in the growing season of 2017 – 325.4 mm and the lowest average air temperature -14.6 °C (*Table 1*).

Statistical analysis

Results of the study were analysed by ANOVA. Significance of sources of variation was checked with the Fisher-Snedecor test and the significance of differences between means was tested using the multiple comparison Tukey's test at the significance level of P = 0.05. Statistical calculations were performed in Excel using the authors' own algorithm based on the split-plot mathematical model.

Results and discussion

The average iron content in tubers was 43.5 $mg \cdot kg^{-1}$ d.m., ranging from 41.5 to 46.4 $mg \cdot kg^{-1}$ (*Table 2*). The research shows that the genetic factor had a significant effect on the iron content in potato tubers. The variety that contained the most of this ingredient was the Honorata variety, followed by Tajfun and Jelly. The influence of varietal properties on iron content is emphasized by Leszczyński and Lisińska (1986), Mikos-Bielak and Sawicka (1992), Gąsior (1996), as well as Sawicka (1996). Among the biostimulators used in the experiment, only the BrunatneBio Złoto biostimulator significantly increased the iron content in the tubers of the tested varieties. The factor that also significantly modified the content of the analysed component were the hydrothermal conditions prevailing during the years of research. High content of iron was found in tubers harvested in 2017 in which the sum of rainfall was 124 and 30 mm than in 2016 and 2015, respectively (*Table 1*). The problems of biostimulators on mineral content in potato tubers were investigated by Wierzbowska et al. (2015). When analysing the effect of Asahi SL, Bio-Algeen S90 and Kelpak SL biostimulators, the authors showed that the iron content in tubers was significantly modified only by the Kelpak SL biostimulator. The opposite direction of changes in iron content was observed by the authors in relation to the Bio-Algeen S90 biostimulator. In the light of the presented research, it should be stated that the iron content in tubers depends on the type of biostimulator and the mechanism of its impact on plants and on hydrothermal conditions. The large amount of rainfall caused that the potato tubers accumulated twice as much iron as in the remaining years. Lombardo et al. (2014) and Griffiths et al. (2012) found that the "mineral profile" can be influenced by the cultivation system. Lipiński et al. (2006) in their research proved that higher soil pH and higher humus content causes iron reduction. Iron affects the proper functioning of the circulatory system, participates in the synthesis of haemoglobin and in the oxidation and delivery of oxygen to tissues (Błoniarz et al., 2005). It is part of cytochrome oxidase, peroxidase and catalase enzymes (Jędrzejczak, 2004). The iron content in potato tubers treated with biostimulators was on average 43.5 $mg \cdot kg^{-1}$ d.m., and the daily norm of this element is 8 mg according to the recommendations of the Academy of Food Science and Nutrition in the USA (Wierzbicka, 2012). Consumption of 100 grams of potatoes covers the daily demand

http://www.aloki.hu ● ISSN 1589 1623 (Print) ● ISSN 1785 0037 (Online)
DOI: http://dx.doi.org/10.15666/aeer/1605_66336641
© 2018, ALÖKI Kft., Budapest, Hungary

for iron in approx. 5.5% of the daily requirement (*Table 3*). The established iron content in potato tubers corresponds to the research of: Prośba-Białczyk and Mydlarski (2000), Rogóż and Trąbczyńska (2009), Sawicka and Mikos-Bielak (2008), Różyło and Pałys (2006), Wierzbicka (2012), Wierzbicka and Trawczyński (2011) and Wierzbowska et al. (2015), who fund iron content in potato tubers from 26.9 $mg \cdot kg^{-1}$ - 91.85 $mg \cdot kg^{-1}$ d.m., while Kabata-Pendias and Pendias (1993) considered 21-58 $mg \cdot kg^{-1}$ of dry matter as the optimal content, while Ostrowska et al. (1991) estimate that the content of this element in potato is 93-188 $mg \cdot kg^{-1}$ of dry matter. The correct ratio of iron to manganese in feeds is assumed to be 2.5:1 (Rogóż, 2009). If it is larger, manganese deficiency is likely (Wierzbicka, 2012; Wierzbowska et al., 2015). In the tests carried out, the ratio was 10:1, which indicates a deficiency of manganese. The content of manganese in tubers treated with biostimulators was on average 4.4 $mg \cdot kg^{-1}$ d.m., which with demand of 1.8-2.3 (Wierzbicka, 2012) per 100 g of tubers realizes the demand for this component in the range of about 1.7% (*Table 3*). The studies carried out show that varietal features were the dominant factor that influenced the formation of manganese content in potato tubers (*Table 4*). The variety that contained the most of this ingredient was the Jelly variety. The observed interaction between the varieties and the years proves the individual reaction of the varieties to the weather conditions in the research years. The highest average manganese content was obtained in the Jelly and Tajfun varieties in 2017 (with the highest rainfall total). Tubers originating from objects treated with biostimulators in relation to the control object were characterized by a significantly higher content of manganese. The content of manganese in tubers was significantly modified by the BrunatneBio Złoto biostimulator. The applied biostimulator reacted to the atmospheric conditions in the years of research as indicated by the object x years interaction. The BrunatneBio Złoto biostimulator caused a significant increase in manganese content in 2017, which turned out to be wet and cold. The level of manganese content in potato tubers in the conducted experiment coincides with that given by other authors – 3.6-15 $mg \cdot kg^{-1}$ of dry mass (Kabata-Pendias and Pendias 1993; Sawicka, 1996; Sykut et al., 1998). In the studies by Mikos-Bielak (1999), the upper limit of the range was exceeded twice, and in Kucharzewski et al. (2002) almost ten times. The Mn concentration of approx. 500 $mg \cdot kg^{-1}$ of dry mass is toxic for most plants (Kucharzewski and Dębowski, 2001). It should be emphasized that Fe and Mn accumulate mainly in the outer layer of the potato tuber, so their excess can be removed by peeling (Mikos-Bielak, 1999). In the research conducted by Wierzbicka and Trawczyński (2011), the average contents of micro-elemenys in the tubers of organic potatoes were equal to: Fe-46.9; Mn-7.3 $mg \cdot kg^{-1}$ d.m. The spatial distribution of minerals in potato tubers is not even (Subramanian et al., 2011; Petryk and Bedla, 2010; Srek et al., 2012). According to Zarzecka (2004), some herbicides cause an increase in manganese in potato tubers. Kaniuczak et al. (2009) found in their research that liming reduces the content of manganese, and mineral fertilization increases the content of Mn in potato tubers. Manganese performs important functions in the plant. It takes part in the process of photosynthesis, the transformation of nitrogen compounds in the plant and in the biosynthesis of vitamin C (Jędrzejczak, 2004). It influences the uptake of phosphorus and iron from the soil. Manganese deficiency in potato delays plant development. In humans, it is responsible for the absorption of vitamins, the formation of connective tissue and bones, metabolism of carbohydrates, lipids and normal brain function (Wierzbicka, 2012).

http://www.aloki.hu ● ISSN 1589 1623 (Print) ● ISSN 1785 0037 (Online)
DOI: http://dx.doi.org/10.15666/aeer/1605_66336641
© 2018, ALÖKI Kft., Budapest, Hungary

Table 2. *Content of iron in tubers of potatoes depending on the biostimulator used*

Objects	Cultivars			Years			Mean
	Honorata	Jelly	Tajfun	2015	2016	2017	
1. Control object	44.6	42.9	44.1	42.5	43.5	45.6	43.9
2. Kelpak SL	43.2	42.0	43.5	41.9	43.5	43.5	43.0
3. Tytanit	42.8	42.1	43.1	41.5	43.1	43.1	42.6
4. GreenOk	44.8	42.4	43.7	42.1	43.5	45.3	43.6
5. BrunatneBio Złoto	45.6	43.5	43.7	43.1	44.3	46.4	44.6
Mean	44.2	42.6	43.6	42.2	43.6	44.8	43.5

$LSD_{0.05}$ for: cultivars – 0.63; objects – 0.31; years – 0.63; interaction: objects x years – 0.54; cultivars x years – 1.1; cultivars x objects – 0.46; cultivars x objects x years – 0.8

Table 3. *Mean daily intake of iron and manganese with diet*

Component	Range in dry matter mean ($mg \cdot kg^{-1}$)	Mean ($mg \cdot kg^{-1}$)	Dietary reference intake/day[1]	Percent of realization	
				Women	Men
Iron (Fe)	41.5-46.4	43.5	8 (mg)	5.5	5.5
Manganese (Mn)	3.5-5.0	4.4	1.8-2.3 (mg)	1.7	2.2

[1]By National Academy of Sciences Food and Nutrition Board USA (Jarosz, 2012)

Table 4. *Content of manganese in tubers of potatoes depending on the biostimulator used*

Objects	Cultivars			Years			Mean
	Honorata	Jelly	Tajfun	2015	2016	2017	
1. Control object	4.4	4.7	4.5	4.2	4.5	4.9	4.5
2. Kelpak SL	4.2	4.4	3.5	3.6	3.8	4.7	4.0
3. Tytanit	4.2	4.5	4.5	4.1	4.2	4.9	4.4
4. GreenOk	4.1	4.5	4.4	4.0	4.2	4.7	4.3
5. BrunatneBio Złoto	4.6	4.8	4.8	4.5	4.7	5.0	4.7
Mean	4.3	4.6	4.3	4.1	4.3	4.8	4.4

$LSD_{0.05}$ for: cultivars – 0.33; objects – 0.43; years – 0.33; interaction: objects x years – 0.75; cultivars x years – 0.58; cultivars x objects – 0.64; cultivars x objects x years – 1.11

Conclusions

The content of iron and manganese in potato tubers was significantly differentiated by the genotype of the variety. The highest concentration of Mn was found in the Jelly variety tubers, and of iron in the Honorata variety tubers. Tubers of plants treated with the BrunatneBio Złoto Cytokiny preparation were characterized by the highest content of iron and manganese. Weather conditions, particularly the high amount of rainfall in 2017, contributed to the increase of iron and manganese in potato tubers.

http://www.aloki.hu ● ISSN 1589 1623 (Print) ● ISSN 1785 0037 (Online)
DOI: http://dx.doi.org/10.15666/aeer/1605_66336641
© 2018, ALÖKI Kft., Budapest, Hungary

REFERENCES

[1] Błoniarz, J., Zaręba, S., Rahnama, M. (2005): Iron and manganese in selected herbs and herbal-fruit teas. – RPZHAW 53(2): 179-188 (in Polish).
[2] Czuba, R. (2000): Micronutrients in modern fertilization systems. – Zesz. Probl. Post. Nauk Roln. 471: 161-169 (in Polish).
[3] Dresow, J. F., Krause, T., Haase, N. U., Loges, R., Heß, J., Böhm, H. (2013): Effect of different defoliation systems of ryegrass–clover on yield and selected quality parameters of organic potatoes (Solanum tuberosum L.) for industrial processing at harvest and after storage. – Potato Research 56: 179-204. DOI: 10.1007/s11540-013-9239-8.
[4] Galdón, B. R., Rodriguez, L. H., Mesa, D. R., Leon, H. L., Perez, N. L., Rodriguez, E. M. R., Romero, C. D. (2012): Differentiation of potato cultivars experimentally cultivated based on their chemical composition and by applying linear discriminant analysis. – Food Chemistry 133: 1241-1248.
[5] Gąsior, J. (1996): Effect of nitrogen fertilization and harvesting time on the content of Iron in potato tubers. – Zesz. Probl. Post. Nauk Roln. 434: 243-248 (in Polish).
[6] Griffiths, A. M., Cook Eggett, D. L., Christensen, M. J. (2012): A retail market study of organic and conventional potatoes (Solanum tuberosum): mineral content and nutritional implications. – Int. J. Food Sci. Nutr. 63(4): 393-401.
[7] Grzyś, E. (2012): The Effect of Selected Biologically Active Substances on Maize Cultivated under Stress Conditions. – Monografie CXLV. Wyd. UP, Wrocław (in Polish).
[8] Jarosz, E. (2012): Nutritional Standards for the Population of Poland. – Institute of Food and Nutrition, Warsaw, pp. 106-107 (in Polish).
[9] Jędrzejczak, R. (2004): Iron and manganese in food. – Rocz. Państ. Zakł. Hig. 55: 13020 (in Polish).
[10] Kabata-Pendias, A., Pendias, H. (1993): Biogeochemistry of Trace Elements. – PWN, Warszawa.
[11] Kaniuczak, J., Hajduk, E., Właśniewski, S. (2009): Effect of liming and mineral fertilization on the content of manganese and zinc in potato tubers and green mass of fodder sunflower cultivated on loess soil. – Zesz. Probl. Post. Nauk Rol. 541: 199-206 (in Polish).
[12] Kucharzewski, A., Dębowski, M. (2001): Evaluation of the State of Contamination of Agricultural Produce in the Area of the Lower Silesia Voivodship. – Stacja Chemiczno-Rolnicza we Wrocławiu, Wrocław, pp. 3-67 (in Polish).
[13] Kucharzewski, A., Nowak, L., Dmowski, Z., Markowska, J. (2002): The content of heavy metals and sulfur in potatoes in Lower Silesia. – Zesz. Probl. Post. Nauk Roln. 489: 491-497 (in Polish).
[14] Kunachowicz, H., Nadolna, I., Iwanow, K., Przygoda, B. (2010): The Nutritional Value of Selected Foods and Typical Dishes. – Wyd. Lekarskie PZWL, Warszawa (in Polish).
[15] Law on Food and Nutrition Safety (2009): Dz. U. 2009, 98, poz. 817.
[16] Leszczyński, W., Lisińska, G. (1986): The effect of nitrogen fertilization and the date of potato planting of Atol, Tisa and Reda varieties on changes in the quality of tubers. – Biul. Inst. Ziemn. 34: 63-72 (in Polish).
[17] Lipiński, W., Franczak, S., Watros, A. (2006): Influence of granulometric composition, pH and organic matter of soil on the content of iron and manganese from wheat grain. – J. Elementol. 11(1): 35-42 (in Polish).
[18] Lombardo, S., Pandino, G., Mauromicale, G. (2014): The mineral profile in organically and conventionally grown "early" crop potato tubers. – Sci. Horticult. 167: 169-173.
[19] Lutaladio, N., Castaidi, L. (2009): Potato: The hidden treasure. – J. Food Comp. Anal. 22: 491-493.
[20] Maciejewski, T., Szukała, J., Jarosz, A. (2007): The impact of the Asahi SL biostimulator on the quality characteristics of potato tubers. – J. Res. Appl. Agric. Eng. 52(3): 109-112 (in Polish).

http://www.aloki.hu ● ISSN 1589 1623 (Print) ● ISSN 1785 0037 (Online)
DOI: http://dx.doi.org/10.15666/aeer/1605_66336641
© 2018, ALÖKI Kft., Budapest, Hungary

[21] Mikos-Bielak, M. (1999): Impact in geNeral in the Districts of Stalowa Wola on the Content of Macro and Micronutrients in Potato Tubers. – Mat. Konf. Ziemniak jadalny i dla przetwórstwa spożywczego czynniki agrotechniczne i przechowalnicze warunkujące jakość. IHAR, Radzików, pp. 189-191 (in Polish).
[22] Mikos-Bielak, M., Sawicka, B. (1992): Zmienność zawartości mikroelementów w bulwach poszczególnych odmian ziemniaków. – VII Symp. Mikroelementy w rolnictwie, pp. 136-140.
[23] Ostrowska, A., Gawliński, S., Szczubiałka, Z. (1991): Methodology and Assessment of Soil and Plant Properties Wyd. – Inst. Ochrony Środowiska, Warszawa (in Polish).
[24] Panda, D., Pramanik, K. B., Naya, R. (2012): Use of sea weed extracts as plant growth regulators for sustainable agriculture. – Int. J. Bioresource and Stress Manag. 3(3): 404-411.
[25] Papenfus, H. B., Kulkarni, M. G., Strik, W. A., Finnie, J. F., van Staden, J. (2013): Effect of a commercial seaweed extract (Kelppak) and polyamines on nutrient-deprived (N, P and K) okra seedlings. – Sci. Horticult. 151: 142-1146.
[26] Petryk, A., Bedla, D. (2010): Evaluation of Pb, Zn, Cr, Fe content in potato tubers and in soil in the commune of Trzebinia. – Inżynieria Ekologiczna 22: 18-24 (in Polish).
[27] Prośba-Białczyk, U., Mydlarski, M. (2000): The influence of habitat conditions and varietal properties on the content of trace elements in potato tubers. – Biuletyn IHAR 213: 45-53 (in Polish).
[28] Rogóż, A. (2009): The content of trace elements in soils and selected root crops. Cz II. The content of manganese and iron. – Zesz. Probl. Post. Nauk Rol. 541(2): 365-373 (in Polish).
[29] Rogóż, A., Trąbczyńska, K. (2009): The content of trace elements in soils and selected root crops. Vol. I. Copper and zinc content. – Zesz. Probl. Post. Nauk Rol. 541(2): 353-363 (in Polish).
[30] Różyło, K., Pałys, E. (2006): Effect of fertilization and soil conditions on the chemical composition of potato tubers and their health condition. – Zesz. Probl. Post. Nauk Rol. 511: 279-286 (in Polish).
[31] Sawicka, B. (1996): They enter the game of manganese and iron in tubers of early potato varieties during the growing season. – Zesz. Probl. Post. Nauk Roln. 434: 225-229 (in Polish).
[32] Sawicka, B., Mikos-Bielak, M. (2008): Modification of Potato Tuber Chemical Composition by Applications of the Asahi SL Biostimulator. – In: Dąbrowski, Z. T. (ed.) Biostimulators in Modern Agriculture. - Solanaceous Crops. Editorial House Wieś Jutra, Warszawa, pp. 61-67.
[33] Spiak, Z. (2000): Micronutrients in agriculture. – Zesz. Probl. Post. Nauk Roln. 471: 29-34 (in Polish).
[34] Srek, P., Hejcman, M., Kunzova, E. (2012): Effect of long-term cattle slurry and mineral N, P and K application on concentrations of N, P, K, Ca, Mg, As, Cd, Cr, Cu, Mn, Ni, Pb and Zn in peeled potato tubers and peels. – Plant Soil Environ. 58(4): 167-173.
[35] Subramanian, N. K., White, P. J., Broadley, M. R., Ramsay, G. (2011): The three-dimensional distribution of minerals in potato tubers. – Ann. Bot. 107(4): 681-691.
[36] Sykut, S., Ruszkowska, M., Wojcieska, U., Kusio, M. (1998): The content of manganese in plants as an indicator of the degree of soil acidification. – Zesz. Probl. Post. Nauk Roln. 456: 233-236.
[37] Whittaker, A., Marotti, I., Dinelli, G., Calamai, L., Romagnoli, S., Manzelli, M., Palchetti, E., Vecchio, V., Benedettelli, S. (2010): The influence of tuber mineral element composition as a function of geographical location on acrylamide formation in different Italian potato genotype. – Journal of the Science of Food and Agriculture 90: 1968-1976. DOI 10.1002/jsfa.4026.

http://www.aloki.hu ● ISSN 1589 1623 (Print) ● ISSN 1785 0037 (Online)
DOI: http://dx.doi.org/10.15666/aeer/1605_66336641
© 2018, ALÖKI Kft., Budapest, Hungary

[38] Wierzbicka, A. (2012): Mineral content of potato tubers grown in the organic system their nutritional value and interaction. – J. of Research and Applications in Agricultural Engineering 57(4): 188-192 (in Polish).
[39] Wierzbicka, A., Trawczyński, C. (2011): Influence of irrigation and soil microorganisms on macro and micronutrient content in organic potato tubers. – Frag. Agron. 28(4): 139-148.
[40] Wierzbowska, J., Cwalina-Ambroziak, B., Głosek, M., Sienkiewicz, S. (2015): Effect of biostimulators on yield and selected chemical properties of potato tubers. – J. Elem. 20(3): 757-768.
[41] Wierzbowska, J., Cwalina-Ambroziak, B., Bowszyc, T., Głosek-Sobieraj, M., Mackiweicz-Walec, E. (2015): Content of microelements in tubers of potato treated with biostimulators. – Pol. J. Natur. Sc. 30(3): 225-234.
[42] Zarzecka, K.(2004): The content of iron and manganese in potato tubers depending on the weed control methods. – Acta Sci. Pol. Agric. 3(1): 165-173 (in Polish).
[43] Żechałko-Czajkowska, A. (1992): Micronutrients in human food. – VII Symp. Mikroelementy w rolnictwie, pp. 20-25 (in Polish).

http://www.aloki.hu ● ISSN 1589 1623 (Print) ● ISSN 1785 0037 (Online)
DOI: http://dx.doi.org/10.15666/aeer/1605_66336641
© 2018, ALÖKI Kft., Budapest, Hungary

RESEARCH ON CARBON EMISSION DIVERSITY FROM THE PERSPECTIVE OF URBANIZATION

ZHENG, D. C.[1,2] – LIU, W. X.[1,2,*] – LI, X. X.[1] – LIN, Z. Y.[1] – JIANG, H.[2]

[1]*Internet Innovation Research Center—The College's Research Base of Humanities and Social Science in Fujian Province, Minjiang University, 350108 Fuzhou, Fujian, China*

[2]*Straits Institute of Minjiang University, 350108 Fuzhou, Fujian, China*

**Corresponding author*
e-mail: 424070881@qq.com; phone: +86-136-8500-6093

(Received 1st Jul 2018; accepted 13th Sep 2018)

Abstract. Urbanization is only a carrier of human activities, and it does not directly affect carbon emissions. Based on the essential relationship of carbon emissions and urbanization, and summarizing the shortcomings of the present research methods, this paper first classifies the degree of urbanization in China by using the multi-index cluster analysis method based on panel data, and then analyzes the influence factors of carbon emissions by the STIRPAT model for different urbanization levels. The results show that the elasticity of factors affecting carbon emissions is quite different under different urbanization levels. The conclusion is that the policy of reducing emissions should be different for different levels of urbanization. Differentiated emission reduction policies are necessary for a vast China.
Keywords: *classification of urbanization, factors of carbon emission, STIRPAT model, entropy weight, multi-index cluster analysis*

Introduction

At present, the greenhouse effect has seriously affected the global climate and has become a serious obstacle in the process of human social development, and carbon dioxide is the most important component of greenhouse gases, and its contribution to the greenhouse effect is more than 60%. It can be seen that the excessive emission of carbon dioxide is the main reason for the greenhouse effect.

Scholars have started a lot of work around the causes of excessive carbon dioxide emissions. They have analyzed the possible factors, including economic growth, income level, industrial structure and so on, and the degree of urbanization is also regarded as an important factor. However, in most of the research work, "urbanization" is regarded as an explanatory variable into the model, which is a one-sided approach. In essence, the extent of carbon emissions depends on changes in human activities. Urbanization is a carrier of changes in human activities, affecting human activities, but it does not directly affect carbon emissions.

Based on the essential relationship between carbon emission and urbanization and the shortcomings of current research methods, the degree of urbanization in China is classified by using the multi-index cluster analysis method based on panel data. The influence factors of carbon emissions are analyzed through the STIRPAT model, and it is found that under different levels of urbanization, the influence of various factors on carbon emissions is quite different. The conclusion is that for provinces and cities with different urbanization levels, the emission reduction policy should be different, and for a vast China, differentiated emission reduction policies are very necessary.

http://www.aloki.hu ● ISSN 1589 1623 (Print) ● ISSN 1785 0037 (Online)
DOI: http://dx.doi.org/10.15666/aeer/1605_66436654
© 2018, ALÖKI Kft., Budapest, Hungary

Basic conception

First of all, the scientific connotation of "urbanization" should be clarified. Cities and towns are only one of the geographic carriers of human activities where people form unique production mode, consumption mode and social mode. In a narrow sense, urbanization is a process of increasing urban population. However, urbanization in a broad sense is a trend of gradual change from a traditional rural society dominated by agriculture to a modern urban society dominated by industry and service industries. It includes the changes in the occupation of the population, the transformation of the industrial structure, and the changes in land and geographical space (Lu, 2007). Urbanization is not only a simple migration of rural population to towns, but also a change in social structure (Poumanyvong and Kaneko, 2010). This is a dynamic process, manifested in the transformation of people in the geographical space of towns and villages. Therefore, using only the proportion of urban population does not fully describe the degree of urbanization.

The level and speed of urbanization are affected and restricted by the socio-economic environment and the natural environment. As Knox and McCarthy (2011) pointed out, "Urbanization is the interaction of a variety of factors, including economic, demographic, political, cultural, technological, environmental, and social, and it is also influenced by two kinds of contingency factors, such as geographical location and historical reasons."(Paraschiv, 2012). Therefore, in different countries and regions, the level and speed of urbanization show great differences.

Urbanization also plays an important role in ecological and social activities, making the natural environment and social environment change. These effects are positive and reverse. On the one hand, urbanization has brought about the increase of urban population, aggravated social and economic activities, resulting in greater demand for energy. At the same time, congested traffic brings congestion on the road. These two factors will cause serious air pollution and waste discharge. On the other hand, urbanization has produced an "agglomeration effect", which has concentrated the scope of social and economic activities and increased public transport at the same time. This can effectively reduce carbon emissions from commutes. Towns and cities are often centers of technological innovation, new technologies and new industries. The birth of these products can often increase production efficiency and reduce unit energy consumption, which can also effectively reduce carbon emissions.

Literature review

There is a correlation between urbanization and carbon emissions, which has become the consensus of researchers and policy makers. A large amount of research work has focused on the impact of urbanization on carbon emissions. If the impact of urbanization is neglected in the prediction of CO_2 emissions and the formulation of energy and environmental policies, the model's forecast results and the effect of the implementation of policies will be seriously affected, and even result in a deviation in the direction of work (Sadorsky, 2014).

The ecological modernization theory founded by Joseph Huber and Martin Jänicke in Germany in the early 1980s pointed out that the ecological environment is inevitably affected by socio-economic activities, and that can be transformed from negative to positive in the process of economic development and social system transformation. Specifically, excessive carbon emissions are unavoidable in the primary and secondary

http://www.aloki.hu ● ISSN 1589 1623 (Print) ● ISSN 1785 0037 (Online)
DOI: http://dx.doi.org/10.15666/aeer/1605_66436654
© 2018, ALÖKI Kft., Budapest, Hungary

stages of development. However, with the further advancement of modernization, the improvement of social environmental awareness, the innovation and application of environmental protection technologies, the scientific nature of urban planning and the adjustment of industrial structure, these factors will all contribute to the reduction of carbon emissions. Sun et al. (2013) studied the total carbon emissions of 76 countries and regions from 1980 to 2007, examined the relationship between the dynamic evolution of urbanization and carbon emissions, and verified the rationality of ecological modernization theory.

The theory of urban environmental change has put forward the opposite view, which is established on the base of a series of researches (Bartone et al., 1994; Lee, 1994; McGranahan et al., 1996; Pugh, 1996; Satterthwaite, 1997). McGranahan (2000) summed up these research results and developed this theory (Marcotullio and Lee, 2003). From the perspective of urban development, these scholars point out that the environmental problems faced by cities are different at each stages of development. Only in the middle and later stages of urban development can carbon emissions become one of the main problems of urban environment.

The problem of urban density was originally concerned by architecture and urban planning. When economists are involved in this field, how urban density affects environmental changes and energy consumption has become an interesting and practical topic, which has evolved a compact city theory. Most scholars supported the idea that compacting cities can bring environmental benefits. They believe that compact cities can bring about the scale effects of urban public facilities such as public transportation, public education and water supply. At the same time, compact cities can also reduce the use of private cars, shorten travel distances, and reduce losses in the power supply, thereby reducing energy consumption and CO_2 emissions. However, some other critics pointed out that compact cities are more likely to cause new problems such as traffic jams and urban heat island effects, resulting in increased CO_2 emissions (Gaigné et al., 2012).

Although the impact of urbanization on carbon emissions has become an important research area for urban economics, in most research work, the level of urbanization is simply measured by the proportion of urban population, and directly enters the model as an explanatory variable (Shahbaz et al., 2016; Yang et al., 2018), which does not accurately portray the true relationship between urbanization and carbon emissions. First, urbanization embodies a comprehensive process of change, and it is not enough to measure only the proportion of urban population. Secondly, using the urbanization level as an explanatory variable directly into the analysis model does not meet the true relationship between the two. The impact of urbanization on carbon emissions plays a role through human activities, and urbanization itself does not have a direct impact on environmental change.

The lack of research has attracted the attention of a few researchers who have put forward new ideas for research. Chikaraishi pointed out in the 2015 study that the relationship between urbanization and environmental change can be described by two relationships: indirect effect and moderating effect. He expressed the two effects by functions as follows: $y = f(\beta, x(z))$ and $y = f(\beta(z), x)$, where y indicates environmental change, x indicates human activity, z indicates urbanization degree, and β indicates the influence of human activities on environmental changes. In the two functions, the former indicates that the explanatory variables (human activities) are influenced by the degree of urbanization, and the latter indicates that the degree of

http://www.aloki.hu ● ISSN 1589 1623 (Print) ● ISSN 1785 0037 (Online)
DOI: http://dx.doi.org/10.15666/aeer/1605_66436654
© 2018, ALÖKI Kft., Budapest, Hungary

urbanization affects the elastic coefficient of human activity - environmental change. And the above three modern urban environmental theories have realized that the impact of urbanization on the environment may have both positive or reverse effects, which means that when the mathematical model determines that urbanization does not have a significant impact on environmental changes in statistical sense, it is in fact possible that the positive and negative effects of urbanization on environmental change are comparable.

Research on carbon emission according to urbanization distiguish based on STIRPAT model

As mentioned earlier, urbanization does not directly affect carbon emissions. People's social and economic activities are the direct cause of carbon emissions. In the process of urbanization, as people's agglomeration activities increase, their social and economic pattern also change, which in turn has a further impact on carbon emissions. Furthermore, in areas with different levels of urbanization, people's socio-economic pattern is naturally very different, and there is a huge difference in the level of carbon emissions among regions.

China has a vast territory with significant difference in social and economic development level among different regions. In order to make a scientific research on the influence factors and the impact of carbon emissions all over the country, a carbon emission difference analysis model based on the urbanization level is established in this paper.

STIRPAT model and its extension

STIRPAT (Stochastic Impacts by Regression on Population, Affluence, and Technology) model is a random model developed from the IPAT equation and has become the most classic model for conducting environmental impact assessments. A large amount of research work is based on it whose function expression is $I_i = aP_i^b A_i^c T_i^d e_i$ (Dietz and Rosa, 1997), where, I, P, A and T respectively denote environmental impact, population, wealth and technological level. The subscript i represents each observation object. The parameter a is regarded as a constant. b, c and d determine the influence of three factors, population, wealth and technology, on the environment, respectively. The residual item e represents the social structure, system and culture that can affect the environment, and other factors that can affect human activities. In explaining the model, technology includes not only the technology itself, but also the social structure, the system, the culture, and all the other factors that can affect human activities. In practical research, STIRPAT models usually appear in logarithmic form for parameter estimation and hypothesis testing.

Based on the STIRPAT model, a series of extensions and modifications on the model can be made. First, the STIRPAT model can add other relevant factors as explanatory variables into the model, among which population structure, urbanization level and industrial structure level are the most frequently introduced variables. Maruotti (2011) and York et al. (2003) considered the variable "proportion of people between 15-65 years old" in the model. Maruotti (2011), York et al. (2003), Zhang (2013), Sadorsky (2014), Poumanyvong and Kaneko (2010), Wang et al. (2016) took into account the influencing factor of urbanization level. Second, the dummy variable can be added to

http://www.aloki.hu ● ISSN 1589 1623 (Print) ● ISSN 1785 0037 (Online)
DOI: http://dx.doi.org/10.15666/aeer/1605_66436654
© 2018, ALÖKI Kft., Budapest, Hungary

the STIRPAT model. The parameters of the dummy variable in the model do not indicate the effect on the environmental change. The "year dummy variable" and "country dummy variable" are two common dummy variables with which the researchers distinguish the impact elasticity of carbon emissions in different years or different countries (Poumanyvong and Kaneko, 2010; Zhang et al., 2013). York et al. (2003) introduced the dummy variable "Whether the subject is in the tropics" to assess the impact of tropical regions on environmental changes. Third, the quadratic term and multiple items can also be added to the model to build nonlinear relationships between variables, which can sometimes make the model more realistic. For instance, Dietz and Rosa (1997) added a quadratic item to the population in an attempt to prove that the environmental changes and population changes are nonlinear, while York et al. (2003) added the quadratic form of per capita GDP.

Classification of urbanization level

China has a vast area and great differences in regional development. Therefore, it is necessary to classify and discriminate the urbanization status.

Population urbanization and land urbanization are two aspects of the process of urbanization. In measuring the level of urbanization, the two factors of population urbanization and land urbanization level have been comprehensively considered in this paper. Regarding the urbanization level of the population, this paper adopts the indicator of "the ratio of urban population to total population" in accordance with international practice. The research work on the level of land urbanization should include the integration of land urbanization of city and established towns. According to the stipulations of the *Regulations for the Statistical Division of Urban and Rural Areas* and the *National New Urbanization Plan (2014-2020)*, the township is an important part of the scope of urbanization. At present, a large number of research work limit the scope of the inspection targets to urban areas, for example, Bai Xianchun used the land index of urban area when adjusting land factors for urbanization level (Bai, 2004) and other scholars use the area of urban built-up areas to conduct research on land factors (*Table 1*). In this paper, the urban and the designated town built-up area are summed up to obtain the urban built-up area, which is used to describe the level of land urbanization. The specific formula is as *Equation 1:*

$$\text{Land urbanization level} = \frac{\text{urban built} - \text{up area} + \text{designated town built} - \text{up area}}{\text{land survey area}} \quad \text{(Eq.1)}$$

Table 1. *Composition and data sources of urbanization classified index*

Urbanization rate	Urban built-up area	Designated town built-up area	Land survey area
%	sq.km	sq.km	Ten thousand hectares
China Statistical Yearbook	China Statistical Yearbook	Statistical yearbook of urban and rural construction in China	China Statistical Yearbook

In this paper, lessons are drawn from the multi-index cluster analysis method of panel data based on entropy weight algorithm designed by Zheng Dachuan in 2016 to classify the level of urbanization. The specific steps are as follows:

http://www.aloki.hu ● ISSN 1589 1623 (Print) ● ISSN 1785 0037 (Online)
DOI: http://dx.doi.org/10.15666/aeer/1605_66436654
© 2018, ALÖKI Kft., Budapest, Hungary

- Measurement of entropy weight of index (*Table 2*). In this paper, the most commonly used discrete degree statistics namely the standard deviation coefficient $CV_{nk} = \sigma_{nk} / \mu_{nk}$ is used to get the entropy weight result.

Table 2. *Entropy weight of each urbanization index*

Index *k*	Level of population urbanization	Level of land urbanization
Entropy weight α_k	0.6113	0.3887

- The Euclidean distance is used to calculate the individual distance of each index D_k separately.
- The full distance of individual is calculated as:

$$D = \sum_{k=1}^{K} \alpha_k D_k \quad \text{(Eq.2)}$$

- Based on *Equation 2,* the type distance measurement is carried out by the sum of squares of deviations (Ward method), and the type of the sample is divided.

According to the results of hierarchical cluster analysis, the level of urbanization in the whole country can be divided into four categories:

- Category I: Beijing, Tianjin, Shanghai
- Category II: Liaoning, Guangdong, Jiangsu, Zhejiang
- Category III: Shanxi, Ningxia, Shaanxi, Jilin, Hubei, Hainan, Shandong, Inner Mongolia, Heilongjiang, Fujian, Chongqing, Hebei, Hunan, Jiangxi, Anhui, Qinghai, Henan, Guangxi, Sichuan and Xinjiang
- Category IV: Guizhou, Yunnan, Gansu

Variable and data selection

Carbon emission accounting

The carbon dioxide emission level is measured according to the terminal consumption of primary energy on the regional energy balance. In this paper, the total CO_2 emissions from the 16 main energy sources are used as the accounting results of carbon emissions (*Table 3*).

Table 3. *The CO_2 emission coefficient of 16 energy sources (Ren, 2014)*

Energy source	Raw coal	Cleaned coal	Other coal washing	Coal briquette	Coke	Coke gas	Blast furnace gas	Other gases
Carbon dioxide emission coefficient (kg-CO_2/kg or kg-CO_2/m^3)	1.9003	2.2829	0.7247	1.7622	2.8604	0.8469	0.1636	0.7091

http://www.aloki.hu ● ISSN 1589 1623 (Print) ● ISSN 1785 0037 (Online)
DOI: http://dx.doi.org/10.15666/aeer/1605_66436654
© 2018, ALÖKI Kft., Budapest, Hungary

Energy source	Crude oil	Gasoline	Kerosene	Diesel	Fuel oil	Liquefied petroleum gas	Refinery dry gas	Natural gas
Carbon dioxide emission coefficient (kg-CO_2/kg or kg-CO_2/m^3)	3.0202	2.9251	3.0179	3.0959	3.1705	3.1013	3.0119	2.1622

Population

In the current research work, the indicators of population variables are usually expressed in terms of total population (Othman and Jafari, 2016; Yang et al., 2018). Some researchers have joined the total number of working age population. This paper holds that population density is an important factor affecting urban carbon emissions, and a higher population density will affect the degree of urban traffic congestion and have a negative impact on carbon emissions. On the other hand, high population density can promote efficient planning of the urban system and bring convenience to people's travel activities. Therefore, in this study, for the population influencing factors described, in addition to the total population, the population density index was specifically added[1].

Treasure

For the factor on wealth in STIRPAT model, almost all research work is described by GDP capita (Dietz and Rosa, 1997; Poumanyvong and Kaneko, 2010; Rozanov et al., 1990), so does this paper. In order to eliminate the interference of inflation, the description of wealth in this paper especially adopts the actual GDP after deducting the price effect according to the GDP index.

Technology

Energy intensity = total energy consumption / GDP, which represents the amount of energy consumed per unit of GDP produced. The greater the value, the lower the technical level. The greater the value of energy intensity, the greater the amount of energy consumed per unit of GDP, which indicates that GDP production is more dependent on energy consumption rather than technological progress; on the contrary, it means that the higher the technological level of wealth creation, the less energy consumption can provide more output.

Analysis of the factors of carbon emissions

The principle of estimation of panel data model is included two categories: fixed effect and random effect among which the random effect RE model is the individual effect model: $y_{it} = x'_{it}\beta + (\alpha_i + \epsilon_{it})$. For a given i, the mixed error term$\mu_i = \alpha_i + \epsilon_{it}$ is related to different t, that is, $\mathrm{Cov}(u_{it}, u_{is}) = \delta_\alpha^2/(\delta_\alpha^2 + \delta_\varepsilon^2)$, for all s≠t.

[1] Population density = total population / total area, usually taking the unit of "person/km^2". In model building, we perform natural logarithm transformation on all variables to reduce the influence of heteroscedasticity. However, the population density of Qinghai Province is less than 1 in all years and cannot be converted logarithmically. Therefore, in the research process of this paper, the unit of population density is taken as "person/10 km^2".

http://www.aloki.hu ● ISSN 1589 1623 (Print) ● ISSN 1785 0037 (Online)
DOI: http://dx.doi.org/10.15666/aeer/1605_66436654
© 2018, ALÖKI Kft., Budapest, Hungary

For regional economic analysis, it should be considered that there is a random effect for a certain region in a continuous period. That is to say, there is correlation between error items at different time points. This development correlation is determined by the inertia of regional social and economic development and the invariance of basic development conditions. Therefore, even if the Hausman test refuses the original hypothesis of the RE model in statistical sense, we still use the random effect model to classify the regional carbon emissions.

Based on the results of the classification of urbanization level in the whole country, the panel data analysis of four categories of provinces was conducted based on random effects in this paper. At the same time, in order to illustrate the necessity of categorical analysis, the national data are specifically estimated by a non-classified random effects model. It is easy to see from *Table 4* whether classifying the level of urbanization has a great influence on the estimation result of the model.

Table 4. *Comparison of estimation results based on random effects model*

	Nationwide	**Category I**	**Category II**	**Category III**	**Category IV**
Ln (total population)	-0.1735	-0.9151	-0.5975	-0.2696	-0.2092
Ln (population density)	0.0038	0.2690	0.1324	0.1157	0.1067
Ln (actual GDP)	1.1556	1.3660	1.5469	1.1394	0.8654
Ln (energy intensity)	1.2528	1.6169	1.8601	1.1691	0.84224

When estimating over the entire country, the total population and the total carbon emissions are inversely related. When the total population increases by one percentage point, CO_2 emissions fall by 0.17%. The population density elasticity of carbon emissions is almost zero, only 0.003%. The GDP elasticity and energy intensity elasticity of carbon emissions are positive, indicating that changes in GDP and energy intensity all over the country will bring about the same direction of CO_2 change.

According to different levels of urbanization, the elasticity of each variable of CO_2 and the estimation of the entire country are the same under different levels of urbanization, which indicates that there is no difference in the basic direction of urbanization between different levels of urbanization. However, in terms of elasticity, there is a great difference according to the level of urbanization.

Under the background of rapid urbanization, people's awareness of the impact of carbon emissions is growing. With the increase of population, the emission of CO_2 is decreasing, while with the improvement of urbanization level, the population elasticity of carbon emissions is increasing progressively. As the first category, the three largest cities of Beijing, Tianjin and Shanghai have the largest population elasticity of carbon emissions, and when the population increases by 1%, CO_2 emissions also drops by nearly 1%. In the third and fourth category provinces with lower urbanization level, the population elasticity of CO_2 is 0.26% and 0.21% respectively. China has become the world's second largest economy today. In China, the level of urbanization has also been greatly improved. At the same time, people's awareness of environmental protection has also been improved. The higher the level of urbanization, the deeper people's understanding of the hazards of carbon emissions, they are also more motivated to take measures to strictly control the impact of population increase on CO2 emissions. However, this does not prove the same conclusion under all conditions. In poor

http://www.aloki.hu ● ISSN 1589 1623 (Print) ● ISSN 1785 0037 (Online)
DOI: http://dx.doi.org/10.15666/aeer/1605_66436654
© 2018, ALÖKI Kft., Budapest, Hungary

countries or regions, people's awareness of environmental protection is low, but the increase in population is likely to lead to an increase in carbon emissions.

The impact of population density on carbon emissions shows a positive effect at all levels of urbanization. That is, regardless of the level of urbanization, the total carbon emissions will increase correspondingly with the increase in population density, and the degree of increase will decrease with the urbanization level. In the first category of cities with the highest level of urbanization, if the population density increases by one percentage point, CO_2 emissions increase by 0.26%; with urbanization levels gradually decreasing, the population density elasticity of CO_2 is 0.13%, 0.11% and 0.106% in order, indicating urban congestion caused by urbanization is a positive factor affecting CO_2 emissions. Regardless of the level of urbanization, the road traffic planning and population distribution planning at this stage can not effectively reduce CO_2 emissions.

With the continuous growth of the regional economy, the resulting economic activities, such as production, sales, transportation and service, have also increased, resulting in the increase of CO_2 emissions, which is also verified in the model's estimation results. In particular, the growth of CO_2 emissions from economic growth is more obvious in areas with relatively fast economic development, such as regions in the first and second categories. In this paper, the carbon emissions of real GDP is carried out. In these two types of regions, the real GDP elasticity of CO_2 is 1.36% and 1.54%, respectively, exceeding 1.13% and 0.86% of the third and fourth categories, which shows that in the more economically developed regions, the high-emission secondary industry is still driving economic growth at the current stage; at the same time, higher economic levels have led to a significant increase in people's economic activity, which has led to more emissions. In the regions of the third and fourth categories, the primary industry still accounts for a large proportion, and people's economic activities are not as good as those in developed regions. Therefore, the GDP elasticity of CO_2 emissions is rather small.

Energy intensity reflects the level of energy consumption needed to create a unit of GDP, and its value reflects the production technology capabilities of a region: the higher the numerical value, the lower the technology level; conversely, it represents a higher level of technology. When estimating the energy intensity elasticity of CO_2 emissions, we found that in the economically developed regions, the elastic index value is relatively large, while in the regions where the economic development level is relatively low, the elasticity level is even smaller, which means that in the economically developed regions, because the secondary industry and the tertiary industry are the pillar industries, when the level of production technology is increased and the energy intensity value is reduced, the CO_2 emissions in the region will be significantly reduced, while in regions with relatively backward economies, the proportion of primary industries is still relatively large, so the reduction in CO_2 emissions brought about by the increase in production technology levels is relatively limited.

Conclusions

How to reduce carbon emissions is an important issue in China at the present stage. In the process of in-depth analysis of the factors affecting carbon emissions, it is necessary to classify and study according to the level of urbanization. The discrepancy of urbanization level will inevitably lead to differences in the elasticity of carbon emission factors. Sometimes, the difference is huge. Through the empirical research in

http://www.aloki.hu ● ISSN 1589 1623 (Print) ● ISSN 1785 0037 (Online)
DOI: http://dx.doi.org/10.15666/aeer/1605_66436654
© 2018, ALÖKI Kft., Budapest, Hungary

this paper, we can see that there are different policy focuses on measures to reduce total carbon emissions for different levels of urbanization.

For the first and second categories of regions with high level of urbanization, they have something in common in policy-making. First of all, restricting population entry does not bring about a reduction in CO_2 emissions. At the same time, because of the congestion in the core aggregation areas of the population, the increase in population density and the increase in economic activity will all increase CO_2 emissions. Therefore, reasonable and scientific urban development planning and population distribution planning are particularly important. Secondly, the industrial restructuring of these two categories of regions has achieved certain results, but the second industry is still the backbone of their development, so it is necessary to continue to optimize and adjust the industrial structure for the emission reduction work in these two regions. The role of technological progress in reducing CO_2 emissions is quite obvious in these two regions. Therefore, encouraging and supporting the application and innovation of these two regions in technology emission reduction is the key area that the two categories of regional governments should attach importance to.

For the third and fourth categories of regions with relatively low level of urbanization, the conclusion is obvious. First, we see that the population elasticity of carbon emissions is also negative, but its absolute value is obviously smaller than the first two categories, which shows that the urban expansion of the two regions is lower because of the weak economic development, and the capacity of the cities to accommodate the new population is lower than that of the first and the second categories. Therefore, accelerating the healthy development of urban social economy is very necessary for these two categories of regions, otherwise, in the near future, the increase in population may lead to the increase in CO_2 emissions. However, in terms of the population density elasticity of CO_2, these two regions are advantageous because the increase in CO_2 emissions caused by the increase in population density is relatively limited. However, it is still necessary to do a good job in urban planning. Second, the impact of GDP growth on CO_2 emissions in these two regions is also relatively small, which seems to be inconsistent with our usual concept. As a matter of fact, the first industry accounts for a relatively large proportion in the industrial structure of these two categories of regions, so the impact of GDP growth on CO_2 emissions is relatively limited. Moreover, due to income level restrictions, the economic activity of these two categories of regions will be weaker than those of the first and second categories of regions, and will result in less emissions. Similarly, in these two categories of areas, the improvement of technological progress has relatively limited impact on reducing CO_2 emissions. Therefore, for these two regions, it is necessary to pay attention to improving the elasticity of technological progress in carbon emissions while optimizing the industrial structure.

In this paper, an analysis model for carbon emissions based on the level of urbanization is established. Based on the level of urbanization, the carbon emission factors and their impact elasticity under different levels of urbanization are scientifically studied in depth. The results of the study proved that “one size fits all” policy development is unable to adapt to different provinces and cities where actual conditions are not the same. This method can also be applied to other countries or regions or worldwide carbon emission studies. Different levels of urbanization will produce different conclusions. But they all prove a conclusion that it is only feasible to formulate

http://www.aloki.hu ● ISSN 1589 1623 (Print) ● ISSN 1785 0037 (Online)
DOI: http://dx.doi.org/10.15666/aeer/1605_66436654
© 2018, ALÖKI Kft., Budapest, Hungary

targeted emission reduction policies based on the actual urbanization level of each province and city and the various factors that affect carbon emissions.

Acknowledgements. The authors gratefully acknowledge financial support from the Natural Science Foundation of Fujian Province (Fund Number: 2016J01337), Major Projects of Social Science Planning in Fuzhou (FundNumber: 2017FZA03) and Education and Scientific Research Projects of Young and Middle-Aged Teachers in Fujian Province. (Fund Number: JAS150459). All errors are our own.

REFERENCES

[1] Bai, X., Ling, K., Guo, C. et al. (2004): Urbanization in China: Horizontal estimation and international comparison. – Urban Issues 2: 23-26.
[2] Bartone, C., Bernstein, J., Leitmann, J. et al. (1994): Toward Environmental Strategies for Cities. Policy Considerations for Urban Environmental Management in Developing Countries. – The World Bank, Washington DC,
[3] Chikaraishi, M., Fujiwara, A., Kaneko, S. et al. (2015): The moderating effects of urbanization on carbon dioxide emissions: A latent class modeling approach. – Technological Forecasting & Social Change 90: 302-317.
[4] Dietz, T., Rosa, E. A. (1997): Effects of population and affluence on CO_2 emissions. – Proceedings of the National Academy of Sciences of the United States of America 94: 175-179.
[5] Gaigné, C., Riou, S., Thisse, J. F. (2012): Are compact cities environmentally friendly? – Social Science Electronic Publishing 72: 123-136.
[6] Knox, P. L., McCarthy, L. M. (2011): Urbanization: Pearson new international edition: An introduction to urban geography. – Pearson.
[7] Lee, Y. S. (1994): Myths of Environmental Management and the Urban Poor. – In: Brennan, E. et al. (eds.) Mega-City Growth and the Future. United Nations University, Tokyo.
[8] Lu, D. (2007): Urbanization process and spatial sprawl in China. – Urban Planning Forum 4: 47-52.
[9] Marcotullio, P. J., Lee, Y. S. F. (2003): Urban environmental transitions and urban transportation systems: a comparison of the North American and Asian experience. – International Development Planning Review 25: 325-354.
[10] Maruotti, A. (2011): The impact of urbanization on CO_2 emissions: Evidence from developing countries. – Cesifo Working Paper 70: 1344-1353.
[11] McGranahan, G. P. et al. (2000): The citizens at risk: from urban sanitation to sustainable cities. – International Journal of Sustainability in Higher Education 24: 455-456.
[12] McGranahan, G., Songsore, J., Kjellen, M. (1996): Sustainability, Poverty and Urban Environmental Transitions. – In: Pugh, C. (ed.) Sustainability, the Environment and Urbanization. Earthscan, London, pp. 103-134.
[13] Othman, J., Jafari, Y. (2016): Identification of the key sectors that produce CO_2 emissions in Malaysia: application of input–output analysis. – Carbon Management 7: 113-124.
[14] Paraschiv, M. (2012): Urbanization: an introduction to Urban Geography, third edition. – Journal of Urban & Regional Analysis 4: 1267-1268.
[15] Poumanyvong, P., Kaneko, S. (2010): Does urbanization lead to less energy use and lower CO_2 emissions? A cross-country analysis. – Ecological Economics 70: 434-444.
[16] Pugh, C. (1996): Sustainability and Sustainable Cities. – In: Pugh, C. (ed.) Sustainability the Environment and Urbanization. Earthscan, London.
[17] Ren, Z. (2014): Research on Regional Differences and Emission Reduction Mechanisms of Carbon Emissions in China. – Capital University of Economics and Business, Beijing.

http://www.aloki.hu ● ISSN 1589 1623 (Print) ● ISSN 1785 0037 (Online)
DOI: http://dx.doi.org/10.15666/aeer/1605_66436654
© 2018, ALÖKI Kft., Budapest, Hungary

[18] Rozanov, B. G., Targulian, V., Orlov, D. S. et al. (1990): The earth as transformed by human action. Global and regional changes in the biosphere over the past 300 years. – Forest Ecology & Management 55: 341-342.
[19] Sadorsky, P. (2014): The effect of urbanization on CO_2, emissions in emerging economies. – Energy Economics 41: 147-153.
[20] Satterthwaite, D. (1997): Sustainable cities or cities that contribute to sustainable development? – Urban Studies 34: 1667-1691.
[21] Shahbaz, M., Loganathan, N., Muzaffar, A. T. et al. (2016): How urbanization affects CO_2, emissions in Malaysia? The application of STIRPAT model. – Renewable & Sustainable Energy Reviews 57: 83-93.
[22] Sun, C., Jin, N., Zhang, X. et al. (2013): Differences in the impact of different urbanization stages on carbon emissions. – Geographical Sciences 33: 266-272.
[23] Wang, Q., Wu, S. D., Zeng, Y. E. et al. (2016): Exploring the relationship between urbanization, energy consumption, and CO_2, emissions in different provinces of China. – Renewable & Sustainable Energy Reviews 54: 1563-1579.
[24] Yang, L., Xia, H., Zhang, X. et al. (2018): What matters for carbon emissions in regional sectors? A China study of extended STIRPAT model. – Journal of Cleaner Production 180: 595-602.
[25] York, R., Rosa, E. A., Dietz, T. (2003): STIRPAT, IPAT and ImPACT: analytic tools for unpacking the driving forces of environmental impacts. – Ecological Economics 46: 351-365.
[26] Zhang, H., Wang, K., Xiang, B. (2013): A study of the differences in the effects of urbanization on CO_2 emissions. – China Population, Resources and Environment 23: 152-157.
[27] Zheng, D., Liu, W., Lin, Z. et al. (2016): New classification method and practical operation of China's urbanization level. – Urban Issue 9: 27-34.

http://www.aloki.hu ● ISSN 1589 1623 (Print) ● ISSN 1785 0037 (Online)
DOI: http://dx.doi.org/10.15666/aeer/1605_66436654
© 2018, ALÖKI Kft., Budapest, Hungary

TREND IN NATURAL ILLUMINANCE LEVELS BY MANN-KENDALL METHOD IN CHONGQING, CHINA

QUAN, L.[1] – HE, Y.[2*] – ZHANG, X.[2]

[1]*Faculty of Chongqing Jianzhu College, 400039 Chongqing, China*
(e-mail: 65771923@qq.com; phone: +86-133-2020-5120)

[2]*Faculty of Architecture and Urban Planning, Chongqing University*
400045 Chongqing, China
(e-mail: 543346273@qq.com – X. Zhang; phone: +86-133-2026-9588)

**Corresponding author*
e-mail: he_ying@cqu.edu.cn

(Received 1st Jul 2018; accepted 13th Sep 2018)

Abstract. Changes in the trend of the total natural light illumination value in Chongqing, China was studied based on solar irradiance data of Chongqing from 1961 to 2010. The overall and inter-annual change trends of annual and monthly total natural light illuminance values were analyzed by Mann-Kendall method, meanwhile the luminous efficacy model was integrated in the analysis of data. The result showed that the basic trend in the change of total illuminance value is due to the reduction of natural light intensity. The change in trend was very obvious, and the alteration occurred in 1974. Monthly total illuminance values in Chongqing had no changed trend in May, in September, in November, a very obvious decreasing trend occurred in January, in July, in August and in December, an obvious trend occurred in February, in April and in October, and a not obvious one in March. At the same time, the annual variation of the total monthly illuminance of natural light fluctuates little in January, in February, in October, in November, and in December, and fluctuates widely in March, in April, in May, in June, in July, in August, and in September. The lowest monthly total illuminance values were observed in January and December, and the highest monthly illuminance values were observed in July and in August. The total natural light illuminance has the highest value in summer, and the lowest value in winter, and a moderate value in spring and in autumn.
Keywords: *solar radiation, luminous efficacy, natural light illuminance, Mann–Kendall method*

Introduction

With shortages of energy resources, it is of great significance to make full use of natural light and pursue ecological and sustainable development. Daylighting climate data are the basis for the application of natural light in buildings; illuminance data are one of the core contents of daylighting climate data. China has obtained illuminance data in a study from 14 cities through two consecutive years of observation of natural light (1983 to 1984) in typical Chinese daylighting climate regions (Wu, 1987a). China was divided into five daylighting climate zones according to natural light distribution and designed daylighting design standards (Wu, 1987a). The International Daylighting Measurement Program (IDMP) was implemented in 1991 to acquire daylighting climate observation data from some cities (including Beijing and Chongqing in China) throughout the world (He et al., 2012). After that, the relevant daylighting climate observation work is basically in a state of stagnation.

As the visible part of solar irradiance, natural light has a close relationship with solar irradiance. Data on solar irradiance are abundant owing to the regular observation project of the meteorological department. Therefore, natural illuminance data can be obtained through solar irradiance. However, luminous efficacy is the key factor in obtaining

http://www.aloki.hu ● ISSN 1589 1623 (Print) ● ISSN 1785 0037 (Online)
DOI: http://dx.doi.org/10.15666/aeer/1605_66556665
© 2018, ALÖKI Kft., Budapest, Hungary

illuminance data from solar irradiance. Luminous efficacy is the ratio of natural illuminance to solar irradiance. Several authors have suggested models to derive the luminous efficacy for different sky condition. Littlefair model, Perez model (Perez et al., 1990), Olseth & Skartveit model, Chung model and Munerer & Kinghorn model (Muneer and Gul, 1998). The starting points and the model structures of these model calculations are different, and the accuracy of different models in different countries and regions is also different (Luo et al., 2011; Wang et al., 2011). Wu (1987a) proposed a monthly and annual luminous efficacy calculation model by combining China's daylighting climate observation data to meet the requirements of daylighting chimate zones and daylighting design. Solar irradiance values throughout the world have changed greatly in recent years as a result of the changing global climate (Zhang et al., 2011), worsening atmospheric pollution (Streets et al., 2008; Wand et al., 2012), and rapid urbanization process (Alpert et al., 2005). Consequently, natural illuminance has also changed (Shen et al., 2008). However, only very few relevant reports examine the changing characteristics and trends of natural illuminance. Since the total illuminance values of natural light varies greatly from year to year, missing values and outliers may occur, the accuracy of ordinary linear regression methods will be affected. The non-parametric test method (Mann–Kendall test method; Kendall, 1975) can reveal the trend of the time series well. It does not require the sample to follow a certain distribution, nor is it subject to a few abnormal values, and does not require statistical analysis. It is suitable for non-normally distributed data and it has been widely used in meteorological research (McBean and Motiee, 2008; Hamed, 2009; Shen, 2010), but it has not applied to analyze the changing natural light illuminance so far. For this reason, in this paper, the Mann–Kendall test method and statistical methods are used to analyze the variation trend of natural light illumination in Chongqing, China.

Chongqing is located in western China, lacking natural light resources, and the use of natural light is particularly important. Therefore, it is necessary to study the natural illuminance of Chongqing to obtain the natural light trend in Chongqing over the years, and then accurately assess the natural light environment in Chongqing. It will provide basic data for the use of natural light, and guide the design and application of natural light.

Data and methods

Although Chongqing has accumulated some annual light climate observation data, more long-term and large-scale light climate observation data are required to understand the changes in Chongqing's daylighting climate. Therefore, it is necessary to use rich irradiance data to obtain illuminance data.

Luminous efficacy model

Irradiance data can be obtained from meteorological observatories, so luminous efficacy K is the key factor in obtaining data on outdoor natural illuminance value. As far as we know (Wu, 1987a; Wang et al., 2011), there are many luminous efficacy models at present. Different models have different model parameters, and their accuracy varies from region to region. How to choose a conversion model suitable for Chongqing is the key to accurately obtain the natural illuminance value. The monthly and annual luminous efficacy model proposed by Wu et al. (1987a) has a relatively high accuracy. Its relevant parameters can be obtained from meteorological observation data suitable for determining daylighting climate characteristics. Therefore, we choose this model as the luminous

http://www.aloki.hu ● ISSN 1589 1623 (Print) ● ISSN 1785 0037 (Online)
DOI: http://dx.doi.org/10.15666/aeer/1605_66556665
© 2018, ALÖKI Kft., Budapest, Hungary

efficacy model. This model was utilized in the present study to obtain natural illuminance values in China. The model considers four factors as parameters. These factors are geographic latitude, altitude, vapor pressure, and sunshine duration. A quaternary simple linear regression equation (*Eq. 1*) was established in this study by integrating annual K values:

$$K_{Gi} = B_i + C_i N + D_i H + E_i \mathrm{e} + F_i S \quad \text{(Eq.1)}$$

In the equation, i is year or month; K_G is the value of annual or monthly luminous efficacy (lx/w·m^{-2}); N is geographic latitude (°); H is altitude (m); e is annual or monthly vapor pressure (hPa); S is monthly for the whole year or monthly average sunshine duration (h); B_i, C_i, D_i, E_i, F_i are equation regression coefficients. The regression coefficients of the equations for the whole year and each month in *Equation 1* can be found in the *Table 1* (Wu, 1987a).

Table 1. *Annual and monthly K_G value equation regression coefficients*

Coefficient	B_i	C_i	D_i	E_i	F_i
Jan	205.5471	-1.7685	-0.0044	-4.8330	-0.1077
Feb	152.6140	-1.2209	-0.0028	-0.0384	0.0188
Mar	204.6445	-1.6917	-0.0053	-3.0371	-0.0590
Apr	198.8032	-1.7017	-0.0042	-1.6187	-0.0388
May	318.8958	-3.1121	-0.0180	-4.4467	-0.1100
Jun	149.2460	0.2505	0.0001	-0.8415	-0.1600
Jul	30.0591	0.9744	0.0107	1.6673	0.0186
Aug	102.8181	0.3733	0.0090	0.6862	-0.0867
Sep	94.6386	0.8336	0.0062	0.3282	-0.1300
Oct	150.4375	-0.4354	0.0038	-0.8060	-0.1176
Nov	309.8648	-3.6607	-0.0108	-5.8644	-0.1480
Dec	13.2985	1.3349	0.0075	4.9952	0.0670
Year	142.1748	-0.3757	0.0008	-0.4147	-0.0853

Data sources

Radiation data, geographic latitude, altitude, vapor pressure, and sunshine hours were obtained from the China National Meteorological Information Center. The data of the center was handed by the "Monthly Meteorological Record Monthly Data Report" published by climate data processing departments of Chinese provinces, municipalities and autonomous regions. All data has undergone rigorous quality control and inspection, and the data quality is guaranteed.

There are two meteorological observation stations in Chongqing city, one of which is Chongqing Station and the other is Shapingba station. The two stations are only 10 km apart, and the different in meteorological conditions is extremely small, so the geographical influence can be ignored. The data of Chongqing station are from 1958 to 1986, and the data of Shapingba station are from 1987 to present. In this paper, the solar radiation annual value, monthly value, sunshine hours, geographical latitude, altitude and average absolute humidity in Chongqing from 1961 to 2012 are come from the two meteorological observation stations and selected as the basic data for the study. All data were quality controlled using quality control methods, including climate limit value or

http://www.aloki.hu ● ISSN 1589 1623 (Print) ● ISSN 1785 0037 (Online)
DOI: http://dx.doi.org/10.15666/aeer/1605_66556665
© 2018, ALÖKI Kft., Budapest, Hungary

allowance value check, internal consistency check, time continuity check and time series consistency check.

Conversion of annual total illuminance data

The annual or monthly luminous efficacy value of Chongqing under different climate conditions (K_{Gi}) can be obtained with *Equation 1*. Combined with the annual or monthly total irradiance value （E_e） in the region, annual or monthly total illuminance data （E_v） in this region can be calculated with *Equation 2*. The distribution of total illuminance values in Chongqing is shown in *Figures 1* and *4*.

$$E_v = K_{Gi} E_e \quad \text{(Eq.2)}$$

Research methods

Mann–Kendal trend analysis

We suppose that time series (x_1, x_2, …, x_n) has no trend. Statistics S is calculated through the following calculation method (*Eq. 3*).

$$S = \sum_{k=1}^{n-1} \sum_{j=k+1}^{n} \mathrm{sgn}(x_j - x_k) \quad \text{(Eq.3)}$$

where S has a normal distribution, a mean value of 0, and variance of $\mathrm{var}(S) = \frac{n(n-1)(2n+5)}{18}$. The standard calculation method for normal statistics is provided below (*Eq. 4*):

$$Z = \begin{cases} \frac{S-1}{\sqrt{\mathrm{var}(S)}} & S > 0 \\ 0 & S = 0 \\ \frac{S+1}{\sqrt{\mathrm{var}(S)}} & S < 0 \end{cases} \quad \text{(Eq.4)}$$

For a given confidence level α in the bilateral trend test, we suppose that the null hypothesis is unacceptable if $|Z| \geq Z_{1-\alpha/2}$. The time series data exhibit an obvious increasing or decreasing trend at a confidence level of α.

Based on the trend test, Sen's method is insignificantly affected by missing data errors or outliers. Using Sen slope calculate *Q'*, if *Q'* is a positive number, indicating that the data has a growing trend; if *Q'* is a negative number, indicating that the data has a downward trend. We can obtain the slope estimate *Q'* by using *Equation 5:*

$$Q' = \mathrm{median}\left(\frac{x_i - x_j}{i - j}\right) \quad \forall j < i \quad \text{(Eq.5)}$$

where $1 < j < i < n$; median represents the median function.

http://www.aloki.hu ● ISSN 1589 1623 (Print) ● ISSN 1785 0037 (Online)
DOI: http://dx.doi.org/10.15666/aeer/1605_66556665
© 2018, ALÖKI Kft., Budapest, Hungary

Mann–Kendall mutation test

We suppose that time series (x_1, x_2, …, x_n) exists. One order series, m_i (Kendall, 1975), is constructed to represent the sample accumulative number of $x_i > x_j$ $(1 < j < i)$. d_k is defined as (*Eq. 6*)

$$d_k = \sum_{i=1}^{k} m_i \quad 2 \le k \le n \tag{Eq.6}$$

The mean value and variance of d_k can be approximately expressed as (*Eqs. 7* and *8*)

$$E(d_k) = \frac{k(k-1)}{4} \tag{Eq.7}$$

$$\mathrm{var}(d_k) = \frac{n(n-1)(2n+5)}{72} \quad 2 \le k \le n \tag{Eq.8}$$

Under the hypothesis that the time series is random and independent, the statistics is defined as (*Eq. 9*)

$$\mathrm{UF}_k = \frac{d_k - E(d_k)}{\mathrm{var}(d_k)} \quad k = 1, 2, ..., n \tag{Eq.9}$$

Given the significance level of α, $|\mathrm{UF}_k| > \mathrm{UF}_{\alpha/2}$ means that the series has an obvious change trend. Tine series x_i is arranged in a reverse order and calculated it with *Equation 7* while ensuring that (*Eq. 10*)

$$\begin{cases} \mathrm{UB}_k = -\mathrm{UF}_k \\ k = n + 1 - k \end{cases} \tag{Eq.10}$$

By analyzing statistical series UF_k and UB_k, the change trend of series x_i can be further analyzed and the mutation time and region can be determined. $UFk > 0$ indicates that the series tends to increase; $UF_k < 0$ indicates that the series tends to decrease. When the series exceed the credibility line, then they exhibit an obvious increasing or decreasing trend. If an intersection point exists between the curves of UF_k and UB_k and falls between the credibility lines, the corresponding time of the intersection point is the starting moment of mutation.

Results

Change trend analysis of annual total illuminance

Based on the series of annual total illuminance values in Chongqing from 1961 to 2010, the statistical values Z obtained through Mann–Kendall trend test method was -3.96. A positive Z value represents an increasing trend, whereas a negative Z value represents a decreasing trend. Absolute Z values equal to or greater than 2.56 indicate that the values passed significance tests with confidence coefficients of 99%. This shows that

http://www.aloki.hu ● ISSN 1589 1623 (Print) ● ISSN 1785 0037 (Online)
DOI: http://dx.doi.org/10.15666/aeer/1605_66556665
© 2018, ALÖKI Kft., Budapest, Hungary

the change trend of the annual total illuminance in Chongqing is decreasing, and the change trend is very obvious. Therefore, the natural annual total illuminance value in Chongqing should be corrected by combining the change trend of the data.

According to the slope (Q') value obtained from the Mann–Kendall trend test (Sen Slope) (*Fig. 1*), the natural annual total illuminance of Chongqing dropped by 2.4×10^8 lx/10a. According to the slope Q' value, compared with the standard value of the natural annual total illuminance in the mid-1980s, the natural annual total illuminance decreases by about 10%. Using the original daylighting illuminance standard value to design will bring greater errors. Therefore, the annual total illuminance standard value of Chongqing should be revised to adapt to the current natural lighting design requirements under current climate conditions in Chongqing.

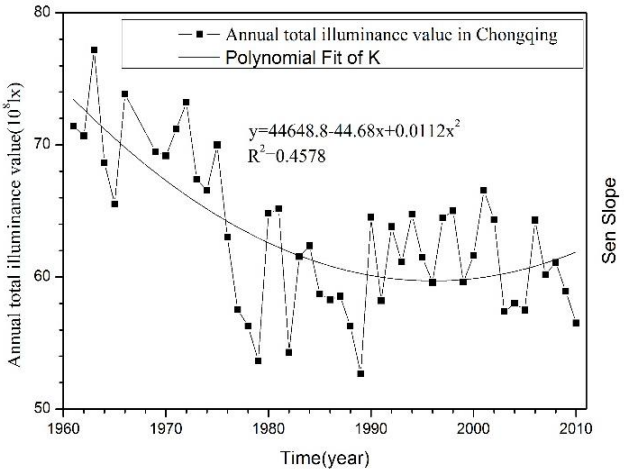

Figure 1. *Changes of annual total illuminance value in Chongqing between 1961 and 2010*

Mutation analysis of annual total illuminance

The annual total illuminance mutation map (shown in *Fig. 2*) of Chongqing was drawn through Mann–Kendall mutation test method. From *Figure 2* we can see that the curves of UF_k and UB_k intersect in 1974, and the intersection point exists between and falls between the credibility lines, the corresponding time of the intersection point is the starting moment of mutation, so the Mutation occurred in 1974. Relevant research findings are also found in other cities in China (He et al., 2013). From *Figure 2* we also find the forward sequence curve (UF_k) is almost below 0. It indicates that the series tends to decrease. The forward sequence curve (UF_k) showed a rapid downward trend after 1974, and passed the 1.96 confidence level critical value. It shows that the decreasing trend became more obvious. After that, the absolute value of statistics in 1979 exceeded 3, and even reached 4.65 in 1989. It shows that the annual total illuminance value of natural light in Chongqing has a very significant downward trend in recent years.

The monthly illuminance distribution and change trend of Chongqing

Total illuminance distribution for each month

Equation 1 is used to calculate the K_{Gi} values for each month of Chongqing from 1961 to 2012, and the monthly illuminance values of each year can be calculated according to *Equation 2*. *Table 2* shows the average value of the total natural light intensity for each

http://www.aloki.hu ● ISSN 1589 1623 (Print) ● ISSN 1785 0037 (Online)
DOI: http://dx.doi.org/10.15666/aeer/1605_66556665
© 2018, ALÖKI Kft., Budapest, Hungary

month from 1961 to 2012 (*Figure 3a*) and the average number of hours of sunshine in each month from 1961 to 2012 (*Figure 3b*).

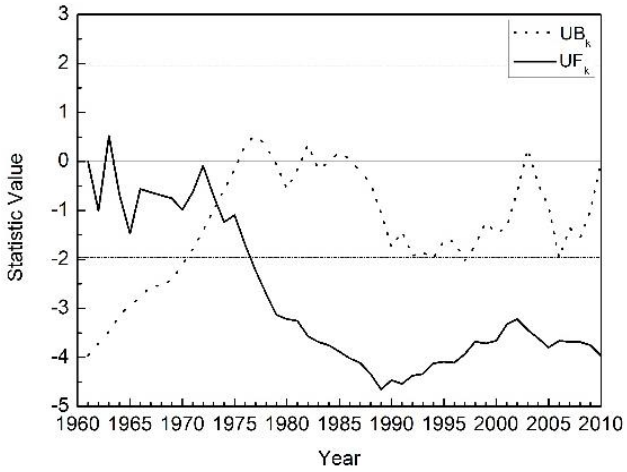

Figure 2. *Mann–Kendall mutation detection of annual total illuminance value in Chongqing*

Table 2. *Average monthly total illuminance and monthly sunshine duration of natural light between 1961 and 2012*

Month	1	2	3	4	5	6	7	8
Illuminance/×10^8 lx	2.01	2.82	4.66	6.32	7.04	7.05	9.19	9.53
Daylight hours/h	27.4	35.8	74.3	103.9	111.7	108	178	193
Month	9	10	11	12	Mean	Std. deviation	Min	Max
Illuminance/×10^8 lx	5.71	3.58	2.54	1.80	5.19	2.70	1.8	9.53
Daylight hours/h	107.8	56.8	41.1	25.1	88.56	55.96	25.1	193

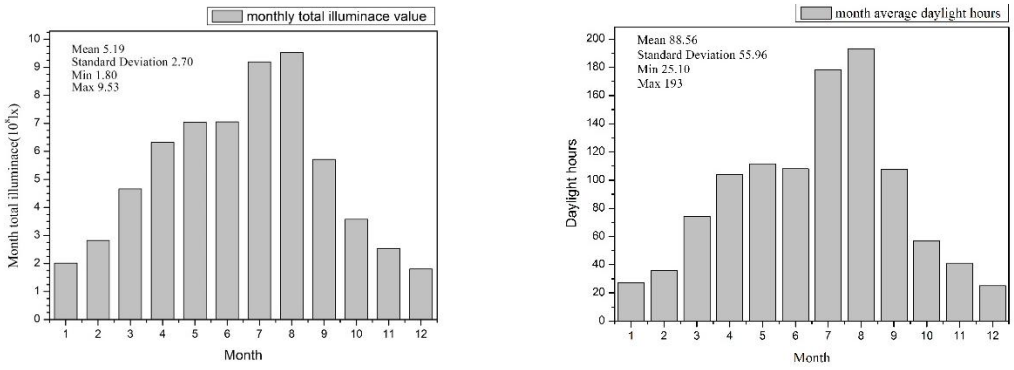

(a) Monthly total illuminance **(b) Monthly sunshine duration**

Figure 3. *Average monthly total illuminance and monthly sunshine duration of natural light between 1961 and 2012*

From *Figure 3* we can see the change trend of the monthly total illuminance in Chongqing is similar to that of the corresponding monthly sunshine duration. The low values of the monthly total illuminance and sunshine duration are observed in

http://www.aloki.hu ● ISSN 1589 1623 (Print) ● ISSN 1785 0037 (Online)
DOI: http://dx.doi.org/10.15666/aeer/1605_66556665
© 2018, ALÖKI Kft., Budapest, Hungary

December and in January. The high values are observed in July and in August. In addition, monthly total illuminance and monthly sunshine duration in summer is the largest; the minimum is in winter; and the middle is in spring and autumn. The total monthly illuminance and sunshine duration in spring are greater than those in autumn. The lowest value of total illumination in December was less than 1/5 of the highest value of total illumination in August, and the average number of sunshine duration in December was even less than 1/7 of the average number of duration of sunshine in August. This also shows that the monthly total illuminance in Chongqing varies with the seasons, with uneven distribution of total natural illuminance in each month. natural light is sufficient in Summer and scarce in winter.

Based on the above analysis, in accordance with the existing daylight design standards, daylighting can fully meet the needs of indoor illuminance, and may lead to the introduction of excessive natural light in summer, so we should pay attention to the orientation of the building windows and shade. In winter, the outdoor natural illumination is low, and due to the impact of climate change, the actual natural illuminance value is often lower than the standard value, which will lead to insufficient indoor illuminance, which will affect the use of building and cause energy waste. Therefore, the window area should be appropriately enlarged, or increase structural measures to increase the amount of natural light introduced into the room to meet the daylight needs.

The change trend of monthly total illuminance

The statistical values *Z*, Sen slope value *Q'*, of monthly total illuminance were obtained through Mann–Kendall trend test method based on the series of monthly total illuminance values in Chongqing (*Table 3*).

Table 3. *Monthly total illumination Mann–Kendall trend test statistics in Chongqing*

Month	**1**	**2**	**3**	**4**	**5**	**6**	**7**	**8**	**9**	**10**	**11**	**12**
Z	-3.07	-1.77	-1.446	-1.738	0.405	-2.19	-2.87	-2.57	0.698	-1.79	-0.731	-3.25
Q'	-0.011	-0.012	-0.012	-0.017	0.006	-0.024	-0.038	-0.033	0.009	-0.015	-0.004	-0.015

A positive *Z* value represents an increasing trend, whereas a negative *Z* value represents a decreasing trend. Absolute Z values equal to or greater than 1.64, 1.96, and 2.56 indicate that the values passed significance tests with confidence coefficients of 90%, 95% and 99%, respectively. *Table 3* shows that in January, in July, in August and in December passed the significance test with a confidence coefficient of 99%, indicating that the change trends in these months are very obvious. In February, in April and in October passed the significance test with a confidence coefficient of 95%, indicating that the change trend in these months is obvious. In March passed the significance test with a confidence coefficient of 90%, indicating that the change trend in the month is not obvious. In May, in September and in November failed to pass the significance test with a confidence coefficient of 90%, which means that no change trend exists.

Slope value Q' represents monthly total illuminance change. A positive Q' value denotes an increasing trend, whereas a negative Q' value denotes a decreasing trend.

http://www.aloki.hu ● ISSN 1589 1623 (Print) ● ISSN 1785 0037 (Online)
DOI: http://dx.doi.org/10.15666/aeer/1605_66556665
© 2018, ALÖKI Kft., Budapest, Hungary

Table 3 and *Figure 4* show that only the monthly total illuminance changes exhibit positive values in May and in September, The other months exhibit a decreasing trend. The monthly total illuminance have large change in July and in August, the change values are -0.38 × 10^8 lx/10a and -3.3 × 10^8 lx/10a. The monthly total illuminance have Minimum change in May and in November, the change values are 0.06 × 10^8 lx/10a and -0.04 × 10^8 lx/10a. The variation trend of monthly total illuminance values in most months in Chongqing is consistent with the variation in annual total illuminance values, that is, the overall trend shows a downward trend. In January, in February, in October, in November, and in December in Chongqing, there are many overcast days, and the sunshine duration are low, therefore, the monthly total illuminance values in these months are stable. But in March, in April, in May, in June, in July, in August and in September, the climate change was relatively large, and the sunshine duration changed greatly. As a result, the monthly total illuminance values in these months were drastically changed.

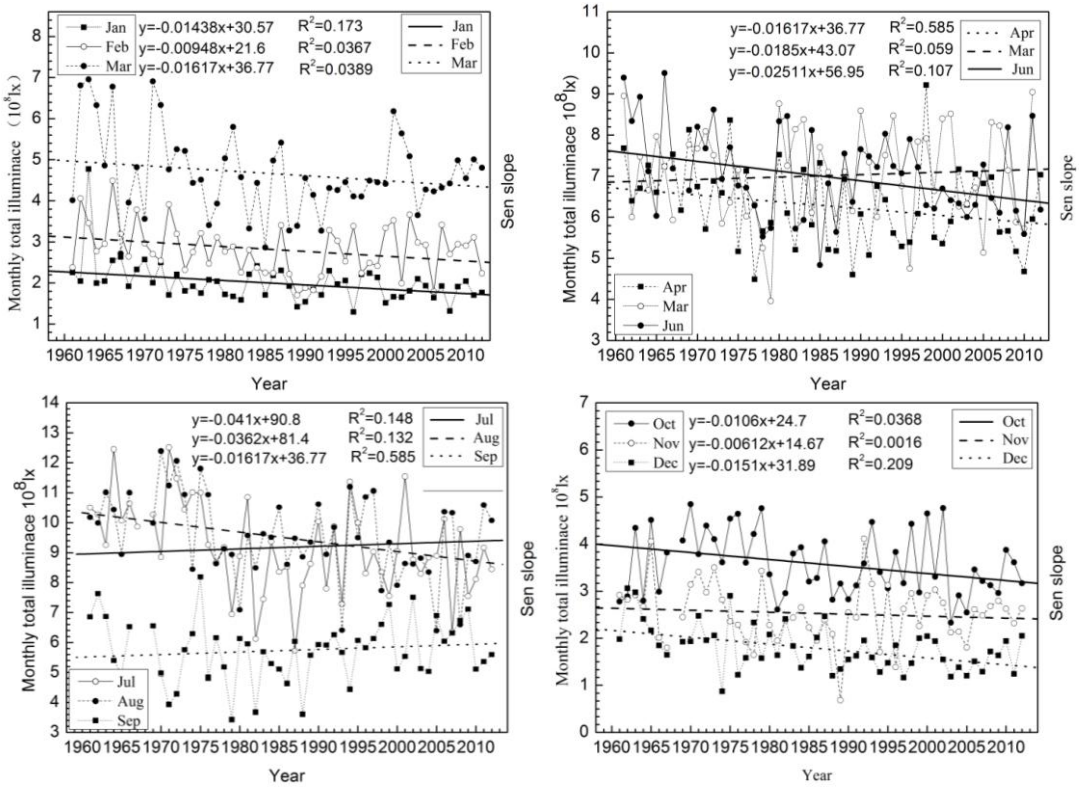

Figure 4. *Variation trend of monthly total illuminance value in Chongqing between 1961 and 2012*

Discussion

Natural light is the visible part of solar radiation; thus, the effects of solar radiation corresponding to meteorological factors also affect natural illumination changes. Solar radiation that reach the ground is influenced by clouds, atmosphere (including basic atmospheric composition, aerosols, and water vapor), and changes in solar radiation. We discuss the influencing factors of natural light illuminance in the following subsections.

http://www.aloki.hu ● ISSN 1589 1623 (Print) ● ISSN 1785 0037 (Online)
DOI: http://dx.doi.org/10.15666/aeer/1605_66556665
© 2018, ALÖKI Kft., Budapest, Hungary

Cloud

Clouds have a significant impact on natural lighting climates. Clouds affect not only the natural light reaching the ground but also the sky luminance distribution. In general, changes in the cloud cover will lead to a decrease or increase in natural light.

Aerosol

Aerosol is another important and complex influencing factor of natural light. Aerosol not only reflects, scatters, or absorbs sunlight but also produces indirect effects by changing the microphysical nature of clouds. The effects of aerosols on sunlight vary. An increase in aerosol content increases atmospheric optical thickness, thus correspondingly reducing the natural illumination that reaches the surface.

Water vapor

Water vapor absorbs sunlight. Research indicates that the global average of columnar water vapor content is 25 mm. For every 1% increase in solar radiation, water vapor content increases from 3 mm to 6 mm (Ramanathan and Vogelmann, 1997). Water vapor changes will have insignificant effects on natural illumination.

Atmospheric molecular scattering and absorption

Atmospheric gas molecules also scatter and absorb sunlight. However, human activity has changed atmospheric gas composition in recent decades (such as CO_2). Given that gas composition has low levels of ingredients in the atmosphere, the effect of atmospheric gas on natural illumination can be neglected.

Solar activity

Solar activity changes are mainly observed by satellite. To date, four independent space-based instruments directly observe total solar irradiance (Fröhlich, 2004). Solar radiation is typically an 11-year cycle and the amount of change is usually small and not more than 1% (Hamed, 2009). Therefore, the effect of solar activity can be ignored.

Conclusion

- Using solar radiation data to obtain natural illuminance data can greatly enrich daylighting climate data.
- The trend of total illuminance value of natural light in Chongqing is very obvious, with a drop of 2.4×10^8 lx/10a, and the mutation occurred in 1974. Therefore, the design standard of daylighting in Chongqing should be revised to meet the needs of daylighting demand.
- Monthly total illuminance values in Chongqing have no change trend in May, in September, in November, very obvious decreasing trend in January, in July, in August and in December, obviously in February, in April and in October, and not obvious in March.
- The annual variation of the total monthly illuminance of natural light fluctuates little in January, in February, in October, in November, and in December, and fluctuates widely in March, in April, in May, in June, in July, in August, and in September.

http://www.aloki.hu ● ISSN 1589 1623 (Print) ● ISSN 1785 0037 (Online)
DOI: http://dx.doi.org/10.15666/aeer/1605_66556665
© 2018, ALÖKI Kft., Budapest, Hungary

Acknowledgements. This work was financially supported by the National Natural Science Foundation of China (Grant No. 51878089), Chongqing Research Program of Basic Research and Frontier Technology (Grant No. cstc 2015jcyjBX0121).

REFERENCES

[1] Alpert, P., Kishcha, P., Kaufman, Y. J. et al. (2005): Global dimming or local dimming: effect of urbanization on sunlight availability. – Geophysical Research Letters 32: L17802.

[2] Fröhlich, C., Lean, J. (2004): Solar radiative output and its variability: evidence and mechanisms. – Astron and Astrophys Rev 12: 273–320. DOI: 10.1007 /s00159-004-0024-1.

[3] Hamed, K. H. (2009): : Exact distribution of the Mann-Kendall trend test statistic for persistent data. – Hydrology 1: 86–94.

[4] He, Y., Mao, H., Quan, L. (2012): Sky luminance distribution types in China. – Journal of Central South University of Technology 3: 777–782.

[5] He et al. (2013): The trend of natural illuminance levels in 14 Chinese cities in the past 50 years. Energy, – Sustainability and Society 3: 22.

[6] Kendall, M. (1975): Multivariate Analysis. – Charles Griffin & Company, London.

[7] Luo, T., Yan, D., Lin, R. et al. (2011): Study and application on the typical yearly daylight illuminance. – China Illuminating Engineering Journal 5: 1–6 [in Chinese].

[8] McBean, E., Motiee, H. (2008): Assessment of impact of climate change on water resources: along term analysis of the Great Lakes of North America. – Hydrol Earth Syst Sci 12: 239–255.

[9] Muneer, T., Gul, I. (1998): Long-term Evaluation of a Meteorological Solar Radiation Model against UK data. – Energy Conversion and Management 3/4: 303–317.

[10] Perez, R., Chen, I., Seals, R. (1990): Modeling daylight availability and irradiance components from direct and global irradiance. – Solar Energy 5: 271–289.

[11] Ramanathan, V., Vogelmann, A. M. (1997): Greenhouse effect, atmospheric solar absorption and the Earths radiation budget: from the Arrhenius-Langley era to the 1990s. – Ambio 26: 38–46.

[12] Shen, W. (2010): Trend analysis of precipitation in northern Xinjiang during 1953–2008. – Journal of Water Resources & Water Engineering 4: 130–134 [in Chinese].

[13] Shen, Y., Zhao, Z., Shi, G. (2008): The Progress in variation of surface solar radiation, factors and probable climate effects. – Advances in Earth Science 9: 915–923 [in Chinese].

[14] Streets, D. G., Yu, C., Wu, Y. et al. (2008): Aerosol trends over China, 1980–2000. – Atmospheric Research 2: 174–182 [in Chinese].

[15] Wand, Z., Han, L., Chen, X., et al. (2012): Characteristics and sources of $PM_{2.5}$ in typical atmospheric pollution episodes in Beijing. – Journal of Safety and Environment 5: 122–126 [in Chinese].

[16] Wang, A., Jin, H., Wang, H. et al. (2011): Obtaining outdoor illuminance values with solar irradiation transformation models. – Journal of Civil, Architectural & Environmental Engineering 3: 88–93 [in Chinese].

[17] Wu, Q. (1987a): The light equivalent of total solar radiation and its application in the calculation of illumination climate. – Acta Meteorologica Sinica 5: 290–296 [in Chinese].

[18] Wu, Q. (1987b): The temporal and spatial distribution of total illumination in China. – Acta Energiae Solaris Sinica 4: 347–351 [in Chinese].

[19] Zhang, Q., Li, Y., Chen, Q. et al. (2011): Temporal and spatial distributions of cloud cover over southwest China in recent 46 years. – Plateau Meteorology 2: 339–348 [in Chinese].

http://www.aloki.hu ● ISSN 1589 1623 (Print) ● ISSN 1785 0037 (Online)
DOI: http://dx.doi.org/10.15666/aeer/1605_66556665
© 2018, ALÖKI Kft., Budapest, Hungary

NET PRIMARY PRODUCTIVITY DYNAMICS AND DRIVING FORCES IN GUANGZHOU CITY, CHINA

WU, Y.[1] – LUO, Z.[2] – WU, Z.[1*]

[1]*School of Geographical Sciences/Guangdong Province Engineering Technology Research for Geographical Conditions Monitoring and Comprehensive Analysis, Guangzhou University 510006 Guangzhou, China*

[2]*South China Institute of Environmental Science, Ministry of Environmental Protection 510535 Guangzhou, China*

**Corresponding author*
e-mail: gzuwzf@163.com

(Received 2nd Jul 2018; accepted 22nd Aug 2018)

Abstract. Urban expansion and land use/land cover change (LULCC), driven primarily by human activities, have significant influences on the environment; in addition, the two factors, together with climate change, have an impact on urban vegetation. This study explored spatiotemporal dynamics of net primary productivity (NPP) and calculated relative contributions of driving factors from 2001 to 2013 in Guangzhou City, China. The effects of climate variables, urban expansion, and subsequent LULCC on interannual NPP variability were analyzed and compared. Results showed that NPP fluctuated and generally declined in Guangzhou over the 13-year study period, especially significant in inner suburbs (southern, eastern, and northern regions ($p < 0.05$), due to increasingly intensive human activities. LULCC, especially the reduction of cropland due to urban sprawl, resulted in significant NPP losses and positive relative impact index (RII) values, which indicated that LULCC played a negative role in NPP accumulation. More than 67.2% of NPP variability was controlled by LULCC in the whole area under study and mean RII values in all regions were higher than 50%, indicating that the influence of LULCC on NPP variability was greater than that of climate change. Particularly noteworthy is the fact that local climate change had a greater influence on NPP in forested areas (e.g. in the northeastern region), but it should not be ignored that RII kept increasing annually in this region and therefore more efforts paid in conservation were required. In conclusion, urban expansion and LULCC across the whole study area are resulted from human activities, and this, rather than climate change, was the primary driving force for the regional reduction in NPP.

Keywords: *net primary productivity, urban expansion, climate change, land use/land cover change (LULCC), human activities*

Introduction

Net primary productivity (NPP), the amount of photosynthetically fixed carbon available to the first heterotrophic level in an ecosystem (Field et al., 1998), is a key component of energy and matter transformation in terrestrial ecosystems. NPP plays an important role in global change and carbon balance as a key regulator of ecological processes, and is often used to quantify ecosystem service values. A decline in vegetation productivity is the primary manifestation of vegetation degradation, and NPP is an important indicator of productivity. In recent years, many studies of NPP have conducted long-term monitoring of vegetation dynamics in terrestrial ecosystems on both local and global scales, and results showed that vegetated ecosystems are susceptible to the effects of climate conditions and human activities, or the combined effects of them (Fu et al., 2013; Zhang et al., 2016; Wu and Wu, 2018; Chao et al., 2018; Fang et al., 2017).

http://www.aloki.hu ● ISSN 1589 1623 (Print) ● ISSN 1785 0037 (Online)
DOI: http://dx.doi.org/10.15666/aeer/1605_66676690
© 2018, ALÖKI Kft., Budapest, Hungary

Climate change influences NPP variability by altering levels of photosynthesis, respiration, and the decomposition of organic carbon in the soil (Gong et al., 2012; Pei et al., 2013b, 2015; Wang et al., 2013). According to the study by Nemani et al. (2003), the increase in global NPP from 1982 to 1999 was partly due to global climate change, and this trend was observed in China over the same period (Piao et al., 2005). NPP variability is highly sensitive to climate change, but the mechanisms involved are complicated (Liang et al., 2014; Ahlström et al., 2012; Gu et al., 2017). Human-induced change, especially urbanization, is another important influencing factor of NPP variability with complex mechanisms (Buyantuyev and Wu, 2012; Zhang et al., 2015; Peng et al., 2016). Growing evidence has shown that urban expansion has a great influence on regional ecosystems due to increased levels of greenhouse gas in the atmosphere, the destruction of the ozone layer, biodiversity loss due to deforestation (Verburg et al., 2002), and the reduction in landscape-level photosynthetic activity (Imhoff et al., 2000). In addition, urban expansion, together with land use/land cover (LULC) change, has dramatically influenced hydrological systems, biogeochemical cycles, and climate (Grimm et al., 2008). This has led to alterations in the distribution, structure, and material cycling of terrestrial ecosystems, ultimately affecting carbon storage and flux (Imhoff et al., 2000; Piao et al., 2009; Hutyra et al., 2011). Urbanization often causes reductions in NPP due to land cover transformation and carbon fixing potential drops greatly when the land converts from cultivated land or forests to developed land, or when a region transforms from a suburban area into an urban area (Zhao et al., 2012; Jiang and Wu, 2015; Chen et al., 2017). Therefore, climate change and human activities are two of the most important driving forces of NPP variability. With aggravating global climate change and increasing human activities, quantifying the effects of different driving factors on vegetation dynamics has become a critical issue for mitigation and management planning. To date, some studies have attempted to quantify relative contributions of climate change or human-induced LULCC to NPP within specific regions (Yan et al., 2016; Xu et al., 2011; Zhang et al., 2016). However, such studies are often lack a spatial quantitative component relating to climate change and LULCC, and they do not take the spatial differences in the impacts of these different driving forces on NPP into account.

Guangzhou City is ideal for the study of climate change and human-induced impacts on NPP because it has hot and humid subtropical monsoon climate that favors year-round vegetation growth. The city has experienced dramatic urbanization and LULCC, which have converted large patches of croplands and woodlands into built-up areas within a matter of a decade or even a few years. Guangzhou's urban development strategy of "southern expansion, northern optimization, eastern advance, western union" in its 11th Five-year Plan will continue to accelerate urban sprawl, which may lead to multiple ecological problems. Some studies have noted that climate variables and human activities have led to a significant change in vegetation productivity in urban areas over a short period, with clear spatial heterogeneity. Accordingly, the study of NPP variability and the driving mechanisms in Guangzhou can be regarded as a representative case for southern China. This paper attempts to achieve the following goals: (1) to examine the spatiotemporal variability in NPP across five regions during 2001-2013; (2) to analyze the effects of climate variables, urban expansion, and subsequent LULCC on NPP; and (3) to reveal the relative contribution of driving forces on NPP accumulation and describe the spatial heterogeneity.

http://www.aloki.hu ● ISSN 1589 1623 (Print) ● ISSN 1785 0037 (Online)
DOI: http://dx.doi.org/10.15666/aeer/1605_66676690
© 2018, ALÖKI Kft., Budapest, Hungary

Material and methods

Study area

Guangzhou City (112°57'E~114°3'E and 22°26'N~23°56'N) is an important political, economic, educational, scientific, and technological center within Guangdong Province and South China (*Fig. 1*). It is located in the north end of the Pearl River Delta region and adjoins the extension of the Nanling Mountains in the north and the South China Sea in the south, with a total land area of 7,434.4 km^2. The topography of Guangzhou consists of hilly areas and plains, with elevation decreasing from northeast to the southwest. It has a subtropical, marine monsoon climate with an annual average temperature of 22 °C and annual precipitation of 1,982.7 mm. Guangzhou has experienced dramatic urbanization due to China's reform and opening up policies. In recent decades, Guangzhou's economy has developed fast, which supports a population of over 12.9 million. Its regional Gross Domestic Product (GDP) has grown from $268.48 billion in 2001 to $1,542.01 billion in 2013 (http://www.gzstats.gov.cn/). According to urban planning (Urban Master Development Plan of Guangzhou (2001-2010); the 10th Five-year Plan (2001-2005) and the 11th Five-year Plan (2006-2010)), the development of Guangzhou was predominantly in five regions, namely the central part, the south, the east, the north, and the northeast (*Fig. 1*). The central region mainly includes old districts with overwhelming urbanization and significant economic development. The southern, eastern, and northern regions are inner suburbs with rapid urban development. The northeastern region is composed of outer suburbs which are mainly dominated by forests and agricultural land, with relatively slower urban development.

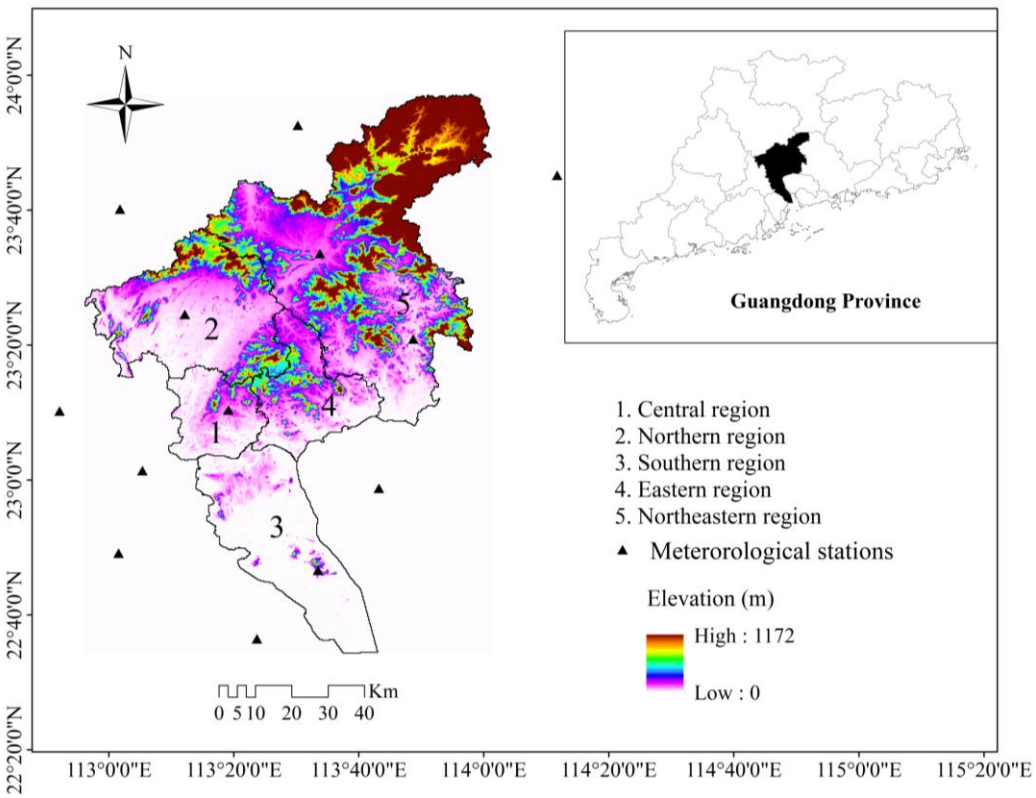

Figure 1. *Location of study area, five regions and topography*

http://www.aloki.hu ● ISSN 1589 1623 (Print) ● ISSN 1785 0037 (Online)
DOI: http://dx.doi.org/10.15666/aeer/1605_66676690
© 2018, ALÖKI Kft., Budapest, Hungary

Data collection and pre-processing

In this study, Terra MODIS data over the study area from 2001 to 2013 were selected for the NPP simulation. Data included 16-day NDVI composites (MOD13Q1) at a spatial resolution of 250 m, monthly land surface temperature (LST) (MOD11C3) at a spatial resolution of 0.05° (5.55 km), and monthly evapotranspiration (ET) and potential evapotranspiration (PET) (MOD16A2) at a spatial resolution of 1 km. All MODIS datasets were downloaded from the National Aeronautics and Space Administration's (NASA) Earth Observation System. The monthly NDVI data were produced from the MODIS 16-day products by using the maximum value composites (MVC) method, which eliminated disturbances from clouds, the atmosphere, and altitude angle, and minimized non-vegetation effects (Tucker et al., 1994). Other MODIS data were aggregated to grid cells at a resolution of 250 m from their original Sinusoidal Projection using the MODIS Reprojection Tool (MRT) to get the same spatial resolution and projected coordinate system as the MODIS-NDVI data. All MODIS data were checked using quality flags from the companion Quality Assurance (QA) images. The MODIS LST products (MOD11C3) were used to estimate air temperature (T_{air}) for the CASA model. Other studies have used this method to estimate T_{air} from MODIS LST data, and confirmed that LST is highly correlated with T_{air} (Vancutsem et al., 2010; Fu et al., 2011; Benali et al., 2012). In this study, T_{air} was estimated using LST data based on cross validation across years (Fu et al., 2011). The results showed that the best model had r^2 values ranging from 0.82 to 0.90 and RMSE values ranging from 1.64 to 2.17 °C, for 2001-2013.

The climate data included monthly mean air temperature, total precipitation, and total solar radiation data derived from 13 meteorological stations in and around Guangzhou. These three weather variables were used to analyze the correlation with NPP and simulate NPP_p. and the percentage of sunlight was derived in order to calculate the total solar radiation for simulating NPPp and NPP. These climate data were then interpolated into raster format at 250 m spatial resolution by using the universal Kriging method to match the MODIS NDVI data. All meteorological data were downloaded from the Chinese National Metrological Information Center/China Meteorological Administration (NMIC/CMA).

Finally, a time series of Landsat images were used to extract land cover over the study areas. Data sources included Landsat Thematic Mapper (TM; bands 1-5 and 7) images acquired on November 2005, December 2006, January 2009, October 2011; Enhanced Thematic Mapper (ETM+; bands 1-5 and 7) images acquired on November 2001 and January 2003; and Operational Land Imager (OLI; bands 2-7) images acquired on December 2013. These images were rectified to the Universal Transverse Mercator (UTM) projection and World Geodetic System 1984 (WGS84) datum. After Line-of-Sight Atmospheric Analysis of Spectral Hypercube (FLAASH) and image mosaicking, the 2001 image was selected as the base image for automatic registration of other images with Root Mean Square Errors (RMSE) of less than 0.5 pixels. Subsequently, the images were masked using the boundary of the Guangzhou Metropolitan area. A maximum likelihood supervised classification approach was used to classify the Landsat images and they were combined with the actual land cover in Guangzhou and the International Geosphere-Biosphere Program (IGBP) schemes. Finally, land cover maps from seven years were classified into 12 categories (*Table 1*). The overall accuracy of the classification results was higher than 82.5%.

http://www.aloki.hu ● ISSN 1589 1623 (Print) ● ISSN 1785 0037 (Online)
DOI: http://dx.doi.org/10.15666/aeer/1605_66676690
© 2018, ALÖKI Kft., Budapest, Hungary

Table 1. *Land use/land cover classification scheme*

LULC types	Description	ε_{max}
EBF	Lands dominated by broadleaf trees with a canopy cover great than 60% and height exceeding 2-m. Almost all trees remain green all year	0.985
ENF	Lands dominated by needleleaf trees with a canopy cover great than 60% and height exceeding 2-m. Almost all trees remain green all year	0.389
MF	Lands with evergreen broadleaf and needleleaf forest	0.475
DBF	Lands dominated by broadleaf trees with a canopy cover great than 60% and height exceeding 2-m. Consists of seasonal broadleaf tree communities with an annual cycle of leaf-on and leaf-off periods	0.692
GL	Lands with herbaceous, tree and shrub cover is less than 10%	0.542
SL	Lands with woody vegetation less than 2-m tall and mainly shrub and lands with herbaceous types of cover, shrub cover is greater than 60%	0.429
WG	Lands with herbaceous and with tree canopy between 10 and 30%	0.542
CL	Lands covered with temporary crops followed by harvest and a bare soil period	0.542
CL&NVM	Lands with a mosaic of croplands, forest, shrub-land, and grasslands in which no one component comprises more than 60% of the landscape	0.542
WB	Oceans, seas, lakes, reservoirs, rivers and dike-pond	0.296
U&BL	Land covered by buildings and other man-made structures	0.196
UL	Exposed soil, sand, rocks, landfill sites, areas of active excavation	0.217

EBF: evergreen broadleaf forests; ENF: evergreen needleleaf forests; MF: mixed forests; DBF: deciduous broadleaf forests; GL: grasslands; SL: shrub lands; WG: woody grasslands; CL: croplands; CL&NVM: cropland/nature vegetation mosaics; U&BL: urban and built-up lands; UL: unused lands; WB: water bodies

NPP estimation

NPP was assessed by using the Carnegie-Ames-Stanford Approach (CASA) model, a parameter-based model based on light use efficiency (Potter et al., 1993). The CASA model can be calculated as the product of the amount of photosynthetic active radiation absorbed (APAR) ($MJ \cdot m^{-2}$) and the actual light use efficiency (ε) ($g\ C \cdot MJ \cdot m^{-1}$) factor. NPP can be expressed as (*Eq. 1*):

$$NPP(x,t) = APAR \times \varepsilon \quad \text{(Eq.1)}$$

where NPP (x, t) ($g\ C \cdot m^{-2}$) is the net primary productivity for grid cell x in month t. The actual light use efficiency (ε) is affected by temperature and water, and can be calculated by using *Equation 2:*

$$\varepsilon(x,t) = T_1(x,t) \times T_2(x,t) \times W(x,t) \times \varepsilon_{max} \quad \text{(Eq.2)}$$

where $T_1(x, t)$ and $T_2(x, t)$ are temperature stress coefficients; $W(x, t)$ is a moisture stress coefficient; and ε_{max} represents the maximum light use efficiency that needs to be simulated for different vegetation types. ε_{max} differs greatly in different situations and is mainly affected by temperature, water availability, soil type, etc. (Prince, 1991). In this paper, the ε_{max} values for different land cover types were adopted from Zhu et al. (2006) who computed ε_{max} according to the principle of minimal error based on simulated NPP and measured ground NPP.

http://www.aloki.hu ● ISSN 1589 1623 (Print) ● ISSN 1785 0037 (Online)
DOI: http://dx.doi.org/10.15666/aeer/1605_66676690
© 2018, ALÖKI Kft., Budapest, Hungary

APAR is the product of *PAR* and the fraction of photosynthetically active radiation (*FPAR*) (Wang et al., 2009), and *PAR* depends on the solar surface radiation (*SOL*) ($MJ \cdot m^{-2}$). Thus, NPP at location *x* and time *t* becomes (*Eq. 3*):

$$NPP(x,t) = FPAR \times SOL \times 0.5 \times T_1(x,t) \times T_2(x,t) \times W(x,t) \times \varepsilon_{max} \quad \text{(Eq.3)}$$

FPAR is defined as a linear function of *NDVI* and the simple ratio (*SR*) (*Eq. 4*):

$$FPAR(x,t) = \alpha FPAR_{NDVI} + (1-\alpha) FPAR_{SR} \quad FPAR \in [0.001, 0.95] \quad \text{(Eq.4)}$$

where α is set to 0.5; $FPAR_{\mathrm{NDVI}}$ and $FPAR_{\mathrm{SR}}$ are FPAR estimated by the *NDVI-FPAR* model (*Eq. 5*) and the *SR-FPAR* model (*Eq. 6*):

$$FPAR(x,t) = \frac{(NDVI(x,t) - NDVI_{i,min}) \times (FPAR_{max} - FPAR_{min})}{(NDVI_{i,max} - NDVI_{i,min})} + FPAR_{\mathrm{min}} \quad \text{(Eq.5)}$$

$$FPAR(x,t) = \frac{(SR(x,t) - SR_{i,min}) \times (FPAR_{max} - FPAR_{min})}{(SR_{i,max} - SR_{i,min})} + FPAR_{\mathrm{min}} \quad \text{(Eq.6)}$$

where $NDVI_{i,\ max}$ and $NDVI_{i,\ min}$ values correspond to 95% and 5% of the *NDVI* population respectively, and *i*; $SR_{i,\ max}$ and $SR_{i,\ min}$ correspond to $NDVI_{i,max}$ and $NDVI_{i,\ min}$ respectively. The relationship between *NDVI* and *SR* can therefore be expressed as (*Eq. 7*):

$$SR(x,t) = \left[\frac{1 + NDVI(x,t)}{1 - NDVI(x,t)}\right] \quad \text{(Eq.7)}$$

SOL is the total solar radiation over time period ($MJ \cdot m^{-2}$), can be calculated based on the percentage of sunshine, namely (*Eq. 8–12*):

$$SOL = \left[a + b \times \frac{n}{N}\right] \times R_a \quad \text{(Eq.8)}$$

$$R_a = S_0 \times \frac{24}{\pi} \times d \times (W_0 \times sin\varphi \times sin\delta + cos\varphi \times cos\delta \times sinW_0) \quad \text{(Eq.9)}$$

$$d = 1/[1 + 0.033 \times cos\ (2\pi \times J/365)] \quad \text{(Eq.10)}$$

$$\delta = 0.409 \times sin\ (2\pi \times J/365 - 1.39) \quad \text{(Eq.11)}$$

$$W_0 = arcos\,(-tan\varphi \times tan\delta) \quad \text{(Eq.12)}$$

where R_a is the vertical incidence of solar radiation from the upper atmosphere; *n/N* is the percentage of sunshine; *a* and *b* are set to 0.191 and 0.758, respectively, according to Hou et al. (1993); S_0 is a solar constant (0.082 $MJ \cdot m^{-2} \cdot min^{-1}$); *d* is a correction factor for the relative distance between Earth and the Sun; δ is solar declination (unit: radians);

http://www.aloki.hu ● ISSN 1589 1623 (Print) ● ISSN 1785 0037 (Online)
DOI: http://dx.doi.org/10.15666/aeer/1605_66676690
© 2018, ALÖKI Kft., Budapest, Hungary

W_0 is the hour angle between sunrise and sunset (unit: radian); φ is geographic latitude (unit: radians), and is set to 0.540; and J is the number of days in a year.

Additionally, $T_1(x, t)$, $T_2(x, t)$ and $W(x, t)$ are the temperature and moisture stress coefficients, and can be calculated as (*Eq. 13–15*):

$$T_1(x,t) = 0.8 + 0.02 \times T_{opt} - 0.0005 \times (T_{opt})^2 \quad \text{(Eq.13)}$$

$$T_2(x,t) = 1.184/[1 + e^{0.2*(T_{opt}-10-T(x))}]/[1 + e^{0.3*(-T_{opt}-10+T(x))}] \quad \text{(Eq.14)}$$

$$W(x,t) = 0.5 + 0.5 \times ET(x,t)/PET(x,t) \quad \text{(Eq.15)}$$

where T_{opt} is the temperature at which *NDVI* reaches its maximum for the whole year, and T_2 falls to half its value at T_{opt} at temperatures 10 °C or 13 °C below T_{opt}. The moisture stress coefficient (W) reflects the influence of the effective water condition of plants and can be used for light utilization. It is determined by regional actual evapotranspiration (*ET*) (mm) and potential evapotranspiration (*PET*) (mm), derived from the MOD16A2 products.

Mann-Kendall trend analysis and Theil–Sen median slope estimator

In the present study, both spatial and temporal NPP change trends were analyzed using a robust non-parametric Mann-Kendall (M-K) method, which is widely applied to long-time series trend analysis of non-normal data (Prince, 1991; Wang et al., 2001, 2015b). It has been reported that the M-K test statistic Z is approximately normally distributed with the sample size $n \geq 8$ (Neeti and Eastman, 2011). A positive or a negative of Z value indicates an increasing or a decreasing trend, which is monotonic (Neeti and Eastman, 2011). The M-K test statistic S is calculated as (*Eq. 16;* Kendall, 1975):

$$S = \sum_{i=1}^{n-1} \sum_{j=i+1}^{n} sgn(x_j - x_i) \quad \text{(Eq.16)}$$

where n is the number of data points; x_i and x_j are the data values in time series i and j ($j > i$), respectively; and $sgn(x_j - x_i)$ is the sine function expressed as (*Eq. 17*):

$$sgn(x_j - x_i) = \begin{cases} 1, if\ x_j - x_i > 0 \\ 0, if\ x_j - x_i = 0 \\ -1, if\ x_j - x_i < 0 \end{cases} \quad \text{(Eq.17)}$$

The variance is computed as (*Eq. 18*):

$$Var(S) = \frac{n(n-1)(2n+5) - \sum_{i=1}^{m} t_i(t_i-1)(2t_i+5)}{18} \quad \text{(Eq.18)}$$

where n is the number of data points, m is the number of tied groups, and t_i denotes the number of ties with extent i. A tied group is a set of sample data that share the same value. In cases where the sample size n > 8, the standard normal test statistic Z_S is calculated (*Eq. 19*) using *Equation 18:*

http://www.aloki.hu ● ISSN 1589 1623 (Print) ● ISSN 1785 0037 (Online)
DOI: http://dx.doi.org/10.15666/aeer/1605_66676690
© 2018, ALÖKI Kft., Budapest, Hungary

$$Z = \begin{cases} \frac{S-1}{\sqrt{Var(S)}}, & if\ S > 0 \\ 0, & if\ S = 0 \\ \frac{S+1}{\sqrt{Var(S)}}, & if\ S < 0 \end{cases} \quad \text{(Eq.19)}$$

In this study, the Z score thresholds used for testing significance over time were 1.96 for the 5% significant level ($\propto = 0.05$), and 2.576 for the 1% significant level ($\propto = 0.01$), which provided both the significance and direction of the trend.

The Theil–Sen median slope estimator for estimating the slope of the trend in a sample with N pairs of data, which is appropriate for assessing the rate of change in a short or noisy time series (Wang et al., 2015a), can be calculated as (*Eq. 20*):

$$\beta_i = Median\left(\frac{x_j - x_k}{j-k}\right) \quad for\ i = 1, \ldots, N \quad \text{(Eq.20)}$$

where x_j and x_k are the data values at times j and k ($j > k$), respectively.

All analyses were conducted using ENVI 5.1 (Exelis Visual Information Solutions, Boulder, CO, USA), ARCGIS 10.2 (ESRI, Redlands, CA, USA), and MATLAB R2014a (The Mathworks, Inc., Natick, MA, USA).

Impacts assessment of LULCC on NPP

Based on the relative impact index (RII) from Wu et al. (2018), we applied RII to assess the impact of LULCC driven by human activities on NPP. RII was calculated based on NPP_{lulcc} and NPP_p, namely (*Eq. 21*):

$$RII = \frac{NPP_{lulcc}}{NPP_p} \times 100\% = \frac{NPP_p - NPP_{lulcc}}{NPP_p} \times 100\% \quad \text{(Eq.21)}$$

where NPP_{lulcc} is the NPP variability that is due to LULCC driven by human activities, and NPP_p is the NPP of potential vegetation. If $RII > 0$, it implies that there is a negative impact of LULCC on NPP and vegetation activity, and if $RII < 0$, it implies that there is either a limited human impact or more effective vegetation protection and management. When $|RII| > 50\%$, it indicates that LULCC is the primary driver of NPP change. For more details about *RII* and the calculation of NPP_p see Wu et al. (2018).

Relative contributions of climate and LULCC on NPP

The correlation between climatic variables (temperature, precipitation and solar radiation) and annual NPP can be expressed as (*Eq. 22*):

$$R_{xy} = \frac{\sum_{i=1}^{n}[(x_i - \bar{x})(y_i - \bar{y})]}{\sqrt{\sum_{i=1}^{n}(x_i - \bar{x})^2 \times \sum_{i=1}^{n}(y_i - \bar{y})^2}} \quad \text{(Eq.22)}$$

where R_{xy} is the correlation coefficients between x and y, x_i and y_i is the value of NPP and climatic variables in the ith year respectively; $\bar{x}$ and $\bar{y}$ is the mean value of NPP and climatic variables from 2001 to 2013.

http://www.aloki.hu ● ISSN 1589 1623 (Print) ● ISSN 1785 0037 (Online)
DOI: http://dx.doi.org/10.15666/aeer/1605_66676690
© 2018, ALÖKI Kft., Budapest, Hungary

The method of Wu et al. (2014) was employed to compare the comprehensive impact of climate change and LULCC on NPP on a spatial scale, using the variation slope of NPP in different situations to quantify and compare the comprehensive impacts. Assuming that the slope of NPP was K_1 and K_2 in the situation of constant climate and constant LULCC respectively, the slope of actual NPP was K, so the impact of climate change and LULCC on NPP can be expressed as $\Delta Cli.NPP = K\text{-}K_1$ and $\Delta LULCC.NPP = K\text{-}K_2$ respectively. The impact of other factors on NPP was $\Delta Inter.NPP = (K_1 + K_2)\text{-}K$. Therefore, the contributions of climate change, LULCC and other factors on NPP change can be described by *Equations 23–25:*

$$Contr_{cli} = \frac{|\Delta Cli.NPP|}{|\Delta LULCC.NPP| + |\Delta Cli.NPP| + |\Delta Inter.NPP|} \times 100\% \quad \text{(Eq.23)}$$

$$Contr_{LULCC} = \frac{|\Delta LULCC.NPP|}{|\Delta LULCC.NPP| + |\Delta Cli.NPP| + |\Delta Inter.NPP|} \times 100\% \quad \text{(Eq.24)}$$

$$Contr_{inter} = 100 - Contr_{cli} - Contr_{LULCC} \quad \text{(Eq.25)}$$

The sum of the contributions of climate change, LULCC and other factors on NPP change is equal to 1. The contributions of the three impact factors can be mapped individually at the pixel scale, and the synthesized impact image can be derived from the three images using a Maxwell Triangle.

Results

NPP model validation

There was little field data on NPP available for validating the CASA model outputs. We compared our simulated average annual NPP values over the period from 2001 to 2013 with MOD17A3 NPP values and other domestic simulation results. As shown in *Figure 2,* there was a strong agreement between our simulated NPP results and MOD17A3 NPP values with a correlation coefficient of 0.860 and a mean relative error of 24.88% across the 118 random sample points. The NPP values from our simulation results were clearly different from those of other studies (*Table 2*), which may have been due to differences in the study range, stand age and density, hydrothermal conditions, vegetation coverage, input data sources, parameter values for the CASA model, and so on.

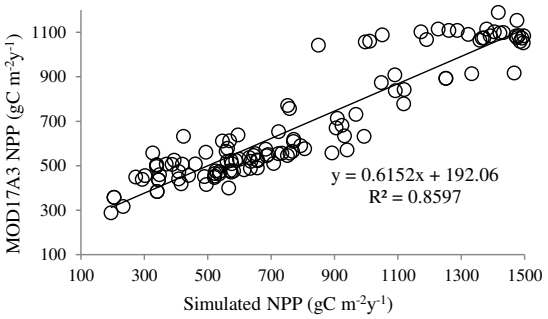

Figure 2. *Correlation between simulated NPP values and MOD17A3 NPP values*

http://www.aloki.hu ● ISSN 1589 1623 (Print) ● ISSN 1785 0037 (Online)
DOI: http://dx.doi.org/10.15666/aeer/1605_66676690
© 2018, ALÖKI Kft., Budapest, Hungary

Table 2 *Comparison of the mean annual NPP ($gC \cdot m^{-2}$) for different land covers and other model output or datasets*

Land cover types*	This study	Ni et al., 2003	Zhu et al., 2007b	Gao et al., 2008	Jiang et al., 2015	Hua, 2009	MOD17A3
EBF	1,327.22	1016.5	985.8	718.0	833.06	1,046.89	913.93
ENF	515.69	395.5	367.1	358.0	519.34	799.53	388.0
MF	595.68	-	347.1	707.0	533.49	874.36	456.0
DBF	827.43	671.8	642.9	472.0	744.7	818.28	622.02
GL	582.00	230.6	382.8	208.0	470.04	384.4	317.0
SL	483.08	364.2	367.7	700.0	524.25	603.94	415.0
WG	634.63	-	465.0	-	-	657.13	398.32
CL	644.06	532.9	426.5	577.0	534.74	416.9	609.91
CL&NVM	661.62	-	-	-	-	-	566.02
WB	250.48	-	-	-	395.18	-	-
U&BL	183.39	-	-	-	384.04	-	-
UL	239.47	-	-	-	514.47	-	-

The full names of the land types match those in *Table 1*

Spatial-temporal dynamics of NPP

The estimated mean NPP had an overall decreasing trend from 2001 to 2013 in Guangzhou (from 807.45 gC m^{-2} in 2001 to 719.84 gC m^{-2} in 2013). From a geographical perspective, the average mean NPP decreased markedly from the northeast to the south and had clear geographic heterogeneity (*Fig. 3a*).

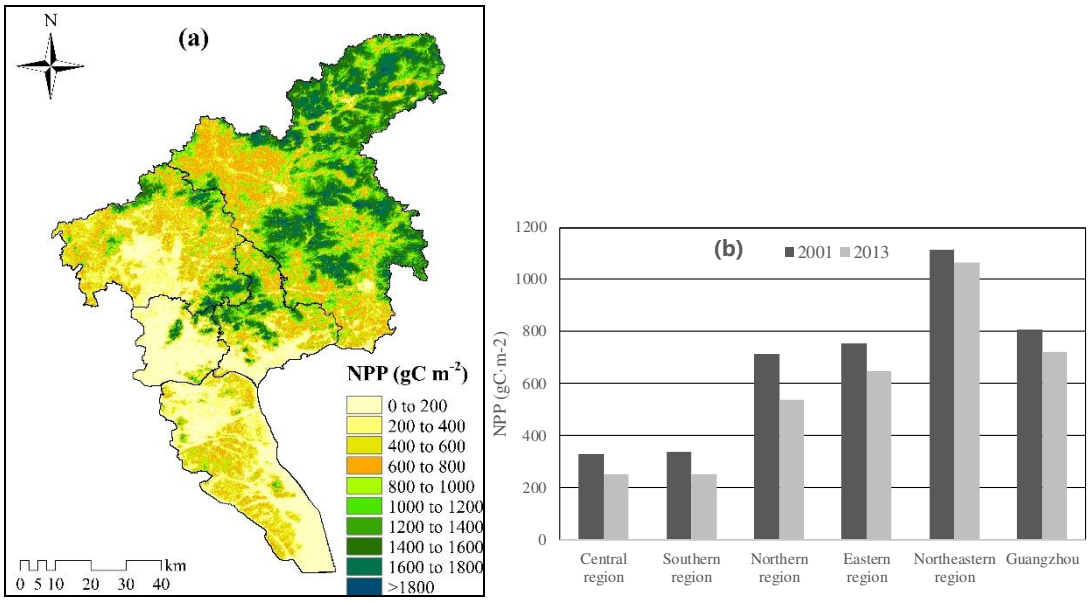

Figure 3. *Spatial pattern of mean NPP during 2001-2013 (a) and NPP variability between 2001 and 2013 in Guangzhou (b)*

For individual grid cells, the annual mean NPP values ranged from 7 gC m^{-2} yr^{-1} in the central region to more than 1189 gC m^{-2} yr^{-1} in the northeastern region. For different

http://www.aloki.hu ● ISSN 1589 1623 (Print) ● ISSN 1785 0037 (Online)
DOI: http://dx.doi.org/10.15666/aeer/1605_66676690
© 2018, ALÖKI Kft., Budapest, Hungary

land cover types, the highest NPP values (greater than 850 gC m^{-2}) were found in forests, which are mainly located in the northeast and the important conservation areas within Guangzhou city. Low NPP values (less than 250 gC m^{-2}) were found in the areas dominated by urban land cover with little green space, implying that NPP was closely related to NDVI and the light use efficiency (ε) of the land cover type. *Fig. 3b* details the changed in NPP from 2001 to 2013 in Guangzhou city and the five regions. Average NPP values across Guangzhou and the five regions between 2001 and 2013 varied significantly and declined sharply by 2013. Estimated NPP values in the northern region decreased the most (175.47 gC m^{-2}), followed by the eastern and southern regions (108.26 gC m^{-2} and 86.52 gC m^{-2} respectively). Values in the northern region also decreased, and the lowest value was 46.90 gC m^{-2}. The pattern overall showed that the order of dynamic changes in annual NPP ranked from high to low was inner suburbs, inner city, and outer suburbs.

To further assess the temporal changes and regional disparity in NPP under changing land cover, land types in Guangzhou city and the five regions were analyzed for 2001, 2005, 2009, and 2013. The results showed that the mean NPP of land cover classes in those regions varied significantly (*Fig. 4*). The lowest NPP values for all land cover types were found in the central region, while land cover in the northeastern region contained more NPP with more than 3,000 gC m^{-2} in all year. The average NPP for all land cover types decreased across the whole study area and all regions, with the most significant decreases occurring in the northern region with a remarkable decline of -183.78 gC m^{-2} between 2001 and 2013, followed by the southern and eastern regions with respective losses of -72.73 gC m^{-2} and -64.95 gC m^{-2}, respectively.

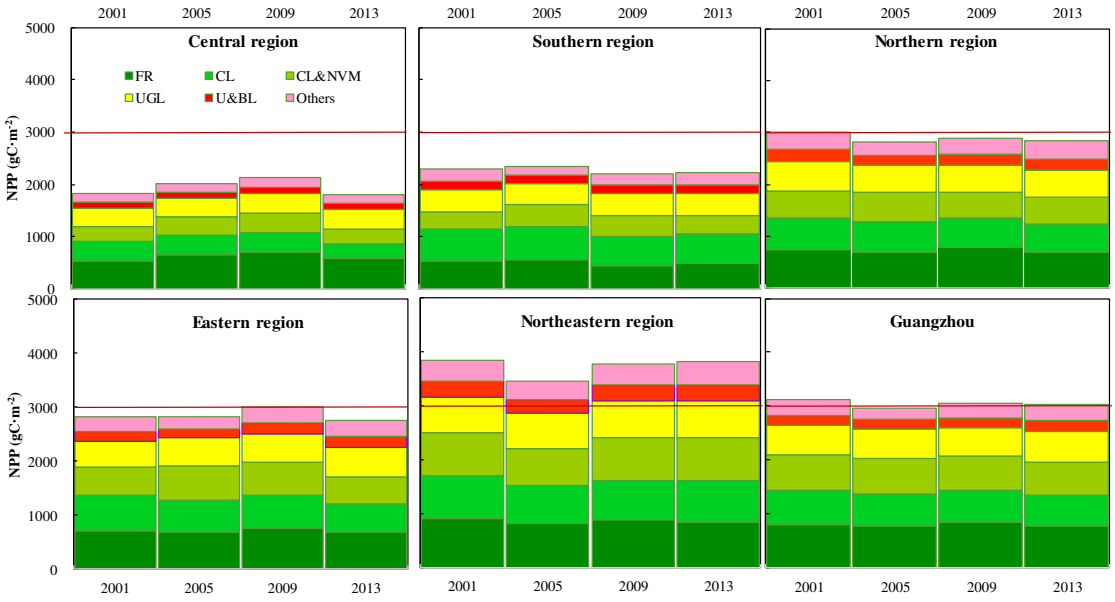

Figure 4. *Changes in the mean NPP across Guangzhou City and its five regions. (FR: forest; CL: croplands; CL&NVM: cropland/nature vegetation mosaics; UGL: urban green lands: mainly includes grasslands: shrub lands and woody lands; U&BL: urban and built-up lands; Others: include water bodies and unused lands)*

Spatial NPP trends and tests for significance across Guangzhou and the five regions were analyzed at the pixel level (*Fig. 5a-b*). Results showed that NPP decreased in all

http://www.aloki.hu ● ISSN 1589 1623 (Print) ● ISSN 1785 0037 (Online)
DOI: http://dx.doi.org/10.15666/aeer/1605_66676690
© 2018, ALÖKI Kft., Budapest, Hungary

regions over the duration of the study (*slope* < 0). About 70.2% of all NPP pixels had a decreasing trend with an average slope of -10.94, and this was especially noticeable in the central part of the northern region and most areas of the southern region. Pixels with a significant decreasing trend ($p < 0.05$) accounted for 19.34% of the total pixels, and only 3.44% of pixels had a significantly increasing trend ($p < 0.05$). Significant negative trends ($p < 0.05$) were mainly observed in the northeastern region (7.75%) and in portions of the northern region (5.34%). Of all pixels with significant positive trends ($p < 0.05$), about 61.01% were concentrated in the forested lands of northeastern region due to relatively less human interference and policy protection measures (e.g., Land Use Master Plan of Guangzhou, 1997-2010); however, the increasing number of pixels with a declining trend in this region cannot be ignored. Moreover, in the five regions where human modifications of land cover occurred the most, the proportion of areas with significant NPP decreases was much higher than the area of increase.

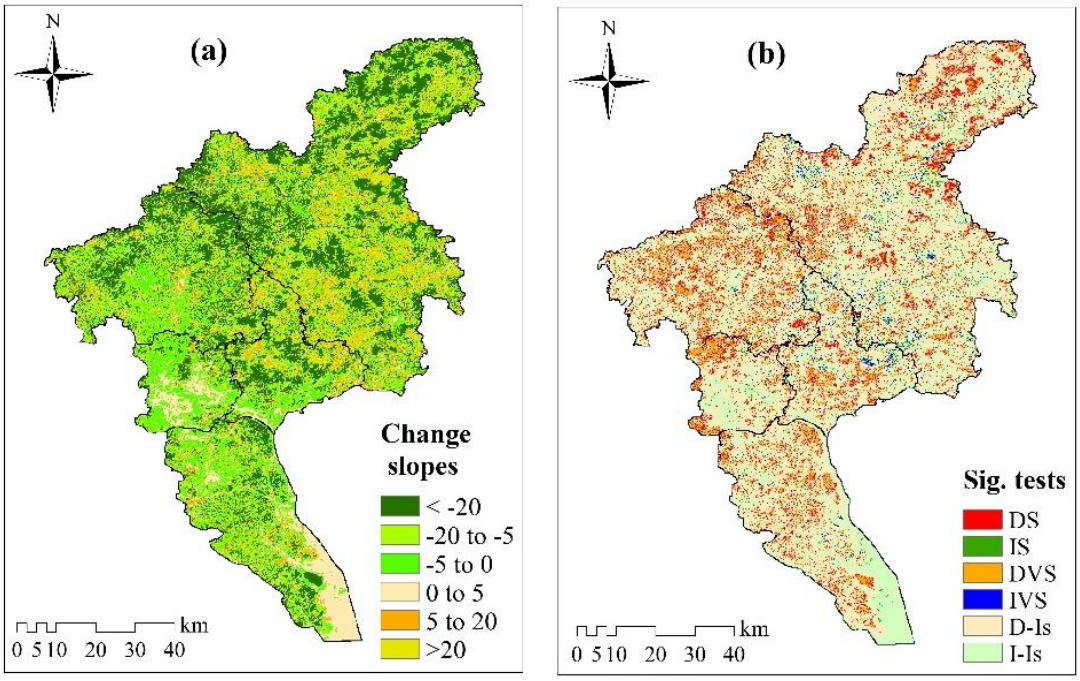

Figure 5. *Change trends (a) and significance tests for NPP (b) from 2001 to 2013. (DS: decreased significantly; IS: increased significantly; DVS: decreased very significantly; IVS: increased very significantly; D-Is: decreased insignificantly; I-Is: increased insignificantly)*

The influence of climate variability on NPP

Correlation analysis was performed between each climate factor (annual mean temperature (TEM), total precipitation (PRE), and total solar radiation (SOL)) and annual mean NPP across Guangzhou City and the five regions from 2001-2013 (*Table 3*). At the 13-year time scale, temperature and solar radiation tended to have positive impacts on NPP over the entire region, while precipitation had a negative relationship that was especially significant in the eastern and northeastern regions. The results indicated that rising temperatures and increasing solar radiation were associated with NPP increases, and solar radiation had a greater effect on NPP than temperature did.

http://www.aloki.hu ● ISSN 1589 1623 (Print) ● ISSN 1785 0037 (Online)
DOI: http://dx.doi.org/10.15666/aeer/1605_66676690
© 2018, ALÖKI Kft., Budapest, Hungary

Table 3. *Correlation coefficients between climate variables and NPP*

Correlation	Central region	Southern region	Northern region	Eastern region	Northeastern region	Guang zhou
R_{NPP-T}	0.530	0.394	0.512	0.351	0.444	0.476
R_{NPP-P}	-0.301	-0.217	-0.166	-0.582*	-0.645*	-0.572*
$R_{NPP-SOL}$	0.654*	0.440	0.644*	0.661*	0.779**	0.304

R_{NPP-T}, R_{NPP-P} and $R_{NPP-SOL}$ are the correlations between NPP and temperature, precipitation and solar radiation, respectively

For further analyzed the influence of each climatic factor (TEM, PRE, SOL) on NPP dynamics, the proportion of areas whose NPP variability was influenced by climate variables were calculated, and those percentages are shown in *Figure 6*. Across the whole study area, the area proportion dominated by solar radiation variation was the largest, being 37.9%, followed by temperature. For the five regions, solar radiation was the most dominant; particularly, the figures in the northern and northeastern regions reached 42.3% and 40.3%, respectively, while the figures in the areas dominated by precipitation were always smaller (less than 30%). These results suggested that the variability in solar radiation in the study area had the greatest influence on NPP, followed by temperature. Furthermore, changes in solar radiation and temperature strongly affected NPP in most areas of Guangzhou, while precipitation was a limiting factor for NPP accumulation due to the regional rainy and humid climate characteristics.

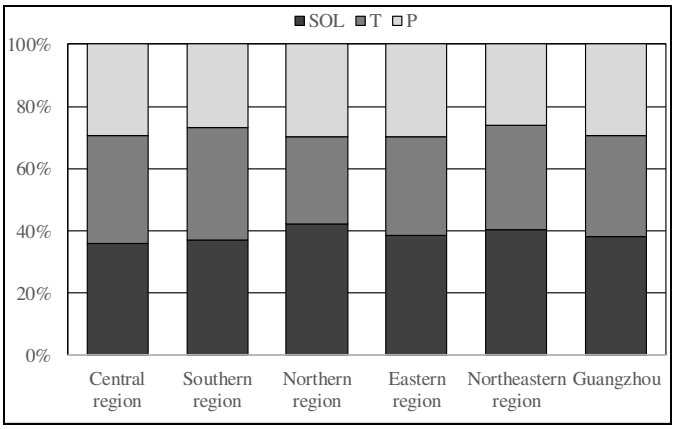

Figure 6. *Pixels percentages dominated by climate variables*

The response of NPP to LULCC

Since 1978, Guangzhou has experienced rapid urbanization and industrialization. A trend of sustained and accelerating development has taken place from 2001 to 2013 (Wu et al., 2016), and there was considerable change in land use types during this period. For example, urban and built-up areas increased by 979.72 km^2 at an annual rate of 8.13%. This was especially pronounced in the southern and eastern regions, where urban land increased by more than 20.0% as cropland decreased significantly in both (*Table 4*). In addition, there was a significant conversion from cropland, forest, and cropland/natural vegetation patches to impervious surface. In most cases, this resulted in significant losses of NPP.

http://www.aloki.hu ● ISSN 1589 1623 (Print) ● ISSN 1785 0037 (Online)
DOI: http://dx.doi.org/10.15666/aeer/1605_66676690
© 2018, ALÖKI Kft., Budapest, Hungary

Results showed that about 0.59 Tg C of NPP was lost due to the transformation from vegetated to non-vegetated areas between 2001 and 2013, and 85.1% of that was due to the conversion to urban land. In the five regions, the most significant losses in total NPP due to the conversion from other land cover types to urban land occurred in the northeastern region (a 42.5% loss), followed by the eastern region (18.6%) and northern region (17.9%). The greatest NPP losses due to conversion to other land cover types, especially urban land, occurred in cropland. This process reduced the carbon sequestration capacity of Guangzhou City. To further illustrate the impacts of urban expansion and cropland reduction on NPP loss, NPP changes in the urban and built-up coverage in 2013 and in the cropland coverage in 2001 during 2001-2013 were analyzed and compared (*Fig. 7*). Results showed that within the coverage of urban and built-up of 2013, urban and built-up areas had increased by 1,133.82 km^2 from 2001 to 2013, resulting a significant NPP loss of 0.55 Tg C of NPP with a decreased rate of 15.73 $gC\ m^{-2}yr^{-1}$ due to the conversion from vegetation to built-up areas over the 13-year period, especially from cropland to construction lands. Based on the cropland coverage of 2001, cropland declined sharply by 746.75 km^2 from 2001 to 2013, and about 320.93 km^2 was swallowed up by urban expansion, this directly led to the decline of the carbon fixation capacity of vegetation. During the 13-year period, NPP decreased significantly with a loss of 0.40 Tg C, and about 0.19 Tg C loss was mainly ascribed to the conversion from cropland to impervious surface. The above analysis showed that in both coverages, NPP decreased very significantly from 2001 to 2013 due to gradually reducing vegetation coverage and increasing built-up lands caused by anthropogenic influence.

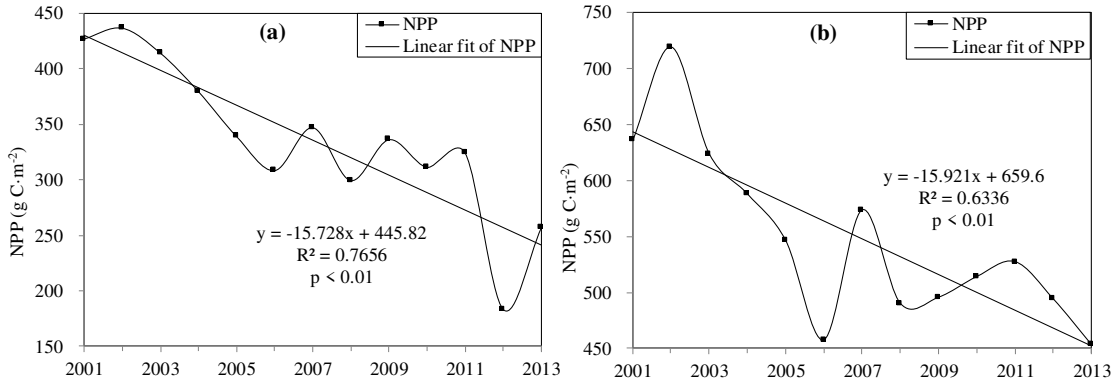

Figure 7. *NPP changes from 2001 to 2013 based on the range of urban and built-up lands in 2013 (a) and cropland in 2001 (b)*

Table 4. *Change in three indices in the five regions from 2001 to 2013*

Region / Indices	Central region	Southern region	Northern region	Eastern region	Northeastern region
ΔU&BL (%)	19.84	20.73	15.85	22.16	6.48
ΔCL (%)	-9.81	-14.36	-6.51	-12.23	-4.90
ΔRII (%)	4.62	6.52	9.19	7.27	5.98

ΔU&BL and ΔCL is the proportion of urban area and cropland change respectively; ΔRII is the difference in RII between 2013 and the 13-year average

http://www.aloki.hu ● ISSN 1589 1623 (Print) ● ISSN 1785 0037 (Online)
DOI: http://dx.doi.org/10.15666/aeer/1605_66676690
© 2018, ALÖKI Kft., Budapest, Hungary

The impacts of LULCC on NPP were further investigated by examining the RII over the whole study area and the five regions from 2001 to 2013. Results showed that more than 91.0% of pixels in whole area had positive RII values and the mean RII value was greater than 50% across all regions, indicating LULCC driven by human activity had a negative influence on NPP and was the primary cause for NPP losses. Moreover, there was a clear increasing trend in RII across the five regions over the 13 years (*Table 4*) that was especially significant in the northern region followed by the eastern and southern regions, which suggested that intense human development radiated outward from the central urban areas to the urban fringe, where the inner suburbs were the first to be affected.

Comparison of the effects of LULC and climate change on NPP

In this study, we measured the relative contributions and synthesized the spatial impacts of climate and LULCC on NPP (*Fig. 8a*). The results showed that there were significant differences between the major factors controlling NPP at the pixel level. Over 13 years in the study area, 67.2% of all pixels had NPP variability that was dominated by LULCC due to increased human activities (*Fig. 8b*).

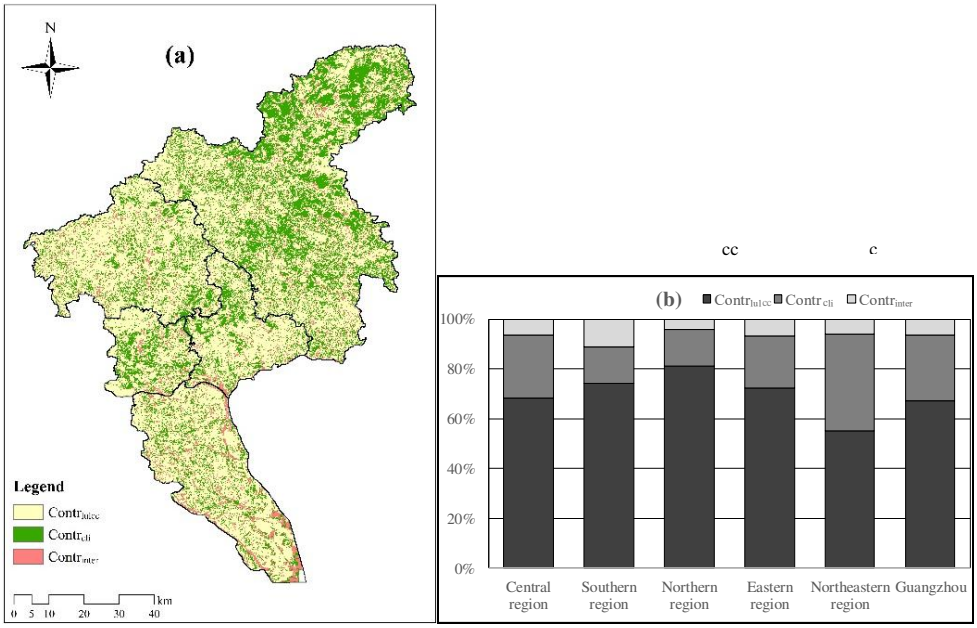

Figure 8. *Spatial distribution (a) and percentages (b) of the relative contributions of climate change, land cover change, and their interaction on NPP. ($Contr_{lulcc}$: contributions of LULCC; $Contr_{cli}$: contributions of climate change; $Contr_{inter}$: contributions of the interaction effects)*

These were mainly distributed in the northern, eastern, and southern regions, indicating that LULCC had a negative influence on NPP. On the other hand, 26.6% of pixels with NPP variability were more sensitive to climate change and mainly concentrated in the northeastern region dominated by forested lands. Only 6.2% of the total pixels were controlled by the interaction of climate and LULCC, and they were mainly concentrated in central region and some areas of southern region. Moreover, the proportion of pixels whose NPP changes were controlled by LULCC was higher than 50.0% across all regions, indicating that LULCC dominated by human activities and had a greater

http://www.aloki.hu ● ISSN 1589 1623 (Print) ● ISSN 1785 0037 (Online)
DOI: http://dx.doi.org/10.15666/aeer/1605_66676690
© 2018, ALÖKI Kft., Budapest, Hungary

influence on NPP variability than climate change, especially in the inner suburbs (about 76.66% of pixels with NPP variability were controlled by LULCC). Overall, results showed that the influence of urban expansion and LULCC on NPP was much greater than the influence of climate, and LULCC was the main cause of reduced NPP in most of the areas under study.

Discussion

Uncertainties in NPP estimates

Compared with MODIS NPP, we found that our simulated NPP values for all land cover types were higher than MOD17A3, which may be because the fact that MODIS NPP is derived at the global scale with diverse climate and vegetation conditions and at a relatively coarse spatial resolution (1 km). The NPP estimates in this study were also very different from previous research studies of NPP change during China's urbanization (*Table 2*), which may be due to the fact that Guangzhou is a southern city with a warmer climate, higher vegetation coverage, and better hydrothermal conditions than that of other cities and the whole country.

In addition, there could be large uncertainties in this NPP estimation due to input data, parameters, model structure, and the applicability of the model (Wu and Wu, 2018). Some parameters (e.g., ε_{max} and *FPAR*) in the CASA model may not be appropriate across all areas of China and the process parameters should be optimized (Wang et al., 2013; Gong et al., 2012; Zhang et al., 2009). Furthermore, there was a large disparity in the spatial resolution of meteorological data and MODIS products in this study, which may have caused bias in NPP estimation. Although we reduced these errors by resampling, further adjustment and higher resolution data may be needed. Additionally, ground NPP data-based site observations of biomass within the study would have been better for validation than MODIS NPP. Overall, there were still some uncertainties in the NPP estimates due to the factors mentioned above, and in future studies, optimization of model parameters and more multisource data validation will be needed to enhance the accuracy of NPP estimation.

Correlation between climate variability and NPP

Climate variables are important factors affecting vegetation conditions, for example, temperature, precipitation and solar radiation can affect the vegetation distribution and NPP dynamics of various biomes at regional, and even local, scales (Dekker et al., 2007; Hu et al., 2009; Zhu et al., 2007a). In this study, the effects of these three climate variables on NPP variability were different, however, negative correlations with NPP and precipitation, and positive correlations with NPP and temperature and solar radiation occurred in all regions (*Table 3*), indicating that precipitation was unfavorable for vegetation growth, while temperature and solar radiation benefited NPP accumulation. This was consistent with Fu et al.'s (2013) study on Guangzhou where an increase in precipitation caused a decrease in temperature and radiation, which reduced the solar radiation exposure and for photosynthesis for photosynthesis in plants and may have decreased the soil organic matter content (Mohamed et al., 2004; Eisfelder et al., 2014; Zhang et al., 2016), resulting in less absorption of photosynthetically active radiation and the accumulation of vegetation biomass (Piao et al., 2003).

http://www.aloki.hu ● ISSN 1589 1623 (Print) ● ISSN 1785 0037 (Online)
DOI: http://dx.doi.org/10.15666/aeer/1605_66676690
© 2018, ALÖKI Kft., Budapest, Hungary

Solar radiation serves as an important energy source for plant photosynthesis, and we found it had a better regression coefficient with NPP than temperature and precipitation across all regions (*Table 3*). This implied that the NPP distribution and production are closely related to climatic variables and always dominated by a single climatic factor (Zhao and Running, 2010; Wu et al., 2014), and in most areas of Guangzhou City, the response of interannual NPP variability to solar radiation was the main controlling factor (*Fig. 6*). The results also have been verified by other studies (Zhang et al., 2014; Liang et al., 2014). Moreover, according to Zhu et al. (2007a), solar radiation had a larger influence on vegetation NPP in the South China compared with temperature and precipitation. Although other environmental factors may also affect NPP variability to some extent, such as soil texture (Pan et al., 1996), topography (Gao et al., 2013), drought (Pei et al., 2013a), CO_2 concentration (Mu et al., 2008), and so on, their effects on NPP were less climatic factors on carbon storage of vegetation (Sui et al., 2013; Gao et al., 2013).

NPP dynamics and associated urbanization and LULCC

Urbanization and subsequent LULC driven by human activities are important factors affecting vegetation dynamics, particularly in highly urbanized areas that are characterized by extremely fragile ecosystems (Wu and Wu, 2018; Zhang et al., 2014; Liu et al., 2018). In this study, NPP exhibited spatial heterogeneity across the whole area under study and decreased in the five regions from 2001 to 2013. Similarity, previous studies found that vegetation was degraded at different levels in Guangzhou in recent decades (Fu et al., 2013; Hu et al., 2009; Wu and Wu, 2018). In our study, a significant reduction in NPP was concentrated in the inner suburbs (southern, eastern, and northern regions; *Fig. 5*), this was mostly because that the amount of urban sprawl increased gradually from center to the periphery from 2001 to 2013 (Wu et al., 2016), and urbanization "hot spots" have moved from the center to the suburbs, resulting in a substantial reduction in vegetation areas and vegetation carbon fixation. Following intense urban development, ecological degradation slows and new urban ecosystems develop (Peng et al., 2016), which always leads to large losses in NPP. Moreover, the significant increase in RII in the inner suburbs implied that vegetation productivity in these areas was still subjected to disturbance by human activities. Most studies have demonstrated that the urban fringe is gradually emerging as the most human-disturbed area and this phenomenon has been observed in most urban areas during urbanization (Xu et al., 2007; Wu et al., 2014; Wu and Wu, 2018). Conversely, increased NPP and smaller RII values were widely distributed in the outer suburbs (northeastern region), which are dominated by mountains and hills with higher elevations, and low population density combined with conservation efforts that have effectively reduced the impacts of humans on vegetation activity. This phenomenon has also been confirmed by other studies (Peng et al., 2016; Hu et al., 2009).

Prior research has verified that different urbanization stages, finance aggregation, and population growth may also be important factors affecting NPP variability (Peng et al., 2016; Lu et al., 2010). Substantial environmental change occurs under increased demand by city dwellers for green space and corresponding ecosystem services. Thus, maintaining green spaces and adaptive urban planning could have benefits for the urban ecosystem and a favorable impact on vegetation productivity. However, it should be noted that growing human activity and urban sprawl are still a serious threat to vegetation NPP accumulation, and more plausible adaptation strategies should be

http://www.aloki.hu ● ISSN 1589 1623 (Print) ● ISSN 1785 0037 (Online)
DOI: http://dx.doi.org/10.15666/aeer/1605_66676690
© 2018, ALÖKI Kft., Budapest, Hungary

employed to cope with the conflict between urban development and ecosystem carbon balance.

Dominant driving forces of NPP variability

Over the 13-year study period, temperature and solar radiation were generally favorable for vegetation growth, whereas human activities had a negative impact. As shown by the absolute values of the contributions made by climate and LULCC, the influence of LULCC on interannual NPP variability in most parts of the area under study was always greater than climate. Notably, negative impacts of LULCC on NPP were most significant in the inner suburbs due to the conversion from vegetated to non-vegetated land, especially from cropland to new urban areas. This finding was in agreement with several studies (Pei et al., 2013b; Fu et al., 2013; Wu et al., 2014; Yang et al., 2015; Liu et al., 2018). A considerable proportion NPP change was undeniably dominated by climate factors in some croplands and wooded areas (e.g. the northeastern region; *Fig. 8*), where LULCC actually caused an increase in NPP. This was closely related to regional land cover types, population and economic conditions, terrain, conservation policies, and so on. In addition to the roles of regional population, economic conditions, and terrain, the effects of protection policies must be acknowledged. For example, the Land Use Master Plan of Guangzhou (1997-2010) effectively prevented excessive losses of agricultural land in this region. The Urban Master Development Strategic Plan of Guangzhou (2010-2020) defined Conghua and Zengcheng (the two districts are mainly in northeastern region) as eco-agricultural and eco-tourism zones, which further promoted the protection of agricultural and forested lands in the northeastern region and contributed to forest carbon accumulation. This limited the NPP reduction caused by climate change.

RII is an effective index for evaluating the effects of LULCC alone, independent of climate change, on NPP. In this study, we used RII to further assess the effects of climate change and LULCC on NPP. The fit curve of frequency by pixels of RII indicated that RII values were mostly positive (*Fig. 9*) in five regions, ranging from 50-90%, indicating that human activity had a negative effect on vegetation productivity and NPP.

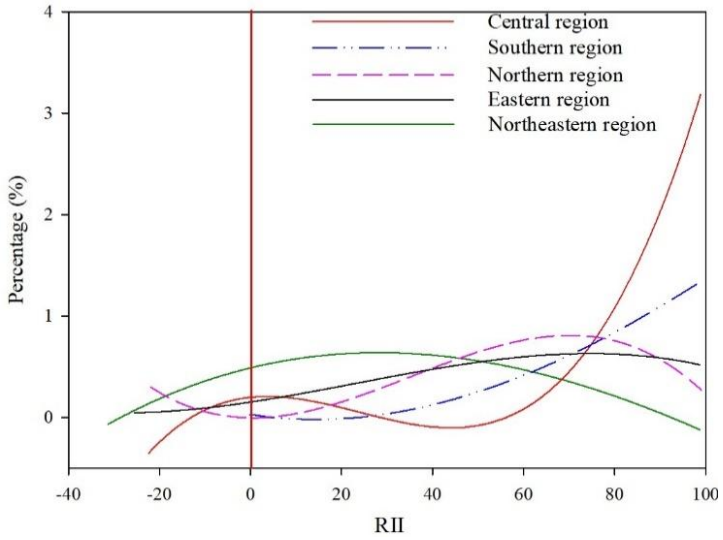

Figure 9. *Fit curve of frequency by pixels of RII in five regions*

http://www.aloki.hu ● ISSN 1589 1623 (Print) ● ISSN 1785 0037 (Online)
DOI: http://dx.doi.org/10.15666/aeer/1605_66676690
© 2018, ALÖKI Kft., Budapest, Hungary

In addition, mean RII values were greater than 50% in all regions and about 77.3% of those pixels were concentrated in the inner suburbs, suggesting that NPP variability was most affected by human activities. These findings were consistent with our results based on the method of Wu et al. (2014). Especially, about 17.12% pixels in RII were less than 0 in northeastern region, which was benefited by the protection policies of agriculture and forested lands. Nonetheless, it is worth noting that the increase in RII over the five regions (*Table 4*) meant that human impacts on NPP through LULCC also increased, and vegetation productivity was affected by human disturbance, especially in inner suburbs. Although the creation and protection of urban green spaces, forests, and wetlands contributed to the increase in NPP, the effects of some protection projects were less than satisfactory. The effectiveness of restoration projects and urban and industrial land use plans should be adjusted to balance environmental conservation and economic development, and more plausible adaptation strategies should be applied to cope with climate change.

Conclusions

NPP is one of the most significant factors characterizing ecosystem structure and function, and can be used to describe the spatiotemporal pattern of urban carbon storage and its driving mechanisms. The current study estimated NPP change in Guangzhou and its five regions from 2001 to 2013 and examined the effects of driving forces on NPP variability in a spatially explicit way. Nonlinear NPP trends indicated that NPP decreased across the study area and most significantly in the inner suburbs (southern, eastern, and northern regions) due to rapid urbanization and human interference, while a slight increase of NPP was concentrated in the western part of the northeastern region. Solar radiation and temperature strongly influenced NPP increases, while precipitation was a limiting factor. NPP reductions were correlated with urban sprawl combined with land conversions from vegetated areas to impervious surface, especially cropland to built-up land. More than 91.0% of pixels had positive RII values, implying that LULCC played a negative role in NPP accumulation.

Comparatively, there were significant differences in the effects of climate change and LULCC on NPP. More than 67.2% of pixels exhibited NPP trends that were dominated by LULCC, and absolute average RII values further confirmed that LULCC had a greater impact than climate change on NPP. The interacting effects of climate change and LULCC led to slight NPP variability. In the northeastern region, about 38.1% of pixel NPP trends were dominated by climate change, but it cannot be ignored that the influence of human activities on vegetation productivity is still increasing and prolonged efforts will be needed to protect and expand environmental resources in this region. The above results revealed that LULCC due to urban expansion, rather than climate variability, was the main cause for regional NPP reductions in Guangzhou.

NPP variability can also be an indicator of urban development intensity and will provide further insights into terrestrial carbon change resulting from urbanization. In particular, the obvious spatial heterogeneity in the effects of LULCC and climate change on NPP change can provide valuable decision support information for ecological conservation and management in this region. Moreover, it is noteworthy that with the increase in impervious surface and decrease in vegetation cover resulting from human activities, the urban heat island effect will likely be intensified and the decline of cultivated land and forest will threaten food security and ecosystem function. Future

http://www.aloki.hu ● ISSN 1589 1623 (Print) ● ISSN 1785 0037 (Online)
DOI: http://dx.doi.org/10.15666/aeer/1605_66676690
© 2018, ALÖKI Kft., Budapest, Hungary

work should aim to improve data resolution and delve further into the mechanisms coupling land use change, climate change and the carbon cycle for a long time. And further work is also needed to identify the mechanisms of cropland NPP and food security to urban expansion.

Acknowledgements. This study was supported by the Natural Science Foundation of Guangdong Province of China (2018A030310069) and the National Natural Science Foundation of China (61806059, 41671430).

REFERENCES

[1] Ahlström, A., Miller, P. A., Smith, B. (2012): Too early to infer a global NPP decline since 2000. – Geophysical Research Letters 39(15): 15403.
[2] Benali, A., Carvalho, A. C., Nunes, J. P., Carvalhais, N., Santos, A. (2012): Estimating air surface temperature in Portugal using MODIS LST data. – Remote Sensing of Environment 124: 108–121.
[3] Buyantuyev, A., Wu, J. G. (2012): Urbanization diversifies land surface phenology in arid environments: Interactions among vegetation, climatic variation, and land use pattern in the Phoenix metropolitan region, USA. – Landscape and Urban Planning 105(1–2): 149–159.
[4] Chao, Z. H., Zhang, P. D., Wang, X. F. (2018): Impacts of urbanization on the net primary productivity and cultivated land change in Shandong Province, China. – Journal of the Indian Society of Remote Sensing 46(2): 1–11.
[5] Chen, T., Huang, Q. H., Liu, M., Li, M. C., Qu, L. A., Deng, S. L., Chen, D. (2017): Decreasing net primary productivity in response to urbanization in Liaoning Province, China. – Sustainability 9(2): 162.
[6] Dekker, S. C., Rietkerk, M., Bierkens Arc, F. P. (2007): Coupling microscale vegetation, soil water and macroscale vegetation, precipitation feedbacks in semiarid ecosystems. – Global Change Biology 13(3): 671–678.
[7] Eisfelder, C., Klein, I., Niklaus, M., Kuenzer, C. (2014): Net primary productivity in Kazakhstan, its spatio-temporal patterns and relation to meteorological variables. – Journal of Arid Environments 103(8): 17–30.
[8] Fang, X., Zhang, C., Wang, Q., Chen, X., Ding, J. L., Karamage, F. (2017): Isolating and quantifying the effects of climate and CO2 changes (1980-2014) on the net primary productivity in arid and semiarid China. – Forests 8(3): 1–19.
[9] Field, C. B., Behrenfeld, M. J., Randerson, J. T., Falkowski, P. (1998): Primary production of the biosphere: integrating terrestrial and oceanic components. – Science 281(5374): 237–40.
[10] Fu, G., Shen, Z. X., Zhang, X. L., Shi, P. L., Zhang, Y. J., Wu, J. S. (2011): Estimating air temperature of an alpine meadow on the Northern Tibetan Plateau using MODIS land surface temperature. – Acta Ecologica Sinica 31(1): 8–13.
[11] Fu, Y. C., Lu, X. Y., Zhao, Y. L., Zeng, X. T., Xia, L. (2013): Assessment impacts of weather and land use/land cover (LULC) change on urban vegetation net primary productivity (NPP) a case study in Guangzhou, China. – Remote Sensing 5(8): 4125–4144.
[12] Gao, Q. Z., Wang, Y. F., Li, Y., Guo, Y. Q., Ganjurjav, Qin, X., Jiang, C. W., Wang, B. (2013): Effects of topography and human activity on the net primary productivity (NPP) of alpine grassland in northern Tibet from 1981 to 2004. – International Journal of Remote Sensing 34(6): 2057–2069.
[13] Gao, Z. Q., Liu, J. Y. (2008): A comparative study of Chinese vegetation net productivity. – Chinese Science Bulletin 53(3): 317–326.

http://www.aloki.hu ● ISSN 1589 1623 (Print) ● ISSN 1785 0037 (Online)
DOI: http://dx.doi.org/10.15666/aeer/1605_66676690
© 2018, ALÖKI Kft., Budapest, Hungary

[14] Gong, W., Wang, L. C., Lin, A. W., Zhang, M. (2012): Evaluating the monthly and interannual variation of net primary production in response to climate in Wuhan during 2001 to 2010. – Geosciences Journal 16(3): 347–355.
[15] Grimm, N. B., Faeth, S. H., Golubiewski, N. E., Redman, C. L., Wu, J., Bai, X., Briggs, J. M. (2008): Global change and the ecology of cities. – Science 319(5864): 756–760.
[16] Gu, F. X., Zhang YD, Huang, M., Guo, Tao, B., Liu, Z. J., Hao, M., Guo, R. (2017): Climate-driven uncertainties in modeling terrestrial ecosystem net primary productivity in China. – Agricultural and Forest Meteorology 246: 123–132.
[17] Hou, G. L., Li, J. Y., Zhang, Y. G. (1993): China Agricultural Climate Resources. – China Renmin University Press, Beijing (in Chinese).
[18] Hu, Y. H., Jia, G. S., Guo, H. D. (2009): Linking primary production, climate and land use along an urban–wildland transect: a satellite view. – Environmental Research Letters 4(4): 044009.
[19] Hua, X. B. (2009): Quantifying the human appropriation of net primary production and analysis of its multi-year changes in Guangdong. – Master Thesis, Sun Yat-sen University (in Chinese).
[20] Hutyra, L. R., Yoon, B., Hepinstall-Cymerman, J., Alberti, M. (2011): Carbon consequences of land cover change and expansion of urban lands: A case study in the Seattle metropolitan region. – Landscape and Urban Planning 103(1): 83–93.
[21] Imhoff, M. L., Tucker, C. J., Lawrence, W. T., Stutzer, D. C. (2000): The use of multisource satellite and geospatial data to study the effect of urbanization on primary productivity in the united states. – IEEE Transactions on Geoscience and Remote Sensing 38(6): 2549–2556.
[22] Jiang, C., Wu, Z. F. (2015): Impacts of urbanization on net primary productivity in the Pearl River Delta, China. – International Journal of Plant Production 9(4): 581–598.
[23] Kendall, M. G. (1975): Rank Correlation Methods. – Griffin, London, UK.
[24] Liang, L., Zhou, S. H., Qin, Z. H., He, K. X., Chen, C., Luo, Y. X., Zhou, X. D. (2014): Drought change trend using MODIS TVDI and its relationship with climate factors in China from 2001 to 2010. – Journal of Integrative Agriculture 13(7): 1501–1508.
[25] Liu, H. Y., Mi, Z. R., Lin, L., Wang, Y. H., Zhang, Z. H., Zhang, F. W., Wang, H., Liu, L. L. (2018): Shifting plant species composition in response to climate change stabilizes grassland primary production. – Proceedings of the National Academy of Sciences 115(16): 4051–4056.
[26] Liu, S. S., Du, W., Su, H., Wang, S. Q., Guan, Q. F. (2018): Quantifying impacts of land-use/cover change on urban vegetation gross primary production: a case study of Wuhan, China. – Sustainability 10(3): 714.
[27] Lu, D. S., Xu, X. F., Tian, H. Q., Moran, E., Zhao, M. S., Running, S. (2010): The effects of urbanization on net primary productivity in Southeastern China. – Environmental Management 46(3): 404–410.
[28] Mohamed, M. A. A., Babiker, I. S., Chen, Z. M., Ikeda, K. Ohta, K., Kato, K. (2004): The role of climate variability in the inter-annual variation of terrestrial net primary production (NPP). – Science of the Total Environment 332(1–3): 123–137.
[29] Mu, Q. Z., Zhao, M. S., Running, S. W., Liu, M. L., Tian, H. Q. (2008): Contribution of increasing CO2 and climate change to the carbon cycle in China's ecosystems. – Journal of Geophysical Research Biogeosciences 113(1): 1–15.
[30] Neeti, N., Eastman, J. R. (2011): A contextual Mann-Kendall approach for the assessment of trend significance in image time series. – Transactions in GIS 15(5): 599–611.
[31] Nemani, R. R., Keeling, C. D., Hashimoto, H., Jolly, W. M. Piper, S. C., Tucker, C. J., Myneni, R. B., Running, S. W. (2003): Climate-driven increases in global terrestrial net primary production from 1982 to 1999. – Science 300(5625): 1560–3.

http://www.aloki.hu ● ISSN 1589 1623 (Print) ● ISSN 1785 0037 (Online)
DOI: http://dx.doi.org/10.15666/aeer/1605_66676690
© 2018, ALÖKI Kft., Budapest, Hungary

[32] Ni, J. (2003): Net primary productivity in forests of China: scaling-up of national inventory data and comparison with model predictions. – Forest Ecology and Management 176(1–3): 485–495.
[33] Pan, Y., Mcguire, A. D., Kicklighter, D. W., Melillo, J. (1996): The importance of climate and soils for estimates of net primary production: a sensitivity analysis with the terrestrial ecosystem model. – Global Change Biology 2(1): 5–23.
[34] Pei, F. S., Li, X., Liu, X. P., Lao, C. H. (2013a): Assessing the impacts of droughts on net primary productivity in China. – Journal of Environmental Management 114(2): 362–371.
[35] Pei, F. S., Li, X., Liu, X. P., Wang, S. J., He, Z. J. (2013b): Assessing the differences in net primary productivity between pre- and post-urban land development in China. – Agricultural and Forest Meteorology 171–172(3): 174–186.
[36] Pei, F. S., Li, X., Liu, X. P., Lao, C. H., Xia, G. R. (2015): Exploring the response of net primary productivity variations to urban expansion and climate change: A scenario analysis for Guangdong Province in China. – Journal of Environmental Management 150(150C): 92–102.
[37] Peng, J., Shen, H., Wu, W., Liu, Y., Wang, Y. (2016): Net primary productivity (NPP) dynamics and associated urbanization driving forces in metropolitan areas: a case study in Beijing City, China. – Landscape Ecology 31(5): 1077–1092.
[38] Piao, S., Fang, J. Y., Zhou, L. M., Zhu, B., Tan, K., Tao, S. (2005): Changes in vegetation net primary productivity from 1982 to 1999 in China. – Global Biogeochemical Cycles 19(2): 1605–1622.
[39] Piao, S. L., Fang, J. Y., Chen, A. P. (2003): Seasonal dynamics of terrestrial net primary production in response to climate changes in China. – Acta Botanica Sinica 45(3): 269–275.
[40] Piao, S. L., Fang, J. Y., Ciais, P., Peylin, P., Huang, Y., Sitch, S., Wang, T. (2009): The carbon balance of terrestrial ecosystems in China. – Nature 458(7241): 1009–1013.
[41] Potter, C. S., Randerson, J. T., Field, C. B., Matson, P. A., Vitousek, P. M., Mooney, H. A., Klooster, S. A. (1993): Terrestrial ecosystem production: A process model based on global satellite and surface data. – Global Biogeochemical Cycles 7(4): 811–841.
[42] Prince, S. D. (1991): A model of regional primary production for use with coarse resolution satellite data. – International Journal of Remote Sensing 12(6): 1313–1330.
[43] Sui, X. H., Zhou, G. S., Zhuang, Q. L. (2013): Sensitivity of carbon budget to historical climate variability and atmospheric CO2 concentration in temperate grassland ecosystems in China. – Climatic Change 117(1–2): 259–272.
[44] Tucker, C. J., Newcomb, W. W., Dregne, H. E. (1994): AVHRR data sets for determination of desert spatial extent. – International Journal of Remote Sensing 15(17): 3547–3565.
[45] Vancutsem, C., Ceccato, P., Dinku, T., Connor, S. J. (2010): Evaluation of MODIS land surface temperature data to estimate air temperature in different ecosystems over Africa. – Remote Sensing of Environment 114(2): 449–465.
[46] Verburg, P. H., Soepboer, W., Veldkamp, A., Limpiada, R., Espaldon, V., Mastura, S. S. A. (2002): Modeling the spatial dynamics of regional land use: the CLUE-S model. – Environmental Management 30(3): 391–405.
[47] Wang, C. Z., Guo, H. D., Zhang, L., Liu, S. Y., Qiu, Y. B., Sun, Z. C. (2015a): Assessing phenological change and climatic control of alpine grasslands in the Tibetan Plateau with MODIS time series. – International Journal of Biometeorology 59(1): 11–2.
[48] Wang, H., Li, X. B., Long, H. L., Zhu, W. Q. (2009): A study of the seasonal dynamics of grassland growth rates in Inner Mongolia based on AVHRR data and a light-use efficiency model. – International Journal of Remote Sensing 30(14): 3799–3815.

http://www.aloki.hu ● ISSN 1589 1623 (Print) ● ISSN 1785 0037 (Online)
DOI: http://dx.doi.org/10.15666/aeer/1605_66676690
© 2018, ALÖKI Kft., Budapest, Hungary

[49] Wang, J., Price, K. P., Rich, P. M. (2001): Spatial patterns of NDVI in response to precipitation and temperature in the central Great Plains. – International Journal of Remote Sensing 22(18): 3827–3844.
[50] Wang, J., Wang, K. L., Zhang, M. Y., Zhang, C. H. (2015b): Impacts of climate change and human activities on vegetation cover in hilly southern China. – Ecological Engineering 81: 451–461.
[51] Wang, L. C., Gong, W., Ma, Y. Y., Zhang, M. (2013): Modeling regional vegetation NPP variations and their relationships with climatic parameters in Wuhan, China. – Earth Interactions 17(4): 1–20.
[52] Wu, S. H., Zhou, S. L., Chen, D. X., Wei, Z. Q., Dai, L., Li, X. G. (2014): Determining the contributions of urbanisation and climate change to NPP variations over the last decade in the Yangtze River Delta, China. – Science of the Total Environment 472: 397–406.
[53] Wu, Y. Y., Li, S. Y., Yu, S. X. (2016): Monitoring urban expansion and its effects on land use and land cover changes in Guangzhou city, China. – Environmental Monitoring and Assessment 188(1): 54.
[54] Wu, Y. Y., Wu, Z. F. (2018): Quantitative assessment of human-induced impacts based on net primary productivity in Guangzhou, China. – Environmental Science and Pollution Research 25(12): 11384–11399.
[55] Xu, C., Liu, M., An, S., Chen, J. M., Yan, P. (2007): Assessing the impact of urbanization on regional net primary productivity in Jiangyin County, China. – Journal of Environmental Management 85(3): 597–606.
[56] Xu, D. Y., Li, C. L., Zhuang, D. F., Pan, J. J. (2011): Assessment of the relative role of climate change and human activities in desertification: a review. – Journal of Geographical Sciences 21(5): 926–936.
[57] Yan, H., Zhan, J., Wu, F., Yang, H. (2016): Effects of climate change and LUCC on terrestrial biomass in the Lower Heihe River Basin during 2001-2010. – Energies 9(4): 9–14.
[58] Yang, L. Y., Zhang, L. B., Li, Y., Wu, S. T. (2015): Water-related ecosystem services provided by urban green space: A case study in Yixing city (China). – Landscape and Urban Planning 136: 40–51.
[59] Zhang, F. Y., Pu, L. J., Huang, Q. (2015): Quantitative assessment of the human appropriation of net primary production (HANPP) in the coastal areas of Jiangsu, China. – Sustainability 7(12): 15857–15870.
[60] Zhang, J. H., Hu, Y. L., Xiao, X. M., Chen, P. S., Han, S. J., Song, G. Z., Yu, G. R. (2009): Satellite-based estimation of evapotranspiration of an old-growth temperate mixed forest. – Agricultural and Forest Meteorology 149(6–7): 976–984.
[61] Zhang, W. T., Huang, B., Luo, D. (2014): Effects of land use and transportation on carbon sources and carbon sinks: a case study in Shenzhen, China. – Landscape and Urban Planning 122(2): 175–185.
[62] Zhang, Y., Zhang, C. B., Wang, Z. Q., Chen, Y. Z., Gang, C. C., An, R., Li, J. H. (2016): Vegetation dynamics and its driving forces from climate change and human activities in the Three-River Source Region, China from 1982 to 2012. – Science of the Total Environment 563–564: 210–220.
[63] Zhang, Y. L., Song, C. H., Zhang, K. R., Cheng, X. L., Zhang, Q. F. (2014): Spatial-temporal variability of terrestrial vegetation productivity in the Yangtze River Basin during 2000-2009. – Journal of Plant Ecology 7(1): 10–23.
[64] Zhao, M., Running, S. W. (2010): Drought-induced reduction in global terrestrial net primary production from 2000 through 2009. – Science 329(5994): 940–943.
[65] Zhao, T. T., Brown, D. G., Fang, H. L., Theobald, D. M. Liu, T., Zhang, T. (2012): Vegetation productivity consequences of human settlement growth in the eastern United States. – Landscape Ecology 27(8): 1149–1165.

http://www.aloki.hu ● ISSN 1589 1623 (Print) ● ISSN 1785 0037 (Online)
DOI: http://dx.doi.org/10.15666/aeer/1605_66676690
© 2018, ALÖKI Kft., Budapest, Hungary

[66] Zhu, W. Q., Pan, Y. Z., He, H., Yu, D. Y., Hu, H. B. (2006): Simulation of maximum light use efficiency for some typical vegetation types in China. – Chinese Science Bulletin 51(4): 457–463.
[67] Zhu, W. Q., Pan, Y. Z., Yang, X. Q., Song, G. B. (2007a): Comprehensive analysis of the impact of climatic changes on Chinese terrestrial net primary productivity. – Chinese Science Bulletin 52(23): 3253–3260.
[68] Zhu, W. Q., Pan, Y. Z., Zhang, J. S. (2007b): Estimation of net primary productivity of Chinese terrestrial vegetation based on remote sensing. – Chinese Journal of Plant Ecology 31(3): 413–424.

http://www.aloki.hu ● ISSN 1589 1623 (Print) ● ISSN 1785 0037 (Online)
DOI: http://dx.doi.org/10.15666/aeer/1605_66676690
© 2018, ALÖKI Kft., Budapest, Hungary

ECONOMIC EFFECT OF CLIMATE ALTERATION ON GRAIN PRODUCTION IN IRAN

SAEI, M.[1,2*] – MOHAMMADI, H.[1] – ZIAEE, S.[1] – BARKHORDARI, S.[3]

[1]*Department of Agricultural Economics, Faculty of Agriculture, University of Zabol, Zabol, Iran*

[2]*Economic, Social and Extension Research Department, Kerman Agricultural and Natural Resources Research and Education Center, AREEO, Kerman, Iran*

[3]*Faculty of Economics, University of Tehran, Tehran, Iran*

**Corresponding author*
e-mail: mahdiyeh.saei@uoz.ac.ir

(Received 2nd Jul 2018; accepted 13th Sep 2018)

Abstract. The present study shows the economic effects of climate alteration on grain (maize, wheat, and rice) production in Iran using a Ricardian method. The model was estimated using the longitudinal data on grain yields and climate variables from 1983-2014. The marginal effects of climate changes on productivity of crops were estimated by applying Panel Corrected Standard Error (PCSE) models. Empirical results showed a considerable hill-shaped correlation between wheat yield and spring and fall rainfalls and temperatures. The joint effect of the spring and fall rainfall and temperature for wheat was significantly negative. For maize, the outcomes showed a considerable hill-shaped correlation between crop productivity and spring precipitation. Moreover, there was a meaningful interaction term between winter rainfall and temperature at 1%. Our results for maize yield were not as robust as those for wheat. For rice, winter temperature had a considerable U-shaped relationship with rice yield, while summer precipitation and temperature had a considerable hill-shaped relationship with yield. The annual marginal impacts of rainfall and temperature for all the crops were positive. The outcomes showed that in Iran, the sensitivity of cereal production to enhance in precipitation levels would be less compared to the increase in temperature.
Keywords: *climate change, grain yield, panel regression, ricardian method*

Introduction

One of the global concern is climate change due to its impending threats to sustainable economic development. The effects of climate variations are more severe on agriculture compared to other economic activities (Stern, 2006; Mendelsohn et al., 2006; Rosenzweig and Iglesias, 1994; Adams et al., 1998; Cline, 2007; Nelson et al., 2009; Kurukulasuriya and Ajwad, 2007; De Salvo et al., 2013). The effects are probably too strong for developing nations, because of their strong dependency on agriculture and absence of economic resources for reducing and adapting to climate alteration (Mendelsohn et al., 2006; Stern, 2006; Nelson et al., 2009). Studies suggests that climate variation will considerably impact the agriculture sector of developing nations, leading to serious consequences in food safety and production. It would also have adverse effects on enormous population along with more effects on poor farmers with small farms.

Review of literature

Many researchers have measured the effects of climate variables on crop yield via simulation models for example CERES-rice, CERES-maize, and EPIC models (Phillips et al., 1996; Rosenzweig et al., 2002; Tan and Shibasaki, 2003) or regression models

http://www.aloki.hu ● ISSN 1589 1623 (Print) ● ISSN 1785 0037 (Online)
DOI: http://dx.doi.org/10.15666/aeer/1605_66916707
© 2018, ALÖKI Kft., Budapest, Hungary

(Mendelsohn et al., 1994; Chang, 2002; Haim et al., 2008). Previous studies have generally employed two major approaches to assess the effect of climate on agriculture: the approach of production function (agronomic model or crop modeling) (Mearns et al., 1997), and the Ricardian approach (Mendelsohn et al., 1994). Employing controlled experiments, the first approach simulates data on crop yields and climate variables in a laboratory. With a precise control and randomized usage of environmental circumstances, this method can anticipate the climatic influences on agriculture yields. However, it does not consider farmers' attitudes towards climate change adaptation. This leads to overestimation of negative effects and underestimation of positive impacts (Adams et al., 1990, 1999; Haim et al., 2008; Mendelsohn et al., 1994). On the contrary, the Ricardian model estimates the association among values of land and agro-climatic variables through cross-sectional information (Kumar and Parikh, 1998; Mendelsohn et al., 1994). The major power of the Ricardian model is that it considers farmers' adaptations which influence land values as measured by farm earnings or net revenue. The model has been used in different countries, namely the USA (Mendelsohn and Dinar, 2003; Mendelsohn et al., 1994), England and Wales (Maddison, 2000); Kenya (Mariara and Karanja, 2007), Taiwan (Chang, 2002), South Africa (Gbetibouo and Hassan, 2005), Cameroon (Moula, 2009), China (Wang et al., 2009), and India and Brazil (Sanghi and Mendelsohn, 2008). Nevertheless, the approach, in its main form, may not be used for most developing countries since there are no influential land markets and reasonable land expenses in these countries.

Although the research about climate outcomes on Iranian agriculture is restricted, it is rising. In coming sections, we review the studies conducted on the influence of climate variation on agricultural crop productivity in developing nations generally, continued by reviewing of studies in Iran.

Liangzhi et al. (2005) studied climate effect on Chinese wheat yields using crop specific cross-section and time series data over 1979-2000 for main wheat generating provinces in China along with climate data like solar radiation, rainfall, and temperature during this period. They observed that 1% enhance in the heat in the germination season of wheat reduced wheat yields by almost 0.3%. They also report that rising temperatures over the two decades prior to their research accounted for a 2.4% reduction in wheat productivities in China while a major growth in wheat yields (i.e., 75%) is induced by increasing application of physical inputs.

Guiteras (2009) estimated the influence of climate variation on Indian agriculture with the feasible generalized least squares (FGLS) approximation method. His results offer that climate variation is probable to impose considerable costs on the Indian economy unless producers can quickly distinguish and adjust with temperature rises. The study also declared that such a quick adaptation might be fewer probable in a developing country, where availability of capital and information for adjustment is limited.

Ayinde et al. (2010) studied climate variation and agricultural crops in Nigeria using time series data. They used descriptive statistics and a Granger causality test analysis as analytical tools. According to their results, the temperature remains relatively constant and has no effect on agricultural output. However, using the Granger causality approach in their research revealed that alterations in precipitation positively affected agricultural crops in Nigeria.

Lee et al. (2012) evaluated the climate variation effects on agricultural crops in Asia over 1998-2007. They applied agricultural crop model and estimated a country-level

http://www.aloki.hu ● ISSN 1589 1623 (Print) ● ISSN 1785 0037 (Online)
DOI: http://dx.doi.org/10.15666/aeer/1605_66916707
© 2018, ALÖKI Kft., Budapest, Hungary

constant impact panel model for agricultural crops by seasonal climate and other input variables. Their outcomes showed that greater temperatures and higher precipitation in summer increased agricultural crops while a decrease in temperatures was dangerous in South and Southeast of Asia. Moreover, they reported that a general enhance in annual temperature decreased agricultural crops in Asia. They stated that adapting to climate alteration through development new varieties with more tolerance to greater temperatures was essential. Moreover, they suggested increasing investments in agricultural productivity and expansion of appropriate adaptation programs or strategies.

Kumar and Sharma (2013) analyzed the climate alteration effects on agriculture sector productivity, the production value, and food safety in India according to secondary information over 1980-2009. They performed a regression analysis with the Cobb-Douglas production type model. They revealed that climate variations had harmful effects on lots of the food and non-food grain products in quantity and production value terms. The reported negative influences of climate alteration on the agricultural crops and food grains value shows food security risks to marginal farming households. Moreover, the research reported an econometric estimating of the state-wise food security measure, revealing the harmful impacts of climatic variations on food safety.

Vaseghi and Esmaeili (2008a) studied the outcomes of climate alteration on agriculture in Iran, using chronological combined series of climate data over 1984-2004 and Ricardian model in 17 provinces and reported that climatic alterations had a considerable and nonlinear impact on net income per hectare of wheat. Moreover, they illustrated that the rise in temperature and fall in precipitation in the following 100 years would cause the decrease in yields per hectare by 41%.

Elsewhere, Vaseghi and Esmaeili (2008b) applied the Ricardian scheme to measure the economic outcomes of climate alteration on maize production in 11 Iranian provinces for 1990 to 2004. They reported that climatic variables had considerable nonlinear effects on net income of maize. In addition, they demonstrated that the increase in temperature and fall in precipitation during the future 100 years would cause a 29% decrease in the maize yield (584 thousand Rials per hectare).

Sabzevary et al. (2012) examined the impacts of climatic variables on dry farming and irrigated wheat yields in selected stations of Hamadan Province, Iran. The investigation was performed by bivariate linear regression technique and the impact of all factors on wheat productivity was compared utilizing explanatory and correlative coefficients. Overall, the dry farming wheat yields index sensitivity to agroclimatic and atmospheric parameters was greater than irrigated wheat.

Pahrizkari et al. (2014) evaluated the climate alteration effect and consuming agricultural inputs (seeds, fertilizers, poisons, machinery) on the irrigated wheat yield over 2001-2013 in Shahrood watershed of Iran. The outcomes showed that increasing temperature over the generation season negatively affected the yield of wheat so that through enhancing the temperature, the yield of this crop has declined by 0.683%. Also, they showed a considerable relation between the yield of wheat and inputs consumption.

Agriculture sector of Iran, despite its decreasing share in countrywide income, counts for almost 18% of national GDP, 85% of the food supply, above 20% of employment, 25% of non-oil products, and 90% of feedstock utilized in agro-industry (NCCOI, 2014). Therefore, incomes of a main group of people depend on agriculture that are in danger because of considerable negative influences of climate alteration on agriculture.

http://www.aloki.hu ● ISSN 1589 1623 (Print) ● ISSN 1785 0037 (Online)
DOI: http://dx.doi.org/10.15666/aeer/1605_66916707
© 2018, ALÖKI Kft., Budapest, Hungary

The objective of this study is, thus, to assess the impacts of climate alteration on the yields of major grain crops (wheat, maize, and rice) of Iran using panel data. In this regard, a Richardian model is employed.

Materials and methods

Wheat growing regions in Iran are divided into four main climates in terms of weather conditions and cultivars: hot and humid, hot and arid, temperate, and cold climate. Irrespective of the growth habits of the cultivars (winter, spring, and intermediate), wheat in Iran is generally grown in autumn. In hot and humid climate, its sowing date is mid-November to mid-December and it is harvested in late-May. In hot and arid climate, it is sown in mid-December and harvested in mid-April. Temperate climate itself is sub-divided into northern and southern regions due to its stretch. In the northern regions, it is sown in late-October to late-November and in the southern regions, it is sown from November 6 until December 6. The harvest time is late-May to late-June. Wheat in cold climate is sown in late-December to mid-October and it is harvested in late-May to early-July.

Maize is a crop of tropics and subtropics and unlike other grains, it requires high temperatures and solar heat from sowing until harvest. In Iran, maize can be grown in most regions (hot, temperate, and cold). It may be sown in spring or summer depending on the regional climate and sowing type. Maize is mainly planted as a second crop after harvesting wheat. The sowing date of maize as the first crop varies from June 10 to June 20, and its sowing date as the second crop is July 11 in temperate regions. In hot regions, summer maize is sown from mid-July to early-August and spring maize is sown from late-February until mid-March. In cold regions, maize is planted in early-May. In all regions, maize is harvested about 4 months later.

Forty percent of total rice production in Iran is accounted for by Mazandaran province. The first crop starts in late-March in all provinces and it is finally harvested in late-July to mid-August. In recent years, farmers in some cities in the north of Iran prepare their farms for the second crop of rice immediately after harvesting the first crop. The second crop is harvested in October-November.

The data

Longitudinal data regarding three major grain yields and climate variables (i.e., rainfall and temperature) from chosen provinces in Iran were applied for estimating the model. The number of provinces selected for all crops was 5 for rice, 15 for wheat, and 9 for maize. The bases of including these provinces in the study have been the ‘major grain-producing provinces’ and accessibility of data for a minimum period of 30 years from1983 to 2014. Data on crop productivity measured in kilograms per hectare (kg/ha) were prepared from the Agricultural Jihad Ministry. Province-level climate information for monthly average temperature and monthly total precipitation were gathered from the Iran Meteorological Organization (IRIMO). Then, the monthly data were applied to group the climate factors into seasonal averages for rainfall and temperature for three crops. Crop productivities are usually reported for the production year, which is resembling to the financial year. So, the years were merged for the simplicity of analysis. Thus, for example, rice yield data in 1982-83 were considered as the yield for the year 1983. Accordingly, climate factors were in accordance with the yield data. Although yields depend on numerous factors, only climate variables (i.e., rain and

http://www.aloki.hu ● ISSN 1589 1623 (Print) ● ISSN 1785 0037 (Online)
DOI: http://dx.doi.org/10.15666/aeer/1605_66916707
© 2018, ALÖKI Kft., Budapest, Hungary

temperature) were noticed in this research. Other factor inputs such as fertilizer, seed, and herbicides could have been involved but these were not existent on a crop-by-crop basis. Data related to the crop productivity and climate variables utilized in the present research are displayed in *Table 1*. According to the descriptive statistics of the model for a 30-year period, the average yield of wheat, maize and rice in Iran are 2920, 5175 and 3826 kg ha^{-1}. In wheat-producing provinces, mean temperature is 14, 27, 16 and 4 °C and mean precipitation is 118, 7, 60 and 122 mm in spring, summer, autumn, and winter, respectively. In the case of maize producing provinces, the mean temperature in these seasons is 17, 29, 18 and 6 °C and the mean precipitation is 100, 2, 54 and 130 mm, respectively. These are 18, 29, 20 and 9 °C and 121, 52, 230 and 235 mm for rice-producing provinces, respectively.

Methodology

The Ricardian log-linear model applied in current research is an empirical method proposed by Mendelsohn et al. (1994) for measuring the economic effect of climate variation on grain production in Iran. The technique was called after Ricardo due to his innovative results that the land value would reveal its net productivity at a situation under perfect competition. This method that predicts the impacts of climate and other factors on land values and farm incomes, has been generally utilized in various researches (Mendelsohn et al., 1994 and 1999; Sanghi and Mendelsohn, 1999; Gbetibouo and Hassan, 2005; Kurukulasuriya and Ajwad, 2007; Mendelsohn and Reinsborough, 2007).

The approximated variations in productivity resulted by alterations in ecological factors are accumulated with the total national effect (Olsen et al., 2000) or combined with an economic scheme for simulating the yield variations welfare effects under diverse climate variation scenarios (Kumar and Parikh, 1998; Chang, 2002). This model provides the probability of accounting the direct influence of climate alteration on crop productivities and the indirect replacement between diverse inputs contain introducing several activities, and other possible adaptations to climate alterations by direct measurement of farm costs or incomes (Deressa and Hassan, 2009). Applying Ricardian method, net incomes were regressed on climate parameters for identifying the effects of climate in explanation of net incomes.

The Ricardian method includes determining a net productivity function of the subsequent form (*Eq. 1*):

$$\pi = \sum P_i Q_i(X, C, Z) - \sum P_x X \qquad \text{(Eq.1)}$$

where π is the net income per hectare, P_i is the price of crop i, Q_i is output of crop i, X represents a purchased inputs vector (excluding land), C represents a climate factors vector, Z represents a vector for other control factors related with the farm including seeds and economic factors like market accessibility, and P_x represents an input prices vector. The producer is expected to select X for maximizing net incomes considering the features of the farm and prices.

Resolving *Equation 1* causes a decreased type model (*Eq. 2*) in which net income is a function of all the exogenous factors P_i, P_x, Z, and C:

http://www.aloki.hu ● ISSN 1589 1623 (Print) ● ISSN 1785 0037 (Online)
DOI: http://dx.doi.org/10.15666/aeer/1605_66916707
© 2018, ALÖKI Kft., Budapest, Hungary

$$\pi = R\,(P_i, P_x, C, Z) \qquad \text{(Eq.2)}$$

The empirical model applied in current research was a log-linear description of the Ricardian methodology (*Eq. 3*):

$$ln\pi = \beta_0 + \beta_1 T + \beta_2 T^2 + \beta_3 P + \beta_4 P^2 + \beta_5 T \times P + \varepsilon \qquad \text{(Eq.3)}$$

where T and P represent vectors for seasonal temperatures and rainfalls, and ε represents an error expression. The square and interaction expressions related to climatic factors are showed in the model to see if there is any nonlinearity in the impacts of mentioned parameters on the crop yield. In the log-linear functional model, the linear coefficients offer approximations for the proportional alteration in π for a change in the climate parameter and the quadratic terms related to rainfall and temperature reveals the nonlinear shape related to the response function between climate and net incomes (*Eq. 3*). When the net income function has a U shape, the quadratic term has a positive value, while in the case of having negative value for the quadratic term, the function has a hill shape. According to agronomic study and earlier cross-sectional analyses, a hill shape for correlation with temperature is expected for the farm value. Since there is a specific temperature at which a specific crop has its optimal growth over the seasons, products frequently show a hill-shaped relation with the yearly temperature. However, the correlation of seasonal climate factors is more complicated and may contain a mix of negative and positive coefficients over seasons. The predicted marginal effect of only one climate factor on net income of the farm assessed at the mean of factor is (*Eq. 4*):

$$(\partial\pi/\partial C_j) = (\alpha_{1j} + 2\beta_{2j} \times \mathrm{C}) \times \pi \qquad \text{(Eq.4)}$$

The alteration in yearly welfare, ΔW, causing by a climate variation from C_0 to C_1 can be calculated as following (*Eq. 5*):

$$\Delta W = \pi(C_1) - \pi(C_0) \qquad \text{(Eq.5)}$$

where π is the expected net income under the coming climate situation, C_1 represents the forecasted level for climate factors (rainfall or temperature), C_0 shows the normal mean temperature under the present climate situation, and ΔW represents the difference between the forecasted value of net income per hectare under the upcoming climate situation and the existing climate situation. Farm-level net-revenues, which reveal the modifications done by farmers for the normal climate conditions, can be employed to evaluate the climate response function. However, no such information is accessible for Iran. Hence, this study uses annual yield in the approximation of climate response function and other descriptive variables are taken in the similar ways. Similar to state level constant impact determined by Kumar (2009) while analyzing Indian agriculture and country-level fixed effects specified by Deschenes and Greenstone (2007) while analysing of US agriculture, we specified a district level constant-effect panel regression in the existing research. The Hausman specification test also confirms for the same. If there is AR cross-sectional dependence along with heteroscedasticity, FGLS with fixed effects was recognized to be an appropriate method of estimation.

http://www.aloki.hu ● ISSN 1589 1623 (Print) ● ISSN 1785 0037 (Online)
DOI: http://dx.doi.org/10.15666/aeer/1605_66916707
© 2018, ALÖKI Kft., Budapest, Hungary

However, one of the disadvantages of FGLS estimation is that it generates excessively optimistic standard error estimates. Furthermore, the estimates are only feasible if N < T, suggesting that there are less number of observations comparing to the number of time period, which is not the case for the three crops. In this regard, Beck and Katz (1995) propose using Panel Corrected Standard Errors (PCSE) models with Monte Carlo analysis. These models work well and yield correct estimates of sampling variability even in the existence of complicated panel error structures. Following Beck and Katz (1995), this study employs the PCSE model for measuring the impacts of climate variation on the yield of major cereal crops in Iran.

Table 1. *Summary statistics of yields and climate variables applied in the Ricardian model. (Source: Research findings)*

	Variables	Unit	N	Mean	Std. dev.	Min.	Max.
Wheat	Yield	(Kg/ha)	480	2919.52	888.54	902.4	5732.81
	Spring temperature	(°C)	480	14.40	4.078	5.83	28.16
	Summer temperature	(°C)	480	27.02	3.74	20.5	38.6
	Fall temperature	(°C)	480	16.33	3.77	10.13	28.33
	Winter temperature	(°C)	480	3.59	4.18	-6.1	15.63
	Spring precipitation	(mm)	480	117.62	63.70	.3	315
	Summer precipitation	(mm)	480	6.98	11.64	0	65.4
	Fall precipitation	(mm)	480	60.18	53.96	0	395.5
	Winter precipitation	(mm)	480	122.51	70.38	4.7	556
Maize	Yield	(Kg/ha)	288	5175.57	2251.49	259.81	11250
	Spring temperature	(°C)	288	16.58	3.78	8.8	28.16
	Summer temperature	(°C)	288	29.05	3.21	22.93	38.6
	Fall temperature	(°C)	288	18.51	3.27	13.66	28.33
	Winter temperature	(°C)	288	6.54	3.45	-3.63	15.63
	Spring precipitation	(mm)	288	100.26	73.75	.3	315
	Summer precipitation	(mm)	288	2.23	4.37	0	26.5
	Fall precipitation	(mm)	288	53.84	61.83	0	395.5
	Winter precipitation	(mm)	288	130.13	83.15	4.1	556
Rice	Yield	(Kg/ha)	160	3826.19	763.81	2001.07	5699.97
	Spring temperature	(°C)	160	17.69	4.31	12.13	28.16
	Summer temperature	(°C)	160	28.97	4.56	22.93	38.6
	Fall temperature	(°C)	160	20.29	3.42	15.2	28.33
	Winter temperature	(°C)	160	9.02	2.59	4.67	15.63
	Spring precipitation	(mm)	160	121.40	82.61	.3	427.8
	Summer precipitation	(mm)	160	51.89	76.68	0	320.4
	Fall precipitation	(mm)	160	229.62	239.82	0	996.4
	Winter precipitation	(mm)	160	235.36	133.90	26.3	598

Results

The independent factors utilized in the scheme are linear, quadratic, and interaction terms between precipitation and temperature. Cross-sectional dependency is detected using Pesaran test. The Wooldridge autocorrelation test signs for the autocorrelation and Wald test signs for the heteroscedasticity. The panel unit root test presents that the

http://www.aloki.hu ● ISSN 1589 1623 (Print) ● ISSN 1785 0037 (Online)
DOI: http://dx.doi.org/10.15666/aeer/1605_66916707
© 2018, ALÖKI Kft., Budapest, Hungary

factors we used are unit root free variables. To overcome the autocorrelation, cross-sectional dependency, and heteroscedasticity problem, we estimated two econometric models: Feasible Generalized Least Squares (FGLS) and Prais-Winsten models with Panel Corrected Standard Errors (PCSE).

Tables 2, 3, and *4* present the outcomes of panel regression with district constant impacts for wheat, maize, and rice crop productivity, respectively. We compared the obtained PCSE and FGLS and, as expected, detected that the standard errors of FGLS are lower comparing to those of PCSE for nearly all estimates. This evidence, compatible with the findings of Beck and Katz (1995), shows that FGLS underestimates the standard errors. Therefore, we study only the PCSE estimates in discussing results and making inferences.

Table 2. *Regression coefficients of climate factors for wheat crop*

	FGLS		**PCSE**	
Variables	**Coefficients**	**Std. err.**	**Coefficients**	**Std. err.**
Constant	7.575***	0.53	7.028***	0.905
Spring temp.	0.0526***	0.020	0.0524	0.039
Spring temp. sq.	-0.0022***	0.0006	-0.0019*	0.0011
Summer temp.	-0.085	0.047	-0.037	0.080
Summer temp. sq.	0.0017**	0.00086	0.00080	0.0014
Fall temp.	0.0938***	0.023	0.080**	0.040
Fall temp. sq.	-0.0024***	0.00066	-0.0020*	0.0011
Winter temp.	0.0186***	0.0047	0.0256***	0.0091
Winter temp. sq.	-0.000052	0.00040	-0.00037	0.00084
Spring prec.	0.0027***	0.00054	0.0035***	0.00099
Spring prec. Sq.	-3.96e-06***	9.42e-07	-5.5e-06***	1.79e-06
Summer prec.	-0.0079	0.0055	-0.0054	0.0096
Summer prec. Sq.	2.44e-06	0.000026	-0.0000109	0.000052
Fall prec.	0.00083**	0.00039	0.00073	0.00077
Fall prec. Sq.	2.12e-06**	8.69e-07	2.88e-06	1.95e-06
Winter prec.	0.00030	0.00020	0.000054	0.00040
Winter prec. Sq.	-3.69e-07	4.88e-07	-2.95e-07	8.15e-07
Spring temp∗prec	-.0000925***	.0000259	-.00011***	.000045
Summer temp∗prec	.0003358	.0002009	.00025	.00032
Fall temp∗prec	-.0000715***	.0000202	-.000074*	.000038
Winter temp∗prec	1.71e-06	.0000182	7.45e-06	.000031
Wald chi2(20)	183.54		65.70	
Prob > *chi*2	0.0000		0.0000	
R^2			0.89	

Log of yield is the dependent variable
***, ** and * indicate significance at 1%, 5%, and 10% levels, respectively

http://www.aloki.hu ● ISSN 1589 1623 (Print) ● ISSN 1785 0037 (Online)
DOI: http://dx.doi.org/10.15666/aeer/1605_66916707
© 2018, ALÖKI Kft., Budapest, Hungary

Impacts of climate factors on wheat yield

Table 2 presents the panel regressions for wheat yield. We discuss the PCSE regression estimates for explaining the influence of climate factors on wheat yield. The R^2 value is 0.89, which demonstrates that the climate variables in the model explain more than two-thirds of alterations in the crop yield. The PCSE regression results specify that the variables of temperature and precipitation in spring, autumn, and winter influenced wheat yield positively, but only the variables of temperature in autumn and winter and precipitation in spring were statistically significant. Further, the variables of the squared temperature of spring and autumn and squared precipitation of spring were negative and statistically significant; this means that the increase in these variables is related to the increase in wheat yield up to a threshold beyond which crop yield is negatively influenced. According to Thapa-Parajuli and Devkota (2016), assuming that all other conditions are constant, the increase in temperature resulted in the increase in wheat yield up to a certain threshold in Nepal. Since wheat in Nepal is sown in cold season, the increase in temperature of this season enhances the yield. The same trend is observed for precipitation. This result is supported by Attri and Rathore's (2003) study in India. Also, interaction between fall and spring climate are usually negative and considerable whereas summer and winter climate interaction impacts are positive but insignificant. Accordingly, the joint effect related to temperature and precipitation for the fall and spring damages the wheat yield significantly. It can be clarified that increasing temperature and precipitation of both fall and spring would cause the significant negative joint climatic impact in wheat yield in Iran. Thus, it can be asserted that the climate variation although initially promotes producing wheat in Iran, this trend terminates following a determined threshold level.

Impacts of climate factors on maize yield

The PCSE outcomes indicate that the increase in temperature and precipitation in spring, summer, and autumn, which are the growing seasons of grain maize in Iran, affects the yield of this crop positively, but only the variables of temperature and precipitation of spring are statistically significant. Also, the yield of maize is negatively and significantly influenced by the squared precipitation of spring and is positively and significantly influenced by the squared precipitation of autumn. So, we can say that the precipitation of spring improves the yield of maize up to a specific threshold and then it affects its yield adversely. Further, the winter precipitation shows a considerable undesirable effect on maize yield. The decrease in crop productivity per hectare with increasing winter precipitation specifies that the available level of rainfall is enough for planting. The interaction term between winter rainfall and temperature is significant at 1%, suggesting that the winter rainfall impact on yield is affected by the degree of temperature and vice versa. We found that our results related to maize yield are not as robust as the findings related to wheat (*Table 3*).

Impacts of climate factors on rice yield

The yield of rice was positively and significantly influenced by the temperature and precipitation of summer, whereas it was negatively and significantly affected by the squared temperature and precipitation of this season. So, it can be said that the increase in these variables entails the enhancement of the crop yield up to a specific threshold, beyond which it starts to be lost. Saravanakumar (2015) indicated that precipitation had

http://www.aloki.hu ● ISSN 1589 1623 (Print) ● ISSN 1785 0037 (Online)
DOI: http://dx.doi.org/10.15666/aeer/1605_66916707
© 2018, ALÖKI Kft., Budapest, Hungary

an inverse U-shaped relationship with rice yield. This implies that more precipitation can improve its yield up to a certain threshold, but further precipitation would influence it negatively. This sort of the quadratic relationship between precipitation and yield has been reported by Chen and Chang (2005) in Taiwan and by Auffhammer et al. (2012) and Gupta et al. (2012) in India. Saravanakumar (2015) reported an inverse U-shaped relationship between temperature and rice yield, too. These findings are in agreement with studies on the effect of higher temperature on rice crop during its vegetative phase (Morita et al., 2004). It has been documented that the increase in temperature over a critical threshold can result in the loss of rice yield (Dash and Hunt, 2007; Geethalakshmi et al., 2011). The temperature of winter had, also, a significant U-shaped relationship with crop yield (*Table 4*).

Table 3. *Regression coefficients of climate factors for maize crop*

	FGLS		**PCSE**	
Variables	**Coefficients**	**Std. err.**	**Coefficients**	**Std. err.**
Constant	5.92**	2.50	2.78	3.81
Spring temp.	0.188***	0.074	0.214*	0.113
Spring temp. sq.	-0.0042**	0.0020	-0.0039	0.0031
Summer temp.	-0.131	0.197	0.022	0.29
Summer temp. sq.	0.0032	0.0034	0.00059	0.0051
Fall temp.	0.204*	0.117	0.237	0.180
Fall temp. sq.	-0.0057*	0.0030	-0.0062	0.0046
Winter temp.	-0.033***	0.025	-0.038	0.042
Winter temp. sq.	-0.00041	0.0017	-0.0023	0.0027
Spring prec.	0.0023	0.0024	0.0066*	0.0038
Spring prec. Sq.	-5.54e-06	3.42e-06	-0.0000128**	5.15e-06
Summer prec.	0.085	0.067	0.142	0.104
Summer prec. Sq.	-0.0012***	0.00041	-0.00073	0.00060
Fall prec.	0.0025**	0.0016	0.0016	0.0026
Fall prec. Sq.	5.21e-06**	2.18e-06	6.84e-06*	3.86e-06
Winter prec.	-0.00090	0.00071	-0.0022**	0.0011
Winter prec. Sq.	1.24e-06	1.32e-06	1.27e-06	1.87e-06
Spring temp∗prec	4.20e-06	.00011	-.00012	.000017
Summer temp∗prec	-.0024	.0024	-.0048	.0037
Fall temp∗prec	-.00016**	.000073	-.00014	.000117
Winter temp∗prec	0.00011*	.000060	0.00028***	.00010
Wald chi2(20)	96.84		65.70	59.97
Prob > *chi*2	0.0000		0.0000	0.0000
R^2			0.54	

Log of yield is the dependent variable
***, ** and * indicate significance at 1%, 5%, and 10% levels, respectively

http://www.aloki.hu ● ISSN 1589 1623 (Print) ● ISSN 1785 0037 (Online)
DOI: http://dx.doi.org/10.15666/aeer/1605_66916707
© 2018, ALÖKI Kft., Budapest, Hungary

Table 4. *Regression coefficients of climate factors for rice crop*

	FGLS		PCSE	
Variables	**Coefficients**	**Std. err.**	**Coefficients**	**Std. err.**
Constant	4.56***	1.52	4.57***	1.83
Spring temp.	-0.073	0.063	-0.055	0.077
Spring temp. sq.	0.00099	0.00177	0.000086	0.0021
Summer temp.	0.253**	0.112	0.23**	0.14
Summer temp. sq.	-0.0040**	0.0019	-0.0035**	0.0025
Fall temp.	0.121	0.107	0.153	0.127
Fall temp. sq.	-0.0023	0.0026	-0.0032	0.0032
Winter temp.	-0.122***	0.045	-0.166***	0.053
Winter temp. sq.	0.0050**	0.0022	0.0085**	0.0027
Spring prec.	-0.0011	0.0012	-0.0017	0.0015
Spring prec. Sq.	2.41e-06**	1.07e-06	2.84e-06**	1.32e-06
Summer prec.	0.0063*	0.0036	0.0055*	0.0042
Summer prec. Sq.	-7.06e-06***	1.72e-06	-8.01e-06***	1.99e-06
Fall prec.	-0.0010	0.00076	-0.0011	0.00090
Fall prec. Sq.	2.23e-07	2.21e-07	3.65e-07	2.64e-07
Winter prec.	-0.0010	0.00062	-0.0010	0.00079
Winter prec. Sq.	4.51e-08	5.11e-07	2.47e-07	6.52e-07
Spring temp∗prec	7.42e-06	.000066	.000036	.000082
Summer temp∗prec	-.00017	.00013	-.00012	.00016
Fall temp∗prec	.000056*	.000034	.000052*	.000041
Winter temp∗prec	0.000099**	.000050	0.000091**	.000065
Wald chi2(20)	98.21		65.70	75.79
Prob > *chi*2	0.0000		0.0000	0.0000
R^2			0.91	

Log of yield is the dependent variable
***, ** and * indicate significance at 1%, 5%, and 10% levels, respectively

To prevent the complicated analysis and explanation of climate factors because of quadratic and interaction terms, the computed marginal effects and elasticities of climate factors are shown in *Tables 5* and *6*, respectively.

Marginal effect analysis

Table 5 presents the marginal effects of seasonal climate factors on cereal grain yields, which were assessed at the average. The magnitudes of the marginal effects show that at current levels of rainfall, enhancing temperature over the summer, fall, and winter seasons boost wheat yield. The marginal increase in spring temperature, however, reduce wheat yield. In addition, a rise in rainfall over the spring, summer, and

http://www.aloki.hu ● ISSN 1589 1623 (Print) ● ISSN 1785 0037 (Online)
DOI: http://dx.doi.org/10.15666/aeer/1605_66916707
© 2018, ALÖKI Kft., Budapest, Hungary

winter seasons causes a positive marginal effect while a rise in rainfall during fall season causes a negative marginal impact on the wheat yield. Also, outcomes indicate that at present levels of rainfall, a rise in summer and spring temperatures would increase maize yield, while the same increase in fall and winter seasons would decrease the yield. Moreover, analyzing season precipitations for maize shows that spring rainfall causes a positive marginal effect but that of other seasons have a negative marginal effect.

Finally, marginal impacts for rice show that rising temperature in spring season has a significantly harmful effect on rice productivity. However, increasing temperatures of summer, fall, and winter has beneficial effects on rice yield. Also, increasing summer and fall precipitation increases rice yield. The annual marginal impacts of temperature and rainfall for each crop are positive.

Table 5. *Marginal effects of climate factors on grain yield*

Crop	Period	Climate variable	
		Temperature	Rainfall
Wheat	Spring	-0.018	0.00063**
	Summer	0.0082	0.0013
	Fall	0.010	-0.00013
	Winter	0.023**	9.14e-06
	Annual	0.024	0.0018
Maize	Spring	0.072***	0.0020***
	Summer	0.046	-0.00011
	Fall	-0.0021	-0.00036
	Winter	-0.032	-0.000059
	Annual	0.083	0.0014
Rice	Spring	-0.047***	-0.00039
	Summer	0.019	0.00098
	Fall	0.035**	0.000063
	Winter	0.0096	-0.00012
	Annual	0.017	0.00053

***, ** and * indicate significance at 1%, 5%, and 10% levels, respectively

Table 6 represents the elasticities of climate factors in the model. The regression coefficients and average values of climate factors were applied for computing elasticities of seasonal temperature and precipitation. The outcomes demonstrate that a 1% rise in temperature over the summer, fall, and winter will enhance yield by 0.027, 0.021, and 0.01%, respectively, while the rise in temperature by 1% during the spring reduces yield by 0.033%. Also, when the spring, summer, and winter precipitations are increased by 1%, wheat yield increases by 0.00063, 0.0013, and 0.000009%, respectively. However, rising rainfall over the fall season decreases yield by 0.00013%. Elasticities of annual climate factors offer that higher temperature and more precipitation increase wheat yield by 0.024% and 0.0018%, respectively.

In the case of maize, the results are different but the impacts of annual climate factors are similar. A 1% rise in temperature over the spring and summer increases yield by 0.139 and 0.157% but the same increase in fall and winter temperatures decrease

http://www.aloki.hu ● ISSN 1589 1623 (Print) ● ISSN 1785 0037 (Online)
DOI: http://dx.doi.org/10.15666/aeer/1605_66916707
© 2018, ALÖKI Kft., Budapest, Hungary

yield by 0.0046 and 0.024%, respectively. Besides, a 1% increase in rainfall during the spring increases yield by 0.0023%. However, rainfall increase over the summer, fall, and winter reduces the maize yield.

Finally, the magnitudes of the elasticities show that a 1% rise in temperature over the summer, fall, and winter seasons would enhance rice productivity by 0.068, 0.087, and 0.01%, respectively. However, the rise in temperature by a 1% during the spring would reduce yield by 0.1%. The sum of elasticities is 0.065 showing that warming up of weather is beneficial for the rice yield. If annual average temperature rises by a 1%, rice yield enhances by 0.065%. Also, outcomes indicate that a 1% rise in rainfall over summer and fall seasons would increase rice yield by 0.0061 and 0.0017%, while the same increase in spring and winter seasons would decrease rice yield by 0.0057 and 0.0035%, respectively. The aggregate effect, i.e., the sum of all seasons, was found to decline the yield by 0.0013%.

As observed, the rainfall impact on product yield is unimportant comparing to the temperature effect. This difference could be because of the application of irrigation to cultivate the crops.

Table 6. *Elasticities of climate factors on the grain yield*

Crop	Period	Climate variable	
		Temperature	Rainfall
Wheat	Spring	-0.033	0.0093**
	Summer	0.027	0.0011
	Fall	0.021	-0.00099
	Winter	0.01**	0.00014
	Annual	0.093	0.094
Maize	Spring	0.139***	0.0023***
	Summer	0.157	-0.000029
	Fall	-0.0046	-0.0022
	Winter	-0.024	-0.0009
	Annual	0.267	0.02
Rice	Spring	-0.1***	-0.0057
	Summer	0.068	0.0061
	Fall	0.087**	0.0017
	Winter	0.01	-0.0035
	Annual	0.065	-0.0013

***, ** and * indicate significance at 1%, 5%, and 10% levels, respectively

Discussion

The present research was conducted based on the Ricardian method to investigate the climate alteration impact on cereal production in Iran with emphasizing on wheat, maize, and rice crops. The outcomes based upon Prais-Winsten models with panels corrected standard errors (PCSEs) estimation offer that climatic change influences cereal production significantly; however, the impact varies across the crops. The marginal effect analysis revealed that a marginal temperature rise over the summer, winter, and fall seasons boost wheat yield, while a marginal temperature rise over the

http://www.aloki.hu ● ISSN 1589 1623 (Print) ● ISSN 1785 0037 (Online)
DOI: http://dx.doi.org/10.15666/aeer/1605_66916707
© 2018, ALÖKI Kft., Budapest, Hungary

spring declines yield level. Also, a rise in rain throughout the spring, winter, and summer seasons have a positive impact while its rise throughout the fall shows a negative marginal influence on the wheat yield. The outcomes are somewhat different for maize from the wheat results. Outcomes demonstrated that at available levels of rainfall, a temperature rise throughout summer and spring seasons would increase maize yield, while the same increase in winter and fall seasons would decrease the yield. Besides, analyzing season precipitations for maize showed that spring rain has a positive marginal effect while that of other seasons show a negative marginal effect. Marginal impacts of rice indicated that rising temperature in spring season has a significantly harmful effect on rice productivity. However, the increase in summer, winter and fall temperatures affect beneficially on rice yield. Also, increasing summer and fall precipitation increases rice yield. The annual marginal effects relating to rainfall and temperature for all the crops are positive.

Furthermore, the outcomes ascertained that the cereal production in Iran are less sensitive to rising precipitation levels than rising temperature levels. This difference could be because of application of irrigation to cultivate the crops. Therefore, the impact of rainfall changes on these products is not fully clear. This result has considerable effects for appropriate adaptation processes and strategies. For instance, these outcomes offer that research on breeding for drought tolerance rather than heat tolerance should shape future agricultural research in the country.

The key outcome of the present analysis is that climate variation is beneficial for main cereal crops in Iran. Considering the results of current study, the crops yields will enhance based on the estimation model. Though the current study demonstrates that climate variation does not threaten the agriculture economy of Iran, this event can be hazardous if unsuitable adaptation policies are implemented. Thus, the agricultural strategies must be taking into account for encouraging farmers to use suitable practices and techniques against climate variation. These strategies should help farmers for developing irrigation approaches, select suitable crops, and face with water shortage. Adaptation can be carried out through different methods. First and main one is the extreme challenge, i.e., teaching farmers about the events of climate variation and its effects. Hence, more effective extension programs are required to promote farmers' awareness of climate variation. Certainly, inhibition of damages can occur through more effective farm planning. Crop insurance, different economic bases of areas dependent on agriculture and developed monitoring/predictions of climate will also enhance adaption of crops cope to future variations. These strategies, however, must considered the large seasonal changeability on the response of crops.

Conclusion

The current paper attempts to estimate the impact of climate alteration on cereal production in Iran. Our results suggests that warmer summers are beneficial to all crops studied in the current work. The effect of warmer springs is harmful to wheat and rice but beneficial to maize. Warmer falls are beneficial for wheat and rice but harmful to maize. Wetter spring have a tendency to enhance yields for wheat and maize and wetter summers increase yields for wheat and rice. The key outcome of the present analysis is that climate variation is beneficial for main cereal crops in Iran. Moreover, the research shows that there are limited data on the economic influence of climate variation on agriculture in Iran and further studies and deeper analyses are needed in this field.

http://www.aloki.hu ● ISSN 1589 1623 (Print) ● ISSN 1785 0037 (Online)
DOI: http://dx.doi.org/10.15666/aeer/1605_66916707
© 2018, ALÖKI Kft., Budapest, Hungary

Acknowledgements. This research was supported by the research fund of University of Zabol Grant code: UOZ-GR-9517-4, whom the authors sincerely thank.

REFERENCES

[1] Adams, R. M., Rosenzweig, C., Pearl, R. M., Ritchie, J. T., McCarl, B. A., Glyer, J. D., Curry, R. B., Jones, J. W., Boote, K. J., Allen, L. H. (1990): Global climate change and U.S. agriculture. – Nature 345: 219-224.

[2] Adams, R. M., Hurd, B. H., Lenhart, S., Leary, N. (1998): Effects of global climate change on agriculture: An interpretative review. – Climate Research 11(1): 19-30.

[3] Adams, R. M., McCarl, B. A., Segerson, K., Rosenzweig, C., Bryant, K. J., Dixon, B. L., Connor, R., Evenson, R. B., Ojima, D. (1999): Economic Effects of Climate Change on U.S. Agriculture. – In: Mendelsohn, R., Neumann, J. E. (eds.) The Impact of Climate Change on the United States Economy. Cambridge University Press, Cambridge, UK, pp. 18-54.

[4] Attri, S. D., Rathore, L. S. (2003): Simulation of impact of projected climate change on wheat in India. – International Journal of Climatology 23: 693-705.

[5] Auffhammer, M., Ramanathan, V., Vincent, J. R. (2012): Climate change, the monsoon, and rice yield in India. – Climatic Change 111(2): 411-424.

[6] Ayinde, O. E., Adewumi, M. O., Ojehomon, V. E. T. (2010): Determinants of technical efficiency and varietal-gap of rice production in Nigeria: A meta-frontier model approach. – A paper prepared for presentation at the International Association of Agricultural Economists Conference, Beijing, China, August 16-22, 2009, pp. 1-21.

[7] Beck, N., Katz, J. N. (1995): What to do (and not to do) with time-series cross-section data. – The American Political Science Review 89(3): 634-647.

[8] Chang, C. C. (2002): The potential impact of climate change on Taiwan's agriculture. – Agriculture Economics 27: 51-64.

[9] Chen, C. C.; Chang, C. C. (2005): The impact of weather on crop yield distribution in Taiwan: Some new evidence from panel data models and implications for crop insurance. – Agricultural Economics 33(3): 503-511.

[10] Cline, W. (2007): Global warming and agriculture: Impact estimates by country. – Journal of Economic Literature 46(2): 448-450.

[11] Deressa, T. T., Hassan, R. M. (2009): Economic impact of climate change on crop production in Ethiopia: Evidence from cross-section measures. – Journal of African Economics 18(4): 529-554.

[12] De Salvo, M., Raffael, R., Moser, R. (2013): The impact of climate change on permanent crops in an Alpine region: a Ricardian analysis. – Agricultural Systems 118: 23-32.

[13] Deschenes, O., Greenstone, M. (2007): The economic impacts of climate change: Evidence from agricultural output and random fluctuations in weather. – The American Economic Review 97(1): 354-385.

[14] Dash, S. K., Hunt, J. C. R. (2007): Variability of climate change in India. – Current Science 93(6): 782-788.

[15] Gbetibouo, G. A., Hassan, R. M. (2005): Measuring the economic impact of climate change on major South African field crops: a Ricardian approach. – Global and Planetary Change 47(2): 143-152.

[16] Geethalakshmi, V., Lakshmanan, A., Rajalakshmi, D., Jagannathan, R., Sridhar, G., Ramaraj, A. P., Bhuvaneswari, K., Gurusamy, L. and Anbhazhagan, R. (2011): Climate change impact assessment and adaptation strategies to sustain rice production in Cauvery basin of Tamil Nadu. – Current Science 101(3): 342-347.

[17] Guiteras, R. (2009): The Impact of Climate Change on Indian Agriculture. – University of Maryland, College Park.

http://www.aloki.hu ● ISSN 1589 1623 (Print) ● ISSN 1785 0037 (Online)
DOI: http://dx.doi.org/10.15666/aeer/1605_66916707
© 2018, ALÖKI Kft., Budapest, Hungary

[18] Gupta, SH., Sen, P., Srinivasan, S. (2012): Impact of climate change on the Indian economy: Evidence from food grain yields. – Working Paper No. 218, Centre for Development Economics, Department of Economics, Delhi School of Economics, New Delhi.
[19] Haim, D., Shechter, M., Berliner, P. (2008): Assessing the impact of climate change on representative field crops in Israel agriculture: A case study of wheat and cotton. – Climate Change 86(3): 425-440.
[20] Kumar, K. (2009): Climate Sensitivity of Indian Agriculture: Do Spatial Effects Matter? – SANDEE Working Papers, 45-09. SANDEE, Kathmandu.
[21] Kumar, K., Parikh, S. (1998): Climate Change Impacts on Indian Agriculture: The Ricardian Approach. – In: Dinar, A., Mendelsohn, R., Evenson, R., Parokh, J., Sanghi, A., Kumar, K., McKinsey, J., Lonergan, S. (eds.) Measuring the Impact of Climate Change on Indian Agriculture. World Bank Technical Report No. 409, World Bank, Washington, DC.
[22] Kumar, A., Sharma, P. (2013): Impact of Climate Variation on Agricultural Productivity and Food Security in Rural India. – Economics Discussion Papers, No 2013-43, Kiel Institute for the World Economy, Kiel, Germany.
[23] Kurukulasuriya, P., Ajwad, M. I. (2007): Application of the Ricardian technique to estimate the impact of climate change on smallholder farming in Sri Lanka. – Climate Change 81: 39-59.
[24] Lee, J., Nadolnyak, D., Hartarska, V. (2012): Impact of climate change on agricultural production in Asian countries: Evidence from panel study. – Paper prepared for presentation at the Southern Agricultural Economics Association Annual Meeting, Birmingham.
[25] Liangzhi, Y., Rosegrant, M. W., Fang, CH., Wood. S. (2005): Impact of Global Warming on Chinese Wheat Productivity. – EPT Discussion Paper 143, International Food Policy Research Institute, Washington, DC.
[26] Maddison, D. (2000): A hedonic analysis of agricultural land prices in England and Wales. – European Review of Agricultural Economics 27(4): 519-532.
[27] Mariara, J. K., Karanja, F. K. (2007): The economic impact of climate change on Kenyan crop agriculture: a Ricardian approach. – Global and Planetary Change 57: 319-330.
[28] Mearns, L. O., Rosenzweig, C., Goldberg, R. (1997): Mean and variance change in climate scenarios: Methods, agricultural applications, and measures of uncertainty. – Climate Change 35(4): 367-396.
[29] Mendelsohn, R., Dinar, A. (2003): Climate, water and agriculture. – Land Economics 79(3): 329-341.
[30] Mendelsohn, R., Reinsborough, M. (2007): A Ricardian analysis of US and Canadian farmland. – Climatic Change 81: 9-17.
[31] Mendelsohn, R., Nordhaus, W. D., Shaw, D. (1994): The impact of global warming on agriculture: a Ricardian analysis. – The American Economic Review 84(4): 753-771.
[32] Mendelsohn, R., Nordhaus, W. D., Shaw, D. (1999): The Impact of Climate Variation on US Agriculture. – In: Mendelsohn, R., Neumann, J. (eds.) The Impact of Climate Change on the United States Economy. Cambridge University Press, Cambridge, UK.
[33] Mendelsohn, R., Dinar, A., Williams, L. (2006): The distributional impact of climate change on rich and poor countries. – Environment and Development Economics 11(2): 159-178.
[34] Morita, S., Shiratsuchi, H., Takahashi, J., Fujita, K. (2004): Effect of high temperature on ripening in rice plant: analysis of the effect of high night and high day temperature applied to the panicle in other parts of the plant. – Japanese Journal of rice Science 73(1): 77-83.
[35] Moula, E. L. (2009): An empirical assessment of the impact of climate change on smallholder agriculture in Cameroon. – Global Planet Change 67(3): 205-208.

http://www.aloki.hu ● ISSN 1589 1623 (Print) ● ISSN 1785 0037 (Online)
DOI: http://dx.doi.org/10.15666/aeer/1605_66916707
© 2018, ALÖKI Kft., Budapest, Hungary

[36] National Climate Change Office of Iran (NCCOI) (2014): Third National Communication to United Nations Framework Convention on Climate Change (UNFCCC). – Department of Environment. Available via: http://climate-change.ir.
[37] Nelson, G. C., Rosegrant, M. W., Koo, J., Robertson, R., Sulser, T., Zhu, T., Ringler, C., Msangi, S., Palazzo, A., Batka, M., Magalhaes, M., Valmonte-Santos, R., Ewing, M., Lee, D. (2009): Climate Change: Impact on Agriculture and Costs of Adaptation. – Food Policy Report, International Food Policy Research Institute, Washington, DC.
[38] Olsen, J. E., Bocher, P. K., Jensen, T. (2000): Comparison of scales of climate and soil data for aggregating simulated yields of winter wheat in Denmark. – Agriculture, Ecosystems and Environment 82(3): 213-28.
[39] Pahizikari, A., Mozaffari, M. M., Hosseini Khodadadi, M. (2014): Economic analysis of climate change on yield of irrigated wheat in Shahrood watershed. – Agricultural and Natural Resources Journal 18(4): 88-100.
[40] Phillips, D. L., Jeffrey, J. L., Rusty, F. D. (1996): Sensitivity of the US corn belt to climate change and elevated CO_2: I. Corn and soybean yields. – Agricultural Systems 52: 481-502.
[41] Rosenzweig, C., Iglesias, A. (eds.) (1994): Implications of Climate Change for International Agriculture: Crop Modelling Study. – US Environmental Protection Agency, Washington.
[42] Rosenzweig, C., Tubiello, F. N., Goldberg, R., Mills, E., Bloomfield, J. (2002): Increased crop damage in the U.S. from excess precipitation under climate change. – Global Environment Change 12: 197-202.
[43] Sabzevary, A., Torkaman, M., Meryanji, Z. (2012): Survey the effect of parameters and meteorological variables in optimal performance of wheat (A case study: Hamedan province). – Journal of Soil Water and Agriculture Science Technology 26(6): 1554-1567.
[44] Sanghi, A., Mendelsohn, R. (1999): The Impact of Global Warming on Brazilian and Indian Agriculture. – Yale School of Forestry and Environmental Sciences, New Haven, CT, USA.
[45] Sanghi, A., Mendelsohn, R. (2008): The impact of global warming on farmers in Brazil and India. – Global Environment Change 18(4): 655-665.
[46] Saravanakumar, V. (2015): Impact of Climate Change on Yield of Major Food Crops in Tamil Nadu, India. – SANDEE Working Papers, WP 91-15. SANDEE, Kathmandu.
[47] Stern, N. (2006): The Economics of Climate Change: The Stern Review. H. M. Treasury, London, TAC (Technical Advisory Committee of the CGIAR) (1992): A Review of CGIAR Priorities and Strategies Draft. – TAC Secretariat, FAO, Rome.
[48] Tan, G., Shibasaki, R. (2003): Global estimation of crop productivity and the impacts of global warming by GIS and EPIC integration. – Ecological Modeling 168(3): 357-370.
[49] Thapa-Parajuli, R. B., Devkota, N. (2016): Impact of climate change on wheat production in Nepal. – Asian Journal of Agricultural Extension, Economics and Sociology 9(2): 1-14.
[50] Vaseghi, E., Esmaeili, A. A. K. (2008a): Investigation of the economic impacts of climate change on Iran agriculture: a Ricardian approach (Case study: wheat). – Journal of Science and Technology of Agriculture and Natural Resources 12(45): 685-696.
[51] Vaseghi, E., Esmaeili, A. A. K. (2008b): Impacts of climate change on land rent: Case study of maize. – Economics and Agriculture Journal 2(3): 47-67.
[52] Wang, J., Mendelsohn, R. O., Dinar, A., Huang, J., Rozelle, S., Zhang, L. (2009): The impact of climate change on China's agriculture. – Agricultural Economics 40: 323-337.
[53] Wooldridge, J. (2002): Econometric Analysis of Cross Section and Panel Data. – MIT Press, Cambridge.

http://www.aloki.hu ● ISSN 1589 1623 (Print) ● ISSN 1785 0037 (Online)
DOI: http://dx.doi.org/10.15666/aeer/1605_66916707
© 2018, ALÖKI Kft., Budapest, Hungary

OPTIMIZATION PROCESS FOR THE REMOVAL OF HEAVY METALS FROM AQUEOUS SOLUTION USING GRAPHENE OXIDE NANOSHEETS AND RESPONSE SURFACE METHODOLOGY

ROUNIASI, N.[1] – MONAVVARI, S. M.[1*] – ABDOLI, M. A.[2] – BAGHDADI, M.[2] – KARBASSI, A. R.[2]

[1]*Department of Environment, Faculty of Natural Resources and Environment, Science and Research Branch, Islamic Azad University, Tehran, Iran*

[2]*School of Environment, College of Engineering, University of Tehran, Tehran, Iran*

**Corresponding author*
e-mail: monavarism@yahoo.com; phone/fax: +98-21-8823-3144

(Received 3rd Jul 2018; accepted 31st Aug 2018)

Abstract. Water pollution due to heavy metals has become a critical problem worldwide. In this study, the removal of chromium(III), cadmium and lead by graphene oxide adsorbent was examined. Graphene oxide nanosheets were synthesized through Hummer's method, and their characteristics were examined using FTIR, XRD, and SEM. The effect of independent variables, pH, contact time and initial concentration of solution on the removal efficiency of Cr(III), $Cd^{2+}$and Pb^{2+} was evaluated according to the experimental Box-Behnken Design using response surface methodology (RSM). Applying quadratic model, the adsorption rate of Cd^{2+} and Pb^{2+} was obtained as 99% and the adsorption rate of Cr(III) was obtained as 98%. ANOVA was applied as statistical analysis of responses. According to FESEM images, the average size of graphene oxide sheets was 1 to 3 μm. After optimization by RSM, adsorption capacities of Cr(III), Pb^{2+} and Cd^{2+} were found to be 38 mg/g, 136 mg/g and 68 mg/g, respectively. Examination of isotherms suggested that Cd^{2+} and Cr(III) adsorptions follow Langmuir, and Pb^{2+} adsorption follows Freundlich isotherm. The results showed that graphene oxide has a good effect on removing Cr(III), Cd^{2+} and Pb^{2+} ions from aqueous solutions. pH of the solution and initial concentration of the contaminant had the highest effect on adsorption of the mentioned heavy metals. The results of RSM analysis showed that the obtained data were in agreement with the predicted model.
Keywords: *adsorption, water pollution, heavy metals, Box-Behnken Design, Langmuir, Freundlich*

Abbreviations: *GO:* Geraphene oxid; *RSM:* Response surface methodology; *FTIR:* Fourier transform infrared; *XRD:* X-ray diffraction; *SEM:* scanning electron microscope; *FESEM:* Field Emission Scanning Electron Microscope; *BBD:* Box-Behnken Design; *EPA:* Environmental Protection Agency ;*Cr:* Chromium; *Cd:* Cadmium; *Pb:* Lead; *pH:* potential hydrogen; *Conc:* Concentration; *PZC:* point of zero charge

Introduction

Growth of urbanization, rapid industrialization of cities and emission of heavy metals in the ecosystem - even at extremely low concentrations - have brought up concerns worldwide. Removal of heavy metals from water and wastewater has been at the center of attention owing to strict regulations on water pollution control in many countries (Amarasinghe and Williams, 2007). Lead, chromium, cadmium, zinc, and nickel are among the most water polluting heavy metals (Yang et al., 2014). Conventional methods for the removal of heavy metals from water include chemical oxidation, chemical precipitation, ion exchange, adsorption, filtration, reverse osmosis, solvent extraction and coagulation-flocculation (Rajasulochana

http://www.aloki.hu ● ISSN 1589 1623 (Print) ● ISSN 1785 0037 (Online)
DOI: http://dx.doi.org/10.15666/aeer/1605_67096729
© 2018, ALÖKI Kft., Budapest, Hungary

and Preethy, 2016). Adsorption method is known to be better than other techniques due to high efficiency, flexibility, simple design, low cost, easy operation and minimum sludge production (Fu and Wang, 2011). The most important characteristics for an adsorbent are high adsorption capacity and rapid adsorption. These can be achieved when the adsorbent possesses a large specific surface area and abundant adsorption sites (Wang et al., 2012). Majority of adsorbents rarely have both of the mentioned characteristics. Therefore, an investigation on new adsorbents which can properly adsorb heavy metals is required (Pan et al., 2009). Among the studied adsorbents, graphene oxide nanoparticles, owing to adsorption capacity and large specific surface area, are applied either independently or along with other adsorbents in order to remove heavy metals from aqueous solutions (Liu et al., 2011; McGrail et al., 2016). Considerable physical properties of graphene include heat superconductivity, extremely high electron mobility (Jiang et al., 2010), high mechanical strength (Yu et al., 2008) and adsorption of some metal ions (Hao et al., 2012). Sitko et al. (2013) examined the adsorption of heavy metal ions from aqueous solutions using graphene oxide, and observed that maximum adsorption occurred at pH ranges of 4-8 for cadmium and 3-7 for lead and chromium. Fan et al. (2013) examined a mixture of graphene oxide and magnetic chitosan (MCGO) as an adsorbent and reached a maximum adsorption capacity of 96% for lead ions. Kumar et al. (2014) studied the removal of lead and arsenic using graphene oxide nanosheets and concluded that graphene oxide is highly efficient in removing heavy metals from aqueous solutions. Among the contaminants, chromium(III), cadmium and lead are the most environment-polluting elements since they are widely used in industry. The efficiency of adsorption processes depends on various parameters such as pH, temperature, type of adsorbent, adsorbent dosage and organic or inorganic contaminants (Liu et al., 2011). The water containing high concentration of chromium may cause serious environmental problems and also skin sensitivity, cancer and DNA damage to humans (Tchounwou et al., 2012). Cadmium is categorized as a carcinogenic element, which leads to lung cancer, kidney diseases, digestive and immune system disorders in human bodies (Jaishankar et al., 2014). According to EPA, lead, after entering the body, does not leave the body and precipitates in blood, skin, organs and tissues including muscles, bones and joints (Huang et al., 2014; Li et al., 2007) and causes environmental pollution with severe toxic effects on human health and other creatures (Uluozlu et al., 2008).

The conducted studies show that graphene oxide nanosheets are the most effective adsorbents used for the removal of heavy metals from aqueous environments and soil. The key reason for using graphene oxide nanosheets in this study is their simultaneous possession of several properties.

In this study, the efficiency of graphene oxide nanosheets in removing chromium(III), cadmium and lead from aqueous solutions was examined. The aim of this study was to evaluate the effect of pH, initial concentration and contact time on graphene oxide adsorption capacity. The variables analyzed by response surface method (RSM) were applied according to Box-Behnken design in order to optimize heavy metals removal from aqueous solutions. Also, absorption isotherm was investigated using Langmuir and Freundlich adsorption isotherms.

http://www.aloki.hu ● ISSN 1589 1623 (Print) ● ISSN 1785 0037 (Online)
DOI: http://dx.doi.org/10.15666/aeer/1605_67096729
© 2018, ALÖKI Kft., Budapest, Hungary

Materials and methods

Materials and instruments

Chemicals applied in the experiments were lab grade. All the chemicals including nitric acid 65% (HNO_3), sulfuric acid 97% (H_2SO_4), hydrogen peroxide 30% (H_2O_2), hydrochloric acid (HCl), sodium hydroxide (NaOH), sodium nitrate ($NaNO_3$), sodium chloride (NaCl), chromium(III) chloride ($CrCl_3$), potassium dichromate ($K_2Cr_2O_7$), potassium permanganate ($KMnO_4$), lead nitrate ($PbNO_3$) and graphite powder were provided by Merck, Germany. Deionized water was used in all the experiments. Synthesis of graphene oxide nanosheets was done using Hettich centrifuge (Model Universal 320 R), an ultrasonic bath (Elmasonic, E 60H Model, Germany) and a heater (IKA 2000 Model, Germany). Moreover, pH was determined by a pH-meter (pH-Meter 765, Germany), and agitation of the samples was carried out using an IKA-werke-KS260C shaker, Germany. The samples containing Cr(III), Cd^{2+} and Pb^{2+} ions were analyzed through ICP (Inductively Coupled Plasma) Varian-OES-710.

Synthesis of graphene oxide

Using the modified Hummer's method (which is suitable to synthesize graphene oxide), the synthesis of graphene oxide was carried out as follows. Initially, 200 mL concentrated sulfuric acid was poured into a 500 mL glass container and its temperature decreased after stirring in an ice-water bath for 30 min. Then, 4 g of sodium nitrate was added to the solution and its temperature decreased after stirring in an ice-water bath for 1 h. Afterward, 4 g of graphite (500 mesh) was added and mixed for 2 h in this condition. 4 g of graphite (500 mesh) was added to the solution and then mixed for 2 h. During 2 h, 24 g of potassium permanganate was added and stirred. The glass container containing the sample was fixed in an oil bath at 38 to 40 °C for 24 h. After removing the oil bath, 640 mL double distilled water was added to reaction container and stirred for 30 min. The reaction stopped by adding 140 mL hydrogen peroxide 30%. The sample was totally settled after three days. After removing the supernatant, the produced graphene oxide was washed four times using HCl (5%) and then filtered through a buchner funnel. The obtained suspension was washed four times using double distilled water. Then the suspension was treated by ultrasound for 30 min. Finally, the obtained brown solid substance was dried in a vacuum oven at 40 °C (Chaiyakun et al., 2012).

Determination of PZC

In order to examine the heavy metals removal more closely, pH of the zero charge point, where the adsorbent surface is electrically neutral and unladen, and also the adsorbent PZC (pH_{PZC}) were measured (Zhao et al., 2011, 2012). In order to measure PZC, 10 flasks containing 0.1 mol/L NaCl solution were used. The initial pH of the solution was adjusted in the range of 1 to 10 using NaOH and HCl 0.1 mol/L. Then, 0.1 g adsorbent was added to each solution, and the electrolyte solution was stirred with the adsorbent for 24 h. After reaching equilibrium, pH of the solutions was measured, ΔpH graph was drawn according to the initial pH, and pH_{PZC} was estimated.

Characterization of graphene oxide nanosheets

Morphology, size and shape of the synthesized adsorbent were examined using a field emission scanning electron microscope (FESEM model MIRA3, TESCAN).

http://www.aloki.hu ● ISSN 1589 1623 (Print) ● ISSN 1785 0037 (Online)
DOI: http://dx.doi.org/10.15666/aeer/1605_67096729
© 2018, ALÖKI Kft., Budapest, Hungary

Characteristics of graphene oxide nanoparticles were determined using an x-ray diffraction model: X'Pert PRO MPD PANalytical. Fourier transform infrared (FTIR) of graphene oxide in the range of 400-4000 cm^{-1} was analyzed using Bruker, Tensor 27, Germany.

Adsorption experiments

All the experiments were conducted in a batch mode. Initially, the solutions containing Cr(III), Cd^{2+} and Pb^{2+} were prepared by adding a certain amount of potassium dichromate, cadmium nitrate and lead nitrate to 1 L of DI water. In order to study the effect of environmental pH on adsorbing metals within the range of 2-6, 0.05 g/L and 0.02 g/L of the synthesized graphene oxide were added to the lead and cadmium-containing solutions and chromium-containing solution, respectively (the initial concentration was within the ranges of 10-100 mg/L for Cd^{2+} and Cr(III) and 50-150 mg/L for lead, and contact time of 5-60 min was allotted to each metal). The solutions were studied by the presented model and stirred on a magnetic stirrer with a constant speed of 200 rpm for a specified time. Finally, the solutions were stabilized as the mentioned time passed. At the next step, the suspension was filtered by centrifugal method and passed through 0.2 µm filters. The heavy metals concentration after adsorption was measured using ICP. Adsorption efficiencies of Cr(III), Pb^{2+} and Cd^{2+} were calculated by *Equation 1* (Belay et al., 2010).

$$R = \frac{(C_0 - C_e)}{C_0} * 100 \quad \text{(Eq.1)}$$

Moreover, adsorption capacity of the synthesized graphene oxide at various heavy metals concentrations was determined using *Equation 2* (Li et al., 2011).

$$Qe = \frac{(C_0 - C_e)V}{m} \quad \text{(Eq.2)}$$

where, R is adsorption removal efficiency, Qe is the amount of the heavy metal adsorbed onto the adsorbent in equilibrium conditions (mg/g), C_0 is the initial concentration of the heavy metal in solution (mg/L), C_e indicates equilibrium concentration of the heavy metal after equilibrium time elapsing (mg/L), V is volume of the solution in liter, and m is mass of the adsorbent in gram.

Experimental design and data analysis

RSM along with experimental techniques was used to assess the relationship among the effective variables in the experiment (Ghafari et al., 2009). ANOVA was applied as a statistical method for analysis of responses. Response surface method was applied according to Box-Behnken design in order to optimize heavy metals removal from aqueous solutions. This method has several advantages such as reducing the number of test steps, time and cost, and saving the consumption materials. This method is used in this study because it can 1) test several levels of testing with different factors, 2) identify how removal efficiencies are affected by changes in the level of pH, initial concentration and contact time (as factors), and 3) specify the optimized combination of adsorbent pH, initial concentration and contact time for the efficient removal of heavy metals.

http://www.aloki.hu ● ISSN 1589 1623 (Print) ● ISSN 1785 0037 (Online)
DOI: http://dx.doi.org/10.15666/aeer/1605_67096729
© 2018, ALÖKI Kft., Budapest, Hungary

In this study, pH of the solution, concentration of contaminants and contact time were chosen as the independent variables affecting the heavy metals removal efficiency and labeled as pH (pH), concentration (conc) and contact time (Time), respectively (*Tables 1A, 2B,* and *3A*). Version 10 of Design-Expert software was used to investigate the effect of independent variables on response surface methodology (adsorption capacity of adsorbent and adsorption efficiency of heavy metals). Designing was carried out using the Box-Behnken design. The number of steps in the experiment was determined using *Equation 3:*

$$N = 2K\left(K-1\right) + C_o \quad \text{(Eq.3)}$$

where, K represents the number of factors investigated and C_o indicates the number of replication for the experiment (Khajeh, 2011). 17 experiments with five replicates at center points were done for each metal. Thus, totally 51 experiments were designed and conducted (Yetilmezsoy et al., 2009). A second-order polynomial regression model equation, which relates the removal efficiency to the investigated factors, can be presented as *Equation 4:*

$$Y = C_{k0} + \sum_{i=1}^{4} C_{ki}x_i + \sum_{i=1}^{4} C_{kii}x_i^2 + \sum_{i<j=2}^{4} C_{kij}x_i x_j \quad \text{(Eq.4)}$$

where, Y is predicted response; C_{k0}, C_{ki}, C_{kii} and C_{kij} are regression coefficients for intercept, linear effects, quadratic effects and double interactions, respectively; and x_i and x_j are coded values of the independent variables (Wu et al., 2012).

In order to evaluate the accuracy of the models, statistical analysis was carried out using ANOVA with p-value ($Prob \leq F < 0.0001$). Adequacy and predictability of the model were examined using lack of fit criterion, R^2 linear regression coefficient of determination, adjusted R^2, adequate precision and residual detection (Wu et al., 2012).

Results and discussion

Characterization of graphene oxide nanosheets

The FESEM images illustrate the morphology of graphene oxide nanosheets (*Fig. 1*). Morphology of the sheet structure of graphene oxide is clear in the images. The size of graphene oxide sheets is approximately 1-3 μm.

As can be seen in *Figure 1,* graphene oxide is semitransparent with some particles and lateral dimensions of several micrometer size and small holes, indicating the production accuracy of the synthesized graphene oxide sheets. FTIR spectra can be categorized into three classes: 2000-4000, 1300-2000 and 800-1300 cm^{-1}. The first class is usually concerned with hydrogen bonded O-H; absorbed H_2O; mostly free O-H; symmetric, dehydration and aliphatic units; and asymmetric stretching vibrations in CH_3, CH_2 or C-H, bonds. The second class includes the most significant oxygen functionalities characterized by N-O and C-O-containing structures. The third class is normally related to various C-O bonds such as those in phenols, hydroxyl groups and ethers (Omar and Moloukhia, 2008). FTIR spectra of graphene oxide nanosheets are indicated in *Figure 2.* For graphene oxide, IR band in the range of 1032 cm^{-1} is assigned to alkoxy C-O groups situated at the edges of the GO nanosheets. In the ranges of 1384

http://www.aloki.hu ● ISSN 1589 1623 (Print) ● ISSN 1785 0037 (Online)
DOI: http://dx.doi.org/10.15666/aeer/1605_67096729
© 2018, ALÖKI Kft., Budapest, Hungary

and 1623 cm^{-1}, it is concerned with carboxyl C-O groups and C=C in stretching vibrations of aromatic structures, respectively. In the ranges of 1694, 2921, and 3422 cm^{-1}, IR band is assigned to stretching CH^2, SP of GO aromatic sheets and OH groups of GO, respectively.

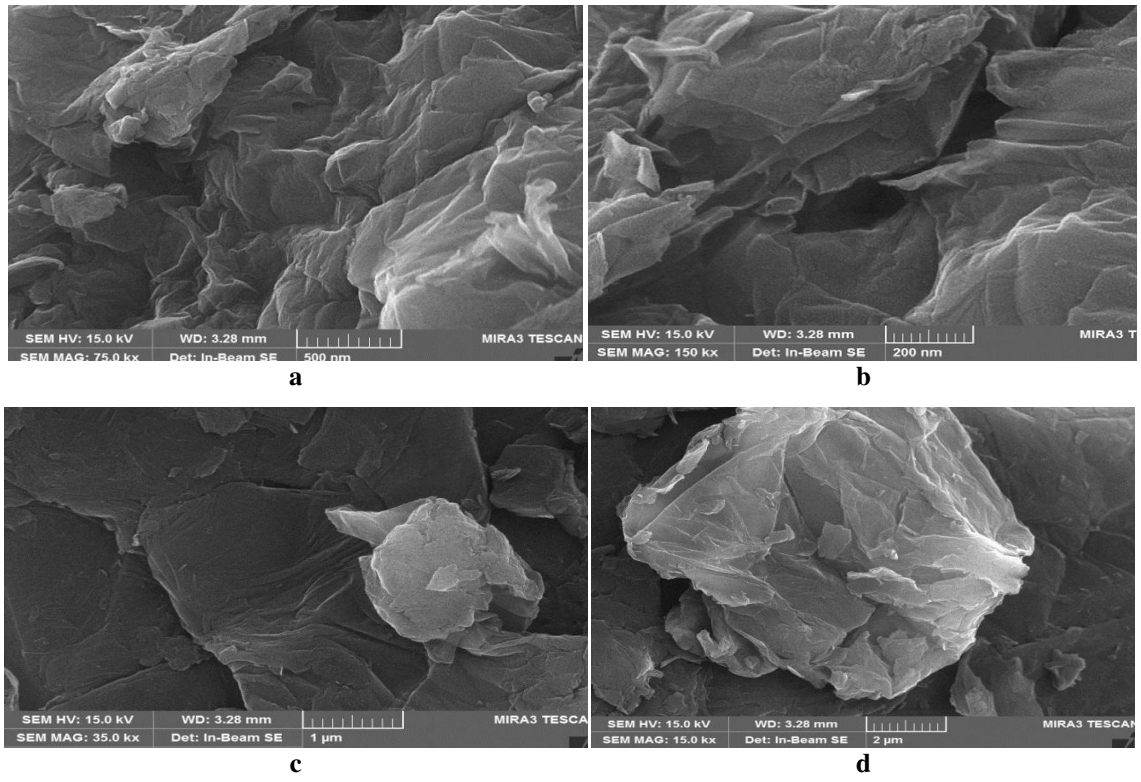

Figure 1. *FESEM image of the graphene oxide: a) 200 nm, b) 500 nm, c)1 µm, and d) 2 µm*

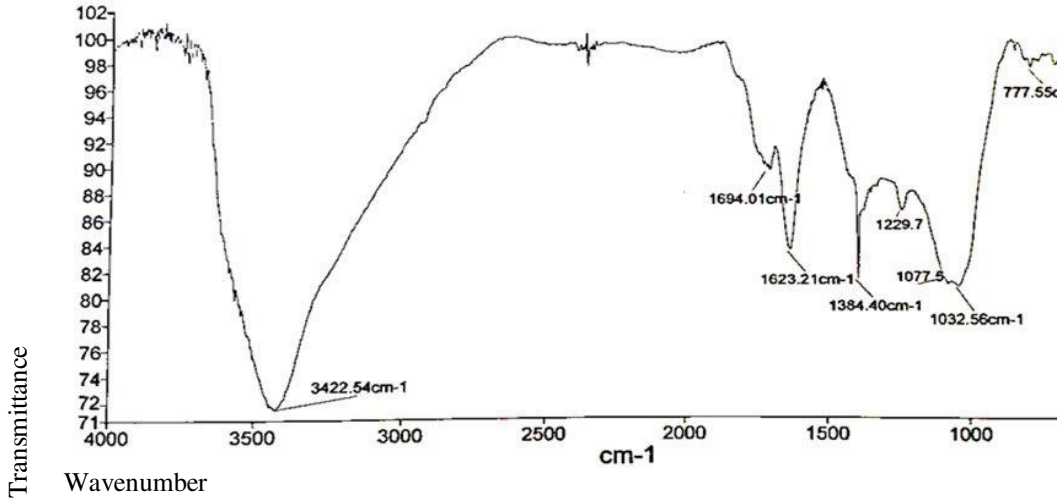

Figure 2. *FTIR spectra of the synthesized graphene oxide*

Figure 3 shows the XRD spectra of GO nanosheets. It is obvious that the synthesized adsorbent has only one intense peak centered at 11.3°.

http://www.aloki.hu ● ISSN 1589 1623 (Print) ● ISSN 1785 0037 (Online)
DOI: http://dx.doi.org/10.15666/aeer/1605_67096729
© 2018, ALÖKI Kft., Budapest, Hungary

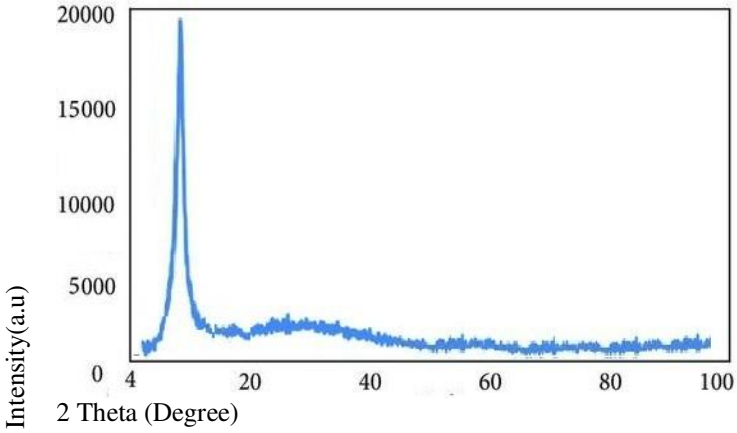

Figure 3. *XRD spectra of the synthesized GO*

Statistical analysis

The model and the quadratic equation were obtained using the Box-Behnken design. The maximum adsorption capacity of each experiment was finally recorded after adding the specified amounts of graphene oxide; adjusting the pH, concentration and time; and conducting the experiments. In order to examine the heavy metals removal, it is necessary to analyze the input data, output parameters, and optimized values.

The statistical significance of the variables was evaluated by analysis of variance (ANOVA) (*Tables 1C, 2C* and *3C*). The F-value implies that the terms in the model have a significant effect on the response. The p-value (<0.0001) indicates that the terms are significant at the probability level of 95% (*Tables 1A, 2A* and *3A*). The p-value of lack of fit (LOF) was not significant compared to the pure error, suggesting that the model fitted well with the experimental data. Adequate precision gives the ratio of signal to noise. The ratios greater than 4 are desirable. The predicted R^2 was in reasonable agreement with the adjusted R^2, which confirm the accuracy of the model (Hu et al., 2013; Tripathi et al., 2009). Software package of Design-Expert 10 version (Minneapolis, USA) was employed to design the experiments and analyze the obtained data.

Cadmium (Cd^{2+})

The following quadratic model was obtained using BBD and indicates the mathematical relation among the variables involved in Cd^{2+} (*Eq. 5*):

$$Qe = -(16.83) + (2.28 \times \text{pH}) + (0.36 \times \text{Conc}) + (0.35 \times \text{Time}) - (0.022 \times \text{pH} \times \text{Conc}) + (7.153 \times \text{pH} \times \text{Time}) + (0.709 \times pH^2\text{Conc}^2) - (5.85 \times \text{Time}^2) \quad \text{(Eq.5)}$$

Plus signs preceding the parameters represent the synergistic effect of the variable, and minus signs indicate a reduction or reverse effect. When the value of one variable increases due to the rise in that of another variable, a positive correlation coefficient is formed, which represents the synergistic effect. On the contrary, when the value of a variable increases due to the reduction in that of another variable, the correlation coefficient is negative (Talib et al., 2017). Considering the parameters and statistical analysis of the model, the R^2 linear regression coefficient value is high (R^2 = 0.9999)

http://www.aloki.hu ● ISSN 1589 1623 (Print) ● ISSN 1785 0037 (Online)
DOI: http://dx.doi.org/10.15666/aeer/1605_67096729
© 2018, ALÖKI Kft., Budapest, Hungary

and it reasonably agrees with the adjusted R^2 value of 0.9999. Consequently, the quadratic model fits the experimental data within the range of operating factors. As the value of R^2 is closer to 1, power of the model will be greater in describing the response variations as a function of independent variables (Zarei et al., 2015). The significance of the predicted model is represented by the F value which equals 16712 for adsorption of Cd^{2+} by the synthesized graphene oxide. The F-value of the model was found to be significant. The value of adequate precision represents the difference between the value of the predicted response and the average value of the prediction error. If this proportion reaches > 4, it will be indicative of adequate signal in the model. According to the results, the mentioned value is 485 for Cd^{2+} adsorption.

Table 1. *Initial factors and values obtained for* Cd^{2+}

A) Independent variables and their levels

Variables	Factor	Unit	Levels		
			–1	**0**	**+1**
pH	pH	-	2	4	6
Conc.	Cd Conc.	mg/L	10	55	100
Time	Time	min.	5	32.5	60

B) RSM design and the observed values

Run	Factor			Qe
	pH	**Cd Conc.**	**Time**	
1	6	55	5	41.7895
2	4	55	32.5	29.8021
3	4	10	60	8.40417
4	6	10	32.5	31.653
5	6	100	32.5	68.349
6	4	55	32.5	29.8015
7	4	55	32.5	30.839
8	2	55	5	14.5829
9	4	55	32.5	30.1014
10	2	10	32.5	14.4269
11	4	100	60	49.4414
12	4	55	32.5	29.7955
13	2	55	60	14.0758
14	4	100	5	48.9891
15	4	10	5	8.31452
16	2	100	32.5	44.51
17	6	55	60	42.8255

Central point: pH = 4, Conc = 55, Time = 32.5 Average = 31.63

C) Analysis of variance for RSM

Factor	SS[a]	dF[b]	MS[c]	F-value	p-value
Model	5021.51	8	627.69	16712.29	< 0.0001
pH	1544.50	1	1544.66	41122.58	< 0.0001
Conc.	3304.98	1	3304.98	87995.61	< 0.0001

http://www.aloki.hu ● ISSN 1589 1623 (Print) ● ISSN 1785 0037 (Online)
DOI: http://dx.doi.org/10.15666/aeer/1605_67096729
© 2018, ALÖKI Kft., Budapest, Hungary

Time	0.15	1	0.15	4.04	0.00794
pH* conc	16.52	1	16.52	439.76	< 0.0001
Conc* time	0.62	1	0.62	16.48	0.0036
pH^2	33.83	1	33.83	900.86	< 0.0001
$Conc.^2$	45.79	1	45.79	1219.44	< 0.0001
$Time^2$	82.53	1	82.53	2197.44	< 0.0001
Residual	0.03	8	0.038		
Lack fit	0.02	4	0.049	1.91	0.2727
Pure error	0.01	4	0.026		

R^2 = 0.9999, Adj. R^2 = 0.9999, Adeq. precision = 485.3
[a]Sum of square
[b]Degree of freedom
[c]Mean square

Lead (Pb^{2+})

Equation 6 indicates the mathematical relations among the input parameters of lead.

$$Qe = -(10975639) + (37.36219 \times pH) + (0.90729 \times Conc) + (1.61406 \times Time) - (0.051692 \times pH \times Conc) - (0.072090 \times pH \times Time) - (1.98777 \times (pH)^2) - (0.20492 \times (Time)^2) \quad \text{(Eq.6)}$$

The linear regression coefficient R^2 value (0.9999) and adjusted R^2 showed the effective removal of Pb^{2+} by graphene oxide and significance of the model for this metal with F = 8141. The obtained adequate precision is 313.

Table 2. *Initial factors and values obtained Pb^{2+}*

A) Independent variables and their levels

Variables	Factor	Unit	Levels		
			-1	0	+1
pH	pH	-	2	4	6
Conc.	Pb Conc.	mg/L	50	100	150
Time	Time	min	5	32.5	60

B) RSM design and the observed values

Run	Factor			Qe
	pH	Pb Conc.	Time	
1	2	100	5	44.4753
2	4	100	32.5	99.8557
3	4	100	32.5	99.1589
4	4	100	32.5	99.5009
5	6	100	5	99.0929
6	4	150	60	118.551
7	6	150	32.5	149.553
8	4	100	32.5	98.8449
9	6	100	60	99.3135

http://www.aloki.hu ● ISSN 1589 1623 (Print) ● ISSN 1785 0037 (Online)
DOI: http://dx.doi.org/10.15666/aeer/1605_67096729
© 2018, ALÖKI Kft., Budapest, Hungary

10	4	50	5	48.7973
11	2	150	32.5	103.863
12	2	100	60	51.6843
13	6	50	32.5	49.5921
14	4	50	60	49.4307
15	4	100	32.5	99.2496
16	2	50	32.5	23.1052
17	4	150	5	112.356

Central point: pH = 4, Conc = 100, Time = 32.5 Average = 85.09

C) Analysis of variance for RSM

Factor	SS[a]	dF[b]	MS[c]	F-value	p-value
Model	16032.24	7	2290.32	8141.96	< 0.0001
pH	2075.12	1	2075.12	7376.94	< 0.0001
Conc.	4492.39	1	4492.39	15970.21	< 0.0001
Time	0.11	1	0.11	0.39	0.5545
pH* conc	45.86	1	45.86	163.02	< 0.0001
pH* time	26.98	1	26.98	95.91	< 0.0001
pH ²	120.86	1	120.86	429.66	< 0.0001
Time ²	589.09	1	589.09	2094.20	< 0.0001
Residual	1.69	6	0.28		
Lack fit	1.11	2	0.56	3.86	0.1146
Pure error	0.058	4	0.14		
Core total	16033.93	17			

R^2 = 0.9999, Adj. R^2 = 0.9998, Adeq. precision = 313.3
[a]Sum of square
[b]Degree of freedom
[c]Mean square

Chromium (Cr(III))

Equation 7 indicates the mathematical relations among the input parameters of chromium.

$$Qe = (4.65520) + (0.68819 \times \text{pH}) - (0.18288 \times \text{Conc}) - (0.098263 \times \text{Time}) + (0.11980 \times \text{pH} \times \text{Conc}) - \left(5.56740 \times (\text{Conc})^2\right) + \left(1.52885 \times (\text{Time})^2\right) \quad \text{(Eq.7)}$$

R^2 value (0.9980) and adjusted R² suggest good removal of Cr(III) by graphene oxide and significance of the model for this metal with F = 655. The obtained adequate precision is 90.

http://www.aloki.hu ● ISSN 1589 1623 (Print) ● ISSN 1785 0037 (Online)
DOI: http://dx.doi.org/10.15666/aeer/1605_67096729
© 2018, ALÖKI Kft., Budapest, Hungary

Table 3. *Initial factors and values obtained for Cr(III)*

A) Independent variables and their elevels

Variable	Factor	Unit	Levels		
			-1	0	+1
pH	pH	-	2	3.25	4.5
Conc.	Cr Conc.	mg/L	10	55	100
Time	Time	Min	5	32.5	60

B) RSM design and the observed values

Run	Factor			Qe
	pH	Cr Conc.	Time	
1	3.25	55	32.5	15.0606
2	3.25	55	32.5	15.0964
3	2	100	32.5	15.0061
4	4.5	100	32.5	36.4972
5	3.25	55	32.5	14.4681
6	4.5	10	32.5	9.52933
7	2	55	5	11.2105
8	3.25	100	60	21.8738
9	3.25	10	5	8.67247
10	3.25	100	5	21.0389
11	4.5	55	5	25.4581
12	3.25	55	32.5	14.9065
13	4.5	55	60	24.5924
14	2	55	60	7.1957
15	3.25	10	60	8.85581
16	2	10	32.5	4.54325
17	3.25	55	32.5	15.6882

Central point: pH = 3.25, Conc = 55, Time = 32.5

C) Analysis of variance for RSM

Factor	SS[a]	dF[b]	MS[c]	F-value	p-value
Model	1000.19	6	166.70	655.0	< 0.0001
pH	386.27	1	386.27	1517.76	< 0.0001
Conc.	243.34	1	243.34	956.15	< 0.0001
Time	6.104e	1	6.104e	0.024	0.8808
pH* conc.	100.49	1	100.49	394.83	< 0.0001
Conc.^{2}	4.13	1	4.13	16.24	0.0038
Time^2	4.41	1	4.41	17.35	0.0031
Residual	2.04	8	0.25		
Lack fit	1.27	4	0.32	1.65	0.3199
Pure error	0.77	4	0.19		

R^2 = 0.9980, Adj. R^2 = 0.9964, Adeq. precision = 90.17
[a]Sum of square
[b]Degree of freedom
[c]Mean square

http://www.aloki.hu ● ISSN 1589 1623 (Print) ● ISSN 1785 0037 (Online)
DOI: http://dx.doi.org/10.15666/aeer/1605_67096729
© 2018, ALÖKI Kft., Budapest, Hungary

Comparative effects of the studied variables on removal efficiency

Figure 4 shows the effect of all the three variables on the removal rate at a point and the response level is visible and comparable in the designing method. Removal efficiency increased with the increase of pH (a) and concentration (b). However, increase in the contact time (c) did not have a significant effect on the value obtained for the heavy metals removal, and a different result was obtained for each metal.

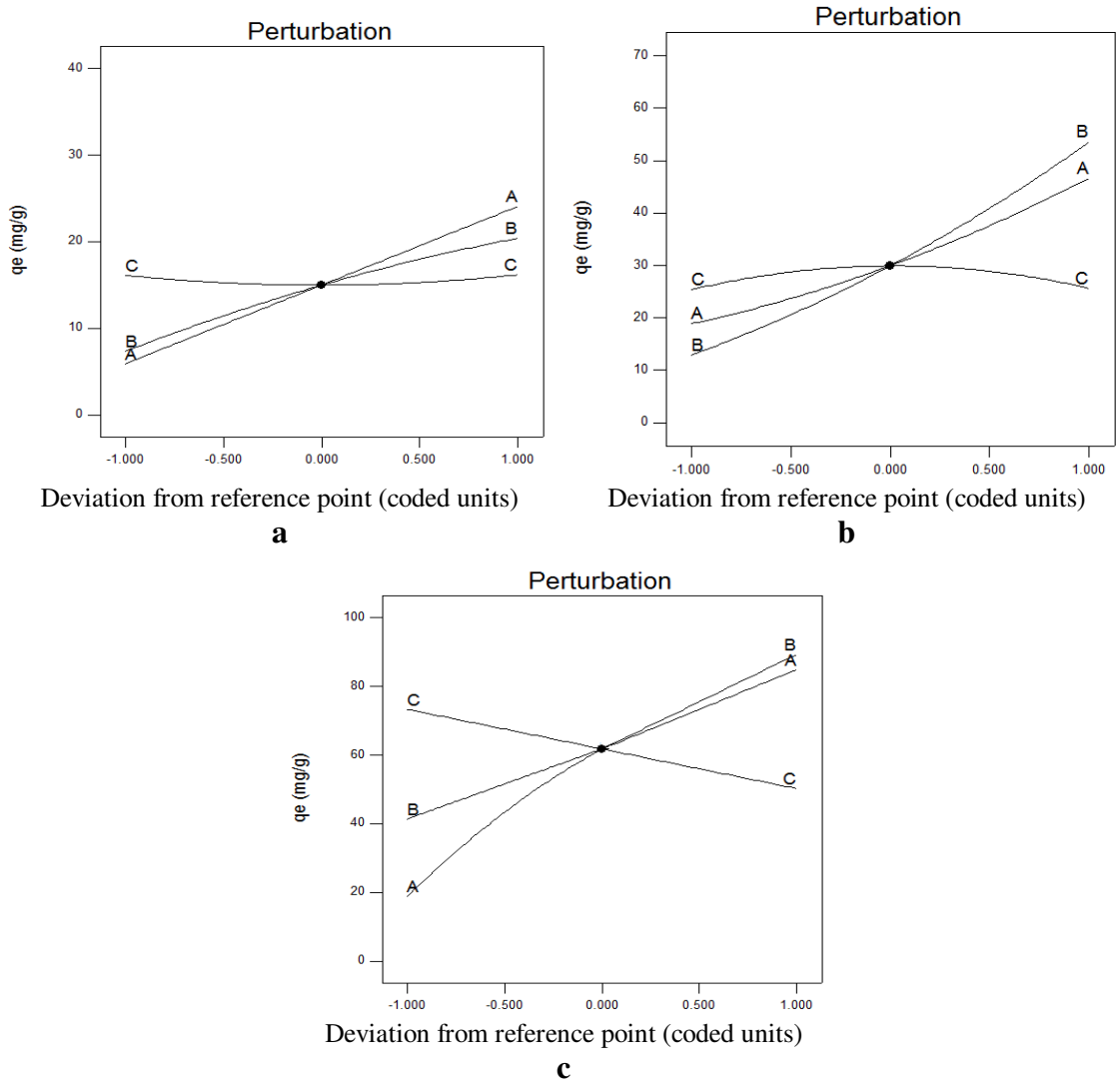

Figure 4. *Perturbation plots of removal by graphene oxide: a) chromium, b) cadmium, c) lead*

Effect of the variables on responses

Effect of pH

pH is a determinant factor in adsorption of Cr(III), Cd^{2+} and Pb^{2+} ions from aqueous solutions (Li and Wang, 2009; Ramkumar et al., 2008). To study the effect of pH on adsorption capacity of graphene oxide, pH of the solution was tested in the ranges of 2-6 for Cd^{2+} and Pb^{2+} and 2-4.5 for Cr(III). Adsorption capacity with contaminant concentration and also the contact time versus pH are illustrated in *Figure 5*. The value

http://www.aloki.hu ● ISSN 1589 1623 (Print) ● ISSN 1785 0037 (Online)
DOI: http://dx.doi.org/10.15666/aeer/1605_67096729
© 2018, ALÖKI Kft., Budapest, Hungary

of pH_{PZC} for synthesized graphene oxide was obtained as 3. When pH of the solution is below 3, the adsorbent surface is positively charged. Any increase in pH leads to change of surface charge from positive to negative. This demonstrates that heavy metals adsorption onto graphene oxide and thereby heavy metals removal are higher in $pH \geq 3$ (Lingamdinne et al., 2008). Results showed that the removal of Cr(III), Cd^{2+} and Pb^{2} by graphene nanoparticles was affected by pH of the solution. In the adsorption process, two ions of OH^- and H^+ are responsible for decomposition (Zarei et al., 2015). For chromium, by raising the initial pH of the solution from 2 to 4.5, the adsorption capacity of graphene oxide increases from 4.5 to 36.5 on a constant trend. As can be seen in *Figure 5a* and *b*, the maximum Cr(III) adsorption occurred at pH = 4.5. Analysis of *Figure 5* indicates that the negatively charged groups on the adsorbent surface and ionization of binding sites in functional groups in the cell wall increase with the increase of pH. Consequently, the removal of Cr(III) ion from aqueous solution and adsorption capacity were increased. Zhang et al. (2018) concluded that pH is the most effective variable in adsorbing chromium, and changes in pH may have a marked effect on kinetic characteristics and adsorption equilibrium. They studied the pH range of 2-11 and demonstrated that the highest adsorption capacity of chromium occurred at the pH range of 3-5 and subsequently the adsorption capacity considerably increased with the increase of pH. Another study was conducted by Jiang et al. (2017) on the effective synthesis of graphite compounds for the effective removal of chromium from aqueous solutions. The mentioned study was carried out in the pH range of 1-9, the initial concentrations of 10-100 mg/L and time duration of 5 to 300 min. The best result was achieved at pH range of 4-6 and concentration of 100 mg/L. By increasing the time from 5 to 180 min, initially the adsorption efficiency increased rapidly and then reached the saturation point (Jiang et al., 2017). According to *Figure 5c* and *d*, the effects of variables on Cd^{2+} adsorption indicate that with the increase of initial pH from 2 to 6, the graphene oxide adsorption capacity increases from 0.2 to 32.2 mg/g. At the first stage, adsorption capacity rapidly increases with the increase of pH from 2 to 4.5. Afterwards, with the increase of pH from 4.5 to 6, the slope of curve constantly increases and the maximum adsorption capacity for Cd^{2+} occurs at pH = 6. According to the tested conditions, cadmium, lead and chromium began to precipitate at pH values greater than 6 and 4.5. Similar results have been reported in other studies, confirming that cadmium and lead begin to precipitate at pH values greater than 6 (Zhao et al., 2011). A study conducted by Sitko et al. (2013) on adsorption of metal ions using graphene oxide revealed that when pH increase from 3 to 4, Cd^{2+} adsorption capacity rapidly increases and becomes constant at pH range of 5-8 (Depci et al., 2012; Zhao et al., 2011). The effects of variables on Pb^{2+} ion are shown in *Figure 5c*. Adsorption increases from 23 to 89.9 mg/g with the increase of initial pH from 2 to 6. At the first step, the adsorption capacity increases quickly with the increase of pH from 2 to 4. Afterwards the adsorption capacity increases with a slight slope with the increase of pH from 4 to 6. According to the results obtained in other studies, Cr(III) and Pb^{2+} adsorptions rapidly increase at the pH range of 2-3, and then the increasing rate slows down (Lingamdinne et al., 2016; Hao et al., 2012). Other studies have shown that most of the Cd^{2+} and Pb^{2+} adsorption processes take place at the pH range of 5.3 to 6, and Cr(III), Cd^{2+} and Pb^{2+} ions start to precipitate at the pH values higher than 6 (Fan et al., 2012; Jafari et al., 2016). As a result, the maximum rate of Pb^{2+} and Cd^{2+} adsorption occurs at pH = 5.5 and the maximum rate of Cr(III) adsorption occurs at pH = 4.5. *Figure 5* indicates the

http://www.aloki.hu ● ISSN 1589 1623 (Print) ● ISSN 1785 0037 (Online)
DOI: http://dx.doi.org/10.15666/aeer/1605_67096729
© 2018, ALÖKI Kft., Budapest, Hungary

effect of pH on time and concentration for Cr(III), Cd^{2+} and Pb^{2+} adsorptions in aqueous solutions.

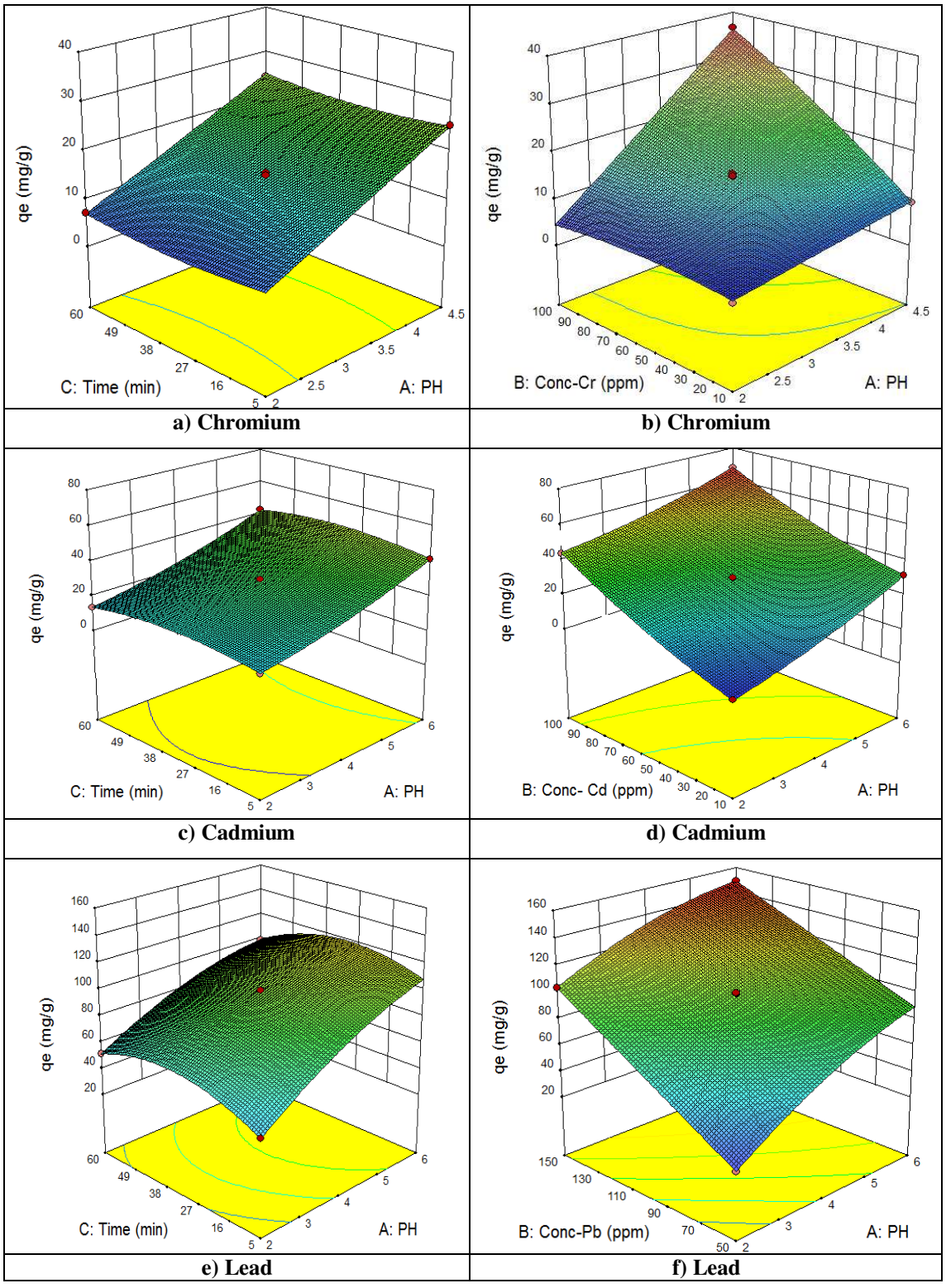

Figure 5. *The 3D response surface for Cr(III): a) pH and time, b) pH and concentration; for Cd^{2+}: c) pH and time, d) pH and concentration; and for Pb^{2+}: e) pH and time, f) pH and concentration*

http://www.aloki.hu ● ISSN 1589 1623 (Print) ● ISSN 1785 0037 (Online)
DOI: http://dx.doi.org/10.15666/aeer/1605_67096729
© 2018, ALÖKI Kft., Budapest, Hungary

Effects of initial concentration and contact time on adsorption capacity

The effect of concentration on adsorption capacity in optimum conditions (25 °C) shows that the adsorption capacity of graphene oxide increases smoothly from 63 to 135 mg/g for Pb^{2+} with the increase of initial concentration from 50 to 150 mg/L. Also, with the increase of initial concentration of the solution from 10 to 100 mg/L, graphene oxide adsorption capacity increases from 5 to 38 mg/g for Cr(III) and from 1.2 to 68 mg/g for Cd^{2+}. As can be seen in *Figure 5,* the maximum adsorption rate took place at high concentrations. This can be due to the fact that increase of adsorbent concentration increases the area of adsorbent and facilitates the access to more adsorbed sites, thus increasing the rate of heavy metals absorption. Due to the large number of sites available for absorption and absorption equilibrium in the initial stage of absorption, the adsorption process progresses steadily (Vasudevan et al., 2011). At different initial concentrations of heavy metals, the adsorption intensity was initially constant; however, over time, minor changes happened, and finally, it reached a constant value. Reaching the equilibrium time, the amount of adsorbed ions did not noticeably change over time. According to surface plots, increase of contact time did not lead to a considerable change in adsorption efficiency. Many studies yet have been done about the effect of initial concentration and contact time of adsorbent on the removal of metal ions. In some studies it has been suggested that the optimum contact time to reach the equilibrium condition for the removal of metal ions is less than 60 min (Barassi et al., 2009; Ramana et al., 2012; Sari and Tuzen, 2009). After optimization, the best values for heavy metals were obtained at pH = 6 for Pb^{2+}, and the maximum adsorption capacity of adsorbent reached 136 mg/g in initial concentration of 128 mg/L and contact time of 30 min. However, for Cd^{2+} ion at pH = 6, the maximum adsorption capacity was 68 mg/g in initial concentration of 100 mg/L and contact time of 33 min. Also, for Cr(III) at pH = 4.5, the maximum adsorption capacity was 37.63 mg/g initial concentration of 100 mg/L and contact time of 6 min. In a similar study, the maximum graphene adsorption capacity for lead was found to be 120 mg/g at pH = 5 and contact time of 30 min (Vasudevan and Lakshmi, 2012). Also, in another study, the maximum adsorption capacity for lead was obtained as 101 mg/g at pH = 6 (Awad et al., 2017). In a study conducted by Sitko et al. (2013) on cadmium, the maximum adsorption capacity was 49 mg/g at pH = 5 and contact time of 120 min. In another study, the maximum graphene oxide adsorption capacity for cadmium (88 mg/g) was obtained in initial concentration of 30 mg/L and a contact time of 30 min (Sheet et al., 2014). In this study, the values obtained as the maximum graphene adsorption capacity for Cr(III), Cd^{2+} and Pb^{2+} were consistent with the findings reported in other studies.

Examination of adsorption isotherms

Isotherm is the most important parameter in the design of adsorption systems. It represents the relation between the adsorption capacity of an adsorbent and the adsorbate concentration. The Langmuir and Freundlich adsorption isotherm models are used in this study. Langmuir isotherm is based on monolayer adsorption and homogeneity of the adsorbate with equal energy on the whole surface of the adsorbent. Contrary to Langmuir isotherm, Freundlich isotherm is on the basis of multilayer adsorption and heterogeneity of the adsorbate on the adsorbent (Jamali et al., 2015). The results of adsorption experiments with different pH values, contact times and initial concentrations of heavy metals have been analyzed using Langmuir and Freundlich

http://www.aloki.hu ● ISSN 1589 1623 (Print) ● ISSN 1785 0037 (Online)
DOI: http://dx.doi.org/10.15666/aeer/1605_67096729
© 2018, ALÖKI Kft., Budapest, Hungary

models. The values of adsorption isotherms are obtained using the equations presented in *Table 4*.

Table 4. *Linear equations and isotherm parameters*

Model		Parameters
Isotherm	Langmuir	$\frac{C_e}{q_e} = \frac{1}{Q^\circ b} + \frac{C_e}{Q^\circ}$
	Frendlich	$\log(q_e) = \log(K_f) + \frac{1}{n}\log(C_e)$

In Langmuir and Freundlich equations, C_e represents equilibrium concentration of heavy metals in mg/L; q_e indicates the amount of heavy metals adsorbed in equilibrium time in mg/g; Q° and b are Langmuir parameters related to the maximum absorption capacity and the energy of absorption correlation, respectively; and K_f and n are Freundlich constants which represent adsorption capacity and desirability of adsorption process, respectively. Values of K_f and n parameters are, respectively, determined through intercept and linear regression slope of $\log(C_e)$ versus $\log(q_e)$. In this model, n-values less than 1 indicate weak adsorption. The values between 1-2 and 2-10 represent difficult and desired adsorption, respectively (Jamali et al., 2015).

Referring to *Table 5,* "n" constant values of 1.9 for Cd^{2+} and Cr(III) and 7.4 for Pb^{2+} show the higher fitness of Freundlich model for Pb^{2+}. R^2 values for Cd^{2+} and Cr(III) obtained from Langmuir isotherm are greater than those obtained from Freundlich model, indicating the higher fitness of Langmuir isotherm for Cd^{2+} and Cr(III). However, Freundlich model has a higher fitness for Pb^{2+} ion (*Fig. 6*). Surface adsorption of Pb^{2+} ions takes place onto the monolayer of the adsorbent surface. Adsorption sites are equally and similarly present on the surface area of the adsorbent (Iram et al., 2010).

Table 5. *Values of adsorption isotherm models*

Heavy metals	Langmuir model			Freundlich model		
	R^2	b (L/mg)	q_{max} (mg/g)	R^2	N	K (mg/g) $(L/mg)^{1/n}$
Cr(III)	0.985	21.32	41.32	0.928	1.94	22.84
Pb^{2+}	0.072	0.031	833.33	0.958	7.42	24.46
Cd^{2+}	0.997	0.264	87.71	0.958	1.94	18.23

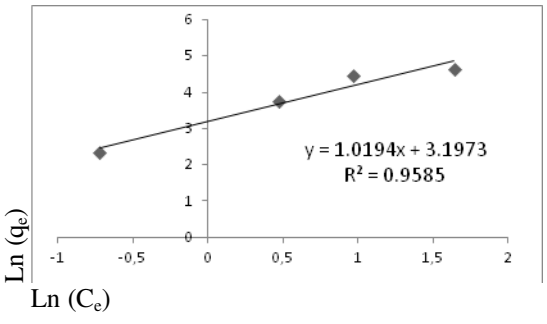

a

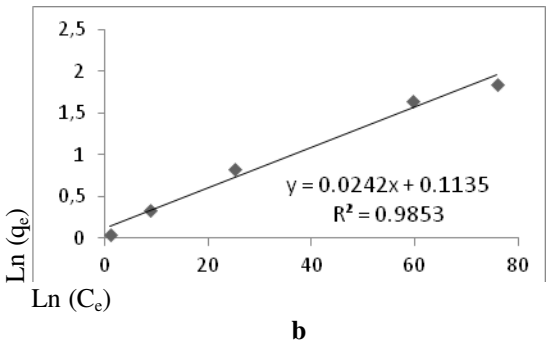

b

http://www.aloki.hu ● ISSN 1589 1623 (Print) ● ISSN 1785 0037 (Online)
DOI: http://dx.doi.org/10.15666/aeer/1605_67096729
© 2018, ALÖKI Kft., Budapest, Hungary

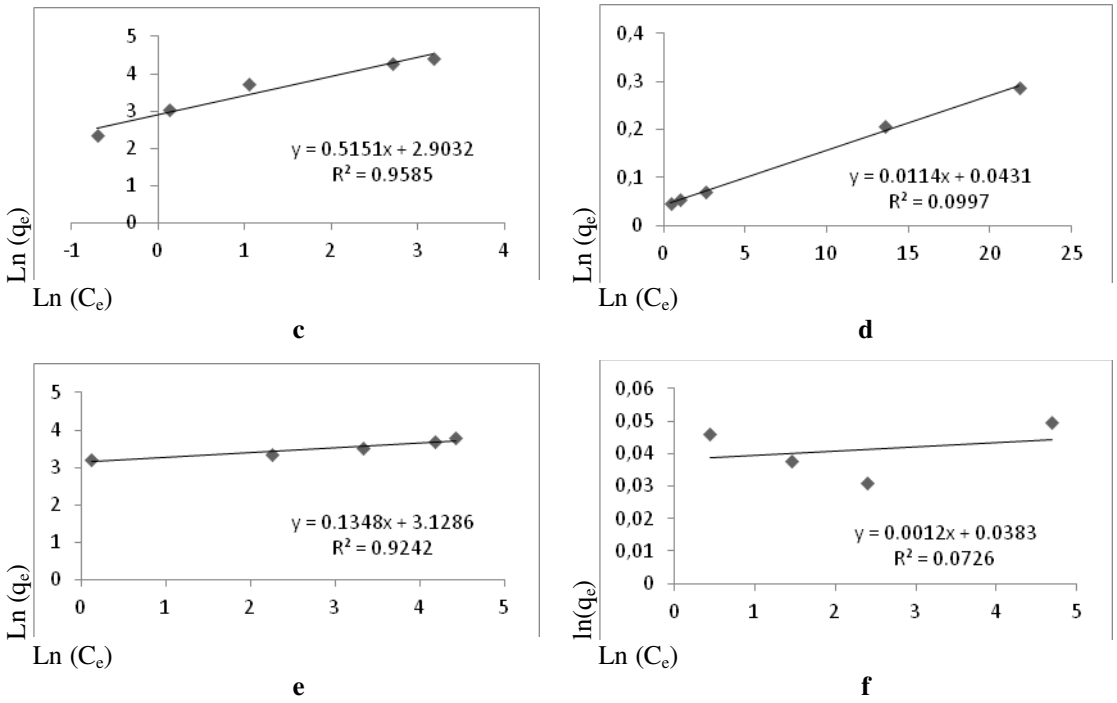

Figure 6. *Adsorption isotherm of graphene oxide: a) Freundlich Cr(III), b) Langmuir Cr(III), c) Freundlich Cd^{2+}, d) Langmuir Cd^{2+}, e) Freundlich Pb^{2+} ion, and f) Langmuir Pb^{2+}*

Conclusion

In the present study, graphene oxide nanoparticles were used to examine the removal of Cr(III), Cd^{2+} and Pb^{2+} which were synthesized by Hummer's method. RSM was used according to the Box-Behnken design to evaluate the effect of independent variables on response function. Properties of the synthesized adsorbent were studied using FESEM, FTIR, and XRD. In FESEM images, the size of graphene oxide sheets was 1 to 3 μm with wrinkled morphology. FTIR spectra were classified into three groups, and it was observed that ranges of alkoxy groups, carboxyl groups, stretching vibration of aromatic, stretching CH_2, aromatic sheets and OH groups of graphene oxide sheets were in agreement with the results of previous studies. XRD spectra exhibited an intense peak at $2\Theta = 11.3^{o}$ for graphene oxide. Some of the effective parameters for the removal of Cr(III), Cd^{2+} and Pb^{2+} were optimized. After optimization, the maximum adsorption capacity of adsorbent reached 136 mg/g for Pb^{2+} at pH = 6, initial concentration of 128 mg/L and contact time of 30 min. However, the maximum adsorption capacity was 68 mg/g for Cd^{2+} ion at pH = 6, initial concentration of 100 mg/L and contact time of 33 min. Also, the maximum adsorption capacity was 37.63 mg/g for Cr(III) at pH = 4.5, initial concentration of 100 mg/L and contact time of 6 min. The high value of R^2 linear regression coefficient was desirable. Values of R^2, adjusted coefficient (Adj. R^2) and predicted coefficient (Pred. R^2) were acceptable. The high value of R^2 linear regression coefficient guarantees the desirability of the presented quadratic equation and is representative of good fitness of the data with the predicted model. According to the results, all linear, quadratic and interaction effects of the variables were significant with a safety factor of 95%, indicating the effect of the variables on Cr(III), Cd^{2+} and Pb^{2+} removal using graphene oxide adsorbents. Adequate precision indicated the noise ratio, and the values greater than 4 represented the desirability of the quadratic equation

http://www.aloki.hu ● ISSN 1589 1623 (Print) ● ISSN 1785 0037 (Online)
DOI: http://dx.doi.org/10.15666/aeer/1605_67096729
© 2018, ALÖKI Kft., Budapest, Hungary

model for prediction. Replicability of the model, with C.V value of less than 10%, indicated a good condition. Values obtained from Langmuir isotherm equation for Cr(III) and Cd^{2+} exhibit the maximum fitness of this model with Cr(III) and Cd^{2+}. However, the values obtained from Freundlich isotherm for Pb^{2+} ions showed the maximum fitness of this isotherm with Pb^{2+} ions. The results showed that graphene oxide was effective in removing heavy metals from aqueous solutions. It was concluded that the adsorption process is a function of pH value, initial concentration of the solution and contact time, and graphene oxide can be effectively used to remove heavy metals from polluted waters. Finfings in this study can be applied in the treatment of industrial wastewater. Further studies should be carried out to investigate the efficiency of the proposed method for the removal of heavy metals at lower concentrations.

Acknowledgements. The authors wish to extend their gratitude to University of Tehran as well as the Islamic Azad University of Hamadan for providing the laboratory and the required experimental equipments.

Conflict of interests. The authors state that there is no conflict of interests regarding publication of this article.

REFERENCES

[1] Amarasinghe, B. M. W. P. K., Williams, R. A. (2007): Tea waste as a low cost adsorbent for the removal of Cu and Pb from wastewater. – Chemical Engineering Journal 132(1-3): 299-309.

[2] Awad, F., AbouZeid, K., El-Maaty, W., El-Wakil, A., El-Shall, M. (2017): Efficient removal of heavy metals from polluted water with High Selectivity for Mercury (II) by 2-Imino-4-thiobiuret–partially reduced graphene oxide (IT-PRGO). – ACS Applied Materials & Interfaces 9(39): 34230-34242.

[3] Barassi, G., Valdés, A., Araneda, C., Basualto, C., Sapag, J., Tapia, C., Valenzuela, F. (2009): Cr (VI) sorption behavior from aqueous solutions onto polymeric microcapsules containing a long-chain quaternary ammonium salt: kinetics and thermodynamics analysis. – Journal of Hazardous Materials 172(1): 262-268.

[4] Belay, A. A. (2010): Impacts of chromium from tannery effluent and evaluation of alternative treatment options. – Journal of Environmental Protection 1(01): 53.

[5] Chaiyakun, S., Witit-Anun, N., Nuntawong, N., Chindaudom, P., Oaew, S., Kedkeaw, C., Limsuwan, P. (2012): Preparation and characterization of graphene oxide nanosheets. – Procedia Engineering 32: 759-764.

[6] Depci, T., Kul, A.R., Önal, Y. (2012): Competitive adsorption of lead and zinc from aqueous solution on activated carbon prepared from Van apple pulp: study in single-and multi-solute systems. – Chemical Engineering Journal 200: 224-236.

[7] Fan, L., Luo, C., Sun, M., Li, X., Qiu, H. (2013): Highly selective adsorption of lead ions by water-dispersible magnetic chitosan/graphene oxide composites. – Colloids and Surfaces B: Biointerfaces 103: 523-529.

[8] Fan, L., Luo, C., Sun, M., Qiu, H. (2012): Synthesis of graphene oxide decorated with magnetic cyclodextrin for fast chromium removal. – Journal of Materials Chemistry 22(47): 24577-24583.

[9] Fu, F., Wang, Q. (2011): Removal of heavy metal ions from wastewaters: a review. – Journal of Environmental Management 92(3): 407-418.

[10] Ghafari, S., Aziz, H. A., Isa, M.H., Zinatizadeh, A. A. (2009): Application of response surface methodology (RSM) to optimize coagulation–flocculation treatment of leachate

http://www.aloki.hu ● ISSN 1589 1623 (Print) ● ISSN 1785 0037 (Online)
DOI: http://dx.doi.org/10.15666/aeer/1605_67096729
© 2018, ALÖKI Kft., Budapest, Hungary

using poly-aluminum chloride (PAC) and alum. – Journal of Hazardous Materials 163(2-3): 650-656.

[11] Hao, L., Song, H., Zhang, L., Wan, X., Tang, Y., Lv, Y. (2012): SiO2/graphene composite for highly selective adsorption of Pb (II) ion. – Journal of Colloid and Interface Science 369(1): 381-387.

[12] Hu, X.-J. Liu, Y.-G., Wang, H., Chen, A.W., Zeng, G.-M., Liu, S., Guo, Y.-M., Hu, X., Li, T.-T., Wang, Y., Zhou, L., Liu, S. (2013): Removal of Cu(II) ions from aqueous solution using sulfonated magnetic graphene oxide composite. – Journal of Separation and Purification Technology 108: 189-195.

[13] Huang, Z., Pan, X. D., Wu, P. G., Han, J. L., Chen, Q. (2014): Heavy metals in vegetables and the health risk to population in Zhejiang, China. – Food Control 36(1): 248-252.

[14] Iram, M., Guo, C., Guan, Y., Ishfaq, A., Liu, H. (2010): Adsorption and magnetic removal of neutral red dye from aqueous solution using Fe3O4 hollow nanospheres. – Journal of Hazardous Materials 181(1-3): 1039-1050.

[15] Jafari Kang, A., Baghdadi, M., Pardakhti, A. (2016): Removal of cadmium and lead from aqueous solutions by magnetic acid-treated activated carbon nanocomposite. – Desalination and Water Treatment 57(40): 18782-18798.

[16] Jaishankar, M., Tseten, T., Anbalagan, N., Mathew, B.B., Beeregowda, K. N. (2014): Toxicity, mechanism and health effects of some heavy metals. – Interdisciplinary Toxicology 7(2): 60-72.

[17] Jamali, H. A., Dindarloo, K. and Nikpey, A. (2015): Optimization of metal working fluids treatment using calcium chloride by response surface methodology. – The Journal of Qazvin University of Medical Sciences 19(2): 46-54.

[18] Jiang, J. W., Lan, J., Wang, J. S., Li, B. (2010): Isotopic effects on the thermal conductivity of graphene nanoribbons: Localization mechanism. – Journal of Applied Physics 107(5): 054314.

[19] Jiang, X., Luo, H., Yin, Y., Zhou, W. (2017): Facile synthesis of MoS 2/reduced graphene oxide composites for efficient removal of Cr (vi) from aqueous solutions. – RSC Advances 7(39): 24149-24156.

[20] Khajeh, M. (2011): Optimization of process variables for essential oil components from Satureja hortensis by supercritical fluid extraction using Box-Behnken experimental design. – The Journal of Supercritical Fluids 55(3): 944-948.

[21] Kumar, S., Nair, R. R., Pillai, P. B., Gupta, S. N., Iyengar, M. A. R., Sood, A. K. (2014): Graphene oxide–MnFe2O4 magnetic nanohybrids for efficient removal of lead and arsenic from water. – ACS Applied Materials & Interfaces 6(20): 17426-17436.

[22] Li, H., Bi, S., Liu, L., Dong, W., Wang, X. (2011): Separation and accumulation of Cu (II), Zn (II) and Cr (VI) from aqueous solution by magnetic chitosan modified with diethylenetriamine. – Desalination 278(1-3): 397-404.

[23] Li, K., Wang, X. (2009): Adsorptive removal of Pb (II) by activated carbon prepared from Spartina alterniflora: equilibrium, kinetics and thermodynamics. – Bioresource Technology 100(11): 2810-2815.

[24] Li, Q., Yu, L. J., Deng, Y., Li, W., Li, M. T., Cao, J. H. (2007): Leaf epidermal characters of Lonicera japonica and Lonicera confuse and their ecology adaptation. – Journal of Forestry Research 18(2): 103-108.

[25] Lingamdinne, L. P., Koduru, J. R., Choi, Y. L., Chang, Y. Y., Yang, J. K. (2016): Studies on removal of Pb (II) and Cr (III) using graphene oxide based inverse spinel nickel ferrite nano-composite as sorbent. – Hydrometallurgy 165: 64-72.

[26] Liu, M., Chen, C., Hu, J., Wu, X., Wang, X. (2011): Synthesis of magnetite/graphene oxide composite and application for cobalt (II) removal. – The Journal of Physical Chemistry C 115(51): 25234-25240.

http://www.aloki.hu ● ISSN 1589 1623 (Print) ● ISSN 1785 0037 (Online)
DOI: http://dx.doi.org/10.15666/aeer/1605_67096729
© 2018, ALÖKI Kft., Budapest, Hungary

[27] McGrail, B. T., Mangadlao, J. D., Rodier, B. J., Swisher, J., Advincula, R., Pentzer, E. (2016): Selective mono-facial modification of graphene oxide nanosheets in suspension. – Chemical Communications 52(2): 288-291.
[28] Omar, H. A., Moloukhia, H. (2008): Use of activated carbon in removal of some radioisotopes from their waste solutions. – Journal of Hazardous Materials 157(2-3): 242-246.
[29] Pan, B., Pan, B., Zhang, W., Lv, L., Zhang, Q., Zheng, S. (2009): Development of polymeric and polymer based hybrid adsorbents for pollutants removal from waters. – Chemical Engineering Journal 151(1-3): 19-29.
[30] Rajasulochana, P., Preethy, V. (2016): Comparison on efficiency of various techniques in treatment of waste and sewage water – A comprehensive review. – Resource-Efficient Technologies 2(4): 175-184.
[31] Ramana, D. V., Reddy, D. H. K., Yu, J. S., Seshaiah, K. (2012): Pigeon peas hulls waste as potential adsorbent for removal of Pb (II) and Ni (II) from water. – Chemical Engineering Journal 197: 24-33.
[32] Ramkumar, J., Chandramouleeswaran, S., Sudarsan, V., Mishra, R. K., Kaushik, C. P., Raj, K., Mukherjee, T., Tyagi, A. K. (2008): Borosilicate glasses modified with organic ligands: A new selective approach for the removal of uranyl ion. – Journal of Hazardous Materials 154(1-3): 513-518.
[33] Sari, A., Tuzen, M. (2009): Kinetic and equilibrium studies of Pb (II) and Cd (II) removal from aqueous solution onto colemanite ore waste. – Desalination 249(1): 260-266.
[34] Sheet, I., Kabbani, A. Holail, H. (2014): Removal of heavy metals using nanostructured graphite oxide, silica nanoparticles and silica/graphite oxide composite. – Energy Procedia 50: 130-138.
[35] Sitko, R., Turek, E., Zawisza, B., Malicka, E., Talik, E., Heimann, J., Gagor, A., Feist, B., Wrzalik, R. (2013): Adsorption of divalent metal ions from aqueous solutions using graphene oxide. – Dalton Transactions 42(16): 5682-5689.
[36] Talib, N. A. A., Salam, F., Yusof, N. A., Ahmad, S. A. A., Sulaiman, Y. (2017): Modeling and optimization of electrode modified with poly (3, 4-ethylenedioxythiophene)/graphene oxide composite by response surface methodology/Box-Behnken design approach. – Journal of Electroanalytical Chemistry 787: 1-10.
[37] Tchounwou, P. B., Yedjou, C. G., Patlolla, A. K., Sutton, D. J. (2012): Heavy Metal Toxicity and the Environment. – In: Luch, A. (ed.) Molecular, Clinical and Environmental Toxicology. Springer, Basel, pp. 133-164.
[38] Tripathi, P., Srivastava, V. C., Kumar, A. (2009): Optimization of an azo dye batch adsorption parameters using Box–Behnken design. – Desalination 249(3): 1273-1279.
[39] Uluozlu, O. D., Sari, A., Tuzen, M., Soylak, M. (2008): Biosorption of Pb (II) and Cr (III) from aqueous solution by lichen (Parmelina tiliaceae) biomass. – Bioresource Technology 99(8): 2972-2980.
[40] Vasudevan, S., Lakshmi, J. (2012): The adsorption of phosphate by graphene from aqueous solution. – RSC Advances 2(12): 5234-5242.
[41] Vasudevan, S., Lakshmi, J., Sozhan, G. (2011): Effects of alternating and direct current in electrocoagulation process on the removal of cadmium from water. – Journal of Hazardous Materials 192(1): 26-34.
[42] Wang, X., Guo, Y., Yang, L., Han, M., Zhao, J., Cheng, X. (2012): Nanomaterials as sorbents to remove heavy metal ions in wastewater treatment. – Environ. Anal. Toxicol 2(7): 1000154.
[43] Yang, Y., Wu, W. Q., Zhou, H. H., Huang, Z. Y., Ye, T. T., Liu, R., Kuang, Y. F. (2014): Adsorption behavior of cross-linked chitosan modified by graphene oxide for Cu (II) removal. – Journal of Central South University 21(7): 2826-2831.

http://www.aloki.hu ● ISSN 1589 1623 (Print) ● ISSN 1785 0037 (Online)
DOI: http://dx.doi.org/10.15666/aeer/1605_67096729
© 2018, ALÖKI Kft., Budapest, Hungary

[44] Yetilmezsoy, K., Demirel, S., Vanderbei, R. J. (2009): Response surface modeling of Pb (II) removal from aqueous solution by Pistacia vera L.: Box–Behnken experimental design. – Journal of Hazardous Materials 171(1-3): 551-562.
[45] Yu, T., Ni, Z., Du, C., You, Y., Wang, Y., Shen, Z. (2008): Raman mapping investigation of graphene on transparent flexible substrate: The strain effect. – The Journal of Physical Chemistry C 112(33): 12602-12605.
[46] Zarei, H., Mahvi, A. H., Nasseri, S., Nabizadeh Noudehi, R, Shemirani, F. (2015): Modeling adsorption on fluoride and application of Box–Behnken design and response surface methodology for arsenic (V) removal from aqueous solution using Nano-Scale Alumina on Multi Walled Carbon Nanotube. – Iranian Journal of Health and Environment 8(3): 309-322.
[47] Zhao, G., Li, J., Ren, X., Chen, C., Wang, X. (2011): Few-layered graphene oxide nanosheets as superior sorbents for heavy metal ion pollution management. – Environmental Science & Technology 45(24): 10454-10462.
[48] Zhao, G., Ren, X., Gao, X., Tan, X., Li, J., Chen, C., Huang, Y., Wang, X. (2011): Removal of Pb (II) ions from aqueous solutions on few-layered graphene oxide nanosheets. – Dalton Transaction 40(41): 10945-10952.
[49] Zhao, G., Wen, T., Yang, X., Yang, S., Liao, J., Hu, J., Shao, D., Wang, X. (2012): Preconcentration of U (VI) ions on few-layered graphene oxide nanosheets from aqueous solutions. – Dalton Transactions 41(20): 6182-6188.
[50] Zhang, K., Li, H., Xu, X., Yu, H. (2018): Synthesis of reduced graphene oxide/NiO nanocomposites for the removal of Cr (VI) from aqueous water by adsorption. – Microporous and Mesoporous Materials 255: 7-14.

http://www.aloki.hu ● ISSN 1589 1623 (Print) ● ISSN 1785 0037 (Online)
DOI: http://dx.doi.org/10.15666/aeer/1605_67096729
© 2018, ALÖKI Kft., Budapest, Hungary

SUCROSE PHOSPHATE SYNTHASE GENE EXPRESSION IN SORGHUM, SWEET SORGHUM AND F5 HYBRID POPULATIONS

JI, Y.[1] – ZHANG, W. T.[1] – PANG, H. B.[1] – LI, X. M.[1] – MA, L. J.[1] – WANG, L. L.[1] – ZHANG, Y.[1] – HUSSAIN, K.[3] – WU, S. W.[2*] – LI, Y. Y.[1*]

[1]*College of Life Science, Shenyang Normal University*
No. 253 Huanghe North Street, Shenyang, Liaoning 110034, China

[2]*College of Science Institute, Shenyang Agricultural University*
No. 120 Dongling Road, Shenyang, Liaoning 110866, China

[3]*Department of Botany, University of Gujrat, HH Campus, Gujrat, Pakistan*

**Corresponding authors*
e-mail: wusuwen001@126.com, yueyinglicn@163.com

(Received 4th Jul 2018; accepted 20th Sep 2018)

Abstract. Sweet sorghum has drought resistance, waterlogging resistance, salt and alkali resistance, wide adaptability and excellent resistance to leaf diseases, and is one of China's important food crops, sugar crops and energy crops. In the face of the energy crisis, as an energy crop, sweet sorghum has a high conversion rate of ethanol, which shows an attractive prospect for development and utilization and has attracted the attention of many countries. One of the main indicators to measure the use value of sweet sorghum is its high sugar content, and it is of great significance to increase the sugar content. In this study, we examined the expression of sucrose phosphate synthase (SPS) in leaves of sweet sorghum and sorghum and found the rules of sugar accumulation in sweet sorghum. The effect of SPS gene expression on sucrose accumulation in sweet sorghum and the factors affecting the difference of sugar content between sweet sorghum and sorghum cultivars were studied. The sweet sorghum LTR102 (as the female in this experiment), and common grain sorghum 654 (as the male), and hybrid F5 high and low sugar individuals were used as experimental materials. The gene expression of sucrose phosphate synthase was detected by real-time PCR. According to the qualitative and quantitative analyses of SPS gene, the SPS gene is not only the key factor for the accumulation of sucrose, but also the factor that causes the difference in sugar content between sweet sorghum and common sorghum. At different growth stages, the high sugar individuals showed superiority in sucrose accumulation, SPS activity and SPS gene expression compared to the other three individuals.
Keywords: *quantitative expression, RT-PCR, sucrose content, developmental stage*

Introduction

With the increasing scarcity of fossil fuels and the increasing environmental pollution, biomass energy has become an increasingly attractive alternative to fossil fuels as a renewable clean energy source, reducing greenhouse gas emissions and supporting agricultural development (Guo et al., 2016). The name "sweet sorghum" is used to distinguish those varieties of sorghum (*Sorghum bicolor* (L.) Moench), which accumulate high concentrations of soluble sugars like sucrose, glucose and fructose in the stem juice, from the common grain sorghum (Rao et al., 2013). Sweet sorghum is a C4 plant with a high photosynthetic rate, and has excellent characteristics such as drought resistance, waterlogging resistance, salt and alkali resistance. It has a short growing period, the use of seeds to reproduce and the amount of seeds used is much lower than that of sugar cane (*Saccharum officinarum*), and is suitable for sowing, so the production cost of sweet sorghum is much lower than that of sugarcane (Luo et al.,

http://www.aloki.hu ● ISSN 1589 1623 (Print) ● ISSN 1785 0037 (Online)
DOI: http://dx.doi.org/10.15666/aeer/1605_67316740
© 2018, ALÖKI Kft., Budapest, Hungary

2012; Zhang et al., 2018). Far lower than sugarcane, and suitable for sowing, so the production cost of sweet sorghum is much lower than sugarcane. And a lot of research has been carried out and will create economic benefits (Luo et al., 2012). At present, sweet sorghum is one of the most promising renewable energy sources. In recent years, sweet sorghum as a sugar crop, feed crop, energy crop and industrial crop has important significance for global economic development and environmental protection (Zhao et al., 2015; Jiang et al., 2012; Tang et al., 2012). Although sweet sorghum varieties have important agronomic traits and invaluable economic values, the high sugar metabolism-related genes have been little known so far (Li et al., 2014). Thus, it is great significance to understand the accumulation pattern of sugar in sweet sorghum and to investigate the effect of SPS gene expression on sucrose accumulation in sweet sorghum and the differences in sugar content between sweet sorghum and sorghum.

Sucrose-phosphate synthase (SPS, EC 2.4.1.14) is a key enzyme in sucrose biosynthesis in both photosynthetic and nonphotosynthetic tissues of plants. It is encoded by different gene families. SPS exists in multiple forms which show differential distributions and functional specializations in the plant tissues. The expression of SPS was higher in sugarcane as compared with maize (*Zea mays* L.), while in contrast no PCR amplification was obtained with the Arabidopsis plants (*Arabidopsis thaliana* (L.) Heynh.) (ElSayed, et al., 2013). At the transcript level, the rice (*Oryza sativa* L.) SPS genes, particularly SPS1, were preferentially expressed in source tissues. Diurnal changes in SPS gene expression, SPS activity, and soluble sugar content in leaf blades were investigated. The expression of all the SPS genes, particularly that of SPS1 and SPS11, tended to be higher at night when the activation state of the SPS proteins was low, and the mRNA levels of SPS1 and SPS6 were negatively correlated with sucrose content. The temporal patterns of SPS gene expression and sugar content under continuous light conditions suggested the involvement of endogenous rhythm and/or sucrose sensing in the transcriptional regulation of SPS genes (Okamura et al., 2011). The association among sucrose content, tree phenology and elevated SPS gene expression also implicates both enzyme and product in regulating poplar developmental processes (Park et al., 2009). SPS activity is highly regulated by hierarchy of mechanisms including transcriptional control (Taneja and Das, 2014). Therefore, to understand the accumulation and metabolism of sugar in plants, it is essential to study the regulation of SPS and gene expression.

Real-time PCR (real-time quantitative PCR technology) can quantify the initial template, it is simple and quick to operate, with strong specificity and high sensitivity. Because the entire process does not require post-processing of PCR products, it can effectively prevent contamination and false positives in the detection process, greatly improving the detection efficiency, and fluorescence quantification can also prevent non-specific amplification by melting curves, probes, etc. Thus, real-time PCR has the tendency to replace conventional PCR. It refers to the addition of fluorescent groups to the PCR reaction system, real-time monitoring of the entire PCR process using fluorescence signal accumulation, and finally the quantitative analyses of unknown templates using standard curves (Hou, 2009). Okamura et al. (2011) investigated the tissue- and developmental stage-specific expression patterns of the rice SPS gene family using real-time RT-PCR techniques. The diurnal changes in SPS gene expression and activity in leaves were also examined. Based on the results presented, predictions of the key transcriptional regulator of each SPS gene were discussed. Therefore, RT-PCR technology plays an important role in the determination of SPS enzyme activity.

http://www.aloki.hu ● ISSN 1589 1623 (Print) ● ISSN 1785 0037 (Online)
DOI: http://dx.doi.org/10.15666/aeer/1605_67316740
© 2018, ALÖKI Kft., Budapest, Hungary

For sweet sorghum, sugar content is an important trait indicator. The study of the correlation between the changes of SPS activity and gene expression and sucrose content is the theoretical basis to find out the factors influencing sugar sorghum accumulation in sweet sorghum. In this study, the relationship between SPS activity and gene expression patterns and sugar accumulation was studied, which provided the theoretical basis for the selection and breeding of sweet sorghum new varieties and the determination of the best harvest stage.

Research design and methods

Plant material

Sweet sorghum LTR102 (as the female parent in this experiment), common grain sorghum 654 (as the male parent) and F5 high and low sugar plants from the cross of the first two were supplied by Liaoning Academy of Agricultural Sciences. Through subculture techniques, the genotypes were continuously purified to screen for high sugar varieties. Three replicates of each treatment were sampled to extract the sugar and determine the sugar content at the seedling stage, jointing stage, heading stage and mature stage.

Determination of SPS activity

The sample (1 g) was homogenized to a fine powder in pre-chilled mortar and added to 2.5 mL phosphate buffer (twice). These supernatant liquor were collected after centrifugation at 10,000xg (4 °C) for 15 min, the reaction mixture contained in a final volume of 50 μL supernatant liquor, 50 μL phosphate buffer, 20 μL $MgCl_2$, 20 μL UDPG and 20 μL 6-phosphate fructose. Then, vibrated it and incubated the tubes for 30 min in a water bath at 30 °C. The reaction was stopped by the addition of 200 μL of NaOH and the tubes placed in a water bath at 100 °C for 10 min. After cooling the tubes to room temperature, the tissue sample was added to 1.5 mL HCl (30%) and 0.5 mL resorcinol and then, the tubes placed in a water bath at 80 °C for 10 min. After cooling the tubes to room temperature, absorbance was measured at 480 nm.

Total RNA extraction and cDNA synthesis

Total RNA was extracted by improved Trizol method. The leaf tissue was homogenized to a fine powder in liquid nitrogen. And then added 1 ml Trizol to each 50-100 mg of tissue, the sample volume should not be exceeded 100 μL at room temperature for 5 min. Then, the leaf tissue was added 0.2 mL chloroform to the tubes and vibrate it for 15 s, static cultivation at room temperature for 5 min. These supernatant liquor were collected after centrifugation at 12,000xg (4 °C) for 15 min and then, collected the supernate into tubes. The samples were added 0.5mL isopropanol at room temperature for 5 min. These samples were collected after centrifugation at 12,000 g (4 °C) for 10 min and then, the supernatant liquor was discarded. The precipitate was added 1 mL ethanol to the tubes to dissolve RNA precipitate. Similarly, the samples were collected after centrifugation at 12,000xg (4 °C) for 5 min. If it used for reverse-transcription PCR, repeat the above steps twice (discard supernatant liquor and dissolve RNA precipitate). Dried for 5-10 min at room temperature. Then dissolved the sample by TE (30-60 μL). Then take analyses of the extracted RNA purity and RNA

http://www.aloki.hu ● ISSN 1589 1623 (Print) ● ISSN 1785 0037 (Online)
DOI: http://dx.doi.org/10.15666/aeer/1605_67316740
© 2018, ALÖKI Kft., Budapest, Hungary

integrity. RNA samples that were diluted 100-fold or 200-fold with RNase to solubilize RNA samples. Absorbance was measured at 260, 280, 230 nm.

Determine the RNA concentration of the original sample: RNA μg/μL = A(260, 280, 230) × 33 × T / 1000. A: Absorbance; T: Dilution times.

After electrophoresis on a 1.0% agarose gel at 90 V for 45 min, the clarity and integrity of the RNA bands were visualized on a gel imager.

Design of SPS primers

Based on the known cDNA sequence of a sweet sorghum SPS3-1 gene coding region (Liu, 2009), primers were designed using Oligo6 software and Primer primier software (Zhang et al., 2004). And it was named SPS-1, β-Actin is the housekeeping gene *(Table 1)*.

Table 1. *Primers for SPS gene amplification*

Primer	Length of primer (bp)	TM	Primer sequence	Amplified length
SPS-1 forward primer	20	58	GGCAAGAAATAGAAGAGCAG	121bp
SPS-1 reverse primer	20	58	ACCATACGAGGCATAAAACG	
Actin-F forward primer	20	58	AGATGGTGTCAGCCACACTG;	210bp
Actin-R reverse primer	20	58	CGAGCTTCTCCTTCATGTCC	

Quantitative PCR systems and conditions

RT-PCR was used to determine the expression of SPS in sweet sorghum. RT-PCR was performed with primers according to *Table 1*. The RNA from all sample was reverse transcribed using QuantiTect Reverse Transcription Kid, primed with 50 pmol of reverse primer (Oligo dT) by following the manufacturer's protocol and carried out in a PTC 100 Peltier Thermal Cycler (MJ Research, Ramsey, MN, USA).

The PCR reaction was performed in a volume of 25 μL containing 10×Buffer (2.5 μL), 25 mg/mL $MgCl_2$ (2.5 μL), 100 μmol/L dNTP (0.5 μL), 5 U/μL Taq enzyme (0.5 μL), 0.2 μmol/L Forward Primer (1.0 μL), 0.2 μmol/L Reverse Primer (1.0 μL), cDNA template (1.0 μL), and sterile ddH_2O added up to the final volume.

This PCR program was performed with initial denaturation at 94 °C for 2 min, (denaturation 94 °C 30 s → annealing 53 °C 20 s → extension 72 °C 80 s) 32 cycles → extension 72 °C 10 min and saved at 4 °C (Yao et al., 2009; Li et al., 2007).

Detection of the expression of SPS using real-time quantitative PCR

Correlation analyses of SPS gene and housekeeping gene expression

In this experiment, Comparative Delta-delta Ct method was used for relative quantitative analyses of the target gene. Dilution of cDNA into 5 gradients (2^2, 2^4, 2^5, 2^6, 2^7), using SYBR Green I real-time PCR of target gene SPS and housekeeping gene β-actin. Create the standard curves for two genes and detect amplification efficiency. By calculating the difference between the two standard curves M (slope) is less than 0.1, it is proved that the relative quantitative analyses can be used.

http://www.aloki.hu ● ISSN 1589 1623 (Print) ● ISSN 1785 0037 (Online)
DOI: http://dx.doi.org/10.15666/aeer/1605_67316740
© 2018, ALÖKI Kft., Budapest, Hungary

Real-time PCR reaction system and conditions

The PCR program was performed with initial denaturation at 95 °C for 15 min, ten cycles of 94 °C for 20 s, 53 °C for 20 s, 72 °C for 80 s with 35 cycles and final 53-95 °C extension for dissolution curve program. Three replicates of each treatment were sampled to set no template negative control. The PCR product was analyzed and subjected to 1% agarose gel electrophoresis to determine the product specificity. The experimental data was processed and analyzed by SPSS software.

Results

Correlation analyses of SPS activity and sucrose content

By measuring the activity of SPS in the leaves of the male and female parents, and the F5 high sugar population and the low sugar population they hybridize, we can understand the changes of SPS among different groups in different periods. The variation of SPS was increased. At the mature stage, the activity of three sweet sorghum varieties (the female parent, high sugar individuals and low sugar individuals) reached the maximum of 14.86, 17.63, 13.76 μmol/h.g.fw, respectively. The SPS activity of the male parent at the mature stage was more minor than the heading stage. In spite of the SPS activity of four species was similar at the seedling stage, the large differences in SPS activity from the jointing stage. The SPS activity of the cross of the high and low sugar individuals grew linearly, the rate of increase in activity was faster than that of the parents and high sugar varieties had the highest SPS activity at mature stage. Analyses of correlation for sucrose and SPS activities in leaves in sorghum and sweet sorghum showed that sucrose was significant positive correlation with SPS activity ($R = 0.763$, $P < 0.01$) (*Fig. 1*).

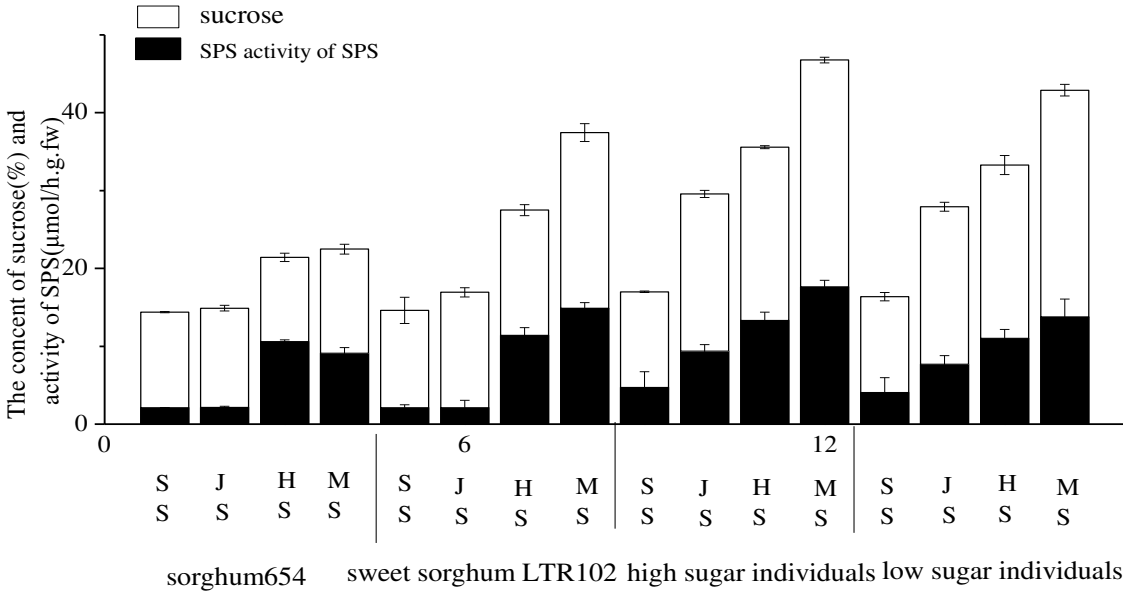

Figure 1. *The relationship between the activity of SPS and sucrose of different group at different growth stages (SS: seeding stages; JS: jointing stages; HS: heading stages; MS: mature stages)*

http://www.aloki.hu ● ISSN 1589 1623 (Print) ● ISSN 1785 0037 (Online)
DOI: http://dx.doi.org/10.15666/aeer/1605_67316740
© 2018, ALÖKI Kft., Budapest, Hungary

Analyses of extraction results of RNA

Agarose gel electrophoresis showed that the RNA extracted by the modified Trizol method had three bands, and the brightness of the 28S bands in the total RNA was about twice that of the 18S band, indicating that it was less degraded during the extraction process. The integrity of the extracted RNA was intact, indicating that the RNA was not contaminated and could be used as a template in the next experiment (*Fig. 2*).

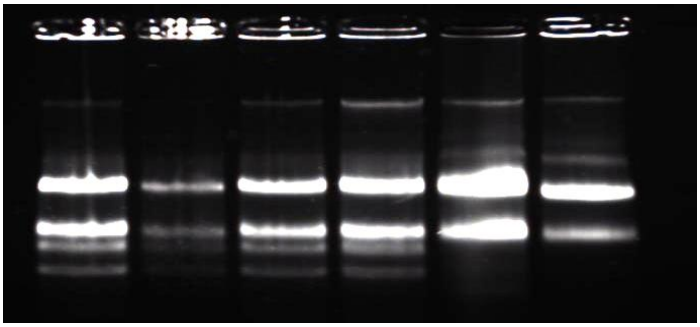

Figure 2. *1% agarose gel electrophoresis of total RNA extracted*

Qualitative analyses of SPS gene expression

At the seedling stage, parents, the SPS gene expression of F5 high and low sugar leaves (*Fig. 3*). In the figure, bands 1 to 4 were used as templates for the cDNAs of paternal, maternal, high-sugar and low-sugar individuals, and β-Actin was a PCR product amplified by primers. The fragment length was about 210 bp. The bands 5 and 6 were used as templates for the cDNAs of the paternal, maternal, high- and low-sugar individuals, and SPS-1 was a PCR product amplified by primers. The fragment length was 121 bp. At the seedling stage, the SPS gene has already begun to express.

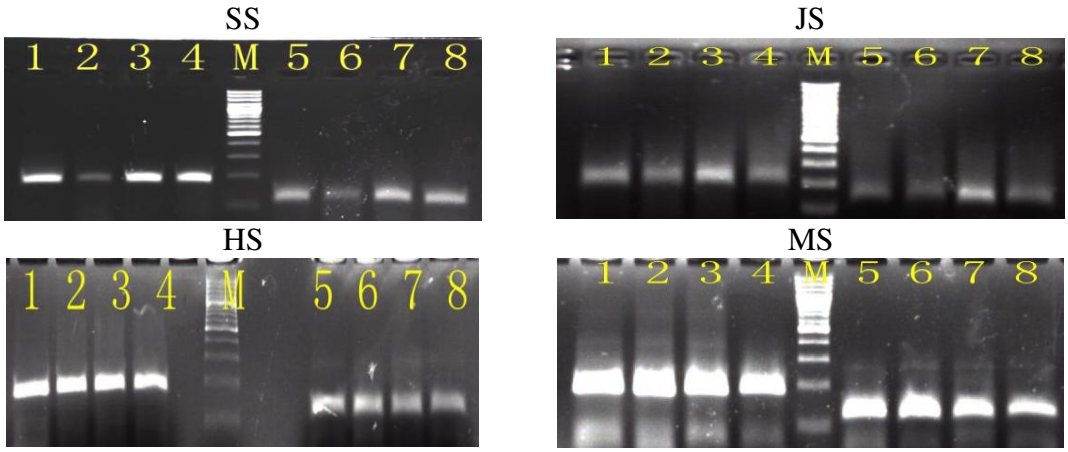

Figure 3. *The electrophoresis of SPS gene and housekeeping genes at developmental stages [top left: SS (seeding stages); top right: JS (jointing stages); bottom left: HS (heading stages); bottom right: MS (mature stages)]*

At the jointing stage, parents, the high sugar individuals showed strong expression, and the SPS gene expression of the paternal parent at the jointing stage was not as

http://www.aloki.hu ● ISSN 1589 1623 (Print) ● ISSN 1785 0037 (Online)
DOI: http://dx.doi.org/10.15666/aeer/1605_67316740
© 2018, ALÖKI Kft., Budapest, Hungary

strong as high sugar individuals. At the heading stage, the brightness and thickness of the target fragment were stronger than those of the previous two stages, indicating that the expression level of the SPS gene was greater than that at the seedling stage and the jointing stage. At the mature stage, the degree of brightness and thickness of the target fragment reached the maximum, which fully demonstrated that the expression level of SPS gene reached a large value during the mature stage (*Fig. 3*).

Using β-Actin and SPS-1 as primers, the desired target fragment can be amplified with clear. From *Figure 3* we can see that the SPS gene can be detected at the seedling stage. With the extension of the growth period, the expression level of SPS gene gradually increases, and the expression level reaches the maximum at the mature stage. This is similar to the variation of sucrose content, and it can be initially demonstrated that the expression of SPS affects the accumulation of sucrose. On the basis of RT-PCR detection was performed to more accurately understand the change pattern of SPS gene.

Quantitative analyses of SPS gene expression

Comparative analyses of quantitative expression of SPS gene at seedling stage

Relative quantitative analyses of SPS gene expression in the parental, F5 high and low sugar individuals at different growth stages was performed using the Comparative Delta-delta Ct method. In comparison with the relative concentration of SPS gene in female leaves, the relative concentration of SPS gene in the high-growth individuals at the seedling stage was higher, which was 1.59 times that of the parental SPS gene. The relative concentration of the parental SPS gene was the minimum and was only half of the parental SPS gene expression *(Table 2)*.

Table 2. *The comparison of different breeds of the SPS gene expression at seedling stage*

Replicate name	GOI CT	Norm. CT	Delta CT	Delta-delta CT	Relative conc.	Calibrator
Male parent	25.44	20.30	5.14	0.88	0.54	
Female parent	27.09	21.97	5.12	0.00	1.00	Yes
High sugar	26.15	21.70	4.45	-0.12	1.59	
Low sugar	25.59	20.51	5.07	0.36	1.03	

Comparative analyses of quantitative expression of SPS gene at jointing stage

At the jointing stage, the relative concentration of SPS gene in the female parent leaves was also used as a control. The parents, F5 high sugar and low sugar plants had little difference in expression at this stage. The highest SPS gene expression level in the high-sugar individual was only 1.25 times that of the minimum low-sugar individual (*Table 3*).

Table 3. *The comparison of different breeds of the SPS gene expression at jointing stage*

Replicate name	GOI CT	Norm. CT	Delta CT	Delta-delta CT	Relative conc.	Calibrator
Male parent	25.44	20.3	5.14	0.24	0.84	
Female parent	27.09	22.19	4.9	0	1.00	Yes
High sugar	26.37	21.45	4.83	-0.07	1.05	
Low sugar	25.59	20.52	5.07	0.18	0.88	

http://www.aloki.hu ● ISSN 1589 1623 (Print) ● ISSN 1785 0037 (Online)
DOI: http://dx.doi.org/10.15666/aeer/1605_67316740
© 2018, ALÖKI Kft., Budapest, Hungary

Comparative analyses of quantitative expression of SPS gene at heading stage

The relative concentration of SPS gene in the paternal leaves was the minimum, and the expression levels in the other three individuals were not significantly different. This indicated that the difference in expression levels of SPS genes between sweet sorghum and sorghum increased from the heading stage. The expression level of SPS gene in sweet sorghum was about 2 times higher than that of sorghum (*Table 4*).

Table 4. *The comparison of different breeds of the SPS gene expression at heading stage*

Replicate name	GOI CT	Norm. CT	Delta CT	Delta-delta CT	Relative conc.	Calibrator
Male parent	24.28	19.09	5.19	0.88	0.54	
Female parent	24.39	20.27	4.31	0.00	1.00	Yes
High sugar	24.46	20.62	4.19	-0.12	1.08	
Low sugar	24.62	19.96	4.66	0.36	0.78	

Comparative analyses of quantitative expression of SPS gene at mature stage

At the mature stage, the relative concentration of SPS gene in the female parent leaves was used as a control. Parents, F5 high-sugar and low-sugar populations had different expression levels at this stage. The expression level of the SPS gene in the maximum high-sugar individual was approximately 15 times that of the minimum low-sugar individual (*Table 5*).

Table 5. *The comparison of different breeds of the SPS gene expression at mature stage*

Replicate name	GOI CT	Norm. CT	Delta CT	Delta-delta CT	Relative conc.	Calibrator
Male parent	27.65	21.96	5.69	1.31	0.40	
Female parent	26.48	22.11	4.38	0.00	1.00	Yes
High sugar	26.07	24.28	1.80	-2.58	5.98	
Low sugar	28.52	23.80	4.73	0.35	0.78	

In summary, the relative concentration of maternal SPS gene was used as a control at each stage. The maximum expression level was high-sugar individuals, and the minimum expression level was the male parent. The order of SPS gene expression from high to low was high-sugar individuals, maternal, low-sugar group and paternal. At the mature stage, this change trend is similar to the accumulation pattern of sucrose and the change of SPS activity. It can be seen that the expression of SPS gene influences the accumulation of sucrose, and the higher the expression level of SPS gene, the higher the sucrose content.

In the test materials selected for this experiment, the male parent was the pure sorghum or hybrid sweet sorghum. At the maturing stage, the SPS gene expression was lowest in the male parent leaves, and it was up to 15 times higher than the high-sugar individual with the maximum expression. It is further explained that the difference in sucrose content is one of the causes of the difference in sugar content between ordinary sorghum and sweet sorghum.

http://www.aloki.hu ● ISSN 1589 1623 (Print) ● ISSN 1785 0037 (Online)
DOI: http://dx.doi.org/10.15666/aeer/1605_67316740
© 2018, ALÖKI Kft., Budapest, Hungary

Discussion and conclusion

Sweet sorghum is an important sugar crop. The accumulation of sweet sorghum sugar is mainly based on sucrose. Comparing the gene expression levels of SPS at different stages of different varieties of sweet sorghum has important significance for increasing the sugar content of sweet sorghum (Ye et al., 2012). In this experiment, the improved Trizol method can propose high-quality, non-polluting RNA easily and rapidly. The qualitative analyses of the sweet sorghum SPS gene revealed that the spectrum detected at the mature stage was the most distinct, and the SPS gene expression reached the maximum level during the mature period. The correlations between sucrose and SPS activity in leaves of sorghum and sweet sorghum were analyzed. The results showed that there was a significant positive correlation between sucrose and SPS activity, and it could be initially proved that SPS gene expression was a factor affecting sucrose content.

The experiment of RNA extraction must always be careful not to degrade RNA (Zong et al., 2011). Compared with conventional PCR technology, real-time fluorescence quantitative PCR technology has high sensitivity, specificity, reproducibility, fast and simple operation, and can directly perform qualitative analyses and quantitative analyses (Liu et al., 2011). Real-time PCR technology is a very effective experimental method and has been widely used in molecular biology, genetic engineering, medical diagnosis and other fields (Ren et al., 2007). In this experiment, by analyzing the correlation between SPS gene and housekeeping gene expression, the dissolution profiles of the two genes were single peaks, indicating that the specificity of the reaction and accurate in the PCR amplification process and there are no non-specific amplifications and primer dimers. It is an ideal dissolution curve, indicating that the selected primers can be applied to Comparative Delta-delta Ct method relative quantitative analyses of parental, F5 high glucose and low sugar populations at different growth stages of SPS gene expression.

By comparing the changes of the relative concentrations of SPS gene in female parent at different growth stages, it can be seen that the change pattern of SPS gene in sweet sorghum is consistent with the variation law of sucrose content and SPS activity, and both of them reach the maximum value at mature stage. Yekai et al. (2012) showed that the highest value of the sorghum SPS enzyme activity appeared in the maturity stage of No. 9, which was consistent with this experiment. The correlation analyses of sucrose and SPS gene relative concentrations in leaves of sorghum and sweet sorghum showed that the relative concentration of sucrose and SPS gene was positively correlated. By understanding the changing pattern of SPS genes and providing theoretical basis for determining the selection and breeding of new sweet sorghum varieties. It is great significance to understand the laws of sugar accumulation in sweet sorghum, the principle of SPS, metabolism and regulation. It is also possible to breed sweet sorghum varieties with high sugar content to guide production practices and have good reference for other crops.

Acknowledgements. The research was partly supported by Major incubating project of Shenyang Normal University.

http://www.aloki.hu ● ISSN 1589 1623 (Print) ● ISSN 1785 0037 (Online)
DOI: http://dx.doi.org/10.15666/aeer/1605_67316740
© 2018, ALÖKI Kft., Budapest, Hungary

REFERENCES

[1] ElSayed, A. E., Boulila, M., Rafudeen, M. S. (2013): Investigation into the expression of sucrose transporters and sucrose phosphate synthase mRNA in different plant species. – Agricultural Research 2(1): 31-42.
[2] Guo, H. X., Wang, F. Y., Li, S., Miao, Y. F. (2016): Effect of different planting density and nitrogen application on growth, biomass and sugar content of sweet sorghum. – Jiangsu Agricultural Sciences 44(4): 152-154.
[3] Hou, Y. (2009): Research progress and application of fluorescence quantitative PCR. – Guizhou Agricultural Sciences 37(6): 29-32.
[4] Jiang, H., Hu, R. F., Zou, J. Q., Li, Y. Y. (2012): Research progress of biomass energy sweet sorghum. – Heilongjiang Agricultural Sciences 2: 139-141.
[5] Li, Y. Y., Liu, Y., Tao, S. Y. (2007): Application of RAPD technology in genome analysis of sweet sorghum varieties. – Journal of Shenyang Normal University (Natural Science) 25(4): 499-502.
[6] Li, Y. Y., Mao, X., Yu, X., Zhang, Y. H., Ma, L. J., Li, X. M., Ma, C. Y., Hao, L. (2014): Development of a high sugar trait-related SCAR marker in sweet sorghum. – International Journal of Agriculture & Biology 3: 668-670.
[7] Liu, C. H. (2011): Research progress and application of real-time fluorescence quantitative PCR. – China Practical Medicine 6(31): 238-240.
[8] Liu, Y. (2009): Cloning of Genes of the Key Enzymes Involved in Sugar Accumulation and Development of Functional Markers in Sweet Sorghum. – Institute of Crop Sciences, CAAS, Beijing China.
[9] Luo, S. (2012): Research progress of sweet sorghum. – Technology and Market 19(4): 292.
[10] Okamura, M., Aoki, N., Hirose, T., Yonekura, M., Ohto, C., Ohsugi, R. (2011): Tissue specificity and diurnal change in gene expression of the sucrose phosphate synthase gene family in rice. – Plant Science 181: 159-166.
[11] Park, J.-Y., Canam, T., Kang, K.-Y., Unda, F., Mansfield, S. D. (2009): Sucrose phosphate synthase expression influences poplar phenology. – Tree Physiology 29: 937-946.
[12] Rao, P. S., Kumar, C. G., Reddy, B. V. S. (2013): Sweet Sorghum: From Theory to Practice. – In: Rao, P. S., Kumar, C. G. (eds.) Characterization of Improved Sweet Sorghum Cultivars. – Springer Briefs in Agriculture, Springer, India, pp: 1-15.
[13] Ren, G. K., Wang, Y. Y. (2007): Research progress of real-time fluorescence quantitative PCR. – Clinical Medicine Practice Journal 16(4): 243-245.
[14] Taneja, D., Das, N. (2014): Molecular cloning, sequence, and expression studies of sucrose-phosphate synthase in the potato (Solanum tuberosum L.) cultivars. – Acta Physiol Plant 36: 2253-2269.
[15] Tang, S. Y., Xi, Z. X., Xie, Q. (2012): Sweet sorghum in the development of bio-energy industry. – Current Biotechnology 2(2): 81-86.
[16] Yao, Y., Chen, Y. S., Li, F. S. (2009): Optimization of RAPD-PCR system and amplification program of dwarf caster. – Chin J Biologicals March 22(3): 284-287.
[17] Ye, K, Zaitunigui Kuerban, Chen, W. (2012): Research on activity of SS and SPS in sweet sorghum sowed on different dates. – Xinjiang Agricultural Science 49(10): 1874-1880.
[18] Zhang, G. Q., Ge, Y. B., Zhang, Z. Y., He, C. G. (2018): A Review of drought resistance of sorghum. – Gansu Agr. Sci. and Techn 6: 67-72.
[19] Zhang, X. Y., Gao, Y. N. (2004): To design PCR primers with Oligo 6 and Primer Premier 5. – China Journal of Bioinformatics 2: 15-46.
[20] Zhao, H., Zhai, G. W., Zou, G. H. (2015): Comparison of substance accumulation and distribution changes between sweet sorghum and ordinary sorghum. – Acta Agriculturae Zhejiangensis 27(1): 7-11.
[21] Zong, C. Z. (2011): Analysis of factors affecting RNA isolation qualities. – Journal of Guangxi Agriculture 26(1): 31-34.

http://www.aloki.hu ● ISSN 1589 1623 (Print) ● ISSN 1785 0037 (Online)
DOI: http://dx.doi.org/10.15666/aeer/1605_67316740
© 2018, ALÖKI Kft., Budapest, Hungary

ALLELOPATHIC POTENTIAL OF *LANTANA CAMARA* AGAINST SELECTED WEEDS OF WHEAT CROP

ANWAR, T.[1] – ILYAS, N.[1] – QURESHI, R.[1*] – MAQSOOD, M.[1] – MUNAZIR, M.[2] – ANWAR, P.[3] – RAHIM, B. Z.[4] – ANSARI, K. A.[5] – PANNI, M. K.[6]

[1]*Department of Botany, Pir Mehr Ali Shah Arid Agriculture University Murree Road, Shamsabad, Rawalpindi 46300, Pakistan*

[2]*Department of Botany, Government College Women University, Sialkot, Pakistan*

[3]*Department of Biochemistry and Molecular Biology, University of Sialkot, Sialkot, Pakistan*

[4]*Department of Botany, Baluchistan University, Quetta 87500, Baluchistan, Pakistan*

[5]*Department of Botany, Shah Abdul Latif University, Khairpur, Sindh, Pakistan*

[6]*Institiue of Biotechnology and Genetic Engineering (IBGE), The University of Agriculture Peshawar 25130, Pakistan*

**Corresponding author*
e-mail: rahmatullahq@yahoo.com

(Received 6th Jul 2018; accepted 31st Aug 2018)

Abstract. The current study was aimed at screening allelopathic potential of *Lantana camara* L. against some noxious weeds (i.e. *Phalaris minor, Avena fatua, Chenopodium album, Euphorbia helioscopia* and *Rumex dentatus*) of wheat crop. The screening test of these weeds was carried out in laboratory on filter paper, soil and agar by three solvent extracts (viz., aqueous, hexane and methanolic) and sandwich method. The methanolic *L. camara* extract significantly suppressed germination percentage of *E. helioscopia*, *P. minor R. dentatus* and *A. fatua* measuring at 65%, 63%, 61% and 60%, respectively. Likewise, *L. camara* significantly suppressed radical length of *A. fatua*, *P. minor and C. album* with 54%, 53% and 52%, respectively compared to the control. Besides, plumule length of *E. helioscopia*, *C. album, R. dentatus* and *A. fatua* was also inhibited at 56%, 55%, 53% and 53%, respectively by *L. camara* methanolic extract. It can be concluded that *L. camara* methanolic extract significantly reduced seed germination, radical and plumule length of selected weeds and have potential to be used in further detailed evaluation for searching bioherbicide from this plant.
Keywords: *allelopathic activity, bio-herbicide, filter paper, noxious weed, sandwich method, screening test, wheat*

Introduction

Wheat (*Triticum aestivum* L.) that belongs to family Poaceae, is one of the most important cereal crops of the world. It provides human nutrition to the most of human populations. Weeds are growing in cultivated crops and compete for light, moisture, other vital elements of nutrition and space and cause low quality and less productivity with raised costs of production (Arafat et al., 2015). Controlling weeds through traditional methods is time consuming with more labor cost. While weed control through synthetic chemicals, is expensive and hazardous that also cause environmental pollution (Dallali et al., 2017). This situation necessitates developing alternate weed management strategies (Thi et al., 2008). Certain plants produce many chemicals which are released by certain processes like, exudation, leaching and

http://www.aloki.hu ● ISSN 1589 1623 (Print) ● ISSN 1785 0037 (Online)
DOI: http://dx.doi.org/10.15666/aeer/1605_67416760
© 2018, ALÖKI Kft., Budapest, Hungary

decomposition, etc. These chemicals can be obtained from different parts of certain plants like, flower, roots, stem and leaves. Such chemicals become a source of allelopathy, commonly called as allelochemicals. Allelopathy is a form of plant interference that can significantly influence ecosystem and agro ecosystem dynamics (Michelangelo et al., 2016). Allelochemicals come from the class of secondary metabolites. These are produced as byproducts in the primary metabolic ways of the plants (Anwar et al., 2013). Like many other natural compounds, these chemicals have the capacity of producing wide array of biological effects and can be quite useful for weed control processes as well as agriculture systems (Zhou et al., 2004).

Lantana camara L. belongs to Verbenaceae family. This plant possessed certain aromatic compounds which can inhibit early growth and seed germination of adjacent plant by outcompeting for soil nutrients and fluctuating micro environment by producing dense thickets (Dobhal et al., 2010). Keeping this in view, this study was undertaken for evaluating allelopathic activity of *L. camara* against some major weeds (viz., *Phalaris minor, Avena fatua, Chenopodium album, Euphorbia helioscopia* and *Rumex dentatus*) of wheat crop.

Materials and methods

Collection and mechanical processing of L. camara

This research was carried out at Plant Physiology Laboratory, Department of Botany, Pir Mehr Ali Shah Arid Agriculture University, Rawalpindi (PMAS-AAUR), Pakistan. The mature leaves of *L. camara* were collected from district Rawalpindi (73° 02' E longitude and 33° 36' N latitude, 508 m above sea level), Punjab, Pakistan and washed for several times under running tap water to remove dust. The same leaves were dried in blotting paper for 4 weeks in shade at room temperature (20-25 °C). The dried leaves were crushed using heavy duty blender (warring Lab.), to make fine powder, passed through mesh size 2 mm and kept in air tight plastic zip lock bags separately at 4 °C (Anwar et al., 2013).

Procurement and surface sterilization of test species seeds

Seeds of some noxious weeds sensitive to herbicide (Shahid et al., 2006) such as *Avena fatua*, *Chenopodium album, Euphorbia helioscopia*, *Phalaris minor* and *Rumex dentatus* and wheat (Wafaq-2001) were procured from the Barani Agricultural Research Institute (BARI), Chakwal (72.7211° E longitude and 32.9309° N latitude), District Rawalpindi, Punjab, Pakistan. These weeds are reported to be the most densely populated weeds of wheat crop (Qureshi and Bhatti, 2001; Qureshi et al., 2009). Seeds were surface sterilized with 2% (w/v) solution of Sodium hypochlorite (NaOCl) for 5-8 min. After disinfection, the seeds were washed several times with distilled water (Anwar et al., 2016).

Studied parameters

Subsequent three growth parameters were used for screening allelopathic potential as follows:

a. Germination percentage
b. Radical length (cm)
c. Plumule length (cm)

http://www.aloki.hu ● ISSN 1589 1623 (Print) ● ISSN 1785 0037 (Online)
DOI: http://dx.doi.org/10.15666/aeer/1605_67416760
© 2018, ALÖKI Kft., Budapest, Hungary

Aqueous extract preparation

An aliquot (10 g) of dried leaf powder of *L. camara* was soaked in 100 ml distilled water in a flask and agitated at room temperature (20-25 °C) for 24 h on an orbital shaker (160 rpm). The extract was strained through muslin cloth and finally filtered through Whatman filter paper No. 1. Aqueous extract was obtained as filtrate of the mixture and final volume was attuned to 100 ml, this gives 10% water extract (Maharjan et al*.,* 2007). This stock solution was then diluted with distilled water to prepare the different concentration of the extract i.e. T_1 (100%), T_2 (75%), T_3 (50%) after Sahu and Devkota (2013). The control was distilled water (0%), indicated as T_4. The extract was stored at 4 °C in pre-disinfected flasks. To evade adulteration and forthcoming chemical modifications, the extracts were ensured to be used within 3-4 days (Anwar et al., 2017a).

Hexane extract preparation

An aliquot (10 g) of dried leaf powder of *L. camara* was mixed with hexane (0.5 L) repeated three times for 6 h on shaker. This extract was filtered, concentrated and dried over a rotary evaporator in pre-weighed flask. The obtained residue was 6.14 g. The stock solution was then diluted with hexane to prepare three concentrations i.e. T_1 (100%), T_2 (75%), T_3 (50%) and T_4 (0% control). These stored at 4 °C in pre-sterilized flasks (Sahu and Devkota, 2013).

Methanolic extract preparation

An aliquot (10 g) of dried leaf powder of *L. camara* placed on shaker with methanol (to extract polar compounds) (0.5 L) repeated three time for 6 h on shaker. This extract was filtered, concentrated, and dried over a rotary evaporator in pre-weighed flask. The obtained residue was 25.29 g. The stock solution was than diluted with methanol to prepare three concentrations i.e. T_1 (100%), T_2 (75%), T_3 (50%) and T_4 (0% control). These stored at 4 °C in pre-sterilized flasks (Sahu and Devkota, 2013).

Bioassay techniques

An aliquot (15 ml) of *L. camara* extract added on 25 g soil per Petri dish and 5 ml extract was added on filter paper per Petri dish while distilled water, hexane and methanol used as control in aqueous, hexane and methanolic extraction respectively. Ten seeds of selected test species were used per Petri dish. Each treatment was replicated for five times. The Petri dishes were wrapped with squash tape, enclosed with Aluminum foil and incubated in the growth chamber (NTS Model MI-25S) at room temperature (20-25 °C) for 15 days. The germination percentages, lengths of radical and plumule were calculated of each test species by comparing with control (Khan et al., 2008).

Sandwich method

The sandwich method was followed after Fujii et al. (2003, 2004). Five ml of 0.75% (w/v) agar (Nalge Nunc Intl., Roskilde, Denmark, gelling temperature 30-31 °C) was poured in each of the six-well (10 cm^2 area /well) into multi-dish plastic plate. The agar solution was left for solidification. *L. camara* leaf powder @ 10 and 50 mg were placed in wells of the plate and were roofed by a thin layer of 0.75% (w/v) agar. After solidification, 10 seeds of each test species were placed on agar gel in each well of the plate. The multi-well plastic plates were then wrapped with the plastic tape and incubated

http://www.aloki.hu ● ISSN 1589 1623 (Print) ● ISSN 1785 0037 (Online)
DOI: http://dx.doi.org/10.15666/aeer/1605_67416760
© 2018, ALÖKI Kft., Budapest, Hungary

in the growth chamber (NTS Model MI-25S) at room temperature (20-25 °C) for 15 days. In the control treatment, only agar gel without dried leaves powder was used as a seed bed for test species seeds. Each treatment was replicated five times. The germination percentages, lengths of radical and plumule for each test species were calculated by comparing with control. An aliquot (10 mg) of dried leaf powder of *L. camara* added on filter paper along with 5 ml distilled water per Petri dish while an aliquot (50 mg) of dried leaf powder of *L. camara* added on 25 g soil along with 15 ml distilled water per Petri dish (Raana et al., 2012). Ten surface sterilized seeds of test species were placed to each sterilized Petri plate. The Petri dishes were wrapped with squash tape, enclosed with Aluminium foil and incubated in the growth chamber (NTS Model MI-25S) at room temperature (20-25 °C) for 15 days. The germination percentages, lengths of radical and plumule were calculated of each test species by comparing with control (Anwar et al., 2017b).

Statistical analysis

A completely randomized design (CRD) with five replications was used for the experiments. The statistical analysis was completed by STATISTIX 9 and means were separated by using Fisher's protected LSD test (Nekonam et al., 2014).

Results

Allelopathic potential of L. camara aqueous extract

Germination percentage

The results revealed that *L. camara* aqueous extract significantly inhibited germination percentage of *R. dentatus* (58%), followed by *E. helioscopia* (56%), *A. fatua* (57%) and *P. minor* (55%) on filter paper, whereas, no significant effect on germination percentage of *T. aestivum* and *C. album* (*Table 1*). The aqueous extract on soil significantly inhibited seed germination of *E. helioscopia* (64%), followed by *P. minor* (63%), *R.* dentatus (61%) and *A. fatua* (60%) as compared to control (*Table 2*). The results further indicated that maximum (96% germination was observed for *T. aestivum* and *C. album* (*Table 1*). Besides, minimum germination was noted for *R. dentatus* (42%) and *E. helioscopia* (36%) on filter paper and soil, respectively (*Tables 1* and *2*). The statistics also recommended that germination percentage reduction of the *R. dentatus, E. helioscopia*, *A. fatua* and *P. minor* was concentration dependent (*Fig. 1a*).

Table 1. *Allelopathic effect of L. camara aqueous extract (AE) on germination percentage of test species on filter paper*

Treatments	Test species					
	T. aestivum	***A. fatua***	***R. dentatus***	***P. minor***	***E. helioscopia***	***C. album***
$T_{1\ AE}$	86^{a}	38^{d}	36^{d}	37^{d}	39^{d}	76^{a}
$T_{2\ AE}$	88^{a}	62^{c}	55c	56^{c}	59^{c}	78^{a}
$T_{3\ AE}$	89^{a}	76^{b}	71^{b}	68^{b}	75^{b}	79^{a}
$T_{4\ AE}$	90^{a}	89^{a}	86^{a}	82^{a}	88^{a}	80^{a}
LSD	17.902	29.46	18.32	19.23	17.957	21.13
F-value	12.13*	18.29*	14.85*	31.44*	31.00*	17.61*

Means followed by different letters within one column differ significantly at P < 5%
*Significant at P < 1%

http://www.aloki.hu ● ISSN 1589 1623 (Print) ● ISSN 1785 0037 (Online)
DOI: http://dx.doi.org/10.15666/aeer/1605_67416760
© 2018, ALÖKI Kft., Budapest, Hungary

Table 2. *Allelopathic effect of L. camara aqueous extract (AE) on germination percentage of test species on soil*

Treatments	Test species					
	T. aestivum	***A. fatua***	***R. dentatus***	***P. minor***	***E. helioscopia***	***C. album***
$T_{1\ AE}$	87^{a}	36^{d}	34^{d}	31^{d}	32^{d}	77^{a}
$T_{2\ AE}$	89^{a}	52^{c}	52^{c}	49^{c}	51^{c}	79^{a}
$T_{3\ AE}$	90^{a}	71^{b}	69^{b}	60^{b}	69^{b}	80^{a}
$T_{4\ AE}$	91^{a}	90^{a}	87^{a}	83^{a}	89^{a}	81^{a}
LSD	18.608	14.197	19.778	17.604	14.541	18.12
F-value	10.89**	42*	13.52*	14.67*	43.98*	14.65*

Means followed by different letters within one column differ significantly at $P < 5\%$
*Significant at $P < 1\%$

Radical length

The data revealed that the highest radical length inhibition activity was exhibited by *A. fatua* (52%), *P. minor* (51%) and *C. album* (49%) in *L. camara* aqueous extract on filter paper. The results further indicated that extract on soil caused significant radical length reduction of *A. fatua* (54%), *P. minor* (53%) and *C. album* (52%) as compared to control. While the radical length of *T. aestivum, R. dentatus* and *E. helioscopia* remained unaffected. The results also illustrated that minimum radical length was noted for *A. fatua* i.e. 48% and 46% on filter paper and soil, respectively (*Tables 3* and *4*). The maximum radical length (97%) was noted for *T. aestivum, R. dentatus* and *E. helioscopia* (*Fig. 1b*).

Plumule length

The data obtained exhibited that the aqueous extract of *L. camara* significantly inhibited the plumule length of *E. helioscopia* (52%), *A. fatua* (50%), *R. dentatus* (50%) and *C. album* (50%) as compared to control on filter paper. There was no significant effect on plumule elongation of *T. aestivum and P. minor*. Likewise, *L. camara* aqueous extract significantly inhibited plumule length of *E. helioscopia* (56%), *C. album* (55%), *R. dentatus* (53%) and *A. fatua* (53%) in soil. The statistical data concluded that minimum plumule length was noted for *E. helioscopia* i.e. 48% and 44% on filter paper and soil, respectively (*Tables 5* and *6*). The statistical figures also proposed that maximum plumule length (96%) was noted for *T. aestivum and P. minor* (*Fig. 1c*).

Table 3. *Allelopathic effect of L. camara aqueous extract (AE) on radical length (cm) of test species on filter paper*

Treatments	Test species					
	T. aestivum	***A. fatua***	***R. dentatus***	***P. minor***	***E. helioscopia***	***C. album***
$T_{1\ AE}$	9.01^{a}	4.46^{d}	8.11^{a}	4.62^{d}	7.15^{a}	4.10^{d}
$T_{2\ AE}$	9.05^{a}	6.71^{c}	8.16^{a}	6.45^{c}	7.19^{a}	5.52^{c}
$T_{3\ AE}$	9.05^{a}	8.02^{b}	8.19^{a}	7.92^{b}	7.22^{a}	6.78^{b}
$T_{4\ AE}$	9.11^{a}	9.25^{a}	8.21^{a}	9.42^{a}	7.28^{a}	8.11^{a}
LSD	1.7087	3.0879	1.0971	0.6573	1.0360	1.0027
F-value	47.38*	18.78*	126.95*	309.12*	128.48*	92.48*

Means followed by different letters within one column differ significantly at $P < 5\%$
*Significant at $P < 1\%$

http://www.aloki.hu ● ISSN 1589 1623 (Print) ● ISSN 1785 0037 (Online)
DOI: http://dx.doi.org/10.15666/aeer/1605_67416760
© 2018, ALÖKI Kft., Budapest, Hungary

Table 4. *Allelopathic effect of L. camara aqueous extract (AE) on radical length (cm) of test species on soil*

Treatments	Test species					
	T. aestivum	***A. fatua***	***R. dentatus***	***P. minor***	***E. helioscopia***	***C. album***
$T_{1\ AE}$	9.14^{a}	4.31^{d}	8.12^{a}	4.52^{d}	7.19^{a}	4.01^{c}
$T_{2\ AE}$	9.19^{a}	5.02^{c}	8.27^{a}	5.65^{b}	7.33^{a}	4.09^{c}
$T_{3\ AE}$	9.21^{a}	7.06^{b}	8.31^{a}	6.29^{b}	7.43^{a}	5.99^{b}
$T_{4\ AE}$	9.25^{a}	9.34^{a}	8.43^{a}	9.65^{a}	7.49^{a}	8.37^{a}
LSD	3.9879	1.8106	1.1918	1.0912	1.0634	0.8063
F-value	19.78*	52.46*	98.97*	83.01*	74.89*	126.70*

Means followed by different letters within one column differ significantly at $P < 5\%$
*Significant at $P < 1\%$

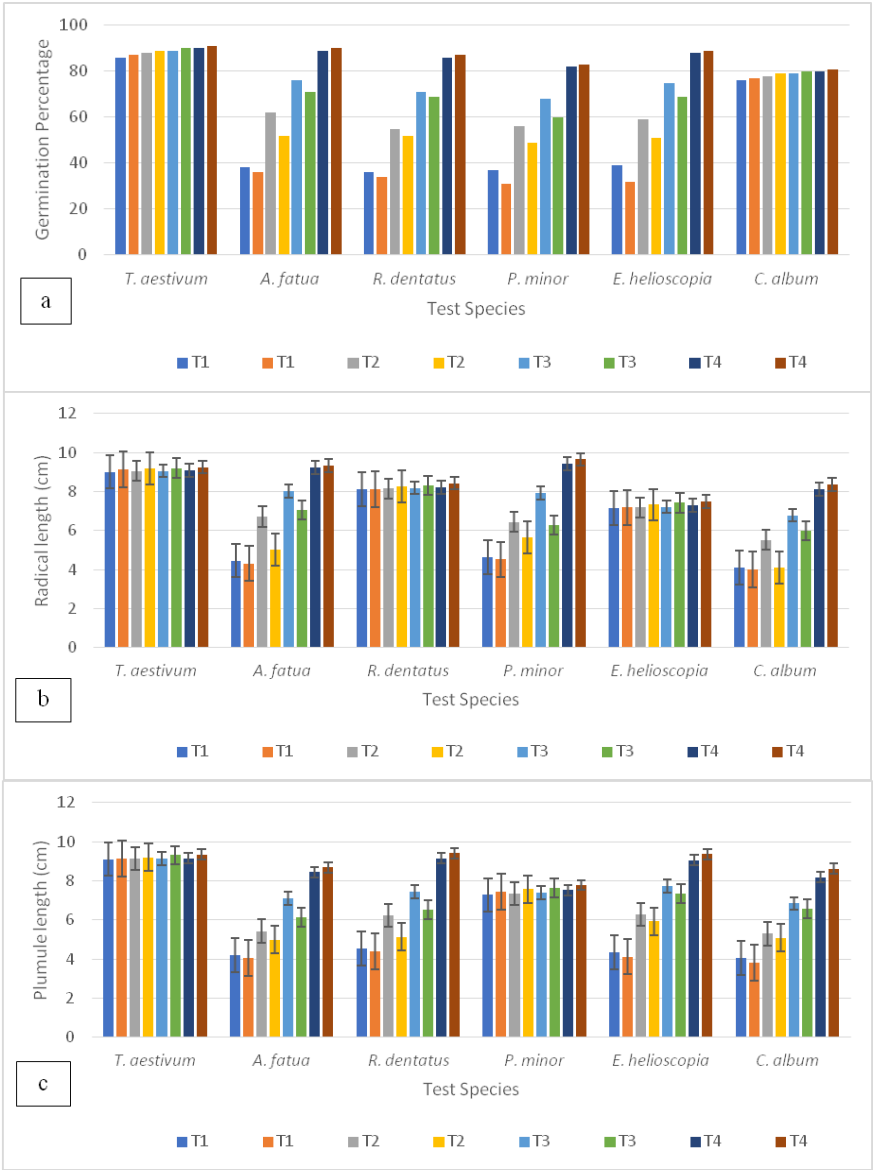

Figure 1. *Allelopathic potential of L. camara aqueous extract against test species on filter paper (FP) and soil (S) on: (a) germination percentage, (b) radical length, (c) plumule length*

http://www.aloki.hu ● ISSN 1589 1623 (Print) ● ISSN 1785 0037 (Online)
DOI: http://dx.doi.org/10.15666/aeer/1605_67416760
© 2018, ALÖKI Kft., Budapest, Hungary

Table 5. *Allelopathic effect of L. camara aqueous extract (AE) on plumule length (cm) of test species on filter paper*

Treatments	Test species					
	T. aestivum	***A. fatua***	***R. dentatus***	***P. minor***	***E. helioscopia***	***C. album***
$T_{1\ AE}$	9.11^{a}	4.20^{d}	4.53^{d}	7.28^{a}	4.33^{d}	4.06^{d}
$T_{2\ AE}$	9.13^{a}	5.43^{c}	6.24^{c}	7.33^{a}	6.28^{c}	5.29^{c}
$T_{3\ AE}$	9.15^{a}	7.09^{b}	7.46^{b}	7.41^{a}	7.73^{b}	6.84^{b}
$T_{4\ AE}$	9.16^{a}	8.45^{a}	9.15^{a}	7.53^{a}	9.06^{a}	8.19^{a}
LSD	1.3210	0.6647	1.0678	0.9468	0.6294	2.9953
F-value	45.63*	238.96*	97.24*	37.04*	197.36*	13.53*

Means followed by different letters within one column differ significantly at $P < 5\%$
*Significant at $P < 1\%$

Table 6. *Allelopathic effect of L. camara aqueous extract (AE) on plumule length (cm) of test species on soil*

Treatments	Test species					
	T. aestivum	***A. fatua***	***R. dentatus***	***P. minor***	***E. helioscopia***	***C. album***
$T_{1\ AE}$	9.13^{a}	4.06^{c}	4.38^{c}	7.43^{a}	4.12^{d}	3.81^{d}
$T_{2\ AE}$	9.21^{a}	4.98^{c}	5.12^{c}	7.58^{a}	5.92^{c}	5.09^{c}
$T_{3\ AE}$	9.32^{a}	6.14^{b}	6.52^{b}	7.64^{a}	7.34^{b}	6.58^{b}
$T_{4\ AE}$	9.34^{a}	8.68^{a}	9.41^{a}	7.78^{a}	9.37^{a}	8.62^{a}
LSD	2.9853	1.2127	0.6756	0.6851	0.8319	0.7647
F-value	12.53*	70.45*	117.35*	245.78*	209.87*	237.96*

Means followed by different letters within one column differ significantly at $P < 5\%$
*Significant at $P < 1\%$

Allelopathic potential of L. camara hexane extract

Germination percentage

There was significant reduction of germination of *E. helioscopia* (35%), followed by *P. minor* (33%) and *A. fatua* (32%) on filter paper (*Table 7*), whereas, no significant effect on the germination of *T. aestivum, R. dentatus* and *C. album,* showing resistance to the extract. The data illustrated that the highest seed germination inhibition was noted for *P. minor* (40%), followed by *A. fatua* (39%) and *E. helioscopia* (38%) by the incorporation of *L. camara* hexane extract into soil. The maximum (97%) germination noted for *T. aestivum, R. dentatus* and *C. album*. In the present study, minimum germination was noted for *E. helioscopia* (65%) and *P. minor* (60%) on filter paper and soil, respectively (*Tables 7* and *8*). The statistics also recommended that allelopathic inhibitory effect was concentration dependent for *E. helioscopia*, *P. minor* and *A. fatua* with concentration increase, suppression potential was gradually enhanced (*Fig. 2a*).

Radical length

The experimental results of the current study indicated that the highest radical length inhibition activity was exhibited by *A. fatua* (38%) and *R. dentatus* (34%) in *L. camara* hexane extract on filter paper. statistical data concluded that hexane extract on soil

http://www.aloki.hu ● ISSN 1589 1623 (Print) ● ISSN 1785 0037 (Online)
DOI: http://dx.doi.org/10.15666/aeer/1605_67416760
© 2018, ALÖKI Kft., Budapest, Hungary

caused significant radical length reduction of *A. fatua* (40%) and *R. dentatus* (39%) as compared to control. The statistics also recommended that radical length of *T. aestivum, P. minor, E. helioscopia* and *C. album* remained unaffected. The results also illustrated that minimum radical length was noted for *A. fatua* i.e. 62% and 66% on filter paper and soil, respectively (*Tables 9* and *10*). The maximum radical length (96%) was noted for *T. T. aestivum, P. minor, E. helioscopia* and *C. album* (*Fig. 2b*).

Table 7. *Allelopathic effect of L. camara hexane extract (HE) on germination percentage of test species on filter paper*

Treatments	Test species					
	T. aestivum	***A. fatua***	***R. dentatus***	***P. minor***	***E. helioscopia***	***C. album***
$T_{1\ HE}$	86^{a}	63^{c}	82^{a}	55^{c}	60^{c}	76^{a}
$T_{2\ HE}$	88^{a}	71^{c}	83^{a}	59^{c}	67^{c}	78^{a}
$T_{3\ HE}$	89^{a}	82^{b}	84^{a}	71^{b}	80^{b}	79^{a}
$T_{4\ HE}$	90^{a}	93^{a}	85^{a}	82^{a}	92^{a}	80^{a}
LSD	19.708	18.890	17.67	19.60	17.435	29.778
F-value	11.89**	17.19*	32.71*	31.19*	21.97*	23.52*

Means followed by different letters within one column differ significantly at $P < 5\%$
*Significant at $P < 1\%$

Table 8. *Allelopathic effect of L. camara hexane extract (HE) on germination percentage of test species on soil*

Treatments	Test species					
	T. aestivum	***A. fatua***	***R. dentatus***	***P. minor***	***E. helioscopia***	***C. album***
$T_{1\ HE}$	89^{a}	58^{d}	84^{a}	50^{c}	58^{c}	78^{a}
$T_{2\ HE}$	90^{a}	68^{c}	85^{a}	58^{c}	64^{c}	80^{a}
$T_{3\ HE}$	91^{a}	80^{b}	86^{a}	68^{b}	74^{b}	81^{a}
$T_{4\ HE}$	92^{a}	95^{a}	87^{a}	84^{a}	94^{a}	82^{a}
LSD	13.554	17.510	16.580	14.744	14.08	19.13
F-value	13.63*	22.36*	51.38*	21.04*	38.81*	31.14*

Means followed by different letters within one column differ significantly at P < 5%
*Significant at P < 1%

Table 9. *Allelopathic effect of L. camara hexane extract (HE) on radical length (cm) of test species on filter paper*

Treatments	Test species					
	T. aestivum	***A. fatua***	***R. dentatus***	***P. minor***	***E. helioscopia***	***C. album***
$T_{1\ HE}$	8.08^{a}	5.63^{d}	5.41^{c}	7.14^{a}	7.06^{a}	8.12^{a}
$T_{2\ HE}$	8.11^{a}	6.78^{c}	6.01^{c}	7.17^{a}	7.08^{a}	8.29^{a}
$T_{3\ HE}$	8.15^{a}	7.89^{b}	7.11^{b}	7.19^{a}	7.10^{a}	8.31^{a}
$T_{4\ HE}$	8.18^{a}	9.04^{a}	8.15^{a}	7.22^{a}	7.11^{a}	8.33^{a}
LSD	2.3332	1.4291	0.8679	1.2428	0.7319	0.8297
F-value	27.95*	23.83*	81.03*	29.85*	219.87*	222.41*

Means followed by different letters within one column differ significantly at P < 5%
*Significant at P < 1%

http://www.aloki.hu ● ISSN 1589 1623 (Print) ● ISSN 1785 0037 (Online)
DOI: http://dx.doi.org/10.15666/aeer/1605_67416760
© 2018, ALÖKI Kft., Budapest, Hungary

Table 10. *Allelopathic effect of L. camara hexane extract (HE) on radical length (cm) of test species on soil*

Treatments	Test species					
	T. aestivum	***A. fatua***	***R. dentatus***	***P. minor***	***E. helioscopia***	***C. album***
$T_{1\ HE}$	8.13^{a}	5.54^{c}	5.01^{c}	7.13^{a}	7.12^{a}	8.22^{a}
$T_{2\ HE}$	8.19^{a}	6.48^{c}	5.89^{c}	7.26^{a}	7.14^{a}	8.39^{a}
$T_{3\ HE}$	8.23^{a}	7.61^{b}	6.99^{b}	7.31^{a}	7.17^{a}	8.41^{a}
$T_{4\ HE}$	8.28^{a}	9.24^{a}	8.25^{a}	7.32^{a}	7.21^{a}	8.43^{a}
LSD	2.4502	0.9978	0.7720	1.1434	0.8468	1.1019
F-value	9.54**	72.85*	102.44*	72.9*	36.04*	86.41*

Means followed by different letters within one column differ significantly at P < 5%
*Significant at P < 1%

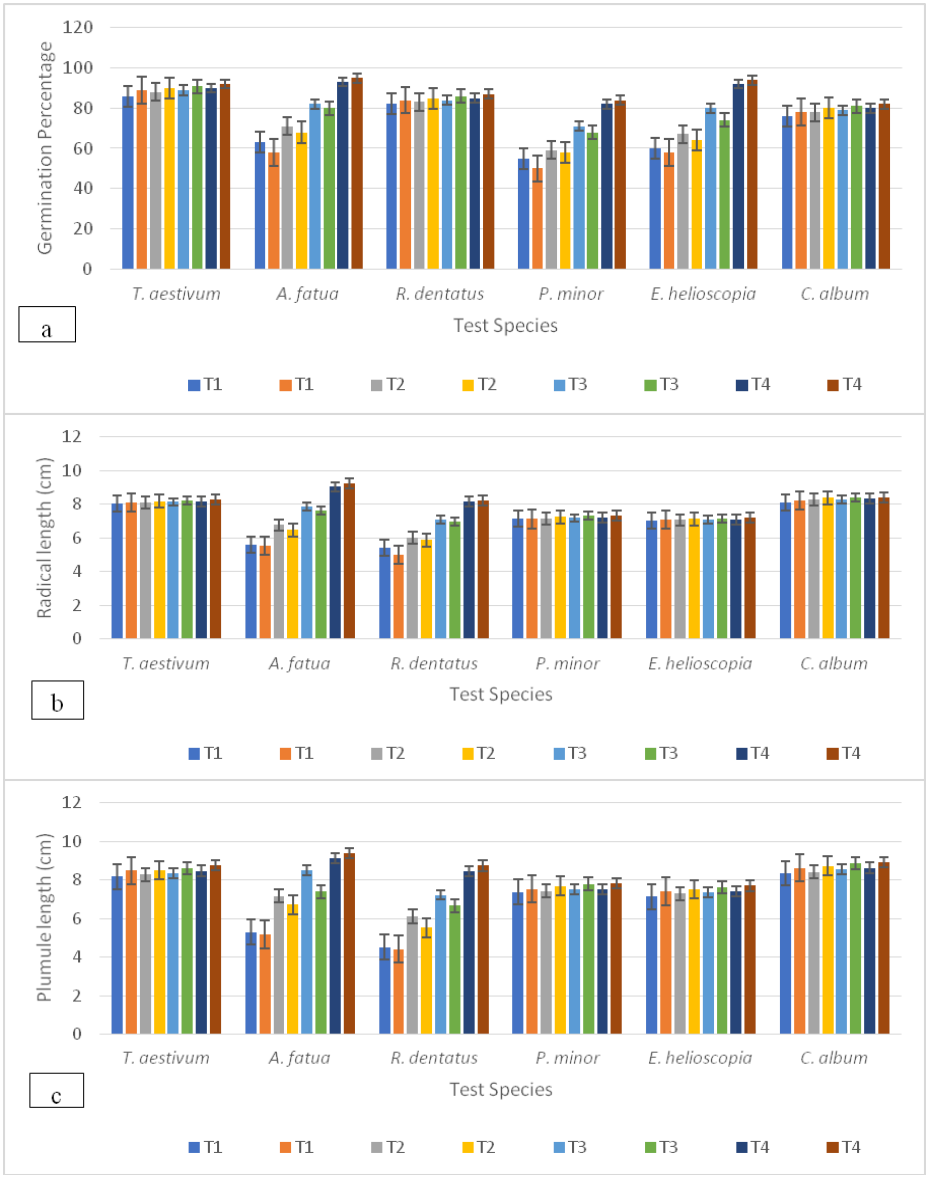

Figure 2. *Allelopathic potential of L. camara hexane extract against test species on filter paper (FP) and soil (S) on: (a) germination percentage (b) radical length (c) plumule length.*

http://www.aloki.hu ● ISSN 1589 1623 (Print) ● ISSN 1785 0037 (Online)
DOI: http://dx.doi.org/10.15666/aeer/1605_67416760
© 2018, ALÖKI Kft., Budapest, Hungary

Plumule length

Analysis of the data revealed that *L. camara* hexane extract significantly inhibited the plumule length of *R. dentatus* (46%) and *A. fatua* (42%) as compared to control on filter paper. Interestingly, there was no significant effect on plumule elongation of *T. aestivum, P. minor, E. helioscopia* and *C. album*. Likewise, *L. camara* hexane extract significantly inhibited plumule length of *R. dentatus* (49%) and *A. fatua* (45%) in soil. The statistical data concluded that minimum plumule length was noted for *R. dentatus* i.e., 54% and 51% on filter paper and soil, respectively (*Tables 11* and *12*). The statistical figures also proposed that maximum plumule length (95%) was noted for *T. aestivum, P. minor, E. helioscopia* and *C. album* (*Fig. 2c*).

Table 11. *Allelopathic effect of L. camara hexane extract (HE) on plumule length (cm) of test species on filter paper*

Treatments	Test species					
	T. aestivum	***A. fatua***	***R. dentatus***	***P. minor***	***E. helioscopia***	***C. album***
$T_{1\ HE}$	8.18^{a}	5.31^{d}	4.53^{d}	7.39^{a}	7.14^{a}	8.34^{a}
$T_{2\ HE}$	8.29^{a}	7.18^{c}	6.12^{c}	7.43^{a}	7.29^{a}	8.43^{a}
$T_{3\ HE}$	8.35^{a}	8.51^{b}	7.23^{b}	7.51^{a}	7.35^{a}	8.55^{a}
$T_{4\ HE}$	8.48^{a}	9.14^{a}	8.45^{a}	7.52^{a}	7.41^{a}	8.63^{a}
LSD	2.1332	1.5092	0.6679	1.5428	0.7497	0.6297
F-value	28.55*	24.81*	84.03*	27.95*	220.41*	221.91*

Means followed by different letters within one column differ significantly at P < 5%
*Significant at P < 1%

Table 12. *Allelopathic effect of L. camara hexane extract (HE) on plumule length (cm) of test species on soil*

Treatments	Test species					
	T. aestivum	***A. fatua***	***R. dentatus***	***P. minor***	***E. helioscopia***	***C. album***
$T_{1\ HE}$	8.49^{a}	5.18^{c}	4.42^{d}	7.54^{a}	7.43^{a}	8.64^{a}
$T_{2\ HE}$	8.51^{a}	6.72^{b}	5.53^{c}	7.69^{a}	7.52^{a}	8.73^{a}
$T_{3\ HE}$	8.62^{a}	7.41^{b}	6.67^{b}	7.79^{a}	7.62^{a}	8.88^{a}
$T_{4\ HE}$	8.78^{a}	9.39^{a}	8.75^{a}	7.82^{a}	7.71^{a}	8.93^{a}
LSD	2.3501	0.8878	0.7630	1.6434	1.3019	0.5319
F-value	9.65**	75.85*	101.54*	73.1*	84.41*	239.87*

Means followed by different letters within one column differ significantly at P < 5%
*Significant at P < 1%

Allelopathic potential of L. camara methanolic extract

Germination percentage

The statistical data exposed that *L. camara* methanolic extract significantly inhibited germination of *R. dentatus* (68%), *A. fatua* (66%), *E. helioscopia* (63%) and *P. minor* (62%) on filter paper, whereas, no significant effect on germination of *T. aestivum* and *C. album* showing resistance against extract. Similarly, *L. camara* methanolic extract on soil significantly suppressed seed germination of *A. fatua* (76%), *E. helioscopia* (73%),

http://www.aloki.hu ● ISSN 1589 1623 (Print) ● ISSN 1785 0037 (Online)
DOI: http://dx.doi.org/10.15666/aeer/1605_67416760
© 2018, ALÖKI Kft., Budapest, Hungary

R. dentatus (70%) and *P. minor* (69%). It was noted that maximum (95%) germination was observed for *T. aestivum* and *C. album*. In the present study, it was recognized that minimum germination was noted for *R. dentatus* (32%) followed by *A. fatua* (24%) on filter paper and soil, respectively (*Tables 13* and *14*). The results revealed that germination reduction of the *R. dentatus, A. fatua, E. helioscopia* and *P. minor* were concentration dependent (*Fig. 3a*).

Table 13. *Allelopathic effect of L. camara methanolic extract (ME) on germination percentage of test species on filter paper*

Treatments	Test species					
	T. aestivum	***A. fatua***	***R. dentatus***	***P. minor***	***E. helioscopia***	***C. album***
$T_{1\ ME}$	88^{a}	31^{d}	28^{d}	32^{d}	33^{d}	78^{a}
$T_{2\ ME}$	90^{a}	56^{c}	58^{c}	54^{c}	51^{c}	80^{a}
$T_{3\ ME}$	91^{a}	75^{b}	74^{b}	69^{b}	70^{b}	81^{a}
$T_{4\ ME}$	92^{a}	91^{a}	88^{a}	84^{a}	90^{a}	82^{a}
LSD	18.65	18.702	15.197	39.778	18.604	16.541
F-value	15.19*	13.13*	42.98*	33.52*	16.67*	45.98*

Means followed by different letters within one column differ significantly at P < 5%
*Significant at P < 1%

Table 14. *Allelopathic effect of L. camara methanolic extract (ME) on germination percentage of test species on soil*

Treatments	Test species					
	T. aestivum	***A. fatua***	***R. dentatus***	***P. minor***	***E. helioscopia***	***C. album***
$T_{1\ ME}$	90^{a}	22^{d}	27^{d}	26^{d}	25^{d}	79^{a}
$T_{2\ ME}$	91^{a}	49^{c}	48^{c}	42^{c}	47^{c}	81^{a}
$T_{3\ ME}$	92^{a}	69^{b}	68^{b}	61^{b}	62^{b}	82^{a}
$T_{4\ ME}$	93^{a}	92^{a}	89^{a}	85^{a}	91^{a}	83^{a}
LSD	11.554	17.857	15.18	14.944	16.480	15.61
F-value	13.83*	31.80*	38.99*	21.14*	51.28*	25.18*

Means followed by different letters within one column differ significantly at P < 5%
*Significant at P < 1%

Radical length

The results obtained in the study indicated that *L. camara* methanolic extract significantly inhibited radical length of *C. album* (60%)*, P. minor* (63%) and *A. fatua* (66%) on filter paper, whereas, no significant effect was noted for *T. aestivum*, *R. dentatus* and *E. helioscopia* showing resistance against extract. Similarly, the applications of extract into soil significantly suppressed radical length of *A. fatua* (68%)*, P. minor* (66%) *C. album* (63%) and *E. helioscopia* (55%) as compared to control (*Tables 15* and *16*). The maximum (96%) radical length was observed for *T. aestivum* and *R. dentatus.* The final data concluded that minimum radical length was noted for *C. album (*40%) and *A. fatua* (32%) on filter paper and soil, respectively (*Fig. 3b*).

http://www.aloki.hu ● ISSN 1589 1623 (Print) ● ISSN 1785 0037 (Online)
DOI: http://dx.doi.org/10.15666/aeer/1605_67416760
© 2018, ALÖKI Kft., Budapest, Hungary

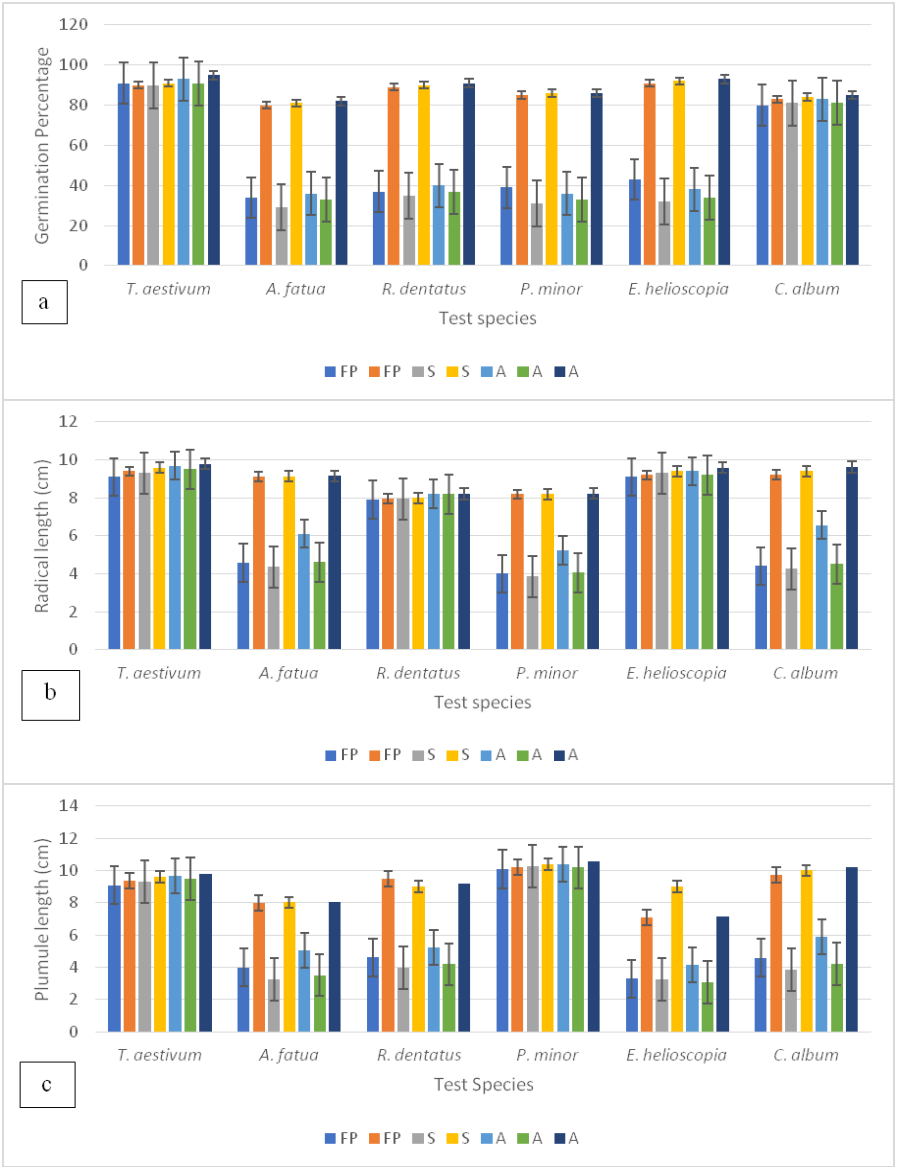

Figure 3. *Allelopathic potential of L. camara leaf powder against test species on filter paper (FP), soil (S) and agar (A) on: (a) germination percentage (b) r*adical length (c) plumule *length*

Table 15. *Allelopathic effect of L. camara methanolic extract (ME) on radical length (cm) of test species on filter paper*

Treatments	Test species					
	T. aestivum	***A. fatua***	***R. dentatus***	***P. minor***	***E. helioscopia***	***C. album***
$T_{1\ ME}$	9.11^{a}	3.18^{d}	8.31^{a}	3.59^{d}	7.49^{a}	3.39^{d}
$T_{2\ ME}$	9.23^{a}	6.24^{c}	8.43^{a}	6.88^{c}	7.51^{a}	5.46^{c}
$T_{3\ ME}$	9.37^{a}	7.93^{b}	8.54^{a}	8.10^{b}	7.63^{a}	7.11^{b}
$T_{4\ ME}$	9.43^{a}	9.49^{a}	8.67^{a}	9.81^{a}	7.69^{a}	8.58^{a}
LSD	3.7879	2.5542	0.8095	1.2569	1.9073	0.9043
F-value	16.78*	23.58*	206.09*	39.32*	27.90*	20.88*

Means followed by different letters within one column differ significantly at P < 5%
*Significant at P < 1%

http://www.aloki.hu ● ISSN 1589 1623 (Print) ● ISSN 1785 0037 (Online)
DOI: http://dx.doi.org/10.15666/aeer/1605_67416760
© 2018, ALÖKI Kft., Budapest, Hungary

Table 16. *Allelopathic effect of L. camara methanolic extract (ME) on radical length (cm) of test species on soil*

Treatments	Test species					
	T. aestivum	***A. fatua***	***R. dentatus***	***P. minor***	***E. helioscopia***	***C. album***
$T_{1\ ME}$	9.46[a]	3.07[c]	8.52[a]	3.35[d]	3.51[a]	3.31[d]
$T_{2\ ME}$	9.51[a]	5.45[b]	8.66[a]	5.28[c]	7.65[a]	4.49[c]
$T_{3\ ME}$	9.61[a]	6.03[b]	8.77[a]	7.31[b]	7.72[a]	6.45[b]
$T_{4\ ME}$	9.65[a]	9.56[a]	8.89[a]	9.99[a]	7.87[a]	8.85[a]
LSD	2.4770	1.740	0.989	1.3125	1.2662	2.420
F-value	18.01*	44.47*	64.33*	121.84*	94.32*	53.72*

Means followed by different letters within one column differ significantly at P < 5%
*Significant at P < 1%

Plumule length

The data obtained exhibited that *L. camara* methanolic extract significantly suppressed the plumule length of *R. dentatus* (63%)*, A. fatua* (63%), *C. album* (61%) and *E. helioscopia* (59%) as compared control on filter paper. Interestingly, there was no significant effect on plumule elongation of *T. aestivum and P. minor*. Likewise, *L. camara* methanolic extract significantly inhibited plumule length of *E. helioscopia* (67%), *R. dentatus* (66%), *A. fatua* (65%) and *C. album* (64%) in soil. The statistical data concluded that minimum plumule length was noted for *R. dentatus* (37%) and *E. helioscopia* (33%) on filter paper and soil, respectively (*Tables 17* and *18*). The statistical figures also proposed that maximum plumule length (96%) was noted for *T. aestivum and P. minor* (*Fig. 3c*).

Allelopathic potential of L. camara leaf powder

Germination percentage

The data revealed that *A. fatua* (60%)*, R. dentatus* (58%), *P. minor* (54%) and *E. helioscopia* (53%) possessed significant germination in *L. camara* leaf powder on filter paper, whereas, no significant effect on germination of *T. aestivum* and *C. album* showing resistance to dry powder. It is also clear from the result that *E. helioscopia* (65%)*, P. minor* (64%)*, A. fatua* (64%) and *R. dentatus* (61%) showed inhibition respectively as compared to control in powder applied into soil. The results also declared that maximum (95%) germination was noted for *T. aestivum* and *C. album.* In the present study, it was demonstrated that minimum germination was noted for *A. fatua* (42%) and *E. helioscopia* (45%) on filter paper and soil, respectively. The experimental results of the current study indicated on agar the highest germination reduction was noted for *E. helioscopia* (59%), followed by *P. minor* (58%), *R. dentatus* (56%) and *A. fatua* (56%) at 10 mg conc. Similarly, the highest germination reduction was noted for *E. helioscopia* (63%), followed by *P. minor* (62%), *A. fatua* (60%) and *R. dentatus* (59%) at 50 mg conc. The statistical data concluded that minimum germination was noted for *E. helioscopia* i.e. 41% and 37% at 10 mg and at 50 mg conc., respectively. The statistics also recommended that with the increase of concentration, the inhibitory effect was progressively increased for *E. helioscopia, P. minor, A. fatua* and *R. dentatus*

http://www.aloki.hu ● ISSN 1589 1623 (Print) ● ISSN 1785 0037 (Online)
DOI: http://dx.doi.org/10.15666/aeer/1605_67416760
© 2018, ALÖKI Kft., Budapest, Hungary

(*Table 19*). The statistical results recommended that the germination %age *T. aestivum* and *C. album* were completely resistant to dry powder (*Fig. 4a*).

Table 17. *Allelopathic effect of L. camara methanolic extract (ME) on plumule length (cm) of test species on filter paper*

Treatments	Test species					
	T. aestivum	***A. fatua***	***R. dentatus***	***P. minor***	***E. helioscopia***	***C. album***
$T_{1\ ME}$	9.33^{a}	3.19^{d}	3.42^{d}	7.31^{a}	3.71^{d}	3.26^{d}
$T_{2\ ME}$	9.41^{a}	5.97^{c}	6.38^{c}	7.44^{a}	6.28^{c}	5.64^{c}
$T_{3\ ME}$	9.50^{a}	7.33^{b}	7.92^{b}	7.59^{a}	7.91^{b}	7.18^{b}
$T_{4\ ME}$	9.59^{a}	8.55^{a}	9.27^{a}	7.61^{a}	9.16^{a}	8.29^{a}
LSD	1.4210	0.6947	1.4678	0.6468	0.9294	1.6091
F-value	43.63*	228.96*	95.24*	35.04*	193.36*	25.73*

Means followed by different letters within one column differ significantly at P < 5%
*Significant at P < 1%

Table 18. *Allelopathic effect of L. camara methanolic extract (ME) on plumule length (cm) of test species on soil*

Treatments	Test species					
	T. aestivum	***A. fatua***	***R. dentatus***	***P. minor***	***E. helioscopia***	***C. album***
$T_{1\ ME}$	9.41^{a}	3.09^{d}	3.27^{d}	7.56^{a}	3.11^{d}	3.11^{d}
$T_{2\ ME}$	9.53^{a}	4.55^{c}	5.79^{c}	7.68^{a}	5.12^{c}	5.23^{c}
$T_{3\ ME}$	9.65^{a}	7.08^{b}	7.12^{b}	7.79^{a}	7.34^{b}	7.09^{b}
$T_{4\ ME}$	9.75^{a}	8.87^{a}	9.59^{a}	7.81^{a}	9.47^{a}	8.73^{a}
LSD	2.8953	1.3127	0.6726	0.6941	0.6419	0.5756
F-value	15.53*	71.45*	117.15*	235.78*	225.87*	119.35*

Means followed by different letters within one column differ significantly at P < 5%
*Significant at P < 1%

Table 19. *Allelopathic effect of L. camara leaf powder on germination percentage of test species*

Treatments		Test species					
Media		***T. aestivum***	***A. fatua***	***R. dentatus***	***P. minor***	***E. helioscopia***	***C. album***
Filter paper	10 mg	91^{a}	34^{b}	37^{b}	39^{b}	43^{b}	80^{a}
	Control	90^{a}	80^{a}	89^{a}	85^{a}	91^{a}	83^{a}
Soil	50 mg	90^{a}	29^{b}	35^{b}	31^{b}	32^{b}	81^{a}
	Control	91^{a}	81^{a}	90^{a}	86^{a}	92^{a}	84^{a}
Agar	10 mg	93^{a}	36^{b}	40^{b}	36^{b}	38^{b}	83^{a}
	50 mg	91^{a}	33^{b}	37^{b}	33^{b}	34^{b}	81^{a}
	Control	95^{a}	82a	91^{a}	86^{a}	93^{a}	85^{a}
LSD		13.622	12.454	16.410	16.07	14.544	16.880
F-value		26.14*	15.63*	21.56*	37.71*	22.14*	54.38*

Means followed by different letters within one column differ significantly at P < 5%
*Significant at P < 1%

http://www.aloki.hu ● ISSN 1589 1623 (Print) ● ISSN 1785 0037 (Online)
DOI: http://dx.doi.org/10.15666/aeer/1605_67416760
© 2018, ALÖKI Kft., Budapest, Hungary

Radical length

The data revealed that *C. album*, *P. minor* and *A. fatua* showing 52%, 5% and 50% radical length inhibition respectively as compared to control in *L. camara* leaf powder on filter paper, whereas, no significant effect on radical length of *T. aestivum, R. dentatus* and *E. helioscopia* showing resistance to dry powder. It is also clear from the result that *C. album, P. minor* and *A. fatua* showed 55%, 53% and 52% radical length inhibition respectively as compared to control in powder applied into soil. The results also declared that maximum (98%) radical length was noted for *T. aestivum, R. dentatus* and *E. helioscopia* (*Table 20*). In the present study, it was demonstrated that minimum radical length was noted for *C. album* i.e. 48% and 45% on filter paper and soil, respectively. The results of the current study indicated on agar the highest radical length reduction was noted for *P. minor* (36%), followed by *A. fatua* (33%) and *C. album* (32%) at 10 mg conc. Similarly, the highest radical length reduction was noted for *C. album* (53%), followed by *P. minor* (51%) *A. fatua* (50%) at 50 mg conc. The statistical data concluded that minimum radical length was noted for *P. minor* (64%) and *C. album* (37%) at 10 mg and at 50 mg conc., respectively (*Fig. 4b*).

Table 20. *Allelopathic effect of L. camara leaf powder on radical length (cm) of test species*

Treatments		**Test species**					
Media		***T. aestivum***	***A. fatua***	***R. dentatus***	***P. minor***	***E. helioscopia***	***C. album***
Filter paper	10 mg	9.1[a]	4.58[b]	7.91[a]	4.01[b]	9.1[a]	4.41[b]
	Control	9.4[a]	9.11[a]	7.98[a]	8.19[a]	9.2[a]	9.21[a]
Soil	50 mg	9.3[a]	4.36[b]	7.94[a]	3.86[b]	9.3[a]	4.26[b]
	Control	9.6[a]	9.13[a]	8.00[a]	8.21[a]	9.4[a]	9.41[a]
Agar	10 mg	9.7[a]	6.12[b]	8.20[a]	5.25[b]	9.4[a]	6.57[b]
	50 mg	9.5[a]	4.61[c]	8.19[a]	4.07[c]	9.2[a]	4.51[c]
	Control	9.8[a]	9.15[a]	8.21[a]	8.23[a]	9.6[a]	9.62[a]
LSD		3.2779	0.8692	0.8236	2.5388	1.503	0.9823
F-value		23.22*	498.76*	266.70*	47.00*	57.71*	66.95*

Means followed by different letters within one column differ significantly at P < 5%
*Significant at P < 1%

Plumule length

The data revealed that *E. helioscopia*, *C. album*, *R. dentatus* and *A. fatua* showing 54%, 53%, 51% and 50% plumule length inhibition respectively as compared to control in *L. camara* leaf powder on filter paper, whereas, no significant effect on plumule length of *T. aestivum* and *P. minor* showing resistance to dry powder. It is also clear from the result that *E. helioscopia, C. album, A. fatua* and *R. dentatus* showed 64%, 61%, 59% and 56% plumule length inhibition respectively as compared to control in powder applied into soil. The results also declared that maximum (98%) plumule length was noted for *T. aestivum* and *P. minor.* In the present study, it was demonstrated that minimum plumule length was noted for *E. helioscopia* i.e. 49% and 36% on filter paper and soil, respectively (*Table 21*). The experimental results of the current study indicated on agar the highest plumule length reduction was noted for *R. dentatus* (43%), followed

http://www.aloki.hu ● ISSN 1589 1623 (Print) ● ISSN 1785 0037 (Online)
DOI: http://dx.doi.org/10.15666/aeer/1605_67416760
© 2018, ALÖKI Kft., Budapest, Hungary

by *E. helioscopia* (42%), *C. album* (42%) and *A. fatua* (37%) at 10 mg conc. Similarly, the highest plumule length reduction was noted for *C. album* (59%), followed by *E. helioscopia* (57%), *A. fatua* (56%) and *R. dentatus* (55%) at 50 mg conc. The statistical data concluded that minimum plumule length was noted for *R. dentatus* (67%) and *C. album* (41%) at 10 mg and at 50 mg conc., respectively (*Fig. 4c*).

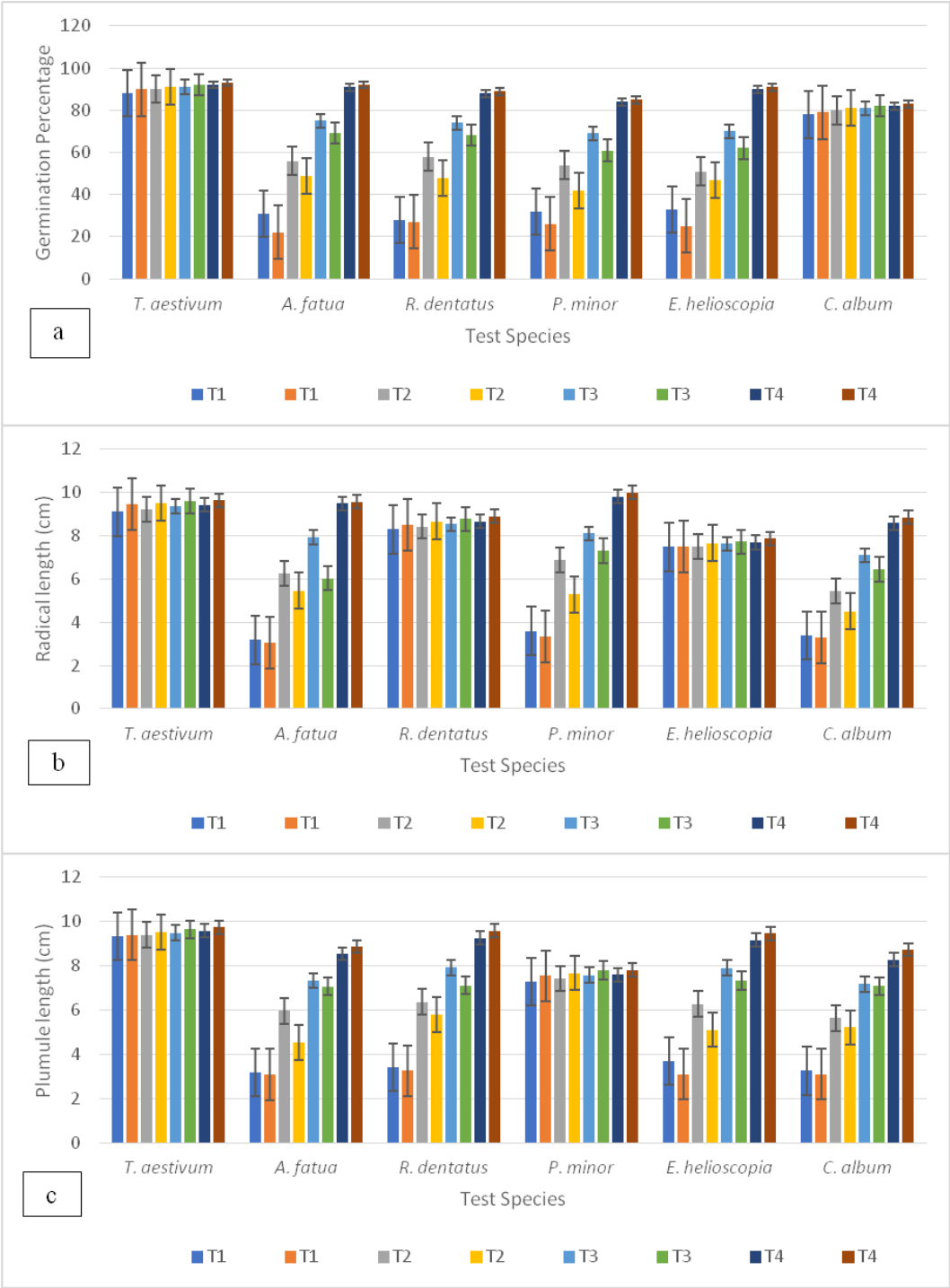

Figure 4. *Allelopathic potential of L. camara methanolic extract against test species on filter paper (FP) and soil (S) on: (a) germination percentage (b) ra*dical length (c) plumule length

http://www.aloki.hu ● ISSN 1589 1623 (Print) ● ISSN 1785 0037 (Online)
DOI: http://dx.doi.org/10.15666/aeer/1605_67416760
© 2018, ALÖKI Kft., Budapest, Hungary

Table 21. *Allelopathic effect of L. camara leaf powder on plumule length (cm) of test species*

Treatments		Test species					
Media		***T. aestivum***	***A. fatua***	***R. dentatus***	***P. minor***	***E. helioscopia***	***C. album***
Filter paper	10 mg	9.1[a]	3.98[b]	4.61[b]	10.1[a]	3.29[b]	4.59[b]
	Control	9.4[a]	8.01[a]	9.48[a]	10.2[a]	7.09[a]	9.71[a]
Soil	50 mg	9.3[a]	3.26[b]	3.94[b]	10.3[a]	3.26[b]	3.86[b]
	Control	9.6[a]	8.03[a]	9.00[a]	10.4[a]	9.01[a]	10.01[a]
Agar	10 mg	9.7[a]	5.02[b]	5.20[b]	10.4[a]	4.15[b]	5.87[b]
	50 mg	9.5[a]	3.51[c]	4.19[c]	10.2[a]	3.06[c]	4.21[c]
	Control	9.8[a]	8.05[a]	9.21[a]	10.6[a]	7.13[a]	10.2[a]
LSD		3.4490	0.9763	1.9841	1.3929	0.9953	0.9834
F-value		21.59*	128.81*	33.17*	65.06*	51.17*	124.10*

Means followed by different letters within one column differ significantly at $P < 5\%$
*Significant at $P < 1\%$

Discussion

Natural herbicides obtained from allelopathic plants can help in reducing usage of synthetic herbicides for weed controlling. Resultantly these may environment friendly better agricultural products as well as alleviate human health concerns (Khan et al., 2014). *Lantana camara* is reported to possess phenolic, alkaloids and aromatic compounds which inhibit the growth and seed germination of adjacent plant by competing soil nutrients and fluctuating micro environment by producing dense thickets (Dobhal et al., 2010). Keeping this in view, the present study was performed for evaluating *L. camara* as allelopathic potential against some major weeds (*Phalaris minor, Avena fatua, Chenopodium album, Euphorbia helioscopia* and *Rumex dentatus*) of wheat crop.

The aqueous extract of *L. camara* significantly inhibited seed germination of *A. fatua* (42%) and *E. helioscopia* (36%) on filter paper and soil, respectively. Besides, there was lowest radical length (cm) in *A. fatua* being the most susceptible weed, while lowermost plumule length was noted in *E. helioscopia*. These results are in-line with past studies. The aqueous extract of *L. camara* significantly suppressed the growth and seed germination of different plant species including agricultural crops (Sharma et al., 2005; Ahmed et al., 2007). Our results were also in accordance with those of Hussain et al. (2011) who reported that leaf extract *L. camara* to be the most toxic for test species. Iramus et al. (2011) had observed that the retardation in root length of *Vigna radiata* was due to inhibitory effect of *L. camara* leaf extract and suppressive effect was concentration dependent. Jabeen and Ahmed (2009) stated that germination and subsequent growth of *Cucurbita pepo* was significantly reduced by leaf aqueous extract of *L. camara*. The germination inhibition was due to allelopathic action of some inhibitory chemical substances excreted by plants. Tadele (2014) described that the potential of leaf aqueous extract of *L. camara* on root and shoot elongation was species specific and concentration dependent. Enyew and Raja (2015) observed that *L. camara* leaf aqueous extract caused significant retardation in root elongation of *Zea mays* that may be attributed to the secondary metabolites produced by the extract. The germination and subsequent growth of *Eichhornia crassipes* was significantly checked

http://www.aloki.hu ● ISSN 1589 1623 (Print) ● ISSN 1785 0037 (Online)
DOI: http://dx.doi.org/10.15666/aeer/1605_67416760
© 2018, ALÖKI Kft., Budapest, Hungary

by aqueous extracts from mature and young leaves of *L. camara*, caused tissues decay and damages in *E. crassipes* (Saxena, 2000).

The analysis of the data of hexane extract indicated that there was significant reduction in germination of *E. helioscopia* (35%), followed by *P. minor* (33%) and *A. fatua* (32%) on filter paper, while lowest radical length was observed in *A. fatua* and the lowermost plumule length in *R. dentatus.* Tadele (2014) stated that leaf hexane extract of *L. camara* significantly decreased germination of *Eragrostis teff*. Padhy et al. (2000) described that growth suppression in seed germination and vigor may be due to the presence secondary metabolites in *L. camara* extract. The allelopathic potential of leaf extracts of *L. camara* different concentrations were retarder to all growth parameters of *Vigna radiata* seeds. The growth of *Setaria italica*, *Lactuca sativa* and *Pennisetum americanum* was significantly checked by all parts of *L. camara* extracts (Hussain et al., 2011).

The methanolic extract of *L. camara* significantly inhibited seed germination of *R. dentatus* (68%)*, A. fatua* (66%)*, E. helioscopia* (63%) and *P. minor* (62%). Besides, the same extract significantly reduced radical length of *A. fatua* and plumule length of *R. dentatus* and *E. helioscopia*. Mishra (2015) presented the similar results and stated that *L. camara* has allelopathic effect on *Lepidium sativum* germination and growth. Ahmed et al. (2007) described the inhibitory potential of *L. camara* in different crops. Mishra (2012) stated that *L. camara* extract checked seed germination of *Parthenium hysterophorus* demonstrating the presence of inhibitory phytochemicals. Oudhia (2000) noticed significant reduction in seed germination of *Melilotus alba* by extract *L. camara*.

The results of sandwich method indicated significant reduction in germination percentage of *A. fatua* and *E. helioscopia* on filter paper and soil by applying *L. camara* leaf powder. There was no inhibitory effect on *T. aestivum, R. dentatus* and *E. helioscopia*. There was minimal radical length in *C. album* and plumule length in *E. helioscopia* that showed the most sensitive weeds against the *L. camara* leaf powder. Some of the studies reported inhibitory effect of *L. camara* on the germination and growth of various crops. The leaf powder of *L. camara* inhibited germination, radical and plumule length of radish and lettuce (Qiaoying et al., 2009), *P. hysterophorus* (Mishra and Singh, 2012), *Albizia procera, Acacia auriculiformis, Paraserianthes falcataria, Amaranthus tricolor, Abelmoschus esculentus, Vigna sinensis, Oryza sativa* and *Cucurbita pepo* (Mishra, 2012). Das et al. (2012) also noticed inhibition linked with the production of allelochemicals from the *L. camara* leaves that inhibit growth of adjacent plants by outcompeting for soil nutrients and altering micro environment by forming dense thickets.

Conclusion

This study was aimed at evaluating allelopathic potential of *L. camara* against some major weeds of wheat crop. The selected solvent extracts (i.e. aqueous, methanolic and ethanolic) and dried leaf materials significantly inhibited seed germination, radical and plumule length of the selected weeds without harming the wheat plants. Among all the tested extract, methanolic ones showed its supremacy in terms of growth and germination inhibition of the studied weeds. It can be concluded that *L. camara* methanolic extract can be explored in future studies in purifying and identifying herbicidal compounds to be used in future herbicidal products development.

http://www.aloki.hu ● ISSN 1589 1623 (Print) ● ISSN 1785 0037 (Online)
DOI: http://dx.doi.org/10.15666/aeer/1605_67416760
© 2018, ALÖKI Kft., Budapest, Hungary

REFERENCES

[1] Ahmed, R., Uddin, M. B., Khan, M. A., Mukul, S. A., Hossain, M. K. (2007): Allelopathic effects of *Lantana camara* on germination and growth behavior of some agricultural crops in Bangladesh. – Journal Forestry Research 18: 301-304.

[2] Anwar, T., Khalid, S., Arafat, Y., Sadia, S., Riaz, S. (2013): Allelopathic suppression of *Avena fatua* and *Rumex dentatus* in associated crops. – Pakistan Journal of Weed Science Research 19: 31-43.

[3] Anwar, T., Khalid, S., Saeed, M., Mazhar, R., Qureshi, H., Rashid, M. (2016): Allelopathic interference of leaf powder and aqueous extracts of hostile weed: *Parthenium hysterophorus* (Asteraceae). – Science International 4: 86-93.

[4] Anwar, T., Khalid, S., Mazhar, R., Qureshi, H., Rashid, M. (2017a): Herbicidal potential of selected species to overcome weed infestation in *Triticum aestivum*, *Zea mays* and *Helianthus annuus*. – Pakistan Journal of Weed Science Research 23: 49-63.

[5] Anwar, T., Khalid, S., Panni, M. K., Qureshi, H., Rashid, M. (2017b): Allelopathic effect of *Euphorbia helioscopia* on *Avena fatua*, *Rumex dentatus*, *Helianthus annuus*, *Zea mays* and *Triticum aestivum*. – Pakistan Journal of Weed Science Research 23: 165-177.

[6] Arafat, Y., Khalid, S., Lin, W., Fang, C., Sadia, S., Ali, N., Azeem, S. J. (2015): Allelopathic evaluation of selected plants extract against broad and narrow leaves weeds and their associated crops. – Academic Journal of Agricultural Research 3: 226-234.

[7] Das, C. R., Mondal, N. K., Aditya, P., Datta, J. K., Banerjee, A., Das, K. (2012): Allelopathic potentialities of leachates of leaf litter of some selected tree species on gram seeds under laboratory conditions. – Asian Journal of Experimental Biological Science 3: 59-65.

[8] Dobhal, P. K., Kohli, R. K., Batish, D. R. (2010): Evaluation of impact of *Lantana camara* L. invasion on four major woody shrubs along Nayar river of Pauri Garhwal in Himalaya. – International Journal of Biodiversity and Conservation 2: 166-172.

[9] Enyew, A., Raja, N. (2015): Allelopathic effect of *Lantana camara* L. leaf powder on germination and growth behavior of maize (*Zea mays* Linn.) and wheat (*Triticum turgidum* Linn.) cultivars. – Asian Journal of Agricultural Research 7: 4-10.

[10] Fujii, Y., Parvez, S. S., Parvez, M. M., Ohmae, Y., Iida, O. (2003): Screening of 239 medicinal plant species for allelopathic activity using sandwich method. – Weed Biology Management 3: 233-241.

[11] Fujii, Y., Shibuya, T., Nakatani, K., Itani, T., Hiradate, S., Parvez, M. M. (2004): Assessment method for allelopathic effect from leaf litter leachates. – Weed Biology Management 4: 19-23.

[12] Hussain, M. I., Gonzalez, L., Reigosa, M. J. (2011): Allelopathic potential of *Acacia melanoxylon* on the germination and root growth of native species. – Weed Biology Management 11: 18-28.

[13] Iramus, S., Moinuddin, A., Syed, T. A. (2011): Allelopathic effect of scarlet pimpernel (*Anagallis arvensis*) on seed germination and radical elongation of mung bean and pearl millet. – Pakistan Journal of Botany 43: 351-355.

[14] Jabeen, N., Ahmed, M. (2009): Possible allelopathic effect of three different weeds on germination and growth of maize (*Zea mays*) cultivars. – Pakistan Journal of Botany 41: 1677-1683.

[15] Khan, I., Ali, Z., Khan, M. I., Hussain, Z., Khan, I. A., Waqas, M., Khan, R. Khan, S. (2014): Allelopathic effects of some weeds on chickpea crop. – Pak. J. Weed Sci. Res. 20: 207-211.

[16] Khan, M. A., Hussain, I., Ahmad, E. (2008): Allelopathic effect of *Eucalyptus* (*Eucalyptus camaldulensis* L.) on germination and seedling growth of (*Triticum aestivum* L.). – Pakistan Journal of Weed Science Research 14: 9-18.

http://www.aloki.hu ● ISSN 1589 1623 (Print) ● ISSN 1785 0037 (Online)
DOI: http://dx.doi.org/10.15666/aeer/1605_67416760
© 2018, ALÖKI Kft., Budapest, Hungary

[17] Maharjan, S., Shrestha, B. B., Jha, P. K. (2007): Allelopathic effects of aqueous extract of *Parthenium hysterophorus* L. on seed germination and seedling growth of some cultivated and wild herbaceous species. – Science World 5: 35-39.
[18] Michelangelo, M. T., Vidal, R. A., Junior, A. A. B., Bittencourt, H. V. H., Filho, S. S. (2016): Allelopathy: driving mechanisms governing its activity in agriculture. – Journal of Plant Interaction 1: 53-60.
[19] Mishra, A. (2012): Allelopathic interaction of *Lantana camara* leaf of extract on growth of *Parthenium hysterophorus* in seedling stage. – International Journal of Plant Science 7: 259-262.
[20] Mishra, A. (2015): Review; allelopathic properties of *Lantana camara*. – Int Res J Basic Clin Stud 3: 13-28.
[21] Mishra, A. Singh R (2012): Allelopathic effect of *Lantana camara* extract of different parts on seed germination of *Parthenium hysterophorus* L. – International Journal of Plant Science 5: 74-75.
[22] Nekonam, M. S., Kraimmojeni, H., Sharifnabi, B., Razmjoo, J., Amini, H., Bahrami, F. (2014): Assessment of some medicinal plants for their allelopathic potential against redroot pigweed (*Amaranthus retroflexus*). – Journal of Plant Protection and Research 54: 90-95.
[23] Oudhia, P. (2000): Allelopathic effects of some obnoxious weeds on germination of *Melilotus alba*. – Legume Research 22: 133-134.
[24] Padhy, B., Patnaik, P. K., Tripathy, A. K. (2000): Allelopathic potential of *Eucalyptus* leaf litter leachate on germination and seedling growth of finger millet. – Allelopathy Journal 7: 69-78.
[25] Qiaoying, Z., Shaolin, P., Yunchun, Z. (2009): Allelopathic potential of reproductive organs of exotic weed *Lantana camara*. – Allelopathy Journal 23: 213-220.
[26] Qureshi, R., Bhatti, G. R. (2001): Determination of weed communities in wheat (*Triticum aestivum* Linn.) crop of District Sukkur. – Pakistan Journal of Botany 33(1): 109-115.
[27] Qureshi, R., Waheed, A., Arshad, M. (2009): Weed communities of wheat crop in district Toba Tek Singh, Pakistan. – Pakistan Journal of Botany 41: 239-245.
[28] Raana, G., Khalid, S., Qureshi, R., Sadia, S., Bajwa, A. A. (2012): Screening and evaluation of *Euphorbia pulcherrima* for weed management. – Pakistan Journal of Weed Science Research 18: 529-539.
[29] Sahu, A., Devkota, A. (2013): Allelopathic effects of aqueous extract of leaves of *Mikania micrantha* H. B. K. on seed germination and seedling growth of *Oryza sativa* L. and *Raphanus sativus* L. – Science World Journal 11: 90-93.
[30] Saxena, M. K. (2000): Aqueous leachate of *Lantana camara* kills water hyacinth. – Journal of Chemical Ecology 26: 2435-2447.
[31] Sharma, G. P., Raghubanshi, A. S., Sing, J. S. (2005): *Lantana* invasion: an overview. – Weed Biology Management 5: 157-167.
[32] Tadele, D. (2014): Allelopathic Effects of Lantana (*Lantana camara* L.) leaf extracts on germination and early growth of three agricultural crops in Ethiopia. – Momona Ethiopian Journal of Science 6: 111-119.
[33] Zhou, Y. H., Yu, J. Q., Huang, L. F., Nogues, S. (2004): The relationship between CO_2 assimilation, photosynthetic electron transport and water-water cycle in chill-exposed cucumber leaves under low light and subsequent recovery. – Plant Cell Environment 27: 1503-1514.

http://www.aloki.hu ● ISSN 1589 1623 (Print) ● ISSN 1785 0037 (Online)
DOI: http://dx.doi.org/10.15666/aeer/1605_67416760
© 2018, ALÖKI Kft., Budapest, Hungary

EFFECT OF NITROGEN FERTILIZATION ON N_2O EMISSION IN DIFFERENT SOIL REACTIONS AND GROWN GRASS SPECIES

GAŁCZYŃSKA, M.[1*] – GAMRAT, R.[2] – BURCZYK, P.[3]

[1]*Department of Chemistry, Microbiology and Environmental Biotechnology, West Pomeranian University of Technology, Słowackiego 17, PL-71-434 Szczecin, Poland*

[2]*Department of Ecology, Environmental Protection and Management, West Pomeranian University of Technology, Słowackiego 17, PL-71-434 Szczecin, Poland*
(e-mail: Renata.Gamrat@zut.edu.pl; phone: +48-91-449-6343)

[3]*Institute of Technology and Life Sciences, Czesława 9, PL-71-504 Szczecin, Poland*
(e-mail: p.burczyk@itp.edu.pl; phone: +48-692-377-439)

**Corresponding author*
e-mail: Malgorzata.Galczynska@zut.edu.pl; phone: +48-91-449-6322

(Received 7th Jul 2018; accepted 6th Sep 2018)

Abstract. This research was carried out in order to determine the effect of fertilization, or lack of it, on N_2O emission in different conditions of soil reaction and grown grass species. The pot experiment was conducted in a randomized block design with three replications in 2014–2016 (Poland). Four grass species were grown in mineral soil under mineral or organic fertilizing (Σ = 150 N kg), or lack of fertilization and different soil reaction. The effect of N-fertilization dose was determined, too. The difference of groundcover density of tested grass species was assessed. The results indicated that N_2O emission was reduced with subsequent doses by 13, 15 and 18% compared with the initial values. The application of mineral fertilization caused a higher increase of the grass biomass than the use of organic fertilizer – without any marked effect of soil reaction. The N_2O emission was influenced by the type and dose of nitrogen fertilization, the reaction of mineral soil and the biomass of the cultivated grasses. With an increase in biomass of grasses, N_2O emission was found to decrease, generally at neutral soil reaction. The highest groundcover density was found for *Festuca pratensis* and *Lolium perenne*, which translated into increased nitrogen uptake and, consequently, reduced N_2O emissions. It was determined as the optimum technique of grassland management for the reduction of N_2O emission.
Keywords: *greenhouse gas, grassland, mineral or organic fertilization, Lolium perenne, Festuca pratensis*

Introduction

Emission of N_2O is considered the most harmful emission depleting the ozone layer and, according to Ravishankara et al. (2009), it will remain such in the 21st century. The global warming potential related to the emission of this compound is 298 times greater than CO_2 emission (Myhre et al., 2013). The dangers of N_2O emission stem from the fact that its amount is not regulated under the Montreal Protocol (MP, 1987). The largest source of emissions of this anthropogenic greenhouse gas is agriculture (Bellido et al., 2015; Mori, 2016). Additionally, at the end of the 19th and the 20th century, the atmospheric accumulation rates of N_2O exceeded the projections regarding agricultural production as limited to N fertilizers and biologically fixed nitrogen fertilizers (Davidson, 2009). Out of agricultural activities, permanent grassland, i.e. meadows and pastures, contribute to a significant amount of nitrous oxide emission due to microbial nitrification and denitrification of nitrogen mineralisation in soil (Mu et al., 2009). From the perspective of environmental protection, management of grassland constitutes

http://www.aloki.hu ● ISSN 1589 1623 (Print) ● ISSN 1785 0037 (Online)
DOI: http://dx.doi.org/10.15666/aeer/1605_67616777
© 2018, ALÖKI Kft., Budapest, Hungary

a challenge as it occupies 40% of the earth's surface and efficient shaping of its effect on the atmosphere is difficult (Maillard et al., 2017).

According to research by Chang et al. (2017), Europe has experienced a greater warming than that presented for the globe since the pre-industrial era and the warming trend is expected to increase at an even faster rate in the 21st century. Climate models for various climate scenarios project an increase of 1–5.5 °C in the annual average temperature in Europe in the period 2071–2100 as compared to 1971–2000. Grassland ecosystems play an important role in the global nitrogen cycle and provide vital ecosystem services for many species. Consequently, numerous activities have been taken to assess the pan-European reaction of grassland to anticipated climate change. The emission of N_2O can be reduced by introducing to soil the appropriate amount of mineral fertilization applicable for a given crop (Shimizu et al., 2013) or by application of manure and its subsequent mineralization (Mori and Hojito, 2015). Bouwman (1996) and Sosulski et al. (2014) identified several factors affecting N_2O emission, including soil conditions, type of crop, nitrogen (N) fertilizer type and soil and crop management. The authors highlight the fact that the observed N_2O emission from mineral soil was higher than from mineral soil – a fact also observed by Aurangojeb (2017). Dobbie et al. (1999) also pointed to the effect of nitrogen fertilization dose, temperature and amount of precipitation on N_2O emission. Signor et al. (2013) stress the role of soil reaction in N_2O emission. In turn, Koncz et al. (2017) examined the influence of grassland management depending on grazing and mowing treatments.

The literature on the subject confirms the increase in N_2O emission with an increase in the applied mineral or organic fertilizer (Bouwman, 1996; Dobbie et al., 1999; Soussana et al., 2007, 2010; Chang et al., 2015; Ciais et al., 2010; Zhang et al., 2010; Koncz et al., 2017; Aurangojeb, 2017). There is no to big information in the recent publications on the effect of split application of N fertilizer on N_2O emission levels in cultivation of species: *Dactylis glomerata* L., *Festuca pratensis* Huds., *F. rubra* L. and *Lolium perenne* L. The search for optimal techniques of grassland management for the purpose of decreasing N_2O emission led the authors of the present paper to conduct the analysis of N_2O emission and biomass of grass in the conditions of split application of nitrogen fertilizer depending on the type of fertilization and soil reaction.

The aim of the study was to determine the effect of applied fertilization, or lack of it, on nitrous oxide emission in different conditions of soil reaction and grown grass.

Material and methods

Experimental design

In the period 2014–2016, a pot experiment was conducted in a greenhouse on Faculty of Environmental Management and Agriculture of West Pomeranian University of Technology in Szczecin, Poland.

The granulometric composition of the soil material in a pot (11 kg each) corresponded to sandy loam (sand: 2–0.05 mm – 60.9%, silt: 0.05–0.002 mm – 35.1%, colloidal clay: 0.002 mm – 4.0%). It was also characterized by slightly acid reaction (pH = 5.9), total organic carbon – 9.6 $g \cdot kg^{-1}$, humus – 16.6 $g \cdot kg^{-1}$, organic substance – 37.6 $g \cdot kg^{-1}$, total nitrogen – 0.75 $g \cdot kg^{-1}$, and low content of available phosphorus – 28 $mg \cdot kg^{-1}$, potassium – 83 $mg \cdot kg^{-1}$ and magnesium – 24 $mg \cdot kg^{-1}$. Each of the four species (*Dactylis glomerata* L., *Festuca pratensis* Huds., *F. rubra* L., *Lolium perenne*

http://www.aloki.hu ● ISSN 1589 1623 (Print) ● ISSN 1785 0037 (Online)
DOI: http://dx.doi.org/10.15666/aeer/1605_67616777
© 2018, ALÖKI Kft., Budapest, Hungary

L.) was sown in an amount of 270 seeds on ¼ of the study area of the pot under the variable fertilization and soil pH conditions.

In order to obtain variability of soil pH, calcium oxide was introduced to half of the pots producing pH = 7.0. In a growing season, the fertiliser was applied to pots three times (every six weeks, starting from the half of May, 10 days after the 1st and 2nd mowing) in two fertilization variants (mineral fertilizer – ammonium nitrate, organic fertilizer – fresh slurry) in the amount of 0.355 g of N per pot, corresponding to 50 kg $N \cdot ha^{-1}$. The control sample were pots with the analysed grass species without fertilization. The experiment was conducted in three repetitions in each subsequent year of the study. At the beginning of the experiment, phosphorus fertilization in the form of superphosphate was applied to all pots in the amount of 40 kg $P_2O_5 \cdot ha^{-1}$. In case of mineral fertilization, potassium level in the soil material was supplemented with a dose of this element in the form of K_2SO_4 to the value determined for fresh slurry, i.e. 4 $kg \cdot m^{-3}$. Pot experiment was arranged in a randomized block design.

Climatic conditions of plant growth

The climate in Szczecin is moderately warm. The average annual temperature is 8.6 °C. During the experiment period of 2014–2016 the temperature varied from 9 to 24 °C, from 9 to 27 °C and from 8 to 26 °C for the respective years. The annual time of sun exposition in this period amounted to 1015 h, 955 h and 1001 h respectively. The grass was grown outdoors under controlled and optimum humidity conditions, i.e. 60% of field water capacity (the TRIME FM P3 Eikelkamp meter). Water deficits were compensated by watering and the pots were protected from atmospheric precipitation.

Measurement of N_2O fluxes

Measurements of nitrogen dioxide emission were conducted with the use of a closed static chamber after a few hours from the application of each different nitrogen fertilizer and before each mowing. Measurements of N_2O were carried out using photoacoustic field gas monitor INNOVA 1412, LumaSense Technologies, Inc.® (Burczyk et al., 2008). N_2O concentration in the chamber was recorded every minute and emission levels were noted every 15 min.

Measurement and analysis of biomass tested grass species

Each year of the experiment, during each of the three mowing treatments, a percentage density of ¼ of the study area covered by each of the tested grass species was determined on the basis of plant density. The assessment of plant density was based on the percentage share of covered area as determined according to step values (26%, 38%, 50%, 63%, 75%, 88%, 100%), partly modelled on Braun-Blanquet method (Dzwonko, 2007). Cut fresh weight (at the height of 1–2 cm) of all the tested grass species grown in each of the 18 pots in the three years of the experiment was weighed on an analytical weight. Additionally, yield of sward was determined for each mowing.

Calculations of N_2O fluxes in optimisation grassland management

The values of N_2O emission in reference to 1 kg yield of the three mowing treatments were calculated according to particular stages of the experiment as presented in *Figure 1*. Total time period covered by the calculations amounted to 4.1 months,

http://www.aloki.hu ● ISSN 1589 1623 (Print) ● ISSN 1785 0037 (Online)
DOI: http://dx.doi.org/10.15666/aeer/1605_67616777
© 2018, ALÖKI Kft., Budapest, Hungary

starting from the application of the 1st dose to 10 days after the last mowing. Determination of the optimum management conditions was based on the calculated smallest N_2O emission in reference to 1 kg of grass biomass for all three mowing treatments.

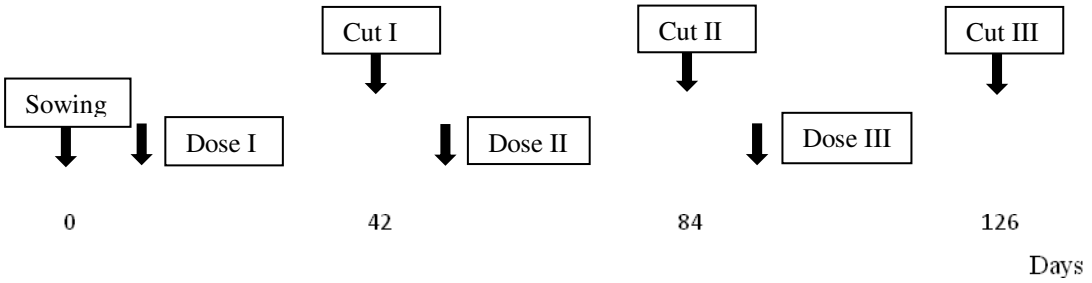

Figure 1. *Scheme of experimental design of the study: a time of sowing and a time application N-fertilizer and measurements of N_2O emission after cutting and application N-fertilizers*

Statistical analysis

Results obtained of N_2O and grass biomass were elaborated statistically with the method of two-factor analysis of variance (ANOVA: 1st factor – type of fertilization, 2nd factor – type of soil reaction) and one-way analysis of variance (dose N-fertilizer) *Statistica 12* software (StatSoft Poland). The linear correlation between analysed gas grass biomass was performer. The significance of differences between mean values and the value of Pearson correlation coefficient were evaluated with the HSD Tukey's test at $P < 0.05$. To assess the area covered by the tested grass species, a radar chart showing mean values of the nine measurement of the area covered by grass was used. Mean value of the area coverage was used for the one-way analysis of variance (grass species).

Results and discussion

Emission of N_2O fluxes from soil and after cutting of grasses

The main threats due to greenhouse gases relate to organic soil, however more and more studies address the issue in relation to mineral soil (Dobbie et al., 1999; Mu et al., 2009; Skiba et al., 2012; Aurangojeb, 2017). The experiment conducted as a part of the present study contributes to the discussion on the role of environmental factors of N_2O emission from mineral soil.

Numerous management techniques are introduced for the purpose of limiting N_2O emission, among others: split application of fertilizer (Weerasekara et al., 2018), introducing legumes to sward (Fuchs et al., 2018), injecting fresh slurry to a specific depth (Webb et al., 2010), control of soil density (Langevin et al., 2015), and the use of nitrification inhibitors (Dai et al., 2013; Duan et al., 2017).

Imer et al. (2013) report that N_2O emission is shaped by the type of climatic zone, type of soil and its pH as well as the source of nitrogen supply to soil. Moreover, emission of nitrogen greenhouse gas is additionally determined by the plant cover of soil. Consequently, lack of the plant cover results in increased emission levels. Linn and

http://www.aloki.hu ● ISSN 1589 1623 (Print) ● ISSN 1785 0037 (Online)
DOI: http://dx.doi.org/10.15666/aeer/1605_67616777
© 2018, ALÖKI Kft., Budapest, Hungary

Doran (1984) reported, that emission of N_2O from N-fertilized, no-tillage soils was 9.4 times greater than with conventional tillage. Nitrous oxide production from nonfertilized soil was slightly greater for no tillage.

Organic nitrogen fertilizers foster the release of significant amount of ammonia and nitrous oxide (Ball et al., 2007). In our conducted experiment, following the first application of fertilizer (50 kg·N·ha^{-1}) to soil without plant cover, the highest N_2O emission levels were recorded in the conditions of acidic soil reaction and application of fresh slurry (*Fig. 2*). Under the same conditions in this experiment, mineral nitrogen fertilization applied in the same dose as organic nitrogen fertilization was found to produce a statistically lower emission of this gas. Emission levels following application of mineral and organic fertilizers to soil material of neutral pH were comparable. In the controlled conditions (without nitrogen fertilization), the value of nitrous oxide emission was approximately 50% lower than the values recorded for each type of fertilization. Merbold et al. (2014) report that following tillage and harrowing there was a pronounced increase in N_2O emission. Žurovec et al. (2017) demonstrated that with fertilization in the amount of 67.5 kg·N·ha^{-1}, reduced soil cultivation, similarly to lack of cultivation treatments, can bring favourable environmental effect due to a decrease in N_2O emission levels as compared with the conventional soil cultivation.

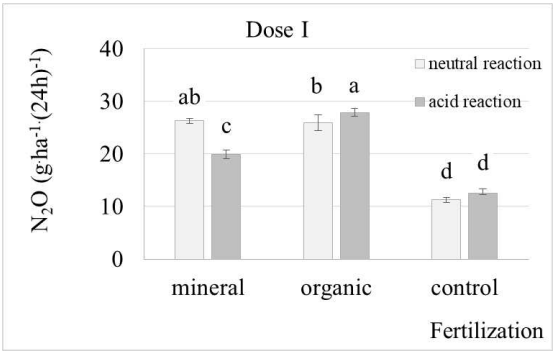

Figure 2. *N_2O emissions from soil without a plant soil cover; different letters (a, b, c, d) indicate significant difference at $P < 0.05$ among different N-fertilizer in the same variety*

Data presented in the literature on the subject show that the highest levels of N_2O emission were recorded on different dates from fertilizer application, for example following a week (Flechard et al., 2007), two weeks (Merbold et al., 2014) or on the day of organic fertilizer application (Imer et al., 2013). In our experiment, the N_2O emission in consecutive doses associated with increasing fertilizer dose (I cut – 50 kg N·ha^{-1} – 24.98 g N_2O ha^{-1} 24 h^{-1}; II cut – 100 kg N·ha^{-1} – 15.22 g N_2O ha^{-1} 24 h^{-1}; III cut – 150 kg N·ha^{-1} – 12.61 g N_2O ha^{-1} 24 h^{-1}) differed significantly ($F = 162$; $P < 0.000$). The measurements of nitrous oxide emission was conducted a few hours after application of nitrogen fertilizer, therefore it is difficult to conclude whether the recorded emission levels were indeed the highest. Following the application of the second dose of nitrogen (*Fig. 3*), it was found that in the controlled conditions the N_2O emission with respect to both types of fertilization was 75% lower. It is important to note that N_2O emission for both fertilizer forms was 50% lower than that recorded in the first measurement. In turn, after the second mowing and application of the third and the last fertilizer dose, N_2O emission was found to decrease, on average, by 20% in both types of fertilization. In the

http://www.aloki.hu ● ISSN 1589 1623 (Print) ● ISSN 1785 0037 (Online)
DOI: http://dx.doi.org/10.15666/aeer/1605_67616777
© 2018, ALÖKI Kft., Budapest, Hungary

control conditions, the values remained at the same level with respect to the effect observed following the application of the second dose. Differences in terms of N_2O emission depending on soil pH to which a given nitrogen fertilizer was applied were not remarkable, yet statistically significant following the 1st and the 2nd mowing and application of the second dose.

In our experiment, the results indicated that N_2O emission was reduced with subsequent doses by 13%, 15% and 18% as compared with the initial values.

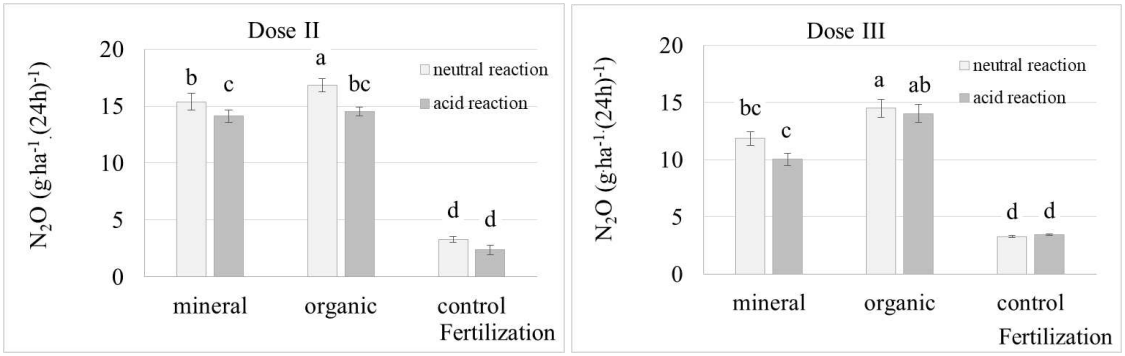

Figure 3. *N_2O emissions under conditions of 10 days after 1st and 2nd cut; different letters (a, b, c, d) indicate significant difference at $P < 0.05$ among different N-fertilizer in the same variety*

Emission of N_2O fluxes from soil after cutting grasses and grasses biomass

Grass seeds need mineral nutrients, including nitrogen, to germinate and grow (Springer, 2017). In our experiment, a 50% reduction in N_2O emission levels was observed on the day of the 1st mowing in comparison with the measurements taken following the application of the first dose of fertilizer (*Figures 2* and *4*). This resulted from nitrogen uptake by developing grass species as well as natural processes in the soil connected with nitrogen cycle and release of its gaseous form to the atmosphere (Kering et al., 2012). In our experiment, the results of N_2O emission on the day of the 1st mowing showed that this parameter was approximately 10 times greater with mineral nitrogen fertilization than organic fertilization or lack of fertilization – in this particular case, regardless of soil material pH (*Fig. 4*). Merbold et al. (2014) observe that following mineral fertilization the emission, as compared with background, increased 4–10 times. The smaller N_2O emission for slurry is due mainly to less inorganic N in slurry as compared with synthetic fertilizer as the same as reported Mori and Hojito (2011) for emission factor of manure. Similarly, the results obtained by Dobbie et al. (1999) show that nitrous oxide fluxes varies widely. In our experiment, fluxes generally increased sharply after N-fertilizer additions before tailing off to very low values, which continued until the next fertilizer addition (*Figs. 2, 3* and *4*).

In our experiment, the N_2O emission in consecutive cuts associated with increasing fertilizer dose (I cut – 50 kg $N \cdot ha^{-1}$ – 3.181 g N_2O ha^{-1} 24 h^{-1}; II cut – 100 kg $N \cdot ha^{-1}$ – 3.687 g N_2O ha^{-1} 24 h^{-1}; III cut – 150 kg $N \cdot ha^{-1}$ – 1.316 g N_2O ha^{-1} 24 h^{-1}) differed significantly ($F = 16.7$; $P < 0.000$). In the conditions of the second mowing in comparison with the first mowing, N_2O emission decreased by 30% with the application of mineral fertilizer, however, there was a ten-fold increase when organic fertilizer was used. The controlled conditions showed a two-fold increase in emission levels (*Fig. 4*). The results of the second moving (12–15 kg N_20-N per 100 kg N) showed higher values

http://www.aloki.hu ● ISSN 1589 1623 (Print) ● ISSN 1785 0037 (Online)
DOI: http://dx.doi.org/10.15666/aeer/1605_67616777
© 2018, ALÖKI Kft., Budapest, Hungary

than that obtained by Dobbie et al. (1999) for cut grassland (0.3–5.8 kg N_20-N per 100 kg N) grown on mineral soils. In the last mowing, in our experiment, N_2O flux following mineral fertilization was almost 33% lower than in the previous cutting, and with organic fertilization the values were 25% lower. The emission from soil without fertilization showed a decrease, however only by 50% (*Fig. 4*).

Another feature of soil which could have an effect on N_2O emission is soil pH which can affect nitrification, denitrification and N_2/N_2O ratio. It is generally believed that N_2O reduction is inhibited at low pH (Bouwman et al., 1993). However, other authors stress that the same soil modified for different pH values showed no measurable differences in terms of N_2O emission. These results are contrary to data obtained by Sajeev et al. (2018) who observed a 21– 55% reduction in N_2O emission due to change in soil pH.

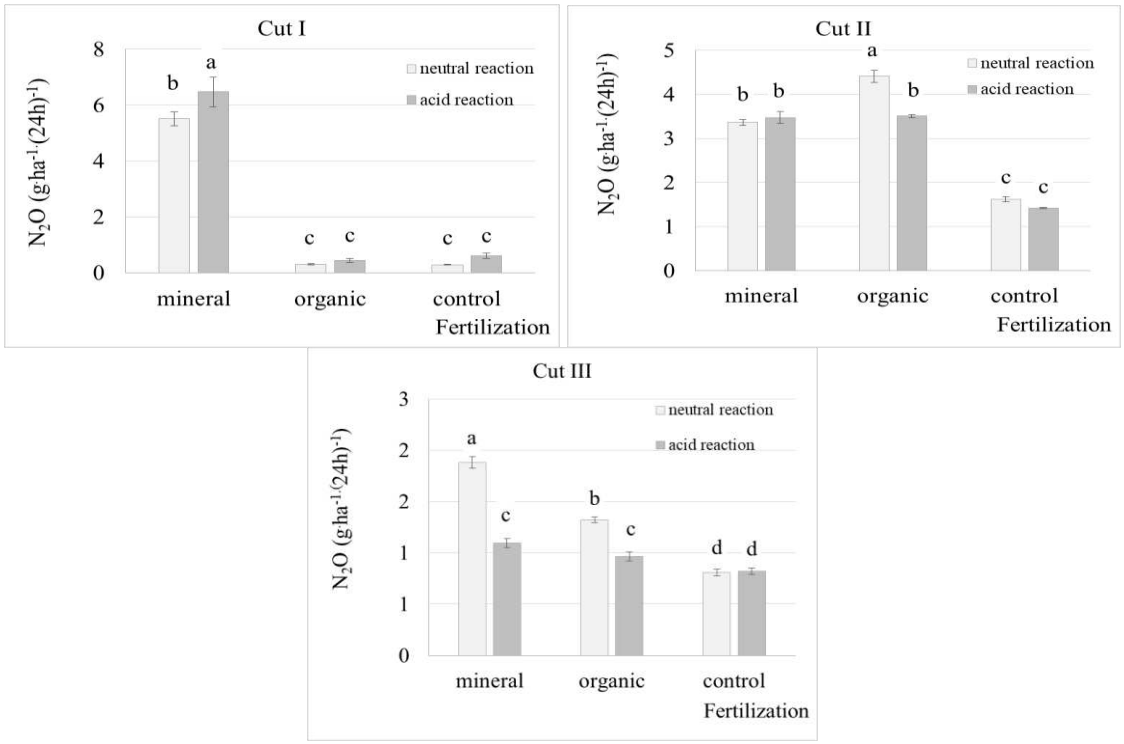

Figure 4. *N_2O emission from soil under I, II and III cut conditions; different letters (a, b, c, d) indicate significant difference at $P < 0.05$ among different N-fertilizer in the same variety*

Signor et al. (2013) demonstrated that N-fertilization implies a higher plant biomass production. In our experiment, on the basis of statistical analysis, it was found that grass biomass was dependent on the type of fertilization and soil material pH. From analysed grasses, *Lolium perenne* L. was provided with very favourable conditions for development with respect to mineral soil, as indicated by other authors (Bernal et al., 1998; Baggs and Blum, 2004; Harkot et al., 2015) and appropriate soil reaction, both slightly acidic as well as neutral, and nitrogen availability (*Fig. 5*). Hebeisen et al. (1997) pointed that high viability of the plant, even in the conditions of low nitrogen availability, is connected with the possibility of developing the root system to a depth of as much as 1.5 m and, therefore, obtaining the element from deeper layers of soil.

http://www.aloki.hu ● ISSN 1589 1623 (Print) ● ISSN 1785 0037 (Online)
DOI: http://dx.doi.org/10.15666/aeer/1605_67616777
© 2018, ALÖKI Kft., Budapest, Hungary

Similarly to ryegrass, the conditions of *Festuca pratensis* Huds. development in our experiment also were favourable as the plant favours compact and medium compact mineral soils with sufficient moisture. Moreover, Borawska-Jarmułowicz et al. (2016) indicated that the plant's root system is well developed and reaches 1.2 m deep into the soil profile. Sosnowski (2012) demonstrated that in the conditions of nitrogen fertilization *Festuca pratensis* Huds., *Lolium perenne* L. and *Dactylis glomerata* L. showed an increase in yield – as is confirmed by the our results obtained in the 1st, 2nd and 3rd mowing treatment with the use of both types of nitrogen fertilization in comparison with the control (*Fig. 5*).

Dactylis glomerata L. shows tolerance to acidic as well as alkaline pH of mineral soil. Due to developing greater number of generative shoots (Borawska-Jarmułowicz et al., 2016), this plant is capable of a specific physiological adaptation to variable levels of mineral nutrients in soil (Crossley and Bradshaw, 1968; Zarzycki and Bedla, 2017) and shows a higher mean average increase in sward height as compared with *Festuca* variation. However, in the conditions of the experiment conducted as a part of this study, the biomass and groundcover density were found to be significantly lower as compared with *Lolium perenne* L. and *Festuca pratensis* Huds (*Fig. 5*).

In comparison to other tested grass species, *Festuca rubra L.* is characterised by a considerably lower growth rate (Zarzycki and Bedla, 2017), which translated into insignificant groundcover density observed in our experiment (*Fig. 5*).

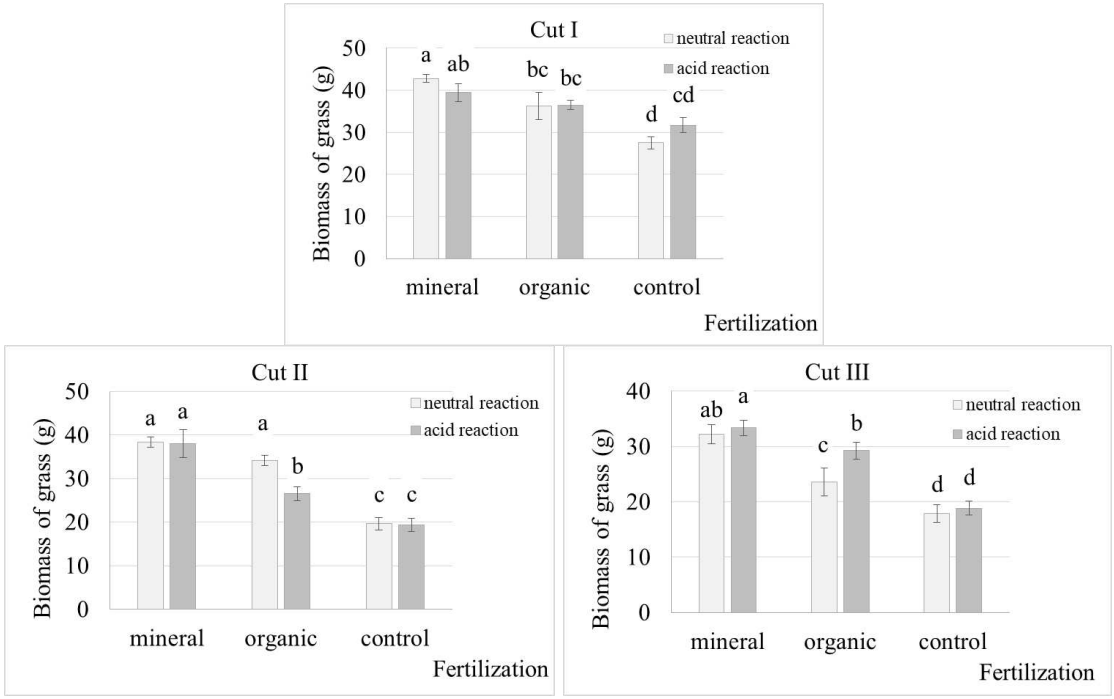

Figure 5. *Grass biomass depending on fertilization and soil reaction in the first, second and third cut; different letters (a, b, c, d) indicate significant difference at $P < 0.05$ among different N-fertilizer in the same variety*

Temperature and duration of sun exposition are important factors for plant yielding. Zhang et al. (2017) pointed that the amount of hours of daily sun exposition has an effect on the yield of grass only in periods of drought. In our experiment, constant soil

http://www.aloki.hu ● ISSN 1589 1623 (Print) ● ISSN 1785 0037 (Online)
DOI: http://dx.doi.org/10.15666/aeer/1605_67616777
© 2018, ALÖKI Kft., Budapest, Hungary

moisture was maintained. The mean air temperature recorded in the subsequent years for the period between seeds sowing and the first cut was 15, 14 and 16 °C, for the period between the first and second cut, respectively 18, 18 and 19 °C, and for the period between second and third cut 18, 19 and 18 °C (*Fig. 6*). Biomass of the analysed grass for given moving treatments was connected with life process of the grown species and air temperature.

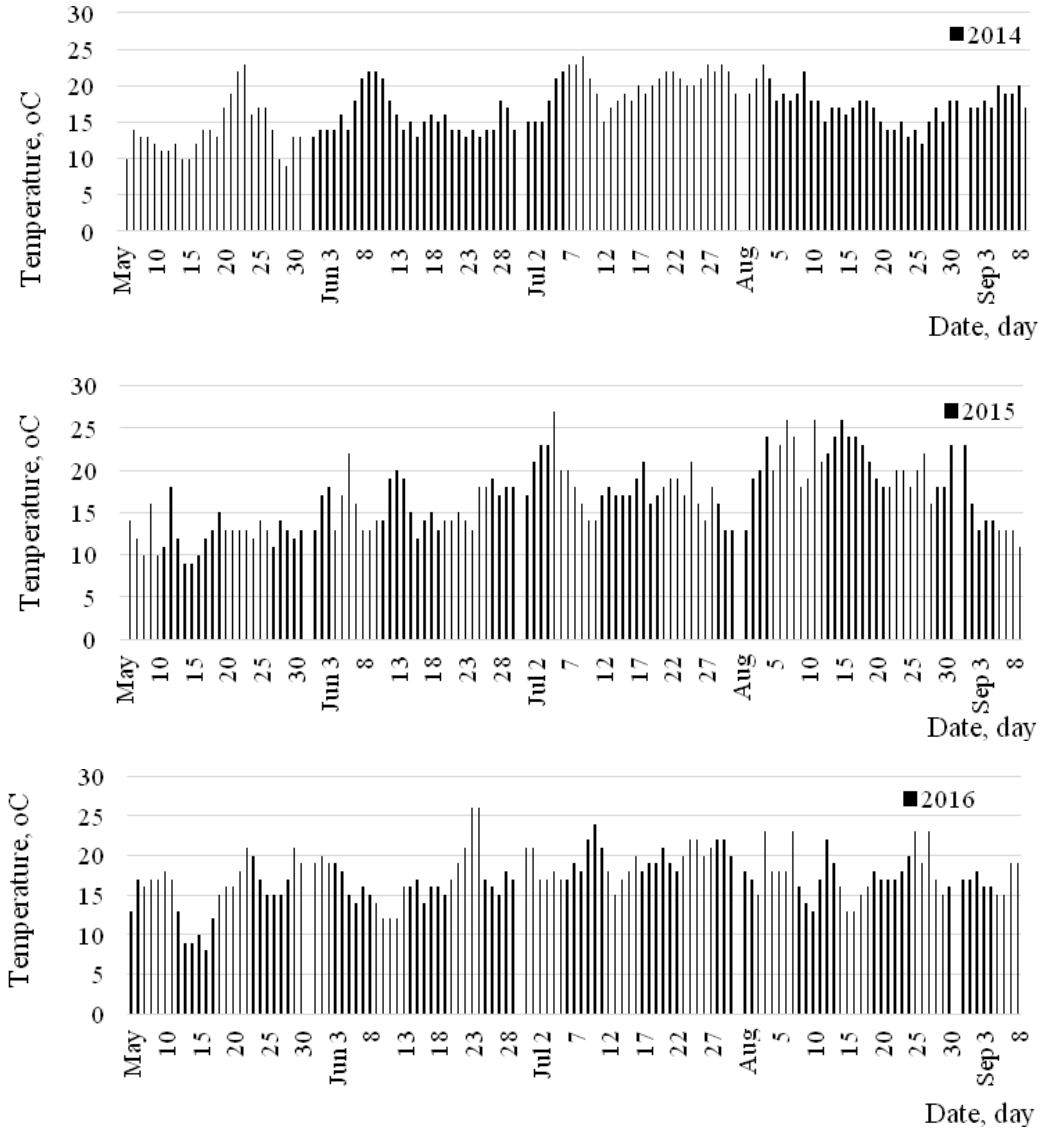

Figure 6. *Average daily air temperature from 16 May to 30 September in 2014–2016*

The lowest biomass yield for each of the mowing treatments was obtained in the conditions without nitrogen fertilization (*Fig. 5*). Markedly increased biomass in acidic soil pH was found only for the first mowing. On average, as compared with the first mowing, biomass showed a 33% and 38% decrease with subsequent mowing treatments. Biomass of the tested grass at application of mineral fertilization was higher than with the use of organic fertilizer – without any marked effect of soil material reaction. In subsequent mowing treatments, under the aforementioned fertilizing

http://www.aloki.hu ● ISSN 1589 1623 (Print) ● ISSN 1785 0037 (Online)
DOI: http://dx.doi.org/10.15666/aeer/1605_67616777
© 2018, ALÖKI Kft., Budapest, Hungary

conditions, biomass showed a decline of 8% and 34%. In the case of organic fertilization, the effect of soil pH on biomass amount was found to be more pronounced. This was observed for the 2nd and 3rd moving with a reverse trend in terms of biomass amount. For subsequent mowing treatments, biomass showed a decrease of 18% and 26%.

Share of grass species in the cover of the study area

From sowing to the last cut the temperature and the number of sunshine hours had a positive effect on the development of grasses. Despite the diversity of the grass species and their sensitivity to temperature variability, optimal habitat conditions, in particular air temperature, were maintained during the experiment. Nevertheless, the rate of growth and sensitivity differed strongly between red fescue and ryegrass as indicated by Jankowska-Huflejt (2013) and Jankowski et al. (2018).

Out of the tested grass species, in the conducted experiment the best yield was obtained for *Festuca pratensis* Huds. and *Lolium perenne* L. *Dactylis glomerata* L. showed substantially worse results and *Festuca rubra* L. the worst. The share of the latter two species amounted to, on average, 1/3 of the biomass obtained from individual mowing treatments.

Generally, for all cuts it was found that *Lolium perenne* L. (average in the range of 75% to 88%) and *Festuca pratensis* Huds. (average in the range of 75% to 88%) significantly ($F = 19904$; $P < 0{,}000$) occupied a larger area than *Dactylis glomerata* L. (average in the range of 50% to 63%) and *Festuca rubra* L. (average in the range of 38% to 50%). The density of the tested grass species showed an increasing tendency in the second mowing, and decreasing in the third as compared to the first mowing treatment (*Fig. 7*). The lowest density in subsequent mowing treatments was recorded for *Festuca rubra* L. (50%/50%/38%), followed by *Dactylis glomerata* L. (63%/63%/50%), and *Lolium perenne* L. with *Festuca pratensis* Huds. (75%/88%/63%). There was no effect of the type of fertilization and soil pH on density of the tested grass species ($P > 0.05$). However, biomass analysis shows that for particular mowing treatments there was a statistically significant effect of fertilization and soil reaction on the development of the tested grass species (*Fig. 5*).

In individual mowing treatments, mean area covered by the tested grass species amounted to 27, 21 and 39% which could affect N_2O emission levels (*Fig. 4*), as is also shown in studies by Linn and Doran (1984). They suggested that this gas emission from non-fertilized soil was slightly greater for no tillage.

Assessment of the relationship between N_2O emission and biomass

It was found that out of 18 variants tested in the course of the experiment, 14 showed a statistically significant linear correlation – 13 out of which were negative (*Table 1*). With an increase in biomass of the tested grass species, N_2O emission was found to decrease, always at neutral soil reaction. In the control conditions and with organic fertilization only in the first mowing treatment there were no significant correlations at acidic pH of soil material. In the case of mineral fertilization, such correlation was recorded in all mowing treatments. Negative correlations confirm the relationship between high nitrogen dependence of species such as *Dactylis glomerata* L. and the resultant decreased N_2O emission alongside an increase in plant biomass – an observation which has also been made by other authors (Abalos et al., 2018).

http://www.aloki.hu ● ISSN 1589 1623 (Print) ● ISSN 1785 0037 (Online)
DOI: http://dx.doi.org/10.15666/aeer/1605_67616777
© 2018, ALÖKI Kft., Budapest, Hungary

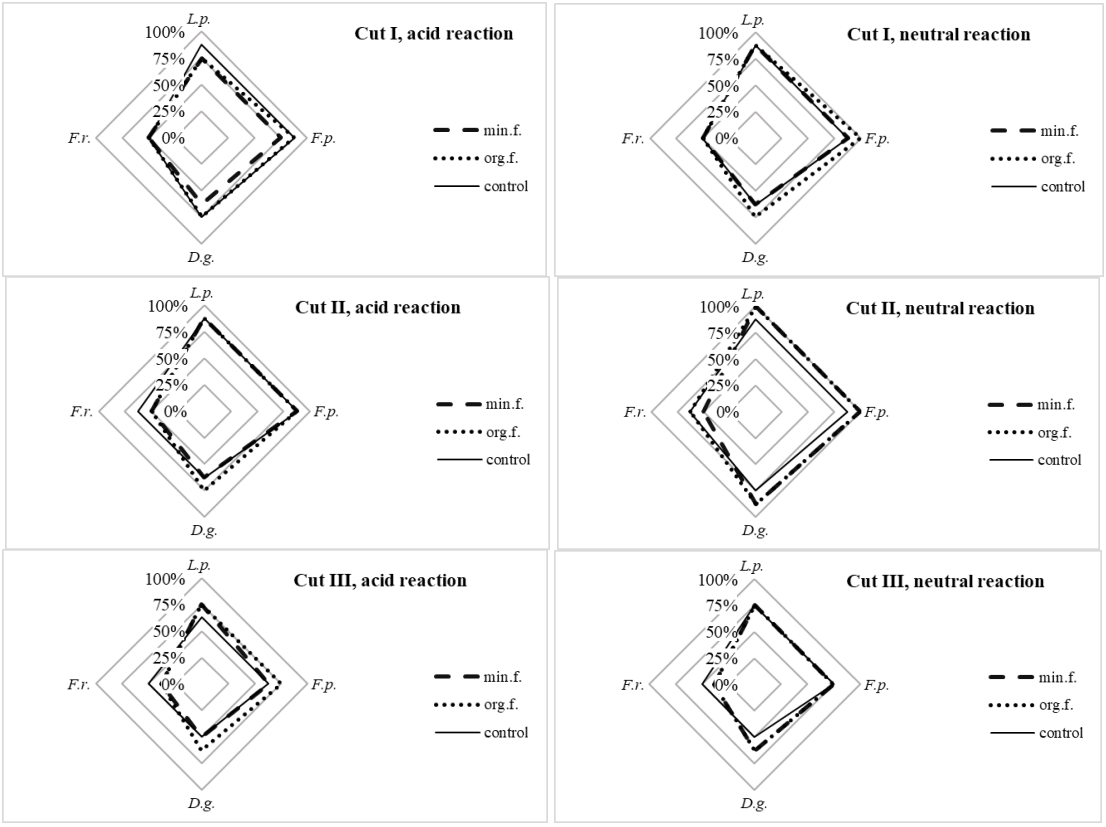

Figure 7. *Percentage of grass species in the coverage of the study surface depending on fertilization and soil reaction in individual cuts; Lolium perenne (L.p.), Festuca pratensis (F.p.), Dactylis glomerata (D.g.), Festuca rubra (F.r.); mineral fertilizer (min.f.), organic fertilizer (org.f.)*

Table 1. *Linear correlation between N_2O emission ($mg \cdot ha^{-1} \cdot (24\ h)^{-1}$) and grass biomass (g)*

Cut	Reaction	Type of fertilization		
		Control	Mineral fertilization	Organic fertilization
I	Neutral	y = 658.9 – 11.73*x r = -0.8053; p = 0.0088	y = 18017 – 163.6*x r = -0.6819; p = 0.0431	y = 644.1 – 9.337*x r = -0.9730; p = 0.00001
	Acid	y = -157.9 + 27.73*x r = 0.8543; p = 0.0034	y = 7030 + 149.9*x; r = 0.1450; p = 0.7097	y = 1080.7 – 17.64*x r = -0.9887; p = 0.00000
II	Neutral	y = 2307 – 35.13*x r = -0.9735; p = 0.00001	y = 4892 – 39.95*x r = -0.6797; p = 0.0440	y = 7453 – 88.94*x r = -0.7593; p = 0.0176
	Acid	y = 1556 – 6.805*x r = -0.6962; p = 0.0372	y = 3952 – 12.56*x r = -0.3062; p = 0.4229	y = 3885 – 14.37*x r = -0.7262; p = 0.0267
III	Neutral	y = 1049 – 13.39*x r = -0.6723; p = 0.0473	y = 2897 – 30.46*x r = -0.9166; p = 0.0005	y = 1562 – 8.186*x r = -0.7100; p = 0.0321
	Acid	y = 1163 – 18.14*x r = -0.7693; p = 0.0154	y = 807.8 + 8.8876*x r = 0.2840; p = 0.4590	y = 1530 – 24.01*x r = -0.8258; p = 0.0061

Statistically significant correlations were underlined

http://www.aloki.hu ● ISSN 1589 1623 (Print) ● ISSN 1785 0037 (Online)
DOI: http://dx.doi.org/10.15666/aeer/1605_67616777
© 2018, ALÖKI Kft., Budapest, Hungary

Annual of N_2O fluxes

Due to specific management strategies, organic farming may have an effect on reduction of greenhouse gases emission – including nitrous oxide (Lorenz and Lal, 2016). Grassland cultivation can mobilize large pools of N in the soil, with the potential for N leaching and N_2O emissions. Numerous studies report various N_2O emission levels from grassland in particular regions of the European Union depending on, among others, manner of use (Ciais et al., 2010; Koncz et al., 2017). For example Soussana et al. (2007) and Flechard et al. (2007) reported that 9 sites reached 1.0 ± 0.5 kg N-N_2O ha^{-1} yr^{-1}. Similar results were obtained by Chang et al. (2015) who demonstrated that indirect N_2O emissions from fertilized grassland soils were 1.2 ± 0.4 kg N-N_2O ha^{-1} yr^{-1}. In turn, Zhang et al. (2010) observed a several times lower N_2O flux from meadows located in mountain regions in the western part of China: 0.26, 0.14 and 0.38 kg N-N_2O ha^{-1} yr^{-1}. Calculated annual emission of our analysed experiment showed very different values (mineral fertilization: acid reaction 0.4–7.3 and neutral reaction 0.7–9.6; organic fertilization: 0.2–10.2 and 0.1–10.5, without fertilization: 0.2–4.6 and 0.1–4.1 N-N_2O ha^{-1} yr^{-1}, respectively).

On the basis of the equation by Bouwman (1996): E = 1 + 1.25 * F, with fertilization dose in the amount of 50 $kg \cdot N \cdot ha^{-1}$, annual N_2O emission level was identified at 63.5 $kg \cdot N \cdot ha^{-1}$. The results of our studies showed that for the first mowing, there was a variability in N_2O emission which was dependent on the type of nitrogen fertilization (Nmin-69.6 $kg \cdot N \cdot ha^{-1}$ and Norg-4.3 $kg \cdot N \cdot ha^{-1}$). The greater was the dose of nitrogen fertilization, the more the results differ from the values calculated with the equation by Bouwman (1996) for mineral soil. A decrease in N_2O flux in subsequent mowing treatments was most likely connected with phenological development of given grass species and with temperature decrease, particularly in the third mowing. The effect of temperature on N_2O emission levels was indicated by, among others, Dobbie et al. (1999), Soussana et al. (2010), Aurangojeb (2017).

Soil pH is another important factor influencing N_2O emissions, because nitrous oxide reductase is inhibited by low pH and in the presence of O_2. Generally, if denitrification is the main source of N_2O, higher pH values decrease the soil N_2O emissions, but if nitrification is the main process of N_2O production, then an increase in the soil pH stimulates the N_2O production (Signor et al., 2013). In our experiment, this effect was observed from the moment of the application of the second fertilizer dose, through the second mowing, third fertilizer dose and third mowing treatment. As emissions increased with temperature and rainfall, Ball et al. (2007) recommended to restrict tillage operations to cool, dry conditions, and being aware of possible soil compaction which may also promote denitrification. Soussana et al. (2010) pointed to the fact that emission factor of N_2O from mowed synthetically fertilised permanent grassland increased in the range from 0.1% to 5.7% alongside an increase in mean average air temperature from 5.2 to 15.8 °C, and atmospheric precipitation in the range 1160–2595 mm yr^{-1}.

Assessment of the possibilities of management optimization on crop of grasses

The search for optimum techniques of grassland management in order to reduce nitrous oxide emission led the authors to conduct the analysis of N_2O flux and biomass of grass due to split application of nitrogen fertilizer. On the basis of estimates and the adopted method of N_2O flux assessment with respect to 1 kg of grass biomass for each

http://www.aloki.hu ● ISSN 1589 1623 (Print) ● ISSN 1785 0037 (Online)
DOI: http://dx.doi.org/10.15666/aeer/1605_67616777
© 2018, ALÖKI Kft., Budapest, Hungary

of the three mowing treatments in a 4.1 month long period, optimum management conditions were determined (*Table 2*). It was found that with the application of 50 $kg \cdot N \cdot ha^{-1}$ dose at the beginning of the experiment, the expected effect can be achieved with the use of mineral fertilizer in a slightly acidic soil material (0.083 g $N_2O \cdot kg^{-1}$ yield grass; 10.9 $Mg \cdot ha^{-1}$ grass yield). An increase in gas emission was recorded using 100 $kg \cdot N \cdot ha^{-1}$ in aggregate, in a system: 1st and 2nd dose – mineral fertilization in a slightly acidic environment (0.096 g $N_2O \cdot kg^{-1}$ grass yield; 13.6 $Mg \cdot ha^{-1}$ grass yield). An even greater increase of the analysed emission was recorded using 150 $kg \cdot N \cdot ha^{-1}$ in a system: 1st, 2nd and 3rd dose – mineral fertilization, always in a slightly acidic environment (0.097 g $N_2O \cdot kg^{-1}$ grass yield; 15.6 $Mg \cdot ha^{-1}$ grass yield).

Table 2. *Emission of N_2O on grass yield and grass yield*

Cut	Reaction	Type of fertilization					
		Control		Mineral fertilization		Organic fertilization	
		N_2O emission (kg $N_2O \cdot kg^{-1}$gy)	Grass yield ($kg \cdot ha^{-1}$)	N_2O emission (kg $N_2O \cdot kg^{-1}$gy)	Grass yield ($kg \cdot ha^{-1}$)	N_2O emission (kg $N_2O \cdot kg^{-1}$gy)	Grass yield ($kg \cdot ha^{-1}$)
I	neutral	0.000094	3875	0.000149	6030	0.000163	5107
	acid	0.000091	4468	0.000126	5561	0.000174	5140
II	neutral	0.000044	2762	0.000098	5395	0.000121	4818
	acid	0.000033	2719	0.000091	5358	0.000134	3732
III	neutral	0.000045	2512	0.000088	4538	0.000144	3316
	acid	0.000045	2653	0.000071	4694	0.000112	4115

Conclusions

In conclusion, the N_2O emission was influenced by the type and dose of nitrogen fertilization, the reaction of mineral soil and the biomass of cultivated grasses. With an increase in biomass of the tested grass species, a decrease in N_2O emission was observed, especially in neutral soil reaction. Among the tested grass species, in the experimental conditions, the highest density of ground coverage was found for *Festuca pratensis* and *Lolium perenne*, which contributed to an increased nitrogen uptake and, consequently, reduced N_2O emissions. It was established as the optimum technique of grassland management in order to reduce N_2O emission. The use of 50 $kg \cdot N \cdot ha^{-1}$ mineral fertilizers resulted in the smallest emission of nitrous oxide per 1 kg of yield in a slightly acidic soil. Second application of the same fertilizer dose induced a 16% increase in emission per 1 kg of yield when the second dose was the mineral fertilizer. When the dose was applied three times (1st, 2nd and 3rd – mineral fertilizer in a slightly acidic environment), the emission increased only by 1% per 1 kg of yield. In the next study we would like to test and describe the influence of soil moisture on N_2O emission.

Acknowledgements. This work was supported by "European Agricultural Fund for Rural Development: Europe investing in rural areas". An article elaborated in the West Pomeranian University of Technology in Szczecin and Institute of Technology and Life Sciences. An article co-financed from the European Union funds under the II Technical Assistance measure: „Krajowa Sieć Obszarów Wiejskich" of the

http://www.aloki.hu ● ISSN 1589 1623 (Print) ● ISSN 1785 0037 (Online)
DOI: http://dx.doi.org/10.15666/aeer/1605_67616777
© 2018, ALÖKI Kft., Budapest, Hungary

Rural Development Programme for 2014-2020, The Managing Authority of the Rural Development Programme for 2014-2020 – the Minister of Agriculture and Rural Development.

REFERENCES

[1] Abalos, D., van Groenigen, J. W., De Deyn, G. B. (2018): What plant functional traits can reduce nitrous oxide emissions from intensively managed grasslands? – Global Change Biology 24(1): e248-e258.

[2] Aurangojeb, M. (2017): Nitrous oxide emissions from drained organic and mineral soil: a study on hemi Boreal Spruce Forest. – Kompendiet AB, Gothenburg.

[3] Baggs, E. M., Blum, H. (2004): CH_4 oxidation and emissions of CH_4 and N_2O from *Lolium perenne* swards under elevated atmospheric CO_2. – Soil Biology and Biochemistry 36(4): 713-723.

[4] Ball, B. C., Watson, C. A., Crichton, I. (2007): Nitrous oxide emissions, cereal growth, N recovery and soil nitrogen status after ploughing organically managed grass/clover swards. – Soil Use and Management 23(2): 145-155.

[5] Bellido, J., Sakai, K., Nakamura, S., Kazuro, M., Okamoto, K., Nakandakari, T. (2015): N_2O emissions from shimajiri-maji (calcaric dark red soil) after applying two chemical fertilizers. – Applied Ecology and Environmental Research 13(2): 339-348.

[6] Bernal, M. P., Navarro, A. F., Sánchez-Monedero, M. A., Roig, A., Cegarra, J. (1998): Influence of sewage sludge compost stability and maturity on carbon and nitrogen mineralization in soil. – Soil Biology and Biochemistry 30(3): 305-313.

[7] Borawska-Jarmułowicz, B., Mastalerczuk, G. Janicka, M. (2016): Evaluation of biological characteristics and yield of selected varieties of *Dactylis glomerata*, *Festuca pratensis* and *Phleum pratense* in pure stands and mixtures. – Grassland Science in Poland 19: 35-50.

[8] Bouwman, A. F. (1996): Direct emission of nitrous oxide from agricultural soils. – Nutrient Cycling in Agroecosystems 46(1): 53-70.

[9] Bouwman, A. F., Fung, I., Matthews, E., John, J. (1993): Global analysis of the potential for N_2O production in natural soils. – Global Biogeochemical Cycles 7(3): 7557-7597.

[10] Burczyk, P., Gamrat, R., Gałczyńska, M. (2008): The use of the photoacoustic field gas monitor for measurement of the concentration of gases in measurements of dinitrogen oxide emission from grassland's soils. – Polish Journal of Environmental Studies 17(3A): 105-108.

[11] Chang, J., Ciais, P., Viovy, N., Vuichard, N., Sultan, B., Soussana, J. F. (2015): The greenhouse gas balance of European grasslands. – Global Change Biology 21(10): 3748-3761.

[12] Chang, J., Ciais, P., Viovy, N., Soussana, J. F., Klumpp, K., Sultan, B. (2017): Future productivity and phenology changes in European grasslands for different warming levels: implications for grassland management and carbon balance. – Carbon Balance and Management 12: 11-21.

[13] Ciais, P., Soussana, J. F., Vuichard, N., Luyssaert, S., Don, A., Janssens, I. A., Piao, S. L., Dechow, R., Lathiere, J., Maignan, F., Wattenbach, M., Smith, P., Ammann, C., Freibauer, A., Schulze, E. D. (2010): The greenhouse gas balance of European grasslands. – Biogeosciences Discussion 7: 5997-6050.

http://www.aloki.hu ● ISSN 1589 1623 (Print) ● ISSN 1785 0037 (Online)
DOI: http://dx.doi.org/10.15666/aeer/1605_67616777
© 2018, ALÖKI Kft., Budapest, Hungary

[14] Crossley, G. K., Bradshaw, A. D. (1968): Differences in response to mineral nutrients of populations of ryegrass, *Lolium perenne* L., and Orchard grass, *Dactylis glomerata* L. – American Society of Agronomy 8(3): 383-387.
[15] Dai, Y., Di, H. J., Cameron, K. C., He, J. Z. (2013): Effects of nitrogen application rate and a nitrification inhibitor dicyandiamide on ammonia oxidizers and N_2O emissions in a grazed pasture soil. – Science of the Total Environment 465: 125-35.
[16] Davidson, E. A. (2009): The contribution of manure and fertilizer nitrogen to atmospheric nitrous oxide since 1860. – Nature Geoscience 2: 659-662.
[17] Dobbie, K. E., McTaggart, I. P., Smith, K. A. (1999): Nitrous oxide emissions from intensive agricultural systems: variations between crops and seasons, key driving variables, and mean emission factors. – Journal of Geophysical Research 104(D21): 891-299.
[18] Duan, Y. F., Kong, X. W., Schramm, A., Labouriau, R., Eriksen, J., Petersen, S. O. (2017): Microbial N transformations and N_2O emission after simulated grassland cultivation: effects of the nitrification inhibitor 3,4-dimethylpyrazole phosphate (DMPP). – Applied and Environmental Microbiology 83(1): 1-18.
[19] Dzwonko, Z. (2007): Guide to phytosociological research. – Instytut Botaniki Uniwersytetu Jagiellońskiego, Sorus, Poznań-Kraków (in Polish).
[20] Flechard, C., Ambus, P., Skiba, U., Rees, R., Hensen, A., van Amstel, A., van den Pol-van Dasselaar, A., Soussana, J., Jones, M., Clifton-Brown, J., Raschi, A., Horvath, L., Neftel, A., Jocher, M., Ammann, C., Leifeld, J., Fuhrer, J., Calanca, P., Thalman, E., Pilegaard, K., Marco, C. D., Campbell, C., Nemitz, E., Hargreaves, K., Levy, P., Ball, B., Jones, S., van de Bulk, W., Groot, T., Blom, M., Domingues, R., Kasper, G., Allard, V., Ceschia, E., Cellier, P., Laville, P., Henault, C., Bizouard, F., Abdalla, M., Williams, M., Baronti, S., Berretti, F., Grosz, B. (2007): Effects of climate and management intensity on nitrous oxide emissions in grassland systems across Europe. – Agriculture, Ecosystems and Environment 121(1-2): 135-152.
[21] Fuchs, K., Hörtnagl, L., Buchmann, N., Eugster, W., Snow, V., Merbold, L. (2018): Management matters: testing a mitigation strategy for nitrous oxide emissions on intensively managed grassland. – Biogeosciences Discussion 15: 5519-5543. https://doi.org/10.5194/bg-15-5519-2018.
[22] Harkot, W. A., Czarnecki, Z., Powroznik, M., Wankowicz, W. (2015): Initial growth and development of selected lawn varieties of *Lolium perenne* in various habitat conditions. – Grassland Science in Poland 18: 99-112.
[23] Hebeisen, T., Lüscher, A., Zanetti, S., Fischer, B., Hartwig, U., Frehner, M., Hendrey, G., Blum, H., Nösberger, J. (1997): Growth response of *Trifolium repens* L. and *Lolium perenne* L. as monocultures and biospecies mixture to free air CO_2 enrichment and management. – Global Change Biology 3(2): 149-160.
[24] Imer, D., Merbold, L., Eugster, W., Buchmann, N. (2013): Temporal and spatial variations of soil CO_2, CH_4 and N_2O fluxes at three differently managed grasslands. – Biogeosciences 10: 5931-5945.
[25] Jankowska-Huflejt, H. (2013): Persistence of grasses varieties and legumes mixtures selected for use grazing in organic farming. – Journal of Research and Applications in Agricultural Enginee 58(3): 229-234.
[26] Jankowski, K., Truba, M., Jankowska, J., Czeluscinski, W., Wiśniewska-Kadżajan, B., Malinowska, E., Koper, O. Góral, P., Kania, P., Matsyura, A. (2018): Effects of soil conditioners on lawn grass growth in different year seasons. – Applied Ecology and Environmental Research 16(4): 3755-3765.
[27] Kering, M. K., Butler, T. J., Biermacher, J. T., Guretzky, J. A. (2012): Biomass yield and nutrient removal rates of perennial grasses under nitrogen fertilization. – Bioenergy Research 5(1): 61-70.
[28] Koncz, P., Pintér, K., Balogh, J., Papp, M., Hidy, D., Csintalan, Z., Molnár, E., Szaniszló, A., Kampfl, G., Horváth, L., Nagy, Z. (2017): Extensive grazing in contrast to mowing is

http://www.aloki.hu ● ISSN 1589 1623 (Print) ● ISSN 1785 0037 (Online)
DOI: http://dx.doi.org/10.15666/aeer/1605_67616777
© 2018, ALÖKI Kft., Budapest, Hungary

climate-friendly based on the farm-scale greenhouse gas balance. – Agriculture, Ecosystems and Environment 240(1): 121-134.

[29] Langevin, B., Génermont, S., Basset-Mens, C., Lardon, L. (2015): Simulation of field NH_3 and N_2O emissions from slurry spreading. – Agronomy for Sustainable Development 35(1): 347-358.

[30] Linn, D. M., Doran, J. W. (1984): Effect of water-filled pore space on carbon dioxide and nitrous oxide production in tilled and non-tilled soils. – Soil Science Society of America Journal 48: 1267-1272.

[31] Lorenz, K., Lal, R. (2016): Environmental impact of organic agriculture. – Advances in Agronomy 139: 99-152.

[32] Maillard, É., Brian, G., McConkey, A., Angers, D. (2017): Increased uncertainty in soil carbon stock measurement with spatial scale and sampling profile depth in world grasslands: a systematic analysis. – Agriculture, Ecosystems and Environment 236(268): 268-276.

[33] Merbold, L., Eugster, W., Stieger, J., Zahniser, M., Nelson, D., Buchmann, N. (2014): Greenhouse gas budget (CO_2, CH_4 and N_2O) of intensively managed grassland following restoration. – Global Change Biology 20(6): 1913-1928.

[34] Mori, A. (2016): Greenhouse gas sink-source functions of grassland ecosystems. – The Japan Agricultural Research Quarterly 50(3): 187-190.

[35] Mori, A., Hojito, M. (2011): Nitrous oxide and methane emissions from grassland treated with bark- or sawdust-containing manure at different rates. – Soil Science and Plant Nutrition 57: 138-149.

[36] Mori, A., Hojito, M. (2015): Effect of dairy manure type and supplemental synthetic fertilizer on methane and nitrous oxide emissions from a grassland in Nasu, Japan. – Soil Science and Plant Nutrition 61(2): 347-358.

[37] MP (1987): The Montreal protocol on substances that deplete the ozone layer. Montreal, 16 September 1987. – Journal of Laws from 1992 98: Item 490 (in Polish).

[38] Mu, Z. J., Huang, A., Kimura, S. D., Jin, T., Wei, S., Hatano, R. (2009): Linking N_2O emission to soil mineral N as estimated by CO_2 emission and soil C/N ratio. – Soil Biology and Biochemistry 41: 2593-2597.

[39] Myhre, G., Shindell, D., Bréon, F. M., Collins, W., Fuglestvedt, J., Huang, J., Koch, D., Lamarque, J.-F., Lee, D., Mendoza, B., Nakajima, T., Robock, A., Stephens, G., Takemura, T., Zhang, H. (2013): Anthropogenic and natural radiative forcing. – In: Stocker, T. F., Qin, D., Plattner, G. K., Tignor, M., Allen, S. K., Boschung, J., Nauels, A., Xia, Y., Bex, V., Midgley, P. M. (eds.) Climate change. University Press, Cambridge, UK, pp. 659-740.

[40] Ravishankara, A. R., Daniel, J. S., Portman, R. W. (2009): Nitrous oxide (N_2O): the dominant ozone-depleting substance emitted in the 21st century. – Science 326(5949): 123-125.

[41] Sajeev, E. P. M., Winiwarter, W., Amon, B. (2018): Greenhouse gas and ammonia emissions from different stages of liquid manure management chains: abatement options and emission interactions. – Journal of Environmental Quality 47(1): 30-41.

[42] Shimizu, M., Hatano, R., Arita, T., Kouda, Y., Mori, A., Matsuura, S., Niimi, M., Jin, T., Desyatkin, A. R., Kawamura, O., Hojito, M., Miyata, A. (2013): The effect of fertilizer and manure application on CH_4 and N_2O emissions from managed grasslands in Japan. – Soil Science and Plant Nutrition 59(1): 69-86.

[43] Signor, D., Cerri, C., Pellegrino, E. (2013): Nitrous oxide emissions in agricultural soils: a review. – Pesq. Agropecuria Trop., Goiânia 43(3): 322-338.

[44] Skiba, U., Jones, S. K., Dragosits, U., Drewer, J., Fowler, D., Rees, R. M., Pappa, V. A., Cardenas, L., Chadwick, D., Yamulki, S., Manning, A. J. (2012): UK emissions of the greenhouse gas nitrous oxide. Philosophical Transactions of the Royal Society. – Biological Sciences 367(1593): 1175-1185.

http://www.aloki.hu ● ISSN 1589 1623 (Print) ● ISSN 1785 0037 (Online)
DOI: http://dx.doi.org/10.15666/aeer/1605_67616777
© 2018, ALÖKI Kft., Budapest, Hungary

[45] Sosnowski, J. (2012): Reaction of *Dactylis glomerata* L., *Festuca pratensis* Huds. and *Lolium perenne* L. to microbiological fertilizer and mineral fertilization. – Acta Scientiarum Polonorum - Agricultura 11(1): 91-98

[46] Sosulski, T., Szara, E., Stępień, W., Szymańska, M. (2014): Nitrous oxide emissions from the soil under different fertilization systems on a long-term experiment. – Plant Soil and Environmental 60(11): 481-488.

[47] Soussana, J. F., Allard, V., Pilegaard, K., Ambus, P., Amman, C., Campbell, C., Ceschia, E., Clifton–Brown, J., Czobel, S., Domingues, R., Flechard, C., Fuhrer, J., Hensen, A., Horvath, L., Jones, M., Kasper, G., Martin, C., Nagy, Z., Neftel, A., Raschi, A., Baronti, S., Rees, R. M., Skiba, U., Stefani, P., Manca, G., Sutton, M., Tuba, Z., Valentini, R. (2007): Full accounting of the greenhouse gas (CO_2, N_2O, CH_4) budget of nine European grassland sites. – Agriculture, Ecosystems and Environment 121: 121-134.

[48] Soussana, J. F., Tallec, T., Blanfor, V. (2010): Mitigation the greenhouse gas balance of ruminant production systems through carbon sequestration in grasslands. – Animal 4: 334-350.

[49] Springer, T. L. (2017): Effect of nitrogen fertilization and residual nitrogen on biomass yield of switchgrass. – Bioenergy Research 10(3): 648-656.

[50] Webb, J., Pain, B., Bittman, S., Morgan, J. (2010): The impacts of manure application methods on emissions of ammonia, nitrous oxide and on crop response - a review. – Agriculture, Ecosystems and Environment 137: 39-46.

[51] Weerasekara, C., Kitchen, N. R., Jose, S., Motavalli, P. P., Bardhan, S., Mitchell, R. B. (2018): Biomass yield of warm-season grasses affected by nitrogen and harvest management. – Agronomy Journal 110: 890-899. DOI: 10.2134/agronj2017.04.0196.

[52] Zarzycki, J., Bedla, D. (2017): The influence of past land-use and environmental factors on grassland species diversity. – Applied Ecology and Environmental Research 15(4): 267-278.

[53] Zhang, F., Qi, J., Li, F. M., Li, C. S., Li, C. B. (2010): Quantifying nitrous oxide emissions from Chinese grasslands with a process-based model. – Biogeosciences 7(6): 2039-2050.

[54] Zhang, Q., Kong, D., Singh, V. P., Shi, P. (2017): Response of vegetation to different timescales drought across China: spatiotemporal patterns, causes and implications. – Global Planetary Change 152: 1-11.

[55] Žurovec, O., Sitaula, B. K., Čustović, H., Žurovec, J., Dörsch, P. (2017): Effects of tillage practice on soil structure, N_2O emissions and economics in cereal production under current socio-economic conditions in central Bosnia and Herzegovina. – PLoS ONE 12(11): e0187681.

http://www.aloki.hu ● ISSN 1589 1623 (Print) ● ISSN 1785 0037 (Online)
DOI: http://dx.doi.org/10.15666/aeer/1605_67616777
© 2018, ALÖKI Kft., Budapest, Hungary

NEW RECORD OF THE ASIATIC WILDCAT (*FELIS SILVESTRIS ORNATA* GRAY 1830) IN NORTHEASTERN ANATOLIA

GÜNDOĞDU, E.* – SARI, A. – ARPACIK, A. – BAŞKAYA, Ş.

Department of Wildlife Ecology and Management, Faculty of Forestry, Karadeniz Technical University, 61080 Trabzon, Turkey
(phone: +90-505-934-3200)

**Corresponding author*
e-mail: ebubekirgundogdu@gmail.com

(Received 8th Jul 2018; accepted 6th Sep 2018)

Abstract. The aim of this study is to determine new distribution records of Asiatic wildcat in Northeastern Turkey. Latest distribution and status of this elusive cat was uncertain due to limited wildlife research in Turkey. This study was conducted in 2015 and 2016. Field studies were carried out based on direct and indirect observations. Besides obtaining camera trap photos, direct observations were conducted by one or two teams, each of which consisting of two wildlife experts. In indirect observations, all tracks, feces, spaw, scrape, urine and food remains were benefited from. As a result of the study, 6 camera trap video records belonging to Asiatic wildcat were obtained. Asiatic wildcat, once regarded as least concern species, is declining rapidly in its natural habitat because of habitat fragmentation followed by the pressure of large predators and excessive use of agricultural pesticides. This present study is an update on current distribution of Asiatic wildcat in Northeastern Anatolia of Turkey.
Keywords: *distribution, camera trap, wildcat, Bingöl, Turkey*

Introduction

There are twenty three recognized species of small wildcats worldwide (Yiqing and Yong, 1990; Nowell and Jackson, 1996; Jutzeler et al., 2010), being relatively primitive types and wild ancestors of domestic cats (Gao, 1987). Very simply, the European wildcat (Felis silvestris Schreber 1777) is distributed throughout Europe except for the northern regions; the African wildcat (*F. s. libyca* Forster 1780) is distributed in all African countries and south-western Asia; the Asiatic wildcat (*F. s. ornata* Gray 1830) is distributed in central and western Asia (Allen, 1938; Ellerman et al., 1951; Gao, 1987; Nowell and Jackson, 1996; Ablimit et al., 2010). The existence of distinguishable phenotypes across this wide distribution, along with apparently considerable local variation (Pocock, 1951; Yamaguchi et al., 2015), has left wildcat taxonomy in a state of confusion for many years (Guggisberg, 1975). The wildcat is a polytypic species with three wild subspecies, the European, African and Asiatic wildcats (Ragni and Randi, 1986, 1991; Wozencraft, 1993; Johnson and O'Brien, 1997). African and European wildcats are closely related and split recently, probably towards the end of the Last Glacial Maximum, as suggested by paleontological, biochemical and molecular data (Davis, 1987; Randi and Ragni, 1991; Masuda et al., 1996). Nowell and Jackson (1994) divided wildcats into three different forms; these three wildcat species seem to be more of a division of subspecies.

Domestic and wildcats can hybridize and generate fertile offspring both in captivity and in nature (Robinson, 1977; Ragni, 1993; Pierpaoli et al., 2003). The wildcats are now distributed worldwide due to deforestation, the spread of agriculture and the eradication of large predators, which have probably favoured the expansion of free-

http://www.aloki.hu ● ISSN 1589 1623 (Print) ● ISSN 1785 0037 (Online)
DOI: http://dx.doi.org/10.15666/aeer/1605_67796785
© 2018, ALÖKI Kft., Budapest, Hungary

ranging, often in sympatry with wildcat populations in Europe and Africa (Nowell and Jackson, 1996).

There are five members of the Felidae family cat species in Turkey. Those are Leopard (*Panthera pardus*), European wildcat (*Felis silvestris*), Jungle cat (*Felis chaus*), Lynx (*Lynx lynx*) and Caracal (*Caracal caracal*) (Sarı, 2018). However, ecology, taxonomy, latest status and correct distribution and population sizes of those species are uncertain due to limited wildlife researches. The present research provided a new distribution record of the Asiatic wildcat in a narrow area of Turkey.

Materials and methods

Study area

Study area is located in Yedisu county of Bingöl province (39°23'52"N; 40°36'39"E) in Northeastern Anatolia, Turkey (*Fig. 1*). Our main goals were to obtain distribution records of Asiatic wildcat from both Turkish and foreign literature and observed by local hunters, wildlife officers and unconfirmed information provided by local people. Therefore, this area was chosen as the study area.

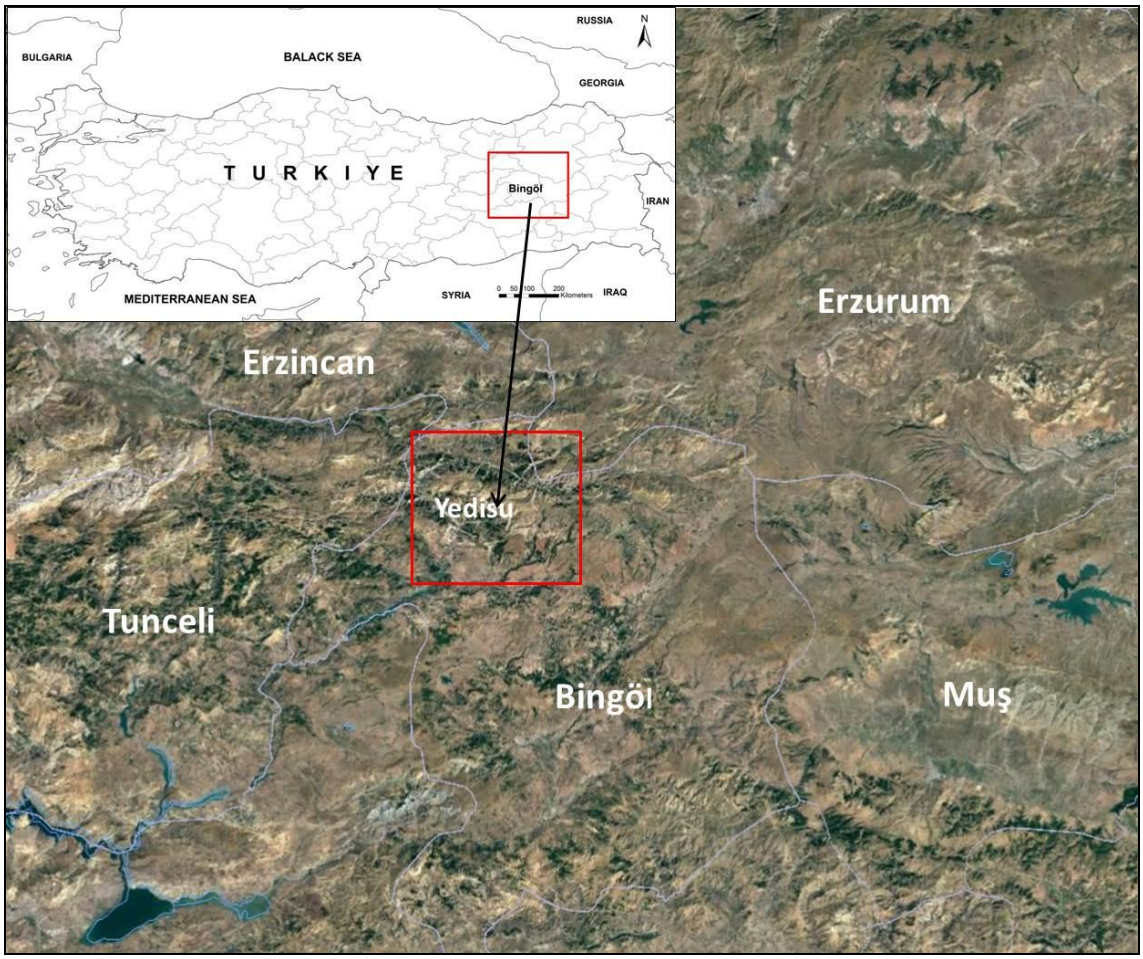

Figure 1. *Location of study area (Google Earth, 2018)*

http://www.aloki.hu ● ISSN 1589 1623 (Print) ● ISSN 1785 0037 (Online)
DOI: http://dx.doi.org/10.15666/aeer/1605_67796785
© 2018, ALÖKI Kft., Budapest, Hungary

The land in the study area is quite rugged and high, with an average elevation of 1500 m. Mountains and hilly areas occupy a very large space. The study area is surrounded by Çavuşlu Mountain (2660 m.) in the east, Devil Mountain (2950 m.) in the south, Bağır Mountain (3173 m.) in the west and Koşan Mountains (3078 m.) in the north. The heights of the high plateaus and plains on the mountains are not below 2000 m. Even most plains are located on over 1000 m from sea level. The upper parts of the mountains cover the glacial lakes and the skirts cover moraine remains. On majority lands of Bingöl province, the dominant climate is continental. Winters are long and harsh, and summers short and hot. Annual mean temperature is 5.1 °C. Considering the course of temperature in the year, the coolest month is January (-9 °C), while the hottest month is August (39 °C). Annual mean precipitation in Bingöl is 32.9 mm. The study area is predominantly the Iranian-Turanian floristic region in terms of vegetation. For this reason, in the regions where the study areas are located, plant societies generally consist of forest and steppe formation. The mountains are covered with sparsely forested, with parts of the southern parts of the mountains are often empty. Scots pine (*Pinus sylvestris*) forests are pure and mixed with a sparse and fragmented spread in the average 1300-2000 m. Oak forests (*Quercus sp.*) are located in the lower part of 1200 m, and Common aspen (Populus tremula) and Silver birch (*Betula pendula*) trees are covered also scattered fragments.

Materials

A total of 21 camera traps which have infrared features were used and placed along the line during the study (*Fig. 2*). Swarovski 10x42 LC binocular and ATS/STS 80 (HD) (20-60x) telescope were used for direct observation. Various digital cameras (3x optical zoom-5.0 Mega Pixels and 12x optical zoom-6.0 Mega Pixels) and video recorder (24x optical zoom) were used to take photographs of species, their habitats and to record observations. Global Positioning System (Magellan Explorist 500L) was employed to record the altitude and coordinates in the field. We also conducted interviews with national park officers, Turkish military services, villagers, and shepherds: field situation in the past, poaching, and whether the species of special interest to the local people was discussed.

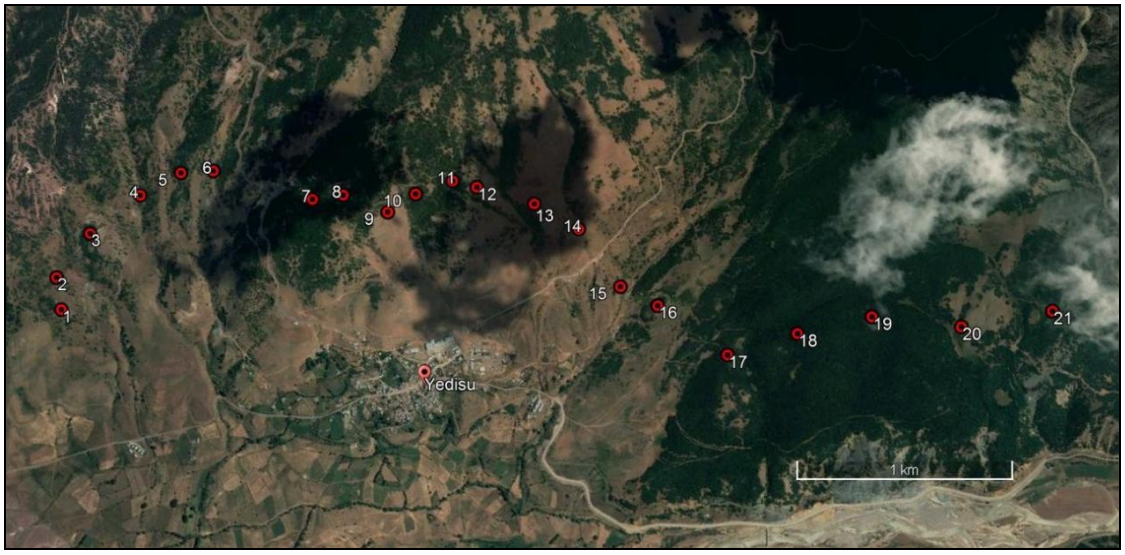

Figure 2. *Location of 21 camera traps (Google Earth, 2018)*

http://www.aloki.hu ● ISSN 1589 1623 (Print) ● ISSN 1785 0037 (Online)
DOI: http://dx.doi.org/10.15666/aeer/1605_67796785
© 2018, ALÖKI Kft., Budapest, Hungary

Methods

Field studies were conducted in 2015 and 2016 within a 150 km^2 area. We focused on making correct identifications of specimens and assessing the accuracy of observations by local hunters, wildlife officers and information provided by local people.

In external appearance Asiatic wildcat can only be confused with European wildcat, which has been characterized by its bushy tail, which ends as a broadly rounded black tip, and long soft fur with relatively conspicuous stripes (Yamaguchi et al., 2004). Asiatic wildcat has a slimmer build than European wildcat, a light brown or grey coloration with dark spots and a slim tail (Yamaguchi et al., 2004; Firouz, 2005; Yamaguchi et al., 2015). It was tried to obtain photographs and video images with camera traps in general. The camera traps were scattered randomly in the study area and were checked at certain times. The locations of camera traps were constantly changed according to tracks and indications obtained in the study area. Besides obtaining camera trap photos, direct observations were conducted by one or two teams, each of which consisting of two experts. In indirect observations, it was benefited from all tracks, feces, spaw, scrape, urine and food remains.

Results and discussion

Although specimens and living individuals of European wildcat have been reported in different parts of Turkey, The Asiatic wildcat records were obtained first in Yedisu, Bingöl in 2016 June. The Asiatic wildcat was only probably distributed in Northeastern of Turkey according to Demirsoy (1996). There is not any data about distribution of the Asiatic wild cat from Demirsoy (1996) in Turkey.

A total of 35625 photos and 161 hours of videos were recorded over 314 nights, making a total of 6594 trap nights for all the camera traps. As a result of the study 6 different camera trap video images belonging to one Asiatic wildcat were obtained. We checked all these data and found them to be *F. s. ornata*. Asiatic wildcat has distinct dark spots on its flanks as seen in the photos (*Fig. 3*). Our findings are in agreement with Ablimit and Khan (2013), that individuals identified in this study have a similar morphological structure with their findings. The coat pattern (color and points) of identified specimen are quite similar with them. Morphological criteria especially helped to resolve these identification problems in our study.

While European wildcats may be confused with domestic or feral cats, distinguishing them from Asiatic wildcat is easy. The wildcat's fur varies from tawny grey to light grey or sand colored, showing pronounced stripes and spots on the flanks, head and limbs, and also distinct rings on the black-tipped tail (Yamaguchi et al., 2004; Firouz, 2005). The European wildcat has been characterized by its bushy tail, which ends as a broadly rounded black tip, and long soft fur with relatively conspicuous stripes (Yamaguchi et al., 2015). The Asiatic wildcat is the least known and inhabits Eurasia from the Middle East to western India, through Central Asia to Mongolia and northwestern China. It is similar to the African wildcat, but is distinguishable by its coat pattern, which consists mainly of distinct dark spots instead of stripes. In most of the Middle East, including Iran, the Asiatic wildcat has spots on its flanks and head, while the coat of the European wild cat is uniformly greyish, without spots (Yamaguchi et al., 2004).

http://www.aloki.hu ● ISSN 1589 1623 (Print) ● ISSN 1785 0037 (Online)
DOI: http://dx.doi.org/10.15666/aeer/1605_67796785
© 2018, ALÖKI Kft., Budapest, Hungary

Domestic and wildcats can interbreed and produce fertile offspring both in captivity and in nature (Robinson, 1977; Ragni, 1993; Pierpaoli et al., 2003). However, Randi and Ragni (1991) determined that the rate of hybridization of domestic cat and wild cats was very low and they used their own large gene pools in breeding. In this study, it is thought that Asiatic cat individuals not hybrid individuals from European wild cat and domestic cat. But this problem is planned to be revealed in the future with another genetic study.

Figure 3. *Camera-trapped video images Asiatic wildcat in the study area*

Considering the habitat type characteristics of the areas belonging to the Asiatic wildcat, it has been determined that the important habitats are degraded Oak forest areas, rocky areas and pasture-grazing areas. These areas consist of grift shrub and trees and steep rocks. This habitat structure provides a number of concealed and escaped areas that can protect the Asiatic wildcat from larger compete predators such as leopard, lynx, wolf and bear.

There is limited information on the seasonal habitat use of Asiatic wildcat. However, it seems that the habitat use of the animal is strongly associated with the movements of its prey and human disturbance. Deforestation, the spread of agriculture and the eradication of large predators have probably favoured the expansion of free-ranging and feral cats, which are now distributed worldwide, often in sympatry with wildcat populations in Europe and Africa (Nowell and Jackson, 1996). The most important threats observed in the study for Asiatic wildcat are the habitat deterioration caused by overgrazing activities and the predatory pressure created by stray dogs and larger carnivore species.

http://www.aloki.hu ● ISSN 1589 1623 (Print) ● ISSN 1785 0037 (Online)
DOI: http://dx.doi.org/10.15666/aeer/1605_67796785
© 2018, ALÖKI Kft., Budapest, Hungary

Conclusions

In Turkey, wildlife studies on mammalian species are still not enough. This is the first documented report of the Asiatic wildcat's distribution from Turkey. As a conclusion, Northeastern Turkey should be thoroughly and regularly studied in order to better understand the Asiatic wildcat status and develop urgent conservation measures in these areas. It is important that further work be carried out to ascertain the size of the remaining Asiatic wildcat population in the other parts of Turkey. Despite the small size of the forest, the area is still rich in both fauna especially rodents and flora. It was observed that the populations of species that may be a food source for the Asiatic wildcat such as European hedgehog (*Erinaceus concolor* Martin 1837), European hare (*Lepus europaeus* Pallas 1778), Common Tortoise (*Testudo graeca* Linnaeus 1758) and Williams's jerboa (*Allactaga williamsi* Thomas 1897) were in very good condition. The Asiatic wildcat being the predator, has an important role in maintaining the health of the ecosystem. Therefore, the population size of the Asiatic wildcat could be used as indicator of sustainable conservation and management of the species in the area. Unknown and population size is critically small, any fatality of Asiatic wildcat individuals may lead to population extinction in the study area. Therefore, more studies should be carried out to investigate the reproduction status and sex composition of the Asiatic wildcat population in the study area. This would help the managers to control the population size over successive years using suitable management techniques.

REFERENCES

[1] Ablimit, A., Khan, B. (2013): Status of Asiatic wild cat and its habitat in Xinjiang Tarim Basin, China. – Open J. Ecology 3(8): 551-558.
[2] Ablimit, A., Khan, B., Masuda, R., Ohdachi, S. (2010): Asiatic wild cat (*Felis silvestris ornata*) is no more a 'Least Concern' species in Xinjiang, China. – Pakistan J. Wildlife 1(2): 57-63.
[3] Allen, G. M. (1938): The mammals of China and Mongolia. – National History of Central Asia 11(1): 312-489.
[4] Davis, S. J. (1987): The Archaeology of Animals. – BT Batsford Ltd., London.
[5] Demirsoy, A. (1996): Turkey's Vertebrates-Mammalians. – Ministry of Forestry: Project No: 90 K 1000: 90.
[6] Ellerman, J. R., Morrison-Scott, R. C. S. (1951): Checklist of Palearctic and Indian Mammals. – British National History Museum, London.
[7] Firouz, E. (2005): The Complete Fauna of Iran. – Tauris, London.
[8] Gao, Y. (1987): Fauna Sinica: Mammalia, Vol 8: Carnivora. – China Scientific Press, Beijing.
[9] Guggisberg, C. W. A. (1975): Wild Cats of the World. – David & Charles, London.
[10] Johnson, W. E., O'Brien, S. J. (1997): Phylogenetic reconstruction of the Felidae using 16S rRNA and NADH-5 mitochondrial genes. – Journal of Molecular Evolution 44: 98-116.
[11] Jutzeler, E., Xie, Y., Vogt, K. (2010): Asian wildcat (*Felis silvestris ornata*). – Cat News Special Issue 5: 42-43.
[12] Masuda, R., Lopez, J. V., Slattery, J. P., Yuhki, N., O'Brien, S. J. (1996): Molecular phylogeny of mitochondrial cytochrome b and 12S rRNA sequences in the Felidae: ocelot and domestic cat lineages. – Molecular Phylogenetics and Evolution 6: 351-365.
[13] Nowell, K., Jackson, P. (1996): Wild Cats: Status, Survey and Conservation Action Plan. – IUCN/Species Survival Commission Cat Specialist Group, Gland, Switzerland.

http://www.aloki.hu ● ISSN 1589 1623 (Print) ● ISSN 1785 0037 (Online)
DOI: http://dx.doi.org/10.15666/aeer/1605_67796785
© 2018, ALÖKI Kft., Budapest, Hungary

[14] Pierpaoli, M., Biro, Z. S., Herrmann, M., Hupe, K., Fernandes, M., Ragni, B. (2003): Genetic distinction of wildcat (*Felis silvestris*) populations in Europe, and hybridisation with domestic cats in Hungary. – Mol. Ecol. 12: 2585-2598.
[15] Pocock, R. I. (1951): Catalogue of the Genus Felis. – British Museum, London.
[16] Ragni, B. (1993): Status and Conservation of the Wildcat in Italy. – In: Seminar on the Biology and Conservation of the Wildcat (*Felis silvestris*), Nancy, France, 23-25 September 1992, Council of Europe, Environmental Encounters 16: 40-41.
[17] Ragni, B., Randi, E. (1986): Multivariate analysis of chraniometric characters in European wildcat, domestic cat and African wild cat (genus Felis). – Zeitschrift für Säugetierkunde 51: 243-251.
[18] Randi, E., Ragni, B. (1991): Genetic variability and biochemical systematics of domestic and wild cat populations (*Felis silvestris*: Felidae). – Journal of Mam. 72: 79-88.
[19] Robinson, R. (1977): Genetics for Cat Breeders. 2nd ed. – Pergamon Press, Oxford.
[20] Sarı, A. (2018): Habitat Use of Leopard (*Panthera pardus*) in Northeastern Anatolia. – Doctorate Thesis. K. T. Ü. Graduate School of Natural and Applied Sciences, Department of Forest Engineering, Trabzon.
[21] Wozencraft, W. C. (1993): Felidae. – In: Wilson, D. E., Reeder, D. M. (eds) Mammal Species of the World: A Taxonomic and Geographic Reference. Smithsonian Institution Press, Washington and London, pp. 290-291.
[22] Yamaguchi, N., Driscoll, C. A., Kitchener, A. C., Ward, J. M., Macdonald, D. W. (2004): Craniological differentiation between European wildcats (*Felis silvestris silvestris*), African wildcats (*F. s. lybica*) and Asian wildcats (*F. s. ornata*): implications for their evolution and conservation. – Biol J Linn Soc 83: 47-63.
[23] Yamaguchi, N., Kitchener, A. C., Driscoll, C. A. (2015): *Felis silvestris*. – The IUCN Red List of Threatened Species, Gland.
[24] Yiqing, M., Yong, M. (1990): On the protection status of cats (Felidae). – Wildl. of China 4: 7-9.

http://www.aloki.hu ● ISSN 1589 1623 (Print) ● ISSN 1785 0037 (Online)
DOI: http://dx.doi.org/10.15666/aeer/1605_67796785
© 2018, ALÖKI Kft., Budapest, Hungary

EVALUATION OF URBAN MULTI-SCALE LANDSCAPE ECOLOGICAL PATTERN BASED ON OPEN SPACE CLASSIFICATION: A CASE STUDY IN XINXIANG, CHINA

MAO, D.[1,2,3] – ZHANG, Y. C.[3] – KONG, D. Z.[2] – HE, S. L.[1,2,3*] – LI, X. Y.[2]

[1]*Postdoctoral Research Base, Henan Institute of Science and Technology Xinxiang, Henan 453003, China*

[2]*College of Forestry, Henan Agriculture University, Zhengzhou, Henan 450002, China*

[3]*School of Horticulture and Landscape Architecture, Henan Institute of Science and Technology, Xinxiang, Henan 453003, China*

**Corresponding author*
e-mail: maoda@foxmail.com

(Received 11th Jul 2018; accepted 13th Sep 2018)

Abstract. The past ten years have been a period of rapid urbanization in China, and are meaningful to evaluate urban landscape ecological pattern of this period. The urban landscape can be divided into the architectural space and 6 types of open space with different functions. Based on this kind of classification, this study used an urban area with 101 km^2 to evaluate landscape ecological pattern. This study chose 4 indices, namely, Patch density, Landscape shape index, Contagion index and Shannon's diversity index. Using ArcGIS and Fragstats, this study evaluated the landscape ecological patterns of various scales and multiple time points in the case area. The study found that at the macro level, except for the Patch density, which has the relatively obvious growth trend, the landscape ecological pattern indices of other overall levels are not significantly different in time series. However, at the micro level, the spatial differentiation characteristics of each index between 1 km^2 spatial units are very obvious and they have great changes according to the different time periods. Therefore, the evaluation of the landscape ecological pattern of the rapidly growing urbanization areas should pay more attention to the spatial unit comparison of the micro level, so as to discover the special areas in the urban space where the landscape ecology is unbalanced and unstable.
Keywords: *open space system, urban geography, landscape ecology, evaluation*

Introduction

Recently, China has witnessed rapid development of urbanization, and various elements in urban space have undergone drastic changes with rapid urbanization process. In this process , Chinese researchers have carried out many studies in combination with the practical situation of China (Chen et al., 2014; Wu et al., 2014). There are a series of problems to urban landscape ecology that need to be solved. Researchers and institutions have paid more attention to the related urban landscape ecological pattern research. It has been pointed out that the landscape ecological pattern of the city is suitable for observation and evaluation through multi-scale and flexible spatial classification (Li et al., 2010; Jun-Hyun et al., 2016; Grafius et al., 2018).

The ecological pattern of urban landscape should be viewed from the macro and micro level. At the macro level, observe the whole change of indicators, and at the micro level, observe the differences of indicators of different spatial units. The city is a spatially heterogeneous, and complex adaptive system. Landscape pattern and its changes are the results of the interaction of natural, social and biological elements

http://www.aloki.hu ● ISSN 1589 1623 (Print) ● ISSN 1785 0037 (Online)
DOI: http://dx.doi.org/10.15666/aeer/1605_67876799
© 2018, ALÖKI Kft., Budapest, Hungary

(Turner, 2003; Forman, 2016). The intensified human activities lead to fragmentation of landscapes, which have a series of impacts on ecosystems, and damage to the health and integrity of ecosystems, bringing about changes in ecosystem service functions. At the macro level, the city is human habitation, and is often used as a continuous construction site in ecological research. Its internal ecological features are different to express in large-scale space. Meanwhile, at the micro level, because the inner city is divided into different lots by artificial roads, its ecological features and ecological functions are very different from the macro scale.

The main reasons for the study of urban landscape ecology at the micro level are the accuracy of data and the classification of spatial elements (Wang, 2010). In the traditional study, many large scale studies regard 30-m square as a basic grid element. These studies juxtapose urban construction land and forest land, fields, water bodies, etc. which are outside the main urban area as large-scale elements, but ignore the complexity and diversity of urban landscape ecology. The essence of ecological function in urban open space system is that the basic space unit is an organic whole which are associated with each other. The urban green space system was once the main research object of urban landscape ecology. But the analysis and optimization of urban green land mostly stay on the classification of lots on drawings. The green space on drawings has a large subjective qualitative component which cannot reflect the ecological effects such as real green coverage in a region at the middle and micro level and cannot quantify the urban landscape ecological pattern.

Landscape ecological classification is the basis and prerequisite for landscape pattern analysis and landscape function evaluation (Xiao et al., 1998). In recent years, the theory of urban open space systems studied by Chinese domestic scholars has made new developments in spatial classification (Wang, 2005; Wang et al., 2012; Wang, 2010; Shao, 2011; Mao et al., 2016a, b). Open space is a general term of surface space outside the building in the city. Therefore, urban landscape can be divided by the most basic architectural space and the open space. At first, the open space is divided into green open space which represents green coverage and gray open space which represents road, square, waste land, etc. (Wang, 2005). With the continuous study of researchers, the open space can be divided into 6 types: green open space, blue open space (Wang, 2010), light gray open space, dark gray open space, yellow green space ("Production land" in the original paper, Shao, 2011) and brown open space. Together with the architectural space, these six types form the basic landscape classification for our study. The meaning of various types of space can be seen in *Table 1*.

Table 1. *Table of landscape ecological elements based on open space classification*

Space classification	Meaning
Green open space	Trees, shrubs, lawns and other cities have plants covered space
Blue open space	Rivers, ditches, lakes and other water bodies in cities
Light grey open space	Piazza, open-air stadium, open car park and outdoor temporary stacking sites
Deep grey open space	Urban traffic space, such as road, track, viaduct, etc.
Brown open space	Bare land, abandoned land, urban space under demolition and construction
Yellowish open space	Agricultural planting areas in urban space
Architectural space	The space occupied by buildings in the city or the space beyond the open space

http://www.aloki.hu ● ISSN 1589 1623 (Print) ● ISSN 1785 0037 (Online)
DOI: http://dx.doi.org/10.15666/aeer/1605_67876799
© 2018, ALÖKI Kft., Budapest, Hungary

This classification method combines the author's thinking on the classification of open space. It has strong identifiability in remote sensing, aerial photography and other resources, and reflects the ecological value of different levels. There were similar practice studies before (Wang, 2010). So study group consider that this open space classification can well reflect the urban landscape pattern. Using this classification method to interpret and classify high-precision satellite imagery cannot only satisfy the macro-scale landscape ecological pattern evaluation, but also meet the micro-scale landscape ecological pattern evaluation.

Case area and data

Case area

The study area is located in Xinxiang City, China. Xinxiang City is located in 35°18' north latitude and 113°54' east longitude, which is one of the core cities of China's Central Plains urban agglomeration (*Fig. 1*). Xinxiang City covers an area of 422 km^2 and a total area of about 140 km^2, with the population of 1.4 million. The research object of this time is the main city of Xinxiang City (*Fig. 2*). It is surrounded by the loop line which is comprised by four roads. It is 101 km^2. The main city area of Xinxiang City is flat and the boundary is composed of four outer loop expressways. It is clear and complete. The traffic in the urban area is basically a square road network. It is an ideal plain landscape ecological city model.

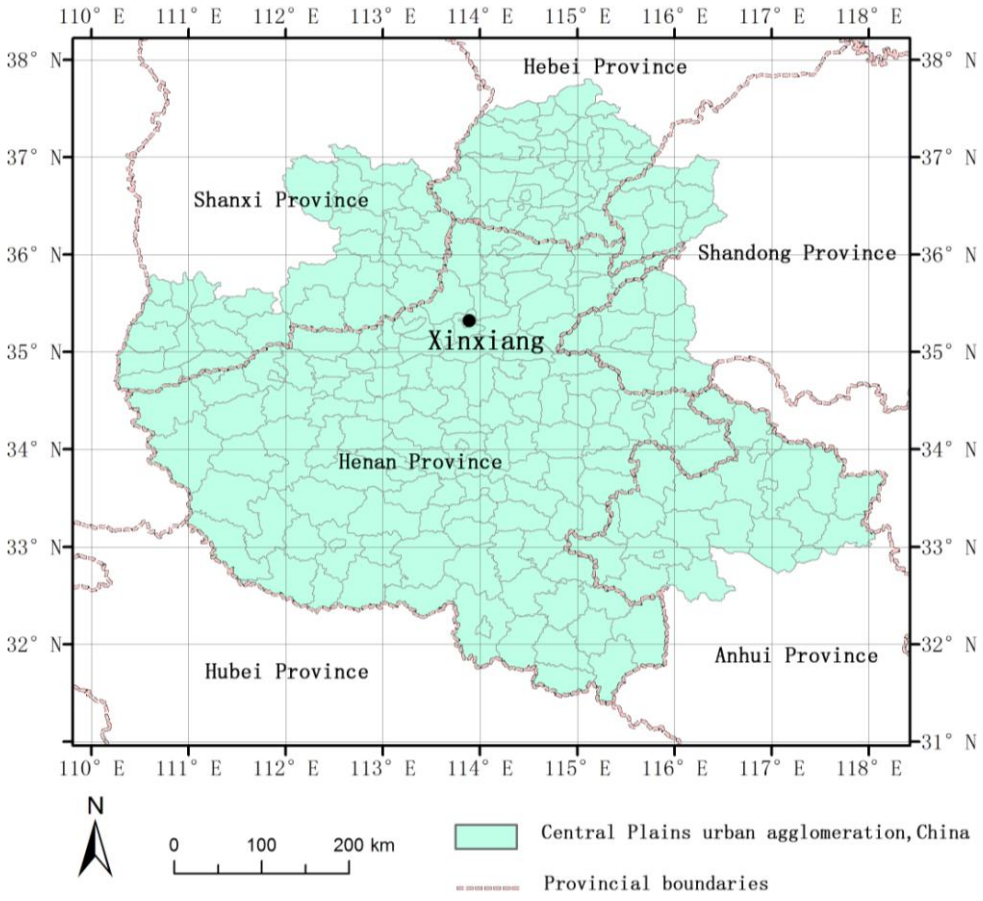

Figure 1. *Location map of Xinxiang and Central Plains urban agglomeration*

http://www.aloki.hu ● ISSN 1589 1623 (Print) ● ISSN 1785 0037 (Online)
DOI: http://dx.doi.org/10.15666/aeer/1605_67876799
© 2018, ALÖKI Kft., Budapest, Hungary

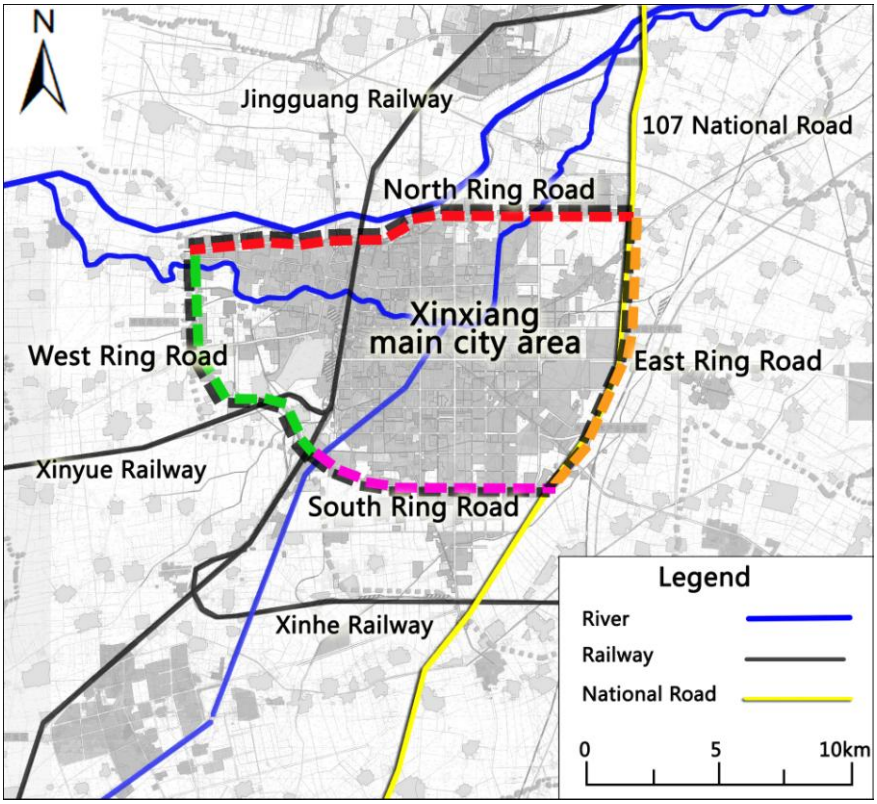

Figure 2. *Map of main city area of Xinxiang*

Case data

The study chose time-series high-definition satellite imagery (mostly with 0.85-m resolution, a small amount with 1.85-m resolution), and comprehensively carried out a variety of methods including visual interpretation, and combined with the basic grid unit for refined opening spatial elements extract in categories, so as to achieve full coverage of urban spatial classifications. Finally, in the case area, the classified data resources of 5 time nodes (2008, 2010, 2012, 2014, and 2016) were obtained. These data can reflect the spatial and temporal evolution of landscape ecology in the last 10 years of Xinxiang City's main urban area in a more detailed and comprehensive way.

Method

Many researchers used remote sensing images and related geospatial data as information sources, and used GIS technology and landscape pattern software to classify and analysis. Wang Shengnan divided open space into green, blue, gray and other types in her doctoral dissertation (Wang, 2010), through landscape ecological pattern analysis and other methods were used to analyze the evolution mechanism of the main city area of Luoyang in the process of rapid urbanization. In Shao Dawei's doctoral dissertation, he used remote sensing data and landscape pattern indicators to analyze the spatial evolution of Nanjing (Shao, 2011). At the same time, it is more common to study urban microcosmic spatial analysis with unit grids (Guo, 2016; Gao, 2014). The unit scale of these studies is basically 1 km^2. These studies provide an important reference to software selection and index selection of this paper.

http://www.aloki.hu ● ISSN 1589 1623 (Print) ● ISSN 1785 0037 (Online)
DOI: http://dx.doi.org/10.15666/aeer/1605_67876799
© 2018, ALÖKI Kft., Budapest, Hungary

Study software

The software used in the research mainly includes ArcGIS and Fragstats. ArcGIS is a most used geographic information software in the world nowadays. By using ArcGIS, various kinds of geographic data can be connected and matched. Transformation between vector data and grid data can also be finished. Fragstats are mainly used to deal with landscape ecological pattern index. There are many softwares for analyzing or simulating landscape ecological pattern, such as Fragstats, Patch Analyst, APACK, SIMMAP, etc. Fragstats is a software for calculating landscape index which was developed by the Department of Forest Science at Oregon State University in America. Because it is free and easy to use, it can support a series of landscape pattern index at three levels: Patch Metrics, Class Metrics and Landscape Metrics. At present, Fragstats is a computer program for quantitative analysis of landscape structure and spatial pattern, which can calculate including landscape area, density, size and difference, edge, shape, core lot, nearest neighbor structure, diversity structure, aggregation and dispersion structure and hundreds of indices which are combined with statistics. There are many cases of landscape ecology research using these two software (Hua et al., 2008; Midha and Mathur, 2010; Kupfer, 2012; Ojoyi et al., 2017; Yan et al., 2018). So choosing these two software is very suitable.

Index selection

Based on the previous research results (Wu, 2007; Hong et al., 2011; Liu et al., 2013), patch density, landscape shape index, contagion index and Shannon's diversity index were selected as analysis indicators in this study.

Patch density

Patch density (PD) is an index of the number of patches divided by the total area (Wu, 2007), and it is generally used to observe landscape fragmentation (see *Eq. 1* for calculation). In the equation, N represents the number of patches and A represents the area. The larger the patch density is, the greater the fragmentation is, so it is regarded as a reverse index in this study.

$$PD = N/A \quad \text{(Eq.1)}$$

Landscape shape index

The landscape shape index (LSI) is the total length of all plaque boundaries in the landscape (m) divided by the square root of the total area of the landscape (m), multiplied by the square correction constant (Wu, 2007; see *Eq. 2* for calculation). In the equation, E is the total length of all patch boundaries in the landscape, and A is the total area of the landscape. In urban space, the high value area of LSI value is usually the area where human activities are dense and the degree of fragmentation is higher.

$$LSI = \frac{0.25E}{\sqrt{A}} \quad \text{(Eq.2)}$$

http://www.aloki.hu ● ISSN 1589 1623 (Print) ● ISSN 1785 0037 (Online)
DOI: http://dx.doi.org/10.15666/aeer/1605_67876799
© 2018, ALÖKI Kft., Budapest, Hungary

Contagion index

Contagion index (CONT) is considered to describe the degree of agglomeration or extension trend of different piecemeal types in the landscape (Wu, 2007; see *Eq. 3* for calculation). In the equation, m is the total number of plaque types, and P_{ij} is the probability that two adjacent grid cells randomly selected belong to type i and j. Like other indicators of ecological pattern, its significance of the Numbers will vary according to the interpretation of different majors and directions. Generally speaking, the high contagion index indicates that a certain dominant block type in the landscape has formed a good connectivity, while the low value indicates that the landscape fragmentation degree is high.

$$CONT = \left[1 + \sum_{i=1}^{m}\sum_{j=1}^{n}\frac{P_{ij}\ln(P_{ij})}{2\ln(m)}\right](100) \quad \text{(Eq.3)}$$

Shannon diversity index

Shannon diversity index (SHDI) is obtained by multiplying the area ratio of various patches by the negative value of the sum of the natural logarithm of that value (Wu, 2007; see *Eq. 4* for calculation). In the equation, m represents the number of species and P_i represents the proportion of individuals belonging to the first species in the sample. In ecology, Shannon's diversity index is a sensitive index, which is generally used to reflect landscape heterogeneity. When the index is 0, it shows that the patch is a single patch, and the greater the value of the patch is, the more balanced each patch is, and the higher the land use degree is.

$$SHDI = -\sum_{i=1}^{m}\left[P_i\ln(P_i)\right] \quad \text{(Eq.4)}$$

Research steps

First item

This research first carries on the analysis from the macroscopic scale. Taking ArcGIS 10.2 as the basic software platform, the vector data of the case area that has been interpreted and classified are projected and converted into grid data of 1 m × 1 m. Loading raster data into fragstats can quickly get macro-scale indicators.

Second item

For the microscopic scale, this study chose to generate 1 km × 1 km grids in the UTM projection coordinate system (*Fig. 3*), and took each grid as the microscopic observation unit of the case area. In *Fig. 3,* for ease of study, the researchers digitally represent the abscissa and alphabetically represent the ordinates of the table. Such grid units can be named, for example, A01, A02, etc. At the same time, In ArcGIS, the generated grid is used to cut the transformed grid data, which will allow you to generate hundreds of separate grid files. Then, the batch processing function in fragstats can be used to quickly analyze and get the index value of each unit.

http://www.aloki.hu ● ISSN 1589 1623 (Print) ● ISSN 1785 0037 (Online)
DOI: http://dx.doi.org/10.15666/aeer/1605_67876799
© 2018, ALÖKI Kft., Budapest, Hungary

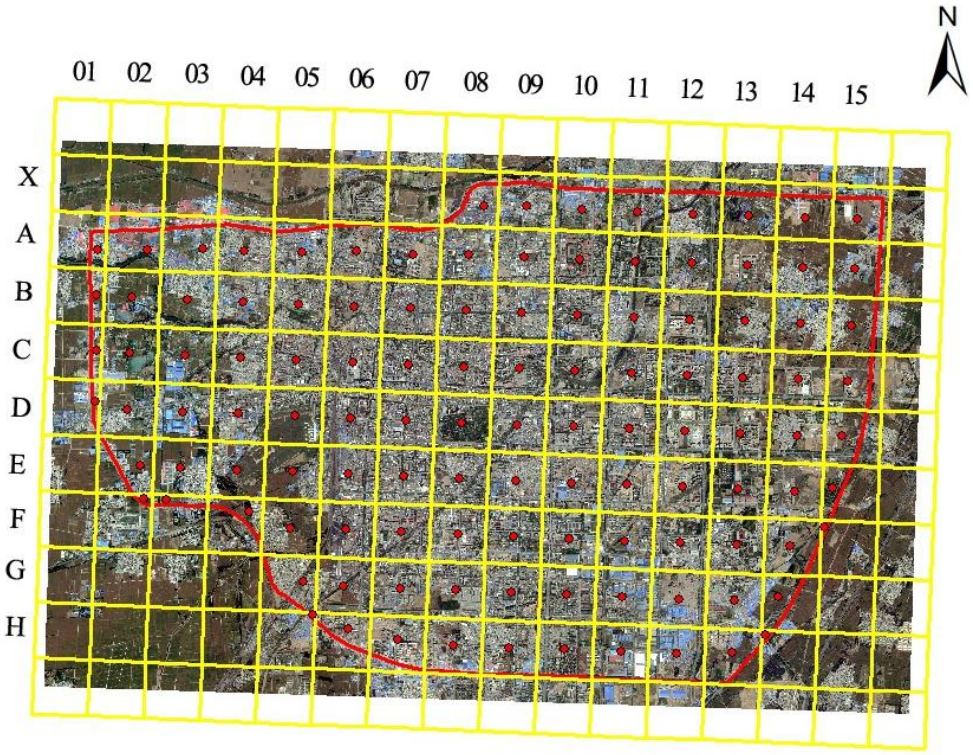

Figure 3. *case area satellite picture divided by 1 km× 1km grid*

Third item

The spatial unit can be connected with the index in ArcGIS by format conversion of the obtained spatial unit index values. By classifying the connection results, the micro-scale landscape ecological pattern of the case area can be visualized in ArcGIS.

Results and analysis

Macro-scale

This study first used software to calculate the indicators for landscape ecological pattern in case area from 2008 to 2012 (*Table 2*). *Table 2* shows that the number of patches in (NP) declined gradually, while it rose overall from 2012 to 2016, which shows that a certain degree of fragmentation of urban space is not a linear change but dynamic development.

Table 2. *Table of indicators for landscape ecological pattern in case area (2008-2016 years)*

YEAR	PD (patch density)	LSI (landscape shape index)	CONT (contagion index)	SHDI (Shannon diversity index)
2008	482.290	167.860	47.355	1.649
2010	468.196	169.820	46.154	1.687
2012	466.767	168.244	47.562	1.637
2014	509.865	177.523	46.086	1.675
2016	493.580	173.527	47.250	1.641

http://www.aloki.hu ● ISSN 1589 1623 (Print) ● ISSN 1785 0037 (Online)
DOI: http://dx.doi.org/10.15666/aeer/1605_67876799
© 2018, ALÖKI Kft., Budapest, Hungary

According to the number of different types of patches, the number of blue patches and yellow-green patches decreased linearly, while the number of other types of patches fluctuated. The change of landscape shape index (LSI) is small, showing a fluctuating and rising state, which indicates that the intervention of artificial behavior on the environment has increased to a certain extent. In 2008-2016, due to the solidification of the boundary of the main urban area, the indexes of the overall level, such as contagion index, Shannon's diversity index and aggregation index, all changed little, and the indicators need to be compared with each other in a downsized scale.

Micro scale

According to *Figure 4,* there are obvious spatial differences. The scale of the value is obtained by determining the global median and then the arithmetical difference. The minimum value of unit's PD increased from 45 in 2008 to more than 100 in 2016, and the maximum value increased from about 1400 in 2008 to more than 1600, indicating that the rapid urbanization has brought about increased spatial fragmentation. There are continuous units with high patch density in the northwest and central part of the main urban area for a long time. These units belong to the living area of the old city and the small industrial factory area, the buildings are mostly low stories, the building density is generally high, and the open space is broken up seriously. Besides, the patch density of the southeast part of the main urban area is relatively low, the building is generally multi-storey, the high level is high, and the open space is relatively complete.

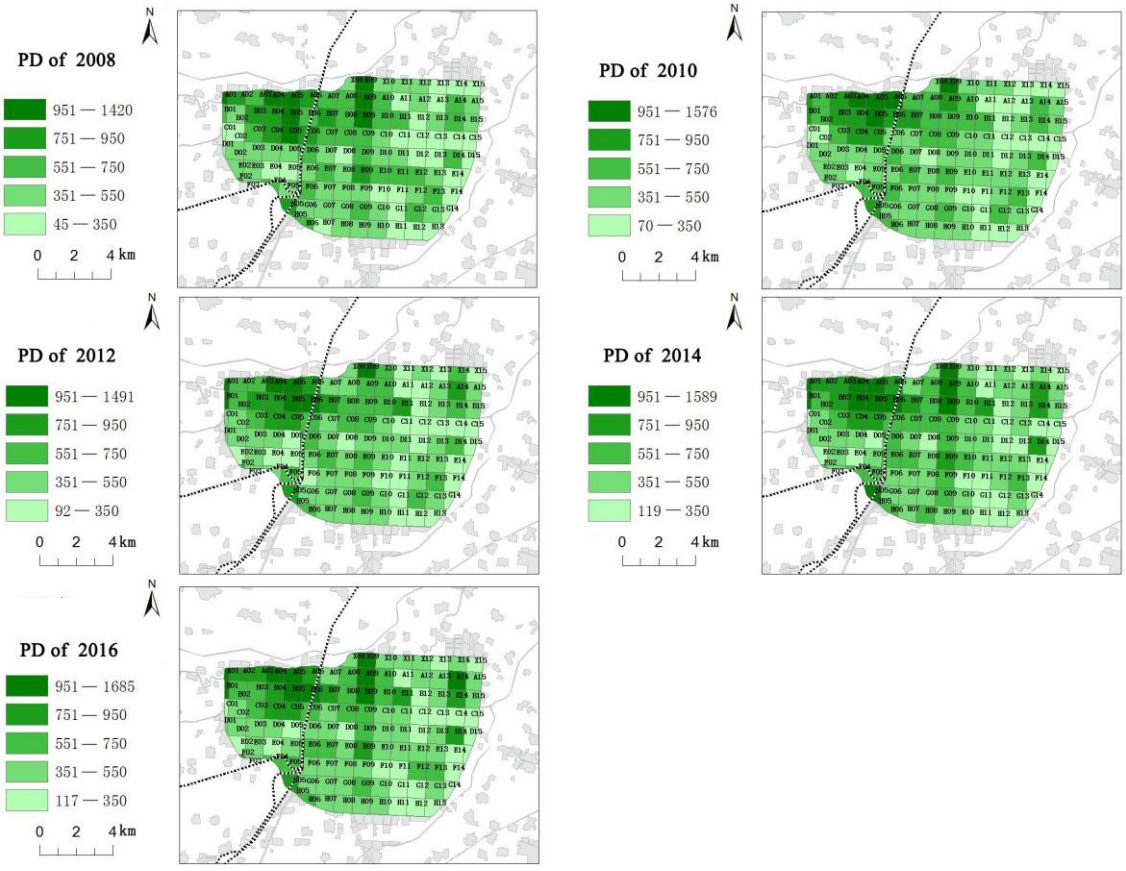

Figure 4. *Pattern maps of patch density based on Xinxiang grid units in 2008-2016*

http://www.aloki.hu ● ISSN 1589 1623 (Print) ● ISSN 1785 0037 (Online)
DOI: http://dx.doi.org/10.15666/aeer/1605_67876799
© 2018, ALÖKI Kft., Budapest, Hungary

From *Figure 5* it can be seen that the difference between the unit and the surrounding area of the people's park is very obvious, and the contrast between the old urban area in the west and the new urban area in the east is also obvious. Green open space, large proportion of yellow and green space landscape shape index are relatively low. Because of the village in the city, the landscape shape index of the east and south of the main urban area is decreasing, while the central and northern land block is in high value for a long time.

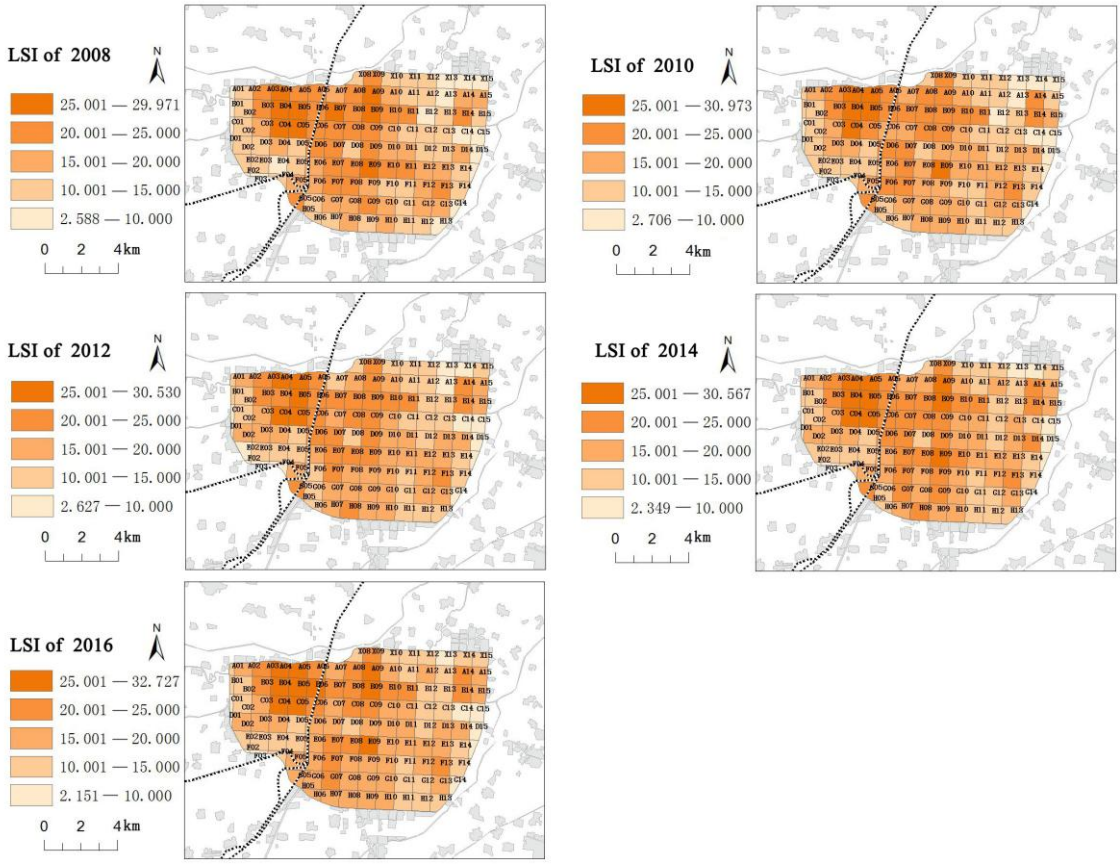

Figure 5. *Pattern maps of Landscape shape index based on Xinxiang grid units in 2008-2016*

From 2008 to 2016, *Figure 6* shows that the high value units of the spreading degree gradually change from the edge of the main urban area to the central zone of the main urban area, which reflects the recent decade of urban construction on the yellow and green space (suburban farmland) erosion. While the contrast between the high value units and the adjacent low value units in the central part of the city is becoming more and more obvious, which reflects that there is still a large imbalance in the urban center area.

According to *Figure 7,* the main urban area of Xinxiang city as a whole presents the distribution pattern of low central area and high surrounding area. And there are obvious low value continuous units around the railway line and in the northeast of the main urban area. The number of very low value units and very high value units has declined in the last decade, which reflects that the urban construction of the main urban area has entered a more stable period.

http://www.aloki.hu ● ISSN 1589 1623 (Print) ● ISSN 1785 0037 (Online)
DOI: http://dx.doi.org/10.15666/aeer/1605_67876799
© 2018, ALÖKI Kft., Budapest, Hungary

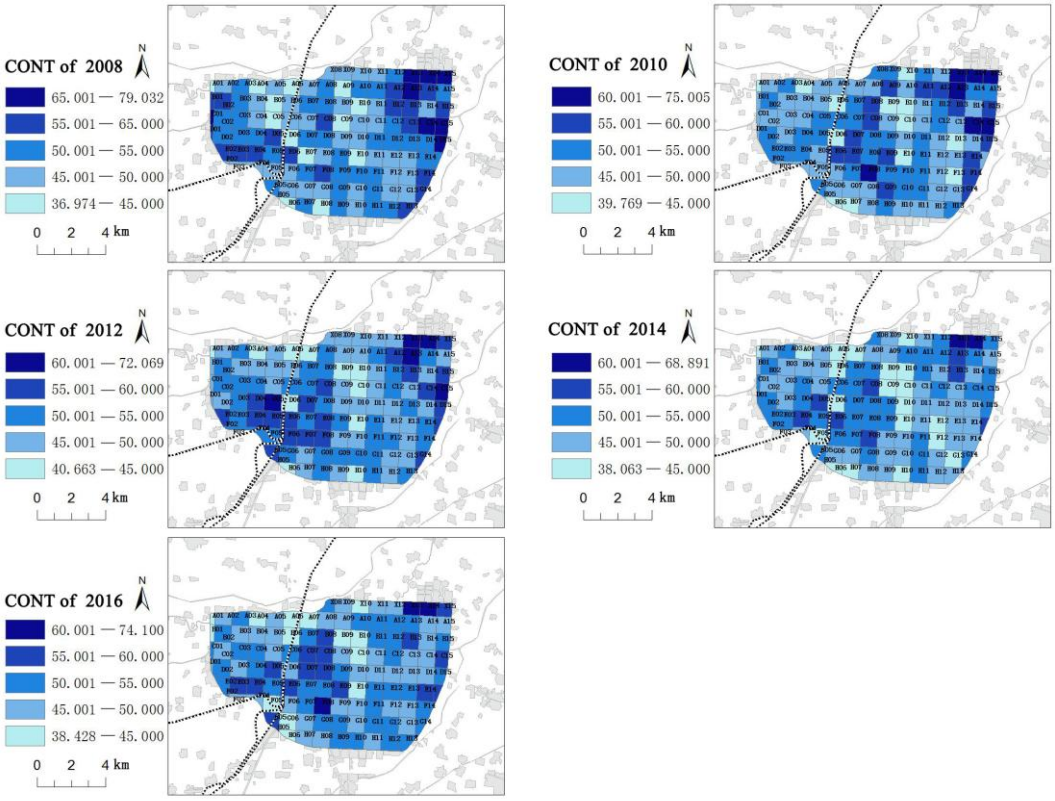

Figure 6. *Pattern maps of contagion index based on Xinxiang grid units in 2008-2016*

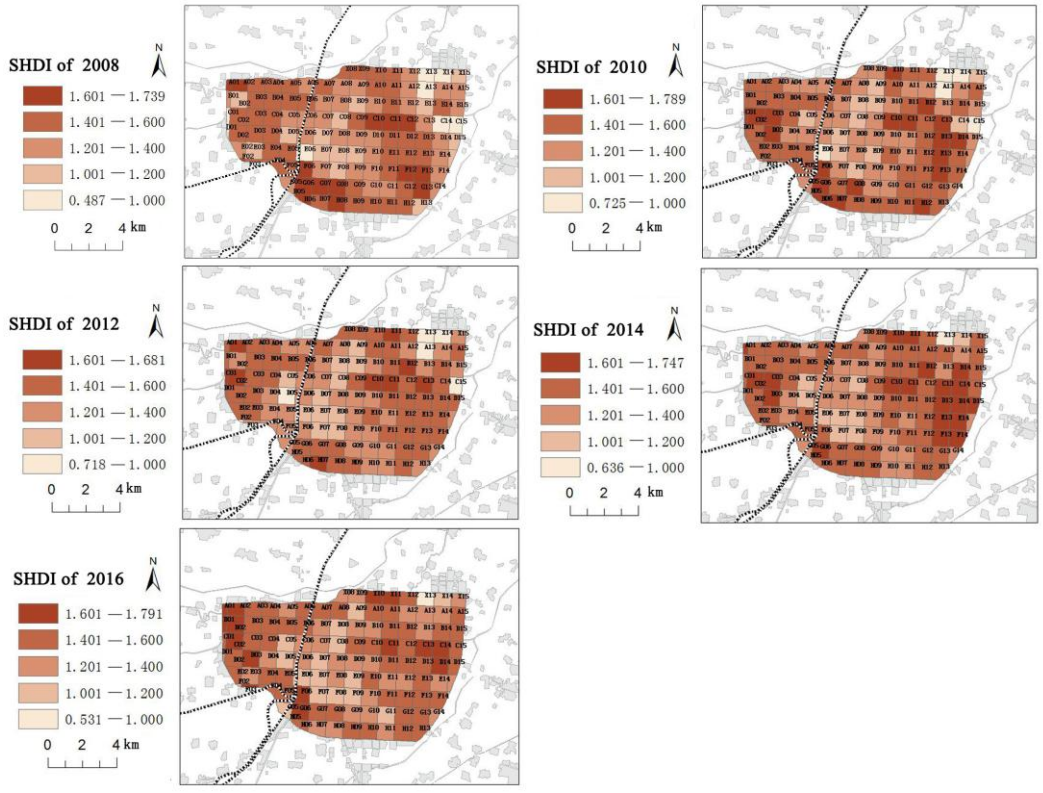

Figure 7. *Pattern maps of Shannon diversity index based on Xinxiang grid units in 2008-2016*

http://www.aloki.hu ● ISSN 1589 1623 (Print) ● ISSN 1785 0037 (Online)
DOI: http://dx.doi.org/10.15666/aeer/1605_67876799
© 2018, ALÖKI Kft., Budapest, Hungary

Comparative analysis

It is found that the landscape ecological pattern in the main urban area of Xinxiang is not consistent in macro scale and micro scale, especially in micro scale. On the one hand, the distribution of green open space and blue open space is not balanced. The green coverage rate of old urban area, shantytown and village in city is very low, and it is the key area of ecological development. On the other hand, brown open space is an important factor affecting urban ecological environment, and its volume is very large. The spatial distribution of the blue open space is quite different, so it is recommended to actively repair the city river and build the ecological corridor. The generation of brown open space occurs more frequently in the process of urban renewal and transformation, and the new construction land is more likely to produce brown open space. Moreover, brown open space is also characterized by a rapid transformation into a green open space. The conversion of green open space and brown open space is also worthy of attention.

Conclusions

The dynamic trajectory of cities can never be fully predicted or controlled, but can and should be influenced or guided in more desirable directions through planning and design activities that are based on urban ecological knowledge and sustainability principles (Ramalho and Hobbs, 2012; Ahern, 2013; Kattel et al., 2013; Wu, 2014; Tanner et al., 2016). For landscape ecological pattern, different scale and precision of observation can obtain different study results. Compared with previous studies, this study is more innovative based on the latest classification of open space and the combination of micro grid units. Based on high resolution image and open space classification, this study classified and extracted the urban space system of the case area. This study analyzed Patch density, Landscape shape index, Contagion index and Shannon's diversity index from the macro level and the micro level. Comparative analysis at the micro level can discover some problem areas that are not found at the macro level. At the micro level, the spatial differentiation characteristics of each index between spatial units are very obvious and they have great changes according to different time period. Therefore, the evaluation of the landscape ecological pattern in the rapidly growing urbanization areas should pay more attention to the spatial unit comparison at the micro level, so as to discover the special areas in the urban space where the landscape ecology is unbalanced and unstable. Urban construction and planning should be able to timely monitor and pay attention to the spatial units with low landscape ecological patterns. These can serve the current "Urban Repair" and "Ecological Restoration" services and improve the overall ecological quality of cities and regions.

REFERENCES

[1] Ahern, J. (2013): Urban landscape sustainability and resilience: the promise and challenges of integrating ecology with urban planning and design. – Landscape Ecology 28(6): 1203-1212.

[2] Chen, L. D., Li, X. Z., Fu, B. J., et al. (2014): Development history and future research priorities of landscape ecology in China. – Acta Ecologica Sinica 34(12): 3129-3141.

http://www.aloki.hu ● ISSN 1589 1623 (Print) ● ISSN 1785 0037 (Online)
DOI: http://dx.doi.org/10.15666/aeer/1605_67876799
© 2018, ALÖKI Kft., Budapest, Hungary

[3] Forman, R. T. T. (2016): Urban ecology principles: are urban ecology and natural area ecology really different? – Landscape Ecology 31(8): 1-10.
[4] Gao, X. W., Fei, X. Y., Zhang. Z. G. et al. (2014): The aggregation degree evaluation of urban park green space based on convolution method. – Acta Ecologica Sinica 34(15): 4446-4453.
[5] Grafius, D. R., Corstanje, R., Harris, J. A. (2018): Linking ecosystem services, urban form and green space configuration using multivariate landscape metric analysis. – Landscape Ecology 33(4): 557-573.
[6] Guo, H. X., Huang, Y., Zhao, D. Q. et al. (2016): Researches on urban compactness based on grid method: a case study of Tianhe District, Guangzhou. – Urban Planning International 31(4): 51-57.
[7] Hong, H. J., Peng, X. C., Chen, Z. L. et al. (2011): The investigation of spatiotemporal patterns of landscape fragmentation during rapid urbanization in Changsha City. – Remote Sensing for Land & Resources (1): 133-137.
[8] Hua, S., Xie, G. X., Shi, L. et al. (2008): Quantitative analysis and optimization of the landscape patterns based on GIS and FRAGSTATS in urban areas: a case in Changsha. – Ecology and Environment 17(4): 1554-1559.
[9] Jun-Hyun, K., Gu, D., Wonmin, S. et al. (2016): Neighborhood landscape spatial patterns and land surface temperature: an empirical study on single-family residential areas in Austin, Texas. – International Journal of Environmental Research & Public Health 13(9): 880.
[10] Kattel, G. R., Elkadi, H., Meikle, H. (2013): Developing a complementary framework for urban ecology. – Urban Forestry & Urban Greening 12(4): 498-508.
[11] Kupfer, J. A. (2012): Landscape ecology and biogeography rethinking landscape metrics in a post-fragstats landscape. – Progress in Physical Geography 36(3): 400-420.
[12] Li, Y., Wang, Y. L., Peng, J. et al. (2010): Assessment of urban land suitability for construction in view of landscape ecology: a case study of Dandong City. – Acta Ecologica Sinica 30(8): 2141-2150.
[13] Liu, Q., Yang, Y., Tian, H. (2013): Quantitative study on urban spatial pattern of lanzhou city from the perspective of landscape ecology. – Journal of Arid Land Resources & Environment 27(1): 47-52.
[14] Mao, D., Liu, Y. P., Wang, F. Z. et al. (2016a): Growth trend analysis of carbon dioxide (CO_2) emissions and urban green open spaces: a case study of Henan, China. – Oxidation Communications 39(4): 3305-3312.
[15] Mao, D., Zhao, M. L., Liu, J. Y. et al. (2016b): Quality evaluation of provincial urban open space system - a case study from Henan Province, China. – RISTI - Revista Iberica de Sistemas e Tecnologias de Informacao (E8): 131-141.
[16] Midha, N., Mathur, P. K. (2010): Assessment of forest fragmentation in the conservation priority Dudhwa landscape, India using FRAGSTATS computed class level metrics. – Journal of the Indian Society of Remote Sensing 38(3): 487-500.
[17] Ojoyi, M. M., Odindi, J., Mutanga, O. et al. (2017): Analysing fragmentation in vulnerable biodiversity hotspots in Tanzania from 1975 to 2012 using remote sensing and FRAGSTATS. – Nature Conservation 16(2): 19-37.
[18] Ramalho, C. E., Hobbs, R. J. (2012): Time for a change: dynamic urban ecology. – Trends in Ecology & Evolution 27(3): 179-188.
[19] Shao, D. W. (2011): Study on the Evolution, Mechanism and Optimization of Urban Open Space Pattern. – Nanjing Normal University, Nanjing.
[20] Tanner, C. J., Adler, F. R., Grimm, N. B. et al. (2016): Urban ecology: advancing science and society. – Frontiers in Ecology & the Environment 12(10): 574-581.
[21] Turner, M. G. (2003): Landscape ecology: the effect of pattern on process. – Annual Review of Ecology & Systematics 20(20): 171-197.
[22] Wang, F. Z. (2005): On the optimization of urban opening spatial system in Chinese cities. – Human Geography 20(2): 1-8+113.

http://www.aloki.hu ● ISSN 1589 1623 (Print) ● ISSN 1785 0037 (Online)
DOI: http://dx.doi.org/10.15666/aeer/1605_67876799
© 2018, ALÖKI Kft., Budapest, Hungary

[23] Wang, F. Z., Wang, S. N., Li, M. (2012): Dynamic evolution and optimization of green open space in Luoyang. – Geographical Research 31(7): 1209-1223.
[24] Wang, S. N. (2010): Analysis & Optimization on Urban Open Space System of Luoyang in Urbanizing Progress. – Henan University, Kaifeng.
[25] Wu, J. (2014): Urban ecology and sustainability: the state-of-the-science and future directions. – Landscape & Urban Planning 125(2): 209-221.
[26] Wu, J. G. (2007): Landscape Ecology: Pattern, Process, Scale and Hierarchy (2nd ed.). – Higher Education Press, Beijing.
[27] Wu, J. G., Xiang, W. N., Zhao, J. (2014): Urban ecology in china: historical developments and future directions. – Landscape & Urban Planning 125(3): 222-233.
[28] Xiao, D. N., Zhong, L. S. (1998): Ecological principles of landscape classification and evaluation. – Chinese Journal of Applied Ecology 9(2): 217-221.
[29] Yan, J. X., Zhang, J. F., Han, Y. (2018): FRAGSTATS based study of urban green space landscape pattern in Handan City. – Journal of Chinese Urban Forestry 16(1): 127-142.

http://www.aloki.hu ● ISSN 1589 1623 (Print) ● ISSN 1785 0037 (Online)
DOI: http://dx.doi.org/10.15666/aeer/1605_67876799
© 2018, ALÖKI Kft., Budapest, Hungary

ALLEVIATION OF WATER STRESS AND PROMOTION OF THE GROWTH OF SUGAR BEET (*BETA VULGARIS* L.) PLANTS BY MULTI-TRAITS RHIZOBACTERIA

KARAGÖZ, H.[1,3] – ÇAKMAKÇI, R.[2] – HOSSEINPOUR, A.[1*] – KODAZ, S.[1]

[1]*Department of Field Crops, Faculty of Agriculture, Atatürk University, 25240 Erzurum, Turkey*

[2]*Department of Agronomy, Faculty of Agriculture, Çanakkale Onsekiz Mart University 17100 Çanakkale, Turkey*

[3]*East Anatolia Agricultural Research Institute, Gezköy-Dadaskent, 25090 Erzurum, Turkey*

**Corresponding author*
e-mail: arash.pour@atauni.edu.tr

(Received 13th Jul 2018; accepted 20th Sep 2018)

Abstract. Drought stress may affect the yield and sucrose accumulation of sugar beet by restricting leaf and root growth**.** The effect of inoculation of nine IAA-producing, N_2-fixing, P-solubilizing and ACC deaminase-containing bacteria on the yield and morpho-physiological parameters of sugar beet under five different water regimes was investigated. The diminishing water supply caused a gradual decrease in the plant growth, chlorophyll contents, root and leaf weight and sugar content, accompanied by increasing activities of drought stress markers (GR, GST, G6PD, 6PGD, MDA and H_2O_2). Although it varied depending on the water regimes and bacterial strains, the results of two pot experiments show that inoculation with multi-traits plant growth promoting bacteria stimulated overall plant growth, including enzyme activity, sugar content, fibrous and storage roots development and leaf yield and the contents of leaf chlorophyll, N, P, K, Ca, Mg, Na, Mn and Zn, but decreased MDA and H_2O_2 contents, which might partly contribute to the activation of the processes involved in the alleviation of the effect of water stress.
Keywords: *water stress, enzyme activity, nutrients uptake, plant growth-promoting bacteria, malondialdehyde content (MDA), hydrogen peroxide (H_2O_2)*

Introduction

Beta vulgaris L. (sugar beet) is a very significant industrial sugar product, and the most significant input for sugar beet production is mineral fertilizer. Sugar beet production demands more water, but recently, stress of water has turn into an important limitation to sugar beet production, causing serious reductions in productivity. Drought is described by the decrease of water content. One of the most widespread environmental factors affecting plant fertility is drought. During the drought, level of water in leaf decrease and turgor is diminished. As result, reduces cell growth and yield with stoma closes. Drought inhibits the photosynthesis of plants, and thus reduces growth and development. Water stress reduces the production rate of dry matter and is considered as one of the major limiting factors for sugar beet root and leaf yield (Pidgeon et al., 2006; Romano et al., 2013). As evidenced, sucrose concentration and photosynthesis extremely responsive to drought because of its activity reduces with the growing water shortage (Bloch et al., 2006).

Plant-growth-promoting rhizobacteria (PGPR) improve many physiological, nutritional, morphological and biochemical plant responses, and thus, it enhances the plant resistance to abiotic and biotic stresses. The inoculation of selected drought-tolerant strains can reduce the yield limitation caused by water deficit and improve the

http://www.aloki.hu ● ISSN 1589 1623 (Print) ● ISSN 1785 0037 (Online)
DOI: http://dx.doi.org/10.15666/aeer/1605_68016813
© 2018, ALÖKI Kft., Budapest, Hungary

ability of plant tolerance to drought stress (Marulanda et al., 2009; Castillo et al., 2013). In this regard, the use of PGPR is seen as a different tactic to induce stress endurance in cultivation. PGPR has skill to fix nitrogen, solubilize inorganic phosphate, generate 1-aminocyclopropane-1-carboxylate (ACC) deaminase and indole acetic acid (IAA), and support plant development. The bacteria which having ACC deaminase can decrease the negative effects of ethylene causing stress of water (Safronova et al., 2006). Under stress conditions in plants, while "stress ethylene" production increases if the bacteria prevent the ethylene synthesis and containing ACC deaminase, plants can reduce the level of ethylene, expected to provide protection against the inhibitory effects of stress in plants (Çakmakçı et al., 2009).

For increase the crop production, we need to selected effective bacteria which plant growth-promoting rhizobacteria. In addition to there are a few number of studies which against water stress using PGPR. Different approaches are required for better water wasting due to the lack of water resources for this reason, this study was governed for research the effect of varied ACC deaminase-containing, IAA-producing, N2-fixing and/or P-solubilizing bacterial species on the growth, antioxidant and pentose phosphate oxidative cycle enzymes, root yield and quality, in the sugar beet, under different water regimes (150%, 100%, 75%, 50%, and 25% of water-holding capacity). In this study, under limited water conditions, we aimed to reduce the loss of quality and efficiency depending on the stress and to increase the water stress resistance of sugar beet by using bacteria inducing the plant growth.

Materials and methods

Bacterial species

The bacterial species *Bacillus subtilis* RC11, *Bacillus subtilis* RC63, *Pseudomonas fluorescens* T26, *Rhodococcus erythropolis* RC9, and *Variovorax paradoxus* RC21 were isolated from the rhizosphere of wild red raspberries, and *Paenibacillus polymyxa* RC05 was isolated from wheat (Çakmakçı et al., 2007, 2009). The other four strains (*Pseudomonas putida* RC310, *Pseudomonas fluorescens* PF8/6, and *Bacillus megaterium* A21/3) were isolated from the rhizosphere of tea (Çakmakçı et al., 2010). Some features of bacteria used in the experiment are given in *Table 1*.

Table 1. *Some features of bacteria used in the experiment*

Used bacterial isolates	IAA-production (μg mL^{-1} OD_{600} $unit^{-1}$)	Nitrogenase activity (nmol C_2H_4, 10^7 cfu h^{-1})	P- solubilization (μg P mL^{-1} d^{-1})	ACC deaminase activity (nmol α-ketobutyrate mg^{-1} protein h^{-1})
Rhodococcus erythropolis RC9	22.6 ± 1.5	0.55 ± 0.11	27.8 ± 1.5	577.8 ± 26.7
Pseudomonas fluorescens T26	23.9 ± 2.1	0.61 ± 0.13	27.7 ± 1.2	796.1 ± 35.2
Paenibacillus polymyxa RC05	32.8 ± 2.6	0.68 ± 0.14	10.1 ± 0.9	682.1 ± 33.7
Bacillus subtilis RC11	29.4 ± 1.8	0.32 ± 0.12	16.6 ± 0.4	539.2 ± 21.2
Variovorax paradoxus RC21	19.4 ± 1.2	0.47 ± 0.12	35.7 ± 2.1	332.6 ± 17.4
Pseudomonas putida RC310	25.9 ± 2.4	0.56 ± 0.15	26.8 ± 1.8	746.2 ± 46.8
Pseudomonas fluorescens PF8/6	20.7 ± 1.5	0.47 ± 0.09	113.5 ± 12.7	223.6 ± 21.7
Bacillus subtilis RC63	29.7 ± 1.9	0.74 ± 0.17	34.6 ± 0.08	972.0 ± 28.3
Bacillus megaterium A21/3	19.5 ± 1.1	0.48 ± 0.16	74.3 ± 1.9	276.3 ± 16.7

Data were means ± standard error of three replicates

http://www.aloki.hu ● ISSN 1589 1623 (Print) ● ISSN 1785 0037 (Online)
DOI: http://dx.doi.org/10.15666/aeer/1605_68016813
© 2018, ALÖKI Kft., Budapest, Hungary

Experiments and growth conditions

This study was established under natural light in green house Department of Field Crops, Faculty of Agriculture, Atatürk University of Erzurum during 2010-2011 production season. Sugar beet seedlings were grown in a greenhouse during the initial period in a night- day cycle of 10-14 h light, 15 to 24 °C, and 60% humidity and during the development period in 15-9 h day-night, 16-28 °C and 55-60% relative humidity. Two different trial sets were established as a factorial arrangement (treatments x water regimes) in randomized complete block design with five replications. Totally 11 applications existed in both test sets; (1) control (no bacteria and no mineral fertilizers), (2) NP-fertilizers (55 mg of N + 40 mg P/kg soil), (3) *R. erythropolis* RC9, (4) *P. fluorescens* T26, (5) *P. polymyxa* RC05, (6) *B. subtilis* RC11, (7) *V. paradoxus* RC21, (8) *P. putida* RC310, (9) *P. fluorescens* PF8/6, (10) *B. subtilis* RC63 and (11) *B. megaterium* A21/3, and five water regimes, randomly distributed into pots filled with equal amounts of soil. The soil was a sandy clay loam with an organic substance content of 3.2%, pH 7.6, present Olsen-phosphorus content of 16.2 mg kg^{-1} and total N content of 15.7 mg kg^{-1}. Replaceable K, Ca, Mg and Na were 448, 3420, 472 and 78 mg kg^{-1}; present Fe, Mn, Zn and Cu contents were 5.9, 9.6, 1.2 and 1.7 ppm. Bacterial inoculation of the seeds was carried out according to Sahin et al. (2004).

Two pots essay were made on sugar beet fully watered (100% of water-holding capacity (WHC)), under waterlogging (150% of the maximum WHC), and continuous moderate (75% and 50% of WHC) and severe water stress (25% of WHC). At the beginning of the experiment, pots were saturated with water to determine the water-holding capacity (WHC) per pot; pots were covered to prevent evaporation and they were left for free drainage. After the drainage was stopped, pots were weighed and WHC was found. After sugar beet was planted, all the pots were irrigated at the rate of 65 ± 5% of WHC to provide the seedling emergence and seedling hold for 3 weeks after planting. After three weeks from planting, different irrigation levels were started to be applied in both sets of experiment. Irrigation applications were determined by the amount of available moisture in the soil. By this method, to determine the available moisture in the soil, the amount of moisture, which can bring WHC to the same soil, was determined and different ratios were discussed for the consummation of the lost moisture. Amount of irrigation water that would be given for each pot determined that difference as coefficient (150% 100, 75%, 50%, 25%) multiplying. The pots were measured every three days), the amount of irrigation water diminishing from each group was completed by adding according to pot's own capacity.

After two weeks from planting, seedlings were thinned in the pots, in each pot, 5 plants were remained in five leaf period for the first and 1 plant was allowed in seven leaf period for the second experiment. Using a chlorophyll meter SPAD-502 (Minolta, Japan), Chlorophyll contents of leaves which the top fourth and fifth was evaluated. The first experiment set was harvested 65 days after sowing and the second set was harvested 130 days after sowing. A t 80 °C, dry weightiness was detected by drying for 48 h. Sugar beets' sugar contents in storage-root were detected during harvesting and it was expressed as a weight per plant.

Definition of enzyme activities and protein concentrations

Leaves which washed three times in total was adjusted as ph 8.0 and Using liquid nitrogen, plant examples were homogenized The activities of glutathione reductase

http://www.aloki.hu ● ISSN 1589 1623 (Print) ● ISSN 1785 0037 (Online)
DOI: http://dx.doi.org/10.15666/aeer/1605_68016813
© 2018, ALÖKI Kft., Budapest, Hungary

(GR; EC 1.8.1.7), glutathione S-transferase (GST; EC 2.5.1.18), glucose-6-phosphate dehydrogenase (G6PD; EC 1.1.1.49) and 6-phosphogluconate dehydrogenase (6PGD; EC 1.1.1.44) were determined with the according to Carlberg and Mannervik (1985), Habig and Jacoby (1981) and Beutler (1984). Each enzyme activity was detected spectrophotometrically (Shimadzu Spectrophotometer UV-1208, Kyoto, Japan) at 25 °C. Protein concentration was calculated according to the method of Bradford (1976) with help to 595 nm absorbance measurement by using as the standard of bovine serum albumin.

Measurement of H_2O_2 and MDA

The content of H_2O_2 was assessed according to the method described by Sairam and Srivastava (2002). The density of H_20_2 was determined spectrophotometrically by reading the absorbance of the titanium-hydro peroxide complex and calculated using a standard curve drawn with a known H_2O_2 concentration. Lipid peroxidation was determined by estimating the malondialdehyde (MDA) content in fresh leaf weight according to the method of Heath and Packer (1968), prepared in 10% trichloroacetic acid containing 0.65% 2-thiobarbituric acid (TBA) and it was heated at 95 °C for 25 min, and then quickly cooled. The concentration of MDA was calculated from the absorbance at 532 nm and expressed as nmol g^{-1} FW.

Macro and micro element content of sugar beet leaf

The leaf samples were dried in the oven at 68 °C for 48 h and milled to 1 mm. Total N was measured by The Kjeldahl method and a Vapodest 10 Rapid Kjeldahl Distillation Unit (Gerhardt, Konigswinter, Germany). Following the extraction process, Macro- (P, K, Ca and Mg) and micro-elements (Fe, Mn, Zn and Cu) were detected by the inductively Coupled Plasma spectrophotometer (Optima 2100 DV, ICP/OES, Perkin-Elmer, Waltham MA, USA).

Statistical analysis

Analysis of variance from SPSS 13.0 (SPSS Inc.) programme was performed on the data obtained from both trials and then in conformity with Duncan's Multiple Range Test, the means were separated. The level of enzyme activities was evaluated in three samples from each replicate.

Results

In terms of sugar beet root dry weight for both harvests (65-day and 130-day harvest), all treatments, except for *P. fluorescens* PF8/6, gave better results compared to control (*Table 2*). According to the average irrigation level, the highest dry root weight was achieved with *P. putida* RC310 and *B. subtilis* RC63 inoculations in both trials. If sugar beet was harvested at early period, it was found that water restriction importantly reduced the root weight. Inoculation with RC310 and RC63 increased fresh and dry leaf weight compared to control and fertilizers, but other inoculations gave the same result with mineral fertilizer. Strains RC310, RC63, RC11, T26, and RC21 were most effective in promoting fresh and dry leaf weight of sugar beet in both trials set. Moreover, these strains were found to be effective in terms of fresh and dry leaf and root weight at water constraint applications at levels of 75%, 50% and 25% of WHC. In

http://www.aloki.hu ● ISSN 1589 1623 (Print) ● ISSN 1785 0037 (Online)
DOI: http://dx.doi.org/10.15666/aeer/1605_68016813
© 2018, ALÖKI Kft., Budapest, Hungary

the excessive water application of both trial sets, primarily IAA-producing and N_2-fixing *P. polymyxa* RC05 and *R. erythropolis* RC9, all bacteria inoculations importantly increased dry root and leaf weight, and the amount of sugar per plant compared to control. Water-stressed plants inoculated with the effective PGPR recorded improved the plant growth in terms of dry root weight, and sugar per plant compared to the un-inoculated, water-stressed plants (*Table 2; Fig. 1*). As an average of the five water regimes, PGPR inoculation increased dry storage root weight by 0.3-41.5% and 2.1-45.6% at the first and second trials, whereas, NP fertilizer increased root weight by 20.2 and 31.8%, respectively, compared with control (*Table 2*). In the application of water at the rate of 25% of WHC, inoculation with RC310 and RC11 achieved an increase respectively of 37.6 and 35.5%, and 43.0 and 39.5% in the trial first and second compared with control. These were, however, higher than 6.1% and 9.2% increases by NP fertilization over control.

Table 2. *The effect of PGPR and fertilizer application on the dry storage root leaf weight of sugar beet in different harvest and under different water regimes*

Treat-ments	Water regimes at first trial set was harvested 65 days after sowing						Water regimes at second trial set was harvested 130 days after sowing					
	WR1	WR2	WR3	WR4	WR5	Mean	WR1	WR2	WR3	WR4	WR5	Mean
Dry storage root weight (g/plant)												
Control	3.46	5.13	3.72	3.20	2.79	3.66 d	45.9	56.7	44.4	37.4	28.6	43.4 d
NP	4.56	7.01	4.14	3.41	2.96	4.40 bc	55.8	89.3	63.4	43.6	34.1	57.2 b
RC9	4.80	5.85	3.42	3.30	2.79	4.03 c	60.2	73.2	42.3	40.1	33.0	49.8 c
T26	4.41	4.86	4.52	4.15	2.92	4.17 bc	55.3	60.8	55.3	51.6	32.0	51.0 c
RC05	4.85	5.61	3.71	3.46	3.34	4.19 bc	60.6	70.3	43.4	43.7	39.0	51.4 c
RC11	4.02	5.51	5.09	3.99	3.78	4.48 b	50.4	69.2	56.5	48.2	39.9	53.0 bc
RC21	4.63	5.22	4.03	3.96	3.31	4.23 bc	58.0	64.2	49.3	47.7	38.5	51.5 c
RC310	4.77	7.51	5.41	4.88	3.84	5.18 a	57.4	90.7	67.2	59.6	40.9	63.2 a
PF8/6	4.67	4.75	3.18	2.78	2.82	3.67 d	58.7	59.5	39.0	33.6	30.6	44.3 d
RC63	4.15	6.46	6.32	5.47	3.02	5.08 a	52.0	83.6	68.0	60.1	35.0	61.9 a
A21/3	4.46	5.82	3.99	3.84	2.89	4.20 bc	55.8	73.0	49.3	46.6	31.9	51.3 c
Mean	4.44 b	5.80 a	4.32 b	3.86 c	3.12 d	4.31	55.5 b	71.9 a	52.6 c	46.5 d	35.3 e	52.4
Dry leaf weight (g/plant)												
Control	5.68	7.94	5.93	5.23	4.58	5.87 e	37.3	51.6	34.8	26.5	27.4	35.5 f
NP	7.43	11.52	9.05	6.43	5.05	7.89 b	39.6	72.1	45.4	33.2	28.8	43.8 bc
RC9	7.76	10.00	5.54	5.91	4.70	6.78 cd	46.1	60.7	33.1	33.5	26.7	40.0 cd
T26	7.75	8.71	7.62	7.29	5.03	7.28 cd	47.0	52.9	45.8	42.7	28.5	43.4 c
RC05	7.76	8.93	5.84	5.48	5.43	6.69 d	42.1	54.2	34.8	28.7	27.4	37.4 ef
RC11	6.41	9.37	8.09	6.72	5.69	7.28 cd	37.8	56.7	48.5	39.3	31.8	42.8 cd
RC21	8.38	9.00	6.73	6.45	5.29	7.17 cd	49.4	54.6	40.3	37.9	27.6	42.0 cd
RC310	7.76	11.54	9.65	8.02	6.60	8.71 a	47.0	70.1	58.1	47.1	37.9	52.0 a
PF8/6	7.87	9.25	6.35	5.50	4.65	6.73 cd	42.4	56.1	37.8	31.4	28.1	39.2d-f
RC63	6.69	10.01	9.19	8.59	5.89	8.07 b	40.0	60.8	55.0	50.2	30.8	47.3 b
A21/3	7.14	10.22	7.17	6.97	5.00	7.30 c	42.6	61.6	42.69	39.6	27.9	42.9 cd
Mean	7.32 b	9.68 a	7.38 b	6.60 c	5.26 d	7.25	42.9 b	59.2 a	43.3 b	37.3 c	29.3 d	41.8

The difference between the averages shown the same letter not important ($p < 0.01$); WR: water regimes

http://www.aloki.hu ● ISSN 1589 1623 (Print) ● ISSN 1785 0037 (Online)
DOI: http://dx.doi.org/10.15666/aeer/1605_68016813
© 2018, ALÖKI Kft., Budapest, Hungary

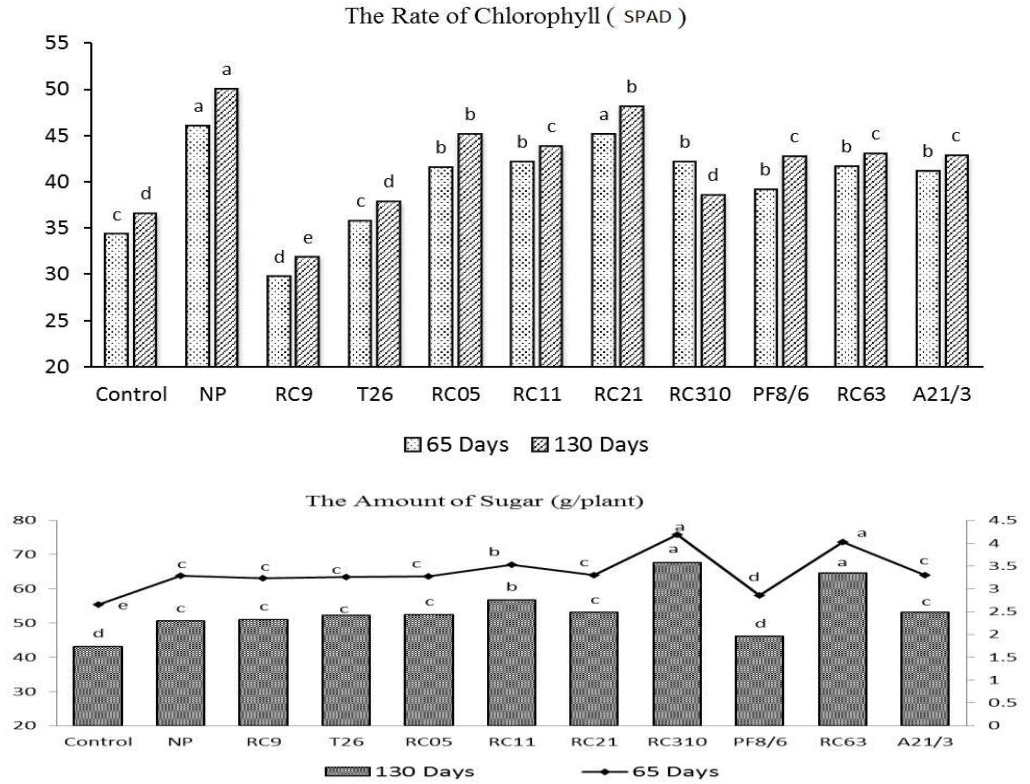

Figure 1. *Effect of PGPR and mineral fertilizer on the chlorophyll content and sugar per plant at the first (65 days) and second trial (130 days) average of five water regimes*

Under waterlogging stress (150% of WHC), sugar beet chlorophyll contents importantly raised NP fertilizer, RC21, A21/3 and RC05 inoculation. The maximum chlorophyll contents in the sugar beet leaves was found after RC21, followed by RC11, RC310 and RC05 inoculations under water stress applied at 75%, 50% and 25% WHC in both experiments (*Fig. 1*). In both trial sets, water stress decreased the chlorophyll contents of sugar beet, and generally, inoculation of the multi traits bacteria under water stress improved the chlorophyll contents, but responses were strain-specific. Chlorophyll content was positively and importantly correlated ($p \leq 0.01$) with dry root weight ($r = 0.35^{**}$), dry leaf weight ($r = 0.36^{**}$) and sugar per plant ($r = 0.34^{**}$) contents.

Of the bacterial inoculations, RC310 and RC63 produced the highest sugar per plant compared to control and mineral fertilizer while other inoculations gave the same result with mineral fertilizer. The highest ACC deaminase-containing RC63, RC310, RC11, and T26 inoculation were found to be effective according to the amount of sugar per plant at water constraint applications with 75%, 50% and 25% WHC (*Fig. 1*).

On average of five water regimes, inoculation of PGPR significantly raised the N and P content leaves of the sugar beet except RC9 and RC05, respectively, compared to control. On the other hand, all bacterial strains tested importantly raised the K, Ca and Zn content of the sugar beet leaf. N and K content were the greatest with RC310 and RC63, whereas maximal P, Ca and Mg was with strain RC21 and A21/3 inoculations (*Table 3*). In addition, six of the strains (RC05, PF8/6, RC6/3, RC310, RC9, and RC21) importantly raised the Mn content of sugar beet plants, but not Fe and Cu concentrations (*Table 3*).

http://www.aloki.hu ● ISSN 1589 1623 (Print) ● ISSN 1785 0037 (Online)
DOI: http://dx.doi.org/10.15666/aeer/1605_68016813
© 2018, ALÖKI Kft., Budapest, Hungary

Table 3. *Effect of mineral fertilizer and plant growth-promoting rhizobacteria (PGPR) on macro- and micro-nutrient concentrations in sugar beet leaves in the first trial set with the average of five water regimes*

Treatments	Macro-nutrient (g kg^{-1} DW)					Micro-nutrient (mg kg^{-1} DW)				
	N	P	K	Ca	Mg	Na	Fe	Cu	Mn	Zn
Control	21.4 g	2.95 b	20.92 e	8.58 c	3.58 c	1672 b-c	142 a	31.8 a	45.6 f	31.5 g
NP	23.5 ef	3.08 ab	22.30 de	8.88 bc	3.70 bc	1696 a-c	137 a-c	28.7 bc	45.6 f	33.9 f
RC9	22.9 fg	3.18 a	23.10 cd	9.09 ab	3.91 ab	1760 ab	128 cd	28.2 bc	51.5 cd	37.7 e
T26	23.1 f	3.16 a	23.26 b-d	9.34 ab	3.80 a-c	1711 a-c	134 a-d	28.2 bc	48.1 ef	38.6de
RC05	23.9 d-f	3.10 ab	23.71 a-d	9.34 ab	3.84 ab	1616 cd	132 b-d	28.6 bc	56.5 a	39.9cd
RC 11	24.1 c-f	3.20 a	23.88 a-d	9.31 ab	3.87 ab	1713 a-c	137 a-c	27.4 c	47.9 ef	44.5 b
RC21	25.6 bc	3.26 a	23.39 a-d	9.49 a	3.99 a	1804 a	127 d	28.7 bc	50.4 de	41.8 c
RC310	27.7 a	3.21 a	24.98 a	9.41 a	3.91 ab	1544 d	138 ab	28.6 bc	52.4 b-d	38.6de
PF8/6	25.2 b-d	3.18 a	22.97 cd	9.43 a	3.77 a-c	1678 bc	139 ab	28.9 bc	55.1 ab	48.2 a
BS63	26.7 ab	3.20 a	24.74 ab	9.46 a	3.83 a-c	1511 d	132 b-d	28.4 bc	54.2 a-c	45.4 b
A21/3	25.0 c-e	3.24 a	23.95 a-c	9.46 a	3.98 a	1543 d	132 b-d	29.3 b	46.7 f	47.6 a
Mean	24.5	3.16	23.38	9.25	3.70	1659	134	29.0	50.4	40.7

Means followed with the same letter within each column are not significant different ($p < 0.05$)

On average of five water regimes, the highest GR activity was found effective at RC05, RC11, RC63 and mineral fertilizer, whereas the highest GST activity was found effective at PF8/6 and T26. Under waterlogging stress, sugar beet GR activity importantly raised after RC21, RC9 and RC11, while G6PD and 6PGD activity importantly raised after RC21, RC9 and RC63 inoculations. Under continuous moderate and severe water stress, the maximum GR activity in sugar beet leaf were found after RC63 inoculation, followed by A21/3, RC11, RC05 and 28/3, whereas the highest levels of GST activity were determined in treatments with PF8/6, followed by T26 and RC9. Moreover, under these stress, G6PD activity was found effective after RC310, RC05, RC21, and RC63; whereas 6PGD in sugar beet leaf was found effective after PF8/6, RC310, RC63, and RC05. In general, under water stress, there was an importantly raise in the enzyme activity in both inoculated and uninoculated treatments. In addition, enzyme activity in the uninoculated plants was lower than that of inoculated plants (*Fig. 2*).

While MDA and H_2O_2 decreased, sugar beet growth, root and leaf weight, sugar per plant and chlorophyll contents also increased. Water deficit treatment importantly raised the drought stress markers (MDA and H_2O_2), which showed the degree of oxidative damage posed with during stress. In all applications, levels of MDA and H_2O_2 were raised because of water stress. Also, when drought treatment, in all treatments show that H_2O_2 and MDA increased, whereas effective bacterial strains (RC310, RC63, RC26, RC11 and RC05) decreased the MDA and H_2O_2 content in the leaf (*Fig. 3*).

Discussion

One of the most negative factors of plant growth is certainly scarcity of water. Drought stress can also occur under irrigated conditions when use or availability of

http://www.aloki.hu ● ISSN 1589 1623 (Print) ● ISSN 1785 0037 (Online)
DOI: http://dx.doi.org/10.15666/aeer/1605_68016813
© 2018, ALÖKI Kft., Budapest, Hungary

irrigation water is restricted (Tarkalson and King, 2017). Sugar beet is considered a drought-tolerant species based on the ability of established plants to survive transient periods of drought and recover when water subsequently becomes available (Wedeking et al., 2017). However, the stage of plant growth that emerged from stress is important to come from above the stress (Tatar et al., 2016). Water-restriction caused important yield losses and this effect was excessive in young plants affected by drought. When a temporary water stress appears at early period, it can be said that it reduces sugar beet root yield importantly. Indeed, when young beet plants were exposed to stress of water, it was found that sugar yield, the rate of photosynthesis and assimilation severely decreased Monti et al. (2006) and storage roots showed significant changes (Hoffmann, 2010). Bacterial activity was found higher than the beet harvested in the early period. Sahin et al. (2004) determined that the bacterial activity was higher at the early development stages. The water stress in growth stage may cause decrease of yield. Sugar beet root weight reduction decreased importantly under drought conditions, but this situation changed according to inoculated bacteria and irrigation level.

Bacterial inoculations and fertilizer application importantly raised fresh and dry leaf weight, and sugar per plant compared to control in the first and second trials. Generally, different PGPR applications give dissimilar response with different application of irrigation. The fact that inoculation of bacteria encouraged the growth of sugar beet leaves was in line with the results of previous researches (Çakmakçı et al., 1999; Schmidt et al., 2004; Shi et al., 2009). Similar to previous research findings (Romano et al., 2013), sugar beet root, leaf development and yield decreased under the water restrictions and drought stress.

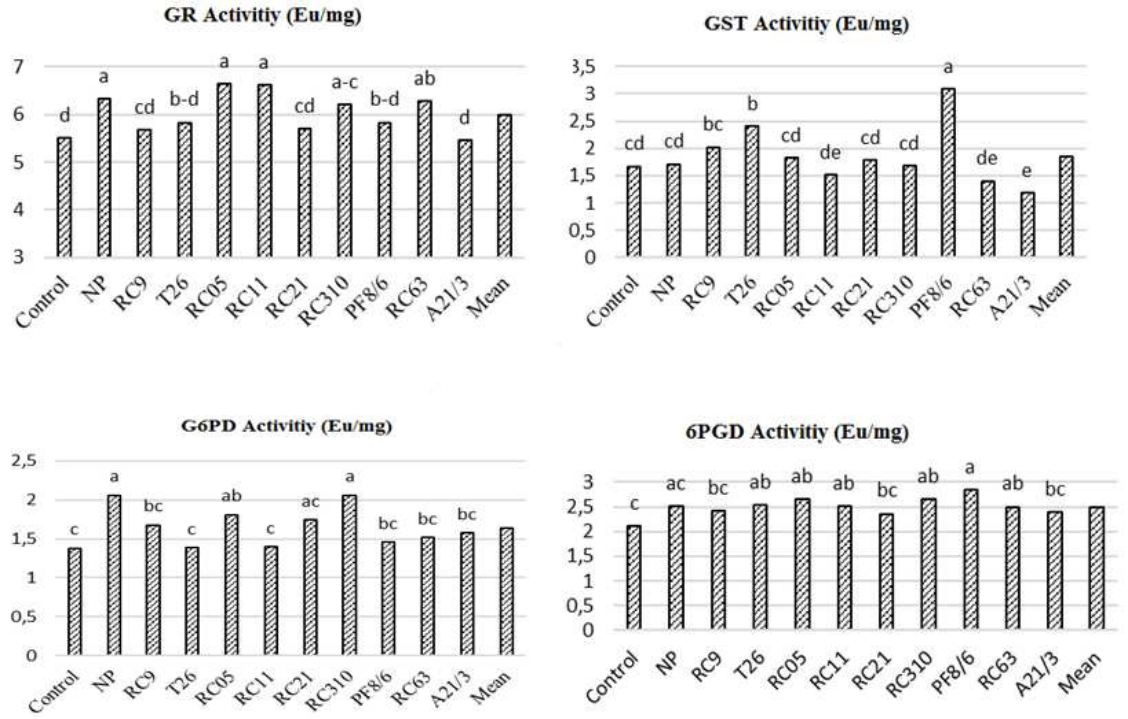

Figure 2. *Effect of PGPR and mineral fertilizer on the activities of anti-oxidant (GR and GST) and pentose phosphate oxidative cycle enzymes (G6PD and 6PGD) in sugar beet leaves in the second trial*

http://www.aloki.hu ● ISSN 1589 1623 (Print) ● ISSN 1785 0037 (Online)
DOI: http://dx.doi.org/10.15666/aeer/1605_68016813
© 2018, ALÖKI Kft., Budapest, Hungary

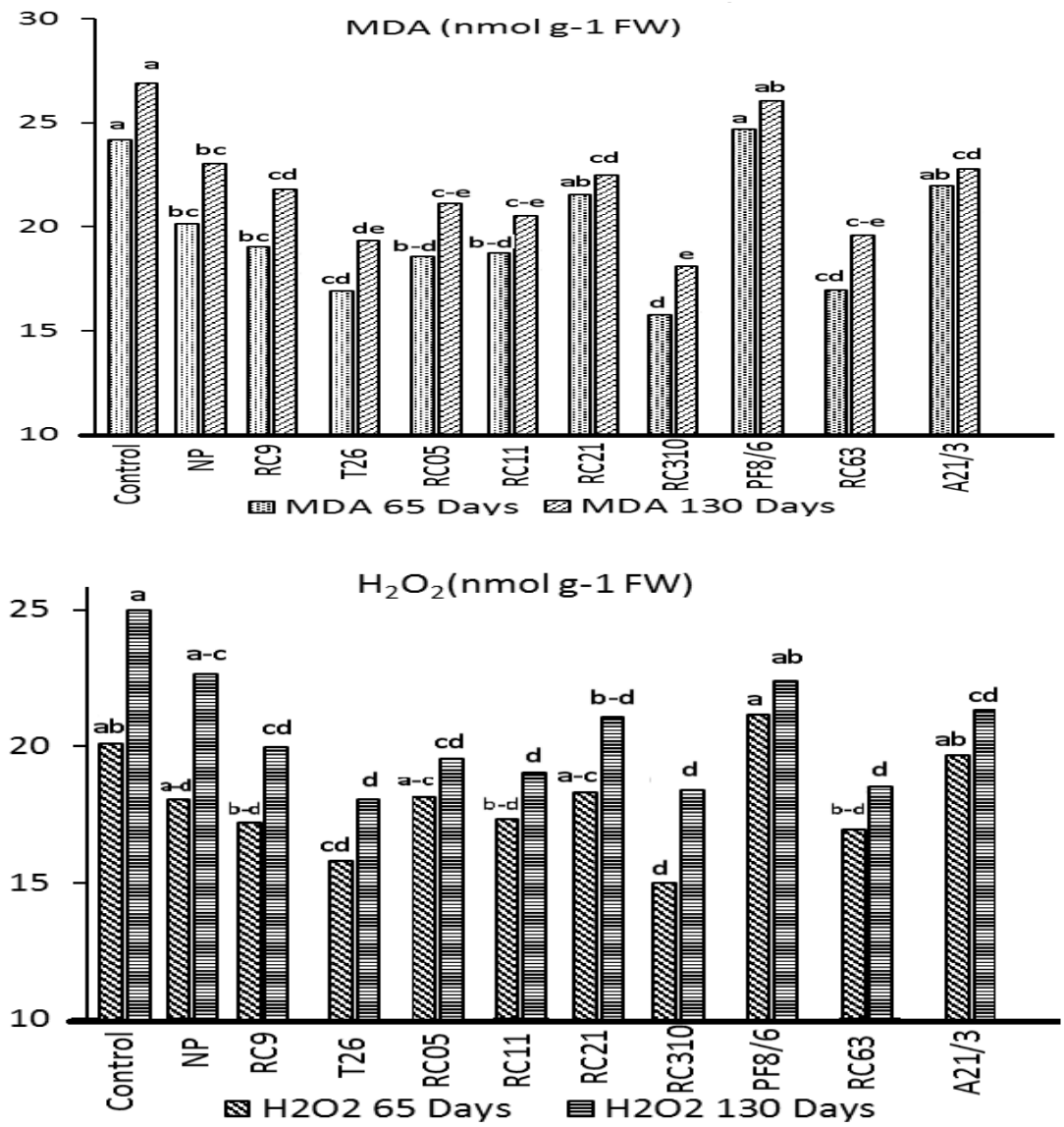

Figure 3. *Effect of PGPR and mineral fertilizer on the malondialdehyde (MDA) and hydrogen peroxide (H_2O_2) content of sugar beet leaves in the first (65 days) and second trial (130 days) average of five water regimes*

Under insufficient water supply, the sucrose concentration was higher than under well-watered conditions. In spite of the fact that sugar content ratio is high proportionally, the amount of sugar per plant is reduced at beet under water stress compared to optimum irrigation applications. Moreover, if water stress limits the use of sucrose in the growth at a higher rate than the decrease in photosynthesis, sugar rate increase can be the main reason of the more sugar in the roots. Drought could increase the sugar content in sugar beet, but reduce the root, leaf and sugar yield and the drought is clearly the main reason for the sugar beet yield losses (Jaggard et al., 1998; Pidgeon et al., 2001). Similarly, sucrose concentration increased with reduced water availability (Bloch et al., 2006). Our results showed that water stress reduced the vegetative growth and fresh weight, it increased sugar percentage and the percentage of fresh weight in root. Although there are a few studies in the literature on the main factor limiting the

http://www.aloki.hu ● ISSN 1589 1623 (Print) ● ISSN 1785 0037 (Online)
DOI: http://dx.doi.org/10.15666/aeer/1605_68016813
© 2018, ALÖKI Kft., Budapest, Hungary

drought sugar yield (Pidgeon et al., 2006; Gobin, 2010), sugar beet's sensitivity to water restrictions and the response have not been studied enough (Habibi et al., 2011). Bacterial inoculation minimized the water stress-imposed effects importantly increasing the sugar per plant in sugar beet, but this changed depending on the inoculation bacteria and level of irrigations.

Reduction in water content due to drought can reduce food intake from soil. whereas application of PGPR increased the uptake of N, P, K, Ca, Mg, Mn and Zn in sugar beet. This parameter showed that using PGPR reduces the negative effects of water constraints in leaf macro- and micro-nutrient contents. Among the bacterial strains, the strains RC310 exhibiting better performance under severe water stress (25% of WHC) conditions was observed to have the highest K content in sugar beet leaf, which correlated well with their increased the amount of sugar per plant and weight of root and leaf (*Tables 2* and *3; Fig. 1*). As reported by Grzebisz et al. (2013), normalization of K intake in case of water stress can provide important advantage against too negative effects of water stress in plant growth and yield. Under drought conditions, increased nutrient uptake could improve water-use efficiency and alleviate drought stress effects on plant growth. Indeed, if nutrient uptake can be increased by using active bacteria, plant growth can be stimulated.

An alternative approach for increasing plant resistance against stress is to raise the plant antioxidant enzymes by using bacteria (Çakmakçı et al., 2007). Our studies show that PGPR can rise GR, GST, 6PGD and G6PD activities, together with the growth sugar beet lıke wheat and spinach plants (Çakmakçı et al., 2007, 2009). Therefore, investigating the ability to enhance enzymes activity in plants by using bacteria, similar to the first and pioneering work is required. Study has clearly demonstrated that some effective bacterial strains can promote plant growth together with antioxidant and oxidative pentose phosphate pathway enzymes in sugar beet under drought conditions. If plant antioxidant enzyme activity can be raised by using bacteria, it is being possible to increase the resistance of plants to stress conditions with plant growth. PGPR inoculation was shown to reduce the negative effects of water stress. Moreover, sugar beet can partly tolerate water stress protecting itself from oxidative damage by the increasing enzymes activities in leaves with the help of bacteria.

Of the bacterial inoculations, high ACC deaminase-containing RC310 and RC63 exhibiting better performance under moderate and severe water stress conditions were observed to have the highest level N and K content in sugar beet leaf, which was correlated well with their increased both fresh and dry weight of leaf and root (*Table 2*), 6PGD and G6PD enzyme activities and decreased both H_2O_2 and MDA content (*Fig. 3*), thus protecting the plants from water stress compared to the other bacteria and control. Increasing potassium and nitrogen by high N_2-fixing, P-solubilizing and for sustain the process of photosynthesis in leaves during drought, bacteria which ACC deaminase-including can decrease lipid peroxidation by rising the activity of antioxidant enzymes and decreasing MDA content. Therefore, Bacteria have nutrient uptake from soil and protect against to pests and diseases, also the bacteria provide protection to plants during water stress and drought.

In our study, drought caused a significant decrease in leaf weight as well as in root weight. Inoculation with PGPR could tolerate a certain degree of slow leaf development caused water constraint and they slowed leaf weight reduction occurred in the mineral fertilization. Positive effects of these selected strains on fresh and dry root and leaf weight, chlorophyll contents, enzyme activities and nutrient uptake of sugar beet plants

http://www.aloki.hu ● ISSN 1589 1623 (Print) ● ISSN 1785 0037 (Online)
DOI: http://dx.doi.org/10.15666/aeer/1605_68016813
© 2018, ALÖKI Kft., Budapest, Hungary

showed the beneficial role of these PGPR, which might be attributed to IAA production, N_2-fixation, P-solubilisation, ACC deaminase activity, or even other non-evaluated PGPR traits that stimulated the plant growth. There are a great number studies that bacteria can provide protection plants against different stresses duo to they have produce IAA and ACC deaminase Glick (2012). Inoculation with IAA-producing Shi et al. (2009) and N_2-fixing and/or P-solubilizing Sahin et al. (2004) bacteria stimulate growth and increased root and sugar yields of sugar beet. Screening of rhizobacteria that show multiple PGP traits suggests that they have better potential in alleviating plant water stress and in improving the growth of sugar beet.

Conclusions

As a result of excess water applications, soil salinization, desertification, the loss of soil due to erosion occur with increasing costs. In addition, programs that provide the maximum production per unit of irrigation water in case of limited water and water constraint conditions in order to reduce the possible decline in production are important. This research has shown that sugar beet cultivation in PGPR can be used to minimize the harmful effects of water stress. Inoculation with ACC deaminase-containing bacteria partially eliminated the effects of water stress on growth, yield and quality of sugar beet. PGPR increases the uptake of plant nutrients (macro and micro). The effective bacterial strain tested in this study improved for enhanced plant growth promotion will be able to reduce the inputs of chemical fertilizers and the negative effect of water stress, and will have a potential to be used as a bio-fertilizer in sustainable and organic sugar beet production. Due to insufficient irrigation water and the high cost of water, in arid and semi-arid regions, inoculation with ACC deaminase containing PGPR can be used to prevent the reduction in yield. The PGPR can encourage plant growth and development, decrease stress sensitivity, and may conduce to the concept of biotechnology application in agriculture. As a result, RC310 and PF8 / 6 bacterial strains used in this study and other useful bacteria can use in organic sugar beet growing and in water-restricted areas. This study will also shed light on researchers working with sugar beets and PGPR. Inspired by this work, researchers can determine how affected of sugar beet by other stress conditions. Also researchers can search to ways to reduce the negative effect of other stress conditions with using PGPR.

REFERENCES

[1] Beutler, E. (1984): Red Cell Metabolism: A Manual of Biochemical Methods (3rd ed.) – Grune & Stratton, Orlando, FL, USA.

[2] Bloch, D., Hoffmann, C. M., Marlander, B. (2006): Impact of water supply on photosynthesis, water use and carbon isotope discrimination of sugar beet genotypes. – European Journal of Agronomy 24: 218–225.

[3] Bradford, M. M. (1976): A rapid and sensitive method for the quantitation of microgram quantities of protein utilizing the principle of protein-dye binding. – Analytical Biochemistry 72: 248–254.

[4] Çakmakçı, R., Kantar, F., Algur, Ö. F. (1999): Sugar beet and barley yields in relation to Bacillus polymyxa and Bacillus megaterium var. phosphaticum inoculation. – Journal of Plant Nutrition and Soil Science 162: 437–442.

http://www.aloki.hu ● ISSN 1589 1623 (Print) ● ISSN 1785 0037 (Online)
DOI: http://dx.doi.org/10.15666/aeer/1605_68016813
© 2018, ALÖKI Kft., Budapest, Hungary

[5] Çakmakçı, R., Erat, M., Erdoğan, Ü., Dönmez, M. F. (2007): The influence of plant growth-promoting rhizobacteria on growth and enzyme activities in wheat and spinach plants. – Journal of Plant Nutrition and Soil Science 170: 288–295.
[6] Çakmakçı, R., Erat, M., Oral, B., Erdoğan, Ü., Şahin, F. (2009): Enzyme activities and growth promotion of spinach by indole-3-acetic acid-producing rhizobacteria. – The Journal of Horticultural Science and Biotechnology 84: 375–380.
[7] Çakmakçı, R., Dönmez, M. F., Ertürk, Y., Erat, M., Haznedar, A., Sekban, R. (2010): Diversity and metabolic potential of culturable bacteria from the rhizosphere of Turkish tea grown in acidic soils. – Plant Soil 332: 299–318.
[8] Carlberg, I., Mannervik, B. (1985): Glutathione reductase. – Methods Enzymol 113: 484–490.
[9] Castillo, P., Escalante, M., Gallardo, M., Alemano, S., Abdala, G. (2013): Effects of bacterial single inoculation and co-inoculation on growth and phytohormone production of sunflower seedlings under water stress. – Acta Physiologiae Plantarum 35: 2299–2309.
[10] Glick, B. R. (2012): Plant growth-promoting bacteria mechanisms and applications. – Scientifica 2012: 1–15.
[11] Gobin, A. (2010): Modelling climate impacts on crop yields in Belgium. – Climate Res 44: 55–68.
[12] Grzebisz, W., Gransee, A., Szczepaniak, W., Diatta, J. (2013): The effects of potassium fertilization on water-use efficiency in crop plants. – Journal of Plant Nutrition and Soil Science 176: 355–374.
[13] Habibi, D., Taleghani, D. F., Oroojnia, S. (2011): Physiological evaluation of sugar beet genotypes under drought stress. – 2nd Int. Con. Chem. Eng. Appl., IPCBEE 23: 96–101, IACSIT Press, Singapore.
[14] Habig, W. H., Jakoby, W. B. (1981): Assays for differentiation of glutathione S-transferases. – Methods in Enzymology 77: 398–405.
[15] Heath, R. L., Packer, L. (1968): Photoperoxidation in isolated chloroplasts I. Kinetics and stoichiometry of fatty acid peroxidation. – Archives of Biochemistry and Biophysics 125: 189–198.
[16] Hoffmann, C. M. (2010): Sucrose accumulation in sugar beet under drought stress. – Journal of Agronomy and Crop Science 196: 243–252.
[17] Jaggard, K. W., Dewar, A. M., Pidgeon, J. D. (1998): The relative effects of drought stress and virus yellows on the yield of sugarbeet in the UK, 1980-95. – The Journal of Agricultural Science 130: 337–343.
[18] Marulanda A, Barea JM, Azcón R (2009): Stimulation of plant growth and drought tolerance by native microorganisms (AM fungi and bacteria) from dry environments: mechanisms related to bacterial effectiveness. – The Journal of Plant Growth Regulation 28: 115–124.
[19] Monti, A., Brugnoli, E., Scartazza, A., Amaducci, M. T. (2006): The effect of transient and continuous drought on yield, photosynthesis and carbon isotope discrimination in sugar beet (*Beta vulgaris* L.). – Journal of Experimental Botany 57: 1253–1262.
[20] Pidgeon, J. D., Werker, A. R., Jaggard, K. W., Richter, G. M., Lister, D. H., Jonse, P. D. (2001): Climatic impact on the productivity of sugar beet (*Beta vulgaris* L.) in Europe 1961-1995. – Agricultural and Forest Meteorology 109: 27–37.
[21] Pidgeon, J. D., Ober, E. S., Qi, A., Clark, C. J. A., Royal, A., Keith, W., Jaggard, K. W. (2006): Using multi-environment sugar beet variety trials to screen for drought tolerance. – Field Crops Research 95: 268–279.
[22] Romano, A., Sorgona, A., Lupini, A., Araniti, F., Stevanato, P., Cacco, G., Abenavoli, M. R. (2013): Morpho-physiological responses of sugar beet (Beta vulgaris L.) genotypes to drought stress. – Acta Physiologiae Plantarum 35: 853–865.
[23] Safronova, V. I., Stepanok, V. V., Engqvist, G. L., Alekseyev, Y. V., Belimov, A. A. (2006): Root-associated bacteria containing 1-aminocyclopropane-1-carboxylate

http://www.aloki.hu ● ISSN 1589 1623 (Print) ● ISSN 1785 0037 (Online)
DOI: http://dx.doi.org/10.15666/aeer/1605_68016813
© 2018, ALÖKI Kft., Budapest, Hungary

deaminase improve growth and nutrient uptake by pea genotypes cultivated in cadmium supplemented soil. – Biology and Fertility of Soils 42: 267–272.

[24] Sahin, F., Çakmakçı, R., Kantar, F. (2004): Sugar beet and barley yields in relation to inoculation with N2-fixing and phosphate solubilizing bacteria. – Plant Soil 265: 123–129.

[25] Sairam, P. K., Srivastava, G. C. (2002): Changes in antioxidant activity in sub-cellular fractions of tolerant and susceptible wheat genotypes in response to long term salt stress. – Plant Science 162: 897–904.

[26] Schmidt, C. S., Agostini, F., Simon, A. M., Whyte, J., Townend, J., Leifert, C., Killham, K., Mullins, C. (2004): Influence of soil type and pH on the colonisation of sugar beet seedlings by antagonistic Pseudomonas and Bacillus strains, and on their control of Pythium damping-off. – European Journal of Plant Pathology 110: 1025–1046.

[27] Shi, Y. W., Lou, K., Li, C. (2009): Promotion of plant growth by phytohormone-producing endophytic microbes of sugar beet. – Biology and Fertility of Soils 45: 645–653.

[28] Tarkalson, D. D., King, B. A. (2017): Effects of tillage and irrigation management on sugarbeet production. – Agronomy Journal 109: 1–11.

[29] Tatar, Ö., Bruck, H., Asch, F. (2016): Photosynthesis and remobilization of dry matter in wheat as affected by progressive drought stress at stem elongation stage. – Journal of Agronomy and Crop Science 202: 292–299.

[30] Wedeking, R., Mahlein, A. K., Steiner, U., Oerke, E. C., Goldbach, H. E., Wimmer, M. A. (2017): Osmotic adjustment of young sugar beets (Beta vulgaris) under progressive drought stress and subsequent rewatering assessed by metabolite analysis and infrared thermography. – Functional Plant Biology 44: 119–133.

http://www.aloki.hu ● ISSN 1589 1623 (Print) ● ISSN 1785 0037 (Online)
DOI: http://dx.doi.org/10.15666/aeer/1605_68016813
© 2018, ALÖKI Kft., Budapest, Hungary

MODELING STEM PROFILE OF CAUCASIAN FIR AND ORIENTAL SPRUCE MIXED STANDS IN TURKEY USING NONLINEAR MIXED-EFFECTS MODELS

ÇAKIR, C. Y.[1] – KAHRİMAN, A.[2*]

[1]*Artvin Regional Directorate Ardanuç Forest District Directorate, 08300 Artvin, Turkey*

[2]*Artvin Çoruh University Faculty of Forestry, 08100 Artvin, Turkey*

**Corresponding author*
e-mail: kaydin61@hotmail.com; phone/fax: +90-466-215-1034

(Received 15th Jul 2018; accepted 20th Sep 2018)

Abstract. The objective of this study is to develop segmented polynomial taper equations using the nonlinear mixed-effects modeling approach for Caucasian fir (*Abies nordmanniana* (Steven) Spach. subsp. *nordmanniana*) - Oriental spruce (*Picea orientalis* (L.) Link.) mixed stands in Artvin-Ardanuç region of Turkey. For this purpose, the data obtained from 213 felled sample trees in total, which are 107 fir and 106 spruce, were used. Jiang et al.'s (2005) stem profile model produced the best prediction results for both tree species. The R^2_{adj}, RMSE, $\bar{E}$, MAE, AIC and BIC values of the model were found as 98.7% and 98.3%, 1.700 and 1.814 cm, 0.143 and 0.167 cm, 1.179 and 1.269 cm, 4142.2 and 3951.7, 4148.5 and 3957.8 for fir and spruce, respectively. Based on AIC, BIC and -2LnL criteria, the model including random-effects in two parameters (b_3 and b_4) were the best for both tree species. This mixed-effects model with two random parameters showed homogeneous residual variance and autocorrelation was almost removed. Mixed-effects models provided much better fits than their fixed model counterparts for both species. In addition, among 12 different calibration choices, the best results were obtained with the choice involving the measurement of five diameters that divide the sample tree measurements into two equal parts for fir and of four diameters that bottom of the sample tree for spruce.
Keywords: *stem diameter, segmented polynomial taper models, calibration, random parameters, Artvin*

Introduction

The correct calculation of the volume of trees and stands, and of the distribution of this volume among different commercial classes, is of great importance when formulating forest management plans and making projections concerning the future of the forestry products sector. Among the methods for the accurate estimation of tree volumes, the most effective and versatile approach is the stem taper model (Jiang et al., 2005; Özçelik and Brooks, 2012). Using this method, detailed estimations can be made of the types of wood that can be obtained from trees in demand under the ever-changing market conditions (Ercanlı and Kahriman, 2013; Kumaş and Kahriman, 2015).

There are two important reasons for the continuous increase in the number of studies on stem taper: The first reason is that the stem forms of all trees are not alike and that a theory has yet to be developed that reflects these differences in form; and the second is that a single method is yet to be developed that considers the changing standards in wood types under the ever-changing market conditions (Newnham, 1992; Diéguez-Aranda et al., 2006; Özçelik and Yaşar, 2015). Thus, it is quite easy to determine both the total stem volume and the merchantable volume using a simple stem taper model.

http://www.aloki.hu ● ISSN 1589 1623 (Print) ● ISSN 1785 0037 (Online)
DOI: http://dx.doi.org/10.15666/aeer/1605_68156833
© 2018, ALÖKI Kft., Budapest, Hungary

Stem profile equations not only identify the stem form but also estimate (i) the total stem volume, (ii) the merchantable stem volume, (iii) the volume of the stem section between any two heights, (iv) the volume of the stem section between any two diameters, (v) the stem diameter at any height, and (vi) the height at any stem diameter (Kozak, 2004; Özçelik et al., 2011).

Many different stem taper models have been developed over the last century, and they can be divided into three categories (Diéguez-Aranda et al., 2006) as follows: simple polynomial taper equations (Demaerschalk, 1972, 1973), variable-form taper equations (Newnham, 1992; Kozak, 2004) and segmented polynomial taper equations (Max and Burkhart, 1976; Parresol et al., 1987; Fang et al., 2000; Jiang et al., 2005). The performances of these stem profile functions vary depending on the tree species studied, the quality of the dataset, and the form and type of the selected model (Sakıcı et al., 2008; Özçelik et al., 2011; Şenyurt et al., 2017). Since the stem taper models that are compatible with the models used in this study divide the tree stem into parts and define each part individually, they can be used to estimate the entire stem profile in the most realistic way possible (Green and Reed, 1985). Another advantage of these stem taper models over other such models is that they can be easily converted into volume equations for the calculation of volumes (Fang et al., 2000).

The diameter data obtained from the various heights of a single tree can be used to develop a stem taper model, which indicates that successive measurement values are interrelated (Özçelik and Yaşar, 2015). In such hierarchical data structures, where each tree has a unique stem development, the problem of "autocorrelation", also known as "serial correlation", may be observed, which means that different items of data are dependent on each other (Leites and Robinson, 2004). Such serial correlations among the sample data may result in the confidence intervals in the parameter estimations concerning stem taper and stem volume equations being estimated with a systematic error, thus affecting the reliability of the model results in an adversely way (Searle et al., 1992; Kurt, 2014). In this regard, for hierarchical data structures in which the assumption of data independence cannot be met, and the problem of serial correlation exists in the data, the use of Nonlinear Mixed-Effects Models is recommended, as this enables the modeling of the variance-covariance matrix structure (Littell et al., 2005).

Regarding their ranges, incremental growth characteristics and economic value, the Caucasian Fir (*Abies nordmanniana* (Steven) Spach. subsp. *nordmanniana*) and the Oriental Spruce (*Picea orientalis* (L.) Link.) are among the leading forest tree species in Turkey. According to the 2015 forest inventory of the General Directorate of Forestry, the total areas covered by fir and spruce are 884,781 ha and 322,857 ha, respectively (General Directorate of Forestry, 2015).

According to the 2015 forest inventory of the General Directorate of Forestry, approximately 38% of forestry areas in Turkey (8,394,788 ha) are mixed forests, while forest inventory data from 2006 states that around 707 m^3 (55%) of the total tree wealth of Turkey is composed of mixed forests (General Directorate of Forestry, 2015), which suggests that mixed forests and mixed stands constitute a significant portion of Turkey's forestry lands.

The objectives of this research were to develop a stem taper and stem volume model that facilitates detailed volume estimations of the mixed stands of Caucasian fir and Oriental spruce that are abundant in the area covered by the Artvin Regional Directorate - Ardanuç Forest District Directorate. We fitted and evaluated taper functions using mixed-effect modelling techniques.

http://www.aloki.hu ● ISSN 1589 1623 (Print) ● ISSN 1785 0037 (Online)
DOI: http://dx.doi.org/10.15666/aeer/1605_68156833
© 2018, ALÖKI Kft., Budapest, Hungary

Material and methods

Study site

In the Artvin-Ardanuç region, where mixed stands of Caucasian fir (*Abies nordmanniana* (Steven) Spach. subsp. *nordmanniana*) and Oriental spruce (*Picea orientalis* (L.) Link.) can be found (40°54'54" - 41°15'31" N, 41°53'47"' - 42°22'52" E), the monthly average temperature varies between 2.8–21.0°C (annual average: 12.3°C), with the lowest temperature varies between +9.5 and -16.1 °C, and the highest temperature reaches 43°C. While annual average precipitation is 700 mm, annual average relative humidity varies between 60 and 70% (Turkish State Meteorological Service, 2016). The climate in Ardanuç is a mixture of continental and Mediterranean climates, where summers are hot and dry, and winters are partially warmer and less rainy than the normal continental climate.

There is around 75,535.4 ha of Caucasian fir, and 44,001.3 ha of Oriental spruce stands in the Artvin Regional Directorate, while 38,810.3 ha of this area is composed of mixed stands of Caucasian fir and Oriental spruce. The area of the mixed stands of Caucasian fir and Oriental spruce in the Ardanuç Forest District Directorate, as the study site, is 6,487.6 ha (General Directorate of Forestry, 2015). The ranges of the Caucasian fir and Oriental spruce mixed stands in Turkey, and the distribution of these two species in the study site are given in *Figure 1*.

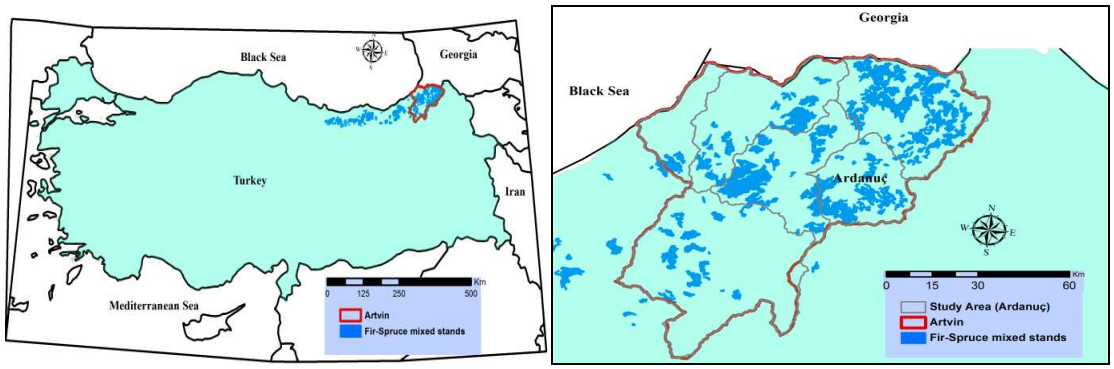

Figure 1. *Location of the study area*

Data

The data were obtained from 213 sample trees felled from the mixed stands of Caucasian fir and Oriental spruce within the boundaries of the Artvin Regional Directorate - Ardanuç Forest District Directorate, with 107 of them being fir and 106 being spruce. In selecting the sample trees, care was taken to ensure that the samples had a balanced distribution of various diameters and heights, and reflected the variation in volume development.

The sample trees used in this study were felled at the stump height level (0.3 m). Their stump diameter (0.30 m) and diameter at breast height (1.30 m) were measured, and after which, their diameter values were measured at 1 m intervals (2.3, 3.3, 4.3 m...). The total height values of the trees were measured with a steel measuring tape. If the tree stems were found to be oddly-shaped rather than cylindrical during measurement, two diameters perpendicular to the stem's cross section were measured, and their average was taken as the diameter measurement.

http://www.aloki.hu ● ISSN 1589 1623 (Print) ● ISSN 1785 0037 (Online)
DOI: http://dx.doi.org/10.15666/aeer/1605_68156833
© 2018, ALÖKI Kft., Budapest, Hungary

The data used in this study were divided randomly into two groups, with one being used in the estimation of the parameters of stem taper models and the other being used in the determination of the calibration responses of such models. Approximately 80% of the data (85 fir and 84 spruce trees) were included in group I as model data, and the remaining 20% (22 fir and 22 spruce trees) were included in group II as control data. *Figures 2* and *3* show a scatter plot of relative diameter of these trees against their corresponding relative height of the data used, for both fitting and validation data sets.

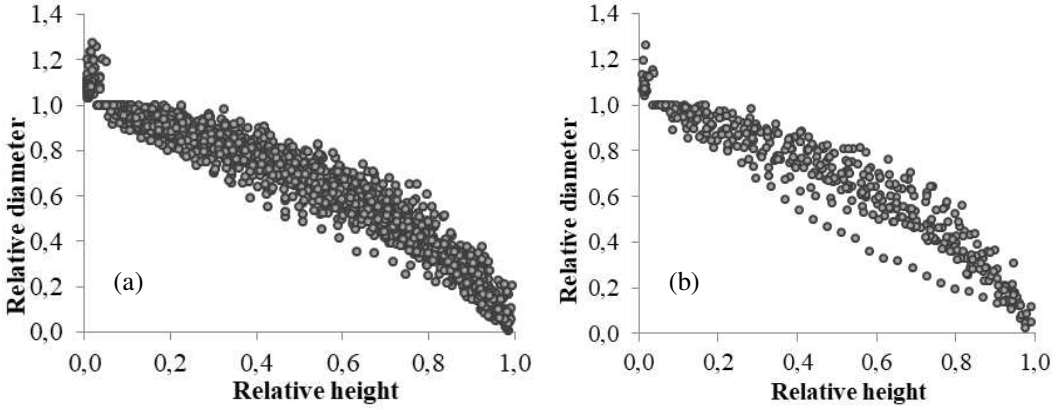

Figure 2. *Plot of the relative height versus relative diameter outside bark for (a) the fitting data points, and (b) the validation data points of Caucasian fir*

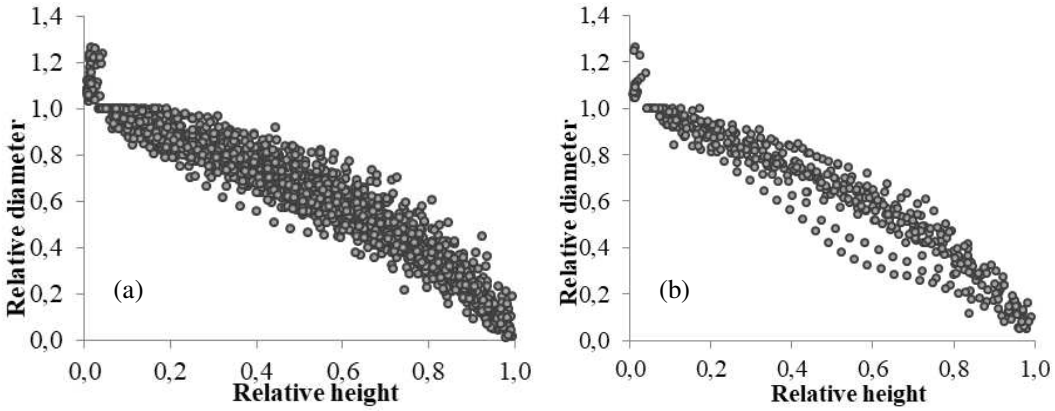

Figure 3. *Plot of the relative height versus relative diameter outside bark for (a) the fitting data points, and (b) the validation data points of Oriental spruce*

Table 1 provides the summary statistics of diameter at breast height, total height, tree volume, diameter outside bark at a height h and height above ground to the measurement point for model fitting and validation data set.

Selection of the best statistical regression models

The estimation of the parameters of these stem taper models was done with the NLIN procedure available in SAS/STAT® 9.3 software (SAS Institute, 2013). In this study, the adjusted coefficient of determination (R^2_{adj}), Root-Mean-Square Error (RMSE), Bias ($\bar{E}$), Mean Absolute Error (MAE), Akaike's Information Criterion (AIC) and

http://www.aloki.hu ● ISSN 1589 1623 (Print) ● ISSN 1785 0037 (Online)
DOI: http://dx.doi.org/10.15666/aeer/1605_68156833
© 2018, ALÖKI Kft., Budapest, Hungary

Schwarz's Bayesian Information Criterion (BIC) were used to evaluate the performance of the stem taper models for both species. It is desired that R^2_{adj} be close to 1 and that the RMSE, $\bar{E}$, MAE, AIC, and BIC values be low (Castedo-Dorado et al., 2006). The model evaluation criteria were as follows (*Eqs. 1–6*):

$$R^2_{adj} = 1 - \frac{(n-1)\sum_{i=1}^{n}(y_i - \hat{y}_i)^2}{(n-p)\sum_{i=1}^{n}(y_i - \bar{y}_i)^2} \quad \text{(Eq.1)}$$

$$RMSE = \sqrt{\frac{\sum_{i=1}^{n}(y_i - \hat{y}_i)^2}{n-p}} \quad \text{(Eq.2)}$$

$$\bar{E} = \frac{\sum_{i=1}^{n}(y_i - \hat{y}_i)}{n} \quad \text{(Eq.3)}$$

$$MAE = \frac{\sum_{i=1}^{n}|y_i - \hat{y}_i|}{n} \quad \text{(Eq.4)}$$

$$AIC = -2\ln(L) + 2k \quad \text{(Eq.5)}$$

$$BIC = -2\ln(L) + k.\ln(n) \quad \text{(Eq.6)}$$

where n is the number of observations; p is the number of coefficient in the model; y_i, $\hat{y}_i$ and $\bar{y}$ are observed, predicted and average observed the diameters outside bark, respectively, k is the number of parameters in the model; L maximum likelihood (ML) value.

Table 1. *Descriptive statistics for Caucasian fir and Oriental spruce sample trees*

Species	Variable	Initial model development (80%)				Model validation (20%)			
		n	Mean	S.D.	Range	n	Mean	S.D.	Range
Caucasian fir	D (cm)	85	33.6	15.5	9.4-66.0	22	35.1	15.8	7.9-65.5
	H (m)	85	21.2	7.5	5.7-39.8	22	21.5	8.0	7.7-40.0
	v (m^3)	85	1.36	1.36	0.03-5.68	22	1.48	1.58	0.03-6.66
	d (cm)	1830	25.5	14.7	0.2-75.0	451	24.0	13.2	1.2-66.3
	h (m)	1830	12.0	8.2	0.3-39.3	451	11.2	7.5	0.3-34.3
Oriental spruce	D (cm)	84	32.6	14.9	8.0-80.0	22	36.6	16.4	8.7-72.1
	H (m)	84	20.2	6.7	6.8-38.5	22	21.3	6.5	7.5-31.1
	v (m^3)	84	1.14	1.24	0.02-6.21	22	1.42	1.22	0.02-4.13
	d (cm)	1703	23.3	13.8	0.4-86.0	466	25.6	14.6	1.0-76.4
	h (m)	1703	11.1	7.5	0.3-38.3	466	11.4	7.4	0.3-30.3

D = diameter at breast height; H = total height; d = diameter outside bark at height h; h = height above ground level, v = tree volume (m^3); n = number of observations; S.D. = standard deviation

The data were randomly divided into two groups as follows: (i) the data used for estimation of the parameters of the mixed-effects stem taper models; and (ii) the data

http://www.aloki.hu ● ISSN 1589 1623 (Print) ● ISSN 1785 0037 (Online)
DOI: http://dx.doi.org/10.15666/aeer/1605_68156833
© 2018, ALÖKI Kft., Budapest, Hungary

used for the calibration of such models. Group I contains approximately 80% of all data (1830 stem diameter measurements of 85 sample fir and 1703 stem diameter measurements of 84 sample spruces), whereas group II contains approximately 20% of all data (451 stem diameter measurements of 22 sample fir and 466 stem diameter measurements of 22 sample spruce).

After identifying the best among the six stem taper models used in this study, the next step was the application of the Mixed-Effects Modeling process on the best stem taper model.

Statistical nonlinear mixed-effect modeling approach

In developing the stem taper models, the diameter values measured along the stem of each tree are used. When these diameter values, which are interdependent (serial correlation "autocorrelation") are used in model development, the principle of data independence, as one of the fundamental assumptions of a regression analysis, is violated (Valentine and Gregorie, 2001), which may result in the confidence intervals of the parameters being estimated with a systematic error, the reliability of model results being adversely affected and erroneous estimations (Ye, 2005). To account for such serial correlations, the mixed-effects approach has been widely recommended in modelling, as this enables the modeling of the variance-covariance matrix structure (Littell et al., 2005).

Unlike in linear and nonlinear regression analyses, the model structure in a mixed-effects modeling approach is based on a structure in which the parameters are divided into two groups, namely parameters for fixed effects and those for random effects. While fixed-effect parameters refer to the general relationships that apply to the entire population, random-effect parameters refer to the variability among the different sampling units (sample trees). The equation structures of the mixed models are given below (*Eq. 7*):

$$Y_{ij} = f(\Phi_i, X_{ij}) + \varepsilon_{ij} \quad \text{(Eq.7)}$$

Here, Y_{ij} denotes the value of the dependent variable measured in the jth measurement on the ith sample tree, X_{ij} the value of the independent variable measured in the jth measurement on the ith sample tree, Φi the parameter values of the model, and $\mathcal{E}_{ij}$ the model errors (Castedo-Dorado et al., 2006; Crecente-Campo et al., 2010). The division of model parameters by mixed models into two groups, namely, fixed-effect and random-effect parameters can be demonstrated with the following formula (*Eq. 8;* Castedo-Dorado et al., 2006).

$$\Phi_i = A_{ij}\beta + B_{ij}b_i \quad \text{(Eq.8)}$$

Here, β is the fixed effect parameter and is calculated for the entire population, while b_i is the random-effect parameter, and indicates the variation among the sample trees. In mixed models, the fundamental assumption for the random-effect parameter and model errors is as follows (*Eqs. 9* and *10*):

$$b_i \sim N(0, D) \quad \text{(Eq.9)}$$

http://www.aloki.hu ● ISSN 1589 1623 (Print) ● ISSN 1785 0037 (Online)
DOI: http://dx.doi.org/10.15666/aeer/1605_68156833
© 2018, ALÖKI Kft., Budapest, Hungary

$$\varepsilon_{ij} \sim N(0, R) \quad \text{(Eq.10)}$$

Here, b_i (random-effect parameter) is normally distributed with an arithmetic mean of 0 and a variance of D, and $\mathcal{E}_{ij}$ (model error) is also normally distributed with an arithmetic mean of 0 and a variance of R. The estimation of the components in these assumptions constitutes a significant aspect of mixed models (Lappi, 1997). While component D is the positive-definite variance-covariance matrix that represents the variation among the sample trees (variation among trees), component R is the variance-covariance matrix that defines the variation among the data obtained from the sample trees (variation within a tree). The formulas of such variance-covariance matrices that define and model the variation both among sample trees and among the data measured on sample trees are shown below (*Eqs. 11* and *12*):

$$D = \begin{bmatrix} \sigma_u^2 & \sigma_{uv}^2 \\ \sigma_{uv}^2 & \sigma_v^2 \end{bmatrix} \quad \text{(Eq.11)}$$

$$R = \sigma^2 I_i \quad \text{(Eq.12)}$$

Here, σ_u^2 denotes the variance of random-effect parameter u, σ_v^2 the variance of random-effect parameter v, σ_{uv}^2 the covariance between the random-effect parameters, σ^2 the value of the model error, and I_i the value of the diagonal matrix defining the non-constant variance, in which the number of rows and columns is equal to the number of items of data to be used for the sample tree on which the mixed-effects model will be applied (Castedo-Dorado et al., 2006; Trincado et al., 2007).

The variance components and fixed parameters of the best compatible nonlinear stem taper model were estimated with PROC NLMIXED procedures of the SAS/ETS 9.3 package (SAS Institute, 2013). Using this method, different random parameter combinations for the best stem taper model were tested. As the criteria for determining the best random-effect parameter combination, Akaike's Information Criterion (AIC), Schwarz's Bayesian Information Criterion (BIC) and twice the negative log-likelihood (-2Ln(L)) were used.

Calibration response

Another important issue that needs to be considered and resolved in mixed-effects modeling is the calibration responses of the model. Calibrated models allow more accurate, consistent and reliable estimations to be made (Castedo-Dorado et al., 2006; Trincado and Burkhart, 2006; Yang et al., 2009; Crecente-Campo et al., 2010; Cao and Wang, 2011). In mixed-effects models, the observed values obtained newly from the sample areas are used to calculate random parameters, and by adding these random parameter values (or subtracting, if negative) to the fixed effect parameter values that apply to the entire population, the parameter values that apply to the sample area in question are calculated. In calibrating mixed models in forestry applications, the Best Linear Unbiased Predictor (BLUPs) method employed first by Lappi (1997) in a forestry study, and also known as Henderson's equations, is used.

The Best Linear Unbiased Predictor (BLUPs) method requires the measurement of a certain amount of new data in the sample area of the growth environment to be calibrated, particularly for the estimation of the random-effect parameter (Crecente-

http://www.aloki.hu ● ISSN 1589 1623 (Print) ● ISSN 1785 0037 (Online)
DOI: http://dx.doi.org/10.15666/aeer/1605_68156833
© 2018, ALÖKI Kft., Budapest, Hungary

Campo et al., 2010). In particular, the determination of which trees (the thickest, thinnest or medium-diameter trees) will be measured in the sample area is referred to as the calibration response of mixed-effects models. For this purpose, random parameters are calculated using a varying number of trees with different qualities, and subsequently, the error values of the estimations made are analyzed. Using this method, the random-effect parameter is estimated by using *Equation 13*.

$$\widehat{b}_i \approx DZ'_i\left(R + Z_i DZ'_i\right)^{-1}\left(Y_i - A_{ij}\beta\right) \quad \text{(Eq.13)}$$

Here, components D and R denote the pre-defined variance-covariance matrices, component Z_i the design matrix for random-effect parameters, and z'_i the inverse of the matrix Z_i. Furthermore, component (Y_i-$A_{ij}\beta$) in the equation above is calculated by subtracting the estimation made using only the fixed effect parameters in the mixed model from the observed value.

To determine the calibration response of the mixed-effects models, the Root-Mean-Squared Error (RMSE), Sum of Squared Error (SSE) and Mean Squared Error (MSE) values were used to identify the option that gives the best result among the compared options (Castedo-Dorado et al., 2006).

Results and discussion

Stem taper model selection

The values for the various model success criteria concerning the stem taper models for both species in this study are given in *Table 3*. As can be seen in *Table 2,* the evaluation of the values concerning the model success criteria identified Model 5, developed by Jiang et al. (2005), as the most successful model for both tree species, explaining 98.7% of the variance in the stem taper estimation for fir trees and 98.3% for spruce trees. The RMSE, $\bar{E}$, MAE, AIC and BIC values of the most successful stem taper equation for firs and spruces were also found to be 1.700 and 1.814 cm, 0.143 and 0.167 cm, and 1.179 and 1.269 cm, 4142.2 and 3951.7, 4148.5 and 3957.8 respectively (*Table 3*).

The equation of Jiang et al. (2005) has produced relatively successful results in the modeling of stem tapers in numerous studies. Using this four-segmented polynomial equation structure (Jiang et al., 2015) to model the stem taper, the adjusted coefficient of determination (R^2_{adj}) and Root-Mean-Square Error (RMSE) values were found to be 98.37% and 1.2798 cm in Jiang et al.'s (2005) study, and 98.4% and 0.7505 for Balsam fir, 98.2% and 0.8517 for Red spruce, and 97.2% and 1.4205 cm for White pine in the study conducted by Li and Weiskittel (2010), 98.13% and 1.3848 cm in the study by Özçelik and Bal (2013), 94.44% and 2.2029 cm in the study by Atalay (2014), 98.43% and 0.9843 cm in the study by Kurt (2014), 97.7% and 1.6302 cm in the study by Kumaş and Kahriman (2015), 92.6% and 2.4190 cm in the study by Doyog et al. (2017), and 97.6% and 1.4755 cm in the study by Şenyurt et al. (2017), respectively.

The parameter estimates, standard error values, t-test values and significance levels within the most successful stem taper model (M5: Jiang et al., 2005) for both species are given in *Table 4*.

http://www.aloki.hu ● ISSN 1589 1623 (Print) ● ISSN 1785 0037 (Online)
DOI: http://dx.doi.org/10.15666/aeer/1605_68156833
© 2018, ALÖKI Kft., Budapest, Hungary

Table 2. *Stem taper functions evaluated based on fitting data*

Model	Expression
M1: Demaerschalk (1972)	$d = b_1 D^{b_2} (H-h)^{b_3} H^{b_4}$
M2: Demaerschalk (1973)	$d = \{b_1 D^2 [(H-h)^{b_2} / (b_3 H^{b_{2+1}} + b_4 H^{b_2})]\}^{0.5}$
M3: Max and Burkhart (1976)	$d = D[b_1(Z-1) + b_2((Z)^2-1) + b_3(a_1 - Z)^2 I_1 + b_4(a_2 - Z)^2 I_2]^{0.5}$ $I_1 = 1, if\ Z \leq a_1; 0\ otherwise \quad I_2 = 1, if\ Z \leq a_2; 0\ otherwise \quad Z = \frac{h}{H}$
M4: Parresol et al. (1987)	$d = D\{Z_i^2(b_1 - b_2 z_1) + (z_i - a)^2 [b_3 + b_4(z_i + 2a)]I\}^{0.5}$ $I = 1, if\ Z \geq a; 0\ otherwise \quad Z = \frac{H-h}{H}$
M5: Jiang et al. (2005)	$d = \left\{ \begin{array}{l} I_S \left[D^2 \left(1 + \frac{\left(1 - \frac{h}{H}\right)^{b_1} - \left(1 - \frac{1,30}{H}\right)^{b_1}}{1 - \left(1 - \frac{1,30}{H}\right)^{b_1}} \right) \right] \\ + I_B \left[D^2 - \frac{(D^2 - F^2)\left(\left(1 - \frac{1,30}{H}\right)^{b_2} - \left(1 - \frac{h}{H}\right)^{b_2} \right)}{\left(1 - \frac{1,30}{H}\right)^{b_2} - \left(1 - \frac{5,30}{H}\right)^{b_2}} \right] \\ + I_T \left[F^2 \left(\left(\frac{h - 5,30}{H - 5,30} - 1 \right)^2 + I_M \left(\frac{1 - b_4}{b_3^2} \right) \left(b_3 - \frac{h - 5,30}{H - 5,30} \right)^2 \right) \right] \end{array} \right\}^{0,5}$ $I_S = 1, if\ h < 1.3; 0\ otherwise \quad I_B = 1, if\ 1.3 \leq h \leq 5.3; 0\ otherwise$ $I_T = 1, if\ h > 5.3; 0\ otherwise \quad I_M = 1, if\ h < (5,30 + b_3(H - 5,30)); 0\ otherwise$
M6: Fang et al. (2000)	$d = c_1 \left[H^{(k-b_1)/b_1} (1-Z)^{(k-\beta)/\beta} \alpha_1^{I_1+I_2} \alpha_2^{I_2} \right]^{0.5}$ $Z = \frac{h}{H} \quad p_1 = \frac{h_1}{H} \quad p_2 = \frac{h_2}{H} \quad I_1 = 1, if\ p_1 \leq q \leq p_2; 0\ otherwise \quad I_2 = 1, if\ p_2 \leq q \leq 1; 0\ otherwise$ $\beta = b_1^{1-(I_1+I_2)} b_2^{I_1} b_3^{I_2} \quad c_1 = \sqrt{\frac{a_1 D^{a_2} H^{a_3 - k/b_1}}{b_1(r_0 - r_1) + b_2(r_1 - a_1 r_2) + b_3(a_1 r_2)}}$ $\alpha_1 = (1-p_1)^{(b_2 - b_1)k/b_1 b_2} \quad \alpha_2 = (1-p_2)^{(b_3 - b_2)k/b_2 b_3}$ $r_0 = \left((1 - h_{st})/H\right)^{k/b_1} \quad r_1 = (1-p_1)^{k/b_1} \quad r_2 = (1-p_2)^{k/b_2}$

d is diameter outside bark at a height h (cm), D is diameter outside bark at breast height (cm), h is height above ground to the measurement point (m), H is total tree height (m), a_1 and a_2 are the join points to be estimated from the sample data for Max and Burkhart (1976) model, a is the join point to be estimated from the sample data for Parresol et al. (1987) model, F diameter outside bark at 5.3 m above ground (cm), h_1 and h_2 are the heights from ground level where the two inflection points assumed in the Fang et al. (2000) model occur, k is equal to π/40 000, a metric constant for converting from diameter squared in square centimeters to cross-sectional area in square meters, h_{st} is stump height (m), a_1-a_3, b_1-b_4, p_1-p_2 are coefficients to be estimated

http://www.aloki.hu ● ISSN 1589 1623 (Print) ● ISSN 1785 0037 (Online)
DOI: http://dx.doi.org/10.15666/aeer/1605_68156833
© 2018, ALÖKI Kft., Budapest, Hungary

Table 3. *Goodness of fit statistics of six taper model for Caucasian fir and Oriental spruce species*

Taper model	Caucasian fir						Oriental spruce					
	R^2_{adj}	RMSE	$\bar{E}$	MAE	AIC	BIC	R^2_{adj}	RMSE	$\bar{E}$	MAE	AIC	BIC
M1	0.979	2.134	0.006	1.58	4503.5	4509.8	0.977	2.082	0.057	1.57	4155.4	4161.6
M2	0.977	2.245	0.192	1.65	4584.6	4590.9	0.975	2.182	0.203	1.63	4224.8	4231.0
M3	0.978	2.162	0.265	1.59	4527.8	4536.6	0.976	2.147	0.311	1.65	4203.8	4212.4
M4	0.972	2.464	0.577	1.84	4728.2	4735.7	0.967	2.503	0.676	1.96	4429.3	4436.7
M5	0.987	1.700	0.143	1.18	4142.2	4148.5	0.983	1.814	0.167	1.27	3951.7	3957.8
M6	0.981	2.035	0.054	1.50	4434.8	4446.2	0.979	2.001	0.138	1.52	4101.3	4112.4

Table 4. *The parameter estimations for the Jiang et al. (2005) taper model*

Parameters	Caucasian fir				Oriental spruce			
	Estimate	Standard error	t value	p	Estimate	Standard error	t value	p
b_1	158.2541	5.8746	26.94	<0.0001	152.8303	6.5333	23.39	<0.0001
b_2	1.3388	0.5260	2.55	0.0110	2.9909	0.7597	3.94	<0.0001
b_3	0.8796	0.0050	177.66	<0.0001	0.9003	0.0054	168.08	<0.0001
b_4	4.0340	0.1203	33.53	<0.0001	4.0662	0.1576	25.80	<0.0001

In the equation of Jiang et al. (2005), it is hard to measure the diameter at a height of 5.30, although this variable can be estimated using the tree's height and diameter at breast height. For both tree species, the equation for estimating the diameter value at a height of 5.30 m using the height and diameter at breast height values is given below (*Eqs. 14* and *15*).

for Caucasian fir $$F_{d5.3} = D\left(0.923 + \left(-0.832\frac{5.27}{H}\right)^2\right) \quad \text{(Eq.14)}$$

for Oriental spruce $$F_{d5.3} = D\left(0.893 + \left(-0.668\frac{5.27}{H}\right)^2\right) \quad \text{(Eq.15)}$$

where $F_{d5.3}$ is diameter at a height of 5.30 m, D is diameter at breast height (cm), and H is total tree height (m).

All parameters in the equations concerning Caucasian fir and Oriental spruce were found to be statistically significant at a significance level of $p < 0.001$. The adjusted coefficients of determination (R^2_{adj}), Root-Mean-Square Error (RMSE), mean errors ($\bar{E}$) and mean absolute errors (MAE)) for both species were found to be 0.986 and 0.987, 1.725 and 1.520 cm, 0.044 and 0.015 cm, and 1.279 and 1.145 cm, respectively.

Nonlinear mixed-effect modeling

In this study, the parameters of the Jiang et al. (2005) equation, as the most successful equation in modeling the diameter of trees along their stem, were also

http://www.aloki.hu ● ISSN 1589 1623 (Print) ● ISSN 1785 0037 (Online)
DOI: http://dx.doi.org/10.15666/aeer/1605_68156833
© 2018, ALÖKI Kft., Budapest, Hungary

estimated through mixed-effects modeling. A test was made of the one, two, three and four-way random-effect parameter combinations of parameters b_1, b_2, b_3 and b_4 of the stem taper model, thus testing a total of 15 different combinations. The Akaike's Information Criterion (AIC), Schwarz's Bayesian Information Criterion (BIC) and twice the negative log-likelihood (-2LnL (L)) were used to determine the best random-effect parameter combination, and the garnered data is presented in *Table 5*.

Table 5. *The goodness-of-fit statistics for different random parameters for the Jiang et al. (2005) taper model*

Random parameters	Caucasian fir				Oriental spruce			
	RMSE	**-2LnL**	**AIC**	**BIC**	**RMSE**	**-2LnL**	**AIC**	**BIC**
b_1	1.657	4090.7	4104.7	4113.5	1.770	3904.4	3918.4	3927.0
b_2	1.706	4137.3	4151.3	4160.1	1.828	3944.8	3958.8	3967.4
b_3	1.239	3629.0	3643.0	3651.8	1.223	3357.4	3371.4	3380.0
b_4	1.196	3572.5	3586.5	3595.3	1.215	3348.2	3362.2	3370.8
b_1,b_2	1.716	4145.2	4163.2	4174.6	1.785	3908.9	3926.9	3937.9
b_1,b_3	1.166	3530.8	3548.8	3560.1	1.144	3258.1	3276.1	3287.1
b_1,b_4	1.119	3465.7	3483.7	3495.1	1.136	3247.3	3265.3	3276.4
b_2,b_3	1.250	3641.6	3659.6	3671.0	1.215	3346.8	3364.8	3375.8
b_2,b_4	1.210	3590.4	3608.4	3619.7	1.208	3338.1	3356.1	3367.2
b_3,b_4	1.100	3439.1	3457.1	3468.5	1.129	3229.1	3247.1	3258.2
b_1,b_2,b_3	1.161	3525.6	3539.6	3548.4	1.125	3233.6	3247.6	3256.2
b_1,b_2,b_4	1.113	3458.6	3472.6	3481.4	1.117	3223.6	3237.6	3246.2
b_1,b_3,b_4	2.817	4918.3	4932.3	4941.1	2.862	3920.8	3934.8	3943.0
b_2,b_3,b_4	2.893	4625.4	4639.4	4648.0	2.983	3426.1	3440.1	3447.8
b_1,b_2,b_3,b_4	2.917	3525.1	3539.1	3546.4	2.302	4191.9	4205.9	4214.4

AIC, BIC and -2LnL values are preferred over coefficients of determination when comparing mixed-effects nonlinear regression models, with regression models that produce smaller information criteria values being considered successful (Castedo-Dorado et al., 2006). As can be seen in *Table 5*, the values of AIC, BIC and -2LnL indicate that the model with random-effect parameters b_3 and b_4 is the most successful for both fir and spruce. Including more than two random parameters either produced failed model convergence or non-significant parameters at a significance level of 0.05 for some variance and covariance parameters and fixed parameters for both species. The parameter estimations of the mixed-effects model are given in *Table 6*.

Also compared nonlinear and mixed effects models to Jiang et al. (2005) stem taper model. These results indicated that all mixed effects models except for the model with random-effect parameters (b_2), (b_1,b_2), (b_1,b_3,b_4), (b_2,b_3,b_4), (b_1,b_2,b_3,b_4) for fir and (b_2), (b_1,b_3,b_4), (b_2,b_3,b_4), (b_1,b_2,b_3,b_4) for spruce provided much better fits than their fixed model counterparts (*Tables 3* and *5*). The reduction rates in AIC and BIC for fir and spruce were 12.8% (1.0-16.5), 13.6% (1.0-18.1) and 12.7% (1.0-16.4%), 13.4% (1.0-18.0) respectively. Mixed effects models were more accurate and precise than those fitted without random effects as root-mean-square error (RMSE) was reduced by 28.2% (2.5-35.5) for fir and 29.5% (2.4-38.4%) for spruce growth prediction. The reduction rates in RMSE, AIC and BIC for fir and spruce were 35.3, 16.2, 16.1% for fir and 37.8, 17.8, 17.7% for spruce with random-effect parameters b_3 and b_4.

http://www.aloki.hu ● ISSN 1589 1623 (Print) ● ISSN 1785 0037 (Online)
DOI: http://dx.doi.org/10.15666/aeer/1605_68156833
© 2018, ALÖKI Kft., Budapest, Hungary

Table 6. *The parameter estimations and variance components with the goodness-of-fit statistics for the selected stem taper model (M5: Jiang et al., 2005)*

Parameters		Caucasian fir				Oriental spruce			
		Estimate	**Standard error**	**t value**	**p**	**Estimate**	**Standard error**	**t value**	**p**
Fixed parameters	b_1	158.26	3.5914	44.07	<0.001	152.90	4.0306	37.93	<0.001
	b_2	1.3388	0.3007	4.95	0.0110	2.9898	0.4588	6.52	<0.001
	b_3	0.8522	0.0034	251.59	<0.001	0.8473	0.0040	211.49	<0.001
	b_4	3.6780	0.1271	28.94	<0.001	3.4051	0.1381	24.65	<0.001
Variance component	σ_u^2	0.0107	0.0014	7.69	<0.001	0.0132	0.0024	5.51	<0.001
	σ_v^2	4.2857	0.7841	5.47	<0.001	3.3346	0.6879	4.85	<0.001
Covariance	σ_{uv}^2	0.1879	0.0296	6.35	<0.001	0.1723	0.0359	4.80	<0.001
Error	σ^2	0.9470	0.0327	28.93	<0.001	1.0648	0.0384	27.74	<0.001

The relative height-error distribution in the nonlinear and mixed-effects models for Caucasian fir and Oriental spruce is given in *Figures 4* and *5,* respectively. For both species, the model with random-effect parameters has a more homogenous error variance structure than that of the nonlinear model at all relative height values (*Figs. 4* and *5*). In other words, as is seen in *Figures 4* and *5,* the error variance values rise in parallel to the relative height values in the nonlinear model but remain constant in the mixed-effects model (Trincado and Burkhart, 2006; Yang et al., 2009; Sharma and Parton, 2009; Özçelik et al., 2011; Özçelik and Yaşar, 2015; Şenyurt et al., 2017).

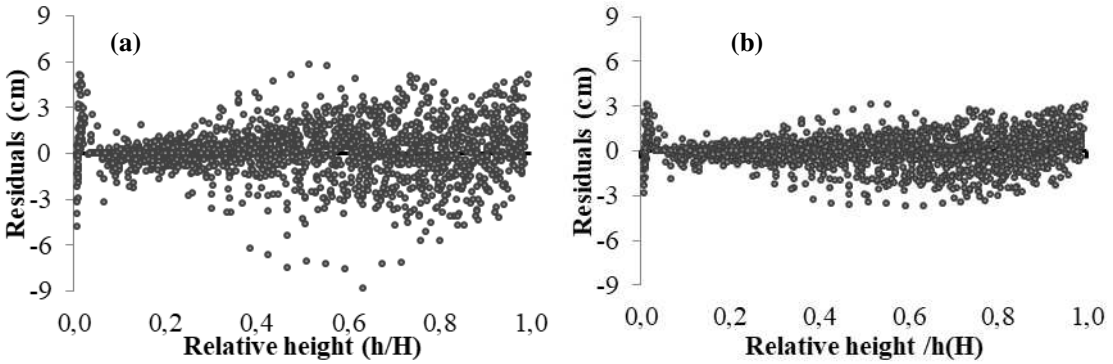

Figure 4. *Residual plots for the (a) nonlinear and (b) mixed effects model for Caucasian fir*

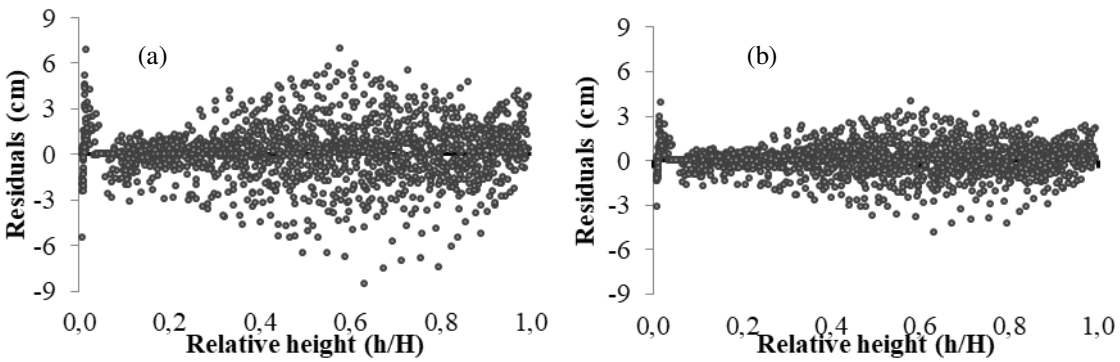

Figure 5. *Residual plots for the (a) nonlinear and (b) mixed effects model for Oriental spruce*

http://www.aloki.hu ● ISSN 1589 1623 (Print) ● ISSN 1785 0037 (Online)
DOI: http://dx.doi.org/10.15666/aeer/1605_68156833
© 2018, ALÖKI Kft., Budapest, Hungary

The error autocorrelations for Lag 1 for Caucasian fir and Oriental spruce are given in *Figures 6* and *7*, respectively. Here, a positive correlation is observed in the nonlinear regression model, and the error-related autocorrelation problem is remedied once the random-effect parameters are added to the model for both species. (*Figs. 6b* and *7b*).

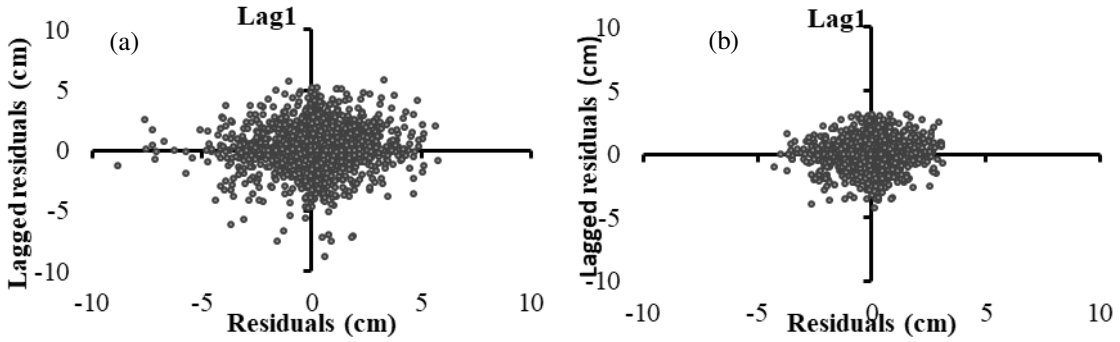

Figure 6. *Residuals plotted against lagged residuals for (a) nonlinear regression Jiang et al. (2005) model and (b) nonlinear mixed effect regression model of Caucasian fir*

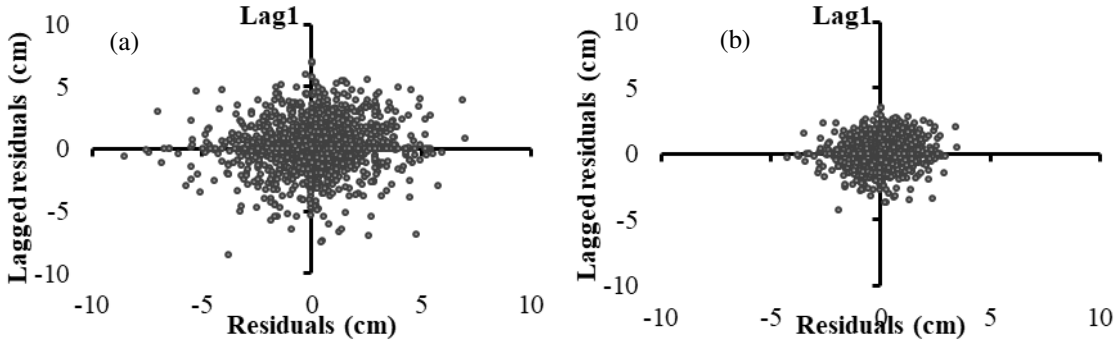

Figure 7. *Residuals plotted against lagged residuals for (a) nonlinear regression Jiang et al. (2005) model and (b) nonlinear mixed effect regression model of Oriental spruce*

As obtained in some studies (Trincado and Burkhart, 2006; Sharma and Parton, 2009; Gomez-Garcia et al., 2013; Özçelik and Yaşar, 2015; Ercanlı, 2015; Şenyurt et al., 2017; Zheng et al., 2017), the error (RMSE) of the models decreased from 1.700 to 1.100 cm for Caucasian fir and from 1.814 to 1.129 cm for Oriental spruce in the transformation of the nonlinear model to the mixed-effects model (*Tables 3* and *5*).

For the compatible stem taper model of Jiang et al. (2005) to set an example for taper estimations through the use of nonlinear mixed-effects regression parameters, the graphical results of the taper estimations for three trees in the small-, medium- and large-diameter classes are given in *Figure 8*. The trees were randomly selected from approximately thin, medium and thick diameters at breast height. The diameters of these trees being 22.4, 38.4 and 60.1 cm for firs and 18.2, 36.1 and 56.1 cm for spruces and the heights are 16.2, 26.8 and 36.1 m for firs and 13.9, 23.0 and 31.2 m for spruces. As seen in *Figure 8*, the mixed-effects model is successful to define the stem form of both Caucasian fir and Oriental spruce trees, and similar results have been obtained in previous studies in which the stem taper model was obtained through mixed-effects modeling (Trincado and Burkhart, 2006; Yang et al., 2009; Sharma and Parton, 2009; Li

http://www.aloki.hu ● ISSN 1589 1623 (Print) ● ISSN 1785 0037 (Online)
DOI: http://dx.doi.org/10.15666/aeer/1605_68156833
© 2018, ALÖKI Kft., Budapest, Hungary

and Weiskittel, 2010; Subedi and Sharma, 2011; Gomez-Garcia et al., 2013; Chiu et al., 2015; Özçelik and Yaşar, 2015; Şenyurt et al., 2017).

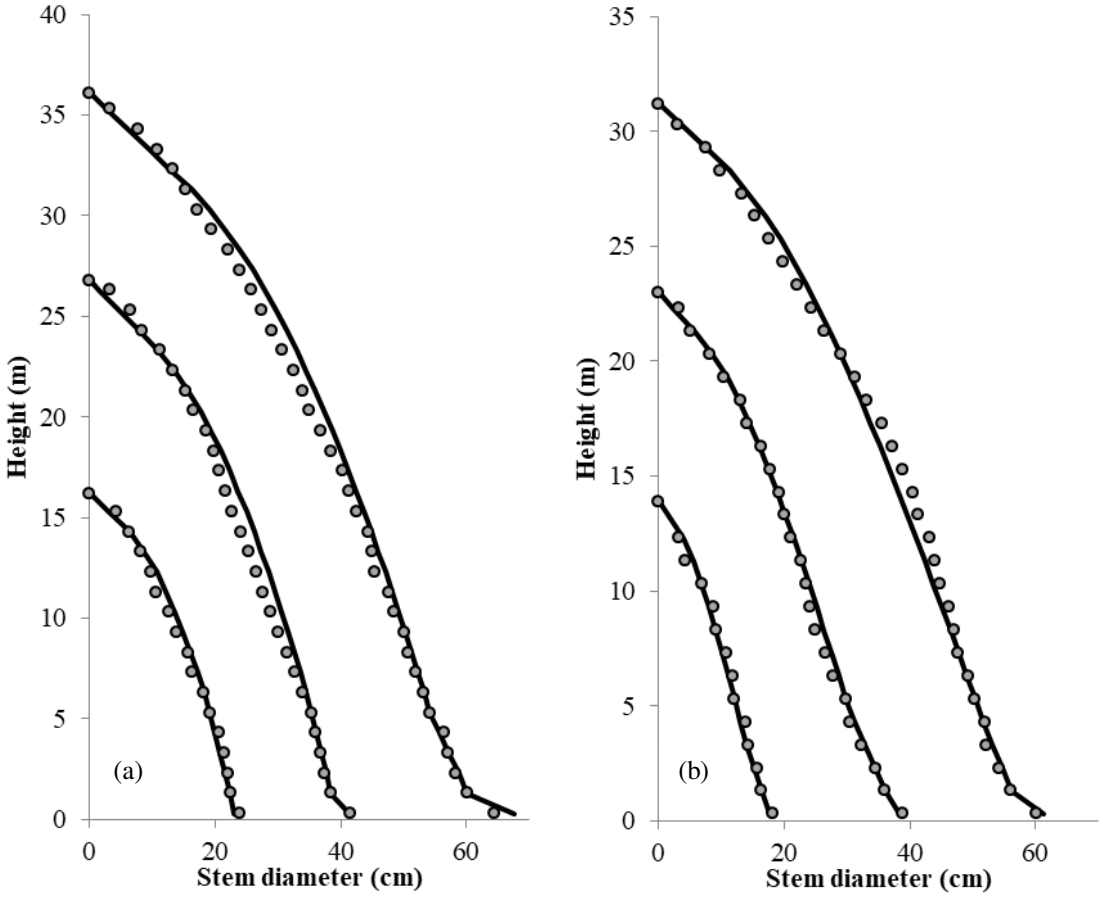

Figure 8. *Stem profile curves of taper equations to three sampled trees using mixed-effect model with b3 and b4 having random effects for (a) Caucasian fir and (b) Oriental spruce*

One of the major steps in the mixed-effects modeling process is the presentation of the calibration responses of the model that is found to be the most successful in modeling the stem taper. For this purpose, the model of Jiang et al. (2005) was calibrated using data related to 22 samples trees from each species that had not been used in the formation of the models or the estimation of parameters. In determining the calibration responses of mixed-effects models, the different scenarios suggested by Garber and Maguire (2003), Trincado and Burkhart (2006), Yang et al. (2009), Sharma and Parton (2009), Özçelik et al. (2011), Cao and Wang (2011), Subedi and Sharma (2011), Gómez-García et al. (2013, 2016), and Şenyurt et al. (2017) were also considered. These calibration response options are as follows: (i, ii, iii) 3, 4 or 5 diameter values at the lowest base section of trees; (iv, v, vi) 3, 4 or 5 diameter values obtained by dividing the measured diameters into two equal parts of sample trees; (vii, viii, ix) 3, 4, or 5 diameter values from the top sections of the trees; (x) a total of 3 diameter values from heights of 0.30 m, 1.30 m and 5.30 m; (xi) a total of 4 diameter values at heights of 0.30 m, 1.30 m, 5.30 m and in the top section of trees; (xii) a total of 5 diameter values from heights of 0.30 m, 1.30 m and 5.30 m, the diameter that divides

http://www.aloki.hu ● ISSN 1589 1623 (Print) ● ISSN 1785 0037 (Online)
DOI: http://dx.doi.org/10.15666/aeer/1605_68156833
© 2018, ALÖKI Kft., Budapest, Hungary

the measured diameter values into two equal parts of tree ($d_{h/2}$) and the diameter of the top section.

With *Equation 13* regarding the Best Linear Unbiased Predictor (BLUP) method, the random-effect parameters for the sample trees were calculated using the SAS program code of Trincado et al. (2007). The random-effect parameter values (parameters u and v) that were calculated in 12 different ways for each sample tree from both species (22 sample trees) were added to parameters b_3 and b_4. As a result, when the values of parameters b_3 and b_4 were changed for each sample tree, different stem taper equations were obtained for these trees. Subsequently, in the calibration of mixed-effects models, the estimations for the diameter values measured along the stems of 22 sample trees were obtained using different stem taper equations, obtained through random parameters, and calculated based on 12 different calibration options. The Sum of the Squared Error (SSE), Mean Squared Error (MSE) and Root-Mean-Squared Error (RMSE) values for the estimations related to the sample trees from each species are given in *Table 7*. The best estimation results from among these calibration options were obtained from the calibration option based on the measurement of five diameters from the middle section of firs (SSE: 451.0, MSE: 0.9999 and RMSE: 1.0090) and four diameters from the stump section of spruces (SSE: 548.0, MSE: 1.1760 and RMSE: 1.0939).

Table 7. *Comparison of the predictive performance for some sampling scenarios*

Calicration scenarios	Caucasian fir			Oriental spruce		
	SSE	**MSE**	**RMSE**	**SSE**	**MSE**	**RMSE**
(i) Three diameter-base of the stem	479.2	1.0626	1.0401	580.1	1.2448	1.1254
(ii) Four diameter-base of the stem	460.3	1.0205	1.0193	548.0	1.1760	1.0939
(iii) Five diameter-base of the stem	460.3	1.0206	1.0193	580.5	1.2457	1.1258
(iv) Three diameter-middle part of stem	451.2	1.0005	1.0093	566.5	1.2157	1.1122
(v) Four diameter-middle part of stem	451.3	1.0008	1.0094	567.7	1.2183	1.1134
(vi) Five diameter-middle part of stem	451.0	0.9999	1.0090	567.1	1.2169	1.1127
(vii) Three diameter-top of stem	458.4	1.0165	1.0173	579.0	1.2426	1.1244
(viii) Four diameter-top of stem	457.4	1.0143	1.0162	577.8	1.2400	1.1232
(ix) Five diameter-top of stem	456.6	1.0124	1.0152	576.7	1.2376	1.1222
(x) Three diameter-$d_{0.30}$, $d_{1.30}$, $d_{5.30}$	491.2	1.0891	1.0530	575.6	1.2353	1.1211
(xi) Four diameter-$d_{0.30}$, $d_{1.30}$, $d_{5.30}$, d_{top}	459.8	1.0196	1.0188	577.0	1.2383	1.1225
(xii) Five diameter-$d_{0.30}$, $d_{1.30}$, $d_{5.30}$,$d_{h/2}$,d_{top}	458.2	1.0160	1.0170	575.3	1.2345	1.1207

Conclusions

In this study, a compatible stem taper model is developed that uses the mixed-effects modeling technique for the mixed stands of Caucasian fir and Oriental spruce in the Artvin-Ardanuç region. To model the stem taper of the trees, six compatible stem taper models developed by Demaerschalk (1972, 1973), Max and Burkhart (1976), Parresol et al. (1987), Fang et al. (2000) and Jiang et al. (2005) were used.

An evaluation of the success criteria values revealed that the model developed by Jiang et al. (2005) was the most accurate in modeling the stem diameter for both species (*Table 3*). The model developed by Jiang et al. (2005) used in this study explains 98.7% of the variance in the stem taper estimation for fir and 98.3% of the variance in the stem

http://www.aloki.hu ● ISSN 1589 1623 (Print) ● ISSN 1785 0037 (Online)
DOI: http://dx.doi.org/10.15666/aeer/1605_68156833
© 2018, ALÖKI Kft., Budapest, Hungary

taper estimation for spruce (*Table 3*). The RMSE values in the most successful stem taper equation for firs and spruces were found to be 1.700 and 1.814 cm, respectively.

The most significant advantage of the mixed-effects modeling technique over conventional regression models is that mixed-effects modeling technique allows the elimination of the problem of autocorrelation among the data and the homogenization of the distribution of error variance. In this study, the autocorrelation problem was all but eliminated using the mixed-effects modeling technique, and the distribution of error variance was transformed into a homogenous structure for all relative height classes. After the addition of the random-effect parameters to the model for both species, the error-related autocorrelation problem was eliminated (*Figs. 6b* and *7b*), and the model with random-effect parameters had a more homogenous error variance structure at all relative height values (*Figs. 4b* and *5b*). Moreover, the decrease in the RMSE values in the mixed-effects modeling approach from 1.700 cm to 1.100 cm for Caucasian fir and 1.814 cm and 1.129 cm for Oriental spruce in the transformation from the nonlinear regression model is another successful aspect. Mixed effects models provided much better fits than their fixed model counterparts for both species.

Calibrated models allow more accurate, consistent and reliable estimations to be made (Trincado and Burkhart, 2006; Yang et al., 2009; Cao and Wang, 2011). The best estimation results from the 12 different calibration options in this study were obtained through the calibration option, which involved the measurement of five diameters from the middle section of firs and four diameters from the stump section of spruces. In studies by different researchers, calibration responses are analyzed using the values of one, two, three, four, or five diameters at various stem heights (Trincado and Burkhart, 2006; Yang et al., 2009; Lejeune et al., 2009; Sharma and Parton, 2009; Özçelik et al., 2011; Gómez-García et al., 2013; Şenyurt et al., 2017).

All of these assessments have shown that successful diameter estimations could be made using the nonlinear mixed-effects modeling technique for the stem diameter estimations of both species in mixed stands of Caucasian fir and Oriental spruce in the Artvin-Ardanuç region. Thus, the success of the diameter estimations has a direct effect on volume estimations. In practical forestry applications, it is more important to accurately estimate the volume of trees than their diameter at breast height diameter. The mixed-effects model approach is substantial, and will allow forest managers to better predict tree volumes to any utilization standard. It is worth noting that when one of the models with a similar level of success in estimation needs to be selected for a specific species in any region, the practical implementation of the method and the preferences of the forest managers is also important.

Acknowledgements. This study was supported by the Scientific Research Projects Unit of Artvin Çoruh University under Project 2016.F10.01.02. This study was produced from a master's thesis prepared by Celal Yavuz ÇAKIR and supervised by Dr. Aydın KAHRİMAN for the Institute of Natural and Applied Science, Artvin Çoruh University, Turkey. The authors wish to thank the other researchers in this project and employees of Ardanuç Forest Enterprise who contributed to this project. We also thank Dr. İlker Ercanlı and Professor Dr. Ramazan Özçelik for their support and contributions. The authors declare that they have no conflict of interest.

http://www.aloki.hu ● ISSN 1589 1623 (Print) ● ISSN 1785 0037 (Online)
DOI: http://dx.doi.org/10.15666/aeer/1605_68156833
© 2018, ALÖKI Kft., Budapest, Hungary

REFERENCES

[1] Atalay, F. (2014): Developing Compatible Taper and Volume Equations for Crimean Pine [*Pinus nigra* Arnold. subsp. *pallasiana* (Lamb.) Holmboe] in Mudurnu-Sırçalı Forest District Enterprise. – MSc Thesis, Çankırı Karatekin University Graduate School of Natural and Applied Sciences, Çankırı.

[2] Cao, Q. V., Wang, J. (2011): Calibrating fixed- and mixed-effects taper equations. – Forest Ecology and Management 262: 671-673. DOI: 10.1016/j.foreco.2011.04.039.

[3] Castedo-Dorado, F., Diéguez-Aranda, U., Barrio, M., Sánchez, M., Gadow, K. V. (2006): A generalized height-diameter model including random components for radiata pine plantations in northeastern Spain. – Forest Ecology and Management 229: 202-213. https://doi.org/10.1016/j.foreco.2006.04.028.

[4] Chiu, C. M., Chien, C. T., Nigh, G. (2015): A comparison of three taper equation formulations and an analysis of the slenderness coefficient for Taiwan incense cedar (*Calocedrus formosana*), – Australian Forestry 78(3): 159-168. DOI: 10.1080/00049158.2015.1051610.

[5] Clark III, A., Souter, R. A., Schlaegel, B. E. (1991): Stem profile equations for southern tree species. – USDA Forest Service Research Paper SE-282.

[6] Crecente-Campo, F., Tomé, M., Soares, P., Diéguez-Aranda, U. (2010): A generalized nonlinear mixed-effects height-diameter model for Eucalyptus globulus L. in northwestern Spain. – Forest Ecology and Management 259: 943-952. DOI: 10.1016/j.foreco.2009.11.036.

[7] Demaerschalk, J. P. (1972): Converting volume equations to compatible taper equations. – Forest Science 18: 241-245.

[8] Demaerschalk, J. P. (1973): Integrated systems for the estimation of tree taper and volume. – Canadian Journal of Forest Research 3: 90-94.

[9] Diéguez-Aranda, U., Castedo-Dorado, F., Alvarez-Gonzalez, J. G., Rojo, A. (2006): Compatible taper function for Scots pine plantations in Northwestern Spain. – Canadian Journal of Forest Research 36: 1190-1205. DOI: 10.1139/X06-008.

[10] Doyog, N. D., Lee, Y. J., Lee, S. (2017): Stem taper equation analysis for Larix kaempferi species in the Central Region of South Korea. – Journal of Sustainable Forestry 36(8): 747-763. https://doi.org/ 10.1080/10549811.2017. 1356737.

[11] Ercanlı, İ. (2015): Nonlinear mixed effect models for predicting relationships between total height and diameter of oriental beech trees in Kestel, Turkey. – Revista Chapingo Serie Ciencias Forestales y del Ambiente 21(1): 185-202. DOI: 10.5154/r.rchscfa.2015.02.006.

[12] Ercanlı, İ., Kahriman, A. (2013): developing stem taper and volume equations using nonlinear mixed effect modeling for Oriental spruce (*Picea orientalis* (L.) Link) and scots pine (*Pinus sylvestris* L.) stands in Trabzon and Giresun Forest Directorate. – The International Symposium for the 50th Anniversary of the Forestry Sector planning in Turkey 26-28 November, Antalya, Turkey. pp 613-621.

[13] Fang, Z., Borders, B. E., Bailey, R. L. (2000): Compatible volume taper models for loblolly and slash pine based on system with segmented-stem form factors. – Forest Science 46: 1-12. https://doi.org/10.1093 /forestscience/46.1.1.

[14] Garber, S. M., Maguire, D. A. (2003): Modeling stem taper of three central Oregon species using nonlinear mixed effects models and autoregressive error structures. – Forest Ecology and Management 179: 507-507. DOI: 10.1016/S0378-1127(02)00528-5.

[15] General Directorate of Forestry. (2015): Forests of Turkey. – Turkey General Directorate of Forest Publications, Ankara, Turkey.

[16] Gómez-García, E., Crecente-Campo, F., Diéguez-Aranda, U. (2013): Selection of mixed-effects parameters in a variable-exponent taper equation for birch trees in northwestern Spain. – Annals of Forest Science 70: 707-715. DOI: 10.1007/s13595-013-0313-9.

http://www.aloki.hu ● ISSN 1589 1623 (Print) ● ISSN 1785 0037 (Online)
DOI: http://dx.doi.org/10.15666/aeer/1605_68156833
© 2018, ALÖKI Kft., Budapest, Hungary

[17] Gómez-García, E., Diéguez-Aranda, U., Özçelik, Ö., Sal-Cando, M., Castedo-Dorado, F., Crecente-Campo, F., Corral-Rivas, J. J., Arias-Rodil, M. (2016): Development of a stem taper function using mixed-effects models for Pinus sylvestris in Turkey: selection of fixed parameters to expand. – Bosque 37(1): 159-167. DOI: 10.4067/S0717-92002016000100015.
[18] Green, E. J., Reed, D. D. (1985): Compatible tree volume and taper functions for pitch pine. – Northern Journal of Applied Forestry 2: 14-16.
[19] Jiang, L., Brooks, J. R., Wang, J. (2005): Compatible taper and volume equations for yellow-poplar in West Virginia. – Forest Ecology and Management 213: 399-409. DOI: 10.1016/j.foreco.2005.04.006.
[20] Kozak, A. (2004): My last words on taper equations. – Forest Chronicle 80: 507-515. DOI: 10.5558/tfc80507-4.
[21] Kumaş, G., Kahriman, A. (2015): Development of compatible taper and volume equations for calabrian pine in Antalya Regional Directorate. – Artvin Çoruh University Journal of Forestry Faculty 17(1): 21-31. DOI: 10.17474/acuofd.13340.
[22] Kurt, A. K. (2014): Developing Stem Taper and Stem Volume Equations using Nonlinear Mixed Effect Modeling Approach for Crimean Pine Stands (*Pinus nigra* Arnold. subsp. *pallasiana* (Lamb.) Holmboe) in Tarsus Forest Enterprise, – MSc Thesis, Çankırı Karatekin University Graduate School of Natural and Applied Sciences, Çankırı.
[23] Lappi, J. (1997): A longitudinal analysis of height–diameter curves. – Forest Science 43: 555-570. DOI: 10.1093/forestscience/43.4.555.
[24] Leites, L. P., Robinson, A. P. (2004): Improving taper equations of Loblolly pine with crown dimensions in a mixed-effects modeling framework. – Forest Science 50(2): 204-212. https://doi.org/10.1093/ forestscience/50.2.204.
[25] Lejeune, G., Ung, C. H., Fortin, M., Guo, X. J., Lambert, M. C., Ruel, J. C. (2009): A simple stem taper model with mixed effects for boreal black spruce. – European Journal of Forest Research 128(5): 505-513.
[26] Li, R., Weiskittel, A. R. (2010): Comparison of model forms for estimating stem taper and volume in the primary conifer species of the North American Acadian Region. – Annals of Forest Science 67(302): 1-16. DOI: 10.1051/forest/2009109.
[27] Littell, R. C., Miliken, G. A., Stroup, W. W., Wolfinger, R. D. (2005): SAS system for mixed models. – SAS Institute Inc., Cary, NC, USA.
[28] Max, T. A., Burkhart, H. E. (1976): Segmented polynomial regression applied to taper equations. – Forest Science 22(3): 283-289. DOI: 10.1093/forestscience/22.3.283.
[29] Newnham, R. M. (1992): Variable-form taper functions for four Alberta tree species. – Canadian Journal of Forest Research 22(2): 210-22. DOI: 10.1139/x92-028.
[30] Özçelik, R., Brooks, J. R. (2012): Compatible volume and taper models for economically important tree species of Turkey. – Annals of Forest Science 69: 105-118. DOI: 10.1007/s13595-011-0137-4.
[31] Özçelik, R., Bal, C. (2013): Effects of adding crown variables in stem taper and volume predictions for black pine. – Turkish Journal of Agriculture and Forestry 37: 231-242. DOI: 10.3906/tar-1206-2.
[32] Özçelik, R., Yaşar, Ü. (2015): Development of stem diameter model for Bormullerian fir (*Abies nordmanniana* (Stev.) subsp. *bormulleriana* (Mattf.)) stands in Ayancık District using mixed effects modeling approach. – Turkish Journal of Forestry 16(2): 86-95.
[33] Özçelik, R., Brooks, J. R., Jiang, L. (2011): Modeling stem profile of Lebanon cedar, Brutian pine, and Cilicia fir in Southern Turkey using nonlinear mixed-effects models. – European Journal of Forest Research 130: 613-621. DOI: 10.1007/s10342-010-0453-5.
[34] Parresol, B. R., Hotvedt, J. E., Cao, Q. V. (1987): A volume and taper prediction system for bald cypress. – Canadian Journal of Forest Research 17: 250-259.
[35] Sakıcı, O. E., Mısır, N., Yavuz, H., Mısır, M. (2008): Stem taper functions for Abies nordmanniana subsp. bornmulleriana in Turkey. – Scandinavian Journal of Forest Reearch 23: 522-533. https://doi.org/ 10.1080/02827580802552453.

http://www.aloki.hu ● ISSN 1589 1623 (Print) ● ISSN 1785 0037 (Online)
DOI: http://dx.doi.org/10.15666/aeer/1605_68156833
© 2018, ALÖKI Kft., Budapest, Hungary

[36] SAS Institute Inc. (2013): SAS/IML 9.3 User's Guide. Cary, USA. – SAS Institute Inc., Cary, NC, USA.
[37] Searle, S. R., Casella, G., Mc Culloch, C. E. (1992): Variance Components. – John Wiley and Sons Inc., Hoboken, NJ, USA.
[38] Şenyurt, M., Ercanlı, İ., Bolat, F. (2017): Taper equations based on nonlinear mixed effect modeling approach for Pinus nigra in Çankırı forests. – Bosque 38(3): 545-554. DOI: 10.4067/S0717-92002017000300012.
[39] Sharma, M., Parton, J. (2009): Modeling stand density effects on taper for Jack pine black spruce plantations using dimensional analysis. – Forest Science 55(3): 268-282.
[40] Subedi, N., Sharma, M. (2011): Applying wavelet-based functional approach in modelling tree taper, – Annals of Forest Science 68: 1039-1048.
[41] Trincado, G., Burkhart, H. E. (2006): A generalized approach for modeling and localizing stem profile curve. – Forest Science 52(6): 670-682.
[42] Trincado, G., Vander-Schaaf, C. L., Burkhart, H. E. (2007): Regional mixed-effects height-diameter models for loblolly pine (*Pinus taeda* L.) plantations. – European Journal Forest Research 126: 253-262. https://doi.org/ 10.1007/s10342-006-0141-7.
[43] Turkish State Meteorological Service (2016): Artvin Meteorological Station Climate Data (1927-2016). – Artvin, Turkey.
[44] Valentine, H. T., Gregoire, T. G. (2001): A switching model of bole taper. – Canadian Journal of Forest Research 31: 1400-1409. DOI: 10.1139/x01-061.
[45] Yang, Y., Huang, S., Meng, S. X. (2009): Development of a tree-specific stem profile model for white spruce: a nonlinear mixed model approach with a generalized covariance structure. – Forestry 82(5): 541-555. DOI: 10.1093/forestry/cpp026.
[46] Ye, S. (2005): Covariance structure selection in linear mixed models for longitudinal data, – MSc Thesis, Department of Bioinformatics and Biostatistics, University of Louisville, Kentucky, USA.
[47] Zheng, C., Wang, Y., Jia, L., Mason, E. G., We, S., Sun, C., Duan, J. (2017): Compatible taper volume models of *Quercus variabilis* Blume forests in north China. – iForest 10: 567-575. https://doi.org/10.3832/ifor2114-010.

http://www.aloki.hu ● ISSN 1589 1623 (Print) ● ISSN 1785 0037 (Online)
DOI: http://dx.doi.org/10.15666/aeer/1605_68156833
© 2018, ALÖKI Kft., Budapest, Hungary

GENETIC DIVERSITY OF WILD RASPBERRY GENOTYPES (*RUBUS IDAEUS* L.) IN NORTH ANATOLIA BASED ON ISSR MARKERS

CEKIC, C.[1*] – CALIS, O.[2] – OZTURK ERDEM, S.[1]

[1]*Department of Horticulture, Faculty of Agriculture, Gaziosmanpaşa University, Tokat, Turkey*

[2]*Department of Plant Protection, Faculty of Agriculture, Akdeniz University, Antalya, Turkey*

**Corresponding author*
e-mail: cetin.cekic@gop.edu.tr

(Received 18th Jul 2018; accepted 20th Sep 2018)

Abstract. The preliminary aim of the study before future breeding program was to reveal usability of ISSR markers to assess genetic diversity and relatedness within raspberry genotypes wildly grown in Northern Turkey. In this study, 19 wild raspberry genotypes collected from Black Sea region in Turkey were used. ISSR PCR analyses were carried on the DNA of genotypes isolated using mini CTAB extraction method. The levels of polymorphism between genotypes were determined using the UBC ISSR primers. A total of 111 bands were obtained from 15 UBC ISSR primers. Out of 111 bands, 101 bands were polymorphic. The number of bands obtained per primer ranged between 3 and 10, the average number of bands were determined as 7.4. The average number of polymorphic bands per primer was 6.73. Similarities and differences between genotypes have been studied at the molecular level. The data used for statistical analysis were obtained by the evaluation of ISSR bands. Similarity coefficient and UPGMA dendrogram were built using the Basic Coordinates Analysis. According to the dendrogram, the genotypes have been divided in two main groups, one small and other large group. While the small group was only comprised of three (A8, A10 and A14) genotypes, the large group included the rest of the genotypes studied.
Keywords: *molecular, polymorphism, dendrogram, raspberry, Turkey*

Introduction

Anatolia is one of the gene resources of the world with its natural flora of hundreds of wild plant forms, and wild forms of strawberry is also very common in most parts of the Turkey, especially in Black Sea coast and on the mountains through the sea cost. The wild ancestors of many plants which now provide staples for mankind still grow this region. Turkey is also the home of wild form of many soft fruits such as raspberry, blackberry. These species are mainly originated from the foothills of the Mountains on Black Sea coast. The wild forms have so much contribution to improve new cultivars. That is why it is so important to describe the wild forms and to establish collection gardens with them (Davis, 1982; Jennings, 1988).

As an important commercial fruit crop, red raspberries (*Rubus idaeus* L.: Rosaceae) are widely grown in all temperate regions of the world and are consumed by local people. Many of the most important modern commercial red raspberry cultivars derive from hybrids or selections from the wild. Black Sea region in northern Turkey is one of the important germplasm centers of this species (Davis, 1982). They grow naturally in high elevations and require moist, rich soils. The plants are usually seen as small, spatially discrete populations over 1000 m altitude, mostly along roadsides, in woodland clearings. *Rubus idaeus* has been an important source of genes for breeding new raspberry varieties (Alice et al., 2001; Marshal et al., 2001). In the development of improved varieties, the main qualities selected for are hardiness, productivity, disease resistance, fruit size, and

http://www.aloki.hu ● ISSN 1589 1623 (Print) ● ISSN 1785 0037 (Online)
DOI: http://dx.doi.org/10.15666/aeer/1605_68356843
© 2018, ALÖKI Kft., Budapest, Hungary

firmness. Scientists have also started using *R. idaeus* as a model plant to develop and apply genetic techniques in the study of perennials, particularly members of the family *Rosaceae* (Graham et al., 1996).

Very few recent studies have attempted to quantify the genetic variation present in raspberry germplasm in Turkey. Ercisli et al. (2008) examined genetic diversity in 11 wild selections with one red raspberry using Amplified Fragment Length Polymorphism (AFLP) markers. There are also several reports on genetic diversity in raspberries from all over the worlds and modern molecular marker techniques are essential in effectively evaluating this germplasm collection as a source of useful genetic material for raspberry breeding programs (Howell et al., 1994; Chwedorzewska et al., 2002; Lund et al., 2003).

The development of molecular biology has resulted in DNA based marker procedures that should lead to a greater understanding of relationships between species and more accurate taxonomic classification. These techniques should also allowed more effective understanding of crop plant's genetic architecture and utilization of genetic diversity by breeders and identification of species and cultivars by means other than morphological characteristics (Graham et al., 1996).

Inter simple sequence repeats (ISSRs) have been shown to provide a powerful, rapid, simple, reproducible and inexpensive means to assess genetic diversity and identify closely related cultivars in many species (Gonzalez et al., 2002) The ISSR technique has been extensively used for several applications in molecular taxonomy, conservation and breeding. ISSR PCR has since been applied for cultivar identification (Charters et al., 1996; Cekic et al., 2001; Haritha et al., 2015; Ayesh, 2017), to detect geneflow and introgression (Allainguillume et al., 1997; Kalyani et al., 2014) and for mapping purposes (Kojima et al., 1998) and genetic diversity analysis (Cekic and Özmen, 2016). Further, ISSR PCR is useful in fingerprint and characterization of accessions and identification of cultivar and varieties (Wolf et al., 1995; Hardik et al., 2016). Against this backdrop, the present work was taken up with an objective to assess the level of genetic variation among 19 raspberry genotypes from Black Sea region in North Anatolia based on ISSR PCR before future breeding program.

Material and methods

Plant material

For research purposes, a total of 19 different raspberry genotypes from Black Sea region in North Anatolia were used. Observed observations showed wild raspberry plants spread from 1200 m above sea level of Turkey, where the forests end and the open fields begin, and on the northern slopes facing the Black Sea, where foliage is common where water leaks from the ground. Coordinates and elevation of the place where the samples are taken are recorded by specifying with Global Positioning System (GPS) (*Table 1*) and these coordinates marked on the map (*Fig. 1*) In addition, plants and surroundings are photographed in terms of ease of identification of the region and plant sample taken in the field.

DNA extraction

Total genomic DNA was extracted according to the cetyltrimethylammonium bromide (CTAB) method (Doyle and Doyle, 1987). DNA sample concentration was determined using a fluorometer employing a Hoechst dye (Hoefer Inc., San Francisco, CA, USA),

http://www.aloki.hu ● ISSN 1589 1623 (Print) ● ISSN 1785 0037 (Online)
DOI: http://dx.doi.org/10.15666/aeer/1605_68356843
© 2018, ALÖKI Kft., Budapest, Hungary

and the DNA samples were diluted to a final concentration of 10 ng/µl with 1 × TE buffer and stored at -20 °C prior to polymerase chain reaction (PCR) amplification.

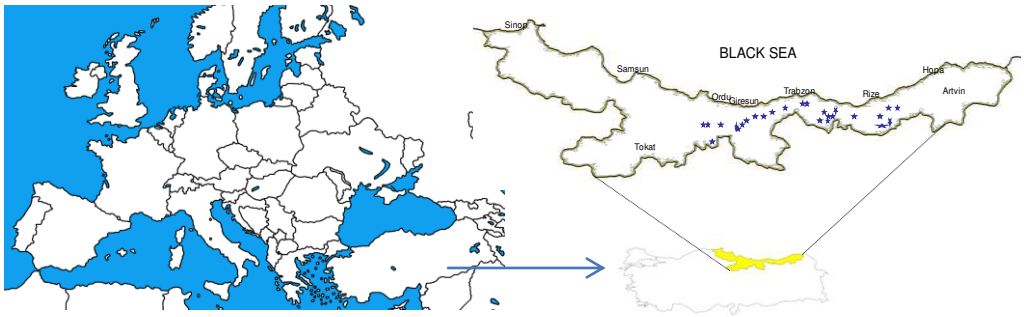

Figure 1. *The localization of Black sea coast in Turkey, where the samples were collected*

Table 1. *The latitudes, longitudes and elevations of the samples taken*

Sample ID	City	Location	Altitude (m)	Latitude	Longitude
A1	*Trabzon*	*Duzkoy*	1505	40° 50.993N	039° 25.963E
A3	*Trabzon*	*Zigana*	1999	40° 38.279N	039° 24.285E
A4	*Trabzon*	*Zigana*	2013	40° 38.409N	039° 24.362E
A5	*Trabzon*	*Sumela*	1732	40° 39.415N	039° 40.913E
A6	*Trabzon*	*Sumela*	1718	40° 39.349N	039° 40.773E
A7	*Trabzon*	*Sumela*	1714	40° 39.358N	039° 40.761E
A8	*Trabzon*	*Sumela*	1718	40° 39.473N	039° 40.730E
A9	*Trabzon*	*Uzungol*	1123	40° 36.470N	040° 23.795E
A10	*Rize*	*Ayder*	1486	40° 56.494N	041° 08.037E
A11	*Rize*	*Ayder*	1584	40° 56.143N	041° 08.252E
A12	*Giresun*	*Kumbet yaylasi*	1381	40° 34.723N	038° 26.411E
A13	*Ordu*	*Turnalik*	1495	40° 41.811N	037° 55.442E
A14	*Ordu*	*Turnalik*	1480	40° 40.582N	037° 55.763E
A15	*Ordu*	*Cambasi*	1730	40° 39.936N	037° 56.344E
A16	*Giresun*	*Bektaş yaylasi*	1623	40° 42.410N	038° 13.910E
A18	*Giresun*	*Bektas inisdibi*	1926	40° 40.133N	038° 15.615E
A19	*Giresun*	*Bektas yaylasi*	1789	40° 40.915N	038° 18.139E
A21	*Rize*	*Cagirankaya*	2043	40° 49.375N	040° 37.886E
A22	*Trabzon*	*Sisdagi*	1775	40° 51.351N	039° 09.087E

ISSR amplification

15 primers that produced clear and reproducible fragments were selected out of a hundred UBC primers, which were previously tested for further analyses. ISSR amplification was performed in a 20 µl volume containing 20 ng genome DNA, 1 × Taq buffer, 2.0 mM $MgCl_2$, 0.2 mM dNTPs, 0.75 µM primer, 0.5 units of Taq DNA polymerase. The amplification reaction consisted of an initial denaturation step at 94 °C for 5 min, followed by 45 cycles of 45 s at 94 °C, annealing at 50 °C–56 °C for 45 s, extension at 72 °C for 90 s, and ended with extension at 72 °C for 7 min. The amplified products were resolved electrophoretically on 2.0% agarose gels run at 100 V in

http://www.aloki.hu ● ISSN 1589 1623 (Print) ● ISSN 1785 0037 (Online)
DOI: http://dx.doi.org/10.15666/aeer/1605_68356843
© 2018, ALÖKI Kft., Budapest, Hungary

1.0 × TBE buffer, visualized by staining with ethidium bromide (0.5 μg/ml), and photographed under ultraviolet light (Charters et al., 1996; Rafalski et al., 1996) The amplifications were repeated twice and only clear repetitive bands were used in data analysis, and molecular weights were estimated using a 100 bp DNA marker (Vivantis).

Data analysis

Alleles were designated on the basis of fragment size; bands were scored as diallelic (1 = band present, 0 = band absent). To assess the genetic variation among the genotypes, the eighteen ISSR markers were analyzed using NTSYS-pc (Rohlf, 2002). The coefficients of genetic similarity for all pair-wise comparisons were computed using Jaccard's coefficient. A similarity matrix was used to create a dendrogram using the unweighted pair group method with arithmetic mean (UPGMA). The observed number of bands, polymorphic band number, polymorphic band ratio per primer, Resolving power (RP value) and Polymorphic information content (PIC) were calculated with the POPGENE software version 1.31 (Yeh et al., 1997) to estimate genetic variation. Polymorphic information content (PIC), the probability in detecting polymorphism by a primer or primer combination between two randomly drawn genotypes was calculated using the formula PIC = 1 - Σpi2, where pi is the frequency of the ith allele (Sehgal et al., 2009); Resolving power (Rp) which is the ability of each primer to detect level of variation between individuals was calculated according to Prevost and Wilkinson (1999): Rp = ΣIb where Ib (band informativeness) takes the values of: $1 - [2|0.5 - p|]$, where p is the proportion of individuals containing the band, and marker index (MI) for each primer was also calculated as a product of two functions - the polymorphic information content and effective multiplex ratio (EMR) (Varshney et al., 2007). Group constellations were also independently developed by using principal component analysis (PCA) to verify the grouping obtained through the dendrogram. PCA further helped in depicting the variation among the genotypes in a three-dimensional mode (McVean, 2009).

Results and discussion

ISSR polymorphism

On the basis of the number, intensity and reproducibility of ISSR bands 15 primers were selected out of a hundred UBC primers, which were previously tested (Cekic et al., 2001). Bands with the same mobility were treated as identical fragments. Weak bands with negligible intensity and smear bands were both excluded from final analysis (*Fig. 2*). Each primer was evaluated for total band number (TBN), polymorphic band number (PBN) and the ratio of polymorphism (PR = PBN/TBN × 100). The amplification of ISSR markers was consistent between repeat PCR runs. The number of polymorphic bands produced ranged from 3 (for primer 889) to 10 (for primers 881 and 888). The number of scored bands varied from four to ten with an average of 7.40 bands per primer and an average of 6.73 polymorphic bands per primer. In total, 101 bands out of 111 derived from 15 primers were polymorphic (*Table 2*). Cao et al. (2000) reported that 50 polymorphic bands were sufficient for determination of differences and similarities between genotypes. With our 101 polymorphic band obtained in our study, it appears to have exited. So that this variability allowed raspberry genotypes to be distinguished on their genetic bases. The polymorphism level with 90% was higher than

http://www.aloki.hu ● ISSN 1589 1623 (Print) ● ISSN 1785 0037 (Online)
DOI: http://dx.doi.org/10.15666/aeer/1605_68356843
© 2018, ALÖKI Kft., Budapest, Hungary

the findings with 69% polymorphism level of Ercisli et al. (2008), where 12 raspberry genotypes in eastern Turkey were analysed by AFLP markers. The average PIC and RP values were 0.25 and 0.41, ranging according to primers from 0.0729 to 0.3515, and from 0.08 to 0.57 for PIC and RP values, respectively (*Table 2*). Chesnokov and Artemyeva (2015) reported that the maximum PIC value is 0.5 for the dominant markers like ISSR, and for the markers with equal distribution in the population the PIC values are higher.

Table 2. *Band number, Polymorphic band number, Polymorphic band ratio (%), PIC (polymorphism information content) and RP (resolving power) values in raspberry genotypes*

ISSR primer code	Primer sequence and anchors	Band number	Polymorphic band number	Polymorphic band ratio (%)	PIC value	RP value
807	*AGAGAGAGAGAGAGAG**T***	10	8	80	0.1844	0.30
856	*ACACACACACACACAC**YA***	9	7	78	0.2092	0.35
881	*GGGTGGGTGGGTGGGT*	10	10	100	0.3227	0.46
888	***BDB**CACACACACACACA*	10	10	100	0.3211	0.49
889	***DBD**ACACACACACACAC*	3	3	100	0.0729	0.08
890	***VHV**GTGTGTGTGTGTGT*	9	7	78	0.2352	0.43
891	***HVH**TGTGTGTGTGTGTG*	5	4	80	0.2516	0.48
808	*AGAGAGAGAGAGAGAG**C***	7	6	86	0.2310	0.45
810	*GAGAGAGAGAGAGAGA**T***	6	6	100	0.2826	0.40
811	*GAGAGAGAGAGAGAGA**C***	6	5	83	0.3021	0.54
826	*ACACACACACACACAC**C***	4	4	100	0.2793	0.34
835	*AGAGAGAGAGAGAGAG**YC***	8	8	100	0.3515	0.57
841	*GAGAGAGAGAGAGAGA**YC***	7	7	100	0.2935	0.48
842	*GAGAGAGAGAGAGAGA**YG***	9	8	89	0.2049	0.33
844	*CTCTCTCTCTCTCTCT**RC***	8	8	100	0.2715	0.41
Average		**7.40**	**6.73**	**91.60**	**0.25**	**0.41**
Total		**111**	**101**			

Cluster analysis

Genetic similarity among varieties was estimated using dissimilarity coefficient matrix based on ISSR bands scored. Pair wise values of dissimilarity coefficients ranged from 0.57 for genotypes with the same scored bands to 0.83 for the most similar genotypes. The dendrogram was constructed based on the similarity matrix, using the unweighted pair group method with arithmetic mean (UPGMA) method (Rohlf, 1992). The 19 raspberry genotypes were divided into two main clusters (*Fig. 3*), in which three genotypes in one group and the rest of the genotypes falling under the other group. While the first major group contained only one subgroup, the second major cluster was further separated into several subgroups. The coefficient values in first subgroup ranged from 0.74-0.83. On the other hand, the similarity of the second varied 0.62 to 0.75 (*Fig. 3*).

http://www.aloki.hu ● ISSN 1589 1623 (Print) ● ISSN 1785 0037 (Online)
DOI: http://dx.doi.org/10.15666/aeer/1605_68356843
© 2018, ALÖKI Kft., Budapest, Hungary

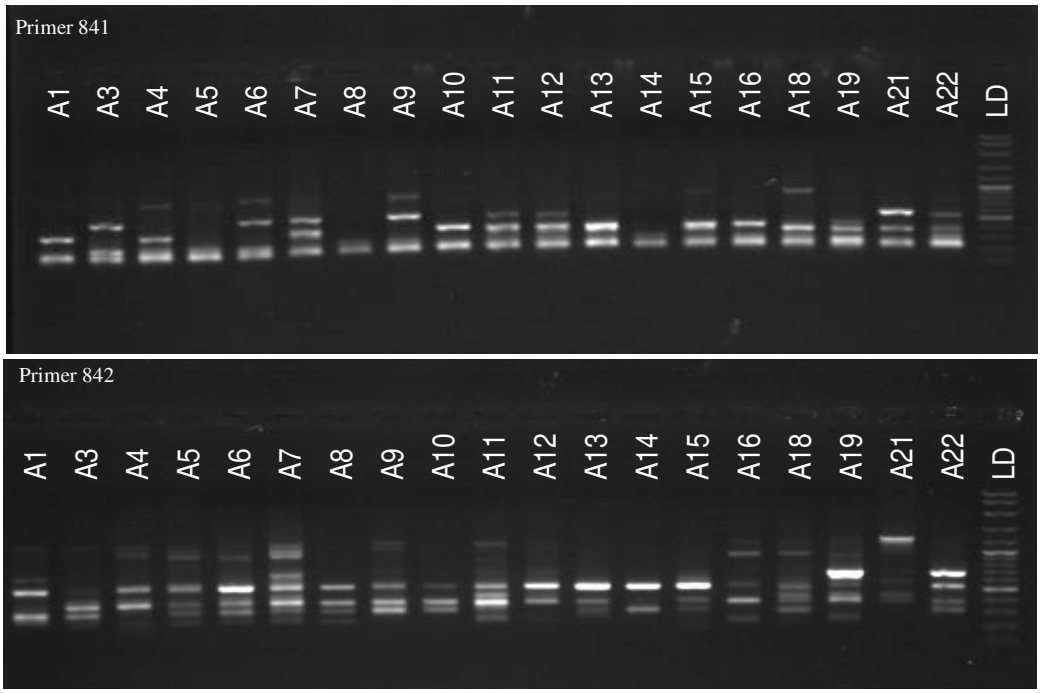

Figure 2. *Agarose gel of polymorphic DNA amplification profiles of different raspberry genotypes obtained with UBC ISSR primer 841 and 842 (LD: 100 bp LADDER -Vivantis)*

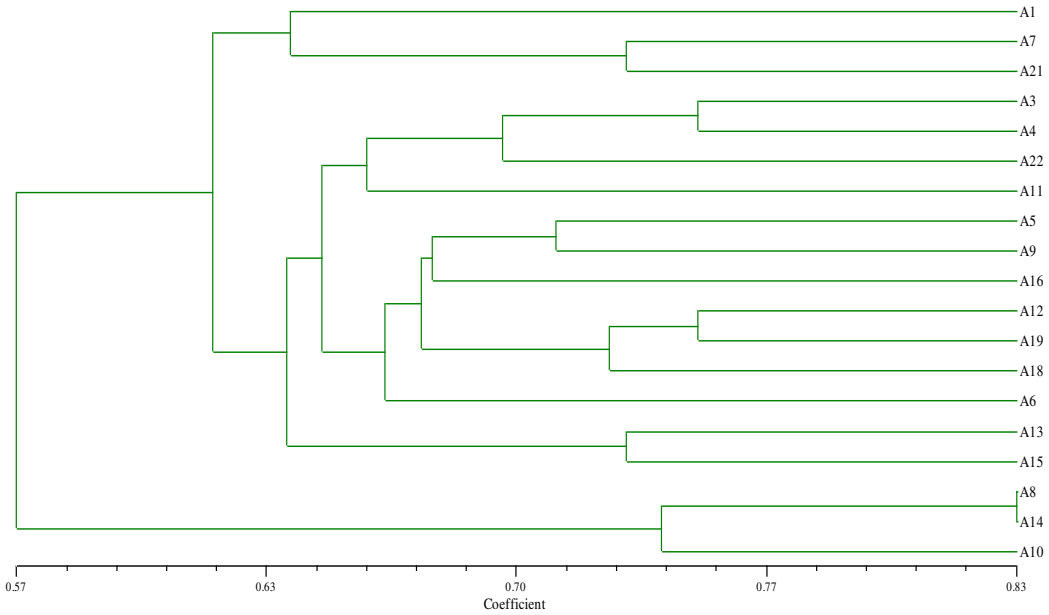

Figure 3. *Dendrogram showing genetic relationships among value of ISSR markers for raspberry genotypes*

Group constellations were also independently developed by using principal component analysis (PCA) to verify the grouping obtained through the dendrogram. PCA further helped in depicting the variation among the genotypes (Asif et al., 2015). The principle component analysis roughly also put the genotypes into two different

http://www.aloki.hu ● ISSN 1589 1623 (Print) ● ISSN 1785 0037 (Online)
DOI: http://dx.doi.org/10.15666/aeer/1605_68356843
© 2018, ALÖKI Kft., Budapest, Hungary

clusters as parallel to the dendrogram of the raspberry genotypes. The small main group consists of the A8, A10 and A14 genotypes which form a different cluster in the PC1-PC2 and PC1-PC3 planes (*Fig. 4a, b*). Although, A8 and A14 were found to be 100% similar in same group of dendrogram, these two genotypes were still apart from each other by the different dimensional view of PCA analysis. On the other hand, while A18 and A19 were differentiated around 26% level in the dendrogram, PCA analysis put these two genotypes very close each other in both PC1-PC2 and PC1-PC3 dimensions (*Fig. 4a, b*).

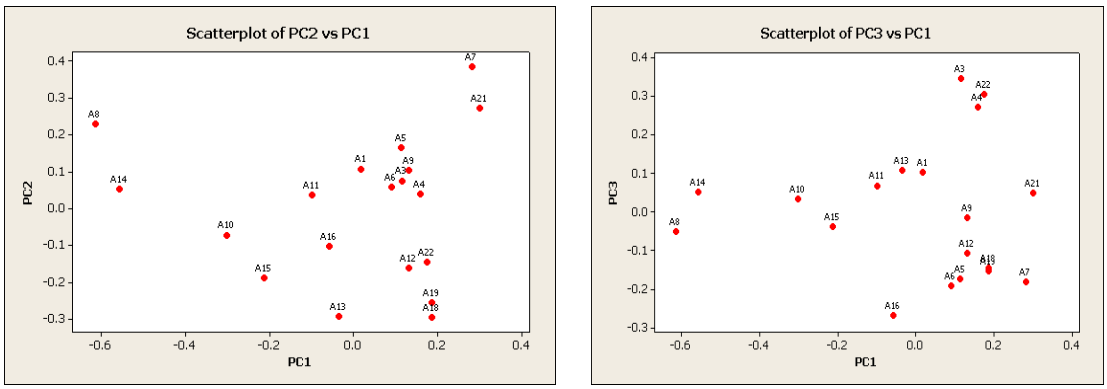

a **b**

Figure 4. *The principle component analysis with three components of raspberry genotypes according to 15 ISSR primers*

Conclusion

Screening of the 19 genotypes of different raspberry genotypes revealed that banding profiles obtained with fifteen ISSR primers were enough to distinguish the diversity among the wild raspberry genotypes. The fifteen ISSR primers we used on 19 raspberry genotypes resulted 101 polymorphic bands, which is much higher than the reports of Cao et al. (2000), where 50 polymorphic bands were sufficient for determination of differences and similarities between genotypes. The results indicated that the ISSR technique is effective to develop genotype specific banding patterns valuable for genotype identification. Since ISSR PCR technique does not require previous DNA sequence information and uses very small quantity of DNA, it is considered as one of the most widely used techniques for genotype identification and genetic diversity studies. The study also revealed that the dendrogram created using UPGMA method and the PCA analysis were complementary, and were useful to use together in diversity studies.

Although no scientific data was recorded regarding the morphological characters of genotypes, the observation of morphologies of genotypes during in collection parcel did not reveal obvious correlation with morphological characters. This work was the first attempt to use ISSR markers to assess genetic diversity and relatedness within raspberry genotypes wildly grown in Norhern Turkey, and the information generated herein may be useful for the improvement of this crop and could serve a promising future for breeding programs in our genetic collection. Further studies examining new molecular markers correlating morphological and pomological characters could explain more completely the diversity within this species.

http://www.aloki.hu ● ISSN 1589 1623 (Print) ● ISSN 1785 0037 (Online)
DOI: http://dx.doi.org/10.15666/aeer/1605_68356843
© 2018, ALÖKI Kft., Budapest, Hungary

REFERENCES

[1] Alice, L. A., Ericsson, T., Eriksen, B., Campbel, C. S. (2001): Hybridization and gene flow between distantly related species of *Rubus* (Rosaceae): Evidence from nuclear ribosomal DNA internal transcribed spacer region sequences. – Systematic Botany 26: 769778.

[2] Allainguillaume, J., Wilkinson, M. J., Clulow, S. A., Barr, S. N. R. (1997): Evidence that genes from the male parent may influence the morphology of potato dihaploids. – Theoretical and Applied Genetics 94(2): 241-248.

[3] Asif, L., Muhammad, B., Syed, B. H., Farah, A. (2015): Estimation of genetic divergence, association, direct and indirect effects of yield with other attributes in cotton (Gossypium hirsutum L.) using biplot correlation and path coefficient analysis. – Tropical Plant Research 2(2): 120-126.

[4] Ayesh, B. M. (2017): Genotyping and molecular identification of date palm cultivars using inter-simple sequence repeat (ISSR) markers. – Methods Mol. Biol. 1638(1): 73-183.

[5] Cao, W., Scoles, G. J., Hucl, P., Chibbar, R. N. (2000): Phylogenetic relationships of five morphological groups of hexaploid wheat (*Triticum aestivum* L. Em Thell) based on RAPD analysis. – Genome 43: 724-727.

[6] Cekic, C., Özmen, Z. S. (2016): Determination of bio-variation among different mulberry species grown in Tokat region by molecular markers. – VII International Scientific Agriculture Symposium, "Agrosym 2016", 6-9 October 2016, Jahorina, Bosnia and Herzegovina. Proceedings, pp.188-192, ref.15.

[7] Cekic, C., Battey, N. H., Wilkinson, M. J. (2001): The potential of ISSR-PCR primer pair combinations for genetic linkage analysis using the seasonal flowering locus in *Fragaria vesca* as a model. – Theoretical and Applied Genetics 103(4): 540-546.

[8] Charters, Y. M., Robertson, A., Wilkinson, M. J., Ramsay, G. (1996): PCR analysis of oilseed rape cultivars (*Brassica napus L ssp oleifera*) using 5'-anchored simple sequence repeat (SSR) primers. – Theoretical and Applied Genetics 92(3-4): 442-447.

[9] Chesnokov, Y. V., Artemyeva, A. M. (2015): Evaluation of the measure of polymorphism information of genetic diversity. – Agricultural Biology 50(5): 571-578.

[10] Chwedorzewska, K. J., Bednarek, P. T., Puchalski, J. (2002): Studies on changes in specific rye genome regions due to seed aging and regeneration. – Cell Mol. Biol. Lett. 7: 569-576.

[11] Davis, P. H. (1982): Flora of Turkey. – Edinburgh University Press, Edinburgh.

[12] Doyle, J. J., Doyle, J. L. (1987): A rapid DNA isolation procedure for small quantities of fresh leaf tissue. – Phytochemical Bulletin 19: 11-15.

[13] Ercisli, S., Badjakov, I., Kondakova, V., Atanassov, A., Todorovska, E. (2008): AFLP-based genetic relationships in wild and cultivated red raspberry genotypes (Rubus Idaeus L.). – Biotechnology & Biotechnological Equipment 22(4): 907-910.

[14] Gonzalez, A., Coulson, A., Brettell, R. (2002): Development of DNA markers (ISSRs) in mango. – Acta Horticulturae (ISHS) 575: 139-143.

[15] Graham, J., McNicol, R. J., McNicol, J. W. (1996): A comparison of methods for the estimation of genetic diversity in strawberry cultivars. – Theoretical and Applied Genetics 93: 402-406.

[16] Hardik, N. L., Dinesh, N. V., Mohamed, M. H., Ragaa, A. E. (2016): Fingerprinting and molecular comparison among two parental strains of Trichoderma spp. and their corresponding fusants produced by protoplast fusion. – Biotechnology & Biotechnological Equipment 30(6): 1065-1074.

[17] Haritha, G., Sudhakar, T., Chandra, T., Ram, T., Divya, B., Sarla, N. (2015): Informative ISSR markers help identify genetically distinct accessions of *Oryza rufipogon* in yield improvement. – Rice Science 23(5): 225-241.

http://www.aloki.hu ● ISSN 1589 1623 (Print) ● ISSN 1785 0037 (Online)
DOI: http://dx.doi.org/10.15666/aeer/1605_68356843
© 2018, ALÖKI Kft., Budapest, Hungary

[18] Howell, E. C., Newbury, H. J., Swennen, R. L., Withers, L. A., Ford–Lloyd, B. V. (1994): The use of RAPD for identifying and classifying *Musa* germplasm. – Genome 37: 328-332.
[19] Jennings, D. L. (1988): Raspberries and Blackberries: Their Breeding, Diseases and Growth. – Academic Press, London.
[20] Kalyani, M., Sarmah, D. K., Deka, M. (2014): High gene flow and genetic diversity in three economically important *Zanthoxylum Sp*p. of Upper Brahmaputra valley zone of NE India using molecular markers. – Meta Gene. 2(C): 706-721.
[21] Kojima, T., Nagaoka, T., Noda, K., Ogihara, Y. (1998): Genetic linkage map of ISSR and RAPD markers in Eikorn wheat in relation to that of RFLP markers. – Theoretical and Applied Genetics 96(1): 37-45.
[22] Lund, B., Ortiz, R., Skovgaard, I. M., Wough, R., Andersen, S. B. (2003): Analysis of potential duplicates in barley gene bank collections using resampling of microsatellite data. – Theoretical and Applied Genetics 106: 11291138.
[23] McVean, G. (2009): A genealogical interpretation of principal components analysis. – PLoS Genetics 5(10): e1000686.
[24] Marshal, B., Harrison, R. E., Graham, J., McNicol, J. W., Wright, G., Squire, G. R. (2001): Spatial trends of phenotypic diversity between colonies of wild raspberry *Rubus idaeus*. – New Phytologist 151: 671682.
[25] Prevost, A., Wilkinson, M. J. (1999): A new system of comparing PCR primers applied to ISSR fingerprinting of potato cultivars. – Theor App Genet. 98: 107-112.
[26] Rafalski, J. A., Vogel, J. M., Morgante, M., Powell, W., Andre, C., Tingey, S. V. (1996): Generating New DNA Markers in Plants. – In: Birren, B., Lai, E. (eds.) Non-Mammalian Genomic Analysis: A Practical Guide. – Academic Press, New York.
[27] Rohlf, F. J. (1992): NTSYS-pc Numerical Taxonomy and Multivariate Analysis System Version 1.8. – Appl. Biostatistics, New York.
[28] Sehgal, D., Rajpa, V. R., Raina, S. N., Sasanuma, T. (2009): Assaying polymorphism at DNA level for genetic diversity diagnostics of the safflower (*Carthamus tinctorius* L.) world germplasm resources. – Genetica 135: 457-470.
[29] Varshney, R. K., Chabane, K., Hendre, P. S., Aggarwal, R. K., Graner, A. (2007): Comparative assessment of EST-SSR, EST-SNP and AFLP markers for evaluation of genetic diversity and conservation of genetic resources using wild, cultivated and elite barleys. – Plant Sci. 173(6): 638-649.
[30] Wolff, K., Zietkiewicz, E., Hofstra, H. (1995): Identification of chrysanthemum cultivars and stability of DNA fingerprint patterns. – Theoretical and Applied Genetics 91(3): 439-447.
[31] Yeh, F. C., Yang, R. C., Boyle, T. B. J., Ye, Z. H., Mao, J. X. (1997): POPGENE the User-Friendly Shareware for Population Genetic Analysis. – Molecular Biology and Biotechnology Centre, University of Alberta, Canada.

http://www.aloki.hu ● ISSN 1589 1623 (Print) ● ISSN 1785 0037 (Online)
DOI: http://dx.doi.org/10.15666/aeer/1605_68356843
© 2018, ALÖKI Kft., Budapest, Hungary

EFFECT OF DIFFERENT STRAWBERRY POLLINATORS ON FRUIT PROPERTIES OF LOCAL OSMANLI STRAWBERRY CULTIVAR IN TURKEY

CEKIC, C.* – CELEBIOGLU, B. – OZTURK ERDEM, S.

Department of Horticulture, Faculty of Agriculture, Gaziosmanpaşa University, Tokat, Turkey

**Corresponding author*
e-mail: cetin.cekic@gop.edu.tr

(Received 18th Jul 2018; accepted 20th Sep 2018)

Abstract. In this study, impact on the fruit characteristics of different pollinators used on the Osmanli strawberry cultivar, which is male sterile and therefore necessarily needs foreign pollination, was studied. In the trial three foreign cultivars, as well as three local varieties obtained from farmers in Northeast of Turkey, where these local varieties were grown with the Osmanli strawberry, were used as pollinators on Osmanli strawberry cultivar. Before pollination, pollen viability and pollen germination capability of pollinator cultivars were determined; and then, the physical properties, photochemical and aroma components of the hybrid fruit of strawberry, as well as the fruits of six parent cultivars used as pollinators, were analyzed. The study showed that the pomological and phytochemical characters as well as aroma components of fruits in Osmanli strawberry can be influenced by the pollinators of its flower. Since the highest aroma components were obtained from Sweet Charlie as pollinator, this cultivar with its well aroma can be used as pollinator on the Osmanli strawberry cultivar.
Keywords: *male sterility, phytochemicals, pollinator, pomology, metaxenia*

Introduction

Strawberries grown in many countries of the world in the soft fruit group are preferred due to their unique aroma, taste and rich nutritional content. There are diploid species *Fragaria vesca* and *Fragaria viridis* in the flora of Turkey. These wild species, together with local and old octoploid F. X ananassa varieties which have been used for many years, constitute the strawberry genetic resources of the country. Local varieties such as the Osmanli (Ottoman) and Arnavutkoy have narrowed and limited production areas by the growing use of more efficient commercial strawberry varieties. Cultured strawberry species have bigger fruits and give higher yields than the wild species, but the local or wild species have better aroma than the commercial varieties in use. Concentration of taste and aroma compounds generally decreases in commercial varieties with increasing fruit size (Zebatakis and Holden, 1997). Quantities of sugars and organic acids are qualitative and quantitative in essence of qualities in fruit. Sugar / acid balance is also a very important issue for breeders. In strawberry fruit, sugar and organic acids are important factors in determining the harvest time and the taste of fruit (Mina et al., 2017). There are many genetic and environmental factors in the formation of strawberry aroma, such as genes controlling some aroma compounds (Jetti et al. (2007), or cultural applications to plants (Loughrin and Kasperbauer, 2002). Osmanli strawberry cultivar which comes to foreground in terms of very good flavor of the local strawberry varieties decreases day by day and faces the danger of disappearance. This local cultivar is morphologically male sterile and a pollinator strawberry is necessary for fruiting.

On the other hand, pollens have effects on endosperm and embryo development (xenia), on the developing maternal tissues of seed or fruit outside the embryo and

http://www.aloki.hu ● ISSN 1589 1623 (Print) ● ISSN 1785 0037 (Online)
DOI: http://dx.doi.org/10.15666/aeer/1605_68456855
© 2018, ALÖKI Kft., Budapest, Hungary

endosperm (metaxenia), or on the carpel tissue (carpoxenia) in foreign-pollinating species. Since pollen sources totally come from outside in self-incompatible and infertile species, fruit quality attributes may vary based on pollen source. The variations in aroma and other fruit quality attributes of Osmanli strawberries may also result from either variation in climate parameters or pollinating species. Therefore, there is a need for a research to elucidate such variations. Various researchers reported effects of pollinator on fruit quality attributes (Gercekcioglu, 1997).

The aroma of strawberry fruit is composed of various esters, alcohols, aldehydes and sulphur compounds and it is originated from degradation of carbohydrates, proteins and fats throughout ripening period (Samykanno et al., 2013).

In this study, in order to determine the effects different pollinators on the fruit characteristics of Osmanli strawberry cultivar, which is male sterile and therefore necessarily needs foreign pollination, three local ('Karacilek', 'Tuylu', 'Deli') and three commercial ('Cabarla', 'Sweet Ann' and 'Sweet Charlie') strawberry varieties were used as pollinators for Osmanli local cultivar. Morphological, phytochemical composition and aroma compounds of the fruits by different pollinators were investigated. Another objective was to determine the role of pollinator and to select proper pollinator or pollinators for Osmanli strawberry cultivar.

Material and method

In the trial, as well as three commercial cultivars ('Cabarla', 'Sweet Ann' and 'Sweet Charlie'), three local varieties ('Karacilek', 'Tuylu', 'Deli') obtained from farmers in North west of Turkey, where these local varieties were grown with the Osmanli strawberry, were used as pollinators on Osmanli strawberry cultivar. Before pollination, pollen viability and pollen germination power of pollinator cultivars were determined; and then, the physical properties, photochemical and aroma components of the hybrid fruit of Osmanli strawberry, as well as the fruits of six parent cultivars used as pollinators, were analyzed. The plants Osmanli seedlings used as mother parent were moved to a temperature-controlled greenhouse into tulle-covered cages and ten Osmanli seedlings were left for open pollination. The flowers over mother parent were emasculated and the flowers were covered with parchment paper. Then throughout following three days, pollinations were performed. Ten pots were used for each pollinator and ten flowers were pollinated for each plant. The non-pollinated fruits were plucked and removed. Pomological measurements such as appearance of calyx flowers, position of calyx with respect to fruits, position of achenes over the fruit, width of the sections without achenes over the fruit, achenity and achene depths were analyzed in accordance with UPOV (The International Union for the Protection of New Varieties of Plants 2012) criteria, which is used for the definition of morphological and pomological characteristics within the species. Fruit mass, fruit width and length was measured and fruits were grouped based on length/width ratio in accordance with Cekic et al. (2003). Fruit external color (cheek and tip), fruit firmness, water soluble dry matter (WSDM) content, pH, titratable acidity, ascorbic acid (vitamin C) content (%), fruit aroma compounds were determined.

Fruit mass was determined through weighing with a precise balance (±0.01 g). Fruit width and length was measured with a digital caliper (±0.05 mm); fruits were grouped based on length/width ratio in accordance with Çekiç et al. (2003). Fruit external color (cheek and tip) was measured with Minolta CR400 color-meter and L, a, b, *Chroma* (C) and Hue (h) values were determined. Fruit firmness was measured in kg/mm^2 with a

http://www.aloki.hu ● ISSN 1589 1623 (Print) ● ISSN 1785 0037 (Online)
DOI: http://dx.doi.org/10.15666/aeer/1605_68456855
© 2018, ALÖKI Kft., Budapest, Hungary

penetrometer vertically penetrating 10 mm into the fruit. Water soluble dry matter (WSDM) content was measured with a portable hand-refractometer. The pH values were measured with a digital pH meter. Titratable acidity was measured with potentiometric titration method. Ascorbic acid (vitamin C) content (%) was measured by using Kromasil (250 × 4.6 mm 100-5C18 5 µm) HPLC column and Perkin Elmer (Series-200) UV detector at 215 nm wave length.

All the observations and analyses were performed in three replications, and carried out in this study were considered as the average of 10 fruits. All the resultant data were subjected to variance analyses and means were compared with LSD multiple comparison test. SAS software was sued in statistical analyses.

Results and discussion

Pollen vigor tests

Before hybridization works, pollen vigor levels of local and standard cultivars to be used as a pollinator for Osmanli cultivar were determined with tri-phenyl tetrazolium chloride (TTC) test. The greatest vigor was observed in Cabarla cultivar (74.4%) and the lowest vigor was observed in Tuylu cultivar (6.7%).

Eti et al. (1995) in a study used 8 different strawberry cultivars and reported pollen vigor levels through TTC test as between 5.07-73.71%. Present values varied between 6.7-74.4% and the present range of vigor was higher than the one reported by Eti et al. (1995).

Success of hybridization and fruit set

From a total of 321 hybridizations, 253 plants were obtained. The most successful hybridization was achieved in Sweet Charlie cultivar (91.4%) and the worst yield was observed in Tuylu cultivar (14.4%). About 78.8% of hybridizations yielded a fruit.

Appearance of calyx leaves and position of calyx with respect to fruit

Appearance of calyx leaves and their position with respect to the fruit are provided in *Table 1* based on UPOV criteria. Since calyx leaves were taken out during emasculation process from the fruit samples obtained from hybridizations with Osmanli cultivar, data about the appearance of calyx leaves were not available for these fruits. Considering the position of calyx with respect to the fruit, it was observed that Cabarla, Sweet Charlie and Karacilek cultivars at the end of hybridization did not presented their own criteria and reflected the characteristics of Osmanli cultivar (buried within the fruit).

Position of achenes over the fruit

Position of achenes over the fruit is provided in *Table 1*. In Sweet Ann and Sweet Charlie cultivars used as pollinator, achenes lost their characteristics of being within the fruit surface and reflected the characteristics of the parent Osmanli cultivar.

Width of the sections without achenes over the fruit

The width of the sections without achenes over the fruit is provided in *Table 1*. In Cabarla and Sweet Ann cultivars, the width of sections without achenes lost their characteristics of being ‘narrow’ and turned into ‘absent or very narrow’ characteristic of

http://www.aloki.hu ● ISSN 1589 1623 (Print) ● ISSN 1785 0037 (Online)
DOI: http://dx.doi.org/10.15666/aeer/1605_68456855
© 2018, ALÖKI Kft., Budapest, Hungary

parent Osmanli cultivar. Besides in Sweet Charlie, Tuylu and Karacilek cultivars, width of the sections without achenes had 'absent or very narrow' characteristics of themselves and parent Osmanli cultivar.

Table 1. *Fruit characteristics of parents and hybrids according to UPOV criteria*

Parents and hybrids	Attitude of sepals	Position of calyx attachment	Position of achenes	Width of band without achenes
Cabarla	Upwards	Level with fruit	Below surface	Medium
Sweet Charlie	Upwards	Level with fruit	Below surface	Absent or very narrow
Sweet Ann	Upwards	Inserted	Below surface	Narrow
Tuylu	Downwards	Inserted	Below surface	Absent or very narrow
Deli	Downwards	Inserted	Below surface	Absent or very narrow
Karacilek	Upwards	Level with fruit	Below surface	Absent or very narrow
Osmanli	Downwards	Inserted	Below surface	Absent or very narrow
Osmanli x Karacilek	X	Inserted	Below surface	Absent or very narrow
Osmanli x Tuylu	X	Inserted	Below surface	Absent or very narrow
Osmanli x Sweet Ann	X	Inserted	Below surface	Absent or very narrow
Osmanli x Cabarla	X	Inserted	Below surface	Absent or very narrow
Osmanli x Sweet Charlie	X	Inserted	Below surface	Absent or very narrow

X: calyx and corolla were totally removed from mother plants while emasculation of stubborn anthers

Fruit mass (g/fruit)

Mean fruit mass values are provided in *Table 2*. Significant differences were observed in fruit mass of strawberry genotypes used in this study at 5% level. The fruits of Osmanli x Tuylu hybrids had the lowest fruit mass values and other hybrids were not significantly different from each other with regard to fruit mass.

Fruit length and width (mm)

Fruit length and widths of strawberry genotypes were measured in accordance with Cekic et al. (2003) (*Table 2*). The greatest fruit length and width were observed in Sweet Ann cultivar. The lowest fruit width was seen in Osmanli x Tuylu hybrid and the lowest fruit length was observed in Tuylu cultivar. The fruits obtained from the pollination of Osmanli cultivar with Karacilek cultivar had the greatest length and width scale.

Length/width ratio

Length/width ratio is one of the pomological characters of strawberry fruits, where the fruit shapes can be like sphere, flattened or cylindrical depending of the ratio. Although the ratio was over 1 in the fruits of cabarla, sweet charlie and sweet ann cultivars, the fruits of Osmanli pollinated with them were flattened with the ratio lower than 1. So, it can be said that pollinators had no effect on the fruit shape of Osmanli cultivar (*Table 2*).

Number of achenes per fruit

Number of achenes per fruit is provided in *Table 2*. The greatest number was observed in Sweet Charlie (301.8) and the lowest number was observed in Osmanli cultivar (59.6). After hybridization with Osmanli cultivar, the greatest number was observed in Osmanli x

http://www.aloki.hu ● ISSN 1589 1623 (Print) ● ISSN 1785 0037 (Online)
DOI: http://dx.doi.org/10.15666/aeer/1605_68456855
© 2018, ALÖKI Kft., Budapest, Hungary

Cabarla hybrids (147.5). With regard to achenity according to 1 (less achenes) – 9 (highly achenes) scale, 'Sweet Charlie' was expressed with 9 and 'Osmanli' was expressed with 1.

Table 2. *Pomological characteristics of fruits*

Parents and hybrids	Weigth* (g/fruit)	Width* (mm)	Length* (mm)	Length/ width*	Fruit firmness* (kg)	Achene number*	Achene number/fruit size*
Cabarla	12.5 b	28.7 a	37.1 a	1.28 ab	1.47 a	242.9 ab	189.59 ab
Sweet Charlie	14.4 b	30.3 a	40.5 a	1.32 a	1.47 a	301.8 a	229.35 a
Sweet Ann	21.9 a	32.2 a	44.0 a	1.36 a	1.18 ab	273.6 a	200.66 ab
Tuylu	2.6 d	18.0 bc	14.9 c	0.83 e	0.59 d	77.7 de	91.50 de
Deli	4.1 cd	19.1 bc	19.5 c	1.02 cd	0.84 bcd	124.5 cde	121.55 cde
Karacilek	9.0 bc	23.6 b	27.6 b	1.13 bc	1.11 abc	189.2 bc	160.68 bc
Osmanli	3.5 cd	20.4 bc	17.9 c	0.87 de	0.62 d	59.6 e	68.86 e
Osmanli x Karacilek	4.1 cd	21.2 bc	17.6 c	0.82 e	0.72 cd	114.4 cde	140.34 bcd
Osmanli x Tuylu	2.6 d	17.4 c	15.6 c	0.89 de	0.81 bcd	60.8 e	68.08 e
Osmanli x Sweet Ann	3.4 cd	19.6 bc	15.4 c	0.78 e	0.65 d	94.3 de	120.97 dce
Osmanli x Cabarla	3.0 cd	18.7 bc	15.6 c	0.82 e	0.69 cd	147.5 cd	177.66 abc
Osmanli x Sweet Charlie	3.8 cd	20.4 bc	17.0 c	0.82 e	0.59 d	143.0 cd	173.45 abc

*The difference between the values indicated by different letters in the same column is significant at the 0.05 probability level

Achene number and Achene number/fruit size

In the strawberry, one component of yield is fruit size, which we have shown to be determined by the number of fertilized ovules (achenes) on the surface and the degree of receptacle expansion associated with each achene. Berry weight is highly correlated with achene spacing and achene number, so that for each value of achene spacing there is a linear relation between berry weight and achene number (Abbot and Webb, 1970). This data was taken to determine the success of fertilization by the different pollinators and the effect of pollinators on the achene numbers. While number/fruit size ratio in the open pollinated Ottoman cultivar was 68.86, this ratio varied between 91.50 (Tuylu) and 229.35(Sweet Charlie) in the pollinators. On the other hand, this ratio ranged from 68.08 to 177.66 on the fruits of Osmanli pollinated with Tuylu and Cabarla, respectively.

Fruit firmness

Fruit surface and flesh firmness are significant factors for transport and storage of strawberries. Fruit firmness values are provided in *Table 2*. Values were significant at 5% level. The greatest firmness was observed in Cabarla cultivar (1.47 kg) and the lowest value was seen in Tuylu cultivar (0.59 kg).

http://www.aloki.hu ● ISSN 1589 1623 (Print) ● ISSN 1785 0037 (Online)
DOI: http://dx.doi.org/10.15666/aeer/1605_68456855
© 2018, ALÖKI Kft., Budapest, Hungary

Özdemir et al. (2007) carried out a study with 7 different strawberry cultivars and reported the greatest firmness for Cabarla cultivar (0.63 kg). Gündüz and Özdemir (2012) also reported Cabarla cultivar as prominent with its fruit firmness. In another study, Osmanli cultivar was reported as the softest cultivar (Özuygur, 2005).

Water soluble dry matter (WSDM) content

WSDM is among the most significant quality criteria for strawberries and it is mostly related to sugar content of the fruits. WSDM directly influences fruit taste. Therefore, high WSDM values are preferred in strawberry fruits. Among the main plants, the greatest WSDM content was observed in Osmanli cultivar. Among the hybrids, Osmanli x Tuylu (12.1%) had the greatest WSDM content. The Sweet Ann cultivar and Osmanli x Sweet Charlie (9.1%) hybrids had the lowest WSDM contents (*Table 3*).

Besides plant genetics, environmental factors also influence WSDM content of the fruits (Shaw, 1988; Galletta and Bringhurst, 1990; Abeytilakarathna et al., 2013). Özdemir et al. (2007) and Macit et al. (2011) reported that 'Cabarla' cultivar had lower WSDM content than the other cultivars.

pH

The pH values of strawberry cultivars are provided in *Table 3*. Gelling of jellies, marmalades and jams, color, taste and aroma of foodstuff and taste, aroma and odor development are closely related to fruit pH levels. Present values were not able to be subjected to statistical analyses because of insufficient number of fruits. Among the hydrides, Osmanli x Tuylu (3.79) had the greatest pH and among the main cultivars, Osmanli (3.67) had the greatest pH value. The lowest pH (3.33) was obtained from Karacilek cultivar.

Sürücü (2010) reported the pH value of Osmanli cultivar as 3.65 and such a value was parallel to the present value.

Table 3. *Phytochemical characteristics of fruits*

Parents and hybrids	Water soluble dry matter (%)*	ph**	Titratable acidity (%)*	Water soluble dry matter/titratable acidity*	Vitamin C content (mg/100g)*
Cabarla	8.8 bc	3.62	0.69 d	12.75 ab	16.77 d
Sweet Charlie	7.4 c	3.42	0.82 cd	9.02 b	23.81 b
Sweet Ann	6.0 d	3.49	0.86 cd	6.97 c	19.23 c
Tuylu	10.3 ab	3.59	1.26 ab	8.17 bc	27.32 a
Deli	8.1 bc	3.60	0.94 c	8.61 bc	19.13 c
Karacilek	11.3 ab	3.33	0.85 cd	13.29 a	19.24 c
Osmanli	12.2 a	3.67	1.08 bc	11.29 ab	27.97 a
Osmanli x Karacilek	9.7 ab	3.40	1.24 ab	7.82 bc	24.44 b
Osmanli x Tuylu	12.1 a	3.79	1.07 b	11.30 ab	***
Osmanli x Sweet Ann	10.8 ab	3.76	1.10 b	9.81 b	***
Osmanli x Cabarla	9.3 ab	3.60	1.15 b	8.08 bc	23.34 b
Osmanli x Sweet Charlie	9.1 b	3.59	1.34 a	6.79 c	24.34 b

*The difference between the values indicated by different letters in the same column is significant at the 0.05 probability level

**The difference between the values is not significant in terms of statistics

***Not enough fruit was available for analysis

http://www.aloki.hu ● ISSN 1589 1623 (Print) ● ISSN 1785 0037 (Online)
DOI: http://dx.doi.org/10.15666/aeer/1605_68456855
© 2018, ALÖKI Kft., Budapest, Hungary

Titration acidity

Titratable acidity values of strawberry cultivars are provided in *Table 3*. A single value was obtained from each cultivar because of insufficient number of fruits from the cultivars. Therefore, results were not subjected to statistical analyses. The greatest acidity was observed in Osmanli x Sweet Charlie (1.34%) hybrid. Among the main cultivars, the greatest acidity was observed in Tuylu cultivar (1.26%). The lowest acidity was observed in Osmanli x Tuylu (1.07%) hybrid. Among the entire cultivars used in this study, Cabarla (0.69%) had the lowest titratable acidity.

Özuygur (2005) in a study reported the lowest titratable acidity for Sweet Charlie (0.75%) cultivar. In that study, titratable acidy of Osmanli cultivar was reported as 0.92% and the value was measured as 1.08% in present study.

WSDM/Acid ratio

The WSDM/acid ratios for experimental cultivars are provided in *Table 3*. The greatest ratio was observed in Karacilek (13.29) and the lowest ratio was observed in Osmanli x Sweet Charlie (6.79) hybrid.

Schöpplein et al. (2002) reported WSDM/acid ratio of 11 strawberry genotypes as between 8.7-12.4. The WSDM/acid ratios varied within a larger range (6.79-13.29) in present study.

Özuygur (2005) in a study reported the WSDM/acid ratio of Osmanli cultivar as 11.12 and such a value was quite close to the present value. Özuygur (2005) reported WSDM/acid ratio of Sweet Charlie as 10.21 and the cultivar had the second greatest ratio after Osmanli cultivar.

Ascorbic acid (vitamin C) content

Ascorbic acid values of parents and hybrids are provided in *Table 3*. The values were found to be significant at 5% level. The greatest value was obtained from Osmanli (27.97 mg/100 g), it was followed by Tuylu cultivar and the lowest value was obtained from Cabarla (16.77 mg/100 g) cultivar. Ascorbic acid values were not able to be obtained from Osmanli x Tuylu and Osmanli x Sweet Ann hybrids because of insufficient number of fruits from these hybrids. The differences in ascorbic acid values of the other three hybrids were not found to be significant.

Hakala et al. (2003) reported vitamin C content of strawberry cultivars as between 32.4-84.7 mg/100 g, but indicated that vitamin C contents of the years were significant. Özuygur (2005) reported the lowest average ascorbic acid content for Osmanli cultivar (26.22 mg/100 g) and reported ascorbic acid content of Sweet Charlie cultivar as 50.88 mg/100 g. Although present values of Osmanli cultivar were close to the ones reported by Özuygur (2005), present values for Sweet Charlie were significantly different. Eti (2006) reported the greatest ascorbic acid content for Sweet Charlie (57.29%) cultivar. Sürücü (2010) reported vitamin C content of Osmanli cultivar as 59 mg/100 g.

Aroma compounds

Mass spectroscopy (MS) library of NIST and WILEY was used for the identification of aroma substances. With regard to number of aroma substances, 15 different substances were identified in Cabarla, 10 in Sweet Charlie, 9 in Tuylu, 7 in Deli, 11 in

http://www.aloki.hu ● ISSN 1589 1623 (Print) ● ISSN 1785 0037 (Online)
DOI: http://dx.doi.org/10.15666/aeer/1605_68456855
© 2018, ALÖKI Kft., Budapest, Hungary

Karacilek, 11 in Osmanli, 8 in Osmanli x Cabarla hybrid and 9 substances in Osmanli x Sweet Charlie hybrid. Data were not able to be obtained for Sweet Ann cultivar.

The greatest lactone content was observed in Deli cultivar, it was respectively followed by Cabarla, Sweet Charlie, Osmanli x Sweet Charlie and the lowest value was seen in Osmanli cultivar. Furaneol (2,5-dimethyl-4-OH-3(2H)-furanone) was identified only in Cabarla (6.65%) cultivar. Furaneol has quite low threshold detection value (10 µg/L; Schieberle and Hoffmann, 1997) and with caramel aroma provided to strawberries, it is a significant aroma substance. The 2,5-dimethyl-4-metoxy-3(2H)-furanon (mesifurane) is a lactone compound with great contributions to strawberry aroma. The greatest amount of this compound was respectively observed in Cabarla, Osmanli and Sweet Charlie cultivars. Schieberle and Hoffmann (1997) reported detection threshold for mesifurane as 25 µg/L and indicated that this compound contributed a fragrance to strawberries.

Acids with high detection thresholds have quite low contributions to general aroma of the fruits. The greatest 'trans cinnamic acid' was observed in Osmanli (29.24%) cultivar, the greatest 'hexanoic acid' was observed in Sweet Charlie (28.39%) cultivar and the greatest 'succinic acid' was observed in Osmanli x Cabarla (20.96%) hybrid. Cinnamic acid was identified only in Osmanli cultivar (1.10). Palmitic acid was identified in Sweet Charlie (2.81) and Osmanli (2.18) cultivars.

Fruit color parameters

Multiple color spaces are often used to define color parameters of fruits. Among them, CIE L*a*b* (CIELAB) specified by International Commission on Illumination is the most common one (Fairchild, 2013) were used to evaluate the skin color parameters (L*, a*, and b*). L* represents lightness (100: white, 0: black), a* indicates the difference between red (+a*) and green (-a*), and b* represents the difference between yellow (+b*) and blue (-b*). Hue angle (h^o) and Chroma (C*) values were derived from a* and b* values. Mean color parameters (L, a, b, *Chroma* and h^0) were measured from the cheeks and tips of the fruits using a Minolta Chroma Meter CR-400 (MinoltaKonica, Japan) on the basis of CIE L*a*b* color space. Equations in the scientific literatures (Viscarra Rossel et al., 2006; Kus et al., 2017) were used for calculations. The differences in color parameters of strawberry genotypes were found to be significant at 5% level. A decrease was observed in 'L' values of all hybrid fruits. The greatest cheek L value was observed in Osmanli x Sweet Ann (49.0) hybrid and the greatest tip L value was observed in Osmanli x Tuylu (50.7) hybrid. As compared to Osmanli cultivar, an increase was observed in 'a' values of all hybrids. Hybrids had greater 'b' values than Osmanli cultivar. Osmanli x Cabarla (30.9) hybrid had the greatest cheek measurement and Osmanli x Karacilek (30.7) hybrid had the greatest tip measurements. *'Chroma'* values of hybrid fruits were higher than Osmanli fruits. While cheek 'h' values of all hybrids were greater than Osmanli cultivar, a decrease was observed in tip 'h' values of Osmanli x Sweet Ann and Osmanli x Sweet Charlie hybrids as compared to Osmanli cultivar. The differences in cheek and tip values of hybrid fruits and Osmanli fruits were not found to be significant (*Table 4*). Özuygur (2005) reported the greatest 'L' and 'h' (60.7 and 81.2) and lowest 'a', 'b' and 'C' (7.2; 47.8 and 48.5) values for Osmanli cultivar and the second greatest 'C' value (78.0) for Sweet Charlie cultivar. Parallel to present findings, Skupien and Osmianski (2004) in a study reported L values as between 35.32 and 41.11. Nunes et al. (1995) indicated high correlations of 'a' values with anthocyanin content of strawberries. Skupien and

http://www.aloki.hu ● ISSN 1589 1623 (Print) ● ISSN 1785 0037 (Online)
DOI: http://dx.doi.org/10.15666/aeer/1605_68456855
© 2018, ALÖKI Kft., Budapest, Hungary

Osmianski (2004) reported negative correlations of 'a' value with pelargonidin-3-glucozid and total pelargonidin contents. Gündüz and Özdemir (2012) observed the brightest fruit external color on 'Osmanli' cultivar and indicated that Sweet Charlie had also sufficient brightness. Kafkas (2004), Serçe et al. (2004), Kıyga (2009), Yılmaz (2009) and Gündüz and Özdemir (2012) reported the greatest 'h' values for 'Osmanli' cultivar.

Table 4. *Color (L, a, b, Chroma ve h^0) values of fruits*

	*L**		*a**		*b**		*Chroma**		*h^0**	
	Cheek	**Tip**	**Cheek**	**Tip**	**Cheek**	**Tip**	**Cheek**	**Tip**	**Cheek**	**Tip**
Cabarla	41.4 ef	45.5 cde	38.5 a	39.7 a	33.4 ab	40.5 a	51.1 a	56.8 a	40.8 c	45.4 bc
Sweet Charlie	39.4 f	41.5 e	37.5 a	38.8 a	32.3 abc	34.5 b	49.6 a	52.1 ab	40.3 c	41.4 c
Sweet Ann	44.8 def	47.3 bcde	35.4 a	38.2 a	38.2 a	41.1 a	52.3 a	56.4 a	47.0 bc	47.0 abc
Tuylu	59.9 a	58.4 a	17.5 c	16.7 b	22.8 d	22.6 e	29.0 c	28.3 d	53.0 ab	53.4 ab
Deli	50.5 bcd	53.0 ab	27.1 b	26.2 b	34.3 ab	34.2 bc	44.3 ab	43.5 bc	53.1 ab	53.8 ab
Karacilek	51.1 bc	51.1 bcd	22.7 bc	23.8 b	29.6 bc	31.4 bcd	38.2 b	40.8 c	56.9 a	57.5 a
Osmanli	53.4 b	52.0 bc	23.3 bc	24.2 b	26.3 cd	27.7 cde	35.3 bc	37.0 cd	49.0 ab	48.9 abc
Osm. x Karacilek	47.7 bcd	48.1 bcde	25.9 bc	24.9 b	30.8 bc	30.7 bcd	40.4 b	39.6 c	49.7 ab	51.0 abc
Osm. x Tuylu	48.6 bcd	50.7 bcd	25.2 bc	25.2 b	29.8 bc	30.6 bcd	39.2 b	40.0 c	49.8 ab	52.0 abc
Osm. x S. Ann	49.0 bcd	50.2 bcd	25.7 bc	24.3 b	30.3 bc	28.2 bcde	39.8 b	37.5 cd	49.6 ab	48.8 abc
Osm. x Cabarla	46.9 cde	44.3 de	25.8 bc	24.4 b	30.9 bc	26.8 de	40.4 b	36.4 cd	50.0 ab	47.6 abc
Osm. x S. Charlie	46.7 cde	46.1 cde	24.5 bc	26.7 b	28.8 bcd	30.4 bcd	37.9 b	40.6 c	49.3 ab	48.2 abc

*The difference between the values indicated by different letters in the same column is significant at the 0.05 probability level

Conclusion

Osmanli strawberries morphologically infertile, but they have stubborn anthers. Therefore to improve the reliability of hybrids, calyx and corolla were totally removed from mother plants while emasculation of anthers. Then, calyx was not observed in hybridized plants. Variation was not observed in achenes over the fruits obtained through all pollinators and thus all fruits reflected achene characteristics of open-pollinating Osmanli cultivar. A similar case was also observed in widths of sections without achenes. In all fruits with controlled pollinators, width of sections without achenes reflected the fruit characteristics of Osmanli cultivar. Fruit size of pollinators did not reflect over the fruits obtained through controlled pollination. Among the pollinators, Tuylu cultivar reduced fruit size as compared to open-pollinating ones and large-fruit pollinators did not increase their fruit size.

Among the Osmanli cultivar and pollinators, Tuylu had the lowest fruit firmness, but the fruits of pollinated Osmanli cultivar had the greatest firmness values. The fruits pollinated by firm-fruits also had soft fruit flesh. Therefore, it was concluded that pollinator had adverse effects on fruit firmness. With regard to pH values of the fruits, there were not significant differences between the fruits of pollinator cultivars and controlled-pollinated Osmanli cultivar. While Osmanli cultivar was the richest in ascorbic acid content, pollinators decreased ascorbic acid contents of Osmanli strawberries. Since Osmanli cultivar is male-infertile and needs a pollinator, Karacilek with the greatest ascorbic acid content may be recommended as a pollinator. The greatest number of aroma compounds was observed in fruits pollinated with Sweet Charlie cultivar, therefore Sweet Charlie may be recommended as a pollinator for Osmanli cultivar prominent with its own aroma.

http://www.aloki.hu ● ISSN 1589 1623 (Print) ● ISSN 1785 0037 (Online)
DOI: http://dx.doi.org/10.15666/aeer/1605_68456855
© 2018, ALÖKI Kft., Budapest, Hungary

As to conclude, pollinator selection is a significant issue for male-infertile Osmanli strawberries. The present study proved that some characteristics of pollinators relatively passed into Osmanli strawberries at different levels in the same year and the effects of pollens on fruits in foreign-pollinating cultivars (metaxenia) were also observed in Osmanli strawberries. Pollinator resulted in changes in fruit pomological and phytochemical characteristics and aroma characteristics which are significant attributes for Osmanli strawberry varied based on pollinators. Although a common known knowledge these terms (xenia, metaxenia, carpoxenia), there is not enough scientific literature on this area. Our study serves some preliminary data about the first effects of pollinators on the fruit. Based on this study, in depth studies should be done on strawberries and other species.

REFERENCES

[1] Abbot, A. J., Webb, R. A. (1970): Achene spacing of strawberries as an aid to calculating potential yield. – Nature 225: 663-664.

[2] Abeytilakarathna, P., Fonseka, R. M., Eswara, J. P., Wijethuga, K. G. N. A. B. (2013): Relationship between total solid content and red, green and blue colour intensity of strawberry (*Fragaria x ananassa* Duch.) fruits. – Journal of Agricultural Sciences - Sri Lanka 8(2): 82-90.

[3] Cekic, C., Gercekcioglu, R., Gunes, M. (2003): Determination of Adaptation Characteristics of Some Strawberry Varieties to Tokat Ecology. – National Kiwi and Soft Fruit Symposium, 23-25 October 2003, Ordu, pp. 221-225.

[4] Eti, S., Paydas, S., Dalaman, O. (1995): Research on pollen quality and quantities in some hybrid strawberry plants. – Turkey II. National Horticulture Congress, 3-6 October 1995, Adana. Volume I (Fruit): 292-296.

[5] Galletta, G. J., Bringhurst, R. S. (1990): Strawberry Management. – In: Galletta, G. J., Himelrick, D. G., Chandler, L. E. (eds.) Small Fruit Crop Management. – Prentice-Hall, Inc., Englewood Cliffs, NJ.

[6] Gerçekçioğlu, R. (1997): Essentials of Fruit Production. – Gaziosmanpaşa University Faculty of Agriculture Publications, Tokat.

[7] Gündüz, K., Özdemir, E. (2012): Earliness index, yield and fruit quality characteristics of some strawberry genotypes of different growing areas. – Ege University, Faculty of Agriculture Publications 49(1): 27-36.

[8] Hakala, M., Lapvetelainen, A., Huopalathi, R., Kallio, H. Tahvonen, R. (2003): Effects of varieties and cultivation conditions on the composition of strawberries. – Journal of Food Composition and Analysis 16(1): 67-80.

[9] Jetti, R. R., Yang, E., Kurnianta, A., Finn, C., Qian, M. C. (2007): Quantification of selected aroma-active compounds in strawberries by headspace solid-phase microextraction gas chromatography and correlation with sensory descriptive analysis. – J Food Sci 72: 487-496.

[10] Kafkas, E. (2004): Determination of Aroma Compounds and Relations between Aroma Compounds and Some Fruit Quality Criteria in Some Strawberry Genotypes. – Çukurova University, Institute of Science, Adana.

[11] Kıyga, Y. (2009): Morphological and Pomological Characterization of Osmanli x Camorosa Strawberry Hybrids. – Mustafa Kemal University, Graduate School of Natural and Applied Sciences, Antakya.

[12] Kus, Z. A., Demir, B., Eski, I., Gurbuz, F., Ercisli, S. (2017): Estimation of the colour properties of apples varieties using neural network. – Erwerbs-Obstbau 59(4): 291-299.

[13] Loughrin, J. H., Kasperbauer, M. J. (2002): Aroma of fresh strawberries is enhanced by ripening over red versus black mulch. – J Agric Food Chem 50(1): 161-5.

http://www.aloki.hu ● ISSN 1589 1623 (Print) ● ISSN 1785 0037 (Online)
DOI: http://dx.doi.org/10.15666/aeer/1605_68456855
© 2018, ALÖKI Kft., Budapest, Hungary

[14] Macit, I., Koç, A., Güler, S., Deligöz, I. (2011): Organic Strawberry Production in the Black Sea Region. Organic Agriculture Research Results. – Turkish Ministry of Agriculture and Rural Affairs, General Directorate of Agricultural Research, Ankara, pp. 87-94.
[15] Mina, K. K., Min-Yeop K., Kwang-Geun L. (2017): Categorization of fruits according to their content of polyphenols and vitamin C, antiradical activity, and quality parameters. – Journal of Food Processing and Preservation 42: 2.
[16] Nunes, M. C. N., Brecht, J. K., Morais, A. M. M. B., Sargent, S. A. (1995): Physical and chemical quality characteristics of strawberry after storage are reduced by a short delay to cooling. – Postharvest Biology and Technology 6: 17-28.
[17] Özdemir, E., Gündüz, K., Serçe, S. (2007): Adaptation of Some New Strawberry Varieties to the Amik Valley Conditions. – Turkey V. National Horticultural Congress, Erzurum, 4-7 September, pp. 20-22.
[18] Özuygur, M. (2005): Determination of Yield, Fruit Quality Criteria and Plant Characteristics in some Native, American and European Strawberry Varieties and Some Hybrid Strawberry Genotypes in Adana Conditions. – Çukurova University, Graduate School of Natural and Applied Sciences, Adana.
[19] Samykanno, K., Pang, E., Marriott, P. J. (2013): Chemical characterisation of two Australian-grown strawberry varieties by using comprehensive two-dimensional gas chromatography-mass spectrometry. – Food Chem. 141: 1997-2005.
[20] Schieberle, P., Hofmann, T. (1997): Evaluation of the character impact odorants in fresh strawberry juice by quantitative measurements and sensory studies on model mixtures. – J. Agric. Food Chem. 45: 227-232.
[21] Schopplein, E., Kruger, E., Rechner, A. (2002): Analytical and sensory qualities of strawberry cultivars. –Acta Hort. 567: 805-807.
[22] Serçe, S., Gündüz, K., Bakan, M., Paydaş, S. (2004): Strawberry gene resources of turkey. – Food and Agriculture 68: 60-64.
[23] Shaw, D. V. (1988): Genotypic variation and genotypic correlation for sugars and organic acids of strawberries. – Journal of the American Society for Horticultural Science 113: 770-774.
[24] Skupien, K., Osmianski, J. (2004): Comparison of six cultivars of strawberries (*Fragaria x ananassa Duch.*) grown in Nortwest Poland. – European Food Research and Technology 219: 66-70.
[25] Sürücü, E. Ö. (2010): Determination of Aroma Matter Compositions of 'Osmanli', 'Camorasa' and 'Seyhun' Strawberry Varieties. – Çukurova University, Graduate School of Natural and Applied Sciences, Adana.
[26] Viscarra Rossel, R. A., Minasny, B., Roudier, P., McBratney, A. B. (2006): Color space models for soil science. – Geoderma 133: 320-337.
[27] Yılmaz, H. (2009): Nutritive Value of Strawberry. – Hasad Publications, İstanbul.
[28] Zebatakis, I., Holden, M. A. (1997): Strawberry Flavor: Analysis and Biosynthesis. – J. Sci. Food and Agric. 74: 421-434.

http://www.aloki.hu ● ISSN 1589 1623 (Print) ● ISSN 1785 0037 (Online)
DOI: http://dx.doi.org/10.15666/aeer/1605_68456855
© 2018, ALÖKI Kft., Budapest, Hungary

THE INVESTIGATION OF COLD TOLERANCE IN COTTONSEED (*GOSSYPIUM HIRSUTUM* L.) GERMINATION

EKINCI, R.

Field Crops Department, Faculty of Agriculture, Dicle University, Diyarbakır, Turkey
(e-mail: remzi.ekinci@dicle.edu.tr; phone: +90-412-248-1000; fax: +90-412-248-1048)

(Received 28th Jul 2018; accepted 26th Sep 2018)

Abstract. This study was carried out to determine the factors affecting the cold tolerance of cotton genotypes and to determine the relationships between cold tolerance and some seed characteristics in 2017. Fourteen cotton varieties belonging to *G. hirsutum* L. were used as material. Cold (15 °C) and normal (30 °C) germination condition parameters and fatty acid composition of the cotton varieties were investigated. Resulting, genetic structure and environmental conditions were effective in terms of fatty acid composition and cold tolerance parameters in addition to need of 21 days which is the time to germinate in cold conditions. Varieties Fantom and Stoneville-453 were the highest mid-tolerant, followed by BA-119, Sayar-314 and Deltapine-499, second degree mid-tolerant, and Berke, Deltaopal, SureGrow-125 and Deltapine-332 were medium tolerant in the third grade while Carmen, Gloria, Flora and Teks varieties were sensitive. Positive relationship was observed between cold tolerance and linolenic acid, stearic acid, saturated fatty acids, saturated/unsaturated fatty acid ratio, 100 seed weight, and seed density while negative relationship was between cold tolerance and oleic acid, linoleic acid, palmitic acid, unsaturated fatty acids, unsaturated/saturated fatty acid ratio, oleic/linolenic acid ratio, oleic/palmitic acid ratio, and linoleic/palmitic acid.
Keywords: *cotton, chilly, stress, fatty acids, correlation*

Introduction

Many ecological factors are involved in the growth and development of cotton plants. The main factors of these are temperature (high and low temperature), humidity, drought, wind and salinity. Germination in cotton seeds begins with water intake and continues with many biochemical and physiological changes such as softening of seed husk, seed swelling and cracking of seed husk by the effect of water (Khan, 2003). Temperature and humidity are very important factors in the germination of cottonseed. If the temperature is insufficient, germination cannot occur and cotton germination is known to be inhibited at low temperatures (Haigh and Barlow, 1997). The optimum germination temperature in cotton seeds is 30-34 °C (Lauterbach et al., 1999; Cole and Wheeler, 1974). For many cotton varieties, the physiological level of zero for germination is 15 °C (Marani and Dag, 1962; Wanjura and Buxton, 1972; Speed et al., 1996). If temperature falls below 15 °C during germination or if the cotton plant remains at temperatures of 10 °C or lower for several hours, long-term irreparable damage to cotton seeds can occur. The most important quality criteria in the seed are high viability and seed vigor (resistance to stress conditions, germination rate, etc.) (McDonald, 1999). Low temperatures cause irregularities and delays in germination and emergence of cotton seeds, resulting in the inability to obtain the desired plant populations in the field.

According to data, from 1970-2016 averaged for many years in Turkey from May to September period (hot period), soil temperature decreases from 5 cm to 10 cm soil depth while in other periods (cold/cool periods) it increases (*Fig. 1*). Cotton is grown between April 15 and May 15 in Diyarbakir/Turkey ecological conditions as a main

http://www.aloki.hu ● ISSN 1589 1623 (Print) ● ISSN 1785 0037 (Online)
DOI: http://dx.doi.org/10.15666/aeer/…..1605_68576872
© 2018, ALÖKI Kft., Budapest, Hungary

crop. The most important factor affecting the sowing date is the temperature of the air and the soil. According to long years average (1970-2016), temperature changes at 5 cm soil depth were 8 °C, 14 °C, 20.5 °C (MGM data) in March, April and May, respectively (*Figs. 1* and *2*). In addition, especially in April and May, low night temperatures in addition to rainfall causing low temperatures in this period are great disadvantages for cotton seeds germination and emergence.

One of the biggest obstacles to early planting and possibility to extent vegetation duration is the problem of germination and emergence at low temperatures. Especially after midnight, there are serious decreases in air temperatures. This affects cotton germination, emergence and seedling growth negatively. The second (re) planting should be done with the low temperature period that occurs after early planting and the lack of sufficient plant population, as well as with stand deficiencies and poor seedling growth in field conditions. The ability of cotton seeds to germinate at low temperatures will ensure that cotton sowing occurs earlier. This will lead to cotton vegetation time to be longer as well as positive development for cotton fiber yield (Sharma et al., 1998; Norfleet et al., 1998; Porter et al., 1997; Tomar et al., 1991; Raju and Kharache, 1994) and quality characteristics (Porter et al., 1997). Also, it will prevent the adverse effects of cotton development due to the low temperatures that occurs after the date of planting in the spring.

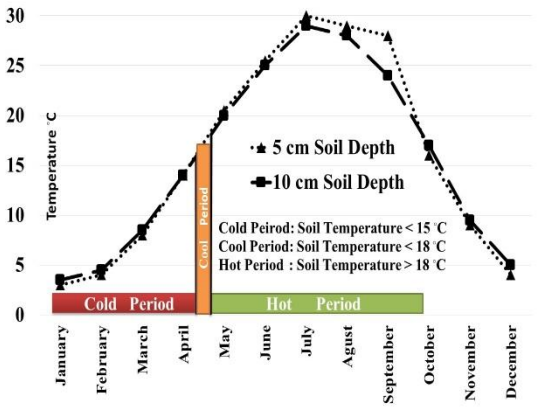

Figure 1. *Temperature change averaged for many years (1970-2016) at 5 cm and 10 cm soil depth (MGM data)*

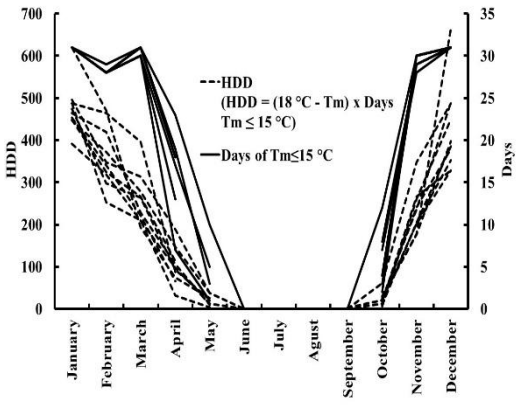

Figure 2. *Change of HDD and T < 15 °C days between 2008-2017 by months*

http://www.aloki.hu ● ISSN 1589 1623 (Print) ● ISSN 1785 0037 (Online)
DOI: http://dx.doi.org/10.15666/aeer/…..1605_68576872
© 2018, ALÖKI Kft., Budapest, Hungary

Germination tests on cold conditions are also a stress test. When seed is subjected to cold stress conditions, this way, its performance against cold stress is examined. Many tests and parameters related to cold tolerance have been explored and used. Germination percentage, germination coefficient, speed of germination index, cold warm vigor index, high cold stress index, vigor index and germination index are the primaries. The cold- warm vigor index developed by Hopper is a very good colt tolerance test (Hopper et al., 1994; Metzer, 1987; Kerby et al., 1989).

Cotton fatty acid composition which is not always constant can vary respect to species, variety and environmental factors (Genter et al., 1957; Zimmerman et al., 1959; Ramey, 1984; Baydar and Turgut, 1999; Karaca and Aytaç, 2012). Temperatures of 15 °C or higher causes phase transition at fatty acid composition of cottonseed and membrane lipids. When the temperature is below 15 °C, the oil crystallizes and the cell membrane loses its fluidity and selective permeability (Hall, 2003). Fatty acid composition in cottonseeds is manifested by low membrane function at low temperatures.

This study was carried out to determine the factors affecting the germination of cotton seeds in cold conditions and to determine the relationship between cold germination tolerance and some seed characteristics of cotton.

Materials and methods

The field study was carried out in the research area of Faculty of Agriculture at Dicle University, in the year of 2016 with 14 cotton (*G. hirsutum* L.) varieties (Teks, Stoneville-453, Stoneville-468, Deltaopal, Deltapine-499, Deltapine-332, BA-119, Carmen, Sayar-314, SureGrow-125, Fantom, Berke, Flora and Gloria).

The experimental area is located (37°890075 N, 40°275785 E) at 670 m above sea level. This region generally is characterized by a semiarid continental climate. The soil temperature change of 5 and 10 cm for long-term (1970-2016) have been presented in *Figure 1*. Change of day degree units (HDD) and T < 15 °C days period 2008-2017 by months have been presented in *Figure 2*. The average relative humidity is about 29.8% and total rainfall is 495 mm. The soil is low in organic matter and phosphorus. It has adequate calcium, potassium, and high clay content (48% to 68%) in the 0 to 160 cm profile. The sowing of cotton seeds was made by machine on 5 May (2016). All plots were treated with 20-20-0 (N-P-K) composite fertilizer to provide 75 kg N ha^{-1} and 75 kg P_2O_5 ha^{-1}. All plots were furrow irrigated regularly. A total of 9 irrigations were applied. Plots were harvested twice by hand. Yield of four rows of plot were weighed and calculated for seed cotton yield. First harvest was done on 20 October (2016); second harvest was done on 12 November (2016).

The germination tests at 15 °C and 30 °C temperatures were carried out in the test laboratories of the Science and Technology Research and Application Center at Dicle University in 2017 with 4 replications according to randomized blocks design. Fatty acid composition of cotton seeds was analyzed with gas chromatography (GC).

Germination tests in cold (CC_{15C}) and normal (standard) conditions (NC_{30C}) were carried out in a temperature controlled growth cabinet having 80-100% humidity. Fifty seeds with 3 replications were placed in a wet paper towels and placed into growth cabinet. Counts were made on days 4, 7, 14 and 21 in both germination tests. At each count, a moist towel was opened and healthy developing seedlings having hypocotyl length of 3.8 cm or more was counted and recorded. The counted seedlings were

http://www.aloki.hu ● ISSN 1589 1623 (Print) ● ISSN 1785 0037 (Online)
DOI: http://dx.doi.org/10.15666/aeer/…..1605_68576872
© 2018, ALÖKI Kft., Budapest, Hungary

removed then the towel rewound and left in the growth cabinet again (Edmisten, 2000; Smith and Varvil, 1984; Tolliver et al., 1997). The parameters of germination coefficient (GC), speed of germination index (SGI), cold warm vigor index (CWVI) and high cold stress index (HCSI) were calculated with the following equations in cold and normal germination conditions.

GC can be calculated as *Equation 1* (Maguire, 1962):

$$GC = \frac{\sum G}{\sum GT} x100 \quad \text{(Eq.1)}$$

SGI was calculated as *Equation 2* (AOSA, 1983, 1990):

$$SGI = \sum \frac{G_n}{T_n} \quad \text{(Eq.2)}$$

where, G represents the number of germinated seeds counted on T day (4, 7, 14 and 21 days).

CWVI was calculated as *Equation 3:*

$$CWVI = GP_{NC7} + GP_{CC21} \quad \text{(Eq.3)}$$

GP represents germinated percentage, NC represents normal condition (30 °C) at 7 day, CC represents cold condition (15 °C) at 21 day. The obtained CWVI value is considered to be excellent over 160, good between 140 and 159, moderate between 139 and 120 and weak if below 120 (Stauss and Hopper, 1983; Baughman et al., 1994, 2011).

HCSI was determined as *Equation 4* (Fischer and Maurer, 1978):

$$HCSI = \frac{\frac{G_{GPNC14} - G_{GPCC14}}{G_{GPNC14}}}{\frac{M_{GPNC14} - M_{GPCC14}}{M_{GPNC14}}} \quad \text{(Eq.4)}$$

where, G: Genotype; M: Means; GPNC14: normal condition (30 °C) germination percent at 14 day; GPCC14: cold condition (15 °C) germination percent at 14 day. HCSI < 0.50 highly cold stress tolerant, 0.50 < HCSI < 1.00 moderately cold stress tolerant and HCSI > 1.00 susceptible.

The values obtained for each parameter were analyzed using JMP 7.0 (Copyright © 2007 SAS Institute Inc.) statistical package program. Means were grouped according to the LSD (0.05) test.

Results

Ratios for oleic acid (C18:1) (%), linoleic acid (C18:2) (%), linolenic acid (C18:3) (%), palmitic acid (C16:0) (%), stearic acid (C18:0) (%), saturated fatty acids (%), unsaturated fatty acids (%), unsaturated/saturated fatty acids, saturated/unsaturated fatty acids, oleic/linoleic acid, oleic/linolenic acid, linoleic/palmitic acid and means for 100

http://www.aloki.hu ● ISSN 1589 1623 (Print) ● ISSN 1785 0037 (Online)
DOI: http://dx.doi.org/10.15666/aeer/…..1605_68576872
© 2018, ALÖKI Kft., Budapest, Hungary

seed weight (g) and seed density (g.ml^{-1}) were given in *Tables 1*, *2*, and *3*. In terms of all the traits examined, varieties were statistically (1%) different than each other.

The ranges and the mean values for oleic acid 14.75-21.90% (18.70%), linoleic acid 36.99-48.95% (44.01%), linolenic acid 0.26-0.50% (0.37%), palmitic acid 20.75-27.75% (24.21%), stearic acid 2.05-3.58% (2.80%), saturated fatty acids 23.76-30.84% (27.00%), unsaturated fatty acids 54.37-70.47% (63.10%), unsaturated/saturated fatty acids ratio 2.05-2.69 (2.35), saturated/unsaturated fatty acids ratio 0.37-0.49 (0.43), oleic/linoleic acid ratio 0.31-0.50 (0.43), oleic/linolenic acid ratio 29.12-78.99 (52.73), oleic/palmitic acid ratio 0.58-1.00 (0.78), linoleic/palmitic acid ratio 1.61-2.06 (1.83) 100 seed weight 9.96-13.30 g (11.34 g), and seed density 1.01-1.15 g.ml^{-1} (1.06 g.ml^{-1}) were measured (*Tables 1, 2* and *3*).

In terms of oleic acid trait, Carmen and Teks varieties; in terms of linoleic acid trait, Carmen, Flora, and Gloria varieties; in terms of linolenic acid and stearic acid traits, Fantom, and Stoneville-453 varieties; in terms of palmitic acid trait, BA-119, Berke, and SureGrow-125 varieties were the group in which the highest values were obtained (*Table 1*).

Table 1. *Percentage of oleic acid (C18:1), linoleic acid (C18:2), linolenic acid (C18:3), palmitic acid (C16:0) and stearic acid (C18:0) of cotton varieties*

Varieties	**(C18:1)(%)**	**(C18:2)(%)**	**(C18:3) (%)**	**(C16:0) (%)**	**(C18:0)(%)**
BA-119	19.57 e	44.57 d	0.38 de	27.67 a	2.94 cd
Berke	20.51 bcd	46.32 cd	0.41 bc	27.75 a	3.09 bc
Carmen	21.24 ab	48.95 a	0.26 i	24.17 de	2.10 h
Deltaopal	20.11 cde	40.39 f	0.30 h	25.09 bcd	2.20 gh
Deltapine-332	19.90 de	46.95 bc	0.26 i	24.25 de	2.05 h
Deltapine-499	20.77 bc	42.79 e	0.40 cd	20.75 g	3.01 c
Fantom	14.75 h	39.51 f	0.50 a	21.26 fg	3.58 a
Flora	14.99 h	47.92 abc	0.34 f	24.65 cd	2.68 ef
Gloria	17.74 f	48.20 ab	0.39 cde	26.03 bc	3.08 bc
Sayar-314	18.23 f	41.21 ef	0.31 gh	22.74 ef	2.34 g
Stoneville-453	16.88 g	36.99 g	0.49 a	21.04 g	3.45 a
Stoneville-468	19.87 de	42.34 e	0.37 e	24.26 de	2.80 de
SureGrow-125	15.35 h	45.06 d	0.43 b	26.35 ab	3.20 b
Teks	21.90 a	44.97 d	0.33 fg	22.80 ef	2.62 f
Means	18.70	44.01	0.37	24.21	2.80
CV (%)	3.14	2.79	4.26	4.45	4.03
Min-Max.	14.75-21.90	36.99-48.95	0.26-0.50	20.75-27.75	2.05-3.58
$LSD_{0.05}$	0.84	1.76	0.02	1.54	0.16
Prob.	**	**	**	**	**

(C18:1): oleic acid, (C18:2): linoleic acid, (C18:3): linolenic acid, (C16:0): palmitic acid, (C18:0): stearic acid, CV: coefficient of variance, $LSD_{0.05}$: least significant difference at 5% level, Prob: probability, * and ** significant at the 5% and 1% probability levels, respectively, means in each column followed by the same letter are not significantly different ($p < 0.05$)

http://www.aloki.hu ● ISSN 1589 1623 (Print) ● ISSN 1785 0037 (Online)
DOI: http://dx.doi.org/10.15666/aeer/…..1605_68576872
© 2018, ALÖKI Kft., Budapest, Hungary

In terms of saturated fatty acids trait, BA-119, Berke, SureGrow-125 varieties; in terms of unsaturated fatty acids trait, Carmen variety; in terms of unsaturated/saturated fatty acids ratio trait, Carmen, Deltapine-332, Deltapine-499, and Teks varieties; in terms of saturated/unsaturated fatty acids ratio trait, BA-119, Berke, and SureGrow-125 varieties; in terms of oleic/linoleic acids ratio trait, Deltaopal, Deltapine-499, and Teks varieties were the group in which the highest values were obtained (*Table 2*).

Table 2. *Percentage of saturated fatty acid, unsaturated fatty acid, and ratio of unsaturated/saturated fatty acids, saturated/unsaturated fatty acids, oleic (C18:1)/linoleic acid (C18:2) of cotton varieties*

Varieties	Sat. fatty acids (%)	Unsat. fatty acids (%)	Unsat./sat. fatty acids rate	Sat./unsat. fatty acids rate	(C18:1)/(C18:2) rate
BA-119	30.61 ab	64.53 cd	2.11 de	0.47 ab	0.43 de
Berke	30.84 a	67.25 b	2.18 cde	0.45 abc	0.44 de
Carmen	26.28 cd	70.47 a	2.68 a	0.37 e	0.43 de
Deltaopal	27.30 c	60.81 fg	2.23 cd	0.44 bc	0.50 a
Deltapine-332	26.31 cd	67.12 b	2.55 a	0.39 e	0.42 e
Deltapine-499	23.76 f	63.97 de	2.69 a	0.37 e	0.48 ab
Fantom	24.85 def	54.77 h	2.20 cde	0.45 bc	0.37 f
Flora	27.33 c	63.26 de	2.31 bc	0.43 cd	0.31 h
Gloria	29.12 b	66.34 bc	2.27 bc	0.43 cd	0.36 f
Sayar-314	25.09 def	59.75 g	2.39 b	0.41 d	0.44 de
Stoneville-453	24.50 ef	54.37 h	2.22 cd	0.45 bc	0.45 cd
Stoneville-468	27.06 c	62.59 ef	2.31 bc	0.43 cd	0.46 bc
SureGrow-125	29.56 ab	60.85 fg	2.05 e	0.49 a	0.34 g
Teks	25.42 de	67.21 b	2.64 a	0.37 e	0.48 ab
Means	27.00	63.10	2.35	0.43	0.43
CV (%)	4.00	2.13	4.52	4.50	4.26
Min-Max.	23.76-30.85	54.37-70.47	2.05-2.69	0.37-0.49	0.31-0.50
$LSD_{0.05}$	1.55	1.93	0.15	0.03	0.03
Prob.	**	**	**	**	**

(C18:1): oleic acid, (C18:2): linoleic acid, CV: coefficient of variance, $LSD_{0.05}$: least significant difference at 5% level, Prob: probability, * and ** significant at the 5% and 1% probability levels, respectively, means in each column followed by the same letter are not significantly different ($p < 0.05$)

In terms of oleic/linoleic rate trait, Carmen, and Deltapine -332 varieties; in terms of oleic/palmitic rate trait, Deltapine-499, and Teks varieties; in terms of linoleic/palmitic rate trait, Carmen, Deltapine-332, Deltapine-499, Flora, and Teks varieties; in terms of 100 seed weight and seed density traits, Fantom, and Stoneville-453 varieties were the group in which the highest values were obtained (*Table 3*).

The average values of germination coefficients (GC_{15} and GC_{30}) (determined by *Eq. 1*), speed of germination index (SGI_{15} and SGI_{30}) (determined by *Eq. 2*), cold-warm

http://www.aloki.hu ● ISSN 1589 1623 (Print) ● ISSN 1785 0037 (Online)
DOI: http://dx.doi.org/10.15666/aeer/…..1605_68576872
© 2018, ALÖKI Kft., Budapest, Hungary

vigor index (CWVI) (determined by *Eq. 3*) and high cold stress index (HCSI) (determined by *Eq. 4*) were given in *Table 4* for cold and normal conditions of cotton constituting the material.

Table 3. *Ratio of oleic (C18:1)/linolenic (C18:3), oleic (C18:1)/palmitic (C16:0), linoleic (C18:2)/palmitic (C16:0), means of 100 seed weight and seed density of cotton varieties*

Varieties	(C18:1)/(C18:3) rate	(C18:1)/(C16:0) rate	(C18:2)/(C16:0) rate	100 seed weight (g)	Seed density ($g.ml^{-1}$)
BA-119	50.81 d	0.70 de	1.61 g	10.96 cd	1.04 c
Berke	49.69 de	0.73 d	1.67 fg	11.42 bc	1.06 bc
Carmen	78.99 a	0.88 b	2.02 a	12.03 b	1.02 d
Deltaopal	67.22 b	0.80 c	1.61 g	10.45 de	1.08 b
Deltapine-332	75.77 a	0.82 c	1.94 abc	10.18 e	1.02 d
Deltapine-499	51.77 d	1.00 a	2.06 a	11.98 b	1.06 bc
Fantom	29.12 h	0.69 de	1.86 bcd	13.3 a	1.13 a
Flora	43.64 f	0.60 e	1.94 abc	10.89 cd	1.02 d
Gloria	45.22 ef	0.68 f	1.85 bcd	10.98 cd	1.01 d
Sayar-314	57.86 c	0.80 c	1.82 cde	11.45 bc	1.07 b
Stoneville-453	33.99 g	0.80 c	1.76 def	13.01 a	1.15 a
Stoneville-468	53.05 d	0.81 c	1.74 defg	10.57 de	1.07 bc
SureGrow-125	35.42 g	0.58 f	1.70 efg	11.48 bc	1.08 b
Teks	65.72 b	0.96 a	1.97 ab	9.96 e	1.02 d
Means	52.73	0.78	1.83	11.34	1.06
CV (%)	5.94	4.98	5.36	4.28	1.55
Min-Max.	29.12-78.99	0.58-1.00	1.61-2.06	9.96-13.30	1.01-1.15
$LSD_{0.05}$	4.48	0.06	0.14	0.69	0.02
Prob.	**	**	**	**	**

(C18:1): oleic acid, (C18:2): linoleic acid, (C18:3): linolenic acid, (C16:0): palmitic acid, CV: coefficient of variance, $LSD_{0.05}$: least significant difference at 5% level, Prob: probability, * and ** significant at the 5% and 1% probability levels, respectively, means in each column followed by the same letter are not significantly different ($p < 0.05$)

In terms of all the traits examined, there were statistical difference of 1% between genotypes. Ranges and mean values for germination coefficient in the cold conditions (GC_{15}), germination coefficient (GC_{30}) under normal conditions, speed of germination index (SGI_{15}) in cold condition, speed of germination index (SGI_{30}) under normal condition, CWVI and HCSI were 5.65-6.23% (5.99%), 11.20-15.03% (13.64%), 1.62-2.45 (1.88%), 7.47-9.06% (8.16%), 110.41-152.45 (130.17), 0.86-1.13 (1.00) (*Table 4*).

In terms of CWVI trait, Fantom, Sayar-314 and Stoneville-453 varieties; in terms of HCSI trait, Flora, Gloria, and Teks varieties; were the group in which the highest values were obtained (*Table 4*).

http://www.aloki.hu ● ISSN 1589 1623 (Print) ● ISSN 1785 0037 (Online)
DOI: http://dx.doi.org/10.15666/aeer/…..1605_68576872
© 2018, ALÖKI Kft., Budapest, Hungary

Table 4. *Percent of GC (15 °C and 30 °C), SGI (15 °C and 30 °C), CWVI and HCSI of cotton varieties*

Varieties	GC 15 °C	GC 30 °C	SGI 15 °C	SGI 30 °C	CWVI	HCSI
BA-119	6.17 ab	14.58 ab	1.86 c	7.47 f	134.10 cd	0.95 g
Berke	6.23 a	14.81 ab	1.89 c	8.98 a	138.45 bc	1.00 ef
Carmen	5.82 de	14.33 a-d	1.82 cd	8.69 ab	114.66 e	1.06 bcd
Deltaopal	6.08 bc	13.86 cde	1.72 de	8.19 bd	127.40 d	1.00 ef
Deltapine -332	5.78 ef	11.51 f	1.69 e	7.61 ef	128.12 d	1.04 cde
Deltapine-499	6.13 ab	15.03 a	1.94 c	8.12 ce	134.54 cd	0.97 fg
Fantom	6.21 ab	13.49 e	2.2 b	7.60 ef	152.45 a	0.86 h
Flora	5.65 f	11.51 f	1.64 e	7.76 df	112.82 e	1.10 ab
Gloria	5.66 f	11.20 f	1.62 e	7.55 f	110.41 e	1.08 abc
Sayar-314	6.12 ab	14.52 abc	2.09 b	8.33 bc	145.35 ab	0.93 g
Stoneville-453	6.16 ab	14.69 ab	2.45 a	9.06 a	150.65 a	0.87 h
Stoneville-468	6.13 ab	13.63 de	1.85 c	7.78 df	128.03 d	0.94 g
SureGrow-125	5.96 cd	14.31 bcd	1.84 cd	8.43 bc	129.56 d	1.02 de
Teks	5.68 f	13.43 e	1.64 e	8.59 ac	115.81 e	1.13 a
Means	5.99	13.64	1.88	8.16	130.17	1.00
CV (%)	1.69	3.67	4.75	4.58	4.25	3.48
Range	5.65-6.23	11.20-15.03	1.62-2.45	7.47-9.06	110.41-152.45	0.86-1.13
$LSD_{0.05}$	0.15	0.72	0.13	0.53	7.91	0.05
Prob.	**	**	**	**	**	**

GC: germination coefficient, SGI: speed of germination index, CWVI: cold warm vigor index, HCSI: high cold stress index, °C: centigrade degree, CV: coefficient of variance, LSD0.05: least significant difference at 5% level, Prob: probability, * and ** significant at the 5% and 1% probability levels, respectively, means in each column followed by the same letter are not significantly different ($p < 0.05$)

Discussion

When the germination rate at 30 °C, considered as the normal germination temperature for cotton plant, was examined, it was determined that the maximum germination occurred on the 7th day, whereas the germination count at 21 day determined to be the maximum germination time at 15 °C, which was considered as the cold condition (*Figs. 3* and *4*). This suggests that low temperature causes delayed of germination time and a significant reduction of germination rate.

Results of the germination coefficient (GC_{15}), speed of germination index (SGI_{15}), cold-warm vigor index (CWVI) and high cold stress index (HCSI) values that are indicative for cold tolerance were parallel to each other. The high values of the GC_{15}, SGI_{15} and CWVI were confirmed by the low HCSS. Our findings had similarity with Tuck et al. (2006).

It is desirable that the CWVI values are high and the HCSI value is low for tolerance to cold. No HCSI value < 0.50 was obtained from the varieties forming the material, and so no cold-tolerant variety was detected. Since 0.50 < HCSI < 1.00 was detected in

http://www.aloki.hu ● ISSN 1589 1623 (Print) ● ISSN 1785 0037 (Online)
DOI: http://dx.doi.org/10.15666/aeer/…..1605_68576872
© 2018, ALÖKI Kft., Budapest, Hungary

Stoneville-453, Fantom, Sayar-314, BA-119, Stoneville-468 and Deltapine-499 varieties, they were called as mid-tolerant but other varieties were susceptible to cold. However, Fantom (0.86) and Stoneville-453 (0.87) varieties were found to be the highest mid-tolerant varieties with the lowest HCSI values (*Table 4; Fig. 8*). BA-119, Sayar-314 and Deltapine-499 varieties showed themselves as medium tolerant varieties at the second level (*Fig. 8*).

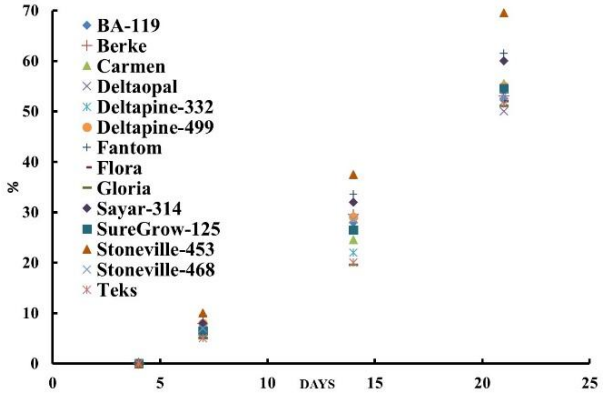

Figure 3. *Germination percentage at cold (15 °C) conditions on days 4, 7, 14 and 21*

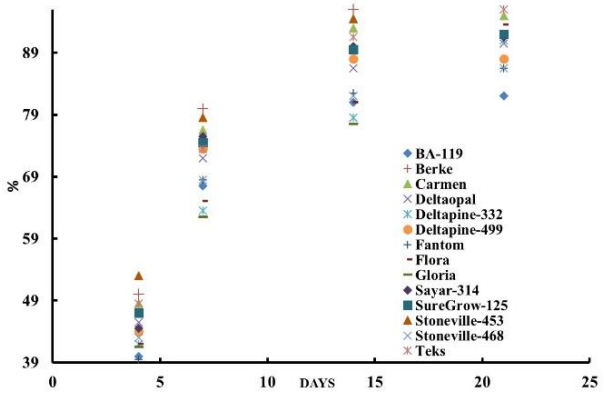

Figure 4. *Germination percentage at standard (30 °C) conditions on days 4, 7, 14 and 21*

Values of CWVI > 160 were not determined, while values of Fantom, Stoneville-453 and Sayar-314 ranged from 140 to 160 that were indicated as *good*. On the other hand, Stoneville-468, BA-119, Deltapine-499, Berke, Deltaopal, SureGrow-125 and Deltapine-332 varieties were found to be *medium* because CWVI values were between 120-140 while Carmen, Gloria, Flora and Teks varieties were *weak* because of values were smaller than 120 (*Table 4; Fig. 8*). Similar results have been obtained with varieties in terms of CWVI and HCSI characteristics.

Among the cotton varieties used were Fantom and Stoneville-453, the highest mid-tolerant, BA-119, Sayar-314 and Deltapine-499 varieties, secondly medium tolerant, Berke, Deltaopal, SureGrow-125 and Deltapine-332 medium tolerant with 3th grade, Carmen, Gloria, Flora and Teks varieties were thought to be sensitive to cold. Our findings are similar to the results of Bartonkowski et al. (1978), Maluf and Tifchelaar (1982), Hailstones and Smith (1988), Speed et al. (1996), Borth (1997), Al-Bahrain and

http://www.aloki.hu ● ISSN 1589 1623 (Print) ● ISSN 1785 0037 (Online)
DOI: http://dx.doi.org/10.15666/aeer/…..1605_68576872
© 2018, ALÖKI Kft., Budapest, Hungary

Khary (2000), Sheikh et al. (2002), Down et al. (2010), Özbek (2011), Karaca and Aytaç (2012), Kaya (2014), Kazmi et al. (2015), Bolek et al. (2016), while those of Dogras et al. (1977) and Lukonge et al. (2007) are different. This difference may be due to the difference in genotype or environmental conditions.

The cold-tolerant genotype in cotton seeds is characterized by high CWVI and low HCSI. It is seen that Fantom and Stoneville-453 varieties where the highest values for linolenic acid, stearic acid, 100 seed weight and seed density traits are obtained are also the highest varieties in which CWVI values are obtained (*Fig. 8*). This suggests that linolenic acids, stearic acids, 100 seed weight and seed density are important properties for CWVI (*Figs. 11* and *13*). The positive correlation between linolenic (r = +0.54**), stearic acids (r = +0.43**), 100 seed weight (r = +0.52**) and seed density (r = +0.77**) with the CWVI supports this situation (*Table 5*). In this case, the amount of high linolenic acids, stearic acids, 100 seed weight and seed density cottonseed, is more tolerant to high cold stress, reveals the result. This suggests that linolenic acids, stearic acids, 100 seed weight and seed density are important properties for CWVI and HCSI (*Figs. 6, 7, 11* and *13*). However, significant positive correlation was found between cold tolerance in the cottonseed and saturated fatty acids (r = +0.22), saturated/unsaturated (r = +0.32), but this was not statistically significant (*Table 5; Figs. 5–14*).

Table 5. *Pearson correlation coefficients to examine the relationship of GC (15 °C and 30 °C), SGI (15 °C and 30 °C), CWVI and HCSI*

Traits	GC_{15}	GC_{30}	SGI_{15}	SGI_{30}	CWVI	HCSI
Oleic acid	-0.01	+0.27*	-0.31*	+0.27	-0.23	+0.30*
Linoleic acid	-0.66**	-0.46**	-0.69**	-0.16	-0.71**	+0.74**
Linolenic acid	+0.45**	+0.28*	+0.59**	+0.08	+0.54**	-0.55**
Palmitic acid	-0.09	-0.12	-0.48**	-0.09	-0.31*	+0.34*
Stearic acid	+0.35**	+0.2	+0.48**	+0.02	+0.43**	-0.44**
Sat. fatty acids	+0.02	+0.08	+0.39**	+0.09	+0.22	-0.25
Unsat. fatty acids	-0.51**	-0.21	-0.69**	+0.02	-0.66	+0.72
Uns./sat. ratio	-0.36**	-0.07	-0.19	+0.09	-0.32	+0.34
Sat./uns. ratio	+0.38**	+0.11	+0.19	+0.07	+0.32	-0.33
Oleic/linoleic	+0.38**	+0.52**	+0.12	+0.35**	-0.20	+0.16
Oleic/linolenic	-0.30*	-0.08	-0.46**	-0.09	-0.42**	+0.45**
Oleic/palmitic	-0.06	+0.32*	-0.05	+0.28*	-0.01	+0.05
Linoleic/palmitic	-0.46**	-0.25	-0.11	-0.06	-0.3*	+0.29*
100 seed weight	+0.45**	+0.39**	+0.72**	+0.21	+0.52**	-0.58**
Seed density	+0.71**	+0.5**	+0.75**	+0.27*	+0.77**	-0.75**

GC: germination coefficient, SGI: speed of germination index, CWVI: cold warm vigor index, HCSI: high cold stress index, °C: centigrade degree, * and ** significant at the 5% and 1% probability levels, respectively

http://www.aloki.hu ● ISSN 1589 1623 (Print) ● ISSN 1785 0037 (Online)
DOI: http://dx.doi.org/10.15666/aeer/…..1605_68576872
© 2018, ALÖKI Kft., Budapest, Hungary

On the other hand, our findings, oleic acid, linoleic acid, palmitic acid, unsaturated fatty acids, unsaturated/saturated, oleic/linoleic, oleic/linolenic, oleic/palmitic, and linoleic/palmitic should be low for high cold tolerance in the cottonseed (*Figs. 9, 10, 12* and *14*). Correlations between CWVI and oleic (r = -0.23), linoleic (r = -0.71**) and palmitic (r = -0.31*) acids, unsaturated fatty acids (r = -0.66), unsaturated/saturated (r = -0.32), oleic/linoleic (r = -0.20), oleic/linolenic (r = -0.42**), oleic/palmitic (r = -0.01), and linoleic/palmitic (r = -0.30*) support this (*Table 5*). All results obtained for CWVI are also supported by HSCI results. The existence of a positive relationship (r = +0.78 **) between HCSI and CWVI confirms this similarity (*Table 5*). Our findings are similar to those of Judith and Christiansen (1976), Carmichael (2007), Özbek (2011), but differ from the findings of Edmisten (2000).

100 seed weight and seed density traits can vary significantly depending on the conditions of growing the cotton plant. As 100 seed weight and seed density increases in favorable growing conditions, it decreases in unfavorable conditions. It is also an indicator of the maturity of the cotton seed. While mature cotton is high in seed density, low value is obtained in immature cotton seeds. This suggests that cold tolerance is influenced not only by the genetic structure of the cotton seed, but also by the environmental conditions and seed maturity of the cotton seed. This reveals the fact that the conditions for growing cotton seeds are of great importance for cold tolerance. Our findings showed similarities with the findings of Bartee and Krieg (1974), Tripathi and Khan (1990), Bolek (2006, 2010) and Pahlavani et al. (2008).

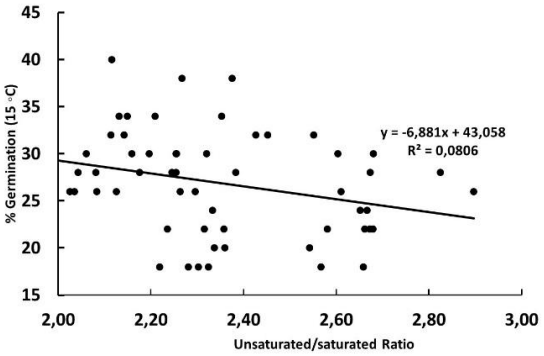

Figure 5. *Relationship between germination percentage and unsat./sat. fatty acids ratio at cold (15 °C)*

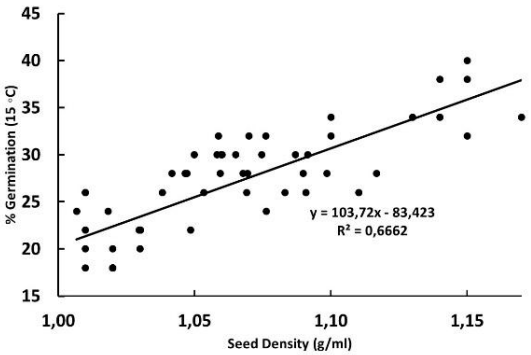

Figure 6. *Relationship between germination percentage and seed density at cold (15 °C)*

http://www.aloki.hu ● ISSN 1589 1623 (Print) ● ISSN 1785 0037 (Online)
DOI: http://dx.doi.org/10.15666/aeer/…..1605_68576872
© 2018, ALÖKI Kft., Budapest, Hungary

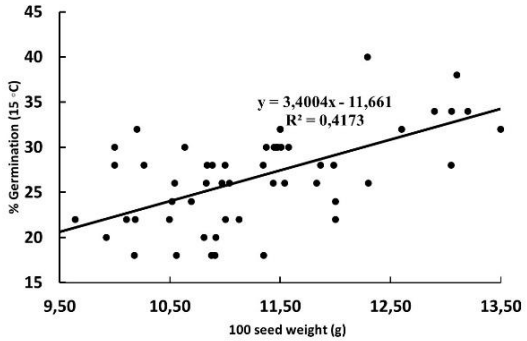

Figure 7. *Relationship between germination percentage and 100 seed weight at cold (15 °C)*

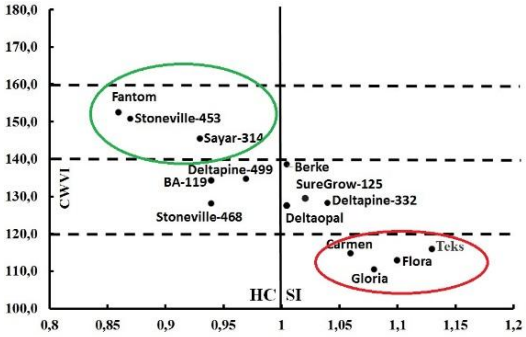

Figure 8. *Relationship between CWVI and HCSI at cold (15 °C)*

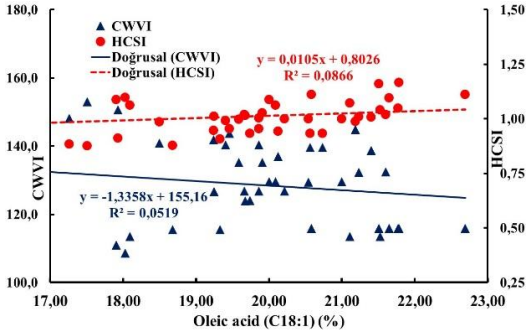

Figure 9. *Relationship between CWVI and C18:1 at cold (15 °C)*

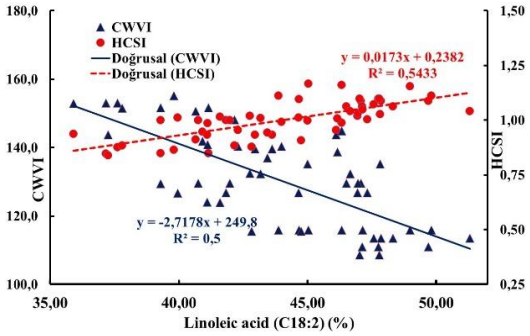

Figure 10. *Relationship between CWVI and C18:2 at cold (15 °C)*

http://www.aloki.hu ● ISSN 1589 1623 (Print) ● ISSN 1785 0037 (Online)
DOI: http://dx.doi.org/10.15666/aeer/…..1605_68576872
© 2018, ALÖKI Kft., Budapest, Hungary

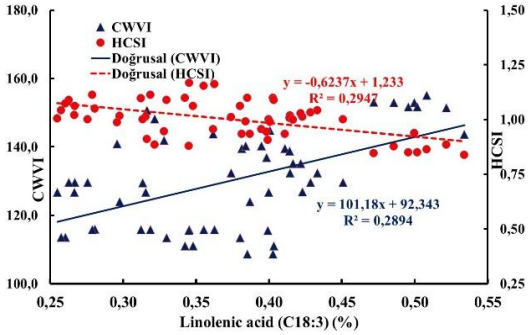

Figure 11. *Relationship between CWVI and C18:3 at cold (15 °C)*

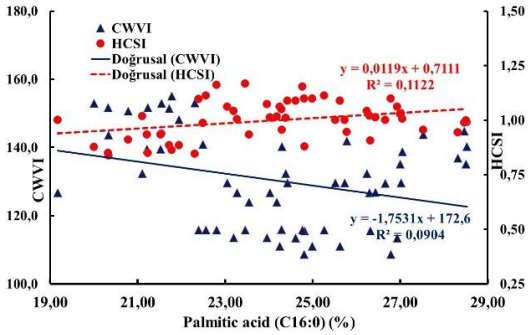

Figure 12. *Relationship CWVI and C16:0 at cold (15 °C)*

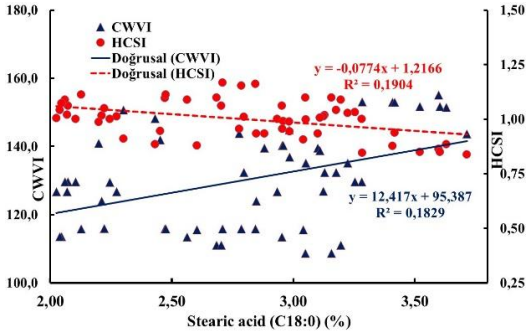

Figure 13. *Relationship between CWVI and C18:0 acid at cold (15 °C)*

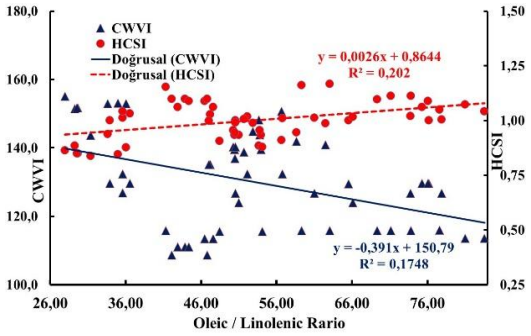

Figure 14. *Relationship between CWVI and oleic/linolenic acid ratio at cold (15 °C)*

http://www.aloki.hu ● ISSN 1589 1623 (Print) ● ISSN 1785 0037 (Online)
DOI: http://dx.doi.org/10.15666/aeer/…..1605_68576872
© 2018, ALÖKI Kft., Budapest, Hungary

Conclusion

Genetic structure and environmental conditions are very effective factors in terms of fatty acid composition and cold tolerance parameters. The cold condition for germination of cotton seed is 15 °C that prolongs the duration up to 21 days which brings with many negativity. There were not cold tolerant variety used in this experiment but cultivars could be ordered as Fantom and Stoneville-453 were the highest medium-tolerant, BA-119, Sayar-314 and Deltapine-499 were the second medium-tolerant, Berke, Deltaopal, SureGrow-125 and Deltapine-332 varieties were medium-tolerant at the third level, while Carmen, Gloria, Flora and Teks varieties were sensitive. In future studies, it is recommended to use Stoneville-453 and Fantom cotton varieties as highest medium-tolerant genotypes and Carmen, Gloria, Flora and Teks cotton varieties as sensitive genotypes. It is recommended that the properties of linolenic acid, stearic acid, saturated fatty acids, saturated/unsaturated fatty acids ratio, 100 seed weight and seed density are high in cotton seeds to reduce cold stress during germination. The CWVI and HCSI features are ideal indicators for cold tolerance.

REFERENCES

[1] Al-Bahrayn, A. M., Al-Khayri, J. M. (2000): Genotype variability in fatty acid composition and chemical characteristic of cotton (*Gossypium hirsutum* L.). Pakistan Journal of Biological Sciences 3: 1778-1780.
[2] AOSA (1983): Association of Official Seed Analysts - Seed Vigor Testing Handbook. – AOSA, East Lasing.
[3] AOSA (1990): Rules for testing seeds. – USA. J. Seed Technol. 12: 1-112.
[4] Bartee, S. N., Krieg, D. R. (1974): Cottonseed density: associated physical and chemical properties of 10 cultivars. –Agronomy Journal 66: 433-435.
[5] Bartkowski, J. E., Katterman, F. R. H., Buxton, R. D. (1978): Influence of exogenous fatty acids on cottonseed germination. –Physiologia Plantarum 44: 153-156.
[6] Baughman, T., Boman, R., Lemon, R. (1994): Cool Warm Test. Texas Cooperative Extension. – The Texas A&M University System, College Station, TX.
[7] Baughman, T., Boman, R., Lemon, R. (2011): Cotton Seed Quality – Where It All Begins. – The Texas A&M University, College Station, TX. http://lubbock.tamu.edu/cotton/pdf/cotseedqual.pdf.
[8] Baydar, H., Turgut, İ. (1999): Variations of fatty acid composition according to some morphological and physiological properties and ecological regions in oilseed plants. – Turkish Journal of Agriculture and Forestry 23(1): 81-86.
[9] Bolek, Y. (2006): Predicting cotton seedling emergence for cold tolerance: *Gossypium barbadense*. – Journal of Agronomy 5(3): 461-465.
[10] Bolek, Y. (2010): Predicting cotton seedling emergence for cold tolerance: *Gossypium hirsutum* L. – Not. Bot. Hort. Agrobot. Cluj 38(1): 134-138.
[11] Bolek, Y., Tekerek, H., Hayat, K., Bardak, A. (2016): Screening of cotton genotypes for protein content, oil and fatty acid composition. – Journal of Agricultural Science 8(5): 107-121.
[12] Borth, T. D. (1997): Genetic and environmental factors affecting the fatty acid composition of polar and non-polar lipids of developing cottonseed. – http://esr.lib.ttu.edu/handle/2346/10811.
[13] Carmichael, D. (2007): Effects of harvest aid materials and timing on planting seed quality. – Submitted to the Graduate Faculty of Texas Tech University, Ph. D. Thesis, Texas.

http://www.aloki.hu ● ISSN 1589 1623 (Print) ● ISSN 1785 0037 (Online)
DOI: http://dx.doi.org/10.15666/aeer/…..1605_68576872
© 2018, ALÖKI Kft., Budapest, Hungary

[14] Cole, D. F., Wheeler, J. E. (1974): Effect of pregermination treatments on germination and growth of cottonseed at suboptimal temperatures. – Crop Science 14: 451-453.
[15] Dogras, C. C., Dilley, D. R., Herner, R. C. (1977): Phospholipid biosynthesis and fatty acid content in relation to chilling injury during germination of seeds. – Plant Physiology 60: 897-902.
[16] Down, M. K., Boykin, D. L., Meredith, W. R., Campbell, B. T., Bourland, F. M., Gannaway, J. R., Glass, K. M., Zhang, J. (2010): Fatty acid profiles of cottonseed genotypes from the national cotton variety trials. – The Journal of Cotton Science 14: 64-73.
[17] Edmisten, K. L. (2000): Cotton seed quality concerns for 2000. – North Carolina State University http://www.cotton.ncsu.edu/ccn/2000/ccn-00-4a.htm. Accessed on 15.05.2011.
[18] Fischer, R. A., Maurer, R. (1978): Drought resistance in spring wheat cultivars. I. Grain yield response. – Aust. J. Agric. Res. 29: 897-907.
[19] Genter, C. F., Eheart, J. F., Linkous, W. N., Collins, F. I. (1957): Factors affecting linolenic and linoleic acid content of soybean oil. – Agron. Jour. 49: 598-597.
[20] Judith, B. S. J., Christiansen, M. N. (1976): Inhibition of linolenic acid synthesis and modification of chilling resistance in cotton seedlings. – Plant Physiology 57(2): 257-259.
[21] Haigh, A. M., Barlow, E. V. R. (1997): Germination and priming of tomato. Carrot and sorghum seeds in a range of osmotica. – J. Amer. Soc. Hort. Sci. 112(2): 210-216.
[22] Hailstones, M. D., Smith, M. T. (1988): Lipid peroxidation in relation to declining vigour in seeds of soya (*Glycine max* L.) and cabbage (*Brassica oleracea* L.). – Journal of Plant Physiology 133: 452-456.
[23] Hall, A. J. (2003): Evaluation of fatty acid composition of cotton germplasm and association with cold tolerance. – Master Thesis, Faculty of Texas Tech University.
[24] Hopper, N. W., Gannaway, J. R., Jividen, G. M., Struve, T. H. (1994): Selection of cold tolerant lines of cotton based on seedling response. – Proceedings of the Beltwide Cotton Conference, National Cotton Council, Memphis, Tennessee.
[25] Karaca, E, Aytaç, S. (2012): The factors affecting on fatty acid composition of oil crops. – J. Fac. Agric. OMU 22(1): 123-131.
[26] Kaya, G. (2014): Impact of seed applications (priming) of fatty acid composition of seed and seed quality and its relations. – Journal of Central Research Institute for Field Crops 17(1-2). http://dergipark.gov.tr/tarbitderg/issue/11504/137023.
[27] Kazmi, S. F., Khan, N. U., Gul, S., Ali, I. (2015): Fatty acid profile of upland cotton genotypes through NIR-Near-Infrared Spectroscopy. – The Journal of Animal & Plant Sciences. 25(1): 212-225.
[28] Kerby, T. A., Keeley, M., Johnson, S. (1989): Weather and seed quality variables to predict cotton seedling emergence. – Agronomy Journal 81: 415-419.
[29] Khan, N. U. (2003): Genetic analysis combining ability and heterotic studies for yield. Its components, fibre and oil quality traits in upland cotton (*G. hirsutum*). – Ph. D. Dissertation. Sindh Agric. Univ., Tandojam, Pakistan.
[30] Lauterbach, B., Krieg, D., Jividen, G., Dugger, P., Richter, D. (1999): Fatty acid compozition of lipid fractions in germinating cotton as affected by temperature. – Proc. Beltwide Cotton Conference 1: 564-565.
[31] Lukonge, E., Labuschagne, M. T., Hugo, A. (2007): The evaluation of oil and fatty acid composition in seed of cotton accessions from various countries. – Journal of the Science of Food and Agriculture 87(2): 340-347.
[32] Maguire, J. D. (1962): Speed of germination-aid in selection and evaluation for seedling emergence and vigor. – Crop Sci. 2: 176-177.
[33] Maluf, W. R., Tigchelaar, E. C. (1982): Relationship between fatty acid composition and low-temperature seed germination in tomato. – Journal of American Society Horticulture Science 107: 620-623.

http://www.aloki.hu ● ISSN 1589 1623 (Print) ● ISSN 1785 0037 (Online)
DOI: http://dx.doi.org/10.15666/aeer/…..1605_68576872
© 2018, ALÖKI Kft., Budapest, Hungary

[34] Marani, A., Dag, J. (1962): Germination of seeds of cotton varieties at low temperatures. – J. Agric. Res. 44: 367-38.
[35] McDonald, M. B. (1999): Seed deterioration: physiology, repair and assesment. – Seed Sci. and Tech. 27: 177-237.
[36] Metzer, R. B. (1987): Seed vigor index-field emergence relationships. – Proc. Cotton Prod. Res. Conf. 1987: 130-131.
[37] Norfleet, M. L., Reeves, L., Burmester, C. H., Monks, C. D. (1998): Optimal planting dates for cotton in the Tennessee Valley of North Alabama. – Field Crops Abst. 51(4).
[38] Özbek, N. (2011): The determination of relationships between lint quality and seed characteristics in cotton (*Gossypium hirsutum* L.). – Ph.D. Thesis, Department of Department of Crop Science, Institute of Science and Technology, Universtiy of Aydın Adnan Mendere, Aydın.
[39] Pahlavani, M. H., Miri, A. A., Kazemi, G. (2008): Response of oil and protein content to seed size in cotton. – International Journal of Agriculture & Biology 10: 643-647.
[40] Porter, P. M., Sullıvan, M. J., Harvey, L. H. (1997): Cotton cultivar response to planting dates on the Southeastern Coastal Plain. – Journal of Production Agriculture 9(2): 223.
[41] Raju, A. R., Kharche, S. G. (1994): Effects of sowing time and plant population on fiber quality of cotton hybrids varieties. – Field Crops Abst. 47(4).
[42] Ramey, N. H. (1984): The oil and nitrogen content of samples from the regional cotton variety tests. – Presented at the 33rd Oilseed Processing Clinic. New Orleans, LA. January 16-17.
[43] Sharma, D., Sarma, N. N., Paul, S. R. (1998): Performance of upland cotton (*Gossypium hirsutum* L.) varieties for early-sowing condition in hill slope of Assam. – Field Crops Abst. 51(5).
[44] Sheikh, S. A., Rustamani, M. A., Keerio, M. I., Memon, N. (2002): Fatty acids composition in germinating cotton seedlings affected by high temperature stress. – Pakistan Journal of Applied Sciences 2(1): 97-99.
[45] Smith, C. W., Varvil, J. J. (1984): Standard and cool germination test compared with field emergence in upland cotton. – Agronomy J. 76: 587-589.
[46] Speed, T. R., Krieg, D. R., Jividen, G. (1996): Relationship between cotton seedling cold tolerance and physical and chemical properties. – Proceedings of the Beltwide Cotton Conference, National Cotton Council, Memphis, TN 2: 1170-1171.
[47] Staus, H. C., Hopper, N. W. (1983): Evaluation of several tests to determine seed quality of cotton. – Proc. Beltwide Cotton Prod. Res. Conf. 1983: 38.
[48] Tolliver, J., Savoy, B. R., Drummond, E. A. (1997): Cool germination test on cotton variability between seed testing laboratories. – Proc. of the Beltwide Cotton Conf 1997: 442-443.
[49] Tomar, S. P. S., Tomar, S. S., Jain, V. K. (1991): Effect of sowing dates. Nitrogen levels and varieties on Hirsutum cotton. – Field Crops Abst. 44(41).
[50] Tripathi, R. S., Khan, M. L. (1990): Effects of seed weight and microsite characteristics on germination and seedling fitness in two species of quercus in a subtropical wet hill forest. – JSTOR Oikos 57(3): 289-296.
[51] Tuck, C. A., Tan, D. K. Y., Bange, M. P., Stiller, W. N. (2006): Cold-tolerance screening for cotton cultivars using germination chill protocols. – http://www.commbank.com.au/.
[52] Wanjura, D. F., Buxton, D. R. (1972): Hypocotyl and radicle elongation of cotton as affected by soil environment. – Agron. J. 64: 431-434.
[53] Zimmerman, D. C., Klosterman, H. J. (1959): The distribution of fatty acids in linseed oil from the word collection of flax varieties. – Proc. North Dakota Acad. Sci. 13: 71-75.

http://www.aloki.hu ● ISSN 1589 1623 (Print) ● ISSN 1785 0037 (Online)
DOI: http://dx.doi.org/10.15666/aeer/…..1605_68576872
© 2018, ALÖKI Kft., Budapest, Hungary

EFFECTS OF TiO_2 NANOPARTICLES ON MAIZE (*ZEA MAYS* L.) GROWTH, CHLOROPHYLL CONTENT AND NUTRIENT UPTAKE

DAĞHAN, H.

Department of Soil Science and Plant Nutrition, Faculty of Agriculture, University of Eskisehir Osmangazi, 26160 Eskisehir, Turkey
(phone: +90-222-324-2991; fax: +90-222-324-2990)

**Corresponding author*
e-mail: hdaghan@ogu.edu.tr

(Received 5th Aug 2018; accepted 28th Sep 2018)

Abstract. Nanotechnology, as the source of new industrial materials, has been widely used in recent years and has appeared in almost every field. Nowadays, nanoparticles are used in many areas like textiles, cosmetics, pharmaceuticals, automotive and defense (military) industries. The usage of nanoparticles has increased in recent years, but their effects on the environment are not exactly known. In this study, TiO_2 nanoparticle (TiO_2-NP) was applied at increasing concentrations (0, 5, 10 and 20 mg L^{-1}) to maize (*Zea mays* L.) plant grown in hydroponic culture at 16 h light/8 h dark, 25/20 °C temperature, 60% humidity and 10 Klux light intensity for 20 days. Application of TiO_2-NP on biomass production, nitrogen (N), phosphorus (P), potassium (K), zinc (Zn), iron (Fe), manganese (Mn), copper (Cu) and chlorophyll contents were investigated. The results showed that the plants' shoot and root biomass and leaf chlorophyll contents were significantly reduced with increasing TiO_2-NP applications. On the other hand, TiO_2-NP applications positively affected macro- (N, P, K) and micronutrients' (Zn, Mn, Cu) concentration except for Fe. Compared to the control treatment, the concentration of Zn, Mn, Cu, N and P significantly increased with the application of TiO_2 nanoparticles. Consequently, TiO_2-NPs treatments have increased nutrient uptake of maize excluding iron while decreased the dry biomass of maize at high doses.
Keywords: *chlorophyll, nanoparticle, maize, phytotoxicity, TiO_2 nanoparticles*

Abbreviations: TEM: Transmission Electron Microscopy; SEM: scanning electron microscopy; DW: dry weight; ICP-MS: inductively coupled plasma mass spectrometry; SPAD: soil-plant analysis development

Introduction

Nanotechnology, one of the most popular scientific disciplines, has been widely used in different branches of science and technology in recent years (Siddiqui et al., 2015; Reddy et al., 2016; Cox et al., 2017). Although today nanotechnology has a billion-dollar industry around the world, ongoing comprehensive research shows that this technology is still in the discovery stage and that technology is expected to grow even further (Reddy et al., 2016; Cox et al., 2017).

Nanoparticles, rare in nature and being used in nanotechnology are widely used in cosmetics, agriculture, industry, technology, transportation, pharmaceutics, and energy due to their different properties (Kavaz, 2011; Rafique et al., 2014; Rastogi et al., 2017). The nano is a word from the Greek and it means very small, tiny. The size of these particles are less than 100 nm and they have unique chemical and physical properties (Du et al., 2011; Doğaroğlu and Köleli, 2017a; Rastogi et al., 2017). These properties of nanoparticles depend on their size, shape, morphology and properties of surface area.

Nanoparticles (NPs) are widely produced to supply increasing industrial demands. Enormous and unlimited use of NPs in recent years has led researchers to investigate this issue, regarding the problems that may arise in practice, and the environmental impact of these problems (Gottschalk et al., 2015; Tolaymat et al., 2015; Reddy et al., 2016).

http://www.aloki.hu ● ISSN 1589 1623 (Print) ● ISSN 1785 0037 (Online)
DOI: http://dx.doi.org/10.15666/aeer/1605_68736883
© 2018, ALÖKI Kft., Budapest, Hungary

Metallic nanoparticles such as TiO_2, ZnO, CuO etc., are the most common nanoparticles used in agriculture and industry. TiO_2-NP is the oxide of the metal titanium (Ti) and belongs to the family of transition metal oxides (Samadi et al., 2014; Lyu et al., 2017). Titanium dioxide is the most-produced nanoparticle (88.000 metric tons/year) after silicon dioxide (SiO_2) in the world (Medina-Velo et al., 2017) and it is used quite wide range areas such as cosmetics, pharmaceuticals, paints, coatings, antibacterial products, textiles (Da Costa and Sharma, 2015; Cox et al., 2017). Because of its intensive usages, its entry into the environment, concentration of soil and water is increasing day by day. There is no data directly published about the toxic concentration of TiO_2 and other metallic nanoparticles in soil and water (Da Costa and Sharma, 2015). But the knowledge about the toxic effect of TiO_2-NPs on the environment is limited and not well known. However, the researches done to evaluate the effects of TiO_2-NPs on the plant are not much. Several studies reported TiO_2 impact on plant development and physiology (Lyu et al., 2017). According to some reports, TiO_2-NPs are beneficial to some organisms and have positive effects on plant growth, chlorophyll synthesis and photosynthesis (Lyu et al., 2017). For instance, in spinach, TiO_2-NPs increased chlorophyll synthesis, photosynthesis and plant dry weight (Zheng et al., 2005; Hong et al., 2005). On the other hand, some investigations have reported that TiO_2-NP has an adverse impact on seed germination and plant growth and may lead to phytotoxicity (Samadi et al., 2014; Ruttkay-Nedecky et al., 2017).

Maize is a cereal plant that has been the most-cultivated crops in the world after wheat and rice. According to the Food and Agriculture Organization (FAO), the world maize harvested area was 1.8 billion hectares with an approximately billion tones production in 2016 (FAO, 2018). For these reasons, maize was used in the current experiment to investigate the effects of TiO_2-NP on growth and development of maize and the possible participation of TiO_2-NP in the food chain.

The toxic effects of nanoparticles such as TiO_2, ZnO, CuO, etc. on the plant were tested in petri-dishes (Lee et al., 2010; Castiglione et al., 2011; Doğaroğlu and Köleli, 2017a, b) or in the agar medium (Lee et al., 2008; Nair and Chung, 2014). These experiments could give very limited information. However, a hydroponic experiment gave more information about the uptake, accumulation of NPs in a different part of plants (shoot and root) and also the impact of these NPs on plants (such as chlorophyll content, plant growth, etc.) in a short time (Pošćić et al., 2016). After seedlings, plants would need essential mineral nutrients in growing media for healthy growth. Because of that reason, hydroponics systems with nutrient supply would be useful for phytotoxicity testing (Song et al., 2013). Because of these advantages, a hydroponic experiment was conducted under controlled climate chamber condition. The effect of TiO_2-NPs on growth, chlorophyll content, and mineral nutrient uptake of maize was investigated.

Materials and methods

The TiO_2 (<100 nm) nanoparticles, used for the hydroponic experiment, were synthesized by Dr Birol Karakaya in Gebze MAM institute.

The identification of TiO_2 nanoparticle as one of the primary nanomaterials by the Organization for Economic Co-operation and Development (OECD) is the most important criterion in selecting the nanoparticles to be used in this study (OECD, 2013). Maize, a widely grown plant, was used as plant material in this study. KERMESS (FAO 600-630) hybrid maize seeds were obtained from the KWS Seed Company.

http://www.aloki.hu ● ISSN 1589 1623 (Print) ● ISSN 1785 0037 (Online)
DOI: http://dx.doi.org/10.15666/aeer/1605_68736883
© 2018, ALÖKI Kft., Budapest, Hungary

The synthesized and characterization of nanomaterials

Titanium dioxide (~30-60 nm) nanoparticles were synthesized by Dr. Birol Karakaya through using a combination of Sol-Gel and hydrothermal synthesis with small changes in traditional methods at a research centre (BME-Kocaeli/Turkey) (Doğaroğlu and Köleli, 2017a). In this study, Variable Pressure Field Emission Scanning Electron Microscope (VP FE-SEM) (Carl Zeiss Supra 55) was used to characterize TiO_2-NPs coated with platinum-palladium. Titanium dioxide nanoparticles coated with platinum-palladium were imaged in SEM and elemental analysis was performed with EDX.

Hydroponic experiment

The maize seeds were germinated in a mixture of peat and perlite (1:1 w/w). When seedlings were getting 2-3 leaves and hairy rooted, they were transferred into the 4.5 L polyethylene pots supplied with the Hoagland nutrient solution medium (Hoagland and Arnon, 1950). The composition of the nutrient solution was as follows; the macronutrients (1 mM KH_2PO_4, 3 mM KNO_3, 0.25 mM $MgSO_4.7H_2O$, 2 mM $Ca(NO_3)_2.4H_2O$ and $2.5x10^{-2}$ mM KCI) and micronutrients (1 µM $MnSO_4.H_2O$, 1 µM $ZnSO_4.H_2O$, 0.25 µM $CuSO_4.H_2O$, 0.25 µM $(NH_4)_6Mo_7O_{24}$, and 0.125 µM H_3BO_3), pH was 5.2. Freshly prepared 0.1 mM Fe EDTA solution was added to each pot for the supply of the iron requirement of the maize plants. The nutrient solution was continuously aerated with a pump (KNF vacuum pump No.22.AN.18). Five maize plants were transferred to the pots and TiO_2-NP was applied with increasing dose 0, 0.5, 10, 20 mg L^{-1} to the nutrient culture. The nutrient solution was changed every 2-3 days. The plants were grown under controlled conditions (16/8 h light/dark period, 25/20 °C, 60% humidity and 10 Klux light intensity) for 20 days. The experiment design was a randomized block method with tree replication.

The effects of TiO_2-NP application on leaf chlorophyll contents were determined by the Konica Minolta SPAD-502 (Konica-Minolta, Japan, 0.06 cm^{-2} measurement area and its accuracy is 1.0 SPAD units) chlorophyll meter. The SPAD-502 calculates the chlorophyll content as soil Plant Analysis Development value (SPAD value). After the chlorophyll measurements, the plants were harvested as shoots and roots part and then washed with distilled water. After that, all samples were dried at 65°C in an oven until reaching a constant weight. The dry weights of plant samples were taken, and then ground in the mixer mill (Retsch MM301) for plant analysis. Plant samples were digested with HNO_3 and H_2O_2 in microwave oven (MarsXpres CEM). Total K, P, Zn, Fe, Cu, and Mn concentrations of the samples were determined by Inductively Coupled Plasma Mass Spectrometry (ICP-MS) (Agilent 7500ce Model). All results were given based on dry plant matter at 65 °C. The nitrogen concentrations of shoots were analyzed according to Bremner and Mulvaney (1982). Certified reference materials (SRM 1573A, SRM 1547) were also analyzed in order to check the accuracy of the extraction technique used in this study.

Statistical analysis

The variance analysis of the results was statistically analyzed by using the IBM SPSS-20 statistical analysis package program. The difference between the averages was grouped by applying the Least Significant Difference (LSD) test.

http://www.aloki.hu ● ISSN 1589 1623 (Print) ● ISSN 1785 0037 (Online)
DOI: http://dx.doi.org/10.15666/aeer/1605_68736883
© 2018, ALÖKI Kft., Budapest, Hungary

Results and discussion

The characterization of TiO_2-NP

The SEM image of synthesized TiO_2-NPs is shown in *Figure 1* and the average size of nanoparticles was found about 30-50 nm^{-1}. The SEM image showed that the TiO_2-NPs tend to agglomerate and this might be based on its hydrophobic surface properties (Nia et al., 2015; Doğaroğlu and Köleli, 2017a). In addition, SEM-EDX showed that Ti, O and C were identified using SEM-EDX (*Fig. 1*).

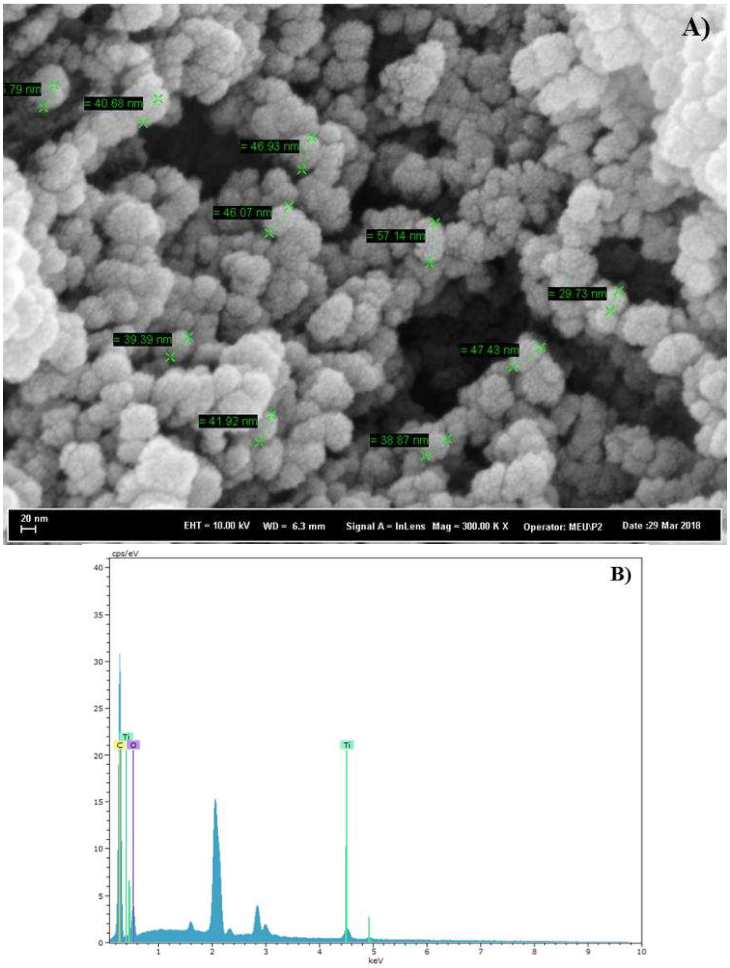

Figure 1. *SEM image and EDX spectrum of synthesized the TiO_2-NPs. Scanning Electron microscopic image of TiO_2-NPs (A) and elemental analysis of the TiO_2-NPs (B)*

Hydroponic experiment

The effects of increasing doses (0, 5, 10 and 20 mg L^{-1}) of TiO_2-NP treatment on maize plants were investigated in hydroponic culture experiment.

Morphological observations and chlorophyll content

Chlorophyll does not only give plants green color, it is also vital for plants. It produces energy and carbohydrates for physiological processes, plant growth, and development (Tan et al., 2017). If chlorophyll damage with any phytotoxicity, plant

http://www.aloki.hu ● ISSN 1589 1623 (Print) ● ISSN 1785 0037 (Online)
DOI: http://dx.doi.org/10.15666/aeer/1605_68736883
© 2018, ALÖKI Kft., Budapest, Hungary

growth also reduces. Generally, the phytotoxicity of nanoparticle negatively affects the physiology and growth of a plant. Physiologically, the chlorophyll content leads to a decrease and this cause decrease in biomass production. The phytotoxic effects of NP-TiO_2 are related to the size, concentration, surface properties of the particles and their effects on germination and chlorophyll content, biomass production and other parameters (Samadi et al., 2014; Doğaroğlu and Köleli, 2017a; Yaqoob et al., 2018). Very slight chlorosis at 5 and 10 mg TiO_2 L^{-1} doses, and moderate chlorosis at 20 mg TiO_2 L^{-1} dose on the leaves of maize were observed (*Fig. 2*). The roots of plants had no significant visual symptoms.

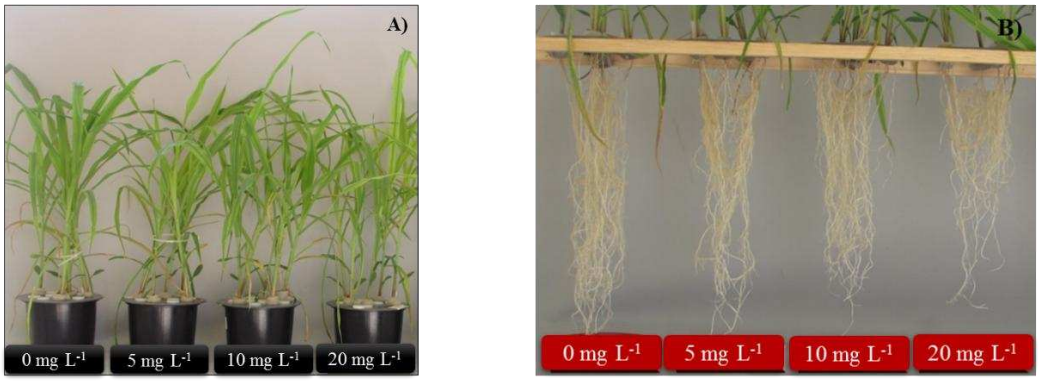

Figure 2. *TiO_2-NP application effects on shoot (A) and root (B) growth of maize*

Increasing TiO_2-NP applications has significantly reduced the chlorophyll contents of old and young leaves (*Fig. 3*). While the highest chlorophyll contents (SPAD Unit) were measured in old and young leaves of the control plants (24.2 and 30.4 respectively) and the lowest chlorophyll content (14.2 SPAD Unit) was measured on old leaves at 20 mg TiO_2 L^{-1} dose ($p \leq 0.01$). Doğaroğlu and Köleli (2017a) had the similar results. They have reported the chlorophyll contents of barley decreased at 20 mg kg^{-1} ZnO-NP and TiO_2-NP treatments. On the contrary to our result, many studies reported that TiO_2-NPs treatments increased photosynthetic activity and chlorophyll content of plants such as spinach (Hong et al., 2005), cucumber (Servin et al., 2012, 2013), Arabidopsis (Lenaghan et al., 2013), rapeseed (Li et al., 2015).

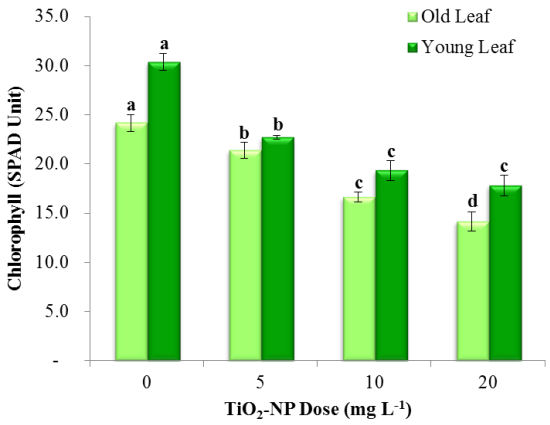

Figure 3. *TiO_2-NP application effects on chlorophyll contents of maize. Letter(s) on each bar show significant level ($p < 0.01$)*

http://www.aloki.hu ● ISSN 1589 1623 (Print) ● ISSN 1785 0037 (Online)
DOI: http://dx.doi.org/10.15666/aeer/1605_68736883
© 2018, ALÖKI Kft., Budapest, Hungary

Dry weight (DW)

The dry weights (DWs) of the shoot and root decreased with the increasing TiO_2-NP application compared to the control treatment plant (*Fig. 4*). Controlled plant was has produced the highest shoot (2.13 g) and root (0.192 g) DWs. The lowest shoot (1.50 g) DW was obtained at 20 mg L^{-1} TiO_2-NP application dose. The root DW decreased up to 10 mg L^{-1} TiO_2 doses; however, DW production increased at 20 mg L^{-1} TiO_2 doses. Because of chlorophyll inhibition, the phytotoxicity of TiO_2-NPs application may be reduced with shoot and root DWs of the plant. In addition, these decreases may depend on the TiO_2-NPs size and surface properties with the application of increasing doses of TiO_2-NPs.

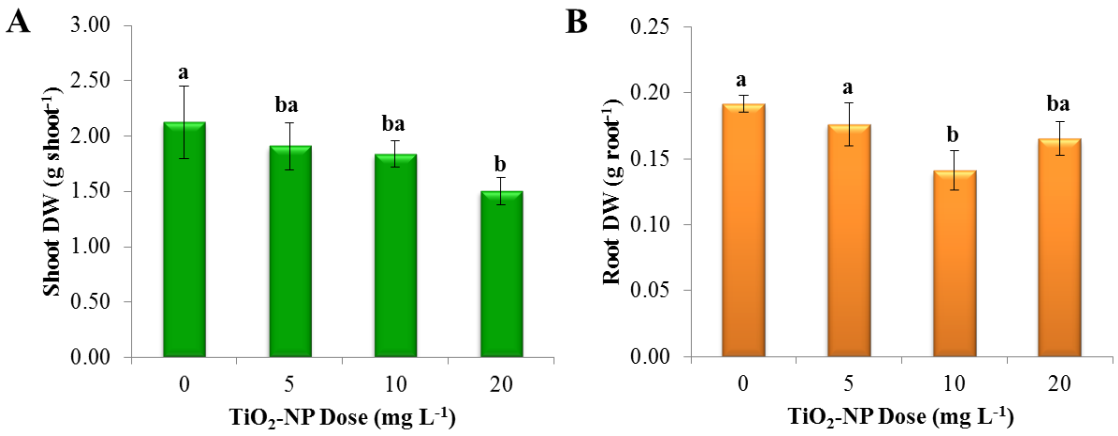

Figure 4. *TiO_2 application effects on shoot (A) and root (B) DWs of maize. Letter(s) on each bar show significant level ($p < 0.05$)*

Asli and Neuman (2009), that the plant leaf growth was inhibited by 300 mg TiO_2 L^{-1} treatment in maize, reported similar finding. Du et al. (2011) reported that the application of TiO_2 and ZnO nanoparticles (10 g TiO_2-NPs and 5 g ZnO-NPs mixed with 110 kg soil separately) reduced wheat growth and enzyme in field conditions. Feizi et al. (2012) investigated the effect of increasing doses of TiO_2-NPs (0, 5, 20, 40, 60 and 80 mg L^{-1}) on the fennel seed germination and early growth. On the contrary, they reported that the total germination percentage increased at 60 mg L^{-1} TiO_2 application after 14 days of seed incubation. The germination of *Zea mays* L. and *Vicia narbonensis* L. seeds were delayed by TiO_2-NPs applied at concentrations ranging from 0.2% to 4.0% for the first 24 hours (Castiglione et al., 2011). Kumar and Udayasoorian (2014) investigated the effect of three different types of nanoparticles (ZnO, TiO_2, and Al_2O_3) on growth parameters (germination percentage, vigor index, shoot and root length) of maize. They found that the highest toxic effect on growth parameters of the 2000 mg L^{-1} dose of the all three nanoparticles suspensions in the order of $ZnO > TiO_2 > Al_2O_3$.

Mineral nutrient concentrations

Unfortunately, many scientists have not analyzed or reported the nutrient concentration of plant after nanoparticle exposure. In fact, the relationship of toxicity (such as heavy metal, NPs, salt etc.) and plant nutrient uptake can be synergistic, antagonistic or neutral. Because of this reason, when the phytotoxic effect of

http://www.aloki.hu ● ISSN 1589 1623 (Print) ● ISSN 1785 0037 (Online)
DOI: http://dx.doi.org/10.15666/aeer/1605_68736883
© 2018, ALÖKI Kft., Budapest, Hungary

nanoparticles is investigated, the mineral nutrient concentration should also be also measured. In this study, the effects of increasing TiO_2-NP doses on macro (N, P and K) and micro (Cu, Fe, Mn and Zn) nutrient element concentrations of the shoot were investigated (*Table 1*) and root (*Table 2*).

Table 1. *The effects of increasing TiO_2-NP application on mineral nutrient concentrations (N, P, K, Zn, Fe, Mn, Cu) in shoots*

Cultivar	TiO_2-NP (mg L^{-1})	N	P	K	Zn	Fe	Mn	Cu
		(%)			(mg kg^{-1})			
Maize	0	2.88 b[§]	0.50 b	7.40	36.8 b	64.3 a	62.0 c	6.49
	5	3.02 b	0.60 a	7.41	44.5 a	56.8 b	75.0 b	6.04
	10	3.24 a	0.62 a	7.52	43.0 a	54.3 bc	77.6 b	6.19
	20	3.20 a	0.64 a	7.69	44.4 a	51.5 c	84.2 a	6.34
Dose	F	17.4**	15.0**	3.20n.s.	5.46*	15.1**	25.6**	2.24n.s.

*$p \leq 0.05$, **$p \leq 0.01$. n.s.: not significant. [§]Means followed by the same letters in a column do not differ significantly by the LSD test ($p < 0.05$)

The shoot nutrient (N, P, K, Zn, Cu, Mn) concentrations were increased with TiO_2-NP applications except for Fe (*Table 1*). The highest N (3.24%), P (0.64%), K (7.69%), Zn (44.5 mg kg^{-1}) and Mn (84.2 mg kg^{-1}) were recorded at the shoot of TiO_2 treatment plants compared to control plant. However, the highest Fe (64.3 mg kg^{-1}) and Cu (6.49 mg kg^{-1}) concentrations were obtained from control plant. While TiO_2-NP applications were positively affecting N, P, K, Zn and Mn uptake, negatively affecting Fe and Cu uptake to the shoot of the plant. All results were significantly important ($p < 0.05$) except for K and Cu concentrations result.

The highest Fe (4618 mg kg^{-1}) concentration was obtained in the roots of maize plant ($p \leq 0.01$) (*Table 2*). However, the highest concentrations of P (1.23%), K (4.80%), Zn (119 mg kg^{-1}), Mn (71.2 mg kg^{-1}), and Cu (48.2 mg kg^{-1}) were obtained at 20 mg L^{-1} TiO_2-NP dose in plant roots. All results were significantly important ($p < 0.01$) except for the Mn concentration result.

Table 2. *The effects of increased TiO_2-NP application on mineral nutrient concentrations (P, K, Zn, Fe, Mn, Cu) in roots*

Cultivar	TiO_2-NP (mg L^{-1})	P	K	Zn	Fe	Mn	Cu
		(%)		(mg kg^{-1})			
Maize	0	1.04 b[§]	3.85 c	93.9 c	4618 a	56.2	39.5 c
	5	0.97 b	4.48 b	109 b	3797 b	62.5	36.4 d
	10	1.05 b	4.34 b	110 b	3350 c	65.7	45.5 b
	20	1.23 a	4.80 a	119 a	1501 d	71.2	48.2 a
Dose	F	23.3**	53.2**	68.5**	493**	3.88n.s.	77.5**

**$p \leq s0.01$. n.s.: not significant. [§]Means followed by the same letters in a column do not differ significantly by the LSD test ($p < 0.05$)

Tan et al. (2017) reported that increasing amount of three different TiO_2-NPs particles (unmodified, hydrophobic, and hydrophilic TiO_2-NPs) affected plant growth

http://www.aloki.hu ● ISSN 1589 1623 (Print) ● ISSN 1785 0037 (Online)
DOI: http://dx.doi.org/10.15666/aeer/1605_68736883
© 2018, ALÖKI Kft., Budapest, Hungary

and mineral nutrition concentration of basil plants. Compared with the control, hydrophobic and hydrophilic TiO_2-NPs significantly reduced seed germination (41% and 59%, respectively); while unmodified and hydrophobic TiO_2-NPs significantly decreased shoot biomass (31% and 37%, respectively). On the other hand, they reported that the unmodified particles increased Cu (104%) and Fe (90%); hydrophilic particles increased Fe (90%); while hydrophobic increased Mn (339%) but reduced Ca (71%), Cu (58%), and P (40%) at 500 mg kg^{-1} soil treatment. Servin et al. (2013) reported that TiO_2-NPs (27 ± 4 nm) treatment (250, 500, and 750 mg kg^{-1}) to the soil were enhanced K and P concentration of cucumber fruit.

Pošćić et al. (2016), studied the application of increasing doses (0, 500 and 1000 mg kg^{-1}) of cerium oxide ($nCeO_2$) and titanium dioxide ($nTiO_2$) nanoparticles effects on the nutrient concentration of barley (*Hordeum vulgare* L). They were obtained significantly increased Ca and significantly decreased sulfur (S) in both $nTiO_2$ treatments. Potassium concentration was decreased at 1000 mg kg^{-1} $nTiO_2$. Manganese and Zn concentrations were increased at 500 mg $nTiO_2$ kg^{-1} treatment.

All these results indicated that there was a relation between TiO_2-NPs and mineral nutrient uptake. On the other hand, NPs size, concentrations, application medium (soil, hydroponic, agar, etc.) are also related to the plant nutrient uptake and toxic effects of NPs on plant physiology and growth.

Concluding remarks

The TiO_2-NP application decreased chlorophyll and plant growth, while interestingly, it enhanced some of the mineral nutrient uptakes such as N, P, and K. This study showed possible toxic effect of TiO_2-NPs on maize growth and physiology. Still, some uptake and toxic effect mechanism of NPs in maize plant is unknown. In the future study, it will be necessary to investigate the effects of phytotoxicity mechanisms, the size distribution of nanoparticles in plant and possible effects of uptake and translocation of nanoparticles by plants.

However, the potential impacts of nanoparticles on agricultural and environmental systems, their transport and mobility in the ecosystem, accumulation and toxicity on plants and the risk of entry of these particles into the food chain need to be investigated in the future especially plants grown in natural environments or in the field.

Acknowledgements. The author acknowledges the financial support of the project by Eskisehir Osmangazi University Scientific Research Fund (BAP, Project No: 201423049). The author would like to thank Dr. Nurdilek Gülmezoğlu and Dr. Nurcan Köleli for their valuable advice, comments, and Dr. Birol Karakaya for preparing the TiO_2-NPs.

Conflict of Interest. The authors have declared no conflict of interest.

REFERENCES

[1] Asli, S., Neumann, P. M. (2009): Colloidal suspensions of clay or titanium dioxide nanoparticles can inhibit leaf growth and transpiration via physical effects on root water transport. – Plant Cell Environment 32: 577-584. DOI: 10.1111/j.1365-3040.2009.01952.x.

http://www.aloki.hu ● ISSN 1589 1623 (Print) ● ISSN 1785 0037 (Online)
DOI: http://dx.doi.org/10.15666/aeer/1605_68736883
© 2018, ALÖKI Kft., Budapest, Hungary

[2] Bremner, J. M., Mulvaney, C. S. (1982): Total Nitrogen. – In: Page, A. L., Miller, R. H., Keeny, D. R. (eds.) Methods of Soil Analysis, American Society of Agronomy and Soil Science Society of America, Madison, pp. 1119-1123.

[3] Castiglione, M. R., Giorgetti, L., Geri, C., Cremonini, R. (2011): The effects of nano-TiO_2 on seed germination, development and mitosis of root tip cells of *Vicia narbonensis* L. and *Zea mays* L. – Journal of Nanoparticle Research 13: 2443-2449. DOI: 10.1007/s11051-010-0135-8.

[4] Cox, A., Venkatachalam, P., Sahi, S., Sharma, N. (2017): Reprint of: Silver and titanium dioxide nanoparticle toxicity in plants: A review of current research. – Plant Physiology and Biochemistry 110: 33-49.

[5] Da Costa, M. V. J., Sharma, P. K. (2015): Influence of titanium dioxide nanoparticles on the photosynthetic and biochemical processes in *Oryza sativa*. – International Journal of Recent Scientific Research 6(1): 2445-2451.

[6] Doğaroglu, Z. G., Köleli, N. (2017a): TiO_2 and ZnO nanoparticles toxicity in barley (*Hordeum vulgare* L.). – Clean Soil, Air, Water 45(11): 1700096 (1-7). DOI: 10.1002/clen.201700096.

[7] Doğaroğlu, Z. G., Köleli, N. (2017b): Effects of TiO_2 and ZnO nanoparticles on germinating and antioxidant system in wheat (*Triticum Aestivum* L.). – Applied Ecology and Environmental Research 15(3): 1499-1510. DOI: 10.15666/aeer/1503_14991510.

[8] Du, W., Sun, Y., Ji, R., Zhu, J., Wu, J., Guo, H. (2011): TiO_2 and ZnO nanoparticles negatively affect wheat growth and soil enzyme activities in agricultural soil. – Journal of Environmental Monitoring 13: 822-828.

[9] FAO (2018): http://www.fao.org/faostat/en/#data/QC/visualize. – Accessed on 04.06.2018.

[10] Feizi, H., Moghaddam, P. R., Shahtahmassebi, N., Fotovat, A. (2012): Impact of bulk and nanosized titanium dioxide (TiO_2) on wheat seed germination and seedling growth. – Biological Trace Element Research 146(1): 101-106. DOI: 10.1007/s12011-011-9222-7.

[11] Gottschalk, F., Nowack, B., Lassen, C., Kjølholt, J., Christensen, F. (2015): Nanomaterials in the Danish environment. Modelling exposure of the Danish environment to selected nanomaterials. – Environmental Project No. 1639, 2015 from the Danish Environmental Protection Agency. http://www2.mst.dk/Udgiv/publications/2015/01/978-87-93283-60-2.pdf.

[12] Hoagland, D. R., Arnon, D. I. (1950): The Water Culture Method for Growing Plants without Soil. – The College of Agriculture, University of California, California Agriculture Experiment Station Circular, Berkeley, 347, pp. 1-32.

[13] Hong, F., Yang, F., Liu, C., Gao, Q., Wan, Z., Gu, F., Wu, C., Ma, Z., Zhou, J., Yang, P. (2005): Influences of nano-TiO_2 on the chloroplast aging of spinach under light. – Biological Trace Element Research 104: 249-60. DOI: 10.1385/BTER: 104: 3: 249.

[14] Kavaz, D. (2011): Nanoparticles. – Nanobülten Magazine, University of Hacettepe 13: 12-19 (in Turkish).

[15] Kumar, K. V., Udayasoorian, C. (2014): Toxicity potential of different metal oxides nanoparticles on germination of maize plant. – Global Journal for Research Analysis (GJRA) 3(1): 116-118.

[16] Lee, C. W., Mahendra, S., Zodrow, K., Li, D., Tsai, Y. C., Braam, J., Alvarez, P. J. (2010): Developmental phytotoxicity of metal oxide nanoparticles to *Arabidopsis thaliana*. – Environmental Toxicology and Chemistry 29(3): 669-675.

[17] Lee, W. M., An, Y. J., Yoon, H., Kweon, H. S. (2008): Toxicity and bioavailability of copper nanoparticlees to the terrestrial plants mung bean (*Phaseolus radiatus*) and wheat (*Triticum aestivum*): plant agar test for water-insoluble nanoparticles. – Environmental Toxicology Chemistry 27: 1915-1921.

[18] Lenaghan, S. C., Li, Y., Zhang, H., Burris, J. N., Stewart, C. N., Parker, L. E., Zhang, M. (2013): Monitoring the environmental impact of TiO_2 nanoparticles using a plant-based

http://www.aloki.hu ● ISSN 1589 1623 (Print) ● ISSN 1785 0037 (Online)
DOI: http://dx.doi.org/10.15666/aeer/1605_68736883
© 2018, ALÖKI Kft., Budapest, Hungary

sensor network. – IEEE Transactions on Nanotechnology 12: 182-189. https://doi.org/10.1109/TNANO.2013.2242089.

[19] Li, J., Naeem, M. S., Wang, X., Liu, L., Chen, C., Ma, N., Zang, C. (2015): Nano-TiO_2 is not phytotoxic as revealed by the oilseed rape growth and photosynthetic apparatus ultrastructural response. – PLoS ONE 10(12): e0143885. https://doi.org/10.1371/journal.pone.0143885.

[20] Lyu, S., Wei, X., Chen, J., Wang, C., Wang, X., Pan, D. (2017): Titanium as a beneficial element for crop production. – Frontiers in Plant Science 8: 597. DOI: 10.3389/fpls.2017.00597.

[21] Medina-Velo, I. A., Peralta-Videa, J. R., Gardea-Torresdey, J. L. (2017): Assessing plant uptake and transport mechanisms of engineered nanomaterials from soil. – MRS Bulletin 42(05): 379-384. DOI: 10.1557/mrs.2017.87.

[22] Nair, P. M. G., Chung, I. M. (2014): Physiological and molecular level effects of silver nanoparticles exposure in rice (*Oryza sativa* L.) seedlings. – Chemosphere 112: 105-113.

[23] Nia, M. H., Rezaei-Tavirani, M., Nikoofar, A. R., Masoumi, H., Nasr, R., Hasanzadeh, H., Jadidi, M., Shadnush, M. (2015): Stabilizing and dispersing methods of TiO_2 nanoparticles in biological studies, – Journal of Paramedical Sciences 6(2): 96-105.

[24] OECD (2013): Organization for Economic Co-operation and Development (OECD). OECD Environment, Health and Safety Publications. – Series on the Safety of Manufactured Nanomaterials, No.37, ENV/JM/MONO (2013) 2. http://search.oecd.org/officialdocuments/displaydocumentpdf/?cote=env/jm/mono(2013)2&doclanguage=en. Accessed on 15.06.2018.

[25] Pošćić, F., Mattiello, A., Fellet, G., Miceli, F., Marchiol, L. (2016): Effects of cerium and titanium oxide nanoparticles in soil on the nutrient composition of barley (*Hordeum vulgare* L.) kernels. – International Journal of Environmental Research and Public Health 13(6): 577. DOI: 10.3390/ijerph13060577.

[26] Rafique, R., Arshad, M., Khokhar, M. F., Qazi, I. A., Hamza, A., Virk, N. (2014): Growth response of wheat to titania nanoparticles application. – NUST Journal of Engineering Sciences 7(1): 42-46.

[27] Rastogi, A., Zivcak, M., Sytar, O., Kalaji, H. M., He, X., Mbarki, S., Brestic, M. (2017): Impact of metal and metal oxide nanoparticles on plant: a critical review. – Frontiers in Chemistry 5: 78. DOI: 10.3389/fchem.2017.00078.

[28] Reddy, P. V. L., Hernandez-Viezcas, J. A., Peralta-Videa, J. R., Gardea-Torresdey, J. L. (2016): Lessons learned: Are engineered nanomaterials toxic to terrestrial plants? – Science of the Total Environment 568: 470-479.

[29] Ruttkay-Nedecky, B., Krystofova, O., Nejdl, L., Adam, V. (2017): Nanoparticles based on essential metals and their phytotoxicity. – Journal of Nanobiotechnology 15(33): 1-19. DOI: 10.1186/s12951-017-0268-3.

[30] Samadi, N., Yahyaabadi, S., Rezayatmand, Z. (2014): Effect of TiO_2 and TiO_2 nanoparticle on germination, root and shoot length and photosynthetic pigments of *Mentha Piperita*. – International Journal of Plant & Soil Science 3(4): 408-418.

[31] Servin, A. D., Castillo-Michel, H., Hernandez-Viezcas, J. A., Diaz, B. C., Peralta-Videa, J. R., Gardea-Torresdey, J. L. (2012): Synchrotron micro-XRF and micro-XANES confirmation of the uptake and translocation of TiO_2 nanoparticles in cucumber (*Cucumis sativus*) plants. – Environmental Science & Technology 46: 7637-7643. https://doi.org/10.1021/es300955b.

[32] Servin, A. D., Morales, M. I., Castillo-Michel, H., Hernandez-Viezcas, J. A., Munoz, B., Zhao, L., Nunez, J. E., Peralta-Videa, J. R., Gardea-Torresdey, J. L. (2013): Synchrotron verification of TiO_2 accumulation in cucumber fruit: A possible pathway of TiO_2 nanoparticle transfer from soil into the food chain. – Environmental Science & Technology 47: 11592-11598.

[33] Siddiqui, M. H., Al-Whaibi, M. H., Firoz, M., Al-Khaishany, M. Y. (2015): Role of Nanoparticles in Plants (Chapter 2). – In: Siddiqui, M. H. et al. (eds.). Nanotechnology

http://www.aloki.hu ● ISSN 1589 1623 (Print) ● ISSN 1785 0037 (Online)
DOI: http://dx.doi.org/10.15666/aeer/1605_68736883
© 2018, ALÖKI Kft., Budapest, Hungary

and Plant Sciences. Springer International Publishing, Switzerland. DOI: 10.1007/978-3-319-14502-0_2.

[34] Song, U., Jun, H., Waldman, B., Roh, J., Kim, Y., Yi, J., Lee, E. J. (2013): Functional analyses of nanoparticle toxicity: A comparative study of the effects of TiO_2 and Ag on tomatoes (*Lycopersicon esculentum*). – Ecotoxicology and Environmental Safety 93: 60-67.

[35] Tan, W., Du, W., Barrios, A. C., Armendariz, Jr. R., Zuverza-Mena, N., Ji, Z., Chang, C. H., Zink, J. I., Fernandez-Viezcas, J. A., Peralta-Videa, J. R, Gardea-Torresdey, J. L. (2017): Surface coating changes the physiological and biochemical impacts of nano-TiO_2 in basil (*Ocimum basilicum*) plants. – Environmental Pollution 222: 64-72.

[36] Tolaymat, T., El Badawy, A., Sequeira, R., Genaidy, A. (2015): A system-of systems approach as a broad and integrated paradigm for sustainable engineered nanomaterials. – Science of the Total Environment 511: 595-607.

[37] Yaqoob, S., Ullah, F., Mehmood, S., Mahmood, T., Ullah, M., Khattak, A., Zeb, M. A. (2018): Effect of waste water treated with TiO_2 nanoparticles on early seedling growth of *Zea mays* L. – Journal of Water Reuse and Desalination 8(3): 424-431. https://doi.org/10.2166/wrd.2017.163.

[38] Zheng, L., Hong, F., Lu, S., Liu, C. (2005): Effect of nano- TiO_2 on strength of naturally aged seeds and growth of spinach. – Biological Trace Element Research 104: 83-92. DOI: 10.1385/BTER:104:1:083.

http://www.aloki.hu ● ISSN 1589 1623 (Print) ● ISSN 1785 0037 (Online)
DOI: http://dx.doi.org/10.15666/aeer/1605_68736883
© 2018, ALÖKI Kft., Budapest, Hungary

CHARACTERIZATION OF *PHYTOPHTHORA CAPSICI* LEONIAN RESISTANCE IN SOME PEPPER GENOTYPES BY PRINCIPAL COMPONENT ANALYSIS

KARIPÇIN, M. Z.[1*] – SEYITOGLU, G.[1] – MIKAIL, N.[2]

[1]*Department of Horticulture, Faculty of Agriculture, Siirt University, 56100 Siirt, Turkey*

[2]*Department of Animal Science, Faculty of Agriculture, Siirt University, 56100 Siirt, Turkey*
(phone: +90-484-212-1111; fax: +90-484-223-1998)

**Corresponding author*
e-mail: zkaripcin@siirt.edu.tr

(Received 30th Jul 2018; accepted 28th Sep 2018)

Abstract. In the study, resistance analyses were performed on pepper lines and genotypes (60 genotypes) of mainly common local genotypes found in the gene pool by classical testing methods. Classical tests were first applied in seedling stage. Second inoculation (the last) was carried out (in the stage of fruit retention) on resistant genotypes determined in the first inoculation. Varieties resistant to *phytophthora capsici* (CM 334 and partially resistant P1, P2 and P4) were also included in the study. Peroxidase and catalase enzyme contents of plant materials have been determined. Scale of 0-5 was applied to inoculated plants. Five pepper properties were measured and used as original variables. The first two principal components accounted for 74% of total variance. Score plots of the first two principal components were used to map genotypes according to their morphological properties. Some relationships between genotypes and their morphological traits were obtained. The results revealed that genotypes of P1, 13 (Urfa), 25 (UKST), 38 (UI), 48 (UKDT), 57 (ANKSB) were partial resistant genotypes while CM334 was fully resistant. To conclude, principal component analysis was shown to be a useful tool for mapping the pepper genotypes in terms of *phytophthora capsici* resistance.
Keywords: *pepper, biotic stress, resist, peroxidase, catalase, PCA*

Introduction

Pepper is one of the species of genus *Capsicum* in the family *Solanaceae*. The genus *Capsicum* is divided into twenty-five different species (Baral and Bosland, 2002). *Capsicum* originates from Mexico, South Peru and Bolivia. Almost all *Capsicum* species are diploid with 12 chromosome pairs (Moscone et al., 1996). *Capsicum annuum*, *Capsicum frutescens*, *Capsicum chinense*, *Capsicum baccatum* and *Capsicum pubescens* were cultured (Pickersgill, 1997). These species are the most important species in terms of economic and nutritional status (Djian-Caporalino et al., 2006).

Phytophthora capsici Leonian (*P. capsici*), is one of the most important soil born plant pathogens in the world and first was found by Fernandez-Pavia and his friends; of the 26 isolates, only 7 were pathogenic on the cucumber. While 24 of them were virulent in pepper, no stable condition was observed in tomato (Pavia et al., 2004). *Phytophthora capsici* causes damages on tissues of root, fruit and leaves of various vegetables (Manohara and Rizal, 2002). Phytophthora species secrete a large number of effectors during the infection of host plants (Stam et al., 2013). Bell pepper succumbed to disease in particularly humid and humid conditions. Only some partially resistant pepper cultivars are commercially available (Candole et al., 2010; Gisbert et al., 2010). Also *Phytophthora blight* caused by *Phytophthora capsici* is a very important disease in vegetable production (crop losses exceeding 50%) on worldwide and selective use of

http://www.aloki.hu ● ISSN 1589 1623 (Print) ● ISSN 1785 0037 (Online)
DOI: http://dx.doi.org/10.15666/aeer/1605_68856901
© 2018, ALÖKI Kft., Budapest, Hungary

fungicides is the main part of disease management programs (Jackson et al., 2012; Sanogo et al., 2012; Yin et al., 2012). *Phytophthora capsici* is an oomycete that causes reductions in the production of capsicum (*Capsicum annuum* L.) worldwide. Nowadays, there are no chilles varieties that are resistant to this pathogen and the fungicides used for its struggle increase the resistance of disease races and increase the environmental damage (Garcia-Rodriguez et al., 2010).

Identification of initial symptoms of disease is very difficult and usually cannot be detected by the producers. Yellowing, fading and falling of leaves on the upper part of pepper plants are the most important and obvious signs of the disease (Ton et al., 2005). When these symptoms were observed, the infection has already reached to the advanced stage and caused root rot. *P. capsici* is very difficult to be controlled and causes a marked decline in pepper yields at pepper producer countries. For example, in Indonesia, root rot reduces 30 to 40% pepper yield in some gardens while in others it may cause 100% loss of yield (Nam, 2012). In Malaysia, more than 95% of pepper production areas have been similarly infected with *P. capsici*, resulting in a 5 to 10% reduction in productivity (Kueh, 1990). Yield loss in India was around 30% (Anandaraj, 2000). Successful management with *P. capsici* cannot be made due to the insufficient biologic information on *P. capsici*. According to the majority of scientists, A1 and A2 are the pathogen reproduction types (Ton, 2005; Hausbeck and Lamour, 2004; Ristaino and Johnston, 1999).

Plant enzymes are involved in defense mechanisms of plants against diseases caused by pathogens. Plant enzymes include antioxidants, such as peroxidase that enhance the cell structure and contribute to the formation of inhibitors in defense and catalyze the formation of lignin and other oxidative phenols. Studies conducted with plants such as pepper, tomato and wheat revealed a significant relationship between enzymes and protection against pathogens (Mohammadi and Kazemi, 2002). Catalase (CAT) enzyme is found in vertebrates, invertebrates, plants, fungi and all aerobic organisms (Bergmeyer and Grassl, 1982). The CAT enzyme has the highest conversion rate among all enzymes (Koç and Üstüm, 2016). The CAT enzyme is inhibited at high light intensity and by H_2O_2 which occur at high concentrations in stressed plant cells (Fridovich, 1986). Peroxidase (POX) is a part of the enzyme complex in the superoxide dismutase and CAT containing plant cell that regulates the level of harmful oxygen radicals formed under unfavorable external conditions. The POX enzyme has been isolated and characterized many times and the amino acid sequence of the enzyme has been revealed (Koç, 2011). The CAT and POX enzymes take part in purification of ROS (cell reactive oxygen species) from toxins. The enzymes disintegrate H_2O_2 and regulate the concentration of H_2O_2 in the cells. The CAT enzyme and different types of POX enzymes catalyze the disintegration of H_2O_2 (Chang et al., 1984). Since the catalase enzyme is not involved in chloroplasts, the breakdown of H_2O_2 in chloroplasts takes place by specific peroxidases (Asada, 1992). Principal component analysis (PCA) is a multivariate analysis technique and is also known as eigenvector analysis. The main objective of a PCA is to reduce the dimensionality of a set of data. This is particularly advantageous if a set of data with many variables lies, in reality, close to a two-dimensional subspace. In this case the data can be plotted with respect to these two dimensions, thus giving a straight forward visual representation of what the data look like, instead of appearing as a large mass of numbers to be digested (Jolliffe, 2002). The PCA is usually applied in environmental and agricultural studies (Panishkan et al., 2012; Yılmaz et al., 2017). The PCA was used to cluster patterns of 60 pepper

http://www.aloki.hu ● ISSN 1589 1623 (Print) ● ISSN 1785 0037 (Online)
DOI: http://dx.doi.org/10.15666/aeer/1605_68856901
© 2018, ALÖKI Kft., Budapest, Hungary

genotypes based on their morphological properties. The aims of this study were to study classification of pepper genotypes according to their morphological and chemical properties by using PCA.

Materials and methods

Materials

Fifty-nine pepper lines in the pepper gene pool of the Siirt University/Turkey, Department of Horticulture and CM334 (Criollos de Morelos 334) resistant to *P. capsici* were used in the experiment (*Table 1*). Fungal material was obtained from Van Yüzüncü Yıl University/Turkey, Faculty of Agriculture, Plant Protection Department. The isolate used is the most aggressive isolate of the strain.

Table 1. *Materials used in the study, fruit shape, hotness and resistance to P. capsici status*

Genotype/ variety No	Shape of fruit	Hotness	Resistance to *P. capsici*	Genotype/ variety No	Shape of fruit	Hotness	Resistance to *P. capsici*
1	B	Not hot	VS	31	C	Hot	S
2	B	Slightly hot	VS	32	SCG	Hot	S
3	C	Hot	PR	33	SCG	Slightly hot	S
4	SCG	Hot	S	34	C	Slightly hot	S
5	C	Hot	S	35	C	Slightly hot	S
6	SCG	Slightly hot	S	36	C	Hot	S
7	SCG	Slightly hot	S	37	C	Slightly hot	S
8	SCG	Hot	S	38	SCG	Hot	PR
9	C	Hot	S	39	SCG	Slightly hot	S
10*	C	Hot	R	40	C	Hot	S
11	C	Hot	S	41	SCG	Slightly hot	S
12	B	Not hot	VS	42	C	Hot	S
13	C	Hot	PR	43	B	Not hot	VS
14	C	Hot	S	44	C	Hot	S
15	SCG	Slightly hot	S	45	B	Not hot	VS
16	SCG	Hot	S	46	C	Hot	S
17	SCG	Not hot	S	47	C	Hot	S
18	C	Hot	S	48	C	Hot	PR
19	C	Hot	S	49	SCG	Slightly hot	S
20	SCG	Hot	S	50	C	Slightly hot	S
21	B	Not hot	VS	51	C	Slightly hot	S
22	SCG	Not hot	S	52	C	Hot	S
23	SCG	Slightly hot	S	53	C	Slightly hot	S
24	C	Slightly hot	S	54	C	Hot	S
25	C	Hot	PR	55	C	Hot	S
26	C	Hot	S	56	SCG	Hot	S
27	SCG	Slightly hot	S	57	C	Hot	PR
28	C	Hot	S	58	C	Hot	S
29	C	Slightly hot	S	59	C	Slightly hot	S
30	B	Not hot	VS	60	C	Slightly hot	S

SCG: Semi Capia-Green; **B:** Bell Pepper, **C:** Capia; **S:** Sensitive; **VS:** Very Sensitive; **PR:** Partially Resistant; **R**: Resistant
*Control genotypes: CM334 (Criollos de Morelos 334)

http://www.aloki.hu ● ISSN 1589 1623 (Print) ● ISSN 1785 0037 (Online)
DOI: http://dx.doi.org/10.15666/aeer/1605_68856901
© 2018, ALÖKI Kft., Budapest, Hungary

Methods

Experimental design and treatments

Field studies were carried out in research and application fields of the Department of Horticulture, Faculty of Agriculture, Siirt University, Turkey. The effects of *P. capsici* on pepper varieties/lines have been investigated in two stages. At the first stage, resistance or sensitivity status of varieties/lines were determined at seedling period. After that, the resistant varieties/lines were selected and the effect of pathogen on plants was investigated in field conditions following the seedling period.

Prior to planting, the pepper seeds were placed in 2% sodium hydroxide solution for 5 min, subjected to surface disinfection, and washed twice using sterile distilled water. Peat was used as seedling growing medium. The experiment was designed with 3 replicates and each replicate included 10 plants.

The seedlings at 3-4 leaf stage were infected with spore solution containing zoospores of *P. capsica*. Seven-day cultures of *P. capsica* (in 9 cm petri dishes) grown in an incubator purely under dark at 25 °C within Potato Dextrose Agar medium were used for this purpose.

Fungi incubation

The petri dishes were left under the light for 2 days to allow sporulation. Twenty mL of sterile distilled water was added in each petri dish and incubated in the refrigerator at 4 °C for 40 min and then kept at room temperature for 30 min. Thus, zoosporogenesis of the fungus has been promoted. The zoospores of *P. capsici* were collected by filtration through two layers of cheesecloth. The zoospores of the fungus were then adjusted with hemocytometer at a concentration of 2×10^6 zoospor ml^{-1}.

Three ml of this solution was taken and inoculated to the surrounding of seedling roots to be inoculated with pathogen. After the first inoculation, the surviving seedlings were inoculated second time as indicated in the first stage. Peroxidase and catalase enzymes of samples taken from the sensitive varieties/lines in the uninoculated control group were also determined.

Enzyme activity assay

Catalase and peroxidase enzyme activities were determined by using Thermo Scientific UV-VIS instrument at Siirt University Science, Technology Application and Research Center. The plant leaf samples taken in accordance with the cold chain rules were broken into pieces with homogenate buffer for 5 min within a homogenizer and centrifuged at 15000 rpm for one hour at + 4°C. Both enzyme activities were measured in 100 µl homogenate of the substrate added to the buffer solution.

Catalase enzyme activity was determined using the method outlined by Jebara et al. (2005). Enzyme activity and enzyme calculation formula are given in *Table 2*. The measurement was performed at 240 nm in a quartz cuvette with 3 repetitions following the calibration of the instrument. The EU / ml values were obtained by calculation.

The activity measurement of peroxidase enzyme was determined spectrophotometrically according to the procedure applied by Şişecioğlu et al. (2010). This procedure is based on the oxidation of guaiacol chromogenic substrate by H_2O_2 and the monitoring the increase in absorbance resulted from colored compound at 470 nm (Şişecioğlu et al., 2010). The enzyme activity and enzyme calculation formula are

http://www.aloki.hu ● ISSN 1589 1623 (Print) ● ISSN 1785 0037 (Online)
DOI: http://dx.doi.org/10.15666/aeer/1605_68856901
© 2018, ALÖKI Kft., Budapest, Hungary

given in *Table 3*. After device calibration, the measurement was made at 470 nm in a quartz cuvette with 3 repetitions. The EU/ml values were determined by calculation.

Table 2. *Catalase enzyme mechanism and enzyme calculation formula*

Catalase: $2H_2O_2 \longrightarrow 2H_2O + O_2$ Calculation of Catalase: EU/ml = 3.45 (pure) Catalase/min (V_E) 3.45 = 240 nm which corresponds to degradation of 3.45 µm dead caused by hydrogen peroxide produced in 3 ml of reaction for absorbance decline from 0.45 to 0.40. df = dilution factor min = time required to decrease absorbance at 240 nm from 0.45 to 0.40. V_E = The amount of enzyme used

Table 3. *Peroxidase enzyme mechanism and enzyme calculation formula*

Peroxidase mechanism: 2Guaiacol + $2H_2O_2 \longrightarrow$ 2oxide guaiacol + $2H_2O$ Calculation of Peroxidase: EU/ml = (Peroxidase, absorbance difference occurs in 1 min) * df / 1*(0.01) df: dilution factor 1: per enzyme / increase in 1 min 0.01: amount of enzyme homogenant used Unit/mg protein: (Unit / ml enzyme) / (mg protein / ml enzyme)

0-5 scale

Disease severity of plants was determined using 0-5 scale after 4, 8, 12 and 16 days of pathogen inoculation. In this evaluation; 0 = no sign of disease; 1 = brown lesions began to appear on lightly faded leaves and body; 2 = disease indication in 30-50% of the plant; 3 = disease symptoms at 50-70% of the plant; 4 = disease symptoms at 70-90% of the plant; 5 = dead plant (Sunwoo et al., 1996; Ozgonen and Erkilic, 2007).

Principal component analysis

The first principal component (PC), y_1 is a linear combination of x_1, x_2, …, x_p (*Eq. 1*):

$$y_1 = a_{11}x_1 + a_{12}x_2 + \cdots + a_{1p}x_p = \sum_{i=1}^{p} a_{1i}x_i \quad \text{(Eq.1)}$$

such that the variance of y_1 is maximized given the constraint that the sum of squared (SS) weights is (*Eq. 2*):

$$\sum_{i=1}^{p} a_{1i}^2 = 1 \quad \text{(Eq.2)}$$

The random variables x_i, can be either deviation from mean scores or standardized scores. If the variance of y_1 is maximized, then so is the SS correlations of y_1 with the original variables x_1, x_2, …, x_p (*Eq. 3*):

$$\sum_{i=1}^{p} r_{y_i x_i}^2 \quad \text{(Eq.3)}$$

http://www.aloki.hu ● ISSN 1589 1623 (Print) ● ISSN 1785 0037 (Online)
DOI: http://dx.doi.org/10.15666/aeer/1605_68856901
© 2018, ALÖKI Kft., Budapest, Hungary

PCA finds the optimal weight vector $(a_{11}, a_{12}, \ldots, a_{1p})$ and the associated variance of y_i which is usually denoted by λ_i. The second PC, y_2, involves finding a second weight vector $(a_{21}, a_{22}, \ldots, a_{2p})$ such that the variance of (*Eq. 4*)

$$y_2 = a_{21}x_1 + a_{22}x_2 + \cdots + a_{2p}x_p = \sum_{i=1}^{p} a_{2i}x_i \quad \text{(Eq.4)}$$

is maximized subject to the constraints that it is uncorrelated with the first PC and (*Eq. 5*)

$$\sum_{i=1}^{p} a_{2i}^2 = 1 \quad \text{(Eq.5)}$$

the results in y2 having the next largest SS correlations with the original variables. The first two PCs together have the highest possible SS multiple correlations (Dunteman, 1989).

Statistical analysis was performed using MINITAB 14 Software.

Results and discussion

Enzymatic component of antioxidative enzymes are important for the formation of antioxidative reactions in plants and in obtaining cell homeostasis for defense system. Antioxidative enzymes are being frequently used in recent transgenic studies to increase the resistance of plants to different stressors. The fruit shape and hotness of peppers may also be an indicative of resistance. The resistance of capia, half-capia-pointed pepper or bell peppers was different. The capia peppers showed resistance to *phytopthora capsici*, while the genotypes or varieties with semi capia-pointed peppers were included in the partially resistant or sensitive or even very sensitive group. The bell pepper genotypes and varieties did not show any resistance to the disease and were found as sensitive or even very sensitive.

The highest peroxidase activity among genotypes investigated was obtained with line 10 (0.0744), and followed by genotypes 3 (0.0568), 38 (0.0540), 57 (0.0533) and 11 (0.0482), respectively. The genotype 10 showed a similar profile (2.9571429) in terms of catalase activity and followed by genotypes 8 (1,5525), 56 (1,5525), 9 (1,514,6341) and 11 (1,444186), respectively (*Tables 4* and *5*). Similar to our findings, Lamour et al. (2012) also showed that CM 334 genotype had resistance to all *P. capsici* isolates.

Seven of the 60 genotypes (genotypes 3, 10, 13, 25, 38, 48 and 57) survived after the first inoculation. Significant disease symptoms were observed in other 53 genotypes and these genotypes died in a short time after the inoculation. Different genotypes resistant to *P. capsici* may be developed when early symptoms are not ignored (Black et al., 1991; Ortega et al., 1995; Pochard et al., 1983). Similar to the findings of Kim et al. (1989), resistance to *P. capsici* increased during 12-leaf period. All other genotypes except 10 genotypes died after the second inoculation. The highest peroxidase enzyme activity was obtained with the seven genotypes survived following the first inoculation (*Tables 4* and *5*). The seedlings were not significantly affected from *P. capsici* at the beginning of their developments. However, when seedlings reached to 4 true leaf stage, the initial symptoms started to appear, and the resistance mechanism was different for the different parts of plants (Bosland and Lindsey, 1991; Sy et al., 2005). The peroxidase enzyme activity was low in very sensitive genotypes, while enzyme activity

http://www.aloki.hu ● ISSN 1589 1623 (Print) ● ISSN 1785 0037 (Online)
DOI: http://dx.doi.org/10.15666/aeer/1605_68856901
© 2018, ALÖKI Kft., Budapest, Hungary

was very high in very resistant genotype (genotype 10-CM 334) and partially resistant genotypes (3, 13, 25, 38, 48 and 57).

Table 4. *Peroxidase activities of the genotypes used in the study*

GNP	Peroxidase (EU/ml)	Std deviation	GNP	Peroxidase (EU/ml)	Std deviation
10	0.074	0.002	51	0.025	0.007
3	0.057	0.001	14	0.022	0.001
38	0.054	0.009	46	0.022	0.004
57	0.053	0.014	42	0.021	0.011
11	0.048	0.001	39	0.021	0.009
13	0.048	0.000	6	0.018	0.001
25	0.048	0.004	29	0.018	0.000
48	0.047	0.007	32	0.017	0.006
34	0.044	0.008	41	0.017	0.005
59	0.043	0.001	18	0.016	0.000
26	0.043	0.025	19	0.015	0.002
28	0.043	0.003	23	0.015	0.001
35	0.041	0.003	33	0.014	0.007
5	0.041	0.001	16	0.013	0.001
54	0.041	0.004	49	0.012	0.003
37	0.041	0.011	43	0.012	0.003
36	0.041	0.008	15	0.011	0.001
58	0.041	0.002	17	0.011	0.000
24	0.040	0.006	22	0.011	0.004
31	0.040	0.009	4	0.011	0.000
55	0.038	0.002	20	0.010	0.000
47	0.038	0.028	27	0.009	0.002
9	0.036	0.002	7	0.009	0.000
40	0.036	0.007	8	0.008	0.001
52	0.033	0.002	30	0.007	0.001
60	0.032	0.002	12	0.006	0.001
50	0.030	0.006	2	0.006	0.000
53	0.030	0.006	45	0.005	0.001
56	0.028	0.008	1	0.005	0.001
44	0.027	0.006	21	0.003	0.000

Although catalase enzyme content was different in some genotypes, similar results were obtained for peroxidase. The peroxidase (POX) content of genotypes that sensitive in the early stage of inoculation had generally high but catalase content significantly varied among these genotypes. The POX enzyme content can be used as a determinant because POX is an oxide-reductive enzyme which stimulates oxidation and suberization of phenols participating in cell wall polysaccharide processes, lignification of host plant cells during defense and provides a reaction against pathogenic substances (Ray et al., 1998). The POX content is very high in stable plant tissues (Breusegem et al., 2001; Lin and Kao, 2001). Lignin accumulation and phenolic compounds have been correlated with the disease. Similar results were also obtained in wheat-*Fusarium graminearum* (Mohammadi and Kazemi, 2002) and cucumber-*Pythium aphanidermatum* (Chen et al., 2000) treatments. The POX is believed to participate in cell wall metabolism (Welinder,

http://www.aloki.hu ● ISSN 1589 1623 (Print) ● ISSN 1785 0037 (Online)
DOI: http://dx.doi.org/10.15666/aeer/1605_68856901
© 2018, ALÖKI Kft., Budapest, Hungary

1993) and production of anti-microbial compounds (Kobayashi et al., 1994) that play a role in healing of wounds. The POX content was tended to increase in resistant variety/line/genotypes (Jung et al., 2006).

Table 5. *Catalase activities of the genotypes used in the study*

GNP	Catalase (EU/ml)	Std deviation	GNP	Catalase (EU/ml)	Std deviation
10	2.96	0.02	43	0.64	0.04
8	1.55	0.05	2	0.62	0.12
56	1.55	0.06	59	0.62	0.07
9	1.51	0.03	52	0.61	0.21
11	1.44	0.03	36	0.60	0.04
13	1.11	0.07	51	0.60	0.02
15	1.11	0.03	19	0.60	0.04
7	1.07	0.08	55	0.60	0.09
3	0.99	0.06	58	0.58	0.07
6	0.99	0.05	26	0.58	0.06
33	0.96	0.03	28	0.58	0.03
29	0.93	0.08	39	0.57	0.05
34	0.91	0.06	30	0.56	0.04
60	0.89	0.13	35	0.54	0.06
38	0.87	0.07	21	0.52	0.04
25	0.84	0.03	48	0.50	0.14
37	0.83	0.04	45	0.50	0.02
41	0.83	0.10	24	0.49	0.05
57	0.83	0.04	40	0.48	0.07
22	0.82	0.03	31	0.47	0.05
53	0.81	0.05	49	0.46	0.04
16	0.78	0.01	44	0.45	0.04
27	0.71	0.03	1	0.43	0.10
47	0.69	0.03	42	0.40	0.24
50	0.69	0.03	5	0.35	0.15
20	0.68	0.13	46	0.34	0.08
17	0.68	0.03	32	0.28	0.07
18	0.68	0.02	12	0.20	0.12
54	0.66	0.02	4	0.13	0.00
14	0.65	0.06	23	0.04	0.08

The scale of 0-5 was used to identify the disease (*Table 6*). Zero stands for no disease symptoms and 5 represents the highest symptoms of disease. The disease was very vigorous and continuous in genotypes with a 5-scale value. Distinction of symptoms required great attention in genotypes received scores between 0 and 5. Some of the genotypes (3, 25 and 38) received high values at the initial assessment whereas their scores were lower at later observations and included in resistant genotypes. Sixteen days after the inoculation, the differences between susceptible and resistant and partially resistant genotypes started to be apparent. The enzyme (peroxidase and catalase) contents were also compatible with the resistance of genotypes. Some genotypes were classified within the sensitive group at initial assessments, whereas they scored lower in the later evaluations, meaning less disease symptoms (i.e. Gayoso et al., 2004; Ray et

http://www.aloki.hu ● ISSN 1589 1623 (Print) ● ISSN 1785 0037 (Online)
DOI: http://dx.doi.org/10.15666/aeer/1605_68856901
© 2018, ALÖKI Kft., Budapest, Hungary

al., 1998; Ponmurugan et al., 2007). Resistance or sensitivity did not follow a linear trend in some genotypes. Genotypes of 28, 35 and 45 were finally determined as susceptible, and despite the deaths at the first inoculation they were classified among the genotypes that responded as if the disease symptoms had improved. The genotypes 3, 25 and 38 received higher scale values at the beginning and followed by lower values at the subsequent observations. The genotype 10 had a 0-scale value in every observation and it was identified as the most resistant plant material without any signs of disease. The genotype 33 showed initial disease symptoms even at the fourth observation following the first inoculation. The enzyme activity content of sensitive genotypes with no stabilized score values do not have also sufficient values for enzyme activity. Inconsistent differences in the scale values may be due to enzyme activity, and this may also a sign of morphological clarification and genetical impurities.

Table 6. *Evaluation of pepper lines and genotypes in first inoculation according to 0-5 scale*

***Capsicuum* spp. genotypes**	**DAYS**				***Capsicuum* spp. genotypes**	**DAYS**			
	4	8	12	16		4	8	12	16
1	0	4	5	5	31	0	2	1	5
2	0	4	5	5	32	0	3	3	5
3	0	0	1	1	33	0	3	4	5
4	0	2	2	5	34	0	2	1	5
5	0	1	1	5	35	0	2	1	5
6	0	1	2	5	36	0	2	1	5
7	0	1	3	5	37	0	2	1	5
8	0	1	3	5	38	0	1	1	3
9	0	1	2	5	39	0	2	3	5
10	0	0	0	0	40	0	2	2	5
11	0	0	1	5	41	0	2	4	5
12	0	3	5	5	42	0	2	3	5
13	0	0	1	2	43	0	1	4	5
14	0	1	3	5	44	0	2	2	5
15	0	1	3	5	45	0	3	5	5
16	0	1	4	5	46	0	2	4	5
17	0	1	4	5	47	0	1	2	5
18	0	3	4	5	48	0	1	1	3
19	0	1	4	5	49	0	2	4	5
20	0	2	3	5	50	0	2	4	5
21	0	1	5	5	51	0	2	3	5
22	0	3	5	5	52	0	1	4	5
23	0	3	4	5	53	0	1	3	5
24	0	2	2	5	54	0	1	3	5
25	0	1	1	2	55	0	1	2	5
26	0	2	1	5	56	0	1	3	5
27	0	2	5	5	57	0	0	1	3
28	0	3	2	5	58	0	1	2	5
29	0	2	3	5	59	0	1	2	5
30	0	3	4	5	60	0	1	3	5

http://www.aloki.hu ● ISSN 1589 1623 (Print) ● ISSN 1785 0037 (Online)
DOI: http://dx.doi.org/10.15666/aeer/1605_68856901
© 2018, ALÖKI Kft., Budapest, Hungary

Significant correlation between POX activity and content of phenolic compound of plants with different families in which pepper is included has been reported (Candole et al., 2012). The peroxidase and similar enzymes trigger the formation and enhancement of the phenolics in the plant cell wall during defense against pathogens (Gayoso et al., 2004).

In some studies, approximately one week after the infection of disease, the increase in peroxidase, as well as phenol contents especially in the stem and leaves of plant, was reported and even the increase reached to the maximum level (Gayoso et al., 2004). The CM334 is a worldwide known resistant genotype (partial wild) against *P. capsica* and has been defined as a resistant genotype in our study based on both peroxidase and catalase contents. The peroxidase activity of resistant CM334 genotype was higher compared to the sensitive genotypes.

Inadequate enzyme activity in sensitive varieties may have caused these genotypes defeating against the disease. Living in a certain period of time for sensitive genotypes despite the disease may be attributed to the consumption rate of phenolic substances. Ponmurugan et al. (2007), it is predicted that it may be aimed at producing some metabolites which may cause the metabolism of the pathogens to be distributed and balanced. The overproduction of ROS (free radicals) and the consumption of antioxidant defenses may cause disruption of oxidant–antioxidant balance and occurrence of oxidative stress in the cells (Koç and Üstün, 2016).

Three morphological (resistance, hotness and fruit shape) and two chemical (peroxidase and catalase) characteristics of pepper genotypes were investigated in this study. The descriptive statistics (mean, standard deviation, minimum, maximum and median) for characteristics were presented in *Table 7*. The relationships among genotypes in terms of characteristics studied were evaluated by principal PCA. The mean and standard deviation values revealed that resistance had the lowest variability and peroxidase and catalase had the highest variability. High coefficient of variability is an indication of the differences in genotypes.

Table 7. *Descriptive statistics of pepper genotypes*

Traits	N of obs.	Mean	Std. dev	Minimum	Median	Maximum	CV (%)
Resistance	60	2.9833	0.5365	1.0000	3.0000	4.0000	17.98
Hotness	60	1.6000	0.7178	1.0000	1.0000	3.0000	44.86
Fruit shape	60	1.5333	0.7003	1.0000	1.0000	3.0000	45.67
Peroxidase	60	0.0274	0.0165	0.0030	0.0260	0.0740	60.22
Catalase	60	0.7389	0.4278	0.0360	0.6435	2.9570	57.90

Each component in the table explains a certain portion of the variability in the data. The higher the proportion, the more variability is explained by the PC. Cumulative proportion is the variability explained by the consecutive PCs. The PCs with the largest eigenvalues were retained to explain the variability. A PC with eigenvalues greater than 1.0 is kept for further analyses. The scree plot enables visual comparison of the eigenvalue sizes (*Fig. 1*). The first two PCs have eigenvalues greater than 1.0 and explain 74% of the variation in the data. The eigenvalues start to form a straight line after the second PC. The amount of variability explained by the two PCs is sufficient hence the first two PCs will be used to explain the variability.

http://www.aloki.hu ● ISSN 1589 1623 (Print) ● ISSN 1785 0037 (Online)
DOI: http://dx.doi.org/10.15666/aeer/1605_68856901
© 2018, ALÖKI Kft., Budapest, Hungary

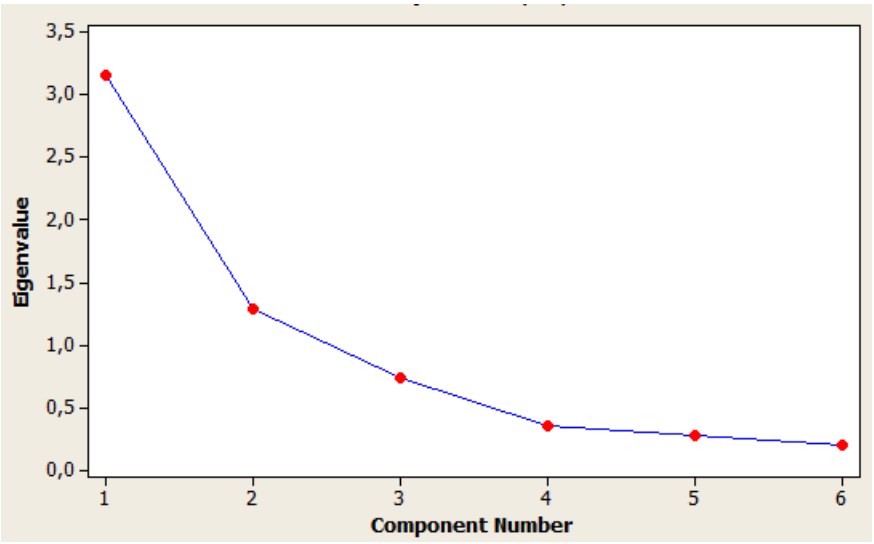

Figure 1. *Scree plot of the eigenvalues*

The PCs are the linear combinations of the original variables that account for the variance in the data. The coefficients indicate the relative weight of each variable in the component. Peroxidase, resistance and fruit shape had the highest influence in PC1 (*Table 8*). The peroxidase and resistance had positive effects in PC1, while fruit shape had negative effect (the effect on ingredient increases as the fruit gets more pointed).

Table 8. *Results of principal component analysis*

Trait	PC1	PC2	PC3	PC4	PC5	PC6
Resistance	0.491860	0.197271	-0.067553	-0.131608	0.491860	0.197271
Hotness	0.440223	-0.051902	0.545261	0.648487	0.440223	-0.051902
Shape of fruit	-0.480311	0.259828	-0.171691	0.208326	-0.480311	0.259828
Genotype	0.116054	-0.718223	-0.580743	0.343676	0.116054	-0.718223
Peroxidase	0.501997	-0.050420	-0.153561	-0.512774	0.501997	-0.050420
Catalase	0.260977	0.610322	-0.554803	0.371071	0.260977	0.610322
Eigenvalues	3.1560	1.2860	0.7356	0.3548	0.2705	0.1972
Proportion %	52.6	21.4	12.3	5.90	4.50	3.30
Cumulative proportion %	52.6	74.0	86.3	92.2	96.7	100.0

The second PC had a large negative association with genotype (71.8%) and positive associations with catalase (61.0%) and fruit shape (25.9%) (*Fig. 2*).

There are a number of variants of the biplot idea, but all give a simultaneous display of n observations and p variables on the same two-dimensional diagram. In one of the variants, the plot of observations is identical to a plot with respect to the first two PCs, but the biplot simultaneously gives graphical information about the relationships between variables. The relative positions of variables and observations, which are plotted on the same diagram, can also be interpreted (Jolliffe, 2002). High positive effects of resistance, peroxidase and hotness on PC1 are seen in biplot figure (*Fig. 2*). In other words, the first component focuses on the hotness, peroxidase and catalase

http://www.aloki.hu ● ISSN 1589 1623 (Print) ● ISSN 1785 0037 (Online)
DOI: http://dx.doi.org/10.15666/aeer/1605_68856901
© 2018, ALÖKI Kft., Budapest, Hungary

contents of plants and resistance to phytophthora disease. The second component is more related to the fruit shape of the plant. The relationships among genotypes grouping based on fruit shape, hotness and resistance are illustrated in the score plots (*Figs. 3–5*).

Figures 3 and *4* show that the genotypes form groups according to these morphological characteristics. Based on resistance parameter, genotypes could be grouped absolutely independently (*Fig. 5*).

The first PC accounts 52.4% and the second PC explains 21.6% of total variation. A model based on the first two principal components accounts for 74.00% of total variance.

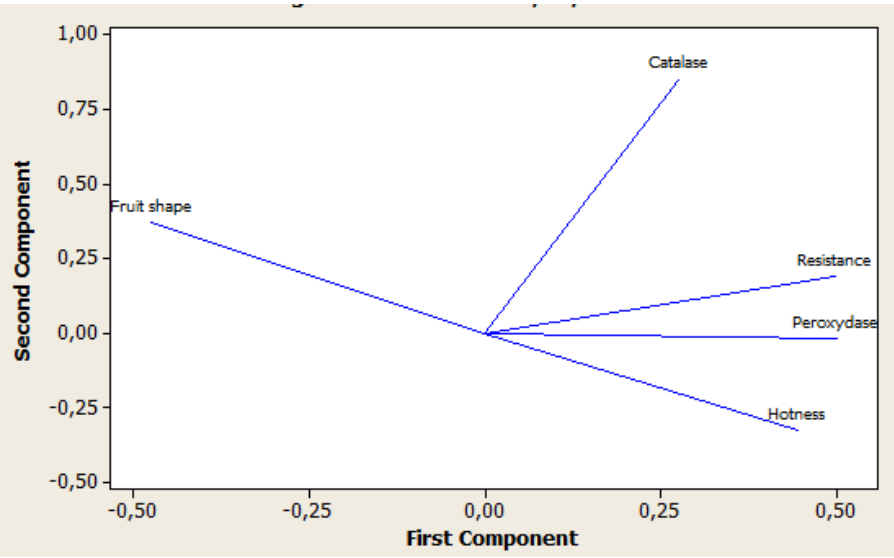

Figure 2. *Biplot analysis of different pepper genotypes*

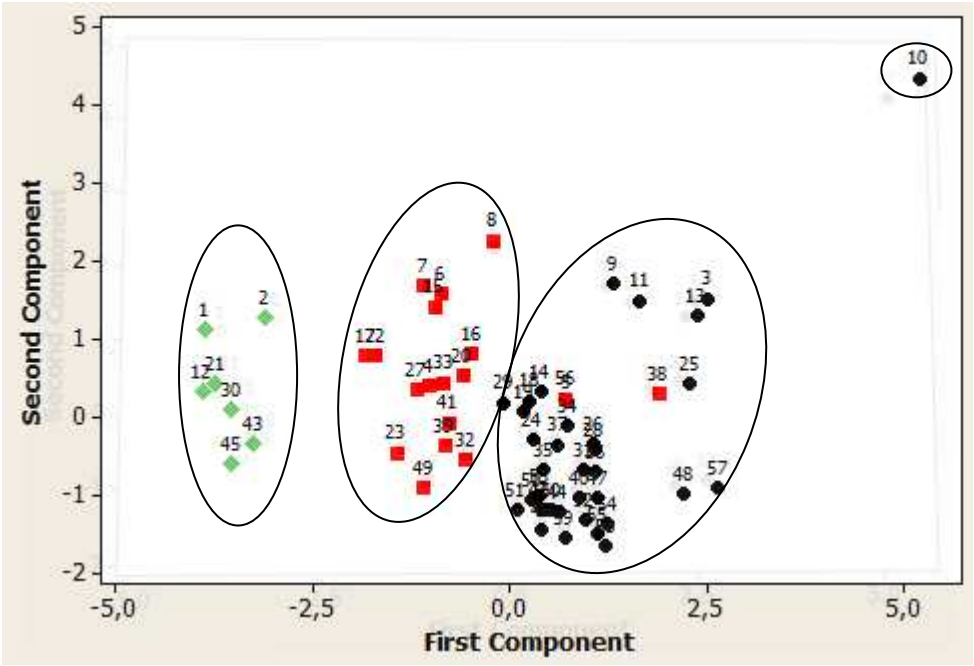

Figure 3. *Score plot of PC1 versus PC2 shows the differentiation of genotypes according to fruit shape (◆ - bell pepper, ■ - semi capia, ● - capia)*

http://www.aloki.hu ● ISSN 1589 1623 (Print) ● ISSN 1785 0037 (Online)
DOI: http://dx.doi.org/10.15666/aeer/1605_68856901
© 2018, ALÖKI Kft., Budapest, Hungary

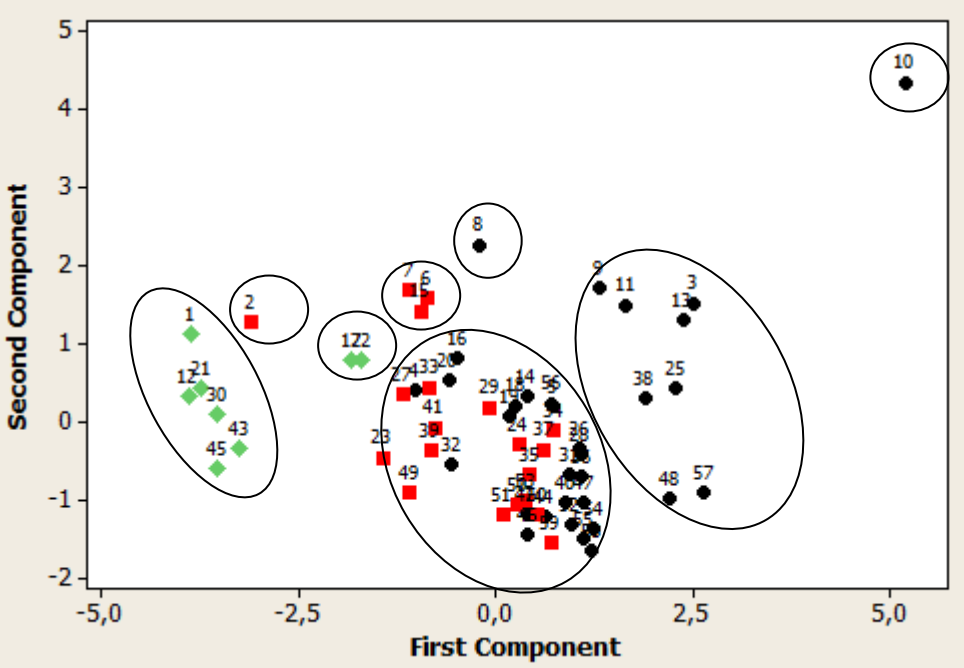

Figure 4. *Score plot of PC1 versus PC2 shows the differentiation of genotypes according to hotness (◆ - not hot, ■ - some hot, ● - hot)*

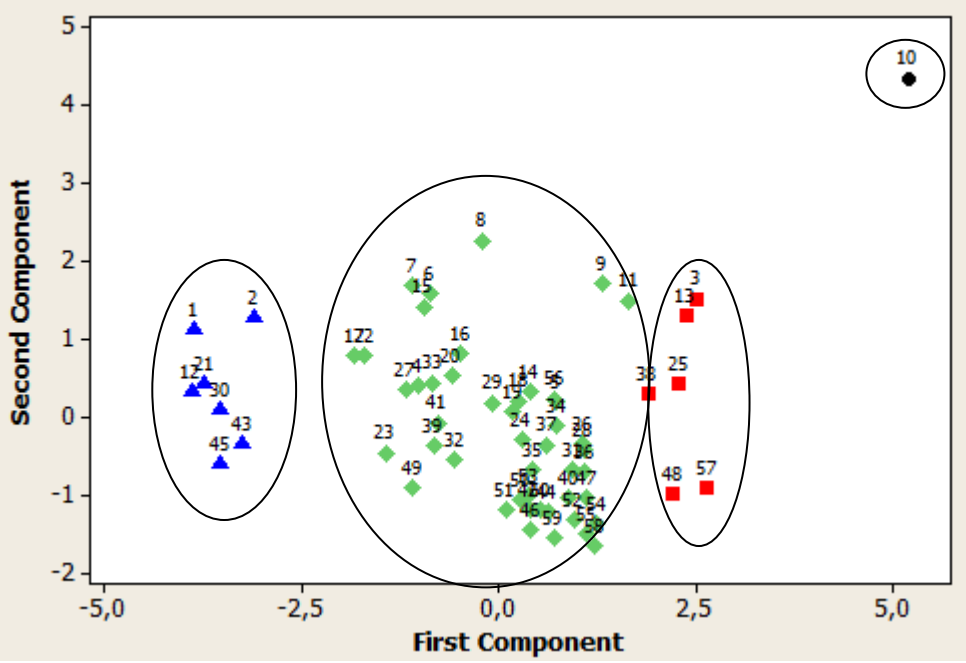

Figure 5. *Score plot of PC1 versus PC2 shows the differentiation of genotypes according to resistance (▲ -very sensitive, ◆ - sensitive, ■ - partially resistant, ● - resistant)*

Most of genotypes died at the first inoculation applying. Few genotypes died in the first two weeks of inoculation. The CM 334 genotype showed resistance in both inoculations and showed no sign of disease as two inoculations. The first inoculation in

http://www.aloki.hu ● ISSN 1589 1623 (Print) ● ISSN 1785 0037 (Online)
DOI: http://dx.doi.org/10.15666/aeer/1605_68856901
© 2018, ALÖKI Kft., Budapest, Hungary

the leaves of the partially endogenous genotypes P1, 13 (Urfa), 25 (UKST), 38 (UID), 48 (UKDT), 57 (ANKSB)] showed weak symptoms. New shoot formation was detected in these genotypes. In the second inoculation, however, these genotypes have also been found at high rates since the first week after the inoculation of the disease indications. Deaths in these genotypes were observed in approximately 2 weeks. The first week after inoculation is important for breeders. As a result of our observations that the genotypes started to show resistance in the first week after inoculation may be breeding material. The yield and fruit qualities of genotypes found to be resistant or very resistant are not available in commercial pepper cultivation. CM 334 genotype has lower fruit quality and yield values. Partly resistant genotypes (deaths in the first two weeks and deaths after second inoculation due to disease) should be used at breeding program because according to Hwang et al. (1996), resistance against *P. capsici* occurs during the last stages of plant development. The genotypes that are resistant (genotype 10 /CM 334) or part-resistant (genotypes 3, 13, 38 and 48) all have the shape of capia fruit. Again, the genotypes listed above have bitter fruits. It was found that the fruits of the fruit-shaped capia and hot were likely to be resistance (*Table 1*). The PCA helped to reveal some relationships between genotypes and morphological properties. The PCA has proved to be a useful approach in characterization of genotypes based on their morphological properties.

Acknowledgements. The authors thank Siirt University Research Funds (BAP) for their financial support.

REFERENCES

[1] Anandaraj, M. (2000): Diseased of Black Pepper. – In: Ravindram, P. N. (ed.). Black Pepper - Piper Nigrum. Medicinal and Aromatic Plants - Industrial Profiles. Harwood Academic Publishers, Netherlands, pp. 239-267.
[2] Asada, K. (1992): Ascorbate peroxidase–a hydrogen peroxide-scavenging enzyme in plants. – Physiologia Plantarum 85(2): 235-241.
[3] Baral, J., Bosland, P. W. (2002a): An update synthesis of the *Capsicum* genus. – Capsicum and Eggplant Newsletter 21: 11-21.
[4] Baral, J., Bosland, P. W. (2002b): Genetic diversity of a Capsicum germplasm collection from Nepal as determined by randomly amplified polymorphic DNA markers. – Journal of the American Society for Horticultural Science 127(3): 318-324.
[5] Bergmeyer, J., Grassl, M. (1982): Methods of Enzymatic Analysis (3rd ed., Vol. I.). – Verlag Chemie, Weinheim.
[6] Black, L. L., Green, S. K., Hartman, G. L., Poulos, J. M. (1991): Pepper Diseases: A Field Guide. – Asian Veg. Res. & Dev. Ctr., Shanhua, Taiwan.
[7] Breusegem, F. V., Vranova, E., Dat, J. F., Inze, D. (2001): The role of active oxygen species in plant signal transduction. – Plant Science 161: 405-414.
[8] Bosland, P. W., Lindsey, D. L. (1991): A seedling screen for Phytophthora root rot of pepper, Capsicum annuum. – Plant Dis. 75: 1048-1050.
[9] Candole, B. L., Conner, P. J., Ji, P. (2010): Screening Capsicum annuum accessions for resistance to six isolates of Phytophthora capsici. – HortScience 45(2): 254-259.
[10] Candole, B. L., Conner, P. J., Ji, P. (2012): Evaluation of phytophthora root rot-resistant Capsicum annuum accessions for resistance to phytophthora foliar blight and phytophthora stem blight. – Agricultural Sciences 3(05): 732.

http://www.aloki.hu ● ISSN 1589 1623 (Print) ● ISSN 1785 0037 (Online)
DOI: http://dx.doi.org/10.15666/aeer/1605_68856901
© 2018, ALÖKI Kft., Budapest, Hungary

[11] Chang, H., Siegel, B. Z., Siegel, S. M. (1984): Salinity-induced changes in isoperoxidases in taro Colocasia esculenta. – Phytochemistry 23(2): 233-235.
[12] Chen, C., Belanger, R. R., Benhamou, N., Paulitz, T. C. (2000): Defense enzymes induced in cucumber roots by treatment with plant growth-promoting rhizobacteria (PGPR) and Pythium aphanidermatum. – Physiological and Molecular Plant Pathology 56(1): 13-23.
[13] Djian-Caporalino, C., Lefebvre, V., Sage-Daubeze A-M., Palloix, A. (2006): Capsicum. – In: Singh, R. J. (ed.) Genetic Resources, Chromosome Engineering, and Crop Improvement: Vegetable Crops (Vol. 3). – Taylor and Francis, Boca Raton, FL.
[14] Dunteman, G. H. (1989): Principal Component Analysis (Vol. 2). – Retrieved from internal-pdf://pca-0493116425/PCA.pdf.
[15] Fernandez-Pavia, S. P., Biles, C. L., Liddell, C. M. (2004): Characterization of Southern New Mexico Phytophthora capsici Leonian isolates from pepper (*Capsicum annuum* L.). – Revista Mexicana de Fitopatología 22(1): 82-89.
[16] Fridovich, I. (1986): Biological effects of the superoxide radical. – Archives of Biochemistry and Biophysics 247(1): 1-11.
[17] García-Rodríguez, M. A., Chiquito-Almanza, E., Loeza-Lara, P. D., Godoy-Hernández, H., Villordo Pineda, E., Pons-Hernández, J. L., ... and Anaya-López, J. L. (2010): Producción de chile ancho injertado sobre criollo de Morelos 334 para el control de *Phytophthora capsici*. – Agrociencia 44(6): 701-709.
[18] Gayoso, C., Pomar, F., Merino, F., Bernal, M. A. (2004): Oxidative metabolism and phenolic compounds in *Capsicum annuum* L. var. *annuum* infected by *Phytophthora capsici* Leon. – Scientia Horticulturae 102(1): 1-13.
[19] Gisbert, C., Sánchez-Torres, P., Raigón, M. D., Nuez, F. (2010): *Phytophthora capsici* resistance evaluation in pepper hybrids: agronomic performance and fruit quality of pepper grafted plants. – Journal of Food, Agriculture & Environment 8(1): 116-121.
[20] Hausbeck, M. K., Lamour, K. H. (2004): *Phytophthora capsici* on vegetable crops: research progress and management challenges. – Plant Disease 88(12): 1292-1301.
[21] Hwang, B. K., Kim, Y. J., Kim, C. H. (1996): Differential interactions of Phytophthora capsici isolates with pepper genotypes at various plant growth stages. – European Journal of Plant Pathology 102(4): 311-316.
[22] Jackson, K. L., Yin, J., Ji, P. (2012): Sensitivity of Phytophthora capsici on vegetable crops in Georgia to mandipropamid, dimethomorph, and cyazofamid. – Plant Disease 96(9): 1337-1342.
[23] Jebara, S., Jebara, M., Liman, F., Aouani, E. (2005): Changes in ascorbate peroxidase, catalase, guaicol peroxidase superoxide dismutase activities in common bean nodules under salt stres. – Journal of Plant Physiology 162: 929-936.
[24] Jolliffe, I. T. (2002): Principal Component Analysis. – http://books.google.com/books?id=_olByCrhjwIC&pgis=1.
[25] Jung, W. J., Jin, Y. L., Park, R. D., Kim, K. Y., Lim, K. T., Kim, T. H. (2006): Treatment of Paenibacillus illinoisensis suppresses the activities of antioxidative enzymes in pepper roots caused by Phytophthora capsici infection. – World Journal of Microbiology and Biotechnology 22(9): 901-907.
[26] Kim, Y. J., Hwang, B. K., Park, K. W. (1989): Expression of age-related resistance in pepper plants infected with Phytophthora capsici. – Plant Dis. 73: 745-747.
[27] Kobayashi, A., Koguchi, Y., Kanzaki, H., Kajiyama, S., Kawazu, K. (1994): A new type of antimicribial phenolic produced by peroxidase and its possible role in the chemical defense systems against plant pathogens. – Journal of Bioscience 49: 411-414.
[28] Koç, E., Üstün, A. S. (2016): Phytophthora capsici Leon. ile enfekte edilen duyarlı ve dayanıklı biber genotiplerinin köklerinde antioksidatif tepkiler ve lipid peroksidasyonu/Antioxidative reactions and lipid peroxidation in roots of susceptible and resistant pepper genotypes infected with Phytophthora capsici Leon. – Erciyes Üniversitesi Fen Bilimleri Enstitüsü Dergisi 28(5).

http://www.aloki.hu ● ISSN 1589 1623 (Print) ● ISSN 1785 0037 (Online)
DOI: http://dx.doi.org/10.15666/aeer/1605_68856901
© 2018, ALÖKI Kft., Budapest, Hungary

[29] Koç, E., Üstün, A. S., İşlek, C., Arıcı, Y. K. (2011): Defence responses in leaves of resistant and susceptible pepper cultivars infected with different inoculum concentrations of Phytophthora capsici Leon. – Scientia Horticulturae 128(4): 434-442 http://dx.doi.org/10.1016/j.scienta.2011.02.008.
[30] Kueh, T. K. (1990): Major Diseases of Black Pepper and Their Management. – The Planter, Kaula Lumpur 66(767): 59-69.
[31] Lamour, K. H., Stam, R., Jupe, J., Huitema, E. (2012): The oomycete broad-host-range pathogen Phytophthora capsici. – Molecular Plant Pathology 13(4): 329-337.
[32] Manohara, D., Rizal, M. (2002): Pests and diseases on pepper in indonesia and their management. – Paper Presented at the Symposium on Pests and Diseases on Pepper, Sarawak, Malaysia.
[33] Lin, C. C., Kao, C. H. (2001): Cell wall peroxidase activity, hydrogen peroxide level and NaCl-inhibited root growth of rice seedlings. – Plant Soil 230: 135-143.
[34] Mohammadi, M., Kazemi, H. (2002): Changes in peroxidase and polyphenol activity in susceptible and resistant wheat heads inoculated with Fusarium graminearum and induced resistance. – Plant Science 162: 491-498.
[35] Moscone, E. A., Lambrou, M., Ehrendorfer, F. (1996): Fluorescent chromosome banding in the cultivated species of *Capsicum* (Solanaceae). – Plant Systematics and Evolution 202: 37-63.
[36] Nam, T. N. T. (2012): Final Report of Project: Research, Supplement of Technical Standar for Black Pepper Production Following GAP in GiaLai. – The Western Highlands Agriculture and Forestry Science Institute, Vietnam.
[37] Ortega, I. M., Bryant, F. C., Drawe, D. L. (1995): Contrasts of esophageal-fistula versus bite-count techniques to determine cattle diets. – Journal of Range Management 48(6): 498-502.
[38] Ozgonen, H., Erkilic, A. (2007): Growth enhancement and *Phytophthora* blight (*Phytophthora capsici* Leonian) control by arbuscular mycorrhizal fungal inoculation in pepper. – Crop Protection 26(11): 1682-1688.
[39] Panishkan, K., Swangjang, K., Sanmanee, N., Sungthong, D. (2012): Principal component analysis for the characterization in the application of some soil properties. – World Acad Sci Eng Technol 6: 727-729.
[40] Pickersgill, B. (1997): Genetic resources and breeding of Capsicum spp. – Euphytica 96: 129-133.
[41] Pochard, E., Malot., P., Domingues, G. (1983): Etude de deux nouvelles sources de resistance a Phytophthora capsici Leon. chez le piment: confirmation de 1'existance de trois composantes distinctes dans la resistance. – Agronomie 3: 333-342.
[42] Ponmurugan P, Baby UI., Rajkumar, R. (2007): Growth, photosynthetic, and biochemical responses of tea cultivars infected with various diseases. – Photosynthetica 45: 143-146.
[43] Ray, H., Douches, D. S., Hammerschmidt, R. (1998): Transformation of potato with cucumber peroxidase: Expression and disease response. – Physiological and Molecular Plant Pathology 53: 93-103.
[44] Ristaino, J. B., Johnston, S. A. (1999): Ecologically based approaches to management of phytophthora blight on bell pepper. – Plant Disease 82(12): 1080-1089.
[45] Sanogo, S., Ji, P. (2012): Integrated management of Phytophthora capsici on solanaceous and cucurbitaceous crops: current status, gaps in knowledge and research needs. – Canadian Journal of Plant Pathology 34(4): 479-492.
[46] Stam, R., Jupe, J., Howden, A. J., Morris, J. A., Boevink, P. C., Hedley, P. E., Huitema, E. (2013): Identification and characterisation CRN effectors in Phytophthora capsici shows modularity and functional diversity. – PloS one 8(3): e59517.
[47] Sunwoo, J. Y., Lee, Y. K., Hwang, B. K. (1996): Induced resistance againstPhytophthora capsici in pepper plants in response to DL-β-amino-n-butyric acid. – European Journal of Plant Pathology 102(7): 663-670.

http://www.aloki.hu ● ISSN 1589 1623 (Print) ● ISSN 1785 0037 (Online)
DOI: http://dx.doi.org/10.15666/aeer/1605_68856901
© 2018, ALÖKI Kft., Budapest, Hungary

[48] Şişecioğlu, M., Gülçin, İ., Çankaya, M., Atasever, A., Şehitoğlu, M. H., Kaya, H. B., Özdemir, H. (2010): Purification and characterization of peroxidase from Turkish black radish (Raphanus sativus L.). – Journal of Medicinal Plants Research 4(12): 1187-1196.
[49] Sy, T., Cote, S., Saavedra, R. (2005): The contagious leader: Impact of the leader's mood on the mood of group members, group affective climate, and group processes. – Journal of Applied Psychology 90: 295-305.
[50] Ton, N. T., Nam, T. N. T., Don, L. D., Tri, M. V., Hieu, N. M., Phuong, N. B. (2005): S the Scientific, Technogogical and Marketing Measures for the Development of Black Pepper Production Serving to Processing and Export. – Final Report of National Research Project. Institute of Agricultural Science for Southern Vietnam, Ho Chi Minh City.
[51] Welinder, K. G. (1992): Superfamily of plant, fungal and bacterial peroxidase. – Curr. Opin. Struct. Biol. 2: 388-393.
[52] Yilmaz, B., Genc, A., Cimen, B., Incesu, M., Yeşiloğlu, T. (2017): Characterization of morphological traits of local and global persimmon varieties and genotypes collected from Turkey. – Turkish Journal of Agriculture and Forestry 41(2): 93-102.
[53] Yin, J., Jackson, K. L., Candole, B. L., Csinos, A. S., Langston, D. B., Ji, P. (2012): Aggressiveness and diversity of *Phytophthora capsici* on vegetable crops in Georgia. – Annals of Applied Biology 160(2): 191-200.

http://www.aloki.hu ● ISSN 1589 1623 (Print) ● ISSN 1785 0037 (Online)
DOI: http://dx.doi.org/10.15666/aeer/1605_68856901
© 2018, ALÖKI Kft., Budapest, Hungary

ANALYSIS OF THE EFFECT OF PLANT DENSITY AND USE OF SELENIUM ON OIL QUALITY AND QUANTITY IN WINTER-PLANTED CANOLA VARIETIES

ZAMAN FASHAMI, M.[1] – DADASHI, M. R.[2*] – SHIRANI-RAD, A. H.[3] – KHORGHAMI, A.[4]

[1]*Agronomy Department, Islamic Azad University, Golestan, Iran*

[2]*Gorgan Branch, Islamic Azad University, Golestan, Iran*

[3]*Seed and Plant Improvement Institute, Karaj, Iran*

[4]*Khoramabad Branch, Islamic Azad University, Lorestan, Iran*

**Corresponding author*
e-mail: mdadashi730@yahoo.com

(Received 29th May 2018; accepted 31st Aug 2018)

Abstract. This study was carried out in Iran to determine the effect of foliar application of Selenium and plant density on oil quality and quantity and fatty acid composition of canola cultivars. The experiment was laid out in a factorial split plot arrangement based on a complete blocked design with three replications at Karaj Seedling and Seed Breeding Institute, Karaj, Iran during 2015 and 2016. Treatments were plant density (40, 60 and 80 plants/area) and foliar application of selenium (0 and 30 $g.l^{-1}$ sodium selenite) in main plots and varieties (Sarigol, Hyola 401, Jacomo, Jerome, and Dalgan) in sub-plots**.** The results showed that year, plant density, selenium, variety treatments, and interaction effect of density*year and cultivar*density had a significant effect on seed yield, oil yield, oil percentage, and fatty acid composition, such as palmitic, linolenic, linoleic, oleic and erusic acids ($P \leq 0.01$). The Dalgan variety had the highest seed and oil yield in 40 plants per square meter (m^2) density (4817.41 and 2134.83 $kg.ha^{-1}$ respectively). Maximum seed oil content (43.78%) was obtained in 40 plants per square density treatment. However, the maximum rates of seed oil yield, palmitic acid, and linoleic acid were observed in Hyola-401 variety, and Jerome variety had the highest linolenic and erusic acid. The palmitic and linolenic acids in Dalgan variety at 40 plants per square treatment had the maximum rate. The findings showed that with increasing of plant density decreased grain yield, oil content and fatty acid compositions. However, application of selenium increased them especially in Dalgan variety. Also the highest seed yield, seed oil content and palmitic acid and lowest amount of linolenic and erusic acids was obtained in Dalgan variety. The maximum linoleic and erusic acid was obtained in Jermco variety. The lowest erusic acid was obtained in 40 plants per square treatment. The results also showed that foliar application of selenium increased seed yield, seed oil yield, palmitic, linolenic and erusic acid compared to non-application of it. In final the present study indicated that increased seed yield, oil content, oil yield and fatty acid quality in 40 plants/area treatment, specially Dalgan variety in Golestan province, Iran.
Keywords: *erusic acid, fatty acids, foliar application, sodium selenate, yield*

Introduction

Canola (*Brassica napus* L.) is an oilseed plant that has a wide range of adaptation to different climates, and has two autumn and spring types and is utilized in the crop rotation programs in different regions (Angadi et al., 2003). In terms of oil production canola is locate after soybean (FAO, 2017). Various canola cultivars' capability to germinate and grow at low temperatures resulted in increasing development of its cultivation in cold regions of the world, including Canada, northern Europe and the cold parts of Asia. This issue has caused several studies to be conducted on this product in

http://www.aloki.hu ● ISSN 1589 1623 (Print) ● ISSN 1785 0037 (Online)
DOI: http://dx.doi.org/10.15666/aeer/1605_69036916
© 2018, ALÖKI Kft., Budapest, Hungary

the cold regions. Following soybean, canola is the second most important source for production of edible oil in the world (FAO, 2017).

The canola seed oil content, quality and components have always been the concern of plant breeders. Fatty acid compounds and unsaturated fatty acids levels controlled genetically controlled but also affected by environmental conditions (Bellaloui et al., 2013). Studies have shown that some environmental factors, such as the temperature and shading (Ruuska et al., 2004), for example, at high plant density per unit area, change the composition of fatty acids. They state that the oil seed produced under shade conditions has less fatty acids than those produced in full sunlight. Today, the canola yield and oil quality have rapidly increased in order to mechanize harvesting, higher yield cultivars introduction, and better agronomic practices (Shahbaz et al., 2018). However, further studies are needed to increase canola oil yield and quality.

Plant density is the most important factor to reach the maximum crops yield. Along with the use of suitable cultivars adapted to the climatic conditions of each area, as well as the maximum use of environmental resources such as light, water, and nutrients, it can allow the result to achieve higher crop yields (Chavan, 1989). However, increasing the plant density reduces the number of stems per plant due to the increase of inter-plant competition, which decreases the number of stems or lateral branches by decreasing the allocated space per plant (Vega et al., 2000). Increasing the plant density results in the single plant yield reduction by reducing the number of sub-branches and the number of pods per plant, but the appropriate increase of plant density will result in compensation of sub-branch and plant yield components' reduction by increasing the number of plants per area (Onofri et al., 1996). In high density rape seed, plant bedding and chlorophyll degradation in the plant increased, resulting in the loss of yield due to inter and intra-plant competition (Morrison et al., 1990). They argued that the reduction of light in the plant community is a major cause of the early leaves senescence, and appropriate density can delay their senescence by having an effect on the leaves emitted radiation. It was reported that with the increasse in plant density, the number of pods per square increased, but the number of seeds per pod and 1000 grain weight linearly decreased that resulted in the decrease of grain yield (Ozer, 2003). Also, Bilgili et al. (2003) and Lythgoe et al. (2001) concluded that the plant density plays a major role in rapeseed grain yield. Canola can adjust its grain yield in a wide range of density. The ability of a plant to compensate of below optimal level density depends on available resources, such as light, water, and nutrients (Angadi et al., 2004). The scores of higher plant density are prevention of the large number of branches and the number of pods in branches that leads to uniform maturity of canola (Malhi and Gill, 2004).

Due to an impact on the growth and development of plants and its presence in antioxidant systems, selenium is recognized as one of the vital elements for human and animal health. While beneficial elements are not involved directly in the metabolism of plants and completing their life cycle, they play a role in improving the vegetative and reproductive growth, especially in environmental or biological stress conditions (Hajibolan, 2012). Recent findings reveal that selenium at low concentrations can enhance oxidative stress resistance by increasing antioxidant capacity, which has a positive effect on the decrease of lipid peroxidation. This indicates the positive impact of selenium in reducing lipid peroxidation and increasing the activity of anti-oxidative enzymes (Seppanen et al., 2003; Xue et al., 2001). Low concentration of selenium has a beneficial impact on the plants' growth and stress resistance through their antioxidant capacity (Turakainen, 2000). The use of selenium leads into an increase in plant height,

http://www.aloki.hu ● ISSN 1589 1623 (Print) ● ISSN 1785 0037 (Online)
DOI: http://dx.doi.org/10.15666/aeer/1605_69036916
© 2018, ALÖKI Kft., Budapest, Hungary

number of pods, number of seeds per pod, biological yield, harvest index and oil percentage and reduced respiration, proline and malondialdehyde (Bybordi, 2016). Seppanen et al. (2003) reported that selenium prevents chlorophyll degradation in environmental stress conditions. Other beneficial impacts of selenium are increasing metabolism of carbohydrates and the stress resistance (Zhu et al., 2004). Haji Boland et al. (2014) showed that the impact of selenium in increasing drought resistance and improving the water relations in canola was related to increasing the water absorption due to development of root, which increased the photosynthesis and forming the soluble sugars. By conducting the studies on the methods of increasing the yield under density conditions, we can provide an appropriate mechanism for improving product yields.

However, information on selenium foliar application and plant density on fatty acid composition changes and oil quality are limited in canola. Therefore, this study was conducted to examine the application of selenium on the seed oil quantity and quality in various winter-planted canola cultivars, in order to reduce the adverse effects of stress resulting from density.

Material and methods

Research location: the present study was conducted in two years of 2015 and 2016 in a 400-ha farm of Karaj Seedling and Seed Breeding Institute, Karaj, Iran (35°49'). The latitude of the location is 35°49'N and its longitude is 51°6'E and its height from sea surface is 1321 m.

Meteorological information: this region is considered among the hot and dry Mediterranean climate regions based on the climate data and amberthermic curve, due to having 150 to 180 dry days in a year. It is also considered a dry humidity regime, due to having cold and wet winters and hot and dry summers. According to the 30-year Karaj meteorological information, the average rainfall is 243 mm per year. In this region, rainfall occurs often in the late fall and early spring. The average annual maximum temperature is seen in July with 28 °C and the average annual minimum temperature is seen in January with 1 °C. The average temperature of this region in a 30-year period is 13.5 °C and the soil temperature is 14.5 °C.

Soil characteristics of the region: according to *Table 1,* soil texture of the region is loamy and clay (*Table 1*).

Table 1. *Soil characteristics in experimental location*

Characteristics	Electrical conductivity (dS/m)	pH	Percentage of neutralized materials	Humidity percentage of saturated clay	Organic carbon (%)	Nitrogen (%)	Phosphorus (Mg/kg)	Potassium (Mg/kg)	Percentage of clay	Percentage of silt	Percentage of sand
Sampling depth (0-30 cm)	1.45	7.9	8.56	36	0.91	0.09	14.7	197	28	47	25
Sampling depth (30-60 cm)	1.24	7.2	8.68	38	0.99	0.07	15.8	155	25	49	26

http://www.aloki.hu ● ISSN 1589 1623 (Print) ● ISSN 1785 0037 (Online)
DOI: http://dx.doi.org/10.15666/aeer/1605_69036916
© 2018, ALÖKI Kft., Budapest, Hungary

According to the results of soil analysis and fertilizer recommendation, we applied fertilizer (a part of the N fertilizer and all of the P and K fertilizer required). We also applied Treflan herbicide (2.5 l/ha) laid uniformly in field. Fertilizer and herbicide were mixed with soil using disk. For the optimal usage of nitrogen, the rest of the required nitrogen fertilizer was used at the beginning of the stem generation and the emergence of the first flower buds. After conducting the experiment, the feeding operation including the control of pests, especially wax aphid, was performed using metasystoxpesticide in accordance with the planting plan and seedling emergence, which was approximately 1.5 l/ha.

Statistical design: the experiment was laid out in a factorial split plot arrangement based on completely randomized block design with three replications. Here, we would plot the plants to the maximum capacity in terms of density and would separate and single out the plants to reach an ideal amount for this experiment. In this experiment, treatments were plant density at three levels of 40, 60 and 80 m^2 and with selenium in two levels of control (lack of foliar application (water) and foliar application with selenium at amounts of 30 $g.l^{-1}$ sodium selenate were placed as a factorial in main plots, and five cultivar such as Sarigol, Hyola 401, Jacomo, Jerome, and Dalgan was placed at sub-plots. Each experimental plot included 6 rows with 30 and 4 cm row to row and plant to plant distance respectively. Middle rows were harvested to seed yield to determination. Irrigation was performed in accordance with the plant requirement using siphon. Foliar application of selenium (30 $g.l^{-1}$ sodium selenite per hectar) applied in two stages, 15 $g.l^{-1}$/ha before rosette and 15 $g.l^{-1}$/ha in the fast stem growth stage and foliar application of water as control. After treatments, a 5 grams seed sample was selected from each plot to determine the amount of the seed oil content using an NMR device. After determining the seed oil percentage, the seed yield was calculated in $kg.ha^{-1}$. Gas chromatography method was used to measure and determine the seed oil fatty acid and its composition (Yang et al., 2009). Statistical analysis was also performed using the SAS 9.1 software. In order to compare the means of the traits, Duncan statistical method was used at the level of 5%.

Results

Seed yield: according to the analysis of variance table, the effect of year, density, variety, and selenium, the interaction effect of variety * density were significant on seed yield ($P \leq 0.01$). Also, the effect of year, block and density were significant on seed oil content, while the interaction of the studied treatments had no significant effect on this trait (*Table 2*). The effect of year, block, density, variety, selenium and interaction effect of variety * density were significant on seed oil yield ($P \leq 0.01$). The results of present study showed that the year, block, density, selenium, variety treatments were significant on fatty acid composition, such as palmitic, linolenic, linoleic, oleic and erusic acids ($P \leq 0.01$). However, the interaction effect of variety * density were significant on all fatty acid composition, except linolenic and oleic acids (*Table 2*).

The results showed that the highest seed yield was obtained in Dalgan variety cultivated in 40 plants per m^2 density (4817.41 $kg.ha^{-1}$), and the lowest seed yield was obtained in Sarigol variety at 80 plant per m^2 density (1519.91 $kg.ha^{-1}$) (*Fig. 1*). Based on the results, the Jerome variety had the lowest seed yield in 40 and 60 plant per m^2 density treatment (3895 and 2541 $kg.m^{-2}$ respectively) (*Fig. 1*). Increasing the plant density decreases seed yield significantly in all varieties.

http://www.aloki.hu ● ISSN 1589 1623 (Print) ● ISSN 1785 0037 (Online)
DOI: http://dx.doi.org/10.15666/aeer/1605_69036916
© 2018, ALÖKI Kft., Budapest, Hungary

The findings of the present study showed that the highest seed oil content was obtained at the 40 plants per square density treatment (43.78%), compared to 80 plants per square density treatment (41.71%) ($P \leq 0.05$) (*Table 3*). However, in 40 plants per square density treatment, the highest seed oil yield, palmitic, linoleic acid, linolenic, oleic and erusic acids were obtained and with increasing the plant density it reduced them significantly (*Table 3*). There are significant reductions in seed yield, seed oil yield, palmitic, linoleic acid, linolenic, oleic and erusic acids by the increase in plant densities (*Table 3*).

Table 2. *Analysis of variance for effect of plant density and application of selenium on seed yield and oil quality of canola varieties*

Source of variations	df	Seed yield (kg/ha)	Seed oil content (%)	Seed oil yield (kg/ha)	Palmitic acid (%)	Linolenic acid (%)	Linoleic acid (%)	Oleic acid (%)	Erusic acid (%)
Year	1	2033944**	53.38**	708886**	8.42**	1.02**	22.66**	15.89 ns	0.004**
Block (year)	4	196524**	21.20*	101354**	0.63**	0.49**	6.23**	23.18**	0.001 ns
Density	2	88636772**	64.22**	18379067**	29.52**	86.01**	183.25**	194.89**	0.43**
Year×density	2	31792 ns	2.53 ns	21324 ns	0.51**	0.02 ns	0.22 ns	0.47 ns	0.00 ns
Selenium	1	1340929**	2.89 ns	283387**	0.39*	0.97**	2.43 ns	2.36 ns	0.01**
Year×selenium	1	1572 ns	0.04 ns	1680 ns	0.00 ns	0.01 ns	0.00 ns	0.00 ns	0.00 ns
Density×selenium	2	167427*	0.17 ns	43175 ns	0.03 ns	0.07 ns	0.31 ns	0.23 ns	0.001 ns
Year×density×selenium	2	6707 ns	0.03 ns	1849 ns	0.01 ns	0.01 ns	0.00 ns	0.00 ns	0.00 ns
Block×year×density×selenium	20	201006	17.11	24449	0.36	0.52	3.12	10.06	0.001
Variety	4	3889155**	3.05 ns	825393**	1.27**	3.79**	8.04**	8.96 ns	0.02**
Variety×density	8	734100**	0.57 ns	156745**	0.26**	0.71**	1.41 ns	1.51 ns	0.003**
Variety×selenium	4	81848 ns	0.04 ns	17.338 ns	0.02 ns	0.04 ns	0.13 ns	0.14 ns	0.00 ns
Year×variety	4	9775 ns	0.11 ns	1667 ns	0.01 ns	0.00 ns	0.02 ns	0.03 ns	0.00 ns
Year×density×variety	8	6752 ns	0.03 ns	1600 ns	0.02 ns	0.02 ns	0.01 ns	0.01 ns	0.00 ns
Year×selenium×variety	4	2274 ns	0.00 ns	679 ns	0.00 ns	0.00 ns	0.00 ns	0.00 ns	0.00 ns
Density×selenium×variety	8	42383 ns	0.02 ns	9653 ns	0.01 ns	0.03 ns	0.05 ns	0.006 ns	0.00 ns
Year×density×selenium×variety	8	2481 ns	0.01 ns	843 ns	0.00 ns	0.00 ns	0.00 ns	0.00 ns	0.00 ns
Total error	96	52358	7.42	18583	0.07	0.11	1.68	6.63	0.00
Coefficient of variations (%)	-	7.46	6.37	10.33	5.3	5.71	6.81	3.97	5.90

*, **, and ns represent significance at the level of 5% and 1%, and non significance, respectively

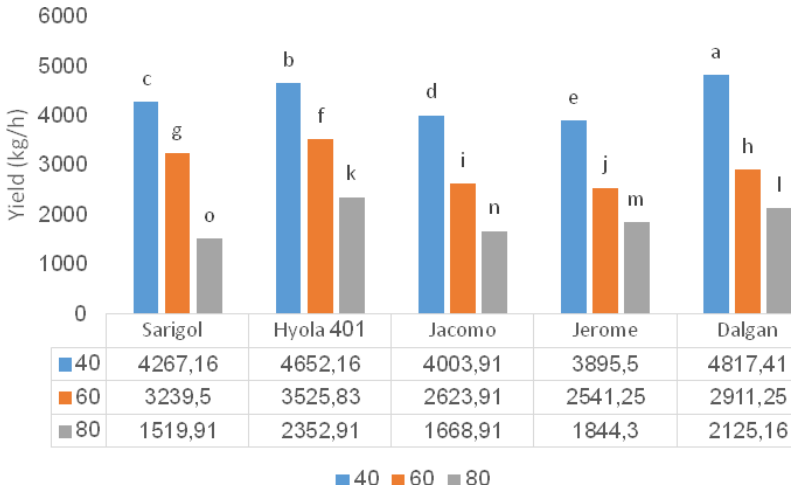

Figure 1. *Effect of different densities on seed yield of canola varieties. (Columns by uncommon letters had significant differences)*

http://www.aloki.hu ● ISSN 1589 1623 (Print) ● ISSN 1785 0037 (Online)
DOI: http://dx.doi.org/10.15666/aeer/1605_69036916
© 2018, ALÖKI Kft., Budapest, Hungary

Table 3. *Effect of different densities on seed yield and fatty acid compounds in the canola varieties*

Density (plant per m^2)	Seed yield (kg/ha)	Seed oil content (%)	Seed oil yield (kg/ha)	Palmitic acid (%)	Linolenic acid (%)	Linoleic acid (%)	Oleic acid (%)	Erusic acid (%)
40	4327.23a	43.782 a	1896.45 a	5.85 a	7.06 a	20.74 a	65.35a	0.39 a
60	2963.35 b	42.6797 b	1267.85 b	5.21 b	5.85 b	18.96 b	63.53 b	0.31 b
80	1902.25c	41.7143 c	793.1c	4.45 c	4.66 c	17.25 c	61.75 c	0.22 c

Means by uncommon letters had significant differences

Foliar application of selenium increased seed yield significantly compared to control (3679.63 $kg.ha^{-1}$) (*Table 4*). Also, The results of the present study showed that application of selenium increases seed oil yield (1358.81 $kg.ha^{-1}$), palmitic (5.21%), linolenic (5.93%) and erusic (0.32%) acids (*Table 4*).

Table 4. *Effect of selenium application on seed yield and fatty acid compounds in the canola varieties*

Selenium	Seed yield (kg/ha)	Seed oil yield (kg/ha)	Palmitic acid (%)	Linolenic acid (%)	Erusic acid (%)
Selenium foliar application	3679.63 a	1358.81 a	5.21 a	5.93 a	0.32 a
Lack of application with foliar application	3152.26 b	1279.46 b	5.12 b	5.78 b	0.30 b

Means by uncommon letters had significant differences

The results showed that the highest amount of seed oil yield (1521 $kg.ha^{-1}$), palmitic acid (5.452%) and linoleic acid (19.62%) were obtained in Hyola-401 variety but the highest linolenic acid (6.17%) and erusic acid (0.33%) were obtained in Jerome variety (*Table 5*). However, the erusic acid, as a negative factor in fatty acid composition in the Dalgan variety, was lower than other varieties (0.29%). There are no significant differences between Jacomo and Jerome varieties in seed yield, seed oil yield, palmitic, linolenic, linoleic and erusic acids. However between Hyola-401 and Dalgan there are no significant differences in palmitic and linoleic acids.

Table 5. *Effect of variety treatment on seed yield and some fatty acid compounds in the canola varieties*

Variety	Seed yield (kg/ha)	Seed oil yield (kg/ha)	Palmitic acid (%)	Linolenic acid (%)	Linoleic acid (%)	Erusic acid (%)
Hyola 401	3510.31a	1521.44 a	5.42 a	5.41d	19.62 a	0.27d
Dalgan	3284.61b	1421.58b	5.29 a	5.65 c	19.30ab	0.29 c
Sarigol	3008.86c	1296.38 c	5.15 b	5.90 b	18.91bc	0.31 b
Jacomo	2765.58 d	1180.03 d	5.01 c	6.14 a	18.56 c	0.33 a
Jerome	2760.36 d	1176.25 d	4.98 c	6.17a	18.53c	0.33 a

Means by uncommon letters had significant differences

http://www.aloki.hu ● ISSN 1589 1623 (Print) ● ISSN 1785 0037 (Online)
DOI: http://dx.doi.org/10.15666/aeer/1605_69036916
© 2018, ALÖKI Kft., Budapest, Hungary

The results showed that the Dalgan variety had the highest oil yield in 40 plants per m^2 density treatment (2134.83 $kg.ha^{-1}$), while Jerome variety had the lowest oil yield at the same density (1686.75 $kg.ha^{-1}$) (*Fig. 2*). However, in 80 plants per square density treatment the Sarigol variety had the lowest seed oil content (628.08 $kg.ha^{-1}$). Based on the results in all varieties, oil yield decreased significantly by the increase in plant density.

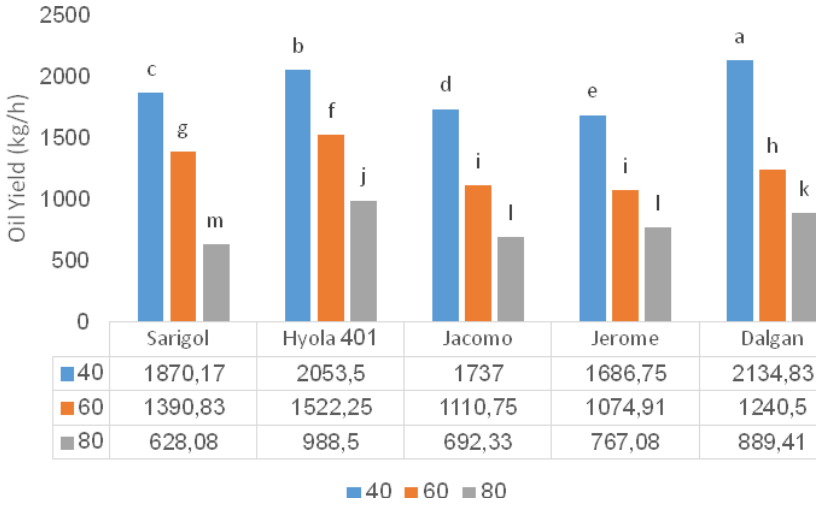

Figure 2. *The interaction effect of different densities on oil yield of canola varieties. (Columns by uncommon letters had significant differences)*

The 40 plants per square treatment had the highest fatty acid composition. The highest palmitic and linolenic acids was observed in Dalgam cultivar at 40 plants per square density treatment with amounts of 6.08 and 66.06, respectively. In addition, the lowest amount of erusic acid (0.18) was obtained in this cultivar with the same density conditions (*Table 6*). The oleic, linolenic and linoleic as three unsaturated fatty acids that oleic and erusic acids significantly decreased with increasing plants density (*Tables 3* and *6*), reaching a a maximum reduction in 80 plant per square density treatment compared with the 60 plant per square treatment. Interaction effect of plant density*variety shows that the highest palmitic acid (6.08%) and oleic acid (66.06%) were obtained in Dalgan variety in 60 plant per square density treatment (*Table 6*). The decrease of these fatty acid compounds result to oil quality reduction. The 40 plants per square density treatment had the lowest erusic acid and in this plant density treatment erusic acids percent in Dalgan, Hyola-401, Sarigol, Jacomo and Jerome varieties were 18, 19, 23, 24 and 25%, respectively (*Table 6*)

Table 6. *Interaction effect of plant density*variety on fatty acid composition in canola varieties*

Density (plant per m^2)	**Variety**	**Palmiticacid** (%)	**Oleic acid** (%)	**Erusic acid** (%)
40	Sarigol	5.79 C	65.21 b	0.23 m
	Hyola 401	6.00 b	65.85 a	0.19 n
	Jacomo	5.70 d	64.86c	0.24 l
	Jerome	5.65 e	64.79 c	0.25 k
	Dalgan	6.08 a	66.06 a	0.18 o

http://www.aloki.hu ● ISSN 1589 1623 (Print) ● ISSN 1785 0037 (Online)
DOI: http://dx.doi.org/10.15666/aeer/1605_69036916
© 2018, ALÖKI Kft., Budapest, Hungary

60	Sarigol	5.42 g	63.96e	0.29 i
	Hyola 401	5.53 f	64.37 d	0.27 j
	Jacomo	4.99 i	63.01 g	0.33 g
	Jerome	4.88 j	62.82 g	0.34 f
	Dalgan	5.24 h	63.49 f	0.31 h
80	Sarigol	4.23 o	63.21 k	0.42 a
	Hyola 401	4.72 k	62.45 h	0.36 e
	Jacomo	4.32 n	61.42 jk	0.41 b
	Jerome	4.40 m	61.61 j	0.40 c
	Dalgan	4.56 l	62.04 i	0.38 d

Means by uncommon letters had significant differences

The palmitic acid content in 2016 was higher than 2015 due to the lower temperature at the grain filling period. In both years, the palmitic acid as a saturated fatty acid decreased linearly with increasing of plant density. The results also showed that palmitic acid decreased significantly by the increase of plant density in both years (*Fig. 3*).

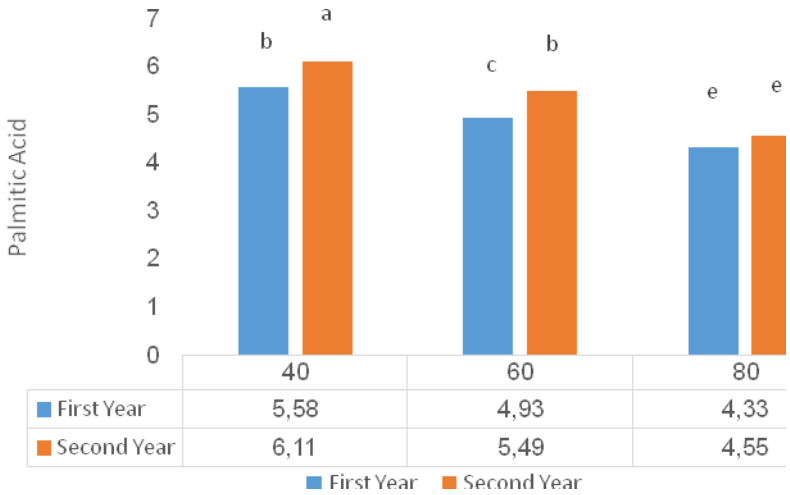

Figure 3. *The effect of different plants density on palmitic acid in canola varieties during 2015-2016. (Columns by uncommon letters had significant differences)*

Discussion

In the present study there are significant differences between varieties in the seed yield. Rezadoost and Rashidi (2003) reported that cultivar had a significant effect on the seed yield ($P \leq 0.01$). Increasing the plant density from 40 to 80 plants per square decreases the seed yield of canola genotypes from 6337 kg.ha^{-1} to 2741 kg.ha^{-1} (Nasiri et al., 2017). Looking at the yield components, including the number of pods per plant, number of seeds per pod and 1000-seed weight, it is seen that all of these traits are affected by factors such as the optimal use of light, nutrients, appropriate density, efficient photosynthesis and the adequate uptake of assimilate materials by plant, which all of them are effective in increasing the seed yield (Wales, 1991). Onofri et al. (1996) found that seed yield per hectare increased with increasing plant density, but an extreme

http://www.aloki.hu ● ISSN 1589 1623 (Print) ● ISSN 1785 0037 (Online)
DOI: http://dx.doi.org/10.15666/aeer/1605_69036916
© 2018, ALÖKI Kft., Budapest, Hungary

increase in the plant density reduced seed yield. The seed yield was reduced in this study as density was increased from 40 to 80 plants per square meter that is in line with findings of Chavan et al. (1989); Patel et al. (1980) and Tanveer et al. (1998) in canola. Increasing the plant population per square in high density plants result in increasing of the inter-plant competition for water and nutrients, and the reduced grain number and weight per plants that laid to the grain yield reduction. Vega et al. (2000) concluded that plant density forced a strong competition for water and nutrient absorption during the grain filling period. This means that the process distributed lower nutrient between grains, therefore allocating less dry matter to physiological sinks at grain filling period. The Jerome variety had the lowest seed yield in 40 and 60 plant per m^2 density. Similarly, Naseri et al. (2012) reported that the thicker density plans (80 plants per m^2) reduced canopy sunlight absorption, assimilation, and transformed them to reproductive sinks that laid to the increasing of competition among plants and seed yield reduction. Chavan et al. (1989) reviled that higher plant densities resulted in seed yield reduction due to the increase of plant elongation and competition. However, in an appropriate density, environmental factors were optimum for higher assimilation then achieving higher seed yield.

Different results have been observed on the effect of plant density on the changes in oil content of oil-seed plants. Danesh-Shahraki et al. (2008) held that the plant density had a significant effect on oil content of canola. The seed oil content was reduced associated with increasing of plant density in canola (Onofri et al., 1996), sunflower (Vega, 2000) and soybean (Wells, 1991). It seems that the low and uniform distribution of plants in a lower plant density reduces the plant competition and better photosynthetic system performance that results in increasing of the seed oil content (Wells, 1991). Onofri et al. (1996) attributed the increasing of oil percent in lower plant density per unit area to the increasing number of pods per plant and the relative grain size reduction.

With regards to this fact that the application of selenium increased grain yield, some researchers founded that the application of selenium increases yield in rapeseed (Zahedi et al., 2009), potato (Turakainen et al., 2004; Germ et al., 2007), lettuce (Ramos et al., 2010) and buckwheat (Ozbolt et al., 2008). Kopsell et al. (2000) founded that foliar application of selenium increases chlorophyll content of *Brassicaoleracea* due to positive effects of leaves' Mg content that led to the increase of the photosynthesis and yield. Selenium delayed leaf senescence (Hawrylak-Nowak et al., 2009), increased plant growth and yield due to the increase of starch storage in chloroplasts (Xue et al., 2001). They also told that the selenium had a protective role for cell water status and adjusted it in a water deficit condition. Germ et al. (2003) holds that the selenium consumption by plants compensate the water deficit that results to increasing of grain yield. Even though selenium is not an essential element for plant growth (Djanaguiraman et al., 2005), the present study indicates that the foliar application of selenium increased the grain yield of canola at 30 $g.l^{-1}.ha^{-1}$. Zahedi et al. (2010) argued that the increase of rapeseed grain yield by foliar application of selenium is due to the increase of number of pods per plant and the number of grain per pods, which are in line with these findings. The application of selenium reduced the water deficit stress damages in potato (Germ et al., 2007) and rapeseed (Valadabadi et al., 2010) and that laid to the increase of biological yield.

The seed oil yield and fatty acid composition increased with the application of selenium. Other researchers such as Davoodi et al. (2016) founded that fatty acid

http://www.aloki.hu ● ISSN 1589 1623 (Print) ● ISSN 1785 0037 (Online)
DOI: http://dx.doi.org/10.15666/aeer/1605_69036916
© 2018, ALÖKI Kft., Budapest, Hungary

composition such as palmitic acid oleic acid, were increased by the foliar application of selenium in canola. Since Linoleic acid is an essential fatty acid for photosynthetic activity (Hugly et al., 1989) and canola pollen development (Mc-Conn and Browse., 1996), selenium application seems to increase the linoleic acid synthesis and the improvement of photosynthetic conditions, which lead to the increase of plant grain yield. However, the increase of seed oil yield might be the result of supply assimiliation at grain filling period which linked with the increase of silique photosynthesis (Shahbaz et al., 2018). They also find that canola oil quality is depended on quantity of oleic, linoleic, and linolenic acids as fatty acid composition. The composition of canola fatty acid has 60–65% oleic acid, 18–20% linoleic acid, 10–10.5% linolenic acid, and less than 3% erusic acid (Rathke et al., 2006). However, it should be noted that the erusic acid is an important indicator for rapeseed oil quality and its edible consumption (Gesgel et al., 2007), and in this study, foliar application of selenium increases erusic acid content.

The Hyola-401 variety had the highest seed oil yield. Naseri et al. (2012) founded the Hyola-401 hybrid had the highest seed yield than Hyola 308, Zarfam and Sarigol cultivars. They argued that the seed yield difference may be due to their genetic properties. Pasbaneslam (2015) evaluated 23 spring and autumn genotypes of canola in terms of seed yield, oil, and seed oil percentage, and he reported a significant difference among the cultivars. They found that there are significant differences between the different genotypes in this state. However differences between varieties in seed yield can be found because of genetic differentiation. The variation of seed yield among the rapeseed varieties may be attributed to their genetic potential (Sana et al., 2003). There are significant differences for seed yield between 29 genotypes of *Brassicanapus* L. (Khehra and Singh, 1988). It seems that the Dalgan variety may be tolerant to environmental factors while others may be susceptible. The amount of seed yield, seed oil content, palmitic acid, linolenic acid, linoleic acid anderusic acid in Jerome variety are equal to Jacomo, and their differences were not significant (*Table 5*). Some researchers such as Das (1998), Baranyk and Zukalova (2000) and Gentent et al. (1996) reported the differences in oil yield and oil content of *brassica* species. The variation in genetic variety make up and genetic background of each variety is the main reason for different amount of seed oil content (Sana et al., 2003). Adaptation characteristics of different varieties to environmental condition are another reason for this phenomenon.

The Dalgan variety was better than other varieties in oil yield at 40 plants per m^2 density. The Sarigol variety had the lowest seed oil content compared to other varieties. The seed oil yield had a negative correlation with seed size (Onofri et al., 1996). High oil yield in 40 plants per square density treatments could be due to the high seed yield (Nasiri et al., 2017). It was reported that the thin density leads to the increase in pod per plant and the reduction of seed size and the increase of seed oil content in thin density (Onofri et al., 1996). Two main factors that affected the canola oil content are genetic and environmental factors (Ozoni and Davaji, 2007). However the higher seed oil yield in Dalgan variety is due to the smaller seed size and the higher number of seed per plant compare to other varieties. In the present study, the seed oil yield reduced at high plant population treatments was due to the reduction of seed yield. The changes of seed yield result correlate to the same direct change of oil yield (Ali and Zhou, 2018). Ozer (2003) reviled that the lower seed size is associated with higher seed oil yield that is in line with these findings. Based on the results, the increase in plant density results in the increase of plant vegetative growth of seedlings, which reduced photo assimilation of

http://www.aloki.hu ● ISSN 1589 1623 (Print) ● ISSN 1785 0037 (Online)
DOI: http://dx.doi.org/10.15666/aeer/1605_69036916
© 2018, ALÖKI Kft., Budapest, Hungary

translocation to reproductive grain sinks then seed oil percentage. Also, increasing of vegetative growth coincide the grain filling period to high temperatures of July and August, which negatively affects the plant metabolism and oil synthesis.

The palmitic and linolenic acids in Dalgam variety were higher than others mainly in 40 plants per square density. The oleic, linolenic and linoleic as well decreased in higher plant densities. The decrease of these fatty acid compounds is the result of oil quality reduction. Nasiri et al. (2017) holds that the highest erusic acid was founded in 80 plants per square that was in line with present findings. Also Fathy et al. (2009) founded that highest palmitic acid and linoleic acid increased by plant density increase, which was in line with present results too. Shahbaz et al. (2018) holds that the content of rapeseed erusic acid was significantly reduced at high plant density compared with to the low plant density. Our study in 2015-2016 indicated that Palmitic acid influenced by plant density and year treatments. The palmitic acid decreased in higher plant density compared to lower densities. However, seed filling period is a crucial stage in oilseed growth, and during grain filling period plant density effects on oil quality, stability, and content. Decreasing the oil content and oil yield in the higher plant density is the main reason for reduction of fatty acid compounds, such as the saturated and unsaturated fatty acids. The higher plant densities result in increasing of vegetative growth and late pod formation in the field condition. The pod shattering due to the nonuniformed pods maturity at higher plant densities leads to seed damage, resulting in low oil quality. Shahabaz et al. (2018) concludes that changes in conversion of carbohydrates into lipids as photosynthetic function negatively affect biosynthesis and accumulation of fatty acids that is founded in higher canola plant density. The unsaturated fatty acids, oleic acid for example, were strongly influenced by environmental changes. The linoleic acid is an important and essential fatty acid for the photosynthetic activity of the plant (Hugly et al., 1989) and the development of canola pollen (Mc-Conn and Browse, 1996). However, because the synthesis of fatty acids is a light-dependent process (Suresha et al., 2013), the increase in plant density reduced their biosynthesis due to the increase of shading in the canopy. The canola grain filling period is one of the most sensitive stages that changes in temperature and sunlight in this period, and it directly affects the fatty acid composition, accumulation of assimilates, and their modification of the source-sink ratio (Gauthier, 2017). Based on Ruuska et al. (2004) seeds produced in shade conditions have a lower fatty acids compared to the seeds of plants fully exposed to the sunlight. Therefore, in this study, the increase of shading in higher plant density treatments led to a decrease in seed oil content and composition of saturated and unsaturated fatty acids in canola.

Conclusion

This study was laid out in order to study the effect of foliar application of selenium on seed yield, quality and quantity of seed oil of canola varieties in three 40, 60 and 80 plant/area treatments. Based on the results, plant density and foliar application of selenium was significant on seed yield, oil production, and fatty acid compositions of canola varieties. The maximum seed yield in canola was founded in foliar application of selenium and low plant density. The amount of two beneficial fatty acids in canola oil including linoleic acid (Omega 6) and oleic acid (Omega 9) was reduced by increasing of plant density treatments. In addition, the application of selenium element reduced harmful fatty acids, such as erusic acid, while it increased the beneficial fatty acids such

http://www.aloki.hu ● ISSN 1589 1623 (Print) ● ISSN 1785 0037 (Online)
DOI: http://dx.doi.org/10.15666/aeer/1605_69036916
© 2018, ALÖKI Kft., Budapest, Hungary

as oleic acid and linoleic acid. Our results showed that the Dalgan had a highest seed yield compared to other varieties. However, these findings suggest that, the Dalgan variety with 40 plant/area along with foliar application of selenium is better treatment to achieving the highest canola seed yield and oil quality in the Golestan province, Iran.

REFERENCES

[1] Angadi, S. V., Cutforth, H. W., McConkey, B. G., Gan, Y. (2003): Yield adjustment by canola grown at different plant population under semiarid conditions. – Crop Science 43: 1358-1366.

[2] Angadi, S. V., Cutworth, H. W., McConkey, B. G., Gan, T. (2004): Early seeding improves the sustainability of canola and mustard production on the Canadian semiarid prairie. – Canadian Journal of Plant Science 84: 705-711.

[3] Baranyk, P., Zukalova, H. (2000): Seed yield, oil content and oil yield of hybrid oilseed rape in the conditions of Czech Republic. – Rostlina Vyroba 46: 521-526.

[4] Bellaloui, N., Hu, Y., Mengistu, A., Kassem, M. A., Abel, C. A. (2013): Effects of foliar boron application on seed composition, cell wall boron, and seed δ15N and δ 13C isotopes in water-stressed soybean plants. – Frontiers in Plant Science 4: 270-281.

[5] Bilgili, U., Sincik, M., Uzan, A., Acikgoz, E. (2003): The influence of row spacing and seeding rat on seed yield and yield components of forge turnip (*Brassica napus L.*). – Journal of Agronomy Crop Science 189(4): 250-254.

[6] Bybordi, A. (2016): Influence of zeolite, selenium and silicon upon some agronomic and physiologic characteristics of canola grown under salinity. – Communications in Soil Science and Plant Analysis 47: 832-850.

[7] Chavan, S., Kanade, A., Shinde, V., Hanvilkar, A. (1989): Effect of dates of sowing, plant density and levels of nitrogen on mustard. – Journal of Maharashtra Agriculture Universities 14: 198-200.

[8] Danesh-Sharaki, A., Kashani, A., Mesgarpour, M., Nabipour, M., Koohi, M. (2008): The effect of density and nitrogen time utilization on some farming agronomic of rapeseed. – Study and Construction in Agriculture & Horticulture 79: 10-17 (in Persian).

[9] Davoodi, A. S., Mirashkari, B., Shiranairad, A. H., Farahush, F., Rashidi, V. (2016): Effect of selenium brecmite application and seed oil quality on rapeseed cultivars. – Journal of Research on Plant Physiology 8 (31): 129-143 (in Persian).

[10] Djanaguiraman, M., Devi, D. D., Shanker, A. K., Sheeba, J. A., Bangarusamy, U. (2005): Selenium - an antioxidative protectant in soybean during senescence. – Plant & Soil 272: 77-86.

[11] Fathy, S., El-Nakhlawy, A., Bakhashwain, A. (2009): Performance of canola (*Brassica napas* L.) seed yield, yield components and seed quality under the effects of four genotypes and nitrogen fertilizer rates. – Meteorology, Environment & Arid Land Agriculture Science 20(2): 33-47.

[12] Food and Agriculture Organization (FAO) (2009): Crop Production Statistics. – http://www.fao.org/docrep/010/ah864e/ah864e00.htm.

[13] Food and Agriculture Organization (FAO) (2017): Food Outlook. Global Market Analysis. – http://www.fao.Food outlook.com.

[14] Gauthier, M., Pelleta, D., Monneya, C., Herreraa, J. M., Rougiera, M. B., Baux, A. (2017): Fatty acids composition of oilseed rape genotypes as affected by solar radiation and temperature. – Field Crops Research 212: 165-174.

[15] Gentent, A., Rakow, G., Roney, J. P., Downey, R. K. (1996): Agronomic performance and seed quality of Ethiopian mustard in Saskatchewan. – Canadian Journal of Plant Science 76: 387-392.

http://www.aloki.hu ● ISSN 1589 1623 (Print) ● ISSN 1785 0037 (Online)
DOI: http://dx.doi.org/10.15666/aeer/1605_69036916
© 2018, ALÖKI Kft., Budapest, Hungary

[16] Germ, M., Kreft, I., Stibilj, V., Urbanc-Bercic, O. (2007): Combined effects of selenium and drought on photosynthesis and mitochondrial respiration in potato. – Plant Physiology & Biochemistry 45: 162-167.
[17] Hajiboland, R. (2012): Effects of Micronutrient Deficiencies on Plants Stress Responses. – In: Parvaiz, A., Prasad, M. N. V. (eds.) Abiotic Stress Responses in Plants: Metabolism, Productivity and Sustainability. – Springer, New York, pp. 282-326.
[18] Hajiboland, R., Kivanfar, N., Jodmand, A., Rezaee, H., Yousefnejad, M. (2014): Effect of selenium treatment on stress tolerance in rapeseed. – Journal of Plant Research 4: 557-568.
[19] Hawrylak-Nowak, B., Matraszek, R., Pogorzelec, M. (2015): The dual effects of two inorganic selenium forms on the growth, selected physiological parameters and macronutrients accumulation in cucumber plants. – Acta Physiologiae Plantarum 37(41): 1-13.
[20] Hugly, S., Kunt, L., Browse, J., Somerville, C. (1989): Enhanced thermal tolerance of photosynthesis and altered chloroplast ultrastructure in a mutant of Arabidopsis deficient in lipid desaturation. – Plant Physiology 90: 1134-1142.
[21] Khehra, M. K., Singh, P. (1988): Sensitivity and performance of some Brassica napus genotypes in stress and non-stress environments. – Crop Improvement India 15: 209-211.
[22] Kopsell, D. A., Randle, W. M., Mills, H. A. (2000): Quantitative, chemically specific imaging of selenium nutrient accumulation in leaf tissue of rapid-cycling Brassica oleracea responds to increasing sodium selenate concentrations. – Journal of Plant Nutrition 23: 927-935.
[23] Lythgoe, B., Norton, R. M., Nicolas, M. E., Conner, D. J. (2001): Compensatory and competitive ability of tow canola cultivars. – International Journal of Agronomy 2: 1-8.
[24] Malhi, S., Gill, K. S. (2004): Placement, rate and source of N, seed row spacing and seeding depth effects on canola production. – Canadian Journal of Plant Science 84: 719-729.
[25] Mc-Conn, M., Browse, J. (1996): The critical requirement for linolenic acid ispollen development, net photosynthesis, in an Arabidopsis mutant. – The Plant Cell 8: 403-416.
[26] Morrison, M. J., McVetty, P. B. E., Scarth, R. (1990): Effect of row spacing and seeding rate on summer rape in southern Manitoba. – Canadian Journal of Plant Science 70: 127-137.
[27] Naseri, R., Kazemi, E., Mahmoodian, L., Mirzae, A., Soleymanifard, A. (2012): Study on effect of different plant density on seed yield, oil and protein content of four canola cultivars in western Iran. – Intentional Journal of Agriculture & Crop Science 4(2): 70-78.
[28] Nasiri, A., Samdaliri, M., Shirani Rad, A., Shahsavari, N., MosaviMirkale, A., Jabbari, H. (2017): Effect of plant density on yield and physiological characteristics of six canola cultivars. – Journal of Scientific Agriculture 1: 249-253.
[29] Onofri, A., Tei, F., Ciriciofolo, E. (1996): Effect of plant density and row spacing on winter oil seed rape yield in the Mediterranean area. – Agricultura Mediterranea 126(1): 40-49.
[30] Ozbolt, L., Kreft, S., Kreft, I., Germ, M., Stibilj, V. (2008): Distribution of selenium and phenolics in buckwheat plants grown from seeds soaked in Se solution and under different levels of UV-B radiation. – Food Chemistry 110: 691-696.
[31] Ozer, H. (2003): The effect of plant population densities on growth, yield and yield components of two spring rapeseed cultivars. – Plant, Soil & Environment 49(9): 422-426.
[32] OzoniDevaji, A., Isfahani, M., Samiazadehlahiji, H., Rabiei, M. (2007): Effect of planting pattern and plant density on grain yield and its components in apetalous and petalled rapeseed (Brassica napus L.) cultivars. – Iranian Journal of Agronomy Sciences 5(1): 50-72 (in Persian with English abstract).

http://www.aloki.hu ● ISSN 1589 1623 (Print) ● ISSN 1785 0037 (Online)
DOI: http://dx.doi.org/10.15666/aeer/1605_69036916
© 2018, ALÖKI Kft., Budapest, Hungary

[33] Pasbaneslam, B. (2015): Investigating the possibility of late canola cultivation in East Azarbaijan. – Journal of Planting & Seed 27(3): 269-284.
[34] Patel, J., Pramar, M. T., Patel, J. C. (1980): Effect of different sowing dates, spacing and plant population on the yield of mustard. – Indian Journal Agronomy 25: 526-527.
[35] Ramos, S. J., Faquin, V., Guilherme, L. R. G., Castro, E. M., Ávila, F. W., Carvalho, G. S., Bastos, C. E. A., Oliveira, C. (2010): Selenium biofortification and antioxidant activity in lettuce plants fed with selenate and selenite. – Plant, Soil & Environment 56(12): 584-588.
[36] Rathke, G. W., Behrens, T., Diepenbrock, W. (2006): Integrated nitrogen management strategies to improve seed yield, oil content and nitrogen efficiency of winter oilseed rape (*Brassica napus*L.): a review. – Agriculture, Ecosystem & Environment 117: 80-108.
[37] Rezadoost, S., Rashidi, M. (2003): Effect of planting date and cultivar on the qualitative and quantitative characteristics of autumn canola. – The 7th Iranian Crop Sciences Congress 24-26. Aug. 2002. Karaj. Iran, pp. 150.
[38] Ruuska, S. A., Schwender, J., Ohlrogge, J. B. (2004): Te capacity of green oilseeds to utilize photosynthesis to drive biosynthetic processes. – Plant Physiology 136: 2700-2709.
[39] Sana, M. A., Ali, M., Malik, A., Saleem, M. F., Rafiq, M. (2003): Comparative yield potential and oil contents of different canola cultivars (*Brassica napus* L.). – Pakistan Journal of Agronomy 2(1): 1-7.
[40] Seppanen, M., Turakianen, M., Hartikainen, H. (2003): The effect of selenium onphotoxidative stress tolerance in potato. – Plant Science 165: 311-319.
[41] Shahbaz, K., Sumera, A., Jie, K., Noman, A., Shahid, M., Din, M., Ali, A., Zhou, G. (2018): Alteration in yield and oil quality traits of winter rapeseed by lodging at different planting density and nitrogen rates. – Nature Scientific Reports 8: 634-464.
[42] Suresha, G., Kumar, S., Santha, I. (2013): Functional expression of *Brassica juncea* oleate desaturase gene ($Bjfad_2$) in *Escherichia coli*. – Biologia 68: 599-605.
[43] Tanveer, S., Khan, N. I., Saeed, F. (1998): Effect of different sowing methods and sowing dates on the grain yield of canola sarson. – Journal of Agricultural Research 36: 145-150.
[44] Turakainen, M., Hartikainen, H., Sppinen, M. M. (2004): Effect of selenium treatments on potato (*Solanum tuberosum* L.) growth and concentrations of soluble sugars and starch. – Journal of Agriculture & Food Chemistry 52: 5378-5382.
[45] Valadabadi, S. A., Shiranirad, A. H., Aliabadi, H. F. (2010): Ecophysiological influences of zeolite and selenium on water deficit stress tolerance in different rapeseed cultivars. – Journal of Ecology & the Natural Environment 2(8).154-159.
[46] Vega, C. R. C., Sadras, V. O., Andrade, F. H., Uhart, S. A. (2000): Reproductive allometry in soybean, maize and sunflower. – Oxford Journal of Life Science Annals of Botany 85: 606-613.
[47] Wells, R. (1991): Soybean growth response to plant density, relationships among canopyphotosynthesis, leaf area and light interception. – Crop Science 31: 755-761.
[48] Xue, T., Hartikainen, H., Piironen, V. (2001): Antioxidative and growth-promotingeffect of selenium on senescing lettuce. – Plant Soil 237: 55-61.
[49] Yang, M., Shi, L., Xu, F. S., Lu, J. W., Wang, Y. H. (2009): Effects of B, Mo, Zn and their interactions on seed yield of rapeseed (*Brassica napus*L.). – Pedosphere 19(1): 53-59.
[50] Zahedi, H., Noormohammadi, G., Shirani-Rad, A. H., Habibi, D., Akbar-Boojar, A. M. (2010): The effect of zeolit and foliar application of selenium on growth, yield and yield components of three canola cultivars under drought stress. – World Applied Sciences Journal 7(2): 255-262.
[51] Zhu, Y. G., Huang, Y., Hu, Y., Liu, Y., Christie, P. (2004): Interaction between selenium and iodine uptake by spinach (*Spinacia oleracea* L.) in solution culture. – Plant & Soil Journal 261: 99-105.

http://www.aloki.hu ● ISSN 1589 1623 (Print) ● ISSN 1785 0037 (Online)
DOI: http://dx.doi.org/10.15666/aeer/1605_69036916
© 2018, ALÖKI Kft., Budapest, Hungary

SPATIAL DISTRIBUTION CHARACTERISTICS OF SOIL ORGANIC MATTER AND NITROGEN UNDER NATURAL CONDITIONS IN YANCHENG COASTAL WETLANDS

XU, Y.[1] – ZHEN, Y.[2] – HAN, S.[1] – ZHANG, H.-B.[1*]

[1]*College of Urban and Planning, Yancheng Teachers University, Yancheng 224007, China*
(e-mail: xeniayy@hotmail.com – Y. Xu, hanshuang412@163.com – S. Han)

[2]*School of Geoscience and Technology, Southwest Petroleum University, Chengdu 610500, China*
(e-mail: zhenyan0824@163.com)

**Corresponding author*
e-mail: yctuzhanghb@163.com; phone: +86-133-7526-7876

(Received 31st May 2018; accepted 27th Sep 2018)

Abstract. SOM (soil organic matter) and N (nitrogen) are important ecological factors in coastal wetland ecosystems. A specific area in Yancheng coastal wetlands was chosen and monitored on the spot in April 2012, spatial distribution characteristics of SOM and N and the relationship between them were analysed. The results showed that the content of SOM and N differs significantly in various vegetation types, their content in *Spartina* marshes is the highest, followed by *Reed* marshes, *Suaeda* marshes and the mudflat. The average content of SOM and N in them were 1.138%, 1.103%, 0.851%, 0.399% and the average value of total nitrogen were 489.935 mg/kg, 369.811 mg/kg, 365.491 mg/kg, and 95.542 mg/kg respectively. Furthermore, SOM and TN (total nitrogen), TN and ammonia nitrogen (NH_3-N) in the coastal wetlands are closely related and fit perfectly for linear regression equation, however, the correlation coefficient for OM (organic matter) and NH_3-N is low and fits well for the cubic curve equation. The specific value of carbon and nitrogen are the highest in the mudflat, followed by *Reed* marshes, *Spartina* marshes and *Suaeda* marshes. The specific value of NH_3-N and TN are the highest in the mudflat and in S*partina* marshes, *Reed* marshes and *Suaeda* marshes are close to it. Vegetation coverage conditions and physiological characteristics of plants are important factors affecting spatial distribution of SOM/N in coastal wetlands.

Keywords: *soil ecological elements, spatial differences, relationship, coastal wetlands, Yancheng National Nature Reserve*

Introduction

Coastal wetlands, in the transition zone of the terrestrial ecosystem and marine ecosystem, is an ecologically sensitive area of fragility (Zhang et al., 2005). Nutrient elements such as OM and N, are not only important components of wetland soil, but also extremely important ecological factors in the wetland ecosystem (Mitsch and Gosselin, 1986). Soil is a space-time continuum with high variability and there are obvious variations in the soil properties at the same time in different space positions (Sun et al., 2010). SOM is an important component of the soil. On the one hand, it shows fertility status of the soil; on the other hand, it also reflects the improvement of soil conditions and climate changes (Li and Wang, 2000; Wang et al., 2002). N as an important indicator of wetland soil nutrient levels (Judith and Jeffery, 2001), can not only reflect nutrient supply situation of the wetland soil and, to some extent, its level of availability; but also strongly correlates with the growth of plants.

Yancheng coastal wetland is one of the few typical coastal wetlands in China and the world, but under the bidirectional action of nature and human, the structure and function

http://www.aloki.hu ● ISSN 1589 1623 (Print) ● ISSN 1785 0037 (Online)
DOI: http://dx.doi.org/10.15666/aeer/1605_69176925
© 2018, ALÖKI Kft., Budapest, Hungary

of ecosystem changed greatly (Liu et al., 2003) and has raised wide attention of scholars. Real-time monitoring and diagnosis of ecosystem health are scientific preventive measures for maintaining the wealth of coastal wetland ecosystem (Zhu et al., 2010). The study of the biodiversity, accumulation and distribution of SOM, chemical processes of P (phosphorus) and N and soil water characteristics in the coastal wetlands had accumulated a series of achievements. (Gao et al., 2004, 2008; Liu et al., 2005; Shen et al., 2005; Mao et al., 2009; Ren et al., 2010). But study on the relationship between soil OM and N in coastal wetlands needs to deepen and expand. In this paper, one typical case area of Yancheng coastal wetlands is selected to reveal the spatial distribution characteristics of SOM and N in coastal wetlands and further elaborate the relationship of OM and N, NH_3-N and TN. It is of scientific and practical significance for deeply understanding the evolution law of the coastal wetland ecosystem, revealing the environmental change of coastal wetlands and promoting the natural exploitation and utilization of coastal wetlands.

Materials and methods

Study area

Yancheng Nature Reserve lies in the middle of Jiangsu coastal area. It is located between 32°20' and 34°37'N latitude and 119°29' and 121°15'E longitude and is bordered by the Yellow Sea to the east. It crosses 6 counties (cities, areas): Dongtai, Dafeng, Tinghu, Binhai, Sheyang and Xiangshui with a coastline of 582 km and a beach wetland area of 45.33 × 104 hm^2, which is the largest western Pacific coast muddy tidal flat wetland. With Xinyanggang River to the north, Doulonggang River to the south, seawall to the west, the core area of Yancheng national natural reserve is the typical long silted wet beach in Jiangsu province and its total land mass is 1.92 × 104 hm^2. The reserve is divided into northern and southern parts by Zhonglugang Road (*Fig. 1*). The northern part, with an area of about 0.52 × 104 hm^2, is a typical artificial management area and is planted a large area of r*eed* marshes. The southern part, with an area of about 1.10 × 104 hm^2, is a typical natural condition control area, whose landscape patterns and ecological processes are mainly affected by the climate, topography, hydrology, soil, vegetation and other natural factors, and it became the typical wetland areas under the control of natural conditions. This paper chose the coastal wetlands under southern natural conditions (Zhonglugang Road to the north, Doulonggang River to the south) as the research area, whose vegetation is from land to sea, in turn is *Reed*, *Suaeda*, *Spartinas* and mudflat.

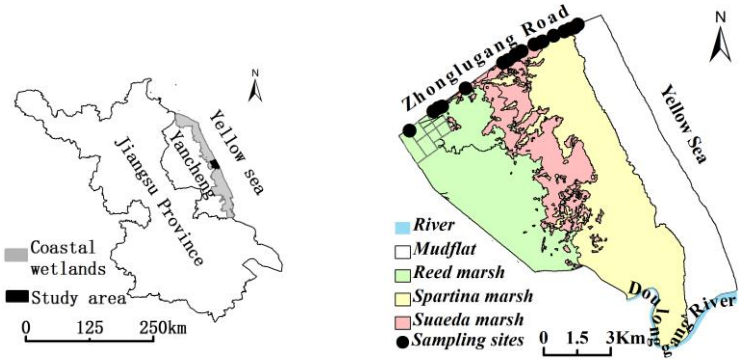

Figure 1. *Location of study area and sample points*

http://www.aloki.hu ● ISSN 1589 1623 (Print) ● ISSN 1785 0037 (Online)
DOI: http://dx.doi.org/10.15666/aeer/1605_69176925
© 2018, ALÖKI Kft., Budapest, Hungary

Data sources and processing

This paper was based on analysis data of research in April 2012. On the south side of Zhonglugang Road in the study area, 17 sample plots are arranged along the direction of land-to-sea. From sea to land were numbered by S1-S17. S1 and S2 are mudflat. S3, S4, S5, S6, S7 are *Spartina* marshes. S8, S9, S10, S11, S12, S13 are *Suaeda* marshes. S14, S15, S16, S17 are *Reed* marshes. The sample is distributed zonally in *Figure 1*. The sample area covered all the vegetation types and the equidistant distribution was basically adopted in each vegetation zone. Each sample plot set three sample points and used the soil collector to collect soil samples of 0-20 cm depth. Each sample column was 10 cm in diameter and 20 cm in height, and three sample columns were taken for mixing. A total of 17 mixed samples were mixed. We brought the samples back for laboratory analysis and recorded the vegetation types of each sample at the same time. After being brought to the laboratory and drying for 7 days, the samples were put into the oven. Under the condition of 50℃ drying to constant weight, further grind the dried sample to make the particle size less than 0.149 mm. The experimental procedures were using the samples to measure the content of organic matter through hydrate thermo - accretion potassium oxidation - colorimetric method. The total content of nitrogen in soil was measured by using concentrated sulfuric acid-indophenol blue colorimetric method. And Ammonia nitrogen in the soil was measured by using indophenol blue colorimetric method. Analyze the field monitoring data with statistic package for social science (SPSS) 19.0 software and single factor variance analysis. Conduct the significant test of difference on the soil OM, TN and NH_3-N. Then, we studied the relationship between OM and TN, OM and NH_3-N, TN and NH_3-N by using the regression analysis method.

Results

The characteristics of SOM\N in the coastal wetland

In the study area, the vegetation zonation is obvious. *Reed* marshes are located above the high tide of spring tide with high vegetation and the average height is above 1.5 m and the coverage is above 90%. *Suaeda* marshes is located in the upper part of the intertidal zone. The plants between the high tide and the average high tide are short, with a height of 0.5-1.2 m and a coverage of about 50%. The *Spartina alterniflora* is located between the mean high tide and the neap tide, with dense vegetation and average height of 2 m, covering degree of 100%. The mudflat is located between the high tide and low tide of the neap tide, almost no vegetation nearly.

The value of the soil OM, TN, NH_3-N is tested by the normal distribution testing in the SPSS 19.0. The data show an approximately normal distribution and are statistically significant. It can be seen from *Table 1:* the content of SOM is between 0.365% and 1.547% and the average level is 0.942%. Its maximum value is in *Spartina* marshes and its minimum value is in the mudflat. There is a moderate degree of variation and the variation coefficient is 36.075%. The content of TN is between 92.316 mg/kg and 908.710 mg/kg, with a mean value of 371.350 mg/kg. Its maximum value is in *Spartina* marshes and its minimum value is in the mudflat. There is a moderate degree of variations and the variation coefficient is 56.314%. The content of NH_3-N is between 3.510 mg/kg and 22.136 mg/kg. Its maximum value is in *Spartina* marshes and its minimum value is in the mudflat as well. Its mean value is 9.101 mg/kg, with a moderate degree of variation and the variation coefficient is 45.872%.

http://www.aloki.hu ● ISSN 1589 1623 (Print) ● ISSN 1785 0037 (Online)
DOI: http://dx.doi.org/10.15666/aeer/1605_69176925
© 2018, ALÖKI Kft., Budapest, Hungary

Table 1. *Characteristics of SOM, TN, NH_3-N in coastal wetlands*

ITEM	MAX	MIN	AVG	SD	CoV
OM/%	1.547	0.365	0.942	0.340	36.075%
TN/mg/kg	908.710	92.316	371.350	209.123	45.872%
NH_3-N/mg/kg	22.136	3.510	9.101	4.175	56.314%

The distribution pattern of SOM\N in coastal wetlands

It can be concluded from the single factor variance analysis of SOM and N in different vegetation types that: the test results of the three indicators are all F > P (alpha = 0.05), which shows that the content of SOM and N differs greatly between different vegetation. It can be seen from *Figure 2* that the content of coastal wetland SOM and TN is characterized by s-type fluctuation from land to sea. That is to say, it shows the characteristic of "high - low - high – low" from *Reed* marshes, *Suaeda* marshes, *Spartina* marshes to the mudflat. The average content of OM is 1.103%, 0.851%, 1.138% and 0.399% respectively and that of TN is 369.811 mg/kg, 365.491 mg/kg, 489.935 mg/kg and 95.542 mg/kg respectively. In addition, the soil NH_3-N turns out to be of the same characteristic of OM and TN in space after being analyzed and the mean values from *Reed* marshes, *Suaeda* marshes to mudflat is 8.731 mg/kg, 7.635 mg/kg, 12.419 mg/kg, 5.943 mg/kg respectively. Overall, differences in SOM and N in vegetation are reflected: *Spartina* marshes>*Reed* marshes> *Suaeda* marshes > the mudflat.

The content of SOM and N is closely related to vegetation types in coastal wetlands. SOM in coastal wetlands is closely related to the sources of SOM like plankton, benthos and plants. Variations in the content of nutrients like soil nitrogen, in a large degree, is mainly related to the factors such as climate, the soil parent material, etc. While in a small degree, it is mainly affected by the differences of vegetation and terrain without taking the differences of climate and soil plant material into consideration. SOM of the mudflat mainly comes from plankton and humus produced by benthos for lack of vegetation growth and the accumulation of nutrients is inferior to the vegetated areas. Not only *Spartina* marshes are affected by the sea, but also *Spartina* plants are tall in height and rich in density and have developed root system, which makes both the ground and underground biomass larger and the OM and N contribution rate high. In non-growing seasons, a lot of litter accumulates on the surface before large amounts of OM and N return into soil for decomposition. What is more, the good expansion ability of *Spartinas* contributes to the obvious increase in the sedimentary rate on the beach surface, the continuous acceleration of the beach face and accumulation of OM and N. On the other hand, the accumulation of SOM in *Spartina* marshes is affected by sea plankton and benthos. Therefore its capacity of enriching OM is much higher than *Reed*, *Suaeda* and the mudflat. While *Suaeda* marshes have lower content of the OM and N because the alkaline lotus have short plants, small and thin roots with low biomass on both the ground and underground and relatively weak accumulation for the OM and N. *Reed* marshes are less affected by seawater and SOM mainly comes from the metabolism and the litter form of humus of reed roots. Compared to *Spartina* marshes, the biomass and expansion ability of reeds is weaker. Furthermore, *Reed* marshes are located in top area of the coastal wetlands, which results in that their underground water level is lower than that of *Spartina* marshes and *Suaeda* marshes and weak soil peat

http://www.aloki.hu ● ISSN 1589 1623 (Print) ● ISSN 1785 0037 (Online)
DOI: http://dx.doi.org/10.15666/aeer/1605_69176925
© 2018, ALÖKI Kft., Budapest, Hungary

accumulation ability. So the OM and N content in general is lower than that of *Spartina* marshes.

On the other hand, studies show that the soil particle size is closely related to the content of OM and N. Because *Spartina* marshes and *Suaeda* marshes have smaller particle size, they have greater chance of hummifications product and root secretions and higher content of OM and N. While where is smaller particle size, there is worse ventilation and water permeability, which affect soil respiration and soil in anaerobic condition for a long time and go against the decomposition of OM andNH_3-N. And that does be good to the fixation of C and N. Meanwhile, the particle size of mudflat and *Suaeda* is large, so the content of SOM and NH_3-N is less (Wang et al., 2013; Hou et al., 2011; Oades, 1998).

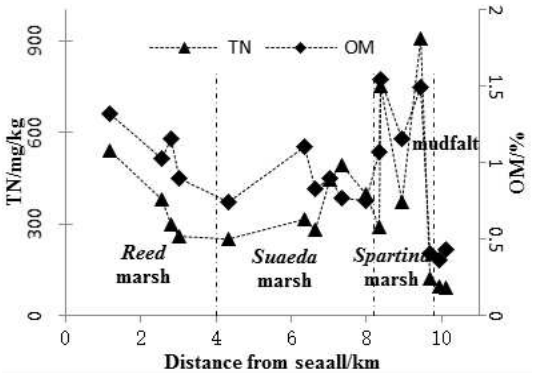

Figure 2. *The OM and TN content of soil in different vegetation*

The relationship between SOM and N in coastal wetlands

By using the SPSS correlation analysis, the conclusion can be drawn that: under the significance level of 0.01, OM and TN, TN and NH_3-N are very close, whose correlation coefficient is 0.825 and 0.858. By using linear regression to analyze the relationship between them, it shows good fitting effect as is shown in *Equations 1* and *2,* while the correlation of SOM and NH_3-N is poorer and its coefficient is 0.688 (the significance level of 0.01). It changes for the reason that NH_3-N in the soil can be directly absorbed by plants in the use of N and easily affected by hydrothermal conditions and biological activities (Deng et al., 2015). So we can use the cubic curve simulation method to express the relationship between them rather than simply using linear regression analysis. The cubic curve simulation method also shows a better fitting effect (*Eq. 3*).

$$OM = 0.444 + 0.001TN \quad \text{(Eq.1)}$$

$$TN = -19.866 + 42.986(NH_3\text{-}N) \quad \text{(Eq.2)}$$

$$OM = 0.905 - 0.125(NH_3\text{-}N) + 0.019(NH_3\text{-}N)^2 - 0.01(NH_3\text{-}N)^3 \quad \text{(Eq.3)}$$

where OM = organic matter; TN = total nitrogen; NH3-N = ammonia nitrogen.

The accumulation and decomposition of SOM directly affect the storage and transformation of N in the soil and play a leading role in the nitrogen content (Xu et al.,

http://www.aloki.hu ● ISSN 1589 1623 (Print) ● ISSN 1785 0037 (Online)
DOI: http://dx.doi.org/10.15666/aeer/1605_69176925
© 2018, ALÖKI Kft., Budapest, Hungary

2015). The distribution characteristics of soil carbon (hereafter referred to as C) and N and SOM and N are entirely different in coastal wetland. As can be seen from the C/N value, The C/N value of the mudflat is the highest whose mean value is 24.326. And the C/ N value in *Spartina* marshes and *Suaeda* marshes are highly close and their averages are 15.986 and 14.350 respectively. The C/ N value in *Reed* marshes, whose average value is 18.115, is higher than that of *Spartina* marshes and lower than that of the mudflat. Studies have shown that (Ge et al., 2010), C and N can reveal the conversion relationship between soil C and N in the process of biological decomposition. If the soil C/ N value is higher than 25, it will indicate that the soil N content cannot meet the needs of the bacteria and bring the accumulation of N content. In addition, the rapid propagation of soil spoilage bacteria can accelerate the decomposition of SOM. The C/ N value of all samples of C and N in this study are less than 25 except one point 27.190 in the mudflat. As can be seen from the mean of different vegetation zone average, only the point 24.326 of mudflat is closest to 25. Therefore, the OM and N accumulation of the mudflat is the weakest. The average value of C/N of *Reed* marshes, *Suaeda* marshes and *Spartina* marshes is lower than 20. This indicates that the degree of humification of coastal wetland soil is the highest, which easily causes the decomposition of OM and the mineralization of organic nitrogenous and it leads to the reduction of C and N value.

NH_3-N is one of the main forms of soil inorganic nitrogen and effective N which can be absorbed directly by the plant. By analyzing the ratio of NH_3-N/TN, it can be concluded that the mudflat has the highest ratio and its average value is 6.141. Besides, the content of NH_3-N/TN in the soil of *Spartina* marshes, *Reed* marshes and *Suaeda* marshes are closer. Their average values are 3.052, 2.161 and 2.399 respectively and it has much to do with the absorption of plants. *Spartina* root system is well-developed and may reach several meters deep underground, so the surface of 0~20 cm soil absorb less HN3-N. Therefore, the NH_3-N/TN in *Spartina* marshes is highest; *Reed* marshes take the second place. The root system of *Suaeda* marshes is undeveloped and its roots are short and mainly concentrated in the 15 to 25 cm soil layer. However, it absorbs much more NH_3-N on a scale of 0-20 cm soil layer. So the value of NH_3-N/TN is the lowest. On the other hand, the vegetation coverage and biomass of *Suaeda* marshes are low, which results in more barren soil under the eluviations (*Fig. 3*).

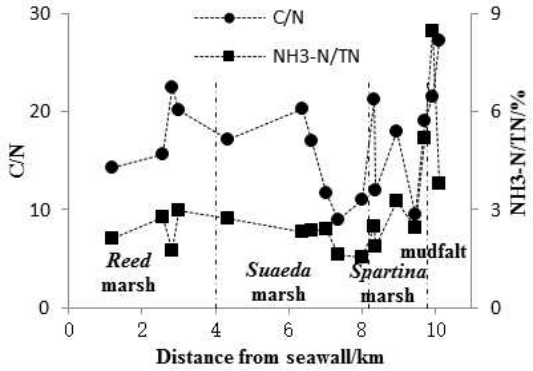

Figure 3. *The NH3-N and C/N of soil in different vegetation*

Discussion

The spatial differences and processes of the soil ecological elements is the basis of exploring the evolution mechanism of in the coastal wetlands. Many studies have

http://www.aloki.hu ● ISSN 1589 1623 (Print) ● ISSN 1785 0037 (Online)
DOI: http://dx.doi.org/10.15666/aeer/1605_69176925
© 2018, ALÖKI Kft., Budapest, Hungary

revealed the response relationship between plant community and environmental factors at the scale of ecosystem (Cui and Yang, 2001; Mao et al., 2009; Yao et al., 2009), which showed that SOM and TN are the main factors that affect the spatial differences of the plant communities in wetlands (Zhang et al., 2009). The spatial differences of the soil ecological factors such as nitrogen, phosphorus, salinity and organic matter were the main content in Yancheng coastal wetlands. There were a series of common achievements, while some were still controversial aspects. Studies on SOM and N are not controversial, the lowest level was in the mudflat, but there were disagreements on whether the highest level was in *Reed* marshes or *Spartina* marshes (Shen et al., 2005; Yao et al., 2009; Zhong et al., 2010). Some studies had showed that the content of OM and N in the surface soil with vegetation distribution is higher than that in the mudflat and the highest value appears in *Spartina* marshes. In the vertical direction, the content decreases gradually from the table down (Mao et al., 2009; Ren et al., 2011). On this basis, the variation of SOM and N in the coastal wetland under natural conditions was further analyzed. The results confirmed that the highest content of the soil OM and N in *Spartina* marshes, and the areas covered by vegetation were higher than the mudflat. The positive correlation between the soil OM and TN was verified, the results showed there was obvious liner relation between them. On the other hand, it was found that the distribution characteristics of the specific value of soil carbon and nitrogen in the coastal wetlands were totally different from them of the soil OM and N. However, some studies showed that the highest C/N ratio appeared in the place where the growth time of *Spartina* was the longest, and the lowest value was the mudflat (Mao et al., 2009). In this paper, the ratio of the soil OM and N in the mudflat was the highest, followed by *Reed* marshes, *Spartina* marshes and *Suaeda* marshes. The ratio of NH_3-N and TN in the mudflat was the highest and the specific value in *Spartina* marshes, *Reed* marshes and *Suaeda* marshes were close. The results indicated that vegetation cover conditions and plant physiological characteristics may be the reasons for the differences of the soil C/N and NH_3-N/TN ratios in the coastal wetlands. However, how SOM, N and vegetation interact and how they are coupled remains to be further studied.

Conclusion

Based on analysis data of research in April 2012, this paper analyzed the spatial distribution features of soil organic matter and nitrogen in Yancheng coastal wetlands under the natural condition and the relationship between soil organic matter, total nitrogen and ammonia nitrogen. The results showed that there were significant differences among different vegetation types. It shows the tendency of decrease from *Spartina* marshes, *Reed* marshes, *Suaeda* marshes to the mudflat. The soil TN and NH_3-N, TN and OM in the coastal wetland were (significance level of 0.01) closely related, the correlation coefficient were 0.825 and 0.858 respectively. The soil OM and NH_3-N correlation was poor, but the fitting effect of the third-order curve equation was good, the curve equation of OM and NH_3-N was as *Equation 3*. The specific value of carbon and nitrogen in the mudflat was the highest and the average value was 24.326. The C/N value in *Spartina* marshes and the *Suaeda* marshes were very close, with the average of 15.986 and 14.350 respectively. The average C/N in *Reed* marshes was only 18.115. The specific value ratio of NH_3-N/TN was the highest in the mudflat, with an average value of 6.141, while the average value of the *Spartina* marshes, *Suaeda* marshes and *Reed* marshes was close, with the average value of 3.052, 2.161 and 2.399 respectively.

http://www.aloki.hu ● ISSN 1589 1623 (Print) ● ISSN 1785 0037 (Online)
DOI: http://dx.doi.org/10.15666/aeer/1605_69176925
© 2018, ALÖKI Kft., Budapest, Hungary

Acknowledgements. This research was supported by National Natural Science Foundation of China (No. 41771199), the Natural Science Foundation of Jiangsu Province, China (Grants No. BK20171277) and the Natural Science Foundation of Jiangsu Higher Education Institutions of China (No.18KJD170001). We gratefully acknowledge Yancheng natural reserve for giving us the opportunity to enter the study area and carry out field works.

REFERENCES

[1] Cui, B. S., Yang, Z. F. (2001): Research advances in wetland ecosystem models. – Advances in Earth Science 16(3): 352-358.

[2] Deng, B. L., Yuan, Z. Y., Wen, W. H. (2015): Distribution patterns and relationship of SOM, total nitrogen and alkaline nitrogen in mountainous meadows of Wugong Mountain. – Jiangsu Agricultural Science 43(11): 414-417.

[3] Gao, J. H., Ou, W. X, Yang, G. S. (2004): Overview on geochemistry process of nitrogen and phosphor in tidal flat wetland. – Wetland Science 2(3): 220-227.

[4] Gao, J. H., Yang, G. H., Ou, W. X. (2008): Analyzing and quantitatively evaluating the organic matter source at different ecologic zones of tidal salt marsh, North Jiangsu Province, China. – Frontier of Environmental Science and Engineering in China 2(1): 81-88.

[5] Ge, G., Xu, Y. H., Zhao, L., Wu, Z. Q., Wu, L. (2010): Spatial distribution characteristics of SOM and nitrogen in the Poyang lake wetland. – Resources and Environment in the Yangtze Basin 19(6): 619-622.

[6] Hou, C. C., Song, C. C., Li, Y. C., Guo, Y. D. (2011): Seasonal dynamics of soil organic carbon and active organic carbon fractions in *Calamagrostis angustifolia* wetlands topsoil under different water conditions. – Environmental Science 32(1): 290-297.

[7] Judith, M. S., Jeffery, C. (2001): Cornwell nitrogen, phosphorus and sulfur dynamics in a low salinity marsh system dominated by *Spartina* alterniflora. – Wetlands 21(4): 629-638.

[8] Li, Z. P., Wang, X. J. (2000): Analysis and evaluation of SOM dynamics at a little region scale. – Scientia Geographica Sinica 20(2): 182-188.

[9] Liu, G. M., Yang, J. S., Jiang, Y. (2005): Salinity characters of soils and groundwater in typical coastal area in Jiangsu Province. – Soils 37(2): 163-168.

[10] Liu, Q. S., Li, Y. F., Zhu, X. D. (2003): Characteristics of coastal wetland ecosystems and their healthy design: a case study from Yancheng Natural Reserve, Jiangsu Province, China. – Acta Oceanologica Sinica 25(3): 143-148.

[11] Mao, Z. G., Wang, G. X., Liu, J. E., Ren, L. J. (2009): Influence of salt marsh vegetation on spatial distribution of soil carbon and nitrogen in Yancheng coastal wetland. – Chinese Journal of Applied Ecology 20(2): 293-297.

[12] Mitsch, J., Gosselin, G. (1986): Wetlands. – Van Nostrand Reinhold Company, New York, pp. 89-125.

[13] Oades, J. M. (1998): The retention of organic matter in soil. – – Biogeochemistry 43: 35-70.

[14] Ren, L. J., Wang, G. X., Qiu, L., Mao, Z. G., Liu, J. (2010): Morphology and biomass distribution of *Spartina* alterniflora growing in different tidal flat habitats in Jiangsu. – Journal of Ecology and Rural Environment 26(3): 220-226.

[15] Ren, L. G., Wang, G. X., Dan, H. E., Mao, Z. G, Liu, J. E. (2011): Spatial distributions of SOM in different vegetation zones of the Yancheng Tidal Flat. – Advances in Marine 29(1): 54-62.

[16] Shen, Y. M., Zeng, H., Wang, H., Liu, Y. M., Chen, Z. Y. (2005): Characteristics of halophyte and associated soil along aggradational muddy coasts in Jiangsu Province. – Acta Eclolgica Sinica 25(1): 1-6.

http://www.aloki.hu ● ISSN 1589 1623 (Print) ● ISSN 1785 0037 (Online)
DOI: http://dx.doi.org/10.15666/aeer/1605_69176925
© 2018, ALÖKI Kft., Budapest, Hungary

[17] Sun, Y. B., Deng, S. Y., Li, D. Z., Song, Y., Li, H. (2010): Spatial distribution and variability of main soil physical and chemical properties in Chongming and affecting factors. – Journal of Ecology and Rural Environment 26(4): 306-312.
[18] Wang, G., Yang, W. B., Wang, G. X., Liu, J. E., Hang, Z. Q. (2013): The effects of *Spartina* alterniflora seaward invasion on soil organic carbon fractions, sources and distribution. – Acta Ecologica Sinica 33(8): 2474-2483.
[19] Wang, S. J., Chen, Y., Li, S. Y. (2002): Balance of SOM in a long-term triple cropping system in paddy fields. – Acta Pedologica Sinica 39(1): 9-15.
[20] Xu, W. X., Zhai, Y., Huang, T., Shi, L. C., Jun, Y. E. (2015): Spatial distribution of SOM and total nitrogen in farmland in Shihezi agricultural areas. – – Chinese Journal of Soil Science 46(6): 1354-1358.
[21] Yao, C., Wan, S. W., Sun, D. L., Qin, P. (2009): Ecological mechanisms of vegetation succession of coastal wetland in Yancheng Nature Reserve. – Acta Ecologica Sinica 29(5): 2203-2210.
[22] Zhang, X. L., Li, P. Y., Li, P., Xu, X. Y. (2005): Present conditions and prospects of study on coastal wetlands in China. – Advances in Marine Science 23(1): 87-95.
[23] Zhang, X. L., Ye, S. Y., Yin, P., Chen, D. J. (2009): Characters and successions of natural wetland vegetation in Yellow River delta. – Ecology and Environmental Sciences 18(1): 292-298.
[24] Zhong, C. Q., Wang, J. X., Xing, W., Zhang, W. K. (2010): Effects of vegetation and hydrological conditions on the profile characteristics of TN, TP and OM in coastal salt marshes in northern Jiangsu Province. – Journal of Beijing Forestry University 32(3): 186—190.
[25] Zhu, Z. M., Feng, B. Y., Liu, L. (2010): Designing of health early-warning indicator system for littoral wetland ecosystems. – Journal of Ecology and Rural Environment 26(5): 436-441.

http://www.aloki.hu ● ISSN 1589 1623 (Print) ● ISSN 1785 0037 (Online)
DOI: http://dx.doi.org/10.15666/aeer/1605_69176925
© 2018, ALÖKI Kft., Budapest, Hungary

CHANGES IN PHYSIOLOGICAL TRAITS AND FATTY ACID COMPOSITION IN SESAME (*SESAMUM INDICUM* L.) CULTIVARS UNDER VARIOUS FOLIAR APPLICATION AND DROUGHT STRESS CONDITIONS

ZAREI, A.[1] – MASOUD SINAKI, J.[2*] – AMINI DEHAGHI, M.[3] – DAMAVANDEI, A.[2]

[1]*Agronomy Department, Damghan Branch, Islamic Azad University, Damghan, Iran*

[2]*Agriculture Faculty, Damghan Branch, Islamic Azad University, Damghan, Iran*

[3]*Faculty of Agriculture, Shahed University, Tehran, Iran*

**Corresponding author*
e-mail: jmsinaki2020@gmail.com

(Received 22nd Jun 2018; accepted 14th Aug 2018)

Abstract. Sesame is a source of excellent vegetable oil (35-63%). The present study aimed to evaluate the effect of phosphorus nano-chelate and chitosan application under end-season drought stress conditions based on split plot-factorial in three replications in the research field of Shahed University in Tehran, Iran during 2015-16 on the cultivation of sesame during summer. Main plots included drought stress in three levels including full irrigation as control (non-stress), irrigation cut-off at 50% seed ripening (75 BBCH), and 50% flowering (65 BBCH) as mild and severe stress levels, respectively. Subplots consisted of spraying treatments at four levels including non-spraying (control), phosphorus nano-chelate (2 ppt), chitosan (3 $g.L^{-1}$), and a combination of phosphorus nano-chelate + chitosan, as well as two cultivars such as sesame Oltan and Naz. Based on the results, the effects of drought stress, foliar application, and cultivar were significant on seed yield, oil and protein contents, peroxidase activity, and palmitic acid content. The highest seed yield was achieved by using phosphorus nano-chelate in Naz cultivar under full-irrigation condition (2114.7 $kg.ha^{-1}$). Severe drought stress caused a decrease in more than 60%, compared to the control treatment. Regarding foliar treatments, the highest percentage of oil was observed in using phosphorus nano-chelate, as well as the integrated use of phosphorus nano-chelate and chitosan, which increased by 12.39 and 14.97%, respectively, compared to the control treatment. Oil content in the seed of Naz cultivar was 7.22% higher than that of Oltan cultivar seed. In addition, the severe drought stress and Naz cultivar had the highest seed protein percentage (23.43 and 22.49%, respectively). The activities of catalase and superoxide dismutase antioxidant enzymes were directly related to an increasing drought stress. Further, Oltan cultivar had the highest activities of SOD and POX enzymes. The highest saturated fatty acids (palmitic and stearic) content were achieved in the non-foliar application (control treatment) in Oltan cultivar. Regarding the interaction effects of foliar treatment and cultivar, the lowest linoleic percentage was achieved in Oltan cultivar under non-foliar treatment and the highest percentage of the acid was observed in other treatments. In conclusion, the foliar application of phosphorus nano-chelate and chitosan improved the quantitative and qualitative yield of sesame and increased the growth and quality under drought stress condition.
Keywords: *enzyme activity, linoleic, oil, palmitic, protein, seed yield, nano fertilizer*

Abbreviations: CAT: catalase, SOD: superoxide dismutase, ROS: reactive oxygen species, POX: peroxidase, ppt: part per thousand, BBCH: Biologische Bundesanstalt, Bundessortenamt, and Chemische Industrie

Introduction

Drought is a major environmental stress affecting plant morphology, physiology, and biochemistry (Shao et al., 2008). Plants can avoid the harmful effects of drought in several ways such as stomata closure, leaf rolling, osmotic adjustments, a reduction in

http://www.aloki.hu ● ISSN 1589 1623 (Print) ● ISSN 1785 0037 (Online)
DOI: http://dx.doi.org/10.15666/aeer/1605_69276944
© 2018, ALÖKI Kft., Budapest, Hungary

the cellular expansion, and alterations of various essential physiological and biochemical processes which can affect growth, productivity, and quality (Farouk and Amany, 2012). Traits are correlated with drought tolerance such as yield components and physiological traits, which are suitable indicators for selecting drought tolerant genotypes in breeding programs in order to reduce the impact of water deficit on crop yield (Almeida et al., 2008). Biochemically, water deficit was observed to stimulate the accumulation of the ROS (Dossa et al., 2017). In order to prevent or alleviate injuries from ROS, plants have evolved an antioxidant defense system including non-enzymatic compounds like ascorbate, glutathione, tocopherol, carotenoids, flavonoids, and enzymes such as SOD, CAT, POX, ascorbate peroxidase, glutathione reductase, and polyphenol oxidase (Agrwal and Pandey, 2004). Yousefzadeh Najafabadi and Ehsanzadeh (2017) reported that the drought stress in the sesame plant led to an increase in carotenoid concentration, CAT, SOD, and POX activities. A large number of studies have focused on the effects of drought stress on sesame yield, yield components, and oil content (Kadkhodaie et al., 2014). However, few studies emphasized the available information regarding the effects of drought stress on the fatty acid compositions of sesame genotypes. For example, Kim et al. (2006) planted 18 cultivars withholding irrigation for only 15 days at flowering and maturity stages and determined the seed oil yield and composition, compared with the well-watered plants as a control. Based on the results, the seed oil content was not significantly affected by drought stress while the oleic acid content increased. However, the linoleic acid content decreased under drought conditions. In another study, Abedi and Pakniyat (2010) reported that drought stress results in increased protein content, phosphorus content, CAT activity, and SOD activity. Jouyban and Moosavi (2012) concluded that an increase in the irrigation interval led to an increase in the protein content of sesame.

Chitosan, known as elicitors, is considered as a natural biopolymer modified from chitin, which is the main structural component of squid pens, cell walls of some fungi and crab shells. They were introduced as a material to improve grain yield under unfavorable conditions due to their bioactivities to plants such as inducing the plant resistance against a wide range of diseases through antifungal, antibacterial, antivirus activities (Wang et al., 2006), stimulating the growth of plants and seed germination (Chandrkrachang, 2002), improving soil fertility and enhancing the mineral nutrient uptake of plant (Dzung, 2007), increasing the content of chlorophylls, photosynthesis, and chloroplast enlargement (Limpanavech et al., 2008), escalating nitrogen fixing nodes related to the species of leguminous plants and reducing the effects of abiotic stress on plants (Dzung et al., 2011).

Nanotechnology provides new interdisciplinary venture into agriculture and food sciences by converging science and engineering. In addition, nanoparticles have potential applications in agriculture system, viz., the detection of pollutants, plant diseases, pests, and pathogens, controlled delivery of pesticide, fertilizers, nutrients, and genetic material, and can act as nano architects in forming and binding soil structure (Ghormade et al., 2011). The excess use of chemical fertilizers causes an irreparable damage to the soil structure, mineral cycles, soil microbial flora, plants, and even more on the food chains across ecosystems leading to heritable mutations in future generations of consumers. Considering the abovementioned issues, the use of nano-fertilizers in agriculture is considered as one of the solutions to the problems (Solanki et al., 2015). Jan et al. (2014) reported that the application of phosphorus plays a vital role

http://www.aloki.hu ● ISSN 1589 1623 (Print) ● ISSN 1785 0037 (Online)
DOI: http://dx.doi.org/10.15666/aeer/1605_69276944
© 2018, ALÖKI Kft., Budapest, Hungary

in forming and translocating carbohydrates, root development, crop maturation, and resistance to disease pathogens.

Sesame (*Sesamum indicum* L.) is an ancient oilseed crop mainly grown in drought-prone environments, which is highly valued due to its high oil yield (~55%), as well as quality and stability (Pathak et al., 2014). Although sesame is considered as drought tolerant crop, the productivity is heavily affected by severe drought stress mainly when it occurs during anthesis (Dossa et al., 2017). Resistance to water stress in sesame is important in many countries with low rainfall (Golestani and Pakniyat, 2015). The fatty acid composition of sesame seed oil determines its commercial value, and drought stress and genotype may affect both the quality and quantity of oil which is extractable by sesame seed processors (Kadkhodaie et al., 2014).

Restricted water resources are considered as a limiting factor for irrigation applications around the world. Therefore, the present study aimed to evaluate the changes in the quality and biochemical traits of two sesame genotypes under drought stress and foliar application of chitosan and phosphorus nano-chelate in second cultivation.

Materials and methods

Plant material and growth conditions

The present study was conducted to investigate the changes in the quality and biochemical traits related to two sesame genotypes under drought stress and foliar application in chitosan and phosphorus nano-chelate in the second cultivation at research field of Shahed University in Tehran, Iran, during 2016. The experiment was conducted during a one-year factorial split plot experiment based on completely randomized block design with three replications. The research farm is located at geographical characteristics of latitude 31° and 36' and longitude 48° and 53' and the height of this area from sea level is equal to 1050 m. The place soil was tested and recognized as silty loam clay soil with pH about 8.10 (*Table 1*).

Table 1. *Some physical and chemical properties of soil in the experimental area (depth of 0-30 cm)*

	Texture	**pH**	**Electrical conductivity ($dS.m^{-1}$)**	**Organic matter (%)**	**Total nitrogen ($mg.kg^{-1}$)**	**Phosphorus ($mg.kg^{-1}$)**	**Potassium ($mg.kg^{-1}$)**	**Iron ($mg.kg^{-1}$)**
Experiment farm	Silty loam clay	8.10	2.00	1.11	1100	16.6	303.6	7.0
Optimum range	Loam and silty loam	6.5-7	1.51	2.00	2000	16.0	350.0	6.6

The experimental factors including drought stress at full irrigation as control (non-stress), mild stress (irrigation cut-off at 50% seed ripping equivalent 75 BBCH) and severe stress (irrigation cut-off at 50% flowering equivalent 65 BBCH) were in the main plots and spraying treatments including non-spraying (control), phosphorus nano-chelate (2 ppt), chitosan (3 $g.L^{-1}$), and the combination of phosphorus nano-chelate + chitosan and Oltan, and Naz single branch sesame cultivars were in the subplots. Based on the available documents, 75 BBCH is equivalent to seed about 50% of the final size

http://www.aloki.hu ● ISSN 1589 1623 (Print) ● ISSN 1785 0037 (Online)
DOI: http://dx.doi.org/10.15666/aeer/1605_69276944
© 2018, ALÖKI Kft., Budapest, Hungary

and 65 BBCH equals to 50% of flower open (Attibayeba et al., 2010). The experimental site and planting farm are presented in *Figure 1* and the climatic and meteorological conditions in *Table 2*.

Figure 1. *Experimental site and planting farm*

Table 2. *Climate and meteorological data during the experiment period*

	Jan	Feb	Mar	Apr	May	Jun	Jul	Auq	Sep	Oct	Nov	Dec
Maximum temperature (°C)	17	18.9	24.2	31.4	35.4	14.4	44	43	37.8	34.4	18.8	16.8
Minimum temperature (°C)	-5.6	-11	0.5	0	13.8	15.4	19	19	15.8	5.4	0.2	2.9
Average temperature (°C)	4.6	4.6	12.2	18.3	24.6	29.2	32	31	27	17.3	8.9	6.2
Total monthly precipitation (mm)	2.5	10.5	14.8	6	9.1	2.3	0.8	0	0	0	8.2	8.4
Average wind speed ($m.s^{-1}$)	3.6	3.8	4.5	4.6	4.5	5.5	5.5	4.1	4	4.6	3.7	3.3
Maximum wind speed ($m.s^{-1}$)	18	13	20	15	26	25	32	14	18	13	14	13

http://www.aloki.hu ● ISSN 1589 1623 (Print) ● ISSN 1785 0037 (Online)
DOI: http://dx.doi.org/10.15666/aeer/1605_69276944
© 2018, ALÖKI Kft., Budapest, Hungary

Regarding each experimental plot, six 3.5-m lines with 50 × 10 cm spacing, and main and subplots were 2 and 1 m, respectively. The seed was planted in late May after harvesting the wheat. Field preparation operations such as plowing, disc and the like were conducted before planting. Then, the first irrigation was given after sowing and the second was performed after 3 days. Accordingly, the irrigation time was determined by using Class A evaporation pan (in 70 mm evapotranspiration) (Shakeri et al., 2015). In the next procedure, irrigation treatments such as irrigation up to 50% flowering and seed ripening were performed after foliar use of nutrients. As for chitosan, chitosan-poly (D-glucosamine) prepared from SIGMA-ALDRICH was 3 $g.L^{-1}$, and a combination of the Khazra nano fertilizer (17% of phosphorus) was used at 2 ppt concentration for phosphorus nano-chelate. Then, spraying with these compounds was conducted at the beginning of flowering and seed ripping. In addition, drought stress treatments were conducted by irrigation at 65 BBCH (severe stress) or 75 BBCH (mild stress).

The extended Biologische Bundesantalt and Chemische (BBCH) scale and its associated decimal code were used to describe the different growth stages of *Sesamum indicum* L.

Seed yield

Seed harvest was done after physiological maturity, which occurred at the beginning of November by considering the browning about 75% of the capsules on the main stem in 50% of the plants. First, the grain yield was calculated based on the unit area and harvesting one square meter of each experimental plot and measuring grain weight (Mehrabi and Ehsanzadeh, 2011).

Seed oil and protein contents

Grain protein measurements were performed using the Bradford method (1976). In addition, the grain oil percentage was conducted by the method proposed by Leiboritz et al. (1987). Oil and protein percentages were multiplied in the seed yield in order to calculate the oil and protein yield.

Seed phosphorous contents

In order to measure the seed, phosphorus percentage was used based on the method proposed by Badigannavar et al. (2015). Finally, the obtained number was included in the standard equation and calculated as the concentration in the plant dry matter.

Protein and antioxidant enzyme assay

Before the leaves became yellowish, ten leaves of each plot were sampled for biochemical traits at the end of the seed ripping. In order to determine the total protein content and enzyme activity, 1 g of plant material was homogenized in 1 M Tris-HCl buffer (pH 6.8). The homogenate was centrifuged in a refrigerated centrifuge at 13000 g for 20 min (SIGMA 3-30K), and the obtained supernatant was used for determining protein assaying and enzyme. All the steps were conducted at 4 °C. Then, the protein content of the extracts was determined according to Bradford's (1976) method by using bovine serum albumin as the standard (Fazeli et al., 2007).

http://www.aloki.hu ● ISSN 1589 1623 (Print) ● ISSN 1785 0037 (Online)
DOI: http://dx.doi.org/10.15666/aeer/1605_69276944
© 2018, ALÖKI Kft., Budapest, Hungary

Catalase assay

The total CAT (EC 1.11.1.6) activity was measured according to the method proposed by Beers and Sizer (1952). The reaction solution consisted of 50 µL of the enzyme extract, 100 mM phosphate buffer (pH 7.0), 0.1 µ M EDTA, and 20 mM H_2O_2 in a total volume of 1.5 mL. Then, the enzyme activity was estimated by decreasing the absorbance of H_2O_2 at 240 nm due to H_2O_2 consumption. In addition, the decrease in H_2O_2 was monitored by reading the absorbance at the latter wavelength through using a UV-visible spectrophotometer (model Lambda 25, PerkinElmer, USA), and quantified by its molar extinction coefficient (36 mM^{-1} cm^{-1}). Finally, the enzyme activity was expressed as µmol H_2O_2 min^{-1} g^{-1} FW.

Peroxidase assay

Peroxidase (POX; EC 1.11.1.7) activity was assayed as described by Aghighi Shahverdi et al. (2018). The reaction mixture consisted of 4 cm3 of 0.2 M acetate buffer (pH 4.8), 0.4 cm^3 of H_2O_2 (3%), 0.2 cm^3 of 20 mM benzidine, and 0.05 cm^3 of enzyme extract. The rate of benzidine oxidation was measured at 530 nm.

Superoxide dismutase assay

The total SOD (EC 1.15.1.1) activity was determined by measuring the ability to inhibit the photochemical reduction of nitroblue tetrazolium (NBT) as described by Beauchamp and Fridovich (1971). The reaction mixture consisted of 0.1 cm^3 enzyme extract, 50 mM potassium phosphate buffer (pH 7.8), 13 mM methionine, 75 µM NBT, 0.1 mM EDTA, and 2 µM riboflavin. First, the test tubes were shaken and placed 30 cm from three 30 W fluorescent lamps. Then, the reduction in NBT was measured by reading absorbance at 560 nm. In the next procedure, blanks and controls were run similarly without any illumination and enzyme, respectively. One unit of SOD was defined as the amount of enzyme which produced a 50% inhibition of NBT reduction under the assay conditions (Fazeli et al., 2007).

Fatty acid compounds

In order to determine the amount of fatty acids, the oil should be extracted without high temperature in order to avoid possible changes in the fatty acid composition. Consequently, 50 g seed (after grinding) was mixed with hexane (1:4 ratio) and placed on a shaker (160 rpm) for 48 hours (Farhoosh et al., 2009). After separating the solvent, it was added to 7 mL methanol potassium 2 M. Then, each sample was injected into a gas chromatography (GC\MASS; Acme 6000, YOUNG LIN, Korea) with a 100 m-length column, an inner diameter of 0.25 mm, and 0.2 µm thickness. By comparing the peak of samples with standard peak and based on the RRT pick (relative retention time), the type of fatty acids was identified and its values were determined through calculating the surface area under the resulting peak curves.

Statistical analysis

ANOVA was used for analyzing the results of total traits by using the SAS 9.4 procedure PROC GLM. The mean comparison of data was done by Duncan's multiple range test at 5% probability level. Finally, correlation coefficients were calculated for each of the traits with the SAS 9.4.

http://www.aloki.hu ● ISSN 1589 1623 (Print) ● ISSN 1785 0037 (Online)
DOI: http://dx.doi.org/10.15666/aeer/1605_69276944
© 2018, ALÖKI Kft., Budapest, Hungary

Results

Seed yield

As shown in *Table 3*, the effect of drought, foliar application, cultivar, and interaction effect of drought × foliar application × cultivar on seed yield was significant. The highest seed yield was achieved by using phosphorus nano-chelate and control treatment in Naz cultivar and full irrigation condition (2114.7 and 2120.3 kg.ha^{-1}, respectively). According to the *Figure 2,* severe drought stress in Naz cultivar had the lowest seed yield (659.4 kg.ha^{-1}). Furthermore, an integrated application of phosphorus nano-chelate and chitosan under severe stress condition caused 4.76 and 10.85% increase in the seed yield of Oltan and Naz cultivars in compared to the mild stress, respectively.

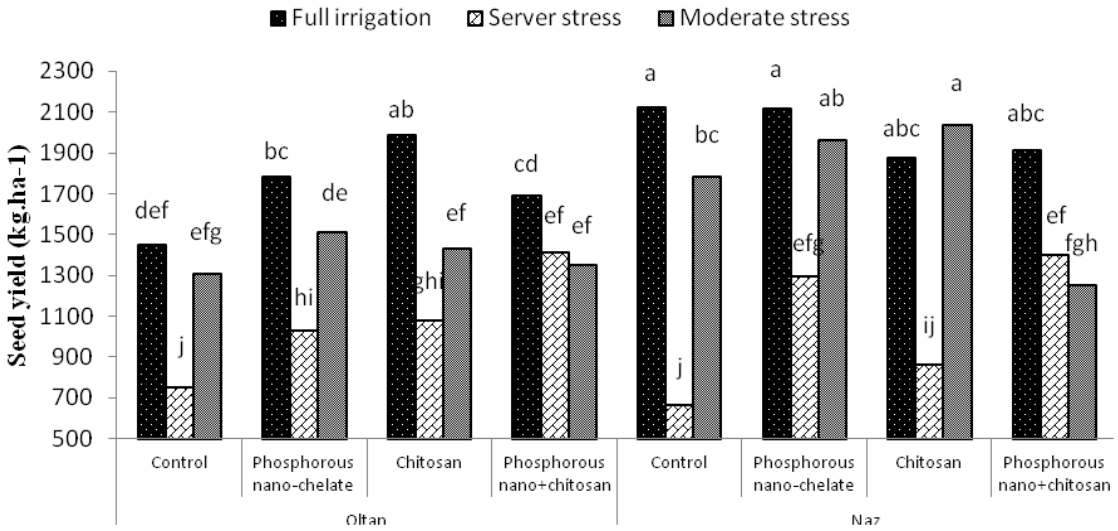

Figure 2. *Interaction effect of drought stress × foliar treatments on the seed yield of sesame. (Means in each column followed by at least one similar letter are not significantly different at 5% probability level by Duncan multiple test)*

Seed oil

The results of ANOVA indicated that the effect of drought stress, spraying and cultivar was significant on oil percentage and oil yield. In addition, the effect of drought × foliar application and drought × cultivar was significant on yielding seed oil (*Table 3*). As shown in *Table 4*, irrigation up to 50% flowering caused the least amount of seed oil. In foliar treatments, the highest oil percentage was observed in using phosphorus nano-chelate as well as the integrated application of phosphorus nano-chelate and chitosan, which increased 12.39 and 14.97%, respectively, compared to the control treatment (*Table 5*). Further, the oil content in the seed of Naz cultivar was 7.22% higher than that of Oltan cultivar seed (*Table 6*). Furthermore, as illustrated in *Figure 3,* based on the mean comparison of interaction effects of drought stress and foliar application, the highest seed oil yield was observed in full irrigation (control) with foliar application of phosphorus nano-chelate (922.3 kg.ha^{-1}) and the lowest mean was achieved in severe drought stress and none-sprayed treatment. Regarding the interaction effect of drought stress in cultivars, the highest oil yield was obtained in Naz cultivar

http://www.aloki.hu ● ISSN 1589 1623 (Print) ● ISSN 1785 0037 (Online)
DOI: http://dx.doi.org/10.15666/aeer/1605_69276944
© 2018, ALÖKI Kft., Budapest, Hungary

under full irrigation (924.03 kg.ha^{-1}). The results indicated that the severe drought stress could reduce oil yield by more than 50%, compared to the control treatment in both cultivars (*Fig. 3*).

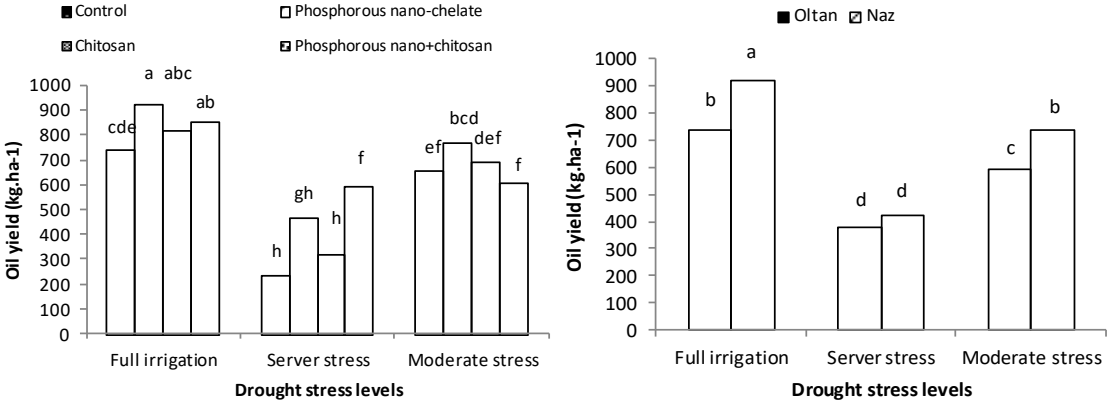

Figure 3. *Interaction effects of drought stress × foliar treatments and drought stress × cultivars on oil yield of sesame. (Means in each column followed by at least one similar letter are not significantly different at 5% probability level by using Duncan multiple test)*

Seed protein

As shown in *Table 3*, drought stress and cultivar could play a role in the percentage and yield of protein. In addition, foliar application, drought × foliar, drought × cultivar, and foliar × cultivar significantly affected protein yield. The severe drought stress level and Naz cultivar had the highest seed protein percentage (23.43 and 22.49%, respectively) (*Tables 4* and *6*). In addition, full irrigation treatment under the foliar application of phosphorus nano-chelate and chitosan (alone and integrated application) resulted in increasing seed protein yield. On the other hand, severe drought stress and non-sprayed treatment had the lowest seed protein yield, which decreased 57.21%, compared to the control treatment (*Fig. 4*). Further, based on the mean comparison interaction effect of drought stress in cultivar, the highest mean was observed in full irrigation in Naz cultivar (*Fig. 4*). The results showed that increasing the level of drought stress caused a significant decrease in seed protein yield.

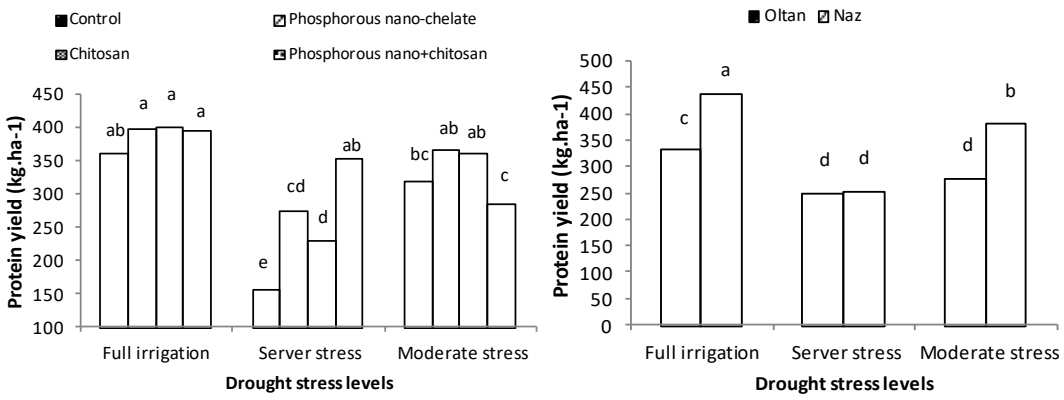

Figure 4. *Interaction effects of drought stress × foliar treatments and drought stress × cultivars on protein yield of sesame. (Means in each column followed by at least one similar letter are not significantly different at 5% probability level by using Duncan multiple test)*

http://www.aloki.hu ● ISSN 1589 1623 (Print) ● ISSN 1785 0037 (Online)
DOI: http://dx.doi.org/10.15666/aeer/1605_69276944
© 2018, ALÖKI Kft., Budapest, Hungary

Table 3. *Results of ANOVA (mean square) for the effect of drought stress and foliar application of phosphorous nano-chelate and chitosan on quality traits, the activity of antioxidant enzymes, fatty acid contents of two sesame cultivars*

Sources of variance	Mean square (MS)													
	df	Seed yield	Oil content	Oil yield	Protein content	Protein yield	Phosphorus content	CAT activity	POX activity	SOD activity	Oleic content	Linoleic content	Palmitic content	Stearic content
Block (B)	2	44149.4 ns	19.3 ns	13893.0 ns	0.57 ns	966.8 ns	0.0016 ns	0.0007 ns	0.009 ns	0.00002 ns	6.31 ns	9.86 ns	3.98 ns	5.13 ns
Drought (D)	2	3996516.8**	404.7**	1150020.8**	59.9**	111556.6 **	0.0064 *	0.91**	0.17 *	0.49 **	3.85 ns	4.93 ns	10.48**	3.69 ns
B × D	4	12049.9	3.8	4658.8	0.75	1093.1	0.00005	0.001	0.01	0.003	23.43	16.02	1.06	0.68
Foliar application (F)	3	232814.7**	227.2**	114094.2**	15.5 ns	18590.2**	0.20**	0.05**	0.11 ns	0.03 ns	10.92ns	9.49 ns	2.47 ns	7.22 *
Cultivar (C)	1	786003.0**	173.0**	324063.0**	54.4 *	90303.6**	0.00004 ns	0.001ns	0.21 *	0.18 **	2.02 ns	19.17*	6.94 *	16.11 *
D × F	6	240058.6**	13.5 ns	52273.6**	1.2 ns	16581.4**	0.001 ns	0.01 ns	0.07 ns	0.011ns	3.28 ns	8.62 ns	3.85 *	5.10 ns
D × C	2	182158.5**	12.9 ns	38123.4*	4.93 ns	20674.6**	0.0001 ns	0.001ns	0.02 ns	0.007ns	1.98 ns	0.22 ns	0.96 ns	0.22 ns
F × C	3	117209.2**	8.1 ns	13825.0ns	3.91 ns	10675.3*	0.001 ns	0.004ns	0.02 ns	0.036ns	9.40 ns	22.37**	11.69 **	15.51**
D × F × C	6	125747.9**	3.7 ns	20469.2 ns	1.94 ns	7519.0 ns	0.00001 ns	0.003ns	0.12 ns	0.023ns	1.79 ns	1.88 ns	1.11 ns	1.67 ns
Error	42	25470.5	18.7	10051.8	7.67	3608.1	0.002	0.006	0.05	0.01	5.83	3.80	1.51	2.33
CV (%)	-	10.63	10.45	15.77	12.8	18.60	16.53	18.29	21.60	22.43	6.02	5.67	10.42	18.34

*, ** Significant at $P < 0.05$ and $P < 0.01$, respectively

Table 4. *The effect of drought stress levels on some of the quality traits and activity of CAT and SOD enzymes*

Drought stress levels	Oil content (%)	Protein content (%)	Phosphorus content (%)	CAT activity (U.mg protein.min^{-1})	SOD activity (U.mg protein.min^{-1})
Full irrigation (non-stress as control)	44.31 ± 1.05 a	20.51 ± 0.46 b	0.28 ± 0.01 a	0.14 ± 0.01 c	0.46 ± 0.01 c
Irrigation up to 50% seed ripping (mild stress)	43.11 ± 0.87 a	20.91 ± 0.64 b	0.29 ± 0.02 a	0.21 ± 0.02 b	0.56 ± 0.03 b
Irrigation up to 50% flowering (severe stress)	36.67 ± 1.21 b	23.43 ± 0.46 a	0.26 ± 0.02 b	0.51 ± 0.01 a	0.75 ± 0.03 a

Means within a column followed by the same letter are not significantly ($P < 0.05$) different according to Duncan multiple test

http://www.aloki.hu ● ISSN 1589 1623 (Print) ● ISSN 1785 0037 (Online)
DOI: http://dx.doi.org/10.15666/aeer/1605_69276944
© 2018, ALÖKI Kft., Budapest, Hungary

Seed phosphorous

As indicated in *Table 3*, the results of ANOVA indicated that drought stress and foliar application could significantly influence on seed phosphorous content. In addition, drought stress caused a 7.14% decrease in seed phosphorous content, compared to the control treatment (*Table 4*). Further, the use of phosphorous nano-chelate had the highest seed phosphorous content (0.43%) while control treatment had the lowest mean in this regard (*Table 5*).

Antioxidants activity

Based on the results in *Table 3*, drought stress played a significant effect on CAT and SOD activities. The activities of these two antioxidant enzymes are consistent with an increase in drought stress. Thus, severe drought stress had the most activity. Regarding the comparison between the spraying treatments, the most catalase activity was related to chitosan application (*Table 5*). Furthermore, a significant difference was observed between cultivars in terms of POX and SOD activities. In addition, Oltan cultivar had the highest activities of SOD (0.79 U.mg protein.min^{-1}) and POX (0.64 U.mg protein.min^{-1}) enzymes (*Table 6*).

Table 5. *The effect of foliar application of phosphorous nano-chelate and chitosan on oil content, phosphorous content, and CAT activity of sesame*

Foliar treatments	Oil content (%)	Phosphorus content (%)	CAT activity (U.mg protein.min^{-1})
Control	38.32 ± 1.43 b	0.19 ± 0.01 d	0.24 ± 0.04 c
Phosphorus nano-chelate	43.74 ± 1.15 a	0.43 ± 0.01 a	0.26 ± 0.04 c
Chitosan	38.33 ± 1.35 b	0.25 ± 0.009 b	0.36 ± 0.03 a
Phosphorus nano-chelate + chitosan	45.07 ± 1.11 a	0.23 ± 0.007 c	0.30 ± 0.04 b

Means within a column followed by the same letter are not significantly ($P < 0.05$) different according to Duncan multiple test

Table 6. *The effect of cultivars od sesame on oil and protein contents, and POX and SOD activities*

Cultivars	Oil content (%)	Protein content (%)	POX activity (U.mg protein.min^{-1})	SOD activity (U.mg protein.min^{-1})
Oltan	39.81 ± 1.08 b	20.75 ± 0.51 b	0.79 ± 0.04 a	0.64 ± 0.03 a
Naz	42.91 ± 0.89 a	22.49 ± 0.39 a	0.68 ± 0.03 b	0.54 ± 0.02 b

Means within a column followed by the same letter are not significantly ($P < 0.05$) different according to Duncan multiple test

Fatty acid composition

Oleic, linoleic, palmitic, and stearic acids are the most important fatty acids measured in the experiment. The results indicated that the effects of cultivar, as well as the interaction of foliar application in cultivar, were significant on the contents of linoleic, palmitic, and stearic acids (*Table 3*). As illustrated in *Figure 5* and *6,* the highest content of saturated fatty acids (palmitic and stearic) was achieved in the non-

http://www.aloki.hu ● ISSN 1589 1623 (Print) ● ISSN 1785 0037 (Online)
DOI: http://dx.doi.org/10.15666/aeer/1605_69276944
© 2018, ALÖKI Kft., Budapest, Hungary

foliar application (control treatment) in Oltan cultivar. In addition, the interaction effect of drought stress and the foliar application was significant on palmitic acid percent (*Table 3*). Further, as shown in *Figure 5,* the highest palmitic acid percent achieved full irrigation treatment under foliar application in chitosan and compound of phosphorous nano-chelate and chitosan. Regarding the interaction effects of foliar treatment and cultivar, the lowest linoleic percentage was achieved in Oltan cultivar under non-foliar treatment and the highest percentage of the acid was observed in other treatments (*Fig. 6*).

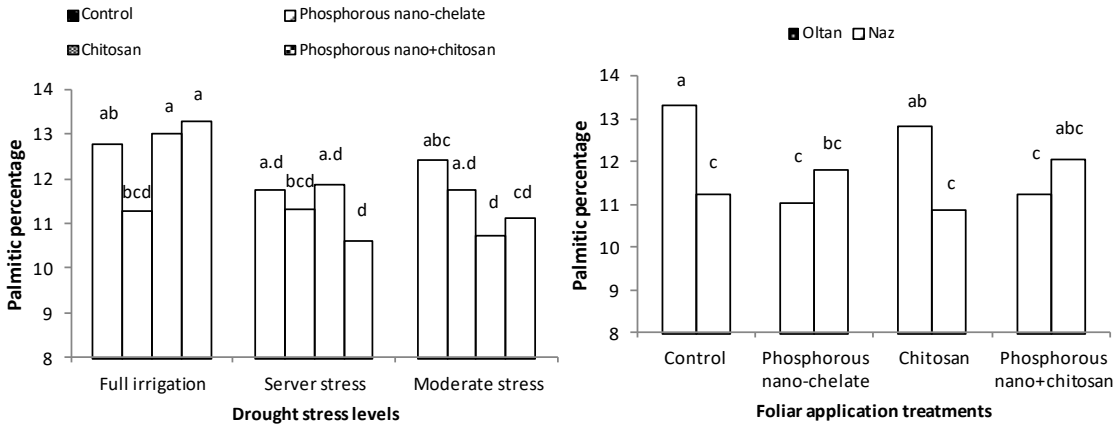

Figure 5. *Interaction effects of drought stress × foliar treatments and foliar treatments × cultivars on palmitic acid percentage. (Means in each column followed by at least one similar letter are not significantly different at 5% probability level, using Duncan multiple test)*

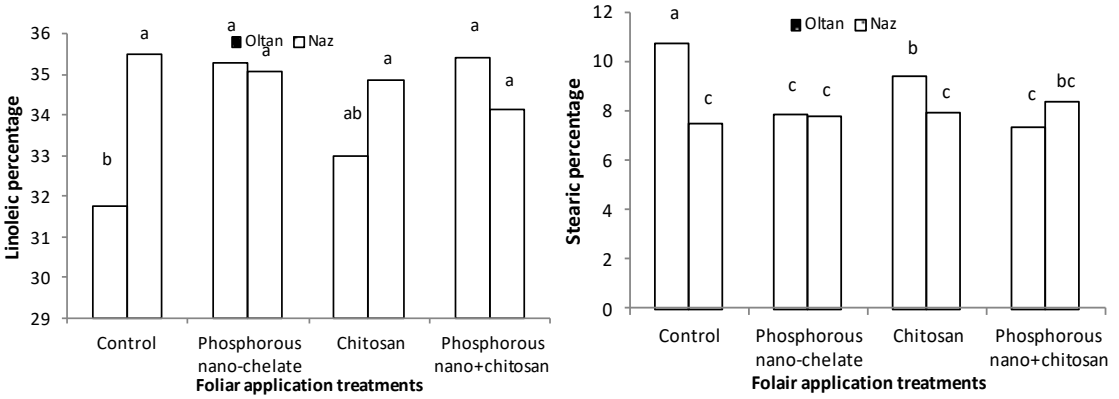

Figure 6. *Interaction effects of foliar treatments × cultivars on linoleic and stearic acids percentage. (Means in each column followed by at least one similar letter are not significantly different at 5% probability level, using Duncan multiple test)*

Correlations among traits

Tables 7 and *8* represent the results of simple correlation in non-drought stress (control) and drought stress conditions, respectively. As shown, qualitative traits such as seed yield, oil content, oil yield, protein content, protein yield, and phosphorous content were positively correlated in both conditions. However, a weak correlation was reported between oil content and protein content although the correlation among grain yield with

http://www.aloki.hu ● ISSN 1589 1623 (Print) ● ISSN 1785 0037 (Online)
DOI: http://dx.doi.org/10.15666/aeer/1605_69276944
© 2018, ALÖKI Kft., Budapest, Hungary

oil and protein yield was very high. Regarding drought stress conditions, no significant correlation was observed between fatty acids content and qualitative traits while positive and negative correlations were observed between the traits in the control condition.

Table 7. *Correlation coefficients among physiological and quality attributes of sesame under non drought stress conditions*

		1	2	3	4	5	6	7	8	9	10	11	12	13
Quality traits	1	1.00												
	2		1.00											
	3	0.85	0.75	1.00										
	4	0.60	0.32	0.66	1.00									
	5	0.94	0.33	0.84	0.88	1.00								
	6		0.32				1.00							
Enzyme activity	7						-0.32	1.00						
	8								1.00					
	9	-0.61		-0.56	-0.95	-0.81				1.00				
Fatty acids quality	10		-0.32		0.32					-0.45	1.00			
	11	0.54		0.45	0.29	0.48	0.31	-0.59				1.00		
	12	-0.39		-0.37	-0.29	-0.37	-0.47	0.56				-0.75	1.00	
	13						-0.51	0.42	-0.50			-0.49	0.65	1.00

Table 8. *Correlation coefficients among physiological and quality attributes of sesame under drought stress conditions*

		1	2	3	4	5	6	7	8	9	10	11	12	13
Quality traits	1	1.00												
	2	0.52	1.00											
	3	0.95	0.75	1.00										
	4				1.00									
	5	0.89	0.48	0.85	0.35	1.00								
	6	0.36		0.36		0.32	1.00							
Enzyme activity	7	-0.56	-0.49	-0.60		-0.52		1.00						
	8				-0.62	-0.41			1.00					
	9	-0.47	-0.46	-0.51	-0.47	-0.64		0.72	0.51	1.00				
Fatty acids quality	10										1.00			
	11								-0.29			1.00		
	12										-0.35	-0.48	1.00	
	13								0.30		-0.45	-0.54		1.00

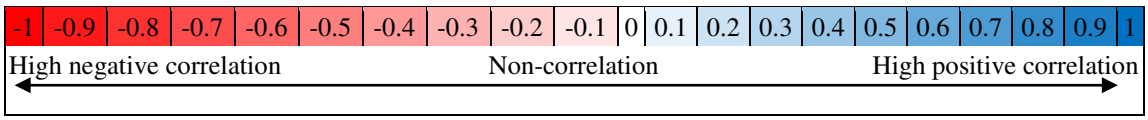

1: Seed yield, 2: Oil content, 3: Oil yield, 4: Protein content, 5: Protein yield, 6: Phosphorous content, 7: CAT activity, 8: POX activity, 9: SOD activity, 10: Oleic content, 11: Linoleic content, 12: Palmitic content, 13: Stearic content

http://www.aloki.hu ● ISSN 1589 1623 (Print) ● ISSN 1785 0037 (Online)
DOI: http://dx.doi.org/10.15666/aeer/1605_69276944
© 2018, ALÖKI Kft., Budapest, Hungary

Discussion

Plants are exposed to environmental stresses during their growth. Drought stress is considered as one of the major abiotic stresses which causes a high reduction in plant growth and yield, which can affect the absorption and transfer of nutrients to the plant (Askari et al., 2018). Thus, the response of two sesame genotypes for lasting drought stress was emphasized in the present study. In addition, the originality of the present research resides in the fact that it is used as an integrated approach by combining agro-morphological, physiological, biochemical and seed quality traits to identify useful genotypes and interesting traits efficiently for planting in drought-prone environments in the south of Tehran, Iran. Based on the results, the severe drought stress led to a decrease in seed yield, oil percentage, oil yield, and plant phosphorus content. In line with the results of the present study, severe or prolonged drought plays a significant role in the productivity by affecting the number of capsules per plant, grain yield and oil yield and quality despite its relative tolerance to drought stress (Kadkhodaei et al., 2014; Dossa et al., 2017). Drought stress through chlorophyllase and peroxidase enzymes activities in plants resulted in reducing the content of chloroplast destruction and chlorophyll. In addition, these physiological changes lead to a reduction in plant growth and yield (Misra and Sricastatva, 2000; Askari et al., 2018).

Sesame seed quality (oil and protein contents) are adversely affected by environments severe drought (Menshah et al., 2006). The results of this study indicated that opposite responses to the changes in the oil content and protein content were found in response to drought stress as severe drought stress led to an increase in protein content and a decrease in the seed oil content (*Table 4*). According to Akinoso et al. (2006), the oil percentage varies with genetic and environmental influences.

The saturated fatty acid such as palmitic (C16:0) and stearic (C18:0) acids and unsaturated fatty acid such as linoleic acid (C18:2) were insignificantly influenced by cultivar and interaction effect of foliar application in cultivar while the effect of drought stress on fatty acids composition, except palmitic acid content, was insignificant (*Table 3*). As illustrated in *Figures 5* and *6,* non-application of nutrient treatment (control) in Oltan cultivar had the highest palmitic and stearic acid contents. In addition, drought stress resulted in decreasing the oil percentage, oleic acid and linoleic acid concentrations of the seeds and increasing the protein percentage, palmitic acid, and stearic acid in safflower seeds (Mohsennia and Jalilian, 2012). Further, genetic, climatic and agronomic factors indicated a significant effect on oil content and composition of sesame. However, oil content and composition are considerably different within different varieties (Yoshida et al., 2007). Fatty acid composition and oil content are exposed to variation by different physiological, ecological and cultural factors. The composition of sesame oil relies on the climatic conditions, soil type, as well as the maturity of plant and variety (El-Khier et al., 2008). Furthermore, the proximate analysis showed a significant variation among the different sesame genotypes which implies that genetic diversity is available among Nigerian sesame (Alege and Mustapha, 2013). Alege et al. (2011) studied three species of sesame from Nigeria by using morphological markers and reported a significant genetic diversity.

The mechanisms of absorption and transfer of nutrients in plants such as mass flow, emission or absorption, and transfer by osmotic phenomena are regarded as all functions of the moisture content of the soil and the expansion of the absorbing root. Regarding the reduced moisture or root expansion, intensity and amount of nutrient uptake undergo some changes (Taiz and Ezeiger, 1998). In the present study, the plant phosphorus

http://www.aloki.hu ● ISSN 1589 1623 (Print) ● ISSN 1785 0037 (Online)
DOI: http://dx.doi.org/10.15666/aeer/1605_69276944
© 2018, ALÖKI Kft., Budapest, Hungary

content decreased by increasing drought stress (*Table 4*). Askari et al. (2018) reported that sever and mild drought stress can reduce phosphorus concentration to 15.96 and 6.96%, respectively, compared to optimal irrigation. The modulation of root development is considered as one of the drought stress effects. On the other hand, root growth is closely related to the absorption of phosphorus and nitrogen from the soil. In such a case, foliar application of phosphorus nano-chelate can compensate for the deficiency of this element and improve the growth, which was consistent with the results of the present study (Askari et al., 2018).

In addition, supplying the plant with its needed nutritional sources could increase its protein and oil percentage. Further, as shown in *Table 5*, practicing the phosphorus nano-chelate fertilizer increased the oil content in this experiment. Furthermore, phosphorus plays a role in increasing the formation of more capsules, and eventually, the formation of more seeds since it can enhance shooting and flowering (Safari Arabi et al., 2018). As a result, an increase in seeds leads to an increase in the oil content. In addition, it can affect the percentage and the yield of sesame oil since better nutrition leads to better photosynthesis during sesame growth and supplying the needed phosphorus fills the pod and seed.

The production of ROS appears to be involved in stress resistance induction (Gill and Tuteja, 2010; Pongprayoon et al., 2013). In order to prevent or alleviate injuries from ROS, plants have evolved an antioxidant defense system including non-enzymatic compounds like ascorbate, glutathione, tocopherol, carotenoids, flavonoids, and enzymes such as SOD, CAT, POX, ascorbate peroxidase, glutathione reductase, and polyphenol oxidase (Agarwal and Pandey, 2004). Based on the results of this study, the higher activity of SOD and CAT in the severe drought stress level indicated that they have a stronger ability to remove ROS (*Table 4*). Increased SOD, POX and CAT activities in response to water stress were reported in some studies (Kukreja et al., 2005). Further, Fazeli et al. (2007) and Kadkhodaie et al. (2014) concluded that more increase of antioxidant enzymes in leaves was related to drought resistance of some sesame genotypes. Furthermore, Cho et al. (2008) reported an improvement in the quality of sunflower by increasing the free radical scavenging activity. In general, the higher POX and SOD activities in Oltan leaves than may suggest the higher efficiency of Oltan under drought condition, compared to those of Naz.

Chitosan is a biopolymer with multiple agricultural applications, which has been shown to enhance plant growth and production yield in many species such as rice (*Oryza sativa* L.), pearl millet (*Pennisetum glaucum* L.), maize (*Zea mays* L.) and many orchid species (Pornpienpakde et al., 2010; Kananont et al., 2010). Furthermore, it was proposed as one potential chemical which can induce drought resistance via improving water use efficiency in the plant, as well as inducing drought resistance (Bittelli et al., 2001; Dzung et al., 2011). The same results were observed in the present experiment.

In addition, based on the results of the present experiment, the highest CAT activity was observed in the foliar application of chitosan which an increase of 33.33%, compared to the control treatment (*Table 5*). The chitosan response in plants is involved in inducing the reactive oxygen species (ROS) scavenging system. The enzyme activity and/or transcript levels of several antioxidant enzymes such as CAT, SOD, and POX were found to be induced by chitosan treatment (Yang et al., 2009; Povero et al., 2011). Further, the application of chitosan prior to drought stress can enhance the antioxidant activities of the SOD and CAT enzymes and decrease electrolyte leakage and production of malondialdehyde (Yang et al., 2009).

http://www.aloki.hu ● ISSN 1589 1623 (Print) ● ISSN 1785 0037 (Online)
DOI: http://dx.doi.org/10.15666/aeer/1605_69276944
© 2018, ALÖKI Kft., Budapest, Hungary

Regarding the results of correlation between traits, more negative correlation was observed between antioxidant enzyme activities (CAT and SOD) and qualitative traits (seed yield, seed oil and protein contents, and phosphorous content) in drought stress conditions, compared to non-drought stress conditions (*Tables 7* and *8*). Dossa et al. (2017) reported a high correlation within the different antioxidative enzyme activities and morphological traits of sesame which is in line with the results of the present study.

Conclusion

In conclusion, the exposure of sesame cultivars to drought resulted in decreasing seed yield, percentage and yield of seed oil, increasing seed protein percentage, CAT and SOD activities, and changing the fatty acids composition. In addition, foliar application of phosphorus nano-chelate and chitosan caused an increase in the seed yield, seed oil yield, and phosphorous content. Further, Naz cultivar was superior to most of the studied traits, compared to Oltan cultivar. Furthermore, the results indicated that sesame planting in warm and dry conditions could produce the appropriate grain yield and oil yield, due to the improvement of the physiological traits including the synthesis of oil and protein, the activity of antioxidant enzymes, and the like. Due to an increase in the content of phosphorus seeds and the improvement of oil and protein content of seeds, phosphorus nano fertilizer increased the quantitative and qualitative attributes of sesame. Finally, planting Naz cultivar under irrigation limited to the foliar application of phosphorus nano-chelate and chitosan is highly recommended to achieve higher performance in warm and dry climates. Study of changes in the quality of fatty acids and their relationship with physiological traits for future research is recommended.

REFERENCES

[1] Abedi, T., Pakniyat, H. (2010): Antioxidant enzyme changes in response to drought stress in ten cultivars of oilseed rape (*Brassica napus* L.). – Czech J. Genet. Plant Breed. 46(1): 27-34.

[2] Agarwal, S., Pandey, V. (2004): Antioxidant enzyme responses to NaCl stress in Cassia angustifolia. – Biol. Plant 48: 555-560.

[3] Aghighi Shahverdi, M., Omidi, H., Tabatabaei, S. J. (2018): Morpho-physiological response of stevia (*Stevia rebaudiana* Bertoni) to salinity under hydroponic culture condition (a case study in Iran). – Applied Ecology and Environmental Research 16(1): 17-28.

[4] Akinoso, R., Igbeka, J. C., Olayanju, T. M. A. (2006): Process optimization of oil expression from Sesame seed (*Sesamum indicum* L.). – The CIGR E. Journal 8: 1-7.

[5] Alege, G. O., Mustapha, O. T. (2013): Assessment of genetic diversity in Nigerian sesame using proximate analysis. – G. J. Biosci. Biotechnol. 2(1): 57-62.

[6] Alege, G. O., Akinyele, B. O., Ayodele, S. M., Ogbode, A. V. (2011): Taxonomic importance of the vegetative and pod characteristics in Nigerian species of sesame. – African Journal of Plant Science 5(3): 213-317.

[7] Almeida, S. M. D., Gonçalves, S. J. A., Enciso, J., Sharma, V., Jifon, J. (2008): Yield components as indicators of drought tolerance of sugarcane. – Sci. Agric. 65: 620-627.

[8] Askari, A., Ardakani, M. R., Vazan, S., Paknejad, F., Hosseini, Y. (2018): The effect of mycorrhizal symbiosis and seed priming on the amount of chlorophyll index and

http://www.aloki.hu ● ISSN 1589 1623 (Print) ● ISSN 1785 0037 (Online)
DOI: http://dx.doi.org/10.15666/aeer/1605_69276944
© 2018, ALÖKI Kft., Budapest, Hungary

absorption of nutrients under drought stress in sesame plant under field conditions. – Applied Ecology and Environmental Research 16(1): 335-357.

[9] Attibayeba, N., Nsika-Mikoko, E., Nkounkon, J. S. (2010): Description of different growth stage of *Sesamum indicum* L. using the extended BBCH scale. – Pakistan Journal of Nutrition 9(3): 235-239.

[10] Badigannavar, A., Girish, G., Ganapathi, T. R. (2015): Genetic variation for seed phosphorus and yield traits in Indian sorghum landraces and varieties. – The Crop Journal 3: 358-365.

[11] Beauchamp, C., Fridovich, I. (1971): Superoxide dismutase: improved assays and assay applicable to acrylamide gels. – Anal. Biochem. 44: 276-278.

[12] Beers, R. F., Sizer, I. W. (1952): A spectrophotometric method for measuring the breakdown of hydrogen peroxide by catalase. – J. Biol. Chem. 195: 133-40.

[13] Bittelli, M., Flury, M., Campbell, G. S., Nichols, E. J. (2001): Reduction of transpiration through foliar application of chitosan. – Agric Meteorol. 107: 167-175.

[14] Bradford, M. M. (1976): A rapid and sensitive method for quantitation of microgram quantities of protein utilizing the principle of protein-dye binding. – Annual Review of Biochemistry 72: 248-254.

[15] Chandrkrachang, S. (2002): The applications of chitin and chitosan in agriculture in Thailand. – Advances in Chitin Science 5: 458-462.

[16] Cho, M. H., No, H. K., Prinyawiwatkul, W. (2008): Chitosan treatments affect growth and selected quality of sunflower sprouts. – J Food Sci. 73: 71-77.

[17] Dossa, K., Yehouessi, J. W., Likeng-Li-Ngue, B., Diouf, D., Liao, B., Zhang, X., Cisse, N., Bell, J. M. (2017): Comprehensive screening of some west and central African sesame genotypes for drought resistance probing by agromorphological, physiological, biochemical and seed quality traits. – Agronomy 83(7): 1-18.

[18] Dzung, N. A. (2007): Chitosan and their derivatives as prospective bio substances for developing sustainable eco-agriculture. – Advances in Chitin Science X: 453-459.

[19] Dzung, N. A., Khanh, V. T. P., Dzung, T. T. (2011): Research on the impact of chitosan oligomers on biophysical characteristics, growth, development and drought resistance of coffee. – Carbohydrate Polymers 84: 751-755.

[20] El-Khier, M. K. S., Ishag, K. E. A., Yagoub, A. E. A. (2008): Chemical composition and oil characteristics of sesame seed cultivars grown in Sudan. – Res. Journal of Agric. and Biol. Sci. 4(6): 761-766.

[21] Farhoosh, R., Hadad Khodaparast, M. H., Sharif, A. (2009): Bene hull oil as a highly stable and antioxidative vegetable oil. – Eur. J. Lipid Sci. Technol. 111: 1259-1265.

[22] Farouk, S., Amany, A. R. (2012): Improving growth and yield of cowpea by foliar application of chitosan under water stress. – Egypt Journal of Biol. 14: 14-26.

[23] Fazeli, F., Ghorbanli, M., Niknam, V. (2007): Effect of drought on biomass, protein content, lipid peroxidation and antioxidant enzymes in two sesame cultivars. – Biologia Plantarum 51(1): 98-103.

[24] Gill, S. S., Tuteja, N. (2010): Reactive oxygen species and antioxidant machinery in abiotic stress tolerance in crop plants. – Plant Physiol Bioc. 48: 909-930.

[25] Golestani, M., Pakniyat, H. (2015): Evaluation of traits related to drought stress in sesame (*Sesamum indicum* L.) genotypes. – Journal of Asian Scientific Research 5(9): 465-472.

[26] Ghormade, V., Deshpande, M. V., Paknikar, K. M. (2011): Perspectives for nano-biotechnology enabled protection and nutrition of plants. – Biotechnol Adv 29: 792-803.

[27] Jan, A., Ali, S., Adail, M., Khan, A. (2014): Growth and yield components of sesame (*Sesamum indicum* L.) as influenced by phosphorus levels under different row spacing. – Journal of Environment and Earth Science 4(22): 150-154.

[28] Jouyban, Z., Moosavi, S. G. (2012): Effect of different irrigation intervals, nitrogen and superabsorbent levels on chlorophyll index, yield and yield components of sesame. – Journal of Food Agric Environ 10(1): 360-364.

http://www.aloki.hu ● ISSN 1589 1623 (Print) ● ISSN 1785 0037 (Online)
DOI: http://dx.doi.org/10.15666/aeer/1605_69276944
© 2018, ALÖKI Kft., Budapest, Hungary

[29] Kadkhodaie, A., Razmjoo, J., Zahedi, M., Pessarakli, M. (2014): Oil content and composition of sesame (*Sesamum indicum* L.) genotypes as affected by irrigation regimes. – J Am Oil Chem Soc 91: 1737-1744.
[30] Kananont, N., Pichyangkura, R., Chanprame, S., Chadchawan, S., Limpanavech, P. (2010): Chitosan specificity for the in vitro seed germination of two Dendrobium orchids (Asparagales: Orchidaceae). – Sci Hortic-Amsterdam 124: 239-247.
[31] Kim, K. S., Ryu, S. N., Chung, H. G. (2006): Influence of drought stress on chemical composition of sesame seed. – Korean J Crop Sci. 51(1): 73-80.
[32] Kukreja, S., Nandval, A. S., Kumar, N., Sharma, S. K., Sharma, S. K., Unvi, V., Sharma, P. K. (2005): Plant water status, H_2O_2 scavenging enzymes, ethylene evolution and membrane integrity of *Cicer arietinum* roots as affected by salinity. – Biol. Plant. 49: 305-308.
[33] Leiboritz, H. E., Benqrson, D. A., Mouqle, P. D., Simpson, K. L. (1987): Effects of Artemia Lipid Fraction on Growth and Survival of Larval in Land Liver Sides. 469-476. – In: Sorgeloss, P., Bengtson, D. A., Deelier, W., Japers, E. (eds.). Artemia Research and Its Application. Universal Press, Wetteven, Belgium.
[34] Limpanavech, P., Chaiyasuta, S., Vongpromek, R., Pichyangkura, R., Khunwasi, C., Chadchawan, S., Lotrakul, P. (2008): Chitosan effects on floral production, gene expression, and anatomical changes in the *Dendrobium orchid*. – Scientia Horticulturae 116: 65-72.
[35] Mehrabi, Z., Ehsanzadeh, P. (2011): Study of physiological characteristics and performance of four sesame cultivars under soil moisture regimes. – Journal of Crop Improvement 13(2): 75-88.
[36] Mensah, J. K., Obadoni, B. O., Eruotor, P. G., Onome-Irieguna, F. (2006): Simulated flooding and drought effects on germination, growth, and yield parameters of sesame (*Sesamum indicum* L.). – African Journal of Biotechnology 5(13): 1249-1253.
[37] Misra, A., Sricastatva, N. K. (2000): Influence of water stress on Japanese mint. – Journal Herbs Spices Medician Plants 7: 51-58.
[38] Mohsennia, O., Jalilian, J. (2012): Response of safflower seed quality characteristics to different soil fertility systems and irrigation disruption. – Inter. Res. Journal of Applied and Basic Sci. 3(5): 968-976.
[39] Pathak, N., Rai, A. K., Kumari, R., Thapa, A., Bhat, K. V. (2014): Sesame crop: an underexploited oilseed holds tremendous potential for enhanced food value. – Agric. Sci. 5: 519-529.
[40] Pongprayoon, W., Roytrakul, S., Pichayangkura, R., Chandchawan, S. (2013): The role of hydrogen peroxide in chitosan-induced resistance to osmotic stress in rice (*Oryza sativa* L.). – Plant Growth Regul. DOI: 10.1007/s10725-013-9789-4.
[41] Pornpienpakde, P., Singhasurasak, R., Pichyangkura, R., Chaiyasap, P., Bunjongrat, R., Chadchawan, S., Limpanavech, P. (2010): Improving the micropropagation efficiency of hybrid *Dendrobium orchids* with chitosan. – Sci Hortic-Amsterdam 124: 490-499.
[42] Povero, G., Loreti, E., Pucciariello, C., Santaniello, A., Tommaso, D. D., Tommaso, G. D., Kapetis, D., Zolezzi, F., Piaggesi, A., Perata, P. (2011): Transcript profile of chitosan-treated Arabidopsis seedling. – J Plant Res. DOI: 10.1007/s10265-010-0399-1.
[43] Safari Arabi, M., Lak, S. H., Modhej, A., Ramzanpour, M. R., Mobasser, H. R. (2018): Interaction of *Pseudomonas fluorescence* bacteria and phosphorus on the quantitative and the qualitative yield of rapeseed (*Brassica napus* L.) cultivars. – Applied Ecology and Environmental Research 16(1): 63-80.
[44] Shakeri, M., Modarres-Sanavy, S. A. M., Amini Dehaghi, M., Tabatabaei, S. A., Moradi-Ghahderijiani, M. (2015): Improvement of yield, yield components and oil quality in sesame (*Sesame indicum* L.) by N-fixing bacteria fertilizers and urea. – Archives of Agronomy and Soil Science 62(4): 547-560.
[45] Shao, H. B., Chu, L. Y., Jaleel, C. A., Zhao, C. X. (2008): Water deficit stress induced anatomical changes in higher plants. – Comptes Rendus Biologies 331: 215-25.

http://www.aloki.hu ● ISSN 1589 1623 (Print) ● ISSN 1785 0037 (Online)
DOI: http://dx.doi.org/10.15666/aeer/1605_69276944
© 2018, ALÖKI Kft., Budapest, Hungary

[46] Solanki, P., Bhargava, A., Chhipa, H., Jain, N., Panwar, J. (2015): Nano-fertilizers and Their Smart Delivery System. – Springer International Publishing, Switzerland. DOI: 10.1007/978-3-319-14024-7_4.
[47] Taiz, L., Ezeiger, H. (1998): Plant Physiology (2nd ed.). – Sinaye Associates Inc., Sonderland, MA.
[48] Wang, Y., He, H. G., Zhou, Y. (2006): Effect of different molecular weight chitosan on several physiological and biochemical characteristics related to plant defense reaction. – Plant Physiology 42: 1109-1111.
[49] Yang, F., Hu, J., Li, J., Wu, X., Qian, Y. (2009): Chitosan enhances leaf membrane stability and antioxidant enzyme activities in apple seedlings under drought stress. – Plant Growth Regul 58: 131-136.
[50] Yoshida, H., Tanaka, M., Tomiyama, Y., Mizushina, Y. (2007): Regional distribution in the fatty acids of triacylglycerols and phospholipids of sesame seeds (*Sesamum indicum* L.). – J. Food Lipids 14: 189-201.
[51] Yousefzadeh Najafabadi, M., Ehsanzadeh, P. (2017): Photosynthetic and antioxidative upregulation in drought-stressed sesame (*Sesamum indicum* L.) subjected to foliar-applied salicylic acid. – Photosynthetica 55(4): 611-622.

http://www.aloki.hu ● ISSN 1589 1623 (Print) ● ISSN 1785 0037 (Online)
DOI: http://dx.doi.org/10.15666/aeer/1605_69276944
© 2018, ALÖKI Kft., Budapest, Hungary

PLANT WASTES FOR REMOVAL OF TOXIC MALACHITE GREEN DYE

AL-AHMARY, K.[1] – ALMHYAWI, S.[1] – AL-TURKUSTANI, A.[1] – EL-GENDY, A.[1,2] – OMAR, H.[3,4*]

[1]*Department of Chemistry, Faculty of Science, University of Jeddah, Jeddah, Saudi Arabia*

[2]*Department of Chemistry, Faculty of Science, Zagazig University, Zagazig, Egypt*

[3]*Department of Biological Science, Faculty of Science, University of Jeddah, Jeddah, Saudi Arabia*

[4]*Department of Botany, Faculty of Science, Tanta University, Tanta, Egypt*

**Corresponding author*
e-mail: hananomar1@yahoo.com; phone: +96-656-567-9599

(Received 27th Jun 2018; accepted 28th Sep 2018)

Abstract. The wastes of *Myoporum laetum* and *Livistona chinensis* leaves were utilized for removal of malachite green dye (MG) from solution. The highest removal for dye was observed with *M. laetum* biomass at pH: 6, temperature: 35 °C, biomass dose: 0.3 g L^{-1} and contact time: 120 min. The different concentrations of MG (5-35%) were highly removed by *M. laetum* (99.28% to 79.31%, respectively) as compared with *L. chinensis* (95.48-69.67%, respectively) at the optimum conditions. The sorption data were represented by Langmuir, Freundlich and Temkin isotherms. Adsorption was established well with isotherms of Langmuir and Freundlich. The study of thermodynamic suggested that the adsorption reaction was endothermic and the sorption of dye onto the biomass proceed in the forward direction and greatly promising process. The removal of dye was characterized by FT-IR analyses and the results confirmed that the groups responsible for the process of dye binding were hydroxyl or amino, and carboxylate or amide. The *M. laetum* cell wall showed a great porosity which permits the passage of dye molecules. The *M. laetum* biomass was more efficient than that of *L. chinensis.* The efficiency of the plant waste for a decolorizing solution containing dye, their abundance in nature and less processing requirements may lead to the emergence of low-cost adsorbents.
Keywords: *dye, plant leaves, equilibrium isotherm, thermodynamic, IR, SEM*

Introduction

Dyes are used in many industries and their extensive use causes pollution. Dyes are more difficult to degrade because they have a complex aromatic structure which makes them more stable (Seshadri et al., 1994). Dyes are toxic, mutagenic and difficult to be analyzed (Hammud, 2011). Thus, when the dye is discharged into waters it can affect the ecological system and human health. Dyes are dangerous to the aquatic living organisms (Vijayaraghavan and Yun, 2008). It causes problems to aquatic groups due to decreasing of light penetration and photosynthesis. The total amount of dyes generated in the world was found to be over 10,000 tons per year (Forgacs et al., 2004).

Malachite green is a dark green and belongs to triphenylmethane family. It is a water-soluble dye and can enter the cells due to their high lipid solubility (Albert, 1979). Malachite green dye is greatly used as a fungicide, bactericide, and antiprotozoal and for staining of cell and tissue samples (Hecht and Endemann, 1998). Malachite green play an important role as a food additive and in the process of paper coloring, silk, cotton, wool, leather, anthelmintic, and detergent (Srivastava et al., 2004). Its oral consumption is carcinogenic so that it is applied externally on ulcers

http://www.aloki.hu ● ISSN 1589 1623 (Print) ● ISSN 1785 0037 (Online)
DOI: http://dx.doi.org/10.15666/aeer/1605_69456962
© 2018, ALÖKI Kft., Budapest, Hungary

and wounds (Clifton-Hadley and Alderman, 1987). Therefore, the presence of malachite green dye in animal milk, fishes, and other foodstuff is very dangerous to the human being (Srivastava et al., 1995). The products formed from degradation of malachite green are not safe and have a carcinogenic effect (Srivastava et al., 2004). Previous studies confirmed that malachite green induced hurts to bones, skin, eyes, liver, kidney, heart, and spleen in animals (Sundarrajan et al., 2000).

In many parts of the world, the dye is still being used. Accordingly, it is important to find methods to eliminate dye from ponds or wastewater. It is important to eliminate dye from the water before its discharging to stream by using an effective treatment technique. The industrial separation method used for the purification of wastewater is the adsorption technique. As compared with other methods, adsorption is the first in terms of cost, ease of design, flexibility, the simplicity of procedure and insensitivity to toxic pollutants (Laxmi and Ahmaruzzaman, 2010). Lately, the use of biomass for removal of dye has been seriously studied as another economical, and feasible technique. The biological treatment is a superior technique for the adsorption due to their ability to remove dyes in a highly concentrated form. Recently, attention has been concentrated on algae (Deokar and Sabale, 2014), bacteria, fungi (Gupta et al., 2015) and plants (Kadirvelu et al*.,* 2003). Adsorption of wastewater dyes by plant material or biomass is an eco-friendly and emerging process for removal of dyes in industrial effluents. The biomass is easy to be removed and can be stored for a long time without decomposition.

It is useful to understand and predict the mobility of toxic substances in the environment. Langmuir model is a common sorption isotherm and depends on reaction hypotheses (Langmuir, 1918). All the sites of adsorption are assumed to be identical, keep one molecule of the compound, energetically, and independent on the quantity of adsorbed. The model of Freundlich is empirical and based on the relation between the quantity of adsorbed and the concentration of remained solute (Freundlich, 1909).

The trees of *Myoporum laetum* and *Livistona chinensis* are found abundantly along streets of Jeddah city in Saudi Arabia. These trees are pruned annually making a huge accumulation and create great environmental problems. Therefore, economic utilization of these trees will be beneficial. The plant leaves can be dried and used as available biomaterials for the elimination of dye from solutions. The present study aimed to evaluate the efficiency of *Myoporum laetum* and *Livistona chinensis* leaves for removal of malachite green from solution. The effect of pH, contact time, dye concentrations, and temperature were determined to optimize the sorption conditions. The data of equilibrium biosorption was explained by Langmuir, Freundlich, and Temkin adsorption isotherm equations. The thermodynamic study, infrared spectroscopy, and scanning electron microscopy were investigated.

Materials and methods

Dye solution

Malachite green ($C_{52}H_{54}N_4O_{12}$) with a purity of 90% and molecular weight of 927.02 was attained from Merck, Germany. One gram of malachite green was dissolved in one liter of deionized water (1 g L^{-1}) to prepare the stock solution. Different concentrations (5, 10, 15, 20, 25, 30 and 35 mg L^{-1}) were prepared from the stock dye solution.

http://www.aloki.hu ● ISSN 1589 1623 (Print) ● ISSN 1785 0037 (Online)
DOI: http://dx.doi.org/10.15666/aeer/1605_69456962
© 2018, ALÖKI Kft., Budapest, Hungary

Preparation of biomass

The waste of *Myoporum laetum* and *Livistona chinensis* leaves were gathered from the streets of Jeddah, during the trimming season of trees in Saudi Arabia. The plant leaves were washed with water and then air dried at the Chemistry Lab., Faculty of Science, King Abdulaziz University. The dry constant was milled and sieved by using a standard sieve of 1.0 mm. The biomass was treated with 0.2% $CaCl_2$, dried at 45 C and then kept until use.

Removal of dye

The bioremoval study was performed for 5 mg L^{-1} dye solution using 0.5 g L^{-1} biomass of leaves in Erlenmeyer flasks. The dye solution and biomass were agitated at 150 rpm for 1 h to detect the optimum factors of temperature, pH, contact time, and weight of biomass for removal of dye. The absorbance of the removed dye was measured by UV-1800 spectrophotometer at 616 nm. The dye removal percentage was represented by *Equation 1*.

$$\text{Removal of dye } (\%) = \frac{Ci - Ce}{Ci} \times 100 \qquad \text{(Eq.1)}$$

where C_i represents the initial dye concentration and C_e is the concentration of dye at equilibrium.

Solution pH, temperature, and contact time

Dye solutions with different pH (2, 4, 6, 8, and 10), temperature (25, 35, 45 and 55 °C), and contact time (ranged from 0.0 to 180 min) were prepared. The optimum conditions of pH, temperature, and contact time for the uptake of dye were estimated by the dry biomass.

Weight of biomass

To obtain the ideal weight of biomass for removal of malachite green from solution, different weights of dry biomass (0.5, 1.0, 1.5, 2.0, 2.5 and 3.0 g L^{-1}) were prepared. At the optimal conditions of pH, temperature, and contact time, the removal of dye from solution was estimated.

Dye concentration

At the optimal condition of pH, temperature, contact time, and biomass, different concentrations of dye (5, 10, 15, 20, 25, 30, and 35 mg L^{-1}) were used to evaluate the efficiency of dry plant leaves for removal of dye from solution.

Adsorption isotherms

The different adsorption isotherms were evaluated at the optimal conditions of pH, temperature, contact time, biomass and dye concentration. The monolayer adsorption was represented by the model of Langmuir isotherm. The Langmuir model (Langmuir, 1918) was stated in *Equation 2*.

http://www.aloki.hu ● ISSN 1589 1623 (Print) ● ISSN 1785 0037 (Online)
DOI: http://dx.doi.org/10.15666/aeer/1605_69456962
© 2018, ALÖKI Kft., Budapest, Hungary

$$\frac{1}{q_e} = \frac{1}{q_m} + \frac{1}{bq_m}\left(\frac{1}{C_e}\right) \quad \text{(Eq.2)}$$

where q_e is the amount dye absorbed onto the biomass (mg g^{-1}), q_m is the Langmuir constant that clarifies the highest capacity (mg g^{-1}), and b is the constant of Langmuir and represent the affinity of binding site (L mg^{-1}), C_e is the concentration of dye in the solution at equilibrium (mg L^{-1}), $1/bq_m$ is the intercept, and $1/q_m$ is the slope.

The affinity of biomass (adsorbent) to dye (adsorbate) was obtained from the factor of dimensionless separation (R_L). The R_L was discussed by Malik (2004) in *Equation 3*.

$$R_L = \frac{1}{1+bC_i} \quad \text{(Eq.3)}$$

The shape of isotherm was found to be favorable ($0 < R_L < 1$), linear ($R_L = 1$), irreversible ($R_L = 0$), or unfavorable ($R_L > 1$),

The unfavorable sorption on dissimilar surfaces and multilayer sorption was described in the Freundlich model (Freundlich, 1906). The Freundlich model was represented in *Equation 4*.

$$\ln q_e = \ln K_F + \frac{1}{n} \ln C_e \quad \text{(Eq.4)}$$

where q_e is the dye adsorbed onto the biomass (mg g^{-1}) at equilibrium, K_F Freundlich isotherm constant (mg g^{-1}), n is the sorption intensity constant, and C_e represents the concentration of dye at equilibrium (mg L^{-1}).

The interactions of indirect adsorbent-adsorbate and the behavior of the adsorption systems on the heterogeneous surfaces was represented by the model of Temkin isotherm (Temkin and Pyzhev, 1940). The model of Temkin was found in *Equation 5*.

$$q_e = \frac{R_T}{b_T} \ln A_T + \frac{R_T}{b_T} \ln C_e \quad \text{(Eq.5)}$$

where R is the gas constant, T is the absolute temperature, b_T is the Temkin isotherm constant (J mol^{-1}), A_T is the Temkin equilibrium constant (L g^{-1}), R_T/b_T is a constant related to the heat of adsorption (J mol^{-1}), and C_e is the concentration of dye (mg L^{-1}) at equilibrium. A_T and b_T were determined from the slope and intercept obtained by plotting q_e versus ln C_e.

Thermodynamic study

The values of thermodynamic were assessed by studying the temperature changes with an equilibrium constant. The following equation illustrates the free energy of the sorption reaction (*Eq. 6*):

$$\Delta G^\circ = -R_T \ln K_c \quad \text{(Eq.6)}$$

where ΔG° represents the variation in free energy (kJ mol^{-1}), R declares the gas constant (8.314 kJ mol^{-1}), T indicates the absolute temperature, and K_c is the equilibrium constant.

http://www.aloki.hu ● ISSN 1589 1623 (Print) ● ISSN 1785 0037 (Online)
DOI: http://dx.doi.org/10.15666/aeer/1605_69456962
© 2018, ALÖKI Kft., Budapest, Hungary

The thermodynamic values were estimated by the change of temperature with the equilibrium constant as found in *Equation 7*.

$$\ln K_c = -\frac{\Delta H^\circ}{R_T} + \frac{\Delta S^\circ}{R} \quad \text{(Eq.7)}$$

where ΔH° represents the enthalpy, and ΔS° is the entropy of the equilibrium process.

Infrared spectroscopy (IR)

The functional groups on the surface of the biomass were characterized by infrared spectrophotometer (Tensor 27, Netherlands).

Scanning electron microscopy (SEM)

Scanning electron microscopy (JEOL, JSM-5200 LV) was used to study the surface of the biomass before and after the treatment with dye.

Results

Influence of pH

As shown in *Figure 1,* the removal of malachite green (5 mg L^{-1}) onto 0.5 g L^{-1} biomass of *Myoporum laetum* and *Livistona chinensis* was increased with increasing the pH values. The removal of dye increased gradually from pH 2 (94.46%) up to pH 6 (99.01%) and then remained constant up to pH 10 by using the biomass of *M. laetum.* However, the removal of dye increased slowly at pH ranged from 4 to 8 (89.73% to 90.62%, respectively) and then highly increased at pH 10 (96.78%) by using *L. chinensis* biomass.

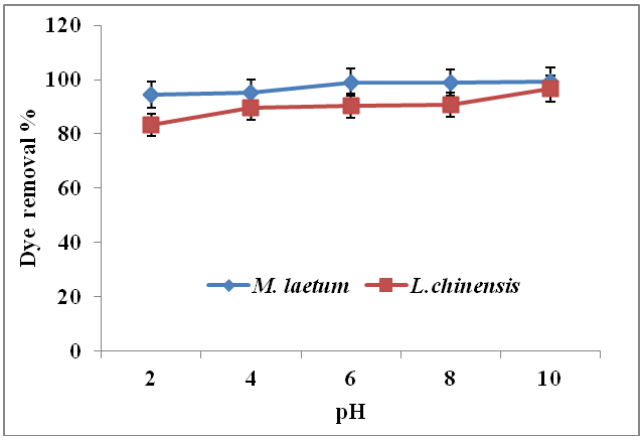

Figure 1. *The effect of different pH values on the removal of malachite green (5 mg L^{-1}) by using the biomass of M. laetum and L. chinensis leaves. The data are the mean of three values ± SD*

Influence of temperature

Figure 2 represents the removal percentage of MG onto the plant biomass (0.5 g L^{-1}) at different temperatures (25, 35, 45, and 55 °C) after 1 h. The results showed that the

http://www.aloki.hu ● ISSN 1589 1623 (Print) ● ISSN 1785 0037 (Online)
DOI: http://dx.doi.org/10.15666/aeer/1605_69456962
© 2018, ALÖKI Kft., Budapest, Hungary

removal of MG increased with increasing temperature up to 35 °C for both biomasses of *M. laetum* (97.67%) and *L. chinensis* (92.32%). With increasing the temperature up to 55 °C, the removal of dye still constant with the biomass of *M. laetum* (97.67%) and decreased with *L. chinensis* biomass (89.46%). It can be noticed that the removal efficiency of MG onto the biomass of *M. laetum* was higher than *M. laetum.* The temperature of 35 °C was chosen as the optimum temperature for the uptake of MG from solution.

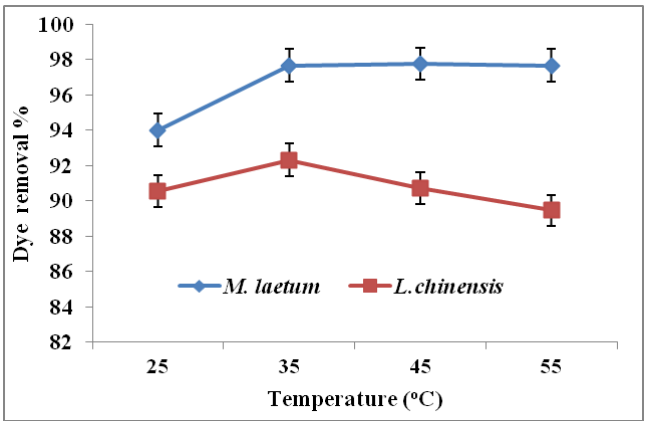

Figure 2. *The effect of different temperatures on the removal of malachite green (5 mg L^{-1}) by using the biomass of M. laetum and L. chinensis leaves. The data are the mean of three values ± SD*

Influence of contact time

The removal of dye (5 mg L^{-1}) at a different time (0.0-180 min) by tested biomass (0.5 g L^{-1}) was explained in *Figure 3*. As shown in the results, the uptake of dye increased with increasing the contact time up to a certain extent. After this point, the removal percentage of MG is not affected. The removal of dye quickly increased through the first 10 min (57%) and then slowly increased until equilibrium at 120 and 160 min for *M. laetum* and *L. chinensis,* respectively. The maximum removal percentages were 96% and 88% by *M. laetum* and *L. chinensis,* respectively.

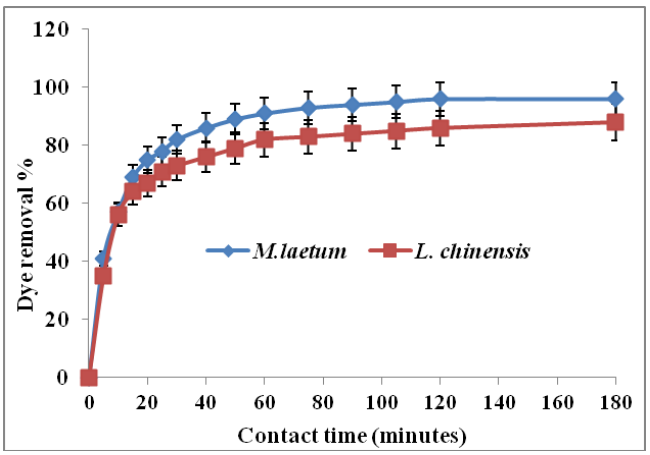

Figure 3. *The effect of contact time on the removal of malachite green (5 mg L^{-1}) by using the biomass of M. laetum and L. chinensis leaves. The data are the mean of three values ± SD*

http://www.aloki.hu ● ISSN 1589 1623 (Print) ● ISSN 1785 0037 (Online)
DOI: http://dx.doi.org/10.15666/aeer/1605_69456962
© 2018, ALÖKI Kft., Budapest, Hungary

Influence of weight of biomass

The removal of MG from solution by 0.1-0.7 g biomass was illustrated in *Figure 4*. The results revealed that the removal of dye was greatly increased with increasing dose of biomass up to 0.3 g of *M. laetum* (99.11%) and 0.4 g of *L. chinensis* (95.98%) and then remained constant. As clear from the results, the biomass of *M. laetum* was more efficient than *L. chinensis* for the uptake of MG.

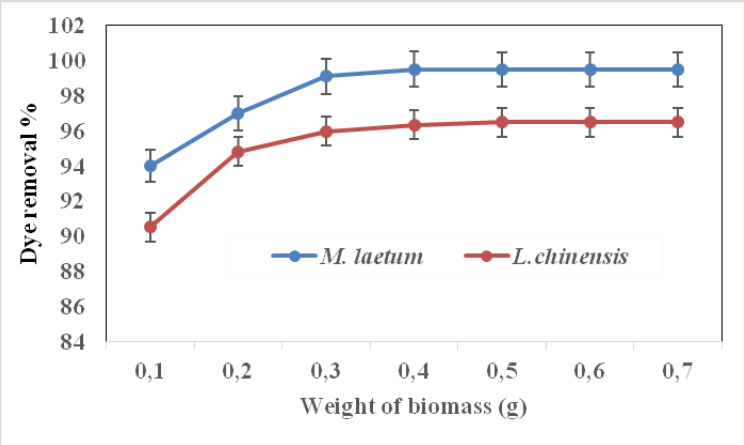

Figure 4. *The effect of different weights of M. laetum and L. chinensi biomasses on the removal of malachite green (5 mg L^{-1}). The data are the mean of three values ± SD*

Influence of dye concentration

The influence of 5-35 mg L^{-1} dye on the uptake of MG was investigated for both biomasses at the optimum conditions (*Fig. 5*). As shown from the above results the most favorable conditions for the removal of MG by using *M. laetum* were observed at pH: 6, temperature: 35 °C, 0.3 g L^{-1} biomass dose and 120 min contact time. However, pH: 10, temperature: 35 °C, 0.4 g L^{-1} biomass dose and 160 min contact time were the optimum condition for the removal of MG by using *L. chinensis*. The results presented that the percentage of MG uptake decreased with increasing the dye concentration from 5 to 35 mg L^{-1}. The maximum uptake of dye (99.28% and 95.48%) was attained at 5 mg L^{-1} by the biomass of *M. laetum* and *L. chinensis*, respectively. However, the biomass of *M. laetum* and *L. chinensis* showed the minimum removal percentage (79.31% and 69.67%, respectively) at 35 mg L^{-1} MG concentration.

Adsorption isotherms

It is important to design the most adsorption system for removal of MG dye. Thus, the equilibrium experimental data for adsorbed MG onto *M. laetum* and *L. chinensis* biomasses were studied using different isotherms of Langmuir and Freundlich and Temkin (*Table 1*). According to Langmuir isotherm, the values of intercept ($1/bq_m$) and slop ($1/q_m$) were attained from the plot of $1/q_e$ against $1/C_e$ for adsorption of MG onto the biomasses of *M. laetum* and *L. chinensis* (Fig. 6a, b). The results in *Table 1* revealed that the maximum capability (q_m) was found to be 50.065 and 42.212 mg g^{-1} for the biomass of *M. laetum* and *L. chinensis,* respectively. It can be noticed that the greatest capacity of adsorption of MG dye was recorded with *M. laetum.* Regarding to the

http://www.aloki.hu ● ISSN 1589 1623 (Print) ● ISSN 1785 0037 (Online)
DOI: http://dx.doi.org/10.15666/aeer/1605_69456962
© 2018, ALÖKI Kft., Budapest, Hungary

results of Langmuir isotherm, the highest binding site affinity (*b*) for MG was observed with *M. laetum* biomass (0.242 L mg^{-1}). The R_L values for both *M. laetum* and *L. chinensis* were found to be 0.176 and 0.106, respectively suggesting that the process of dye sorption is favorable (*Table 1*).

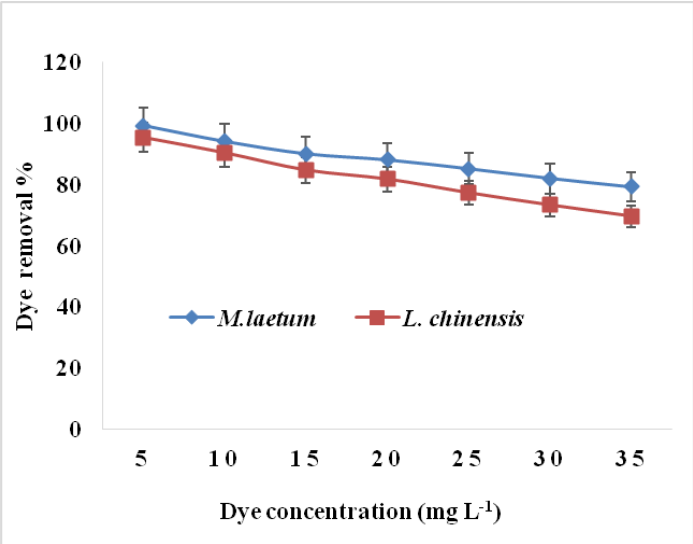

Figure 5. *Removal of different concentrations of malachite green by using the biomass of M. laetum and L. chinensis leaves under the optimal conditions. The data are the mean of three values ± SD*

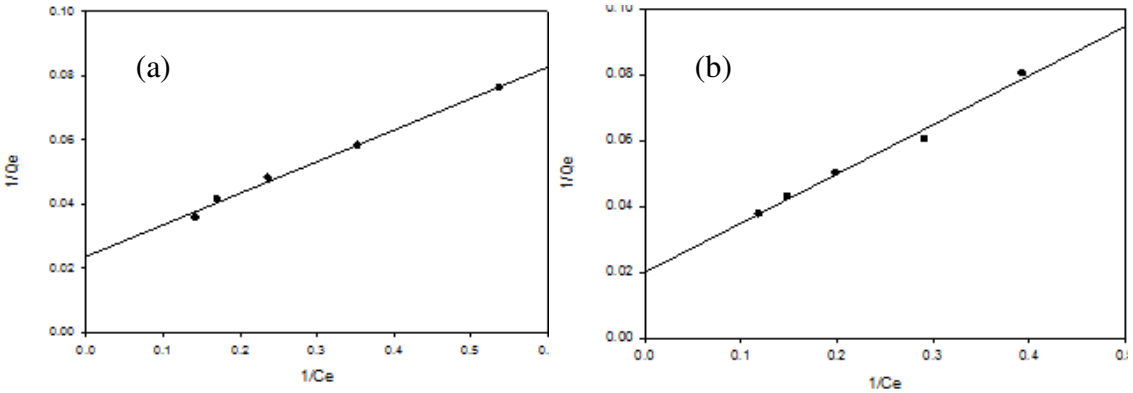

Figure 6. *The linear plots of Langmuir isotherm for adsorption of malachite green onto the biomass of M. laetum (a) and L. chinensis leaves (b)*

With regard to Freundlich isotherm, the results showed that the plotting of ln *qe* versus ln *Ce* give a straight line with a slope of 1/n and intercept of ln K_F for adsorption of MG onto the tested biomasses (*Fig. 7a, b*). The values of *n* were found to be 1.839 and 1.655 for *M. laetum* and *L. chinensis*, respectively (*Table 1*). As a general, MG is favorably adsorbed onto the tested biomass where $n > 1$. The adsorption capacity (K_F) for *M. laetum* (9.497 mg g^{-1}) was higher than that of *L. chinensis* (7.419 mg g^{-1}). Therefore, *M. laetum* biomass obtained the greatest binding affinity and adsorption capacity for MG as compared with the biomass of *L. chinensis*.

http://www.aloki.hu ● ISSN 1589 1623 (Print) ● ISSN 1785 0037 (Online)
DOI: http://dx.doi.org/10.15666/aeer/1605_69456962
© 2018, ALÖKI Kft., Budapest, Hungary

Table 1. *Parameters of Langmuir, Freundlich and Temkin isotherms for adsorption of malachite green onto the biomass of M. laetum and L. chinensis leaves*

Isotherm		*M. laetum*	*L. chinensis*
Langmuir	q_m (mg g^{-1})	50.065	42.212
	b (L mg^{-1})	0.242	0.134
	R_L	0.176	0.106
	R^2	0.97	0.97
Freundlich	K_F (mg g^{-1})	9.497	7.419
	n	1.839	1.655
	R^2	0.97	0.99
Temkin	A_T (L mg^{-1})	1.791	1.590
	b_T	233.34	246.33
	R^2	0.86	0.94

q_m: Langmuir constant, b: affinity of binding site, R_L: dimensionless separation factor, R^2: linear correlation coefficient, K_F: Freundlich isotherm constant, n: sorption intensity constant, A_T: Temkin isotherm equilibrium binding constant, b_T: Temkin isotherm constant

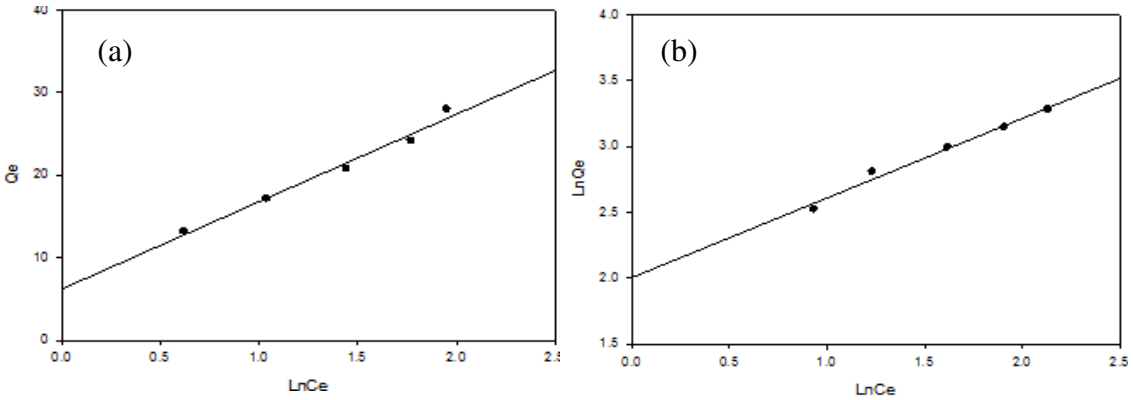

Figure 7. *The linear plots of Fruendlich isotherm for adsorption of malachite green onto the biomass of M. laetum (a) and L. chinensis leaves (b)*

According to the Temkin isotherm, the constant of A_T and b_T for sorption of MG by *M. laetum* and *L. chinensis* dry leaves were attained from the slop of q_e against ln C_e (*Fig. 8a, b*). The results demonstrated that A_T was 1.791 and 1.590 L mg^{-1} for *M. laetum* and *L. chinensis* biomass, respectively (*Table 1*). The b_T values were 233.34 and 246.33 for *M. laetum* and *L. chinensis* biomasses, respectively.

The results showed that the Langmuir isotherm for *M. laetum* biomass was linear within the entire studied concentration of dye with a linear correlation coefficient ($R^2 = 0.97$), suggesting that the data fit quite well with Langmuir model. The Langmuir isotherm confirms the monolayer sorption of MG by *M. laetum* biomass and heterogonous active sites distribution on the adsorbent. Depending on the great values of the correlation coefficient ($R^2 = 0.97$), the Freundlich model was also established to be a favorable model for explanation of the adsorption performance of MG by *M. laetum* biomass. Based on these results, it can be noticed that the adsorption of dye was well fitted by both Langmuir and Freundlich models for the biomass of *M. laetum.* It

http://www.aloki.hu ● ISSN 1589 1623 (Print) ● ISSN 1785 0037 (Online)
DOI: http://dx.doi.org/10.15666/aeer/1605_69456962
© 2018, ALÖKI Kft., Budapest, Hungary

can be concluded that both homogenous and heterogonous adsorption takes place throughout the process.

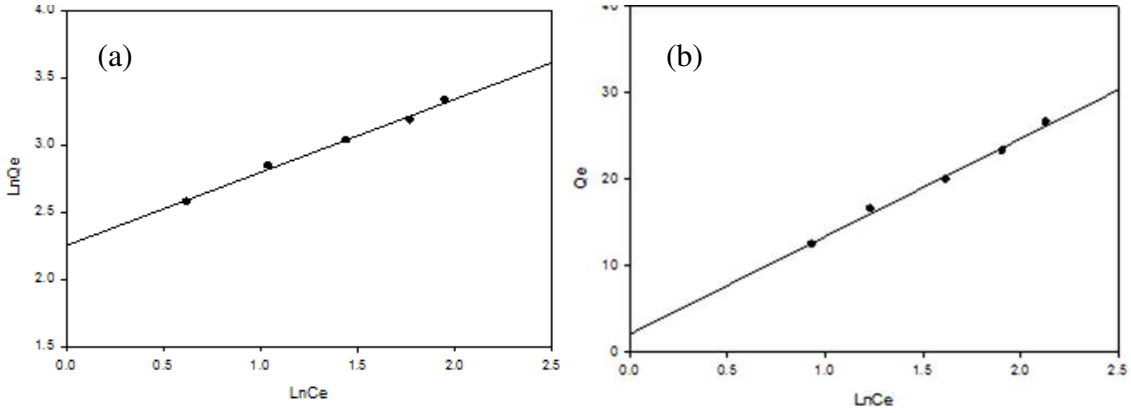

Figure 8. *The linear plots of Temkin isotherm for adsorption of malachite green onto the biomass of M. laetum (a) and L. chinensis leaves (b)*

As compared with other isotherms, the highest value of the correlation coefficient ($R^2 = 0.99$) was observed with the biomass of *L. chinensis*. This result clarified that the Freundlich model was the most favorable to describe the adsorption equation data for *L. chinensis* biomass.

According to Temkin isotherm, the correlation coefficients (R^2) of *M. laetum* and *L. chinensis* biomasses were ranged between 0.86 and 0.94, respectively (*Table 1*). This result elucidated that Temkin equation represents the poor fit as compared with the other isotherms for both biomasses.

Thermodynamic study

In the present study, the values of thermodynamic were given in *Table 2*. The ΔG° was determined as -6.3 kJ mol^{-1} and -4.8 kJ mol^{-1} for *M. laetum* and *L. chinensis*, respectively. The highest affinity for removal of MG by the biomass of *M. laetum* may be returned to the highest value of $-\Delta G^\circ$ as compared with *L. chinensis* biomass. The sorption process of MG by the tested biomass was spontaneous and highly favorable due to the negative values of ΔG°. The values of ΔH° and ΔS° were represented by 8.5 kJ mol^{-1} and 49 kJ mol^{-1}, respectively for *M. laetum* and 7.3 kJ mol^{-1} and 40 kJ mol^{-1}, respectively for *L. chinensis* (*Table 2*).

IR spectral analysis

The IR spectral analysis of raw biomass of *M. laetum* showed different functional groups at 3435 cm^{-1} due to –OH and –NH stretching, at 2923 cm^{-1} attributed to C-H stretching vibration, at 1627 cm^{-1} assigned to $–COO^-$ stretching or amide I and amide II and finally at 1035 cm^{-1} due to N-H bending vibration or C-OH stretching vibration of alcohol (*Fig. 9a*). However, the IR spectrum of *M. laetum* biomass after dye sorption (*Fig. 9b)* exhibited change in the position and intensity of adsorption bands at 3435, 1627 and 1037 cm^{-1} due to hydroxyl or amino groups, and carboxylate or amide groups. These results showed the contribution of these groups in the biosorption of MG dye by *M. laetum* biomass.

http://www.aloki.hu ● ISSN 1589 1623 (Print) ● ISSN 1785 0037 (Online)
DOI: http://dx.doi.org/10.15666/aeer/1605_69456962
© 2018, ALÖKI Kft., Budapest, Hungary

Table 2. *Parameters of thermodynamic and activation energy for adsorption of malachite green onto the biomass of M. laetum and L. chinensis leaves*

Plant	ΔG° (kJ mol^{-1})	ΔH° (kJ mol^{-1})	ΔS° (kJ mol^{-1})
M. laetum	-6.3	8.5	49
L. chinensis	-4.8	7.3	40

ΔG°: variation in free energy, ΔH°: enthalpy of equilibrium, ΔS°: entropy of equilibrium

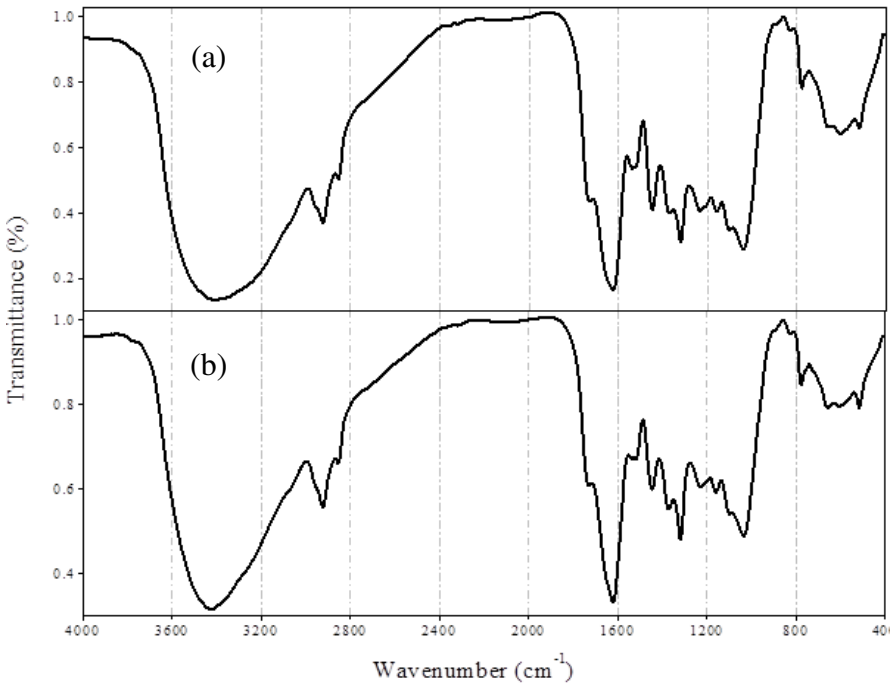

Figure 9. *FTIR spectrum of M. laetum biomass before (a) and after (b) adsorption of malachite green*

The IR spectrum of raw biomass of *L. chinensis* (*Fig. 10a*) exhibited a broad peak for adsorption at 3436 cm^{-1} attributable to -OH and -NH stretching vibration, 2923 cm^{-1} due to stretching vibration of C-H, 1631 cm^{-1} caused by COO^{-} group or amide group and 1034 cm^{-1} assigned to N-H bending or stretching vibration of C-OH. The adsorption bands after dye treatments revealed some changes in the position and intensity of the above absorption bands especially at 1631 cm^{-1} due to carboxylate or amide groups which confirm the participation of these groups in dye biosorption by *L. chinensis* biomass (*Fig. 10b*).

Scanning electron microscopy micrographs (SEM)

Evaluation of the morphological changes on the surface of *M. laetum* biomass, which is the most efficient for sorption of MG dye adsorption, was performed by using scanning electron microscopy. Before the removal of MG by the biomass, the cells were rich with high porous structure exhibited hole-like (*Fig. 11a*). The surface of the biomass cells became rough and meanders after the removal of dye ions, due to precipitation of dye ions around the cell surface (*Fig. 11b*).

http://www.aloki.hu ● ISSN 1589 1623 (Print) ● ISSN 1785 0037 (Online)
DOI: http://dx.doi.org/10.15666/aeer/1605_69456962
© 2018, ALÖKI Kft., Budapest, Hungary

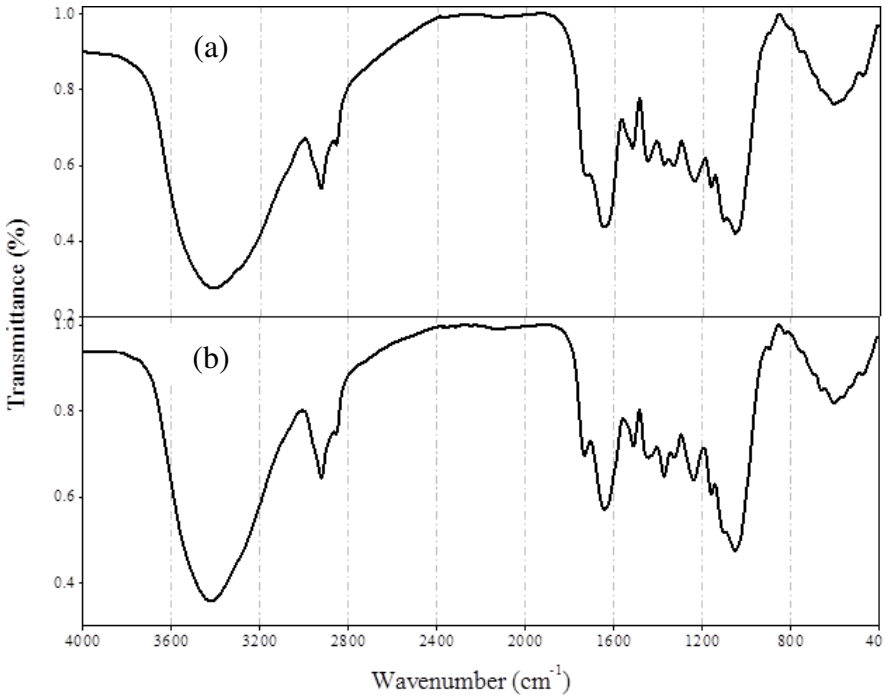

Figure 10. *FTIR spectrum of L. chinensis biomass (a) before and (b) after adsorption of malachite green*

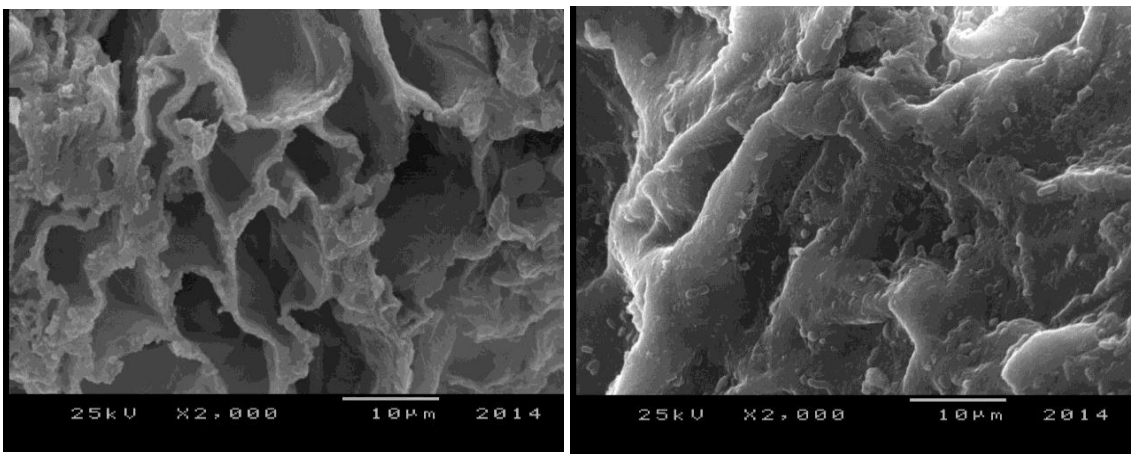

a **b**

Figure 11. *Scanning electron microscopy micrographs of M. laetum surface before (a) and after (b) adsorption of malachite green*

Discussion

The waste materials of the dry leaves of the plant can be used for the removal process of dye. The removal process was found to be affected by the pH values of the dye solution. In agreement with the current result, Anbia and Ghaffari (2011) showed that the uptake of malachite green from solution using adsorbent was found to increase at high pH. They reported that the pH effects on the charge, functional groups, and ionization degree on the biomass active sites, in addition to the chemistry of dye solution. The MG is a cationic basic dye and contains a negatively charged chloride ion,

http://www.aloki.hu ● ISSN 1589 1623 (Print) ● ISSN 1785 0037 (Online)
DOI: http://dx.doi.org/10.15666/aeer/1605_69456962
© 2018, ALÖKI Kft., Budapest, Hungary

a positive charged organic ion, and a positive nitrogen ion. The color intensity and stability of MG structure were found to be affected by the pH value (Mall et al., 2006). They showed that the pH range 3-7 made the color of MG stable, and the reduction of color increased with increasing pH from 7 to 11 in the solution of MG.

The pH value of the solution effect on the functional groups on the active sites of the biomass and the degree of ionization of dye which effects on the process of uptake (Nandi et al., 2009). MG is protonated in the acidic medium and deprotonated at high values of pH. The low removal of MG at acidic pH may be related to the competition between the abundant hydrogen ions, adsorption sites on the biomass and the dye cations. In our study, the great adsorption of MG at pH 8-10 may be related to the changes in the structure of MG molecules as mentioned by Sun and Tomkinson (2001). Maurya et al. (2006) found that deprotonating of different functional groups of the biomass lead to an increase in the removal dye.

The results showed that the removal of MG by the tested biomass increased with increasing temperature. This result indicates that high temperature is favorable for the removal of MG from aqueous solution. The rate of diffusion of the dye molecules is a temperature dependent process. In accordance with the present result, Demierege et al. (2015) showed that the biosorption of dye by using mushroom stump wastes increased with increasing temperature from 20 °C to 50 °C due to the increase in surface activity and kinetic energy of dye molecules. Increase in temperature may increase the mobility of the large dye ion and consequently increase the adsorption process (Singla et al., 2016). A sufficient energy is required for a number of molecules to make an interaction with the active site at the surface (Doğan and Alkan, 2003). An increase in temperature causes fast diffusion of dye molecules across the internal pores of the adsorbent particles and the external boundary layer due to the less resistance of viscous forces in the aqueous solution (Banerjee and Chattopadhyaya, 2017). The increase in adsorption capacity may be due to the enlargement of the pore size of adsorbents at high temperature (Demirbas et al., 2008).

The present result indicated that removal of MG dye by using the tested biomasses showed an increase with increasing contact time through the first minutes and then slowly increased until equilibrium. The uptake of dye does not increase with more increase in contact time as a result of the accumulation of dye on the available sites of adsorption on biomass material (Eren, 2009; Singla et al., 2016). The biomass of *M. laetum* reached equilibrium earlier than and that of *L. chinensis.* This result suggests that there are a higher affinity and stronger electrostatic force of attraction between MG dye and the binding-sites and functional groups on the wall surface of *M. laetum* biomass as compared with that of *L. chinensis.* The uptake of dye returned to the great number of active and vacant sites on the adsorbent surface at equilibrium time (Vijayaraghavan et al., 2008). Ashish et al. (2017) showed that the removal of MG dye occurs at the high-speed rate by *Limonia acidissima* (98.87%) after 3.30 h of equilibrium time. Malik et al. (2007) suggested that a monolayer of dye is formed on the surface of the biomass, and the rate of the dye uptake is controlled by the rate of transported dye from the exterior to the interior site of the biomass. This result suggests that there are a higher affinity and stronger electrostatic force of attraction between MG dye and the binding-sites and functional groups on the wall surface of the biomass.

As shown in the results, the removal of dye was greatly increased with increasing the weight of biomass up to certain limits and then remained constant. At first, the rate of dye removal has been found to be rapid and slowed down as the biomass dose increased

http://www.aloki.hu ● ISSN 1589 1623 (Print) ● ISSN 1785 0037 (Online)
DOI: http://dx.doi.org/10.15666/aeer/1605_69456962
© 2018, ALÖKI Kft., Budapest, Hungary

(Salleh et al., 2003; Omar et al., 2018). This can be explained depending on the fact that, at a lower weight of biomass the dye is more available and due to this, the removal of dye per unit weight of biomass is higher. In addition, the increase in the adsorbent dose leads to an increase in the adsorbed dye due to increases in the number of available adsorption sites and the surface area of adsorbent (Mane et al., 2007). As clear from the results, the biomass of *M. laetum* was more efficient than *L. chinensis* in the removal of dye. This may be returned to the availability of more binding sites on the surface of *M. laetum* biomass.

The removal of dye decreased gradually with increasing dye concentration at the optimum condition as shown in the present study. This result may be returned to the increase in the gradient pressure between solution and biomass which drive the dye molecules from the solution to the surface of the biomass (Rasool and Lee, 2015). The decrease in the removal capacity with increasing dye concentration may be due to the higher quantity of adsorbate than the adsorbent dose (Chen and Zhao, 2009). At high concentration of dye, the available sites of sorption became fewer as compared to the concentration of dye and so the uptake of dye is associated with the initial concentration of dye.

Equations of equilibrium isotherm were used to illustrate experimental absorption data. These equations parameters and the thermodynamic properties explain both the mechanism of sorption and adsorbent affinity. Graphically it is likely to elucidate the isotherm of equilibrium adsorption by plotting liquid phase concentration against solid phase concentration. It is necessary to determine the foremost acceptable correlation for the equilibrium curve, to enhance the design of an adsorption system to eliminate dyes from effluents. Consequently, the association of equilibrium data using theoretical and experimental equation is essential for the sorption interpretation and expectation of the adsorption range.

According to the Langmuir isotherm results, the *M. laetum* biomass recorded the greatest affinity of the binding site (b) to MG. In addition, the R_L low values elucidated that the removal of MG was favorable by the biomass. The low value of R_L means high adsorbent to adsorbate affinity (Jelinek et al., 2015). Depending on the high values of linear correlation coefficient (R^2), the models of Langmuir and Freundlich were found to be more favorable for explaining the sorption MG onto *M. laetum* and *L. chinensis* biomass. In addition, homogeneous and heterogeneous adsorption energy occurred throughout the removal of MG by the biomass. Hii et al. (2011) confirmed that the high values of the linear correlation coefficient ($R^2 > 0.95$) of each model of Langmuir and Freundlich are favorable for a description of the sorption of the dye by *Aristaeomorpha foliacea*. The confirmation of Langmuir and Freundlich isotherms to the sorption study showed that the tested biomass may exhibit monolayer adsorption and heterogeneous surface conditions (Kumari and Abraham, 2007). The results of Temkin isotherm proposed that the heat of molecule adsorption decreased linearly in the layer. Fil (2016) reported that the negative value of $\Delta G°$ for all temperatures proposed that the adsorption process was spontaneous. The ΔH° within the range of 0.5-20.9 kJ mol^{-1} means that the removal of MG by tested biomass was physical biosorption (Ahmet and Mustafa, 2008). The positive ΔS° values represent the decrease in the degree of freedom on the adsorbent surface during MG sorption process.

The IR analysis explained that the interaction between the biomass and MG were ionic between MG and carboxylate group, and coordinate bond was found between MG and the lone pair of electrons on the -OH or $-NH_2$ groups. In addition, forces of van der

http://www.aloki.hu ● ISSN 1589 1623 (Print) ● ISSN 1785 0037 (Online)
DOI: http://dx.doi.org/10.15666/aeer/1605_69456962
© 2018, ALÖKI Kft., Budapest, Hungary

Waals between nonpolar groups of biomass and MG, and ion-dipole interaction between the negative dipole end of the carbonyl group and MG. According to the results of IR, the changes in the position of functional groups on the tested biomass after treatment with MG confirmed the contribution of these groups in the dye removal as suggested by Jayaraj et al. (2011). Zhai et al. (2014) explained that the plant cell walls consist of carbohydrate, protein, lignin, hemicellulose, cellulose microfibrils and aromatic compounds. These molecules on the surface of the cell have carboxyl, amino, phosphate, thiol, and sulfhydryl functional groups (Tüzün et al., 2005).

The surface of the tested biomass became rough and meanders after exposure to the ions of MG because of the precipitation of dye at the surface of the biomass cell. This result may be due to the linkage of dye ions with the functional groups of cell surface and replacement of the ions for some of the cations in the cell wall matrix. The differences in the morphology and the structure of the biomass cell wall lead to the presence of differences in the efficiency of dye removal. The increase of dye removal may be related to the pores on the surface of plant biomass which allow the free passage of dye molecules (Deokar, 2016). The irregular surface of biomass cells, make the sorption of solution ions possible on different parts of these materials.

Conclusions

The color removal of dye from wastewater is a matter of concern due to its toxicity. The easily available and low-cost biomass such as the waste of *M. laetum* and *L. chinensis* leaves were found to have the unlimited capacity for the removal of MG and thus decrease the toxic effect of dye in the solution. The efficiency of *M. laetum* biomass was higher than *L. chinensis* biomass for adsorption of MG. The present study confirmed that the plant biomaterial which is discarded as a waste can be used for the removal of dyes from wastewater and make the water cleaner for various uses. This is an economical and environmentally-friendly alternative to various other methods that use a large number of chemicals to treat wastewater.

REFERENCES

[1] Ahmet, S., Mustafa, T. (2008): Biosorption of total chromium from aqueous solution by red algae (*Ceramium virgatum*): equilibrium, kinetic and thermodynamic studies. – Journal of Hazardous Materials 160: 349-355.
[2] Albert, A. (1979): Selective Toxicology. Sixth ed. – Chapman and Hall, London.
[3] Anbia, M., Ghaffari, A. (2011): Removal of malachite green from dye wastewater using mesoporous carbon adsorbent. – Journal of the Iranian Chemical Society 8: S67-S76.
[4] Ashish, S., Sartape, A., Aniruddha, M., Mandhare, A., Vikas, V., Jadhav, B., Prakash, D., Raut, B., Mansing, A., Anuse, A., Sanjay, S., Kolekar, S. (2017): Removal of malachite green dye from aqueous solution with adsorption technique using *Limonia acidissima* (wood apple) shell as low cost adsorbent. – The Arabian Journal of Chemistry 10: 3229-3238.
[5] Banerjee, S., Chattopadhyaya, M. (2017): Adsorption characteristics for the removal of a toxic dye, tartrazine from aqueous solutions by a low cost agricultural by-product. – The Arabian Journal of Chemistry 10: 1629-1638.
[6] Chen, H., Zhao, J. (2009): Adsorption study for removal of Congo red anionic dye using organo-attapulgite. – Adsorption 15: 381-389.

http://www.aloki.hu ● ISSN 1589 1623 (Print) ● ISSN 1785 0037 (Online)
DOI: http://dx.doi.org/10.15666/aeer/1605_69456962
© 2018, ALÖKI Kft., Budapest, Hungary

[7] Clifton-Hadley, R. S., Alderman, D. J. (1987): The effects of malachite green on proliferative kidney disease. – Journal of Fish Diseases 10: 101-107.
[8] Demierege, S., Toptas, A., Ayan, E., Yasa, I., Yanik, J. (2015): Removal of textile dyes from aqueous solutions by biosorption on mushroom stump wastes. – Chemistry and Ecology DOI: 10.1080/02757540.2014.976209.
[9] Demirbas, E., Kobya, M., Sulak, M. T. (2008): Asorption kinetics of a basic dye from aqueous solutions onto apricot stones activated carbon. – Bioresource Technology 99: 5368-5373.
[10] Deokar, R. R. (2016): *Enteromorpha intestinalis*: low cost biosorbents for biosorption methylene blue. – International Journal of Recent Scientific Research 7: 9291-9297.
[11] Deokar, R. R., Sabale, A. B. (2014). Biosorption of methylene blue from aqueous solution on to green seaweeds. – International Journal of Recent Scientific Research 5: 347-351.
[12] Doğan, M., Alkan, M. (2003): Adsorption kinetics of methyl violet onto perlite. – Chemosphere 50: 517-528.
[13] Eren, E. (2009): Investigation of a basic dye removal from aqueous solution onto chemically modified *Unye bentonite*. – Journal of Hazardous Materials 166: 88-93.
[14] Fil, B. A. (2016): Isotherm, kinetic, and thermodynamic studies on the adsorption behavior of malachite green dye onto montmorillonite clay. – Particulate Science and Technology 34: 118-126.
[15] Forgacs, E., Cserháti, T., Oros, G. (2004): Removal of synthetic dyes from wastewaters: a review. – Environment International 30: 953-971.
[16] Freundlich, H. M. F. (1906): Over the adsorption in solution. – The Journal of Physical Chemistry 57: 358-371.
[17] Gupta, V. K., Khamparia, S., Tyag, I., Jaspal, D., Malviya, A. (2015): Decolorization of mixture of dyes: A critical review. – Global Journal of Environmental Science and Management 1: 71-94.
[18] Hammud, H. H. (2011): Biosorption studies of methylene blue by Mediterranean algae *Carolina* and its chemically modified forms. Linear and nonlinear models' prediction based on statistical error calculation. – International Journal of Chemistry 3: 147-163.
[19] Hecht, T., Endemann, F. (1998): The impact of parasites, infections and disease on the development of aquaculture in sub-Saharan Africa. – Journal of Applied Ichthyology 14: 213-221.
[20] Hii, S. L., Estrop, L. L., Wong, C. L. (2011): Adsorption of reactive blue 4 onto the chemically modified red seaweed *Amphiroa foliacea*: equilibrium, kinetics and modeling studies. – International Journal of Physical Science 6: 7171-7182.
[21] Jayaraj, R., Mohan, M. C., Prasath, P. M., Khan, T. H. (2011): Malachite green dye removal using the seaweed *Enteromorpha*. – European Journal of Chemistry 8: 649-656.
[22] Jelínek, L., Procházková, G., Quintelas, C., Beldíková, E., Brányik, T. (2015): *Chlorella vulgaris* biomass enriched by biosorption of polyphenols. – Algal Research 10: 1-7.
[23] Kadirvelu, K., Kavipriya, M., Karthika, C., Radhika, M., Vennilamani, N., Pattabhi, S. (2003) Utilization of various agricultural wastes for activated carbon preparation and application for the removal of dyes and metal ions from aqueous solutions. – Bioresource Technology 87: 129-132.
[24] Kumari, K., Abraham, T. (2007): Biosorption of anionic textile dyes by nonviable biomass of fungi and yeast. – Bioresource Technology 98: 1704-1710.
[25] Langumuir, I. (1918): The adsorption of gases on plane surfaces of glass, mica and platinum. – Journal of the American Chemical Society 40: 1361-1403.
[26] Laxmi, G. S., Ahmaruzzaman, M. (2010): Adsorption technique for the removal of phenolic compounds from wastewater using low-cost natural adsorbents. – Assam University Journal of Science and Technology: Physical Sciences and Technology 5: 156-166.

http://www.aloki.hu ● ISSN 1589 1623 (Print) ● ISSN 1785 0037 (Online)
DOI: http://dx.doi.org/10.15666/aeer/1605_69456962
© 2018, ALÖKI Kft., Budapest, Hungary

[27] Malik, P. K. (2004): Dye removal from wastewater using activated carbon developed from sawdust: adsorption equilibrium and kinetics. – Journal of Hazardous Materials 113: 81-88.
[28] Malik, R., Ramteke, D. S., Wate, S. R. (2007): Adsorption of malachite green on groundnut shell waste based powdered activated carbon. – Waste Management 27: 1129-1138.
[29] Mall, I. D., Srivastava, V. C., Kumar, G. V. A., Mishra, I. M. (2006): Characterization and utilization of mesoporous fertilizer plant waste carbon for adsorptive removal of dyes from aqueous solution. – Colloids and Surfaces A: Physicochemical and Engineering Aspects 278: 175-187.
[30] Mane, V. S., Mal, I. D., Srivastava, V. C. (2007): Use of bagasse fly ash as an adsorbent for the removal of brilliant green dye from aqueous solution. – Dyes and Pigments 73: 269-278.
[31] Maurya, N. S., Mittal, A. K., Cornel, P., Rother, E. (2006): Biosorption of dyes using dead macro fungi: Effect of dye structure, ionic strength and pH. – Bioresource Technology 97: 512-521.
[32] Nandi, B., Goswami, A., Purkait, M. (2009): Removal of cationic dyes from aqueous solutions by kaolin: kinetic and equilibrium studies. – Applied Clay Science 42: 583-590.
[33] Omar, H., El-Gendy, A., Al-Ahmary, K. (2018): Bioremoval of toxic dye by using different marine macroalgae. – Turkish Journal of Botany 42: 15-27. DOI: 10.3906/bot-1703-4.
[34] Rasool, K., Lee, D. S. (2015): Characteristics, kinetics and thermodynamics of Congo red biosorption by activated sulfidogenic sludge from an aqueous solution. – International Journal of Environmental Science and Technology 12: 571-580.
[35] Salleh, M. A., Mahmoud, D. K., Karim, W. A., Idris, A. (2003): Cationic and anionic dye adsorption by agricultural solid wastes: A comprehensive review. – Desalination 280: 1-13.
[36] Seshadri, S., Bishop, P. L., Agha, A. M. (1994): Anaerobic/aerobic treatment of selected Azo dyes in wastewater. – Waste Management 14: 127-137.
[37] Singla, S., Kaushal, J., Mahajan, P. (2016): Removal of dyes from wastewater by plant waste: a review. – International Journal of Advanced Research in Science, Engineering and Technology 5: 228-239.
[38] Srivastava, S. J., Singh, N. D., Srivastava, A. K., Sinha, R. (1995): Acute toxicity of malachite green and its effects on certain blood parameters of a catfish, *Heteropneustes fossilis*. – Aquatic Toxicology 31: 241-247.
[39] Srivastava, S., Sinha, R., Roy, D. (2004): Toxicological effects of malachite green. – Aquatic Toxicology 66: 319-329.
[40] Sun, R., Tomkinson, J. (2001): Fractional separation and physico-chemical analysis of lignins from the black liquor of oil palm trunk fiber pulping. – Separation and Purification Technology 24: 529-539.
[41] Sundarrajan, M., Frenandis, A. Z., Subrahmanyam, G., Prabhudesai, S., Krishnamurthy, S. C., Rao, K. V. (2000): Overexpression of G1/S cyclins and PCNA and their relationship to tyrosine phosphorylation and dephosphorylation during tumor promotion by metanil yellow and malachite green. – Toxicology Letters 116: 119-130.
[42] Temkin, M. J., Pyzhev, V. (1940): Kinetics of ammonia synthesis on promoted iron catalysts. – Acta Physicochimica U. S. S. R 12: 217-222.
[43] Tüzün, I., Bayramoğlu, G., Yalçın, E., Başaran, G., Çelik, G., Arıca, M. Y. (2005): Equilibrium and kinetic studies on biosorption of Hg(II), Cd(II) and Pb(II) ions onto micro algae *Chlamydomonas reinhardtii*. – Journal of Environmental Management 77: 85-92.
[44] Vijayaraghavan, K., Yun, Y. S. (2008): Biosorption of C. I. reactive black 5 from aqueous solution using acid-treated biomass of brown seaweed *Laminaria* sp. – Dyes and Pigments 76: 726-732.

http://www.aloki.hu ● ISSN 1589 1623 (Print) ● ISSN 1785 0037 (Online)
DOI: http://dx.doi.org/10.15666/aeer/1605_69456962
© 2018, ALÖKI Kft., Budapest, Hungary

[45] Vijayaraghavan, K., Mao, J., Yun, Y. S. (2008): Biosorption of methylene blue from aqueous solution using free and polysulfone-immobilized *Corynebacterium glutamicum*: Batch and column studies. – Bioresource Technology 99: 2864-2871.
[46] Zhai, S., Horikawa, Y., Imai, T., Sugiyama, J. (2014): Cell wall ultrastructure of palm leaf fibers. – The International Association of Wood Anatomists 35: 127-137.

http://www.aloki.hu ● ISSN 1589 1623 (Print) ● ISSN 1785 0037 (Online)
DOI: http://dx.doi.org/10.15666/aeer/1605_69456962
© 2018, ALÖKI Kft., Budapest, Hungary

NEXUS OF AGRICULTURE, GDP, POPULATION AND CLIMATE CHANGE: CASE OF SOME EURASIAN COUNTRIES AND TURKEY

DOĞAN, H. G.

Department of Agricultural Economics, Agricultural Faculty, Kirsehir Ahi Evran University
40100 Kirsehir Province, Turkey
(e-mail: hg.dogan@ahievran.edu.tr; phone: +90-386-280-4869)

(Received 7th Jul 2018; accepted 20th Sep 2018)

Abstract. Climate has an important role in the life processes of living creatures economically, socially and biologically. It affects several sectors and is affected by several sectors. Climate events are known to have changed since the second millennium and today it stands out as a problem that humanity has to face. Climate change has to be evaluated together with the global warming phenomenon. The most important factor causing global warming is the CO_2 concentration. This study examines the effects of variables including the share of the agricultural fields within total area, agricultural added value, GDP and population on the CO_2 release within the scale of the Eurasian Region and Turkey. The study covers the period between 1993 and 2016 years. Econometric models like ADF unit square test, ARDL and VECM were used. According to the obtained results, the effect of population was determined to be greater than that of the other variables in both regions. All of the variables under study had an increasing effect on CO_2 release in the long term in the Eurasian Region, while the share of the agricultural areas within total area and the GDP variables had an effect to reduce CO_2 release. This different situation is directly related to the size of the agricultural production in the Eurasian Region and Turkey and to the awareness level of the people. As a result, awareness of the individuals as well as of the state rulers on environmental destruction or environmental cost in particular in all works is considered to be important. On the other hand, it is necessary to plan agricultural production system within an environmental dimension and this needs to become a state policy. However, when creating these policies, one should avoid practices causing any difficulty in meeting the food demand of the population or causing excessive increases in food prices, such as the results when agriculture was affected by the climate events. Otherwise, there may be undesired consequences like food deficiency and corresponding deterioration of the macroeconomic balances of countries.
Keywords: *CO_2, ARDL, VECM, Eurasia, Turkey*

Introduction

Climate is an important environmental element affecting life on Earth (Carson, 1999). However, it has significantly changed in recent years. The change process started with the industrial revolution continued with the burning of fossil fuels and with human activities. It leads to the phenomenon of global warming. Climate change affects every stage of our lives, especially physical and natural environment (Özdemir et al., 2017). Global warming and climate change have important effects on the economies of developed and developing countries. It is stated that the concerned economic effects may reach to enormous levels if the necessary measures to reduce release and measures for compliance are not taken. The global warming and climate change have directly or indirectly affected all regions of the world in recent years. The sensible effects are more visible in the last few decades. These effects are expected to increase further in years to come. In other words, global warming and climate change is a global phenomenon at present (Gafari et al., 2014). The primary accountable element of the said phenomenon is human activity. Human activities cause global warming and increase the greenhouse gas release that leads to great changes in global climate. Several extreme events may occur due to climate change. These include irregular precipitation periods, irregular wind directions, increased level of drought,

http://www.aloki.hu ● ISSN 1589 1623 (Print) ● ISSN 1785 0037 (Online)
DOI: http://dx.doi.org/10.15666/aeer/160569636976
© 2018, ALÖKI Kft., Budapest, Hungary

desertification, and changes in underground and surface water levels (Angel, 2008). Technological development and welfare increase have been an important factor in greenhouse gas release. The basic sources for the greenhouse concentration can be defined with the use of fossil fuels in sectors like electricity generation, agricultural production and transportation. It is stated that the result may have huge negative regional, country based and global effects (Janjua et al., 2014). These effects occur with the accumulation of the greenhouse gases. Scientists agree on the fact that the basic cause of this problem is due to greenhouse gases like CO_2.

According to the present calculation, it is estimated that only a 1 °C increase in global warming will lead to an annual economic cost of 2 trillion dollars in 2050. According to a study conducted in EU, the cumulative global economic cost of global warming may reach to Euro 74 trillion (Bayraç and Doğan, 2016). It has been a significant increase in the amount of greenhouse gas in the atmosphere since the industrial revolution. Since 1750, the CO_2 level in the atmosphere increased nearly by 30% and reached from 280 ppm to 380 ppm. Today, CO_2 concentration increases around by 1.5 ppm every year. Therefore, it is necessary to keep the atmospheric greenhouse concentrations under control through various methods (Bayraç and Doğan, 2016). There are main sectors causing greenhouse gas release. *Figure 1* includes sectoral greenhouse gas releases at a global scale. As shown in *Figure 1,* the greenhouse gas releases are caused by industry (21%), transportation (14%), buildings (6%), agriculture and forestry and other field uses (24%), power and heat generation (25%), and other energy generation (10%) (IPCC, 2014a).

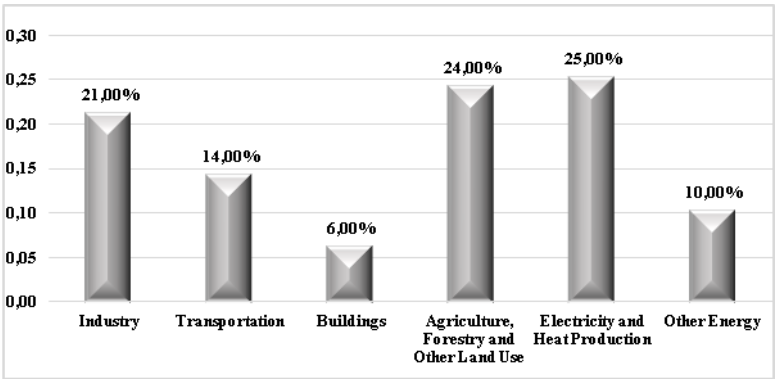

Figure 1. *Sectoral greenhouse release (IPCC, 2014a)*

Sectoral greenhouse releases stated by IPCC are in one aspect directly related to the energy consumption. It is estimated that the total global energy supply will double between 2004 and 2020 (Kaygusuz, 2009). On sectoral basis, energy sources may vary and substitute each other. It is stated that the 24% coal share in 2004 will increase to 36% in 2020 and substitute oil in certain extent. After such a substitution, the CO_2 release is expected to increase three times between 2004 and 2020 (Kaygusuz, 2009).

Climate change affects various economic sectors including agriculture, forestry, water, industry, tourism, energy and even finance and insurance markets with agriculture being the most sensitive to these changes (Hosseini et al., 2013). Agricultural sector is affected more by the climate events than the others. It is a high risk sector as it is inherently based on natural conditions. Agricultural sector has dynamics causing climate change and it has a decisive role for production and sustainability in both short term and long term (Gafari et al., 2014). It is proportionally

http://www.aloki.hu ● ISSN 1589 1623 (Print) ● ISSN 1785 0037 (Online)
DOI: http://dx.doi.org/10.15666/aeer/160569636976
© 2018, ALÖKI Kft., Budapest, Hungary

the second biggest sector contributing to the greenhouse release (IPCC, 2014b). The greenhouse gas emission in the agriculture sector contributing by 24% is caused by soil processing during production process and animal activities, heat and electrical energy generation, agricultural equipment, inorganic manure, agricultural chemicals and fossil fuels used in tractors and other transportation vehicles. ABD emission statistics report that the agricultural sector is directly responsible for greenhouse release. Soil management is defined to be the most important dynamic in the sector (Holly, 2015). Reynolds and Wenzlau (2012) reported that the agriculture sector has a 14 to 30% contribution to the total greenhouse emission due to irrigation and nitrogen rich fertilizers. In another aspect, agriculture is a sector that is affected by climate change. That is, it both causes and is significantly affected by climate change and global warming. The agricultural sector is highly dependent on climate events. This dependency directly affects food supply, agricultural food products and sectoral economic performance (Holly, 2015; Sakurai et al., 2014; Kang et al., 2009; Magadza, 2000).

As stated by World Bank (2016a, b), global agricultural sector produces CO_2, CH_4 and N_2O. However, the CH_4 and N_2O concentration are lower than the CO_2 concentration. CO_2 concentration had a 40% increase from 1750 to 2014 (IPCC, 2014b). United Nations Food and Agriculture Organization (FAO) states that the agricultural sector has a potential to reach an 80 to 88% reduction in the CO_2 emissions it causes at the moment (Reynolds and Wenzlau, 2012). Based on this result, it can be considered that environmental damage is not a must for economic and agricultural growth. Several attempts have been made to find a scientific answer to this question. It is emphasized that growth increase depends on various factors including energy consumption, food demand and land usage and leads to increases in CO_2 emissions. However, the agricultural sector contributes to the greenhouse release by producing CO_2 and causes global warming while it helps to reduce the CO_2 level by producing more O_2 through plantation (Khasman et al., 2016). It is clear that proper approaches are necessary for the organization of this two-way action-reaction process.

Humanity faces increasing threats with respect to global warming and climate change every day on one hand, and food demand and economic growth quests on the other. When we take a liveable world as a priority, energy consumption, considered among the main contaminants, becomes a focal point in this matter. Therefore, there has been a demand for empirical studies on energy consumption, economic growth and their environmental costs. When we look at the results obtained from the said studies, we notice the presence of strong relation between these variables that are studied. Since the last quarter of the second millennium, that is within period of oil wars and thereafter, scientific studies happened to have different dimensions with the Kyoto Protocol. These research studies indicate the fact that the studies on energy economy and environment economy cover a very important field. However, the results highlight the necessity to increase the energy consumption to ensure the targeted growth rates despite the potential environmental cost (Tiwari, 2011). The present study intends to bring a perspective from the agricultural dimension to the greenhouse effect, which is one of the main causes of global warming and climate change. Eurasian countries and Turkey were selected as the study region. It is intended to compare two regions with different population growth and economic structures. Despite these differences, it is aimed to study the comparative conditions of the two regions that are within the same geopolitical frame. The variables that are studied include two important variables.

http://www.aloki.hu ● ISSN 1589 1623 (Print) ● ISSN 1785 0037 (Online)
DOI: http://dx.doi.org/10.15666/aeer/160569636976
© 2018, ALÖKI Kft., Budapest, Hungary

Because, agriculture has an effect to reduce both global warming and climate change while it has also an effect to increase global warming and climate change by greenhouse gas release (Bayraç and Doğan, 2016). In addition, the variables including population and national income per capita were examined in the study as the other important determinants. As it was already mentioned, the main reason of the global warming and climate change process has a human root.

Figures 2 and *3* include the development trend of the Eurasian countries and Turkey between the years 1993 and 2016 years with respect to the variables under the study.

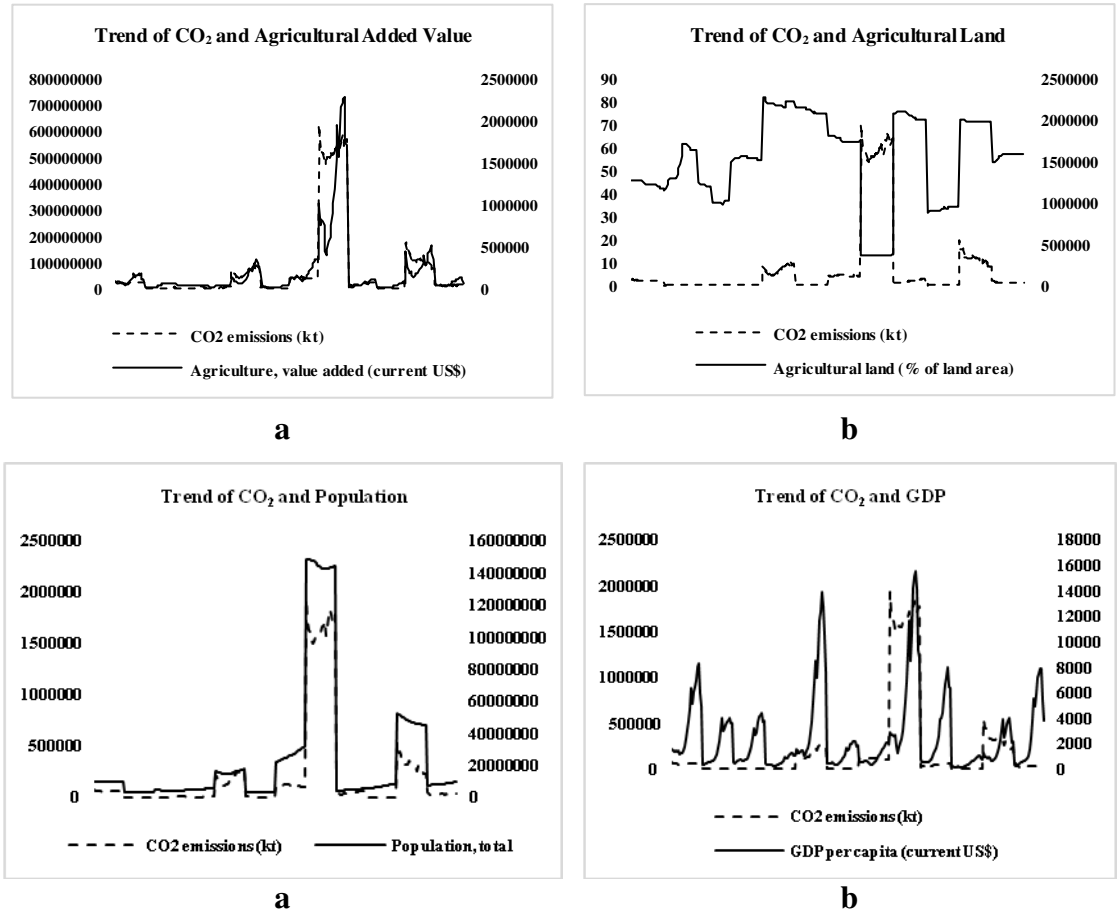

Figure 2. *The interaction among agricultural added value (a), agricultural land (b), population (c) and GDP (d) and CO_2 in Eurasian countries (Wolrdbank, 2017). Note: X-axis represents the Eurasian countries (12 countries) between 1993 and 2016 years*

When we examine the trend of variables in the Eurasian countries between 1993 and 2016 years, the trends of CO_2 and other variables are similar with the direction of the coefficients obtained from the econometric results. It is possible to see in *Figure 2* that agricultural added value, population and GDP have movements in the same direction. This simultaneous trend differs only in the Russian Federation within the panel addressed with respect to agricultural field. The reason is that agricultural production is very low in the Russian Federation (average share of the agricultural added value within GDP between 1993 and 2016 years is 4.88%; the lowest among 12 countries within the Eurasian region (World Bank, 2017). It can be said that the other factors increasing the

http://www.aloki.hu ● ISSN 1589 1623 (Print) ● ISSN 1785 0037 (Online)
DOI: http://dx.doi.org/10.15666/aeer/160569636976
© 2018, ALÖKI Kft., Budapest, Hungary

CO_2 level in the Russian Federation are more effective. However, it cannot be said that this is valid for all of the panel.

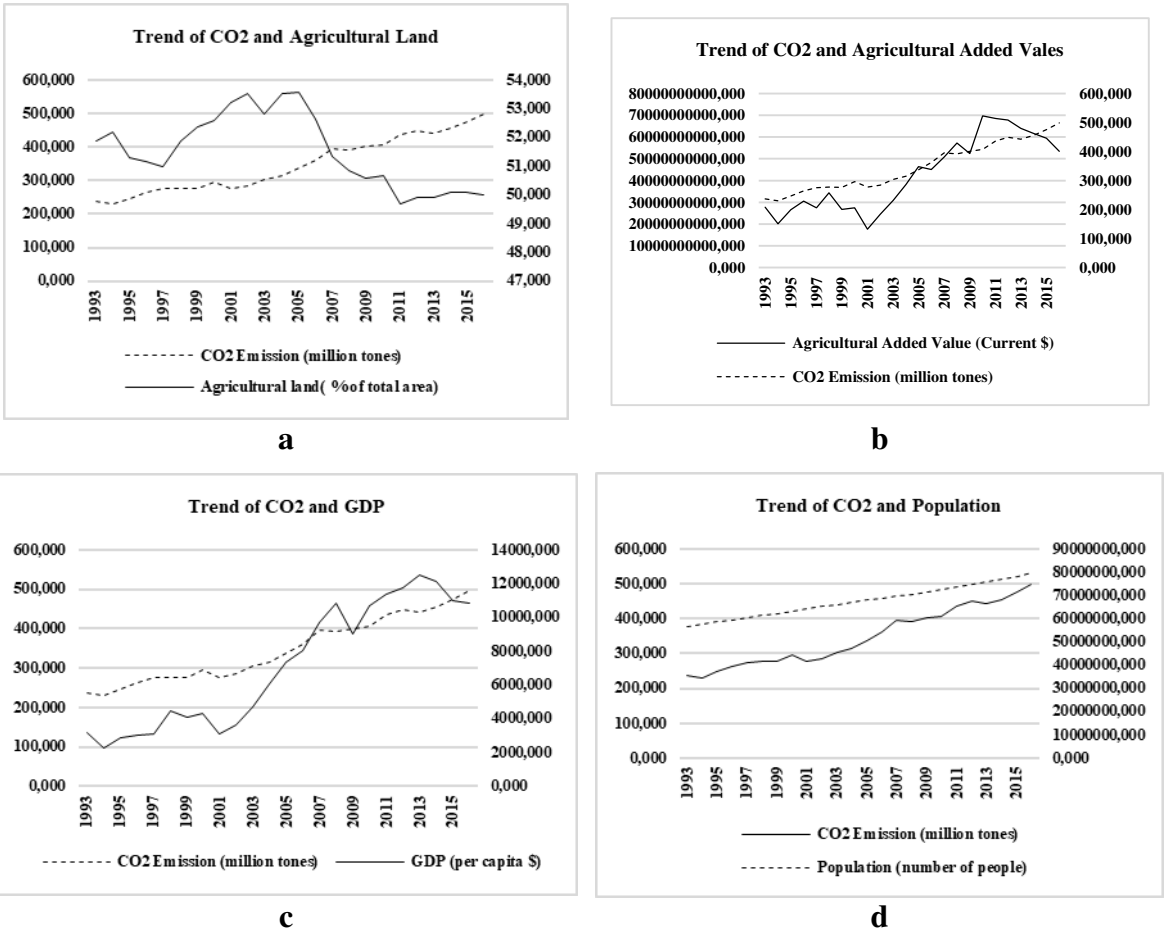

Figure 3. *The interaction among agricultural land (a), Agricultural added value (b), GDP (c), population (d) and CO_2 in Turkey (World Bank, 2017). Note: X-axis represents between 1993 and 2016 years*

Figure 3 indicates the interaction between CO_2 release in Turkey and agricultural area, agricultural added value, population and GDP. Accordingly, the long time trend of the variables develops in the same trend as CO_2. However, the interaction of agricultural fields and CO_2 should be kept different from this framework because the increase in CO_2 release continues even if the share of the agricultural fields has a decreasing trend after 2005. This can be linked to the fact that the agricultural fields in Turkey face urbanization and housing despite they are under the status of agricultural production.

Materials and methods

In the study, factors affecting CO_2 release in Eurasian countries and Turkey were investigated. The study involved the years between 1993 and 2016 years. These factors are the share of agricultural areas in total area, agricultural added value, GDP and population. Eurasia is defined from United Kingdom to Japan in the literature. It includes 103 countries (Anonymous, 2018). This concept was firstly used by Alexander

http://www.aloki.hu ● ISSN 1589 1623 (Print) ● ISSN 1785 0037 (Online)
DOI: http://dx.doi.org/10.15666/aeer/160569636976
© 2018, ALÖKI Kft., Budapest, Hungary

von Humbolt in 1849 (İşyar, 2013). Although there is no consensus on the scope of this concept, there are many approaches that cover various countries. Countries emerging after the dissolution of the Soviet Union are also located within this region. It can be said that they are intensely related to each other in terms of culture, politics and economics. Therefore, in this study, 12 countries with similar characteristics were named as the Eurasian region. These are Belarus, Armenia, Georgia, Kazakhstan, Kyrgyzstan, Moldova, Uzbekistan, Russia, Tajikistan, Turkmenistan, Ukraine and Azerbaijan. Panel data analysis was used for the modelling of 12 countries while time series analysis was used in the econometric modelling for Turkey. *Table 1* includes the symbols and data sources of the variables.

Table 1. *Symbols and data sources of the variables used in the study*

Name of the variable	Symbol	Unit	Data source
CO_2	Y	For Eurasia; kgtonnes/for Turkey; million tones	World Bank, Turkstat
Share of agricultural fields within total area	χ	% of land area	World Bank
Agricultural added value	σ	current US$	World Bank
GDP per capita	λ	current US$	World Bank
Population	δ	Total number of people	World Bank

Full logarithmic form was chosen in the study for the variables used in the model. The functional relation between the CO_2 level and other variables can be expressed as follows in *Equation 1:*

$$\ln Y = f(\ln \chi, \ln \sigma, \ln \lambda, \ln \delta) \quad \text{(Eq.1)}$$

The factors causing the long term greenhouse gas effect in both the Eurasian Region and Turkey were analysed by means of the following economic models:

- Unit root test (ADF)
- Autoregressive distributed lag bound test (ARDL)
- Vector error correction model (VECM)

Unit root test is used to carry out the stability studies of the series. Stability tests are carried out to avoid the spurious regression problem. Several studies in the literature revealed the necessity to carry out the unit root tests (Maddala and Shaowen, 1999; Kao and Chiang, 2000; Hadri, 2000; Choi, 2001; Levin et al., 2002; Im, 2003). There are several types of the unit root test. However, basically the unit root tests are based on the ADF principle. This study also used the ADF unit root test. The notation of the ADF test statistics can be stated as follows in *Equation 2:*

$$\Delta X_t = \beta_0 + \beta_1 t + \beta_i X_{t-1} + \sum_{j=1}^{n} Y_i \Delta X_{t-j} + e_t \quad \text{(Eq.2)}$$

In *Equation 2,* $\beta 0$ refers to fixed term; t refers to deterministic trend; n refers to lag length and e_t refers to stochastic term. The results of the ADF test statistics are

http://www.aloki.hu ● ISSN 1589 1623 (Print) ● ISSN 1785 0037 (Online)
DOI: http://dx.doi.org/10.15666/aeer/160569636976
© 2018, ALÖKI Kft., Budapest, Hungary

compared by means of the MacKinnon critical value. Stability of the series is decided by accepting/rejecting according to the importance levels of 1%, 5% and 10% (MacKinnon, 1996).

Autoregressive distributed lag (ARDL) and vector error correction model (VECM)

The frequently used models in the literature are the Engle-Granger model (1987) based on the error term in the co-integration tests, Johansen model (1988) and Johansen & Jesilius model (1990) based on system approach (Altıntaş, 2013). However, stability approach at the I(0) level of all variables provides validity of these methods (Pesaran and Shin, 1995; Pesaran et al., 2001). The advantage of the ARDL approach is that it can carry out the co-integration test without considering the integration levels of the variables. There are basically 3 important points to pay attention to in the method. I-limit test procedure is easy and it is possible to carry out co-integration relation test after determining the lag length contrary to the multivariable co-integration methods like Johansen and Juselius (1990). II-limit test procedure does not require the preliminary tests of the variables included in the unit root test model, which is different from the co-integration techniques of Johansen and Juselius (1990). The limit test can be applied regardless of the fact that the models in the series are at the I(2) level, I(0) level and I(1) level or mutually co-integrated at the same level. III-limit test is very effective for small or limited sample clusters.

Equations 3, 4, 5, 6 and *7* include the limit test models of the 4 independent variables that were adapted to the study and the notations based on the estimation of the unlimited error correction model by the OLS method.

$$\Delta \ln Y = \beta_0 + \sum_{i=1}^{m} \beta_{1i} \Delta \ln Y_{t-i} + \sum_{i=0}^{m} \beta_{2i} \Delta \ln \chi_{t-i} + \sum_{i=0}^{m} \beta_{3i} \Delta \ln \sigma_{t-i} + \sum_{i=0}^{m} \beta_{4i} \Delta \ln \lambda_{t-i} + \sum_{i=0}^{m} \beta_{5i} \Delta \ln \delta_{t-i} + a1 \ln Y_{t-1}\, a2 \ln \chi_{t-1} + a3 \ln \sigma_{t-1} + a4 \ln \lambda_{t-1} + a5 \ln \delta_{t-1} + u_t \quad \text{(Eq.3)}$$

$$\Delta \ln \chi = V_0 + \sum_{i=1}^{m} \beta_{1i} \Delta \ln \chi_{t-i} + \sum_{i=0}^{m} \beta_{2i} \Delta \ln Y_{t-i} + \sum_{i=0}^{m} \beta_{3i} \Delta \ln \sigma_{t-i} + \sum_{i=0}^{m} \beta_{4i} \Delta \ln \lambda_{t-i} + \sum_{i=0}^{m} \beta_{5i} \Delta \ln \delta_{t-i} + a1 \ln Y_{t-1}\, a2 \ln \chi_{t-1} + a3 \ln \sigma_{t-1} + a4 \ln \lambda_{t-1} + a5 \ln \delta_{t-1} + u_t \quad \text{(Eq.4)}$$

$$\Delta \ln \sigma = K_0 + \sum_{i=1}^{m} \beta_{1i} \Delta \ln \sigma_{t-i} + \sum_{i=0}^{m} \beta_{2i} \Delta \ln Y_{t-i} + \sum_{i=0}^{m} \beta_{3i} \Delta \ln \chi_{t-i} + \sum_{i=0}^{m} \beta_{4i} \Delta \ln \lambda_{t-i} + \sum_{i=0}^{m} \beta_{5i} \Delta \ln \delta_{t-i} + a1 \ln Y_{t-1}\, a2 \ln \chi_{t-1} + a3 \ln \sigma_{t-1} + a4 \ln \lambda_{t-1} + a5 \ln \delta_{t-1} + u_t \quad \text{(Eq.5)}$$

$$\Delta \ln \lambda = Z_0 + \sum_{i=1}^{m} \beta_{1i} \Delta \ln \lambda_{t-i} + \sum_{i=0}^{m} \beta_{2i} \Delta \ln \chi_{t-i} + \sum_{i=0}^{m} \beta_{3i} \Delta \ln \sigma_{t-i} + \sum_{i=0}^{m} \beta_{4i} \Delta \ln Y_{t-i} + \sum_{i=0}^{m} \beta_{5i} \Delta \ln \delta_{t-i} + a1 \ln Y_{t-1}\, a2 \ln \chi_{t-1} + a3 \ln \sigma_{t-1} + a4 \ln \lambda_{t-1} + a5 \ln \delta_{t-1} + u_t \quad \text{(Eq.6)}$$

$$\Delta \ln \delta = Q_0 + \sum_{i=1}^{m} \beta_{1i} \Delta \ln \delta_{t-i} + \sum_{i=0}^{m} \beta_{2i} \Delta \ln \chi_{t-i} + \sum_{i=0}^{m} \beta_{3i} \Delta \ln \sigma_{t-i} + \sum_{i=0}^{m} \beta_{4i} \Delta \ln \lambda_{t-i} + \sum_{i=0}^{m} \beta_{5i} \Delta \ln Y_{t-i} + a1 \ln Y_{t-1}\, a2 \ln \chi_{t-1} + a3 \ln \sigma_{t-1} + a4 \ln \lambda_{t-1} + a5 \ln \delta_{t-1} + u_t \quad \text{(Eq.7)}$$

In *Equations 3, 4, 5, 6* and *7* Δ refers to the difference processor, and m refers to lag length. Information criteria like AIC, SC, FPE and HQ are used to determine the lag

http://www.aloki.hu ● ISSN 1589 1623 (Print) ● ISSN 1785 0037 (Online)
DOI: http://dx.doi.org/10.15666/aeer/160569636976
© 2018, ALÖKI Kft., Budapest, Hungary

length. Here, the lag length providing the smallest critical value is determined to be the lag length of the model. The process continues by passing to the next lag value like the first smallest value, the second smallest value … etc until reaching to the model without autocorrelation. The significance of the one-lag level values of the variables is tested to determine the presence of long term co-integration between the variables by using the F-test. H_0 hypothesis indicates that there is no co-integration between the variables in the Equations 3-7 and it is formed as follows: H_0: a1 = a2 = a3 = a4 = a5. The alternative hypothesis H_1 which indicates the presence of co-integration is formed as follows: H_1: a1 ≠ a2 ≠ a3 ≠ a4 ≠ a5. In the study, co-integration between series was searched and then the long term ARDL model on the greenhouse release and error correction model (VECM) was estimated.

The VECM model allows the estimation of the short and long term flexibilities as well as the deviation coefficient from the balance taking place between the variables (Enders, 2008). In addition, the VECM analysis allows the removal of the spurious regression problem that may occur between the dependent and descriptive variables. *Equations 8, 9, 10, 11* and *12* include a corresponding VECM model (Granger, 1988).

$$\Delta \ln Y = \beta_0 + \sum_{i=1}^{m} \beta_{1i} \Delta \ln Y_{t-i} + \sum_{i=0}^{m} \beta_{2i} \Delta \ln \chi_{t-i} + \sum_{i=0}^{m} \beta_{3i} \Delta \ln \sigma_{t-i} + \sum_{i=0}^{m} \beta_{4i} \Delta \ln \lambda_{t-i} + \sum_{i=0}^{m} \beta_{5i} \Delta \ln \delta_{t-i} + \Psi ECM_{t-1} + \varepsilon_t \quad \text{(Eq.8)}$$

$$\Delta \ln \chi = V_0 + \sum_{i=1}^{m} \beta_{1i} \Delta \ln \chi_{t-i} + \sum_{i=1}^{m} \beta_{2i} \Delta \ln Y_{t-i} + \sum_{i=1}^{m} \beta_{3i} \Delta \ln \sigma_{t-i} + \sum_{i=1}^{m} \beta_{4i} \Delta \ln \lambda_{t-i} + \sum_{i=1}^{m} \beta_{5i} \Delta \ln \delta_{t-i} + \Psi ECM_{t-1} + u_t \quad \text{(Eq.9)}$$

$$\Delta \ln \sigma = K_0 + \sum_{i=1}^{m} \beta_{1i} \Delta \ln \sigma_{t-i} + \sum_{i=1}^{m} \beta_{2i} \Delta \ln Y_{t-i} + \sum_{i=1}^{m} \beta_{3i} \Delta \ln \chi_{t-i} + \sum_{i=1}^{m} \beta_{4i} \Delta \ln \lambda_{t-i} + \sum_{i=1}^{m} \beta_{5i} \Delta \ln \delta_{t-i} + \Psi ECM_{t-1} + v_t \quad \text{(Eq.10)}$$

$$\Delta \ln \lambda = Z_0 + \sum_{i=1}^{m} \beta_{1i} \Delta \ln \lambda_{t-i} + \sum_{i=1}^{m} \beta_{2i} \Delta \ln \chi_{t-i} + \sum_{i=1}^{m} \beta_{3i} \Delta \ln \sigma_{t-i} + \sum_{i=1}^{m} \beta_{4i} \Delta \ln Y_{t-i} + \sum_{i=1}^{m} \beta_{5i} \Delta \ln \delta_{t-i} + \Psi ECM_{t-1} + z_t \quad \text{(Eq.11)}$$

$$\Delta \ln \delta = Q_0 + \sum_{i=1}^{m} \beta_{1i} \Delta \ln \delta_{t-i} + \sum_{i=1}^{m} \beta_{2i} \Delta \ln \chi_{t-i} + \sum_{i=1}^{m} \beta_{3i} \Delta \ln \sigma_{t-i} + \sum_{i=1}^{m} \beta_{4i} \Delta \ln \lambda_{t-i} + \sum_{i=1}^{m} \beta_{5i} \Delta \ln Y_{t-i} + \Psi ECM_{t-1} + k_t \quad \text{(Eq.12)}$$

Equations 8, 9, 10, 11 and *12* are analyzed and interpretation is possible depending on the fact that the ECM coefficient is both statistically significant and negative or positive.

Empirical results

The presence of unit root in the series was searched first before evaluating the relation between CO_2 and other variables in short and long term. *Table 2* includes the unit root test results related to the variables that were examined.

http://www.aloki.hu ● ISSN 1589 1623 (Print) ● ISSN 1785 0037 (Online)
DOI: http://dx.doi.org/10.15666/aeer/160569636976
© 2018, ALÖKI Kft., Budapest, Hungary

Table 2. *Unit root test*

	ADF							
	Eurasia				Turkey			
	Individual intercept		Individual intercept and trend		Intercept		Intercept and trend	
	Level	1st Dif.	Level	1st Dif.	Level	1st Dif.	Level	1st Dif.
Y	0.65	-9.20*	-3.57*	-7.22*	-0.58	-3.60*	-2.25	-3.50***
χ	-0.12	-3.79*	1.63	-2.21*	-0.71	-3.75*	-1.37	-3.68**
σ	1.97	-5.84*	-0.62	-2.93*	-1.15	6.08*	-2.32	-5.99*
λ	1.97	-2.92*	1.88	-2.78*	-0.82	-5.72*	-2.27	-5.78*
δ	1.06	-2.29*	-1.55***	-2.17*	1.68	-3.17**	-5.21*	-3.47***

*, ** and *** mean significant, respectively, at 1%, 5% and 10%. According to SIC. Y: CO_2, χ: share of agricultural fields within total area, σ: agricultural added value, λ: GDP per capita, δ: population

According to the unit root test results which reveal whether the variables are affected by the past values, all of the variables are not stable at I(0) level per Individual Intercept in the Eurasian countries. However, they are stable at I(1) level.

Individual intercept and trend are stable at the CO_2 and population I(0) level while the other variables are not stable. At I(1) level, all variables were determined to be stable. A similar case can also be stated for Turkey. According to Intercept, all variables are not stable at I(0) level. And they are all stable at I(1) level. According to Intercept and Trend, population is stable at I(0) level, while all variables are stable at I(1) level.

According to the results of the unit root test, the ARDL test can be applied if one of the variables under study is stable at I(0) level, the other is stable at I(1) level. *Table 3* includes the results of the ARDL model established for the Eurasian countries and Turkey.

Table 3. *ARDL long run results*

Eurasia			Turkey	
Dependent variable: Y **ARDL (1,1,1,1,1)**			**Dependent variable:** Y **ARDL (2,2,2,2,2)**	
Long-run coefficient			**Long-run coefficient**	
Independent variable	**Coefficient**	**t-stat**	**Coefficient**	**t-stat**
χ	0.53	2.65*	-1.83	-111.15*
σ	0.15	3.64*	0.07	23.02**
λ	0.06	2.03**	-0.04	-10.74***
δ	1.34	8.50*	1.98	181.50*

ARDL maximum lags were specified as automatic selection. *, ** and *** mean significant, respectively, at 1%, 5% and 10%. Y: CO_2, χ: share of agricultural fields within total area, σ: agricultural added value, λ: GDP per capita, δ: population

According to the results of ARDL, all variables examined in the Eurasian countries were considered to be statistically important in the long run. The share of the agricultural fields within the total area, agricultural added value, 1% increase in GDP

http://www.aloki.hu ● ISSN 1589 1623 (Print) ● ISSN 1785 0037 (Online)
DOI: http://dx.doi.org/10.15666/aeer/160569636976
© 2018, ALÖKI Kft., Budapest, Hungary

and population increase the CO_2 level by 0.53 %, 0.15 %, 0.06 % and 1.34 % respectively. All variables studied in Turkey were considered to be statistically important. It was determined that the CO_2 level decreases by 1.83% as the share of the agricultural fields within the total area increases by 1%. In fact, this is related with the decreasing size of the agricultural fields in Turkey in recent years. As shown in *Figure 3,* the share of the agricultural fields within the total area decreased gradually after 2005. However, the forest areas in Turkey had an 11% increase during the study period despite the decreasing agricultural fields (Turkstat, 2018). The basic cause of this negative relation was dimensioned in this aspect. The positive relation between the agricultural added value and the CO_2 level gives the idea that the wrong practices in the agricultural production activities create environmental pressure. However, the negative relation between the agricultural added value and the CO_2 level can be explained with the environmentally improving effect of the agricultural sector (Khashman et al., 2016). That is, it can be said that the increase in agricultural fields may contribute to the decrease of the greenhouse effect and the destruction created thereby. A similar reverse directional relation is also seen in GDP. GDP is one of the most important parameters used to express the development levels of countries. The trend of GDP has significantly increased in recent years under the conditions of Turkey. According to the result, a 1% increase in GDP causes a decrease of 0.04% in the CO_2 level. It can be considered to be a result in line with the reverse relation appearing after the peak point of the Environmental Kuznets Curve (EKC) suggested by Simon Kuznets in 1958. As known, the peak point of EKC is stated as the level of awareness of the individuals (Kuznets, 1955). Under the conditions of Turkey, a 1% increase in population can be explained by a 1.98% increase in the CO_2 level.

Short and long term causalities were determined with the Vector Error Correction Model for the variables affecting the CO_2 level for the Eurasian countries and Turkey. Suitable lag length was determined before conducting the VECM causality analysis. Suitable lag length is given in *Table 4*.

Table 4. *Lag length criteria for VAR model*

	Lag	**LogL**	**LR**	**FPE**	**AIC**	**SC**	**HQ**
Eurasia	1	1745.681	NA	8.29e-14	-15.93224	-15.54158	-15.77441
	2	2103.077	681.6993	3.82e-15*	-19.00997*	-18.22866*	-18.69432*
	3	2124.706	40.25422*	3.94e-15	-18.97876	-17.80679	-18.50528
	Lag	**LogL**	**LR**	**FPE**	**AIC**	**SC**	**HQ**
Turkey	0	159.3997	NA	5.52e-13	-14.03633	-13.78837	-13.97792
	1	315.6009	227.2018	3.91e-18	-25.96372	-24.47593	-25.61324
	2	390.2824	74.68146*	6.52e-20*	-30.48022*	-27.75261*	-29.83767*

According to the results of the lag length criteria, the lag length for the Panel VECM created for the Eurasia countries was 2, and the lag length for the Panel VECM created for Turkey was 2 as well. *Table 5* includes the long and short term causality results obtained for the Eurasian countries and Turkey after determining suitable lag length.

http://www.aloki.hu ● ISSN 1589 1623 (Print) ● ISSN 1785 0037 (Online)
DOI: http://dx.doi.org/10.15666/aeer/160569636976
© 2018, ALÖKI Kft., Budapest, Hungary

Table 5. *VECM approach short run causality*

	Eurasia short-run causality					**Long run ECT**
	D(Y)	**D(χ)**	**D(σ)**	**D(δ)**	**D(λ)**	
D(Y)	-	0.9744	3.0233	1.0030	0.0907	-0.0141*
D(χ)	1.2823	-	0.3571	5.9735**	0.4358	-0.0001
D(σ)	1.0367	2.5298	-	2.7246	11.1840*	0.0240*
D(δ)	0.1642	0.1535	2.5210	-		-0.0001
D(λ)	0.7102	0.2088	0.1517	0.5529	-	0.0270*
	Turkey short run causality					**Long run ECT**
D(Y)	-	0.2016	0.1261	3.1334***	0.001	-1.325**
D(χ)	2.004	-	6.346*	0.679	5.276**	-0.297
D(σ)	1.330	0.043	-	8.353*	0.032	-7.972*
D(δ)	3.104***	3.540***	2.943***	-	1.875	0.009
D(λ)	1.703	0.422	1.472	3.535***	-	-5.717***

*,** and *** mean significant, respectively, at 1%, 5% and 10%. Y: CO_2, χ: share of agricultural fields within total area, σ: agricultural added value, λ: GDP per capita, δ: population

According to the results of the VECM approach Short Run Causality relation, a causality relation was determined in the Eurasia countries in the short term from the agricultural fields to population and from the agricultural added value to GDP. In the long term, it is possible to see the effect of the agricultural added value and GDP. It can be said that the 0.014% difference between the observed value and realized value of the CO_2 level would disappear within a period. In other words, the relevant imbalance can only disappear after 71 years if the conditions are maintained this way. When we look at the situation in Turkey, a causality relation was determined in the short term from the CO_2 level to population, from the agricultural fields to GDP, from the agricultural added value to population, from population to CO_2, agricultural fields and agricultural added value, and from GDP to population. Long term effect of agricultural added value and GDP are determined. It can be said that the 1.325% difference between the observed value and the realized value of the CO_2 level will disappear after a period. In other words, the CO_2 level will be balanced every 9 months if the conditions in Turkey are maintained this way.

Discussion and conclusion

There is an increasing trend in the global release of greenhouse gas. This increase is contributed by the countries of the world by various rates. The condition in the Eurasian region which is examined in the present study is different. Overall a decrease is observed in the region despite countries among the Eurasian countries showed increases and decreases between 1993 and 2016 years. This decrease is at the level of 13.91% (World Bank, 2017). In Turkey, there was an increase of 110% during the period of the study (Turkstat, 2018). The share of the agricultural fields within total area, agricultural added value, effect of GDP and population were analyzed by means of ARDL and VECM in order to determine this increase and decrease.

http://www.aloki.hu ● ISSN 1589 1623 (Print) ● ISSN 1785 0037 (Online)
DOI: http://dx.doi.org/10.15666/aeer/160569636976
© 2018, ALÖKI Kft., Budapest, Hungary

Accordingly, all variables studied in the Eurasian region have an effect increasing the CO_2 level in the long run. Population was determined to be the most effective variable. Similarly, population is considered to be the primary cause affecting the CO_2 level under the conditions of Turkey. According to the results of the VECM analysis, in the Eurasian Region, the long-term deviations are eliminated in the short term, albeit with a very small proportion. As it can be seen from the results of the VECM analysis, it can be said that long term deviations in Turkey is not balanced in any way. When we consider the population increases in the period under study, a population increase of 2.16% took place in the whole Eurasian region, while this increase was 40.22% in Turkey in the same period (World Bank, 2017). Another effective variable determined after population was the share of agricultural fields within the total area. A linear relation was determined between the share of the agricultural fields and CO_2 release in the Eurasian region while there was a negative directional relation in Turkey. However, the share of the agricultural fields within the total area of the Eurasian region was 55.09% between 1993 and 2006 while this value was 51.53% in Turkey. However, the cultivation status of the total agricultural fields, ratio of the forest lands and the product patterns in the agricultural fields are different in the Eurasian region and Turkey. Mostly the product group of grains are cultivated in the Eurasian region with intensive agriculture every year. However, the share of the agricultural fields within total area during the period of the study has gradually decreased in Turkey despite heavy agricultural activities. Soilless agriculture, environment friendly production systems and corresponding policy actions were taken as well. This is totally related to the intention of agriculture to reduce greenhouse gas release. While a one-way causality was determined between the agricultural fields and population in the Eurasian region in the short run, there was no such causality in Turkey. When we look at long term causality, long term deviation in the Eurasia Region does not appear to be reversible in the short run. With regards to the agricultural added value, effects increasing CO_2 release were determined in both regions, and balancing long term deviations in the short run was considered to be statistically important. GDP is another variable with differences between regions. There is a positive directional and linear relation between GDP and environmental destruction in the underdeveloped countries while it is possible to see a negative directional relation in the developing or developed countries. This can be explained by the presence of the individuals in the country under the study and the policies implemented for that purpose. Turkey consists of a structure which is, even partly, more developed, has higher income level and possesses social awareness. This difference can be seen in the reports of the United Nations development plans.

In summary, the quality and sustainability of the world we live in and the life conditions in the world are dependent on humans. Human-induced deterioration is also expressed in scientific studies (Kadıoğlu, 2002; Türe, 2003). For example, every year, a result of human activities CO_2 level increases by 3 billion tons (Bozoğlu et al., 2003; Karakaya and Özçağım, 2004). Environmental cost should definitely be taken into consideration while carrying out both agricultural activities and other income generating activities. All countries of the world should ensure conscientious individuals and informed development processes. Contributions should be made to raise awareness and improve education in underdeveloped countries and regions. States and policy makers should implement the laws on environmental issues and make them enforceable. All relevant ministries and organizations should be extremely sensitive and definitely take

http://www.aloki.hu ● ISSN 1589 1623 (Print) ● ISSN 1785 0037 (Online)
DOI: http://dx.doi.org/10.15666/aeer/160569636976
© 2018, ALÖKI Kft., Budapest, Hungary

steps in their action plans to protect environmental plans. In conclusion, a destructed environment, polluted water and atmosphere affect all humans.

REFERENCES

[1] Altıntaş, H. (2013): Türkiye'de petrol fiyatları, ihracat ve reel döviz kuru ilişkisi: ARDL sınır testi yaklaşımı ve dinamik nedensellik analizi. – Uluslararası Yönetim İktisat ve İşletme Dergisi 9(19): 1-30.
[2] Angel, J. (2008): Potential Impacts of Climate Change on Water Availability. – Illinois State Water Survey, Institute of Natural Resource Sustainability, Champaign, IL.
[3] Anonymous (2018): https://en.wikipedia.org/wiki/List_of_Eurasian_countries_by_population.
[4] Bayraç, N., Doğan, E. (2016): Türkiye'de İklim Değişikliğinin Tarım Sektörü Üzerine Etkileri. – Eskişehir Osmangazi Üniversitesi İİBF Dergisi, Nisan 11(1): 23-48.
[5] Bozoğlu, B., Keskin, B., Çavdar, S. (2003): Küresel Isınma. – 6. Çevre Sorunları Öğrenci Yaklaşımları Sempozyumu Nisan 2003, Mersin.
[6] Carson, D. J. (1999): Climate modelling: achievements and prospects. – Quarterly Journal of Royal Meteorological Society 125: 1-28.
[7] Choi, I. (2001): Unit root tests for panel data. – J Int Money Financ 20: 249-272.
[8] Enders, W. (2008): Applied Econometric Time Series. – John Wiley & Sons, Hoboken, NJ.
[9] Engle, R. F., Granger, C. W. (1987): Co-integration and error correction: representation, estimation, and testing. – Econometrica: Journal of the Econometric Society 251-276.
[10] Gafari, SH., Galalinasab, M., Ervani, H. (2014): Assessing the economic impact of climate change on agriculture. – National Conference on Climate Change and Sustainable Development of Agriculture and Natural Resources Engineering, Tehran.
[11] Granger, C. W. (1988): Some recent development in a concept of causality. – Journal of Econometrics 39(1-2): 199-211.
[12] Hadri, K. (2000): Testing for stationarity in heterogeneous panel data. – Econometric Journal 3: 148-161.
[13] Holly, R. (2015): The Complicated Relationship between Agriculture and Climate Change. – http://investigatemidwest.org/2015/07/09/thecomplicated-relationship-between-agriculture-and-climate-change/.
[14] Hosseini, S. S., Nazari, M. R., Araghinejad, S. (2013): Investigate of climate change effects on the agricultural sector, with emphasis on the implementation of the strategies in this section. – Iran Agricultural Economics and Development Research 1: 1-16.
[15] Im, K., Pesaran, M., Shin, Y. (2003): Testing for unit roots in heterogeneous panels. – J Econom 115: 53-74.
[16] IPCC (2014a): IPCC Fifth Assessment Report: Climate Change 2014 (AR5). – IPCC, Geneva.
[17] IPCC (2014b): Climate Change 2014: Synthesis Report. Contribution of Working Groups I, II and III to the Fifth Assessment Report of the. – IPCC, Geneva.
[18] Janjua, P. Z., Samad, G., Khan, N. (2014): Climate change and wheat production in Pakistan; autoregressive distributed lag approach, NJAS. – Wageningen Journal of Life Sciences 68: 13-19.
[19] Johansen, S. (1988): Statistical analysis of cointegration vectors. – Journal of Economic Dynamics and Control 12(1): 231-54.
[20] Johansen, S., Juselius, K. (1990): Maximum likelihood estimation and inference on cointegration with application to the demand for money. – Oxford Bulletin of Economics and Statistics 52: 169-210.
[21] Kadıoğlu, M. (2001): Bildiğimiz Havaların Sonu Küresel İklimDeğişimi ve Türkiye. – Güncel Yayıncılık, İstanbul.

http://www.aloki.hu ● ISSN 1589 1623 (Print) ● ISSN 1785 0037 (Online)
DOI: http://dx.doi.org/10.15666/aeer/160569636976
© 2018, ALÖKI Kft., Budapest, Hungary

[22] Kang, Y., Khan, S., Ma, X. (2009): Climate change impacts on crop yield, crop water productivity and food security. A review. – Prog. Nat. Sci. 19(12): 1665-1674.
[23] Kao, C., Chiang, M. (2000): On the estimation and inference of a cointegrated regression in panel data. – Adv Econom 15: 179-222.
[24] Karakaya, E., Özçağım, M. (2004): Sürdürülebilir kalkınma ve iklim değişikliği: Uygulanabilecek iktisadi araçların analizi. – Kırgızistan-Türkiye Manas Üniversitesi I. Maliye Konferansı 16 Nisan, Bişkek.
[25] Kaygusuz, K. (2009): Energy and environmental issues relating to greenhouse gas emissions for sustainable development in Turkey. – Renewable and Sustainable Energy Reviews 13: 253-270.
[26] Khashman, A., Khashman, Z., Mammadli, S. (2016): Arbitration of Turkish agricultural policy impact on CO_2 emission levels using neural networks. – Procedia Computer Science 102: 583-587.
[27] Kuznets, S. (1955): Economic growth and income inequality. – The American Economic Review 45(1): 1-28.
[28] Levin, A., Lin, C., Chu, C. (2002): Unit root tests in panel data: asymptotic and finite sample properties. – J Econom. 108: 1-24.
[29] Maddala, G., Shaowen, W. (1999): Comparative study of unit root tests with panel data and a new simple test. – Oxf Bull Econ Stat 61: 631-652.
[30] Magadza, C. (2000): Climate change impacts and human settlements in Africa: prospects for adaptation. – Environ. Monit. Assess. 61: 193-205.
[31] MacKinnon, J. G. (1996): Numerical distribution functions for unit root and cointegration tests. – J. Applied Econ. 11: 601-618.
[32] Pesaran, H., Shin, Y. (1995): An Autoregressive Distributed Lag Modelling Approach to Cointegration Analysis. – In: Strom, S., Holly, A., Diamond, A. (eds.) Centennial Volume of Ranger Frisch. Cambridge University Press, Cambridge.
[33] Pesaran, H., Shin, Y., Smith, R. J. (2001): Bound testing approaches to the analysis of long run relationship. – Journal of Applied Econometrics 16(3): 289-326.
[34] Reynolds, L., Wenzlau, S. (2012): Climate-friendly agriculture and renewable energy: working hand-in-hand toward climate mitigation. – Renewable Energy World, 21 December 2012.
[35] Sakurai, Y., Song, K., Tachibana, S., Takahashi, S. (2014): Volitional enhancement of firing synchrony and oscillation by neuronal operant conditioning: interaction with neurorehabilitation and brain-machine interface. – Front. Syst. Neurosci. 8: 1-11.
[36] Özdemir, F., Küçükçongar, M., Arısoy, R.Z., Öztürk, E., Önder, M., Kan, M., Kınacı, İ., Yılmaz, T., Yorgancılar, M., and Şahin, M., 2017. Agricultural Drought Perception and Its Socio-Economic Impacts in KOP Region Project Report (in Turkish), Ministry of Development, KOP Regional Development Agencies and The Ministry of Food Agriculture and Livestock, Konya.
[37] Tiwari, A. K. (2011): Primary energy consumption, CO_2 emissions and economic growth: evidence from India. – SEE Journal 6(2): 95-113.
[38] Türe, E. (2003): Küresel Isınma ve Temiz Enerjiler. – III. Atmosfer Bilimleri Sempozyumu 19-21 Mart Haliç Üniversitesi, İstanbul.
[39] Turkstat (2018): www.tuik.gov.tr.
[40] World Bank (2016a): World Development Indicators: Agricultural Methane Emissions. – http://data.worldbank.org/indicator/EN.ATM.METH.KT.CE.
[41] World Bank (2016b): World Development Indicators: Agricultural Nitrous Oxide Emissions. – http://data.worldbank.org/indicator/EN.ATM.NOXE.AG.ZS.
[42] World Bank (2017): http://databank.worldbank.org/data/reports.aspx?source=world-development-indicators.

http://www.aloki.hu ● ISSN 1589 1623 (Print) ● ISSN 1785 0037 (Online)
DOI: http://dx.doi.org/10.15666/aeer/160569636976
© 2018, ALÖKI Kft., Budapest, Hungary

THE SHEEP TRACKS OF TRANSHUMANCE IN THE APULIA REGION (SOUTH ITALY): STEPS TO A STRATEGY OF AGRICULTURAL LANDSCAPE CONSERVATION

CAMMERINO, A. R. B.[1] – BISCOTTI, S.[2] – DE IULIO, R.[3] – MONTELEONE, M.[1*]

[1]Department of Agriculture, Food and Environment, University of Foggia
Via Napoli, 24 - 71122 Foggia, Italy
(phone: +39-881-589-223)

[2]Land Planning Office of Foggia Province, Via Telesforo, 53 - 71122 Foggia, Italy
(phone: +39-881-791-347)

[3]Department of Humanities, Literature, Cultural Heritage, Education Sciences,
Via Arpi, 176 - 71121 Foggia, Italy

**Corresponding author*
e-mail: massimo.monteleone@host.domain; phone: +39-881-589-223

(Received 10th Jul 2018; accepted 3rd Sep 2018)

Abstract. Transhumance is a very old form of pastoralism where livestock is moved seasonally between higher and lower pastures. The historical sheep track represents a valuable ecological asset that needs to be maintained. This study consisted in the agro-ecological characterization of the sheep tracks landscape and the detection of areas having higher conservation value. A planning framework was arranged and the sheep track system of the Apulia region (Italy) was characterized with the support of a Geographic Information System. Plain areas, mainly associated with transhumance in the past, are today much less involved in the residual presence of these sheep tracks; conversely, the most abundant presence and the best conservation status was detected in the hilly and marginal agricultural areas. Moreover, those biotopes having prevailing semi-natural traits closely associated with transhumance are today under-represented in the landscape and largely surpassed in extent by biotopes pertaining to agricultural land use. This work is a preliminary step in detecting the traits of the residual sheep track network in Apulia. Actions are required converging in a preservation plan that supports the recovery of the sheep track system according to an integrated land management perspective. Therefore, a new dimension in the sheep track conservation should be accomplished, not related to pastoralism, but able to deliver ecological services and promoting rural development in marginal areas.
Keywords: *agroecological planning, analytic hierarchy procedure (AHP), corine biotopes; geographical information system (GIS), high nature value farmland (HNV), land ecological network (LEN)*

Introduction

Transhumance is a very old form of pastoralism consisting in the seasonal movement of livestock and herders between higher pastures, in summer, and lower pastures, during winter (Ruiz and Ruiz, 1986). In Southern Italy, since the 15th century, long and grassy paths were connecting Abruzzo and Molise (in the Central Apennines) to the Southern Apulia region (down to the Tavoliere plain), and then in the reverse way (de Iulio and Biscotti, 2015). *Figure 1* provides a general representation of all the historical sheep tracks once traceable in Southern Italy. This practice dates back to time immemorial, but a long documented history is also available. In the middle of the 15th century, no less than 3.0 million sheep and 30 thousand shepherds travelled annually along the transhumance paths, while in the 17th century the sheep were about 5.5 million (de Iulio and Biscotti, 2015). Transhumance was practiced until the 1950-1960s, and abandoned

http://www.aloki.hu ● ISSN 1589 1623 (Print) ● ISSN 1785 0037 (Online)
DOI: http://dx.doi.org/10.15666/aeer/1605_69777000
© 2018, ALÖKI Kft., Budapest, Hungary

later, at least according to the original model, while much shorter trips of herds are still observed (between higher pastures in summer and lower valleys in winter), albeit quite rarely.

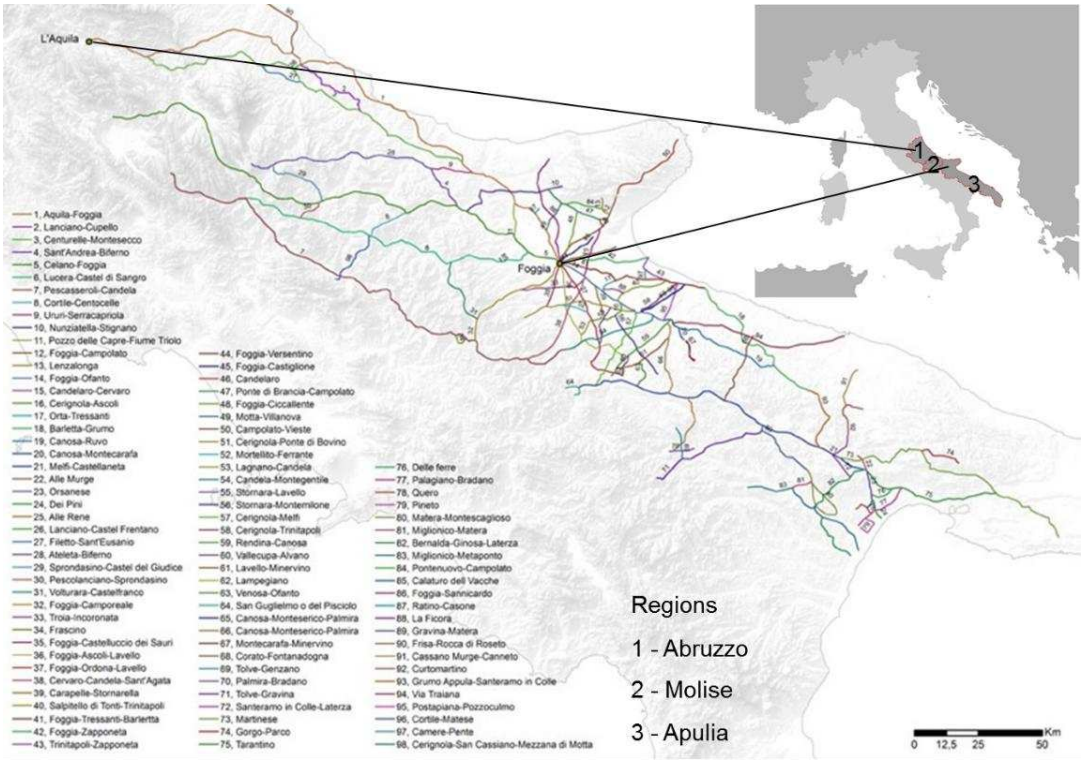

Figure 1. *Comprehensive map of the historical South Italian transhumance network. The name and dislocation of the most important sheep tracks in the three involved Italian regions (Abruzzo, Molise and Apulia, respectively) are displayed. (Adaptation from: I tratturi (n. d.): http://www.leviedeitratturi.com/i-tratturi/)*

Transhumance took place in several areas of the world and in almost every continent, particularly in Europe and Western Asia. These grassy routes travelled by drovers and herds assumed specific names in the language of various regions: *tratturi* in Italy, *cañadas* in Spain, *carraires* in France and *drumul oierilor* in Romania, all having the same features and functions (Paone, 2006).

The main *tratturi* (the so-called "royal" paths) have a precise width of 111 m, and are generally longer than 100 km, crossing longitudinally the southern part of the Italian peninsula. Secondary paths (named *tratturelli*) and lower order "branches", connecting the higher order paths, complete the dense and intricate sheep track network (*Fig. 1*).

Over the centuries, flocks, but also herds, were following this complex network of sheep tracks that developed progressively, adapting to the natural shape of the landscape. This provided the environmental "warp" to a "weft" made of relevant historical and cultural heritage. Natural environment and human culture, affecting each other, are closely interconnected and represent the two main landscape dimensions driving the coevolution processes. A vast scientific literature highlights the strategic importance of this landscape heritage, also with respect to the Mediterranean regions, including the relevant remaining of historical rural infrastructures, such as routes and lanes, stone-made terraces, field enclosures, ancient buildings and architectures, and

http://www.aloki.hu ● ISSN 1589 1623 (Print) ● ISSN 1785 0037 (Online)
DOI: http://dx.doi.org/10.15666/aeer/1605_69777000
© 2018, ALÖKI Kft., Budapest, Hungary

much more (Moreira et al., 2006; Brown et al., 2007; Cullotta and Barbera, 2011; Petanidou et al., 2008). Historically, transhumance has created a truly peculiar agricultural landscape, as clearly demonstrated by Melini et al. (2014) who presented an interesting case study in Molise, a southern region of Italy. Large open fields, lean (steppic) pastures, *maquis* and *garrigue* shrubland, animal resting places, woods and glades, single or clustered trees with broad and shadowing canopies, dry stone walls serving as land ownership boundaries, etc. are all elements jointly characterizing this landscape systems. One of the key features of this type of landscape is its strong semi-natural trait, resulting from the limited human interference, apart grazing management. Both over- and under-grazing may represent degrading factors leading to ecological disruption, but when grazing was well managed, semi-natural ecosystems resulted from a dynamic equilibrium between wildlife and human activities (Pykälä, 2000; Sutherland, 2002). Today, these landscapes are recognised as key habitats for maintaining biodiversity in the European agricultural areas (Bakker, 1989; Poschlod and Bonn, 1998; Pykälä, 2000).

Semi-natural ecosystems, with specific reference to permanent pastures, are a treasure chest of exceptional biodiversity and are the source for the majority of the environmental public goods generated by European farming (EC, 2014). This considering, they are fundamentally different from pastures under more intensive agricultural use (Beaufoy et al., 2011) and need to be protected from land use change due both to intensification, with the consequent conversion into arable land, and abandonment, frequently followed by natural afforestation. Indeed, the rapid technological changes experienced by more intensive agricultural practices proved to be one of the major threats to biodiversity in the last decades (Luoto et al., 2003; Butler et al., 2007), thereby altering the composition, structure and function of these valuable agro-ecosystems (Vitousek et al., 1997; Kremen and Ostfeld, 2005). On the other hand, a widespread agricultural land abandonment due to extra-marginal economic conditions can result in forest transition (Kauppi et al., 2006). Land intensification and land dereliction are the combined, double-sided process largely explaining the current agricultural land-use changes. Therefore, halting the loss of these semi-natural ecosystems, and specifically permanent pastures, is a key action for stopping the decline of biodiversity in Europe as a whole.

Transhumance, being connected to pasture maintenance and utilization, particularly along the sheep track network, largely contributed in forming a valuable set of pastoral landscapes and associated habitats. Some of these habitats are crucial, today, for the conservation of many “endangered” animal and vegetal species (Garzon, 2001), i.e. species which has been categorized as likely to become extinct.

The importance played by the sheep track system formed with transhumance in the conservation of semi-natural ecosystems and its associated biodiversity have been rarely analysed (Olea and Mateo-Tomás, 2009). Despite being present in many European countries, from Balkans to Scotland, this practice is currently a declining activity in Europe (Ruiz and Ruiz, 1986; Liberatori and Penteriani, 2001) due to the shift from old and traditional breeding practices to modern ones.

Although transhumance, today, is no longer carried out, Mediterranean countries retain significant traces of these sheep tracks, together with historical and cultural artefacts linked to transhumance. Therefore, the legacy of such a peculiar resource should be considered a valuable regional asset that needs to be properly maintained and relaunched through a systemic strategy, made of both conservation and valorization,

http://www.aloki.hu ● ISSN 1589 1623 (Print) ● ISSN 1785 0037 (Online)
DOI: http://dx.doi.org/10.15666/aeer/1605_69777000
© 2018, ALÖKI Kft., Budapest, Hungary

altogether promoting new or renewed forms of rural development in those involved areas.

Generally, *tratturi* have the juridical status of public property and are preserved thanks to specific regulations protecting cultural heritage. After the 1930s, they were included in the enfranchisement law. Agriculture thus began to occupy the space of the traditional greenways that, until then, were under protection by numerous national regulations (Russo, 2002). In 1977, with the Presidential Decree n. 616 (Art. 66), sheep routes and tracks passed under the authority of the regional governments.

The management of this asset in the Apulia region is, today, in charge of the Regional Land Property Department that recently endorsed a new regulation framework (L.R. 4/2013) through which the entire regional sheep track system should be characterized and classified in order to promote, soon after, integrated actions of recovery and development. The first need (preliminary to every other kind of analyses and measures) was to consider the current conservation status of the sheep track system, discerning those portions still able to be recognized and not yet impaired from those stretches degraded by now and irremediably lost.

As part of a more general planning procedure on the sheep track network in the Apulia Region, the present study was specifically focused on the agroecological analysis and landscape characterization. This task was assigned to the University of Foggia (Department of Agriculture, Food and Environment) in collaboration with other institutional entities, forming a panel that included experts from the public administration of the Apulia Region (Land Property Department), the Foggia Province (Planning Department), the National Ministry of Cultural Heritage (Department of archaeology, fine arts and landscape). Colleagues from the Polytechnic University of Bari, specialized in architectural design (Department of Engineering and Architecture) and from the University of Foggia, specialized on cultural anthropology (Department of Humanistic Studies, Letters, Cultural Heritage) coordinated the team and contributed to the work, financially supported by the Apulia Regional Administration.

In parallel with the agroecological analysis, other studies and investigations were performed, involving this wide range of experts and scholars, mostly considering the current territorial arrangement of the land ownership, a survey of historical records and remaining, traditions and cultural heritage, arts and historical buildings, and much more.

The specific objective of the present study was to identify, characterize, classify and select land areas pertaining to the sheep track regional network, having higher conservation value according to agroecological criteria, still in good status of maintenance, and featuring less intensive farming practices or semi-natural conditions, similar (at least approximately) to the original landscapes at the times of transhumance.

The purpose of collecting a significant amount of information and defining a coherent and comprehensive framework of knowledge was considered a precondition, the final goal being developing an effective planning model to address the establishment of a protected natural area (called “Sheep track regional park”) to be connected to the regional ecological network and the “Natura 2000” (Habitat Directive 92/43/CEE) biodiversity system.

The study area

The study area is the Apulia region, placed in the Southeast of Italy and about 20.000 km^2 wide. It can be divided into 11 sub-regions according to the Regional

http://www.aloki.hu ● ISSN 1589 1623 (Print) ● ISSN 1785 0037 (Online)
DOI: http://dx.doi.org/10.15666/aeer/1605_69777000
© 2018, ALÖKI Kft., Budapest, Hungary

Landscape Plan (PPTR, 2013). This subdivision takes into account the geo-morphological, hydrological, environmental, as well as the anthropic and cultural traits of the region. Over the centuries, all these assorted characteristics contributed to the development of a landscape heritage consisting of a wide range of natural and semi-natural environments (habitats and species), as documented by several national and regional publications (ISPRA, 2013; PPTR, 2013). The typical climate is Mediterranean, although several peculiar local conditions can be detected. Altitude varies from 0 to about 1,200 m above the sea level. The region is mostly characterized by plain areas (53%), while hilly and mountainous surface covers the remaining part (47%). *Figure 2* displays the 11 sub-regions together with the Apulian sheep track network.

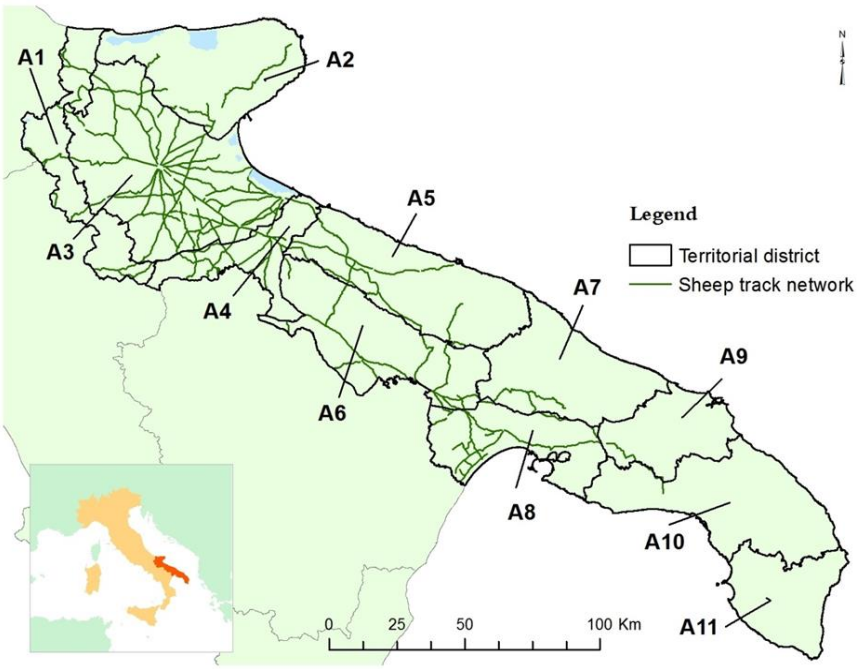

Figure 2. *Map of the Apulian sheep track network. Sub-regions according to the Apulian Landscape Plan are also represented. Monti Dauni (A1), Gargano (A2), Tavoliere (A3), Ofanto (A4), Puglia Centrale (A5), Alta Murgia (A6), Murgia dei Trulli (A7), Arco Ionico Tarantino (A8), Campagna Brindisina (A9), Tavoliere del Salento (A10), Salento delle Serre (A11)*

Material and methods

A landscape planning procedure is the methodological approach carried out in this work. It was applied to a peculiar set of agriculture, natural and semi-natural ecosystems (defined "biotopes"). A Geographic Information System (GIS) supported the analysis and allowed the processing of georeferred information, thus obtaining properly designed thematic maps. The software "ArcGis 10.1" was used for these purposes.

After a survey of the land use/land cover databases available from both regional and national digital cartographic portals, the Apulian Biotope Map (ISPRA, 2013) was the one selected to be used in the analysis. This database is focused on the spatial representation of the ecological and naturalistic traits of lands, specifically considering the range of ecosystems and biotopes detected in the region. This kind of information was judged particularly fitted to the scope of the considered land planning procedure.

http://www.aloki.hu ● ISSN 1589 1623 (Print) ● ISSN 1785 0037 (Online)
DOI: http://dx.doi.org/10.15666/aeer/1605_69777000
© 2018, ALÖKI Kft., Budapest, Hungary

Schematically, the applied methodology is composed of a sequence of steps, as represented in *Figure 3*. Starting from the historical sheep track network (step 1), the spatial analysis was restricted to a buffer zone of 1 km outlined around each path of the network (step 2).

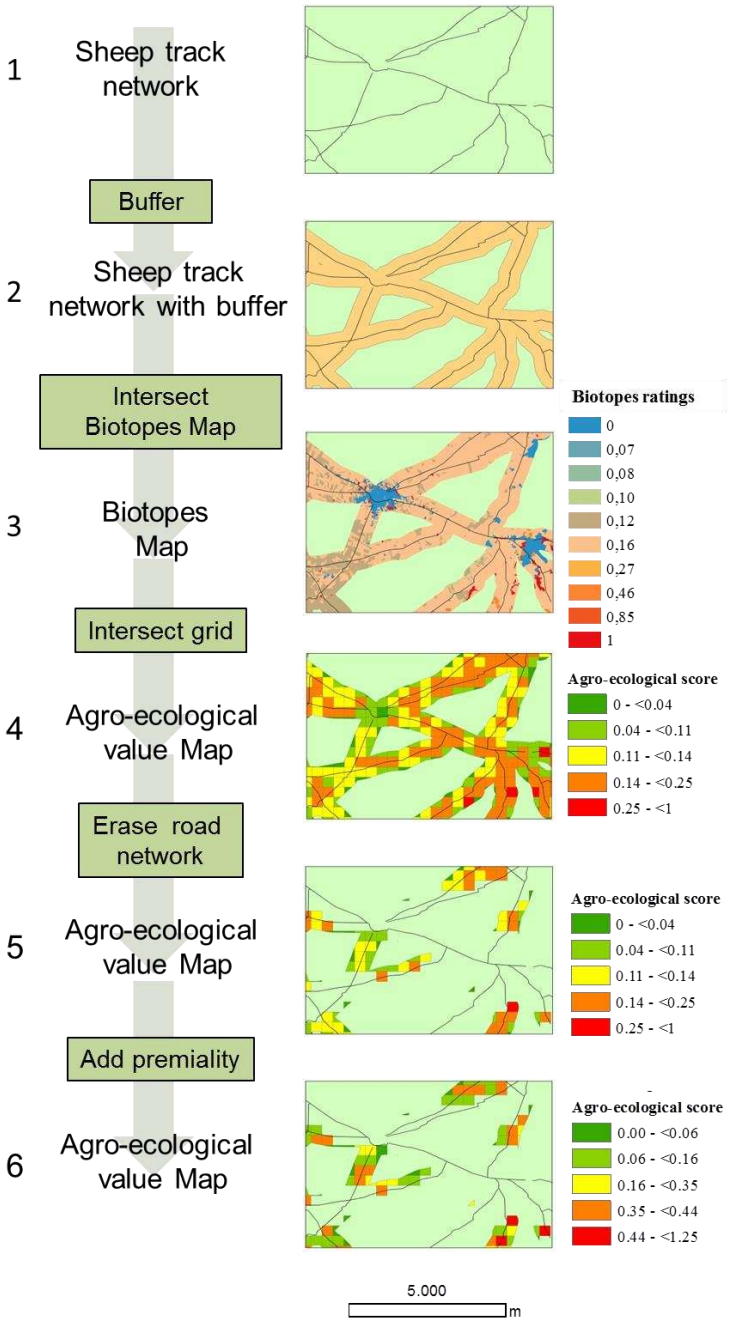

Figure 3. *Flow chart explaining the six consecutive steps of the applied methodology: identification of sheep track network (step 1); creation of a buffer area around the sheep paths (step 2); spatial intersection between the buffer area and the biotope map (step 3); overlapping with a grid to define the agro-ecological score for each mesh (step 4); erasing of the modern road network (step 5); adding premiality for those meshes belonging to protected areas (step 6). Concerning step 3, the exact rating assigned to the 11 biotope categories is reported (see the legend), while about steps from 4 to 6, the agroecological scores (see the legends) are partitioned according to a quintile distribution*

http://www.aloki.hu ● ISSN 1589 1623 (Print) ● ISSN 1785 0037 (Online)
DOI: http://dx.doi.org/10.15666/aeer/1605_69777000
© 2018, ALÖKI Kft., Budapest, Hungary

The biotope units within the buffer areas were selected. Then, an aggregation of the original biotope categories was performed, thus identifying 11 biotope categories (or biotope "categories"), in total. Each cluster was ranked with respect to all the others by assigning an "agroecological rating", ranging from 0 to 1, according to the opinion of experts who have adopted a set of shared criteria. The applied ranking procedure is a rearrangement of the methodology by Berthoud et al. (1989) originally developed to define the environmental naturalness value for conservation priorities.

The Biotope Map was obtained accordingly (step 3). A grid with a squared mesh of 1 km by side was overlapped to the Biotope Map. The surface fraction of each biotope occurring in every cell of the mesh was determined. Then, the "agroecological score" of every cell was computed as the average rating of all the featuring biotopes, each weighted by its corresponding surface fraction. A quintile classification of the cell-scores was performed (each class having 20% of the total number of cells), and 5 consecutive score-classes were therefore identified. In this way, the Agroecological Value Map was obtained (step 4). Those stretches of the sheep tracks currently no longer physically recognizable or irrecoverably impaired were discarded and consequently removed from the map (step 5). This occurred when a complete overlapping between a sheep truck path and a modern road segments was detected. Finally, the "agroecological score" was increased only for those cells placed inside protected natural areas. A score re-classification (according to the same quintile breakdown) was consequently performed (step 6).

Some critical methodological features of the applied procedure probably need to be better clarified. The following are further explanations, by bullet points, about these issues:

(A) *Biotope data source and their aggregation*. The Apulian Biotope Map (ISPRA, 2013) was obtained at 1:50.000 scale, it accounts for 80 detected habitats, arranged according to the European classification system called CORINE Biotopes. In the CORINE system, each habitat is classified within a hierarchical structure made of several embedded levels. The Apulian Biotope Map reached the 6th hierarchical level of habitat classification. Considering all the habitats featured in the sheep track network, a clustering of them was arranged, according to similarity criteria. In this way, 11 aggregated biotope categories were defined, each with a larger or smaller number of habitats. *Table A1* (see *Appendix*) reports this clustering. The categories "woods and forests" is the one with the larger number of habitats (16), followed by "meadows and pastures" (7), "dunal vegetation" (7), "bush and garrigue" (6), "riparian vegetation areas" (6). For the sake of simplicity, the habitats listed in *Table A1* are reported only with their CORINE Biotope code, while the specific name assigned to each habitat is reported in *Table A2* (see *Appendix*), according to the CORINE biotopes (Version 2000) database. A detailed description of these habitats can be found in ISPRA (2013).

(B) *Spatial scale of the analysis* (reason why a 1 km mesh-size). The appropriate size of the landscape analysis may vary according with the objectives of the work. The main advantage of using a grid of regular mesh superimposed to the regional digital map in the GIS assisted procedure is represented by the equal area of each cell, thus creating statistically similar units across the area being analysed. The choice of 1 km as the mesh size of the grid overlapped to the Biotope Map was associated to the corresponding size of 1 km of the buffer applied to both sides of each sheep track. Considering that the largest *tratturo*, the first order sheep track, was originally 111 m width, the buffer dimension is about nine time larger. This should be considered a proper dimension to

http://www.aloki.hu ● ISSN 1589 1623 (Print) ● ISSN 1785 0037 (Online)
DOI: http://dx.doi.org/10.15666/aeer/1605_69777000
© 2018, ALÖKI Kft., Budapest, Hungary

perform a planning analysis at regional scale, an optimal trade off allowing capturing both good amount of internal variability as well as heterogeneity of biotopes among adjacent cells of the grid.

(C) *Biotopes ranking procedure* (how coherently evaluating the rating distance between pairs of biotope categories). An Analytic Hierarchy Procedure (AHP) was applied (Saaty, 2008) with the main goal of estimating the correct rating to be assigned to each biotope category or, in other words, valuing the distance, in terms of a quantitative rating, between the agroecological values of all possible pairs of biotope categories. In this kind of analysis, expert judgement played a key role in estimating the relative importance of a biotope category with respect to another (Delivand et al. 2015). Therefore, a panel of 10 experts belonging to the "Regional Committee on the Sheep track Network" and mostly composed by naturalists, ecologists and agronomists, was asked to perform the AHP under the coordination of the Authors. In other words, each single expert was asked to compare the biotope categories two by two, according to the following set of criteria (Spitaleri et al. 1991):

a) Level of naturalness (fully artificial, semi-artificial, semi-natural; fully natural although of secondary origins)
b) Degree of diversity (low, medium, high richness of species)
c) Rarity status (low, medium, high number of species demanding protection or precious biocenosys)
d) Biotope representativeness (presence of endemic species or species associations characterizing the Mediterranean type of environment)

Consecutive pairwise comparison between criteria produced a resulting symmetric matrix of judgment (Delivand et al. 2015). In this way, the AHP generates a "weight" for each evaluation criterion: the higher the weight, the more important the corresponding criterion. Then, for each criterion, a "value" to every biotope category was assigned, again according to the AHP expert pairwise comparisons: the higher the "value", the better the performance of the biotope category with respect to the considered criterion. Finally, the AHP combines the criteria "weights" and the biotope "values", thus determining a global "rating" for each biotope category, and a consequent ranking. Saaty (2008) presents a complete description on how to lay out and solve AHP analysis (matrix operations, eigenvalue extraction and normalization). When many pairwise comparisons are performed, some inconsistencies may typically arise. The AHP incorporates an effective technique for checking the consistency of the evaluations made by the experts when building each of the pairwise comparison matrices. The technique relies on the computation of an index called "consistency ratio" (CR). A perfectly consistent expert should always obtain CR = 0, but small values of inconsistency may be tolerated. If CR is smaller or equal to 0.1 the combination of weights or the combination of biotope values should be considered satisfactory. Differently, some pair comparisons have to be revised (Saaty, 2008; Ying et al., 2007).

(D) *Reason why long stretches of the sheep track network were discarded*. By using the geo-referred database and comparing the historical sheep track system with the modern road network it was observed that, today, not only secondary roads but also highways and main national roads of intense motorized traffic are overlaid to the original sheep paths. Roads have physically occupied the original settlement of the sheep paths and roadside facility services their adjacent areas. This happens both quite often and for long distances, thus representing a very serious impairment, almost

http://www.aloki.hu ● ISSN 1589 1623 (Print) ● ISSN 1785 0037 (Online)
DOI: http://dx.doi.org/10.15666/aeer/1605_69777000
© 2018, ALÖKI Kft., Budapest, Hungary

irreversible, to the integrity of the sheep path system. Therefore, whenever such conditions were detected and stretches of the sheep track were no longer physically discernible, it was determined not to consider them furthermore in the analysis and to remove them from the processing map.

(E) *Reward assigned to cells inside natural protected areas*. Those cells of the mesh whose surface was inside protected natural areas (both National and Regional Parks, as well as SCI and SPA of "Natura 2000" network) were rewarded by increasing of 0.25 their "agroecological score". The total score of each cell was therefore re-classified into new 5 intervals, according to the corresponding quintile.

Having conveniently prepared the comprehensive set of spatial data useful for the analysis, the final step of the analytical procedure was the following: cells belonging to the upper score class (i.e. those corresponding to the highest agroecological scores) were selected and further examined. These cells were appropriately mapped at a smaller scale, and studied, more in detail, in their biotope composition. Considering those remaining cells, the percentage of land assigned to each biotope categories was determined as well as the percentage of land attributed to each Apulian sub-region; a combination of the two factors (biotope category and sub-region) was also analysed in terms of surface fraction allotted to each biotope category in each sub-region. A double entry table was then obtained and the corresponding matrix was processes through a factorial analysis. The outcomes of this multivariate statistical procedure were very useful in detecting the main characters of the agricultural landscape of the region with respect to the areas pertaining to the sheep track network.

Results

The main findings related to the ranking of the biotope categories, the selected areas to be preserved and their characteristics and distribution among the territorial districts are presented below.

Ranking of biotope categories

Figure 4 reports the 11 clustered biotope categories ranked according to their agroecological "rating" assigned by the expert panel as the result of the AHP.

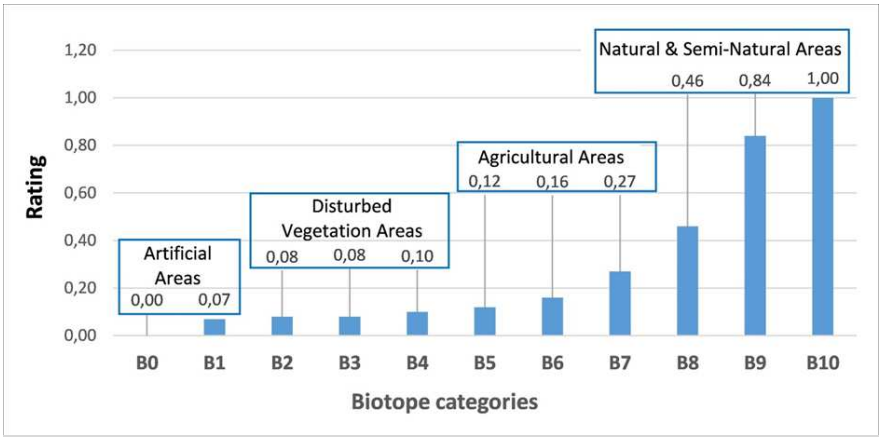

Figure 4. *Rank of the agroecological "rating" assigned to biotope categories by the expert panel as a result of the Analytic Hierarchy Procedure (AHP). More details about the applied procedure and the list of biotopes are available in the Appendix*

http://www.aloki.hu ● ISSN 1589 1623 (Print) ● ISSN 1785 0037 (Online)
DOI: http://dx.doi.org/10.15666/aeer/1605_69777000
© 2018, ALÖKI Kft., Budapest, Hungary

As a general outcome, lower ratings were assigned to artificial biotope categories, while higher ratings were associated to natural and semi-natural biotopes. Finally, the ratings of farmland biotopes are placed in a central position along the ranking (the complete list of the detected biotopes in reported in *Tables A1* and *A2* in the *Appendix*).

However, the main interesting comment to *Figure 4* is not the ranking *per se*, but the relative rating distance between biotope categories. The highest agroecological rating, indeed, was attributed to "meadows and pasture" (B10), followed by "bush and garrigue" (B9). Those biotope categories (such as permanent pasture, grassland and other semi-natural vegetation types) are clearly associated to transhumance. Their remarkable rating (1.00 and 0.84, respectively) is considerably higher than that of other natural or semi-natural biotopes, represented by "woods and forests" (B8), whose rating was estimated equal to 0.46, i.e. approximately half the values of B10 and B9. This impressive difference, detected by the joint expert evaluation, can be justified in the light of the so called "forest transition" process. Land abandonment (especially in traditional agricultural landscapes) and forest expansion often lead to lower landscape heterogeneity with negative effects on biodiversity, particularly for those species benefitting from open habitats and edge environment (Giampietro, 1997; Marull et al., 2010 and 2014). Biotope B10 is characterized by the presence of priority habitat types (i.e. habitat types in danger of disappearance) with single species or plant associations that, according to the Directive 92/43/CEE, need special protection. These species are represented by *Brachypodium retusum*, *Brachypodium ramosum*, *Trachynia distachya*, *Bromus madritensis* e *Lagurus ovatus*. Moreover, these species are often associated with the presence of rare wild orchids. Biotope B9 is frequently present in 'Natura 2000' areas (Habitat Directive 92/43/CE) that are part of an ecological network of protected zones, safeguarded against potentially damaging developments.

These considerations, largely prevailing among the experts, motivated the biotope ranking, and the lower ecological rating attributed to wood and forest as compared to pasture, garigue, maquis and meadows.

Moreover, among biotope categories associated to farmland, a higher rating was credited to "complex cultivation patterns" (B7), agricultural systems characterized by higher heterogeneity as compared to "tree crops" (B6) and "annual crops" (B5), more specialized farming systems. B7, indeed, is a traditional form of agricultural land utilization, marked by a rich assortment of crop patterns and diversified cultivation managements, strictly associated with higher biodiversity degrees, preserving and attracting wild species, both animals and plants. Finally, lower ratings were assigned to other biotope categories considered of poorer agroecological relevance, being artificial habitats, or habitats frequently subjected to human disturbance, or in any case habitats difficult to correlate with pastoral use, although natural or semi-natural.

Selected fractions of the original sheep track network

Figure 5 represents the outcome of the overall analytical procedure. The results obtained consist in the selection and location on the map of those areas characterized by the highest agroecological value within the sheep track network of the Apulia region (identified as "red" colored spots on the map). The geographical distribution of these areas appears self-evident and leads to make further assessment about the most involved sub-regions as well as about the most represented biotope categories (see the following sub-sections).

http://www.aloki.hu ● ISSN 1589 1623 (Print) ● ISSN 1785 0037 (Online)
DOI: http://dx.doi.org/10.15666/aeer/1605_69777000
© 2018, ALÖKI Kft., Budapest, Hungary

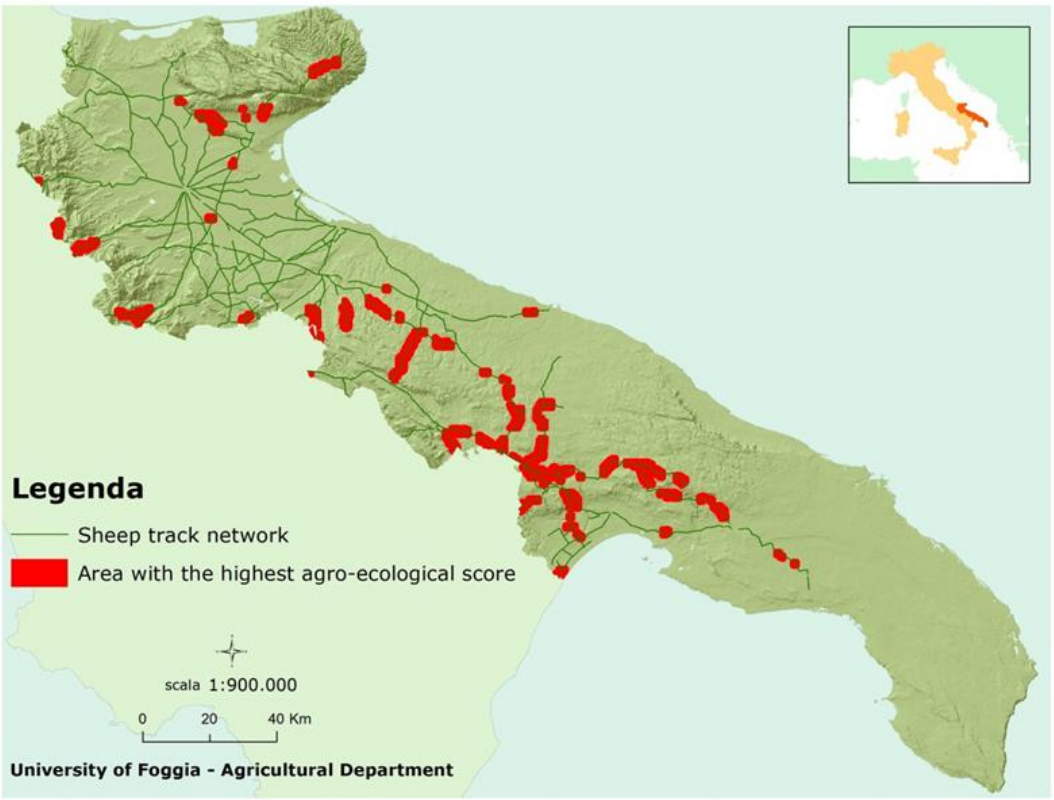

Figure 5. *Outcome of the planning analysis. Geographical dislocation of the selected portions of the sheep track network of the Apulia region credited with the highest agroecological score*

Considering the total historical sheep track network in the region, approximately 51% of the pertaining areas were excluded from the original system due to irreversible impairments and loss of physical integrity of the paths. Approximately, another 38% was discarded considering that these areas showed lower agroecological value (below the upper quintile assumed as benchmark). Therefore, the remaining 11% is the relative amount of the original network that was considered deserving specific attention through protective policies and development strategies. From about 350 thousand hectares originally assigned to the network, roughly 170 thousand hectares are still functional and clearly detectable, while 40 thousand hectares are the surfaces in the best agroecological conditions (totals reported in *Table 1*).

Surface breakdown by sub-regions

Table 1 reports the absolute and relative surface coverage of the sheep track network by sub-regions. Column TA1 accounts for the total area pertaining to the buffer zone considering the historical sheep track network, while column TA2 reports its breakdown percentages. Column RA1 offers the remaining areas of the buffer zone after the exclusion of the impaired and degraded lands that showed overlapping stretches with the road network (highways and main national roads), while Column RA2 reports its breakdown percentages. Finally, Column SA1 represents the selected areas of the buffer zone, i.e. those lands belonging to the class with the highest agroecological score, while Column SA2 reports its breakdown percentages.

http://www.aloki.hu ● ISSN 1589 1623 (Print) ● ISSN 1785 0037 (Online)
DOI: http://dx.doi.org/10.15666/aeer/1605_69777000
© 2018, ALÖKI Kft., Budapest, Hungary

Table 1. *Absolute and relative surface coverage of the sheep track network by sub-regions. The following variables are considered: total buffer area (TA); remaining buffer area after the exclusion of the portions overlapping with the road network (RA); selected buffer area having the highest agroecological score (SA)*

Apulian sub-regions	Code	Total area		Remaining area		Selected area	
		(ha)	(%)	(ha)	(%)	(ha)	(%)
		TA1	TA2	RA1	RA2	SA1	SA2
Monti Dauni	A1	22,523	6.37	11,923	6.88	4,194	10.44
Gargano	A2	20,536	5.81	9,123	5.26	3,582	8.91
Tavoliere	A3	142,823	40.42	65,758	37.92	456	1.13
Ofanto	A4	33,603	9.51	15,503	8.94	1,609	4.00
Puglia centrale	A5	37,594	10.64	17,933	10.34	3,033	7.55
Alta Murgia	A6	39,691	11.23	22,581	13.02	17,217	42.85
Murgia dei trulli	A7	13,442	3.80	9,060	5.22	4,966	12.36
Arco Jonico Tarantino	A8	34,604	9.79	16,542	9.54	4,849	12.07
Campagna brindisina	A9	5,834	1.65	3,336	1.92	9	0.02
Tavoliere Salentino	A10	2,708	0.77	1,661	0.96	265	0.66
Salento delle Serre	A11	-	-	-	-	-	-
Total (Apulia Region)		**353,358**	**100.00**	**173,420**	**100.00**	**40,180**	**100.00**

With reference to the historical areas of the network, about 40% of the overall buffer area falled within Tavoliere (*Table 1,* A2). Only other three sub-regions showed quite high percentages, approximately in the range 9-11%, i.e. Alta Murgia, Puglia Centrale and Arco Jonico Tarantino. About the remaining not degraded areas of the network (*Table 1,* RA2), Tavoliere significantly decreased its surface contribution to approximately 38% of the total, while Alta Murgia increased its contribution reaching about 13%; approximately the same was observed considering Murgia dei Trulli, with a percentage that increased to 5%. Radically different are the percentages that marked the best agroecological areas of the network, i.e. those finally selected (*Table 1,* SA2). In this case, Tavoliere collapsed to 1% only, while Alta Murgia impressively increased its allocation to roughly 43%; quite remarkable are the percentages contributed by Murgia dei Trulli and Arco Jonico Tarantino (approximately 12%), together with Monti Dauni that reached the 10% of the total surface of the network. The most important transformation to be considered in comparing the sheep track initial condition (i.e. the historical network) with the final one (the selected agroecological network) is the drastic overturning in the surface contribution of Tavoliere and Alta Murgia. The former almost disappeared in its contribution, while the latter became unconditionally the most relevant. What was observed, indeed, is part of a wider "modernization" process also involving the transformation of the agricultural landscapes from several decades until now. Agricultural intensification and the expansion of built areas rarefied the agroecological zones of higher value in the plains (Tavoliere) and concentrated these residual but valuable agro-ecosystems in the inner areas of the region (Alta Murgia), more hilly and mountainous. These latter areas, mostly characterized by marginal agricultural systems, show still suitable conditions for the persistence of such extensive ecosystems. The same kind of transformation was observed also considering other internal and marginal sub-regions, such as Monti Dauni and Gargano, whose surface

http://www.aloki.hu ● ISSN 1589 1623 (Print) ● ISSN 1785 0037 (Online)
DOI: http://dx.doi.org/10.15666/aeer/1605_69777000
© 2018, ALÖKI Kft., Budapest, Hungary

contribution has shown an increase from the initial condition (the historical network) to the final one (the selected network). Other two sub-regions showed similar surface fraction increases, i.e. Murgia dei Trulli and Arco Jonico Salentino, respectively.

Table 2 was derived from *Table 1,* but is useful to highlight other specific traits about the agricultural landscape dynamic and its transformation processes over the last decades. Having fixed equal to 100, in each sub-region, the total surface of the sheep track network, *Table 2* gives the share of "land losses" (Column LL) in consequence of degradation processes due to the road network entirely covering the sheep paths, together with the share of "land discarded" (Column LD) in consequence of agroecological impoverishment due to farmland intensification. The residual share, pertaining to the "land selected" (reported in Column LS), account for the relative extent of the sheep track network still in good ecological conditions (and therefore selected in the course of the planning procedure).

Two different dimensions of the comprehensive process of landscape deterioration were considered:

i) Land "consumption" (LL) related to human settlements and infrastructures (expansion of built-up area and road constructions, in particular), on the one hand;
ii) Degraded land (LD) due to over-exploitation for agricultural intensive use, on the other hand.

Table 2. *Shares of land surface pertaining to the sheep track network by sub-regions. The following classes are considered: buffer area losses due to road network overlapping (LL); buffer area discarded due to lower agroecological score (LD); buffer area selected because of higher agroecological conditions (LS)*

Apulian sub-regions	**Code**	**Land losses LL (%)**		**Land discarded LD (%)**		**Land selected LS (%)**	
Tavoliere	A3	53.96	*	45.72	*	0.32	
Ofanto	A4	53.86	*	41.35	*	4.79	
Puglia centrale	A5	52.30	*	39.63	*	8.07	
Alta Murgia	A6	43.11		13.51		43.38	*
Murgia dei trulli	A7	32.60		30.46		36.94	*
Monti Dauni	A1	47.06		34.32		18.62	*
Gargano	A2	55.57	*	26.99		17.44	*
Arco Jonico Tarantino	A8	52.20	*	33.79		14.01	
Campagna brindisina	A9	42.82		57.03	*	0.15	
Tavoliere Salentino	A10	38.65		51.56	*	9.79	
Salento delle Serre	A11	-		-		-	
Average (Apulia Region)		**47.21**		**37.44**		**15.35**	

Percentages marked by a star are higher than the average value of the class

The sub-regional areas of the network where the two landscape degradation typologies jointly occurred (both LL and LD), resulted in very limited percentages of areas still ecologically valuable to be selected (LS). This condition was detected in sub-regions such as Tavoliere (A3), Ofanto (A4) and Puglia Centrale (A5). It is worth

http://www.aloki.hu ● ISSN 1589 1623 (Print) ● ISSN 1785 0037 (Online)
DOI: http://dx.doi.org/10.15666/aeer/1605_69777000
© 2018, ALÖKI Kft., Budapest, Hungary

noting that these sub-regions are flat areas marked by intensive agriculture and large and expanding urban centers. The opposite was shown in the case of Alta Murgia (A6) and Murgia dei trulli (A7), where the two degradation processes limitedly affected the agricultural landscape (neither LL, nor LD) or, their incidence was below the average regional value. Murgia, indeed, is one of the inner and marginal areas of the Apulia region, today largely included into a National Natural Park. The same trend, but somewhat lower, is observed also considering Monti Dauni (A1), another inner area of the Apulia region. This double effect explains the highest (in A6 and A7) and relatively high (in A1) surfaces selected at the end of the planning procedure in the mentioned sub-regions. Intermediate conditions also occurred, such as Gargano (A2) and Arco Jonico Tarantino (A8), marked by higher landscape degradation due to road infrastructures rather than agricultural intensification (LL, but not LD). Campagna Brindisina (A9) and Tavoliere Salentino (A10), conversely, showed a higher degradation level related to agriculture intensification coupled with a lower than average damage to the sheep track network due to road construction (not LL, but LD).

Surface breakdown by biotope categories

Considering the selected areas of the sheep track network (the areas represented as "red spots" in *Fig. 5*), the most abundant biotope category, in terms of covered surfaces, corresponds to "Complex cultivation patterns" (B7), accounting for 47% of the total considered network (*Table 3*). Far behind, that is to say much less represented than the former, are biotopes such as Tree crops (B6), about 18%, then followed by "Woods and forests" (B8), together with "Meadows and pastures" (B10), both around 15% of the total surface. The other biotope categories showed very limited diffusion and can be considered negligible in this discussion.

Table 3. *Biotope categories with codes, their corresponding surface coverage and percentage breakdown with respect to the total selected area*

Biotope categories	Code	Biotope areas (ha)	Biotope percentages (%)
Complex cultivation patterns	B7	18,937	47.13
Tree crops	B6	7,055	17.56
Woods and Forests	B8	6,232	15.51
Meadows and pastures	B10	5,986	14.90
Annual crops	B5	1,087	2.70
Bush and garrigue	B9	648	1.61
Riparian vegetation areas	B4	235	0.58
Total		**40,180**	**100.00**

The ranking process and the selection procedure assigned the maximum rating to "Meadows and pastures" (B10 = 1.00) as compared to other biotope categories (B8 = 0.46; B7 = 0.27; B6 = 0.16), in order to get the presence of these semi-natural ecosystems as much as possible, considering their strict relevance in association with transhumance. The supposed consequence was to include this biotope category, with all its inherent habitats, within the selected portion of the sheep track network, the one with the best agroecological value. The outcomes of the analysis were both unexpected and worrisome. B10, indeed, is much less represented in terms of surface, while agricultural

http://www.aloki.hu ● ISSN 1589 1623 (Print) ● ISSN 1785 0037 (Online)
DOI: http://dx.doi.org/10.15666/aeer/1605_69777000
© 2018, ALÖKI Kft., Budapest, Hungary

land use (B7 and B6) and forest cover (B8) are the most abundant biotope categories observed along the sheep track network, and specifically in that fraction of the network selected because of the best agroecological conditions. The presented data confirmed, from a different perspective, the well-known progressive trend in pasture rarefaction and forestry expansion, together with farmland. Considering farmland, however, the ecosystem quality is significantly increased due to the large surface fraction of "Complex cultivation patterns" (B7) as compared to "Tree crops" (B6) and "Annual crops" (B5).

Surface breakdown by sub-regions and biotope categories

Table 4 shows the percentage breakdown of the surfaces allocated to every biotope featuring within each sub-regions. These data arrangement allows an accurate characterization of the Apulia region, specifically concerning the "red spots" of higher agroecological value.

Table 4. *Breakdown of relative surface coverage allotted to every biotope category (Bi) within each sub-region (Ai). All the reported values are expressed in percentages*

Apulian sub-regions	Code	B4	B5	B6	B7	B8	B9	B10
Monti Dauni	A1	0.11	3.51	1.42	67.77	19.39	0.00	7.79
Gargano	A2	0.03	11.66	10.08	5.80	46.14	2.27	24.02
Tavoliere	A3	1.88	65.73	3.28	0.00	3.10	0.00	26.01
Ofanto	A4	11.29	13.81	21.03	26.90	0.44	0.36	26.17
Puglia Centrale	A5	0.00	0.00	64.48	20.92	1.67	0.67	12.26
Alta Murgia	A6	0.05	0.00	11.56	62.39	5.93	0.00	20.06
Murgia dei Trulli	A7	0.00	0.00	5.73	46.38	46.27	1.41	0.21
Arco Jonico Tarantino	A8	0.59	0.00	39.34	36.27	7.74	9.71	6.36
Campagna Brindisina	A9	0.00	0.00	60.05	0.00	0.00	0.00	39.95
Tavoliere Salentino	A10	0.00	0.00	51.77	5.96	0.00	0.00	42.27
Salento delle Serre	A11	0.00	0.00	0.00	0.00	0.00	0.00	0.00

The same double entry table (reported in *Table 4*) was also the matrix employed in performing a "factor analysis" based on variables correlations. The first two independent and uncorrelated factors were selected, considering that their corresponding eigenvalues were higher than 1. This multivariate procedure accounted for 60% of the total variance (F1 35% and F2 25%, respectively). The resulting "biplot" is shown in *Figure 6*.

Very clearly, Tavoliere (A3) is predominantly associated to Annual crops (B5), confirmed by the high percentage of B5 in A3 (62%) in *Table 4*. Alta Murgia (A6) and Monti Dauni (A1) are the territorial districts where Complex cultivation patterns (B7) is the dominant biotope (B7 > 60%). Murgia dei Trulli (A7) presents a hybrid condition, with a similar share of "Complex cultivation patterns" (B7), on one hand, and "Woods and forest" (B8), on the other one (B7 = B8 = 46%). Gargano (A2) is mainly characterized by a larger occurrence of "Woods and forest" (B8 = 46%). Puglia centrale (A5) is characterized by a considerable prevalence of "Tree crops" (B6 = 64%), while Arco Jonico Tarantino (A8) showed a remarkable combination between "Tree crops" (B6 = 39%) and "Bush and garrigue" (B9 = 10%), respectively. Campagna Brindisina

http://www.aloki.hu ● ISSN 1589 1623 (Print) ● ISSN 1785 0037 (Online)
DOI: http://dx.doi.org/10.15666/aeer/1605_69777000
© 2018, ALÖKI Kft., Budapest, Hungary

(A9) and Tavoliere Salentino (A10) are characterized by a combination of Tree crops (B6 = 52 and 60%, respectively) together with "Meadows and pasture" (B10 = 42 and 40%, respectively). Ofanto (A4) is strictly associated with "Riparian vegetation areas" (B4 = 11%), although shows a high incidence of "Complex cultivation pattern" (B7 = 27%) and "Meadows and pasture" (B10 = 26%). Lastly, Salento delle Serre does not present any significant portions of the sheep track network within its land.

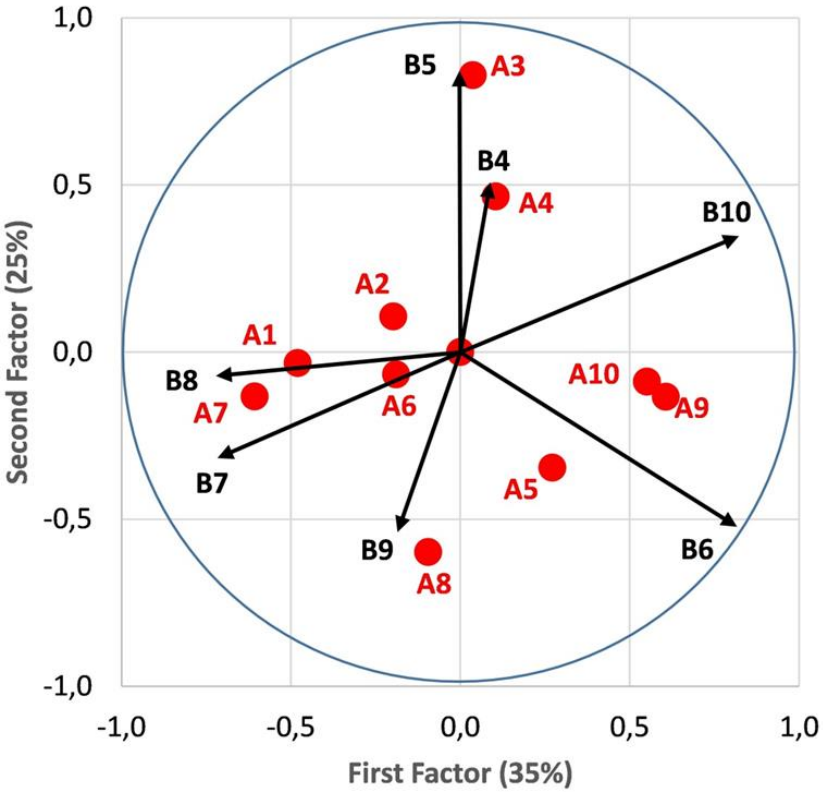

Figure 6. *Biplot of the factor analysis representing both the scores (points) and the factorial weights (arrows). Each point in the graph corresponds to one of the Apulian sub-regions (11 in total). A11 is not represented in the plot because scored zero (see Table 4)*

Discussion

This study performed an agroecological characterization of the sheep track landscape of the Apulian region and the identification of areas with higher conservation value was the subsequent goal.

Two overturning results came out from the analysis of the selected sheep track network: the first pertains to geography, while the second is related to biotopes.

1) The best conservation status of the sheep track network was detected in Alta Murgia (a hilly and marginal agricultural area), whereas sub-regions such as Tavoliere, but also Monti Dauni and Gargano, that were the geographical areas historically associated with transhumance and pastoralism are, today, much less involved in the conservation of these ancient sheep and shepherd paths. Unfortunately, in these latter sub-regions, large portions of the network are fragmented, hidden, covered, impaired and partially ruined by road construction and roadside infrastructures. Alternatively,

http://www.aloki.hu ● ISSN 1589 1623 (Print) ● ISSN 1785 0037 (Online)
DOI: http://dx.doi.org/10.15666/aeer/1605_69777000
© 2018, ALÖKI Kft., Budapest, Hungary

land conversion to intensive agricultural systems is the other factor affecting the ecological integrity of the lands along the sheep tracks.

2) Despite a higher agroecological rating was attributed to those biotope categories with prevailing semi-natural traits and in strict association with transhumance, the biotopes with the highest occurrence and the largest extents were those pertaining to agricultural systems and, in particular, "Complex cultivation patterns" (B7). Surprisingly, "Meadows and pastures" (B10) as well as "Bush and garrigue" (B9) are under-represented in terms of surface and outnumbered in terms of units by "Woods and forests" (B8) and "Tree crops" (B6).

Among agricultural systems, B7 should be considered very valuable in preserving a high degree of biodiversity, strongly connected to cultivation practices and strictly dependent on farming management, this latter being clearly based on extensive agricultural systems. The agricultural traits shown by B7 are very similar to "type 2" High Nature Value Farmland (HNVF), sensu Andersen et al. (2003). This type of HNVF, indeed, are characterized by a farming landscape with a large proportion of semi-natural vegetation (wood, forests, meadows and pastures) which insists in a rich mosaic of arable and/or tree crops. Such inherently biodiversity and rich farming systems, including livestock, arable, permanent crop or mixed farming, usually rely on traditional low intensity practices (Andersen et al., 2003; Beaufoy et al., 1994; EEA, 2004; Pedroli et al., 2007; Van Doorn and Elbersen, 2012). Low grazing densities of livestock, the use of fallow inserted in a sequence of arable crops, low inputs of fertilizing nutrients per unit of cultivated area, reduced use of agrochemicals and rainfed condition in arable and permanent crop systems are the main features (Beaufoy et al., 1994; Van Doorn and Elbersen, 2012). Such farming systems are referred to as HNVF since they contribute to maintain natural habitats and viable populations of wild species of the highest conservation value, together with the diversity of the land cover types (Beaufoy et al., 1994; Bignal and McCracken, 1996, 2000; Henle et al., 2008; Plieninger and Bieling, 2013).

The conservation of the sheep track landscapes is just one *tessera* of a complex mosaic that relates to the need of preserving the agricultural landscape as a whole. A socio-geographical double bound is observed: agricultural abandonment in marginal, hilly sub-regions (and the consequent forest expansion), on the one hand; agricultural intensification on flat, alluvial and fertile areas (and the consequent competition with urban expansion), on the other hand. They shall be considered the two sides of the same coin. The sheep track landscape is affected by exactly the same risks and the same threats.

The abandoning of pastures at higher altitudes has led to an expansion of woodland areas, and the loss of open spaces, which are important not only for the landscape itself, but also for biodiversity conservation. Conversely, the areas on the plain have been affected by urban expansion and the loss of traditional crop and inter-cropping, with a notable worsening of the landscape quality (Agnoletti et al., 2011).

With respect to agricultural abandonment, some authors suggest that forest expansion should be favored given their potential for slowing down soil erosion, improving water quality, and mitigate climate change through carbon sequestration (Rudel et al., 2005). Similarly, some authors judge land abandonment an opportunity for biodiversity conservation. While American ecologists and naturalists are commonly more focused on the conservation of post-abandonment ecosystems, European landscape ecologists generally consider land abandonment, and the consequent secondary naturalization

http://www.aloki.hu ● ISSN 1589 1623 (Print) ● ISSN 1785 0037 (Online)
DOI: http://dx.doi.org/10.15666/aeer/1605_69777000
© 2018, ALÖKI Kft., Budapest, Hungary

process, mainly as a threat (Marull et al., 2015). The uncontrolled expansion of unmanaged forests leads to social and ecological negative impacts, causes damages to biodiversity (Marull et al., 2015) and increases wildfire hazard (Pausas et al., 2008).

Concerning agricultural intensification/extensification dynamics, depending on the cultivation management, farming systems may entail either a decrease or an increase in biological diversity (Marull et al., 2015). It is generally recognized, today, that farm systems may provide environmental services as well as productive goods. In this respect, ensuring both agricultural production and ecological services might trigger the well-known "sparing" vs. "sharing" opposite strategies (Marull et al., 2015):

i) The land-sparing approach is based on increasing agricultural intensification in some areas so as to devote the others to nature conservation and forest transition (Green et al., 2005; Matson and Vitousek, 2006); conversely:
ii) The land-sharing approach is based on a wildlife-friendly farming able to provide complex agroecological matrices connected with natural sites that jointly maintain high species richness at landscape level (Bengston et al., 2003; Marull et al., 2010; Perfecto and Vandermeer, 2010; Tscharntke et al., 2012).

This latter strategy (i.e. the land sharing approach) can be seen allied with the strategy of HNVF identification and protection; extensive farmland and semi-natural ecosystems are the most important indicators in selecting HNVF. Sound ecological sheep tracks can be considered the very first candidate to be identified as HVVF, thus providing very useful ecological services, including regulatory, support, cultural and aesthetic functions (Lomba et al., 2014), i.e. positive externalities and environmental benefits. Preserving at least some selected portions of the sheep tracks implies keeping farming systems that use traditional agricultural practices.

Another relevant dimension pertaining to the protection of the sheep track network is related to the cultural heritage it represents and the historical legacy that should be transmitted to future generations.

According to Oppermann et al. (2012), the characteristics of HNVF landscapes make them central to the European identity and culture. Following these characteristics, HNVF landscape are considered, at least throughout Europe, "cultural" landscape (Plieninger and Bieling, 2012). If this is true with respect to HNVF (and no doubt, it is), then, even more this applies to the sheep track landscapes.

Considering the historical and cultural values of the agricultural landscape, the Italian Ministry of Agricultural Food and Forestry Policies recently started a survey for the compilation of a National Catalogue of Historical Rural Landscapes. It aims at creating a list of landscapes having historical importance in terms of significance, integrity and vulnerability (www.reterurale.it). A valuable site ("Pasture of Northern Alta Murgia") linked to transhumance was identified in Apulia, characterized by the presence of large, open, semi-grazed pastures and small rural buildings, remains of the *tratturo* "Melfi-Castellaneta" that crossed the area. Another relevant example concerns the Molise region that applied the *tratturi* system to the UNESCO world heritage, considering them a combined work of nature and man, areas including outstanding value from the historical, aesthetic, ethnological and anthropological point of view.

One of the main problems with the conservation and valorization of the Italian rural landscapes, is the lack of perception of their importance, both among the public administrators and civil society. Anyway, their protection should not to be postponed any longer. Above all, what is needed is to promote their active but sustainable

http://www.aloki.hu ● ISSN 1589 1623 (Print) ● ISSN 1785 0037 (Online)
DOI: http://dx.doi.org/10.15666/aeer/1605_69777000
© 2018, ALÖKI Kft., Budapest, Hungary

utilization, i.e. their original function as well as alternative forms of development. This means that the key to a sustainable future for semi-natural farmland (including the sheep tracks) is their socio-economic viability and the possibility to find a stable or growing market for local products and services. Nature, history, culture are important component of the product panel.

Conclusion

Maintaining the sheep track network areas and the ecosystem services they can offer is a way to preserve, synergistically, not only relevant biotopes but also a complex and long lasting cultural system, traditionally linked to transhumance. The analysis worked out in this paper was performed at regional scale, in the frame of a planning assignment by the Apulian Land Property Department. The work achieved its target: an agroecological characterization of the sheep track landscape connected to transhumance was carried out and the selection and location on the map of those portions of the network characterized by the highest agroecological value was thus obtained.

This work should be considered a preliminary, although essential step to promote further actions, mostly in terms of policy measures, to encourage the recovery and requalification of the sheep track system in a perspective of both integrated land management and rural development.

Acknowledgements. The Apulia Regional Administration - Land Property Department, supported this research. The authors are very grateful to the Regional Administration for the coordination of the activity performed by the "Regional Committee on the Sheep Track Network". Heartfelt thanks are also addressed to all the colleagues of the same Committee.

REFERENCES

[1] Agnoletti, M., Cargnello, G., Gardin, L., Santoro, A., Bazzoffi, P., Sansone, L., Pezza, L., Belfiore, N. (2011): Traditional landscape and rural development: comparative study in three terraced areas in northern, central and southern Italy to evaluate the efficacy of GAEC standard 4.4 of cross compliance. – Italian Journal of Agronomy (6)(s1): 16.

[2] Andersen, E., Baldock, D., Bennett, H., Beaufoy, G., Bignal, E., Brouwer, F., Elbersen, B., Eiden, G., Godeschalk, F., Jones, G., McCracken, D., Nieuwenhuizen, W., van Eupen, M., Hennekens, S., Zervas, G. (2003): Developing a High Nature Value Farming Area Indicator. – Internal Report for the European Environment Agency. IEEP, London.

[3] Bakker, J. P. (1989): Nature Management by Grazing and Cutting. On the Ecological Significance of Grazing and Cutting Regimes Applied to Restore Former Species-Rich Grassland Communities in the Netherlands. – Kluwer Academic Publishers, Dordrecht.

[4] Beaufoy, G., Baldock, D., Clarke, J. (1994): The Nature of Farming - Low Intensity Farming Systems in Nine European Countries. – IEEP, London.

[5] Beaufoy, G., Jones, G., Kazakova, Y., McGurn, P., Poux, X., Stefanova, V. (2011): Permanent Pastures and Meadows: Adapting CAP Pillar 1 to Support Public Goods. – European Forum for Nature Conservation and Pastoralism (EFNCP) and the Grasslands Trust, Derwentside.

[6] Bengtsson, J., Angelstam, P., Elmqvist, T., Emanuelsson, U., Folke, C., Ihse, M., Moberg, F., Nystrom, M. (2003): Reserves, resilience and dynamic landscapes. – Ambio 32(6): 389-396.

http://www.aloki.hu ● ISSN 1589 1623 (Print) ● ISSN 1785 0037 (Online)
DOI: http://dx.doi.org/10.15666/aeer/1605_69777000
© 2018, ALÖKI Kft., Budapest, Hungary

[7] Berthoud, G., Duelli, P., Burnand, J. D. (1989): Méthode d'évaluation du potentiel écologique des mileux. – Programme national SOL, Liebefeld.
[8] Bignal, E. M., McCracken, D. I. (1996): Low-intensity farming systems in the conservation of the countryside. – Journal of Applied Ecology 33: 413-424.
[9] Bignal, E. M., McCracken, D. I. (2000): The nature conservation value of European traditional farming systems. – Environmental Reviews 8: 149-171.
[10] Brown, R. D., Lafortezza, R., Corry, R. C., Leal, D. B., Sanesi, G. (2007): Cultural Patterns as a Component of Environmental Planning and Design. – In: Hong, S. K., Nakagoshi, N., Fu, B., Morimoto, Y. (eds.) Landscape Ecological Applications in Man-influenced Areas: Linking Man and Nature Systems. Springer, New York, pp. 395-415.
[11] Butler, S. J., Vickery, J. A., Norris, K. (2007): Farmland biodiversity and the footprint of agriculture. – Science 315: 381-384.
[12] CORINE biotopes (Version 2000): Database. – https://www.eea.europa.eu/data-and-maps/data/corine-biotopes (access date: 1st June 2018).
[13] Cullotta, S., Barbera, G. (2011): Mapping traditional cultural landscapes in the Mediterranean area using a combined multi-disciplinary approach: Method and application to Mount Etna (Sicily; Italy). – Landscape and Urban Planning 100(1-2): 98-108.
[14] De Iulio, R., Biscotti, S. (2015): Il mosaico delle mappe di Agatangelo della Croce. – In: Volpe, G. (ed.) Tratturi di Puglia, risorse per il futuro. Claudio Grenzi Editore, Foggia, pp. 131-136.
[15] Delivand, M. K., Cammerino, A. R. B., Garofalo. P., Monteleone, M. (2015): Optimal locations of bioenergy facilities, biomass spatial availability, logistics costs and GHG (greenhouse gas) emissions: a case study on electricity productions in South Italy. – Journal of Cleaner Production 99: 129-139.
[16] EC European Commission (2014): Farming for Natura (2000): Guidance on how to support Natura 2000 farming systems to achieve conservation objectives, based on Member States good practice experiences. – http://ec.europa.eu/environment/nature/natura2000/management/docs/FARMING%20FOR%20NATURA%202000-final%20guidance.pdf (access date: 1st June 2018).
[17] EEA (2004): High nature value farmland. – European Environmental Agency Report1/2004.
[18] Garzón, J. (2001): Importancia de la trashumancia para la conservación de los ecosistemas en España. – Boletín de la Institución Libre de Enseñanza 40-41: 35-60.
[19] Giampietro, M. (1997): Socioeconomic constraints to farming with biodiversity. – Agriculture, Ecosystems and Environment 62: 145-167.
[20] Green, R. E., Cornell, S. J., Scharlemann, J. P. W., Balmford, A. (2005): Farming and the fate of wild nature. – Science 307: 550-551.
[21] Henle, K., Alard, D., Clitherow, J., Cobb, P., Firbank, L., Kull, T., McCracken, D., Moritz, R. F. A., Niemela, J., Rebane, M., Wascher, D., Watt, A., Young, J. (2008): Identifying and managing the conflicts between agriculture and biodiversity conservation in Europe. – Agriculture, Ecosystems and Environment 124: 60-71.
[22] ISPRA (2013): Il Sistema Carta della Natura della Regione Puglia. – Rapporto ISPRA, Rome.
[23] Kauppi, P. E., Ausubel, J. H., Fang, J., Mather, A. S., Sedjo, R. A., Waggoner, P. E. (2006): Returning forests analyzed with the forest identity. – Proceedings of the National Academy of Sciences of the United States of America 103(46): 17574-17579.
[24] I tratturi (n. d.): http://www.leviedeitratturi.com/i-tratturi. – Access date: 1st June 2018.
[25] Kremen, C., Ostfeld, R. S. (2005): A call to ecologists: measuring, analyzing, and managing ecosystem services. – Frontiers in Ecology and the Environment 3: 540-548.
[26] Liberatori, F., Penteriani, V. (2001): A long-term analysis of the declining population of the Egyptian vulture in the Italian peninsula: distribution, habitat preference, productivity and conservation implications. – Biological Conservation 101: 381-389.

http://www.aloki.hu ● ISSN 1589 1623 (Print) ● ISSN 1785 0037 (Online)
DOI: http://dx.doi.org/10.15666/aeer/1605_69777000
© 2018, ALÖKI Kft., Budapest, Hungary

[27] Lomba, A., Guerra, C. A., Alonso, J. M., Honrado, J. P., Jongman, R. H. G., McCracken, D. (2014): Mapping and monitoring high nature value farmlands: challenges in European landscape. – Journal of Environmental Management 143: 140-50.
[28] Luoto, M., Pykälä, J., Kuussaari, M. (2003): Decline of landscape-scale habitat and species diversity after the end of cattle grazing. – Journal for Nature Conservation 11: 171-178.
[29] Marull, J., Pino, J., Tello, E., Cordobilla, M. J. (2010): Social metabolism, landscape change and land-use planning in the Barcelona Metropolitan Region. – Land Use Policy 27: 497-510.
[30] Marull, J., Tello, E., Wilcox, P., Coll, F., Pons, M., Warde, P., Valldeperas, N., Ollés, A. (2014): Recovering the land-use history behind a Mediterranean edge environment: The importance of cultural landscapes in biological conservation. – Applied Geography 54: 1-17.
[31] Marull, J., Font, C., Tello, E., Fullana, N., Domene, E., Pons, M., Galàn, E. (2015): Towards an energy–landscape integrated analysis? Exploring the links between socio-metabolic disturbance and landscape ecology performance (Mallorca, Spain, 1956-2011). – Landscape Ecology 31(2): 317-336.
[32] Matson, P. A., Vitousek, P. M. (2006): Agricultural Intensification: will land spared from farming be land spread for nature? – Conservation Biolology 20(3): 709-710.
[33] Melini, M., Adducchio, D., Ciliberti, D., Di Felice, G. (2014): Landscape conservation and valorization by satellite imagery and historic maps. The case of Italian transhumance routes. – European Journal of Remote Sensing 47: 375-387.
[34] Moreira, F., Queiroz, I., Aronson, J. (2006): Restoration principles applied to cultural landscapes. – Journal for Nature Conservation 14(3-4): 217-224.
[35] Habitat Directive 92/43/CEE: http://ec.europa.eu/environment/nature/legislation/habitatsdirective/index_en.htm. – Access date: 1st June 2018.
[36] Olea, P. P., Mateo-Tomás, P. (2009): The role of traditional farming practices in ecosystem conservation: The case of transhumance and vultures. – Biological Conservation 142: 1844-1853.
[37] Opperman, R., Beaufoy, G., Jones, G. (2012): High Nature Value Farming in Europe. 35 European Countries – Experiences and Perspectives. – Verlag Regionalkultur, Ubstadt-Weiher, Germany.
[38] Paone, N. (2006): Molise in Europa: tratturi, cañadas, drailles, drumurile oierilos. – Cosmo Iannone, Isernia, Italy.
[39] Pausas, J. G., Llovet, J., Rodrigo, A., Vallejo, R. (2008): Are wildfires a disaster in the Mediterranean basin? A review. – International Journal of Wildland Fires 17(6): 713-723.
[40] Pedroli, B., Van Doorn, A., De Blust, G., Paracchini, M. L., Wascher, D., Bunce, F. (2007): Europe's Living Landscapes. – Essays on Exploring Our Identity in the Countryside. Landscape Europe/KNNV.
[41] Perfecto, I., Vandermeer, J. (2010): The agroecological matrix as alternative to the land-sparing/agriculture intensification model. – Proceeding of National Academy of Science USA 107(13): 5786-5791.
[42] Petanidou, T., Kizos, T., Soulakellis, N. (2008): Socioeconomic dimensions of changes in the agricultural landscape of the Mediterranean basin: a case study of the abandonment of cultivation terraces on Nisyros Island, Greece. – Environmental Management 41(2): 250-266.
[43] Plieninger, T., Bieling, C. (2012): Resilience and the Cultural Landscape: Understanding and Managing Change in Human-Shaped Environments. – Cambridge University Press, Cambridge.
[44] Plieninger, T., Bieling, C. (2013): Resilience-based perspectives to guiding high nature value Farmland through socioeconomic change. – Ecology and Society 18(4): 20.

http://www.aloki.hu ● ISSN 1589 1623 (Print) ● ISSN 1785 0037 (Online)
DOI: http://dx.doi.org/10.15666/aeer/1605_69777000
© 2018, ALÖKI Kft., Budapest, Hungary

[45] Poschlod, P., Bonn, S. (1998): Changing dispersal processes in the central European landscape since the last ice age: an explanation for the actual decrease of plant species richness in different habitats? – Acta Botanica Neerlandica 47: 27-44.
[46] PPTR (2013): Piano Paesaggistico Territoriale Regione Puglia. – http://www.paesaggio.regione.puglia.it (access date: 1st June 2018).
[47] Pykälä, J. (2000): Mitigating human effects on European biodiversity through traditional animal husbandry. – Conservation Biology 14: 705-712.
[48] Rudel, T. K., Coomes, O., Moran, E., Achard, F., Angelsen, A., Xu, J., Lambin, E. (2005): Forest transitions: towards a global understanding of land use change. – Global Environmental Change 15: 23-31.
[49] Ruiz, M., Ruiz, J. P. (1986): Ecological history of transhumance in Spain. – Biological Conservation 37: 73-86.
[50] Russo, S. (2002): Tra Abruzzo e Puglia. La transumanza dopo la Dogana. – Franco Angeli, Milano.
[51] Saaty, T. L. (2008): Decision making with the analytic hierarchy process. – International Journal of Services Science 1: 83-98.
[52] Spitaleri, R. M., Napoleone, I. (1991): A numerical approach for the evaluation of biotopes for conservational purposes. – Coenoses 6(3): 169-171.
[53] Sutherland, W. J. (2002): Conservation biology. - Openness in management. – Nature 418: 834-835.
[54] Tscharntke, T., Clough, Y., Wanger, T. C., Jackson, L., Motzke, I., Perfecto, I., Vandermeer, J., Whitbread, A. (2012): Global food security, biodiversity conservation and the future of agricultural intensification. – Biological Conservation 151: 53-59.
[55] Van Doorn, A. M., Elbersen, B. S. (2012): Implementation of High Nature Value Farmland in Agri-environmental Policies: What Can Be Learned from Other EU Member States? – Alterra Report. Alterra, Wageningen.
[56] Vitousek, P. M., Mooney, H. A., Lubchenco, J., Melillo, J. M. (1997): Human domination of Earth's ecosystems. – Science 277: 494-499.
[57] Ying, X., Guang-Ming, Z., Gui-Qiu, C., Lin, T., Ke-Lin, W., You, H. D. (2007): Combining AHP with GIS in synthetic evaluation of eco-environment quality. A case study of Hunan Province, China. – Ecological Modeling 209: 97-109.

APPENDIX

Table A1. *Clustered biotope categories and list of their corresponding biotopes identified according to the CORINE Biotope codes*

Biotope codes	Biotope categories	Pertaining biotopes (identified with the CORINE Biotope codes)
B0	Artificial areas	86.1 – 86.3 – 86.41
B1	Artificial vegetated areas	83.31 – 83.322 – 85.1
B2	Dunal vegetation	15.1 – 15.83 – 16.1 – 16.21 – 16.28 – 16.29 – 18.22
B3	Bare rock	62.11
B4	Riparian vegetation areas	22.1 – 24.225 – 24.53 – 44.14 – 44.61 – 53.1 - 89
B5	Annual crops	82.1
B6	Tree crops	83.11 – 83.15 – 83.16 – 83.21
B7	Complex cultivation patterns	83.2
B8	Woods and forests	32.11 – 41.18 – 41.41 – 41.782 – 41.737B 41.7511 – 41.7512 – 41.782 – 41.86 -41.9 – 42.84 – 45.1 – 45.31 – 45.324 – 45.42 – 83.325
B9	Bush and garrigue	31.81 – 31.863 – 32.211 – 32.219 – 32.4 – 32.6
B10	Meadows and pastures	31.8A – 34.323 – 34.326 – 34.5 – 34.75 – 34.81 – 84.6

http://www.aloki.hu ● ISSN 1589 1623 (Print) ● ISSN 1785 0037 (Online)
DOI: http://dx.doi.org/10.15666/aeer/1605_69777000
© 2018, ALÖKI Kft., Budapest, Hungary

Table A2. *Complete list of biotopes featuring in the Apulian Biotope Map, properly clustered according to the aggregation criteria applied in the work. The Corine Biotope cedes are also displayed*

Biotope categories	Corine biotope codes	Biotope names
B0 Artificial areas	86.1	Towns
	86.3	Active industrial sites
	86.41	Quarries
B1 Artificial vegetated areas	85.1	Large parks
	83.31	Conifer plantations
	83.322	Eucalyptus plantations
B2 Dunal vegetation	15.1	Annual salt pioneer swards
	16.1	Sand beaches
	16.21	Shifting dunes
	15.83	Clay areas with accelerated erosion
	16.28	Dune sclerophyllous scrubs
	16.29	Wooded dunes
	18.22	Mediterraneo-Pontic sea-cliff communities
B3 Bare rock	62.11	Western EU-Mediterranean and oro-Iberian calcareous cliffs
B4 Riparian vegetation areas	22.1	Permanent ponds and lakes
	24.53	Mediterranean river mud communities
	44.14	Mediterranean tall willow galleries
	44.61	Mediterranean riparian poplar forests
	24.225	Mediterranean river gravel communities
	53.1	Reed beds
	89	Industrial lagoons and reservoirs, canals
B5 Annual crops	82.1	Unbroken intensive cropland
B6 Tree crops	83.11	Olive groves
	83.15	Fruit orchards
	83.16	Citrus orchards
	83.21	Vineyards
B7 Complex cultivation patterns	82.3	Complex cultivation patterns
B8 Woods and forests	41.9	Chestnut woods
	41.18	Southern Italian beech forests
	41.41	Medio-European ravine forests
	45.1	Olive-carob forests
	45.42	Italian kermes oak woodland
	45.31A	Southern Italian holm-oak forests
	41.737B	Eastern sub-Mediterranean white oak woods
	41.86	Thermophilous ash woods
	42.84	Aleppo pine forests
	41.782	Apulian Trojan oak woods
	45.324	Italian supra-Mediterranean holm-oak forests
	83.325	Other broad-leaved tree plantations
	41.7511	Southern Italic Quercus cerris woods
	41.7512	Southern Italic Quercus frainetto woods
	32.11	Evergreen oak matorral

http://www.aloki.hu ● ISSN 1589 1623 (Print) ● ISSN 1785 0037 (Online)
DOI: http://dx.doi.org/10.15666/aeer/1605_69777000
© 2018, ALÖKI Kft., Budapest, Hungary

B9 Bush and garrigue	32.4	Western meso-Mediterranean calcicolous garrigues
	32.6	Supra-Mediterranean garrigues
	31.81	Medio-European rich-soil thickets
	32.211	Oleo-lentisc brush
	32.219	Thermo-Mediterranean kermes oak brushes
	31.863	Supra-Mediterranean bracken fields
B10 Meadows and pastures	84.6	Sardinian woody pasture (Dehesa)
	34.323	Middle European Brachypodium semi-dry grasslands
	34.326	Sub-Mediterranean Mesobromion
	34.75	Eastern sub-Mediterranean dry grasslands
	34.81	Mediterranean subnitrophilous grass communities
	34.5	Mediterranean xeric grasslands
	31.8A	Tyrrhenian sub-Mediterranean deciduous thickets

http://www.aloki.hu ● ISSN 1589 1623 (Print) ● ISSN 1785 0037 (Online)
DOI: http://dx.doi.org/10.15666/aeer/1605_69777000
© 2018, ALÖKI Kft., Budapest, Hungary

OPTIMIZATION AND COMPARISON OF THE EFFECTS OF VERMICOMPOST AND CONVENTIONAL FERTILIZATION ON SPINACH (*SPINACIA OLERACEA* L.) GROWTH

ALTUNTAS, O.* – DURAK, A. – KUCUK, R.

Department of Horticulture, Agriculture Faculty, Turgut Ozal University, Malatya, Turkey

**Corresponding author*
e-mail: ozlem.altuntas@ozal.edu.tr, ozaltuntas01@gmail.com; phone: +90-422-846-1255; fax: +90-422-846-1225

(Received 10th Jul 2018; accepted 20th Sep 2018)

Abstract. Vermicompost helps soil to retain water, regulate soil temperature and structure, and helps solve the soil's nutrient problem. The aim of our study was to compare chemical fertilization with different rates of vermicompost treatments in terms of growth properties, yield, and nutrient element content of spinach (*Spinacia oleracea* L.). We also determined the appropriate rate of vermicompost application for spinach. The experiment was repeated in two successive seasons with five treatments in the experiment: (1) control, (2) 1 ton vermicompost/ha, (3) 2 tons vermicompost/ha, (4) 3 tons vermicompost/ha, and (5) chemical fertilization. To assess the effect of the treatments in spinach, soil analysis (soil texture, pH, EC (Electrical Conductivity), percent of calcium carbonate, organic matter, and macro and micro elements), plant height and yield of spinach plants, and plant nutrient element analysis of spinach leaves were performed. Evaluation of the results indicated that vermicompost had positive impacts on the soil and the plant; the best treatment rate was 3 t/ha. This vermicompost application rate resulted in a 149% yield increase compared with the chemical fertilizer treatment.
Keywords: *earthworm, vermicompost, Spinacia oleracea, organic fertilizers, yield, nutrient elements content*

Introduction

The main objective of agricultural production is to provide food enough to meet requirements of population in good quality that will not harm health of human beings. For this purpose, it requires the development and application of new inputs and technologies. New agricultural technologies, including agrochemicals (fertilizers, pesticides, etc.) and intercropping, are being randomly used to improve the success of modern agriculture. Some of these technologies are causing our soils to become ill, environmental pollution, increased pest resistance in weeds, insects, and pathogens, and toxic residue in our food (Narwal, 2010). Fertilizing and irrigation are the main inputs in agricultural production. Prior to any kind of agricultural production, artificial fertilizer is applied to eliminate nutritional deficiencies in the soil. For an effective fertilizing process, improving the availability of the nutrients supplied by fertilizers is equally significant as the fertilizer treatment. Nowadays, human and public health and environmental protection is becoming more important and in this case, using of organic manure is getting higher. Organic matter has a fairly high importance on soil productivity and soil serves several functions. For this reason, farmers preserve resources to minimize the artificial inputs from outside the farm, and manage pests (weeds, insects, nematodes, and pathogens) via internal regulating mechanisms based on ecological principles and processes (Stinner and House, 1987). Organic agriculture is often proposed as a solution for producing food with reduced environmental impact

http://www.aloki.hu ● ISSN 1589 1623 (Print) ● ISSN 1785 0037 (Online)
DOI: http://dx.doi.org/10.15666/aeer/1605_70017016
© 2018, ALÖKI Kft., Budapest, Hungary

(Tilman, 1998; Scialabba and Hattam, 2002). Even though it constitutes less than 1% of global agricultural land and less than 5% of retail sales in most high-income countries (Willer and Lernoud, 2015), it represents one of the fastest growing food sectors (Seufert et al., 2017).

Vermicompost, the excreta of the earthworm, can improve the health and nutrients of the soil. Vermicompost helps manage waste as a valuable compost and biocontrol agent. In soil quality improvement, using vermicompost waste is better compared to traditional compost and landfill (Joshi et al., 2015). Vermicompost helps with soil water retention, regulation of soil temperature and structure, enhances the soil with nutrient elements, and increases the biomass and community structure of the microbial population (Vivas et al., 2009).

Vermicomposting consists of a simple biotechnological composting process. Here, certain earthworms were used to improve the waste conversion process to yield a better product. This mesophilic process used microorganisms and earthworms that are active between 10 and 32 °C, which are not ambient values; however, these are the values in moist organic material. This process is faster than composting. The reason for this is that the material passes through the earthworm's gut, then a transformation occurs that results with earthworm's castings (worm manure) that are rich in microbial activity and plant growth regulators and fortified with pest repellence attributes. Briefly, earthworms can transform garbage into "gold" (Gandhi et al., 1997; Julka, 2001). Vermicompost has 1.5–2.2% nitrogen (N), 1.8–2.2% phosphorus (P), and 1.0–1.5% potassium (K) on average. The organic carbon content is between 9.15 and 17.98%, and has micronutrients such as sodium (Na), calcium (Ca), zinc (Zn), sulphur (S), magnesium (Mg), and iron (Fe) (Adhikary, 2012).

Spinach (*Spinacia oleracea* L.) is a significant source of organominerals, such as vitamin B complex, ascorbic acid, vitamin A, and carotin (Bhattacharjee et al., 1998). Spinach is used in a variety of meals, such salad and with cooked meat and vegetable dishes (Molerock and Correll, 2008). Spinach best grows in cool climates, in an optimum temperature range of 7 and 24 °C. The minimum temperature for spinach seed germination is 2 °C (Molerock and Correll, 2008).

Crop yield quality and size are mostly affected by fertilization (Jablonska-Ceglarek and Rosa, 2001), so fertilizers with different mineral constituents create differences in the yield and nutritional quality of the crop. Nitrogen is the nutrient that most strongly affects nutritional quality differences in crops. Simultaneously treatment with organic and inorganic fertilizer has been found to be the most effective at improving crop production (Chaoui et al., 2003). Organic foods are often seen as healthier and more nutritious and better in quality compared with conventionally grown foods (Kansal et al., 1981).

Due to its short vegetation period and high market demand during winter, the amount of spinach production increases each year. Spinach is a vegetable whose leaves are eaten, thus the treatment of fertilizers and pesticides used during its growth requires special attention. This study was performed to determine the impacts of different rates of vermicompost application on soil properties, yield, and some growth properties and nutrient element contents in the leaves of spinach. Also, vermicompost treatments with and without artificial fertilizers were compared in terms of the properties mentioned above. We believe that this is a healthy and environment-friendly production technique for both the soil and crop, and especially in leafy vegetables such as spinach.

http://www.aloki.hu ● ISSN 1589 1623 (Print) ● ISSN 1785 0037 (Online)
DOI: http://dx.doi.org/10.15666/aeer/1605_70017016
© 2018, ALÖKI Kft., Budapest, Hungary

Materials and methods

Experiment location

The experiment was performed at the research station belonging to Turgut Ozal University, Agriculture Faculty, Department of Horticulture, Battalgazi, Malatya, Turkey (38°25'22" N and 38°21'30" E) in two consecutive years: spring (from March to May) and fall (from October to April) 2015. The study area is located 790 m above the sea level. The soil of the study area has an A-Bw–C1-C2 horizon with a soil temperature typical of mesic soil, an acidic moisture regime, and is classified as Aridisol Ordo, Orthid sub Ordo, and Camborthid big group. The soils in the experimental area were clean with no pesticide residues as no planting had occurred in the experimental area for a long time. For the second growing period in the experiment, a location that was not cultivated in the first year was used. Soil analyses were performed both prior to seed sowing (no treatment) and also after harvesting for V300 (3 tons vermicompost/ha) treatment in the first (spring) season.

Plant material

As plant material, the Sprinter F_1 spinach cultivar with high market quality, flat leaf surface, wide oval shape, bright green color, bump foliar, medium stem with high yield potential, and fast growth was used in the experiment (*Fig. 1*).

Figure 1. *Sprinter F_1 is spinach cultivar that used in the experiment*

Experimental layout

In spring 2015, two months elapsed from sowing the spinach seeds to the harvest time; the time elapsed in fall was around six months. In this study, the experiment was repeated in two successive seasons: the first experiment covered the spring season from March 19 to May 14, 2015, for a total of 56 days, and the second experiment covered the autumn-winter-early spring seasons from October 8, 2015 to April 17, 2016, for a total of 192 days. The Malatya climate data during the spinach growing season in the field are provided in *Table 1*.

http://www.aloki.hu ● ISSN 1589 1623 (Print) ● ISSN 1785 0037 (Online)
DOI: http://dx.doi.org/10.15666/aeer/1605_70017016
© 2018, ALÖKI Kft., Budapest, Hungary

Table 1. *Average climate data in Malatya, Turkey during the 2015 and 2016 growing season*

	October	November	December	January	February	March	April	May	June
Average temperature (°C)	15.4	7.8	2.0	−0.4	1.4	6.7	13.0	18.1	23.2
Average highest temperature (°C)	21.3	12.5	5.4	3.1	5.3	11.5	18.3	23.9	29.5
Average lowest temperature (°C)	9.8	3.9	−0.9	−3.4	−2.2	2.1	7.5	11.9	16.1
Average sun bathing time (hour)	7.3	5.2	3.1	3.2	4.2	5.4	7.2	9.2	11.4
Average rainy days	6.7	8.6	10.8	10.9	10.7	11.0	10.7	10.0	4.7
Monthly total rainfall amount (mm)	35.9	42.0	39.9	42.1	40.7	48.9	54.7	44.5	17.1

Experimental design

The experiment had a random block design with five treatments and three replications. For each replication, treatment size was 5 × 5 m = 25 m^2 and the total area used in the experiment excluding edge effects was 375 m^2. Since the experimental area is small, spinach seeds were planted by spreading, and the space between the rows and over rows was 30 cm and 2–3 cm, respectively, by rarefying the plants after emergence. Seeding density was 375 g seed in each area (10 kg per ha).

Fertilizer treatments in the experiment were as follows: (1) control without fertilizer (WF), (2) 1 ton (1000 kg) vermicompost/ha (V100), (3) 2 tons (2000 kg) vermicompost/ha (V200), (4) 3 tons (3000 kg) vermicompost/ha (V300), and (5) chemical fertilization (CF). The CF treatment included a mixture of pure N 1 kg/ha, 1 kg/ha phosphorus (P_2O_5), and 1.2 kg/ha potassium (K_2O), by calculating chemical fertilizers (Şalk et al., 2008). Vermicompost was produced in our faculty and is not commercial. After the production, pre-experiments were carried out to determine the dose in pepper, tomatoes, lettuce and spinach growing. In the results of spinach; we were not found significant difference between 3 tons of vermicompost treatment per hectare and 4 tons of vermicompost treatment per hectare in terms of plant growth and yield. For this reason, we preferred 3 tons of vermicompost/ha dose at the highest level in vermicompost treatments in this study.

In the spring growing period (Experiment 1), fertilizer treatments were applied into the soil two days prior to sowing as base fertilizer. In the fall growing period (Experiment 2), fertilization was performed in two parts: the first treatment was two days before sowing and the second treatment occurred during the first week of March after the cold winter days. Vermicompost was applied in solid form at the same time as chemical fertilization. In spring, all treatments were applied before sowing once as base fertilizer and in the fall season, it was split into parts: half prior to planting and the rest in the first week of March.

http://www.aloki.hu ● ISSN 1589 1623 (Print) ● ISSN 1785 0037 (Online)
DOI: http://dx.doi.org/10.15666/aeer/1605_70017016
© 2018, ALÖKI Kft., Budapest, Hungary

Vermicompost preparation

In the experiment, solid vermicompost produced at Turgut Ozal University was used. Vermicompost was produced by *Eisenia foetida* worms called Red California worms. We also used farm manure. We placed the worms inside the farm manure. Vermicomposting is a mesophilic process where the farm manure passes through the earthworm gut, and changes the physical and chemical structures of the farm manure occurs through this process, which results in earthworm castings (worm manure). The worm gut activity is similar to a small composting tube that mixes conditions and inoculates residues (Abbot and Parker, 1981). A synergistic relationship exists between moisture, pH, and microbial populations in the gut, creating an excellent byproduct appears (Becker, 1991). Every day, worms swallow large soil amounts that have organic substances (germs, plants, and animal debris). They then grind these in their gizzard and digest them in intestine with the help of enzymes (Scheu, 1987). Then, solid forms of vermicompost were applied to the spinach-growing soil. The properties of vermicompost used in the experiment are outlined in *Table 2*.

Table 2. *Some selected physical and chemical properties of the vermicompost used in the experiment (Durak et al., 2017)*

Property	Value
pH	8.89
$CaCO_3$	11.30%
Organic matter	55%
EC	0.009 mmhos /cm
Total nitrogen	2.55%
P (combustion)	9376.46 ppm
P (Olsen method-plant available phosphorous)	2193 ppm
K (Dry combustion method)	11263.10 ppm
K (Soluble in ammonium acetate)	4635 ppm
Ca (Combustion method)	24366.60 ppm
Ca (Soluble in ammonium acetate)	2072.25 ppm
Mg (Dry combustion)	4894.80 ppm
Fe (Dry combustion)	3797.45 ppm
Mn (Dry combustion)	275.08 ppm
Zn (Dry combustion)	94.95 ppm

Soil analyses

Soil analyses were performed both prior to planting and after harvesting. Soil texture analyses was performed according to the Bouyoucos hydrometer method (Gee and Bauder, 1986). pH and electrical conductivity (EC) were measured in soil water solution (1:2.5) using a pH meter with glass electrode and EC meter, respectively (Richards, 1954). Calcium carbonate ($CaCO_3$) (%) was measured using a Scheibler Calcimeter (Allison and Moodie, 1965). Soil organic matter was measured according to the modified Walkley-Black method with the soil available in terms of phosphorous (mg kg^{-1}) by measuring P in the extracts after $NaHCO_3$ extraction using a spectrometer (Olsen and Dean, 1965). Extractable potassium (mg 100 g^{-1}) was determined in a flame

http://www.aloki.hu ● ISSN 1589 1623 (Print) ● ISSN 1785 0037 (Online)
DOI: http://dx.doi.org/10.15666/aeer/1605_70017016
© 2018, ALÖKI Kft., Budapest, Hungary

photometer in the extracts obtained after soils were shaken and centrifuged with 1 N (Normality) ammonium acetate three times (Knudsen et al., 1982). Total and extractable Fe, Zn, Cu, and Mn (mg kg^{-1}) in the extracts were determined by shaking soil HNO_3 and HCI mixtures (Baker and Amacher, 1982) and diethylenetriaminepentaacetic acid (DTPA) solution using an Atomic Adsorption Spectrometer and filtered using Whatman 42 filter paper (Lindsay and Norvell, 1978).

Plant analyses and measurements

Plant heights of 10 randomly selected plants from each replicate were measured and averaged. The roots of the spinach were separated from the aboveground biomass when determining fresh matter yield. For yield measurements, plants at harvesting time were harvested with their roots and weighed after roots were washed and separated from the aboveground biomass. The final yields were obtained as kg m^{-2}. For the analyses of the nutrients in plant leaves, 10 mature leaves were randomly selected from each replication and were first washed with tap water, later with pure water, and left for air drying. Dried leaves were grinded in a mill and prepared for analyses (Kacar, 1995; Kacar and Inal, 2008).

For nitrogen analyses, a modified Kjeldahl method was used (Kacar, 1995; Kacar and Inal, 2008). Phosphorous, in dried and grinded plant samples, was measured in the extracts prepared according to dry combustion. P in the extracts was determined with the Vanado Molibdo Phosphoric Yellow Color method using a spectrophotometer. For measurement of K content, a flame photometer was used to measure K in the extracts obtained by extracting the plants burned in ash furnace using 3 N HCI as previously described (Plank, 1992). Fe, Mn, Mg, and Zn contents in the plant were determined using an Atomic Adsorption Spectrometer after the plants were burnt according to the dry combustion method (Kacar, 1995; Kacar and Inal, 2008; Karaman et al., 2012).

Data analyses

Experiments were performed over two successive seasons according to a randomized block design with three replications. The data obtained each season were subjected to analysis of variance (ANOVA) using the SPSS statistical program (SPSS version 20). The data were subjected to factorial analysis of variance, and means were separated by a Duncan's Post Hoc Test with a 5% level of significance ($p < 0.05$).

There were no significant interactions and differences between two growing season; therefore, the data belongs to Experiment 1 and Experiment 2 were pooled. Accordingly, the results have not presented separately.

Results

The results of both soil and also plant analyses in two successive growing seasons (spring and fall growing period) were very close to each other. For this reason, the results presented in the study were obtained by averaging the values of both.

Soil analyses results

The results of soil analyses performed both prior to sowing (no treatment) and after harvesting in V300 treatment area (3 tons/ha) are presented in *Table 3*.

http://www.aloki.hu ● ISSN 1589 1623 (Print) ● ISSN 1785 0037 (Online)
DOI: http://dx.doi.org/10.15666/aeer/1605_70017016
© 2018, ALÖKI Kft., Budapest, Hungary

Table 3. *Some physical and chemical properties of experimental area soils prior to planting (no treatment) and after harvesting (in V300 treatment) in the spring season*

Season	Texture	pH	Salt (mmhos/cm)	CaCO3 (%)	Soil organic matter (%)	P (ppm)	K (ppm)	Ca (ppm)	Mg (ppm)	Fe (ppm)	Mn (ppm)	Zn (ppm)	Cu (ppm)
BS	Clay loam	7.49 ±0.21	0.005 ±0.001	39.9 ±0.2	1.92 ±0.12	9.00 ±0.91	526.15 ±12.12	4038.46 ±29.31	689.18 ±24.22	0.59 ±0.09	6.42 ±0.71	0.58 ±0.11	2.55 ±0.45
AH	Clay loam	7.45 ±0.23	0.006 ±0.001	39.9 ±0.3	1.97 ±0.13	7.58 ±0.77	497.73 ±10.09	4200.00 ±37.14	765.53 ±34.53	0.63 ±0.09	21.9 ±1.14	0.68 ±0.09	2.85 ±0.24

BS: Before sowing (no treatment); AH: After harvesting

Differences in the results of the analyses performed in soil samples obtained before planting and after harvesting were observed and pH decreased within the short growing period. Similarly, a decline was observed in salt content. Due to plant uptake, potassium and phosphorous contents of the soils decreased whereas organic matter levels increased (*Table 3*).

Plant height and yield production of spinach

We observed that spinach height and yield were better in the vermicompost treatments compared with both the control and chemical fertilizer treatments (*Figs. 2* and *3*). Total spinach yield was statistically different at a $p < 0.01$ significance level in V200 and V300 vermicompost treatments compared with the control (*Fig. 3*). According to the evaluation of plant heights, V300 treatment was found statistically different at the $p < 0.05$ significance level (*Fig. 2*). V300 treatment had higher values recorded than other treatments.

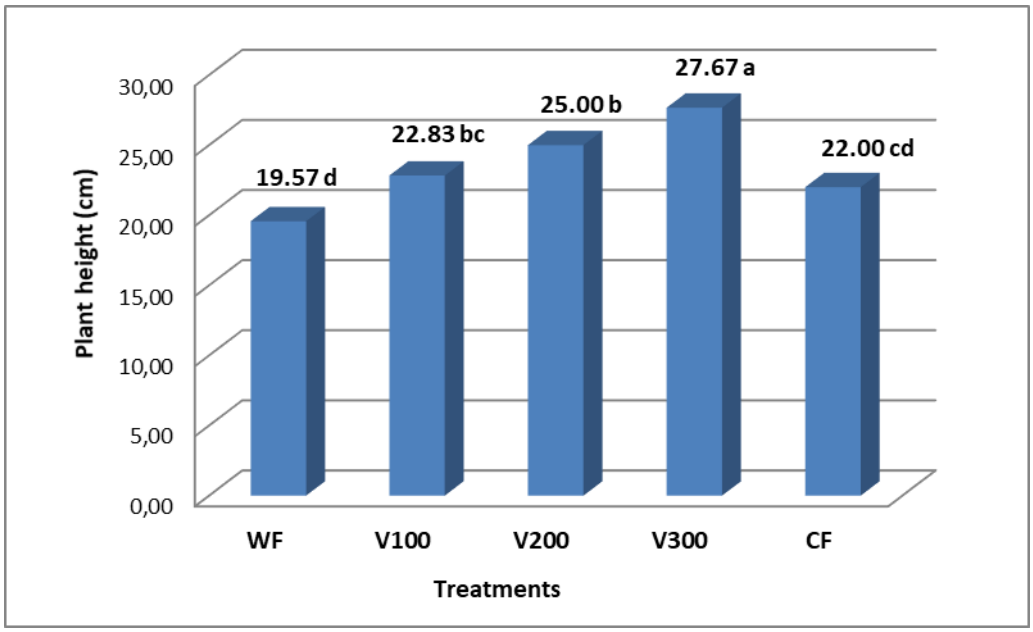

Figure 2. *Average plant heights of the control treated with chemical fertilizer and vermicompost at different application rates. The means followed by different letters are significantly different ($p < 0.05$). WF: control without fertilizer, V100: 1 ton vermicompost/ha, V200: 2 tons vermicompost/ha, V300: 3 tons vermicompost/ha, and CF: chemical fertilizer*

http://www.aloki.hu ● ISSN 1589 1623 (Print) ● ISSN 1785 0037 (Online)
DOI: http://dx.doi.org/10.15666/aeer/1605_70017016
© 2018, ALÖKI Kft., Budapest, Hungary

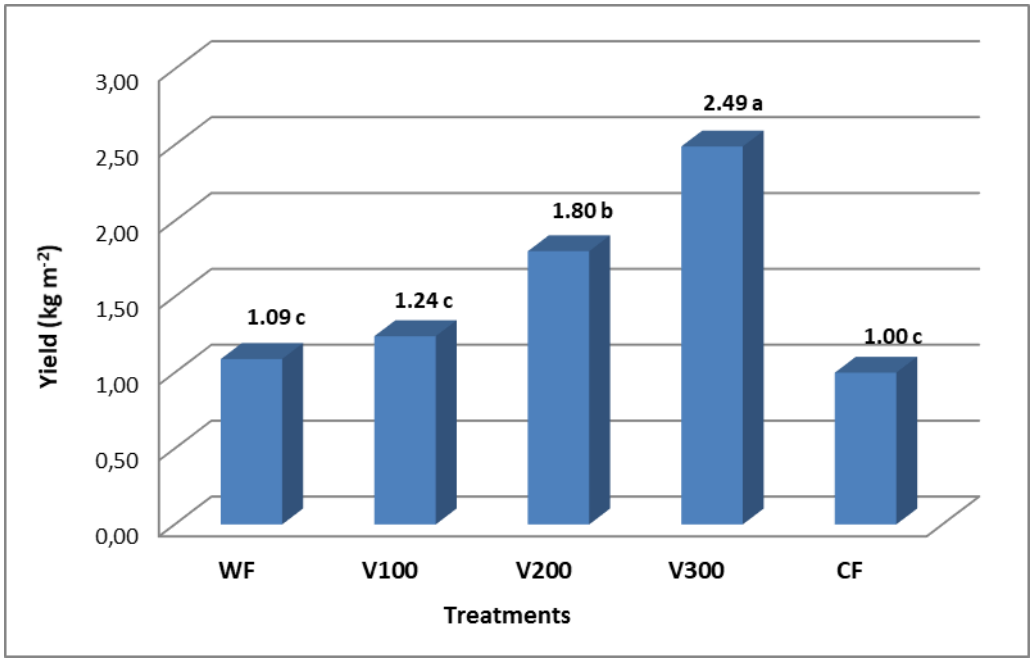

Figure 3. *Crop yields of vermicompost and chemical fertilizer at different rates and control areas. The means followed by different letters are significantly different ($p < 0.01$). WF: control without fertilizer, V100: 1 ton vermicompost/ha, V200: 2 tons vermicompost/ha, V300: 3 tons vermicompost/ha, and CF: chemical fertilizer*

The highest yield was obtained with the V300 treatment followed by the V200 treatment. The yields obtained with V100, CF, and WF treatments were closer to each other, and therefore, they were grouped together (*Fig. 3*).

Nutrient contents of plant leaves

As seen in *Table 4,* all nutrients except Fe were within the adequate limits for spinach. The main reasons for the high Fe content were that the experimental area had not been used for agriculture for a long time, and the higher Fe uptakes from vermicompost. In terms of N content, no difference was observed among the treatments. The lowest nitrogen content was recorded in the controls with no fertilizer treatment. In statistical evaluation, the V100 treatment was grouped with the treatment with no fertilizer. The highest nitrogen content was determined in the chemical fertilizer treatment areas, followed by the V300 then V200 treatments.

P content ranged between 0.23 and 0.36%. The lowest P content was recorded in the treatments with no fertilizer, whereas the values in other treatments were found close to each other. There were no statistically significant differences among treatments.

The K content of the leaves ranged between 2.12 and 6.03%. These differences were found to be statistically significant. The lowest K content was found in the treatments with no fertilizer, whereas the highest values were determined in the treatments where only chemical fertilizers were applied. V100 treatment was grouped with the WF treatment. V200 and V300 treatments were also grouped together.

Ca content of different fertilizer treatments were not found to be statistically significant and they ranged between 0.68 and 0.81% in the study.

http://www.aloki.hu ● ISSN 1589 1623 (Print) ● ISSN 1785 0037 (Online)
DOI: http://dx.doi.org/10.15666/aeer/1605_70017016
© 2018, ALÖKI Kft., Budapest, Hungary

Table 4. *Average nutrient contents of plant leaves treated with Vermicompost, chemical fertilizer at different doses and the controls*

Treatments	N (%)	P (%)	K (%)	Ca (%)	Mg (%)	Fe (ppm)	Mn (ppm)	Zn (ppm)	Cu (ppm)
WF	2.76 c	0.23	2.12 b	0.68	0.49 b	201.3 c	42.5	23.9	5.6
V100	3.28 c	0.32	3.21 b	0.80	0.57 ab	434.9 b	48.9	40.2	5.8
V200	4.01 b	0.36	4.77 ab	0.78	0.75 a	561.5 a	64.5	45.6	6.9
V300	4.86 ab	0.36	4.97 ab	0.81	0.79 a	534.3 a	68.2	53.8	7.3
CF	4.93 a	0.32	6.03 a	0.76	0.65 a	496.4 a	58.7	44.4	7.5
Adequate range for spinach	4.0–6.0	0.3–0.6	5.0–8.0	0.7–1.2	0.6–1.0	60–200	30–250	25–100	5–25

The means in the columns followed by different letters are significantly different ($p < 0.05$). WF: control without fertilizer, V100: 1 ton vermicompost/ha, V200: 2 tons vermicompost/ha, V300: 3 tons vermicompost/ha, and CF: chemical fertilizer

According to nutrient analyses results of the leaves, the Mg content of the leaves differed among fertilizer treatments and these differences were statistically significant. The highest Mg content (0.79%) was found in V300 treatment, followed by V200 and CF (0.75–0.65%), and these three treatments were grouped together. The lowest Mg content (0.49%) was determined in the WF treatment, whereas the V100 treatment with 0.57% was the intermediate group.

The evaluation of the results of the micronutrients in spinach leaves showed that the V300 and V200 treatments provided better results than other treatments. Among the micronutrients, the Fe content impacted the micronutrients significantly ($p < 0.05$) in the treatments. Fe content was the highest in the V200, V300, and CF treatments followed by the V100 treatment, whereas the lowest values were recorded in the WF treatment. In the spinach leaves, the Mn levels ranged between 42.5 and 68.2 ppm, Zn content from 23.9 to 53.8 ppm, and Cu content from 5.6 to 7.5 ppm, depending on different treatments. Differences in the contents of the Mn, Zn, and Cu were not found to be statistically significant ($p < 0.05$).

Discussion

Vermicompost treatment enhanced the quality parameters of the soil in this study. Castings slow-released nutrients that were ready for the plants. Castings include plant nutrients, which dissolve slowly instead of immediate nutrient leaching, as they are encased in a mucus membrane secreted by the worms. The product has excellent soil structure, porosity, aeration, and water retention capabilities, which may insulate plant roots against extreme temperature values, decrease erosion, and control weeds (Suhane, 2007). According to the results of the soil analysis in our study, the pH was reduced in the soil and the organic matter was increased by vermicompost application. Spinach plants had uptake potassium and phosphorus more with vermicompost treatments, so the amount of phosphorus and potassium in the soil was decreased.

Red worm castings have high humus content, which causes soil particles to be converted into clusters to form a channel for air by improving the capacity to retain water. When there are worms, the compacted soil is regenerated and the water

http://www.aloki.hu ● ISSN 1589 1623 (Print) ● ISSN 1785 0037 (Online)
DOI: http://dx.doi.org/10.15666/aeer/1605_70017016
© 2018, ALÖKI Kft., Budapest, Hungary

penetration is enhanced at a rate of more than 50% (Ghabbour, 1973; Capowiez et al., 2009). In this study, vermicompost has provided nutrients to be better uptake by the spinach plant by increasing the proportion of humus in the soil. The humic acid in humus forms binding sites for plant nutrients like calcium, iron, potassium, sulfur, and phosphorus. Humic acid also enhances the plant growth although at a slower rate (Canellas et al., 2002), and is essential for plants from three aspects: (1) enabling the plant to extract nutrients from soil, (2) helping the plant to dissolve minerals that were not dissolved for delivering organic matter to plants for use, and (3) stimulating root growth. Even the chemical fertilizers are more effective when humus is present in the soil (Li and Li, 2010). Bacteria, enzymes, and remnants of plant materials not digested by worms exist in worm castings, which are actually biologically active mounds. The microbial activities of useful microorganisms in the castings are considerable, with rates 1–20 times greater than in normal soil (Edwards, 1995). Nitrogen-fixing and phosphate solubilizing bacteria, known as the actinomycetes and mycorrhizal fungi, are among useful soil microorganisms stimulated by earth worms (Scheu, 1987). Castings also slow-release nutrients ready for plants and include plant nutrients encased in mucus membranes (Edwards, 1995).

In this study, macro and micro nutrient contents of spinach leaves were found to be higher in vermicompost treatments than WF and CF treatments. The micro and macro nutrient contents of spinach in the areas treated with vermicompost were always higher compared with those treated with mineral components, which can be explained by the release and availability of the micronutrients after mineralization of organic materials. Additionally, microorganisms in the rhizosphere area provided by vermicompost treatment increased the availability of nutrients, such as N and K, by improving nitrogen fixation and biological solubilization of P (Mackey et al., 1982). Fe content was determined high when compared with reference values for spinach, which may be attributed to the fact that no agricultural activity had been performed in the study area.

According to the results of previous studies, vermicompost treatments were increased nutrient element contents in the leaves of plants. Pant et al. (2009) reported relatively higher micro nutrient (B, Zn, Fe, Mn, and Cu) content in the tissues of pak choi (*Brassica rapa*) in the areas treated with non-treated vermicompost tea than those treated with aerated vermicompost tea and vermicompost tea combined with microbial enhancer and controls. Vermicompost treatment increased nutrient content in different parts of other plants, such as N, P, K, Zn, Fe, Mn, and Cu content in geranium (*Pelargonium* species); average N, P, K, and Mg content of plant tissue of *Amaranthus* species; and N, P, K, and Ca content of groundnut (*Arachis hypogaea*) and marigold (*Tagetes*) plant; K, Zn, Ca, and Fe content in the stem and root tissues of Lilium plant; K and Ca content of marigold (*Tagetes*) plants; total N (%) of spinach; and P content in the leaves of maize (*Zea mays*) (Peyvast et al., 2007; Uma and Malathi, 2009; Shadanpour et al., 2011; Chand et al., 2011; Mycin et al., 2010; Gutie'rrez-Miceli et al., 2008; Moghadam et al., 2012). Uptake of P and K by African marigold (*Tagetes*) and uptake of K, Ca, and Mg by Setaria grass plants increased with vermicompost treatment (Jaworska and Kmiecik, 1999; Mackey et al., 1982). Increases in uptake and availability of nutrients were explained by improved soil environment and humic acid released after vermicompost treatment (Mycin et al., 2010; Stevenson, 1991; Nardi et al., 2002).

In our study, the reason for the improvement of soil properties and increase of nutrient element contents in the spinach leaves due to vermicompost treatments; it can be said that the increase of soil humus and microbial activity in vermicompost

http://www.aloki.hu ● ISSN 1589 1623 (Print) ● ISSN 1785 0037 (Online)
DOI: http://dx.doi.org/10.15666/aeer/1605_70017016
© 2018, ALÖKI Kft., Budapest, Hungary

applications is the result of decrease of pH value. Hence, the plant height and yield of the plants in the vermicompost treatments were found to be higher than control and chemical treatments.

According to the results of this study, with the highest plant height values obtained in V300 treatment in mind, the treatments of V200, V100, CF, and WF followed these values, in decreasing order. The plant height results for V300 treatment were determined to be 29% higher than WF treatment and 20% higher than CF treatment.

In similar study results, vermicompost treatments were found to increase plant height. Peyvast et al. (2008) investigated the effect of four different application rates (0, 10, 20, and 30%) of vermicompost obtained from cattle dung on spinach (*Spinacia oleracea*) under greenhouse conditions. The highest and the lowest plant heights in spinach were obtained with the 10% and 0% vermicompost treatments, respectively, and the plant heights of 14.30 and 14.16 cm were obtained with 20% and 30% vermicompost treatments, respectively. Although the treatments of all three vermicompost rates compared to the control increased the plant heights, these increases were not statistically significant. In potato (*Solanum tuberosum*), the highest plant height was obtained through incorporating a mixture of vermicompost and 100% NPKS (chemical fertilizers) into soil (Alam et al., 2007). Taller plants in *Abelmoschus esculentus* were obtained with vermicompost prepared from *perithecium* compared to control (only soil) and soil treated with the recommended dose of chemical fertilizers (Vijaya et al., 2008). Crossandra (*Crossandra undulaefolia*) had higher plant heights when it was grown in pots treated with water and hyacinth vermicompost compared to when grown in the control pots and in pots treated with water hyacinth compost (Gajalakshmi and Abbasi, 2002). A six t/ha vermicompost treatment improved the plant height of eggplant (*Solanum melongena*) compared to control without vermicompost (Moraditochaee et al., 2011).

In some of the previous studies, the growth responses of plants in vermicompost was claimed to resemble hormone-induced activity, which is related to high nutrient levels, humic acid, and humate in vermicompost (Edwards and Burrows, 1988; Atiyeh et al., 2000a). A positive vermicompost effect includes stimulated seed germination in some plants like green gram (Karmegam et al., 1999), tomato (Atiyeh, 2000b; Zaller, 2007), petunia (Arancon et al., 2008), and pine trees (Lazcano et al., 2010). Also, vermicompost enhances vegetative growth by stimulating shoot and root development (Edwards et al., 2004) and the morphology of the seedling by increasing leaf area and root branching (Lazcano et al., 2009) Vermicompost has been demonstrated to stimulate plant flowering and increase the number and biomass of flowers (Arancon et al., 2008; Atiyeh et al., 2002) and increase fruit yield (Singh et al., 2008; Atiyeh et al., 2000b; Arancon et al., 2004a, b).

According to the results of this study, the highest yield was obtained in V300 treatment. The V300 treatment was followed by V200, V100, WF and CF respectively. The yield results for V300 treatment were determined to be 56% higher than WF treatment and 60% higher than CF treatment.

In previous similar studies, yield was determined higher in vermicompost treatments. Earlier research reported that vermicompost treatment increased the total yield of potato (Alam et al., 2007), two cultivars (Sultan and Storm) of cucumber (*Cucumis sativus*) (Azarmi et al., 2009; Singh et al., 2008), strawberry (*Fragaria X ananassa*) (Singh et al., 2008), *Abelmoschus esculentus* (Vijaya and Seethalakshmi, 2011), lettuce (*Lactuca sativa*) (Papathanasiou et al., 2012), and *Amaranthus* species (Uma and Malathi, 2009),

http://www.aloki.hu ● ISSN 1589 1623 (Print) ● ISSN 1785 0037 (Online)
DOI: http://dx.doi.org/10.15666/aeer/1605_70017016
© 2018, ALÖKI Kft., Budapest, Hungary

the fruit yield of eggplant (*Solanum melongena*) (Alam et al., 2007), in marketable yields of tomato (*Lycopersicum esculentum*) (Uma and Malathi, 2009), fruits of okra (*Abelmoschus esculentus*) (Ansari and Sukhraj, 2010), and increased the harvest index of crossandra (*C. undulaefolia*) (Gajalakshmi and Abbasi, 2002). In addition, vermicompost treatments improved the oil yields of geranium (*Pelargonium* species) (Chand et al., 2011) and *Matricaria chamomilla* (Hadi et al., 2011).

Conclusions

Ecological agriculture, which is synonymous with sustainable agriculture, improves the fertility of the soil and creates a secondary income source for farmers, while focusing on total food protection and on the farm–human ecosystem. Vermicompost has potential to be applied in ecological agriculture systems. We believe that plant growth, yield and soil properties are enhanced by the application of vermicompost given our study results. In this respect, vermicompost could be applied in the near future as an alternative agriculture supplement combined with inorganic fertilizers. Spinach (*Spinacia oleracea* L.) is a unique crop as a vegetable with a relatively short growing period with high yield potential. In the present study, vermicompost positively impacted spinach yield and other plant parameters, as well as soil organic matter, as supported by the results of soil analyses, and plant analyses and measurements. Evaluation of the results indicated that vermicompost had positive impacts on the soil and the plant. The best treatment application rate was 3 tons vermicompost/ha. The study results suggest that the use of vermicompost for commonly consumed vegetables would increase the parameters and future experiments should be conducted for other vegetable species.

Acknowledgements. We thank Inonu University Scientific Research Projects Directorate for their financial support.

Conflict of Interests. The authors declare no conflict of interests.

REFERENCES

[1] Abbot, I., Parker, C. A. (1981): Interactions between earthworms and their soil environments. – Soil Biol. Biochem. 13: 191-197.
[2] Adhikary, S. (2012): Vermicompost, the story of organic gold: A review. – Agric. Sci. 3: 905.
[3] Alam, M. N., Jahan, M. S., Ali, M. K. Ashraf, M. A. Islam, M. K. (2007): Effect of vermicompost and chemical fertilizers on growth, yield and yield components of potato in Barind soils of Bangladesh. – J. Appl. Sci. Res.3: 1879-1888.
[4] Allison, L. E., Moodie, C. D. (1965): Carbonate. – In: Black, C. A. (ed.) Methods of Soil Analysis. American Society of Agronomy, Madison, WI, USA.
[5] Ansari, A. A., Sukhraj, K. (2010): Effect of vermiwash and vermicompost on soil parameters and productivity of okra (*Abelmoschus esculentus*) in Guyana. – Afr. J. Agric. Res. 5: 1794-1798.
[6] Arancon, N. Q., Edwards, C. A., Atiyeh, R. (2004a): Effects of vermicomposts produced from food waste on the growth and yields of greenhouse peppers. – Bioresour. Technol. 93: 139-144.
[7] Arancon, N. Q., Edwards, C. A., Bierman, P. (2004b): Influences of vermicomposts on field strawberries: Effects on growth and yields. – Bioresour. Technol. 93: 145-153.

http://www.aloki.hu ● ISSN 1589 1623 (Print) ● ISSN 1785 0037 (Online)
DOI: http://dx.doi.org/10.15666/aeer/1605_70017016
© 2018, ALÖKI Kft., Budapest, Hungary

[8] Arancon, N. Q., Edwards, C. A., Babenko, A., Cannon, J., Galvis, P., Metzger, J. D. (2008): Influences of vermicomposts, produced by earthworms and microorganisms from cattle manure, food waste and paper waste, on the germination, growth and flowering of petunias in the greenhouse. – Appl. Soil Ecol. 39: 91-99. DOI: 10.1016/j.apsoil. 2007.11.010.
[9] Atiyeh, R. M., Subler, S., Edwards, C. A., Bachman, G., Metzger, J. D., Shuster, W. (2000a): Effects of Vermi-composts and Composts on Plant Growth in Horticultural Container Media and Soil. – Pedobiologia 44: 579-590.
[10] Atiyeh, R. M., Arancon, N. Q., Edwards, C. A., Metzger, J. D. (2000b): Influence of earthworm-processed pig manure on the growth and yield of green house tomatoes. – Bioresour. Technol. 75: 175-180.
[11] Atiyeh, R. M., Arancon, N., Edwards, C. A., Metzger, J. D. (2002): The influence of earthworm-processed pig manure on the growth and productivity of marigolds. – Bioresour. Technol. 81: 103-108. DOI: 10.1016/S0960-8524(01)00122-5.
[12] Azarmi, R., Giglou, M. T., Hajieghrari, B. (2009): The effect of sheep-manure vermicompost on quantitative and qualitative properties of cucumber (*Cucumis sativus* L.) grown in the greenhouse. – Afr. J. Biotechnol. 8: 19.
[13] Baker, D. E., Amacher, M. C. (1982): Nickel, Copper, Zinc, and Cadmium. – In: Page, A. L., Miller, R. H., Keeney, D. R. (eds.) Methods of Soil Analysis (2nd ed.) ASA, SSSA, Madison, WI, USA.
[14] Becker, B. (1991): The Benefits of Earthworms. – Nat. Food Farm.12.
[15] Bhattacharjee, S., Dasgupta, P., Paul, A. R., Ghosal, S., Padhi, K. K., Pandey, L. P. (1998): Mineral element composition of spinach. – J. Sci. Food Agric. 77: 456-458.
[16] Canellas, L. P., Olivares, F. L., Okorokova, A. L., Fa-canha, R. A. (2002): Humic acids isolated from earth-worm compost enhance root elongation, lateral root emergence, and plasma membrane H^+—ATPase activity in maize roots. – J. Plant Physiol. 130: 1951-1957.
[17] Capowiez, Y., Cadoux, S., Bouchand, P., Roger-Estrade, J., Richard, G., Boizard, H. (2009): Experimental evidence for the role of earthworms in compacted soil regeneration based on field observations and results from a semi-field experiment. – Soil Biol. Biochem. 41: 711-717.
[18] Chand, S., Pandey, A., Anwar, M., Patra, D. D. (2011): Influence of integrated supply of vermicompost, biofertilizer and inorganic fertilizer on productivity and quality of rose scented geranium (*Pelargonium species*). – Indian J. Nat. Prod. Resour. 2: 375-382.
[19] Chaoui, H. I., Zibilske, L. M., Ohno, T. (2003): Effects of earthworms casts and compost on soil microbial activity and plant nutrient availability. – Soil Biology and Bio Chemistry 35: 295-302.
[20] Durak, A., Altuntaş, Ö., Kutsal, İ. K., Işık, R., Karaat, F. E. (2017): The effects of vermicompost on yield and some growth parameters of lettuce. – Turk. J. Agric. Food Sci. Technol. 5: 1566-1570.
[21] Edwards, C. A. (1995): Historical overview of vermicomposting. – Biocycle 36: 56-58.
[22] Edwards, C. A., Burrows, I. (1988): The Potential of Earthworms Composts as Plant Growth Media. – In: Edward, C. A., Neuhauser, E. F. (eds.) Earthworms in Waste and Environmental Management. SPB Academic Publishing, The Hague, The Netherlands.
[23] Edwards, C. A., Domínguez, J., Arancon, N. Q. (2004): The Influence of Vermicomposts on Plant Growth and Pest Incidence. – In: Shakir, S. H., Mikhaïl, W. Z. A. (eds.) Soil Zoology for Sustainable Development in the 21st Century. Self-published, Cairo, Egypt.
[24] Gajalakshmi, S., Abbasi, S. A. (2002): Effect of the application of water hyacinth compost/vermicompost on the growth and flowering of Crossandra undulaefolia, and on several vegetables. – Bioresour. Technol. 85: 197-199.
[25] Gandhi, M., Sangwan, V., Kapoor, K. K., Dilbaghi, N. (1997): Composting of household wastes with and without earthworms. – Environ. Ecol. 15: 432-434.

http://www.aloki.hu ● ISSN 1589 1623 (Print) ● ISSN 1785 0037 (Online)
DOI: http://dx.doi.org/10.15666/aeer/1605_70017016
© 2018, ALÖKI Kft., Budapest, Hungary

[26] Gee, G. W., Bauder, J. W. (1986): Particle-Size Analysis. – In: Klute, A. (ed.) Methods of Soil Analysis (2nd ed., Part 1). Physical and Mineralogical Methods. Agron. Monogr. 9; ASA–SSA, Madison, WI, USA.
[27] Ghabbour, S. I. (1973): Earthworm in agriculture: A modern evaluation. – Indian Rev. Ecol. Biol. Soc. 111: 259-271.
[28] Gutie'rrez-Miceli, F. A., Moguel-Zamudio, B., Abud-Archila, M., Gutie'rrez-Oliva, V. F., Dendooven, L. (2008): Sheep manure vermicompost supplemented with a native diazotrophic bacteria and mycorrhizas for maize cultivation. – Bioresour. Technol. 99: 7020-7026.
[29] Hadi, M. R. H. S., Darz, M. T., Ghandehari, Z., Riazi, G. (2011): Effects of vermicompost and amino acids on the flower yield and essential oil production from Matricaria chamomile L. – J. Med. Plants Res. 5: 5611-5617.
[30] Jablonska-Ceglarek, R., Rosa, R. (2001): Production effects of green fertilizers in the form of forecrops in vegetable cultivation. – Electron. J. Pol. Agric. Univ. Ser. Hortic. 4.
[31] Jaworska, G., Kmiecik, W. (1999): Effect of the date of harvest on the selected traits of the chemical composition of spinach (*Spinacia oleracea* L.) and New Zealand spinach (*Tetragonia expansa* Murr.). – Acta Agrar. Silv. Ser. Agrar. 37.
[32] Joshi, R., Singh, J., Vig, A. P. (2015): Vermicompost as an effective organic fertilizer and biocontrol agent: Effect on growth, yield and quality of plants. – Rev. Environ. Sci. Biotechnol. 14: 137-159.
[33] Julka, J. M. (2001): Earthworm Diversity and Its Role in Agroecosystem. VII National Symposium on Soil Biology and Ecology. – Bangalore University of Agricultural Sciences, Bangalore, pp. 13-17.
[34] Kacar, B. (1995): Soil Analysis. – Chemical Analyses of Plant and Soil: III. – Agriculture Faculty, Ankara University, Turkey.
[35] Kacar, B., Inal, A. (2008): Plant Analysis. – Nobel Press, Ankara, Turkey.
[36] Kansal, B. D., Singh, B., Bajaj, K. L., Kaur, G. (1981): Effect of different levels of nitrogen and farmyard manure on yield and quality of spinach (*Spinacea oleracea* L.). – Plant Foods Hum. Nutr. 31: 163-170.
[37] Karaman, M. R., Adiloglu, A., Brohi, R., Günes, A., İnal, A., Kaplan, M., Zengin, M. (2012): Bitki besleme (Plant Nutrition). – Dumat Ofset, Ankara (Gübretaş Rehber Kitaplar Dizisi, Gubretas Guidebook Series 2.)
[38] Karmegam, N., Alagumalai, K., Daniel, T. (1999): Effect of vermicompost on the growth and yield of green gram (*Phaseolus aureus* Roxb.). – Trop. Agric. 76: 143-146.
[39] Knudsen, D., Peterson, G. A., Pratt, P. F. (1982): Lithium, sodium, and potassium. – In: Page, A. L. (ed.) Methods of Soil Analysis; Part 2. Chemical and Microbiological Properties, (methodsofsoilan2). American Society of Agronomy, Madison, WI, USA, pp. 225-246.
[40] Lazcano, C., Arnold, J., Tato, A., Zaller, J. G., Domín-guez, J. (2009): Compost and vermicompost as nursery pot components: Effects on tomato plant growth and morphology. – Span. J. Agric. Res. 7: 944-951.
[41] Lazcano, C., Sampedro, L., Zas, R., Domínguez, J. (2010): Vermicompost enhances germination of the mari-time pine (*Pinus pinaster* Ait.). – New For. 39: 387-400. DOI: 10.1007/s11056-009-9178-z.
[42] Li, K., Li, P. Z. (2010): Earthworms helping economy, improving ecology and protecting health. – Int. J. Environ. Eng. 10: 354-365.
[43] Lindsay, W. L., Norvell, W. A. (1978): Development of a DTPA soil test for zinc, iron, manganese, and copper. – Soil Sci. Soc. Am. J., 42: 421-428.
[44] Mackey, A. D., Syres, J. A., Greeg, P. E. H. (1982): Plant availability of phosphorus in superphosphate and phosphate rock as influenced by earthworms. – Soil Biochem. 14: 281-287.

http://www.aloki.hu ● ISSN 1589 1623 (Print) ● ISSN 1785 0037 (Online)
DOI: http://dx.doi.org/10.15666/aeer/1605_70017016
© 2018, ALÖKI Kft., Budapest, Hungary

[45] Moghadam, A. R. L., Ardebili, Z. O., Saidi, F. (2012): Vermicompost induced changes in growth and development of Lilium Asiatic hybrid var. Navona. – Afr. J. Agric. Res. 7: 2609-2621.
[46] Molerock, T. E., Correll, J. C. (2008): Vegetables I. *Asteracea, Brassicaceae, Chenopodicaceae*, and *Cucurbitaceae*. – Prohens, J., Nuez, F. (eds.) Handbook of Plant Breeding. Springer, Berlin, Germany.
[47] Moraditochaee, M., Bozorgi, H. R., Halajisani, N. (2011): Effects of vermicompost application and nitrogen fertilizer rates on fruit yield and several attributes of eggplant (*Solanum melongena* L.) in Iran. – World Appl. Sci. J. 15: 174-178.
[48] Mycin, T. R., Lenin, M., Selvakumar, G., Thangadurai, R. (2010): Growth and nutrient content variation of groundnut Arachis hypogaea L. under vermicompost application. – J. Exp. Sci. 1: 12-16.
[49] Nardi, S., Pizzeghello, D., Muscolo, A., Vianello, A. (2002): Physiological effects of humic substances on higher plants. – Soil Biol. Biochem. 34: 1527-1536.
[50] Narwal, S. S. (2010): Allelopathy in ecological sustainable organic agriculture. – Allelopath. J. 25: 51-72.
[51] Olsen, S. R., Dean, L. A. (1965): Phosphorus. – In: Black, C. A. (ed.) Methods of Soil Analysis, Part 2. American Society of Agronomy, Madison, WI, USA.
[52] Pant, A. P., Radovich, T. J. K., Hue, N. V., Talcott, S. T., Krenek, K. A. (2009): Vermicompost extracts influence growth, mineral nutrients, phytonutrients and antioxidant activity in pak choi (*Brassica rapa* cv. Bonsai, Chinensis group) grown under vermicompost and chemical fertilizer. – J. Sci. Food Agric. 89: 2383-2392.
[53] Papathanasiou, F., Papadopoulos, I., Tsakiris, I., Tamoutsidis, E. (2012): Vermicompost as a soil supplement to improve growth, yield and quality of lettuce (*Lactuca sativa* L.). – J. Food Agric. Environ. 10: 677-682.
[54] Peyvast, G., Olfati, J. A., Madeni, S., Forghani, A. (2007): Effect of vermicompost on the growth and yield of spinach (*Spinacia oleracea* L.). – J. Food Agric. Environ. 6: 132-135.
[55] Peyvast, G., Olfati, J. A., Madeni, S., Forghani, A., Samizadeh, H. (2008): Vermicompost as a soil supplement to improve growth and yield of parsley. – Int. J. Veg. Sci. 14: 82-92.
[56] Plank, M. J. (1992): U.S. Shoring Shield. – U.S. Patent No. 5,096,334.
[57] Richards, L.A. (1954): Diagnosis and Improvement of Saline Alkali Soils. – USDA Handbook, No: 60. United States Department of Agriculture, Washington, DC, USA.
[58] Şalk, A., Arın, L., Deveci, M., Polat, S. (2008): Özel sebzecilik. – Tekirdağ, Turkey.
[59] Scheu, S. (1987): Microbial activity and nutrient dynamics in earthworms casts. – J. Biol. Fertil. Soil. 5: 230-234.
[60] Scialabba, N., Hattam, C. (2002): Organic Agriculture, Environment and Food Security. – Environment and Natural Resources Series. Food and Agriculture Organization of the United Nations (FAO), Rome.
[61] Seufert, V., Ramankutty, N., Mayerhofer, T. (2017): What is this thing called organic?– How organic farming is codified in regulations. – Food Policy 68: 10-20.
[62] Shadanpour, F., Mohammadi, T. A., Hashemi, M. K. (2011): Marigold: The possibility using vermicompost as the growth medium. – J. Ornam. Hortic. Plants 1: 153-160.
[63] Singh, R., Sharma, R. R., Kumar, S., Gupta, R. K., Patil, R. T. (2008): Vermicompost substitution influences growth, physiological disorders, fruit yield and quality of strawberry (*Fragaria* × *ananassa* Duch.). – Bioresour. Technol. 99: 8507-8511.
[64] Stevenson, F. J. (1991): Organic Matter—Micronutrient Reactions in Soil. – In: Mortvedt, J. J., Cox, F. R., Shuman, L. M., Welch, R. M. (eds.) Micronutrients in Agriculture. Soil Science Society of America, Madison, MI, USA.
[65] Stinner, B. R., House, G. J. (1987): Role of ecology in lower input, sustainable agriculture: An introduction. – Am. J. Altern. Agric. 2: 146-147.
[66] Suhane, R. K. (2007): Vermicompost. – Rajendra Agriculture University, Pusa, India.
[67] Tilman, D. (1998): The greening of the green revolution. – Nature 396: 211-212.

http://www.aloki.hu ● ISSN 1589 1623 (Print) ● ISSN 1785 0037 (Online)
DOI: http://dx.doi.org/10.15666/aeer/1605_70017016
© 2018, ALÖKI Kft., Budapest, Hungary

[68] Uma, B., Malathi, M. (2009): Vermicompost as a soil supplement to improve growth and yield of Amaranthus species. – Res. J. Agric. Biol. Sci. 5: 1054-1060.
[69] Vijaya, D., Padmadevi, S. N., Vasanda, S., Meerabhai, R. S., Chellapandi, P. (2008): Vermicompost induced changes in growth and development of Lilium Asiatic hybrid var. – Navona J. Org. Syst. 3: 51-56.
[70] Vijaya, K. S., Seethalakshmi, S. (2011): Contribution of Parthenium vermicompost in altering growth, yield and quality of *Alelmoschus esculentus* (I) Moench. – Adv. Biotechnol. 11: 44-47.
[71] Vivas, A., Moreno, B., Garcia-Rodriguez, S., Benitez, E. (2009): Assessing the impact of composting and vermicomposting on bacterial community size and structure, and microbial functional diversity of an olive-mill waste. – Bioresource Technology 100(3): 1319-1326.
[72] Willer, H., Lernoud, J. (2015): The World of Organic Agriculture - Statistics and Emerging Trends 2015. – FiBL & IFOAM Frick, Switzerland.
[73] Zaller, J. G. (2007): Vermicompost as a substitute for peat in potting media: Effects on germination, biomass alloca-tion, yields and fruit quality of three tomato varieties. – Sci. Hortic. 112: 91-199. DOI: 10.1016/j.scienta.2006.12.023.

http://www.aloki.hu ● ISSN 1589 1623 (Print) ● ISSN 1785 0037 (Online)
DOI: http://dx.doi.org/10.15666/aeer/1605_70017016
© 2018, ALÖKI Kft., Budapest, Hungary

EVALUATION OF HIGH TEMPERATURE TOLERANCE AND PHYSIOLOGICAL RESPONSES OF DIFFERENT ANOECTOCHILUS GERMPLASM RESOURCES

MEI, Y.[1,2,3#] – QIU, D.[2,3#] – XIAO, S.[1,*] – CHEN, D.[1,4*]

[1]*Horticulture and Landscape College, Hunan Agricultural University, Changsha 410128, China*

[2]*Crops Research Institute, Guangdong Academy of Agricultural Sciences Guangzhou 510640, China*

[3]*Key Laboratory of Crops Genetics and Improvement of Guangdong Province Guangzhou 510640, China*

[4]*Guangdong Key Laboratory of Tea Plant Resources Innovation and Utilization Guangzhou 510640, China*

**Corresponding authors*
e-mail: 23952650030@qq.com (S. Xiao), dongchen1113@sohu.com (D. Chen)

[#]These authors contributed equally to this work.

(Received 18th Jul 2018; accepted 27th Sep 2018)

Abstract. *Anoectochilus* genus is a precious Chinese medicinal plant. High temperature is among the critical factors that threatens plant growth in the *Anoectochilus* genus. The experiment was conducted at Key Laboratory of Crops Genetics and Improvement of Guangdong Province, Guangzhou, China. Two lab experiments were conducted to evaluate the high temperature tolerance of different *Anoectochilus* germplasm resource and the physiological responses of high-temperature-resistant and sensitive *Anoectochilus* to high temperature. Heat injury index, recovery index, soluble protein contents, proline content, malondialdehyde (MDA) content, relative electrical conductivity (REC), superoxide dismutase (SOD) activity, and catalase (CAT) activity were investigated. The results showed that, the recovery index was strongly negatively correlated with the heat injury index. The mean heat injury index at 6 h, 12 h, 24 h, 30 h and 36 h under high temperature were 5.17%, 16.90%, 39.96%, 53.70% and 70.61%, respectively. Five high-temperature-resistant species of *Anoectochilus* were selected. Compared with high-temperature-sensitive species of *Anoectochilus* germplasm, the high-temperature-resistant *Anoectochilus* germplasm had higher SOD activity, proline content and lower REC, CAT activity, MDA, and soluble protein content. REC, SOD activity and soluble protein content were strongly related to heat injury index. In conclusion, REC, SOD activity and soluble protein content are important attributes that could help to screen out the high temperature tolerant varieties of *Anoectochilus*.
Keywords: *Anoectochilus, high temperature stress, heat injury index, physiological indexes, enzymatic activity*

Introduction

Anoectochilus is an important medicinal plant species in China and recognized as ‘golden grass’ and/or ‘the king of medicine’ due to its high medicinal value. It has notable anti-inflammatory effects (Zhang et al., 2007; Du et al., 2008). *Anoectochilus* plants generally have substantial concentrations of polysaccharides, alkaloids, flavonoids, amino acids and organic acids etc. (Zheng et al., 2013; Shao et al., 2014). The extracts of *Anoectochilus* had been reported to cure diabetes, hypertension, tumor, nephritis, fever, snakebite, chest and abdominal pain etc. (Du et al., 2003; Fang et al., 2008). Therefore, *Anoectochilus* was endowed with high edible, medicinal as well as ornamental value.

http://www.aloki.hu ● ISSN 1589 1623 (Print) ● ISSN 1785 0037 (Online)
DOI: http://dx.doi.org/10.15666/aeer/1605_70177031
© 2018, ALÖKI Kft., Budapest, Hungary

The *Anoectochilus* species required cool, humid, low-light environment for its optimum growth. Generally, most of the *Anoectochilus* species were sensitive to high temperature. The optimum temperature for the growth of *Anoectochilus* was ranging from 18 °C to 25 °C, and ≥ 70% relative humidity whereas temperature over 30 °C inhibited the growth of *Anoectochilus*. So, it was important to enhance the heat resistance for the introduction and breeding of new *Anoectochilus* varieties. However, the high-temperature-resistance ability of the different *Anoectochilus* species are still unknown. Moreover, no study has yet been reported the evaluation of the high-temperature-resistance ability of the different *Anoectochilus* species.

How does the *Anoectochilus* respond under high temperature? Like other plants, the *Anoectochilus* plant might activate some physiological and biochemical responses to avoid high temperature damage (He et al., 2004). MDA, proline and soluble protein are important osmoregulator substances in plants under stress conditions. Enhancement in the activities of antioxidants such as superoxide dismutase (SOD) and catalase (CAT) improved plant stress tolerance. For example, Wang et al. (2018) indicated that amino acids and soluble proteins are important for Hard Fescue to resist heat stress. For lettuce seedlings, the malondialdehyde (MDA), proline and soluble sugar contents in leaf were associated with heat stress (Han et al., 2013). The activities of SOD, CAT and peroxidase (POD), as well as the contents of MDA in *Rhododendron lapponicum* leaves were assumed as key physiological indexes in response to heat stress (Li et al., 2018). Rivero et al. (2015) reported that high temperature stress on tomato plants would cause the increase of SOD whilst decrease in CAT activities. Zhang et al. (2017) suggested that *C. nitidissima* plants might have some level of tolerance to high temperature period that might be related to the growing period of the plants. Chen et al. (2016) showed that the leaves of gerbera cultivars had a phenotypic response to heat treatment, as a consequence of increased relative electrical conductivity (REC), decreased soluble protein, and accumulated MDA and proline in leaves. Tian et al. (2011) reported that the marigold cultivars increased SOD, POD and CAT activities, and increased MDA contents and REC in response to high temperature stress. To date, very few studies had been conducted to investigate the physiological responses of *Anoectochilus* under high-temperature stress. Therefore, present study was aimed to establish a method to evaluate high-temperature-resistance of *Anoectochilus* species by evaluating the heat injury index and recovery index of different *Anoectochilus* species, and to investigate the physiological responses of *Anoectochilus* under high-temperature stress.

Materials and methods

Plant materials and growth

Thirty-two *Anoectochilus* genus species were collected from different provinces of China (*Table 1*) by the Southern Medicine Research Group of Crop Research Institute, Guangdong Academy of Agricultural Sciences. The plant samples were grown under greenhouse conditions for 6 months. Uniform seedlings with 8~9 cm height, 3~4 leaves, and 2~3 healthy roots were selected. The seedlings were then transplanted to a 6 cm × 6 cm × 6 cm plastic planting container, 1 plant per container. For high temperature treatment, the container was filled with cultivation substrates (peat: vermiculite = 1:2 (V:V)).

http://www.aloki.hu ● ISSN 1589 1623 (Print) ● ISSN 1785 0037 (Online)
DOI: http://dx.doi.org/10.15666/aeer/1605_70177031
© 2018, ALÖKI Kft., Budapest, Hungary

Table 1. *The resource information of the 32 species of Anoectochilus genus*

Species	Time of collection	Location
NYJ1	2013.08	Fuzhou, Fujian
NYJ2	2013.08	Fuzhou, Fujian
NYJ3	2013.08	Fuzhou, Fujian
NYJ4	2013.08	Fuzhou, Fujian
NYJ5	2010.06	Fuzhou, Fujian
NYJ6	2013.08	Fuzhou, Fujian
NYJ7	2010.06	Fuzhou, Fujian
NYJ8	2013.07	Qujing, Yunnan
NYJ9	2013.07	Qujing, Yunnan
NYJ10	2014.05	Guangzhou, Guangdong
NYJ11	2010.06	Fuzhou, Fujian
NYJ12	2013.08	Fuzhou, Fujian
NYJ13	2012.09	Nankunshan, Guangdong
NYJ14	2012.09	Nankunshan, Guangdong
NYJ15	2012.09	Nankunshan, Guangdong
NYJ16	2014.11	Shenzhen, Guangdong
NYJ17	2013.08	Fuzhou, Fujian
NYJ18	2014.11	Heyuan, Guangdong
NYJ19	2014.11	Heyuan, Guangdong
NYJ20	2015.1	Longyan, Fujian
NYJ21	2015.1	Longyan, Fujian
NYJ22	2014.12	Jinxiu, Guangxi
NYJ23	2014.12	Jinxiu, Guangxi
NYJ24	2015.1	Sanming, Fujian
NYJ25	2013.08	Fuzhou, Fujian
NYJ26	2015.1	Sanming, Fujian
NYJ27	2015.1	Longyan, Fujian
NYJ28	2015.12	Heyuan, Guangdong
NYJ29	2015.12	Qingyuan, Guangdong
NYJ30	2016.03	Mangshi, Yunnan
NYJ31	2015.1	Beiliu, Guangxi
NYJ32	2015.1	Meizhou, Guangdong

Experiment 1: High temperature treatment for thirty-two Anoectochilus genus species

High temperature treatment stress was imposed at Key Laboratory of Crops Genetics and Improvement of Guangdong Province, Crop Research Institute of Guangdong Academy of Agricultural Sciences. The high temperature treatment processes were as follows: before high temperature treatment, all plants were grown in an artificial climate incubator with a day/night temperature of 25 °C /18 °C, light intensity of 2000 Lx 12 h day/night cycle, and relative humidity of 80% for 15 days. The plants were watered

http://www.aloki.hu ● ISSN 1589 1623 (Print) ● ISSN 1785 0037 (Online)
DOI: http://dx.doi.org/10.15666/aeer/1605_70177031
© 2018, ALÖKI Kft., Budapest, Hungary

once per day at 20 ml per plant. Then, the plants were transferred to incubator with day/night temperature of 43 °C /38 °C, illumination intensity of 2000 Lx 12 h day/night cycle, and relative humidity of 80%. The heat injury index of different species of *Anoectochilus* were determined at 6 h, 12 h, 24 h, 30 h, and 36 h as described by Li et al. (2009). After that, all the plants were subjected to incubation with a day/night temperature of 25 °C /18 °C, light intensity of 2000 Lx 12 h day/night cycle, and relative humidity of 80% for 15 days and the recovery index was investigated according to Jia and Chen (2005). The heat injured plants were separated into five levels: level 0, no injured leaves, green; level 1, drooping leaves, leaves' color were normal; level 2, the tip of the leaves wilted; level 3, 50% of the leaves wilted; level 4, almost all the leaves wilted; level 5, the whole plant died. The calculation of heat injury index was according to the following formula: heat injury index = ∑(number of plant at different injury level × injury level) injury level / (the highest injury level × total number of plants) × 100%. For calculation of recovery index, the plants were separated into different levels: level 0, the whole plant died; level 1, stems kept erecting, dry leaves, plants were unable to recover; level 3, the whole plant recovered and grew well. The recovery index was calculated as the following formula: recovery index = ∑(number of plant at different recovery level × recovery level) injury level / (the highest recovery level × total number of plants) × 100%.

Experiment 2: Physiological responses of high-temperature-resistant and sensitive Anoectochilus

The fresh plant sample (5.0 g) of all the plant species was collected at 6 h, 12 h, 24 h, 30 h, and 36 h under high temperature treatment, soaked in liquid nitrogen for 1 min, and then immediately stored at -80 °C for the determination of physiological indexes. The physiological indexes, i.e. soluble protein contents, proline content, malondialdehyde (MDA) content, relative electrical conductivity (REC), and the activities of superoxide dismutase (SOD) and catalase (CAT) were determined to test the high-temperature-resistance and sensitivity of *Anoectochilus*.

Measurement of soluble protein contents

Soluble protein contents were estimated according to the methods devised by Bradford (1976) using G-250, the absorbance was read at 595 nm and the concentration was expressed as $mg \cdot g^{-1}$.

Determination of proline content

Proline contents were determined according to the method of Bates et al. (1973) by evaluating the absorbance of the red chromophore in the toluene fraction at 520 nm and the amount of proline was estimated by comparing with a standard curve and expressed as $\mu g \cdot g^{-1}$.

Determination of malondialdehyde (MDA) content

The malondialdehyde (MDA) content was measured by the method of Chen and Wang (2006). MDA reacted with thiobarbituric acid (TBA), the absorbance of the reaction solutions were recorded at 532 nm, 600 nm, and 450 nm. The final result of MDA was expressed as nmol·g.

http://www.aloki.hu ● ISSN 1589 1623 (Print) ● ISSN 1785 0037 (Online)
DOI: http://dx.doi.org/10.15666/aeer/1605_70177031
© 2018, ALÖKI Kft., Budapest, Hungary

Determination of relative electrical conductivity (REC)

The plant leaves were thoroughly washed with deionized water. The leaf sample was then put into a clean beaker with 30 ml of deionized water and kept under vacuum for 15 min. The electrical conductivity was measured and marked as EC1. The leaves were then heated in boiling water for 20 min and then cooled at room temperature. The electrical conductivity was investigated again and marked as EC2. The formula for the calculation of the relative electrical conductivity (REC) calculation was: REC = (EC1/EC2) × 100%.

Determination of superoxide dismutase (SOD) activity

The superoxide dismutase activity was measured by using Nitro blue tetrazolium (NBT) method, after the reaction, the color change was measured at 560 nm, and one unit of SOD activity was equal to the volume of extract needed to cause 50% inhibition of the color reaction. The enzyme activity was expressed as $U \cdot g^{-1}$ (Wang et al., 2009).

Determination of catalase (CAT) activity

Catalase activity was determined by the method of Wang et al. (2009), 50 μl of enzyme extract was added to the reaction solution system containing 1 ml 0.3% H_2O_2 and 1.95 ml H_2O, the absorbance change at 240 nm was recorded for calculating CAT activity. The enzyme activity was expressed as $U \cdot g^{-1}$.

Statistical analysis

The data were analyzed using statistical software SPSS V 18.1; the differences amongst means were separated by using least significant difference (LSD) test at 5% probability level. Microsoft Excel was used for graphical representation.

Results

Experiment 1

Heat injury index and recovery index

The heat injury index investigated at 6 h, 12 h, 24 h, 30 h and 36 h, under high temperature treatment and the recovery index at 15 d after high temperature treatment was shown in *Table 2*. The heat injury index in different species of *Anoectochilus* was different, a wide range of heat injury index was detected at 6 h (0. 00%- 15.33%), 12 h (0. 00%- 58.00%), 24 h (2.00%- 74.67%), 30 h (2.00- 78.00%) and 36 h (37.33-94.00%) under high temperature. The mean heat injury index at 6 h, 12 h, 24 h, 30 h and 36 h under high temperature were 5.17%, 16.90%, 39.96%, 53.70% and 70.61%, respectively. At 30 h of high temperature treatment, over 75% of the *Anoectochilus* species had a heat injury index higher than 50%. At 36 h of high temperature treatment, over 80% of the *Anoectochilus* species had a heat injury index higher than 60.00%. The recovery index at 15 d after recovery was ranging from 0.00% to 74.44%, with a mean of 23.85%. Over 80% of the *Anoectochilus* species had a recovery index lower than 40.00%. Overall, the *Anoectochilus* species, like NYJ2, NYJ6, NYJ14, NYJ21 and NYJ24 were high-temperature-resistant species of *Anoectochilus*, and others were high-temperature-sensitive species of *Anoectochilus*.

http://www.aloki.hu ● ISSN 1589 1623 (Print) ● ISSN 1785 0037 (Online)
DOI: http://dx.doi.org/10.15666/aeer/1605_70177031
© 2018, ALÖKI Kft., Budapest, Hungary

Table 2. *The heat injury index and recovery index of 32 species of Anoectochilus genus under heat stress*

Species	Heat injury index					Recovery index
	6 h	12 h	24 h	30 h	36 h	15 d
NYJ1	7.33	11.33	45.33	59.33	74.00	22.22
NYJ2	0.00	0.67	2.00	14.00	40.67	74.44
NYJ3	8.67	18.07	38.00	58.67	67.33	38.89
NYJ4	6.67	24.67	49.33	62.00	76.67	22.22
NYJ5	7.33	20.00	50.00	68.00	79.33	0.00
NYJ6	0.00	0.00	2.00	12.67	37.33	67.78
NYJ7	8.67	22.67	51.30	63.33	75.33	5.56
NYJ8	4.00	18.00	42.00	53.33	67.33	31.11
NYJ9	6.00	22.00	47.33	60.67	77.33	17.78
NYJ10	4.67	14.00	40.67	52.67	64.00	28.89
NYJ11	6.67	14.67	58.67	62.00	80.67	5.56
NYJ12	6.00	24.67	46.67	61.33	78.00	21.11
NYJ13	2.67	10.00	36.67	39.33	66.67	34.44
NYJ14	0.67	0.67	4.00	15.33	39.33	60.00
NYJ15	3.33	16.00	38.00	41.00	64.67	32.22
NYJ16	4.67	24.00	39.33	62.00	73.33	12.22
NYJ17	3.33	12.67	36.67	54.67	70.67	30.00
NYJ18	15.33	54.00	77.33	74.00	88.66	0.00
NYJ19	12.67	58.00	74.67	71.33	87.33	0.00
NYJ20	6.00	10.67	46.00	68.00	91.00	4.44
NYJ21	0.67	2.00	2.67	15.33	44.67	51.11
NYJ22	10.60	16.67	46.00	67.33	94.00	3.33
NYJ23	1.33	16.00	47.33	63.33	72.00	31.11
NYJ24	0.67	4.00	6.00	15.33	42.00	44.44
NYJ25	8.00	21.33	48.00	68.00	84.67	0.00
NYJ26	2.00	14.67	42.67	66.00	74.00	12.22
NYJ27	9.33	18.67	45.33	68.00	83.33	2.22
NYJ28	2.00	8.00	34.00	59.33	70.67	33.33
NYJ29	1.33	14.00	42.00	59.33	68.00	31.11
NYJ30	2.67	13.33	48.66	56.00	69.33	31.11
NYJ31	9.33	22.67	50.67	64.00	80.67	0.00
NYJ32	2.67	12.67	39.33	62.67	76.67	14.44
Mean	5.17	16.90	39.96	53.70	70.61	23.85

Experiment 2

From the 32 species, one high-temperature-resistant and one high-temperature-sensitive *Anoectochilus* was selected to investigate the physiological response of the different *Anoectochilus*.

http://www.aloki.hu ● ISSN 1589 1623 (Print) ● ISSN 1785 0037 (Online)
DOI: http://dx.doi.org/10.15666/aeer/1605_70177031
© 2018, ALÖKI Kft., Budapest, Hungary

Relative electrical conductivity (REC)

Before high temperature treatment, the two species had similar levels of REC. With high temperature treatment, NYJ2 had lower REC than NYJ18. At 6 h, 12 h, 24 h, 30 h and 36 h under high temperature treatment, the REC was significantly higher than CK for NYJ2. For NYJ18, at 6 h under high temperature treatment, the REC level was slightly higher than CK, while at 12 h, 24 h, 30 h and 36 h under high temperature treatment, the REC increased rapidly and significantly and it was higher than CK (*Fig. 1*).

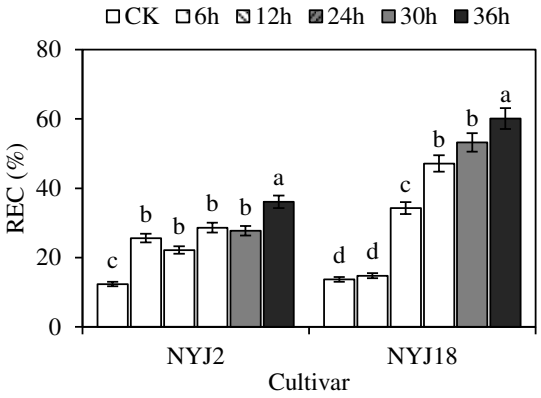

Figure 1. *Effect of high temperature stress on the relative electrical conductivity (REC) in high-temperature-resistant Anoectochilus germplasm (NYJ2) and high-temperature-sensitive Anoectochilus germplasm (NYJ18). Vertical bars with different lower case letters above are significantly different at P = 0.05 by LSD tests. Capped bars represent SD*

Superoxide dismutase (SOD) activity

For NYJ2, the SOD activity at 6 h, 12 h, 24 h and 30 h under high temperature treatment was significantly higher than CK. At 36 h under high temperature treatment, the SOD activity was similar to that in CK. For NYJ18, compared with CK, the SOD activity at 6 h, 12 h, 24 h and 36 h under high temperature treatment was significantly decreased. The SOD activity at 36 h under high temperature treatment was slightly decreased. The SOD activity in NYJ2 was higher than in NYJ18 (*Fig. 2*).

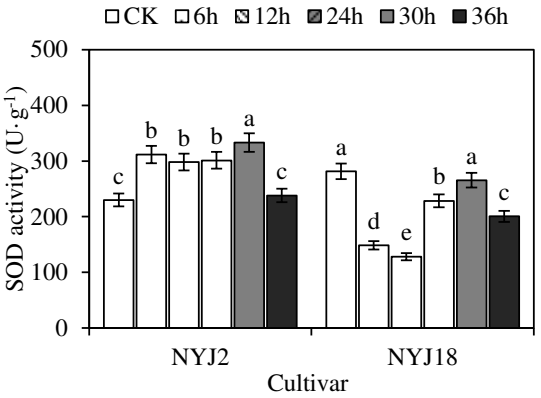

Figure 2. *Effect of high temperature stress on SOD activity in high-temperature-resistant Anoectochilus germplasm (NYJ2) and high-temperature-sensitive Anoectochilus germplasm (NYJ18). Vertical bars with different lower case letters above are significantly different at P = 0.05 by LSD tests. Capped bars represent SD*

http://www.aloki.hu ● ISSN 1589 1623 (Print) ● ISSN 1785 0037 (Online)
DOI: http://dx.doi.org/10.15666/aeer/1605_70177031
© 2018, ALÖKI Kft., Budapest, Hungary

Catalase (CAT) activity

The CAT activity in NYJ2 was lower than in NYJ18. The CAT activity at 6 h, 12 h under high temperature treatment was slightly decreased for NYJ2, whilst the CAT activity at 24 h, 30 h and 36 h under high temperature treatment was dramatically decreased. For NYJ18, short time high temperature treatment (6 h) did not affect CAT activity, but at 12 h, 24 h, 30 h, and 36 h high temperature treatment, the CAT activity was decreased linearly (*Fig. 3*).

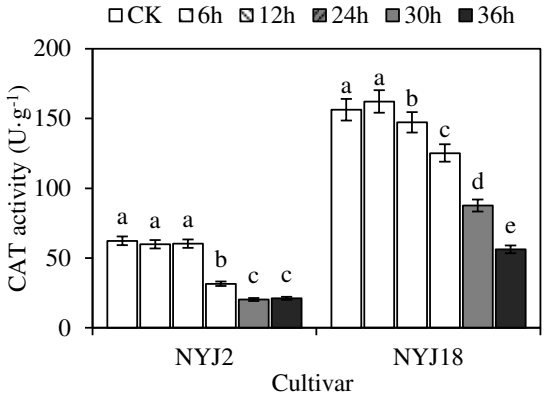

Figure 3. *Effect of high temperature stress on CAT activity in high-temperature-resistant Anoectochilus germplasm (NYJ2) and high-temperature-sensitive Anoectochilus germplasm (NYJ18). Vertical bars with different lower case letters above are significantly different at P = 0.05 by LSD tests. Capped bars represent SD*

Malondialdehyde (MDA) content

The MDA content in NYJ2 was lower than in NYJ18. As temperature increased, the MDA content in the plant was increased. For NYJ2, in the 6 h high temperature treatment the MDA content was slightly increased, in the 30 h high temperature treatment the MDA content reached a peak, then decreased in the 36 h high temperature treatment. For NYJ18, the MDA content increased gradually when high temperature treatment time increased (*Fig. 4*).

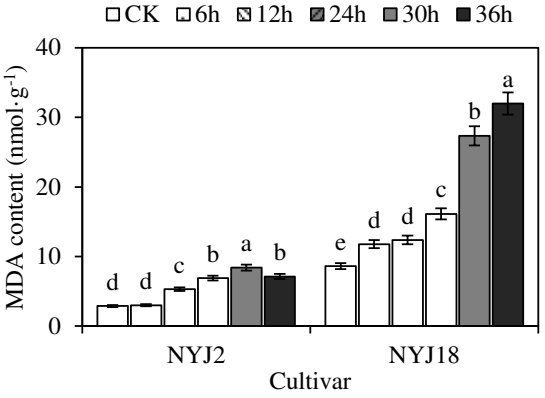

Figure 4. *Effect of high temperature stress on malondialdehyde (MDA) content in high-temperature-resistant Anoectochilus germplasm (NYJ2) and high-temperature-sensitive Anoectochilus germplasm (NYJ18). Vertical bars with different lower case letters above are significantly different at P = 0.05 by LSD tests. Capped bars represent SD*

http://www.aloki.hu ● ISSN 1589 1623 (Print) ● ISSN 1785 0037 (Online)
DOI: http://dx.doi.org/10.15666/aeer/1605_70177031
© 2018, ALÖKI Kft., Budapest, Hungary

Proline content

With increase in temperature, the proline content in NYJ2 increased gradually, and was significantly higher than CK. For NYJ18, the proline content was significantly decreased in the 6 h high temperature treatment only. At 12 h, 24 h 30 h, and 36 h under high temperature treatment, the proline content was substantially improved (*Fig. 5*).

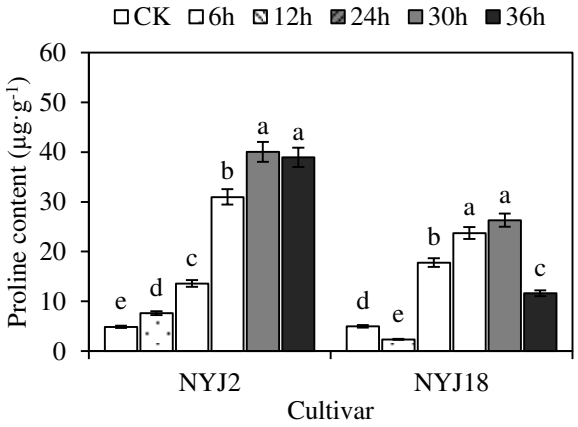

Figure 5. *Effect of high temperature stress on proline content in high-temperature-resistant Anoectochilus germplasm (NYJ2) and high-temperature-sensitive Anoectochilus germplasm (NYJ18). Vertical bars with different lower case letters above are significantly different at P = 0.05 by LSD tests. Capped bars represent SD*

Soluble protein content

Exposure of high temperature stress for short duration (6 h, 12 h and 24 h) did not significantly affect soluble protein content in NYJ2. At 30 h and 36 h high temperature treatment, the soluble protein content was significantly increased in NYJ2 whereas, for NYJ18, at 6 h high temperature treatment, the soluble protein content was decreased significantly. With increased duration of high temperature, the soluble protein contents were increased (*Fig. 6*).

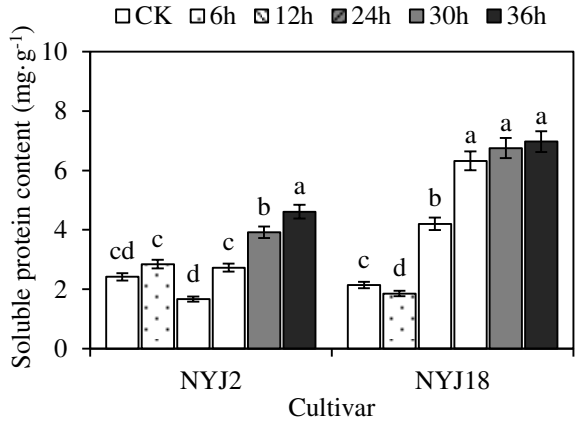

Figure 6. *Effect of high temperature stress on soluble protein content in high-temperature-resistant Anoectochilus germplasm (NYJ2) and high-temperature-sensitive Anoectochilus germplasm (NYJ18). Vertical bars with different lower case letters above are significantly different at P = 0.05 by LSD tests. Capped bars represent SD*

http://www.aloki.hu ● ISSN 1589 1623 (Print) ● ISSN 1785 0037 (Online)
DOI: http://dx.doi.org/10.15666/aeer/1605_70177031
© 2018, ALÖKI Kft., Budapest, Hungary

Correlation analysis

The recovery index showed a significant negative correlation relationship with heat injury index at 6 h (-0.7675**), 12 h (-0.6687**), 24 h (-0.8566**), 30 h (-0.8894**), and 36 h (-0.9291**), respectively (*Table 3*). The heat injury index was significantly associated with REC (0.9186**), SOD activity (0.8699**), and soluble protein content (0.9442**) for both high-temperature-resistant and sensitive *Anoectochilus* germplasm (*Table 4*). For high-temperature-resistant *Anoectochilus* germplasm (NYJ2), a significant positive correlation relationship between heat injury index and soluble protein content (0.8741*) was investigated (*Table 5*). For high-temperature-sensitive *Anoectochilus* germplasm (NYJ18), the heat injury index was significantly associated with REC (**0.9783****), MDA content (-0.8241*), and soluble protein content (**0.9695****) (*Table 6*).

Table 3. *Correlation analysis between heat injury index and recovery index*

Investigated index	Recovery index at 15d	Heat injury index 6 h	Heat injury index 12 h	Heat injury index 24 h	Heat injury index 30 h	Heat injury index 36 h
Recovery index at 15 d	1.0000	-0.7675**	-0.6687**	-0.8566**	-0.8894**	-0.9291**
Heat injury index 6 h	-0.7675**	1.0000	0.8167**	0.7813**	0.6926**	0.7623**
Heat injury index 12 h	-0.6687**	0.8167**	1.0000	0.8292**	0.6653**	0.6636**
Heat injury index 24 h	-0.8566**	0.7813**	0.8292**	1.0000	0.9171**	0.9021**
Heat injury index 30 h	-0.8894**	0.6926**	0.6653**	0.9171**	1.0000	0.9519**
Heat injury index 36 h	-0.9291**	0.7623**	0.6636**	0.9021**	0.9519**	1.0000

Significant correlations at **p < 0.01

Table 4. *Correlation analysis between the investigated indexes for both high-temperature-resistant and sensitive Anoectochilus germplasm*

Investigated index	Heat injury index	REC (%)	SOD activity ($U \cdot g^{-1}$)	CAT activity ($U \cdot g^{-1}$)	MDA content (nmol/g)	Proline content ($\mu g \cdot g^{-1}$)	Soluble protein content ($mg \cdot g^{-1}$)
Heat injury index	1.0000	0.9186**	0.8699**	-0.4571	0.1295	0.2410	0.9442**
REC (%)	0.9186**	1.0000	0.8417**	-0.1427	-0.1792	0.3998	0.9554**
SOD activity ($U \cdot g^{-1}$)	0.8699**	0.8417**	1.0000	-0.3337	0.1518	0.0502	0.8279**
CAT activity ($U \cdot g^{-1}$)	-0.4571	-0.1427	-0.3337	1.0000	-0.6031*	0.3406	-0.1872
MDA content (nmol/g)	0.1295	-0.1792	0.1518	-0.6031*	1.0000	-0.5853*	-0.1062
Proline content ($\mu g \cdot g^{-1}$)	0.2410	0.3998	0.0502	0.3406	-0.5853*	1.0000	0.4018
Soluble protein content ($mg \cdot g^{-1}$)	0.9442**	0.9554**	0.8279**	-0.1872	-0.1062	0.4018	1.0000

Significant correlations at *p < 0.05 and **p < 0.01

http://www.aloki.hu ● ISSN 1589 1623 (Print) ● ISSN 1785 0037 (Online)
DOI: http://dx.doi.org/10.15666/aeer/1605_70177031
© 2018, ALÖKI Kft., Budapest, Hungary

Table 5. *Correlation analysis between the investigated indexes for high-temperature-resistant Anoectochilus germplasm*

Investigated index	Heat injury index	REC (%)	SOD activity ($U \cdot g^{-1}$)	CAT activity ($U \cdot g^{-1}$)	MDA content ($nmol \cdot g^{-1}$)	Proline content ($\mu g \cdot g^{-1}$)	Soluble protein content ($mg \cdot g^{-1}$)
Heat injury index	1.0000	0.7381	0.5615	-0.3608	-0.7247	0.7130	0.8741*
REC (%)	0.7381	1.0000	0.6988	0.2077	-0.7803	0.7974	0.7244
SOD activity ($U \cdot g^{-1}$)	0.5615	0.6988	1.0000	0.3369	-0.9155*	0.9620**	0.5820
CAT activity ($U \cdot g^{-1}$)	-0.3608	0.2077	0.3369	1.0000	-0.1482	0.2003	-0.1143
MDA content ($nmol \cdot g^{-1}$)	-0.7247	-0.7803	-0.9155*	-0.1482	1.0000	-0.9876**	-0.8287*
Proline content ($\mu g \cdot g^{-1}$)	0.7130	0.7974	0.9620**	0.2003	-0.9876**	1.0000	0.7665
Soluble protein content ($mg \cdot g^{-1}$)	**0.8741***	0.7244	0.5820	-0.1143	-0.8287*	0.7665	1.0000

Significant correlations at *p < 0.05 and **p < 0.01

Table 6. *Correlation analysis between the investigated indexes for high-temperature-sensitive Anoectochilus germplasm*

Investigated index	Heat injury index	REC (%)	SOD activity ($U \cdot g^{-1}$)	CAT activity ($U \cdot g^{-1}$)	MDA content ($nmol \cdot g^{-1}$)	Proline content ($\mu g \cdot g^{-1}$)	Soluble protein content ($mg \cdot g^{-1}$)
Heat injury index	1.0000	0.9783**	0.8082	-0.0252	-0.8241*	0.7524	0.9695**
REC (%)	**0.9783****	1.0000	0.8901*	0.1310	-0.9126*	0.7246	0.9904**
SOD activity ($U \cdot g^{-1}$)	0.8082	0.8901*	1.0000	0.1805	-0.9831**	0.4295	0.8452*
CAT activity ($U \cdot g^{-1}$)	-0.0252	0.1310	0.1805	1.0000	-0.2541	0.2149	0.2168
MDA content ($nmol \cdot g^{-1}$)	**-0.8241***	-0.9126*	-0.9831**	-0.2541	1.0000	-0.4417	-0.8757*
Proline content ($\mu g \cdot g^{-1}$)	0.7524	0.7246	0.4295	0.2149	-0.4417	1.0000	0.7895
Soluble protein content ($mg \cdot g^{-1}$)	**0.9695****	0.9904**	0.8452*	0.2168	-0.8757*	0.7895	1.0000

Significant correlations at *p < 0.05 and **p < 0.01

Discussion

In this study, we applied the high temperature treatment method to evaluate the high-temperature-resistance of *Anoectochilus* species. In this method, the recovery index was strongly negatively correlated with heat injury indices for *Anoectochilus* species (*Table 3*). The mean heat injury index at 6 h, 12 h, 24 h, 30 h and 36 h under high temperature were 5.17%, 16.90, 39.96%, 53.70% and 70.61%, respectively. Over 80% of the *Anoectochilus* species were high-temperature-sensitive, five high-temperature-resistant species of *Anoectochilus* (NYJ2, NYJ6, NYJ14, NYJ21 and NYJ24) were identified (*Table 2*).

http://www.aloki.hu ● ISSN 1589 1623 (Print) ● ISSN 1785 0037 (Online)
DOI: http://dx.doi.org/10.15666/aeer/1605_70177031
© 2018, ALÖKI Kft., Budapest, Hungary

The REC and MDA content of the two species of *Anoectochilus* genus were apparently increased with the increase of high temperature stress. Han et al. (2013) indicated that high temperature could lead to increased membrane permeability and membrane lipid peroxidation. The REC increased as a consequence of increasing membrane permeability which led to extracellular electrolyte leakage. In our study, REC and MDA content of the high-temperature-sensitive NYJ18 increased more than that of high-temperature-resistant NYJ2.

In addition, when both high-temperature-resistant *Anoectochilus* germplasm resource (NYJ2) and high-temperature-sensitive *Anoectochilus* germplasm resource (NYJ18) were pooled together, the heat injury index significantly associated to REC (0.9186**). For high-temperature-sensitive *Anoectochilus* germplasm resource (NYJ18), the heat injury index significantly associated to REC (0.9783**) and MDA content (-0.8241*). It could be seen that the heat injury index of different breedings of *Anoectochilus* were significantly positively correlated with REC. The high-temperature-sensitive species had strong negative relation to MDA content (Peng et al., 2012). Therefore, by comparing the increase range of REC and MDA content of two species to identify their high-temperature-resistant ability, which was consistent with the conclusions of most research on other plants (Lin et al., 2014; Li et al., 2015).

For anti-enzyme activity, SOD could reduce superoxide radicals into hydrogen peroxide, while CAT could trigger the conversion of hydrogen peroxide into water and oxygen (Xu et al., 2006). In this study, the results showed that CAT activity in both species of *Anoectochilus* decreased under heat stress, and in high-temperature-sensitive NYJ18 it decreased more rapidly than in high temperature tolerant NYJ2. The SOD activity of the high-temperature-sensitive NYJ18 decreased rapidly at the beginning of stress treatment; while the SOD activity for high temperature tolerant NYJ2 increased. Moreover, when both high-temperature-resistant *Anoectochilus* germplasm resource (NYJ2) and high-temperature-sensitive *Anoectochilus* germplasm resource (NYJ18) were pooled together, the heat injury index significantly associated with SOD activity (0.8699**). SOD was resistant to membrane lipid peroxidation and maintenance of membrane structure integrity, and these were great significance (Lin et al., 2014). The changes of SOD and CAT activity with high temperature treatment time in this study were consistent with other researches (Jiang et al., 2008; Peng et al., 2012; Can et al., 2016).

Soluble protein and proline in leaves act as osmotic adjustment substances, and are beneficial to the maintenance of cell structure and function under stress. Previous study suggested that soluble protein and proline were active oxygen scavengers, which had a protective effect on plant cells (Can et al., 2016). With time and stress level increased, within a certain temperature range, the accumulation of free proline was positively correlated with the stress intensity (Liu et al., 2001; Sun et al., 2006). In this study, the proline content of the high-temperature-resistant NYJ2 was significantly higher than that of high-temperature-sensitive NYJ18 in the late stress stage and the proline content in the high-temperature-sensitive NYJ18 significantly decreased. In addition, the soluble protein content of NYJ2 and NYJ18 decreased in a certain range at the beginning of stress treatment (before 12 h), and then increased with the prolongation of stress time. The soluble protein content of high-temperature-resistant NYJ2 was significantly lower than that of high-temperature-sensitive NYJ18. Moreover, when we pooled both high-temperature-resistant *Anoectochilus* germplasm resource (NYJ2) and high-temperature-sensitive *Anoectochilus* germplasm resource (NYJ18) together, the

http://www.aloki.hu ● ISSN 1589 1623 (Print) ● ISSN 1785 0037 (Online)
DOI: http://dx.doi.org/10.15666/aeer/1605_70177031
© 2018, ALÖKI Kft., Budapest, Hungary

heat injury index significantly associated with soluble protein content (0.9442**). For high-temperature-resistant *Anoectochilus* germplasm resource (NYJ2), the heat injury index significantly associated with soluble protein content (0.8741*). For high-temperature-sensitive *Anoectochilus* germplasm resource (NYJ18), the heat injury index significantly associated with soluble protein content (0.9695**). Thus, soluble protein content might be important for identifying high-temperature-resistance of *Anoectochilus* species.

Conclusion

In conclusion, the recovery index was strongly negatively correlated with the heat injury index. The mean heat injury index at 6 h, 12 h, 24 h, 30 h and 36 h under high temperature were 5.17%, 16.90, 39.96%, 53.70% and 70.61%, respectively. Over 80% of the *Anoectochilus* species were high-temperature-sensitive, five high-temperature-resistant species of *Anoectochilus* (NYJ2, NYJ6, NYJ14, NYJ21 and NYJ24) were identified. Compared with high-temperature-sensitive species of *Anoectochilus* germplasm, the high-temperature-resistant *Anoectochilus* germplasm had higher SOD activity, proline content and lower REC, CAT activity, MDA, and soluble protein content. The heat injury index was significantly associated with REC, SOD activity, and soluble protein content for both high-temperature-resistant and sensitive *Anoectochilus* germplasm. For high-temperature-resistant *Anoectochilus* germplasm, heat injury index was significantly related to soluble protein content. For high-temperature-sensitive *Anoectochilus* germplasm, the heat injury index was significantly associated with REC, MDA content and soluble protein content. This study is important to understand the heat-resistant mechanism and the breeding of new varieties of *Anoectochilus*. Further studies on molecular basis regarding heat-resistance of *Anoectochilus* is needed.

Acknowledgements. This study was supported by Guangdong Science and Technology Plan Project (No: 2014A020208071); Qingyuan Science and Technology Plan Project (No: 2015A014).

Author contributions. Yu Mei, Daoshou Qiu, Shengen Xiao, Dong Chen designed the research, Yu Mei and Daoshou Qiu performed the experiments and collected the data, Yu Mei and Shengen Xiao analyzed the data and wrote the manuscript, Dong Chen edited the manuscript and provided guidance during experimentation.

REFERENCES

[1] Bates, L. S., Waldren, R. P., Teare, I. D. (1973): Rapid determination of free proline for water stress studies. – Plant and Soil 39: 205-207.
[2] Bradford, M. M. (1976): A rapid and sensitive method for the quantitation of microgram quantities of protein utilizing the principle of protein-dye binding. – Anal Biochem 72: 248-254.
[3] Can, V. T., Luo, C., He, X., Dong, L., Do, M. P. (2016): Effect of high temperature stress on physiology indices of Mango seedlings. – Chinese Journal of Tropical Crops 37(1) 53-58.
[4] Chen, J. X., Wang, X. F. (2006): Plant Physiology Experiment Instructions. – South China University of Technology (SCAU) Press, Guangzhou, China.

http://www.aloki.hu ● ISSN 1589 1623 (Print) ● ISSN 1785 0037 (Online)
DOI: http://dx.doi.org/10.15666/aeer/1605_70177031
© 2018, ALÖKI Kft., Budapest, Hungary

[5] Chen, W., Zhu, X., Han, W., Wu, Z., Lai, Q. (2016): Morphological, physiological and biochemical responses of gerbera cultivars to heat stress. – Korean Journal of Horticultural Science & Technology 34(1): 1-14.
[6] Du, X. M., Sun, N. Y., Hayashi, J., Chen, Y., Sugiura, M., Shoyama, Y. (2003): Hepatoprotective and antihyperliposis activities of in vitro cultured *Anoectochilus formosanus*. – Phytotherapy Research 17(1): 30-33.
[7] Du, X. M., Irino, N., Furusho, N., Hayashi, J., Shoyama, Y. (2008): Pharmacologically active compounds in the *Anoectochilus* and *Goodyera* species. – Journal of Natural Medicines 62(2): 132-148.
[8] Fang, H. L., Wu, J. B., Lin, W. L., Ho, H. Y., Lin, W. C. (2008): Further studies on the hepatoprotective effects of *Anoectochilus formosanus*. – Phytotherapy Research 22(3): 291-296.
[9] Han, Y., Fan, S., Zhang, Q., Wang, Y. (2013): Effect of heat stress on the MDA, proline and soluble sugar content in leaf lettuce seedlings. – Agricultural Sciences 4(5B): 112-115.
[10] He, C. N., Wang, C. L., Guo, S. X., Xiao, P. G. (2004): Advances on chemical compositions and pharmacological studies of *Anoectochilus* Blume (*Orchidaceae*). – Chinese Pharm J 39: 81-84.
[11] Jia, K., Chen, G. (2005): Tolerance of different eggplant varieties at seedling stage to high temperature stress. – Chinese Journal of Ecology 24(4): 398-401
[12] Jiang, C., Hu, Y., Qin, J., Wang, Y., Zhang, M. (2008): Research in effect of high temperature on physiological indexes of varieties in China rose. – Seed 6: 31-34.
[13] Li, W., Xiao, X., Lv, L. (2015): Morphological response to heat stress and screening of assessment indexes for heat tolerance in eggplant. – Chinese Journal of Tropical Crops 36(6): 1142-1146.
[14] Li, X., Luo, L., Hua, Z. (2018): Physiological and biochemical responses of rhododendron lapponicum to heat stress. – Acta Agriculturae Boreali-occidentalis Sinica 27(2): 253-259.
[15] Li, Z., Sun, B., Luo, S., Li, Z. (2009): Morphological response to heat stress and screening of assessment indexes for heat tolerance in eggplant (*Solanum melogena* L.) in South China. – Journal of Plant Genetic Resources 10(2): 244-248.
[16] Lin, X., Shi, M., Lin, S. (2014): Effects of high-temperature stress on chlorophyll fluorescence parameters, SOD activity and electrolyte leakage of *Anoectochilus* roxburghii (Wall.) Lindl. and *Anoectochilus* formosanus Hayata. – Chinese Journal of Tropical Crops 35(6): 1137-1142.
[17] Liu, Y., Li, H., Xiao, D. (2001): The accumulation of free proline in mosses under high temperature stress. – Journal of Jishou University (Natural Science Edition) 22(1): 1-3.
[18] Peng, H., Gao, Y., Du, H., Qian, H., Wang, P. (2012): Effect of heat stress on related physiological indexes of pansy cultivar seedling. – Journal of Shanghai Jiaotong University (Agricultural Science) 30(6): 66-71.
[19] Rivero, R. M., Ruiz, J. M., Romero, L. (2015): Oxidative metabolism in tomato plants subjected to heat stress. – Journal of Pomology & Horticultural Science 79(4): 560-564.
[20] Shao, Q., Wang, H., Guo, H., Zhou, A., Huang, Y., Sun, Y., Li, M. (2014): Effects of shade treatments on photosynthetic characteristics, chloroplast ultrastructure, and physiology of *Anoectochilus roxburghii.* – PloS One 9(2): e85996.
[21] Sun, Y., Wang, S., Li, Y., Chen, S., Zhou, G. (2006): Study on effect of high temperature stress on physiological Characteristics of coptis chinensis Franch. – Chinese Agricultural Science Bulletin 22(4): 236-238.
[22] Tian, Z., Wang, F., Zhang, W., Zhao, X. (2011): Effects of heat stress on growth and physiology of marigold cultivars. – Acta Horticulturae Sinica 38(10): 1947-1954.
[23] Wang, J., Yuan, B., Xu, Y., Huang, B. (2018): Differential responses of amino acids and soluble proteins to heat stress associated with genetic variations in heat tolerance for hard fescue. – Journal of the American Society for Horticultural Science 143(1): 45-55.

http://www.aloki.hu ● ISSN 1589 1623 (Print) ● ISSN 1785 0037 (Online)
DOI: http://dx.doi.org/10.15666/aeer/1605_70177031
© 2018, ALÖKI Kft., Budapest, Hungary

[24] Wang, W. B., Kim, Y. H., Lee, H. S., Kim, K. Y., Deng, X. P., Kwak, S. S. (2009): Analysis of antioxidant enzyme activity during germination of alfalfa under salt and drought stresses. – Plant Physiology and Biochemistry 47(7): 570-577.
[25] Xu, S., Li, J., Zhang, X., Wei, H., Cui, L. (2006): Effects of heat acclimation pretreatment on changes of membrane lipid peroxidation, antioxidant metabolites, and ultrastructure of chloroplasts in two cool-season turfgrass species under heat stress. – Environmental and Experimental Botany 56(3): 274-285.
[26] Zhang, W., Zou, F., Chen, J., Liu, B., Huang, Y., Zhao, Y. (2017): Effect of high temperature stress on physiological indexes of heat tolerance in *Camellia nitidissima* Chi. – Subtropical Agriculture Research 13(2): 88-92.
[27] Zhang, Y., Cai, J., Ruan, H., Pi, H., Wu, J. (2007): Antihyperglycemic activity of kinsenoside, a high yielding constituent from *Anoectochilus roxburghii* in streptozotocin diabetic rats. – Journal of Ethnopharmacology 114(2): 141-145.
[28] Zheng, C. F., Pan, Y. T., Cai, W. Y., Yuan, X. N., Gao, F. (2013): Identification and determination of flavonoids in *Anoectochilus roxburghii* (Wall.) Lindl by HPLC-UV-MS/MS. – Natural Product Research and Development 25: 1381-1386.

http://www.aloki.hu ● ISSN 1589 1623 (Print) ● ISSN 1785 0037 (Online)
DOI: http://dx.doi.org/10.15666/aeer/1605_70177031
© 2018, ALÖKI Kft., Budapest, Hungary

THE EFFECT OF SYNTHETIC GROWTH REGULATORS ON SELECTED PARAMETERS OF *MEDICAGO* X *VARIA* T. MARTYN AND *TRIFOLIUM PRATENSE* L. NUTRITIONAL VALUE

SOSNOWSKI, J.* – KRÓL, J.

Department of Grassland and Green Areas Creation, Siedlce University of Natural Sciences and Humanities, Prusa 14 Street, 08-110 Siedlce, Poland
(phone: +48-25-643-1318)

**Corresponding author*
e-mail: jacek.sosnowski@uph.edu.pl

(Received 23rd Jul 2018; accepted 28th Sep 2018)

Abstract. The aim of the paper is to study the effects of auxin and cytokinin, synthetic growth regulators, on selected parameters of hybrid alfalfa and red clover nutritional value. The experiment was conducted at the experimental facility of Siedlce University of Natural Sciences and Humanities between 2014 and 2016. In the autumn of 2014 plastic cylinders with no bottom, 40 cm high and with the diameter of 36 cm, were sunk 30 cm deep into the ground, with spacing of 0.8 × 0.8 m. They were filled with the soil of the anthropogenic order. Experimental factors: plant species - hybrid alfalfa and red clover, growth regulator - control (distilled water), indole-3-butric acid (auxin), 6-benzyloaminopuryn (cytokinin), indole-3-butric acid + 6-benzylaminopuryn. After plants in each cylinder were harvested their chemical analysis was carried out. Dry matter digestibility (%) and total protein, crude fibre concentration in dry matter (g kg^{-1}) was determined with the NIRS method using the Buchi NIRFlex N-500 spectrometer. The results of the multi-factor experiment with 24 experimental units were processed statistically using repeated measures analysis of variance. Growth regulators affected the content of protein and crude fibre in plant matter in different wayes. Cytokinin and a mixture of hormones reduced the concentration of protein relative to the control, but fibre share increased. Auxin had no significant effect on these features.
Keywords: *auxin, cytokinin, Fabaceae, total protein, crude fibre, dry mater digestibility*

Introduction

Auxin and cytokinin are important plant hormones regulating such important physiological processes as nutrient transport (Jenik and Barton, 2005). Additionally, according to many authors (Jenik and Barton, 2005; Cheng et al., 2006, 2007; Weijers et al., 2006), natural plant hormones take part in root elongation, which, in turn, affects the rate of nutrient absorption from the soil. It was confirmed by other studies that plant growth regulators containing synthetic hormones stimulate root system growth too, increasing nutrient uptake form the soil (Hwang and Sakakibara, 2006). Ali et al. (2008) reported that auxins are leading factors in this process, acting as signals informing about the state of physiological processes in cells and about growing demand for nutrients, this way attracting them. Thus, high quantities of soil nutrients are absorbed by the roots, and big amounts of them are transported from vegetative to generative parts.

According to Nowak and Wróbel (2010a, b) chemicals and mineral fertilizers can no longer be used in rising quantities to increase agricultural productivity, which is why there is a need to look for other substances affecting plant growth. The authors' opinion is that such growth regulators should increase production potential in unfavourable climatic and in other adverse conditions, not conducive to the growth and development of a particular plant species. Von Richthofen (2006) pointed out that those products would be very important in the case of *Fabaceae* plants, with their unstable growth and

http://www.aloki.hu ● ISSN 1589 1623 (Print) ● ISSN 1785 0037 (Online)
DOI: http://dx.doi.org/10.15666/aeer/1605_70337043
© 2018, ALÖKI Kft., Budapest, Hungary

sensitivity to weather conditions. Among growth regulators there are synthetic plant hormones that have been used both in agriculture and horticulture for quite a few years (Czapla et al., 2005; Nowak and Wróbel, 2010a, b; Wierzbowska and Bowszys, 2008)

For economic and environmental reasons *Fabacea* plants like lucerne (*Medicago* x *varia* T. Martyn) and clover (*Trifolium pratense* L.) are worth considering for cultivation in larger areas. Those plants make it possible to limit mineral fertiliser use, and, besides, they contribute to activation and movement of many nutrients in the soil (Wilczek et al., 2006). Additionally, *Fabaceae* plants grown together with grass species as mixtures improve physical and chemical properties of the soil, positively affecting its structure, fertility, biological activity of microflora, and movement of nutrients from lower to upper layers (Gaweł and Żurek, 2003). Wild growing clover (*Trifolium pratense* L.) has been known for a long time, mainly as a medicinal plant (Booth et al., 2006). High content of polyphenols and isoflavones belonging to the group of phytoestrogens such as daidzein, genistein, formononetin and biochanin makes it an antioxidant plant (Surh et al., 2006). Present in *Fabaceae* plants Polyphenol compounds positively affect human health, for example, mitigating menopause symptoms, preventing development of cardiovascular disease, and lowering a risk of some cancer forms (Thompson et al., 2007). High-protein PX (protein-xanthophyll) concentrate is an alfalfa product which may become widely used in animal nutrition, while EFL (extract fleur lucerne) produced form concentrated alfalfa juice is used in human nutrition. For their yield to be high and to contain high protein content, plants used to produce PX should be grown in good conditions, without weeds. All chemical treatments should be applied according to the withdrawal period, to maintain high standards of health and safety (Plaza et al., 2003; Karwowska et al., 2010). Both of the above substances are produced by extracting proteins, macronutrients, and vitamins from alfalfa juice, with indigestible elements removed earlier (Brito et al., 2007).

The aim of the paper is to study the effects of auxin and cytokinin, synthetic growth regulators, on selected parameters of *Medicago* x *varia* T. Martyn and *Trifolium pratense* L. nutritional value. The purpose of the experiment was to assess the impact of indole-3-butyric acid (synthetic auxin), 6-benzyloaminopuryn (synthetic cytokinin), and their mixture on total protein and crude fibre content, and dry mater digestibility of selected plants.

Material and methods

Experimental conditions

The experiment was conducted at the experimental facility of Siedlce University of Natural Sciences and Humanities (52°10’03”N; 22°17’24”E; Poland) between 2014 and 2016. In the autumn of 2014 plastic cylinders with no bottom, 40 cm high and with the diameter of 36 cm, were sunk 30 cm deep into the ground, with spacing of 0.8 × 0.8 m. They were filled with the soil of the anthropogenic order, culture earth type, hortiolse subtype, and the granulometric composition of loamy sand. Before the experiment was set up, organic carbon (C_{org}) concentration in the soil was 13.50 g kg^{-1} DM, with total nitrogen concentration of 1.30 g kg^{-1} DM. The ratio of C:N was 10.4:1, and soil pH of 6.8 was close to neutral. The soil had high content of phosphorus and magnesium, while available forms of potassium were of medium quantities. Because of relatively high content of nutrients mineral fertilizers were not used.

http://www.aloki.hu ● ISSN 1589 1623 (Print) ● ISSN 1785 0037 (Online)
DOI: http://dx.doi.org/10.15666/aeer/1605_70337043
© 2018, ALÖKI Kft., Budapest, Hungary

Plastic sheeting was spread between the plants to prevent weeds from sprouting. Next, 10 seeds were planted into each cylinder. After germination, when seedlings had 3-10 leaves, three best looking plants were selected for further research, while the others were removed. In the growing seasons of 2015 and 2016 plants reached their full potential to be harvested three times when 30-40% alfalfa and clover plants were in the bloom stage. The experiment was set up in a split-plot design with three replications (*Fig. 1*).

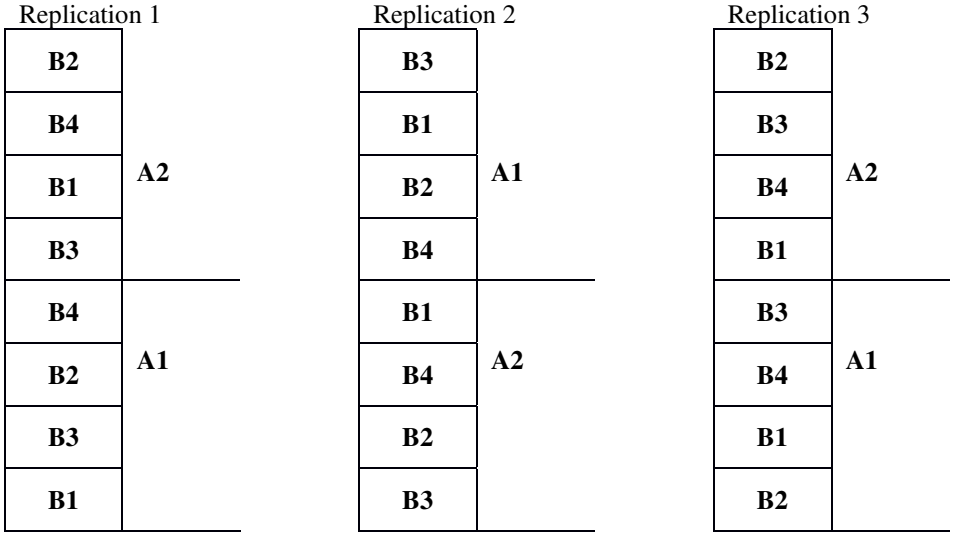

Figure 1. *The outlay of the experiment. Plants: A1 - hybrid alfalfa, A2 - red clover. Treatments: B1 - control, B2 - auxin; B3 - cytokinin, B4 - auxin + cytokinin*

Experimental factors:

- Plant species: hybrid alfalfa (*Medicago* x *varia* T. Martyn) var. Kometa and red clover (*Trifolium pratense* L.) var. Krynia;
- Growth regulator (applied as a spray): K – control (distilled water), A – indole-3-butric acid (IBA – synthetic auxin), C - 6-benzyloaminopuryn (BAP - synthetic cytokinin), AC - indole-3-butric acid + 6-benzylaminopuryn (IBA+BAP at a rate of 1:1).

Plants were treated twice during each growing cycle:

- Hybrid alfalfa – the first treatment after the development of the first internode, the other when the first flower buds were visible outside leaves;
- Red clover – the first treatment after the appearance of the first branches, the other when the first florescence emerged.

For the plants to be thoroughly covered, 0.2 dm^3 of spraying liquid was used per one cylinder with growth regulator concentration of 30 mg dm^{-3}. The control unit was treated with the same amount of distilled water.

After plants in each cylinder were harvested their chemical analysis was carried out. Dry matter digestibility (%) and total protein, crude fibre concentration in dry matter (g kg^{-1}) was determined with the NIRS method using the Buchi NIRFlex N-500 spectrometer.

http://www.aloki.hu ● ISSN 1589 1623 (Print) ● ISSN 1785 0037 (Online)
DOI: http://dx.doi.org/10.15666/aeer/1605_70337043
© 2018, ALÖKI Kft., Budapest, Hungary

Weather conditions

Sielianinov's hydrothermal coefficient was calculated in order to determine temporal variation of meteorological conditions and their effects on vegetation. The hydrothermal coefficient (K) was calculated on the basis of monthly sums of precipitation (P) and a sum of monthly air temperatures (t), using the following formula (Skowera and Puła, 2004):

$$K=P/0.1\sum t$$

Values of Selianinov's hydrothermal coefficient (K) are presented in *Table 1*. It was assumed that extreme conditions took place when its value was below 0.7 and above 2.5 (Skowera and Puła, 2004).

Table 1. *The value of Sielianinov's hydrothermal coefficient (K) in the growing season*

Years	Months						
	April	**May**	**June**	**July**	**August**	**September**	**October**
2014	1.36 (o)	1.87 (mw)	1.64 (mw)	0.59 (sd)	1.92 (mw)	0.64 (sd)	0.12 (ed)
2015	1.22 (md)	2.63 (sw)	0.87 (d)	1.08 (md)	0.18 (ed)	1.46 (o)	1.94 (mw)
2016	1.89 (mw)	0.82 (d)	1.02 (md)	2.15 (w)	1.05 (md)	0.36 (ed)	7.65 (ew)

$K \leq 0.4$ extreme drought (ed). $0.4 < K \leq 0.7$ severe drought (sd). $0.7 < K \leq 1.0$ drought (d). $1.0 < K \leq 1.3$ moderate drought (md). $1.3 < K \leq 1.6$ optimal (o). $1.6 < K \leq 2.0$ moderately wet (mw). $2.0 < K \leq 2.5$ wet (w). $2.5 < K \leq 3.0$ severely wet (sw). $K > 3.0$ extremely wet (ew)
2014 - the year in which the experiment was established, 2015 and 2016 - years of full use of experience

Optimal temperature and moisture conditions were only in April 2014 and in September 2015. In the remaining months of the growing periods they were not as favourable, varying from extremely dry in August 2015 to extremely wet in May 2014. Throughout the experiment the best conditions were at the beginning of each growing season. It can be concluded that the most difficult situation for plants was in 2015, when, apart from May and the end of the growing season, the weather ranged from moderately dry to extremely dry. The growing season of 2016 was characterized by a lack of a period with optimal conditions for plant growth. A high level of precipitation in July (K = 2.15) and drought in most of the remaining months hindered proper growth and development of plants.

Statistical analysis

The results of the multi-factor experiment with 24 experimental units were processed statistically using repeated measures analysis of variance; the same forage parameters were measured during each growing cycle. The Fisher-Snedecor test was done to determine the significance of the effect of experimental factors on the parameters. Tukey's test was used to compare differences between means at the $LSD_{0.05}$ significance level. All the calculations were made with the Statistica 13 – 2017 program. In tables

http://www.aloki.hu ● ISSN 1589 1623 (Print) ● ISSN 1785 0037 (Online)
DOI: http://dx.doi.org/10.15666/aeer/1605_70337043
© 2018, ALÖKI Kft., Budapest, Hungary

homogenous groups are marked with letters. Means in lines and columns marked with the same letters are not significantly different.

Results and discussion

Total protein concentration (*Table 2*), an average for treatments, was in a statistically significant way higher in hybrid alfalfa (199 g kg^{-1}) than in red clover (176 g kg^{-1}). The concentration in red clover was lower but at close levels during both growing seasons; similar results were recorded by Ćwintal and Kościelecka (2005) in their experiment on diploid and tetraploid red clover agricultural value. Throughout the experiment protein concentration was the highest in the second year, also in alfalfa, with 203 g kg^{-1}.

Table 2. *The effect of growth regulators on total protein concentration (g kg^{-1} DM)*

Treatments	Year		Means
	2015	2016	
Treatment effect			
K	194 Aa	185 Aa	189 a
A	187 Aa	190 Aa	189 a
C	181 Ab	190 Aa	186 b
AC	185 Ab	187 Aa	186 b
Species effect			
Hybrid alfalfa	195 Ba	203 Aa	199 a
Red clover	179 Ab	173 Ab	176 b
Means	187 A	188 A	

Means followed by the same lowercase letters in columns are not significantly different. Means followed by the same capital letters in lines are not significantly different.
K - control (distilled water), A - synthetic auxin, C - synthetic cytokinin, AC - synthetic auxin + synthetic cytokinin

Growth regulators diversified total protein concentration in dry matter. It was the highest in plants from units treated with auxin and from the control, with the identical value of 189 g kg^{-1}. Cytokinin and a mixture of auxin with cytokinin resulted in statistically significant reductions of protein content in the biomass. Average annual protein content values were similar throughout the experiment, but there were some differences between harvests (see below). Gaweł and Żurek (2003) studying protein content in three varieties of alfalfa demonstrated opposite results, with its decrease in consecutive years. Low total protein content in the present experiment resulted from longer growing cycles, which was a consequence of three harvests instead of four. Andrzejewska et al. (2013) found that delaying alfalfa harvest time from the beginning of the flower budding stage to the flowering stage resulted in a decrease in protein content by, on average, 20 g kg^{-1}. In addition, the authors discovered that this delay caused an increase in the amount of fibre.

In the present experiment there was some diversification of total protein content in plants caused by an interaction between the effect of a regulator and a harvest (*Table 3*). The highest average total protein content for both species was in the first harvest (202 g kg^{-1}), and it was lower in the second (188 g kg^{-1}) and third (172 g kg^{-1}).

http://www.aloki.hu ● ISSN 1589 1623 (Print) ● ISSN 1785 0037 (Online)
DOI: http://dx.doi.org/10.15666/aeer/1605_70337043
© 2018, ALÖKI Kft., Budapest, Hungary

Table 3. *The effect of growth regulators on total protein concentration in harvests (g kg^{-1} DM)*

Treatments	Harvest		
	1	2	3
Treatment effect			
K	212 Aa	187 Ba	170 Ca
A	199 Ab	195 Aa	173 Bc
C	201 Aab	188 Aab	167 Ba
AC	197 Ab	181 Ba	180 Ba
Species effect			
Hybrid alfalfa	214 Aa	198 Ba	185 Ca
Red clover	190 Ab	178 Bb	160 Cb
Means	202 A	188 B	172 C

Means followed by the same lowercase letters in columns are not significantly different. Means followed by the same capital letters in lines are not significantly different
K - control (distilled water), A - synthetic auxin, C - synthetic cytokinin, AC - synthetic auxin + synthetic cytokinin

The above differences were statistically significant. Those findings were comparable with results provided by Wilczek et al. (2005a). Wilczek et al. (2005a, b) examined selected varieties of hybrid alfalfa and alfalfa (*Medicago sativa* L.) and found total protein content in those plants at the level of 170-220 g kg^{-1} DM. In turn, Stochmal et al. (2000) identified general protein content in legume plants as190 g kg^{-1} DM.

Hybrid alfalfa had higher average concentration of crude fibre (239 g kg^{-1}) than red clover (*Table 4*). This concentration in red clover was in a statistically significant way similar in both growing seasons (2015 – 214 g kg^{-1}; 2016 – 216 g kg^{-1}). Crude fibre content was diversified by growth regulators, and it was on average the highest in forage from units treated with cytokinin (234 g kg^{-1}) and with a mixture of auxin and cytokinin (231 g kg^{-1}). In the control unit and in the one with auxin there was statistically significant reduction of crude fibre concentration, by, on average, 5.1%.

Table 4. *The effect of growth regulators on crude fibre concentration (g kg^{-1} DM)*

Treatments	Year		Means
	2015	2016	
Treatment effect			
K	225 Ab	219 Ab	222 b
A	219 Ab	221 Ab	220 b
C	237 Aa	231 Ba	234 a
AC	232 Aa	231 Aa	231 a
Species effect			
Hybrid alfalfa	243 Aa	235 Ba	239 a
Red clover	214 Ab	216 Ab	215 b
Means	228 A	225 A	

Means followed by the same lowercase letters in columns are not significantly different. Means followed by the same capital letters in lines are not significantly different
K - control (distilled water), A - synthetic auxin, C - synthetic cytokinin, AC - synthetic auxin + synthetic cytokinin

http://www.aloki.hu ● ISSN 1589 1623 (Print) ● ISSN 1785 0037 (Online)
DOI: http://dx.doi.org/10.15666/aeer/1605_70337043
© 2018, ALÖKI Kft., Budapest, Hungary

As an average for both species crude fibre content underwent substantial variation as a result of regulator and harvest interaction (*Table 5*). In the first and second harvests auxin caused a statistically significant decline in fibre concentration, to 207 and 231 g kg^{-1}. In the third harvest the regulator also caused a decrease, but this trend was not statistically significant. The experiment confirmed the view of differences in fibre content between consecutive harvests. Forage from the first and third harvests had a better nutritional value because fibre content was in a statistically significant way lower than in the second one. This tendency in consecutive harvests was confirmed by other authors (Wilczek et al., 2005a, b).

Table 5. *The effect of growth regulators on crude fibre concentration in harvests (g kg^{-1} DM)*

Treatments	Harvest		
	1	2	3
Treatment effect			
K	221 ABa	235 Abc	210 Bb
A	207 Bb	231 Ac	223 Aab
C	222 Ba	251 Aa	230 Ba
AC	226 ABa	246 Aab	223 Bab
Species effect			
Hybrid alfalfa	225 Ba	261 Aa	230 Ba
Red clover	213 Aa	220 Ab	213 Ab
Means	219 B	241 A	221 B

Means followed by the same lowercase letters in columns are not significantly different. Means followed by the same capital letters in lines are not significantly different
K - control (distilled water), A - synthetic auxin, C - synthetic cytokinin, AC - synthetic auxin + synthetic cytokinin

According to Gaweł (2009) proper digestibility of plant material should be around 65%. Dry matter digestibility (*Table 6*), i.e. percentage of nutrients absorbed by the digestive system, was significantly higher in red clover (52.7%) than in alfalfa hybrid (50.5%), with a statistically significantly increase in the latter plant in the second year. This result was confirmed by the research of Gaweł (2012), when digestibility of alfalfa mixtures with grasses was also the highest in the second year.

Generally, throughout the research growth regulators did not affect red clover and hybrid alfalfa digestibility, with its average annual values remaining similar with no statistically significant differences. However, there were differences between harvests during the same growing season (*Table 7*). The lowest value, average for the species and the regulator, was in the biomass of the second harvest (48.2%), while plant material from the first and third ones had statistically significantly higher digestibility, 53% and 53.6%, respectively. The highest digestibility of all samples was in alfalfa treated with growth regulators in the third harvest (55.5%), and the lowest in the second (45.2%). In red clover dry-matter digestibility in the second and third harvests remained at a similar level and was significantly lower than the values in the first one.

According to Gaweł and Żurek (2003) the number of growing cycles in a growing season had a marked effect on plant digestibility. This was closely related to the development stage at the harvest time and the pace of plant senescence. Overall, low digestibility of hybrid alfalfa and red clover in the present study resulted from the three

http://www.aloki.hu ● ISSN 1589 1623 (Print) ● ISSN 1785 0037 (Online)
DOI: http://dx.doi.org/10.15666/aeer/1605_70337043
© 2018, ALÖKI Kft., Budapest, Hungary

harvests in the growing season. Gaweł (2009, 2012) reported that with four harvests read clover had dry matter digestibility of 72%, and growing this species in a mixture of grasses raised it to 75%.

Table 6. *The effect of growth regulators on digestibility (%)*

Treatments	Year		Means
	2015	2016	
Treatment effect			
K	52.0 Aa	53.2 Aa	52.6 a
A	51.6 Aa	51.5 Aa	51.5 a
C	49.9 Aa	51.9 Aa	50.9 a
AC	50.4 Aa	52.5 Ba	51.4 a
Species effect			
Hybrid alfalfa	49.8 Bb	51.2 Ab	50.5 b
Red clover	52.1 Aa	53.3 Aa	52.7 a
Means	51.0 B	52.2 A	

Means followed by the same lowercase letters in columns are not significantly different. Means followed by the same capital letters in lines are not significantly different
K - control (distilled water), A - synthetic auxin, C - synthetic cytokinin, AC - synthetic auxin + synthetic cytokinin

Table 7. *The effect of growth regulators on digestibility of forage in individual harvests (%)*

Treatments	Harvest		
	1	2	3
Treatment effect			
K	52.0 ABa	51.2 Ba	54.6 Aa
A	54.7 Aa	48.0 Bb	51.9 ABa
C	52.1 Aa	47.2 Bb	53.4 Aa
AC	53.2 Aa	46.5 Bb	54.5 Aa
Species effect			
Hybrid alfalfa	50.8 Bb	45.2 Cb	55.5 Aa
Red clover	55.2 Aa	51.2Ba	51.6 Bb
Means	53.0 A	48.2 B	53.6 A

Means followed by the same lowercase letters in columns are not significantly different. Means followed by the same capital letters in lines are not significantly different
K - control (distilled water), A - synthetic auxin, C - synthetic cytokinin, AC - synthetic auxin + synthetic cytokinin

In the first harvest of the first and second years (*Fig. 2*) the highest dry matter digestibility was on units treated with auxin, but the values were not significantly higher than those obtained on units with other treatments.

In the second harvest of the second year (2016) it was highest on the control and on units with cytokinin. Other treatments decreased this value. In turn, in the third harvest of the second year the highest dry matter digestibility was on the unit treated with a mixture of auxin with cytokinin, and it was statistically significantly higher than the

http://www.aloki.hu ● ISSN 1589 1623 (Print) ● ISSN 1785 0037 (Online)
DOI: http://dx.doi.org/10.15666/aeer/1605_70337043
© 2018, ALÖKI Kft., Budapest, Hungary

values on other units. It should be noted that that growing season was characterized by extreme weather conditions. September 2016 was extremely dry and October extremely wet (*Table 1*). Such a large diversity of weather conditions could have impacted the effect of hormone mixtures on plants. It can be concluded that because of the September drought in 2016 a mixture of auxin with cytokinin stimulated total protein accumulation in plants, limiting accumulation of fibrous substances. The consequence of this was a big increase in plant dry matter content. In turn, extremely wet October (monthly rainfall of 161.2 mm) with low temperatures (daily average temperature of 7.2 °C) slowed down accumulation of protein and of non-digestible substances.

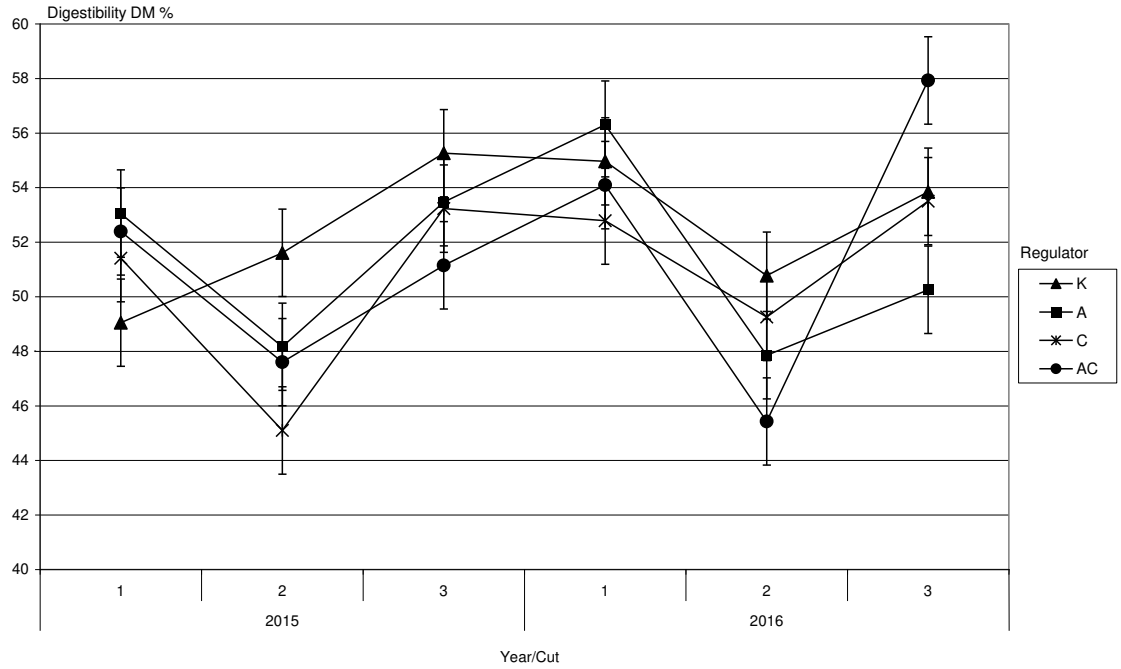

Figure 2. *The effect of growth regulators on digestibility of forage in individual harvests (%)*

Conclusions

1. Exogenous growth regulators in different ways affected the content of protein and crude fibre in plant dry matter.
2. Cytokinin and a mixture of hormones reduced the concentration of protein relative to the control, but fibre share increased. Auxin had no significant effect on these features.
3. Overall, growth regulators did not change dry matter digestibility, but there were differences between harvests.
4. The experiment did not prove that the quality of plant material improved as a result of the application of synthetic auxin, cytokinin, and mixtures of these compounds.

Acknowledgements. The research carried out under the theme No 357/13/S was financed by the science grant of the Ministry of Science and Higher Education.

http://www.aloki.hu ● ISSN 1589 1623 (Print) ● ISSN 1785 0037 (Online)
DOI: http://dx.doi.org/10.15666/aeer/1605_70337043
© 2018, ALÖKI Kft., Budapest, Hungary

REFERENCES

[1] Ali, B., Hayat, S., Hasan, S., Ahmad, A. (2008): A comparative effect of IAA and 4-Cl-IAA on growth, nodulation and nitrogen fixation in *Vigna radiata* (L.) – Acta Physiol. Plant. 30: 35-41.

[2] Andrzejewska, J., Albrecht, K. A., Jendrzejczak, E. (2013): Plant height and feed value of alfalfa in different development stages and cuts. – Fragm. Agron. 30(2): 14-22.

[3] Booth, N. L., Overk, C. R., Yao, P., Totura, S., Deng, Y., Hedayat, A. S., Bolton, J. L., Pauli, G. F., Farnsworth, R. (2006): Seasonal variation of red clover (*Trifolium pratense* L.) isoflavones and estrogenic activity. – J. Agric. Food Chem. 54: 1277-1282.

[4] Brito, A. F., Broderic, G. A, Olmos Colmenero, J. J., Reynal, S. (2007): Effects of feeding formatetreated alfalfa silage or red clover silage on omasal flow of nutrients and microbial protein synthesis in lactating dairy cows. – J. Dairy Sci. 90: 1392-1404.

[5] Cheng, Y., Dai, X., Zhao, Y. (2006): Auxin biosynthesis by the YUCCA Flavin monooxygenases controls the formation of floral organs and vascular tissues in Arabidopsis. – Genes & Development 20: 1790-1799.

[6] Cheng, Y., Dai, X., Zhao, Y. (2007): Auxin synthesized by the YUCCA flavin monooxygenases is essential for embryogenesis and leaf formation in Arabidopsis. – The Plant Cell. 19: 2430-2439.

[7] Ćwintal, M., Kościelecka, D. (2005): The influence of the way of sowing and amount of seeds on the density structure, yielding and quality of diploid and tetraploid red clover in the year of sowing Part I. Density structure of plants and shoots. – Biul. IHAR 237/238: 237-248.

[8] Czapla, J., Stasiulewicz, L., Nogalska, A. (2005): Spring triticale yield as dependent upon growth regulators, applied alone or in combinations with magnesium sulphate – Acta Sci. Pol. Agricultura 4(2): 29-36.

[9] Gaweł, E. (2009): Yielding of red clover and lucerne mixtures with grasses on the ecological farms. – J. Res. Appl. Agric. Eng. 54(3): 97-86.

[10] Gaweł, E. (2012): Nutritive value of lugume-grass mixtures cultivated in organic farms. – J. Res. Appl. Agric. Eng. 57(3): 91-97.

[11] Gaweł, E., Żurek, J. (2003): Nutritional value of selected lucerne cultivars. – Biul. IHAR 225: 167-174.

[12] Hwang, I., Sakakibara, H. (2006): Cytokinin biosynthesis and perception. – Physiologia Plantarum 126: 528-538.

[13] Jenik, P. D., Barton, M. K. (2005): Surge and destroy: the role of auxin in plant embryogenesis. – Development 132: 3577-3585.

[14] Karwowska, M., Stadnik, J., Dolatowski, Z. J., Grela, R. E. (2010): Effect of protein-xanthophylls (PX) concentrate of alfalfa supplementation on physico-chemical properties of turkey breast and thigh muscles during ageing. – Meat Science 82(2): 486-490.

[15] Nowak, A., Wróbel, J. (2010a): The effect of growth regulators on content of assimilation pigment in leaves of three soybean cultivars (*Glycine max* L. Merr). – Rośliny Oleiste-Oilseed Crops 31: 351-359.

[16] Nowak, A., Wróbel, J. (2010b): Impact of selected growth regulators on yielding of soybean (*Glycine max* L. Merr) in control requirements of substrate moisture. – Rośliny Oleiste-Oilseed Crops 31: 124-132.

[17] Plaza, L., De Ancos, B., Cano, M. P. (2003): Nutritional and health-related compounds in sprouts and seeds of soybean (*Glycine max*), wheat (*Triticum aestivum*. L) and alfalfa (*Medicago sativa*) treated by a new drying method. – Eur Food Res Technol. 216: 138-144. DOI 10.1007/s00217-002-0640-9.

[18] Rylott, P. D., Smith, M. L. (1990): Effects of applied growth substances on pod set in broad beans (*Vicia faba* var. major). – J. Agri. Sci. 114: 41-47.

[19] Skowera, B., Puła, J. (2004): Pluviometric extreme conditions in spring season in Poland in the years 1971-2000. – Acta Agrophys. 3(1): 171-177.

http://www.aloki.hu ● ISSN 1589 1623 (Print) ● ISSN 1785 0037 (Online)
DOI: http://dx.doi.org/10.15666/aeer/1605_70337043
© 2018, ALÖKI Kft., Budapest, Hungary

[20] Stochmal, A., Simonet, A. M., Macias, F. A., Oliviera, M. A., Abreu, J. M., Nash, R., Oleszek, W. (2000): Acylated apigenin glycosides from alfalfa (*Medicago sativa* L.) var. Artal. – Phytochemistry 57: 1223-1226.
[21] Surh, J., Kim, M. J., Koh, E., Kim, Y-K. L., Kwon, H. (2006): Estimated intakes of isoflavones and coumestrol in Korean population. – Int. J. Food. Sci. Nutr. 57(5/6): 325-344.
[22] Thompson, C. J., Pitter, M. H., Ernst, E. (2007): *Trifolium pretense* isoflavones in the treatment of menopausal hot flushes. – Phytomedicine 14: 153-159.
[23] Von Richthofen, J. S. (2006): What do European farmers think about grain legumes. – Grain Legumes 45: 14-15.
[24] Weijers, D., Schlereth, A., Ehrismann, J. S., Schwank, G., Kientz, M., Jurgens, G. (2006): Auxin triggers transient local signaling for cell specification in Arabidopsis embryogenesis. – Dev. Cell. 10: 265-270.
[25] Wierzbowska, J., Bowszys, T. (2008): Effect of growth regulators applied together with different phosphorus fertilization levels on the content and accumulation of potassium, magnesium and calcium in spring wheat. – J. Elementol. 13(1): 411-422.
[26] Wilczek, M., Ćwintal, M., Kornas-Czuczwar, B., Koper, R. (2006): Influence of pre-sowing laser stimulation and microelement nutrition (B, Mo) on yielding of seed of tetraploid red clover during four-year performance. – Acta Agrophys. 8(3): 735-743.
[27] Wilczek, M., Koper, R., Ćwintal, M., Korniłłowicz-Kowalska, T. (2005a): Germination capacity and health status of alfalfa seeds after laser treatment. – Int. Agrophysics 19(1): 85-89.
[28] Wilczek, M., Koper, R., Ćwintal, M., Korniłłowicz-Kowalska, T. (2005b): Germination capacity and health status of hybrid alfalfa seeds after laser treatment. – Int. Agrophysics 19(3): 257-261.

http://www.aloki.hu ● ISSN 1589 1623 (Print) ● ISSN 1785 0037 (Online)
DOI: http://dx.doi.org/10.15666/aeer/1605_70337043
© 2018, ALÖKI Kft., Budapest, Hungary

POLLINATORS OF *PULSATILLA GRANDIS* WENDER. IN SOUTHERN BAKONY (HUNGARY)

MÉSZÁROS, T.[1*] – JÓZAN, ZS.[2]

[1]*Department of Plant Sciences and Biotechnology, Georgikon Faculty, University of Pannonia Keszthely, Festetics u. 7, 8360 Hungary (phone: +36-83-545-095; fax +36-83-545-058)*

[2]*Mernye, Rákóczi Ferenc u. 5, 7453 Hungary*

**Corresponding author e-mail: meszarost773@gmail.com*

(Received 23rd Jul 2018; accepted 5th Oct 2018)

Abstract. Sexual reproduction plays an important role in the maintenance of the genetic variability of plant species. In the case of entomophilous species (like *Pulsatilla grandis*) pollinators are needed to this way of propagation. It is important to have complete knowledge on the pollinators to understand the biology of plant species. Our aim was to collect information about the pollinators of *P. grandis*, as there is no available data on the pollinators of this endangered species. We studied the flower-visiting species in 2017 and 2018 on the Csatár Hill near Veszprém (Hungary) in a population of about 2000 individuals of *P. grandis*. The number of collected *Apis mellifera* individuals (239) was the highest followed by *Bombus* (31 individuals) and *Andrena* (15 individuals) species. *Lasioglossum, Polistes* and *Priocnemis* species were collected as well. We collected 5 male insects which visit the flowers only for nectar but they can help the self-pollination as they are searching for nectar in the flower. We recorded the most intense flower visitation between 10-11 a.m. Our new results can help to develop the conservation strategy of *P. grandis*.
Keywords: *flower-visiting insects, Apis mellifera, Bombus, pollen, nectar*

Introduction

The frequency and intensity of grazing is decreasing due to the decline in livestock farming. As a result the diversity of semi-natural grasslands is decreasing as well. The species number of plants and insects is dwindling in these habitats (Walker and Pinches, 2011). Biodiversity influences ecosystem services in some semi-natural landscapes (Lowenstein et al., 2015). Having enough information about the pollination strategy of rare and endangered species is a key factor to develop protection and management strategies. However, our knowledge is imperfect even in the case of intensively studied species (Denisow et al., 2014a; Gostin, 2011). In the case of metapopulations it is especially important to know the plant-pollinator interactions and the requirements of effective gene flow to maintain healthy populations of rare and endangered species (Schemske et al., 1994). Sexual reproduction is essential from genetic and evolutional aspects. It contributes to the inter- and intrapopulation genetic variability of individuals (Charlesworth and Charlesworth, 1987). Fructification rate and seed set depends on fertilization which is the result of pollination, so the effectiveness of pollination is a key factor in the reproduction success of entomophilous species (Larson and Barrett, 2000). The plant-pollinator interactions are very complex and can be influenced by many factors in addition to environmental ones (Denisow et al., 2014a). In the temperate climate zone about 80% of plant species is pollinated by insects. Both cultivated and wild species are important elements of pollination systems (Strzałkowska et al., 2016). In

http://www.aloki.hu ● ISSN 1589 1623 (Print) ● ISSN 1785 0037 (Online)
DOI: http://dx.doi.org/10.15666/aeer/1605_70457062
© 2018, ALÖKI Kft., Budapest, Hungary

the case of early spring flowering species the number of pollinators is low. The number of flower-visitations by insects is limited due to unfavourable weather conditions (Kratochwil, 1988). In early spring pollen is an especially important protein source for insects (Moquet et al., 2015). The demand for nectar and pollen increases quickly in early spring by bee-like insects (Denisow, 2006). The pollen is needed to forage the brood to reach the proper family size. *Pulsatilla grandis* is a valuable and threatened species of semi-dry grasslands. This species is a significant pollen source for bees as it is flowering in early spring. The morphology and ecology of *Pulsatilla* species also promote the pollination by insects (Zimmermann, 1935). They attract insects with their bell-shaped, actinomorphic flowers and lots of yellow stamens (Walker and Pinches, 2011; Essl, 2005). In the case of partly opened flowers the pollinators first touch the pistils so they can be fertilized with the pollen carried from another plant. While in the case of older, fully opened flowers the bees land on tepals, so they first touch the stamens and after that the pistils (Zimmermann, 1935). Some authors classified *Pulsatilla* species as pollen producing plants, having a lot of stamens but producing no nectar, similar to other species of the *Ranunculaceae* family. Although Weryszko-Chmielewska and Sulborska (2011) proved that the staminodes of *Pulsatilla* flowers produce nectars, so they function as nectaries. Staminodes are much smaller than stamens and have a simple structure. They can be found on the basis of the androecium. The nectar is produced when the pistil is ready for fertilization. Insects have to reach the basis of androecium to reach the nectar. Meanwhile they support fertilization as they touch the stigma. The pollen production of *Pulsatilla* species is 4.22-9.16 g/m^2, so they are significant pollen sources. These species produce more pollen than other early spring perennials (Strzałkowska-Abramek et al., 2016). *Pulsatilla grandis* has different strategies to ensure the efficient pollination. It can close its flowers in the case of unfavourable weather conditions (rain, wind) until the flowers are not pollinated (Sauberer and Panrok, 2015). Most anthers of *Pulsatilla* flowers open in the warmest hours of the day, which is typical of many other early spring species as well (Denisow et al., 2014b, 2015). Pollen emission round midday is advantageous for early spring plants and increases the number of insect visitations (Strzałkowska et al., 2016). The anthers open one after the other. So the flower produces pollen during a long period of time and the ratio of fertilization is higher. This long period of pollen emission is important from population genetic aspect. The number of pollinators, carrying pollen from other individuals, increases as well, so the genetic variability of the next generation multiplies (Kratochwil, 1988). Because the flying distance of pollinator insects is about 10 km, the gene flow between distant populations is not probable (Walker, 2011). *Pulsatilla vulgaris* Mill. is a related species occurring in Western Europe. The success of its reproduction is considerably influenced by the pollination of insects and the spread of pollen depends on the flying distance of pollinators. There is a positive correlation between the foraging distance and the size of pollinator species. Bumblebee species which also visit its flowers has longer foraging range and provide gene flow between distant populations as well (Hensen et al., 2005; Walther-Hellwig and Frankl, 2000; Osborne et al., 2008). It was observed that besides bumblebees honey bees have longer flying distances as well (Steffan-Dewenter and Kuhn, 2003), therefore these insects have significant role in the pollination of populations living in fragmented habitats.

Insects visit *Pulsatilla* species both for nectar and pollen (*Table 1*). However, the visiting *Apoidea* species do not fertilize the flowers in every cases, some of them are nectar robbers (Kratochwil, 1988).

http://www.aloki.hu ● ISSN 1589 1623 (Print) ● ISSN 1785 0037 (Online)
DOI: http://dx.doi.org/10.15666/aeer/1605_70457062
© 2018, ALÖKI Kft., Budapest, Hungary

Our aim was the collect information about the pollinators of *P. grandis*, as there is no available data on the pollinators of this endangered species.

Table 1. *Pollinators of the Pulsatilla genus and Pulsatilla vulgaris*

Taxon	Pollinator	Comment	Reference
Pulsatilla genus	*Apis mellifera* Linnaeus, 1758 *Bombus terrestris* (Linnaeus, 1758)	Mainly visited by honey bees (*Apis mellifera* Linnaeus, 1758) for pollen and nectar	Zimmermann (1935)
Pulsatilla genus	Honey bees and bumble bee species	Pollen and nectar collection	Weryszko-Chmielewska and Sulborska (2011)
P. vulgaris		Nectar collecting bees	Weryszko-Chmielewska and Sulborska (2011)
P. vulgaris	*Lasioglossum lineare* (Schenck, 1869), *Andrena bicolor* Fabricius, 1775	Solitary bees are the main pollinators	Kratochwil (1988)
P. vulgaris	*Halictidae* family, *Andrena* genus		Sauberer and Panrok (2015)
P. vulgaris	*Apis* and *Bombus* species		Walker (2011), Walker and Pinches (2011)
P. vulgaris	*Halictus fulvicornis* (Kirby,1802), *H. tumulorum* (L.1758), *H. albipes* (Fab. 1781), *H. flavipes* (Fab. 1787), *H. leucopus* (Kirby, 1802), *Osmia bicolor* (Schrank, 1781), and *Bombus agrorum* (Fab. 1787) [=*B. pascuorum* (Scopoli, 1763)]	Great Britain	Wells and Barling (1971)

Materials and methods

Study species

Pulsatilla grandis Wender. is a Natura 2000 species, wich is listed in the Annex II and Annex IV of the Habitats Directive of the European Commission (Council Directive 92/43/EEC) (Randic et al., 2013). Its range is Pannonian type, i.e. distributed from Western Ukraine to Austria and the Czech Republic (Sauberer and Panrok, 2015). It is listed as a threatened species, e.g. in Germany, Czech Republic, Slovenia, Slovakia and Ukraine (Dostalova and Király, 2013).

This perennial species of dry grasslands is flowering in early spring. Its attractive flowers are pollinated by insects.

Its flowers open in late February or early March. The leaves develop at the end of flowering. After flowering the peduncle elongates bearing the fruit over the layer of other plants which helps the dispersion of seeds by wind (Kaligaric et al., 2006; Sauberer and Panrok, 2015).

http://www.aloki.hu ● ISSN 1589 1623 (Print) ● ISSN 1785 0037 (Online)
DOI: http://dx.doi.org/10.15666/aeer/1605_70457062
© 2018, ALÖKI Kft., Budapest, Hungary

Flowers are mainly cross-pollinated but in the lack of allogamy self-pollination is also possible (Walker and Pinches, 2011; Zimmermann, 1935; Lindell, 1998).

Study area

The pollinators of *P. grandis* were studied on the calcareous rocky steppes of the Csatár Hill (N47.107830, E17.848507) (*Figs. 1, 2* and *3*), near Veszprém in Southern Bakony (Hungary). The summit of this dolomite hill is 340 metres above sea level. This population of *P. grandis* contains more thousand individuals. The botanical values of the area are threatened by the expansion of weekend houses.

Measuring pollinators

The pollinators were studied in the spring of 2017 and 2018. The methods were different in the two years. On the 25 March 2017 we observed three fully-opened flowers of an individual and one fully-opened flower of another one. On the 28th March 2017 three fully-opened flowers of an individual were studied (no other flower visitation was recorded). The flower-visitations were recorded through 18 h from between 9 a.m. and 5 p.m. on both days. The weather was sunny and windless on both days.

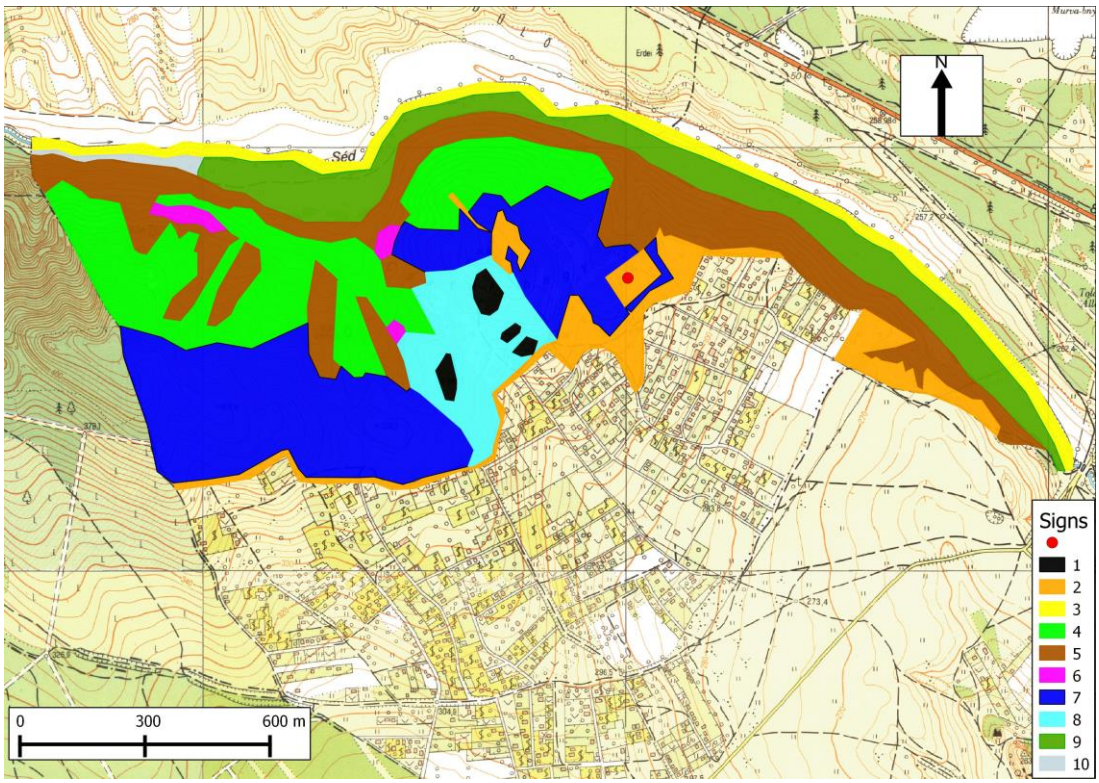

Figure 1. *Vegetation map of the Csatár Hill (vegetation types were classified according to Borhidi (2003)). Legend: red point: experimental site, 1: Seselio leucospermi-Festucetum pallentis Zólyomi (1936) 1958, 2: Chrysopogono-Caricetum humilis Zólyomi (1950) 1958, 3: Aegopodio-Alnetum V. Kárpáti, I. Kárpáti & Jurko 1961, 4: Mercuriali-Tilietum Zólyomi & Jakucs in Zólyomi 1958, 5: Daphno laureolae-Fagetum (Isépy 1970) Borhidi in Borhidi & Kevey 1996, 6: Fago ornetum Zólyomi (1950) 1958, 7: Vicio sparsiflorae-Quercetum pubescentis Zólyomi ex Borhidi et Kevey 1996, 8: Cotino-Quercetum pubescentis Soó (1931) 1932, 9: Arvum et ager incultum, 10: Urtico-Convolvuletum Görs & T. Müll. 1969*

http://www.aloki.hu ● ISSN 1589 1623 (Print) ● ISSN 1785 0037 (Online)
DOI: http://dx.doi.org/10.15666/aeer/1605_70457062
© 2018, ALÖKI Kft., Budapest, Hungary

Figure 2. *Experimental site. (Photo: T. Mészáros, date: 11.03.2017)*

Figure 3. *Experimental site. (Photo: T. Mészáros, date: 10.05.2018)*

http://www.aloki.hu ● ISSN 1589 1623 (Print) ● ISSN 1785 0037 (Online)
DOI: http://dx.doi.org/10.15666/aeer/1605_70457062
© 2018, ALÖKI Kft., Budapest, Hungary

Photos were taken about the flower visiting insects to identify them and record the time of visitation. With this method it was possible for pollinators to visit the flowers more times. However this method was not effective enough. Only a little ratio of visitations was recorded and identified. At the same time only these results show that some pollinators visit the same plant individuals repeatedly. Those individuals that were not identified reliably are not included in the results of this study. In 2018 we studied a 3800 square metres area. The number of *P. grandis* individuals was about 2600. The pollinators were collected in glasses every hour. An insect collecting nest (30 cm in diameter) was used to collect the insects individually and then put them in the glasses. We studied the area through 20 h on 2-10 April (1-3 people collected simultaneously). The length of observation (25 h) and sampling (20 h) were different as there were periods when no pollinators visited the plants (*Table 2*). The study days were sunny and windless, excepting 4 April which was a sunny but very windy day. The individuals were identified with a binocular microscope by Zs. Józan. The collected individuals were identified according to following literature: Andrenidae species: Schmid-Egger and Scheuckl (1977), Apis mellifera and Bombus species: Móczár (1957), Halictidae species: Móczár (1967) and Ebmer (1970), Osmia species: Móczár (1958), Vespidae species: Móczár (1995), Pompilidae species: Wolf (1972) and for all species: Schmiedeknecht (1930).

Table 2. *Flower visitations of Pulsatilla grandis (2018)*

Date	Length of observation (h)	Length of sampling (h)
2 April	3 p.m.-6 p.m.	3 p.m.-6 p.m.
3 April	9 a.m.-4 p.m.	10 a.m.-4 p.m.
4 April	9 a.m.-4 p.m.	10 a.m.-3 p.m.
8 April	9 a.m.-4 p.m.	10 a.m.-3 p.m.
10 April	11 a.m.-12 a.m.	11 a.m.-12 a.m.
Total:	**25**	**20**

a.m. = before noon, p.m. = after noon

Besides the cited publications distribution data of species are based on the unpublished studies of Zs. Józan who studied and collected pollinators through 5 decades in the Bakony Hills, Western and Southern Transdanubia. Flower-visitation data was collected by the author and Jenő Papp. The specimens of collected insects are preserved in the Rippl-Rónai Museum (Kaposvár, Hungary) and in the Natural History Museum of the Bakony Hills (Zirc, Hungary).

Results

In 2017 we recorded 31 flower-visitations of *Aculeata* (6 species) species (*Table 3*). *Apis mellifera* was the most frequent (80% of all visitations) pollinator of *P. grandis*. The *Bombus* genus was the second most frequent with 12%. The flower-visitations of *Andrena* and *Lasioglossum* species were not significant, both representing 3%.

We recorded the most visitations between 10-11 a.m., followed by the period between 11-12 a.m. *Apis* species visited the flowers between 9 a.m and 3 p.m., the *Bombus* species between 10 a.m. and 3 p.m., the *Andrena* species between 11-12 a.m.,

http://www.aloki.hu ● ISSN 1589 1623 (Print) ● ISSN 1785 0037 (Online)
DOI: http://dx.doi.org/10.15666/aeer/1605_70457062
© 2018, ALÖKI Kft., Budapest, Hungary

while the *Lasioglossum* species between 12-1 p.m. There was no visitation between 1-2 p.m.

Table 3. *Aculeata pollinators of Pulsatilla grandis in decreasing frequency (2017)*

Species	Sex	Number of flower-visitations (during 18 h)	Time of flower visitation
Apis mellifera Linnaeus, 1758	Worker	25	9 a.m.-1 p.m., 2-3 pm.
Bombus lapidarius (Linnaeus, 1758)	♀	2	11-12 a.m., 2-3 p.m.
Bombus pascuorum (Scopoli, 1763)	♀	1	10-11 a.m.
Andrena bicolor (Fabricius, 1775)	♀	1	11-12 a.m.
Lasioglossum fulvicorne (Kirby, 1802)	♀	1	12-1 p.m.
Bombus haematurus (Kriechbaumer, 1870)	♀	1	12-1 p.m.
Total:		**31**	

♀ = female, a.m. = before noon, p.m. = after noon

In 2018 23 species (299 individuals) were collected (*Table 4*). *Apis mellifera* was the most frequent (80% of all visitations) pollinator of *P. grandis*. It was followed by the *Bombus* genus with 10%. The ratio of *Andrena* species was only 5% (*Table 5*).

Table 4. *Aculeata pollinators of Pulsatilla grandis in decreasing frequency (2018)*

Species	Number of individuals	Sex	Time of flower visitation
Apis mellifera (Linnaeus, 1758)	239	Worker	10 a.m.-6 p.m.
Bombus lapidarius (Linnaeus, 1758)	8	♀	11 a.m.-1 p.m., 2-3 pm.
Andrena bicolor (Fabricius, 1775)	6	5 ♀ + 1 ♂	10-11 a.m., 12-2 p.m.
Bombus pratorum (Linnaeus, 1761)	6	♀	12-5 p.m.
Bombus haematurus (Kriechbaumer, 1870)	5	♀	10-12 a.m., 3-4 p.m., 5-6 p.m.
Bombus hypnorum (Linnaeus, 1758)	5	♀	10-11 a.m., 12-2 p.m.
Osmia cornuta (Latreille, 1805)	5	4 ♀+1 ♂	12-2 p.m.
Bombus terrestris (Linnaeus, 1758)	4	♀	10 a.m.-2 p.m.
Andrena gravida (Imhoff, 1832)	3	2 ♀+1 ♂	12-2 p.m., 3-4 p.m.
Bombus pascuorum (Scopoli, 1763)	2	♀	11-12 a.m., 1-2 p.m.
Lasioglossum laterale (Brullé, 1832)	2	♀	11 a.m-1 p.m.
Osmia bicolor (Schrank, 1781)	2	♀	12-12 p.m.
Polistes nimpha (Christ, 1791)	2	♀	12-1 p.m.
Andrena bimaculata (Kirby, 1802)	1	♂	2-3 p.m.
Andrena bluethgeni (Stöckhert, 1930)	1	♀	11-12 a.m.
Andrena dorsata (Kirby, 1802)	1	♀	11-12 a.m.
Andrena jacobi (Perkins, 1921)	1	♂	4-5 p.m.
Andrena nitida (Müller, 1776)	1	♀	12-1 p.m.
Andrena vaga (Panzer, 1799)	1	♀	1-2 p.m.
Bombus ruderarius (Müller, 1776)	1	♀	12-1 p.m.
Lasioglossum bluethgeni (Ebmer, 1971)	1	♀	2-3 p.m.
Lasioglossum xanthopus (Kirby, 1802)	1	♀	11-12 a.m.
Priocnemis mimula (Wesmael, 1851)	1	♀	2-3 p.m.
Total:	**299**		**10 a.m -6 p.m.**

♀ = female, ♂ = male, a.m. = before noon, p.m. = after noon

http://www.aloki.hu ● ISSN 1589 1623 (Print) ● ISSN 1785 0037 (Online)
DOI: http://dx.doi.org/10.15666/aeer/1605_70457062
© 2018, ALÖKI Kft., Budapest, Hungary

Table 5. *Aculeata pollinators (genus) of Pulsatilla grandis in decreasing frequency (2018)*

Genus	Number of individuals	Ratio of all flower visits (%)
Apis	239	79.9
Bombus	31	10.4
Andrena	15	5.0
Osmia	7	2.3
Lasioglossum	4	1.3
Polistes	2	0.7
Priocnemis	1	0.3
Total:	**299**	**100**

We observed the most flower-visitation between 10-11 a.m., followed by the period between 12-1 p.m. (*Table 6*). *Apis* and *Bombus* species visited the flowers between 10 a.m. and 6 p.m., while *Andrena* species between 10 a.m. and 5 p.m.

Table 6. *Temporal distribution of Pulsatilla grandis pollinators (2018, daylight saving time)*

Time	Number/hour	Ratio (%)
10-11 a.m.	66	22.0
11-12 a.m.	55	18.4
12-1 p.m.	60	20.1
1-2 p.m.	40	13.4
2-3 p.m.	25	8.4
3-4 p.m.	16	5.3
4-5 p.m.	26	8.7
5-6 p.m.	11	3.7
Total:	**299**	**100**

a.m. = before noon, p.m. = after noon

We collected the most number of insects (34 individuals) on 8 April between 10-11 a.m., while we collected the fewest (1 individual) on 10 April between 10-11 a.m. There was no visitation before 10 a.m. We recorded visitations between 4-6 p.m. only on the first few days. Later no visitation was observed after 4 p.m.

We found 5 males besides the females and workers (*Andrena bicolor, A. gravida, A. bimaculata, A. jacobi, Osmia cornuta).*

Three quarters of bee-like species collected from *P. grandis* have a wide range (Palearctic, Western Palearctic and Eurosiberian). One quarter of the species occurs in certain regions of Europe, and only 15% lives in the Mediterranean with a range extending to Central Europe.

The ratio of species preferring warm habitats (eremophil) was only 20%. The species of cool and wet habitats represented 35%. Most of the species (45%) are eurytopic.

The species are polilectic, except *Andrean vaga* which is an oligolectic species. According to the studies of Zs. Józan in the Bakony Hills, Western and Sothern Transdanubia 45% of species visited less than 25 plant species, 30% visited 26-50 species, 10% visited 51-75 species, while 15% visited more than 76 plant species for pollen or nectar.

http://www.aloki.hu ● ISSN 1589 1623 (Print) ● ISSN 1785 0037 (Online)
DOI: http://dx.doi.org/10.15666/aeer/1605_70457062
© 2018, ALÖKI Kft., Budapest, Hungary

Collected species

Apidae

Apis mellifera Linnaeus, 1758

It was the most dominant pollinator species. Our only social bee species that has perennial colonies. It is a eurytopic species (Móczár, 1957), its subspecies can be found worldwide (Móczár, 1957). The workers visit practically the flowers of every plant species that produce pollen or nectar (unpublished data of the author). In early spring they visit the catkins of *Salix* species (*Salix caprea, Salix cinerea*) which produce a high amount of pollen. *P. grandis* seems to be a good source of pollen and nectar as well. The pollen baskets of specimens collected from its flowers were full of pollen. After winter the workers feed the first larvae generation with this protein rich forage. From the end of March they start to visit the flowers of fruit trees, so the visitation of other plants become less significant. It has economic and ecological significance (Rand et al., 2015).

Bombus haematurus Kriechbaumer, 1870

This bumblebee species has Ponto-Mediterranean range (Móczár, 1957). Its number has been increasing rapidly in Hungary in the last decades. The species was first observed in Hungary in 1990 in the Mecsek Hills. Later about 40 occurrences have been recorded in the Bakony Hills, Transdanubian Hills, Mecsek Hills, Villányi Hills, furthermore in Vas County and near Bősárkány (North Hungary) (Józan, 1995, 1996b, 1998, 2000a, 2003, 2006, 2009, 2016, 2017). Sárospataki et al. (2004) classified the species as rare and highly threatened. However, the studies of recent years show it is not so rare. It is also supported by the fact that the species was observed together with other common species on the Csatár Hill. Visited plant species: *Rubus idaeus, R. fruticosa, Geum urbanum* (Rosaceae), *Vicia grandiflora* (Fabaceae), *Galeobdolon luteum, Lamium purpureum, L. maculatum* (Labiatae), *Symphytum officinale* (Boraginaceae), *Corydalis cava, Lonicera* sp., *Philadelphus coronarius* (other plant families) (Józan, 2009, 2017).

Bombus hypnorum (Linnaeus, 1758)

B. hypnorum is a Eurosiberian bumblebee which prefers habitats with cool and humid microclimate (Móczár, 1953, 1957). It is moderately rare in Hungary (Móczár, 1953; Sárospataki et al., 2004). The species has been observed in 30 localities in Hungary from Bősárkány through the Bakony Hills, the Transdanubian Hills, the Mecsek Hills until the Villányi Hills (Józan, 1990, 1992a, 1995, 1996a, 1998, 2000a, 2000b, 2001, 2006, 2016, 2017). Visited plant species: *Rubus idaeus, Rosa sp.* (Rosaceae), *Lamium maculatum* (Labiatae), *Calendula officinalis, Cirsium arvense* (Asteraceae), *Anchusa officinalis, Echium vulgare* (Boraginaceae), and *Berberis vulgare, Epilobium montanum, Knautia drymeia, Lycium barbarum, Salix cinerea, Symphoricarpus albus, Philadelphus coronarius* (other plant families) (Józan, 2017).

Bombus lapidarius (Linnaeus, 1758)

It is a common eurytopic species living in the Western-Palearctic range (Móczár, 1953, 1957; Sárospataki et al., 2004). It is common everywhere in Hungary. It has been found in lots of localities during our studies (Józan, 1985, 1992a, 1992b, 1995, 1996a, 1996b, 1998, 2000a, 2000b, 2001, 2002, 2003, 2006, 2009, 2016, 2017). Its pollination

http://www.aloki.hu ● ISSN 1589 1623 (Print) ● ISSN 1785 0037 (Online)
DOI: http://dx.doi.org/10.15666/aeer/1605_70457062
© 2018, ALÖKI Kft., Budapest, Hungary

was recorded on 50 plant species of 23 plant families. Most of the species belong to the Fabaceae, Labiatae and Asteraceae families (Józan, 2009, 2016, 2017).

Bombus pascuorum (Scopoli, 1763)

It is a eurytopic Eurosiberian bumblebee species (Móczár, 1953, 1957; Sárospataki et al., 2004). *B. pascuorum* is the most common bumblebee species in Hungary according to our studies (Józan, 1990, 1992a, 1992b, 1995, 1996a, 1998, 2000a, 2000b, 2001, 2006, 2009, 2014, 2016, 2017). It has been collected from 70 plant species of 22 plant families (Józan, 2009, 2016, 2017).

Bombus pratorum (Linnaeus, 1761)

B. pratorum lives in habitats with cool and humid microclimate. Its range is of Eurosiberian type (Móczár, 1953, 1957). *B. pratorum* was classified as moderately rare in Hungary (Sárospataki et al., 2004). During our faunistic studies it has been collected from 40 localities in Transdanubia (Józan, 1990, 1992a, 1996a, 2000b, 2001, 2002, 2006, 2017). Visited plant species: *Rubus idaeus* (Rosaceae), *Astragalus onobrychis, Trifolium pratense* (Fabaceae), *Aegopodium podagraria, Anthriscus sylvestris* (Apiaceae), *Ajuga reptans, Galeobdolon luteum, Marrubium peregrinum, Salvia nemorosa* (Labiatae), *Centaurea jacea, C. micranthos, Taraxacum officinale* (Asteraceae), *Stellaria* sp. (Caryophyllaceae), *Echium vulgare, Pulmonaria officinalis, Symphytum officinale, S. tuberosum* (Boraginaceae), other plant families: *Allium ursinum, Berberis vulgaris, Cerinthe minor, Geranium* sp., *Knautia arvensis, K.. drymeia, Melampyrum nemorosum, Ribes rubrum, Solanum nigrum, Symphoricarpus albus* (Józan, 2017).

Bombus ruderarius (Müller, 1776)

It is a eurytopic bumble bee species with a Western Palearctic range (Móczár, 1957). It is moderately common in Hungary (Móczár, 1953; Sárospataki et al., 2004). We have found this species in many different localities during our faunistic studies (Józan, 1990, 1992a, 1992b, 1995, 1996a, 1996b, 1998, 2000a, 2000b, 2001, 2002, 2006, 2009, 2016, 2017). It has been collected from more than 40 species of 14 plant families (Józan, 2009, 2017).

Bombus terrestris (Linnaeus, 1758)

It is a eurytopic bumble bee species that occurs in the Palearctic region (Móczár, 1957). It is very common in every part of Hungary (Józan, 2001; Móczár, 1953; Sárospataki et al., 2004). It has been collected from 110 localities (Józan, 1985, 1990, 1992a, 1992b, 1995, 1996a, 1996b, 1998, 2000a, 2000b, 2001, 2002, 2003, 2006, 2009, 2014, 2015, 2016, 2017). Its pollination has been observed on nearly 100 species of 35 plant families. Most significant families were the Fabaceae, Labiatae and Asteraceae (Józan, 2009, 2016, 2017).

Andrenidae

Andrena bicolor Fabricius, 1775

This Eastern Palearctic mining bee species prefers cool and humid habitats (Dylewska, 1987; Móczár, 1957). *A. bicolor* is moderately common in Hungary (Móczár and Warncke, 1972). It has two generations per year, the first being on the wing in spring and the second in summer (Schmid-Egger and Scheuchl, 1977). It has

http://www.aloki.hu ● ISSN 1589 1623 (Print) ● ISSN 1785 0037 (Online)
DOI: http://dx.doi.org/10.15666/aeer/1605_70457062
© 2018, ALÖKI Kft., Budapest, Hungary

been found in nearly 100 localities during our faunistic studies (Józan, 1990, 1992a, 1992b, 1996a, 1996b, 1998, 2000a, 2000b, 2001, 2002, 2003, 2006, 2009, 2014, 2016, 2017). It has been collected from 35 species of 15 plant families. The summer generation visits mainly the flowers of *Campanula* species (Schmid-Egger and Scheuchl, 1977; Józan, 2009, 2016, 2017).

Andrena bimaculata (Kirby, 1802)

A. bimaculata is an eurytopic mining bee species that is widespread in the Palearctic region. It has two generations per year (Dylewska, 1987; Schmid-Egger and Scheuhl, 1977). It is common in Hungary (Móczár and Warncke, 1972; Józan, 2011). It has been collected from more than 130 localities (Józan, 1985, 1990, 1992a,1992b,1995, 1996a, 1996b, 1998, 2000a, 2000b, 2001, 2003, 2009, 2014, 2016, 2017). It has been observed on 36 species of 13 plant families. The spring generation swarms mainly on the catkins of *Salix* species (Schmid-Egger and Scheuchl, 1977; Józan, 2009, 2016, 2017).

Andrena bluethgeni Stöckhert, 1930

The range of this species is not well-known. It has been found in Central and Northern Europe (Schmid-Egger and Scheuchl, 1977). It is very rare in Hungary. In the last century it was collected only from 4 localities near Budapest and from one locality in the North Hungarian Mountains (Móczár and Warncke, 1972). In the last decades we have observed it in six localities of the Balaton Uplands, near Esztergom, in the Zákány Hills and in Külső-Somogy (Józan, 1992a, 2000b, 2016). Visited plant species: *Amygdalus communis, Cerasus vulgare, Prunus cerasifera, P. spinosa* (Rosaceae)*, Capsella bursa-pastoris* (Cruciferae)*, Acer platanoides* (Aceraceae) (Józan, 2016).

Andrena dorsata (Kirby, 1802)

A. dorsata is a eurytopic Western Palearctic mining bee species with two generations (Dylewska, 1987). It is common in Hungary. It has been collected from more than 200 localities during our faunistic studies (Józan,1985, 1990, 1992a, 1992b, 1995, 1996a, 1996b, 1998, 2000a, 2000b, 2002, 2003, 2006, 2009, 2014, 2016, 2017). It has been noted on nearly 100 species of 27 plant families. Most of them belong to the Rosaceae, Cruciferae and Asteraceae families (Józan, 2009, 2016, 2017).

Andrena gravida Imhoff, 1832

A. gravida is a widespread mining bee species in Europe (Dylewska, 1987). Its only generation flies from early spring until May. It is common in Hungary (Móczár and Warncke, 1972). It has been found in nearly 150 localities (Józan, 1990, 1992a, 1992b, 1995, 1996a, 1996b, 1998, 2000a, 2000b, 2001, 2002, 2003, 2006, 2009, 2016, 2017). It has been collected from more than 50 species of 25 plant families. Most of them are members of the Rosaceae and Cruciferae families (Józan, 2009, 2016, 2017).

Andrena jacobi Perkins, 1921

It is a Western Palearctic species with one generation swarming in spring (Dylewska, 1987). It is moderately common in Hungary (Móczár and Warncke, 1972). We have found it in 84 localities during our studies (Józan, 1990, 1992a, 1992b, 1995, 1996a, 1996b, 1998, 2000a, 2000b, 2001, 2017) It has been collected from 24 species of 12 plant families. It has mainly visited the species of Rocaseae family (Józan, 2017).

http://www.aloki.hu ● ISSN 1589 1623 (Print) ● ISSN 1785 0037 (Online)
DOI: http://dx.doi.org/10.15666/aeer/1605_70457062
© 2018, ALÖKI Kft., Budapest, Hungary

Andrena nitida (Müller, 1776)

A. nitida has the same range as the former species (Dylewska, 1987). Its only generation flies in the spring months. It is quite common in Hungary (Móczár and Warncke, 1972). It has been found in nearly 130 localities (Józan, 1990, 1992a, 1992b, 1995, 1996a, 1996b, 1998, 2000b, 2001, 2002, 2003, 2009, 2015, 2016, 2017). It has visited more than 50 species of 25 plant families. Most of them are members of Rosaceae and Cruciferae families (Józan, 2016, 2017).

Andrena vaga Panzer, 1799

A. vaga is a mining bee species that lives in Southern Europe (Dylewska, 1987). It flies in early spring. It is not rare in Hungary but not abundant (Móczár and Warncke, 1972). It has been collected from 60 localities in the last decades (Józan, 1985, 1990, 1992a, 1995, 1996a, 1996b, 1998, 2000b, 2001, 2003, 2006, 2015, 2016, 2017). Visited plant species: *Prunus spinosa, Sorbus intermedia* (Rosaceae), *Lamium purpureum* (Labiatae), *Salix cinerea, S. rosmarinifolia* (Salicaceae) (Józan, 2016, 2017).

Halictidae

Lasioglossum bluethgeni Ebmer, 1971

L. bluethgeni is a Pontomediterranean sweat bee species (Ebmer, 1988; Móczár, 1967). It has two generations. The spring generation contains only of females. It has been observed in many locations in Hungary, but it is not common. It has been collected from 35 Transdanubian localities in the last decades (Józan, 1992b, 1995, 1996a, 1998, 2000b, 2006, 2009, 2015, 2016, 2017). It has visited the flowers of the following species: *Anthriscus cerefolium, A. sylvestris, Daucus carota, Pastinaca sativa* (Apiaceae), *Capsella bursa-pastoris, Rorippa amphibia, Lepidium draba* (Cruciferae), *Hieratium* sp. (Asteraceae), *Echium vulgare, Lithospermum purpureo-coeruleum* (Boraginaceae), other families: *Cotinus coggygria, Dictamnus albus, Scabiosa ochroleuca* (Józan, 2009).

Lasioglossum fulvicorne Kirby, 1802

It is a eurotypic species with a Palearctic range (Ebmer, 1988; Móczár,1967). It is rare in Hungary. It has been collected only from Nagybajom (Józan, 1992a), Tótújfalu (Józan, 1995), Kővágószőlős (Józan, 1996a) and Zics (Józan, 2000b). Visited plant species: *Anthemis austriaca, Berteroa incana, Capsella bursa-pastoris, Dorycnium germanicum, Ficaria verna, Orlaya grandiflora.*

Lasioglossum laterale (Brullé, 1832)

This sweat bee species occurs in the Northern part of the Mediterranean (Ebmer, 1988; Móczár, 1967). It has two generations. The spring generation contains only of females. It is moderately common in Hungary (Móczár, 1967). It has been collected from more than 70 localities in the Bakony Hills and in the southern part of Transdanubia (Józan, 1990, 1992a, 1995, 1996a, 1996b, 1998, 2000a, 2000b, 2003, 2006, 2009, 2017). It has been collected from 20 species of 10 plant families.

Lasioglossum xanthopus (Kirby, 1802)

L. xanthopus is a Wester Palearctic species (Ebmer, 1988; Móczár, 1967). It also has two generations. The spring generation contains only of females. It is moderately common in Hungary (Móczár, 1967). We have found it in less localities than the former

http://www.aloki.hu ● ISSN 1589 1623 (Print) ● ISSN 1785 0037 (Online)
DOI: http://dx.doi.org/10.15666/aeer/1605_70457062
© 2018, ALÖKI Kft., Budapest, Hungary

species (Józan, 1992a, 1995, 1998, 2000a, 2000b, 2003, 2016, 2017). According to our observations it does not occurs abundantly in any type of habitat. It has been recorded on 24 species of 13 plant families. The distribution of species was quite equal between families (Józan, 2016, 2017).

Megachilidae

Osmia bicolor (Schrank, 1781)

It is a widespread species in Europe. It swarms in spring and nests in snail shells (Móczár, 1958). It is moderately common in Hungary (Móczár, 1958). It has been collected from 75 Transdanubian localities (Józan, 1985, 1990, 1992a, 1992b, 1995, 1996a, 1996b, 1998, 2000b, 2003, 2006, 2009, 2015, 2016). It has been recorded on 22 species of 15 plant families. Most of them are member of the Rosaceae family (Józan, 2009, 2014, 2016, 2017).

Osmia cornuta (Latreille, 1805)

It is a widespread species ranging from the northern part of the Mediterranean to Central Europe. It is common in Hungary (Móczár,1958). It nests in hollow stems or other holes. The cells are separated with mud (Móczár, 1958). The males are often on wings in early March foraging on *Salix* catkins (author's observation). It rarely can be seen in May. It was collected from 16 species of 14 plant families. Most of them are member of the Rosaceae family (Józan, 2009, 2016, 2017).

Pompilidae

Priocnemis mimula Wesmael, 1851

It is a Palearctic pompilid species. It is distributed mainly in the hilly and mountainous regions of Hungary. It is common but not abundant (Móczár, 1956). It is a parasitoid species. It visits the flowers for nectar (Móczár, 1956). It has a limited role in pollination due to the lack of body hairs.

Vespidae

Polistes nimpha (Christ, 1791)

It is a Palearctic Vespidae species. It is very common in Hungary. First it feeds the larvae with nectar and other sweet saps. Later the larvae feed on chopped insects (Móczár, 1995). Its role in pollination is similar to the former species.

Discussion

Apis mellifera was the main pollinator of *P. grandis* in both years of our study. It was followed by *Bombus* species. The high number of *Apis mellifera* can be partly explained by the fact that an apiary can be found 300 meters from the population of *P. grandis*. The fruit trees of the Csatár Hill were not blossoming at the time of early *P. grandis* flowering, so the studied flowers were the only pollen sources for *Apis mellifera*. The significant role of honey bees in successful fructification was observed in the case of later flowering orchid species as well (Biró et al., 2015).

Apis and *Bombus* species had the longest collecting period in both years, which can be explained with the fact that both genus contains eurytopic species.

http://www.aloki.hu ● ISSN 1589 1623 (Print) ● ISSN 1785 0037 (Online)
DOI: http://dx.doi.org/10.15666/aeer/1605_70457062
© 2018, ALÖKI Kft., Budapest, Hungary

In 2018 early spring was cold, so a large number of insects visited the flowers of *Pulsatilla* on 4 April even in windy weather.

In 2018 the mornings were quite cool so the flowers were not visited before 10 a.m. In the first days of our study the insects collected pollen until 6 p.m. but later their activity decreased in late afternoon which is the consequence of the long winter as well.

Males visit the flowers only for nectar. They do not have special collecting hairs, so the probability of carrying pollen from a flower to another is lower. In the lack of allogamy *P. grandis* can reproduce with self-pollination as well (Walker and Pinches, 2011; Zimmermann, 1935; Lindell, 1998). As a consequence, male insects can help the pollination of this species too. They can carry the pollen of the same plant to the stigma as they searching for nectar in the flower.

It is normal that the ratio of eremophil bee species was low (20%) in the early spring aspect.

In comparison with the observations of Kratochwil (1988) on *P. vulgaris* we found mainly social bee species (*Apis mellifera, Bombus*), while *Andrena* and *Osmia* species were the most frequent among solitary species. *Andrena bicolor* was the most frequent species of the genus in our study as well. We did not collect *Lasioglossum lineare*, but we found *L. fulvicorne*, *L. laterale* and *L. xanthopus*. Two non-*Apoidea Hymenoptera* species was collected: *Priocnemis mimula* and *Polistes nimpha*.

Our results support the observations of Weryszko-Chmielewska and Sulborska (2011) on *Pulsatilla* species as Bee-like species were the main pollinators of *P. grandis*.

The studies of Sauberer and Panrok (2015) on *Pulsatilla* species showed different results from our observations on *P. grandis*. We collected only 1-2 individuals of 4 Halictidae species (*L. fulvicorne, L. laterale and L. xanthopus*) and the number of individuals of *Apis* and *Bombus* species was significantly higher than the number of individuals of the *Andrena* genus.

Our results meet the observations of Zimmermann (1935), Walker (2011) and Walker and Pinches (2011): *Apis mellifera* and *Bombus* species were the most frequent pollinators. However, in our case *B. lapidarius* was the most frequent species of the genus instead of *Bombus terrestris* (Zimmermann, 1935).

Compared to the results of Wells and Barling (1971) we collected only 1-2 *Bombus pascuorum* and *Osmia bicolor*.

Pulsatilla species produce pollen in early spring when the activity of Aculeata species is starting as well. They attract the insects with a huge amount of pollen and some nectar.

Pulsatilla species have many strategies to ensure the success of allogamy, especially in the case of early flowering species.

As the seed dispersal distances are short the gene flow ensured by pollination plays an important role in the maintenance of the genetic variability of populations. Therefore, the significance of pollinators is high (Hensen et al., 2005).

In our former studies we found significant differences between the number of fruits in the different *P. grandis* populations in the southern part of Bakony Hills (Mészáros T. in prep.) which can indicate the important role of pollinators as well. According to our studies a large number of pollinators have visited the flowers of *P. grandis*. The success of fructification can depend not only on the number of pollinators but on habitat parameters or weather conditions as well. As a consequence, further studies are needed to determine the role of the studied insects in the success of fructification.

http://www.aloki.hu ● ISSN 1589 1623 (Print) ● ISSN 1785 0037 (Online)
DOI: http://dx.doi.org/10.15666/aeer/1605_70457062
© 2018, ALÖKI Kft., Budapest, Hungary

Conclusion

No special plant-pollinator relation was found between the studied species and its pollinators. This result is not surprising as only 1-2% of bee species are specialists. Most of the bee species feed on more plant species and most of the plant species are visited by many insects.

The number of bees has decreased considerably in the last decades which can be caused by the changes in landscape structure and the retreat of visited plant species, so the pollination crisis is becoming more obvious (Potts et al., 2010; Biesmeijer et al., 2007). Besides the retreat of food plants the increasing presence of dangerous chemicals reduces the number of pollinators as well (Dainese et al., 2018).

The early flowering of *P. grandis* is very important for bees appearing in early spring as these flowers are the first food sources for them after the pupa stage. In this period of the year only a few plant species produces pollen. After the flowering of *P. grandis* its pollinators (which have longer life cycle than the flowering period of *P. grandis*) visit other plant species occurring in increasing number, so the bees can choose from more food sources. We can speak about mutual dependency as pollinators are necessary for successful fertilization (and with that for the maintenance of genetic diversity of populations), and the flowers *P. grandis* are food sources for early pollinators. Either the decrease of pollinators or early flowering plant populations influences the relation negatively.

With our study we filled the gap of missing information about the pollinators of *P. grandis* and would like to draw attention to the key role of early flowering plant species in the maintenance of bee diversity. In the lack of these species even the non-specialist pollinators can not maintain their populations. Therefore it is important to conserve and maintain the populations of early flowering plant species.

Acknowledgements. We would like to thank Mrs. Józan, Dénes Péteri and Gábor Barad for their help in insect collection. We would like to thank Judit Bódis and István Galambos for their comments on the manuscript. The publication is supported by the EFOP-3.6.3-VEKOP-16-2017-00008 project. The project is co-financed by the European Union and the European Social Fund.

REFERENCES

[1] Biesmeijer, J. C., Roberts, S. P. M., Reemer, M., Ohlemüller, R., Edwards, M., Peeters, T., Schaffers, A. P., Potts, S. G., Kleukers, R., Thomas, C. D., Settele, J., Kunin, W. E. (2006): Parallel declines in pollinators and insect-pollinated plants in Britain and the Netherlands. – Science 313: 351-354.

[2] Biró, É., Bódis, J., Nagy, T., Tökölyi, J., Molnár, V. A. (2015): Honeybee (*Apis mellifera*) mediated increased reproductive success of a rare deceptive orchid. – Applied Ecology and Environmental Research 13(1): 181-192. DOI: 10.15666/aeer/1301_181192.

[3] Borhidi, A. (2003): Magyarország növénytársulásai. – Akadémiai Kiadó, Budapest.

[4] Charlesworth, D., Charlesworth, B. (1987): Inbreeding depression and its evolutionary consequences. – Ann Rev Ecol Syst. 18(1): 237-268.

[5] Dainese, M., Riedlinger, V., Holzschuh, A., Kleijn, D., Scheper, J., Steffan-Dewenter, I. (2018): Managing trap- nesting bees as crop pollinators: Spatiotemporal effects of floral resources and antagonists. – J Appl Ecol 2018(55): 195-204. DOI: 10.1111/1365-2664.12930.

[6] Denisow, B., Wrzesień, M. (2006): The study of blooming and pollen efficiency of *Adonis vernalis* L. in xerothermic plant communities. – J. Apic. Sci. 50(1): 25-32.

http://www.aloki.hu ● ISSN 1589 1623 (Print) ● ISSN 1785 0037 (Online)
DOI: http://dx.doi.org/10.15666/aeer/1605_70457062
© 2018, ALÖKI Kft., Budapest, Hungary

[7] Denisow, B., Wrzesien, M., Cwener, A. (2014a): Pollination and floral biology of *Adonis vernalis* L.(Ranunculaceae)–a case study of threatened species. – Acta Societatis Botanicorum Poloniae 83(1): 29-37.
[8] Denisow, B., Strzałkowska-Abramek, M., Bożek, M., Jeżak, A. (2014b): Early spring nectar and pollen and insect visitor behavior in two *Corydalis species (Papaveraceae)*. – J. Apic. Sci. 58(1): 93-102.
[9] Denisow, B., Pogroszewska, E., Laskowska, H. (2015): The effect of silicon on nectar and pollen production in Hosta Tratt. 'Krossa Regal'. – Acta Sci. Pol. Hortorum Cultus 14(4): 131-142.
[10] Dostalova, A., Király, G. (2013): Pulsatilla grandis. – The IUCN Red List of Threatened Species 2013: e.T162014A5530433. http://dx.doi.org/10.2305/IUCN.UK.2011-1.RLTS.T162014A5530433.en.
[11] Du Rand, E. E., et al. (2015): Detoxification mechanisms of honey bees (Apis mellifera) resulting in tolerance of dietary nicotine. – Sci. Rep. 5: 11779. DOI: 10.1038/srep11779.
[12] Dylewska, M. (1987): Die Gattung *Andrena* Fabricius *(Andrenidae, Apoidea)* in Nord- und Mitteleuropa. – Acta Zoologica Cracoviensa 30/12: 359-708.
[13] Ebmer, A. W. (1970): Die Bienen des Genus Halictus Latr. s. l. im Grossraum von Linz (Hymenoptera, Apidae) Teil II. – Naturkundliches Jahbuch der Stadt Linz 1970: 19-82.
[14] Ebmer, A. W. (1988): Kritische Liste der nicht-parasitischen Halictidae Österreichs mit Berücksichtigung aller mitteleuropäischen Arten (Insecta: *Hymenoptera: Apoidea: Halictidae*). – Linzer biologische Beiträge 20/2: 527-711.
[15] Essl, F. (2005): Bestandesentwicklung, Vegetationsanschluss und Gefährdungssituation der Gewöhnlichen Küchenschelle (*Pulsatilla vulgaris* MILL.) in Österreich von 1991-2005. – Linzer biologische Beiträge 37(2): 1145-1176.
[16] Gostin, I. N.(2011): Anatomical and micromorphological peculiarities of *Adonis vernalis* L. (*Ranunculaceae*). – Pak J Bot 43: 811-820.
[17] Hensen, I., Oberprieler, C., Wesche, K. (2005): Genetic structure, population size, and seed production of *Pulsatilla vulgaris (Ranunculaceae)* in Central Germany. – Flora 200: 3-14.
[18] Józan, Zs. (1985): A Barcsi borókás fullánkos *(Hymenoptera, Aculeata)* faunája. – II. Dunántúli Dolgozatok (A) Természettudományi Sorozat 5: 177-192.
[19] Józan, Zs. (1990): A Zselic méhszerű *(Hymenoptera), Apoidea* faunájának alapvetése. – Janus Pannonius Múzeum Évkönyve 34(1989): 81-92.
[20] Józan, Zs. (1992a): A Boronka-melléki Tájvédelmi Körzet fullánkos hártyásszárnyú *(Hymenoptera, Aculeata)* faunájának alapvetése. – Dunántúli Dolgozatok (A) Természettudományi Sorozat 7: 163-210.
[21] Józan, Zs. (1992b): A Béda-Karapancsa Tájvédelmi Körzet fullánkos hártyásszárnyú *(Hymenoptera, Aculeata)* faunájának alapvetése. – Dunántúli Dolgozatok (A) Természettudományi Sorozat 6: 219-246.
[22] Józan, Zs. (1995): Adatok a tervezett Duna-Dráva Nemzeti Park fullánkos hártyásszárnyú *(Hymenoptera, Aculeata)* faunájának ismeretéhez. – Dunántúli Dolgozatok (A) Természettudományi Sorozat 8: 99-115.
[23] Józan, Zs. (1996a): A Mecsek méhszerű faunája *(Hymenoptera, Apoidea)*. – Janus Pannonius Múzeum Évkönyve 40(1995): 29-43.
[24] Józan Zs. (1996b): A Baláta környék fullánkos hártyásszárnyú faunájának *(Hymenoptera, Aculeata)* alapvetése. – Somogyi Múzeumok Közleményei 12: 271-297.
[25] Józan, Zs. (1998): A Duna-Dráva Nemzeti Park fullánkos hártyásszárnyú *(Hymenoptera, Aculeata)* faunája. – Dunántúli Dolgozatok (A) Természettudományi Sorozat 9: 291-327.
[26] Józan, Zs. (2000a): A Villányi-hegység fullánkos hártyásszárnyú *(Hymenoptera, Aculeata)* faunája. – Dunántúli Dolgozatok (A) Természettudományi Sorozat 10: 267-283.
[27] Józan, Zs. (2000b): Külső-Somogy méhszerű *(Hymenoptera, Apoidea)* faunája. – Somogyi Múzeumok Közleményei 14: 307-330.

http://www.aloki.hu ● ISSN 1589 1623 (Print) ● ISSN 1785 0037 (Online)
DOI: http://dx.doi.org/10.15666/aeer/1605_70457062
© 2018, ALÖKI Kft., Budapest, Hungary

[28] Józan, Zs. (2001): Somogy megye fullánkos hártyásszárnyú *(Hymenoptera, Aculeata)* faunája. – Natura Somogyiensis 1: 269-293.
[29] Józan, Zs. (2002): Az Őrség és környéke fullánkos hártyásszárnyú faunájának alapvetése *(Hymenoptera, Acuelata)*. – Praenorica Folia Historico-Naturalia 6: 59-96.
[30] Józan, Zs. (2003): A Látrányi Puszta Természetvédelmi Terület fullánkos hártyásszárnyú *(Hymenoptera, Aculeata)* faunája. – Natura Somogyiensis 5: 209-233.
[31] Józan, Zs. (2006): A Mecsek fullánkos hártyásszárnyú faunája *(Hymenoptera, Acueata)*. – Folia Comloensis 15: 219-238.
[32] Józan, Zs. (2009): A cserszegtomaji Gyötrös-tető fullánkos hártyásszárnyú *(Hymenoptera: Aculeata)* faunájának alapvetése. – In: Entomológia: kutatás, szemléletformálás, ismeretterjesztés – Móczár László köszöntése 95. születésnapján. – Szegedi Tudományegyetem Ökológiai Tanszéke, Szeged, pp. 119-135.
[33] Józan, Zs. (2014): Adatok Simontornya fullánkos *(Hymenoptera, Aculeata)* faunájához. – In: Szita, É. et al. (eds.) Simontornya ízeltlábúi – In memoriam Pillich Ferenc. – Magyar Biodiverzitás-kutató Társaság, Budapest, pp. 117-129.
[34] Józan, Zs. (2015): A Barcsi borókás fullánkos faunája, III *(Hymenoptera: Aculeata)*. – Natura Somogyiensis 26: 95-108.
[35] Józan, Zs. (2016): A balatonfüredi Tamás-hegy fullánkos hártyásszárnyú *(Hymenoptera, Aculeata)* faunája. – Natura Somogyiensis 30: 47-70.
[36] Józan, Zs. (2017): A Tihanyi Tájvédelmi Körzet fullánkos hártyásszárnyú *(Hymenoptera, Aculeata)* faunája II. – Folia Musei Historico-Naturalis Bakonyiens is 34: 99-130.
[37] Kaligaric, M., Skornik, S., Ivancic, A., Rebeusek, F., Sternberg, M., Kramberger, B., Sencic, L. (2006): Germination and survival of endangered *Pulsatilla grandis (Ranunculaceae)* after artificial seeding, as affected by various disturbances. – Israel Journal of Plant Sciences 54: 9-17.
[38] Kratochwil, A. (1988): Zur Bestäubungsstrategie von *Pulsatilla vulgaris* MILL. – Flora 181: 261-324.
[39] Larson, B. M. H., Barrett, S. C. H.(2000): A comparative analysis of pollen limitation in flowering plants. – Biological Journal of the Linnean Society 69(4): 503-520.
[40] Lindell, T. (1998): Breeding systems and crossing experiments in *Anemone patens* and in the *Anemome pulsatilla* group *(Ranunculaceae)*. – Nord. J. Bot. 18: 549-561.
[41] Lowenstein, D. M., Matteson, K. C., Minor, E. S. (2015): Diversity of wild bees supports pollination services in an urbanized landscape. – Oecologia 179: 811. https://doi.org/10.1007/s00442-015-3389-0.
[42] Moquet, L., Mayer, C., Michez, D., Wathelet, B., Jacquemart, A.-L. (2015): Early spring floral foraging resources for pollinators in wet heathlands in Belgium. – Journal of Insect Conservation 9: 1-12. DOI: 10.1007/s10841-015-9802-5.
[43] Móczár, M. (1953): A dongóméhek (*Bombus* Latr.) faunakatalógusa (Cat. Hym. IV.). – Folia Entomologica Hungarica VI/5: 197-228.
[44] Móczár, L. (1956): Pókölődarázs alkatúak – *Pompiloidea.* – In: Székessy, V. (ed.) Magyarország Állatvilága (Fauna Hungariae) XIII/5. Akadémiai Kiadó, Budapest.
[45] Móczár, M. (1957): Méhfélék – *Apidae*. – In: Székessy, V. (ed.) Magyarország Állatvilága (Fauna Hungariae) XIII/13. Akadémiai Kiadó, Budapest.
[46] Móczár, M. (1958): Művészméhek – *Megachilidae.* – In: Székessy, V. (ed.) Magyaroság Állatvilága (Fauna Hungariae) XIII/12. Akadémiai Kiadó, Budapest.
[47] Móczár, M. (1967): Karcsúméhek – *Halictidae.* – In: Székessy, V. (ed.) Magyarország Állatvilága (Fauna Hungariae) XIII/11. Akadémiai Kiadó, Budapest.
[48] Móczár, L., Warncke, K. (1972): Faunenkatalog der Gattung Andrena Fabricius (Cat. Hym. XXVI). – Acta Biologica Szeged 18(1-4): 185-221.
[49] Móczár, L. (1995): Redősszárnyúdarázs szerűek – *Vespoidea.* – In: Székessy, V. (ed.) Magyarország Állatvilága (Fauna Hungariae) XIII/B/6. Akadémiai Kiadó, Budapest.

http://www.aloki.hu ● ISSN 1589 1623 (Print) ● ISSN 1785 0037 (Online)
DOI: http://dx.doi.org/10.15666/aeer/1605_70457062
© 2018, ALÖKI Kft., Budapest, Hungary

[50] Osborne, J. L., Martin, A. P., Carreck, N. L., Swain, J. L., Knight, M. E., Goulson, D., Hale, R. J., Sanderson, R. A. (2008): Bumblebee flight distances in relation to the forage landscape. –Journal of Animal Ecology 77: 406-415.
[51] Potts, S. G., Biesmeijer, J. C., Kremen, C., Neumann, P., Schweiger, O., Kunin, W. E. (2010): Global pollinator declines: trends, impacts and drivers. – Trends Ecol Evol 25: 345-363.
[52] Randic, M., Brkljacic, A., Lukac, G., Kremer, D. (2013): New localities of rare NATURA 2000 species: *Pulsatilla grandis* Wender., *Genista holopetala* (Koch) Bald. and *Cypripedium calceolus* L. in the NW Dinarides in Croatia. – Natura Croatica 22(1): 95-109.
[53] Sárospataki, M., Novák, I., Molnár, V. (2004): Hazai poszméhfajok (*Bombus* spp.) veszélyeztetettsége és védelmük szükségessége. – Természetvédelmi Közlemények 11: 299-307.
[54] Sauberer, N., Panrok, A. (2015): Verbreitung und Bestandessituation der Großen Kuhschelle (*Pulsatilla grandis*) am Alpenostrand in Niederösterreich und Wien. – Biodiversität und Naturschutz in Ostösterreich BCBEA 1(2): 262-289.
[55] Schemske, D. W., Husband, B. C., Ruckelshaus, M. H., Goodwillie, C., Parker, I. M., Bishop, J. G. (1994): Evaluating approaches to the conservation of rare and endangered plants. – Ecology 75(3): 584-606.
[56] Schmid-Egger, C., Scheuchl, E. (1997): Illustrierte Bestimmungstabellen der Wildbienen Deutschlands und Österreichs, Band III: Andrenidae. – Eigenverlag, Velden/Vils.
[57] Schmiedeknecht, O. (1930): Hymenopteren Nord- und Mitteleuropas, mit Einschluss von England, Südschweiz, Südtirol und Ungarn. – Verlag von Gustav Fischer, Jena.
[58] Steffan-Dewenter, I., Kuhn, A. (2003): Honeybee foraging in differentially structured landscapes. – Proceedings of the Royal Society of London Series B–Biological Sciences 270: 569-575.
[59] Strzałkowska-Abramek, M., Jachuła, J., Dmitruk, M., Pogroszewska, E. (2016): Flowering phenology and pollen production of three early spring *Pulsatilla species*. – Acta Sci. Pol. Hortorum Cultus 15(6): 333-346.
[60] Walker, K. (2011): *Pulsatilla vulgaris* (L.) Mill. – https://www.scribd.com/document/296701252/Pulsatilla-vulgaris-Plantlifedossier-FINAL-Apr11-pdf (downloaded 25.03.2018).
[61] Walker, K. J., Pinches, C. E. (2011): Reduced grazing and the decline of *Pulsatilla vulgaris* Mill. (Ranunculaceae) in England, UK. – Biological Conservation 144: 3098-3105.
[62] Walther-Hellwig, K. and Frankl, R. (2000): Foraging habitats and foraging distances of bumblebees, *Bombus* spp. (Hym., Apidae), in an agricultural landscape. – J. Appl. Entomol. 124: 299-306.
[63] Wells, T. C. E., and Barling, D. M. (1971): Biological Flora of the British Isles. *Pulsatilla vulgaris* Mill. (*Anemone Pulsatilla* L.) – The Journal of Ecology 59(1): 275-292.
[64] Weryszko-Chmielewska, E. and Sulborska, A. (2011): Staminodial nectary structure in two *Pulsatilla* (L.) species. – Acta Biologica Cracoviensia Series Botanica 53(2): 94-103.
[65] Wolf, H. (1972): Pompilidae – In: Sauter, W. (ed.): Insecta Helvetica, Fauna 5. Hymenoptera. Entomologische Gesellschaft, Zürich, pp. 1-176.
[66] Zimmermann, W. (1935): Genetische Untersuchungen an *Pulsatilla* I-III. – Flora oder Allgemeine Botanische Zeitung 129(2): 158-234.

http://www.aloki.hu ● ISSN 1589 1623 (Print) ● ISSN 1785 0037 (Online)
DOI: http://dx.doi.org/10.15666/aeer/1605_70457062
© 2018, ALÖKI Kft., Budapest, Hungary

THE EFFECT OF SUPER-ABSORBENT POLYMER AND SOWING DEPTH ON GROWTH AND YIELD INDICES OF POTATO (*SOLANUM TUBEROSUM* L.) IN HAMEDAN PROVINCE, IRAN

SALAVATI, S.[1] – VALADABADI, S. A.[1*] – PARVIZI, K. H.[2] – SAYFZADEH, S.[1] – HADIDI MASOULEH, E.[1]

[1]*Department of Agronomy, College of Agriculture, Takestan Branch, Islamic Azad University Takestan, Iran*
(phone: +98-81-3826-6448)

[2]*Horticulture Crops Research Department, Hamedan Agricultural and Natural Resources Research and Education Center, AREEO, Hamedan, Iran*
(phone: +98-81-3437-3587)

**Corresponding author*
e-mail: dr.valadabady@yahoo.com; phone: +98-28-3527-0130

(Received 24th Jul 2018; accepted 5th Oct 2018)

Abstract. In order to evaluate the effect of using super-absorbent polymer (SAP) on quantitative yield and growth indices of potato in autumn sowing, an experiment was conducted in Hamedan city, Hamedan province, Iran during two crop years. The experiment was conducted as split split plot based on randomized complete block design (RCBD) with three replications. Treatments include sowing depth (10, 15, 20 and 25 cm), potato cultivars (Sante, Fontane, and Agria) and SAP (non-application and application). The use of SAP in all three cultivars led to an increase in stem diameter, crop height and tuber yield and resulted in a decrease in the percentage of tuber dry weight. The results of growth indices showed that in all three cultivars, the use of SAP led to an increase in leaf area index (LAI), in leaf area duration (LAD) and in crop growth rate (CGR). The LAI and LAD increased with increasing depth and use of SAP. The highest LAI and LAD were obtained under conditions of using SAP at three depths. At all sowing depth, the use of SAP resulted in an increase in *CGR* relative to the non-use of SAP.
Keywords: *Agria, Sante, superabsorbent polymer, tuber yield, Fontane*

Introduction

Drought is one of the biggest challenges in the agricultural sector of Iran. Almost 90% of the regions in Iran are considered to have arid and semi-arid climates (Bannayan et al., 2010). In this respect, we must apply methods that can improve better water use efficiency (WUE) and do not damage the sustainable production of potato (*Solanum tuberosum* L.) as important crop in these regions (Parvizi and GhadamiFiroozabadi, 2015). Reports showed that drought stress induces a wide range of physiological and biochemical changes in crops (Garg et al., 2012; Maksup et al., 2014). In general, dehydration in crops increases cell volume, cell division, cell growth and crop dry weight, and reduces them relatives to non-stress conditions (Sirousmehr et al., 2014).

Potato is currently the fourth most important food crop in the world after wheat, rice, and corn (FAO, 2008). The area under potato cultivation in Iran in 2013 was 190,000 hectares and its yield in area under potato cultivation in Iran was reported as over 29,2623 kg/ha in 2013 (FAO, 2013). Several studies indicated that potato is sensitive to drought stress in all growth stages, especially the tuber formation stage due to the shallow roots with limited expansion and its inability to absorb water from lower depths (Ayas, 2013; Shock et al., 2013). Increasing the use of this crop in the food industry in

http://www.aloki.hu ● ISSN 1589 1623 (Print) ● ISSN 1785 0037 (Online)
DOI: http://dx.doi.org/10.15666/aeer/1605_70637078
© 2018, ALÖKI Kft., Budapest, Hungary

line with the growing world's population made the farmers and agricultural specialists to approach the production of this product to its genetic potential by eliminating nutrient deficiencies and managing the correct use of water and fertilizers (Haase et al., 2007).

In terms of total tuber yield, the early-season to mid-season cultivars of Marfona, Arinda, Fresco and Sante are superior to other cultivars. In general, the early-season to mid-season cultivars of Sante and Faresco and the late-season cultivars of Agria, Columbus, Timothy, Satina and Julianus are more suitable for potato cultivation and production in Hamedan Province (Parvizi, 2008).

The use of superabsorbent polymers (SAP) is one of the strategies to reduce the effect of drought stress especially in semi-arid regions of Iran. SAP are water-friendly gels which the water inside it is slowly evacuated and the soil remains moist for a long time after water absorption and drying the environment gradually (Ghooshchi, 2015). SAP in agriculture reduce the number of irrigation up to 50%, increase the water and nutrition storage capacity of the soil for a long time, make the uniform use of water for crops, cause the faster and more favorable root growth, decrease the soil nutrient leaching, reduce the irrigation costs, increase the cationic exchange capacity of the soil, maximize the production potential of crop production, provide moisture in the upper layer of the soil, and increase the faster and more healthy growth of crops, especially in very hot and dry areas (Yazdani et al., 2007; He and Zhang, 2005). In a study, the use of SAP led to the increase of crop height, stem diameter, grain yield and biomass yield (Islam et al., 2011). In another study, the effect of organic and SAP on leaf chlorophyll index and their interaction effect on stomatal and nitrogen conductivity were statistically significant. In this study, the use of SAP increased the percentage of phosphorus in potato tubers (Rashidi et al., 2015).

Another method of management of potato yield increase is determining the appropriate sowing depth playing an essential role in forming the number of stolons and potato aerial stem and ultimately the final yield of potato (Ezekiel, 1992). The sowing depth determines the status and changes in the soil heat and moisture and is a criterion for soil resistance to the primary bud exit from the soil. Abducting the suitable sowing growth causes a delay in the rate of emergence or weakness of the seedlings (Acquaah, 2005). Several research results showed the significant effect of sowing depth on potato yield (Esehaghbeygi, 2010; Arab et al., 2011). Although in the autumn sowing, there will be a risk of frozen tubers under the soil if there is a severe cold weather but this possibility will decrease if the tubers are sown deeply. Thus, the autumn sowing of potato in temperate and semi-temperate regions is of great importance for some reasons such as reduced water consumption, higher sales prices, optimal utilization and maximum utilization of fall and winter precipitation resources and can be appropriate to change the pattern of sowing (Hassanpanah, 2016). The present study aimed at evaluating the effect of using moisture superabsorbent on growth and yield indices of autumn potato with different depths to reduce the adverse effects of drought stress.

Materials and methods

This experiment was carried out during two crop years of 2015-2016 and 2016-2017 at Ekbatan Research Station, Hamedan Agricultural and Natural Resources Research Center, Hamedan city, Hamedan province, (34° 88' North, 48° 53' West and 1731 m above sea level) which is located in the west of Iran (*Fig. 1*).

http://www.aloki.hu ● ISSN 1589 1623 (Print) ● ISSN 1785 0037 (Online)
DOI: http://dx.doi.org/10.15666/aeer/1605_70637078
© 2018, ALÖKI Kft., Budapest, Hungary

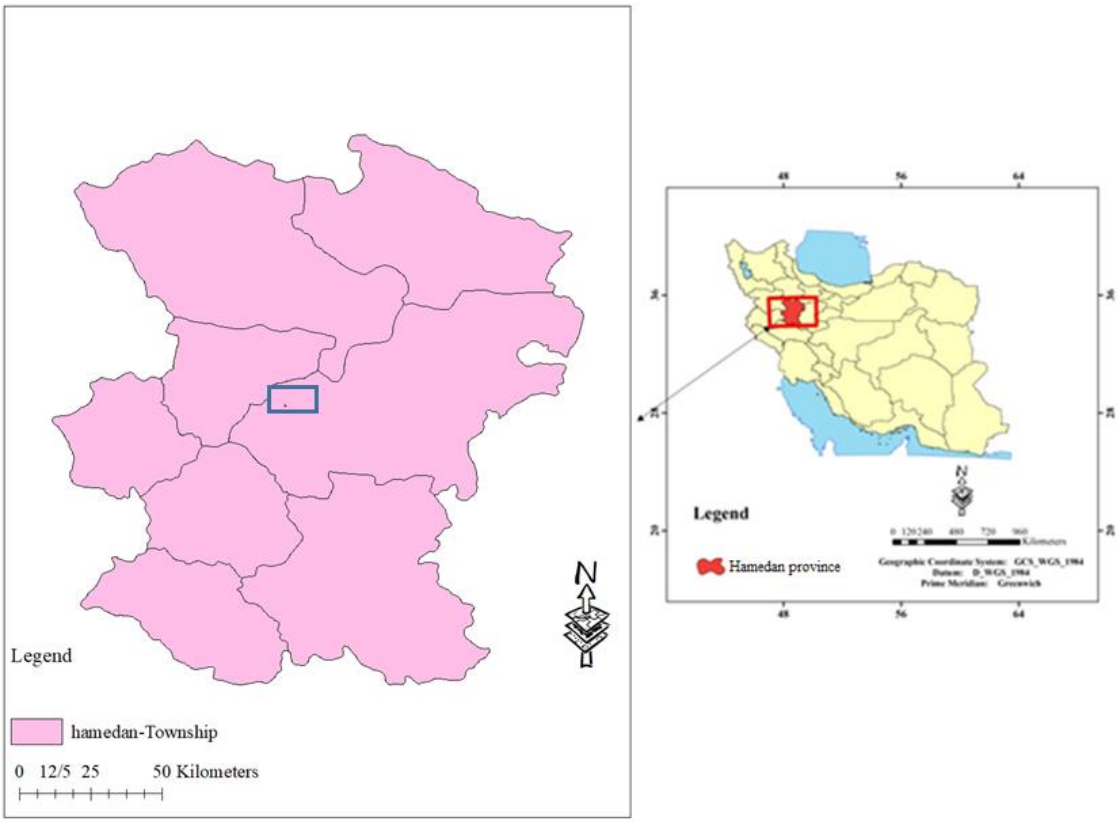

Figure 1. *The location of the experiment area, Hamedan city, Hamedan province, Iran*

The experiment was conducted as split plot based on randomized complete block design (RCBD) with three replications. The main factor included the sowing depth at four levels (10, 15, 20 and 25 cm), the subplots included the potato cultivar at three levels (early-season Sante, mid-season Fontane, and late-season Agria) and the sub-subplot included the use of SAP as 80 kg / ha and at two levels (without using (control) and using SAP). Before the cultivation, sampling was carried out with a depth of 0-30 cm to determine the physical and chemical characteristics of soil in the test site and the full specifications are presented in *Table 1*. Tillage was carried out in the autumn. After land levelling, a plot of 14 m^2 was started. Each plot included 3 rows of planting at a distance of 75 cm and a length of 6 m, the block spacing was one meter and the crop spacing in each row was 25 cm.

Table 1. *Experimental farm soil specification*

Soil depth	Soil texture	pH	EC	Nitrogen percentage	Absorbable phosphorus (mg/kg)	Absorbable potassium (mg/kg)
0-30	Clay loam	7.8	1.8	0.35	4.8	386.3

Fertilizer application was performed based on soil analysis. Accordingly, 250 kg of ammonium phosphate and 150 kg of potassium sulfate per hectare were used. Before sowing, the seed tubers were disinfected by Rural T. S fungicide (52.5% wettable

http://www.aloki.hu ● ISSN 1589 1623 (Print) ● ISSN 1785 0037 (Online)
DOI: http://dx.doi.org/10.15666/aeer/1605_70637078
© 2018, ALÖKI Kft., Budapest, Hungary

powder). The SAP was distributed to 80 kg/ha at the time of sowing the tubers in cultivation grooves. Sowing the tubers was carried out on November 20th and the tubers were under the soil and in sleep throughout the winter. In the spring and before the buds leave the soil, the first turn of the weed control was carried out with paraquat (Gramaxone) herbicide (3 liters per hectare). Then, the weed control was carried out manually by observing the first weed and continued until the product was ripe. Irrigation was carried out as droplets and tapes. When the crop height reached 10-15 cm, the cultivator and soil were carried out at the foot of the crops. During the grazing time, the complete fertilization of Humex micro fertilizer (at 3,000) was carried out in one turn while Urea fertilization was carried out as topdressing in two turns (mobbing and flowering stages). In flowering stage, the traits such as number of stems per crop, crop height and stem diameter were measured.

At the time of harvesting after random sampling from a square meter, the marginal effect was removed and the resulting tubers were weighed to obtain the tuber yield in kilograms per square meter. In order to calculate the percentage of tuber dry matter from each plot, three tubers were randomly weighed thoroughly after washing, then they were cut into thin chips and placed in an oven at 70 °C for 48 h. Then, they were weighed again and the percentage of tuber dry matter was calculated by dividing the dry weight of the tubers by their initial weight multiplied by 100. For measurements of growth indices, 1 m^2 of each plot were randomly selected from the central rows in plots. The remaining rows (except the border rows) were used for taking periodic plant samples. The sampling was done at 185, 192, 199 and 205 days after sowing. Then, the crops were dried in an oven at 75 °C for 48 h to be weighed. The rate of leaf area index (*LAI*), crop growth rate (*CGR*) and leaf area duration (*LAD*) were obtained from the *Equations 1– 3,* respectively (Taiz and Zeiger, 2006):

$$LAI = \frac{LA_1 + LA_2}{2} \times \frac{1}{GA} \quad \text{(Eq.1)}$$

$$CGR = \frac{W_2 - W_1}{GA(t_2 - t_1)} \quad \text{(Eq.2)}$$

$$LAD = \left(\frac{LAI_1 + LAI_2}{2}\right)(t_2 - t_1) \quad \text{(Eq.3)}$$

where $LA_2 + LA_1$ is total leaf area, GA is ground area $W_2 - W_1$ is dry weight changes, $t_2 - t_1$ is sampling time interval and $LAI_1 + LAI_2$ is total leaf area at time interval of $t_2 - t_1$.

The data obtained from the experiment were analysed by SAS statistical program (v.9.12) and the averages ere compared by Duncan's multiple range test at the 5% level. The charts were drawn by Excel (2010) software.

Results

The number of days up to 50% germination

The results of compound analysis indicated the significant effect of year (Y), sowing depth (D), cultivar (C), superabsorbent application use (S) and interaction between cultivar, depth and SAP in cultivar and depth at 1% level on the number of days up to 50% germination (*Table 2*). The results showed that number of days up to 50% germination was significantly affected by years (*Table 3*).

http://www.aloki.hu ● ISSN 1589 1623 (Print) ● ISSN 1785 0037 (Online)
DOI: http://dx.doi.org/10.15666/aeer/1605_70637078
© 2018, ALÖKI Kft., Budapest, Hungary

Table 2. *The analysis of compound variance for the effect of cultivar, sowing depth, and superabsorbent use on some potato traits*

Change sources	Df	Number of days to germination	Number of stems per crop	Stem diameter at flowering time	Crop height at flowering time	Tuber yield	Tuber dry matter
Year (Y)	1	286.17**	3.60**	2.097**	200.88**	10.39**	197.0407**
Repetition(R)(Y)	4	24.49	0.04	0.021	12.10	0.18	4.7807
Depth (D)	3	98.71**	0.62**	0.309**	46.72**	49.90**	116.3769**
Y*D	3	0.11ns	0.01ns	0.009ns	0.06ns	0ns	0.0002ns
R*D(Y)	12	19.70	0.03	0.005	5.24	0.41	1.0554
Cultivar (C)	2	1265.81**	36.41**	0.179**	3454.51**	8.17**	40.4527**
D*C	6	42.12**	0.04ns	0.222**	68.31**	9.79**	7.7951**
Y*C	2	0.21ns	0.02ns	0.004ns	1.91ns	0ns	0.0001ns
Y*D*C	6	1.32ns	0.06ns	0.003ns	0.32ns	0ns	0.0001ns
R*D*C (Y)	32	17.79	0.06	0.003	2.99	0.28	1.6067
Superabsorbent(S)	1	91.84**	1.28**	0.700**	309.58**	35.44**	313.7075**
Y*S	1	0.17ns	0.02ns	0.002ns	1.18ns	0ns	0.0016ns
D*S	3	23.85ns	0.08ns	0.047**	15.86**	1.04*	3.6122ns
Y*D*S	3	0.34ns	0.09ns	0.002ns	0.43ns	0ns	0.0002ns
C*S	2	21.34ns	0.19*	0.021**	14.89*	0.47ns	2.4021ns
Y*C*S	2	0.88ns	0.06ns	0.005ns	0.39ns	0ns	0.0001ns
D*C*S	6	24.30**	0.08ns	0.04**	19.26**	1.24**	8.9846**
Y*D*C*S	6	0.82ns	0.02ns	0.003ns	1.19ns	0ns	0.0001ns
Error	48	6.09	0.04	0.003	2.35	0.31	1.7108
c.v	-	10.58	4.63	4.52	4.66	8.05	6.64

ns, *, and **: insignificant and significant at levels of 5% and 1%, respectively

Table 3. *The effect of years on evaluated parameters in potato plant*

Years	Number of days to germination	Number of stems per crop	Stem diameter at flowering time (cm)	Crop height at flowering time (cm)	Tuber yield (kg/m^2)	Tuber dry matter (%)
2015-016	154^b	4.54^b	1.15^b	31^b	6.69^b	18^b
2016-017	157^a	4.86^a	1.39^a	34^a	7.23^a	20^a

Values with the different letters are significantly different according to Duncan's multiple range test at $P < 0.05$

Crop height

Effect of year (Y), sowing depth (D), cultivar (C), superabsorbent use (S), and mutual effects of sowing depth and SAP, cultivar and sowing depth and interaction effect of sowing depth, cultivar and SAP at 1% level and interaction effect of cultivar and SAP was significant at crop height ($p < 0.05$) (*Table 2*).

Stem diameter

The results of compound analysis showed that stem diameter under the effect of year (Y), sowing depth (D), cultivar (C), superabsorbent use application (S) and interaction

http://www.aloki.hu ● ISSN 1589 1623 (Print) ● ISSN 1785 0037 (Online)
DOI: http://dx.doi.org/10.15666/aeer/1605_70637078
© 2018, ALÖKI Kft., Budapest, Hungary

of sowing depth and SAP, cultivar and sowing depth, cultivar and SAP and interactions of sowing depth, cultivar and SAP were at 1% level (*Table 2*).

The number of stems per crop

The results of variance analysis showed the significant effect of year (Y), sowing depth (D), cultivar (C), use of super adsorbent (S) at 1% level, and interaction of cultivar and SAP on the number of stems per crop at 5% level (*Table 2*).

Tuber yield

The results of compound analysis showed the significant effect of year (Y), sowing depth (D), cultivar (C), use of super adsorbent (S) and interaction of sowing depth and cultivar and SAP, cultivar and sowing depth at 1% and interaction between SAP and sowing depth at 5% level on the tuber yield (*Table 2*). The results showed that tuber yield was significantly affected by years (*Table 3*).

Percentage of dry matter

The results of compound analysis showed that the dry matter percentage of the tuber was significantly ($P < 0.01$) affected by year (Y), sowing depth (D), cultivar (C), and superabsorbent use (S). Meanwhile, the interaction effect of cultivar and sowing depth as well as the interaction effect of sowing depth, cultivar and SAP were significant at 1% level (*Table 2*).

Discussion

The number of days up to 50% germination

The results of comparing the three-sided interaction between sowing depth, cultivar and SAP showed that the maximum number of days to 50% germination in Agria cultivar was obtained with a depth of 25 cm with a SAP use (165 days). The use of SAP with sowing depths of 10, 15 and 25 cm resulted in significant increase of days to 50% germination in Agria cultivar while this situation did not occur in two other cultivars (*Fig. 2*). It should be noted that the survival rate of tubers and their germination percentage were insignificant at 10 cm depth of all cultivars especially Agria cultivar due the frozen tubers.

Crop height

The results of mean comparison showed that the highest crop height in Agria cultivar was obtained at a depth of 15 cm with a SAP use (46 cm), which increased 9.5% than the use of SAP at the same depth and cultivar (Agria). In general, the use of SAP in all three cultivars resulted in a significant increase in crop height relative to non-use of SAP (*Fig. 3*).

The decrease in stem height with water deficit during the growing season and in the absence of SAP use is consistent with the results of research by Motalebifard et al. (2014). Cell growth is the most sensitive stage under the influence of water stress. The size of organs is limited by decreasing cell growth and the first palpable effect due to water deficiency in the crops is shown by decreasing leaf size and crop height (Kirank et al., 2003). The results of studies by Jahan et al. (2013) and Islam et al. (2011) showed

http://www.aloki.hu ● ISSN 1589 1623 (Print) ● ISSN 1785 0037 (Online)
DOI: http://dx.doi.org/10.15666/aeer/1605_70637078
© 2018, ALÖKI Kft., Budapest, Hungary

the positive effect of SAP on crop height which is consistent with the results of this research.

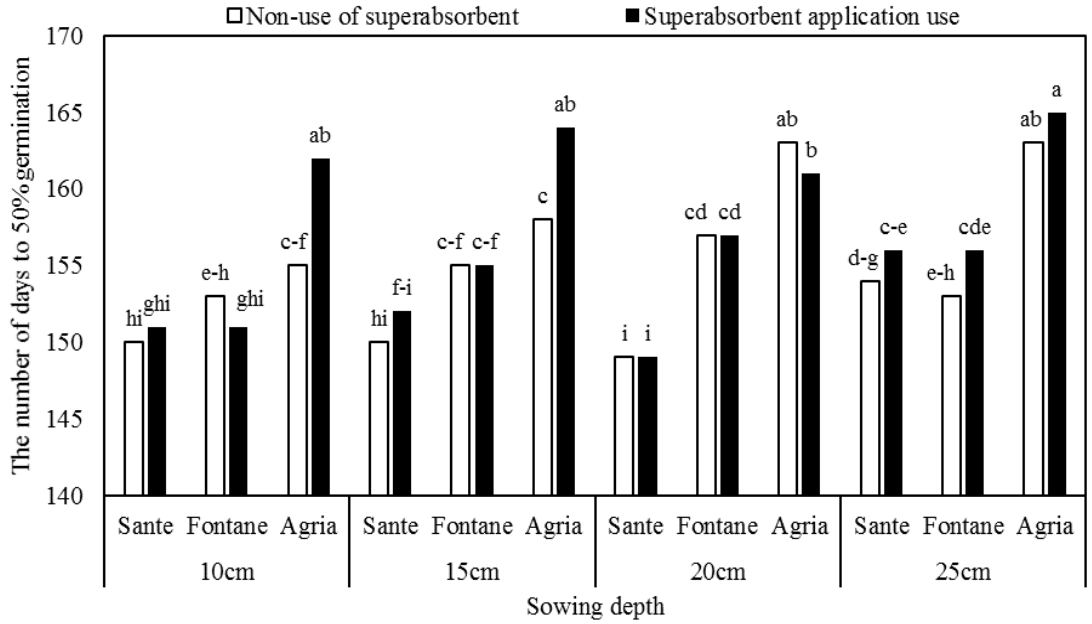

Figure 2. *The interaction of cultivar (Sante, Fontane and Agria), sowing depth (10, 15, 20 and 25 cm), and superabsorbent (application and non-application) on the number of days to 50% germination in potato. At each treatment, values with the different letters are significantly different according to Duncan's multiple range test at P < 0.05*

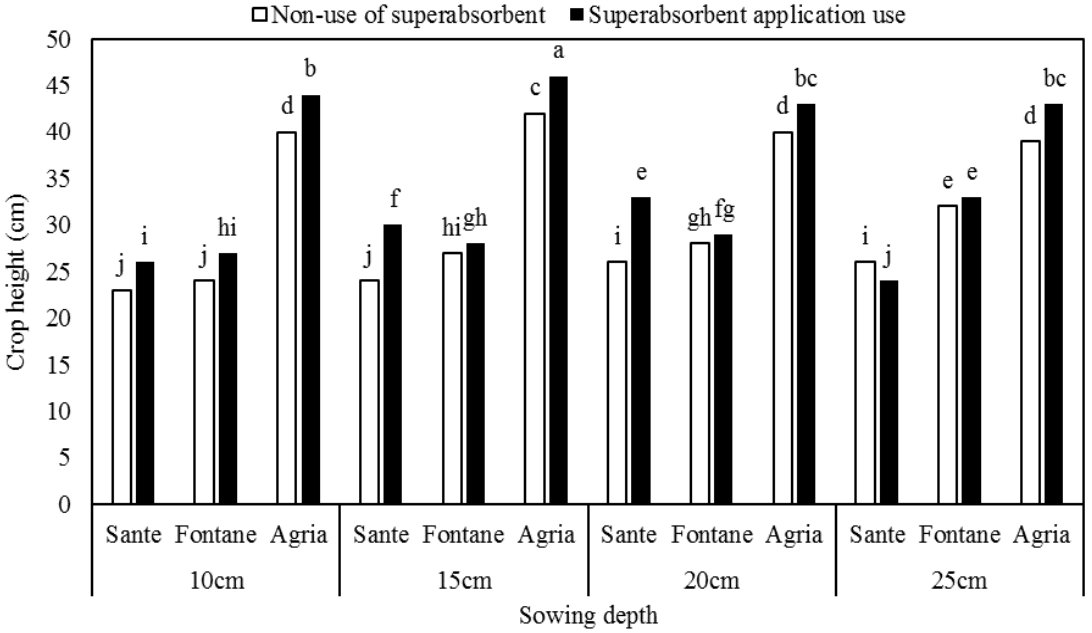

Figure 3. *The interaction of cultivar (Sante, Fontane and Agria), sowing depth (10, 15, 20 and 25 cm), and superabsorbent (application and non-application) on crop height of potato at flowering time. At each treatment, values with the different letters are significantly different according to Duncan's multiple range test at P < 0.05*

http://www.aloki.hu ● ISSN 1589 1623 (Print) ● ISSN 1785 0037 (Online)
DOI: http://dx.doi.org/10.15666/aeer/1605_70637078
© 2018, ALÖKI Kft., Budapest, Hungary

Stem diameter

With the significance of the interaction of sowing depth, cultivar and SAP, it was found that the highest stem diameter was Sante cultivar at a depth of 10 cm with the use of SAP (1.55 cm) and Agria cultivar at a depth of 20 Cm with the use of SAP (1.57 cm). In general, the use of SAP in all three cultivars resulted in a significant increase in stem diameter (*Fig. 4*).

The number of stems per crop

The significance of interaction between cultivars and SAP showed that in Sante and Agria, the use of SAP resulted in a significant increase in number of stems per crop. However, the use of SAP had no significant effect on number of stems per crop in Fontane cultivar (*Fig. 5*).

Tuber yield

The highest tuber yield was in the Fontane cultivar at a depth of 25 cm with SAP use. In general, the use of SAP in all three cultivars and different sowing depths resulted in a significant increase in tuber yield relative to non-use of SAP (*Fig. 6*). In this regard, the potato yield under the sowing depth (greater than 20 cm depending on the sowing conditions) was increased (Ezekiel, 1992). The results of Esehaghbeygi's study (2010) indicated that cultivar and sowing depth had a significant effect on the yield of potato and dry matter.

Extreme leaf area reduction of radiation absorption, as well as the reduction of photosynthetic yields result in the loss of dry matter and yield under drought stress conditions.

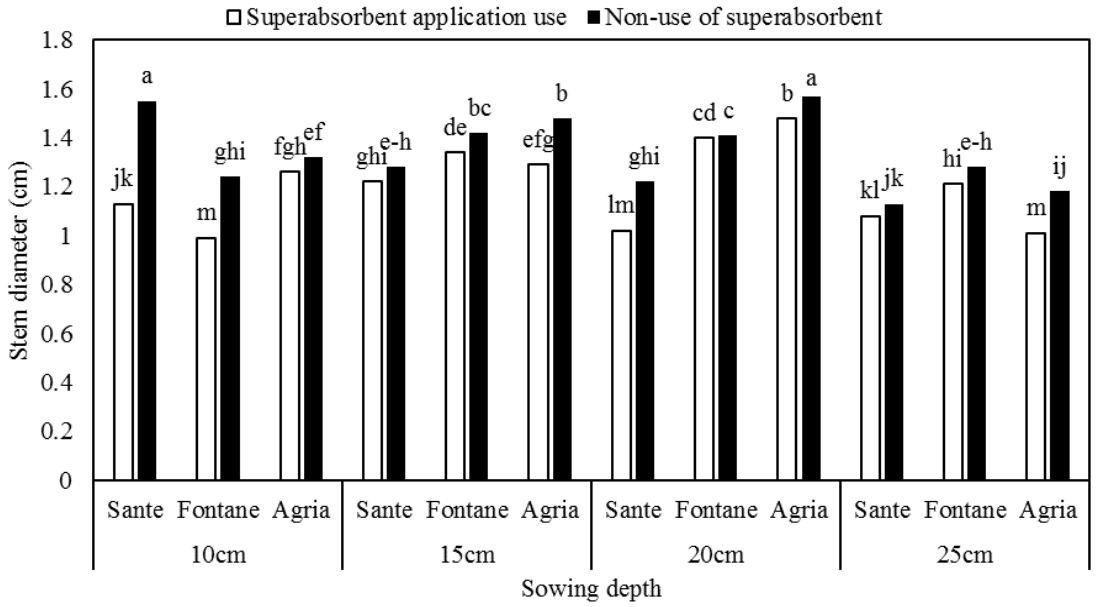

Figure 4. *The interaction of cultivar (Sante, Fontane and Agria), sowing depth (10, 15, 20 and 25 cm), and superabsorbent (application and non-application) on stem diameter of potato at flowering time. At each treatment, values with the different letters are significantly different according to Duncan's multiple range test at $P < 0.05$*

http://www.aloki.hu ● ISSN 1589 1623 (Print) ● ISSN 1785 0037 (Online)
DOI: http://dx.doi.org/10.15666/aeer/1605_70637078
© 2018, ALÖKI Kft., Budapest, Hungary

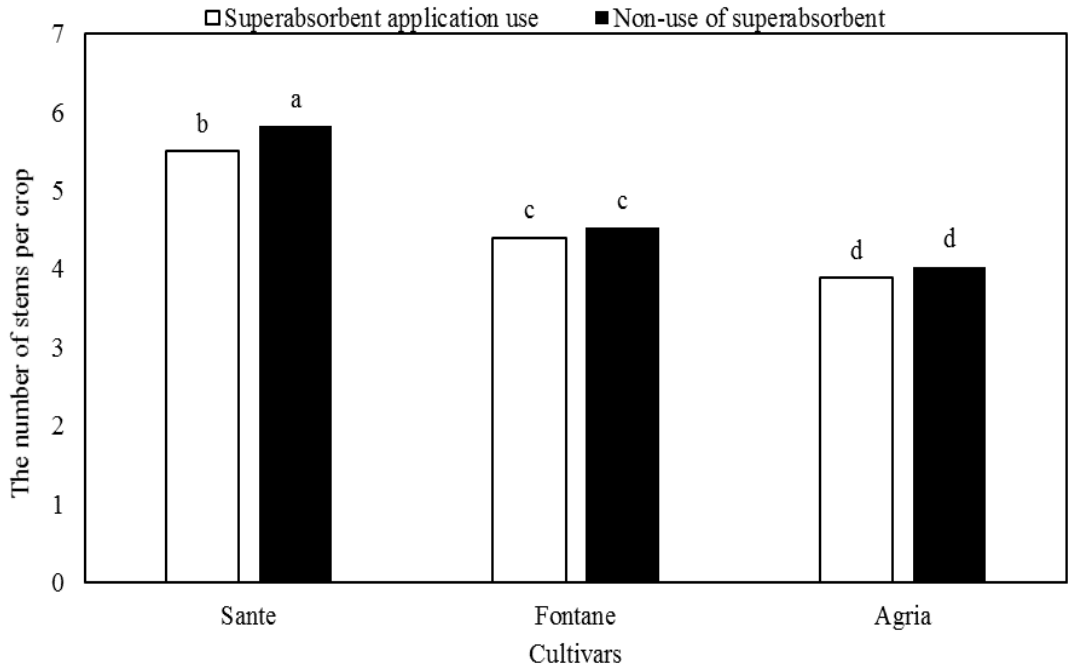

Figure 5. *The interaction of cultivar (Sante, Fontane and Agria) and superabsorbent (application and non-application) on the number of stems in potato at flowering time. At each treatment, values with the different letters are significantly different according to Duncan's multiple range test at P < 0.05*

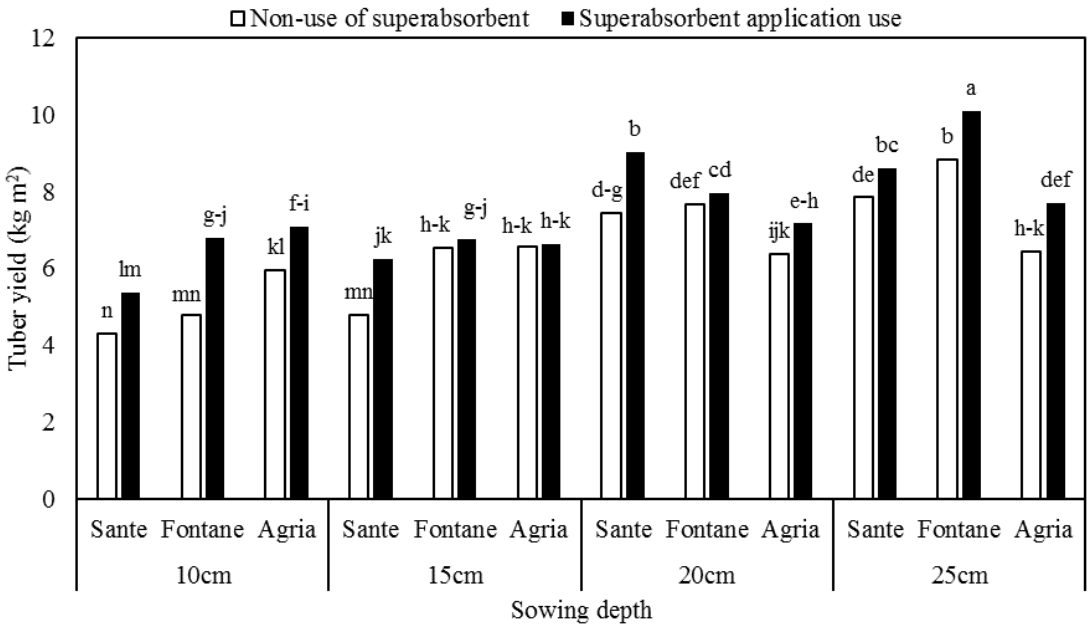

Figure 6. *The interaction of cultivar (Sante, Fontane and Agria), sowing depth (10, 15, 20 and 25 cm), and superabsorbent (application and non-application) on potato tuber yield. At each treatment, values with the different letters are significantly different according to Duncan's multiple range test at P < 0.05*

http://www.aloki.hu ● ISSN 1589 1623 (Print) ● ISSN 1785 0037 (Online)
DOI: http://dx.doi.org/10.15666/aeer/1605_70637078
© 2018, ALÖKI Kft., Budapest, Hungary

In this relation, King et al. (2004) stated that the soil water deficit in the mid and late stages of potato tuber yield could reduce the tuber yield. SAP can increase the growth and yield of crops by increasing the absorption and maintenance of water in soil, storage of nitrogen, phosphorus, sulfur and exchangeable cations, as well as increasing ventilation by improving soil structure (Nazarli et al., 2010). Other researchers reported a decrease in yield, yield components including number of tubers per crop, and the average weight of the tuber per crop, as well as reduced water use efficiency due to the application of water stresses (Alva et al., 2012; Liu et al., 2006; Ayas, 2013).

Percentage of dry matter

With significance of interaction between cultivar, sowing depth, use of SAP, it was determined that the highest percentage of dry matter in Sante and Fontane cultivars was cultured at 10 cm depth without using SAP. In general, the use of SAP and increasing the sowing depth in all three cultivars resulted in a significant decrease in the percentage of dry matter, while their variation was not uniform (*Fig. 7*).

Several studies showed that the percentage of dry matter of the tubers increases with decreasing irrigation, drought stress, and reducing yield (Ayas and Korukcu, 2010; Ayas, 2013; Porter et al., 1999). It seems that the reason for increasing dry matter percentage due to drought stress is to reduce the potential of water around the root and water deficit of the crop resulting in less water being directed to the tissues of the crop while the percentage of dry matter of the tubers increased (Bagheri et al., 2016).

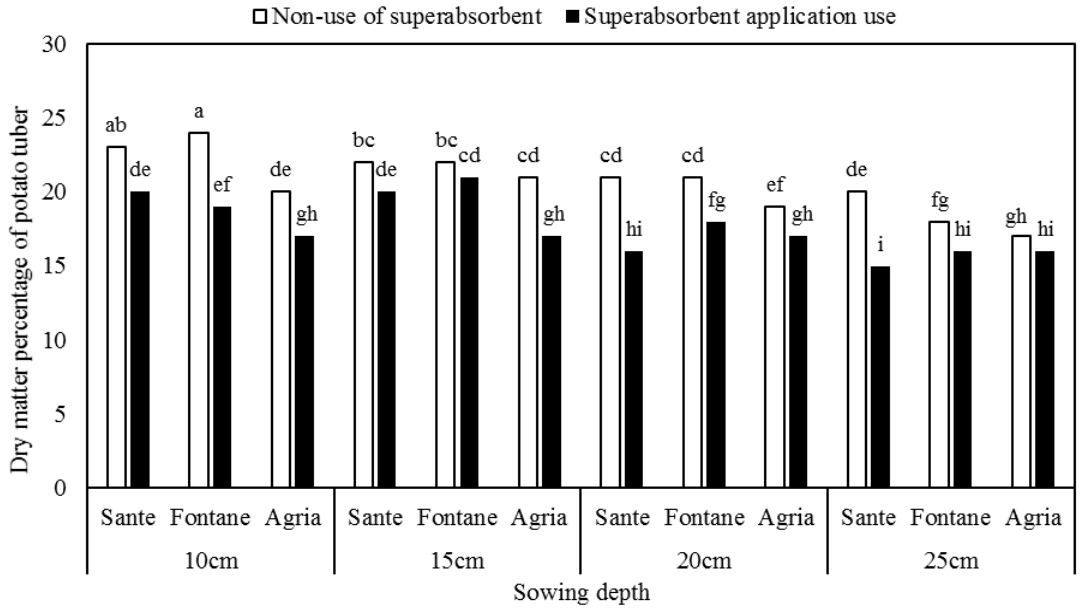

Figure 7. *The interaction of cultivar (Sante, Fontane and Agria), sowing depth (10, 15, 20 and 25 cm), and superabsorbent (application and non-application) on dry matter percentage of potato tuber. At each treatment, values with the different letters are significantly different according to Duncan's multiple range test at $P < 0.05$*

Leaf area index (LAI) and leaf area duration (LAD)

The results showed that in all three cultivars, the use of SAP led to an increase in leaf area index and leaf area duration. The highest leaf area index in Sante and Agria

http://www.aloki.hu ● ISSN 1589 1623 (Print) ● ISSN 1785 0037 (Online)
DOI: http://dx.doi.org/10.15666/aeer/1605_70637078
© 2018, ALÖKI Kft., Budapest, Hungary

cultivars was obtained with SAP use (*Figs. 8* and *9*). In Sante cultivar at 10 cm depth, leaf area index and leaf area duration were lower than other treatments. Increasing the sowing depth to 20 cm in Sante cultivar resulted in an increase in leaf area index. In other treatments, this trend was the same (*Figs. 10* and *11*). *LAI* and *LAD* levels increased with increasing SAP depth and use. The highest rate of these two traits was obtained under the conditions of SAP use at three depths of 15, 20, and 25 cm. The amount of *LAI* and *LAD* at sowing depth of 10 cm was less than three other depths (*Figs. 12* and *13*).

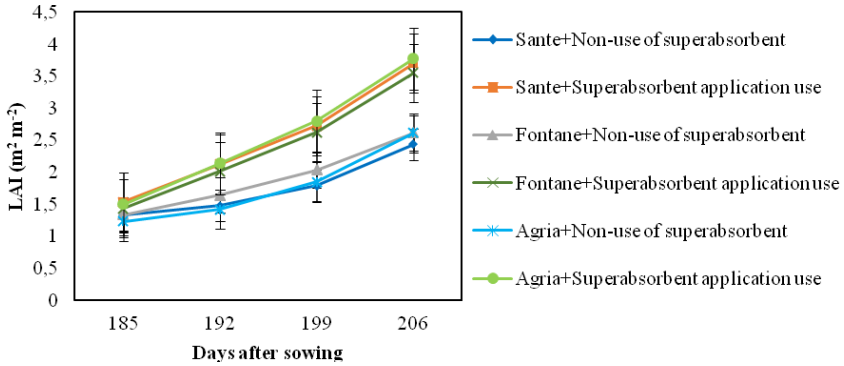

Figure 8. *The effects of cultivar and superabsorbent use on the leaf area index of potato (LAI). Bars represent standard errors of three replicate*

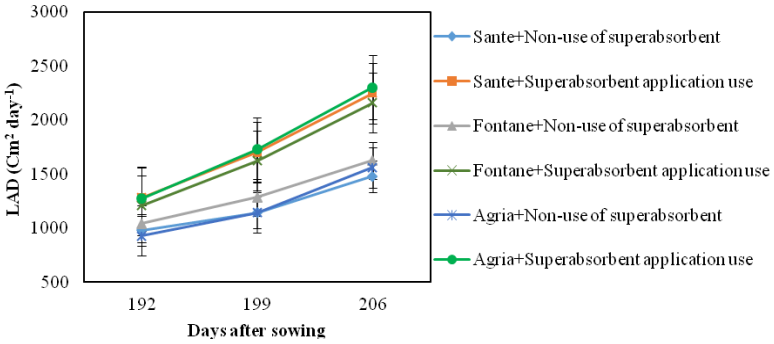

Figure 9. *The effects of cultivar and superabsorbent use on the leaf area duration of potato (LAD). Bars represent standard errors of three replicate*

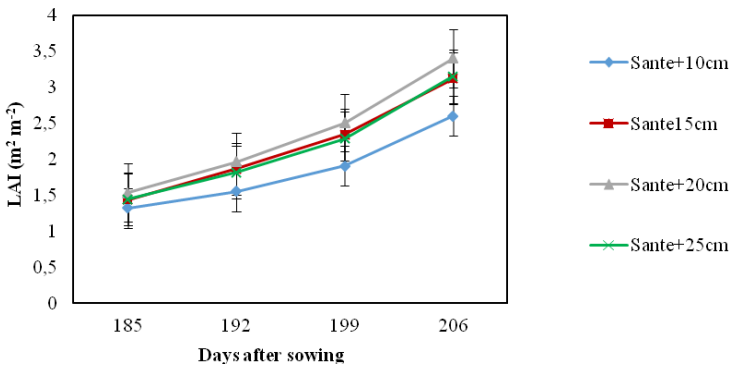

Figure 10. *The effects of sowing depth on the leaf area index of potato (LAI). Bars represent standard errors of three replicate*

http://www.aloki.hu ● ISSN 1589 1623 (Print) ● ISSN 1785 0037 (Online)
DOI: http://dx.doi.org/10.15666/aeer/1605_70637078
© 2018, ALÖKI Kft., Budapest, Hungary

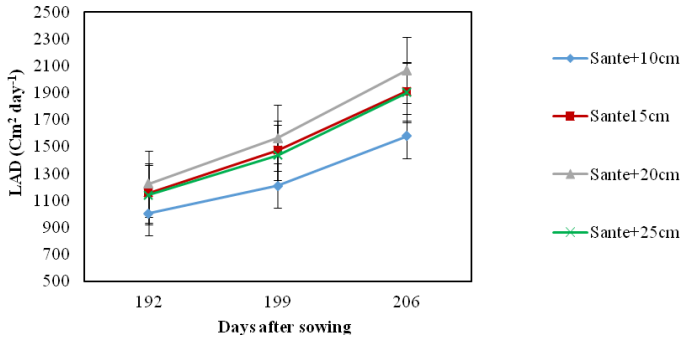

Figure 11. *The effects of sowing depth on the leaf area duration of potato (LAD). Bars represent standard errors of three replicate*

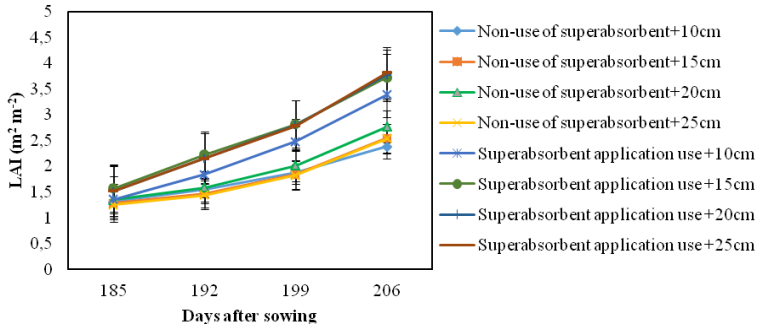

Figure 12. *The effects of superabsorbent use and sowing depth on the leaf area index of potato (LAI). Bars represent standard errors of three replicate*

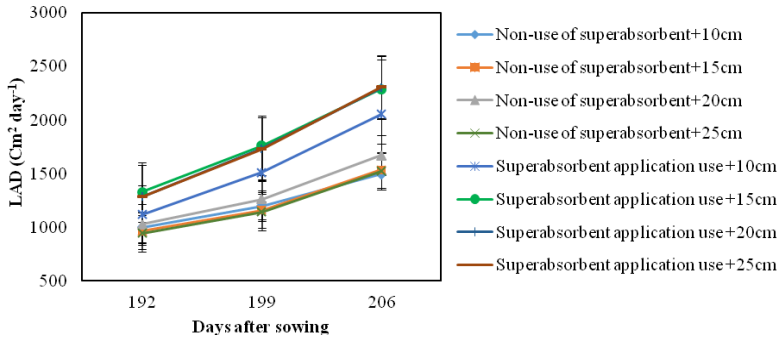

Figure 13. *The effects of superabsorbent use and sowing depth on the leaf area duration of potato (LAD). Bars represent standard errors of three replicate*

Drought stress can reduce leaf area and photosynthesis (Ierna and Mauromicale, 2006). The study results of FazeliRostampour (2013) showed that the use of SAP and supply of needed water up to 80% increased the leaf area index and leaf area duration.

Crop growth rate (CGR)

The effects of cultivar and SAP use indicated that in all three cultivars, the use of superabsorbent n led to an increase in *CGR* (*Fig. 14*). In Sante cultivar at 10 cm depth,

http://www.aloki.hu ● ISSN 1589 1623 (Print) ● ISSN 1785 0037 (Online)
DOI: http://dx.doi.org/10.15666/aeer/1605_70637078
© 2018, ALÖKI Kft., Budapest, Hungary

CGR was less than other treatments during the growing season. Increasing the depth of cultivation in the Sante cultivar led to an increase in *CGR* (*Fig. 15*). In each of the four depths, the SAP use resulted in an increase in *CGR* compared with the absence of SAP use. The highest *CGR* was obtained under the conditions of SAP use at three depths of 15, 20 and 25 cm (*Fig. 16*).

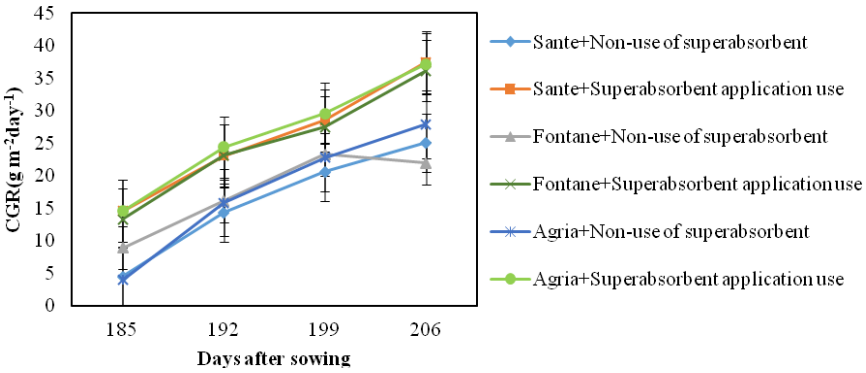

Figure 14. *The effect of cultivar and superabsorbent use on potato growth rate (CGR). Bars represent standard errors of three replicate*

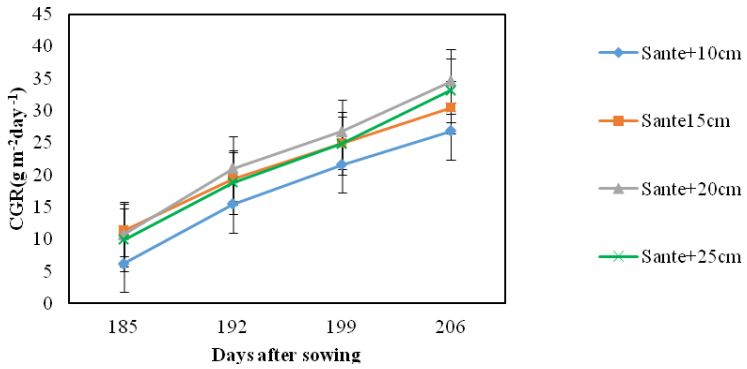

Figure 15. *The effect of cultivar and sowing depth on potato growth rate (CGR). Bars represent standard errors of three replicate*

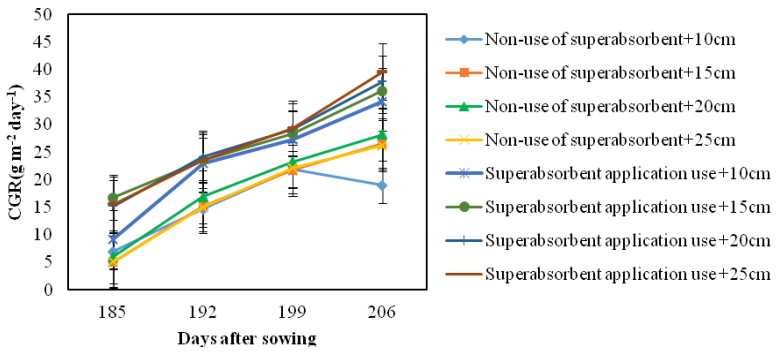

Figure 16. *The effect of superabsorbent use and sowing depth on crop growth rate (CGR). Bars represent standard errors of three replicate*

http://www.aloki.hu ● ISSN 1589 1623 (Print) ● ISSN 1785 0037 (Online)
DOI: http://dx.doi.org/10.15666/aeer/1605_70637078
© 2018, ALÖKI Kft., Budapest, Hungary

Higher the LAI and the adequate absorption of radiation results in higher production rates and higher growth rates. Reducing the leaf water potential results in the reduced growth rate of the product due to the increase in respiration rate associated with the increase in plant temperature and reduction of the intensity of photosynthesis (Evans, 1978).

Conclusion

In conclusion, increasing the sowing depth to 25 cm resulted in increasing the number of days to 50% germination, number of stems per crop, and tuber yield. However, increasing the sowing depth resulted in the reduced tuber dry weight. In general, the use of superabsorbent in all three cultivars and at different sowing depths resulted in a significant increase in tuber yield relative to the non-use of superabsorbent. The results of growth indices showed that in all three cultivars, the use of superabsorbent led to an increase in leaf area index, in leaf area duration, and in crop growth rate. Based on the results of this study and durability of superabsorbent polymer in soil, we can say that using superabsorbent under different sowing depth conditions can increase the potato yield and productivity.

REFERENCES

[1] Acquaah, G. (2005): Principles of Crop Production: Theory, Techniques, and Technology. Second edition. – Pearson Prentice Hall, New Jersey, USA.
[2] Alva, A. K., Ren, H., Moore, A. D. (2012): Water and nitrogen management effects on biomass accumulation and partitioning in two potato cultivars. – American Journal of plant Sciences 3(1): 164-170.
[3] Arab, H. R., Afshari, H., Samdaliri, M., Laei, GH., Toudar, S. R. (2011): The effect of planting date, depth and density on yield and yield components of potato in Shahrood (Iran). – Journal of Research in Agricultural Science 7(2): 141-149.
[4] Ayas, S. (2013): The effects of different regimes on potato (*Solonum tuberosum* L. Hermes) yield and quality characteristics under unheated greenhouse conditions. – Bulgarian Journal of Agricultural Science 19(1): 87-95.
[5] Ayas, S., Korukcu, A. (2010): Water-yield relationships in deficit irrigated potato. – Journal of Agricultural Factulty of Uludag University 24(2): 23-26.
[6] Bagheri, H. R., Qarineh, M. H., Bakhshande, A. S., Tayyi, J., Mehnatkesh, A. S., Andrzian, B. (2016): Effects of water deficit and different nitrogen fertilizer levels on yield, yield components and water use efficiency of potato (*Solanum tuberosum* L.). – Environmental Stresses in Crop Science 9(1): 1-14.
[7] Bannayan, M., Sanjani, S., Alizadeh, A., Lotfabadi, S., Mohammadian, A. (2010): Association between climate indices, aridity index, and rainfed crop yield in northeast of Iran. – Field Crops Research 118(2): 105-114.
[8] Esehaghbeygi, A. (2010): The effect of cultivation depth and variety on the yield and properties of potato tuber. – Journal of Plant Productions 33(1): 67-74.
[9] Evans, L. T. (1978): Crop Physiology: Some Case Histories. First edition. – Cambridge University Press, Cambridge, UK.
[10] Ezekiel, R., Bhargava, S. C. (1992): Nitrogen distribution within the potato plant in relation to planting date under short day conditions. – Indian Journal of Plant Physiology 35(2): 130-139.

http://www.aloki.hu ● ISSN 1589 1623 (Print) ● ISSN 1785 0037 (Online)
DOI: http://dx.doi.org/10.15666/aeer/1605_70637078
© 2018, ALÖKI Kft., Budapest, Hungary

[11] FazeliRostampour, M. (2013): Effects of irrigation regimes and polymer on dry matter yield and several physiological traits of forage sorghum var 'Speedfeed'. – African Journal of Biotechnology 12(51): 7074-7080.
[12] FAO (2008): FAOSTAT. Statistic Database. – http://faostat.fao.org/.
[13] FAO (2013): FAOSTAT. Statistic Database. – http://faostat.fao.org/.
[14] Garg, B., Lata, C., Prasad, M. (2012): A study of the role of gene TaMYB2 and an associated SNP in dehydration tolerance in common wheat. – Molecular Biology Reports 39(12): 10865-10871.
[15] Ghooshchi, F. (2015): Investigation the possibility of decreasing the damage due to irrigation-cut tension on physiological characteristics and corn quality by applying the super absorbent polymer. – Crop Physiology Journal 7(27): 85-94.
[16] Haase, T., Schuler, C., Heb, J. (2007): The effects of different N and K sources on tuber nutrient uptake, total graded yield of potatoes (*Solanum tuberosum* L.) for processing. – Agronomy Journal 26(3): 187-193.
[17] Hassanpanah, D. (2016): The most suitable of cultivars and planting depth for potato autumn sowing in various regions of Ardabil province. – Ardabil Agricultural Extension Coordination Management 115: 1-16.
[18] He, X. S., Zhang, F. D. (2005): Characteristics and performance of water-absorbent polymer coated urea. – Plant Nutrition and Fertilizer Science 12(3): 334-339.
[19] Ierna, A., Mauromicale, G. (2006): Physiological and growth response to moderate water deficit of off-season potatoes in a Mediterranean environment. – Agricultural Water Management 82(1-2): 193-209.
[20] Islam, M. R., Xue, X., Mao, S., Zhao, X., Eneji, A. E., Hu, Y. (2011): Superabsorbent polymers (SAP) enhance efficient and eco-friendly production of corn (*Zea mays* L.) in drought affected areas of northern china. – African Journal of Biotechnology 10(24): 4887-4894.
[21] Jahan, M., Kamayestani, N., Ranjbar, F. (2013): Assay for applying super absorbent polymer in a low input corn (*Zea mays* L.) production system aimed to reduce drought stress under Mashhad conditions. – Agroecology 5(3): 272-281.
[22] King, B. A., Stark, G. C., Love, S. (2004): Potato Production with Limited Water Supplies. – Agricultural Experiment Station Publications, University of Idaho, United States of America, pp. 1-8.
[23] Kirnak, H., Gencoglan, C., Degirmenci, V. (2003): Effect of deficit irrigation on yield and growth of second crop corn in Harran Plain conditions. – Journal of Agricultural Faculty of Ataturk University 34(2): 117-123.
[24] Liu, F., Shahnazari, A., Anderson, M. N., Jacobsen, S. E., Jensen, Ch. R. (2006): Effects of deficit irrigation (DI) and partial root drying (PRD) on gas exchange, biomass partitioning, and water use efficiency in potato. – Scientia Horticulturae 109(2): 113-117.
[25] Maksup, S., Roytrakul, S., Supaibulwatana, k. (2014): Physiological and comparative proteomic analyses of Thai jasmine rice and two check cultivars in response to drought stress. – Journal of Plant Interactions 9(1): 43-55.
[26] Motalebifard, R., Najafi, N., Oustan, Sh., Nayshabori, M. R., Valizadeh, M. (2014): Effect of soil moisture, phosphorus and zinc levels on the growth attributes of potato, greenhouse conditions. – Iranian Journal of Soil and Water Research 45(1): 75-86.
[27] Nazarli, H., Zardashti, M. R., Darvishzadeh, R., Najafi, S. (2010): The effect of water stress and polymer on water use efficiency, yield and several morphological traits of sunflower under greenhouse condition. – Notulae Scientia Biologicae 2(4): 53-58.
[28] Parvizi, K. (2008): Evaluation of quantitative and qualitative traits of late and early ripening advanced potato cultivars. – Pajouhesh & Sazandegi 21(2): 80-90.
[29] Parvizi, K., GhadamiFiroozabadi, A. (2015): Evaluation the effect of water deficit methods on quantitative and qualitative traits of new potato cultivar. – Iranian Journal of Field Crops Research 13(3): 637-650.

http://www.aloki.hu ● ISSN 1589 1623 (Print) ● ISSN 1785 0037 (Online)
DOI: http://dx.doi.org/10.15666/aeer/1605_70637078
© 2018, ALÖKI Kft., Budapest, Hungary

[30] Porter, G. A., Opena, G. B., Bradbury, W. B., McBurnie, J. C., Sisson, J. A. (1999): Soil management and supplemental irrigation effects on potato: I. Soil properties, tuber yield, and quality. – Agronomy Journal 91(3): 416-425.
[31] Rashidi, N., Arji, A., Gardkane, M., Kashi, A. (2015): Effect of organic and superabsorbent cultures on physiological and biochemical properties of potato cultivars 'Marfona' in Kermanshah. – Journal of Horticultural Science 28(4): 453-463.
[32] Shock, C. C., Shock, B. M., Welch, T. (2013): Strategies for efficient irrigation water use. – Oregon State University, Sustainable Agriculture Techniques EM8783: 1-7.
[33] Sirousmehr, A., Arabi, J., Asgharipour, M. R. (2014): Effect of drought stress levels and organic manures on yield, essential oil content and some morphological characteristics of sweet basil (*Ocimum basilicum*). – Advances in Environmental Biology 8(4): 880-885.
[34] Taiz, L., Zeiger, E. (2006): Plant Physiology. Fourth edition. – Sinauer Associates, Sunderland, Massachusetts, USA.
[35] Yazdani, F., Allahdadi, I., Akbari, G. A., Behbahani, M. R. (2007): Effect of different rates of superabsorbent polymer (Tarawat A200) on soybean yield and yield components (*Glycine max* L.). – Pajouhesh & Sazandegi 20(2): 167-174.

http://www.aloki.hu ● ISSN 1589 1623 (Print) ● ISSN 1785 0037 (Online)
DOI: http://dx.doi.org/10.15666/aeer/1605_70637078
© 2018, ALÖKI Kft., Budapest, Hungary

EFFECTS OF POTASSIUM ON PHENOLOGICAL, PHYSIOLOGICAL AND AGRONOMIC TRAITS OF MAIZE (*ZEA MAYS* L.) UNDER HIGH NITROGEN NUTRITION WITH OPTIMUM AND REDUCED IRRIGATION

SHAH, T.[1,2] – KHAN, H.[1] – NOOR, M. A.[3*] – GHONEIM, A.[4] – WANG, X.[5*]– SHER, A.[6] – NASIR, M.[7] – BASAHI, M. A.[8]

[1]*Department of Agronomy, University of Agriculture, Peshawar, Pakistan*

[2]*Key Laboratory of Oil Crop Biology and Genetic Improvement, Oil Crops Research Institute of the Chinese Academy of Agricultural Sciences, Wuhan, Hubei, China*

[3]*Institute of Crop Sciences, Chinese Academy of Agricultural Sciences, Key Laboratory of Crop Physiology and Ecology, Ministry of Agriculture, 100081 Beijing, China*

[4]*Department of Soil Sciences, College of Food and Agricultural Sciences, King Saud University, P.O. Box 2460, Riyadh 11451, Saudi Arabia*

[5]*College of Life Sciences, Yan'an University, 716000 Yan'an, Shaanxi, China*

[6]*School of Agronomy, Anhui Agricultural University, Hefei 230036, Anhui, China*

[7]*College of Natural Resources and Environment, Northwest Agriculture and Forestry University, 712100 Yangling, China*

[8]*Dept. of Biology, College of Science & Arts, Sajir, Shaqra University P.O. Box-33, 11961 Shaqra, Saudi Arabia*

**Corresponding authors*
e-mail: mehmood2017@gmail.com (M. A. Noor); wangxiukang@126.com (X. Wang)

(Received 30th Jul 2018; accepted 8th Oct 2018)

Abstract. Potassium (K) as a macro nutrient governs important physiological mechanisms ensuring optimum plant growth and produce quality. An experiment was conducted during the summer of 2017 to study the effects of potassium application on maize under high nitrogen (N) nutrition with optimum and reduced irrigations. The experiment was comprised of three factors, viz. two irrigation levels (optimum, reduced), three potassium levels (80, 120 and 160 kg ha^{-1}) and four nitrogen levels (100, 150, 200 and 250 kg ha^{-1}). Two separate trials were carried out in randomized complete block design (RCBD), one under optimum (five irrigations) and another under reduced irrigation (three irrigations). One control plot (0K, 0N) was used under each replication for both trials. Optimum irrigation had resulted in maximum days of tasseling, silking, physiological maturity, crop growth rate (CGR), net assimilation rate (NAR), absolute growth rate (AGR), plant height, grains ear^{-1}, thousand grains weight, biological yield, grain yield, chlorophyll contents and shelling percentage. High N (250 kg ha^{-1}) delayed tasseling, silking and physiological maturity and resulted in maximum growth, physiological traits and biological yields. However, 150 kg N ha^{-1} had resulted in maximum number of ears m^{-2}, number of grains ear^{-1}, thousand grains weight and grain yield. While 100 kg N ha^{-1} had resulted in early tasseling, silking and physiological maturity. Potassium fertilization at the rate of 160 kg ha^{-1} delayed phenology and recorded with maximum growth rates, improved physiology and maximum yield traits and grain yield. However, the treatment 120 kg K ha^{-1} remained almost statistically similar to the 160 kg K ha^{-1} for most of the parameters. In the case of control vs rest, generally the performance of the control plot was poor. Hence, 150 kg N ha^{-1} with 120 kg K ha^{-1} under optimum irrigation is recommended for optimum productivity of maize crop.

Keywords: *fertilizer rate, maize, deficit irrigation, ear characteristics, grain yield*

http://www.aloki.hu ● ISSN 1589 1623 (Print) ● ISSN 1785 0037 (Online)
DOI: http://dx.doi.org/10.15666/aeer/1605_70797097
© 2018, ALÖKI Kft., Budapest, Hungary

Introduction

Maize (*Zea mays* L.) is the third most important cereal crop in Pakistan after wheat and rice and ranks second in Khyber Pakhtunkhwa province after wheat. Maize is cultivated in Pakistan on 64% irrigated and 36% on rainfed land (Ahmad and Rashid, 2003). Implementation and adoption of the new production technologies had increased the maize production per unit area due to balance use of agriculture inputs and new methods (Amanullah, 2004).

Improper application of the synthetic fertilizers in Khyber Pakhtunkhwa is the main cause of low yield of maize (Amanullah et al., 2014). In Pakistan only tobacco crop receive potassium due to industrial requirement while farmers do not apply potassium to wheat and maize in general. Deficiency of potassium is reported in most of the Pakistani soils due to multiple cropping systems (Ahmad and Rashid, 2003). Potassium is used by the crops in large amounts (Mengel et al., 2001; White and Karley, 2010). A soil deficient in potassium results in reduced plant photosynthesis (Wang et al., 2015a), which is the main cause of low yield of maize (Amanullah and Khalid, 2016), sunflower (Amanullah and Khan, 2010) and brassica (Amanullah et al., 2011).

Potassium is the primary major nutrient which is a non-structural component of the plant body. After nitrogen it is the second most abundant nutrient in plant tissues generally 1-3% by weight. It is very important for the transport of assimilates in plant cells and activates more than 60 different enzymes. Potassium increases plant tolerance to frost and heat injuries, droughts and enhances the resistance to diseases, different pest incidence and keeps anion balance in plants (Wang et al., 2013). The most important role of K^+ in plants is the osmoregulation which maintains turgor pressure in the cell, crucial for cell elongation and hence the growth and regulation of stomatal opening and closing, affecting carbon dioxide intake by photosynthesis process and transpirational cooling (Marschner, 1995). Potassium is a macro nutrient which is important for the growth of plants. Comparatively the large amounts of mineral potassium are present in the Pakistani soil which is non-soluble, and only a small amount is available to plants. Optimum amount of potassium in the soil in case of water scarcity comparatively enhances deposition of total dry matter in the crops compared to soils with less potassium regimes (Rosenstock et al., 2016). Potassium regulates stomata which in turn enhance photosynthesis (Marschner, 2012). Moreover, the root growth is supported by the crucial role of potassium in the transportation of photosynthetic products (Romheld and Kirkby, 2010).

Being a macro-nutrient, nitrogen is essential for the plant health and acts as a growth-limiting nutrient (Noor, 2017; Wang et al., 2018). Nitrogen is the major part of several essential organic compounds such as amino acids, proteins, coenzymes, nucleic acids, chlorophyll, cytochrome, ribosomes and many vitamins (Noorka et al., 2009, 2011). Among various grasses, maize is the grass whose nitrogen requirements for optimum grain yield is very high (Noor, 2017). Certain metabolic processes of the plants depend on the role of nitrogen in plants (Wang et al., 2015b). During the whole grain-filling stage, it aids to keep the kernels active, affecting the size and number of improved kernels (Huber et al., 1994). Usually nitrogen demand of maize is very different, and approximately 0-250 kg N ha^{-1} is the range for economically optimal nitrogen rates (EONR) (Scharf et al., 2006). Therefore, it is imperative to manage nitrogenous fertilizers accurately (Noor, 2017), but the capacity to determine the exact EONR had been kept comparatively elusive.

http://www.aloki.hu ● ISSN 1589 1623 (Print) ● ISSN 1785 0037 (Online)
DOI: http://dx.doi.org/10.15666/aeer/1605_70797097
© 2018, ALÖKI Kft., Budapest, Hungary

A sufficient amount of water in the soil is important for the growth and development of crops, recovery of water loss through transpiration and as a transport medium for nutrients to roots (Wang et al., 2018). Scarce availability of water to crops in the soil leads to drought. Acute water deficiency reduces water use and hence crop yield. There are three big processes by which maize yield is limited by water scarcity in the soil: (i) decreased absorption of the incident photosynthetically active radiation by canopy, (ii) reduced radiation use efficiency, (iii) decreased harvest index (Earl and Davis, 2003).

To know and keeping in mind the importance of potassium, in case of high nitrogen nutrition impact on maize lodging under optimum and reduced irrigations, the present experiment was designed and conducted to find out optimum level of potassium for improved growth and yield traits by minimizing lodging losses, enhancing resistance to drought and to figure out the best nitrogen level for higher maize productivity in the agro-climatic conditions of Peshawar, Pakistan.

Materials and methods

Site description

Field experiments were conducted to study the response of spring planted maize hybrid, at Agronomy Research Farm, The University of Agriculture Peshawar, Pakistan, during the summer of 2017. The research farm is located at 34.01°N, 71.35°E, at an altitude of 350 m above sea level in the Peshawar valley (*Fig. 1*). Peshawar is located about 1600 km north of the Indian Ocean and has semiarid climate. The research farm is irrigated by the Warsak canal from Kabul River. The soil of the farm is clay loam in texture, alkaline (pH 8.2), and calcareous, with a low organic matter content of 8.7 (g kg^{-1}) and low concentrations of extractable phosphorus of 6.57 mg kg^{-1} and exchangeable potassium (AB-DTPA) of 121 (mg kg^{-1}). The climate of the area is semiarid where the mean annual rainfall is very low (300 to 500 mm), 60–70% rainfall occurs in summer, while the remaining 30–40% rainfall occurs in winter.

Experimental treatments and management practices

Two trials, one with optimum irrigation (I) (I = 5 irrigations) and another with reduced irrigation (I_2 = 3 irrigations) were carried out in randomized complete block design (RCBD). Nitrogen (N_1 = 100, N_2 = 150, N_3 = 200 and N_4 = 250 kg ha^{-1}) and potassium (K_1 = 80, K_2 = 120 and K_3 = 160 kg ha^{-1}) were applied in combination to both experiments with three replications. Each replication was added with an unfertilized plot (0N, 0K). CS-220 variety of maize was sown on 18th May 2017 with a sub-plot area of 3 m × 4 m, which was consisted of 70 cm apart 3 m long 5 rows. Seeds were planted at the rate of 35 kg ha^{-1}. Before seed bed preparation, presoaking irrigation of 100 mm was given. When the soil reached at field capacity, seedbed was prepared. Subsequently, five irrigations (75 mm each) were applied at VE, V6, V12, V18 and R1 stages of maize for optimum irrigation treatment. For the reduced irrigation, three irrigations (75 mm each) were applied at VE, V12 and R1 stages of maize. Muriate of potash (MOP) was used as a source of potassium which contains 60% K_2O, Similarly N was applied as urea (46% N). Source of phosphorus was triple super phosphate (TSP) at the rate of 90 kg ha^{-1}. Potash and phosphorus were applied as a whole at the planting time, whereas half split of nitrogen was applied at planting and the other half at V6 stage (knee height). Weeds were controlled by applying herbicide Primixtra gold (S-

http://www.aloki.hu ● ISSN 1589 1623 (Print) ● ISSN 1785 0037 (Online)
DOI: http://dx.doi.org/10.15666/aeer/1605_70797097
© 2018, ALÖKI Kft., Budapest, Hungary

Metolachlor 400 g/L, Atrazine 320 g/L) at rate of 2000 ml ha^{-1} two weeks after sowing maize crop. On the basis of calibration for experimental area, 250 l ha^{-1} water was used for the herbicide application. Furadan (Carbofuran) was applied at rate of 10 kg ha^{-1} with second irrigation and 10 kg ha^{-1} with the third irrigation. During the whole growing season, uniform agronomic techniques were performed in all sub plots.

Figure 1. *Location of the study site in the Peshawar city of Pakistan. (Modified from the source: www.surveyofpakistan.gov.pk)*

Harvesting of whole plots was done manually on 15th August 2017. After harvesting, plants were kept in the field for three days and then tied into bundles and stacked in the sun light for 3 weeks for sun-drying. After 3 weeks the ears of the whole plot were husked and allowed to dry in sunshine for two days. After sun-drying, husked ears were threshed by maize sheller and subsequent calculations were done to determine grain yields.

Measurements

Phenological parameters

Days to tasseling data were recorded by counting days from planting date to the date when 50% plants had produced tassels in each plot. Days to silking data were figured out in each plot by counting the number of days from sowing date to the date when 50% silks

http://www.aloki.hu ● ISSN 1589 1623 (Print) ● ISSN 1785 0037 (Online)
DOI: http://dx.doi.org/10.15666/aeer/1605_70797097
© 2018, ALÖKI Kft., Budapest, Hungary

were appeared. Data on days to physiological maturity were recorded by counting the number of days between sowing date and the date when 50% plants in each plot get matured. The sign of physiological maturity i.e. dark brown/black abscission layer appearance in the base of seed was considered. For recording plant height (cm) with the help of meter rod, five plants were randomly chosen at silking stage in each sub-plot and then averaged.

Physiological traits

For calculating CGR (Crop Growth Rate, g m^{-2} d^{-1}), one meter long row from side rows in each experimental unit was harvested and plants were oven-dried for 72 h at 70 °C to calculate their dry weight at, (1) V6 leaf stage, (2) Blister stage, and (3) R6 (Physiological maturity) stage. Formula used was:

$$CGR\ (g\ m^{-2}\ d^{-1}) = [(W_2 - W_1) / (T_2 - T_1) \times (1 / GA)]$$

where, W_1 = Initial weight at 27th day after sowing; W_2 = Last weight at 98th day after sowing; T_1 = Initial date 18th May 2017 (Sowing); T_2 = 30th August 2017 (Harvesting); GA = Row to row distance (0.75 cm) × plant to plant distance (20 cm) × number of plants (five plants)

Similarly, for absolute growth rate (AGR) one meter long row was selected from each plot was harvested and oven-dried for 72 h at 70 °C and then dry weight was determined at various growth stages viz. (1) V6 leaf stage, (2) Blister stage, and (3) R6 stage. AGR was figured out by the following formula:

$$AGR\ (g\ m^{-2}\ d^{-1}) = W_2 - W_1 / T_2 - T_1$$

where, W_1 = weight at 27th day after sowing; W_2 = weight at 98th day after sowing; T_1 = date 18th May 2017 (sowing); T_2 = 15th August (harvesting).

Net assimilation arte (NAR) was calculated similarly as for CGR in each sub plot by selecting one meter long row from border rows, and harvested and oven-dried at 70 °C for 72 h. Dry weight was found out at two growth stages, (1) V6 stage, and (2) R6 stage (physiological maturity). The following formula was used for NAR:

$$NAR\ (g\ m^{-2}\ d^{-1}) = [W_2 - W_1 / T_2 - T_1] \times [\ln L_2 - \ln L_1 / L_2 - L_1]$$

where, W_1 = weight at 27th day after sowing; W_2 = weight at 98th day after sowing; T_1 = date 18th May 2017 (sowing); T_2 = 15th August 2017 (harvesting); L_1 = Initial leaf area at 18th May 2017; L_2 = final leaf area at 15th August 2017.

Chlorophyll contents at different stages

From each experimental unit, five plants and three leaves per plant were randomly selected and sampled. The chlorophyll contents were measured out on three locations per leaf with chlorophyll meter (Model: SPAD-502, Minolta, Japan) and then averaged.

Yield and yield attributes

Ten ears were randomly chosen and sampled from each experimental unit and grains were counted and averaged. From these sampled ears, 1000 grains were randomly

http://www.aloki.hu ● ISSN 1589 1623 (Print) ● ISSN 1785 0037 (Online)
DOI: http://dx.doi.org/10.15666/aeer/1605_70797097
© 2018, ALÖKI Kft., Budapest, Hungary

selected and weight was measured by electronic balance. At R6 stage, three central rows in each experimental unit were harvested manually by keeping sufficient border plants, fresh weight was measured and then sun-dried for 7 d and after that their dry weight was recorded. For calculating grain yield, all the ears from sun-dried plants of three central rows for each plot were threshed and weighed for calculating grain and biological yields, and for ear characteristics. The grain yields were adjusted to 15.5% grain moisture content and then presented. For each treatment, shelling percentage was estimated with the following formula:

$$\text{Shelling percentage} = \text{Grain weight of 10 ears} / \text{Total weight of 10 ears} \times 100$$

Statistical analysis

Data were statistically analyzed by analysis of variance (ANOVA) procedure suitable for randomized complete block design. Means were compared using least significant difference (LSD) test at 0.05 probability level, when F-values were significant (Steel et al., 1996). Interaction graphs were made through Sigma plot software (version 12.5).

Results

Phenological parameters

Irrigation, nitrogen, potassium and control vs rest significantly affected number of days to tasseling of maize, whereas all the interactions were found non-significant (*Table 1*). Means values of the data indicated that optimum irrigation significantly enhanced days to tasseling compared with reduced irrigation. Results revealed that lower N (100 kg ha^{-1}) resulted in early tasseling. Days to tasseling were delayed with increase in nitrogen and maximum days to tasseling were noted with 250 kg N ha^{-1}. Potassium fertilization at the rate of 120 kg ha^{-1} showed maximum days to tasseling which were statistically same to 160 kg K ha^{-1} treatment, while less days to tasseling were recorded with 80 kg K ha^{-1}. Fertilized plots resulted in more days to tasseling compared with control plots.

Results revealed that days to silking were significantly influenced by nitrogen, potassium and control vs rest comparison, whereas irrigation and all the interactions were found non-significant (*Table 2*). Mean values for nitrogen showed that lower N (120 kg ha^{-1}) resulted in early silking, while delayed silking was observed with nitrogen application at the rate of 250 kg ha^{-1}. Maximum days to silking were noted with 160 kg K ha^{-1} while less days to silking were recorded with potassium fertilization at the rate of 80. Data regarding physiological maturity was also effected by all treatments, while all the interactions were non-significant (*Table 1*). Optimum irrigation resulted in late physiological maturity compared to reduced irrigation. Mean values for nitrogen reported that minimum days to physiological maturity were observed with lower N (100 kg ha^{-1}) which were statistically identical to 150 kg N ha^{-1}. Increase in N had delayed the maturity and more days to physiological maturity were recorded for 250 kg N ha^{-1}. Potassium fertilization at the rate of 160 kg ha^{-1} delayed physiological maturity while early maturity was observed with 80 kg K ha^{-1}.

http://www.aloki.hu ● ISSN 1589 1623 (Print) ● ISSN 1785 0037 (Online)
DOI: http://dx.doi.org/10.15666/aeer/1605_70797097
© 2018, ALÖKI Kft., Budapest, Hungary

Table 1. *Phenology of maize hybrid as influenced by fertilization of potassium and nitrogen under optimum and reduced irrigation*

	Days to tasseling	**Days to silking**	**Days to physiological maturity**	**Plant height (cm)**
Potassium levels (kg ha^{-1})				
80	49 b	56 b	93 c	192.3
120	50 a	56 b	94 b	191.9
160	50 a	57 a	95 a	192.3
LSD (0.05)	0.5	0.3	0.6	ns
Nitrogen levels (kg ha^{-1})				
100	48 c	55 d	93 c	188.2 c
150	49 b	56 c	93 c	191.3 b
200	51 a	57 b	95 b	193.2 b
250	51 a	58 a	97 a	195.9 a
LSD (0.05)	0.6	0.4	0.7	2.6
Irrigation (I)				
Optimum	50	57	95	193.5
Reduced	49	56	94	190.8
LSD (0.05)	**	ns	**	**
Control	47	54	89	185.5
Rest	50	57	94	192.2
Interactions	Significance level			
N x K	ns			
K x I	ns			
N x I	ns			
K x N x I	ns			

Means followed by different letter(s) of the same category are statistically significant using least significant differences (LSD) test at $P \leq 0.05$. **: Significant at 0.05% probability. ns: non-significant

Plant height was also affected significantly due to irrigation and N treatments, whereas potassium and all the interactions were found non-significant (*Table 1*). Taller plants were produced by optimum irrigated plots. Mean values of the data revealed that nitrogen application at the rate of 100 kg ha^{-1} resulted in shortest plants. Plant height increase with each increment of N and significantly tallest plants were recorded with 250 kg N ha^{-1}. The tallest plants were produced with 160 kg K ha^{-1} treatment. Fertilized plots produced taller plants as compared to control plots.

Growth parameters

All the treatments had significantly affected the growth parameters at different stages, while all the interactions were found non-significant (*Table 2*). Results showed that S1 (1st sampling stage) recorded with higher crop growth rate than S2 (2nd sampling stage). Mean values of the data indicated that optimum irrigation significantly increased the crop growth rate compared to reduced irrigation treatment. Mean values for nitrogen revealed that lower N (100 kg ha^{-1}) resulted in less crop growth rate. Crop growth rate increased with increase in N and significantly higher crop growth rate was recorded for 250 kg N ha^{-1}. Potassium application at the rate of 160 kg ha^{-1} resulted in more crop

http://www.aloki.hu ● ISSN 1589 1623 (Print) ● ISSN 1785 0037 (Online)
DOI: http://dx.doi.org/10.15666/aeer/1605_70797097
© 2018, ALÖKI Kft., Budapest, Hungary

growth rate while less crop growth rate was observed with 80 kg K ha^{-1}. The treatment 120 kg K ha^{-1} was statistically similar to the highest K application treatment. Fertilized plots resulted in more crop growth rate compared to control plots.

Table 2. *Growth indices of maize hybrid as influenced by fertilization of potassium and nitrogen under optimum and reduced irrigation*

	Crop growth rate (g m^{-2} day^{-1})	**Absolute growth rate (g m^{-2} day^{-1})**	**Net assimilation rate (g m^{-2} day^{-1})**
Potassium levels (kg ha^{-1})			
80	14.59 b	7.59 b	2.10 b
120	15.28 ab	8.22 ab	2.22 a
160	16.17 a	9.24 a	2.23 a
LSD (0.05)	1.12	1.06	0.11
Nitrogen levels (kg ha^{-1})			
100	14.12 b	7.03 c	1.95 d
150	14.55 b	7.55 bc	2.10 c
200	15.60 b	8.68 b	2.26 b
250	17.13 a	10.13 a	2.42 a
LSD (0.05)	1.29	1.23	0.13
Irrigation			
Optimum	15.37	8.46	2.2
Reduced	14.85	7.82	2.07
LSD (0.05)	*	*	***
Stages			
S1	16.91 a	9.91 a	2.20 a
S2	13.30 b	6.37 b	2.07 b
LSD (0.05)	***	***	***
Control	12.19	5.62	1.56
Rest	15.35	8.35	2.18
Interactions	Significance level	Interactions	Significance level
S x I	ns	I x N	ns
K x N	ns	I x K x N	ns
S x K	ns	S x I x K	ns
S x N	ns	S x I x N	ns
S x K x N	ns	S x I x K x N	ns
I x K	ns		

Means followed by different letter(s) of the same category are statistically significant using least significant differences (LSD) test at $P \leq 0.05$. *, ***: Significant at 0.05% probability. ns: non-significant

All treatments and stages significantly affected absolute growth rate (AGR) of maize, while all the interactions were found non-significant (*Table 2*). Results showed that S1 produce more AGR than S2. Mean values of the data indicated that optimum irrigation significantly produced more AGR. AGR increased with increase in N and significantly more values were recorded with 250 kg N ha^{-1}. Potassium application at the rate of 160 kg ha^{-1} was found with maximum AGR, and was similar to 120 kg K ha^{-1}.

http://www.aloki.hu ● ISSN 1589 1623 (Print) ● ISSN 1785 0037 (Online)
DOI: http://dx.doi.org/10.15666/aeer/1605_70797097
© 2018, ALÖKI Kft., Budapest, Hungary

Almost same trend was found for net assimilation rate (NAR) of maize (*Table 2*). Results showed that S1 produce more NAR than S2. Amongst N treatments, 250 kg N ha^{-1} was found maximum and K application at the rate of 160 kg ha^{-1} resulted in maximum NAR, and was to 120 kg K ha^{-1}.

Chlorophyll contents at different stages

All the treatments and the control vs rest significantly affected chlorophyll contents at tasseling stage of maize, while all the interactions were found non-significant (*Table 3*). Lower N (100 kg ha^{-1}) resulted in less chlorophyll contents at tasseling stage. Whereas, 250 kg N ha^{-1} produced maximum chlorophyll contents at tasseling stage. Optimum irrigation and the potassium application at the rate of 160 kg ha^{-1} resulted in more chlorophyll contents at tasseling stage.

Table 3. *Chlorophyll contents (SPAD values) of maize hybrid as influenced by fertilization of potassium and nitrogen under optimum and reduced irrigation*

	Chlorophyll content at tasseling	**Chlorophyll content at silking**	**Chlorophyll content at grain formation**
Potassium levels (kg ha^{-1})			
80	50 c	52 c	48 c
120	53 b	55 b	51 b
160	56 a	58 a	54 a
LSD (0.05)	3	3	3
Nitrogen levels (kg ha^{-1})			
100	46 d	48 d	44 d
150	50 c	52 c	48 c
200	53 b	55 b	51 b
250	62 a	64 a	60 a
LSD (0.05)	3	3	3
Irrigation			
Optimum	53	55	51
Reduced	52	54	50
LSD (0.05)	**	**	**
Control	44	46	42
Rest	53	55	51
Interactions		Significance level	
N x K		ns	
K x I		ns	
N x I		ns	
K x N x I		ns	

Means followed by different letter(s) of the same category are statistically significant using least significant differences (LSD) test at $P \leq 0.05$. **: Significant at 0.05% probability. ns: non-significant

Almost the same results pattern for treatments were found for the SPAD values at later stages of silking and grain formation, as recorded for tasseling stage. We observed that silking stage was recorded with maximum SPAD values (chlorophyll contents) as compared to other two stages (*Table 3*).

http://www.aloki.hu ● ISSN 1589 1623 (Print) ● ISSN 1785 0037 (Online)
DOI: http://dx.doi.org/10.15666/aeer/1605_70797097
© 2018, ALÖKI Kft., Budapest, Hungary

Yield and yield attributes

Data concerning grains ear^{-1} of maize showed that all the treatments (I, N, K) significantly influenced grains ear^{-1}, whereas all the interactions were found non-significant (*Table 4*). More number of grains ear^{-1} were produced by optimum irrigated plots. N fertilization at the rate of 100 kg ha^{-1} produced less grains ear^{-1}. Grains ear^{-1} increased with increase in nitrogen up to 150 kg ha^{-1}. Thereafter, no increase in grains ear^{-1} were observed with further increase in N level. Maximum number of grains ear^{-1} were produced when potassium was applied at the rate of 160 kg ha^{-1} which was statistically similar with 120 kg K ha^{-1}. Fertilized plots produced more grains ear^{-1} in contrast to unfertilized plots.

Table 4. *Agronomic traits of maize hybrid as influenced by fertilization of potassium and nitrogen under optimum and reduced irrigation*

	Grains ear^{-1}	**1000-grain weight (g)**	**Biological yield (kg ha^{-1})**	**Shelling percentage (%)**	**Grain yield (kg ha^{-1})**
Potassium levels (kg ha^{-1})					
80	373 b	241 b	10752 b	75.50 c	3847 c
120	382 a	247 a	11260 a	78.60 b	4068 a
160	386 a	246 a	11145 a	81.78 a	3981 b
LSD (0.05)	6	3.4	188	2.77	50
Nitrogen levels (kg ha^{-1})					
100	350 c	232 c	10493 c	71.58 d	3515 d
150	397 a	251 a	11111 b	75.61 c	4193 a
200	386 b	247 b	11281 ab	78.92 b	4121 b
250	388 b	249 ab	11323 a	88.42 a	4031 c
LSD (0.05)	7	3.9	204	3.19	58
Irrigation					
Optimum	384	248	11179	79.08	4059
Reduced	378	241	10924	78.18	3871
LSD (0.05)	**	**	**	**	**
Control	354	225	8802	69.5	2388
Rest	381	245	11052	78.63	3965
Interactions					
N x K	ns	ns	**(*Fig. 2*)	ns	**(*Fig. 3*)
K x I	ns	ns	ns	ns	ns
N x I	ns	ns	ns	ns	ns
K x N x I	ns	ns	ns	ns	ns

Means followed by different letter (s) of the same category are statistically significant using least significant differences (LSD) test at $P \leq 0.05$. **: significant at 0.05% probability. ns: non-significant

Irrigation (I), nitrogen (N), potassium (K), control vs rest and K x N interaction significantly affected thousand grains weight of maize, whereas other interactions were found non-significant (*Table 4*). Optimum irrigation significantly produced heavier grains compared to reduced irrigation. Whereas, lower N (100 kg N ha^{-1}) resulted in lighter grains. Grain weight increases with increase in N up to 150 kg N ha^{-1} which was statistically similar with 250 kg N ha^{-1}. Thereafter, no increase in thousand grains

http://www.aloki.hu ● ISSN 1589 1623 (Print) ● ISSN 1785 0037 (Online)
DOI: http://dx.doi.org/10.15666/aeer/1605_70797097
© 2018, ALÖKI Kft., Budapest, Hungary

weight was noted with increase in N level. Potassium application at the rate of 120 kg ha^{-1} resulted in more thousand grains weight which was statistically similar to 160 kg K ha^{-1}.

Irrigation (I), nitrogen (N), potassium (K), control vs rest and K × N interaction significantly affected biological yield of maize (*Table 4*). Optimum irrigation remained superior in this regard. Mean values for nitrogen revealed that lower N resulted in less biological yield. Biological yield increase with increase in N and significantly more biological yield was recorded with 250 kg N ha^{-1} which was statistically similar with 200 kg N ha^{-1}. Potassium application at the rate of 120 kg ha^{-1} resulted in more biological yield which was statistically similar to 160 kg K ha^{-1}. K × N interaction represented that application of K at the rate of 80 kg ha^{-1} × 100 kg N ha^{-1} produced less biological yield. Biological yield increased up to 80 kg K ha^{-1} × 150 kg N ha^{-1}. Thereafter, no increase in biological yield was noted with increase in N level. In case of 120 kg K x N, biological yield increased linearly with increase in N up to 200 kg N ha^{-1}, thereafter a slight decrease in biological yield was noted with increase in N level up to 250 kg ha^{-1}. Similarly in case of 160 kg K x N, biological yield increased linearly with increase in N up to 150 kg N ha^{-1}, thereafter a slight increase in biological yield was noted with increase in N level up to 250 kg ha^{-1} (*Fig. 2*).

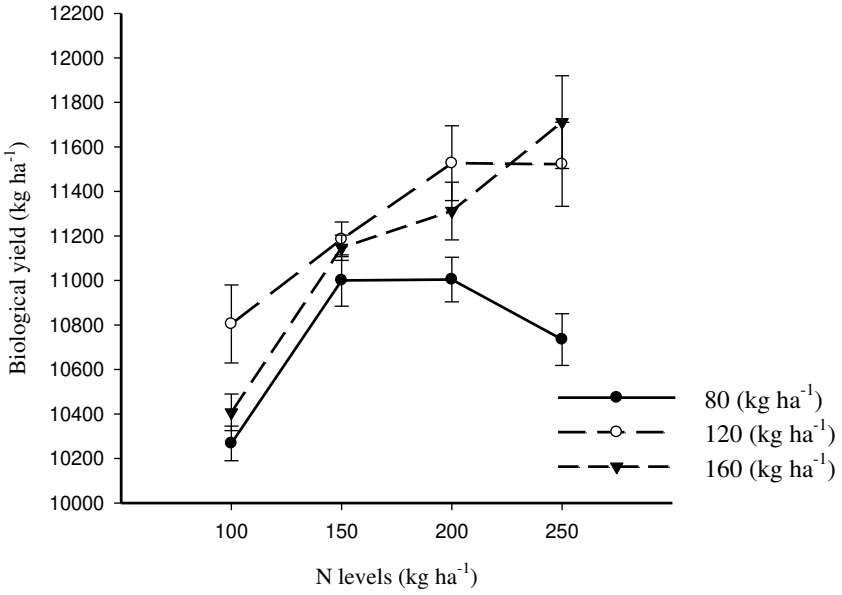

Figure 2. *Interactive response of K and N on biological yield (kg ha^{-1})*

Irrigation (I), nitrogen (N), potassium (K), control vs rest and K x N interaction significantly affected grain yield of maize, whereas other interactions were found non-significant (*Table 4*). K × N interaction represented that application of K at the rate of 80 kg ha^{-1} × 100 kg N ha^{-1} produced less grain yield. Grain yield increased up to 80 kg K ha^{-1} × 150 kg N ha^{-1}. Thereafter, no increase in grain yield was noted with increase in N level. In case of 120 kg K × N, grain yield increased with increase in N up to 150 kg N ha^{-1}, thereafter a slight decrease in grain yield was noted with increase in N level up to 250 kg ha^{-1}. Similarly in case of 160 kg K × N, grain yield increased with increase in N up to 150 kg N ha^{-1}, thereafter a slight decrease in grain yield was noted with increase in N level up to 250 kg ha^{-1} (*Fig. 3*).

http://www.aloki.hu ● ISSN 1589 1623 (Print) ● ISSN 1785 0037 (Online)
DOI: http://dx.doi.org/10.15666/aeer/1605_70797097
© 2018, ALÖKI Kft., Budapest, Hungary

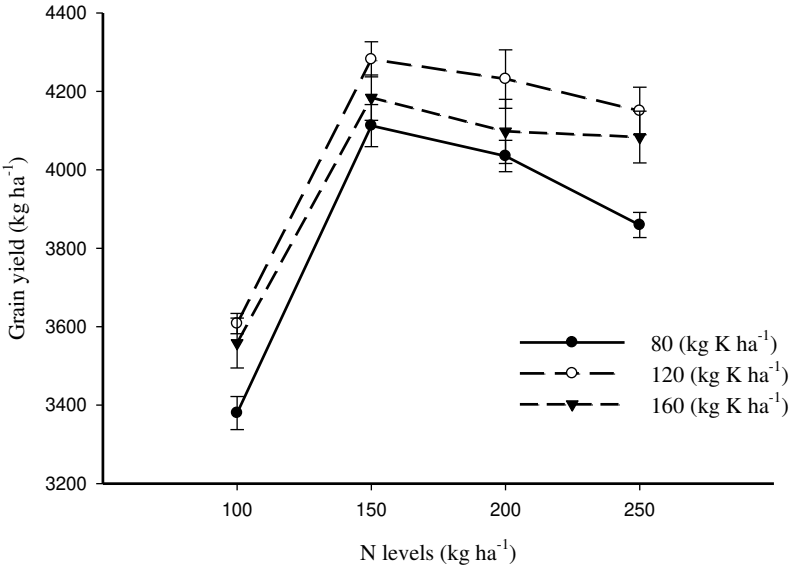

Figure 3. *Interactive response of K and N on grain yield (kg ha^{-1})*

Irrigation (I), nitrogen (N), potassium (K) and control vs rest significantly affected shelling percentage of maize, while all the interactions were found non-significant (*Table 4*). Optimum irrigation significantly recorded with maximum shelling percentage. Shelling percentage increased with increase in N and significantly more shelling percentage was recorded with 250 kg N ha^{-1}. Potassium application at the rate of 160 kg ha^{-1} resulted in more shelling percentage while less shelling percentage was observed with 80 kg K ha^{-1}. Fertilized plots resulted in more shelling percentage compared with control plots.

Discussion

Effect of N and K on phenology of maize under optimum and reduced irrigation

Delayed tasseling was observed with higher levels of nitrogen and potash. This delayed phenology with increasing N levels could be attributed to the impact of N on vegetative growth of maize crop, and photosynthetic performance (Ma et al., 2015), that might had increased leaf longevity and ultimately phenological development (Wang et al., 2017). These results are in full accordance with that of Peng et al. (2017) who observed delayed phenology with higher levels of N. Likewise, delayed tasseling under high level of potassium could be attributed to the role of potassium in stomata regulation and photosynthetic activity (Shah et al., 2017). These results were supported by Zamir et al. (2015) who observed delayed tasseling from plots having higher levels of potash. The optimum irrigation level had delayed days to tasseling in comparison with reduced irrigation which could be attributed to hormonal changes and greater availability of N and K (Alfredo and Setter, 2000). Delayed silking in plots treated with higher levels of N might be attributed to vigorous vegetative growth in response to higher nitrogen use efficiency that might had delayed the silking (Sharifi and Namvar, 2016). These results are also supported by Muller et al. (2017), as they observed delayed silking with increasing levels of N. Delayed silking with higher levels of K are further evidenced by Aslam et al. (2014).

http://www.aloki.hu ● ISSN 1589 1623 (Print) ● ISSN 1785 0037 (Online)
DOI: http://dx.doi.org/10.15666/aeer/1605_70797097
© 2018, ALÖKI Kft., Budapest, Hungary

Delayed maturity in plots treated with higher levels of N could be attributed to prolonged vegetative growth. This prolong vegetative growth might be attributed to retention of green leaf, higher chlorophyll contents, and greater photosynthetic performance (Zhang et al., 2014). Higher rates of N delayed leaf senescence and uphold extended photosynthetic performance that might have delayed the maturity (Arif et al., 2012). These results are in line with that of Ali et al. (2012), who observed delayed physiological maturity from plots treated with higher N levels. The delayed maturity under higher K levels could be attributed to improved water use efficiency and higher uptake of nutrients that extended the vegetative growth and delayed maturity (Hati et al., 2006). These results are in line with Iqbal et al. (2016), who observed delayed physiological maturity with higher K levels. Although plant height is genetically controlled character however, it is also influenced from environment and management practices (Achieng et al., 2010). Taller plants in plots treated with higher levels of N might be related to impact of N on enzymatic and photosynthetic activities as well as cell division and stem elongation (Cechin and Fumis, 2004). The report of Achieng et al. (2010) are in full accord with our finding. The taller plants obtained from optimum irrigation could be attributed to better physiological activities and improved plant growth (Gaveh et al., 2011). Our results are also in line with that of Cakir (2004).

Effect of N and K on growth indices of maize under optimum and reduced irrigation

The higher crop growth rate in response to optimum nitrogen application is attributed to higher leaf area and leaf area index and higher chlorophyll contents (Azarpour et al., 2014). The higher level of nitrogen promotes hormonal activities in plants that enhance the vegetative growth and leaves enlargement (Azarpour et al., 2014). The higher crop growth rate in early stages compared to later stages of plant development is supported by Peng et al. (2017). The higher CGR means greater dry matter is accumulated by plants per unit area per unit time as a result of enhanced photosynthetic efficiency which might increase in response to higher levels of potassium application and optimum irrigation (Inthichack et al., 2012). These results are supported by Antony and Singandhupe (2004) who observed greater plant growth and final yield in response to optimum irrigation regime. Al-Omran et al. (2010) reported that optimum water supply is essential for higher crop growth, which is in accordance with our findings.

The higher net accumulation rate and absolute growth rate of maize crop was observed from application of higher levels of N and K as well as optimum irrigation. The higher concentration of nitrogen and potassium might had increased enzymatic activities responsible for translocation of assimilates towards the economic portion (Zhong et al., 1997). The higher rates of N and K had increased the dry matter of plants through increased photosynthates production that might had increased the net accumulation rates. Likewise optimum irrigation might had improved the leaf longevity that might results in optimum NAR compared with reduced irrigation (Amanullah and Khalid, 2016). These results are in line with that of Azizian and Sepaskah et al. (2014). The maximum shelling percentage of maize crop was observed from higher levels of nitrogen and potash as well as optimum irrigation treatment was due to optimum leaf area and chlorophyll contents that might had increased the physiological parameters i.e. CGR, NAR and AGR, thus resulting in maximum translocation of assimilates towards the economic portion. This higher translocation of assimilates might had improved the shelling percentage. These results are further supported by the findings of Shah et al. (2017).

http://www.aloki.hu ● ISSN 1589 1623 (Print) ● ISSN 1785 0037 (Online)
DOI: http://dx.doi.org/10.15666/aeer/1605_70797097
© 2018, ALÖKI Kft., Budapest, Hungary

Effect of N and K on chlorophyll contents of maize under optimum and reduced irrigation

The increased chlorophyll contents of maize leaf in response to increasing levels of nitrogen might be attributed to the impact of nitrogen on leaf growth and leaf area (Bojovic and Markovic, 2009). The same authors reported a high correlation between nitrogen application and leaf chlorophyll contents. It was reported that nitrogen is the structural element of protein and chlorophyll molecule, and its higher concentrations had proved to increase the chloroplast formation and leaf photosynthetic efficiency (Shah et al., 2017). Hokmalipour and Darbandi (2011) reported that nitrogen fertilization activates the enzymes associated with chlorophyll formation thus results in higher concentration of chlorophyll than control plots. These results are in full accordance with that of Ciompi et al. (1996) and Zhao et al. (2005). The higher chlorophyll contents in plots treated with higher levels of potassium might be associated with better nitrogen uptake under higher N levels (Peng et al., 2017). Potassium is essential for chlorophyll formation, stomatal conductance and RuBP case activities, thus it had great impact on photosynthesis (Liu et al., 2009). These results are further supported by Shah et al. (2017). The maximum chlorophyll content in response to optimum irrigation is supported by Liu et al. (2005).

Effect of N and K on agronomic traits of maize under optimum and reduced irrigation

Number of grains ear^{-1} was significantly affected by N, K and irrigation levels. Optimum number of grains ear^{-1} was recorded from plots having 180 kg N ha^{-1}. This increase could be attributed to greater seed row ear^{-1} and number of grains row^{-1} (Hokmalipour and Darbandi, 2011) and maximum dry matter accumulation. These results are supported by Shah et al. (2017). The K fertilization has likely to increase the water use efficiency of crops under water limited conditions and hence increased the dry matter production and its ultimate partitioning towards the reproductive part of the plant, that might had increased the number of grains ear^{-1} (Iqbal et al., 2016). These results are supported by Shah et al. (2017) who observed higher number of grains ear^{-1} from increasing K levels.

Higher thousand grains weight and grain yield from plots treated with 180 kg N ha^{-1} might be attributed to higher chlorophyll contents associated with higher leaf area, that might had increased the photosynthetic efficiency and assimilates production and its availability during grains filling stage (Manzoor et al., 2006). The higher assimilates production through photosynthesis and its efficient partitioning towards the grain might had increased the yield and yield components of maize (Khan et al., 2014b). These results are fully supported by the results reported by Hokmalipour and Darbandi (2011). The increased yield and yield components of maize in response to higher levels of K might be attributed to the role of K in increasing water use efficiency that might had increased the cell division, improved plant growth and efficiently translocate the photosynthates towards the grains (Shah et al., 2017). However Enujeke (2013) reported that accumulation of proteins and other reserves food might be the cause for increased yield. The probable reason for optimum yield with higher K levels could be more leaf area, delayed maturity and improved yield attributes (Iqbal et al., 2016), due to stabilized stomatal regulation, greater carbon dioxide assimilation and the more carbohydrate production (Zeidan and Kramany, 2001). The increase in grain yield with

http://www.aloki.hu ● ISSN 1589 1623 (Print) ● ISSN 1785 0037 (Online)
DOI: http://dx.doi.org/10.15666/aeer/1605_70797097
© 2018, ALÖKI Kft., Budapest, Hungary

optimum irrigation have also been reported by Pandey et al. (2000) and Khan et al. (2014a). The combination of N and K had boosted 1000 grains weight and grain yield than their sole use. This increase in grain yield is also supported by the study of Shah et al. (2017).

The maximum biological yield in response to increasing levels of nitrogen might be attributed to better vegetative growth, greater leaf area and dry matter production (Keivanrad and Zandi, 2012) probably due to lower completion of plants for N and more even distribution of assimilates (Zangani et al., 2006). These results are in line with that of Imran et al. (2015), who observed maximum biological yield from higher doses of N fertilizer. Likewise the stover and biological yield was increased with increasing levels of potassium which might be attributed to the better plant growth due to the possible role of potassium in water balance, maintenance of turgor pressure, transportation of assimilates and disease resistance (Brar and Tiwari, 2004). The report of Hosinkhani et al. (2013) was also found in accordance with our findings. Shah et al. (2017) also reported similar results as ours. The optimum irrigation had increased the biological yield in comparison with reduced irrigation which might be explained with proper plant growth and better development due to moisture availability at sensitive stages of phonological development (Ngwako and Mashiqa, 2013). These results are supported by Hussain et al. (1996). The increase in biological yield with integrated use of N and P was supported by Khan et al. (2014a). Brar and Tiwari (2004) also observed the increase in biological yield of maize from integrated use of N and P, and attributed this increase to greater nitrogen use efficiency.

Conclusion

On the basis of findings obtained in present work, it is concluded that optimum irrigation produced optimum plant growth, yield and yield attributes in maize. Application of 120 kg K ha^{-1} had resulted in higher grain yields and yield components. Whereas, application of 150 kg N ha^{-1} boosted maize yield and yield components to their optimum levels. Based on the results, application of 120 kg K ha^{-1} along with 150 kg N ha^{-1} is recommended for obtaining optimum growth, yield and yield attributes under optimum irrigation (five irrigations) for maize in agro-climatic conditions of the Peshawar, Pakistan. To strengthen our results, future studies should focus on optimizing the fertilizer (N, P, K) rates by estimating the nutrient use efficiencies, with special emphasis on agronomic- and physiological-use efficiency for the maize hybrids being cultivated in major areas of Pakistan. In addition to nutrient recovery analysis, the data pertaining to the plant organ nutrient analysis for N, P and K under different planting densities are vital for the Pakistani maize production system.

Acknowledgements. The publication of present work was supported by the National Key Research and Development Program of China (grant no. 2017YFC0504704) and the National Natural Science Foundation of China (51669034, 41761068, 51809224).

REFERENCES

[1] Achieng, J. O., Ouma, G., Odhiambo, G., Muyekho, F. (2010): Effect of farmyard manure and inorganic fertilizers on maize production on Alfisols and Ultisols in Kakamega, western Kenya. – Agri. Bio. J. North America 1(4): 430-439.

http://www.aloki.hu ● ISSN 1589 1623 (Print) ● ISSN 1785 0037 (Online)
DOI: http://dx.doi.org/10.15666/aeer/1605_70797097
© 2018, ALÖKI Kft., Budapest, Hungary

[2] Ahmad, N., Rashid, M. (2003): Fertilizers and their use in Pakistan. Extension Bulletin. – NDFC. Islamabad.
[3] Alfredo, A. C. A., Setter, T. L. (2000): Response of cassava to water deficit: Leaf area growth and abscisic acid. – Crop Sci. 40: 131-137.
[4] Ali, M., Ali, A., Tahir, M., Yaseen, M. (2012): Growth and yield response of hybrid maize through integrated phosphorus management. – Pak. J. Life Soc. Sci. 10(1): 59-66.
[5] Al-Omran, A. M., Al-Harbi, A. R., Wahb-Allah, M. A., Nadeem, M., Al-Eter, A. (2010): Impact of irrigation water quality, irrigation systems, irrigation rates and soil amendments on tomato production in sandy calcareous soil. – Turkish J. Agri. For. 34(1): 59-73.
[6] Amanullah (2004): Physiology partitioning of assimilates and yield of maize as affected by plant density rate and timing of nitrogen application. – Doctoral Dissertation, University of Agricultural, Peshawar, Pakistan.
[7] Amanullah, Khalid, S. (2016): Integrated Use of Phosphorus, Animal Manures and Biofertilizers Improve Maize Productivity under Semiarid Condition. – In: Larramendy, M. L., Soloneski, S. (eds.) Organic Fertilizers - From Basic Concepts to Applied Outcomes. InTech, Rijeka, pp. 137-155.
[8] Amanullah, Khan, M. W. (2010): Interactive effect of potassium and phosphorus on grain quality and profitability of sunflower in Northwest Pakistan. – Pedosphere 21(4): 532-538.
[9] Amanullah, Hassan, M., Malhi, S. S. (2011): Seed yield and yield components response of rape (*B. napus*) versus mustard (*B. juncea*) to sulfur and potassium fertilizer application in Northwest Pakistan. – J. Plant Nutr. 34(8): 1164-1174.
[10] Amanullah, Kakar, K. M., Khan, A., Khan, I., Shah, Z., Hussain, Z. (2014): Growth and yield response of maize (*Zea mays* L.) to foliar NPK-fertilizers under moisture stress condition. – Soil Environ. 33: 116-123.
[11] Antony, E., Singandhupe, R. B. (2004): Impact of drip and surface irrigation on growth, yield and WUE of capsicum (*Capsicum annum* L.). – Agric. Water Manag. 65(2): 121-132.
[12] Arif, M., Ali, K., Munsif, F., Ahmad, W., Ahmad, A., Naveed, K. (2012): Effect of biochar, FYM and nitrogen on weeds and maize phenology. – Pak. J. Weed Sci. Res. 18(4): 475-484.
[13] Aslam, M., Zamir, M. S. I., Afzal, I., Amin, M. (2014): Role of potassium in physiological functions of spring maize (*Zea mays* L.) grown under drought stress. – J. Anim Plant Sci. 24(5): 1452-1465.
[14] Azarpour, E., Moraditochaee, M., Bozorgi, H. R. (2014): Effect of nitrogen fertilizer management on growth analysis of rice cultivars. – Int. J. Biosci. 4(5): 35-47.
[15] Azizian, A., Sepaskhah, A. R. (2014): Maize response to different water, salinity and nitrogen levels: agronomic behavior. – Int. J. Plant Prod. 8(1): 107-130.
[16] Bojović, B., Marković, A. (2009): Correlation between nitrogen and chlorophyll content in wheat (*Triticum aestivum* L.). – Kragujevac J. Sci. 31: 69-74.
[17] Brar, M. S., Tiwari, K. N. (2004): Boosting seed cotton yields in Punjab with potassium: A review. – Better Crops 88(3): 28-31.
[18] Cakir, R. (2004): Effect of water stress at different development stages on vegetative and reproductive growth of corn. – Field Crops Res. 89(1): 1-16.
[19] Cechin, I., de Fátima Fumis, T. (2004): Effect of nitrogen supply on growth and photosynthesis of sunflower plants grown in the greenhouse. – Plant Sci. 166(5): 1379-1385.
[20] Ciompi, S., Gentili, E., Guidi, L., Soldatini, G. F. (1996): The effect of nitrogen deficiency on leaf gas exchange and chlorophyll fluorescence parameters in sunflower. – Plant Sci. 118(2): 177-184.
[21] Earl, H. J., Davis, R. F. (2003): Effect of drought stress on leaf and whole canopy radiation use efficiency and yield of maize. – Agron J. 95(3): 688-696.

http://www.aloki.hu ● ISSN 1589 1623 (Print) ● ISSN 1785 0037 (Online)
DOI: http://dx.doi.org/10.15666/aeer/1605_70797097
© 2018, ALÖKI Kft., Budapest, Hungary

[22] Enujeke, E. C. (2013): Effects of variety and spacing on growth characters of hybrid maize. – Asian J. Agri. Rur. Dev. 3: 296-310.
[23] Gaveh, E. A., Timpo, G. M., Agodzo, S. K., Shin, D. H. (2011): Effect of irrigation, transplant age and season on growth, yield and irrigation water use efficiency of the African eggplant. – Hort. Environ. Biotech. 52(1): 13-28.
[24] Hati, K. M., Mandal, K. G., Misra, A. K., Ghosh, P. K., Bandyopadhyay, K. K. (2006): Effect of inorganic fertilizer and farmyard manure on soil physical properties, root distribution, and water-use efficiency of soybean in Vertisols of central India. – Biores. Tech. 97(16): 2182-2188.
[25] Hokmalipour, S., Darbandi, M. H. (2011): Effects of nitrogen fertilizer on chlorophyll content and other leaf indicate in three cultivars of maize (*Zea mays* L.). – World App. Sci. J. 15(12): 1780-1785.
[26] Hosinkhani, A., M., Panahi Kordlaghari, K., Balouchi, H. R. (2013): Effects of potassium and iron nutrient elements on the quantity yield of Shariar wheat cultivar in Boyerahmad Reign. – Annals Biol Res. 4(4): 56-60.
[27] Huber, J. L., Redinbaugh, M. G., Huber, S. C., Campbell, W. H. (1994): Regulation of maize leaf nitrate reductase activity involves both gene expression and protein phosphorylation. – Plant Physiol. 106(4): 1667-1674.
[28] Hussain, G., Al-Jaloud, A. A., Karimulla, S. (1996): Effect of treated effluent irrigation and nitrogen on yield and nitrogen use efficiency of wheat. – Agric. Water Manag. 30(2): 175-184.
[29] Imran, S, Arif, M., Khan, A., Khan, M. A., Shah, W. et al. (2015): Effect of nitrogen levels and plant population on yield and yield components of maize. – Adv. Crop Sci. Tech. 3: 170. DOI: 10.4172/2329-8863.1000170.
[30] Inthichack, P., Nishimura, Y., Fukumoto, Y. (2012): Effect of potassium sources and rates on plant growth, mineral absorption, and the incidence of tip burn in cabbage, celery, and lettuce. – Hort. Environ. Biotech. 53(2): 135-142.
[31] Iqbal, S., Guber, A. K., Khan, H. Z. (2016): Estimating nitrogen leaching losses after compost application in furrow irrigated soils of Pakistan using HYDRUS-2D software. – Agric. Water Manag. 168: 85-95.
[32] Keivanrad, S., Delkhosh, B., Shirani Rad, A. H., Zandi, P. (2012): The Effect of different rates of nitrogen and plant density on qualitative and quantitative traits of Indian mustard. – Adv. Environ. Biol. 6(1): 145-152.
[33] Khan, F., Khan, S., Fahad, S., Faisal, S., Hussain, S., Ali, S., Ali, A. (2014a): Effect of different levels of nitrogen and phosphorus on the phenology and yield of maize varieties. – American J. Plant Sci. 5(17): 2582.
[34] Khan, S. A., Mulvaney, R. L., Ellsworth, T. R. (2014b): The potassium paradox: Implications for soil fertility, crop production and human health. – Renewable Agri. Food Sys. 29(1): 3-27.
[35] Liu, J., Chen, F., Olokhnuud, C., Glass, A. D. M., Tong, Y., Zhang, F., Mi, G. (2009): Root size and nitrogen-uptake activity in two maize (*Zea mays* L.) inbred lines differing in nitrogen-use efficiency. – J. Plant Nutr. Soil Sci. 172(2): 230-236.
[36] Liu, X. J., Mosier, A. R., Halvorson, A. D., Zhang, F. S. (2005): Tillage and nitrogen application effects on nitrous and nitric oxide emissions from irrigated corn fields. – Plant Soil 276(1-2): 235-249.
[37] Ma, S. Y., Liu, Y. N., Wang, Y. Q., Qin, Y. N., Liu, H. L., Peng, Z. P. (2015): Study on the characters of living condition and nutrient balance of high-yield wheat and maize rotation system in Hebei province. – J. Agric. Univ. 38: 8-13.
[38] Marschner, H. (1995): Mineral Nutrition of Higher Plants. Ed. 2. – Academic Press, London.
[39] Marschner, P., Rengel, Z. (2012): Nutrient Availability in Soils. – In: Marschner, H. (ed.) Mineral Nutrition of Higher Plants (Third Edition). Elsevier/Academic Press, London, pp. 315-330.

http://www.aloki.hu ● ISSN 1589 1623 (Print) ● ISSN 1785 0037 (Online)
DOI: http://dx.doi.org/10.15666/aeer/1605_70797097
© 2018, ALÖKI Kft., Budapest, Hungary

[40] Mengel, K., Kirkby, E. A., Kosegarten, H., Appel, T. (2001): Potassium. – In: Mengel, K., Kirkby, E. A. (eds.) Principles of Plant Nutrition (Vol. 2). Springer, Dordrecht, pp. 481-511.
[41] Mueller, S. M., Camberato, J. J., Messina, C., Shanahan, J., Zhang, H., Vyn, T. J. (2017): Late-split nitrogen applications increased maize plant nitrogen recovery but not yield under moderate to high nitrogen rates. – Agron. J. 109: 2689-2699.
[42] Ngwako, S., Mashiqa, P. K. (2013): The effect of irrigation on the growth and yield of winter wheat (*Triticum aestivum* L.) cultivars. – Int. J. Agri. Crop Sci. 5(9): 976.
[43] Noor, M. A. (2017): Nitrogen management and regulation for optimum NUE in maize–A mini review. – Cogent Food & Agri. 3(1): 1348214.
[44] Noorka, I. R., Rehman, S., Haidry, J. R., Khaliq, I., Tabassam, S., Din, M. (2009): Effect of water stress on physico-chemical properties of wheat (*Triticum aestivum* L.). – Pak. J. Bot. 41(6): 2917-2924.
[45] Noorka, I. R., Hafiz, S. I., El-Bramawy, M. A. S. (2011): Response of sesame to population densities and nitrogen fertilization on newly reclaimed sandy soils. – Pak. J. Bot. 43(4): 1953-1958.
[46] Pandey, R. K., Maranville, J. W., Admou, A. (2000): Deficit irrigation and nitrogen effects on maize in a Sahelian environment. I. Grain yield and yield components. – Agric Water Manag. 46: 1-13.
[47] Peng, Z., Liu, Y., Li, Y., Abawi, Y., Wang, Y., Men, M., An-Vo, D.-A. (2017): Responses of nitrogen utilization and apparent nitrogen loss to different control measures in the wheat and maize rotation system. – Front. Plant Sci. 8: 160
[48] Romheld, V., Kirkby, E. A. (2010): Research on potassium in agriculture: Needs and prospects. – Plant Soil 335: 155-180.
[49] Rosenstock, N. P., Berner, C., Smits, M. M., Krám, P., Wallander, H. (2016): The role of phosphorus, magnesium and potassium availability in soil fungal exploration of mineral nutrient sources in Norway spruce forests. – New Phytol 211(2): 542-553.
[50] Scharf, P. C., Brouder, S. M., Hoeft, R. G. (2006): Chlorophyll meter readings can predict nitrogen need and yield response of corn in the north-central USA. – Agron. J. 98(3): 655-665.
[51] Shah, T., Khan, A. Z., Numan, M., Ahmad, W., Zahoor, M., Ullah, M., Jalal, A. (2017): Nutrient uptake and yield of wheat varieties as influenced by foliar potassium under drought condition. – Cercetari Agron. Moldova 50(2): 5-20.
[52] Sharifi, R. S., Namvar, A. (2016): Effects of time and rate of nitrogen application on phenology and some agronomical traits of maize (*Zea mays* L.). – Biologija 62(1): 35-45.
[53] Steel, R. G. D., Torrie, J. H. Dickey, D. (1996): Principals and Procedures of Statistics. – Mc Graw Hill, USA.
[54] Wang, M., Zheng, Q., Shen, Q., Guo, S. (2013): The critical role of potassium in plant stress response. – Int. J. Mol. Sci. 14(4): 7370-7390.
[55] Wang, X. G., Zhao, X. H., Jiang, C. J., Li, C. H., Shan, C. O. N. G., Di, W. U., Wang, C. Y. (2015): Effects of potassium deficiency on photosynthesis and photoprotection mechanisms in soybean (*Glycine max* (L.) Merr.). – J. Integ. Agri. 14(5): 856-863.
[56] Wang, X., Li, Z., Xing, Y. (2015): Effects of mulching and nitrogen on soil temperature, water content, nitrate-N content and maize yield in the Loess Plateau of China. – Agric. Water Manag. 161: 53-64.
[57] Wang, S., Wang, Z., Gu, J. (2017): Variation patterns of fine root biomass, production and turnover in Chinese forests. – J. For. Res. 28: 1185-1194.
[58] Wang, X., Fan, J., Xing, Y., Xu, G., Wang, H., Deng, J., Wang, Y., Zhang, F., Li, P., Li, Z. (2018a): The Effects of Mulch and Nitrogen Fertilizer on the Soil Environment of Crop Plants. – Adv. Agron. 153, https://doi.org/10.1016/bs.agron.2018.08.003.
[59] Wang, X., Yue, Y., Noor, M. A., Hou, H., Zhou, B., Ma, W., Zhao, M. (2018b): Tillage time affects soil hydro-thermal properties, seedling growth and yield of maize (*Zea mays* L.). – App. Eco. Environ. Res. 6007-6023.

http://www.aloki.hu ● ISSN 1589 1623 (Print) ● ISSN 1785 0037 (Online)
DOI: http://dx.doi.org/10.15666/aeer/1605_70797097
© 2018, ALÖKI Kft., Budapest, Hungary

[60] White, P. J., Karley, A. J. (2010): Potassium. – In: Hell, R., Mendel, R.-R. (eds.) Cell Biology of Metals and Nutrients. Springer, Berlin, Heidelberg, pp. 199-224.
[61] Zamir, M. S. I., Aslam, M., Javeed, H. M. R. (2015): Influence of potassium levels on the phenology of maize (*Zea mays* L.) hybrids grown under drought stress. – Pak. J. Life Soc. Sci. 13(2): 1-7.
[62] Zangani, E., Kashani, A., Fathi, G. H., Mesgarbashi, M. (2006): Effect and efficiency of nitrogen levels on quantitative and qualitative yield and yield components of two cultivars of rapeseed in Ahwaz region. – Iranian J. Agric. Sci. 37(1): 39-45.
[63] Zeidan, M. S., Kramany, M. F. E. (2001): Effect of organic manure and slow-release N-fertilizers on the productivity of wheat in sandy soil. – Agron. Hung. 49: 379-385.
[64] Zhang, S., Sadras, V., Chen, X., Zhang, F. (2014): Water use efficiency of dryland maize in the Loess Plateau of China in response to crop management. – Field Crops Res. 163: 55-63.
[65] Zhao, D., Reddy, K. R., Kakani, V. G., Reddy, V. R. (2005): Nitrogen deficiency effects on plant growth, leaf photosynthesis, and hyperspectral reflectance properties of sorghum. – Europ. J. Agron. 22(4): 391-403.
[66] Zhong, N. W., Song, Z. Y., Yong, L. X. (1997): The effect of different K sources on yield and quality of some vegetable crops. – Acta Agric. Zhejiangesis 9(3): 143-148.

http://www.aloki.hu ● ISSN 1589 1623 (Print) ● ISSN 1785 0037 (Online)
DOI: http://dx.doi.org/10.15666/aeer/1605_70797097
© 2018, ALÖKI Kft., Budapest, Hungary

THE EFFECT OF ECOLOGICAL SITE PROPERTIES ON THE MAJOR ESSENTIAL OIL COMPONENTS OF THE CRIMEAN JUNIPER LEAVES

GÜLSOY, S.* – MERDIN, A.

Faculty of Forestry, Isparta University of Applied Sciences, 32260 Isparta, Turkey
(phone: +90-505-547-0196; fax: +90-246-211-3948)

**Corresponding author*
e-mail: srkngulsoy@gmail.com

(Received 31st Jul 2018; accepted 28th Sep 2018)

Abstract. This study explores the relationship between environmental factors and the main essential oil components in the leaves of Crimean juniper (*Juniperus excelsa* M. Bieb.), which is commonly distributed in rocky and stony land with shallow soil conditions in the Mediterranean region of Turkey. After the leaf samples collected from 20 plots were dried, essential oil components were detected by GC-MS method. α-Pinene (81.3%), myrcene (5.2%) and limonene (4.5%) were found to be the major components, respectively. Relations between these major components and environmental factors (physiographic, climatic and soil factors) were questioned by Pearson correlation analysis, cluster analysis and principal component analysis. According to statistical analysis results; α-pinene bio18, altitude and pH were found to have a negative relationship. The limonene component showed a negative relationship with latitude and clay, but showed a positive correlation with pH.
Keywords: *environmental factors, climate, principal component analysis, major components, Mediterranean region*

Introduction

Due to various biochemically active substances contained by their miscellaneous organs such as leaves, cones, bark, roots and flowers, the taxa of juniper are amongst the important medicinal and aromatic plant species distributed in forests (Topçu et al., 2005). Therefore, it has been used by people not only as food and spice but also for multiple purposes such as beverage, perfumery, cosmetics, aromatherapy and medicine for treatment of some diseases since ancient times (Ložienė and Venskutonis, 2016). With the development of new technologies in recent years, juniper species just like many other medicinal and aromatic plant species can now be processed with more modern techniques and they can be used more comprehensive in different forms, e.g. such as food, medicine, pharmaceuticals and cosmetics (Faydaoğlu, and Sürücüoğlu, 2011).

It is possible to explain properties of the medical and aromatic plants with the biochemical substances they contain. Juniper species are characterized by intense essential oils they contain in different organs, and several volatile components in the essential oils. Therefore, many studies have been conducted in the scientific literature regarding the essential oil yield and components of juniper species in recent years (Bakkour et al., 2013; Höferl et al., 2014; Fejér et al., 2018).

In Turkey's forests, which cover an area of around 22.3 million hectares, juniper species are represented by 11 different taxa in 7 species belonging to 3 different sections (Fakir, 2014). In Turkey, out of these taxa, *Juniperus excelsa* M. Bieb. (Crimean juniper) has the widest distribution area (Göze et al., 2017). Around the

http://www.aloki.hu ● ISSN 1589 1623 (Print) ● ISSN 1785 0037 (Online)
DOI: http://dx.doi.org/10.15666/aeer/1605_70997113
© 2018, ALÖKI Kft., Budapest, Hungary

world, it is distributed in Macedonia, Aegean and Greek Islands, Asia Minor and Caucasia; while it has the widest distribution especially in the Mediterranean Region and Western Taurus range in Turkey. The distribution range of Crimean juniper extends through the steppe areas into the inner parts of Anatolia. The anthropogenic impacts throughout the history resulted in the destruction of this species in the Mediterranean forest (Fontaine et al., 2007). On the other hand, the seed dormancy and germination problems which are considered to be a general juniper-related issue has led to challenges in the regeneration of Crimean juniper in natural habitats until recently (Gülsoy and Özkan, 2013).

Crimean juniper is of ecological importance for Turkey's forests and has been used in food, pharmaceutical, medicine, preservation and perfume industries due to several chemical substances they contain in their cones, leaves and barks such as other juniper species. It is known that especially the essential oils this species contains in its organs, add value to the plant in medicinal and aromatic terms. The products such as juniper oils and juniper essence that are obtained through distillation from various organs are reported to add industrial value to this species. In particular, the extracts of the species is expressed to be the effect of anti-inflammatory, anti-microbial, antiseptic, anti-termite, insecticide, hypotensive, diuretic, antioxidant, antibacterial and antispasmodic (Moein et al., 2010; Orhan, et al., 2012; Adams et al., 2013; Göze et al., 2017).

As one can understand from the abovementioned information, Crimean juniper is an important forest tree species but also a crucial plant with its biochemical substances. Therefore, there are many studies in the literature regarding various biochemical substances of the species and its medicinal-aromatic properties. However, there is no study that explores the relationship between the ecology of the species and the main essential oil components it contains. Nevertheless, it is argued that the biochemical properties of plants vary depending on different methods applied, which part of the plant is used, maturity period, growing method and genetic factors as well as ecological conditions (Gende et al., 2010). This study aimed to identify the ecological habitat conditions of this species distributed in the Lakes District in the Mediterranean Region of Turkey. Another important intention of the study was to introduce the interactions between the environmental factors and the major essential oil components. Thus, the study aimed at obtaining significant information about the impacts on the essential oil components in the leaves depending on the ecological site conditions of this species. It is suggested that the results of this study will lead to further scientific studies on this topic.

Material and methods

Study area

This study was conducted at 20 Crimean juniper sites selected is located within the Lakes District extending from 38°25'-36°06 northern latitudes and 29°30'-32°34' eastern longitudes in the southwest of Turkey (*Fig. 1*).

The predominant bedrock formations in the study area are mainly limestone and dolomite. The main soil types are red, brown or reddish-brown forest soils of the terra-rossa type developed on karst landforms that lead to variations in soil characteristics in the district (Sandler et al., 2015). Soil depth is generally thin with a thickness of 0-40 cm on slopes and rarely deep a thickness of up to 100 cm in depressions. According to the data recorded for many years in the region, the average annual rainfall is

http://www.aloki.hu ● ISSN 1589 1623 (Print) ● ISSN 1785 0037 (Online)
DOI: http://dx.doi.org/10.15666/aeer/1605_70997113
© 2018, ALÖKI Kft., Budapest, Hungary

approximately 600-1300 mm and the average annual temperature varies between 12-20 °C. A subtropical Mediterranean climate generally characterized by hot and dry summer months and warm wet winter months prevails in coastal zones near the Mediterranean Sea, low-altitude locations and the sea-facing slopes of the mountains, while the transition climate from Mediterranean climate to continental climate is observed in areas distant from the sea and at higher elevations (Benli, 2016).

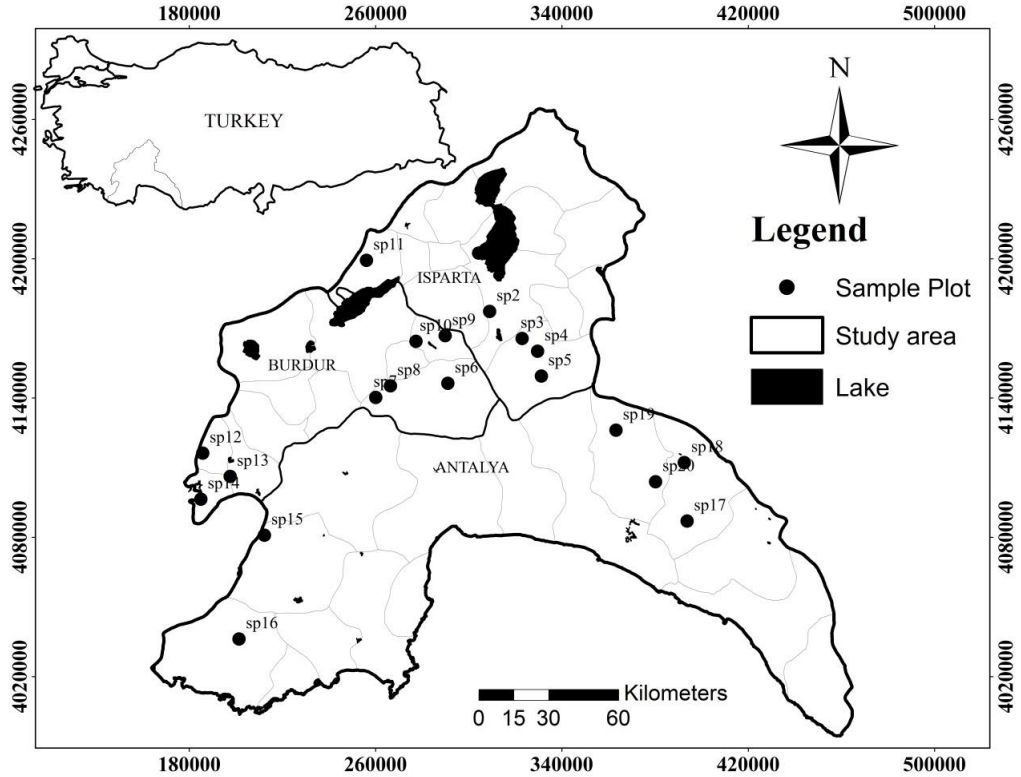

Figure 1. *Location map of the sample plots in the study area*

Data collection

Crimean juniper leaves used in this study were obtained from 20 sampling plots in the Lakes District of Turkey. These plots were selected from the sites free from human impact, fungal and insect damage. Leaves samplings were collected from the last year's shoots on the northern aspects of the plants. In addition to leaf sampling, several ecological measurements were conducted in each sampling plot in order to find the associations of the essential oil components to be derived from the leaves with environmental factors. First, latitude, longitude and elevation (m) values were recorded using GPS while the aspect of hillside (°) was recorded using a compass and the slope (%) was measured with a clinometer. The surface stoniness (%) of the land was estimated using the iron rod penetration method at 10 points randomly selected within each sampling plot (Eriksson and Holmgren, 1996). Furthermore, landform and slope position were recorded through observations in the sampling plots. The depth of the mineral soil was measured in hand-excavated pits and bedrock formations were determined from geological maps compiled by General Directorate of Mineral Research and Exploration.

http://www.aloki.hu ● ISSN 1589 1623 (Print) ● ISSN 1785 0037 (Online)
DOI: http://dx.doi.org/10.15666/aeer/1605_70997113
© 2018, ALÖKI Kft., Budapest, Hungary

The climate maps were obtained from the database developed by Fick and Hijmans (2017) at global scale and edited with the Global Mapper at the local scale. The boundaries of the sampling plots were matched with the pixels of the maps of climate variables according to the GPS coordinates, climate data for each plots were obtained from these maps.

Before the statistical assessments, a digital elevation model (DEM) was created from the topographic database. Radiation index, heat index and topographic position index for each sampling plot were calculated using this DEM. At this stage; the radiation index equation (*Eq. 1*)

$$RI = \frac{[1-\cos((\pi/180)(Q-30))]}{2} \quad \text{(Eq.1)}$$

that can be applied to intermediate distance from equator line to 60° north latitude, slope degree less than 90°, and all aspects of hillsides was used (McCune and Keon, 2002). RI varies between 0 and 1, and the approximation of this value to 1 indicates the long duration of sunshine in the plot. Then, heat index values with *Equation 2:*

$$\text{HI} = 1 + \cos((45°\text{-aspect degree})/\text{slope degree}) \quad \text{(Eq.2)}$$

were calculated (Beers et al., 1966). HI varies between -1 and 1, and the approximation of this value to 1 indicates hotter points in the field.

The elevation value of the pixel on which the sampling plot is located on the map and the elevation differences of the other pixels adjacent to that sampling plot were used to calculate the topographic position index (TPI) values for each sampling plot (Weiss, 2001). Last, the distance between the sampling plots and the borders of the lakes and sea located in the study site was calculated on the basis of the distance that would result from the landform on DEM. For this step, ArcMap 10.2 software was used. For both measurements, "distance point to line/polygon" command was used for measurements in each sampling plot on the basis of the closest polygon and line to the points (Mert et al., 2013).

The soil samples (0-5 cm) were taken among of the trees from which leaf samples were collected in the field. After the soil samples were air-dried and ground, they were passed through the sieve (2 mm). The soils were analysed at the Laboratory of Süleyman Demirel University Faculty of Agriculture - Soil Department. Particle size of the soils was determined by using Bouyoucos's hydrometer method (Bouyoucos, 1951). Field capacity was measured by a pressure plate device (Cassell and Nielson, 1986). Soil pH level was determined through pH metre with glass electrode according to Jackson (1958). In addition, organic matter content in soils was determined by modified Walkley-Black method according to Jackson's procedure (1958). The carbonate contents ($CaCO_3$) in soil samples were measured with a Scheibler Calcimeter using volumetric method (Bush, 1970). Finally, after saturating soils with Na-acetate, they were extracted with ammonium acetate and the extracted sodium was read in the atomic absorption spectrophotometer and their cation exchange capacity was found (Chapman, 1965).

As a result 42 different environmental variables were identified and codes with maximum 6 characters were assigned to these variables for statistical assessment (*Table 1*).

http://www.aloki.hu ● ISSN 1589 1623 (Print) ● ISSN 1785 0037 (Online)
DOI: http://dx.doi.org/10.15666/aeer/1605_70997113
© 2018, ALÖKI Kft., Budapest, Hungary

Table 1. *Variables used during statistical analysis and the assigned codes*

Variables	Code	Variables	Code	Variables	Code
Latitude	latitu	pH	pH	Distance to nearest sea border (km)	nsea
Longitude	lngitu	Lime	lime	Annual mean temperature (°C)	bio1
Elevation (m)	elvtn	Organic matter (%)	orgmat	Max temperature of warmest month (°C)	bio5
Slope degree (°)	slope	Electrical conductivity (dScm-1)	ec	Min temperature of coldest month (°C)	bio6
Radiation index	rdinx	Cation exchange capacity (me/100 g)	cec	Mean temperature of wettest quarter (°C)	bio8
Surface stoniness (%)	surfst	Sodium Na+ (me/100 g)	na	Mean temperature of driest quarter (°C)	bio9
Soil depth	sdepth	Potassium K+ (me/100 g)	k	Mean temperature of warmest quarter (°C)	bio10
Land surface shape	lshape	Calcium Ca++ (me/100 g)	ca	Mean temperature of coldest quarter (°C)	bio11
Slope position	sposit	Magnesium Mg++ (me/100 g)	mg	Annual precipitation (mm)	bio12
Landform	landfm	Field capacity (%)	fieldc	Precipitation of wettest month (mm)	bio13
Bedrock formation	bedrck	Wilting point (%)	wiltpo	Precipitation of driest month (mm)	bio14
Sand (%)	sand	Topographic position index	tpi	Precipitation of wettest quarter (mm)	bio16
Clay (%)	clay	Heat index	hindx	Precipitation of driest quarter (mm)	bio17
Silt (%)	silt	Distance to the nearest lake (km)	nlake	Precipitation of warmest quarter (mm)	bio18

The leaves collected from the field were stored to air-dry for 2 months under laboratory conditions in summer period of 2015. Then, the air-dried samples were placed in metal containers and dried in oven at 35 °C until reaching a constant weight. The adsorption of essential oil components was carried out using Solid Phase Microextraction Technique (SPME) by a fibre (Spietelun et al., 2013). For desorption of essential oil components, fibre was immersed onto injection port for 5 more minutes. The percentage of the essential oil components were determined by Gas Chromatography-Mass Spectrometry (GC/MS) analysis. In the GC/MS device, the column temperature was started at 40 °C for 2 min. It was then heated to 250 °C with an increase rate of 4 °C per minute and kept at 250 °C for 5 min.

Statistical analysis

During statistical assessments, factor analysis was firstly performed for the bio-climate variables considered to have a high correlation probability**.** In order to determine the bilateral relationships between the environmental variables and major essential components, Pearson Correlation Analysis was applied. To determine how the sampling plots were grouped in terms of the major components, cluster analysis was performed (Sarstedt and Mooi, 2014). Finally, Principal Components Analysis (PCA) was applied to identify the direction of the relationships between the major essential oil components that were the dependent variables and the environmental factors that were the independent variables (Bro and Smilde, 2014). SPSS Version 21.0 and PC-ORD Version 6.0 software were used in statistical analysis process.

Results and discussion

The mean elevation of 20 sampling plots selected at different locations was 1273 m, while the elevation of the highest sampling plot was 1920 m and that of the lowest sampling plot was 475 m. The mean inclination of the sampling plots was 27 degrees with plots consisting of both flat and steep inclination. The radiation index values ranged from 0.005 to 0.999. The topographic position index of the sampling plots varied from -0.438 to 0.954. The heat index values ranged from 0.013 to 2.00. As for the

http://www.aloki.hu ● ISSN 1589 1623 (Print) ● ISSN 1785 0037 (Online)
DOI: http://dx.doi.org/10.15666/aeer/1605_70997113
© 2018, ALÖKI Kft., Budapest, Hungary

landforms of the sampling plots, 40% had flat terrain while 60% had undulating terrain. 55% of the sampling plots were located on upper slopes, 20% were located on medium slopes, 15% were located on lower slopes and 10% were on bottom lands. According to the landform characteristics, 2 different types of data were recorded in the study site, out which 90% were rocky and stony while 10% were flat. The mean stoniness percentage of the sampling plots was found to be 47.8%. With regard to the bedrock characteristics, limestone was dominant (80%) in the areas where *J. excelsa* was distributed.

Depth of the sampling plots ranged from 4 cm to 120 cm with a mean soil depth of 46 cm. The results of the chemical analysis conducted on topsoil (0-5 cm) samples revealed that the percentage of sand in the sampling plots ranged from 16.5% to 54.4%, percentage of clay ranged from 4.7% to 44.2%, while the dust percentage ranged from 25.9% to 52.9% according to the texture analysis. As for the acidity-alkalinity of the soils sampled from the sampling plots, pH value ranged from 7.1 to 8.5. With regard to the lime content ($CaCo_3$) of the soil, it was found the highest with 68.9% in one of the sampling plots, while it ranged from 1.29% to 6.72% at the other sampling plots. The amount of organic matter ranged from 2.7% to 13.4%. The mean cation exchange capacity (CEC) of the soils collected from 20 sampling plots was found to be 55.8 me/100 g. The lowest cation exchange capacity was found to be 19.5 me/100 g, while the highest was 102.8 me/100 g. Average field capacity of the soils collected from the sampling plots was 36.8%. The lowest field capacity was found to be 21.7%, while the highest was found 56.7%. The exchangeable cations from the biggest to the smallest in the soils collected from the sampling plots were Ca^{++} (85.5 me/100 g), Na^{+} (16.2 me/100 g), Mg^{++} (9.3 me/100 g) and K^{+} (8.9 me/100 g).

With regard to a total of 41 essential oil components obtained from the leaves of *J. excelsa*, α-pinene was the component with the highest amount with a mean value of 81.3% v/w. α-pinene was followed by myrcene with 6.2% v/w and limonene with 4.5% v/w (Gülsoy and Merdin, 2017). The total percentage of the remaining 38 component was 8.0% v/w, therefore, α-pinene, myrcene and limonene were defined as the primary essential oil constituents in the leaves of Crimean juniper.

If there is a very high correlation between the independent variables, explaining the relations in the environment becomes a complex. The bio-climate data used in this study are highly correlated with each other. By applying factor analysis, climate variables with the highest correlation coefficient with the components can be determined. As a result of this process, relationships are made through these representative variables. Other climate parameters are evaluated with an indirect interpretation. For this purpose, factor analysis was applied among the bio-climate variables in this study.

The factor analysis applied to bio-climate variables revealed that bio12 and bio18 variables had the highest correlation coefficient. Therefore, only these two variables were used in the subsequent statistical assessment as they had the highest explanation capacity instead of using all bio-climate variables (*Table 2*).

The correlation analysis applied to the relationship between the environmental variables and major essential oil components revealed that α-pinene had a negative correlation with elevation (r = -0.505) and bio18 (r = -0.451). Limonene, however, had a negative correlation with latitude (r = -0.526). Myrcene did not have any statistically significant correlation with any environmental factors. Finally, α-pinene that was subjected to correlation analysis with soil variables had a statistically significant negative correlation with pH (r =-0.444) while limonene had a negative correlation with

http://www.aloki.hu ● ISSN 1589 1623 (Print) ● ISSN 1785 0037 (Online)
DOI: http://dx.doi.org/10.15666/aeer/1605_70997113
© 2018, ALÖKI Kft., Budapest, Hungary

clay (r = -0.475) and a positive correlation with pH (r = 0.448). Myrcene showed no significant relationship with any of the soil variables.

Table 2. *The correlation coefficients of the variables according to the factor analysis applied to the bio-climate variables on component 1 and component 2*

Variables	Component 1	Component 2
bio1	0,940	-0,300
bio5	0,744	-0,624
bio6	0,943	-0,199
bio8	0,948	-0,276
bio9	0,939	-0,332
bio10	0,926	-0,37
bio11	0,948	-0,276
bio12	0,657	**0,736**
bio13	0,714	0,690
bio14	-0,921	-0,012
bio16	0,715	0,691
bio17	-0,902	-0,048
bio18	**-0,954**	-0,098
bio19	0,715	0,691

After the correlation and factor analyses, cluster analysis (according to Jacard index and Flexible Beta (= 0.25) Cluster Group Linkage Method) was performed in order to find out how the amount of major components were grouped on the basis of the sampling plots. The dendrogram showing the groups of sampling plots according to the cluster analysis is presented in *Figure 2*.

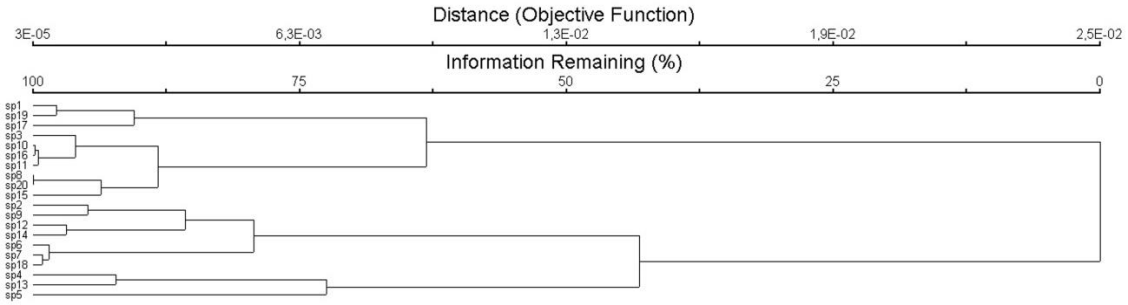

Figure 2. *Dendrogram showing the cluster analysis applied to the major essential oil components (sp: sample plot)*

The dendrogram shows that division starts at the division line of 40%, after which the sampling plots were clearly divided into 2 groups. 10 sampling plots were in cluster group 1 (sp1, sp3, sp8, sp10, sp11, sp15, sp16, sp17, sp19, sp20), while the other 10 sampling plots were in cluster group 2 (sp2, sp4, sp5, sp6, sp7, sp9, sp12, sp13, sp14, sp18). This suggests that this might be due to the different effects of locations on major essential oil components. Therefore, in order to determine to what extent this difference between the locations was represented by the environmental variables of the sampling

http://www.aloki.hu ● ISSN 1589 1623 (Print) ● ISSN 1785 0037 (Online)
DOI: http://dx.doi.org/10.15666/aeer/1605_70997113
© 2018, ALÖKI Kft., Budapest, Hungary

plots, PCA was conducted. Through the analysis, the eigenvalues of the axes, variance percentages and percentage values of cumulative variance were calculated (*Table 3*).

Table 3. *Eigenvalues of the axes and variance percentages in the PCA applied to major essential components*

Eigenvalue	% of variance	Cumulative% of variance	Broken-stick eigenvalue	Eigenvalue
Axis1	**1,807**	**60,249**	**60,249**	**1,833**
Axis2	0,886	29,531	89,780	0,833
Axis3	0,307	10,220	100,00	0,333

The prerequisite to interpret the axis values found through the PCA analysis is that the eigenvalue coefficient of the relevant axis is smaller than the Broken-stick eigenvalue coefficient. *Table 3* shows that Axis1 which explains 60.2% of the total variance fulfils this criterion. In Axis 2, however, the Broken-stick eigenvalue coefficient explains 29.5% of the total variance although its numerical value is higher than the eigenvalue. These two axes together explain 89.7% of the total variance. Therefore, it would be right to make an interpretation principally over Axis 1 and partially over Axis 2 in order to explain the associations during the PCA applied between the major components and environmental variables.

The correlation coefficients of Principal Component Axes with major essential oil components (Pearson and Kendall correlations) are presented in *Table 4.*

Table 4. *Eigenvalues of the axes and variance percentages in the PCA applied to major essential components*

Major components	Axis1	Axis2
	r	**r**
α-pinene	**0.710**	**0.648**
Myrcene	**-0.684**	**0.682**
Limonene	**-0.914**	-0.007

The table shows that α-pinene (r:0.710) which was the most intense components in the leaves of Crimean juniper had a significantly positive correlation with Axis 1, limonene (r:-0.914) and myrcene (r:-0.684) had a negative correlation with the same axis. On the other hand, α-pinene (r:0.648) and myrcene (r:0.682) had a positive correlation with Axis 2.

Data matrixes regarding the physiographical-climate and soil variables developed to determine the correlations between the essential oil components and environmental factors were transferred to the PCA separately. First, the correlation between the physiographical-climate variables and major components was determined (*Table 5*).

The results showed that latitude (r:0.506) had the highest correlation with PCA Axis 1, while topographic position index (r:-0.499), elevation (r:-0.469) and precipitation of the hottest quarter (r:-0.457) had the statistically highest correlation with Axis 2. A simple interpretation on Axis 1 reveals that α-pinene's intensity increased in the plants in areas where latitude rose, while to the contrary myrcene and limonene decreased. The interpretation made on Axis 2 showed that myrcene and α-pinene decreased in areas

http://www.aloki.hu ● ISSN 1589 1623 (Print) ● ISSN 1785 0037 (Online)
DOI: http://dx.doi.org/10.15666/aeer/1605_70997113
© 2018, ALÖKI Kft., Budapest, Hungary

where elevation, topographic position index and precipitation of the hottest quarter increased. Results of the correlations of the major components on the ordination indices are shown in *Figure 3*.

Table 5. *Correlation coefficients between physiographical climate factors and PCA Axis 1-2*

Variables	Axis1	Axis2
	r	r
latitu	**0.506**	-0.048
lngitu	0.002	-0.229
elvtn	-0.328	**-0.469**
nlake	0.264	0.245
nsea	-0.007	-0.230
slope	0.244	0.073
rdinx	0.044	-0.162
surfst	0.099	0.226
lshape	0.119	0.156
sposit	-0.024	0.32
landfm	-0.044	0.22
hindx	-0.157	0.273
tpi	-0.061	**-0.499**
bio12	0.323	0.024
bio18	-0.249	**-0.457**

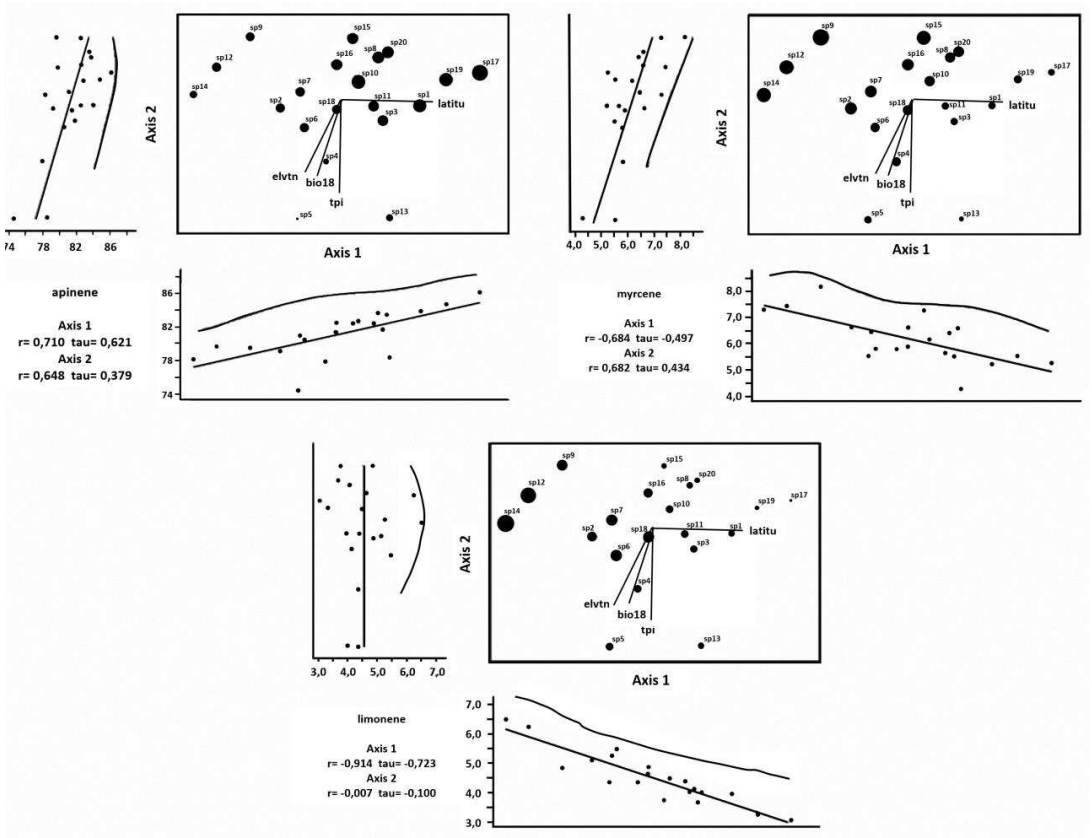

Figure 3. *Correlation between major essential oil components and physiographical-climate factors on PCA Axis 1-2*

http://www.aloki.hu ● ISSN 1589 1623 (Print) ● ISSN 1785 0037 (Online)
DOI: http://dx.doi.org/10.15666/aeer/1605_70997113
© 2018, ALÖKI Kft., Budapest, Hungary

The correlation coefficients between Axis 1-2 and soil factors are presented in *Table 6* and the ordination graphs of the sampling plots according to these correlations are shown in *Figure 4*.

Table 6. *Correlation coefficients between the soil characteristics and PCA Axis 1-2*

Variables	Axis1	Axis2
	r	r
sand	-0.366	0.159
clay	**0.430**	-0.025
silt	0.100	-0.235
sdepth	0.050	0.113
bedrck	0.108	-0.024
pH	-0.032	-0.008
lime	0.079	-0.058
orgmat	-0.041	-0.151
ec	0.270	-0.118
cec	-0.277	-0.081
na	-0.148	-0.114
k	0.056	**-0.480**
ca	-0.176	-0.042
mg	-0.008	-0.299
fieldc	0.018	-0.072
wiltpo	-0.142	-0.113

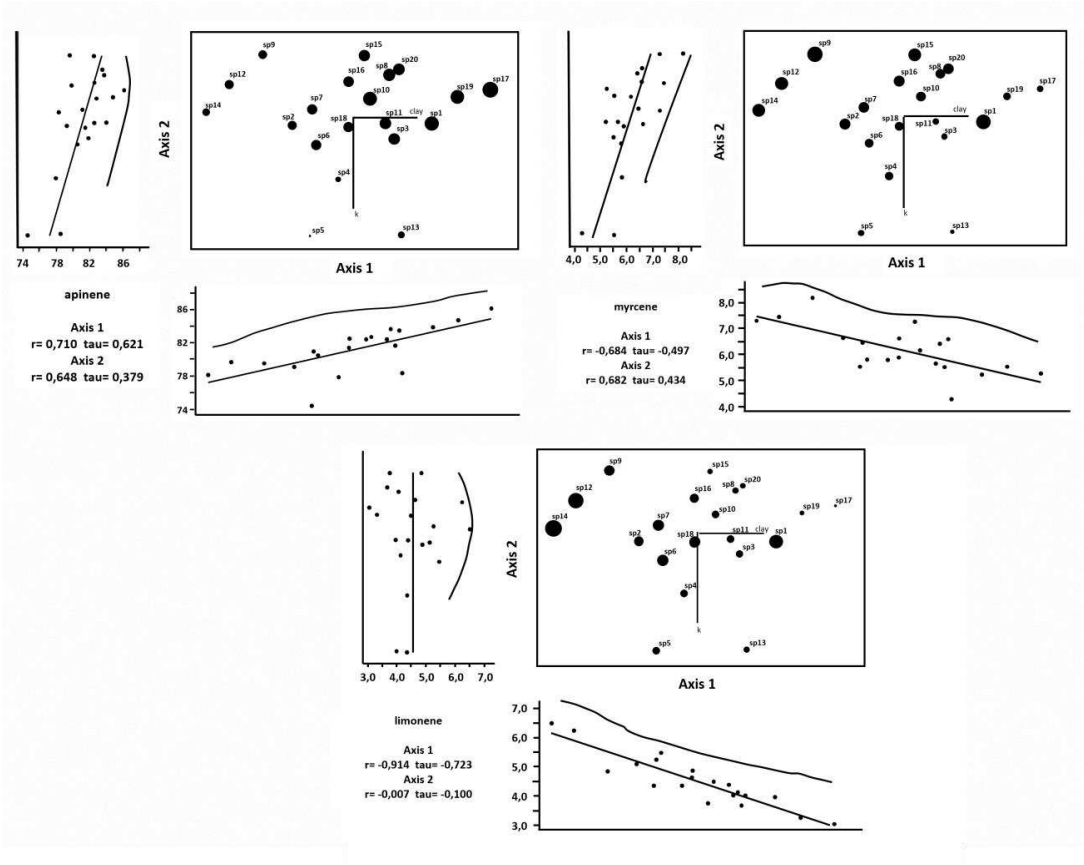

Figure 4. *Correlation between major essential oil components and soil factors on PCA Axis 1-2*

http://www.aloki.hu ● ISSN 1589 1623 (Print) ● ISSN 1785 0037 (Online)
DOI: http://dx.doi.org/10.15666/aeer/1605_70997113
© 2018, ALÖKI Kft., Budapest, Hungary

As shown in *Figure 4,* a statistically significant correlation was found between PCA Axis 1 and clay only (r = 0.430) and between Axis 2 and potassium only (r = -0.480). Clay percentage had a positive correlation with α-pinene out of the essential oil components in the Crimean juniper leaves on Axis 1, which was the most explanatory one, and a negative correlation with myrcene and limonene.

In this study, the essential oil components in the leaves of Crimean juniper which has a considerable distribution area both in Turkey and across the world and the environmental variables were associated. Ecological site conditions in areas where the species is distributed at elevations between 500-2000 m in moderately and highly mountainous parts are that limestone is dominant with rocky-stony landform, mainly on upper slopes and undulating terrain. The mean radiation index and temperature index of the sampling plots show that the species is found mainly on the very shadowy and humid aspects but also prefer sunny aspects as soon as it finds the appropriate site conditions at the combination of other ecological factors. In general, these areas are very inclined, steep and precipitous and had shallow or moderately deep soils in terms of absolute soil depth. In a study conducted to explore the ecology of the species in the region, it was found that its distribution increased at an elevation of 800-1800 m where the surface stoniness intensified under dry climate conditions, while the ecological tolerance of Crimean juniper was higher especially on the shady aspects of these environments compared to *Cedrus libani* A. Rich and *Pinus nigra* Arnold (Özkan et al., 2010). In general, it was stated that Crimean juniper that is referred to as a cold and drought tolerant species (Sarangzai et al., 2015) preferred mainly the humid environments in the northern and western aspects of the inner parts of the Mediterranean Region of Turkey (Fontaine et al., 2007). On the other hand, it was also underlined that especially higher elevations and areas with valley characteristics were more appropriate for the distribution of this species compared to the lower elevations and flat terrains (Fisher and Gardner, 1995). Furthermore, it is known that Crimean juniper trees could adapt to areas with typical Mediterranean climate with hot summers and frost in winter under shallow soil conditions in the rocky and stony terrains of the very inclined or steep lands without suffering from any damage. That is because Crimean juniper is known to convert the restricted absolute depth conditions into physiologically appropriate forms by taking advantage of the cracked structure of the bedrock which is mainly dominated by limestone in these types of environments (Gülsoy and Özkan, 2013). Therefore we can conclude that the findings of this study regarding the distribution of this species are in accordance with other published studies.

The dominant soil type of the topsoil included in this study (0-5 cm) was loam and its derivatives, while they were classified as rich and humic soils in terms of organic matter content. In direct proportion to the rich humus content, the field capacity of these soils and wilting point were found to be high and the soils have a granular structure in general. Moreover, with respect to lime content, nearly all of these soils were classified as carbonated, poorly alkaline and saline-free soils. The pH of the soils collected from juniper sites were found to be mildly alkaline and the most common cation in the soils was Ca^{++}, which can be explained by the high lime percentage depending on the limestone bedrock (Gülser et al., 2012).

In the study, forty one compounds were identified from the leaves of Crimean juniper and quantified, with α-pinene (81.3%), myrcene (5.2%) and limonene (4.5%) being the major components. All major components identified belonged to the monoterpene class. Topçu et al. (2005) found that the major essential components in

http://www.aloki.hu ● ISSN 1589 1623 (Print) ● ISSN 1785 0037 (Online)
DOI: http://dx.doi.org/10.15666/aeer/1605_70997113
© 2018, ALÖKI Kft., Budapest, Hungary

leaves of Crimean juniper consists of α- pinene (29.7%), cedrol (25.3%) and α-murolene (4.4%), respectively. Furthermore, in another studies conducted in Iran and in south-east of R. Macedonia, α-pinene (32.3%, 33.8%) and cedrol (13.1%, 24.4%) were found as major components in the leaves essential oil of Crimean juniper (Emami et al., 2011; Sela et al., 2015). On the contrary, Sela et al. (2015) found that sabinene and thujone were the predominant essential oil components in the samples from south-western part of R. Macedonia. In a different study, α-pinene (36.0%), β- pinene (30.2%) and limonene (12.6%) were found as the major components in the leaves of the species (Nadir et al., 2013). It is clear that α-pinene was found to be the major component in almost all of these studies, while differences were observed between the percentages of α-pinene and those of the other components. This difference is considered to be due to the location where the samples were collected, harvest season, maturity stage and genetic factors (Salehi et al., 2010; Adams et al., 2013). As a matter of fact, it has been stated that these types of factors are also effective in the several chemical properties such as the phenolic content, antioxidant and sugar levels of plants (Ali et al., 2011; Skrovankova et al., 2015).

Finally, with regard to the association between the percentages of major essential oil components in the sampling plots and the environmental factors, the cluster and principal component analyses showed that primarily latitude as well as clay percentage and secondarily topographical position index, elevation and climate factors might have an effect. Adams et al. (2013) reported a partial effect of geographical variations in the essential oil components of Crimean juniper leaves sampled from Greece, Bulgaria, Turkey and Cyprus. No other study was found in the literature that explored the association between the essential oil properties of Crimean juniper leaves and environmental factors.

Conclusions

In conclusion, the findings of this study exhibited that environmental factors can have an impact on the essential oil components of the plants, whereas they are not so explanatory. The reason is that factors such as especially genetic variation of plant species, time of sample collection and methods applied have an impact on the type and percentage of these components in addition to the environmental factors as mentioned before. Therefore, there is a need for further studies with established standards on this matter in order to obtain clearer and precise results. It is possible that some secondary metabolites, such as volatile oils, can be assessed in some cases, such as climate change, environmental pollution etc., if clearer information is obtained from these studies.

Acknowledgements. We would like to thank Süleyman Demirel University Scientific Research Projects Coordination Unit for supporting our study under the project number SDÜ-BAPKB-4116-YL1-14. Moreover, the soil data were obtained simultaneously with the project numbered TUBİTAK-112O814, for which we would also like to thank the relevant institutions and persons.

REFERENCES

[1] Adams, R. P., Tashev, A. N., Baser, K. H. K., Christou, A. K. (2013): Geographic variation in volatile leaf oils of *Juniperus excelsa* M. Bieb. – Phytologia 95(4): 279-285.

http://www.aloki.hu ● ISSN 1589 1623 (Print) ● ISSN 1785 0037 (Online)
DOI: http://dx.doi.org/10.15666/aeer/1605_70997113
© 2018, ALÖKI Kft., Budapest, Hungary

[2] Ali, L., Svensson, B., Alsanius, B. W., Olsson, M. E. (2011): Late season harvest and storage of Rubus berries-Major antioxidant and sugar levels. – Scientia Horticulturae 129: 376-381.
[3] Bakkour, Y., El-Achi, N., Tabcheh, M., El-Nakat, H., El-Omar, F. (2013): Chemical composition and antioxidant activities of the essential oils from green and ripe berries of *Juniperus excelsa* growing in Lebanon. – International Journal of Pharmacy and Life Sciences 4: 2362-2367.
[4] Beers, T. W. Dress, P. E. Wensel, L. C. (1966): Notes and observations: aspect transformation in site productivity research. – Journal of Forestry 64: 691-692.
[5] Benli, H. (2016): Potential application of solar water heaters for hot water production in Turkey. – Renewable and Sustainable Energy Reviews 54: 99-109.
[6] Bouyoucos, G. J. (1951): A recalibration of the hydrometer method for making mechanical analysis of soils. – Agronomy Journal 43: 434-438.
[7] Bro, R., Smilde, A. K. (2014): Principal component analysis. – Analytical Methods 6(9): 2812-2831.
[8] Bush, P. R. (1970): A rapid method for the determination of carbonate carbon and organic carbon. – Chemical Geology 6: 59-62.
[9] Cassell, D. K., Nielson, D. R. (1986): Field Capacity and Available Water Capacity. – In: Klute, A. (ed.) Agronomy No. 9: Methods of Soil Analysis: Physical and mineralogical methods. Am. Soc. Agron. and Soil Sci. Soc. Am., Madison, WI, pp. 911-913.
[10] Chapman, H. D. (1965): Cation-Exchange Capacity. – In: Black, C. A. (ed.) Methods of Soil Analysis. Part 2. Chemical and Microbiological Properties. American Society of Agronomy, Madison, WI, pp. 891-901.
[11] Emami, A. S., Abedindo, B. F., Khayyat, M. H. (2011): Antioxidant activity of the essential oils of different parts of *Juniperus excelsa* M. Bieb. *subsp. excelsa and J. excelsa* M. Bieb. *subsp. polycarpos* (K. Koch) Takhtajan (*Cupressaceae*). – Iran Journal of Pharmaceutical Research 10: 799-810.
[12] Eriksson, C. P., Holmgren, P. (1996): Estimating stone and boulder content in forest soils evaluating the potential of surface penetration methods. – Catena 28: 121-134.
[13] Fakir, H. (2014): Türkiye'nin Doğal-Egzotik Ağaç ve Çalıları. – Turkish General Directorate of Forestry Publication No. 1, Ankara, pp. 673-702.
[14] Faydaoğlu, E., Sürücüoğlu, M. S. (2011): History of the use of medical and aromatic plants and their economic importance. – Kastamonu Univ. Journal of Forestry Faculty 11: 52-67.
[15] Fejér, J., Gruľová, D., Elıašová, A., Kron, I., De Feo, V. (2018): Influence of environmental factors on content and composition of essential oil from common juniper ripe berry cones (*Juniperus communis* L.). – Plant Biosystems - An International Journal Dealing with all Aspects of Plant Biology. DOI: 10.1080/11263504.2018.1435577.
[16] Fick, S. E., Hijmans, R. J. (2017): WorldClim 2: new 1-km spatial resolution climate surfaces for global land areas. – International Journal of Climatology 37(12): 4302-4315.
[17] Fisher, M., Gardner, A. S. (1995): The status and ecology of a *Juniperus excelsa subsp. polycarpos* woodland in the northern mountains of Oman. – Vegetatio 119: 33-51.
[18] Fontaine, M., Aerts, R., Özkan, K., Mert, A., Gülsoy, S., Süel, H., Waelkens, M., Muys, B. (2007): Elevation and exposition rather than soil types determine communities and site suitability in Mediterranean mountain forests of southern Anatolia, Turkey. – Forest Ecology and Management 247: 18-25.
[19] Gende, L., Maggi, M., Van Baren, C., Di Leo, A., Bandoni, A., Fritz, R., Eguaras, M. (2010): Antimicrobial and miticide activities of Eucalyptus globulus essential oils obtained from different Argentine regions. – Spanish Journal of Agricultural Research 8(3): 642-650.
[20] Göze, I., Göze, Ö. F., Yelkovan, I., Çetinus, Ş. A., Saygin, H., Ercan, N. (2017): The Review of certain ın vivo antioxidant effects on essential oils of *Origanum minutiflorum*

http://www.aloki.hu ● ISSN 1589 1623 (Print) ● ISSN 1785 0037 (Online)
DOI: http://dx.doi.org/10.15666/aeer/1605_70997113
© 2018, ALÖKI Kft., Budapest, Hungary

O Schwarz-Ph Davis, *Juniperus excelsa* Bieb. subsp. *excelsa* and histopathologic changes. – Revista Brasileira de Ciência Avícola 19(2): 333-338.

[21] Gülser, F., Çığ, A., Türkoğlu, N. (2012): The Determination of nutrient contents of native juniper (*Juniperus excelsa* Bieb.) and soil properties of plant growing areas in Van. – Iğdır University Journal of the Institute of Science and Technology 2: 93-98.

[22] Gülsoy, S., Merdin, A. (2017): Essential oil yield and components of juniper (*Juniperus excelsa* Bieb.) leaves. – Bilge International Journal of Science and Technology Research 1(2): 119-128.

[23] Gülsoy, S. Özkan, K. (2013): Determination of environmental factors and ındicator plant species for site suitability assessment of Crimean juniper in the Acipayam District, Turkey. – Sains Malaysiana 42: 1449-1457.

[24] Höferl, M., Stoilova, I., Schmidt, E., Wanner, J., Jirovetz, L., Trifonova, D., Krastev, L., Krastanov, A. (2014): Chemical composition and antioxidant properties of Juniper berry (*Juniperus communis* L.) essential oil. Action of the essential oil on the antioxidant protection of Saccharomyces cerevisiae model organism. – Antioxidants 3(1): 81-98.

[25] Jackson, M. L. (1958): Soil Chemical Analysis. –Prentice-Hall, Inc. Englewood Cliffs, NJ.

[26] Ložienė, K., Venskutonıs, P. R. (2016): Juniper (*Juniperus communis* L.) Oils. – In: Preedy, V. (ed.) Essential Oils in Food Preservation Flavor and Safety. Academic Press, Amsterdam, pp. 495-500.

[27] McCune, B., Keon, D. (2002): Equations for potential annual direct incident radiation and heat load. – Journal of Vegetation Science 13: 603-606.

[28] Mert, A., Şentürk, Ö., Güney, C. O., Akdemir, D., Özkan, K. (2013): Mapping of Some Distal Variables Available for Mapping Habitat Suitabilities of the Species: A Case Study of Buldan District. – In: Atalay, İ., Efe, R. (eds.) GeoMed 2013 The 3rd International Geography Symposium, 10-13 June, 2013, Kemer Antalya, pp. 210,.

[29] Moein, M. R., Ghasemi, Y., Moein, S., Nejati, M. (2010): Analysis of antimicrobial, antifungal and antioxidant activities of *Juniperus excelsa* M. B. subsp. *polycarpos* (K. Koch) Taghtajan essential oil. – Pharmacognosy Research 2(3): 128-131.

[30] Nadir, M., Rasheed, M., Ahmed, A. (2013): Comparative studies on the phytochemistry of essential oil from needles and berries of *Juniperus excelsa* M. Bieb. – Journal of the Chemical Society of Pakistan 35(2): 438-443.

[31] Orhan, N., Akkol, E., Ergun, F. (2012): Evaluation of anti inflammatory and antinociceptive effects of some Juniperus species growing in Turkey. – Turkish Journal of Biology 36: 719-726.

[32] Özkan, K., Gulsoy, S., Aerts, R., Muys, B. (2010): Site properties for Crimean juniper (*Juniperus excelsa*) in semi-natural forests of south western Anatolia, Turkey. – Journal of Environmental Biology 31: 97-100.

[33] Salehi, S. P., Mirzaa, M., Calagaria, M., Adams, R. P. (2010): Effects drying and harvest season on the essential oil composition from foliage and berries of Juniperus excelsa. – Industrial Crops and Products 32: 83-87.

[34] Sandler, A., Meunier, A., Velde, B. (2015): Mineralogical and chemical variability of mountain red/brown Mediterranean soils. – Geoderma 239: 156-167.

[35] Sarangzai, A. M., Siddiqui, M. F., Ahmed, M., Hussain, M. I., Laghari, S. K., Ahmed, A. (2015): Relationship between soil properties and natural regeneration pattern of Juniperus excelsa forest in Ziarat, Balochistan. – Pakistan Journal of Botany 47(3): 905-910.

[36] Sarstedt, M., Mooi, E. (2014): Cluster Analysis. – In: Mooi, E., Sarstedt, M. (eds.) A Concise Guide to Market Research. Springer, Berlin, Heidelberg, pp. 273-324.

[37] Sela, F., Karapandzova, M., Stefkov, G., Cvetkovıkj, I., Kulevanova, S. (2015): Chemical composition and antimicrobial activity of essential oils of *Juniperus excelsa* Bieb. (Cupressaceae) grown in R. Macedonia. – Pharmacognosy Research 7(1): 74-80.

http://www.aloki.hu ● ISSN 1589 1623 (Print) ● ISSN 1785 0037 (Online)
DOI: http://dx.doi.org/10.15666/aeer/1605_70997113
© 2018, ALÖKI Kft., Budapest, Hungary

[38] Skrovankova, S., Sumczynski, D., Mlcek, J., Jurikova, T., Sochor, J. (2015): Bioactive compounds and antioxidant activity in different types of berries. – International Journal of Molecular Sciences 16(10): 24673-24706.
[39] Spietelun, A., Marcinkowski, Ł., De La Guardia, M., Namieśnik, J. (2013): Recent developments and future trends in solid phase microextraction techniques towards green analytical chemistry. – Journal of Chromatography 1321: 1-13.
[40] Topçu, G., Gören, A. C., Bilsel, G., Bilsel, M., Çakmak, O., Schilling, J., Kinston, D. G. I. (2005): Cytotoxic activity and essential oil composition of leaves and berries of *Juniperus excelsa*. – Pharmaceutical Biology 43: 125-128.
[41] Weiss, A. (2001): Topographic position and landforms analysis. –Poster Presentation, ESRI User Conference, San Diego, CA, pp. 200-200.

http://www.aloki.hu ● ISSN 1589 1623 (Print) ● ISSN 1785 0037 (Online)
DOI: http://dx.doi.org/10.15666/aeer/1605_70997113
© 2018, ALÖKI Kft., Budapest, Hungary

UNVEILING PICOEUKARYOTIC DIVERSITY AND DISTRIBUTION IN THE BAY OF LARGE RESERVOIR SYSTEM

LI, Y. T.[1,2*] – LIU, K. S.[1*] – HOU, Y. Y.[1] –YU, J. J.[1] – DUAN, Y. H.[1] – LIU, X. X.[1] – HOU, J. J.[1**] – BI, Y. H.[3**]

[1]*Hubei Key Laboratory of Edible Wild Plants Conservation and Utilization, Hubei Normal University, Cihu Road, Huangshigang District, Huangshi, Hubei Province, 435002 China*

[2]*Bengbu University, Bengbu 233030, China*

[3]*State Key Laboratory of Freshwater Ecology and Biotechnology, Institute of Hydrobiology, The Chinese Academy of Sciences, Wuhan 430072, China*

**The first two authors made equal contributions to this paper.*

***Corresponding authors (contributed equally)*
J. J. Hou – e-mail: hjj6681@163.com, phone: +86-714-651-1613
Y. H. Bi – e-mail: biyh@ihb.ac.cn, phone: +86-276-878-0016

(Received 1st Aug 2018; accepted 5th Oct 2018)

Abstract. Few studies have reported about the diversity and distribution of picoeukaryotes in the ecosystem of reservoir bay. In this study, Sanger-based clone libraries of 18S rRNA gene were used to determine the picoeukaryotic diversity of three sampling sites; these sites were located across the Xiangxi Bay of Three Gorges Reservoir, China. The sampling sites were monitored across all four seasons in 2013. We identified 13 phyla in Xiangxi Bay. In this experimental survey, we found that picoeukaryotic community was dominated by three main phyla, namely, Cryptophyta, Chlorophyta, and Ciliophora (69.9% of clones in all). Moreover, the remaining 10 phyla showed a relative abundance of less than 6%. In Xiangxi Bay, the seasonal variability of communities overwhelms spatial patterns; upper reaches exhibited highest species diversity, whereas middle reaches exhibited lowest species diversity. The community temporal stability had decreased from upstream to downstream. Primary producers were dominant in all the sample sites, irrespective of the season. In Xiangxi Bay upstream, terrestrial microbes may be integral components of the microbial community assembly. In Xiangxi Bay, the distribution pattern of picoeukaryotes might have been affected by the mainstream of Three Gorges Reservoir.
Keywords: *picoeukaryotes, microbial diversity, 18S rDNA, tributary bay, distribution pattern*

Introduction

Picoeukaryotes are widely distributed in aquatic environments, contributing significantly to biomass and primary production (Li, 1994; Caron et al., 2012). They are core members of aquatic microbial food webs and play a fundamental role in biogeochemical cycling (Massana et al., 2011). This indicates that they play an important role in maintaining the balance of water ecosystems (Biegala et al., 2003; Vaulot et al., 2008). Many studies have reported about the unexpected diversity of picoeukaryotes in Open Ocean, coastal areas, and estuaries (Massana et al., 2011; Wu et al., 2014; Farnelid et al., 2016).

Some studies have determined the diversity of picoeukaryotes in freshwater systems. In oligotrophic systems, picoeukaryotes are very important primary producers of biomass (Stenuite et al., 2009). Moreover, a high level of picoeukaryote diversity was recorded in mesotrophic lakes (Lepère et al., 2008; Lefèvre et al., 2008). Recent studies have reported that picophytoplankton is an important primary producer in eutrophic

http://www.aloki.hu ● ISSN 1589 1623 (Print) ● ISSN 1785 0037 (Online)
DOI: http://dx.doi.org/10.15666/aeer/1605_71157128
© 2018, ALÖKI Kft., Budapest, Hungary

estuaries, contributing significantly to the total phytoplankton biomass (Murrell and Lores, 2004; Gaulke et al., 2010). In another study, researchers found that pico-phytoplankton abundance was quite high in rivers; it was almost equivalent to that in lakes and oceans (Contant and Pick, 2013). Currently, molecular techniques are used for surveying the diversity of picoeukaryotes that inhabit rivers (Thomasa et al., 2012), freshwater lakes (Zhao et al., 2011), and shallow aquatic environments (Simon et al., 2015a, b). However, we have little information about the diversity and distribution of picoeukaryotes, which thrive in an ecosystem of reservoir bay.

The Three Gorges Reservoir is located in the lower section of the upper reaches of Yangtze River in China (Han et al., 2015). The Xiangxi River is one of the longest rivers in the Three Gorges Reservoir region. After constructing the Three Gorges Dam, the Xiangxi River was transformed into Xiangxi Bay (Holbach et al., 2015). In this study, we used Sanger-based clone libraries of 18S rRNA gene to determine the picoeukaryote diversity of three sampling sites, which were present along the Xiangxi Bay of the Three Gorges Reservoir; the picoeukaryote diversity was monitored across all the four seasons in 2013. We addressed the following basic questions: what is the picoeukaryotic diversity in the bay of a large reservoir? Does the mainstream reservoir affect the distribution pattern of picoeukaryote in the bay?

Materials and methods

Sample collection and environmental data

Water samples were collected from downstream (XX01, 30°97'32.28"N, 110°75'80.59"E), midstream (XX04, 31°11'06.06"N, 110°77'57.14"E) and upstream (XX07, 31°18'96.64"N, 110°75'33.75"E) of Xiangxi Bay of the Three Gorges Reservoir of China in February (winter), April (spring), August (summer), and October (autumn) of 2013 (*Fig. 1*). The linear distance between the XX01 and XX07 sample sites was approximately 26 km.

Water samples were collected at a depth of 0.5 m beneath the water surface using a 5-L sampler and pre-filtered through 5 μm pore-size polycarbonate filters (Millipore) followed by filtration onto GF/F filters (0.7 μm, Whatman) for molecular analyses. Samples were immediately frozen in liquid nitrogen and stored at -80 °C until analysis.

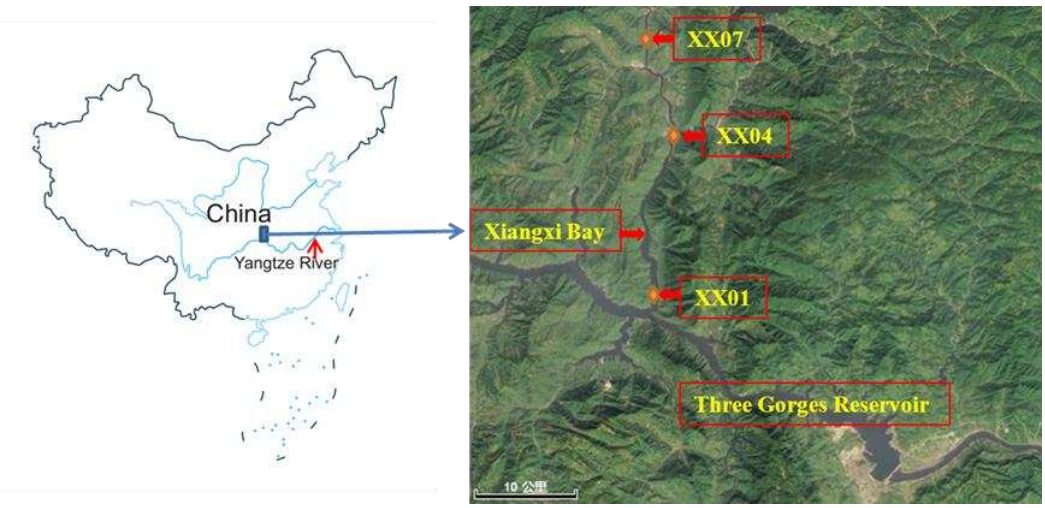

Figure 1. *Map of study area and sampling site*

http://www.aloki.hu ● ISSN 1589 1623 (Print) ● ISSN 1785 0037 (Online)
DOI: http://dx.doi.org/10.15666/aeer/1605_71157128
© 2018, ALÖKI Kft., Budapest, Hungary

Physical and chemical factors, such as water temperature (WT), dissolved oxygen (DO), pH and turbidity, were measured in situ. Concentrations of total nitrogen (TN), orthophosphate (P-PO_4, PO43-), nitrate (N-NO_3, NO3-), total phosphorus (TP), Chemical Oxygen Demand (COD), Oxidation-Reduction Potential (ORP), water transparency (SD) and ammonium (N-NH_4, NH4+) were measured using standard methods, as described previously (Huang et al., 1999). The trophic states of the Xiangxi Bay in different sample sites and seasons were determined by comprehensive nutritional status index (trophic level index, TLI) using the values of TN, TP and SD (Tian et al., 2017). Trophic states are set as follows: $TLI \leq 30$, oligotrophic; $30 < TLI \leq 50$, mesotrophic; $50 < TLI \leq 60$, slightly eutrophic; $60 < TLI \leq 70$, moderately eutrophic; $TLI > 70$, highly eutrophic (Meng and Zhao, 2007).

DNA extraction and clone library construction

DNA was extracted from filters using a previously described method (Countway et al., 2005). Near full-length 18S rDNA fragments were amplified by polymerase chain reaction （PCR） using the eukaryotic-specific primers Euk328f/Euk329r (Euk328f: 5'-ACCTGGTTGATCCTGCCAG-3', Euk329r: 5'-TGATCCTTCYGCAGGTTCAC-3') (Moon-van der Staay et al., 2000). PCR was carried out under the following conditions: 35 cycles (denaturation at 94 °C for 30 s, annealing at 55 °C for 45 s, extension at 72 °C for 2 min) proceeded by 3 min denaturation at 94 °C and followed by 8 min extension at 72 °C. 18S rDNA clone libraries were constructed using the pGEM®-T Easy Vector Systems (Promega) following the instructions provided by the manufacturer.

Amplified ribosomal DNA restriction analysis (ARDRA)

Positive clones from each library were screened by re-amplifying the 18S rDNA by PCR as described above, except that 0.1 μl of the culture of *Escherichia coli* containing the insert was used as a template. Positive PCR product was digested with *Hae*III (Fermentas). Gel electronic images were visualized by means of ChemiDoc XRS (Bio-Rad), images were analyzed with Image Lab software v. 3.0 (Bio-Rad). Clones with the same ARDRA pattern were grouped and considered as the same operational taxonomic unit (OTU).

Statistical analyses

Based on the result of ARDRA analysis, a library coverage value was computed according to the literature (Dang et al., 2008). Diversity indexes (Shannon and Pielou evenness) were also calculated. The Shannon diversity index is an index that is commonly used to characterize species diversity in a community. Pielou's evenness refers to how close in numbers each species in an environment are. The Kruskal-Wallis test was used for comparison between multiple groups. Bray-Curtis (temporal) dissimilarity based on relative abundance data OTUs was used as indices of the temporal turnover of community. The community structures were compared with non-metric multidimensional scaling (NMDS) using Bray-Curtis distances. The significance of the observed differences was determined by permutational multivariate analysis of variance (PERMANOVA) based on Bray-Curtis distance measurements with 999 permutations. NMDS and. the Bray-Curtis dissimilarity between pairwise samples was

http://www.aloki.hu ● ISSN 1589 1623 (Print) ● ISSN 1785 0037 (Online)
DOI: http://dx.doi.org/10.15666/aeer/1605_71157128
© 2018, ALÖKI Kft., Budapest, Hungary

calculated on the basis of OTU abundances. All these analyses were done using the R package vegan.

Analysis based on sequence

One or several representative clones of each ARDRA pattern were partially sequenced (Majorbio, China). Colonies were sequenced using the Euk 528F primer (5'-GCGGTAATTCCAGCTCCAA-3') (Elwood et al., 1985). All sequences obtained were edited to exclude the primer sequence using Lasergene.v7.1 (DNAStar Inc), and checked for chimerical structures using the CHECK-CHIMERA program on the Ribosomal Database Project (http://rdp.cme.msu.edu/html/). In order to determine the phylogenetic affiliation, all non-chimeric sequences were aligned using the online automatic SILVA Incremental Aligner SINA v1.2.11 (http://www.arb-silva.de/aligner/) to identify known sequences with a high degree of similarity. Phyla that differed significantly ($q < 0.05$) for two groups were identified using White's non-parametric t-test with Storey's multiple testing correction in the STAMP software version 2.1 (Parks et al., 2014). Similarity percentage analysis (SIMPER) was used to assessing which taxa are primarily responsible for an observed difference between groups. SIMPER were carried out using PAST 3.18 (Hammer et al., 2001).

Correlations between picoeukaryotic communities and environmental factors were analyzed using the canonical correlation analysis (CCA) using R package vegan. CCA was performed using the relative abundance data of phyla (except rare phyla) and environmental factors. Significant environmental variables were chosen by the manual forward selection procedure, followed by Monte Carlo permutation tests (1000 iterations).

Nucleotide sequence accession number

The 18S rRNA gene sequences determined have been deposited in the GenBank database under accession numbers KX998709 - KX998893.

Results

Environmental characterization

The physicochemical parameters of water samples were present in *Table A1* in the *Appendix*. Among these parameters, statistically significant difference was observed in only TN values of the three sample sites ($p = 0.036$, Kruskal-Wallis tests). On the whole, the concentration of TN had increased gradually from upstream to downstream. Except for autumn, the TLI of the three sampling sites was greater than 50 through the year (*Table A1, Fig. A1*). The median TLI of three sampling sites (XX01, XX04, and XX07) was 51.57, 57.74, and 57.54, respectively (*Fig. A1*).

18S rDNA clone libraries

In total, 12 clone libraries were constructed for the three sample sites. Approximately 85–105 clones were isolated from each clone library; these clones were then subjected to ARDRA analysis. In total, ARDRA analysis was performed on 1116 clones; these clones were clustered into 240 OTUs. In each sample, the number of OTUs ranged from 18 to 59. The coverage of respective libraries ranged from 63% to 91% (*Table 1*). The

http://www.aloki.hu ● ISSN 1589 1623 (Print) ● ISSN 1785 0037 (Online)
DOI: http://dx.doi.org/10.15666/aeer/1605_71157128
© 2018, ALÖKI Kft., Budapest, Hungary

distribution of OTUs varied according to seasons or different sample sites. Only 31 OTUs appeared at all sites. Furthermore, only 6 OTUs appeared throughout the year (*Fig. A2*).

Table 1. *Summary of ARDRA analysis of the 12 clone libraries*

Season	Sample sites	No. of RFLP types	Coverage	Shannon-Wiener	Pielou evenness
Spring	XX01	40	78.70%	4.65	0.87
	XX04	18	90.00%	3.17	0.76
	XX07	59	68.47%	5.52	0.94
Summer	XX01	36	68.42%	4.64	0.89
	XX04	44	71.27%	4.94	0.90
	XX07	35	72.50%	4.47	0.86
Autumn	XX01	29	90.76%	3.54	0.71
	XX04	48	68.13%	5.29	0.85
	XX07	55	63.16%	5.51	0.95
Winter	XX01	42	71.59%	4.93	0.93
	XX04	23	80.00%	4.10	0.91
	XX07	48	78.99%	5.04	0.90

The Shannon index and Pielou evenness index of 12 clone libraries were calculated (*Table 1*). The Shannon index peaked in upstream (XX07 site), and they were least in the middle reaches (XX04 site) of Xiangxi Bay (*Fig. A1*). No statistically significant difference was observed in the diversity index of the three sample sites; moreover, no statistically significant difference was observed for the four seasons of the year (all $p > 0.09$, Kruskal-Wallis test).

Picoeukaryotic community composition

We obtained 185 high-quality sequences after removing all low-quality, unassembled, and potentially chimeric sequences. We performed phylogenetic analyses on 12 samples; the analyses results indicate that there were 13 phyla in these 12 samples (*Fig. 2*). Moreover, analyses results indicate that these libraries were dominated by Cryptophyta and Chlorophyta (32.4% and 21.5% of the total 910 clones respectively), followed by Ciliophora (16%) and Bacillariophyta (5.9%), Chrysophyta (3.3%). Telonemia, Pyrrhophyta, and Cercozoa were the three groups of picoeukaryotes, which were present in extremely low proportions. Besides, we also detected a very small amount of Haptophyta (1 sequence, 1 clone). Moreover, some kinds of fungi (Chytridiomycota, Cryptomycota, and Basidiomycota) and fungus-like (Oomycota) taxa were also detected in this study. The relative abundance of these fungi and fungus-like taxa was very low at the three sample sites. In these libraries, a significant number of sequences (37 sequences, 16.5% of the total 910 clones) were not affiliated with any formal taxa.

Among the Cryptophyta, an overwhelming majority belonged to Cryptomonadales (39 sequences); we also identified six sequences that were affiliated to uncultured Kathablepharidae. The Chlorophyta sequences were grouped into four taxa:

http://www.aloki.hu ● ISSN 1589 1623 (Print) ● ISSN 1785 0037 (Online)
DOI: http://dx.doi.org/10.15666/aeer/1605_71157128
© 2018, ALÖKI Kft., Budapest, Hungary

Chlorophyceae, Chlorodendrophyceae, Mamiellophyceae, and Trebouxiophyceae. Among them, Chlorophycea was the most abundant taxon (26 of 35 Chlorophyta sequence). The Ciliophora sequences were grouped into three taxa: uncultured Choreotrichia, Litostomatea, and Prostomatea. Among them, uncultured Choreotrichia was the most abundant taxon (20 of 40 Ciliophora sequence). All the six sequences of Bacillariophyta belonged to the taxon Mediophyceae. Chrysophyta contained different types of sequences: three sequences were affiliated to the taxon Chrysophyceae, while one sequence was affiliated to Nannochloropsis. Telonemia consisted of four sequences, which were affiliated to the taxon Telonema (Shalchian-Tabrizi et al., 2006).

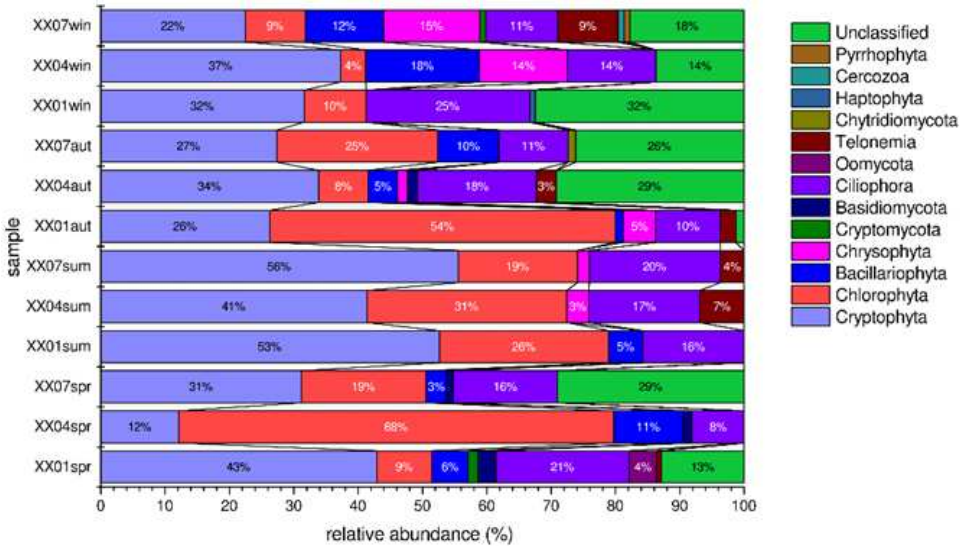

Figure 2. *Distribution of the phyla in all samples. Spr: spring, sum: summer, aut: autumn, win: winter*

Community structure across space and time

From winter to spring, the structure of picoeukaryotic communities changed slightly; a different picoeukaryotic community structure was observed from summer to autumn, with slight variation in composition. Seasonal patterns were detected by NMDS analyses (*Fig. 3*). By performing PERMANOVA analyses, we found that the composition of picoeukaryotic communities was significantly different across all the four seasons (p = 0.0011); however, there was no significant difference between the composition of picoeukaryotic communities of three sample sites (p = 0.9937). By SIMPER analysis, we observed the seasonal differences were mainly attributed to appreciable seasonal fluctuations in the relative abundance of dominant phyla. The seasonal differences were mainly observed in following phyla: Chlorophyta (24.41%), Cryptophyta (20.3%), and Ciliophora (12.25%).

In Xiangxi Bay, picoeukaryotes were unevenly distributed across the three sample sites; moreover, the distribution of picoeukaryotes also changed across the four seasons. By determining the Bray-Curtis dissimilarity matrix of all the samples, we found that the community temporal stability decreased from upstream to downstream (*Fig. 4*). By STAMP analysis, we found that Basidiomycota has a significantly higher abundance in spring than in summer ($q < 0.01$) (*Fig. 5*). No significant variations were observed in the composition of the phyla, regardless of the sample site.

http://www.aloki.hu ● ISSN 1589 1623 (Print) ● ISSN 1785 0037 (Online)
DOI: http://dx.doi.org/10.15666/aeer/1605_71157128
© 2018, ALÖKI Kft., Budapest, Hungary

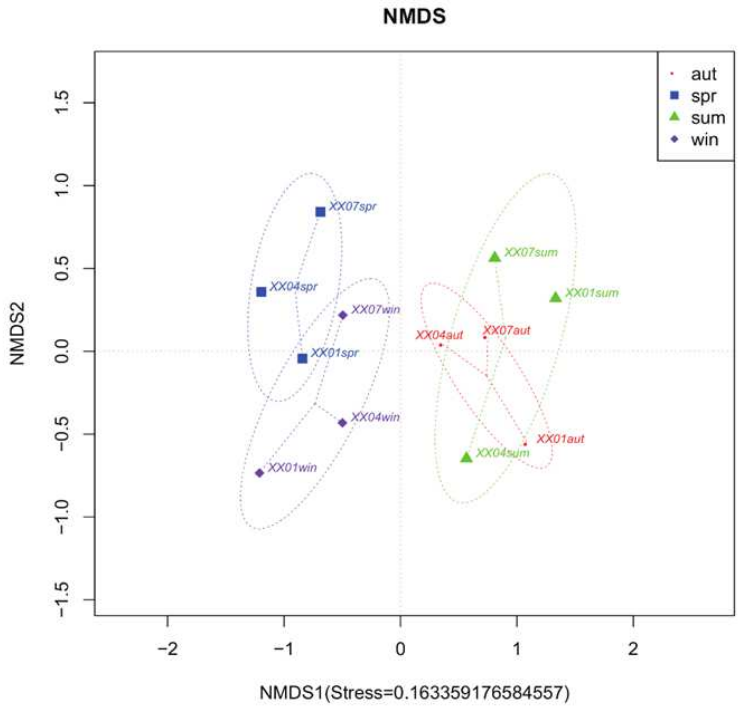

Figure 3. *Non-metric MultiDimensional Scaling (NMDS) plot based on Bray-Curtis distances*

Picoeukaryotic communities in relation to environmental variables

The results of CCA analysis indicate that abundances of specific taxa depended upon environmental variables (*Fig. 6*). The first two axes accounted for 35.3% of the variance. The abundances of Chrysophyta and Bacillariophyta were negatively related to pH and turbidity. The distribution of Bacillariophyta was greater in the area with higher concentration of N–NH_4. The distribution of Chrysophyta was concentrated in the least turbid area, which had lower values of N–NH_4.

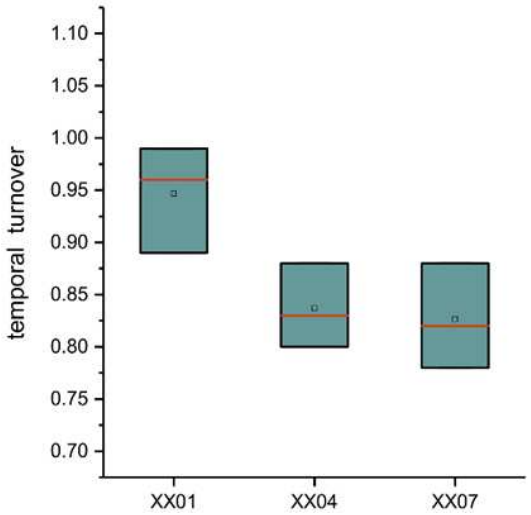

Figure 4. *Boxplot of spring-summer, summer-autumn and autumn-winter pairwise dissimilarity (temporal turnover) coefficient of the three sample sites. Median is indicated by the red center lines, arithmetic average is indicated by the black hollow circle*

http://www.aloki.hu ● ISSN 1589 1623 (Print) ● ISSN 1785 0037 (Online)
DOI: http://dx.doi.org/10.15666/aeer/1605_71157128
© 2018, ALÖKI Kft., Budapest, Hungary

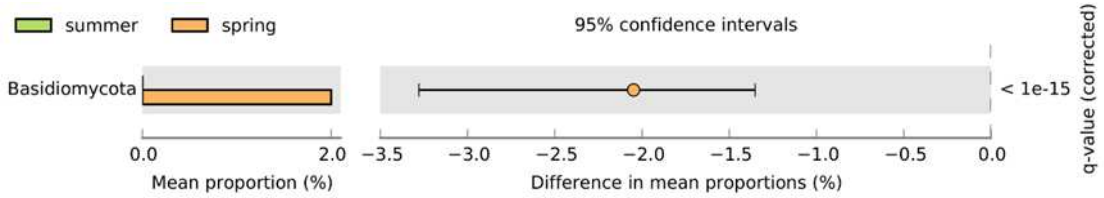

Figure 5. *Phyla that was significantly different between two seasons*

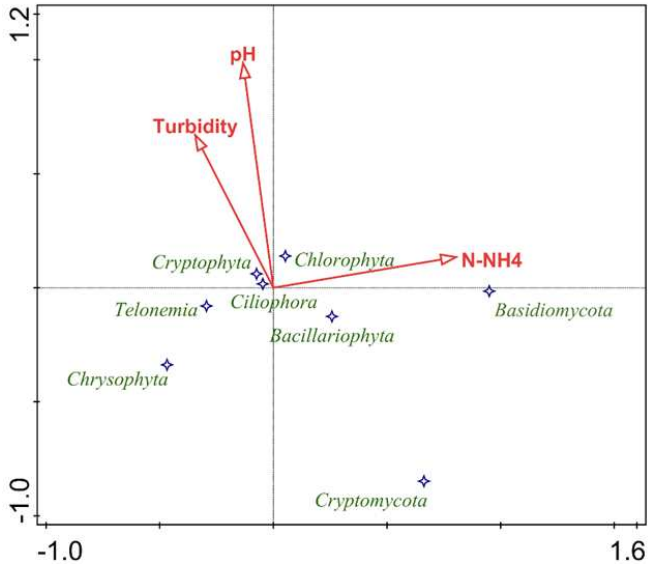

Figure 6. *Canonical correspondence analysis (CCA) plot for the environmental parameters and the picoeukaryotic communities. N-NH4: ammonium*

Discussion

In this study, we found that TLI was the highest in middle reaches (XX04 site) and least in the downstream (XX01 site) of Xiangxi Bay (*Fig. A1*). There is water exchange between the Three Gorges Reservoir mainstream and its tributaries (Liu et al., 2012; Huang et al., 2014). Owing to water exchange, nutrients are supplied from the Three Gorges Reservoir mainstream to the Xiangxi Bay (Yang et al., 2015). Water exchange occurs frequently at the river mouth; however, the time of water retention is short (Liu et al., 2012). Consequently, the middle reaches of Xiangxi Bay were replenished with several nutrients (Ji et al., 2010). Therefore, middle reaches of Xiangxi Bay have the highest TLI.

Previous studies have reported that the diversity of species decreases with eutrophication (Baho et al., 2017; Cook et al., 2018). Therefore, the diversity index was lowest in middle reaches of Xiangxi Bay (*Fig. A1*). Surprisingly, the diversity index was highest at the upstream (XX07 site) of Xiangxi Bay, but its trophic level was higher than the downstream of Xiangxi Bay. With the flows of water, soil, litter, and anthropogenic materials were transported in and around rivers. These materials got easily mixed with the resident microbial communities (Mansour et al., 2018). Recently, several studies have been carried out on different water ecosystems; these studies have reported that terrestrial microbes show significant abundance in the microbial communities of headwater ecosystems (Crump et al., 2012; Besemer et al., 2013; Ruiz-

http://www.aloki.hu ● ISSN 1589 1623 (Print) ● ISSN 1785 0037 (Online)
DOI: http://dx.doi.org/10.15666/aeer/1605_71157128
© 2018, ALÖKI Kft., Budapest, Hungary

González et al., 2015). In the upstream sampling site, microbial diversity could be structured by inoculating the microbes from terrestrial sources; these microbes would contribute to community assembly. This may be the reason for the differences in the diversity of picoeukaryotic communities, which are found in the down and upper reaches of Xiangxi Bay.

The upstream of Xiangxi Bay had the highest diversity index, while the midstream of Xiangxi Bay had the lowest diversity index (*Fig. A1*). Before the construction of the Three Gorges Reservoir, the diversity index of Xiangxi River was lower down-stream (Kuang et al., 2004). This implies that the distribution pattern of plankton diversity has changed to some extent after the construction of the Three Gorges Reservoir. Furthermore, our results indicate that diversity indices of summer and winter were greater than those of spring and autumn (*Fig. A3*). Similar results have been presented by researchers in previous studies (Zhang et al., 2017). Previous studies have proved that the mainstream of Three Gorges Reservoir significantly influences its tributaries in spring and autumn seasons: this is because water is discharged from the mainstream of Three Gorges Reservoir during spring season; moreover, water is impounded into the same reservoir during autumn (Li et al., 2012). After analyzing the diversity indices and temporal turnover of picoeukaryotic communities, we infered that the Three Gorges Reservoir does impact plankton diversity of its tributaries.

The concentration of $N–NO_3$ is much higher than that of $N–NH_4$ in Xiangxi Bay (*Table A1*). The results of ordination analysis prove that Bacillariophyta had a positive relationship with $N–NH_4$. In the presence of sufficient nutrients, diatoms are generally $N–NO_3$ opportunists (Donald et al., 2011; Glibert and Wilkerson, 2014). Some studies have reported that diatoms are distributed in the area, which has higher concentration of $N–NH_4$ values (Zhao et al., 2013). Therefore, further studies must be conducted to determine whether elevated levels of $N–NH_4$ favor the growth of pico-diatoms in Xiangxi Bay. Chrysophyta often grows in highly transparency water, which has low organic content (Lin et al., 2003). In this survey, Chrysophyta appear in less turbid areas, which have comparatively lower concentration of $N–NH_4$. The relative abundance of Chrysophyta was much greater in oligotrophic lakes than in Xiangxi Bay. This indicates that eutrophication affects the composition of plankton communities in different water bodies.

In summary, water exchange between Xiangxi Bay and Three Gorges Reservoir mainstream may affected the distribution pattern of biodiversity and nutritional state of Xiangxi Bay. So, middle reaches of Xiangxi Bay have the highest TLI. Furthermore, upper reaches exhibited highest species diversity, whereas middle reaches exhibited lowest species diversity. In Xiangxi Bay, the seasonal variability of communities overwhelms spatial patterns. The community temporal stability had decreased from upstream to downstream. In the upstream sampling site, microbial diversity could be structured by inoculating the microbes from terrestrial sources.

Acknowledgements. This research was supported by the National Natural Science Foundation of China (41171045) and the Research Fund for Science and Technology Inovation Team of University (T201504).

http://www.aloki.hu ● ISSN 1589 1623 (Print) ● ISSN 1785 0037 (Online)
DOI: http://dx.doi.org/10.15666/aeer/1605_71157128
© 2018, ALÖKI Kft., Budapest, Hungary

REFERENCES

[1] Baho, D. L., Drakare, S., Johnson, R. K., Allen, C. R., Angeler, D. G. (2017): Is the impact of eutrophication on phytoplankton diversity dependent on lake volume/ecosystem size? – Journal of Limnology 76: 199-210.
[2] Besemer, K., Singer, G., Quince, C., Bertuzzo, E., Sloan, W., Battin, T. J. (2013): Headwaters are critical reservoirs of microbial diversity for fluvial networks. – Proceedings of the Royal Society B: Biological Sciences 280: 20131760.
[3] Biegala, I. C., Not, F., Vaulot, D., Simon, N. (2003): Quantitative assessment of picoeukaryotes in the natural environment by using taxon-specific oligonucleotide probes in association with tyramide signal amplification-fluorescence in situ hybridization and flow cytometry. – Applied and Environmental Microbiology 6: 5519-5529.
[4] Caron, D., Countway, P., Jones, A., Kim, D., Schnetzer, A. (2012): Marine protistan diversity. – Annual Review of Marine Science 4: 467-493.
[5] Contant, J., Pick, F. R. (2013): Picophytoplankton during the ice-free season in five temperate-zone rivers. – Journal of Plankton Research 35: 553-565.
[6] Cook, S. C., Housley, L., Back, J. A., King, R. S. (2018): Freshwater eutrophication drives sharp reductions in temporal beta diversity. – Ecology 99: 47-56.
[7] Countway, P. D., Gast, R. J., Savai, P., Caron, D. A. (2005): Protistan diversity estimates based on 18S rDNA from seawater incubations in the Western North Atlantic. – Journal of Eukaryotic Microbiology 52: 95-106.
[8] Crump, B. C., Amaral-Zettler, L. A., Kling, G. W. (2012): Microbial diversity in arctic freshwaters is structured by inoculation of microbes from soils. – The ISME Journal 6: 1629-1639.
[9] Dang, H. Y., Li, T. G., Chen, M. G., Huang, G. Q. (2008): Cross-ocean distribution of rhodobacterales bacteria as primary surface colonizers in temperate coastal marine waters. – Applied and Environmental Microbiology 74: 52-60.
[10] Donald, D. B., Bogard, M. J., Finlay, K., Leavitt, P. R. (2011): Comparative effects of urea, ammonium, and nitrate on phytoplankton abundance, community composition, and toxicity in hypereutrophic freshwaters. – Limnology and Oceanography 56: 2161-2175.
[11] Elwood, H. J., Olsen, G. J., Sogin, M. L. (1985): The small-subunit ribosomal RNA gene sequences from the Hypotrichou Ciliates Oxytricha nova and Stylonychia pustulata. – Molecular Biology and Evolution 2: 399-410.
[12] Farnelid, H. M., Turk-Kubo, K. A., Zehr, J. P. (2016): Identification of associations between bacterioplankton and photosynthetic picoeukaryotes in coastal waters. – Frontiers in Microbiology 7: 339.
[13] Gaulke, A. K., Wet, M. S., Paerl, H. W. (2010): Picophytoplankton: a major contributor to planktonic biomass and primary production in a eutrophic, river-dominated estuary. – Estuarine, Coastal and Shelf Science 90: 45-54.
[14] Glibert, P. M., Wilkerson, F. P. (2014): Phytoplankton communities from San Francisco Bay Delta respond differently to oxidized and reduced nitrogen substrates even under conditions that would otherwise suggest nitrogen sufficiency. – Frontiers in Marine Science 1: 1-16.
[15] Hammer, Ø., Harper, D. A. T., Ryan, P. D. (2001): PAST: Paleontological statistics software package for education and data analysis. – Palaeontologia Electronica 4: 9.
[16] Han, L. F., Gao, B., Zhou, H. D., Xu, D. Y., Wei, X., Gao, L. (2015): The spatial distribution, accumulation and potential source of seldom monitored trace elements in sediments of Three Gorges Reservoir, China. – Scientific Reports 5: 16170.
[17] Holbach, A., Bi, Y., Yuan, Y., Wang, L., Zheng, B., Norra, S. (2015): Environmental water body characteristics in a major tributary backwater of the unique and strongly seasonal Three Gorges Reservoir, China. – Environmental Science: Processes & Impacts 17: 1641-53.

http://www.aloki.hu ● ISSN 1589 1623 (Print) ● ISSN 1785 0037 (Online)
DOI: http://dx.doi.org/10.15666/aeer/1605_71157128
© 2018, ALÖKI Kft., Budapest, Hungary

[18] Huang, X. F., Chen, W. M., Cai, Q. M. (1999): Survey, observation and analysis of lake ecology. – China Standard Press, Beijing, pp. 45-79 (in Chinese).
[19] Huang, Y. L., Zhang, P., Liu, D. F., Yang, Z. J., Ji, D. B. (2014): Nutrient spatial pattern of the upstream, mainstream and tributaries of the Three Gorges Reservoir in China. – Environmental Monitoring and Assessment 186: 6833-6847.
[20] Ji, X. P., Liu, D. F., Huang, Y. L., Ji, D. B., Yi, Z. Q. (2010): Dynamic characteristics of nutrients in Xiangxi Bay and converse impact from mainstream in drainage period of the Three Gorges Reservoir. – Chinese Journal of Environmental Engineering 4: 2687-2693 (in Chinese).
[21] Kuang, Q. J., Hu, Z. Y., Zhou, G. J., Ye, L., Cai, Q. H. (2004): Investigation on phytoplankton in Xiangxi River Watershed and the evaluation of its water quality. – Plant Science Journal 22: 507-513 (in Chinese).
[22] Lefèvre, E., Roussel, B., Amblard, C., Sime-Ngando, T. (2008): The molecular diversity of freshwater picoeukaryotes reveals high occurrence of putative parasitoids in the plankton. – PLOS ONE 3: e2324.
[23] Lepère, C., Domaizon, I., Debroas, D. (2008): Unexpected importance of potential parasites in the composition of the freshwater small-eukaryote community. – Applied and Environmental Microbiology 74: 2940-2949.
[24] Li, W. K. W. (1994): Primary production of prochlorophytes, cyanobacteria, and eucaryotic ultraphytoplankton: measurements from flow cytometric sorting. – Limnology and Oceanography 39: 169-175.
[25] Li, Y., Liu, D. F., Kong, S., Ji, D. B., Yang, Z. J., Chen, Y. Y. (2012): Comparative analysis of the impact of discharging and impounding process of Three Gorges Reservoir on the algal bloom in the Xiangxi Bay. – Acta Scientiae Circumstantiae 32: 1882-1893 (in Chinese).
[26] Lin, Q. Q., Hu, R., Duan, S. S., Han, B. P. (2003): Reservoir trophic states and the response of plankton in Guangdong Province. – Acta Ecologica Sinica 23: 1101-1108 (in Chinese).
[27] Liu, L., Liu, D. F., Johnson, D. M., Yi, Z. Q., Huang, Y. L. (2012): Effects of vertical mixing on phytoplankton blooms in Xiangxi Bay of Three Gorges Reservoir: Implications for management. – Water Research 46: 2121-2130.
[28] Mansour, I., Heppell, C. M., Ryo, M., Rillig, M. C. (2018): Application of the microbial community coalescence concept to riverine networks. – Biological Reviews https://doi.org/10.1111/brv.12422.
[29] Massana, R., Pernice, M., Bunge, J. A., Campo, J. D. (2011): Sequence diversity and novelty of natural assemblages of picoeukaryotes from the Indian Ocean. – The ISME Journal 5: 184-195.
[30] Meng, C. H., Zhao, B. (2007): Study on the trend of eutrophication after impounding in Three Gorges Reservoir. – Journal of Agro-Environment Science 26: 863-867.
[31] Moon-van der Staay, S. Y., van der Staay, G. W. M., Guillou, L., Vaulot, D., Claustre, H., Medlin, L. K. (2000): Abundance and diversity of prymnesiophytes in the picoplankton community from the equatorial Pacific Ocean inferred from 18S rDNA sequences. – Limnology and Oceanography 45: 98-109.
[32] Murrel, M. C., Lores, E. M. (2004): Phytoplankton and zooplankton seasonal dynamics in a subtropical estuary: importance of cyanobacteria. – Journal of Plankton Research 26: 371-382.
[33] Parks, D., Tyson, G. W., Hugenholtz, P., Beiko, R. G. (2014): STAMP: statistical analysis of taxonomic and functional profiles. – Bioinformatic 30: 3123-3124.
[34] Ruiz-González, C., Niño-García, J. P., del Giorgio, P. A. (2015): Terrestrial origin of bacterial communities in complex boreal freshwater networks. – Ecology Letters 18: 1198-1206.
[35] Shalchian-Tabrizi, K., Eikrem, W., Klaveness, D., Vaulot, D., Minge, M., Le Gall, F., Romari, K., Throndsen, J., Botnen, A., Massana, R., Thomsen, H., Jakobsen, K. (2006):

http://www.aloki.hu ● ISSN 1589 1623 (Print) ● ISSN 1785 0037 (Online)
DOI: http://dx.doi.org/10.15666/aeer/1605_71157128
© 2018, ALÖKI Kft., Budapest, Hungary

Telonemia, a new protist phylum with affinity to chromist lineages. – Proceedings of the Royal Society B: Biological Sciences 273: 1833-1842.

[36] Simon, M., Jardillier, L., Deschamps, P., Moreira, D., Restoux, G., Bertolino, P., López-García, P. (2015a): Complex communities of small protists and unexpected occurrence of typical marine lineages in shallow freshwater systems. – Environmental Microbiology 17: 3610-3627.

[37] Simon, M., López-García, P., Deschamps, P., Moreira, D., Restoux, G., Bertolino, P., Jardillier, L. (2015b): Marked seasonality and high spatial variability of protist communities in shallow freshwater systems. – The ISME Journal 9: 1943-1951.

[38] Stenuite, S., Tarbe, A. L., Sarmento, H., Unrein, F., Pirlot, S., Sinyinza, D., Thill, S., Lecomte, M., Leporcq, B., Gasol, J. M., Descy, J. P. (2009): Photosynthetic picoplankton in Lake Tanganyika: biomass distribution patterns with depth, season and basin. – Journal of Plankton Research 31: 1531-1544.

[39] Thomasa, M. C., Selingerb, L. B., Inglisa, G. D. (2012): Seasonal diversity of planktonic protists in Southwestern Alberta Rivers over a 1-year period as revealed by terminal restriction fragment length polymorphism and 18S rRNA gene library analyses. – Applied and Environmental Microbiology 78: 5653-5660.

[40] Tian, W., Zhang, H. Y., Zhao, L., Zhang, F. F., Huang, H. (2017): Phytoplankton diversity effects on community biomass and stability along nutrient gradients in a eutrophic lake. – International Journal of Environmental Research and Public Health 14: 95.

[41] Vaulot, D., Eikrem, W., Viprey, M., Moreau, H. (2008): The diversity of small eukaryotic phytoplankton (<3μm) in marine ecosystems. – FEMS Microbiology Ecology 32: 95-820.

[42] Wu, W. X., Huang, B. Q., Zhong, C. (2014): Photosynthetic picoeukaryote assemblages in the South China Sea from the Pearl River estuary to the SEATS station. – Aquatic Microbial Ecology 71: 271-284.

[43] Yang, L., Liu, D. F., Huang, Y. L., Yang, Z. J., Ji, D. B., Song, L. X. (2015): Isotope analysis of the nutrient supply in Xiangxi Bay of the Three Gorges Reservoir. – Ecological Engineering 77: 65-73.

[44] Zhang, J. L., Zheng, B. H., Liu, D. F., Wang, L. J., Tan, Q. R. (2017): Succession pattern of phytoplankton of Daning River in the Three Gorges Reservoir and its driving factors. – Environmental Science 38: 535-546 (in Chinese).

[45] Zhao, B. Y., Chen, M. J., Sun, Y., Yang, J. X., Chen, F. Z. (2011): Genetic diversity of picoeukaryotes in eight lakes differing in trophic status. – Canadian Journal of Microbiology 57: 115-126.

[46] Zhao, Z., Mi, T., Xia, L., Yan, W. M., Jiang, Y., Gao, Y. Z. (2013): Understanding the patterns and mechanisms of urban water ecosystem degradation: phytoplankton community structure and water quality in the Qinhuai River, Nanjing City, China. – Environmental Science and Pollution Research 20: 5003-5012.

http://www.aloki.hu ● ISSN 1589 1623 (Print) ● ISSN 1785 0037 (Online)
DOI: http://dx.doi.org/10.15666/aeer/1605_71157128
© 2018, ALÖKI Kft., Budapest, Hungary

APPENDIX

Table A1. *Physical and environmental characteristics of the sampling stations. Spr: spring, sum: summer, aut: autumn, win: winter. WT: water temperature, DO: dissolved oxygen, TN: total nitrogen, P-PO4: orthophosphate, N-NO3: nitrate, TP: total phosphorus, N-NH4: ammonium, COD: chemical oxygen demand, ORP: oxidation-reduction potential, TLI: trophic level index*

	XX01spr	XX04spr	XX07spr	XX01sum	XX04sum	XX07sum	XX01aut	XX04aut	XX07aut	XX01win	XX04win	XX07win
TP(mg/L)	0.20	0.24	0.41	0.08	0.15	0.26	0.07	0.08	0.05	0.15	0.17	0.20
P-PO_4(mg/L)	0.16	0.14	0.27	0.10	0.01	0.05	0.07	0.06	0.04	0.13	0.17	0.19
N-NH_4(mg/L)	0.12	0.14	0.04	0.02	0.05	0.07	0.03	0.03	0.03	0	0	0.02
N-NO_3(mg/L)	1.54	0.80	0.11	1.00	0.84	0.12	1.47	1.22	1.11	1.73	1.39	1.33
TN(mg/L)	1.77	1.24	0.91	1.6	2.17	1.34	1.55	1.47	1.19	1.84	1.47	1.45
COD(mg/L)	1.13	1.94	3.76	2.59	3.76	3.69	1.86	1.86	2.18	1.2	1.24	1.28
WT(°C)	17.40	18.70	21.10	29.60	28.70	29.50	24.50	24	24.10	12.80	12.20	12.4
DO(mg/L)	7.96	12.3	18	12.5	8.16	15.6	7.7	7.3	7.81	9.18	9.74	9.01
ORP(mV)	255	211.7	192.1	61.2	61.6	48.1	104.6	95.2	88.7	304.1	295.7	298
pH	8.24	8.83	9.43	9.31	9.08	9.75	8.68	8.81	8.85	8.19	8.34	8.28
Turbidity(NTU)	1.30	5.80	6.10	8.20	18	17.80	1.40	2.40	2.10	1.20	1.10	1.20
TLI	50.71	60.97	62.25	54.41	61.44	64.46	49.58	51.7	48.95	52.44	54.52	52.83

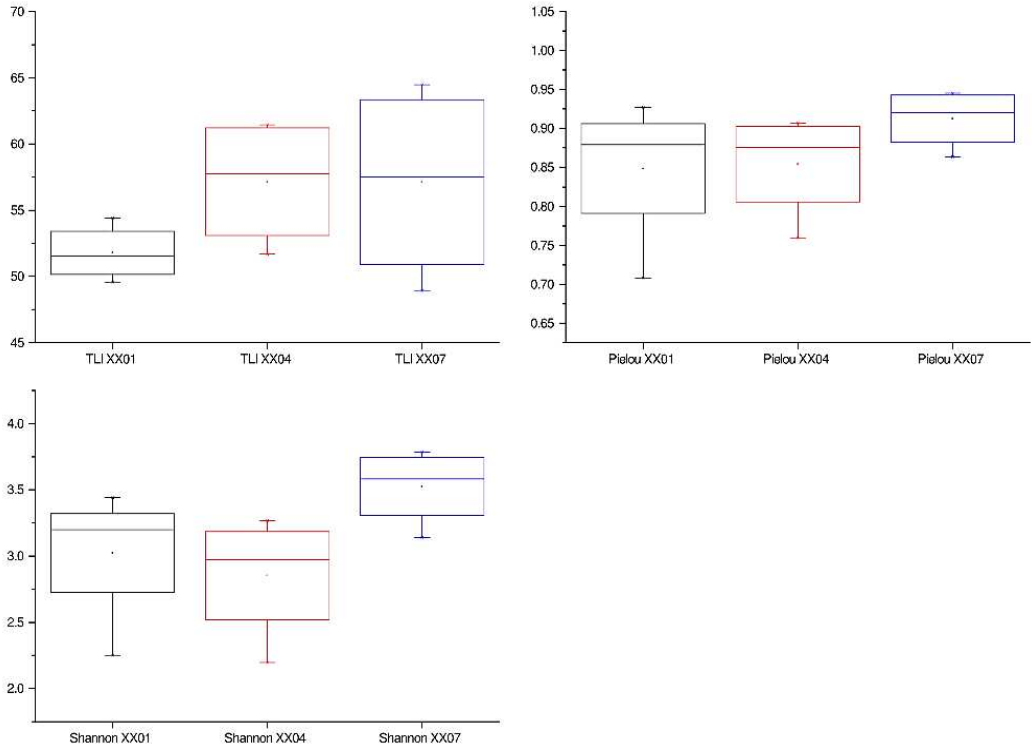

Figure A1. *Nutritional status and diversity index plot. TLI: trophic level index. Median is indicated by the center lines, arithmetic average is indicated by the hollow circle*

http://www.aloki.hu ● ISSN 1589 1623 (Print) ● ISSN 1785 0037 (Online)
DOI: http://dx.doi.org/10.15666/aeer/1605_71157128
© 2018, ALÖKI Kft., Budapest, Hungary

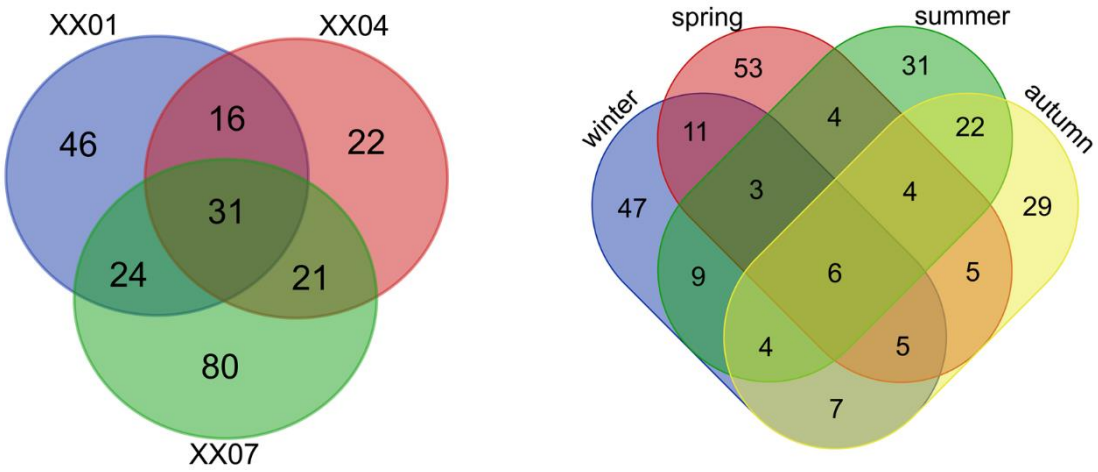

Figure A2. *Venn diagrams showing shared and unique season and sample sites OTUs based on clone libraries*

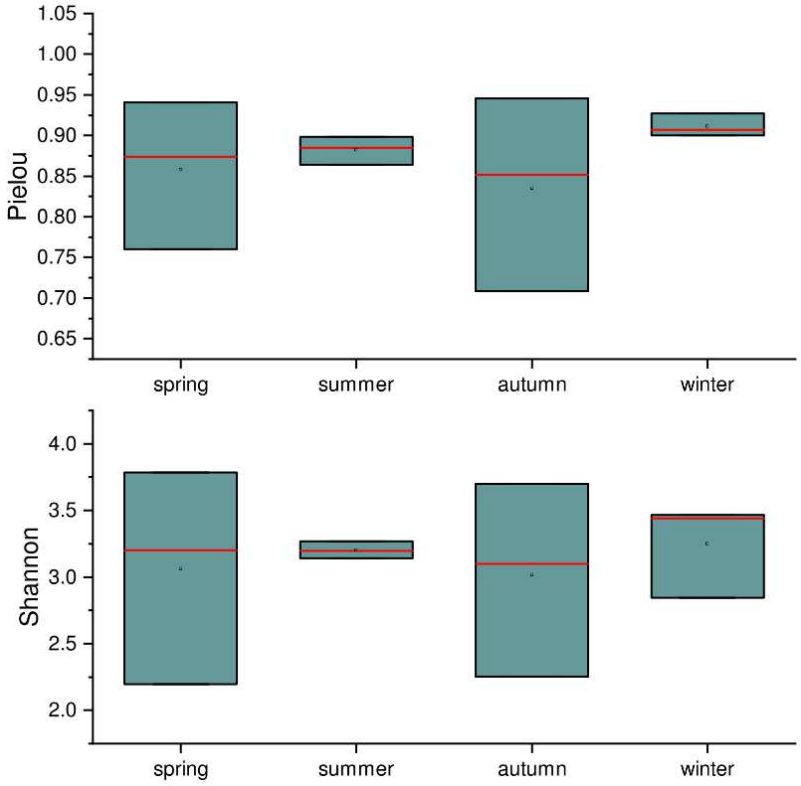

Figure A3. *Boxplot of the Shannon and Pielou evenness indexes among the four seasons. Median is indicated by the red center lines, arithmetic average is indicated by the black hollow circle*

http://www.aloki.hu ● ISSN 1589 1623 (Print) ● ISSN 1785 0037 (Online)
DOI: http://dx.doi.org/10.15666/aeer/1605_71157128
© 2018, ALÖKI Kft., Budapest, Hungary

CHANGING POTENTIAL DISTRIBUTION OF GRAY WOLF UNDER CLIMATE CHANGE IN LAKE DISTRICT, TURKEY

SUEL, H.[1*] – MERT, A.[2] – YALCINKAYA, B.[2]

[1]*Department of Forestry, Sütçüler Vocational School, University of Applied Science Isparta 32950 Isparta, Turkey*

[2]*Department of Wildlife Ecology and Management, Faculty of Forestry, University of Applied Science Isparta, 32260 Isparta, Turkey*
(e-mail: ahmetmert@isparta.edu.tr, bernayalcinkaya48@gmail.com)

**Corresponding author*
e-mail: halilsuel@isparta.edu.tr; phone: +90-530-153-0577; fax: +90-246-351-2901

(Received 1st Aug 2018; accepted 28th Sep 2018)

Abstract. The increase of human activities in recent years has led to many adverse effects and accelerated climate change at an important level. Therefore, it is very important to know how species will be affected by climate change. This study aimed to determine how the distribution of Gray wolf (*Canis lupus*), one of the most important predator species in the ecosystem, will be affected by climate change. The study was carried out using presence data of this species in the Lake District and the changes in the habitats and distribution of Gray wolf according to the RCP 4.5 and RCP 8.5 (HADGEM2-ES) climate scenarios. We conducted mapping and modelling of the current habitat preferences of Gray wolf using MaxEnt method based on the bioclimatic features derived from the Worldclim. 4 bioclimatic variables (BIO12, BIO13, BIO16 and BIO19), and 3 environmental variables (slope, ruggedness, topographic position index) were used in the study. The model and maps of the Gray wolf were compared with the future climate scenarios. In conclusion, it is projected that habitats which are determined as suitable for Gray Wolf will decline significantly due to climate change.
Keywords: *climate change, GIS, Canis lupus, HADGEM2-ES, MaxEnt*

Introduction

Adverse effects of global climate change on ecological systems are increasing day by day. One of the most striking results of global climate change is that Earth's climate has warmed by about 0.6°C over the past century and it is estimated that it will increase by 1.4-5.8°C in the next century. Regional changes have also been observed in rainfall and humidity levels in the proportion to the rising global temperature (Bellard et al., 2012; Collins et al., 2013; Trenberth et al., 2014).

Changes in the climate are presented in the report prepared by the IPCC (Intergovernmental Panel on Climate Change) and made available to researchers. The data is updated by the IPCC periodically and different scenarios for the future are presented. The last of these reports (IPCC 5th Assessment Report) was announced to the world in Sweden in September 2013 (IPCC, 2013). A report on climate change in Turkey was also prepared by Turkey's State Meteorological Service. In this report, regional climate projections produced by downscaling methods for Turkey were based on global models in the CIMIP5 (Coupled Model Intercomparison Project Phase 5) project and the RCP (Representative Concentration Pathways) scenarios created for the IPCC 5th Assessment Report. RCP 4.5 (which we can describe as moderate) and RCP 8.5 (which we can characterize as pessimistic) were selected. According to the temperature and rainfall projections obtained using HadGEM2-ES (Hadley Centre

http://www.aloki.hu ● ISSN 1589 1623 (Print) ● ISSN 1785 0037 (Online)
DOI: http://dx.doi.org/10.15666/aeer/1605_71297137
© 2018, ALÖKI Kft., Budapest, Hungary

Global Environment Model version 2- Earth System) based on RCP 4.5 scenario for Turkey, it is estimated that temperatures in 2050 will have limited to rise approximately 2 C and precipitation will have decreased by nearly 20% throughout the whole country. It is also expected that in 2070 temperatures will have increased by 4 C and precipitation will have decrease decreased by 40% especially in summer. According to the temperature and rainfall projections produced using HadGEM2-ES based on RCP 8.5 scenario for Turkey, it is predicted that in 2050, temperatures will have increased by about 5 C and precipitation will have decreased by about 50%, in 2070 temperatures will have increased by 6°C, especially in the summer, and rainfall will have decreased by 50% especially in summer (Akcakaya et al., 2013; Demir et al., 2013; Demircan et al., 2017).

The changes in precipitation and temperatures will affect all living organisms. Most of the research on this subject has focused on plant species and wild animals because these species can easily be affected by climate change challenges and respond in different ways to this situation (Bellard et al., 2012; Gamfeldt et al., 2013). Therefore, the reactions of all species in the food chain to climate change need to be evaluated for sustainability of ecosystems. For this reason, conservationists and researchers need to detect species that are likely to be most affected by the impacts of climate change in order to minimize biodiversity losses due to climate change and the most appropriate approaches should be selected. Therefore, many recent studies have concentrated on modelling species based on ecological needs and projecting those needs onto modelled future climate regimes to predict future potential distributions (Braunisch et al., 2013; Domisch et al., 2013; Porfirio et al., 2014; Pacifici et al., 2015).

Large predators which constitute the top of the food chain are among the most affected species by changes in precipitation and temperature (Gilman et al., 2010). Gray wolves (*Canis lupus*) may be the most affected large mammalian carnivore by the mentioned negative factors in Turkey.

In addition, these species are in a wide range of motion, especially for searching for food. It is thought that these behaviours often lead them to conflict with humans and livestock, thereby increasing extinction risk (Behdarvand et al., 2014; Ripple et al., 2014). When previous studies on this species in Turkey are examined, it is seen that these studies are limited and generally were carried on population estimates. In these studies, it is stated that the number of individuals belonging to this species is about 5000-7000 (Can, 2008; Akbaba and Ayas, 2012). Contrary to traditional studies, species distribution maps created using modeling techniques for protection of these species are an important basis for conservationists (Guisan et al., 2013; Fourcade et al., 2014). The MaxEnt method, which is one of the modelling techniques used to identify high-quality habitats and determine the ecological factors that are effective in the distribution of species, is a widely preferred modelling and mapping method (Phillips et al., 2004; Barbet-Massin et al., 2012; Mesler, 2015). In this study, it is thought that this method will be useful in estimating the potential distribution of Gray wolf under climate change and monitoring the differences that may occur in future distribution.

The aims of the present study carried out in Lake District are as follows: i) to take inventory of Gray wolf in this area, ii) to determine the climatic factors and environmental variables affecting the distribution of Gray wolf for the present iii) to determine the appropriate habitats for the species by creating the current potential distribution map, and iv) to determine the future potential distribution of species taking future climate scenarios into account (RCP 4.5 and RCP 8.5 scenarios).

http://www.aloki.hu ● ISSN 1589 1623 (Print) ● ISSN 1785 0037 (Online)
DOI: http://dx.doi.org/10.15666/aeer/1605_71297137
© 2018, ALÖKI Kft., Budapest, Hungary

Materials and methods

Site description

The study area, Lake District, is located in the Western Mediterranean Region between 38°25'-36°06' N latitudes and 29°30'-32°34' E longitudes according to the UTM coordinate system in Turkey (*Fig. 1*). In terms of climate characteristics, the study area has a very high variation, especially depending on elevation differences. It is possible to say that the average annual precipitation values in the region are between 600-1300 mm and the annual mean temperature values vary between 12°C and 20°C. The summer drought period in the region lasts for approximately 2-4 months. In general, the area has a transitional climate between the Mediterranean climate and the continental climate. Red pine (*Pinus brutia* Ten.), Black pine (*Pinus nigra* Arnold.), various oak species, and juniper species are dominant forest trees in the region.

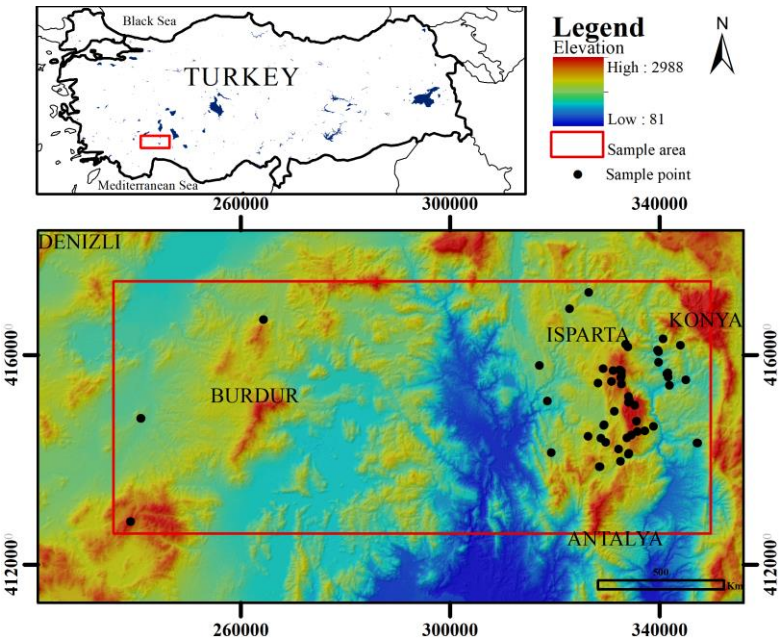

Figure 1. *Geographical location of the study area and presence data of Gray wolf*

Sampling method

Tracks and signs of Gray wolf were recorded on field cards by using indirect inventory techniques during the field study. Thus, from 2014 to 2016, feeding signs, footprints, faeces, burrows, and signs of predation belonging to Gray wolf were recorded as presence data at 59 sample points by using absence-presence inventory techniques (Baddeley, 1985).

Data and statistical evaluation

Scenarios and projections (*Table 1*) updating at regular intervals were presented in the report prepared by the IPCC and made available to researchers (IPCC, 2013). In this study, 2 of 4 different scenarios, namely RCP 4.5 (which we can describe as moderate) and RCP 8.5 which we can characterize as pessimistic, were selected to create habitat suitability maps of Gray wolf for future scenarios.

http://www.aloki.hu ● ISSN 1589 1623 (Print) ● ISSN 1785 0037 (Online)
DOI: http://dx.doi.org/10.15666/aeer/1605_71297137
© 2018, ALÖKI Kft., Budapest, Hungary

Table 1. *Types of representative concentration pathways (RCP's) (based on IPCC, 2013)*

Name of RCP's	Radiative forcing	Time	Pathway shape	Concentration (ppm)	Emissions (Kyoto Protocol's greenhouse gases)
RCP 8.5	>8.5 W/m2	In 2100	Rising	> ~1370 CO2-eq in 2100	Rising continues until 2100
RCP 6.0	~6.0 W/m2	At stabilization after 2100	Stabilization without overshoot	~850 CO2-eq (at stabilization after 2100)	Decline in the last quarter of century
RCP 4.5	~4.5 W/m2	At stabilization after 2100	Stabilization without overshoot	~650 CO2-eq (at stabilization after 2100)	Decline from the mid-century
RCP2.6-PD*	~3.0 W/m2	Peak at before 2100 and then decline	Peak and decline	Peak at ~490 CO2-eq before 2100 and then decline	Decline in the first quarter of century

Climate maps were obtained primarily for modelling and mapping. In order to create these maps, 19 different bioclimatic data (available at http://www.worldclim.org) generated by Hijmans et al. (2005) was downloaded in ascii format on a world scale, and then was cut according to the scale of the study area and made ready for use. In the same way, the bioclimatic data to be used in future scenarios (2050, HadGEM2-ES RCP 4.5 and 8.5 scenarios; 2070, HadGEM2-ES RCP 4.5 and 8.5 scenarios) were prepared.

In the next step, maps of environmental variables were created with ArcMap 10.2 software. Firstly, slope, aspect, and elevation maps were created by digital elevation model (DEM) of the study area. Topographic position index, landform position index, ruggedness index, roughness index, topographic convergence index, hill shade index, solar illumination index (6am, 8am, 10am, noon, 2pm, 4pm, 6pm, 8pm), and solar radiation index were then created. Finally, aspect suitability index (ASI) (*Eq. 1*), radiation index (RI) (*Eq. 2*) and heat index (SI) values are calculated and mapped. Finally, using different equations; aspect suitability index (ASI), radiation index (RI) and heat index (HI) (*Eq. 3*) values are calculated and mapped using different equations. The equations for these indices are as follows:

$$\mathrm{ASI} = \cos(Amax - A) + 1 \quad \text{(Eq.1)}$$

$$\mathrm{RI} = \frac{[1 - \cos((\pi/180)(Q - 30))]}{2} \quad \text{(Eq.2)}$$

$$\mathrm{HI} = \cos(A - Amax) * \tan\left(radian(slope)\right) \quad \text{(Eq.3)}$$

where the value of Amax is 202.50. A, refers to the radian value of aspect. Q refers to aspect. The value of π was taken as 3.14159265.

Bioclimatic variables have a high correlation with each other (Süel, 2014). If there is a high correlation between the variables, accuracy and reliability of obtained models decrease. For this reason, Pearson correlation analysis and factor analysis were applied to bioclimatic variables by SPSS software.

MaxEnt 3.4.1 software was used for the determination and modelling of the variables that are effective in the distribution of Gray wolf. For the analysis, the data matrix consisting of bioclimatic variables and environmental variables was recorded as "ascii" file. The presence data of Gray wolf was saved as "csv" file. The data was analyzed via cross validation with 90% training data of the model, 10% test data, and 10 replications. The success of the obtained models was assessed according to area under the curve

http://www.aloki.hu ● ISSN 1589 1623 (Print) ● ISSN 1785 0037 (Online)
DOI: http://dx.doi.org/10.15666/aeer/1605_71297137
© 2018, ALÖKI Kft., Budapest, Hungary

(AUC) values in the receiver operating characteristic (ROC) curve. If the model's AUC value is close to 1, the model is perfect. If it is closer to 0.7, it is descriptive; however, if it is 0.5, the model is invalid (Phillips et al., 2004).

As a result of this analysis, the current potential distribution model of the Gray wolf was obtained and the variables affecting the distribution were determined. This model was then simulated for 2050 (HadGEM2-ES RCP 4.5 and 8.5 scenario) and 2070 (HadGEM2-ES RCP 4.5 and 8.5 scenario).

Results

Presence data of Gray wolf was recorded in 59 sampling points. Pearson correlation analysis and factor analysis were applied to climatic variables due to high correlations among them.

As a result of the factor analysis, four different bioclimatic variables with the best representation ability were obtained: BIO12 (Annual Precipitation), BIO13 (Precipitation of Wettest Month), BIO16 (Precipitation of Wettest Quarter) and BIO19 (Precipitation of Coldest Quarter).

13 different current potential distribution models were obtained for the Gay wolf and the 13th model was chosen as the most suitable model according to AUC values in the ROC curve. The training data AUC value is 0.937 and the test data AUC value is 0.920 for this model (*Fig. 2*). When the variables affecting the distribution of Gray wolf in the conclusion model were examined, BIO12 (23%), BIO13 (18.5%), and BIO16 (21.3%) were determined as bioclimatic factors and heat index (14%), aspect (12.4%), and topographic position index (10.8%) were determined as environmental variables.

As a result of simulating the variables obtained in the current habitat suitability model for Gray wolf into the future scenarios, a model with AUC training value of 0.942 and AUC test value of 0.939 was obtained (*Fig. 3*).

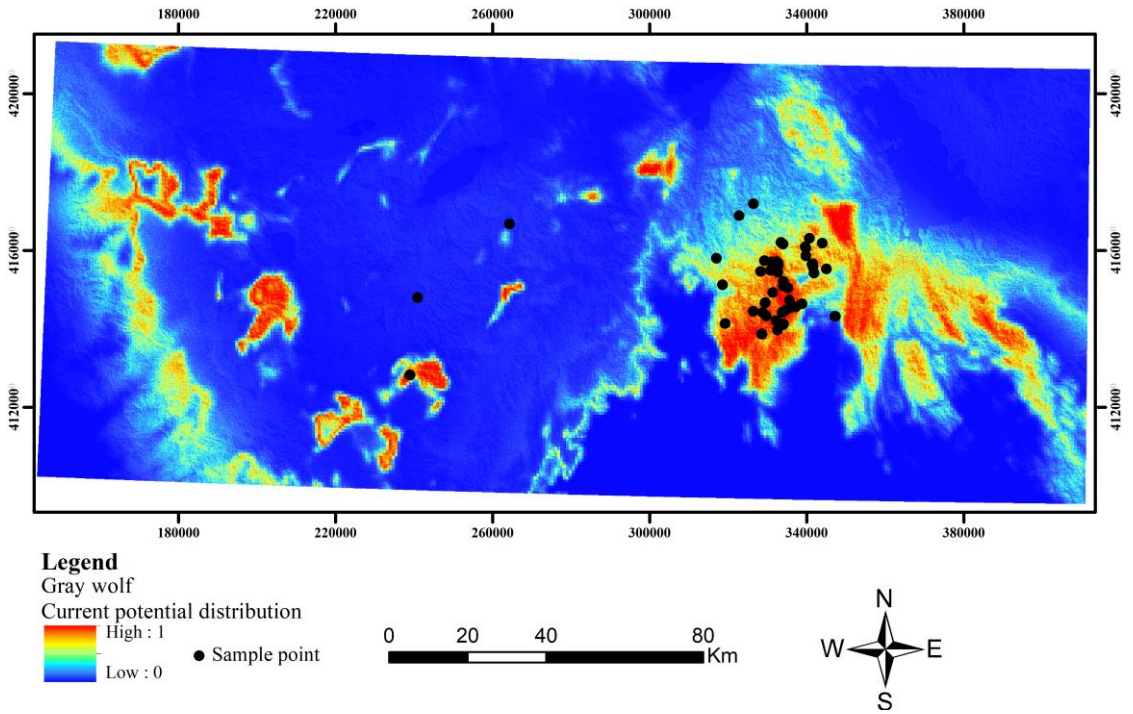

Figure 2. *Current habitat suitability maps of Gray wolf*

http://www.aloki.hu ● ISSN 1589 1623 (Print) ● ISSN 1785 0037 (Online)
DOI: http://dx.doi.org/10.15666/aeer/1605_71297137
© 2018, ALÖKI Kft., Budapest, Hungary

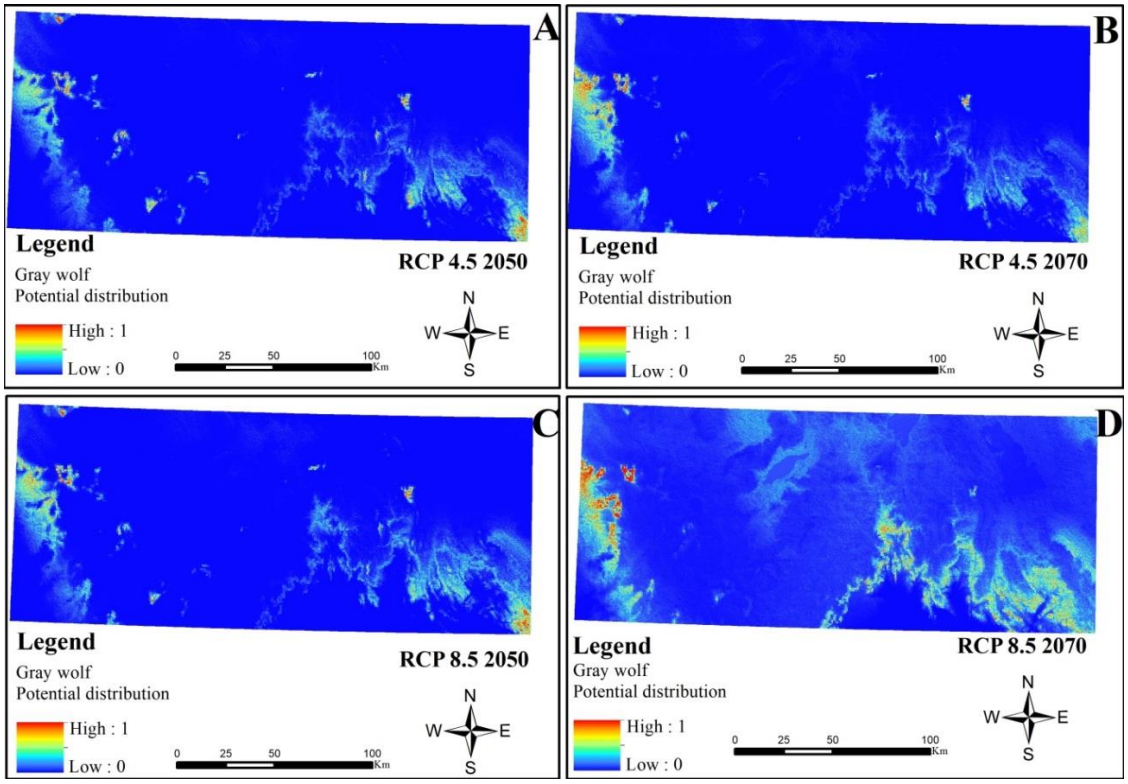

Figure 3. *Habitat suitability maps of Gray wolf for future scenarios. A: HADGEM2-ES RCP 4.5 2050, B: HADGEM2-ES RCP 4.5 2070, C: HADGEM2-ES RCP 8.5 2050, D: HADGEM2-ES RCP 8.5 2070*

Discussion

When the current habitat suitability model for Gray wolf is examined using variables ((BIO12 (23%), BIO13 (18.5%), BIO16 (21.3%), heat index (14%), aspect (12.4%), topographic position index (10.8%)) which formed the model, it is determined that precipitation and temperature are the most important factors limiting the distribution of this species According to *Figure 2*, high zones and the eastern part of the study area are more preferred by this species (red coloured areas in maps). However, when the habitat suitability maps (*Fig. 3*) generated for HADGEM2-ES RCP 4.5 (2050; 2070) and HADGEM2-ES RCP 8.5 (2050; 2070) are examined, it is seen that there would be a significant change in distribution. In other words, depending on climate change, the distribution of the Gray wolf will be affected and the species will migrate in search of a different habitat.

According to the scenario RCP 4.5 2050 (HADGEM2-ES), there is a decrease in the distribution of the wolves, a deviation towards the interior and coastal areas at the same time. A similar change is also observed in the habitat suitability map created for the RCP 4.5 2070 (HADGEM2-ES) scenario (*Fig. 3*). However, according to the scenario RCP 4.5 2070 (HADGEM2-ES), this distribution is concentrated towards the western part of the area, whereas the current habitat suitability map shows a distribution in the eastern part of the area. It is thought that the rise in temperature and the decrease in precipitation will cause these changes (Larsen and Ripple, 2006). At the same time, prey species, which are preferred by target species in the field, should be taken into account as to how they will react to possible changes in the future climate. When

http://www.aloki.hu ● ISSN 1589 1623 (Print) ● ISSN 1785 0037 (Online)
DOI: http://dx.doi.org/10.15666/aeer/1605_71297137
© 2018, ALÖKI Kft., Budapest, Hungary

studies on feeding behaviour of the target species in literature are examined, it is stated that they move seasonally by following migratory prey species in their region due to nutritional needs despite being a non-immigrant species (Hof et al., 2012; Metz et al., 2012). In view of this information, it is thought that the hunting species in the area may be another important factor for the change in the distribution of the target from east to west according to the HADGEM2-ES RCP 4.5 scenarios. Diet types of this species vary depending on age, sex, and season. There are also several conditions (weather conditions, the vulnerability of prey species, and wolf density in the region etc.) limiting food availability of Gray wolf (Stahler et al., 2006; Metz et al., 2012).

When habitat suitability maps created according to the scenarios of HADGEM2-ES RCP 8.5, 2050, and 2070 are examined, it is predicted that the potential distribution of goal species in the region will reduce considerably and the distribution will shift to the west and north-west. It is seen that in studies conducted on the general behavior of the species, before setting a new territory or joining any wolf pack, the male wolf can move about 113 km and their females can move about 78 km. In some cases, they can even show a distribution over 840 km. It is also known that the species prefer to habitat as high as possible, avoiding human influence (Treves and Karanth, 2003).

It is estimated that Gray wolf with high metabolic demand and long distance mobility (Walker and Churchill, 2014) can use coastal areas of the region for any reason such as diet and reach up to Central Anatolia. As can be seen from the HADGEM2-ES RCP 8.5 scenarios, especially in the habitat conformity map created for 2070, it is proven that coastal area is suitable for distribution of this species. However, it is also probable that human activity which is increasing in coastal areas especially in summer months will limit the movement of the species. To sum up, Gray wolf has to be able to force itself to more movement in order to reduce the effect of negative conditions that will occur in the climate and to be able to return to higher parts where it will feel safe and secure after satisfying its basic needs. According to the habitat suitability maps obtained for both scenarios, it is seen that the results support each other and the distribution of Gray wolf in the region will be affected negatively.

Conclusion

In conclusion, it is predicted that Gray wolf's habitats will be affected by climate change in the future; however, this situation can be tolerated by the high mobility of this species. Nevertheless, it is clearly seen that there are significant differences between the current potential distribution areas shown in *Figure 2* and the potential distribution areas determined for the future scenarios in *Figure 3*. Due to decreases in the suitable habitats, it is expected that the conflict of this species with human and other animal groups will increase. To sum up, present study should be supported by more detailed studies performed by determining all the variables affecting the habitat in order to prevent the extinction of this species.

Acknowledgements. We thank to project 4123- YL1-14 supported by the Coordination Unit for Scientific Research Projects, Süleyman Demirel University.

http://www.aloki.hu ● ISSN 1589 1623 (Print) ● ISSN 1785 0037 (Online)
DOI: http://dx.doi.org/10.15666/aeer/1605_71297137
© 2018, ALÖKI Kft., Budapest, Hungary

REFERENCES

[1] Akbaba, B., Ayas, Z. (2012): Camera trap study on inventory and daily activity patterns of large mammals in a mixed forest in north-western Turkey. – Mammalia 76(1): 43-48.

[2] Akcakaya, A., Eskioglu, O., Atay, H., Demir, O. (2013): Yeni senaryolar ile Türkiye için iklim değişikliği projeksiyonları. – Meteoroloji Genel Müdürlüğü Matbaası, Turkey.

[3] Barbet-Massin, M., Jiguet, F., Albert, C. H., Thuiller, W. (2012): Selecting pseudo-absences for species distribution models: How, where and how many? – Methods in Ecology and Evolution 3(2): 327-338.

[4] Baddeley, C. J. (1985): Assessments of wild animal abundance. – Forest Research Institute Bulletin 106: 1-46.

[5] Behdarvand, N., Kaboli, M., Ahmadi, M., Nourani, E., Mahini, A. S., Aghbolaghi, M. A. (2014): Spatial risk model and mitigation implications for wolf–human conflict in a highly modified agroecosystem in western Iran. – Biological Conservation 177: 156-164.

[6] Bellard, C., Bertelsmeier, C., Leadley, P., Thuiller, W., Courchamp, F. (2012): Impacts of climate change on the future of biodiversity. – Ecology Letters 15(4): 365-377.

[7] Braunisch, V., Coppes, J., Arlettaz, R., Suchant, R., Schmid, H., Bollmann, K. (2013): Selecting from correlated climate variables: a major source of uncertainty for predicting species distributions under climate change. – Ecography 36(9): 971-983.

[8] Can, O. E. (2008): Camera trapping large mammals in Yenice Forest habitats: A feasibility study for camera trapping large mammals in Yenice Forests, Turkey. – Doctoral Dissertation, Orta Doğu Teknik University, Ankara, Turkey.

[9] Collins, M., Knutti, R., Arblaster, J., Dufresne, J. L., Fichefet, T., Friedlingstein, P., Gao, X., Gutowski, W. J., Johns, T., Krinner, G., Shongwe, M., Tebaldi, C., Weaver, A. J., Wehner, M. (2013): Long-term Climate Change: Projections, Commitments and Irreversibility. – In: Stocker, T. F., Qin, D., Plattner, G. K., Tignor, M., Allen, S. K., Boschung, J., Nauels, A., Xia, Y., Bex, V., Midgley, P. M. (eds.) Climate Change 2013: The Physical Science Basis. Contribution of Working Group I to the Fifth Assessment Report of the Intergovernmental Panel on Climate Change. Cambridge University Press, Cambridge, UK and New York.

[10] Demir, O., Atay, H., Eskioglu, O., Tuvan, A., Demircan, M., Akcakaya, A. (2013): RCP 4. 5 Senaryosuna göre Türkiye'de sıcaklık ve yağış projeksiyonları. – III. Türkiye İklim Değişikliği Kongresi-TIKDEK, 3-5.

[11] Demircan, M., Gurkan, H., Eskioglu, O., Arabaci, H., Coskun, M. (2017): Türkiye için iklim değişikliği projeksiyonları: Üç model ve iki senaryo. – Türkiye Su Bilimleri ve Yönetimi Dergisi 1(1): 22-43.

[12] Domisch, S., Araújo, M. B., Bonada, N., Pauls, S. U., Jähnig, S. C., Haase, P. (2013): Modelling distribution in European stream macroinvertebrates under future climates. – Global Change Biology 19(3): 752-762.

[13] Fourcade, Y., Engler, J. O., Rodder, D., Secondi, J. (2014): Mapping species distributions with MaxEnt using a geographically biased sample of presence data: A performance assessment of methods for correcting sampling bias. – PloS One 9(5): e97122.

[14] Gamfeldt, L., Snäll, T., Bagchi, R., Jonsson, M., Gustafsson, L., Kjellander, P., Ruiz-Jaen, C. M., Froberg, M., Stendahl, J., Philipson, D. C., Andersson, E., Westerlund, B., Andrén, H., Moberg, F., Moen, J., Bengtsson, J. (2013): Higher levels of multiple ecosystem services are found in forests with more tree species. – Nature Communications 4: 1340.

[15] Gilman, S. E., Urban, M. C., Tewksbury, J., Gilchrist, G. W., Holt, R. D. (2010): A framework for community interactions under climate change. – Trends in Ecology & Evolution 25(6): 325-331.

[16] Guisan, A., Tingley, R., Baumgartner, J. B., Naujokaitis-Lewis, I., Sutcliffe, P. R., Tulloch, A. I., Regan, J. T., Brotons, L., Mcdonald-Madden, E., Mantyka-Pringle, C., Martin, G. T., Rhodes, R. J., Maggini, R., Setterfield, A. S., Elith, J., Schwartz, W. M.,

http://www.aloki.hu ● ISSN 1589 1623 (Print) ● ISSN 1785 0037 (Online)
DOI: http://dx.doi.org/10.15666/aeer/1605_71297137
© 2018, ALÖKI Kft., Budapest, Hungary

Wintle, A. B., Broennimann, O., Austin, M., Ferrier, S., Kearney, R. M., Possingham, P. H., Buckley, M. Y. (2013): Predicting species distributions for conservation decisions. – Ecology Letters 16(12): 1424-1435.

[17] Hijmans, R. J., Cameron, S. E., Parra, J. L., Jones, P. G., Jarvis, A. (2005): Very high resolution interpolated climate surfaces for global land areas. – International Journal of Climatology 25(15): 1965-1978.

[18] Hof, A. R., Jansson, R., Nilsson, C. (2012): How biotic interactions may alter future predictions of species distributions: future threats to the persistence of the arctic fox in Fennoscandia. – Diversity and Distributions 18(6): 554-562.

[19] IPCC (Intergovernmental Panel on Climate Change) (2013): Climate Change: The Physical Science Basis. Summary for Policy Makers. – http://www.ipcc.ch/ (accessed on 01.03.2018).

[20] Larsen, T., Ripple, W. J. (2006): Modeling Gray wolf (*Canis lupus*) habitat in the Pacific Northwest, USA. – Journal of Conservation Planning 2(1): 30-61.

[21] Mesler, J. I. (2015): Modeling habitat suitability and connectivity of Gray wolf (*Canis lupus*) populations in the Pacific Northwest. – Doctoral Dissertation, Humboldt State University, Arcata, CA.

[22] Metz, M. C., Smith, D. W., Vucetich, J. A., Stahler, D. R., Peterson, R. O. (2012): Seasonal patterns of predation for gray wolves in the multi-prey system of Yellowstone National Park. – Journal of Animal Ecology 81(3): 553-563.

[23] Pacifici, M., Foden, W. B., Visconti, P., Watson, J. E., Butchart, S. H., Kovacs, K. M., Scheffers, R. B., Hole, G. D., Martin, G. T., Akcakaya, R. H., Corlett, R. T., Huntley, B., Bickford, D., Carr, A. J., Hoffmann, A. A., Midgley, F. G., Pearce-Kelly, P., Pearson, G. R., Williams, E. S., Willis, G. S., Young, B., Rondinini, C. (2015): Assessing species vulnerability to climate change. – Nature Climate Change 5(3): 215.

[24] Phillips, S. J., Dudík, M., Schapire, R. E. (2004): A maximum entropy approach to species distribution modeling. – Proceedings of the Twenty-First International Conference on Machine Learning, Banff, Alberta, Canada, pp. 655-662.

[25] Porfirio, L. L., Harris, R. M., Lefroy, E. C., Hugh, S., Gould, S. F., Lee, G., Bindoff, L. N., Mackey, B. (2014): Improving the use of species distribution models in conservation planning and management under climate change. – PLoS One 9(11): e113749.

[26] Ripple, W. J., Estes, J. A., Beschta, R. L., Wilmers, C. C., Ritchie, E. G., Hebblewhite, M., Schmitz, O. J. (2014): Status and ecological effects of the world's largest carnivores. – Science 343(6167): 151-162.

[27] Stahler, D. R., Smith, D. W., Guernsey, D. S. (2006): Foraging and feeding ecology of the Gray wolf (*Canis lupus*): lessons from Yellowstone National Park, Wyoming, USA. – The Journal of Nutrition 136(7): 1923-1926.

[28] Süel, H. (2014): Mapping habitat suitability of game animals in Sütçüler district, Isparta. – Doctoral Dissertation, Suleyman Demirel University, Isparta.

[29] Trenberth, K. E., Dai, A., Van Der Schrier, G., Jones, P. D., Barichivich, J., Briffa, K. R., Sheffield, J. (2014): Global warming and changes in drought. – Nature Climate Change 4(1): 17.

[30] Treves, A., Karanth, K. U. (2003): Human-carnivore conflict and perspectives on carnivore management worldwide. – Conservation Biology 17(6): 1491-1499.

[31] Walker, C. S., Churchill, S. E. (2014): Territory Size in *Canis lupus*: Implications for Neandertal Mobility. – In: Carlson, K., Marchi, D. (eds.) Reconstructing Mobility. Springer, Boston, MA.

http://www.aloki.hu ● ISSN 1589 1623 (Print) ● ISSN 1785 0037 (Online)
DOI: http://dx.doi.org/10.15666/aeer/1605_71297137
© 2018, ALÖKI Kft., Budapest, Hungary

QUALITY CHARACTERISTICS OF THE MIXTURES OF SOME WARM SEASON PERENNIAL GRASSES WITH ALFALFA (*MEDICAGO SATIVA* L.) UNDER IRRIGATED CONDITIONS IN THE MEDITERRANEAN REGION OF TURKEY

CINAR, S.[1,2*] – HATIPOGLU, R.[3] – AVCI, M.[4] – GUNDEL, F. D.[5] – AKTAS, A.[5]

[1]*Department of Horticulture and Field Crops, Faculty of Agriculture, Kyrgyz-Turkish Manas University, Bishkek, Kyrgyzstan*

[2]*Department of Plant and Animal Production, Technical Vocational School, Kilis 7 Aralik University, Kilis, Turkey*

[3]*Department of Field Crops, Faculty of Agriculture, Cukurova University, Adana, Turkey*

[4]*Faculty of Plant Production and Technology, Nigde Omer Halisdemir University Nigde, Turkey*

[5]*East Mediterranean Agricultural Research Institue, Adana, Turkey*

**Corresponding author*
e-mail: scinar01@hotmail.com

(Received 3rd Aug 2018; accepted 8th Oct 2018)

Abstract. This study was conducted to determine forage quality characteristics of duo (alfalfa + one grass) and trio (alfalfa + two grasses) mixtures of some warm season perennial grass species such as dallis grass (*Paspalum dilatatum* Poir.), Rhodes grass (*Chloris gayana* L.), Bermuda grass (*Cynodon dactylon* (L.) Pers.) Guineae grass (*Panicum maximum* Jacq.), blue couch grass (*Digitaria didactyla* Willd) and finger grass (*Digitaria milanjiana* (Rendle) Stapf) with alfalfa as well as their pure sowings under irrigated conditions in the Mediterranean region of Turkey during 2010-2012 growing seasons. In the study, crude protein contents, crude protein yields, acid detergent fiber contents (ADF), neutral detergent fiber contents (NDF), digestible dry matter contents (DDM) and relative feed values (RFV) of the mixtures and pure sowings were determined. The experimental design was completely randomized block design with three replications. The results of the study showed that there were significant differences among mixtures and pure sowings in the forage quality characteristics. The highest crude protein yield (3948.5) kg ha^{-1}) was obtained from the mixture of dallis grass + alfalfa. The highest crude protein ratio (20.5%), DDM ratio (68.3%) and RFV (170.88) was obtained from the pure alfalfa. The highest ADF (40.2%) and NDF (70.9%) was obtained from the pure Guinea grass. From the results of the study, it was concluded that Bermuda grass, Rhodes grass, blue couch grass and dallis grass could be used to establish of duo and trio pasture mixtures with alfalfa, having long grazing season and giving high hay quality. Before the establishment of such pasture mixtures, it is needed to search for proper mixture ratios and proper management techniques of the mixtures.
Keywords: *warm season perennial grasses, alfalfa, mixture, forage quality, ADF, NDF, RFV*

Introduction

Quality forage for livestock is produced from natural pastures and forage crops grown under field conditions worldwide. Legume–grass mixtures are easily established in degenerated pasture or field conditions. Legumes are rich in terms of protein contents, whereas grasses have higher carbohydrate contents and can benefit from the nitrogen fixed by legumes when they are grown together. Thus, legume–grass mixtures

http://www.aloki.hu ● ISSN 1589 1623 (Print) ● ISSN 1785 0037 (Online)
DOI: http://dx.doi.org/10.15666/aeer/1605_71397154
© 2018, ALÖKI Kft., Budapest, Hungary

may be more productive than monoculture grasses. Alfalfa (*Medicago sativa* L.) is grown under both irrigated and dry conditions and it may be more productive in mixtures with grasses. Several studies reported that alfalfa–grass mixtures resulted in higher yields and higher nutritional quality as compared with grasses alone (Albayrak and Turk, 2011).

The advantages of cool season legumes in cool season pastures and hay lands have been well documented, but there is little information on mixing legumes with warm season grasses. Some researchers reported that growing warm-season grasses with legumes resulted in higher dry matter yields than pure sowings (Aganoglu, 1985; Blanchet et al., 1995; Larbi et al., 1995; Gettle et al., 1996; Tessema and Baars, 2006; Cinar and Hatipoglu, 2014).

Mediterranean region of the Turkey experiences long periods of drought, especially in mid-summer. High temperatures and low precipitation are detrimental to production of cool season forages. Lack of productivity of cool season pastures during the summer months often results in overgrazing. Perennial warm season grasses produce their yields in midsummer, which could provide forage production during that period (Jung et al., 1978).

Methods to effectively establish and manage some warm season grasses for yield have been characterized for Mediterranean conditions (Cinar and Hatipoglu, 2014). Using the potential of these species to provide a dependable pasture forage supply during summer months warrants investigation of options to enhance their quality.

Rhodes grass is one of the main sub-tropical grasses and is widely grown in Africa, Australia, Japan and South America as well as in the Middle East under irrigation for both forage and soil conservation purposes. Dallis grass is a summer-active perennial grass native to the humid sub-tropics of southern Brazil, Argentina and Uruguay. It is now widespread in many areas of the world, and is capable of very high production under suitable conditions. Bermuda grass has been widely used in tropical and warm temperate regions as a pasture grass and is one of the major turf grasses in the world. Blue couch grass is similar to Bermuda grass. It differs from Bermuda grass in its shorter, broader leaf and its distinctive bluish colour (Skerman and Riveros, 1990).

Guinea grass is widely distributed in the tropical and sub-tropical areas of the world. It can produce over 20 tons dm ha^{-1} but suffers from drought when dry matter production can be reduced to as low as 40% of its yield potential. Guinea grass responds well to cutting and grazing, and is fairly pest resistant (Nung and Binh, 2014).

Finger grass is a native of tropical Eastern and Southern Africa, from Ethiopia down to South Africa. It is found in semiarid to wet equatorial areas, with average annual rainfall between 450 to 1700 mm. It grows in grasslands on sandy loam soils and in open woodlands on heavy black or sandy soils. An annual dry matter yield of up to 15 t/ha has been achieved from well fertilized finger grass. It is very palatable to all types of stock as green feed, dry feed or as hay. It can be used in mixed pastures or as a hay crop. It should not be grazed in the wet season of establishment (Cameron et al., 2010).

This study was conducted to determine forage quality of duo (one grass + alfalfa) and trio (two grass + alfalfa) mixtures of some perennial warm season grass species such as dallis grass (*Paspalum dilatatum* Poir.), Rhodes grass (*Chloris gayana* L.), Bermuda grass (*Cynodon dactylon* (L.) Pers.) Guineae grass (*Panicum maximum* Jacq.), blue couch grass (*Digitaria didactyla* Willd) and finger grass (*Digitaria milanjiana* (Rendle) Stapf) with alfalfa (*Medicago sativa* L.) as well as their pure sowings under irrigated conditions in the Mediterranean region of Turkey.

http://www.aloki.hu ● ISSN 1589 1623 (Print) ● ISSN 1785 0037 (Online)
DOI: http://dx.doi.org/10.15666/aeer/1605_71397154
© 2018, ALÖKI Kft., Budapest, Hungary

This paper was prepaired from a part of data obtained from the research conducted to determine the forage yields and qualities of duo (one grass + alfalfa) and trio (two grass + alfalfa) mixtures of some perennial warm season grass species such as dallis grass (*Paspalum dilatatum* Poir.), Rhodes grass (*Chloris gayana* L.), Bermuda grass (*Cynodon dactylon* (L.) Pers.), Guineae grass (*Panicum maximum* Jacq.), blue couch grass (*Digitaria didactyla* Willd) and finger grass (*Digitaria milanjiana* (Rendle) Stapf) with alfalfa (*Medicago sativa* L.) as well as their pure growings under irrigated conditions in Mediterranean region of Turkey. A paper from data related to the yields and some other characteristics of the mentioned mixtures as well as pure growings had been published (Cinar et al., 2014).

Materials and methods

Materials

The study was carried out during 2011 and 2012 years in Adana province (36°51'N, 35°20'E, elevation 12 m), located in the Mediterranean region of Turkey (*Fig. 1*).

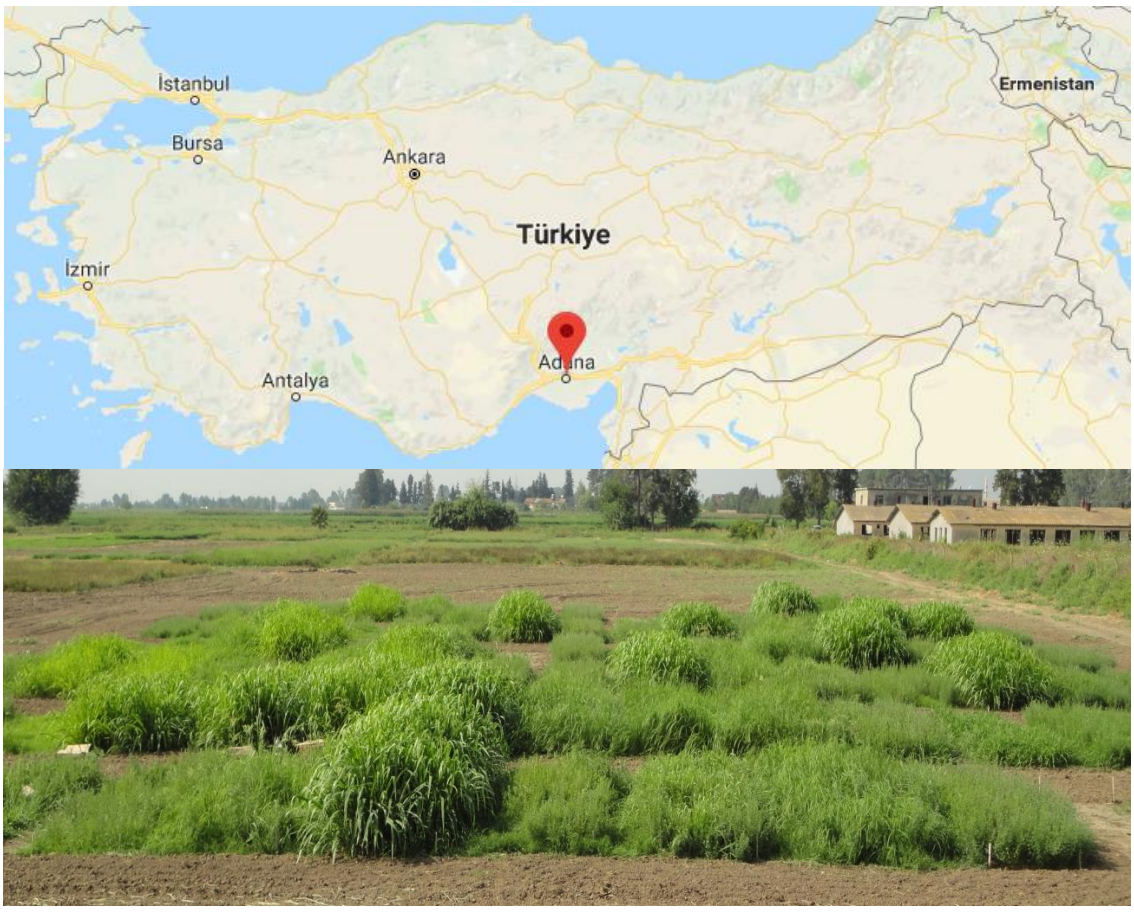

Figure 1. *The map of Turkey and picture of study area*

The experimental area has typically Mediterranean climate with hot and dry summer and heavy precipitation during winter. According to the average of long years, the coolest month is January with a monthly mean temperature of 9.9 °C and the hottest

http://www.aloki.hu ● ISSN 1589 1623 (Print) ● ISSN 1785 0037 (Online)
DOI: http://dx.doi.org/10.15666/aeer/1605_71397154
© 2018, ALÖKI Kft., Budapest, Hungary

month is July with 29.7 °C. The total precipitation was higher in 2011 (687.7 mm) and in 2012 (1048.8 mm) compared with the longterm precipitation mean (647.1 mm). The means of the temperature and relative humidity during the experimental period were close to the long-term means (Anonymous, 2013).

The research area has a flat land; its soil texture is classified as silty clay with slightly alkaline, which contained medium organic matter, poor phosphorus (P), zinc (Zn) and calcium (Ca) contents (Anonymous, 2011).

Dallis grass (*Paspalum dilatatum* Poir.), Rhodes grass (*Chloris gayana* L.), Bermuda grass (*Cynodon dactylon* (L.) Pers.) Guineae grass (*Panicum maximum* Jacq.), blue couch grass (*Digitaria didactyla* Willd), finger grass (*Digitaria milanjiana* (Rendle) Stapf) and alfalfa (*Medicago sativa* L.) were used as experimental material. In the research, duo and trio mixtures of the mentioned grass species with alfalfa as well as their pure sowings were studied.

Methods

The experiment was established according to the randomized complete block design with three replications. There were 28 treatment plots in each block. Each plot consisted of 6 rows each 5 m in length. The row spacing was 25 cm. The seeding rates for dallis grass, Rhodes grass, Bermuda grass, Guineae grass, finger grass, blue couch grass and alfalfa in pure sowing were 11 kg ha^{-1}, 4 kg ha^{-1}, 10 kg ha^{-1}, 6 kg ha^{-1}, 8 kg ha^{-1}, 8 kg ha^{-1} and 10 kg ha^{-1}, respectively. Seed mixtures consisted of 30% alfalfa and 70% grasses. Seed ratio of each grass species in trio mixtures was 35%. The seeds of alfalfa and grass species were sown in the same rows. Sowing was done by hand on May 28th 2011. Plots were fertilized with 100 kg ha^{-1} N and 100 kg ha^{-1} P at sowing (Avci, 2000). The plots were irrigated once after each harvest. The harvest time was based on the 10% flowering stage of alfalfa (Cinar et al., 2014). The plots were harvested at 5 cm cutting height. The plots were harvested 3 and 5 times during the growing season of 2011 and 2012, respectively.

All samples were dried at 70 °C for 48 h and weighed. The samples from the mixture plots were hand-separated to the mixture components before the drying. Dry matter content was determined from ground samples dried at 105 °C for 24 h (Sleugh et al., 2000).

Contents of crude protein, acid detergent fiber (ADF) and neutral detergent fiber (NDF) of samples were determined using Infrared Reflectance Spectroscopy (NIRS) (Hoy et al., 2002; Aydin et al., 2010). NIRS was calibrated using software program coded IC-0904 FE hay and fresh forage.

Crude protein yield (CPY), digestible dry matter yield (DDMY), dry matter intake (DMI), digestible dry matter (DDM) and relative feed value (RFV) were estimated according to the following equations adapted from Sheaffer et al. (1995) (*Eqs. 1–4*):

$$DMI = 120 / (NDF\%) \text{ dry matter basis} \quad \text{(Eq. 1)}$$

$$DDM = 88.9 - (0.779 \times ADF\% \text{ dry matter basis}) \quad \text{(Eq. 2)}$$

$$RFV = (DDM\% \times DMI)/1.29 \quad \text{(Eq. 3)}$$

$$CPY = \text{Crude protein content } (CP\%) \times \text{dry matter yield } (DMY) \quad \text{(Eq. 4)}$$

http://www.aloki.hu ● ISSN 1589 1623 (Print) ● ISSN 1785 0037 (Online)
DOI: http://dx.doi.org/10.15666/aeer/1605_71397154
© 2018, ALÖKI Kft., Budapest, Hungary

Relative feed value (RFV) was calculated by multiplying digestible dry matter by dry matter intake and then dividing by 1.29 (Schroeder, 1994).

Statistical analyses

The experimental design was completely randomized block design with three replications. Data were analyzed by using MSTATC software program (V.1.2, Michigan State University, USA). The differences between means were separated by Duncan multiple range test ($P \leq 0.05$) (Steel and Torrie, 1960).

Results

Crude protein ratio and crude protein yield

The results of the variance analysis showed that the crude protein ratio was influenced by pure sowings and mixtures as well as years. Year x treatment (pure sowings and mixtures) interaction was also statistically significant. Average crude protein ratios in the second year were significantly higher than that in the first year (*Table 1*). The alfalfa sown in April, normally sown in November under Mediterranean conditions, produced lower hay yield than that sown in November in the first year. Therefore contribution of the alfalfa on the yield of the mixtures was significantly lower than those in the second year. Lower alfalfa ratio in the hay yields of mixtures in the first year resulted in the lower averaged crude protein ratio than those in the second year.

In the first year, crude protein content of alfalfa dry matter was statistically significant higher than those of the other pure sowings and all of the mixtures (*Table 1*). The mixtures GG+A gave significantly lower crude protein ratio than pure sowings and other mixtures.

In the second year, the mixture of RG+FG+A produced dry matter with statistically significant higher crude protein content than the all of the pure sowings with the exception alfalfa and all of the other mixtures with the exceptions of RG+GG+A, GG+A, A, FG+A, BG+A, DG+A, RG+A, GG+FG+A, GG+BCG+A and RG+BCG+A. On the other hand, pure sowing of Guinea grass gave significantly lower crude protein content than the pure sowing of Rhodes grass and all of the mixtures. All of the pure sowings of the grasses gave the dry matter with statistically significant lower crude protein content than the pure sowing of alfalfa and all of the mixtures.

According to the averaged values over two years, the highest crude protein ratio was obtained from pure sown alfalfa. Pure sowings of Guinea grass produced the dry matter with significantly lower crude protein content than the other pure sowings and mixtures.

The results of the variance analysis showed that the crude protein yield was influenced by pure sowings and mixtures as well as years. Year x treatment interaction was also statistically significant. The averaged crude protein yield in first year was significantly lower than those in the second year (*Table 2*). The variation in the crude protein yield of the pure sowings and mixtures depending on the years was due to the variation in dry matter yield and crude protein ratio (Cinar et al., 2014; *Table 1*).

In the first year of the experiment, the mixture of RG+A gave statistically significant higher crude protein yield than the pure growings of Bermuda grass and blue couch grass and the mixtures of GG+A, BCG+A, GG+BCG+A and GG+FG+A. In the second year, the mixture of alfalfa + dallis grass gave significantly higher crude protein yield

http://www.aloki.hu ● ISSN 1589 1623 (Print) ● ISSN 1785 0037 (Online)
DOI: http://dx.doi.org/10.15666/aeer/1605_71397154
© 2018, ALÖKI Kft., Budapest, Hungary

than the pure sowings and the other mixtures with the exception of the alfalfa + Bermuda grass mixture.

Table 1. *Crude protein ratios (%) of dry matters from pure sowings and alfalfa-grass mixtures*

Mixture or pure sowing	Years		Average
	2011	2012	
Bermuda grass (BG)	10.6 fg*	9.9 ı	10.3 m
Dallis grass (DG)	12.8 e	10.1 ı	11.4 kl
Rhodes grass (RG)	9.6 gh	12.4 h	11.0 lm
Guinea grass (GG)	8.1 hı	9.5 ı	8.8 n
Blue couch grass (BCG)	11.0 e-g	10.4 ı	10.7 lm
Finger grass (FG)	9.8 gh	10.3 ı	10.1 m
Alfalfa (A)	20.4 a	20.7 a-d	20.5 a
BG+A	16.6 bc	20.0 a-e	18.3 b
DG+A	15.8 b-d	20.4 a-d	18.1 bc
RG+A	11.1 e-g	20.1 a-e	15.6 fg
GG+A	7.0 ı	20.8 a-c	13.9 hı
BCG+A	17.1 b	19.0 ef	18.0 bc
FG+A	16.5 b-d	20.4 a-d	18.4 b
BG+DG+A	17.0 b	19.6 c-f	18.3 b
BG+RG+A	12.0 ef	19.4 d-f	15.7 fg
BG+GG+A	8.7 hı	15.9 g	12.3 jk
BG+BCG+A	15.1 cd	18.9 ef	17.0 c-e
BG+FG+A	14.7 d	19.5 c-f	17.1 c-e
DG+RG+A	10.6 fg	18.9 ef	14.8 gh
DG+GG+A	8.1 hı	18.5 f	13.3 ıj
DG+BCG+A	16.9 bc	19.4 d-f	18.1 bc
DG+FG+A	16.0 b-d	19.0 ef	17.5 b-d
RG+GG+A	8.3 hı	21.1 ab	14.7 gh
RG+BCG+A	12.7 e	19.9 a-e	16.3 ef
RG+FG+A	11.8 ef	21.2 a	16.5 d-f
GG+BCG+A	8.7 hı	19.9 a-e	14.3 hı
GG+FG+A	8.3 hı	21.1 ab	14.7 gh
FG+BCG+A	15.2 b-d	19.8 b-f	17.5 b-d
Average	**12.5 B+**	**17.7 A**	**15.1**

*Means with the same letter in a column are not statistically different from each other according to the Duncan test at $P \leq 0.05$

+Means with the same letter in the row are not statistically different from each other at $P \leq 0.05$

According to the averaged values over two years, the highest crude protein yield was obtained from the mixture of alfalfa + dallis grass. The crude protein yield of this mixture was statistically significant higher than those of all of pure growings and all of the mixtures with the exceptions of the mixtures of Bermuda grass + alfalfa, finger grass + alfalfa, Rhodes grass + alfalfa.

http://www.aloki.hu ● ISSN 1589 1623 (Print) ● ISSN 1785 0037 (Online)
DOI: http://dx.doi.org/10.15666/aeer/1605_71397154
© 2018, ALÖKI Kft., Budapest, Hungary

Table 2. *Crude protein yields (kg ha^{-1}) of pure sowings and alfalfa-grass mixtures*

Mixture or pure sowing	Years		Average
	2011	2012	
Bermuda grass (BG)	1134.0 e*	603.0 kl	868.5 j
Dallis grass (DG)	1779.0 a-e	826.0 kl	1302.5 ıj
Rhodes grass (RG)	1751.0 a-e	1318.0 jk	1534.5 hı
Guinea grass (GG)	1945.0 a-d	241.0 l	1093.0 ıj
Blue couch grass (BCG)	1292.0 de	559.0 kl	925.5 j
Finger grass (FG)	1560.0 a-e	408.0 l	984.0 j
Alfalfa (A)	1608.0 a-e	4514.0 c-f	3061.0 cd
BG+A	2019.0 a-c	5685.0 ab	3852.0 a
DG+A	1927.0 a-d	5970.0 a	3948.5 a
RG+A	2223.0 a	4859.0 b-e	3541.0 a-c
GG+A	1331.0 c-e	3147.0 gh	2239.0 fg
BCG+A	1502.0 b-e	4384.0 c-f	2943.0 de
FG+A	2140.0 ab	5053.0 b-d	3596.5 ab
BG+DG+A	1748.0 a-e	4500.0 c-f	3124.0 b-d
BG+RG+A	1622.0 a-e	5060.0 b-d	3341.0 b-d
BG+GG+A	1720.0 a-e	2064.0 ıj	1892.0 gh
BG+BCG+A	1670.0 a-e	4487.0 c-f	3078.5 cd
BG+FG+A	1555.0 a-e	4963.0 b-d	3259.0 b-d
DG+RG+A	1966.0 a-d	4733.0 c-e	3349.5 b-d
DG+GG+A	1938.0 a-d	3758.0 fg	2848.0 de
DG+BCG+A	1518.0 a-e	5118.0 bc	3318.0 b-d
DG+FG+A	1780.0 a-e	4320.0 c-f	3050.0 cd
RG+GG+A	1851.0 a-d	3114.0 gh	2482.5 ef
RG+BCG+A	1883.0 a-d	4060.0 ef	2971.5 de
RG+FG+A	2081.0 ab	3806.0 fg	2943.5 de
GG+BCG+A	1450.0 b-e	2697.0 hı	2073.5 fg
GG+FG+A	1344.0 c-e	2628.0 hı	1986.0 gh
FG+BCG+A	1719.0 a-e	4192.0 d-f	2955.5 de
Average	**1716.0 B+**	**3467.0 A**	**2591.5**

*Means with the same letter in a column are not statistically different from each other according to the Duncan test at $P \leq 0.05$

+Means with the same letter in the row are not statistically different from each other at $P \leq 0.05$

ADF and NDF ratios

The results of the variance analysis showed that ADF and NDF contents of the dry matter were statistically significant influenced by pure sowing and mixtures as well as the years. Interaction of the years and treatments was also statistically significant. The averaged ADF content over the pure sowings and mixtures in the first year was significantly higher than those in the second year (*Table 3*). In the first year, contribution of the warm season grasses on the hay yield of the mixtures was higher than those in the second year. The grasses contain generally higher ADF than alfalfa

http://www.aloki.hu ● ISSN 1589 1623 (Print) ● ISSN 1785 0037 (Online)
DOI: http://dx.doi.org/10.15666/aeer/1605_71397154
© 2018, ALÖKI Kft., Budapest, Hungary

(Linn and Martin, 1999). Therefore averaged ADF content of the dry matter in the first year was significantly higher than those in the second year.

In the first year and as the averaged values over the two years, alfalfa gave the dry matter with significantly lower ADF content than the other pure sowings and all of the mixtures. In the second year, alfalfa was the treatment among the treatments producing dry matter with low ADF content. In contrast to this, Guinea grass produced the dry matter with significantly higher ADF content than the other pure sowings and all of the mixtures in the second year and as the averaged values over the two years. It was among the treatments with high ADF content in the first year.

Table 3. *ADF ratios (%) of dry matters from pure sowings and alfalfa-grass mixtures*

Mixture or pure sowing	Years		Average
	2011	2012	
Bermuda grass (BG)	31.6 i-k*	32.1 c-e	31.9 e-h
Dallis grass (DG)	34.1 f-h	34.8 b	34.5 bc
Rhodes grass (RG)	36.6 de	34.9 b	35.8 b
Guinea grass (GG)	40.2 ab	39.2 a	39.7 a
Blue couch grass (BCG)	31.1 jk	33.0 bc	32.1 e-g
Finger grass (FG)	34.8 e-g	32.9 b-d	33.8 cd
Alfalfa (A)	25.6 n	27.3 jk	26.5 n
BG+A	28.6 lm	29.2 f-j	28.9 k-m
DG+A	31.1 jk	29.2 f-j	30.2 h-k
RG+A	35.5 ef	29.5 f-j	32.5 d-f
GG+A	41.0 a	28.0 ı-k	34.5 bc
BCG+A	27.7 m	28.2 ı-k	28.0 mn
FG+A	29.7 k-m	30.1 e-ı	29.9 ı-l
BG+DG+A	27.8 m	28.9 g-j	28.4 lm
BG+RG+A	33.3 g-ı	29.7 f-j	31.5 f-ı
BG+GG+A	38.6 bc	28.2 ı-k	33.4 c-e
BG+BCG+A	28.6 lm	29.8 e-ı	29.2 j-m
BG+FG+A	29.9 kl	30.2 e-ı	30.0 ı-l
DG+RG+A	35.8 ef	31.0 c-g	33.4 c-e
DG+GG+A	39.5 a-c	28.5 h-k	34.0 cd
DG+BCG+A	29.6 k-m	30.7 d-h	30.1 h-k
DG+FG+A	31.0 jk	31.5 c-f	31.2 f-ı
RG+GG+A	39.3 a-c	26.3 k	32.8 c-f
RG+BCG+A	32.6 h-j	28.8 g-j	30.7 g-j
RG+FG+A	34.4 f-h	28.5 h-k	31.5 f-ı
GG+BCG+A	38.3 b-d	28.8 g-j	33.5 c-e
GG+FG+A	38.0 cd	27.7 ı-k	32.9 c-f
FG+BCG+A	28.5 lm	29.4 f-j	28.9 k-m
Average	**33.3 A+**	**30.2 B**	**31.8**

*Means with the same letter in a column are not statistically different from each other according to the Duncan test at $P \leq 0.05$

+Means with the same letter in the row are not statistically different from each other at $P \leq 0.05$

http://www.aloki.hu ● ISSN 1589 1623 (Print) ● ISSN 1785 0037 (Online)
DOI: http://dx.doi.org/10.15666/aeer/1605_71397154
© 2018, ALÖKI Kft., Budapest, Hungary

The averaged NDF ratio of dry matter in the first year was significantly higher than those in the second year (*Table 4*). As mentioned above, higher grass ratio in the hay yield of the mixtures in the first year than that in the second year resulted in higher NDF content in the first year.

Table 4. *NDF ratios (%) of dry matters from pure sowings and alfalfa grass-mixtures*

Mixture or pure sowing	Years		Average
	2011	2012	
Bermuda grass (BG)	64.9 bc*	62.7 c	63.8 b
Dallis grass (DG)	63.4 b-d	64.8 bc	64.1 b
Rhodes grass (RG)	67.2 ab	66.7 ab	67.0 a
Guinea grass (GG)	68.5 ab	68.2 a	68.3 a
Blue couch grass (BCG)	63.6 b-d	62.6 c	63.1 b
Finger grass (FG)	63.3 b-d	60.0 d	61.7 b
Alfalfa (A)	36.4 h	38.2 l	37.3 k
BG+A	49.9 e-g	40.8 g-k	45.3 h-j
DG+A	52.9 ef	40.4 h-l	46.7 hı
RG+A	64.8 bc	40.4 h-l	52.6 c-f
GG+A	70.0 a	38.7 kl	54.3 cd
BCG+A	48.5 fg	39.2 j-l	43.9 ıj
FG+A	46.7 g	40.5 g-l	43.6 j
BG+DG+A	50.6 e-g	40.6 g-l	45.6 h-j
BG+RG+A	61.6 cd	41.7 e-j	51.7 d-f
BG+GG+A	67.1 ab	41.9 e-ı	54.5 cd
BG+BCG+A	51.7 ef	40.4 h-l	46.1 h-j
BG+FG+A	53.9 e	41.4 f-j	47.6 gh
DG+RG+A	64.5 b-d	43.8 ef	54.2 cd
DG+GG+A	67.9 ab	42.1 e-ı	55.0 c
DG+BCG+A	51.3 e-g	43.0 e-g	47.2 h
DG+FG+A	49.2 e-g	44.2 e	46.7 hı
RG+GG+A	68.3 ab	38.8 kl	53.5 c-e
RG+BCG+A	59.6 d	41.8 e-j	50.7 ef
RG+FG+A	60.8 cd	39.5 ı-l	50.2 fg
GG+BCG+A	65.3 a-c	42.0 e-ı	53.7 c-e
GG+FG+A	67.1 ab	38.7 kl	52.9 c-f
FG+BCG+A	52.6 ef	42.7 e-h	47.7 gh
Average	**59.0 A+**	**45.9 B**	**52.5**

*Means with the same letter in a column are not statistically different from each other according to the Duncan test at $P \leq 0.05$

+Means with the same letter in the row are not statistically different from each other at $P \leq 0.05$

Digestible dry matter content

The results of the variance analysis showed that the digestible dry matter ratio was influenced by pure sowings and mixtures as well as years. Year x treatment interaction

http://www.aloki.hu ● ISSN 1589 1623 (Print) ● ISSN 1785 0037 (Online)
DOI: http://dx.doi.org/10.15666/aeer/1605_71397154
© 2018, ALÖKI Kft., Budapest, Hungary

was also statistically significant. Averaged digestible dry matter ratios in the second year were significantly higher than that in the first year (*Table 5*).

The digestible dry matter ratio is calculated using the ADF values and is inversely proportional. ADF ratios are higher in the second year than in the first year. Therefore, the rate of digestible dry matter in the second year is higher than in the first year.

In the first year, digestible dry matter ratio of alfalfa was significantly higher than those of the other pure sowings and all of the mixtures with the exception of BCG+A and BG+DG+A (*Table 5*). Pure sowing of Guinea grass produced dry matter with significantly lower digestibility ratio than the other pure sowings and all of the mixtures with the exceptions of the mixtures containing Guinea grass.

Table 5. *Digestible dry matter ratios (%) of dry matters from pure sowings and alfalfa-grass mixtures*

Mixture or pure sowing	Years		Average
	2011	2012	
Bermuda grass (BG)	64.3 c-h*	63.9 g-ı	64.1 f-k
Dallis grass (DG)	62.3 g-k	61.8 j	62.1 mn
Rhodes grass (RG)	60.4 k-n	61.7 j	61.0 n
Guinea grass (GG)	57.6 o	58.4 k	58.0 o
Blue couch grass (BCG)	64.7 c-g	63.2 ıj	63.9 g-l
Finger grass (FG)	61.8 ı-k	63.3 h-j	62.6 k-n
Alfalfa (A)	69.0 a	67.6 ab	68.3 a
BG+A	66.6 bc	66.2 b-f	66.4 b-d
DG+A	64.7 c-g	66.2 b-f	65.4 c-g
RG+A	61.2 ı-l	65.9 b-f	63.6 h-m
GG+A	57.0 o	67.1 a-c	62.0 mn
BCG+A	67.3 ab	66.9 a-d	67.1 ab
FG+A	65.8 b-e	65.5 c-g	65.6 b-f
BG+DG+A	67.3 ab	66.3 b-e	66.8 bc
BG+RG+A	63.0 f-j	65.8 b-f	64.4 f-j
BG+GG+A	58.9 m-o	66.9 a-d	62.9 j-m
BG+BCG+A	66.6 bc	65.6 c-g	62.4 l-n
BG+FG+A	65.6 b-e	65.4 c-g	66.1 b-e
DG+RG+A	61.1 j-m	64.8 e-ı	65.5 c-g
DG+GG+A	58.1 no	66.7 a-e	62.9 j-m
DG+BCG+A	65.9 b-d	65.0 d-h	62.4 l-n
DG+FG+A	64.8 c-f	64.4 f-ı	65.4 c-g
RG+GG+A	58.3 no	68.4 a	64.6 e-ı
RG+BCG+A	63.5 d-ı	66.5 b-e	63.4 ı-m
RG+FG+A	62.1 h-k	66.7 a-e	65.0 d-h
GG+BCG+A	59.1 l-o	66.5 b-e	64.4 f-j
GG+FG+A	59.3 l-o	67.3 a-c	62.8 j-m
FG+BCG+A	63.4 e-j	65.9 b-f	64.6 e-ı
Average	62.8 B+	65.3 A	64.1

*Means with the same letter in a column are not statistically different from each other according to the Duncan test at $P \leq 0.05$

+Means with the same letter in the row are not statistically different from each other at $P \leq 0.05$

http://www.aloki.hu ● ISSN 1589 1623 (Print) ● ISSN 1785 0037 (Online)
DOI: http://dx.doi.org/10.15666/aeer/1605_71397154
© 2018, ALÖKI Kft., Budapest, Hungary

In the second year, the mixture of RG+GG+A produced the dry matter with significantly higher digestibility ratio than all of the pure sowings with the exception of alfalfa and all of the mixtures with the exceptions of GG+A, GG+FG+A, BCG+A, BG+GG+A, DG+GG+A and RG+FG+A All of the pure sowings of the grasses gave the dry matter with significantly lower digestibility ratio than the pure sowing of alfalfa.

Some of our findings are consistent with those above mentioned, some of them are incompatible. The differences between our finding and that of previous studies could be due to the ecological differences, varieties, mixes, practices applied.

Relative feed value (RFV)

The results of the variance analysis showed that RFV was statistically significant influenced by pure sowings and mixtures as well as years. Year x mixture interaction was also statistically significant. The averaged RFV over the pure sowings and mixtures significantly changed depending on the years. The averaged RFV in the second year was significantly higher than those in first year (*Table 6*). The higher alfalfa contribution to the hay yield of the mixtures in the second year as compared to the first year resulted in higher RFV in second year. RFV is inversely proportional to the ADF and NDF. Therefore higher averaged RFVs were obtained in the second year in which ratios of NDF and ADF were lower than those in the first year.

In the first year of the experiment and as averaged value over the years, pure sown alfalfa produced the dry matter with significantly higher RFV than the other pure sowings and all of the mixtures. In the second year, the mixtures of DG+A, RG+A, GG+A, BCG+A, RG+GG+A, RG+FG+A and GG+FG+A gave dry matters with RFVs being not statistically significant different from that of Alfalfa dry matter.

Discussion

It was determined that crude protein content of pure growing alfalfa was significantly higher than those of pure growing grasses and generally higher than the mixtures of grasses with alfalfa. Previous studies have also shown that alfalfa contains significantly more protein than grasses and that grass+legume mixtures contain more crude protein than the pure sowing grasses (Spandl and Hesterman, 1997; Avci, 2000; Albayrak and Ekiz, 2005; Cinar and Hatipoglu, 2014).

Nutrient value of a mixture forage relatively depends on the botanical composition and harvesting time. The results indicated that CP contents of dry matter of the mixtures were generally lower than 16-18% which requires supplementary feeding to obtain high performance from milk cows (Baytekin and Gul, 2009).

According to the two years averaged values, alfalfa gave significantly higher crude protein yield than the pure growing grasses. Conrad and Martz (1985), Rohweder and Keuren (1985), Spandl and Hesterman (1997) reported also that alfalfa has higher dry matter and crude protein yield than grasses. Some of the duo mixture of grasses with alfalfa such as BG+A, DG+A and FG+A produced significantly higher crude protein yield than pure growing alfalfa. This was due to the higher dry matter yields of those mixtures. This result was consistent with that of Albayrak and Turk (2011).

http://www.aloki.hu ● ISSN 1589 1623 (Print) ● ISSN 1785 0037 (Online)
DOI: http://dx.doi.org/10.15666/aeer/1605_71397154
© 2018, ALÖKI Kft., Budapest, Hungary

Table 6. *RFVs of pure sowings and alfalfa-grass mixtures*

Mixture or pure sowing	Years		Average
	2011	2012	
Bermuda grass (BG)	92.2 e-h*	94.8 j	93.5 k
Dallis grass (DG)	91.5 e-h	88.6 j	90.1 k
Rhodes grass (RG)	83.7 f-j	64.5 l	74.1 l
Guinea grass (GG)	78.2 ıj	79.7 k	78.9 l
Blue couch grass (BCG)	94.7 e-g	94.0 j	94.3 k
Finger grass (FG)	90.8 e-ı	98.1 j	94.5 k
Alfalfa (A)	176.5 a	165.1 a	170.8 a
BG+A	124.5 b-d	151.0 b-h	137.8 b-d
DG+A	113.7 d	152.3 a-g	133.0 c-f
RG+A	88.1 e-j	152.0 a-g	120.0 g-j
GG+A	75.8 j	161.3 a-d	118.6 h-j
BCG+A	129.7 bc	159.3 a-e	144.5 b
FG+A	131.5 b	150.4 b-h	141.0 bc
BG+DG+A	124.0 b-d	145.6 e-ı	134.8 b-e
BG+RG+A	95.5 ef	146.9 e-ı	121.2 g-j
BG+GG+A	81.6 g-j	148.6 c-ı	115.1 j
BG+BCG+A	121.1 b-d	151.4 a-h	136.3 b-e
BG+FG+A	113.5 d	147.2 e-ı	130.4 c-g
DG+RG+A	88.0 e-j	137.7 hı	112.9 j
DG+GG+A	79.7 h-j	147.3 e-ı	113.5 j
DG+BCG+A	120.0 b-d	140.7 g-ı	130.4 c-g
DG+FG+A	122.9 b-d	135.6 ı	129.3 d-h
RG+GG+A	79.4 h-j	164.3 ab	121.8 g-j
RG+BCG+A	99.1 e	148.0 d-ı	123.6 f-j
RG+FG+A	95.4 ef	157.0 a-f	126.2 e-ı
GG+BCG+A	84.1 f-j	147.1 e-ı	115.6 ıj
GG+FG+A	82.4 f-j	162.3 a-c	122.3 f-j
FG+BCG+A	118.0 cd	143.5 f-ı	130.8 c-g
Average	**102.7 B+**	**136.9 A**	**119.8**

*Means with the same letter in a column are not statistically different from each other according to the Duncan test at $P \leq 0.05$

+Means with the same letter in the row are not statistically different from each other at $P \leq 0.05$

In the study, alfalfa gave the dry matter with significantly lower ADF and NDF contents than the other pure sowings and generally lower than those of all of the mixtures. In contrast to this, Guinea grass produced the dry matter with significantly higher ADF and NDF contents than the other pure sowings and all of the mixtures. The reasons of the higher ADF and NDF contents of Guinea grass could be development stage of the plant at the harvest (Anonymous, 2012) as well as the lower leaf- stem ratio (Pinkerton and Cross, 1992). The ADF concentration refers to the cell wall portion of the forage. The portion consist of cellulose and lignin. The ADF value is important because it describes the ability of an animal to digest the forage. As the ADF increases, the digestibility of the forage usually decreases. The NDF value refers to the total cell

http://www.aloki.hu ● ISSN 1589 1623 (Print) ● ISSN 1785 0037 (Online)
DOI: http://dx.doi.org/10.15666/aeer/1605_71397154
© 2018, ALÖKI Kft., Budapest, Hungary

wall, composed of the ADF fraction plus hemicellulose. NDF value is important in ration formulation because it reflects the amount of forage that the animal can consume. As the NDF percentage increases, the dry matter intake will generally decrease (Joachim and Jung, 1997; Albayrak et al., 2011). Horner et al. (1985) determined ADF content of alfalfa as 35.3 - 41.1% while Cassida et al. (2000) reported it as 29.7 - 33.5%. ADF content of the mixture of Rhodes grass + white sweet clover was reported by Corletto et al. (2009) as 37.0%. Horner et al. (1985) determined NDF content of alfalfa as 46.0% while Cassida et al. (2000) reported it as 37.8 - 42.0%. Jeranyama and Garcia (2004) reported a NDF value of 54% for the mixture of alfalfa + grasses of mixtures. Tessema and Baars (2006) determined NDF values for Rhodes grass and for the mixture of alfalfa + Rhodes grass as 55.7% and 46.9%, respectively. Lemus (2009) reported a NDF value of 67.2 - 67.6% for dallis grass. Cinar et al. (2014) reported a ADF, NDF value of the 40.2%, 70.9% for dallis grass respectively.

Some of our findings are consistent with those above mentioned, some of them are incompatible. Differences between the findings may be due to differences in climatic conditions, under which researches were conducted, and management techniques applied in the experimental plots (Linn and Martin, 1999; Belyea et al., 1999; Bani et al., 2007).

According to the averaged values over two years, the highest digestible dry matter ratio was obtained from pure sown alfalfa. It was significantly higher than those of all of the other pure sowings and all of the mixtures with the exception of the mixture BCG+A. Pure sowings of Guinea grass produced the dry matter with significantly lower digestibility ratio than the other pure sowings and mixtures. Alfalfa's ADF content is lower than those of grasses. As the proportion of alfalfa in the mixture increases, the ADF ratio decreases and the digestibility increases (Joachim and Jung, 1997; Cinar and Hatipoglu, 2014). Felicity et al. (1996) determined DDM content of dallis grass as 63.6% while Cook et al. (2005) 57.0-63.0%. Cinar and Hatipoglu (2014) reported DDM ratio values of alfalfa, dallis grass, Bermuda grass, Rhodes grass, DG+A, BG+A, RG+A, RG+DG+A, BG+DG+A, RG+BG+A 68.1%, 57.6%, 63.1%, 60.7%, 63.0%, 66.3%, 63.4%, 62.6%, 65.1%, 63.1% respectively.

Relative feed value (RFV) has been used for years to compare the quality of legume and legume/grass hays and silages. Having one index to price hay and predict animal performance has been very useful for livestock producers and hay farmers. Forages with an RFV value over 151, between 150-125, 124-103, 102-87, 86-75, and less than 75 are categorized as prime, premium, good, fair, poor and rejected, respectively (Kiraz, 2011; Uzun, 2010; Cinar et al., 2014). According to these index values, hay of pure sowing alfalfa is classified as prime while hays of the mixtures of Bermuda grass+alfalfa, dallis grass+alfalfa, blue couch grass+alfalfa, finger grass+alfalfa, Bermuda grass+dallis grass+alfalfa, Bermuda grass+blue couch grass+alfalfa, Bermuda grass+finger grass+alfalfa, dallis grass+blue couch grass+alfalfa, dallis grass+finger grass+alfalfa, Rhodes grass+finger grass+alfalfa, finger grass+blue couch grass+alfalfa are classified as premium.

Conclusions

It was concluded that, the mixtures of Bermuda grass+alfalfa, dallis grass+alfalfa, blue couch grass+alfalfa, finger grass+alfalfa, Bermuda grass+finger grass+alfalfa, dallis grass+blue couch grass+alfalfa, dallis grass+finger grass+alfalfa, Bermuda

http://www.aloki.hu ● ISSN 1589 1623 (Print) ● ISSN 1785 0037 (Online)
DOI: http://dx.doi.org/10.15666/aeer/1605_71397154
© 2018, ALÖKI Kft., Budapest, Hungary

grass+dallis grass+alfalfa, Rhodes grass+finger grass+alfalfa and finger grass+blue couch grass+alfalfa could be grown for the feeding of high yielding dairy cows in Mediterranean climatical conditions. On the other hand, additional researches on the seed mixture ratios, fertilization and harvest time should be conducted in order to increase the forage quality of the mentioned mixtures.

REFERENCES

[1] Aganoglu, V. (1985): A research on the possibility of growing Rhodes grass (*Chloris gayana* Kunth) and alfalfa (*Medivago sativa* L.) in mixture under Cukurova conditions. – Msc Thesis, Field Crops Department of Institute for Natural and Applied Sciences, Cukurova University, Adana.

[2] Albayrak, S., Ekiz, H. (2005): An investigation on the establishment of artificial pasture under Ankara's ecological conditions. – Turk J Agric For 29: 69-74.

[3] Albayrak, S., Türk, M. (2011): Effects of fertilization on forage yield and quality of crested wheatgrass (*Agropyron cristatum* L. Gaertn.). – Bulgarian Journal of Agricultural Science 17(5): 642-648.

[4] Albayrak, S., Turk, M., Yuksel, O. Yilmaz, M. (2011): Forage yield and the quality of perennial legume-grass mixtures under rainfed conditions. – Notulae Botanicae Horti Agrobotanici Cluj 39(1): 114-118.

[5] Anonymous (2011): Chemical Analysis Results. – University of Cukurova Laboratory of Soil Science, Faculty of Agriculture, Adana, Turkey.

[6] Anonymous (2012): *Paspalum dilatatum* Poir. – www.tropicalforages.info (accessed January 10, 2012).

[7] Anonymous (2013): Meteorological data for Adana. – http://www.wunderground.com (accessed December 12, 2014).

[8] Avci, M. (2000): Determining Suitable Mixtures of Cool Season Perennial Grasses and Legumes for Establishment of Short Term Pastures in Cukurova Region. – Department of Field Crops, Institute of Natural and Applied Sciences, Cukurova University, Adana.

[9] Aydin, N., Mut, Z., Mut, H., Ayan, İ. (2010): Effect of autumn and spring sowing dates on hay yield and quality of oat (*Avena sativa* L.) genotypes. – Journal of Animal and Veterinary Advances 9(10): 1539-1545.

[10] Bani, P., Minuti, A., Luraschi, A. O., Ligabue, M., Ruozzi, F. (2007): Genetic and Enviromental Influences on In Vitro Digestibility of Alfalfa. – Italian Journal of Animal Science 6(1): 251-253.

[11] Baytekin, H., Gül, İ. (2009): Forage Crops Harvest, Hay Yield and Storage. – In: Avcıoğlu, R., Hatipoğlu, R., Karadağ, Y. (eds.) Forage. Cilt III. TÜGEM, Emre p, İzmir, pp. 121-141.

[12] Belyea, R., Restrepo, R., Martz, F., Ellersieck, M. (1999): Effect of year and cutting on equations for estimating net energy of alfalfa. – Journal of Dairy Science 82(9): 1943-1949.

[13] Blanchet, K. M., George, J. R., Gettle, R. M., Buxton, D. R., Moore, K. J. (1995): Establishment and persistence of legumes interseeded into switchgrass. – Agron. J. 87: 935-941.

[14] Cameron, A. G., Lemcke, B. (2010): Pasture species sowing guide for the top end. – http://www.nt.gov.au/d/Content/File/p/Pasture/544.pdf (accessed April 20, 2014).

[15] Cassida, K. A., Griffin, T. S., Rodriguez, J., Patching, S. C., Hesterman, O. B., Rust, S. R. (2000): Protein degradability and forage quality in maturing alfalfa, red clover and birdsfoot trefoil. – Crop Science 40: 209-215.

http://www.aloki.hu ● ISSN 1589 1623 (Print) ● ISSN 1785 0037 (Online)
DOI: http://dx.doi.org/10.15666/aeer/1605_71397154
© 2018, ALÖKI Kft., Budapest, Hungary

[16] Cinar, S., Hatipoğlu, R. (2014): Quality characteristics of the mixtures of some warm season perennial grasses with alfalfa Medicago sativa L. under irrigated conditions of Cukurova. – Turkish Journal of Field Crops 20(1): 31-37.
[17] Cinar, S. Hatipoğlu, R., Gundel, F., Aktaş, A., Avci, M. (2014): Performances of Some Perennial Warm Season Grasses Alfalfa Medicago sativa L Mixtures Under Mediterranean Conditions Turkish Journal of Field Crops. – Turkish Journal of Field Crops 19(2): 212-218.
[18] Conrad, H. R., Martz, F. A. (1985): Forages for Dairy Cattle. – In: Heath, E., Barns, F., Metcalfe, S. (eds.) Forages. Iowa State University Press, Iowa, pp. 550-559.
[19] Cook, B. G., Pengelly. B. C., Brown, S. D., Donnelly, J. I., Eagles, D. A., Franco, M. A., Hanson, J, Mullen. B. F., Partrıdge, I. J., Peters, M., Schultze Kraft, R. (2005): Tropical Forages: an Interactive Selection Tool. – CSIRO, DPI & F (Qld), CIAT and ILRI, Brisbane, Australia.
[20] Corletto, A., Cazzato, E., Ventricelli, P., Cesentino, S. L., Gresta, F., Testa, G., Maiorana, M., Fornaro, F., De Giorgio, D. (2009): Performance of perennial tropical grasses in different mediterannean environments in southern Italy. – Tropical Grasslands 43: 129-138. www.tropicalgrasslands.asn.au/.
[21] Felicity, S. J., Mcnabb, W. C., Peters, J. S., Barry, T. N., Campbell, B. D., Ulyatt, M. J. (1996): Nutritive value of subtropical grasses invading North Island pastures. – Proceedings of the New Zealand Grassland Association 57: 203-206.
[22] Gettle, R. M., George, J. R., Blanchet, K. M., Buxton, D. R., Moore, K. J. (1996): Frost-seeding legumes into established switchgrass. Establishment, density, persistence, and sward composition. – Agron. J. 88: 98-103.
[23] Horner, L. J., Bush, J., Adams, G. D., Taliaferro, C. M. (1985): Comparative nutritional value of eastern gama grass and alfalfa hay for dairy cows. – Journal of Dairy Science 68: 15-26.
[24] Hoy, M. D., Moore, K. J., George, J. R., Brummer, E. E. (2002): Alfalfa yield and quality as influenced by establishment method. – Agron. J. 94: 65-71.
[25] Jeranyama, P., Garcia, A. (2004): Understanding relative feed value (RFV) and relative forage quality (RFQ). – http://pubstorage.sdstate.edu/AgBio_Publications/articles/ExEx8149.pdf (accessed May 20, 2014).
[26] Joachim, H., Jung, G. (1997): Analysis of forage fiber and cell walls in ruminant nutrition. – Journal of Nutrition 127: 810-813.
[27] Jung, G. A., Gross, C. F., Kocher, R. E., Burdette, L. A., Sharp, W. C. (1978): Warm season range grasses extend beef cattle forage. – Penn. Agric. Exp. Stn. Sci. Agric. 64: 211-219.
[28] Kiraz, A. B. (2011): Determination of relative feed value of some legume hays harvested at flowering stage. – Asian Journal of Animal Veterinary Advances 6(5): 525-530.
[29] Larbi, A., J. Lazier, Ochang, J., Addie, A. (1995): Dry matter production of thirteen tropical legumes in association with rhodes grass (Chloris gayana cv. Callide) on an acid soil in Etiopia. – Tropical Grasslands Volume 29: 88-91.
[30] Lemus, R. (2009): Seeding warm season perennial grasses. – Forage News, Mississippi State University Extension Service, March, 2009.
[31] Linn, J. G., Martin, N. P. (1999): Forage quality tests and interpretations. – http://extension.umn.edu/distribution/livestocksystems/ID2637.html (accessed June 10, 2014).
[32] Nung, H. V., Binh, L. H. (2014): Forage productivity of guinea grass in different farming systems. – http://www.fao.org/ag/agp/agpc/doc/publicat/VIET95/V95_97.PDF (accessed April 15, 2014).
[33] Pinkerton, B. W., Cross, D. L. (1992): Forage quality. – http://www.clemson.edu/ psapublishing/ Pages/AGRO/forage16.pdf (accessed June 15, 2014).

http://www.aloki.hu ● ISSN 1589 1623 (Print) ● ISSN 1785 0037 (Online)
DOI: http://dx.doi.org/10.15666/aeer/1605_71397154
© 2018, ALÖKI Kft., Budapest, Hungary

[34] Rohweder, D. A., Keuren, R. W. (1985): Permanent Pastures. – In: Heath, E., Barns, F., Metcalfe, S. (eds.) Forages. Iowa State University Press, Iowa, pp. 487-495.
[35] Schroeder, J. W. (1994): Forage nutrition for ruminants. – AS-1250. www.ag.ndsu.edu.tr.
[36] Sheaffer, C. C., Peterson, M. A., Mccalin, M., Volene, J. J., Cherney, J. H., Johnson, K. D., Woodward, W. T., Viands, D. R. (1995): Acid detergent fiber, neutral detergent fiber concentration and relative feed value. – North American Alfalfa Improvement Conference, Minneapolis.
[37] Skerman, P. J., Riveros, F. (1990): Tropical Grasses. – Plant Production and Protection Series 23. FAO, Rome.
[38] Sleugh, B., Moore, K. J., George, J. R., Brummer, E. C. (2000): Binary legume grass mixtures improve forage yield, quality, and seasonal distribution. – Agron. J. 92: 24-29. DOI: 10.2134/agronj2000.92124.
[39] Spandl, E., Hesterman, O. B. (1997): Forage quality and alfalfa characteristics in binary mixtures of alfalfa and Bromegrass or Timothy. – Crop Science 37: 1581-1585.
[40] Steel, R. G. D., Torrie, J. H. (1960): Principles and Procedures of Statistics with Special Reference to the Biological Sciences. – Mc Graw-Hill, London.
[41] Tessema, Z., Baars, R. M. T. (2006): Chemical composition dry matter production and yield dynamics of tropical grasses mixed with perennial forage legumes. – Tropical Grasslands Volume 40: 150-156.
[42] Uzun, F. (2010): Changes in hay yield and quality of bulbous barley at different phenological stages. – Turk. J. Agric. For. 34: 1-9.

http://www.aloki.hu ● ISSN 1589 1623 (Print) ● ISSN 1785 0037 (Online)
DOI: http://dx.doi.org/10.15666/aeer/1605_71397154
© 2018, ALÖKI Kft., Budapest, Hungary

THE COUPLING RELATIONSHIP BETWEEN TROPICAL UPPER SEA TEMPERATURE FIELD AND EAST ASIAN SUMMER MONSOON

LI, X.[1] – TU, S.[2,*] – KANG, X.[1] – HUANG, X.[2]

[1]*Civil Aviation Flight University of China, 618307 Guanghan, China*

[2]*Faculty of Information Technology, Beijing University of Technology, 100124 Beijing, China*

**Corresponding author*
e-mail: sstu@bjut.edu.cn

(Received 3rd Aug 2018; accepted 28th Sep 2018)

Abstract. In order to study the variability of the upper sea temperature in the tropical Pacific and Indian Oceans and reveal their coupling relationship with East Asian summer monsoon circulation, the singular value decomposition is employed to reveal the variation of 120 m sea temperature in the tropical Pacific and Indian Oceans, the main modalities of anomalous activities of the East Asian summer monsoon, and their mutual relation. The results show that during the summer of years with strong summer monsoon, the western Pacific subtropical high is weak and its location is northerly. In years with strong summer monsoon, the sinking movement of vertical velocity anomalies in East Asia weakens the Meiyu front and vice versa. When the 850 hPa east trade winds in the equatorial central and eastern Pacific Ocean are enhanced, the middle Indian Ocean and the western Pacific Ocean show westerly anomalies. Meanwhile, if the meridional wind anomalies on both sides of the equator in the central Indian Ocean/ eastern Pacific and East Asia show a clear convergent and divergent pattern, respectively, the corresponding 120 m sea temperature shows a La Niña state and is easy to trigger the strong East Asian summer monsoon.
Keywords: *singular value decomposition, 850 hPa wind filed, the tropical Pacific, El Niño state, 120 m sea temperature*

Introduction

Located in the East Asian monsoon region, China shows a typical monsoon climate. The monsoon in China shows large interannual variability leading to frequent droughts and floods (Hao et al., 2016). Therefore, it is of great practical significance to study the variability and main impacting factors of East Asian summer monsoon (EASM). The strength of the EASM is closely related to the subtropical high, the atmospheric circulation in tropics and mid-high latitudes, and the thermal effects of the Tibetan Plateau (Duan et al., 2008; Li et al., 2016). The anomaly of sea temperature is the most important for the prediction of EASM among the above factors (Zhang and Li, 2004). It impacts the precipitation in the monsoon region by impacting the monsoon circulation (Zhang et al., 1999). In the tropical oceans, the El Niño-Southern Oscillation (ENSO) is a strong signal of air-sea interactions. Studies have shown that the ENSO has an important impact on the EASM as well as the climate of China. The warming period of El Niño affects the strength and the burst time of the EASM, thereby affecting the amount of summer precipitation in East Asia (Feng et al., 2011; Zhou et al., 2012; Zhang et al., 2017). Many studies about the variability of the EASM have been conducted based on the sea surface temperature (SST). However, the subsurface sea temperature is less affected by the sea-air interface and has more significant interannual variation compared to the SST, thus, it has a large impact on the continued development of the climate. Chen et al. (2011, 2012) studied the interannual and interdecadal

http://www.aloki.hu ● ISSN 1589 1623 (Print) ● ISSN 1785 0037 (Online)
DOI: http://dx.doi.org/10.15666/aeer/1605_71557170
© 2018, ALÖKI Kft., Budapest, Hungary

variability of subsurface ocean temperature anomalies in the tropical Pacific and their impacts on the climate anomalies in China using the variation of sea temperature in the thermocline. They found that the subsurface sea temperature affects the variation of EASM by affecting the subtropical high and the trough-ridge system in mid-high latitudes. Recent studies also show that there is a mutual interaction between the subsurface sea temperature anomalies in the western Pacific warm pool and the ENSO cycle (Li and Li, 2014; Shan et al., 2016; Li et al., 2017).

The above studying areas are mostly in the tropical Pacific Ocean, which cannot reveal the characteristic that the cold and warm center from the tropical Eastern Indian Ocean to the western Pacific Ocean is an integral system (Cai et al., 2005). The direct relationship between the EASM circulation field and the tropical subsurface sea temperature field is also rarely discussed. Therefore, the aim of this study is to reveal the general pattern of forecasting the EASM and the ENSO. Considering the areas from the tropical Indian Ocean to the Pacific Ocean, a singular value decomposition (SVD) method is employed to study the variation of tropical subsurface sea temperature and the EASM and discuss the coupling relationship between them.

Data and method

The data used in this study is the monthly anomalies of global upper sea temperature (1955-2003) produced by Scripps/NODC Joint Environmental Data Analysis Center (JEDAC) and downloaded from the Nanjing Atmospheric Data Service Center. It is a 5° × 2° dataset covering 60°S-60°N with 11 vertical layers at depths of 0, 20, 40, 60, 80, 120, 160, 200, 240, 300, and 400 m. The data from 30°S-40°N in the Indo-Pacific region is selected for this study. The 2.5° × 2.5° 850 hPa monthly mean data from the National Centers for Environmental Prediction/ National Center for Atmospheric Research (NCEP/NCAR) reanalysis are also selected.

The methods employed here include the synthetic analysis and the SVD. SVD is a method for analyzing the correlation between two element fields, that is, several pairs of correlative spatial distributions of the two element fields. Such spatial distribution can explain the cross-covariance of the two fields to the greatest extent (John et al., 1992). Its main advantage is that it is universal in the diagnostic analysis of the time-space coupled signals in meteorological fields. It is more effective than the natural orthogonal function and the typical correlation method when analyzing the connection between two different element fields and is a powerful tool to study the spatiotemporal relationship between two sequences of element fields (Ding and Jiang, 1995).

Circulation characteristics in years with strong/weak EASM

An Index of EASM (IEASM) defined by Zhang et al. (Zhang et al., 2003) is the difference between the anomalies of 850 hPa zonal wind in East Asian tropical monsoon trough (10°~20°N, 100°~150°E) and East Asian subtropical zone (25°~35°N, 100°~150°E) in June, July, and August. That is, IEASM = U850 hPa (10°~20° N, 100°~150°E) - U850 hPa (25°~35°N, 100°~150°E). A higher IEASM means a stronger summer monsoon and vice versa. This paper selected the data from 1955 to 1998. After standardizing, the years with the normalized IEASM > 1 are defined as the years with strong EASM and those with normalized IEASM < -1 are defined as the years with weak EASM. The years with strong/weak EASM are calculated by the above method,

http://www.aloki.hu ● ISSN 1589 1623 (Print) ● ISSN 1785 0037 (Online)
DOI: http://dx.doi.org/10.15666/aeer/1605_71557170
© 2018, ALÖKI Kft., Budapest, Hungary

which are listed in *Table 1*. The rest of years are considered as the years with normal EASM.

Table 1. *The years with strong/weak EASM defined by IEASM*

Strong/weak	Years					
EASM	1967	1972	1974	1978	1981	1984
Strong	1985	1986	1994	1997	2001	2002
EASM	1955	1956	1959	1969	1980	1983
Weak	1988	1995	1998			

In order to understand the variation characteristics of circulation in years with strong/weak EASM, a synthesis analysis is conducted using the years of strong and weak EASM to explore the variation of atmospheric circulation field during the EASM. *Figure 1a* and *b* are the summer (July) 850 hPa anomalous wind field for years with strong and weak EASM, respectively. In *Figure 1a,* the western Pacific subtropical high in the northern hemisphere (corresponding to the cyclonic circulation anomaly) is weaker than normal and its location is more northerly with the axis at 25°N. The Australia high in the southern hemisphere (corresponding to the anti-cyclonic circulation anomaly) is also weaker than normal, but its weakening intensity is far less than that of the western Pacific subtropical high. This corresponds to an air pressure anomaly field which has high and low values in the south and north, respectively, which forms a strong southeast and southwest anomalous airflow across the equator strengthening the EASM circulation. At 45°E, the northward Somalia jet across the equator further strengthens the EASM circulation. Therefore, the easterly airflow from the south side of the western Pacific subtropical high, the cross-equatorial southerly airflow from 105°~120° E in the southern hemisphere, and the westerly airflow from the Indian Ocean come together and form the southeasterly and southwesterly airflows. The southeasterly airflow is a subtropical monsoon airflow while the southwesterly airflow is a tropical monsoon airflow, both providing the warm and wet southerly airflow for East Asian monsoon zone. East Asia to the east of 100°E, the Korean peninsula, and Japan are all affected by these airflows, and they are also the main water vapor source for the summer precipitation in Eastern China. When this northward warm wet airflow meets the cold air from the circulation of mid-high latitude, a type of subtropical monsoon called Meiyu front is formed (Qin and Wang, 2015). In *Figure 1b,* the anomaly of the circulation field is almost opposite to that in *Figure 1a*. The western Pacific subtropical high in the northern hemisphere (corresponding to the anti-cyclonic circulation anomaly) is stronger than normal and is more southerly with the axis at 20°N, while the Australia high in the southern hemisphere (corresponding to the cyclonic circulation anomaly) is stronger than normal, but its strengthening intensity is far less than that of the western Pacific subtropical high. This corresponds to an air pressure anomaly field with high and low values in the north and south, respectively, which forms a strong northeast and northwest anomalous airflow across the equator weakening the EASM circulation. Therefore, the years with strong and weak EASM have significant differences in the tropospheric low-level circulation field: In the summer of years with strong/weak EASM, the tropical region in East Asia-Pacific shows a closed cyclonic/anti-cyclonic circulation anomaly corresponding to a weaker/stronger western Pacific subtropical high. Gong and He (2002) and Liu and Guo

http://www.aloki.hu ● ISSN 1589 1623 (Print) ● ISSN 1785 0037 (Online)
DOI: http://dx.doi.org/10.15666/aeer/1605_71557170
© 2018, ALÖKI Kft., Budapest, Hungary

(2005) found that the geo-potential height field in East Asia shows negative anomalies during the period when EASM is stronger while the situation is opposite when EASM is weak. Zhang and Wang (2006) and Wu and Zhang (2011) pointed out that the EASM circulation is stronger/weaker when cyclonic/anti-cyclonic circulation anomalies occur in the tropical monsoon region of East Asia, which is in line with the results in this study.

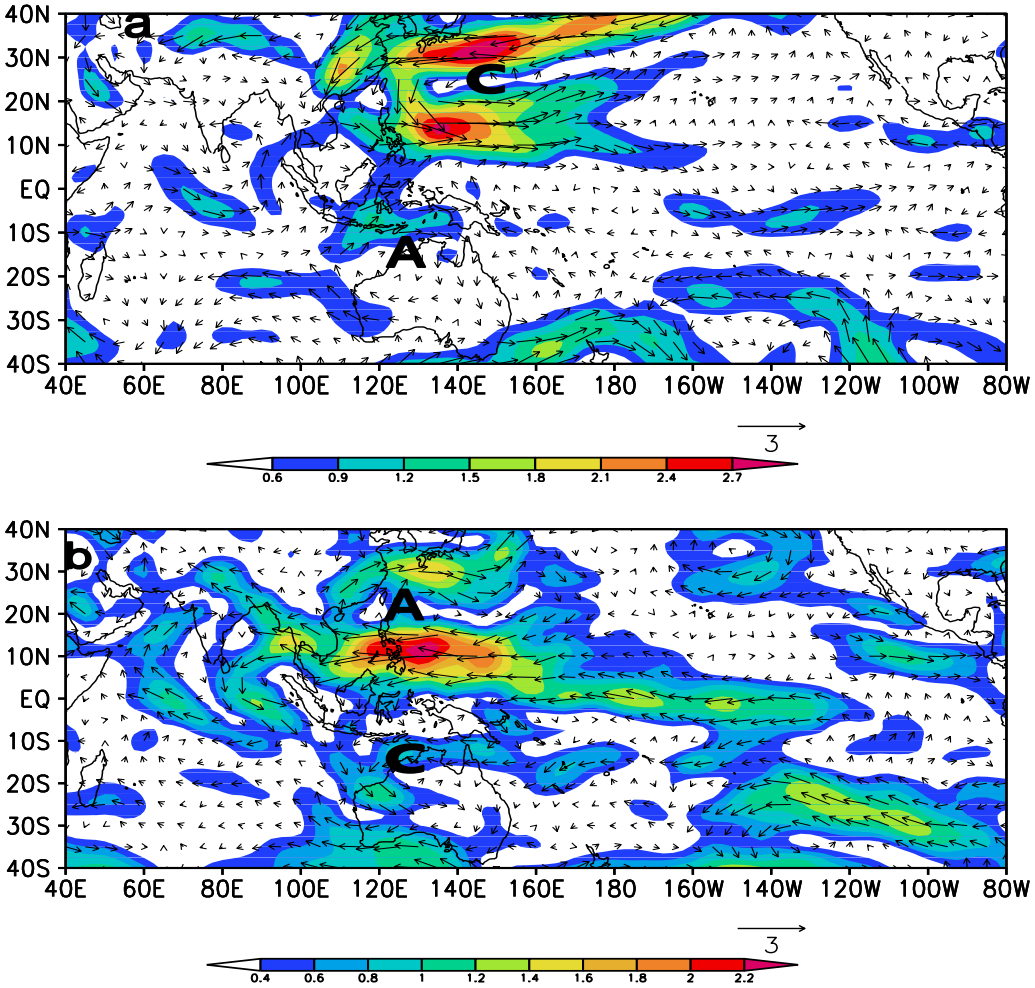

Figure 1. *The anomalies of the 850 hPa wind field (unit: m/s) in the summer of years with (a) strong and (b) weak EASM. A: anti-cyclone; C: cyclone*

In order to further understand the characteristics of circulation in the East Asian monsoon region during the summer of years with strong and weak EASM. *Figure 2a* and *b* show the mean longitude-height profiles of the vertical velocity anomalies in 25°~35°N in the East Asian monsoon region during the summer of years with strong and weak EASM, respectively. In the years with strong EASM (*Fig. 2a*), the vertical velocity from the near ground to the upper level in 110°~140°E shows anomalies of sinking movement, and the upward movement in the summer Meiyu front area (25°~35°N, 110°~140°E) is weakened, indicating the weakening of the Meiyu front intensity in East Asia. In the years with weak EASM (*Fig. 2b*), the vertical velocity from the near ground to the upper level in 110°~140°E shows anomalies of upward

http://www.aloki.hu ● ISSN 1589 1623 (Print) ● ISSN 1785 0037 (Online)
DOI: http://dx.doi.org/10.15666/aeer/1605_71557170
© 2018, ALÖKI Kft., Budapest, Hungary

movement, and strong upward movement appears in the Meiyu front area (25°~35°N, 110°~140°E), leading to the of strengthening of the Meiyu front intensity in East Asia. Thus, the vertical velocity anomalies in East Asia are significantly different in the summers of years with strong and weak EASM. In the years with strong/weak EASM, the vertical velocity anomalies in East Asia are downward/upward, weakening/strengthening the Meiyu front.

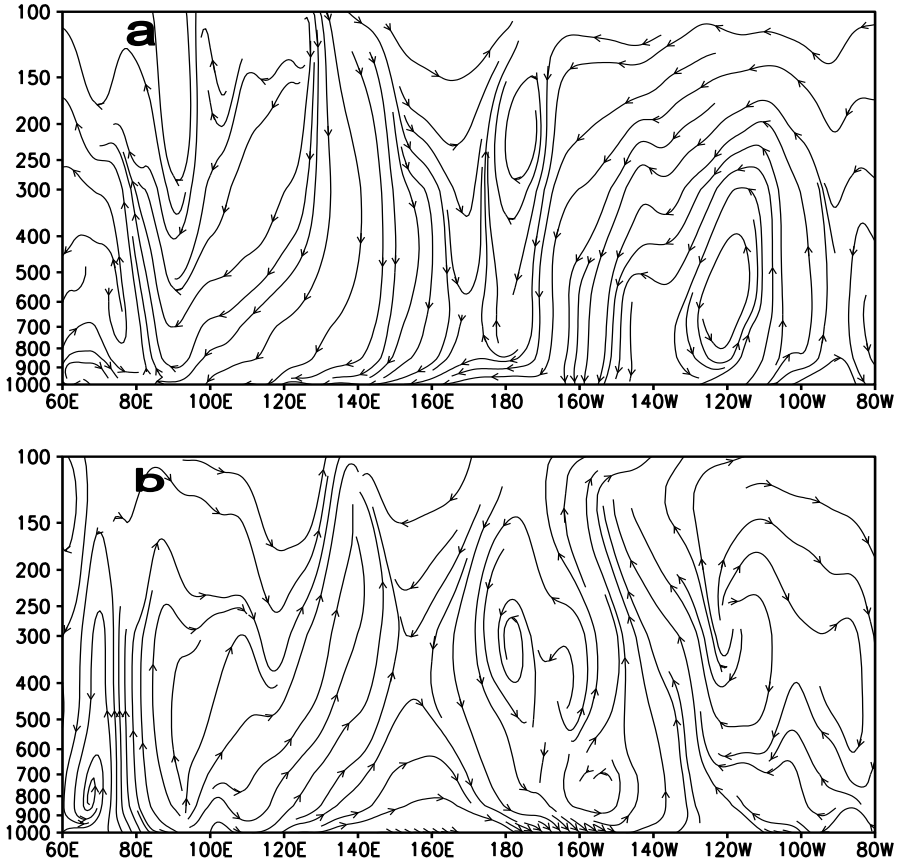

Figure 2. *Mean longitude-height profiles of the vertical velocity anomalies in 25~35°N in the East Asian monsoon region during the summer of years with (a) strong and (b) weak EASM*

Results

Coupling relationship between subsurface sea temperature and 850 hPa wind field

According to Li et al. (2018), the 120 m layer in the equatorial region from the central Indian Ocean to the western Pacific Ocean and the 40 m layer in the equatorial eastern Pacific Ocean have the highest correlation with the IEASM. Since the distributions of the correlation field in the eastern Pacific are roughly the same in the layers of 40 m and 120 m, the relationship between the 120 m sea temperature and the summer monsoon reflects the relationship between subsurface sea temperature and the EASM in most regions from the tropical Pacific to the Indian Ocean. Meanwhile, in order to analyzing the Pacific as a whole system without splitting the east and the western Pacific, the 120 m layer sea temperature in winter (January) is selected to discuss the coupling relation between 120 m layer sea temperature and the 850 hPa wind field using SVD in order to understand the covariation of the sea temperature field

http://www.aloki.hu ● ISSN 1589 1623 (Print) ● ISSN 1785 0037 (Online)
DOI: http://dx.doi.org/10.15666/aeer/1605_71557170
© 2018, ALÖKI Kft., Budapest, Hungary

and the wind field during the same period. *Figure 3* shows the left and right heterogeneous correlation graphs and time coefficients of the first mode of SVD selecting the winter 120 m normalized sea temperature anomalies as the left field and the normalized 850 hPa zonal wind anomalies as the right field. *Table 2* shows the corresponding main information of the first three modes of SVD. It can be seen from *Table 2* that the first mode interprets 39.98% of the total covariance, reflecting the main coupling characteristics between the 120 m layer sea temperature field and the 850 hPa zonal wind field. For the first three modes, the correlations between time coefficients of the left and the right singular vectors are high and this correlation is significant at 0.001 confidence level. Therefore, a detailed analysis is conducted on the heterogeneous correlation field of the first mode.

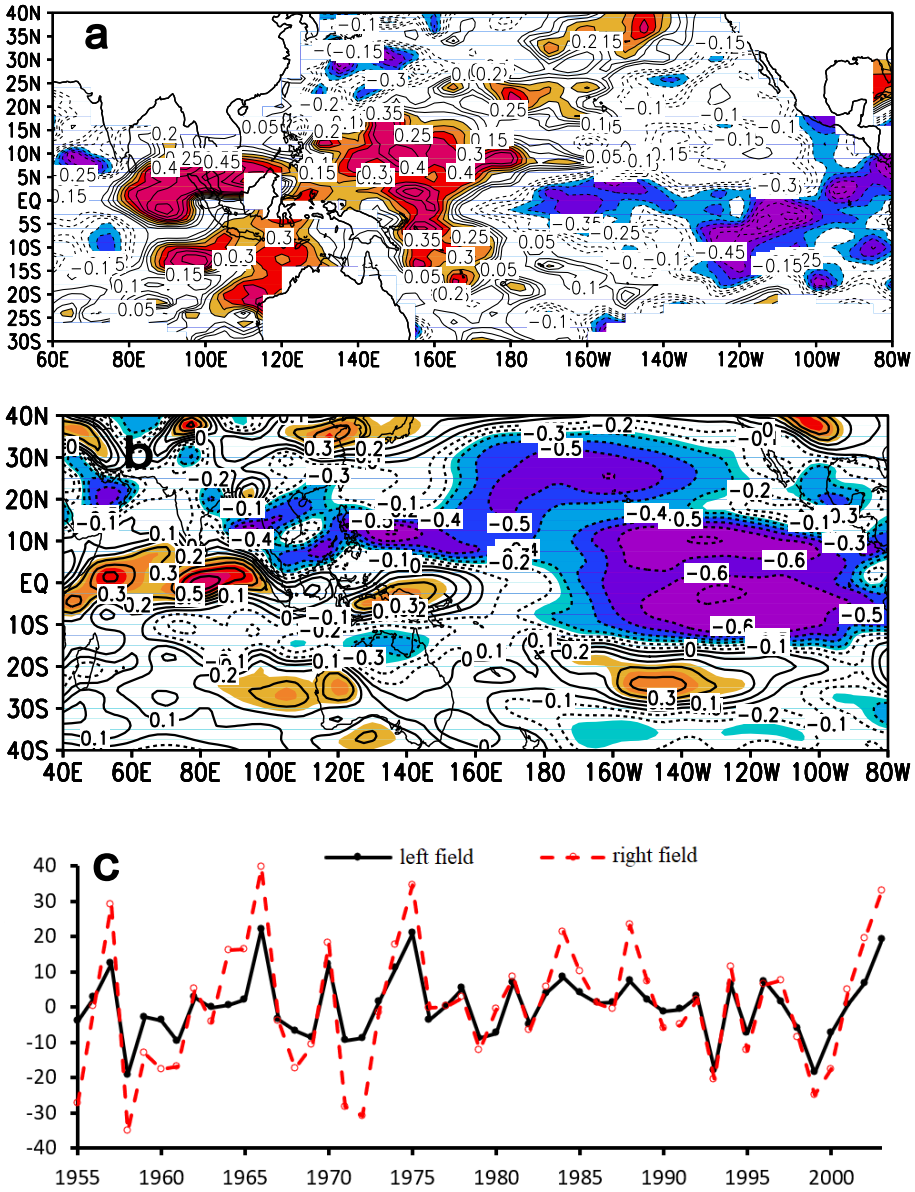

Figure 3. *Heterogeneous correlation graphs between winter 120 m sea temperature field and 850 hPa zonal wind field: (a) left field, (b) right field, and (c) time coefficient. The shadow means the values significant at 0.1 confidence level*

http://www.aloki.hu ● ISSN 1589 1623 (Print) ● ISSN 1785 0037 (Online)
DOI: http://dx.doi.org/10.15666/aeer/1605_71557170
© 2018, ALÖKI Kft., Budapest, Hungary

Table 2. *Information of the first three modes of SVD between sea temperature field and zonal wind field*

Sequence number	Correlation coefficients	The sum of squares of the interprets covariance%	Accumulation of the sum of squares of the interprets covariance%
1	0.91	39.98	39.98
2	0.90	8.71	48.69
3	0.92	5.59	54.28

In *Figure 3a,* the region from the equatorial eastern Indian Ocean to the western Pacific shows positive anomalies of sea temperature, with the center of the positive values located in 10°S~10°N, 80°~170°E. The correlation coefficient in the southern part of the Bay of Bengal, the region from Sumatra to the southern part of the South China Sea, and the equatorial ocean near 160°E reach 0.5 (significant at 0.001 confidence level). Most of the equatorial eastern Pacific shows negative anomalies. The absolute value of the maximum correlation coefficient is comparable with the corresponding values from the equatorial eastern Indian Ocean to the western Pacific. The absolute value of the correlation coefficient of the negative anomalies in the equatorial central Indian Ocean is lower. In *Figure 3b,* the zonal wind in the equatorial central and eastern Pacific shows easterly anomalies and the eastward trade wind is enhanced. Its negative center is located in 10°S~10°N, 150°~100°W with the maximum correlation coefficient of 0.7 (significant at 0.001 confidence level). The region from the equatorial central Indian Ocean to the western Pacific Ocean shows westerly anomalies indicating the existence of westerly jets (Ke et al., 2015). The positive center of this region is in 5°S~5°N, 50°~100°E with the maximum correlation coefficient of 0.5 (significant at 0.001 confidence level). As the modal correlation coefficient is positive, the time coefficients of the left and right fields share the same positive and negative phase on average (*Fig. 3c*). When the time coefficient is strongly positive, the trade wind in the equatorial central and eastern Pacific Ocean is enhanced. The region from center Indian Ocean to the western Pacific Ocean shows westerly anomalies. Meanwhile, the sea temperature in the region from the equatorial eastern Indian Ocean to the western Pacific Ocean becomes higher while the sea temperature in the central Indian Ocean and the eastern Pacific becomes lower, showing a La Niña state. On the contrary, when the time coefficient is strongly negative, the trade wind in the equatorial central and eastern Pacific Ocean is weakened. The region from center Indian Ocean to the western Pacific Ocean shows easterly anomalies. Meanwhile, the sea temperature in the region from the equatorial eastern Indian Ocean to the western Pacific Ocean becomes lower while the sea temperature in the central Indian Ocean and the eastern Pacific becomes higher, showing an El Niño state. Besides, the time coefficients show that the trends of the two fields are in generally consistent and both of them show clear characteristics of interannual variability.

Figure 4 shows the left and right heterogeneous correlation graphs and time coefficients of the first mode of SVD selecting the winter 120 m normalized sea temperature anomalies as the left field and the normalized 850 hPa meridional wind anomalies as the right field. *Table 3* shows the corresponding main information of the first three modes of SVD. It can be seen from *Table 3* that the first mode interprets

http://www.aloki.hu ● ISSN 1589 1623 (Print) ● ISSN 1785 0037 (Online)
DOI: http://dx.doi.org/10.15666/aeer/1605_71557170
© 2018, ALÖKI Kft., Budapest, Hungary

38.45% of the total covariance, reflecting the main coupling characteristics between the 120 m layer sea temperature field and the 850 hPa meridional wind field. For the first three modes, the correlations between time coefficients of the left and the right singular vectors are high. Therefore, an analysis is conducted on the heterogeneous correlation field of the first mode. In *Figure 4a,* the equatorial eastern Pacific shows positive anomalies of sea temperature. The center of the positive values located in 10°S~5°N, 170°~110°W with the maximum correlation coefficient of 0.4 (significant at 0.01 confidence level) while the correlation coefficients in the region of positive anomalies in the equatorial central Indian Ocean are low. The region from the equatorial eastern Indian Ocean to the western Pacific shows negative anomalies of sea temperature, with the center of the negative values located in 5°~15°N, 110°~150°E. The maximum of the correlation coefficient is comparable with that in the equatorial eastern Pacific Ocean. In *Figure 4b,* the meridional wind in the eastern Pacific Ocean to the north of the equator shows northerly anomalies with the maximum correlation coefficient of 0.6 (significant at 0.001 confidence level) while that to the south of the equator shows southerly anomalies. Therefore, the meridional wind anomaly is convergent from both hemispheres to the equatorial eastern Pacific Ocean, which is conducive to the accumulation of the warm water near the equatorial eastern Pacific Ocean. Similarly, the meridional wind in the equatorial central Indian Ocean shows northerly and southerly anomalies to the north and south of the equator, respectively, which is also conducive to the accumulation of the warm water near the central Indian Ocean. East Asia (110°~130°E) shows southerly and northerly anomalies to the north and south of the equator, respectively, which is divergent and is not conducive to the accumulation of the warm water near the equatorial western Pacific Ocean. As the modal correlation coefficient is positive, when the time coefficients of the left and right fields are strongly positive, the meridional wind anomalies on the two sides of the equator are convergent in the central Indian Ocean and eastern Pacific Ocean but divergent in East Asia. In this condition, the sea temperature in the central Indian Ocean and eastern Pacific Ocean increases while the sea temperature in the region from the eastern Indian Ocean to the western Pacific Ocean decreases, showing an El Niño state. On the contrary, when the time coefficients of the left and right fields are strongly negative, the meridional wind anomalies on the two sides of the equator are divergent in the central Indian Ocean and eastern Pacific Ocean but convergent in East Asia. In this condition, the sea temperature in the central Indian Ocean and eastern Pacific Ocean decreases while the sea temperature in the region from the eastern Indian Ocean to the western Pacific Ocean increases, showing a La Niña state. The time coefficients (*Fig. 4c*) show that the trends of the two fields are in generally consistent and both of them show clear characteristics of interannual variability.

Table 3. *Information of the first three modes of SVD between sea temperature field and meridional wind field*

Sequence number	Correlation coefficients	The sum of squares of the interprets covariance%	Accumulation of the sum of squares of the interprets covariance%
1	0.93	38.45	38.45
2	0.91	9.27	47.72
3	0.91	6.92	54.64

http://www.aloki.hu ● ISSN 1589 1623 (Print) ● ISSN 1785 0037 (Online)
DOI: http://dx.doi.org/10.15666/aeer/1605_71557170
© 2018, ALÖKI Kft., Budapest, Hungary

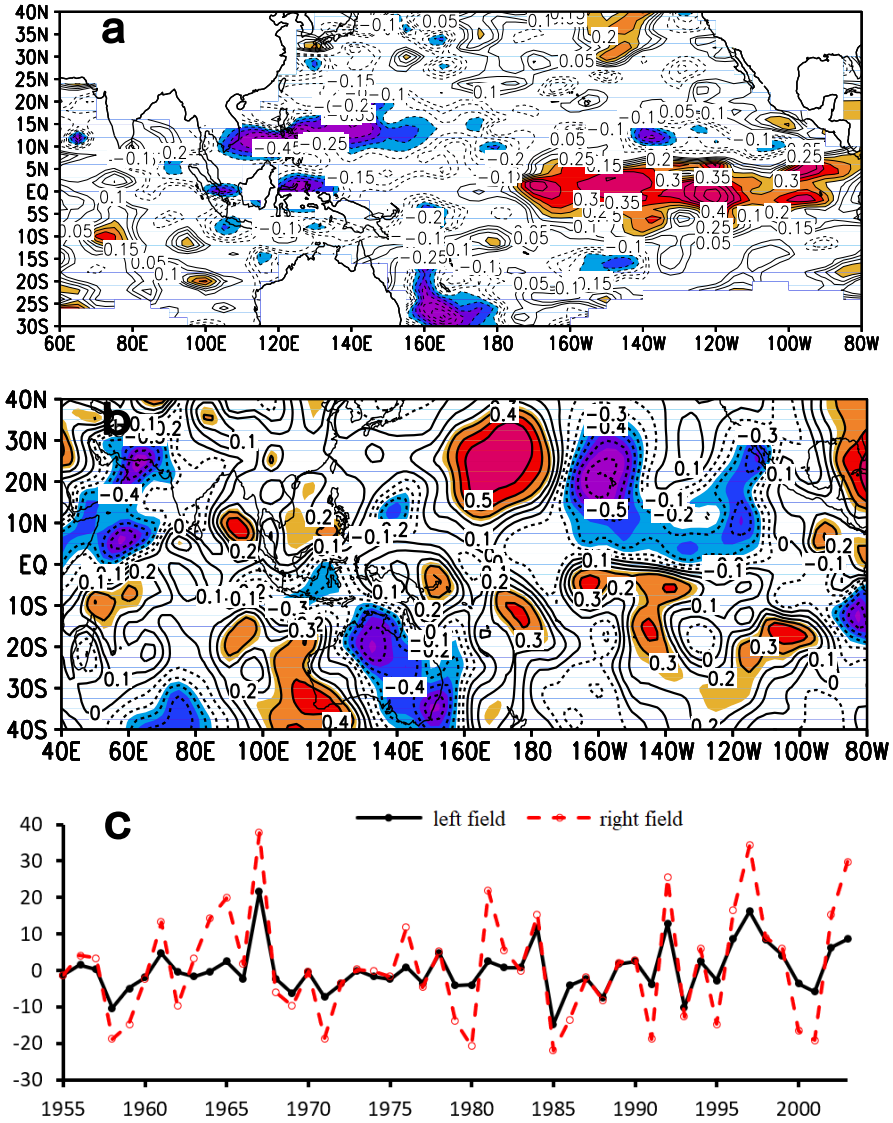

Figure 4. *Heterogeneous correlation graphs between winter 120 m sea temperature field and 850 hPa meridional wind field: (a) left field, (b) right field, and (c) time coefficient. The shadow means the values significant at 0.1 confidence level*

Coupling relationship between subsurface sea temperature in tropical Pacific-Indian Ocean and EASM circulation

The correlation coefficients are calculated between the IEASM and the sea temperature anomalies in the region from the tropical Pacific Ocean to the tropical Indian Ocean. The calculation is conducted month by month and layer by layer from 0 to 400-m depth. It is found that the IEASM has high correlations with the sea temperature anomalies in the equatorial region from the central Indian Ocean to the eastern Pacific Ocean and these correlations change with time. The correlation is the highest when the sea temperature field leads and lags the monsoon for six months and four months, respectively, and the distribution characteristics are significant (Li et al., 2018; Guo et al., 2018). It can be seen that the tropical subsurface sea temperature affects the intensity of EASM by affecting the atmospheric circulation in East Asian,

http://www.aloki.hu ● ISSN 1589 1623 (Print) ● ISSN 1785 0037 (Online)
DOI: http://dx.doi.org/10.15666/aeer/1605_71557170
© 2018, ALÖKI Kft., Budapest, Hungary

while the variation of EASM also affects the distribution of the sea temperature field. To further understand the coupling relationship between 120 m sea temperature field and EASM circulation field, the SVD is conducted between these two fields for the conditions that the sea temperature field leads and lags the EASM circulation field for six months and four months, respectively.

Coupling relationship when subsurface sea temperature field leads wind field

Figure 5 shows the left and right heterogeneous correlation graphs and time coefficients of the first mode of SVD selecting the winter (January) 120 m normalized sea temperature anomalies as the left field and the summer (July) normalized 850 hPa wind field anomalies as the right field. *Table 4* shows the corresponding main information of the first three modes of SVD. It can be seen from *Table 4* that the first mode interprets 37.92% of the total covariance, reflecting the main coupling characteristics between the 120 m layer sea temperature field and the 850 hPa wind field. For the first three modes, the correlations between time coefficients of the left and the right singular vectors are high (significant at 0.001 confidence level). Therefore, an analysis is conducted on the heterogeneous correlation field of the first mode.

Table 4. *Information of the first three modes of SVD between sea temperature field and wind field*

Sequence number	Correlation coefficients	The sum of squares of the interprets covariance %	Accumulation of the sum of squares of the interprets covariance %
1	0.92	37.92	37.92
2	0.90	10.03	47.95
3	0.91	7.45	55.40

In the right field in *Figure 5a,* the region from the equatorial eastern Indian Ocean to the western Pacific shows westerly anomalies. The region locates in 0°~15°N, 70°~180°E, and the highest correlation is found around 80°~150°E with the maximum correlation coefficient of 0.8 (significant at 0.001 confidence level), which is in line with the latitudinal band and eastward stretch of the westerly jet in summer during the years with strong EASM. Meanwhile, the western Pacific subtropical high in the northern hemisphere (corresponding to the anti-cyclonic circulation anomaly) is weaker than normal, indicating that the EASM circulation is strengthened. In the corresponding left field in *Figure 5b,* the region from the equatorial eastern Indian Ocean to the western Pacific shows positive anomalies of sea temperature centered in 10°S~10°N, 100°~170°E. The correlation coefficients in the south of the Bay of Bengal and the equatorial ocean near 160°E are 0.4 which is significant at 0.01 confidence level. Most regions in the equatorial central Indian Ocean and the equatorial eastern Pacific Ocean show negative anomalies, and the absolute value of the maximum correlation coefficient is lower than that in the region from the equatorial eastern Indian Ocean to the western Pacific. According to *Figure 5c,* when the time coefficient is strongly positive, the sea temperature in the region from the equatorial eastern Indian Ocean to the western Pacific Ocean becomes higher while the sea temperature in the central Indian Ocean and the eastern Pacific becomes lower in winter, showing a La Niña state.

http://www.aloki.hu ● ISSN 1589 1623 (Print) ● ISSN 1785 0037 (Online)
DOI: http://dx.doi.org/10.15666/aeer/1605_71557170
© 2018, ALÖKI Kft., Budapest, Hungary

As the sea temperature leads the monsoon for six months, the EASM in La Niña years will be stronger than normal. On the contrary, when the time coefficient is strongly negative, the sea temperature in the region from the equatorial eastern Indian Ocean to the western Pacific Ocean becomes lower while the sea temperature in the central Indian Ocean and the eastern Pacific becomes higher in winter, showing an El Niño state and leading to a weaker EASM. Besides, the time coefficients show that the trends of the two fields are in generally consistent and both of them show clear characteristics of interannual variability.

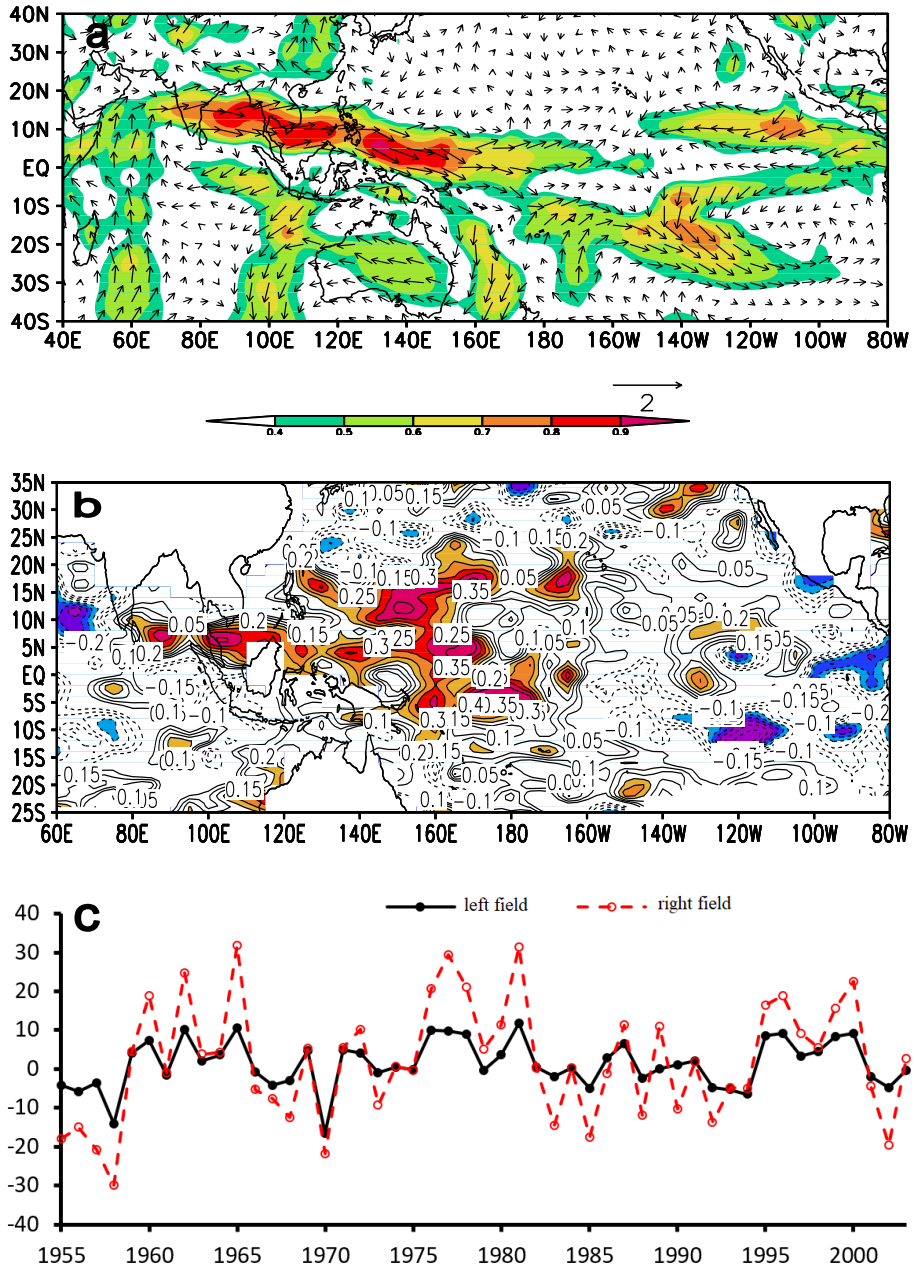

Figure 5. *Heterogeneous correlation graphs between 120 m sea temperature field and 850 hPa meridional wind field when sea temperature leads the wind for six months: (a) left field, (b) right field, and (c) time coefficient. The shadow means the values significant at 0.1 confidence level*

http://www.aloki.hu ● ISSN 1589 1623 (Print) ● ISSN 1785 0037 (Online)
DOI: http://dx.doi.org/10.15666/aeer/1605_71557170
© 2018, ALÖKI Kft., Budapest, Hungary

Coupling relationship when subsurface sea temperature field lags wind field

Figure 6 shows the left and right heterogeneous correlation graphs and time coefficients of the first mode of SVD selecting the winter (November) 120 m normalized sea temperature anomalies as the left field and the summer (July) normalized 850 hPa wind field anomalies as the right field. *Table 5* shows the corresponding main information of the first three modes of SVD. It can be seen from *Table 5* that the first mode interprets 40.15% of the total covariance, reflecting the main coupling characteristics between the 120 m layer sea temperature field and the 850 hPa wind field. For the first three modes, the correlations between time coefficients of the left and the right singular vectors are high. An analysis is conducted on the heterogeneous correlation field of the first mode. The distribution of the right field in *Figure 6a* is similar to that in *Figure 5a,* indicating the strengthening of EASM circulation. In the corresponding left field in *Figure 6b,* the equatorial eastern Pacific Ocean shows positive anomalies in sea temperature while the positive anomalies in the equatorial eastern Indian Ocean are relatively low. The highest correlation is found in 5°S~5°N, 160°~120°W with the maximum correlation coefficient of 0.4 (significant at 0.01 confidence level). The region from the equatorial eastern Indian Ocean to the western Pacific shows negative anomalies, with the absolute value of the maximum correlation coefficient similar to that in the equatorial eastern Pacific Ocean. According to *Figure 6c,* when the time coefficient is strongly positive, the EASM is stronger than normal. As sea temperature lags monsoon for four months, the sea temperature in the region from the equatorial eastern Indian Ocean to the western Pacific Ocean becomes lower while the sea temperature in the central Indian Ocean and the eastern Pacific becomes higher in autumn and winter, showing an El Niño state. On the contrary, when the time coefficient is strongly negative, the EASM is weaker than normal. The sea temperature in the region from the equatorial eastern Indian Ocean to the western Pacific Ocean becomes higher while the sea temperature in the central Indian Ocean and the eastern Pacific becomes lower in autumn and winter, showing a La Niña state. The time coefficients show that the trends of the two fields are also in generally consistent and both of them show clear characteristics of interannual variability.

Table 5. *Information of the first three modes of SVD between sea temperature field and wind field*

Sequence number	Correlation coefficients	the sum of squares of the interprets covariance %	Accumulation of the sum of squares of the interprets covariance %
1	0.90	40.15	40.15
2	0.91	12.49	52.64
3	0.88	7.88	60.52

Discussion

The covariation of the sea temperature field and the wind field can be summarized as follow: When the 850 hPa trade wind in the equatorial central and eastern Pacific Ocean increases/decreases, the region from the central Indian Ocean to the western Pacific Ocean shows westerly/easterly anomalies, or the meridional wind anomalies on the two sides of the equator are convergent/divergent in the central Indian Ocean and eastern

http://www.aloki.hu ● ISSN 1589 1623 (Print) ● ISSN 1785 0037 (Online)
DOI: http://dx.doi.org/10.15666/aeer/1605_71557170
© 2018, ALÖKI Kft., Budapest, Hungary

Pacific Ocean but divergent/convergent in East Asia. The corresponding 120 m sea temperature in the region from the eastern Indian Ocean to the western Pacific Ocean increases/decreases, and the sea temperature in the central Indian Ocean and eastern Pacific Ocean decreases/ increases, showing a La Niña/El Niño state.

From the lead-lag SVD above, it is found that: When the sea temperature in the region from the central Indian Ocean to the western Pacific Ocean is higher/lower than normal and the sea temperature in the central Indian Ocean and the eastern Pacific Ocean is lower/higher than normal, a La Niña/El Niño state will be shown. After that, the EASM is stronger/weaker than normal, and the increase/decrease of EASM circulation leads to an El Niño/La Niña state in the tropical Pacific and Indian oceans in autumn and winter. This result is consistent with (Ke et al., 2015) and (Guo et al., 2018), further verifying the relationship between the subsurface sea temperature and the EASM.

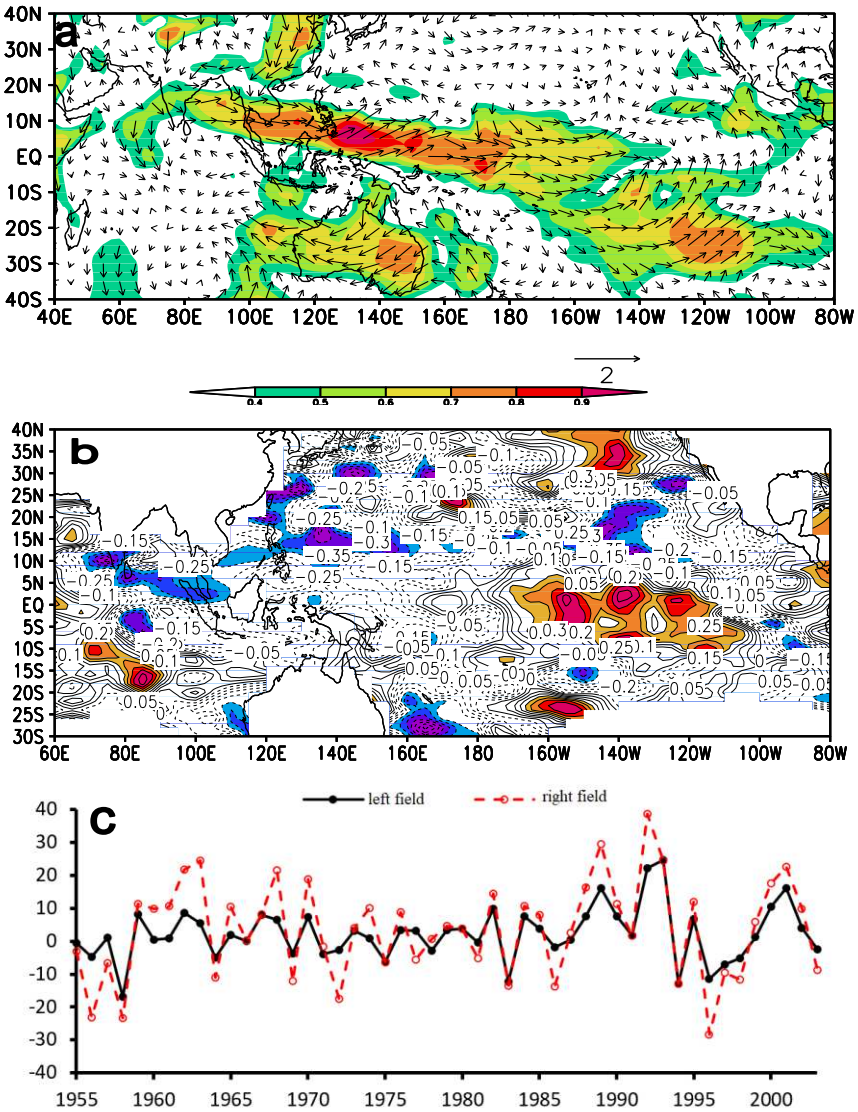

Figure 6. *Heterogeneous correlation graphs between winter 120 m sea temperature field and 850 hPa meridional wind field when sea temperature lags the wind for four months: (a) left field, (b) right field, and (c) time coefficient. The shadow means the values significant at 0.1 confidence level*

http://www.aloki.hu ● ISSN 1589 1623 (Print) ● ISSN 1785 0037 (Online)
DOI: http://dx.doi.org/10.15666/aeer/1605_71557170
© 2018, ALÖKI Kft., Budapest, Hungary

In summary, the distribution of tropical subsurface sea temperature anomalies has an impact on the interannual variation of the EASM while the anomalies of EASM change the thermal state of the ocean. There is a mutual interaction between the EASM and the subsurface sea temperature in the tropical region from the Pacific Ocean to the Indian Ocean. The tropical subsurface sea temperature anomalies are an important reference for predicting the variation of EASM. However, this study only focuses on the subsurface sea temperature of the tropical ocean. More parameters which are representative of the ocean characteristics (such as heat capacity and salinity) (Yang et al., 2017) are needed for the future work. Meanwhile, the mechanism of interaction between the EASM and the subsurface sea temperature in the tropical Pacific and Indian Ocean needs to be further explored.

Conclusions

This study analyzes the interannual variation and circulation characteristics of the IEASM. The characteristics of the subsurface sea temperature anomaly field and the EASM anomaly field in the tropical Indian and Pacific Ocean are investigated, and their coupling relationship is discussed in this study. It turned out that:

The intensity of the EASM has obvious interannual variability. The IEASM defined by Zhang et al. (2003) during the years with strong/weak EASM are analyzed, and the result shows that the tropospheric low-level circulation is significantly different in the years with strong and weak EASM. In the summer years with strong/weak EASM, the western Pacific subtropical high is located more north/south than usual, and the tropical region in East Asia and the Pacific Ocean shows closed cyclonic/anti-cyclonic anomaly circulation, and the western Pacific subtropical high is weak/strong than normal.

The characteristics of the integral circulation in the EASM region during the years with strong and weak EASM show that the vertical velocity anomalies in the EASM region are significantly different during the summer of the year with strong and weak EASM. The vertical velocity anomalies in East Asia are downward/upward during the years with strong and weak EASM leading to a weaker/stronger Meiyu front.

The covariation of the sea temperature field and the wind field is: When the 850 hPa trade wind in the equatorial central and eastern Pacific Ocean increases/decreases, the region from the central Indian Ocean to the western Pacific Ocean shows westerly/easterly anomalies, or the meridional wind anomalies on the two sides of the equator are convergent/divergent in the central Indian Ocean and eastern Pacific Ocean but divergent/convergent in East Asia. The corresponding 120 m sea temperature in the region from the eastern Indian Ocean to the western Pacific Ocean increases/decreases, and the sea temperature in the central Indian Ocean and eastern Pacific Ocean decreases/ increases, showing a La Niña/El Niño state.

When the winter 120 m sea temperature in the region from the equatorial eastern Indian Ocean to the western Pacific is higher than normal and that in the central Indian Ocean and the eastern Pacific Ocean is lower than normal, which means the distribution of the sea temperature is a La Niña state, it is easy to be with strong EASM, and the distribution of the sea temperature tends to turn into an El Niño state during the autumn and winter. In contrast, when the winter 120 m sea temperature in the region from the equatorial eastern Indian Ocean to the western Pacific is lower than normal and the that in the central Indian Ocean and the eastern Pacific Ocean is higher than normal, which means the distribution of the sea temperature is an El Niño state, it is easy to be with

http://www.aloki.hu ● ISSN 1589 1623 (Print) ● ISSN 1785 0037 (Online)
DOI: http://dx.doi.org/10.15666/aeer/1605_71557170
© 2018, ALÖKI Kft., Budapest, Hungary

weak EASM, and the distribution of the sea temperature tends to turn into a La Niña state during the autumn and winter.

Acknowledgements. This work was supported in part by the China Civil Aviation Flight Technology and Flight Safety Research Base Open Fund Project (F2016KF02).

REFERENCES

[1] Cai, Y., Zhang, J., Yu, W. (2005): An analysis of temperature anomaly in 0-400 m layer of equatorial Indian and Pacific Oceans. – Journal of Tropical Oceanography 24(4): 60-66.
[2] Chen, Y., Zhao, Y., Wang, F., et al. (2011): The decadal variability of tropic subsurface ocean temperature anomaly and its impact on climate of China. – Journal of Tropical Meteorology 27(6): 785-796.
[3] Chen, Y., Zhao, Y., Feng, J., et al. (2012): ENSO cycle and climate anomaly in China. – Chinese Journal of Oceanology and Limnology 30(6): 985-1000.
[4] Ding, Y., Jiang, Z. (1995): Generality of singular value decomposition in diagnostic analysis of meteorological field. – Acta Meteorologica Sinica 54(3): 365-372.
[5] Duan, A., Wu, G., Liang, X. (2008): Influence of the Tibetan Plateau on the summer climate patterns over Asia in the IAP/LASG SAMIL model. – Advances in Atmospheric Sciences 25(4): 518-528.
[6] Feng, J., Chen, W., Tam, C., et al. (2011): Different impacts of El Nino and El Nino Modoki on China rainfall in the decaying phases. – International Journal of Climatology 31(14): 2091-2101.
[7] Gong, D., He, X. (2002): Interdecadal change in Western Pacific subtropical high and climatic effects. – Acta GeographicaSinica 57(2): 185-193.
[8] Guo, S., Li, F., Ge, F. (2018): A strong correlation between pacific subsurface ocean temperature and East Asian summer monsoon. – Transactions of Atmospheric Sciences 41(1): 103-112.
[9] Hao, L., Ding, Y., Min, J. (2016): Relationship between summer monsoon change in East Asia and abnormal summer rainfall in North China. – Plateau Meteor 35(5): 1280-1289.
[10] John, M., Catherine, S., Christopher, S. (1992): Singular value decomposition of wintertime sea surface temperature and 500 mb height anomalies. – Journal of Climate 5(6): 561-576.
[11] Ke, Z., Hua, L., Zhong, L., et al. (2015): The influence of sea surface temperature anomaly on the East Asian summer monsoon strength and its precursor. – Journal of Applied Meteorological Science 26(5): 536-544.
[12] Li, W., Zhang, R., Sun, C., et al. (2016): Recent research advances on the interannual-interdecadal variations of drought/flood in South China and associated causes. – Journal of Applied Meteorological Science 27(5): 577-591.
[13] Li, X., Li, C. (2014): Occurrence of two types of El Nino events and the subsurface ocean temperature anomalies in the equatorial Pacific. – Chinese Science Bulletin 59(21): 2098-2107.
[14] Li, X., Xu, F., Chen, H., et al. (2017): Correlation analysis of the cycle process between the Western Pacific warm pool and ENSO during 1980－2016. – Journal of Marine Meteorology 37(3): 85-94.
[15] Li, X., Tu, S., Tang, Y., et al. (2018): Correlation analysis of East Asian summer monsoon and subsurface ocean temperature from the Pacific Ocean to the Indian Ocean in the tropics. – Applied Ecology and Environmental Research 16(1): 81-96.

http://www.aloki.hu ● ISSN 1589 1623 (Print) ● ISSN 1785 0037 (Online)
DOI: http://dx.doi.org/10.15666/aeer/1605_71557170
© 2018, ALÖKI Kft., Budapest, Hungary

[16] Liu, Y., Guo, Y. (2005): Impact of pressure system anomaly over mid high latitude on the interdecadal change of East Asia summer monsoon. – Plateau Meteorology 24(2): 129-135.
[17] Qin, Y., Wang, P. (2015): Anomalies of the ascending branch structure in the Hadley cell over the Eastern Asia monsoon region and their impacts on the precipitation in the Yangtze River basin in summer. – Journal of Tropical Meteorology 31(4): 467-474.
[18] Shan, C., Li, Y., Ren, R., et al. (2016): Characteristics of the West Pacific warm pool thermal condition and its effects on the ENSO events based on the GODAS data. – Journal of the Meteorological Sciences 36(5): 674-680.
[19] Wu, B., Zhang, R. (2011): Interannual variability of the East Asian summer monsoon and its association with the anomalous atmospheric circulation over the mid-high latitudes and external forcing. – Acta Meteorologica Sinica 69(2): 219-233.
[20] Yang, X., Wu, X., Xu, J. (2017): A Review on the upper ocean heat and salt content in the Western Pacific warm pool. – Transactions of Oceanology and Limnology (5): 18-30.
[21] Zhang, Q., Wang, Y. (2006): The response of East Asian monsoon circulation between winter and summer to sea surface temperature over the Pacific Ocean. – Climatic and Environmental Research 11(4): 487-498.
[22] Zhang, Q., Tao, S., Chen, L. (2003): The inter-annual variability of east Asian summer monsoon indices and its association with the pattern of general circulation over East Asia. – Journal of Meteorological Research 61(4): 559-568.
[23] Zhang, R., Li, Q. (2004): Impact of sea temperature variability of tropical oceans on East Asian monsoon. – Meteorological Monthly 30(12): 22-26.
[24] Zhang, R., Sumi, A., Kimoto, M. (1999): A diagnostic study of the impact of El Nino on the precipitation in China. – Adv. Atmos. Sci. 16(2): 229-241.
[25] Zhang, R., Min, Q., Su, J. (2017): Impact of El Nino on atmospheric circulations over East Asia and rainfall in China: Role of the anomalous western North Pacific anticyclone. – Science China: Earth Sciences 47(5): 544-553.
[26] Zhou, W., Chen, W., Wang, D. (2012): The implications of El Nino–Southern Oscillation signal for South China monsoon climate. – Aquatic Ecosystem Health & Management 15(1): 14-19.

http://www.aloki.hu ● ISSN 1589 1623 (Print) ● ISSN 1785 0037 (Online)
DOI: http://dx.doi.org/10.15666/aeer/1605_71557170
© 2018, ALÖKI Kft., Budapest, Hungary

EXAMINING THE RELATIONSHIP BETWEEN FINANCIAL DEVELOPMENT, SUSTAINABLE ECONOMIC OPPORTUNITY AND ECOLOGICAL FOOTPRINT IN SADC COUNTRIES

OLOWU, G.[1*] – BEIN, M.[1] – OLASEHINDE-WILLIAMS, G.[2]

[1]*Faculty of Economics and Administrative Sciences, Cyprus International University Haspolat via Mersin 10, Turkey*

[2]*Department of Economics, Eastern Mediterranean University, Famagusta via Mersin 10, Turkey*

**Corresponding author*
e-mail: olowugbolahan@gmail.com; phone: +90-392-671-1111 (ex 2227); fax +90-392-671-1130

(Received 3rd Aug 2018; accepted 28th Sep 2018)

Abstract. The study empirically investigates the relationship between financial development, sustainable economic opportunity and ecological footprint in Southern African Development Community (SADC) countries. The research was carried out utilizing time series data on financial access (bank branches per 100,000 adults), financial depth (private credit by deposit money banks to GDP), financial efficiency (bank return on equity percentage, after tax), financial stability (bank Z-score), composite index for financial development, ecological footprint indicator and sustainable economic opportunity. Bootstrap panel causality procedure based on meta-analysis in heterogeneous mixed panels was employed to test causal effects. The empirical results indicate the following; (i) causality between financial development, sustainable economic opportunity and ecological footprint varies across countries with different conditions, which leads to the conclusion that SADC countries are heterogeneous in nature, (ii) for the entire panel, financial development causally affects both sustainable economic opportunity and ecological footprint, and (iii) for the entire panel, sustainable economic opportunity causally affects ecological footprint. The findings suggest introduction of modern financial institutions, especially depository and investment institutions that will stimulate financial services and not only provide funds for investments in human and physical capital required to improve sustainable economic opportunity in SADC countries, but also make funds available for research and development of more efficient ecofriendly technologies.
Keywords: *Africa, bootstrap panel Granger causality test, environment, funds, growth*

Introduction

The main aim of this research is to empirically analyze and find answers to the following questions in relation to Southern African Development Community (SADC) countries; (i) is there any statistically significant causal relationship between financial development, sustainable economic opportunity and ecological footprint in the regional bloc? (ii) is there any statistically significant causal relationship between financial development, sustainable economic opportunity and the ecological footprint in the individual member countries?

The authors believe that finding answers to these questions will aid policy makers in these countries in economic planning, positioning of the countries for opportunities that are sustainable without losing sight of environmental degradation issues.

Crucial to the development of economically sustainable livelihoods strategies is an in-depth understanding of markets and the facilitation of stronger, fairer relationships between government policies in creating development opportunity, for citizens and corporations. A financially viable enterprise should therefore benefit local communities

http://www.aloki.hu ● ISSN 1589 1623 (Print) ● ISSN 1785 0037 (Online)
DOI: http://dx.doi.org/10.15666/aeer/1605_71717190
© 2018, ALÖKI Kft., Budapest, Hungary

today without entirely sacrificing the future environment (Rousseau and Wachtel, 2011; Feng et al., 2018).

Variables of socio-economic growth in recent times generally include two basic components–sustainability and inclusiveness of opportunity (Acemoglu and Wolitzky, 2015). Sustainable economic opportunity is about being commercially viable and attractive to development today, bearing the future in mind. It is the aggregation and transformation of various capitals, from human, natural, produced, and social capital into financial capital as a means of achieving economic development and growth (Mo Ibrahim Foundation, 2018).

Financial development is advancement of financial systems (financial markets, banks and various financial intermediaries) in quality, quantity and efficiency. It is the output of the depth, access and efficiency of the financial sector (Ang and McKibbin, 2007; Huang and Wang, 2017). Countries always put in place policies, institutions, and measures that create, widen and deepen effective financial markets and intermediaries so that capital and financial services can be easily available (World Economic Forum, 2012). Financial capital is often utilized to the detriment of sustainability which is long term. Most financial and commercial activities are usually aimed at short term gains and immediate profit (Sofia et al., 2011).

Ecological footprint is a measurement of how much nature still exists, and how much has been used up. It measures the ecological assets that a given population requires to produce the natural resources it consumes. It is an extensive detailing of demand and supply of nature, in supporting commercial activities. The ecological footprint is an instrument of projection to track the consumption of land and/or living resources and the carbon-based waste of human populations (Baabou et al., 2017; Global Footprint Network, 2018).

Over the past two decades, extant literature has revealed that financial sector activities and environmental resources have significant impact on economic performance of societies (Li et al., 2016). Unsurprisingly, research interest in this area continues to grow. An extensive body of literature exists on the inter-relations between financial development and economic activity. They are grouped into 4 broad categories; (i) those that provide evidence in support of the supply-leading theory which states that economic growth is preceded by financial development. The theory suggests that financial development induces improvements in savings and investment efficiency which in turn drives economic growth (Ang, 2008; Körner and Schnabel, 2009; Bojanic, 2012; Pradhan et al., 2014; Li et al., 2015), (ii) those that support the demand-following theory which states that economic growth drives the demand for financial services. The theory asserts that growth in the real sector of an economy raises the demand for supporting financial services and this in turn induces growth in the financial sector (Liang and Jian-Zhou, 2006; Ang and McKibbin, 2007; Panopoulou, 2009), (iii) those that are in alignment with the neutrality hypothesis. This group of literature posits that there is no significant relationship between the financial sector and economic growth (Al-Yousif, 2002; Mukhopadhyay et al., 2011), and (iv) the group of studies that affirm the existence of a feedback relationship (feedback hypothesis). The feedback hypothesis argues that improved financial sector performance positively affects economic growth and increased economic growth in turn causes an increase in demand for financial services (Wolde-Rufael, 2009; Pradhan et al., 2013).

The economic activity-environment nexus has mostly been tested within the environmental Kuznets curve (EKC) framework which examines the impact of

http://www.aloki.hu ● ISSN 1589 1623 (Print) ● ISSN 1785 0037 (Online)
DOI: http://dx.doi.org/10.15666/aeer/1605_71717190
© 2018, ALÖKI Kft., Budapest, Hungary

economic growth on single pollution indicators such as CO_2, SO_2, NO_X and CO and asserts that there is an inverted U-shaped relationship between economic performance and pollution. The hypothesis suggests that pollution increases alongside industrialization during the early stages of economic growth up to a point beyond which higher economic growth leads to the introduction of more efficient technologies, better environmental regulations and higher environmental expenditures (Acar and Asici, 2017). Recent examples of such EKC studies include Lau et al. (2014), Onafowora and Owoye (2014), Al-Mulali et al. (2015), Apergis and Ozturk (2015), Chang (2015), Tang and Tan (2015), Azam and Khan (2016), Kang et al. (2016), Li et al. (2016), and Gill et al. (2017).

Overall, studies on economic activity, financial development and the environment display the following limitations. First, many of them only investigate the effect of either financial development or economic growth on environmental quality. They do not examine all 3 variables within a unified framework. Second, most of the studies only carry out one-way examinations of the effect of either financial development or economic growth on environmental quality. They mostly neglect the possibility of feedback relationships. Third, most of them adopt very narrow measures of these 3 variables. For example, financial development is mostly proxied with these three measures: domestic credit to private sector, banking sector credit and financial domestic credit. These measures of financial development are indicators of financial depth. They ignore other important aspects of financial sector performance such as financial access, financial efficiency and financial stability. Similarly, environmental quality is mostly measured with degree of pollution. However, the impacts of economic activities are wide-ranging and multidimensional, such that it cannot be sufficiently accounted for using one-dimensional pollution indicators (Wackernagel et al., 2002). Also, economic performance is most commonly measured through economic growth which largely ignores economic opportunities that contribute to a prosperous and equitable society. Finally, previous studies also mostly neglect the issues of cross-sectional dependency and cross-country heterogeneity. According to Chang et al. (2013), the importance of cross-country heterogeneity and cross-sectional dependency cannot be over emphasized. Although each country may sustain its own dynamics in economic development, economic or financial instability in one country often spreads to other countries through economic integration and trade.

In this context, this study's contributions to literature are as follows. First, the relationship between financial development, economic performance and the environment is examined via bootstrap panel Granger causality tests of Emirmahmutoglu and Kose (2011) in SADC countries. With this test, it is possible to detect Granger causality in the entire panel as well as in each of the individual countries contained in the panel. Furthermore, with this test, the pre-test bias associated with testing for stationarity and co-integration is avoided. Second, panel causality modeling which controls for country-specific differences and cross-country dependency is followed. Third, various dimensions of financial development–financial access, financial depth, financial efficiency and financial stability–as well as an aggregate index of these 4 measures is considered. Moreover, ecological footprint, a multidimensional indicator of environmental state, is used in this study. Furthermore, rather than adopt economic growth as the measure of economic performance, the degree of sustainable economic opportunity is used instead.

http://www.aloki.hu ● ISSN 1589 1623 (Print) ● ISSN 1785 0037 (Online)
DOI: http://dx.doi.org/10.15666/aeer/1605_71717190
© 2018, ALÖKI Kft., Budapest, Hungary

SADC countries

Southern African Development Community (SADC) consists of 15 countries whose main objectives are; achievement of development and economic growth, poverty alleviation, enhancement of standard and quality of life through regional integration, evolution of common political values, systems and institutions, promotion of peace and security, promotion of self-sustaining development on the basis of collective self-reliance and interdependence among Member States, achievement of complementarity between national and regional strategies and programmes, maximization of productive employment and utilization of resources of the Region, achievement of sustainable utilization of natural resources and effective protection of the environment, and consolidation of the long standing historical, social and cultural affinities and links among the people of the Region.

The sources of GDP in SADC are industry (32%), agriculture (17%), and service sector, with the largest share (52%). This regional bloc has shown signs of economic improvement over the past decade. The regional bloc includes four countries officially classified as middle-income countries–Botswana, Mauritius, Namibia and South Africa (www.sadc.int/about-sadc/overview/sadc-facts-figures).

The rest of this study is structured as follows: data and empirical methodology, results, discussions and conclusion.

Data and empirical methodology

Data

The study sample consists of time series data on 13 of the 15 SADC countries over the period 2000-2016. Seychelles and Zimbabwe are left out of the sample due to insufficient data. In the analysis, data on financial access (bank branches per 100,000 adults), financial depth (private credit by deposit money banks to GDP), financial efficiency (bank returns on equity %, after tax) and financial stability (bank Z-score) provided by the World Bank and accessed at http://www.worldbank.org/en/publication/gfdr/data/global-financial-development-database are used. These 4 measures are then further aggregated into a single composite index for financial development using principal component analysis (PCA) given as (*Eq. 1*):

$$p_i = \sum_{i=1}^{n} a_{ij} x_i \quad \text{(Eq.1)}$$

where: $p_i = p_1, p_2, \ldots, p_k$ represent the principal Components, a_{ij} stand for component loadings and x refers to the original measures. Differences in measurement units were controlled for by using the variables in their standardized forms. The composite index is constructed with the formula (*Eq. 2*):

$$CI = \sum_{i=1}^{n} a_{ij} \frac{x_{ij}}{\sigma(x)_i} \quad \text{(Eq.2)}$$

where: CI is the composite index for financial development and σ is the standard deviation.

http://www.aloki.hu ● ISSN 1589 1623 (Print) ● ISSN 1785 0037 (Online)
DOI: http://dx.doi.org/10.15666/aeer/1605_71717190
© 2018, ALÖKI Kft., Budapest, Hungary

The ecological footprint indicator provided by (Global Footprint Network, 2018) is used as the measure of environment condition. Ecological footprint sums the use of six categories of productive surface areas: cropland, grazing land, fishing grounds, built-up land, forest area, and carbon demand on land and land area. It is expressed in units of global hectares (gha).

Data on sustainable economic opportunity is from the Ibrahim Index of African Governance (IIAG) online database. The sustainable economic opportunity index consists of four sub-categories (public management, business environment, infrastructure and rural sector), made up of 29 indicators, from 18 different data sources.

The descriptive statistics for the SADC countries included in the analysis are presented in *Table 1*.

Table 1. *Summary statistics*

Panel A: Financial development index				
Country	**Mean**	**Std. Dev**	**Minimum**	**Maximum**
Angola	11.589	1.237	9.278	14.155
Botswana	9.136	1.545	6.150	11.260
DR Congo	5.037	1.333	3.120	9.2700
Lesotho	7.886	0.847	5.960	9.2800
Madagascar	5.552	0.745	4.200	6.9400
Malawi	9.691	1.093	8.350	12.060
Mauritius	18.184	4.334	11.390	27.610
Mozambique	3.629	1.175	2.640	7.4100
Namibia	17.621	15.769	7.530	45.210
South Africa	16.153	7.366	11.360	40.040
Swaziland	14.554	4.005	5.4600	18.280
Tanzania	10.606	1.500	8.8200	13.820
Zambia	2.252	0.379	1.763	3.131
Panel	10.121	7.110	1.763	45.210
Panel B: Sustainable economic opportunity				
Angola	28.093	3.575	23.400	32.700
Botswana	66.237	1.935	63.300	68.800
DR Congo	28.862	3.396	24.200	35.100
Lesotho	47.387	1.860	44.500	50.300
Madagascar	42.525	3.084	36.300	47.500
Malawi	48.126	2.336	45.500	52.000
Mauritius	72.380	5.654	66.600	79.900
Mozambique	46.640	1.790	44.100	49.900
Namibia	60.600	2.357	57.500	63.800
South Africa	66.206	2.574	62.400	69.300
Swaziland	46.340	3.408	41.800	50.700
Tanzania	50.133	1.506	46.100	52.500
Zambia	48.493	1.690	45.700	51.700
Panel	50.209	13.288	23.400	79.900

http://www.aloki.hu ● ISSN 1589 1623 (Print) ● ISSN 1785 0037 (Online)
DOI: http://dx.doi.org/10.15666/aeer/1605_71717190
© 2018, ALÖKI Kft., Budapest, Hungary

Panel C: Ecological footprint				
Angola	0.600	0.191	0.410	0.980
Botswana	1.702	0.174	1.360	2.040
DR Congo	0.465	0.015	0.430	0.480
Lesotho	0.903	0.046	0.830	0.990
Madagascar	0.594	0.026	0.540	0.640
Malawi	0.444	0.046	0.360	0.510
Mauritius	1.754	0.212	1.400	2.080
Mozambique	0.486	0.049	0.430	0.600
Namibia	2.829	0.979	1.898	5.702
South Africa	1.957	0.141	1.660	2.170
Swaziland	1.216	0.254	0.660	1.450
Tanzania	0.722	0.066	0.660	0.870
Zambia	0.495	0.057	0.430	0.590
Panel	1.094	0.782	0.360	5.702

In *Table 1,* the lowest mean financial development value (2.252) reported for Zambia shows the country has the least developed financial sector over the period considered, and the highest mean financial development value (18.184) reported for Mauritius indicates the country has the best developed financial sector for the period considered. Mauritius again turns out as the best performing country in terms of sustainable economic opportunity (72.380) while Angola has the poorest performance (28.093). Average demand of nature is highest in Namibia (2.829) and lowest in Malawi (0.444).

Methodology

Bootstrap panel Granger casualty test

This study applies the bootstrap panel causality procedure based on meta-analysis in heterogeneous mixed panels proposed by Emirmahmutoglu and Kose (2011). The test is an extension of the Toda and Yamamoto (1995) approach to testing coefficient restrictions in a level VAR model for an integrated or cointegrated process. The test does not require the variables in the underlying VAR system to be stationary. It may therefore be applied to panels consisting of stationary, non-stationary, cointegrated and non-cointegrated series (Seyoum et al., 2014). Pre-test bias associated with testing for stationarity and cointegration is therefore avoided. The method employs a modified Wald (MWALD) test in a lag augmented VAR (LA-VAR) which has a conventional asymptotic chi-square distribution when a VAR (p + dmax) is estimated, where p is the lag order and dmax is the maximal order of integration suspected to occur in the process. The system of equations for the panel causality tests include two sets of equations specified as follows:

$$Y_{1,t} = \alpha_{1,1} + \sum_{i=1}^{ly_1+dmax_j} \beta_{1,1,i} Y_{1,t-i} + \sum_{i=1}^{lx_1+dmax_j} \delta_{1,1,i} X_{1,t-i} + \sum_{i=1}^{lz_1+dmax_j} \gamma_{1,1,i} Z_{1,t-i} + \varepsilon_{1,1,t} \quad \text{(Eq.1a)}$$

$$Y_{2,t} = \alpha_{1,2} + \sum_{i=1}^{ly_1+dmax_j} \beta_{1,2,i} Y_{2,t-i} + \sum_{i=1}^{lx_1+dmax_j} \delta_{1,2,i} X_{2,t-i} + \sum_{i=1}^{lz_1+dmax_j} \gamma_{1,2,i} Z_{2,t-i} + \varepsilon_{1,2,t} \quad \text{(Eq.1b)}$$

http://www.aloki.hu ● ISSN 1589 1623 (Print) ● ISSN 1785 0037 (Online)
DOI: http://dx.doi.org/10.15666/aeer/1605_71717190
© 2018, ALÖKI Kft., Budapest, Hungary

$$Y_{N,t} = \alpha_{1,N} + \sum_{i=1}^{ly_1+dmax_j} \beta_{1,N,i} Y_{N,t-i} + \sum_{i=1}^{lx_1+dmax_j} \delta_{1,N,i} X_{N,t-i} + \sum_{i=1}^{lz_1+dmax_j} \gamma_{1,N,i} Z_{N,t-i} + \varepsilon_{1,N,t} \quad \text{(Eq.1n)}$$

$$X_{1,t} = \alpha_{2,1} + \sum_{i=1}^{ly_2+dmax_j} \beta_{2,1,i} Y_{1,t-i} + \sum_{i=1}^{lx_2+dmax_j} \delta_{2,1,i} X_{1,t-i} + \sum_{i=1}^{lz_2+dmax_j} \gamma_{2,1,i} Z_{1,t-i} + \varepsilon_{2,1,t} \quad \text{(Eq.2a)}$$

$$X_{2,t} = \alpha_{2,2} + \sum_{i=1}^{ly_2+dmax_j} \beta_{2,2,i} Y_{2,t-i} + \sum_{i=1}^{lx_2+dmax_j} \delta_{2,2,i} X_{2,t-i} + \sum_{i=1}^{lz_2+dmax_j} \gamma_{2,2,i} Z_{2,t-i} + \varepsilon_{2,2,t} \quad \text{(Eq.2b)}$$

$$X_{N,t} = \alpha_{2,N} + \sum_{i=1}^{ly_2+dmax_j} \beta_{2,N,i} Y_{N,t-i} + \sum_{i=1}^{lx_2+dmax_j} \delta_{2,N,i} X_{N,t-i} + \sum_{i=1}^{lz_2+dmax_j} \gamma_{2,N,i} Z_{N,t-i} + \varepsilon_{2,N,t} \quad \text{(Eq.2n)}$$

and

$$Z_{1,t} = \alpha_{3,1} + \sum_{i=1}^{ly_3+dmax_j} \beta_{3,1,i} Y_{1,t-i} + \sum_{i=1}^{lx_3+dmax_j} \delta_{3,1,i} X_{1,t-i} + \sum_{i=1}^{lz_3+dmax_j} \gamma_{3,1,i} Z_{1,t-i} + \varepsilon_{3,1,t} \quad \text{(Eq.3a)}$$

$$Z_{2,t} = \alpha_{3,2} + \sum_{i=1}^{ly_3+dmax_j} \beta_{3,2,i} Y_{2,t-i} + \sum_{i=1}^{lx_3+dmax_j} \delta_{3,2,i} X_{2,t-i} + \sum_{i=1}^{lz_3+dmax_j} \gamma_{3,2,i} Z_{2,t-i} + \varepsilon_{3,2,t} \quad \text{(Eq.3b)}$$

$$Z_{N,t} = \alpha_{3,N} + \sum_{i=1}^{ly_3+dmax_j} \beta_{3,N,i} Y_{N,t-i} + \sum_{i=1}^{lx_3+dmax_j} \delta_{3,N,i} X_{N,t-i} + \sum_{i=1}^{lz_3+dmax_j} \gamma_{3,N,i} Z_{N,t-i} + \varepsilon_{3,N,t} \quad \text{(Eq.3n)}$$

In the system of *Equations 1, 2* and *3,* $Y_{i,t}$, i = 1,…,N denotes financial development (access, depth, efficiency, stability and overall index, respectively), $X_{i,t}$, i = 1,…,N denotes sustainable economic opportunity and . N represents the number of countries included in the panel (j = 1,…, N), $Z_{i,t}$, i = 1,…,N is ecological footprint. t refers to the time period (t = 1,…,T), l is the lag length and $dmax_j$ stands for the maximal order of integration.

The possible alternative causal relations that could be detected for each country and the entire panel are (i) One-way Granger causality from X to Y when all $\beta_{2,j,i}$s are zero, but not all $\delta_{1,j,i}$s are zero. (ii) One-way Granger causality from Y to X when all $\delta_{1,j,i}$s are zero, but not all $\beta_{2,j,i}$s are zero. (iii) Two-way Granger causality between X and Y if some of the $\delta_{1,j,i}$s and $\beta_{2,j,i}$s are not zero. (iv) One-way Granger causality from Z to Y when all $\beta_{3,j,i}$s are zero, but not all $\gamma_{1,j,i}$s are zero. (v) One-way Granger causality from Y to Z when all $\gamma_{1,j,i}$s are zero, but not all $\beta_{3,j,i}$s are zero. (vi) Two-way Granger causality between Z and Y if some of the $\gamma_{1,j,i}$s and $\beta_{3,j,i}$s are not zero. (vii) One-way Granger causality from Z to X when all $\delta_{3,j,i}$s are zero, but not all $\gamma_{2,j,i}$s are zero. (viii) One-way Granger causality from X to Z when all $\gamma_{2,j,i}$s are zero, but not all $\delta_{3,j,i}$s are zero. (ix) Two-way Granger causality between Z and X if some of the $\gamma_{2,j,i}$s and $\delta_{3,j,i}$s are not zero.

The Emirmahmutoglu and Kose (2011) Granger causality test employs the Fisher (1932) meta-analysis statistical procedure. It conducts N number of separate time series tests, and combines the significant individual p-values in a single panel test statistic. The test statistic has a chi-square distribution with 2N degrees of freedom. The Fisher test statistic (λ) is specified as (*Eq. 4*):

$$\lambda = -2 \sum_{i=1}^{N} ln_{(pi)} \;\; i = 1,2, \ldots, N \quad \text{(Eq.4)}$$

pi denotes the p-value for the Wald statistic of the ith cross section.

In the presence of cross sectional dependency, the limit distribution of the Fisher test statistic becomes invalid. The test deals with this problem through the bootstrap approach. Readers are referred to Emirmahmutoglu and Kose (2011) for the detailed

http://www.aloki.hu ● ISSN 1589 1623 (Print) ● ISSN 1785 0037 (Online)
DOI: http://dx.doi.org/10.15666/aeer/1605_71717190
© 2018, ALÖKI Kft., Budapest, Hungary

bootstrap procedure. In line with Emirmahmutoglu and Kose (2011), *Equations 1, 2* and *3* are estimated and the panel Granger causality tests with bootstrap critical values are executed (*Eq. 5*).

$$LM = \sum_{i=1}^{N-1}\sum_{j=i+1}^{N} T_{ij}\hat{p}_{ij}^2 \rightarrow \chi^2 \frac{N(N-1)}{2} \quad \text{(Eq.5)}$$

where $\hat{p}_{ij}^2$ = correlation coefficients from residuals

Pesaran (2004) Scaled LM test: Pesaran (2004) developed a scaled version of the LM test which is more efficient than the Breusch-Pagan (1980) LM test for data series with large N. Under the null of no cross-sectional dependence, the LM statistic is as follows (*Eq. 6*):

$$LM_s = \sqrt{\frac{1}{N(N-1)}}\sum_{i=1}^{N-1}\sum_{j=i+1}^{N}(T_{ij}\hat{p}_{ij}^2 - 1) \rightarrow N(0,1) \quad \text{(Eq.6)}$$

Pesaran (2004) CD test: a major flaw of the previous tests is that they suffer from size distortion especially when N is large and T is small. To deal with this limitation, Pesaran (2004) developed a more general alternative test statistic that provides valid results for large panels by averaging pairwise correlation coefficients $\hat{p}_{ij}$. For the null of no cross-sectional dependence, the LM test statistic for dependence is given as (*Eq. 7*):

$$CD_p = \sqrt{\frac{2}{N(N-1)}}\sum_{i=1}^{N-1}\sum_{j=i+1}^{N} T_{ij}\,\hat{p}_{ij} \rightarrow N(0,1) \quad \text{(Eq.7)}$$

Tests for slope homogeneity

Cross-country heterogeneity is also an issue of importance when employing bootstrap panel causality tests. Presence of slope heterogeneity in the data series is an indication that economic occurrences observed in one of the SADC countries are not necessarily replicated in the other SADC countries. The Pesaran and Yamagata (2008) standardized version of the Swamy (1970) homogeneity test was applied. The modified version of the Swamy (1970) test is computed as (*Eq. 8*):

$$\tilde{S} = \sum_{i=1}^{N}(\hat{\beta}_i - \hat{\beta}_{WFE})' X_i' \frac{M_T X_i}{\tilde{\sigma}_i^2}(\hat{\beta}_i - \hat{\beta}_{WFE}) \quad \text{(Eq.8)}$$

where $\hat{\beta}_i$=Pooled OLS estimator, $\hat{\beta}_{WFE}$ = weighted fixed effect pooled estimator and $\tilde{\sigma}_i^2$ is the estimator. The standard dispersion statistics is computed as (*Eq. 9*):

$$\tilde{\Delta} = \sqrt{N}\left(\frac{N^{-1}\tilde{S} - k}{2k}\right) \quad \text{(Eq.9)}$$

Alternatively, the bias adjusted version of the standard dispersion statistics may be computed (*Eq. 10*):

$$\tilde{\Delta}_{Adj} = \sqrt{N}\left(\frac{N^{-1}\tilde{S} - E(\tilde{z}_{it})}{\sqrt{var}(\tilde{z}_{it})}\right) \quad \text{(Eq.10)}$$

Both statistics are tested under the null of slope homogeneity.

http://www.aloki.hu ● ISSN 1589 1623 (Print) ● ISSN 1785 0037 (Online)
DOI: http://dx.doi.org/10.15666/aeer/1605_71717190
© 2018, ALÖKI Kft., Budapest, Hungary

Results

Table 2 reports the results of cross-sectional dependence tests (LM, LM_S and CD_P) obtained from estimating *Equations 6, 7* and *8*. The results from LM and LM_S tests clearly show that the null hypothesis of no cross-sectional dependence is rejected for all variables at ($p < 0.01$) significance level, whereas the results from CD_p test show that the null of no cross-sectional dependence is rejected for depth, stability, financial index and sustainable economic opportunity at ($p < 0.01$) level of significance, and for access at ($p < 0.1$) level of significance. Both efficiency and ecological footprint turn out as insignificant under the CD_p test. The results overwhelmingly indicate that there is cross-sectional dependence among the SADC countries. Therefore, shocks are transmitted across the SADC economies. *Table 2* also reports the results from the slope homogeneity tests ($\hat{\Delta}, \hat{\Delta}_{adj}$). Based on the delta and the bias adjusted delta statistics, the null hypothesis of slope homogeneity is rejected for financial depth, financial efficiency, overall financial index, ecological footprint and sustainable economic opportunity. This suggests that individual SADC countries possess unique economic characteristics. The bootstrap panel Granger causality approach can thus be applied.

Table 2. *Cross-sectional dependence and homogeneous test results*

Variables	Cross-sectional dependence tests			Slope homogeneity tests	
	LM (Eq.5)	LM_S (Eq.6)	CD_P (Eq.7)	$\hat{\Delta}$ (Eq.8)	$\hat{\Delta}_{adj}$ (Eq.9)
Access	194.256***	9.308***	-1.345*	1.114	1.236
Depth	134.804***	4.548***	4.874***	2.456***	2.725***
Efficiency	135.590***	4.611***	-0.799	1.857**	2.060**
Stability	120.212***	3.380***	4.441***	1.143	1.268
Fin. index	230.785***	12.233***	3.277***	1.199*	1.330*
Ecological footprint	123.202***	3.619***	-0.722	3.075***	3.412***
Sustainable economic opportunity	125.343***	3.790***	-1.843***	4.420***	4.903***

*, ** and *** indicate significance at 0.1, 0.05 and 0.001 significance levels, respectively

Tables 3–7 below report the test statistics for the causality tests between financial development (overall index, access, depth, efficiency and stability, respectively) and sustainable economic opportunity for each SADC country, and for the entire panel. The main focus is on the outcomes involving the overall financial index. The test results indicate that at country level, the causality between financial development and sustainable economic opportunity varies across countries with different conditions. For example, significant Granger causality from overall financial development index to sustainable economic opportunity exists in Botswana, Mauritius and Namibia. Significant Granger causality in the other direction exists in DR Congo, Malawi and Mozambique. A significant feedback relationship only exists in South Africa. At the panel level, significant one-way causality is detected running from the overall financial development index to sustainable economic opportunity.

http://www.aloki.hu ● ISSN 1589 1623 (Print) ● ISSN 1785 0037 (Online)
DOI: http://dx.doi.org/10.15666/aeer/1605_71717190
© 2018, ALÖKI Kft., Budapest, Hungary

When the overall index is disaggregated into its components, at the country level, the following results are found. Significant one-way causality from; financial access to sustainable economic opportunity in Botswana, DR Congo, Mauritius, Mozambique, Namibia and South Africa, from sustainable economic opportunity to financial access in Angola, from financial depth to sustainable economic opportunity in Mozambique, South Africa and Swaziland, from sustainable economic opportunity to financial depth in Angola, DR Congo and Tanzania, from financial efficiency to sustainable economic opportunity in Angola, Namibia, South Africa and Swaziland, from sustainable economic opportunity to financial efficiency in Lesotho and Madagascar, from financial stability to sustainable economic opportunity in Botswana, DR Congo, Mauritius, Namibia and South Africa, and from sustainable economic opportunity to financial stability in DR Congo, Lesotho, Malawi, Mozambique and Zambia. Bidirectional causal relationships are however detected between financial access and sustainable economic opportunity in Lesotho, between financial depth and sustainable economic opportunity in Madagascar, Malawi, Mauritius and Namibia, between financial efficiency and sustainable economic opportunity in Malawi and Mozambique, and between financial stability and sustainable economic opportunity in Madagascar, South Africa and Tanzania. At the panel level, significant one-way causality from financial access and financial efficiency to sustainable economic opportunity is found, whereas a significant feedback relationship is detected between financial depth and sustainable economic opportunity and between financial stability and sustainable economic opportunity.

Table 3. *Granger causality between financial development (index) and sustainable economic opportunity*

H0: financial development (index) does not Granger cause sustainable economic opportunity		**H0: sustainable economic opportunity does not Granger cause financial development (index)**	
Countries	**Wald statistic**	**Countries**	**Wald statistic**
Angola	0.059	Angola	2.628
Botswana	6.999***	Botswana	0.062
DR Congo	0.612	DR Congo	28.153***
Lesotho	2.144	Lesotho	2.740*
Madagascar	2.339	Madagascar	0.879
Malawi	1.461	Malawi	23.596***
Mauritius	3.646**	Mauritius	0.098
Mozambique	0.311	Mozambique	41.915***
Namibia	4.826**	Namibia	0.245
South Africa	35.555***	South Africa	43.658***
Swaziland	2.704	Swaziland	2.970
Tanzania	1.161	Tanzania	0.182
Zambia	0.834	Zambia	0.022
Panel	77.256**	Panel	158.424

*, ** and *** indicate significance at 0.1, 0.05 and 0.001 significance levels, respectively

http://www.aloki.hu ● ISSN 1589 1623 (Print) ● ISSN 1785 0037 (Online)
DOI: http://dx.doi.org/10.15666/aeer/1605_71717190
© 2018, ALÖKI Kft., Budapest, Hungary

Table 4. *Granger causality between financial development (access) and sustainable economic opportunity*

H0: financial development (access) does not Granger cause sustainable economic opportunity		**H0: sustainable economic opportunity does not Granger cause financial development (access)**	
Countries	**Wald statistic**	**Countries**	**Wald statistic**
Angola	0.615	Angola	8.265***
Botswana	6.999***	Botswana	0.062
DR Congo	24.705***	DR Congo	4.281
Lesotho	21.873***	Lesotho	7.771**
Madagascar	2.339	Madagascar	0.879
Malawi	3.963	Malawi	0.036
Mauritius	3.646**	Mauritius	0.098
Mozambique	3.496**	Mozambique	0.541
Namibia	5.824**	Namibia	0.189
South Africa	12.895***	South Africa	0.930
Swaziland	8.155***	Swaziland	0.057
Tanzania	1.161	Tanzania	0.182
Zambia	0.900	Zambia	0.076
Panel	108.526**	Panel	0.568

*, ** and *** indicate significance at 0.1, 0.05 and 0.001 significance levels, respectively

Table 5. *Granger causality between financial development (depth) and sustainable economic opportunity*

H0: financial development (depth) does not Granger cause sustainable economic opportunity		**H0: sustainable economic opportunity does not Granger cause financial development (depth)**	
Countries	**Wald statistic**	**Countries**	**Wald statistic**
Angola	2.925	Angola	25.486***
Botswana	1.386	Botswana	1.056
DR Congo	0.612	DR Congo	28.154***
Lesotho	3.078	Lesotho	1.076
Madagascar	8.685**	Madagascar	8.467**
Malawi	17.019***	Malawi	19.902***
Mauritius	13.246***	Mauritius	30.121***
Mozambique	4.224***	Mozambique	0.551
Namibia	9.996**	Namibia	10.829**
South Africa	7.237*	South Africa	1.748
Swaziland	16.643***	Swaziland	0.271
Tanzania	6.050	Tanzania	11.689***
Zambia	3.794	Zambia	3.589
Panel	84.040*	Panel	131.834**

*, ** and *** indicate significance at 0.1, 0.05 and 0.001 significance levels, respectively

http://www.aloki.hu ● ISSN 1589 1623 (Print) ● ISSN 1785 0037 (Online)
DOI: http://dx.doi.org/10.15666/aeer/1605_71717190
© 2018, ALÖKI Kft., Budapest, Hungary

Table 6. *Granger causality between financial development (efficiency) and sustainable economic opportunity*

H0: financial development (efficiency) does not Granger cause sustainable economic opportunity		**H0: sustainable economic opportunity does not Granger cause financial development (efficiency)**	
Countries	**Wald statistic**	**Countries**	**Wald statistic**
Angola	13.430***	Angola	0.404
Botswana	1.476	Botswana	4.676
DR Congo	1.085	DR Congo	2.601
Lesotho	3.657	Lesotho	11.187**
Madagascar	1.755	Madagascar	3.679*
Malawi	22.468***	Malawi	27.576***
Mauritius	3.154	Mauritius	4.538
Mozambique	7.460*	Mozambique	8.627**
Namibia	4.423**	Namibia	0.796
South Africa	23.677***	South Africa	0.536
Swaziland	8.349**	Swaziland	5.257
Tanzania	3.635	Tanzania	0.425
Zambia	0.623	Zambia	3.262
Panel	94.378*	Panel	69.049

*, ** and *** indicate significance at 0.1, 0.05 and 0.001 significance levels, respectively

Table 7. *Granger causality between financial development (stability) and sustainable economic opportunity*

H0: financial development (stability) does not Granger cause sustainable economic opportunity		**H0: sustainable economic opportunity does not Granger cause financial development (stability)**	
Countries	**Wald statistic**	**Countries**	**Wald statistic**
Angola	2.439	Angola	1.742
Botswana	30.035***	Botswana	1.309
DR Congo	8.451**	DR Congo	14.939***
Lesotho	2.672	Lesotho	68.804***
Madagascar	16.370***	Madagascar	7.234*
Malawi	1.787	Malawi	11.989***
Mauritius	7.592***	Mauritius	2.594
Mozambique	1.883	Mozambique	6.382*
Namibia	4.826**	Namibia	0.245
South Africa	70.341***	South Africa	41.103***
Swaziland	3.513	Swaziland	5.731
Tanzania	23.042***	Tanzania	49.592***
Zambia	0.244	Zambia	7.091***
Panel	161.827**	Panel	190.694**

*, ** and *** indicate significance at 0.1, 0.05 and 0.001 significance levels, respectively

http://www.aloki.hu ● ISSN 1589 1623 (Print) ● ISSN 1785 0037 (Online)
DOI: http://dx.doi.org/10.15666/aeer/1605_71717190
© 2018, ALÖKI Kft., Budapest, Hungary

In *Tables 8–12* below, the causality results for the relationship between financial development (overall index, access, depth, efficiency and stability, respectively) and ecological footprint at country and panel levels are reported. Again, the focus is on the outcomes from the overall financial development index. At country level, it is discovered that causality varies with different conditions. Significant Granger causality from overall financial development index to ecological footprint exists in DR Congo, Namibia and Swaziland. Significant one-way causality in the other direction exists in Mauritius and Mozambique. Significant feedback relationship exists in Lesotho, Madagascar, Malawi and South-Africa. At the panel level, one-way causality from overall financial development index to ecological footprint is found.

When the overall financial development index is disaggregated into its components, at country level, one-way causal effect is detected from financial access to ecological footprint in Angola, Mozambique, Namibia, Swaziland and Zambia, from ecological footprint to financial access in DRC, Mauritius and South Africa, from financial depth to ecological footprint in Botswana, DRC Congo, Madagascar and Mauritius, from ecological footprint to financial depth in Angola, Tanzania and Zambia, from financial efficiency to ecological footprint in Malawi, Mauritius and Tanzania, from ecological footprint to financial efficiency in Namibia and Swaziland, from financial stability to ecological footprint in DR Congo, Namibia, South Africa and Zambia, and from ecological footprint to financial stability in Lesotho. Bidirectional causal effects are also detected between financial access and ecological footprint in Madagascar and Malawi, between financial depth and ecological footprint in Lesotho, Malawi, Mozambique, Namibia and Swaziland, and between financial stability and ecological footprint in Malawi, Mauritius, Swaziland and Tanzania. At the panel level, causality is found running only from financial access to ecological footprint.

Table 8. *Granger causality between financial development (index) and ecological footprint*

H0: financial development (index) does not Granger cause ecological footprint		**H0: ecological footprint does not Granger cause financial development (index)**	
Countries	**Wald statistic**	**Countries**	**Wald statistic**
Angola	5.431	Angola	2.187
Botswana	0.787	Botswana	1.756
DR Congo	3.212*	DR Congo	2.495
Lesotho	13.793***	Lesotho	2.804*
Madagascar	26.075***	Madagascar	11.904***
Malawi	13.907***	Malawi	14.675***
Mauritius	6.202	Mauritius	6.020**
Mozambique	1.93	Mozambique	20.474***
Namibia	2.970*	Namibia	0.002
South-Africa	11.230**	South-Africa	12.542***
Swaziland	17.114**	Swaziland	2.756
Tanzania	2.125	Tanzania	2.502
Zambia	2.709	Zambia	0.187
Panel	100.121*	Panel	2.756

*, ** and *** indicate significance at 0.1, 0.05 and 0.001 significance levels, respectively

http://www.aloki.hu ● ISSN 1589 1623 (Print) ● ISSN 1785 0037 (Online)
DOI: http://dx.doi.org/10.15666/aeer/1605_71717190
© 2018, ALÖKI Kft., Budapest, Hungary

Table 9. *Granger causality between financial development (access) and ecological footprint*

H0: financial development (access) does not Granger cause ecological footprint		**H0: ecological footprint does not Granger cause financial development (access)**	
Countries	**Wald statistic**	**Countries**	**Wald statistic**
Angola	8.930***	Angola	0.065
Botswana	0.787	Botswana	1.756
DR Congo	2.785	DR Congo	29.065***
Lesotho	0.712	Lesotho	1.639
Madagascar	26.075***	Madagascar	45.053***
Malawi	3.571*	Malawi	4.254**
Mauritius	6.202	Mauritius	22.274***
Mozambique	4.263*	Mozambique	1.598
Namibia	3.354**	Namibia	0.056
South Africa	2.407	South Africa	3.737*
Swaziland	19.896***	Swaziland	3.683
Tanzania	2.125	Tanzania	2.502
Zambia	2.871*	Zambia	0.261
Panel	92.743*	Panel	117.991

*, ** and *** indicate significance at 0.1, 0.05 and 0.001 significance levels, respectively

Table 10. *Granger causality between financial development (depth) and ecological footprint*

H0: financial development (depth) does not Granger cause ecological footprint		**H0: ecological footprint does not Granger cause financial development (depth)**	
Countries	**Wald statistic**	**Countries**	**Wald statistic**
Angola	5.431	Angola	12.095***
Botswana	3.736*	Botswana	1.543
DR Congo	3.212*	DR Congo	2.495
Lesotho	13.793***	Lesotho	18.873***
Madagascar	11.585***	Madagascar	1.087
Malawi	13.907***	Malawi	7.756*
Mauritius	6.390*	Mauritius	5.853
Mozambique	27.401***	Mozambique	9.045**
Namibia	69.097 ***	Namibia	25.824***
South Africa	1.787	South Africa	0.092
Swaziland	7.815**	Swaziland	7.109*
Tanzania	5.558	Tanzania	9.794**
Zambia	1.658	Zambia	7.078**
Panel	155.431	Panel	94.677

*, ** and *** indicate significance at 0.1, 0.05 and 0.001 significance levels, respectively

http://www.aloki.hu ● ISSN 1589 1623 (Print) ● ISSN 1785 0037 (Online)
DOI: http://dx.doi.org/10.15666/aeer/1605_71717190
© 2018, ALÖKI Kft., Budapest, Hungary

Table 11. *Granger causality between financial development (efficiency) and ecological footprint*

H0: financial development (efficiency) does not Granger cause ecological footprint		**H0: ecological footprint does not Granger cause financial development (efficiency)**	
Countries	**Wald statistic**	**Countries**	**Wald statistic**
Angola	1.421	Angola	0.064
Botswana	0.777	Botswana	0.836
DR Congo	0.916	DR Congo	0.682
Lesotho	0.622	Lesotho	2.385
Madagascar	3.430	Madagascar	3.433
Malawi	10.652***	Malawi	0.702
Mauritius	9.868**	Mauritius	2.662
Mozambique	3.229	Mozambique	3.433
Namibia	1.046	Namibia	6.675***
South Africa	2.200	South Africa	0.170
Swaziland	6.413	Swaziland	18.066***
Tanzania	3.077*	Tanzania	0.231
Zambia	1.462	Zambia	2.439
Panel	51.938	Panel	45.391

*, ** and *** indicate significance at 0.1, 0.05 and 0.001 significance levels, respectively

Table 12. *Granger causality between financial development (stability) and ecological footprint*

H0: financial development (stability) does not Granger cause ecological footprint		**H0: ecological footprint does not Granger cause financial development (stability)**	
Countries	**Wald statistic**	**Countries**	**Wald statistic**
Angola	1.087	Angola	8.232
Botswana	0.514	Botswana	3.306
DR Congo	20.352***	DR Congo	5.033
Lesotho	4.279	Lesotho	10.230**
Madagascar	6.235	Madagascar	1.369
Malawi	23.191***	Malawi	10.934**
Mauritius	11.913***	Mauritius	18.154***
Mozambique	1.930	Mozambique	3.768
Namibia	2.970*	Namibia	0.002
South Africa	11.230**	South Africa	4.676
Swaziland	17.114***	Swaziland	9.811**
Tanzania	28.073***	Tanzania	9.970**
Zambia	25.873***	Zambia	3.324
Panel	134.210	Panel	70.200

*, ** and *** indicate significance at 0.1, 0.05 and 0.001 significance levels, respectively

http://www.aloki.hu ● ISSN 1589 1623 (Print) ● ISSN 1785 0037 (Online)
DOI: http://dx.doi.org/10.15666/aeer/1605_71717190
© 2018, ALÖKI Kft., Budapest, Hungary

With respect to the causal relations between sustainable economic opportunity and ecological footprint, as reported in *Table 13,* one-way causal effect from sustainable economic opportunity to ecological footprint is detected in Madagascar, Mozambique, Namibia and Tanzania at the country level. One-way causality in the opposite direction is however detected in Mauritius while a feedback relationship between both variables is uncovered in Angola, South Africa and Swaziland.

Table 13. *Granger causality between sustainable economic opportunity and ecological footprint*

H0: sustainable economic opportunity does not Granger cause ecological footprint		**H0: ecological footprint does not Granger cause sustainable economic opportunity**	
Countries	**Wald statistic**	**Countries**	**Wald statistic**
Angola	12.593***	Angola	6.507*
Botswana	0.654	Botswana	0.141
DR Congo	2.216	DR Congo	0.403
Lesotho	0.368	Lesotho	2.421
Madagascar	33.985***	Madagascar	3.161
Malawi	3.651	Malawi	6.493
Mauritius	4.304	Mauritius	196.026***
Mozambique	17.640***	Mozambique	4.324
Namibia	5.084**	Namibia	0.194
South Africa	4.013**	South Africa	5.203**
Swaziland	14.688***	Swaziland	133.019***
Tanzania	4.117**	Tanzania	0.613
Zambia	3.981	Zambia	2.074
Panel	103.569***	Panel	351.836

*, ** and *** indicate significance at 0.1, 0.05 and 0.001 significance levels, respectively

Discussion

Findings from this study bring to the fore some interesting issues. First, the very ambitious agenda set by the SADC at inception include amongst others; regional integration, evolution of common political values, systems and institutions, achievement of complementarity between national and regional programmes and strategies, interdependence among member states, and strengthening and consolidation of historical, social and cultural affinities and links among people of the region. The presence of cross-sectional dependence in the region shows that the regional bloc has succeeded to a great extent in achieving these goals. The presence of country-specific heterogeneity however suggests that the region still has a long way to go before full integration is achieved. This is further confirmed by the dissimilar patterns of causality noticeable across the SADC.

Second, the dissimilar patterns of causality also suggest that a one size fits all approach to dealing with issues surrounding the interaction between financial development, sustainable economic opportunity and ecological footprint is not feasible in the SADC. In places where causality runs from financial development to sustainable

http://www.aloki.hu ● ISSN 1589 1623 (Print) ● ISSN 1785 0037 (Online)
DOI: http://dx.doi.org/10.15666/aeer/1605_71717190
© 2018, ALÖKI Kft., Budapest, Hungary

economic opportunity, the financial system is able to stimulate the economy (supply-leading theory). As for countries where causality runs in the opposite direction, the financial system simply responds to improvements in the economy (demand-following theory). In countries where causality runs in both directions, a vicious cycle in which financial development triggers improvements in the economy which in turn further triggers financial development is experienced. In countries where no significant causality is detected, the neutrality theory holds. The economy cannot be improved through financial development neither can better economic performance drive financial development.

Third, it is also quite significant that the dimensions of financial development (access, depth, efficiency and stability) that are causally related to sustainable economic opportunity vary from country to country.

Fourth, concerning the relationship between sustainable economic opportunity and ecological footprint, the energy-led growth hypothesis holds true in countries where causality is detected from ecological footprint to sustainable economic opportunity. In such countries, energy is a necessary production factor and expansion of energy use will improve the economy, whereas in countries where causality is from sustainable economic opportunity ecological footprint, the conservation hypothesis holds true. In such places, energy plans may be implemented without the impacts on the economy.

Conclusion

In this paper, causal relationship between financial development, sustainable economic opportunity and ecological footprint in SADC countries during the period during the period 2000–2016 was examined. The use of bootstrap panel Granger causality tests of Emirmahmutoglu and Kose (2011), the adoption of ecological footprint, a multidimensional indicator of environmental condition, the introduction of sustainable economic opportunity and the consideration of various dimensions of financial development–financial access, financial depth, financial efficiency and financial stability–as well as an aggregate index of these 4 measures represent the main contribution of this paper. The empirical results indicate the following; first, that causality between financial development, sustainable economic opportunity and ecological footprint varies across countries with different conditions, and leads to the conclusion that SADC countries are heterogeneous in nature.

Second, that financial development causally affects sustainable economic opportunity. This supports the findings of Liang and Jian-Zhou (2006), Ang and McKibbin (2007), Panopoulou (2009), and Li et al. (2015). All these researches have revealed that financial development supports economic growth through channeling of credits. For example, Li et al. (2015), while investigating the relationship between financial development, environmental quality and economic growth in 102 countries, clearly indicated that financial development has an effect on economic growth and could be used in the production function of economic models, with sustainable economic opportunity being a measure of economic performance.

That financial development causally affects ecological footprint aligns with the position of Tamazian et al. (2009) and Charfeddine and Khediri (2016). Extant literature suggests that financial sector and the environment may be positively or negatively correlated. On one hand, a well-developed financial sector may assist the energy sector in adopting more efficient, ecofriendly technologies that help lower environmental

http://www.aloki.hu ● ISSN 1589 1623 (Print) ● ISSN 1785 0037 (Online)
DOI: http://dx.doi.org/10.15666/aeer/1605_71717190
© 2018, ALÖKI Kft., Budapest, Hungary

degradation (Charfeddine and Khediri, 2016). Financial development may also cause improvements in the environment through funding of environmental projects at reduced funding costs (Tamazian et al., 2009).

Third, that sustainable economic opportunity causally affects ecological footprint. This is in agreement with the conclusions reached by Jensen (1996) that economic activity affects environmental conditions. Economic activities may also lead to increase in manufacturing activities, resulting in greater industrial pollution and environmental degradation (Jensen, 1996). The findings of Jensen (1996) is hung on the pollution haven hypothesis that industries that produce increased pollution are most likely to move to environments with flexible regulations on environmental pollution.

Policy recommendations

On the basis of the findings made in this study, the following policy recommendations are made:

In SADC countries where the supply-leading theory is confirmed, policy makers need to give more attention to political, legal and regulatory determinants of financial development since financial development can be used as a tool for achieving sustainable economic development. It will be in the interest of such countries to introduce modern financial institutions, especially depository and investment institutions that will stimulate financial services in terms of access, depth, efficiency and stability. Furthermore, each country should focus mainly on improving the dimensions of financial development (access, depth, efficiency or stability) that causally affect their sustainable economic opportunity.

Policy makers in SADC countries where the demand-following theory is confirmed need to quickly come to the realization that all efforts directed towards financial system development will not be worthwhile in the long-run, and more effort should instead be directed toward achieving a better economy.

In SADC countries where the energy-led hypothesis is confirmed, energy conservation policies designed to reduce greenhouse gas emissions to combat global warming may be counterproductive because they harm the economy. On the other hand, in SADC countries where the conservation hypothesis holds, energy conservation policies may be implemented without significant impact on economic performance.

REFERENCES

[1] Acar, S., Asici, A. A. (2017): Nature and economic growth in Turkey: what does ecological footprint imply? – Middle East Development Journal 9(1): 101-115.

[2] Acemoglu, D., Wolitzky, A. (2015): Sustaining Cooperation: Community Enforcement vs. Specialized Enforcement (No. w21457). – National Bureau of Economic Research, Cambridge, MA. DOI: 10.3386/w21457.

[3] Al-Mulali, U., Saboori, B. and Ozturk, I. (2015): Investigating the environmental Kuznets curve hypothesis in Vietnam. – Energy Policy 76: 123-131.

[4] Al-Yousif, Y. K. (2002): Financial development and economic growth: another look at the evidence from developing countries. – Review of Financial Economics 11(2): 131-150.

[5] Ang, J. B. (2008): What are the mechanisms linking financial development and economic growth in Malaysia? – Economic Modelling 25(1): 38-53.

http://www.aloki.hu ● ISSN 1589 1623 (Print) ● ISSN 1785 0037 (Online)
DOI: http://dx.doi.org/10.15666/aeer/1605_71717190
© 2018, ALÖKI Kft., Budapest, Hungary

[6] Ang, J. B., McKibbin, W. J. (2007): Financial liberalization, financial sector development and growth: evidence from Malaysia. – Journal of Development Economics 84(1): 215-233. DOI: 10.1016/j.jdeveco.2006.11.006.
[7] Apergis, N., Ozturk, I. (2015): Testing environmental Kuznets curve hypothesis in Asian countries. – Ecological Indicators 52: 16-22.
[8] Azam, M., Khan, A. Q. (2016): Testing the Environmental Kuznets Curve hypothesis: A comparative empirical study for low, lower middle, upper middle and high income countries. – Renewable and Sustainable Energy Reviews 63: 556-567.
[9] Baabou, W., Grunewald, N., Ouellet-Plamondon, C., Gressot, M. and Galli, A. (2017): The ecological footprint of Mediterranean cities: awareness creation and policy implications. – Environmental Science & Policy 69: 94-104.
[10] Bojanic, A. N. (2012): The impact of financial development and trade on the economic growth of Bolivia. – Journal of Applied Economics 15(1): 51-70.
[11] Breusch, T. S. and Pagan, A. R. (1980): The Lagrange multiplier test and its applications to model specification in econometrics. – The Review of Economic Studies 47(1): 239-253.
[12] Chang, M. C. (2015): Room for improvement in low carbon economies of G7 and BRICS countries based on the analysis of energy efficiency and environmental Kuznets curves. – Journal of Cleaner Production 99: 140-151.
[13] Chang, T., Cheng, S. C., Pan, G., and Wu, T. P. (2013): Does globalization affect the insurance markets? Bootstrap panel Granger causality test. – Economic Modelling 33: 254-260.
[14] Charfeddine, L., Khediri, K. B. (2016): Financial development and environmental quality in UAE: Cointegration with structural breaks. – Renewable and Sustainable Energy Reviews 55: 1322-1335.
[15] Emirmahmutoglu, F., Kose, N. (2011): Testing for Granger causality in heterogeneous mixed panels. – Economic Modelling 28(3): 870-876.
[16] Feng, Y., Chen, H., Tang, J. (2018): The impacts of social responsibility and ownership structure on sustainable financial development of China's energy industry. – Sustainability 10(2): 301. DOI: 10.3390/su10020301.
[17] Fisher, A. G. (1932): Fundamental presupposition for successful economic planning. – Economic Record 8(3): 88-98. DOI: 10.1111/j.1475-49321932.tb00737. x.
[18] Gill, A. R., Viswanathan, K. K., Hassan, S. (2017): A test of environmental Kuznets curve (EKC) for carbon emission and potential of renewable energy to reduce greenhouses gases (GHG) in Malaysia. – Environment, Development and Sustainability 20(3): 1-12. DOI: 10.1016/j.rser.2017.05.247.
[19] Global Footprint Network National Footprint Accounts. (2018): https://data.footprintnetwork.org.
[20] Huang, Y., Wang, X. (2017): Building an efficient financial system in China: a need for stronger market discipline. – Asian Economic Policy Review 12(2): 188-205. DOI: 10.1111/aepr.12173.
[21] Jensen, V. M. (1996): Trade and Environment: The Pollution Haven Hypothesis and the Industrial Flight Hypothesis; Some Perspectives on Theory and Empirics. – University of Oslo, Centre for Development and the Environment, Oslo.
[22] Kang, Y. Q., Zhao, T., Yang, Y. Y. (2016): Environmental Kuznets curve for CO2 emissions in China: a spatial panel data approach. – Ecological Indicators 63: 231-239.
[23] Körner, T., Schnabel, I. (2009): When do state-owned banks hamper economic growth? – 7th Workshop on "Money, Banking and Financial Markets," Halle Institute for Economic Research.
[24] Lau, L. S., Choong, C. K., Eng, Y. K. (2014): Investigation of the environmental Kuznets curve for carbon emissions in Malaysia: Do foreign direct investment and trade matter? – Energy Policy 68: 490-497.

http://www.aloki.hu ● ISSN 1589 1623 (Print) ● ISSN 1785 0037 (Online)
DOI: http://dx.doi.org/10.15666/aeer/1605_71717190
© 2018, ALÖKI Kft., Budapest, Hungary

[25] Li, S., Zhang, J., Ma, Y. (2015): Financial development, environmental quality and economic growth. – Sustainability 7(7): 9395-9416.
[26] Li, T., Wang, Y., Zhao, D. (2016): Environmental Kuznets curve in China: new evidence from dynamic panel analysis. – Energy Policy 91: 138-147.
[27] Liang, Q., Jian-Zhou, T. (2006): Financial development and economic growth: Evidence from China. – China Economic Review 17(4): 395-411.
[28] Mo Ibrahim Foundation (2018): http://mo.ibrahim.foundation.
[29] Mukhopadhyay, B., Pradhan, R. P., Feridun, M. (2011): Finance–growth nexus revisited for some Asian countries. – Applied Economics Letters 18(16): 1527-1530.
[30] Onafowora, O. A., Owoye, O. (2014): Bounds testing approach to analysis of the environment Kuznets curve hypothesis. – Energy Economics 44: 47-62.
[31] Panopoulou, E. (2009): Financial variables and euro area growth: A non-parametric causality analysis. – Economic Modelling 26(6): 1414-1419.
[32] Pesaran, M. H. (2004): General Diagnostic Tests for Cross Section Dependence in Panels. – CESifo Working Paper Series No. 1229; IZA Discussion Paper No. 1240. http://ssrn.com/abstract=572504.
[33] Pesaran, M. H., Yamagata, T. (2008): Testing slope homogeneity in large panels. – Journal of Econometrics 142(1): 50-93.
[34] Pradhan, R. P., Dasgupta, P., Samadhan, B. (2013): Finance, development and economic growth in BRICS: A panel data analysis. – Journal of Quantitative Economics 11(1-2): 308-322.
[35] Pradhan, R. P., Tripathy, S., Chatterjee, D., Zaki, D. B., Mukhopadhyay, B. (2014): Development of banking sector and economic growth: The ARF experience. – Decision 41(3): 245-259.
[36] Rousseau, P. L., Wachtel, P. (2011): What is happening to the impact of financial deepening on economic growth? – Economic Inquiry 49(1): 276-288. DOI: 10.1111/j.1465-7295.2009. 00197.
[37] Seyoum, M., Wu, R., Lin, J. (2014): Foreign direct investment and trade openness in Sub-Saharan economies: A panel data granger causality analysis. – South African Journal of Economics 82(3): 402-421.
[38] Sofia, A., Ghulam, S., Zakir, H. (2011): Relationship between financial sector development and sustainable economic development: time series analysis from Pakistan. – International Journal of Economics and Finance 3(1). DOI: 10.5539/ijef. v3n1p262.
[39] Southern African Development Community (2018): https://www.sadc.int/about-sadc/overview/sadc-facts-figures.
[40] Swamy, P. A. (1970): Efficient inference in a random coefficient regression model. – Econometrica: Journal of the Econometric Society 311-323.
[41] Tamazian, A., Chousa, J. P., Vadlamannati, K. C. (2009): Does higher economic and financial development lead to environmental degradation: evidence from BRIC countries. – Energy Policy 37(1): 246-253.
[42] Tang, C. F., Tan, B. W. (2015): The impact of energy consumption, income and foreign direct investment on carbon dioxide emissions in Vietnam. – Energy 79: 447-454.
[43] Toda, H. Y., Yamamoto, T. (1995): Statistical inference in vector auto regressions with possibly integrated processes. – Journal of Econometrics 66(1-2): 225-250.
[44] Wackernagel, M., Schulz, N. B., Deumling, D., Linares, A. C., Jenkins, M., Kapos, V., Randers, J. (2002): Tracking the ecological overshoot of the human economy. – Proceedings of the National Academy of Sciences 99(14): 9266-9271.
[45] Wolde-Rufael, Y. (2009): Re-examining the financial development and economic growth nexus in Kenya. – Economic Modelling 26(6): 1140-1146.
[46] World Economic Forum (2012): World economic forum global competitiveness report. – http://www3.weforum.org/docs/WEF_GlobalCompetitivenessReport_2012-13.pdf.

http://www.aloki.hu ● ISSN 1589 1623 (Print) ● ISSN 1785 0037 (Online)
DOI: http://dx.doi.org/10.15666/aeer/1605_71717190
© 2018, ALÖKI Kft., Budapest, Hungary

THE EFFECTS OF SHADING TREATMENTS ON THE PLANT GROWTH RATE OF SOME VARIETIES OF ASTER FLOWERS (*DAHLIA* SPP.) IN THE ECOLOGIC CONDITIONS OF TOKAT (TURKEY)

YAZICI, K.* – GUNES, S.

Department of Horticulture, Faculty of Agriculture, Gaziosmanpasa University
Taslıciftlik Campus, 60000 Tokat, Turkey
(phone: +90-545-645-1035; fax: +90-252-1616-2184)

**Corresponding author*
e-mail: k-yazici-karaman@hotmail.com

(Received 3rd Aug 2018; accepted 28th Sep 2018)

Abstract. Aster flowers belong to the Asteraceae family which has approximately 1.000 genera, and a number of species approaching 25.000. It is the largest family of the flowering plants and has spread to almost every region of the world, except for Antarctica. Considering the relatively low number of studies in the literature regarding the subject, this study was conducted to determine the shading requirements of the *Dahlia* spp. The experimental tests were conducted in the facilities of the "Agricultural Applications and Research Directorate" of Gaziosmanpasa University in the city of Tokat. Observations and measurements were made regarding the yield, flower diameter, plant height, plant stem diameter, pedicle length, pedicle width, number of buds, bud diameter, and lifetime-in-pot properties of the *Le Castel, Seattle, Babylon Purple*, and *Gloriosa* genera of the *Dahlia* spp. The results obtained indicate that the tested shading practices (35% and 55%) have resulted in increased performances compared to the control group in terms of yield and quality. Between the genera, *Le Castel* genus has given better results compared to others in terms of yield in both 35% and 55% shading. In pedicle length, *Babylon Purple* genus has given better results with 35% shading, while *Gloriosa* was the best in that regard with 55% shading. For the flower diameter property, the best results (249.05 mm) were obtained in the third measurement by *Babylon Purple* with 35% shading practice. As a result, the difference between plant diameters of the genera under the shading practices were found to be statistically significant, and that 35% shading practice was ideal for all the genera tested.
Keywords: *ornamental plant, bulbous plants, aster, growing, Klux*

Introduction

Bulbous and tuber plants have attractive flowers with interesting shapes and colors, and they bloom relatively early (Yazici and Gülgün, 2016). Especially towards the end of winter months, their flowers bloom as soon as the snow melts away, which makes them a tell-tale sign of the spring. They are also grown with relative ease. All these reasons have made them one of the most commonly used plants in gardens and parks all around the world (Mathew, 1987; Mathew and Swindells, 1994; Leeds, 2000). In Turkey, around 700 flower bulb species grow naturally (Karagüzel et al., 2007). As the significance of the diversity and richness of Turkey's flora was recognized by authorities of other countries, the flower bulbs were gathered from the wilds with the purpose of exhibiting them in botanical gardens. This practice transformed into commercial purposes over time, and the level of destruction of their natural habitats increased.

http://www.aloki.hu ● ISSN 1589 1623 (Print) ● ISSN 1785 0037 (Online)
DOI: http://dx.doi.org/10.15666/aeer/1605_71917202
© 2018, ALÖKI Kft., Budapest, Hungary

Amongst bulbous plants, Aster flower of the Asteraceae family is especially preferred as an outdoor ornamental flower. Most of the plants in this family are annual or biennial flowers, and very few are in bush or tree forms. The flowers have the shape of stars, while the leaves are either simple or are compound leaves in the shape of badges (Kim et al., 1992; Villasenor and Martiez, 2018). Aster flowers have around 30 prominent species and around 20.000 breeds. The flower naturally grows in the Central America continent, especially in the high mountains of Mexico. The flowers bloom in summer and fall. The stems are of brier type, while the roots are tuberous. 27 species of it can be found in nature. Some of these species may reach up to 8-9 meters height, while others are scrubs (Brickell, 1992; Hessayon, 1993; Mc Claren, 2004; Alp, 2008). Starting in July, they continue to bloom flowers, until the arrival of the first cold-weather waves. In temperate regions, they bloom much earlier, and the variation of their plant height and flower shapes and sizes increase. Their flowers can be of many shapes: simple, lotus, anemone, powder puff, orb, semi-cactus, cactus, decorative, orchid, or peony. In addition to the shades of blue, the flowers also contain all of the warmer colors. There are very few literature studies in Turkey regarding the Aster flower. Since it is a plant that can be produced relatively easy due to its large bulb resembling a potato, it is a good candidate for commercial use in the ornamental plant sector.

This study aims to evaluate the adaptation capabilities of the ornamental plant known as the Aster flower (*Dahlia* spp) and to determine the shading practices most suitable for the plant under the ecological conditions Kazova plains of the city of Tokat. A secondary objective is to determine the suitability of the Aster flower (*Dahlia* spp.) for plant design. Hopefully, this study will be able to determine optimal shading practices for the plant and act as a precursor for the growers that want to grow ornamental plants as the city of Tokat. We believe a new plant can thus be introduced to the ornamental plant design patterns places similar to Tokat ecological conditions, and *Dahlia* spp. can become an important part of decorative flowers. In addition, it could also contribute to application appropriate shading, varieties and to develop different studies in similar climatic conditions areas.

Literature review

American Dahlia Society officially lists 15 colors for the Dahlia: bicolor, bronze, dark blend, dark pink, dark red, flame blend, lavender, light blend, orange, pink, purple, red, variegated, white, and yellow. It can be used as a cut flower, or as an ornamental plant for outdoor environments. Those grown from the tubers have large flowers, while those grown from seeds have smaller ones (Evans, 1998; Mc Claren, 2004; Önay, 2007; Romer, 2008).

Hertogh and Nard (1992) and Mc Claren (2004) state that Aster flowers have flat receptacles, and that while the flowers on the edge are tongue-like in form while the ones on inner areas are more tubular. The flowers have a wide variation of colors. The leaves are bilateral, are of single or three bodies, and have serrated edges. Aster flowers are quite varying both in flower form and in color. It is also possible that a layered type aster flower can transform into a semi-layered form, along with a change in its color. The ones with two colors may lose one color over time. It is also reported by these researchers that the same plant may grow flowers of a different color over different branches.

http://www.aloki.hu ● ISSN 1589 1623 (Print) ● ISSN 1785 0037 (Online)
DOI: http://dx.doi.org/10.15666/aeer/1605_71917202
© 2018, ALÖKI Kft., Budapest, Hungary

In another shading practice study, the effects of shading on the rooting properties of the "Choot Hashani", "Orpheo" and "Lavanta Perfection" genera of the Dahlia spp. were evaluated. Natural light density has caused about 50% rooting reduction in the "Orpheo" slips, while it had no effect on the rooting rate of the "Lavanta Perfection" slips (Brian and Halevy, 1973). Shading during daylight hours has caused longer internodes for the "Orhpeo" genus only, while it had no effect on the rooting rate. On the other hand, the same shading has caused increased rooting for the "Choot Hashani" genus. Shading the bases of the slips has caused rooting percentage and roots per slip to increase significantly. The variance in response to shading is still being discussed, and the shading practices for these genera were determined to have influence only when applied to the rooting area. It is being surmised that shading incentivizes the weedy character of the rooting area, resulting in improved rooting (Brian and Halevy, 1973).

According to another study; excessive sunlight, high temperature, low humidity and sunlight caused problems in *Dahlia* spp., but the amount and intensity of sunlight should be adjusted to increase the flower stalk length and flower color quality with shading applications (Lumpkin and Lumpkin, 2005). According to another study on dahlia; different levels and combination of bio fertilizers and organic manures was applied to assess the vegetative, floral and yield characteristics of dahlia. The experiment was laid out in randomised block design with ten treatments and three replications. The maximum plant height (65.07 cm), number of primary branches (9.67), number of leaves (33.67), plant spread (43.73 cm), number of flowers (8.13), duration of flowering (10.53), flower yield ha-1 (33.65), weight of tuber (56.67 g), number of tubers (4.87) and tuber yield (13.80 t ha^{-1}) were produced in the treatment. (Pandey et al., 2017). The experiment of Verma and Kulkarni (2017) was laid out in simple randomized block design with three replication and twenty treatments on dahlia. Significant differences for all growth and yield parameters were found among different genotypes of dahlia. Maximum plant height (122.38 cm), number of branches (13.15), stem girth (1.48 cm) plant spread (59.12 cm) and intermodal length (18.04 cm) were recorded in genotype Hiranmoyee whereas, maximum leaf area (1909.78 cm^2) was recorded in genotype Barakanchari. Maximum number of flowers per plant (25.30) was found in genotype Hiranmoyee whereas, maximum flower yield per plant (g) was found in Song of India (718.72 g).

Materials and methods

The study was conducted in the fields of Center of Agricultural Research and Applications in the city of Tokat (Turkey), under the ecological conditions of the Kazova plains in the year 2018. After harvest, the plants were left to pot life in the laboratories of Gaziosmanpaşa University Faculty of Agriculture Department of Garden Plants.

Materials

The plants which had the most commonly sought-after colors were used in the study: white and pink speckled yellow-red and yellowish-orange. The plant has great potential for use in ornamental plant sector, especially as an outdoor environment ornament. The plant materials for the study were obtained from Konya Asya Lale Production Company, which were mostly created by hybridization of *D. pinnata* and

http://www.aloki.hu ● ISSN 1589 1623 (Print) ● ISSN 1785 0037 (Online)
DOI: http://dx.doi.org/10.15666/aeer/1605_71917202
© 2018, ALÖKI Kft., Budapest, Hungary

D. coccinea species. The types obtained and used in the study are given in *Figure 1a–d.* Also photographs from the experimental field are *Figure 2a* and *b*.

a **b** **c** **d**

Figure 1. a. *Seattle,* ***b.*** *Babylon Purple,* ***c.*** *Le Castel,* ***d.*** *Gloriosa*

a **b**

Figure 2. *Photographs from the experimental field*

Method

Dahlia spp. tubers were planted to the garden belonging to the GUTAM (Gaziosmanpaşa University Agricultural Application and Research Center) in three different shading applications (open, 35%, and 55% shading). The light intensities in the applications were measured by light meter (400,000 Lux / 40,000 FC) at 12:30 pm. Light intensities at three different points were measured and averaged. These averages were 97.6 Klux in open area, 66.8 Klux in 35% shading and 48.1 Klux in 55% shading. The growth environment was loamy-sand garden soil. Considering that the flowers are relatively large, the plants were seeded in a 50 × 50 cm grid, to a depth of 15 cm. Each repeat had 8 tubers and there were a total of three repeats, separated into two rows. A total of 288 *Dahlia* spp. tubers were thusly used. The tests were repeated three times with "parcels divided by randomized blocks" method, and each repeat had 8 tubers. After the variance analysis, the averages were compared using Duncan test (Düzgüneş et al., 1987).

http://www.aloki.hu ● ISSN 1589 1623 (Print) ● ISSN 1785 0037 (Online)
DOI: http://dx.doi.org/10.15666/aeer/1605_71917202
© 2018, ALÖKI Kft., Budapest, Hungary

Results

Phenological findings

Vegetation period

This period was defined as the time it takes for 50% of the tubers after seeding to grow into plants that reach the soil surface. The Aster flower tubers that were sown on May 26 vegetated on June 11, in 15 days.

Inflorescence period

This period was defined as the time it takes for 50% of the plants flowering after being sown. The non-shaded (control group) tubers that were sown on May 16 flowered 35 days later, in the 1st of July, while those under 35% shading flowered 40 days later in 6th of July and those under 55% shading flowered 44 days later, on July 10th.

Floral period

This period was defined as the time it takes for 50% of the plant flowers to wither and fall. The plants that were not shaded which bloomed in 6th of July kept their flowers for a period of 85 days, till the 29th of September, while those under 35% shading kept their flowers for 96 days and those under 55% shading kept them for 103 days.

Leaf coloration period (days)

The leaf coloration was observed on the flowers for a total of 141 days, from the day 50% of the plants reached their vegetation period (June 11) till October 30th.

Abscission period

This period was defined as the time it took for 50% of the leaves to fall and was determined as 158 days from the plants' vegetation (June 11) till November 16th.

Morphological observations

Yield (pcs)

Inspected independent from the type, the general averages indicate that shaded plants yielded more flowers in the first harvest, compared to the control group. Those under 35% shading yielded an average of 20.58 flowers and achieved better flower yields compared to those in the control group and the 55% shaded group. The plants under 35% and 55% shading yielded significantly more yields in second and third harvests, compared to non-shaded plants. When the interaction between the flower genera and the shading level are inspected, it can be seen that the Seattle and Babylon Purple flowers under 35% shading yielded more flowers (with 15.66 and 17.66 units respectively), compared to the control and 55% shaded plants *(Fig. 3a).*

Flower diameter (mm)

Inspected independent of plant type, the plants under shading achieved higher flower diameters compared to non-shaded plants. Inspection of interaction between the shading application and plant genera reveals that *Le Castel, Seattle*, and *Babylon Purple* plants in the control group bloomed flowers with a significantly lower diameter in the first

http://www.aloki.hu ● ISSN 1589 1623 (Print) ● ISSN 1785 0037 (Online)
DOI: http://dx.doi.org/10.15666/aeer/1605_71917202
© 2018, ALÖKI Kft., Budapest, Hungary

control (25th of July) compared to shaded groups, with 121.25, 157.69, and 249.38 mm, respectively. In the third measurement (25th of September), the plants under shading application (*Le Castel, Seattle, Babylon Purple*, and *Gloriosa*) were found to have larger-diameter flowers compared to the control group. When the plant genera are compared to each other, Le Castel is found to be the one with the lowest flower diameter (121.25 mm), while Babylon Purple had the largest flower diameter (249.38 mm). The difference between *Seattle* and *Gloriosa* types were found to be insignificant (157.69 and 165.35 mm respectively). Le Castel plants under 35% and 55% shading had the smallest diameter flowers, while *Babylon Purple's* under shading had the largest (*Fig. 3b).*

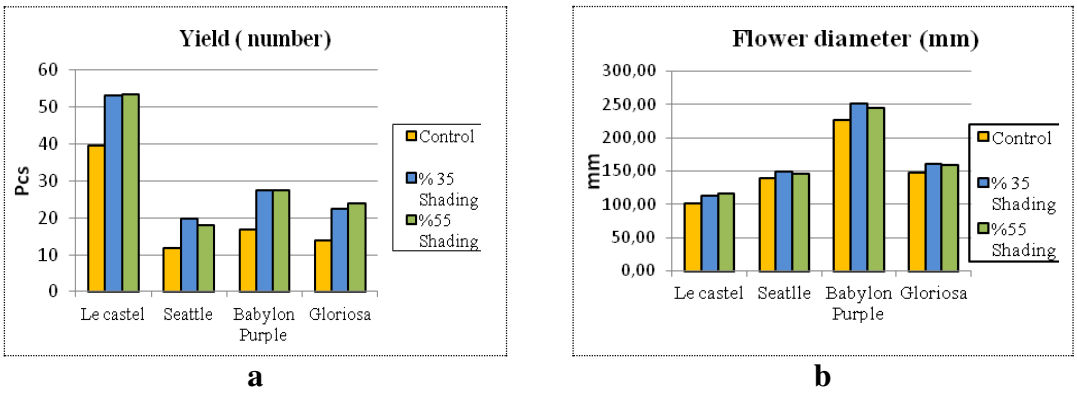

a **b**

Figure 3. a. *The yied in Dahlia spp. some varieties.* ***b.*** *The flower diameter in Dahlia spp. some varieties*

Pedicle length (cm)

Inspected independent of plant type, the plants under 35% and 55% shading were found to have significantly longer pedicles in all three harvests compared to the control group plants. When the interaction between the flower genera and shading levels are inspected in this regard, it can be seen that *Le Castel* and *Seattle* type flowers of the control group had significantly shorter pedicles (23.5 and 20.92 cm, respectively) compared to shaded plants. The *Babylon Purple* plants under 35% shading, and *Gloriosa* plants under 55% shading achieved significantly longer pedicle lengths compared to the plants in the control group, with 34.24 and 32.35 cm, respectively. Regarding the shading application's effect on the plant genera, 35% and 55% shaded *Babylon Purple* flowers, and 55% shaded *Gloriosa* flowers were found to have significantly longer pedicles overall, with 34.24, 30.97, and 32.35 cm, respectively (*Table 1*).

Pedicle width (mm)

Inspected independent of plant type, the plants under 55% shading had significantly wider pedicles (6.56 mm) compared to the plants in 35% shading and control group. In the second harvest measurement, the plants under 55% shading had wider pedicles compared to the control group as well (5.15 and 4.86 mm, respectively). No significant difference was found between the pedicle widths of the flowers in the third measurement. Inspection of shading application with the plant genera reveals that Le Castels under 35% shading had thinner pedicles (3.77 mm) compared to those under no

http://www.aloki.hu ● ISSN 1589 1623 (Print) ● ISSN 1785 0037 (Online)
DOI: http://dx.doi.org/10.15666/aeer/1605_71917202
© 2018, ALÖKI Kft., Budapest, Hungary

shading, or under 55% shading. Babylon Purple plants under 55% shading, on the other hand, were found to have wider pedicles (8.60 mm) compared to control and 35% shaded groups in the first measurement in 25th of July. The Babylon Purple plants also had wider pedicles (6.22 mm) in the second measurement (25th of August) compared to other groups as well. In the third measurement, Le Castel plants of the third measurement under 35% and 55% shading were found to have significantly thinner pedicles compared to other types as well (*Table 1*).

Table 1. *Statistical data of the pedicle length and pedicle width of Dahlia spp. some varieties*

Pedicle length									
Varieties	**Harvest 1**			**Harvest 2**			**Harvest 3**		
	Control	**35% shading**	**55% shading**	**Control**	**35% shading**	**55% shading**	**Control**	**35% shading**	**55% shading**
Le Castel	23.50bB	28.06bA	28.14bA	20.60bB	24.96cA	25.23cA	19.37bB	26.61aA	27.32aA
Seattle	20.92cB	27.98bA	28.62bA	14.65cB	27.14bA	26.89bcA	12.94cB	26.25aA	27.86aA
Babylon Purple	29.45aB	34.24aA	30.97aAB	25.60aB	29.17aA	28.31bAB	24.31aB	26.75aA	26.35aA
Gloriosa	27.74aB	30.78bAB	32.35aA	25.82aB	29.16aA	30.47aA	23.14aB	27.46aA	27.37aA
General average	25.40B	30.27A	29.71A	21.67B	27.61A	27.43A	19.54B	26.76A	27.27A
Pedicle width									
Varieties	**Harvest 1**			**Harvest 2**			**Harvest 3**		
	Control	**35% shading**	**55% shading**	**Control**	**35% shading**	**55% shading**	**Control**	**35% shading**	**55% shading**
Le Castel	4.22bA	3.77bB	4.29cA	3.47bA	3.89bA	3.62cA	3.11bA	3.31bA	3.23bA
Seattle	6.90aA	6.65aA	6.55bA	5.41aA	5.55aA	5.28bA	5.12aA	5.34aA	4.96aA
Babylon Purple	6.62aB	6.68aB	8.60aA	5.22aB	5.56aAB	6.22aA	4.85aA	5.13aA	5.91aA
Gloriosa	6.84aA	6.42aA	6.91bA	5.34aA	5.34aA	5.56abA	4.95aA	5.04aA	5.24aA
General average	6.14B	5.88B	6.56A	4.86B	5.09AB	5.15A	4.48A	4.70A	4.81A

Bud (gemma) count (pcs)

When the average bud count is inspected independent of the plant type, the first harvest's plants under 35% shading had more buds (4.45) compared to the control and 55% shading groups. In the second and third harvests' measurements, the plants in the control group developed significantly fewer buds compared to 35% and 55% shaded plants. The inspection of interaction between shading practices and the plant types reveals that *Seattle* and *Babylon Purple* plants developed more buds (2.54 and 3.20 respectively) compared to the control and 55% shading group plants in the first harvest's measurements made in 25th of July. Le Castel plants in the first harvest measurement developed more buds (7.62) compared to others (*Fig. 4a).*

Bud diameter (mm)

Type-independent inspection of the averages reveal that 35% and 55% shaded plants have developed larger flower buds compared to the control group. The 35% shaded

http://www.aloki.hu ● ISSN 1589 1623 (Print) ● ISSN 1785 0037 (Online)
DOI: http://dx.doi.org/10.15666/aeer/1605_71917202
© 2018, ALÖKI Kft., Budapest, Hungary

plants of the second harvest have developed significantly larger buds compared to the 55% shaded plants. The inspection of interaction between plant types and shading practices reveals that the control group *Babylon Purple* plants of the first harvest of 25th of July have developed smaller flower buds (28.75 mm) compared to the 35% and 55% shaded plants. 35% shaded *Le Castel* and *Gloriosa* plants of the second harvest of 25th of August, on the other hand, developed larger buds (19.45 mm and 27.44 mm respectively) compared to others. The plants under 35% and 55% shading of the third harvest (*Le Castel, Seattle, Babylon Purple* and *Gloriosa*) have developed significantly larger buds compared to the control group plants. For plant types, the largest buds were developed by the 35% shaded *Babylon Purple* plants of the first harvest (31.70 mm), while *Le Castels* developed the smallest buds (21.79 mm) (*Fig. 4b).*

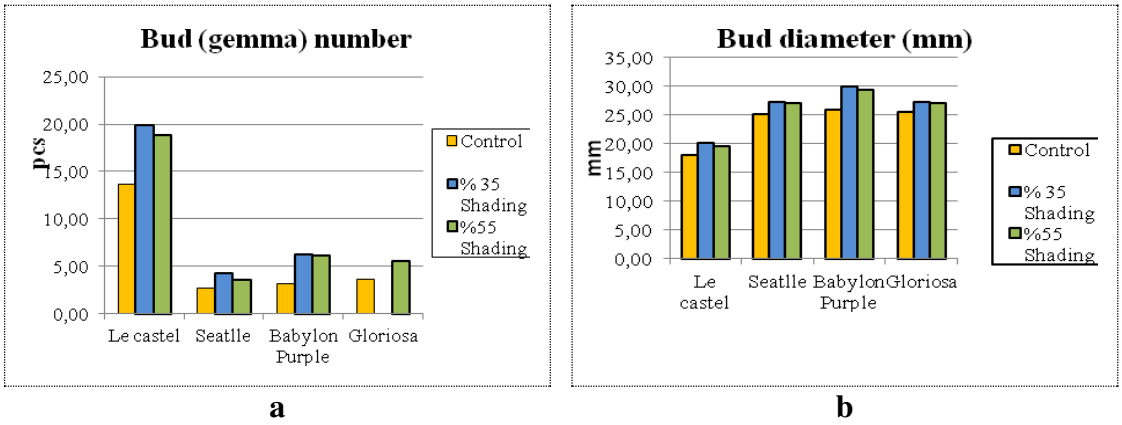

Figure 4. a. *The bud number in Dahlia spp. some varieties.* ***b.*** *The bud diameter in Dahlia spp. some varieties*

Plant height (cm)

When the averages are inspected independent of plant type, 35% shaded plants were found to have developed higher (77.14 cm) compared to the control and 55% shaded groups in the first harvest. In the second harvest, shaded plants reached a higher size compared to the control group. In the third harvest, the longest plants were developed by the 35% shaded plants (133.54 cm), while the smallest ones were developed by the control group (110 cm). The analysis of type-shading interaction reveals that the *Le Castel* plants of the control group in the second harvest of 25th of August developed shorter plants (96.37 cm) compared to the ones in the 55% shaded group (111.66 cm.) *Seattle* plants under 55% shading developed to be longer (92.27 cm) compared to the control group plants (64.56 cm). *Babylon Purple* and *Gloriosa* plants of the control group were shorter (120.93 cm and 113.53 cm, respectively) compared to the shaded ones. *Le Castel* plants developed longer (111.66 cm) compared to *Seattle* plants (92.27 cm). The *Gloriosa* plants of the third harvest under 35% shading grew to be longer (151.55 cm) compared to the *Le Castels (Fig. 5).*

Stem diameter (mm)

Type-independent evaluations reveal no significant variation in terms of stem diameter. When the effects of shading application on various types of plants are inspected, it can be seen that *Gloriosa* plants under 35% shading in the first harvest of

http://www.aloki.hu ● ISSN 1589 1623 (Print) ● ISSN 1785 0037 (Online)
DOI: http://dx.doi.org/10.15666/aeer/1605_71917202
© 2018, ALÖKI Kft., Budapest, Hungary

25th of July have developed larger stems (15.60 mm) compared to the *Le Castel* (11.29 mm) plants. No significant differences were observed between 55% shaded *Seattle* (18.23 mm) and *Babylon Purple* (18.39 mm) plants. The second harvest's (25th of August) Le Castel plants developed thinner stems (12.11 mm) compared to the Seattle plants (18.01 mm). *Gloriosa's* under 35% shading developed larger stems (17.94 mm) compared to the *Le Castel's* (11.55 mm). No significant difference was observed between 55% shaded *Babylon Purple* and *Gloriosa* plant stem diameters (22.23 mm and 18.72 mm respectively). The Seattle plants of the third harvest (25th of September) developed larger stems (20.26 mm) compared to the Le Castel plants (13.83 mm). Le Castel plants under 35% shading developed thinner stems (13.31 mm) compared to other plants. No significant difference was observed between 55% shaded Babylon Purple and Gloriosa plants (23.94 mm and 22.79 mm, respectively) (*Fig. 6a*).

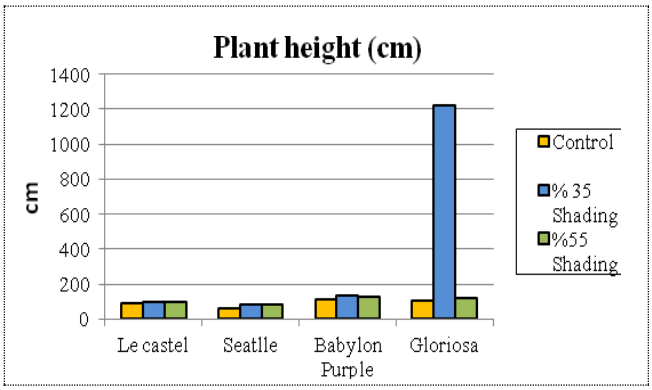

Figure 5. *The plant height number in Dahlia spp. some varieties*

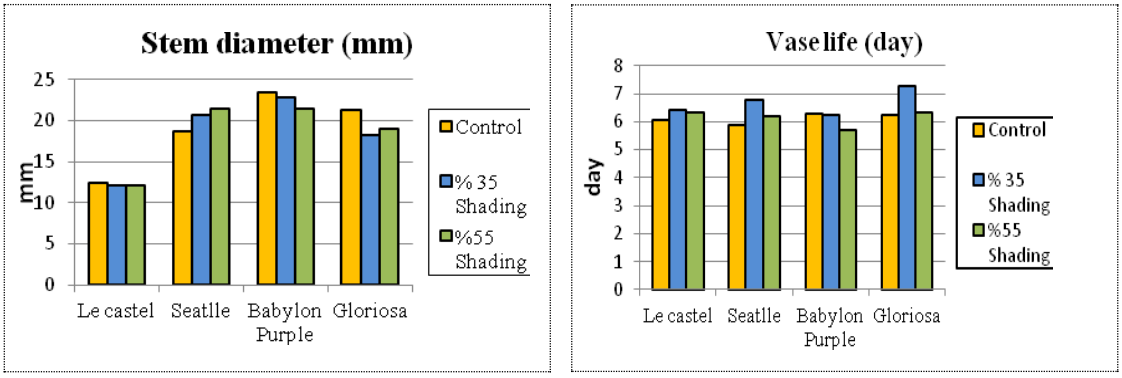

a **b**

Figure 6. a. *The stem number in Dahlia spp. some varieties.* ***b.*** *The vase life in Dahlia spp. some varieties*

Vase life (day)

The vase life of flowers is commercially important because of storage. After the harvest, fading time of flower was examined in pure water. Type-independent inspection reveals that 35% shaded plants had significantly more vase lifetimes compared to control and 55% shaded groups in the first and second harvests, and in total average. Type and shading based inspection reveal that 35% shaded *Le Castel* and

http://www.aloki.hu ● ISSN 1589 1623 (Print) ● ISSN 1785 0037 (Online)
DOI: http://dx.doi.org/10.15666/aeer/1605_71917202
© 2018, ALÖKI Kft., Budapest, Hungary

Gloriosa flowers of the first harvest of 27th of July have survived longer in the vases (6.58 and 7.41 days respectively) compared to control and 55% shading groups. Amongst the flowers of the second harvest of 27th of August, the Seattle flowers of 35% shading survived longer in a vase (6.91 days) compared to other groups. On average, Seattle and Gloriosa flowers under 35% shading were found to survive longer in a vase (6.79 and 7.29 days respectively) compared to control and 55% shading (*Fig. 6b*).

Discussion

The evaluations on the collected data reveal that shading practices (35% and 55%) have resulted in positive developments regarding total yield and some quality criteria compared to the control group. In terms of yield, the inspection of shading practices reveals that the plants of second and third harvests have developed more flowers compared to the control group when 35% and 55% shading was applied. Evaluation of the plant types in terms of yield (*Le Castel*, *Seattle*, *Babylon Purple*, *Gloriosa*) reveal that Le Castel plants were significantly yielding compared to other plants in all three harvests. Amongst the third harvest plants, Le Castels under 55% shading yielded the highest amount of flowers (85.33). According to the study of Akçal (2016), plants subjected to 16 h of photo-period under 40% shading displayed a more uniform development and resulted in more compact flowers suitable for decorations. Similarly, the results of our study indicate that 14-15 h of photo-period under 35% shading result in more uniformly developed plants which were more suitable for use as outdoors ornamentals.

The results also indicate that 35% and 55% shading practices also increase the plant height and flower diameter. This is similar to the findings of Yanming Dent et al. (2012), which indicates that 20-50% shading for Jasmine (*Jasminum sambac Aiton*) plants have resulted in increased vegetative growth and yield. Similarly, both the 35% and 55% shading practices in our study resulted in better vase lifetime, stem diameter, plant height and yield. The study of Malta (2016) also report similar results, in which 35% and 55% shading practices for tulips (*Tulipa gesneriana L.*) have resulted in better properties in terms of flower lifetime, pedicle length, flower diameter and corm size.

Pedicle length is an especially important property for the cut flower sector. In terms of pedicle length, the plants under 35% and 55% shading were found to have developed longer pedicles compared to the control group plants in general. Even though *Babylon Purple* and *Gloriosa* types have similar properties in this regard, the *Babylon Purple* type flowers have developed the longest pedicles (32.24 cm) in the first harvest under 35% shading.

When all these criteria are evaluated together, it can be surmised that shading practices of 35% and 55% result in increased yields for the Aster flower overall. In some climate-related events like rainfalls, the 55% shaded plants were found to have developed form irregularities towards their centers. Considering all of these, we report that the ideal point lies in 35% shading for the Aster flowers in places such as Tokat Kazova conditions.

Conclusion

Although it is known that the Dahlia's need shadow what kind of dahlia to how much shadow (Klux) are important. As shown in this study, the responses of the varieties to

http://www.aloki.hu ● ISSN 1589 1623 (Print) ● ISSN 1785 0037 (Online)
DOI: http://dx.doi.org/10.15666/aeer/1605_71917202
© 2018, ALÖKI Kft., Budapest, Hungary

shadow applications were found to be significant. After this study, the amount of shade should be taken into consideration in landscaping applications for Dahlia's. In addition, the use of varieties (*Bayblon purple Seattle, Glorissa, Le castel*) should be evaluated according to their development in the shade in the light of the obtained data.

Acknowledgements. This study is a part of Ms. thesis and is supported with the project no 2017-49 by Tokat Gaziosmanpasa University Coordinator of Scientific Research and Projects.

REFERENCES

[1] Akçal, A. (2016): Cyclamen hederifolium Aiton.'un sera koşullarında farklı fotoperiyot ve gölgeleme uygulamalarına tepkisi. – ÇOMÜ Zir. Fak. Derg. (COMU J. Agric. Fac.) 2015: 3(2): 79-89.
[2] Alp, Ş. (2008): Yıldız çiçeği-dahlia (Dahlia ssp.) yetiştiriciliği, sınıflandırılması ve kullanımı Bağbahçe 17 (Mayıs-Haziran 2008). – Yüzüncü Yıl Üniversitesi, Tuşba/Van, Turkey.
[3] Biran, İ., Halevy, H. A. (1973): Stock plant shading and rooting of dahlia cuttings. – Scientia Horticulturae 1(2): 125-131.
[4] Brickell, C. (1992): Encyclopedia of Gardening. – The Royal Horticultural Society, London.
[5] De Hertogh, A., Le Nard, M. (1992): The Physiology of Flower Bulbs. – Elsevier, Amsterdam.
[6] Düzgünes, O., Kesici, T., Kavuncu, O., Gürbüz, F. (1987): Araştırma ve deneme metotları. – Ankara Üniv. Ziraat Fak. Yayınları: 1021, Ders Kitabı, Ankara.
[7] Evans, E. (1998): Dahlias for the Home Landscape. – Department of Horticultural Science, Cooperative Extension Service, North Carolina State University College of Agriculture & Life Sciences, North Carolina.
[8] Hessayon, D. G. (1993): The Flowers Expert. – Pbi, Waltham Cross.
[9] Karagüzel, Ö., Aydinşakir, K., Kaya, A. S. (2007): Dünyada Ve Türkiye'de Çiçek Soğanları Sektörünün Durumu. – Derim Dergisi 24(1): 1-10.
[10] Kim, K. J., Jansen, R. K., Wallace, R. S., Michaels, H. J., Andalmer, J. D. (1992): Phylogenetic implications of RBLe sequence variation in the asteracea. – Annals of Missouri Botanical Garden 79: 428-445.
[11] Leeds, R. (2000): The Plant Finder's Guide to Early Bulbs. – David and Charles, Newton Abott, UK.
[12] Lumpkin (2005): http://www.dahlias.net/dahwebpg/Gardens/Lumpkin/Lumpkin.htm. – Accessed on 05.02.2018.
[13] Malta, S. (2016): Farklı yetiştirme ortamları, lokasyon ve gölge uygulamalarının lale (Tulipa gesneriana L.) 'de bitki gelişimi ve kalite özelliklerine etkisi. – Gaziosmanpaşa Üniversitesi, Fen Bilimleri Enstitüsü, Y. lisans Tezi.
[14] Mathew, B. (1987): Flowering Bulbs for the Garden. – Kew Gardening, London.
[15] Mathew, B., Swindells, P. (1994): The Garden's Guide to Bulbs. – Reed International Books Limited, London.
[16] McClaren, B. (2004): Encyclopedia of Dahlias. – Timber Press, Portland, OR.
[17] Önay, G. (2007): Bahçem ve ben. Amatör Bahçıvanın El Kitabı. Dördüncü Basım. – Remzi Kitabevi, Turkey.
[18] Pandey, S. K., Kumari, S., Singh, D., Singh, K. V., Prasad, M. (2017): Effect of biofertilizers and organic manures on plant growth, flowering and tuber production of dahlia (Dahlia variabilis L.) Cv. S.P . Kamala. – Int. J. Pure App. Biosci. 5(2): 549-555.
[19] Romer, J. (2008): Growing Dahlias. – Instructional Technology Center, Iowa State University, Ames, IA.

http://www.aloki.hu ● ISSN 1589 1623 (Print) ● ISSN 1785 0037 (Online)
DOI: http://dx.doi.org/10.15666/aeer/1605_71917202
© 2018, ALÖKI Kft., Budapest, Hungary

[20] Verma, J., Kulkarni, B. S. (2017): Evaluation of dahlia genotypes for growth and yield characters under dry zone of Karnataka, India. – International Journal of Current Microbiology and Applied Sciences 6(11): 402-409.
[21] Villasenor, J. L., Martiez, R. R. (2018): A new species of Dahlia (Astrecea, Coreopsideae) from the state of Oaxaca Mexico. – Phytotaxa 362(2): 239-243.
[22] Yanming, D., Quinsong, S., Congcong, L., Xiaoqing, Y., Risheng, T. (2012): Differential responses of double petal and multi petal jasmine to shading: II. Morphology, anatomy and physiology. – Scientia Horticultureae 144: 19-28.
[23] Yazici, K., Gülgün, B. (2016): Importance of *Lilium candidum* (white lily) growth in ecological conditions of turkey as a potential for landscape and food sector in Tokat. – Journal of Ecosystem and Ecology Science 6(3): 243-250.

http://www.aloki.hu ● ISSN 1589 1623 (Print) ● ISSN 1785 0037 (Online)
DOI: http://dx.doi.org/10.15666/aeer/1605_71917202
© 2018, ALÖKI Kft., Budapest, Hungary

CROP LOAD REGULATION WITH CHEMICAL THINNERS IN DEVECI PEAR (*PYRUS COMMUNIS* L.)

KAÇAL, E.

Department of Fruit Breeding and Genetic, Fruit Research Institute, 32500 Eğirdir, Isparta, Turkey
(e-mail: emel.vural@gmail.com; phone: +90-246-313-2420-112; fax: +90-246-313-2425)

(Received 3rd Aug 2018; accepted 28th Sep 2018)

Abstract. The efficacy of three different doses of ammonium thiosulfate (ATS), potassium thiosulfate (KTS) and BA (6-benzyladenine) on fruit quality, yield and return bloom was evaluated in this present experiment on 'Deveci' pear (*Pyrus communis,* L.). All treatments were compared to an unsprayed control and hand fruit thinning. The highest fruit set was achieved with BA treatments. It was significantly reduced in KTS rates compared to control and other thinning treatments. KTS sprays create a statistically significant increase in fruit diameter and fruit weight, while ATS and BA have had no dramatic effect. Hand fruit thinning has resulted in heavier fruit at harvest similar to KTS with 2%. Thinners increased the percentage of fruit to ≥75 mm in diameter and proportions to 250-500 g fruit weight. In the control trees, the ratio of fruit to ≥75 mm diameter was 57%, the 75% or more of which was in hand thinning and chemical thinners. The proportion of fruits within 250-500 g fruit weight group was found in the highest KTS doses. No physiological disorder as bitter pit, water core, and aging disorder and phytotoxicity were observed in fruit samples. Study results show that 2% KTS significantly reduce crop load and increased fruit quality in 'Deveci' pear. Therefore, it can be used as an alternative to hand fruit thinning in the 'Deveci' pear to achieve high fruit quality. But, neither flower nor fruit thinners induced return bloom in 'Deveci' pear.
Keywords: *alternate bearing, 6-BA, blossom thinners, fruit quality, yield efficiency*

Introduction

Turkey is among the top 10 pear producers in the world with 420.000 tons of pear production. Although pears are grown throughout the country, production is mainly focused around the Southern Marmara, Northern Mediterranean and Central Anatolia Regions. Many different varieties of pears are grown in Turkey. Most popular pear varieties are 'Santa Maria', 'Deveci', 'Akca', 'Mustafabey', 'Williams', 'Kieffer', and 'Ankara'. 'Deveci', which is an Anatolian origin, is one of the major pear varieties produced in Turkey. It constitutes 20% of production (Atalaysun, 2016) and is very popular among consumers because of having large fruit and high consumption quality. 'Deveci' is a variety with biennial bearing. If there is no thinning in the "on year", no flower may be in the next year. Alternate bearing or biennial bearing is common in temperate fruit trees such as apple, pistachio, pear and olive. Genetic predisposition has an important role in the occurrence of alternate bearing, but it is possible to reduce it with plant nutrition practices and crop load management. Crop load management is one of the most important horticultural practices for sustainable fruit quality and quantity (Yıldırım and Koyuncu, 2004). Thinning applications can be performed in different phenological periods such as buds, flowers and fruits by different methods. Flower thinning is practiced to maximize crop value and promote return bloom when compared to fruitlet thinning. Early thinning will conserve photosynthetic reserves by reducing competition between all organs throughout the tree. Flower thinning can be conducted mechanically or chemically. But in practice, the most common method is the use of chemical thinners. Chemical blossom thinners are caustic and reduce fruit set by

http://www.aloki.hu ● ISSN 1589 1623 (Print) ● ISSN 1785 0037 (Online)
DOI: http://dx.doi.org/10.15666/aeer/1605_72037212
© 2018, ALÖKI Kft., Budapest, Hungary

damaging different parts of the flower and prevent fertilization (Fallahi and Willemsen, 2002). Several chemicals like ATS, KTS, armothin, etc. have been identified to reduce fruit set when applied at the flowering time. Chemical fruit thinning is achieved by plant growth regulators such as BA, NAA, NAD when the fruits reach a certain size. Hand fruit thinning, one of the applications in crop load management, is not economical for industrial countries since it increases labour costs and is a time-consuming practice (Bangerth and Quinlan, 2000). Therefore, the interest in chemical thinners has also increased steadily.

Apple is the main fruit species in which thinning studies are widely performed due to high expectation of fruit quality and the tendency to alternate bearing. Many apple varieties have been tested for their response to chemical thinners in different ecologies. However, limited studies are available in the literature on pear. Crop load studies with chemicals have been conducted on 'Nijisseiki', 'Hosui', 'Conference', 'Forelle', 'Bartlett', 'Williams', 'Abbate Fetel', 'Williams Bon Chretien' and 'Packams Triumph' pears (McArtney and Wells, 1995; Maas and van der Steeg, 2011; Kirstein, 2015; Greene, 2012; Theron, 2011; Bound, 2015). The effects of Ethephon, NAA, BA, ABA, Metamitron, and ATS have been investigated in these studies. In the present work, it was evaluated the efficacy of three rates of ATS, KTS, and BA on fruit quality, crop load and return bloom in 'Deveci' pear grown on the Quince A rootstock.

Materials and methods

Study area and plant material

This study was conducted on the Fruit Research Institute (37°49'1"9N, 30°52'23"E), Eğirdir, Isparta, Turkey in 2017-2018 vegetation periods. Isparta has favourable conditions for temperate fruit growing. It is very important apple production region within Turkey; it leading producer with about 25% of total. The Institute is located between Eğirdir and Kovada Lakes. The location is the transitional zone between the Mediterranean and the continental climate. The study area is 917 m above sea level. The average temperature is 12.2 °C and the annual rainfall is 564.3 mm (1929-2017). Some of the meteorological data recorded in the study area (37°48'52"N, 30°52'30"E) are presented in *Table 1*.

Table 1. *The recorded monthly meteorological data of the experimental area (2017 year)*

	Jan.	**Feb.**	**Mar.**	**Apr.**	**May**	**June**	**July**	**Aug.**	**Sept.**	**Oct.**	**Nov.**	**Dec.**
Avg. temp. (°C)	0.57	1.52	7.6	10.9	15.21	19.28	23.38	22.78	19.57	12.23	6.91	5.37
Min. temp. (°C)	-4.38	0.87	1.05	3.97	8.43	11.73	14.65	14.77	9.53	5.19	0.75	1.06
Max. temp. (°C)	5.51	2.16	14.15	17.83	22	26.83	32.11	30.78	29.61	19.27	13.06	9.68
Avg. hum. (%)	76.24	70.8	65.89	61.61	67.91	66.75	49.27	61.38	56.49	69.99	82.8	85.96
Total rainfall (mm)	188.6	0.65	88	84.2	73	60.8	0.4	24.6	0.8	82.8	81	181.6

'Deveci' pear tree, 16-year-old, at a spacing of 4.0 x 2 m in north-south rows on Quince A rootstock, was selected as experimental trees. 'Deveci' trees grow semi-vigour and are semi-spreading. The number of days between full bloom and harvest is 150-160. Ripening season is around 15-20 October. Eleven applications including

http://www.aloki.hu ● ISSN 1589 1623 (Print) ● ISSN 1785 0037 (Online)
DOI: http://dx.doi.org/10.15666/aeer/1605_72037212
© 2018, ALÖKI Kft., Budapest, Hungary

unsprayed control (no thinning), hand fruit thinning (HFT) just after June drops (one fruitlet left per cluster), ammonium thiosulfate (ATS) (1.0%, 2.0%, 3.0%), potassium thiosulfate (KTS) and BA (6-benziyladenine) (Exilis®) (100, 125 and 150 mg l^{-1}) were designed. The applications were performed by spraying on the predetermined healthy trees by handgun sprayer. All sprays were applied to the whole tree and no surfactant was used. Detailed information about experiments is given in *Table 2*.

Table 2. *Thinning practices, application time and date*

Treatments	Doses	Application period	Application date
Control	-	-	-
HFT	-	After June drop (one fruit was left in each flower cluster)	06.06.2017
ATS	1% 2% 3%	Full bloom (70-80%)	19.04.2017
KTS	1% 2% 3%		
BA	100 mg l^{-1} 125 mg l^{-1} 150 mg l^{-1}	10-12 mm fruit diameter	12.05.2017

The experimental area was irrigated twice a week by drip irrigation and the fertilizers were given based on the soil analysis results. The soil of the experimental area was loamy-clay. It contains 2.8% organic matter. During the trial, orchard management practices were carried routinely and spray program was followed for plant health.

Measurements

Fruits were harvested at commercial harvest time in 16.10.2017. Ten fruits were selected randomly per tree for fruit quality measurements such as fruit length (mm), fruit diameter (mm), fruit weight (g), fruit flesh firmness (N), soluble solid contents (SSC) and titratable acidity (TA). A total of 120 fruits were analysed in each application. Fruit samples were also assessed for physiological disorders. They were graded into various sizes and weight classes. Different groups were formed between 100-500 g for fruit weight and 65-90 mm for fruit diameter.

All flower clusters were counted to determine fruit set ratio at pink bloom stage and the number of fruits per tree. The yield was recorded in each tree at harvest. During the winter period, the stem diameter was measured at a height of 15 cm from the graft union and the trunk cross-sectional area (TCSA) as calculated (πr^2).

A few days after application, macroscopic observations were made for phytotoxic effects of thinners on tree organs. This trial was planned for two vegetation years and no thinning applications could be made because of alternate bearing in 2018. Thus, flowers were only counted for return bloom in 2018. During the spraying period, meteorological data were taken in order to determine the effects of temperature and relative humidity on thinning mode of chemicals (*Fig. 1*).

http://www.aloki.hu ● ISSN 1589 1623 (Print) ● ISSN 1785 0037 (Online)
DOI: http://dx.doi.org/10.15666/aeer/1605_72037212
© 2018, ALÖKI Kft., Budapest, Hungary

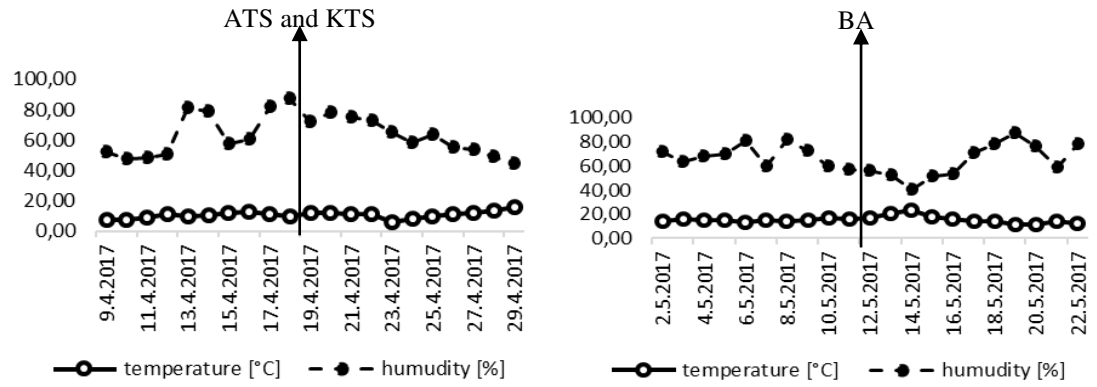

Figure 1. *Temperature and relative humidity in the application period*

Statistical analysis

Experiments were arranged in a randomized complete block design with four replicates, three trees were used for each replicate. Statistical procedures were performed using statistical analysis systems SPSS software. Duncan's multiple range test was used for means separation at a significance level of 5%.

Results and discussion

Fruit set and cropping

In this study, fruit set was affected by treatments. Differences among treatments on fruit set and cropping were significantly at 5% level. It is tended to decline with increased rates of KTS. ATS at 3% and KTS at 3% spraying significantly reduced fruit set, whereas BA did not. This data is not overlapping with findings of Chabikwa (2008), Bound and Mitchell (2002), Curetti et al. (2011) and Bertelsen (2002) on 'Early Bon Chretien', 'Packam's Triumph', 'Williams' and 'Clara Frijs' pears for BA. But these results are similar to Greene (2012) who works on 'Bartlett' pear. Low temperatures at application time could reduce BA efficiency. The highest ATS rate caused approximately 42.86% reduction in fruit set in comparison with untreated control. That was 52.29% compared to 125 mg l^{-1} BA. In BA and ATS, yield was higher than KTS doses and the highest yield was obtained from ATS as 2%. ATS and KTS reduced yield at harvest as 3% and 1% respectively. But, the lowest fruit yield with the 30.89 kg $tree^{-1}$ was taken from hand fruit thinning trees. 100 mg l^{-1} BA was the best practice for yield efficiency compared to untreated control and others (*Table 3*).

Fruit quality

Significant differences were found among treatments on fruit quality parameters in comparison with the unsprayed control. All thinning practices increase fruit quality statistically ($P \leq 0.05$) at varying rates compared to control. KTS sprays increased fruit diameter and fruit weight, while ATS and BA had no significant effect. Hand fruit thinning has resulted in heavier fruit at harvest similar to KTS as 2% (*Table 4*). ATS doses used in this study, being a promising thinner for 'Packham's Triumph' (Bound, 2015) and 'Clara Frijs' (Bertelsen, 2002) pears, were not as effective as hand fruit thinning and KTS doses on the fruit quality.

http://www.aloki.hu ● ISSN 1589 1623 (Print) ● ISSN 1785 0037 (Online)
DOI: http://dx.doi.org/10.15666/aeer/1605_72037212
© 2018, ALÖKI Kft., Budapest, Hungary

Table 3. *Effect of thinners on fruit set and cropping*

Treatments	Doses	Fruit set (fruitlets/100 flower clusters)	Yield (kg tree^{-1})	Yield efficiency (kg cm^{-2})
Control	-	11.85abc*	38.83abc	0.17ab
HFT	-	9.20abc	30.89c	0.14ab
ATS	1%	10.99abc	42.80abc	0.17ab
	2%	11.69abc	47.19a	0.12b
	3%	6.77c	31.68bc	0.13b
KTS	1%	10.05abc	31.39c	0.13b
	2%	9.73abc	38.15abc	0.15ab
	3%	8.56bc	36.15abc	0.16ab
BA	100 mg l^{-1}	12.59ab	41.76abc	0.19a
	125 mg l^{-1}	14.19a	44.41ab	0.17ab
	150 mg l^{-1}	11.29abc	34.28bc	0.15ab

*Means in columns followed by the same letters are not significantly different at 5% level

Table 4. *Effects of treatments on some fruit quality parameters*

Treatments	Doses	Fruit width (mm)	Fruit weight (g)	Shape index	Fruit flesh firmness (N)
Control	-	76.57d*	222.58e	0.90abc	43.73f
HFT	-	80.85ab	263.60a	0.89bc	43.96f
ATS	1%	78.50c	237.04de	0.89bc	45.84cde
	2%	78.36cd	239.68bcde	0.90abc	49.80a
	3%	80.09abc	257.39abc	0.89bc	47.91b
KTS	1%	80.29abc	258.61ab	0.91ab	46.84bcd
	2%	81.67a	267.13a	0.88c	46.37bcd
	3%	79.65abc	251.21abcd	0.89bc	47.44bc
BA	100 mg l^{-1}	79.49bc	249.09abcd	0.92a	45.20def
	125 mg l^{-1}	79.47bc	241.42bcde	0.89bc	46.29bcd
	150 mg l^{-1}	78.59c	237.94cde	0.89bc	44.57ef

*Means in columns followed by the same letters are not significantly different at 5% level

ATS increased fruit diameter and fruit weight 3% relative to other ATS rates. Multiple applications of the ATS may also have a better thinning effect on the 'Deveci' variety, such as 'Packham's Triumph' (Bound and Mitchell, 2002). Compared to ATS and unsprayed control, KTS doses gave good results on fruit quality. However, the 2% KTS was more effective than the 1% KTS and 3% KTS. BA applications were made when the fruit diameter was 8-12 mm. Although the doses of 50-200 mg l^{-1} have been used in practice, the thinning effect of 100-150 mg l^{-1} BA has been found promising for some varieties. Theron et al. (2011) reported that the application of 100-150 mg l^{-1} BA on 8-12 mm fruit diameter in 'Early Bon Chretien' pear greatly reduced fruit set and that the thinning effect of 150 mg l^{-1} BA was higher. In the literature, although the positive effects of BA on fruit thinning in pear are mentioned, it is reported that some pear varieties do not respond to fruit thinning applications. Reactions of varieties to

http://www.aloki.hu ● ISSN 1589 1623 (Print) ● ISSN 1785 0037 (Online)
DOI: http://dx.doi.org/10.15666/aeer/1605_72037212
© 2018, ALÖKI Kft., Budapest, Hungary

chemical thinners may differ. Greene (2012) informed that BA was not effective in 'Bartlett's' pear, while Maas and Van der Steeg (2011) in 'Conference', Bound (2015), in 'Packham's Triumph' and Bertelsen (2002) in 'Clara Frijs' pear could be recommended for thinning. In 'Forelle' pear variety, BA + NAA applications reduced fruit set more than single applications of BA (Kirstein, 2015). In our study, although BA treatments increased fruit quality compared to control, they did not exceed KTS, ATS and hand fruit thinning with regards to efficacy. It is thought that this situation may be related to the climatic conditions at the time of application with the variety response. This is because the air temperature in the application period was around 15 °C, which is the limit value for BA. Low temperatures during the application period may have overshadowed the effectiveness of the BA. In contrast, Bregoli et al. (2006) stated that the effect of BA may be related to the king fruit size rather than climatic conditions. In this study, BA treatments were made 24 days after full bloom when the fruit diameter reached 10-12 mm. It is also possible that the phenological period at the time of application may not be suitable for BA in Deveci, or BA alone may be inadequate for a good thinning effect. As a matter of fact, Kurnaz et al. (1992) suggested that NAA and Carbaryl applications in 'Deveci' pear are not enough alone to be as effective as hand fruit thinning on fruit weight and size.

The fruit flesh firmness in ATS reached the highest value of 2%, but it was significantly ($P \leq 0.05$) reduced in control and hand fruit thinning fruits. It is thought that the fruits of this application have more cells, but these cells do not reach sufficient size because of high crop load. The positive effect of ATS on fruit flesh firmness has also been reported in previous studies in apples (Bound and Wilson, 2007). SSC values obtained in the current study were classified according to the applications. As a result of a yield decrease, SSC was higher in 3% ATS and hand fruit thinning. Reductions in SSC with high crop load may have been the result of reductions in soluble carbohydrates, increased competition for assimilate between plant organs resulting from increased crop load. Similar findings were reported by Coneva and Cline (2006) in 'Redhaven' peaches. SSC is increasing due to the increase of ATS doses. Titratable acidity was unaffected by thinning (*Table 5*).

Table 5. *Effects of treatments on soluble solids content and titratable acidity*

Treatments	Doses	SSC	TA %
Control	-	12.4bc*	0.2ns
HFT	-	13.6a	0.3
ATS	1%	12.5bc	0.3
	2%	12.8abc	0.3
	3%	13.7a	0.3
KTS	1%	13.1abc	0.3
	2%	12.5bc	0.2
	3%	13.2abc	0.2
BA	100 mg l^{-1}	13.3abc	0.3
	125 mg l^{-1}	12.3c	0.3
	150 mg l^{-1}	13.5ab	0.2

*Means in columns followed by the same letters are not significantly different at 5% level
ns: not significant

http://www.aloki.hu ● ISSN 1589 1623 (Print) ● ISSN 1785 0037 (Online)
DOI: http://dx.doi.org/10.15666/aeer/1605_72037212
© 2018, ALÖKI Kft., Budapest, Hungary

Fruit size in 'Deveci' pear is an important trait, and it is linked to eating quality. Fruit juiciness and crispness reduce when fruit size decreases. It was determined that in control trees where no application was made, the fruit diameter and weight, as well as the fruit flesh firmness, decreased (*Table 4*). The eating quality of these fruits is also lower relative to large fruits. The effect of thinners on fruit diameter distribution was different. The chemical thinners increased the percentage of fruit to ≥75 mm in diameter. In control trees, the ratio of fruit to ≥75 mm was 57%, where ATS 2% and KTS 3% were 69%. In KTS 2%, 80% of the fruits have ≥75 mm. Fruit rate of to ≥85 mm was found to be higher in hand fruit thinning and KTS at 2% (*Fig. 2*). The effect of KTS sprays on fruit size was the greatest.

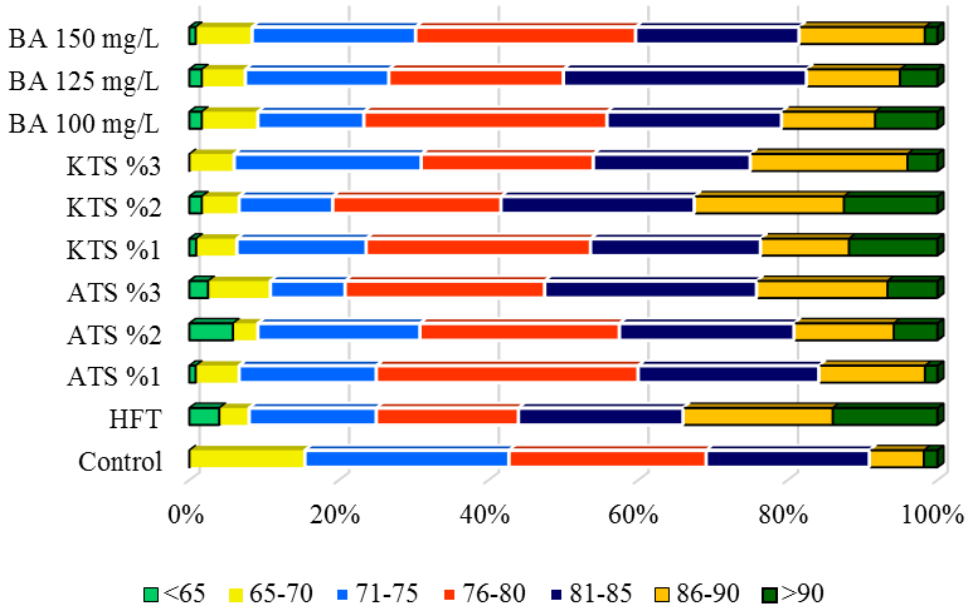

Figure 2. *Effects of thinners on fruit size distribution (mm)*

'Deveci' pear can produce fruit up to 1500 g depending on the nutrition conditions and crop load. Although fruit size is an important factor for 'Deveci', over a certain size, it is not preferred by consumers. Ideal fruit weight for 'Deveci' is approximately between 250 and 450 g. The fruits above 450 g are not demanded. The fruit weight of 250 g and above in KTS was higher than the other. Among the KTS doses, 2% KTS was the most effective with 59.2%. Hand fruit thinning was followed with 57% to KTS. The lowest fruit rate was found in control with 32.7%, while doses of ATS 1% and BA 150 mg l^{-1} were beyond all applications, except control trees. In BA applications, 50% of the fruits reached to 100-250 g fruit weights (*Table 6*). The reduction of fruit size in 'Deveci' following application of BA contradicts the findings of Curetti et al. (2011) for 'Williams'.

Return bloom

Early thinning before seed development could increase return bloom. Also, crop load significantly affects it (Melan and Gjerde, 1993). This is particularly important for varieties showing alternate bearing. However, thinners positively affected the fruit quality in 'Deveci', they reduced return bloom dramatically in the second year of the

http://www.aloki.hu ● ISSN 1589 1623 (Print) ● ISSN 1785 0037 (Online)
DOI: http://dx.doi.org/10.15666/aeer/1605_72037212
© 2018, ALÖKI Kft., Budapest, Hungary

experiment. Similar findings were found by Bound and Mitchell (2002) in 'Packham's Triumph' pear with ATS at 2%. According to Forshey (1986), varieties showing alternate bearing generally do not respond to chemical thinners. In 2017, the highest number of flowers was recorded in the KTS 3%. This was followed by ATS 2% and ATS 3%. The number of flowers in the hand fruit thinning and BA 100 mg l^{-1} was lower, but the highest flower number was obtained from these applications in 2018 (*Fig. 3*). However, the efficiency of BA on return bloom was not at optimum level. This response is likely to be related to dose, application time, varietal characteristics or weather conditions. Additionally, spur leaf damage might be prevented to the formation of flower buds (Luckwill, 1970).

Table 6. *Effects of thinners on fruit weight distribution (g)*

	100-150	**150-200**	**200-250**	**250-300**	**300-350**	**350-400**	**400-450**	**450-500**
Control	8.2	33.6	25.5	25.5	3.6	1.8	1.8	0.0
HFT	5.0	21.0	17.0	28.0	16.0	7.0	4.0	2.0
ATS 1%	1.7	25.0	38.3	19.2	12.5	2.5	0.8	0.0
ATS 2%	7.5	23.3	25.0	26.7	11.7	2.5	2.5	0.8
ATS 3%	6.7	16.7	22.5	29.2	15.0	5.8	2.5	1.7
KTS 1%	1.8	19.1	31.8	23.6	10.9	7.3	3.6	1.8
KTS 2%	3.3	16.7	20.8	27.5	20.0	8.3	3.3	0.0
KTS 3%	3.0	26.0	25.0	22.0	16.0	5.0	1.0	2.0
BA 100 mg l^{-1}	2.5	15.8	40.0	23.3	13.3	4.2	0.8	0.0
BA 125 mg l^{-1}	5.0	22.5	30.8	23.3	15.0	3.3	0.0	0.0
BA 150 mg l^{-1}	3.4	25.2	31.9	25.2	10.9	3.4	0.0	0.0

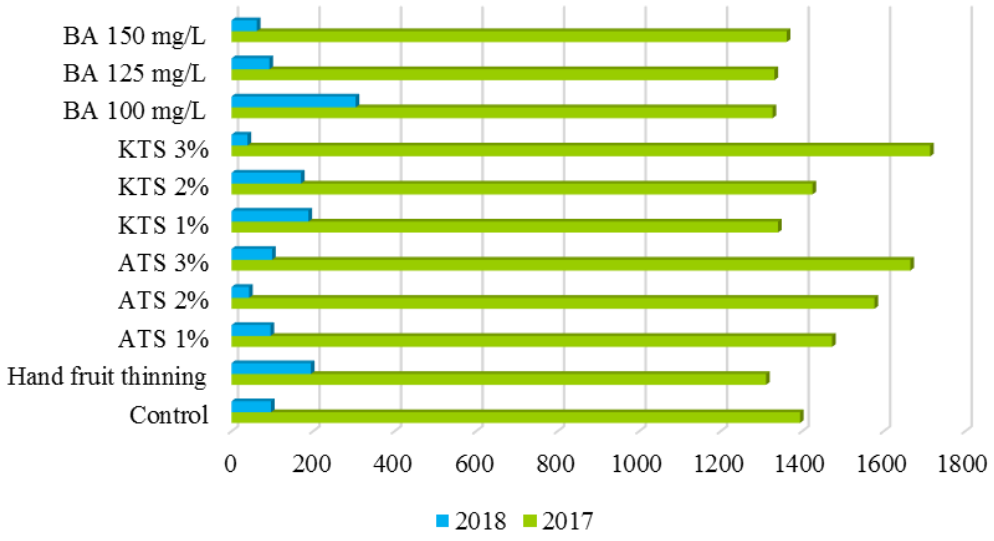

Figure 3. *Effects of thinners on flower number in 2017 and 2018 years*

Phytotoxicity and physiological disorders

Blossom thinners as ATS and KTS are caustic and they can cause damage on the development of spur leaves or other parts of the tree (Webster, 2002; Grenee, 2002).

http://www.aloki.hu ● ISSN 1589 1623 (Print) ● ISSN 1785 0037 (Online)
DOI: http://dx.doi.org/10.15666/aeer/1605_72037212
© 2018, ALÖKI Kft., Budapest, Hungary

Factors such as weather conditions, high concentrations and variety characteristics often affect the thinners' response and damage ratio on the flower, spur leaves, young branches and fruits (Forshey, 1986; Kaçal and Koyuncu, 2012). Previous studies reported that high doses of ATS result in serious damage (Sanders and Looney, 1993; Janoudi and Flore, 2005). Phytotoxic effect of ATS than high doses, the previous day from the time of application occurred in cool, humid, and rainy weather (Schupp and Greene (2002). However, Bound and Jones (2004) performed that rates of 3% ATS or higher doses caused foliar damage and bud death. KTS and ATS doses showed symptoms of leaf burning and chlorosis on spur leave a few days after application in this study resulting from low temperate and high humidity, but they did not affect fruit size. This damage has increased with increasing doses. No phytotoxicity was found in BA applications.

BA can cause russet on the fruit skin. This condition was observed by Greene (2002) on Bartlett pear. But in the case of excessive thinning, physiological disorders such as bitter pit and water core in fruits are likely to occur when the increase in fruit size and nutritional conditions are taken into account. However, during the experiment, no physiological disorder as bitter pit, water core, and aging disorder and phytotoxicity were observed.

Conclusion

Efficacy of ATS, KTS, and BA on the fruit quality and return bloom in 'Deveci' pear was evaluated in this experiment. Flower thinners reduce fruit set and yield and increase fruit quality. But neither flower nor fruit thinners induced return bloom. There is no record about what is the optimum fruit number for next year cropping and high fruit quality in 'Deveci'. Further detailed crop load studies should be done on 'Deveci' pear. Dose, application times, chemicals and combined use of either flower or fruit thinners, single applications or the sequential use of ATS and KTS should further be tested to create a thinning schedule for pear growers.

REFERENCES

[1] Atalaysun, M. (2016): Turkey fresh deciduous fruits report. – Gain Report TR6051.
[2] Bangerth, F., Quinlan, J. (2000): Editorial preface. – Plant Growth Regulation 31(1–2): v–vi.
[3] Bertelsen, M. G. (2002): Benzyladenine and other thinning agents for pear cv. 'Clara Frijs'. – J. Amer. Pomol. Soc. 56: 149–155.
[4] Bound, S. A. (2015): Optimizing crop load and fruit quality of 'Packham's Triumph' pear with ammonium thiosulfate, ethephon and 6-benzyladenine. – Scientia Hort. 192: 187–196.
[5] Bound, S. A., Jones, K. M. (2004): Ammonium thiosulphate as a blossom thinner of 'Delicious' apple, 'Winter Cole' pear and 'Hunter' apricot. – Australian Journal of Experimental Agriculture 44: 931–937.
[6] Bound, S. A., Mitchell, L. (2002): The effect of blossom desiccants on crop load of Packham's Triumph pear. – Acta Horticulturae 596: 729–733.
[7] Bound, S. A., Wilson, S. J. (2007): Ammonium thiosulfate and 6-benzyladenine improve the crop load and fruit quality of 'Delicious' apples. – Australian Journal of Experimental Agriculture 47: 635–644.

http://www.aloki.hu ● ISSN 1589 1623 (Print) ● ISSN 1785 0037 (Online)
DOI: http://dx.doi.org/10.15666/aeer/1605_72037212
© 2018, ALÖKI Kft., Budapest, Hungary

[8] Bregoli, A. M., Fabbroni, C., Vancini, R., Galliano, A., Costa, G. (2006): Results obtained on the efficacy of 6-BA alone, and in combination with other thinning agents from different apple producing areas of northern Italy Anna Maria. – Journal of Fruit and Ornamental Plant Research 14: 23–38.
[9] Chabikwa, T. G. (2008): Chemical thinning of European pear cultivars (Pyrus communis, L.). – Master of Science Dissertation, Stellenbosch University, South Africa.
[10] Coneva, E. D., Cline, A. (2006): Blossom thinners reduce crop load and increase fruit size and quality of peaches. – HortScience 41: 1253–1258.
[11] Curetti, M., Rodríguez, R., Magdalena, C., Rodríguez, A. (2011): Effect of concentration, application volume and addition of a surfactant on response to benzyladenine as thinning agent in 'Williams' pears. – Acta Horticulturae 909: 395–40.
[12] Fallahi, E., Willemsen, K. M. (2002): Blossom thinning of pome and stone fruit. – Hortscience 7: 474–477.
[13] Forshey, C. G. (1986): Chemical fruit thinning of apples. – New York's Food and Life Sciences Bulletin, Number 116. New York State Agricultural Experiment Station, Geneva, a Division of the New York State College of Agriculture and Life Sciences, Cornell University, Ithaca.
[14] Greene, D. W. (2002): Chemicals, timing and environmental factors involved in thinner efficacy on apple. – HortScience 37: 477–481.
[15] Greene, D. W. (2012): Influence of abscisic acid and benzyladenine on fruit set and fruit quality of 'Bartlett' pears. – HortScience 47: 1607–1611.
[16] Janoudi, A., Flore, J. A. (2005): Application of ammonium thiosulfate for blossom thinning in apples. – Scientia Horticulturae 104: 161–168.
[17] Kaçal, E., Koyuncu, F. (2012): Use of chemical blossom thinners in 'Jerseymac' and 'Jonagold' apples. – Bulgarian Journal of Agricultural Science 18: 898–904.
[18] Kirstein, D. L. (2015): Mechanical thinning of Pome Fruit. – Doctoral Dissertation, Stellenbosch University, South Africa.
[19] Kurnaz, Ş., Özcan, M., Kopuzoğlu, N., Demirsoy, H. (1992): Effects of NAA, Carbaryl and hand thinning application on Deveci pear cultivar grown in Samsun. – Bahçe 21: 3–8.
[20] Luckwill, L. C. (1970): The Control of Growth and Fruitfulness of Apple Trees. – In: Luckwill, L. C., Cutting, C. V. (eds.) Physiology of Tree Crops. Academic Press, London.
[21] Maas, F. M., Van der Steeg, P. A. H. (2011): Crop load regulation in 'Conference' pears. – Acta Horticulturae 909: 369–380.
[22] McArtney, S. J., Wells, G. H. (1995): Chemical thinning of Asian and European pear with ethephon and NAA. – New Zealand Journal of Crop and Horticultural Science 23: 73–84.
[23] Meland, M., Gjerde, B. (1993): The effect of hand thinning on return bloom of Summerred and Aroma apples. – Acta Horticulturae 349: 219–222.
[24] Sanders, M., Looney, N. E. (1993): Ammonium thiosulphate (ATS) - a fertilizer that thins. – Tree Fruit Leader 2(1): 1-3.
[25] Schupp, J. R., Greene, D. W. (2002): Thinning McIntosh apple trees with blossom thinners, with and without post-bloom NAA: A report to the New England Tree Fruit Growers Research Committee. – Fruit Notes 67: 9–12.
[26] Theron, K. I., Chakbiwa, T. G., Lötze, G. F. A. (2011): Evaluation of 6-Benzyladenine (BA) and Naphthylacetamide (NAD) as post-bloom thinning compounds for 'Early Bon Chrétien' pear. – Acta Horticulturae 909: 387–394.
[27] Webster, T. (2002): Current approved thinning strategies for apples and pears and recent thinning research trials in Europe. – The Compact Fruit Tree 35: 73–76.
[28] Yıldırım, F., Koyuncu, F. (2004): Development of chemical thinning in apples. – Derim 21: 44–53. http://www.dergipark.gov.tr/download/article-file/52912.

http://www.aloki.hu ● ISSN 1589 1623 (Print) ● ISSN 1785 0037 (Online)
DOI: http://dx.doi.org/10.15666/aeer/1605_72037212
© 2018, ALÖKI Kft., Budapest, Hungary

EFFECTS OF LAND COVERS ON HYDRO-PHYSICAL SOIL CHARACTERISTICS IN SEMI-ARID ENVIRONMENTS: THE CASE OF GUMUSHANE-SIRAN, TURKEY

USTA, A. – YILMAZ, M.* – KOCAMANOĞLU, Y. O. – GENÇ, E.

Faculty of Forestry, Karadeniz Technical University, 61080 Trabzon, Turkey

**Corresponding author*
e-mail: yilmaz61@ktu.edu.tr ; phone: +90-462-377-2854; ORCID: 0000-0002-9552-993X

(Received 4th Aug 2018; accepted 4th Oct 2018)

Abstract. Land degradation is already one of the major problems affecting the world. Land degradation by soil erosion is one of the most serious ecological problems and environmental issues in many sites of arid and semiarid regions. There has been an increasing concern regarding the semiarid highlands of Turkey that degradation of these ecosystems results in excessive soil erosion, ecosystem degradation, and loss of natural resources. This paper, therefore, explores the impact of land cover in a linkage to the soil erodibility indices and some soil properties of Koruluk (Gümüşhane-Turkey) dam watershed. Soil samples were taken from soil profiles opened in 78 sample pilots among the lands which border each other in the same altitude levels and same slopes on the andesite-basalt bedrock in the southern aspect group according to 0-10 cm and 10-20 cm depths. Sand, silt, clay, soil organic matter, dispersion ratio, erosion ratio, structural stability index, aggregate stability, clay dispersion ratio, field capacity, available water capacity, bulk density, total porosity, soil pH and electrical conductivity analyses were performed in soil samples. The results obtained about land cover were tested by variance analysis. The relationships between the selected soil characteristics were determined by correlation analysis. Degraded scotch pine forest soils were observed to be more susceptible to erosion compared to degraded oak forests and open space areas. Consequently, it was revealed that soils that developed from similar parent material in semi-arid ecosystem and under all land covers were susceptible to erosion. The fact that the watershed supplies Koruluk dam built for irrigation water production makes these results quite significant. Agricultural activities are very important in the protection and continuity of the socio-economic situation of local people. The continuity of agricultural activities, in one respect, is associated with the availability of irrigation in this semi-arid region. Therefore, priority should be given to the necessary rehabilitation, planning and management studies in Koruluk dam watershed, and the results of this study should be considered.
Keywords: *Koruluk dam, degraded forests, semi-arid, erodibility indices, soil properties*

Introduction

Soil erosion is an ecological, environmental, economic, social and serious problem. This not only causes land degradation and reduction of soil fertility but also significantly affects the public health and sustainable development in rural areas (Tang, 2004; Zheng et al., 2004; Jing et al., 2005). Soil erosion is a natural process that continues depending on physiographic and climatic factors. However, it is the accelerated erosion that reduces soil fertility, decreases its quality, adversely affect water quality and management. Erosion can be accelerated through human activities. Surface mining, forestry, agriculture and construction are the major activities (Lal, 2001).

The trigger for accelerated erosion in arid and semi-arid areas is loss of vegetation cover. This exposes soils to wind and water erosion, loss of soils decreases the potential for vegetation production. The end result is a decrease in the carrying capacity of the rangeland and productivity of forests. Despite being in arid and semi-arid areas the

http://www.aloki.hu ● ISSN 1589 1623 (Print) ● ISSN 1785 0037 (Online)
DOI: http://dx.doi.org/10.15666/aeer/1605_72137229
© 2018, ALÖKI Kft., Budapest, Hungary

erosion is largely a result of infrequent but heavy rainfall events. The erosion of soils exacerbates soil degradation. Soil quality decreases along with the erosion, especially structural units become weakened. In others, erosion may lead to decline in soil quality and set in motion the degradative trend. Soil erosion can be a manifestation of soil degradation because it involves physical removal of soil in a vertical and/or horizontal direction and degrades soil quality (Lal, 2001). Soil physical processes involve decline in soil structure leading to an increase in bulk density, decrease in total and macroporosity reduction in infiltration, increase in runoff, and exacerbation in erosion by water and wind.

Turkey is one of the countries that are most affected by erosion and are susceptible to land/soil degradation and drought because of its geomorphological structure, physiographic, edaphic and climatic characteristics. Sediment occurring in active erosion areas leads to major flooding, drainage and deposit losses in stream beds, base-agricultural lands, dams and reservoirs by accumulating. The reservoirs and dam built with big investments lose their function due to the runoffs and the soil material moved by the rivers and are in danger of being inactivate before their economic life. About 65 of the total area of Turkey has a semi-arid and arid characteristic (ÇEM, 2011). Drinking and potable water needs in arid and semi-arid regions are met by the dams and reservoirs. Arid and semiarid areas are considered fragile environments where vegetation cover is scarce and where soil erosion processes occur rapidly and severely after rainfall events fall in these areas. However, even under those conditions, the importance of native vegetation is very significant in the regulation of surface hydrological processes.

Land cover affects the occurrence and the intensity of runoff and soil erosion (Chen et al., 2001; Wei et al., 2007). Proper management of land cover patterns may greatly improve soil properties, leading to reduced soil erosion to the recommended threshold limits (Fu, 1989; Chen et al., 2003). Improved physical soil characteristics can also positively affect the establishment of vegetation (Kosmas et al., 2000). Land cover systems might lead to changes in a number of soil characteristics and soil erosion processes (Bao-hua et al., 2003; Costa et al., 2003).

Four dams and four reservoirs were established in Gümüshane region where the study was conducted. Koruluk dam watershed, one of these dams, has become susceptible to erosion and deterioration by the destruction of vegetation cover by local people as well as the effect of geomorphological and climatological characters. Being aware of erosion trends, physical and chemical characteristics of watershed soils is quite important for the rehabilitation works to be conducted in these areas and measures to be taken.

The aim of this study is to investigate the hydro-physical characteristics and some erosion trends of Koruluk Dam watershed soils in Gümüşhane-Şiran region which is located in semi-arid region in Turkey's Eastern Black Sea Region depending on land cover changes.

Material and method

Study area

Study area is located in Gümüşhane province in northeast of Turkey. Koruluk dam, which was built for irrigation, is located in the northern part of Gümüşhane-Şiran district and is 7 km away from there (*Fig. 1*).

http://www.aloki.hu ● ISSN 1589 1623 (Print) ● ISSN 1785 0037 (Online)
DOI: http://dx.doi.org/10.15666/aeer/1605_72137229
© 2018, ALÖKI Kft., Budapest, Hungary

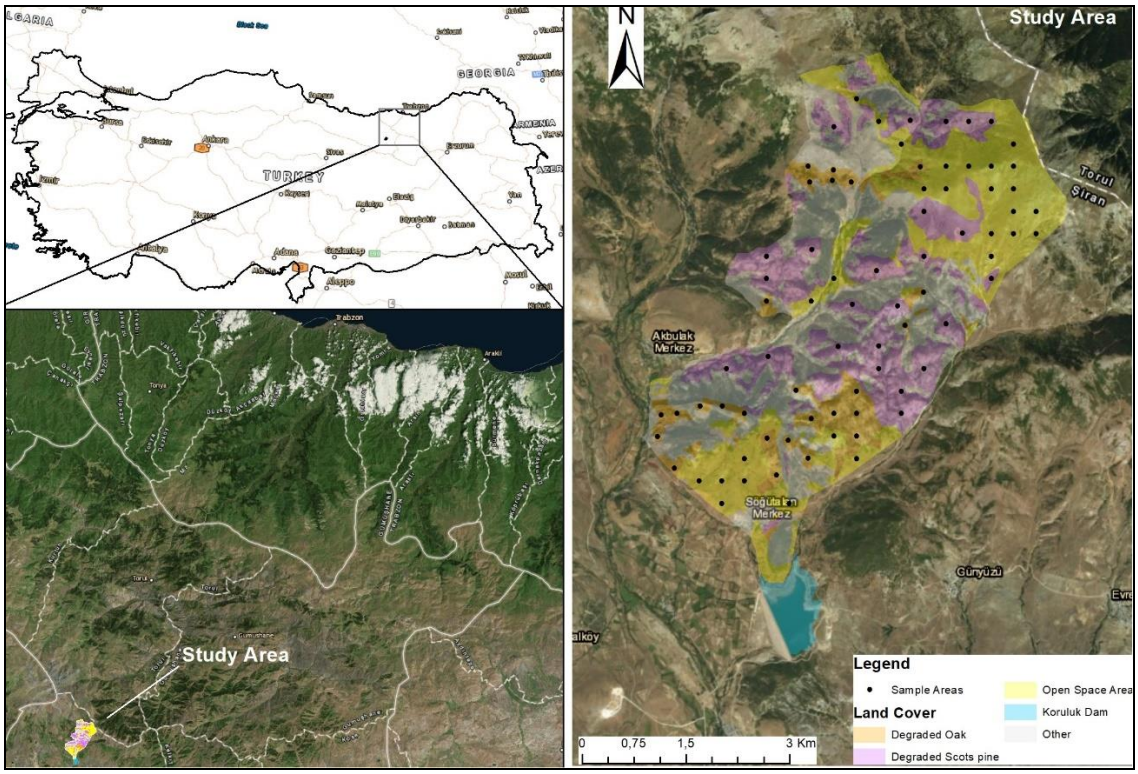

Figure 1. *Location of study area*

The construction of the dam was carried out between 1990-2005. The lake area is 0.7 km^2 in normal water elevation. Total irrigation area of the dam used for for the irrigation of agricultural areas near the dam is 3447 ha. Erenkaya, Şiran, Çal, Söğütalan, Örenkale, Sarıca, Koyunbaba, Günbatur and Bilgili villages benefit from Koruluk dam fed by Ceviz stream for irrigation.

In the study area, eocene aged andesite-basalt volcanic rocks are surfaced (Baykal, 1952). The data of Kelkit meteorological station (1965-1989) close to Şiran district were used in determining the climatic type of the study area. According to Thornthwaite climate analysis, the study area has a climatic type which is "close to the continental climate with little or no excess water semi-arid at low temperature (microthermal) indicated by DC'2db'2" symbol". Some climate data according to Thornthwaite method were given in *Table 1*.

Table 1. *Climate analysis according to Thornthwaite method (Thornthwaite, 1948)*

	Months												
Climate data	**I**	**II**	**III**	**IV**	**V**	**VI**	**VII**	**VIII**	**IX**	**X**	**XI**	**XII**	**Annual**
Average temp, °C	-8.0	-5.3	0.9	7.2	11.7	14.8	18.5	18.2	14.4	8.5	2.7	-3.7	6.7
Average precip, mm	22.4	24.0	35.7	52.2	50.0	44.5	10.3	8.9	17.3	30.8	27.5	25.0	348.6
Potential evapo, mm	0.0	0.0	4.5	39.6	72.1	92.3	117.4	108.1	75.2	40.9	11.2	0.0	561.3
Water defiency, mm	-	-	-	-	-	-	77.0	99.2	57.9	10.1	-	-	244.3
Water surplus, mm	-	-	18.9	12.6	-	-	-	-	-	-	-	-	31.6

http://www.aloki.hu ● ISSN 1589 1623 (Print) ● ISSN 1785 0037 (Online)
DOI: http://dx.doi.org/10.15666/aeer/1605_72137229
© 2018, ALÖKI Kft., Budapest, Hungary

Soil sampling and analyses

Sample pilots were taken from on soils developed from volcanic rocks and from south aspect. Average slopes and altitudes of the sample pilots are close to each other (*Table 2*).

Table 2. *Geomorphological characteristics of the areas under different land cover*

	Degraded oak forest	**Open space area**	**Degraded scotch pine forest**
Average slope (%)	31	35	38
General aspect	South	South	South
Average altitude (m)	1770	1820	1815
Parent material	Andesite-basalt	Andesite-basalt	Andesite-basalt

Sample pilots in the study area were determined by the selection sampling method as 26, 28 and 24 pieces, respectively, including degraded oak forest, open space area and degraded scotch pine forest. Total of the 78 sample plots, 25 of them were received in Işık (2016). The soil was sampled at two different depths: 0–10 cm (surface layer) and 10–20 cm (subsurface layer). Statistical analyses and assessments were carried out for surface layer, subsurface layer and average of profile (0-10 cm, 10-20 cm depths and 0-20 cm depth).

Particle size distribution (2-mm) and soil organic carbon (0.5 mm) were determined using disturbed soil samples using the Bouyoucos hydrometer method (Bouyoucos, 1962; Gülçur, 1974) and the modified Walkley-Black wet oxidation procedure, respectively. Soil organic matter (SOM) was calculated by multiplying soil organic carbon by 1.72 (Nelson and Sommers, 1982; Arp, 1999). Soil pH were measured using the procedures outlined by Arp (1999) and Page et al. (1982), for bulk density (BD) and total porosity (TP) by Blake and Hartge (1986) and Danielson and Sutherland (1986). Dispersion ratio (DR) was determined according to the methods described by Middleton (1930). The clay and silt fractions obtained by chemical dispersion were taken as total clay (TC) and total silt (TS), while water dispersible clay (WDC) was obtained as above except that no chemical dispersant was used. Colloid-moisture equivalent ratio (C-MER) and erosion ratio (ER) (Özhan, 2004), available water capacity (AWC) (Karaöz, 1989), aggregate stability (AS) (Le Bissonnais, 1996) and structure stability index (SSI) (Leo, 1963) were also determined.

Statistical analyses

Analyses of variance (ANOVA) were performed to determine the effects of land cover on the chemical and hydro-physical properties of the soil. Significant differences between variables were determined by Student-Newman-Keuls test. Correlation analysis was used to determine relationships between erodibility indices and hydro-physical properties of soils. Statistical analyses were performed using SPSS (2011).

Results

The change of average of the soil samples taken from two depth levels of soil profiles (0-10 cm and 10-20 cm and 0-20 cm) according to land cover was tested by

http://www.aloki.hu ● ISSN 1589 1623 (Print) ● ISSN 1785 0037 (Online)
DOI: http://dx.doi.org/10.15666/aeer/1605_72137229
© 2018, ALÖKI Kft., Budapest, Hungary

analysis of variance. The selected soil characteristics of Koruluk dam watershed soils are statistically different compared to land cover ($p < 0.05$ and $p < 0.001$) (*Tables 3, 4, 5*).

Table 3. *Change of erodibility indices, physical and chemical properties of the topsoils under land covers (0-10 cm soil depths)*

	Land covers		
	Degraded oak forest	**Open space area**	**Degraded scotch pine forest**
Chemical soil properties			
SOM (%)	2.38±1.34 b	2.30±1.70 b	1.40±1.21 a
pH	6.88±0.56 b	6.18±0.18 a	6.31±0.53 a
EC (µs/cm)	64.5±46.8 b	41.8±22.9 a	46.3±39.5 a
Physical soil properties			
BD	1.19±0.12 a	1.19±0.09 a	1.20±0.08 a
TP	55.7±6.4 b	57.1±5.3 b	47.0±10.5 a
Sand	78.4±10.5 a	79.3±6.3 a	82.8±5.5 a
Silt	9.3±4.2 b	10.7±2.9 b	7.3±1.8 a
Clay	12.3±6.9 a	10.0±3.9 a	9.9±5.2 a
FC	20.4±3.7 a	24.5±7.9 b	18.9±3.9 a
AWC	7.47±1.12 a	9.81±2.76 b	8.21±2.06 a
Erodibility indices			
AS (%)	52.2±16.7 b	46.8±9.5 a	45.8±10.5 a
SSI (%)	14.52±10.3 b	12.95±5.0 b	9.78±3.1 a
DR	38.3±17.6 a	31.1±12.9 ab	43.4±10.7 bc
C-MER	0.56±0.29 b	0.38±0.10 a	0.57±0.22 b
ER	88.2±56.1 a	89.1±74.7 a	92.9±58.1 a
WDC	3.30±1.31 b	1.61±1.38 a	2.92±1.59 b

Different letters indicate significant differences ($p < 0.05$).

The soils collected from different land covers showed significant difference ($p < 0.001$) with respect to average SOM content open space areas had the highest content of soil (2.22%) followed by degraded oak forest (2.01%), while the level of SOM in degraded scotch pine forest was very low (1.30%) (*Table 5*).

There is no difference between land covers in terms of BD values. Degraded scotch pine forest soils have the highest average BD values (1.18 g/cm^3) in terms of BD average values (*Table 5*). Total porosity values of Koruluk dam watershed are statistically different according to land cover ($p < 0.001$). The average AS value is minimum in degraded scotch pine forest soils and maximum in degraded oak forest soils. AS values are statistically different according to land cover ($p < 0.001$). The highest silt content of soils presents in open space area soils (11.0%) and is different from degraded oak forest and degraded scotch pine forest soils. While open space area and degraded oak forests are in the same group in the average sand contents of soils, the habitats dominated by degraded scotch pine forests are different with the highest values. The lowest average sand content was found in open space areas. There are significant differences in the soil fractions by percentage among land covers ($p < 0.05$, $p < 0.001$). The clay content in environments in which degraded oak exists is higher than open

http://www.aloki.hu ● ISSN 1589 1623 (Print) ● ISSN 1785 0037 (Online)
DOI: http://dx.doi.org/10.15666/aeer/1605_72137229
© 2018, ALÖKI Kft., Budapest, Hungary

space area and degraded scotch pine forests, degraded oak forest soils are similar with open space area soils and different from degraded scotch pine forest soils. DR from erodibility indices is greater than the limit value of 15 in soils under every three land covers. The highest DR values were found in degraded scotch pine forest soils and also the soils under this land cover are susceptible to erosion. However, degraded scotch pine forest soils are more susceptible to erosion. The study area soils vary according to land cover in terms of average DR values (*Table 5*).

ER values of soils are greater than the limit value of 10 in areas under all land cover, and soils were observed to be more susceptible to erosion in terms of this erosion index value. The highest average ER value was found in degraded oak forest soils (*Table 5*). No statistical difference was found according to land cover types in terms of the average ER values of soils. Although there was no difference in soils taken from the surface layer, ER values of subsurface layer were statistically different. All land covers are susceptible to erosion because its C-MER values are lower than the limit value of 1.5. C-MER values are statistically different; and open space area soils are present in two groups as separately with degraded scotch pine forest soils and degraded oak forest soils (*Table 5*). DR values are at the highest level in degraded scotch pine forest soils with the lowest clay+silt amounts (%17.5), and at the lowest level in open space area soils with high clay+silt amounts (%22.7) (*Table 5*).

Table 4. *Change of erodibility indices, physical and chemical properties of the subsoils under land covers (10-20 cm depths)*

	Land covers		
	Degraded oak forest	**Open space area**	**Degraded scotch pine forest**
Chemical soil properties			
SOM (%)	1.51±0.67 a	2.13±1.30 b	1.14±1.18 a
pH	6.77±0.28 b	6.03±0.21 a	6.06±0.36 a
EC (µs/cm)	51.5±32.3 a	46.1±25.1 a	40.8±25.8 a
Physical soil properties			
BD (gr/cm^3)	1.15±0.15 a	1.10±0.08 a	1.16±0.05 a
TP (%)	52.6±9.5 a	60.7±4.1 b	51.6±5.1 a
Sand (%)	78.2±15.6 a	75.0±6.7 a	82.1±2.9 a
Silt (%)	7.3±4.81 a	11.4±2.1 b	8.7±3.1 a
Clay (%)	14.5±11.1 b	13.5±5.2 b	9.2±1.8 a
FC (%)	24.8±7.8 b	26.9±11.2 b	16.4±2.12 a
AWC (%)	8.05±2.3 a	9.46±2.6 a	8.22±0.82 a
Erodibility indices			
AS (%)	60.9±13.4 c	52.5±7.0 b	43.9±8.8 a
SSI (%)	15.95±15.0 b	18.46±6.7 b	11.67±2.3 a
DR	35.1±18.7 b	25.8±9.9 a	42.7±10.5 b
C-MER	0.61±0.42 a	0.52±0.20 a	0.60±0.07 a
ER	96.8±78.9 bc	58.2±26.2 a	73.1±23.9 ab
WDC	3.03±1.128 b	1.96±1.32 a	2.73±1.27 b

Different letters indicate significant differences ($p < 0.05$).

http://www.aloki.hu ● ISSN 1589 1623 (Print) ● ISSN 1785 0037 (Online)
DOI: http://dx.doi.org/10.15666/aeer/1605_72137229
© 2018, ALÖKI Kft., Budapest, Hungary

Table 5. *Change of erodibility indices, physical and chemical properties of the soils under land covers (average of 0-20 cm depths)*

	Land covers		
	Degraded oak forest	**Open space area**	**Degraded scotch pine forest**
Chemical soil properties			
SOM (%)	2.01±1.81 b	2.22±1.52 b	1.30±1.19 a
pH	6.83±0.47 b	6.11±0.21 a	6.20±0.42 a
EC (µs/cm)	58.9±41.4 b	43.8±23.8 a	44.1±34.4a
Physical soil properties			
BD (gr/cm^3)	1.17±0.12 a	1.14±0.09 a	1.18±0.07 a
TP (%)	54.5±5.8 c	58.9±7.0 b	48.8±9.0 a
Sand (%)	78.3±12.8 a	77.4±6.8 a	82.5±4.6 b
Silt (%)	8.5±4.5 a	11.0±2.6 b	7.9±2.5 a
Clay (%)	13.2±8.9 bc	11.6±4.8 ab	9.6±4.2 a
FC (%)	22.3±6.22 c	25.6±9.5 b	17.9±3.5 a
AWC (%)	7.72±1.77 a	9.65±2.71 b	8.21±1.66 a
Erodibility indices			
AS (%)	55.6±16.0 c	49.6±8.8 b	45.0±9.8 a
SSI (%)	15.13±12.5 b	15.45±6.8 b	10.54±2.9 a
DR	37.1±17.9 b	28.5±11.7 a	43.1±10.5 c
C-MER	0.57±0.34 b	0.45±0.17 a	0.58±0.17 b
ER	91.5±65.5 a	73.6±40.9 a	85.0±48.0 a
WDC	3.19±1.30 b	1.78±1.36 a	2.84±1.45 b

Different letters indicate significant differences ($p < 0.05$).

Relationships between some soil properties of 0-20 cm depths as the average of two depths (0-20 cm, 10-20 cm) and hydro-physical characteristics were tested by correlation analysis. In the correlation analysis carried out among soil properties selected in the study area which was susceptible to erosion, significant positive relationships were observed between SSI values and soil pH, SOM, C-MER, silt and clay amounts, and significant negative relationships were observed between DR, ER, BD and sand amounts (*Table 6*).

Statistically significant and important relationships were found between the aggregate stabilities of the study area soils and some soil characteristics (*Table 6*). There are positive correlations between AS values of the soils and C-MER, SSI, pH, SOM, Clay and FC values; and there are negative correlations between DR, ER, BD, sand values.

Discussion

SOM values of open space areas and degraded oak forest top soils are higher than degraded scotch pine forest. SOM values in open space areas and degraded oak forests are statistically similar and different from degraded scotch pine forest soils ($p < 0.001$). In degraded oak forests, while SOM values showed a decrease of approximately 37% in

http://www.aloki.hu ● ISSN 1589 1623 (Print) ● ISSN 1785 0037 (Online)
DOI: http://dx.doi.org/10.15666/aeer/1605_72137229
© 2018, ALÖKI Kft., Budapest, Hungary

subsurface layer compared to surface layer, there is a decrease of 19% in degraded scotch pine forests. This decrease in the value of the SOM will reduce erosion resistance (Wu and Tiessen, 2002). DR, ER values of open space areas with high SOM content are lower, and SSI values are higher. The average FC and AWC are also high in open space area soils with high average of SOM content (*Table 4*). The easier weathering of meadow grass and annual plants in open space areas raised the SOM content compared to Oak and Scotch Pine litters. Increased SOM improves aggregation, water-holding capacity, nutrient-retention capacity and ion exchange capacity in soils. SOM is one of the most important factors that determine the soil structural properties (Abdollahi et al., 2014), an important criterion in terms of susceptibility to erosion (Boix-Fayos et al., 1998; Marti et al., 2001; Castro et al., 2002; Sarah, 2005; Le Bissonnais et al., 2007). The presence of SOM by 2% is an important threshold in terms of soil erosion due to AS (Oades, 1988; Cerda, 1996). Indeed, organic matter content of 60% of soil samples which is the subject of the research is lower than 2%, and the aggregate stability of this land is relatively low. Therefore, it can be said that watershed soils are quite susceptible to erosion.

Table 6. *The correlations between hydro-physical characteristics and soil properties (average of 0-20 cm depth)*

	Sand	**Clay**	**Silt**	**SOM**	**FC**	**pH**	**EC**
AS (%)	-0.422**	0.530**	0.073	0.279**	0.260**	0.410**	0.146*
Sand (%)		-0.946**	-0.818**	-0.198*	-0.321**	-0.052	0.270
Clay (%)			0.587**	0.101	0.265**	0.191*	0.360
Silt (%)				0.316**	0.332**	-0.208*	-0.145*
SOM (%)					0.478**	0.120	0.139*
FC (%)						-0.155	-0.051
pH							0.272**
	DR	**SSI**	**WDC**	**BD**	**TP**	**C-MER**	**ER**
AS (%)	-0.616**	0.557**	0.057	-0.620**	0.084	0.542**	-0.520**
Sand (%)	0.545**	-0.933**	-0.306**	0.596**	-0.162*	-0.799**	0.681**
Clay (%)	-0.500**	0.891**	0.411**	-0.546**	0.115*	0.886**	-0.667**
Silt (%)	-0.474**	0.747**	0.033**	-0.518**	0.202**	0.448**	-0.515**
SOM (%)	-0.407**	0.339**	-0.255*	-0.502**	0.312**	-0.088	-0.127
FC (%)	-0.355**	0.303**	-0.172*	-0.443**	0.296*	-0.201*	0.012
pH	-0.181*	0.131	0.485**	-0.133	-0.027	0.398*	-0.042
EC	-0.127*	0.085	-0.154*	0.046	0.083	0.180**	-0.216**
DR		-0.714**	0.234*	0.625**	-0.204*	-0.392**	0.712**
SSI			0.137	-0.675**	0.168*	0.771**	-0.713**
WDC				-0.210*	-0.018	0.479**	-0.162*
BD (gr/lt)					-0.368**	-0.333**	0.637**
TP (%)						-0.189	-0.143*
C-MER							-0.681**

AS: Aggregate stability, SOM: Soil organic matter, FC: Field capacity, EC: Electrical conductivity, DR: Dispersion ratio, SSI: Structural stability index, WDC: Water dispersible clay, BD: Bulk density TP: Total porosity, C-MER: Colloid-moisture equivalent ratio, **: Correlation is significant at the 0.01 level (2-tailed), *: Correlation is significant at the 0.05 level (2- tailed)

http://www.aloki.hu ● ISSN 1589 1623 (Print) ● ISSN 1785 0037 (Online)
DOI: http://dx.doi.org/10.15666/aeer/1605_72137229
© 2018, ALÖKI Kft., Budapest, Hungary

Open space area and degraded scotch pine forest soils are similar in terms of soil reaction and more acidic than degraded oak forest soils. This situation may have emerged as a result of further leaching of open space area and degraded scotch pine forest soils. This will be understood when soil pH at surface layer and subsurface are compared (*Tables 3, 4,* and *5*). Reasonably higher pH of the degraded scotch pine forests was primarily due to presence of base cations (Ca^{++}, Mg^{++}, K^{+} and Na^{+}) associated in the soils. The fact that the oak litter had a slightly acid character and that the clay colloids in the soil (the average clay content is higher in degraded oak forest soils) adsorbed the base cations affected the high soil pH in degraded oak forests compared to other lands. Because the potential evaporation in the region is higher than the amount of rainfall, the water entering the soil during rainy season moves downwardly for a while (*Table 1*). With the start of the arid period, the deep water moves the dissolved salts to topsoil layers by evaporating and can increase the pH of the topsoil. This is even more evident in degraded oak forests where the average land slope and altitude are low. Acidity increases in the top layer in open space area soils as a result of root respiration of intense herbaceous plants. Soil pH is lower in degraded scotch pine forest soils due to acidic origin litter compared to degraded oak forest soils.

Although soil texture is not as effective as SOM on AS (Tisdall and Oades, 1982; Metzger et al., 1987; Roberson and Firestone, 1991; Canton et al., 2009), the clay fraction of soil is an important criterion on the aggregate strength (Balcı, 1996) and has a considerable impact on erosion trends. Clay content of the soils checks the structural stability of the soil (Gollany et al., 1991; Payne, 1992). In case of a decrease of structural stability and structural strength of the soil, soils undergo physical degradation (Sahani and Behera, 2001). The average clay content of Koruluk dam watershed are in degraded scotch pine forest, open space areas and degraded oak forest soils, respectively, including 9.6%, 11.6% and 13.2%. It is reported that land cover is effective on the clay content (Okatan et al., 2010; Yılmaz et al., 2015) and that the soils with clay content ranging between 9-30% are more susceptible to erosion (Nkana and Tonye, 2003). The clay content of the majority of soils in the research area remains in these ranges (2.7–36.0%), and soils under all land covers were found to be susceptible to erosion. All land covers showed more clay in the lower depth (10-20 cm) compared to the upper soil. While passing from top depth to lower depth, clay content increased in degraded oak forests by 20% and in open space areas by 35% (*Tables 3* and *4*). It decreased in degraded scotch pine forest by about 8%. The increase in clay content in open space area and degraded oak forests and decrease in degraded scotch pine forest when going down from land cover on the same parent material and the same aspect to the lower depth levels in soil profiles can be explained in two ways. Firstly, litter decomposition is slow as the average altitude of degraded scotch pine forests is higher. In this case, lesser amount of water can enter the soil, and the movement of fine material in the soil could not take place. Second one is the decrease of decomposition reactions in the soil depending on the altitude as going down to soil depths. In open space areas and degraded oak forests, the presence of a layer that can transmit the soil by absorbing water that can reach on the soil especially in winter and spring seasons with abundant precipitation allowed the movement of clay from top soil to the lower soil in these areas, even if just a bit. Again, in the areas on these two land covers, SOM amount in the topsoil facilitated the movement of clay to sub soils by increasing soil permeability. The fact that the slope degrees of degraded oak forests and open space

http://www.aloki.hu ● ISSN 1589 1623 (Print) ● ISSN 1785 0037 (Online)
DOI: http://dx.doi.org/10.15666/aeer/1605_72137229
© 2018, ALÖKI Kft., Budapest, Hungary

areas are less than degraded scotch pine forests is effective in increasing the amount of water that can enter into soil.

In semi-arid and arid regions with low degree of coverage of the vegetation such as the research area, soil erosion trends can significantly be affected by physiographic-topographical features which are effective in the formation and development of soil, and the land cover. Within the scope of the study, the erosion trend values of soils developing under similar climatic conditions in the same parent material were found to be different. Probably, these differences resulted from the factors such as land cover type, altitude and land slope degree. These factors changed the other soil characteristics such as pore volume, BD and AS of the soil due to the mechanical composition of the soil. Pore size distribution and connectivity together with BD, aggregation and AS is important soil property that can be to a great extent influenced by the land degradation and soil erosion.

Degraded scotch pine forest soils had higher BD than the adjacent soils under degraded oak forests and open space areas for the average of two different depths. BD was generally higher in subsurface than surface soils (*Table 5*). This situation is more obvious in soil profiles taken from open space areas and degraded oak forests. A decrease occurred in BD with the accumulation of clay moved from top soil in sub soil horizons (10-20 cm). In degraded scotch pine forests, the BD remained approximately same as there was no significant change between the clay and silt content, amount of SOM, total porosity of the top soils with sub soils.

Many researchers reported that there are strong relationships between BD of soil and SOM content (Aşkın and Özdemir, 2003; Morisada et al., 2004; Leifeld et al., 2005; Perie and Ouimet, 2008). Curtis and Post (1964) stated a negatif correlation between SOM and BD. Sharma and Qahar (1989) and Gupta et al. (2010) determined the strongest correlation between BDs and SOM among the data attained from the analysis results. We obtained similar results with strong negative correlation ($r = -0.757$, $p < 0.001$) between SOM and BD of soil samples. In the research area, it was observed that DR, ER values were high, SSI, AS and C-MER values were lower in degraded scotch pine forest where SOM content was low, and BD was high. The increase in BD values increased the erosion sensitivity indices and decreased the endurance indices. Significant positive relationships were observed between BD values and DR and ER values as $r = 0.630$, $p < 0.001$ and $r = 638$, $p < 0.001$, respectively. Chaudhari et al. (2013) determined strong positive relationships in BD values and DR and ER values in their study ($r = 0.792$, $p < 0.001$ and $r = 0.663$, $p < 0.001$). Along with the increase of BD of soil, SSI, AS, C-MER and TP values decreased, and this decrease was statistically significant (*Table 6*).

The total porosity of degraded scotch pine forest soils that was more susceptible to erosion remained the lowest. Water erosion and soil loss are expected to be less in open space area and degraded oak forest soils with high pore volume, and soil losses are expected to be more in degraded scotch pine forest soils with low pore volume. The low total porosity and low amounts of organic material of degraded scotch pine forest top soils (0-10 cm) may increase soil loss. The highest pore volume values were found in open space area soils where the average SOM is high. Dense rooting system of the open space areas grasses may account for the difference in TP of the 10–20 cm layer between the degraded scotch pine forest, degraded oak forest and open space areas soils. Vegetation increases SOM, TP, and reduces BD and soil erodibility (Igwe, 2003). In

http://www.aloki.hu ● ISSN 1589 1623 (Print) ● ISSN 1785 0037 (Online)
DOI: http://dx.doi.org/10.15666/aeer/1605_72137229
© 2018, ALÖKI Kft., Budapest, Hungary

open space areas soils, high total porosity and amounts of SOM could reduce soil erosion by facilitating the entry of water into the soil with infiltration.

The main soil characteristics of soils affecting the aggregate stabilities are soil texture, clay mineralogy, SOM content, type and concentration of cations and sesquioxide contents (Le Bissonnais, 1996). However, general soil properties most closely correlated with soil AS are the contents of clay and SOM (Canasveras et al., 2010; Jozefaciuk and Czachor, 2014; Waruru et al., 2016). Clay particles are considered as cementing agents for aggregation because of their high specific surface area, cation exchange capacity, and consequently, high physical and chemical activity. SOM content can affect soil structure as well as soil AS various ways (Besalatpour et al., 2013). The topography and vegetation characteristics indirectly affect the aggregate stability (Canton et al., 2009). Furthermore, slope and aspect may influence the rate of weathering and erodibility of soils and thus soil aggregate stability (Bronick and Lal, 2005). The study area soils are susceptible to erosion under all land covers, and the erosion trends of open space area soils are lower in terms of DR, ER, WDC values. The average AS values were observed to be 49.6% in open space area soils, and the erosion trend values were higher in open space area soils and were 55.6% in degraded oak forest soils.

In other words, it is remarkable that the aggregate stability of degraded oak forest soils with higher erosion potential in terms of some parameters than open space area soils was found to be higher. It is thought that the fact that soil reaction (soil pH) was higher in degraded oak forest soils influenced high AS values. The increase in soil reaction decreases the clay dispersion (Amezketa and Araqües, 1995; Lipiec et al., 2018), therefore, increases the aggregate stability. The main factors affecting the clay dispersion and clay clotting in the soil are the electrolyte concentration (EC), solution pH and sodium adsorption ratio (Shainberg and Letey, 1984; Suarez et al., 1984). Low electrolyte concentrations increase the clay dispersion and adversely affect the soil structure. It is well known that low electrolyte concentrations have adverse effects on hydraulic conductivity and infiltration ratio (Shainberg et al., 1987; Quirk, 1986; Abu-Sharar et al., 1987; Shainberg and Singer, 1990; Rengasamy and Olsson, 1991). The fact that the electrical conductivity values, a measure of the electrolyte concentration in soil solution, are maximum in degraded oak forest soils have an effect on high average aggregate stability values in these soils. When *Tables 2, 3* and *4* are analyzed, it can be seen that the average SSI values of degraded oak forest soils with the highest average AS values are high.

The erosion trends values of soils vary depending on the soil's mechanical composition, infiltration capacity, the soil structure and the organic and chemical characteristics of the soil (Wishmeier and Smith, 1978; Canga, 1998). Texture is an important factor affecting erodibility values, but structure, SOM, and permeability also contribute (Mitchell and Bubenzer, 1980; Goldman et al., 1986). The change of sand, silt and clay fractions ratios forming the mechanical composition of the soils is very important because it changes the erosion trend values of the soils. High amount of sand and low amount of silt and clay increase the erosion trends of soils (Yılmaz et al., 2015). There are positive correlations between erosion trend values and the coarse fractions in the soil (Korkanç, 2003; Erol, 2004; Koiter et al., 2017). Soils under all land cover are susceptible to erosion in terms of DR, ER and C-MER values (*Tables 3, 4 and 5*).

http://www.aloki.hu ● ISSN 1589 1623 (Print) ● ISSN 1785 0037 (Online)
DOI: http://dx.doi.org/10.15666/aeer/1605_72137229
© 2018, ALÖKI Kft., Budapest, Hungary

The clay+silt amounts of soils affect the erosion resistance since they are effective on SOM and water holding capacity. DR, one of the most important erodibility indicators, varies between 13.1 and 71.7. There are studies in which the DR values change between 13-69 (Igwe, 2003) and 26-95 (Korkanç, 2003).

Results of this study indicated that dispersion ratios varied according to the land cover ($p < 0.05$). Soils of the open space area had a smaller and significant DR than rest of the soils developed from the other land covers, which had statistically similar values. On the other hand, having DR on greater than %15, all land covers produced soils susceptible to water erosion.

In addition to these erodibility indices, SSI values are also used for the structural stability of soils. SSI values is an indicator of stable soil aggregates and thus higher SSI values, better will be the soil structure and higher will be the stable soil aggregates (Rudramurty et al., 2007). Structural stability has been used to evaluate the sensitivity of soils to erosion (Darboux and Le Bissonnais, 2006). The soils with the structural stability value of less than 40% are classified as strongly erodible soils, and the soils with higher structural stability value are classified as moderately erodible soils (Leo, 1963). Based on these erosion indices values, the study area soils are in the strongly erodible soils. SSI value is maximum in open space area soils by 15.43 and minimum in degraded scotch pine forest soils by 10.54. SSI values were found to be statistically different according to land covers. Open space area and degraded oak forest soils are similar, and degraded scotch pine forest soils are different (*Tables 3, 4* and *5*). It is well established that addition of SOM can not only reduce BD and increase water holding capacity and soil structure stability (Mikha et al., 2006). The fact that the structural stability index values of soils were found to be very low may be due to the low organic matter and clay content of the soil. SOM and clay content are the main abiotic binding agents in the formation and stabilization of aggregates (Tisdall and Oades, 1982; Chenu et al., 2000; Duchicela et al., 2012; Portella et al., 2012; Carrizo et al., 2015). The SOM of 60% of study area soils were found to be lower than 2%. These low values in SOM may adversely affect the AS. Kay and Angers (Kay and Angers, 1999) stated that a minimum of 2% SOC was necessary to maintain SSI and observed that if SOC content was between 1.2-1.5%, stability declined rapidly. In case of higher amounts of SOM, an increase can be expected in the SSI. Boix-Fayos et al. (2001) showed that a threshold of 3-3.5% SOC had to be attained to achieve increases in AS; no effects on AS were observed in soils below this threshold.

The clay contents of the soil are considered to be more effective on the increase or decrease of structural stability index in soils with higher amount of organic matter than this threshold value. In the studies carried out by Yılmaz et al. (2015, 2008), the structure stability indices of the soils with clay amount ranging from 8.5% to 15.7% varied between 14.5 and 25, the structure stability indices of the soils with clay amount ranging from 40.6% to 47.8% varied between 41.0 and 50.9. It is reported that SSI values of the soils of different land covers with average amount of clay ranging from 17.8% to 22.9% vary between 22.3 and 29.3 (Yılmaz et al., 2008).

Conclusions

The land cover has been destroyed in Koruluk dam watershed which was built to meet the irrigation water needs of the local community on Ceviz stream (Gümüşhane-Şiran). It was determined that degraded oak forest, degraded scotch pine forests and

http://www.aloki.hu ● ISSN 1589 1623 (Print) ● ISSN 1785 0037 (Online)
DOI: http://dx.doi.org/10.15666/aeer/1605_72137229
© 2018, ALÖKI Kft., Budapest, Hungary

open space areas were susceptible to erosion in sub watershed close to the dam reservoir.

In all study area, watershed lands are faced with effective erosion because they lack the protective vegetation cover. Active erosion in watershed lands threatens the economic life of dam reservoir and surrounding irrigation reservoirs. Protective vegetation cover should be created in areas close dam reservoir and residential areas by means of performing afforestation with the types such as rose hip and mayflower that will yield money for the local people and with oak in higher altitudes, and by grassing open spaces with appropriate types (such as *Trifolium repense, Trifolium pratense, Dactylis glomerata, Festuca drymeja, Onobrychis sativa, Lolium perenne, Lotus corniculatus and Bromus inermis*). If lands susceptible to erosion in the dam watershed are not restored with a continuous vegetation cover, dam reservoirs will complete their economic life in a shorter time due to the soil erosion that will occur. This study scientifically revealed that natural vegetation has significant effects on local water, soil conservation and ecological restoration management in a semi-arid ecosystem.

Further research is needed to determine the degree of improvement that vegetation can play an important role on soil porosity, bulk density, soil infiltration, soil structural properties (structural and aggregate stability) and soil erodibility indices. In this study area, the relationship between the function and the structure of the artificial vegetation should also be one of the focus points of future research.

REFERENCES

[1] Abdollahi, L., Schjønning, P., Elmholt, S., Munkholm, L. J. (2014): The effects of organic matter application and intensive tillage and traffic on soil structure formation and stability. – Soil and Tillage Research 136: 28-37.

[2] Abu-Sharar, T. M., Bingham, F. T., Rhoades, J. D. (1987): Stability of soil aggregates as affected by electrolyte concentration and composition. – Soil Science Society of America Journal 51: 309-314.

[3] Amezketa, E., Aragües, R. (1995): Flocculation-dispersion behaviour of arid-zone soil clays as affected by electrolyte concentration and composition. – Invest Agrar: Prod Prot Veg. 10(1): 101-112.

[4] Arp, P. A. (1999): Soils for Plant Growth, Field and Laboratory Manual. – Faculty of Forestry and Environmental Management, University of New Brunswick, Canada.

[5] Aşkın, T., Özdemir, N. (2003): Soil bulk density as related to soil particle size distribution and organic matter content. – Agriculture 9(2): 52-55.

[6] Balcı, A. N. (1996): Soil Conservation. – Istanbul University Faculty of Forestry, Publication no: 3947-439, Istanbul, Turkey (in Turkish).

[7] Bao-hua, Z., Yu-rong, H., Hong-yi, Z., Gen-wei, C. (2003): The features of soil aggregation and its eco-environmental effects under different subalpine forests on the east slope of Gongga Mountain, China. – Journal of Forestry Research 14(1): 80-82.

[8] Baykal, F. (1952): Geological investigations in Kelkit-Siran. – General Directorate of Mineral Research and Exploration, Compilation Report No. 2205, Ankara, Turkey (in Turkish).

[9] Besalatpour, A. A., Ayoubi, S., Hajabbasi, M. A., Mosaddeghi, M. R., Schulin, R. (2013): Estimating wet soil aggregate stability from easily available properties in a highly mountainous watershed. – Catena 111: 72-79.

[10] Blake, G. R., Hartge, K. H. (1986): Particle Density – In: Klute, A. (ed.). Methods of Soil Analysis. Part 1, 2nd edn. American Society of Agronomy, Inc. Soil Science Society of America, Madison, WI, pp. 377-381.

http://www.aloki.hu ● ISSN 1589 1623 (Print) ● ISSN 1785 0037 (Online)
DOI: http://dx.doi.org/10.15666/aeer/1605_72137229
© 2018, ALÖKI Kft., Budapest, Hungary

[11] Boix-Fayos, C., Calvo-Cases, A., Imeson, A. C., Soriano-Soto, M. D., Tiemessen, I. R. (1998): Spatial and short-term temporal variations in runoff, soil aggregation and other soil properties along a Mediterranean climatological gradient. – Catena 33: 123-128.
[12] Boix-Fayos, C., Calvo-Cases, A., Imeson, A. C., Soriano-Soto, M. D. (2001): Influence of soil properties on the aggregation of some Mediterranean soils and the use of aggregate size and stability as land degradation indicators. – Catena 44: 47-67.
[13] Bouyoucos, G. J. (1962): Hydrometer method improved for making particle size analyses of soils. – Agronomy Journal 54: 464-465.
[14] Bronick, C. J., Lal, R. (2005) Soil structure and management: a review. – Geoderma 124: 3-22.
[15] Canasveras, J. C., Barron, V., Del Campillo, M. C., Torrent. J., Gomez. J. A. (2010): Estimation of aggregate stability indices in Mediterranean soils by diffuse reflectance spectroscopy. – Geoderma 158: 78-84.
[16] Canga, M. R. (1998): Soil Erosion and Conservation. – Faculty of Agriculture, Ankara University, Ankara.
[17] Canton, Y., Sole-Benet, A., Asensio, C., Chamizo, S., Puigdefabregas, J. (2009): Aggregate stability in range sandy loam soils: relationships with runoff and erosion. – Catena 77: 192-199.
[18] Carrizo, M. E., Alesso, C. A., Cosentino, D., Imhoff, S. (2015): Aggregation agents and structural stability in soils with different texture and organic carbon contents. – Scientia Agricola 72(1): 75-82.
[19] Castro Filho, C., Lourenço, A., Guimaraes, M. D. F., Fonseca, I. C. B. (2002): Aggregate stability under different soil management systems in a red latosol in the state of Parana, Brazil. – Soil and Tillage Research 65(1): 45-51.
[20] ÇEM (2011): Arid and Semi-Arid Areas Management Workshop Final Declaration and Notifications. – ÇEM, Nevşehir (in Turkish). http://www.cem.gov.tr/erozyon/Libraries/su/Kurak_ve_Yarı_Kurak_Alan_Yönetimi_Çalıştayı-nevşehir-Ürgüp.sflb.ashx (accessed 2018 March 29).
[21] Cerda, A. (1996): Soil aggregate stability in three Mediterranean environments. – Soil Technology 9(3): 133-140.
[22] Chaudhari, P. R., Ahire, D. V., Ahire, V. D., Chkravarty, M., Maity, S. (2013): Soil bulk density as related to soil texture, organic matter content and available total nutrients of Coimbatore soil. – International Journal of Scientific and Research Publications 3(2): 1-8.
[23] Chen, L., Wang, J., Fu, B., Qiu, Y. (2001): Land-use change in a small catchment of northern Loess Plateau, China. – Agriculture, Ecosystems & Environment 86(2): 163-172.
[24] Chen, L., Messing, I., Zhang, S., Fu, B., Ledin, S. (2003): Land use evaluation and scenario analysis towards sustainable planning on the Loess Plateau in China-case study in a small catchment. – Catena 54(1): 303-316.
[25] Chenu, C., Le Bissonnais, Y., Arrouays, D. (2000): Organic matter influence on clay wettability and soil aggregate stability. – Soil Science Society of America Journal 64(4): 1479-1486.
[26] Costa, M. H., Botta, A., Cardille, J. A. (2003): Effects of large-scale changes in land cover on the discharge of the Tocantins River, Southeastern Amazonia. – Journal of Hydrology 283(1): 206-217.
[27] Curtis, R. O., Post, B. W. (1964): Estimating bulk density from organic matter content in some vermont forest soils. – Soil Sci. Soc. Am. Proc. 28: 285-286.
[28] Danielson, R. N., Sutherland, P. L. (1986): Porosity. – In: Klute, A. (ed.) Methods of Soil Analysis. Part 1, 2nd edn. American Society of Agronomy, Inc. Soil Science Society of America, Madison, WI, pp. 443-460.
[29] Darboux, F., Le Bissonnais, Y. (2006): Changes in Structural Stability with Soil Surface Degradation. Consequences for Soil Erosion Processes. – In: EGU, European

http://www.aloki.hu ● ISSN 1589 1623 (Print) ● ISSN 1785 0037 (Online)
DOI: http://dx.doi.org/10.15666/aeer/1605_72137229
© 2018, ALÖKI Kft., Budapest, Hungary

Geosciences Union (ed.) General Assembly 2006, Vol. 8. Copernicus Publications, Göttingen, Germany.
[30] Duchicela, J., Vogelsang, K. M., Schultz, P. A., Kaonongbua, W., Middleton, E. L., Bever, J. D. (2012): Non-native plants and soil microbes: potential contributors to the consistent reduction in soil aggregate stability caused by the disturbance of North American grasslands. – New Phytologist 196(1): 212-222.
[31] Erol, A. (2004): Effect of hydro-physical soil properties on soil formation factors in Kose Creek Watershed in Gumushane. – PhD Thesis. Istanbul University Graduate School of Natural & Applied Sciences, Istanbul, Turkey (in Turkish).
[32] Fu, B. (1989): Soil erosion and its control in the Loess Plateau of China. – Soil Use and management 5(2): 76-82.
[33] Goldman, S. J., Jackson, K., Bursztynsky, T. A. (1986): Erosion and Sediment Control Handbook. – McGraw-Hill, New York, USA.
[34] Gollany, H. T., Schumacher, T. E., Evenson, P. D., Lindstrom, M. J., Lemme, G. D. (1991): Aggregate stability of an eroded and desurfaced Typic Argiustoll. – Soil Science Society of America Journal 55(3): 811-816.
[35] Gülçur, F. (1974): Physical and chemical soil analysis methods. – Istanbul University Faculty of Forestry Publications, No: 201, Istanbul, Turkey (in Turkish).
[36] Gupta, R. D., Arora, S., Gupta, G. D., Sumberia, N. M. (2010): Soil physical variability in relation to soil erodibility under different land uses in foothills of Siwaliks in NW India. – Tropical Ecology 51(2): 183-197.
[37] Igwe, C. A. (2003): Erodibility of soils of the upper rainforest zone, southeastern Nigeria. – Land Degradation & Development 14(3): 323-334.
[38] Işık, S. (2016): Investigation of some hydro-physical properties in degraded forest areas in Gümüşhane-Şiran Location. Master's thesis. – Karadeniz Technical University, Trabzon, Turkey[In Turkish].
[39] Jing, K., Wang, W. Z., Zheng, F. L. (2005): Soil Erosion and Environment in China. – Science Press, Beijing (in Chinese).
[40] Jozefaciuk, G., Czachor, H. (2014): Impact of organic matter, iron oxides, alumina, silica and drying on mechanical and water stability of artificial soil aggregates. Assessment of new method to study water stability. – Geoderma 221: 1-10.
[41] Karaöz, M. Ö. (1989): Methods of analysis for some soil chemical properties (pH, carbonate, salinity, organic matter, total nitrogen, available phosphorus). – Istanbul University, Faculty of Forestry. Series B 39: 64-82 (in Turkish).
[42] Kay, B. D., Angers, D. A. (1999): Soil Structure. – In: Sumner, M. E. (ed.) Handbook of Soil Science. CRC Press, Boca Raton, USA, pp. A-229-A-276.
[43] Koiter, A. J., Owens, P. N., Petticrew, E. L., Lobb, D. A. (2017): The role of soil surface properties on the particle size and carbon selectivity of interrill erosion in agricultural landscapes. – Catena 153: 194-206.
[44] Korkanç, S. Y. (2003): Land use problems and recommended solutions in the vicinity of Bartın (A case study of Iskalan Creek Watershed). – PhD Thesis, Istanbul University Graduate School of Natural & Applied Sciences, Istanbul, Turkey (in Turkish).
[45] Kosmas, C., Gerontidis, S., Marathianou, M. (2000): The effect of land use change on soils and vegetation over various lithological formations on Lesvos (Greece). – Catena 40(1): 51-68.
[46] Lal, R. (2001): Soil degradation by erosion. – Land Degradation & Development 12(6): 519-539.
[47] Le Bissonnais, Y. (1996): Aggregate stability and assessment of soil crustability and erodibility: I. Theory and methodology. – European Journal of Soil Science 47(4): 425-437.
[48] Le Bissonnais, Y., Blavet, D., De Noni, G., Laurent, J. Y., Asseline, J., Chenu, C. (2007): Erodibility of Mediterranean vineyard soils: relevant aggregate stability methods and significant soil variables. – European Journal of Soil Science 58(1): 188-195.

http://www.aloki.hu ● ISSN 1589 1623 (Print) ● ISSN 1785 0037 (Online)
DOI: http://dx.doi.org/10.15666/aeer/1605_72137229
© 2018, ALÖKI Kft., Budapest, Hungary

[49] Leifeld, J., Bassin, S., Fuhrer, J. (2005): Carbon stocks in Swiss agricultural soils predicted by land-use, soil characteristics, and altitude. – Agriculture, Ecosystems & Environment 105(1): 255-266.
[50] Leo, W. M. (1963): A rapid method for estimating structural stability of soils. – Soil Science 96: 342-346.
[51] Lipiec, J., Czyż, E. A., Dexter, A. R., Siczek, A. (2018): Effects of soil deformation on clay dispersion in loess soil. – Soil and Tillage Research 184: 203-206.
[52] Martí, C., Badia, D., Buesa, M. A. (2001): Determinación de la estabilidad estructural de sue-los del altoaragón por tamizado en húmedo y lluvıa sımulada. – Edafología 8: 21-30 (in Spanish).
[53] Metzger, L., Levanon, D., Mingelgrin, U. (1987): The effect of sewage sludge on soil structural stability: microbiological aspects. – Soil Science Society of America Journal 51(2): 346-351.
[54] Middleton, H. E. (1930): Properties of soils which influence soil erosion No. 178. – US Dept. of Agriculture, Washington, DC.
[55] Mikha, M. M., Vigil, M. F., Liebig, M. A., Bowman, R. A., Mcconkey, B., Deibert, E. J., Pikul, J. L. (2006): Cropping system influences on soil chemical properties and soil quality in the Great Plains. – Renewable Agriculture and Food Systems 21(1): 26-35.
[56] Mitchell, J. K., Bubenzer, G. D. (1980): Soil Loss Estimation. – In: Kirkby, M. J., Morgan, R. P. C. (eds): Soil Erosion. John Wiley and Sons Ltd., London, pp. 17-62.
[57] Morisada, K., Ono, K., Kanomata, H. (2004): Organic carbon stock in forest soils in Japan. – Geoderma 119(1): 21-32.
[58] Nelson, D. W., Sommers, L. (1982): Total Carbon, Organic Carbon, and Organic Matter. – In: Page, A. L. et al. (eds.) Methods of Soil Analysis. Part 2. Chemical and Microbiological Properties, No. 9, American Society of Agronomy, Inc. Soil Science Society of America, Madison, WI, pp. 539-579.
[59] Nkana, J. C. V., Tonye, J. (2003): Assessment of certain soil properties related to different land-use systems in the Kaya watershed of the humid forest zone of Cameroon. – Land Degrad. Dev. 14: 57-67.
[60] Oades, J. M. (1988): The retention of organic matter in soils. – Biogeochemistry 5: 35-70.
[61] Okatan, A., Aydin, M., Usta, A., Yılmaz, M. (2010): Effects of land use type on hydro-physical properties of soils in the Torul dam basin-Gumushane, Turkey. – Fresenius Environmental Bulletin 19(12b): 3230-3241.
[62] Özhan, S. (2004): Watershed Management. – Istanbul University Faculty of Forestry, Publication no: 482. Istanbul, Turkey (in Turkish).
[63] Page, A. L., Miller, R. H., Keeney, D. R. (1982): Methods of Soil Analysis. Part 2. Chemical and Microbiological Properties. – American Society of Agronomy, Inc. Soil Science Society of America, Madison, WI, Soil Science Society of America, Madison, Wisconsin.
[64] Payne, D. (1992): Estructura del suelo, laboreo y comportamiento mecánico. – In: Urbano, P., Rojo, C. (eds.) Condiciones del suelo y desarrollo de las plantas según Russell. Ediciones Mundi-Prensa, Madrid, pp. 395-430 (in Spanish).
[65] Perie, C., Ouimet, R. (2008): Organic carbon, organic matter and bulk density relationships in boreal forest soils. – Canadian Journal of Soil Science 88(3): 315-325.
[66] Portella, C. M. R., Guimaraes, M. D. F., Feller, C., Fonseca, I. C. D. B., Tavares Filho, J. (2012): Soil aggregation under different management systems. – Revista Brasileira de Ciencia do Solo 36(6): 1868-1877.
[67] Quirk, J. P. (1986): Soil permeability in relation to sodicity and salinity. – Phil. Trans. R. Soc. Lond. A. 316(1537): 297-317.
[68] Rengasamy, P., Olsson, K. A. (1991): Sodicity and soil structure. – Aust. J. Soil Res. 29: 935-932.

http://www.aloki.hu ● ISSN 1589 1623 (Print) ● ISSN 1785 0037 (Online)
DOI: http://dx.doi.org/10.15666/aeer/1605_72137229
© 2018, ALÖKI Kft., Budapest, Hungary

[69] Roberson, E. B., Firestone, M. K. (1991): Cover crop management of polysaccharide-mediated aggregation in an orchard soil. – Soil Science Society of America Journal 55(3): 734-739.
[70] Rudramurthy, H. V., Puttaiah, E. T., Gurumurthy, B. R. (2007): Structural stability index of soils under different land use systems in southern transitional zone of Karnataka. – Karnataka J. Agric. Sci. 20(1): 126-127.
[71] Sahani, U., Behera, N. (2001): Impact of deforestation on soil physicochemical characteristics, microbial biomass and microbial activity of tropical soil. – Land Degradation & Development 12(2): 93-105.
[72] Sarah, P. (2005): Soil aggregation response to long-and short-term differences in rainfall amount under arid and Mediterranean climate conditions. – Geomorphology 70(1): 1-11.
[73] Shainberg, I., Letey, J. (1984): Response of soils to sodic and saline conditions. – California Agriculture 52(2): 1-57.
[74] Shainberg, I., Singer, M. J. (1990): Soil Responses to Saline and Sodic Conditions. Ch. 5. – In: Tanji, K. K. (ed.). Agricultural Salinity Assessment and Management. ASCE Manuals and Reports on Engineering Practice, No. 71, Am. Soc. Civil Eng., New York.
[75] Shainberg, I., Keren, R., Alperovitch, N., and Goldstein, D. (1987): Effect of exchangeable potassium on the hydraulic conductivity of smectite-sand mixtures. – Clays and Clay Min. 35: 305-310.
[76] Sharma, P. D., Qahar, A. Q. (1989): Characterisation of some Outer Himalayan protected and eroded forest soils. – Journal of the Indian Society of Soil Science 37: 113-120.
[77] SPSS (2011): Version 15.0. – SPSS, Chicago, IL.
[78] Suarez, D. L., Rhoades, J. D., Lavado, R., Grieve, C. M. (1984): Effect of pH on saturated hydraulic conductivity and soil dispersion. – Soil Sci. Soc. Am. J. 48: 50-55.
[79] Tang, K. L. (2004): Soil and water conservation in China. – Science Press, Beijing (in Chinese).
[80] Thornthwaite, C. W. (1948): An approach toward a rational classification of climate. – Geographical Review 38(1): 55-94.
[81] Tisdall, J. M., Oades, J. (1982): Organic matter and water-stable aggregates in soils. – European Journal of Soil Science 33(2): 141-163.
[82] Waruru, B. K., Shepherd, K. D., Ndegwa, G. M., Sila, A. M. (2016): Estimation of wet aggregation indices using soil properties and diffuse reflectance near infrared spectroscopy: An application of classification and regression tree analysis. – Biosystems Engineering 152: 148-164.
[83] Wei, W., Liding, C., Bojie, F., Zhilin, H., Dongping, W., Lida, G. (2007): The effect of land uses and rainfall regimes on runoff and soil erosion in the semi-arid loess hilly area. – China Journal of Hydrology 335(3-4): 247-258.
[84] Wischmeier, W. H., Smith, D. D. (1978): Predicting Rainfall Erosion Losses - A Guide to Conservation Planning. – USDA, Hyattsville, Maryland, USA.
[85] Wu, R., Tiessen, H. (2002): Effect of land use on soil degradation in alpine grassland soil, China. – Soil Science Society of America Journal 66(5): 1648-1655.
[86] Yilmaz, M., Yilmaz, F., Karagul, R., Altun, L. (2008): Changes in erodibility indices and some soil properties according to parent materials and land use regimes in erfelek dam creek watershed (Sinop, Turkey). – Fresenius Environmental Bulletin 17(12A): 2083-2090.
[87] Yilmaz, M., Usta, A., Çakir, G., Kahveci, S. N. I. (2015): The effects of land use type on soil erodibility indices in Galyan-Atasu dam watershed, Trabzon, NE Turkey. – Fresenius Environmental Bulletin 24(3B): 1082-1090.
[88] Zheng, F. L., Yang, Q. K., Wang, Z. L. (2004): Water erosion prediction model. – Research of Soil and Water Conservation 11(4): 13-24 (in Chinese, with English abstract).

http://www.aloki.hu ● ISSN 1589 1623 (Print) ● ISSN 1785 0037 (Online)
DOI: http://dx.doi.org/10.15666/aeer/1605_72137229
© 2018, ALÖKI Kft., Budapest, Hungary

FLOODING TREATMENT RESTRAINS VOLUNTEER RICE GERMINATION AND SEEDLING GROWTH

LUO, H. W.[1,2#] – DU, B.[1,2#] – ZHENG, A. X.[1#] – LAI, R. F.[1] – YOU, Z. S.[1] – WANG, M.[1] – WANG, Z. M.[3] – HE, L. X.[1,2] – ZHANG, T. T.[1,2] – TANG, X. R.[1,2*]

[1]*Department of Crop Science and Technology, College of Agriculture, South China Agricultural University, Guangzhou 510642, PR China*

[2]*Scientific Observing and Experimental Station of Crop Cultivation in South China, Ministry of Agriculture, Guangzhou 510642, PR China*

[3]*Key Laboratory of Key Technology for South Agricultural Machine and Equipment, Ministry of Education, Guangzhou 510642, PR China*

[#]*These authors have contributed equally to this work.*

**Corresponding author*
e-mail: luohaowen@stu.scau.edu.cn

(Received 7th Aug 2018; accepted 5th Oct 2018)

Abstract. Volunteer rice is a global problem in rice production, especially conservation tillage. Here volunteer rice from four rice cultivars viz. *Xiangyaxiangzhan*, *Meixiangzhan*, *Changnongjing 1* and *Yliangyou1173* was treated with different flooding treatments. Two weeks of water flooding were applied at four depths: 2.0-2.5 cm (F1), 3.0-3.5 cm (F2), 4.5-5 cm (F3) and 6.0-6.5 cm (F4). A control was set by maintaining the soil wet as normal farmer practice of this region. It was found volunteer rice germination was more reduced with increased submergence levels, while treatments F3 and F4 both decreased the germination index and germination energy greatly for all rice varieties. Flooding treatments also reduced the seedling rate and inhibited the growth of volunteer seedling. Treatments F3 and F4 decreased seedling rates of *Changnongjing 1* and *F2 generation of Yliangyou1173* to zero, while the flooding treatment induced the malonaldehyde accumulation and altered the activities of peroxidase, superoxide and catalase in seedlings for all rice varieties. Hence, we suggest 2-week flooding at soil depth 6 cm after the harvest of early-season rice in South China in order to prevent the harvest loss in late-season rice caused by volunteer rice.
Keywords: *rice, flood, seed germination, rice seedling, anti-oxidative enzyme*

Introduction

Oryza sativa L. (Rice), one of the main crops and a staple food, contributes to 35%-75% of caloric intake by about 3 billion people worldwide. During the rice production, the primary considerations are the yield and grain quality, which can be affected by many factors, especially volunteer rice. As a common problem in paddy field, volunteer rice emerges from the previous crop (Gealy and Gressel, 2005; Warwick et. al., 2005; Street et al., 1995) because of shattered seeds or harvest loss. The severity of this global problem in rice production differs depending mostly on the region, cultivating measures and cultivars planted. Volunteer rice in temperate regions germinates either before winter (October-November) or in spring (April-May) (Sudianto et al., 2013). Seeds of volunteer plants could be harvested with the cultivated rice. The grains of volunteer rice from a different variety or plant type that matures earlier or later would reduce the overall milling quality (Singh et al., 2016a).

http://www.aloki.hu ● ISSN 1589 1623 (Print) ● ISSN 1785 0037 (Online)
DOI: http://dx.doi.org/10.15666/aeer/1605_72317242
© 2018, ALÖKI Kft., Budapest, Hungary

In tropics and subtropics, since volunteer rice germinates after the harvest, farmers take mechanical or chemical control measures to eliminate or lower the interference with the succeeding or ratooned rice. Volunteer rice is regarded as a weed phenologically and morphologically different from the planted cultivar and has lower yield and grain quality. Furthermore, volunteer rice from hybrid rice is a segregating plant that competes with crop and reduces grain yield and rice quality, thus decreasing the final productivity of paddy field and the overall level of grain quality. Thus, volunteer rice from conventional varieties is considered less influential than that from hybrid or weedy rice. Moreover, volunteer seeds from herbicide- resistant rice such as Clearfield rice^{TM} could even become the agent for resistant gene flow between rice cultivars and natural weedy rice by outcrossing (Shivrain et al., 2007; Gressel and Valverde, 2010; Gealy et al., 2003. Normally, less than 1% cross pollination happens between cultivars and weedy populations (Cao et al., 2006), but introgressed crop genes are able to persist in weedy population indefinitely (Ellstrand et al., 1999). Therefore, the outcrosses can promote the rise to weedy type population, which then competes with the rice cultivar and contaminates the rice, inducing economic losses.

In recent years, conservation tillage is increasingly recognized and accepted since tranditional tillage is faced by many limitations, such as poor soil structure and negative effect on soil organism. Organic farmers in Europe have great interest in conservation tillage (Peigné et al., 2018). There are many practices, including direct seeding without any tillage, or tillage at depth down to 15-20 cm. The rice root system and soil nitrogen can accumulate in the surface soil layer in zero-tillage compared with conventional tillage (Triplett and Dick, 2008; Huang et al., 2016). During rice production in China, zero-tillage has become increasingly popular for its benefits of saving fuel, labor and equipment and conserving soil (Huang et al., 2011). However, conservation tillage is still limited by many urgent problems, including volunteer rice. In South China, rice normally grows twice each year, in March (early season) and in July (late season) (Kong et al., 2017). In conservation tillage, the volunteer rice from early season easily germinates and seedlings in late season because the paddy fields are not ploughed. As a result, the volunteer plants would compete with the rice cultivar for nutrients and sunshine. Meanwhile, because of the commensalism between volunteer plants and the rice cultivar, the rice population becomes denser and prone to inducing various diseases and insect pests, which will complicate rice management and reduce the yield and grain quality of late season rice.

As reported, winter-flood reduced the germination rate of volunteer rice (Singh et al., 2016a), indicating flood treatment could be an effective means to deal with volunteer rice in double-cropping rice in South China. Under the hypothesis that flood treatment can reduce the germination of volunteer rice and the growth of volunteer seedlings, we conducted experiments in artificial weather boxes.

Materials and methods

Seed materials

Seeds from two fragrant rice cultivars (*Meixiangzhan*, *Xiangyaxiangzhan*), one japonica rice cultivar (*Changnongjing 1,* Yangtze University, Hubei, China) and the F2 generation of hybrid rice (*Yliangyou1173*) were used as the experimental

http://www.aloki.hu ● ISSN 1589 1623 (Print) ● ISSN 1785 0037 (Online)
DOI: http://dx.doi.org/10.15666/aeer/1605_72317242
© 2018, ALÖKI Kft., Budapest, Hungary

materials (Those cultivars were well-known and widely grown in South China). Seeds of early season rice were collected from College of Agriculture, South China Agricultural University, Guangzhou, China. All seeds were obtained from the upper parts of panicle.

Flood treatment and growth conditions

Normally, there was about two weeks between the harvest of early season and transplantation of late season rice in South China. Hence, after sowing seeds into soil-containing plastic pots (100× 80 × 20 cm^3; 500 seeds in each pot), we began the 2-week flood treatments as follows:

CK: soil was contained wet without any water layer at soil surface.

F1, *F2*, F3, F4: 2.0-2.5, 3-3.5, 4.5-5, 6-6.5 cm water layer were maintained at soil surface, respectively.

After the treatments F1, F2, F3 and F4, the water layers were drained off and all the pots contained wet soil without any water layer for a week in order to determinate the seedling rate and some biochemical indicators. The temperature for germination and growth was 33 °C in the day and 27 °C at night under 1200X yellow light. The experimental soil was sandy loam containing 1.443% total nitrogen, 24.56% organic matter, 0.927% total phosphorous and 18.220% total potassium at pH 6.54.

Seed bioassay

After sowing, the germination of each treatment was observed daily for 7 days according to the Association of Official Seed Analysis (Wiesner, 1990). The number of days to reach 50% germination (T_{50}) was calculated by a devised method with modification (Farooq et al., 2013):

$$T50 = ti + \frac{\left(\frac{N}{2} - ni\right)(tj - ti)}{nj - ni}$$

where N is the final number of emerged seeds; n_i and n_j are the cumulative numbers of emerged seeds at time t_i and t_j respectively when $n_i < N/2 < n_j$.

Mean germination time (MGT) was calculated as follows (Ellis, 1981):

$$MGT = \Sigma Dn / \Sigma n$$

where n is the number of emerged seeds on day D, which is counted from the beginning of emergence.

Germination index (GI) was calculated according to the equation of Association of Official Seed Analysis:

$$GI = \frac{\text{No. of emerged seeds}}{\text{Days of first count}} + \ldots\ldots + \frac{\text{No. of emerged seeds}}{\text{Days of final count}}$$

http://www.aloki.hu ● ISSN 1589 1623 (Print) ● ISSN 1785 0037 (Online)
DOI: http://dx.doi.org/10.15666/aeer/1605_72317242
© 2018, ALÖKI Kft., Budapest, Hungary

The energy of germination (*GE*) was observed on the 3rd day after sowing. This percentage of germinating seeds 3 d after sowing is relative to the total number of seeds tested (Ruan et al., 2002).

The radicle and plumule lengths of twenty seedlings randomly selected from each experimental unit were measured 7 d after sowing. Three weeks after sowing, seedling rate was recorded while 30 seedlings randomly selected from each experimental unit were measured for fresh weight and then oven-dried at 80 °C for 48 h to determine the dry biomass.

Biochemical analyses

After malonaldehyde (MDA) reacted with thiobarbital acid, absorbance of solutions was recorded at 532, 600, and 450 nm. The MDA content (μmol/L) was determined as = 6.45(OD532 −OD600) − 0.56OD450 (Pan, 2013), and final result was expressed as μmol/g FW.

The superoxide (SOD, EC 1.15.1.1) activity was detected according to Zhang (Zhang et al., 2008). The reaction mixture contained 1.75 ml of sodium phosphate buffer (SPB, pH 7.8), 0.3 ml of 130 $mM \cdot l^{-1}$ methionine buffer, 0.3 ml of 750 $\mu mol \cdot l^{-1}$ nitroblue tetrazolium (NBT) buffer, 0.3 ml of 100 $\mu mol \cdot l^{-1}$ ethylene diamine tetraacetic acid disodium (EDTA-Na_2) buffer, 0.3 ml of 20 $\mu mol \cdot l^{-1}$ lactoflavin and 0.05 ml of enzyme extract. The color change was measured at 560 nm after the reaction. One unit of activity was equal to the volume of extract needed to inhibit 50% of the color reaction. The peroxidase (POD EC1.11.1.7) activity was examined according to Yu (Xia et al., 2009). Enzyme extract (50 μl) was added to the reaction solution which contained 1 ml of 0.3% H_2O_2, 0.95 ml of 0.2% guaiacol, and 1 ml of 50 $mM \cdot l^{-1}$ SPB (pH 7.0). The absorbance was read at 470 nm. One unit of POD activity was expressed as the absorbance increase because of guaiacol oxidation by 0.01 (U/g FW). Catalase (CAT, EC 1.11.1.6) activity was measured according to Aebi (1984). An aliquot of enzyme extract (50 μl) was added to the reaction solution containing 1 ml of 0.3% H_2O_2 and 1.95 ml of SPB and, the absorbance was recorded at 240 nm. One unit of CAT activity was expressed as the absorbance decrease by 0.01 (U/g FW).

Statistical analyses

Data were analyzed using Statistix 8.1 (Analytical Software, Tallahassee, FL, USA) while differences among means were separated by using least significant difference (LSD) test at the 5% probability level. Graphical representation was conducted via Sigma Plot 14.0 (Systat Software Inc., California, USA).

Results

Germination rate

Flooding treatment significantly affected the emergence of volunteer rice. The germination of seeds started after 3 days in both treatments F3 and F4 for all rice varieties (*Fig. 1*). For *Xiangyaxiangzhan*, the speeds of germination were not significantly different among treatments CK, F1 and F2, but were significantly slowed down after treatments F3 and F4. Similar trend was found in *Meixiangzhan*.

http://www.aloki.hu ● ISSN 1589 1623 (Print) ● ISSN 1785 0037 (Online)
DOI: http://dx.doi.org/10.15666/aeer/1605_72317242
© 2018, ALÖKI Kft., Budapest, Hungary

For both *Changnongjing 1* and *F2 generation of Yliangyou1173*, the trend of speed germination was recorded as: CK > F1 > F2 > F3 > F4.

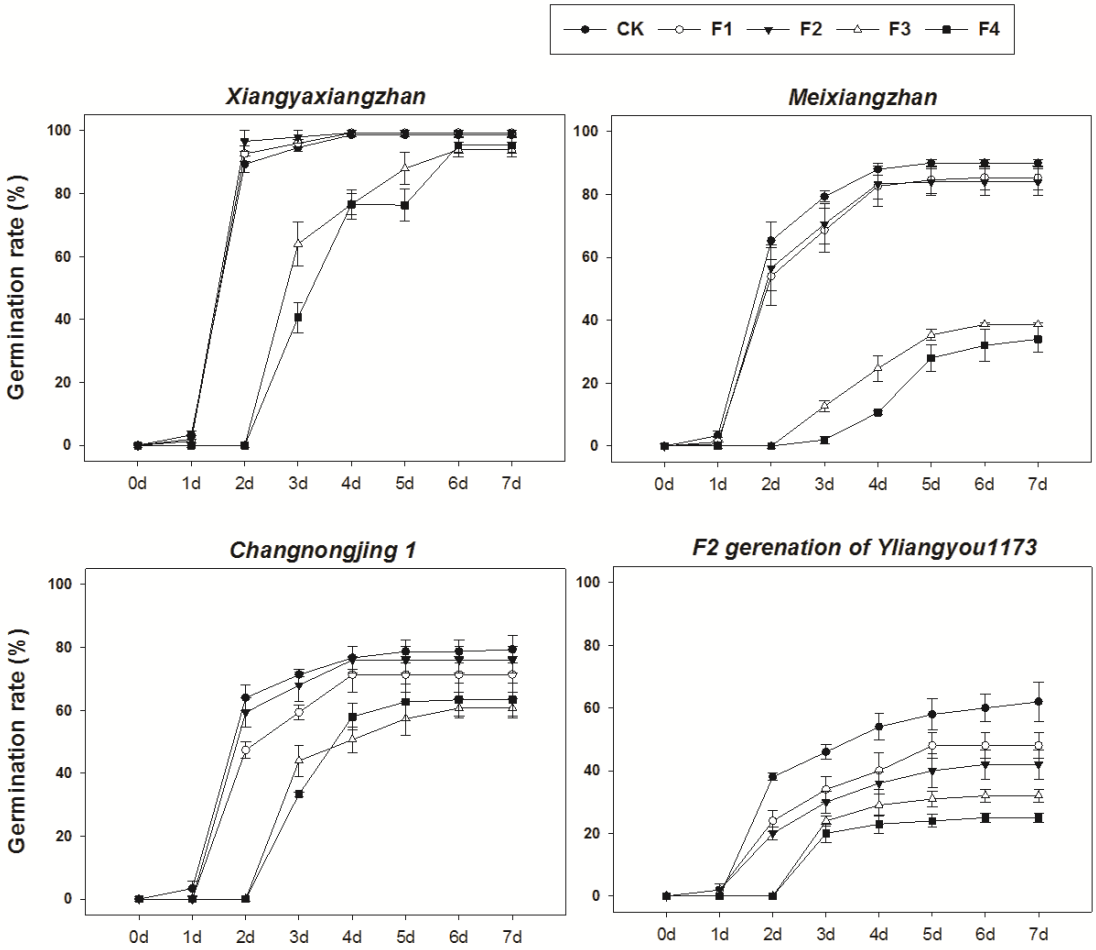

Figure 1. *Effects of flood treatments on germination rate of volunteer rice*

Emergence attributes

Flooding treatments influenced germination vigor significantly (*Table 1*). Treatments F3 and F4 both decreased the GI, GE, lengths of radicle and plumule, but increased the MGT and T_{50} significantly for all rice varieties. For *Xiangyaxiangzhan*, GIs in F3 and F4 declined by 43.56% and 47.72%, respectively, and GEs in F3 and F4 decreased by 22.29% and 22.37%, respectively, compared with CK. For *Meixiangzhan*, the lowest GI, GE and FGP were found in F4; Compared with CK, GIs in F3 and F4 decreased by 77.42% and 85.32%, respectively, while 71.97% and 87.88% lower were recorded in F3 and F4, respectively. For *Changnongjing 1*, no significant difference between treatments F3 and F4 was found in GI, GE or FGP, while GI, GE and FGP significantly all declined in F3 and F4. For *F2 generation of Yliangyou1173*, the changing trend of GI, GE and FGP was recorded as: CK > F1 > F2 > F3 > F4, while F3 and F4 prolonged MGT and T_{50} significantly. Furthermore, F1 and F2 treatments did not significantly affect FGP for *Xiangyaxiangzhan*, *Meixiangzhan* or *Changnongjing 1* whilst both F3 and F4 decreased the lengths of radicle and plumule for all 4 varieties compared with CK.

http://www.aloki.hu ● ISSN 1589 1623 (Print) ● ISSN 1785 0037 (Online)
DOI: http://dx.doi.org/10.15666/aeer/1605_72317242
© 2018, ALÖKI Kft., Budapest, Hungary

Table 1. *Effects of flooding treatments on the germination vigor of volunteer rice*

Treatments		MGT (d)	T_{50} (d)	GI	GE (%)	FGP (%)	Radicle length (cm)	Plumule length (cm)
Xiangyaxiangzhan	CK	4.53±0.02c	1.50±0.03c	77.25±1.57a	98.67±0.67a	98.67±0.67ab	5.35±1.06bc	4.27±0.16b
	F1	4.53±0.02c	1.52±0.03c	77.56±0.96a	99.33±0.67a	99.33±0.67a	7.68±0.59a	5.72±0.71a
	F2	4.50±0.02c	1.48±0.02c	79.22±0.96a	99.33±0.67a	99.33±0.67a	5.98±0.25b	5.32±0.42a
	F3	5.19±0.05b	2.75±0.07b	43.60±2.23b	76.67±4.67b	94.00±2.31b	4.37±0.64cd	3.09±0.44c
	F4	5.32±0.02a	3.28±0.04a	40.38±1.74b	76.59±3.33b	95.33±2.40ab	3.58±0.41d	3.70±0.49bc
Meixiangzhan	CK	4.63±0.04c	1.63±0.08c	65.15±2.83a	88.00±2.00a	90.00±1.15a	6.12±1.06a	4.68±0.40a
	F1	4.72±0.08c	1.80±0.13c	57.62±5.34a	82.67±6.36a	85.33±3.71a	2.92±0.35b	3.20±0.73bc
	F2	4.69±0.04c	1.75±0.08c	58.09±4.73a	83.33±4.81a	84.00±4.16a	4.42±0.71b	4.30±0.49ab
	F3	5.45±0.08b	3.63±0.27	14.71±0.83b	24.67±4.06b	38.67±0.67b	4.38±0.43b	2.41±0.44c
	F4	5.80±0.04a	4.38±0.03	9.56±1.24b	10.67±0.67c	34.00±4.00b	4.51±0.92ab	3.22±0.74bc
Changnongjing 1	CK	4.58±0.04c	1.55±0.02d	59.23±1.50a	76.67±3.71a	79.33±4.37a	7.48±0.73a	3.72±0.18a
	F1	4.69±0.06b	1.76±0.09c	48.81±2.36b	71.33±5.70a	71.33±5.70abc	5.80±0.56b	2.22±0.13b
	F2	4.63±0.02bc	1.64±0.02cd	55.03±3.56ab	76.00±4.16a	76.00±4.16ab	5.50±1.03b	2.28±0.32b
	F3	5.16±0.03a	2.70±0.05b	28.79±2.31c	50.67±4.06b	60.67±2.96c	2.37±0.21c	1.68±0.33c
	F4	5.23±0.02a	2.95±0.06a	28.87±2.01c	58.00±4.16b	63.33±5.21bc	2.12±0.04c	1.05±0.17d
F2 generation of Yliangyou1173	CK	4.76±0.03b	1.81±0.06c	39.15±2.48a	3.20±0.40ab	62.00±6.24a	4.33±0.85a	3.20±0.40ab
	F1	4.83±0.06b	2.14±0.12b	29.90±3.54b	3.98±0.46a	48.00±4.04b	4.32±0.75a	3.98±0.46a
	F2	4.81±0.06b	2.08±0.10bc	26.00±1.92b	3.03±0.61b	42.00±4.62bc	3.33±0.77ab	3.03±0.61b
	F3	5.13±0.02a	2.67±0.02a	15.68±1.25c	3.15±0.33ab	32.00±2.08cd	3.10±0.29ab	3.15±0.33ab
	F4	5.11±0.06a	2.65±0.08a	12.48±1.24c	2.73±0.15b	25.00±1.53d	2.40±0.21b	2.73±0.15b

Figures not sharing the same letters differ significantly at P = 0.05 (the same below). FGP: final germination percentage

Seedling quality

Flooding treatments reduced the seedling quality of volunteer rice significantly. The trend of seedling rate was recorded as: CK > F1 > F2 > F3 > F4 for both *Xiangyaxiangzhan* and *Meixiangzhan* (*Table 2*). In treatments F1 and F2 compared with CK, seedling rate was 81.51% and 81.94% lower in *Changnongjing 1*, respectively, while 43.55 and 57.98 lower in *F2 generation of Yliangyou1173*, respectively. No seed could grow or develop into a whole seedling in F3 or F4 for either *Changnongjing 1* or *F2 generation of Yliangyou1173*. Moreover, dry weights were 5.2%, 10.09%, 45.15% and 39.58% lower in F1, F2, F3 and F4 respectively for *Xiangyaxiangzhan*, respectively. For *Meixiangzhan*, the trend of dry weight was recorded as: CK > F1 > F2 > F3 > F4. Both F1 and F2 decreased the dry weight in *Changnongjing 1* and *F2 generation of Yliangyou1173*.

MDA contents and anti-oxidant responses of seedlings

Flooding treatments influenced the anti-oxidative activities in terms of POD, SOD and CAT, and caused oxidative damage by increasing lipid per-oxidation (MDA content). For *Xiangxiangzhan*, MDA contents in F1, F2, F3 and F4 were 19.39%, 10.20%, 36.73% and 64.29% higher, respectively. POD and CAT activities in F1 and F2 all were higher than CK while lower in F3 and F4. Similar discussion was found in *Meixiangzhan*. For *Meixiangzhan*, MDA contents were 12.33, 11.53, 37.09 and 85.11% higher in F1, F2, F3 and F4, respectively. Highest and lowest SOD activity were recorded in F2 and F4, respectively. For *Changnongjing 1* and *F2 generation of Yliangyou1173*, both F1 and F2 treatments reduced the activities of POD, SOD and CAT while promoting the production of MDA (*Table 3*).

http://www.aloki.hu ● ISSN 1589 1623 (Print) ● ISSN 1785 0037 (Online)
DOI: http://dx.doi.org/10.15666/aeer/1605_72317242
© 2018, ALÖKI Kft., Budapest, Hungary

Table 2. *Effect of flood treatments on seedling quality of volunteer rice*

Treatments		Seedling rate (%)	Fresh weight (mg)	Dry weight (mg)
Xiangyaxiangzhan	CK	98.67±0.67a	63.43±1.26a	9.22±0.21a
	F1	88.67±1.77b	57.87±1.41ab	8.75±0.13a
	F2	65.67±3.48c	64.50±0.79a	8.29±0.29a
	F3	64.33±3.48c	45.80±1.01c	5.06±0.35b
	F4	48.67±3.71d	53.28±4.89bc	5.57±0.90b
Meixiangzhan	CK	90.00±1.15a	97.92±1.81a	15.62±0.61a
	F1	74.00±6.11b	83.81±2.34ab	11.37±0.28b
	F2	68.00±4.00b	78.55±3.96b	10.30±0.12b
	F3	26.00±1.56c	66.88±5.21b	7.81±0.58c
	F4	18.67±2.52c	72.12±10.69b	6.86±0.54c
Changnongjing 1	CK	79.33±4.37a	105.62±2.13a	14.58±1.34a
	F1	14.67±0.67b	62.29±1.72b	8.48±0.38b
	F2	14.33±2.33b	57.45±2.01c	7.86±0.12b
	F3	0	-	-
	F4	0	-	-
F2 generation of Yliangyou1173	CK	62.00±6.24a	85.24±1.88a	8.80±0.31a
	F1	35.00±2.65b	32.31±1.45b	3.48±0.28b
	F2	26.05±2.10b	34.19±1.10b	3.35±0.24b
	F3	0	-	-
	F4	0	-	-

Table 3. *Effects of flood treatments on MDA contents and anti-oxidant responses of seedlings*

Treatments		POD ($U \cdot g^{-1} \cdot min^{-1}$)	SOD (U·g-1)	CAT (U·g-1·min-1)	MDA (umol·g-1)
Xiangyaxiangzhan	CK	124.33±2.60c	178.67±2.91b	160.59±2.91c	3.27±0.12c
	F1	133.67±0.89b	185.67±2.02ab	169.25±1.54b	3.90±0.17bc
	F2	145.02±4.04a	193.33±2.34a	179.32±3.13a	3.60±0.06c
	F3	105.33±2.73d	164.79±3.18c	143.10±2.39d	4.47±0.26b
	F4	89.33±1.45e	147.15±4.09d	125.61±1.70e	5.38±0.24a
Meixiangzhan	CK	113.33±2.71c	201.74±4.09b	153.59±3.80c	3.76±0.14c
	F1	122.09±1.08b	213.81±3.78a	162.25±1.64b	4.22±0.20bc
	F2	134.15±3.06a	216.51±2.81a	172.32±4.37a	4.19±0.13bc
	F3	94.33±2.13d	187.17±2.17c	136.10±2.80d	5.15±0.30b
	F4	78.33±0.96e	174.00±1.53d	118.61±2.86e	6.96±0.28a
Changnongjingone	CK	154.33±2.19a	238.46±3.11a	190.59±4.05a	2.11±0.03c
	F1	131.25±1.45b	164.12±5.17b	137.00±4.16b	6.40±0.29b
	F2	104.67±1.86c	128.00±5.19c	118.76±4.36c	7.77±0.19a
	F3	-	-	-	-
	F4	-	-	-	-
F2 generation of Yliangyou1173	CK	107.67±1.91a	143.00±2.08a	132.85±2.08a	5.13±0.15c
	F1	84.33±2.91b	115.84±2.09b	106.00±1.33b	8.45±0.19b
	F2	67.61±1.79c	97.55±4.10c	87.63±3.14c	10.08±0.38a
	F3	-	-	-	-
	F4	-	-	-	-

http://www.aloki.hu ● ISSN 1589 1623 (Print) ● ISSN 1785 0037 (Online)
DOI: http://dx.doi.org/10.15666/aeer/1605_72317242
© 2018, ALÖKI Kft., Budapest, Hungary

Correlation analysis

Seedling rate was significantly and positively correlated with dry weight, POD, SOD, CAT, GI, GE, and FGP (*Table 4*). Significant positive correlations were also observed among GI, GE and FGP, but negative correlations were found between MDA and seedling rate and between T_{50} and FGP.

Table 4. *Relationship between seedling rate, anti-oxidant responses and seed bioassay*

Index	Seedling rate	Dry weight	POD	SOD	CAT	MDA	GI	GE	T_{50}	FGP
Dry weight	0.600*									
POD	0.585*	0.679**								
SOD	0.585*	0.805**	0.749**							
CAT	0.742**	0.731**	0.919**	0.904**						
MDA	-0.778**	-0.715**	-0.754**	-0.878**	-0.920**					
GI	0.759**	0.526*	0.797**	0.452	0.735**	-0.597*				
GE	0.735**	0.466	0.749**	0.423	0.699**	-0.605*	0.962**			
T_{50}	-0.522*	-0.424	-0.650**	-0.155	-0.449	0.212	-0.807**	-0.732**		
FGP	0.739**	0.394	0.666**	0.424	0.676**	-0.659**	0.884**	0.967**	-0.554*	
Plumule length	0.716**	0.263	0.413	0.357	0.543*	-0.482	0.644**	0.560*	-0.382	0.555*

Significant correlations as *P < 0.05 and **P < 0.01

Discussion

Volunteer rice is a global problem of rice production, especially in conservation tillage. In the United States, areas of rice growing normally begin to be flooded from early autumn after the rice harvest until the tillage operations in spring (Fogliatto et al., 2010) because anaerobic environment could limit the germination and growth of abundant weeds such as weedy rice (Bird et al., 2002). The present study confirms this view by showing the decline of emergence properties of volunteer rice in flooding treatments. Specifically, the germination speed slowed as the water layer increased, especially F3 and F4. Once the water layer was over 4.5 cm, the time to start germination was extended and the quantity of eventually germinated volunteer rice was weakened. Flooding treatment significantly altered the germination characteristics of volunteer rice. Since the seed germination and seedling establishment phase is highly vulnerable to injury, disease and stress, we believe this phase is a key time period to prevent harvest loss caused by volunteer rice. Germination vigor is driven by the ability of plant embryos, embedded in seeds, to resume the metabolic activity in a coordinated and sequential manner (Rajjou et al., 2012). The germination vigor can be evaluated using many indexes. We observed that as water layer rose in flooding treatments, MGT and T_{50} were prolonged for most rice varieties while the GI and GE reduced. Both F4 and F3 significantly influenced volunteer rice germination by minimizing the germination rate, and drastically declined both radicle and plumule lengths for all rice varieties. These results agreed with Prakash (Rajjou et al., 2012) who found rice germination was further reduced with the rise of submergence levels. In addition, the volunteer rice from *Xiangyaxiangzhan* was strongly tolerant against submergence. The FGPs in F1, F2, F3 and F4 were all not significantly different from those in CK. Thus,

http://www.aloki.hu ● ISSN 1589 1623 (Print) ● ISSN 1785 0037 (Online)
DOI: http://dx.doi.org/10.15666/aeer/1605_72317242
© 2018, ALÖKI Kft., Budapest, Hungary

Xiangyaxiangzhan might be one of the tolerant genotypes against flooding stress. The flooding tolerance during germination is a complicated process involving many mechanisms. Ismail already identified several genotypes with higher flooding tolerance during germination (Ismail et al., 2009). However, the submergence tolerance during germination is associated with the flooding tolerance during the vegetative stage, as reported in the sensitivity of FR13A, a landrace that is most tolerant of complete inundation during this stage (Ella et al., 2003; Jackson and Ram, 2003).

We also noticed flooding treatment greatly reduced seedling rate and dry matter weight. As reported similarly, flooding treatments decreased root, shoot and total dry matter production in all rice cultivars and with more reduction in higher than lower flooding levels (5 vs. 1 cm) (Prakash et al., 2016a). These results indicate the seeds of volunteer rice even under the flooding environment could germinate successfully, but the chance of developing into whole normal seedlings was very low, which was greatly embodied by the zero seedling rates of both *Changnongjing 1* and *F2 generation of Yliangyou1173* in treatments F3 and F4. After 3 weeks of treatment, MDA production in volunteer seedlings was enhanced with the increasing submergence level. The MDA over-accumulation might be attributed to oxidation of polyunsaturated fatty acids (e.g., lineolenic acids, galacto- and phosphp-lipid components), which are critical in the functional and structural characteristics of thylakoid membranes and the arrangement of reaction centers of photosystems (Elshintinawy, 2000). MDA also reacts with free amino acids to even form ethylene in cellular membranes (Rakwal et al., 2003; Jiang and Zhang, 2002). Thus, MDA accumulation is a key indicator of oxidative stress, which is characteristic of intercellular and intracellular membranes and hence intensifies the ion leakage through cell membranes (Dash and Mohanty, 2002). In this study, the improvement of MDA content meant flooding treatment caused submergence stress and some oxidative damage to volunteer seedlings. Furthermore, the anti-oxidative enzymatic activities all differed maong the flooding conditions. Anti-oxidant plays an important role in quenching reactive oxygen species. For example, when superoxide radicals accumulate in organisms, SOD is responsible for breakdown and then POD and CAT are involved in scavenging H_2O_2 (Sairam et al., 2000). In the present study, treatments F1 and F2 both enhanced the activities of POD, SOD and CAT for both *Xiangyaxiangzhan* and *Meixiangzhan*, whilst F3 and F4 greatly decreased the anti-oxidative enzymatic activities. The main reason might be that lower flooding level (1.5-3.5 cm) already caused oxidative stress to rice seedlings, but the damage could be mitigated by the anti-oxidant regulation of seedlings. Thus volunteer seedlings under lower submergence level would activate the anti-oxidation mechanism in order to prevent the oxidant damage caused by flooding stress. However, under higher flooding level (4.5-6.5 cm), the submergence stress during germination and seedling development already caused irreversible damage and even destroyed the anti-oxidative system, so that the POD, SOD and CAT activities decreased while the MDA content increased greatly. Moreover, *Changnongjing 1* and *F2 generation of Yliangyou1173* were sensitive to flooding stress so that the anti-oxidative enzymatic activities declined in F1 and F2.

Conclusion

In conclusion, long-term (2 weeks) flooding treatment significantly limited or even prevented the germination and growth of volunteer rice, while treatment F4 (6.0-6.5 cm)

http://www.aloki.hu ● ISSN 1589 1623 (Print) ● ISSN 1785 0037 (Online)
DOI: http://dx.doi.org/10.15666/aeer/1605_72317242
© 2018, ALÖKI Kft., Budapest, Hungary

was the most effective because of the lowest seedling rate. In order to prevent the harvest loss in late season rice caused by volunteer rice and further investigation should be at the field trials, the possible effects of flooding on the late-season rice production should be studied before the real application.

Acknowledgements. This study was funded by National Natural Science Foundation of China (31271646), The World Bank Loan Agricultural Pollution Control Project in Guangdong (0724-1510A08N3684) and (2017LM1098). The authors declare no conflicts of interest.

REFERENCES

[1] Aebi, H. (1984): Catalase in vitro. – Methods Enzymol 105: 121-126.
[2] Bird, J. A., Eagle, A. J., Horwath, W. R., Hair, M. W., Zibert, E. E., Van, K. C. (2002): Long-term studies find benefits, challenges in alternative rice straw management. – California Agriculture 56: 69-75.
[3] Cao, Q., Bao-Rong, L. U., Xia, H., Rong, J., Sala, F., Spada, A., Grassi, F. (2006): Genetic diversity and origin of weedy rice (Oryza sativa f. spontanea) populations found in north-eastern China revealed by simple sequence repeat (SSR) markers. – Annals of Botany 98: 1241-1252.
[4] Dash, S., Mohanty, N. (2002): Response of seedlings to heat-stress in cultivars of wheat: Growth temperature-dependent differential modulation of photosystem 1 and 2 activity, and foliar antioxidant defense capacity. – Journal of Plant Physiology 159: 49-59.
[5] Ella, E. S., Kawano, N., Yamauchi, Y., Tanaka, K., Ismail, A. M. (2003): Blocking ethylene perception enhances flooding tolerance in rice seedlings. – Functional Plant Biology 30: 813-819.
[6] Ellis, R. (1981): The quantification of ageing and survival in orthodox seeds. – Seed Science & Technology 9: 373-409.
[7] Ellstrand, N. C., Prentice, H. C., Hancock, J. F. (1999): Gene flow and introgression from domesticated plants into their wild relatives. – Horizontal Gene Transfer 30: 539-563.
[8] Elshintinawy, F. (2000): Structural and functional damage caused by boron deficiency in sunflower leaves. – Photosynthetica 36: 565-573.
[9] Farooq, M., Basra, S. M. A., Hafeez, K., Warriach, E. A. (2013): Influence of high- and low-temperature treatments on seed germination and seedling vigor of coarse and fine rice. – Custom Integrated Circuits Conference, 1992, Proceedings of the IEEE, 12.2.1-12.2.4.
[10] Fogliatto, S., Vidotto, F., Ferrero, A. (2010): Effects of winter flooding on weedy rice (Oryza sativa L.). – Crop Protection 29: 1232-1240.
[11] Gealy, D. R., Gressel, J. (2005): Gene Movement Between Rice (Oryza sativa) and Weedy Rice (Oryza sativa). A U.S. Temperate Rice Perspective. – In: Gressel, J. (ed.) Crop Ferality and Volunteerism. CRC Press, Boca Raton, FL, pp. 323-354.
[12] Gealy, D. R., Mitten, D. H., Neil, R. J. (2003): Gene flow between red rice (Oryza sativa) and herbicide-resistant rice (O. sativa): implications for weed management. – Weed Technology 17: 627-645.
[13] Gressel, J., Valverde, B. E. (2010): A strategy to provide long-term control of weedy rice while mitigating herbicide resistance transgene flow, and its potential use for other crops with related weeds. – Pest Management Science 65: 723-731.
[14] Huang, M., Ibrahim, M. D., Xia, B., Zou, Y. (2011): Significance, progress and prospects for research in simplified cultivation technologies for rice in China. – Journal of Agricultural Science 149: 487-496.

http://www.aloki.hu ● ISSN 1589 1623 (Print) ● ISSN 1785 0037 (Online)
DOI: http://dx.doi.org/10.15666/aeer/1605_72317242
© 2018, ALÖKI Kft., Budapest, Hungary

[15] Huang, M., Zhou, X., Chen, J., Cao, F., Zou, Y., Jiang, L. (2016): Factors contributing to the superior post-heading nutrient uptake by no-tillage rice. – Field Crops Research 185: 40-44.
[16] Ismail, A. M., Ella, E. S., Vergara, G. V., Mackill, D. J. (2009): Mechanisms associated with tolerance to flooding during germination and early seedling growth in rice (Oryza sativa). – Annals of Botany 103: 197-209.
[17] Jackson, M. B., Ram, P. C. (2003): Physiological and molecular basis of susceptibility and tolerance of rice plants to complete submergence. – Ann Bot 91: 227-241.
[18] Jiang, M., Zhang, J. (2002): Water stress-induced abscisic acid accumulation triggers the increased generation of reactive oxygen species and up-regulates the activities of antioxidant enzymes in maize leaves. – Journal of Experimental Botany 53: 2401-2410.
[19] Kong, L., Ashraf, U., Cheng, S., Rao, G., Mo, Z., Tian, H., Pan, S., Tang, X. (2017): Short-term water management at early filling stage improves early-season rice performance under high temperature stress in South China. – European Journal of Agronomy 90: 117-126.
[20] Pan, S. (2013): Roles of plant growth regulators on yield, grain qualities and antioxidant enzyme activities in super hybrid rice (Oryza sativa L.). – Rice 6: 1-10.
[21] Peigné, J., Vian, J. F., Payet, V., Saby, N. (2018): Soil fertility after 10 years of conservation tillage in organic farming. – Soil & Tillage Research 175: 194-204.
[22] Prakash, M., Sunilkumar, B., Narayanan, G. S., Gokulakrishnan, J., Anandan, R. (2016): Seed germination and seedling growth of rice varieties as affected by flooding stress. – Indian Journal of Agricultural Research 50. DOI: 10.18805/ijare.v50i3.10748.
[23] Rajjou, L., M. Duval, Gallardo, K., Catusse, J., Bally, J., Job, C., Job, D. (2012): Seed germination and vigor. – Annual Review of Plant Biology 63: 507-533.
[24] Rakwal, R., Agrawal, G. K., Kubo, A., Yonekura, M., Tamogami, S., Saji, H., Iwahashi, H. (2003): Defense/stress responses elicited in rice seedlings exposed to the gaseous air pollutant sulfur dioxide. – Environmental & Experimental Botany 49: 223-235.
[25] Ruan, S., Xue, Q., Tylkowska, K. (2002): The influence of priming on germination of rice (Oryza sativa L.) seeds and seedling emergence and performance in flooded soil. – Seed Science & Technology 30: 61-67.
[26] Sairam, R. K., Srivastava, G. C., Saxena, D. C. (2000): Increased antioxidant activity under elevated temperatures: a mechanism of heat stress tolerance in wheat genotypes. – Biologia Plantarum 43: 245-251.
[27] Shivrain, V. K., Burgos, N. R., Anders, M. M., Rajguru, S. N., Moore, J., Sales, M. A. (2007): Gene flow between Clearfield rice and red rice. – Crop Protection 26: 349-356.
[28] Singh, V., Burgos, N., Singh, S., Abugho, S., Earnest, L., Gbur, E., Scott, R. (2016a): Herbicide and winter flood treatments for controlling volunteer rice off-season. – Crop Protection 79: 87-96.
[29] Singh, V., Burgos, N. R., Singh, S., Gealy, D. R., Gbur, E. E., Caicedo, A. L. (2016b): Impact of volunteer rice infestation on yield and grain quality of rice. – Pest Management Science 73: 604.
[30] Street, J. E., Teresiak, H., Boykin, D. L., Allen, R. L. (1995): Interaction between timings and doses of quinclorac in rice. – Weed Research 35: 75-79.
[31] Sudianto, E., Song, B. K., Ting-Xiang, N., Saldain, N. E., Scott, R. C., Burgos, N. R. (2013): Clearfield ® rice: its development, success, and key challenges on a global perspective. – Crop Protection 49: 40-51.
[32] Triplett, G. B., Dick, W. A. (2008): No-tillage crop production: a revolution in agriculture! – Agronomy Journal 100: 153-S165.
[33] Warwick, S. I., Stewart, C. N. J., Gressel, J. (2005): Crops come from wild plants - how domestication, transgenes, and linkage together shape ferality. – Crop Ferality & Volunteerism 36: 30.
[34] Wiesner, L. (1990): Rules for Testing Seeds. Rev. – Information Systems Division, National Agricultural Library, Beltsville, MD, Washington, DC.

http://www.aloki.hu ● ISSN 1589 1623 (Print) ● ISSN 1785 0037 (Online)
DOI: http://dx.doi.org/10.15666/aeer/1605_72317242
© 2018, ALÖKI Kft., Budapest, Hungary

[35] Xia, X. J., Wang, Y. J., Zhou, Y. H., Yuan, T., Mao, W. H., Kai, S., Asami, T., Chen, Z. X., Yu, J. Q. (2009): Reactive oxygen species are involved in brassinosteroid-induced stress tolerance in cucumber. – International Journal of Rock Mechanics & Mining Sciences & Geomechanics Abstracts 150: 801-814.
[36] Zhang, W. F., Zhang, F., Raziuddin, R., Gong, H. J., Yang, Z. M., Lu, L., Ye, Q. F., Zhou, W. J. (2008): Effects of 5-aminolevulinic acid on oilseed rape seedling growth under herbicide toxicity stress. – Journal of Plant Growth Regulation 27: 159-169.

APPENDIX

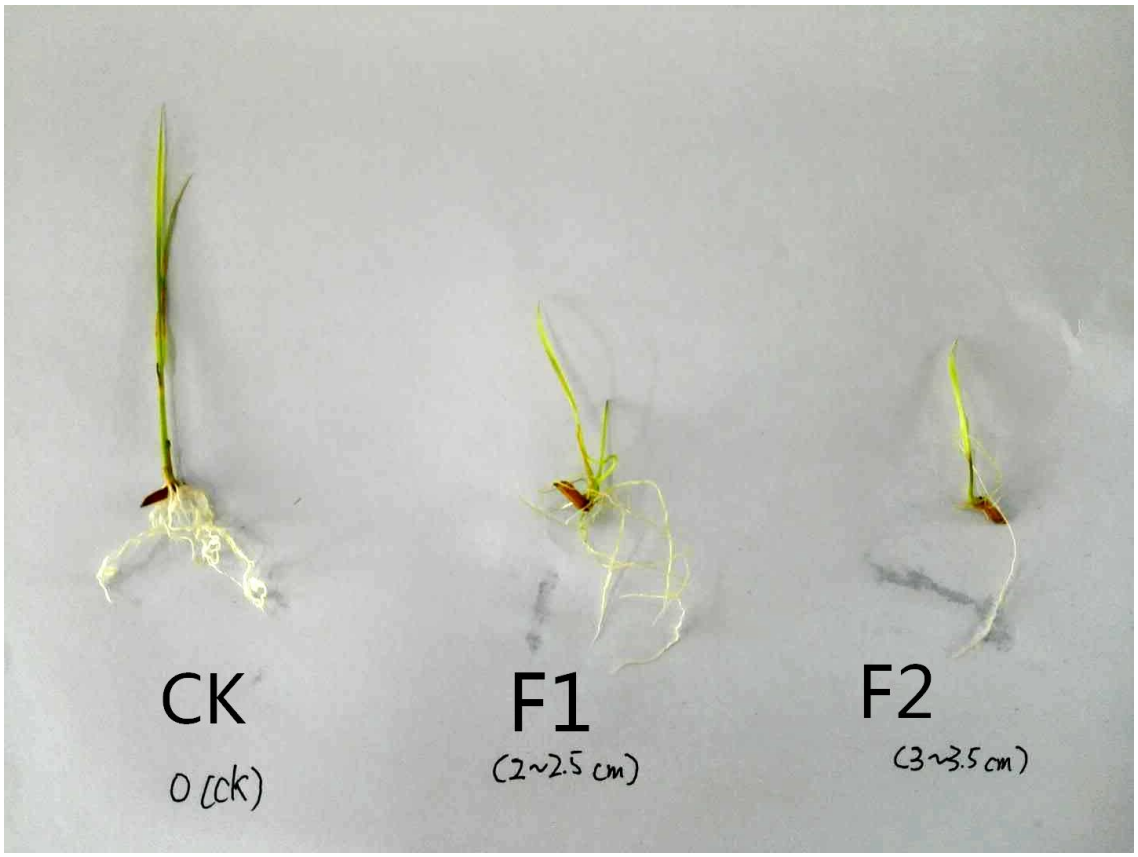

http://www.aloki.hu ● ISSN 1589 1623 (Print) ● ISSN 1785 0037 (Online)
DOI: http://dx.doi.org/10.15666/aeer/1605_72317242
© 2018, ALÖKI Kft., Budapest, Hungary

EFFECTS OF CALCIUM AND UV-C TREATMENTS ON PHYSICAL AND BIOCHEMICAL QUALITY ATTRIBUTES OF PEPPER THROUGHOUT COLD STORAGE

ÇAVUŞOĞLU, Ş.

Department of Horticulture, Faculty of Agriculture, Van Yuzuncu Yil University, Van, Turkey
(e-mail: seydacavusoglu@yyu.edu.tr; phone: +90-444-5065-21685)

(Received 8th Aug 2018; accepted 5th Oct 2018)

Abstract. Effects of pre-harvest calcium chloride and post-harvest UV-C (200–280 nm ultraviolet light) treatments on pepper fruits (*Capsicum annuum* L. cv. Mertcan F1) were investigated in this study. Calcium treatments usually delay softening in horticultural crops. UV-C treatments prevent decay on fruit surface. However, instead of these physical attributes, changes in the chemical composition of fruit were investigated in this study. Experimental treatments were arranged as control (without any treatments), UV-C, Ca and Ca + UV-C. Treated fruits were stored in a cold storage at 0 °C and 95% relative humidity for 10 days. Samples were taken in every 2 days of the storage and pH, titratable acidity (TA), soluble solids content (SSC), color change, total phenolic content (TPC) and total antioxidant capacity (TAC) were determined. All experimental treatments all increased SSC, titratable acidity, total phenolic content and total antioxidant capacity. Particularly, treatments containing Ca yielded the greatest increases in SSC and titratable acidity. UV-C + Ca treatment preserved the color intensity (chroma - C) the best (32.85). Total phenolic content and total antioxidant capacity had the least change with UV-C treatment. UV-C + Ca was recommended as the best treatment keeping quality attributes of 'cv. Mertcan F1' pepper throughout the cold storage for 10 days. Such 10-day extension is a significant criterion for pepper storage and marketing.
Keywords: *Capsicum annuum L., antioxidant, total phenolic content, postharvest*

Introduction

Turkey has ecologically quite available conditions for pepper farming. It is possible to grow peppers all year-long in Turkey. Annual productions, yield levels and quality attributes are all greater than world averages (Vural and et al., 2000; Gunay, 2005). Turkey produces 2,127,944 tons of pepper annually and such an amount constitutes about 7% of world production (32,324,345 tons). Following China and Mexico, Turkey has the third place in world pepper production (FAOSTAT, 2014). Despite high production volumes, deficiency in storage and packaging techniques causes significant losses in fresh peppers. As it is a quickly rotting product, storage and delivery to markets are vital issues for peppers (Erdogmus et al., 2015).

Pepper (*Capsicum annuum* L.) is originated from tropical and sub-tropical countries of America and it is an essential vegetable for healthy life. Fruits are quite rich in biological agents such as vitamins, antioxidants and other phytochemicals. Fruits are consumed in various ways; as fresh vegetable in salads, fried, cooked with meat or olive oil, as pepper paste, pickle and spice (Vural et al., 2000; Frank et al., 2005; Crosby, 2008). Peppers are also rich in antioxidants, ascorbic acid, carotenoid and vitamin E, thus used in prevention of some cancer cases, heart diseases and cardiovascular diseases (Simonne et al., 1997; Salk et al., 2008).

http://www.aloki.hu ● ISSN 1589 1623 (Print) ● ISSN 1785 0037 (Online)
DOI: http://dx.doi.org/10.15666/aeer/1605_72437252
© 2018, ALÖKI Kft., Budapest, Hungary

Peppers have non-climacteric fruits (Watkins, 2002) and thus they are not significantly influenced by post-harvest ethylene synthesis. Besides, fresh pepper fruits have quite high water contents shortening their shelf life and speeding up deteriorations. Especially when the pepper fruits were kept in room conditions, the physiological deterioration is most likely to be caused by water loss, congestion and wrinkles. Consumers prefer peppers with a firm and fresh appearance. Therefore, in order to maintain the quality of peppers, like other products, they must be kept in cold storages with high relative humidity and low temperatures. Fresh pepper fruits can be stored between 7 to 10 C° and 90-95% relative humidity for 1-3 weeks (Hardenburg et al., 1986; Snowdon, 1992). This time period can be extended up to 35-45 days by modified atmosphere packages (Rodov et al., 1995; Halloran et al., 2000; Demirdoven et al., 2006). Cold damage is the most important factor restricting the preservation of peppers in cold storages. Low temperatures below 7–10 C° cause softening, shrinkage, drying and pathological disorders in peppers, which severely reduce the quality and acceptability of the product (Mercier et al., 2001; Nyanjage et al., 2005).

Calcium facilitates calcium pectate formation on cell walls, thus increases fruit firmness. Such a case then facilitates the preservation of the product for a long period. Besides, as in many vegetables, calcium also prevents blossom-end rotting in peppers. Pre and post-harvest calcium treatments delay aging during the storage and marketing stages and these treatments do not have any negative effects on appearance (Lester and Grusak, 2000; Hernandez-Munoz, 2006; Chen et al., 2011). Ca treatments generally reduce respiration and metabolic activity in fruits. As a result, the breakdown of carbohydrates were delayed and increasing of soluble solids content (SSC) in peppers were decreased (Rao et al., 2011).

Erdogmus et al. (2015) reported that post-harvest application of 2% $CaCl_2$ to the 'cv. Yalova Yağlık 28' pepper at 0 C° and 90% relative humidity resulted in 11.6% weight loss after 30 days of storage and a decrease was the lowest as compared to the other applications. Rao et al. (2011) immersed fresh sweet 'Indra' peppers into 0.5, 1.0 and 1.5% calcium chloride solutions for 15 min and stored peppers at 10 °C and 25 °C for 18 days in polyethylene packages. Researchers reported that significant effects of 1.5% calcium chloride treatment on SSC, titratable acidity (TA) and pH ($p < 0.05$) and weight loss both during the storage and the shelf life. It was concluded that fruits could be stored for up to 71 days without significant losses in taste.

Ultraviolet-C (UV-C) is a technology commonly used in surface and water disinfection as well as in fruit juice pasteurization (Koutchma et al., 2016). Recent studies showed that UV-C light stimulated the formation of secondary metabolites when it was applied as an abiotic stressor to the plants (Alothman et al., 2009). UV-light treatments increased antioxidants and total phenolics of red peppers during the storage (Andrade-Cuvi, 2011; Perez-Ambrocio et al., 2018). Vicente et al. (2005) applied UV-C light to 'Zafiro' pepper with red color and stored peppers in a cold storage at 10 C° and 90% relative humidity for 18 days. The 7 kJm^{-2} UV-C treatments better preserved color parameters, carotenoid levels and fruit firmness and reduced decay rates, but did not affect the changes in SSC values. UV-C treatments had lower total phenolic content. Abbasi et al. (2015) applied UV-C (3 and 5 min at 254 nm), the edible coatings aleo gel, ginger oil and chitosan to 'Royal Wonder' bell pepper at different rates and stored treated fruits

http://www.aloki.hu ● ISSN 1589 1623 (Print) ● ISSN 1785 0037 (Online)
DOI: http://dx.doi.org/10.15666/aeer/1605_72437252
© 2018, ALÖKI Kft., Budapest, Hungary

at 8-9 C° and 80-85% relative humidity for 24 days. Researchers reported that 5-min UV-C treatments better preserved fruit firmness, SSC, color parameters, ascorbic acid contents and titratable acidity. UV-C (short-wave ultraviolet radiation) is a chemical-free method and it provides longer-lasting, high-quality preservation of products by preventing or eliminating the development of pathogens.

This study investigated the effects of alternative environment-friendly methods (calcium and UV-C treatments) on preservation of quality attributes of fresh peppers throughout the cold storage. Shelf life of fresh peppers is quite short due to softening, water loss and decay. Extension of the shelf life for a few days is very important for the marketing of the product. Number of studies on calcium and UV-C treatments in peppers is quite limited. Thus, the primary objective of the present study was set as to extend shelf life of fresh peppers with calcium and UV-C treatments.

Materials and methods

Fruit material

The 'cv. Mertcan F1'(*Capsicum annum* L.) peppers used in this study were obtained from a producer farm in the Kazanlı distict in Mersin province, Turkey (36° 49' 14.5956" and 34° 45' 22.0536"), toward the end of the production period spanning October 2016 to January 2017. This pepper is a sweet and early type. It is cultivated in greenhouses at 40 cm × 50 cm spacing by fertilization and drip irrigation. Peppers were transported by air-conditioned vehicles to The Post-harvest Laboratory of Van Yuzuncu Yil University, Faculty of Agriculture, Department of Horticulture. Initially, pH, SSC, titratable acidity, color parameters, total phenolic content and total antioxidant capacity were measured before placing the peppers into cold storage.

Experimental plan

The pepper fruits to be used in experiments were packed due to the fact that it is cheap and lightweight in styrofoam packs of 0.5 kg, 30 fruits in each and 2 replications for each treatment, and then they were placed in cardboard boxes of 5 kg. Experimental treatments were arranged as; a-) Control, b-) UV-C, c-) Ca and d-) Ca+UV-C. For pre-harvest Ca treatments, 12.1% commercial calcium fertilizer (DRT speedfol calcium) was applied for 2 days and 1 hour per week at 500 cc/da rate of application.

UV-C was applied as specified by Vicente et al. (2005); 30 fruits were placed on a sterile plastic tray 30 cm below 4 sterile UV-C lamps (TUV G30T8, 30 W, Philips, Argentina) with 254 nm light emission and applied at 14 kJm^{-2}. In order to get better light during the application, the peppers were manually rotated around the surface three times. The radiation intensity was measured by a digital UV radiometer (Cole-Parmer Instrument Company, Vernon Hills, Ill.).

Fruits were stored at 0 °C and 95% relative humidity for 10 days and they were analyzed in every 2 days.

The SSC ratio was measured with a digital refractometer (Atago, Tokyo, Japan) and the results were expressed in Brix. Titratable acidity was measured as the

http://www.aloki.hu ● ISSN 1589 1623 (Print) ● ISSN 1785 0037 (Online)
DOI: http://dx.doi.org/10.15666/aeer/1605_72437252
© 2018, ALÖKI Kft., Budapest, Hungary

quantity of 0.1 N NaOH solution consumed in titration until a pH values of 8.2 and the results were expressed as citric acid percentage. Fruit color changes were measured with a Minolta colormeter (Model CR-400; Osoka, Japan). L shows brightness (0 black, 100 white), 'a' shows green color change (60 green, +60 red), b bluish change (-60 blue, +60 yellow), C color intensity (low values indicate dark color) and h (hue) angle value (0 red-violet, 90 yellow, 180 blue-green, 270 blue).

In order to find the total phenolic content; 5 g fresh pepper tissue was extracted with 25 ml of 80% methanol and homogenized at medium speed in a homogenizer (Ika Ultra-Turrax T25 Basic, Germany) for 2 min. Then the mixture was kept in dark for 14-16 hours at 4 °C. Samples were filtered through filter papers and tubed. Samples were stored at -20 °C until the analyses. Total phenolic content was determined by a spectrophotometer (Varian Bio 100, Australia) in accordance with Swain and Hillis' method (1959), in which the Folin-Ciocaltaeu calorimetric method was modified. The absorbance of the samples in the spectrophotometer at wavelength of 725 nm was identified, and total phenolic content was expressed as Gallic acid equivalent (GAE) mg/100 g fresh weight (FW).

Antioxidant capacity specified by Benzie and Starin (1996), Ferric Reducing Antioxidant Power (FRAP), was used to determine the total antioxidant capacity. The absorbance of the samples in the spectrophotometer at a wavelength of 593 nm was identified and the total antioxidant capacity was expressed as μmol trolox equivalent (TE) / g FW.

Experimental data were subjected to variance analysis with SPSS 11.5 software in accordance with randomized sampling design. Means were compared with Duncan's multiple range test at $p < 0.05$. LSD (Least Significant Differences) test was used to analyze the differences between treatments and intervals.

Results and discussion

The titratable acidity values of the 'cv. Mertcan F1' pepper fruits increased slightly with Ca and post-harvest UV-C treatments during the 10-day storage period (*Table 1*). The effects of all treatments on TA were found to be insignificant ($p > 0.05$). It can also be stated that increase in TA and SSC was resulted from loss of water in fresh peppers in time. Despite the slight increases in TA, as stated by Rao et al. (2011), use of fruit organic acid in respiration slowed down the conversion of carbon dioxide and water. Parallel to present findings, Erdogmus et al. (2015) reported insignificant changes in 1% and 2% $CaCl_2$ – treated 'Yalova Yaglik 28' pepper fruits throughout the storage for 15 and 30 days at 7.5 °C with 90% relative humidity (RH). Likewise, Rao et al. (2011) found that 1.5% $CaCl_2$ treatments preserved TA of 'Indra' fresh sweet peppers during storage during 18 days at 10 °C and 25 °C shelf life as compared to the control fruits. Such slight changes in TA ensure that pepper taste could be preserved for a long time.

The pH values of 'cv. Mertcan F1' pepper fruits did not change much in the first 8 days of storage, while the values decreased in the last 2 days (*Table 1*). Similar to present study, Rao et al. (2011) applied calcium to peppers, Abbasi et al. (2015) applied UV-C to 'Royal Wonder' bell peppers and they both indicated insignificant effects of experimental treatments on pH values of the peppers

http://www.aloki.hu ● ISSN 1589 1623 (Print) ● ISSN 1785 0037 (Online)
DOI: http://dx.doi.org/10.15666/aeer/1605_72437252
© 2018, ALÖKI Kft., Budapest, Hungary

throughout the storage. In present study, slight increase in titratable acidity at the end of storage was effective in reducing the pH values.

The effects of treatments and storage periods on SSC ratios were also found to be insignificant ($p > 0.05$). There was a slight increase in SSC ratios in all treatments as compared to the initial values (*Table 1*). The UV-C applications of Vicente et al. (2005) to 'Zafiro' pepper and Abbasi et al. (2015) to 'Royal Wonder' bell pepper and $CaCl_2$ application of Rao et al. (2011) to 'Indra' sweet pepper preserved the SSC values as it was in present study. The SSC increase was high at the beginning due to water loss. With the progress of ripening throughout the storage, inherent sugar is used for respiration, thus increase in SSC slowed down toward to end of storage.

As compared to the initial values, color lightness (L*) values decreased in control and Ca treatments and brightness values increased in UV-C and Ca + UV-C treatments during the first 2 days and then decreased until the 4th day. At the end of the 10th day, the effects of all treatments on brightness was not found to be significant ($p > 0.05$). The change in brightness values was irregular in all treatments and they all had different results (*Table 1* and *Fig. 1*). Such changes in color parameters were attributed different maturity levels at harvest. Abbasi et al. (2015) reported that UV-C treatments did not have significant effects on L* values of 'Royal Wonder' bell pepper. In present study, despite fluctuations during cold storage, there was no significant change in the initial value of L* during the 10 days of storage. As indicated also by Abbasi et al. (2015), such insignificant effects of UV-C treatments were because of the chemical structure of the wax layer over the cuticle and its effects on the reflection of light.

Table 1. *Effects of Ca and UV-C treatments on pH, titratable acidity (TA), soluble solids content (SSC), pH, total phenolic content (TPC), total antioxidant capacity (TAC) and color parameters (L*, a*, b*, C and h^o) of pepper fruits stored at 0 °C and 90-95% relative humidity for 10 days*

Parameter	Storage time	Control	Control+UV	Ca	Ca+UV
pH	0	6.610 ± 0.010 A a	6.425± 0.175A a	6.220± 0.180Aab	6.360± 0.210A a
	2	6.310 ± 0.010 A b	6.400 ±0.030A a	6.460± 0.010A a	6.015± 0.135B a
	4	6.065 ± 0.025 A b	6.105 ±0.205A a	6.055± 0.045A b	6.405 ±0.265A a
	6	6.160 ± 0.010 A b	6.205 ±0.005A a	6.305± 0.025Aab	6.220 ±0.110A a
	8	6.240 ± 0.060 B b	6.450 ±0.040A a	6.485± 0.035A a	6.440 ±0.040A a
	10	5.795 ± 0.155 A c	6.055 ±0.145A a	6.055± 0.165A b	5.900 ±0.070A a
SSC	0	3.950 ± 0.050 A a	3.850 ±0.150A a	4.050± 0.350A a	4.400 ±0.200A a
	2	3.950 ± 0.350 A a	4.100 ±0.500A a	4.250± 0.050A a	4.450 ±0.050A a
	4	4.350 ± 0.150 A a	4.050 ±0.350A a	4.550± 0.250A a	4.650 ±0.250A a
	6	4.050±0.350 A a	4.350 ±0.150A a	4.450± 0.150A a	4.700± 0.300A a
	8	4.300 ± 0.200A a	4.450 ±0.150A a	4.500± 0.200A a	4.700± 0.200A a
	10	4.400 ± 0.000A a	4.300 ±0.000A a	4.450±0.050Aa	4.600± 0.200A a
TE	0	0.029 ± 0.003A c	0.032± 0.000A a	0.029± 0.003Acd	0.032± 0.000A c
	2	0.029 ± 0.003A c	0.032 ±0.000A a	0.032± 0.000Acd	0.029 ±0.003A c
	4	0.035 ± 0.003A bc	0.042 ±0.010A a	0.026± 0.000A d	0.042 ±0.003A b
	6	0.035 ± 0.003A bc	0.035 ±0.003A a	0.035± 0.003Abc	0.042 ±0.003A b
	8	0.042 ± 0.003A b	0.042 ±0.003A a	0.042± 0.003Aab	0.045± 0.000A ab
	10	0.048 ± 0.003A a	0.048 ±0.003A a	0.048± 0.003A a	0.051± 0.000A a

http://www.aloki.hu ● ISSN 1589 1623 (Print) ● ISSN 1785 0037 (Online)
DOI: http://dx.doi.org/10.15666/aeer/1605_72437252
© 2018, ALÖKI Kft., Budapest, Hungary

L*	0	40.255±1.725A ab	40.215 ±0.415A ab	41.330±0.010A a	40.075± 0.645A ab
	2	39.730 ± 0.470B ab	41.310 ±0.420A a	40.15±0.32ABab	40.640± 0.320AB a
	4	38.685 ± 0.435B b	39.685 ±0.165A b	38.170± 0.090Bb	38.310± 0.020B ab
	6	42.050 ± 0.010A a	40.070 ±0.350B ab	39.905± 0.655Bab	41.705± 0.145A a
	8	41.185 ± 0.165A ab	40.870±0.290ABab	41.620± 0.370A a	38.925± 0.935B ab
	10	34.630 ± 0.400A c	35.520 ±0.550A c	33.495± 1.535A c	36.125± 2.395A b
a*	0	-17.685 ± 0.445A bc	-16.930 ±0.070A c	-17.370± 0.120A b	-16.835± 0.005A bc
	2	-160.630±0.370A bc	-17.430 ±0.140A c	-16.560 ±0.070A b	-16.775 ±0.365A bc
	4	-16.290± 0.120A bc	-16.760 ±0.240Abc	-16.175± 0.275A b	-16.090 ±0.070A b
	6	-17.120±0.330A bc	-16.550 ±0.140A b	-16.510± 0.260A b	-16.940 ±0.350A bc
	8	-18.015± 0.465A c	-18.340 ±0.000A d	-18.590± 0.170A b	-17.440± 0.400A c
	10	-13.930± 0.730A a	-15.060 ±0.380A a	-13.070± 1.570A a	-13.290± 0.400A a
b*	0	27.340 ±0.090A ab	25.670 ±B cd0.520	27.105± 0.185A b	25.010± 0.310B ab
	2	24.725± 0.865ABcd	27.595 ±0.205A ab	24.450± 0.000AB c	25.215± 1.175AB ab
	4	24.925±0.365A bcd	26.590 ±0.580A bc	24.640± 0.980A c	24.520 ±0.210Ab
	6	26.660 ±0.740A abc	24.460 ±0.090ABd	23.980± 0.470B c	25.350 ±0.660AB ab
	8	28.625±1.045A a	29.240 ±0.110A a	29.800± 0.840A a	27.055± 0.465A a
	10	23.325±0.565A d	24.930 ±0.880A cd	23.235± 1.005A c	24.335± 0.305A b
Chroma (C*)	0	32.580 ±0.310A ab	30.755 ±0.465B cd	32.195± 0.215A ab	30.150± 0.260B ab
	2	29.805± 0.925ABbc	32.650 ±0.240A b	29.535± 0.035B bc	30.295± 1.185AB ab
	4	29.785± 0.375A bc	31.435 ±0.615A bc	29.485± 0.965A bc	29.340± 0.220A bc
	6	31.695 ± 0.795A ab	29.560 ±0.150ABd	29.120± 0.530B bc	30.495± 0.735AB ab
	8	33.845± 1.115 A a	34.520 ±0.090A a	35.140± 0.810A a	32.200± 0.610A a
	10	27.185± 0.865A c	29.130 ±0.950A d	26.725± 1.605A c	27.850± 0.000A c
Hue angle (h^o)	0	123.120± 0.430A a	123.530 ±0.430A b	122.710± 0.050A a	123.995± 0.325A a
	2	124.050± 0.400A a	122.390 ±0.040B c	124.180± 0.110A a	123.795± 0.605AB a
	4	123.285± 0.115A a	122.320 ±0.190A c	123.450± 0.620A a	123.460± 0.020A a
	6	122.835± 0.275C a	124.475±0.095ABa	124.630± 0.070A a	123.865± 0.185Ba
	8	122.505 ±0.465A ab	122.125 ±0.105A c	122.145±0.385Aab	123.035± 0.045A a
	10	120.850±0.850A b	121.135 ±0.295A d	119.370 ±1.840A b	118.800± 1.010A a
TPC	0	55.663± 0.000A a	55.163 ±1.375A a	55.788 ±1.125A a	57.662± 7.250A a
	2	60.100± 0.563A a	59.100 ±3.562A a	62.787 ±8.125A a	57.788± 0.000A a
	4	65.163± 0.250A a	58.038 ±4.375A a	61.600 ±13.062A a	62.162± 0.375A a
	6	65.350± 9.812A a	65.538 ±5.250A a	65.788 ±3.625A a	68.225± 1.188A a
	8	68.975± 1.937A a	57.413 ±0.000B a	63.225 ±4.812AB a	64.288± 0.000AB a
	10	67.788± 2.250A a	57.350 ±8.062A a	62.287 ±3.000A a	65.663± 5.875A a
TAC	0	15.892 ±0.000A a	15.517 ±0.542A a	14.433 ±0.792A a	15.767± 1.292A a
	2	16.142± 0.083A a	15.767 ±1.292A a	15.350 ±0.000A a	15.433± 1.125A a
	4	16.558± 0.083A a	15.683 ±3.542A a	18.142 ±2.667A a	17.433± 1.042A a
	6	20.850± 5.958A a	18.350 ±3.458A a	21.350 ±2.042A a	19.892± 0.500A a
	8	20.183± 0.000A a	16.267± 0.875A a	18.058 ±2.833A a	15.517± 1.375A a
	10	18.142 ±0.917A a	15.642± 3.167A a	17.975 ±1.083A a	18.850± 3.292A a

SEM: Standard error of mean

A, B, C →: In the same row, different upper cases indicate statistically significant differences between the groups ($p < 0.05$)

a, b, c ↓: In the same column, different lower cases indicate statistically significant differences between the storage time ($p < 0.05$)

http://www.aloki.hu ● ISSN 1589 1623 (Print) ● ISSN 1785 0037 (Online)
DOI: http://dx.doi.org/10.15666/aeer/1605_72437252
© 2018, ALÖKI Kft., Budapest, Hungary

The chroma (C*) values decreased in all treatments until the 6th day of storage, and then increased. At the end of the storage, the greatest chroma was observed in Ca treatments and the lowest value was observed in Ca + UV-C treatments with also the lowest initial chroma values. It can be stated based on present findings that Ca + UV treatments kept maturity going because had the least change and therefore in long-term pepper fruit storage, these treatments may be more effective than the other treatments. There is a decrease in h angle values in all treatments after the 6th day of storage (*Table 1* and *Fig. 1*). At the end of the 10-day storage, the lowest h angle value was obtained from Ca treatments and the greatest value was obtained from UV-C treatments. The effects of present treatments on a* values were not found to be significant ($p > 0.05$) throughout the storage period. Since a* values indicate the color change from green to red, control treatments were less effective than the other treatments. The effects of treatments on b* values were found to be significant only on 6th day of storage ($p < 0.05$) (*Table 1* and *Fig. 1*). Perez-Ambrocio et al. (2018) applied UV-C to Habanero chili pepper at various times and kept pepper fruits at 0 °C for 35 days. Contrary to present findings, researchers reported slightly increasing L* and a* values and decreasing b* values with UV-C treatments. Such differences were mainly resulted from differences in pepper types and harvest times.

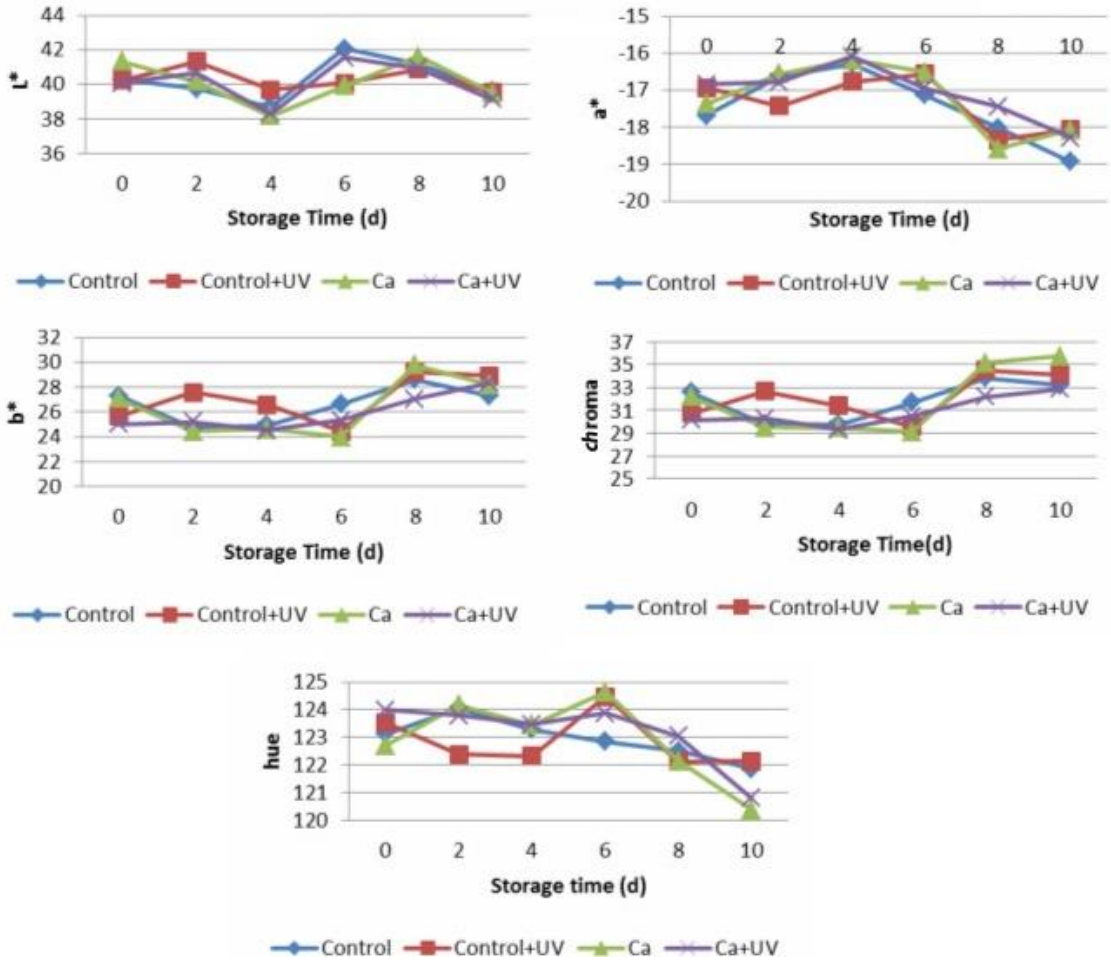

Figure 1. *Color parameters of pepper treated with Ca and UV-C light at the beginning and end of 10-day storage*

http://www.aloki.hu ● ISSN 1589 1623 (Print) ● ISSN 1785 0037 (Online)
DOI: http://dx.doi.org/10.15666/aeer/1605_72437252
© 2018, ALÖKI Kft., Budapest, Hungary

The effects of treatments and storage periods on total phenolic content and total antioxidant capacity of pepper were also not found to be significant ($p > 0.05$). In all treatments, a slight increase was observed in total phenolic content and total antioxidant capacity of the samples until the 6th day of storage, but afterwards a decrease was observed as compared to the initial values (*Table 1* and *Fig. 2*). Such an increase was an expected case as the physiological and pathological deterioration will increase with the prolongation of the cold storage period. Castro-Concha et al. (2014) investigated total phenolic content and antioxidant capacities of 'Habanero' (*Capsicum chinense*) peppers at different maturity levels and Perez-Ambrocio et al. (2018) applied UV-C to the same pepper cultivar for 0.5 and 3 min and both reported increased total phenolics and antioxidants. Such findings conflict with the present ones because of differences in pepper types and cultivation places. Researchers also indicated that 'Habanero' chili pepper had greater quantities of phenolics in research countries than in Mexico.

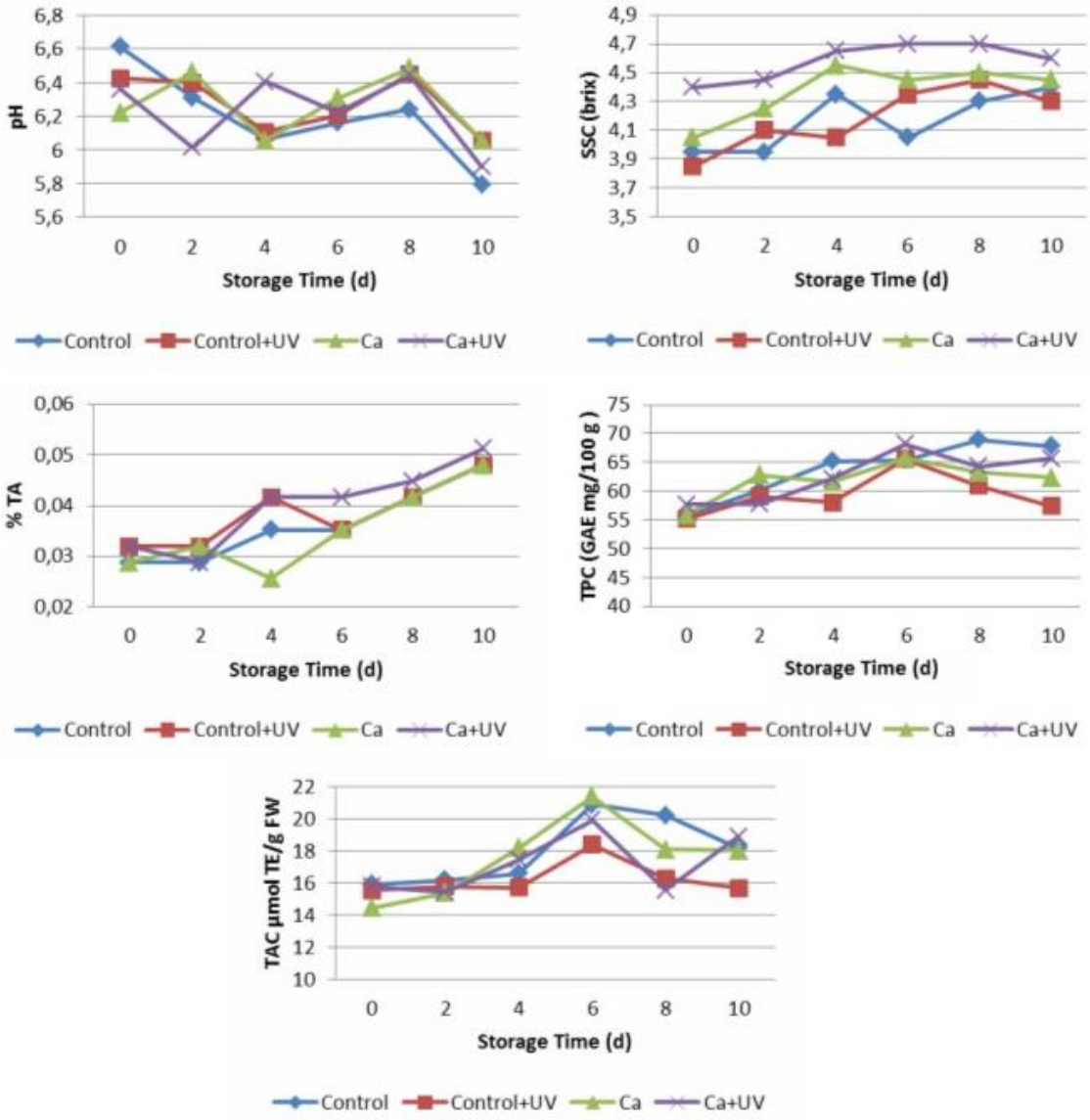

Figure 2. *The pH, titratable acidity (TA), soluble solids content (SSC), total phenolic content (TPC) and total antioxidant capacity (TAC) of 'cv. Mertcan F1' pepper for 10-day storage*

http://www.aloki.hu ● ISSN 1589 1623 (Print) ● ISSN 1785 0037 (Online)
DOI: http://dx.doi.org/10.15666/aeer/1605_72437252
© 2018, ALÖKI Kft., Budapest, Hungary

Conclusion

In general, Ca + UV-C treatments were found to be the most successful treatments for preservation of quality attributes throughout the cold storage. As compared to the initial values, Ca + UV-C treatments yielded the lowest changes in quality attributes after 10 days of storage. The Ca + UV-C treatments also reduced color changes and increased total phenolic content and total antioxidant capacity of the plants. Present findings revealed that UV-C treatments slowed the increase in total phenolic content and total antioxidant capacity. Therefore, it can be stated that Ca + UV-C treatments were quite effective in storage of peppers for longer periods and better quality.

As a result, since the post-harvest UV-C treatments do not contain any chemicals and pre-harvest Ca treatments have no adverse effect on human health, they can reliably be used in pepper storage for longer periods without significant losses in quality attributes.

Acknowledgements. This research received no specific grant from any funding agencies in the public, commercial, or none-profit sectors.

REFERENCES

[1] Abbasi, N. A., Ashraf, S., Ali, I., Butt, S. J. (2015): Enhancing storage life of bell pepper by UV-C irradiation and edible coatings. – Pak. J. Agri. Sci. 52(2): 403–411.
[2] Alothman, M., Bhat, R., Karim, A. A. (2009): Effects of radiation processing on phytochemicals and antioxidants in plant produce. – Trends Food Sci. Tech. 20: 201–212.
[3] Andrade-Cuvi, M. J., Vicente, A. R., Concellón, A., Chaves, A. R. (2011): Changes in red pepper antioxidants as affected by UV-C treatments and storage at chilling temperatures. – LWT-Food Sci. Technol. 44: 1666–1671.
[4] Benzie, I. E. F., Strain, J. J. (1996): The ferric reducing ability of plasma (FRAP) as a measure of "antioxidant power": the FRAP assay. – Analytical Biochemistry 239: 70–76.
[5] Castro-Concha, L. A., Tuyub-Che, J., Moo-Mukul, A., Vazquez-Flota, F. A., Miranda-Ham, M. L. (2014): Antioxidant capacity and total phenolic content in fruit tissues from accessions of *Capsicum chinense* Jacq. (Habanero pepper) at different stages of ripening. – Sci. World J. 1–5.
[6] Chen, F., Liu, H., Yang, H., Lai, S., Cheng, X., Xin Y, Yang, B., Hou, H., Yao, Y., Zhang, S., Bu, G., Deng, Y. (2011): Quality attributes and cell wall properties of strawberries (*Fragaria annanassa* Duch.) under calcium chloride treatment. – Food Chem. 126: 450–459.
[7] Crosby, K. M. (2008): Pepper. In: Prohens, J., Nuez, F. (Eds.), Vegetables, II: Fabaceae, Liliaceae, Umbelliferae, and Solanaceae. – Springer, New York.
[8] Demirdoven, A., Batu, A., Ece, A. (2006): Biberin modifiye atmosferde paketlenerek depolanmasi. – Gıda Teknolojileri Elektronik Dergisi 1: 1–7.
[9] Erdogmus, A. O., Kaynas, K., Kaya, S. (2015): Kirmızi biberde (*Capsicum annuum*L. cv. Kapya) bazi hasat sonrasi uygulamalarin depolama kalitesi uzerine etkileri. – COMÜ Zir. Fak. Derg. 3 (2): 45–53.
[10] FAOSTAT (2014): FAO Statistical Database. – http:// http://www.fao.org/faostat/en/#data/QC. Accessed on 11 December 2015.
[11] Frank, C. A., Nelson, R. G., Simonne, E. H., Behe, B. K., Simonne, A. H. (2005): Consumer preferences for color, price and vitamin C content of bell peppers. – HortScience 36: 795–800.
[12] Gunay, A. (2005): Sebze yetiştiriciliği, Cilt II. – Meta Basimevi, İzmir.
[13] Halloran, N., Yanmaz, R., Kasim, M. U., Kasim, R. (2000): Modified atmospheric storage of 'Kandil' bell pepper cultivar. – Gida. 25(2): 129–132.

http://www.aloki.hu ● ISSN 1589 1623 (Print) ● ISSN 1785 0037 (Online)
DOI: http://dx.doi.org/10.15666/aeer/1605_72437252
© 2018, ALÖKI Kft., Budapest, Hungary

[14] Hardenburg, R. E., Watada, A. E., Wang, C. Y. (1986): The Commercial Storage of Fruits, Vegetables and Florist and Nursery Stocks. Agriculture Handbook 66. – U.S. Dept. Agric. Research Service, Washington.
[15] Hernandez-Munoz, P., Almenar, E., Ocio, M. J., Gavara, R. (2006): Effect of calcium dips and chitosan coatings on postharvest life of strawberries (*Fragaria ananassa*). – Postharvest Biol. Technol. 39: 247–253.
[16] Koutchma, T., Popović, V., Ros-Polski, V., Popielarz, A. (2016): Effects of ultraviolet light and high-pressure processing on quality and health-related constituents of fresh juice products. – Compr. Rev. Food Sci. F. 15: 844–867.
[17] Lester, G. E., Grusak, M. A. (2000): Postharvest application of chelated and non-chelated calcium dip treatments to commercially grown honey dew melons: effects on peel attribute tissue calcium concentration, quality, and consumer preference following storage. – Hortic. Technol. 11: 561–566.
[18] Mercier, J., Baka, M., Reddy, B., Corcuff, R., Arul, J. (2001): Shortwave ultraviolet irradiation for control of decay caused by Botrytis cinerea in bell pepper: induced resistance and germicidal effects. – J. Am. Soc. Hort. Sci. 126: 128–133.
[19] Nyanjage, M., Nyalala, S. P. O., Illa, A. O, Mugo, B. W, Limbe, A. E, Vulimu, E. M. (2005): Extending post-harvest life of sweet pepper (*Capsicum annum* L.'California Wonder') with modified atmosphere packaging and storage temperature. – Agric. Trop. Subtrop. 38: 28–34.
[20] Pérez-Ambrocio, A., Guerrero-Beltrán, J. A., Aparicio-Fernández, X., Ávila-Sosa, R., Hernández-Carranza, P., Cid-Pérez, S., Ochoa-Velasco, C. E. (2018): Effect of blue and ultraviolet-C light irradiation on bioactive compounds and antioxidant capacity of habanero pepper (*Capsicum chinense*) during refrigeration storage. – Postharvest Biology and Tech. 135: 19–26.
[21] Rao, R. T. V., Gol, N. B., Shah, K. K. (2011): Effect of postharvest treatments and storage temperatures on quality and shelf life of sweet pepper (*Capsicum annum* L.). – Scientia Hoticulturae 132: 18–26.
[22] Rodov, V., Ben-Yehoshua, S., Fierman, T., Fang, D. (1995): Modified-humidity packaging reduces decay of harvested 'Red Bell' pepper fruit. – HortScience 30(2): 299–302.
[23] Salk, A., Arın, L., Deveci, M., Polat, S. (2008): Ozel sebzecilik. – Namik Kemal Universitesi Ziraat Fakultesi Basimevi, Tekirdag.
[24] Simonne, A. H., Simonne, E. H., Eitenmiller, R. R., Mills, H. A., Green, N. R. (1997): Ascorbic acid and provitamin A contents in unusually colored bell peppers (*Capsicum annuum* L.). – J. Food Comp. Anal. 10: 299–311.
[25] Snowdon, A. L. (1992): Color atlas of postharvest diseases and disorders of fruit and vegetables (Vol. 2). – Walfe Publishing, Aylesbury.
[26] Swain, T., Hillis, W. E. (1959): The phenolic constituents of *Prunus domestica*. I.— The quantitative analysis of phenolic constituents. – Journal of the Science of Food and Agriculture 10: 63–68.
[27] Vicente, A. R., Pineda, C., Lemoine, L., Civello, P. M., Martinez, G. A., Chaves, A. R. (2005): UV-C treatments reduce decay, retain quality and alleviate chilling injury in pepper. – Postharvest Biology and Tech. 35: 69–78.
[28] Vural, H., Esiyok, D., Duman, İ. (2000): Kultur sebzeleri (Sebze yetiştirme). – Ege Universitesi Basimevi, İzmir.
[29] Watkins, C. B. (2002): Ethylene Synthesis, Mode of Action Consequences and Control. – In: Knee, M. (ed.) Fruit Quality and Its Biological Basis. Sheffield Academic Press, Sheffield.

http://www.aloki.hu ● ISSN 1589 1623 (Print) ● ISSN 1785 0037 (Online)
DOI: http://dx.doi.org/10.15666/aeer/1605_72437252
© 2018, ALÖKI Kft., Budapest, Hungary

RHIZOBACTERIAL SWITCHING TOWARDS CLIMATE SMART AGROECOSYSTEMS

KAUSHAL, M.[1*] – KAUSHAL, R.[2]

[1]*International Institute of Tropical Agriculture*
Plot No. 25, Mikocheni B, Coca Cola Road, Dar es Salaam 34441, Tanzania

[2]*Department of Soil Science, Dr. Y. S. Parmar University of Horticulture and Forestry*
Nauni, Solan, Himachal Pradesh 173230, India

**Corresponding author*
email: kaushal.mbg@gmail.com

(Received 11th Aug 2018; accepted 4th Oct 2018)

Abstract. Climate smart agriculture is defined as a systematic and synergetic ingress for transformation and reorientation of agricultural development under constrained environment with climate risks. Enhanced plant productivity and reduced microbial respiratory C can potentially mitigate the rising of the atmospheric CO_2 however we are currently in shortfall of efficient routes to accomplish these objectives. Under future climate scenarios of exalted CO_2, rhizosphere microbes may serve important links in mediating plant productivity and soil C/N dynamics with optimization of root-soil interface mechanisms to achieve CSA goals. Study was undertaken to precisely quantify microbial biomass-carbon and microbial activity of rhizosphere region of cauliflower (*Brassica oleracea var. botrytis*) at two different agro-climatic zones. A native bacterial strain *Bacillus pumilus* isolated from cauliflower rhizosphere was employed that enhanced plant growth, nutrient uptake with improved soil nutrient status. Microbial biomass carbon (119.8 mg MB-C/ 100 g soil) was the highest with the application of *Bacillus pumilus* and 75% NP fertilizers at both locations. Moreover, the microbial activity was found to be the highest (0.18 mg CO_2/ g soil) with the same consortium up to 48 h and then followed a sudden decreasing trend. The results clearly suggest that *Bacillus pumilus* strains as bio-inoculants can be successfully employed for maintaining soil health being useful in context of climate smart agriculture goals.
Keywords: *Bacillus pumilus, microbial biomass, soil microbial activity, Pearson's correlation, principal component analysis*

Introduction

The hastily growing world population which is expected to be 8.9 billion by 2050 (UN, 2015), raised an alarming situation of increasing food demand. In a study done by Center for Study of Carbon Dioxide and Global Change revealed that about 70-100% increase in crop production is requisite to feed this consistently rising population (UN, 2015). Intensive farming, a tool of elevated yield however, promotes the use of chemical fertilizers and pesticides at peak levels with rapid existence of pests and diseases. When used frantically, these fertilizers and pesticides get accumulated in soil and in water leading to adverse impact on livestock and on human health, as well as on our ecosystem (Liu et al., 2012). Depletion of soil nutrients, diversification of croplands, genetic diversity and augmentation to global warming are the other well-known associated obstacles of intensive agriculture. Thus, considering long-term emphasis of soil quality and fertility there is an increasing interest in the use of climate smart agritechnology that can enhance crop yield as well as ensures sustainability and resilience (Hamilton et al., 2016). Climate smart agriculture (CSA) may be defined as a synergetic approach to transform and reorient agricultural development and security

http://www.aloki.hu ● ISSN 1589 1623 (Print) ● ISSN 1785 0037 (Online)
DOI: http://dx.doi.org/10.15666/aeer/1605_72537270
© 2018, ALÖKI Kft., Budapest, Hungary

under the horrified situation of climate change (Khatri-Chhetri et al., 2017). Sustainable productivity, enhanced resilience or adaptation and Green house gases (GHGs) mitigation are identified as the three interlinked pillars requisite to engender these agricultural food security goals. To achieve desired goals of food productivity, adaptation and GHG mitigation CSA approaches must involve the appropriate inclusion of beneficial bacteria. Revitalising soil quality is a major aspect of sustainable agriculture. Technologies like use of plant growth promoting microbes serves as a boon to crops with multifarious attributes. Despite of the restoration of soil fertility, rhizosphere microbes are lending with other perks such as stimulation of plant growth, boosting crop yield and resistance against diversified soil borne pathogens. Plant growth-promoting rhizobacteria (PGPR) can arouse plant growth by direct (fixation of nitrogen, solubilization of phosphorus etc.) or indirect (antibiosis, induction of systemic resistance etc.) mechanisms (Kaushal and Wani, 2016). Some of the common PGPR include genera *Acinetobacter, Alcaligenes, Arthrobacter, Azospirillum, Azotobacter, Bacillus pumilus, Beijerinckia, Burkholderia, Enterobacter, Erwinia, Flavobacterium, Rhizobium*, and *Serratia* (Anandaraj and Dinesh, 2008). Various studies have shown positive effects of PGPR on cereals (Shaharoona et al., 2006), fruits (Kavino et al., 2010) and vegetables (Kaushal et al., 2017) when either used alone or in combination with fertilizers for enhancing crop yields and have committed to the progress of sustainable agricultural systems. Impacts of PGPR on growth and yield parameters have been widely investigated, slight clue exists on the effects of PGPR on sensitive biochemical and microbial indices reflecting soil quality. Besides extra sensitive to environmental stress biochemical properties imparts rapid and authentic values on soil quality (Ding, 2010). The biochemical parameters comprise of the variables that are directly associated to microbial activity such as microbial biomass C and respiration. Microbial biomass C and respiration are considered as potential indicators of soil quality and management impacts (Dinesh and Ghoshal, 2013). Moreover, ameliorated microbial biomass C boosts plant productivity and reduced microbial respiratory C loss could potentially mitigate increasing atmospheric CO_2 concentrations. Nevertheless, our understanding of PGPR interactions with plants to regulate microbial biomass C and microbial respiration in the rhizosphere is still limited. We evaluated the effect of *Bacillus pumilus* inoculation with reduced applications of N and P on productivity of cauliflower and soil nutrient status under North Western Himalayas. *Bacillus pumilus* with 75% NP, improves cauliflower yield (by 27.65%) over recommended dose of fertilizers through several different mechanisms, such as enhancement of nutrient uptake and the suppression of plant diseases (Kaushal and Kaushal, 2015). Here, we hypothesized that use of PGPR along with reduced application of fertilizers (NP) would attenuate such negative impacts of sole NPK use on beneficial soil microbiota and their related functions.

Hence, the objective of the study was to figure out the impacts of *Bacillus pumilus* (native strains of PGPR isolated from cauliflower rhizosphere) applied with reduced application of NP fertilizers (urea and muriate of potash) on microbial biomass C and microbial activity (CO_2 evolution). Another objective was to determine the correlations between yield parameters of cauliflower, soil nutrient status and inoculated population of native strain impacting microbial biomass and activity.

http://www.aloki.hu ● ISSN 1589 1623 (Print) ● ISSN 1785 0037 (Online)
DOI: http://dx.doi.org/10.15666/aeer/1605_72537270
© 2018, ALÖKI Kft., Budapest, Hungary

Materials and methods

Site description

The study was conducted at two locations (Dr. Y. S. Parmar University of Horticulture and Forestry, Nauni, Solan and Regional Horticultural Research Station, Kullu) of Himachal Pradesh that belongs to North-Western Himalayan region of India as presented in *Figure 1*. Experiments was replicated twice at both locations in each year 2010 and 2011. Both locations differ slightly in geographical characteristics, physico-chemical and microbiological properties of soil as presented in *Table 1*. Rhizosphere soil sampling was done before sowing (Mar 2010 and 2011) and after harvest (May 2010 and 2011) of field trails at both locations replicated twice. Three randomized soil samples were collected from each plot to make one composite sample (100 g) with the help of a soil augur and up to a depth of 15-20 cm from all the treated plots and every replicated experiment.

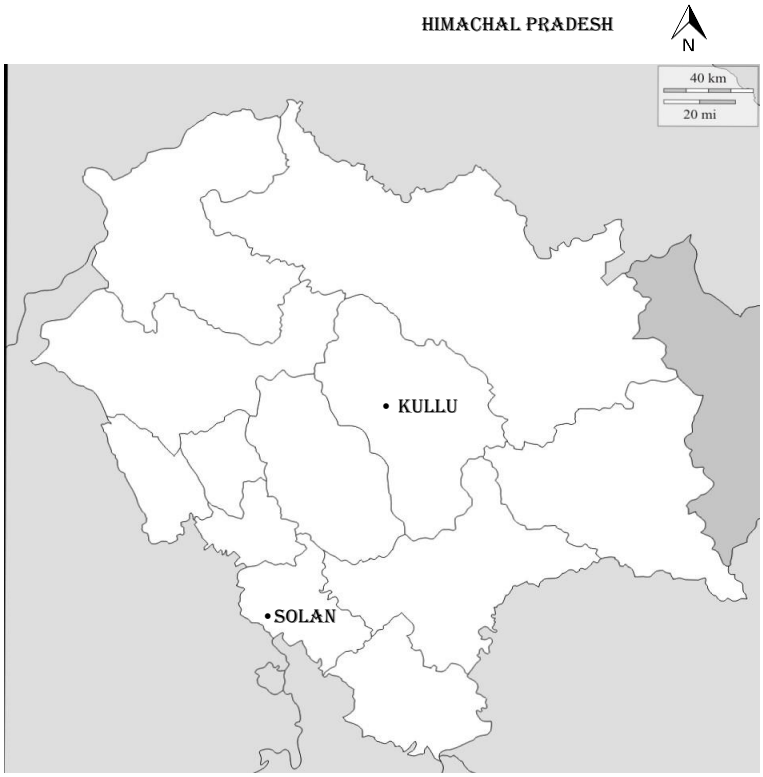

Figure 1. *Study area and sampling locations of rhizospheric soil samples*

Plant growth promoting rhizobacterial attributes of Bacillus pumilus

Isolated native bacterial strain from cauliflower (*Brassica oleracea var. botrytis*) was tested for its in vitro efficacy in ideal laboratory conditions before the field experimentations (Jan – Mar 2010) at Soil Microbiology Laboratory, Department of Soil Science and Water Management, Dr. Y S Parmar University of Horticulture and Forestry, Solan – India. Isolate was tested for major plant growth promoting attributes including P-solubilization, Indole acetic acid (IAA), siderophore and Hydrogen cyanide (HCN) production and antagonistic activities against phytopathogens (Kaushal et al.,

http://www.aloki.hu ● ISSN 1589 1623 (Print) ● ISSN 1785 0037 (Online)
DOI: http://dx.doi.org/10.15666/aeer/1605_72537270
© 2018, ALÖKI Kft., Budapest, Hungary

2016). Nitrogen fixation ability of native bacterial strain was also quantified indirectly by acetylene reduction assay (ARA) method and compared to standard strain (procured from the Institute of Microbial Technology, Chandigarh) of *Azotobacter chroococcum* (Hardy et al., 1968).

Table 1. *General characteristics of both locations (Solan and Kullu)*

Parameters/characteristics	Solan	Kullu
Longitude	77.0967° E	77.1095° E
Latitude	30.9045° N	31.9579° N
Altitude	1502 m	1279 m
pH	6.76	6.71
Electrical conductivity (EC) (dSm^{-1})	0.47	0.34
Bulk density (BD) (g cm^{-3})	1.04	1.50
Organic matter (OM) (%)	1.16	1.03
Nitrogen (N) (kg/ha)	301.7	313.6
Phosphorus (P) (kg/ha)	41.00	86.00
Potassium (K) (kg/ha)	195.3	191.7
Total microbial counts Nutrient agar (NA) (10^4 × cfu/g soil)	185.67	107.00

Field efficacy of Bacillus pumilus inoculation

Based on in vitro plant growth promoting traits and N_2-fixing abilities, field studies were conducted twice at both locations with *Bacillus pumilus* and reduced application of N and P fertilizers (Kaushal and Kaushal, 2015). The treatments: T1 (Uninoculated control), T2 (*Bacillus pumilus* +25% NP), T3 (*Bacillus pumilus* +50% NP), T4 (*Bacillus pumilus* +75% NP), T5 (*Bacillus pumilus* +100% NP), T6 (100% NPK), T7 (75% NPK), T8 (50% NP), T9 (*Bacillus pumilus*-inoculation) and T10 (Recommended dose of fertilizers) were arranged in randomized complete block design (RCBD) and replicated thrice. Calcium ammonium nitrate (25% N) and single super phosphate (16% P_2O_5) were the sources of nitrogen and phosphorus, respectively. Bacterial cell suspension (at OD 540 nm 1.00) of 72 h old cultures, grown in 10% nutrient broth, was used as inoculum. Data were collected on the growth and yield parameters of cauliflower, soil nutrient status and rhizospheric as well as endophytic microbial population and analysed over recommended dose of fertilizers. We used 20 plants/treated plot for analysing the data and each plant is harvested manually and recorded for growth and yield parameters which includes number of non-wrapper leaves, curd diameter and curd weight.

Efficacy of Bacillus pumilus inoculation on soil microbial biomass and microbial activity (CO2 evolution)

We analysed the incremental growth of microbial biomass-carbon and microbial activity (CO_2 evolution) over time. The fumigation–extraction method was used to analyse soil microbial biomass-C (CMIC) (Vance et al., 1987). Microbial activity was measured as the CO_2 evolved from moist soil, adjusted to 55% water holding capacity, and pre-incubated for 7 days at 20 °C in the dark. The CO_2 evolution was then measured

http://www.aloki.hu ● ISSN 1589 1623 (Print) ● ISSN 1785 0037 (Online)
DOI: http://dx.doi.org/10.15666/aeer/1605_72537270
© 2018, ALÖKI Kft., Budapest, Hungary

for the next 7 days using NaOH traps and titration with HCl and the metabolic quotient (qCO_2) was calculated (Salamanca et al., 2002).

Statistical analysis

All samples were measured in triplicate. The selected variables were compared between the tested soils using a one-way ANOVA. Significant differences were detected at the 0.05 level. Correlations between all measurable variables (plant, soil and microbial) were estimated using Pearson's r with $p < 0.05$ significance threshold. Principal components analysis (PCA) was conducted to determine and clarify the relationship between plant, soil and microbial parameters.

Results and discussion

Plant growth promoting rhizobacterial traits of Bacillus pumilus

Bacillus pumilus was the native bacterial strain isolated from rhizosphere of cauliflower. Our earlier published results confirmed that this strain displayed a very high ability towards most of the plant growth promoting attributes (Kaushal et al., 2017).

The isolate (*Bacillus pumilus*) produced a significantly higher concentration P-solubilization (664.33 µg/mL), IAA (29.67 µg/mL), maximum (51.36%) siderophore unit and HCN production (*Fig. 2*).

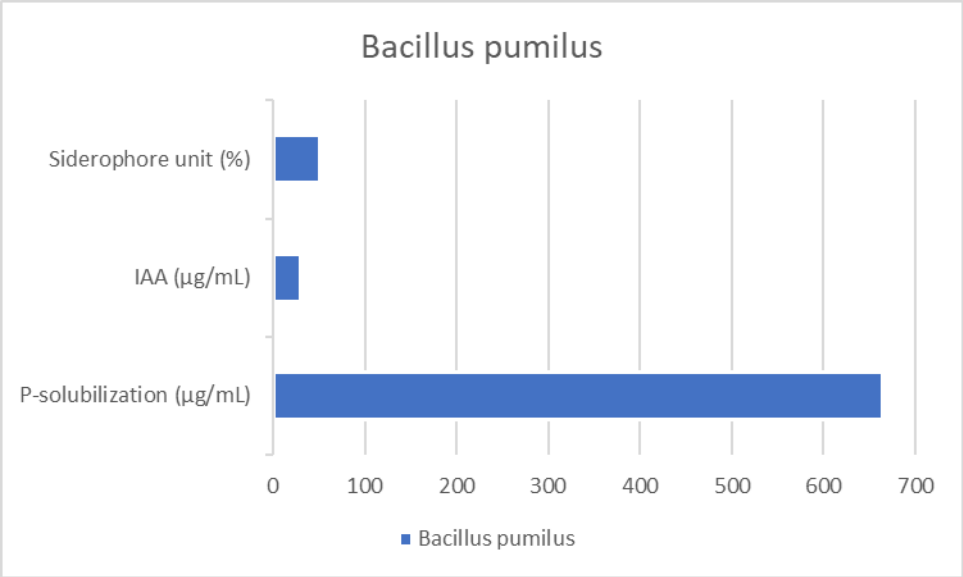

Figure 2. *Plant growth promoting activities of selected bacterial isolates (Bacillus pumilus). *Significance < 0.05*

Inorganic phosphate is solubilized by rhizosphere microbes with the production of organic acids and chelating oxo-acids from sugar (Cao et al., 2017). Thus, most quantitative analysis to evaluate the efficacy of phosphate-solubilizing bacteria due to the production of organic acids into surrounding medium are based on lowering pH (Bini et al., 2011). IAA produced by *B. pumilus* can enhance plant growth which was

http://www.aloki.hu ● ISSN 1589 1623 (Print) ● ISSN 1785 0037 (Online)
DOI: http://dx.doi.org/10.15666/aeer/1605_72537270
© 2018, ALÖKI Kft., Budapest, Hungary

the same as synthetic PGRs produced (Dasri et al., 2016). Siderophore and HCN production was also exhibited by *Bacillus pumilus* used as potential biocontrol agent of Fusarium in tomato (Heidarzadeh and Baghaee-Ravari, 2016). With regards to antagonistic activity against *Sclerotinia sclerotiorum*, culture filtrate of *Bacillus pumilus* exhibited very high antifungal antibiotic activity with an inhibition zone ranged from 20.2 to 22.4 mm. Our results are agreement with other researchers., who demonstrated that *Bacillus pumilus* strain is a promising biological control agent for control against Sclerotinia stem rot (Gao et al., 2014). *Bacillus pumilus* also showed higher nitrogenase activity, i.e., 437.26 ηmole C_2H_4 h^{-1} mg^{-1} protein (109 mg of N_2 fixed/ha/d), as compared to standard of *Azotobacter chroococcum*, i.e., 372.85 ηmole C_2H_4 h^{-1} mg^{-1} protein (93.0 mg of N_2 fixed/ha/d). In support to our results, a representative strain of *Bacillus pumilus* was identified that is also able to fix atmospheric N_2 as determined by the acetylene-dependent production assay (Castellano-Hinojosa et al., 2016).

Field efficacy of Bacillus pumilus inoculation

Our earlier published results confirmed that bio-inoculation of *Bacillus pumilus* at 75% of N and P fertilizers significantly enhanced all the growth and yield parameters of cauliflower such as number of non-wrapper leaves, curd weight and curd diameter (Kaushal and Kaushal, 2015).

Field experiment data of two years for both locations (replicated twice) revealed that bio inoculation of *Bacillus pumilus* along with 75% NP increased curd yield by 27.65% over recommended dose of fertilizers along with the saving of 25% NP (*Fig. 3*). Application of beneficial microbes to crop plants enhanced the fixation of atmospheric N, organic decomposition and augmented the soil properties by production of bioactive compounds such as vitamins, phytohormones which accelerated plant growth and yield (Upadhyay et al., 2012). The increase in levels of chemical fertilizers (NP) along with the bio-inoculation of *Bacillus pumilus* significantly enhanced NPK content in plants. Two years data (each replicated twice) revealed that N contents increased by 4.46% and 3.29%, P contents 0.49% and 0.57%, K contents 3.84% and 3.02% over uninoculated controls at Kullu and Solan, respectively. Uptake of N (77.14 kg/ha and 90.86 kg/ha) and P (35.28 kg/ha and 26.22 kg/ha) also boosted significantly with progressive increase in the supply of N and P nutrients along with bio-inoculation of *Bacillus pumilus* to the crop in both the years and locations. As far as ameliorations in plants nutrient status is concerned, enhanced nutrients like N, P and K might be due to enhanced vegetative growth and improved soil health leading to increased root formation. Studies reported enhanced N, P and K constituent of plant which might be attributed to presence of abundant number of soil microorganisms, microbial respiration and microbial biomass C and align with the findings of other researchers (Liu et al., 2012; Santibanez and Varnero, 2014). In addition, increased level of P might be due to presence of adequate organic acids which were released after organic matter decomposition and subsequently help in the solubilization of the indigenous phosphates. It was interesting to note that larger the total rhizosphere population, more is the accumulation of nitrogen, phosphorus and potassium contents in plants. Soil physico-chemical and nutrient status, i.e. pH, electrical conductivity (EC), bulk density (BD), organic matter (OM), N, P, K, was also assessed after harvest of crop (*Fig. 3*). Concentration of nutrients increased in soil with the combined use of *Bacillus pumilus* and NP fertilizers. The available nutrient contents N and P were increased by 2.56-32.00% and 6.66-40.72%, respectively over control. Bio-inoculation of *Bacillus*

http://www.aloki.hu ● ISSN 1589 1623 (Print) ● ISSN 1785 0037 (Online)
DOI: http://dx.doi.org/10.15666/aeer/1605_72537270
© 2018, ALÖKI Kft., Budapest, Hungary

pumilus not only improved the nutritional content particularly NPK of plants but also increased their uptake significantly over uninoculated control. This increase may be attributed to atmospheric nitrogen fixation, phosphate solubilization in the rhizosphere by *Bacillus pumilus*. The higher concentration of soil available nutrients with conjoint use of *Bacillus pumilus* and NP fertilizers may be attributed to well develop root system, significant improvement in soil physical properties and metabolic activity as well as rhizospheric and endophytic microbial population (Kaushal and Wani, 2016). The microbial analysis performed at the harvest of crop in each year at both the locations. The data revealed higher population of rhizospheric and endophytic bacteria in duly inoculated plots as compare to uninoculated control. The highest 162.5×10^8 cfu/g soil and 158.8×10^8 cfu/g soil rhizospheric population was recorded at Kullu and Solan, respectively. The lowest total bacterial counts were recorded under uninoculated control at both the locations. Also, endophytic bacterial population was highest 106.4×10^1 cfu/g root (Kullu) and 108.8×10^1 cfu/g root (Solan). At both the locations, the lowest endophytic bacterial counts were recorded with uninoculated control. The rhizosphere is a niche of beneficial microflora. Higher root exudation, OC, N and moisture content in amended organic fertilizers mechanized the microbes for their proliferation (Nagar et al., 2016). Decomposition of root tissue contribute ample energy in terms of C and N for the multiplication of bacteria enabling the growth of heavy microbial population (Singh et al., 2012). Moreover, increase in beneficial microbial population may be because of balanced water supply, particulate organic matter and presence of respirable substances (Majumdar et al., 2014). The study revealed that bio-inoculation of *Bacillus pumilus* supplied plots improved the cauliflower yield, physico-chemical properties of soil leading to enhanced soil microbiome (*Fig. 3*).

Efficacy of Bacillus pumilus inoculation on soil microbial biomass and microbial activity (CO2 evolution)

Soil microbial biomass-carbon (SMBC) was significantly higher in *Bacillus pumilus* + 75% NP plots (*Figs. 4* and *5*). This might be due to enhanced mineralization of organic leading to increased microbial activity (Nagar et al., 2016) as revealed in our studies also. SMBC at Kullu was 119.8 mg MB-C/ 100 g soil and Solan was 117.6 mg MB-C/ 100 g soil both with bio-inoculation of *Bacillus pumilus* + 75% of N and P fertilizers as presented in *Figures 4* and *5*. Similarly, various studies displayed that increased population of *Azotobacter*, PSB, soil enzymes, OC exhibited positive correlation with SMBC (Majumdar et al., 2014). Moreover, significiant improvement in SMBC in our experiments might be due to more stimulation in associated microbial populations. Treatments consisting of *Bacillus pumilus* bio-inoculation and chemical fertilizers (NP) increased the CO_2 evolution up to 48 h of incubation period and then followed a decreasing trend with the increase in incubation period at both the locations. However, the maximum CO_2-evolution was recorded 0.18 mg CO_2/ g soil (Kullu) and 0.17 mg CO_2/ g soil (Solan) with bio-inoculation of *Bacillus pumilus* + 75% of N and P fertilizers as presented in *Figures 6* and *7*. The basal soil respiration gives an estimate of total microbial activity, reflecting both the quantity and quality of the carbon sources (Liu et al., 2012). In present study, higher soil respiration sustained our notion that the rhizosphere soils had a dominant soil microbial activity, implying accelerated decomposition of organic residues that makes nutrients available for the consequent stimulation of heterotrophic microorganisms as observed by other researchers (Fall et

http://www.aloki.hu ● ISSN 1589 1623 (Print) ● ISSN 1785 0037 (Online)
DOI: http://dx.doi.org/10.15666/aeer/1605_72537270
© 2018, ALÖKI Kft., Budapest, Hungary

al., 2012). Moreover, the lower soil microbial metabolic quotient (qCO_2) displayed lower soil chemical stress to microbes, more worthwhile C utilization ability, low energy demand in microbial biomass supply and improved soil quality (Gonzalez-Quinones et al., 2011). Our results also suggested that inorganic fertilization did not increase soil respiration. Similar effects on soil respiration due to inorganic fertilization has been found when N fertilizer was added, possibly from the elimination of the decomposition of soil organic carbon due to reduction in microbial biomass (Yang et al., 2010; Ge et al., 2012).

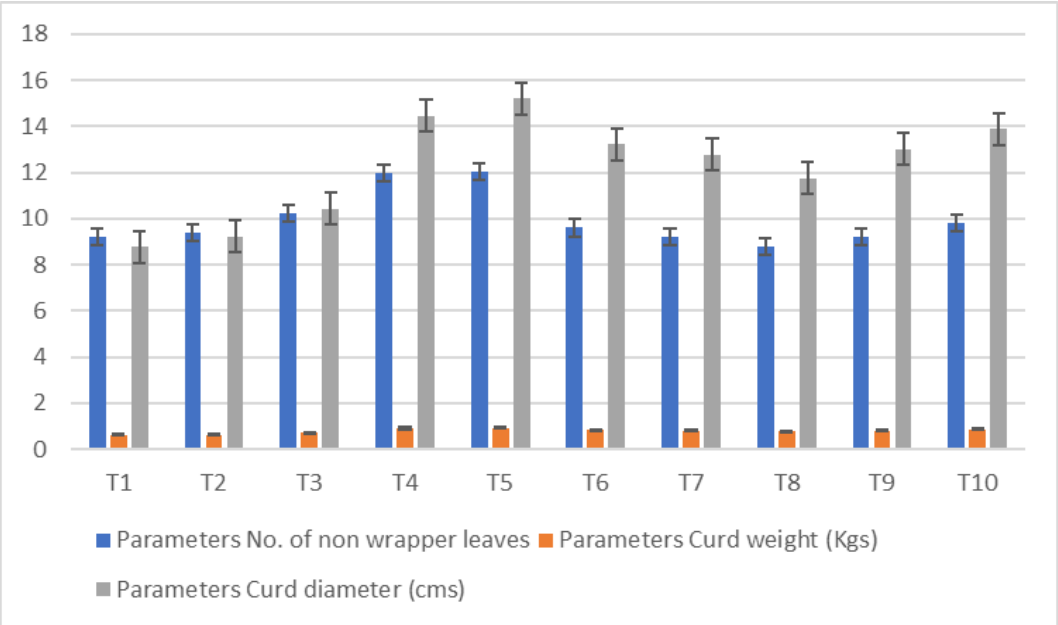

a

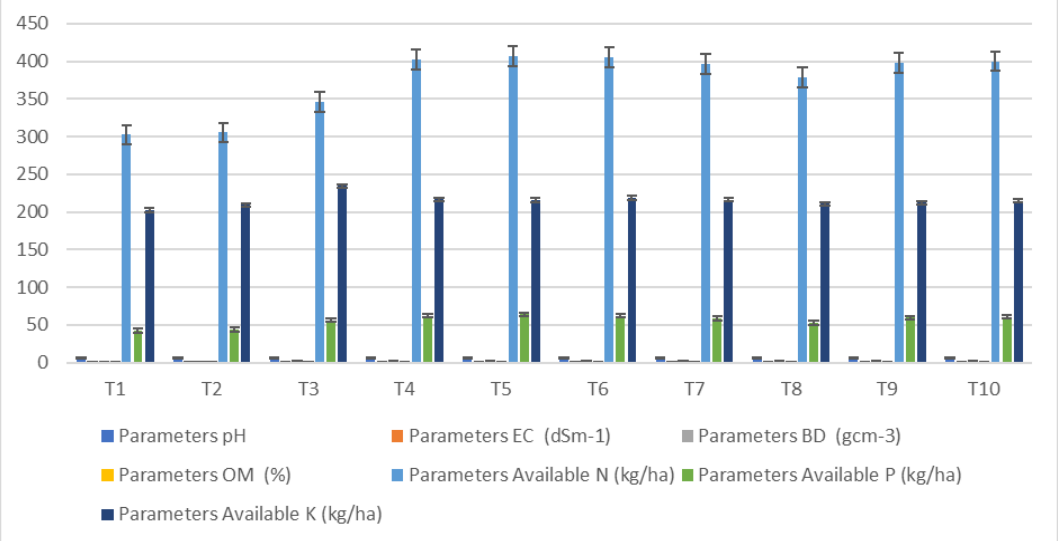

b

Figure 3. *Impact of selected bacterial isolates (Bacillus pumilus) on (a) plant and (b) soil parameters. T1 (uninoculated control), T2 (Bacillus pumilus + 25% NP), T3 (Bacillus pumilus + 50% NP), T4 (Bacillus pumilus + 75% NP), T5 (Bacillus pumilus + 100% NP), T6 (100% NPK), T7 (75% NPK), T8 (50% NP), T9 (Bacillus pumilus-inoculation) and T10 (recommended dose of fertilizers) *Significance < 0.05*

http://www.aloki.hu ● ISSN 1589 1623 (Print) ● ISSN 1785 0037 (Online)
DOI: http://dx.doi.org/10.15666/aeer/1605_72537270
© 2018, ALÖKI Kft., Budapest, Hungary

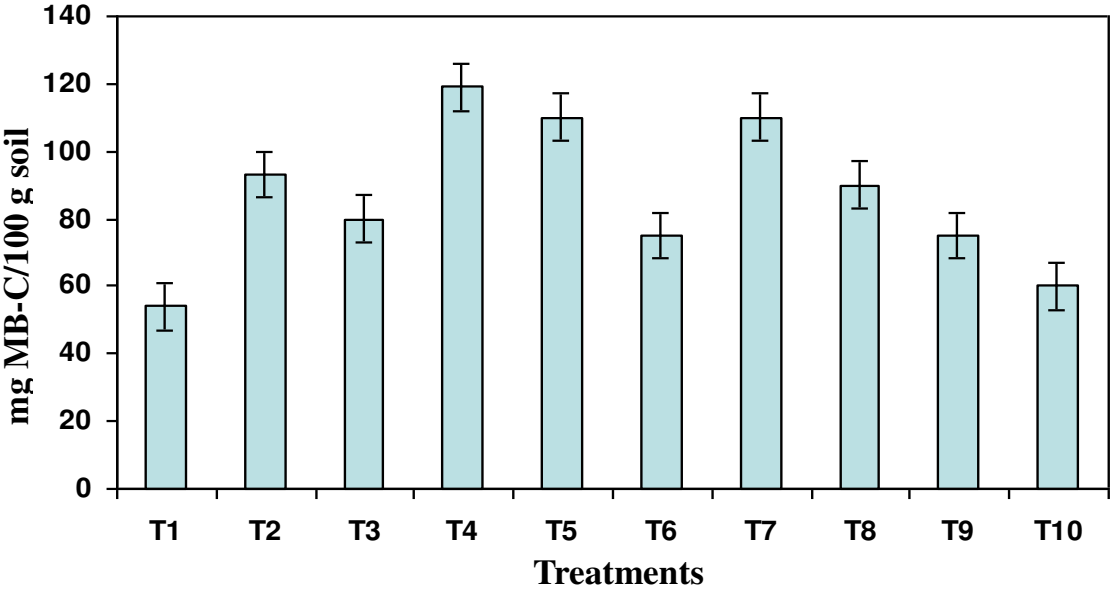

Figure 4. *Impact of bio-inoculation of Bacillus pumilus on microbial biomass-carbon at Solan. T1 (uninoculated control), T2 (Bacillus pumilus + 25% NP), T3 (Bacillus pumilus + 50% NP), T4 (Bacillus pumilus + 75% NP), T5 (Bacillus pumilus + 100% NP), T6 (100% NPK), T7 (75% NPK), T8 (50% NP), T9 (Bacillus pumilus-inoculation) and T10 (recommended dose of fertilizers). *Significance < 0.05*

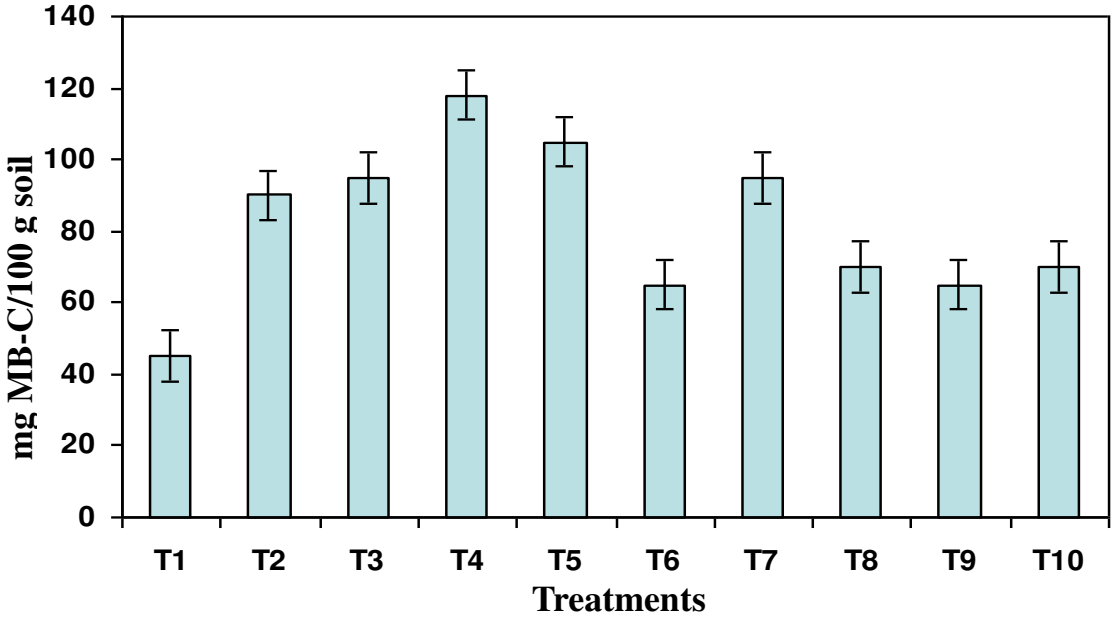

Figure 5. *Impact of bio-inoculation of Bacillus pumilus on microbial biomass-carbon at Solan. T1 (uninoculated control), T2 (Bacillus pumilus + 25% NP), T3 (Bacillus pumilus + 50% NP), T4 (Bacillus pumilus + 75% NP), T5 (Bacillus pumilus + 100% NP), T6 (100% NPK), T7 (75% NPK), T8 (50% NP), T9 (Bacillus pumilus-inoculation) and T10 (recommended dose of fertilizers). *Significance < 0.05*

http://www.aloki.hu ● ISSN 1589 1623 (Print) ● ISSN 1785 0037 (Online)
DOI: http://dx.doi.org/10.15666/aeer/1605_72537270
© 2018, ALÖKI Kft., Budapest, Hungary

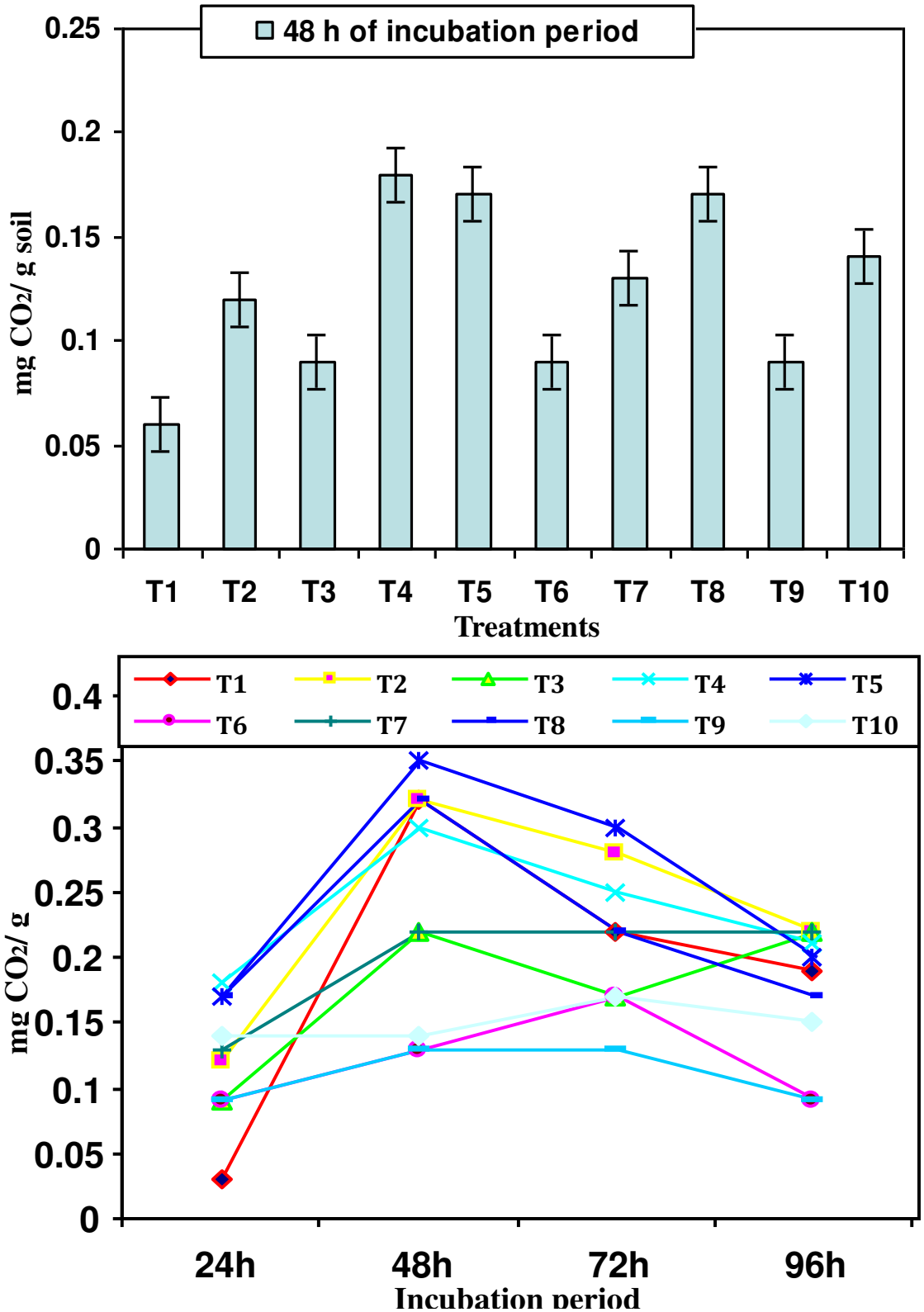

Figure 6. *Impact of bio-inoculation of Bacillus pumilus on microbial activity (CO_2 evolution) at Kullu. T1 (uninoculated control), T2 (Bacillus pumilus + 25% NP), T3 (Bacillus pumilus + 50% NP), T4 (Bacillus pumilus + 75% NP), T5 (Bacillus pumilus + 100% NP), T6 (100% NPK), T7 (75% NPK), T8 (50% NP), T9 (Bacillus pumilus-inoculation) and T10 (recommended dose of fertilizers). *Significance < 0.05*

http://www.aloki.hu ● ISSN 1589 1623 (Print) ● ISSN 1785 0037 (Online)
DOI: http://dx.doi.org/10.15666/aeer/1605_72537270
© 2018, ALÖKI Kft., Budapest, Hungary

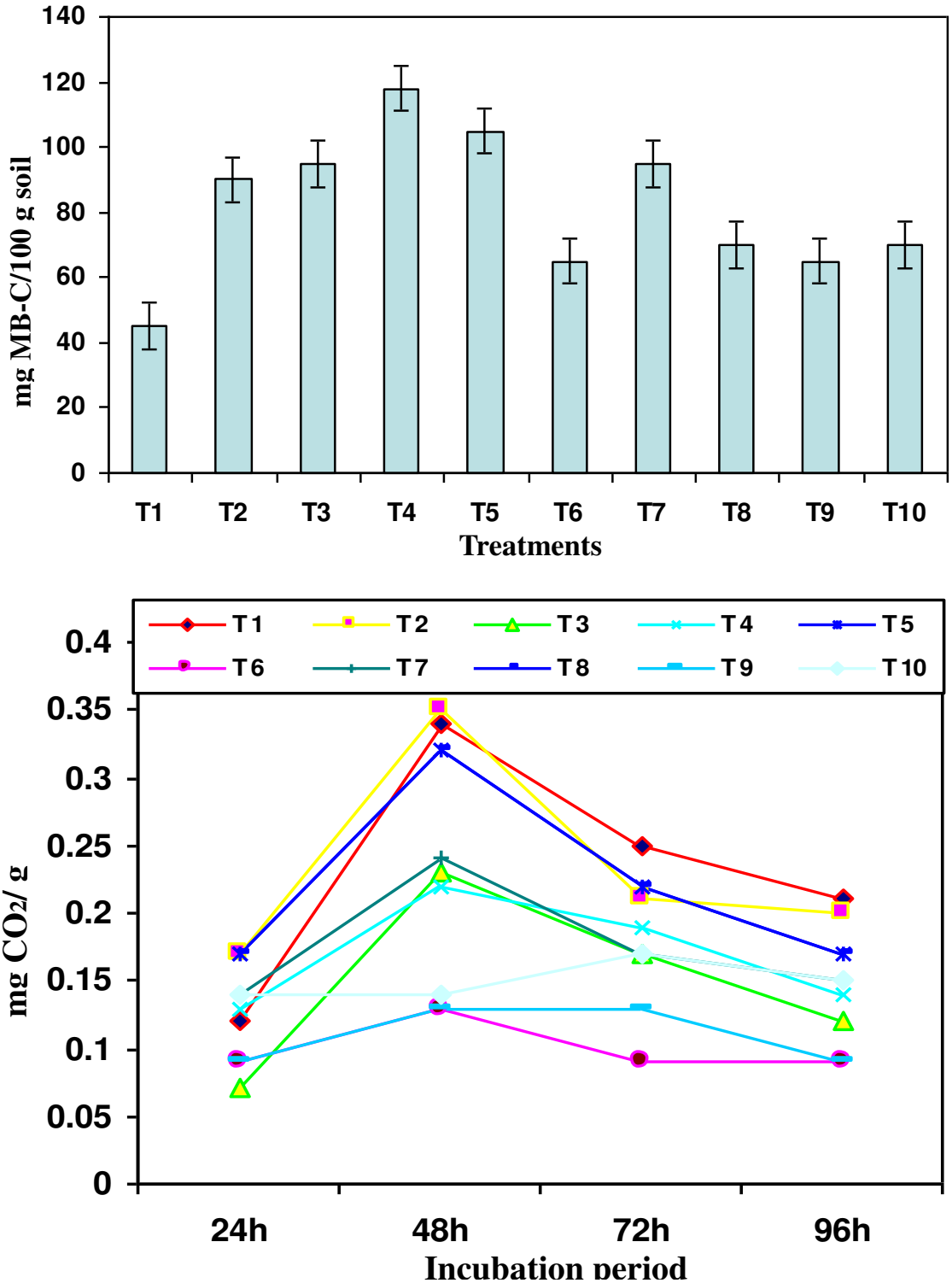

Figure 7. *Impact of bio-inoculation of Bacillus pumilus on microbial activity (CO_2 evolution) at Kullu. T1 (uninoculated control), T2 (Bacillus pumilus + 25% NP), T3 (Bacillus pumilus + 50% NP), T4 (Bacillus pumilus + 75% NP), T5 (Bacillus pumilus + 100% NP), T6 (100% NPK), T7 (75% NPK), T8 (50% NP), T9 (Bacillus pumilus-inoculation) and T10 (recommended dose of fertilizers). *Significance < 0.05*

http://www.aloki.hu ● ISSN 1589 1623 (Print) ● ISSN 1785 0037 (Online)
DOI: http://dx.doi.org/10.15666/aeer/1605_72537270
© 2018, ALÖKI Kft., Budapest, Hungary

Correlations analysis

Pearson correlation matrix revealed that many plant, soil and microbial variables were significantly correlated with each other The plant parameters, i.e. number of non-wrapper leaves, curd diameter, curd weight, curd yield, curd depth, soil physico-chemical, i.e. pH, EC, BD, OM, N, P, K, rhizospheric and endophytic bacterial population was significantly correlated at 5% level of significance at Kullu as given in *Table 2*. Significant positive correlation exists between curd diameter-N, P ($r = 0.49$, 0.48 respectively), curd diameter-rhizospheric bacterial population ($r = 0.42$), curd diameter-endophytic bacterial population ($r = 0.38$), curd weight-N, P ($r = 0.65$, 0.73, respectively), curd weight-rhizospheric bacterial population ($r = 0.35$), curd weight-endophytic bacterial population ($r = 0.50$), curd yield-N, P ($r = 0.65$, 0.73 respectively), curd yield-rhizospheric bacterial population ($r = 0.35$) curd yield-endophytic bacterial population ($r = 0.50$), curd depth-N, P ($r = 0.50$, 0.51 respectively), curd depth-rhizospheric bacterial population ($r = 0.32$), curd depth-endophytic bacterial population ($r = 0.33$), N-rhizospheric bacterial population ($r = 0.42$), P-rhizospheric bacterial population ($r = 0.43$), P-endophytic bacterial population ($r = 0.32$) and between K-endophytic bacterial population ($r = 0.53$). The plant parameters, i.e. number of non-wrapper leaves, curd diameter, curd weight, curd yield, curd depth, soil physico-chemical, i.e. pH, EC, BD, OM, N, P, K, rhizospheric and endophytic bacterial population was significantly correlated at 5% level of significance at at Solan as given in *Table 3*. Significant positive correlation exists between number of non-wrapper leaves-N, P ($r = 0.32$, 0.52 respectively), number of non-wrapper leaves-rhizospheric bacterial population ($r = 0.41$), curd diameter-N, P ($r = 0.47$, 0.59 respectively), curd diameter-rhizospheric bacterial population ($r = 0.46$), curd diameter-endophytic bacterial population ($r = 0.35$), curd weight-N, P ($r = 0.76$, 0.84 respectively), curd weight-rhizospheric bacterial population ($r = 0.38$), curd yield-N, P ($r = 0.76$, 0.84, respectively), curd yield-rhizospheric bacterial population ($r = 0.38$), curd depth-N, P ($r = 0.52$, 0.68, respectively), curd depth-rhizospheric bacterial population ($r = 0.37$), P-rhizospheric bacterial population ($r = 0.47$) and between P-endophytic bacterial population ($r = 0.31$). In our results, positive correlation between plant, soil and bacterial variables was obtained which showed a considerably positive relationship. Enhanced SMBC might be one of the determinant factor of this positive relationship. Moreover, as predicted in our findings, MBC is the important source of C supplying higher energy to the microbes leading to enhanced metabolic activities (Liu et al., 2017). The rhizosphere microbial community is recognized to be closely related to soil health and quality (Raaijmakers and Mazzola, 2016). The positive correlation between N-rhizospheric bacterial population ($r = 0.42$), P-rhizospheric bacterial population ($r = 0.43$), P-endophytic bacterial population ($r = 0.32$) and between K-endophytic bacterial population ($r = 0.53$) revealed in the field experiments corresponds with many previous studies, suggesting that the soil quality is directly related to bacterial population occurrence and could therefore be used as an indicator for soil fertility prediction. Moreover, bio-inoculation of *Bacillus pumilus* significantly induce the community shift of culturable bacteria in the rhizosphere soil leading to improved soil microbial biomass. From a long-term perspective, appropriate application of *Bacillus pumilus* can improve the soil quality and fertility. This comprises both nutrients (e.g., aggregation of organic matter) and structure (e.g., aggregates accumulation), which is conductive to agricultural sustainable development. The results also suggested a positive effect of N application on microbial biomass-C. After N application, N

http://www.aloki.hu ● ISSN 1589 1623 (Print) ● ISSN 1785 0037 (Online)
DOI: http://dx.doi.org/10.15666/aeer/1605_72537270
© 2018, ALÖKI Kft., Budapest, Hungary

availability increased and consequently microbes immobilized N, which subsequently increased microbial biomass-C (Chaparro et al., 2014). A clear positive effect of combined application of *Bacillus pumilus* and NP on microbial biomass and microbial activity was observed. Microbial activity also varies considerably among the treatments including control. The metabolic quotient (soil respiration per unit of microbial biomass) reflects the maintenance energy requirement of soil microbes and can be a relative measure of how efficiently the soil microbial biomass is utilizing C resources, as well as the degree of substrate limitation for soil microbes (Xun et al., 2016). The results in this study did show changes in the microbial pool that would suggest changes in microbial biomass-C and activity as well (*Tables 2* and *3*). In contrast, combined application of *Bacillus pumilus* and NP treatments indicated relatively highly efficient microbial community and better use of the available organic substrates. On the contrary, the Pearson's correlation indicated strongly positive correlation between microbial biomass and plant and soil parameters (*Tables 2* and *3*). All the soil factors controlling microbial biomass-C had significant effects on microbial respiration (CO_2 evolution) as described by the correlation analysis.

Principal components analysis was used to determine the factors related to soil microbial properties. The two components (PC1 and PC2) explained 63.54% and 12.82% of the total variance. The PC1 and PC2 were chosen to draw a biplot, because of explaining 76.36% of the total variance together as presented in *Figure 8*. PCA was weighted by physico-chemical (pH, EC, BD, OM, N, P and K), which exhibited a more powerful influence on discrimination in soil samples and microbiological (rhizospheric and endophytic bacterial population) variables together with growth and yield components. Thus, PCA allowed us to detect the subtle differences in plant, soil physical-chemical and microbial factors among the studied parameters. Additionally, the high soil organic matter (SOM) and N contents as material basis largely contribute to the high microbial biomass and basal respiration. Also, changes in SOM and N application affects soil microbial biomass (SOM/N ∝ SMBC). As far as soil quality is concerned, microbial diversity should be well considered when vast of N fertilizer was added to soils in agricultural practice.

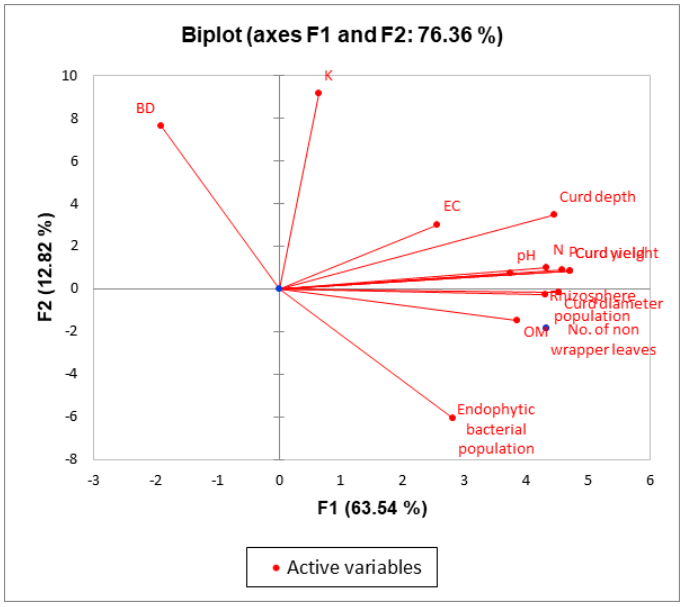

Figure 8. *PCA-ordination biplot of plant, soil and microbial parameters*

http://www.aloki.hu ● ISSN 1589 1623 (Print) ● ISSN 1785 0037 (Online)
DOI: http://dx.doi.org/10.15666/aeer/1605_72537270
© 2018, ALÖKI Kft., Budapest, Hungary

Table 2. *Pearson's correlation coefficient (r value) between plant, soil parameters, rhizospheric and endophytic population under field conditions experiment at Kullu (n = 30)*

Parameters	No. non wrapper leaves	Curd diameter	Curd weight	Curd yield	Curd depth	pH	Electrical conductivity (EC)	Bulk density (BD)	Organic matter (OM)	Nitrogen (N)	Phosphorus (P)	Potassium (K)	Rhizospheric bacterial population	Endophytic bacterial population
No. non wrapper leaves	1.00													
Curd diameter	0.49*	1.00												
Curd weight	0.28	0.64*	1.00											
Curd yield	0.28	0.64*	1.00	1.00										
Curd depth	0.21	0.68*	0.61*	0.61*	1.00									
pH	0.11	-0.04	-0.01	-0.01	0.005	1.00								
Electrical conductivity (EC)	0.15	-0.03	-0.02	-0.02	-0.18	0.14	1.00							
Bulk density (BD)	-0.12	-0.04	0.07	0.07	-0.002	-0.15	-0.01	1.00						
Organic matter (OM)	-0.04	0.06	0.16	0.16	0.01	-0.03	0.08	-0.04	1.00					
Nitrogen (N)	0.09	0.49*	0.65*	0.65*	0.50*	0.13	-0.05	0.09	0.35*	1.00				
Phosphorus (P)	0.17	0.48*	0.73*	0.73*	0.51*	0.14	-0.007	0.16	0.30*	0.88*	1.00			
Potassium (K)	-0.10	-0.10	-0.13	-0.13	-0.07	0.02	0.12	-0.03	-0.05	-0.17	0.07	1.00		
Rhizospheric bacterial population	0.17	0.42*	0.35*	0.35*	0.32*	0.13	0.16	-0.13	0.12	0.42*	0.43*	0.09	1.00	
Endophytic bacterial population	0.27	0.38*	0.50*	0.50*	0.33*	-0.001	-0.05	-0.05	-0.02	0.29	0.32*	-0.002	0.53*	1.00

*Significant correlation at $\alpha = .05$ level

http://www.aloki.hu ● ISSN 1589 1623 (Print) ● ISSN 1785 0037 (Online)
DOI: http://dx.doi.org/10.15666/aeer/1605_72537270
© 2018, ALÖKI Kft., Budapest, Hungary

Table 3. *Pearson's correlation coefficient (r value) between plant, soil parameters, rhizospheric and endophytic population under field conditions experiment at Solan (n = 30)*

Parameters	No. non wrapper leaves	Curd diameter	Curd weight	Curd yield	Curd depth	pH	Electrical conductivity (EC)	Bulk density (BD)	Organic matter (OM)	Nitrogen (N)	Phosphorus (P)	Potassium (K)	Rhizospheric bacterial population	Endophytic bacterial population
No. non wrapper leaves	1.00													
Curd diameter	0.35*	1.00												
Curd weight	0.45*	0.54*	1.00											
Curd yield	0.45*	0.54*	1.00	1.00										
Curd depth	0.36*	0.40*	0.57*	0.57*	1.00									
pH	-0.17	0.26	0.21	0.21	-0.06	1.00								
Electrical conductivity (EC)	0.08	0.07	0.18	0.18	0.19	0.11	1.00							
Bulk density (BD)	0.09	-0.23	-0.02	-0.02	0.09	-0.22	0.09	1.00						
Organic matter (OM)	0.04	0.12	0.27	0.27	0.21	0.18	0.39*	0.04	1.00					
Nitrogen (N)	0.32*	0.47*	0.76*	0.76*	0.52*	0.22	0.13	-0.19	0.17	1.00				
Phosphorus (P)	0.52*	0.59*	0.84*	0.84*	0.68*	0.20	0.14	-0.17	0.26	0.83*	1.00			
Potassium (K)	0.07	-0.09	0.06	0.06	-0.07	0.17	0.15	-0.02	0.12	0.06	0.07	1.00		
Rhizospheric bacterial population	0.41*	0.46*	0.38*	0.38*	0.37*	0.10	0.07	-0.15	0.26	0.26	0.47*	0.05	1.00	
Endophytic bacterial population	0.22	0.35*	0.22	0.22	0.26	-0.12	-0.14	-0.04	0.08	0.26	0.31*	-0.05	0.42*	1.00

*Significant correlation at $\alpha = .05$ level

http://www.aloki.hu ● ISSN 1589 1623 (Print) ● ISSN 1785 0037 (Online)
DOI: http://dx.doi.org/10.15666/aeer/1605_72537270
© 2018, ALÖKI Kft., Budapest, Hungary

Conclusion

The inference could be drawn that inclusion of rhizobacteria in CSA ensures win win results of enhanced sustainable productivity, resilience and reduced GHG emissions. The conjoint application of *Bacillus pumilus* + NP (75%) showed higher impacts on plant productivity as well as soil fertility. Plant nutrients (N, P and K) and microbial population registered manifold improvement in organically sound (*Bacillus pumilus* + NP) plots as compared to control. SMBC was found to be higher in *Bacillus pumilus* + 75% NP treated plots as compared to other treatment plots. Similar trends were recorded in the bacterial (rhizospheric and endophytic) populations. A significant reduction in CO_2 evolution was recorded after 48 h of incubation in the treatments receiving *Bacillus pumilus* bio-inoculation. Therefore, based on these findings it is concluded that this fertilization regime (*Bacillus pumilus* + NP) not only could produce a good yield but also offers an opportunity for savings of fertilizers and mitigation of soil pollution. Despite the information gained from this detailed study, other relationships needed to know turnover rates of microbial biomass and microbial activity for which detail work using isotope dating is in progress.

REFERENCES

[1] Anandaraj, M., Dinesh, R. (2008): Use of Microbes for Spices Production. – In: Parthasarathy, V. A., Kandiannan, K., Srinivasan, V. (eds.) Organic Spices. New India Publishing Agency, New Delhi, pp. 101-132.

[2] Bini, Y. K., Anandaraj, M., Dinesh, R., Silna, N., Kumar, A. (2011): Evaluation of PGPR strains for growth and disease suppression in ginger (*Zingiber officinale Rosc*.). – Proceedings of 2nd Asian PGPR Conference, Beijing, China.

[3] Cao, Y., Halane, M. K., Gassmann, W., Stacey, G. (2017): The role of plant innate immunity in the legume-Rhizobium symbiosis. – Annual Review of Plant Biology 68: 535-561.

[4] Castellano-Hinojosa, A., Correa-Galeote, D., Palau, J., Bedmar, E. J. (2016): Isolation of N_2-fixing rhizobacteria from *Lolium perenne* and evaluating their plant growth promoting traits. – Journal of Basic Microbiology 56: 85-91.

[5] Chaparro, J. M., Badri, D. V., Vivanco, J. M. (2014): Rhizosphere microbiome assemblage is affected by plant development. – ISME Journal 8: 790-803.

[6] Dasri, K., Munglue, P., Rattana, K., Sangchanjiradet, S. (2016): The effects of IAA produced by *Bacillus pumilus* A1_YM_1 on growth of orchids under micropropagation. – Khon Kaen Agriculture Journal 44: 832-837.

[7] Dinesh, R., Ghoshal Chaudhuri, S. (2013): Soil biochemical/microbial indices as ecological indicators of land use change in mangrove forests. – Ecological Indicators 32: 253-258.

[8] Ding, W., Yu, H., Cai, Z., Han, F., Xu, Z. (2010): Responses of soil respiration to N fertilization in a loamy soil under maize cultivation. – Geoderma 155: 381-389.

[9] Fall, D., Diouf, D., Zoubeirou, A. M., Bakhoum, N., Faye, A., Sall, S. N. (2012): Effect of distance and depth on microbial biomass and mineral nitrogen content under *Acacia senegal* (L.) Wild. trees. – Journal of Environment Management 95: S260-S264.

[10] Gao, X., Han, Q., Chen, Y., Qin, H., Huang, L., Kang, Z. (2014): Biological control of oilseed rape Sclerotinia stem rot by *Bacillus subtilis* strain Em7. – Biocontrol Science and Technology 24: 39-52.

http://www.aloki.hu ● ISSN 1589 1623 (Print) ● ISSN 1785 0037 (Online)
DOI: http://dx.doi.org/10.15666/aeer/1605_72537270
© 2018, ALÖKI Kft., Budapest, Hungary

[11] Ge, X., Xiao, W., Zeng, L., Huang, Z., Huang, L. L., Tan, B. W. (2012): Relationships between soil nutrient contents and soil enzyme activities in *Pinus massoniana* stands with different ages in Three Gorges Reservoir Area. – Chinese Journal of Applied Ecology 23: 445-451.
[12] Gonzalez-Quinones, V., Stockdale, E., Banning, N., Hoyle, F., Sawada, Y., Wherrett, A. D., Jones, D. L., Murphy, D. V. (2011): Soil microbial biomass-Interpretation and consideration for soil monitoring. – Soil Research 49: 287-304.
[13] Hamilton, C. E., Bever, J. D., Labbe, J., Yang, X. H., Yin, H. F. (2016): Mitigating climate change through managing constructed microbial communities in agriculture. – Agriculture Ecosystem and Environment 216: 304-308.
[14] Hardy, R. W., Holsten, R., Jackson, E., Burns, R. (1968): The acetylene-ethylene assay for N_2 fixation: laboratory and field evaluation. – Plant Physiology 43: 1185-1207.
[15] Heidarzadeh, N., Baghaee-Ravari, S. (2016): Application of *Bacillus pumilus* as a potential biocontrol agent of Fusarium wilt of tomato. – Archives of Phytopathology and Plant Protection 48: 13-16.
[16] Kaushal, M., Kaushal, R. (2015): Acetylene reductase activity and molecular characterization of plant growth promoting rhizobacteria to know efficacy in integrated nutrient management system. – Indian Journal of Biotechnology 14: 221-227.
[17] Kaushal, M., Wani, S. P. (2016): Plant-growth-promoting rhizobacteria: drought stress alleviators to ameliorate crop production in drylands. – Annals of Microbiology 66: 35-42.
[18] Kaushal, M., Kumar, A., Kaushal, R. (2017): *Bacillus pumilus* strain YSPMK11 as plant growth promoter and bicontrol agent against *Sclerotinia sclerotiorum*. – 3 Biotech. 7: 90.
[19] Kavino, M., Harish, S., Kumar, N., Saravanakumar, D., Samiyappan, R. (2010): Effect of chitinolytic PGPR on growth, yield and physiological attributes of banana (*Musa* spp.) under field conditions. – Applied Soil Ecology 45: 71-77.
[20] Khatri-Chhetri, A., Aggarwal, P. K., Joshi, P. K., Vyas, S. (2017): Farmer's prioritization of climate smart agriculture (CSA) technologies agricultural system. – Agricultural Systems 157: 184-191.
[21] Liu, N., Zhang, Y., Chang, S., Kan, H., Lin, L. (2012): Impact of grazing on soil carbon and microbial biomass in typical steppe and desert steppe of Inner Mongolia. – PloS One 7: e36434.
[22] Liu, Y., Li, R., Wang, J., Zhang, X., Jia, R., Gao, Y., Peng, H. (2017): Increased enzymatic hydrolysis of sugarcane bagasse by a novel glucose and xylose stimulated β-glucosidase from *Anoxybacillus flavithermus* subsp. *yunnanensis* E13T. – BMC Biochemistry 18: 4.
[23] Majumdar, B., Saha, A. R., Ghorai, A. K., Sarkar, S. K., Chowdhury, H., Kundu, D. K., Mahapatra, B. S. (2014): Effect of fertilizer treatments on jute (*Chorchorus olitorius*), microbial dynamics in its rhizosphere and residual fertility status of soil. – Indian Journal of Agricultural Sciences 84: 503-508.
[24] Nagar, N. K., Goud, V. V., Kumar, R., Kumar, R. (2016): Effect of organic manures and crop residue management on physical, chemical and biological properties of soil under pigeon pea based intercropping system. – International Journal of Science 6: 101-113.
[25] Raaijmakers, J. M., Mazzola, M. (2016): Soil immune responses. – Science 352: 1392-1393.
[26] Salamanca, E., Raubuch, M., Joergensen, R. G. (2002): Relationships between soil microbial indices in secondary tropical forest soils. – Applied Soil Ecology 21: 211-219.
[27] Santibanez, C., Varnero, M. T. (2014): Evaluation of chanar seed cake from biodiesel production as a soil amendment. – Journal of Soil Science and Plant Nutrition 14: 129-138.
[28] Shaharoona, B., Arshad, M., Zahir, Z. A., Khalid, A. (2006): Performance of Pseudomonas spp. containing ACC-deaminase for improving growth and yield of maize

http://www.aloki.hu ● ISSN 1589 1623 (Print) ● ISSN 1785 0037 (Online)
DOI: http://dx.doi.org/10.15666/aeer/1605_72537270
© 2018, ALÖKI Kft., Budapest, Hungary

(Zea mays L.) in the presence of nitrogenous fertilizer. – Soil Biology and Biochemistry 38: 2971-2975.

[29] Singh, A., Singh, V. K., Chandra, R., Srivastava, P. C. (2012): Effect of integrated nutrient management on pigeon pea-based intercropping system and soil properties in mollisols of the Tarai Region. – Journal of Indian Society of Soil Science 60: 38-44.

[30] United Nations, Department of Economic and Social Affairs, Population Division (2015): World Population Prospects: The 2015 Revision. – UN, New York.

[31] Upadhyay, A. K., Bahadur, A., Singh, J. (2012): Effect of organic manures and biofertilizers on yield, dry matter partitioning and quality traits of cabbage (*Brassica oleracea* var. *capitata*). – Indian Journal of Agricultural Sciences 82: 31-34.

[32] Vance, E. D., Brookes, P. C., Jenkinson, D. S. (1987): An extraction method for measuring soil microbial biomass C. – Soil Biology and Biochemistry 19: 703-707.

[33] Xun, W., Zhao, J., Xue, C., Zhang, G., Ran, W., Wang, B., Shen, Q., Zhang, R. (2016): Significant alteration of soil bacterial communities and organic carbon decomposition by different long-term fertilization management conditions of extremely low productivity arable soil in South China. – Environmental Microbiology 18: 1907-1917.

[34] Yang, K., Zhu, J., Zhang, M., Yan, Q., Sun, O. J. (2010): Soil microbial biomass carbon and nitrogen in forest ecosystems of Northeast China: a comparison between natural secondary forest and larch plantation. – Journal of Plant Ecology 3: 175-182.

http://www.aloki.hu ● ISSN 1589 1623 (Print) ● ISSN 1785 0037 (Online)
DOI: http://dx.doi.org/10.15666/aeer/1605_72537270
© 2018, ALÖKI Kft., Budapest, Hungary

EFFECTS OF LOW TEMPERATURES ON ENZYME ACTIVITY, CHLOROPHYLL AND ION CONTENTS IN COMMON BEAN GENOTYPES

KABAY, T.

Ercis Vocational School, Van Yuzuncu Yil University, Van, Turkey
(e-mail: tkabay@yyu.edu.tr; phone: +90-532-205-1624; fax: +90-432-225-1104)

(Received 14th Aug 2018; accepted 15th Oct 2018)

Abstract. Low temperatures slow down plant growth and development and generate physiological damages on plants. Metabolism of largely produced and consumed common bean (*Phaseolus vulgaris* L.) plants decelerates at temperatures below 15 °C. This study was carried out at Van Yuzuncu Yil University in Van province of Turkey with limited vegetation period due to its cold climate in winter. In this study, the bean plants were subjected to low temperature stress and catalase (CAT), super oxide dismutase (SOD), ascorbate peroxidase (APX) enzyme activities, malondialdehyde (MDA), chlorophyll-a, chlorophyll-b and total chlorophyll, K, Ca, and Mg ion contents of low temperature stress-tolerant Yakutiye and Ç30 and low temperature stress-sensitive Zulbiye and Ç13 bean genotypes were measured on 25th, 30th, 35th and 40th days of low temperature stress. Four bean seeds were sown in 2-liter pots filled with 2:1 peat:perlite mixture as to have 2 plants in each pot. The pots were irrigated with Hoagland nutrient solution. Low temperature stress plants were sown on 15th of March with low outdoor temperatures. In control group, been seeds were sown on 25th of April and plant samples were taken in again 5-day intervals in 4 periods (25th, 30th, 35th and 40th days of growth). Significant differences were observed in enzyme activities, chlorophyll contents and ion contents of low temperature-tolerant and sensitive bean genotypes in 4 measurement periods.
Keywords: *abiotic stress, biochemical characteristics, nutrient, Phaseolus vulgaris, physiological characteristics*

Introduction

In terrestrial climate zones, low bean yields are generally attributed to prominent climate conditions of the regions. Seed germination in beans largely depends on genotypes and quite a few genotypes are able to well-germinate at temperatures below 10 °C. In vegetables, low temperatures at root zone generate a stress in water absorption of the roots (Sakamoto and Suzuki, 2015). Beans are generally sensitive to cold temperatures, thus germination rates and percentages decrease at low soil temperatures in spring. Water absorption damage increases because of rapid water intake and ultimately seedling formation greatly weakened. In cold climates, temperatures often go below 15 °C during the initial growth stages of the seedlings and such low temperatures then negatively influence seedling growth and development (Elkoca et al., 2005). Plants develop different mechanism against cold stress-induced damages and ultimate die outs or to provide cold-tolerance. Exothermic effects of inner and intra cell frost formation on plants are categorized as physical changes in cell membranes throughout cold-stress period, cold resistance and acclimatization and biochemical changes throughout the cold acclimatization (changes in some soluble substances in plant extract, lipid composition of cell membranes, protein contents, enzyme activity and antioxidant systems (Aslantaş et al., 2010).

Abiotic stress factors negatively affect several crops. Significant decreases were reported in photosynthesis rates and chlorophyll contents of pea plants when the plants were subjected to 45 °C temperature for 24 h (Georgieva et al., 2007). Decreasing

http://www.aloki.hu ● ISSN 1589 1623 (Print) ● ISSN 1785 0037 (Online)
DOI: http://dx.doi.org/10.15666/aeer/1605_72717287
© 2018, ALÖKI Kft., Budapest, Hungary

chlorophyll, K and Ca contents and increasing MDA, CAT, SOD and APX activities were reported for bean and tomato plants under drought and high temperatures (Terzi et al., 2010; Kabay and Şensoy, 2016, 2017; Alp and Kabay, 2017).

It was reported in a previous study investigating the effects of low temperature stress on physiological characteristics of tomato genotypes that cold stress reduced chlorophyll and dry matter content of young and old leaves and wakened antioxidative systems of the plants (Gökmen, 2006). Low temperatures were reported to increase antioxidant enzyme and MDA content of rapeseed plants (Xian et al., 2017). Low temperatures increase chlorophyll and weight losses of cabbages and increased reactive oxygen species (Soengas et al., 2018).

It was indicated in another study carried out with cold stress-resistant and sensitive sugar cane cultivars that sensitive cultivar had greater root length and root volume than the resistant cultivar, but cell structure was destructed in both cultivars and cold stress-induced plants had greater MDA, proline, soluble sugar, soluble protein, POD and SOD activity than the control plants (Sun et al., 2017).

It was reported in another study investigating the effects of cold stress on rye and wheat seedlings that cold stress increased antioxidant enzyme activities, proline, sugar and anthocyanins contents of both species (Kolupaev et al., 2016).

Significant decreases were reported in malondialdehyde, proline, peroxidase and catalase activities of control and transgenic tomato plants under cold and low temperature stress (Yu et al., 2015). Xintaimici and Jinyan cucumber (*Cucumis sativus* L.) cultivars were subjected to two different temperature regimes (15/15 °C and 25/18 °C) under low light intensity and significant increases were reported in leaf superoxide dismutase and guaiacol peroxidase activities of both cultivars and less increases were reported in leaf catalase activity (Xu et al., 2008). Ogweno et al. (2009) reported different photosynthetic physiological responds of tomato leaves to moderate and low temperature stress. Huang et al. (2018) reported decreasing net photosynthetic rate and chlorophyll contents of Akihime and Benihoppe strawberry cultivars under cooling stress. Researchers also reported that foliar selenium (Se) sprays relieved the decrease in net photosynthetic rate and chlorophyll content and increased malondialdehyde and hydrogen peroxide content under stress conditions. Do et al. (2018) reported increasing ascorbate peroxidase (APX) and superoxide dismutase (SOD) activities of melon and pumpkin plants when they were subjected to 12/7 °C (day/night) low temperatures for 0–72 h. Li et al. (2018) reported that cold stress increased the accumulation of reactive oxygen species (ROS) and resulted in an oxidative stress, such a case then decreased photosynthetic processes of tea leaves, but melatonin treatments reduced antioxidant potential and oxidative stress and increased photosynthetic capacity. Bilska-kos et al. (2017) reported that low temperatures (14/12 °C) altered pectin content and osmatic potential of maize leaf cells and ultimately altered cell membrane composition. Zhou et al. (2017) reported significant decreases in fresh and dry weights, leaf areas and relative water contents of tomato cultivars under drought stress as compared to the control plants. While significant increases were reported in antioxidant compound quantities of tomato plants, decreases were reported in chlorophyll contents (Gökmen, 2006). It was reported in study carried out to determine yield and total temperature demands of bean plants at different growth stages that the greatest yield was obtained from early July sowings and yields decreased as the sowing time approached to autumn (Yoldaş and Eşiyok, 2009). High and low temperatures (15/8, 20/13, 28/21, 33/23 and 36/26 °C) were applied to tomato plants

http://www.aloki.hu ● ISSN 1589 1623 (Print) ● ISSN 1785 0037 (Online)
DOI: http://dx.doi.org/10.15666/aeer/1605_72717287
© 2018, ALÖKI Kft., Budapest, Hungary

and it was observed that temperature stress negatively influenced plant growth and development and nutrient uptake (Sung et al., 2015).

This study was carried out to determine the effects of low temperature stress on enzyme activity, chlorophyll, K, Ca and Mg contents of low temperature tolerant (Yakutiye and Ç30) and sensitive (Zulbiye and Ç13) common bean (*Phaseolus vulgaris* L.) genotypes.

Materials and methods

This study was conducted to determine the effects of low temperature stress on common bean genotypes. The study carried out at the Greenhouses of Van Yuzuncu Yil University Erciş Vocational Collage of Turkey and the plant analyses were carried out at laboratories of the Agricultural Faculty of the same university. Catalase (CAT), super oxide dismutase (SOD), ascorbate peroxidase (APX) enzyme activities, malondialdehyde (MDA), chlorophyll-a, chlorophyll-b and total chlorophyll, K, Ca, and Mg ion contents of low temperature stress-resistant Yakutiye and Ç30 and low temperature stress-sensitive Zulbiye and Ç13 bean genotypes (*Fig. 1*) were measured on 25th, 30th, 35th and 40th days of low temperature stress. For low temperature stress, bean seeds were sown in 2-liter pots filled with 2:1 peat:perlite mixture on 15th of March with low outdoor temperatures in a plastic covered high tunnels. Four seeds were placed in each pot as to have 2 plants in each pot. Pots were irrigated with Hoagland nutrient solution. The initial samples were taken from 25-days old plants and high tunnel cover was removed. Plants were then exposed to outdoor conditions and plant samples were taken in 5-day intervals (25th, 30th, 35th and 40th days) in 4 periods. High-tunnel temperature was 16.76 °C in day time and 15.28 °C at night. When the tunnel cover was removed, day temperature was measured as 12.67 °C and night temperature was measured as 8.43 °C by Hobo temperature data loggers. In control group, bean seeds were sown on 25th of April into the pots placed in a high-tunnel and plant samples were taken in again 5-day intervals on 25th, 30th, 35th and 40th days of growth. Throughout the experiments, day temperature was measured as 27.44 °C and night temperature was measured as 16.87 °C. The analyses performed on plant samples are provided below.

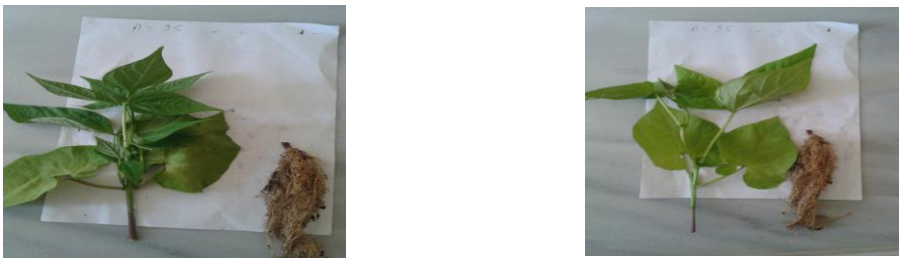

Control Low temperature

Figure 1. *A view of control and low temperature stressed plant sample*

Mineral element analyses

At the end of 25th, 30th, 35th and 40th days after sowing, representative control and low temperature stress-treated plants were harvested, the shoot were initially dried at open places for two days and then dried in an oven at 65 °C for 48 h. About 200 mg of

http://www.aloki.hu ● ISSN 1589 1623 (Print) ● ISSN 1785 0037 (Online)
DOI: http://dx.doi.org/10.15666/aeer/1605_72717287
© 2018, ALÖKI Kft., Budapest, Hungary

dry shoot samples were ground and subjected to pre-digestion in ethyl alcohol and then burned to ash in an ash oven at 550 °C. Resultant ash was dissolved in 3.3% HCl, filtered through blue-band filter paper. K, Ca and Mg readings were performed in an atomic absorption device at Scientific Research and Implementation Center of Yüzüncü Yıl University (Kacar, 1994; Kacar and İnal, 2008).

Lipid peroxidation

Lipid peroxidation of the plants generally expressed as malondialdehyde (MDA) content. About 0.5 g leaf sample was homogenized in 10 ml 0.1% trichloric acid (TCA) and resultant homogenate was centrifuged at 15000 rpm for 5 min. About 1 ml was taken from the clear portion of the centrifuged sample and supplemented with 0,5% tiobarbituric acid (TBA) dissolved in 4 ml 20% TCA. The mixture was kept at 95 °C for 30 min and instantly cooled in ice-bath. Cooled sample was then centrifuged at 10000 rpm for 10 min and absorbance readings were performed in clear portion at 532 and 600 nm wave lengths. The following equation was used to calculate malondialdehyde (MDA) content of the samples (Heath and Packer, 1968; Sairam and Saxena, 2000):

$$\text{MDA (nmol ml-1)} = [(A532-A600)/155\ 000]\ 10^6$$

Antioxidative enzyme analyses

About 1 g frozen leaf sample was homogenized in 5 ml cold 0.1 M Na-phosphate, 0.5 mM Na-EDTA and 1 mM ascorbic acid mixture (pH: 7.5) and the resultant homogenate was centrifuged at 18000 rpm and 4 °C for 30 min. Ascorbate peroxidase (AP) activity of the resultant homogenate was instantly determined. For catalase (CAT) and superoxide dismutase (SOD) activities, 1 g frozen leaf sample was homogenized in 5 ml cold 0.1 M Na-phosphate and 0.5 mM Na-EDTA mixture (pH: 7.5). Resultant homogenate was centrifuged at 18000 rpm and 4 °C for 30 min. A portion of homogenate was used to determine CAT activity instantly and the remaining portion was kept at -20 °C for SOD activity (Jebara et al., 2005; Bagcı, 2010).

Catalase (CAT) activity

Catalase activity was determined through monitoring the inhibition of H_2O_2 at 240 nm. As the reaction solution, 0.05 M phosphate buffer (KH_2PO_4) and 1.5 mM H_2O_2 mixture was used (pH: 7.0). About 2.5 ml reaction solution was mixed with 0.2 ml plant extract. Readings were performed in a spectrophotometer at 0 and 60th seconds. Reaction was initiated with the addition of 0.1 ml enzyme extract. Assessments were made by taking the change in absorbance within a minute into consideration (Jebara et al., 2005; Bagcı, 2010).

Superoxide dismutase (SOD) activity

SOD activity was determined through monitoring te inhibition of nitroblue tetrazolium (NBT) at 560 nm wave length. As a reaction solution, 50 mM Na-phosphate buffer (Na_2HPO_4 x H_2O_2), 0.1 mM Na- EDTA, 33 µM NBT, 5 µM riboflavin and 13 mM methionine mixture was used (pH: 7.0). About 2.5 ml reaction solution was mixed with 0.1 or 0.2 ml plant extract. Reaction was performed by keeping at 25 °C

http://www.aloki.hu ● ISSN 1589 1623 (Print) ● ISSN 1785 0037 (Online)
DOI: http://dx.doi.org/10.15666/aeer/1605_72717287
© 2018, ALÖKI Kft., Budapest, Hungary

under 75 µmol m-2 s-1 (40 W) light for 10 min. Control solution without enzyme supplementation was kept at dark for the same duration. Readings were performed in control and reaction solution at 560 nm. SOD activity was identified as the activity reducing 50% of NTB (Rahnama and Ebrahimzadeh, 2005).

Ascorbate peroxidase (APX) activity

Ascorbate peroxidase (APX) activity was measured through ascorbic acid-induced inhibition of H_2O_2 at 290 nm. As the reaction solution, 50 mM phosphate buffer (KH_2PO_4), 0.5 mM ascorbic acid, 0.1 mM EDTA and 1.5 mM H_2O_2 mixture was used (pH: 7.0). About 3 ml reaction solution was mixed with 0.1 ml plant extract. Readings were performed in a spectrophotometer at 290 nm in 0 and 60th seconds. Reaction was initiated with 0.1 ml enzyme addition. Assessments were made by taking the changes in absorbance within a minute into consideration (Sairam et al., 2005).

Chlorophyll

0.25 g samples from the third leaf of the plant were homogenized in 80% acetone in a place where the light does not directly come out, then the extract completed to 25 ml with acetone after filtering. Prepared samples were read at 663 nm and 645 nm wavelength and calculated by the following formula ((Lichtenthaler, 1983; Amira, 2011).

$$\text{Chlorophyll a (mg/g)} = (12.7 * 663\ \text{nm}) – (2.69 * 645\ \text{nm}) * V / W*10000$$

$$\text{Chlorophyll b (mg/g)} = (22.91 * 645\ \text{nm}) – (4.68 * 663\ \text{nm}) * V / W*10000$$

$$\text{Total Chlorophyll} = \text{Chlorophyll a} + \text{Chlorophyll b}$$

Statistical analysis

Experiments were conducted in randomized plots – factorial experimental design. Experimental data were subjected to variance analysis and significant means were compared with Duncan's multiple range test (Yesilova and Denizhan, 2016). Statistical analyses were performed by using SAS 9.4 software (SAS, 2018).

Results

In the present study, quite significant differences were observed between the control plants and cold stress-treated plants. Cold stress reduced chlorophyll a, chlorophyll-b and total chlorophyll contents and such decreases were greater in sensitive genotypes than in tolerant genotypes (*Tables 1–3*). Under low temperature stress, the greatest chlorophyll a, chlorophyll-b and total chlorophyll contents were obtained from the 1st period of Ç30 common bean genotype (chlorophyll-a: 0.468 mg g^{-1} FW, chlorophyll-b: 0.188 mg g^{-1} FW, and total chlorophyll: 0.657 mg g^{-1} FW) and the lowest chlorophyll-a (0.206 mg g^{-1} FW), chlorophyll-b (0.106 mg g^{-1} FW) and total chlorophyll content (0.312 mg g^{-1} FW) were obtained from the 4th period of Ç13 genotype (*Tables 1–3*). Considering the effects of low temperature on total chlorophyll content, the greatest total chlorophyll content of 0.697 mg g^{-1} FW in the 1st period of low temperature-tolerant Ç30 bean genotype decreased to 0.578 mg g^{-1} FW in the 2nd period and

http://www.aloki.hu ● ISSN 1589 1623 (Print) ● ISSN 1785 0037 (Online)
DOI: http://dx.doi.org/10.15666/aeer/1605_72717287
© 2018, ALÖKI Kft., Budapest, Hungary

decreased to 0.481 mg g^{-1} FW in the 4th period. In Yakutiye (Y) bean cultivar, total chlorophyll content of 0.616 mg g^{-1} FW in the 1st period decreased to 0.581 mg g^{-1} FW in the 2nd period and decreased to 0.460 mg g^{-1} FW in the 4th period. On the other hand, in low temperature-sensitive Ç13 bean genotype, total chlorophyll content of 0.633 mg g^{-1} FW in the 1st period decreased to 0.582 mg g^{-1} FW in the 2nd period and decreased to 0.312 mg g^{-1} FW in the 4th period. In low temperature-sensitive Zulbiye (Z) bean cultivar, total chlorophyll content of 0.631 mg g^{-1} FW in the 1st period decreased to 0.563 mg g^{-1} FW in the 2nd period and decreased to 0.326 mg g^{-1} FW in the 4th period (*Table 3*). In control plants, chlorophyll a, chlorophyll b and total chlorophyll contents increased in all 4 periods. The period-dependent differences in chlorophyll contents of the control and low temperature treatments were found to be significant (*Table 4*). Chlorophyll a+b values of the control treatments were identified as 0.731 mg g^{-1} FW for Ç30, 0.734 mg g^{-1} FW for Ç13, 0.727 mg g^{-1} FW for Yakutiye and 0.653 mg g^{-1} FW for Zulbiye. Chlorophyll a+b values of the low temperature treatments were identified as 0.562 mg g^{-1} FW for Ç30, 0.482 mg g^{-1} FW for Ç13, 0.541 mg g^{-1} FW for Yakutiye and 0.475 mg g^{-1} FW for Zulbiye (*Table 4*).

Table 1. *Change in chlorophyll a (mg g^{-1} FW) content of common bean genotypes under low temperature stress in 4 periods*

Genotype	Period 1 (day 25th)	Period 2 (day 30th)	Period 3 (day 35th)	Period 4 (day 40th)
Control				
Ç30	0.485d*	0.472de	0.508c	0.535ab
Yakutiye	0.460ef	0.480d	0.514c	0.534ab
Ç13	0.455eg	0.472de	0.522bc	0.541a
Zulbiye	0.356ı	0.418h	0.439	0.446fg
Low temperatures				
Ç30	0.468a*	0.412d	0.378e	0.337g
Yakutiye	0.439b	0.424cd	0.362f	0.326g
Ç13	0.458a	0.434bc	0.276h	0.206j
Zulbiye	0.456a	0.416d	0.255ı	0.217j

*Means in control and low temperature followed by the same letter are not significantly different ($P < 0.05$)

Table 2. *Change in chlorophyll b (mg g^{-1} FW) content of bean (Phaseolus vulgaris) genotypes under low temperature stress in 4 periods*

Genotype	Period 1 (day 25th)	Period 2 (day 30th)	Period 3 (day 35th)	Period 4 (day 40th)
Control				
Ç30	0.212g*	0.224ef	0.234cd	0.251a
Yakutiye	0.209g	0.221f	0.241bc	0.249ab
Ç13	0.223f	0.232ce	0.243ab	0.247ab
Zulbiye	0.233ce	0.228df	0.243ab	0.246ab
Low temperatures				
Ç30	0.188a*	0.168c	0.149de	0.143e
Yakutiye	0.176b	0.154d	0.148de	0.134f
Ç13	0.176b	0.147de	0.124g	0.106h
Zulbiye	0.175b	0.147de	0.125g	0.108h

*Means in control and low temperature followed by the same letter are not significantly different ($P < 0.05$)

http://www.aloki.hu ● ISSN 1589 1623 (Print) ● ISSN 1785 0037 (Online)
DOI: http://dx.doi.org/10.15666/aeer/1605_72717287
© 2018, ALÖKI Kft., Budapest, Hungary

Table 3. *Change in chlorophyll a + b (mg g^{-1} FW) content of bean (Phaseolus vulgaris) genotypes under low temperature stress in 4 periods*

Genotype	Period 1 (day 25th)	Period 2 (day 30th)	Period 3 (day 35th)	Period 4 (day 40th)
Control				
Ç30	0.697de*	0.696df	0.742c	0.787a
Yakutiye	0.669g	0.701de	0.756bc	0.784a
Ç13	0.678fg	0.705d	0.765b	0.788a
Zulbiye	0.589ı	0.647h	0.682eg	0.693df
Low temperatures				
Ç30	0.657a*	0.581d	0.528f	0.481h
Yakutiye	0.616c	0.578d	0.511g	0.460ı
Ç13	0.633b	0.582d	0.401j	0.312m
Zulbiye	0.631b	0.563e	0.379k	0.326l

*Means in control and low temperature followed by the same letter are not significantly different (P < 0.05)

Table 4. *Change in chlorophyll a, b and chlorophyll a+b content of control and low temperature stress treatments*

Genotype	Chlorophyll a		Chlorophyll b		Chlorophyll a+b	
	Control	Low temperatures	Control	Low temperatures	Control	Low temperatures
Ç30	0.439d*	0.399a*	0.230b*	0.162a*	0.731a*	0.562a*
Yakutiye	0.461c	0.388b	0.230b	0.154b	0.727a	0.541b
Ç13	0.496b	0.343c	0.237a	0.138c	0.734a	0.482c
Zulbiye	0.514a	0.336d	0.238a	0.139c	0.653b	0.475c

*Means in each column followed by the same letter are not significantly different (P < 0.05)

There were differences in ion contents of the 1st and the 4th period and K, Ca and Mg contents decreased at the end of 4th period as compared to the 1st period. Such decreases were greater in low temperature sensitive bean plants (*Tables 5–7*). Under low temperature stress, the greatest K content (1.530%) was obtained from the 1st period of Zulbiye been genotype and the lowest K content (1.170%) was obtained from the 4th period of Ç13 bean genotype. The greatest Ca content (3.365%) was obtained from the 1st period of Zulbiye bean genotype and the lowest Ca content (1.645%) was obtained from the 4th period of Zulbiye bean genotype. The greatest Mg content (0.410%) was obtained from the 1st period of Zulbiye bean genotype, the lowest Mg content was obtained from the 4th period of again Zulbiye bean genotype (*Tables 6–7*).

As compared to the 1st period, plant K, Ca and Mg ion contents of the control groups increased at the end the 4th period. The K contents of Ç30, Yakutiye, Zulbiye and Ç13 genotypes were found to be significant under low temperature stress. The K content of 1.467% in the 1st period of Ç30 genotype decreased to 1.420% in the 2nd period, but placed in the same statistical group as Yakutiye (Y) cultivar with a K value of 1.442%. K contents also decreased in the 3rd and 4th periods, Ç30 and Zulbiye (Z) bean cultivar were placed in the same statistical group. K content of Ç30 bean genotype decreased to

http://www.aloki.hu ● ISSN 1589 1623 (Print) ● ISSN 1785 0037 (Online)
DOI: http://dx.doi.org/10.15666/aeer/1605_72717287
© 2018, ALÖKI Kft., Budapest, Hungary

1.263% in the 4th period and K content of Zulbiye cultivar of the same statistical group decreased to 1.275%. The decreases in K content of Yakutiye bean cultivar in the 2nd and 3rd periods were not found to be significant (*Table 5*).

Table 5. *Change in potassium (K) content (%) of common bean genotypes under low temperature stress in 4 periods*

Genotype	Period 1 (day 25th)	Period 2 (day 30th)	Period 3 (day 35th)	Period 4 (day 40th)
Control				
Ç30	3.370c*	3.382c	3.407b	3.44a.
Yakutiye	3.265fg	3.282ef	3.292e	3.30e
Ç13	3.337d	3.365c	3.265fg	3.415b
Zulbiye	3.222ı	3.132j	3.237hı	3.257gh
Low temperatures				
Ç30	1.467c*	1.420d	1.335f	1.263g
Yakutiye	1.530b	1.442d	1.425d	1.335f
Ç13	1.422d	1.367e	1.232h	1.170ı
Zulbiye	1.567a	1.510b	1.263g	1.275g

*Means in control and low temperature followed by the same letter are not significantly different ($P < 0.05$)

With regard to Ca content of bean genotypes under low temperature stress, Ç30 genotype and Yakutiye (Y) bean cultivar were placed in the same statistical group in the 1st period of stress (Ç30: 3.475%; Y: 3.502%). Ç13 genotype and Zulbiye (Z) bean cultivar were also placed in the same statistical group (Ç13: 3.665%; Z: 3.647%). There were decreases in Ca contents of the bean genotypes also in the 2nd period of the low temperature stress. Ç30, Ç13 and Yakutiye bean genotypes were placed in the same statistical group. As compared to the 1st and 2nd periods, Ca contents decreased in the 3rd period (Ç30: 2.842%; Y: 3.357%; Ç13: 2.900%; Z: 2.695%) and in the 4th period (Ç30: 2.635%; Y: 2.785%; Ç13: 1.865%; Z: 1.645%) (*Table 6*).

Table 6. *Change in calcium (Ca) content (%) of bean (Phaseolus vulgaris) genotypes under low temperature stress in 4 periods*

Genotype	Period 1 (day 25th)	Period 2 (day 30th)	Period 3 (day 35th)	Period 4 (day 40th)
Control				
Ç30	3.562hi*	3.512k	3.612e	3.657cd.
Yakutiye	3.640d	3.677c	3.705b	3.522jk
Ç13	3.583fh	3.573gh	3.542ıj	3.593eg
Zulbiye	3.603ef	3.750a	3.575gh	3.462l
Low temperatures				
Ç30	3.475ac*	3.405bc	2.842de	2.635f
Yakutiye	3.502ac	3.400bc	3.357c	2.785df
Ç13	3.665a	3.565ab	2.900d	1.865g
Zulbiye	3.647a	3.400bc	2.695ef	1.645h

*Means in control and low temperature followed by the same letter are not significantly different ($P < 0.05$)

http://www.aloki.hu ● ISSN 1589 1623 (Print) ● ISSN 1785 0037 (Online)
DOI: http://dx.doi.org/10.15666/aeer/1605_72717287
© 2018, ALÖKI Kft., Budapest, Hungary

While the differences in magnesium (Mg) contents of Ç30, Y and Z bean (*Phaseolus vulgaris*) genotypes were not found to be significant in the 1st period (Ç30: 0.362%; Y: 0.380%; Z: 0.382%) and in the 2nd period (Ç30: 0.262%; Y: 0.280%; Z: 0.285%) and they were placed in the same statistical group, but Ç13 genotype was found to be significantly different from the other groups. Magnesium content of genotypes decreased in the 3rd period, but all genotypes were placed in the same statistical group. In the 4th period of low temperature stress, decrease in Mg contents of Ç30, Ç13 and Y bean (*Phaseolus vulgaris*) genotypes (Ç30: 0.195%; Y: 0.195%; Ç13: 0.190%) were not found to be significant and they were all placed in the same statistical group, but Zulbiye (Z) bean genotype with an Mg content of 0.182% was found to be significantly different from the other genotypes (*Table 7*). Period-dependent differences in K, Ca and Mg contents of control and low temperature treatments were found to be significant (*Table 8*). K contents of control groups were identified as Ç30: 3.41%, Ç13: 3.34%, Yakutiye: 3.29% and Zulbiye: 3.21% and K contents of low temperature treatments were identified as Ç30: 1.37%, Ç13: 1.29%, Yakutiye: 1.43% and Zulbiye: 1.40% (*Table 8*).

Table 7. *Change in magnesium (Mg) content (%) of bean (Phaseolus vulgaris) genotypes under low temperature stress in 4 periods*

Genotype	Period 1 (day 25th)	Period 2 (day 30th)	Period 3 (day 35th)	Period 4 (day 40th)
Control				
Ç30	0.407dh*	0.435ce	0.510a	0.382fh
Yakutiye	0.385eh	0.422df	0.500a	0.365h
Ç13	0.397dh	0.447bd	0.475ac	0.390eh
Zulbiye	0.367gh	0.417dg	0.485ab	0.305ı
Low temperatures				
Ç30	0.362b*	0.262d	0.227e	0.195f
Yakutiye	0.380b	0.280d	0.230e	0.195f
Ç13	0.410a	0.310c	0.222e	0.190f
Zulbiye	0.385b	0.285d	0.237e	0.185f

*Means in control and low temperature followed by the same letter are not significantly different ($P < 0.05$)

Table 8. *Change in K (%), Ca (%) and Mg (%) content of control and low temperature stress treatments*

Genotype	K		Ca		Mg	
	Control	Low temperatures	Control	Low temperatures	Control	Low temperatures
Ç30	3.41a*	1.37c*	3.59b*	3.09b*	0.433ac*	0.261b*
Yakutiye	3.29c	1.43a	3.63a	3.26a	0.418a	0.271b
Ç13	3.34b	1.29d	3.57c	2.99c	0.427a	0.283a
Zulbiye	3.21d	1.40b	3.59b	2.85d	0.393b	0.273ab

*Means in each column followed by the same letter are not significantly different ($P < 0.05$)

http://www.aloki.hu ● ISSN 1589 1623 (Print) ● ISSN 1785 0037 (Online)
DOI: http://dx.doi.org/10.15666/aeer/1605_72717287
© 2018, ALÖKI Kft., Budapest, Hungary

Significant differences were observed in MDA contents of the bean plants in 4 periods and increases were observed at the end of 4th period as compared to the 1st period. Such increases were greater in low temperature sensitive bean genotypes (*Table 9*). Similar changes were also observed in CAT, SOD and APX antioxidative enzyme activities. Increases were observed in CAT, SOD and APX activities of the bean genotypes in 4 periods. Increases were greater in the 4th period as compared to the 1st period and increases were also greater in low temperature-sensitive bean genotypes (*Tables 10–13*).

Table 9. *Change in malondialdehyde (MDA nmol g^{-1} FW) content of bean (Phaseolus vulgaris) genotypes under low temperature stress in 4 periods*

Genotype	Period 1 (day 25th)	Period 2 (day 30th)	Period 3 (day 35th)	Period 4 (day 40th)
Control				
Ç30	5.662b*	5.663b	5.713ab	5.735ab.
Yakutiye	5.691b	5.643b	5.719ab	5.732ab
Ç13	5.634b	5.899a	5.786ab	5.813ab
Zulbiye	5.662b	5.615b	5.767ab	5.799ab
Low temperatures				
Ç30	5.613l*	5.925h	5.954g	6.106e
Yakutiye	5.685j	5.881ı	5.981g	6.114e
Ç13	5.646k	6.057f	6.249c	6.325b
Zulbiye	5.668jk	6.217d	6.255c	6.373a

*Means in control and low temperature followed by the same letter are not significantly different ($P < 0.05$)

Table 10. *Change in superoxide dismutase (SOD unit g^{-1} FW) content of bean (Phaseolus vulgaris) genotypes under low temperature stress in 4 periods*

Genotype	Period 1 (day 25th)	Period 2 (day 30th)	Period 3 (day 35th)	Period 4 (day 40th)
Control				
Ç30	105.025fh*	107.158cg	109.449c	118.930b
Yakutiye	107.980cf	104.642gh	109.248cd	118.768b
Ç13	103.910h	106.278dh	109.200cd	121.815a
Zulbiye	103.884h	105.388eh	108.235ce	122.059a
Low temperatures				
Ç30	102.226e*	116.015d	121.513c	144.875b
Yakutiye	101.283e	116.510d	119.986dc	146.259b
Ç13	102.829e	124.475c	122.594c	157.812a
Zulbiye	102.738e	124.662c	124.193c	157.873a

*Means in control and low temperature followed by the same letter are not significantly different ($P < 0.05$)

Despite the insignificant differences in malondialdehyde (MDA) activity of the control groups in the 1st and 2nd periods, the MDA activity of Ç13 genotype was

http://www.aloki.hu ● ISSN 1589 1623 (Print) ● ISSN 1785 0037 (Online)
DOI: http://dx.doi.org/10.15666/aeer/1605_72717287
© 2018, ALÖKI Kft., Budapest, Hungary

identified as 5.899 nmol g^{-1} FW in the 2nd period. Significant increases were observed in MAD activities of the bean genotypes in the first two periods of low temperature stress (*Table 9*). The increase in MAD activity continued in the 3rd period, Ç30 (5.954 nmol g^{-1} FW) and Y (5.981 nmol g^{-1} FW) genotypes were placed in the same statistical group, Ç13 (6.248 nmol g^{-1} FW) and Z (6.255 nmol g^{-1} FW) were also placed in the same statistical group (*Table 7*). Such increases also continues in the 4th period of low temperature stress, Ç30 bean genotype (6.106 nmol g^{-1} FW) and Y bean cultivar (6.114 nmol g^{-1} FW) were placed in the same statistical group, Ç13 genotype had an MDA activity of 6.325 nmol g^{-1} FW and Zulbiye bean cultivar had an MDA activity of 6.373 nmol g^{-1} FW (*Table 9*).

Table 11. *Change in catalase (CAT mmol g^{-1}) content of bean (Phaseolus vulgaris) genotypes under low temperature stress in 4 periods*

Genotype	Period 1 (day 25th)	Period 2 (day 30th)	Period 3 (day 35th)	Period 4 (day 40th)
Control				
Ç30	0.176d*	0.186c	0.193bc	0.196b
Y	0.175d	0.184c	0.193b	0.197b
Ç13	0.171e	0.186c	0.194 b	0.210a
Z	0.167f	c0.185h	0.196b	0.214a
Low temperatures				
Ç30	0.172h*	0.184f	0.203df	0.217c
Y	0.176gh	0.187f	0.203df	0.224b
Ç13	0.178g	0.193e	0.216c	0.244a
Z	0.176g	0.186f	0.215c	0.245a

*Means in control and low temperature followed by the same letter are not significantly different ($P < 0.05$)

Table 12. *Change in ascorbate peroxidase (APX mmol g^{-1} FW) content of bean (Phaseolus vulgaris) genotypes under low temperature stress in 4 periods*

Genotype	Period 1 (day 25th)	Period 2 (day 30th)	Period 3 (day 35th)	Period 4 (day 40th)
Control				
Ç30	0.733l*	0.759ıj	0.781f	0.812d
Yakutiye	0.755j	0.763gh	0.793e	0.826c
Ç13	0.747k	0.0.766g	0.778f	0.855a
Zulbiye	0.756j	0.771g	0.791e	0.836b
Low temperatures				
Ç30	0.759i*	0.766h	0.903e	0.928d
Yakutiye	0.731k	0.771h	0.873f	0.923d
Ç13	0.747j	0.784g	1.124b	1.162a
Zulbiye	0.742j	0.785g	1.116c	1.167a

*Means in control and low temperature followed by the same letter are not significantly different ($P < 0.05$)

http://www.aloki.hu ● ISSN 1589 1623 (Print) ● ISSN 1785 0037 (Online)
DOI: http://dx.doi.org/10.15666/aeer/1605_72717287
© 2018, ALÖKI Kft., Budapest, Hungary

Table 13. *Change in MDA (nmol g^{-1} FW), CAT (mmol g^{-1} FW), SOD (unit g^{-1} FW) and APX (mmol g^{-1} FW) content of control and low temperature stress treatments*

Genotype	MDA		CAT		SOD		APX	
	Control	Low temperatures	Control	Low temperatures	Control	Low temperatures	Control	Low temperatures
Ç30	5.68b*	5.89d*	0.188b	0.194d*	110.14a*	121.16b*	0.771c*	0.839b*
Yakutiye	5.69ab	5.92c	0.0.187b	0.197c	110.16a	121.01b	0.784b	0.824c
Ç13	5.78a	6.07b	0.190a	0.208a	110.31a	127.17a	0.786ab	0.954a
Zulbiye	5.71ab	6.13a	0.190a	0.205b	109.89a	127.36a	0.788a	0.952a

*Means in each column followed by the same letter are not significantly different (P < 0.05)

The changes in superoxide dismutase (SOD) activity of the bean genotypes under low temperature stress were not found to be significant in the 1st period and they were all placed in the same statistical group. In the 2nd period, Zulbiye (124.662 unit g^{-1} FW) and Ç13 (124.475 unit g^{-1} FW) bean genotypes were placed in the same statistical group and Yakutiye (116.510 unit g^{-1} FW) and Ç30 (116.015 unit g^{-1} FW) bean genotypes were placed in the same statistical group. In the 4th period of low temperature stress, greater increases were observed in the SOD activities of Ç13 (157.812 unit g^{-1} FW) and Zulbiye (157.873 unit g^{-1} FW) genotypes (*Table 10*). With regard to catalase (CAT) activity in the 1st period of low temperature stress, Ç13 (0.178 mmol g^{-1} FW) and Zulbiye (0.176 mmol g^{-1} FW) bean genotypes were placed in the same statistical group, but Yakutiye (0.176 mmol g^{-1} FW) and Ç30 (0.172 mmol g^{-1} FW) bean genotypes were significantly different from the other genotypes. A slight increase was observed in CAT activities of the genotypes in the 2nd period of low temperature stress, but differences in CAT activities of the genotypes, except for Ç13, were not found to be significant. In the 3rd period of stress, Ç30 and Yakutiye genotypes had a CAT activity of 0.203 mmol g^{-1} FW, Ç13 genotypes had a CAT activity of 0.216 mmol g^{-1} FW and Zulbiye genotype had a value of 0.215 mmol g^{-1} FW. The differences among the genotypes were not significant, thus they were all placed in the sme statistical group. In the 4th period of low temperature stress, the differences in CAT activities of the genotypes (Ç30: 0.217 mmol g^{-1} FW; Y: 0.224 mmol g^{-1} FW; Ç13: 0.244 mmol g^{-1} FW; Z: 0.245 mmol g^{-1} FW) were found to be significant (*Table 11*). With regard to ascorbate peroxidase (APX) activity of the 1st period, Ç13 (0.747 mmol g^{-1} FW) and Zulbiye (0.742 mmol g^{-1} FW) bean genotypes were placed in the same statistical group, thus the difference between them were not significant. Yakutiye (0.731 mmol g^{-1} FW) and Ç30 (0.759 mmol g^{-1} FW) bean genotypes were found to be significantly different from the other genotypes. In the 2nd period of stress, there was a slight increase in APX activity of the sensitive and tolerant genotypes and the differences in APX activity of sensitive and tolerant genotypes were found to be significant. There were significant differences in APX activity of the genotypes in the 3rd (Ç30: 0.903 mmol g^{-1} FW; Y: 0.873 mmol g^{-1} FW; Ç13: 1.124 mmol g^{-1} FW; Z: 1.116 mmol g^{-1} FW) and 4th (Ç30: 0.928 mmol g^{-1} FW; Y: 0.923 mmol g^{-1} FW; Ç13: 1.162 mmol g^{-1} FW; Z: 1.167 mmol g^{-1} FW) period of low temperature stress (*Table 12*).

Period-dependent differences in MDA, CAT, SOD and APX activity of control and low temperature treatments were found to be significant. Low temperature-tolerant Yakutiye cultivar had the values of MDA: 5.69 nmol g^{-1} FW, CAT: 0.187 mmol/g FW,

http://www.aloki.hu ● ISSN 1589 1623 (Print) ● ISSN 1785 0037 (Online)
DOI: http://dx.doi.org/10.15666/aeer/1605_72717287
© 2018, ALÖKI Kft., Budapest, Hungary

SOD: 110.16 unit g^{-1} FW, APX: 0.784 mmol g^{-1} FW in control treatments and had the values of MDA: 5.92 nmol g^{-1} FW, CAT: 0.197 mmol g^{-1} FW, SOD: 121.01 unit g^{-1} FW, APX: 0.824 mmol g^{-1} FW in low temperature treatments. Low temperature-sensitive Zulbiye cultivar had the values of MDA: 5.71 nmol g^{-1} FW, CAT: 0.190 mmol g^{-1} FW, SOD: 109.89 unit g^{-1} FW, APX: 0.788 mmol g^{-1} FW in control treatments and had the values of MDA: 6.13 nmol g^{-1} FW, CAT: 0.205 mmol g^{-1} FW, SOD: 127.36 unit g^{-1} FW, APX: 0.952 mmol g^{-1} FW in low temperature treatments.

Significant findings were obtained for investigated parameters of present study both in control and low temperature stress treatments. Among the investigated parameters, decreases were observed in chlorophyll and ion contents of the genotypes in 4 periods and increases were observed in MDA, CAT, SOD and APX activity of the genotypes. The differences between the genotypes and between the periods were found to be significant.

Discussion

Some significant recession is observed in plant growth and development under low temperatures. This recession is greater in low temperature-sensitive genotypes. In the present study, changes in chlorophyll, K, Ca, and Mg contents and lipid peroxidation (MDA), catalase (CAT), superoxide dismutase (SOD) and ascorbate peroxidase (APX) activities of low temperature-tolerant and sensitive bean (*Phaseolus vulgaris*) genotypes were investigated in four different periods of low temperature stress. Present findings were quite similar with the findings of the earlier studies.

There were decreases in chlorophyll a, chlorophyll b and total chlorophyll contents of tolerant and sensitive genotypes in four periods *(Tables 1–3)*. Such decreases were greater in low temperature sensitive Ç13 and Zulbiye (Z) genotypes than in low temperature-tolerant Ç30 and Yakutiye (Y) bean genotypes. There were also significant differences in investigated parameters of the control and low temperature treatments of four periods (*Table 4*). Decreases were reported in chlorophyll a, chlorophyll b and total chlorophyll contents of bean and tomato plants under abiotic stress conditions (Terzi et al., 2010; Kabay and Şensoy, 2016, 2017; Alp and Kabay, 2017). Similar findings were reported in literature about the effects of different low temperatures. It was reported in a previous study investigating the effects of low temperature stress on physiological characteristics of tomato genotypes that cold stress reduced chlorophyll and dry matter content of young and old leaves (Gökmen, 2006). Low temperatures increased chlorophyll and weight losses of cabbages (Soengas et al., 2018). Cold stress decreased photosynthetic processes of tea leaves, but melatonin treatments reduced antioxidant potential and oxidative stress and increased photosynthetic capacity (Li et al., 2018). Low temperatures (14/12 °C) altered osmatic potential of maize leaf cells and ultimately altered cell membrane composition (Bilska-kos et al., 2017).

In control groups, significant increases were observed in potassium (K), calcium (Ca) and Magnesium (Mg) content of bean (*Phaseolus vulgaris*) genotypes in four periods. The changes in K, Ca and MG content of bean genotypes under low temperature stress were also found to be significant and K, Ca and Mg contents decreased in four periods. Such decreases were greater in stress-sensitive genotypes (*Tables 5–7*). The decreases in K content of Yakutiye (Y) bean cultivar in the 2nd and 3rd periods were not found to be significant. The decreases in K content of cv. Zulbiye in the 3rd and 4th periods were also not found to be significant (*Table 5*). The changes in Ca and Mg contents were

http://www.aloki.hu ● ISSN 1589 1623 (Print) ● ISSN 1785 0037 (Online)
DOI: http://dx.doi.org/10.15666/aeer/1605_72717287
© 2018, ALÖKI Kft., Budapest, Hungary

found to be significant in the 4th period of stress (*Tables 6* and *7*). Throughout 4 periods, changes in K, Ca and Mg content of bean genotypes in control and low temperature treatments were found to be significant and ion contents decreased under low temperature stress (*Table 8*).

It was reported that low temperature stress negatively influenced leaf cells of maize plants (Bilska-kos et al., 2017). Low soil temperatures in spring negatively influence seedling growth and development of sensitive bean plants (Elkoca et al., 2005). Low temperature stress was reported to have negative effects on cold stress-resistant and sensitive sugar cane cultivars (Sun et al., 2017). It was reported in study carried out to determine total temperature demands of bean plants at different growth stages that the greatest yield was obtained from early July sowings and yields decreased as the sowing time approached to autumn (Yoldaş and Eşiyok, 2009). High and low temperatures (15/8, 20/13, 28/21, 33/23 and 36/26 °C) were applied to tomato plants and it was observed that temperature stress negatively influenced plant growth and development and nutrient uptake (Sung et al., 2015). In vegetables, low temperatures at root zone generate a stress in water absorption of the roots (Sakamoto and Suzuki, 2015). Decreasing chlorophyll, K and Ca contents were reported for bean and tomato plants under abiotic stress (Terzi et al., 2010; Kabay and Şensoy, 2016; Zhou et al., 2017; Uzal and Yasar, 2017; Kabay et al., 2017; Alp and Kabay, 2017)

Significant differences were observed in MDA contents of the bean plants in 4 periods and increases were observed at the end of 4th period as compared to the 1st period. Such increases were greater in low temperature sensitive bean genotypes (*Table 7*). Similar changes were also observed in CAT, SOD and APX antioxidative enzyme activities. Increases were observed in CAT, SOD and APX activities of the bean genotypes in 4 periods. Increases were greater in the 4th period as compared to the 1st period and increases were also greater in low temperature-sensitive bean genotypes (*Table 9–12*). With regard to MDA activity, there were significant differences both between the bean genotypes and between the stress periods (*Table 9*). There were significant differences in superoxide dismutase (SOD) activity of the bean genotypes in the 4th period of stress. However, the differences in SOD activity of Ç13 and Zulbiye genotypes were not significant different in the 2nd and 3rd period of the stress (*Table 10*). There were significant differences in catalase (CAT) activity of both the bean genotypes and the stress periods (*Table 11*). The changes in CAT activity of Ç30 and Yakutiye bean genotypes were not found to be significant in 2nd and 3rd period of stress (*Table 11*). The differences in ascorbate peroxidase (APX) activity of both the genotypes and the stress periods were also found to be significant (*Table 12*). Both the control and the low temperature treatments yielded significant differences in MDA, CAT, SOD and APX activity of the bean genotypes. Significant increases were observed in MDA, CAT, SOD and APX activities under low temperature stress (*Table 13*). Xintaimici and Jinyan cucumber (*Cucumis sativus* L.) cultivars were subjected to two different temperature regimes (15/15 °C and 25/18 °C) under low light intensity and significant increases were reported in leaf superoxide dismutase and less increases were reported in leaf catalase activity (Xu et al., 2008). Increasing ascorbate peroxidase (APX) and superoxide dismutase (SOD) activities of melon and pumpkin plants were reported under low temperature conditions (Do et al., 2018).

In process of cold resistance, plants develop different mechanisms against cold stress-induced damages and ultimate die outs or develop such mechanisms to provide cold-tolerance such as physical changes in cell membranes, changes in some soluble

http://www.aloki.hu ● ISSN 1589 1623 (Print) ● ISSN 1785 0037 (Online)
DOI: http://dx.doi.org/10.15666/aeer/1605_72717287
© 2018, ALÖKI Kft., Budapest, Hungary

substances in plant extract, lipid composition of cell membranes, protein contents, enzyme activity and antioxidant systems and plant nutrients (Aslantaş et al., 2010). It was reported in a previous study investigating the effects of low temperature stress on physiological characteristics of tomato genotypes that young and old leaves of the plants were found to be insufficient in antioxidative systems (Gökmen, 2006). Low temperatures were reported to increase antioxidant enzyme and MDA content of rapeseed plants (Xian et al., 2017). Low temperatures increased chlorophyll and weight losses of cabbages and increased reactive oxygen species (Soengas et al., 2018). In a previous study carried out with cold stress resistant and sensitive sugar cane cultivar, cell structure was destructed and cold stress-induced plants had greater MDA, proline, soluble sugar, soluble protein, POD and SOD activity than the control plants (Sun et al., 2017). It was reported in another study investigating the effects of cold stress on rye and wheat seedlings that cold stress increased antioxidant enzyme activities, proline, sugar and anthocyanins contents of both species (Kolupaev et al., 2016). Significant decreases were reported in malondialdehyde, proline, peroxidase and catalase activities of control and transgenic tomato plants under cold and low temperature stress (Yu et al., 2015). While significant increases were reported in antioxidant compound quantities of tomato plants, decreases were reported in chlorophyll contents (Gökmen, 2006). In present study, significant decreases were observed in chlorophyll, K, Ca and Mg contents and increases were observed in MDA, CAT, SOD and APX activities of bean genotypes under low temperature conditions. Present findings were mostly well complied with the results of similar earlier studies.

Conclusion

Significant differences were observed in chlorophyll contents, enzyme activities and ion contents of low temperature-resistant and sensitive common bean (*Phaseolus vulgaris*) genotypes throughout cold stress treatments. The decrease in chlorophyll-a, chlorophyll-b, total chlorophyll, K, Ca and Mg contents were greater in low temperature-sensitive bean plants than in low temperature-tolerant plants.

With the progress of cold stress, the MDA content of sensitive genotypes were greater than the MAD contents of tolerant genotypes. On the other hand, tolerant genotypes had greater CAT, SOD and APX antioxidant enzyme activities than the sensitive genotypes. Present findings proved one more time the suitability of the parameters selected to determine the effects of low temperature stress for selection of drought stress-tolerant bean genotypes.

REFERENCES

[1] Alp, Y., Kabay, T. (2017): The effect of drought stress on plant development in some native and commercial tomato genotypes. – Yuzuncu Yil University Journal of Agricultural Sciences 27(3): 387-395.

[2] Amira, M. S., Qados, A. (2011): Effect of salt stress on plant growth and metabolism of bean plant Vicia faba (L.). – Journal of the Saudi Society of Agricultural Sciences 10: 7-15.

[3] Aslantaş, R., Karakurt, H., Karakurt, Y. (2010): The cellular and molecular mechanisms on resistance to low temperatures in plants. – Ataturk University Journal of the Faculty of Agriculture 41(2).

http://www.aloki.hu ● ISSN 1589 1623 (Print) ● ISSN 1785 0037 (Online)
DOI: http://dx.doi.org/10.15666/aeer/1605_72717287
© 2018, ALÖKI Kft., Budapest, Hungary

[4] Bagcı, E. G. (2010): Identification of drought-induced oxidative stress in chickpea with physiological and biochemical parameters. – Unpublished Ph. D. Thesis, Ankara University Faculty of Science.
[5] Bilska-Kos, A., Solecka, D., Dziewulska, A., Ochodzki, P., Jończyk, M., Bilski, H., Sowiński, P. (2017): Low temperature caused modifications in the arrangement of cell wall pectins due to changes of osmotic potential of cells of maize leaves (Zea mays L.). – Protoplasma 254(2): 713-724.
[6] Do, T. H., Nguyen, H. C., Lin, K. H. (2018): The responses of antioxidant system in bitter melon, sponge gourd, and winter squash under flooding and chilling stresses. – AIP Conference Proceedings 1954(1): 020001.
[7] Elkoca, E., Kantar, F., Eleman, G., Şat, İ. G. (2005): Determination of cold resistant dry bean (Phaseolus vulgaris l.) genotypes under field conditions. – Atatürk University Journal of the Faculty of Agriculture 36(1).
[8] Georgieva, K., Szigeti, Z., Sarvari, E., Gaspar, L., Maslenkova, L., Peeva, V., Tuba, Z. (2007): Photosynthetic activity of homoiochlorophyllous desiccation tolerant plant Haberlea rhodopensis during dehydration and rehydration. – Planta. 225(4): 955-964.
[9] Gökmen, Ö. Ö. (2006): Investigation of antioxidative mechanisms of domateste cold stress. – Unpublished Ph. D. Thesis, Cukurova Institute of Natural and Applied Sciences.
[10] Huang, C., Qin, N., Sun, L., Yu, M., Hu, W., Qi, Z. (2018): Selenium improves physiological parameters and alleviates oxidative stress in strawberry seedlings under low-temperature stress. – International Journal of Molecular Sciences 19(7): 1913.
[11] Heath, R. L., Packer, L. (1968): Photoperoxidation in isolated chloroplasts: II. role of electron transfer. – Archives of Biochemistry and Biophysics 125(3): 850-857.
[12] Jebara, S., Jebara, M., Liman, F., Aouani, E. (2005): Changes in ascorbate peroxidase, catalase, guaicol peroxidase and superoxide dismutase activities in common bean nodules under salt stres. – J. of Plant Physiol. 162: 929-936.
[13] Kabay, T., Şensoy, S. (2016): Drought stress-induced changes in enzymes, chlorophyll and ions of some bean genotypes. – Yuzuncu Yıl University Journal of Agricultural Sciences 26(3): 380-395.
[14] Kabay, T., Şensoy, S. (2017): Enzyme, chlorophyll and ion changes in some common bean genotypes by high temperature stress. – Ege University Journal of Agricultural Sciences 54(4): 429-437.
[15] Kabay, T., Erdinç, Ç., Şensoy, S. (2017): Effects of drought stress on plant growth parameters membrane damage index and nutrient content in common bean genotypes. – The Journal of Animal and Plant Sciences. 27(3). Page: 940-952.
[16] Kacar, B. (1994): Plant and Soil Chemical Analysis; III: Soil Analysis. – Issue No. 3, A. Ü. Agriculture Foundation, Ankara.
[17] Kacar, B., Inal, A. (2008): Plant Analysis. – Nobel Press, Ankara.
[18] Kolupaev, Y. E., Yastreb, T. O., Oboznyi, A. I., Ryabchun, N. I., Kirichenko, V. V. (2016): Constitutive and cold-induced resistance of rye and wheat seedlings to oxidative stress. – Russian Journal of Plant Physiology 63(3): 326-337.
[19] Kuşvuran, Ş. (2010): Relationships between physiological mechanisms for drought and salinity tolerance of melons. – Unpublished Ph. D. Thesis, Çukurova University Institute of Natural and Applied Sciences.
[20] Li, X., Wei, J. P., Scott, E. R., Liu, J. W., Guo, S., Li, Y., Han, W. Y. (2018): Exogenous melatonin alleviates cold stress by promoting antioxidant defense and redox homeostasis in camellia sinensis L. – Molecules 23(1): 165.
[21] Lichtenthaler, H. K., Wellburn, A. R. (1983): Determinations of total careteonids and chlorophylls a and b of leaf extracts in different solvents. – Biomchem. Soc. Transac. 11: 591-592.
[22] Ogweno, J. O., Song, X. S., Hu, W. H., Shi, K., Zhou, Y. H., Yu, J. Q. (2009): Detached leaves of tomato differ in their photosynthetic physiological response to moderate high and low temperature stress. – Scientia Horticulturae 123(1): 17-22.

http://www.aloki.hu ● ISSN 1589 1623 (Print) ● ISSN 1785 0037 (Online)
DOI: http://dx.doi.org/10.15666/aeer/1605_72717287
© 2018, ALÖKI Kft., Budapest, Hungary

[23] Rahnama, H., Ebrahimzadeh, H. (2005): The effect of NaCl on antioxidant enzyme activities in potato seedlings. – Biol. Planta. 49: 93-97.
[24] Sairam, R. K., Saxena, D. C. (2000): Oxidative stres and antioksidants in wheat genotypes: possible mechanism of water stres tolerance. – J. Agron. and Crop Sci. 184: 55-61.
[25] Sairam, R. K., Srivastava, G. C., Agarwal, S., Meena, R. C. (2005): Differences in antioxidant activity in response to salinity stress in tolerant and susceptible wheat genotypes. – Biol. Planta. 49: 85-91.
[26] SAS (2018): SAS/Stat Software Hangen and Enhanced. – SAS Institute Incorporation, Cary, NC.
[27] Sakamoto, M., Suzuki, T. (2015): Effect of root-zone temperature on growth and quality of hydroponically grown red leaf lettuce (Lactuca sativa L. cv. Red Wave). – American Journal of Plant Sciences 6(14): 2350.
[28] Soengas, P., Rodríguez, V. M., Velasco, P., Cartea, M. E. (2018): Effect of temperature stress on antioxidant defenses in brassica oleracea. – ACS Omega 3(5): 5237-5243.
[29] Sun, B., Liu, G. L., Phan, T. T., Yang, L. T., Li, Y. R., Xing, Y. X. (2017): Effects of cold stress on root growth and physiological metabolisms in seedlings of different sugarcane varieties. – Sugar Tech 19(2): 165-175.
[30] Sung, J., Lee, S., Lee, Y., Ha, S., Song, B., Kim, T., Krishnan, H. B. (2015): Metabolomic profiling from leaves and roots of tomato (Solanum lycopersicum L.) plants grown under nitrogen, phosphorus or potassium-deficient condition. – Plant Science 241: 55-64.
[31] Uzal, O., Yasar, F. (2017): Effects of Ga3 hormone treatments on ion uptake and growth of pepper plants under cadmium stress. – Applied Ecology and Environmental Research 15(4): 1347-1357.
[32] Terzi, R., Sağlam, A., Kutlu, N., Nar, H., Kadioğlu, A. (2010): Impact of soil drought stress on photochemical efficiency of photosystem II and antioxidant enzyme activities of Phaseolus vulgaris cultivars. – Turkish Journal of Botany 34(1) 1-10.
[33] Xian, M., Luo, T., Khan, M. N., Hu, L., Xu, Z. (2017): Identifying differentially expressed genes associated with tolerance against low temperature stress in Brassica napus through transcriptome analysis. – International Journal of Agriculture Biology 19(2).
[34] Xu, P. L., Guo, Y. K., Bai, J. G., Shang, L., Wang, X. J. (2008): Effects of long-term chilling on ultrastructure and antioxidant activity in leaves of two cucumber cultivars under low light. – Physiologia Plantarum 132(4): 467-478.
[35] Yesilova, A., Denizhan, E. (2016): Modelling mite counts using Poisson and negative binomial. – Fresenius Environmental Bulletin. 25: 5062-5066.
[36] Yoldas, F., Esiyok, D. (2009): The influence of temperature on growth and yield of green beans for processing. – International Journal of Agricultural Research 4(3): 124-130.
[37] Yu, X. H., Juan, J. X., Gao, Z. L., Zhang, Y., Li, W. Y., Jiang, X. M. (2015): Cloning and transformation of inducer of CBF expression1 (ICE1) in tomato. – Genet Mol Res. 14: 13131-13143.
[38] Zhou, R., Kjær, K. H., Rosenqvist, E., Yu, X., Wu, Z., Ottosen, C. O. (2017): Physiological response to heat stress during seedling and anthesis stage in tomato genotypes differing in heat tolerance. – Journal of Agronomy and Crop Science 203(1): 68-80.

http://www.aloki.hu ● ISSN 1589 1623 (Print) ● ISSN 1785 0037 (Online)
DOI: http://dx.doi.org/10.15666/aeer/1605_72717287
© 2018, ALÖKI Kft., Budapest, Hungary

A NOVEL APPROACH FOR DROUGHT CHARACTERIZATION BASED ON PERFORMANCE-ORIENTED SPI: AN ILLUSTRATIVE CASE OF SOUTHEASTERN ANATOLIA REGION, TURKEY

YILMAZ, B.

Manisa Vocational School of Technical Sciences, Manisa Celal Bayar University, Sehit Prof. Dr. Ilhan Varank Campus, 45140 Yunusemre, Manisa, Turkey
(e-mail: baris.yilmaz@cbu.edu.tr)

(Received 26th Aug 2018; accepted 11th Oct 2018)

Abstract. Drought is a main water-related natural hazard due to its features, sensitivities and effects to all sectors. According to climate change scenarios, drought hazards are expected to be more devastating, especially in arid and semi-arid regions. Drought characterization is essential to be aware of expected negative effects of droughts as well as to devise water management plans including possible mitigation measures. To this end, many drought indices have been developed for drought analysis, one of which is the Standardized Precipitation Index (SPI) that is widely used worldwide. In this study, a new drought index is proposed, namely the Drought Power Index (DPI), based on the SPI with orientation by reliability-resilience-vulnerability (RRV) concept. The use of the RRV approach with the SPI time series empowers the drought characterization by considering the frequency of drought event, drought recovery period as well as the severity of droughts-once a drought has occurred. Since the drought is identified as an unfavorable phenomenon, the DPI ranges from 0 to 1 where the higher values indicate higher drought devastating features (probability, duration and extremity of drought) and vice versa. The proposed approach is illustrated with reference to the Southeastern Anatolia Region, Turkey. The long-term (1970-2017) monthly precipitation data of eight meteorological stations under the operation of General Directorate of Meteorological Services of Ministry of Forestry and Water Affairs are used in the study. The 12-month SPI time series, which were later used for calculations of DPI, were obtained by the use of SPI_SL_6 software. The study revealed that there has been an increasing trend in DPI values in the basin, especially after 1993. It is concluded that the DPI is a valuable indicator for (i) spatially and temporally evaluating the drought characteristics, (ii) analysing meteorological, agricultural and hydrological drought severity with its coherent capability with SPI, (iii) ranking the regions in accordance with the drought vulnerability conditions.
Keywords: *drought power index (DPI), indicators, reliability, resilience, vulnerability*

Introduction

Drought is an important natural disaster, which has a wide range of negative impacts on the environment, agriculture and the economy (Man and Modra, 2008; Acikgoz, 2011; Konyali and Kiper, 2012; Gurel and Sener, 2012). It can be defined as a prolonged period of time beginning with a decrease in precipitation amount in a given region and a certain time interval; however, it is not possible to make a general definition due to its complexity, spatial and temporal variation and impacts (Heim, 2002; Wilhite and Glanz, 1985; Maracchi, 2000; Tate and Gustard, 2000; Tsakiris et al., 2007). The general approach to quantify the droughts is using indices. World Meteorological Organization (WMO) and Global Water Partnership (GWP) have given a wide and detailed literature and findings of drought indices for researchers in the domains of meteorology, hydrology, agricultural research and application, remote sensing, and water resources management (WMO and GWP, 2016). Depending on their structure, characteristics and their ability to fulfil certain criteria, some of them are used

http://www.aloki.hu ● ISSN 1589 1623 (Print) ● ISSN 1785 0037 (Online)
DOI: http://dx.doi.org/10.15666/aeer/1605_72897303
© 2018, ALÖKI Kft., Budapest, Hungary

for a wide range of applications, while others are intended to address drought related issues in specific systems (Tigkas et al., 2018).

The Standardized Precipitation Index (SPI), suggested by McKee et al. (1993), is a broadly used drought index. In 2009, WMO recommended SPI as the main meteorological drought index that countries should use to monitor and follow drought conditions (Hayes et al., 2011).

Although it is considered as a meteorological drought index originally, it is also used in numerous studies related to hydrological and agricultural droughts. Within a broad perspective, the studies have shown that the SPI is a valuable tool to assess drought events (Ionita et al., 2016; Mishra and Desai, 2005; Szalai and Szinell, 2000; Panaitescu et al., 2014; Lloyd-Hughes and Saunders, 2002; Cancelliere et al., 2007), to detect spatial and temporal droughts (Vicente-Serrano, 2006; Livada and Assimakopoulos, 2007), to reveal recurrent floods (Seiler et al., 2002), to manage water resources in basin scale (Shokoohi and Morovati, 2011; Zhang et al., 2009) and to assess drought impact on crop production (Labudova et al., 2017; Chen et al., 2016).

On the other hand, the EPA (US Environmental Protection Agency) has proposed the use of integrated assessments of watershed health to assist managers with identifying healthy watersheds and prioritizing candidate watersheds for protection and restoration (EPA, 2014). Here, the use of performance indicators (PIs), which is a fundamental concept for developing new ways to assess and manage environmental resources, can help watershed managers to understand the behavior of the droughts.

In this study, a new drought index, the Drought Power Index (DPI), is proposed, based on the SPI with orientation by reliability-resilience-vulnerability concept (RRV), which is first used by Hashimoto et al. (1982) for evaluation of water resources system performance. The use of the RRV approach with the SPI time series empowers the drought characterization by considering the frequency of drought event, drought recovery period as well as the severity of droughts-once a drought has occurred. Additional PIs, namely maximum extent and maximum duration of drought are also added to the formulation of the DPI. These performance indicators are all valuable to judge the effects of climate change in a given watershed. Therefore, it differ from other indices (e.g. SPI) by its capability to reveal the increasing (decreasing) devastating potential of droughts, as well as the propensity of droughts in the watershed. In addition, the DPI serves to that EPA's proposition by its inherent hybrid approach. Since the drought is identified as an unfavorable phenomenon, the DPI ranges from 0 to 1 where the higher values indicate higher drought devastating features. The proposed approach is illustrated with reference to the eight different provinces in the Southeastern Anatolia Region, Turkey. By the use of DPI, it is aimed to provide a better identification of regional drought characteristic.

Materials and methods

Study area and data

The Southeastern Anatolia Region (SAR) covers 9 provinces (Adıyaman, Batman, Diyarbakır, Gaziantep, Kilis, Mardin, Siirt, Şanlıurfa and Şırnak) located on the Euphrates-Tigris Basin and upper Mesopotamia plains *(Fig. 1)*.

The SAR provinces constitute approximately 10.7% of Turkey's total population (80.8 million, in 2018), and covers 9.7 of country's surface area, 780.6×10^3 km^2 (GAP, 2018). In general, the summer season in the region is very hot and under the influence

http://www.aloki.hu ● ISSN 1589 1623 (Print) ● ISSN 1785 0037 (Online)
DOI: http://dx.doi.org/10.15666/aeer/1605_72897303
© 2018, ALÖKI Kft., Budapest, Hungary

of dry and warm tropical air mass while the winter is warm and rainy. The average annual rainfall varies between 400 mm and 700 mm, and the mean annual temperature is about 18 °C, due to the high summer temperatures that approach 40 °C in daytime. The SAR holds 20% of the economically irrigable area of Turkey, while accounts for 28% of total water potential. In the fertile lands, the agriculture is the main activity, so the drought has vital importance on socio-economic development.

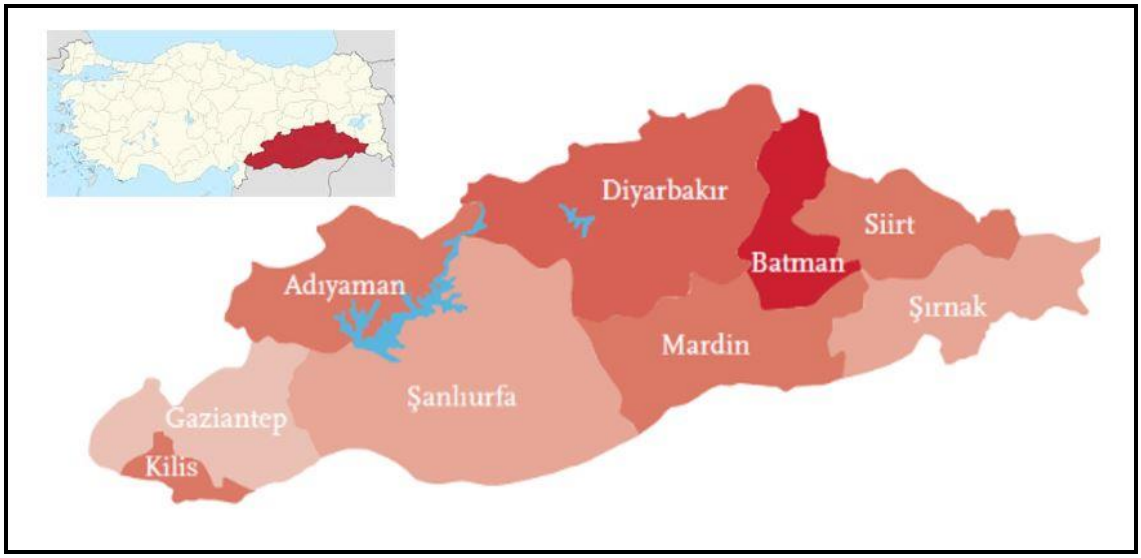

Figure 1. *Location of the Southeastern Anatolia Region (SAR) and provinces in the SAR*

In this study, although it was intended to calculate the DPI for the entire region, due to lack of adequate and reliable data for Şırnak, it is excluded from the analyses, and DPI values are calculated for the remaining eight provinces. *Table 1* shows the geographical co-ordinates of the meteorological stations chosen in the SAR. The precipitation data monitored in the meteorological stations between 1970 and 2017 were obtained from the General Directorate of Meteorological Services of Ministry of Forestry and Water Affairs. The statistical parameters of monthly precipitation at eight stations during the study period are presented in *Table 2*.

Table 1. *The meteorological stations in the SAR*

Stations	Station ID	Latitude (N)	Longitude (E)	Elevation (m)	Annual precip. (mm)
Mardin	17275	37.3103	40.7284	1040	638
Şanlıurfa	17270	37.1608	38.7863	550	431
Siirt	17210	37.9319	41.9354	895	676
Kilis	17262	36.7085	37.1123	640	481
Batman	17282	37.8636	41.1562	610	470
Gaziantep	17261	37.0585	37.3510	854	557
Adıyaman	17265	37.7553	38.2775	672	682
Diyarbakır	17280	37.8973	40.2027	674	475

http://www.aloki.hu ● ISSN 1589 1623 (Print) ● ISSN 1785 0037 (Online)
DOI: http://dx.doi.org/10.15666/aeer/1605_72897303
© 2018, ALÖKI Kft., Budapest, Hungary

Table 2. *Statistical parameters of precipitation during the 1970-2017 period*

Months		Mardin	Şanlıurfa	Siirt	Kilis	Batman	Gaziantep	Adıyaman	Diyarbakır
January	Min (mm)	2.10	0.90	10.00	14.10	5.60	29.40	7.00	0.70
	Max (mm)	233.10	192.40	196.80	197.30	128.00	235.60	333.50	142.80
	Avg. (mm)	101.76	73.76	80.50	77.59	57.67	92.09	126.18	62.28
	SD(mm)	61.48	43.86	37.79	45.83	26.67	45.69	69.92	33.92
	Skewness	0.46	0.50	0.77	1.11	0.38	1.04	0.71	0.23
	Kurtosis	0.45	0.48	0.74	1.07	0.37	1.01	0.69	0.22
February	Min (mm)	11.20	1.80	16.70	2.00	13.00	1.00	1.00	3.80
	Max (mm)	241.70	176.90	189.10	146.20	141.30	196.60	233.00	151.80
	Avg. (mm)	104.25	66.80	94.16	69.66	65.40	81.18	99.21	66.12
	SD(mm)	59.07	41.18	41.24	33.15	29.96	45.23	53.85	32.40
	Skewness	0.60	0.87	0.56	0.08	0.59	0.60	0.46	0.75
	Kurtosis	0.58	0.85	0.54	0.08	0.57	0.58	0.45	0.73
March	Min (mm)	15.30	3.20	13.20	5.70	0.60	5.10	4.90	1.50
	Max (mm)	266.10	297.40	271.30	186.20	259.40	247.40	348.50	210.30
	Avg. (mm)	94.99	62.38	103.75	65.65	73.45	71.79	88.66	67.20
	SD(mm)	56.66	50.50	53.09	40.89	43.93	47.70	62.94	40.50
	Skewness	1.47	2.24	0.84	1.19	1.66	1.33	1.73	1.15
	Kurtosis	1.42	2.17	0.81	1.15	1.60	1.29	1.67	1.12
April	Min (mm)	4.90	0.90	0.70	0.30	0.40	1.90	3.90	1.80
	Max (mm)	259.60	235.60	238.50	170.00	193.90	203.10	223.90	209.00
	Avg. (mm)	78.33	47.27	100.07	47.05	69.27	56.35	67.98	65.13
	SD(mm)	56.66	41.75	53.23	34.69	41.44	43.31	45.27	44.83
	Skewness	1.44	2.37	0.86	1.52	0.58	1.45	1.03	1.21
	Kurtosis	1.40	2.30	0.84	1.47	0.56	1.41	1.00	1.17
May	Min (mm)	0.00	0.00	2.00	0.00	0.00	1.40	1.80	0.00
	Max (mm)	196.80	109.70	291.10	95.10	192.30	126.80	146.80	152.60
	Avg. (mm)	41.39	25.30	60.03	25.30	41.57	30.63	37.95	41.11
	SD(mm)	45.13	27.65	54.38	20.31	39.63	24.81	35.04	34.86
	Skewness	2.10	1.36	2.02	0.94	1.88	1.44	1.68	1.14
	Kurtosis	2.04	1.32	1.95	0.91	1.82	1.39	1.63	1.11
June	Min (mm)	0.00	0.00	0.00	0.00	0.00	0.00	0.00	0.00
	Max (mm)	79.00	31.30	36.60	50.20	35.40	28.60	51.10	39.80
	Avg. (mm)	6.30	4.63	10.12	8.70	8.55	7.49	8.52	9.45
	SD(mm)	12.41	6.06	8.59	11.60	6.84	6.91	10.26	9.92
	Skewness	4.76	2.47	1.13	2.05	1.63	1.12	2.09	1.20
	Kurtosis	4.61	2.40	1.09	1.99	1.58	1.09	2.02	1.16
July	Min (mm)	0.00	0.00	0.00	0.00	0.00	0.00	0.00	0.00
	Max (mm)	31.00	9.70	22.20	15.00	7.50	46.00	10.50	6.10
	Avg. (mm)	2.10	1.09	2.56	2.15	1.06	5.06	1.55	0.80
	SD(mm)	4.85	1.81	3.87	3.45	1.38	8.61	2.00	0.95
	Skewness	5.20	3.78	3.44	2.65	3.53	3.96	2.70	4.08
	Kurtosis	5.04	3.66	3.33	2.57	3.42	3.84	2.62	3.95
August	Min (mm)	0.00	0.00	0.00	0.00	0.00	0.00	0.00	0.00
	Max (mm)	7.00	26.00	13.90	80.90	13.70	75.50	16.90	3.80

http://www.aloki.hu ● ISSN 1589 1623 (Print) ● ISSN 1785 0037 (Online)
DOI: http://dx.doi.org/10.15666/aeer/1605_72897303
© 2018, ALÖKI Kft., Budapest, Hungary

	Avg. (mm)	0.79	1.43	1.68	4.60	1.14	3.59	1.14	0.54
	SD(mm)	1.36	3.86	2.54	12.36	2.00	10.70	2.47	0.84
	Skewness	3.77	5.90	3.20	5.59	5.64	6.73	5.80	2.95
	Kurtosis	3.65	5.72	3.10	5.41	5.46	6.51	5.61	2.85
September	Min (mm)	0.00	0.00	0.00	0.00	0.00	0.00	0.00	0.00
	Max (mm)	15.50	83.20	35.50	48.10	38.10	54.70	44.70	68.20
	Avg. (mm)	2.99	4.59	5.88	6.70	4.73	8.27	6.69	5.56
	SD(mm)	3.36	12.37	7.10	8.96	7.24	12.65	9.62	11.09
	Skewness	2.26	5.85	2.94	2.78	3.69	2.52	2.09	4.37
	Kurtosis	2.19	5.66	2.85	2.69	3.58	2.44	2.02	4.24
October	Min (mm)	0.10	0.00	0.80	0.30	1.30	2.30	1.00	0.00
	Max (mm)	178.10	124.00	189.60	106.30	114.20	118.00	162.80	148.10
	Avg. (mm)	32.64	25.45	49.27	33.91	30.37	39.15	45.58	33.44
	SD(mm)	36.02	29.74	43.49	26.75	25.62	30.86	37.74	33.88
	Skewness	2.04	1.57	1.58	1.20	1.14	1.20	1.22	1.40
	Kurtosis	1.98	1.52	1.53	1.16	1.10	1.16	1.19	1.36
November	Min (mm)	1.10	0.70	1.30	2.00	0.40	3.10	0.00	1.90
	Max (mm)	189.80	187.70	213.80	179.40	146.80	214.30	232.80	123.10
	Avg. (mm)	69.35	46.58	81.06	58.14	53.65	66.33	73.17	53.60
	SD(mm)	46.98	32.78	53.02	36.80	35.17	39.20	45.53	28.33
	Skewness	0.72	1.79	0.91	1.35	1.04	1.33	1.03	0.34
	Kurtosis	0.70	1.74	0.88	1.31	1.01	1.29	1.00	0.33
December	Min (mm)	3.80	0.10	6.90	0.00	0.50	0.10	0.30	0.00
	Max (mm)	337.80	179.10	278.20	196.30	162.00	259.40	331.60	162.00
	Avg. (mm)	103.37	71.73	86.92	81.31	63.36	94.61	125.28	70.06
	SD(mm)	77.51	41.57	58.45	45.55	38.93	55.12	75.71	43.56
	Skewness	1.13	0.41	1.17	0.67	0.55	1.01	0.61	0.38
	Kurtosis	1.10	0.40	1.13	0.65	0.53	0.98	0.59	0.36

Standardized precipitation index (SPI)

The SPI is a powerful index with easy calculation steps as well as flexible time scales (e.g. 1, 3, 6, 12, 24 months). One of the main advantages of SPI is that it use only precipitation data. The index quantifies the precipitation deficit and surplus, taking into account the time series of cumulative precipitation for various reference periods. First, a Gamma distribution (two parametric) is fitted to precipitation data, and then it is transformed into a normal distribution. Therefore, the average of SPI values is 0, and the standard deviation is 1. For the studied area and studied period, one can identify the wet and dry conditions in accordance with the classification scale of SPI (*Table 3*).

It should be noted that, there has been studies which use different statistical distributions (Tsakiris and Vangelis, 2004; Angelidis, 2012), however Guttman (1999) showed that there are only minor differences in the results of SPI with respect to magnitude, duration and extent of drought. Since the SPI is a well-known index, the detailed calculation steps are not given here, however, it can be found in several papers (Mishra and Desai, 2005; Dashtpagerdi et al., 2015). In addition, the SPI software used in this study (SPI_SL_6.exe) could be download from the link given in the WMO (2012).

http://www.aloki.hu ● ISSN 1589 1623 (Print) ● ISSN 1785 0037 (Online)
DOI: http://dx.doi.org/10.15666/aeer/1605_72897303
© 2018, ALÖKI Kft., Budapest, Hungary

Table 3. *Classifications scale for SPI values (McKee et al., 1993)*

SPI values	Drought class
2.00 ≤	Extremely wet
1.99 to 1.50	Severely wet
1.49 to 1.00	Moderately wet
0.99 to (−0.99)	Near normal
(−1.0) to (−1.49)	Moderately dry
(−1.5) to (−1.99)	Severely dry
−2.00 ≥	Extremely dry

Performance indicators (PIs) for the SPI time series

The PIs are generally used to evaluate water management alternatives and/or to enable the comparison of decisions (Hashimoto et al., 1982). They can be simple averages (e.g. average of deficits), simple ratios (e.g. cost/benefit) and probability of time-based or volume based reliability.

In this study, the SPI-12 (12 month-SPI time series) were evaluated with five PIs defined as reliability, resilience, vulnerability, maximum extent and maximum duration. This procedure can be illustrated by considering any selected indicator C, whose time series of values is denoted as C_t, where the simulated period, t, extends to some future time, T (*Fig. 2*). To define reliability and resilience PIs, a single limit of unsatisfactory is assigned to SPI ≤ 0 for SPI-12 time series, which demonstrates the deficit from the mean amount of precipitation.

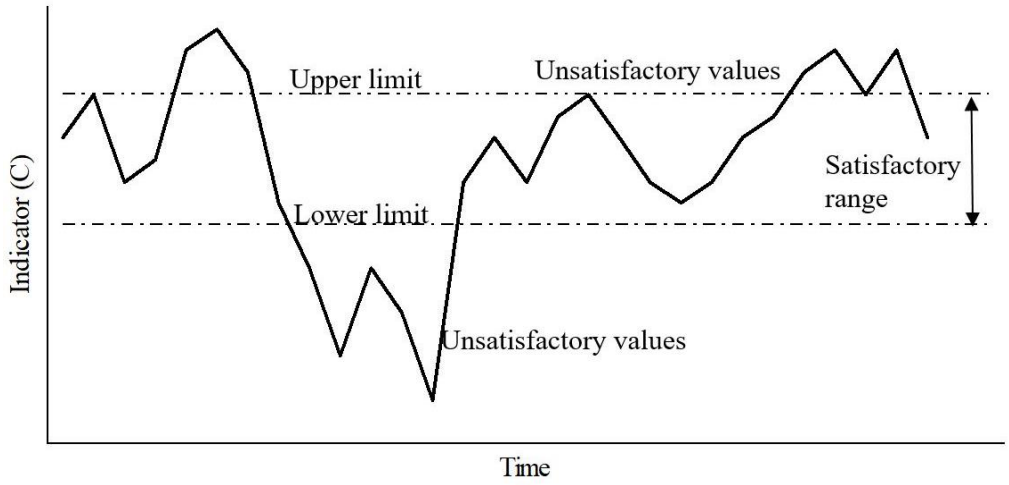

Figure 2. *Illustration for reliability, resilience and vulnerability concept*

Reliability (REL) is defined as the probability that any particular C_t value will be within the range of values considered satisfactory, and is calculated in accordance with *Equation 1*.

$$REL=\frac{(\text{Number of satisfactory } C_t \text{values, SPI>0})}{(\text{Total number of simulated period})} \quad \text{(Eq.1)}$$

http://www.aloki.hu ● ISSN 1589 1623 (Print) ● ISSN 1785 0037 (Online)
DOI: http://dx.doi.org/10.15666/aeer/1605_72897303
© 2018, ALÖKI Kft., Budapest, Hungary

Resilience (RES) is an indicator describing the speed of recovery from an unsatisfactory condition. It is the probability that a satisfactory value C_{t+1} will follow an unsatisfactory Ct value, and is calculated according to *Equation 2.*

$$RES=\frac{(\text{Number of times a satisfactory } C_{t+1} \text{ value follows an unsatisfactory } C_t \text{ value})}{(\text{Total number of unsatisfactory values, SPI}\leq 0)} \quad \text{(Eq.2)}$$

Although several definitions are possible for the vulnerability (Sandoval-Solis et al., 2011), in this study it is expressed as the probability of exceeding a certain threshold. Here, VUL is obtained by using the following relation that accounts the *"drought events"* (SPI ≤ -1), and *"severe and extreme drought events*" where the SPI ≤ -1.50 (*Eq. 3*).

$$VUL=\frac{(\text{Total number of severe and extreme drought events, SPI}\leq -1.5)}{(\text{Total number of drought events, SPI}\leq -1.0)} \quad \text{(Eq.3)}$$

The maximum extent (ME) of the drought is calculated by dividing the minimum SPI that is experienced in the study period, by -4 (*Eq. 4*). Here, an assumption is made as the worst-case drought magnitude, SPI = -4.0. It should be noted that, it could be determined in accordance with the experts' and decision makers' opinions.

$$ME=\frac{(\text{min SPI that is experienced in time})}{(\text{worst-case drought magnitude , assumptive SPI}=-4.0)} \quad \text{(Eq.4)}$$

The maximum duration (MD) is considered as the ratio of maximum duration of continuous droughts to the worst-case drought duration (D), which is accepted as 3 years (36 months) long drought period in this study (*Eq. 5*). It is thought as a threshold after which the devastating socio-economic effects may occur in agriculture sector.

$$MD=\frac{(\text{max duration of continuous droughts})}{(\text{worst-case drought duration , assumptive D}=36 \text{ months})} \quad \text{(Eq.5)}$$

Drought power index (DPI)

The DPI can be calculated by combining the REL, RES, VUL, ME and MD indicators as suggested by various researchers (Hashimoto et al., 1982; Sandoval-Solis et al., 2011; Maity et al., 2013). In this study, the DPI is proposed as a geometric average of *M* performance indicator (C_m^i) for the ith province in accordance with Sandoval-Solis et al. (2011) as given in *Equation 6.*

$$DPI_i=\left[\prod_{m=1}^{M} C_m^i\right]^{1/M} \quad \text{(Eq.6)}$$

Here, since the drought is identified as an unfavorable phenomenon, the indicators have to be arranged in accordance to their criteria type (minimizing or maximizing). For example, the reliability indicator is a maximizing indicator even if we calculate sustainability (maximizing reliability is a desired situation). However, in this proposed index where the main aim is to determine the devastating effects of drought with a single numeric (the power of droughts), the reliability is considered as a minimizing indicator. Therefore, the REL indicator is added to the geometric average formula as (1-REL). The same approach is applied for all five indicators, and the DPI is defined by

http://www.aloki.hu ● ISSN 1589 1623 (Print) ● ISSN 1785 0037 (Online)
DOI: http://dx.doi.org/10.15666/aeer/1605_72897303
© 2018, ALÖKI Kft., Budapest, Hungary

the following formula (*Eq. 7*) for the i^{th} province. The indicator (C_m^i) in the below equation must have a scale from 0-1, and undesirable criteria values tend to 1. In addition, more indicator can be included in DPI.

$$DPI_i=\left[(1\text{-}REL^i)*(1\text{-}RES^i)*VUL^i*ME^i*MD^i\right]^{1/5} \quad \text{(Eq.7)}$$

Decision scale of the DPI

The DPI is a valuable tool to demonstrate the drought character of the given region. However, a decision scale has to be proposed to evaluate the variations of drought character spatially and temporally. Since the drought power index does not mean the same thing for all water users, the proposed scale is flexible in accordance with the decision makers' preferences. To this end, the personal conversations with the water managers and crop yield experts in SAR are addressed the decision scale with the limits of indicators and the drought character (*Table 4*).

Table 4. *Indicator limits and decision scale*

Preferences of status	REL	RES	VUL	ME	MD	DPI range	Drought character
Very bad	0.40	0.40	0.80	0.80	0.80	0.71–1.00	Very strong (VS)
Bad	0.50	0.50	0.60	0.60	0.60	0.56–0.70	Strong (S)
Normal	0.70	0.70	0.40	0.40	0.40	0.36–0.55	Normal (N)
Good	0.80	0.80	0.20	0.20	0.20	0.20–0.35	Weak (W)
Very good	1.00	1.00	0.00	0.00	0.00	0.00–0.19	Very weak (VW)

Results and discussion

The assessment of the SPI-12 time series

The SPI-12 values obtained by the monthly precipitation data corresponding the eight provinces in the SAR are given in *Figure 3*. As can be seen, the most of year (approx. 70%) are counted in normal conditions, however the extreme droughts have occurred in 1973-1975 and 2007-2010 periods in almost all provinces. Generally, the basin has experienced severe droughts in 1990-1992 and 2000-2002. It leaps out that record extreme droughts (SPI-12 < -3.0) are monitored at Şanlıurfa, Batman and Gaziantep in 1973, at Kilis in 2014 and again at Batman in 2008. The year 1988 can be concluded as an extreme wet year in the basin. The percentile distributions of drought severities were analyzed by dividing the study period in two separate periods, 1970-1993 and 1970-2017 (*Table 5*). Although the SPI-12 time series is different from each other, it is possible to say that percentile of total droughts (total of moderate, severe and extreme droughts) has been increased in Mardin, Şanlıurfa and Kilis, due to the increasing number of severe and extreme droughts after 1993. Those results are in accordance with the slope of the regression line given in *Figure 3.*

Assessment of the DPI

To make an evaluation that base on the log-term drought conditions, the PIs and the DPI scores of each province were calculated (*Table 6).* The two different evaluation period constitute better understanding the variation in the drought character of the

http://www.aloki.hu ● ISSN 1589 1623 (Print) ● ISSN 1785 0037 (Online)
DOI: http://dx.doi.org/10.15666/aeer/1605_72897303
© 2018, ALÖKI Kft., Budapest, Hungary

provinces. The REL scores are slightly decreasing in the SAR (except Batman and Diyarbakır) that means the annual total precipitation gets less since the time elapsed. The reduction in precipitation amount is more evident in Mardin, where the probability of getting more than average annual precipitation is decreased from 70 to 53%.

The RES is similar for reliability, so the number of continuous droughts is increasing while the individual droughts are decreasing. This is another important result for the region because continuous droughts are more devastating for the socio-economic development in an agricultural dominant region. Again, the decreasing in the resilience indicator is determined significantly for Mardin, and none of the provinces get an increment in that performance indicator.

In this study, the vulnerability measures the percentage of severe and extreme droughts in all drought events. Şanlıurfa, Batman and Adıyaman are in good status from the view of vulnerability. In other words, the severe and extreme droughts are in a shift towards moderate drought in these provinces; however, for the rest of the region, especially in Kilis and Siirt, the opposite is valid.

Table 5. *Percentiles of droughts (%) for 1970-1993 and 1970-2017 periods*

Drght. catg.	Mardin		Şanlıurfa		Siirt		Kilis		Batman		Gaziantep		Adıyaman		Diyarbakır	
	(1)	(2)	(1)	(2)	(1)	(2)	(1)	(2)	(1)	(2)	(1)	(2)	(1)	(2)	(1)	(2)
Ext. wet	4	2	1	3	5	4	1	2	3	2	0	2	1	0	1	1
Sev. wet	7	3	5	2	4	2	7	5	2	3	5	3	6	6	6	4
Mod. wet	9	7	5	5	3	7	7	10	7	9	9	11	10	15	9	10
Normal	68	74	80	76	71	70	70	70	72	70	73	69	69	63	67	68
Mod. dry (a)	7	7	3	7	13	10	10	6	9	9	7	8	6	10	11	9
Sev. dry (b)	4	3	1	3	3	5	3	4	4	4	1	3	4	4	2	3
Ext. dry (c)	1	4	5	4	1	2	2	3	3	3	5	4	4	2	4	5
Total number of droughts (a+b+c)	12	14	9	14	17	17	15	13	16	16	13	15	14	16	17	17

(1) 1970-1993, (2) 1970-2017

Table 6. *The PIs and the DPI for 1970-1993 and 1970-2017 periods*

Province	REL[1]	REL[2]	RES[1]	RES[2]	VUL[1]	VUL[2]	ME[1]	ME[2]	MD[1]	MD[2]	DPI[1]	DPI[2]
Mardin	0.70	0.53	0.15	0.09	0.42	0.49	0.55	0.76	0.28	0.61	0.44 (N)	0.63 (S)
Şanlıurfa	0.58	0.54	0.20	0.14	0.71	0.51	0.83	0.86	0.28	0.33	0.56 (S)	0.57 (S)
Siirt	0.55	0.53	0.13	0.12	0.26	0.41	0.65	0.69	0.58	0.67	0.52 (N)	0.60 (S)
Kilis	0.50	0.46	0.09	0.09	0.35	0.52	0.66	0.79	0.22	0.36	0.47 (N)	0.59 (S)
Batman	0.52	0.52	0.12	0.11	0.44	0.43	0.77	0.84	0.33	0.36	0.54 (N)	0.56 (S)
Gaziantep	0.58	0.53	0.15	0.14	0.44	0.49	0.85	0.83	0.25	0.33	0.51 (N)	0.56 (S)
Adıyaman	0.50	0.49	0.11	0.10	0.54	0.39	0.69	0.72	0.33	0.33	0.56 (S)	0.53 (N)
Diyarbakır	0.51	0.53	0.12	0.12	0.38	0.48	0.66	0.72	0.31	0.58	0.51 (N)	0.61 (S)

[1]1970-1993, [2]1970-2017, (N) normal, (S) strong

http://www.aloki.hu ● ISSN 1589 1623 (Print) ● ISSN 1785 0037 (Online)
DOI: http://dx.doi.org/10.15666/aeer/1605_72897303
© 2018, ALÖKI Kft., Budapest, Hungary

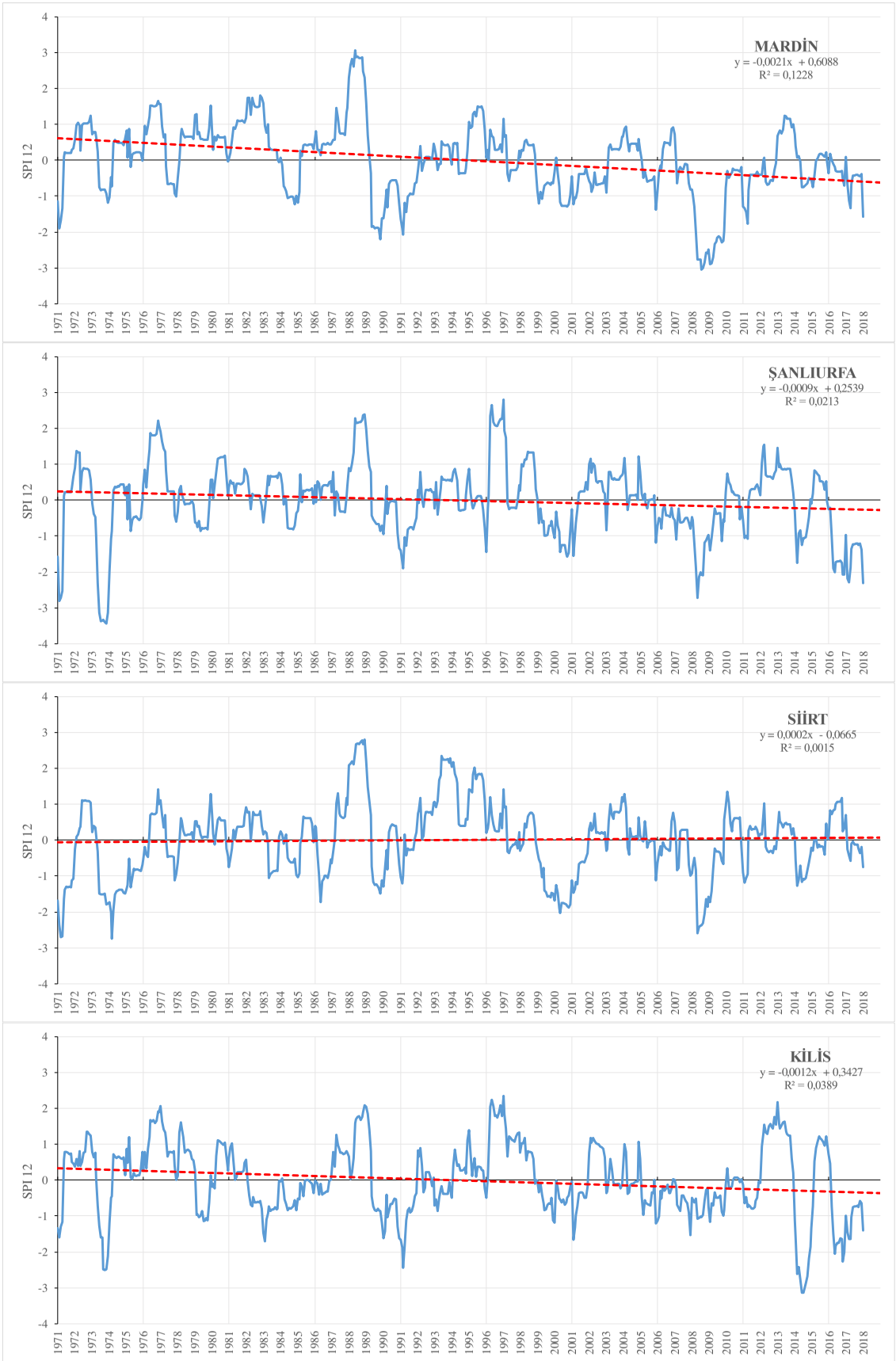

APPLIED ECOLOGY AND ENVIRONMENTAL RESEARCH 16(5):7289-7303.
http://www.aloki.hu ● ISSN 1589 1623 (Print) ● ISSN 1785 0037 (Online)
DOI: http://dx.doi.org/10.15666/aeer/1605_72897303
© 2018, ALÖKI Kft., Budapest, Hungary

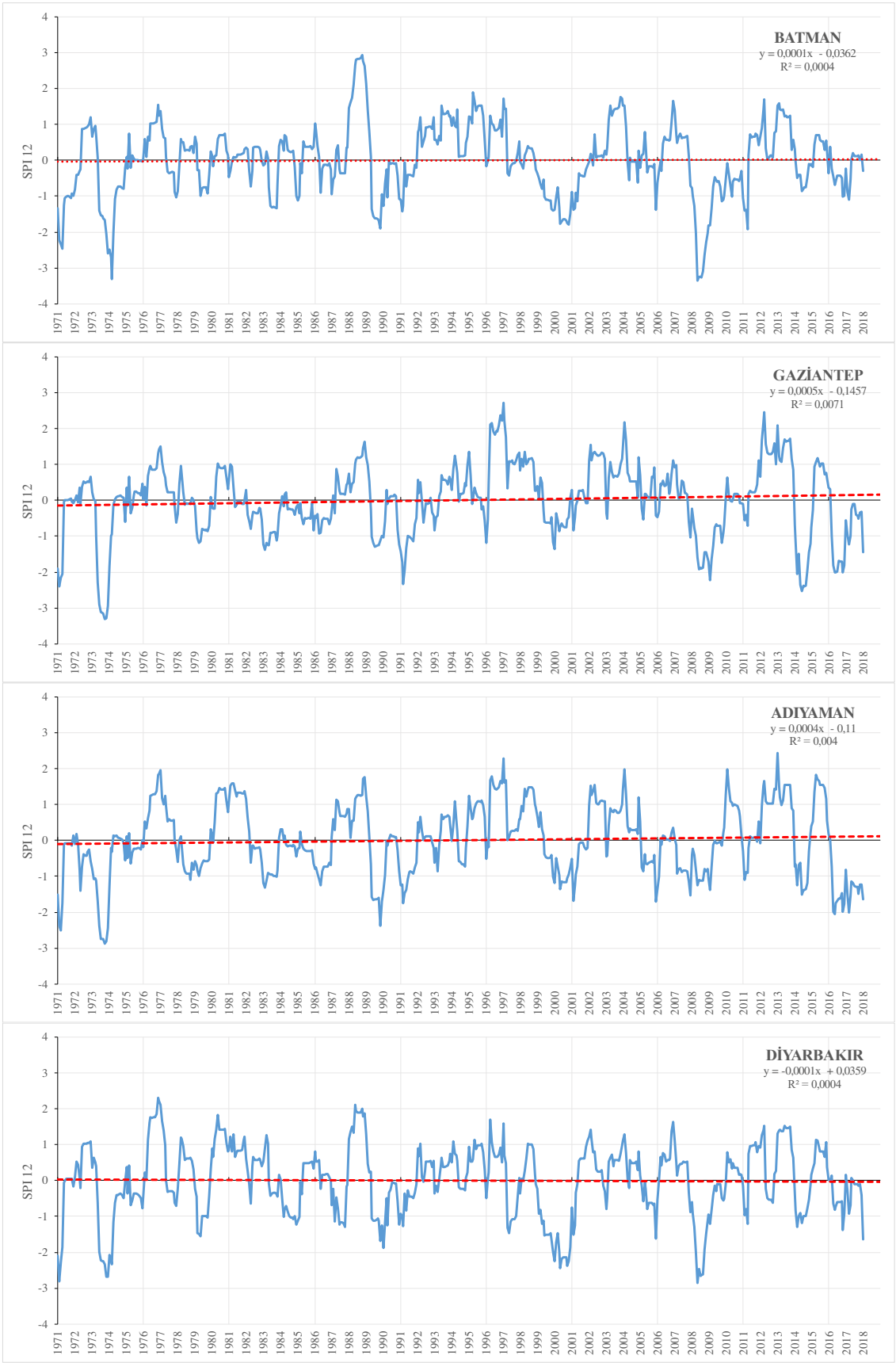

Figure 3. *The SPI-12 time series of provinces in SAR*

http://www.aloki.hu ● ISSN 1589 1623 (Print) ● ISSN 1785 0037 (Online)
DOI: http://dx.doi.org/10.15666/aeer/1605_72897303
© 2018, ALÖKI Kft., Budapest, Hungary

Şanlıurfa, Batman and Gaziantep have the worst scores for the ME due to the minimum SPI-12 values (-3.45), (-3.35) and (-3.31), respectively. Since the worst-case drought magnitude assumed as SPI-12 = -4.0, the maximum extent indicator results higher values 0.86, 0.84 and 0.83, respectively. As seen in *Figure 3,* the extreme droughts have observed in recent years in Batman, Kilis, Mardin and Diyarbakır, and that is why the significant increase in ME for the relevant provinces.

The MD is an important indicator in the proposed index since it detects the longest drought duration relatively. Siirt, Mardin and Diyarbakır has experienced the longest continuous drought durations 24, 22, and 21 months between 1970 and 2017, respectively. Excluding Adıyaman, it is clear from the increasing MD values that the longer droughts have experienced after 1993 for the other provinces.

Considering the end of 2017, the droughts were characterized as strong in seven provinces and normal in Adıyaman. When we compare the DPI values for 1970-1993 and 1970-2017, it is clear that there is an increase in the drought power generally. The DPI increase 43% and 25% for Mardin and Kilis, respectively. The ranking of provinces according to DPI scores for (1970-1993) and (1970-2017) revealed interesting results (*Table 7*). Due to the droughts after 1993, the orders of Mardin and Diyarbakır have moved from bottom to top in the ranking list. Adıyaman seems to lose drought power relative to the first period due to the environmental effects of Atatürk Dam, the biggest dam in Turkey with its 817 km^2 reservoir surface and under operation since 1992.

The results of the Southeastern Anatolia Region case which is in line with the findings of other researches (Sönmez et al., 2005; Oruç, 2017) are revealed that the region is under the threat of intense droughts. Moreover, it is obvious that the droughts have gained power after 1993. The increasing in drought power is more evident in Mardin, Diyarbakır, Siirt and Kilis, according to the DPI as well as the DPI rankings. Therefore, starting from these relevant provinces, the more efficient drought management plans integrated with water management policies are needed to overcome or reduce the negative effects of droughts in the region.

Table 7. *The DPI rankings of provinces*

Rankings	DPI (1970-1993)	DPI (1970-2017)
1	Şanlıurfa	Mardin
2	Adıyaman	Diyarbakır
3	Batman	Siirt
4	Siirt	Kilis
5	Gaziantep	Şanlıurfa
6	Diyarbakır	Batman
7	Kilis	Gaziantep
8	Mardin	Adıyaman

Before concluding, it is worthwhile to mention here that the most critical factor in the RRV approach is the threshold selection process, as by using a different threshold, the results will be different. In the DPI formulation, a reasonable procedure (regional experts' opinions) is proposed to identify the failure thresholds and the performance limits to obtain the decision scale. More research is needed into choosing the threshold level for different hydroclimatic regions. Towards this aim, sensitivity analysis, which

http://www.aloki.hu ● ISSN 1589 1623 (Print) ● ISSN 1785 0037 (Online)
DOI: http://dx.doi.org/10.15666/aeer/1605_72897303
© 2018, ALÖKI Kft., Budapest, Hungary

was beyond the scope of the present paper, is suggested as a tool to assess the sensitivity of the DPI to different SPI thresholds.

However, the DPI withstand the RRV framework approach, which has the ability to combine and quantify performance indicators. That is a key advantage of the DPI. Moreover, in recent years, more attention is given to the development of hybrid frameworks that could provide more reliable assessments with greater clarity and consistency. With its composite design, the DPI also fits well to that concept also, and can capture the long-term drought characteristics. Additionally, the DPI only needs the precipitation data that are relatively easy to obtain and process. In other words, the DPI also carries the advantages of the SPI.

Conclusions

In this study, the Drought Power Index (DPI), a modification of widely used SPI with performance indicators, is proposed. It aims to enhance the standardized precipitation index in characterizing drought's devastation power by logging the historical data. The DPI is a single metric to assess the historical drought characteristics base on the given performance indicators. It allows to evaluate the droughts by (i) considering the probability of occurrence, (ii) the speed of recovery once a drought occur, (iii) the relative frequency of severe and extreme droughts, (iv) maximum magnitude of experienced drought and (v) maximum duration of continuous droughts in a single metric. The selection of the time periods in SPI according to growing season of the main crops in the region as well as the decision makers' preferences on threshold values could make the DPI flexible and adaptable for the different drought management policies. Since it characterizes the drought power, it would provide additional insights for the studies dealing with socio-economic droughts, ecologic droughts as well as agricultural risk and insurance.

The presented case study is indicative to represent the DPI. It is noted that the use of the index in different watersheds should provide consensus on the effectiveness and the applicability of the proposed index. Moreover, the main recommendations on this approach include the application of the proposed approach to different time scales of SPI (e.g. monthly, seasonal or crop specific vegetation months for rainfed crops), investigation of the responses of the performance indicators to different SPI thresholds and application of this framework using other drought indices (e.g. Reconnaissance Drought Index). The further studies will reveal conclusions that are more comprehensive, and will help water authorities to assess existing situations, plan for future scenarios, implement processes and thus increase efficiency of the investments.

REFERENCES

[1] Acikgoz, F. E. (2011): Potential effects of global climate changes on field vegetable growing in the Thrace region. – Journal of Environmental Protection and Ecology 12(1): 240-244.

[2] Angelidis, P., Maris, F., Kotsovinos, N., Hrissanthou, V. (2012): Computation of drought index SPI with alternative distribution functions. – Water Resources Management 26(9): 2453-2473.

http://www.aloki.hu ● ISSN 1589 1623 (Print) ● ISSN 1785 0037 (Online)
DOI: http://dx.doi.org/10.15666/aeer/1605_72897303
© 2018, ALÖKI Kft., Budapest, Hungary

[3] Cancelliere, A., Mauro, G. D., Bonaccorso, B., Rossi, G. (2007): Drought forecasting using the standardized precipitation index. – Water Resources Management 21(5): 801-819.
[4] Chen, T., Xia, G., Liu, T., Chen, W., Chi, D. (2016): Assessment of drought impact on main cereal crops using a standardized precipitation evapotranspiration index in Liaoning province, China. – Sustainability 8: 1069. DOI: 10.3390/su8101069
[5] Dashtpagerdi, M. M., Kousari, M. R., Vagharfard, H., Ghonchepour, D., Hosseini, M. E., Ahani, H. (2015): An investigation of drought magnitude trend during 1975-2005 in arid and semi-arid regions of Iran. – Environment Earth Sciences 73(3): 1231-1244.
[6] EPA (Environmental Protection Agency) (2014): Wisconsin Integrated Assessment of Watershed Health. – EPA 841-R-14-001. http://www.epa.gov/healthywatersheds.
[7] GAP (Southeastern Anatolia Project Regional Development Administration) (2018): Latest stage in GAP. – Retrieved from: http://www.gap.gov.tr/gap-ta-son-durum-sayfa-32.html#
[8] Gurel, A., Senel, Z. (2012): Global climate change and adaptations in agriculture. – Journal of Environmental Protection and Ecology 13(1): 56-60.
[9] Guttman, N. B. (1999): Accepting the standardized precipitation index: A calculation algorithm. – Journal of the American Water Resources Association 35(2): 311-322.
[10] Hashimoto, T., Stedinger, J. R., Loucks, D. P. (1982): Reliability, resiliency, and vulnerability criteria for water resource system performance evaluation. – Water Resources Research 18(1): 14-20.
[11] Hayes, M. J., Svoboda, M., Wall, N., Widhalm, M. (2011): The Lincoln declaration on drought indices: Universal meteorological drought index recommended. – American Meteorological Society 92(4): 485-488.
[12] Heim, R. R. Jr. (2002): A review of twentieth-century drought indices used in the United States. – American Meteorological Society 83(8): 1149-1165.
[13] Ionita, M., Scholz, P., Chelcea, S. (2016): Assessment of droughts in Romania using the standardized precipitation index. – Natural Hazards 81(3): 1483-1498.
[14] Konyali, S., Kiper, T. (2012): Effect of climate changes on agricultural product quantity and yield and its reflection on sustainable development. The case of the Thrace region. – Journal of Environmental Protection and Ecology 13(1): 392-397.
[15] Labudova, L., Labuda, M., Takac, J. (2017): Comparison of SPI and SPEI applicability for drought impact assessment on crop production in the Danubian lowland and the east Slovakian lowland. – Theoretical and Applied Climatology 128(1-2): 491-506.
[16] Livada, I., Assimakopoulos, V. D. (2007): Spatial and temporal analysis of drought in Greece using the standardized precipitation index (SPI). – Theoretical and Applied Climatology 89(3-4): 143-153.
[17] Lloyd-Hughes, B., Saunders, M. A. (2002): A drought climatology for Europe. – International Journal of Climatology 22(13): 1571-1592.
[18] Maity, R., Sharma, A., Kumar, D. N., Chanda, K. (2013): Characterizing drought using the reliability-resilience-vulnerability concept. – Journal of Hydrologic Engineering 18(7): 859-869.
[19] Man, T. E., Modra, C. (2008): Drought impact of environment and agricultural products. – Journal of Environmental Protection and Ecology 9(1): 70-76.
[20] Maracchi, G. (2000): Agricultural Drought – A Practical Approach to Definition, Assessment and Mitigation Strategies. – In: Vogt, J. V., Somma, F. (ed.) Drought and Drought Mitigation in Europe. Advances in Natural and Technological Hazards Research. Kluwer Academic Publishers, Dordrecht.
[21] McKee, T. B., Doesken, N. J., Kleist, J. (1993): The relationship of drought frequency and duration to time scales. – Proceedings of the AMS 8th Conference on Applied Climatology, Anaheim, CA, USA, pp. 179-184.
[22] Mishra, A., Desai, V. (2005): Spatial and temporal drought analysis in the Kansabati River basin, India. – International Journal of River Basin Management 3(1): 31-41.

http://www.aloki.hu ● ISSN 1589 1623 (Print) ● ISSN 1785 0037 (Online)
DOI: http://dx.doi.org/10.15666/aeer/1605_72897303
© 2018, ALÖKI Kft., Budapest, Hungary

[23] Oruç. N. (2017): Drought analysis of the Southeast Anatolia Region. – M.Sc. Thesis, Pamukkale University, Institute of Science, Turkey.
[24] Panaitescu, L., Ilie, C., Lungu, M. L., Popescu, M., Lungu, D., Nita, S. (2014): Risk assessment modern approach to the phenomenon of drought and aridity in central and south Dobrudja. – Journal of Environmental Protection and Ecology 15(1): 110-122.
[25] Sandoval-Solis, S., Mckinney, D. C., Loucks, D. P. (2011): Sustainability index for water resources planning and management. – Journal of Water Resources Planning and Management 137(5): 381-390.
[26] Seiler, R. A., Hayes, M., Bressan, L. (2002): Using the standardized precipitation index for flood risk monitoring. – International Journal of Climatology 22(11): 1365-1376.
[27] Shokoohi, A., Morovati, R. (2011): Basinwide comparison of RDI and SPI within an IWRM framework. – Water Resources Management 29(6): 2011-2026.
[28] Sönmez, F. K., Kömüscü, A. Ü., Erkan, A., Turgu, E. (2005): An analysis of spatial and temporal dimension of drought vulnerability in turkey using the standardized precipitation index. – Natural Hazards 35(2): 243-264.
[29] Szalai, S., Szinell, C. (2000): Comparison of Two Drought Indices for Drought Monitoring in Hungary-A case study. – In: Vogt, J. V., Somma, F. (ed.) Drought and Drought Mitigation in Europe. Advances in Natural and Technological Hazards Research. Kluwer Academic Publishers, Dordrecht.
[30] Tate, E. L., Gustard, A. (2000): Drought Definition: A Hydrological Perspective. – In: Vogt, J. V., Somma, F. (ed.) Drought and Drought Mitigation in Europe. Advances in Natural and Technological Hazards Research. Kluwer Academic Publishers, Dordrecht.
[31] Tigkas, D., Vangelis, H., Tsakiris, G. (2018): Drought characterization based on an agriculture-oriented standardized precipitation index. – Theoretical and Applied Climatology. DOI/10.1007/s00704-018-2451-3.
[32] Tsakiris, G., Pangalou, D., Vangelis, H. (2007): Regional drought assessment based on the reconnaissance drought index (RDI). – Water Resources Management 21(5): 821-833.
[33] Tsakiris, G., Vangelis, H. (2004): Towards a drought watch system based on spatial SPI. – Water Resources Management 18(1): 1-12.
[34] Vicente-Serrano, S. M. (2006): Spatial and temporal analysis of droughts in the Iberian Peninsula (1910-2000). – Hydrological Sciences Journal 51(1): 83-97.
[35] Wilhite, D. A., Glantz, M. H. (1985): Understanding the drought phenomenon: the role of definitions. – Water International 10: 111-120.
[36] WMO (World Meteorological Organization). (2012): Standardized Precipitation Index User Guide. – WMO No: 1090, Geneva, Switzerland.
[37] WMO and GWP (World Meteorological Organization and Global Water Partnership). (2016): Handbook of drought indicators and indices. Integrated drought management programme (IDMP), Integrated drought management tools and guidelines series 2, no 1173. – WMO, Geneva, Switzerland.
[38] Zhang, Q., Chong-Yu, X., Zengxin, Z. (2009): Observed changes of drought/wetness episodes in the Pearl River basin, China, using the standardized precipitation index and aridity index. – Theoretical and Applied Climatology 98(1-2): 89-99.

http://www.aloki.hu ● ISSN 1589 1623 (Print) ● ISSN 1785 0037 (Online)
DOI: http://dx.doi.org/10.15666/aeer/1605_72897303
© 2018, ALÖKI Kft., Budapest, Hungary

HERITABILITY OF END-USE QUALITY AND BIOFORTIFICATION CHARACTERISTICS IN LINE X TESTER BREAD WHEAT (*Triticum aestivum* L.) CROSSES

KUTLU, I.

Department of Biosystem Engineering, Faculty of Agriculture, Eskisehir Osmangazi University 26160 Eskisehir, Turkey
(e-mail: ikutlu@ogu.edu.tr; phone: +90-222-3242991; fax: +90-222-3242990)

(Received 29th Aug 2018; accepted 11th Oct 2018)

Abstract. Wheat (*Triticum aestivum* L.) is an important resource of dietary energy and protein for the growing world population and its potential to reduce micronutrient-related malnutrition can be increased via improving the genetically micronutrient-rich wheat varieties. The study aimed to evaluate "line x tester" bread wheat hybrids in terms of the physical quality criteria affecting wheat flour yield, protein and biofortification associated nutrient element contents. In addition, it was tried to determine the gene effects that play a role in the inheritance of biofortification and end-use quality traits. Twenty-eight F_1 hybrids which were obtained by crossing seven lines and four testers were evaluated along with parents in Eskisehir, Turkey during 2016-17 growing period for mentioned traits. It has been determined that the effects of non-additive genes are dominant in the inheritance of the traits examined. It would be wise to leave the selection for these properties to future generations. In addition, appropriate parents and promising crosses were identified by looking at their parents' general combination abilities and specific combination abilities and heterosis values of the crosses. The results obtained were also supported by the principal component analyses. Consequently, the DH22 line is appropriate for breeding programs for high end-use quality and biofortified capacity. "DH20xHarmankaya", "DH22xHarmankaya", "DH21xAltay" and "DH18xAltay" are promising crosses for biofortification and end-use quality.
Keywords: *zinc and iron concentration, kernel dimensions, protein rate, color values, gene action, malnutrition*

Introduction

Wheat (*Triticum aestivum* L.) is one of the cereals with the highest production worldwide and its traits such as easy marketing, transportation, storage and processing facilities encourage wheat cultivation. This intense and unending interest in wheat farming has also intensified plant breeding efforts to make the agricultural characteristics of wheat more suitable to consumer demands. Until today, major improvements in yield, processing and end-use quality of wheat has been obtained with agronomy and plant breeding. Despite this advancement, common food shortages maintain, there are a lot of undernourished people in the world today, predominantly in the developing countries. The changes in the yield potential of today's wheat varieties and the rapidly decreasing genetic potential, which are caused by the changing climatic conditions, make the breeding studies indispensable. Maintaining grain quality besides yield under climate change is critical for human nutrition, end-use functional traits and commercial value of wheat (Nuttall et al., 2017).

Grain quality is defined by a range of physical and compositional characters which are important end-use requirements and commercial value. Physical characteristics of the wheat kernel, including grain weight, dimensions, shape and hardness, influence the classification, milling, transportation, storage and market value of bread wheat (Maphosa et al., 2014). Grain color that can be included in physical quality characters of the kernel is also a frequently used parameter for the classification of wheat and quality

http://www.aloki.hu ● ISSN 1589 1623 (Print) ● ISSN 1785 0037 (Online)
DOI: http://dx.doi.org/10.15666/aeer/1605_73057326
© 2018, ALÖKI Kft., Budapest, Hungary

determination. Market classes of bread wheat are based in part on white or red kernel color. Color is of extensive significance in food preference, and it may be a guarantee of purity and trueness to the preferred type (Graham et al., 1999). The compositional characteristics include protein concentration and composition of other nutrients. Grain protein concentration and composition determine nutritional and end-use characters of dough mixing and rheological traits including loaf volume, dough strength, extensibility, breakdown and development time all of which influence the activity of the bread making process and product quality (Nuttall et al., 2017). Macro and micronutrient elements such as phosphor (P), potassium (K), copper (Cu), iron (Fe) and zinc (Zn) in the other nutrients constituting the grain composition are important components determining grain quality.

Cereal crops which are an important source of minerals and other nutrients for humans supply 44% of the daily intake of Fe (15% from bread), 25% of Zn (11% from bread) and 31% of Cu (14% from bread) (Henderson et al., 2003). Especially, high Zn and Fe concentrations in bread wheat are important quality characters because they could reduce micronutrient malnutrition-related problems in the developing world (Velu et al., 2012). Iron is an necessary element for nearly all alive organisms as it plays a role in a wide diverse of metabolic processes, including haemoglobin formation, deoxyribonucleic acid (DNA) synthesis, oxygen and electron transport (Abbaspour et al., 2014). In addition, Zn is one of the most important trace elements whose significance to health is increasingly appreciated. It has three major biological roles, as catalyst, structural, and regulatory ion in the organism and its deficiency may play an important role in the appearance of diseases (Chasapis et al., 2012). One of the minerals required for human nutrition is also Cu, which can create negative health effects in case both deficiency and excess (Stern et al., 2007). Potassium is one of the essential nutrients in the human body with the regulatory effect of blood pressure. It is important because of requiring in human nutrition, also it provide increased in quality of edible parts of crops and crop yield (He and MacGregor, 2008). Plant breeding to reduce the extent of mineral nutrient deficiencies and especially increase micronutrient concentrations such as Fe and Zn in cereal grain is named genetic biofortification and it is the most sustainable approach and a widely accepted strategy for this aim (Cakmak, 2008).

Grain quality is influenced by genotype, environment and agronomic practise. There is strong genetic control over physical kernel features like shape, thickness and volume just as functional properties of wheat such as grain hardness, protein content and composition (Ferreira et al., 2012). Grain color is also a simply inherited feature and can be easily combined with high-yielding traits (Graham et al., 1999). Over all, the understanding gene action play role in heritability of milling and end-use characteristics will provide a powerful tool for developing breeding strategies for overcoming the effects of climate change to grain quality. Knowing type of gene effect in the formation of a character is important to determine the breeding method to be able to improve the mentioned feature. In addition, improving biofortified wheat varieties which have desirable nutritional quality, protein content, processing quality and higher grain yield will provide reduction for undernourishment and malnutrition at developing countries.

It has been endeavored providing more crop yield and quality alternatives to farmers in developed varieties with conventional breeding. However, nutritional value of crop has been usually disregarded. Present genetic variation, heritability of characters, gene action, relationship among traits, and the availability of diagnostic tools and screening

http://www.aloki.hu ● ISSN 1589 1623 (Print) ● ISSN 1785 0037 (Online)
DOI: http://dx.doi.org/10.15666/aeer/1605_73057326
© 2018, ALÖKI Kft., Budapest, Hungary

techniques are criteria mostly used to define candidate characters and estimate potential genetic gains. Breeding for enhanced micronutrient content should performed basically depend on accompanying agronomic or end-use traits to be adopted by farmers and consumers. The availability of genetic variation for micronutrient density is necessary for determining the applicability of obtaining meaningful enhancement through conventional breeding. If there is adequate genetic variation, breeders can utilize transgressive segregation, additive gene effects and heterosis to develop micronutrient density (Pfeiffer and McClafferty, 2007). When the required genetic variation is not available, combining through hybridization is frequently used by plant breeders to create genetic variation. The breeder would like to recognize the parental and cross offspring in these newly developed cross populations in terms of desired characteristics in early generations and to choose those with superior characteristics. Knowing heritability and type of gene effect in the characters to be transferred, general and specific combination abilities of selected parents is important to determine breeding method and facilitate cultivar development studies. "Line x tester" analysis is frequently used as an easy and powerful statistical approach for determining combining ability of genotypes in plant breeding (Aslam et al., 2014).

The main purpose of the study was to identify the best parents and promising crosses according to general and specific combining ability of them for physical and chemical quality traits to determine the potential of desirable end-use quality and biofortification properties in bread wheat. In addition, determination of gene effects that play role in inheritance of these traits related to quality and biofortification was aimed.

Materials and methods

Plant material and experimental design

In the study, plant materials are seven doubled haploid (DH) wheat lines gained from the F_2 generation of hybrids between 33IBSWN-S-244, Tosunbey and Mufitbey, four registered cultivars (Altay 2000, Bezostaja-1, Harmankaya 99, Kate A-1) and twenty-eight crosses obtained from them. Hybridization method was line x tester mating design. The 39 genotypes were grown in randomized complete block design with three replications. The field experiment was conducted at Eskisehir Osmangazi University Agriculture Faculty research areas, Eskisehir, Turkey in 2016-17 growing season. The plots consisted of four rows which are 1 m long with 20 plants and distance between rows was 30 cm. Standard practices used by the breeding programs were applied as agronomic practices. Wheat grain was harvested at crop maturity and grain samples were analysed in terms of physical and chemical properties.

Physical kernel properties

Three principal kernel dimensions (length, width and thickness) were measured using a digital caliper (Neiko, 01409A, made in USA) reading to an accuracy of 0.01 (mm). Kernel length was accepted as the longest line through the grain, which almost always runs from the embryo to the distal end, and kernel width was the longest line through the grain at a 90° angle to the length, while kernel thickness was determined the longest line through the grain that is perpendicular to both the length and the width. Then, kernel sphericity (KS) and volume (KV) were calculated using the following equations:

http://www.aloki.hu ● ISSN 1589 1623 (Print) ● ISSN 1785 0037 (Online)
DOI: http://dx.doi.org/10.15666/aeer/1605_73057326
© 2018, ALÖKI Kft., Budapest, Hungary

$$KS = ((LWT)^{1/3}) / L * 100 \quad \text{(Mohsenin, 1986)}$$

$$KV = 4 / 3.\Pi.LWT \quad \text{(Weisstein, 2018)}$$

In these equations, L, W, T indicated length, width and thickness, respectively. Kernel hardness (KH) was determined as SKCS hardness index (HI) using the Single Kernel Characterization System 4100 (SKCS) (Perten Instruments, North America, Inc., Springfield, IL, USA). Similarly, kernel weight was measured using a sample of 300 kernels (Method 55-31) and then calculated thousand kernel weights (AACCI, 2000). The hectolitre weight was determined using a 250 ml volume hectolitre scale (Loyka H Hectolitre scales).

The kernel color of wheat genotypes was determined using Granular Attachment CR-A50 with Konica Minolta Chroma Meter CR-400 for each replicate. The CIE (Commission Internationale De L'eclairage) L (lightness), CIE a (red– green) and CIE b (yellow–blue) were read using a D65 light source and the observer angle at 2°. The tristimulus values of CIE L, a and b readings were calibrated against a standard white plate (Y = 84.8; x = 0.3199; y = 0.3377).

Chemical kernel properties

Kernel nitrogen (N) content was determined by the Kjeldahl method (Kirk and Sawyer, 1991), and then total protein content (%) calculated by multiplying the N percentage by 5.7. The ground samples were turned into ash at 500 °C in furnace for 5 h and then dissolved in 3.3% HCl and analyzed for K, Zn, Fe and Cu by using atomic absorption spectrometer (Analytic-Jena novAA 350, Germany) according to Balint et al. (2001). To check the related elemental measurements, reference tomato leaf samples from National Institute of Standards and Technology (Gaithersburg, MD, USA) were used. Phosphorus concentrations of these samples were measured colorimetrically according to the Barton (1948) method. The analysis results were confirmed by NIST Reference Material 8436 Status Wheat Flour.

Statistical analyses

The analyses of variance, general combining ability (GCA), specific combining ability (SCA), variance of additive and dominant gene effects based on variances of general and specific combination abilities and broad and narrow sense heritability were calculated according to Falconer (1980), using the TarPopGen Statistical Package Program developed by Ozcan (1999). The magnitude of heterosis over mid parent value and over better parent value (heterobeltiosis) was estimated according to the method suggested by Chiang and Smith (1967) and Fonseca and Patterson (1968), respectively.

The raw data of variables into distinct principal factors representing the different proportions of the data variability was transformed with principal component analysis (PCA). Thus, it was provided data reduction and transforming the raw data into principal components. PCA factors were equal to the number of studied variables which were 17 initial in this study, then these factors was transformed the raw data into six factors with the pattern that first factor contributed the most variability. The first six factors have effectively transformed the raw data, extracted significant variability and considerable for further data analysis due to having more than 1.0 eigenvector values. Maximum iterations for convergence were 25; and the variamax rotation method was

http://www.aloki.hu ● ISSN 1589 1623 (Print) ● ISSN 1785 0037 (Online)
DOI: http://dx.doi.org/10.15666/aeer/1605_73057326
© 2018, ALÖKI Kft., Budapest, Hungary

applied. The other factors had eigenvector value less than 1.0 not effective in order to interpret the results. However, evaluation of the first four factors instead of the first six factors resulted in a more meaningful grouping. Bi-plot was drawn by using principal factors, which have most of variability. Bi-plot was two dimensional scatter diagrams which depicted the scattering pattern of genotypes and traits. The maximum, minimum and mean values of genotypes for each trait were shown as box-plot. These analyses carried out with psych" R package (R version 3.3.1).

Results and discussion

End-use quality of parents and hybrids

The maximum, minimum and mean values of psychical kernel characteristic for "line x tester" bread wheat crosses were shown in *Figure 1*. For all genotypes, values of psychical kernel traits were ranged 5.97-7.12 mm for kernel length, 2.29-3.15 mm for kernel width, 2.86-3.45 mm for kernel thickness, 163.59-311.52% for kernel volume, 55.58-61.75% for kernel spherecity, 31.66-42.36 g for thousand kernel weights and 74.35-81.33 kg for hectolitre weight. The best parents among the testers were Harmankaya for kernel length while Bezostaja-1 for all psychical kernel traits. Among the lines, DH18 for kernel length, DH19 for kernel hardness and DH6 for hectolitre weight, while DH20 had the best performance for many of psychical kernel traits. Variation of crosses for these traits were quite small and mostly between their parents. "DH6 x Harmankaya", "DH22 x Harmankaya", "DH19 x Altay", "DH19 x Kate" and "DH20 x Bezostaja" were remarkable crosses for these traits (*Fig. 1*).

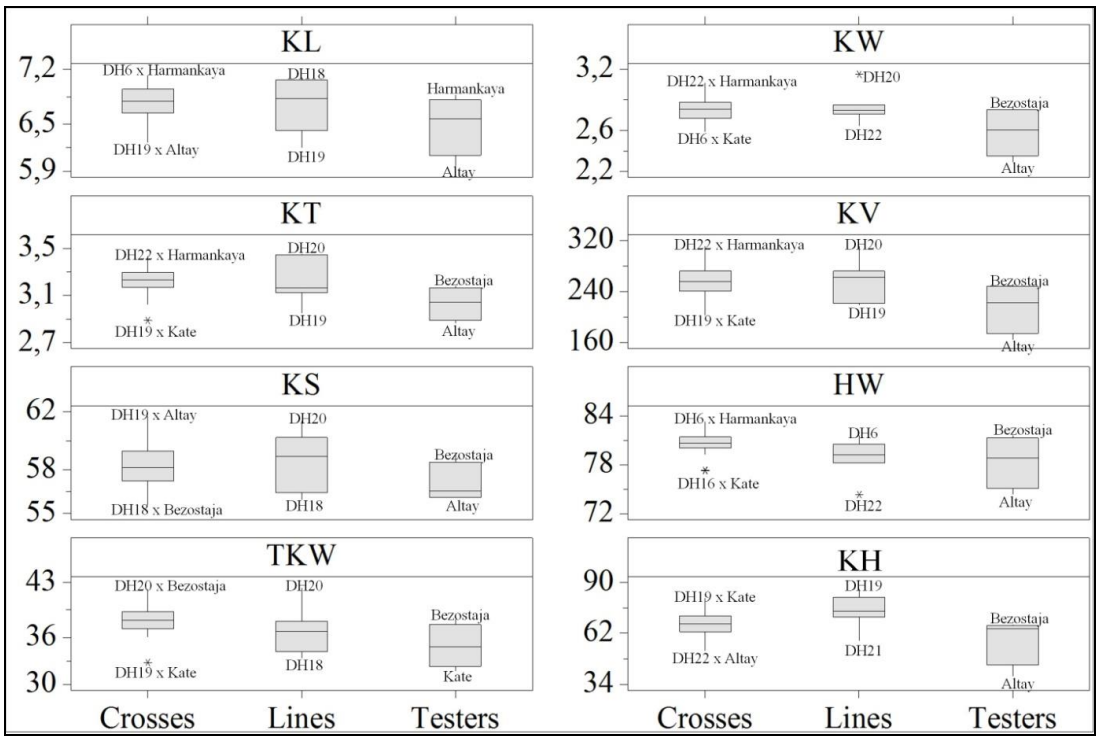

Figure 1. *Maximum, minimum and mean values of psychical kernel characteristic for line x tester bread wheat crosses. KL: kernel length (mm), KW: kernel width (mm), KT: kernel thickness (mm), KV: kernel volume (%), KS: kernel sphericity (%), HW: hectolitre weight (kg), TKW: thousand kernel weight (g), KH: kernel hardness (SKCS-HI)*

http://www.aloki.hu ● ISSN 1589 1623 (Print) ● ISSN 1785 0037 (Online)
DOI: http://dx.doi.org/10.15666/aeer/1605_73057326
© 2018, ALÖKI Kft., Budapest, Hungary

Kernel length, width, thickness, sphericity and volume affect the amount of flour. Because can be extracted in milling more flour, it is preferred with large, round and plump grain than small, thin and shrivelled grain (Maphosa et al., 2014). Thousand kernel weights that is an important component of grain yield is one of the physical factors that are indicative of grain size and determines grain quality and it is very important to focus on breeding studies (Korkut et al., 2001). Hectolitre weight is an important physical quality element used in wheat standards. As it increases, the amount of dry matter and flour increase (Schuler et al., 1995). If considered to the observed values, it is thought that the flour yield and milling quality of the mentioned genotypes and therefore the market values may be higher. Kernel hardness, in other words, the texture of wheat, has a great influence on the quality and general processing properties of bread wheat (Ponce-García et al., 2016). Hardness affects milling and if grain is harder, starch content is more damaged. Gas retention capacity, fermentation tolerance, water absorption, energy consumption in the mill increase (Hruskova and Svec, 2009). In the grain hardness measurements made with SKCS, hard wheat scores are around 75 and soft wheat scores 30 and below. According to this, genotypes DH6, DH16, DH19, DH22, "DH6 x Kate", "DH16 x Bezostaja", "DH19 x Harmankaya" and "DH19 x Kate" belong to the hard wheat class.

The L color value of the crosses, lines and tester measured in the kernel ranged from 43.93 to 56.94, with an average of 49.19. The line DH18, the tester Altay and their cross have the highest values (53.98, 56.94 and 56.73, respectively), it has been the lowest with the "DH21 x Harmankaya", Kate and DH19 (*Fig. 2*). In terms of a value in kernel, "DH20 x Altay" had the highest value (13.20), while "DH22 x Bezostaja" was the last value with 10.84 and the average of the genotypes was 12.01. The b value of the kernel was determined as the lowest 20.12 in "DH16 x Bezostaja", while as the highest 26.65 in "DH20 x Altay". The average of genotypes was 22.96 and the all lines were exceeding the average, while only one tester (Altay) exceeded it (*Fig. 2*).

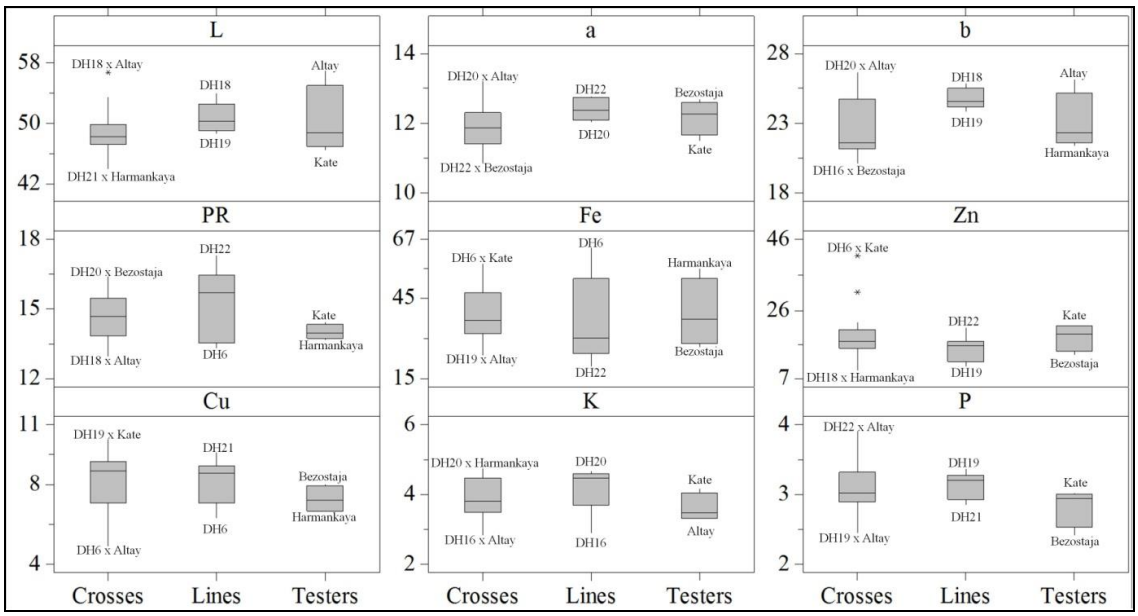

Figure 2. *Maximum, minimum and mean values of chemical kernel characteristic for line x tester bread wheat crosses. L: lightness, a: red-green, b: yellow-blue, PR: protein rate (%), Fe: iron (mg kg^{-1}), Zn: zinc (mg kg^{-1}), Cu: copper (mg kg^{-1}), K: potassium (mg kg^{-1}), P: phosphorous (mg kg^{-1})*

http://www.aloki.hu ● ISSN 1589 1623 (Print) ● ISSN 1785 0037 (Online)
DOI: http://dx.doi.org/10.15666/aeer/1605_73057326
© 2018, ALÖKI Kft., Budapest, Hungary

Kernel color serves as the basis for segregating wheat grain into classes. Wheat grains have white, yellow and red colors. These color differences are generally are caused by color materials present in different parts of the grain and genotypic differences. The fact that the grain is normal and light indicates that the grain is solid, thin-crusted and soft, and that it is normal and dark color indicates that the grain belongs to the hard wheat variety. When the observation values were examined, it was seen clearly that L value is low and a value is high for genotypes with high hardness and protein rate. Namely, dark colored and red grained genotypes had harder and higher protein. Although high protein contents and taking a long time pre-harvest sprouting resistance has been associated with red kernel color in wheat, white kernel color in wheat is preferred for the principal foods made from wheat in some countries (De Peuw and McCetc, 1988). Therefore, breeding programs are planned according to consumer demands for wheat kernel color.

Protein and mineral contents of genotypes

It is desirable that the amount of protein that plays a role in the occurring of wheat quality is least 11% for bread and 9% for biscuits. As shown in *Figure 2,* among parents, the highest protein content (17.30%) was found in the DH22 and the lowest protein content (13.30%) was detected in the DH6 line. Among the crosses, "DH20 x Bezostaja" had the highest value with 16.38%. McNeal et al. (1965) reported that F_1 crosses shown a lower mean value than parents in terms of protein content, while Perenzin et al. (1992) informed that they had higher protein content than their parents. In this study, cross combinations were usually among parental values.

Genetic variation for Zn and Fe is quite limited in registered wheat cultivars, so they are not useful for usage in breeding programs (Cakmak et al., 2004; Zhao and McGrath, 2009; Gomez-Becerra et al., 2010). However, the desired genetic diversity can be created by a suitable hybridization program. In this study, Fe (19.40-63.94 mg Fe kg^{-1}) and Zn (9.29-41.43 mg Zn kg^{-1}) had the largest variation among the examined micronutrients. Similar results were found by Gomez-Becerra et al. (2010). The highest Fe concentration was detected in DH6 line, the cross "DH6 x Kate" and tester Harmankaya followed it with 57.91 and 56.05 mg kg^{-1}, respectively. Zinc concentrations varied between 9.29 and 41.43 and mean values was 18.30 mg kg^{-1}. "DH6 x Kate" among the crosses, Kate between the testers and DH22 between the lines were remarkable genotypes (*Fig. 2*).

Copper concentrations of wheat genotypes ranged from 4.90 to 10.30 and the mean Cu concentration was 8.04 mg kg^{-1}. The best genotypes were "DH19 x Kate" and DH21, while the least Cu concentration was detected "DH6 x Altay". Mean values of K and P concentrations were around 4.0 and 3.0 mg kg^{-1} and there were narrow variations among genotypes. The highest K concentration was found "DH20 x Harmankaya" with 4.75 mg kg^{-1}, while the highest P concentration was 3.92 mg kg^{-1} in "DH22 x Altay". DH20 and DH19 were promising parents for high K and P concentrations (*Fig. 2*).

"Line x tester" variance analyses and estimates of genetic components

The results of "line x tester" variance analysis for each character of genotype and cross combinations are given in *Table 1*. In the analysis of the variance of the traits examined, the squares of all the genotypes (treatment) were found to be significant, while the parents had a statistically significant variation with respect to all other features except the a value.

http://www.aloki.hu ● ISSN 1589 1623 (Print) ● ISSN 1785 0037 (Online)
DOI: http://dx.doi.org/10.15666/aeer/1605_73057326
© 2018, ALÖKI Kft., Budapest, Hungary

Table 1. *Line x tester variance analysis for each character of genotype and hybrid combinations*

VK	DF	Kernel length (mm)	Kernel width (mm)	Kernel thickness (mm)	Kernel volume (%)	Kernel sphericity (%)	Kernel hardness (HI)	Thousand kernel weight (g)	Hectolitre weight (kg)	L	a	b	Protein rate (%)	Fe mg kg^{-1}	Zn mg kg^{-1}	Cu mg kg^{-1}	P mg kg^{-1}	K mg kg^{-1}
Replication	2	0.00^{ns}	0.01^{ns}	0.02^{ns}	428.27^{ns}	1.53^{ns}	10.63^{ns}	5.06^{ns}	0.30^{ns}	2.86^{ns}	0.16^{ns}	1.27^{ns}	0.00^{ns}	2.6^{ns}	0.04^{ns}	0.60^{ns}	0.04^{ns}	0.23^{ns}
Treatment	38	0.22**	0.07**	0.06**	2659.90**	7.05**	245.92**	17.26**	10.73**	26.04**	1.03**	11.72**	3.35**	360.09**	106.56**	6.27**	0.35**	0.96**
Parents	10	0.37**	0.14**	0.10**	4604.31**	10.45**	533.50**	25.56**	19.94**	26.60**	0.43^{ns}	7.27**	5.40**	640.75**	49.06**	3.56**	0.22**	1.12**
Interaction	1	0.47**	0.12**	0.14**	6361.97**	0.61^{ns}	128.50^{ns}	99.60**	78.00**	92.99**	3.98**	60.99**	0.44**	137.41**	171.63**	0.88^{ns}	0.17**	0.00^{ns}
Crosses	27	0.15**	0.04**	0.05**	1802.63**	6.03**	143.76*	11.14^{ns}	4.83**	23.35**	1.14**	11.54**	2.70**	264.39**	125.45**	7.45**	0.40**	0.94**
Lines	6	0.28*	0.04^{ns}	0.06^{ns}	2054.97^{ns}	10.10**	252.14**	21.78*	7.60^{ns}	28.61*	1.42**	2.49^{ns}	7.77**	514.79*	128.76^{ns}	25.97**	0.74^{ns}	3.68**
Testers	3	0.24^{ns}	0.11*	0.08^{ns}	3321.27^{ns}	20.11**	581.91**	18.34^{ns}	2.93^{ns}	94.11**	5.42**	85.40**	0.28^{ns}	213.58^{ns}	63.13^{ns}	1.66^{ns}	0.23^{ns}	0.27^{ns}
Line x Tester	18	0.09**	0.03**	0.04**	1465.40**	2.32**	34.61^{ns}	6.39^{ns}	4.22**	9.80**	0.34^{ns}	2.2^{ns}	1.41**	189.39**	134.73**	2.25**	0.32**	0.14**
Error	76	0.003	0.003	0.003	53.70	0.38	85.04	7.45	1.39	4.08	0.49	1.73	0.01	0.91	2.04	1.01	0.02	0.05
GC																		
σ^2GCA/σ^2SCA		0.03	0	0	0.02	0.13	-0.08	-0.30	0.01	0.16	-0.03	1.20	0.06	0.03	-0.01	0.28	0.2	0.58
σ^2A		0.003	0	0	14.99	0.165	4.85	0.21	0.03	0.60	0.04	0.413	0.06	3.33	-0.41	0.23	0.004	0.04
σ^2D		0.029	0.10	0.01	470.57	0.647	-16.81	-0.35	0.94	1.91	-0.05	0.173	0.46	62.83	44.23	0.41	0.10	0.03
H^2		0.99	0.96	0.95	0.98	0.95	0.49	0.70	0.77	0.86	0.68	0.87	0.99	0.99	0.98	0.86	0.95	0.95
h^2		0.09	0	0	0.03	0.14	0.07	0.05	0.01	0.09	0.08	0.18	0.11	0.05	-0.01	0.14	0.03	0.33
CLV (%)		41.73	19.68	27.80	25.33	37.22	38.97	43.46	34.97	27.23	27.68	4.80	63.98	43.27	22.81	77.42	40.68	86.86
CTV (%)		18.02	28.89	18.36	20.47	37.07	44.97	18.30	6.74	44.78	52.66	82.22	1.15	8.98	5.59	2.47	6.45	3.16
CLxTV (%)		40.24	51.42	53.84	54.19	25.70	16.05	38.24	58.29	27.99	19.66	12.98	34.87	47.76	71.60	20.11	52.86	9.97

*p ≤ 0.05, **p ≤ 0.01. GCA: general combining ability; SCA: specific combining ability, σ^2A: additive gene variance, σ^2D: dominance gene variance, H^2: broad sense heritability, h^2: narrow sense heritability, CLV: contribution of lines to variance, CTV: contribution of testers to variance, CLV: contribution of lines x testers interaction to variance

http://www.aloki.hu ● ISSN 1589 1623 (Print) ● ISSN 1785 0037 (Online)
DOI: http://dx.doi.org/10.15666/aeer/1605_73057326
© 2018, ALÖKI Kft., Budapest, Hungary

When considering at the mean squares of the crosses; there were statistically significant differences according to 5% level of importance of kernel hardness and 1% of importance for other properties while thousand kernel weights was non-significant. Among the varieties used as a line, level of 1% statistically significant differences were found for kernel sphericity, kernel hardness, a value, protein ratio, Cu and K concentrations; and level of significant was 5% for kernel length, thousand kernel weight, L value and Fe concentration. Among the varieties used as tester, kernel width, kernel sphericity, kernel hardness and color values statistically significant variation was found. Among the variances belonging to the "line x tester" interaction, significant differences were found with respect to all examined traits except for kernel hardness, thousand kernel weight, a and b values.

When the proportional relations of the general and specific combination ability variance estimates of the examined properties and the variance components of the additive and dominance are examined, dominant gene effects were dominated in inheritance of b values; while "additive x dominant" gene interaction were prominent in inheritance of kernel hardness, thousand kernel weight, a value and Zn concentration. The selection efficiency is concerned with the magnitude of narrow sense heritability in the segregating populations. It was found very low narrow sense heritability degrees for the characters examined in the study (*Table 1*). This situation indicated that there is very low additive variance in this population and the selection should be postponed to further generations.

Previous researchers (Khan et al., 2010; Istipliler et al., 2015; Kumar et al., 2017) who have detected low narrow sense heritability and dominant gene effects for features such as thousand kernel weight, hectolitre weight, kernel hardness and protein rate, have indicated that the waiting of future generations for selection would be appropriate. Lines, testers, and "line x tester" interaction contributed to combinations' variances was found highly different in examined traits. The contributions of the lines to kernel sphericity, thousand kernel weight, protein rate, Cu and K concentrations were defined as highest, while to kernel length and Fe concentration were found closer to "line x tester" interaction. The contributions of testers were found in highest kernel hardness and color values. It is remarkable that there was much more variation in traits which had the highest "line x tester" interactions such as kernel width, kernel thickness, kernel volume, hectolitre weight, Zn and P concentrations.

General combining abilities of parents

General combining ability effects of the lines, testers or individual line performances are useful tools for selecting the cross parents in cross pollinated plants. GCA effects of the lines and testers used in the research can be seen at *Table 2* for observed traits. The negative GCA effects were generally observed for kernel dimensions. Genotypes DH22 and Harmankaya showed a positive and significant GCA for all kernel dimensions traits, while genotypes DH19 and Kate had negative and significant GCA effects. This situation showed that in the combinations which include these two genotypes had relatively small kernels. All parents had significant GCA effects for kernel volume. However, it can be realized that positive and significant GCA effects increasing the kernel volume are more than negative GCA effects. The DH22, which had the highest positive and significant GCA effect, increased the kernel volume in the combinations in which it took a place (*Table 2*). Therefore, the line Harmankaya and the tester DH22 were the most suitable parents for increasing this trait due to their high GCA effects.

http://www.aloki.hu ● ISSN 1589 1623 (Print) ● ISSN 1785 0037 (Online)
DOI: http://dx.doi.org/10.15666/aeer/1605_73057326
© 2018, ALÖKI Kft., Budapest, Hungary

Table 2. *General combining ability of parents used as lines and testers*

Lines	Kernel length (mm)	Kernel width (mm)	Kernel thickness (mm)	Kernel volume (%)	Kernel sphericity (%)	Kernel hardness (HI)	Thousand kernel weight (g)	Hectolitre weight (kg)	L	a	b	Protein rate (%)	Fe mg kg^{-1}	Zn mg kg^{-1}	Cu mg kg^{-1}	P mg kg^{-1}	K mg kg^{-1}
DH6	0.02	0.01	0.07**	7.21**	0.30	1.48	-0.36	0.89*	-0.97	-0.22	-0.52	-0.66**	11.60**	2.41**	-2.98**	-0.20**	-0.30**
DH16	-0.01	-0.04**	-0.02	-6.32**	-0.39*	1.61	0.45	-1.29**	0.72	-0.39	-0.71	0.00	6.30**	0.98*	-0.28	-0.05	-0.69**
DH18	0.09**	-0.06**	-0.04**	-6.52**	-1.24**	-5.13	1.09	1.01**	2.71**	-0.21	0.33	-1.27**	-2.72**	-4.97**	0.86**	-0.24**	-0.47**
DH19	-0.28**	-0.06**	-0.10**	-23.33**	0.65**	8.27**	-2.15**	-0.34	0.87	0.16	-0.12	-0.15**	-4.94**	3.20**	-0.16	-0.08*	-0.24**
DH20	-0.09**	0.05**	0.05**	5.29*	1.19**	-0.81	1.27	-0.42	-0.34	0.33	0.35	1.08**	-6.69**	-3.70**	0.05	0.02	0.45**
DH21	0.19**	0.04*	-0.04*	7.33**	-1.06**	-0.32	-1.39	0.04	-1.77**	0.54**	0.28	0.23**	-1.40**	-0.80	1.04**	0.06	0.62**
DH22	0.08**	0.07**	0.08**	16.34**	0.54**	-5.09	1.10	0.11	-1.22*	-0.21	0.39	0.77**	-2.15**	2.88**	1.47**	0.50**	0.63**
SE	0.02	0.01	0.02	2.12	0.18	2.66	0.79	0.34	0.58	0.20	0.38	0.04	0.28	0.41	0.29	0.04	0.06
Testers																	
Altay	-0.11**	0.07**	0.04**	4.45**	1.37**	-7.32**	0.06	-0.17	3.16**	0.72**	2.97**	-0.07*	-4.17**	-1.03**	-0.35	-0.09**	-0.00
Bezostaja-1	-0.01*	-0.01	-0.03*	-4.19*	-0.24	2.95	-0.14	0.01	-0.80	-0.47**	-1.34**	0.03	0.57**	-0.74*	0.18	-0.04	-0.15**
Harmankaya	0.14**	0.04**	0.06**	14.65**	-0.18	-0.18	1.18	0.51*	-1.22**	-0.10	-1.17**	-0.11**	0.03	-0.83**	-0.09	-0.02	0.03
Kate A-1	-0.02**	-0.09**	-0.07**	-14.91**	-0.95**	4.56*	-1.10	-0.35	-1.14*	-0.14	-0.46	0.15**	3.57**	2.59**	0.26	0.15**	0.12**
SE	0.01	0.01	0.01	1.60	0.13	2.01	0.60	0.26	0.44	0.15	0.29	0.03	0.21	0.31	0.22	0.03	0.05

*p ≤ 0.05, **p ≤ 0.01. SE: standard error

http://www.aloki.hu ● ISSN 1589 1623 (Print) ● ISSN 1785 0037 (Online)
DOI: http://dx.doi.org/10.15666/aeer/1605_73057326
© 2018, ALÖKI Kft., Budapest, Hungary

GCA effects of kernel sphericity ranged from -1.24 to 1.37. The negative and significant was observed four parents while three parents had positive and significant GCA effects. When the GCA of parents were examined in terms of kernel hardness value, DH19 and Kate showed positive and significant GCA effect at 1% and 5% level, while Altay showed negative and significant GCA effect at 1% level. GCA effect of other parents was found to be insignificant. Negligible positive and negative effects were observed between lines and testers for thousand kernel weight. Besides, it can be seen that one of the lines called DH19 had negative and significant GCA effect for thousand kernel weight. The GCA effect, which reflects the additive gene effect, was found to be positive and significant in the DH6 and DH18 genotypes among the lines and in the Harmankaya variety as a tester, while the negative and significant GCA effect was observed in the DH16 line for hectolitre weight (*Table 2*). DH6, DH22 and Harmankaya genotypes having positive GCA effect on all of these properties are potential to be used as parents in breeding studies to improve flour yield and milling quality of bread wheat. For the L value affecting the lightness or darkness of grain color, the GCA effects were generally negative. Combinations of DH18 and Altay parents showing a positive and significant GCA value may be expected to be darker. The GCA values for a value, a indicator for red color, ranged from -0.47 to 0.72. Bezostaja had negative values, while two of the three parent significant GCA effects were found a positive value. None of the lines for b value had significant GCA effect, whereas three of the tester showed significant positive and negative GCA effect (*Table 2*). It would be appropriate to use DH21 to obtain darker and red kernels, and to use the Altay genotypes as a parent for light colored and white kernels.

When GCA values for protein rate are examined, it was seen that four parents have a positive, five parents have a negative GCA value and the DH20 had the highest GCA effect. While the lowest GCA effect was obtained from the DH18, the effect of the DH16 was calculated to be zero (*Table 2*). It can be concluded that parents with a positive GCA effect have the potential to increase the protein rate and transfer these characteristics to future generations. GCA values calculated for Fe and Zn contents were found statistically significant in almost all of the parents. DH18, DH20, DH21 and Altay genotypes showing a negative GCA value in terms of Fe content also had a negative value for Zn content. While DH6, DH16 and Kate with positive GCA values for both Fe and Zn contents may be suitable parents to improve these properties, DH19 and DH22 have the potential to increase Zn content and Bezostaja has the potential to be suitable parents for breeding programs to increase Fe content. Three of the four lines that detected the significant GCA effect for Cu content had a positive value, indicating that they had a Cu content enhancing effect. Among the parents with important GCA effect for P and K, DH22 and Kate had positive values for both elements (*Table 2*). Parent Kate was a good combiner for protein rate and biofortified crops indicating that this genotype could be the best candidate as one of the parental lines to improve any of these features.

Specific combining abilities and heterosis values of hybrids

Although specific combining ability (SCA) is generally suggested for cross pollinated species such as corn or rye (Longin et al., 2013; Istipliler et al., 2015), SCA effects can be used to select homozygous lines that show transgressive segregation. Significant SCA, heterosis and heterobeltiosis values of physical kernel properties were determined both positive and negative (*Table 3*). This condition indicates that the presence of adequate variation in this population and this cross population contains suitable materials that can be used in breeding studies.

http://www.aloki.hu ● ISSN 1589 1623 (Print) ● ISSN 1785 0037 (Online)
DOI: http://dx.doi.org/10.15666/aeer/1605_73057326
© 2018, ALÖKI Kft., Budapest, Hungary

Table 3. *Specific combining ability, heterosis and heterobeltiosis values of crosses for physical kernel properties*

Crosses	Kernel length (mm)			Kernel width (mm)			Kernel thickness (mm)			Kernel volume (%)			Kernel sphericity (%)			Kernel hardness (HI)		
	SCA	HT	HB	SCA	HT	HB	SCA	HT	HB	SCA	HT	HB	SCA	HT	HB	SCA	HT	HB
DH6 x Altay	0.08*	5.76**	-0.90	0.13**	19.23**	9.06**	0.07*	7.76**	-1.45	20.65**	33.04**	6.52**	0.80*	4.86**	3.16**	-0.32	-2.85	-29.88**
DH6 x Bezostaja	-0.02	0.65	-0.85	-0.02	-0.69	-2.09	-0.05	-2.97**	-6.78**	-7.20	-3.01**	-6.89**	-0.26	-1.64**	-1.76*	0.34	-5.47	-17.25
DH6 x Harmankaya	0.18**	4.01**	3.64**	0.03	6.12**	4.74**	0.03	2.95**	-1.99	12.15**	13.58**	7.14**	-0.60	0.35	-1.97*	-1.10	-12.61*	-22.52**
DH6 x Kate	-0.23**	-1.92**	-4.18**	-0.14**	-2.15**	-6.38**	-0.05	-1.19	-8.13**	-25.60**	-5.78**	-17.60**	0.06	0.25	-2.16*	1.08	-1.71	-14.52
DH16 x Altay	-0.13**	4.31**	-0.31	0.01	12.77**	3.12*	-0.04	5.55**	0.02	-6.91	22.69**	2.84	0.58	3.16**	1.25	4.34	9.78	-19.06*
DH16 x Bezostaja	0.21**	5.85**	5.25**	0.17**	4.13**	2.70	0.11**	2.92**	2.67*	32.24**	13.47**	11.56**	0.59	-1.47**	-1.47	2.91	1.90	-8.12
DH16 x Harmankaya	-0.12**	1.16**	-1.26*	-0.13**	-1.63*	-2.95	-0.04	2.15**	0.94	-20.19**	1.69	1.57	-0.41	-0.65	-3.06**	-4.35	-13.49**	-20.97*
DH16 x Kate	0.04	3.91**	3.64**	-0.05	-0.90	-5.22**	-0.02	0.95	-2.67*	-5.14	3.72**	-4.43	-0.76*	-2.50**	-4.96**	-2.90	-3.21	-13.32
DH18 x Altay	0.09**	4.78**	-3.59**	0.03	11.76**	1.62	0.08**	9.66**	4.52**	13.34**	26.16**	2.40	0.12	3.68**	2.83**	-1.90	-4.28	-26.37**
DH18 x Bezostaja	0.05	0.69*	-2.70**	-0.02	-3.78**	-4.51**	-0.13**	-4.62**	-4.97**	-9.46*	-7.43**	-9.58**	-1.17**	-3.35**	-5.90**	0.90	-3.76	-8.02
DH18 x Harmankaya	-0.13**	-1.53**	-3.10**	-0.04	0.06	-1.88	-0.00	3.25**	2.64	-9.59*	1.66	-2.45	0.46	2.14**	1.91*	-2.18	-14.09**	-16.73
DH18 x Kate	-0.01	0.29	-3.88**	0.03	0.99	-3.98*	0.04	2.96**	-0.15	5.72	3.70**	-7.88**	0.59	1.11*	0.99	3.18	2.70	-2.55
DH19 x Altay	-0.11**	3.03**	1.10	0.01	10.13**	-0.73	0.11**	12.46**	10.78**	3.91	27.04**	11.15**	1.50**	5.43**	2.47**	3.08	17.64**	-13.68
DH19 x Bezostaja	-0.04	0.55	-2.66**	-0.06	-5.73**	-5.92**	-0.04	-0.62	-4.23**	-9.56*	-5.90**	-11.93**	-0.48	-2.52**	-3.49**	-6.47	-2.64	-12.80
DH19 x Harmankaya	0.25**	5.27**	0.11	0.08*	3.70**	0.73	0.10**	8.06**	5.10**	22.38**	18.06**	12.42**	-0.32	0.25	-3.13**	1.42	2.49	-7.00
DH19 x Kate	-0.10**	0.18	-2.21**	-0.03	-2.00*	-7.67**	-0.16**	-2.39**	-2.67	-16.73**	-4.02**	-7.19*	-0.69	-1.61**	-5.02**	1.97	11.78*	-0.55
DH20 x Altay	-0.15**	0.22	-6.25**	-0.15**	2.23**	-11.80**	-0.11**	1.53*	-7.06**	-27.84**	0.77	-23.16**	-0.80*	1.45**	-2.30**	-2.62	0.21	-23.75**
DH20 x Bezostaja	0.03	-0.34	-2.01**	0.01	-4.54**	-9.30**	0.08*	0.34	-3.50**	8.62*	-4.87**	-14.23**	0.36	-1.15**	-3.04**	0.83	0.79	-5.08
DH20 x Harmankaya	0.09**	0.85*	0.67	0.02	0.09	-7.32**	0.07*	3.91**	-0.99	11.32**	4.48**	-7.31**	0.03	0.80	-3.48**	5.58	1.73	-2.87
DH20 x Kate	0.03	0.11	-2.37**	0.12**	1.62*	-8.59**	-0.04	-1.17	-8.03**	7.90	-0.74	-17.90**	0.41	0.25	-4.10**	-3.79	-2.85	-9.17
DH21 x Altay	0.18**	8.04**	-0.35	0.08**	17.13**	5.83**	0.03	7.84**	2.67*	17.97**	33.92**	8.23**	-0.36	2.67**	2.28*	-0.42	22.02**	1.42
DH21 x Bezostaja	-0.01	1.65**	-1.53*	-0.03	-1.22	-1.29	0.05	1.20	0.94	1.34	1.60	-1.29	0.17	-1.15**	-3.34**	-1.05	11.32*	5.30
DH21 x Harmankaya	-0.32**	-2.49**	-3.80**	-0.11**	0.72	-1.91	-0.21**	-3.32**	-4.00**	-39.06**	-5.09**	-9.41**	-0.21	0.81	0.58	-0.58	5.35	-1.70
DH21 x Kate	0.14**	4.32**	0.25	0.05	4.78**	-1.04	0.13**	5.77**	2.46	19.75**	14.94**	1.61	0.40	0.63	0.31	2.05	19.96**	14.30
DH22 x Altay	0.03	9.29**	5.44**	-0.11**	14.99**	7.27**	-0.14**	6.99**	2.52	-21.12**	33.48**	57.19**	-1.84**	1.06*	-0.36	-2.15	-7.31	-29.74**
DH22 x Bezostaja	-0.22**	1.56**	0.00	-0.05	2.59**	-0.94	-0.02	3.28**	2.33	-15.98**	7.48**	1.35	0.80*	0.91*	0.45	2.54	-3.51	-9.62
DH22 x Harmankaya	0.06	6.12**	2.60**	0.15**	15.33**	14.40**	0.06	9.96**	10.00**	23.00**	34.57**	29.12**	1.05**	3.98**	1.92*	1.21	-11.14*	-15.62
DH22 x Kate	0.14**	7.70**	6.93**	0.01	8.46**	5.93**	0.11**	9.88**	7.15**	14.10**	28.32**	23.14**	-0.01	0.91*	-1.19	-1.59	-6.45	-13.00
SE (SCA)	0.03			0.03			0.03			4.23			0.36			5.32		

*p ≤ 0.05, **p ≤ 0.01. SCA: specific combining ability, HT: heterosis, HB: heterobeltiosis, SE: standard error

http://www.aloki.hu ● ISSN 1589 1623 (Print) ● ISSN 1785 0037 (Online)
DOI: http://dx.doi.org/10.15666/aeer/1605_73057326
© 2018, ALÖKI Kft., Budapest, Hungary

The highest SCA values for kernel length, width, thickness, volume, sphericity and hardness were determined as 0.25 (DH19 x Harmankaya), 0.17 (DH16 x Bezostaja), 0.13 (DH21 x Kate), 32.24 (DH16 x Bezostaja), 1.50 (DH19 x Altay), 5.58 (DH20 x Harmankaya), respectively. Most of the cross combinations for these traits had a positive heterosis value indicating the presence of dominance in the direction of increasing these traits, while most heterobeltiosis values were negative. The heterosis express as percent deviation of cross from its mid-parental value, whereas heterobeltiosis was as percent superiority of cross in comparison to the best parent. Therefore, effective selection of desirable recombinants from crosses with significant high heterobeltiosis value is more likely to be. "DH22 x Kate" for kernel length, "DH22 x Harmankaya" for kernel width, "DH19 x Altay" for kernel thickness, "DH22 x Altay" for kernel volume, "DH6 x Altay" for kernel sphericity and "DH21 x Kate" for kernel hardness had the highest and desirable heterobeltiosis value. It was observed that "DH16 x Bezostaja", "DH20 x Harmankaya" and "DH21 x Kate" combinations had positive and significant SCA effects for all physical kernel properties (*Table 3*). Besides that, these combinations had the positive heterosis and heterobeltiosis values. Kernel size, volume, sphericity and hardness provide important information about flour yield. It was determined that the flour yield of large sized and hard kernel was higher and that the amount of grain protein was not decreased during milling (Dziki and Laskowski, 2005). In parents and crosses, those with positive and significant combination abilities, heterosis and heterobeltiosis values can be recommended for use in breeding studies to increase of kernel size, hardness and therefore to increase yield of flour.

"DH6 x Harmankaya", "DH18 x Altay" and "DH22 x Kate" crosses, which have a high SCA effect value, can be pursued for a thousand kernel weight, although all crosses have non-significant SCA effect. The heterosis values of the crosses for thousand kernel weight ranged from -4.02% (DH6 x Bezostaja) to 21.44% (DH18 x Altay) and the number of positive and significant heterosis value was detected thirteen. Four of the significant heterobeltiosis crosses were positive (*Table 4*). The highest heterobeltiosis was determined in the "DH18 x Altay" cross, followed in "DH18 x Harmankaya". Crosses showing positive heterobeltiosis can be considered as promising because heterobeltiosis is an indication of a performance exceeding both parents. For the hectolitre weight, the SCA effects of crosses varied between -1.80 (DH16 x Altay) and 1.89 (DH16 x Bezostaja). Half of the crosses showed a negative SCA effect while the other half showed a positive SCA effect. Only the DH16 cross series had statistically significant SCA effect. Two of the crosses (DH16 x Altay and DH16 x Kate) were found to be significant negative and the other two positive. When the heterosis values of the crosses were examined, significant values were calculated for 5% negative in a cross, 1% negative in a cross, and non-significant values in six crosses. All other crosses showed positive and significant heterosis. The heterobeltiosis values of the crosses were found to be statistically insignificant, and "DH22 x Altay" and "DH22 x Kate" combinations showed a positive significant value (*Table 4*). When the SCA values and heterosis-heterobeltiosis values of the crosses are considered together; the combination of "DH16 x Altay", "DH18 x Altay", "DH19 x Harmankaya", "DH20 x Kate" and "DH21 x Kate" should be followed as promising crosses in order to increase the hectolitre weight. Since, hectolitre weight and thousand kernel weight are one of the indicators of flour yield (Pomeranz, 1964); the wheat genotypes which have high thousand kernel weight and hectolitre weight are preferred in the flour industry. Hence "DH6 x Harmankaya", "DH18 x Altay", "DH19 x Altay", "DH19 x Harmankaya" and "DH22 x Kate" combinations are preferable for flour industry with their positive SCA, heterosis and heterobeltiosis values for both thousand kernel weight and hectolitre weight.

http://www.aloki.hu ● ISSN 1589 1623 (Print) ● ISSN 1785 0037 (Online)
DOI: http://dx.doi.org/10.15666/aeer/1605_73057326
© 2018, ALÖKI Kft., Budapest, Hungary

Table 4. *Specific combining ability, heterosis and heterobeltiosis values of crosses for thousand kernel weight, hectolitre weight and color values*

Crosses	Thousand kernel weight (g)			Hectolitre weight (kg)			L			a			b		
	SCA	HT	HB	SCA	HT	HB	SCA	HT	HB	SCA	HT	HB	SCA	HT	HB
DH6 x Altay	-0.12	6.71*	2.83	0.57	5.02	0.29	-3.15**	-11.03**	-16.26**	-0.24	-2.20	-3.01	0.04	-0.51	-4.29
DH6 x Bezostaja	-1.70	-4.02	-5.95	-1.19	-1.63	-1.64	0.64	-4.29*	-5.43	0.16	-9.88**	-10.48*	0.47	-8.96**	-12.51**
DH6 x Harmankaya	1.50	12.14**	10.27	1.27	2.88	1.98	1.43	-0.96	-4.72	0.51	-2.21	-3.54	0.52	-6.14*	-11.60*
DH6 x Kate	0.32	8.43	0.87	-0.65	1.23	-1.43	1.08	-3.49*	-5.25	-0.43	-7.56**	-11.41*	-1.04	-11.75**	-15.10**
DH16 x Altay	0.44	8.60**	2.94	-1.80**	1.43	-1.07	0.95	-2.33	-6.09*	0.09	0.91	-0.05	0.07	-2.38	-4.92
DH16 x Bezostaja	-0.46	-0.27	-0.60	1.89**	1.63	-0.52	0.18	-4.05*	-7.25*	-0.02	-11.18**	-13.31**	-0.34	-14.46**	-18.79**
DH16 x Harmankaya	-0.73	6.31*	2.79	1.58*	2.78	1.47	-1.05	-4.85**	-10.39**	-0.29	-8.44**	-8.83	0.30	-9.20**	-15.49**
DH16 x Kate	0.76	10.01**	0.74	-1.67*	-0.62	-1.13	-0.08	-4.64**	-8.39**	0.22	-1.73	-4.16	-0.03	-9.48**	-13.97**
DH18 x Altay	1.56	21.44**	20.12**	0.87	6.33	2.23	2.22	2.29	-0.37	-0.13	0.42	-0.41	0.71	2.06	1.51
DH18 x Bezostaja	-1.47	5.26	-1.56	-0.14	0.51	-0.19	-1.92	-5.59**	-9.91**	-0.22	-11.40**	-13.42**	-0.37	-12.16**	-18.25**
DH18 x Harmankaya	0.52	19.07**	15.39*	-0.27	1.85	1.67	0.11	0.07	-6.93*	0.06	-4.21	-4.48	-0.47	-10.17**	-18.00**
DH18 x Kate	-0.61	15.73**	12.78*	-0.45	2.38	0.37	-0.41	-2.73	-7.74*	0.29	0.25	-2.37	0.13	-6.52**	-12.91**
DH19 x Altay	0.87	8.50*	8.39	0.21	4.60	1.36	0.51	0.76	-6.60*	-0.07	2.82	2.61	0.30	2.67	-1.80
DH19 x Bezostaja	0.22	-0.19	-5.60	-1.04	-1.49	-2.95	-1.21	-2.72	-3.13	-0.27	-9.83**	-10.97*	-0.19	-9.53**	-12.55**
DH19 x Harmankaya	1.12	10.14**	8.00	0.50	1.94	1.30	-0.78	-0.04	-2.30	0.36	0.23	-0.51	0.45	-4.09	-9.14*
DH19 x Kate	-2.21	-0.37	-4.04	0.33	2.48	1.28	1.47	2.71	2.49	-0.01	-0.31	-3.88	-0.57	-7.44**	-10.42*
DH20 x Altay	-1.66	-0.83	-10.50*	-0.04	4.34	1.26	-0.07	-5.50**	-9.76**	0.26	8.42**	7.14	0.82	5.17	2.00
DH20 x Bezostaja	2.80	4.55	-0.43	-0.04	-0.19	-1.81	1.59	-2.66	-5.26	0.42	-1.60	-4.17	0.08	-7.75**	-12.05**
DH20 x Harmankaya	-1.00	1.87	-6.31	-0.81	0.36	-0.42	-0.16	-4.51**	-9.46**	-0.42	-3.43	-4.05	-0.13	-6.06*	-12.22**
DH20 x Kate	-0.13	3.43	-9.64	0.89	3.26	2.20	-1.35	-8.60**	-11.60**	-0.25	0.54	-1.75	-0.76	-7.66**	-11.88**
DH21 x Altay	-0.14	3.10	-1.24	-0.49	3.47	-0.39	-1.65	-8.68**	-15.02**	-0.14	3.84	2.15	-0.78	-3.23	-4.40
DH21 x Bezostaja	1.14	0.21	-1.22	0.49	0.22	-0.60	2.75*	-0.44	-0.45	0.30	-3.60	-3.77	0.94	-6.23**	-12.17**
DH21 x Harmankaya	-1.81	-0.48	-2.72	-1.34	-0.55	-0.60	-1.72	-7.97**	-10.41**	-0.36	-3.94	-6.02	-0.12	-8.16**	-15.65**
DH21 x Kate	0.81	6.14	-1.81	1.34	3.55	1.66	0.61	-4.90**	-5.50	0.20	3.14	-1.94	-0.04	-6.71**	-12.54**
DH22 x Altay	-0.94	8.89**	5.24	0.68	9.30	9.30**	1.19	-2.94	-9.07**	0.24	0.78	-0.94	-1.17	-2.54	-5.46
DH22 x Bezostaja	-0.53	3.33	0.94	0.03	3.56	-1.09	-2.03	-9.73**	-10.36**	-0.37	-14.84**	-15.05**	-0.59	-10.42**	-14.62**
DH22 x Harmankaya	0.41	13.54**	11.99*	-0.93	3.92	0.09	2.16	0.56	-2.79	0.15	-6.00*	-8.10	-0.56	-7.75**	-13.80**
DH22 x Kate	1.07	15.28**	7.56	0.22	6.26	4.16**	-1.33	-8.43**	-9.65**	-0.02	-4.98*	-9.72*	2.31**	5.61*	0.77
SE	1.58			0.68			1.17			0.40			0.76		

*p ≤ 0.05, **p ≤ 0.01. SCA: specific combining ability, HT: heterosis, HB: heterobeltiosis, SE: standard error

http://www.aloki.hu ● ISSN 1589 1623 (Print) ● ISSN 1785 0037 (Online)
DOI: http://dx.doi.org/10.15666/aeer/1605_73057326
© 2018, ALÖKI Kft., Budapest, Hungary

All SCA values calculated for kernel color values were statistically insignificant and mostly negative. For the L value, significant SCA value were detected as negative only for the "DH6 x Altay" cross and only the "DH22 x Kate" had positive and significant SCA value for the b value cross (*Table 4*). Similarly, the heterosis and heterobeltiosis values of the grain color had negative values for almost all crosses. This result pointed to the presence of colors that turned darker and turned from white to red in the examined population. Red and white kernel color is controlled by three independent, homoeologous genes. Red color is dominant to white, and a single locus containing the dominant allele is sufficient to result in red color. The degree of red color is additive, with genotypes homozygous dominant at all three loci having the darkest red color, and only those homozygous recessive at all three genes being white. Therefore, the genetics of kernel color makes problematic to conversion of red to white kernel color (Sherman et al., 2008). The "DH19 x Kate" cross has to be followed as a cross for lighter grain color, "DH20 x Altay" for increasing the redness and "DH18 x Altay", "DH20 x Altay" and "DH22 x Kate" crosses for increasing the yellowness.

When the SCA effects of protein rate were examined, it was seen that the values changed between -0.81 and 0.93 and that the SCA effects were positive and significant in 13 crosses, insignificant in 3 crosses, and negative and significant values in others (*Table 5*). Thirteen of the cross combinations had positive and significant, while 11 had negative and significant heterosis. The highest heterosis value was detected in "DH21 x Altay" cross with 10.15%. The heterobeltiosis values determined positively in 6 of the crosses were statistically significant in 4 crosses. It can be suggested DH20 and DH22 lines with a high observation average, positive GCA effect value for high protein bread wheat breeding. Within the crosses, "DH20 x Bezostaja", "DH22 x Kate", "DH22 x Harmankaya", "DH20 x Harmankaya", "DH21 x Altay", "DH21 Harmankaya", "DH6 x Altay" crosses showing high observation values, high positive SCA effect, high heterosis and heterobeltiosis can be considered as promising combinations. There were ten, nine, two, seven and one combinations relating to Fe, Zn, Cu, P and K which had positive and significant SCA effects, respectively. In terms of Fe content, the majority of the crosses have exceeded the mean of parents and have positive and significant heterosis values, while nine crosses exceeding the superior parent have been identified (*Table 5*). Twelve of twenty-two crosses which had significant heterosis values was detected positive value for Zn content, and the heterobeltiosis values of seven of them were also positive. Most of the crosses for Cu, P, and K content exceed mean of parents, while the crosses that detected significant heterobeltiosis were mostly negative. "DH19 x Kate" for Cu content, "DH21 x Bezostaja", "DH21 x Harmankaya", "DH22 x Altay", "DH22 x Harmankaya" and "DH22 x Kate" crosses for P content are combinations that should be considered with both positive SCA values and high heterosis and heterobeltiosis values (*Table 5*). Crop improvement activities focus, first, on exploring the available genetic diversity for Fe, Zn. At the same time (or during subsequent screening), agronomic and end-use features are characterized (Pfeiffer and McClafferty, 2007). The combinations "DH6 x Kate", "DH20 x Bezostaja", "DH21 x Bezostaja" and "DH22 x Altay" came into prominence as promising combinations in terms of the Fe and Zn content and it can be possible to obtain biofortified lines by carrying these combinations to next generations.

http://www.aloki.hu ● ISSN 1589 1623 (Print) ● ISSN 1785 0037 (Online)
DOI: http://dx.doi.org/10.15666/aeer/1605_73057326
© 2018, ALÖKI Kft., Budapest, Hungary

Table 5. *Specific combining ability, heterosis and heterobeltiosis values of crosses for protein rate and concentrations of nutrient elements*

Crosses	Protein rate (%)			Fe (mg kg^{-1})			Zn (mg kg^{-1})			Cu (mg kg^{-1})			P (mg kg^{-1})			K (mg kg^{-1})		
	SCA	HT	HB	SCA	HT	HB	SCA	HT	HB	SCA	HT	HB	SCA	HT	HB	SCA	HT	HB
DH6 x Altay	-0.80**	-3.62**	-5.79**	6.13**	-0.30	-17.53**	-6.80**	-18.85**	-21.85**	0.14	-24.45**	-26.58*	0.04	-6.79**	-9.78**	0.03	-7.09**	-19.87**
DH6 x Bezostaja	0.58**	7.00**	4.32**	-8.62**	-5.61**	-33.17**	-5.37**	3.43	-4.96	-0.27	-29.69**	-37.19**	0.10	6.42**	-6.49	0.14	-8.34**	-20.72**
DH6 x Harmankaya	-0.38**	0.10	-1.22	-1.07	-17.10**	-22.21**	-5.20**	-18.14**	-28.36**	0.60	-13.24*	-15.57	-0.03	-5.84**	-9.89**	-0.34**	-19.01**	-27.31**
DH6 x Kate	0.60**	6.24**	2.03**	3.56**	20.34**	-9.43**	17.36**	17.79**	89.42**	-0.48	-30.45**	-37.10**	-0.11	-4.79**	-7.14*	0.17	-10.33**	-14.14**
DH16 x Altay	0.93**	4.73**	-1.20	-7.60**	-6.33**	-19.42**	-0.45	26.73**	6.28	-0.45	2.08	-0.76	0.12	0.08	-3.50	-0.42**	-8.99**	-14.78**
DH16 x Bezostaja	-0.59**	-5.13**	-10.28**	-1.36*	57.53**	48.25**	1.41	63.25**	52.86**	0.20	8.73	2.35	0.03	8.68**	-4.82	0.15	4.38	-2.57
DH16 x Harmankaya	-0.64**	-5.34**	-11.51**	4.49**	16.01**	-10.79**	2.14*	27.94**	-0.94	0.65	22.10**	18.55	-0.52**	-17.41**	-21.25**	0.01	0.86	-9.42
DH16 x Kate	0.30**	0.19	-3.84**	4.47**	71.43**	65.70**	-3.10**	15.97**	-10.66	-0.41	3.28	-1.50	0.37**	15.12**	11.86**	0.25	2.46	-13.35**
DH18 x Altay	-0.37**	-5.73**	-7.07**	-7.13**	-46.52**	-51.85**	1.93*	0.62	-14.12*	0.14	12.82*	-0.95	0.07	-3.28	-4.09	0.16	0.13	-7.57
DH18 x Bezostaja	-0.19**	-3.97**	-5.58**	8.14**	14.61**	-13.52**	2.31**	21.01**	15.62*	-0.35	4.39	-0.47	0.17*	12.53**	2.58	0.02	-7.85**	-14.67**
DH18 x Harmankaya	0.36**	0.29	-0.19	-6.60**	-44.79**	-46.67**	-3.97**	-45.21**	-56.92**	0.21	17.19**	2.78	-0.12	-6.23**	-6.53	-0.06	-8.96**	-12.25**
DH18 x Kate	0.20**	-1.79**	-4.90**	5.59**	7.92**	-12.67**	-0.28	-4.09	-24.97**	-0.00	10.93*	4.39	-0.12	-2.25	-3.82	-0.12	-14.21**	-16.95**
DH19 x Altay	0.31**	-1.24**	-7.45**	-6.44**	-28.56**	-43.53**	-4.97**	16.54**	-6.90	-1.46**	-19.05**	-27.50**	-0.49**	-22.72**	-27.18**	-0.13	1.31	-4.04
DH19 x Bezostaja	0.63**	1.29**	-4.85**	-0.88	33.34**	27.61**	-1.97*	63.01**	44.28**	0.51	4.97	2.30	-0.08	0.76	-13.56**	0.02	1.31	-3.73
DH19 x Harmankaya	-0.13	-3.67**	-10.54**	13.38**	18.60**	-14.98**	9.75**	94.87**	44.61**	-1.14	-11.20*	-20.57*	0.18*	1.83	-5.10	0.02	2.06	1.06
DH19 x Kate	-0.81**	-8.87**	-13.12**	-6.07**	12.14**	-1.75	-2.80**	36.52**	0.84	2.09**	26.86**	22.00*	0.40**	12.17**	6.49	0.09	-1.01	-6.66
DH20 x Altay	-0.12	2.33**	-5.56**	8.07**	6.43**	-13.04**	2.84**	2.06	-1.69	1.34*	16.81**	1.92	0.02	-1.88	-6.42	0.06	11.26**	-4.93
DH20 x Bezostaja	0.62**	7.57**	-0.48	-0.57	22.28**	22.15**	1.81*	10.52**	1.55	-0.15	-3.54	-8.66	0.26**	17.87**	2.22	-0.34**	-2.69	-16.62**
DH20 x Harmankaya	0.11	4.44**	-4.46**	-3.43**	-29.58**	-48.12**	1.49	-15.12**	-25.71**	-0.11	1.80	-11.27	-0.23**	-6.74**	-12.04**	0.34**	14.38**	1.64
DH20 x Kate	-0.61**	-1.16**	-7.23**	-4.06**	8.76**	-0.96	-6.13**	-37.87**	-45.95**	-1.08	-12.50*	-18.21	-0.05	2.84	-1.17	-0.06	0.51	-4.77
DH21 x Altay	0.78**	10.15**	8.37**	-5.62**	-23.29**	-33.12**	-2.85**	-17.47**	-17.62**	0.40	12.74*	-4.47	-0.15	0.90	-1.24	0.18	19.52**	2.76
DH21 x Bezostaja	-0.42**	2.04**	0.66	9.84**	67.00**	54.84**	5.28**	47.36**	31.07**	0.25	8.58	-0.46	0.03	20.59**	11.26**	-0.04	10.06**	-5.11
DH21 x Harmankaya	0.14*	6.29**	3.59**	-4.30**	-23.13**	-40.22**	-1.25	-16.90**	-24.92**	-0.14	9.45	-7.35	0.46**	25.72**	24.49**	-0.04	10.47**	-1.20
DH21 x Kate	-0.50**	0.73*	0.54	0.08	30.62**	28.23**	-1.18	0.24	-10.00	-0.50	2.25	-7.43	-0.34**	1.68	-1.24	-0.10	4.37*	-0.42
DH22 x Altay	-0.73**	-6.41**	-15.54**	12.58**	48.39**	8.60**	10.31**	61.21**	46.77**	-0.11	19.13**	5.85	0.39**	26.11**	20.96**	0.12	20.21**	4.53
DH22 x Bezostaja	-0.62**	-5.30**	-14.35**	-6.55**	35.01**	16.76**	-3.47**	1.88	-16.61**	-0.19	15.07**	11.17	-0.50**	8.94**	-5.04	0.05	14.44**	-0.20
DH22 x Harmankaya	0.55**	2.40**	-8.39**	-2.47**	-8.31**	-38.29**	-2.96**	-15.20**	-15.77**	-0.07	23.34**	9.46	0.26**	25.48**	19.02**	0.06	14.84**	3.95
DH22 x Kate	0.81**	3.15**	-5.37**	-3.56**	43.27**	14.66**	-3.88**	-4.23	-5.54	0.38	24.56**	18.75	-0.14	16.00**	12.12**	-0.23	3.19	-0.27
SE	0.07			0.55			0.82			0.58			0.08			0.13		

*p ≤ 0.05, **p ≤ 0.01. SCA: specific combining ability, HT: heterosis, HB: heterobeltiosis, SE: standard error

http://www.aloki.hu ● ISSN 1589 1623 (Print) ● ISSN 1785 0037 (Online)
DOI: http://dx.doi.org/10.15666/aeer/1605_73057326
© 2018, ALÖKI Kft., Budapest, Hungary

Selection of genotypes and breeding strategy for grain quality and biofortified capacity

Principal component analysis (PCA) is a method which defined plant properties which contributed most to the present variation within a group of genotypes. In addition, it helps breeders for genetic advancement of characters that have low heritability specifically in early generations via indirect selection, just as the selection of parental lines for breeding purpose (Golparvar et al., 2006; Ahmadizadeh and Felenji, 2011). Cumulative variability of four factors was 26.01%, 41.49%, 56.22% and 69.32%, respectively (*Table 6*). Different characters have different pattern of contribution for principal components. For PC1, all characters were positively contributing except L, b, Zn, P and Cu, whereas for PC2 only six component were positively contributing, also for PC3 and PC4, seven component were negatively contributing (*Table 7*).

Kernel length, kernel width, kernel thickness, kernel volume, thousand kernel weight and hectolitre weight constituted the first component so called physical kernel characters which had the highest factors loadings. Kernel hardness, L, a, b values which can be called as the color properties were the second component, and the third and fourth components included the kernel sphericity, protein rate and nutrient elements.

Table 6. *Eigen value and contribution of the principal component axes towards variation in line x tester bread wheat hybrids*

Component	Initial			Variamax rotation		
	Eigenvalues	Variance (%)	Cumulative (%)	Eigenvalues	Variance (%)	Cumulative (%)
1	4.512	26.543	26.543	4.422	26.012	26.012
2	3.208	18.871	45.414	2.632	15.482	41.494
3	2.370	13.942	59.355	2.503	14.723	56.217
4	1.694	9.963	69.319	2.227	13.102	69.319
5	1.343	7.899	77.218			
6	1.025	6.029	83.246			
7	0.713	4.195	87.441			
8	0.590	3.469	90.910			
9	0.484	2.846	93.756			
10	0.357	2.099	95.854			
11	0.264	1.556	97.410			
12	0.191	1.124	98.535			
13	0.127	0.748	99.282			
14	0.069	0.407	99.689			
15	0.051	0.300	99.989			
16	0.002	0.010	99.999			
17	0.000	0.001	100.000			

http://www.aloki.hu ● ISSN 1589 1623 (Print) ● ISSN 1785 0037 (Online)
DOI: http://dx.doi.org/10.15666/aeer/1605_73057326
© 2018, ALÖKI Kft., Budapest, Hungary

Table 7. *Eigen value and contribution of the principal component axes towards variation in line x tester bread wheat hybrids*

	PC1	PC2	PC3	PC4
Kernel length	**0.681**	-0.150	-0.552	0.302
Kernel width	**0.893**	0.060	0.222	0.152
Kernel thickness	**0.925**	-0.001	0.056	-0.058
Kernel volume	**0.969**	-0.006	-0.056	0.151
Kernel sphericity	0.471	0.198	**-0.745**	-0.239
Kernel hardness	0.120	**-0.573**	-0.308	-0.121
Thousand kernel weight	**0.750**	0.014	0.136	-0.015
Hectolitre weight	**0.650**	-0.150	-0.516	-0.111
L	-0.187	**0.752**	0.063	-0.292
a	0.066	**0.723**	0.175	0.134
b	-0.029	**0.879**	0.173	0.048
Protein rate	0.042	-0.094	**-0.813**	0.437
Fe	0.016	-0.334	**0.635**	-0.232
Zn	-0.208	-0.403	**0.127**	0.126
Cu	-0.021	0.153	-0.044	**0.769**
P	-0.051	-0.220	0.228	**0.655**
K	0.237	0.010	0.094	**0.785**

Bi-plot analysis was performed based on two principal components for relationships between variables and genotypes (*Fig. 3*). Genotypes and variables were presented in single bi-plot graph to further simplify the visualization. Physical kernel characters, protein rate, color values and Fe content contributed maximum towards the total variability present in the evaluated germplasm. Therefore, these traits might be considered selecting effectively of parents for hybridization program to improvement of genetic potential in bread wheat kernel quality in the population as well as to develop elite lines or new F_1 crosses. Moreover, selection of the genotypes had high kernel quality and biofortified capacity should be suggested as one of the best breeding strategy for genetic advancement of bread wheat. According to bi-plot graph, there was high variability in the examined genotypes. “DH20 x Altay”, “DH19 x Altay”, DH20, DH22, “DH21 x Altay”, “DH20 x Bezostaja”, “DH18 x Altay”, “DH22 x Harmankaya” and “DH20 x Harmankaya” can be identified as the best genotypes as these genotypes grouped in positive part as well as they can be easily identified as distinct or farthest from the rest of the genotype groups of the bi-plot (*Fig. 3*). Genotypes “DH6 x Harmankaya”, “DH20 x Harmankaya” and “DH22 x Harmankaya” were reflected much better performance compared to the rest of genotypes for physical kernel characters. The “DH6 x Kate” genotype, had high Fe and Zn content, can be specifically selected to breed biofortified variety.

http://www.aloki.hu ● ISSN 1589 1623 (Print) ● ISSN 1785 0037 (Online)
DOI: http://dx.doi.org/10.15666/aeer/1605_73057326
© 2018, ALÖKI Kft., Budapest, Hungary

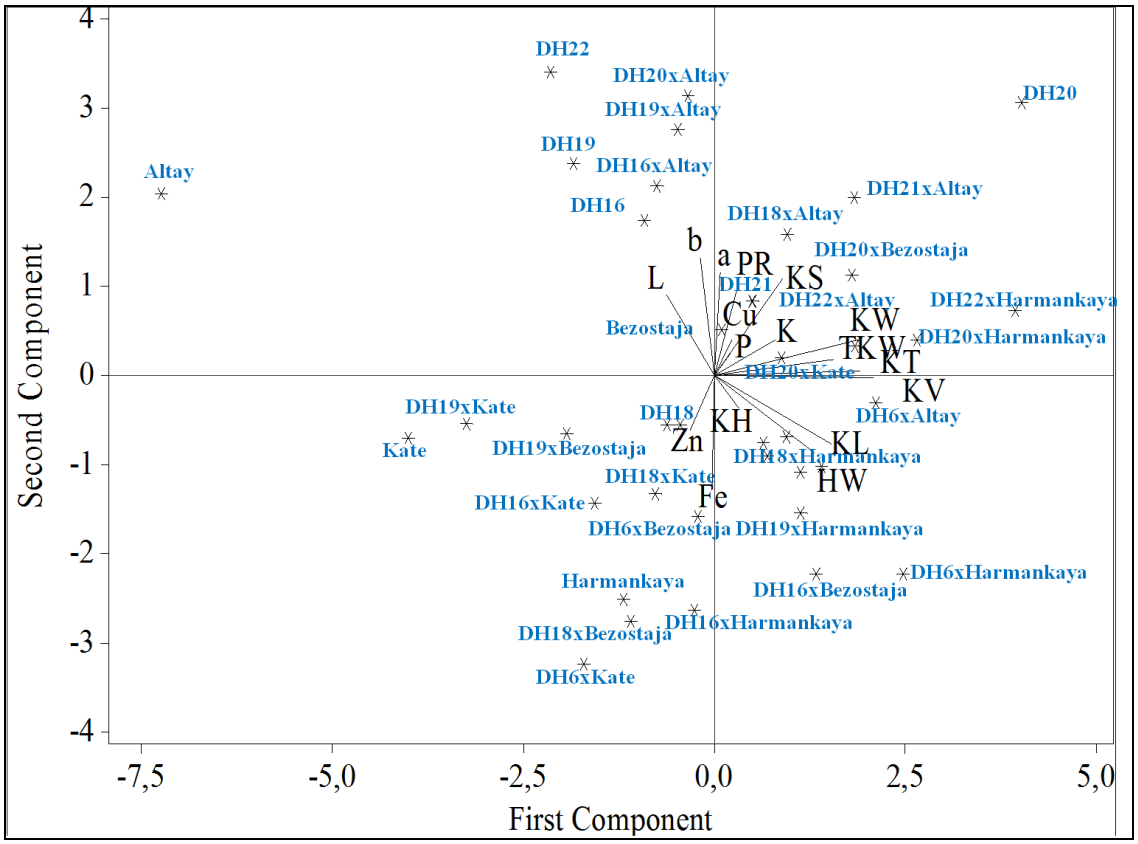

Figure 3. *Principal component bi-plot of 39 bread wheat genotypes between 17 kernel quality characters. (Contribution of first component = 26.01%, second component = 15.48%)*

Conclusions

The population examined in this study has sufficient variation to be assessed in breeding programs in terms of both end-use quality characteristics and biofortification. The predominance of non-additive type of gene actions clearly showed that selection of superior crops should be delayed to F_4 or F_5 generations. The lines DH6, DH22 and the tester Harmankaya were good combiners for the flour yield and milling quality. The lines DH21, DH22 and the tester Kate were good combiners for protein rate and biofortified crops. The DH22 line, in particular, is well-suited to be a favourite of breeding programs for this purpose with both end-use quality and biofortified capacity. "DH6 x Harmankaya", "DH20 x Harmankaya", "DH22 x Harmankaya", "DH6 x Kate", "DH20 x Altay", "DH19 x Altay", "DH21 x Altay", "DH20 x Bezostaja" and "DH18 x Altay" was found as the best crosses to all examined traits. Because "DH20 x Harmankaya", "DH22 x Harmankaya", "DH21 x Altay" and "DH18 x Altay" had both the best SCA and they grouped in positive part of the bi-plot, these crosses are particularly important as promising crosses for biofortification and end-use quality.

It is clear that genetic biofortification offer sustainable solutions to the escalating micronutrient-related malnutrition problems. However, biofortified crops must also be suitable for producers and consumer demands. Therefore, biofortification and end-use quality traits are highly complementary. This research provides general information about the inheritance of wheat quality, and plant breeding strategies for the bioavailability of micronutrients in modern cultivars. This information will light on the

http://www.aloki.hu ● ISSN 1589 1623 (Print) ● ISSN 1785 0037 (Online)
DOI: http://dx.doi.org/10.15666/aeer/1605_73057326
© 2018, ALÖKI Kft., Budapest, Hungary

molecular researches about genes controlled these properties, functional genomic analyzes and the creation of association maps in the future. In addition, examined wheat population has a potential occurring both high quality and nourishing candidate varieties for the countries with high malnutrition prevalence in the near future.

REFERENCES

[1] AACCI (2000): Approved Methods of the American Association of Cereal Chemists Methods, 08-01, 32-23, 32-32, 44-19, 46-30, 55-10, 55-31 (10th ed.). – The Association, St. Paul, MN, U. S. A.
[2] Abbaspour, N., Hurrell, R., Kelishadi, R. (2014): Review on iron and its importance for human health. – Journal of Research in Medical Sciences: The Official Journal Of Isfahan University Of Medical Sciences 19(2): 164.
[3] Ahmadizadeh, M., Felenji, H. (2011): Evaluation diversity among potato cultivars using agro-morphological and yield components in fall cultivation of Jiroft area. – American-Eurasian Journal of Agriculture and Environmental Science 11(5): 655-662.
[4] Aslam, R., Munawar, M., Salam, A. (2014): Genetic architecture of yield components accessed through line × tester analysis in wheat (*Triticum aestivum* L.). – Universal Journal of Plant Science 2(5): 93-96.
[5] Bálint, A. F., Kovács, G., Erdei, L., Sutka, J. (2001). Comparison of the Cu, Zn, Fe, Ca and Mg contents of the grains of wild, ancient and cultivated wheat species. – Cereal Research Communications 29(3-4): 375-382.
[6] Barton, C. J. (1948): Photometric analysis of phosphate rock. – Anal. Chem. 20(11): 1068-1073.
[7] Cakmak, I. (2008): Enrichment of cereal grains with zinc: agronomic or genetic biofortification? – Plant and Soil 302(1-2): 1-17.
[8] Cakmak, I., Torun, A., Millet, E., Feldman, M., Fahima, T., Korol, A. Nevo, E., Braun, H. J., Özkan, H. (2004): *Triticum dicoccoides*: an important genetic resource for increasing zinc and iron concentration in modern cultivated wheat. – Soil Sci. Plant Nutr. 50: 1047e1054.
[9] Chasapis, C. T., Loutsidou, A. C., Spiliopoulou, C. A., Stefanidou, M. E. (2012): Zinc and human health: an update. – Archives of Toxicology 86(4): 521-534.
[10] Chiang, M. S., Smith, J. D. (1967): Diallel analysis of inheritance of quantitative characters in grain sorghum. I. heterosis and inbreeding depression. – Can. Journal Genetic Cytology 9: 44-51.
[11] De Peuw, R. M., McCetc, T. N. (1988): Utilization of sodium hydroxide to assess kernel color and its inheritance in eleven spring wheat varieties. – Can. J. Plant Sci. 68: 323-329.
[12] Dziki, D., Laskowski, J. (2005): Wheat kernel physical properties and milling process. – Acta Agrophysica 6(1): 59-71.
[13] Falconer, D. S. (1980): Introduction to Quantitative Genetics. – Oliver and Boyd Ltd., London.
[14] Ferreira, M. S. L., Martre, P., Mangavel, C., Girousse, C., Rosa, N. N., Samson, M., More, M. (2012): Physicochemical control of durum wheat grain filling and glutenin polymer assembly under different temperature regimes. – J. Cereal Sci. 56: 58-66.
[15] Fonseca, S. M., Patterson, F. L. (1968): Hybrid vigor in a seven parent diallel cross in common winter wheat (*Triticum aestivum* L.). – Crop. Science 8: 85-88.
[16] Golparvar, A. R., Ghasemi-Pirbalouti, A., Madani, H. (2006): Genetic control of some physiological attributes in wheat under drought stress conditions. – Pakistan Journal of Biological Sciences 9(8): 1442-1446.
[17] Gomez-Becerra, H. F., Erdem, H., Yazici, A., Tutus, Y., Torun, B., Ozturk, L., Cakmak, I. (2010): Grain concentrations of protein and mineral nutrients in a large collection of

http://www.aloki.hu ● ISSN 1589 1623 (Print) ● ISSN 1785 0037 (Online)
DOI: http://dx.doi.org/10.15666/aeer/1605_73057326
© 2018, ALÖKI Kft., Budapest, Hungary

spelt wheat grown under different environments. – Journal of Cereal Science 52(3): 342-349.

[18] Graham, R., Senadhira, D., Beebe, S., Iglesias, C., Monasterio, I. (1999): Breeding for micronutrient density in edible portions of staple food crops: conventional approaches. – Field Crops Research 60(1-2): 57-80.

[19] He, F. J., MacGregor, G. A. (2008): Beneficial effects of potassium on human health. – Physiologia Plantarum 133(4): 725-735.

[20] Henderson, L., Irving, K., Gregory, J. (2003): The National Diet & Nutrition Survey: Adults Aged 19–64 Years. Vol. 3. – Her Majesty's Stationery Office, London.

[21] Hruskova, M., Svec, I. (2009): Wheat hardness in relation to other quality factors. – Czech J. Food Science 27: 240-248.

[22] Istipliler, D., Ilker, E., Tonk, F. A., Civi, G., Tosun, M. (2015): Line x tester analysis and estimating combining abilities for yield and some yield components in bread wheat. – Turk. J. Field Crops 20(1): 72-77.

[23] Khan, A. A., Iqbal, M., Ali, Z., Athar, M. (2010): Diallelic analysis of quantitative traits in hexaploid wheat (*Triticum aestivum* L.). – Plant Biosystems 144(2): 373-380.

[24] Kirk, S., Sawyer, R. (1991): Pearson's Composition and Analysis of Foods (Ed. 9). – Longman Group Ltd., Harlow, UK.

[25] Korkut, K. Z., Baser, I., Bilgin, O. (2001): Genotypic and phenotypic variability, heritability and phenotypic correlation for yield and yield components in bread wheat varieties. – Acta Agronomica Hungarica 49(3): 237-242.

[26] Kumar, B., Bharadwaj, D. N., Singh, L., Gupta, S. K. (2017): Estimation of combining ability in F_1 and F_2 generations of diallel crosses in winter wheat (*Triticum aestivum* L. Em. Thell). – Int. J. Curr. Microbiol. App. Sci. 6(12): 1432-1444.

[27] Longin, C. F., Gowda, M., Mühleisen, J., Ebmeyer, E., Kazman, E., Schachschneider, R., Schacht, J., Kirchhoff, M., Zhao, Y., Reif, J. C. (2013): Hybrid wheat: quantitative genetic parameters and consequences for the design of breeding programs. – Theor. Appl. Genet. 126(11): 2791-2801.

[28] Maphosa, L., Langridge, P., Taylor, H., Parent, B., Emebiri, L. C., Kuchel, H., Reynolds, M. P., Chalmers, K. J., Okada, A., Edwards, J., Mather, D. E. (2014): Genetic control of grain yield and grain physical characteristics in a bread wheat population grown under a range of environmental conditions. – Theor Appl Genet. 127: 1607-1624.

[29] McNeal, F. H., Balridge, D. E., Berg, M. A., Watson, C. A. (1965): Evaluation of three hard red spring wheat crosses for heterosis. – Crop Science 5: 399-400.

[30] Mohsenin, N. N. (1986): Physical Properties of Plant and Animal Materials. 2nd ed. – Gordon and Breach, New York.

[31] Nuttall, J. G., O'Leary, G. J., Panozzo, J. F., Walker, C. K., Barlow, K. M., Fitzgerald, G. J. (2017): Models of grain quality in wheat – A review. – Field Crops Research 202: 136-145.

[32] Ozcan, K. (1999): Developing of a statistical package program for population genetics. – PhD. Thesis, University of Aegean, Institute of Science, Izmir.

[33] Perenzin, M., Pogna, N. E., Borghi, B. (1992): Combining ability for bread making quality in wheat. – Can. J. Plant Science 72: 743-754.

[34] Pfeiffer, W. H., McClafferty, B. (2007): HarvestPlus: Breeding Crops for Better Nutrition. – Crop Sci. 47(S3): S88–S105.

[35] Pomeranz, Y. (1964): Wheat Chemistry and Technology (edited). – American Association of Cereal Chemists, St. Paul, Minnesota.

[36] Ponce-García, N., Ramírez-Wong, B., Escalante-Aburto, A., Torres-Chávez, P. I., de Dios Figueroa-Cárdenas, J. (2016): Mechanical Properties in Wheat (*Triticum aestivum*) Kernels Evaluated by Compression Tests: A Review. – Viscoelastic and Viscoplastic Materials, InTech, Rijeka.

http://www.aloki.hu ● ISSN 1589 1623 (Print) ● ISSN 1785 0037 (Online)
DOI: http://dx.doi.org/10.15666/aeer/1605_73057326
© 2018, ALÖKI Kft., Budapest, Hungary

[37] Schuler, S. F., Bacon, R. K., Finney, P. L., Gbur, E. E. (1995): Relationship of test weight and kernel properties to milling and baking quality in soft red winter wheat. – Crop Science 35(4): 949-953.
[38] Sherman, J. D., Souza, E., See, D., Talbert, L. E. (2008): Microsatellite markers for kernel color genes in wheat. – Crop Science 48(4): 1419-1424.
[39] Stern, B. R., Solioz, M., Krewski, D., Aggett, P., Aw, T., Baker, S., Crump, K., Dourson, M., Haber, L., Hertzberg, R., Keen, C., Meek, B., Rudenko, L., Schoeny, R., Slob, W., Starr, T. (2007): Copper and human health: biochemistry, genetics, and strategies for modeling dose-response relationships. – Journal of Toxicology and Environmental Health, Part B. 10(3): 157-222.
[40] Velu, G., Singh, R. P., Huerta-Espino, J., Peña, R. J., Arun, B., Mahendru-Singh, A., YaqubMujahid, M., Sohu, V. S., Mavi, G. S., Crossa, J., Alvarado, G., Joshi, A. K., Pfeiffer, W. H. (2012): Performance of biofortified spring wheat genotypes in target environments for grain zinc and iron concentrations. – Field Crops Research 137: 261-267.
[41] Weisstein, E. W. (2018): Ellipsoid. – *MathWorld*—A, Wolfram Web Resource. http://mathworld.wolfram.com/Ellipsoid.html. Access date: 25.07.2018.
[42] Zhao, F. J., McGrath, S. P. (2009): Biofortification and phytoremediation. – Curr. Opin. Plant Biol. 12: 373e380.

http://www.aloki.hu ● ISSN 1589 1623 (Print) ● ISSN 1785 0037 (Online)
DOI: http://dx.doi.org/10.15666/aeer/1605_73057326
© 2018, ALÖKI Kft., Budapest, Hungary

DEFINING THE EQUILIBRIUM CONDITION IN A MIXED-SPECIES UNEVEN-AGED FOREST IN SCOTLAND

CAMERON, A. D.* – JANO, G.

Institute of Biological and Environmental Sciences, University of Aberdeen, Cruickshank Building, St. Machar Drive, Aberdeen AB22 3UU, Scotland (phone: +44-1224-272-000)

**Corresponding author e-mail: a.d.cameron@abdn.ac.uk; phone: +44-1224-272-673*

(Received 27th Aug 2018; accepted 15th Oct 2018)

Abstract. Transforming even-aged planted forests into uneven-aged, vertically diverse structures often implies that an equilibrium or sustainable condition will eventually be reached where the stand structure and species composition remains relatively constant over time. However, identifying the equilibrium condition is complicated by the complex dynamics of diverse forest structures. In this study four 'sustainability' indices—stand structure, stocking density, species diversity and increment—were applied over a 20 year period in a long-term permanent sample plot within an uneven-aged forest in Scotland to determine whether the equilibrium condition has been achieved. The Shannon Index of species diversity highlighted a gradual shift towards shade tolerating species. Transition periods (average time for all trees in one diameter class to move into next higher diameter class) of shade tolerating species declined with increasing diameter (trees growing more quickly), whereas the opposite trend was found with light demanding species highlighting competition pressures. However, evaluation of the q value, Lorenz curves, Gini coefficient and Stand Density Index revealed values comparable with those found in long-established Central European uneven-aged forests and suggests that, while subtle changes in species composition are occurring, the forest is within the range of parameters indicated for the equilibrium condition.

Keywords: *uneven-aged silviculture, Lorenz curves, Gini coefficient, Stand Density Index, Shannon Index*

Introduction

In many regions of the world, forest cover is dominated by even-aged plantation forests characterised by uniform canopies often of pure coniferous species. There has been increasing pressure in recent years to develop forest ecosystems that are more structurally and species diverse (e.g. Spiecker, 2003), and that are more adaptable to the potential threats of a changing climate (e.g. Millar et al., 2007). The move from predominately clear cutting management (removal of all trees from an area of forest) towards a more ecological or natural approach (i.e. 'uneven-aged', 'irregular', 'selection', 'plenter' or 'close-to-nature' forests) has required a better understanding of the mechanisms of regeneration and seedling/sapling development of species within structurally diverse canopies. Uneven-aged forests are generally described as having vertically varied structures usually comprising a mix of species ranging from new seedlings to mature stems growing within the same space and where a certain level of canopy cover is maintained in perpetuity. The expectation is that these forests will eventually reach a stage of development where, following each harvesting cycle, they revert to the same condition that is often defined as the 'equilibrium' (i.e. 'sustainable', 'stable' or 'balanced') state (e.g. Meyer, 1943; Smith, 1962; Bormann and Likens, 1994; Schütz, 2001). While no forest ecosystem can be regarded as being permanent as

http://www.aloki.hu ● ISSN 1589 1623 (Print) ● ISSN 1785 0037 (Online)
DOI: http://dx.doi.org/10.15666/aeer/1605_73277344
© 2018, ALÖKI Kft., Budapest, Hungary

a result of climatic and human influences that impact over the long lifespans of most forest trees (von Denton, 2011), there remains a desire amongst foresters to achieve some form of equilibrium in uneven-aged forests. This is seen as being important if only to demonstrate that the silvicultural systems used are capable of maintaining a range of economic and environmental services and that these have some degree of permanence.

Determining the equilibrium condition within uneven-aged forests is complicated by the fact that it requires objective, easy-to-use measures that define ways in which management practices influence the relatively complex dynamics of diverse forest structures. O'Hara et al. (2007) pointed out that as forest stands move closer towards a vertically-diverse uneven-aged structure, variations in stand characteristics become more difficult to observe. They suggested four 'sustainability criteria'—stand structure, stand density, species diversity and increment—that they assert are capable of identifying subtle changes in the dynamics of uneven-aged forests. Maintaining the constancy of these measures should ensure that uneven-aged structures achieve a state that could be described as sustainable or in equilibrium, even accepting that some fluctuations are inevitable. Identifying the equilibrium condition would therefore require recurrent assessments of the same area of forest over a period of time to observe whether the equilibrium criteria have been realised.

Distribution of tree size is most commonly used to describe the condition of uneven-aged forests although it is not without its critics. The structure of uneven-aged forests was first objectively studied by de Liocourt (1898) through his negative exponential relationship between stem number and diameter (high number of small trees declining exponentially to a few large trees), and continues to be widely seen as a target for uneven-aged stands with the perception that it is both stable and creates 'natural' forest structures (Larsen, 1995). The shape of the negative exponential distribution is expressed by the ratio of decline in number of trees with increasing diameter known as the q value (Meyer, 1952). However, use of the q value and the underlying negative exponential relationship has been challenged by those who believe that it places too great an importance on the stem number-diameter distribution in decisions on uneven-aged stand structure and management (e.g. O'Hara, 1998; Schütz and Pommerening, 2013). A study of Central European uneven-aged stands by O'Hara and Gersonde (2004) indicated that there are more trees in the highest and lowest diameter classes than suggested by the q value due to the low growth of the small diameter classes requiring a high number of stems to allow diameter advancement. Once these small stems are released by canopy opening, their increment increases causing a sharp decline in the diameter distribution of the medium size classes. When the trees are larger, mortality declines while diameter class advancement continues to be high resulting in a slower decline in stem number. O'Hara et al. (2007) proposed that Lorenz curves (Lorenz, 1905) and related Gini coefficients (Gini, 1909) are more effective in analysing stand structure since they determine the equality of the population of trees in a stand rather than just the shape of diameter distributions (Weiner and Solbrig, 1984). Lorenz curves were originally developed to analyse economic data, but are widely used in studying forest structure. Lorenz curves define number and size as proportions of the tree population and make the method suitable for comparing stands of different size ranges and those that do not accurately follow the negative exponential distribution or reveal a variable q value; a situation common to most if not all uneven-aged stand structures. The Gini coefficient is a measure of the size of inequality in a stand (Weiner

http://www.aloki.hu ● ISSN 1589 1623 (Print) ● ISSN 1785 0037 (Online)
DOI: http://dx.doi.org/10.15666/aeer/1605_73277344
© 2018, ALÖKI Kft., Budapest, Hungary

and Solbrig, 1984) and is considered to be better than other measures in analysing tree size diversity (Lexerød and Eid, 2006).

Stand density is an important measure of sustainability since successful regeneration and recruitment are dependent on the understorey light environment (Jenkins and Chambers, 1989; Philip, 1994; Mitchell and Popovich, 1997) and is usually represented as the number of trees or basal area per hectare. Foresters commonly adjust stocking density at harvesting interventions by altering basal area (cross-sectional area of all trees per hectare) as a means of effecting changes such as increasing levels of regeneration or to favour certain species in the regeneration mix. Successful regeneration in uneven-aged spruce-fir forests generally requires a basal area of no more than 27-33 $m^2 ha^{-1}$ (Schütz, 2002). A basal area no more than 27 $m^2 ha^{-1}$ has been found to be required for successful regeneration of both intermediate and shade tolerant species (Mailly and Kimmins, 1997; Drever and Lertzmann, 2003; Schütz and Pommerening, 2013), and a lower limit of around 20 $m^2 ha^{-1}$ has been suggested as the point at which competing vegetation inhibits regeneration (Ralston et al., 2004). Species diversity in the understorey, therefore, is strongly influenced by the direction of management in determining an appropriate basal area. An 'equilibrium' basal area and stocking density would have to be set at a level that permits continuous regeneration and recruitment into the canopy, ideally of the preferred species.

While basal area has been widely used to control level of canopy cover, it needs to be considered along with stocking density (number of trees per hectare) to provide a more accurate measure of 'site occupancy' since the maximum basal area that a forest stand can attain increases with tree diameter (Zeide, 2005). Site occupancy is usually expressed as the stand density index (SDI) (Reineke, 1933) and allows objective comparisons to be made between stands at different stages of development. Although SDI was originally developed as a stand density assessment method for single-species, even-aged stands, it has been adapted for use in uneven-aged stands with the aim of controlling stand density through balancing growth among the diameter classes (Sterba and Monserud, 1993; Woodall et al., 2005; Yang et al., 2018).

Many researchers argue that a better determinant of the equilibrium condition is increment, particularly within the saplings and lower diameter classes that will eventually become the future canopy trees (Meyer, 1952; Sterba, 2004; Schütz and Pommerening, 2013). It is suggested that the equilibrium state would require a similar number of trees growing into each diameter class from the next lower class and also trees growing out of the diameter class plus those that are harvested or die (Schütz, 1975). The problem with this approach is that data on tree removals are often unavailable or not recorded using a consistent method to estimate increment across the diameter classes (O'Hara et al., 2007). However, an indicator of the productivity of the standing trees in uneven-aged stands can be derived from increment cores to calculate 'transition periods', defined as the average number of years required for all trees in one diameter class to rise into the next higher diameter class (Čavlović et al., 2006). A feature of long established uneven-aged stands is that transition times decline (i.e. increment increases) with increasing diameter due to young trees in the partially shaded understorey emerging into the canopy where more light is available (Smith et al., 1997).

There have been very few investigations attempting to define the equilibrium condition in spite of the fact that it is a central premise of forest sustainability. The aim of the current study was to determine whether sustainability measures based on stem number and diameter, tree density, species diversity and increment (after O'Hara et al.,

http://www.aloki.hu ● ISSN 1589 1623 (Print) ● ISSN 1785 0037 (Online)
DOI: http://dx.doi.org/10.15666/aeer/1605_73277344
© 2018, ALÖKI Kft., Budapest, Hungary

2007) can identify the equilibrium condition. These measures were applied to data collected over a 20 year period from a one hectare permanent sample plot in a rare example of an uneven-aged experimental forest comprising a geographically diverse range of native, Continental European, and North American species, located in Scotland. The stages of this study were analysed as follows: 1) examination of temporal changes in the stem number-diameter distributions, Lorenz curves and Gini coefficients; 2) analysis of increment across diameter classes using transition periods; 3) examination of temporal shifts in canopy and understorey species composition calculated using the Shannon Index of species diversity, and 4) examination of the relationship between stand density and understorey species composition.

Materials and methods

Study area and permanent sample plot

The research site is located within Faskally Research Forest, Perthshire, Scotland (56°42'39.4"N, 3°45'45.5"W) (*Fig. 1*). The research forest is at 120 m altitude and has a moist temperate climate with a mean annual precipitation of 900 mm. The geology comprises Dalradian mica schist parent material overlain with brown earth and ironpan soils. The conversion of the forest was started in 1953 in a mature mixed stand of planted Norway spruce (*Picea abies* (L.) Karst.), Scots pine (*Pinus sylvestris* L.), European larch (*Larix decidua* Mill.), Douglas fir (*Pseudotsuga menziesii* (Mirb.) Franco) and European beech (*Fagus sylvatica* L.). Gaps were opened in the canopy within a 25 hectare area of the forest and planted with Douglas fir, Norway spruce, western hemlock (*Tsuga heterophylla* (Raf.) Sarg.), European beech, Scots pine, European larch and silver birch (*Betula pendula* Roth). Further details on the background of the experimental site are reported in Cameron (2007).

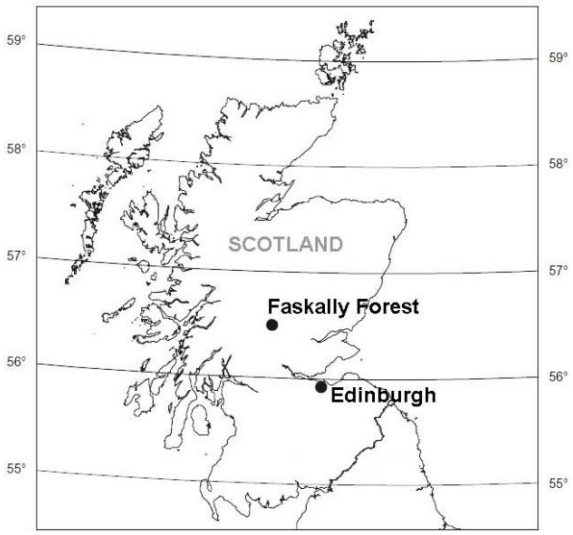

Figure 1. *Geographical location of study area*

A one hectare permanent sample plot was established in 1997 and complete inventories of the plot (all trees counted and measured) were carried out at this time and

http://www.aloki.hu ● ISSN 1589 1623 (Print) ● ISSN 1785 0037 (Online)
DOI: http://dx.doi.org/10.15666/aeer/1605_73277344
© 2018, ALÖKI Kft., Budapest, Hungary

subsequently in 2003, 2009 and 2015 corresponding with the six-year cutting cycles with the harvesting interventions occurring the year prior to the inventories. Permanent sample plots are favoured as a method of evaluating whether planned management objectives have been applied and whether management interventions have led to the intended structural changes towards a predefined target (Sterba and Ledermann, 2006). It is the principle of re-measuring exactly the same section of forest over time that gives this approach its precision in comparison with random plot surveys. The current study used data from all previous inventories of the one hectare permanent sample plot.

Diameter distributions

At each inventory, species and stem diameter (DBH – diameter at breast height measured at 1.3 m from ground level) of all the canopy trees (≥8 cm DBH) were recorded using diameter tapes based on methods described by Philip (1994). The diameter distributions of the canopy trees were recorded by five centimetre diameter classes based on the mid-point of the class, e.g. 10 cm class (8-12 cm), 15 cm class (13-17 cm) and so on (Philip, 1994). The average diminution quotient q for the canopy trees was calculated by dividing the number of trees in each diameter class by the number of trees in the next higher class.

Regeneration

A each inventory, a separate survey of seedlings and saplings (≥0.1 m tall, <8 cm DBH) was made using randomly set out 2 × 2 m sample grids (Cameron, 2007; Cameron and Hands, 2010; Cameron and Prentice, 2016). In the 2015 inventory, the regeneration was split into seedlings (≥0.1 m tall, <3 cm DBH) and saplings (3-7 cm DBH) to provide more detailed information on levels of recruitment into the canopy.

Seedlings and saplings were separated into shade tolerating (shade and intermediate tolerant) and light demanding species. Shade tolerating species have the capacity to germinate, establish, survive and grow in the shade of other plants, whereas light demanding species require full or nearly full light to achieve these attributes. Levels of shade tolerance of species used in this study were based on studies of relative shade tolerance (e.g. Mailly and Kimmins, 1997; Minore, 1979; Schütz, 2002; Drever and Lertzmann, 2003; Hale, 2004; Petritan et al., 2007; Schütz and Pommerening, 2013; Drössler et al., 2017). A summary of the data from the four inventories is shown in *Tables 1* and *2*.

Lorenz curves, Gini Coefficients and Stand Density Index (SDI)

Lorenz curves are derived by plotting cumulative relative number of trees against the corresponding cumulative relative diameter or basal area with the upper limit set by the largest tree. Lorenz curves were plotted from data from the full inventories. Curves are generated by ranking the trees by the cumulative proportion of number of trees (y-axis) against the cumulative proportion of both DBH class and basal area (x-axis) (*Eq. 1*).

$$L(F) = \frac{\int_0^F x(F_1)dF_1}{\int_0^1 x(F_1)dF_1} \quad \text{(Eq.1)}$$

where $L(F)$ = Lorenz curve, F = cumulative proportion of trees, $F(x)$ = cumulative distribution function and $x(F)$ = inverse cumulative distribution function.

http://www.aloki.hu ● ISSN 1589 1623 (Print) ● ISSN 1785 0037 (Online)
DOI: http://dx.doi.org/10.15666/aeer/1605_73277344
© 2018, ALÖKI Kft., Budapest, Hungary

Table 1. *Number of canopy trees (≥ 8 cm DBH) by species, basal area and q value within the one hectare permanent sample plot measured in 1997, 2003, 2009 and 2015. (Source: Cameron and Prentice, 2016)*

Species	Number of trees ha^{-1}			
	1997	**2003**	**2009**	**2015**
Pseudotsuga menziesii	222	174	119	112
Picea abies	116	130	71	55
Larix decidua	86	39	58	43
Pinus sylvestris	83	46	52	36
Tsuga heterophylla	32	15	6	6
Abies procera	0	0	2	2
Betula pendula	97	71	59	56
Fagus sylvatica	30	29	15	19
Acer pseudoplatanus	0	0	2	4
Sorbus aucuparia	0	0	0	3
Ilex aquifolium	0	0	0	1
Total number of trees ha^{-1}	666	504	384	337
Basal area (m^2 ha^{-1})	32	27	28	26
q value	1.6	1.5	1.4	1.4

Table 2. *Number of seedlings (≥0.1 m tall, <3 cm DBH) and saplings (3-7 cm DBH) within the one hectare permanent sample plot measured in 1997, 2003, 2009 and 2015. Seedlings and saplings are split in the 2015 inventory. S = shade tolerant, I = intermediate tolerance, L = light demanding. (Source: Cameron and Prentice, 2016)*

Species	Shade tolerance	Seedlings and saplings ha^{-1}				
		1997	**2003**	**2009**	**2015**	
					Seedlings	**Saplings**
Pseudotsuga menziesii	I	197	401	542	958	27
Picea abies	I	158	339	500	1042	69
Larix decidua	L	53	92	83	83	13
Pinus sylvestris	L	0	0	42	167	0
Tsuga heterophylla	S	3	278	1417	1833	41
Picea sitchensis	I	0	31	0	0	1
Abies grandis	S	0	0	126	250	0
Abies procera	S	0	0	42	42	0
Fagus sylvatica	S	244	247	1208	1417	52
Betula pendula	L	33	0	208	125	2
Sorbus aucuparia	I	0	0	167	1083	3
Acer pseudoplatanus	I	0	0	125	0	0
Ilex aquifolium	S	0	0	0	42	1
Total		688	1388	4460	7042	209

The Gini coefficient measures the ‘bow’ of the Lorenz curve, and equals the area between the curve and the line of equality (45°) divided by the total area of the triangle

http://www.aloki.hu ● ISSN 1589 1623 (Print) ● ISSN 1785 0037 (Online)
DOI: http://dx.doi.org/10.15666/aeer/1605_73277344
© 2018, ALÖKI Kft., Budapest, Hungary

below the 45° line. The Gini coefficient ranges from a minimum value of 0, where all values are equal, to a theoretical maximum of 1 representing total inequality (an infinite population where all individuals except one have a value of 0) (Weiner and Solbrig, 1984; *Eq. 2*).

$$G = 1 - \sum_{k=1}^{n}(X_k - X_{k-1})(Y_k + Y_{k-1}) \quad \text{(Eq.2)}$$

where G = Gini coefficient, X_k = cumulated proportion of diameter class variable for k = 0,…,n, with $X_0 = 0$, $X_n = 1.$, Y_k = cumulated proportion of stem number, for k = 0,…,n, with $Y_0 = 0$, $Y_n = 1$.

A high Gini coefficient indicates that the distribution of diameters or basal areas is very heterogeneous whereas a low Gini coefficient indicates more homogenous stands with a limited spread of tree sizes. Uneven-aged forest stands would expected to have higher and more stable values of Gini coefficient than even-aged stands (O'Hara et al., 2007).

Stand density index (SDI) is defined as the number of trees per hectare when the quadratic mean diameter of the stand is established at the index value of 25 cm (Reineke, 1933). SDI was determined for each inventory by calculating the index for each individual diameter class then summing for the whole stand (Woodall et al., 2005; *Eq. 3*):

$$SDI = \sum TPHi \left(\frac{DBHi}{25}\right)^{1.6} \quad \text{(Eq.3)}$$

where SDI = Stand Density Index, DBH_i = midpoint of the ith diameter class (cm) and TPH_i = number of trees per hectare in the ith diameter class.

Shannon Indices of species diversity

Shannon Indices (Spellerberg and Fedor, 2003) were calculated for the canopy trees and understorey regeneration using data of the broadleafs and conifers, and shade tolerating and light demanding species (from *Table 2*) using the formula (*Eq. 4*):

$$SI = -\sum_{i=1}^{n} p_i * \ln p_i \quad \text{(Eq.4)}$$

where SI = Shannon Index and p_i = proportion of the total number of trees. SI increases with increasing number of trees and increasing number of species. It is therefore sensitive to both species richness and species evenness.

Transition periods and annual recruitment

Transition periods (after Čavlović et al., 2006) were calculated from a sample of 90 trees randomly selected within the one hectare permanent sample plot in the spring of 2017. To ensure a representative sample of stem sizes, stratified random sampling was carried out across three size classes (small trees 8-25 cm DBH, medium trees 25-40 cm DBH, large trees >40 cm DBH). The species and DBH were recorded and increment cores removed from the outer 30 mm of each sample tree. Cores were taken at 1.3 m height on the north side of each tree and the number of annual rings in the first 25 mm from the bark were counted. Transition periods (years for all trees in a diameter class to move into the next diameter class) were calculated for each diameter class from the

http://www.aloki.hu ● ISSN 1589 1623 (Print) ● ISSN 1785 0037 (Online)
DOI: http://dx.doi.org/10.15666/aeer/1605_73277344
© 2018, ALÖKI Kft., Budapest, Hungary

increment cores. Transition period for the 10 cm class was calculated using the formula (*Eq. 5*):

$$T_{10} = \frac{10(DBH_{ul} - DBH)}{2(\frac{25}{N_{rings}})} \quad \text{(Eq.5)}$$

where T_{10} = transition period for the 10 cm DBH class, DBH_{ul} = upper limit of the DBH class and N_{rings} = number of rings in the outer 25 mm of each core. Pearson's correlations (r) were determined between transition period and DBH class. Annual recruitment into the 10 cm DBH class was calculated using the formula (*Eq. 6*):

$$R_{10} = \frac{(N_5 + N_{10})}{2T_{10}} \quad \text{(Eq.6)}$$

where R_{10} = annual recruitment into the 10 cm DBH class (trees per hectare), N_5 = number of trees in the 5 cm DBH class (3-7 cm), N_{10} = number of trees in the 10 cm DBH class (8-12 cm) and T_{10} = transition period for the 10 cm DBH class (years).

Results

Analysis of stand structure

The shape of the stem number-diameter distribution has changed over the four inventories of the permanent sample plot with a 'flattening' of the curve (*Fig. 2*) as a result of a reduction in tree density (*Table 1*) mainly in the smaller size categories.

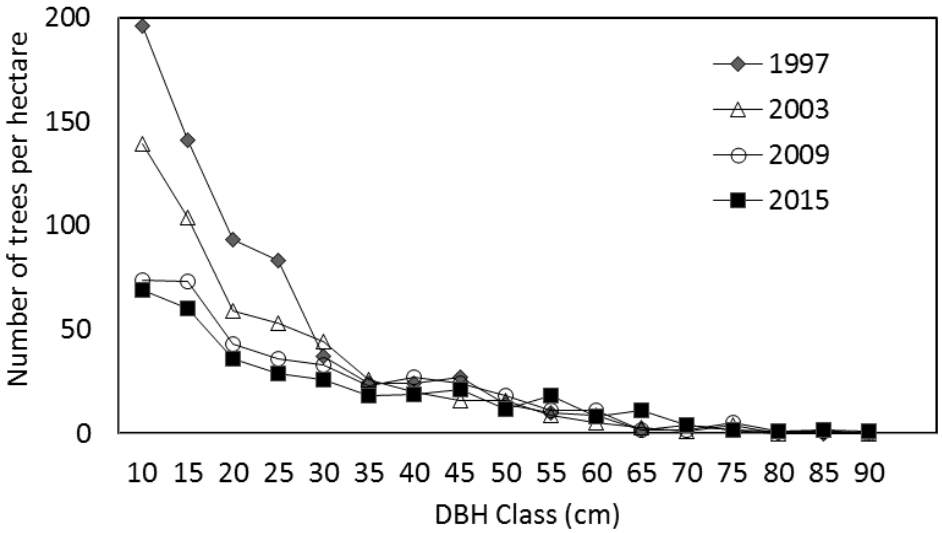

Figure 2. *Diameter distribution of canopy trees (≥8 cm DBH) recorded in the one hectare permanent sample plot in 1997, 2003, 2009 and 2015*

The current stem number-diameter distribution (2015 inventory) shows an approximate exponential relationship when compared with an 'idealised' negative exponential curve fitted to the data (*Fig. 3*).

http://www.aloki.hu ● ISSN 1589 1623 (Print) ● ISSN 1785 0037 (Online)
DOI: http://dx.doi.org/10.15666/aeer/1605_73277344
© 2018, ALÖKI Kft., Budapest, Hungary

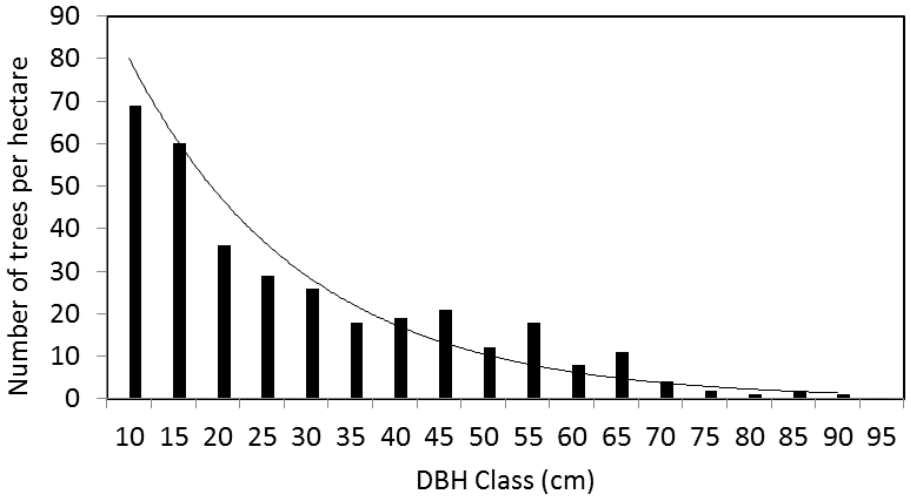

Figure 3. *Diameter distribution of canopy trees (≥8 cm DBH) measured in 2015 (fitted 'ideal' negative exponential curve* $y = 103.16e^{-0.253x}$*)*

The Lorenz curves indicate that a change in shape of the cumulative distribution of DBH and number of trees has occurred between 1997 and 2015 inventories (*Fig. 4*) with the curves becoming flatter particularly in the last two inventories of 2009 and 2015. The declining Gini coefficients (calculated from DBH) indicate that the heterogeneity of the stand has increased between 1997 and 2015 (*Table 3*). Lorenz curves derived from basal area and cumulative proportion of number of trees in the 2009 and 2015 inventories show a clear shift from one of side of the equality line (45°) to the other (*Fig. 4*) reflecting a shift in the impact of the smaller trees towards the larger trees in the basal area distribution. The movement of the Gini coefficients (calculated from basal area) towards zero highlights the greater balance between smaller and larger trees by the 2015 inventory (*Table 3*). SDI, a measure of the occupancy of the stand, shows a decline from 629 to 485 between the 1997 and 2015 inventories (*Table 3*), and reflects the overall reduction in 'site occupancy' by the canopy trees over this period.

Table 3. *Gini coefficients and Stand Density Indices (SDI) calculated from inventories of 1997, 2003, 2009 and 2015*

	Year of inventory			
	1997	**2003**	**2009**	**2015**
Gini coefficient (DBH)	0.66	0.64	0.53	0.50
Gini coefficient (basal area)	0.25	0.15	0.10	0.01
SDI (uneven-aged formula)	629	516	508	485

Proportion of shade tolerating and light demanding species in the canopy

An examination of the proportions of shade tolerating and light demanding coniferous and broadleaved species by diameter class from the 2015 inventory of the

http://www.aloki.hu ● ISSN 1589 1623 (Print) ● ISSN 1785 0037 (Online)
DOI: http://dx.doi.org/10.15666/aeer/1605_73277344
© 2018, ALÖKI Kft., Budapest, Hungary

permanent sample plot indicates that nearly 80% of species in the 10 cm diameter class are shade tolerating and dominated by conifers (*Fig. 5*).

Species diversity

The Shannon Index (SI) for the understorey species diversity was at its lowest at the start of the study in 1997 (SI = 1.43), and has steadily increased by 2015 (SI = 1.91) (*Fig. 6*). The SI of canopy tree diversity has not varied greatly over the four inventories and this is evident when split by shade tolerance and by conifers and broadleafs. The SI of the understorey species (*Fig. 7b*) indicates that the diversity of shade tolerating species has increased in the understorey while the Index for light demanding species has remained relatively stable. Diversity of coniferous species in the understorey has gradually increased since 1997, whereas diversity of broadleaved species has fluctuated slightly although remaining relatively stable in 2009 and 2015.

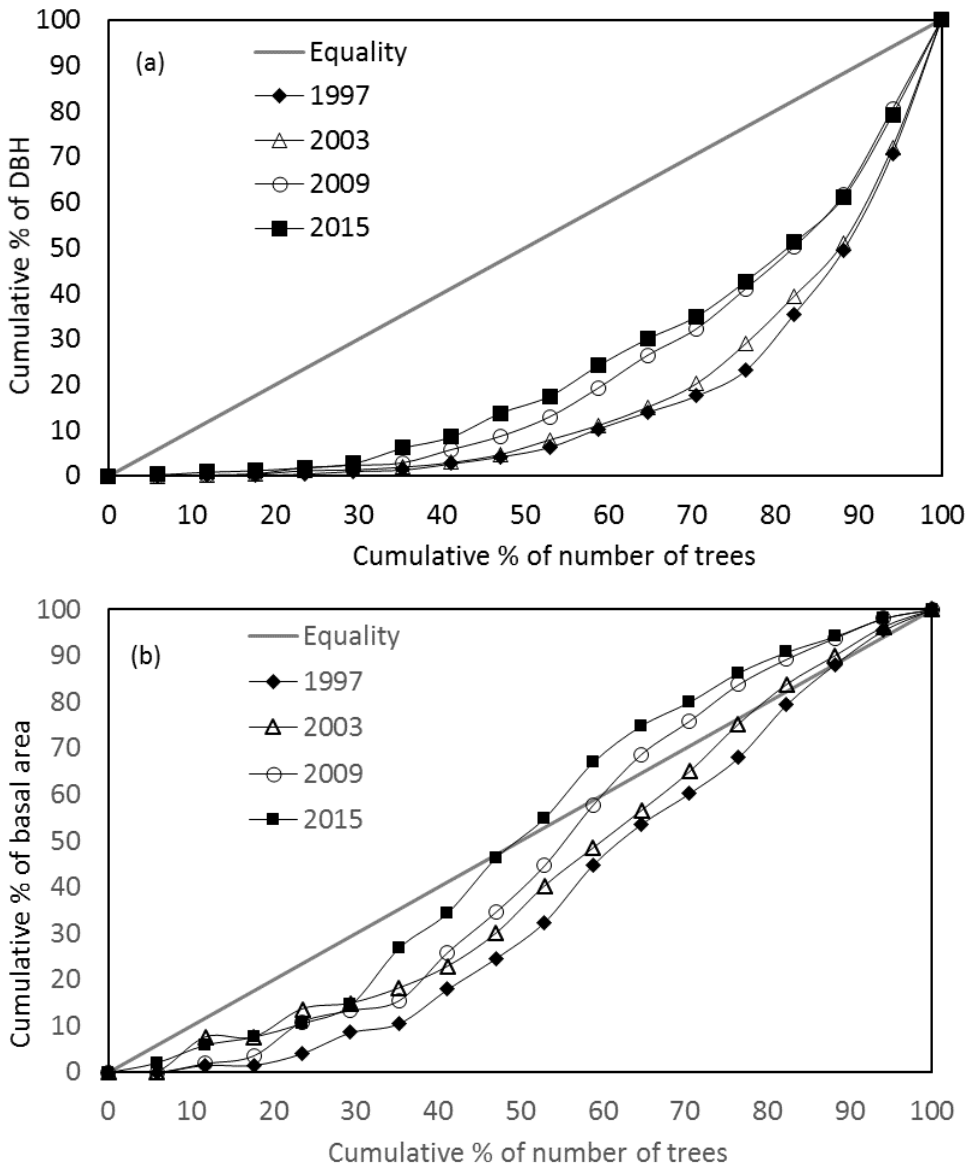

Figure 4. *Lorenz curves for cumulative % of DBH (diameter at 1.3 m)(a) and basal area (b) against number of trees measured in1997, 2003, 2009 and 2015*

http://www.aloki.hu ● ISSN 1589 1623 (Print) ● ISSN 1785 0037 (Online)
DOI: http://dx.doi.org/10.15666/aeer/1605_73277344
© 2018, ALÖKI Kft., Budapest, Hungary

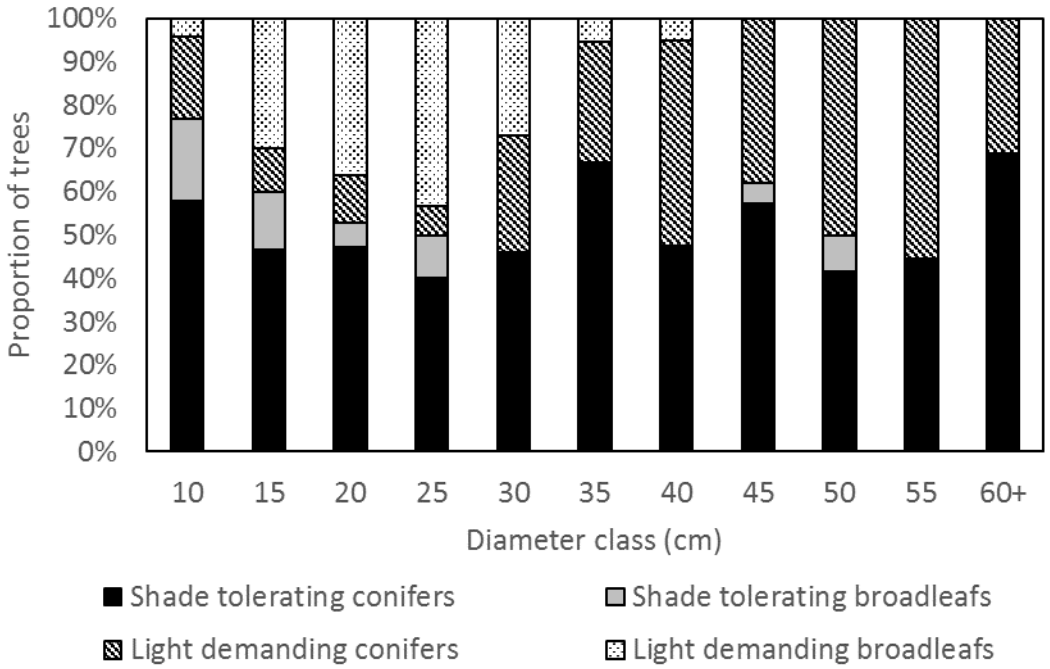

Figure 5. *Proportional distributions of coniferous and broadleaved canopy trees (DBH ≥ 8 cm) relative to their shade tolerance measured in 2015*

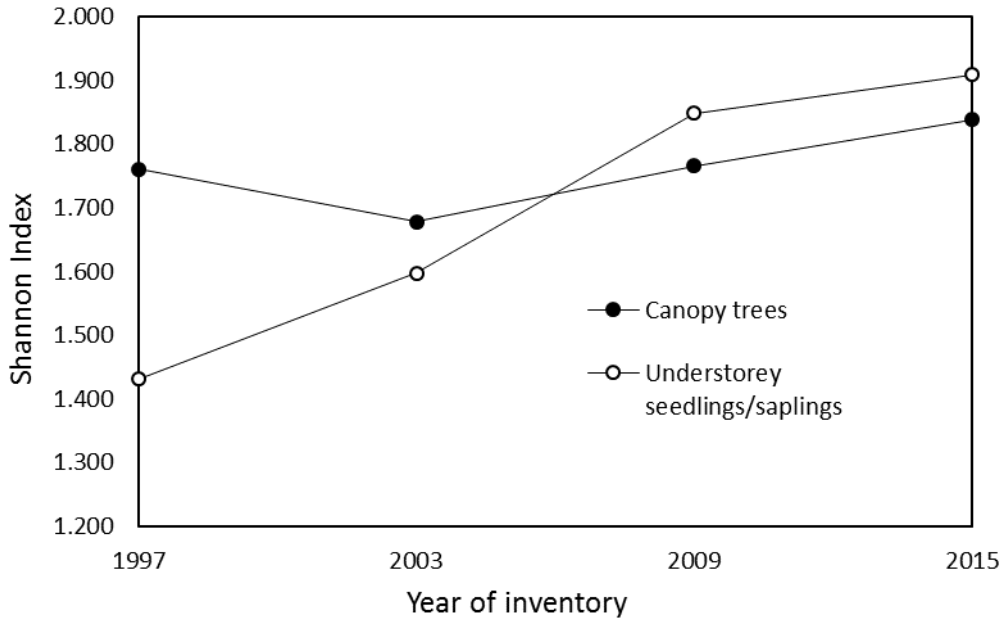

Figure 6. *Shannon Index for diversity of canopy trees and understorey seedlings and saplings measured in 1997, 2003, 2009 and 2015 (y axis truncated)*

Recruitment of shade tolerating and light demanding species

Transition periods for the shade tolerating species declined with tree size indicating faster growth as the trees become larger (*Fig. 8*). The opposite trend was observed for light demanding species with the tendency for growth of these trees to decline with

http://www.aloki.hu ● ISSN 1589 1623 (Print) ● ISSN 1785 0037 (Online)
DOI: http://dx.doi.org/10.15666/aeer/1605_73277344
© 2018, ALÖKI Kft., Budapest, Hungary

increasing diameter. The average levels of annual recruitment were considerably higher for shade tolerating species in comparison with light demanding species indicating that more trees were being recruited into each diameter class (*Table 4*).

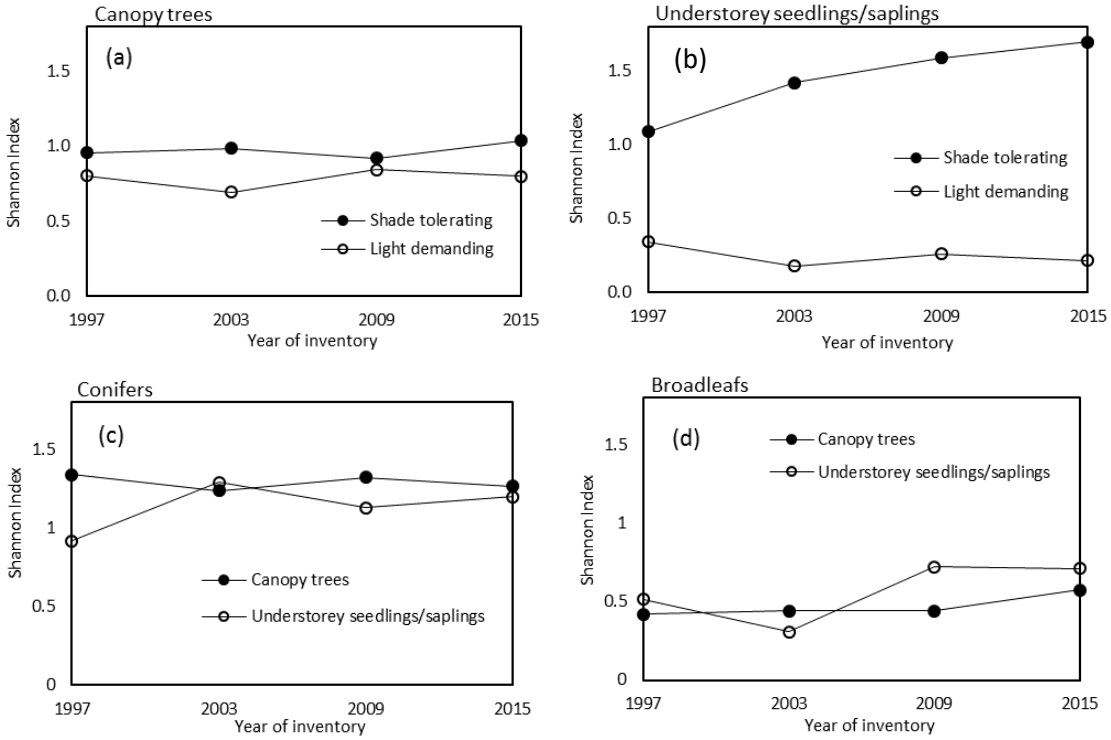

Figure 7. *Shannon Index of diversity of species by shade tolerance in the canopy (a) and understorey (b), and separated by conifers (c) and broadleafs (d) measured in 1997, 2003, 2009 and 2015*

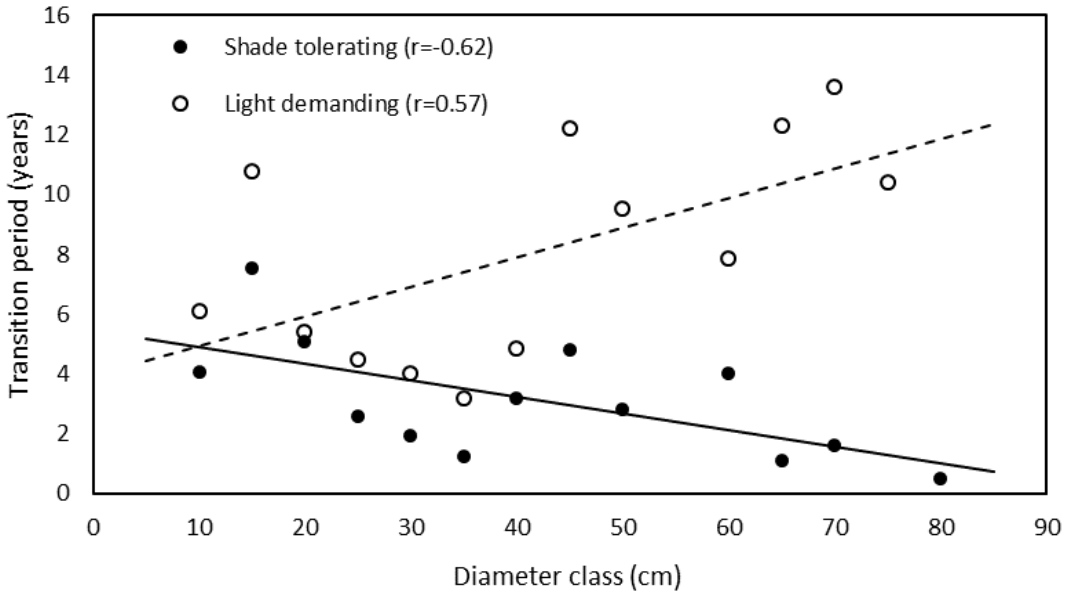

Figure 8. *Transition periods by diameter class and trend lines for shade tolerating (solid line) and light demanding (dashed line) species*

http://www.aloki.hu ● ISSN 1589 1623 (Print) ● ISSN 1785 0037 (Online)
DOI: http://dx.doi.org/10.15666/aeer/1605_73277344
© 2018, ALÖKI Kft., Budapest, Hungary

Table 4. *Annual recruitment by diameter class for light demanding and shade tolerating species in 2015*

Diameter class (cm)	Annual recruitment (trees ha^{-1} year^{-1})	
	Light demanding	Shade tolerating
10	3.770	28.448
15	2.269	5.159
20	2.037	6.809
25	0.556	10.742
30	0.875	11.897
35	1.406	12.800
40	1.546	3.125
45	0.984	1.771
50	0.944	2.857
55	0.953	-
60	0.527	1.500
65	0.221	5.909
70	0.096	3.750
75	-	-
80	-	-
85	-	0.139
Mean	1.24	7.30

Discussion and conclusion

While results indicate that the negative exponential relationship of the stem number-diameter distribution represents the all-aged, all-sized structure widely recognised in uneven-aged 'plenter' forests, Schütz (2002) pointed out that due to natural stand differentiation as a result of competition between species and individual trees, evidence of diameter variation is not on its own a valid indicator of age range or vertical structure. Using Lorenz curves based on stem diameter has highlighted a flattening of the stem number-diameter distribution with each inventory underlining the decline in the number of trees in the smaller diameter classes relative to the larger tree sizes. The associated decline in the Gini coefficients has shown that the diameter distribution has become less heterogeneous since the start of the study indicating a slight decline in the number of smaller trees. Nevertheless, the value of the Gini coefficient at the last inventory in 2015 (0.50) is in the middle of the range reported for uneven-aged boreal forests (0.44-0.57) (Lexerød and Eid, 2006) and within the range for plenter stands in Central Europe (O'Hara et al., 2007) (~ 0.4-0.7). These observations suggest that a Gini coefficient of around 0.50 is probably representative of a relatively stable uneven-aged stand structure. Significantly higher values would indicate greater inequality suggesting too many small or large trees or a diameter distribution deviating substantially from the negative exponential curve. Too small a Gini coefficient would indicate a substantial flattening of the negative exponential distribution that would result in too few trees in the smaller size classes for adequate recruitment into the higher classes and the stand may become unsustainable. When the Lorenz curves and Gini coefficients are calculated using cumulative basal area, the Lorenz curves representing the last two inventories have moved across the 'equality line' due to the greater effect of the bigger

http://www.aloki.hu ● ISSN 1589 1623 (Print) ● ISSN 1785 0037 (Online)
DOI: http://dx.doi.org/10.15666/aeer/1605_73277344
© 2018, ALÖKI Kft., Budapest, Hungary

trees within the population as a direct result of the reduction of trees in the smaller size categories following the 1997 inventory. The associated Gini coefficient has been reduced to close to zero or equality indicating a relative balance in basal areas across the size classes, a distribution that has been suggested as potentially demonstrating a sustainable or equilibrium state (Cameron, 2007).

Since SDI (stand density index) has not been used widely in uneven-aged, mixed species forests (Woodall et al., 2005), comparable data are limited. Although there has been a decline in SDI, stocking density and basal area (representing a reduction in site occupancy) over the four inventories of this study, values from the 2015 inventory are surprisingly similar to those reported by Adamic et al. (2017) for managed, uneven-aged forests in Slovenia (values for current study in parentheses): SDI = 504 (485), stocking density (trees ha^{-1}) = 345 (337) and basal area (m^2 ha^{-1}) = 29 (26), indicating that site occupancy is probably within an acceptable range to maintain a steady stream of regeneration and recruitment into the canopy.

While species diversity of the canopy trees over the study period has not changed greatly, mainly due to the relatively small proportion of the canopy removed at each harvesting intervention, species diversity in the understorey has increased and this is entirely formed of shade tolerating species. This is a widely recognised feature of uneven-aged forests where the partially shaded conditions favour shade tolerance in the understorey species. These species are also growing faster than light demanding species with higher annual recruitment in all diameter classes, and further emphasises the favourable environment for shade tolerating species. The few light demanding species that do move into the canopy are subject to competition for crown development limiting their growth potential as observed through the increasing transition periods (trees growing more slowly with increasing size) whereas transition periods are declining (trees growing faster with increasing size) with shade tolerating species. This trend in the transition periods of shade tolerating species is consistent with the development of trees in uneven-aged stands where young trees emerge from the shaded understorey environment moving up into the canopy where higher light levels and more space permit canopy expansion and greater growth (Knuchel, 1953; Assmann, 1970; Smith et al., 1997).

The gradual shift towards shade tolerating species observed at the study site is unlikely to influence current stand structure if continuous regeneration and recruitment into the lower classes balance losses through competition and harvesting. It has been suggested that the dominance of shade tolerating species in uneven-aged forests is due to their greater resilience to changing environmental conditions within the understorey, with some species of *Abies* and *Picea* capable of surviving in a quasi-stationary state for a long time until they are released by the presence of small canopy gaps (Whitmore, 1989, Schütz, 2002). This allows the density of trees in uneven-aged stands to be relatively high (Schütz and Pommerening, 2013), which further increases the competitive pressure on light demanding species. In the longer term, what is lost from the population of light demanding species is likely to be balanced by an increase in shade tolerating species leaving overall species diversity largely unchanged.

Claiming that an uneven-aged forest has reached an equilibrium condition often implies that some optimum or target structure has to be first determined and that this structure remains in a relatively stable condition over some accepted period of time. However, deciding on a timescale over which a level of constancy in structure and function of uneven-aged stands indicating a sustainable state has never been

http://www.aloki.hu ● ISSN 1589 1623 (Print) ● ISSN 1785 0037 (Online)
DOI: http://dx.doi.org/10.15666/aeer/1605_73277344
© 2018, ALÖKI Kft., Budapest, Hungary

satisfactorily resolved. It could be argued that the timescale over which the current study was carried out is too short to indicate an equilibrium condition; yet the longer the observation period becomes, the more likely that influences of climate and management direction will force change anyway (e.g. von Detten, 2011), and this raises the issue of whether it is realistic to set target equilibrium structures in the first place. O'Hara et al. (2007) found that long-term uneven-aged forests in Central Europe showed significant variation in stand structure, stocking density, species diversity and increment over periods of decades, and suggested that these forests are still evolving and that there is no single ideal structure. They stated that the resilience of uneven-aged forests may be due more to the flexibility of predominantly shade tolerant species in vertically diverse stands (Ibid.) than a rigorous approach to management with the aim of maintaining stable stand structures over time. Sterba (2004) suggested several equilibrium conditions are possible for uneven-aged stands and that there is no one ideal stand structure. Criticism of rigid definitions of optimal stand structures is not new and Henri Biolley, who was instrumental in the early development of selection systems, emphasised that uneven-aged stands should not be developed by reference to theoretical size-class distributions and instead should be managed on purely silvicultural grounds (Biolley, 1934). A flexible interpretation of the equilibrium condition would suggest that the current structure of the uneven-aged stand in this study is close to an equilibrium state even if it is accepted that a very gradual shift in species composition will inevitably take place; a view supported by Sterba (2004) who pointed out that stable diameter distributions do not necessarily show stable species distributions.

Unless there is a dramatic change in canopy cover that would influence the future passage of regeneration and recruitment into the canopy, there is no reason why the uneven-aged forest in this study under the current management regime will not continue long into the future as a relatively stable, vertically-structured, species-diverse stand. This study has also demonstrated that species from diverse geographic origins appear to be capable of forming relatively stable vertically-structured stands. This is important where foresters feel the need to diversify the species composition within their forests using a wide range of alternative species as a means of building resilience to a changing climate (Linder and Cramer, 2002; Woods, 2003; Pretzsch, 2003; Cameron, 2015). Future research will continue to focus on the gradual evolution of this forest in terms of structural diversity and tree species composition with the aim of determining whether a final stable forest structure can be achieved. The experimental site will also be used in future studies to estimate the net primary production of structurally diverse forests in terms of their potential to sequester atmospheric carbon, and how this compares with even-aged forest structures.

Acknowledgements. The authors wish to thank the staff of Tay Forest District, Forestry Commission Scotland for their support in carrying out this study.

REFERENCES

[1] Adamic, M., Diaci, J., Rozman, A., Hladnik, D. (2017): Long-term use of uneven-aged silviculture in mixed mountain Dinaric forest: a comparison of old-growth and managed stands. – Forestry 90: 279-291.
[2] Assmann, E. (1970): Principles of Forest Yield Study. – Pergamon Press, Oxford.

http://www.aloki.hu ● ISSN 1589 1623 (Print) ● ISSN 1785 0037 (Online)
DOI: http://dx.doi.org/10.15666/aeer/1605_73277344
© 2018, ALÖKI Kft., Budapest, Hungary

[3] Biolley, H. (1934): Nombres d'arbres et régimes de futaies. – Journal Forestier Suisse 4-8: 27-33.
[4] Bormann, F. H., Likens, G. E. (1994): Pattern and Process in a Forested Ecosystem: Disturbance, Development and the Steady State Based on the Hubbard Brook Ecosystem Study. – Springer-Verlag, Berlin.
[5] Cameron, A. (2007): Determining the sustainable normal irregular condition: A provisional study on a transformed, irregular mixed species stand in Scotland. – Scandinavian Journal of Forest Research 22: 13-21.
[6] Cameron, A. D. (2015): Building resilience into Sitka spruce (*Picea sitchensis* [Bong.] Carr.) forests in Scotland in response to the threat of climate change. – Forests 6: 398-415.
[7] Cameron, A. D., Hands, M. O. R. (2010): Developing a sustainable irregular structure: an evaluation of three inventories at 6-year intervals in an irregular mixed-species stand in Scotland. – Forestry 83: 469-475.
[8] Cameron, A. D., Prentice, L. (2016): Determining the sustainable irregular condition: an analysis of an irregular mixed-species selection stand in Scotland based on recurrent inventories at 6-year intervals over 24 years. – Forestry 89: 208-214.
[9] Čavlović, J., Božić, M., Boncina, A. (2006): Stand structure of an uneven-aged fir-beech forest with an irregular diameter structure: modelling the development of the Belevine forest, Croatia. – European Journal of Forest Research 125: 325-333.
[10] De Liocourt, F. (1898): De L'aménagement des sapinieres. – Bulletin de la Société forestière de Franche-Compté et des Provinces de l'Est: 396-409.
[11] Drever, C. R., Lertzman, K. P. (2003): Effects of a wide gradient of retained tree structures on understorey light in coastal Douglas fir forests. – Canadian Journal of Forest Research 33: 137–146.
[12] Drössler, L., Fahlvik, N., Wysocka, N., Hjelm, K., Kuehne, C. (2017): Natural regeneration in a multi-layered *Pinus sylvestris-Picea abies* forest after target diameter harvest and soil scarification. – Forests 8: 35-49.
[13] Gini, C. (1909): Concentration and dependency ratios (in Italian). – English translation in Rivista di Politica Economica 87 (1997): 769–789.
[14] Hale, S. E. (2004): Managing light to encourage natural regeneration in British conifer forests. – Forestry Commission Information Note 63. Forestry Commission, Edinburgh.
[15] Jenkins, M. W., Chambers, J. L. (1989): Understorey light levels in mature hardwood stands after partial overstorey removal. – Forest Ecology and Management 26: 247-256.
[16] Knuchel, H. (1953): Planning and Control in the Managed Forest (English translation by M. L. Anderson). – Oliver & Boyd, Edinburgh and London.
[17] Larsen, J. B. (1995): Ecological stability for forests and sustainable silviculture. – Forest Ecology and Management 73: 85-96.
[18] Lexerød, N. L., Eid, T. (2006): An evaluation of different diameter diversity indices based on criteria related to forest management planning. – Forest Ecology and Management 222: 17-28.
[19] Lindner, M., Cramer, W. (2002): Wälder und Forstwirtschaft Deutschlands im globalen Wandel: Eine interdisziplinäre Wirkungsanalyse (German forest sector under global change: An interdisciplinary impact assessment). – Forstwissenschaftliches Zentralblatt 121: 3–17.
[20] Lorenz, M. O. (1905): Methods of measuring the concentration of wealth. – American Statistical Association 9: 209–219.
[21] Mailly, D., Kimmins, J. P. (1997): Growth of *Pseudotsuga menziesii* and *Tsuga heterophylla* seedlings along a light gradient: resource allocation and morphological acclimation. – Canadian Journal of Botany 75: 1424–1435.
[22] Meyer, H. A. (1943): Management without rotation. – Journal of Forestry 41: 126–132.
[23] Meyer, H. A. (1952): Structure, growth and drain in balanced uneven-aged forests. – Journal of Forestry 50: 85-92.

http://www.aloki.hu ● ISSN 1589 1623 (Print) ● ISSN 1785 0037 (Online)
DOI: http://dx.doi.org/10.15666/aeer/1605_73277344
© 2018, ALÖKI Kft., Budapest, Hungary

[24] Millar, C. I., Stephenson, N. L., Stephens, S. L. (2007): Climate change and forest of the future: managing in the face of uncertainty. – Ecological Applications 17: 2145-2151.
[25] Minore, D. (1979): Comparative Autecological Characteristics of Northwestern Tree Species: A Literature Review (Gen. Tech. Rep. PNW-87). – US Department of Agriculture Forest Service, Washington, DC.
[26] Mitchell, J. E., Popovich, S. J. (1997): Effectiveness of basal area for estimating canopy cover of ponderosa pine. – Forest Ecology and Management 95: 45-51.
[27] O'Hara, K. L. (1998): Silviculture for structural diversity: a new look at multi-aged systems. – Journal of Forestry 96: 4-10.
[28] O'Hara, K. L., Gersonde, R. F. (2004): Stocking control concepts in uneven-aged silviculture. – Forestry 77: 131-143.
[29] O'Hara, K. L., Hasenauer, H., Kindermann, G. (2007): Sustainability in multi-aged stands: an analysis of long-term plenter systems. – Forestry 80: 163-181.
[30] Petritan, A. M., von Lupke, B., Petritan, I. C. (2007): Effects of shade on growth and mortality on maple (*Acer pseudoplatanus*), ask (*Fraxinus excelsior*) and beech (*Fagus sylvatica*) seedlings. – Forestry 80: 397-412.
[31] Philip, M. S. (1994): Measuring Trees and Forests. 2nd ed. – CAB International, Wallingford.
[32] Pretzsch, H. (2003): The elasticity of growth in pure and mixed stands of Norway spruce (*Picea abies* (L.) Karst.) and common beech (*Fagus sylvatica* L.). – Journal of Forest Science 49: 491–501.
[33] Ralston, R., Buongiorno, J., Fried, J. S. (2004): Potential yield, return and tree diversity of managed, uneven aged Douglas fir stands. – Silva Fennica 38: 55–70.
[34] Reineke, L. H. (1933): Perfecting a stand-density index for even-aged stands. – Journal of Agricultural Research 46: 627-638.
[35] Schütz, J. P. (1975): Dynamique et conditions d'équilibre de peuplements jardinés sur les stations de la hêtraie à sapin. – Schweizerische Zeitschrift für Forstwesen 126: 637-670.
[36] Schütz, J. P. (2001): Opportunities and strategies of transforming regular forests to irregular forests. – Forest Ecology and Management 151: 87–94.
[37] Schütz, J. P. (2002): Silvicultural tools to develop irregular and diverse forest structures. – Forestry 75: 329-337.
[38] Schütz, J. P., Pommerening, A. (2013): Can Douglas fir (*Pseudotsuga menziesii* (Mirb.) Franco) sustainably grow in complex forest structures? – Forest Ecology and Management 303: 175-183.
[39] Smith, D. M. (1962): The Practice of Silviculture. 7th edn. – Wiley, New York.
[40] Smith, D. M., Larson, B. C., Kelty, M. J., Ashton, P. M. S. (1997): The Practice of Silviculture: Applied Forest Ecology. – John Wiley and Sons, New York.
[41] Spellerberg, I. F., Fedor, P. J. (2003): A tribute to Claude Shannon (1916–2001) and a plea for more rigorous use of species richness, species diversity and the 'Shannon–Wiener' Index. – Global Ecology and Biogeography 12: 177-179.
[42] Spiecker, H. (2003): Silvicultural management in maintaining biodiversity and resistance of forests in Europe – temperate zone. Journal of Environmental Management 67: 55-65.
[43] Sterba, H. (2004): Equilibrium curves and growth models to deal with forests in transition to uneven-aged structure - application in two sample stands. – Silva Fennica 38: 413-423.
[44] Sterba, H., Monserud, R. A. (1993): The maximum density concept applied to uneven-aged mixed stands. – Forest Science 39: 432-452.
[45] Sterba, H., Ledermann, T. (2006): Inventory and modelling for forests in transition from even-aged to uneven-aged management. – Forest Ecology and Management 224: 278-285.
[46] von Detten, R. (2011): Sustainability as a guideline for strategic planning? The problem of long-term forest management in the face of uncertainty. – European Journal of Forest Research 130: 451-465.

http://www.aloki.hu ● ISSN 1589 1623 (Print) ● ISSN 1785 0037 (Online)
DOI: http://dx.doi.org/10.15666/aeer/1605_73277344
© 2018, ALÖKI Kft., Budapest, Hungary

[47] Weiner, J., Solbrig, O. T. (1984): The mean and measurement of size hierarchies in plant populations. – Oecologia 61: 334-336.
[48] Whitmore, T. C. (1989): Canopy gaps and the two major groups of forest trees. – Ecology 70: 536-538.
[49] Woodall, C. W., Miles, P. D., Vissage, J. S. (2005): Determining maximum stand density index in mixed species stands for strategic-scale stocking assessments. – Forest Ecology and Management 216: 367-377.
[50] Woodall, C. W., Miles, P. D., Vissage, J. S. (2016): Determining maximum stand density index in mixed-species stands for strategic-scale stocking assessments. – Forest Ecology and Management 216: 367-377.
[51] Woods, A. J. (2003): Species diversity and forest health in northwest British Columbia. – Forest Chronicle 79: 892–897.
[52] Yang, T. R., Lam, T. Y., Kershaw, J. A. (2018): Developing relative stand density index for structurally complex mixed species cypress and pine forests. – Forest Ecology and Management 409: 425-433.
[53] Zeide, B. (2005): How to measure stand density. – Trees 19: 1-14.

http://www.aloki.hu ● ISSN 1589 1623 (Print) ● ISSN 1785 0037 (Online)
DOI: http://dx.doi.org/10.15666/aeer/1605_73277344
© 2018, ALÖKI Kft., Budapest, Hungary